World Journal of Gastroenterology®

Volume 13 Number 1
January 7, 2007

National Journal Award
2005

The WJG Press

The WJG Press, Apartment 1066 Yishou Garden, 58 North Langxinzhuang Road, PO Box 2345, Beijing 100023, China
Telephone: +86-10-85381892
Fax: +86-10-85381893
E-mail: wjg@wjgnet.com
http: //www.wjgnet.com

ISSN 1007-9327 CN 14-1219/R Local Post Offices Code No. 82-261

World Journal of Gastroenterology www.wjgnet.com Volume 13 Number 1 Jan 07 2007

ISSN 1007-9327
CN 14-1219/R

World Journal of Gastroenterology®

Indexed and Abstracted in:

Current Contents®/Clinical Medicine, Science Citation Index Expanded (also known as SciSearch®) and Journal Citation Reports/Science Edition, *Index Medicus*, MEDLINE and PubMed, Chemical Abstracts, EMBASE/Excerpta Medica, Abstracts Journals, *Nature Clinical Practice Gastroenterology and Hepatology*, CAB Abstracts and Global Health.
ISI JCR 2003-2000 IF: 3.318, 2.532, 1.445 and 0.993.

Volume 13 Number 1
January 7, 2007

World J Gastroenterol
2007 January 7; 13(1): 1-164
Online Submissions
www.wjgnet.com/wjg/index.jsp
www.wjgnet.com
Printed on Acid-free Paper

A Weekly Journal of Gastroenterology and Hepatology

World Journal of Gastroenterology®

Editorial Board

2007-2009

Published by The WJG Press, PO Box 2345, Beijing 100023, China
Fax: +86-10-85381893 E-mail: wjg@wjgnet.com http://www.wjgnet.com

The *World Journal of Gastroenterology* Editorial Board consists of 903 members, representing a team of worldwide experts in gastroenterology and hepatology. They are from 54 countries, including Albania (1), Argentina (2), Australia (26), Austria (9), Belarus (1), Belgium (13), Brazil (1), Bulgaria (1), Canada (19), Chile (1), China (49), Croatia (2), Czech(1), Denmark (5), Egypt (3), Finland (4), France (34), Germany (96), Greece (3), Hungary(2), Iceland (1), India (6), Iran (2), Ireland (4), Israel (6), Italy (71), Japan (161), Lebanon(3), Lithuania (1), Macedonia(1), Malaysia (3), Mexico (3), Monaco (1), Netherlands (20), New Zealand (1), Nigeria(1), Norway(3), Pakistan(1), Poland (6), Portugal (2), Russia (3), Serbia (1), Singapore (3), Slovakia (1), Slovenia (1), South Africa (1), South Korea (13), Spain (29), Sweden (9), Switzerland (11), Turkey (7), United Arab Emirates(1), United Kingdom (61), and United States (192).

Louis Libbrecht, *Leuven*
Etienne M Sokal, *Brussels*
Gert A Van Assche, *Leuven*
Yvan Vandenplas, *Brussels*
Eddie Wisse, *Keerbergen*

Brazil
Heitor Rosa, *Goiania*

Bulgaria
Zahariy Krastev, *Sofia*

Canada
Fernando Alvarez, *Québec*
Olivier Barbier, *Québec*
Matthew Bjerknes, *Toronto*
Frank J Burczynski, *Winnipeg*
Michael F Byrne, *Vancouver*
Wang-Xue Chen, *Ottawa*
Hugh J Freeman, *Vancouver*
Chantal Guillemette, *Québec*
Samuel S Lee, *Calgary*
Gary A Levy, *Toronto*
John K Marshall, *Ontario*
Donna-Marie McCafferty, *Calgary*
Thomas I Michalak, *St. John's*
Gerald Y Minuk, *Manitoba*
Morris Sherman, *Toronto*
Alan BR Thomson, *Edmonton*
EF Verdu, *Ontario*
John L Wallace, *Calgary*
Eric M Yoshida, *Vancouver*

Chile
Silvana Zanlungo, *Santiago*

China
Henry LY Chan, *Hongkong*
Xiao-Ping Chen, *Wuhan*
Zong-Jie Cui, *Beijing*
Da-Jun Deng, *Beijing*
Sheung-Tat Fan, *Hong Kong*
Jin Gu, *Beijing*
De-Wu Han, *Taiyuan*
Ming-Liang He, *Hong Kong*
Wayne HC Hu, *Hong Kong*
Chee-Kin Hui, *Hong Kong*
Ching Lung Lai, *Hong Kong*
Kam Chuen Lai, *Hong Kong*
James YW Lau, *Hong Kong*
Yuk Tong Lee, *Hong Kong*
Suet Yi Leung, *Hong Kong*
Wai-Keung Leung, *Hong Kong*
Jing-Yun Ma, *Beijing*
Lun-Xiu Qin, *Shanghai*
Qin Su, *Beijing*
Wai-Man Wong, *Hong Kong*
Hong Xiao, *Beijing*
Dong-Liang Yang, *Wuhan*
Winnie Yeo, *Hong Kong*
Yuan Yuan, *Shenyang*
Man-Fung Yuen, *Hong Kong*
Jian-Zhong Zhang, *Beijing*
Xin-Xin Zhang, *Shanghai*
Shu Zheng, *Hangzhou*

Croatia
Tamara Cacev, *Zagreb*
Marko Duvnjak, *Zagreb*

Czech
Milan Jirsa, *Praha*

Denmark
Peter Bytzer, *Copenhagen*
Hans Gregersen, *Aalborg*
Jens H Henriksen, *Hvidovre*
Fin Stolze Larsen, *Copenhagen*
SØren MØller, *Hvidovre*

Egypt
Abdel-Rahman El-Zayadi, *Giza*
Sanaa Moharram Kamal, *Cairo*
Ayman Yosry, *Cairo*

Finland
Irma Elisabet Jarvela, *Helsinki*
Katri Maria Kaukinen, *Tampere*
Minna Nyström, *Helsinki*
Pentti Sipponen, *Espoo*

France
Bettaieb Ali, *Dijon*
Corlu Anne, *Rennes*
Denis Ardid, *Clermont-Ferrand*
Charles Paul Balabaud, *Bordeaux*
Jacques Belghiti, *Clichy*
Pierre Brissot, *Rennes*
Patrice Philippe Cacoub, *Paris*
Franck Carbonnel, *Besancon*
Laurent Castera, *Pessac*
Bruno Clément, *Rennes*
Jacques Cosnes, *Paris*
Thomas Decaens, *Cedex*
Francoise Lunel Fabiani, *Angers*
Gérard Feldmann, *Paris*
Jean Fioramonti, *Toulouse*
Catherine Guettier, *Villejuif*
Chantal Housset, *Paris*
Juan Lucio Iovanna, *Marseille*
Rene Lambert, *Lyon*
Philippe Mathurin, *Lille*
Tamara Matysiak–Budnik, *Paris*
Francis Mégraud, *Bordeaux*
Richard Moreau, *Clichy*
Thierry Piche, *Nice*
Raoul Poupon, *Paris*
Jean Rosenbaum, *Bordeaux*
Jose Sahel, *Marseille*
Jean-Philippe Salier, *Rouen*
Jean-Yves Scoazec, *Lyon*
Khalid Ahnini Tazi, *Clichy*
Baumert F Thomas, *Strasbourg*
MC Vozenin-brotons, *Villejuif*
Jean-Pierre Henri Zarski, *Grenoble*
Jessica Zucman-Rossi, *Paris*

Germany
HD Allescher, *Garmisch-Partenkirchen*
Martin Anlauf, *Kiel*
Rudolf Arnold, *Marburg*
Max G Bachem, *Ulm*
Thomas F Baumert, *Freiburg*
Daniel C Baumgart, *Berlin*
Hubert Blum, *Freiburg*
Thomas Bock, *Tuebingen*
Katja Breitkopf, *Mannheim*
Dunja Bruder, *Braunschweig*
Markus W Büchler, *Heidelberg*
Christa Buechler, *Regensburg*
Reinhard Buettner, *Bonn*
Elke Cario, *Essen*
Uta Dahmen, *Essen*
CF Dietrich, *Bad Mergentheim*
Rainer Josef Duchmann, *Berlin*
Paul Enck, *Tuebingen*
Fred Fändrich, *Kiel*
Ulrich Robert Fölsch, *Kiel*
Helmut Friess, *Heidelberg*
Peter R Galle, *Mainz*
Nikolaus Gassler, *Aachen*
Andreas Geier, *Aachen*
Dieter Glebe, *Giessen*
Burkhard Göke, *Munich*
Florian Graeple, *Tuebingen*
Axel M Gressner, *Aachen*
Veit Gülberg, *Munich*
Rainer Haas, *Munich*
Eckhart Georg Hahn, *Erlangen*
Stephan Hellmig, *Kiel*
Martin Hennenberg, *Bonn*
Johannes Herkel, *Hamburg*
Klaus Herrlinger, *Stuttgart*
Eberhard Hildt, *Berlin*
Joerg C Hoffmann, *Berlin*
Ferdinand Hofstaedter, *Regensburg*
Werner Hohenberger, *Erlangen*
RG Jakobs, *Ludwigshafen*
Jutta Keller, *Hamburg*
Andrej Khandoga, *Munich*
Sibylle Koletzko, *München*
Stefan Kubicka, *Hannover*
Joachim Labenz, *Siegen*
Frank Lammert, *Bonn*
Thomas Langmann, *Regensburg*
Christian Liedtke, *Aachen*
Matthias Löhr, *Mannheim*
Christian Maaser, *Muenster*
Ahmed Madisch, *Dresden*
Michael Peter Manns, *Hannover*
Stephan Miehlke, *Dresden*
Sabine Mihm, *Göttingen*
Silvio Nadalin, *Essen*
Markus F Neurath, *Mainz*
Johann Ockenga, *Berlin*
Florian Obermeier, *Regensburg*
Gustav Paumgartner, *Munich*
Ulrich Ks Peitz, *Magdeburg*
Markus Reiser, *Bochum*
Steffen Rickes, *Magdeburg*
Gerhard Rogler, *Regensburg*
Tilman Sauerbruch, *Bonn*
Dieter Saur, *Munich*
Andreas Schäffler, *Regensburg*
Hans Scherubl, *Berlin*
Joerg Schirra, *Munich*
Roland M Schmid, *München*
AG Schreyer, *Regensburg*
Tobias Schroeder, *Essen*
Hans Seifert, *Oldenburg*
Manfred V Singer, *Mannheim*
Gisela Sparmann, *Rostock*
Jurgen M Stein, *Frankfurt*
Ulrike Susanne Stein, *Berlin*
Manfred Stolte, *Bayreuth*
Christian P Strassburg, *Hannover*
WR Stremmel, *Heidelberg*
Harald F Teutsch, *Ulm*
Robert Thimme, *Freiburg*
HL Tillmann, *Leipzig*
Tung-Yu Tsui, *Regensburg*
Axel Ulsenheimer, *Munich*
Patrick Veit, *Essen*
Fritz E von Veizsacker, *Berlin*
Claudia Veltkamp, *Heidelberg*
Siegfried Wagner, *Deggendorf*
Henning Walczak, *Heidelberg*
Fritz von Weizsacker, *Berlin*
Jens Werner, *Heidelberg*
Bertram Wiedenmann, *Berlin*
Reiner Wiest, *Regensburg*
Stefan Wirth, *Wuppertal*
Stefan JP Zeuzem, *Homburg*

Greece
Elias A Kouroumalis, *Heraklion*
Ioannis E Koutroubakis, *Heraklion*
Spiros Sgouros, *Athens*

Hungary

Peter Laszlo Lakatos, *Budapest*
Zsuzsa Szondy, *Debrecen*

Iceland

H Gudjonsson, *Reykjavik*

India

KA Balasubramanian, *Vellore*
Sujit K Bhattacharya, *Kolkata*
Yogesh K Chawla, *Chandigarh*
Radha K Dhiman, *Chandigarh*
Sri Prakash Misra, *Allahabad*
ND Reddy, *Hyderabad*

Iran

Reza Malekzadeh, *Tehran*
Seyed Alireza Taghavi, *Shiraz*

Ireland

Billy Bourke, *Dublin*
Ronan A Cahill, *Cork*
Anthony P Moran, *Galway*

Israel

Simon Bar-Meir, *Hashomer*
Abraham Rami Eliakim, *Haifa*
Yaron Ilan, *Jerusalem*
Avidan U Neumann, *Ramat-Gan*
Yaron Niv, *Pardesia*
Ran Oren, *Tel Aviv*

Italy

Giovanni Addolorato, *Roma*
Luigi E Adinolfi, *Naples*
Domenico Alvaro, *Rome*
V Annese, *San Giovanni Rotond*
Adolfo Francesco Attili, *Roma*
Giovanni Barbara, *Bologna*
Gabrio Bassotti, *Perugia*
Pier Maria Battezzati, *Milan*
Stefano Bellentani, *Carpi*
Luca Saverioq Belli, *Milan*
Antomio Benedetti, *Ancona*
Mauro Bernardi, *Bologna*
Livia Biancone, *Rome*
Luigi Bonavina, *Milano*
Flavia Bortolotti, *Padova*
Giuseppe Brisinda, *Rome*
Giovanni Cammarota, *Roma*
Antonino Cavallari, *Bologna*
Giuseppe Chiarioni, *Valeggio*
Michele Cicala, *Rome*
Amedeo Columbano, *Cagliari*
Massimo Conio, *Sanremo*
Dario Conte, *Milano*
Gino Roberto Corazza, *Pavia*
Francesco Costa, *Pisa*
Antonio Craxi, *Palermo*
Roberto De Giorgio, *Bologna*
Giovanni D De Palma, *Naples*
Fabio Farinati, *Padua*
Francesco Feo, *Sassari*
Stefano Fiorucci, *Perugia*
Andrea Galli, *Firenze*
Valeria Ghisett, *Turin*
Gianluigi Giannelli, *Bari*
Edoardo G Giannini, *Genoa*
Paolo Gionchetti, *Bologna*
Mario Guslandi, *Milano*
Pietro Invernizzi, *Milan*
Giacomo Laffi, *Firenze*
Giovanni Maconi, *Milan*
Lucia Malaguarnera, *Catania*
ED Mangoni, *Napoli*
Giulio Marchesini, *Bologna*
Fabio Marra, *Florence*
Marco Marzioni, *Ancona*
Giuseppe Montalto, *Palermo*
Giovanni Monteleone, *Rome*
Giovanni Musso, *Torino*
Gerardo Nardone, *Napoli*
Valerio Nobili, *Rome*
Luisi Pagliaro, *Palermo*
Fabrizio R Parente, *Milan*
F Perri, *San Giovanni Rotondo*
Raffaele Pezzilli, *Bologna*
A Pilotto, *San Giovanni Rotondo*
Mario Pirisi, *Novara*
Paolo Del Poggio, *Treviglio*
Gabriele Bianchi Porro, *Milano*
Piero Portincasa, *Bari*
Bernardino Rampone, *Siena*
Claudio Romano, *Messina*
Marco Romano, *Napoli*
Gerardo Rosati, *Potenza*
Mario Del Tacca, *Pisa*
Pier Alberto Testoni, *Milan*
Enrico Roda, *Bologna*
Domenico Sansonno, *Bari*
Vincenzo Savarino, *Genova*
Roberto Testa, *Genoa*
Dino Vaira, *Bologna*

Japan

Kyoichi Adachi, *Izumo*
Yasushi Adachi, *Sapporo*
Taiji Akamatsu, *Matsumoto*
Sk Md Fazle Akbar, *Ehime*
Takafumi Ando, *Nagoya*
Akira Andoh, *Otsu*
Taku Aoki, *Tokyo*
Masahiro Arai, *Tokyo*
Tetsuo Arakawa, *Osaka*
Yasuji Arase, *Tokyo*
Masahiro Asaka, *Sapporo*
Hitoshi Asakura, *Tokyo*
Takeshi Azuma, *Fukui*
Yoichi Chida, *Fukuoka*
Takahiro Fujimori, *Tochigi*
Jiro Fujimoto, *Hyogo*
Kazuma Fujimoto, *Saga*
Mitsuhiro Fujishiro, *Tokyo*
Yoshihide Fujiyama, *Otsu*
Hirokazu Fukui, *Tochigi*
Hiroyuki Hanai, *Hamamatsu*
Kazuhiro Hanazaki, *Nagano*
Naohiko Harada, *Fukuoka*
Makoto Hashizume, *Fukuoka*
Tetsuo Hayakawa, *Nagoya*
Kazuhide Higuchi, *Osaka*
Keisuke Hino, *Ube*
Keiji Hirata, *Kitakyushu*
Yuji Iimuro, *Nishinomiya*
Kenji Ikeda, *Tokyo*
Fumio Imazeki, *Chiba*
Yutaka Inagaki, *Kanagawa*
Yasuhiro Inokuchi, *Yokohama*
Haruhiro Inoue, *Yokohama*
Masayasu Inoue, *Osaka*
Akio Inui, *Kagoshima*
Hiromi Ishibashi, *Nagasaki*
Shunji Ishihara, *Izumo*
Toru Ishikawa, *Niigata*
Kei Ito, *Sendai*
Masayoshi Ito, *Tokyo*
Hiroaki Itoh, *Akita*
Ryuichi Iwakiri, *Saga*
Yoshiaki Iwasaki, *Okayama*
Hiroshi Kaneko, *Aichi-Gun*
Shuichi Kaneko, *Kanazawa*
Takashi Kanematsu, *Nagasaki*
Mitsuo Katano, *Fukuoka*
Junji Kato, *Sapporo*
Mototsugu Kato, *Sapporo*
Shinzo Kato, *Tokyo*
Norifumi Kawada, *Osaka*
Sunao Kawano, *Osaka*
Mitsuhiro Kida, *Kanagawa*
Yoshikazu Kinoshita, *Izumo*
Tsuneo Kitamura, *Chiba*
Seigo Kitano, *Oita*
Kazuhiko Koike, *Tokyo*
Norihiro Kokudo, *Tokyo*
Satoshi Kondo, *Sapporo*
Shoji Kubo, *Osaka*
Shigeki Kuriyama, *Kagawa*
Masato Kusunoki, *Tsu Mie*
Katsunori Iijima, *Sendai*
Shin Maeda, *Tokyo*
Masatoshi Makuuchi, *Tokyo*
Osamu Matsui, *Kanazawa*
Yasuhiro Matsumura, *Chiba*
Yasushi Matsuzaki, *Tsukuba*
Kiyoshi Migita, *Omura*
Tetsuya Mine, *Kanagawa*
Hiroto Miwa, *Hyogo*
Masashi Mizokami, *Nagoya*
Yoshiaki Mizuguchi, *Tokyo*
Motowo Mizuno, *Hiroshima*
Morito Monden, *Suita*
Hisataka S Moriwaki, *Gifu*
Yasuaki Motomura, *Iizuka*
Yoshiharu Motoo, *Kanazawa*
Kazunari Murakami, *Oita*
Kunihiko Murase, *Tusima*
Masahito Nagaki, *Gifu*
Masaki Nagaya, *Kawasaki*
Yuji Naito, *Kyoto*
Hisato Nakajima, *Tokyo*
Hiroki Nakamura, *Yamaguchi*
Shotaro Nakamura, *Fukuoka*
Mikio Nishioka, *Niihama*
Shuji Nomoto, *Nagoya*
Susumu Ohmada, *Maebashi*
Masayuki Ohta, *Oita*
Tetsuo Ohta, *Kanazawa*
Kazuichi Okazaki, *Osaka*
Katsuhisa Omagari, *Nagasaki*
Saburo Onishi, *Nankoku*
Morikazu Onji, *Ehime*
Satoshi Osawa, *Hamamatsu*
Masanobu Oshima, *Kanazawa*
Hiromitsu Saisho, *Chiba*
Hidetsugu Saito, *Tokyo*
Yutaka Saito, *Tokyo*
Isao Sakaida, *Yamaguchi*
Michiie Sakamoto, *Tokyo*
Yasushi Sano, *Chiba*
Hiroki Sasaki, *Tokyo*
Iwao Sasaki, *Sendai*
Motoko Sasaki, *Kanazawa*
Chifumi Sato, *Tokyo*
Shuichi Seki, *Osaka*
Hiroshi Shimada, *Yokohama*
Mitsuo Shimada, *Tokushima*
Tomohiko Shimatan, *Hiroshima*
Hiroaki Shimizu, *Chiba*
Ichiro Shimizu, *Tokushima*
Yukihiro Shimizu, *Kyoto*
Shinji Shimoda, *Fukuoka*
Tooru Shimosegawa, *Sendai*
Tadashi Shimoyama, *Hirosaki*
Ken Shirabe, *Iizuka*
Yoshio Shirai, *Niigata*
Katsuya Shiraki, *Mie*
Yasushi Shiratori, *Okayama*
Masayuki Sho, *Nara*
Yasuhiko Sugawara, *Tokyo*
Hidekazu Suzuki, *Tokyo*

Minoru Tada, *Tokyo*
Tadatoshi Takayama, *Tokyo*
Tadashi Takeda, *Osaka*
Koji Takeuchi, *Kyoto*
Kiichi Tamada, *Tochigi*
Akira Tanaka, *Kyoto*
Eiji Tanaka, *Matsumoto*
Noriaki Tanaka, *Okayama*
Shinji Tanaka, *Hiroshima*
Wei Tang, *Tokyo*
Kyuichi Tanikawa, *Kurume*
Akira Terano, *Shimotsugagun*
Hitoshi Togash, *Yamagata*
Kazunari Tominaga, *Osaka*
Takuji Torimura, *Fukuoka*
Minoru Toyota, *Sapporo*
Akihito Tsubota, *Chiba*
Shingo Tsuji, *Osaka*
Takato Ueno, *Kurume*
Shinichi Wada, *Tochigi*
Hiroyuki Watanabe, *Kanazawa*
Toshio Watanabe, *Osaka*
Yuji Watanabe, *Ehime*
Chun-Yang Wen, *Nagasaki*
Koji Yamaguchi, *Fukuoka*
Takayuki Yamamoto, *Yokkaichi*
Takashi Yao, *Fukuoka*
Masashi Yoneda, *Tochigi*
Hiroshi Yoshida, *Tokyo*
Masashi Yoshida, *Tokyo*
Norimasa Yoshida, *Kyoto*
Kentaro Yoshika, *Toyoake*
Masahide Yoshikawa, *Kashihara*

Lebanon
Bassam N Abboud, *Beirut*
Ala I Sharara, *Beirut*
Joseph Daoud Boujaoude, *Beirut*

Lithuania
Limas Kupcinskas, *Kaunas*

Macedonia
Vladimir Cirko Serafimoski, *Skopje*

Malaysia
Andrew Seng Boon Chua, *Ipoh*
Khean-Lee Goh, *Kuala Lumpur*
Jayaram Menon, *Sabah*

Mexico
Garcia-Compean Diego, *Monterrey*
Saúl Villa-Treviño, *México*
JK Yamamoto-Furusho, *México*

Monaco
Patrick Rampal, *Monaco*

Netherlands
Ulrich Beuers, *Amsterdam*
Gerd Bouma, *Amsterdam*
Lee Bouwman, *Leiden*
Rick Greupink, *Groningen*
Janine K Kruit, *Groningen*
Ernst Johan Kuipers, *Rotterdam*
Ton Lisman, *Utrecht*
Yi Liu, *Amsterdam*
Servaas Morré, *Amsterdam*
Chris JJ Mulder, *Amsterdam*
Michael Müller, *Wageningen*
Amado Salvador Peña, *Amsterdam*
Robert J Porte, *Groningen*
Ingrid B Renes, *Rotterdam*
Andreas Smout, *Utrecht*
RW Stockbrugger, *Maastricht*
Luc JW van der Laan, *Rotterdam*
Karel van Erpecum, *Utrecht*
GP VanBerge-Henegouwen, *Utrecht*

New Zealand
Ian David Wallace, *Auckland*

Nigeria
Samuel Babafemi Olaleye, *Ibadan*

Norway
Trond Berg, *Oslo*
Tom Hemming Karlsen, *Oslo*
Helge Lyder Waldum, *Trondheim*

Pakistan
Muhammad S Khokhar, *Lahore*

Poland
Tomasz Brzozowski, *Cracow*
Robert Flisiak, *Bialystok*
Hanna Gregorek, *Warsaw*
DM Lebensztejn, *Bialystok*
Wojciech G Polak, *Wroclaw*
Marek Hartleb, *Katowice*

Portugal
MP Cecília, *Lisbon*
Miguel Carneiro De Moura, *Lisbon*

Russia
Vladimir T Ivashkin, *Moscow*
Leonid Lazebnik, *Moscow*
Vasiliy I Reshetnyak, *Moscow*

Serbia
DM Jovanovic, *Sremska Kamenica*

Singapore
Bow Ho, *Kent Ridge*
Khek-Yu Ho, *Singapore*
Francis Seow-Choen, *Singapore*

Slovakia
Anton Vavrecka, *Bratislava*

Slovenia
Sasa Markovic, *Ljubljana*

South Africa
Michael C Kew, *Parktown*

South Korea
Byung Ihn Choi, *Seoul*
Ho Soon Choi, *Seoul*
M Yeo, *Suwon*
Sun Pyo Hong, *Gyeonggi-do*
Jae J Kim, *Seoul*
Jin-Hong Kim, *Suwon*
Myung-Hwan Kim, *Seoul*
Chang Hong Lee, *Seoul*
Jong Kyun Lee, *Seoul*
Eun-Yi Moon, *Seoul*
Jae-Gahb Park, *Seoul*
Dong Wan Seo, *Seoul*
Dong jin Suh, *Seoul*

Spain
Juan G Abraldes, *Barcelona*
Agustin Albillos, *Madrid*
Raul J Andrade, *Málaga*
Luis Aparisi, *Valencia*
Fernando Azpiroz, *Barcelona*
Ramon Bataller, *Barcelona*
Josep M Bordas, *Barcelona*
Xavier Calvet, *Sabadell*
Andres Cardenas, *Barcelona*
Vicente Carreño, *Madrid*
Jose Castellote, *Barcelona*
Antoni Castells, *Barcelona*
Vicente Felipo, *Valencia*
Juan C Garcia-Pagán, *Barcelona*
Jaime Bosch Genover, *Barcelona*
Jaime Guardia, *Barcelona*
Angel Lanas, *Zaragoza*
María Isabel Torres López, *Jaén*
José M Mato, *Derio*
Juan F Medina, *Pamplona*
MA Muñoz-Navas, *Pamplona*
Julian Panes, *Barcelona*
Miguel Minguez Perez, *Valencia*
Miguel Perez-Mateo, *Alicante*
Josep M Pique, *Barcelona*
Jesus M Prieto, *Pamplona*
Sabino Riestra, *Pola De Siero*
Luis Rodrigo, *Oviedo*
Manuel Romero-Gómez, *Sevilla*

Sweden
Curt Einarsson, *Huddinge*
Ulf Hindorf, *Lund*
Hanns-Ulrich Marschall, *Stockholm*
Lars Christer Olbe, *Molndal*
Matti Sallberg, *Stockholm*
Magnus Simrén, *Göteborg*
Xiao-Feng Sun, *Linköping*
Ervin Tóth, *Malmö*
Weimin Ye, *Stockholm*

Switzerland
Chrish Beglinger, *Basel*
Pierre A Clavien, Zurich
Jean-Francois Dufour, *Bern*
Franco Fortunato, *Zürich*
Jean Louis Frossard, *Geneva*
Gerd A Kullak-Ublick, *Zurich*
Pierre Michetti, *Lausanne*
Francesco Negro, *Genève*
Bruno Stieger, *Zurich*
Arthur Zimmermann, *Berne*
Radu Tutuian, *Zurich*

Turkey
Yusuf Bayraktar, *Ankara*
Figen Gurakan, *Ankara*
Aydin Karabacakoglu, *Konya*
Serdar Karakose, *Konya*
Hizir Kurtel, *Istanbu*
Osman Cavit Ozdogan, *Istanbul*
Cihan Yurdaydin, *Ankara*

United Arab Emirates
Sherif M Karam, *Al-Ain*

United Kingdom
David Adams, *Birmingham*
NK Ahluwalia, *Stockport*
CG Antoniades, *London*
Anthony TR Axon, *Leeds*
Qasim Aziz, *Manchester*
Nicholas M Barnes, *Birmingham*
Jim D Bell, *London*
Mairi Brittan, *London*
Simon Scott Campbell, *Manchester*
Simon R Carding, *Leeds*
Paul Jonathan Ciclitira, *London*
Tatjana Crnogorac-Jurcevic, *London*
Amar Paul Dhillon, *London*
Emad M El-Omar, *Aberdeen*
Annette Fristscher-Ravens, *London*
Elizabeth Furrie, *Dundee*

Daniel Richard Gaya, *Edinburgh*
Subrata Ghosh, *London*
William Greenhalf, *Liverpool*
Indra Neil Guha, *Southampton*
Peter Clive Hayes, *Edinburgh*
Gwo-Tzer Ho, *Edinburgh*
Anthony R Hobson, *Salford*
Stefan G Hübscher, *Birmingham*
Robin Hughes, *London*
Pali Hungin, *Stockton*
David Paul Hurlstone, *Sheffield*
Janusz AZ Jankowski, *Oxford*
Brian T Johnston, *Belfast*
David EJ Jones, *Newcastle*
Michael A Kamm, *Harrow*
Peter Karayiannis, *London*
Laurens Kruidenier, *Harlow*
Patricia F Lalor, *Birmingham*
Hong-Xiang Liu, *Cambridge*
K E L McColl, *Glasgow*
Stuart AC McDonald, *London*
Dermot Patrick Mcgovern, *Oxford*
Giorgina Mieli-Vergani, *London*
Nikolai V Naoumov, *London*
John P Neoptolemos, *Liverpool*
James Neuberger, *Birmingham*
Mark S Pearce, *Newcastle Upon Tyne*
D Mark Pritchard, *Liverpool*
Stephen E Roberts, *Swansea*
Marco Senzolo, *Padova*
Soraya Shirazi-Beechey, *Liverpool*
Robert Sutton, *Liverpool*
Simon D Taylor-Robinson, *London*
Ulrich Thalheimer, *London*
Nick Paul Thompson, *Newcastle*
David Tosh, *Bath*
Frank Ivor Tovey, *London*
Chris Tselepis, *Birmingham*
Diego Vergani, *London*
Geoffrey Warhurst, *Salford*
Peter James Whorwell, *Manchester*
Karen Leslie Wright, *Bath*
Min Zhao, *Foresterhill*

United States

Gary A Abrams, *Birmingham*
Golo Ahlenstiel, *Bethesda*
James E Allison, *Oakland*
B S Anand, *Houston*
Frank A Anania, *Atlanta*
Gavin Edward Arteel, *Louisville*
Jasmohan Singh Bajaj, *Milwaukee*
Jamie S Barkin, *Miami Beach*
Kim Elaine Barrett, *San Diego*
Marc Basson, *Detroit*
Nancy Baxter, *Minneapolis*
Timothy R Billiar, *Pittsburgh*
Edmund J Bini, *New York*
Jennifer D Black, *Buffalo*
Herbert L Bonkovsky, *Farmington*
Andrea D Branch, *New York*
Robert S Bresalier, *Houston*
Alan L Buchman, *Chicago*
Alan Cahill, *Philadelphia*
John M Carethers, *San Diego*
David L Carr-Locke, *Boston*
Ravi S Chari, *Nashville*
Jiande Chen, *Galveston*
Xian-Ming Chen, *Rochester*
Ramsey Chi-man Cheung, *Palo Alto*
William D Chey, *Ann Arbor*
John Y Chiang, *Rootstown*
Parimal Chowdhury, *Arkansas*
Raymond T Chung,Boston
James M Church, *Cleveland*
Mark G Clemens, *Charlotte*
Vincent Coghlan, *Beaverton*
David Cronin II, *New Haven*
John Cuppoletti, *Cincinnati*
Peter V Danenberg, *Los Angeles*
Kiron Moy Das, *New Brunswick*
Deborah L Diamond, *Seattle*
Peter Draganov, *Florida*
Bijan Eghtesad, *Cleveland*
Hala El-Zimaity, *Houston*
Michelle Embree-Ku, *Providence*
Ronnie Fass, *Tucson*
Mark A Feitelson, *Philadelphia*
Ariel E Feldstein, *Cleveland*
Alessandro Fichera, *Chicago*
Chris E Forsmark, *Gainesville*
Chandrashekhar R Gandhi, *Pittsburgh*
Susan L Gearhart, *Baltimore*
Xupeng Ge, *Boston*
John P Geibel, *New Haven*
Jean-Francois Geschwind, *Baltimore*
Ignacio Gil-Bazo, *New York*
Shannon S Glaser, *Temple*
Ajay Goel, *Dalla*
Julia Butler Greer, *Pittsburgh*
David R Graham, *Houston*
Anna S Gukovskaya, *Los Angeles*
Sanjeev Gupta, *Bronx*
David J Hackam, *Pittsburgh*
Stephen B Hanauer, *Chicago*
Gavin Harewood, *Rochester*
Alan W Hemming, *Gainesville*
Samuel B Ho, *San Diego*
Hongjin Huang, *Alameda*
Jamal A Ibdah, *Columbia*
Atif Iqbal, *Omaha*
Hajime Isomoto, *Rochester*
Hartmut Jaeschke, *Tucson*
Dennis M Jensen, *Los Angeles*
Leonard R Johnson, *Memphis*
Peter James Kahrilas, *Chicago*
AN Kalloo, *Baltimore*
Neil Kaplowitz, Los Angeles
Jonathan D Kaunitz, *Los Angeles*
Ali Keshavarzian, *Chicago*
Miran Kim, *Providence*
Joseph B Kirsner, *Chicago*
Leonidas G Koniaris, *Miami*
Burton I Korelitz, *New York*
Robert J Korst, *New York*
Richard A Kozarek, *Seattle*
Michael Kremer, *Chapel Hill*
Shiu-Ming Kuo, *Buffalo*
Daryl Tan Yeung Lau, *Galvesto*
Joel E Lavine, *San Diego*
Dirk J van Leeuwen, *Lebanon*
Glen A Lehman, *Indianapolis*
Alex B Lentsch, *Cincinnati*
Andreas Leodolter, *La Jolla*
Gene LeSage, *Houston*
Ming Li, *New Orleans*
Zhiping Li, *Baltimore*
LM Lichtenberger, *Houston*
GR Lichtenstein, *Philadelphia*
Otto Schiueh-Tzang Lin, *Seattle*
Martin Lipkin, *New York*
Edward V Loftus, *Rocheste*
Robin G Lorenz, *Birmingham*
JD Luketich, *Pittsburgh*
Henry Thomson Lynch, *Omaha*
Patrick M Lynch, *Houston*
Peter J Mannon, *Bethesda*
John Frank Di Mari, *Texas*
John M Mariadason, *Bronx*
WM Mars, *Pittsburgh*
Laura E Matarese, *Pittsburgh*
Lynne V McFarland, *Washington*
Kevin McGrath, *Pittsburgh*
Howard Mertz, *Nashville*
George W Meyer, *Sacramento*
G Michalopoulos, *Pittsburgh*
James Michael Millis, *Chicago*
Smruti Ranjan Mohanty, *Chicago*
Satdarshan Singh Monga, *Pittsburgh*
Timothy H Moran, *Baltimore*
Steven F Moss, *Providence*
Masaki Nagaya, *Boston*
Laura Eleanor Nagy, *Cleveland*
Hiroshi Nakagawa, *Philadelphia*
Douglas B Nelson, *Minneaplis*
Brant K Oelschlager, *Washington*
Curtis T Okamoto, *Los Angeles*
Stephen JD O'Keefe, *Pittsburgh*
Dimitry Oleynikov, *Omaha*
Natalia A Osna, *Omaha*
Stephen J Pandol, *Los Angeles*
Pankaj Jay Pasricha, *Gaveston*
Zhiheng Pei, *New York*
Michael A Pezzone, *Pittsburgh*
CS Pitchumoni, *New Brunswiuc*
Jay Pravda, *Gainesville*
M Raimondo, *Jacksonville*
GS Raju, *Galveston*
Murray B Resnick, *Providence*
Adrian Reuben, *Charleston*
Douglas K Rex, *Indianapolis*
Victor E Reyes, *Galveston*
Richard A Rippe, *Chapel Hill*
Marcos Rojkind, *Washington*
Hemant Kumar Roy, *Evanston*
Shawn David Safford, *Norfolk*
NJ Shaheen, *Chapel Hill*
Stuart Sherman, *Indianapolis*
Shivendra Shukla, *Columbia*
Alphonse E Sirica, *Virginia*
Shanthi V Sitaraman, *Atlanta*
Shanthi Srinivasan, *Atlanta*
Michael Steer, *Boston*
Gary D Stoner, *Columbus*
Liping Su, *Chicago*
Christina Surawicz, *Seattle*
Gyongyi Szabo, *Worcester*
Yvette Taché, *Los Angeles*
Seng-Lai Tan, *Seattle*
Andrzej Tarnawski, *Long Beach*
Andrzej S Tarnawski, *Orange*
K-M Tchou-Wong, *New York*
Neil D Theise, *New York*
PJ Thuluvath, *Baltimore*
Swan Nio Thung, *New York*
Natalie J Torok, *Sacramento*
RA Travagli, *Baton Rouge*
G Triadafilopoulos, *Stanford*
James F Trotter, *Denver*
Chung-Jyi Tsai, *Lexington*
Hugo E Vargas, *Scottsdale*
Scott A Waldman, *Philadelphia*
Jian-Ying Wang, *Baltimore*
Steven David Wexner, *Weston*
Keith Tucker Wilson, *Baltimore*
Jacqueline L Wolf, *Boston*
Jackie Wood, *Ohio*
George Y Wu, *Farmington*
Jian Wu, *Sacramento*
Samuel Wyllie, *Houston*
Wen Xie, *Pittsburgh*
Yoshio Yamaoka, *Houston*
Francis Y Yao, *San Francisco*
Min You, *Indianapolis*
Zobair M Younossi, *Virginia*
Liqing Yu, *Winston-Salem*
David Yule, *Rochester*
Ruben Zamora, *Pittsburgh*
Michael E Zenilman, *New York*
Zhi Zhong, *Chapel Hill*

National Journal Award
2005

World Journal of Gastroenterology®

Volume 13 Number 1
January 7, 2007

The WJG Press

Contents

World Journal of Gastroenterology
Volume 13 **Number** 1 **January** 7, 2007

Contents

Responsible E-Editor for this issue: Wen-Hua Ma

C-Editor for this issue: Gianfranco Alpini, PhD, Professor

Responsible S-Editor for this issue: Jing Wang

World Journal of Gastroenterology (*World J Gastroenterol , WJG*), a leading international journal in gastroenterology and hepatology, has an established reputation for publishing first class research on esophageal cancer, gastric cancer, liver cancer, viral hepatitis, colorectal cancer, and *H pylori* infection, providing a forum for both clinicians and scientists, and has been indexed and abstracted in Current Contents®/Clinical Medicine, Science Citation Index Expanded (also known as SciSearch®) and Journal Citation Reports/Science Edition, *Index Medicus*, MEDLINE and PubMed, Chemical Abstracts, EMBASE/Excerpta Medica, Abstracts Journals, *Nature Clinical Practice Gastroenterology and Hepatology*, CAB Abstracts and Global Health. ISI JCR 2003-2000 IF: 3.318, 2.532, 1.445 and 0.993. *WJG* is a weekly journal published by The WJG Press. The publication date is on 7th, 14th, 21st, and 28th every month. The *WJG* is supported by The National Natural Science Foundation of China, No. 30224801 and No.30424812, which was founded with a name of *China National Journal of New Gastroenterology* on October 1,1995, and renamed as *WJG* on January 25, 1998.

PUBLISHED BY
The WJG Press

PRINTED BY
Printed in Beijing on acid-free paper by Beijing Kexin Printing House

 Print ISSN 1007-9327
CN 14-1219/R.

EDITORIAL OFFICE
World Journal of Gastroenterology,
The WJG Press, Apartment 1066 Yishou Garden, 58 North Langxinzhuang Road, PO Box 2345, Beijing 100023, China
Telephone: +86-10-85381892
Fax: +86-10-85381893
E-mail: wjg@wjgnet.com
http://www.wjgnet.com

SUBSCRIPTION AND AUTHOR REPRINTS
Jing Wang
The WJG Press, Apartment 1066 Yishou Garden, 58 North Langxinzhuang Road, PO Box 2345, Beijing 100023, China
Telephone: +86-10-85381892
Fax: +86-10-85381893
E-mail: j.wang@wjgnet.com
http://www.wjgnet.com

SUBSCRIPTION INFORMATION
Institutional Price Print-2007: USD 1500.00
Personal Price Print-2007: USD 700.00

INSTRUCTIONS TO AUTHORS
Full instructions are available online at http://www.wjgnet.com/wjg/help/instructions.jsp. If you do not have web access please contact the editorial office.

PO Box 2345, Beijing 100023, China
www.wjgnet.com
wjg@wjgnet.com

World J Gastroenterol 2007 January 7; 13(1): 1-7
World Journal of Gastroenterology ISSN 1007-9327

EDITORIAL

Nutritional modulation of the inflammatory response in inflammatory bowel disease- From the molecular to the integrative to the clinical

Gary E Wild, Laurie Drozdowski, Carmela Tartaglia, M Tom Clandinin, Alan BR Thomson

Gary E Wild, Department of Medicine, Division of Gastroenterology, McGill University, Montreal, Quebec; Department of Anatomy and Cell Biology, McGill University, Montreal, Quebec, Canada
Laurie Drozdowski, Alan BR Thomson, Division of Gastroenterology, University of Alberta, Edmonton, Alberta, Canada
Carmela Tartaglia, Department of Physiology, McGill University, Montreal, Quebec, Canada
M Tom Clandinin, Department of Agriculture, Foods and Nutrition, University of Alberta, Edmonton, Alberta, Canada
Correspondence to: Dr. Alan BR Thomson, Zeidler Ledcor Center, 130, University Campus, Edmonton, AB T6G 2X8, Canada. alan.thomson@ualberta.ca
Telephone: +1-780-4926490 Fax: +1-780-4927964
Received: 2006-07-30 Accepted: 2006-10-05

Abstract

Nutrient deficiencies are common in patients with inflammatory bowel disease (IBD). Both total parenteral and enteral nutrition provide important supportive therapy for IBD patients, but in adults these are not useful for primary therapy. Dietary intervention with omega-3 polyunsaturated fatty acids contained in fish oil may be useful for the care of IBD patients, and recent studies have stressed the role of PPAR on NFκB activity on the potential beneficial effect of dietary lipids on intestinal function.

Key words: Crohn's disease; Ulcerative colitis; Enteral nutrition; Parenteral nutrition; Glutamine; Fiber; Long chain fatty acids

Wild GE, Drozdowski L, Tartaglia C, Clandinin MT, Thomson ABR. Nutritional modulation of the inflammatory response in inflammatory bowel disease- From the molecular to the integrative to the clinical. *World J Gastroenterol* 2007; 13(1): 1-7

http://www.wjgnet.com/1007-9327/13/1.asp

INTRODUCTION

Inflammatory bowel disease (IBD) is a term used to denote inflammation of the gastrointestinal mucosa of unknown etiology. There are a number of hypotheses pertaining to the development and perpetuation of IBD. Three major theories emerge from the literature. The first implicates a persistent intestinal infection[1-3]; the second proposes that IBD is a consequence of a defective mucosal barrier to luminal antigens[4,5]; and the third suggests a dysregulated host immune response to ubiquitous antigens[4,6]. It is believed that IBD has both genetic and environmental components, and is immunologically mediated[4,7-9]. Data from IBD patients concerning cytokine profiles, permeability defects, response to treatment, and natural history of disease all indicate a heterogeneous group of illnesses that fall under the headings of ulcerative colitis (UC) and Crohn's disease (CD). Previous epidemiological data covering diet in UC and CD are conflicting, partly due to this heterogeneity of the diseases, difficulty in obtaining reliable data and publication bias such as negative structures of breastfeeding[10].

NUTRITION IN IBD

Specific antibody isotypes to major milk proteins are found in both UC and CD patients. In CD, the antibodies correlate with disease activity[11]. Although ethnic origin[12], and not the IBD disease state, appears to be the main determinant of lactose intolerance, the avoidance of dairy products by IBD patients is extensive[13]. Lack of breastfeeding in infancy has been associated with CD but not UC. In addition, increased carbohydrate consumption has been documented in CD[14]. Others have alluded to a lack of dietary fiber as a predisposing factor for IBD[15]. The development of UC has also been associated with high intakes of monounsaturated fatty acids (MUFA), n6 polyunsaturated fatty acids (n6 PUFA), sulphur-containing diets and vitamin B6[16].

Deficiencies

IBD is associated with a number of nutritional deficiencies including anemia, hypoalbuminemia, hypomagnesia, hypocalcemia and hypophosphatemia, as well as deficiencies in folic acid, niacin, Vitamins A, B12, C, and D as well as deficiencies of iron, zinc, copper[17]. It is not clear if low levels of micronutrients are one of the results of disease or one of primary importance. Plasma antioxidant concentrations are reduced in IBD patients, particularly those with active disease[18]. Antioxidant activity, assessed by measuring selenium concentrations and erythrocyte

glutathione peroxidase activity, is inversely correlated with inflammatory biomarkers, including TNFα[19]. Hyperhomocysteinemia is more common in patients with IBD, and is associated with reduced serum, concentrations of vitamin B12, folate and B6[20].

Several mechanisms contribute to the malnutrition observed in IBD patients. Firstly, there is a decrease in the oral intake of nutrients because of abdominal pain and anorexia. Secondly, the mucosal inflammation and associated diarrhea leads to a loss of protein, blood, minerals, electrolytes and trace elements. Thirdly, multiple resections or bacterial overgrowth may have an adverse nutritional effect; and lastly, the pharmacological therapies may also lead to malnutrition. For example, sulfasalazine reduces folic acid absorption, and corticosteroids decrease calcium absorption as well as negatively affecting protein metabolism[21]. Alterations in energy metabolism may result in increased resting energy expenditure and lipid oxidation in IBD patients[22,23]. The consequences of malnutrition are numerous, and include reductions in bone mineral density[24], as well as growth retardation and delayed sexual maturity in children[25]. Osteoporosis may also be implicated as a result of proinflammatory cytokine profiles.

Nutritional therapy can take on a number of forms which include Total Parenteral Nutrition (TPN) and Total Enteral Nutrition (TEN). The diets used are elemental, polymeric, and exclusion diets. Elemental diets contain nutrients reduced to their basic components: amino acids for proteins, glucose for carbohydrates, and short-chain triglycerides for fats. Polymeric formulas contain whole proteins for nitrogen, glucose polymers for carbohydrates and long-chain triglycerides for starch or fat, respectively[17].

Total parenteral nutrition (TPN)

The use of TPN for the management of IBD is based on certain theoretical advantages: bowel rest is beneficial because it diminishes motor and transport function of the diseased bowel[26,27]; a decrease in antigenic stimulation will eliminate the immunologic responses to food, especially in the presence of impaired intestinal permeability[28-30]; TPN fosters protein synthesis in the intestine which leads to cell renewal, healing, and reversal of impaired immunocompetence.

Ostro and co-workers[31] demonstrated remission rates of 63% to 89% with TPN in a large retrospective series of CD patients who were refractory to conventional medical management. However, Matuchansky *et al*[32] emphasized that there were high relapse rates (40%-62%) after 2 years. It has been suggested that TPN be used only in a nutritionally supportive role[33,34]. In UC, there is no evidence for better outcome with TPN[35,36]. Although remission rates of 9% to 80% have been reported, TPN given to patients with severe colitis appears to only be beneficial as perioperative nutritional support. In patients with mild disease, TPN is more effective but is not better than steroid therapy, and thus the invasiveness and cost of TPN are unjustified. Any benefits associated with TPN may be due to the administration of nutrients, and not bowel rest, as bowel rest alone has no effect on disease activity[37]. Therefore, although TPN has a role in patients with a non-functioning intestine or the short bowel syndrome due to excessive resections, TPN is of limited use as a primary therapy in IBD. This is not intended to be an extensive review of TPN, but it should be cautioned that even in expert centres, TPN is associated with complications such as sepsis and cholestatic liver disease.

Total enteral nutrition (TEN), elemental and defined formula diets

TEN excludes potential toxic dietary factors and antigenic exposure, since there are only amino acids, glucose or oligosaccharides and low lipid content. TEN is not associated with cholestasis, biliary sludge or gallstone formation, as is seen with TPN. Atrophy of the small intestinal mucosa has been observed in animal models receiving long-term TPN, but this atrophy is prevented with TEN. In addition, a 6-wk TPN treatment in dogs resulted in marked reduction in pancreatic weight, a decrease in small intestinal mass, and a decrease in intestinal disaccharidase activity in dogs[38]. For this reason, TEN is preferable to TPN.

The topic of nutrition in GI disorders occurring in IBD has been reviewed recently[39,40]. When compared to TPN, enteral nutrition yielded similar results of preventing and combating malnutrition[35,36,41]. Although Voitk *et al*[42] proposed that elemental diets may be an effective therapy for IBD, enteral nutrition as a primary therapy has failed to yield consistent results in numerous clinical trials. It is true that a number of trials have shown remission rates in CD patients receiving elemental diets, similar to the rates observed with steroid therapy[43-54]. However, it is noteworthy that significantly better remission rates were observed in patients receiving steroid treatment versus elemental diets when including all the diet group drop outs (i.e., on an intent-to-treat basis). The question remains as to the best way of analyzing the results when a large percentage of patients receiving diet therapy drop out because of unpalatibility or intolerance. Furthermore, some studies have shown no difference with elemental diets when compared to steroid therapy[48,52]. In children, elemental diets were associated with greater linear growth, while in adults these diets preserve nitrogen balance[55,56]. The role of nutritional therapy in the context of pediatric onset illness has been reviewed[57]. Thus, enteral nutrition is easier to use, is less expensive, and is a better alternative to TPN. Unfortunately, its unpalatability limits patient compliance, but with strong encouragement this may be partially overcome.

The fat composition of enteral diets may influence the results which are obtained in the various clinical trials. Elemental diets have a low fat content, while most polymeric diets generally contain more fat including more linoleic acid, which is a precursor for the synthesis of potentially proinflammatory eicosanoids[58].

Defined formula diets are usually more palatable and less expensive than are the elemental diets. While some investigators report no differences between elemental and defined formula diets in patients with acute CD[49,59,60], Giaffer *et al*[61] found elemental diets to be more effective

in active CD. A randomized double-blind trial in Crohn's patients demonstrated that elemental and polymeric (defined) diets, differing only in their source of nitrogen, were equally effective in reducing the Crohn's disease activity index (CDAI), and in inducing clinical remission[62]. Although defined formula diets provide less bowel rest, they have the potential advantage of exposing the GI tract to the usual dietary substrates, which allow thereby for the full expression of intestinal, biliary and pancreatic activity[63]. In animal studies, it has also been observed that luminal nutrition has trophic influences on the gut[64].

Is there a beneficial effect of supplementing polymeric formulas with TGF-β1[65]? In pediatric CD, reductions in proinflammatory cytokine concentrations and mRNA, paired with an up-regulation of TGF-β mRNA, was associated with improved macroscopic and microscopic mucosal inflammation. A meta-analysis and a Cochrane review have demonstrated that in adults, corticosteroids are more effective than enteral diet therapy[48-50]. It is unclear what is the role of nutritional therapy in adults with CD[51-53], although there is some evidence in Japan that enteral nutrition enjoys support as primary therapy[53]. In contrast to the generally agreed role in adults of enteral nutrition being useful to improve the patient's nutritional status as its main benefit, in children with CD enteral nutrition has a much clearer benefit to improve clinical, biochemical and growth parameters[55], and may as well have a steroid sparing effect[56,57].

Glutamine, fiber and fatty acids

Diets high in glutamine, an important source of energy for enterocytes and the preferred fuel of the small intestine[66,67], have been used with variable success. Glutamine probably exerts its trophic effects on the small intestine by increasing protein synthesis, and generating alanine as a substrate for enteric gluconeogenesis[68]. There is evidence that glutamine protects the small intestinal mucosa during critical illness[69,70]. However, oral glutamine supplements do not restore to normal the increased permeability seen in patients with CD, and these supplements do not beneficially affect the patients' CDAI or C-reactive protein (CRP) levels[71]. Similarly, a randomized controlled trial demonstrated that no benefit was associated with the intake of glutamine-enriched polymeric formulas in children with CD[72].

In animal studies, dietary fiber has been implicated in maintaining the integrity of the intestine, and in preventing the bacterial translocation from the gut to the mesenteric lymph nodes[73,74]. Short chain fatty acids (SCFA, C1 to C6 organic fatty acids), are produced by the fermentation of dietary polysaccharides by the normal anaerobic bacteria in the colon. These SCFA are a source of energy for the colonocytes, in addition to their enhancing sodium and water absorption and promoting blood flow[75,76]. Reduced levels of SCFA, particularly butyrate, and a defect in the oxidation of butyrate by colonocytes, have been proposed as a mechanism in the pathogenesis of IBD[77,78]. Evidence to support this hypothesis includes the observation that the oxidation of ^{13}C-labelled butyrate is lower in patients with active UC as compared to healthy controls[79]. However, Simpson and co-workers failed to demonstrate differences between UC patients and controls in the oxidation of rectally administered ^{13}C-labelled butyrate[80].

TPN supplemented with SCFA enhanced functional adaptation to intestinal resection in rats. It remains to be determined if patients with short bowel syndrome may benefit from SCFA[81].

Butyrate (C4 fatty acid) administered to UC patients resulted in remission rates comparable to corticosteroids and mesalamine[82]. In patients with CD, both intestinal biopsies and lamina propria cells cultured with butyrate had significantly reduced levels of inflammatory cytokines (TNF), possibly due to a reduction in NFκB activation and IκB degradation[83].

Eicosanoids are inflammatory mediators, and have been implicated in the pathogenesis of chronic inflammatory lesions in the bowel. Specimens from patients with IBD show increased eicosanoid formation[84]. High dietary intake of omega-6 polyunsaturated fatty acids (PUFAs), which reduces omega-3 intake, may contribute to IBD development[85]. The benefits of fish oil, which contain n3 fatty acids, have been shown in some inflammatory diseases such as psoriasis and rheumatoid arthritis. Epidemiological observations of the low prevalence of IBD in Japanese and Inuit populations consuming high n3 fatty acid fish provided a rationale for the use of n3 fatty acids in IBD. The n3 fatty acids are believed to compete with n6 fatty acids as precursors of eicosanoid synthesis. The n3 products are series 5 leukotrienes, which have less physiological activity than do the arachidonate- derived series 4 counterparts. Thus, fish oil may have an anti-inflammatory effect.

Rats fed with fish oil which had TNBS-induced inflammatory lesions in the bowel showed less prostaglandin- and leukotriene-mediated immune response[86]. Parenteral lipid emulsions enriched with n3 fatty acids reduce diarrhea, attenuate morphological changes, and decrease colonic concentrations of inflammatory mediators in an animal model of acetic acid induced colitis[87].

Loeschke *et al*[88] performed a placebo-controlled trial of n3 fatty acids in the prevention of relapse in UC. Patients in remission who received n3 fatty acids experienced fewer relapses than did those receiving placebo. Unfortunately, the beneficial results of this study did not persist throughout the length of the 2 year study, possibly due to decreased compliance over time. In a multicenter placebo controlled relapse prevention trial, Belluzzi *et al*[89] found a significant reduction in the relapse rate in CD patients given a special formulation designed to allow delayed ileal release of n3 fatty acids. A fish oil diet has been shown to increase eicosapentanoic and docosahexanoic acids in the intestinal mucosal lipids of IBD patients, as well as showing a decrease in arachadonic acid. An increase in the synthesis of leukotriene B5 as well as a 53% decrease of leukotriene B4 was shown in UC patients, whereas the fish oil treatment showed a nonsignificant trend to faster remission[90,91]. Fish oil supplementation results in clinical improvement of active mild to moderate disease, but was not associated with a significant decrease in leukotriene B4 production[84]. Thus, fish oil supplementation of the diet may provide some short-term benefit to patients with CD

or UC. The use of probiotics and prebiotics has received much attention; the interested reader is referred to recent reviews in this area[40].

Fatty acids and gene expression

The effect of fatty acids on gene expression was previously thought to result largely from alterations in membrane phospholipids or eicosanoid production. More recently, the discovery of nuclear receptors; such as peroxisome proliferator-activated receptors (PPARs), and their regulation by fatty acids, has changed this view. PPARs are ligand activated transcription factors that upon heterodimerization with the retinoic X receptor (RXR), recognize PPAR response elements in the promoter regions of various genes, and subsequently affect gene transcription. PPARs bind various ligands including nonsteroidal anti-inflammatory drugs (NSAIDS), thiazolidinediones (antidiabetic agents) as well as PUFAs and their metabolites[92-96]. Several subtypes of the receptor have been identified (α,δ,γ) and these are differentially expressed in a variety of tissues. PPARγ is expressed in intestinal tissue, with the highest abundance detected in the colon[97].

PPARγ has been implicated in the regulation of inflammation, and has become a potential therapeutic target in the treatment of inflammatory disorders, including IBD. It has been suggested that patients with UC have a mucosal deficit in PPARγ that may contribute to the development of their disease. Indeed, analysis of mRNA and protein from colonic biopsies shows reduced PPARγ in UC patients when compared to either Crohn's patients or healthy controls[98].

Using colon cancer lines, it has been shown that PPAR ligands attenuate cytokine gene expression by inhibiting NF-κB via an IκB dependent mechanism[99]. A number of other studies suggest that PPAR activators inhibit COX2 by interference with NF-κB[100-102]. PPARs inhibit the AP-1 signaling pathway[103], and interact with the Jun[104] and STAT signaling pathways[105].

Animal studies support the role of PPAR in intestinal inflammation. Thiazolidinedione ligands for PPAR markedly reduced colonic inflammation in a mouse model of IBD[99]. PPAR+/- and RXR +/- mice display enhanced susceptibility to TNBS-induced colitis[106]. The administration of PPAR and RXR agonists synergistically reduce TNBS-induced colitis, with improved macroscopic and histologic scores, reductions in TNFα and IL-1β mRNA, and decreased NF-κB DNA binding activity.

Although clinical data is limited, the results of an open label study using rosiglitazone, a PPARγ ligand as therapy for UC, showed that 27% of patients achieved remission after 12 wk of therapy[107]. Thus, PPARγ ligands may represent a novel therapy for UC, and double-blind, placebo-controlled, randomized trials are warranted.

Of considerable interest, the ability to modulate PPAR nutritionally has been studied. Dietary PUFA have dramatic effects on gene expression through the regulation of several transcription factors, including PPAR. Fatty acid regulation of PPAR was first noted by Gottlicher *et al*[108]. A diverse array of fatty acids, eicosanoids, and fatty acid metabolites have been shown to activate PPAR[94-96]. Both PPARα and PPARγ bind mono- and polyunsaturated fatty acids at levels, which are found in human serum[95]. Thus, the anti-inflammatory effects of n3 PUFA may involve PPAR and interference with NFκB, rather than simply alterations in eicosanoid synthesis.

Clinical Implications

It is widely accepted that nutritional deficiencies are common in patients with CD and UC, and these need to be anticipated, identified and treated. There are no specific diets which can be recommended for all patients with IBD; diet therapy needs to be individualized. TPN or TEN may be necessary to restore nutritional balance in selected IBD patients with malnutrition, but in adults these interventions do not provide a primary option to modify disease activity. The omega-3 PUFAs contained in fish oil may reduce disease activity in UC and CD when used in the short term in conjunction with standard medical therapy. Their mechanism of action may be to enhance the activity of the nuclear receptors PPAR (peroxisome proliferator-activated receptors) in the intestine, inhibiting the AP-1 signaling pathway and NF-κB, attenuating proinflammatory cytokine gene expression. Future research will focus on the identification and use of specific dietary lipids to reduce intestinal inflammatory activity and to maintain long-term disease remission.

ACKNOWLEDGMENTS

The authors thank Ms. Lori Ingram for her excellent editorial assistance.

REFERENCES

1 **Liu Y**, van Kruiningen HJ, West AB, Cartun RW, Cortot A, Colombel JF. Immunocytochemical evidence of Listeria, Escherichia coli, and Streptococcus antigens in Crohn's disease. *Gastroenterology* 1995; **108**: 1396-1404
2 **Sartor R**. Microbial factors in the pathogenesis of Crohn' s disease, ulcerative colitis and experimental intestinal inflammation. Baltimore: Williams & Wilkins, 1995
3 **Wakefield AJ**, Ekbom A, Dhillon AP, Pittilo RM, Pounder RE. Crohn's disease: pathogenesis and persistent measles virus infection. *Gastroenterology* 1995; **108**: 911-916
4 **Sartor RB**. Current concepts of the etiology and pathogenesis of ulcerative colitis and Crohn's disease. *Gastroenterol Clin North Am* 1995; **24**: 475-507
5 **Sartor RB**. Pathogenesis and immune mechanisms of chronic inflammatory bowel diseases. *Am J Gastroenterol* 1997; **92**: 5S-11S
6 **MacDermott RP**. Alterations in the mucosal immune system in ulcerative colitis and Crohn's disease. *Med Clin North Am* 1994; **78**: 1207-1231
7 **Podolsky DK**. Inflammatory bowel disease (1) *N Engl J Med* 1991; **325**: 928-937
8 **Podolsky DK**. Inflammatory bowel disease (2) *N Engl J Med* 1991; **325**: 1008-1016
9 **Yang H**, Rotter J. The genetics of inflammatory disease. Baltimore: Williams & Wilkins, 1994
10 **Wurzelmann JI**, Lyles CM, Sandler RS. Childhood infections and the risk of inflammatory bowel disease. *Dig Dis Sci* 1994; **39**: 555-560
11 **Knoflach P**, Park BH, Cunningham R, Weiser MM, Albini B. Serum antibodies to cow's milk proteins in ulcerative colitis and Crohn's disease. *Gastroenterology* 1987; **92**: 479-485
12 **De Palma GD**, Catanzano C. Removable self-expanding

metal stents: a pilot study for treatment of achalasia of the esophagus. *Endoscopy* 1998; **30**: S95-S96
13 **Bernstein CN**, Ament M, Artinian L, Ridgeway J, Shanahan F. Milk tolerance in adults with ulcerative colitis. *Am J Gastroenterol* 1994; **89**: 872-877
14 **Matsui T**, Iida M, Fujishima M, Imai K, Yao T. Increased sugar consumption in Japanese patients with Crohn's disease. *Gastroenterol Jpn* 1990; **25**: 271
15 **Kelly DG**, Fleming CR. Nutritional considerations in inflammatory bowel diseases. *Gastroenterol Clin North Am* 1995; **24**: 597-611
16 **Geerling BJ**, Dagnelie PC, Badart-Smook A, Russel MG, Stockbrügger RW, Brummer RJ. Diet as a risk factor for the development of ulcerative colitis. *Am J Gastroenterol* 2000; **95**: 1008-1013
17 **Dudrick SJ**, Latifi R, Schrager R. Nutritional management of inflammatory bowel disease. *Surg Clin North Am* 1991; **71**: 609-623
18 **D'Odorico A**, Bortolan S, Cardin R, D'Inca' R, Martines D, Ferronato A, Sturniolo GC. Reduced plasma antioxidant concentrations and increased oxidative DNA damage in inflammatory bowel disease. *Scand J Gastroenterol* 2001; **36**: 1289-1294
19 **Reimund JM**, Hirth C, Koehl C, Baumann R, Duclos B. Antioxidant and immune status in active Crohn's disease. A possible relationship. *Clin Nutr* 2000; **19**: 43-48
20 **Romagnuolo J**, Fedorak RN, Dias VC, Bamforth F, Teltscher M. Hyperhomocysteinemia and inflammatory bowel disease: prevalence and predictors in a cross-sectional study. *Am J Gastroenterol* 2001; **96**: 2143-2149
21 **Lewis JD**, Fisher RL. Nutrition support in inflammatory bowel disease. *Med Clin North Am* 1994; **78**: 1443-1456
22 **Azcue M**, Rashid M, Griffiths A, Pencharz PB. Energy expenditure and body composition in children with Crohn's disease: effect of enteral nutrition and treatment with prednisolone. *Gut* 1997; **41**: 203-208
23 **Mingrone G**, Capristo E, Greco AV, Benedetti G, De Gaetano A, Tataranni PA, Gasbarrini G. Elevated diet-induced thermogenesis and lipid oxidation rate in Crohn disease. *Am J Clin Nutr* 1999; **69**: 325-330
24 **Bjarnason I**, Macpherson A, Mackintosh C, Buxton-Thomas M, Forgacs I, Moniz C. Reduced bone density in patients with inflammatory bowel disease. *Gut* 1997; **40**: 228-233
25 **Griffiths AM**, Nguyen P, Smith C, MacMillan JH, Sherman PM. Growth and clinical course of children with Crohn's disease. *Gut* 1993; **34**: 939-943
26 **Fischer JE**, Foster GS, Abel RM, Abbott WM, Ryan JA. Hyperalimentation as primary therapy for inflammatory bowel disease. *Am J Surg* 1973; **125**: 165-175
27 **Reilly J**, Ryan JA, Strole W, Fischer JE. Hyperalimentation in inflammatory bowel disease. *Am J Surg* 1976; **131**: 192-200
28 **Dudrick SJ**, MacFadyen BV Jr, Daly JM. Management of inflammatory bowel disease with parenteral hyperalimentation. In: Clearfield HR, Dinoso VP Jr, editors. Gastrointestinal emergencies. New York: Grune & Stratton, 1976: 193-199
29 **Jones VA**, Dickinson RJ, Workman E, Wilson AJ, Freeman AH, Hunter JO. Crohn's disease: maintenance of remission by diet. *Lancet* 1985; **2**: 177-180
30 **Suzuki I**, Kiyono H, Kitamura K, Green DR, McGhee JR. Abrogation of oral tolerance by contrasuppressor T cells suggests the presence of regulatory T-cell networks in the mucosal immune system. *Nature* 1986; **320**: 451-454
31 **Ostro MJ**, Greenberg GR, Jeejeebhoy KN. Total parenteral nutrition and complete bowel rest in the management of Crohn's disease. *JPEN J Parenter Enteral Nutr* 1985; **9**: 280-287
32 **Matuchansky C**. Parenteral nutrition in inflammatory bowel disease. *Gut* 1986; **27** Suppl 1: 81-84
33 **Payne-James JJ**, Silk DB. Total parenteral nutrition as primary treatment in Crohn's disease--RIP? *Gut* 1988; **29**: 1304-1308
34 **Shiloni E**, Coronado E, Freund HR. Role of total parenteral nutrition in the treatment of Crohn's disease. *Am J Surg* 1989; **157**: 180-185
35 **Dickinson RJ**, Ashton MG, Axon AT, Smith RC, Yeung CK, Hill GL. Controlled trial of intravenous hyperalimentation and total bowel rest as an adjunct to the routine therapy of acute colitis. *Gastroenterology* 1980; **79**: 1199-1204
36 **McIntyre PB**, Powell-Tuck J, Wood SR, Lennard-Jones JE, Lerebours E, Hecketsweiler P, Galmiche JP, Colin R. Controlled trial of bowel rest in the treatment of severe acute colitis. *Gut* 1986; **27**: 481-485
37 **Greenberg GR**, Fleming CR, Jeejeebhoy KN, Rosenberg IH, Sales D, Tremaine WJ. Controlled trial of bowel rest and nutritional support in the management of Crohn's disease. *Gut* 1988; **29**: 1309-1315
38 **Hughes CA**, Bates T, Dowling RH. Cholecystokinin and secretin prevent the intestinal mucosal hypoplasia of total parenteral nutrition in the dog. *Gastroenterology* 1978; **75**: 34-41
39 **Stratton RJ**, Smith TR. Role of enteral and parenteral nutrition in the patient with gastrointestinal and liver disease. *Best Pract Res Clin Gastroenterol* 2006; **20**: 441-466
40 **O'Sullivan M**, O'Morain C. Nutrition in inflammatory bowel disease. *Best Pract Res Clin Gastroenterol* 2006; **20**: 561-573
41 **González-Huix F**, Fernández-Bañares F, Esteve-Comas M, Abad-Lacruz A, Cabré E, Acero D, Figa M, Guilera M, Humbert P, de León R. Enteral versus parenteral nutrition as adjunct therapy in acute ulcerative colitis. *Am J Gastroenterol* 1993; **88**: 227-232
42 **Voitk AJ**, Echave V, Feller JH, Brown RA, Gurd FN. Experience with elemental diet in the treatment of inflammatory bowel disease. Is this primary therapy? *Arch Surg* 1973; **107**: 329-333
43 **Axelsson C**, Jarnum S. Assessment of the therapeutic value of an elemental diet in chronic inflammatory bowel disease. *Scand J Gastroenterol* 1977; **12**: 89-95
44 **Lochs H**, Steinhardt HJ, Klaus-Wentz B, Zeitz M, Vogelsang H, Sommer H, Fleig WE, Bauer P, Schirrmeister J, Malchow H. Comparison of enteral nutrition and drug treatment in active Crohn's disease. Results of the European Cooperative Crohn's Disease Study. IV. *Gastroenterology* 1991; **101**: 881-888
45 **Malchow H**, Steinhardt HJ, Lorenz-Meyer H, Strohm WD, Rasmussen S, Sommer H, Jarnum S, Brandes JW, Leonhardt H, Ewe K. Feasibility and effectiveness of a defined-formula diet regimen in treating active Crohn's disease. European Cooperative Crohn's Disease Study III. *Scand J Gastroenterol* 1990; **25**: 235-244
46 **O'Brien CJ**, Giaffer MH, Cann PA, Holdsworth CD. Elemental diet in steroid-dependent and steroid-refractory Crohn's disease. *Am J Gastroenterol* 1991; **86**: 1614-1618
47 **Okada M**, Yao T, Yamamoto T, Takenaka K, Imamura K, Maeda K, Fujita K. Controlled trial comparing an elemental diet with prednisolone in the treatment of active Crohn's disease. *Hepatogastroenterology* 1990; **37**: 72-80
48 **O'Moráin C**, Segal AW, Levi AJ. Elemental diet as primary treatment of acute Crohn's disease: a controlled trial. *Br Med J* (Clin Res Ed) 1984; **288**: 1859-1862
49 **Raouf AH**, Hildrey V, Daniel J, Walker RJ, Krasner N, Elias E, Rhodes JM. Enteral feeding as sole treatment for Crohn's disease: controlled trial of whole protein v amino acid based feed and a case study of dietary challenge. *Gut* 1991; **32**: 702-707
50 **Rocchio MA**, Cha CJ, Haas KF, Randall HT. Use of chemically defined diets in the management of patients with acute inflammatory bowel disease. *Am J Surg* 1974; **127**: 469-475
51 **Saverymuttu S**, Hodgson HJ, Chadwick VS. Controlled trial comparing prednisolone with an elemental diet plus non-absorbable antibiotics in active Crohn's disease. *Gut* 1985; **26**: 994-998
52 **Teahon K**, Bjarnason I, Pearson M, Levi AJ. Ten years' experience with an elemental diet in the management of Crohn's disease. *Gut* 1990; **31**: 1133-1137
53 **Teahon K**, Smethurst P, Pearson M, Levi AJ, Bjarnason I. The effect of elemental diet on intestinal permeability and inflammation in Crohn's disease. *Gastroenterology* 1991; **101**: 84-89
54 **Heuschkel RB**, Menache CC, Megerian JT, Baird AE. Enteral

nutrition and corticosteroids in the treatment of acute Crohn's disease in children. *J Pediatr Gastroenterol Nutr* 2000; **31**: 8-15
55 **Sanderson IR**, Boulton P, Menzies I, Walker-Smith JA. Improvement of abnormal lactulose/rhamnose permeability in active Crohn's disease of the small bowel by an elemental diet. *Gut* 1987; **28**: 1073-1076
56 **Sanderson IR**, Udeen S, Davies PS, Savage MO, Walker-Smith JA. Remission induced by an elemental diet in small bowel Crohn's disease. *Arch Dis Child* 1987; **62**: 123-127
57 **Ruemmele FM**, Roy CC, Levy E, Seidman EG. Nutrition as primary therapy in pediatric Crohn's disease: fact or fantasy? *J Pediatr* 2000; **136**: 285-291
58 **O'Morain C**, O'Sullivan M. Nutritional support in Crohn' s disease: current status and future directions. *J Gastroenterol* 1995; **30** Suppl 8: 102-107
59 **Rigaud D**, Cosnes J, Le Quintrec Y, René E, Gendre JP, Mignon M. Controlled trial comparing two types of enteral nutrition in treatment of active Crohn's disease: elemental versus polymeric diet. *Gut* 1991; **32**: 1492-1497
60 **Royall D**, Wolever TM, Jeejeebhoy KN. Evidence for colonic conservation of malabsorbed carbohydrate in short bowel syndrome. *Am J Gastroenterol* 1992; **87**: 751-756
61 **Giaffer MH**, North G, Holdsworth CD. Controlled trial of polymeric versus elemental diet in treatment of active Crohn's disease. *Lancet* 1990; **335**: 816-819
62 **Verma S**, Kirkwood B, Brown S, Giaffer MH. Oral nutritional supplementation is effective in the maintenance of remission in Crohn's disease. *Dig Liver Dis* 2000; **32**: 769-774
63 **Levine GM**, Deren JJ, Steiger E, Zinno R. Role of oral intake in maintenance of gut mass and disaccharide activity. *Gastroenterology* 1974; **67**: 975-982
64 **Weser E**, Heller R, Tawil T. Stimulation of mucosal growth in the rat ileum by bile and pancreatic secretions after jejunal resection. *Gastroenterology* 1977; **73**: 524-529
65 **Fell JM**, Paintin M, Arnaud-Battandier F, Beattie RM, Hollis A, Kitching P, Donnet-Hughes A, MacDonald TT, Walker-Smith JA. Mucosal healing and a fall in mucosal pro-inflammatory cytokine mRNA induced by a specific oral polymeric diet in paediatric Crohn's disease. *Aliment Pharmacol Ther* 2000; **14**: 281-289
66 **Souba WW**, Smith RJ, Wilmore DW. Glutamine metabolism by the intestinal tract. *JPEN J Parenter Enteral Nutr* 1985; **9**: 608-617
67 **Windmueller HG**, Spaeth AE. Uptake and metabolism of plasma glutamine by the small intestine. *J Biol Chem* 1974; **249**: 5070-5079
68 **Higashiguchi T**, Hasselgren PO, Wagner K, Fischer JE. Effect of glutamine on protein synthesis in isolated intestinal epithelial cells. *JPEN J Parenter Enteral Nutr* 1993; **17**: 307-314
69 **Burke DJ**, Alverdy JC, Aoys E, Moss GS. Glutamine-supplemented total parenteral nutrition improves gut immune function. *Arch Surg* 1989; **124**: 1396-1399
70 **Souba WW**, Herskowitz K, Klimberg VS, Salloum RM, Plumley DA, Flynn TC, Copeland EM. The effects of sepsis and endotoxemia on gut glutamine metabolism. *Ann Surg* 1990; **211**: 543-549; discussion 549-551
71 **Den Hond E**, Hiele M, Peeters M, Ghoos Y, Rutgeerts P. Effect of long-term oral glutamine supplements on small intestinal permeability in patients with Crohn's disease. *JPEN J Parenter Enteral Nutr* 1999; **23**: 7-11
72 **Akobeng AK**, Miller V, Stanton J, Elbadri AM, Thomas AG. Double-blind randomized controlled trial of glutamine-enriched polymeric diet in the treatment of active Crohn's disease. *J Pediatr Gastroenterol Nutr* 2000; **30**: 78-84
73 **Jacobs LR**, Lupton JR. Effect of dietary fibers on rat large bowel mucosal growth and cell proliferation. *Am J Physiol* 1984; **246**: G378-G385
74 **Spaeth G**, Berg RD, Specian RD, Deitch EA. Food without fiber promotes bacterial translocation from the gut. *Surgery* 1990; **108**: 240-246; discussion 246-247
75 **Roediger WE**, Moore A. Effect of short-chaim fatty acid on sodium absorption in isolated human colon perfused through the vascular bed. *Dig Dis Sci* 1981; **26**: 100-106
76 **Sakata T**. Stimulatory effect of short-chain fatty acids on epithelial cell proliferation in the rat intestine: a possible explanation for trophic effects of fermentable fibre, gut microbes and luminal trophic factors. *Br J Nutr* 1987; **58**: 95-103
77 **Roediger WE**. The colonic epithelium in ulcerative colitis: an energy-deficiency disease? *Lancet* 1980; **2**: 712-715
78 **Chapman MA**, Grahn MF, Boyle MA, Hutton M, Rogers J, Williams NS. Butyrate oxidation is impaired in the colonic mucosa of sufferers of quiescent ulcerative colitis. *Gut* 1994; **35**: 73-76
79 **Den Hond E**, Hiele M, Evenepoel P, Peeters M, Ghoos Y, Rutgeerts P. In vivo butyrate metabolism and colonic permeability in extensive ulcerative colitis. *Gastroenterology* 1998; **115**: 584-590
80 **Simpson EJ**, Chapman MA, Dawson J, Berry D, Macdonald IA, Cole A. *In vivo* measurement of colonic butyrate metabolism in patients with quiescent ulcerative colitis. *Gut* 2000; **46**: 73-77
81 **Tappenden KA**, Thomson AB, Wild GE, McBurney MI. Short-chain fatty acid-supplemented total parenteral nutrition enhances functional adaptation to intestinal resection in rats. *Gastroenterology* 1997; **112**: 792-802
82 **Senagore AJ**, MacKeigan JM, Scheider M, Ebrom JS. Short-chain fatty acid enemas: a cost-effective alternative in the treatment of nonspecific proctosigmoiditis. *Dis Colon Rectum* 1992; **35**: 923-927
83 **Segain JP**, Raingeard de la Blétière D, Bourreille A, Leray V, Gervois N, Rosales C, Ferrier L, Bonnet C, Blottière HM, Galmiche JP. Butyrate inhibits inflammatory responses through NFkappaB inhibition: implications for Crohn's disease. *Gut* 2000; **47**: 397-403
84 **Aslan A**, Triadafilopoulos G. Fish oil fatty acid supplementation in active ulcerative colitis: a double-blind, placebo-controlled, crossover study. *Am J Gastroenterol* 1992; **87**: 432-437
85 **Shoda R**, Matsueda K, Yamato S, Umeda N. Epidemiologic analysis of Crohn disease in Japan: increased dietary intake of n-6 polyunsaturated fatty acids and animal protein relates to the increased incidence of Crohn disease in Japan. *Am J Clin Nutr* 1996; **63**: 741-745
86 **Vilaseca J**, Salas A, Guarner F, Rodríguez R, Martínez M, Malagelada JR. Dietary fish oil reduces progression of chronic inflammatory lesions in a rat model of granulomatous colitis. *Gut* 1990; **31**: 539-544
87 **Campos FG**, Waitzberg DL, Habr-Gama A, Logullo AF, Noronha IL, Jancar S, Torrinhas RS, Fürst P. Impact of parenteral n-3 fatty acids on experimental acute colitis. *Br J Nutr* 2002; **87** Suppl 1: S83-S88
88 **Loeschke K**, Ueberschaer B, Pietsch A, Gruber E, Ewe K, Wiebecke B, Heldwein W, Lorenz R. n-3 fatty acids only delay early relapse of ulcerative colitis in remission. *Dig Dis Sci* 1996; **41**: 2087-2094
89 **Belluzzi A**, Brignola C, Campieri M, Pera A, Boschi S, Miglioli M. Effect of an enteric-coated fish-oil preparation on relapses in Crohn's disease. *N Engl J Med* 1996; **334**: 1557-1560
90 **Hawthorne AB**, Daneshmend TK, Hawkey CJ, Belluzzi A, Everitt SJ, Holmes GK, Malkinson C, Shaheen MZ, Willars JE. Treatment of ulcerative colitis with fish oil supplementation: a prospective 12 month randomised controlled trial. *Gut* 1992; **33**: 922-928
91 **Hillier K**, Jewell R, Dorrell L, Smith CL. Incorporation of fatty acids from fish oil and olive oil into colonic mucosal lipids and effects upon eicosanoid synthesis in inflammatory bowel disease. *Gut* 1991; **32**: 1151-1155
92 **Lehmann JM**, Moore LB, Smith-Oliver TA, Wilkison WO, Willson TM, Kliewer SA. An antidiabetic thiazolidinedione is a high affinity ligand for peroxisome proliferator-activated receptor gamma (PPAR gamma). *J Biol Chem* 1995; **270**: 12953-12956
93 **Lehmann JM**, Lenhard JM, Oliver BB, Ringold GM, Kliewer SA. Peroxisome proliferator-activated receptors alpha and gamma are activated by indomethacin and other non-steroidal anti-inflammatory drugs. *J Biol Chem* 1997; **272**: 3406-3410

94 **Delerive P**, Furman C, Teissier E, Fruchart J, Duriez P, Staels B. Oxidized phospholipids activate PPARalpha in a phospholipase A2-dependent manner. *FEBS Lett* 2000; **471**: 34-38
95 **Kliewer SA**, Sundseth SS, Jones SA, Brown PJ, Wisely GB, Koble CS, Devchand P, Wahli W, Willson TM, Lenhard JM, Lehmann JM. Fatty acids and eicosanoids regulate gene expression through direct interactions with peroxisome proliferator-activated receptors alpha and gamma. *Proc Natl Acad Sci USA* 1997; **94**: 4318-4323
96 **Forman BM**, Chen J, Evans RM. Hypolipidemic drugs, polyunsaturated fatty acids, and eicosanoids are ligands for peroxisome proliferator-activated receptors alpha and delta. *Proc Natl Acad Sci USA* 1997; **94**: 4312-4317
97 **Mansén A**, Guardiola-Diaz H, Rafter J, Branting C, Gustafsson JA. Expression of the peroxisome proliferator-activated receptor (PPAR) in the mouse colonic mucosa. *Biochem Biophys Res Commun* 1996; **222**: 844-851
98 **Desreumaux P**, Ernst O, Geboes K, Gambiez L, Berrebi D, Müller-Alouf H, Hafraoui S, Emilie D, Ectors N, Peuchmaur M, Cortot A, Capron M, Auwerx J, Colombel JF. Inflammatory alterations in mesenteric adipose tissue in Crohn's disease. *Gastroenterology* 1999; **117**: 73-81
99 **Su CG**, Wen X, Bailey ST, Jiang W, Rangwala SM, Keilbaugh SA, Flanigan A, Murthy S, Lazar MA, Wu GD. A novel therapy for colitis utilizing PPAR-gamma ligands to inhibit the epithelial inflammatory response. *J Clin Invest* 1999; **104**: 383-389
100 **Ricote M**, Huang J, Fajas L, Li A, Welch J, Najib J, Witztum JL, Auwerx J, Palinski W, Glass CK. Expression of the peroxisome proliferator-activated receptor gamma (PPARgamma) in human atherosclerosis and regulation in macrophages by colony stimulating factors and oxidized low density lipoprotein. *Proc Natl Acad Sci USA* 1998; **95**: 7614-7619
101 **Staels B**, Koenig W, Habib A, Merval R, Lebret M, Torra IP, Delerive P, Fadel A, Chinetti G, Fruchart JC, Najib J, Maclouf J, Tedgui A. Activation of human aortic smooth-muscle cells is inhibited by PPARalpha but not by PPARgamma activators. *Nature* 1998; **393**: 790-793
102 **Marx N**, Bourcier T, Sukhova GK, Libby P, Plutzky J. PPARgamma activation in human endothelial cells increases plasminogen activator inhibitor type-1 expression: PPARgamma as a potential mediator in vascular disease. *Arterioscler Thromb Vasc Biol* 1999; **19**: 546-551
103 **Delerive P**, Martin-Nizard F, Chinetti G, Trottein F, Fruchart JC, Najib J, Duriez P, Staels B. Peroxisome proliferator-activated receptor activators inhibit thrombin-induced endothelin-1 production in human vascular endothelial cells by inhibiting the activator protein-1 signaling pathway. *Circ Res* 1999; **85**: 394-402
104 **Sakai M**, Matsushima-Hibiya Y, Nishizawa M, Nishi S. Suppression of rat glutathione transferase P expression by peroxisome proliferators: interaction between Jun and peroxisome proliferator-activated receptor alpha. *Cancer Res* 1995; **55**: 5370-5376
105 **Zhou YC**, Waxman DJ. STAT5b down-regulates peroxisome proliferator-activated receptor alpha transcription by inhibition of ligand-independent activation function region-1 trans-activation domain. *J Biol Chem* 1999; **274**: 29874-29882
106 **Desreumaux P**, Dubuquoy L, Nutten S, Peuchmaur M, Englaro W, Schoonjans K, Derijard B, Desvergne B, Wahli W, Chambon P, Leibowitz MD, Colombel JF, Auwerx J. Attenuation of colon inflammation through activators of the retinoid X receptor (RXR)/peroxisome proliferator-activated receptor gamma (PPARgamma) heterodimer. A basis for new therapeutic strategies. *J Exp Med* 2001; **193**: 827-838
107 **Lewis JD**, Lichtenstein GR, Stein RB, Deren JJ, Judge TA, Fogt F, Furth EE, Demissie EJ, Hurd LB, Su CG, Keilbaugh SA, Lazar MA, Wu GD. An open-label trial of the PPAR-gamma ligand rosiglitazone for active ulcerative colitis. *Am J Gastroenterol* 2001; **96**: 3323-3328
108 **Göttlicher M**, Widmark E, Li Q, Gustafsson JA. Fatty acids activate a chimera of the clofibric acid-activated receptor and the glucocorticoid receptor. *Proc Natl Acad Sci USA* 1992; **89**: 4653-4657

S- Editor Liu Y **L- Editor** Alpini GD **E- Editor** Ma WH

PO Box 2345, Beijing 100023, China
www.wjgnet.com
wjg@wjgnet.com

World J Gastroenterol 2007 January 7; 13(1): 8-13
World Journal of Gastroenterology ISSN 1007-9327

EDITORIAL

Dieter Glebe, PhD, *Series Editor*

Recent advances in hepatitis B virus research: A German point of view

Dieter Glebe

Dieter Glebe, Institute of Medical Virology, Justus-Liebig University of Giessen, Giessen, Germany
Correspondence to: Dieter Glebe, Institute of Medical Virology, Justus-Liebig University of Giessen, Frankfurter Str. 107, D-35392 Giessen,
Germany. dieter.glebe@viro.med.uni-giessen.de
Telephone: +49-641-9941203 Fax: +49-641-9941209
Received: 2006-12-07 Accepted: 2006-12-12

Abstract

More than 30 years after the discovery of human hepatitis B virus (HBV) this virus remains to be one of the major global health problems. In infected adolescents or adults, 5%-10% will lead to a chronic carrier state, whereas in infected neonates up to 90% develop chronicity. It is estimated that about 370 million people are chronic carriers of HBV worldwide. In many regions of the world, chronic HBV infection is still the major cause of liver cirrhosis and hepatocellular carcinoma. During the last 30 years, many steps of the viral life cycle have been unravelled, mainly due to cloning, sequencing and expression of the genomic DNA extracted from HBV virions. This has lead to the development of a safe and efficient vaccine and sensitive tests for HBV surface protein (HBsAg) allowing reliable diagnosis and screening of blood products. More recently, a growing number of reverse transcriptase inhibitors have been developed. However, together with these improvements new deficiencies in prevention and cure of HBV infections are becoming apparent. Although HBV is a DNA virus, it is highly variable under immunity or drug induced selection pressure, resulting in vaccine-related escape mutants and drug resistance. To overcome these challenging problems new antivirals and optimised vaccines have to be developed.

Key words: Hepatitis B virus; Molecular biology; Viral life cycle; Animal system; Antiviral therapy

Glebe D. Recent advances in hepatitis B virus research: A German point of view. *World J Gastroenterol* 2007; 13(1): 8-13

http://www.wjgnet.com/1007-9327/13/8.asp

The discovery of the Australian antigen by Baruch S. Blumberg, which is now known as "hepatitis B virus surface antigen" (HBsAg), in the late 1960's opened the field of HBV research towards an understanding of an ancient scourge. During the following decades, many research groups all over the world worked successfully to unravel the life cycle of HBV. In Germany, the virologists Heinz Schaller, Peter H. Hofschneider, and Reiner Thomssen initiated HBV research and provided a profound impact on our understanding of the molecular biology of this virus. Among the clinicians; the names of Karl-Hermann Meyer zum Büschenfelde and Wolfgang Gerok are to be mentioned as founders of hepatitis B research. Moreover, in their labs, but also in other groups, students and scientists became inspired to work on this fascinating virus. Since then, an active and growing community of HBV virologists has been established in Germany. In this highlight topic a collection of reviews written by those scientists and clinicians is presented. The articles cover nearly all fields of hepadnaviral research, from attachment and entry to genome replication, maturation, pathology, animal models and antiviral therapy. The aim of this collection is to bring together recent findings in basic virological and clinical HBV research in order to provide a valuable reference for both hospital hepatologists and basic scientists.

Hepatitis B virus is the prototype member of the family *hepadnaviridae* that can be divided into the *orthohepadnaviruses* of mammals and the *avihepadnaviruses* of birds. To date, the *orthohepadnaviruses* are found only in humans and primates and in a special family of the *sciuridae*, namely North-American woodchucks and some squirrel species. Primate HBV were found in old world primates like chimpanzees, gorillas, gibbons, orangutans, and in one new world primate, the woolly monkey. In the review "Taxonomy and genotypes of Hepatitis B Virus", Stephan Schaefer reports that HBV sequences from old world primates are closely related and cluster in monophyletic groups, while the HBV sequence isolated from woolly monkeys (WMHBV) is more divergent[1]. Human HBV is further subdivided into several genotypes. To date, 8 genotypes (called A-H) that differ by definition in at least 8% of their complete genome have been found. The genotypes can be further divided into 24 sub-genotypes that differ by at least 4% from each other. Interestingly, no sub-genotypes have been described for genotype E and G. The fact that genotype E is common in West Africa, but absent in Americans of African origin from Venezuela and Brazil has led to the speculation of a recent genesis of genotype E. The geo-

graphic origin of genotype G is less clear, however a high prevalence of this genotype has been described in Mexico. Both, the genotypes and sub-genotypes show distinct virological and epidemiological properties. As an example, liver cirrhosis was detected in a greater number of patients chronically infected with HBV genotype C than genotype B in Japan. The same was also detected for the prevalence of hepatocellular carcinoma in these patients. Interestingly, detailed analysis of HBV genomes revealed recombination events between different genotypes. Hybrids between genotype B and C, A and D are very common in certain regions and distinct intergenomic recombination breakpoint hotspots were detected (e.g. the preS1/S2 region and the 3'-end of the surface gene). B/C recombinants occur in Japan and C/D recombinants in Tibet. However, the mechanisms underlying these potential recombination events are still unknown. In contrast to HIV or RNA viruses, recombination during replication is unlikely, because reverse transcription of only one RNA genome occurs within the capsid. Thus, it seems also possible that the described changes are the result of an adaptation to distinct genetic disposition in different human populations. Taking into consideration that a chronic HBV carrier can produce up to 10^{13} virions per day together with a high error rate of HBV reverse transcriptase, the HBV quasispecies can substitute every nucleotide of the small 3.2 kb genome within one patient every day. This favours very fast adaptation of the virus to a changing environment, and may result in modular adaptations within distinct segments of the genome.

Soon after the discovery of hepatitis B virus, it was shown that not only humans but also chimpanzees may test positive for this agent. Furthermore, artificial infection of chimpanzees, but also other apes like gibbons and orangutans with serum from HBV-infected patients induces acute and chronic infections related to human disease. Nevertheless, a strong species specificity of hepatitis B virus was observed, since it was not possible to induce HBV-infection in other mammals. Since then, many efforts have been made to establish a small non-primate animal model for HBV infection *in vivo* as described in the review "Viral and cellular determinants involved in hepadnaviral entry" in this topic highlight[2]. The finding that *Tupaia belangeri*, a small non-primate mammal from Southeast-Asia is susceptible to HBV and HDV raises doubt in the strict host specificity of HBV. Besides the *in vivo* infection, which is usually self-limiting and does not lead to chronic infection, the use of primary Tupaia hepatocyte cultures for *in vitro* infection has greatly improved the field. For many years, primary human hepatocyte cultures, obtained after surgical liver resection were the only possibilities to study infectivity of HBV *in vitro*. However, working with these scarcely available cell cultures is not easy and optimal HBV infection is highly dependent on artificial additives like dimethylsulfoxide (DMSO) and polyethyleneglycol (PEG) for optimal infection. Furthermore, susceptibility of these cultures varies strongly. Primary hepatocyte cultures from *Tupaia belangeri* have overcome these limitations both in availability and susceptibility. Furthermore, the infection is possible without the addition of DMSO and PEG. Most established hepatoma cell lines allow HBV production, but only after transfection of HBV DNA. Nevertheless, in 2001, a new hepatoma cell line called HepaRG was established that could be infected with HBV. However this feature is achieved only after prolonged cultivation in medium containing DMSO and other additives.

Experiments 20 years ago using synthetic peptides gave the first hint on the importance of the preS1 domain for viral infectivity. Later it was confirmed that the first 77 aminoacids of this domain are necessary for HBV infectivity, together with the N-terminal myristoylation at Glycin-2. Combining these important features, it turned out that these myristoylated preS1-peptides inhibited HBV infection at nanomolar concentrations *in vitro*. The exact role of myristoylation during the entry process of HBV is still not clear. It might enhance receptor recognition by insertion of the acyl chain into membranes of the receptor-complex. Interestingly, a so called myristoyl-switch is a well known element of viral entry mechanism used by non-enveloped viruses, like picornaviruses and reoviruses. Using a set of different myristoylated preS1-peptides the preS1 sequence responsible for this inhibition was further narrowed down to 10 aminoacids (NPLGFFPDHQ) in position 9-18 of preS1. Even single point mutations within this region abolish the inhibitory potential of preS1 peptides and when introduced into the viral surface proteins, also destroy infectivity of the virus completely.

The MHBs of HBV seem to be dispensable for infectivity of HBV and HDV. However, antibodies raised against the preS2 region that is an integral part of MHBs and LHBs could inhibit infection both *in vivo* and *in vitro*. Controversies exist about a role of a putative translocative motive (TLM) within the carboxyterminal part of preS2 and its importance for infectivity of HBV. However, no function of this sequence has been attributed to infection with HDV that uses HBV surface protein for infection.

The S-domain contributes to the main part of HBV surface proteins, but from the data obtained by use of myristoylated preS1 peptides, we know that the S-domain is not involved in initial binding to target cells. Nevertheless, antibodies raised against this domain are neutralising and contribute to protection against HBV infection in most cases. However, antibodies against the so-called antigenic domain (residues 100-160 that are also generated by the current S-containing vaccines) may not protect against naturally occurring escape-mutants that are frequently selected, e.g. by antiviral treatment. Since we now are aware that these antibodies will not counteract the binding of the virus to its target cells, the preS1 domain containing the minimal interaction site ought to be included into the vaccine. An unsolved problem is the identity of the still undetected high affinity receptor for HBV. An update of the still growing list of potential receptor candidates is listed in this reviews series, but none of them has ever been shown to be relevant for HBV infection.

Inspired by the presumption that the infection process of all hepadnaviruses may follow similar pathways, many labs used the more easy accessible duck hepatitis B virus (DHBV) infection system to study hepadnaviral entry *in vitro*. Although also restricted to primary hepatocyte cultures, this system is, compared to primary human hepatocyte cultures, relatively easy and accessible. Like in

HBV, the preS-domain of large surface protein of DHBV contributes to infection together with its N-terminal myristoylation. Furthermore, the preS-domain binds to a 180 kDa membrane protein and this binding can be inhibited by neutralizing preS-antibodies. Further work identified the gp180/p170 protein as carboxypeptidase D (CPD), a transmembrane protein with enzymatic activity. While substantial evidence supports the essential role of CPD for the DHBV infection process, expression of CPD in non-susceptible cells did not make these cells susceptible towards DHBV. Therefore, the first attachment partners for DHBV are still unknown. Furthermore, this molecule seems to be restricted to *avihepadnaviruses*, since the human homolog of CPD does not contribute to the HBV infection process. Therefore we have to be aware of the possible differences of entry mechanism of *avi-* and *orthohepadnaviruses*. Nevertheless with easy accessible *in vitro* infection systems for HBV available (primary Tupaia hepatocytes and the HepaRG cell line) it should now be possible to characterize cellular attachment factors and entry receptors for HBV.

After uptake, the viral genome has to be transported through the cytoplasm to the nucleus where active transcription can take place. As discussed by Kann *et al*[3]. evaluation of the transport modes of HBV from the plasma membrane to the nucleus is not easy since at least the early steps of attachment and entry are very species specific and usually need primary human or Tupaia hepatocytes. After uptake of the virus in a yet unknown compartment, the viral envelope proteins mediate fusion of viral and cellular membranes that results in delivery of the viral capsid into the cytoplasm. The capsid, harbouring the viral DNA, covalently linked to the viral polymerase must then be transported into the nucleus of the host cell. To study HBV capsid transport without an infection, isolated HBV capsids have to be either analysed within permeabilized cells or microinjected into *Xenopus laevis* oocytes. Both systems are very artificial and time-consuming. However, in the review of Kann *et al*, an easy *in vitro* system is described that allows analysis of intracellular transport after artificial entry of the capsids. The authors replaced the viral surface proteins of the virus by lipids, normally used for protein transfection. The lipids form an artificial membrane that allows fusion with the cellular plasma membrane and release of the viral capsid into the living cell. In fact, lipofection of HBV capsids isolated from virions allows "infection" of cells that are non-susceptible to the whole, complete virus. First, the core particles are transported *via* microtubuli towards the microtubule-organising centre, located at the perinuclear region of the cell. The viral capsid, containing a nuclear localisation signal interacts with the adaptor proteins importin alpha and beta. Importin beta facilitates contact with the nuclear pore and translocation into the nuclear pore. Interestingly, despite complete translocation, the core particles seem to be stuck at the end of their voyage through the nuclear pore, in a structure called "nuclear basket". Within the nuclear basket, the breakdown of the capsid and the release of the viral DNA into the nucleus should be facilitated. However, many questions are still unanswered, e.g. what determines the arrest of the core particle within the nuclear basket and genome release?

Once within the nucleus of the infected cells, the viral HBV genome is converted into a stable form that allows continuous production of progeny virus and is not lost during cell division. Jürgen Beck and Michael Nassal, give an overview of the hepadnaviral genome replication, starting from the conversion of the incoming viral genome with its circular, but only partially double stranded (rcDNA) to the very stable covalently closed circular DNA (cccDNA)[4]. The rc-DNA form of the HBV genome contains diverse modifications (e.g. the polymerase-protein covalently linked to the 5'end of the (-)-DNA strand) that have to be removed before generation of cccDNA that can serve as a matrix for proper transcription. Experimentally, this is difficult to investigate, since detection of cccDNA in the presence of high amounts of rcDNA is not trivial. Furthermore, cccDNA is present only in low amounts in infected hepatocytes (from 10-50 genomes per cells). Nevertheless, the episomal cccDNA is very stable (half-life > 30-60 d for DHBV infected ducks) and can therefore even persist during effective antiviral therapy. A detailed understanding of rc- to cccDNA conversion and its inhibition would therefore be desirable. The HBV cccDNA serves as the template for all viral RNAs that are transcribed by cellular RNA polymerase II. Interestingly, the reverse transcription step of HBV requires the specific packaging of the pregenomic HBV RNA together with the viral polymerase (containing reverse transcriptase, DNA polymerase and primase domains) into newly formed capsids. Therefore, the authors describe the newly formed capsid as a "dynamic replication machine" that puts the compartmentalization of genome amplification, known from other viruses, to its extreme. Besides the capsid, viral reverse transcriptase and pregenomic RNA, additional factors are essential for hepadnaviral replication. New methods that use *in vitro* reconstitution of purified components are beginning to reveal that cellular chaperones (e.g. heat shock proteins, hsps) are essential factors for viral polymerase-protein activation. Cell-free reconstitution systems will allow scientists to systematically study the factors necessary for hepadnaviral replication.

The review by Volker Bruss summarizes our current knowledge about hepatitis B virus morphogenesis[5]. Envelopment of mature core particles depends on the presence of HBV surface proteins that are synthesized at the endoplasmatic reticulum (ER). HBV envelope proteins contain three related co-carboxyterminal surface proteins. Common to all three proteins is the 226 aminoacids long small surface protein (SHBs). Aminoterminal addition of the 55 aminoacid long preS2-domain results in the middle surface protein (MHBs), while further aminoterminal addition of the preS1-domain (109 or 118 aminoacids, depending on the genotype) are found in large surface protein (LHBs). During synthesis at the ER, the SHBs builds a conformation that results in exposure of aminoacids around 99 to 169 to the ER lumen resulting in N-glycosylation of half of the S proteins at asparagine (asn) 146. After budding, this loop is located at the surface of virions and subviral particles and carries the major conformational epitope of the HBV surface proteins. The M-Protein, in addition to the

S-domain, is always N-glycosylated at asn-4 in preS2 and also present on the viral surface. The preS2-domain is also O-glycosylated at threonine (thr) 37, but interestingly only in genotypes B-H, since genotype A lacks thr-37. However, the overall function of this O-glycosylation for the viral life cycle is still unknown. Moreover, the function of the M-protein by itself is still not clear. Absence of the M-protein does neither suppress virion formation nor impede viral infectivity. However, the M-protein seems to have an evolutionary advantage for the virus, since it is conserved through all *orthohepadnaviruses*. The preS2-domain is a further integral building block of the large surface antigen (LHBs) by further aminoterminal addition of the preS1-domain to the preS2-domain. The preS1-domain has a dual function: the aminoterminal domain is necessary for attachment and entry of the virus, while the carboxyterminus together with aminoterminal part of preS2 is used for envelopment. Interestingly, the preS-domains of the LHBs are cytosolic during translation but half of the preS chains of LHBs are believed to translocate after translation. How the preS domains cross the membrane is still unknown, however cytosolic and ER-specific chaperones are believed to be involved in this process. In addition, the preS1-domain is myristoylated at Glycin-2, a modification that is not necessary for viral morphogenesis, but important for efficient viral infection. Even without involvement of the core particle, the surface proteins can bud from a post-ER, pre-Golgi compartment and build subviral particles that do not contain a viral capsid or DNA and are therefore non-infectious. In the case of HBV, they are built in the form of spheres and filaments and can reach concentrations that are 10 000-fold higher than the virions. Interestingly, the L-protein cannot build particles by itself, but needs S or M protein for proper segregation. Moreover, the LHBs can induce a dose-dependent inhibition of particle release even in the presence of SHBs. A massive storage of HBV envelope proteins in turn can lead to massive cell stress causing cell death or cancer. The significance of the secretion inhibition function of LHBs for the viral life cycle is still not clear. However, it seems to be dependent on the myristoylation of preS1 domain of LHBs since blocking of LHBs myristoylation abolishes the storage phenomenon of LHBs.

Hepatocellular carcinoma (HCC) is one of the most frequent malignant tumors world-wide. Behind lung and stomach cancer, HCC is the one of the leading cause of cancer death. In the review by Joachim Lupberger and Eberhard Hildt, titled "HBV Induced Oncogenesis", the authors discuss the relation of chronic HBV infections and HCC and describe the epidemiology of HBV-associated HCC[6]. Epidemiological data state that chronic HBV carriers have a more than 25 times higher risk of developing HCC, while the molecular mechanism underlying the development of HBV-associated HCC are still not clear. The authors distinguish between direct effects and indirect effects caused by the integration of HBV-DNA into the host genome. In contrast to retroviruses, integration of viral HBV-DNA is not necessary for the viral replication. However, almost all HBV-associated HCCs contain integrated HBV DNA. The integrated viral genomes are rearranged or contain deletions, and cannot lead to viable progeny. However, they may exert an effect on key regulators of the cell cycle. Of special interest in this respect is the frequent integration of woodchuck hepatitis B virus into the N-myc2 gene of the host cells of North-American woodchucks in WHV-related HCC. In HBV-associated HCC however, site-specific integration of HBV genome is a rare event. One indirect effect of integrated HBV-DNA is transcription of HBV open reading frames that remain conserved even after integration. Of special interest is the HBx protein, a small polypeptide that is produced at very low levels in HBV infected hepatocytes. A large number of possible functions have been ascribed to this still enigmatic protein. Initially described as a transcriptional activator, the authors discuss interference of HBx with different signal transduction cascades. Furthermore, HBx was found to interfere with DNA repair and might therefore account for an increase of critical cellular mutations that might increase the risk of developing HCC. Besides the HBx, a special form of the HBV surface protein was found in HBV-infected hepatocytes of HCC patients. The middle surface protein (MHBs) was found to be C-terminally deleted in its S-domain (MHBst) that in turn results in an altered topology of the aminoterminal preS2 domain. While the preS2-domain of wildtype MHBs is located in the lumen of the endoplasmatic reticulum (ER) and is glycosylated at asparagine 4, the preS2-domain of the truncated form is in the cytoplasm. This results in interaction of preS2 with protein kinase C (PKC) and permanent activation of Raf/MEK/ERK signal transduction cascades that might exert a tumor promoter-like function. In line with this, transgenic mice expressing MHBst develop liver tumors. However, a more detailed understanding of the molecular mechanism in HBV-associated HCC development is needed.

In general the infection with HBV can lead to a wide spectrum of clinical manifestations, e.g. self-limited acute or fulminant hepatitis, asymptomatic infection, or chronic hepatitis with progression to liver cirrhosis that can lead to hepatocellular carcinoma (HCC). In their review, Baumert *et al*[7] focus on the impact of virus-host interactions for the pathogenesis of HBV infection and associated liver disease. Both, viral factors and host immune response are discussed. One of the major viral factors are certain HBV mutants that are associated with distinct clinical manifestations, altering the natural course of the infection and confer resistance to antiviral agents, e.g. inhibitors of HBV reverse transcriptase. The authors focus mainly on pre-core (pre-C) stop codon mutations resulting in loss of hepatitis B e antigen (HBeAg) and core-promoter mutations that enhance viral replication. The pre-C stop codon mutation is clinically recognized mainly in patients with chronic and fulminant hepatitis but is also detected in asymptomatic HBV carriers or self-limiting hepatitis. In all these patients, HBeAg, a soluble and secreted form of the core-protein cannot be synthesized any more, despite active viral replication. Therefore the authors argue that HBeAg may play an important role for the interaction of the virus with the host immune system, e.g. HBeAg might have an immunomodulatory function. In line with this, HBeAg might predispose neonates born to HBV-

infected mothers to develop persistent HBV infection by establishing T-cell tolerance to HBeAg and HBcAg *in utero*. Core-promoter mutations are mainly found in patients with an aggressive course of disease like fulminant hepatitis B. Those mutations result in a viral phenotype that shows enhanced viral replication in cell culture and might alter viral kinetics and influence cellular immune response *in vivo*. This might result in more severe liver injuries and possibly fulminant hepatitis. Despite the effect of viral variants, the host immune response is the key player in the onset of liver disease. The authors describe that HBV does not induce strong immune response during the early onset of infection. At the onset of HBV clearance an influx of T cells into the liver occurs, but this is not typically associated with strong liver disease, suggesting non-cytopathic mechanisms for viral clearance that is CD8+ dependent and IFN gamma associated. Weeks later, final elimination of HBV-infected liver cells occurs, presumably by a strong T-cell response with associated liver disease during acute self-limited HBV infection. The absence of a strong T-cell response is detected in patients with chronic hepatitis B. The precise mechanism that contributes to the failure of virus-specific T cell response is still not clear and is discussed by the authors.

Hepatitis B virus is the prototype virus of the family of *hepadnaviridae* that is further divided into the *orthohepadnaviruses* of the mammals and the *avihepadnaviruses* of the birds. The review of Funk *et al*[8], describes avian hepatitis B viruses as an important animal model for the understanding of the life cycle of *hepadnaviridae*. Since the discovery of duck hepatitis B viruses (DHBV) in 1980 many other *avihepadnaviruses* have been characterized in various bird species including cranes and herons. The genomic and structural organization is very similar in human HBV and DHBV. Like HBV, DHBV replicate their DNA genome by reverse transcription of an RNA intermediate. Similar to HBV is their narrow host range, e.g. DHBV infects only distinct duck and goose species but not chicken. Both viruses infect mainly hepatocytes and share a similar life cycle. Nevertheless there are differences that have to be taken into consideration when comparing results obtained from HBV or DHBV systems. First of all, the transmission of infection in ducks occurs mainly vertically, while horizontal transmission is uncommon in contrast to human HBV. Although nearly all of DHBV infected ducks develop chronicity, none or very mild hepatitis is detected and no hepatocellular carcinoma occurs. Furthermore, the DHBV envelope is composed of only two surface proteins [large (L) and small (S) surface proteins] and lacks the middle surface protein (MHBs) found in HBV and other *orthohepadnaviruses*. Unlike the envelope proteins of HBV, DHBV L and S-proteins are not glycosylated, but the DHBV L-protein is phosphorylated, a modification that is absent in HBV L-protein. Another difference is the open reading frame (ORF) for the X-protein. For DHBV, only a cryptic X-like ORF has been described, but apparently lacks a functional role in DHBV *in vivo*. Despite these limitations, DHBV infection of ducks has been an important animal model for the understanding of the biology of hepadnaviral infections, due to the ready availability of susceptible ducks.

Because of the various limitations of the duck hepatitis B infection model like absence of a strong immune pathogenesis leading to the development of liver cirrhosis and HCC, infection of woodchucks (*Marmota monax*) with woodchuck hepatitis B virus (WHV) represents a well-accepted model for many aspects of pathogenesis of human HBV infection. In their review, the authors Stephan Menne and Paul J. Cote describe in detail the woodchuck animal model of orthohepadnaviral infections[9]. WHV, as HBV, is a member of the genus *orthohepadnavirus*. In nature, transmission of the virus occurs vertically and horizontally. Similar to HBV, infections of adult woodchucks with WHV results mainly in resolution and only 5% of infected animals progress to chronicity. Experimental infection of newborn woodchucks results in up to 75% to chronic infection, which is similar to the high properties of neonates born to HBV-infected mothers to develop persistent HBV infection. Chronic WHV infection is associated with life-long active viral replication and disease progression to chronic hepatitis and HCC in these animals. However, unlike chronic HBV infections, there is no naturally occurring e-antigen to anti-e seroconversion and step-down of viral replication. The high viral replication and the very high load of surface antigen and continuous presence of e-antigen in chronic WHV-infected woodchucks might therefore play a major role in disease progression that leads to a nearly 100% risk of these animals to acquire a HCC. However, even after recovery from acute WHV-infection a higher risk of HCC remains (up to 20%), when compared to uninfected woodchucks. Interestingly, the authors could show that WHV replication could be reactivated in serologically long-term resolved adult woodchucks by immunosuppression with cyclosporine A. These experiments support the hypothesis that replication-competent WHV (or HBV in humans) is able to persist years after recovery from acute hepatitis and is controlled by an intact host immune system. The observation in the woodchuck model is supported by recently described fatal reactivation of recovered HBV-infected persons during active immune suppression. The woodchuck could therefore be a very helpful model to study the mechanism of a possible long life persistence of HBV even after serological recovery from acute hepatitis. However, compared to humans, the immune system of woodchucks is not well characterized. Nevertheless, the woodchuck model has very much expanded our knowledge of immune pathogenesis of acute and chronic hepadnaviral infections. Chronically WHV-infected woodchucks have proven to be an invaluable tool for preclinical screening of antiviral drugs against chronic HBV infections of men. Of the many studies with nucleoside and nucleotide analogues tested so far in the woodchuck, telbivudine and clevudine are the most potent with a 8 log10/mL reduction in serum viremia after daily administration of 10 mg/kg for 4 wk, respectively. In addition, continuous treatment with clevudine also delayed the development of HCC significantly. The antiviral activity of tenofovir is much lower under same conditions with only 1.2 log10/mL reduction in serum viremia after 4 wk and is more or less comparable to those of lamivudine and adefovir in the woodchuck model. Furthermore, the authors describe in detail further immunological studies in neonatal

and adult WHV-infected woodchucks that might help to identify the factors responsible for the switch from acute to chronic infection. First results showed that under some conditions, a combination of long-term antiviral drug treatment and therapeutic vaccination can break humoral and cellular immune tolerance in chronic WHV-infected woodchucks, when compared with antiviral monotherapy. The woodchuck animal model of chronic HBV infection is therefore an invaluable tool to study viral pathogenesis and host immune responses.

Despite the existence of a HBV vaccine, more than 370 million people are chronically infected with HBV worldwide, leading to chronic liver disease and development of HCC in many cases. Therefore the overall goal of an antiviral therapy for these cases would be the cure of chronic HBV. However with the current antiviral drugs this might not be achievable in all cases within the near future. In the review by Hans L. Tillmann, the aims of today's antiviral therapy against chronic HBV are summarized[10]. That is, first of all, prevention of liver disease and development of HCC in these patients by control and suppression of HBV replication. The author discusses in detail the different types of chronic HBV and their treatment parameters. For antiviral therapy, only interferon alpha (IFN α) and inhibitors against the reverse transcriptase of HBV are currently available. With standard IFN α, seroconversion from HBe to anti-HBe is induced in 20%-40% of patients 24 wk post-treatment. In chronic HBV patients with a HBeAg negative phenotype, patients showed a good response under IFN α treatment for 6-12 mo but a sustained response was usually not observed in the majority of cases. Unfortunately, longer treatment is usually limited by strong side effects, e.g. flu-like symptoms. Pegylation of IFN α, leading to a longer half life of the modified interferon has similar efficacy, but in general the sustained response for both, standard and pegylated interferon seems to be dependent on the HBV genotype. In contrast to the side effects of interferons, inhibitors of HBV reverse transcriptase can be used for prolonged antiviral therapy. Many of the nucleotides or nucleosides analogues against HBV were developed and used in HIV therapy. Lamivudine, also called 3TC, inhibits HBV reverse transcriptase very efficiently and usually results in viral suppression of 5-6 log10 copies/mL after one year of treatment. Prolonged Lamivudine treatment may contribute to seroconversion of HBe to anti-HBe within 50% of patients after 4 years of therapy. The major problem with prolonged Lamivudine, but also other reverse transcriptase inhibitors is occurrence of drug resistance due to the selection of HBV mutants. The mutations occur mainly within the YMDD-motive of the C-domain of the viral polymerase, however other mutations are also described. The high variability of the HBV reverse transcriptase together with a high replication rate of HBV and the slow kinetics of viral clearance lead to rapid selection of mutants under drug selection pressure that results in development of resistance during continuous therapy. For Lamivudine, up to 70% resistance has been described after 4 years of treatment. This leads to viral breakthrough and progression of liver disease. The author notes that it is therefore necessary to perform early diagnostics of drug resistance and to adapt antiviral therapy prior to breakdown of liver function. Even more important is that the new antiviral in use must not show cross-resistance to the HBV mutants selected by the former antiviral, e.g. telbivudine and emtricitabine have been reported to show a similar resistance mutation profile like Lamivudine.

For the future, it will be necessary to have antivirals on hand that inhibit different steps of the viral life cycle. Rational targets might be inhibitors of attachment and entry, conversion from rcDNA to cccDNA, capsid assembly, envelopment and secretion of viral particles. For attachment and entry, it has been shown that acylated preS1 peptides block HBV infection *in vitro* and in animal models. Based on these results a potent inhibitor of viral infection (Myrcludex B) is currently being developed.

REFERENCES

1 **Schaefer S**. Hepatitis B virus taxonomy and hepatitis B virus genotypes. *World J Gastroenterol* 2007; **13**: 14-21
2 **Glebe D**, Urban S. Viral and cellular determinants involved in hepadnaviral entry. *World J Gastroenterol* 2007; **13**: 22-38
3 **Kann M**, Schmitz A, Rabe B. Intracellular transport of hepatitis B virus. *World J Gastroenterol* 2007; **13**: 39-47
4 **Beck J**, Nassal M. Hepatitis B virus replication. *World J Gastroenterol* 2007; **13**: 48-64
5 **Bruss V**. Hepatitis B virus morphogenesis. *World J Gastroenterol* 2007; **13**: 65-73
6 **Lupberger J**, Hildt E. Hepatitis B virus-induced oncogenesis. *World J Gastroenterol* 2007; **13**: 74-81
7 **Baumert TF**, Thimme R, von Weizsäcker F. Pathogenesis of hepatitis B virus infection. *World J Gastroenterol* 2007; **13**: 82-90
8 **Funk A**, Mhamdi M, Will H, Sirma H. Avian hepatitis B viruses: molecular and cellular biology, phylogenesis, and host tropism. *World J Gastroenterol* 2007; **13**: 91-103
9 **Menne S**, Cote PJ. The woodchuck as an animal model for pathogenesis and therapy of chronic hepatitis B virus infection. *World J Gastroenterol* 2007; **13**: 104-124
10 **Tillmann HL**. Antiviral therapy and resistance with hepatitis B virus infection. *World J Gastroenterol* 2007; **13**: 125-140

S- Editor Liu Y **L- Editor** Alpini GD **E- Editor** Liu WF

PO Box 2345, Beijing 100023, China
www.wjgnet.com
wjg@wjgnet.com

World J Gastroenterol 2007 January 7; 13(1): 14-21
World Journal of Gastroenterology ISSN 1007-9327

TOPIC HIGHLIGHT

Dieter Glebe, PhD, *Series Editor*

Hepatitis B virus taxonomy and hepatitis B virus genotypes

Stephan Schaefer

Stephan Schaefer, Abteilung für Virologie, Institut für Medizinische Mikrobiologie, Virologie und Hygiene, Universität Rostock, Schillingallee 70, D-18057 Rostock, Germany
Correspondence to: Stephan Schaefer, Abteilung für Virologie, Institut für Medizinische Mikrobiologie, Virologie und Hygiene, Universität Rostock Schillingallee 70, D-18057 Rostock, Germany. stephan.schaefer@med.uni-rostock.de
Telephone: +49-381-4945920 Fax: +49-381-4945925
Received: 2006-09-01 Accepted: 2006-10-12

Abstract

Hepatitis B virus (HBV) is a member of the hepadnavirus family. Hepadnaviruses can be found in both mammals (orthohepadnaviruses) and birds (avihepadnaviruses). The genetic variability of HBV is very high. There are eight genotypes of HBV and three clades of HBV isolates from apes that appear to be additional genotypes of HBV. Most genotypes are now divided into subgenotypes with distinct virological and epidemiological properties. In addition, recombination among HBV genotypes increases the variability of HBV. This review summarises current knowledge of the epidemiology of genetic variability in hepadnaviruses and, due to rapid progress in the field, updates several recent reviews on HBV genotypes and subgenotypes.

Key words: Orthohepadnavirus; Avihepadnavirus; Hepatitis B virus; Genotype, Subgenotype; Recombination

Schaefer S. Hepatitis B virus taxonomy and hepatitis B virus genotypes. *World J Gastroenterol* 2007; 13(1): 14-21

http://www.wjgnet.com/1007-9327/13/14.asp

INTRODUCTION

Hepatitis B virus (HBV) is the prototype member of a steadily growing family of viruses called hepadnaviruses[1]. Hepadnaviruses can be found in both mammals (orthohepadnaviruses) and birds (avihepadnaviruses). HBV, the hepadnavirus infecting humans, is classified into eight genotypes today. HBV genotypes differ by at least 8%[2]. Since the first definition of the genotypes A, B, C and D[2], genotypes E[3], F[4], G[5] and H[6] have been detected. Due to the genetic diversity of HBV, numerous subgenotypes of HBV have been described[7] (Table 1). HBV subgenotypes differ by at least 4%[8].

HBV genotypes and most subgenotypes show a distinct geographic distribution. In Asia, where there is a high prevalence of HBV carriers, strong evidence suggests that HBV genotypes influence the course of disease. Several recent reviews have summarised knowledge on different aspects of HBV genotypes[7-12] and on hepadnaviruses that infect species other than homo sapiens[13-15]. This review will update recent developments in understanding HBV genotypes and taxonomy.

TAXONOMY

HBV is a partially double stranded virus that uses reverse transcriptase in its replication cycle. Thus, HBV is similar to many retroviruses found in animals and pararetroviruses in plants[16,17].

After cloning and sequencing the HBV genome[18], several related viruses were discovered in woodchucks (Marmota monax)[19], ground squirrels (Spermophilus beecheyi)[20] and pekin duck (Anas domesticus)[21]. Subsequently, numerous new viruses that are similar to HBV were found in mammals and birds and have been cloned (Tables 1 and 2). All these viruses are classified in the family of hepadnaviridae, including the genus orthohepdnavirus (mammals; Figure 1), and the genus avihepadnavirus (birds; Figure 2). In addition to the avihepadnaviruses listed in Table 2, five new hepadnaviruses were cloned from exotic duck and goose species; i.e., the Chiloe wigeon, mandarin duck, puna teal, Orinoco sheldgoose, and ashy-headed sheldgoose. Sequence comparisons revealed that 4 virus isolates were closely related to existing isolates of duck hepatitis B virus (DHBV), while the mandarin duck virus was closely related to Ross goose hepatitis B virus[22].

In chimpanzees, gorillas, orangutans and gibbons new putative members of hepadnaviridae were discovered and sequenced completely[14]. It is now widely accepted that primate hepadnaviruses are indigenous to their hosts. Because hepadnaviruses isolated from apes are grouped as HBV genotypes in phylogenetic analyses, it has been suggested that isolates from apes should be named following the nomenclature used for immune deficiency viruses[23] (Table 1), e.g. HBV found in chimpanzees should be called HBVcpz. With only 5% divergence from the chimpanzee HBV isolates, the HBV isolate from gorilla is categorized in the HBV genotype (Figure 3, unpublished

Table 1 Orthohepadnaviruses and their host

	Host	Ref.
Hepatitis B Virus	Man *Homo sapiens sapiens*	[75]
Chimpanzee Hepatitis B Virus	Chimpanzee *Pan troglodytes*	[76]
Gibbon Hepatitis B Virus	White handed gibbon *Hylobates lar*	[77]
Orangutan Hepatitis B Virus	Orangutan *Pongo pygmaeus pygmaeus*	[78]
Gorilla Hepatitis B Virus	Gorilla *Gorilla gorilla*	[79]
Woolly Monkey Hepatitis B Virus	Woolly monkey *Lagothrix lagotricha*	[80]
Woodchuck Hepatitis Virus	Woodchuck *Marmota monax*	[19]
Ground Squirrel Hepatitis Virus	Ground Squirrel *Spermophilus beecheyi*	[20]
Arctic Squirrel Hepatitis Virus	Arctic Squirrel *Spermophylus parryi kennicotti*	[81]

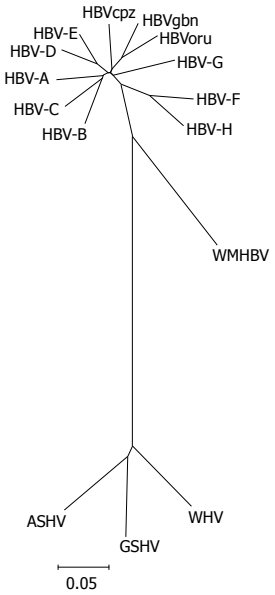

Figure 1 Phylogenetic tree of orthohepadnaviruses. Complete genomes of HBV genotypes A (X02763), B (D00330), C (M12906), D (V01460), E (X75657), F (X69798), G (AF160501) and H (AY090454); HBVcpz (D00220), HBVoru (NC 002168), and HBVgbn (U46935) were aligned using clustal w with orthohepadnavirus genomes from woolly monkey (AF046996) woodchuck (J02442), ground squirrel (K02715) and the tentative member from arctic squirrel (nc_001719). The alignment was tested with the neighbour-joining method.

Table 2 Avihepadnaviruses and their host

	Host	Ref.
Duck Hepatitis B Virus DHBV	Pekin duck *Anas domesticus*	[21]
Grey Teal Hepatitis B Virus (GTHBV)	Grey Teal *Anas gibberifrons gracilis*	[82]
Heron Hepatitis B Virus (HHBV)	Heron *Adrea cinerea*	[83]
Maned Duck Hepatitis B Virus (MDHBV)	Maned Duck *Chenonetta jubata*	[82]
Ross Goose Hepatitis Virus (RGHV)	Ross Goose *Anser rossi*	[4]
Snow Goose Hepatitis B Virus (SGHBV)	Snow Goose *Anser caerulescens*	[84]
Stork Hepatitis B Virus (STHBV)	White Stork *Ciconia ciconia*	[85]
Crane Hepatitis B Virus (CHBV)	Demoiselle cranes *Anthropoides virgo* Grey crowned cranes *Balearica regulorum*	[86]

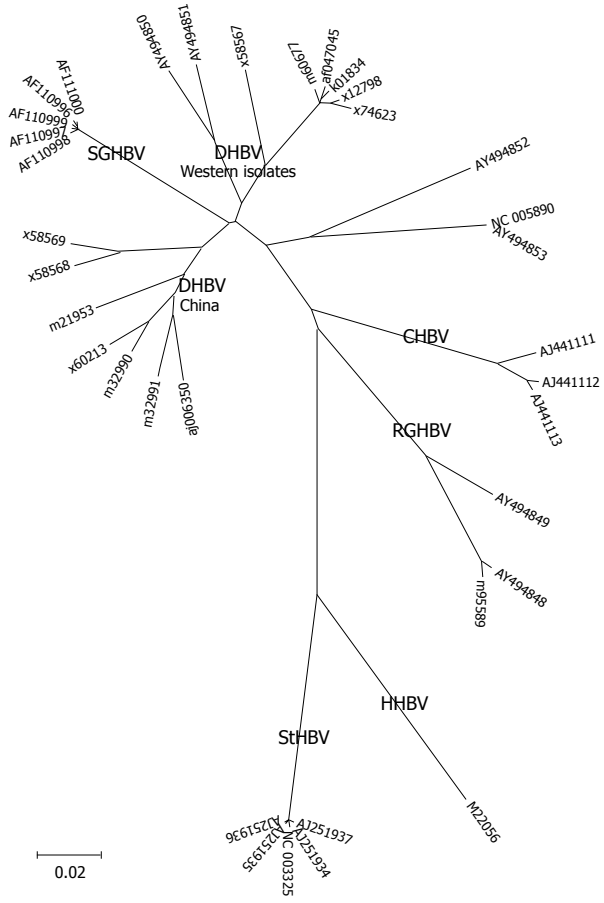

Figure 2 Phylogenetic tree of the genus avihepadnavirus.

results). Thus, three HBV genotypes from apes can now be differentiated. The chimpanzee and gorilla isolates from Africa are categorized as one genotype, i.e., HBVcpz. The isolates from the South-East-Asian apes, gibbon and orang-utan, are categorized into two genotypes, i.e., HBVgbn and HBVoru, respectively. These genotypes diverge by 8%. Within the gibbon genotype, distinct strains of HBV circulating in geographically separated populations have been described[24].

Avihepdnaviruses are the most distant relatives of HBV with a nucleic acid homology of only 40%. WHV and GSHV as mammalian hepadnaviruses are more closely related to HBV and differ by only 17%. Complete WHV and GSHV genomes from GenBank show a high degree of homology and only one genotype is listed[25-27]. However, using degenerate primers, several variant WHV isolates from wild-captured woodchucks were found that showed high divergence with sequencing of small parts of the genome[28]. DHBV has two genotypes, in contrast to WHV and GSHV, which have a narrow host range and geographical distribution[25,26], DHBV is found in different avian species with independent isolates in many countries

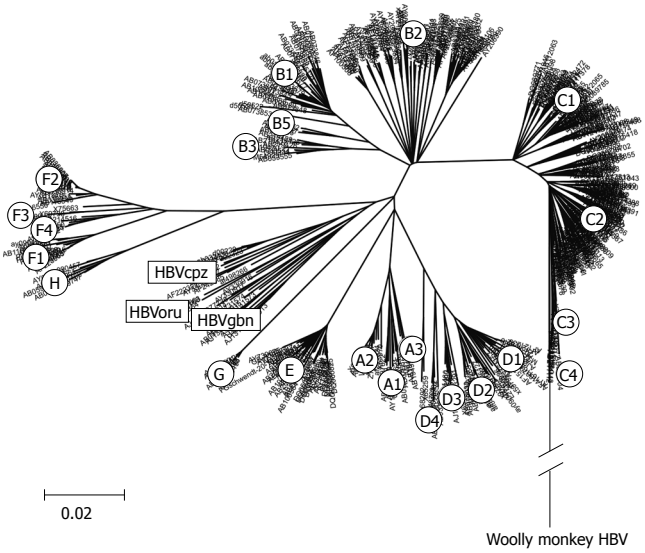

Figure 3 Phylogenetic tree of complete HBV genomes. An alignment of 601 complete HBV sequences was performed with Clustal X in the program DNAstar. The alignment was further analysed by boot-strapping using the Neighbourhood-Joining method contained in MEGA version 3.1[104].

Figure 4 Geographic distribution of HBV genotypes and subgenotypes.

around the world[29] (Figure 4).

Human HBV can be grouped into eight genotypes (based on more than 8% difference)[7,9-12]. Several attempts have been made to reconstruct the evolution of hepadnaviruses[30-34]. Estimating the rate of synonymous substitutions for HBV to be 4.57×10^{-5} per site per year, DHBV has been proposed to have diverged about 30 000 years ago from a common ancestor while GSHV and WHV should have diverged about 10 000 years ago from HBV and the HBV serotypes would be separated by about 3000 years[31]. However, as long as we are not able to accurately estimate the mutation rate of HBV over centuries or even millennia, it is not possible to calculate a time point for the separation of HBV genotypes or hepadnaviral species.

HBV GENOTYPES AND SUBGENOTYPES

HBV genotypes differ by more than 8%[2,3]. Phylogenetic analyses using alignments of whole genomes have shown that 8 genotypes, called A, B, C, D, E, F, G and H, of HBV can be distinguished[7,11,12,35] (Figure 1). In general, HBV isolates found in apes diverge similarly to HBV genotypes in phylogenetic analyses and have been named HBVcpz, -oru, -gor and -gbn for their host's, i.e. chimpanzee, orang-utan, gorilla and gibbon, respectively (Table 1)[23]. However, as elucidated above, the isolate from gorillas is always categorized into the chimpanzee clade.

A prototypic HBV genome may have a length of 3215 nt, as found in HBV genotypes B, C, F and H. Due to deletions and insertions (Table 3), the other HBV genotypes differ slightly in length of genome (Table 3). Thus HBV genotype G with 3248 nt. is 66 nt longer than genotype D with 3182 bp.

Extensive phylogenetic analyses have shown that HBV genotypes can be further subdivided into subgenotypes (Table 4). HBV subgenotypes differ by at least 4%[8]. In

Table 3 Fundamental properties of genomes and differences between HBV genotypes

Genotype	Genome length in bp	ORF-differences
A	3221	Insertion of aa 153 and 154 in HBc
B	3215	
C	3215	
D	3182	Deletion of aa 1-11 in preS1
E	3212	Deletion of aa 11 in preS1
F	3215	
G	3248	Insertion of 12 aa in HBc Deletion of aa 11 in preS1
H	3215	

Table 4 HBV subgenotypes and geographic prevalence

	Subgenotype	Synonyms	Geographic origin	Ref.
A	A1	Aa, A'	Africa, (Asia, South America)	[41,87]
	A2	Ae, A-A'	Europe	
	A3	Ac	Gabon, Cameroon	[88,89]
	(A4)		Mali	[59]
	(A5)		Nigeria	[59]
B	B1	Bj	Japan	[67,90]
	B2	Ba	Asia without Japan	
	B3		Indonesia, Philippines	[7]
	B4		Vietnam	[7]
	B5		Philippines	[91,92]
C	C1	Cs	South East Asia (Vietnam, Myanmar, Thailand, Southern China)	[37-39]
	C2	Ce	Far East (Korea, Japan, Northern China)	
	C3		Micronesia	[7]
	C4		Australia	[93]
	C5		Philippines, Vietnam	[92,94]
D	D1		Mongolia, Belarus, Europe?	
	D2		India?	
	D3		South Africa, East India, Serbia	[40,41]
	D4		Australia	[93]
	D5		East India	[40]
F	F1		South and Central America	[95,96]
	F2		South America	[4]
	F3		Bolivia	[97,98]
	F4		Argentina	[97,98]

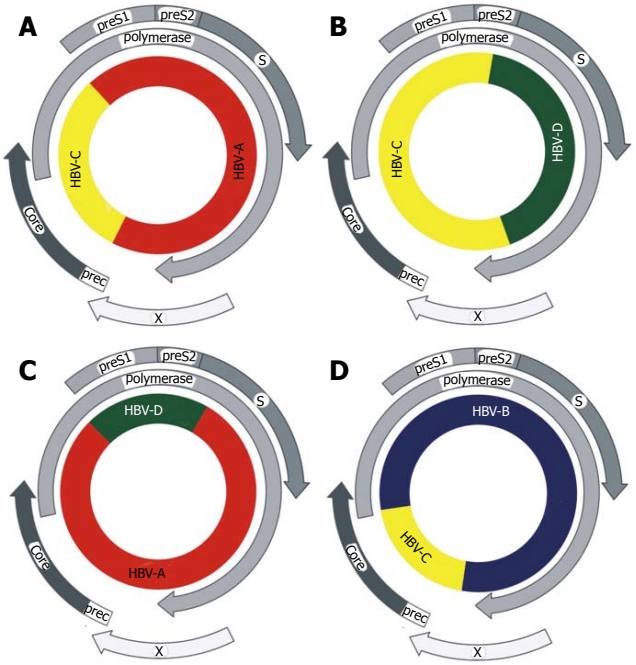

Figure 5 Schematic genome organisation of recombinants between HBV genotypes. HBV recombinants were described from materials sampled in **A**: Vietnam[99]; **B**: Tibet[68]; **C**: Africa[100] and **D**: Asia[67]. The ORF coding for the HBV proteins are shown as arrows, the inner circle represents the HBV genome.

Table 5 Examples for recombination events between of HBV genotypes

Genotype of		Recombination Breakpoint		No. in literature	Ref.
Backbone	Insert	5′	3′		
A	C	1801	2865	3	[99]
A	D	2895	327		
		2820	386-586	3	[100]
		?	670		
B	C	1740-1838	2443- 2485	41	[67,73,101,102]
B	C	3120	3171	1	[60]
		3060	3191	1	
		2910	2950	1	
C	B	1731-1838	2437- 2479	1	[102]
D	A	129	2339	3	[73,101,102]
		495	780		
		822	1775		
G	C	1860	2460	1	[103]
A	E	882	1060	1	[88]

genotypes A, B and C, epidemiological data show that the respective subgenotype pairs A1/A2 (formerly termed Aa/Ae)[36], B1/B2 (formerly Bj/Ba)[36] and C1/C2 (formerly Cs/Ce)[37-39] differ substantially in many virological and probably some clinical parameters. Subgenotypes also show distinct geographic distribution (Figure 3). However, this is not true for genotype D with subgenotypes D1, D2 and D3 being described as widespread in the world; e.g. D3 was found in Asia (East India)[40], South Africa[41] and Europe (Serbia) (Stanojevic *et al,* unpublished results).

Except for genotype E and G, all HBV genotypes can be divided into subgenotypes. The absence of subgenotypes in HBV genotype E has been assumed to be the consequence of a recent genesis for genotype E[42-45]. Furthermore, genotype E is not present in Americans of African origin from Venezuela and Brazil[46,47]. The case for HBV genotype G appears to be less clear. Genotype G was originally found in the USA, France[5] and Germany[48]. Later, partial sequencing of HBV genes pointed to a high prevalence of HBV genotype G in Mexico[49]. Nevertheless, the geographic origin of HBV genotype G remains unknown[50]. To date only a limited number of complete HBV genotype G sequences have been deposited in GenBank that are not classified into subgenotypes.

DOUBLE INFECTIONS AND RECOMBINANTS

Double infections with two different HBV genotypes have been known since typing was done serologically[51,52]. Subsequently, evidence of super infection with HBV isolates of the same or different genotype was described in chronic HBV patients[53]. Super infection was accompanied by acute exacerbation of the chronic disease. Additional observations came from patients treated with interferon. Before treatment, HBV genotype A was prevalent. After treatment and relapse, a switch of the genotype to HBV genotype D was described[54,55].

Using different methods for genotyping, several reports described high rates of double infection with two different HBV genotypes in all parts of the world. Using these methods double infections have been found in 4.4%[56], 10.9%[57], 12.5%[58], 14.1% (Kirschberg *et al,* unpublished results), 17.3%[59] and 17.5%[60] of HBV infected patients. Even triple infections with HBV of genotype A, B and C have been described in 0.9% of HBV infected intravenous drug users[60].

Infection with HBV of genotype G seems to be associated very often with an infection of HBV genotype A[61]. This was found in 4 individuals from the USA and in one patient from France[62].

Coinfection with two different HBV genotypes in one patient may lead to an exchange of genetic material between the two strains. However, with current knowledge of HBV replication, the mechanism for this supposed recombination remains enigmatic. No mechanism can be envisioned that would allow an exchange of genetic material between two hepadnaviral genomes at the level of transcription. Nevertheless, numerous authors described changes in the genome of HBV that appear to be the consequences of a recombinatorial event (Figure 5 and Table 5).

Two recent works have comprehensively analysed the prevalence of events in the HBV genome that are reminiscent of recombinations[63,64]. About 87% of the putative recombinants were B/C (120) and A/D (29) hybrids. The other recombinants comprised A/B/C, A/C, A/E, A/G, C/D, C/F, C/G, C/U (U for unknown genotype) and B/C/U hybrids. Genotypes A and C showed a higher recombination tendency than did

other genotypes. The results also demonstrated region priority and breakpoint hot spots in the intergenotype recombination. Recombination breakpoints were found to be concentrated mainly in the vicinity of the DR1 region (nt 1640-1900), the preS1/S2 region (nt 3150-100), the 3' -end of the Core gene (nt 2330-2450) and the 3'-end of the Surface gene (nt 650-830)[63,64].

Recombination events between human and chimpanzee[65]or gibbon[63] HBV sequences have also been described. Discrepant genotyping results from different parts of the genome are indicative of a recombination between genotype A and F[66]. Even mosaic genomes with sequences derived from three different genotypes have been described[59,64].

Some recombinants among HBV genotypes have become the dominant subgenotype prevalent in certain geographic regions. Recombination between genotypes B and C has led to the generation of two different strains with distinct geographic distribution[67]. Strains of genotype B without recombination are found in Japan (subgenotype B1), whereas strains with recombination between genotype B and C are found throughout Asia (subgenotype B2), sparing Japan[67]. Recombinants between HBV genotypes C and D are the leading HBV subgenotype in Tibet[68-70].

It remains open for discussion whether the observed exchanges are the consequence of direct genetic recombination taking place between two HBV strains or if they are the consequence of fast adaptation of HBV to a certain genetic and immunologic environment in different human populations in the world. The high replication capacity of HBV with a release of up to 10^{13} viral particles per day[71,72] and the high error rate of the viral polymerase, lead to the production of HBV genomes with all possible single mutations and double mutations of every nucleotide of the HBV genome every day[72]. Thus, a fast adaptation of HBV to a new environment is also a possibility.

A hypothetical mosaicism of the HBV genome has already been proposed by Bowyer and Sim[73]. This work and later works described most HBV genotypes as a modular genome[63] that represents a mixture of small segments coming from many different HBV genotypes. If we expand on this observation, the HBV genome may be made up of a number of allelic modules with different properties; e.g. different binding sites for transcription factors or antigenic epitopes. Thus, a certain combination of these modules would make up an HBV genotype. The findings of Fischer *et al*[74]are in support of this speculation. The authors described genotype specific activation or repression of HBV enhancer II, preCore-pregenomic promoter by the transcription factor COUP-TF1.

CONCLUSION

HBV has been recognised as a prototype member of a family of viruses infecting mammals and birds. Due to its high replication capacity and the high error rate of the viral reverse transcriptase, HBV is able to adapt to the host's environment. This adaptation has led to the emergence of eight genotypes in humans and three closely related genotypes in apes. The human genotypes have further diverged into at least 24 subgenotypes, with certainly many more to come, and a plethora of recombinants. From the analysis of recombinants there are indications that at least one more genotype remains to be detected.

REFERENCES

1 **Mason WS**, Burrell CJ, Casey J, Gerlich WH, Howard CR, Kann M, Newbold J, Schaefer S, Taylor JM, Will H Hepadnaviridae. in: Fauquet CM, Mayo MA, Maniloff J, Desselberger U, Ball LA (eds). Virus Taxonomy. Eighth Report of the International Committee on Taxonomy of Viruses. Amsterdam: Elsevier, 2005

2 **Okamoto H**, Tsuda F, Sakugawa H, Sastrosoewignjo RI, Imai M, Miyakawa Y, Mayumi M. Typing hepatitis B virus by homology in nucleotide sequence: comparison of surface antigen subtypes. *J Gen Virol* 1988; **69** (Pt 10): 2575-2583

3 **Norder H**, Couroucé AM, Magnius LO. Complete genomes, phylogenetic relatedness, and structural proteins of six strains of the hepatitis B virus, four of which represent two new genotypes. *Virology* 1994; **198**: 489-503

4 **Naumann H**, Schaefer S, Yoshida CF, Gaspar AM, Repp R, Gerlich WH. Identification of a new hepatitis B virus (HBV) genotype from Brazil that expresses HBV surface antigen subtype adw4. *J Gen Virol* 1993; **74** (Pt 8): 1627-1632

5 **Stuyver L**, De Gendt S, Van Geyt C, Zoulim F, Fried M, Schinazi RF, Rossau R. A new genotype of hepatitis B virus: complete genome and phylogenetic relatedness. *J Gen Virol* 2000; **81**: 67-74

6 **Arauz-Ruiz P**, Norder H, Robertson BH, Magnius LO. Genotype H: a new Amerindian genotype of hepatitis B virus revealed in Central America. *J Gen Virol* 2002; **83**: 2059-2073

7 **Norder H**, Couroucé AM, Coursaget P, Echevarria JM, Lee SD, Mushahwar IK, Robertson BH, Locarnini S, Magnius LO. Genetic diversity of hepatitis B virus strains derived worldwide: genotypes, subgenotypes, and HBsAg subtypes. *Intervirology* 2004; **47**: 289-309

8 **Kramvis A**, Kew MC. Relationship of genotypes of hepatitis B virus to mutations, disease progression and response to antiviral therapy. *J Viral Hepat* 2005; **12**: 456-464

9 **Chu CJ**, Lok AS. Clinical significance of hepatitis B virus genotypes. *Hepatology* 2002; **35**: 1274-1276

10 **Kramvis A**, Kew M, François G. Hepatitis B virus genotypes. *Vaccine* 2005; **23**: 2409-2423

11 **Miyakawa Y**, Mizokami M. Classifying hepatitis B virus genotypes. *Intervirology* 2003; **46**: 329-338

12 **Schaefer S**. Hepatitis B virus: significance of genotypes. *J Viral Hepat* 2005; **12**: 111-124

13 **Schaefer S**, Tolle T, Lottmann S, Gerlich W. Animal Models and Experimental Systems in Hepatitis B Virus Research. in: Koshy R, Caselmann W (eds). Hepatitis B Virus: Molecular Mechanisms in Disease and Novel Strategies for Therapy. London: Imperial College Press, 1998: 51-74

14 **Robertson BH**, Margolis HS. Primate hepatitis B viruses - genetic diversity, geography and evolution. *Rev Med Virol* 2002; **12**: 133-141

15 **Burda MR**, Günther S, Dandri M, Will H, Petersen J. Structural and functional heterogeneity of naturally occurring hepatitis B virus variants. *Antiviral Res* 2001; **52**: 125-138

16 **Abravaya K**, Huff J, Marshall R, Merchant B, Mullen C, Schneider G, Robinson J. Molecular beacons as diagnostic tools: technology and applications. *Clin Chem Lab Med* 2003; **41**: 468-474

17 **Li MD**, Bronson DL, Lemke TD, Faras AJ. Phylogenetic analyses of 55 retroelements on the basis of the nucleotide and product amino acid sequences of the pol gene. *Mol Biol Evol* 1995; **12**: 657-670

18 **Galibert F**, Mandart E, Fitoussi F, Tiollais P, Charnay P.

Nucleotide sequence of the hepatitis B virus genome (subtype ayw) cloned in E. coli. *Nature* 1979; **281**: 646-650
19 **Summers J**, Smolec JM, Snyder R. A virus similar to human hepatitis B virus associated with hepatitis and hepatoma in woodchucks. *Proc Natl Acad Sci USA* 1978; **75**: 4533-4537
20 **Marion PL**, Oshiro LS, Regnery DC, Scullard GH, Robinson WS. A virus in Beechey ground squirrels that is related to hepatitis B virus of humans. *Proc Natl Acad Sci USA* 1980; **77**: 2941-2945
21 **Mason WS**, Seal G, Summers J. Virus of Pekin ducks with structural and biological relatedness to human hepatitis B virus. *J Virol* 1980; **36**: 829-836
22 **Guo H**, Mason WS, Aldrich CE, Saputelli JR, Miller DS, Jilbert AR, Newbold JE. Identification and characterization of avihepadnaviruses isolated from exotic anseriformes maintained in captivity. *J Virol* 2005; **79**: 2729-2742
23 **Bartholomeusz A**, Schaefer S. Hepatitis B virus genotypes: comparison of genotyping methods. *Rev Med Virol* 2004; **14**: 3-16
24 **Sall AA**, Starkman S, Reynes JM, Lay S, Nhim T, Hunt M, Marx N, Simmonds P. Frequent infection of Hylobates pileatus (pileated gibbon) with species-associated variants of hepatitis B virus in Cambodia. *J Gen Virol* 2005; **86**: 333-337
25 **Marion PL** Ground Squirrel Hepatitis Virus. in: MacLachlan A (ed). Molecular Biology of the Hepatitis B Virus. Boca Raton: CRC Press, 1991: 39-51
26 **Paronetto F**, Tennant BC. Woodchuck hepatitis virus infection: a model of human hepatic diseases and hepatocellular carcinoma. *Prog Liver Dis* 1990; **9**: 463-483
27 **Roggendorf M**, Tolle TK. The woodchuck: an animal model for hepatitis B virus infection in man. *Intervirology* 1995; **38**: 100-112
28 **Huang Z**, Buckwold VE. A TaqMan PCR assay using degenerate primers for the quantitative detection of woodchuck hepatitis virus DNA of multiple genotypes. *Mol Cell Probes* 2005; **19**: 282-289
29 **Schödel F**, Weimer T, Fernholz D, Schneider R, Sprengel R, Wildner G, Will H The Biology of Avian Hepatitis B Viruses. In: MacLachlan A (editor). Molecular Biology of the Hepatitis B Virus. Boca Raton: CRC Press, 1991: 53-80
30 **Bollyky PL**, Holmes EC. Reconstructing the complex evolutionary history of hepatitis B virus. *J Mol Evol* 1999; **49**: 130-141
31 **Orito E**, Mizokami M, Ina Y, Moriyama EN, Kameshima N, Yamamoto M, Gojobori T. Host-independent evolution and a genetic classification of the hepadnavirus family based on nucleotide sequences. *Proc Natl Acad Sci USA* 1989; **86**: 7059-7062
32 **Simmonds P**. The origin and evolution of hepatitis viruses in humans. *J Gen Virol* 2001; **82**: 693-712
33 **Simmonds P**. Reconstructing the origins of human hepatitis viruses. *Philos Trans R Soc Lond B Biol Sci* 2001; **356**: 1013-1026
34 **Fares MA**, Holmes EC. A revised evolutionary history of hepatitis B virus (HBV). *J Mol Evol* 2002; **54**: 807-814
35 **Chu CJ**, Hussain M, Lok AS. Hepatitis B virus genotype B is associated with earlier HBeAg seroconversion compared with hepatitis B virus genotype C. *Gastroenterology* 2002; **122**: 1756-1762
36 **Sugauchi F**, Kumada H, Acharya SA, Shrestha SM, Gamutan MT, Khan M, Gish RG, Tanaka Y, Kato T, Orito E, Ueda R, Miyakawa Y, Mizokami M. Epidemiological and sequence differences between two subtypes (Ae and Aa) of hepatitis B virus genotype A. *J Gen Virol* 2004; **85**: 811-820
37 **Chan HL**, Tsui SK, Tse CH, Ng EY, Au TC, Yuen L, Bartholomeusz A, Leung KS, Lee KH, Locarnini S, Sung JJ. Epidemiological and virological characteristics of 2 subgroups of hepatitis B virus genotype C. *J Infect Dis* 2005; **191**: 2022-2032
38 **Huy TT**, Ushijima H, Quang VX, Win KM, Luengrojanakul P, Kikuchi K, Sata T, Abe K. Genotype C of hepatitis B virus can be classified into at least two subgroups. *J Gen Virol* 2004; **85**: 283-292
39 **Tanaka Y**, Orito E, Yuen MF, Mukaide M, Sugauchi F, Ito K, Ozasa A, Sakamoto T, Kurbanov F, Lai CL, Mizokami M. Two subtypes (subgenotypes) of hepatitis B virus genotype C: A novel subtyping assay based on restriction fragment length polymorphism. *Hepatol Res* 2005; **33**: 216-224
40 **Banerjee A**, Kurbanov F, Datta S, Chandra PK, Tanaka Y, Mizokami M, Chakravarty R. Phylogenetic relatedness and genetic diversity of hepatitis B virus isolates in Eastern India. *J Med Virol* 2006; **78**: 1164-1174
41 **Kimbi GC**, Kramvis A, Kew MC. Distinctive sequence characteristics of subgenotype A1 isolates of hepatitis B virus from South Africa. *J Gen Virol* 2004; **85**: 1211-1220
42 **Fujiwara K**, Tanaka Y, Orito E, Ohno T, Kato T, Sugihara K, Hasegawa I, Sakurai M, Ito K, Ozasa A, Sakamoto Y, Arita I, El-Gohary A, Benoit A, Ogoundele-Akplogan SI, Yoshihara N, Ueda R, Mizokami M. Distribution of HBV genotypes among HBV carriers in Benin:phylogenetic analysis and virological characteristics of HBV genotype E. *World J Gastroenterol* 2005; **11**: 6410-6415
43 **Huy TT**, Ishikawa K, Ampofo W, Izumi T, Nakajima A, Ansah J, Tetteh JO, Nii-Trebi N, Aidoo S, Ofori-Adjei D, Sata T, Ushijima H, Abe K. Characteristics of hepatitis B virus in Ghana: full length genome sequences indicate the endemicity of genotype E in West Africa. *J Med Virol* 2006; **78**: 178-184
44 **Kramvis A**, Restorp K, Norder H, Botha JF, Magnius LO, Kew MC. Full genome analysis of hepatitis B virus genotype E strains from South-Western Africa and Madagascar reveals low genetic variability. *J Med Virol* 2005; **77**: 47-52
45 **Mulders MN**, Venard V, Njayou M, Edorh AP, Bola Oyefolu AO, Kehinde MO, Muyembe Tamfum JJ, Nebie YK, Maiga I, Ammerlaan W, Fack F, Omilabu SA, Le Faou A, Muller CP. Low genetic diversity despite hyperendemicity of hepatitis B virus genotype E throughout West Africa. *J Infect Dis* 2004; **190**: 400-408
46 **Motta-Castro AR**, Martins RM, Yoshida CF, Teles SA, Paniago AM, Lima KM, Gomes SA. Hepatitis B virus infection in isolated Afro-Brazilian communities. *J Med Virol* 2005; **77**: 188-193
47 **Quintero A**, Martínez D, Alarcón De Noya B, Costagliola A, Urbina L, González N, Liprandi F, Castro De Guerra D, Pujol FH. Molecular epidemiology of hepatitis B virus in Afro-Venezuelan populations. *Arch Virol* 2002; **147**: 1829-1836
48 **Vieth S**, Manegold C, Drosten C, Nippraschk T, Günther S. Sequence and phylogenetic analysis of hepatitis B virus genotype G isolated in Germany. *Virus Genes* 2002; **24**: 153-156
49 **Sánchez LV**, Maldonado M, Bastidas-Ramírez BE, Norder H, Panduro A. Genotypes and S-gene variability of Mexican hepatitis B virus strains. *J Med Virol* 2002; **68**: 24-32
50 **Lindh M**. HBV genotype G-an odd genotype of unknown origin. *J Clin Virol* 2005; **34**: 315-316
51 **Hess G**, Arnold W, Koesters W, Biswas R, Hütteroth TH, zum Büschenfelde KH. Simultaneous presence of HBsAg and anti-HBs in the serum of different subtypes (serological and immunofluorescent studies). *Z Immunitatsforsch Immunobiol* 1977; **153**: 143-151
52 **Tabor E**, Gerety RJ, Smallwood LA, Barker LF. Coincident hepatitis B surface antigen and antibodies of different subtypes in human serum. *J Immunol* 1977; **118**: 369-370
53 **Kao JH**, Chen PJ, Lai MY, Chen DS. Acute exacerbations of chronic hepatitis B are rarely associated with superinfection of hepatitis B virus. *Hepatology* 2001; **34**: 817-823
54 **Gerner PR**, Friedt M, Oettinger R, Lausch E, Wirth S. The hepatitis B virus seroconversion to anti-HBe is frequently associated with HBV genotype changes and selection of preS2-defective particles in chronically infected children. *Virology* 1998; **245**: 163-172
55 **Hannoun C**, Krogsgaard K, Horal P, Lindh M. Genotype mixtures of hepatitis B virus in patients treated with interferon. *J Infect Dis* 2002; **186**: 752-759
56 **Ding X**, Gu H, Zhong ZH, Zilong X, Tran HT, Iwaki Y, Li TC, Sata T, Abe K. Molecular epidemiology of hepatitis viruses and genotypic distribution of hepatitis B and C viruses in Harbin, China. *Jpn J Infect Dis* 2003; **56**: 19-22
57 **Kato H**, Orito E, Sugauchi F, Ueda R, Koshizaka T, Yanaka S, Gish RG, Kurbanov F, Ruzibakiev R, Kramvis A, Kew MC, Ahmad N, Khan M, Usuda S, Miyakawa Y, Mizokami M. Frequent coinfection with hepatitis B virus strains of distinct

genotypes detected by hybridization with type-specific probes immobilized on a solid-phase support. *J Virol Methods* 2003; **110**: 29-35

58 **Osiowy C**, Giles E. Evaluation of the INNO-LiPA HBV genotyping assay for determination of hepatitis B virus genotype. *J Clin Microbiol* 2003; **41**: 5473-5477

59 **Olinger CM**, Venard V, Njayou M, Oyefolu AO, Maïga I, Kemp AJ, Omilabu SA, le Faou A, Muller CP. Phylogenetic analysis of the precore/core gene of hepatitis B virus genotypes E and A in West Africa: new subtypes, mixed infections and recombinations. *J Gen Virol* 2006; **87**: 1163-1173

60 **Chen BF**, Kao JH, Liu CJ, Chen DS, Chen PJ. Genotypic dominance and novel recombinations in HBV genotype B and C coinfected intravenous drug users. *J Med Virol* 2004; **73**: 13-22

61 **Kato H**, Orito E, Gish RG, Bzowej N, Newsom M, Sugauchi F, Suzuki S, Ueda R, Miyakawa Y, Mizokami M. Hepatitis B e antigen in sera from individuals infected with hepatitis B virus of genotype G. *Hepatology* 2002; **35**: 922-929

62 **Kremsdorf D**, Garreau F, Capel F, Petit MA, Brechot C. *In vivo* selection of a hepatitis B virus mutant with abnormal viral protein expression. *J Gen Virol* 1996; **77** (Pt 5): 929-939

63 **Simmonds P**, Midgley S. Recombination in the genesis and evolution of hepatitis B virus genotypes. *J Virol* 2005; **79**: 15467-15476

64 **Yang J**, Xing K, Deng R, Wang J, Wang X. Identification of Hepatitis B virus putative intergenotype recombinants by using fragment typing. *J Gen Virol* 2006; **87**: 2203-2215

65 **Magiorkinis EN**, Magiorkinis GN, Paraskevis DN, Hatzakis AE. Re-analysis of a human hepatitis B virus (HBV) isolate from an East African wild born Pan troglodytes schweinfurthii: evidence for interspecies recombination between HBV infecting chimpanzee and human. *Gene* 2005; **349**: 165-171

66 **Gutiérrez C**, Devesa M, Loureiro CL, León G, Liprandi F, Pujol FH. Molecular and serological evaluation of surface antigen negative hepatitis B virus infection in blood donors from Venezuela. *J Med Virol* 2004; **73**: 200-207

67 **Sugauchi F**, Orito E, Ichida T, Kato H, Sakugawa H, Kakumu S, Ishida T, Chutaputti A, Lai CL, Ueda R, Miyakawa Y, Mizokami M. Hepatitis B virus of genotype B with or without recombination with genotype C over the precore region plus the core gene. *J Virol* 2002; **76**: 5985-5992

68 **Cui C**, Shi J, Hui L, Xi H, Zhuoma G. The dominant hepatitis B virus genotype identified in Tibet is a C/D hybrid. *J Gen Virol* 2002; **83**: 2773-2777

69 **Wang Z**, Liu Z, Zeng G, Wen S, Qi Y, Ma S, Naoumov NV, Hou J. A new intertype recombinant between genotypes C and D of hepatitis B virus identified in China. *J Gen Virol* 2005; **86**: 985-990

70 **Zeng G**, Wang Z, Wen S, Jiang J, Wang L, Cheng J, Tan D, Xiao F, Ma S, Li W, Luo K, Naoumov NV, Hou J. Geographic distribution, virologic and clinical characteristics of hepatitis B virus genotypes in China. *J Viral Hepat* 2005; **12**: 609-617

71 **Nowak MA**, Bonhoeffer S, Hill AM, Boehme R, Thomas HC, McDade H. Viral dynamics in hepatitis B virus infection. *Proc Natl Acad Sci USA* 1996; **93**: 4398-4402

72 **Brechtbuehl K**, Whalley SA, Dusheiko GM, Saunders NA. A rapid real-time quantitative polymerase chain reaction for hepatitis B virus. *J Virol Methods* 2001; **93**: 105-113

73 **Bowyer SM**, Sim JG. Relationships within and between genotypes of hepatitis B virus at points across the genome: footprints of recombination in certain isolates. *J Gen Virol* 2000; **81**: 379-392

74 **Fischer SF**, Schmidt K, Fiedler N, Glebe D, Schüttler C, Sun J, Gerlich WH, Repp R, Schaefer S. Genotype-dependent activation or repression of HBV enhancer II by transcription factor COUP-TF1. *World J Gastroenterol* 2006; **12**: 6054-6058

75 **Dane DS**, Cameron CH, Briggs M. Virus-like particles in serum of patients with Australia-antigen- associated hepatitis. *Lancet* 1970; **1**: 695-698

76 **Vaudin M**, Wolstenholme AJ, Tsiquaye KN, Zuckerman AJ, Harrison TJ. The complete nucleotide sequence of the genome of a hepatitis B virus isolated from a naturally infected chimpanzee. *J Gen Virol* 1988; **69** (Pt 6): 1383-1389

77 **Norder H**, Ebert JW, Fields HA, Mushahwar IK, Magnius LO. Complete sequencing of a gibbon hepatitis B virus genome reveals a unique genotype distantly related to the chimpanzee hepatitis B virus. *Virology* 1996; **218**: 214-223

78 **Warren KS**, Heeney JL, Swan RA, Heriyanto EJ. A new group of hepadnaviruses naturally infecting orangutans (Pongo pygmaeus). *J Virol* 1999; **73**: 7860-7865

79 **Grethe S**, Heckel JO, Rietschel W, Hufert FT. Molecular epidemiology of hepatitis B virus variants in nonhuman primates. *J. Virol.* 2000; **74**: 5377- 5381

80 **Lanford RE**, Chavez D, Brasky KM, Burns RB, Rico-Hesse R. Isolation of a hepadnavirus from the woolly monkey, a New World primate. *Proc Natl Acad Sci USA* 1998; **95**: 5757-5761

81 **Testut P**, Renard CA, Terradillos O, Vitvitski-Trepo L, Tekaia F, Degott C, Blake J, Boyer B, Buendia MA. A new hepadnavirus endemic in arctic ground squirrels in Alaska. *J Virol* 1996; **70**: 4210-4219

82 **Li L**, Dixon RJ, Gu X, Newbold JE: Comparison of the sequences of the Grey Teal, Maned Duck and Duck Hepatitis B Viruses. In The molecular biology of Hepatitis B Virus. The United States: University of California San Diego, 1998: 13

83 **Sprengel R**, Kaleta EF, Will H. Isolation and characterization of a hepatitis B virus endemic in herons. *J Virol* 1988; **62**: 3832-3839

84 **Chang SF**, Netter HJ, Bruns M, Schneider R, Frölich K, Will H. A new avian hepadnavirus infecting snow geese (Anser caerulescens) produces a significant fraction of virions containing single-stranded DNA. *Virology* 1999; **262**: 39-54

85 **Pult I**, Netter HJ, Fröhlich K, Kaleta EF, Will H: Identification, structural and functional analysis of a new avian Hepadnavirus from storks (STHBV). In The molecular biology of Hepatitis B Virus. The United States: University of California San Diego, 1998: 2

86 **Prassolov A**, Hohenberg H, Kalinina T, Schneider C, Cova L, Krone O, Frölich K, Will H, Sirma H. New hepatitis B virus of cranes that has an unexpected broad host range. *J Virol* 2003; **77**: 1964-1976

87 **Kramvis A**, Weitzmann L, Owiredu WK, Kew MC. Analysis of the complete genome of subgroup A' hepatitis B virus isolates from South Africa. *J Gen Virol* 2002; **83**: 835-839

88 **Kurbanov F**, Tanaka Y, Fujiwara K, Sugauchi F, Mbanya D, Zekeng L, Ndembi N, Ngansop C, Kaptue L, Miura T, Ido E, Hayami M, Ichimura H, Mizokami M. A new subtype (subgenotype) Ac (A3) of hepatitis B virus and recombination between genotypes A and E in Cameroon. *J Gen Virol* 2005; **86**: 2047-2056

89 **Makuwa M**, Souquière S, Telfer P, Apetrei C, Vray M, Bedjabaga I, Mouinga-Ondeme A, Onanga R, Marx PA, Kazanji M, Roques P, Simon F. Identification of hepatitis B virus subgenotype A3 in rural Gabon. *J Med Virol* 2006; **78**: 1175-1184

90 **Sugauchi F**, Orito E, Ichida T, Kato H, Sakugawa H, Kakumu S, Ishida T, Chutaputti A, Lai CL, Gish RG, Ueda R, Miyakawa Y, Mizokami M. Epidemiologic and virologic characteristics of hepatitis B virus genotype B having the recombination with genotype C. *Gastroenterology* 2003; **124**: 925-932

91 **Nagasaki F**, Niitsuma H, Cervantes JG, Chiba M, Hong S, Ojima T, Ueno Y, Bondoc E, Kobayashi K, Ishii M, Shimosegawa T. Analysis of the entire nucleotide sequence of hepatitis B virus genotype B in the Philippines reveals a new subgenotype of genotype B. *J Gen Virol* 2006; **87**: 1175-1180

92 **Sakamoto T**, Tanaka Y, Orito E, Co J, Clavio J, Sugauchi F, Ito K, Ozasa A, Quino A, Ueda R, Sollano J, Mizokami M. Novel subtypes (subgenotypes) of hepatitis B virus genotypes B and C among chronic liver disease patients in the Philippines. *J Gen Virol* 2006; **87**: 1873-1882

93 **Sugauchi F**, Mizokami M, Orito E, Ohno T, Kato H, Suzuki S, Kimura Y, Ueda R, Butterworth LA, Cooksley WG. A novel variant genotype C of hepatitis B virus identified in isolates from Australian Aborigines: complete genome sequence and phylogenetic relatedness. *J Gen Virol* 2001; **82**: 883-892

94 **Cavinta L**, Sun J, Zarnekow M, Barzaga N, Schaefer S. New

hepatitis B virus subgenotype C5 from the Philippines. submitted
95 **Kato H**, Fujiwara K, Gish RG, Sakugawa H, Yoshizawa H, Sugauchi F, Orito E, Ueda R, Tanaka Y, Kato T, Miyakawa Y, Mizokami M. Classifying genotype F of hepatitis B virus into F1 and F2 subtypes. *World J Gastroenterol* 2005; **11**: 6295-6304
96 **Norder H**, Arauz-Ruiz P, Blitz L, Pujol FH, Echevarria JM, Magnius LO. The T(1858) variant predisposing to the precore stop mutation correlates with one of two major genotype F hepatitis B virus clades. *J Gen Virol* 2003; **84**: 2083-2087
97 **Devesa M**, Rodríguez C, León G, Liprandi F, Pujol FH. Clade analysis and surface antigen polymorphism of hepatitis B virus American genotypes. *J Med Virol* 2004; **72**: 377-384
98 **Huy TT**, Ushijima H, Sata T, Abe K. Genomic characterization of HBV genotype F in Bolivia: genotype F subgenotypes correlate with geographic distribution and T(1858) variant. *Arch Virol* 2006; **151**: 589-597
99 **Hannoun C**, Norder H, Lindh M. An aberrant genotype revealed in recombinant hepatitis B virus strains from Vietnam. *J Gen Virol* 2000; **81**: 2267-2272
100 **Owiredu WK**, Kramvis A, Kew MC. Hepatitis B virus DNA in serum of healthy black African adults positive for hepatitis B surface antibody alone: possible association with recombination between genotypes A and D. *J Med Virol* 2001; **64**: 441-454
101 **Bollyky PL**, Rambaut A, Harvey PH, Holmes EC. Recombination between sequences of hepatitis B virus from different genotypes. *J Mol Evol* 1996; **42**: 97-102
102 **Morozov V**, Pisareva M, Groudinin M. Homologous recombination between different genotypes of hepatitis B virus. *Gene* 2000; **260**: 55-65
103 **Suwannakarn K**, Tangkijvanich P, Theamboonlers A, Abe K, Poovorawan Y. A novel recombinant of Hepatitis B virus genotypes G and C isolated from a Thai patient with hepatocellular carcinoma. *J Gen Virol* 2005; **86**: 3027-3030
104 **Kumar S**, Tamura K, Nei M. MEGA3: Integrated software for Molecular Evolutionary Genetics Analysis and sequence alignment. *Brief Bioinform* 2004; **5**: 150-163

S- Editor Liu Y **L- Editor** Lutze M **E- Editor** Ma WH

PO Box 2345, Beijing 100023, China
www.wjgnet.com
wjg@wjgnet.com

World J Gastroenterol 2007 January 7; 13(1): 22-38
World Journal of Gastroenterology ISSN 1007-9327

TOPIC HIGHLIGHT

Dieter Glebe, PhD, *Series Editor*

Viral and cellular determinants involved in hepadnaviral entry

Dieter Glebe, Stephan Urban

Dieter Glebe, Institute of Medical Virology, Justus-Liebig University of Giessen, Frankfurter Str. 107, D-35392 Giessen, Germany
Stephan Urban, Department of Molecular Virology, Otto Meyerhof Zentrum, University of Heidelberg, Im Neuenheimer Feld 350, D-69120 Heidelberg, Germany
Supported by grant SFB535/A2 from DFG, EU QLK 2000-01476 and DFG UR72/1-3, UR72/1-4
Correspondence to: Dieter Glebe, Institute of Medical Virology, Justus-Liebig University of Giessen, Frankfurter Str. 107, D-35392 Giessen,
Germany. dieter.glebe@viro.med.uni-giessen.de
Telephone: +49-641-9941203 Fax: +49-641-9941209
Received: 2006-09-11 Accepted: 2006-12-07

Abstract

Hepadnaviridae is a family of hepatotropic DNA viruses that is divided into the genera *orthohepadnavirus* of mammals and *avihepadnavirus* of birds. All members of this family can cause acute and chronic hepatic infection, which in the case of human hepatitis B virus (HBV) constitutes a major global health problem. Although our knowledge about the molecular biology of these highly liver-specific viruses has profoundly increased in the last two decades, the mechanisms of attachment and productive entrance into the differentiated host hepatocytes are still enigmatic. The difficulties in studying hepadnaviral entry were primarily caused by the lack of easily accessible *in vitro* infection systems. Thus, for more than twenty years, differentiated primary hepatocytes from the respective species were the only *in vitro* models for both *orthohepadnaviruses* (e.g. HBV) and *avihepadnaviruses* (e.g. duck hepatitis B virus [DHBV]). Two important discoveries have been made recently regarding HBV: (1) primary hepatocytes from tree-shrews; i.e., *Tupaia belangeri*, can be substituted for primary human hepatocytes, and (2) a human hepatoma cell line (HepaRG) was established that gains susceptibility for HBV infection upon induction of differentiation *in vitro*. A number of potential HBV receptor candidates have been described in the past, but none of them have been confirmed to function as a receptor. For DHBV and probably all other avian hepadnaviruses, carboxypeptidase D (CPD) has been shown to be indispensable for infection, although the exact role of this molecule is still under debate. While still restricted to the use of primary duck hepatocytes (PDH), investigations performed with DHBV provided important general concepts on the first steps of hepadnaviral infection. However, with emerging data obtained from the new HBV infection systems, the hope that DHBV utilizes the same mechanism as HBV only partially held true. Nevertheless, both HBV and DHBV *in vitro* infection systems will help to: (1) functionally dissect the hepadnaviral entry pathways, (2) perform reverse genetics (e.g. test the fitness of escape mutants), (3) titrate and map neutralizing antibodies, (4) improve current vaccines to combat acute and chronic infections of hepatitis B, and (5) develop entry inhibitors for future clinical applications.

Key words: Hepatitis B virus; Duck hepatitis B virus; Infection models; Receptor; Viral attachment; *Tupaia belangeri*; HepaRG; Carboxypeptidase D

Glebe D, Urban S. Viral and cellular determinants involved in hepadnaviral entry. *World J Gastroenterol* 2007; 13(1): 22-38

http://www.wjgnet.com/1007-9327/13/22.asp

INTRODUCTION

The first step in virus infection is an energy independent attachment of the infectious particle to an accessible structure exposed at the host cell surface. Primary attachment, often characterized by low affinity and reversibility, is usually followed by the passage of the virion to a more specific receptor, which mediates further steps of entry. Both initial attachment and specific receptor recognition often contribute to host specificity and tissue tropism. For enveloped viruses, receptor binding is followed by fusion of the virus with either the plasma or an endosomal membrane. Fusion within intracellular vesicles is regularly triggered by acidification. The universal mechanism of membrane fusion requires conformational changes of virus-encoded fusion proteins leading to a physical approximation and finally merging of viral and cellular membranes[1]. A detailed understanding of receptor binding and membrane fusion is of general interest for molecular virologists and it also provides the basis for therapeutics that interfere with the early steps of infection, as has been successfully accomplished for HIV[2].

HBV and related animal viruses form the family *hepadnaviridae*, which are small, enveloped DNA viruses that cause acute and chronic liver infection. They are

divided into the *orthohepadnaviruses* of mammals and *avihepadnaviruses* of birds[3] (see also the review on HBV taxonomy and genotypes by S. Schaefer in this series). HBV is a serious global infectious diseases and it is assumed that 2 billion people have had contact with that virus[4]. The infection can lead to a chronic carrier state in 5%-10% of immunocompetent adults and up to 90% of infected neonates. Chronic HBV infection is the major cause of liver cirrhosis and hepatocellular carcinoma in numerous regions of the world[5]. While the viral life cycle is still not fully understood, a safe and efficient vaccine has been developed and sensitive tests for HBV surface protein (HBsAg) now allow for reliable diagnosis and screening of blood products. Present therapeutic regimens for HBV address either the host immune system (α-interferon [IFNα]) or inhibit reverse transcription of the viral pregenomic RNA by nucleoside inhibitors (Lamivudine, Adefovir, Entecavir). The latter provoke the selection of resistant or even cross-resistant mutants that will become increasingly problematic to therapeutic control in the future (see also review "Antiviral therapy and resistance of hepatitis B virus infection" by H.L. Tillmann in this series).

To overcome these challenges, antiviral substances that target different replication steps; e.g. inhibitors of viral entry or improved vaccines that counteract the current escape-mutants, are becoming increasingly important. In the past, however, the lack of feasible HBV *in vitro* infection systems hampered investigations aiming in this direction. The only immunocompetent *in vivo* model that could be used for studies related to the infectivity of the virus was based on primary human hepatocytes (PHH) and those of the chimpanzee, which were limited in availability.

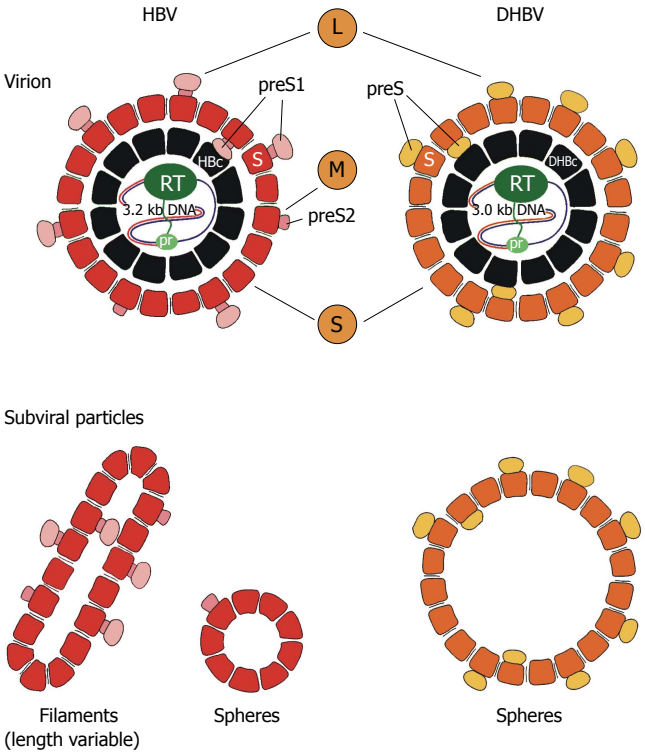

Figure 1 Schematic presentation of human (HBV) and duck (DHBV) hepatitis B virus. The viral DNA is drawn as a single or double line. The viral polymerase is depicted with the primer domain (pr) and the reverse transcription domain (RT). The nucleocapsid (core or HBc/DHBc) is shown in black. Reported encapsidated cellular proteins are omitted. For HBV the surface proteins L, M and S are shown with the S-domain, the preS2-domain and the preS1-domain, whereas for DHBV, L- and S-surface proteins with preS and S-domain are depicted. St, truncated form of DHBV S-surface protein. Non-infectious subviral particles of HBV are shown in filamentous and spherical form and in larger spheroids in the case of DHBV.

ORGANIZATION OF THE HEPADNAVIRAL ENVELOPE

A hallmark of hepadnaviral infection is the constitutive secretion of nucleocapsid-free subviral particles (SVP), mainly composed of the hepadnaviral envelope proteins (large and small in the case of DHBV and large, middle, and small for HBV). HBV-SVPs exist as 22 nm spheres or filaments of the same diameter but variable in length. The HB virions appear in electron microscopy after negative staining as spheres of 45 nm. Virions and SVP contain variable proportions of the three co-carboxyterminal surface (glyco)-proteins; i.e., the large (LHBs), middle (MHBs) and small (SHBs) surface proteins (Figure 1). The SHBs protein is the major component of the virion envelope and the subviral HBsAg particles, while virions and filaments contain more LHB proteins than spheres[6]. In contrast DHBV and DHBV-SVPs are similar in size and shape (55-60 nm)[7] and contain a similar ratio of both envelope proteins (L:S = 1:5). In addition DHBV incorporates a processed version of the DHBs protein consisting of only the two N-terminal transmembrane domains of S and are therefore called S^t[8]. The hepadnaviral surface proteins are products of a single open reading frame and distinguished by three (HBV) or two (DHBV) domains. HBV comprises: preS1 (108 or 119 aa depending on the genotype) only in LHBs, preS2 (55 aa) in LHBs and MHBs, and S (226 aa) common to all three HBs proteins (Figure 2A). All three proteins bear within the S-domain a potential N-glycosylation site (NG) at Asn-146, which is only partially utilised. The second N-glycosylation site at Asn-4 in the preS2-domain is modified in MHBs but not in LHBs[6]. In addition to N-glycans, the preS2 domain of most *orthohepadnaviruses* contains O-glycans[9]. The preS2 domain of both LHBs and MHBs contains a single mucin-type O-glycan (OG) at Thr-37 in genotypes B-H. O-glycans are absent in genotype A, because the O-glycosylation site at Thr-37 is exchanged to Asp in genotype A for an unknown reason[10]. Although potential N- and O-glycosylation sites within the preS1 domain are present, none of them are used due to the cytoplasmic exposition of preS1 during synthesis. In contrast, the two DHBV envelope proteins L (preS+S) and S remain unglycosylated during secretion, but DHBV-L becomes phosphorylated[11] (for more details see review "Avian hepatitis B viruses: molecular and cellular biology, phylogenesis and host tropism" by Funk *et al* in this series). The N-termini of probably all hepadnaviral L-proteins contain recognition sequences that lead to myristoylation at Gly-2[12] while, at least in HBV, more carboxyterminal parts serve as envelopment signals for cytoplasmic core particles[13,14]. Several lines of evidence indicate that hepadnaviral L-proteins adopt dual topologies with half of their preS-domains located inside the particle,

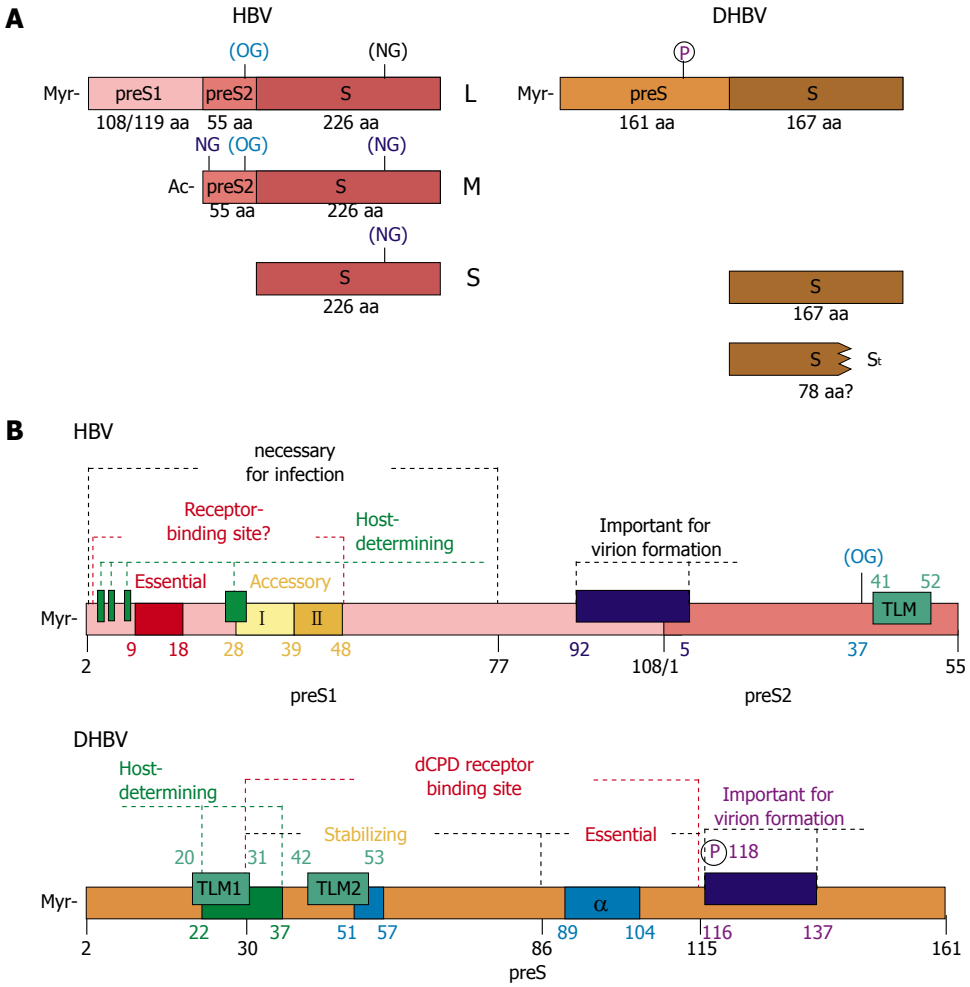

Figure 2 Surface proteins of HBV and DHBV. (**A**) Schematic organisation of the three surface proteins of HBV and the two surface proteins of DHBV. For HBV, used N- and O-glycosylation sites (NG and OG) are shown, (parenthesis indicate partial glycosylation). DHBV surface proteins are non-glycosylated, but the L-protein is phosphorylated at position 118 within its preS-domain. The L-protein of HBV and DHBV is myristoylated (Myr) at Gly-2 of the N-terminus of preS1 or preS, respectively. In case of HBV the preS1-domain encodes for 108 or 119 amino acids, depending on the genotype. The preS2-domain of MHBs is N-terminally acetylated (Ac) and is 55 amino acids long, while a preS2-domain and therefore a special M-protein is missing in DHBV. (**B**) Schematic presentation of preS-domains of HBV and DHBV important for virion formation and viral entry. The host-determining regions are depicted in green. The potential receptor binding site within the preS1-domain of HBV is shown with the essential domain (aa 9-18) and the two accessory domains (aa 28-39 and 39-48, respectively). For DHBV, the carboxypeptidase D (dCPD) binding site is depicted with the essential and stabilizing domains. Alpha helical domains are shown in blue (α). Reported trans-location motives (TLM) are marked in boxes. In DHBV preS, two TLMs are predicted (TLM1 and TLM2). TLM1 overlaps with the host-determining region, while TLM2 is located within the stabilizing sequence of the dCPD receptor binding site. In the case of HBV, the carboxyterminus of the 55 aa long preS2-domain was reported to contain a single TLM. The numbering of HBV preS1 is for genotype D (108 aa). P, phosphorylation site; OG, O-glycosylation; myr, myristoylation.

while the other half is located on the outside[15-18]. Virions and SVP particles bud to a lumen of a post-ER, pre-Golgi intermediate compartment. Therefore the particles contain lipids derived from intracellular compartments, rather than from the plasma membrane. The SHBs subunits of HBV and the subviral particles in the blood are highly cross-linked by disulfide-bonds and do not disassemble in the presence of detergents, unless the disulfide bonds are opened. Interestingly, this tight network of disulfide bridges is not found in DHBV particles. Those can easily be solubilised in mild detergents and both types of surface proteins do not form heterodimeric complexes (unpublished results).

CELL CULTURE SYSTEMS FOR VIRUS PRODUCTION AND ENTRY ANALYSIS

It is known that after artificial delivery of replication competent DNA constructs, later steps of the viral life cycle are not rigidly host-restricted. Transfection of hepatoma cell lines[19-21] or mouse liver cells[22] with replication-competent HBV/DHBV genomes results in the production and secretion of infectious virions. The same holds true for HBV transgenic mice[23]. Furthermore, lipofection of mature core particles, isolated from serum-derived virions into non-permissive hepatoma cells resulted in a full replication cycle of HBV[24]. This suggests that species-specificity of infection is determined at an early step; e.g. viral attachment, entry or fusion. Interestingly, productive infection not only depends on the species origin but also on the state of differentiation of the same cell line. This has been impressively demonstrated in HepaRG cells, which gain susceptibility towards HBV infection only several weeks after induction of differentiation[25]. In case of primary tupaia, human or duck hepatocyte cultures, susceptibility is achieved about one day after attachment

of the perfused and already differentiated hepatocytes, but is lost during prolonged culturing. Since binding and virus accumulation in HepaRG cells is similar in both, differentiated and undifferentiated cells (unpublished data) the restriction may not be caused by the bare presence or absence of a host entry molecule but might be complicated due to the polarisation state of the differentiated cell.

PRIMARY HEPATOCYTE CULTURES AND RELIABLE MARKERS FOR INFECTION

For many years, cultures of primary human hepatocytes (PHH), obtained by immediate perfusion of liver pieces after surgical resection, were the only cells to study viral infectivity[26]. PHH are not easy to handle, cannot be propagated *in vitro* and need particular growth factors for maintenance of their differentiated state[27]. Moreover, the efficiency of HBV infection of PHH *in vitro* was reported to be low leading to only a few percent of cells being infected and a negligible spread within the cell culture. Thus, virus amplification is not achievable. This can be counteracted to some extent by the addition of dimethylsulfoxide (DMSO) during cultivation and the use of 4% polyethylene glycol (PEG) during infection[28-31]. In contrast, infection of PDH with DHBV leads to a spread of infection to virtually every cell in the culture even when very low initial virus titers were supplied. A major drawback of PHH is their limited availability and the heterogeneity in quality with different liver cell preparations resulting in varying susceptibilities towards HBV infection. Furthermore, susceptibility is limited during culture (5-7 d) when DMSO or hydrocortisone is omitted[26,29,30]. Fortunately, primary hepatocyte cultures from *Tupaia belangeri* (PTH) can be infected with HBV as efficiently as PHH cultures of good quality. In contrast to PHH, PTH can also be infected with a primate hepadnavirus from woolly monkey (WMHBV)[32]. Nevertheless, the host range of PTH is restricted to human and primate HBV, since productive infection with rodent hepatitis B virus (woodchuck hepatitis B virus, WHV) is not possible[32].

Hepadnaviruses are non-cytopathic and do not induce conspicuous morphological changes of infected cells. Thus, detection and quantification of infectious virions cannot be achieved by simple virological methods; e.g. plaque test. In general, verification of *in vitro* HBV/DHBV infection should be done by quantification of different markers of an established HBV infection. Conversion of the relaxed circular (rc) DNA genomes of the incoming virus to covalently closed circular (ccc) DNA within the nucleus of an infected hepatocyte is the first marker of a productive HBV/DHBV infection, but is difficult to detect. The amount of cccDNA in just newly infected hepatocytes is very small compared to the large amounts of viral input DNA (as rcDNA), usually needed for efficient *in vitro* infection. Furthermore, DNA-containing particles are also taken up by cells that are not susceptible to infection. This is especially problematic when using embryonic duck hepatocyte preparations because they contain a high percentage of non-parenchymal cells (e.g. antigen-presenting liver sinusoidal endothelial cells). However, quantitative real-time PCR protocols are available that amplify specifically cccDNA, but not rcDNA. With these protocols, specific detection of small amounts of cccDNA is possible, even in the presence of a large excess of rcDNA within infected hepatocytes[24,33]. Verification of specific HBV infection can also be achieved by detection of viral mRNA extracted from cells by either Northern Blot hybridisation or quantitative RT-PCR, usually resulting in higher sensitivity. Less demanding is the detection of secreted viral antigens; i.e., HBeAg or HBsAg, 9-12 d post infection, which could be done by commercially available ELISAs[33,34]. Especially when using enriched or highly purified viral inocula, HBeAg should be the marker of choice, since it is not present in the viral input, in contrast to HBsAg. However, since HBsAg can be detected with higher sensitivity than HBeAg it can be used as a marker, provided that several medium exchanges have been performed prior to the measurement, optimally between day 9-12[33,35]. This is necessary to get rid of input HBsAg, which is released from cells even after removal of the inoculum. There are several reports of alleged infections that determine HBsAg 2 d post infection in the supernatant spuriously assuming that this is progeny viral antigen[36,37]. Using optimized methods, the current detection limit in the PTH-system for purified HBV from human plasma is one HBV particle per hepatocyte in culture plates with 10^5 cells[33,34]. Addition of PEG and DMSO during infection is not necessary to achieve optimal infectivity in PTH[38], as was reported to be beneficial to increase HBV infection of PHH[26,29]. Therefore, *Tupaia belangeri* represent a valuable tool to overcome the restrictions associated with PHH .

HEPATIC CELL LINES

To become independent in the utilization of primary hepatocyte cultures, many groups explored the potentiality of human hepatoma cell lines for infection experiments. HepG2 cells were employed extensively for binding and infection experiments. HepG2-cells exhibit some features of differentiated liver parenchymal cells; e.g. expression of serum albumin[39], and are successfully used for the production of virions after stable or transient transfection of HBV DNA[19,40]. Several studies reported specific binding and uptake of HBV by HepG2 cells[41-46], however, no productive infection was observed by these researchers. In contrast, Bchini *et al*[47] and Paran *et al*[48] reported successful detection of viral antigens upon infection of HepG2 cells that were cultivated with, inter alia, DMSO and 5-aza-2´-deoxycytidine. Unfortunately, these results could not be reproduced by others. In order to search for an explanation for the refractoriness of HepG2 cells towards HBV, Qiao *et al*[43] supposed an inability of the incoming HBV core particles to reach the nucleus, while overexpression of serine protease inhibitor Kazal (SPIK) was suggested by another group[49]. The discovery that the addition of 2% DMSO into the culture medium of primary rat hepatocytes upholds their differentiated state through maintenance of hepatocyte specific detoxification enzymes (e.g. cytochrome P450) was a milestone for hepatic pharmacology[50]. Since hepadnaviral infection depends on the differentiated state of the hepatocyte, this method was

Table 1 Described binding partners for HBV preS1-domain. Numbering of aminoacids (aa) are given for HBV genotype D

Domain	aa	Described interaction partners/binding factors for HBV	Ref.
preS1	10-36	Hepatoma cells bind to preS1 peptide. Inhibition by peptide-antisera	[41]
	19-25	Binding of recombinant subviral particles containing preS1 to human liver. Inhibition by anti-preS1 aa19-25	[142]
	10-36	PreS1-peptide binding not limited to liver cells, also on extrahepatic sites	[143]
	10-36	Partial homology of preS1 aa10-36 with IgA. HBV entry via IgA-binding receptor?	[144]
	18-25	PreS1 aa18-25 crossreact with IgA alpha-1 chain, IgA and HBV use related receptors?	[145]
	10-36	PreS1 aa10-36 binding to 31 kDa protein on HepG2 cells	[146]
	10-36	PreS1-peptide aa10-36 binds to Interleukin 6 (IL6) but not IL3, IL5 and IL7	[147]
	10-36	CHO cells transfected with IL6 cDNA acquire binding sites for preS1 peptide aa10-36	[148]
	10-36	Isolation of 44 kDa protein (HBV-BP) from HepG2 plasma membranes. Homology to SCCA1, human squamous cell carcinoma antigen 1 (human serpin)	[46]
	preS1-GST	Isolation of p80 binding protein from human hepatocytes. Needs preS1 aa12-20/82-90 for binding. p80 binding also to rat hepatocytes	[149]
	preS1	Anti-idiotypic antisera of antibody inhibiting binding of HBV to HepG2. 35kDa protein homology to Glycerinaldehyde-3-phoshate-dehydrgenase (GAPD)	[150,151]
	preS1/ preS2	50 kDa serum glycoprotein interferes with binding of preS1 and preS2 mabs. Soluble form of plasma membrane Protein on human hepatocytes	[152]
	preS1	Yeast two-hybrid assay I: preS1 domain and human liver cDNA library. Isolation of two unknown proteins.	[153]
	preS1	Yeast two-hybrid assay II: preS1 domain and human liver cDNA library. Isolation of cytoplasmic "nascent polypeptide-associated complex alpha polypeptide" (NACA)	[154]
	HBV particles	Asialoglycoproteinreceptor (ASGPR) Ⅰ: preS1-but not preS2-mabs inhibited binding of HBV to ASGPR. SHBs did not bind to ASGPR	[44]
	HBV particles	Asialoglycoproteinreceptor (ASGPR) Ⅱ: HBV uptake by HepG2 and HuH7 (ASGPR+), but not CHO (ASGPR-)	[45]
	HBV particles	Asialoglycoproteinreceptor (ASGPR) Ⅲ: Desialylated HBV only binds to HepG2. Uptake only by susceptible primary human hepatocytes	[155]
	HBV particles	Asialoglycoproteinreceptor (ASGPR) Ⅳ: Increased HBV uptake by HepG2 after desialyation results in HBV infection	[156]

also successfully used for HBV and DHBV infection after preparation of human and duck hepatocytes[26,29,51]. While the method of induced HBV-susceptibility of long-term DMSO-treated hepatoma cell lines was not successful in established hepatoma cell lines (e.g. HepG2 or HuH7), evidence for this principle has been shown for a new hepatoma cell line (HepaRG). This cell line, established from a liver tumour of a female patient suffering from hepatocarcinoma and chronic hepatitis C infection, was shown to become susceptible to HBV and HDV infection upon treatment with DMSO and hydrocortisone[25,52]. The necessity of long term induction of HepaRG differentiation by DMSO and hydrocortisone prior to infection is time consuming, however, it provides the opportunity to decipher cellular determinants of hepatocyte differentiation and their influence on HBV infection for the first time.

In summary, the optimal system for the study of hepadnaviral attachment and entry *in vitro* are primary hepatocyte cultures of Pekin ducks and humans, the latter being very limited in supply and heterogeneous in quality and susceptibility to HBV. Primary hepatocyte cultures from *Tupaia belangeri* and the newly established HepaRG cells can overcome these limitations and provide a nearly unlimited supply of HBV-susceptible hepatic cells for various experimental settings.

CELLULAR AND VIRAL BINDING FACTORS CRUCIAL FOR HBV INFECTIVITY

During the last 25 years, numerous reports on a variety of possible cellular HBV binding partners, involving all three HBV surface proteins, have been published (Tables 1 and 2). Many researchers tried to isolate HBV binding components from plasma membranes of either primary human hepatocytes or established hepatic cell lines (e.g. HepG2) with the help of HBV-peptides or complete (subviral-) particles. In contrast to the DHBV-model discussed later in this review, none of these potential HBV-binding factors has ever been convincingly shown to be essential in HBV entry[53].

FUNCTION OF THE PRES1 DOMAIN

In 1986, Neurath *et al*[41] reported that a synthetic preS1 peptide, comprising amino acids 21-47 and corresponding to amino acids 10-36 in genotype D, E and G binds HepG2 cells and also inhibits HBV binding to this cell line. Furthermore, antibodies directed against this peptide compete with binding of HBV particles to HepG2 cells. They could, however, not show the relevance of their findings for the infection process. These early data were consistent with functional studies of Le Seyec *et al*[54], demonstrating that preS1 amino acids 3-77 of the HBV L-protein are essential for infectivity. In two independent studies, it was further shown that acylation of glycine 2 of preS1 with myristic acid is necessary for efficient hepadnaviral infection[55,56]. Interestingly, a synthetic peptide representing this essential 77 preS1-amino acids, including the N-terminal myristic acid moiety, was able to block HBV infection when added to the medium during infection[25]. Similarly, DHBV infection was sensitive against N-terminal preS-peptides DHBVpreS2-41. Surprisingly the inhibitory activity could be drastically increased by N-terminal myristoylation[57]. The effect of myristoylation

Table 2 Described binding partners for HBV preS2 and S-domains

Domain	aa	Described interaction partners/binding factors for HBV	Ref.
preS2		Binds to polymerised human serum albumin (pHSA). pHSA has affinity to hepatocytes	[157]
		Preincubation of human liver membranes with pHSA induced binding of rec. HBsAg/preS2	[158]
		Natural pHSA only present in minor amount in serum	[159]
	3-16	Natural monomeric HSA binds to preS2 domain aa 3-16	[160]
	3-16	Binding site for pHSA	[161]
	2-24	Polyclonal antisera against preS2 peptide (2-24) neutralised HBV infection of chimpanzees	[71]
	14-32	Immunisation of chimpanzees with preS2 peptide (14-32) protected against infection	[162]
	3-16	PreS2 antisera against aa 3-16 inhibited infection completely, others only partially	[33]
S		Human apolipoprotein H (apo H) binds to small surface protein (SHBs)	[163,164]
		SHBs binds endonexin Ⅱ, now called annexin V	[165]
		Overexpression of annexin V in rat hepatoma cells supported HBV-infection	[166]
		Yeast-derived SHBs alone did not bind to HBV-susceptible hepatocytes	[34]

on the inhibitory potential of preS1 lipopeptides for human HBV[25] was also shown using PTHs[34], and HepaRG cells[58] confirming the fact that myristoylation of the preS-domain of hepadnaviral L-proteins is essential for infectivity, but also indicating that this modification seems to play a role in the context of extracellular inhibition by a peptide. Furthermore, it turned out that the inhibitory activity of the preS1 lipopeptides is dependent on the hydrophobicity of the N-terminal acyl residues. Stepwise increased inhibitory potential of the lipopeptides could be achieved by increasing the chain length from C5 (pentanoyl) to C14 (myristoyl), C16 (palmitoyl) and C18 (stearoyl)[34,58]. The role of the N-terminal myristoylation of preS1 during attachment and entry of HBV is still unclear. One explanation might be that the interaction of preS1 and its receptor might be enhanced by an insertion of myristic acid into the membranes or the receptor. Exposure of a myristoylated peptide or protein ("myristoyl-switch") after attachment is a known element of viral entry mechanisms for some nonenveloped viruses, such as picornaviruses[59] and reoviruses[60].

Using a set of myristoylated HBV preS1 peptides of variable length, the attachment site of HBV was further narrowed down[34]. The data obtained using PTH suggest that: (1) residues containing the first 8 amino acids of preS1 (19 in genotype A) are dispensable, (2) residues in aa 9-18 are essential, (3) residues within aa 19-28 are dispensable, whereas iv) residues of aa 29-48 enhance infection inhibition (Figure 2B). Similar results were obtained in HepaRG cells and PHH in the presence or absence of PEG[58]. Introducing an *E. coli*-based expression system for the production of myristoylated preS-fusion proteins, Engelke *et al*[35] verified that region 9-18 is essential for virion infectivity and identified single amino acids (aa 11, 12, 13 for geno-type D) within this region that are crucial for infection inhibition. Recombinant HBV particles carrying the same point mutations are not infectious. Interestingly, hepatitis delta virus (HDV), an RNA virus that replicates in HBV infected hepatocytes and packages its ribonucleoprotein into the HBV envelope (for a recent review see[61]) can be inhibited by acylated HBV preS-derived peptides with the same specificity[35]. Thus HDV uses at least one common step for entering hepatocytes and is therefore also suitable to study HBV entry events. Surprisingly, HBV-preS1 lipopeptides containing amino acids between aa 49 until aa 78 (the region that has been shown to be important for infectivity of virions[54]) did not further increase but weakened infection inhibition[34,58]. Thus this part of the L-protein may play a role in a different step of infection process. Segment 9-18 is highly conserved with only 3 exchanges in 330 positions of the eleven HBV-genotypes, while in the other segments of 10 aa between aa 1 and 48 there are 4-8 times more exchanges. The unexpected finding that internal deletions of the preS1 sequence 20-27, containing the epitope of the neutralizing monoclonal antibody (mab) MA18/7[6,62]. within lipopeptides 2-48, did not drastically affect infection-inhibition. PreS1-region 20-48 was speculated to contain major B-cell epitopes[63]. Indeed, mab KR359 neutralized HBV infectivity for PHH and binds to aa 19-26[64], whereas another neutralizing mab KR127 binds to aa 37-45. Furthermore, humanised mab KR127 inhibited HBV infection in chimpanzees[65]. Obviously, the binding of mabs to these epitopes hinders the attachment although the essential sequence element needed for infection is elsewhere. While the behaviour of the inhibitory preS1-peptides was very similar in the Tupaia system[34] and PHH/HepaRG cells[58] one point was worth mentioning: the preS1 sequence 20-27 was necessary for full inhibitory potency of the preS1 (2-48) peptide in HepaRG cells. A possible explanation might be that the receptor molecule(s) on Tupaia hepatocytes has binding sites for aa 9-18 and 28-48 comparable to the human receptor(s) but differs with the human binding site at aa 20-27. In a similar approach, Barrera *et al*[66] reported that the preS1-region involved in infection-inhibition of HDV spans residues 5-20 of preS1. However, they needed much higher concentrations of myristoylated preS1 peptides for inhibition in their study (> 5 μmol/L) than in the HBV studies using PTH[34], PHH (< 1 nmol/L)[58] and HepaRG[35]. However this discrepancy might be related to the peptide preparation the authors used, since myristoylated recombinant preS1-proteins obtained from a baculovirus expression system had much higher and comparable specific activities.

The remarkable potency of infection-interference, using acylated preS1-peptide 2-48 at (sub-) nanomolar concentrations, was demonstrated by the kinetics of the peptides using both PTH and HepaRG cells. Even short preincubation periods (30 min) of peptides (100 nmol/L) with the cells are sufficient to block subsequent infection and to induce non-susceptibility of the cells for hours[34,58]. Interestingly, infection could also be blocked by myristoylated peptides (100 nmol/L) after attachment of the viral inoculum at 4℃ had occurred[34]. These experiments supported the assumption that the peptides inhibited infection through binding to the hepatocytes (there possibly addressing a specific receptor), rather than with the virus, although we can presently not exclude the possibility that the peptide might address virions at a specific site on the cell. Using immunohistochemistry, we could demonstrate specific binding of HBV preS1 2-48 peptides to PTH, but not to primary rat hepatocytes or other hepatoma cell lines, such as mouse AML12[34]. The binding was considerably increased when using the respective acylated variants. The binding of the myristoylated HBV-preS-peptides could also prevent binding of highly purified HBV preS1-containing subviral particles, whereas preincubation with myristoylated preS peptides from avian hepadnaviruses did not[34]. However, inhibition of binding required micromolar concentrations of peptides, rather than nanomolar concentrations needed for inhibition of infection[34]. This discrepancy suggested presence of a more abundant low-affinity receptor for HBV on hepatocytes.

This low affinity receptor might be a sulphated glycan, because interaction of HBV and PHH is inhibited by heparin[67]. Furthermore, HBV binds to heparin *in vitro* and could be purified from the plasma of HBV-infected patients by heparin-sepharose columns[68]. Unfortunately, these reports could not clarify the relevance of this interaction for infection. Recently, we could show that HBV infection could be specifically blocked by preincubation of purified virus with heparin, or by treatment of PTH and HepaRG cells with heparinase (unpublished data). Since heparan sulphate proteoglycanes (HSPGs) are enriched in the liver within the space of Dissé, one may speculate that HBV is trapped by liver-specific HSPGs, serving as low-affinity receptors similar to the interaction and entry of apolipoprotein E lipoprotein remnants by liver HSPGs[69]. Specific entry of the virus may subsequently require passage to a yet undefined high affinity receptor(s), which can be blocked by the acylated preS1-derived peptides.

FUNCTION OF THE PRES2 DOMAIN

The M protein of HBV is not essential for infectivity[70], although antibodies against the N-terminal part of preS2 inhibited almost completely HBV infection in PTH cultures[33]. Similar results were reported for polyclonal antisera against HBV preS2 peptides (residue 1-24) *in vivo*[71]. The preS2-domain is present in both M- and L-protein (Figure 2A). However, due to the cytosolic orientation of the preS-domain in L-protein, N-glycosylation at Asn-4 of the preS2-domain occurs only in the M-protein[16,72]. In accordance with this, one of several preS2-antibodies (Q19/10), recognizing aa 1-6 in a glycan dependent manner, strongly bound to the N-terminal part of preS2, but showed the lowest neutralisation potential of all preS2-mabs used in the study[33]. Possibly, the preferential binding of mab Q19/10 to the preS2-domain of MHBs is responsible for the strongly reduced neutralisation potential, which is in agreement with the dispensability of MHBs for infectivity[70]. Furthermore, the HBV M-protein is not essential for infectivity of hepatitis delta virus[73]. A direct role of the N-terminal part of preS2 domain of L-protein for infectivity is still under debate. The carboxyterminal part contains a cell permeable translocation motf (TLM), which was suggested to be involved in HBV entry (Figure 2B)[74]. However, recombinant HBV variants with disturbed or lacking TLM sequence within the preS2 domain of LHBs are still infectious in PHH cultures[75]. The dispensability of the TLM sequence during the entry process of HBV was also detected using the hepatitis delta virus system that uses HBV surface proteins for viral entry. The infectivity of recombinant hepatitis delta virus, containing only the large and small HBV surface proteins, was not affected by the absence or presence of a TLM-sequence within the preS2-domain of the LHBs (Sureau *et al*, Taylor *et al*, personal communication).

FUNCTION OF THE S-DOMAIN

The observation that binding of HBV surface proteins to PTH cultures could be inhibited specifically by myristoylated preS1 peptides[34] argues against a predominant role of the S-domain in initial binding to hepatocytes. PreS1-rich subviral particles from human plasma bound specifically to more than 70% of cultured primary hepatocytes[33,34], while subviral particles containing only S-protein, did not[34]. Addition of the preS1-sequence 2-48 to the S-domain of these particles restored the binding to PTH up to wild-type levels[34]. The main function of the S-domain is morphogenesis, but it contains several elements that participate in entry. The main point is that antibodies against the S-domain (as generated by current S-containing vaccines) could neutralise infection *in vivo* and *in vitro*[33,76-78]. Furthermore, the presence of escape-mutants in HBV-infected patients positive for anti-HBs[79,80] demonstrates the importance of the antigenic domain (residue 100-170) of SHBs for viral spread *in vivo*. Since the S-domain does not contribute directly to binding, the question arises how these antibodies are able to neutralize infection. The S-domain contains 8 Cys residues within the antigenic loop that form inter- and intramolecular disulfide bonds[81,82], resulting in high molecular weight multiprotein complexes[83], while the preS-domain does not contain Cys and forms linear epitopes. We found that a mab recognizing a conformational S-epitope could completely neutralise infection of PTH, while a mab recognising a linear S-epitope failed to inhibit infection completely (90% inhibition)[33]. Therefore, distinct amino acids within the correctly folded antigenic loop of the S-domain might be essential for the uptake process of HBV leading to productive infection. Support for this

assumption comes from infection experiments with HDV, carrying mutant HBV S-proteins in their envelopes. Although short internal deletions, within the antigenic loop of the S-domain (residues 104 to 163), had no effect on HDV morphogenesis, virions with S-deletions between residues 118 and 129 showed reduced infectivity on PHH and HepaRG cells. Single amino acid exchanges within this domain revealed a sequence 119 to 124 (GPCRTC) to be most important for infectivity[52]. This domain contains a CXXC-motive, known to be the active site in protein-disulfide isomerase and related enzymes, involved in catalyzing disulfide-bridge exchanges. In murine leukaemia virus surface proteins, the receptor-binding subunit (SU) domain contains a CXXC motive that is activated after receptor-binding of the envelope transmembrane (TM) subunit. This leads to isomerisation of SU-TM disulfide-bonds and fusion-activation within the TM subunit[84,85]. Whether a CXXC-motive is actively involved in fusion in the case of HDV or HBV, or whether this region binds to a (co)-receptor, is currently unclear.

A clear function in entry can be ascribed to the first transmembrane sequence of the S-domain. It has sequence similarity to type 1 fusion peptides and replacement of the corresponding sequence in influenza virus hemagglutinin with HBV transmembrane sequences confers hemifusion activity of the resulting chimeric influenza virus hemagglutinin[86]. As recently proven for DHBV only the S-domain of the L-protein but not the S-protein itself provides the function of fusion[87]. This observation suggests that the topology of the S-domain in L-protein is different from that of the S-protein. For HBV, this difference is also recognizable in the glycosylation pattern. 50% of SHBs, 30% of MHBs, but 90% of LHBs are N-glycosylated in the S-domain[6].

EARLY EVENTS IN DHBV INFECTION

For more than 20 years, the duck hepatitis B virus model system was successfully used to study hepadnaviral replication. Until recently, one of the exclusive advantages of this system was the possibility to systematically investigate the early events of infection. Even though difficult, a routine preparation of PDH from newly hatched Pekin ducklings, or embryonic hepatocytes from fertilized eggs, has been successfully established in many laboratories to perform *in vitro* infection and infection inhibition studies[51,88]. Guided by the supposition that insights into the DHBV entry process also illuminate the HBV early infection events, a series of studies have been performed, however, only some of them provided satisfactory answers so far. In the following pages we would like to concentrate on the following major issues: (1) What are the roles of the two multifunctional viral envelope proteins, L and S, in entering the hepatocyte and which of their subdomains are involved? (2) Which cellular components have been described to be functionally implicated in these processes? (3) How and where does fusion of the viral and cellular membranes occur and which part of the viral envelope protein acts as a fusion promoter? (4) Which endocytic route is mandatory for the virus in order to productively deliver its nucleocapsid to the nucleus? (5) What determines host specificity of avian hepadnaviruses? (6) Why is the susceptibility of cells towards DHBV infection restricted to differentiated, resting hepatocytes? (7) Finally, taking into account the first functional insights into the HBV entry processes using the recently established *in vitro* systems (HepaRG cells and PTH), we would like to critically scrutinize the question whether there is justified hope that further insights into the DHBV entry processes are relevant for HBV, especially regarding the development of inhibitors for infection.

THE ROLE OF THE DIFFERENT ENVELOPE PROTEINS IN DHBV ENTRY

Soon after the discovery of DHBV and the possibility of replicating the virus *in vitro* using PDH[89,90], several groups characterized DHBV structural proteins biochemically and immunologically, including those that constitute the membranous envelope[91,92]. One approach was the recombinant expression of DHBV-preS fusion proteins to generate antisera. These sera detected two unglycosylated 35 and 37 kDa envelope proteins (the L-protein and its phosphorylated form), co-immunopreciptitated a 17 kDa protein under native conditions (which was identified as the DHBV S-protein by microsequencing) and were able to neutralize DHBV infection *in vitro*[92,93]. Further investigations concentrating on posttranslational modifications of L- and S-proteins and the possible functional implications for DHBV replication revealed, that the N-terminal Glycin-2 of the preS-domain of the DHBV L-protein becomes myristoylated during protein synthesis (Figure 2A)[94]. In addition to myristoylation the DHBV L-protein becomes partially phosphorylated preferentially at Serin 118 in its preS-domain (Figure 2B)[11,95,96]. Both modifications are not required for assembly and secretion of virions. However, while mutations in the phosphorylation sites did not interfere with infectivity of DHBV *in vitro* and *in vivo*[97] the prevention of myristoylation resulted in a loss of infectivity of the mutant in ducklings and a drastically reduced potential to infect PDH *in vitro*[94], (our unpublished results). These findings indicate that at least parts of the DHBV-preS domain, including its N-terminal modification by myristic acid, are involved in virus entry. Functional epitope mapping of mouse mabs obtained after immunization with DHBV particles or recombinant proteins supported this idea[93,98-104]. Three epitopes within the preS domain recognized by neutralizing antibodies were characterized, the first one covering a central part including amino acids 82-109, the second one including a more N-terminal part, amino acids 12-30, and a third part between amino acids 123-137.

The first direct evidence for the participation of the preS-domain of the DHBV L-protein for virus entry came from infection competition experiments using recombinant SVPs composed of only the DHBV L- or DHBV S-protein. These particles were purified from yeast and displayed significant differences in their ability to compete with DHBV infection of PDH with only the L-particles being active[105]. The investigators further showed that only the preS/S-containing particles bind

hepatocytes, supporting the view that the preS-domain as a part of DHBV L plays a pivotal role in attachment and infection of hepatocytes. Following this experimental strategy, Urban *et al* demonstrated that *E. coli*-derived preS-polypeptides, devoid of both the N-terminal myristoyl moiety and the hydrophobic TM-containing S-domain, specifically inhibit DHBV infection *in vitro* with IC_{50}s of about 800 nmol/L. Using a set of terminal and internal deletion mutants it became evident that an uninterrupted innermost preS-domain (amino acids 30-115), including epitopes recognized by neutralizing antibodies, is required for infection inhibition. Since the preS-polypeptide derived from the heron hepatitis B virus (HHBV) also competed with DHBV infection (despite an amino acid variation of 50%), it was evident that the addressed step cannot be responsible for the observed species specificity (see below) between these two avian hepadnaviruses. The striking correlation of the infection competition activity of DHBV-preS polypeptides with their ability to bind duck carboxypeptidase D (including the binding of HHBV preS to dCPD) suggested that it is this molecule which is addressed and inactivated at the surface of hepatocytes[106,107]. Interestingly a second peptide, consisting of the N-terminal 41 amino acids DHBV preS, devoid of CPD-binding and requiring myristoylation of Gly-2 for efficient inhibitory activity (IC_{50} = 200 nmol/L), was identified subsequently[57]. Pre-incubation experiments showed that the peptide addresses a cellular component. Antibodies raised against this peptide and recognizing amino acids 12-23 were able to efficiently block DHBV infection and immunoprecipitate particles indicating that this N-terminal preS-part is exposed on the particle surface and required for infection[108].

Until today, little is known about the role of the DHBV S-protein in DHBV entry. In contrast to the HBV S-protein, DHBV-S is smaller and does not include the antigenic loop, called *a* determinant, which bears epitopes involved in the protective immune response acquired upon vaccination against HBV. Indirect evidence for the involvement of DHBV-S in entry came from the observation that antibodies recognizing the DHBV S-protein, although rarely induced by immunization with DHBV particles[92], can neutralize DHBV-infection of PDH[100]. However, it is not clear if the antibodies directly prevent molecular contacts needed for infection or if they interfere with the formation of preS-dependent interactions by steric hinderance. Both single point mutations within TM-1 of S, resulting in a reduction of hydrophobicity, or the complete replacement of DHBV TM-1 by the HBV TM-1 had no effect on DHBV infectivity (in contrast to the effect the same mutations had when introduced in the TM-1 of L)[100]. It has recently been shown that, besides L- and S-proteins, the DHBV envelope contains a third 10 kDa membrane protein termed S_t[8]. It is a truncated version of the DHBV S-protein, consisting of TM-1, the internal cystein loop and a part of TM-2. S_t, however, seems to play a key role as a chaperone in L-protein translocation. Unfortunately, to date, no further systematic approaches aiming to identify S-specific amino acids that lead to non-infectious virions have been undertaken.

CELLULAR MOLECULES INVOLVED IN DHBV ENTRY

Based on accumulating evidence that the preS-domain plays crucial roles in DHBV infection and also possibly mediates binding to the hepatocyte, Kuroki *et al*[109] performed a biochemical approach for receptor identification and detected a 180 kDa membrane protein in ^{35}S-labeled duck hepatocyte extracts that co-immunoprecipitated with DHBV particles or recombinant envelope proteins. They showed that binding requires only the DHBV-preS part and can be inhibited by neutralizing preS-antibodies. Continuous work by this group and independent efforts by Tong *et al* using GST-preS fusion proteins for affinity purification, identified gp180 or p170 (as named by Tong and co-worker) as the prototype member of a new class of regulatory trans-Golgi network (TGN)-resident carboxypeptidases, soon afterwards termed carboxypeptidase D (CPD)[110,111]. Duck CPD (dCPD) like all other CPDs identified so far, consists of three luminal/extracellular carboxypeptidase E like domains of about 50 kDa each, one transmembrane domain and a highly conserved cytoplasmic tail required for accurate retrieval to the TGN[110,112]. While two of the three luminal/extracellular domains bind Zn^{2+}-ions and exhibit enzymatic carboxypeptidase activity towards yet unidentified cellular proteins that cross the secretory pathway[110,113], the membrane proximal C-domain of dCPD is enzymatically inactive and binds DHBV preS with very high affinity[110,114,115]. However, although the C-domains of human CPD and mouse CPD are homologous to each other and to the dCPD-C domain[116] they do not interact with DHBV preS. Chicken CPD, by comparison, displays only a very weak binding[117]. Interestingly Spangenberg *et al*[117] succeeded in rescuing the binding of DHBV preS to the human CPD C-domain by the introduction of a short dCPD-C domain-derived sequence (amino acids 920-949). Thus, since dCPD is essential for DHBV infection, species specificity could at least partially be explained by the potential of the viral preS-domain to bind CPD.

There is striking experimental evidence that dCPD serves a crucial role in DHBV infection: (1) recombinant DHBV-preS peptides, which are able to bind dCPD *in vitro,* are also active as inhibitors of DHBV infection in PDH[106,107]. (2) soluble dCPD as well as antibodies against dCPD block DHBV infection[115,118]. (3) adenoviral transfer of a dCPD mutant lacking the cytoplasmic TGN-retrieval signal into PDH, abolishes DHBV infection of the transduced cells[119]. (4) dCPD is greatly and selectively down regulated in DHBV infected duck livers and in infected PDH, which is a possible way to exclude superinfection[120], although there is evidence for a second dCPD-independent mechanism[121]. (5) a set of DHBV single point mutants that are deficient in dCPD binding lost their infectivity (unpublished data). However, despite this compelling evidence, it has not been possible to render non-susceptible cell lines that support replication of the viral genome (e.g. LMH cells) susceptible by expression of dCPD[106]. This indicates that either (an) additional factor(s) is/are missing in the dCPD-transduced cell line or that the remarkable and still enigmatic dependency of

hepadnaviral infections on a resting differentiated state of the hepatocyte provide additional constraints that must be overcome as well.

Following the identification of dCPD as a putative DHBV-receptor, extensive work from several groups addressed issues on the sequence requirements of the DHBV preS-domain in order to bind dCPD, as well as details in the mode of dCPD/DHBVpreS interaction[106,111,115,118,122]. Although the results of binding analyses are divergent to some extent, the variations are explainable by the dissimilar techniques that have been applied by the different authors. All findings, however, indicate that a central preS-sequence including amino acids 87-115 (containing major epitopes recognized by neutralizing antibodies) is indispensable for dCPD binding (Figure 2B). The disturbance of the integrity of this sequence abrogated binding entirely. Using quantitative real-time surface plasmon resonance spectroscopy, it became clear that sequences located N-terminal to this essential part (including amino acids 30-86) contribute to the complex stability in a sequence dependent manner, making the interaction of DHBV preS and the C-domain of dCPD to one of the strongest interactions between a viral ligand and a cellular protein[115]. Concerning the mode of interaction, two aspects are noteworthy: First, binding of preS induces conformational changes not only in the viral ligand but also in dCPD. Together with the unusual finding that preS binding to the dCPD C-domain occurs in close proximity to the cellular membrane, the preS-induced dCPD conformational changes indicate that dCPD may play an important role in the fusion of the viral and cellular membrane. If this holds true DHBV entry into hepatocytes would exemplify a novel type of a viral entry mechanism, involving the recruitment of a cellular protein to act as a fusion mediator. However, this hypothesis remains to be supported. Secondly, an extensive 2D NMR structural analysis of the DHBV preS-subdomain that binds dCPD (amino acids 30-115) revealed a mostly unstructured protein with only a short sequence within the essential binding site (amino acids 89-104,) exhibiting the tendency to form an alpha helix (Figure 2B). This is consistent with the observation that a DHBV preS-polypeptide can be treated repeatedly with denaturing agents without losing the ability to bind dCPD with an unaffected K_D of 1.5 nmol/L at 37℃[115]. Thus, the dCPD-binding domain of DHBV represents the first example of a viral protein belonging to the group of intrinsically unstructured/disordered proteins[123] and in that way differs from the well ordered structures found on the surfaces of other enveloped viruses; e.g. influenza virus hemaglutinin or HIV gp120. Structural analyses performed with the whole HBV preS1-polypeptide, as well as with myristoylated N-terminal preS1 peptide fragments, lead to similar results (unpublished data).

Immunization of mice using whole duck hepatocytes and subsequent screening of mabs with respect to their potential to inhibit DHBV binding to and infection of PDH, Guo and Pugh isolated two IgMs exhibiting both activities[124]. They immunoprecipitated a 55 kDa cellular protein that is also detectable in other tissues of ducks and in other birds. Unfortunately, this interesting observation has not been followed up and it therefore remains an open question if the 55 kDa protein represents a primary attachment factor that might be part of the viral entry machinery into hepatocytes.

Following the identification of dCPD as a putative receptor Li *et al*[125] identified a 120 kDa protein preferentially found in liver, pancreas and kidney that displayed binding activity only to some N-terminally and C-terminally truncated variants of GST-preS fusion proteins. Binding depends on the two crucial arginine residues at positions 101 and 102. Purification and mass spectroscopic analysis of p120 identified it as the P-subunit of glycin decarboxylase (GDC), which is an enzyme involved in mitochondrial amino acid metabolism[126]. Recombinant expressed GDC was located to some extent at the cell surface and bound truncated preS-fusion proteins with comparable specificity as the endogenous GDC. Downmodulation of GDC-levels in PDH, either by prolonged cultivation or expression of antisense RNA, resulted in a reduced susceptibility towards infection. Duck GDC has therefore been proposed to act as a co-factor in DHBV infection after proteolytic processing of the DHBV L-protein[127]. Although, the proposed concept of proteolytic activation of the L-protein during entry is attractive, the role of GDC in DHBV infection cannot be exclusive since a DHBV mutant carrying the point mutation R101H is fully infectious, although the respective mutation abolished binding to GDC[108].

MOLECULES INVOLVED IN MEMBRANE FUSION OF DHBV WITH THE HEPATOCYTE MEMBRANE

In contrast to viruses enclosing type 1 fusion proteins on their surface (e.g. HIV, Influenza, Ebola virus), hepadnaviruses do not encode a classical fusion peptide sequence, which becomes proteolytically released from an envelope protein precursor during secretion. It has therefore been hypothesized that instead they use the internally located hydrophobic transmembrane domain 1 (TM-1) as a fusion peptide, similar to the type 2 fusion proteins found in HCV, and alphaviruses[128]. Evidence for this assumption came from experiments with DHBV subviral particles that, upon low pH-treatment, expose hydrophobic domains on their surface, thereby increasing their ability to bind membranes[129]. An elegant subsequent analysis, including reverse genetics, demonstrated that lowering the hydrophobicity of TM-1 in the L- but not the S-protein through alanine substitutions resulted in a loss of DHBV infectivity[87]. Thus, TM-1 serves (a) distinct function(s) in DHBV L- when compared to the DHBV S-protein, with clear involvement in the fusion process on the part of the L-protein.

Subsequent to the observation that a short, possibly amphipatic helix in the C-terminal part of the HBV preS2-domain consisting of amino acids 41-52 is capable of translocating fused proteins, such as GFP or nucleic acids across cellular membranes[74], Stoeckl *et al* predicted two such structural motifs (called trans-location motifs, TLM) also in the N-terminal third of the DHBV preS-domain

(amino acids 20-31 and 42-53, Figure 2B). These two sequence elements are notably conserved among all avian hepadnaviruses. Amino acids 22-41 have previously been shown to be important for a dCPD-independent inhibition of infection mediated by myristoylated DHBV and HHBV preS-peptides[57]. Exchange of 4 highly conserved amino acids in the first motif (D1-mutant) or 3 conserved amino acids in the second motif (D2-mutant) or the concurrent exchange of 7 amino acids (D-1/D2-mutant) resulted in a reduced secretion (D1 mutant) and a loss of infectivity (all mutants) in embryonic hepatocytes, emphasizing the importance of both segments for infection. Interestingly, all mutants bind to and are internalized into cells but cannot be released from an endosomal compartment. This observation supports the preceding idea that the N-terminal preS-part functions at an event downstream of receptor binding and uptake. Based on the loss of the TLM-activity of the mutated sequence, the authors hypothesize that escape from the endosome does not follow a classical fusion mechanism but proceeds via direct translocation of the nucleocapsid and generalize this mechanism for all hepadnaviruses. Although attractive as a model, this hypothesis lacks direct evidence (e.g. that introduction of other TLMs, such as HIV-Tat, can replace the DHBV sequence) and is also not supported by the observation that mutated virions lacking the preS2-containing TLM of the HBV L-protein are infectious *in vitro*[75]. It is also difficult to explain how amino acids 20-53 can contribute to host discrimination between DHBV and HHBV if they provide only a functional TLM in both avian hepadnaviruses (Figure 2B)[130]. Moreover, it has been shown that amino acids 42-51 of TLM-2 as part of DHBV preS does not form an alpha-helix[115]. Thus, the inability of the described DHBV mutants to escape the endosome might be a consequence of the disruption of the interaction with the proposed co-factor and not the disturbance of a TLM-function.

ENDOCYTIC ROUTES USED BY DHBV

Although DHBV infection of PDH is efficient with respect to the percentage of cells that can be synchronously infected, our knowledge of the endocytic routes utilized by the viral particle is still rudimentary. This relates on the one hand to the fact that resting PDH cannot be efficiently transfected by routinely used protocols, making investigations with dominant negative mutants of the endocytic pathway complicated. On the other hand, the low percentage of virus particles that bind to hepatocytes, even when high multiplicities of genome equivalents "MGEs" are offered in the medium[105,131], requires very sensitive methods for a direct visualization of DHBV uptake in hepatocytes by fluorescence microscopy[87]. Consequently, most of our knowledge on the DHBV uptake route comes from results with chemical drugs that are known to interfere with specific intracellular events, which have previously been used to decipher entry routes of other viruses (e.g. binding to charged surface molecules, endosomal acidification, trafficking along microtubules, actin cytoskeleton integrity).

Regarding the question whether productive DHBV infection requires endocytosis and intracellular trafficking events, including acidification as a prerequisite for fusion, early experiments using the lysomotropic reagents ammonium chloride, chloroquine and monensin lead to contradictory results. While Offensperger *et al*[132] showed that infection was abolished with ammonium chloride and chloroquine, Rigg and Schaller reported the contrary[133]. Following DHBV particle uptake using confocal microscopy, Chojnacki *et al* convincingly demonstrated recently that DHBV particles co-localize with fluorescently labeled transferrin in an endosomal compartment 2 h after attachment. The addition of bafilomycin A1, which is a potent inhibitor of vacuolar proton ATPases, at different time points during/after infection clearly showed that transit to the late endosomal compartment is required for infection[87]. Within this compartment, the activation of the DHBV envelope into a fusion competent state is probably not solely triggered by a pH decrease, explaining to some extent the earlier conflicting results, but might include events like CPD-binding and proteolytic cleavage of viral surface proteins. This is consistent with the observation by Breiner and Schaller who, while successfully applying an adenoviral transduction system for PDH, demonstrated that recombinant expression of CPD-mutants lacking the complete TGN retrieval signal abrogated DHBV infection[119]. PH-independent fusion and the dependence of productive infection on endosomal trafficking events have also been confirmed by an independent study[134]. Although there is still some debate on whether the authentic DHBV uptake route into hepatocytes proceeds via dCPD or if dCPD acts at a later stage, these results allow little doubt that accurate vesicular trafficking towards the late endosome, where fusion is expected to occur, is a prerequisite for productive DHBV infection. Using a semiquantitative PCR-based binding assay and chemicals that are known to interfere either with infection of hepadnaviruses or the formation and maintenance of microtubuli and the actin cytoskeleton, Funk *et al* showed that suramin, which is a highly charged urea-derivative and well-known inhibitor of DHBV, RSV and interestingly also HDV infection[135], decreases binding of DHBV to hepatocytes. The authors estimated the number of DHBV binding sites on hepatocytes to be about 10^4/cell, which is remarkably low when compared to other viruses[131]. They further showed that infection at some post-entry step depends on microtubular integrity and that spread in cell culture proceeds via polar egress of new virions from the infected cell[136].

WHAT DETERMINES HOST SPECIFICITY OF AVIAN HEPADNAVIRUSES?

Hepadnaviruses are principally characterized by a narrow host range, restricting *in vivo* infections to only closely related species of their natural hosts. Well-known examples are the restriction of natural HBV infection to humans and chimpanzees. Similar observations have also been made for avian hepadnaviruses. As far as we know, productive DHBV infection exclusively occurs in Pekin

ducks. Related species, such as the Muscovy duck, do not support *in vivo* infection. This *in vivo* species specificity is to some extent reflected by the restricted susceptibility of the respective hepatocyte cultures (e.g., DHBV infects hepatocytes of Pekin ducks but not those from Muscovy ducks or chickens). Interestingly, this is not observed when replication competent viral genomes are artificially transferred into cell lines of different origin. This is best exemplified by the observation that infectious DHBV particles can be produced even in the human hepatoma cell line HuH7[137,138]. It has therefore been assumed that some early step in infection (e.g., attachment, entry, fusion) determines the host range of hepadnaviruses and that the liver specific factors needed for genome replication and virus assembly are not decisive. Comparing the binding of DHBV particles to hepatocytes from Pekin ducks with hepatocytes from Muscovy ducks or chicken hepatocytes and fibroblasts, Pugh *et al* provided evidence for this assumption showing that the difference in susceptibility corresponds to the ability to bind virions and subviral particles. The loss of susceptibility towards infection during prolonged cultivation correlated with a reduction of binding capacity of cells.

The discovery of the heron hepatitis B virus (HHBV) and its property to be not infectious for Pekin ducks and PDH[139], opened the way to investigate host specificity on a molecular level. In that line, Ishikawa and Ganem produced pseudotyped heron hepatitis B viruses (HHBV) with envelopes consisting of HHBV-S and chimeras of the DHBV and HHBV L-protein[130]. They showed that the replacement of the HHBV-preS domain with DHBV-preS rescued the infectivity of HHBV in PDH. This indicated that the preS-domain determines host range without the need for a species-specific "cross-talk" between L- and S-proteins. Further fine mapping revealed that a sequence element containing amino acids 22-37 is sufficient to overcome host restriction *in vitro*[130], (Ishikawa, personal communication). Similar experiments have also been performed with HBV particles that were pseudotyped with chimeric L-proteins carrying WMHBV preS-sequences. Chouteau *et al*[140] found that HBV pseudotyped with a WMHBV envelope lost their infectivity for PHH *in vitro*. However, substitution of only the first 30 amino acids of HBV preS1 could restore infectivity of the chimera, indicating that a short N-proximal region in the L-protein harbors a determinant that contributes to the species specificity of HBV.

Although these data accentuate host restriction of hepadnaviruses as a general theme of this virus family, some unexpected recent observations complicate our understanding. One observation identifies a new hepadnavirus isolated from crown cranes which, despite its close relation to HHBV, infects PDH[12]. Another observation demonstrates that primary hepatocytes from *Tupaia belangeri*, belonging to the order *Scandentia*, are susceptible for HBV infection *in vitro*[32]. Taken together, host specificity of hepadnaviruses is to some extent determined by an early step in infection involving the adaptation of the N-terminal preS-domain of the L-protein to an unknown cellular factor. Moreover, there might be additional viral and host determinants that are to be identified.

WHY IS SUSCEPTIBILITY TOWARDS DHBV INFECTION RESTRICTED TO DIFFERENTIATED, RESTING HEPATOCYTES?

Another hallmark of hepadnaviral infection is its restriction to differentiated resting hepatocytes. Although some attempts have been undertaken there is no proliferating cell line available that supports DHBV infection. The recently described HepaRG cell line, which is the first to support the full replication cycle of HBV, is also not susceptible in a non-differentiated state[25]. HepaRG cells become susceptible for infection only after prolonged treatment with hydrocortisone and DMSO (this process needs at least 2 wk). This induced susceptibility does not correlate with enhanced binding of HBV to differentiated cells. In fact, other hepatoma cell lines, although not susceptible towards infection, bind and accumulate HBV much better than HepaRG cells (unpublished data). This remarkable behavior is supplemented by the observation that initial amplification of cccDNA after *in vitro* infection of embryonic duck hepatocytes increases by the progression of the cell cycle[141]. Thus we have to assume that, in addition to the bare presence or absence of receptor molecules, unknown differentiation-specific and cell cycle-dependent factors of hepatic origin are important key players that are involved in early restriction events.

DO INSIGHTS INTO THE DHBV ENTRY PROCESSES HELP US TO UNDERSTAND HBV INFECTION?

Having now readily available *in vitro* systems to study HBV infection, important questions, such as the nature of the HBV receptor(s) or the characterization of the HBV entry pathway and its inhibition, can now be studied. These investigations are influenced by the results and concepts obtained from the DHBV studies. Just a few examples shall be mentioned: (1) The establishment of transduction systems for PTH, PHH and HepaRG cells will allow us to inspect the relevance of known endocytic pathways for HBV infection. (2) Using highly purified virus preparations, we may further be able to directly follow attachment and entry using sensitive microscopic techniques. (3) The application of microarray-based gene expression profiling will help us identify genes that are becoming up- or down-regulated during differentiation of HepaRG-cells and may therefore also be important regulators of the HBV replication cycle. (4) Having a set of well characterized preS-peptides that interfere with infection, it will be possible to identify the molecule(s) they address. However, it is of utmost importance to be aware of the possible differences in the uptake strategy that might have evolved in the two genera ortho- and avihepadnaviruses with their prototypic members HBV and DHBV, respectively. Two already known examples illustrate this. First, the discovery of dCPD as an important cellular factor for avihepadnavirus infection raised the

question of whether the human homologue plays a similar role in HBV infection. We have performed extensive studies related to that question (e.g., an infection inhibition experiment using soluble human CPD or anti-human CPD antibodies, investigations on whether transfection of human CPD promotes uptake of purified HBV, binding assays using HBV preS and human CPD *etc*.). None of these experiments gave any hint that this molecule is involved in HBV infection (unpublished data). Secondly, Chojnaki *et al*[87] provided unquestionable evidence that DHBV infection depends on the intracellular transport of virions from the early to the late endosome and is thereby blocked by bafilomycin A1. In contrast, HBV infection of HepaRG cells is not influenced by this drug (unpublished results) indicating, along with other evidence, that the two hepadnaviruses enter hepatocytes via different endocytic pathways.

PERSPECTIVES

Since the cloning of the HBV genome, and the discovery of related viruses in the animal kingdom, many aspects of the hepadnaviral life cycle have been unravelled with the help of established hepatoma cell lines and the transfection of replication competent genomes. These cell lines were, however, not suitable for infection experiments, possibly due to the lack of one or more unknown factors required for infection. A huge and still growing list of binding partners for HBV and DHBV have been reported since then, however, none of them have been convincingly shown to be related to HBV infection, and only Carboxypeptidase D has been shown to play a crucial role for the infection of avihepadnaviruses. For over 20 years, primary human hepatocytes were the only possible *in vitro* system for studying HBV infections, which created strong limitations. These limitations have become obsolete with the discovery of the HepaRG cell line and the usability of PTH instead of PHH to study HBV infection in an accurate manner. Although both systems bear their specific difficulties (e.g., Tupaias have to be bred in captivity, and HepaRG cells require a laborious protocol in order to render them susceptible for infection) this should be manageable.

With these models it will be possible to characterise cellular attachment factors and entry receptors for HBV. It will further be possible to decipher the entry pathway(s) of HBV and thereby to relate this important pathogen to other viruses.

In light of the discovery of a crucial domain within the preS1 part of the L-protein, the available HBV vaccines have to be improved. Although the current vaccine has been shown to be safe and effective, it consists only of S-protein containing recombinant particles and relies solely on the generation of protective antibodies recognizing this part of the viral surface protein, which as we now know do not counteract binding of the virus to its target cells. This allows the emergence of escape mutants, frequently arising especially under antiviral therapy, with reverse transcriptase inhibitors (e.g. lamivudine). Inclusion of the preS1 sequences into vaccines should therefore directly protect against infection.

The discovery of HBV preS1-derived lipopeptides as potent inhibitors of HBV entry will not only stimulate further investigations aiming to decipher the early infection events, they also represent a novel antiviral approach for the treatment of acute and chronic hepatitis B and hepatitis delta, similar to the HIV-peptide entry-inhibitor T20 (also called *enfuvirtide* and *fuzeon*). However, compared to T-20, the most active HBV inhibitor (HBVpreS/2-48$^{\text{stearoyl}}$ and also called Myrcludex B) approximately displays a 1000 fold higher specific activity. This substance, which is presently under preclinical development, could be very useful for post-exposure prophylaxis or the inhibiting of re-infection after liver transplantation. Whether efficient entry inhibition will also be beneficial in the treatment of chronic HBV and HDV infections, alone or in combination with current therapies, is an interesting objective to be addressed in a clinical trial in the near future.

ACKNOWLEDGMENTS

The authors thank Wolfram H Gerlich for critical reading of the manuscript.

REFERENCES

1 **Kielian M**, Rey FA. Virus membrane-fusion proteins: more than one way to make a hairpin. *Nat Rev Microbiol* 2006; **4**: 67-76
2 **Briz V**, Poveda E, Soriano V. HIV entry inhibitors: mechanisms of action and resistance pathways. *J Antimicrob Chemother* 2006; **57**: 619-627
3 **The International Committee on Taxonomy of Viruses.** Available from: URL: http://www.ncbi.nlm.nih.gov/ICTVdb/Ictv/index.htm
4 **World Health Organization**. Available from: URL: http://www.who.int/csr/disease/hepatitis/HepatitisB_whocdscsrlyo2002_2.pdf
5 **Beasley RP**, Hwang LY, Lin CC, Chien CS. Hepatocellular carcinoma and hepatitis B virus. A prospective study of 22 707 men in Taiwan. *Lancet* 1981; **2**: 1129-1133
6 **Heermann KH**, Goldmann U, Schwartz W, Seyffarth T, Baumgarten H, Gerlich **WH**. Large surface proteins of hepatitis B virus containing the pre-s sequence. *J Virol* 1984; **52**: 396-402
7 **Chen LB**, Chen PL, Wang GL, Song XT, Li YF, Liu CY, Jia KM. Ultrastructural study of hepatitis B virus in biliary epithelial cells of duck liver. *Chin Med J (Engl)* 1990; **103**: 447-450
8 **Grgacic EV**, Anderson DA. St, a truncated envelope protein derived from the S protein of duck hepatitis B virus, acts as a chaperone for the folding of the large envelope protein. *J Virol* 2005; **79**: 5346-5352
9 **Tolle TK**, Glebe D, Linder M, Linder D, Schmitt S, Geyer R, Gerlich WH. Structure and glycosylation patterns of surface proteins from woodchuck hepatitis virus. *J Virol* 1998; **72**: 9978-9985
10 **Schmitt S**, Glebe D, Tolle TK, Lochnit G, Linder D, Geyer R, Gerlich WH. Structure of pre-S2 N- and O-linked glycans in surface proteins from different genotypes of hepatitis B virus. *J Gen Virol* 2004; **85**: 2045-2053
11 **Grgacic EV**, Anderson DA. The large surface protein of duck hepatitis B virus is phosphorylated in the pre-S domain. *J Virol* 1994; **68**: 7344-7350
12 **Prassolov A**, Hohenberg H, Kalinina T, Schneider C, Cova L, Krone O, Frölich K, Will H, Sirma H. New hepatitis B virus of cranes that has an unexpected broad host range. *J Virol* 2003; **77**: 1964-1976
13 **Bruss V**. A short linear sequence in the pre-S domain of the

large hepatitis B virus envelope protein required for virion formation. *J Virol* 1997; **71**: 9350-9357
14 **Ponsel D**, Bruss V. Mapping of amino acid side chains on the surface of hepatitis B virus capsids required for envelopment and virion formation. *J Virol* 2003; **77**: 416-422
15 **Swameye I**, Schaller H. Dual topology of the large envelope protein of duck hepatitis B virus: determinants preventing pre-S translocation and glycosylation. *J Virol* 1997; **71**: 9434-9441
16 **Bruss V**, Lu X, Thomssen R, Gerlich WH. Post-translational alterations in transmembrane topology of the hepatitis B virus large envelope protein. *EMBO J* 1994; **13**: 2273-2279
17 **Lambert C**, Prange R. Chaperone action in the posttranslational topological reorientation of the hepatitis B virus large envelope protein: Implications for translocational regulation. *Proc Natl Acad Sci USA* 2003; **100**: 5199-5204
18 **Lambert C**, Prange R. Dual topology of the hepatitis B virus large envelope protein: determinants influencing post-translational pre-S translocation. *J Biol Chem* 2001; **276**: 22265-22272
19 **Sells MA**, Chen ML, Acs G. Production of hepatitis B virus particles in Hep G2 cells transfected with cloned hepatitis B virus DNA. *Proc Natl Acad Sci U S A* 1987; **84**: 1005-1009
20 **Shih CH**, Li LS, Roychoudhury S, Ho MH. In vitro propagation of human hepatitis B virus in a rat hepatoma cell line. *Proc Natl Acad Sci USA* 1989; **86**: 6323-6327
21 **Condreay LD**, Aldrich CE, Coates L, Mason WS, Wu TT. Efficient duck hepatitis B virus production by an avian liver tumor cell line. *J Virol* 1990; **64**: 3249-3258
22 **Yang PL**, Althage A, Chung J, Chisari FV. Hydrodynamic injection of viral DNA: a mouse model of acute hepatitis B virus infection. *Proc Natl Acad Sci USA* 2002; **99**: 13825-13830
23 **Guidotti LG**, Matzke B, Schaller H, Chisari FV. High-level hepatitis B virus replication in transgenic mice. *J Virol* 1995; **69**: 6158-6169
24 **Rabe B**, Glebe D, Kann M. Lipid-mediated introduction of hepatitis B virus capsids into nonsusceptible cells allows highly efficient replication and facilitates the study of early infection events. *J Virol* 2006; **80**: 5465-5473
25 **Gripon P**, Rumin S, Urban S, Le Seyec J, Glaise D, Cannie I, Guyomard C, Lucas J, Trepo C, Guguen-Guillouzo C. Infection of a human hepatoma cell line by hepatitis B virus. *Proc Natl Acad Sci USA* 2002; **99**: 15655-15660
26 **Gripon P**, Diot C, Thézé N, Fourel I, Loreal O, Brechot C, Guguen-Guillouzo C. Hepatitis B virus infection of adult human hepatocytes cultured in the presence of dimethyl sulfoxide. *J Virol* 1988; **62**: 4136-4143
27 **Runge DM**, Runge D, Dorko K, Pisarov LA, Leckel K, Kostrubsky VE, Thomas D, Strom SC, Michalopoulos GK. Epidermal growth factor- and hepatocyte growth factor-receptor activity in serum-free cultures of human hepatocytes. *J Hepatol* 1999; **30**: 265-274
28 **Gripon P**, Diot C, Guguen-Guillouzo C. Reproducible high level infection of cultured adult human hepatocytes by hepatitis B virus: effect of polyethylene glycol on adsorption and penetration. *Virology* 1993; **192**: 534-540
29 **Galle PR**, Hagelstein J, Kommerell B, Volkmann M, Schranz P, Zentgraf H. In vitro experimental infection of primary human hepatocytes with hepatitis B virus. *Gastroenterology* 1994; **106**: 664-673
30 **Mabit H**, Vons C, Dubanchet S, Capel F, Franco D, Petit MA. Primary cultured normal human hepatocytes for hepatitis B virus receptor studies. *J Hepatol* 1996; **24**: 403-412
31 **Schulze-Bergkamen H**, Untergasser A, Dax A, Vogel H, Büchler P, Klar E, Lehnert T, Friess H, Büchler MW, Kirschfink M, Stremmel W, Krammer PH, Müller M, Protzer U. Primary human hepatocytes--a valuable tool for investigation of apoptosis and hepatitis B virus infection. *J Hepatol* 2003; **38**: 736-744
32 **Köck J**, Nassal M, MacNelly S, Baumert TF, Blum HE, von Weizsäcker F. Efficient infection of primary tupaia hepatocytes with purified human and woolly monkey hepatitis B virus. *J Virol* 2001; **75**: 5084-5089
33 **Glebe D**, Aliakbari M, Krass P, Knoop EV, Valerius KP, Gerlich WH. Pre-s1 antigen-dependent infection of Tupaia hepatocyte cultures with human hepatitis B virus. *J Virol* 2003; **77**: 9511-9521
34 **Glebe D**, Urban S, Knoop EV, Cag N, Krass P, Grün S, Bulavaite A, Sasnauskas K, Gerlich WH. Mapping of the hepatitis B virus attachment site by use of infection-inhibiting preS1 lipopeptides and tupaia hepatocytes. *Gastroenterology* 2005; **129**: 234-245
35 **Engelke M**, Mills K, Seitz S, Simon P, Gripon P, Schnölzer M, Urban S. Characterization of a hepatitis B and hepatitis delta virus receptor binding site. *Hepatology* 2006; **43**: 750-760
36 **Payan C**, Cottin J, Lemarie C, Ramont C. Inactivation of hepatitis B virus in plasma by hospital in-use chemical disinfectants assessed by a modified HepG2 cell culture. *J Hosp Infect* 2001; **47**: 282-287
37 **Gong ZJ**, De Meyer S, Roskams T, van Pelt JF, Soumillion A, Crabbé T, Yap SH. Hepatitis B virus infection in microcarrier-attached immortalized human hepatocytes cultured in molecularporous membrane bags: a model for long-term episomal replication of HBV. *J Viral Hepat* 1998; **5**: 377-387
38 **Köck J**, Glebe D Hepatitis B virus infection of primary Tupaia hepatocytes. in: Von Weizsäcker F, Roggendorf M (eds). Models of viral hepatitis. Basel: Karger, 2005: **25**: 96-105
39 **Knowles BB**, Howe CC, Aden DP. Human hepatocellular carcinoma cell lines secrete the major plasma proteins and hepatitis B surface antigen. *Science* 1980; **209**: 497-499
40 **Ladner SK**, Otto MJ, Barker CS, Zaifert K, Wang GH, Guo JT, Seeger C, King RW. Inducible expression of human hepatitis B virus (HBV) in stably transfected hepatoblastoma cells: a novel system for screening potential inhibitors of HBV replication. *Antimicrob Agents Chemother* 1997; **41**: 1715-1720
41 **Neurath AR**, Kent SB, Strick N, Parker K. Identification and chemical synthesis of a host cell receptor binding site on hepatitis B virus. *Cell* 1986; **46**: 429-436
42 **Petit MA**, Dubanchet S, Capel F, Voet P, Dauguet C, Hauser P. HepG2 cell binding activities of different hepatitis B virus isolates: inhibitory effect of anti-HBs and anti-preS1(21-47). *Virology* 1991; **180**: 483-491
43 **Qiao M**, Macnaughton TB, Gowans EJ. Adsorption and penetration of hepatitis B virus in a nonpermissive cell line. *Virology* 1994; **201**: 356-363
44 **Treichel U**, Meyer zum Büschenfelde KH, Stockert RJ, Poralla T, Gerken G. The asialoglycoprotein receptor mediates hepatic binding and uptake of natural hepatitis B virus particles derived from viraemic carriers. *J Gen Virol* 1994; **75** (Pt 11): 3021-3029
45 **Treichel U**, Meyer zum Büschenfelde KH, Dienes HP, Gerken G. Receptor-mediated entry of hepatitis B virus particles into liver cells. *Arch Virol* 1997; **142**: 493-498
46 **De Falco S**, Ruvoletto MG, Verdoliva A, Ruvo M, Raucci A, Marino M, Senatore S, Cassani G, Alberti A, Pontisso P, Fassina G. Cloning and expression of a novel hepatitis B virus-binding protein from HepG2 cells. *J Biol Chem* 2001; **276**: 36613-36623
47 **Bchini R**, Capel F, Dauguet C, Dubanchet S, Petit MA. In vitro infection of human hepatoma (HepG2) cells with hepatitis B virus. *J Virol* 1990; **64**: 3025-3032
48 **Paran N**, Geiger B, Shaul Y. HBV infection of cell culture: evidence for multivalent and cooperative attachment. *EMBO J* 2001; **20**: 4443-4453
49 **Lu X**, Block T. Study of the early steps of the Hepatitis B Virus life cycle. *Int J Med Sci* 2004; **1**: 21-33
50 **Muakkassah-Kelly SF**, Bieri F, Waechter F, Bentley P, Stäubli W. Long-term maintenance of hepatocytes in primary culture in the presence of DMSO: further characterization and effect of nafenopin, a peroxisome proliferator. *Exp Cell Res* 1987; **171**: 37-51
51 **Pugh JC**, Summers JW. Infection and uptake of duck hepatitis B virus by duck hepatocytes maintained in the presence of dimethyl sulfoxide. *Virology* 1989; **172**: 564-572
52 **Jaoudé GA**, Sureau C. Role of the antigenic loop of the hepatitis B virus envelope proteins in infectivity of hepatitis

delta virus. *J Virol* 2005; **79**: 10460-10466
53 **Glebe D**. Attachment sites and neutralising epitopes of hepatitis B virus. *Minerva Gastroenterol Dietol* 2006; **52**: 3-21
54 **Le Seyec J**, Chouteau P, Cannie I, Guguen-Guillouzo C, Gripon P. Infection process of the hepatitis B virus depends on the presence of a defined sequence in the pre-S1 domain. *J Virol* 1999; **73**: 2052-2057
55 **Bruss V**, Hagelstein J, Gerhardt E, Galle PR. Myristylation of the large surface protein is required for hepatitis B virus in vitro infectivity. *Virology* 1996; **218**: 396-399
56 **Gripon P**, Le Seyec J, Rumin S, Guguen-Guillouzo C. Myristylation of the hepatitis B virus large surface protein is essential for viral infectivity. *Virology* 1995; **213**: 292-299
57 **Urban S**, Gripon P. Inhibition of duck hepatitis B virus infection by a myristoylated pre-S peptide of the large viral surface protein. *J Virol* 2002; **76**: 1986-1990
58 **Gripon P**, Cannie I, Urban S. Efficient inhibition of hepatitis B virus infection by acylated peptides derived from the large viral surface protein. *J Virol* 2005; **79**: 1613-1622
59 **Hogle JM**. Poliovirus cell entry: common structural themes in viral cell entry pathways. *Annu Rev Microbiol* 2002; **56**: 677-702
60 **Liemann S**, Chandran K, Baker TS, Nibert ML, Harrison SC. Structure of the reovirus membrane-penetration protein, Mu1, in a complex with is protector protein, Sigma3. *Cell* 2002; **108**: 283-295
61 **Taylor JM**. Hepatitis delta virus. *Virology* 2006; **344**: 71-76
62 **Sominskaya I**, Pushko P, Dreilina D, Kozlovskaya T, Pumpen P. Determination of the minimal length of preS1 epitope recognized by a monoclonal antibody which inhibits attachment of hepatitis B virus to hepatocytes. *Med Microbiol Immunol* 1992; **181**: 215-226
63 **Hu WG**, Wei J, Xia HC, Yang XX, Li F, Li GD, Wang Y, Zhang ZC. Identification of the immunogenic domains in HBsAg preS1 region using overlapping preS1 fragment fusion proteins. *World J Gastroenterol* 2005; **11**: 2088-2094
64 **Maeng CY**, Ryu CJ, Gripon P, Guguen-Guillouzo C, Hong HJ. Fine mapping of virus-neutralizing epitopes on hepatitis B virus PreS1. *Virology* 2000; **270**: 9-16
65 **Hong HJ**, Ryu CJ, Hur H, Kim S, Oh HK, Oh MS, Park SY. In vivo neutralization of hepatitis B virus infection by an anti-preS1 humanized antibody in chimpanzees. *Virology* 2004; **318**: 134-141
66 **Barrera A**, Guerra B, Notvall L, Lanford RE. Mapping of the hepatitis B virus pre-S1 domain involved in receptor recognition. *J Virol* 2005; **79**: 9786-9798
67 **Ying C**, Van Pelt JF, Van Lommel A, Van Ranst M, Leyssen P, De Clercq E, Neyts J. Sulphated and sulphonated polymers inhibit the initial interaction of hepatitis B virus with hepatocytes. *Antivir Chem Chemother* 2002; **13**: 157-164
68 **Zahn A**, Allain JP. Hepatitis C virus and hepatitis B virus bind to heparin: purification of largely IgG-free virions from infected plasma by heparin chromatography. *J Gen Virol* 2005; **86**: 677-685
69 **Futamura M**, Dhanasekaran P, Handa T, Phillips MC, Lund-Katz S, Saito H. Two-step mechanism of binding of apolipoprotein E to heparin: implications for the kinetics of apolipoprotein E-heparan sulfate proteoglycan complex formation on cell surfaces. *J Biol Chem* 2005; **280**: 5414-5422
70 **Fernholz D**, Galle PR, Stemler M, Brunetto M, Bonino F, Will H. Infectious hepatitis B virus variant defective in pre-S2 protein expression in a chronic carrier. *Virology* 1993; **194**: 137-148
71 **Neurath AR**, Kent SB, Parker K, Prince AM, Strick N, Brotman B, Sproul P. Antibodies to a synthetic peptide from the preS 120-145 region of the hepatitis B virus envelope are virus neutralizing. *Vaccine* 1986; **4**: 35-37
72 **Schmitt S**, Glebe D, Alving K, Tolle TK, Linder M, Geyer H, Linder D, Peter-Katalinic J, Gerlich WH, Geyer R. Analysis of the pre-S2 N- and O-linked glycans of the M surface protein from human hepatitis B virus. *J Biol Chem* 1999; **274**: 11945-11957
73 **Sureau C**, Guerra B, Lee H. The middle hepatitis B virus envelope protein is not necessary for infectivity of hepatitis delta virus. *J Virol* 1994; **68**: 4063-4066
74 **Oess S**, Hildt E. Novel cell permeable motif derived from the PreS2-domain of hepatitis-B virus surface antigens. *Gene Ther* 2000; **7**: 750-758
75 **Le Seyec J**, Chouteau P, Cannie I, Guguen-Guillouzo C, Gripon P. Role of the pre-S2 domain of the large envelope protein in hepatitis B virus assembly and infectivity. *J Virol* 1998; **72**: 5573-5578
76 **Iwarson S**, Tabor E, Thomas HC, Goodall A, Waters J, Snoy P, Shih JW, Gerety RJ. Neutralization of hepatitis B virus infectivity by a murine monoclonal antibody: an experimental study in the chimpanzee. *J Med Virol* 1985; **16**: 89-96
77 **Ogata N**, Cote PJ, Zanetti AR, Miller RH, Shapiro M, Gerin J, Purcell RH. Licensed recombinant hepatitis B vaccines protect chimpanzees against infection with the prototype surface gene mutant of hepatitis B virus. *Hepatology* 1999; **30**: 779-786
78 **Shearer MH**, Sureau C, Dunbar B, Kennedy RC. Structural characterization of viral neutralizing monoclonal antibodies to hepatitis B surface antigen. *Mol Immunol* 1998; **35**: 1149-1160
79 **Carman WF**, Zanetti AR, Karayiannis P, Waters J, Manzillo G, Tanzi E, Zuckerman AJ, Thomas HC. Vaccine-induced escape mutant of hepatitis B virus. *Lancet* 1990; **336**: 325-329
80 **Nainan OV**, Khristova ML, Byun K, Xia G, Taylor PE, Stevens CE, Margolis HS. Genetic variation of hepatitis B surface antigen coding region among infants with chronic hepatitis B virus infection. *J Med Virol* 2002; **68**: 319-327
81 **Mangold CM**, Streeck RE. Mutational analysis of the cysteine residues in the hepatitis B virus small envelope protein. *J Virol* 1993; **67**: 4588-4597
82 **Mangold CM**, Unckell F, Werr M, Streeck RE. Secretion and antigenicity of hepatitis B virus small envelope proteins lacking cysteines in the major antigenic region. *Virology* 1995; **211**: 535-543
83 **Gilbert RJ**, Beales L, Blond D, Simon MN, Lin BY, Chisari FV, Stuart DI, Rowlands DJ. Hepatitis B small surface antigen particles are octahedral. *Proc Natl Acad Sci USA* 2005; **102**: 14783-14788
84 **Wallin M**, Ekström M, Garoff H. Isomerization of the intersubunit disulphide-bond in Env controls retrovirus fusion. *EMBO J* 2004; **23**: 54-65
85 **Wallin M**, Ekström M, Garoff H. The fusion-controlling disulfide bond isomerase in retrovirus Env is triggered by protein destabilization. *J Virol* 2005; **79**: 1678-1685
86 **Berting A**, Fischer C, Schaefer S, Garten W, Klenk HD, Gerlich WH. Hemifusion activity of a chimeric influenza virus hemagglutinin with a putative fusion peptide from hepatitis B virus. *Virus Res* 2000; **68**: 35-49
87 **Chojnacki J**, Anderson DA, Grgacic EV. A hydrophobic domain in the large envelope protein is essential for fusion of duck hepatitis B virus at the late endosome. *J Virol* 2005; **79**: 14945-14955
88 **Galle PR**, Schlicht HJ, Kuhn C, Schaller H. Replication of duck hepatitis B virus in primary duck hepatocytes and its dependence on the state of differentiation of the host cell. *Hepatology* 1989; **10**: 459-465
89 **Mason WS**, Aldrich C, Summers J, Taylor JM. Asymmetric replication of duck hepatitis B virus DNA in liver cells: Free minus-strand DNA. *Proc Natl Acad Sci USA* 1982; **79**: 3997-4001
90 **Summers J**, Mason WS. Replication of the genome of a hepatitis B--like virus by reverse transcription of an RNA intermediate. *Cell* 1982; **29**: 403-415
91 **Pugh J**, Zweidler A, Summers J. Characterization of the major duck hepatitis B virus core particle protein. *J Virol* 1989; **63**: 1371-1376
92 **Schlicht HJ**, Kuhn C, Guhr B, Mattaliano RJ, Schaller H. Biochemical and immunological characterization of the duck hepatitis B virus envelope proteins. *J Virol* 1987; **61**: 2280-2285
93 **Pugh JC**, Sninsky JJ, Summers JW, Schaeffer E. Characterization of a pre-S polypeptide on the surfaces of infectious avian hepadnavirus particles. *J Virol* 1987; **61**: 1384-1390
94 **Macrae DR**, Bruss V, Ganem D. Myristylation of a duck hepatitis B virus envelope protein is essential for infectivity but not for virus assembly. *Virology* 1991; **181**: 359-363

95 **Borel C**, Sunyach C, Hantz O, Trepo C, Kay A. Phosphorylation of DHBV pre-S: identification of the major site of phosphorylation and effects of mutations on the virus life cycle. *Virology* 1998; **242**: 90-98

96 **Rothmann K**, Schnölzer M, Radziwill G, Hildt E, Moelling K, Schaller H. Host cell-virus cross talk: phosphorylation of a hepatitis B virus envelope protein mediates intracellular signaling. *J Virol* 1998; **72**: 10138-10147

97 **Grgacic EV**, Lin B, Gazina EV, Snooks MJ, Anderson DA. Normal phosphorylation of duck hepatitis B virus L protein is dispensable for infectivity. *J Gen Virol* 1998; **79** (Pt 11): 2743-2751

98 **Chassot S**, Lambert V, Kay A, Godinot C, Roux B, Trepo C, Cova L. Fine mapping of neutralization epitopes on duck hepatitis B virus (DHBV) pre-S protein using monoclonal antibodies and overlapping peptides. *Virology* 1993; **192**: 217-223

99 **Chassot S**, Lambert V, Kay A, Godinot C, Trepo C, Cova L. Identification of major antigenic domains of duck hepatitis B virus pre-S protein by peptide scanning. *Virology* 1994; **200**: 72-78

100 **Cheung RC**, Robinson WS, Marion PL, Greenberg HB. Epitope mapping of neutralizing monoclonal antibodies against duck hepatitis B virus. *J Virol* 1989; **63**: 2445-2451

101 **Lambert V**, Fernholz D, Sprengel R, Fourel I, Deléage G, Wildner G, Peyret C, Trépo C, Cova L, Will H. Virus-neutralizing monoclonal antibody to a conserved epitope on the duck hepatitis B virus pre-S protein. *J Virol* 1990; **64**: 1290-1297

102 **Pugh JC**, Di Q, Mason WS, Simmons H. Susceptibility to duck hepatitis B virus infection is associated with the presence of cell surface receptor sites that efficiently bind viral particles. *J Virol* 1995; **69**: 4814-4822

103 **Sunyach C**, Rollier C, Robaczewska M, Borel C, Barraud L, Kay A, Trépo C, Will H, Cova L. Residues critical for duck hepatitis B virus neutralization are involved in host cell interaction. *J Virol* 1999; **73**: 2569-2575

104 **Yuasa S**, Cheung RC, Pham Q, Robinson WS, Marion PL. Peptide mapping of neutralizing and nonneutralizing epitopes of duck hepatitis B virus pre-S polypeptide. *Virology* 1991; **181**: 14-21

105 **Klingmüller U**, Schaller H. Hepadnavirus infection requires interaction between the viral pre-S domain and a specific hepatocellular receptor. *J Virol* 1993; **67**: 7414-7422

106 **Breiner KM**, Urban S, Schaller H. Carboxypeptidase D (gp180), a Golgi-resident protein, functions in the attachment and entry of avian hepatitis B viruses. *J Virol* 1998; **72**: 8098-8104

107 **Urban S**, Breiner KM, Fehler F, Klingmüller U, Schaller H. Avian hepatitis B virus infection is initiated by the interaction of a distinct pre-S subdomain with the cellular receptor gp180. *J Virol* 1998; **72**: 8089-8097

108 **Schmut N:** Analysis of Carboxypeptidase D-independent and -dependent steps in the duck hepatitis B virus infection. University of Heidelberg, Germany; Available from: URL: http://www.ub.uni-heidelberg.de/archiv/6552, 2006

109 **Kuroki K**, Cheung R, Marion PL, Ganem D. A cell surface protein that binds avian hepatitis B virus particles. *J Virol* 1994; **68**: 2091-2096

110 **Kuroki K**, Eng F, Ishikawa T, Turck C, Harada F, Ganem D. gp180, a host cell glycoprotein that binds duck hepatitis B virus particles, is encoded by a member of the carboxypeptidase gene family. *J Biol Chem* 1995; **270**: 15022-15028

111 **Tong S**, Li J, Wands JR. Interaction between duck hepatitis B virus and a 170-kilodalton cellular protein is mediated through a neutralizing epitope of the pre-S region and occurs during viral infection. *J Virol* 1995; **69**: 7106-7112

112 **Eng FJ**, Varlamov O, Fricker LD. Sequences within the cytoplasmic domain of gp180/carboxypeptidase D mediate localization to the trans-Golgi network. *Mol Biol Cell* 1999; **10**: 35-46

113 **Eng FJ**, Novikova EG, Kuroki K, Ganem D, Fricker LD. gp180, a protein that binds duck hepatitis B virus particles, has metallocarboxypeptidase D-like enzymatic activity. *J Biol Chem* 1998; **273**: 8382-8388

114 **Urban S**. Binding of duck carboxypeptidase D to duck hepatitis B virus. *Methods Mol Med* 2004; **95**: 199-212

115 **Urban S**, Schwarz C, Marx UC, Zentgraf H, Schaller H, Multhaup G. Receptor recognition by a hepatitis B virus reveals a novel mode of high affinity virus-receptor interaction. *EMBO J* 2000; **19**: 1217-1227

116 **Ishikawa T**, Murakami K, Kido Y, Ohnishi S, Yazaki Y, Harada F, Kuroki K. Cloning, functional expression, and chromosomal localization of the human and mouse gp180-carboxypeptidase D-like enzyme. *Gene* 1998; **215**: 361-370

117 **Spangenberg HC**, Lee HB, Li J, Tan F, Skidgel R, Wands JR, Tong S. A short sequence within domain C of duck carboxypeptidase D is critical for duck hepatitis B virus binding and determines host specificity. *J Virol* 2001; **75**: 10630-10642

118 **Urban S**, Kruse C, Multhaup G. A soluble form of the avian hepatitis B virus receptor. Biochemical characterization and functional analysis of the receptor ligand complex. *J Biol Chem* 1999; **274**: 5707-5715

119 **Breiner KM**, Schaller H. Cellular receptor traffic is essential for productive duck hepatitis B virus infection. *J Virol* 2000; **74**: 2203-2209

120 **Breiner KM**, Urban S, Glass B, Schaller H. Envelope protein-mediated down-regulation of hepatitis B virus receptor in infected hepatocytes. *J Virol* 2001; **75**: 143-150

121 **Walters KA**, Joyce MA, Addison WR, Fischer KP, Tyrrell DL. Superinfection exclusion in duck hepatitis B virus infection is mediated by the large surface antigen. *J Virol* 2004; **78**: 7925-7937

122 **Ishikawa T**, Kuroki K, Lenhoff R, Summers J, Ganem D. Analysis of the binding of a host cell surface glycoprotein to the preS protein of duck hepatitis B virus. *Virology* 1994; **202**: 1061-1064

123 **Tompa P**. Intrinsically unstructured proteins. *Trends Biochem Sci* 2002; **27**: 527-533

124 **Guo JT**, Pugh JC. Monoclonal antibodies to a 55-kilodalton protein present in duck liver inhibit infection of primary duck hepatocytes with duck hepatitis B virus. *J Virol* 1997; **71**: 4829-4831

125 **Li JS**, Tong SP, Wands JR. Characterization of a 120-Kilodalton pre-S-binding protein as a candidate duck hepatitis B virus receptor. *J Virol* 1996; **70**: 6029-6035

126 **Li J**, Tong S, Wands JR. Identification and expression of glycine decarboxylase (p120) as a duck hepatitis B virus pre-S envelope-binding protein. *J Biol Chem* 1999; **274**: 27658-27665

127 **Li J**, Tong S, Lee HB, Perdigoto AL, Spangenberg HC, Wands JR. Glycine decarboxylase mediates a postbinding step in duck hepatitis B virus infection. *J Virol* 2004; **78**: 1873-1881

128 **Lu X**, Block TM, Gerlich WH. Protease-induced infectivity of hepatitis B virus for a human hepatoblastoma cell line. *J Virol* 1996; **70**: 2277-2285

129 **Grgacic EV**, Schaller H. A metastable form of the large envelope protein of duck hepatitis B virus: low-pH release results in a transition to a hydrophobic, potentially fusogenic conformation. *J Virol* 2000; **74**: 5116-5122

130 **Ishikawa T**, Ganem D. The pre-S domain of the large viral envelope protein determines host range in avian hepatitis B viruses. *Proc Natl Acad Sci USA* 1995; **92**: 6259-6263

131 **Funk A**, Mhamdi M, Lin L, Will H, Sirma H. Itinerary of hepatitis B viruses: delineation of restriction points critical for infectious entry. *J Virol* 2004; **78**: 8289-8300

132 **Offensperger WB**, Offensperger S, Walter E, Blum HE, Gerok W. Inhibition of duck hepatitis B virus infection by lysosomotropic agents. *Virology* 1991; **183**: 415-418

133 **Rigg RJ**, Schaller H. Duck hepatitis B virus infection of hepatocytes is not dependent on low pH. *J Virol* 1992; **66**: 2829-2836

134 **Funk A**, Mhamdi M, Hohenberg H, Will H, Sirma H. pH-independent entry and sequential endosomal sorting are major determinants of hepadnaviral infection in primary hepatocytes. *Hepatology* 2006; **44**: 685-693

135 **Petcu DJ**, Aldrich CE, Coates L, Taylor JM, Mason WS. Suramin inhibits in vitro infection by duck hepatitis B virus, Rous sarcoma virus, and hepatitis delta virus. *Virology* 1988; **167**: 385-392

136 **Funk A**, Hohenberg H, Mhamdi M, Will H, Sirma H. Spread of hepatitis B viruses in vitro requires extracellular progeny and may be codetermined by polarized egress. *J Virol* 2004; **78**: 3977-3983

137 **Galle PR**, Schlicht HJ, Fischer M, Schaller H. Production of infectious duck hepatitis B virus in a human hepatoma cell line. *J Virol* 1988; **62**: 1736-1740

138 **Pugh JC**, Yaginuma K, Koike K, Summers J. Duck hepatitis B virus (DHBV) particles produced by transient expression of DHBV DNA in a human hepatoma cell line are infectious in vitro. *J Virol* 1988; **62**: 3513-3516

139 **Sprengel R**, Kaleta EF, Will H. Isolation and characterization of a hepatitis B virus endemic in herons. *J Virol* 1988; **62**: 3832-3839

140 **Chouteau P**, Le Seyec J, Cannie I, Nassal M, Guguen-Guillouzo C, Gripon P. A short N-proximal region in the large envelope protein harbors a determinant that contributes to the species specificity of human hepatitis B virus. *J Virol* 2001; **75**: 11565-11572

141 **Borel C**, Schorr O, Durand I, Zoulim F, Kay A, Trepo C, Hantz O. Initial amplification of duck hepatitis B virus covalently closed circular DNA after in vitro infection of embryonic duck hepatocytes is increased by cell cycle progression. *Hepatology* 2001; **34**: 168-179

142 **Pontisso P**, Ruvoletto MG, Gerlich WH, Heermann KH, Bardini R, Alberti A. Identification of an attachment site for human liver plasma membranes on hepatitis B virus particles. *Virology* 1989; **173**: 522-530

143 **Neurath AR**, Strick N, Sproul P, Ralph HE, Valinsky J. Detection of receptors for hepatitis B virus on cells of extrahepatic origin. *Virology* 1990; **176**: 448-457

144 **Neurath AR**, Strick N. Antigenic mimicry of an immunoglobulin A epitope by a hepatitis B virus cell attachment site. *Virology* 1990; **178**: 631-634

145 **Pontisso P**, Ruvoletto MG, Tiribelli C, Gerlich WH, Ruol A, Alberti A. The preS1 domain of hepatitis B virus and IgA cross-react in their binding to the hepatocyte surface. *J Gen Virol* 1992; **73** (Pt 8): 2041-2045

146 **Dash S**, Rao KV, Panda SK. Receptor for pre-S1(21-47) component of hepatitis B virus on the liver cell: role in virus cell interaction. *J Med Virol* 1992; **37**: 116-121

147 **Neurath AR**, Strick N, Sproul P. Search for hepatitis B virus cell receptors reveals binding sites for interleukin 6 on the virus envelope protein. *J Exp Med* 1992; **175**: 461-469

148 **Neurath AR**, Strick N, Li YY. Cells transfected with human interleukin 6 cDNA acquire binding sites for the hepatitis B virus envelope protein. *J Exp Med* 1992; **176**: 1561-1569

149 **Ryu CJ**, Cho DY, Gripon P, Kim HS, Guguen-Guillouzo C, Hong HJ. An 80-kilodalton protein that binds to the pre-S1 domain of hepatitis B virus. *J Virol* 2000; **74**: 110-116

150 **Petit MA**, Capel F, Dubanchet S, Mabit H. PreS1-specific binding proteins as potential receptors for hepatitis B virus in human hepatocytes. *Virology* 1992; **187**: 211-222

151 **Duclos-Vallée JC**, Capel F, Mabit H, Petit MA. Phosphorylation of the hepatitis B virus core protein by glyceraldehyde-3-phosphate dehydrogenase protein kinase activity. *J Gen Virol* 1998; **79** (Pt 7): 1665-1670

152 **Budkowska A**, Quan C, Groh F, Bedossa P, Dubreuil P, Bouvet JP, Pillot J. Hepatitis B virus (HBV) binding factor in human serum: candidate for a soluble form of hepatocyte HBV receptor. *J Virol* 1993; **67**: 4316-4322

153 **Harvey TJ**, Macnaughton TB, Park DS, Gowans EJ. A cellular protein which binds hepatitis B virus but not hepatitis B surface antigen. *J Gen Virol* 1999; **80** (Pt 3): 607-615

154 **Li D**, Wang XZ, Ding J, Yu JP. NACA as a potential cellular target of hepatitis B virus preS1 protein. *Dig Dis Sci* 2005; **50**: 1156-1160

155 **Glebe D**, Gerlich WH. Study of the endocytosis and intracellular localization of subviral particles of hepatitis B virus in primary hepatocytes. *Methods Mol Med* 2004; **96**: 143-151

156 **Owada T**, Matsubayashi K, Sakata H, Ihara H, Sato S, Ikebuchi K, Kato T, Azuma H, Ikeda H. Interaction between desialylated hepatitis B virus and asialoglycoprotein receptor on hepatocytes may be indispensable for viral binding and entry. *J Viral Hepat* 2006; **13**: 11-18

157 **Machida A**, Kishimoto S, Ohnuma H, Baba K, Ito Y, Miyamoto H, Funatsu G, Oda K, Usuda S, Togami S. A polypeptide containing 55 amino acid residues coded by the pre-S region of hepatitis B virus deoxyribonucleic acid bears the receptor for polymerized human as well as chimpanzee albumins. *Gastroenterology* 1984; **86**: 910-918

158 **Pontisso P**, Petit MA, Bankowski MJ, Peeples ME. Human liver plasma membranes contain receptors for the hepatitis B virus pre-S1 region and, via polymerized human serum albumin, for the pre-S2 region. *J Virol* 1989; **63**: 1981-1988

159 **Dash S**, Rao KV, Joshi B, Nayak NC, Panda SK. Significance of natural polymerized albumin and its receptor in hepatitis B infection of hepatocytes. *Hepatology* 1991; **13**: 134-142

160 **Krone B**, Lenz A, Heermann KH, Seifer M, Lu XY, Gerlich WH. Interaction between hepatitis B surface proteins and monomeric human serum albumin. *Hepatology* 1990; **11**: 1050-1056

161 **Sobotta D**, Sominskaya I, Jansons J, Meisel H, Schmitt S, Heermann KH, Kaluza G, Pumpens P, Gerlich WH. Mapping of immunodominant B-cell epitopes and the human serum albumin-binding site in natural hepatitis B virus surface antigen of defined genosubtype. *J Gen Virol* 2000; **81**: 369-378

162 **Itoh Y**, Takai E, Ohnuma H, Kitajima K, Tsuda F, Machida A, Mishiro S, Nakamura T, Miyakawa Y, Mayumi M. A synthetic peptide vaccine involving the product of the pre-S(2) region of hepatitis B virus DNA: protective efficacy in chimpanzees. *Proc Natl Acad Sci USA* 1986; **83**: 9174-9178

163 **Mehdi H**, Kaplan MJ, Anlar FY, Yang X, Bayer R, Sutherland K, Peeples ME. Hepatitis B virus surface antigen binds to apolipoprotein H. *J Virol* 1994; **68**: 2415-2424

164 **Mehdi H**, Yang X, Peeples ME. An altered form of apolipoprotein H binds hepatitis B virus surface antigen most efficiently. *Virology* 1996; **217**: 58-66

165 **Hertogs K**, Leenders WP, Depla E, De Bruin WC, Meheus L, Raymackers J, Moshage H, Yap SH. Endonexin II, present on human liver plasma membranes, is a specific binding protein of small hepatitis B virus (HBV) envelope protein. *Virology* 1993; **197**: 549-557

166 **Gong ZJ**, De Meyer S, van Pelt J, Hertogs K, Depla E, Soumillion A, Fevery J, Yap SH. Transfection of a rat hepatoma cell line with a construct expressing human liver annexin V confers susceptibility to hepatitis B virus infection. *Hepatology* 1999; **29**: 576-584

S- Editor Liu Y **L- Editor** Lutze M **E- Editor** Liu WF

PO Box 2345, Beijing 100023, China
www.wjgnet.com
wjg@wjgnet.com

World J Gastroenterol 2007 January 7; 13(1): 39-47
World Journal of Gastroenterology ISSN 1007-9327

TOPIC HIGHLIGHT

Dieter Glebe, PhD, *Series Editor*

Intracellular transport of hepatitis B virus

Michael Kann, André Schmitz, Birgit Rabe

Michael Kann, CNRS-REGER (UMR 5097), Université Bordeaux 2, 146 rue Léo Saignat, F-33076 Bordeaux Cedex, France
André Schmitz, Birgit Rabe, Institute of Medical Virology, Frankfurter Str. 107, D-35392 Giessen, Germany
Supported by the Deutsche Forschungsgemeinschaft (DFG; SFB 535 TP B5, DFG KA 1193/5-2 and Graduiertenkolleg "Biochemie von Nukleoproteinkomplexen"), by the European Community ('Combined immune and gene therapy for chronic hepatitis' 5th call for Quality of Life and Management of Living Resources, Key Action 2, Control of infectious diseases) and the Canadian Institute of Health Research and the Natural Sciences and Engineering Research Council of Canada
Correspondence to: Michael Kann, MD, CNRS-REGER (UMR 5097), Bat 3A, Université Bordeaux 2, 146 rue Léo Saignat, F-33076 Bordeaux Cedex, France. michael.kann@u-bordeaux2.fr
Telephone: +33-5-57574876 Fax: +33-5-57571766
Received: 2006-08-03 Accepted: 2006-11-21

Abstract

For genome multiplication hepadnaviruses use the transcriptional machinery of the cell that is found within the nucleus. Thus the viral genome has to be transported through the cytoplasm and nuclear pore. The intracytosolic translocation is facilitated by the viral capsid that surrounds the genome and that interacts with cellular microtubules. The subsequent passage through the nuclear pore complexes (NPC) is mediated by the nuclear transport receptors importin α and β. Importin α binds to the C-terminus of the capsid protein that comprises a nuclear localization signal (NLS). The exposure of the NLS is regulated and depends upon genome maturation and/or phosphorylation of the capsid protein. As for other karyophilic cargos using this pathway importin α interacts with importin β that facilitates docking of the import complex to the NPC and the passage through the pore. Being a unique strategy, the import of the viral capsid is incomplete in that it becomes arrested inside the nuclear basket, which is a cage-like structure on the karyoplasmic face of the NPC. Presumably only this compartment provides the factors that are required for capsid disassembly and genome release that is restricted to those capsids comprising a mature viral DNA genome.

Key words: Hepatitis B virus; Capsid; Intracellular transport; Microtubules; Nuclear pore; Importin; Nuclear localization signal; Nuclear basket

Kann M, Schmitz A, Rabe B. Intracellular transport of hepatitis B virus. *World J Gastroenterol* 2007; 13(1): 39-47

http://www.wjgnet.com/1007-9327/13/39.asp

INTRODUCTION

Eukaryotic cells are divided into different compartments and viruses have to get access to the compartment that provides the cellular machinery for replication. Unlike bacteriophages that "just" have to pass the bacterial wall and membrane all viruses that infect eukaryotic cells have to travel through the cell to reach the place of replication. Dependent upon the virus and the type of genome, the machinery of DNA replication, transcription and RNA processing may be required. Gaining access to the nucleus where these factors are found requires active transport since passive diffusion is ineffective.

Although summarized by the term "intracellular transport" one has to differentiate between the intracytoplasmic transport towards the nucleus and the passage through the nuclear envelope into the karyoplasm. Nucleic acids are not karyophilic *per se*. Thus proteins attached to the viral genome must interact with cellular factors that facilitate the different transport processes. As intracytosolic and nuclear transport are based on different mechanisms it is evident that the interacting domains on the viral proteins have to be exposed in a coordinated manner. Moreover an effective virus, meaning a virus with a good particle-infectious unit ratio, has to release its genome from surrounding proteins only after termination of the various transport steps preventing abortion of the infection process. It has to be considered that the analysis of the underlying principles is not only important for analysis of potential drug targets for treatment of individual viral infections but also for creation of efficient vectors in gene therapy.

OVERVIEW ON INTRACYTOSOLIC TRANSPORT PRINCIPLES

The need for active and directed intracytosolic transport results from the high viscosity of the cytoplasm. Protein concentrations of 170-350 mg/mL, RNA concentrations of 30 μg/mL[1] and micro compartmentalization evoke a viscosity 10 to 100 fold higher than the viscosity of water[2].

In consequence diffusion processes are enormously reduced so that only particles with diameters below 50 nm significantly diffuse[3]. Obviously such a passive movement is incompatible with efficient trafficking of organelles. Eukaryotic cells thus provide different active transport machineries that are not only used by large structures but even by small macromolecules as it was shown for the heat shock protein 90 (Hsp90)/glucocorticoid receptor β (GRβ) complex[4] and the human tumour suppressor protein p53[5]. It is thus likely that structures as the HBV capsid with a diameter of 36 nm (80 % of the capsids that show a T = 4 symmetry, 20 % exhibit a T = 3 symmetry and a diameter of 32 nm[6,7]) use the same active cellular transport pathways towards the nucleus.

Most investigations on intracytosolic transport of viruses are done by adding inhibitors to cells during infection. To prevent misinterpretations it is important to realize the variety of cellular processes that are affected. Eukaryotic cells provide two active cytoplasmic transport systems based on microfilaments (MF) and microtubules (MT). Microfilaments have diameters of 5-9 nm and are double-stranded helical polymers of the ATPase actin. They form linear bundles, 2D networks and 3D gels and are most highly concentrated underneath the plasma membrane. Microfilaments are dynamic polar structures with a fast-growing plus-end and a relatively inert, slow-growing minus-end. They stabilize the cell structure and are involved in cell movement e.g. by filopodia and lamellopodia. With a velocity of 2-6 mm/d transport via MF is slow[8,9] and generally thought to serve as the transport pathway for short distances.

Beside its role in transport actin is also involved in the internalization and/or formation of endocytic vesicles. In clathrin-mediated endocytosis a functional actin cytoskeleton enhances the internalization of the clathrin-coated vesicles but without being obligatory[10-12]. In phagocytosis and macropinocytosis local actin polymerization at the cytosolic site of the plasma membrane is required for vesicle formation as well as actin depolymerization[13-16]. Similarly, releasing of caveolin-coated vesicles into the cytoplasm depends on actin polymerization and depolymerization in caveolae-mediated endocytosis[17,18].

Microtubules are hollow cylinders of 11-13 protofilaments made of the GTPase α- and β-tubulin. MT are 25 nm in diameter and like MF they have a highly dynamic, fast-growing plus-end and a less dynamic minus-end, which is typically attached to a microtubule-organizing centre (MTOC). MT surround the nucleus and extend from the perinuclear MTOC to the cell periphery. They are thought to be the major long-range transport system[9] allowing a velocity of 3-5 mm per hour (HSV 1 capsids, retrograde)[19].

For both MT and MF two different mechanisms of transport exist (Figure 1) using polymerization (filament growth)/depolymerization (filament shrinkage) or motor proteins[20]. In the first mechanism the cargo binds dynamically *via* adapter proteins to one end of a growing or shortening filament and can be pushed or pulled in the given direction. Mitotic chromosomes for example bind at its kinetochor *via* a dynein/dynactin-complex to the plus-end of the kinetochor-MT[21-23]. Depolymerization at the plus-end as well as depolymerization at the minus-end directs the chromosomes to the minus-end that is fixed at the spindle pole. Phagosomes[24,25], macropinosomes[26,27] endosomes and lysosomes[27,28] are able to cross the cytosol by the help of a polymerizing actin tail comparable to the movement of the bacteria *listeria monocytogenes*[29-31] and the nuclear polyhedrosis virus (NPV) capsid[32-34].

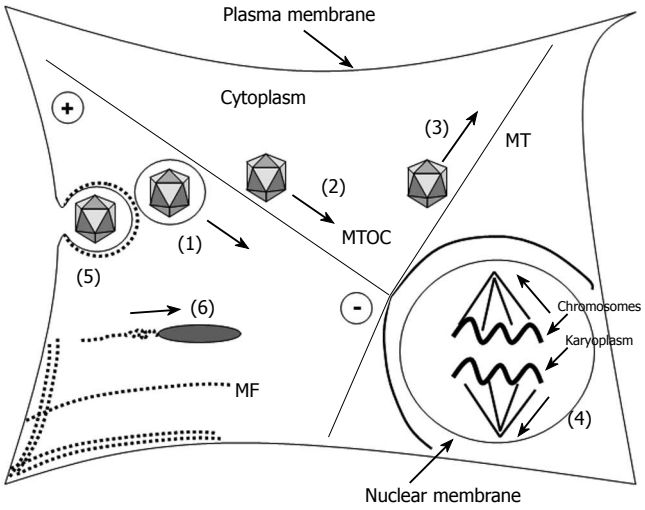

Figure 1 Participation of microtubules and microfilaments in transport processes. Transport processes are indicated as bold arrows. Microtubules (MT, bold lines) have a highly dynamic plus-end and a less dynamic minus-end that is located at the microtubule-organizing (MTOC). They participate in the transport of (1) organelles, e.g. endosomes, (2) direct retrograde transport of capsids via the dynein motor protein complex (adenovirus, HSV 1, parvoviruses), (3) direct anterograde transport of progeny HSV 1 capsids by conventional kinesin, and (4) participate in chromosome segregation upon mitosis. Microfilaments (MF), depicted as dotted lines participate (5) in separation of endocytotic vesicles from the plasma membrane and (6) *via* polymerization in transport of e.g. *Listeria* monocytogenes and nuclear polyhedrosis virus (NPV).

However the most commonly used transport strategy for macromolecules, mRNA, RNPs (ribonucleoprotein complexes), cellular organelles and vesicles along polar MF or MT involves motor protein complexes, namely myosins, kinesins and dyneins[20,35-38]. These cargo specific filament binding proteins exhibit a motor domain (ATPase) and move ATP-dependent and unidirectional along the stable filaments. Dependent upon the involved filament and transport direction different motor protein complexes are used. Class VI myosins are unconventional myosins which move towards the minus-end of MF[39]. They are involved in the transport of clathrin-coated vesicles from the plasma membrane into the inner cell[40,41]. Class I and class V myosins in contrast migrate towards the plus-end of MF[20,35]. Myosin I mediates transport of membranes whereas myosin V is responsible for the transport of organelles, as e.g. recycling endosomes towards the plasma membrane[20,42,43]. In addition myosin V can transport cargos along MT[44] thus linking both transport systems.

The MT specific kinesins can be distinguished upon the localization of the conserved motor domain into conventional kinesins, which have an N-terminal motor domain and that direct cargos in the anterograde direction

towards the plus-end of the MT (i.e. towards the cell periphery)[20,36]. They participate in the intracellular transport and localization of different cellular membrane organelles, as the extension of the ER (endoplasmatic reticulum) from the nucleus towards the cell periphery[45,46]. In addition, conventional kinesins are used in directing progeny capsids of herpes simplex virus 1 (HSV 1) in the anterograde direction[47].

Unconventional kinesins, which have a C-terminal motor domain move in contrast towards the minus-end of MT. They mediate axonal MT transport of vesicles and organelles[36].

The cytoplasmic dynein is commonly associated with the cofactor dynactin (dynactin-complex)[48] transporting cellular vesicles (endosomes and caveolin-negative vesicles[49-52] and macromolecules (e.g. tumor suppressor protein p53[5]) in the retrograde direction towards MT minus-end (the MTOC). Apparently the dynein-complex is frequently used in transport of viral capsids towards the nucleus as it was shown for adenoviruses[53-55], parvoviruses[56-59] and HSV 1 upon infection[47,60].

INTRACYTOSOLIC TRANSPORT OF HBV CAPSIDS

With the exception of NPV all viruses being analyzed so far make use of the MT transport system for their transport towards the nucleus[61]. This includes large viruses that have to travel long distances as the herpes simplex virus 1 (HSV 1;[47]) that has to be transported for centimeters between the axon end and the cell body and parvoviruses (18-26 nm)[56,58,62] that are below the diffusion limit inside the cytoplasm.

Evaluating the transport mode of hepatitis B virus is however not trivial as the entry mechanism is not fully understood. This is mainly caused by a lack of an appropriate and effective *in vitro* infection system that allows study of the early steps of the hepadnaviral life cycle. As described in "Viral and cellular determinants involved in hepadnaviral entry" hepadnaviruses enter the cells in vesicles[63] but do not need acidification for infection[64]. This step that normally occurs upon endocytosis has a major effect on viral structures as described for adeno- and parvoviruses[57,65,66]. The altered structure distinguishes capsids that have passed endocytosis from progeny capsids that are newly synthesized. The different exposed epitopes allow variant interactions so that incoming capsids are targeted to the nucleus while progeny capsids are not.

As such an acid-induced conformational change is missing in the hepadnaviral life cycle the viral capsids released from the endosomal pathway and the newly synthesized progeny capsids have the same structure. Consequently both types of capsid can participate in nuclear transport of the viral genome.

The restrictions of the experimental systems for analysis of hepadnaviral viral infections are most likely caused by an insufficient entry. It was thus a self suggested idea to replace the viral surface proteins by a lipid shell as it is done in protein transfection (lipofection)[67]. The lipids fuse with the plasma membrane and release the capsids into the cytoplasm. For studying the intracellular transport of the hepadnaviral capsid lipofection has the advantage that no cellular transport vesicles are involved.

In fact lipofection of hepatoma cells yielded in a highly productive HBV infection similar to the *in vivo* efficiency.

As lipofection is independent upon receptors high amounts of capsids could be loaded on the cells. This allows one to follow the fate of the capsids and of the viral genomes by microscopical techniques[67] showing that the capsids accumulated at the nuclear envelope after 15 min. As diffusion can be assumed to take 1 h (for calculation see[9]), these data imply a directed active capsid transport towards the nucleus. Released viral genomes occurred exclusively inside the karyoplasm suggesting site-specific disintegration at the nuclear envelope. The use of the MT depolymerizing drug nocodazole inhibits accumulation of capsids at the nuclear envelope and the release of genomes suggesting that genome liberation requires transport to the nucleus.

The microscopical finding of an active MT-mediated transport towards the nucleus was supported analysing the effect of nocodazole on the hepadnaviral life-cycle. It was demonstrated that MT are essential for formation of nuclear DNA (cccDNA that occurs only after repair of the partially double stranded DNA genome within the nucleus) and for amplification of viral DNA via synthesis of progeny mature capsids.

The use of the MT transport system was confirmed in another experimental system in which capsids were injected into the cytosol of *Xenopus laevis* oocytes. Due to the longer transport distances 30 min are required for the capsids to reach the nucleus upon injection at the pole of the oocyte opposed the nucleus. Assuming a distance of 0.5 mm that has to be bridged this period is consistent with the cytosolic transport of HSV 1 capsids that traverse the cytoplasm with 3-5 mm per hour (retrograde transport,[9]). As electron microscopy was used as read-out for capsid localization these data could show that the capsids did not bind to undefined sites of the nuclear envelope but to the nuclear pore complexes (NPC)[68]. However, when anti tubulin-antibodies were preinjected the arrival of the capsids at the NPCs was inhibited confirming that even in cells only distantly related to human hepatocytes the same transport system is used.

Although conclusive, it must be considered that all the observations described above were not done in the "authentic primary" cells and that a liver-specific factor may alter e.g. the place of genome release and lead to another transport model that does not involve the capsid. However, the generation of capsids with a translocation motif (TLM) fused to the N-terminus of the capsid protein recently gave further support[69]. These capsids were still capable of encapsidating the polymerase and the pregenome so that mature DNA capsids were generated being able to initiate an HBV infection in primary human hepatocytes. Although the mode of uptake by a TLM remains controversial-directly penetrating the plasma membrane or using transporters[70]-a clear uptake of the capsids could be observed, resulting in accumulation in the

perinuclear region. This uptake was not observed when wild-type capsids were used being contradictory to most recent results of others[71]. Irrespectively of this divergence the location of the TLM capsids at the perinuclear region where the MTOC is situated supports that the MT were used for transport towards the nucleus.

An open question not being answered for any cargo that uses MT transport for reaching the nucleus is derived from the polarity and arrangement of the MT. As their minus-end is not directly located at the NPC but attached to the MTOC the cargo must cross the distance between the MTOC and the nucleus. There are observations that even for this short gap passive diffusion is not likely: HSV 1 capsids show an equal distribution around the nucleus after infection and do not accumulate at those NPCs adjacent to the MTOC[47]. However, the mechanism of this translocation remains open.

GENERAL MECHANISM OF NUCLEAR TRANSPORT

Viruses that replicate in the nucleus of non-dividing cells have to traverse the nuclear envelope. For this reason nuclear proteins pass the nuclear pore complexes (NPCs). NPCs are large proteinaceous structures consisting of 30 different proteins[72], collectively termed nucleoporins (Nups). Nucleoporins exist in multiples copies, forming a complex of estimated 125 MD[73]. Many nucleoporins contain distinct domains of phenylalanine-glycine (FG) repeats, which mediate the main interaction between nucleoporins and soluble transport receptors. The NPC consists of a central ring-like framework with 8-fold symmetry, representing the part of the complex that is embedded in the nuclear envelope (NE) Attached to a cytoplasmic ring moiety 8 cytoplasmic filaments form an initial docking side for transport complexes. On the karyoplasmic face, 8 fibres form the cage-like structure of the nuclear basket[74]. The central framework is a ring-like assembly built around a central pore through which the exchange of macromolecules occurs. The dimension of the nuclear pore restricts complexes to a diameter of 39 nm including their shell of transport receptors[68]; a size that is exceeded by most viruses or subviral particles.

NPCs regulate the traffic of proteins and nucleic acids into and out of the nucleus[75]. Substrates smaller than roughly 9 nm in size, including ions, metabolites and proteins, travel through the NPC in a diffusion-controlled and energy independent manner[76].

Most nuclear cargos exhibit signals that interact with nuclear transport receptors of the importin β superfamily, comprising importins and transportins. All members of this family exhibit an N-terminal RanGTP-binding domain which is important for dissociating receptor and cargo (reviewed by[77]). There is a variety of different signals that are recognized as exemplified by the M9 domain, bound by transportin, polypeptides of basic amino acids that represent an importin β binding domain (IBB) and "classical" nuclear localization signals (NLSs) that show the consensus sequence K(K/R)X(K/R)[78]. The classical NLS does not directly bind to the transport-mediating receptor importin β (Imp β) but requires an adapter molecule, importin α (Imp α), which connects NLS and - *via* its IBB- Imp β.

The driving force of nuclear import and export is determined by the different concentrations of RanGTP in the nucleus versus the cytoplasm. RanGTP that is enriched in the karyoplasm, interacts with the transport receptors of the import complex, leading to dissociation of cargo and receptor. While the cargo diffuses deeper into the karyoplasm, the RanGTP-receptor complex becomes exported to the cytoplasm.

Hepadnaviral genomes have to enter the nucleoplasm for replication. As hepatocytes are terminally differentiated cells that do not divide they cannot wait until the cell undergoes mitosis as most retroviruses-excluding HIV-do. As karyophilic proteins the capsids use the nuclear pore complex to get for access to the nucleoplasm.

NUCLEAR IMPORT OF HEPADNAVIRAL GENOMES

Nucleic acids are not karyophilic *per se*. Therefore one or more proteins attached to the genome must interact with cellular nuclear import receptors. In case of the hepadnaviruses three models, each involving a different mediator, may play a crucial role in the nuclear import of the HBV genome: (1) The viral polymerase of the Hepatitis B virus. The enzyme is covalently attached to the viral genome and probably contains a hidden NLS. Expression of the polymerase in eukaryotic cells revealed that the protein stays cytoplasmic[79] but extraction of this complex from mature virions showed that it enters the nucleus[80]. However, the procedure of extraction requires harsh treatment and thus structure altering methods. (2) Some of the heat shock proteins as Hsc70 or Hsp90 activating the polymerase[81-84] and (3) the capsid proteins surrounding the viral replication complex.

The lipofection experiments described above, show that released viral DNA is exclusively present within the nucleus. The release is combined with the accumulation of capsids at the nuclear envelope. It thus has to be concluded that if the polymerase mediates nuclear import the release of the import complex must occur at the nuclear envelope, probably after docking of the capsids to the nuclear pore. Examples for such a pathway are the HSV 1 capsid that becomes opened upon the interaction of a penton with the NPC and adenovirus 2 that releases the complex of DNA and associated proteins at the pore[47,85-88].

The polymerase-associated heat shock proteins may act in a similar manner. For example, the interaction with Hsc70 that exhibits a nuclear transport capacity is established[84]. The capsid-nuclear envelope interaction was more extensively investigated in cell biological assays and in microinjection experiments using oocytes of *Xenopus laevis*. Another experimental design is based on Digitonin permeabilized cells most commonly used in studying nuclear import reactions in detail. Digitonin permeabilizes only cholesterol containing membranes as e.g. the plasma membrane and membranes of mitochondria. Other membranes as the nuclear and ER membrane remain

unaffected[89]. In general adhesive cells are analysed under conditions where they attach to the surface of a glass cover slip thus the Digitonin has to be removed by washing steps. The washing removes the soluble cytosolic proteins (and some small nuclear proteins that rapidly diffuse out of the nucleus) including the cellular nuclear transport factors. Consequently these factors have to be replaced either by addition of selected import factors or in form of a cytosolic extract. However, as the nuclear transport capacity is conserved this process can be transferred to the *in vivo* situation presupposed that the subjected cargo with its modification is physiological.

Microinjection in the cytoplasm is another established technique. For electron microscopy *Xenopus laevis* oocytes are frequently used as the huge dimensions of the nucleus allow the analysis of multiple sections. Since nuclear import is phylogenetically well conserved the results are transferable to other cell types as long as no embryogenesis related processes are affected.

These assays and biochemical analyses have been used to analyse the nuclear import of the hepadnaviral genome in more detail. Using permeabilized cells it was shown that the HBV capsid protein contains an NLS within its C-terminal domain. This domain is hidden in the lumen of RNA-containing capsids expressed in *E. coli* and in eukaryotically expressed capsids devoid of the polymerase[90,91]. These capsids failed to interact with nuclei of permeabilized cells. However, the exposure of the C-terminus on the capsid surface was shown to be linked to genome maturation as *in vitro* studies revealed[90]. Interestingly, the exposure could be initiated in RNA-containing capsids expressed in *E. coli* when the C-terminus was *in vitro* phosphorylated by protein kinase C[92] or protein kinase A[93]. These observations strengthen the idea that phosphorylation and genome maturation are linked. The impact of the exposed C-termini for nuclear pore complex association becomes evident by cleavage experiments in which the C-termini were removed from mature capsids followed by subjection of the capsids to Digitonin-permeabilized cells. According with the hypothesis of a capsid-mediated NPC docking the capsids and the necessity of exposed NLS to the digested capsids failed to interact with the nuclei. Consistently with the identification of an NLS on the capsid protein importin β was found to be the mediator of NPC interaction, requiring importin α as an adapter protein.

Most fascinating is the different import behaviour between capsids that have undergone genome maturation to a different extent. Capsids with an immature DNA genome interacted with the NPCs but remained associated with the pores while subjecting mature capsids to the permeabilized cells resulted in a nuclear capsid stain and released viral genomes within the nucleus.

Based on these data all three import models-polymerase, heat shock proteins or capsid mediation-could be true. The mature capsids could interact with the NPC releasing their genome followed by import of the genome mediated by the polymerase or heat shock proteins. The dissociated capsid subunits enter the nucleus as they apparently do in HBV infected individuals. The immature capsids could have been just more stable thus failing to disintegrate and to release the genome.

Alternatively, only the mature capsids that expose more NLS may have become surrounded by enough nuclear transport receptors to pass a hydrophobic mesh caused by the crosslinking of hydrophobe FxFG repeats of nucleoporins. Only these capsids interact with the factors required for genome release.

To differentiate between the models further investigations were initiated to follow the fate of the capsids at the NPC. Surprisingly, electron microscopy after microinjection into *Xenopus laevis* oocytes showed that not only the mature capsids passed the pore and entered the nuclear basket but also immature capsids that apparently failed to diffuse deeper into the karyoplasm. Consistent with the experiments in permeabilized cells, RNA containing capsids did not interact with the NPCs.

For the model of nuclear import these findings implied that apparently the capsids mediated the passage through the nuclear pore into the nuclear basket. Here only the mature capsids disintegrated while the immature capsid stay arrested. Hypothetically this arrest can increase efficiency of HBV infection, assuming that genome maturation proceeds in these capsids.

BEYOND NUCLEAR IMPORT

Hepadnaviral polymerases can only successfully synthesize the full length viral DNA when interacting with the capsid proteins. In fact, recent studies on the phosphorylation sites of the HBV capsid protein show that one serine residue (Ser 157) has to be phosphorylated for pregenome packaging while serine 164 is required for allowing DNA synthesis[94,95]. The highly efficient infections by hepadnaviruses thus imply that the genome release is well coordinated in that only capsids with a mature genome disintegrate. The factor however that apparently is only present within the nucleus remains unknown. Incubations of mature capsids with nuclear extracts failed to induce significant genome release while permeabilized hepatoma cells only require minutes to release thousands of HBV genomes per nucleus. Furthermore a liver-specific factor must be assumed as genome release is more efficient in permeabilized hepatoma- than in HeLa cells. *In vivo*, this conclusion is supported by observations of Untergasser *et al*[96], who observed that cccDNA generation does not occur upon infection of dendritic cells with chimera of HBV and adenovirus.

Another open question is raised by the high copy number of empty capsids found in the nuclei of HBV infected hepatocytes or in hepatocytes of mice that are transgenic for HBV. Apparently they are not derived from capsids that have transported the genome into the nucleus as the half-life of the genome-as different data in the literature are (ranging from 3 d[97], 55 d[98] to a non-relevant degradation[99])-do not explain their frequent abundance. However, the capsid protein is strongly over expressed with regard to the number of viruses and capsids that participate in nuclear entry of the viral genome. Apparently capsid proteins have a nuclear transport capacity by their NLS, which is not hidden as long as

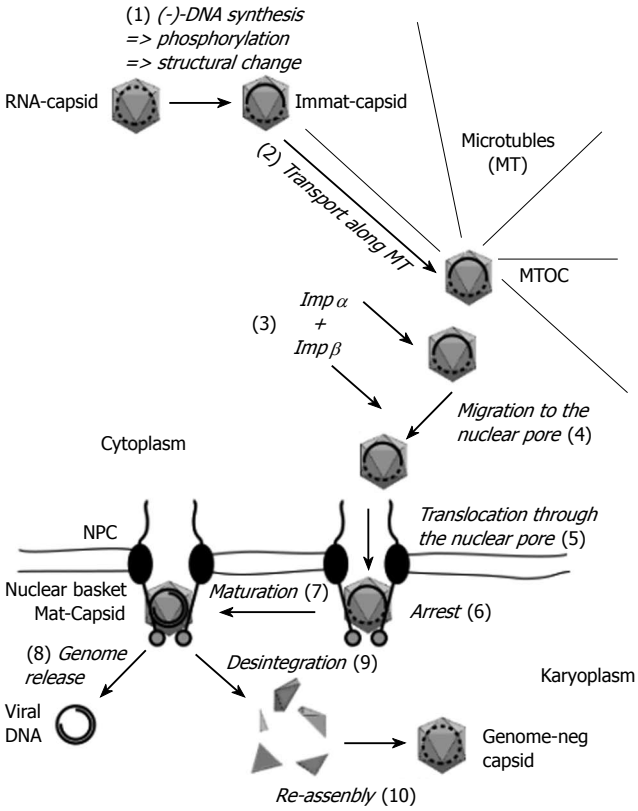

Figure 2 Hepadnaviral trafficking within the cell. Capsids are drawn as grey icosahedra. Immat-Capsid, immature capsid, Mat-Capsid, mature capsid. The nucleic acid found within the capsids is depicted as a dotted line (RNA) or a full line (DNA). The arrows present movements (2, 4, 5, 8) or changes of the capsid (1, 7, 9, 10). Further explanations are given in the text.

they are not assembled to particles. Based on the results described above one must thus conclude that not capsids but the supernumerous capsid proteins or their assembly intermediates are imported. In accordance with consistent biochemical data of all groups studying the assembly process, it must be proposed that the capsid proteins do not need any other protein for assembly. The only driving force is the affinity to each other being supported by their interaction with other components as e.g. RNA. It is thus likely that after import of high numbers of capsid proteins into the nucleus the threshold concentration is reached resulting in rapid assembly to particles.

Nonetheless, one has to ask why the capsid proteins do not become arrested in the nuclear basket as the immature capsids. One can assume that assembled capsids can interact with at least eight basket proteins, most likely the nucleoporin 153[100], that are arresting the capsid. Although the answer remains experimentally open a protein monomer in contrast is restricted to one interaction that is in competition with the thousands of proteins that pass the nuclear pore every second.

The meaning of the nuclear assembly is unsolved. It might be just a side effect caused by the intrinsic assembly ability of the capsid. However, as the capsid proteins interact preferentially with single stranded nucleic acids the assembly may prevent interference with the cellular transcription and RNA export machinery thus reducing toxicity of the virus and ensuring a long life of the infected cell for persistent virus production.

SUMMARIZING THE TRAFFICKING OF HEPADNAVIRAL CAPSID AND GENOME

The summary of the current knowledge on the nuclear import of the hepadnaviral genome is depicted in Figure 2. It must be considered however that there are several elements as e.g. the co-ordination of the transport processes that are yet unknown. (1) Upon genome maturation and phosphorylation the hepadnaviral capsids undergo a structural change that leads to exposure of increasing numbers of the C-termini that are part of the capsid protein. (2) The capsids are transported towards the microtubule-organizing centre (MTOC), which is located at the perinuclear region. (3) As the exposed C-terminal domain exhibits a nuclear localization signal the probability of an interaction with the adaptor protein importin α increases. As in the physiological import of karyophilic proteins this complex is bound by importin β. Whether this acquisition already occurs during the MT-mediated transport or (4) during the unknown passage from the MTOC to the nucleus remains open. (5) Importin β next facilitates docking to the cytosolic fibres of the nuclear pore and translocation of the complex into the nuclear basket. (6) After dissociation of the nuclear import receptors from the capsid the capsid most likely interacts with a protein of the basket. (7) While immature capsids stay arrested and may continue with genome maturation, (8) mature capsids that are less stable release the genome with the associated proteins into the nucleus where genome repair takes place. (9) Supernumerous capsid proteins that result from disintegration can diffuse deeper into the karyoplasm where (10) they re-assemble after the capsid protein concentration reaches the threshold concentration for assembly.

REFERENCES

1 **Kehlenbach RH**. In vitro analysis of nuclear mRNA export using molecular beacons for target detection. *Nucleic Acids Res* 2003; **31**: e64
2 **Janmey PA**, Weitz DA. Dealing with mechanics: mechanisms of force transduction in cells. *Trends Biochem Sci* 2004; **29**: 364-370
3 **Luby-Phelps K**. Physical properties of cytoplasm. *Curr Opin Cell Biol* 1994; **6**: 3-9
4 **Zhang X**, Clark AF, Yorio T. Heat shock protein 90 is an essential molecular chaperone for nuclear transport of glucocorticoid receptor beta. *Invest Ophthalmol Vis Sci* 2006; **47**: 700-708
5 **Giannakakou P**, Sackett DL, Ward Y, Webster KR, Blagosklonny MV, Fojo T. p53 is associated with cellular microtubules and is transported to the nucleus by dynein. *Nat Cell Biol* 2000; **2**: 709-717
6 **Crowther RA**, Kiselev NA, Böttcher B, Berriman JA, Borisova GP, Ose V, Pumpens P. Three-dimensional structure of hepatitis B virus core particles determined by electron cryomicroscopy. *Cell* 1994; **77**: 943-950
7 **Kenney JM**, von Bonsdorff CH, Nassal M, Fuller SD. Evolutionary conservation in the hepatitis B virus core structure: comparison of human and duck cores. *Structure* 1995; **3**: 1009-1019
8 **Brady ST**. Molecular motors in the nervous system. *Neuron*

1991; **7**: 521-533
9 **Sodeik B**. Mechanisms of viral transport in the cytoplasm. *Trends Microbiol* 2000; **8**: 465-472
10 **Fujimoto LM**, Roth R, Heuser JE, Schmid SL. Actin assembly plays a variable, but not obligatory role in receptor-mediated endocytosis in mammalian cells. *Traffic* 2000; **1**: 161-171
11 **Brodsky FM**, Chen CY, Knuehl C, Towler MC, Wakeham DE. Biological basket weaving: formation and function of clathrin-coated vesicles. *Annu Rev Cell Dev Biol* 2001; **17**: 517-568
12 **Apodaca G**. Endocytic traffic in polarized epithelial cells: role of the actin and microtubule cytoskeleton. *Traffic* 2001; **2**: 149-159
13 **Greenberg S**. Signal transduction of phagocytosis. *Trends Cell Biol* 1995; **5**: 93-99
14 **Greenberg S**, Grinstein S. Phagocytosis and innate immunity. *Curr Opin Immunol* 2002; **14**: 136-145
15 **Ridley AJ**, Paterson HF, Johnston CL, Diekmann D, Hall A. The small GTP-binding protein rac regulates growth factor-induced membrane ruffling. *Cell* 1992; **70**: 401-410
16 **Dowrick P**, Kenworthy P, McCann B, Warn R. Circular ruffle formation and closure lead to macropinocytosis in hepatocyte growth factor/scatter factor-treated cells. *Eur J Cell Biol* 1993; **61**: 44-53
17 **Pelkmans L**, Püntener D, Helenius A. Local actin polymerization and dynamin recruitment in SV40-induced internalization of caveolae. *Science* 2002; **296**: 535-539
18 **Pelkmans L**, Helenius A. Endocytosis via caveolae. *Traffic* 2002; **3**: 311-320
19 **Lycke E**, Kristensson K, Svennerholm B, Vahlne A, Ziegler R. Uptake and transport of herpes simplex virus in neurites of rat dorsal root ganglia cells in culture. *J Gen Virol* 1984; **65** (Pt 1): 55-64
20 **Kreis TE**, Vale R. Guidebook to the Cytoskeletal and Motor Proteins. 2nd ed. Oxford: Oxford University Press, 1999
21 **Echeverri CJ**, Paschal BM, Vaughan KT, Vallee RB. Molecular characterization of the 50-kD subunit of dynactin reveals function for the complex in chromosome alignment and spindle organization during mitosis. *J Cell Biol* 1996; **132**: 617-633
22 **Mitchison TJ**, Salmon ED. Poleward kinetochore fiber movement occurs during both metaphase and anaphase-A in newt lung cell mitosis. *J Cell Biol* 1992; **119**: 569-582
23 **Waters JC**, Mitchison TJ, Rieder CL, Salmon ED. The kinetochore microtubule minus-end disassembly associated with poleward flux produces a force that can do work. *Mol Biol Cell* 1996; **7**: 1547-1558
24 **Zhang F**, Southwick FS, Purich DL. Actin-based phagosome motility. *Cell Motil Cytoskeleton* 2002; **53**: 81-88
25 **Desjardins M**, Griffiths G. Phagocytosis: latex leads the way. *Curr Opin Cell Biol* 2003; **15**: 498-503
26 **Merrifield CJ**, Moss SE, Ballestrem C, Imhof BA, Giese G, Wunderlich I, Almers W. Endocytic vesicles move at the tips of actin tails in cultured mast cells. *Nat Cell Biol* 1999; **1**: 72-74
27 **Taunton J**. Actin filament nucleation by endosomes, lysosomes and secretory vesicles. *Curr Opin Cell Biol* 2001; **13**: 85-91
28 **Taunton J**, Rowning BA, Coughlin ML, Wu M, Moon RT, Mitchison TJ, Larabell CA. Actin-dependent propulsion of endosomes and lysosomes by recruitment of N-WASP. *J Cell Biol* 2000; **148**: 519-530
29 **Tilney LG**, DeRosier DJ, Tilney MS. How Listeria exploits host cell actin to form its own cytoskeleton. I. Formation of a tail and how that tail might be involved in movement. *J Cell Biol* 1992; **118**: 71-81
30 **Tilney LG**, DeRosier DJ, Weber A, Tilney MS. How Listeria exploits host cell actin to form its own cytoskeleton. II. Nucleation, actin filament polarity, filament assembly, and evidence for a pointed end capper. *J Cell Biol* 1992; **118**: 83-93
31 **Tilney LG**, Portnoy DA. Actin filaments and the growth, movement, and spread of the intracellular bacterial parasite, Listeria monocytogenes. *J Cell Biol* 1989; **109**: 1597-1608
32 **Charlton CA**, Volkman LE. Penetration of Autographa californica nuclear polyhedrosis virus nucleocapsids into IPLB Sf 21 cells induces actin cable formation. *Virology* 1993; **197**: 245-254
33 **Lanier LM**, Slack JM, Volkman LE. Actin binding and proteolysis by the baculovirus AcMNPV: the role of virion-associated V-CATH. *Virology* 1996; **216**: 380-388
34 **Lanier LM**, Volkman LE. Actin binding and nucleation by Autographa california M nucleopolyhedrovirus. *Virology* 1998; **243**: 167-177
35 **Mermall V**, Post PL, Mooseker MS. Unconventional myosins in cell movement, membrane traffic, and signal transduction. *Science* 1998; **279**: 527-533
36 **Goldstein LS**, Philp AV. The road less traveled: emerging principles of kinesin motor utilization. *Annu Rev Cell Dev Biol* 1999; **15**: 141-183
37 **Schroer TA**. Motors, clutches and brakes for membrane traffic: a commemorative review in honor of Thomas Kreis. *Traffic* 2000; **1**: 3-10
38 **López de Heredia M**, Jansen RP. mRNA localization and the cytoskeleton. *Curr Opin Cell Biol* 2004; **16**: 80-85
39 **Wells AL**, Lin AW, Chen LQ, Safer D, Cain SM, Hasson T, Carragher BO, Milligan RA, Sweeney HL. Myosin VI is an actin-based motor that moves backwards. *Nature* 1999; **401**: 505-508
40 **Buss F**, Arden SD, Lindsay M, Luzio JP, Kendrick-Jones J. Myosin VI isoform localized to clathrin-coated vesicles with a role in clathrin-mediated endocytosis. *EMBO J* 2001; **20**: 3676-3684
41 **Buss F**, Luzio JP, Kendrick-Jones J. Myosin VI, a new force in clathrin mediated endocytosis. *FEBS Lett* 2001; **508**: 295-299
42 **Lapierre LA**, Kumar R, Hales CM, Navarre J, Bhartur SG, Burnette JO, Provance DW, Mercer JA, Bähler M, Goldenring JR. Myosin vb is associated with plasma membrane recycling systems. *Mol Biol Cell* 2001; **12**: 1843-1857
43 **Altschuler Y**, Hodson C, Milgram SL. The apical compartment: trafficking pathways, regulators and scaffolding proteins. *Curr Opin Cell Biol* 2003; **15**: 423-429
44 **Rogers SL**, Gelfand VI. Myosin cooperates with microtubule motors during organelle transport in melanophores. *Curr Biol* 1998; **8**: 161-164
45 **Lee C**, Chen LB. Dynamic behavior of endoplasmic reticulum in living cells. *Cell* 1988; **54**: 37-46
46 **Terasaki M**. Recent progress on structural interactions of the endoplasmic reticulum. *Cell Motil Cytoskeleton* 1990; **15**: 71-75
47 **Sodeik B**, Ebersold MW, Helenius A. Microtubule-mediated transport of incoming herpes simplex virus 1 capsids to the nucleus. *J Cell Biol* 1997; **136**: 1007-1021
48 **Karki S**, Holzbaur EL. Cytoplasmic dynein and dynactin in cell division and intracellular transport. *Curr Opin Cell Biol* 1999; **11**: 45-53
49 **Aniento F**, Emans N, Griffiths G, Gruenberg J. Cytoplasmic dynein-dependent vesicular transport from early to late endosomes. *J Cell Biol* 1993; **123**: 1373-1387
50 **Gruenberg J**, Griffiths G, Howell KE. Characterization of the early endosome and putative endocytic carrier vesicles in vivo and with an assay of vesicle fusion in vitro. *J Cell Biol* 1989; **108**: 1301-1316
51 **Oda H**, Stockert RJ, Collins C, Wang H, Novikoff PM, Satir P, Wolkoff AW. Interaction of the microtubule cytoskeleton with endocytic vesicles and cytoplasmic dynein in cultured rat hepatocytes. *J Biol Chem* 1995; **270**: 15242-15249
52 **Valetti C**, Wetzel DM, Schrader M, Hasbani MJ, Gill SR, Kreis TE, Schroer TA. Role of dynactin in endocytic traffic: effects of dynamitin overexpression and colocalization with CLIP-170. *Mol Biol Cell* 1999; **10**: 4107-4120
53 **Leopold PL**, Kreitzer G, Miyazawa N, Rempel S, Pfister KK, Rodriguez-Boulan E, Crystal RG. Dynein- and microtubule-mediated translocation of adenovirus serotype 5 occurs after endosomal lysis. *Hum Gene Ther* 2000; **11**: 151-165
54 **Suomalainen M**, Nakano MY, Keller S, Boucke K, Stidwill RP, Greber UF. Microtubule-dependent plus- and minus end-directed motilities are competing processes for nuclear targeting of adenovirus. *J Cell Biol* 1999; **144**: 657-672

55 **Suomalainen M**, Nakano MY, Boucke K, Keller S, Greber UF. Adenovirus-activated PKA and p38/MAPK pathways boost microtubule-mediated nuclear targeting of virus. *EMBO J* 2001; **20**: 1310-1319

56 **Suikkanen S**, Aaltonen T, Nevalainen M, Välilehto O, Lindholm L, Vuento M, Vihinen-Ranta M. Exploitation of microtubule cytoskeleton and dynein during parvoviral traffic toward the nucleus. *J Virol* 2003; **77**: 10270-10279

57 **Vihinen-Ranta M**, Wang D, Weichert WS, Parrish CR. The VP1 N-terminal sequence of canine parvovirus affects nuclear transport of capsids and efficient cell infection. *J Virol* 2002; **76**: 1884-1891

58 **Vihinen-Ranta M**, Yuan W, Parrish CR. Cytoplasmic trafficking of the canine parvovirus capsid and its role in infection and nuclear transport. *J Virol* 2000; **74**: 4853-4859

59 **Suikkanen S**, Sääjärvi K, Hirsimäki J, Välilehto O, Reunanen H, Vihinen-Ranta M, Vuento M. Role of recycling endosomes and lysosomes in dynein-dependent entry of canine parvovirus. *J Virol* 2002; **76**: 4401-4411

60 **Döhner K**, Wolfstein A, Prank U, Echeverri C, Dujardin D, Vallee R, Sodeik B. Function of dynein and dynactin in herpes simplex virus capsid transport. *Mol Biol Cell* 2002; **13**: 2795-2809

61 **van Loo ND**, Fortunati E, Ehlert E, Rabelink M, Grosveld F, Scholte BJ. Baculovirus infection of nondividing mammalian cells: mechanisms of entry and nuclear transport of capsids. *J Virol* 2001; **75**: 961-970

62 **Vihinen-Ranta M**, Kalela A, Mäkinen P, Kakkola L, Marjomäki V, Vuento M. Intracellular route of canine parvovirus entry. *J Virol* 1998; **72**: 802-806

63 **Funk A**, Mhamdi M, Lin L, Will H, Sirma H. Itinerary of hepatitis B viruses: delineation of restriction points critical for infectious entry. *J Virol* 2004; **78**: 8289-8300

64 **Köck J**, Borst EM, Schlicht HJ. Uptake of duck hepatitis B virus into hepatocytes occurs by endocytosis but does not require passage of the virus through an acidic intracellular compartment. *J Virol* 1996; **70**: 5827-5831

65 **Christensen J**, Cotmore SF, Tattersall P. A novel cellular site-specific DNA-binding protein cooperates with the viral NS1 polypeptide to initiate parvovirus DNA replication. *J Virol* 1997; **71**: 1405-1416

66 **Cotmore SF**, D'abramo AM, Ticknor CM, Tattersall P. Controlled conformational transitions in the MVM virion expose the VP1 N-terminus and viral genome without particle disassembly. *Virology* 1999; **254**: 169-181

67 **Rabe B**, Glebe D, Kann M. Lipid-mediated introduction of hepatitis B virus capsids into nonsusceptible cells allows highly efficient replication and facilitates the study of early infection events. *J Virol* 2006; **80**: 5465-5473

68 **Panté N**, Kann M. Nuclear pore complex is able to transport macromolecules with diameters of about 39 nm. *Mol Biol Cell* 2002; **13**: 425-434

69 **Brandenburg B**, Stockl L, Gutzeit C, Roos M, Lupberger J, Schwartlander R, Gelderblom H, Sauer IM, Hofschneider PH, Hildt E. A novel system for efficient gene transfer into primary human hepatocytes via cell-permeable hepatitis B virus-like particle. *Hepatology* 2005; **42**: 1300-1309

70 **Futaki S**. Oligoarginine vectors for intracellular delivery: design and cellular-uptake mechanisms. *Biopolymers* 2006; **84**: 241-249

71 **Cooper A**, Shaul Y. Clathrin-mediated endocytosis and lysosomal cleavage of hepatitis B virus capsid-like core particles. *J Biol Chem* 2006; **281**: 16563-16569

72 **Cronshaw JM**, Krutchinsky AN, Zhang W, Chait BT, Matunis MJ. Proteomic analysis of the mammalian nuclear pore complex. *J Cell Biol* 2002; **158**: 915-927

73 **Reichelt R**, Holzenburg A, Buhle EL, Jarnik M, Engel A, Aebi U. Correlation between structure and mass distribution of the nuclear pore complex and of distinct pore complex components. *J Cell Biol* 1990; **110**: 883-894

74 **Lim RY**, Aebi U, Stoffler D. From the trap to the basket: getting to the bottom of the nuclear pore complex. *Chromosoma* 2006; **115**: 15-26

75 **Görlich D**, Kutay U. Transport between the cell nucleus and the cytoplasm. *Annu Rev Cell Dev Biol* 1999; **15**: 607-660

76 **Paine PL**, Moore LC, Horowitz SB. Nuclear envelope permeability. *Nature* 1975; **254**: 109-114

77 **Ström AC**, Weis K. Importin-beta-like nuclear transport receptors. *Genome Biol* 2001; **2**: REVIEWS3008

78 **Kalderon D**, Richardson WD, Markham AF, Smith AE. Sequence requirements for nuclear location of simian virus 40 large-T antigen. *Nature* 1984; **311**: 33-38

79 **Yao E**, Gong Y, Chen N, Tavis JE. The majority of duck hepatitis B virus reverse transcriptase in cells is nonencapsidated and is bound to a cytoplasmic structure. *J Virol* 2000; **74**: 8648-8657

80 **Kann M**, Bischof A, Gerlich WH. In vitro model for the nuclear transport of the hepadnavirus genome. *J Virol* 1997; **71**: 1310-1316

81 **Beck J**, Nassal M. Efficient Hsp90-independent in vitro activation by Hsc70 and Hsp40 of duck hepatitis B virus reverse transcriptase, an assumed Hsp90 client protein. *J Biol Chem* 2003; **278**: 36128-36138

82 **Hu J**, Anselmo D. In vitro reconstitution of a functional duck hepatitis B virus reverse transcriptase: posttranslational activation by Hsp90. *J Virol* 2000; **74**: 11447-11455

83 **Kose S**, Furuta M, Koike M, Yoneda Y, Imamoto N. The 70-kD heat shock cognate protein (hsc70) facilitates the nuclear export of the import receptors. *J Cell Biol* 2005; **171**: 19-25

84 **Mandell RB**, Feldherr CM. The effect of carboxyl-terminal deletions on the nuclear transport rate of rat hsc70. *Exp Cell Res* 1992; **198**: 164-169

85 **Ojala PM**, Sodeik B, Ebersold MW, Kutay U, Helenius A. Herpes simplex virus type 1 entry into host cells: reconstitution of capsid binding and uncoating at the nuclear pore complex in vitro. *Mol Cell Biol* 2000; **20**: 4922-4931

86 **Greber UF**, Suomalainen M, Stidwill RP, Boucke K, Ebersold MW, Helenius A. The role of the nuclear pore complex in adenovirus DNA entry. *EMBO J* 1997; **16**: 5998-6007

87 **Granzow H**, Weiland F, Jöns A, Klupp BG, Karger A, Mettenleiter TC. Ultrastructural analysis of the replication cycle of pseudorabies virus in cell culture: a reassessment. *J Virol* 1997; **71**: 2072-2082

88 **Saphire AC**, Guan T, Schirmer EC, Nemerow GR, Gerace L. Nuclear import of adenovirus DNA in vitro involves the nuclear protein import pathway and hsc70. *J Biol Chem* 2000; **275**: 4298-4304

89 **Adam SA**, Marr RS, Gerace L. Nuclear protein import in permeabilized mammalian cells requires soluble cytoplasmic factors. *J Cell Biol* 1990; **111**: 807-816

90 **Rabe B**, Vlachou A, Panté N, Helenius A, Kann M. Nuclear import of hepatitis B virus capsids and release of the viral genome. *Proc Natl Acad Sci USA* 2003; **100**: 9849-9854

91 **Zlotnick A**, Cheng N, Stahl SJ, Conway JF, Steven AC, Wingfield PT. Localization of the C terminus of the assembly domain of hepatitis B virus capsid protein: implications for morphogenesis and organization of encapsidated RNA. *Proc Natl Acad Sci USA* 1997; **94**: 9556-9561

92 **Kann M**, Sodeik B, Vlachou A, Gerlich WH, Helenius A. Phosphorylation-dependent binding of hepatitis B virus core particles to the nuclear pore complex. *J Cell Biol* 1999; **145**: 45-55

93 **Vlachou A.** Untersuchung von Wechselwirkungen zwischen Hepatitis B Virus Nukleocapsiden und dem Zellkern. Biologie: Giessen, 1999

94 **Gazina EV**, Fielding JE, Lin B, Anderson DA. Core protein phosphorylation modulates pregenomic RNA encapsidation to different extents in human and duck hepatitis B viruses. *J Virol* 2000; **74**: 4721-4728

95 **Melegari M**, Wolf SK, Schneider RJ. Hepatitis B virus DNA replication is coordinated by core protein serine phosphorylation and HBx expression. *J Virol* 2005; **79**: 9810-9820

96 **Untergasser A**, Zedler U, Langenkamp A, Hösel M, Quasdorff

M, Esser K, Dienes HP, Tappertzhofen B, Kolanus W, Protzer U. Dendritic cells take up viral antigens but do not support the early steps of hepatitis B virus infection. *Hepatology* 2006; **43**: 539-547

97 **Civitico GM**, Locarnini SA. The half-life of duck hepatitis B virus supercoiled DNA in congenitally infected primary hepatocyte cultures. *Virology* 1994; **203**: 81-89

98 **Zhu Y**, Yamamoto T, Cullen J, Saputelli J, Aldrich CE, Miller DS, Litwin S, Furman PA, Jilbert AR, Mason WS. Kinetics of hepadnavirus loss from the liver during inhibition of viral DNA synthesis. *J Virol* 2001; **75**: 311-322

99 **Moraleda G**, Saputelli J, Aldrich CE, Averett D, Condreay L, Mason WS. Lack of effect of antiviral therapy in nondividing hepatocyte cultures on the closed circular DNA of woodchuck hepatitis virus. *J Virol* 1997; **71**: 9392-9399

100 **Schmitz A**, Schwarz A, Panté N, Rabe B, Kann M. Retention of hepatitis B virus capsids in the nuclear basket by interaction with the nucleoporin 153. *submitted* 2006

S- Editor Liu Y **L- Editor** Alpini GD **E- Editor** Ma WH

PO Box 2345, Beijing 100023, China
www.wjgnet.com
wjg@wjgnet.com

World J Gastroenterol 2007 January 7; 13(1): 48-64
World Journal of Gastroenterology ISSN 1007-9327

TOPIC HIGHLIGHT

Dieter Glebe, PhD, *Series Editor*

Hepatitis B virus replication

Juergen Beck, Michael Nassal

Juergen Beck, Michael Nassal, Department of Internal Medicine II / Molecular Biology, University Hospital Freiburg, Germany
Supported by grants from the Deutsche Forschungsgemeinschaft and the European Community. Some of the own work described is part of the activities of the European Community sponsored network of excellence on antiviral drug resistance, ViRgil (contract LSHM-CT-2004-503359)
Correspondence to: Dr. Michael Nassal, Department of Internal Medicine II/Molecular Biology, University Hospital Freiburg, Hugstetter Street 55, D-79106 Freiburg, Germany. nassal2@ukl.uni-freiburg.de
Telephone: +49-761-2703507 Fax: +49-761-2703507
Received: 2006-08-01 Accepted: 2006-11-14

Abstract

Hepadnaviruses, including human hepatitis B virus (HBV), replicate through reverse transcription of an RNA intermediate, the pregenomic RNA (pgRNA). Despite this kinship to retroviruses, there are fundamental differences beyond the fact that hepadnavirions contain DNA instead of RNA. Most peculiar is the initiation of reverse transcription: it occurs by protein-priming, is strictly committed to using an RNA hairpin on the pgRNA, ε, as template, and depends on cellular chaperones; moreover, proper replication can apparently occur only in the specialized environment of intact nucleocapsids. This complexity has hampered an in-depth mechanistic understanding. The recent successful reconstitution in the test tube of active replication initiation complexes from purified components, for duck HBV (DHBV), now allows for the analysis of the biochemistry of hepadnaviral replication at the molecular level. Here we review the current state of knowledge at all steps of the hepadnaviral genome replication cycle, with emphasis on new insights that turned up by the use of such cell-free systems. At this time, they can, unfortunately, not be complemented by three-dimensional structural information on the involved components. However, at least for the ε RNA element such information is emerging, raising expectations that combining biophysics with biochemistry and genetics will soon provide a powerful integrated approach for solving the many outstanding questions. The ultimate, though most challenging goal, will be to visualize the hepadnaviral reverse transcriptase in the act of synthesizing DNA, which will also have strong implications for drug development.

Key words: Chaperone-mediated reverse transcription; HBV cccDNA; Hepadnavirus, P protein; Pregenomic RNA; Protein-priming; reverse transcriptase; RNA encapsidation signal

Beck J, Nassal M. Hepatitis B virus replication. *World J Gastroenterol* 2007; 13(1): 48-64

http://www.wjgnet.com/1007-9327/13/48.asp

INTRODUCTION

A hallmark of hepatitis B virus (HBV) replication is protein-primed reverse transcription, related to, but mechanistically distinct from, retroviral replication. This review will focus on the various genome transformations that occur during the replication cycle, with emphasis on the cis-elements on the one hand, and the trans-acting factors known or thought to be involved on the other. A general outline of the chain of events during hepadnaviral replication has been established, mainly using transfection of cloned HBV DNA into a few suitable cell lines, and has been the subject of several reviews[1-6]. Much less clear than what happens is, however, how these various steps are achieved and regulated.

Several features of HBV make resolving such mechanistic questions exquisitely difficult: Foremost, until recently, no *in vitro* systems were available to reconstitute individual replication steps under controlled conditions; conversely, there are no simple infection systems to follow the consequences of mutation-induced *in vitro* phenotypes in the context of authentic virus replication. Secondly, for various of the viral components and mechanisms no precedents exist such that drawing conclusions *in silico*, or by analogy to experimentally more tractable systems, is of limited value. Finally, there is a general lack of structural information on the involved viral factors, in particular on P protein, the viral reverse transcriptase. Fortunately, duck HBV (DHBV), the type member of the *avihepadnaviridae*, provides a valuable model system[7]. Although it differs from HBV in some details, the general features of genome replication are highly conserved; in fact, that hepadnaviruses replicate through reverse transcription has been established with DHBV[8]. Beyond allowing feasible *in vitro* and *in vivo* infection studies, the crucial initiation step of DHBV reverse transcription has recently been

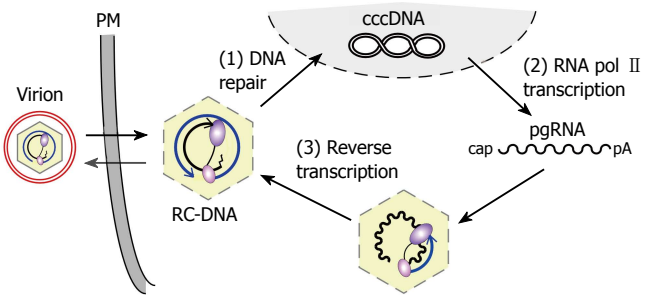

Figure 1 Replication cycle of the hepadnaviral genome. Enveloped virions infect the cell, releasing RC-DNA containing nucleocapsids into the cytoplasm. RC-DNA is transported to the nucleus, and repaired to form cccDNA (1). Transcription of cccDNA by RNA polymerase Ⅱ (2) produces, amongst other transcripts (not shown), pgRNA. pgRNA is encapsidated, together with P protein, and reverse transcribed inside the nucleocapsid (3). (+)-DNA synthesis from the (-)-DNA template generates new RC-DNA. New cycles lead to intracellular cccDNA amplification; alternatively, the RC-DNA containing nucleocapsids are enveloped and released as virions. PM, plasma membrane.

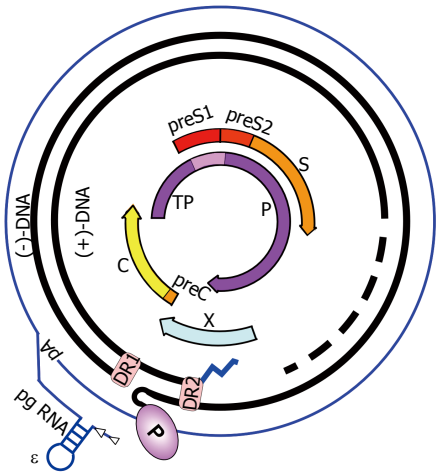

Figure 2 HBV genome organization. The partially double-stranded, circular RC-DNA is indicated by thick black lines, with P covalently linked to the 5′ end of the (-)-DNA, and the RNA primer (zigzag line) at the 5′ end of (+)-DNA. The dashed part symbolizes the heterogeneous lengths of the (+)-strands. DR1 and DR2 are the direct repeats. The outer circle symbolizes the terminally redundant pgRNA with ε close to the 5′ end, and the poly-A tail at the 3′ end. The precore mRNA is nearly identical, except it starts slightly upstream. The relative positions of the open reading frames for core (C), P, preS/S, and X are shown inside. TP, Terminal protein domain of P.

reconstituted in the test tube. On many occasions, we will therefore refer to data obtained with this model virus, and add what is available for human HBV.

OVERVIEW OVER THE HEPADNAVIRAL GENOME REPLICATION CYCLE

Replication of the hepadnaviral genome can broadly be divided into three phases (Figure 1): (1) Infectious virions contain in their inner icosahedral core the genome as a partially double-stranded, circular but not covalently closed DNA of about 3.2 kb in length (relaxed circular, or RC-DNA); (2) upon infection, the RC-DNA is converted, inside the host cell nucleus, into a plasmid-like covalently closed circular DNA (cccDNA); (3) from the cccDNA, several genomic and subgenomic RNAs are transcribed by cellular RNA polymerase Ⅱ; of these, the pregenomic RNA (pgRNA) is selectively packaged into progeny capsids and is reverse transcribed by the co-packaged P protein into new RC-DNA genomes. Matured RC-DNA containing-but not immature RNA containing-nucleocapsids can be used for intracellular cccDNA amplification, or be enveloped and released from the cell as progeny virions. Below we discuss these genome conversions, with emphasis on the reverse transcription step, and particularly its unique initiation mechanism.

RC-DNA TO cccDNA CONVERSION

Persistent viral infections require that the viral genome be present in the infected cell in a stable form that is not lost during cell division, and which therefore can be used for the continuous production of progeny genomes. Many DNA virus genomes harbor replication origins allowing them to directly exploit the cellular replication machinery for amplification; retroviruses integrate a terminally duplicated linear version of their DNA genome into the host genome, such that it is replicated along with the chromosomes. For hepadnaviruses, the genome persists, instead, as a nuclear, episomal covalently closed circle, i.e. the cccDNA. The circular form obviates the need for terminal redundancy in that, on the circle, the core promoter/enhancer Ⅱ is placed in front of the start sites for the genomic RNAs; conversely, in typical HBV expression vectors the cloned hepadnaviral DNA is interrupted by plasmid sequences, such that the control regions need to be duplicated[9].

Distinct features of the RC-DNA (Figure 2) are (1), only the (-)-DNA strand (with opposite polarity to the mRNAs) is complete whereas the (+)-strands comprise a cohort of less than full-length molecules; (2), the 5′ end of the (-)-DNA is covalently linked to P protein; (3) the 5′ end of the (+)-strand consists of an RNA oligonucleotide, derived from the pgRNA, which served as the primer for (+)-strand synthesis. For cccDNA formation, all these modifications need to be removed, and both strands need to be covalently ligated.

How this is achieved is not well understood, in particular because unambiguous cccDNA detection in the presence of excess RC-DNA is not technically trivial, not even by PCR approaches[10]. Also, whenever overlength HBV constructs are involved, e.g. upon transduction of cells with HBV carrying adeno-[11] or baculoviruses[12], caution is indicated because homologous recombination could provide for a virus replication independent mechanism of cccDNA formation.

Direct infection avoids this problem but as yet only limited data are available. Earlier evidence obtained with the DHBV-primary duck hepatocyte (PDH) infection system suggested that the activity of the viral P protein is not required for cccDNA generation[13]; however, more recent data using infection with HBV of primary tupaia hepatocytes[14,15] indicate that reverse transcriptase inhibitors can strongly reduce, though not completely block, cccDNA formation[16]. This would be in line with a

role for P protein in the process, probably the completion of the (+)-strands. However, the other steps towards cccDNA are likely to require cellular activities, as suggested by the apparent lack of cccDNA, despite formation of infectious virions, in non-authentic host cells such as hepatocytes from HBV transgenic mice[17]. However, low level cccDNA generation in mice has been reported in certain experimental settings[18,19].

Naturally hepadnavirus infected hepatocytes contain up to 50 or more copies of cccDNA[20], probably in the form of histone-containing minichromosomes[21]. This amplification occurs intracellularly[22,23] in that progeny RC-DNA genomes, like the initially infecting genome, undergo nuclear import and cccDNA conversion (Figure 1). Together with the long half-life (30 to 60 d for DHBV[20,24]), this ensures that cccDNA is not lost during cell division, and even persists during effective antiviral therapy[25]. Nuclear transport, and enveloped virion formation appear to be competing events, such that late in infection, when sufficient amounts of envelope proteins become available, further cccDNA amplification ceases[26]. A recent analysis on the single cell level revealed that the cccDNA copy number in DHBV infected PDH is not uniform and fluctuates over time; about 90% of the cells contained between 1 and 17 copies, the rest more than 17 copies[27,28]. Cells with only one copy may allow segregation of daughter cells containing no cccDNA. This could explain the apparent, though probably less than complete[29], disappearance of cccDNA during spontaneous clearance of HBV infection. However, therapeutic cccDNA elimination from the chronically infected liver remains a major issue even with the latest generation antivirals[30,31]; further investigations into the mechanism of cccDNA formation, and possibly breakdown, are clearly warranted.

FROM cccDNA TO PREGENOMIC RNA

All known hepadnaviral RNAs, i.e. the subgenomic RNAs as well as the greater-than-genome length pgRNA and precore RNA, are transcribed by cellular RNA polymerase Ⅱ (the enzyme responsible for cellular mRNA synthesis) using cccDNA as the template. All contain 5′ cap structures, all are 3′ terminally poly-adenylated at a common site, and all serve as mRNAs for viral gene products. Spliced transcripts do exist, and even can be packaged into progeny virions[32,33], yet their functional role is still obscure although for DHBV splice site mutants appear to have defects[34]. The extent of splicing appears to be controlled in DHBV by a long-range RNA secondary structure[35], and in HBV by the post-transcriptional regulatory element (PRE)[36].

The transcript relevant for virus replication is the pregenomic RNA (pgRNA), encompassing the entire genome length plus a terminal reduncancy of, in HBV, about 120 nt that contains a second copy each of the direct repeat 1 (DR1) and the ε signal, plus the poly-A tail (Figure 3A). The pgRNA starts immediately after the precore initiator codon. Its first essential role is that as mRNA for the core protein and the reverse transcriptase;

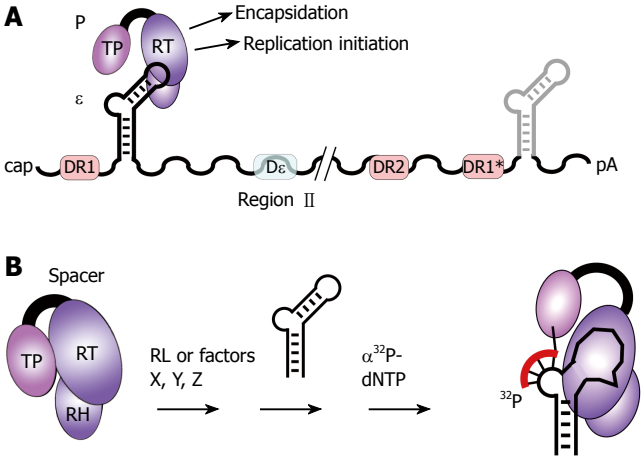

Figure 3 The pgRNA as substrate for P protein. **A**: pgRNA organization. The pgRNA is shown with some major cis-elements, i.e. ε (hairpin structure), DR1, DR2, and DR1*; DHBV, but not HBV, requires for encapsidation an additional cis-element (Dε region Ⅱ). Binding of P protein to 5′ ε, but not 3′ ε, initiates pgRNA encapsidation and replication; **B**: In vitro priming assay. P protein with its Terminal protein (TP), reverse transcriptase (RT), and RNase H (RH) domains can be activated by reticulocyte lysate (RL), or individual factors (X, Y, Z), to bind ε; ε may be supplied as small RNA covering just the hairpin structure. Upon addition of α^{32}P-dNTPs, P uses ε as template to copy 3 to 4 nt from the ε bulge region; by the covalent linkage of the 5′ nt to a tyrosine residue in TP, P protein becomes radioactively labeled, providing a sensitive assay for activity. In vitro priming does thus far not work with human HBV P protein and ε RNA.

unlike retroviral Gag-Pol proteins, P is expressed as a separate polypeptide by an unconventional mechanism[37]. Secondly, pgRNA is the template for generation of new DNA genomes by reverse transcription. The 5′ terminally extended precore RNA contains the initiator codon of the preC region and gives rise to the 25 kDa precore precursor protein of secreted 17 kDa HBeAg. It is unsuited as a pregenome, and is excluded from participating in replication on the level of encapsidation[38].

Of note, RNA polymerase Ⅱ transcription could contribute, in addition to reverse transcription, to hepadnaviral genome variability. Its extent is, however, unclear because the error rate of RNA polymerase Ⅱ is not firmly established and strongly affected by some of the subunits in the holo-enzyme complex[39,40].

CAPSID-ASSISTED REVERSE TRANSCRIPTION OF pgRNA

The next crucial step in hepadnaviral replication is the specific packaging of pgRNA, plus the reverse transcriptase, into newly forming capsids. Key actors are cis-elements on the pgRNA, most notably the encapsidation signal ε, and P protein which binds to ε. This interaction, in a still poorly understood fashion, mediates recruitment of core protein dimers and thus leads to packaging of the pgRNA-P complex. Remarkably, the precore RNA is not packaged although it contains all of the sequence comprising the pgRNA. Likely, active translation from the upstream precore ATG through the ε sequence prevents the P-ε interaction[38]. This implies, in turn, that P binding to ε on the pgRNA interferes with

translation of the core ORF, and evidence supporting this view has been forwarded for DHBV[41].

Once pgRNA and P protein are being encapsidated a second key function of the P-ε interaction is brought to bear, namely the initiation of reverse transcription. At this stage the first DNA nucleotide (nt) is covalently linked to P protein, extended into a complete (-) strand DNA, and (+) strand DNA synthesis ensues, giving rise to a new molecule of RC-DNA; the various immature DNA forms *in statu nascendi* are termed replicative intermediates, visible as a broad multiple band pattern in Southern blots from intracellular DNA.

Completion of reverse transcription before leaving the cell marks another fundamental difference to retroviruses which, except for foamyviruses[42], are secreted as virions containing two copies of RNA; an evolutionary rationale may be that DNA synthesis in the infected cell allows hepadnaviruses the intracellular genome amplification cycle as an alternative to proviral integration for stable virus genome propagation. Yet another difference is that hepadnaviral reverse transcription occurs largely, if not exclusively, in intact nucleocapsids rather than in retrovirus-like reverse transcription complexes which typically lack a continuous core shell[43,44].

Although compartmentalization of the genome amplification process is emerging as a common theme of several classes of RNA and reverse transcribing viruses[45], the hepadnaviral strategy appears as an extreme variation, considering the space restrictions imposed on the replicating complex inside the geometrically defined capsid lumen. Either the RT must slide along the entire 3 kb template, or the template must be pulled through the RT´s active site; at the same time the nucleic acid is most likely in contact with the Arg-rich C termini of the core protein subunits. In fact, capsids from core protein variants lacking part of this region still package pgRNA but appear unable to produce full-length RC-DNA; instead they preferentially reverse transcribe the fraction of spliced genomic RNAs[46,47]. Phosphorylation/dephosphorylation events at the S and T residues in the nucleic acid binding domain clearly accompany genome maturation[48], and mutations affecting the core phosphorylation status[46,49] can influence DNA synthesis in various ways. Outside capsids, or in the absence of core protein, apparently no full-length DNA can be formed.

Together these observations support the view of the capsid as a dynamic replication machine. A recent cryo electron microscopic comparison between recombinant, bacterial RNA containing capsids and authentic genome harboring nucleocapsids indeed showed some structural differences[50]; a complementary study on mutant recombinant cores revealed an enormous flexibility of the capsid structure[51]. Switching between different structural states could well be involved in supporting the progress of DNA synthesis.

The heterogeneous lengths of the (+)-strand DNAs generated by capsid-assisted reverse transcription may result from a non-identical supply of dNTPs inside individual nucleocapsids at the moment of their enclosure by the dNTP-impermeable envelope. This predicts that intracellular cores produced in the absence of envelopment should contain further extended (+)-DNAs. Alternatively, space restrictions in the capsid lumen could prevent (+)-strand DNA completion; in this view, further (+)-strand elongation after infection of a new cell might destabilize the nucleocapsid and thus be involved in genome uncoating.

CIS-ELEMENTS AND TRANSACTING FACTORS ESSENTIAL FOR HEPADNAVIRAL REPLICATION

The absolute requirements for replication are a template nucleic acid, plus an enzyme that is able to read the template information and use it for synthesis of a complementary nucleic acid. Clearly, these basic components are the pgRNA (and later the (-)-strand DNA) and P protein. However, generation of a functional genome also depends critically on precise start and end points, provided by cis-elements on the template (Figure 3A); a further specialty of P protein is its strict dependence, for activity, on cellular factors, namely heat shock proteins (Hsp´s) or chaperones (see below).

Most initial knowledge on the cis- and trans-factors involved in hepadnaviral replication was derived by transient transfection of mutant viral genomes into stable hepatoma cell lines. This system faithfully mimics several of the authentic replication steps, however its complexity precluded elucidation of many mechanistic details. The recent establishment of *in vitro* systems, culminating in the complete *in vitro* reconstitution of active DHBV replication initiation complexes from purified components[52-54], overcame these restrictions (see below). It should be noted, however, that such minimal systems have their own limitations; for instance, the crucial role of the proper capsid environment for RC-DNA formation has not yet been modeled *in vitro*, and HBV P protein has thus far proven refractory to *in vitro* reconstitution of DNA synthesis activity. Hence which of the two approaches is more useful depends on the question addressed, and where ever possible they should be combined.

STRUCTURE OF THE RNA ENCAPSIDATION SIGNAL ε

The best understood cis-element on the hepdnaviral pgRNA is ε (Figure 4), a stem-loop structure initially defined as the sequence from the 5´ end of HBV pgRNA that P-dependently mediated encapsidation of pgRNA, and also of heterologous transcripts to which it was fused[55]; later, the P-ε interaction was found to constitute the first step in initiation of reverse transcription[56-58]; hence ε also acts as the replication origin (Figure 3A).

The hairpin structure of ε (Figure 4A) was confirmed by secondary structure analyses[59,60], and its importance was established by following the effects of site-directed mutants on the packaging efficacy in transfected cells[59-63]. Furthermore, the ε sequence is highly conserved in other mammalian hepadnaviruses, as well as between different

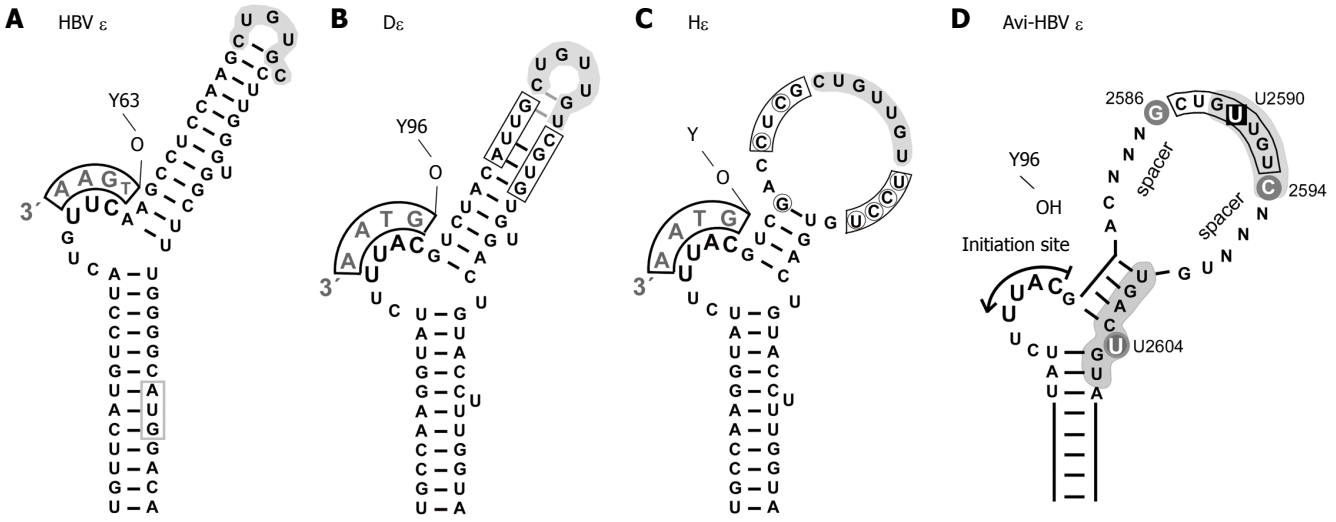

Figure 4 Secondary structures of hepadnaviral ε signals. **A**: HBV ε. The entire hairpin, including in the upper stem region, is stably base-paired; formation of a stable tri-loop, as indicated, is confirmed by direct NMR analysis[68]. The conventional annotation for the loop sequence is high-lighted by grey shading. The bulge-templated DNA oligonucleotide and the priming Y63 are indicated; **B**: DHBV ε. The overall 2D structure is similar to that of HBV ε, including a largely base-paired upper stem[69], as confirmed by preliminary NMR data. The boxed positions were randomized in a SELEX approach, and P binding individuals were selected from the corresponding RNA library[71]; **C**: HHBV ε (Hε). Hε shows substantial sequence variation to **D**: (encircled nt), leading to a largely open upper stem structure; **D**: Generalized secondary structure of an avihepadnaviral ε signal. The scheme summarizes major determinants for productive interaction with P protein[71]. Grey background indicates nt positions that are probably in contact with protein. The bulge and its immediate vicinity, particularly the tip of the lower stem, are essential for P binding whereas the loop appears critically involved in the transition to a productive initiation complex[109]. U2590 > C or U2604 > G mutations abrogate, or strongly reduce, P binding whereas G2586 and C2594 do not affect binding but are important for priming. The major role of the nt termed N may be to provide a proper spacing to the bulge element; their sequence is not important as long as formation of highly stable base-pairing is prevented.

HBV isolates[64,65]. An illustrating example are the HBV precore variants in which HBeAg synthesis is prevented by stop mutations in the ε overlapping precore region. The only mutations causing this phenotype found in nature are those which maintain a stable ε secondary structure[66,67].

It should be noted that RNA secondary structure (2D) analysis provides a mere description of the base-pairing pattern. Hence a true mechanistic understanding requires knowledge of the three-dimensional (3D) structure. The structure of the HBV ε upper stem, recently solved by nuclear magnetic resonance (NMR) techniques[68], revealed that the apical loop consists actually of only 3 nt (as in Figure 4A). This analysis is currently extended to determining the 3D structure of the entire stem-loop, which seems to form a nearly contiguous double-helix (S. Flodell, M. Petersen, F. Girard, J. Zdunek, K. Kidd-Ljunggren, J. Schleucher and S. Wijmenga; submitted); of particular interest will be the structure of the bulge region which is the template for the first few nt of (-)-DNA (see below). Thermodynamic calculations as well as experimental melting curves indicate that the entire HBV ε structure, including the upper stem, is highly stable. Notably, however, in DHBV rearranging this structure is necessary for the RNA to act as a template (see below). Determining the ε RNA structure in the complex with P protein is therefore the ultimate, yet demanding, goal.

Despite limited sequence homology to HBV ε, DHBV ε (Dε) has a similar secondary structure[69] with a bulge and an apical loop (Figure 4B), which suggested that this structure is a common trait of all hepadnaviruses. Surprisingly, the corresponding ε signal (Hε) from the related heron HBV (HHBV) has much reduced base-pairing in the upper stem region (Figure 4C), yet it functionally interacts with DHBV P protein *in vitro* whereas HBV ε does not[70].

Selection, from a library of RNAs with partially randomized upper stems for individuals able to bind to *in vitro* translated DHBV P protein (see Cell-free reconstitution of hepadnaviral replication initiation) revealed the absence of base-pairing in the upper stem region as a common theme (Figure 4D)[71]. Some of the selected P-binding RNAs supported *in vitro* priming while others did not, confirming that a productive interaction, leading to DNA synthesis, requires more than mere physical binding (see below). Hence for avihepadnaviral ε signals an open upper stem structure is beneficial for both physical and productive binding to P; in fact, deliberate Dε stabilization strongly reduces P binding[71]. This is one line of evidence that structural reshaping of the upper stem is a crucial event for initiation of DNA synthesis. Independent support comes from preliminary NMR and melting curve data for wt Dε RNA, according to which the upper stem is the least stable region (F. Girard, O. Ottink, M. Tessari and S. Wijmenga, to be submitted). This marked difference to the highly stable HBV ε structure may be related to the *in vitro* inactivity of the HBV P protein[72].

The functional consequences of mutations affecting ε and other recognized cis-elements are discussed in more detail below. Of note is, however, whereas the HBV ε stem-loop alone is sufficient to mediate encapsidation of heterologous RNAs[62,73], DHBV pgRNA encapsidation requires additional elements. "Region Ⅱ"[74], several hundred nt downstream of 5′ ε, and the intervening sequence[75] may be operative *via* long-range RNA

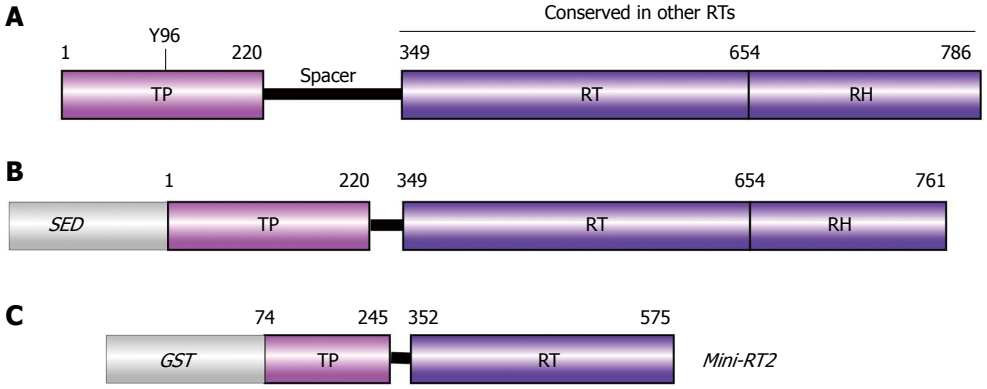

Figure 5 Domain structure of P protein. **A**: Authentic DHBV P protein. Numbers are aa positions for DHBV P protein. The priming Tyr residue Y96 is indicated; **B**: Typical recombinant P protein construct. For solubility, a heterologous solubility enhancing domain (*SED*) such as NusA, GrpE, or *GST* is required, and a short stretch of C terminal aa must be removed. Deletion of the spacer has no negative effects on *in vitro* activity; **C**: Mini-RT2. This heavily truncated recombinant DHBV P protein requires mild detergent, but no chaperones for priming activity.

interactions[76]; why a similar element is dispensable for HBV pgRNA packaging is unclear.

Even HBV ε, however, does not act as a completely autonomous encapsidation element. The 3´ copy of ε cannot substitute for 5´ ε in the context of otherwise authentic pgRNA[77] (although its DHBV counterpart is useable for DHBV P interaction in *in vitro* translation;[78]). Furthermore, 5´ ε mediates encapsidation of heterologous RNAs only up to a limited distance from the 5´ end (about 65 nt), and seems to require the 5´ cap structure[79]. Hence the 5´ cap and factors bound to it appear to have a role in the process, possibly in concert with the 3´ poly-A tail and its associated cellular proteins[80]; this may explain why attempts to reconstitute encapsidation by simultaneous *in vitro* translation of P and core protein from uncapped, non-poly-adenylated RNAs in reticulocyte lysate (RL) were thus far unsuccessful.

An unexplored issue is whether the ε hairpin, or other base-paired regions on the pgRNA, would be substrates for cellular dsRNA recognizing systems such as Toll-like receptor 3 (TLR3) or retinoic acid inducible gene I (RIG-I) which play important roles in innate immune responses against viral infection[81,82], or for enzymes involved in processing of cellular hairpin RNAs such as the microRNA precursors[83]. Direct screens identified a 65 kDa nuclear protein[84] of unknown sequence and, more recently, a novel large RNA-binding ubiquitin ligase, hRUL138[85], as potential cellular ε RNA interaction partners. However, their roles in the viral life-cycle are not known. Also, any cellular ε-binding factor would have to cope with the physical sequestration of pgRNA into nucleocapsids.

P PROTEIN STRUCTURE

The P ORF, covering nearly 80% of the hepadnaviral genome (Figure 2), has a coding capacity of about 830 aa for HBV, and about 790 aa for DHBV (Figure 5). There is no indication for downstream processing of the primary translation products. In further contrast to retroviruses, hepadnaviral virions contain probably just one P protein molecule per particle[86], in line with the covalent linkage to the genome. In transfected cells, P appears to be produced in excess, such that most molecules are not capsid associated[87-89]; they have a short half-life, and are bound to large cytoplasmic structures; their function, if any, is unclear.

Bioinformatic[90] and genetic analyses showed the presence in all P proteins, of two conserved domains, namely the polymerase/reverse transcriptase (RT) domain, and the C-terminal RNase H (RH) domain. Both are necessary as structural components for pgRNA encapsidation[73]. An absolutely hepadnavirus-specific feature is, however, the Terminal Protein (TP) domain at the N terminus, separated from the RT domain by a highly variable, and dispensable, spacer[91]. TP was first identified as the (-)-DNA linked protein[92] and later was shown to provide a specific Y residue to which the first nt of the (-)-DNA becomes covalently linked (Y96 in DHBV TP;[93,94]; Y63 in HBV TP[95]).

At present, no direct structural information on any hepadnaviral P protein is available although homology-based models for the RT[96] and RH domain[97] have been proposed. The RT model is in accord with drug resistance data, and it is supported by mutational analysis of the putative dNTP pocket of DHBV P protein where a single aromatic residue (F451) was shown to have a homologous role in dNTP versus rNTP discrimination as Y115 in HIV-1 RT[98]; replacement of the bulky F451 by smaller residues conferred to the protein a low but clearly detectable RNA polymerase activity. However, outside the active site the accuracy of the modeled structure is unknown. Hence direct structure determination of the RT and RH domains remains a major objective.

This holds even more for the TP domain, which shares no significant sequence similarity to any other protein in the data base, not even to the few other terminal proteins involved in viral genome replication, such as the VPg in picornaviruses[99], or the terminal proteins of adenovirus[100] and the bacteriophage ϕ29[101]; moreover, those TP proteins are not covalently linked to their polymerases.

Structure determination requires a source for sufficient amounts of pure, soluble protein which proved to be immensely difficult for P protein. Eventually, this problem was partly overcome by slight modifications in the primary sequence of DHBV P and particularly by adding solubility mediating fusion partners such as GrpE, NusA, or GST[53,102,103]. However, although such fusions (Figure 5B) display activity (see below) they appear to be present as "soluble aggregates" which are unsuited for crystallization.

Particularly TP, when expressed in *E. coli*, is completely insoluble on its own, mostly due to a hydrophobic region

in the C terminal part. By selection from a pool of TP variants with random mutations we could isolate several TP variants, harboring fewer hydrophobic residues in this region, as monodispersely soluble proteins (J. Beck and M. Nassal, unpublished data). Interestingly, the same region was recently implicated to contain a molecular contact site, possibly for the RT domain[104], as suggested by the ability of separate TP and RT/RH domains to trans-complement each other[53,95,105]. Since replacing several conserved hydrophobic regions at a time may affect TP function the challenge will be to find, for crystallization, mutants that combine solubility with functional activity. However, being at the heart of hepadnaviral replication, solving the structure of TP is one of the big current challenges.

CELL-FREE RECONSTITUTION OF HEPADNAVIRAL REPLICATION INITIATION

Cell-free systems are inherently much more manipulatable than intact cells. The first such system to investigate the mechanism of hepadnaviral reverse transcription was based on the observation that DHBV P protein, *in vitro* translated in rabbit RL, became radioactively labeled when the translation reaction was supplied with α^{32}P-dNTPs[78]- as expected if the initial step of reverse transcription, i.e. covalent attachment of the first nucleotide to P protein, had occurred ("*in vitro* priming"; Figure 3B). In fact, the 3´ copy of Dε present on the P protein mRNA was shown to be the template for limited elongation; the role of ε, though only the 5´ copy, as authentic genome replication origin was confirmed for DHBV[56,57], and finally also HBV[58].

The *in vitro* translation system has been used extensively to functionally analyze P protein as well as Dε mutants, particularly because Dε can be added as a separate short RNA covering just the hairpin structure ("trans-priming"). Human HBV P protein and ε, however, show no enzymatic activity in this setting.

THE P-ε COMPLEX: DETERMINANTS FOR BINDING, PRIMING AND ENCAPSIDATION

A first - though not the only-requirement for a productive P-ε interaction is specific binding. In many RNA-protein interactions, structural diversity and hence specificity is achieved by deviations from a fully base-paired double-helical structure[106], e.g. by interspersed single-stranded bulges and loops. Indeed, the Dε bulge structure (but not its actual sequence, unless it affects structure) is absolutely necessary for P binding. Mutants in the upper stem (see Figure 4B) which favor stable non-bulged structures do not bind to P[70]. Similarly critical is the sequence and structure at the junction between the lower stem and the bulge: Mutation of the unpaired U2604 opposite the bulge to G substantially reduced binding (and nearly abolished priming)[71]. At the tip base-pair of the lower stem, base identity of G2605, but not base-pairing itself, is important; in addition, most ribose residues in Dε could be replaced by deoxyribose residues, except in the two top base pairs of the lower stem and in the bulge residue templating the first nt of (-)-DNA[107]. Hence this small region contains an essential base- and backbone dependent determinant for P-interaction (Figure 4D), likely because it forms, together with the bulge, a distinct three-dimensional recognition surface for P protein.

In the apical loop, various mutations had no drastic effects on P binding, suggesting the loop is not principally required for complex formation (though probably involved in forming a priming competent structure; see below). An exception is U2590 replacement of which by C abrogated binding[70,108]. However, deletion of this residue did not affect binding, and the negative effect of the U2590C mutation was partially rescued by an additional G to A mutation at the neighboring position 2589[61]. A direct 3D structure comparison between wild-type Dε, currently underway (S.S. Wijmenga, personal comm.), and the U2590C mutant RNA may help to explain this complex phenotype.

The existence of Dε RNA variants which bind P but have a much reduced or no template activity indicated that a productive P-ε interaction requires more than binding[61,70,71]. 2D structure comparisons of free versus P bound RNAs provide compelling evidence that the ability of an RNA to undergo a specific conformational shift is such a decisive additional feature[109]. Several base-paired nt in the upper stem of Dε become highly accessible to nucleases once bound to P; similar changes are not seen with priming-deficient variants. Hence it is likely that the RNA, after an initial binding step, must experience an induced-fit alteration into a new structure, and that only this is usable as a template. Non-productive complexes, by contrast, appear to be trapped at the initial binding stage. Foot-printing analysis further revealed that in productive, but not non-productive, complexes the 3' half of the loop plus 3´ adjacent nt are protein bound, as are the unpaired U opposite the bulge and the nt at the tip of the lower stem (Figure 4D). Hence although the loop nucleotides may not be strictly required for initial binding, they probably provide a protein binding site that becomes crucial in the transition to a priming-active complex.

Also P protein undergoes structural alterations in this process. Proteolysis of *in vitro* translated DHBV P protein yielded a distinct proteolytic fragment only in the presence of priming-competent but not priming-inactive RNA variants[108,110]. Hence RNA and P protein mutually alter each others conformation, likely to properly arrange the ε template region and the priming Y residue of TP in the active site of the RT domain.

Notably, of the various P binding RNAs only those that are priming-active also support pgRNA encapsidation. Hence the abilities to initiate reverse transcription, to package pgRNA, and to adopt a distinct RNA-P protein complex conformation appear strictly coupled. In effect, this represents a quality control mechanism ensuring that only RNAs suitable as templates for reverse transcription are packaged. The current methods to analyze these replication-relevant structural changes have a very limited resolution; ultimately, biophysical examination of a priming-active complex will be required, and its

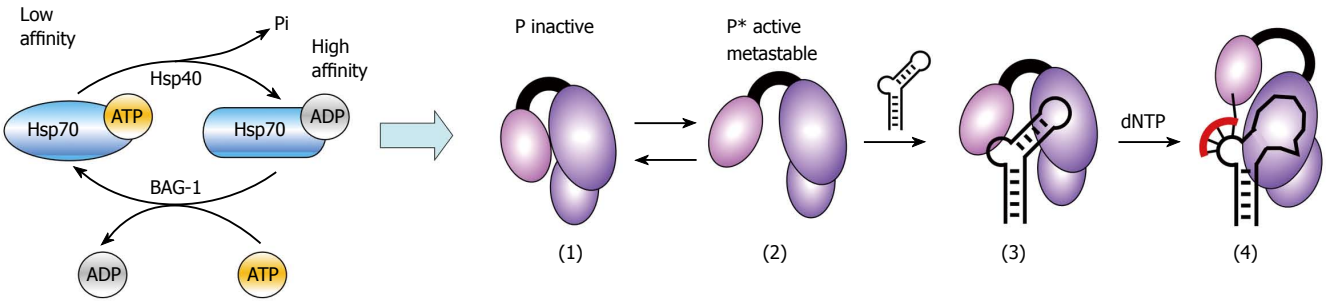

Figure 6 Model for Hsp40/Hsp70 mediated in vitro activation of P protein. The low ATPase activity of Hsp70 is stimulated by Hsp40, yielding high substrate affinity Hsp70/ADP. A new cycle of substrate release and folding requires exchange of the ADP for new ATP which is stimulated by nucleotide exchange factors such as BAG-1. This ATP-dependent Hsp70 cycling applies to the chaperone´s global folding activities but likely also to P activation: in the inactive state of P (1), the ε RNA binding pocket is inaccessible; Hsp40/Hsp70 activation creates active P* (2) which is able to bind ε RNA (3); P* is metastable, and decays to the inactive state (1) within minutes. Maintaining a steady-state level of P* requires constant re-activation by Hsp40/Hsp70 and thus a continuous supply of fresh ATP. Complexes containing priming-competent ε RNAs (3) undergo induced-fit rearrangements in the RNA and the protein, enabling them to initiate DNA synthesis upon dNTP addition (4). Several Dε variants bind P but do not act as template; most likely they are trapped at stage (3). The same may hold for human HBV P protein complexes with HBV ε RNA.

comparison with non-productive complexes should be most revealing. However, several significant obstacles will have to be overcome for this approach, not the least being the strict dependence of DHBV P protein activity on additional cellular factors (see below).

This holds even more for active initiation complexes of human HBV. Insect cell expressed HBV P exerted a low but clearly detectable polymerase activity, with part of the DNA products covalently linked to TP as expected from authentic initiation[111]. The system revealed some important features, such as the priming role of Y63 in HBV TP[95], trans-complementation between TP and RT/RH domains[95], and even some nucleocapsid formation by co-expression of core protein[112]. Disturbingly, however, various of these activities were not strictly ε dependent, and they could not be reconstituted after (partial) purification of the P protein. Whether insect cells contain some RNA that can substitute for ε has not been clarified. *In vitro* translated HBV P protein shows no priming activity in reticulocyte lysate and not even in lysates from Huh7 cells (J. Beck and M. Nassal, unpublished data) which support replication when transfected with HBV. Recently, however, Hu *et al*[72] reported a partial but important progress in that they were able to demonstrate specific binding-though not priming-for HBV P and ε in an *in vitro* reconstitution system (see next paragraph).

IN VITRO RECONSTITUTION OF REPLICATION INITIATION FROM PURIFIED COMPONENTS

One aspect for *in vitro* translation of P protein was, at the time, the lack of alternative ways to recombinantly produce the protein. Surprisingly, wheat germ extract versus rabbit RL translated DHBV P protein had a much reduced priming activity, suggesting the mammalian RL provided additional essential factors[113]. These turned out to be cellular chaperones, which are abundantly present in RL. Apart from Hsp60 chaperonins[114] (GroEL in bacteria), Hsp70 (DnaK in bacteria) and Hsp90 constitute the major chaperone systems. Hsp70 assists folding of many newly synthesized polypeptides, refolding of misfolded proteins resulting, e.g., from heat-shock, and protein translocation through membranes[115-117]. Hsp90 has also broad but more specialized folding functions[118], usually if not exclusively in concert with Hsp70; the two systems are linked *via* the Hsp70/Hsp90 organizing protein Hop. By analogy to the activation of nuclear hormone receptors[119] it was proposed that Hsp90 plus its small co-chaperone p23 are the essential factors for P protein activation[113,120]. However, the complex overall composition and the high chaperone content of RL compared to the minute amounts of P protein precluded a clear-cut distinction.

This was overcome when DHBV P protein became accessible in larger quantities by expressing, in *E. coli*, slightly modified variants[53,102], in particular as fusions with solubility enhancing heterologous domains (Figure 5B). Such recombinant P proteins could now be added to the RL system and showed activity. Finally, because the translation function of RL was not required any longer, it became possible to systematically analyze the chaperone requirements for P protein activation with purified individual components.

In this way we could demonstrate that DHBV P can efficiently be activated *in vitro* by Hsp40 and Hsp70 plus ATP as an energy source, without the need for Hsp90 or other cofactors[54]. The primary reaction product is an RNA binding-competent form of P protein (P*) that decays quickly in the absence of ε RNA but, in its presence, accumulates in an initiation-competent form (Figure 6).

Maintaining P in its activated P* form requires a constant supply of ATP[54], and the same holds for the general folding activity of Hsp70[117]. This suggested that P activation represents a special form of Hsp70 mediated folding in which the chaperone, rather than helping P from an unfolded into a stable folded state, affects the equilibrium between the inactive P ground state and the metastable activated P* form. Of note, bacterial DnaK has been shown to interact, physiologically, with a few folded, as opposed to misfolded, proteins such as the transcription factor σ32[121,122].

Hsp70 chaperoning is a cyclic ATP-driven process[117].

Hsp70 binds ATP and in this form exerts low affinity to folding substrates (Figure 6, left). ATP hydrolysis then generates the high affinity Hsp70/ADP form. In the presence of substrate, the weak Hsp70 ATPase activity is stimulated up to 1000 fold by Hsp40 and related J-domain proteins (named after the prototypic *E. coli* Hsp40, DnaJ;[123]), explaining the important role of Hsp40. Initiating a new folding cycle requires reconversion of Hsp70/ADP into Hsp70/ATP, i.e. replacement of the bound ADP by fresh ATP; otherwise Hsp70 would be trapped and not be available for acting on new substrate molecules. Spontaneous nt exchange is slow but strongly enhanced by nucleotide exchange factors (NEFs). This predicted that addition of BAG-1, an established NEF of Hsp70[124], to the minimal *in vitro* reconstitution system should enhance the formation of P* molecules. Indeed, we observed a strong BAG-1 dependent increase in priming-active P molecules, but not with a BAG-1 mutant unable to interact with Hsp70. Hence ADP-ATP exchange on Hsp70 is the rate limiting step in the *in vitro* priming reaction (M. Stahl, M. Retzlaff, M. Nassal and J. Beck, submitted). A working model for the Hsp40/Hsp70 activation of DHBV P protein is shown in Figure 6.

Though these data are clear-cut, Hu and colleagues, using a similar experimental set-up though a different (i.e. GST) DHBV P fusion protein, reported that in their *in vitro* system P activation was strictly dependent on the additional presence of Hsp90 and the Hsp70/Hsp90 adaptor protein Hop, with the Hsp90 co-chaperone p23 enhancing the reaction rate[52].

In our system, Hop and Hsp90 do have a stimulatory- but not an essential-effect (in a similar range as BAG-1), particularly at low P protein concentrations. In addition, the specific nature of the Hsp40 used can affect activation efficiency. Eukaryotic cells contain numerous Hsp40-like (or J-domain) proteins[125]; all contain the about 70 aa long J-domain which mediates interaction with Hsp70. Hsp70 activation of P protein appears to proceed selectively with the Hdj1 variant of Hsp40 but not Hdj2 or its yeast homolog Ydj1. With Ydj1, Hop and Hsp90 may become essential for detectable activation. Why different Hsp40s have different effects is currently unclear because all Hsp40s can stimulate the Hsp70 ATPase activity; however, there are different ways of how a substrate can enter the folding complex: either it is bound directly by Hsp70, or it is presented to Hsp70 by the Hsp40-like protein[123]. Therefore, the various additional domains present in different J-domain proteins could effect the formation of P* *via* different pathways. Hence in summary, P activation *in vitro* is fundamentally dependent on Hsp70/Hsp40 but can be enhanced by additional factors, including Hop/Hsp90.

Interestingly, the strict chaperone dependence of DHBV P protein activity was relieved by an extensive C terminal truncation that removed the entire RH domain and some 75 aa from the RT domain; the only requirement for priming activity (though restricted to the very first DNA primer nt) of this truncated Mini-RT 2 protein (Figure 5C) was the presence of mild detergent[126]. This suggests that in full-length P protein C terminal parts somehow block the ε RNA binding site, and that this occlusion is removed by the chaperone action[102,127].

Where exactly the chaperones bind to P and which conformational rearrangements they induce is unclear. Using *in vitro* translated DHBV P protein in RL Tavis *et al*[110] noted the ε-dependent generation of a papain- and trypsin-resistant fragment covering mainly the RT domain. Taking advantage of the simple, defined composition of the *in vitro* reconstitution system we could directly investigate the effects of Hsp40 and Hsp70 on P protein conformation. Limited V8 protease digestion revealed specific chaperone- and ATP-dependent cleavages in the C terminal part of TP (between aa 164 and 199). Hence this TP region is inaccessible in non-activated P protein but becomes exposed in P* (M. Stahl, J. Beck and M. Nassal, unpublished data). The functional relevance of this conformational alteration is supported by its correlation with the ability of P to bind ε RNA, and the shielding of the same region from protease attack as long as the Dε RNA is bound; furthermore, the larger fragment encompasses two residues, K182 and R183, which are essential for RNA binding. These data support the model shown in Figure 6. Inclusion of Hop and Hsp90 in this assay should now allow one to monitor whether these, or additional factors, have differential effects on P conformation, or whether they mainly stabilize the changes already established by Hsp40/Hsp70.

Extending the scope of the *in vitro* reconstitution system, Hu and colleagues recently demonstrated that specific binding to ε by the human HBV P protein also appears to be controlled by cellular chaperones[72,128]. On the ε RNA side, the region immediately surrounding the bulge was essential but the apical loop was not. This was surprising given that the loop is essential for pgRNA encapsidation and initiation of replication in intact cells. However, in light of the above described DHBV data, it may just be a drastic manifestation that mere physical binding is not sufficient for a productive interaction; this is further supported in that only about half the P protein sequence was required for RNA binding, with even the catalytic YMDD motif being dispensable. Apparently, the crucial second step, which in Dε involves rearranging the upper stem and the loop, does not occur in the reconstituted HBV P protein-ε complexes, possibly due to the high stability of this region in HBV ε. Finding conditions under which HBV P protein exerts authentic ε-dependent *in vitro* priming-activity remains therefore another major challenge in HBV biology.

IMPORTANCE OF CHAPERONES FOR HEPADNAVIRUS REPLICATION IN INTACT CELLS

Both the Hsp70 and the Hsp90 chaperoning activities are subject to regulation by a multitude of co-chaperones[117,129]. Hence which of the *in vitro* reconstitutable processes is the relevant one inside cells is not trivial to address, in particular because the chaperones are crucial for very many fundamental and regulatory cellular processes. For

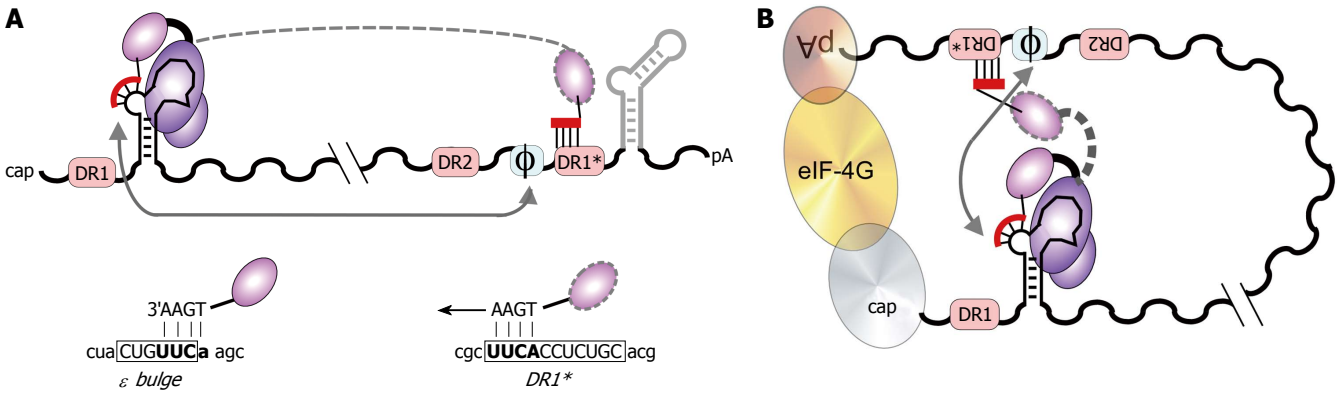

Figure 7 DNA primer translocation (first template switch). P copies 3 to 4 nt from the 5´ ε bulge, yielding the TP-linked DNA oligonucleotide which is translocated to the complementary motif in the 3´ proximal DR1*. **A**: Linear representation. DR1* is nearly 3 kb apart from 5´ ε in primary sequence, and numerous other UUCA motifs are not used as acceptors. ϕ denotes a newly identified cis-element with partial sequence complementarity to the 5´ half of ε. 3´ ε (light grey) is dispensable. The HBV specific sequences in the ε bulge, and in DR1* are shown below in capitals, flanking sequences in lower case; **B**: Models for juxtaposition of 5´ ε and DR1*. A general mechanism would be closed loop formation[80] of the pgRNA by cap-binding and poly-A binding factors (ovals), e.g. *via* elongation initiation factor 4G (eIF-4G; large oval). More specifically, ε might base-pair with ϕ[146,147], as indicated by the grey arrows. In such an arrangement, a small movement, rather than a big jump, of TP with the bound DNA primer (dashed outline) would suffice for specific translocation to DR1*.

instance, geldanamycin (GA), an inhibitor of Hsp90, strongly interfered with DHBV replication in transfected cells at a concentration of 10 ng/mL whereas significant reduction of the *in vitro* priming activity required much higher concentrations[113]. Therefore, the antiviral effect in cells might be indirect, perhaps *via* one of the cellular kinases that are regulated by Hsp90[130]. Such effects on the cell make it also difficult to imagine that chaperone inhibitors could therapeutically be used against HBV infection without causing severe adverse effects. That GA analogs, nonetheless, exert tumor-specific therapeutic value[131] is probably due to the selective presence, in cancer cells, of Hsp90 in a high GA affinity state[132]. Whether this also holds for HBV infected cells is not known.

Various additional chaperones have, in part indirectly, been implicated in affecting P protein, for instance Hsp60[133-135] and the Hsp90 family member GRP94[136]; however, GRP94 is an endoplasmic reticulum (ER) resident protein for which a role in P protein activation is difficult to imagine. Overexpression of p50/cdc37, a co-chaperone of Hsp90 involved in activation of several signal transduction kinases, stimulated DHBV replication in transfected cells and a dominant negative mutant of p50/cdc37 inhibited DHBV P protein priming *in vitro*[137]. Again, the physiological relevance of these observations remains to be confirmed.

One possible solution would be to map the contact sites of the various chaperones on P protein using biochemical and biophysical methods, and then to generate P mutants with specific interaction defects. Monitoring their replication phenotypes in transfected, or better in infected, cells should then allow to narrow down which of the various reported interactions are truly significant for virus propagation *in vivo*.

Though we have stressed the uniquely strict chaperone-dependence of hepadnaviral P protein activation, there is accumulating evidence that other polymerases are also affected by chaperones. Probably the closest analogy exists to telomerase, the cellular reverse transcriptase that maintains chromosome end integrity[138,139]. However, also the DNA polymerase of Herpes simplex virus[140], and the RNA polymerases of flock house virus[141] and influenza virus appear to require chaperone assistance[142,143]. Closely watching progress in those areas might also provide clues as to the mechanism of chaperone-assisted hepadnavirus replication; however, for polymerases without a similarly sophisticated protein-primed initiation mode the chaperones could act at rather different levels.

DNA PRIMER TRANSLOCATION AND (-)-DNA COMPLETION

In contrast to initiation, the subsequent steps for RC-DNA formation are currently not amenable to *in vitro* analysis, and they appear intimately related to the proper environment of intact nucleocapsids. Hence reverse genetics is still the most rewarding approach to address these equally puzzling and complex events.

The initial model of hepadnaviral (-)-DNA formation assumed that synthesis would start inside the 3´ copy of DR1 (DR1*), for HBV at the motif 5´ UUCA. As discussed above, the complementary sequence 3´ AAGT at the 5´ end of (-)-DNA is instead copied from the UUCA motif in the ε bulge (Figure 7A). Hence the oligonucleotide bound to TP must specifically be translocated to the 3´ DR1*, nearly 3 kb apart from 5´ ε. Given that there are about 20 further UUCA motifs on the pgRNA, and that even fewer than 4 nt of identity between the template region in ε and the target site in DR1* are sufficient for specific transfer[58], additional elements ensuring proper translocation must be operating. One model is that DR1* and 5´ ε are brought into close proximity (Figure 7B). A general mechanism would be closed-loop formation of the pgRNA *via* cellular proteins such as elongation initiation factor 4G (eIF-4G) which links 5´ cap and 3´ poly-A binding proteins[80]. A recent more specific model is a long-range RNA interaction between ε and a new cis-element ("ϕ" or "β5") slightly upstream of DR1* that is involved in proper (-)-DNA synthesis[144-146]; it contains a sequence that

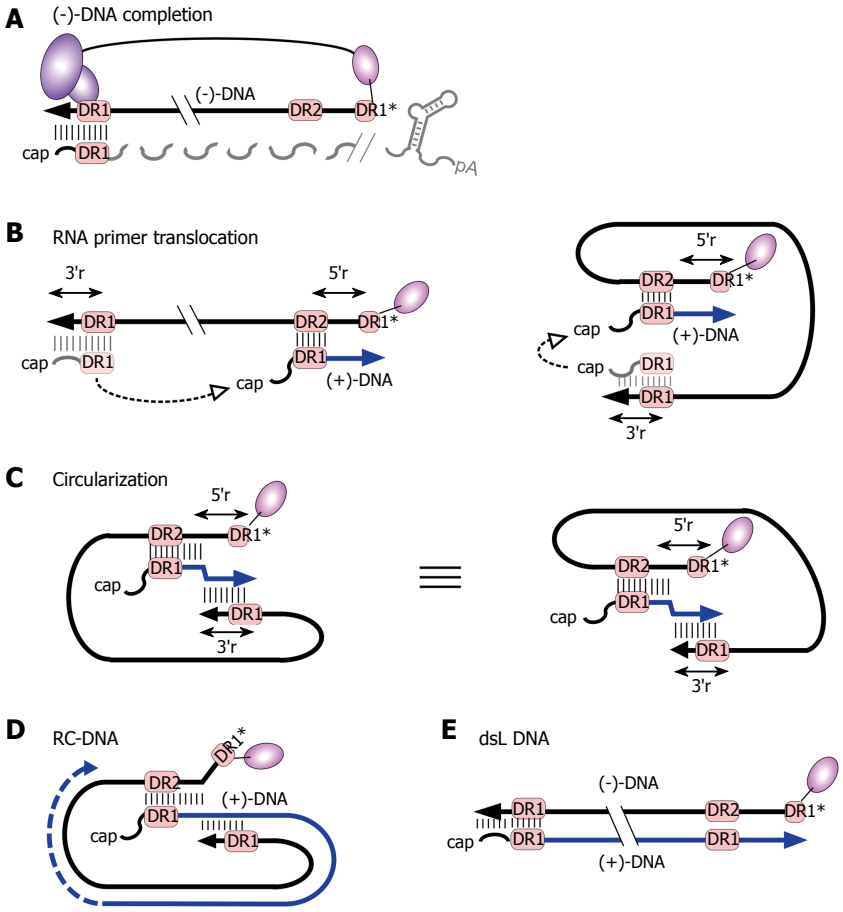

Figure 8 RC-DNA formation. **A**: (-)-DNA completion. The DNA primer, still linked to TP, is extended from DR1* to the 5′ end of pgRNA. The RNA is simultaneously degraded by the RH domain, except for its capped 5′ terminal region including 5′ DR1; the fate of the poly-adenylated 3′ end is unclear; **B**: RNA primer translocation (second template switch). The RNA primer translocates to DR2, and is extended to the 5′ end of (-)-DNA. 3′ r and 5′ r denote an about 10 nt redundancy on the (-)-DNA. As above, several cis-elements appear to promote close proximity of the DR1 donor and the DR2 acceptor, as schematically indicated in the right hand figure; **C**: Circularization (third template switch). Having copied 5′ r, the growing 3′ end of the (+)-DNA switches to 3′ r on the (-)-DNA, enabling further elongation. This reaction must involve juxtaposition of 5′ r and 3′ r. For easier comprehension, the switch is also depicted on the basis of the representation shown on the right of Figure 8B; both are topologically equivalent; **D**: RC-DNA. Extension on the (-)-DNA template creates a set of (+)-DNA strands of various length; **E**: Double-stranded linear (dsL) DNA. This minor DNA form originates when the RNA primer, having failed to translocate to DR2, is extended from its original position ("in *situ* priming").

is partially complementary to the 5′ half of ε. Mutations affecting the base-pairing potential between the two sequences can, indeed, influence the efficiency of (-)-DNA synthesis[147]. Exactly how an ε-ϕ interaction would aid in primer translocation is unclear because base-pairing would simultaneously affect the proper ε structure, implying some temporal regulation. Similar ϕ elements have been proposed to be present in the other hepadnaviruses[146]; for DHBV we noted, however, that Dε mutants with reduced potential base-pairing to the supposed ϕ element showed no obvious (-)-DNA synthesis defects ([71] and K. Dallmeier, B. Schmid and M. Nassal, unpublished data).

The primer translocation process must also involve remodeling of the P-ε complex; the priming Y residue of TP must give way to the growing DNA oligonucleotide, then ε must be replaced by DR1* as the template. Hence P, like other protein-priming polymerases, must have distinct initiation and elongation modes. The recently solved structure of the bacteriophage ϕ29 DNA-dependent DNA polymerase with its (separately expressed) terminal protein[101] gives an impression of the dynamic changes that have to occur. ϕ29 uses for protein priming an S residue in one of three distinct TP domains. In the initiation mode, the priming domain mimics the primer-template nucleic acid that occupies the same site during elongation. The initiation reaction continues until 6 to 10 nt have been attached; at this time the priming domain is pushed out of the polymerase´s active site, marking the transition to elongation mode. Similar events must happen in P protein. Notably, initiation of ϕ29 replication does not start at the very terminal template nt; rather the (identical) penultimate nt is copied. Next, the copied nt slips back to the terminal template position, and the penultimate nt is copied again; adenovirus uses a similar mechanism[100]. Interestingly, such slip-back and re-copying can also occur with HBV P protein on mutant ε templates[58]. A full understanding, however, will obligatorily require high resolution structural data on the hepadnaviral replication complex.

Notably, the single-stranded (-)-DNA is an intermediate that, as in retroviral replication, could be a target for cytidine deamination, and consequently inhibition of replication, by APOBEC enzymes[148]. APOBEC3G, one of several family members, has indeed been reported to interfere with HBV replication[149], however, the mechanism does not involve editing[150]. Also, expression of the corresponding APOBEC mRNA is low in hepatic cells, although it might be inducible[151]. Further research is needed to clarify whether any of the APOBEC enzymes is genuinely involved in the innate response against HBV infection. At any rate, sequestration into intact nucleocapsids of this potentially vulnerable single-stranded DNA replication intermediate may be an efficient counter-defense of HBV.

(+)-STRAND DNA SYNTHESIS AND CIRCULARIZATION

The end product of (-)-DNA synthesis is a unit length DNA copy of the pgRNA from its 5′ end to, in HBV, the UUCA motif in the 3′ DR1* (Figure 8A); hence it contains a small, about 10 nt, terminal redundancy ("r"). Most of

the pgRNA template is degraded concomitantly to (-)-DNA synthesis by the RNase H domain of P. The fate of the non-copied 3´ end of the pgRNA from DR1* to the polyA tail is not exactly known. It seems to be underrepresented in the packaged RNA, both in DHBV[152], and in HBV with mutations in the nucleic acid binding domain of the core protein[46]. Whether some of these 3´ ends are never completely encapsidated, or whether they dissociate out of the capsid, has not yet conclusively been shown.

Well established is, however, that the 5´ terminal about 15 to 18 nt of the pgRNA including the 5´ DR1 sequence are spared from degradation, probably because the active site of RH is halted at this distance when the RT domain reaches the template 5´ end[153]. This capped 5´ RNA oligo is essential as primer for (+)-DNA synthesis. Extension of the RNA from its original position ("in situ priming") gives rise to a double-stranded linear (dsL) DNA (Figure 8E) which occurs to a small percentage in all hepadnaviruses[154]. Lacking the core promoter/enhancer for pgRNA translation upstream of the pgRNA start site it is unsuited for virus propagation but may be of pathogenic potential[155]. For RC-DNA formation, the RNA primer must be transferred to the 3´ proximal DR2 (Figure 8B); pgRNAs with improper 5´ ends, not containing the DR1 sequence in the RNA primer, fail to undergo this essential second template switch. Why the RNA primer predominantly jumps to DR2 although its complementarity to the initial site is larger (more than 15 versus 11 or 12 nt) is not obvious. An interesting explanation has been proposed for DHBV, according to which burying part of the 5´ DR1 sequence in a competing intramolecular hairpin structure effectively shortens the sequence available for hybridization with the RNA primer[156].

From its new location on DR2 the RNA primer is extended towards the P bound 5´ end of the (-)-DNA, including the 5´ r redundancy. Further elongation requires a third template switch, i.e. circularization (Figure 8C). In effect, the growing (+)-DNA end is transferred from 5´ r to 3´ r on the (-)-DNA template from where it can further be extended to yield RC-DNA (Figure 8D).

Though sequence identity between 5´ r and 3´ r is important, additional cis-elements are again required to ensure efficient RNA primer translocation and circularization. Using quantitative genetic techniques, the Loeb laboratory has defined, mostly in DHBV, several such cis-elements on the (-)-DNA[144,156-161], e.g. 3E, M, and 5E, which are located at both termini and in the middle of pgRNA. Collectively, these data provide evidence that these cis-elements, *via* long range base-pairing, allow for a close juxtaposition of the corresponding donor and acceptor sites, and thus facilitate the proper template switches (Figure 8B, right panel). How this is achieved inside the replicating nucleocapsid is not easily envisaged. Also, we noted that chimeric heron-duck HBVs are less sensitive than DHBV to reduced base-pairing in some of these elements (K. Dallmeier and M. Nassal, unpublished). There is evidence, however, that similar potentially base-pairing cis-elements are present in human HBV[144, 162] and assist in circularization (E. Lewellyn and D.D. Loeb, pers. comm.).

Hence intramolecular base-pairing is probably an important mechanism that ensures proper shaping of the viral genome for the various template switches that eventually yield RC-DNA. More details than is possible to show here can be found in informative schematic representations in references[144,160].

CONCLUSIONS AND PERSPECTIVES

Since the original discovery that hepadnaviruses replicate through reverse transcription numerous novel and unique aspects of the replication process have been unraveled by using reverse genetics in transfected cells. Indisputably, this system will continue to be an important tool in future HBV research; in some cases because even a cancer-derived stable cell line mimics many aspects of the complex natural environment for viral replication, allowing to look into the interplay between virus replication and cellular networks by genomics and/or proteomics; in others because we have currently no alternative due to the complexity of the interactions between the viral components themselves. An example is the control of the various template switches during RC-DNA generation by long-range nucleic acid interactions which apparently can only occur, and be monitored, in the context of assembled nucleocapsids.

For a mechanistic understanding, however, cell-free systems are indispensable. Two striking examples for their power are the discovery of the replication origin function of ε and the chaperone-dependence of P protein activation; both would have gone unnoticed for a long time without the *in vitro* translation system. To disentangle these multifactorial processes on the molecular level, *in vitro* reconstitution from purified components is the approach of choice. Despite the bewildering complexity of the chaperoning systems, it will now be possible, starting from relatively simply composed systems, to systematically add-in additional factors and monitor their contributions to P protein activation; this should, *inter alia*, help answer the pressing question why human HBV P protein shows no enzymatic activity under conditions where its DHBV counterpart is active. An *in vitro* activity assay for HBV P protein would also be an important screening tool for better HBV antivirals. Similarly rewarding should be the development of *in vitro* systems that address other steps of the viral replication cycle, foremost perhaps inclusion of the core protein into the now available replication initiation systems.

Ultimately, structural biophysics needs to enter the field. At this time the HBV core protein, without its nucleic acid binding domain, is the only hepadnavirus component for which a high resolution structure is available[163]. Fortunately, 3D structural analyses of the ε element are well underway, and at least individual domains of the P protein may become amenable to direct structure investigations. The most exciting, though also most challenging aim given its multifactorial composition, will be to obtain high resolution data for the P protein-ε RNA complex, caught in the act of DNA synthesis. However, the relevance of any such biophysical and biochemical

data will have to be corroborated in the context of the complete virus replication cycle, whenever possible in an *in vivo* setting.

Finally, although the complex interactions between viral, and viral and cellular, components may seem of foremost interest for basic HBV biology, they also hold the keys for novel, and more efficacious therapies of chronic hepatitis B. The few currently approved anti-HBV drugs are all nucleos(t)idic inhibitors of the reverse transcriptase. Their long-term efficacy is limited by the virtually unavoidable emergence of resistant HBV variants[30]; any new compounds with the same mechanism of action will also face this problem, which will be aggravated by cross-resistance, particularly against different analogs of the same natural nucleotide. Each of the steps in the HBV replication cycle that is now being elucidated in molecular detail provides new, unconventional targets for interference. Replication initiation alone depends on many specific interactions, including the TP and RT/RH domains of P protein, ε RNA, and different chaperones. Blocking any of these interactions, e.g. by small molecules binding to, and altering the structure of ε or preventing chaperone binding to P, would abolish reverse transcription by mechanisms entirely different from that of nucleoside analogs. Knowledge of the 3D structure of P would allow to design better nucleosidic as well as non-nucleoside inhibitors, and additional opportunities will certainly arise once the process of cccDNA formation is better understood. Especially in combination with conventional antivirals, such potential new drugs should greatly increase the chances for curing, rather than just controlling, chronic hepatitis B.

REFERENCES

1 **Nassal M**, Schaller H. Hepatitis B virus replication. *Trends Microbiol* 1993; **1**: 221-228
2 **Nassal M**, Schaller H. Hepatitis B virus replication--an update. *J Viral Hepat* 1996; **3**: 217-226
3 **Nassal M**. Hepatitis B virus replication: novel roles for virus-host interactions. *Intervirology* 1999; **42**: 100-116
4 **Nassal M**. Macromolecular interactions in hepatitis B virus replication and particle formation. In: Cann AJ, ed. Frontiers in Molecular Biology: DNA virus replication. Oxford: Oxford University Press, 2000: 1-40
5 **Ganem D**, Schneider R. Hepadnaviridae: The Viruses and Their Replication. In: Knipe DM, Howley PM, eds. Fields Virology. 4th ed. Philadelphia: Lippincott Williams & Wilkins, 2001: 2923-2969
6 **Seeger C**, Mason WS. Hepatitis B virus biology. *Microbiol Mol Biol Rev* 2000; **64**: 51-68
7 **Schultz U**, Grgacic E, Nassal M. Duck hepatitis B virus: an invaluable model system for HBV infection. *Adv Virus Res* 2004; **63**: 1-70
8 **Summers J**, Mason WS. Replication of the genome of a hepatitis B--like virus by reverse transcription of an RNA intermediate. *Cell* 1982; **29**: 403-415
9 **Protzer U**, Nassal M, Chiang PW, Kirschfink M, Schaller H. Interferon gene transfer by a hepatitis B virus vector efficiently suppresses wild-type virus infection. *Proc Natl Acad Sci USA* 1999; **96**: 10818-10823
10 **Sun D**, Nassal M. Stable HepG2- and Huh7-based human hepatoma cell lines for efficient regulated expression of infectious hepatitis B virus. *J Hepatol* 2006; **45:** 636-645
11 **Ren S**, Nassal M. Hepatitis B virus (HBV) virion and covalently closed circular DNA formation in primary tupaia hepatocytes and human hepatoma cell lines upon HBV genome transduction with replication-defective adenovirus vectors. *J Virol* 2001; **75**: 1104-1116
12 **Isom HC**, Abdelhamed AM, Bilello JP, Miller TG. Baculovirus-mediated gene transfer for the study of hepatitis B virus. *Methods Mol Med* 2004; **96**: 219-237
13 **Köck J**, Schlicht HJ. Analysis of the earliest steps of hepadnavirus replication: genome repair after infectious entry into hepatocytes does not depend on viral polymerase activity. *J Virol* 1993; **67**: 4867-4874
14 **Köck J**, Nassal M, MacNelly S, Baumert TF, Blum HE, von Weizsäcker F. Efficient infection of primary tupaia hepatocytes with purified human and woolly monkey hepatitis B virus. *J Virol* 2001; **75**: 5084-5089
15 **von Weizsäcker F**, Köck J, MacNelly S, Ren S, Blum HE, Nassal M. The tupaia model for the study of hepatitis B virus: direct infection and HBV genome transduction of primary tupaia hepatocytes. *Methods Mol Med* 2004; **96**: 153-161
16 **Köck J**, Baumert TF, Delaney WE, Blum HE, von Weizsäcker F. Inhibitory effect of adefovir and lamivudine on the initiation of hepatitis B virus infection in primary tupaia hepatocytes. *Hepatology* 2003; **38**: 1410-1418
17 **Guidotti LG**, Matzke B, Schaller H, Chisari FV. High-level hepatitis B virus replication in transgenic mice. *J Virol* 1995; **69**: 6158-6169
18 **Raney AK**, Eggers CM, Kline EF, Guidotti LG, Pontoglio M, Yaniv M, McLachlan A. Nuclear covalently closed circular viral genomic DNA in the liver of hepatocyte nuclear factor 1 alpha-null hepatitis B virus transgenic mice. *J Virol* 2001; **75**: 2900-2911
19 **Takehara T**, Suzuki T, Ohkawa K, Hosui A, Jinushi M, Miyagi T, Tatsumi T, Kanazawa Y, Hayashi N. Viral covalently closed circular DNA in a non-transgenic mouse model for chronic hepatitis B virus replication. *J Hepatol* 2006; **44**: 267-274
20 **Zhu Y**, Yamamoto T, Cullen J, Saputelli J, Aldrich CE, Miller DS, Litwin S, Furman PA, Jilbert AR, Mason WS. Kinetics of hepadnavirus loss from the liver during inhibition of viral DNA synthesis. *J Virol* 2001; **75**: 311-322
21 **Bock CT**, Schwinn S, Locarnini S, Fyfe J, Manns MP, Trautwein C, Zentgraf H. Structural organization of the hepatitis B virus minichromosome. *J Mol Biol* 2001; **307**: 183-196
22 **Tuttleman JS**, Pourcel C, Summers J. Formation of the pool of covalently closed circular viral DNA in hepadnavirus-infected cells. *Cell* 1986; **47**: 451-460
23 **Wu TT**, Coates L, Aldrich CE, Summers J, Mason WS. In hepatocytes infected with duck hepatitis B virus, the template for viral RNA synthesis is amplified by an intracellular pathway. *Virology* 1990; **175**: 255-261
24 **Addison WR**, Walters KA, Wong WW, Wilson JS, Madej D, Jewell LD, Tyrrell DL. Half-life of the duck hepatitis B virus covalently closed circular DNA pool in vivo following inhibition of viral replication. *J Virol* 2002; **76**: 6356-6363
25 **Ganem D**, Prince AM. Hepatitis B virus infection--natural history and clinical consequences. *N Engl J Med* 2004; **350**: 1118-1129
26 **Summers J**, Smith PM, Horwich AL. Hepadnavirus envelope proteins regulate covalently closed circular DNA amplification. *J Virol* 1990; **64**: 2819-2824
27 **Zhang YY**, Zhang BH, Theele D, Litwin S, Toll E, Summers J. Single-cell analysis of covalently closed circular DNA copy numbers in a hepadnavirus-infected liver. *Proc Natl Acad Sci USA* 2003; **100**: 12372-12377
28 **Zhang YY**, Theele DP, Summers J. Age-related differences in amplification of covalently closed circular DNA at early times after duck hepatitis B virus infection of ducks. *J Virol* 2005; **79**: 9896-9903
29 **Le Mire MF**, Miller DS, Foster WK, Burrell CJ, Jilbert AR. Covalently closed circular DNA is the predominant form of duck hepatitis B virus DNA that persists following transient infection. *J Virol* 2005; **79**: 12242-12252

30 **Zoulim F**. Antiviral therapy of chronic hepatitis B. *Antiviral Res* 2006; **71**: 206-215
31 **Zoulim F**. Entecavir: a new treatment option for chronic hepatitis B. *J Clin Virol* 2006; **36**: 8-12
32 **Terré S**, Petit MA, Bréchot C. Defective hepatitis B virus particles are generated by packaging and reverse transcription of spliced viral RNAs in vivo. *J Virol* 1991; **65**: 5539-5543
33 **Sommer G**, van Bömmel F, Will H. Genotype-specific synthesis and secretion of spliced hepatitis B virus genomes in hepatoma cells. *Virology* 2000; **271**: 371-381
34 **Obert S**, Zachmann-Brand B, Deindl E, Tucker W, Bartenschlager R, Schaller H. A splice hepadnavirus RNA that is essential for virus replication. *EMBO J* 1996; **15**: 2565-2574
35 **Loeb DD**, Mack AA, Tian R. A secondary structure that contains the 5′ and 3′ splice sites suppresses splicing of duck hepatitis B virus pregenomic RNA. *J Virol* 2002; **76**: 10195-10202
36 **Heise T**, Sommer G, Reumann K, Meyer I, Will H, Schaal H. The hepatitis B virus PRE contains a splicing regulatory element. *Nucleic Acids Res* 2006; **34**: 353-363
37 **Sen N**, Cao F, Tavis JE. Translation of duck hepatitis B virus reverse transcriptase by ribosomal shunting. *J Virol* 2004; **78**: 11751-11757
38 **Nassal M**, Junker-Niepmann M, Schaller H. Translational inactivation of RNA function: discrimination against a subset of genomic transcripts during HBV nucleocapsid assembly. *Cell* 1990; **63**: 1357-1363
39 **Gnatt AL**, Cramer P, Fu J, Bushnell DA, Kornberg RD. Structural basis of transcription: an RNA polymerase II elongation complex at 3.3 A resolution. *Science* 2001; **292**: 1876-1882
40 **Nesser NK**, Peterson DO, Hawley DK. RNA polymerase II subunit Rpb9 is important for transcriptional fidelity in vivo. *Proc Natl Acad Sci USA* 2006; **103**: 3268-3273
41 **Cao F**, Tavis JE. Suppression of mRNA accumulation by the duck hepatitis B virus reverse transcriptase. *Virology* 2006; **350**: 475-483
42 **Delelis O**, Lehmann-Che J, Saïb A. Foamy viruses--a world apart. *Curr Opin Microbiol* 2004; **7**: 400-406
43 **Fassati A**, Goff SP. Characterization of intracellular reverse transcription complexes of human immunodeficiency virus type 1. *J Virol* 2001; **75**: 3626-3635
44 **Iordanskiy S**, Berro R, Altieri M, Kashanchi F, Bukrinsky M. Intracytoplasmic maturation of the human immunodeficiency virus type 1 reverse transcription complexes determines their capacity to integrate into chromatin. *Retrovirology* 2006; **3**: 4
45 **Ahlquist P**. Parallels among positive-strand RNA viruses, reverse-transcribing viruses and double-stranded RNA viruses. *Nat Rev Microbiol* 2006; **4**: 371-382
46 **Köck J**, Nassal M, Deres K, Blum HE, von Weizsäcker F. Hepatitis B virus nucleocapsids formed by carboxy-terminally mutated core proteins contain spliced viral genomes but lack full-size DNA. *J Virol* 2004; **78**: 13812-13818
47 **Le Pogam S**, Chua PK, Newman M, Shih C. Exposure of RNA templates and encapsidation of spliced viral RNA are influenced by the arginine-rich domain of human hepatitis B virus core antigen (HBcAg 165-173). *J Virol* 2005; **79**: 1871-1887
48 **Perlman DH**, Berg EA, O'connor PB, Costello CE, Hu J. Reverse transcription-associated dephosphorylation of hepadnavirus nucleocapsids. *Proc Natl Acad Sci USA* 2005; **102**: 9020-9025
49 **Melegari M**, Wolf SK, Schneider RJ. Hepatitis B virus DNA replication is coordinated by core protein serine phosphorylation and HBx expression. *J Virol* 2005; **79**: 9810-9820
50 **Roseman AM**, Berriman JA, Wynne SA, Butler PJ, Crowther RA. A structural model for maturation of the hepatitis B virus core. *Proc Natl Acad Sci USA* 2005; **102**: 15821-15826
51 **Böttcher B**, Vogel M, Ploss M, Nassal M. High plasticity of the hepatitis B virus capsid revealed by conformational stress. *J Mol Biol* 2006; **356**: 812-822
52 **Hu J**, Toft D, Anselmo D, Wang X. In vitro reconstitution of functional hepadnavirus reverse transcriptase with cellular chaperone proteins. *J Virol* 2002; **76**: 269-279
53 **Beck J**, Nassal M. Reconstitution of a functional duck hepatitis B virus replication initiation complex from separate reverse transcriptase domains expressed in Escherichia coli. *J Virol* 2001; **75**: 7410-7419
54 **Beck J**, Nassal M. Efficient Hsp90-independent in vitro activation by Hsc70 and Hsp40 of duck hepatitis B virus reverse transcriptase, an assumed Hsp90 client protein. *J Biol Chem* 2003; **278**: 36128-36138
55 **Junker-Niepmann M**, Bartenschlager R, Schaller H. A short cis-acting sequence is required for hepatitis B virus pregenome encapsidation and sufficient for packaging of foreign RNA. *EMBO J* 1990; **9**: 3389-3396
56 **Wang GH**, Seeger C. Novel mechanism for reverse transcription in hepatitis B viruses. *J Virol* 1993; **67**: 6507-6512
57 **Tavis JE**, Perri S, Ganem D. Hepadnavirus reverse transcription initiates within the stem-loop of the RNA packaging signal and employs a novel strand transfer. *J Virol* 1994; **68**: 3536-3543
58 **Nassal M**, Rieger A. A bulged region of the hepatitis B virus RNA encapsidation signal contains the replication origin for discontinuous first-strand DNA synthesis. *J Virol* 1996; **70**: 2764-2773
59 **Knaus T**, Nassal M. The encapsidation signal on the hepatitis B virus RNA pregenome forms a stem-loop structure that is critical for its function. *Nucleic Acids Res* 1993; **21**: 3967-3975
60 **Pollack JR**, Ganem D. An RNA stem-loop structure directs hepatitis B virus genomic RNA encapsidation. *J Virol* 1993; **67**: 3254-3263
61 **Pollack JR**, Ganem D. Site-specific RNA binding by a hepatitis B virus reverse transcriptase initiates two distinct reactions: RNA packaging and DNA synthesis. *J Virol* 1994; **68**: 5579-5587
62 **Rieger A**, Nassal M. Distinct requirements for primary sequence in the 5′- and 3′-part of a bulge in the hepatitis B virus RNA encapsidation signal revealed by a combined in vivo selection/in vitro amplification system. *Nucleic Acids Res* 1995; **23**: 3909-3915
63 **Fallows DA**, Goff SP. Mutations in the epsilon sequences of human hepatitis B virus affect both RNA encapsidation and reverse transcription. *J Virol* 1995; **69**: 3067-3073
64 **Laskus T**, Rakela J, Persing DH. The stem-loop structure of the cis-encapsidation signal is highly conserved in naturally occurring hepatitis B virus variants. *Virology* 1994; **200**: 809-812
65 **Lok AS**, Akarca U, Greene S. Mutations in the pre-core region of hepatitis B virus serve to enhance the stability of the secondary structure of the pre-genome encapsidation signal. *Proc Natl Acad Sci USA* 1994; **91**: 4077-4081
66 **Kramvis A**, Kew MC. Structure and function of the encapsidation signal of hepadnaviridae. *J Viral Hepat* 1998; **5**: 357-367
67 **Guarnieri M**, Kim KH, Bang G, Li J, Zhou Y, Tang X, Wands J, Tong S. Point mutations upstream of hepatitis B virus core gene affect DNA replication at the step of core protein expression. *J Virol* 2006; **80**: 587-595
68 **Flodell S**, Schleucher J, Cromsigt J, Ippel H, Kidd-Ljunggren K, Wijmenga S. The apical stem-loop of the hepatitis B virus encapsidation signal folds into a stable tri-loop with two underlying pyrimidine bulges. *Nucleic Acids Res* 2002; **30**: 4803-4811
69 **Beck J**, Bartos H, Nassal M. Experimental confirmation of a hepatitis B virus (HBV) epsilon-like bulge-and-loop structure in avian HBV RNA encapsidation signals. *Virology* 1997; **227**: 500-504
70 **Beck J**, Nassal M. Sequence- and structure-specific determinants in the interaction between the RNA encapsidation signal and reverse transcriptase of avian hepatitis B viruses. *J Virol* 1997; **71**: 4971-4980
71 **Hu K**, Beck J, Nassal M. SELEX-derived aptamers of the duck hepatitis B virus RNA encapsidation signal distinguish critical

and non-critical residues for productive initiation of reverse transcription. *Nucleic Acids Res* 2004; **32**: 4377-4389
72 **Hu J**, Boyer M. Hepatitis B virus reverse transcriptase and epsilon RNA sequences required for specific interaction in vitro. *J Virol* 2006; **80**: 2141-2150
73 **Bartenschlager R**, Junker-Niepmann M, Schaller H. The P gene product of hepatitis B virus is required as a structural component for genomic RNA encapsidation. *J Virol* 1990; **64**: 5324-5332
74 **Calvert J**, Summers J. Two regions of an avian hepadnavirus RNA pregenome are required in cis for encapsidation. *J Virol* 1994; **68**: 2084-2090
75 **Ostrow KM**, Loeb DD. Characterization of the cis-acting contributions to avian hepadnavirus RNA encapsidation. *J Virol* 2002; **76**: 9087-9095
76 **Ostrow KM**, Loeb DD. Chimeras of duck and heron hepatitis B viruses provide evidence for functional interactions between viral components of pregenomic RNA encapsidation. *J Virol* 2004; **78**: 8780-8787
77 **Rieger A**, Nassal M. Specific hepatitis B virus minus-strand DNA synthesis requires only the 5′ encapsidation signal and the 3′-proximal direct repeat DR1. *J Virol* 1996; **70**: 585-589
78 **Wang GH**, Seeger C. The reverse transcriptase of hepatitis B virus acts as a protein primer for viral DNA synthesis. *Cell* 1992; **71**: 663-670
79 **Jeong JK**, Yoon GS, Ryu WS. Evidence that the 5′-end cap structure is essential for encapsidation of hepatitis B virus pregenomic RNA. *J Virol* 2000; **74**: 5502-5508
80 **Mangus DA**, Evans MC, Jacobson A. Poly(A)-binding proteins: multifunctional scaffolds for the post-transcriptional control of gene expression. *Genome Biol* 2003; **4**: 223
81 **Wagner H**, Bauer S. All is not Toll: new pathways in DNA recognition. *J Exp Med* 2006; **203**: 265-268
82 **Meylan E**, Tschopp J. Toll-like receptors and RNA helicases: two parallel ways to trigger antiviral responses. *Mol Cell* 2006; **22**: 561-569
83 **Cullen BR**. Transcription and processing of human microRNA precursors. *Mol Cell* 2004; **16**: 861-865
84 **Perri S**, Ganem D. A host factor that binds near the termini of hepatitis B virus pregenomic RNA. *J Virol* 1996; **70**: 6803-6809
85 **Kreft SG**, Nassal M. hRUL138, a novel human RNA-binding RING-H2 ubiquitin-protein ligase. *J Cell Sci* 2003; **116**: 605-616
86 **Bartenschlager R**, Schaller H. Hepadnaviral assembly is initiated by polymerase binding to the encapsidation signal in the viral RNA genome. *EMBO J* 1992; **11**: 3413-3420
87 **Yao E**, Schaller H, Tavis JE. The duck hepatitis B virus polymerase and core proteins accumulate in different patterns from their common mRNA. *Virology* 2003; **311**: 81-88
88 **Yao E**, Tavis JE. Kinetics of synthesis and turnover of the duck hepatitis B virus reverse transcriptase. *J Biol Chem* 2003; **278**: 1201-1205
89 **Cao F**, Tavis JE. Detection and characterization of cytoplasmic hepatitis B virus reverse transcriptase. *J Gen Virol* 2004; **85**: 3353-3360
90 **Xiong Y**, Eickbush TH. Origin and evolution of retroelements based upon their reverse transcriptase sequences. *EMBO J* 1990; **9**: 3353-3362
91 **Radziwill G**, Tucker W, Schaller H. Mutational analysis of the hepatitis B virus P gene product: domain structure and RNase H activity. *J Virol* 1990; **64**: 613-620
92 **Bartenschlager R**, Schaller H. The amino-terminal domain of the hepadnaviral P-gene encodes the terminal protein (genome-linked protein) believed to prime reverse transcription. *EMBO J* 1988; **7**: 4185-4192
93 **Weber M**, Bronsema V, Bartos H, Bosserhoff A, Bartenschlager R, Schaller H. Hepadnavirus P protein utilizes a tyrosine residue in the TP domain to prime reverse transcription. *J Virol* 1994; **68**: 2994-2999
94 **Zoulim F**, Seeger C. Reverse transcription in hepatitis B viruses is primed by a tyrosine residue of the polymerase. *J Virol* 1994; **68**: 6-13
95 **Lanford RE**, Notvall L, Lee H, Beames B. Transcomplementation of nucleotide priming and reverse transcription between independently expressed TP and RT domains of the hepatitis B virus reverse transcriptase. *J Virol* 1997; **71**: 2996-3004
96 **Das K**, Xiong X, Yang H, Westland CE, Gibbs CS, Sarafianos SG, Arnold E. Molecular modeling and biochemical characterization reveal the mechanism of hepatitis B virus polymerase resistance to lamivudine (3TC) and emtricitabine (FTC). *J Virol* 2001; **75**: 4771-4779
97 **Allen MI**, Deslauriers M, Andrews CW, Tipples GA, Walters KA, Tyrrell DL, Brown N, Condreay LD. Identification and characterization of mutations in hepatitis B virus resistant to lamivudine. Lamivudine Clinical Investigation Group. *Hepatology* 1998; **27**: 1670-1677
98 **Beck J,** Vogel M, Nassal M. dNTP versus NTP discrimination by phenylalanine 451 in duck hepatitis B virus P protein indicates a common structure of the dNTP-binding pocket with other reverse transcriptases. *Nucleic Acids Res* 2002; **30**: 1679-1687
99 **Ferrer-Orta C**, Arias A, Escarmís C, Verdaguer N. A comparison of viral RNA-dependent RNA polymerases. *Curr Opin Struct Biol* 2006; **16**: 27-34
100 **de Jong RN**, van der Vliet PC, Brenkman AB. Adenovirus DNA replication: protein priming, jumping back and the role of the DNA binding protein DBP. *Curr Top Microbiol Immunol* 2003; **272**: 187-211
101 **Kamtekar S**, Berman AJ, Wang J, Lázaro JM, de Vega M, Blanco L, Salas M, Steitz TA. The phi29 DNA polymerase: protein-primer structure suggests a model for the initiation to elongation transition. *EMBO J* 2006; **25**: 1335-1343
102 **Hu J**, Anselmo D. In vitro reconstitution of a functional duck hepatitis B virus reverse transcriptase: posttranslational activation by Hsp90. *J Virol* 2000; **74**: 11447-11455
103 **Beck J**, Nassal M. In vitro reconstitution of epsilon-dependent duck hepatitis B virus replication initiation. *Methods Mol Med* 2004; **95**: 315-325
104 **Cao F**, Badtke MP, Metzger LM, Yao E, Adeyemo B, Gong Y, Tavis JE. Identification of an essential molecular contact point on the duck hepatitis B virus reverse transcriptase. *J Virol* 2005; **79**: 10164-10170
105 **Lanford RE**, Kim YH, Lee H, Notvall L, Beames B. Mapping of the hepatitis B virus reverse transcriptase TP and RT domains by transcomplementation for nucleotide priming and by protein-protein interaction. *J Virol* 1999; **73**: 1885-1893
106 **Chen Y**, Varani G. Protein families and RNA recognition. *FEBS J* 2005; **272**: 2088-2097
107 **Schaaf SG**, Beck J, Nassal M. A small 2′-OH- and base-dependent recognition element downstream of the initiation site in the RNA encapsidation signal is essential for hepatitis B virus replication initiation. *J Biol Chem* 1999; **274**: 37787-37794
108 **Tavis JE**, Ganem D. Evidence for activation of the hepatitis B virus polymerase by binding of its RNA template. *J Virol* 1996; **70**: 5741-5750
109 **Beck J**, Nassal M. Formation of a functional hepatitis B virus replication initiation complex involves a major structural alteration in the RNA template. *Mol Cell Biol* 1998; **18**: 6265-6272
110 **Tavis JE**, Massey B, Gong Y. The duck hepatitis B virus polymerase is activated by its RNA packaging signal, epsilon. *J Virol* 1998; **72**: 5789-5796
111 **Lanford RE**, Notvall L, Beames B. Nucleotide priming and reverse transcriptase activity of hepatitis B virus polymerase expressed in insect cells. *J Virol* 1995; **69**: 4431-4439
112 **Seifer M**, Hamatake R, Bifano M, Standring DN. Generation of replication-competent hepatitis B virus nucleocapsids in insect cells. *J Virol* 1998; **72**: 2765-2776
113 **Hu J,** Seeger C. Hsp90 is required for the activity of a hepatitis B virus reverse transcriptase. *Proc Natl Acad Sci USA* 1996; **93**: 1060-1064
114 **Tang YC**, Chang HC, Roeben A, Wischnewski D, Wischnewski

N, Kerner MJ, Hartl FU, Hayer-Hartl M. Structural features of the GroEL-GroES nano-cage required for rapid folding of encapsulated protein. *Cell* 2006; **125**: 903-914
115 **Hartl FU**, Hayer-Hartl M. Molecular chaperones in the cytosol: from nascent chain to folded protein. *Science* 2002; **295**: 1852-1858
116 **Young JC**, Agashe VR, Siegers K, Hartl FU. Pathways of chaperone-mediated protein folding in the cytosol. *Nat Rev Mol Cell Biol* 2004; **5**: 781-791
117 **Mayer MP**, Bukau B. Hsp70 chaperones: cellular functions and molecular mechanism. *Cell Mol Life Sci* 2005; **62**: 670-684
118 **Young JC**, Moarefi I, Hartl FU. Hsp90: a specialized but essential protein-folding tool. *J Cell Biol* 2001; **154**: 267-273
119 **Pratt WB**, Galigniana MD, Morishima Y, Murphy PJ. Role of molecular chaperones in steroid receptor action. *Essays Biochem* 2004; **40**: 41-58
120 **Hu J,** Toft DO, Seeger C. Hepadnavirus assembly and reverse transcription require a multi-component chaperone complex which is incorporated into nucleocapsids. *EMBO J* 1997; **16**: 59-68
121 **Guisbert E**, Herman C, Lu CZ, Gross CA. A chaperone network controls the heat shock response in E. coli. *Genes Dev* 2004; **18**: 2812-2821
122 **Takaya A**, Matsui M, Tomoyasu T, Kaya M, Yamamoto T. The DnaK chaperone machinery converts the native FlhD2C2 hetero-tetramer into a functional transcriptional regulator of flagellar regulon expression in Salmonella. *Mol Microbiol* 2006; **59**: 1327-1340
123 **Hennessy F**, Nicoll WS, Zimmermann R, Cheetham ME, Blatch GL. Not all J domains are created equal: implications for the specificity of Hsp40-Hsp70 interactions. *Protein Sci* 2005; **14**: 1697-1709
124 **Brehmer D**, Rüdiger S, Gässler CS, Klostermeier D, Packschies L, Reinstein J, Mayer MP, Bukau B. Tuning of chaperone activity of Hsp70 proteins by modulation of nucleotide exchange. *Nat Struct Biol* 2001; **8**: 427-432
125 **Walsh P**, Bursać D, Law YC, Cyr D, Lithgow T. The J-protein family: modulating protein assembly, disassembly and translocation. *EMBO Rep* 2004; **5**: 567-571
126 **Wang X**, Qian X, Guo HC, Hu J. Heat shock protein 90-independent activation of truncated hepadnavirus reverse transcriptase. *J Virol* 2003; **77**: 4471-4480
127 **Cho G**, Suh SW, Jung G. HBV polymerase interacts independently with N-terminal and C-terminal fragments of Hsp90beta. *Biochem Biophys Res Commun* 2000; **274**: 203-211
128 **Hu J**, Flores D, Toft D, Wang X, Nguyen D. Requirement of heat shock protein 90 for human hepatitis B virus reverse transcriptase function. *J Virol* 2004; **78**: 13122-13131
129 **Bracher A**, Hartl FU. Hsp90 structure: when two ends meet. *Nat Struct Mol Biol* 2006; **13**: 478-480
130 **Pratt WB**, Toft DO. Regulation of signaling protein function and trafficking by the hsp90/hsp70-based chaperone machinery. *Exp Biol Med (Maywood)* 2003; **228**: 111-133
131 **Workman P**. Altered states: selectively drugging the Hsp90 cancer chaperone. *Trends Mol Med* 2004; **10**: 47-51
132 **Kamal A**, Thao L, Sensintaffar J, Zhang L, Boehm MF, Fritz LC, Burrows FJ. A high-affinity conformation of Hsp90 confers tumour selectivity on Hsp90 inhibitors. *Nature* 2003; **425**: 407-410
133 **Park SG**, Jung G. Human hepatitis B virus polymerase interacts with the molecular chaperonin Hsp60. *J Virol* 2001; **75**: 6962-6968
134 **Park SG**, Lim SO, Jung G. Binding site analysis of human HBV pol for molecular chaperonin, hsp60. *Virology* 2002; **298**: 116-123
135 **Park SG**, Lee SM, Jung G. Antisense oligodeoxynucleotides targeted against molecular chaperonin Hsp60 block human hepatitis B virus replication. *J Biol Chem* 2003; **278**: 39851-39857
136 **Kim SS**, Shin HJ, Cho YH, Rho HM. Expression of stable hepatitis B viral polymerase associated with GRP94 in E. coli. *Arch Virol* 2000; **145**: 1305-1320
137 **Wang X**, Grammatikakis N, Hu J. Role of p50/CDC37 in hepadnavirus assembly and replication. *J Biol Chem* 2002; **277**: 24361-24367
138 **Holt SE**, Aisner DL, Baur J, Tesmer VM, Dy M, Ouellette M, Trager JB, Morin GB, Toft DO, Shay JW, Wright WE, White MA. Functional requirement of p23 and Hsp90 in telomerase complexes. *Genes Dev* 1999; **13**: 817-826
139 **Keppler BR**, Grady AT, Jarstfer MB. The biochemical role of the heat shock protein 90 chaperone complex in establishing human telomerase activity. *J Biol Chem* 2006; **281**: 19840-19848
140 **Burch AD**, Weller SK. Herpes simplex virus type 1 DNA polymerase requires the mammalian chaperone hsp90 for proper localization to the nucleus. *J Virol* 2005; **79**: 10740-10749
141 **Kampmueller KM**, Miller DJ. The cellular chaperone heat shock protein 90 facilitates Flock House virus RNA replication in Drosophila cells. *J Virol* 2005; **79**: 6827-6837
142 **Momose F**, Naito T, Yano K, Sugimoto S, Morikawa Y, Nagata K. Identification of Hsp90 as a stimulatory host factor involved in influenza virus RNA synthesis. *J Biol Chem* 2002; **277**: 45306-45314
143 **Deng T**, Sharps J, Fodor E, Brownlee GG. In vitro assembly of PB2 with a PB1-PA dimer supports a new model of assembly of influenza A virus polymerase subunits into a functional trimeric complex. *J Virol* 2005; **79**: 8669-8674
144 **Liu N**, Ji L, Maguire ML, Loeb DD. cis-Acting sequences that contribute to the synthesis of relaxed-circular DNA of human hepatitis B virus. *J Virol* 2004; **78**: 642-649
145 **Shin MK**, Lee J, Ryu WS. A novel cis-acting element facilitates minus-strand DNA synthesis during reverse transcription of the hepatitis B virus genome. *J Virol* 2004; **78**: 6252-6262
146 **Tang H**, McLachlan A. A pregenomic RNA sequence adjacent to DR1 and complementary to epsilon influences hepatitis B virus replication efficiency. *Virology* 2002; **303**: 199-210
147 **Abraham TM**, Loeb DD. Base pairing between the 5′ half of epsilon and a cis-acting sequence, phi, makes a contribution to the synthesis of minus-strand DNA for human hepatitis B virus. *J Virol* 2006; **80**: 4380-4387
148 **Harris RS**, Liddament MT. Retroviral restriction by APOBEC proteins. *Nat Rev Immunol* 2004; **4**: 868-877
149 **Turelli P**, Mangeat B, Jost S, Vianin S, Trono D. Inhibition of hepatitis B virus replication by APOBEC3G. *Science* 2004; **303**: 1829
150 **Rösler C**, Köck J, Kann M, Malim MH, Blum HE, Baumert TF, von Weizsäcker F. APOBEC-mediated interference with hepadnavirus production. *Hepatology* 2005; **42**: 301-309
151 **Bonvin M**, Achermann F, Greeve I, Stroka D, Keogh A, Inderbitzin D, Candinas D, Sommer P, Wain-Hobson S, Vartanian JP, Greeve J. Interferon-inducible expression of APOBEC3 editing enzymes in human hepatocytes and inhibition of hepatitis B virus replication. *Hepatology* 2006; **43**: 1364-1374
152 **Ostrow KM**, Loeb DD. Underrepresentation of the 3′ region of the capsid pregenomic RNA of duck hepatitis B virus. *J Virol* 2004; **78**: 2179-2186
153 **Loeb DD**, Hirsch RC, Ganem D. Sequence-independent RNA cleavages generate the primers for plus strand DNA synthesis in hepatitis B viruses: implications for other reverse transcribing elements. *EMBO J* 1991; **10**: 3533-3540
154 **Staprans S**, Loeb DD, Ganem D. Mutations affecting hepadnavirus plus-strand DNA synthesis dissociate primer cleavage from translocation and reveal the origin of linear viral DNA. *J Virol* 1991; **65**: 1255-1262
155 **Bill CA**, Summers J. Genomic DNA double-strand breaks are targets for hepadnaviral DNA integration. *Proc Natl Acad Sci USA* 2004; **101**: 11135-11140
156 **Habig JW**, Loeb DD. The conformation of the 3′ end of the minus-strand DNA makes multiple contributions to template switches during plus-strand DNA synthesis of duck hepatitis B virus. *J Virol* 2003; **77**: 12401-12411
157 **Havert MB**, Loeb DD. cis-Acting sequences in addition to donor and acceptor sites are required for template switching during synthesis of plus-strand DNA for duck hepatitis B virus. *J Virol* 1997; **71**: 5336-5344

158 **Havert MB**, Ji L, Loeb DD. Analysis of duck hepatitis B virus reverse transcription indicates a common mechanism for the two template switches during plus-strand DNA synthesis. *J Virol* 2002; **76**: 2763-2769
159 **Habig JW,** Loeb DD. Template switches during plus-strand DNA synthesis of duck hepatitis B virus are influenced by the base composition of the minus-strand terminal redundancy. *J Virol* 2003; **77**: 12412-12420
160 **Liu N**, Tian R, Loeb DD. Base pairing among three cis-acting sequences contributes to template switching during hepadnavirus reverse transcription. *Proc Natl Acad Sci USA* 2003; **100**: 1984-1989
161 **Mueller-Hill K**, Loeb DD. cis-Acting sequences 5E, M, and 3E interact to contribute to primer translocation and circularization during reverse transcription of avian hepadnavirus DNA. *J Virol* 2002; **76**: 4260-4266
162 **Lee J**, Shin MK, Lee HJ, Yoon G, Ryu WS. Three novel cis-acting elements required for efficient plus-strand DNA synthesis of the hepatitis B virus genome. *J Virol* 2004; **78**: 7455-7464
163 **Wynne SA**, Crowther RA, Leslie AG. The crystal structure of the human hepatitis B virus capsid. *Mol Cell* 1999; **3**: 771-780

S- Editor Liu Y **L- Editor** Alpini GD **E- Editor** Ma WH

PO Box 2345, Beijing 100023, China
www.wjgnet.com
wjg@wjgnet.com

World J Gastroenterol 2007 January 7; 13(1): 65-73
World Journal of Gastroenterology ISSN 1007-9327

TOPIC HIGHLIGHT

Dieter Glebe, PhD, *Series Editor*

Hepatitis B virus morphogenesis

Volker Bruss

Volker Bruss, Department of Virology, University of Göttingen, Kreuzbergring 57, Göttingen 37075, Germany
Correspondence to: Volker Bruss, Department of Virology, University of Göttingen, Kreuzbergring 57, Göttingen 37075, Germany. vbruss@gwdg.de
Telephone: +49-551-395759 Fax: +49-551-394471
Received: 2006-07-31 Accepted: 2006-10-04

Abstract

The hepatitis B virus (HBV) particle consists of an envelope containing three related surface proteins and probably lipid and an icosahedral nucleocapsid of approximately 30 nm diameter enclosing the viral DNA genome and DNA polymerase. The capsid is formed in the cytosol of the infected cell during packaging of an RNA pregenome replication complex by multiple copies of a 21-kDa C protein. The capsid gains the ability to bud during synthesis of the viral DNA genome by reverse transcription of the pregenome in the lumen of the particle. The three envelope proteins S, M, and L shape a complex transmembrane fold at the endoplasmic reticulum, and form disulfide-linked homo- and heterodimers. The transmembrane topology of a fraction of the large envelope protein L changes post-translationally, therefore, the N terminal domain of L (preS) finally appears on both sides of the membrane. During budding at an intracellular membrane, a short linear domain in the cytosolic preS region interacts with binding sites on the capsid surface. The virions are subsequently secreted into the blood. In addition, the surface proteins can bud in the absence of capsids and form subviral lipoprotein particles of 20 nm diameter which are also secreted.

Key words: Hepatitis B virus morphogenesis; HBsAg; Hepatitis B virus capsid; Virus envelopment

Bruss V. Hepatitis B virus morphogenesis. *World J Gastroenterol* 2007; 13(1): 65-73

http://www.wjgnet.com/1007-9327/13/65.asp

INTRODUCTION

In vitro systems for efficient production of hepatitis B virus (HBV) capsids and subviral particles and for experimental examination of their morphogenesis are available. These systems allowed to draw a quite detailed, although still fragmentary, picture of these processes. However, *in vitro* production of virions by transfection of certain cell lines derived from hepatocellular carcinomas, such as HepG2 or Huh7, with cloned genomic HBV DNA[1,2] or by *in vitro* infection[3] is still quite inefficient, and this hampers many approaches to study the morphogenesis of the complete virus. In natural HBV infections one single hepatocyte in the liver releases 1 to 10 viruses per day[4]. *In vitro* the production rate seems to be similar. Therefore, the direct observation of HBV budding by electron microscopy or the characterization of the process by biochemical approaches is difficult to achieve[5]. It seems that the virus production rate in duck hepatitis B virus (DHBV) infection is higher at least *in vitro*, making these techniques suitable for studying DHBV morphogenesis[6].

THE HBV CAPSID FORMATION AND STRUCTURE

The C protein forming the shell of the HBV capsid consists of 183 or 185 amino acid (aa) residues depending on the genotype. The protein is relatively conserved among HBV isolates[7]. It can be expressed in a broad range of pro- and eukaryotic cell types and self-assembles into capsids. The first step is the formation of homodimers[8] linked by a disulfide bridge between the cystein residue 61[9,10]. Higher oligomers containing chaperons have been described[11] but the pathway leading from dimers to complete capsids has not been elucidated in more detail. In the final capsid, the inter-dimer interactions are rather weak[12]. Two different types of capsids are formed[13]: particles with an icosahedral T = 3 symmetry have a diameter of 30 nm and consist of 90 C dimers, whereas particles with an icosahedral T = 4 symmetry are larger (the diameter is 34 nm) and contain 120 C dimers. Both particle species can also be found in infected human liver[14]. In infectious virions, T = 4 capsids have been found[15].

The primary amino acid (aa) sequence of the C protein can be divided into two parts (Figure 1): the N-terminal 149 or 151 aa (depending on the genotype) form the so called assembly domain because this part of the protein is sufficient to direct the self-assembly of capsids. The C-terminal 34 aa are dispensable for capsid formation, rich in arginine residues, and involved in packaging of the pregenome/reverse transcriptase complex. Deletion of this domain abolishes the encapsidation of nucleic acid[16].

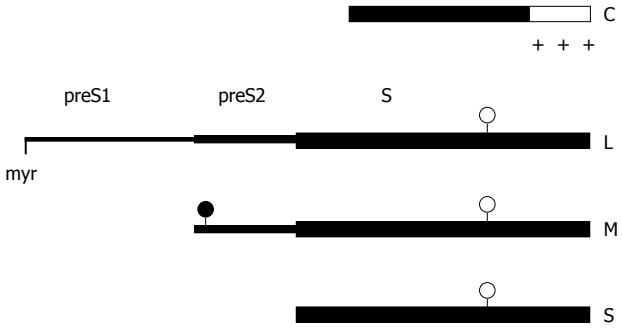

Figure 1 Linear map of the main structural HBV proteins. The C-terminal region (open box) of the capsid protein C is rich in arginine residues (+). The sequence of the small envelope S is also present at the C termini of the M and L protein. The two larger envelope proteins contain the additional N-terminal preS2 and preS2 + preS1 domain, respectively. The L protein is myristylated at glycin 2 (myr), the preS2 domain of M is N-glycosylated (filled circles), and the S domain of all 3 proteins is partially N-glycosylated (open circles).

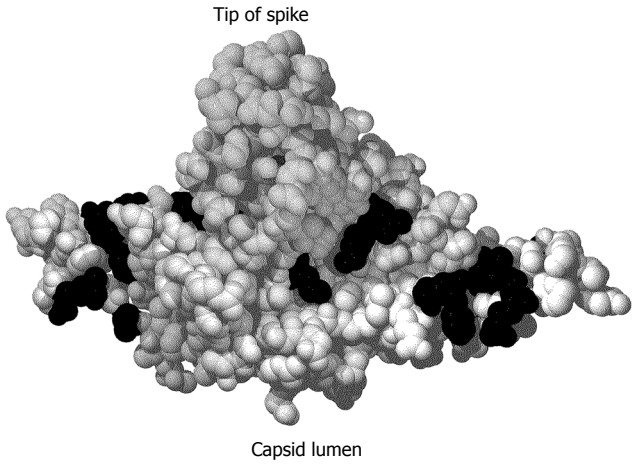

Figure 2 Crystal structure of a C-terminally truncated C protein dimer[21]. The spike protrudes upwards. The lumen of the capsid would be below the figure. Mutational analysis identified aa (shown in black) where the mutation was compatible with capsid formation and viral DNA synthesis in the lumen of the particle but blocked nucleocapsid envelopment[121].

Expression of the C-terminally truncated C protein in *E coli* produces high amounts of T = 4 capsids and relatively little T = 3 particles[17]. Using this material a model for the folding of the C protein in the capsid first at lower resolution by cryo-electron microscopy[18,19] and finally after crystallization at a resolution of 3.3 Å[20,21] has been proposed. The C protein dimer forms a structure like an upside down "T". The horizontal bar mediates the inter-dimer contacts with 5 and 6 dimers arranged around the 5-fold and quasi 6-fold symmetry axes, respectively, and the vertical bar forms a spike protruding outwards from the capsid surface (Figure 2). The tip of the spike forms the major epitope of the capsid antigen (HBcAg). The capsid shell contains pores with a diameter between 12 Å and 15 Å. These pores allow the diffusion of nucleotides into and out of the capsid lumen during the synthesis of the viral DNA genome.

The arginine-rich domain is not present in the capsid crystals but thought to interact with the viral genome in the lumen of the particle[16,22,23]. However, a monoclonal antibody directed against this region binds to intact HBV capsids[24], and trypsin can clip off this domain from approximately half of the C protein chains in recombinant HBV capsids (Daniela Lieder, PhD thesis, Goettingen, 2002). It therefore seems possible that the C-terminal region of one fraction of C proteins reach into the lumen of the particle, while the domains from the other fraction appear on the external surface of the same particle. The peptide at the boundary between the assembly and arginine-rich domains of C forms a mobile array[25] and may allow an extreme mobility of the C terminal domain.

Capsid formation during recombinant expression of the C protein requires a higher concentration of C protein dimers relative to nucleocapsid formation in the context of an infection[26]. During authentic capsid formation, not only the viral pregenomic RNA bound to the viral P protein[27-30] but also cellular factors such as chaperones[31-33] and a protein kinase phosphorylating serine residues in the arginine-rich domain of C[34-37] are encapsidated. Apparently, the threshold concentration of C dimers needed for the initiation of capsid formation is lowered by one or more of these factors. This mechanism assures the efficient encapsidation of replication complexes and prevents that large amounts of empty capsids are formed in the presence of free replication complexes.

C proteins from human and woodchuck HBV can form mixed capsids, while this is not possible between human and duck C proteins[38] which are less homologous. Foreign protein domains can be incorporated into capsids when fused to the N or C terminus or at the tip of the spike[39-44]. The assembly of HBV capsids can be blocked by low molecular weight compounds, possibly offering new options for antiviral treatments in the future[45-48].

THE HBV ENVELOPE PROTEINS

The HBV envelope contains three related viral surface proteins. They are expressed from one open reading frame (ORF) referred to as E containing 389 or 400 codons depending on the genotype and three start sites for translation[49] (Figure 1). Transcription is initiated at a promoter upstream of the ORF and, in addition, at an internal promoter upstream of the second translation initiation site[50]. Translation of the larger mRNA yields the large envelope protein (L) consisting of 389 or 400 aa. Translation of the shorter transcripts gives rise to the middle sized, 281 aa long M protein and, in addition, to the small S protein consisting of 226 aa[51] depending on which translation initiation site is used. The aa sequence present at the C termini of L and M is identical to the S protein and is referred to as the S domain. The 55 aa long additional N-terminal domain of M being central in L is called preS2, and the 108 or 119 aa long N-terminal domain unique to L is named preS1. The E ORF of avian hepadnaviruses contains only 2 start codons, therefore, these viruses possess only two envelope proteins (L and S).

Like typical membrane proteins, the HBV envelope proteins are synthesized at the endoplasmic reticulum (ER). They gain a relatively complex topology (Figure 3). Insertion of the S protein into the ER membrane is initiated by an N-terminal signal sequence (aa 8 to

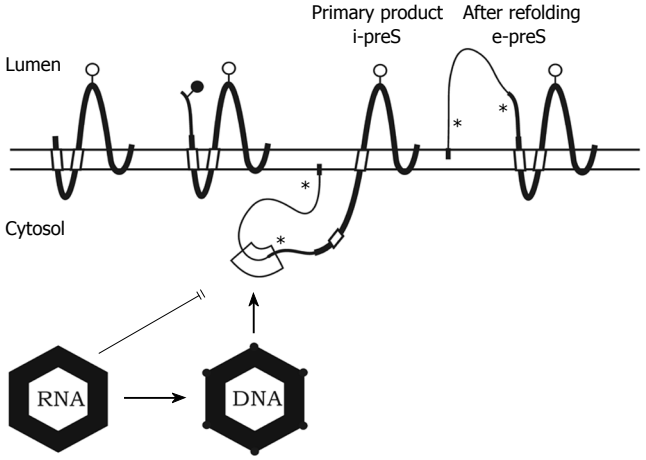

Figure 3 Transmembrane topology of the HBV envelope proteins and model for envelope-capsid interaction. The transmembrane folding of the S protein is determined by an N-terminal and an internal signal shown as open boxes. The C-terminal domain is hydrophobic and probably embedded in the lipid bilayer (horizontal open bar). The C terminus is oriented towards the ER lumen. The folding of the M protein is similar to S. The preS2 domain of M (thinner line) is located in the ER lumen. In the initial folding of the L protein, the preS domains are located in the cytosol (i-preS). Whether the N-terminal myristate group (filled box) is inserted into the membrane as shown here is unknown. After refolding approximately half of the L chains expose the preS domains at the luminal side of the membrane (e-preS). Open and filled circles: see Figure 1. Asterisks indicate potential but unused N-glycosylation sites in preS of L. A domain in i-preS (boxed area) and in the cytosolic loop of S may interact with the capsid during budding. Immature capsids containing pregenomic RNA are not capable to bud. During viral DNA synthesis, the capsid shell changes (indicated by filled circles at the edges) and becomes competent for envelopment.

22) which is, however, not cleaved by the host's signal peptidase. A second signal (aa 80 to 98) directs the translocation of the peptide chain downstream of this signal through the ER membrane into the ER lumen[52], whereas the region upstream of the signal remains in the cytosol. The signal itself anchors the protein as a transmembrane domain in the lipid bilayer. The C-terminal hydrophobic 57 aa of S are believed to be embedded in the ER membrane. Foreign domains fused to the C terminus of S are oriented towards the ER lumen, suggesting that the C terminus of S is also oriented toward this compartment[52]. This configuration causes the region between residues 23 and 79 to form a loop at the cytosolic side of the ER membrane, whereas the loop between aa 99 and approximately 169 is on the luminal side. The luminal loop carries the major conformational epitope of the HBV surface protein antigen (HBsAg) and is N-glycosylated in approximately half of the S molecules at asparagine (asn) residue 146[53]. After budding the HBsAg epitopes are located at the external surface of viral particles.

The transmembrane topology of the M protein is identical to S. The N-terminal preS2 domain (55 aa) is translocated into the ER lumen probably by the action of the first signal in the S domain[54]. The M protein is N-glycosylated at asn 4[55]. In addition, the preS2 domain is O-glycosylated in some but not all HBV genotypes[56].

Glycine residue 2 of the L protein is myristylated[57]. The preS1 and preS2 domains at the N terminus of L initially remain at the cytosolic side of the ER membrane during L translation (i-preS conformation). The central signal in the S domain of L anchors the protein in the ER membrane and causes the translocation of downstream sequences. Therefore, asn 146 in the S domain of L is partially N-glycosylated, while asn 4 of the preS2 as well as a further potential N-glycosylation site in preS1 remain unmodified (Figure 3). These sites are used when the N terminus of L is forced to cotranslationally translocate by the artificial fusion of a signal sequence to the N terminus of preS1[58].

In about half of the L chains, the transmembrane topology changes after translation[59-63]. The preS domains then appear on the luminal side of the ER membrane (e-preS conformation). Probably the N-terminal signal in the S domain crosses the membrane in this conformation similar to the M and S proteins. How the preS domains move post-translationally through the membrane is not known. Cytosolic chaperones like Hsc70 bind to preS1 and deletion of the binding site causes cotranslational translocation of preS[64-66]. Luminal chaperones binding to the e-preS domain[67] could support this process. It might be possible that oligomerized S domains form a channel in the membrane for the preS transport[68]. For HBV, the S and M proteins are not required for the translocation process[69], whereas the S protein is essential for DHBV[70,71]. In DHBV, a C-terminally truncated S protein has been described to fulfil a chaperone function during preS translocation[72]. These facts suggest that the preS translocation mechanism might be different between HBV and DHBV[73]. Both L isoforms have their own function: in the e-preS conformation, the preS1 and preS2 domains of L are exposed on the surface of virions and participate in virus receptor binding[74,75], while in the i-preS conformation, the preS1 and preS2 domains of L are internal in the virion and probably important for contacting the nucleocapsid (see below). In addition, the i-preS domain can activate a variety of promoter elements[76]; however, the significance of this function is not clear.

The S domain but not the preS domain contains multiple cystein residues. Cystein residues in the luminal loop crosslink the envelope proteins with each other by multiple disulfide bridges. Shortly after synthesis, disulfide-linked homo- and heterodimers between S, M, and L proteins can be found[77,78]. The cytosolic loop contains 4 cystein residues. Mutational analysis demonstrated that the exchange of 1 out of 3 of the 4 cysteine residues in this loop by a serine residue blocked subviral particle formation[79]. However, these cysteins are not involved in disulfide bridge formation in subviral particles[77], and a covalent modification of these sites, for example, by fatty acid acylation, has not been found[57]. The DHBV L protein is partially phosphorylated[80,81], mainly at serine 118[82]. However, mutational analyses could not demonstrate an essential role for this modification in the DHBV life cycle[83]. Phosphorylation of the HBV L protein could not be found.

SUBVIRAL PARTICLES

The HBV surface proteins are not only incorporated into virion envelopes. Rather, they also bud very efficiently

from intracellular, post-ER pre-Golgi membranes[84,85] without envelopment of capsids, appear as subviral quasi-spherical or filamentous lipoprotein particles in the lumen of the compartment, and are released from the cell by secretion. The quasi-spherical particles have a diameter of 20 nm and an octahedral symmetry[86], the filaments have variable lengths. Subviral particles are highly over-expressed relative to virions and reach a 10 000-fold higher concentration in serum. Subviral particles and virions carry identical surface antigens (HBsAg), although the protein composition is not identical. Spherical subviral particles contain only low amounts of L protein, whereas the relative amount of L is higher in filaments and even higher in the virion envelope[49]. It is assumed that the massive HBsAg overproduction influences the host's immune system in a way that is advantageous for the virus.

Recombinant expression of the S protein (e.g. in yeast) yields highly immunogenic intracellular 20-nm HBsAg particles which can be used as an active vaccine against hepatitis B[87]. S protein expressed in mammalian cells is efficiently secreted as 20-nm HBsAg particles. How the protein escapes the membrane and mobilizes lipid during subviral particle formation is unclear. Chaperons, such as calnexin[88] and BiP[67], bind to S and support the maturation of the protein. The relative amount of lipid is only 25% by weight in subviral particles[89], suggesting that the lipid is not organized as in a conventional membrane bilayer.

The M protein essentially behaves like the S protein with respect to subviral particle formation. However, the L protein can not be secreted from cells when expressed by itself. In fact, the L protein causes a dose-dependant inhibition of particle release when coexpressed with the S protein[90,91] and a storage of subviral particles in the ER lumen[88]. This can cause cell stress and even cell death or cancer[92,93]. The significance of the secretion inhibition function of L for the viral life cycle has remained unclear. This function can be abolished by blocking L myristylation (e.g. by a point mutation of the acceptor glycine residue) or by the deletion of the N-terminal 19 aa of preS1[94-96]. Also, the fusion of a secretion signal to the N terminus of L forcing the protein to exclusively generate the e-preS conformation abrogates secretion inhibition[58]. This, however, is different for the DHBV L protein[97].

Host proteins are efficiently excluded during the morphogenesis of subviral particles. Even the HBV and DHBV S proteins sharing 25% identical aa do not form mixed particles during coexpression[98]. However, this is possible with the more closely related S proteins from HBV and the woodchuck hepatitis B virus (WHV). Apparently, the S protein subunits interact tightly with each other during 20 nm particle formation. However, foreign protein domains can be incorporated into subviral HBsAg particles when they are fused to the S protein[99,100].

CAPSID MATURATION

During HBV nucleocapsid formation, the RNA pregenome is packaged into the particle's lumen and first converted into single stranded and than into partially double-stranded DNA. While nucleocapsids showing all stages of the viral DNA synthesis can be found within cells, secreted virions contain only rather mature circular, partially double-stranded DNA[101,102]. Therefore, it was proposed that early RNA-containing capsid can not be incorporated into virions and that the viral DNA synthesis is associated with a structural change in the capsid shell that allows only mature capsids to be enveloped[103]. This hypothesis was supported by several genetic experiments. C-terminal truncations of the DHBV core protein blocked viral DNA synthesis and also inhibited capsid envelopment[104]. Missense mutations inhibited the reverse transcriptase activity of HBV and DHBV P protein and locked nucleocapsids in an immature state. The incorporation of these capsids into virions was greatly reduced[105,106]. Using a synchronized DHBV replication system, it was shown that envelopment of capsids happened only late in the replication cycle[107].

The nature of the maturation signal has only been described insufficiently. A comparison of capsids containing RNA and DNA by cryo-electronmicroscopy revealed structural differences[15]. There is also evidence that the phosphorylation state of the arginine-rich domain of the C protein might be part of the signal[108-110]. A validation of this hypothesis by a genetic approach is not suitable because substitutions of phosphorylation sites with alanine or glutamic/aspartic acid also influence pregenome packaging and DNA synthesis[111]. Interestingly, the point mutation of isoleucine 97 to leucine in the C protein caused the envelopment of immature capsids[112]. The side chain of this residue is located in the inner space of the spike and close to a hydrophobic pocket showing structural differences in mature *versus* immature capsids[15]. Possibly, the I97L mutation induces a conformational change causing a constitutive or early expression of the envelopment signal. An additional point mutation (P130T) in a quite distant area of the core protein restored the wild-type phenotype[113], demonstrating the complex nature of the maturation signal for envelopment.

The exclusion of immature nucleocapsids from envelopment causes only replication-competent capsids to become part of virions. This may be one reason for the high specific infectivity of DHBV which is close to the optimum of 1 infectious particle per virion[114]. Also for HBV the specific infectivity seems to be very high[115].

The disassembly of capsids occurs in the basket of nuclear pores upon nuclear transport of the viral genome[116] either during infection or intracellular amplification of the viral genome copy number. Capsid destabilization can also be induced by a tumor necrosis factor alpha-mediated non-cytopathic pathway and may play a role as an antiviral mechanism in natural infections[117].

CAPSID ENVELOPMENT AND VIRION FORMATION

In contrast to retroviruses or togaviruses, it is difficult to directly observe the envelopment of HBV capsid by electron microscopy probably because budding events are less frequent in the available *in vitro* expression systems.

It has even not been clarified whether the HBV envelope contains lipid, although this seems to be likely due to the composition of subviral HBsAg particles. Nevertheless, based on the molecular characterization of HBV formation (see below), it is assumed that hepatitis B virions are formed by budding in analogy to other enveloped viruses.

Mature hepadnaviral nucleocapsids originate in the cytosol. How the capsids move to post-ER, pre-Golgi membranes where the envelopment by the surface proteins supposedly occurs[84,85] is unknown. For DHBV capsids, there is evidence that mature capsids lacking C protein hyperphosphorylation, like capsids in virions, attach to intracellular membranes independent of viral envelope proteins[118]. Immature capsids are hyperphosphorylated and do not bind. This observation suggests that the discrimination between immature and mature capsids happens during the transport of the particle to budding sites before the contact to envelope proteins is established.

Several enveloped viruses utilize a host cell machinery for budding of vesicles into the lumen of so-called multivesicular bodies for their own virus budding[119,120]. Viral capsid proteins interact with the host factor of this pathway via so-called late domains. The HBV C protein contains the sequence PPAY (aa 129-132) exposed on the capsid surface[21] resembling the late domain motif PPXY. However, mutations at this site either blocked capsid formation or reproduced the wild-type phenotype[121]. Therefore, future experiments have to decide whether this pathway is involved in HBV morphogenesis.

The envelopment of HBV capsids strictly depends on viral envelope proteins[122-124] in contrast to type C retroviruses or lentiviruses where mutants blocked in envelope protein expression still release capsids wrapped with a lipid layer. A natural HBV point mutant unable to express the M protein was isolated from a patient and demonstrated that this protein is not required[125], whereas suppression of L or S expression impeded virion formation[122,123]. An L construct with an N-terminally fused secretion signal generating only the e-preS conformation was secreted as a component of subviral particles[126] but failed to support virion formation[58]. Apparently, the i-preS conformation of L exposing the preS domain at the cytosolic side of the ER was essential for nucleocapsid envelopment. This finding is compatible to a model where this part of the L protein contains regions (matrix domains) mediating a contact to the capsid required for budding.

In DHBV, the L protein influences the fate of cytoplasmic capsids[124,127]. If the L protein is absent, capsids deliver the viral genome to the nucleus like in the initial infection of the cell and amplify the intracellular viral genome copy number, whereas capsids are mainly secreted as enveloped virions when the L protein is present. This function mapped to aa 116 to 137 of the 161 aa long DHBV preS domain[128]. A similarly short linear stretch between aa 103 and 124 (or aa 92 and 113 depending on the genotype) genetically mapping in HBV preS was found to be important for virion formation[129]. The exchange of two adjacent aa by alanine residues in this area also prevented nucleocapsid envelopment.

Therefore, it is hypothesized that this part of L interacts with the capsid during envelopment and serves the function of a matrix domain similar to the cytoplasmic tail of the alpha virus E2 protein[130]. This model is supported by an HBV double point mutant where the I97L C protein mutation causing the envelopment of relatively immature capsids is suppressed by the A119F mutation in the putative matrix domain of L[131]. Also *in vitro* binding assays, using HBV envelope-derived peptides and liver-derived as well as recombinant capsids favour the model[132]. These results also suggest that the discrimination between immature and mature capsids might not occur on the level of capsid-envelope protein interactions. As aforementioned, this selection may happen during surface protein-independent membrane association of capsids.

The loop between the first and second transmembrane region in the S protein is also located at the cytoplasmic side of intracellular membranes and may establish a contact between envelope and capsid. Indeed, short deletions in the C-terminal half of this loop inhibited virion but not 20-nm particle formation[133]. However, point mutations (substitutions of two adjacent aa by alanine residues) in this area were not sufficient to block envelopment (V. Bruss, umpublished).

Potential binding sites on the capsid for envelope protein domains have also been mapped by mutational analyses. A screening of random insertions and deletions in the C protein[134] identified a few mutations allowing nucleocapsid formation and genome synthesis but blocking nucleocapsid envelopment[135]. A similar phenotype was found for naturally occurring HBV mutants isolated from chronically infected virus carriers[136]. Eleven point mutations generated on the basis of the crystal structure of the HBV capsid also induced a loss of nucleocapsid envelopment[121] (Figure 2). They are clustered around the base of the spike and in the grove between spikes. The minimal distance from the matrix domain in the preS region of L to the transmembrane region in the S domain of L allowing virion formation as mapped by deletion mutagenesis[137] is sufficient to allow the matrix domain to reach these sites on the capsid surface. Mutations at the tip or stem of the spike had no impact on capsid envelopment. However, HBV budding from transfected cells can be suppressed by a peptide binding to the tip of the spike[138,139], possibly by steric hindrance.

As in the case of subviral 20-nm particles, the incorporation of foreign proteins into the virion envelope is strictly suppressed. Host membrane proteins could not be detected in virions and even envelope proteins from avian hepadnaviruses do not mix. However, the L protein from WHV can substitute with low efficiency for the HBV L protein in HBV morphogenesis[98]. The matrix domains of WHV and HBV L protein are highly conserved in contrast to the matrix domains of DHBV and HBV L. Foreign domains can be integrated into the HBV envelope by fusion to the N terminus of the S protein and addition of an N-terminal secretion signal[122]. This configuration results in a transmembrane topology similar to the M protein with the preS2 domain substituted by the foreign

sequence. When coexpressed with wild-type virus, the chimeric protein is phenotypically mixed into virions and the foreign domain is exposed on the virus surface.

REFERENCES

1 **Acs G**, Sells MA, Purcell RH, Price P, Engle R, Shapiro M, Popper H. Hepatitis B virus produced by transfected Hep G2 cells causes hepatitis in chimpanzees. *Proc Natl Acad Sci USA* 1987; **84**: 4641-4644

2 **Yaginuma K**, Shirakata Y, Kobayashi M, Koike K. Hepatitis B virus (HBV) particles are produced in a cell culture system by transient expression of transfected HBV DNA. *Proc Natl Acad Sci USA* 1987; **84**: 2678-2682

3 **Gripon P**, Rumin S, Urban S, Le Seyec J, Glaise D, Cannie I, Guyomard C, Lucas J, Trepo C, Guguen-Guillouzo C. Infection of a human hepatoma cell line by hepatitis B virus. *Proc Natl Acad Sci USA* 2002; **99**: 15655-15660

4 **Nowak MA**, Bonhoeffer S, Hill AM, Boehme R, Thomas HC, McDade H. Viral dynamics in hepatitis B virus infection. *Proc Natl Acad Sci USA* 1996; **93**: 4398-4402

5 **Roingeard P**, Sureau C. Ultrastructural analysis of hepatitis B virus in HepG2-transfected cells with special emphasis on subviral filament morphogenesis. *Hepatology* 1998; **28**: 1128-1133

6 **Funk A**, Hohenberg H, Mhamdi M, Will H, Sirma H. Spread of hepatitis B viruses in vitro requires extracellular progeny and may be codetermined by polarized egress. *J Virol* 2004; **78**: 3977-3983

7 **Chain BM**, Myers R. Variability and conservation in hepatitis B virus core protein. *BMC Microbiol* 2005; **5**: 33

8 **Zhou S**, Standring DN. Hepatitis B virus capsid particles are assembled from core-protein dimer precursors. *Proc Natl Acad Sci USA* 1992; **89**: 10046-10050

9 **Nassal M**, Rieger A, Steinau O. Topological analysis of the hepatitis B virus core particle by cysteine-cysteine cross-linking. *J Mol Biol* 1992; **225**: 1013-1025

10 **Zheng J**, **Schödel** F, Peterson DL. The structure of hepadnaviral core antigens. Identification of free thiols and determination of the disulfide bonding pattern. *J Biol Chem* 1992; **267**: 9422-9429

11 **Lingappa JR**, Martin RL, Wong ML, Ganem D, Welch WJ, Lingappa VR. A eukaryotic cytosolic chaperonin is associated with a high molecular weight intermediate in the assembly of hepatitis B virus capsid, a multimeric particle. *J Cell Biol* 1994; **125**: 99-111

12 **Ceres P**, Zlotnick A. Weak protein-protein interactions are sufficient to drive assembly of hepatitis B virus capsids. *Biochemistry* 2002; **41**: 11525-11531

13 **Crowther RA**, Kiselev NA, Böttcher B, Berriman JA, Borisova GP, Ose V, Pumpens P. Three-dimensional structure of hepatitis B virus core particles determined by electron cryomicroscopy. *Cell* 1994; **77**: 943-950

14 **Kenney JM**, von Bonsdorff CH, Nassal M, Fuller SD. Evolutionary conservation in the hepatitis B virus core structure: comparison of human and duck cores. *Structure* 1995; **3**: 1009-1019

15 **Roseman AM**, Berriman JA, Wynne SA, Butler PJ, Crowther RA. A structural model for maturation of the hepatitis B virus core. *Proc Natl Acad Sci USA* 2005; **102**: 15821-15826

16 **Gallina A**, Bonelli F, Zentilin L, Rindi G, Muttini M, Milanesi G. A recombinant hepatitis B core antigen polypeptide with the protamine-like domain deleted self-assembles into capsid particles but fails to bind nucleic acids. *J Virol* 1989; **63**: 4645-4652

17 **Zlotnick A**, Cheng N, Conway JF, Booy FP, Steven AC, Stahl SJ, Wingfield PT. Dimorphism of hepatitis B virus capsids is strongly influenced by the C-terminus of the capsid protein. *Biochemistry* 1996; **35**: 7412-7421

18 **Conway JF**, Cheng N, Zlotnick A, Wingfield PT, Stahl SJ, Steven AC. Visualization of a 4-helix bundle in the hepatitis B virus capsid by cryo-electron microscopy. *Nature* 1997; **386**: 91-94

19 **Böttcher B**, Wynne SA, Crowther RA. Determination of the fold of the core protein of hepatitis B virus by electron cryomicroscopy. *Nature* 1997; **386**: 88-91

20 **Zlotnick A**, Palmer I, Kaufman JD, Stahl SJ, Steven AC, Wingfield PT. Separation and crystallization of T = 3 and T = 4 icosahedral complexes of the hepatitis B virus core protein. *Acta Crystallogr D Biol Crystallogr* 1999; **55**: 717-720

21 **Wynne SA**, Crowther RA, Leslie AG. The crystal structure of the human hepatitis B virus capsid. *Mol Cell* 1999; **3**: 771-780

22 **Nassal M**. The arginine-rich domain of the hepatitis B virus core protein is required for pregenome encapsidation and productive viral positive-strand DNA synthesis but not for virus assembly. *J Virol* 1992; **66**: 4107-4116

23 **Zlotnick A**, Cheng N, Stahl SJ, Conway JF, Steven AC, Wingfield PT. Localization of the C terminus of the assembly domain of hepatitis B virus capsid protein: implications for morphogenesis and organization of encapsidated RNA. *Proc Natl Acad Sci USA* 1997; **94**: 9556-9561

24 **Machida A,** Ohnuma H, Tsuda F, Yoshikawa A, Hoshi Y, Tanaka T, Kishimoto S, Akahane Y, Miyakawa Y, Mayumi M. Phosphorylation in the carboxyl-terminal domain of the capsid protein of hepatitis B virus: evaluation with a monoclonal antibody. *J Virol* 1991; **65**: 6024-6030

25 **Watts NR**, Conway JF, Cheng N, Stahl SJ, Belnap DM, Steven AC, Wingfield PT. The morphogenic linker peptide of HBV capsid protein forms a mobile array on the interior surface. *EMBO J* 2002; **21**: 876-884

26 **Seifer M**, Zhou S, Standring DN. A micromolar pool of antigenically distinct precursors is required to initiate cooperative assembly of hepatitis B virus capsids in Xenopus oocytes. *J Virol* 1993; **67**: 249-257

27 **Hirsch RC**, Lavine JE, Chang LJ, Varmus HE, Ganem D. Polymerase gene products of hepatitis B viruses are required for genomic RNA packaging as wel as for reverse transcription. *Nature* 1990; **344**: 552-555

28 **Bartenschlager R**, Schaller H. Hepadnaviral assembly is initiated by polymerase binding to the encapsidation signal in the viral RNA genome. *EMBO J* 1992; **11**: 3413-3420

29 **Lott L**, Notvall L, Lanford RE. Transcomplementation of core and polymerase functions of the woolly monkey and human hepatitis B viruses. *Virology* 2003; **308**: 330-339

30 **Lott L**, Beames B, Notvall L, Lanford RE. Interaction between hepatitis B virus core protein and reverse transcriptase. *J Virol* 2000; **74**: 11479-11489

31 **Beck J**, Nassal M. Efficient Hsp90-independent in vitro activation by Hsc70 and Hsp40 of duck hepatitis B virus reverse transcriptase, an assumed Hsp90 client protein. *J Biol Chem* 2003; **278**: 36128-36138

32 **Wang X**, Grammatikakis N, Hu J. Role of p50/CDC37 in hepadnavirus assembly and replication. *J Biol Chem* 2002; **277**: 24361-24367

33 **Hu J**, Flores D, Toft D, Wang X, Nguyen D. Requirement of heat shock protein 90 for human hepatitis B virus reverse transcriptase function. *J Virol* 2004; **78**: 13122-13131

34 **Kann M**, Gerlich WH. Effect of core protein phosphorylation by protein kinase C on encapsidation of RNA within core particles of hepatitis B virus. *J Virol* 1994; **68**: 7993-8000

35 **Kau JH**, Ting LP. Phosphorylation of the core protein of hepatitis B virus by a 46-kilodalton serine kinase. *J Virol* 1998; **72**: 3796-3803

36 **Daub H**, Blencke S, Habenberger P, Kurtenbach A, Dennenmoser J, Wissing J, Ullrich A, Cotten M. Identification of SRPK1 and SRPK2 as the major cellular protein kinases phosphorylating hepatitis B virus core protein. *J Virol* 2002; **76**: 8124-8137

37 **Enomoto M**, Sawano Y, Kosuge S, Yamano Y, Kuroki K, Ohtsuki K. High phosphorylation of HBV core protein by two alpha-type CK2-activated cAMP-dependent protein kinases in vitro. *FEBS Lett* 2006; **580**: 894-899

38 **Chang C**, Zhou S, Ganem D, Standring DN. Phenotypic mixing between different hepadnavirus nucleocapsid proteins reveals C protein dimerization to be cis preferential. *J Virol* 1994; **68**: 5225-5231

39 **Ulrich R**, Nassal M, Meisel H, Krüger DH. Core particles of hepatitis B virus as carrier for foreign epitopes. *Adv Virus Res* 1998; **50**: 141-182
40 **Skamel C**, Ploss M, Böttcher B, Stehle T, Wallich R, Simon MM, Nassal M. Hepatitis B virus capsid-like particles can display the complete, dimeric outer surface protein C and stimulate production of protective antibody responses against Borrelia burgdorferi infection. *J Biol Chem* 2006; **281**: 17474-17481
41 **Nassal M**, Skamel C, Kratz PA, Wallich R, Stehle T, Simon MM. A fusion product of the complete Borrelia burgdorferi outer surface protein A (OspA) and the hepatitis B virus capsid protein is highly immunogenic and induces protective immunity similar to that seen with an effective lipidated OspA vaccine formula. *Eur J Immunol* 2005; **35**: 655-665
42 **Geldmacher A**, Skrastina D, Borisova G, Petrovskis I, Krüger DH, Pumpens P, Ulrich R. A hantavirus nucleocapsid protein segment exposed on hepatitis B virus core particles is highly immunogenic in mice when applied without adjuvants or in the presence of pre-existing anti-core antibodies. *Vaccine* 2005; **23**: 3973-3983
43 **Ulrich R**, Koletzki D, Lachmann S, Lundkvist A, Zankl A, Kazaks A, Kurth A, Gelderblom HR, Borisova G, Meisel H, Krüger DH. New chimaeric hepatitis B virus core particles carrying hantavirus (serotype Puumala) epitopes: immunogenicity and protection against virus challenge. *J Biotechnol* 1999; **73**: 141-153
44 **Kratz PA**, Bottcher B, Nassal M. Native display of complete foreign protein domains on the surface of hepatitis B virus capsids. *Proc Natl Acad Sci USA* 1999; **96**: 1915-1920
45 **Deres K**, Schröder CH, Paessens A, Goldmann S, Hacker HJ, Weber O, Krämer T, Niewöhner U, Pleiss U, Stoltefuss J, Graef E, Koletzki D, Masantschek RN, Reimann A, Jaeger R, Gross R, Beckermann B, Schlemmer KH, Haebich D, Rübsamen-Waigmann H. Inhibition of hepatitis B virus replication by drug-induced depletion of nucleocapsids. *Science* 2003; **299**: 893-896
46 **Stray SJ**, Bourne CR, Punna S, Lewis WG, Finn MG, Zlotnick A. A heteroaryldihydropyrimidine activates and can misdirect hepatitis B virus capsid assembly. *Proc Natl Acad Sci USA* 2005; **102**: 8138-8143
47 **Stray SJ**, Johnson JM, Kopek BG, Zlotnick A. An in vitro fluorescence screen to identify antivirals that disrupt hepatitis B virus capsid assembly. *Nat Biotechnol* 2006; **24**: 358-362
48 **Asif-Ullah M**, Choi KJ, Choi KI, Jeong YJ, Yu YG. Identification of compounds that inhibit the interaction between core and surface protein of hepatitis B virus. *Antiviral Res* 2006; **70**: 85-90
49 **Heermann KH**, Goldmann U, Schwartz W, Seyffarth T, Baumgarten H, Gerlich WH. Large surface proteins of hepatitis B virus containing the pre-s sequence. *J Virol* 1984; **52**: 396-402
50 **Cattaneo R**, Will H, Hernandez N, Schaller H. Signals regulating hepatitis B surface antigen transcription. *Nature* 1983; **305**: 336-338
51 **Sheu SY**, Lo SJ. Preferential ribosomal scanning is involved in the differential synthesis of the hepatitis B viral surface antigens from subgenomic transcripts. *Virology* 1992; **188**: 353-357
52 **Eble BE**, MacRae DR, Lingappa VR, Ganem D. Multiple topogenic sequences determine the transmembrane orientation of the hepatitis B surface antigen. *Mol Cell Biol* 1987; **7**: 3591-3601
53 **Peterson DL**, Nath N, Gavilanes F. Structure of hepatitis B surface antigen. Correlation of subtype with amino acid sequence and location of the carbohydrate moiety. *J Biol Chem* 1982; **257**: 10414-10420
54 **Eble BE**, Lingappa VR, Ganem D. The N-terminal (pre-S2) domain of a hepatitis B virus surface glycoprotein is translocated across membranes by downstream signal sequences. *J Virol* 1990; **64**: 1414-1419
55 **Stibbe W**, Gerlich WH. Structural relationships between minor and major proteins of hepatitis B surface antigen. *J Virol* 1983; **46**: 626-628
56 **Schmitt S**, Glebe D, Tolle TK, Lochnit G, Linder D, Geyer R, Gerlich WH. Structure of pre-S2 N- and O-linked glycans in surface proteins from different genotypes of hepatitis B virus. *J Gen Virol* 2004; **85**: 2045-2053
57 **Persing DH**, Varmus HE, Ganem D. The preS1 protein of hepatitis B virus is acylated at its amino terminus with myristic acid. *J Virol* 1987; **61**: 1672-1677
58 **Bruss V**, Vieluf K. Functions of the internal pre-S domain of the large surface protein in hepatitis B virus particle morphogenesis. *J Virol* 1995; **69**: 6652-6657
59 **Bruss V**, Lu X, Thomssen R, Gerlich WH. Post-translational alterations in transmembrane topology of the hepatitis B virus large envelope protein. *EMBO J* 1994; **13**: 2273-2279
60 **Prange R**, Streeck RE. Novel transmembrane topology of the hepatitis B virus envelope proteins. *EMBO J* 1995; **14**: 247-256
61 **Ostapchuk P**, Hearing P, Ganem D. A dramatic shift in the transmembrane topology of a viral envelope glycoprotein accompanies hepatitis B viral morphogenesis. *EMBO J* 1994; **13**: 1048-1057
62 **Swameye I**, Schaller H. Dual topology of the large envelope protein of duck hepatitis B virus: determinants preventing pre-S translocation and glycosylation. *J Virol* 1997; **71**: 9434-9441
63 **Guo JT**, Pugh JC. Topology of the large envelope protein of duck hepatitis B virus suggests a mechanism for membrane translocation during particle morphogenesis. *J Virol* 1997; **71**: 1107-1114
64 **Lambert C**, Prange R. Chaperone action in the posttranslational topological reorientation of the hepatitis B virus large envelope protein: Implications for translocational regulation. *Proc Natl Acad Sci USA* 2003; **100**: 5199-5204
65 **Löffler-Mary H**, Werr M, Prange R. Sequence-specific repression of cotranslational translocation of the hepatitis B virus envelope proteins coincides with binding of heat shock protein Hsc70. *Virology* 1997; **235**: 144-152
66 **Prange R**, Werr M, Löffler-Mary H. Chaperones involved in hepatitis B virus morphogenesis. *Biol Chem* 1999; **380**: 305-314
67 **Cho DY**, Yang GH, Ryu CJ, Hong HJ. Molecular chaperone GRP78/BiP interacts with the large surface protein of hepatitis B virus in vitro and in vivo. *J Virol* 2003; **77**: 2784-2788
68 **Berting A**, Hahnen J, Kröger M, Gerlich WH. Computer-aided studies on the spatial structure of the small hepatitis B surface protein. *Intervirology* 1995; **38**: 8-15
69 **Lambert C**, Prange R. Dual topology of the hepatitis B virus large envelope protein: determinants influencing post-translational pre-S translocation. *J Biol Chem* 2001; **276**: 22265-22272
70 **Grgacic EV**. Identification of structural determinants of the first transmembrane domain of the small envelope protein of duck hepatitis B virus essential for particle morphogenesis. *J Gen Virol* 2002; **83**: 1635-1644
71 **Grgacic EV**, Kuhn C, Schaller H. Hepadnavirus envelope topology: insertion of a loop region in the membrane and role of S in L protein translocation. *J Virol* 2000; **74**: 2455-2458
72 **Grgacic EV**, Anderson DA. St, a truncated envelope protein derived from the S protein of duck hepatitis B virus, acts as a chaperone for the folding of the large envelope protein. *J Virol* 2005; **79**: 5346-5352
73 **Lambert C**, Mann S, Prange R. Assessment of determinants affecting the dual topology of hepadnaviral large envelope proteins. *J Gen Virol* 2004; **85**: 1221-1225
74 **Urban S**, Gripon P. Inhibition of duck hepatitis B virus infection by a myristoylated pre-S peptide of the large viral surface protein. *J Virol* 2002; **76**: 1986-1990
75 **Gripon P**, Cannie I, Urban S. Efficient inhibition of hepatitis B virus infection by acylated peptides derived from the large viral surface protein. *J Virol* 2005; **79**: 1613-1622
76 **Hildt E**, Saher G, Bruss V, Hofschneider PH. The hepatitis B virus large surface protein (LHBs) is a transcriptional activator. *Virology* 1996; **225**: 235-239
77 **Wounderlich G**, Bruss V. Characterization of early hepatitis B virus surface protein oligomers. *Arch Virol* 1996; **141**: 1191-1205
78 **Mangold CM**, Unckell F, Werr M, Streeck RE. Secretion and antigenicity of hepatitis B virus small envelope proteins lacking cysteines in the major antigenic region. *Virology* 1995; **211**:

535-543
79 **Mangold CM**, Streeck RE. Mutational analysis of the cysteine residues in the hepatitis B virus small envelope protein. *J Virol* 1993; **67**: 4588-4597
80 **Grgacic EV**, Anderson DA. The large surface protein of duck hepatitis B virus is phosphorylated in the pre-S domain. *J Virol* 1994; **68**: 7344-7350
81 **Rothmann K**, Schnölzer M, Radziwill G, Hildt E, Moelling K, Schaller H. Host cell-virus cross talk: phosphorylation of a hepatitis B virus envelope protein mediates intracellular signaling. *J Virol* 1998; **72**: 10138-10147
82 **Borel C**, Sunyach C, Hantz O, Trepo C, Kay A. Phosphorylation of DHBV pre-S: identification of the major site of phosphorylation and effects of mutations on the virus life cycle. *Virology* 1998; **242**: 90-98
83 **Grgacic EV**, Lin B, Gazina EV, Snooks MJ, Anderson DA. Normal phosphorylation of duck hepatitis B virus L protein is dispensable for infectivity. *J Gen Virol* 1998; **79** (Pt 11): 2743-2751
84 **Huovila AP**, Eder AM, Fuller SD. Hepatitis B surface antigen assembles in a post-ER, pre-Golgi compartment. *J Cell Biol* 1992; **118**: 1305-1320
85 **Patzer EJ**, Nakamura GR, Simonsen CC, Levinson AD, Brands R. Intracellular assembly and packaging of hepatitis B surface antigen particles occur in the endoplasmic reticulum. *J Virol* 1986; **58**: 884-892
86 **Gilbert RJ**, Beales L, Blond D, Simon MN, Lin BY, Chisari FV, Stuart DI, Rowlands DJ. Hepatitis B small surface antigen particles are octahedral. *Proc Natl Acad Sci USA* 2005; **102**: 14783-14788
87 **McAleer WJ**, Buynak EB, Maigetter RZ, Wampler DE, Miller WJ, Hilleman MR. Human hepatitis B vaccine from recombinant yeast. *Nature* 1984; **307**: 178-180
88 **Xu Z**, Bruss V, Yen TS. Formation of intracellular particles by hepatitis B virus large surface protein. *J Virol* 1997; **71**: 5487-5494
89 **Gavilanes F**, Gonzalez-Ros JM, Peterson DL. Structure of hepatitis B surface antigen. Characterization of the lipid components and their association with the viral proteins. *J Biol Chem* 1982; **257**: 7770-7777
90 **Persing DH**, Varmus HE, Ganem D. Inhibition of secretion of hepatitis B surface antigen by a related presurface polypeptide. *Science* 1986; **234**: 1388-1391
91 **Ou JH**, Rutter WJ. Regulation of secretion of the hepatitis B virus major surface antigen by the preS-1 protein. *J Virol* 1987; **61**: 782-786
92 **Xu Z**, Jensen G, Yen TS. Activation of hepatitis B virus S promoter by the viral large surface protein via induction of stress in the endoplasmic reticulum. *J Virol* 1997; **71**: 7387-7392
93 **Chisari FV**, Ferrari C. Hepatitis B virus immunopathogenesis. *Annu Rev Immunol* 1995; **13**: 29-60
94 **Gazina E**, Gallina A, Milanesi G. Common localization of retention determinants in hepatitis B virus L protein from different strains. *J Gen Virol* 1996; **77** (Pt 12): 3069-3075
95 **Kuroki K**, Russnak R, Ganem D. Novel N-terminal amino acid sequence required for retention of a hepatitis B virus glycoprotein in the endoplasmic reticulum. *Mol Cell Biol* 1989; **9**: 4459-4466
96 **Prange R**, Clemen A, Streeck RE. Myristylation is involved in intracellular retention of hepatitis B virus envelope proteins. *J Virol* 1991; **65**: 3919-3923
97 **Gazina EV**, Lin B, Gallina A, Milanesi G, Anderson DA. Intracellular retention of duck hepatitis B virus large surface protein is independent of preS topology. *Virology* 1998; **242**: 266-278
98 **Gerhardt E**, Bruss V. Phenotypic mixing of rodent but not avian hepadnavirus surface proteins into human hepatitis B virus particles. *J Virol* 1995; **69**: 1201-1208
99 **Lambert C**, Thomé N, Kluck CJ, Prange R. Functional incorporation of green fluorescent protein into hepatitis B virus envelope particles. *Virology* 2004; **330**: 158-167
100 **Bruss V**, Ganem D. Mutational analysis of hepatitis B surface antigen particle assembly and secretion. *J Virol* 1991; **65**: 3813-3820
101 **Mason WS**, Aldrich C, Summers J, Taylor JM. Asymmetric replication of duck hepatitis B virus DNA in liver cells: Free minus-strand DNA. *Proc Natl Acad Sci USA* 1982; **79**: 3997-4001
102 **Weiser B**, Ganem D, Seeger C, Varmus HE. Closed circular viral DNA and asymmetrical heterogeneous forms in livers from animals infected with ground squirrel hepatitis virus. *J Virol* 1983; **48**: 1-9
103 **Summers J,** Mason WS**.** Replication of the genome of a hepatitis B-like virus by reverse transcription of an RNA intermediate. *Cell* 1982; **29**: 403-415
104 **Yu M**, Summers J. A domain of the hepadnavirus capsid protein is specifically required for DNA maturation and virus assembly. *J Virol* 1991; **65**: 2511-2517
105 **Gerelsaikhan T**, Tavis JE, Bruss V. Hepatitis B virus nucleocapsid envelopment does not occur without genomic DNA synthesis. *J Virol* 1996; **70**: 4269-4274
106 **Wei Y**, Tavis JE, Ganem D. Relationship between viral DNA synthesis and virion envelopment in hepatitis B viruses. *J Virol* 1996; **70**: 6455-6458
107 **Perlman D**, Hu J. Duck hepatitis B virus virion secretion requires a double-stranded DNA genome. *J Virol* 2003; **77**: 2287-2294
108 **Yu M**, Summers J. Multiple functions of capsid protein phosphorylation in duck hepatitis B virus replication. *J Virol* 1994; **68**: 4341-4348
109 **Yu M**, Summers J. Phosphorylation of the duck hepatitis B virus capsid protein associated with conformational changes in the C terminus. *J Virol* 1994; **68**: 2965-2969
110 **Perlman DH**, Berg EA, O'connor PB, Costello CE, Hu J. Reverse transcription-associated dephosphorylation of hepadnavirus nucleocapsids. *Proc Natl Acad Sci USA* 2005; **102**: 9020-9025
111 **Gazina EV**, Fielding JE, Lin B, Anderson DA. Core protein phosphorylation modulates pregenomic RNA encapsidation to different extents in human and duck hepatitis B viruses. *J Virol* 2000; **74**: 4721-4728
112 **Yuan TT**, Sahu GK, Whitehead WE, Greenberg R, Shih C. The mechanism of an immature secretion phenotype of a highly frequent naturally occurring missense mutation at codon 97 of human hepatitis B virus core antigen. *J Virol* 1999; **73**: 5731-5740
113 **Yuan TT**, Shih C. A frequent, naturally occurring mutation (P130T) of human hepatitis B virus core antigen is compensatory for immature secretion phenotype of another frequent variant (I97L). *J Virol* 2000; **74**: 4929-4932
114 **Jilbert AR**, Miller DS, Scougall CA, Turnbull H, Burrell CJ. Kinetics of duck hepatitis B virus infection following low dose virus inoculation: one virus DNA genome is infectious in neonatal ducks. *Virology* 1996; **226**: 338-345
115 **Barker LF**, Murray R. Relationship of virus dose to incubation time of clinical hepatitis and time of appearance of hepatitis--associated antigen. *Am J Med Sci* 1972; **263**: 27-33
116 **Rabe B**, Vlachou A, Panté N, Helenius A, Kann M. Nuclear import of hepatitis B virus capsids and release of the viral genome. *Proc Natl Acad Sci USA* 2003; **100**: 9849-9854
117 **Biermer M**, Puro R, Schneider RJ. Tumor necrosis factor alpha inhibition of hepatitis B virus replication involves disruption of capsid Integrity through activation of NF-kappaB. *J Virol* 2003; **77**: 4033-4042
118 **Mabit H**, Schaller H. Intracellular hepadnavirus nucleocapsids are selected for secretion by envelope protein-independent membrane binding. *J Virol* 2000; **74**: 11472-11478
119 **von Schwedler UK**, Stuchell M, Müller B, Ward DM, Chung HY, Morita E, Wang HE, Davis T, He GP, Cimbora DM, Scott A, Kräusslich HG, Kaplan J, Morham SG, Sundquist WI. The protein network of HIV budding. *Cell* 2003; **114**: 701-713
120 **Freed EO**. Viral late domains. *J Virol* 2002; **76**: 4679-4687
121 **Ponsel D**, Bruss V. Mapping of amino acid side chains on the surface of hepatitis B virus capsids required for envelopment and virion formation. *J Virol* 2003; **77**: 416-422
122 **Bruss V**, Ganem D. The role of envelope proteins in hepatitis B virus assembly. *Proc Natl Acad Sci USA* 1991; **88**: 1059-1063

123 **Ueda K**, Tsurimoto T, Matsubara K. Three envelope proteins of hepatitis B virus: large S, middle S, and major S proteins needed for the formation of Dane particles. *J Virol* 1991; **65**: 3521-3529
124 **Summers J**, Smith PM, Huang MJ, Yu MS. Morphogenetic and regulatory effects of mutations in the envelope proteins of an avian hepadnavirus. *J Virol* 1991; **65**: 1310-1317
125 **Fernholz D**, Stemler M, Brunetto M, Bonino F, Will H. Replicating and virion secreting hepatitis B mutant virus unable to produce preS2 protein. *J Hepatol* 1991; **13** Suppl 4: S102-S104
126 **Prange R**, Werr M, Birkner M, Hilfrich R, Streeck RE. Properties of modified hepatitis B virus surface antigen particles carrying preS epitopes. *J Gen Virol* 1995; **76** (Pt 9): 2131-2140
127 **Summers J**, Smith PM, Horwich AL. Hepadnavirus envelope proteins regulate covalently closed circular DNA amplification. *J Virol* 1990; **64**: 2819-2824
128 **Lenhoff RJ**, Summers J. Coordinate regulation of replication and virus assembly by the large envelope protein of an avian hepadnavirus. *J Virol* 1994; **68**: 4565-4571
129 **Bruss V**. A short linear sequence in the pre-S domain of the large hepatitis B virus envelope protein required for virion formation. *J Virol* 1997; **71**: 9350-9357
130 **Cheng RH**, Kuhn RJ, Olson NH, Rossmann MG, Choi HK, Smith TJ, Baker TS. Nucleocapsid and glycoprotein organization in an enveloped virus. *Cell* 1995; **80**: 621-630
131 **Le Pogam S**, Shih C. Influence of a putative intermolecular interaction between core and the pre-S1 domain of the large envelope protein on hepatitis B virus secretion. *J Virol* 2002; **76**: 6510-6517
132 **Poisson F**, Severac A, Hourioux C, Goudeau A, Roingeard P. Both pre-S1 and S domains of hepatitis B virus envelope proteins interact with the core particle. *Virology* 1997; **228**: 115-120
133 **Löffler-Mary H**, Dumortier J, Klentsch-Zimmer C, Prange R. Hepatitis B virus assembly is sensitive to changes in the cytosolic S loop of the envelope proteins. *Virology* 2000; **270**: 358-367
134 **Koschel M**, Thomssen R, Bruss V. Extensive mutagenesis of the hepatitis B virus core gene and mapping of mutations that allow capsid formation. *J Virol* 1999; **73**: 2153-2160
135 **Koschel M**, Oed D, Gerelsaikhan T, Thomssen R, Bruss V. Hepatitis B virus core gene mutations which block nucleocapsid envelopment. *J Virol* 2000; **74**: 1-7
136 **Le Pogam S**, Yuan TT, Sahu GK, Chatterjee S, Shih C. Low-level secretion of human hepatitis B virus virions caused by two independent, naturally occurring mutations (P5T and L60V) in the capsid protein. *J Virol* 2000; **74**: 9099-9105
137 **Kluge B**, Schläger M, Pairan A, Bruss V. Determination of the minimal distance between the matrix and transmembrane domains of the large hepatitis B virus envelope protein. *J Virol* 2005; **79**: 7918-7921
138 **Dyson MR**, Murray K. Selection of peptide inhibitors of interactions involved in complex protein assemblies: association of the core and surface antigens of hepatitis B virus. *Proc Natl Acad Sci USA* 1995; **92**: 2194-2198
139 **Böttcher B**, Tsuji N, Takahashi H, Dyson MR, Zhao S, Crowther RA, Murray K. Peptides that block hepatitis B virus assembly: analysis by cryomicroscopy, mutagenesis and transfection. *EMBO J* 1998; **17**: 6839-6845

S- Editor Liu Y **L- Editor** Kumar M **E- Editor** Ma WH

PO Box 2345, Beijing 100023, China
www.wjgnet.com
wjg@wjgnet.com

World J Gastroenterol 2007 January 7; 13(1): 74-81
World Journal of Gastroenterology ISSN 1007-9327

TOPIC HIGHLIGHT

Dieter Glebe, PhD, *Series Editor*

Hepatitis B virus-induced oncogenesis

Joachim Lupberger, Eberhard Hildt

Joachim Lupberger, Eberhard Hildt, University of Freiburg, Department of Internal Medicine II, Hugstetter Str. 55, D-79106 Freiburg, Germany
Correspondence to: Eberhard Hildt, University of Freiburg, Department of Internal Medicine II, Hugstetter Str. 55, Freiburg D-79106, Germany. eberhard.hildt@uniklinik-freiburg.de
Telephone: +49-761-2703510
Received: 2006-07-27 Accepted: 2006-09-28

Abstract

Hepatocellular carcinoma (HCC) is one of the most common cancers in the world with an annual incidence of more than 500 000 in the year 2000. Its incidence is rising in many countries. Recently, it has been estimated that about 53% of HCC cases in the world are related to hepatitis B virus (HBV). The epidemiological association of HBV with HCC is well established. In recent studies, it was revealed that HBsAg carriers have a 25-37 times increased risk of developing HCC as compared to non-infected people. At present, HBV-associated carcinogenesis can be seen as a multi-factorial process that includes both direct and indirect mechanisms that might act synergistically. The integration of HBV DNA into the host genome occurs at early steps of clonal tumor expansion. The integration has been shown in a number of cases to affect a variety of cancer-related genes and to exert insertional mutagenesis. The permanent liver inflammation, induced by the immune response, resulting in a degeneration and regeneration process confers to the accumulation of critical mutations in the host genome. In addition to this, the regulatory proteins HBx and the PreS2 activators that can be encoded by the integrate exert a tumor promoter-like function resulting in positive selection of cells producing a functional regulatory protein. Gene expression profiling and proteomic techniques may help to characterize the molecular mechanisms driving HBV-associated carcinogenesis, and thus potentially identify new strategies in diagnosis and therapy.

Key words: Hepatitis B virus; Hepatocellular carcinoma; Regulatory proteins; Signal transduction

Lupberger J, Hildt E. Hepatitis B virus-induced oncogenesis. *World J Gastroenterol* 2007; 13(1): 74-81

http://www.wjgnet.com/1007-9327/13/74.asp

INTRODUCTION

With an estimate of more than 500 000 incidences in the year 2000 hepatocellular carcinoma (HCC) is one of the most frequent malignant tumors worldwide and its incidence is rising in many countries[1-4]. Despite being the 5th most frequent cancer in the world, HCC is the third leading cause of cancer death behind lung and stomach cancer. The high mortality associated with HCC is due to its unresponsiveness to treatment in many cases and symptoms of HCC often are recognized lately[5]. When viewed as estimated age-adjusted incidence rates of liver cancer per 100 000 men, the figures ranged as follows: in Asia, from 35.5 in Eastern Asia, 18.3 in South-eastern Asia to 5.6 in Western Asia; in Africa, from 24.2 in Middle Africa, 14.4 in Eastern Africa, 13.5 in Western Africa, 6.2 in Southern Africa to 4.9 in Northern Africa; in Europe, from 9.8 in Southern Europe, 5.8 in Eastern and Western Europe to 2.6 in Northern Europe; and to values of 4.8 in South America; 4.1 in North America; 3.6 in Australia/New Zealand and, finally, 2.1 in central America. In all regions, the rates recorded were two to three times higher in men than in women.

These significant differences in the geographic distribution of HCC incidence have led to identify chronic HBV infection as a leading risk factor for HCC[6-9]. Recently, it has been estimated that about 53% of HCC cases in the world are related to HBV[3]. The lifetime risk to develop a HCC was found to be increased even in patients that have cleared hepatitis B virus surface antigen (HBsAg) or with an occult HBV infection. Further risk factors include chronic HCV infection, exposure to aflatoxin B_1, alcohol abuse, obesity and diabetes. Aflatoxin B_1 (AFB_1) is a fungal metabolite that contaminates the food supply in certain areas of the world. It is produced by *Aspergillus flavus* and related fungi that grow on improperly stored foods, such as corn, rice and peanuts. AFB_1 requires metabolic conversion to its *exo*-8,9-epoxide in order to damage DNA. Coexistence of these risk factors, such as HBV and HCV infection or HBV infection and aflatoxin B_1, increases the relative risk of HCC development[11-13]. While a variety of risk factors have been identified in the last years, here a short review describing the current state of knowledge of the molecular pathogenesis of HBV-associated HCC

is given. A focus of this review will be on the role of the HBV-regulatory proteins in this process.

EPIDEMIOLOGY OF HBV-ASSOCIATED HCC

The epidemiological association of HBV with HCC is well established. In recent studies, it was revealed that HBsAg carriers have 25-37 times increased risk of developing HCC as compared to non-infected people[14,15]. Moreover, it was analyzed in more detail whether the viral status of the patients are correlated with the risk of developing HCC. HBV has been designated eight genotypes (A-H) based on genetic divergence. Each genotype has a distinct geographical and ethnic distribution. While genotypes B and C are prevalent in Asia, genotypes A and D occur frequently in Africa, Europe and India. There are conflicting data about the influence of HBV genotypes on HCC development[16-18]. Recent studies from Taiwan provide profound evidence for hepatitis B virus e antigen (HBeAg)-positive patients that HBV genotype C causes a more aggressive disease course as compared to genotype B[19-21]. On the other hand, there are reports from Taiwan describing that more than 50% of the HBV-related HCC patients are infected with genotype B. A study on Taiwanese pediatric patients with chronic HBV infection, who were followed for 15 years, showed that genotype B was identified in 74% of the children with HBV-associated HCC[22]. A further interesting observation is the prevalence of the T1762/A1764 mutation in the basal core promoter region which increases with the progression of liver disease. Since this mutation seems to be associated with HCC development, it might represent a helpful prognostic biomarker[23,24].

The risk of HCC seems to be elevated with increasing HBV viral load[25]. Therefore, it is important to consider that most epidemiological analyses were based only on HBsAg positivity. A recent study revealed that the relative risk of HCC was increased by 6-fold among patients who were positive for both HBsAg and HBeAg, compared to those who were positive for HBsAg alone[15]. Based on this, it can be concluded that HBeAg could be an additional useful marker for risk of developing HCC, since HBeAg reflects productive HBV replication.

DIRECT EFFECTS TRIGGERED BY THE INTEGRATION OF HBV-DNA INTO THE HOST GENOME

Integration is not essential for the viral replication but it allows persistence of the viral genome. Almost all of the HBV-associated HCCs harbor chromosomally integrated HBV DNA[26-28]. In many cases, these integrated viral genomes are characterized by rearrangements and/or partial deletions. HBV integration can induce deletions in the host chromosome at the integration site[29]. Based on these observations, it was tempting to speculate that the integration event *per se* causes a deregulation of key regulators of cell cycle control. This cis-hypothesis (place of integration = place of function) seems to be supported by the woodchuck hepatitis B virus (WHV)-related HCC. Here, insertions of WHV-DNA into the c-myc or, preferentially the N-myc2 gene, have been frequently detected[30-34]. However, in case of the HBV-associated HCC, site-specific integration of the HBV genome or integration of the HBV genome into known oncogenes seems to be a rare event. Interesting examples are the integration of HBV DNA in a cyclin A gene[35], in the retinoic acid receptor beta gene, in the mevalonate kinase gene or in the sarco/endoplasmic reticulum calcium ATPase1 gene[28,36].

It was recently confirmed, using a PCR-based approach, that HBV insertion into cellular genes is a frequent event that occurs early during HBV infection even after acute self-limiting hepatitis[37] and that integration can occur in genes regulating cellular signal transduction cascades, proliferation control and cell viability. Recently, hTERT (human telomerase reverse transcriptase) that is part of the telomerase ribonuclear protein complex was found to be targeted in different HBV-associated HCCs[28,38,39].

In light of these recent data, it will be an important issue to reconsider the role of the integration process for HBV-associated carcinogenesis. A helpful tool will be combining the analysis of putative HBV-specific integration sites with functional genomics of HBV-associated HCCs[40].

INDIRECT EFFECTS OF INTEGRATED HBV-DNA: HBX AND THE PRES2 ACTIVATOR FAMILY

HBx

In most integrated subviral HBV genomes, the open reading frame for HBx or PreS2 regulatory protein is conserved and can be transcribed[41]. The HBx gene is conserved among all mammalian hepadnaviruses. HBx is a small polypeptide (17 kDa) that is produced at very low levels during chronic and acute hepatitis. Recently, a HBx-like regulatory protein was identified for duck hepatitis B virus (DHBV)[42]. Since the time when HBx initially was described to act as a transcriptional activator[43,44], a variety of functions have been ascribed to the still enigmatic HBx[45,46]. While the X protein is essential for viral replication in case of WHV[47], there are conflicting results about the relevance of HBx for the viral life cycle in case of HBV. There are reports describing that expression of the viral genome occurs independently from HBx functionality[48-50]; other papers describe a relevance of HBx for HBV replication[51]. In transgenic mouse models harboring an overgenomic HBV integrate, it could be observed that HBV replication does not depend on the presence of a functional HBx[52]. Comparable results were obtained in cell culture models based on huh-7 cells[48,50] while in case of HepG2 cells a reduction in HBx-deficient HBV genomes could be observed[53,54]. Moreover, infection experiments of primary *tupaia* hepatocytes revealed that HBx-deficient HBV particles are infectious (J. Köck, personal communication).

HBx activates a broad variety of different promoter elements. Based on the pleiotropic nature of the HBx-dependent transcriptional regulation, it was concluded that HBx interferes with signaling cascades upstream from the transcription complex. These signaling cascades trigger activation of transcription factors like AP-1 (activator protein-1), NF-κB (nuclear factor kappa B), SP1, and oct-1[46,55]. HBx affects the expression of a variety of genes that are involved in the control of the cell cycle, proliferation or apoptosis. From the beginning, HBx was considered as a crucial viral protein for the process of HBV-associated carcinogenesis[45,56-58] and this might have affected the focus of HBx research. In light of the putative role of HBx for viral carcinogenesis, the major focus of many research projects has been and is the interference of HBx with signal transduction cascades that affect the control of the cell cycle, proliferation or apoptosis. However, one should consider that selective over-expression of HBx reflects a situation that is different from the situation in an infected cell expressing the complete HBV genome. For example, it is well established that HBx is able to promote cellular proliferation[59]. On the other hand, it was shown that expression of the complete HBV genome that harbors the HBx and the PreS2 regulatory protein inhibits cell cycle progression[60] (Figure 1).

The analysis of HBx/protein kinase C (PKC) interaction is such an example for many reports analyzing the interference of HBx with signaling cascades and correlating this with a putative role of HBx for HBV-associated carcinogenesis. There are conflicting reports about the interference of HBx with PKC signaling. On the one hand, there are reports describing an HBx-dependent activation of PKC, mediated by an elevated DAG level in HBx-producing cells. In these studies, PKC is considered as an essential factor for the HBx-dependent activation of NF-kB or AP-1[61,62]. Other reports provide evidence that HBx neither affects activity of PKC nor that PKC is essential for HBx-dependent transcriptional activation[63-65]. The interesting aspect of an HBx-dependent activation of PKC is that a conclusive model for the role of HBx in the process of HBV-dependent carcinogenesis can be deduced. According to the two-step model of carcinogenesis[66] (initiation and promotion), the HBx-dependent activation of PKC could exert a tumor promoter-like function[61]. Independent from the point whether or not the HBx-dependent activation of PKC exerts a tumor promoter-like function, there is profound experimental evidence from experiments with transgenic mice that HBx indeed could exert a tumor promoter-like function. Irradiation of HBx transgenics or exposure of these transgenics to mutagens (diethylnitrosamine) caused a significant increase in the amount of pre-neoplastic lesions as compared to the wild-type control animals[67,68]. Apart from this, a variety of HBx transgenic mouse models were established, but only in one model system so far direct formation of liver cancer could be observed[69].

A tumor promoter-like function of HBx does not necessarily require an activation of PKC. Other pathways as the activation of c-Raf-1-MEK/MAP2 (mitogen-activated protein kinase 2) kinase cascade could fulfill this function as well. Starting with the finding that HBx increases the Ras/GTP complex formation and thereby activates the c-Raf-1 signal transduction cascade[70], more and more data were collected elucidating the interference of HBx with signaling cascades upstream of Ras. One of the next steps was the observation that Src is activated in HBx-producing cells[71,72], followed by the observation that HBx is able to activate the cytosolic Ca^{2+}-dependent praline-rich tyrosine kinase 2 (Pyk)[54]. Pyk is able to activate Src. A recent report describes an HBx-dependent activation of FAK (focal adhesion kinase), a well known regulator of Src kinases[53]. The activation of these signaling cascades requires the presence of HBx in an extranuclear compartment. On the other hand, there is evidence that a fraction of HBx is localized within the nucleus. The subcellular distribution of HBx is still a matter of debate. There are reports providing evidence that HBx is localized in the cytoplasm as well as in the nucleus[49,73]. The different localizations are associated with different functions. HBx localized in the cytoplasm is able to modulate intracellular signal transduction cascades as described above. Moreover, an association of HBx with the outer membrane of mitochondria that induces oxidative stress was described[74-76]. HBx localized in the nucleus is suggested to interfere directly with transcription factors or to exert a transcription factor-like function. A direct interaction with CREB (cAMP responsive element–binding protein) and ATF-2 (activating transcription factor 2) resulting in their increased DNA binding affinity[77] was reported as well as an interaction with RNA polymerase Ⅱ in the transcription complex[78,79].

In addition to the interaction of HBx with the transcription machinery, there is evidence that HBx interferes at multiple steps with DNA repair and so confers to an increase of critical mutations. HBx was found to bind to DDB1[80,81], a subunit of the damaged DNA binding protein that is bound to damaged DNA, the first step in nucleotide excision repair. In cell culture experiments indeed the expression of HBx significantly inhibited the ability of cells to repair damaged DNA.

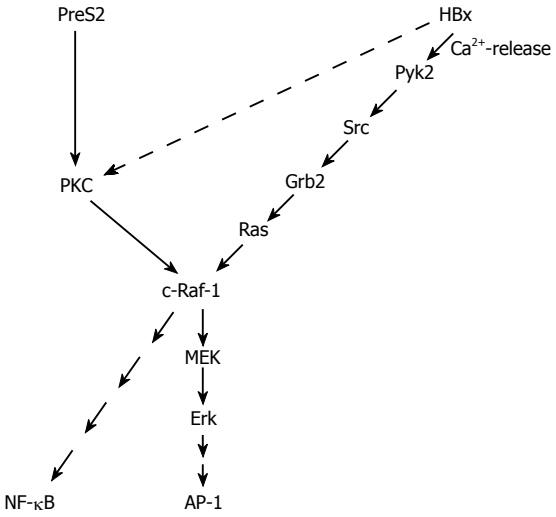

Figure 1 Major signaling pathways activated by the regulatory proteins HBx and PreS2 of HBV.

Therefore, it was tempting to speculate that HBx could confer by this to an increase in the amount of critical mutations in the host genome[80]. However, analysis of mutation frequency in HBx transgenic mice did not corroborate this hypothesis[82]. Other reports focus on the interaction of HBx with p53. On the one hand, it has been shown an indirect inhibition of p53 by HBx: HBx causes a transcriptional repression of the human p53 gene[83]. On the other hand, there is evidence for the capacity of HBx to bind to p53[84,85]. However, if the intracellular amounts of HBx and p53 are considered, there exists a tremendous excess of p53 as compared to HBx in the hepatocytes. The physiological significance of the direct p53/HBx interaction remains questionable.

The family of the PreS2 activators

Apart from the HBx-regulatory protein, the HBV genome encodes a second family of regulatory proteins: the PreS2 activators. Based on a subcloned HBV integrate of the human hepatoma cell line huH4[86] and of an integrate isolated from an HBV-associated HCC[87], preS/S genes that were truncated at the 3´ end were identified[41]. These preS/S^t genes encoded for C-terminally truncated surface proteins (MHBs^t) that display a regulatory protein function. Initial analysis revealed that generation of the regulatory protein function requires at least deletion of the last transmembrane region in the S-domain (transmembrane region 3)[88-91]. This results in C-terminally truncated MHBs molecules that are endoplasmic reticulum (ER)-membrane associated by the remaining transmembrane regions I and Ⅱ of the S domain[92,93]. A prototype of the ER-membrane-associated MHBs^t activator is encoded by the integrate isolated from the human hepatoma cell line huH4[86]. This integrate is truncated at ntHBV 221 of the HBV genome resulting in a C-terminally truncated MHBs protein at amino acid (aa) 76 (MHBs^{t76}). A detailed analysis revealed that a variety of differences exist between the structural protein MHBs and its C-terminally truncated variant MHBs^t. In contrast to the structural protein MHBs and the regulatory variants, MHBs^t are not secreted and lack the glycosylation at asparagine (asn) 4 of the PreS2 domain[92]. The intracellular retention of ER-membrane-associated MHBs^t proteins gave raise to the hypothesis that the observed activator function is due to ER stress, induced by intracellular retention and subsequent accumulation in the ER[93-96]. More detailed analysis revealed, however, that the structural protein MHBs and the regulatory protein MHBs^t differ in the topology of the PreS2 domain[97]. In case of the structural protein, the PreS2 domain faces the lumen of the endoplasmic reticulum and in accordance with this glycosylation at asn 4 can occur. In case of the activator protein MHBs^t, the PreS2 domain directs into the cytoplasm. This explains the lack of N-glycosylation at asn 4. The PreS2 domain facing the cytoplasm interacts with cytosolic binding partners, thereby triggering intracellular signal transduction cascades. In accordance with this, a minimal PreS2 activator was identified lacking any membrane insertion domain (MHBs^{t55})[88,67,98]. This minimal activator encompasses the complete PreS2 domain and is localized within the cytoplasm. Since the PreS2 domain is sufficient to exert the regulatory protein function, this class of regulatory proteins was designated PreS2 activator. The family of PreS2- regulatory proteins encompasses the membrane-associated regulatory proteins, such as MHBs^{t76} or MHBs^{t167}, and the non-membrane-associated short proteins, such as PreS2 domain (MHBs^{t55}). There is no functional difference between the ER and the cytoplasmatically localized Pres2 activators clearly arguing against the ER-overload hypothesis[97].

The PreS1-PreS2 domain of the large hepatitis B virus surface protein (LHBs) displays a dual membrane topology[99-101]. In one fraction of LHBs, the first transmembrane region that is located at the beginning of the S-domain (aa 8-21) is used: in this case, the PreS1-PreS2 domain of LHBs faces the lumen of the endoplasmic reticulum. In case of the other fraction, this transmembrane region is not used, resulting in a PreS1-PreS2 domain that directs into the cytoplasm. As described above, the cytoplasmic orientation of the PreS2 domain in case of the MHBs^t proteins is causative for their regulatory protein function. In accordance with this, LHBs displays a regulatory protein function[102] and belongs to the family of PreS2 activator proteins.

The PreS2 activators bind PKC-α in the cytoplasm. This interaction with PKC results in a DAG (1, 2, sn diacylglycerol)-independent activation of PKC and phosphorylation of the PreS2 domain. The activation of PKC is transduced by the c-Raf-1/MEK/ERK (extracellular signal-regulated kinase) signal transduction cascade[63]. This signal transduction cascade can exert a tumor promoter-like function according to the classical two-step model of carcinogenesis[66]. Indeed, transgenic mice expressing the PreS2 activator MHBs^{t76} develop liver tumors at an age above 10 mo. Although the MHBs^{t76} protein is produced in very small but clearly detectable amounts in the MHBs^{t76} transgenic mice, a permanent activation of the Raf-1/MEK/ERK signal transduction cascade can be observed, resulting in an increased proliferation rate of the hepatocytes. The fact that MHBs^{t76} is produced in very small amounts ensures that the observed effects are not due to any overload-associated effects. The tumor formation in these mice can be explained by the permanent activation signal transduction cascades that exert a tumor promoter-like function[63]. Since tumor formation is observed in older animals, it can be assumed that during the aging process critical mutations are accumulated (initiation) and then the tumor promoter function positively selects these cells.

In case of the LHBs-transgenics, tumor formation can be observed as well[103]. In these mice, a very strong overproduction of the LHBs protein occurs, resulting in an intracellular accumulation of the protein and subsequent formation of ground glass hepatocytes. This permanent accumulation results in a situation comparable to a storage disease. Tumor formation in these transgenics was explained by the resulting permanent inflammation[103-105]. In light of the observation that LHBs can act as a regulatory protein, however, the regulatory protein function that is immanent to LHBs should be considered as an additional factor conferring to tumor formation in these mice. The overload-associated stress

and inflammation results in the formation of critical mutations (initiation) and the permanent activation of the PKC/Raf/MEK/ERK signal transduction cascade which exerts a tumor promoter-like function.

Immune pathogenesis of HCC

A major factor in the process of HBV-associated HCC development is the immune system[104,106,107]. The relevance of a chronic, virus-specific immune response for development of HBV-associated carcinoma was shown in an elegant experiment from F. Chisari`s laboratory[108]. Transgenic mice that produce non-cytopathic amounts of HBsAg were used. In these mice, immunologic tolerance against the transgene product can be observed. In accordance with this, no evidence of the liver disease was observed. These mice were subjected to thymectomy and lethally irradiated. One group was reconstituted with the bone marrow and spleen cells derived from non-transgenic littermates that were vaccinated with a recombinant HBsAg encoding vaccinia virus resulting in HBsAg-specific cytotoxic T lymphocytes (CTLs) and antibodies. The other group was reconstituted with the bone marrow and spleen cells derived from transgenic donors that were immunologically tolerant.

In this animal model, the development of hepatitis and later of chronic hepatitis and finally HCC development could be exclusively observed in the mice that were reconstituted with the bone marrow and spleen cells derived from the vaccinated non-transgenic animals, but not in the control groups. Based on this, it was concluded that the immune system-mediated chronic inflammation of the liver, continuous cell death and subsequent cell proliferation might increase the frequency of genetic alterations and the risk of cancer[104,109-111]. This scenario is not exclusively restricted to HBV. Chronic inflammation, degeneration and regeneration are common to a variety of human liver diseases, such as glycogen storage disease or alcoholism or HCV infection, that can finally result in liver carcinoma development[5]. This means that an ineffective immune response can be the principal oncogenic factor during a chronic HBV infection in man. In other words, the same T-cell response can have complete different effects: if the T cell response is strong enough, HBV can be eliminated from the liver, if not, a pro-carcinogenic effect can be induced by permanently triggering necro-inflammatory disease without resulting in a final eradication of HBV from the liver. An interesting aspect is that the nucleoside analogue on lamivudine in patients with chronic hepatitis B can induce the recovery of antiviral T cell responses. However, restoration of HBV-specific T cell reactivity is only transient. The transient nature of the immune reconstitution may represent a favorable condition for virus reactivation once lamivudine therapy is withdrawn.

CONCLUSION

At present, HBV-associated carcinogenesis can be seen as a multi-factorial process that includes both direct and indirect mechanisms that might act synergistically. The integration of HBV DNA into the host genome occurs at early steps of clonal tumor expansion. The integration has been shown in a number of cases to affect a variety of cancer-related genes and to exert insertional mutagenesis. The permanent liver inflammation resulting in a degeneration and regeneration process confers to the accumulation of critical mutations in the host genome. In addition, the regulatory proteins HBx and the PreS2 activators that can be encoded by the integrate can exert a tumor promoter-like function, resulting in positive selection of cells producing a functional regulatory protein.

Based on new technologies, including gene expression profiling and proteomics, it should be possible to further reveal the molecular mechanisms underlying HBV-associated HCC development and to identify novel diagnostic markers as well as therapeutic and preventive targets.

REFERENCES

1 **El-Serag HB**. Hepatocellular carcinoma: recent trends in the United States. *Gastroenterology* 2004; **127**: S27-S34
2 **Llovet JM**, Burroughs A, Bruix J. Hepatocellular carcinoma. *Lancet* 2003; **362**: 1907-1917
3 **Parkin DM**, Bray FI, Devesa SS. Cancer burden in the year 2000. The global picture. *Eur J Cancer* 2001; **37** Suppl 8: S4-S66
4 **Shibuya K**, Mathers CD, Boschi-Pinto C, Lopez AD, Murray CJ. Global and regional estimates of cancer mortality and incidence by site: II. Results for the global burden of disease 2000. *BMC Cancer* 2002; **2**: 37
5 **Blum HE**. Hepatocellular carcinoma: therapy and prevention. *World J Gastroenterol* 2005; **11**: 7391-7400
6 **Ahn SH**, Park YN, Park JY, Chang HY, Lee JM, Shin JE, Han KH, Park C, Moon YM, Chon CY. Long-term clinical and histological outcomes in patients with spontaneous hepatitis B surface antigen seroclearance. *J Hepatol* 2005; **42**: 188-194
7 **Evans AA**, O'Connell AP, Pugh JC, Mason WS, Shen FM, Chen GC, Lin WY, Dia A, M'Boup S, Dramé B, London WT. Geographic variation in viral load among hepatitis B carriers with differing risks of hepatocellular carcinoma. *Cancer Epidemiol Biomarkers Prev* 1998; **7**: 559-565
8 **Montalto G**, Cervello M, Giannitrapani L, Dantona F, Terranova A, Castagnetta LA. Epidemiology, risk factors, and natural history of hepatocellular carcinoma. *Ann N Y Acad Sci* 2002; **963**: 13-20
9 **Pollicino T**, Squadrito G, Cerenzia G, Cacciola I, Raffa G, Craxi A, Farinati F, Missale G, Smedile A, Tiribelli C, Villa E, Raimondo G. Hepatitis B virus maintains its pro-oncogenic properties in the case of occult HBV infection. *Gastroenterology* 2004; **126**: 102-110
10 **Block TM**, Mehta AS, Fimmel CJ, Jordan R. Molecular viral oncology of hepatocellular carcinoma. *Oncogene* 2003; **22**: 5093-5107
11 **Kew MC**. Synergistic interaction between aflatoxin B1 and hepatitis B virus in hepatocarcinogenesis. *Liver Int* 2003; **23**: 405-409
12 **Olivier M**, Hussain SP, Caron de Fromentel C, Hainaut P, Harris CC. TP53 mutation spectra and load: a tool for generating hypotheses on the etiology of cancer. *IARC Sci Publ* 2004; **(157)**: 247-270
13 **Velázquez RF**, Rodríguez M, Navascués CA, Linares A, Pérez R, Sotorríos NG, Martínez I, Rodrigo L. Prospective analysis of risk factors for hepatocellular carcinoma in patients with liver cirrhosis. *Hepatology* 2003; **37**: 520-527
14 **Hassan MM**, Hwang LY, Hatten CJ, Swaim M, Li D, Abbruzzese JL, Beasley P, Patt YZ. Risk factors for hepatocellular carcinoma: synergism of alcohol with viral hepatitis and diabetes mellitus. *Hepatology* 2002; **36**: 1206-1213

15 **Yang HI**, Lu SN, Liaw YF, You SL, Sun CA, Wang LY, Hsiao CK, Chen PJ, Chen DS, Chen CJ. Hepatitis B e antigen and the risk of hepatocellular carcinoma. *N Engl J Med* 2002; **347**: 168-174
16 **Kao JH**. Hepatitis B viral genotypes: clinical relevance and molecular characteristics. *J Gastroenterol Hepatol* 2002; **17**: 643-650
17 **Orito E**, Mizokami M. Hepatitis B virus genotypes and hepatocellular carcinoma in Japan. *Intervirology* 2003; **46**: 408-412
18 **Sugauchi F**, Kumada H, Acharya SA, Shrestha SM, Gamutan MT, Khan M, Gish RG, Tanaka Y, Kato T, Orito E, Ueda R, Miyakawa Y, Mizokami M. Epidemiological and sequence differences between two subtypes (Ae and Aa) of hepatitis B virus genotype A. *J Gen Virol* 2004; **85**: 811-820
19 **Chen CH**, Lee CM, Lu SN, Changchien CS, Eng HL, Huang CM, Wang JH, Hung CH, Hu TH. Clinical significance of hepatitis B virus (HBV) genotypes and precore and core promoter mutations affecting HBV e antigen expression in Taiwan. *J Clin Microbiol* 2005; **43**: 6000-6006
20 **Kao JH**, Chen PJ, Lai MY, Chen DS. Hepatitis B virus genotypes and spontaneous hepatitis B e antigen seroconversion in Taiwanese hepatitis B carriers. *J Med Virol* 2004; **72**: 363-369
21 **Yu MW**, Yeh SH, Chen PJ, Liaw YF, Lin CL, Liu CJ, Shih WL, Kao JH, Chen DS, Chen CJ. Hepatitis B virus genotype and DNA level and hepatocellular carcinoma: a prospective study in men. *J Natl Cancer Inst* 2005; **97**: 265-272
22 **Ni YH**, Chang MH, Wang KJ, Hsu HY, Chen HL, Kao JH, Yeh SH, Jeng YM, Tsai KS, Chen DS. Clinical relevance of hepatitis B virus genotype in children with chronic infection and hepatocellular carcinoma. *Gastroenterology* 2004; **127**: 1733-1738
23 **Kuang SY**, Jackson PE, Wang JB, Lu PX, Muñoz A, Qian GS, Kensler TW, Groopman JD. Specific mutations of hepatitis B virus in plasma predict liver cancer development. *Proc Natl Acad Sci USA* 2004; **101**: 3575-3580
24 **Liu CJ**, Chen BF, Chen PJ, Lai MY, Huang WL, Kao JH, Chen DS. Role of hepatitis B viral load and basal core promoter mutation in hepatocellular carcinoma in hepatitis B carriers. *J Infect Dis* 2006; **193**: 1258-1265
25 **Iloeje UH**, Yang HI, Su J, Jen CL, You SL, Chen CJ. Predicting cirrhosis risk based on the level of circulating hepatitis B viral load. *Gastroenterology* 2006; **130**: 678-686
26 **Beasley RP**, Hwang LY, Lin CC, Chien CS. Hepatocellular carcinoma and hepatitis B virus. A prospective study of 22 707 men in Taiwan. *Lancet* 1981; **2**: 1129-1133
27 **Brechot C**, Pourcel C, Louise A, Rain B, Tiollais P. Presence of integrated hepatitis B virus DNA sequences in cellular DNA of human hepatocellular carcinoma. *Nature* 1980; **286**: 533-535
28 **Paterlini-Bréchot P**, Saigo K, Murakami Y, Chami M, Gozuacik D, Mugnier C, Lagorce D, Bréchot C. Hepatitis B virus-related insertional mutagenesis occurs frequently in human liver cancers and recurrently targets human telomerase gene. *Oncogene* 2003; **22**: 3911-3916
29 **Thorgeirsson SS**, Grisham JW. Molecular pathogenesis of human hepatocellular carcinoma. *Nat Genet* 2002; **31**: 339-346
30 **Bruni R**, D'Ugo E, Villano U, Fourel G, Buendia MA, Rapicetta M. The win locus involved in activation of the distal N-myc2 gene upon WHV integration in woodchuck liver tumors harbors S/MAR elements. *Virology* 2004; **329**: 1-10
31 **Buendia MA**. Hepatitis B viruses and cancerogenesis. *Biomed Pharmacother* 1998; **52**: 34-43
32 **Fourel G**, Trepo C, Bougueleret L, Henglein B, Ponzetto A, Tiollais P, Buendia MA. Frequent activation of N-myc genes by hepadnavirus insertion in woodchuck liver tumours. *Nature* 1990; **347**: 294-298
33 **Hsu T**, Möröy T, Etiemble J, Louise A, Trépo C, Tiollais P, Buendia MA. Activation of c-myc by woodchuck hepatitis virus insertion in hepatocellular carcinoma. *Cell* 1988; **55**: 627-635
34 **Jacob JR**, Sterczer A, Toshkov IA, Yeager AE, Korba BE, Cote PJ, Buendia MA, Gerin JL, Tennant BC. Integration of woodchuck hepatitis and N-myc rearrangement determine size and histologic grade of hepatic tumors. *Hepatology* 2004; **39**: 1008-1016
35 **Wang J**, Chenivesse X, Henglein B, Bréchot C. Hepatitis B virus integration in a cyclin A gene in a hepatocellular carcinoma. *Nature* 1990; **343**: 555-557
36 **Bréchot C**, Gozuacik D, Murakami Y, Paterlini-Bréchot P. Molecular bases for the development of hepatitis B virus (HBV)-related hepatocellular carcinoma (HCC). *Semin Cancer Biol* 2000; **10**: 211-231
37 **Murakami Y**, Saigo K, Takashima H, Minami M, Okanoue T, Bréchot C, Paterlini-Bréchot P. Large scaled analysis of hepatitis B virus (HBV) DNA integration in HBV related hepatocellular carcinomas. *Gut* 2005; **54**: 1162-1168
38 **Horikawa I**, Barrett JC. cis-Activation of the human telomerase gene (hTERT) by the hepatitis B virus genome. *J Natl Cancer Inst* 2001; **93**: 1171-1173
39 **Hytiroglou P**, Theise ND. Telomerase activation in human hepatocarcinogenesis. *Am J Gastroenterol* 2006; **101**: 839-841
40 **Thorgeirsson SS**, Lee JS, Grisham JW. Functional genomics of hepatocellular carcinoma. *Hepatology* 2006; **43**: S145-S150
41 **Schlüter V**, Meyer M, Hofschneider PH, Koshy R, Caselmann WH. Integrated hepatitis B virus X and 3' truncated preS/S sequences derived from human hepatomas encode functionally active transactivators. *Oncogene* 1994; **9**: 3335-3344
42 **Chang SF**, Netter HJ, Hildt E, Schuster R, Schaefer S, Hsu YC, Rang A, Will H. Duck hepatitis B virus expresses a regulatory HBx-like protein from a hidden open reading frame. *J Virol* 2001; **75**: 161-170
43 **Twu JS**, Schloemer RH. Transcriptional trans-activating function of hepatitis B virus. *J Virol* 1987; **61**: 3448-3453
44 **Wollersheim M**, Debelka U, Hofschneider PH. A transactivating function encoded in the hepatitis B virus X gene is conserved in the integrated state. *Oncogene* 1988; **3**: 545-552
45 **Cougot D**, Neuveut C, Buendia MA. HBV induced carcinogenesis. *J Clin Virol* 2005; **34** Suppl 1: S75-S78
46 **Zhang X**, Zhang H, Ye L. Effects of hepatitis B virus X protein on the development of liver cancer. *J Lab Clin Med* 2006; **147**: 58-66
47 **Zoulim F**, Saputelli J, Seeger C. Woodchuck hepatitis virus X protein is required for viral infection *in vivo*. *J Virol* 1994; **68**: 2026-2030
48 **Blum HE**, Zhang ZS, Galun E, von Weizsäcker F, Garner B, Liang TJ, Wands JR. Hepatitis B virus X protein is not central to the viral life cycle *in vitro*. *J Virol* 1992; **66**: 1223-1227
49 **Hafner A**, Brandenburg B, Hildt E. Reconstitution of gene expression from a regulatory-protein-deficient hepatitis B virus genome by cell-permeable HBx protein. *EMBO Rep* 2003; **4**: 767-773
50 **Stöckl L**, Berting A, Malkowski B, Foerste R, Hofschneider PH, Hildt E. Integrity of c-Raf-1/MEK signal transduction cascade is essential for hepatitis B virus gene expression. *Oncogene* 2003; **22**: 2604-2610
51 **Melegari M**, Wolf SK, Schneider RJ. Hepatitis B virus DNA replication is coordinated by core protein serine phosphorylation and HBx expression. *J Virol* 2005; **79**: 9810-9820
52 **Reifenberg K**, Nusser P, Löhler J, Spindler G, Kuhn C, von Weizsäcker F, Köck J. Virus replication and virion export in X-deficient hepatitis B virus transgenic mice. *J Gen Virol* 2002; **83**: 991-996
53 **Bouchard MJ**, Wang L, Schneider RJ. Activation of focal adhesion kinase by hepatitis B virus HBx protein: multiple functions in viral replication. *J Virol* 2006; **80**: 4406-4414
54 **Bouchard MJ**, Wang LH, Schneider RJ. Calcium signaling by HBx protein in hepatitis B virus DNA replication. *Science* 2001; **294**: 2376-2378
55 **Waris G**, Siddiqui A. Regulatory mechanisms of viral hepatitis B and C. *J Biosci* 2003; **28**: 311-321
56 **Chan HL**, Sung JJ. Hepatocellular carcinoma and hepatitis B virus. *Semin Liver Dis* 2006; **26**: 153-161
57 **Koike K**, Tsutsumi T, Fujie H, Shintani Y, Kyoji M. Molecular mechanism of viral hepatocarcinogenesis. *Oncology* 2002; **62**

Suppl 1: 29-37
58 **Staib F**, Hussain SP, Hofseth LJ, Wang XW, Harris CC. TP53 and liver carcinogenesis. *Hum Mutat* 2003; **21**: 201-216
59 **Madden CR**, Slagle BL. Stimulation of cellular proliferation by hepatitis B virus X protein. *Dis Markers* 2001; **17**: 153-157
60 **Friedrich B**, Wollersheim M, Brandenburg B, Foerste R, Will H, Hildt E. Induction of anti-proliferative mechanisms in hepatitis B virus producing cells. *J Hepatol* 2005; **43**: 696-703
61 **Kekulé AS**, Lauer U, Weiss L, Luber B, Hofschneider PH. Hepatitis B virus transactivator HBx uses a tumour promoter signalling pathway. *Nature* 1993; **361**: 742-745
62 **Luber B**, Lauer U, Weiss L, Höhne M, Hofschneider PH, Kekulé AS. The hepatitis B virus transactivator HBx causes elevation of diacylglycerol and activation of protein kinase C. *Res Virol* 1993; **144**: 311-321
63 **Hildt E**, Munz B, Saher G, Reifenberg K, Hofschneider PH. The PreS2 activator MHBs(t) of hepatitis B virus activates c-raf-1/Erk2 signaling in transgenic mice. *EMBO J* 2002; **21**: 525-535
64 **Lucito R**, Schneider RJ. Hepatitis B virus X protein activates transcription factor NF-kappa B without a requirement for protein kinase C. *J Virol* 1992; **66**: 983-991
65 **Murakami S**, Cheong J, Ohno S, Matsushima K, Kaneko S. Transactivation of human hepatitis B virus X protein, HBx, operates through a mechanism distinct from protein kinase C and okadaic acid activation pathways. *Virology* 1994; **199**: 243-246
66 **Boutwell RK**. The function and mechanism of promoters of carcinogenesis. *CRC Crit Rev Toxicol* 1974; **2**: 419-443
67 **Madden CR**, Finegold MJ, Slagle BL. Hepatitis B virus X protein acts as a tumor promoter in development of diethylnitrosamine-induced preneoplastic lesions. *J Virol* 2001; **75**: 3851-3858
68 **Zhu H**, Wang Y, Chen J, Cheng G, Xue J. Transgenic mice expressing hepatitis B virus X protein are more susceptible to carcinogen induced hepatocarcinogenesis. *Exp Mol Pathol* 2004; **76**: 44-50
69 **Kim CM**, Koike K, Saito I, Miyamura T, Jay G. HBx gene of hepatitis B virus induces liver cancer in transgenic mice. *Nature* 1991; **351**: 317-320
70 **Benn J**, Schneider RJ. Hepatitis B virus HBx protein activates Ras-GTP complex formation and establishes a Ras, Raf, MAP kinase signaling cascade. *Proc Natl Acad Sci USA* 1994; **91**: 10350-10354
71 **Klein NP**, Bouchard MJ, Wang LH, Kobarg C, Schneider RJ. Src kinases involved in hepatitis B virus replication. *EMBO J* 1999; **18**: 5019-5027
72 **Klein NP**, Schneider RJ. Activation of Src family kinases by hepatitis B virus HBx protein and coupled signaling to Ras. *Mol Cell Biol* 1997; **17**: 6427-6436
73 **Sirma H**, Weil R, Rosmorduc O, Urban S, Israël A, Kremsdorf D, Bréchot C. Cytosol is the prime compartment of hepatitis B virus X protein where it colocalizes with the proteasome. *Oncogene* 1998; **16**: 2051-2063
74 **Huh KW**, Siddiqui A. Characterization of the mitochondrial association of hepatitis B virus X protein, HBx. *Mitochondrion* 2002; **1**: 349-359
75 **Lee YI**, Hwang JM, Im JH, Lee YI, Kim NS, Kim DG, Yu DY, Moon HB, Park SK. Human hepatitis B virus-X protein alters mitochondrial function and physiology in human liver cells. *J Biol Chem* 2004; **279**: 15460-15471
76 **Waris G**, Huh KW, Siddiqui A. Mitochondrially associated hepatitis B virus X protein constitutively activates transcription factors STAT-3 and NF-kappa B via oxidative stress. *Mol Cell Biol* 2001; **21**: 7721-7730
77 **Maguire HF**, Hoeffler JP, Siddiqui A. HBV X protein alters the DNA binding specificity of CREB and ATF-2 by protein-protein interactions. *Science* 1991; **252**: 842-844
78 **Haviv I**, Shamay M, Doitsh G, Shaul Y. Hepatitis B virus pX targets TFIIB in transcription coactivation. *Mol Cell Biol* 1998; **18**: 1562-1569
79 **Haviv I**, Vaizel D, Shaul Y. pX, the HBV-encoded coactivator, interacts with components of the transcription machinery and stimulates transcription in a TAF-independent manner. *EMBO J* 1996; **15**: 3413-3420
80 **Becker SA**, Lee TH, Butel JS, Slagle BL. Hepatitis B virus X protein interferes with cellular DNA repair. *J Virol* 1998; **72**: 266-272
81 **Wentz MJ**, Becker SA, Slagle BL. Dissociation of DDB1-binding and transactivation properties of the hepatitis B virus X protein. *Virus Res* 2000; **68**: 87-92
82 **Madden CR**, Finegold MJ, Slagle BL. Expression of hepatitis B virus X protein does not alter the accumulation of spontaneous mutations in transgenic mice. *J Virol* 2000; **74**: 5266-5272
83 **Lee SG**, Rho HM. Transcriptional repression of the human p53 gene by hepatitis B viral X protein. *Oncogene* 2000; **19**: 468-471
84 **Elmore LW**, Hancock AR, Chang SF, Wang XW, Chang S, Callahan CP, Geller DA, Will H, Harris CC. Hepatitis B virus X protein and p53 tumor suppressor interactions in the modulation of apoptosis. *Proc Natl Acad Sci USA* 1997; **94**: 14707-14712
85 **Ueda H**, Ullrich SJ, Gangemi JD, Kappel CA, Ngo L, Feitelson MA, Jay G. Functional inactivation but not structural mutation of p53 causes liver cancer. *Nat Genet* 1995; **9**: 41-47
86 **Kekulé AS**, Lauer U, Meyer M, Caselmann WH, Hofschneider PH, Koshy R. The preS2/S region of integrated hepatitis B virus DNA encodes a transcriptional transactivator. *Nature* 1990; **343**: 457-461
87 **Caselmann WH**, Meyer M, Kekulé AS, Lauer U, Hofschneider PH, Koshy R. A trans-activator function is generated by integration of hepatitis B virus preS/S sequences in human hepatocellular carcinoma DNA. *Proc Natl Acad Sci USA* 1990; **87**: 2970-2974
88 **Lauer U**, Weiss L, Hofschneider PH, Kekulé AS. The hepatitis B virus pre-S/S(t) transactivator is generated by 3′ truncations within a defined region of the S gene. *J Virol* 1992; **66**: 5284-5289
89 **Levrero M**, Balsano C, Avantaggiati ML, Natoli G, Chirillo P, De Marzio E, Collepardo D, Costanzo A. Characterization of the hepatitis B virus transactivators: a possible direct role of the virus in the development of hepatocellular carcinoma. *J Surg Oncol Suppl* 1993; **3**: 34-36
90 **Natoli G**, Avantaggiati ML, Balsano C, De Marzio E, Collepardo D, Elfassi E, Levrero M. Characterization of the hepatitis B virus preS/S region encoded transcriptional transactivator. *Virology* 1992; **187**: 663-670
91 **Natoli G**, Balsano C, Avantaggiati ML, De Marzio E, Artini M, Collepardo D, Elfassi E, Levrero M. Truncated pre-S/S proteins transactivate multiple target sequences. *Arch Virol Suppl* 1992; **4**: 65-69
92 **Hildt E**, Urban S, Lauer U, Hofschneider PH, Kekulé AS. ER-localization and functional expression of the HBV transactivator MHBst. *Oncogene* 1993; **8**: 3359-3367
93 **Meyer M**, Caselmann WH, Schlüter V, Schreck R, Hofschneider PH, Baeuerle PA. Hepatitis B virus transactivator MHBst: activation of NF-kappa B, selective inhibition by antioxidants and integral membrane localization. *EMBO J* 1992; **11**: 2991-3001
94 **Caselmann WH**, Renner M, Schlüter V, Hofschneider PH, Koshy R, Meyer M. The hepatitis B virus MHBst167 protein is a pleiotropic transactivator mediating its effect via ubiquitous cellular transcription factors. *J Gen Virol* 1997; **78** (Pt 6): 1487-1495
95 **Jüngst C**, Cheng B, Gehrke R, Schmitz V, Nischalke HD, Ramakers J, Schramel P, Schirmacher P, Sauerbruch T, Caselmann WH. Oxidative damage is increased in human liver tissue adjacent to hepatocellular carcinoma. *Hepatology* 2004; **39**: 1663-1672
96 **Xu Z**, Jensen G, Yen TS. Activation of hepatitis B virus S promoter by the viral large surface protein via induction of stress in the endoplasmic reticulum. *J Virol* 1997; **71**: 7387-7392
97 **Hildt E**, Urban S, Hofschneider PH. Characterization of essential domains for the functionality of the MHBst transcriptional activator and identification of a minimal MHBst activator. *Oncogene* 1995; **11**: 2055-2066
98 **Hildt E**, Urban S, Eckerskorn C, Hofschneider PH. Isolation

of highly purified, functional carboxy-terminally truncated hepatitis B virus middle surface protein activators from eucaryotic expression systems. *Hepatology* 1996; **24**: 502-507
99 **Bruss V**, Lu X, Thomssen R, Gerlich WH. Post-translational alterations in transmembrane topology of the hepatitis B virus large envelope protein. *EMBO J* 1994; **13**: 2273-2279
100 **Ostapchuk P**, Hearing P, Ganem D. A dramatic shift in the transmembrane topology of a viral envelope glycoprotein accompanies hepatitis B viral morphogenesis. *EMBO J* 1994; **13**: 1048-1057
101 **Prange R**, Streeck RE. Novel transmembrane topology of the hepatitis B virus envelope proteins. *EMBO J* 1995; **14**: 247-256
102 **Hildt E**, Saher G, Bruss V, Hofschneider PH. The hepatitis B virus large surface protein (LHBs) is a transcriptional activator. *Virology* 1996; **225**: 235-239
103 **Chisari FV**, Klopchin K, Moriyama T, Pasquinelli C, Dunsford HA, Sell S, Pinkert CA, Brinster RL, Palmiter RD. Molecular pathogenesis of hepatocellular carcinoma in hepatitis B virus transgenic mice. *Cell* 1989; **59**: 1145-1156
104 **Chisari FV**. Rous-Whipple Award Lecture. Viruses, immunity, and cancer: lessons from hepatitis B. *Am J Pathol* 2000; **156**: 1117-1132
105 **Dunsford HA**, Sell S, Chisari FV. Hepatocarcinogenesis due to chronic liver cell injury in hepatitis B virus transgenic mice. *Cancer Res* 1990; **50**: 3400-3407
106 **Rehermann B**. Immune responses in hepatitis B virus infection. *Semin Liver Dis* 2003; **23**: 21-38
107 **Rehermann B**, Nascimbeni M. Immunology of hepatitis B virus and hepatitis C virus infection. *Nat Rev Immunol* 2005; **5**: 215-229
108 **Nakamoto Y**, Guidotti LG, Kuhlen CV, Fowler P, Chisari FV. Immune pathogenesis of hepatocellular carcinoma. *J Exp Med* 1998; **188**: 341-350
109 **Chisari FV**, Pinkert CA, Milich DR, Filippi P, McLachlan A, Palmiter RD, Brinster RL. A transgenic mouse model of the chronic hepatitis B surface antigen carrier state. *Science* 1985; **230**: 1157-1160
110 **Ferrari C**, Missale G, Boni C, Urbani S. Immunopathogenesis of hepatitis B. *J Hepatol* 2003; **39** Suppl 1: S36-S42
111 **Visvanathan K**, Lewin SR. Immunopathogenesis: role of innate and adaptive immune responses. *Semin Liver Dis* 2006; **26**: 104-115

S- Editor Liu Y **L- Editor** Kumar M **E- Editor** Ma WH

PO Box 2345, Beijing 100023, China
www.wjgnet.com
wjg@wjgnet.com

World J Gastroenterol 2007 January 7; 13(1): 82-90
World Journal of Gastroenterology ISSN 1007-9327

TOPIC HIGHLIGHT

Dieter Glebe, PhD, *Series Editor*

Pathogenesis of hepatitis B virus infection

Thomas F Baumert, Robert Thimme, Fritz von Weizsäcker

Thomas F Baumert, Robert Thimme, Fritz von Weizsäcker, Department of Medicine II, University of Freiburg, Freiburg, Germany
Thomas F Baumert, INSERM U748, Université Louis Pasteur Strasbourg, France
Fritz von Weizsäcker, Schlosspark-Klinik, Charité, Humboldt University, Berlin, Germany
Correspondence to: Fritz von Weizsäcker, MD, Department of Medicine I, Schlosspark Klinik, Teaching Hospital of the Charité, Humboldt University, Heubnerweg 2, D-14059 Berlin, Germany. fritz.weizsaecker@schlosspark-klinik.de
Telephone: +49-30-32641302 Fax: +49-30-32641300
Received: 2006-08-02 Accepted: 2006-11-04

Abstract

Infection with hepatitis B virus (HBV) leads to a wide spectrum of clinical presentations ranging from an asymptomatic carrier state to self-limited acute or fulminant hepatitis to chronic hepatitis with progression to cirrhosis and hepatocellular carcinoma. Infection with HBV is one of the most common viral diseases affecting man. Both viral factors as well as the host immune response have been implicated in the pathogenesis and clinical outcome of HBV infection. In this review, we will discuss the impact of virus-host interactions for the pathogenesis of HBV infection and liver disease. These interactions include the relevance of naturally occurring viral variants for clinical disease, the role of virus-induced apoptosis for HBV-induced liver cell injury and the impact of antiviral immune responses for outcome of infection.

Key words: Host response; Viral hepatitis; Mutants; Pathogenesis; Resistance

Baumert TF, Thimme R, von Weizsäcker F. Pathogenesis of hepatitis B virus infection. *World J Gastroenterol* 2007; 13(1): 82-90

http://www.wjgnet.com/1007-9327/13/82.asp

MOLECULAR VIROLOGY OF HEPATITIS B VIRUS INFECTION

Hepatitis B virus (HBV) is a small DNA virus and belongs to a group of hepatotropic DNA viruses (hepadnaviruses)[1,2]. The virus consists of a nucleocapsid and an outer envelope composed mainly of three hepatitis B surface antigens (HBsAgs) that play a central role in the diagnosis of HBV infection. The nucleocapsid contains hepatitis B core antigen (HBcAg), a DNA polymerase-reverse transcriptase, the viral genome as well as cellular proteins[1,2].

The genome consists of a partially double-stranded circular DNA molecule of about 3200 base pairs in length with known sequence as well as genetic organization. The pre-surface 1 [pre-S1]/pre-surface 2 [pre-S2]/and surface genes [S] code for the various HBsAgs. The protein encoded by the pre-core [pre-C]/core gene [C] undergoes post-translational modification to yield hepatitis B e antigen (HBeAg), which is a seromarker for high viral replication[2]. The core gene codes for HBcAg, the major structural protein of the nucleocapsid. Finally, the X gene codes for the hepatitis B x antigen (HBxAg). HBxAg has been shown to be a potent transactivator of cellular and viral genes. A variety of interactions with cellular proteins has been proposed as potential targets of HBxAg. The precise functions of HBxAg, however, in the viral life cycle and the natural course of HBV infection remain to be established. In addition to the known viral genes, several *cis*- and *trans*-acting genetic elements involved in the fine control of gene expression, RNA packaging and viral replication have been identified[1,2].

The viral DNA polymerase-reverse transcriptase is encoded by the polymerase gene [P] and is of central importance for viral replication. Different from all known mammalian DNA viruses, hepadnaviruses replicate *via* reverse transcription of a RNA intermediate[3,4], the pregenomic RNA, which is a strategy central to the life cycle of RNA retroviruses. Similarities and differences between retroviral and hepadnaviral replication have been defined[1]. Based on the unique replication cycle of HBV, antiviral therapeutic strategies aimed at the reverse transcription of HBV RNA or at HBV reverse transcriptase have been successfully used as antivirals to treat HBV infection[5-13].

VIRAL VARIANTS AND PATHOGENESIS OF INFECTION

Evidence has been accumulating that certain HBV mutants are associated with unique clinical manifestations, may affect the natural course of the infection and confer

resistance to antiviral agents (Table 1)[14-17]. Naturally occurring mutations in the context of various genotypes have been identified in the structural and non-structural genes as well as regulatory elements of the virus. The best characterized mutants are the pre-core (pre-C) stop codon mutations resulting in a loss of hepatitis B e antigen[18], defined clusters of mutations in the core promoter resulting in enhanced viral replication[19-21], and mutations in the reverse transcriptase/polymerase genes conferring resistance to antivirals[16,22]. Furthermore, several mutations in the HBV surface gene have been identified which alter the antigenicity of the viral surface proteins (HBsAg) and structure of the viral envelope[15,23].

Table 1 HBV variants and their potential impact for pathogenesis of HBV infection

HBV region	Mutation	Molecular phenotype	Clinical relevance
Pre-S/S	Pre-S1/ pre-S2/ S-promotor	Misassembly	Fibrosing cholestatic hepatitis
	S	Alteration of B- and T-cell epitopes	Vaccine escape
	S splicing		Immune escape
			Diagnostic escape
Pre-C	Pre-C-stop	Loss of HBeAg	Severe hepatitis
			HBeAg-deficiency
Core	Core	Alteration of T-cell epitopes	Viral persistence
			Severe hepatitis
RT/Pol	Pol	Replication deficiency	Viral latency
			Viral persistence
	Pol	Resistance to antivirals	Therapy escape
Regulatory Elements	Core promotor	Enhanced replication and core expression	Severe hepatitis
			Modulation of drug resistance
		Decreased HBeAg synthesis	HBeAg seronegativity
	Enhancer I	Decreased replication	Chronic hepatitis

HBV genomic region, mutation, molecular phenotype and clinical relevance are indicated.

HBeAg variants and HBeAg-seronegativity

One of the first HBV mutations clinically recognized and functionally characterized was the pre-C stop codon mutation, resulting in a loss of HBeAg. Not all patients with chronic hepatitis B become HBV DNA negative, despite seroconversion from HBeAg to anti-HBe. Numerous studies have shown that these patients are infected with a pre-C/C mutant[24,25]. This mutant has a translation stop codon at the end of the pre-C gene. Thus, the pre-C/C fusion protein, a precursor of HBeAg, cannot be synthesized. In these patients, therefore, viral replication may persist despite elimination of HBeAg and seroconversion to anti-HBe. While the loss of HBeAg appears irrelevant for the biology of the virus, it may play an important role in the interaction of the virus with the immune system. Secreted HBeAg has been proposed to have an immunoregulatory function *in utero* by establishing T-cell tolerance to HBeAg and HBcAg that may predispose neonates born to HBV-infected mothers to develop persistent HBV infection[26]. Recent studies have further demonstrated an immunomodulatory role of HBeAg in antigen presentation and recognition by $CD4^+$ T-cells[27]. The selection of HBeAg mutants in the host may be due in part to immunomodulatory properties of HBeAg resulting in a survival advantage for the virus[28]. Whether and how this mutation - either alone or in combination with other mutations - affects the clinical course of HBV infection is still unclear.

Of interest in this respect is the observation that pre-C stop codon mutants are found not only in patients with fulminant hepatitis[18,29-32] or chronic active hepatitis B[24,25,33-35], but also in asymptomatic HBV carriers[32] or acute, self-limited hepatitis [36]. In the woodchuck model, the pre-C stop codon mutation was found to exert no effect on viral replication or the severity of liver disease. Infections with the pre-C stop codon mutant, however, did not take a chronic course[37]. Interestingly, in the duck hepatitis B virus model the pre-C stop codon mutant replicates less well and is overgrown by wild-type virus during the natural course of coinfection[38].

Core promoter variants and enhanced viral replication

During the last couple of years mutations have been identified in regulatory genetic elements of the HBV genome. Several independent studies have identified and functionally characterized distinct mutations clustered in enhancer Ⅱ of the HBV core promotor. Core promoter mutations are predominantly found in patients with a more aggressive course of disease such as fulminant[19,39-41] or chronic hepatitis B[21,33,42-45]. Some of the patients have a decrease or loss of HBeAg[39,43].

A common hallmark of core promoter mutations is the biological phenotype of enhanced viral replication in transfected hepatoma cell lines[19,21,33,39-44] and primary hepatocytes[20]. The most prevalent mutant comprises a double mutation (A to T at nucleotide 1764 and G to A at nucleotide 1766, nucleotide numbering according to[46] located at the 3`end of enhancer Ⅱ of the basal core promotor being present in up to 80% of individuals chronically infected with HBV[47].

Several other core promotor mutations in immuncompromized patients and severe or fulminant liver disease have been identified[41,42,45]. A common phenotype of these mutations seems to be the enhanced viral encapsidation by altering the balance between pre-C and C RNA transcript levels[42]. Several of these mutations have been shown to create additional transcription factor (HNF-1, HNF-3, HNF-4 or C/EBP) binding sites[41,42,48]. The magnitude of mutant-induced enhancement of viral replication seems to be dependent on the HBV subtype/genotype[40,49].

The phenotype of enhanced viral replication may be the reason why core promoter mutants seem to be selected in immunosuppressed patients or patients with chronic hepatitis. Interestingly, one study suggested the presence of core promotor mutations was significantly associated with the development of hepatocellular carcinoma (HCC)[50]. Furthermore, the high-replication phenotype of viral strains containing core promotor mutations may play a role in the pathogenesis of more aggressive or severe disease associated with these mutations. Interestingly, the

transmission of a high-replication strain containing two core promotor mutations and the pre-C mutation to HBV-naive patients has resulted in an outbreak of fulminant fatal hepatitis[19]. Enhanced viral replication with the concomitant increase in viral protein expression may result in a differential immune response as well as a more rapid and widespread infection in naive patients[19,20,40]. Altered viral kinetics accompanied by a more vigorous cellular immune response may be important mechanisms resulting in more severe liver injury and potentially fulminant hepatitis. Another factor contributing to fulminant hepatic failure associated with defined core promoter mutations may be hepatocyte apoptosis induced by the HBV variant[20]. Since not all patients with fulminant hepatitis are infected with HBV strains exhibiting a high-replication phenotype[51] additional mechanisms for the pathogenesis of fulminant hepatitis likely exist[52].

Variants of HBsAg and immune escape

A variety of mutations have been identified in the HBV structural genes resulting in differential antigen recognition and immune response[53]. During the course of a passive-active HBV immunization program in southern Italy, several children were infected with HBV despite a primary response to the HBsAg vaccine. Molecular analyses showed that one of these children was infected with a HBV mutant[54,55]. This mutant exhibited a defect in the S region of the HBV genome (glycine (Gly) to arginine (Arg) at amino acid position 145) with loss of the group-specific antigenic determinant a, which is the main target of the vaccine response. Further biological characterization of this mutant in the context of replication-competent viral genomes revealed that this mutation also results in impaired S secretion and decreased virion stability[56]. This viral mutant was able to escape the immune surveillance and thereby resulted in an infection despite the presence of anti-HBs antibodies ('vaccine escape mutant'). Similar mutants have been detected in Japan[57] and the Gambia[58] and presumably occur world-wide[53]. Consistent with these initial observations, a recent study demonstrated the accumulation of HBsAg a determinant mutants during the implementation of universal vaccination programs in Taiwan[59]. In contrast to these epidemiological observations, a study in the chimpanzee model using currently available US-licensed HBV vaccines demonstrated protection against the 'classical' vaccine escape (Gly-145-Arg) mutant *in vivo*. This study provides strong evidence that immunization with recombinant HBV vaccines stimulates anti-HBs that is broadly reactive and protects the host efficiently from infection with HBV strains containing the Gly-145-Arg mutant[60]. Since this study only evaluated the protective properties of licensed HBV vaccines against the Gly-145-Arg mutant, it does not exclude the possibility that other genuine vaccine escape mutants result in immunization failure[60]. Further studies are needed to address this issue. In addition to immune escape on the B cell level, vaccine escape mediated by defined HBsAg epitopes can occur on the T cell level[61]. Taken together, these findings indicate, that careful epidemiologic monitoring of vaccine failure caused by infection with HBV mutants may be crucial for the success of global immunization strategies.

'Immune escape mutants' have also been reported in patients after liver transplantation for HBV-related chronic liver disease who had received monoclonal or polyclonal anti-HBs antibodies to prevent reinfection of the graft[62-65]. 'Immune escape mutants' have also been identified in anti-HBs positive individuals[57,66].

In addition to 'vaccine escape mutants' and 'immune escape mutants', 'diagnosis escape mutants' have been described, since most of the HBsAg detection assays are based on anti-HBs antibodies[57,67]. Diagnostic escape may also be the result of a posttranscriptional effect of viral mutations on HBsAg expression as described by Hass *et al* in an elegant study isolating a naturally occurring mutation targeting splicing of subgenomic RNA[68,69]. The emergence of these variants may potentially contribute to occult HBsAg-negative HBV infection[70].

Mutations have further been detected in the pre-S1 or pre-S2 regions of the HBV genome. Their clinical significance is as yet unknown, however. Since the preS1 region appears to be important for the very first steps of viral infection[71,72], it is conceivable that variants affecting this region may also affect the biological phenotype of the virus by altering its ability to bind or infect hepatocytes. A pre-S2 defective HBV variant has been associated with fulminant hepatitis B[73]. A cluster of mutations in the S promotor (two deletions and a point mutation in the regulatory element CCAAT) isolated from a patient with fibrosing cholestatic hepatitis after HBV reinfection of the transplanted liver has been shown to result in virus retention and misassembly[74,75]. Furthermore, a recent study demonstrates evidence that patients with progressive liver disease have a higher frequency of pre-S deletion[76]. HBsAg variants resulting in a defect or impairment in virion secretion have also been described in severe and fulminant hepatitis B[56,77].

Mutations conferring resistance to antiviral therapy

In recent years polymerase gene mutants have been identified in patients treated with antiviral drugs, resulting in drug resistance, respectively[78]. Lamivudine, a nucleoside analogue, is a potent inhibitor of HBV replication and is clinically used as an antiviral for the treatment of chronic hepatitis B and advanced HBV-induced liver disease[11,12,79,80]. Adefovir is an alternative nucleotide analogue previously licensed for the treatment of chronic hepatitis B[9,10]. Other nucleoside analogues currently under clinical investigations include entecavir, emtricitabine, clevudine and telbivudine[16,78]. Several of these drugs act as chain-terminators during the synthesis of the nascent DNA strand, thereby terminating viral replication[16]. Other nucleoside or nucleotide analogues such as adefovir and entecavir interfere with priming and minus-strand DNA elongation[16]. Adefovir and-to a lesser extent-lamivudine also target initial plus-strand DNA repair[81].

The selection of drug resistant mutants depends on several factors. As the viral polymerase is subjected to a spontaneous error rate, viral mutants accumulate during the natural course of the disease. When an antiviral pressure is applied, the mutations exhibiting the best replication capacity in the presence of the drug

are selected. The mutant spread depends on its level of intrinsic resistance and on its replicative fitness[16]. This may explain in part why the peaks of drug resistance observed with lamivudine (23% at year one and up to 65% at year five of treatment[82,83]) and with adefovir dipivoxil (2% at two years and 3.9% at three years of treatment[84,85]) are different.

These mutant viral genomes are characterized by selective amino acid changes in various domains of the HBV reverse transcriptase/polymerase. In particular, lamivudine resistance has been extensively studied. The reverse transcriptase polymerase of HBV and HIV share a common and highly conserved tyrosine, methionine, aspartate, aspartate (YMDD) nucleotide-binding motif in the catalytic domain of the enzyme. Similar to the development of lamivudine-resistant HIV mutants, lamivudine treatment of patients with chronic HBV infection results in drug-resistant strains, characterized by YMDD to YIDD (tyrosine, isoleucin, aspartate, aspartate; "M204I") or YVDD (tyrosine, valine, aspartate, aspartate; "M204V") mutations in the catalytic C-domain of the reverse transcriptase[16,86]. Interestingly, the mutant genomes exhibited lower levels of replication when compared with wild-type genomes[87]. Further studies identified additional mutations in the neighboring B domain (V173L and L180M[88]). Interestingly, these mutations can restore partially the replication capacity of the C-domain mutations[88].

In contrast to lamivudine, viral resistance to adefovir appears to be mediated pre-dominantly by a mutation in the D-domain[84]. The N236T mutation confers only a 5-10-fold resistance to adefovir[84], which may explain the delayed emergence of this mutant[16]. Another mutation A181V located in the B-domain has been described[16]. Three recently isolated cases of primary adefovir resistance were due to a mutation comprising I233V. Interestingly, the viral variants containing this mutation were sensitive to tenofovir[22]. Drug resistance due to viral mutations in the reverse transcriptase/polymerase represents an important clinical issue in the management of chronic hepatitis B and may ultimately require the development of novel treatment approaches including the combination of various antiviral strategies[16,78].

In summary, a large variety of HBV mutations associated with various pathological conditions as well as drug resistance have been isolated and described in detail[15]. Studies *in vitro* as well as *in vivo* have defined the functional relevance of several viral mutants. Furthermore, these studies provided important clues for the understanding of the impact of these mutants on the pathogenesis of disease and the molecular characterization of drug resistance. Functional studies of mutants in established and emerging HBV *in vivo* models[89] may ultimately allow confirmation of the relationship between defined mutations and their clinical relevance[15].

MECHANISMS OF HBV-INDUCED LIVER DISEASE: APOPTOSIS

The induction of apoptosis is a hallmark of many viruses infecting humans. Although HBV is considered as a non-cytopathic virus[14], hepadnavirus-induced apoptosis and cytopathic effects have been described in several experimental model systems: First, a duck hepatitis B variant containing a single amino acid change in the large surface antigen resulting in accumulation of cccDNA resulted in a strong cytopathic effect in hepatocytes in *vitro* and *in vivo*[90-92]. In this system, the level of viral replication and cccDNA formation correlated with cytopathic effects in infected hepatocytes[90]. Second, intracellular retention of the HBV large surface protein has been shown to induce apoptosis in cell lines[93,94]. In this model overexpression of the large surface antigen resulted in cellular vacuolization and apoptosis of transfected hepatoma cells[94]. Third, the HBX protein has been suggested to induce apoptosis in both a p53-dependent and p53-independent manner[95-97]. Exploring the mechanism of these previous observations, a recent study has elegantly demonstrated that HBX interacts with c-FLIP, a key regulator of the death-inducing signaling complex[96]. Recruitment of c-FLIP to the death-inducing signaling complex is inhibited by HBX resulting in hyperactivation of caspase-8 and caspase-3 by death signals[96]. Finally, a viral variant containing two core promoter mutations associated with fulminant hepatitis has been shown to induce apoptosis in primary Tupaia hepatocytes[20]. Interestingly, in the latter model induction of apoptosis was independent of viral replication suggesting that viral protein synthesis was sufficient for the virus-induced hepatocyte cell death. Since the two core promoter mutations resulted in two amino acid changes of the HBX protein, the HBX protein may be a potential candidate mediating this effect[20]. Further studies in animal model systems are needed to elucidate the impact of HBV-induced apoptosis for HBV-induced liver injury[20].

IMMUNOPATHOGENESIS OF HBV INFECTION

Apart from direct biological effects of viral variants (Table 1) there is growing consensus that the host immune response, especially the virus-specific T cell response[98], is the key determinant influencing the course of disease and the onset of liver disease.

Successful immune response.

A genomic array analysis using liver RNA obtained at multiple time points after HBV infection in chimpanzees demonstrated that HBV did not induce any genes during entry and expansion[99], suggesting it is a stealth virus early in the infection. In contrast, a large number of T cell-derived IFN-gamma-regulated genes were induced in the liver during viral clearance[99], reflecting the impact of an adaptive T cell response that inhibits viral replication and kills infected cells, thereby terminating the infection. These results are in agreement with several studies performed in acutely infected patients suggesting an important role of the adaptive T cell response[98,100-105]. Indeed, several studies have shown that the peripheral blood cytotoxic T lymphocyte (CTL) response to HBV is polyclonal and multispecific in patients with acute viral hepatitis and that

it persists indefinitely after recovery, when it is maintained by continued antigenic stimulation by residual virus that persists, apparently harmlessly, in healthy convalescent individuals[106]. In contrast, the CTL response to HBV is relatively weak in patients with chronic HBV infection, except during spontaneous disease flares or interferon (IFN) induced recovery, when it is readily detectable[101,104]. These earlier studies have been confirmed by using new techniques, such as the tetramer technology. By using this approach, Maini *et al*[100] could, for example, show that multispecific HBV-specific $CD8^+$ T cell responses are detectable during the acute phase of self-limited infection and decline thereafter. Of note, a recent study could also demonstrate that HBV-specific $CD8^+$ T cells accumulate in the infected organ, i.e., the liver, where they remain detectable at high frequencies even after HBsAg seroconversion[107].

Studies in the HBV transgenic mouse model revealed that, in addition to causing viral hepatitis, virus-specific T cells as well as NK and NKT cells can abolish HBV expression and replication without killing the hepatocytes and that this antiviral activity is mediated by interferon gamma (IFNγ) and tumor necrosis factor alpha (TNFα)[104,108,109] (Figure 1). Importantly, studies in the chimpanzee model indicated that the same events are operative during natural infection. Indeed, in these studies it was shown that the early phase of HBV clearance was temporally associated with the appearance of CD3, CD8 and IFNγ in the liver, which reflects the influx of T cells into the liver[110]. Of note, there was only limited liver disease during this time although almost 100% of hepatocytes were infected, clearly suggesting that noncytopathic mechanisms were active during this early phase of viral clearance. In contrast, the final elimination of the virus that occurred several weeks later occurred in the presence of significant liver disease, indicating the presence of cytopathic effector functions that are probably mediated by virus-specific T cells[110].

To determine which subset of T cells is responsible for viral clearance and liver disease, the course of HBV infection in chimpanzees that were depleted of its $CD4^+$ or $CD8^+$ cells was monitored[111]. Depletion of $CD4^+$ cells did not significantly alter the course of infection. In contrast to the minor effects observed during CD4-depletion, CD8-depletion greatly prolonged the infection and delayed the onset of viral clearance and liver disease until $CD8^+$ T cells reappeared in the circulation and virus-specific $CD8^+$ T cells entered the liver[111]. Indeed, in the absence of $CD8^+$ cells, the duration of peak infection was prolonged and the time of onset of the initial decrease in HBV DNA levels and increase in serum ALT activity was delayed. In addition, the time required for both the first phase of viral clearance and for the final elimination of the virus was markedly delayed and prolonged in the CD8-depleted animal. It is important to note that the reappearance of $CD8^+$ cells correlated with the appearance of IFNγ producing virus-specific $CD8^+$ T cells in the liver, the onset of a mild liver disease, the appearance of IFNγ mRNA in the liver and a 50 fold reduction in total liver HBV DNA[111]. These results suggest that HBV

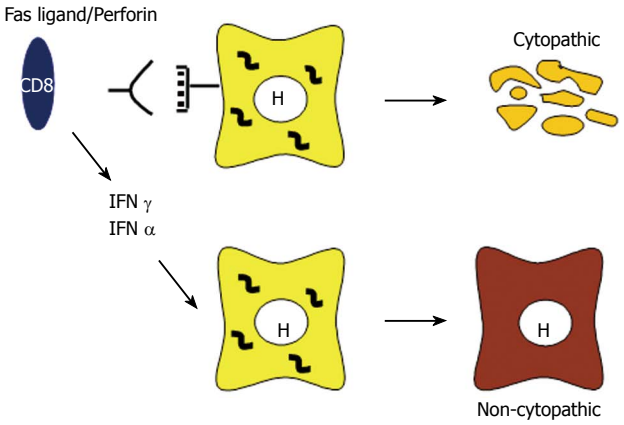

Figure 1 Cytopathic and non-cytopathic T cell responses against HBV infection.

replication is inhibited early and non-cytopathically in a CD8 dependent and probably IFNγ associated manner. The final elimination of the virus occurred several months later and was associated with a rebound of $CD8^+$ cells to baseline levels, a surge of the intrahepatic $CD8^+$ T cell response, a surge in intrahepatic IFNγ mRNA and a surge in sALT activity. Thus, these results demonstrate that intrahepatic HBV-specific $CD8^+$ T cells are required for rapid viral clearance during acute HBV infection. In addition, the data suggest the existence of dual antiviral functions that overlap temporally during natural infection but can be clearly separated by CD8 depletion: a primarily noncytolytic $CD8^+$ dependent mechanism that may be mediated by IFNγ and a primarily cytolytic mechanism that clears the remaining infected cells. It is also important to note that virus-specific $CD8^+$ T cells display oscillating effector functions during the course of infection that seem primarily influenced by the interaction of the T cells with the antigen-presenting cells[112,113].

T cell failure

In contrast to the strong and multispecific T cell responses observed during acute self-limited HBV infection, patients with chronic hepatitis B tend to have weak and narrowly focused immune responses[98]. The mechanisms that contribute to the failure of the virus-specific T cell response in chronically infected patients are only poorly understood and may include T cell deletion, anergy, exhaustion, ignorance and T cell dysfunction. HBV establishes chronic hepatitis mainly by vertical transmission from HBV infected mothers to neonates. The immunomodulatory effects of the HBeAg might play a role in this setting since it has been shown to be tolerable to T cells in transgenic mice. An important mechanism for the development of viral persistence in adults may be the development of viral escape mutations. Of note, mutational inactivation of B-cell and T cell epitopes has been demonstrated in chronic HBV infection but it seems to occur much less compared to the hepatitis C virus[101,104,114]. Little information is currently available about the intrahepatic T cell response during chronic HBV infection. Of note, one study showed functional, tetramer positive $CD8^+$ T cells in the blood and the liver of

chronically HBV infected patients. However, the number of intrahepatic HBV-specific, tetramer-positive T cells did not differ between HBeAg negative patients with normal ALT levels and HBeAg positive patients with increased ALT levels, even though the intrahepatic cellular infiltrate was greater in the latter group[115]. These results suggest a differential contribution of HBV-specific and HBV non-specific bystander lymphocytes in the pathogenesis of chronic hepatitis. T cell dysfunction might also contribute to viral persistence. For example, Reignat *et al*[116] have shown that HBsAg-specific $CD8^+$ T cells display abnormal HLA/ peptide tetramer binding properties in contrast to HBcAg-positive $CD8^+$ T cells. A high viral load may be one important factor that contributes to T cell failure. In this regard, it is important to note that antiviral treatment can overcome $CD8^+$ T cell hypo-responsiveness in subjects with chronic HBV infection, suggesting that the T cells are present but suppressed[117,118]. First evidence suggests that next to high viral loads and a lack of virus-specific $CD4^+$ T cell help, regulatory T cells may contribute to this T cell suppression[119,120]. Clearly, additional studies are required to better understand the complex host-virus interactions that determine the outcome of HBV infection.

CONCLUSION

Virus-host interactions, especially the virus-specific T cell response, are the key factors accounting for the pathogenesis of HBV infection. Viral variants may influence the course of disease and deserve special attention in the setting of antiviral therapy, immune escape and reactivation during immunosuppressive therapy.

REFERENCES

1 **Nassal M**. Hepatitis B virus replication: novel roles for virus-host interactions. *Intervirology* 1999; **42**: 100-116
2 **Hollinger FB**, Liang TJ. Hepatitis B virus. In: Knipe DM, Howley PM. Fields Virology. Philadelphia: Lippincott Williams and Wilkins, 2001: 2971-3036
3 **Summers J**, Mason WS. Replication of the genome of a hepatitis B-like virus by reverse transcription of an RNA intermediate. *Cell* 1982; **29**: 403-415
4 **Bartenschlager R**, Schaller H. The amino-terminal domain of the hepadnaviral P-gene encodes the terminal protein (genome-linked protein) believed to prime reverse transcription. *EMBO J* 1988; **7**: 4185-4192
5 **Feld J**, Locarnini S. Antiviral therapy for hepatitis B virus infections: new targets and technical challenges. *J Clin Virol* 2002; **25**: 267-283
6 **Tong MJ**, Tu SS. Treatment of patients with chronic hepatitis B with adefovir dipivoxil. *Semin Liver Dis* 2004; **24** Suppl 1: 37-44
7 **Wright TL**. Clinical trial results and treatment resistance with lamivudine in hepatitis B. *Semin Liver Dis* 2004; **24** Suppl 1: 31-36
8 **van Bömmel F**, Wünsche T, Mauss S, Reinke P, Bergk A, Schürmann D, Wiedenmann B, Berg T. Comparison of adefovir and tenofovir in the treatment of lamivudine-resistant hepatitis B virus infection. *Hepatology* 2004; **40**: 1421-1425
9 **Marcellin P**, Chang TT, Lim SG, Tong MJ, Sievert W, Shiffman ML, Jeffers L, Goodman Z, Wulfsohn MS, Xiong S, Fry J, Brosgart CL. Adefovir dipivoxil for the treatment of hepatitis B e antigen-positive chronic hepatitis B. *N Engl J Med* 2003; **348**: 808-816
10 **Hadziyannis SJ**, Tassopoulos NC, Heathcote EJ, Chang TT, Kitis G, Rizzetto M, Marcellin P, Lim SG, Goodman Z, Wulfsohn MS, Xiong S, Fry J, Brosgart CL. Adefovir dipivoxil for the treatment of hepatitis B e antigen-negative chronic hepatitis B. *N Engl J Med* 2003; **348**: 800-807
11 **Liaw YF**, Sung JJ, Chow WC, Farrell G, Lee CZ, Yuen H, Tanwandee T, Tao QM, Shue K, Keene ON, Dixon JS, Gray DF, Sabbat J. Lamivudine for patients with chronic hepatitis B and advanced liver disease. *N Engl J Med* 2004; **351**: 1521-1531
12 **Dienstag JL**, Schiff ER, Wright TL, Perrillo RP, Hann HW, Goodman Z, Crowther L, Condreay LD, Woessner M, Rubin M, Brown NA. Lamivudine as initial treatment for chronic hepatitis B in the United States. *N Engl J Med* 1999; **341**: 1256-1263
13 **Ganem D**, Prince AM. Hepatitis B virus infection--natural history and clinical consequences. *N Engl J Med* 2004; **350**: 1118-1129
14 **Baumert TF**, Blum HE. Hepatitis B virus mutations: molecular biology and clinical relevance. *Vir Hep Rev* 2000; **6**: 177-192
15 **Baumert TF**, Barth H, Blum HE. Genetic variants of hepatitis B virus and their clinical relevance. *Minerva Gastroenterol Dietol* 2005; **51**: 95-108
16 **Zoulim F**. Mechanism of viral persistence and resistance to nucleoside and nucleotide analogs in chronic hepatitis B virus infection. *Antiviral Res* 2004; **64**: 1-15
17 **Pawlotsky JM**. The concept of hepatitis B virus mutant escape. *J Clin Virol* 2005; **34** Suppl 1: S125-S129
18 **Liang TJ**, Hasegawa K, Rimon N, Wands JR, Ben-Porath E. A hepatitis B virus mutant associated with an epidemic of fulminant hepatitis. *N Engl J Med* 1991; **324**: 1705-1709
19 **Baumert TF**, Rogers SA, Hasegawa K, Liang TJ. Two core promotor mutations identified in a hepatitis B virus strain associated with fulminant hepatitis result in enhanced viral replication. *J Clin Invest* 1996; **98**: 2268-2276
20 **Baumert TF**, Yang C, Schürmann P, Kock J, Ziegler C, Grüllich C, Nassal M, Liang TJ, Blum HE, von Weizsäcker F. Hepatitis B virus mutations associated with fulminant hepatitis induce apoptosis in primary Tupaia hepatocytes. *Hepatology* 2005; **41**: 247-256
21 **Buckwold VE**, Xu Z, Chen M, Yen TS, Ou JH. Effects of a naturally occurring mutation in the hepatitis B virus basal core promoter on precore gene expression and viral replication. *J Virol* 1996; **70**: 5845-5851
22 **Schildgen O**, Sirma H, Funk A, Olotu C, Wend UC, Hartmann H, Helm M, Rockstroh JK, Willems WR, Will H, Gerlich WH. Variant of hepatitis B virus with primary resistance to adefovir. *N Engl J Med* 2006; **354**: 1807-1812
23 **Kann M**, Gerlich WH. Hepatitis B. in: Collier L, Balows, A. Sussmann, M. Topley Wilson's Microbiology and Microbial Infections. London: Edward Arnold Ltd, 2005
24 **Brunetto MR**, Stemler M, Bonino F, Schodel F, Oliveri F, Rizzetto M, Verme G, Will H. A new hepatitis B virus strain in patients with severe anti-HBe positive chronic hepatitis B. *J Hepatol* 1990; **10**: 258-261
25 **Akahane Y**, Yamanaka T, Suzuki H, Sugai Y, Tsuda F, Yotsumoto S, Omi S, Okamoto H, Miyakawa Y, Mayumi M. Chronic active hepatitis with hepatitis B virus DNA and antibody against e antigen in the serum. Disturbed synthesis and secretion of e antigen from hepatocytes due to a point mutation in the precore region. *Gastroenterology* 1990; **99**: 1113-1119
26 **Milich DR**, Jones JE, Hughes JL, Price J, Raney AK, McLachlan A. Is a function of the secreted hepatitis B e antigen to induce immunologic tolerance in utero? *Proc Natl Acad Sci USA* 1990; **87**: 6599-6603
27 **Milich DR**. Do T cells "see" the hepatitis B core and e antigens differently? *Gastroenterology* 1999; **116**: 765-768
28 **Diepolder HM**, Ries G, Jung MC, Schlicht HJ, Gerlach JT, Gr ner N, Caselmann WH, Pape GR. Differential antigen-processing pathways of the hepatitis B virus e and core proteins. *Gastroenterology* 1999; **116**: 650-657
29 **Kosaka Y**, Takase K, Kojima M, Shimizu M, Inoue K, Yoshiba M, Tanaka S, Akahane Y, Okamoto H, Tsuda F. Fulminant hepatitis B: induction by hepatitis B virus mutants defective in the precore region and incapable of encoding e antigen.

Gastroenterology 1991; **100**: 1087-1094
30 **Omata M**, Ehata T, Yokosuka O, Hosoda K, Ohto M. Mutations in the precore region of hepatitis B virus DNA in patients with fulminant and severe hepatitis. *N Engl J Med* 1991; **324**: 1699-1704
31 **Igaki N**, Nakaji M, Moriguchi R, Akiyama H, Tamada F, Oimomi M, Goto T. An outbreak of fulminant hepatitis B in immunocompromised hemodialysis patients. *J Gastroenterol* 2003; **38**: 968-976
32 **Liu CJ**, Kao JH, Lai MY, Chen PJ, Chen DS. Precore/core promoter mutations and genotypes of hepatitis B virus in chronic hepatitis B patients with fulminant or subfulminant hepatitis. *J Med Virol* 2004; **72**: 545-550
33 **Tacke F**, Gehrke C, Luedde T, Heim A, Manns MP, Trautwein C. Basal core promoter and precore mutations in the hepatitis B virus genome enhance replication efficacy of Lamivudine-resistant mutants. *J Virol* 2004; **78**: 8524-8535
34 **Carman WF**, Jacyna MR, Hadziyannis S, Karayiannis P, McGarvey MJ, Makris A, Thomas HC. Mutation preventing formation of hepatitis B e antigen in patients with chronic hepatitis B infection. *Lancet* 1989; **2**: 588-591
35 **Naoumov NV**, Schneider R, Grötzinger T, Jung MC, Miska S, Pape GR, Will H. Precore mutant hepatitis B virus infection and liver disease. *Gastroenterology* 1992; **102**: 538-543
36 **Mphahlele MJ**, Shattock AG, Boner W, Quinn J, McCormick PA, Carman WF. Transmission of a homogenous hepatitis B virus population of A1896-containing strains leading to mild resolving acute hepatitis and seroconversion to hepatitis B e antigen antibodies in an adult. *Hepatology* 1997; **26**: 743-746
37 **Chen HS**, Kew MC, Hornbuckle WE, Tennant BC, Cote PJ, Gerin JL, Purcell RH, Miller RH. The precore gene of the woodchuck hepatitis virus genome is not essential for viral replication in the natural host. *J Virol* 1992; **66**: 5682-5684
38 **Chuang WL**, Omata M, Ehata T, Yokosuka O, Hosoda K, Imazeki F, Ohto M. Coinfection study of precore mutant and wild-type hepatitis B-like virus in ducklings. *Hepatology* 1994; **19**: 569-576
39 **Sato S**, Suzuki K, Akahane Y, Akamatsu K, Akiyama K, Yunomura K, Tsuda F, Tanaka T, Okamoto H, Miyakawa Y, Mayumi M. Hepatitis B virus strains with mutations in the core promoter in patients with fulminant hepatitis. *Ann Intern Med* 1995; **122**: 241-248
40 **Baumert TF**, Marrone A, Vergalla J, Liang TJ. Naturally occurring mutations define a novel function of the hepatitis B virus core promoter in core protein expression. *J Virol* 1998; **72**: 6785-6795
41 **Pult I**, Chouard T, Wieland S, Klemenz R, Yaniv M, Blum HE. A hepatitis B virus mutant with a new hepatocyte nuclear factor 1 binding site emerging in transplant-transmitted fulminant hepatitis B. *Hepatology* 1997; **25**: 1507-1515
42 **Günther S**, Piwon N, Iwanska A, Schilling R, Meisel H, Will H. Type, prevalence, and significance of core promoter/enhancer II mutations in hepatitis B viruses from immunosuppressed patients with severe liver disease. *J Virol* 1996; **70**: 8318-8331
43 **Okamoto H**, Tsuda F, Akahane Y, Sugai Y, Yoshiba M, Moriyama K, Tanaka T, Miyakawa Y, Mayumi M. Hepatitis B virus with mutations in the core promoter for an e antigen-negative phenotype in carriers with antibody to e antigen. *J Virol* 1994; **68**: 8102-8110
44 **Parekh S**, Zoulim F, Ahn SH, Tsai A, Li J, Kawai S, Khan N, Trépo C, Wands J, Tong S. Genome replication, virion secretion, and e antigen expression of naturally occurring hepatitis B virus core promoter mutants. *J Virol* 2003; **77**: 6601-6612
45 **Preikschat P**, Günther S, Reinhold S, Will H, Budde K, Neumayer HH, Krüger DH, Meisel H. Complex HBV populations with mutations in core promoter, C gene, and pre-S region are associated with development of cirrhosis in long-term renal transplant recipients. *Hepatology* 2002; **35**: 466-477
46 **Raney AK**, Johnson JL, Palmer CN, McLachlan A. Members of the nuclear receptor superfamily regulate transcription from the hepatitis B virus nucleocapsid promoter. *J Virol* 1997; **71**: 1058-1071
47 **Li J**, Buckwold VE, Hon MW, Ou JH. Mechanism of suppression of hepatitis B virus precore RNA transcription by a frequent double mutation. *J Virol* 1999; **73**: 1239-1244
48 **Zheng Y**, Li J, Ou JH. Regulation of hepatitis B virus core promoter by transcription factors HNF1 and HNF4 and the viral X protein. *J Virol* 2004; **78**: 6908-6914
49 **Lamberts C**, Nassal M, Velhagen I, Zentgraf H, Schröder CH. Precore-mediated inhibition of hepatitis B virus progeny DNA synthesis. *J Virol* 1993; **67**: 3756-3762
50 **Kao JH**, Chen PJ, Lai MY, Chen DS. Basal core promoter mutations of hepatitis B virus increase the risk of hepatocellular carcinoma in hepatitis B carriers. *Gastroenterology* 2003; **124**: 327-334
51 **Sterneck M**, Kalinina T, Günther S, Fischer L, Santantonio T, Greten H, Will H. Functional analysis of HBV genomes from patients with fulminant hepatitis. *Hepatology* 1998; **28**: 1390-1397
52 **Bartholomeusz A**, Locarnini S. Hepatitis B virus mutants and fulminant hepatitis B: fitness plus phenotype. *Hepatology* 2001; **34**: 432-435
53 **Zuckerman JN**, Zuckerman AJ. Mutations of the surface protein of hepatitis B virus. *Antiviral Res* 2003; **60**: 75-78
54 **Carman WF**, Zanetti AR, Karayiannis P, Waters J, Manzillo G, Tanzi E, Zuckerman AJ, Thomas HC. Vaccine-induced escape mutant of hepatitis B virus. *Lancet* 1990; **336**: 325-329
55 **Waters JA**, Kennedy M, Voet P, Hauser P, Petre J, Carman W, Thomas HC. Loss of the common "A" determinant of hepatitis B surface antigen by a vaccine-induced escape mutant. *J Clin Invest* 1992; **90**: 2543-2547
56 **Kalinina T**, Iwanski A, Will H, Sterneck M. Deficiency in virion secretion and decreased stability of the hepatitis B virus immune escape mutant G145R. *Hepatology* 2003; **38**: 1274-1281
57 **Yamamoto K**, Horikita M, Tsuda F, Itoh K, Akahane Y, Yotsumoto S, Okamoto H, Miyakawa Y, Mayumi M. Naturally occurring escape mutants of hepatitis B virus with various mutations in the S gene in carriers seropositive for antibody to hepatitis B surface antigen. *J Virol* 1994; **68**: 2671-2676
58 **Fortuin M**, Karthigesu V, Allison L, Howard C, Hoare S, Mendy M, Whittle HC. Breakthrough infections and identification of a viral variant in Gambian children immunized with hepatitis B vaccine. *J Infect Dis* 1994; **169**: 1374-1376
59 **Hsu HY**, Chang MH, Liaw SH, Ni YH, Chen HL. Changes of hepatitis B surface antigen variants in carrier children before and after universal vaccination in Taiwan. *Hepatology* 1999; **30**: 1312-1317
60 **Ogata N**, Cote PJ, Zanetti AR, Miller RH, Shapiro M, Gerin J, Purcell RH. Licensed recombinant hepatitis B vaccines protect chimpanzees against infection with the prototype surface gene mutant of hepatitis B virus. *Hepatology* 1999; **30**: 779-786
61 **Bauer T**, Weinberger K, Jilg W. Variants of two major T cell epitopes within the hepatitis B surface antigen are not recognized by specific T helper cells of vaccinated individuals. *Hepatology* 2002; **35**: 455-465
62 **McMahon G**, Ehrlich PH, Moustafa ZA, McCarthy LA, Dottavio D, Tolpin MD, Nadler PI, Ostberg L. Genetic alterations in the gene encoding the major HBsAg: DNA and immunological analysis of recurrent HBsAg derived from monoclonal antibody-treated liver transplant patients. *Hepatology* 1992; **15**: 757-766
63 **Carman WF**, Trautwein C, van Deursen FJ, Colman K, Dornan E, McIntyre G, Waters J, Kliem V, Müller R, Thomas HC, Manns MP. Hepatitis B virus envelope variation after transplantation with and without hepatitis B immune globulin prophylaxis. *Hepatology* 1996; **24**: 489-493
64 **Protzer-Knolle U**, Naumann U, Bartenschlager R, Berg T, Hopf U, Meyer zum Büschenfelde KH, Neuhaus P, Gerken G. Hepatitis B virus with antigenically altered hepatitis B surface antigen is selected by high-dose hepatitis B immune globulin after liver transplantation. *Hepatology* 1998; **27**: 254-263
65 **Ghany MG**, Ayola B, Villamil FG, Gish RG, Rojter S, Vierling JM, Lok AS. Hepatitis B virus S mutants in liver transplant

recipients who were reinfected despite hepatitis B immune globulin prophylaxis. *Hepatology* 1998; **27**: 213-222
66 **Lu M**, Lorentz T. De novo infection in a renal transplant recipient caused by novel mutants of hepatitis B virus despite the presence of protective anti-hepatitis B surface antibody. *J Infect Dis* 2003; **187**: 1323-1326
67 **Jongerius JM**, Wester M, Cuypers HT, van Oostendorp WR, Lelie PN, van der Poel CL, van Leeuwen EF. New hepatitis B virus mutant form in a blood donor that is undetectable in several hepatitis B surface antigen screening assays. *Transfusion* 1998; **38**: 56-59
68 **Hass M**, Hannoun C, Kalinina T, Sommer G, Manegold C, Günther S. Functional analysis of hepatitis B virus reactivating in hepatitis B surface antigen-negative individuals. *Hepatology* 2005; **42**: 93-103
69 **Baumert TF**, Köck J, Blum HE. A novel target of hepatitis B virus mutations: splicing of surface RNA. *Hepatology* 2005; **42**: 21-23
70 **Chemin I**, Trépo C. Clinical impact of occult HBV infections. *J Clin Virol* 2005; **34** Suppl 1: S15-S21
71 **Glebe D**, Urban S, Knoop EV, Cag N, Krass P, Grün S, Bulavaite A, Sasnauskas K, Gerlich WH. Mapping of the hepatitis B virus attachment site by use of infection-inhibiting preS1 lipopeptides and tupaia hepatocytes. *Gastroenterology* 2005; **129**: 234-245
72 **Engelke M**, Mills K, Seitz S, Simon P, Gripon P, Schnölzer M, Urban S. Characterization of a hepatitis B and hepatitis delta virus receptor binding site. *Hepatology* 2006; **43**: 750-760
73 **Pollicino T**, Zanetti AR, Cacciola I, Petit MA, Smedile A, Campo S, Sagliocca L, Pasquali M, Tanzi E, Longo G, Raimondo G. Pre-S2 defective hepatitis B virus infection in patients with fulminant hepatitis. *Hepatology* 1997; **26**: 495-499
74 **Bock CT**, Tillmann HL, Maschek HJ, Manns MP, Trautwein C. A preS mutation isolated from a patient with chronic hepatitis B infection leads to virus retention and misassembly. *Gastroenterology* 1997; **113**: 1976-1982
75 **Bock CT**, Tillmann HL, Manns MP, Trautwein C. The pre-S region determines the intracellular localization and appearance of hepatitis B virus. *Hepatology* 1999; **30**: 517-525
76 **Chen BF**, Liu CJ, Jow GM, Chen PJ, Kao JH, Chen DS. High prevalence and mapping of pre-S deletion in hepatitis B virus carriers with progressive liver diseases. *Gastroenterology* 2006; **130**: 1153-1168
77 **Kalinina T**, Riu A, Fischer L, Will H, Sterneck M. A dominant hepatitis B virus population defective in virus secretion because of several S-gene mutations from a patient with fulminant hepatitis. *Hepatology* 2001; **34**: 385-394
78 **Durantel D**, Brunelle MN, Gros E, Carrouée-Durantel S, Pichoud C, Villet S, Trepo C, Zoulim F. Resistance of human hepatitis B virus to reverse transcriptase inhibitors: from genotypic to phenotypic testing. *J Clin Virol* 2005; **34** Suppl 1: S34-S43
79 **Lai CL**, Chien RN, Leung NW, Chang TT, Guan R, Tai DI, Ng KY, Wu PC, Dent JC, Barber J, Stephenson SL, Gray DF. A one-year trial of lamivudine for chronic hepatitis B. Asia Hepatitis Lamivudine Study Group. *N Engl J Med* 1998; **339**: 61-68
80 **Marcellin P**, Lau GK, Bonino F, Farci P, Hadziyannis S, Jin R, Lu ZM, Piratvisuth T, Germanidis G, Yurdaydin C, Diago M, Gurel S, Lai MY, Button P, Pluck N. Peginterferon alfa-2a alone, lamivudine alone, and the two in combination in patients with HBeAg-negative chronic hepatitis B. *N Engl J Med* 2004; **351**: 1206-1217
81 **Köck J**, Baumert TF, Delaney WE, Blum HE, von Weizsäcker F. Inhibitory effect of adefovir and lamivudine on the initiation of hepatitis B virus infection in primary tupaia hepatocytes. *Hepatology* 2003; **38**: 1410-1418
82 **Lok AS**, Lai CL, Leung N, Yao GB, Cui ZY, Schiff ER, Dienstag JL, Heathcote EJ, Little NR, Griffiths DA, Gardner SD, Castiglia M. Long-term safety of lamivudine treatment in patients with chronic hepatitis B. *Gastroenterology* 2003; **125**: 1714-1722
83 **Lau DT**, Khokhar MF, Doo E, Ghany MG, Herion D, Park Y, Kleiner DE, Schmid P, Condreay LD, Gauthier J, Kuhns MC, Liang TJ, Hoofnagle JH. Long-term therapy of chronic hepatitis B with lamivudine. *Hepatology* 2000; **32**: 828-834
84 **Angus P**, Vaughan R, Xiong S, Yang H, Delaney W, Gibbs C, Brosgart C, Colledge D, Edwards R, Ayres A, Bartholomeusz A, Locarnini S. Resistance to adefovir dipivoxil therapy associated with the selection of a novel mutation in the HBV polymerase. *Gastroenterology* 2003; **125**: 292-297
85 **Marcellin P**, Chang TT, Lim SG, Sievert W, Tong M, Arterburn S, Xiong S, Brosgart CL, Currie G. Long term efficacy and safety of adefovir dipivoxil in HBeAg+ chronic hepatitis B patients: increasing serologic, virologic and biochemical response over time. *Hepatology* 2004; **41**: A1135
86 **Allen MI**, Deslauriers M, Andrews CW, Tipples GA, Walters KA, Tyrrell DL, Brown N, Condreay LD. Identification and characterization of mutations in hepatitis B virus resistant to lamivudine. Lamivudine Clinical Investigation Group. *Hepatology* 1998; **27**: 1670-1677
87 **Melegari M**, Scaglioni PP, Wands JR. Hepatitis B virus mutants associated with 3TC and famciclovir administration are replication defective. *Hepatology* 1998; **27**: 628-633
88 **Delaney WE**, Yang H, Westland CE, Das K, Arnold E, Gibbs CS, Miller MD, Xiong S. The hepatitis B virus polymerase mutation rtV173L is selected during lamivudine therapy and enhances viral replication *in vitro*. *J Virol* 2003; **77**: 11833-11841
89 **Dandri M**, Volz TK, Lütgehetmann M, Petersen J. Animal models for the study of HBV replication and its variants. *J Clin Virol* 2005; **34** Suppl 1: S54-S62
90 **Lenhoff RJ**, Summers J. Construction of avian hepadnavirus variants with enhanced replication and cytopathicity in primary hepatocytes. *J Virol* 1994; **68**: 5706-5713
91 **Lenhoff RJ**, Luscombe CA, Summers J. Competition in vivo between a cytopathic variant and a wild-type duck hepatitis B virus. *Virology* 1998; **251**: 85-95
92 **Lenhoff RJ**, Luscombe CA, Summers J. Acute liver injury following infection with a cytopathic strain of duck hepatitis B virus. *Hepatology* 1999; **29**: 563-571
93 **Bruss V**. Revisiting the cytopathic effect of hepatitis B virus infection. *Hepatology* 2002; **36**: 1327-1329
94 **Foo NC**, Ahn BY, Ma X, Hyun W, Yen TS. Cellular vacuolization and apoptosis induced by hepatitis B virus large surface protein. *Hepatology* 2002; **36**: 1400-1407
95 **Su F**, Theodosis CN, Schneider RJ. Role of NF-kappaB and myc proteins in apoptosis induced by hepatitis B virus HBx protein. *J Virol* 2001; **75**: 215-225
96 **Kim KH**, Seong BL. Pro-apoptotic function of HBV X protein is mediated by interaction with c-FLIP and enhancement of death-inducing signal. *EMBO J* 2003; **22**: 2104-2116
97 **Chirillo P**, Pagano S, Natoli G, Puri PL, Burgio VL, Balsano C, Levrero M. The hepatitis B virus X gene induces p53-mediated programmed cell death. *Proc Natl Acad Sci USA* 1997; **94**: 8162-8167
98 **Chisari FV**. Cytotoxic T cells and viral hepatitis. *J Clin Invest* 1997; **99**: 1472-1477
99 **Wieland S**, Thimme R, Purcell RH, Chisari FV. Genomic analysis of the host response to hepatitis B virus infection. *Proc Natl Acad Sci USA* 2004; **101**: 6669-6674
100 **Maini MK**, Boni C, Ogg GS, King AS, Reignat S, Lee CK, Larrubia JR, Webster GJ, McMichael AJ, Ferrari C, Williams R, Vergani D, Bertoletti A. Direct ex vivo analysis of hepatitis B virus-specific CD8(+) T cells associated with the control of infection. *Gastroenterology* 1999; **117**: 1386-1396
101 **Rehermann B**, Nascimbeni M. Immunology of hepatitis B virus and hepatitis C virus infection. *Nat Rev Immunol* 2005; **5**: 215-229
102 **Thimme R**, Chang KM, Pemberton J, Sette A, Chisari FV. Degenerate immunogenicity of an HLA-A2-restricted hepatitis B virus nucleocapsid cytotoxic T-lymphocyte epitope that is also presented by HLA-B51. *J Virol* 2001; **75**: 3984-3987
103 **Urbani S**, Boni C, Missale G, Elia G, Cavallo C, Massari M, Raimondo G, Ferrari C. Virus-specific CD8+ lymphocytes share the same effector-memory phenotype but exhibit functional differences in acute hepatitis B and C. *J Virol* 2002; **76**: 12423-12434

104 **Wieland SF**, Chisari FV. Stealth and cunning: hepatitis B and hepatitis C viruses. *J Virol* 2005; **79**: 9369-9380
105 **Webster GJ**, Reignat S, Maini MK, Whalley SA, Ogg GS, King A, Brown D, Amlot PL, Williams R, Vergani D, Dusheiko GM, Bertoletti A. Incubation phase of acute hepatitis B in man: dynamic of cellular immune mechanisms. *Hepatology* 2000; **32**: 1117-1124
106 **Penna A**, Artini M, Cavalli A, Levrero M, Bertoletti A, Pilli M, Chisari FV, Rehermann B, Del Prete G, Fiaccadori F, Ferrari C. Long-lasting memory T cell responses following self-limited acute hepatitis B. *J Clin Invest* 1996; **98**: 1185-1194
107 **Sprengers D**, van der Molen RG, Kusters JG, De Man RA, Niesters HG, Schalm SW, Janssen HL. Analysis of intrahepatic HBV-specific cytotoxic T-cells during and after acute HBV infection in humans. *J Hepatol* 2006; **45**: 182-189
108 **Guidotti LG**, Ishikawa T, Hobbs MV, Matzke B, Schreiber R, Chisari FV. Intracellular inactivation of the hepatitis B virus by cytotoxic T lymphocytes. *Immunity* 1996; **4**: 25-36
109 **Guidotti LG**, Chisari FV. Noncytolytic control of viral infections by the innate and adaptive immune response. *Annu Rev Immunol* 2001; **19**: 65-91
110 **Guidotti LG**, Rochford R, Chung J, Shapiro M, Purcell R, Chisari FV. Viral clearance without destruction of infected cells during acute HBV infection. *Science* 1999; **284**: 825-829
111 **Thimme R**, Wieland S, Steiger C, Ghrayeb J, Reimann KA, Purcell RH, Chisari FV. CD8(+) T cells mediate viral clearance and disease pathogenesis during acute hepatitis B virus infection. *J Virol* 2003; **77**: 68-76
112 **Boettler T**, Panther E, Bengsch B, Nazarova N, Spangenberg HC, Blum HE, Thimme R. Expression of the interleukin-7 receptor alpha chain (CD127) on virus-specific CD8+ T cells identifies functionally and phenotypically defined memory T cells during acute resolving hepatitis B virus infection. *J Virol* 2006; **80**: 3532-3540
113 **Isogawa M**, Furuichi Y, Chisari FV. Oscillating CD8(+) T cell effector functions after antigen recognition in the liver. *Immunity* 2005; **23**: 53-63
114 **Rehermann B**, Pasquinelli C, Mosier SM, Chisari FV. Hepatitis B virus (HBV) sequence variation of cytotoxic T lymphocyte epitopes is not common in patients with chronic HBV infection. *J Clin Invest* 1995; **96**: 1527-1534
115 **Maini MK**, Boni C, Lee CK, Larrubia JR, Reignat S, Ogg GS, King AS, Herberg J, Gilson R, Alisa A, Williams R, Vergani D, Naoumov NV, Ferrari C, Bertoletti A. The role of virus-specific CD8(+) cells in liver damage and viral control during persistent hepatitis B virus infection. *J Exp Med* 2000; **191**: 1269-1280
116 **Reignat S**, Webster GJ, Brown D, Ogg GS, King A, Seneviratne SL, Dusheiko G, Williams R, Maini MK, Bertoletti A. Escaping high viral load exhaustion: CD8 cells with altered tetramer binding in chronic hepatitis B virus infection. *J Exp Med* 2002; **195**: 1089-1101
117 **Boni C**, Bertoletti A, Penna A, Cavalli A, Pilli M, Urbani S, Scognamiglio P, Boehme R, Panebianco R, Fiaccadori F, Ferrari C. Lamivudine treatment can restore T cell responsiveness in chronic hepatitis B. *J Clin Invest* 1998; **102**: 968-975
118 **Boni C**, Penna A, Ogg GS, Bertoletti A, Pilli M, Cavallo C, Cavalli A, Urbani S, Boehme R, Panebianco R, Fiaccadori F, Ferrari C. Lamivudine treatment can overcome cytotoxic T-cell hyporesponsiveness in chronic hepatitis B: new perspectives for immune therapy. *Hepatology* 2001; **33**: 963-971
119 **Stoop JN**, van der Molen RG, Baan CC, van der Laan LJ, Kuipers EJ, Kusters JG, Janssen HL. Regulatory T cells contribute to the impaired immune response in patients with chronic hepatitis B virus infection. *Hepatology* 2005; **41**: 771-778
120 **Franzese O**, Kennedy PT, Gehring AJ, Gotto J, Williams R, Maini MK, Bertoletti A. Modulation of the CD8+-T-cell response by CD4+ CD25+ regulatory T cells in patients with hepatitis B virus infection. *J Virol* 2005; **79**: 3322-3328

S- Editor Liu Y **L- Editor** Lutze M **E- Editor** Ma WH

PO Box 2345, Beijing 100023, China
www.wjgnet.com
wjg@wjgnet.com

World J Gastroenterol 2007 January 7; 13(1): 91-103
World Journal of Gastroenterology ISSN 1007-9327

TOPIC HIGHLIGHT

Dieter Glebe, PhD, *Series Editor*

Avian hepatitis B viruses: Molecular and cellular biology, phylogenesis, and host tropism

Anneke Funk, Mouna Mhamdi, Hans Will, Hüseyin Sirma

Anneke Funk, Mouna Mhamdi, Hans Will, Hüseyin Sirma, Department of General Virology, Heinrich-Pette-Institut für experimentelle Virologie und Immunologie an der Universität Hamburg, Hamburg, Germany
Supported by the Freie und Hansestadt Hamburg and the Bundesministerium für Gesundheit und Soziale Sicherung; grants from DFG and by the German Competence Network for Viral Hepatitis (Hep-Net), funded by the German Ministry of Education and Research (BMBF), Grant No. TP13.1
Correspondence to: Hüseyin Sirma, Department of General Virology, Heinrich-Pette-Institut für experimentelle Virologie und Immunologie an der Universität Hamburg, PO Box 201652, Hamburg 20206, Germany. sirma@hpi.uni-hamburg.de
Telephone: +49-40-48051226 Fax: +49-40-48051222
Received: 2006-09-11 Accepted: 2006-11-25

Abstract

The human hepatitis B virus (HBV) and the duck hepatitis B virus (DHBV) share several fundamental features. Both viruses have a partially double-stranded DNA genome that is replicated via a RNA intermediate and the coding open reading frames (ORFs) overlap extensively. In addition, the genomic and structural organization, as well as replication and biological characteristics, are very similar in both viruses. Most of the key features of hepadnaviral infection were first discovered in the DHBV model system and subsequently confirmed for HBV. There are, however, several differences between human HBV and DHBV. This review will focus on the molecular and cellular biology, evolution, and host adaptation of the avian hepatitis B viruses with particular emphasis on DHBV as a model system.

Key words: Hepadnavirus; Pararetroviruses; Evolution; Host range; Genome; Structure, Virions; Subviral particles; *In vitro* and *in vivo* infection; Transport; Fusion; Endocytosis; Hepatocellular differentiation; cccDNA; Gene expression; Morphogenesis and secretion

Funk A, Mhamdi M, Will H, Sirma H. Avian hepatitis B viruses: Molecular and cellular biology, phylogenesis, and host tropism. *World J Gastroenterol* 2007; 13(1): 91-103

http://www.wjgnet.com/1007-9327/13/91.asp

INTRODUCTION

Full understanding of the molecular biology of the human hepatitis B virus (HBV) is hampered by a variety of experimental restrictions. There is no small animal model system available for infection studies and only few aspects of the viral life cycle are accessible to biochemical methods. A complete viral infection cycle mimicking natural HBV infection *in vitro* could only be achieved until recently with primary human hepatocytes. The disadvantages of this system are: (1) restricted accessibility to the cells, (2) infection inefficiency and (3) high variability in infection assays. The recent establishment of the HepaRG cell line is therefore a major breakthrough and allows HBV infection studies under defined conditions for the first time[1].

This review will focus on one of two established animal virus models; i.e., the DHBV model system. The human HBV and DHBV share several fundamental features. Both viruses have a partially double-stranded DNA genome that is replicated via an RNA intermediate and the coding open reading frames (ORFs) overlap extensively. In addition, the genomic and structural organization, as well as replication and biological characteristics, are very similar in both viruses. They both infect hepatocytes preferentially and have a very similar life cycle. Most of the key features of hepadnaviral infection were first discovered in the DHBV model system and subsequently confirmed for HBV. This includes replication of the viral genome by reverse transcription of a RNA intermediate[2], mechanisms of covalently closed circular (ccc) DNA formation and amplification[3], details of reverse transcription[4], and determinants of host tropism[5].

In light of the above mentioned austerities for HBV, the DHBV model of hepatitis B virus infection remains a convenient and reliable system that offers several unique advantages. Most importantly, steady availability and highly reproducible infection of primary duck hepatocytes (PDHs) provide the optimal basis for *in vitro* and *in vivo* studies of the molecular and cellular biology of hepatitis B virus infection under defined and controlled conditions. In addition, the chicken hepatoma cell line LMH produces progeny virus after transfection with cloned, mutant or wt DHBV genomes, which can be used to infect PDHs or ducks[6].

Thus, the DHBV model system is a unique system that allows elucidation of the hepadnaviral life cycle in considerable detail. However, there are several differences

Table 1 Comparison of HBV and DHBV

	HBV	DHBV
Natural host	Human	Pekin duck
Related viruses	WM-HBV, WHV	HHBV, SGHBV
Pathogenicity		
Chronic infection	yes	yes
Liver injury	yes	no
Experimental systems		
Cell transfection	yes	yes
In vitro infection	yes	yes
Transgenic mouse	yes	no
Small animal model	no	yes

WMHBV: woolly monkey HBV; WHV: woodchuck HBV; HHBV: heron HBV; SGHBV: snow goose HBV.

between human HBV and DHBV. First of all, DHBV infection normally results in chronicity since the virus is transmitted from the hen to the egg (see[7] and references therein). This infection usually does not lead to liver injury and the infected duck remains healthy throughout life. When an adult duck is infected, the infection is usually eliminated. When HBV is transmitted from mother to child, it also often results in chronic infection. However, in a large number of cases, this leads to liver injury and development of hepatocellular carcinoma or cirrhosis. When an adult is infected, this can either result in fulminant, acute or chronic hepatitis when the virus is not eliminated. Another difference between DHBV and HBV is expression of the X protein (for further differences see Table 1). This regulatory protein, with not fully understood function, is expressed by HBV from a conventional ORF, but in DHBV, an unusual cryptic ORF is used.

In the last two decades, parts of the hepadnaviral life cycle, especially the replication strategy, could be undeceived in considerable detail. In contrast, there is very little information available on the infectious entry or secretion pathway. The cellular partners involved in cell-virus interactions at these stages of infection remain unidentified and the molecular determinants of host specificity, hepatotropism and the nature of the receptor complex still await discovery.

For more information about human HBV and the other corresponding model systems please see the comprehensive reviews in this issue.

AVIAN HEPATITIS B VIRUSES

The duck hepatitis B virus was discovered in 1980 by William Mason and colleagues[8]. They found a virus very similar to HBV in about 10% of Pekin ducks from two different sources in the USA and they pointed out that no abnormal level of mortality or signs of hepatitis were found in the infected ducks. Naturally occurring DHBV infections have been reported in Pekin ducks and related species from China, USA, Canada, Europe, India, and South Africa[9-11].

Since then, avihepadnaviruses have been detected in various duck species[10] including exotic ducks and geese[10] (DHBV), in snow geese[12] (SGHBV), a Ross' goose

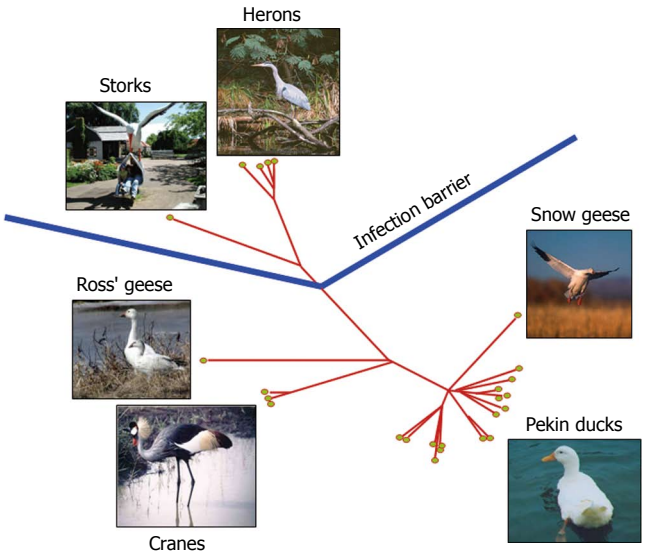

Figure 1 Phylogenetic tree of avian hepadnaviruses and related hosts. Phylogenetic relationship of all known avian hepadnaviruses based on preS/S gene sequence. The corresponding natural hosts are also indicated.

(RGHBV, GenBank Acc.No. M95589), white storks[13] (STHBV), demoiselle and grey crowned cranes[14] (CHBV) as well as grey herons[15] (HHBV). Like their mammalian counterparts, avihepadnaviruses have a rather narrow host range. For instance, DHBV infects only certain duck and goose species but neither infects Muscovy ducks nor chickens[16]. Little is known about the host range of HHBV or STHBV. Despite its substantial sequence homology with DHBV, HHBV does not infect ducks and only very inefficiently primary duck hepatocytes[15]. Recently, we reported that cranes are naturally infected with a hepatitis B virus, designated CHBV[14]. Cranes are phylogenetically very distant from ducks and are more closely related to herons and storks (Figure 1). Interestingly however, CHBV infects primary duck hepatocytes with similar efficiency as DHBV. Collectively this and related data suggest that the host range of hepadnaviruses cannot be simply predicted based on the evolutionary relatedness of their respective hosts. For a comprehensive sequence comparison and a phylogenetic tree of the host birds see[14].

Phylogenetic analysis of the various isolates demonstrated a rather high variability among DHBV strains, whereas genomes from other avihepadnaviruses, such as stork or crane hepatitis B virus, appear less variable. HHBV infection occurs not only in captive grey herons, but also with high prevalence in free-living birds. We have detected HHBV in another heron species (great blue heron) as well as in two of its sub-species (great white heron and Würdemann's heron). Thus, the virus persists in free-living birds and is an endogenous virus of several heron species.

DHBV will certainly remain the most important avihepadnavirus for research purposes since the infection system with PDHs and the important research tools are well established. It is possible to generate mutant viruses after transfection of cloned DHBV genomes into the chicken hepatoma cell line LMH[6]. Thus, different mutations can be studied not only concerning their effects

on replication but also on infection efficiency and events. In addition, *in vivo* infections can be performed in ducks without the need to establish expensive handling facilities and without risk. In these ducks not only the host range of hepadnaviruses can be studied in considerable detail (in addition to *in vitro* studies), but also the activity and toxicity of antiviral substances can be addressed[17].

THE AVIHEPADNAVIRAL LIFE CYCLE: AN OVERVIEW

Avian hepatitis B viruses belong to the family of DNA viruses that replicate their DNA genome by reverse transcription of an RNA intermediate. Thus, they belong, together with the cauliflower mosaic virus, to the group of pararetroviruses that do not integrate their genome into host cell chromosomes.

A schematic view of the DHBV genome and structure of virions is shown in Figure 2. The genome of DHBV has an unusual design. It consists of a ca. 3000 bp partially double-stranded DNA. The circularity of the genome is achieved by overlapping cohesive 5' ends[18]. The coding negative strand is complete and even has a short terminal redundancy but is not covalently closed. Its 5' end is covalently attached to the viral polymerase P[19]. The positive strand is not complete but encompasses between 40% and 85% of the genome[20]. However, the length of the gap varies among different hepadnaviruses and is smallest in DHBV[18]. Attached at the 5' end of the positive strand is a short ribooligonucleotide, which is a remnant of the pregenomic RNA (pgRNA)[21]. Both 5' terminal structures function as primers during viral replication[21]. As another particularity, the viral genome has two direct repeats (DR) with a length of 11 base pairs that have important functions in replication.

The viral genome organization is very compact and economic. All nucleotides have a coding function in at least one of the four open reading frames (ORFs). Regulatory sequences such as enhancers and promoters, as well as several cis-acting elements, overlap with coding regions. The first ORF encodes the surface proteins L and S, the second codes for the capsid protein as well as the e-antigen, the third for the polymerase and a cryptic fourth for the X protein[22].

Two different types of spherical viral particles can be detected in the serum of infected ducks: infectious virus particles (virions) with a diameter between 40 and 60 nm and subviral particles (SVPs) with a diameter between 30 and 60 nm, which lack the 27 nm nucleocapsid, including the viral genome[23]. After transfection of cell lines, a third particle entity can be detected in the cell culture supernatant. These cells secrete so called 'naked capsids' lacking the viral envelope for unknown reasons.

The virus is surrounded by a lipid envelope, which presumably originates from the host cell endoplasmic reticulum (ER) membrane, and contains both viral surface proteins. For HBV, it has been shown that the membrane is rich in phosphatidyl choline (60% of all lipids) as well as cholesterol (30% of all lipids)[24] and thus differs from the lipid composition of the cellular ER membrane,

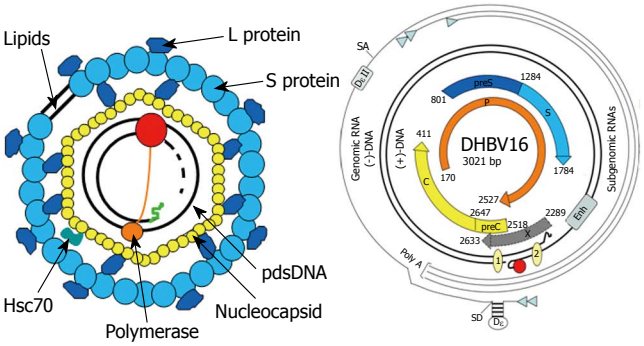

Figure 2 Virion structure and genome organization of avian hepadnaviruses. The viral envelope is derived from hepatocellular membranes and contains the viral surface proteins S and L. It covers the nucleocapsid harbouring the viral genome with the covalently linked terminal protein domain (TP, orange circle) of the polymerase (P, red circle) and cellular proteins like Hsc70. The genome is organized as depicted. The various transcripts are indicated by thin lines with the small arrowhead indicating the start sites. The partially double stranded, viral DNA with the covalently bound TP domain of P (red circle) is symbolized by the thicker lines. The numbered circles 1 and 2 on the viral DNA represent the direct repeats (DR). Enh represents the enhancer domain. The ORFs encoding core (C), polymerase (P), and the surface proteins (preS and S) are symbolized by thick arrows. Epsilon (Dε) is the stem loop structure on the pgRNA which acts as an encapsidation signal and replication origin. The second encapsidation element DεII is unique to avian hepatitis B viruses, since the mammalian counterparts lack this RNA structure. SD and SA represent the major splice donor and acceptor sites, respectively.

implicating that lipids are actively selected for the viral membrane. In total, the amount of lipids in comparison to the amount of protein is very small, in SVPs the weight ratio is about 1:4[25]. Thus, the lipids in the viral envelope are presumably not forming a lipid bilayer but protein aggregates seem to be separated through short lipid regions[26]. This strongly restricts the lateral mobility of the envelope components. The lipid composition of the DHBV envelope remains to be determined.

SVPs largely consist of the viral surface proteins S and L, which are incorporated into the envelope. They do not contain viral DNA and are thus not infectious. This entity is secreted from infected cells in excess compared to virions. It is assumed that per virion 1000 to 10 000 SVPs are secreted[27]. SVPs can compete with viral binding and thus infection[28]. In contrast, it has been shown that SVPs enhance infection when a very low multiplicity of infection (MOI) is used, which indicates an important role in the viral life cycle[29].

Complete virions contain an icosahedral capsid inside the envelope, which is about 35 nm in diameter as seen in cryo-electron microscopy or 27 nm in negative stain pictures and consists of 240 subunits of core protein[30]. The nucleocapsid holds the viral DNA genome with the covalently attached polymerase.

Cellular components can additionally be packed into viral particles. This is the case for Hsc70, which was detected in large amounts[31]. The identity and function of other proteins of cellular origin are still unknown.

A schematic view of the viral life cycle is shown in Figure 3. The life cycle of DHBV starts with attachment of the viral particles to their receptor/receptor complex on the surface of the target host cell. This is mediated by the preS domain of the viral L protein that binds to

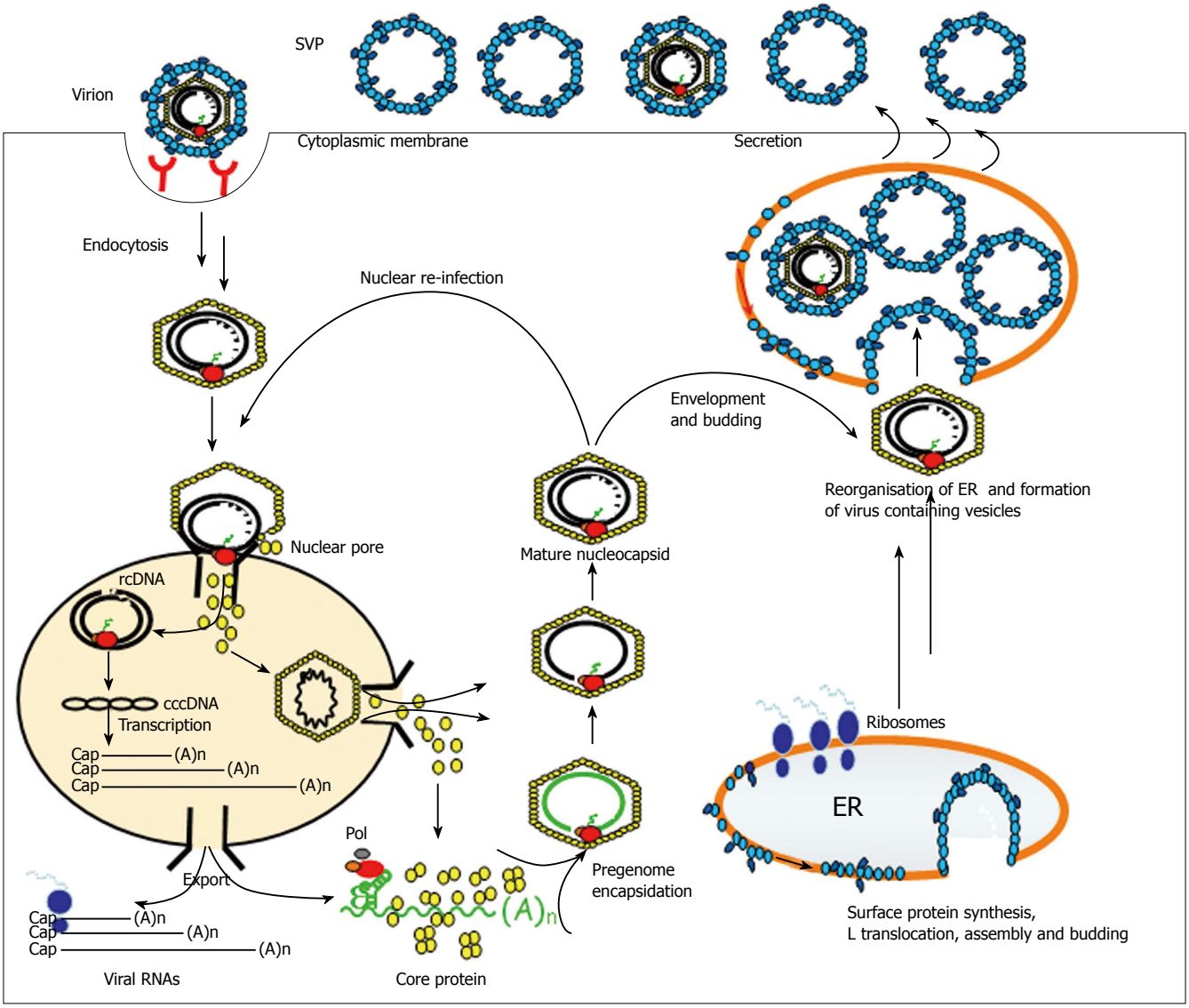

Figure 3 Model of the hepadnaviral life cycle. The hepadnaviral particle binds the hepatocyte via a specific receptor complex/molecule. It then enters the cell via endocytosis and is transported intracellularly in a MT-dependent fashion. After release out of the endosomal compartment, the nucleocapsid containing the viral DNA binds the nuclear pore complex and the viral genome is released into the nucleus. It is also possible that the whole nucleocapsid enters the nucleus and releases the viral DNA inside. Afterwards, the viral rcDNA is converted into cccDNA and viral transcripts are made. These are exported into the cytosol where the pgRNA is packaged together with the viral polymerase into the nucleocapsid. Inside the capsid, the RNA is reverse transcribed into the viral DNA genome. These matured nucleocapsids can then either be transported to the nucleus to add to the cellular cccDNA pool or they interact with viral surface proteins on the cellular ER membrane. There, the nucleocapsid buds into the lumen of the ER and is then transported in a yet undefined fashion to the cell surface where the viral particle is released into the cell exterior.

unknown cellular receptor compounds. After binding, viral particles are taken up into the cell by receptor-mediated endocytosis[32-34]. Then, the nucleocapsid is released from the endosomal compartment into the cytosol. It is currently under discussion whether a low endosomal pH is necessary for this release. The cytoplasmic nucleocapsids are then transported to the nucleus to initiate productive infection. This transport strongly depends on active microtubules (MT) but not on actin[27].

After reaching the nuclear membrane, the core protein is presumably phosphorylated and exposes a nuclear localization signal. This results in binding of nuclear factors; e.g., importins, to the capsid, which leads to uptake of the whole complex into the nucleus[35]. However, disassembly of the capsid near the nuclear membrane and subsequent transport of the viral DNA into the nucleus cannot be excluded.

In the nucleus, the relaxed form of the viral genome, the rcDNA (relaxed circular), is converted into the covalently closed, circular form (cccDNA). This is only possible after removal of the 5'-terminal structures (protein and RNA), repair of the gap and covalent ligation of the strands by cellular proteins. The cccDNA is usually not incorporated into the host genome but is organized in nucleosomes in the form of an episome[36].

Transcription of the viral genome is mediated by the cellular RNA polymerase Ⅱ[37]. *In vivo*, three different viral RNA classes could be identified, which are all polyadenylated and posses a cap structure[21]. They all have the same 3' end since only one polyadenylation site is present in the viral genome but have different 5' ends due to different transcription initiation sites. The different viral

RNAs are transported into the cytoplasm and translated. The two longest RNAs (3.5 kb), which stretch the whole genome, have two different functions. They code for the viral proteins core, the polymerase and e-antigen but one also serves as the pregenome[21]. Part of the 3.5 kb mRNA is spliced and serves as mRNA for L protein synthesis. A second class of viral RNAs (2.1 kb) encodes for the large surface protein, and the third class (1.8 kb) codes for the small surface protein, which is the most abundant one. The identity of the X-encoding RNA is unknown.

After export into the cytosol, the viral RNAs are translated and the viral surface proteins are directly inserted into the ER membrane. Once inserted, they can autonomously form subviral particles or interact with capsids to form virions.

In the cytosol, core protein dimers interact with each other and self assemble with the viral polymerase and the pgRNA into ribonucleoprotein complexes[38]. The pgRNA is packaged upon a chaperone-mediated interaction of the polymerase with the stem loop structure epsilon (ε). This structure also serves as the replication origin for the reverse transcription. Prior to packaging, the core protein is phosphorylated[39]. It is currently unclear whether reverse transcription initiates during ribonucleoprotein complex formation or after assembly of the capsid. However, when the pgRNA is inside the capsid, the particles mature, e.g. the RNA is reverse transcribed into the viral DNA genome and the core proteins are dephosphorylated[2,40]. The mature capsids interact with the viral surface proteins at the membrane of the ER and bud into the lumen, thus forming complete virions. The enveloped virions are then presumably transported through the constitutive secretion pathway to the cell surface and are released there. Alternatively, mature capsids can be transported to the nucleus and add to the cccDNA pool. After a successful infection, between one and 20 cccDNA molecules can be detected inside the nucleus[41]. This re-infection cycle preferentially occurs during establishment of an infection when the levels of large surface protein are low[42]. After a successful infection, the levels of L inside the cell rise and capsids preferentially form virions and are secreted.

In the absence of mature capsids and due to the autonomous budding activity of the viral surface proteins, subviral particles are formed. S as well as L proteins seem to accumulate in membrane domains of the ER where they reach quite high densities. When they reach a critical density, they presumably bud into the ER lumen and form subviral particles.

DHBV PROTEINS AND THEIR BASIC FUNCTIONS IN VIRAL ENTRY, REPLICATION, AND MORPHOGENESIS

Core protein and e-antigen

The viral core protein fulfils several opposing functions during the different stages of the viral life cycle; e.g., nucleic acid binding and assembly opposed to disassembly and nucleic acid release. These diverse functions are partly regulated by: (1) subcellular localization, (2) quaternary structure and (3) posttranslational modification by phosphorylation and dephosphorylation of its C-terminus.

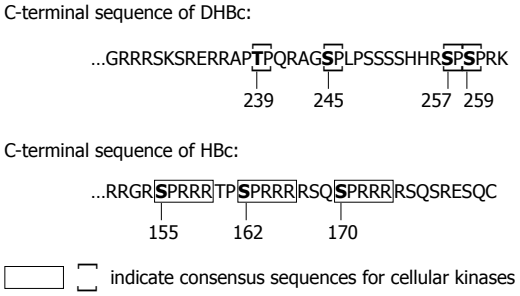

Figure 4 Phosphorylation sites of the viral core protein. The C-terminal sequence of the core proteins from DHBV and HBV are shown. Red brackets indicate the phosphorylation motifs, bold letters indicate the phosphorylated amino acid residue.

The viral nucleocapsid is composed of dimeric subunits of the viral core protein (DHBc) with a molecular weight of 32 kDa. The N-terminal region of the core protein (up to about 144 aa) is acetylated[43] and sufficient for assembly of the capsid shell[44,45]. The carboxyterminal end of the protein, the so called C-terminal domain (CTD), is extremely basic and binds nucleic acids. This is essential for packaging of the pgRNA into the nucleocapsid as well as progression of reverse transcription within[44,46]. In addition, a nuclear localization signal is present between aa 184 and 226 along with a nuclear export signal[47].

The major phosphorylation sites in the core protein are mapped to the arginine-rich C-terminus. This domain contains consensus sequences for different cellular kinases, such as PKC, SRPK1 and SRPK2 (Figure 4). Furthermore, Thr174 is highly conserved and is a cdc2 kinase phosphorylation site. Compared to the extracellular core protein, intracellular core is highly phosphorylated. Mutational analysis of the major phosphorylation sites revealed that individual or combined substitution had no overt effect on pgRNA packaging. However, the S245A mutant was deficient in genome maturation[48]. It has been shown that the CTD contains several phosphosites, which are heterogeneously phosphorylated intracellularly and hypophosphorylated or non-phosphorylated in the secreted virion[40,43]. This dephosphorylation, which occurs as nucleocapsids mature (meaning that the pgRNA is reverse transcribed into the rcDNA genome), is thought to be a maturation signal that results in secretion of only fully matured virions containing the DNA genome[43]. In addition, it has been shown that binding of hepadnaviral capsids to the nuclear pore complex depends on the phosphorylation status of the core protein[35]. The kinases or phosphatases implicated in these steps are not known. This is also true for the fate of the nucleocapsids after nuclear binding; it is not known whether they disassemble at the nuclear pore and thereafter release the viral DNA or if they are transported through the nuclear pore and then disassemble.

DHBc has the autonomous ability to assemble into particulate structures, which is dependent on the DHBc concentration[49]. The nucleocapsid is a dynamic structure and subject to regulated conformational transitions. Formation of progeny virions requires stable

nucleocapsids, whereas during viral entry, the incoming viral structure must disassemble and release the viral genome. Furthermore, reverse transcription of the viral genome occurs within the capsid and it is thought that this is linked with structural rearrangements in the capsid.

The ultrastructural analysis of the HBV core protein revealed that the monomeric form is dominated by a long alpha-helical hairpin structure[45]. The first step of capsid formation is the homodimerization of two core protein monomers that arrange in a way that leads to an antiparallel order, which results in an almost exact twofold symmetry. As a result, the characteristic spike on the capsid surface is formed by a compact four helix bundle. These spikes are the regions that interact in the virion with the viral envelope structures. Preliminary 3D reconstruction of the DHBV capsid suggests that the protein forms T-shaped dimers similar to the human core protein (M. Nassal, personal communication).

The open reading frame that encodes DHBc also codes for a nonstructural viral protein, which is the DHBe or precore. This e-antigen is, compared to the DHBc, truncated at the C-terminus and extended on the N-terminus. In addition it contains a type I signal recognition sequence. It is translocated into the ER during synthesis where the signal recognition sequence is cleaved and the C-terminus removed. After this processing, e-antigen is transported through the Golgi complex and secreted from the infected cell[50,51]. It has been shown that the e-antigen is glycosylated[50]. The glycosylation pattern seems to differ among the different avian hepadnaviruses and even among different isolates of DHBV due to the presence of different numbers of N-glycosylation sites. This is, for instance, obvious in a recent study of HHBV e-antigen that has one glycosylation site. This resulted in two bands in immunoblot analysis (one for glycosylated and for non-glycosylated e-antigen), while CHBV e-antigen with two N-glycosylation sites showed three bands on the immunoblot[14].

DHBe can be detected in the serum of infected ducks[52] and serves as a marker for efficient viral replication. Its exact function is unknown, but it has been shown that it plays no essential role in viral replication, morphogenesis or infectivity[53]. However, it seems to play a role in the establishment of chronic infections[54] and its absence may confer a growth advantage of precore-minus mutants over wildtype virus[55].

Polymerase

The viral polymerase is a multifunctional protein of about 90 kDa in size. It has a DNA-dependent DNA polymerase activity/domain to fill the gap in the viral DNA during replication[56] and an RNaseH activity/domain to selectively digest RNA from an RNA-DNA-hybrid molecule[57], as it has been shown for HBV. It also has reverse transcriptase (RT) activity to transcribe the RNA pregenome into the DNA genome during replication[2]. The polymerase homology domain is centrally located, whereas the RNaseH homology domain is located near the C-terminus of the protein. Viruses with point mutations in these regions are either defective for viral DNA synthesis or only allow negative-strand but not positive-strand DNA synthesis[56]. Most N-terminal sections of the polymerase domain are spacer regions without any other apparent function[58]. Most N-terminal sections are the region implicated in the covalent linkage of the P protein to the viral DNA often referred to as terminal protein.

In the process of viral genome replication, during which the pregenomic RNA is transcribed into the genomic DNA, the different domains can assert their different functions. The pgRNA is transcribed from the viral cccDNA by cellular polymerase Ⅱ. This RNA is then transported into the cytosol and binds the viral polymerase and the core proteins. The polymerase recognizes the epsilon and another downstream region on the viral RNA and binds there with the help of cellular proteins like Hsp90[59]. Inside the particle, the RNA is transcribed into the negative strand DNA by the RT domain of the polymerase. This process is primed by the protein itself and tyrosine 96 of the P protein serves as a primer[60]. This results in covalent attachment of the nascent DNA strand onto the terminal protein part of the polymerase. After attachment of about 4 nucleotides, this DNA product is transferred to the DR1 sequence on the viral pgRNA. This is possible since the epsilon signal and the DR1 share a 4 nucleotide identity. From this position, the DNA negative strand is elongated by the conventional mechanism[61,62]. As this elongation proceeds, the template RNA is degraded by the RNaseH activity of the viral polymerase[2,63]. The end product of this reaction is a negative-stranded DNA, which is terminally redundant by about 8 nucleotides.

Positive strand synthesis is initiated at DR2 and primed by a short oligoribonucleotide, which is a remnant from the pgRNA[64]. This primer is transferred to a complementary region at the 5' end of the negative strand DNA for positive strand synthesis. From there, synthesis of the positive strand proceeds.

Sometimes (in about 1% to 5% of cases) the primer fails to translocate. This results in a process called *in situ* priming, where a fully duplex linear DNA is the end product[65]. This is a dead end for viral replication but may be the cause for integration of some viral genomes into the chromosomal DNA of the host cell.

Elongation of the positive strand proceeds until the 5' end of the negative strand is reached. Then, an intramolecular strand transfer is needed to complete positive strand synthesis. This happens after circularization of the genome, which is possible because of the short redundancies at each strand end. After the circularization, positive strand synthesis can proceed. Usually elongation does not proceed until the end of the template is reached. In the case of DHBV, normally about 80% of the positive strands complete elongation[20].

Envelope proteins

The multiple functions of the viral envelope proteins are reflected by the domain organization and unique biochemical features. The DHBV envelope proteins are encoded by a single ORF consisting of the preS and S domain. The viral envelope proteins are inserted into the membrane of the virus that originated from intracellular membranes (presumably the ER) of the infected cell. In the case of DHBV, these envelope proteins are the small

protein S, which constitutes about 80% of total envelope proteins, and the large protein L, which constitutes about 20%[66,67]. S protein is thus the most abundant protein in the viral envelope. It determines the envelope curvature and is indispensable for both budding and secretion of viral particles. Both viral surface proteins are unique compared to other viral surface proteins in their relatively complex structure and topology[68]. They have a molecular weight of 18 and 36 kDa, respectively, and are anchored in the membrane by several transmembrane domains. The C-terminus of both proteins are identical, while L is N-terminally extended by 161 aa compared to S. The length of this extension varies with the isolate. This unusual organisation results from differential transcription of a single ORF[67] (Figure 2).

The L protein is modified with myristic acid at its N-terminal glycine after removal of the first amino acid methionine, which presumably anchors the protein in the membrane in addition to the transmembrane domains[69]. This myristoylation is required for infectivity of the virus but not for assembly[69]. Unlike the envelope protein of HBV, DHBV L and S are not modified by N-glycosylation although they contain consensus glycosylation sites. In contrast, it has been shown that the DHBV L protein (p36) is the only surface protein that is phosphorylated[70,71]. This phosphorylation occurs at serine 118 by an ERK-type MAP kinase and is not essential for viral replication, particle formation or infectivity[71].

As transmembrane proteins, L and S are incorporated cotranslationally into the ER membrane. The proteins have four transmembrane domains (TM1 to TM4) that anchor them in the membrane and consist of membrane-spanning hydrophobic alpha-helices (Figure 5). In addition, the preS domain of the L protein contains two translocation motifs (TLM), which are 12 amino acid encompassing domains that form an amphipathic alpha helix[32]. TLMs mediate an energy- and receptor-independent transfer of peptides, nucleic acids and proteins when fused to them across membranes without affecting their integrity[72]. The DHBV-TLMs are located between amino acids 20-31 (TLM1) and 42-53 (TLM2) and required for viral infectivity.

Worth mentioning is the dual topology of the L protein[73]. After cotranslational insertion of the protein into the cellular membrane, part of the proteins changes the topology (Figure 5). This leads to exposure of the N-terminus to the cytosolic side of the membrane in about half of the L proteins while the other half has the N-terminus directed to the luminal side[74]. In this way, the protein can fulfil two different functions: it can interact with the cellular receptor on the outside of the virus and it can interact with the nucleocapsid on the inside. Whether S also adopts a dual topology remains to be determined.

The viral surface proteins are able to autonomously form subviral particles without the help of an interacting nucleocapsid. The exact mechanism of this phenomenon is not known, yet it is assumed that the proteins interact with each other to form microdomains in the ER membrane from which they bud when they reach a critical density. A prerequisite for this budding activity would be a tight interaction of the viral surface proteins with the membrane lipids and a membrane bending activity. When

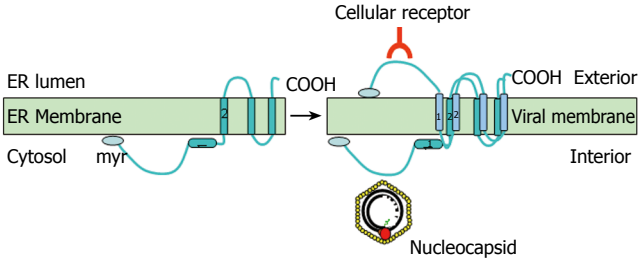

Figure 5 Dual topology of the viral surface protein L. The L protein is inserted into the ER membrane during synthesis with transmembrane domain 2 being inserted into the membrane. Half of the proteins then change their topology and insert the transmembrane domain 1 into the ER membrane. After this change and formation of the virus, L can exert its two basic functions; interaction with the nucleocapsid on the cytosolic preS domain and interaction with the host cell receptor on the surface of the viral particle.

L protein is expressed without the S component, particles are formed inside the cells, but are not secreted. This retention and secretion defect can be overcome by co-expression of the S protein[75]. This implies an important function for the S protein in secretion of viral particles.

Another function of the L protein is regulation of cccDNA amplification. As mentioned above, cccDNA is the replication template for all hepadnaviruses. It is a prerequisite for maintaining chronic infection of hepatocytes and is the main obstruction during antiviral therapy since it is mostly not eliminated from the cells. The amount of cccDNA inside the host cell nucleus is thus of great importance for the virus. To maintain its replication template in the nucleus, it re-infects and this process is regulated in an elaborate manner by the large viral surface protein[76]. During the early stage of infection when the amount of L protein is low inside the cell, mature core particles preferentially infect the nucleus to add to the cccDNA pool. Concomitant with the increase in cccDNA, the levels of L increase. This leads to redirection of the mature capsids into the secretory pathway and reduces cccDNA amplification.

The L protein is also responsible for superinfection exclusion, which prevents hepadnaviral infection of already infected hepatocytes[77]. This phenomenon was first ascribed to downregulation of the putative viral receptor protein gp180. This has not been confirmed and it has been suggested that superinfection exclusion may result from a role of L as a regulator of intracellular trafficking[77].

The L protein not only plays a role in viral morphogenesis or cccDNA amplification, but it is also implicated in additional regulatory functions such as signalling[71]. The cytosolically exposed preS domain of the L protein has the potential to activate gene expression from cellular promoter elements in *trans*. It is also phosphorylated by ERK2 at serine 118, which is induced by various stimuli and may play a role in intracellular virus-host crosstalk[71].

X protein

One major difference between the avian and mammalian hepatitis B viruses is the presence of an ORF called X in the latter. The function of this regulatory protein is still far from being understood. Recently it has been reported

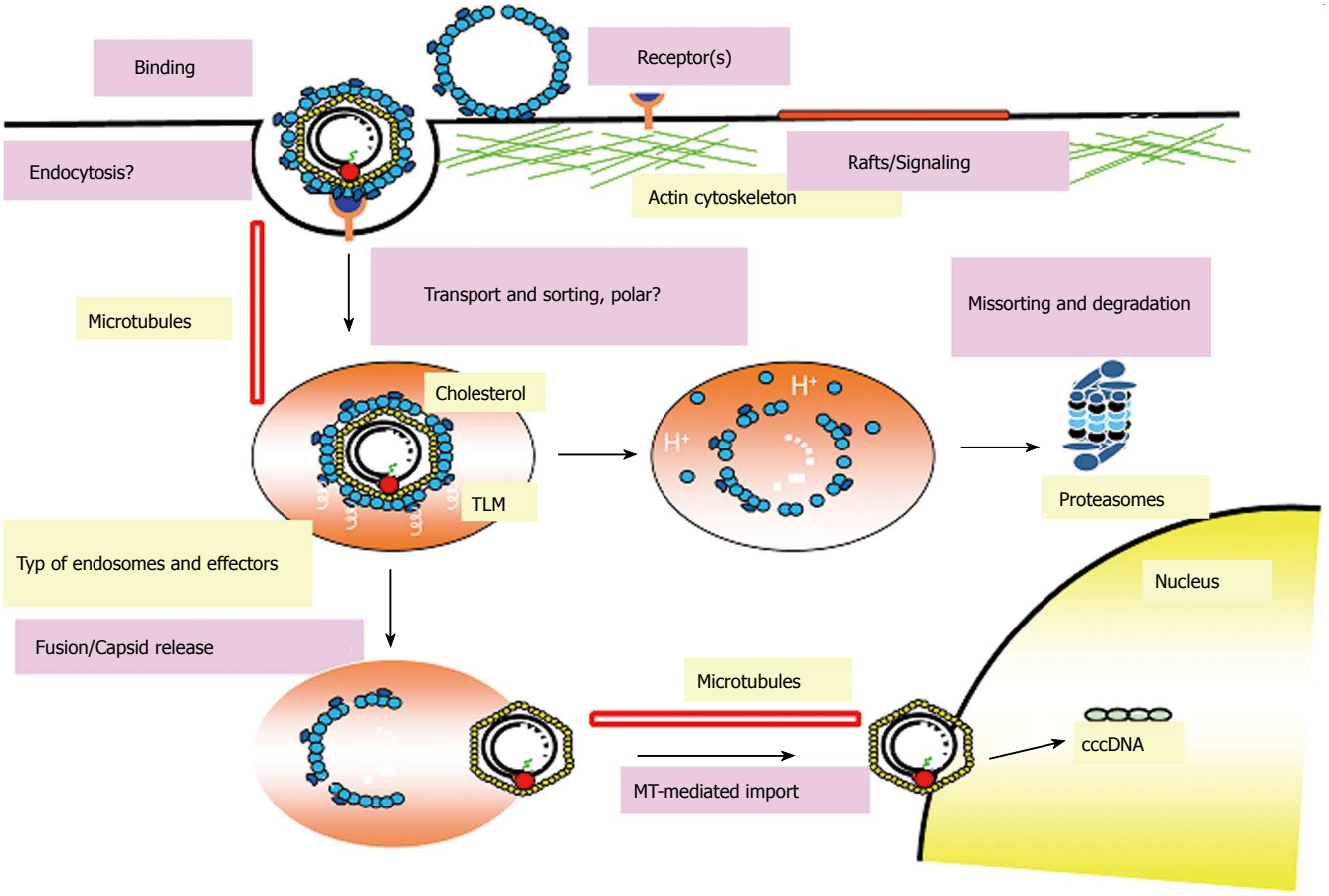

Figure 6 Current model for entry and intracellular trafficking of DHBV. The hepadnaviral life cycle starts with the attachment of virions to specific binding sites on the surface of hepatocytes mediated by the preS region of the large viral envelope protein L. Afterwards the virus enters the cell via endocytosis and resides in an endocytic vesicle which is transported in a MT-dependent and probably polar fashion. The endosomal release of the incoming particle requires the activity of the vacuolar H^+-ATPase and presumably the cholesterol of the viral envelope. After release, the particle is transported in a MT-dependent fashion mediated by dynein/dynactin to the nucleus and initiates infection after release of the viral genome at the nuclear membrane or within the nucleus. However, the majority of viral particles is missorted and degraded by the proteasome and other cellular proteases.

that X protein enhances the replication of transfected HBV genomes[78]. DHBV lacks an apparent X-ORF. But a cryptic X-like ORF has recently been reported[22]. *In vivo* experiments have suggested no functional role for this gene product in DHBV short term infection[79].

DHBV INFECTION

In vitro infection

Hepadnaviruses can only efficiently infect primary hepatocytes with the exception of the recently published HepaRG cell line, which can be infected with the human HBV[1]. Thus, primary hepatocyte cultures have to be established for use with hepadnaviruses. In the case of DHBV, either primary fetal or adult hepatocytes can be used. Fetal hepatocytes can be obtained easily from the livers of non-hatched duck embryos. These are digested with collagenase, washed and plated. This results in a mixed culture containing hepatocytes as well as other cells of the liver, which are the non-parenchymal cells, such as macrophages, sinusoidal endothelial cells, and fibroblasts. Alternatively, primary duck hepatocyte cultures can be obtained from adult ducks by liver perfusion. This results in a rather homogenous suspension of cells containing high amounts of hepatocytes (up to 90%) compared to non-parenchymal cells. Compared to primary human hepatocytes, PDHs are about 20 times more permissive to hepadnaviral infection.

The cells are cultured in a standard medium containing hydrocortisone, insulin as well as DMSO. The DMSO is important for maintaining differentiation and thus infectability of the cells[80]. Under these culture conditions, the cells remain infectable for up to 2 weeks in culture and viral spread occurs. The DMSO as well as omitting serum from the cell culture medium are essential conditions for maintaining cellular infectability since addition of serum to the cultures decreases the amount of cellular receptor proteins on the cell surface[81].

Research with the *in vitro* model of DHBV infection has lead to the discovery of many different features of the hepadnaviral life cycle. However, while factors involved in the early and most vulnerable steps of the viral life cycle (Figure 6) have been identified for a variety of viruses, little is known for hepadnaviruses (for a review see[7] and references therein).

Hepatoma cell lines, which can replicate the viral DNA and produce progeny virus after transfection of the viral genome into the nucleus, are not permissive for infection with the virus itself[82]. This phenomenon led to the assumption that the absence of a viral receptor or

receptor complex on the cell surface of these cells is the major determinant for infection. Great effort was invested to identify these molecules. But to date, the molecules responsible for the viral uptake that leads to productive infection are still unknown, although carboxypeptidase D (gp180) has been shown to specifically interact with the viral L protein and leads to internalization of viral particles after heterologous expression[83-85]. However, this did not lead to productive infection of these cells. In addition, the protein has been shown to not only bind DHBV, but also the viral surface protein from heron HBV, which does not infect PDHs, and this protein is not liver specific. It thus cannot be the determinant for viral host range or tissue specificity. This shows that either additional factors are required for the infection or that gp180 plays no role in the productive uptake and binding of the virus.

Initial binding of hepadnaviral particles seems to involve a component with low affinity without saturation and a component with high affinity and saturation[28]. This indicates that the binding involves at least two determinants and thus components. Several competition experiments with recombinant preS peptides, neutralizing antibodies and SVPs showed that the preS region of the viral L protein is essential for viral binding and the establishment of an infection[26,28,86,87]. In addition, it has been shown that preS peptides that were myristoylated were much more efficient in preventing DHBV infection than non-myristoylated peptides, which indicates that the myristoylation of L plays an important role during infection[86].

To gain more insight into the enigmatical early steps of hepadnaviral infection, we recently characterized the early attachment and entry events of DHBV infection in PDHs[27]. To do so, we established a sensitive, PCR-based assay that allowed us to investigate viral binding and entry. This binding and entry assay showed that only a small proportion of the inoculum binds to the cell surface of hepatocytes. Also the overall number of particles that bind to the cell surface is quiet low, after 2 h at 4℃, only up to 10 virions and 10 000 SVPs per cell were detectable. This indicates that the number of hepatocellular surface binding sites is about 10 000 per cell. Binding was prevented by the use of neutralizing antibodies as well as suramin, which also prevented viral infection showing that the detected binding sites are relevant for productive infection.

The steps after viral binding also remain quite elusive. It was shown years ago that the kinetics of DHBV uptake is unusual since binding and entry seem to be very slow. For a maximal infection efficiency, cells have to be incubated with the virus up to 16 h[80]. We have recently shown that viral uptake indeed needs an unusually long time period[27]. 1 h after attachment only about 70% of bound DHBV was taken up and internalization was complete within 3 h. This shows that virus uptake itself takes a relatively long time period, but since after 3 h all bound virions were internalized, uptake is very efficient. In contrast, viral trafficking inside the cell does not seem to be efficient since a high proportion of viral particles are degraded after viral entry into the cell and thus cannot establish infection[34].

It has been shown previously that DHBV entry into PDHs requires energy, which indicates that cellular and/or viral processes actively take place and that DHBV is presumably entering the cell via endocytosis[33,34]. Studies addressing the pH-dependency of DHBV infection by the use of chemical substances that increase endosomal pH led to contradicting results[33,88-90]. However, the weight of data favours pH-independent entry as well as an endocytic mechanism and shows that the virus does not require passage through a highly acidic compartment. The effect of the vATPase inhibitors seem to be due more to effects on viral trafficking inside the cell than on the endosomal pH alone[34].

After the virus is taken up by the cell via endocytosis, it has to be transported to the nucleus to establish infection. In the nucleus, the viral rcDNA is converted into the cccDNA. This conversion is detectable within the first 24 h after virus inoculation[27,91]. Thus, after efficient viral uptake there is an unusually long gap of 13 to 17 h before the appearance of nuclear viral cccDNA. This gap suggests that there is a rate-limiting post entry step that preceeds cccDNA formation, which involves viral uncoating and nuclear genome transport, or is required for rc- to cccDNA conversion. The intracellular transport has been shown to be independent of the actin skeleton, which in contrast seems to restrict entry, and is strictly dependent on the microtubule (MT) network of the cell[27]. Overexpression of dynamitin, a cofactor subunit of the motor protein complex dynactin-dynein, which mediates transport along microtubules, also reduced DHBV infection (our unpublished data). To date it remains unknown whether the MT-dependent transport of the virus (or the nucleocapsid alone) occurs only at the stage of the endosome or if the virus alone also interacts with microtubules.

To deliver the viral DNA into the nucleus, it has to be released from the viral particle and, prior to that, the viral particle has to be released from the endosomal compartment it resides in. It has been shown that this involves an unusual mechanism that depends on the integrity of a so called TLM[32]. The TLM thus mediates release of the viral particle out of the endosome into which it initially entered.

The infectious entry pathway of hepadnaviruses appears to involve a series of highly coordinated and directional steps leading to the nuclear delivery of viral genomes essential for the establishment of a productive infection. These steps may, alone or in combination, determine the species and host cell tropism common to all hepadnaviruses.

In vivo infection

DHBV-infected ducks exhibit age-related outcomes of infection, which is similar to HBV-infected humans. In principle, hepadnaviruses have the ability to cause either a transient or chronic infection. When infected with DHBV, young ducks develop persistent infection whereas adult ducks become transiently infected and eliminate the virus[92]. These different outcomes are viral dose dependent; persistent infection in young ducks develops more frequently with higher doses of virus[92]. In some cases, dependent on age and infection with a given mutant,

experimental infections can cause symptoms of a liver inflammation[93]. It has been shown that one genome equivalent is sufficient to infect a duckling and that spread of the virus within the liver is very efficient: 14 d after inoculation, virtually all hepatocytes were infected[94]. In addition, it has been shown that the difference between the infection outcome in older and neonatal ducks depends on the production of neutralizing antibodies against the virus[95]. The rapid production of neutralizing antibodies in older ducks led to an efficient inhibition of viral spread in the liver.

The duck hepatitis B virus infects Chinese domestic and American pekin ducks as well as geese. Normally, infection takes place through vertical transmission from the infected hen to the eggs and results in a chronic infection that is without symptoms and is tolerated by the immune system[23]. The virus then replicates in the egg yolk sack and is transferred to the embryonic hepatocytes by day 6 of development[96]. Thus, all offspring from an infected hen are DHBV-positive.

When DHBV infection is persistent in the duck, viral replication mainly occurs in the hepatocytes of the liver. Usually, the level of viral replication is then very high, with most hepatocytes infected and expressing the viral antigens. This is also reflected in the amount of viral antigens circulating in the blood stream. Up to 10^{10} virions and 10^{13} SVPs can be detected per ml of serum[97].

In vivo infections with DHBV are often used to study the growth kinetics of viral mutants[79]. This allows elucidation of specific mutations in the viral genome on the behaviour of this respective mutant in their natural host. In contrast to the *in vitro* situation, the role of the immune system and the spread of the virus within the infected liver can be assessed.

It has been shown that the addition of lipopolysaccharides (LPS, endotoxin) to PDH cultures inhibited DHBV replication efficiently[98]. This was due to the release of interferon alpha and gamma from non-parenchymal cells (i.e. Kupffer cells, resident macrophages of the liver). The exact mechanism behind this phenomenon is not known.

HOST SPECIFICITY

All known hepadnaviruses are strongly, but not exclusively, cell type specific and have a narrow host range restricting them to their natural host and a few closely related species (Figure 1). DHBV, for example, infects only certain duck and goose species, but either does not or very inefficiently infects chicken or Muscovy ducks, respectively. Despite its substantial sequence homology with DHBV, the heron HBV (HHBV) does not infect PDHs. Although ducks and duck-derived primary hepatocytes are virtually non-permissive for HHBV, substitution of a region of the HHBV-specific preS domain of the L protein by the corresponding sequence from DHBV overcomes this species barrier. As a consequence, the pseudotyped HHBV virions can efficiently infect primary duck hepatocytes[5]. The same is true for mammalian hepadnaviruses, as shown for woolly monkey hepatitis B virus pseudotyped with a small stretch of preS1 sequence from HBV, which was

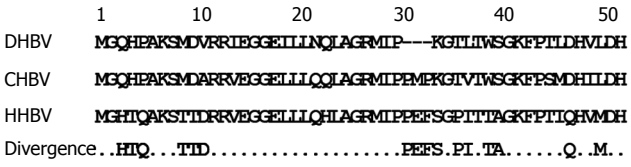

Figure 7 Sequence comparison of the viral L protein from different hepadnaviruses. The first 50 amino acids of the preS domain of hepadnaviral L from duck, crane, and heron HBV are shown. The divergent amino acids are shown in the lowest lane.

then infectious for human hepatocytes. Thus, although the sequence of this region is very divergent among the different hepadnaviruses, the biological functions seem to be conserved. The so called host-determining region (HDR) in the preS part of the avian L protein was mapped to amino acids 22 to 90, and an exchange of this small region also changed the species specificity[5]. These studies clearly indicate that the block to cross-species infection by hepadnaviruses is destined at the level of infectious viral entry. A small domain within the preS region of the L protein plays a pivotal role in host discrimination.

We showed that cranes are naturally infected with a novel hepadnavirus, designated crane HBV (CHBV)[14]. Phylogenetically, cranes are very distant from ducks and are closely related to herons and storks. However, we found that CHBV infects PDHs with similar efficiency as DHBV, indicating a rather broad host range of this virus at least *in vitro*. Whether CHBV can establish chronic infection in ducks *in vivo* and is as non-pathogenic as DHBV remains to be elucidated. Interestingly, comparison between the HDR of DHBV and the HDR of CHBV reveals a short insert of 3 amino acids (PMP) in the CHBV L protein, a sequence similar but not identical to the analogous region of HHBV and STHBV, whereas all other known duck and goose hepadnaviruses have no such insert (Figure 7). It remains to be shown which sequence features of the L protein are responsible for the unusual broad host range of CHBV and at which level of infection the block in cross-species infection is determined.

Accordingly, comparative genomic and subgenomic sequence alignment from different avihepadnaviruses facilitates the prediction of specific properties of each virus and helps to gain insight into the mechanisms controlling species specificity and host adaptation.

CHEMOTHERAPY AND VACCINATION

Antiviral drugs currently in use for therapy of chronic hepatitis B are nucleoside analogues and interferon. These therapies are unsatisfactory since the virus is usually not eliminated from the infected patient and resistant viruses frequently appear after treatment with nucleoside analogues. These data show the need for additional therapies and therapeutic strategies. The therapeutic effect of new vaccination strategies as well as chemotherapeutic agents can be assessed with the DHBV model system.

A long-term study showed that treatment of persistently infected ducks with 0.1 mg/kg per day of entecavir resulted in a rapid 4-log drop in serum DHBV

surface antigen[99]. However, a rapid rebound of levels of DHBV DNA and antigens in serum and liver was observed when entecavir was discontinued. When entecavir was administered at the time of DHBV inoculation, it was not effective to prevent infection but it led to a significant suppression of viral spread even after withdrawal of the drug[100]. Thus, short term suppression of DHBV infection shortly after infection provides the opportunity for the immune response to successfully control the infection.

Immunotherapy using DNA vaccines has been proposed as a way to improve viral clearance via the induction of an effective immune response. It has been shown that a DNA vaccine expressing DHBV surface antigens induces high levels of antibodies directed against these antigens, which protected or partially protected the animals against a challenge with DHBV[101]. This suggests that DNA vaccines may be an alternative to conventional vaccines for inducing immune response and protection against infection.

ACKNOWLEDGMENTS

We apologize to those authors whose work we could not cite directly due to space limitations. The authors are indebted to Claudia Franke (Heinrich-Pette-Institute, Hamburg, Germany) for providing the picture of core protein phosphorylation.

REFERENCES

1 **Gripon P**, Rumin S, Urban S, Le Seyec J, Glaise D, Cannie I, Guyomard C, Lucas J, Trepo C, Guguen-Guillouzo C. Infection of a human hepatoma cell line by hepatitis B virus. *Proc Natl Acad Sci USA* 2002; **99**: 15655-15660
2 **Summers J**, Mason WS. Replication of the genome of a hepatitis B--like virus by reverse transcription of an RNA intermediate. *Cell* 1982; **29**: 403-415
3 **Tuttleman JS**, Pourcel C, Summers J. Formation of the pool of covalently closed circular viral DNA in hepadnavirus-infected cells. *Cell* 1986; **47**: 451-460
4 **Wang GH**, Seeger C. The reverse transcriptase of hepatitis B virus acts as a protein primer for viral DNA synthesis. *Cell* 1992; **71**: 663-670
5 **Ishikawa T**, Ganem D. The pre-S domain of the large viral envelope protein determines host range in avian hepatitis B viruses. *Proc Natl Acad Sci USA* 1995; **92**: 6259-6263
6 **Condreay LD**, Aldrich CE, Coates L, Mason WS, Wu TT. Efficient duck hepatitis B virus production by an avian liver tumor cell line. *J Virol* 1990; **64**: 3249-3258
7 **Ganem D**, Schneider RJ. Hepadnaviridae: The viruses and their replication. In: Knipe DM, Howley PM, editors. Fields Virology. Volume 2. Philadelphia: Lippincott, Williams & Wilkins, 2001; 2923-2969
8 **Mason WS**, Seal G, Summers J. Virus of Pekin ducks with structural and biological relatedness to human hepatitis B virus. *J Virol* 1980; **36**: 829-836
9 **Munshi A**, Mehrotra R, Panda SK. Characterisation of the Indian strain of duck hepatitis B virus (DHBV) and development of a carrier duck colony for antiviral drug testing. *Trop Gastroenterol* 1994; **15**: 77-85
10 **Triyatni M**, Ey P, Tran T, Le Mire M, Qiao M, Burrell C, Jilbert A. Sequence comparison of an Australian duck hepatitis B virus strain with other avian hepadnaviruses. *J Gen Virol* 2001; **82**: 373-378
11 **Mangisa NP**, Smuts HE, Kramvis A, Linley CW, Skelton M, Tucker TJ, De La M Hall P, Kahn D, Jilbert AR, Kew MC. Molecular characterization of duck hepatitis B virus isolates from South African ducks. *Virus Genes* 2004; **28**: 179-186
12 **Chang SF**, Netter HJ, Bruns M, Schneider R, Frölich K, Will H. A new avian hepadnavirus infecting snow geese (Anser caerulescens) produces a significant fraction of virions containing single-stranded DNA. *Virology* 1999; **262**: 39-54
13 **Pult I**, Netter HJ, Bruns M, Prassolov A, Sirma H, Hohenberg H, Chang SF, Frölich K, Krone O, Kaleta EF, Will H. Identification and analysis of a new hepadnavirus in white storks. *Virology* 2001; **289**: 114-128
14 **Prassolov A**, Hohenberg H, Kalinina T, Schneider C, Cova L, Krone O, Frölich K, Will H, Sirma H. New hepatitis B virus of cranes that has an unexpected broad host range. *J Virol* 2003; **77**: 1964-1976
15 **Sprengel R**, Kaleta EF, Will H. Isolation and characterization of a hepatitis B virus endemic in herons. *J Virol* 1988; **62**: 3832-3839
16 **Pugh JC**, Simmons H. Duck hepatitis B virus infection of Muscovy duck hepatocytes and nature of virus resistance *in vivo*. *J Virol* 1994; **68**: 2487-2494
17 **Offensperger WB**, Offensperger S, Keppler-Hafkemeyer A, Hafkemeyer P, Blum HE. Antiviral activities of penciclovir and famciclovir on duck hepatitis B virus in vitro and *in vivo*. *Antivir Ther* 1996; **1**: 141-146
18 **Lien JM**, Petcu DJ, Aldrich CE, Mason WS. Initiation and termination of duck hepatitis B virus DNA synthesis during virus maturation. *J Virol* 1987; **61**: 3832-3840
19 **Gerlich WH**, Robinson WS. Hepatitis B virus contains protein attached to the 5′ terminus of its complete DNA strand. *Cell* 1980; **21**: 801-809
20 **Landers TA**, Greenberg HB, Robinson WS. Structure of hepatitis B Dane particle DNA and nature of the endogenous DNA polymerase reaction. *J Virol* 1977; **23**: 368-376
21 **Seeger C**, Ganem D, Varmus HE. Biochemical and genetic evidence for the hepatitis B virus replication strategy. *Science* 1986; **232**: 477-484
22 **Chang SF**, Netter HJ, Hildt E, Schuster R, Schaefer S, Hsu YC, Rang A, Will H. Duck hepatitis B virus expresses a regulatory HBx-like protein from a hidden open reading frame. *J Virol* 2001; **75**: 161-170
23 **Urban MK**, O'Connell AP, London WT. Sequence of events in natural infection of Pekin duck embryos with duck hepatitis B virus. *J Virol* 1985; **55**: 16-22
24 **Gavilanes F**, Gonzalez-Ros JM, Peterson DL. Structure of hepatitis B surface antigen. Characterization of the lipid components and their association with the viral proteins. *J Biol Chem* 1982; **257**: 7770-7777
25 **Sonveaux N**, Thines D, Ruysschaert JM. Characterization of the HBsAg particle lipid membrane. *Res Virol* 1995; **146**: 43-51
26 **Satoh O**, Imai H, Yoneyama T, Miyamura T, Utsumi H, Inoue K, Umeda M. Membrane structure of the hepatitis B virus surface antigen particle. *J Biochem* 2000; **127**: 543-550
27 **Funk A**, Mhamdi M, Lin L, Will H, Sirma H. Itinerary of hepatitis B viruses: delineation of restriction points critical for infectious entry. *J Virol* 2004; **78**: 8289-8300
28 **Klingmüller U**, Schaller H. Hepadnavirus infection requires interaction between the viral pre-S domain and a specific hepatocellular receptor. *J Virol* 1993; **67**: 7414-7422
29 **Bruns M**, Miska S, Chassot S, Will H. Enhancement of hepatitis B virus infection by noninfectious subviral particles. *J Virol* 1998; **72**: 1462-1468
30 **Nassal M**, Schaller H. Hepatitis B virus replication. *Trends Microbiol* 1993; **1**: 221-228
31 **Hildt M**. Zelluläre Funktionen während der frühen und späten Schritte im Infektionszyklus des Enten Hepatitis B Virus. Dissertation der Naturwissenschaftlich-Mathematischen Gesamtfakultät der Ruprecht-Karls-Universität Heidelberg. Germany: University of Heidelberg, 1996
32 **Stoeckl L**, Funk A, Kopitzki A, Brandenburg B, Oess S, Will H, Sirma H, Hildt E. Identification of a structural motif crucial for infectivity of hepatitis B viruses. *Proc Natl Acad Sci USA* 2006; **103**: 6730-6734
33 **Köck J**, Borst EM, Schlicht HJ. Uptake of duck hepatitis B virus into hepatocytes occurs by endocytosis but does not require

passage of the virus through an acidic intracellular compartment. *J Virol* 1996; **70**: 5827-5831
34 **Funk A**, Mhamdi M, Hohenberg H, Will H, Sirma H. pH-independent entry and sequential endosomal sorting are major determinants of hepadnaviral infection in primary hepatocytes *Hepatology* 2006; **44**: 685-693
35 **Kann M**, Sodeik B, Vlachou A, Gerlich WH, Helenius A. Phosphorylation-dependent binding of hepatitis B virus core particles to the nuclear pore complex. *J Cell Biol* 1999; **145**: 45-55
36 **Newbold JE**, Xin H, Tencza M, Sherman G, Dean J, Bowden S, Locarnini S. The covalently closed duplex form of the hepadnavirus genome exists in situ as a heterogeneous population of viral minichromosomes. *J Virol* 1995; **69**: 3350-3357
37 **Rall LB**, Standring DN, Laub O, Rutter WJ. Transcription of hepatitis B virus by RNA polymerase II. *Mol Cell Biol* 1983; **3**: 1766-1773
38 **Zhou S**, Standring DN. Hepatitis B virus capsid particles are assembled from core-protein dimer precursors. *Proc Natl Acad Sci USA* 1992; **89**: 10046-10050
39 **Gazina EV**, Fielding JE, Lin B, Anderson DA. Core protein phosphorylation modulates pregenomic RNA encapsidation to different extents in human and duck hepatitis B viruses. *J Virol* 2000; **74**: 4721-4728
40 **Pugh J**, Zweidler A, Summers J. Characterization of the major duck hepatitis B virus core particle protein. *J Virol* 1989; **63**: 1371-1376
41 **Zhang YY**, Zhang BH, Theele D, Litwin S, Toll E, Summers J. Single-cell analysis of covalently closed circular DNA copy numbers in a hepadnavirus-infected liver. *Proc Natl Acad Sci USA* 2003; **100**: 12372-12377
42 **Lenhoff RJ**, Summers J. Coordinate regulation of replication and virus assembly by the large envelope protein of an avian hepadnavirus. *J Virol* 1994; **68**: 4565-4571
43 **Perlman DH**, Berg EA, O'connor PB, Costello CE, Hu J. Reverse transcription-associated dephosphorylation of hepadnavirus nucleocapsids. *Proc Natl Acad Sci USA* 2005; **102**: 9020-9025
44 **Nassal M**. The arginine-rich domain of the hepatitis B virus core protein is required for pregenome encapsidation and productive viral positive-strand DNA synthesis but not for virus assembly. *J Virol* 1992; **66**: 4107-4116
45 **Böttcher B**, Wynne SA, Crowther RA. Determination of the fold of the core protein of hepatitis B virus by electron cryomicroscopy. *Nature* 1997; **386**: 88-91
46 **Yu M**, Summers J. A domain of the hepadnavirus capsid protein is specifically required for DNA maturation and virus assembly. *J Virol* 1991; **65**: 2511-2517
47 **Mabit H**, Breiner KM, Knaust A, Zachmann-Brand B, Schaller H. Signals for bidirectional nucleocytoplasmic transport in the duck hepatitis B virus capsid protein. *J Virol* 2001; **75**: 1968-1977
48 **Yu M**, Summers J. Multiple functions of capsid protein phosphorylation in duck hepatitis B virus replication. *J Virol* 1994; **68**: 4341-4348
49 **Pollack JR**, Ganem D. An RNA stem-loop structure directs hepatitis B virus genomic RNA encapsidation. *J Virol* 1993; **67**: 3254-3263
50 **Standring DN**, Ou JH, Masiarz FR, Rutter WJ. A signal peptide encoded within the precore region of hepatitis B virus directs the secretion of a heterogeneous population of e antigens in Xenopus oocytes. *Proc Natl Acad Sci USA* 1988; **85**: 8405-8409
51 **Garcia PD**, Ou JH, Rutter WJ, Walter P. Targeting of the hepatitis B virus precore protein to the endoplasmic reticulum membrane: after signal peptide cleavage translocation can be aborted and the product released into the cytoplasm. *J Cell Biol* 1988; **106**: 1093-1104
52 **Schlicht HJ**, Salfeld J, Schaller H. The duck hepatitis B virus pre-C region encodes a signal sequence which is essential for synthesis and secretion of processed core proteins but not for virus formation. *J Virol* 1987; **61**: 3701-3709
53 **Schneider R**, Fernholz D, Wildner G, Will H. Mechanism, kinetics, and role of duck hepatitis B virus e-antigen expression in vivo. *Virology* 1991; **182**: 503-512
54 **Milich D**, Liang TJ. Exploring the biological basis of hepatitis B e antigen in hepatitis B virus infection. *Hepatology* 2003; **38**: 1075-1086
55 **Zhang YY**, Summers J. Enrichment of a precore-minus mutant of duck hepatitis B virus in experimental mixed infections. *J Virol* 1999; **73**: 3616-3622
56 **Kaplan PM**, Greenman RL, Gerin JL, Purcell RH, Robinson WS. DNA polymerase associated with human hepatitis B antigen. *J Virol* 1973; **12**: 995-1005
57 **Radziwill G**, Tucker W, Schaller H. Mutational analysis of the hepatitis B virus P gene product: domain structure and RNase H activity. *J Virol* 1990; **64**: 613-620
58 **Chang LJ**, Hirsch RC, Ganem D, Varmus HE. Effects of insertional and point mutations on the functions of the duck hepatitis B virus polymerase. *J Virol* 1990; **64**: 5553-5558
59 **Hu J**, Flores D, Toft D, Wang X, Nguyen D. Requirement of heat shock protein 90 for human hepatitis B virus reverse transcriptase function. *J Virol* 2004; **78**: 13122-13131
60 **Weber M**, Bronsema V, Bartos H, Bosserhoff A, Bartenschlager R, Schaller H. Hepadnavirus P protein utilizes a tyrosine residue in the TP domain to prime reverse transcription. *J Virol* 1994; **68**: 2994-2999
61 **Tavis JE**, Ganem D. RNA sequences controlling the initiation and transfer of duck hepatitis B virus minus-strand DNA. *J Virol* 1995; **69**: 4283-4291
62 **Tavis JE**, Ganem D. Evidence for activation of the hepatitis B virus polymerase by binding of its RNA template. *J Virol* 1996; **70**: 5741-5750
63 **Will H**, Reiser W, Weimer T, Pfaff E, Büscher M, Sprengel R, Cattaneo R, Schaller H. Replication strategy of human hepatitis B virus. *J Virol* 1987; **61**: 904-911
64 **Lien JM**, Aldrich CE, Mason WS. Evidence that a capped oligoribonucleotide is the primer for duck hepatitis B virus plus-strand DNA synthesis. *J Virol* 1986; **57**: 229-236
65 **Staprans S**, Loeb DD, Ganem D. Mutations affecting hepadnavirus plus-strand DNA synthesis dissociate primer cleavage from translocation and reveal the origin of linear viral DNA. *J Virol* 1991; **65**: 1255-1262
66 **Pugh JC**, Sninsky JJ, Summers JW, Schaeffer E. Characterization of a pre-S polypeptide on the surfaces of infectious avian hepadnavirus particles. *J Virol* 1987; **61**: 1384-1390
67 **Schlicht HJ**, Kuhn C, Guhr B, Mattaliano RJ, Schaller H. Biochemical and immunological characterization of the duck hepatitis B virus envelope proteins. *J Virol* 1987; **61**: 2280-2285
68 **Bruss V**, Gerhardt E, Vieluf K, Wunderlich G. Functions of the large hepatitis B virus surface protein in viral particle morphogenesis. *Intervirology* 1996; **39**: 23-31
69 **Macrae DR**, Bruss V, Ganem D. Myristylation of a duck hepatitis B virus envelope protein is essential for infectivity but not for virus assembly. *Virology* 1991; **181**: 359-363
70 **Grgacic EV**, Anderson DA. The large surface protein of duck hepatitis B virus is phosphorylated in the pre-S domain. *J Virol* 1994; **68**: 7344-7350
71 **Rothmann K**, Schnölzer M, Radziwill G, Hildt E, Moelling K, Schaller H. Host cell-virus cross talk: phosphorylation of a hepatitis B virus envelope protein mediates intracellular signaling. *J Virol* 1998; **72**: 10138-10147
72 **Oess S**, Hildt E. Novel cell permeable motif derived from the PreS2-domain of hepatitis-B virus surface antigens. *Gene Ther* 2000; **7**: 750-758
73 **Bruss V**, Lu X, Thomssen R, Gerlich WH. Post-translational alterations in transmembrane topology of the hepatitis B virus large envelope protein. *EMBO J* 1994; **13**: 2273-2279
74 **Lambert C**, Prange R. Dual topology of the hepatitis B virus large envelope protein: determinants influencing post-translational pre-S translocation. *J Biol Chem* 2001; **276**: 22265-22272
75 **Gazina EV**, Lin B, Gallina A, Milanesi G, Anderson DA. Intracellular retention of duck hepatitis B virus large surface protein is independent of preS topology. *Virology* 1998; **242**: 266-278
76 **Summers J**, Smith PM, Huang MJ, Yu MS. Morphogenetic and

regulatory effects of mutations in the envelope proteins of an avian hepadnavirus. *J Virol* 1991; **65**: 1310-1317
77 **Walters KA**, Joyce MA, Addison WR, Fischer KP, Tyrrell DL. Superinfection exclusion in duck hepatitis B virus infection is mediated by the large surface antigen. *J Virol* 2004; **78**: 7925-7937
78 **Bouchard MJ**, Wang LH, Schneider RJ. Calcium signaling by HBx protein in hepatitis B virus DNA replication. *Science* 2001; **294**: 2376-2378
79 **Meier P**, Scougall CA, Will H, Burrell CJ, Jilbert AR. A duck hepatitis B virus strain with a knockout mutation in the putative X ORF shows similar infectivity and in vivo growth characteristics to wild-type virus. *Virology* 2003; **317**: 291-298
80 **Pugh JC**, Summers JW. Infection and uptake of duck hepatitis B virus by duck hepatocytes maintained in the presence of dimethyl sulfoxide. *Virology* 1989; **172**: 564-572
81 **Pugh JC**, Di Q, Mason WS, Simmons H. Susceptibility to duck hepatitis B virus infection is associated with the presence of cell surface receptor sites that efficiently bind viral particles. *J Virol* 1995; **69**: 4814-4822
82 **Hirsch R**, Colgrove R, Ganem D. Replication of duck hepatitis B virus in two differentiated human hepatoma cell lines after transfection with cloned viral DNA. *Virology* 1988; **167**: 136-142
83 **Kuroki K**, Cheung R, Marion PL, Ganem D. A cell surface protein that binds avian hepatitis B virus particles. *J Virol* 1994; **68**: 2091-2096
84 **Breiner KM**, Urban S, Schaller H. Carboxypeptidase D (gp180), a Golgi-resident protein, functions in the attachment and entry of avian hepatitis B viruses. *J Virol* 1998; **72**: 8098-8104
85 **Urban S**, Schwarz C, Marx UC, Zentgraf H, Schaller H, Multhaup G. Receptor recognition by a hepatitis B virus reveals a novel mode of high affinity virus-receptor interaction. *EMBO J* 2000; **19**: 1217-1227
86 **Urban S**, Gripon P. Inhibition of duck hepatitis B virus infection by a myristoylated pre-S peptide of the large viral surface protein. *J Virol* 2002; **76**: 1986-1990
87 **Urban S**, Breiner KM, Fehler F, Klingmüller U, Schaller H. Avian hepatitis B virus infection is initiated by the interaction of a distinct pre-S subdomain with the cellular receptor gp180. *J Virol* 1998; **72**: 8089-8097
88 **Offensperger WB**, Offensperger S, Walter E, Blum HE, Gerok W. Inhibition of duck hepatitis B virus infection by lysosomotropic agents. *Virology* 1991; **183**: 415-418
89 **Rigg RJ**, Schaller H. Duck hepatitis B virus infection of hepatocytes is not dependent on low pH. *J Virol* 1992; **66**: 2829-2836
90 **Chojnacki J**, Anderson DA, Grgacic EV. A hydrophobic domain in the large envelope protein is essential for fusion of duck hepatitis B virus at the late endosome. *J Virol* 2005; **79**: 14945-14955
91 **Köck J**, Schlicht HJ. Analysis of the earliest steps of hepadnavirus replication: genome repair after infectious entry into hepatocytes does not depend on viral polymerase activity. *J Virol* 1993; **67**: 4867-4874
92 **Jilbert AR**, Botten JA, Miller DS, Bertram EM, Hall PM, Kotlarski J, Burrell CJ. Characterization of age- and dose-related outcomes of duck hepatitis B virus infection. *Virology* 1998; **244**: 273-282
93 **Freiman JS**, Jilbert AR, Dixon RJ, Holmes M, Gowans EJ, Burrell CJ, Wills EJ, Cossart YE. Experimental duck hepatitis B virus infection: pathology and evolution of hepatic and extrahepatic infection. *Hepatology* 1988; **8**: 507-513
94 **Jilbert AR**, Miller DS, Scougall CA, Turnbull H, Burrell CJ. Kinetics of duck hepatitis B virus infection following low dose virus inoculation: one virus DNA genome is infectious in neonatal ducks. *Virology* 1996; **226**: 338-345
95 **Zhang YY**, Summers J. Rapid production of neutralizing antibody leads to transient hepadnavirus infection. *J Virol* 2004; **78**: 1195-1201
96 **Tagawa M**, Robinson WS, Marion PL. Duck hepatitis B virus replicates in the yolk sac of developing embryos. *J Virol* 1987; **61**: 2273-2279
97 **Lenhoff RJ**, Luscombe CA, Summers J. Competition in vivo between a cytopathic variant and a wild-type duck hepatitis B virus. *Virology* 1998; **251**: 85-95
98 **Klöcker U**, Schultz U, Schaller H, Protzer U. Endotoxin stimulates liver macrophages to release mediators that inhibit an early step in hepadnavirus replication. *J Virol* 2000; **74**: 5525-5533
99 **Foster WK**, Miller DS, Marion PL, Colonno RJ, Kotlarski I, Jilbert AR. Entecavir therapy combined with DNA vaccination for persistent duck hepatitis B virus infection. *Antimicrob Agents Chemother* 2003; **47**: 2624-2635
100 **Foster WK**, Miller DS, Scougall CA, Kotlarski I, Colonno RJ, Jilbert AR. Effect of antiviral treatment with entecavir on age- and dose-related outcomes of duck hepatitis B virus infection. *J Virol* 2005; **79**: 5819-5832
101 **Triyatni M**, Jilbert AR, Qiao M, Miller DS, Burrell CJ. Protective efficacy of DNA vaccines against duck hepatitis B virus infection. *J Virol* 1998; **72**: 84-94

S- Editor Liu Y **L- Editor** Lutze M **E- Editor** Ma WH

PO Box 2345, Beijing 100023, China
www.wjgnet.com
wjg@wjgnet.com

World J Gastroenterol 2007 January 7; 13(1): 104-124
World Journal of Gastroenterology ISSN 1007-9327

TOPIC HIGHLIGHT

Dieter Glebe, PhD, *Series Editor*

The woodchuck as an animal model for pathogenesis and therapy of chronic hepatitis B virus infection

Stephan Menne, Paul J Cote

Stephan Menne, Department of Clinical Sciences, College of Veterinary Medicine, Cornell University, Ithaca, New York, United States
Paul J Cote, Department of Microbiology and Immunology, Georgetown University Medical Center, Washington, DC, United States
Supported by contract N01-AI-05399 to the College of Veterinary Medicine, Cornell University from the National Institute of Allergy and Infectious Diseases. PC and SM also have been supported by contract N01-AI-95390 to the Georgetown University Medical Center, Georgetown University from the National Institute of Allergy and Infectious Diseases
Correspondence to: Stephan Menne, PhD, Department of Clinical Sciences, College of Veterinary Medicine, Veterinary Medical Center, Cornell University, Ithaca, New York 14853, United States. sm119@cornell.edu
Telephone: +1-607-2533280 Fax: +1-607-2533289
Received: 2006-07-28 Accepted: 2006-10-04

Abstract

This review describes the woodchuck and the woodchuck hepatitis virus (WHV) as an animal model for pathogenesis and therapy of chronic hepatitis B virus (HBV) infection and disease in humans. The establishment of woodchuck breeding colonies, and use of laboratory-reared woodchucks infected with defined WHV inocula, have enhanced our understanding of the virology and immunology of HBV infection and disease pathogenesis, including major sequelae like chronic hepatitis and hepatocellular carcinoma. The role of persistent WHV infection and of viral load on the natural history of infection and disease progression has been firmly established along the way. More recently, the model has shed new light on the role of host immune responses in these natural processes, and on how the immune system of the chronic carrier can be manipulated therapeutically to reduce or delay serious disease sequelae through induction of the recovery phenotype. The woodchuck is an outbred species and is not well defined immunologically due to a limitation of available host markers. However, the recent development of several key host response assays for woodchucks provides experimental opportunities for further mechanistic studies of outcome predictors in neonatal- and adult-acquired infections. Understanding the virological and immunological mechanisms responsible for resolution of self-limited infection, and for the onset and maintenance of chronic infection, will greatly facilitate the development of successful strategies for the therapeutic eradication of established chronic HBV infection. Likewise, the results of drug efficacy and toxicity studies in the chronic carrier woodchucks are predictive for responses of patients chronically infected with HBV. Therefore, chronic WHV carrier woodchucks provide a well-characterized mammalian model for preclinical evaluation of the safety and efficacy of drug candidates, experimental therapeutic vaccines, and immunomodulators for the treatment and prevention of HBV disease sequelae.

Key words: Woodchuck; Woodchuck hepatitis virus; Hepatitis B virus; Neonatal-acquired infection; Adult-acquired infection; Resolution; Chronicity; Humoral immune response; Cellular immune response; Antiviral therapy; Immunotherapy; Combination therapy; Hepatocellular carcinoma

Menne S, Cote PJ. The woodchuck as an animal model for pathogenesis and therapy of chronic hepatitis B virus infection. *World J Gastroenterol* 2007; 13(1): 104-124

http://www.wjgnet.com/1007-9327/13/104.asp

INTRODUCTION

Infection of adult humans with the hepatitis B virus (HBV) results characteristically in self-limited hepatic disease with recovery based on serological and clinical parameters. Progression to chronic HBV infection occurs infrequently in infected adults, but HBV infections often persist in unvaccinated infants born to HBV-carrier mothers. Chronic HBV infection can lead to chronic hepatitis, liver cirrhosis, and hepatocellular carcinoma (HCC) later in life. Estimates indicate that more than 2 billion people worldwide have serological evidence of previous or current HBV infection, with at least 350 million chronic carriers, and an overall mortality rate from HBV-induced liver disease of 1.2 million deaths per year[1]. Although highly effective vaccines are licensed and have been in use since the early 1980's to prevent HBV infection in neonates and adults, the large reservoir of chronic HBV

carriers currently remaining could benefit immensely from the timely development of effective antiviral and/or immunotherapies that cure the infection or reduce the risk of disease progression.

Evidence from HBV-infected humans, and from animal models of HBV (i.e., HBV-transgenic mice, chimpanzees, pekin ducks, and woodchucks), indicate that the success or failure of humoral and cellular immune responses to the virus determine the initial outcome of acute HBV infection (i.e., as self-limited versus chronic), and that defective responses appear to play a role in the progression of chronic HBV infection (i.e., to chronic hepatitis, cirrhosis, and possibly HCC)[2-10]. Self-limited infections by HBV involving successful immune responses represent by far the more favorable outcome. Chronic HBV infections, where immune responses have failed or are sub-optimal for virus clearance, represent a daunting challenge to successful therapy against a background of continuing disease progression. Current treatment strategies for chronic HBV infection are suboptimal when compared to the curative process observed in self-limited HBV infection. Understanding the prevention and pathogenesis of HBV infection has advanced greatly through clinical studies in humans, and through experimental studies in the chimpanzee model of HBV infection; however, neither of these models is well-suited for the routine testing of therapeutic strategies for treatment of chronic HBV infection.

Woodchuck hepatitis virus (WHV) is a naturally occurring hepadnavirus of the Eastern woodchuck (*Marmota monax*) (Figure 1). WHV was described initially in 1977 at the Penrose Zoo in Philadelphia in a colony of woodchucks where high rates of chronic hepatitis and HCC had been observed[11]. Several strains of WHV have been identified since then, which are all very closely related genetically[12-16], but which may induce differing proportions of chronic infections in neonatal woodchucks[17]. WHV, and another HBV-like virus, the duck hepatitis B virus (DHBV)[18-20] have been used most extensively in the modeling of HBV infection and antiviral therapy (for previous reviews see[21-24]).

Research using the woodchuck began in 1978 and it was developed further into a laboratory model by 1980 when a woodchuck breeding colony was established at Cornell University. Early progress in model development at the Georgetown and Cornell Universities involved: (1) the production and validation of reagents and assays for WHV and for disease markers, (2) the characterization of infectious WHV inocula that induced predictably high rates of chronic infection when inoculated in neonatal woodchucks, and (3) basic studies of the natural history of virologic responses and tumor development associated with experimental infection of neonatal and adult woodchucks. Since 1988, the neonatal chronic WHV infection model has been applied primarily in the testing of antiviral nucleoside analogues for chronic HBV infection (for previous reviews see[10,25-30]).

Early studies in woodchucks also involved the testing of conventional vaccines for the prevention of acute, self-limited WHV infection in neonatal and adult woodchucks[28], and also for prevention of the chronic outcome and HCC in the vaccinated neonates challenged with higher doses of inoculum to enable breakthrough infections[31,32]. Immunomodulation of acute and chronic WHV infections using immunosuppressive drugs, such as cyclosporine A[33,34], was performed to gain an initial understanding of the role of the woodchuck immune response in the outcome and maintenance of WHV infection. The focus of investigations using the woodchuck has ranged widely since 1980, with flexible emphasis on both model development and model application in many areas of HBV research. These included viral and disease pathogenesis, and the prevention and treatment of HBV infection and disease sequelae (including HCC) using vaccines, antiviral drug candidates, and immunomodulators alone and in combination. The purpose of this review is to highlight the woodchuck as an animal model for pathogenesis and therapy of chronic HBV infection.

Figure 1 Eastern woodchuck (Marmota monax).

NATURAL HISTORY OF WHV INFECTION AND DISEASE

Experimental infection of woodchucks with WHV is a well-accepted model for many aspects of the pathogenesis of human HBV infection[7,10,26-29,35-38]. Recent studies of the host response of woodchucks to WHV infection and therapy have revealed numerous parallels to the immunopathogenesis of HBV infection. Certain immune markers in woodchucks cannot be analyzed currently to the same extent as those in mice and in humans. However, the patterns and profiles of those immune responses measured thus far in the woodchuck model are highly consistent with the underlying immunologic mechanisms defined in humans.

Experimental infection of neonatal or adult woodchucks with WHV7P1[17], a well characterized inoculum of WHV, produces predictable proportions of acute, self-limited (i.e., resolved) infections versus chronic infections. This mimics the effects of age on outcome of HBV infection in humans[3,4]. In adult woodchucks, WHV7P1 infections result mainly in resolution, with less than 5% of woodchucks progressing to chronicity[17] (Figure 2).

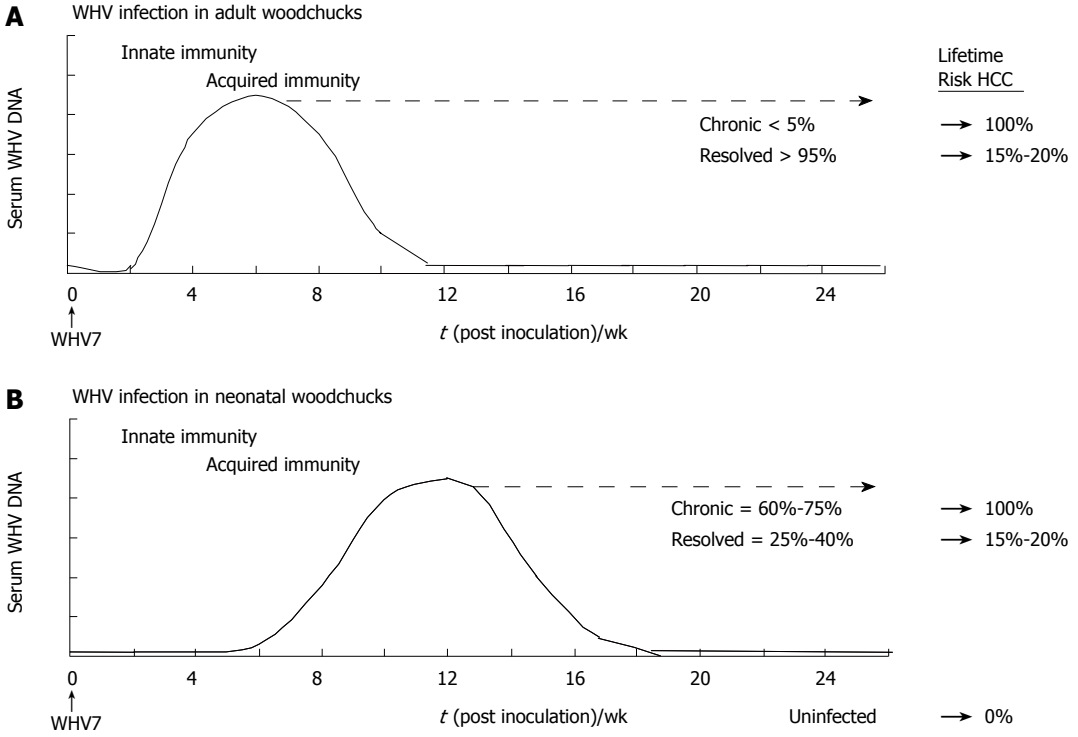

Figure 2 Schematic profiles for serum viremia in adult and neonatal models of experimental WHV infection. **A**: Adult woodchucks. Adult woodchucks born to WHV-negative dams are infected with 1 x 10^7 woodchuck infectious doses 50% of a defined WHV inoculum by the intravenous route. The proportions of chronic and resolved outcomes of adult woodchucks usually are less than 5% and more than 95%, respectively. The lifetime risk for the development of HCC in established chronic and resolved WHV infections is 100% and 15%-20%, respectively; **B**: Neonatal woodchucks. Neonatal woodchucks born to WHV-negative dams are infected with 5 x 10^6 woodchuck infectious doses 50% of a defined WHV inoculum by the subcutaneous route. The proportions of chronic and resolved outcomes range between 60%-75% and 25%-40%, respectively. The lifetime risk for the development of HCC in established chronic and resolved WHV infections is 100% and 15%-20%, respectively. HCC in uninfected, WHV-negative woodchucks is not observed. Approximate time intervals for the development of innate and acquired immunity are shown.

However, transient suppression of cellular immune responses with cyclosporine A (CsA) during the incubation and acute phase of adult WHV infections results in 92% of these infections progressing to the chronic outcome; with CsA given only during the incubation period and very early acute stage (0 to 4 wk post infection), the result is up to 50% chronic outcomes in adult WHV infections[33,34]. This shows the importance and timing of early immune responses in the resolution of acute WHV infection. Experimental immunosuppression, however, does not necessarily mimic natural processes associated with the progression to chronic infection.

Most chronic HBV infections occur as a result of neonatally-acquired infection[39-41]. Experimental infection of neonatal woodchucks with WHV7P1 usually results in a 60%-75% frequency of chronic carriers and a 25%-40% frequency of naturally recovered infections[17] (Figure 2). Viral and host response kinetics are relatively uniform when neonatal woodchucks are inoculated with WHV7P1 in the spring of the year, thus enabling statistical modeling of serologic and hepatic responses using samples collected in successive years. Such features also enable co-temporal comparisons of early acute phase immune responses before the self-limited and chronic outcomes become evident serologically, which can help to differentiate and identify the underlying mechanisms involved in the onset versus maintenance of chronic WHV infection[42-46] (Figure 3).

Chronic WHV infection involves life-long active viral replication and inevitable disease progression to chronic hepatitis and HCC[35,47-50]. In chronically infected woodchucks, there is no naturally occurring e-antigen to anti-e seroconversion and associated step-down of viral replication (i.e., as is commonly seen in chronic HBV infection; e.g.,[51-54]). In general, the high viral replication and high surface antigen and e-antigen loads present in the chronic WHV carrier appear to play a role in the maintenance of immunologic tolerance, and are associated with disease progression to HCC[43-45,55-57].

Self-limited WHV infection involves a relatively complete shut down of viral replication and a nearly complete clearance of virus from the system with full recovery. It has been suggested that trace amounts of residual WHV genomes often detected in long-term recovered woodchucks in liver, serum, and in peripheral blood mononuclear cells (PBMC), could actually represent an alternate form of persistent viral infection[58-65]. Residual HBV DNA has been documented also for humans recovered from self-limited HBV infection (e.g.,[66-71]). In woodchucks, even recovery from acute WHV infection incurs a discernable lifetime risk of HCC (5%-20%) when compared to control seronegative woodchucks (i.e., uninfected with WHV); however, this risk is significantly lower compared to the lifetime risk of HCC in chronic

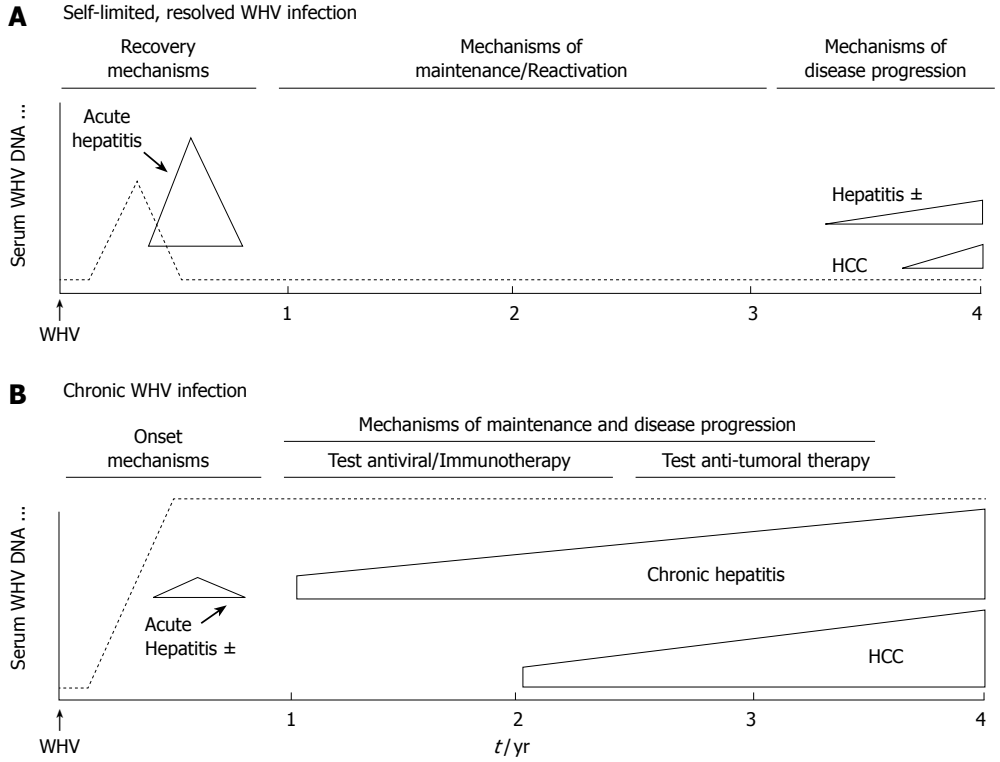

Figure 3 Schematic profiles for viremia, acute hepatitis, and disease progression in the neonatal model of experimental WHV infection. **A**: Self-limited, resolved WHV infection; **B**: Chronic WHV infection. Neonatal woodchucks born to WHV-negative dams are infected experimentally at 3 d of age with 5 x 10^6 woodchuck infectious doses 50% of a defined WHV inoculum by the subcutaneous route. Approximate time intervals for self-limited acute hepatitis and progressive chronic hepatitis are shown. Use of the neonatal WHV infection model enables co-temporal comparisons of acute self-limiting and chronic outcome of WHV infections as they develop. Comparison of acute phase events at early time points before or near the times when self-limited, resolved and chronic outcomes begin to segregate based on serologic criteria allows the definition of immune mechanisms involved in progression toward recovery versus chronicity. Comparison at later time points enables the investigation of mechanisms that are important in the maintenance of the established WHV infection state and that lead to disease progression and tumor development. During this time the established chronic WHV carrier woodchucks are used mainly for the testing of antiviral nucleosides, immunotherapeutic strategies, and for the prevention of onset and development of HCC.

WHV carrier woodchucks, which is essentially 100%[58,72] (Figure 2). Such results provide direct experimental evidence for the carcinogenicity of WHV and, by analogy, for HBV where chronic infection also is associated with HCC.

In a recent study, we examined the reactivation of WHV replication and the generation of infectious WHV in long-term resolved adult woodchucks during experimental immunosuppression with CsA (Menne *et al*, unpublished data). Administration of CsA to serologically recovered woodchucks with evidence of residual WHV DNA in liver and PBMC, and with durable recall cellular immune responses of PBMC to WHV antigens, resulted in a transient reactivation of WHV replication during CsA treatment. This supports the idea that replication-competent WHV (and by analogy, HBV) can persist for many years after recovery from acute viral hepatitis, possibly as part of a continuing process. That is, the virus may be controlled by virus-specific immune responses that are primed continuously by trace amounts of virus and viral antigens. In any case, the presence of long-term recall cellular immune responses with mutual persistence of residual WHV covalently closed circular DNA (WHV cccDNA) is significant to the durability of recovery responses over the long term for the stable control of replication and shut down of the infectious process. The apparent lack (or need) of such immune responses with the apparent loss of WHV cccDNA is significant to the extent of viral immune clearance possible in recovery. One implication from the above studies is how much a relatively successful antiviral and/or immunotherapy for chronic HBV or WHV infection will improve the prospects for disease outcome beyond that observed in natural recovery from infection.

MOLECULAR VIROLOGY STUDIES

WHV is classified as a member of the genus *Orthohepadnavirus*, family Hepadnaviridae[73]. The genetic organization of WHV is similar to that of HBV and other mammalian hepadnaviruses, and their biological properties and replicative strategies are essentially the same[74]. Filaments and spherical particles are found in the serum of WHV-infected woodchucks which are composed of the envelope protein of the virus. Complete virions are 42 to 45 nm in diameter and are composed of an exterior envelope protein (WHV surface antigen; WHsAg), an inner nucleocapsid or core protein (WHcAg), and, within the nucleocapsid, the DNA genome[75,76]. The replicative cycle of WHV seems to be identical to that of HBV[75-78]. The role of cccDNA as the template for viral transcription, the mechanism of replenishment of the cccDNA pool,

and the control of this pathway by surface antigen, have been investigated mainly using DHBV. For some studies, full-length clones of the WHV genome, cut and ligated to form a supercoiled cccDNA, have been used for *in vivo* molecular studies since direct injection into the hepatic parenchyma of woodchucks results in productive WHV infection[79]. Only a brief overview is provided below for background purposes.

During infection, HBV enters the hepatocyte, but the mechanism is poorly understood. No hepatocyte receptor has yet been defined for HBV, although studies suggest that the virus-cell recognition may be mediated all or in part by specific sequences located in the pre-S1 region of the large envelope protein. However, with numerous other potential envelope recognition sites for the cell suggested from *in vivo* neutralization studies with monoclonal antibodies, and the fact that antibodies elicited by vaccines to only the small envelope protein provide protective immunity, we are a long way from understanding the mechanisms of antibody-mediated neutralization of HBV attachment, entry, and uncoating during infection. It is known that the circular, partially double-stranded DNA genome makes its way to the nucleus where the partial DNA strand (i.e., positive strand) is completed via the endogenously linked virion reverse transcriptase-DNA polymerase, and the now fully circularized double strand is then ligated into a cccDNA. The cccDNA serves as the key template for viral mRNA transcription via the cellular RNA polymerase Ⅱ. One of the viral mRNAs (slightly larger than the genome length transcript) becomes encapsidated into maturing core particles along with the virion polymerase, where it is then reverse transcribed into the viral negative strand DNA *via* the RNA-dependent DNA polymerase activity of the encapsidated enzyme. The viral polymerase then uses its DNA-dependent DNA polymerase activity to partially complete the positive strand DNA to about 50%-75%, and this non-covalently closed circularized DNA is found in mature virions of HBV and WHV. Envelope acquisition occurs at the endoplasmic reticulum (ER) and mature virions are secreted from hepatocytes. Hepadnaviruses are not directly cytotoxic to infected cells.

Amplification and replenishment of cccDNA in the nucleus of the infected hepatocyte occurs when a portion of the maturing core particles complete positive strand DNA synthesis and are cycled back to the nucleus (i.e., instead of through the ER) where the new double strand DNA is processed into cccDNA. In HBV, most immunostaining of core is found in the nucleus, whereas in WHV, the core staining is primarily cytoplasmic, and not detected in the nucleus. This suggests a process of newly synthesized cytoplasmic core particles carrying out reverse transcription, partial or complete positive strand synthesis, and occasional re-entry into the nucleus for amplification of cccDNA (alternatively, cytoplasmic core staining may reflect incoming virus, but this seems far less likely). For HBV, cytoplasmic cores may go undetectable by immunostaining, and the denser staining of core particles within the nucleus may reflect maturation of HBV core particles there, with exit to the ER for envelope acquisition via a different cellular pathway. In established carrier woodchucks, WHV virions often circulate in 10- to 100-fold greater concentrations than do HBV virions in human chronic carriers. This may relate to the differential immuno-localization of core particles in the two models.

Transition of viral DNA to RNA during the life cycle of WHV has similarities to that of retroviruses[75,78], but integration of viral DNA into the host genome is not, however, essential for replication of hepadnaviruses, as is the case with retroviruses. Persistence of episomal cccDNA in infected hepatocytes is considered stable and this is problematic for its removal from the system, which appears to require elimination of the infected hepatocyte. It therefore represents the main target for attaining complete eradication of hepadnavirus from the system. When hepadnaviral DNA does integrate into host cell DNA, it is usually truncated and rearranged, and can target any number of sites in cellular DNA[80,81], some or all of which may be important in hepatocarcinogenesis. Morphological and molecular virological studies of the liver have shown that virtually 100% of hepatocytes become infected after experimental WHV infection[82]. Although replicative forms are cleared rapidly during recovery, WHV cccDNA persisted in a certain proportion of woodchucks long after evidence of WHV replication had ceased. That said, recovery is indeed durable and protective against disease progression in the vast majority of cases. On the other hand, persistence of the episomal cccDNA in chronic HBV (and WHV) infections remains a major conundrum in attempts to clear the virus via various therapeutic approaches (see below).

HBV generally is considered a hepatotropic virus, but hepadnavirus DNA can also be detected in extrahepatic tissues. For example, DHBV is often found replicating in the pancreas of ducks. HBV and WHV appear to infect the lymphatic system, although the exact significance of this observation is not well understood[58,60-63,65,83-86]. Some studies suggest that WHV replication and spread in the lymphatic compartment can proceed independently, even before infection of the liver[60,86]. Quiescent (non-replicating) WHV DNA molecules in PBMC from chronic WHV carriers can be activated to form replicative intermediates by stimulation of PBMC with lipopolysaccharide (LPS)[62]. The cell-free supernatants from LPS-stimulated WHV carrier PBMC (but not those from the unstimulated carrier PBMC) contain newly replicated infectious WHV that induce-acute hepatitis in WHV-susceptible adult woodchucks[84].

WHV quiescence versus replication in the lymphatic compartment may vary depending on the state of the host lymphatic target cell (i.e., resting, dividing, circulating in blood, within lymphatic tissue, *etc.*). WHV DNA can be detected in bone marrow cells as early as one month post neonatal WHV infection, but the first signs of WHV replication in PBMC, lymph nodes, and spleens occur during the acute stage of hepatic infection[83]. During recovery lymphatic WHV replication subsides to a quiescent state (or approaches complete elimination). In chronic infections, WHV replication also becomes quiescent in circulating PBMC, but often continues in the

spleen[83], and the quiescent WHV in PBMC often can be activated upon *ex vivo* stimulation using LPS, as indicated above[62,84]. More recent published studies indicate that long-term recovered woodchucks can also harbor infectious DNA in PBMC[58].

From the above, woodchucks recovering from acute WHV infection and those progressing to chronicity seem to have similar PBMC infection profiles, and in both cases the PBMC respond robustly in proliferation assays to polyclonal mitogens such as ConA, PHA, and LPS[44,55,87-89]. Even with similar PBMC WHV DNA profiles, the PBMC proliferative responses to viral antigens are generally more robust in the recovery outcome compared to the chronic outcome[44,55,56,87-90]. Thus, immune response function in viral infection does not appear to be affected adversely by the ongoing lymphatic infection. In fact, lymphatic infection by WHV, either acutely or in chronic WHV carriers, does not result in any lymphadenopathy, lymphopenia, lymphoma, or generalized immunodeficiency enabling opportunistic infections. As with natural recovery, therapy of chronic WHV infection presumes to target all reservoirs and molecular forms of the virus in both the lymphatic system and liver.

IMMUNOLOGICAL STUDIES

Resolution of experimental WHV infection in both neonatal and adult woodchucks involves a self-curative process with appropriate virus-specific immune responses in the periphery and liver (Figure 3). Natural recovery perhaps represents a benchmark for the possible induction of antiviral and/or immunotherapeutic effects in chronic WHV carriers. Specific activation of humoral and cellular immune responses is a prerequisite for viral clearance during acute HBV infection in adult patients, as reported in numerous studies[2-4,9,91]. However, the kinetic development of these responses during the early incubation and acute stages of adult HBV infection, and their influence on the course and outcome of infection, are less well characterized in humans, since patients usually do not present with clinical symptoms immediately after HBV transmission (except for a few rare cases involving known exposure times; e.g.,[92]).

Studies of self-limited WHV infection reveal numerous virus and host response patterns analogous to self-limited HBV infection[61,79,82,83,85,88,89,93-105]. In general, resolution of WHV infection in both the neonatal and adult settings is characterized by: (1) a transient peak of WHV DNA and antigen detection in serum and liver during the acute phase of infection, (2) timely and appropriate cell-mediated immunity (CMI) to viral antigens, (3) acute viral hepatitis with limited liver injury, (4) a transient peak and subsequent normalization of serum aminotransferases, and (5) seroconversion to virus-neutralizing antibodies, all leading to a substantial clearance of virus and viral antigens from the blood and liver. The humoral immune response to viral antigens (i.e., WHcAg and WHsAg) during resolution is associated with the development of robust titers of anti-core (anti-WHc), and of virus-neutralizing, protective, anti-surface antibodies (anti-WHs) with the onset and waning of the acute phase, all usually within several weeks after experimental infection[17,42].

In adult woodchucks, the CMI associated with recovery is characterized by activation of PBMC detected by *in vitro* stimulation of PBMC with WHsAg, WHcAg, and synthetic peptides of both antigens[87-90,93,94,106]. The successful PBMC response to WHcAg is associated co-temporally with viral clearance from serum, and this has been mapped extensively to several key epitopes of the WHcAg[87,93]. In fact, immunization with the dominant WHcAg epitope sequence between amino acids 97 to 110 significantly dampens acute WHV infections in adult woodchucks following experimental challenge with WHV, when compared to infections in unvaccinated control woodchucks[87]. Mapping of the PBMC responses to WHsAg and WHV x antigen (WHxAg) during the acute phase of resolution have been in progress.

The CMI to viral antigens during the acute phase in neonatal woodchucks experimentally infected with cWHV8P1 (from which neonates resolve more frequently) is similar to that in resolving adult woodchucks, which is independent of the WHV inoculum used[44]. Robust PBMC responses to WHcAg, WHsAg, and WHxAg, and to several non-overlapping core peptides, are associated temporally with the clearance of WHV DNA and WHsAg from serum. Detailed analysis of the WHcAg-specific PBMC responses revealed a broad recognition of several WHcAg epitopes representing apparently distinct regions of this antigen. Similar to adult WHV infections, neonatal woodchucks develop PBMC responses to important WHcAg peptides (residues 97 to 110, residues 100-113)[44].

In the liver, the CMI during resolution of adult WHV infection is characterized by moderate to marked hepatic inflammation and liver injury involving increased CD3- (cluster of differentiation 3) positive T lymphocyte accumulation, and apoptosis and regeneration of hepatocytes[96,97]. These events are accompanied by marked elevations of CD3, CD4, and CD8 mRNA expression and increased expression of the T-helper lymphocyte (Th)-type 1 cytokine mRNAs interferon gamma (IFN-γ) and tumor necrosis factor alpha (TNF-α), and of the IFN-γ -inducible oligoadenylate synthetase (2'-5'-OAS) mRNA[96,97]. *In vitro* testing of cell-mediated killing of hepatocytes revealed activation of both FasL- (ligand for the apoptosis-inducing factor Fas) and perforin-dependent pathways during resolution, and a comparative analysis demonstrated that acute hepatitis, but not established chronic WHV infection, is associated with elevated hepatocyte killing as a consequence of increased activation of the perforin-dependent pathway[95]. Further acute phase studies of adult self-limiting WHV infections are in progress to better define the kinetic interrelationships between mRNA expression in liver and PBMC mRNA expression *ex vivo* or following *in vitro* stimulation with antigens.

Neonatal WHV infections can be studied prospectively, in proportionate and adequate numbers of woodchucks, as the dichotomy in outcome proceeds dynamically in real time toward recovery versus chronicity. As with recovering WHV infections in adult woodchucks, resolution of

neonatal WHV infection is associated with moderate hepatic inflammation and liver injury and accumulation of CD3-positive T-lymphocytes[42,43]. Hepatic inflammation is characterized further by significant accumulation of CD3, CD4, and CD8 mRNAs, with elevated expression of the Th-type 1 cytokine mRNAs IFN-γ and TNF-α, and of the intracellular transcription factor STAT4 (signal transactivator of transcription) and T-bet (T box expressed in T lymphocytes) mRNAs, and also of Fas ligand and perforin mRNAs. When taken together, the results indicate that both non-cytolytic and cytolytic clearance of WHV-infected hepatocytes is occurring[43,45,46]. The results from the above studies suggest further that early virus-specific CMI in both the periphery and liver play a pivotal role in resolution of acute WHV infection in neonatal and adult woodchucks, and that the responses to WHcAg and to selected core peptides are instrumental in controlling viral infection.

Although immune responsiveness has been well-characterized in the periphery and liver of established HBV chronic carriers during chronic hepatitis, the actual acute phase responses associated with the early onset of chronic HBV infection are less well understood. Lack of immune responsiveness to HBV antigens in some HBV carriers may ensue with the establishment of the carrier state and have little to do with the early onset at a time when other individuals may recover normally. Moreover, chronic hepatitis is defective by definition, when compared with the acute hepatitis that results in recovery, because the chronic inflammation is incapable of clearing the hepatic infection and lends itself only to progressive liver disease. Adult patients presenting with acute hepatitis B are often well into the infection and only rarely progress to chronic infection. Studies of the early onset of chronic HBV infection in humans after neonatal transmission have obvious limitations. While studies in established chronic HBV carriers show defective immune responses associated with tolerance and chronic hepatitis and a failure to clear the infection[2-4,9,91], it is unclear whether such deficient responses are representative of the primary acute phase responses that predispose to the chronic outcome. Understanding how the chronic infection first becomes established kinetically near the time of the acute stage of infection could lead to the identification of important cause-effect relationships that will facilitate the rational development of therapies for successfully treating established chronic infections.

For testing the hypothesis that chronic WHV infection develops due to a diminished host response to acute infection, co-temporal comparisons were performed in the neonatal WHV infection model[7,17,42-46,107-109]. Using a bank of control and WHV-infected liver specimens that were obtained surgically at two acute phase time points of neonatal WHV infection (wk 8 and 14) and that were assigned to recovered or carrier woodchucks once outcome was known based on later serological profiles, the early onset of the chronic WHV carrier state (compared to co-temporal resolving infections) was characterized by: (1) higher acute phase viral loads in liver (at wk 8 and 14 post infection), (2) diminished acute hepatitis (at wk 14), (3) detectable but significantly diminished hepatic inflammation (at wk 14), and (4) reduced liver injury (at wk 14)[42,43,45,46]. This was associated further with: (1) absent or suboptimal intrahepatic accumulation of CD3, CD4, and CD8 mRNAs, and (2) reduced expression of Th-type 1 cytokine mRNAs, especially IFN-γ and TNF-α, along with the key Th-type 1 transcription factor T-bet[43,45,46]. This represented an early primary deficiency in the Th-type 1 response in liver to acute WHV infection, and was not associated with any local antagonistic Th-type 2 immunoregulation[45].

Studies in the peripheral blood using serial measurements of PBMC responses in neonatal woodchucks experimentally infected with WHV7P1 or cWHV8P1 have shown thus far that all neonates with resolving infections had robust acute phase PBMC responses to WHcAg and to the key epitope of this antigen (core residues 97-110), with the majority of woodchucks also responding to WHsAg and WHxAg[44]. In contrast, prospective carriers responded less frequently or not at all, with only about one-third responding to WHcAg, and among these, only about half responded to the key core epitope and to other WHV antigens. Detailed mapping of the PBMC responses to WHcAg revealed that the epitopes recognized were localized to distinct regions of this antigen and were different from those recognized during resolving WHV infections[44]. In the prospective carriers with minimal acute phase PBMC responses to WHcAg, viremia and antigenemia developed later, and viral and antigen loads were lower compared to those seen in prospective carriers without any evidence of virus-specific PBMC responses[44]. In any case the levels of viremia and antigenemia in these prospective carriers were much higher than in neonates with resolving WHV infections[44]. Interestingly, the fact that virus-specific PBMC responses were undetectable in the majority of prospective carriers indicates an early genesis for the CMI defect commonly observed later in established chronic WHV infection[55,56,87-90,94]. Further studies to correlate the molecular immunologic responses of PBMC based on leukocyte surface marker and cytokine mRNA expression with outcome of neonatal WHV infection are in progress.

Established chronic HBV infection is associated with increased viral load and risk of severe liver disease sequelae[2-4,9,91]. Chronic HBV infections resulting from neonatal transmissions are characterized by T cell immunotolerance to viral antigens throughout most of life until end-stage disease, but may exhibit occasional exacerbations of liver disease before this time[51,110-114]. T cell proliferative responses to viral antigens in adult-acquired chronic HBV infections can be variable during disease progression, but are usually less responsive, except during periodic transient flare reactions and with seroconversion to anti-e antibodies (e.g.,[52-54,115,116]).

Studies in woodchucks indicate that viral antigen-specific CMI during established chronic WHV infection is also defective, similar to that observed in HBV infection[45,55,56,87-89,94]. In the neonatal woodchuck, following an occasional, early and transient, but suboptimal acute hepatitis, WHV chronic carriage is characterized for some

time with minimal chronic persistent hepatitis, and little or no liver injury based on serum enzyme markers up through at least 15 mo post infection[46]. This progresses subsequently to more active hepatitis and liver injury just before or at the time of HCC onset and tumor growth[46,47,49,50,55,57]. PBMC remain essentially immunotolerant to WHV antigens throughout all of the chronic phase of neonatal WHV infection, including end stage disease[55,56,87,89,90,94]. The baseline expression of Th-type 1 cytokines in liver that is usually observed during the chronic phase can sometimes increase above normal with progressive chronic hepatitis (usually with increased TNF-α and less IFN-γ)[45,97], but without affecting clearance of the infection. Less is known of the CMI in documented adult-acquired chronic WHV infections, but the apparent greater degree of chronic hepatitis in this setting may suggest some exception to the fully tolerant state as leading to and maintaining the chronic infection[96]. Indeed, some leukocyte surface and cytokine markers become elevated in liver during acute hepatitis in adult woodchucks that eventually become chronic carriers, although to a lesser extent than seen during the acute phase of woodchucks that resolve.

THERAPEUTIC STUDIES

Antiviral drugs

Woodchucks with experimentally induced chronic WHV infection have been used successfully in the empiric screening and preclinical assessment of antiviral drugs being developed for treatment of chronic HBV infection (for previous reviews see[21,24,25,30,35,117]). Current strategies aim to suppress viral replication in liver and the concentration of viral DNA in serum during chronic HBV infection (i.e., reduce viral load) by treatment with nucleoside and nucleotide analogues. As indicated above, it has been difficult to target the viral cccDNA directly in this process, and so potent inhibition of viral replication is the main means to reduce viral load in blood and tissues, and perhaps diminish replenishment of cccDNA indirectly, until cells harboring this intermediate can turnover or be eliminated by immune responses. Accordingly, lifelong therapy with antiviral drugs is currently the accepted procedure, even though this often results in the selection of drug-resistant mutants (i.e., mutations of the polymerase gene), which has been observed and modeled in the woodchuck (e.g.,[118-122]).

Before testing in woodchucks, potential drug candidates are screened for antiviral activity against HBV in the 2.2.15 cell system, a HepG2 cell line that is engineered to produce HBV constitutively[123]. Drugs with significant antiviral activity *in vitro* also have been tested in a HBV-transgenic mouse model designed and validated for this purpose[124]. However, drug efficacy in an *in vivo* infection model is most usually assessed in the woodchuck model. Most nucleoside analogues with intermediate antiviral activity *in vitro* against HBV had comparable antiviral activity against WHV in woodchucks, but some exceptions exist. For example, fialuridine (D-FIAU) had modest activity *in vitro*, and potent antiviral activity in woodchucks; however, this was associated with a marked and delayed hepatotoxicity characterized by microvesicular steatosis and mitochondrial injury[125], similar to the unfortunate hepatotoxic effects this drug had in humans, where it was first tested[126].

In recent years, numerous nucleoside and nucleotide analogues designed to inhibit HBV replication were tested in the woodchuck model (e.g.,[125,127-140]. Some of these nucleoside analogues had demonstrated antiviral efficacy in chronic WHV carrier woodchucks, such as lamivudine (3TC, Epivir)[21,120,141-143], adefovir dipivoxil (ADV, Hepsera)[144,145], and entecavir (ETV, Baraclude)[139,146], and are now approved by the FDA for treatment of chronic HBV infection. Other nucleoside analogues, also having activity in woodchucks against WHV, are used for the treatment of human immunodeficiency virus (HIV), such as tenofovir disoproxil fumarate (TDF, Viread)[147] and emtricitabine (FTC, Coviracil)[148-150], and still others are in advanced clinical testing, such as telbivudine (LdT)[151-153], valtorcitabine (val-LdC)[151-153], and clevudine (L-FMAU)[55,56,122,150,154-156]. FDA approval of these drugs for treatment of chronic HBV infection is expected in the near future (in fact, telbivudine was approved most recently). Table 1 summarizes the antiviral activities of these second and third-generation nucleosides in chronic WHV carrier woodchucks that were reported in selected studies. We note here in these experiments that viral recrudescence following cessation of drug is often a function of being unable to completely suppress viral replication sufficiently during a given treatment, or significantly enough over time in order to allow cells containing cccDNA to turnover or be eliminated by the immune response.

Lamivudine is a moderately potent antiviral drug in woodchucks and is without toxicity during daily, oral administration for up to 24 wk[21,141,157], and even longer[142]. The average reduction in serum WHV DNA after 4 or 12 wk of treatment with different doses (1, 5, or 15 mg/kg bodyweight) was approximately 2.5 and 1.5 logs, respectively. The average time to recrudescence of viral replication after drug withdrawal was within 1 to 2 wk. In woodchucks, lamivudine also has been shown to act synergistically both with alpha-interferon and with famciclovir[141,157]. An antiviral activity comparable to lamivudine has been reported for adefovir[144]. Daily oral administration of adefovir for 12 wk with doses of 5 and 15 mg/kg resulted in a reduction in serum viremia of 1.7 or 2.5 logs, respectively. Viral recrudescence after drug withdrawal occurred within 6 wk. No toxicity associated with administration of adefovir was observed. The antiviral activity of tenofovir in woodchucks[147] is comparable to those of lamivudine and adefovir. The reduction in serum WHV DNA observed after 4 wk of daily, oral treatment with tenofovir doses of 5 and 15 mg/kg was 1.5 or 1.2 logs, respectively. After drug withdrawal viral recrudescence occurred within 1 to 4 wk and treatment was without any evidence of drug-associated toxicity.

A higher antiviral activity on chronic WHV infection was reported for emtricitabine[149]. Daily oral treatment for 4 wk with doses of 10 or 30 mg/kg reduced serum viremia by 3.2 and 4.9 logs, respectively. Recrudescence of viral replication occurred within 1 to 2 wk after drug withdrawal.

Table 1 Antiviral activities of second and third-generation nucleosides and nucleotides in the woodchuck model of chronic HBV infection

Antiviral drug	Oral dose (mg/kg per day)	Treatment duration (wk)	Follow up duration (wk)	Serum WHV DNA reduction (log)	Time to viral recrudescence (wk)	Drug-associated toxicity	Other viral markers	Ref.
Lamivudine	1	24	24	1.5	within 1-2	none	WHV RI red. (3-fold) no WHV RNA red. no serum WHsAg red.	[141]
	5	4	12	3.4	within 1	none	WHV RI red. (4-fold) no WHV RNA red. no serum WHsAg red.	[21]
	5	12	12	1.9	within 1-2	none	WHV RI red. (3-fold) no WHV RNA red. no serum WHsAg red.	[157]
	15	4	12	5.4	within 1	none	WHV RI red. (12-fold) no WHV RNA red. no serum WHsAg red.	[21]
Adefovir	5	12	6	1.7	within 6	none		[144]
	15	12	6	2.5	within 6	none		[144]
Entecavir	0.02	12	12	7-8[1]	within 2-10	none	WHV RI red. in individual animals to undetectable levels	[139]
	0.1	12	12	7-8	within 6-10	none	WHV RI red. in most animals to undetectable levels	[139]
Tenofovir	5	4	12	1.5	within 1-4	none	no WHV RI red. no WHV RNA red. no serum WHsAg red.	[147]
	15	4	12	1.2	within 1-4	none	no WHV RI red. no WHV RNA red. no serum WHsAg red.	[147]
Emtricitabine	3	4	12	1.4	within 1-2	none	WHV RI red. (3-fold) no WHV RNA red. no serum WHsAg red.	[149]
	10	4	12	3.2	within 1-2	none	WHV RI red. (13-fold) no WHV RNA red. no serum WHsAg red.	[149]
	30	4	12	4.9	within 1-2		WHV RI red. (80-fold) no WHV RNA red. no serum WHsAg red.	[149]
	20[2]	4	4	1.4	within 1-2	none		[148]
	30[2]	4	4	1.8	within 1-2	none	WHV RI red. (2-fold)	[148]
Telbivudine	10	4	8	8	within 4-8	none	serum WHsAg red.	[151-153]
Valtorcitabine	10	4	8	4-6	within 1-8	none		[151-153]
Clevudine	3	4	12	9.2	within 2-10	none	WHV RI red. (28-fold) no WHV RNA red. serum WHsAg red. (2-fold)	[154]
	10	4	12	8.2	within 8-12[3]	none	WHV RI red. (68-fold) WHV RNA red. (2.7-fold) serum WHsAg red. (4-fold) WHV cccDNA red. (2-6-fold or to undetectable levels)	[154]

[1]Two of 6 woodchucks with modest reduction in serum WHV DNA of approximately 2.0 logs were not included. [2]Dosage was given twice daily by intraperitoneal administration. [3]One woodchuck had suppressed serum WHV DNA at the end of the study. WHV RI, hepatic WHV DNA replicative intermediates; WHV RNA, intrahepatic WHV RNA; red., reduction.

A dose of emtricitabine of 3 mg/kg in this study was less efficacious, but was comparable to those observed with 20 and 30 mg/kg, administered twice daily, intraperitoneally, for 4 wk[148]. There was no toxicity associated with this drug treatment. A more remarkable antiviral activity was obtained with valtorcitabine in chronic WHV carrier woodchucks after daily oral administration for 4 wk with a dose of 10 mg/kg[151-153]. In this case, serum WHV DNA became reduced by 4 to 6 logs with no evidence of drug-associated toxicity at the dose used. The time to recrudescence of viral replication after drug withdrawal was as little as 1 wk, but extended to 8 wk in many of the animals. Entecavir had an even higher antiviral activity in woodchucks[139]. Daily oral administration of entecavir for 12 wk at a dose of 0.02 mg/kg resulted in a reduction in serum viremia of 7 to 8 logs in 4 of 6 treated woodchucks (2 of the 6 treated woodchucks had only a modest antiviral effect). Recrudescence of viral replication after drug

withdrawal occurred in as little as 2 wk, but was extended to 10 wk in several of the animals. Administration of entecavir at a dose of 0.1 mg/kg reduced serum viremia by 7 to 8 logs and viral recrudescence was observed within 6 to 10 wk. No toxicity associated with drug treatment was reported.

The most potent antiviral drugs that have been tested so far in woodchucks are telbivudine and clevudine. Daily oral administration of telbivudine for 4 wk at a dose of 10 mg/kg resulted in an 8 log reduction in serum viremia and viral recrudescence was observed within 4 to 8 wk after drug withdrawal[151,152]. Daily oral administration of clevudine for 4 wk at doses of 3 or 10 mg/kg reduced serum viremia by 9.2 and 8.2 logs, respectively[154]. With the lower dose of clevudine viral recrudescence after drug withdrawal was observed within 2 to 10 wk. The higher dose delayed viral recrudescence and serum WHV DNA concentrations reached pretreatment levels within 8 to 12 wk, and in one woodchuck, serum viremia was still suppressed at the end of the study. No toxicity was associated with the above short-term treatments using either telbivudine or clevudine.

The above studies in the woodchuck model demonstrate that a significant antiviral effect on chronic WHV infection could be achieved with all drugs. The relative antiviral efficacy against WHV, at the doses administered and for the duration of treatment used, was clevudine $\geqslant$ telbivudine $\geqslant$ entecavir > valtorcitabine $\geqslant$ emtricitabine $\geqslant$ tenofovir = adefovir = lamivudine. A prolonged suppression of WHV replication after drug withdrawal was achieved with clevudine, telbivudine, entecavir, and valtorcitabine, and the magnitude of these responses was often associated indirectly with transient or sustained reductions in WHV cccDNA potentially enabling some turnover of residually infected cells. The favorable safety and efficacy profile obtained thus far in the woodchuck model using relatively short-term treatments with clevudine, telbivudine, and valtorcitabine suggest that these drugs should be of value in the long-term control of chronic HBV infection in humans and support their continued clinical development.

The preclinical evaluation of antiviral drugs for treatment of lamivudine-resistant HBV infection has been modeled in woodchucks by the experimental induction of lamivudine-resistant WHV with nine or more months of lamivudine treatment, followed by continued therapy with lamivudine along with the new drug candidate of interest[122,145]. Prolonged treatment with lamivudine led to the establishment of drug-resistant WHV mutants, characterized mainly by mutations in the B domain of the WHV polymerase gene (i.e., HBV mutations occur in B and C domains). Supplemental daily oral treatment of these circulating B domain mutants with adefovir or clevudine (10 mg/kg per day, 12 wk and 7 wk, respectively) demonstrated that both drugs could suppress replication of these lamivudine-resistant WHV mutants. In a different study, lamivudine-resistant mutants of WHV were found to be cross-resistant to treatment with clevudine[122]. Studies are in progress using engineered lamivudine-resistant mutants of WHV that mimic the additional polymerase C domain mutants observed in human HBV patients treated with lamivudine.

In addition to the testing of drugs in woodchucks for antiviral effects, applications also have been extended to the testing of entecavir, clevudine, or lamivudine for efficacy against disease progression[30,142,146,155]. Extended lamivudine treatment of woodchucks with chronic WHV infection delayed the development of HCC and significantly extended survival of woodchucks in one study[142]. In that study, twenty 8-mo-old chronic WHV carrier woodchucks were treated throughout the rest of their lifetime with lamivudine (5 mg and then 15 mg/kg, orally, daily). Twenty placebo control WHV carrier woodchucks were included for comparison. Serum WHV DNA decreased by 4 to 5 logs in lamivudine-treated carrier woodchucks, with an antiviral effect that was sustained for more than one year with continued treatment. Importantly, there was a significant delay in time to onset of HCC and death due to HCC among lamivudine-treated woodchucks compared to placebo controls. In another study of lamivudine in WHV carrier woodchucks, no delay in hepatocarcinogenesis was observed with treatment, most likely because drug treatment began when woodchucks were at an older age, was of shorter duration, and less of an antiviral effect on serum WHV DNA was observed[120]. In both studies, lamivudine resistance developed that was associated with a high frequency of mutation in the WHV polymerase gene B domain[118,121].

In another study, long-term oral treatment with entecavir[146] in 8-mo-old woodchucks at 0.5 mg/kg per day for 8 wk, and then with a weekly dose of 0.5 mg/kg for 14 or 36 mo, produced sustained antiviral responses in half of the woodchucks treated for 14 mo, and in 80% of the woodchucks treated for 36 mo (i.e., reduced serum viremia of 5 to 8 logs). Here, the drug-treated woodchucks had marked reduction in viral load and did not develop HCC during the next 2 years follow-up. Compared in this case with historical controls, entecavir treatment significantly delayed the development of HCC and prolonged survival.

In another study, clevudine was administered orally to chronic WHV carrier woodchucks at 10 mg/kg per day for 32 wk[30,55,56,155] starting at 1 to 2 years of age. Half of the clevudine-treated woodchucks and half of the placebo recipients then received 4 doses of a conventional WHsAg vaccine (alum-adsorbed, formalin-inactivated WHsAg) during the next 16 wk. Combination treatment with clevudine and vaccine resulted in a sustained antiviral effect with reductions in serum viremia of more than 8 logs in many cases (Figure 4), and prevented the development of HCC altogether in up to 38% of treated woodchucks. In a subset of the woodchucks studied, where clevudine or placebo treatment was initiated at 1 year of age (and the data analyzed independent of combination with WHsAg vaccine), the development of HCC in clevudine-treated woodchucks was delayed significantly and long-term survival after 4 years likewise was increased significantly compared to woodchucks that did not receive clevudine. These studies show that chemotherapy with antiviral drugs can delay and reduce disease progression in chronic carrier woodchucks, and also show the correlation between

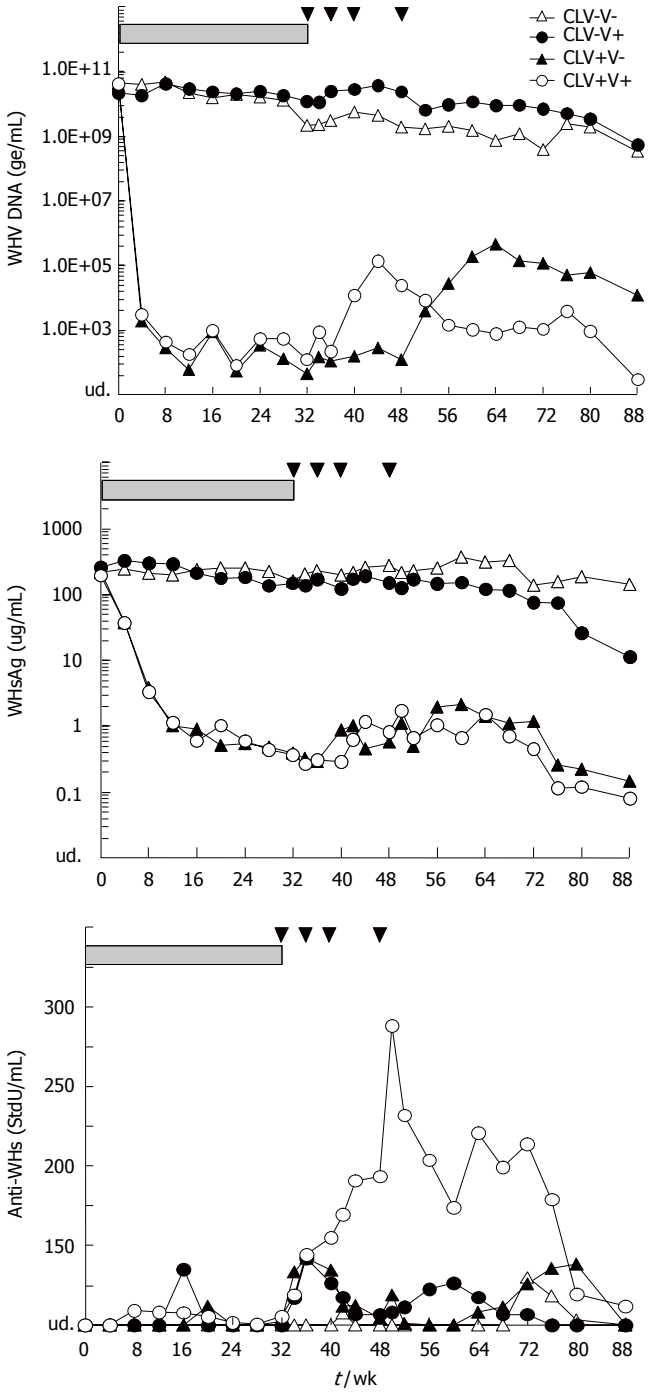

Figure 4 Combination treatment with clevudine and WHsAg vaccine suppresses serum viremia and antigenemia and induces a humoral response in chronic WHV carrier woodchucks. Changes in serum WHV DNA, serum WHsAg, and anti-WHs antibodies of chronic carriers in response to treatment with placebo (CLV-V-), vaccine (CLV-V+), drug (CLV+V-), and combination of drug and vaccine (CLV+V+) are shown. Horizontal bars denote the period of clevudine (CLV) administration for 32 wk. Arrowheads represent the 4 immunizations (V) using 50 μg doses of an alum-adsorbed, formalin-inactivated WHsAg vaccine at wk 32, 36, 40, and 48. WHVge, WHV genomic equivalents (virion or WHV DNA-containing particles).

reduced viral load and reduced disease progression, with noteworthy implications for HBV therapy in humans.

In addition to nucleoside or nucleotide analogues, various other compounds of organic and plant origin have been tested in woodchucks for their antiviral activity (e.g.,[141,158-161]), but these will not be discussed in detail in this review. Direct testing of anti-tumor agents against established HCC in woodchucks is also possible[162-164], but has not been fully developed to date.

Immunotherapy

The main goal of basic immunological studies described above in neonatal and adult WHV-infected woodchucks is to identify and differentiate factors that cause and maintain chronic infection from those that result from chronic carriage. By better defining cause-effect relationships, it should be possible to develop and test rational immunotherapies that can induce immune responses in the established chronic carrier that mimic those in recovery from WHV infection. In this way, it should be possible to enhance the immune elimination of cells harboring viral cccDNA (and/or control its level and expression), as occurs with successful immune responses leading to recovery.

As indicated in the sections above, chronicity as an outcome of neonatal WHV infection appears to result from a failed or suboptimal primary immune response relatively early during the acute phase of infection in the periphery and in the liver. The onset of chronic infection (compared to resolution) is characterized by deficiencies in the CD8-positive cytolytic T lymphocyte (CTL) response, and reduced expression of Th-type 1 cytokines and intracellular transcription factors, minimal acute hepatitis, and humoral and cellular immunologic tolerance to viral antigens[42-46]. Negative immunoregulation of the intrahepatic Th-type 1 response by excessive intrahepatic Th-type 2 immune responses is not a defining factor in this outcome[45,46]. Chronicity then appears to develop due to reduced immune-mediated clearance of infected hepatocytes by both non-cytolytic and cytolytic processes[45,46]. The above studies indicate further that early induction of immune tolerance may be a factor in the onset of chronic neonatal WHV infection, and a similar mechanism may be involved in the onset of chronic HBV infection in unvaccinated infants born to HBV-carrier mothers. This may include the deletion of higher affinity virus-specific T cells by negative selection of precursor T cells in the thymus (central tolerance), or clonal anergy or exhaustion of virus-specific T cells that escaped early negative selection in the thymus, which are then rendered unresponsive due to higher viral and antigen loads (peripheral tolerance).

Several studies have used WHV-naïve woodchucks for testing experimental vaccines, including conventional and DNA vaccines, and adjuvants, for later therapeutic vaccination of chronic WHV carrier woodchucks. In these studies antibody responses against WHsAg or WHcAg were induced[31,55,87,165-172], and partial or full protection against viral infection and disease by challenge with WHV was observed[31,87,165,166,168-172]. A few studies also determined that cellular immune responses were induced in addition to the humoral responses[87,168-171].

Unlike when WHV-naive woodchucks are immunized, the detection of free anti-WHs in serum of WHV carriers vaccinated with WHsAg is more problematic due to an excess of WHsAg in the serum samples. However, positive

Table 2 Immunotherapeutic approaches in the woodchuck model of chronic HBV infection

Treatment	Outcome	Additional results	Ref.
Vaccination			
WHsAg vaccine/adjuvant	Anti-WHs response	CMI to WHsAg	[55,56,155]
WHsAg vaccine/adjuvant	Anti-WHs response (antibodies mainly directed against preS region)		[173]
WHsAg vaccine/Th peptide epitope	Anti-WHs response Transient serum WHV DNA red. in a few animals (1 log)	Two woodchucks died	[174]
Cytokines			
IFN-α (adenoviral vector)	Transient serum WHV DNA red. (1 log)	Transient WHV RI red. (1 log)	[181]
IFN-α (adeno-associated viral vector)	Transient serum WHV DNA red. (2 logs) Sustained serum WHV DNA red. in 2 animals		[182]
IFN-γ (adenoviral vector)	No antiviral effect		[181]
Adoptive immunotransfer			
Liver transplantation	Serum WHV DNA red.	WHV RI red., WHV RNA red.	[188]
Combination treatment			
Lamivudine + WHsAg vaccine/ Th peptide epitope	No additional benefit beyond lamivudine-induced antiviral effect	CMI to WHsAg/WHcAg	
Lamivudine + β-galactosidase (adenoviral vector)	Transient but sustained serum WHV DNA red. (> 1 log) in addition to lamivudine-induced antiviral effect	WHV RI red., WHV cccDNA red., WHV RNA red.	[191]
Clevudine + β-galactosidase/+ IFN-γ/+ IFN-α (adenoviral vector)	Transient but sustained serum WHV DNA red. in addition to clevudine-induced antiviral effect	WHV RI red.	[156]
Clevudine + emtricitabine + IFN-γ (adenoviral vector)	No additional benefit beyond clevudine + emtricitabine-induced antiviral effect	Increased liver inflammation with IFN-γ	[150]
Clevudine + WHsAg vaccine	Anti-WHs response Sustained serum WHV DNA red. (> 6 to 8 log)	WHV cccDNA red., CMI to WHsAg/WHcAg Delay in onset of disease progression	[55,56,155]

WHV RI, hepatic WHV DNA replicative intermediates; WHV cccDNA, covalently closed circular WHV DNA, WHV RNA, intrahepatic WHV RNA; red., reduction.

signals for anti-WHs can often be detected by enzyme immunoassay under these conditions, even though it may be complexed in native serum. This is because of the exchange of bound anti-WHs between WHsAg in the sample solution, and the WHsAg adsorbed to the solid phase assay matrix. Unvaccinated WHV carriers rarely if ever show detectable anti-WHs of this nature, even though they may have some complexed anti-WHs in serum. Thus, the vaccination of WHV carriers with WHsAg most likely increases the levels of anti-WHs in complex, which enables its subsequent detection (at generally low levels) in the various enzyme immunoassay formats. Assays able to detect anti-WHs in complex with WHsAg are being developed to better study such responses.

One approach to immunotherapy is to modulate the deficient humoral and cellular immune responses of chronic HBV carriers by conventional vaccination (Table 2). In one study chronic WHV carrier woodchucks received up to 6 immunizations with a serum-derived WHsAg vaccine that was adsorbed to aluminum salt and contained monophosphoryl lipid A[173]. Following immunization, all of the carrier woodchucks developed an antibody response against WHsAg that was directed mainly against the WHV preS region, but there was little in the way of positive CMI to the antigen used in the vaccine. Despite the induction of anti-WHs antibodies, serum levels of WHV DNA and WHsAg in vaccinated carriers remained unchanged. This was consistent with another study in which four doses of an alum-adsorbed, formalin-inactivated WHsAg vaccine were administered[55,56,155]. In the latter study, CMI to WHsAg and WHsAg peptides was detected in the majority of vaccinated carriers, but, again, there was little effect on serum viral load (Figures 4 and 5). Therapeutic vaccination of chronic WHV carrier woodchucks with a serum-derived WHsAg in combination with an experimental adjuvant (i.e., a peptide carrying a Th epitope from sperm whale myoglobin) induced anti-WHs antibody responses and minor transient reductions in serum WHV DNA in a few of the vaccinated carriers[174]. Caution in the use of this therapeutic WHsAg vaccine was recommended, however, since some of the carriers died during the vaccinations. Such adverse effects could have been related to the experimental adjuvant and/or to liver disease present in the woodchucks at entry into the study. The results from these studies indicate that immunization of chronic WHV carrier woodchucks with WHsAg can partially induce (or boost) B cell responses to WHsAg. Additional modulation, however, seems necessary for inducing a response profile that resembles that observed during resolution of WHV infection.

Another approach to immunotherapy of chronic HBV infection involves direct reconstitution of the deficient Th-type 1 immune responses in the liver to mimic natural recovery from infection. Cytokines such as IFN-γ and TNF-α have been reported to have direct, non-cytolytic antiviral effects in HBV transgenic mice[8,175-177]. However,

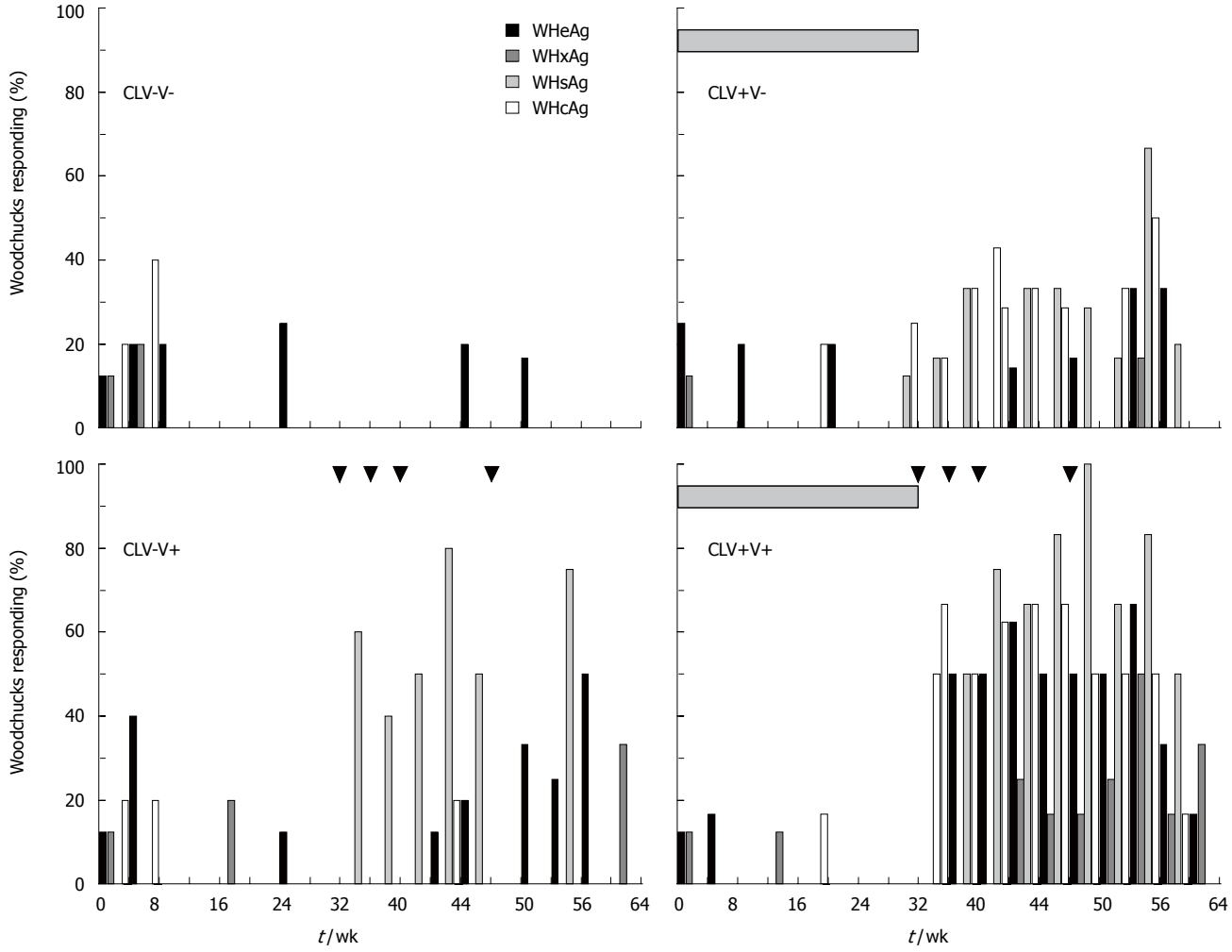

Figure 5 Combination treatment with clevudine and WHsAg vaccine enhances and expands the pattern of cell-mediated immune responses to WHV antigens in chronic WHV carrier woodchucks. Changes in the PBMC responses to WHsAg, WHcAg, WHeAg, and WHxAg of chronic carriers in response to treatment with placebo (CLV-V-), vaccine (CLV-V+), drug (CLV+V-), and combination of drug and vaccine (CLV+V+) are shown. Horizontal bars denote the period of clevudine (CLV) administration for 32 wk. Arrowheads represent the 4 immunizations (V) using 50 μg doses of an alum-adsorbed, formalin-inactivated WHsAg vaccine at wk 32, 36, 40, and 48.

increased expression of these cytokines can occur in established chronic WHV carriers with progressing chronic hepatitis and liver injury[45,96,97,178], but with little concurrent reduction in viral replication. This indicates that additional responses would be important to developing a more complete therapeutic effect resembling recovery. Recent studies have shown that woodchuck IFN-γ (and TNF-α) does not significantly deplete WHV RNA or WHV DNA replicative intermediates *in vitro* in virus-infected primary hepatocytes from chronic carriers[179]. Other studies in primary hepatocyte cultures from established WHV carriers suggest that expression of IFN-γ from a transfected plasmid (and also of TNF-α) can induce partial host response profiles with similarity to recovering liver, and also impair a later step in viral replication by a non-cytolytic mechanism that is probably mediated by TNF-α[180].

The effects of woodchuck IFN-α and IFN-γ on WHV replication were determined *in vivo* in a recent study in chronic WHV carrier woodchucks using an adenoviral vector for the expression of these cytokines[181]. Following vector administration directly into the liver, a slight but transient reduction in intrahepatic WHV DNA replication and in serum WHV DNA of about 1 log was obtained with the IFN-α expressing vector. The intrahepatic expression of IFN-γ, however, had no effect on WHV, thus leading to the conclusion that hepatocytes of chronic WHV carrier woodchucks may be functionally altered in their response to IFN-γ or resistant to this cytokine. In another study, the administration of woodchuck IFN-α using an adeno-associated viral vector for intrahepatic delivery of this cytokine into chronic WHV carrier woodchucks had a significant antiviral effect in that serum WHV DNA was reduced by 2 logs on average (range 1.5 to 4 logs)[182]. The antiviral effect observed was transient in the majority of woodchucks, but two woodchucks appeared to have sustained suppression in serum WHV DNA concentration. The results from these studies indicate that *in vivo* therapeutic gene delivery to augment the deficient Th-type 1 cytokine responses in liver may restore some of the failed antiviral and immunologic functions in human chronic HBV infection.

Another approach to immunotherapy of chronic HBV infection involves the restoration and stimulation

of higher-affinity Th and CTL clones in the periphery (or locally in the liver). Rather than to supplement a specific cytokine deficiency, it may be possible to reconstitute a complete and successful cellular immune response to acute infection by transfer of autologous or histocompatible T cell clones. The efficacy of the latter approach has been demonstrated in recent clinical studies of lymphocompatible bone marrow or PBMC transplantation from HBV-recovered or anti-HBV immunized donors into chronic carrier recipients (e.g.,[183-187]). Studies of cell-based therapies in chronic WHV carrier woodchucks involving adoptive lymphocyte transfer from vaccinated or WHV-resolved donors are in progress using neonatal-infected carrier woodchucks made lymphocompatible with their sires by co-injection of parental bone marrow and/or lymphocytes at birth. Later, after the neonates become established WHV carriers, they are re-administered parental lymphocytes therapeutically that were primed in the parent by immunization or recovery from acute WHV infection (Menne *et al*, unpublished data). Recently, another approach involving adoptive immunotransfer *via* liver transplantation from vaccinated WHV-naïve woodchucks into chronic carrier woodchucks was tested[188]. Following vaccination of donor woodchucks with DNA plasmids encoding WHcAg, WHsAg, and WHsAg in combination with a plasmid expressing IFN-γ livers were transplanted into recipient woodchucks, and the therapeutic effect determined. Two of 3 recipient carriers demonstrated a reduction in serum WHV DNA below the limit of detection by Southern hybridization analysis immediately following transplantation that lasted for up to 7 wk. WHV DNA in serum samples was detected when a more sensitive PCR assay was used. Nevertheless, the reductions in serum viremia were consistent with parallel reductions in intrahepatic levels of WHV RNA and DNA replicative intermediates.

Combination therapy

The high viral and antigen loads in serum during the chronic phase of infection are believed to maintain immunologic tolerance in established carrier woodchucks[55,56]. In some cases, treatment with antiviral drug alone may unmask host immune responses as seen during treatment of adult-acquired chronic HBV infection with lamivudine[189,190]; however, such responses appear sub-optimal for bringing about a complete recovery phenotype. To facilitate the emergence of the host immune response from a tolerant state maintained by high antigen load, combination therapy with a nucleoside analogue followed by modulation of the deficient immune responses represents a promising approach. Such an approach might even be able to improve upon natural recovery by creating optimal conditions for more rapid and complete eradication of viral cccDNA from the system.

In one study, chronic WHV carrier woodchucks were treated with lamivudine at a relatively high daily dose of 200 mg/kg given orally for 23 wk[143]. At the time, WHV DNA and WHsAg serum levels had declined by 3 to 5 logs or 1 log, respectively, woodchucks were vaccinated with three doses of a serum-derived WHsAg in combination with a peptide carrying a Th epitope from sperm whale myoglobin. In contrast to a previous study[174], therapeutic vaccination did not induce detectable anti-WHs antibody responses in carriers; the levels of viremia and antigenemia remained nearly unchanged from that achieved by drug treatment, and they returned to pretreatment levels following drug withdrawal. One important finding of this study was that the combination of lamivudine and vaccine, but not treatment with drug alone, induced CMI to WHsAg and WHcAg, presumably by shifting the cytokine profile from Th-type 2 to that of Th-type 0/1.

In another study chronic WHV carrier woodchucks received lamivudine treatment for 6 mo, again at a relatively high dose (200 mg/kg per day, oral) in order to reduce serum WHV DNA by 1 to 3 logs, and were then superinfected with an adenoviral vector expressing β-galactosidase[191]. Compared to control woodchucks, combination treatment resulted in further reductions of serum WHV DNA (10-20-fold) in the majority of woodchucks. The vector itself induced local immune responses in liver, and a bystander antiviral effect was observed on intrahepatic WHV DNA, WHV cccDNA, and WHV RNA that correlated with the inflammatory responses involving increased intrahepatic expression of woodchuck leukocyte markers and cytokines. The suppression of WHV replication was transient, but prolonged compared to woodchucks receiving lamivudine monotherapy. Similar results were obtained following superinfection of chronic WHV carriers with adenoviral vectors expressing IFN-γ, TNF-α, or β-galactosidase in combination with orally administered clevudine at 10 mg/kg per day[156]. Adenovirus superinfection led to declines in the intrahepatic WHV DNA levels, but a long-term benefit of combination treatment over clevudine alone was not observed. However, in contrast to monotherapy with lamivudine[191], recrudescence of WHV replication was deltayed until 14 wk after withdrawal of clevudine.

The antiviral effect of a combination of two nucleoside analogues in addition to an adenoviral vector expressing IFN-γ also has been tested in chronic WHV carrier woodchucks[150]. Woodchucks received clevudine and emtricitabine simultaneously at daily oral doses of 10 mg/kg and 30 mg/kg, respectively, for 8 wk, with two intravenous injections of the vector at wk 4 and 8. Combination treatment with clevudine and emtricitabine resulted in an antiviral effect on WHV replication, with reductions in serum viremia by 4 logs, and associated declines in intrahepatic levels of WHV DNA replicative intermediates and WHV cccDNA. The antiviral effect was sustained in a few woodchucks following drug withdrawal. The additional administration of the adenoviral vector led to increased liver inflammation, but enhancements of the antiviral effect compared to combination treatment with clevudine and emtricitabine were not observed.

In our study in chronically WHV-infected woodchucks described above[55,56,155], combination therapy with clevudine (10 mg/kg per day, oral, 32 wk), followed by 4 doses of a conventional WHsAg vaccine (alum-adsorbed, formalin-inactivated WHsAg), enhanced the virus-specific CMI to WHsAg, and resulted in additional

collateral responses to other viral antigens (Figures 4 and 5). Vaccination alone elicited low-level antibody responses to WHsAg in most woodchucks but did not affect serum WHV DNA or WHsAg levels compared to placebo-treated control woodchucks. Chronic WHV carrier woodchucks treated first with clevudine to reduce serum WHV DNA (> 6 to 8 log reduction) and WHsAg (> 50- to 500-fold reduction), and then vaccinated, developed a more robust anti-WHs antibody response. After vaccination, WHsAg-specific CMI was shown in both vaccinated groups, but was significantly enhanced in woodchucks treated initially with clevudine, and was broadened to include responses to WHcAg and to selected peptide epitopes of WHcAg and WHsAg.

Thus, the long-term drug treatment combined with therapeutic vaccination was shown to break humoral and cellular immune tolerance in treated WHV carrier woodchucks better than the component monotherapies, and to produce a more complete immune response profile resembling that in recovery from acute WHV infection, including an associated and marked reduction in the concentration of WHV cccDNA in liver. While the inclusion of vaccine after clevudine treatment did not result in a significant further antiviral effect beyond that of clevudine alone (i.e., clevudine is so potent that further antiviral effects would be difficult to measure), the combination therapy did have an additive benefit over the monotherapies in delaying the onset and occurrence of disease progression, including chronic hepatitis and HCC[30,155]. The results of this study suggest that the delay in the onset of chronic hepatitis and HCC is due to the uniformly high degree of suppression of viral load, especially the expression of viral antigens in serum and liver, any of which could act to maintain immune tolerance during chronic carriage. Longer term protection against the onset or development of HCC then appeared to be a function of the improved cellular and humoral immune responsiveness to viral antigens, which could no longer serve as endogenous tolerogens after reduction by drug.

CONCLUSIONS

The woodchuck animal model of chronic HBV infection has been valuable in determining the mechanisms of hepadnavirus replication and for studies of viral pathogenesis including associated disease sequelae and host immune responses. Continued modeling of early acute phase immune responses leading to resolution versus chronicity in the neonatal woodchuck may help to identify useful predictive markers of outcome that will facilitate the early identification of the carrier state, and the rational development of antiviral and/or immunotherapies for established chronic HBV infection. Colony-born woodchucks infected as neonates with well-characterized inocula also enable the evaluation of efficacy and toxicity of new types of prophylaxis or therapy under controlled experimental conditions in a relevant animal model within a reasonable time frame. Continued testing of new therapeutic approaches empirically and rationally in the woodchuck model will ultimately improve the chances for successful therapeutic eradication of established chronic HBV infection and its disease sequelae.

ACKNOWLEDGMENTS

The authors graciously acknowledge the support of Drs. Bud C Tennant (Cornell University) and John L Gerin (Georgetown University).

REFERENCES

1 **Vryheid RE**, Kane MA, Muller N, Schatz GC, Bezabeh S. Infant and adolescent hepatitis B immunization up to 1999: a global overview. *Vaccine* 2000; **19**: 1026-1037
2 **Bertoletti A**, Ferrari C. Kinetics of the immune response during HBV and HCV infection. *Hepatology* 2003; **38**: 4-13
3 **Chisari FV**, Ferrari C. Hepatitis B virus immunopathology. *Springer Semin Immunopathol* 1995; **17**: 261-281
4 **Chisari FV**. Rous-Whipple Award Lecture. Viruses, immunity, and cancer: lessons from hepatitis B. *Am J Pathol* 2000; **156**: 1117-1132
5 **Jilbert AR**, Kotlarski I. Immune responses to duck hepatitis B virus infection. *Dev Comp Immunol* 2000; **24**: 285-302
6 **Menne S**, Tennant BC. Unraveling hepatitis B virus infection of mice and men (and woodchucks and ducks). *Nat Med* 1999; **5**: 1125-1126
7 **Cote PJ**, Toshkov I, Nakamura I, Menne S, Korba B, Tennant B, Gerin J. Chronicity as an outcome of experimental neonatal woodchuck hepatitis virus infection results from a deficient type 1 immune response to acute infection. In: Margolis HS, Alter MJ, Liang TJ, Dienstag JL, editors. Viral hepatitis and liver diseases: proceedings of the 10th international symposium on viral hepatitis and liver disease. Atlanta: International Medical Press Ltd, 2002: 280-285
8 **Chisari FV**. Hepatitis B virus transgenic mice: models of viral immunobiology and pathogenesis. *Curr Top Microbiol Immunol* 1996; **206**: 149-173
9 **Guidotti LG**, Chisari FV. Noncytolytic control of viral infections by the innate and adaptive immune response. *Annu Rev Immunol* 2001; **19**: 65-91
10 **Menne S**, Cote PJ. The woodchuck as an emerging animal model for immunopathogenesis and immunotherapy of human HBV infection. In: Recent research developments in virology, vol. 5. Kerala, India: Transworld Research Network, 2003: 117-141
11 **Summers J**, Smolec JM, Snyder R. A virus similar to human hepatitis B virus associated with hepatitis and hepatoma in woodchucks. *Proc Natl Acad Sci USA* 1978; **75**: 4533-4537
12 **Cummings IW**, Browne JK, Salser WA, Tyler GV, Snyder RL, Smolec JM, Summers J. Isolation, characterization, and comparison of recombinant DNAs derived from genomes of human hepatitis B virus and woodchuck hepatitis virus. *Proc Natl Acad Sci USA* 1980; **77**: 1842-1846
13 **Galibert F**, Chen TN, Mandart E. Nucleotide sequence of a cloned woodchuck hepatitis virus genome: comparison with the hepatitis B virus sequence. *J Virol* 1982; **41**: 51-65
14 **Kodama K**, Ogasawara N, Yoshikawa H, Murakami S. Nucleotide sequence of a cloned woodchuck hepatitis virus genome: evolutional relationship between hepadnaviruses. *J Virol* 1985; **56**: 978-986
15 **Cohen JI**, Miller RH, Rosenblum B, Denniston K, Gerin JL, Purcell RH. Sequence comparison of woodchuck hepatitis virus replicative forms shows conservation of the genome. *Virology* 1988; **162**: 12-20
16 **Girones R**, Cote PJ, Hornbuckle WE, Tennant BC, Gerin JL, Purcell RH, Miller RH. Complete nucleotide sequence of a molecular clone of woodchuck hepatitis virus that is infectious in the natural host. *Proc Natl Acad Sci USA* 1989; **86**: 1846-1849
17 **Cote PJ**, Korba BE, Miller RH, Jacob JR, Baldwin BH, Hornbuckle WE, Purcell RH, Tennant BC, Gerin JL. Effects

of age and viral determinants on chronicity as an outcome of experimental woodchuck hepatitis virus infection. *Hepatology* 2000; **31**: 190-200
18 **Mandart E**, Kay A, Galibert F. Nucleotide sequence of a cloned duck hepatitis B virus genome: comparison with woodchuck and human hepatitis B virus sequences. *J Virol* 1984; **49**: 782-792
19 **Mason WS**, Seal G, Summers J. Virus of Pekin ducks with structural and biological relatedness to human hepatitis B virus. *J Virol* 1980; **36**: 829-836
20 **Omata M**, Uchiumi K, Ito Y, Yokosuka O, Mori J, Terao K, Wei-Fa Y, O'Connell AP, London WT, Okuda K. Duck hepatitis B virus and liver diseases. *Gastroenterology* 1983; **85**: 260-267
21 **Korba BE**, Cote P, Hornbuckle W, Tennant BC, Gerin JL. Treatment of chronic woodchuck hepatitis virus infection in the Eastern woodchuck (Marmota monax) with nucleoside analogues is predictive of therapy for chronic hepatitis B virus infection in humans. *Hepatology* 2000; **31**: 1165-1175
22 **Main J**, McCarron B, Thomas HC. Treatment of chronic viral hepatitis. *Antivir Chem Chemother* 1998; **9**: 449-460
23 **De Clercq E**. Perspectives for the treatment of hepatitis B virus infections. *Int J Antimicrob Agents* 1999; **12**: 81-95
24 **Zoulim F**. Evaluation of novel strategies to combat hepatitis B virus targetting wild-type and drug-resistant mutants in experimental models. *Antivir Chem Chemother* 2001; **12** Suppl 1: 131-142
25 **Tennant BC**, Gerin JL. The woodchuck model of hepatitis B virus infection. *ILAR J* 2001; **42**: 89-102
26 **Roggendorf M**, Tolle TK. The woodchuck: an animal model for hepatitis B virus infection in man. *Intervirology* 1995; **38**: 100-112
27 **Paronetto F**, Tennant BC. Woodchuck hepatitis virus infection: a model of human hepatic diseases and hepatocellular carcinoma. *Prog Liver Dis* 1990; **9**: 463-483
28 **Gerin JL**, Tennant BC, Ponzetto A, Purcell RH, Tyeryar FJ. The woodchuck animal model of hepatitis B-like virus infection and disease. *Prog Clin Biol Res* 1983; **143**: 23-28
29 **Cote PJ**, Gerin JL. The woodchuck as a model of hepadnavirus infection, pathogenesis and therapy. *Forum Trends Exp Clin Med* 1996; **6**: 131-159
30 **Tennant BC**, Toshkov IA, Peek SF, Jacob JR, Menne S, Hornbuckle WE, Schinazi RD, Korba BE, Cote PJ, Gerin JL. Hepatocellular carcinoma in the woodchuck model of hepatitis B virus infection. *Gastroenterology* 2004; **127**: S283-S293
31 **Gerin JL**, Tennant BC, Popper H, Tyeryar FJ, Purcell RH. The woodchuck model of hepadnavirus infection and disease. In: Brown F, Chanock R, Lerner R, editors. Vaccines 86: new approaches to immunization. Cold Spring Harbor: Cold Spring Harbor Laboratory, 1986: 383-386
32 **Cote PJ**, Korba BE, Tennant BC, Gerin JL. Immunopathogenesis and immunomodulation of woodchuck hepatitis virus infection In: Hollinger FB, Lemon SM, Margolis HS, editors. Viral hepatitis and liver disease. Baltimore: Williams & Wilkins, 1991: 483-486
33 **Cote PJ**, Korba BE, Baldwin B, Hornbuckle WE, Tennant BC, Gerin JL. Immunosuppression with cyclosporine during the incubation period of experimental woodchuck hepatitis virus infection increases the frequency of chronic infection in adult woodchucks. *J Infect Dis* 1992; **166**: 628-631
34 **Cote PJ**, Korba BE, Steinberg H, Ramirez-Mejia C, Baldwin B, Hornbuckle WE, Tennant BC, Gerin JL. Cyclosporin A modulates the course of woodchuck hepatitis virus infection and induces chronicity. *J Immunol* 1991; **146**: 3138-3144
35 **Tennant BC**. Animal models of hepadnavirus-associated hepatocellular carcinoma. *Clin Liver Dis* 2001; **5**: 43-68
36 **Michalak TI**. Occult persistence and lymphotropism of hepadnaviral infection: insights from the woodchuck viral hepatitis model. *Immunol Rev* 2000; **174**: 98-111
37 **Robinson WS**. Molecular events in the pathogenesis of hepadnavirus-associated hepatocellular carcinoma. *Annu Rev Med* 1994; **45**: 297-323
38 **Gerin JL**, Cote PJ, Korba BE, Tennant BC. Hepadnavirus-induced liver cancer in woodchucks. *Cancer Detect Prev* 1989; **14**: 227-229
39 **Chang MH**. Chronic hepatitis virus infection in children. *J Gastroenterol Hepatol* 1998; **13**: 541-548
40 **Norkrans G**. Epidemiology of hepatitis B virus (HBV) infections with particular regard to current routes of transmission and development of cirrhosis and malignancy. *Scand J Infect Dis Suppl* 1990; **69**: 43-47
41 **Ghendon Y**. Perinatal transmission of hepatitis B virus in high-incidence countries. *J Virol Methods* 1987; **17**: 69-79
42 **Cote PJ**, Toshkov I, Bellezza C, Ascenzi M, Roneker C, Ann Graham L, Baldwin BH, Gaye K, Nakamura I, Korba BE, Tennant BC, Gerin JL. Temporal pathogenesis of experimental neonatal woodchuck hepatitis virus infection: increased initial viral load and decreased severity of acute hepatitis during the development of chronic viral infection. *Hepatology* 2000; **32**: 807-817
43 **Nakamura I**, Nupp JT, Cowlen M, Hall WC, Tennant BC, Casey JL, Gerin JL, Cote PJ. Pathogenesis of experimental neonatal woodchuck hepatitis virus infection: chronicity as an outcome of infection is associated with a diminished acute hepatitis that is temporally deficient for the expression of interferon gamma and tumor necrosis factor-alpha messenger RNAs. *Hepatology* 2001; **33**: 439-447
44 **Menne S**, Roneker CA, Roggendorf M, Gerin JL, Cote PJ, Tennant BC. Deficiencies in the acute-phase cell-mediated immune response to viral antigens are associated with development of chronic woodchuck hepatitis virus infection following neonatal inoculation. *J Virol* 2002; **76**: 1769-1780
45 **Wang Y**, Menne S, Jacob JR, Tennant BC, Gerin JL, Cote PJ. Role of type 1 versus type 2 immune responses in liver during the onset of chronic woodchuck hepatitis virus infection. *Hepatology* 2003; **37**: 771-780
46 **Wang Y**, Menne S, Baldwin BH, Tennant BC, Gerin JL, Cote PJ. Kinetics of viremia and acute liver injury in relation to outcome of neonatal woodchuck hepatitis virus infection. *J Med Virol* 2004; **72**: 406-415
47 **Ponzetto A**, Forzani B. Animal models of hepatocellular carcinoma: hepadnavirus-induced liver cancer in woodchucks. *Ital J Gastroenterol* 1991; **23**: 491-493
48 **Seeger C**, Baldwin B, Hornbuckle WE, Yeager AE, Tennant BC, Cote P, Ferrell L, Ganem D, Varmus HE. Woodchuck hepatitis virus is a more efficient oncogenic agent than ground squirrel hepatitis virus in a common host. *J Virol* 1991; **65**: 1673-1679
49 **Gerin JL**. Experimental WHV infection of woodchucks: an animal model of hepadnavirus-induced liver cancer. *Gastroenterol Jpn* 1990; **25** Suppl 2: 38-42
50 **Popper H**, Roth L, Purcell RH, Tennant BC, Gerin JL. Hepatocarcinogenicity of the woodchuck hepatitis virus. *Proc Natl Acad Sci USA* 1987; **84**: 866-870
51 **Hsu HY**, Chang MH, Hsieh KH, Lee CY, Lin HH, Hwang LH, Chen PJ, Chen DS. Cellular immune response to HBcAg in mother-to-infant transmission of hepatitis B virus. *Hepatology* 1992; **15**: 770-776
52 **Ferrari C**, Penna A, Bertoletti A, Valli A, Antoni AD, Giuberti T, Cavalli A, Petit MA, Fiaccadori F. Cellular immune response to hepatitis B virus-encoded antigens in acute and chronic hepatitis B virus infection. *J Immunol* 1990; **145**: 3442-3449
53 **Tsai SL**, Chen PJ, Lai MY, Yang PM, Sung JL, Huang JH, Hwang LH, Chang TH, Chen DS. Acute exacerbations of chronic type B hepatitis are accompanied by increased T cell responses to hepatitis B core and e antigens. Implications for hepatitis B e antigen seroconversion. *J Clin Invest* 1992; **89**: 87-96
54 **Marinos G**, Torre F, Chokshi S, Hussain M, Clarke BE, Rowlands DJ, Eddleston AL, Naoumov NV, Williams R. Induction of T-helper cell response to hepatitis B core antigen in chronic hepatitis B: a major factor in activation of the host immune response to the hepatitis B virus. *Hepatology* 1995; **22**: 1040-1049

55 **Menne S**, Roneker CA, Tennant BC, Korba BE, Gerin JL, Cote PJ. Immunogenic effects of woodchuck hepatitis virus surface antigen vaccine in combination with antiviral therapy: breaking of humoral and cellular immune tolerance in chronic woodchuck hepatitis virus infection. *Intervirology* 2002; **45**: 237-250

56 **Menne S**, Roneker CA, Korba BE, Gerin JL, Tennant BC, Cote PJ. Immunization with surface antigen vaccine alone and after treatment with 1-(2-fluoro-5-methyl-beta-L-arabinofuranosyl)-uracil (L-FMAU) breaks humoral and cell-mediated immune tolerance in chronic woodchuck hepatitis virus infection. *J Virol* 2002; **76**: 5305-5314

57 **Korba BE**, Cote PJ, Gerin JL, Menne S, Toshkov IA, Tennant BC. Therapy with Clevudine followed by vaccine delays the progression of WHV-induced hepatitis and hepatocellular carcinoma in chronically-infected woodchucks. *Hepatology* 2001; **34**: 583 Part 582 Suppl

58 **Michalak TI**, Pardoe IU, Coffin CS, Churchill ND, Freake DS, Smith P, Trelegan CL. Occult lifelong persistence of infectious hepadnavirus and residual liver inflammation in woodchucks convalescent from acute viral hepatitis. *Hepatology* 1999; **29**: 928-938

59 **Mulrooney PM**, Michalak TI. Quantitative detection of hepadnavirus-infected lymphoid cells by in situ PCR combined with flow cytometry: implications for the study of occult virus persistence. *J Virol* 2003; **77**: 970-979

60 **Lew YY**, Michalak TI. In vitro and in vivo infectivity and pathogenicity of the lymphoid cell-derived woodchuck hepatitis virus. *J Virol* 2001; **75**: 1770-1782

61 **Korba BE**, Cote PJ, Wells FV, Baldwin B, Popper H, Purcell RH, Tennant BC, Gerin JL. Natural history of woodchuck hepatitis virus infections during the course of experimental viral infection: molecular virologic features of the liver and lymphoid tissues. *J Virol* 1989; **63**: 1360-1370

62 **Korba BE**, Cote PJ, Gerin JL. Mitogen-induced replication of woodchuck hepatitis virus in cultured peripheral blood lymphocytes. *Science* 1988; **241**: 1213-1216

63 **Korba BE**, Wells F, Tennant BC, Cote PJ, Gerin JL. Lymphoid cells in the spleens of woodchuck hepatitis virus-infected woodchucks are a site of active viral replication. *J Virol* 1987; **61**: 1318-1324

64 **Korba BE**, Wells F, Tennant BC, Yoakum GH, Purcell RH, Gerin JL. Hepadnavirus infection of peripheral blood lymphocytes in vivo: woodchuck and chimpanzee models of viral hepatitis. *J Virol* 1986; **58**: 1-8

65 **Coffin CS**, Michalak TI. Persistence of infectious hepadnavirus in the offspring of woodchuck mothers recovered from viral hepatitis. *J Clin Invest* 1999; **104**: 203-212

66 **Yuki N**, Nagaoka T, Yamashiro M, Mochizuki K, Kaneko A, Yamamoto K, Omura M, Hikiji K, Kato M. Long-term histologic and virologic outcomes of acute self-limited hepatitis B. *Hepatology* 2003; **37**: 1172-1179

67 **Blum HE**, Liang TJ, Galun E, Wands JR. Persistence of hepatitis B viral DNA after serological recovery from hepatitis B virus infection. *Hepatology* 1991; **14**: 56-63

68 **Michalak TI**, Pasquinelli C, Guilhot S, Chisari FV. Hepatitis B virus persistence after recovery from acute viral hepatitis. *J Clin Invest* 1994; **93**: 230-239

69 **Penna A**, Artini M, Cavalli A, Levrero M, Bertoletti A, Pilli M, Chisari FV, Rehermann B, Del Prete G, Fiaccadori F, Ferrari C. Long-lasting memory T cell responses following self-limited acute hepatitis B. *J Clin Invest* 1996; **98**: 1185-1194

70 **Rehermann B**, Ferrari C, Pasquinelli C, Chisari FV. The hepatitis B virus persists for decades after patients' recovery from acute viral hepatitis despite active maintenance of a cytotoxic T-lymphocyte response. *Nat Med* 1996; **2**: 1104-1108

71 **Yotsuyanagi H**, Yasuda K, Iino S, Moriya K, Shintani Y, Fujie H, Tsutsumi T, Kimura S, Koike K. Persistent viremia after recovery from self-limited acute hepatitis B. *Hepatology* 1998; **27**: 1377-1382

72 **Korba BE**, Wells FV, Baldwin B, Cote PJ, Tennant BC, Popper H, Gerin JL. Hepatocellular carcinoma in woodchuck hepatitis virus-infected woodchucks: presence of viral DNA in tumor tissue from chronic carriers and animals serologically recovered from acute infections. *Hepatology* 1989; **9**: 461-470

73 **Gust ID**, Burrell CJ, Coulepis AG, Robinson WS, Zuckerman AJ. Taxonomic classification of human hepatitis B virus. *Intervirology* 1986; **25**: 14-29

74 **Ganem D**. Hepadnaviridae: the viruses and their replication. In: Fields BN, Knipe DM, Howley PM, editors. Fields virology, 3rd ed. Philadelphia: Lippincott-Raven, 1996: 2703-2737

75 **Ganem D,** Varmus HE. The molecular biology of the hepatitis B viruses. *Annu Rev Biochem* 1987; **56**: 651-693

76 **Tiollais P,** Pourcel C, Dejean A. The hepatitis B virus. *Nature* 1985; **317**: 489-495

77 **Seeger C**, Ganem D, Varmus HE. Biochemical and genetic evidence for the hepatitis B virus replication strategy. *Science* 1986; **232**: 477-484

78 **Summers J**. The replication cycle of hepatitis B viruses. *Cancer* 1988; **61**: 1957-1962

79 **Chen HS**, Miller RH, Hornbuckle WE, Tennant BC, Cote PJ, Gerin JL, Purcell RH. Titration of recombinant woodchuck hepatitis virus DNA in adult woodchucks. *J Med Virol* 1998; **54**: 92-94

80 **Mason WS**, Jilbert AR, Summers J. Clonal expansion of hepatocytes during chronic woodchuck hepatitis virus infection. *Proc Natl Acad Sci USA* 2005; **102**: 1139-1144

81 **Summers J**, Jilbert AR, Yang W, Aldrich CE, Saputelli J, Litwin S, Toll E, Mason WS. Hepatocyte turnover during resolution of a transient hepadnaviral infection. *Proc Natl Acad Sci USA* 2003; **100**: 11652-11659

82 **Kajino K**, Jilbert AR, Saputelli J, Aldrich CE, Cullen J, Mason WS. Woodchuck hepatitis virus infections: very rapid recovery after a prolonged viremia and infection of virtually every hepatocyte. *J Virol* 1994; **68**: 5792-5803

83 **Korba BE**, Brown TL, Wells FV, Baldwin B, Cote PJ, Steinberg H, Tennant BC, Gerin JL. Natural history of experimental woodchuck hepatitis virus infection: molecular virologic features of the pancreas, kidney, ovary, and testis. *J Virol* 1990; **64**: 4499-4506

84 **Korba BE**, Cote PJ, Shapiro M, Purcell RH, Gerin JL. In vitro production of infectious woodchuck hepatitis virus by lipopolysaccharide-stimulated peripheral blood lymphocytes. *J Infect Dis* 1989; **160**: 572-576

85 **Korba BE**, Gowans EJ, Wells FV, Tennant BC, Clarke R, Gerin JL. Systemic distribution of woodchuck hepatitis virus in the tissues of experimentally infected woodchucks. *Virology* 1988; **165**: 172-181

86 **Michalak TI**, Mulrooney PM, Coffin CS. Low doses of hepadnavirus induce infection of the lymphatic system that does not engage the liver. *J Virol* 2004; **78**: 1730-1738

87 **Menne S**, Maschke J, Tolle TK, Lu M, Roggendorf M. Characterization of T-cell response to woodchuck hepatitis virus core protein and protection of woodchucks from infection by immunization with peptides containing a T-cell epitope. *J Virol* 1997; **71**: 65-74

88 **Cote PJ**, Gerin JL. In vitro activation of woodchuck lymphocytes measured by radiopurine incorporation and interleukin-2 production: implications for modeling immunity and therapy in hepatitis B virus infection. *Hepatology* 1995; **22**: 687-699

89 **Menne S**, Maschke J, Tolle T, Kreuzfelder E, Grosse-Wilde H, Roggendorf M. Determination of peripheral blood mononuclear cell responses to mitogens and woodchuck hepatitis virus core antigen in woodchucks by 5-bromo-2'-deoxyuridine or 2[3H]adenine incorporation. *Arch Virol* 1997; **142**: 511-521

90 **Gujar SA**, Michalak TI. Flow cytometric quantification of T cell proliferation and division kinetics in woodchuck model of hepatitis B. *Immunol Invest* 2005; **34**: 215-236

91 **Ferrari C**, Penna A, DegliAntoni A, Fiaccadori F. Cellular immune response to hepatitis B virus antigens. An overview. *J Hepatol* 1988; **7**: 21-33

92 **Webster GJ**, Reignat S, Maini MK, Whalley SA, Ogg GS, King

A, Brown D, Amlot PL, Williams R, Vergani D, Dusheiko GM, Bertoletti A. Incubation phase of acute hepatitis B in man: dynamic of cellular immune mechanisms. *Hepatology* 2000; **32**: 1117-1124

93 **Menne S**, Maschke J, Lu M, Grosse-Wilde H, Roggendorf M. T-Cell response to woodchuck hepatitis virus (WHV) antigens during acute self-limited WHV infection and convalescence and after viral challenge. *J Virol* 1998; **72**: 6083-6091

94 **Menne S**, Maschke J, Klaes R, Grosse-Wilde H, Roggendorf M. Cellular immune response of woodchucks to woodchuck hepatitis virus surface protein during acute WHV infection. In: Rizzetto M, Purcell R, Gerin J, Verme G, editors. Viral hepatitis and liver diseases: proceedings of the IX triennial international symposium on hepatitis viruses and liver disease. Torino: Edizoni Minerva Medica, 1997: 453-457

95 **Hodgson PD**, Grant MD, Michalak TI. Perforin and Fas/Fas ligand-mediated cytotoxicity in acute and chronic woodchuck viral hepatitis. *Clin Exp Immunol* 1999; **118**: 63-70

96 **Hodgson PD**, Michalak TI. Augmented hepatic interferon gamma expression and T-cell influx characterize acute hepatitis progressing to recovery and residual lifelong virus persistence in experimental adult woodchuck hepatitis virus infection. *Hepatology* 2001; **34**: 1049-1059

97 **Guo JT**, Zhou H, Liu C, Aldrich C, Saputelli J, Whitaker T, Barrasa MI, Mason WS, Seeger C. Apoptosis and regeneration of hepatocytes during recovery from transient hepadnavirus infections. *J Virol* 2000; **74**: 1495-1505

98 **Jacob JR**, Ascenzi MA, Roneker CA, Toshkov IA, Cote PJ, Gerin JL, Tennant BC. Hepatic expression of the woodchuck hepatitis virus X-antigen during acute and chronic infection and detection of a woodchuck hepatitis virus X-antigen antibody response. *Hepatology* 1997; **26**: 1607-1615

99 **Chemin I**, Vermot-Desroches C, Baginski I, Lamelin JP, Hantz O, Jacquet C, Rigal D, Trepo C. Monitoring of early events of experimental woodchuck hepatitis infection: studies of peripheral blood mononuclear cells by cytofluorometry and PCR. *FEMS Immunol Med Microbiol* 1993; **7**: 241-249

100 **Feitelson MA**, Clayton MM. X antigen/antibody markers in hepadnavirus infections. Antibodies to the X gene product(s). *Gastroenterology* 1990; **99**: 500-507

101 **Feitelson MA**, Clayton MM, Blumberg BS. X antigen/antibody markers in hepadnavirus infections. Presence and significance of hepadnavirus X gene product(s) in serum. *Gastroenterology* 1990; **98**: 1071-1078

102 **Michalak TI**, Lin B, Churchill ND, Dzwonkowski P, Desousa JR. Hepadna virus nucleocapsid and surface antigens and the antigen-specific antibodies associated with hepatocyte plasma membranes in experimental woodchuck acute hepatitis. *Lab Invest* 1990; **62**: 680-689

103 **Tyler GV**, Summers JW, Synder RL. Woodchuck hepatitis virus in natural woodchuck populations. *J Wildl Dis* 1981; **17**: 297-301

104 **Lindberg J**, Pichoud C, Hantz O, Vitvitski L, Grimaud JA, Gilbert JM, Joubert L, Frommel D, Trepo C. Woodchuck hepatitis virus infection: serologic and histopathologic course and outcome. *Eur J Clin Microbiol* 1985; **4**: 59-61

105 **Ponzetto A**, Cote PJ, Ford EC, Purcell RH, Gerin JL. Core antigen and antibody in woodchucks after infection with woodchuck hepatitis virus. *J Virol* 1984; **52**: 70-76

106 **Menne S**, Cote PJ. Measurement of cell-mediated immune response in woodchucks. *Methods Mol Med* 2004; **96:** 27-36

107 **Menne S**, Wang Y, Butler SD, Gerin JL, Cote PJ, Tennant BC. Real-time polymerase chain reaction assays for leukocyte CD and cytokine mRNAs of the Eastern woodchuck (Marmota monax). *Vet Immunol Immunopathol* 2002; **87**: 97-105

108 **Nakamura I**, Nupp JT, Rao BS, Buckler-White A, Engle RE, Casey JL, Gerin JL, Cote PJ. Cloning and characterization of partial cDNAs for woodchuck cytokines and CD3epsilon with applications for the detection of RNA expression in tissues by RT-PCR assay. *J Med Virol* 1997; **53**: 85-95

109 **Cote PJ**, Nakamura I, Bellezza C, Tennant BC, Gerin JL. Immunobiology of the woodchuck and woodchuck hepatitis virus infection. In: Rizzetto M, Purcell R, Gerin J, Verme G, editors. Viral hepatitis and liver diseases: proceedings of the IX triennial international symposium on hepatitis viruses and liver disease. Torino, Italy: Edizoni Minerva Medica, 1997: 157-163

110 **Chisari FV**, Ferrari C. Hepatitis B virus immunopathogenesis. *Annu Rev Immunol* 1995; **13**: 29-60

111 **Abbott WG**, Geursen A, Fraser JD, Marbrook J, Skinner MA, Tan PL. The influence of a maternal chronic hepatitis B virus infection on the repertoire of transcribed T-cell receptor beta chain variable region genes in human cord blood. *Hepatology* 1995; **22**: 1034-1039

112 **Itoh Y**, Okanoue T, Sakamoto S, Nishioji K, Kashima K. The effects of prednisolone and interferons on serum macrophage colony stimulating factor concentrations in chronic hepatitis B. *J Hepatol* 1997; **26**: 244-252

113 **Zielińska W**, Paszkiewicz J, Korczak A, Własiuk M, Zółtowska A, Szutowicz A, Cummins JM, Georgiades JA. Treatment of fourteen chronic active HBsAg+, HBeAg+ hepatitis patients with low dose natural human interferon alpha administered orally. *Arch Immunol Ther Exp* (Warsz) 1993; **41**: 241-251

114 **Hsu HY**, Chang MH, Ni YH, Lee PI. Cytokine release of peripheral blood mononuclear cells in children with chronic hepatitis B virus infection. *J Pediatr Gastroenterol Nutr* 1999; **29**: 540-545

115 **Jung MC**, Diepolder HM, Spengler U, Wierenga EA, Zachoval R, Hoffmann RM, Eichenlaub D, Frösner G, Will H, Pape GR. Activation of a heterogeneous hepatitis B (HB) core and e antigen-specific CD4+ T-cell population during seroconversion to anti-HBe and anti-HBs in hepatitis B virus infection. *J Virol* 1995; **69**: 3358-3368

116 **Löhr HF**, Weber W, Schlaak J, Goergen B, Meyer zum Buschenfelde KH, Gerken G. Proliferative response of CD4+ T cells and hepatitis B virus clearance in chronic hepatitis with or without hepatitis B e-minus hepatitis B virus mutants. *Hepatology* 1995; **22**: 61-68

117 **Zoulim F**, Berthillon P, Guerhier FL, Seigneres B, Germon S, Pichoud C, Cheng YC, Trepo C. Animal models for the study of HBV infection and the evaluation of new anti-HBV strategies. *J Gastroenterol Hepatol* 2002; **17** Suppl: S460-S463

118 **Tatti KM**, Korba BE, Stang HL, Peek S, Gerin JL, Tennant BC, Schinazi RF. Mutations in the conserved woodchuck hepatitis virus polymerase FLLA and YMDD regions conferring resistance to lamivudine. *Antiviral Res* 2002; **55**: 141-150

119 **Yamamoto T**, Litwin S, Zhou T, Zhu Y, Condreay L, Furman P, Mason WS. Mutations of the woodchuck hepatitis virus polymerase gene that confer resistance to lamivudine and 2′ -fluoro-5-methyl-beta-L-arabinofuranosyluracil. *J Virol* 2002; **76**: 1213-1223

120 **Mason WS**, Cullen J, Moraleda G, Saputelli J, Aldrich CE, Miller DS, Tennant B, Frick L, Averett D, Condreay LD, Jilbert AR. Lamivudine therapy of WHV-infected woodchucks. *Virology* 1998; **245**: 18-32

121 **Zhou T**, Saputelli J, Aldrich CE, Deslauriers M, Condreay LD, Mason WS. Emergence of drug-resistant populations of woodchuck hepatitis virus in woodchucks treated with the antiviral nucleoside lamivudine. *Antimicrob Agents Chemother* 1999; **43**: 1947-1954

122 **Zhu Y**, Yamamoto T, Cullen J, Saputelli J, Aldrich CE, Miller DS, Litwin S, Furman PA, Jilbert AR, Mason WS. Kinetics of hepadnavirus loss from the liver during inhibition of viral DNA synthesis. *J Virol* 2001; **75**: 311-322

123 **Korba BE**, Gerin JL. Use of a standardized cell culture assay to assess activities of nucleoside analogs against hepatitis B virus replication. *Antiviral Res* 1992; **19**: 55-70

124 **Morrey JD**, Korba BE, Sidwell RW. Transgenic mice as a chemotherapeutic model for hepatitis B virus infection. *Antivir Ther* 1998; **3**: 59-68

125 **Tennant BC**, Baldwin BH, Graham LA, Ascenzi MA, Hornbuckle WE, Rowland PH, Tochkov IA, Yeager AE, Erb HN, Colacino JM, Lopez C, Engelhardt JA, Bowsher RR, Richardson FC, Lewis W, Cote PJ, Korba BE, Gerin JL.

Antiviral activity and toxicity of fialuridine in the woodchuck model of hepatitis B virus infection. *Hepatology* 1998; **28**: 179-191

126 **Kleiner DE**, Gaffey MJ, Sallie R, Tsokos M, Nichols L, Mk-Kenzie R, Straus SE, Hoofnagle JH. Histopathologic changes associated with fialuridine hepatotoxicity. *Mod Pathol* 1997; **10**: 192-199

127 **Lewis W**, Griniuviene B, Tankersley KO, Levine ES, Montione R, Engelman L, de Courten-Myers G, Ascenzi MA, Hornbuckle WE, Gerin JL, Tennant BC. Depletion of mitochondrial DNA, destruction of mitochondria, and accumulation of lipid droplets result from fialuridine treatment in woodchucks (Marmota monax). *Lab Invest* 1997; **76**: 77-87

128 **Josephson L**. Severe toxicity of fialuridine (FIAU). *N Engl J Med* 1996; **334**: 1135-1136; author reply 1137-1138

129 **Fourel I**, Hantz O, Watanabe KA, Jacquet C, Chomel B, Fox JJ, Trepo C. Inhibitory effects of 2′-fluorinated arabinosylpyrimidine nucleosides on woodchuck hepatitis virus replication in chronically infected woodchucks. *Antimicrob Agents Chemother* 1990; **34**: 473-475

130 **Le Guerhier F**, Pichoud C, Jamard C, Guerret S, Chevallier M, Peyrol S, Hantz O, King I, Trépo C, Cheng YC, Zoulim F. Antiviral activity of beta-L-2′,3′-dideoxy-2′,3′-didehydro-5-fluorocytidine in woodchucks chronically infected with woodchuck hepatitis virus. *Antimicrob Agents Chemother* 2001; **45**: 1065-1077

131 **Zahm FE**, d'Urso N, Bonino F, Ponzetto A. Treatment of woodchuck hepatitis virus infection in vivo with 2′, -3′-dideoxycytidine (ddC) and 2′,-3′-dideoxycytidine monophosphate coupled to lactosaminated human serum albumin (L-HSA ddCMP). *Liver* 1996; **16**: 88-93

132 **Korba BA**, Xie H, Wright KN, Hornbuckle WE, Gerin JL, Tennant BC, Hostetler KY. Liver-targeted antiviral nucleosides: enhanced antiviral activity of phosphatidyl-dideoxyguanosine versus dideoxyguanosine in woodchuck hepatitis virus infection in vivo. *Hepatology* 1996; **23**: 958-963

133 **Zahm FE**, Bonino F, Giuseppetti R, Rapicetta M. Antiviral activity of ganciclovir, 9-(1,3-dihydroxy-2-propoxymethyl) guanine against woodchuck hepatitis virus: quantitative measurement of woodchuck hepatitis virus DNA using storage phosphor technology. *Ital J Gastroenterol Hepatol* 1998; **30**: 510-516

134 **Chu CK**, Boudinot FD, Peek SF, Hong JH, Choi Y, Korba BE, Gerin JL, Cote PJ, Tennant BC, Cheng YC. Preclinical investigation of L-FMAU as an anti-hepatitis B virus agent. *Antivir Ther* 1998; **3**: 113-121

135 **Hostetler KY**, Beadle JR, Hornbuckle WE, Bellezza CA, Tochkov IA, Cote PJ, Gerin JL, Korba BE, Tennant BC. Antiviral activities of oral 1-O-hexadecylpropanediol-3-phosphoacyclovir and acyclovir in woodchucks with chronic woodchuck hepatitis virus infection. *Antimicrob Agents Chemother* 2000; **44**: 1964-1969

136 **Hurwitz SJ**, Tennant BC, Korba BE, Gerin JL, Schinazi RF. Pharmacodynamics of (-)-beta-2′,3′-dideoxy-3′-thiacytidine in chronically virus-infected woodchucks compared to its pharmacodynamics in humans. *Antimicrob Agents Chemother* 1998; **42**: 2804-2809

137 **Enriquez PM**, Jung C, Josephson L, Tennant BC. Conjugation of adenine arabinoside 5′-monophosphate to arabinogalactan: synthesis, characterization, and antiviral activity. *Bioconjug Chem* 1995; **6**: 195-202

138 **Ponzetto A**, Fiume L, Forzani B, Song SY, Busi C, Mattioli A, Spinelli C, Marinelli M, Smedile A, Chiaberge E. Adenine arabinoside monophosphate and acyclovir monophosphate coupled to lactosaminated albumin reduce woodchuck hepatitis virus viremia at doses lower than do the unconjugated drugs. *Hepatology* 1991; **14**: 16-24

139 **Genovesi EV**, Lamb L, Medina I, Taylor D, Seifer M, Innaimo S, Colonno RJ, Standring DN, Clark JM. Efficacy of the carbocyclic 2′-deoxyguanosine nucleoside BMS-200475 in the woodchuck model of hepatitis B virus infection. *Antimicrob Agents Chemother* 1998; **42**: 3209-3217

140 **Choi JR**, Cho DG, Roh KY, Hwang JT, Ahn S, Jang HS, Cho WY, Kim KW, Cho YG, Kim J, Kim YZ. A novel class of phosphonate nucleosides. 9-[(1-phosphonomethoxycycloprop yl)methyl]guanine as a potent and selective anti-HBV agent. *J Med Chem* 2004; **47**: 2864-2869

141 **Korba BE**, Cote P, Hornbuckle W, Schinazi R, Gangemi JD, Tennant BC, Gerin JL. Enhanced antiviral benefit of combination therapy with lamivudine and alpha interferon against WHV replication in chronic carrier woodchucks. *Antivir Ther* 2000; **5**: 95-104

142 **Peek SF**, Toshkov I, Erb H, Schinazi R, Korba B, Cote P, Gerin J, Tennant B. Lamivudine (2,3-dideoxy-3-thiacytidine,3TC) delays the onset of hepatocellular carcinoma (HCC) and increases survival in the woodchuck model of chronic hepatitis B virus (HBV) infection. *Hepatology* 2002; **36**: 1855 Part 1852 Suppl

143 **Hervás-Stubbs S**, Lasarte JJ, Sarobe P, Vivas I, Condreay L, Cullen JM, Prieto J, Borrás-Cuesta F. T-helper cell response to woodchuck hepatitis virus antigens after therapeutic vaccination of chronically-infected animals treated with lamivudine. *J Hepatol* 2001; **35**: 105-111

144 **Cullen JM**, Li DH, Brown C, Eisenberg EJ, Cundy KC, Wolfe J, Toole J, Gibbs C. Antiviral efficacy and pharmacokinetics of oral adefovir dipivoxil in chronically woodchuck hepatitis virus-infected woodchucks. *Antimicrob Agents Chemother* 2001; **45**: 2740-2745

145 **Jacob JR**, Korba BE, Cote PJ, Toshkov I, Delaney WE, Gerin JL, Tennant BC. Suppression of lamivudine-resistant B-domain mutants by adefovir dipivoxil in the woodchuck hepatitis virus model. *Antiviral Res* 2004; **63**: 115-121

146 **Colonno RJ**, Genovesi EV, Medina I, Lamb L, Durham SK, Huang ML, Corey L, Littlejohn M, Locarnini S, Tennant BC, Rose B, Clark JM. Long-term entecavir treatment results in sustained antiviral efficacy and prolonged life span in the woodchuck model of chronic hepatitis infection. *J Infect Dis* 2001; **184**: 1236-1245

147 **Menne S**, Cote PJ, Korba BE, Butler SD, George AL, Tochkov IA, Delaney WE, Xiong S, Gerin JL, Tennant BC. Antiviral effect of oral administration of tenofovir disoproxil fumarate in woodchucks with chronic woodchuck hepatitis virus infection. *Antimicrob Agents Chemother* 2005; **49**: 2720-2728

148 **Cullen JM**, Smith SL, Davis MG, Dunn SE, Botteron C, Cecchi A, Linsey D, Linzey D, Frick L, Paff MT, Goulding A, Biron K. In vivo antiviral activity and pharmacokinetics of (-)-cis-5-fluoro-1-[2-(hydroxymethyl)-1,3-oxathiolan-5-yl]cytosine in woodchuck hepatitis virus-infected woodchucks. *Antimicrob Agents Chemother* 1997; **41**: 2076-2082

149 **Korba BE**, Schinazi RF, Cote P, Tennant BC, Gerin JL. Effect of oral administration of emtricitabine on woodchuck hepatitis virus replication in chronically infected woodchucks. *Antimicrob Agents Chemother* 2000; **44**: 1757-1760

150 **Jacquard AC**, Nassal M, Pichoud C, Ren S, Schultz U, Guerret S, Chevallier M, Werle B, Peyrol S, Jamard C, Rimsky LT, Trepo C, Zoulim F. Effect of a combination of clevudine and emtricitabine with adenovirus-mediated delivery of gamma interferon in the woodchuck model of hepatitis B virus infection. *Antimicrob Agents Chemother* 2004; **48**: 2683-2692

151 **Standring DN**, Bridges EG, Placidi L, Faraj A, Loi AG, Pierra C, Dukhan D, Gosselin G, Imbach JL, Hernandez B, Juodawlkis A, Tennant B, Korba B, Cote P, Cretton-Scott E, Schinazi RF, Myers M, Bryant ML, Sommadossi JP. Antiviral beta-L-nucleosides specific for hepatitis B virus infection. *Antivir Chem Chemother* 2001; **12** Suppl 1: 119-129

152 **Bryant ML**, Bridges EG, Placidi L, Faraj A, Loi AG, Pierra C, Dukhan D, Gosselin G, Imbach JL, Hernandez B, Juodawlkis A, Tennant B, Korba B, Cote P, Marion P, Cretton-Scott E, Schinazi RF, Sommadossi JP. Antiviral L-nucleosides specific for hepatitis B virus infection. *Antimicrob Agents Chemother* 2001; **45**: 229-235

153 **Bryant ML**, Bridges EG, Placidi L, Faraj A, Loi AG, Pierra C, Dukhan D, Gosselin G, Imbach JL, Hernandez B, Juodawlkis A, Tennant B, Korba B, Cote P, Cretton-Scott E, Schinazi RF,

Sommadossi JP. Anti-HBV specific beta-L-2'-deoxynucleosides. *Nucleosides Nucleotides Nucleic Acids* 2001; **20**: 597-607

154 **Peek SF**, Cote PJ, Jacob JR, Toshkov IA, Hornbuckle WE, Baldwin BH, Wells FV, Chu CK, Gerin JL, Tennant BC, Korba BE. Antiviral activity of clevudine [L-FMAU, (1-(2-fluoro-5-methyl-beta, L-arabinofuranosyl) uracil)] against woodchuck hepatitis virus replication and gene expression in chronically infected woodchucks (Marmota monax). *Hepatology* 2001; **33**: 254-266

155 **Korba BE**, Cote PJ, Menne S, Toshkov I, Baldwin BH, Wells FV, Tennant BC, Gerin JL. Clevudine therapy with vaccine inhibits progression of chronic hepatitis and delays onset of hepatocellular carcinoma in chronic woodchuck hepatitis virus infection. *Antivir Ther* 2004; **9**: 937-952

156 **Zhu Y**, Cullen JM, Aldrich CE, Saputelli J, Miller D, Seeger C, Mason WS, Jilbert AR. Adenovirus-based gene therapy during clevudine treatment of woodchucks chronically infected with woodchuck hepatitis virus. *Virology* 2004; **327**: 26-40

157 **Korba BE**, Cote P, Hornbuckle W, Schinazi R, Gerin JL, Tennant BC. Enhanced antiviral benefit of combination therapy with lamivudine and famciclovir against WHV replication in chronic WHV carrier woodchucks. *Antiviral Res* 2000; **45**: 19-32

158 **Block TM**, Lu X, Mehta AS, Blumberg BS, Tennant B, Ebling M, Korba B, Lansky DM, Jacob GS, Dwek RA. Treatment of chronic hepadnavirus infection in a woodchuck animal model with an inhibitor of protein folding and trafficking. *Nat Med* 1998; **4**: 610-614

159 **Bartholomew RM**, Carmichael EP, Findeis MA, Wu CH, Wu GY. Targeted delivery of antisense DNA in woodchuck hepatitis virus-infected woodchucks. *J Viral Hepat* 1995; **2**: 273-278

160 **Blumberg BS**, Millman I, Venkateswaran PS, Thyagarajan SP. Hepatitis B virus and primary hepatocellular carcinoma: treatment of HBV carriers with Phyllanthus amarus. *Vaccine* 1990; **8** Suppl: S86-S92

161 **Gerin JL,** Korba BE, Cote PJ, Tennant BC. A preliminary report of a controlled study of thymosin alpha-1 in the woodchuck model of hepadnavirus infection. *Adv Exp Med Biol* 1992; **312**: 121-123

162 **Pützer BM**, Stiewe T, Rödicker F, Schildgen O, Rühm S, Dirsch O, Fiedler M, Damen U, Tennant B, Scherer C, Graham FL, Roggendorf M. Large nontransplanted hepatocellular carcinoma in woodchucks: treatment with adenovirus-mediated delivery of interleukin 12/B7.1 genes. *J Natl Cancer Inst* 2001; **93**: 472-479

163 **Bilbao R**, Gérolami R, Bralet MP, Qian C, Tran PL, Tennant B, Prieto J, Bréchot C. Transduction efficacy, antitumoral effect, and toxicity of adenovirus-mediated herpes simplex virus thymidine kinase/ ganciclovir therapy of hepatocellular carcinoma: the woodchuck animal model. *Cancer Gene Ther* 2000; **7**: 657-662

164 **Gouillat C,** Manganas D, Zoulim F, Vitrey D, Saguier G, Guillaud M, Ain JF, Duque-Campos R, Jamard C, Praves M, Trepo C. Woodchuck hepatitis virus-induced carcinoma as a relevant natural model for therapy of human hepatoma. *J Hepatol* 1997; **26**: 1324-1330

165 **Roos S**, Fuchs K, Roggendorf M. Protection of woodchucks from infection with woodchuck hepatitis virus by immunization with recombinant core protein. *J Gen Virol* 1989; **70** (Pt 8): 2087-2095

166 **Schödel F**, Neckermann G, Peterson D, Fuchs K, Fuller S, Will H, Roggendorf M. Immunization with recombinant woodchuck hepatitis virus nucleocapsid antigen or hepatitis B virus nucleocapsid antigen protects woodchucks from woodchuck hepatitis virus infection. *Vaccine* 1993; **11**: 624-628

167 **Cote PJ**, Shapiro M, Engle RE, Popper H, Purcell RH, Gerin JL. Protection of chimpanzees from type B hepatitis by immunization with woodchuck hepatitis virus surface antigen. *J Virol* 1986; **60**: 895-901

168 **García-Navarro R**, Blanco-Urgoiti B, Berraondo P, Sánchez de la Rosa R, Vales A, Hervás-Stubbs S, Lasarte JJ, Borrás F, Ruiz J, Prieto J. Protection against woodchuck hepatitis virus (WHV) infection by gene gun coimmunization with WHV core and interleukin-12. *J Virol* 2001; **75**: 9068-9076

169 **Siegel F**, Lu M, Roggendorf M. Coadministration of gamma interferon with DNA vaccine expressing woodchuck hepatitis virus (WHV) core antigen enhances the specific immune response and protects against WHV infection. *J Virol* 2001; **75**: 5036-5042

170 **Lu M**, Hilken G, Kruppenbacher J, Kemper T, Schirmbeck R, Reimann J, Roggendorf M. Immunization of woodchucks with plasmids expressing woodchuck hepatitis virus (WHV) core antigen and surface antigen suppresses WHV infection. *J Virol* 1999; **73**: 281-289

171 **Lu M**, Isogawa M, Xu Y, Hilken G. Immunization with the gene expressing woodchuck hepatitis virus nucleocapsid protein fused to cytotoxic-T-lymphocyte-associated antigen 4 leads to enhanced specific immune responses in mice and woodchucks. *J Virol* 2005; **79**: 6368-6376

172 **Argentini C**, Giuseppetti R, D'Ugo E, La Sorsa V, Tritarelli E, Orobello S, Canitano A, Glück R, Rapicetta M. A pre-S/S CHO-derived hepatitis B virus vaccine protects woodchucks from WHV productive infection. *Vaccine* 2005; **23**: 3649-3656

173 **Lu M**, Klaes R, Menne S, Gerlich W, Stahl B, Dienes HP, Drebber U, Roggendorf M. Induction of antibodies to the PreS region of surface antigens of woodchuck hepatitis virus (WHV) in chronic carrier woodchucks by immunizations with WHV surface antigens. *J Hepatol* 2003; **39**: 405-413

174 **Hervás-Stubbs S**, Lasarte JJ, Sarobe P, Prieto J, Cullen J, Roggendorf M, Borrás-Cuesta F. Therapeutic vaccination of woodchucks against chronic woodchuck hepatitis virus infection. *J Hepatol* 1997; **27**: 726-737

175 **Guidotti LG**, Guilhot S, Chisari FV. Interleukin-2 and alpha/beta interferon down-regulate hepatitis B virus gene expression in vivo by tumor necrosis factor-dependent and -independent pathways. *J Virol* 1994; **68**: 1265-1270

176 **Guidotti LG**, Borrow P, Hobbs MV, Matzke B, Gresser I, Oldstone MB, Chisari FV. Viral cross talk: intracellular inactivation of the hepatitis B virus during an unrelated viral infection of the liver. *Proc Natl Acad Sci USA* 1996; **93**: 4589-4594

177 **Guidotti LG**, Ishikawa T, Hobbs MV, Matzke B, Schreiber R, Chisari FV. Intracellular inactivation of the hepatitis B virus by cytotoxic T lymphocytes. *Immunity* 1996; **4**: 25-36

178 **Schildgen O**, Fiedler M, Dahmen U, Li J, Lohrengel B, Lu M, Roggendorf M. Fluctuation of the cytokine expression in the liver during the chronic woodchuck hepatitis virus (WHV) infection is not related to viral load. *Immunol Lett* 2006; **102**: 31-37

179 **Lu M**, Lohrengel B, Hilken G, Kemper T, Roggendorf M. Woodchuck gamma interferon upregulates major histocompatibility complex class I transcription but is unable to deplete woodchuck hepatitis virus replication intermediates and RNAs in persistently infected woodchuck primary hepatocytes. *J Virol* 2002; **76**: 58-67

180 **Wang Y**, Jacob JR, Menne S, Bellezza CA, Tennant BC, Gerin JL, Cote PJ. Interferon-gamma-associated responses to woodchuck hepatitis virus infection in neonatal woodchucks and virus-infected hepatocytes. *J Viral Hepat* 2004; **11**: 404-417

181 **Fiedler M**, **Rödicker** F, Salucci V, Lu M, Aurisicchio L, Dahmen U, Jun L, Dirsch O, Pützer BM, Palombo F, Roggendorf M. Helper-dependent adenoviral vector-mediated delivery of woodchuck-specific genes for alpha interferon (IFN-alpha) and IFN-gamma: IFN-alpha but not IFN-gamma reduces woodchuck hepatitis virus replication in chronic infection in vivo. *J Virol* 2004; **78**: 10111-10121

182 **Berraondo P**, Ochoa L, Crettaz J, Rotellar F, Vales A, Martínez-Ansó E, Zaratiegui M, Ruiz J, González-Aseguinolaza G, Prieto J. IFN-alpha gene therapy for woodchuck hepatitis with adeno-associated virus: differences in duration of gene expression and antiviral activity using intraportal or intramuscular routes. *Mol Ther* 2005; **12**: 68-76

183 **Ilan Y**, Nagler A, Shouval D, Ackerstein A, Or R, Kapelushnik J, Adler R, Slavin S. Development of antibodies to hepatitis B virus surface antigen in bone marrow transplant recipient following treatment with peripheral blood lymphocytes from immunized donors. *Clin Exp Immunol* 1994; **97**: 299-302

184 **Ilan Y**, Nagler A, Adler R, Tur-Kaspa R, Slavin S, Shouval D. Ablation of persistent hepatitis B by bone marrow transplantation from a hepatitis B-immune donor. *Gastroenterology* 1993; **104**: 1818-1821

185 **Lau GK**, Suri D, Liang R, Rigopoulou EI, Thomas MG, Mullerova I, Nanji A, Yuen ST, Williams R, Naoumov NV. Resolution of chronic hepatitis B and anti-HBs seroconversion in humans by adoptive transfer of immunity to hepatitis B core antigen. *Gastroenterology* 2002; **122**: 614-624

186 **Lau GK**, Liang R, Lee CK, Yuen ST, Hou J, Lim WL, Williams R. Clearance of persistent hepatitis B virus infection in Chinese bone marrow transplant recipients whose donors were anti-hepatitis B core- and anti-hepatitis B surface antibody-positive. *J Infect Dis* 1998; **178**: 1585-1591

187 **Brugger SA**, Oesterreicher C, Hofmann H, Kalhs P, Greinix HT, Müller C. Hepatitis B virus clearance by transplantation of bone marrow from hepatitis B immunised donor. *Lancet* 1997; **349**: 996-997

188 **Dahmen U**, Dirsch O, Li J, Fiedle M, Lu M, Rispeter K, Picucci M, Broelsch CE, Roggendorf M. Adoptive transfer of immunity: a new strategy to interfere with severe hepatitis virus reinfection after woodchuck liver transplantation. *Transplantation* 2004; **77**: 965-972

189 **Boni C**, Bertoletti A, Penna A, Cavalli A, Pilli M, Urbani S, Scognamiglio P, Boehme R, Panebianco R, Fiaccadori F, Ferrari C. Lamivudine treatment can restore T cell responsiveness in chronic hepatitis B. *J Clin Invest* 1998; **102**: 968-975

190 **Boni C**, Penna A, Ogg GS, Bertoletti A, Pilli M, Cavallo C, Cavalli A, Urbani S, Boehme R, Panebianco R, Fiaccadori F, Ferrari C. Lamivudine treatment can overcome cytotoxic T-cell hyporesponsiveness in chronic hepatitis B: new perspectives for immune therapy. *Hepatology* 2001; **33**: 963-971

191 **Zhou T**, Guo JT, Nunes FA, Molnar-Kimber KL, Wilson JM, Aldrich CE, Saputelli J, Litwin S, Condreay LD, Seeger C, Mason WS. Combination therapy with lamivudine and adenovirus causes transient suppression of chronic woodchuck hepatitis virus infections. *J Virol* 2000; **74**: 11754-11763

S- Editor Liu Y **L- Editor** Alpini GD **E- Editor** Ma WH

PO Box 2345, Beijing 100023, China
www.wjgnet.com
wjg@wjgnet.com

World J Gastroenterol 2007 January 7; 13(1): 125-140
World Journal of Gastroenterology ISSN 1007-9327

TOPIC HIGHLIGHT

Dieter Glebe, PhD, *Series Editor*

Antiviral therapy and resistance with hepatitis B virus infection

Hans L Tillmann

Hans L Tillmann, University of Leipzig, Philipp-Rosenthal Street 27, Leipzig 04103, Germany
Supported by the German BMBF and Network for competence in viral hepatitis
Correspondence to: Hans L Tillmann, Professor of Medicine, University of Leipzig, Philipp-Rosenthal Street 27, Leipzig 04103, Germany. hans.tillmann@medizin.uni-leipzig.de
Telephone: +49-341-9712231 Fax: +49-341-9712209
Received: 2006-09-11 Accepted: 2006-10-13

Abstract

Hepatitis B virus (HBV) infection is still the most common cause of hepatocellular carcinoma and liver cirrhosis world wide. Recently, however, there has been quite dramatic improvement in the understanding of HBV associated liver disease and its treatment. It has become clear that high viral replication is a major risk factor for the development of both cirrhosis and hepatocellular carcinoma. Early studies have shown lamivudine lowers the risk of HBV associated complications. There are currently three nucleos(t)ides licensed, in addition to interferon, and there are more drugs coming to the market soon. Interferon or its pegylated counterpart are still the only options for treatment with defined end points, while nucleos(t)ides therapy is used mostly for long term treatment. Combination therapies have not been shown to be superior to monotherapy in naïve patients, however, the outcome depends on how the end point is defined. Interferon plus lamivudine achieves a higher viral suppression than either treatment alone, even though Hbe-seroconversion was not different after a one year treatment. HBV-genotypes emerge as relevant factors, with genotypes "A" and "B" responding relatively well to interferon, achieving up to 20% HBsAg clearance in the case of genotype "A". In addition to having a defined treatment duration, interferon has the advantage of lacking resistance selection, which is a major drawback for lamivudine and the other nucleos(t)ides. The emergence of resistance against adefovir and entecavir is somewhat slower in naïve compared to lamivudine resistant patients. Adefovir has a low resistance profile with 3%, 9%, 18%, and 28% after 2, 3, 4, and 5 years, respectively, while entecavir has rarely produced resistance in naïve patients for up to 3 years.

Key words: Hepatitis B; Antiviral therapy; Resistance; Interferon; Nucleosides; Nucleotides

Tillmann HL. Antiviral therapy and resistance with hepatitis B virus infection. *World J Gastroenterol* 2007; 13(1): 125-140

http://www.wjgnet.com/1007-9327/13/125.asp

INTRODUCTION

Even though hepatitis B virus (HBV) infection is a preventable disease through vaccination, an estimated 2 billion people are HBV infected, with more than 350 million HBsAg positive and considered as carriers or actively infected[1]. As with hepatitis C, only about one third of the patients that are HBsAg positive require antiviral therapy because of active HBV replication and associated liver disease determined by elevated liver enzymes. Recently, it was demonstrated that, at least in Asian males older than 30 years of age, there is a viral load related risk of hepatocellular carcinoma[2]. This would suggest that antiviral therapy might be indicated even in the absence of active liver disease to decrease the risk of developing hepatocellular carcinoma.

There are different potential mechanisms for how HBV can be inhibited. Mechanisms include an antiviral and immune modulating approach with substances like interferon, a purely antiviral approach inhibiting the HBV polymerase with substances like acyclovir, ganciclovir, and more recently lamivudine, adefovir, entecavir, telbivudine, and several not yet licensed drugs. Interestingly, most of the antivirals studied for HBV were derived from herpes virus or HIV drug development. Thus many of these substances are active against both HBV and HIV, as HBV likewise to HIV replicates *via* an error-prone viral reverse transcriptase. This cross-reactivity must be kept in mind because patients with an HIV infection must never be treated with a monotherapy for HIV, i.e. lamivudine, tenofovir. The reverse transcriptase of HBV and HIV displays similarities, including a so called YMDD motif. Thus, in any patient undergoing HBV-specific treatment, which might also act against HIV, an HIV test should be recommended. Furthermore, if HBV needs to be treated while HIV does not need to be treated, entecavir, telbivudine, and interferon are the primary options. Future options also might include new approaches such as the inhibition of

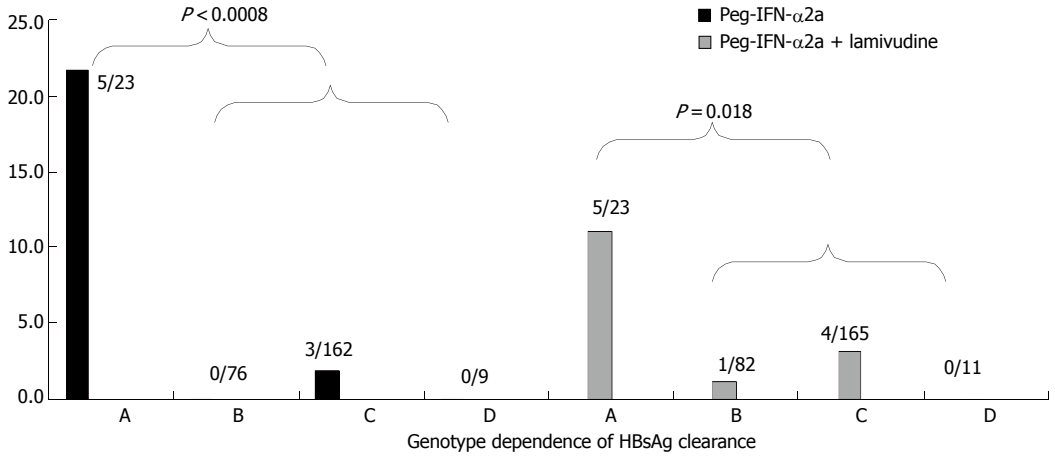

Figure 1 HBsAg seroconversion occurs more frequently on HBV gentoype "A" compared to the other Genotypes. Date given in percent (%). Adapted from Lau GK, *et al*. *N Engl J Med* 2005.

viral entry by using a peptide that is competitive with HBV binding.

Among the earliest substances to be used in man were interferon, acyclovir (previously shown to ameliorate Herpes Simplex Virus I associated encephalitis), as well as vidarabine and ARA-A[3-5]. Even though promising, these agents, except for interferon, were subsequently shown to have minor potency in controlled trials and/or had significant side effects prohibiting further development[6,7]. Similarly, a combination of interferon with these "antiviral" agents did not improve the efficacy of interferon[8]. Ganciclovir, which is effective against cytomegalovirus, has also been evaluated for effectiveness against HBV[9], but was subsequently not developed further because more potent drugs were emerging.

GOALS OF THERAPY FOR HBV INFECTION

The main goal of antiviral therapy is to prevent the development of liver failure, due to either acute fulminant hepatitis or chronic hepatitis B with subsequent liver cirrhosis, the emergence of hepatocellular carcinoma, and HBV transmission. All of these can likely be achieved by suppressing HBV replication, which thereby leads to the remission of liver disease activity and infectivity.

In patients with wild type virus infection, the primary goal of antiviral therapy is to achieve seroconversion from HBeAg to the corresponding anti-HBe antibody (i.e. HBe seroconversion) because this immunologic event is associated with reduced risk for progression of liver disease[10]. Noteworthy, a prior decline in viral load is mandatory to obtain HBe seroconversion, which is subsequently required to also achieve seroconversion from HBsAg to the homologous anti-HBs antibody (i.e. HBs seroconversion). This, however, is achieved less frequently and its likelihood, as that of HBe-Seroconversion, might be genotype related (Figure 1)[11].

HBeAg can be negative in the presence of ongoing high viral replication. In patients with HBeAg negative chronic hepatitis B, pre-core mutants can be detected, which are characterised by an inability to produce HBeAg in detectable quantities (Core-promoter mutations) or show a failure to produce HBeAg (start codon mutations or mutations towards a stop codon typically in the second to last codon of the pre-core region). Available antiviral agents are effective in suppressing HBV replication but in many cases they are not capable of inducing a sustained response after treatment cessation. Therefore, the main objective of therapy is to control viral replication to prevent ALT flares and/or induce remission of disease.

TREATMENT OUTCOME PARAMETERS

Treatment responses have been poorly defined in the past and different studies use different endpoints, thereby making clear comparisons troublesome. In an approach to unify treatment outcome measurements, the European consensus conference in 2002 defined different types of responses[12]; i.e., an initial response, an on-treatment or maintained response, and the sustained response when antiviral treatment has been stopped. The virological response is defined by the decline in HBV DNA below 10^4 or 10^3 copies/mL, the biochemical response by the normalization of ALT levels, and the histological response (HAI score) by the improvement in the inflammatory activity or fibrosis indices. The combined response is defined by the improvement in ALT levels and decrease in viral load while the complete response is characterized by the combination of the decrease in viral load, the normalization of ALT levels, the occurrence of an HBe- or HBs-seroconversion, and an improvement of liver disease at histology.

The treatment response is also defined based on the duration of therapy. An initial response is characterized by at least 1 $\log_{10}$ copies/mL decrease in viral load compared to the baseline value at wk 12 of therapy. The maintained response is defined by a low viral load during therapy. Depending on the use of nucleoside analogue or interferon, there is no agreed threshold to define the maintained response. Usually, a decrease of viral load below 10^4 copies/mL is associated with an improvement of liver histology. However, with nucleoside analogs, the lower the viral load, the lower the risk to develop viral drug resistance. It seems to emerge that viral load shall decrease to $< 3 \log_{10}(10^3)$ copies/mL. The end of treatment response is defined by the response observed at the end of therapy, if there was a decision to stop treatment. A relapse is defined by the increase in viral load after treatment

cessation. The sustained response is conventionally defined by the maintenance of the response 6 mo after drug withdrawal. Finally, a breakthrough is an increase of the viral load of at least 1log after initial response (see also resistance).

To enable better comparison of different studies in the future the following data should always be reported within a given study: HBeAg loss & HBeAg seroconversion to anti-HBe; HBsAg loss & HBsAg seroconversion to anti-HBs; End of treatment results, and if applicable at 6 mo follow-up; HBV-DNA log reduction within defined time points e.g. at wk 12 and 24; Number of patients not achieving a 1 or 2 log reduction within 12 and 24 wk; Mean and median log reduction; Achieved HBV DNA reduction to absolute values, such as below 400 copies (100 IU/mL)and below 50 copies (12.5 IU/mL); HBV-Genotypes.

If new assays become available, the studies should report data in a way that is comparable to former studies.

INDICATION OF ANTIVIRAL THERAPY

Treatment goals and knowledge of the natural history of disease are important for deciding who needs treatment. Two studies have shown that Asian males who are older than 30 years and HBeAg positive[13] or have a high viral load have a 10% risk of developing a hepatocellular carcinoma or cirrhosis[2,122]. In these patients, antiviral strategies seem justified even in the absence of liver disease. In contrast to HCV, HBV can lead to hepatocellular carcinoma in absence of advanced fibrosis/cirrhosis. However, whether these data that were derived from an Asian population can be translated to other regions of the world with different HBV genotypes and ethnic backgrounds appears questionable. There was no difference in survival and liver related death in European HBsAg positive blood donors *vs* HBsAg negative blood donors[14]. Based on the present knowledge of the natural history of chronic HBV hepatitis and on the efficacy of antiviral drugs, antiviral therapy of chronic HBV infection is indicated in patients with chronic hepatitis B in the immunoactive phase characterized by high levels of viral replication and elevated serum ALT levels (Table 1). Liver histology usually shows inflammatory activity and variable degrees of liver fibrosis depending on the duration of the disease. Since continuing HBV replication and elevation of ALT levels reflect a significant risk of disease progression towards liver cirrhosis and hepatocellular carcinoma[15,16], antiviral therapy is indicated to decrease viral load, normalize ALT levels and induce a remission of the liver disease.

There are two main forms of chronic HBsAg positive hepatitis, which are distinguished by their HBeAg status. The HBeAg positive form is associated with a so-called wild type virus infection, HBsAg and HBeAg positivity, high HBV DNA levels, usually > 10^6 copies/mL, and elevated ALT levels. The HBeAg negative form is associated with core promoter and/or pre-core mutant virus infection, HBsAg positivity and HBeAg negativity (most patients have anti-HBe antibody), HBV DNA levels that are fluctuating but are usually > 10^4 copies/mL, and elevated ALT levels that may also fluctuate over time.

Table1 Indication for observing and treating HBV

	HBV-DNA levels	ALT status	Therapy/ Observation	
HBeAg +	> 10^5	Normal	Observe	
HBeAg +	> 10^5	Elevated	Yes	IFN, Antivirals
HBeAg +	> 10^4	Normal	Observe	
HBeAg -	> 10^4	Elevated	Yes	Antivirals, IFN
HBeAg -	> 10^4	Normal	Observe	
Pregnancy	> 10^9 geq/mL	Irrelevant	Yes	Antivirals
HBsAg + chemotherapy	Irrelevant	Irrelevant	Yes	Antivirals
HBsAg -				
Anti-HBc + chemotherapy	Positive	Irrelevant	Observe, treat in case of HBs-Ag appearance	Antivirals
Advanced fibrosis	irrelevant	Elevated	Always	Antivirals
Transplanted patients	> 10^4		Consider Treatment	Antivirals
Asian male	> $10^{5/6}$	Irrelevant	Yes	Antivirals

Treatment endpoints differ depending on the form of chronic hepatitis B.

It is currently not recommended to treat patients who are in the immunotolerant phase. They are defined serologically by HBsAg positivity, HBeAg positivity, high HBV DNA levels (usually higher than 10^8 copies/mL), and normal serum ALT levels. They usually have no liver damage or only minimal liver disease at liver biopsy examination, but they are highly infectious. The results of clinical trials for interferon alpha or nucleoside analogs indicate that patients with high HBV DNA load and normal ALT levels have almost no chance of HBeAg seroconversion. However, patients should be monitored on a regular basis to diagnose a break in immune tolerance characterized by an elevation in ALT levels and a decline in viral load, which may reflect the onset of liver damage and represent an indication for antiviral therapy. In addition, being a 30 years old Asian male with a viral load above 10^6 might also serve as an indication because of the 10% change of developing a HCC or liver cirrhosis in ten years[2,121]. However, this prediction probably cannot be transferred to women and to European patients.

The other category of patients with chronic HBV infection who should not be treated are HBsAg inactive carriers. Their virologic profile is characterized by HBsAg positivity, HBeAg negativity, anti-HBe antibody positivity, persistently low HBV DNA levels (< 10^4 copies/mL), and normal ALT levels. Liver histology usually shows no or minimal damage and the risk of progressing liver disease is considered to be minimal as long as ALT levels remain normal and viraemia is below 10^4 copies/mL. It is currently recommended that these patients should not be treated but should be followed carefully every 3 to 6 mo to promptly diagnose reactivation of viral replication and ALT exacerbations. When their values have been stable for 2 years, one can consider extending their monitoring intervals to 12 mo intervals.

In the case of advanced fibrosis, the recommendation

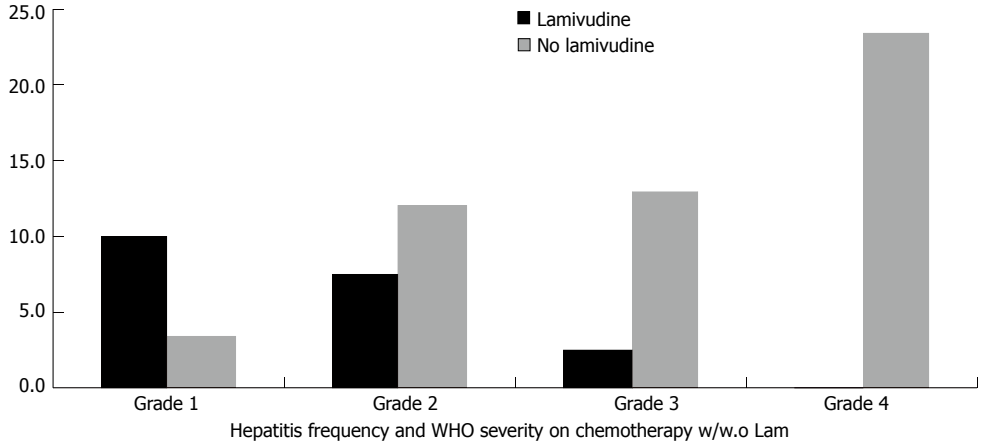

Figure 2 Pre-emptive lamivudine is associated with lower frequency and lower severity of hepatitis during chemotherapy. Date given in percent (%). Adapted from Li YH, *et al. Cancer* 2006.

is to initiate every patient on antivirals to prevent further deterioration of their liver disease independent of disease activity at least in the presence of HBV-DNA. Certainly, when fibrosis regresses during treatment an interruption might be considered.

Another clear indication for antiviral treatment is prevention of reactivation on chemotherapy, where lamivudine has been associated with lower frequency and lower disease severity of hepatitis (Figure 2)[17]. To a lesser extent, antiviral therapy seems indicated in late pregnancy in women with a high viral load[18,19], but formal clinical studies have not yet been published.

General outcome predictors

Some pre-treatment factors have been identified that predict responses to therapy. They may be useful in treatment decisions and drug choices. The results of clinical trials have shown that high ALT values (> 3 × ULN) are always predictive of a higher chance of HBeAg-seroconversion. In addition, a low viral load (< 10^7 copies/mL equivalent to 35 pg/mL) is predictive of a favourable response to standard or pegylated interferon. In addition, likewise to HCV though to a lesser extent, there is emerging evidence that HBV-genotypes are associated with treatment responses. While genotypes seem to be of no relevance for nucleos(t)ide therapy, there is ample evidence that the HBV genotypes A (versus D) and B (versus C) are associated with a better response to interferon therapy. HBsAg-seroconversion might be strongly associated with genotype A[20].

STANDARD INTERFERON ALPHA

A sustained response, defined by HBe seroconversion 24 wk post-treatment, is induced by subcutaneous administration of standard interferon in 20% to 40% of patients depending on patient characteristics; while only 5% to 10% of patients seronconvert in the placebo group[21,22]. Spontaneous HBe seroconversion is part of the natural history of the disease and is believed to be driven by the host immune response; in all clinical trials the spontaneous rate of HBe-seroconversion ranges from 5% to 10% per year. Patients with high ALT levels, a high HAI score, and low HBV DNA levels have a higher chance of HBe seroconversion (> 40%). While responses to HCV associated interferon therapy are usually associated with an immediate drop in both HCV-RNA and ALT, response to interferon with HBV is, especially in responders, associated with a marked increase of ALT in conjunction with a decrease of serum HBV DNA during the second or third month of therapy. The former reflects the immunological response leading to clearance of the virus and might also be associated with the vanishing immunosuppression caused by HBV itself. Clearance of HBsAg and seroconversion to anti-HBs is a late event; the percentage of patients who became HBsAg-negative after seroconverting to anti-HBe varied widely (7%-65%) for follow-ups of 3-4 years[23,24]. The European consensus conference recommended using a regimen of 5 MU daily or 10 MU thrice weekly for 24 wk[12]. However, due to the frequency of side effects at these high doses of interferon, 5-6 MU interferon thrice weekly may be an optimal choice to allow the continuation of therapy. Side effects are frequent and numerous but usually mild and reversible after treatment withdrawal.

HBeAg negative patients with active hepatitis B are mostly infected with the so called pre-core mutant. Trials using 6-12 mo of interferon therapy in that patient population showed that, regardless of interferon dosage, there was a good response while on therapy (inhibition of HBV-DNA, normalization of ALT) but relapses post-therapy were common and observed in a majority of patients. These initial studies indicated that therapy, therefore, should not rely on courses of interferon less than 1 year. Long-term administration for at least 2 years showed clinical benefit in terms of viral suppression and ALT normalization. Approximately 30% of patients may present a sustained response after treatment withdrawal when the interferon course was sufficiently long to maintain the suppression of viral replication[25]. However, side effects and poor tolerance to interferon administration limit its prolonged use in this form of chronic hepatitis B.

RESULTS OF PEGYLATED INTERFERON ALPHA

Pegylation is binding a pegylated side chain to interferon leading to a 12 or 40 kD molecule, i.e., PEG-IFN-α2b, and Peg-IFN-α2a respectively, which increases the half life of interferon making a once weekly application feasible and sufficient. These pegylated interferons have proven

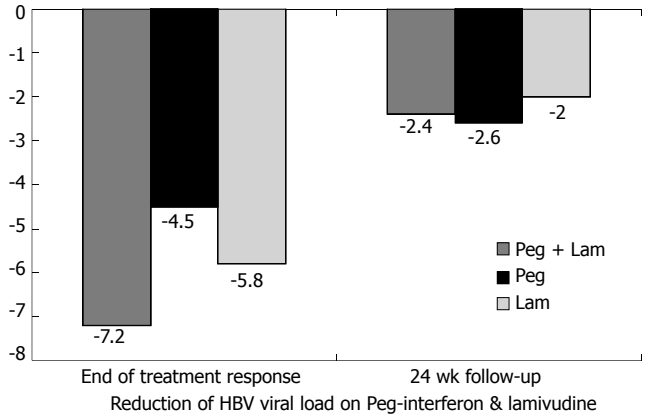

Figure 3 Viral load reduction at the end of treatment and at 24 wk follow-up in the different treatment arms. Adapted from Lau GK, *et al. N Engl J Med* 2005.

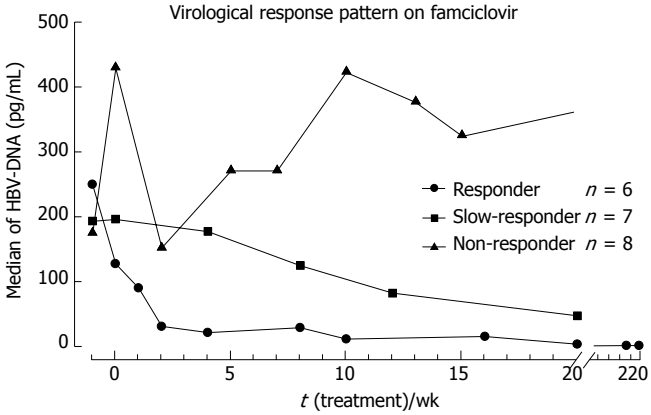

Figure 4 Different response pattern on famciclovir. Adapted from Tillmann HL *et al. Hepatology* 1998.

to not only increase convenience by enabling once weekly dosing but they have also improved efficacy dramatically in hepatitis C. Thus, it was a logical consequence to also evaluate them in Hepatitis B. A phase II study evaluated the efficacy of 90, 180 and 270 μg of PEG-IFN-α2a for 24 wk in comparison to a standard interferon-α2a 4.5MU three times per week[26]. This dose of standard interferon 3 times per week, however, has to be considered to be inappropriate at that time.

In the subsequent phase Ⅲ trials the antiviral effect of pegylated IFN-α2a (40 kDa) or -α2b (12 kDa) administration was evaluated for 48 wk (versus 24 wk used previously and considered as standard care). These trials have shown a HBe seroconversion rate of approximately 30% 6 mo post-treatment[11,27]. However, standard interferon was not a comparator in that study; only lamivudine was tested. Interestingly, a HBs seroconversion rate of 3%-5% was observed at the end of follow-up, while clearance of HBsAg was observed in up to 7% of patients with high genotype dependence (Figure 1). Tolerance and the nature and frequency of side effects for pegylated interferon alpha were generally similar to that of standard interferon in historic controls. Flu like syndrome, inflammatory skin reaction at the injection site and neutropenia were more frequent with pegylated than with standard interferon. Interestingly, depression, which occurs in about 30% of HCV patients during treatment, was reported to be lower than 3%. Even though viral suppression at the end of follow-up was similar for Peg-IFN-α2a and Peg-IFN-α2a plus lamivudine, the end of treatment viral suppression was significantly more pronounced in combination therapy (Figure 3) based on the given confidence intervals.

NUCLEOS(T)IDE ANALOGUES

While interferon usually leads to some side effects, such as flu like symptoms, the various nucleos(t)ides are characterised by few side effects, at least at the licensed dose.

Famciclovir

The first nucleos(t)ide studied in a larger trial was famciclovir, which was developed as a treatment for acyclovir resistant herpes simplex virus I infection. Famciclovir was subsequently shown to also have some HBV-activity *in vitro* and was thus developed for HBV therapy. In both liver and heart transplant patients, famciclovir has proven to ameliorate liver disease, despite only moderate virological response in most of the patients[28-30]. Basically three different patterns of response were determined in our transplant patients. A third of the patients responded well, a third showed slow response and another third did not show any response (Figure 4). Interestingly, the responders showed a clear virological response, which rarely exceeded one log reduction within three months, while transaminases and liver function deterioration were ameliorated.

A controlled trial also proved efficacy[31], but the drug is relatively expensive to produce and lamivudine was emerging as a more potent and less expensive drug. Nevertheless there was a clinical response despite relatively moderate viral suppression of 70%, which is equivalent to less than a 1 log reduction. Some of the patients showed marked and clear improvement in liver function after having had a continuous decrease in liver function prior to initiation of famciclovir (Figure 5).

Despite promising results in liver[28,29] and heart transplant[30] patients, famciclovir was not developed further after the potency of lamivudine became evident. All of the patients responding slowly or not responding to famciclovir showed immediate and more marked response to lamivudine, as did the patients developing resistance on famciclovir[32].

Lamivudine

Lamivudine (3TC) has been developed for inhibiting the reverse transcriptase of HIV[33], but as HBV's life cycle also requires a functioning reverse transcriptase, lamivudine was investigated and proven to be effective in inhibiting HBV as well, both *in vitro* and *in vivo*[34]. Several phase Ⅲ trials have demonstrated the antiviral efficacy of lamivudine administration in patients with HBeAg positive[35,36] and HBeAg negative chronic hepatitis B in doses of 100 to 300 mg/d[37]. The higher doses used in HIV have not proven to be more efficacious[38-40], even though their potential in preventing resistance has not been determined. Advantages of lamivudine are oral administration, an excellent safety

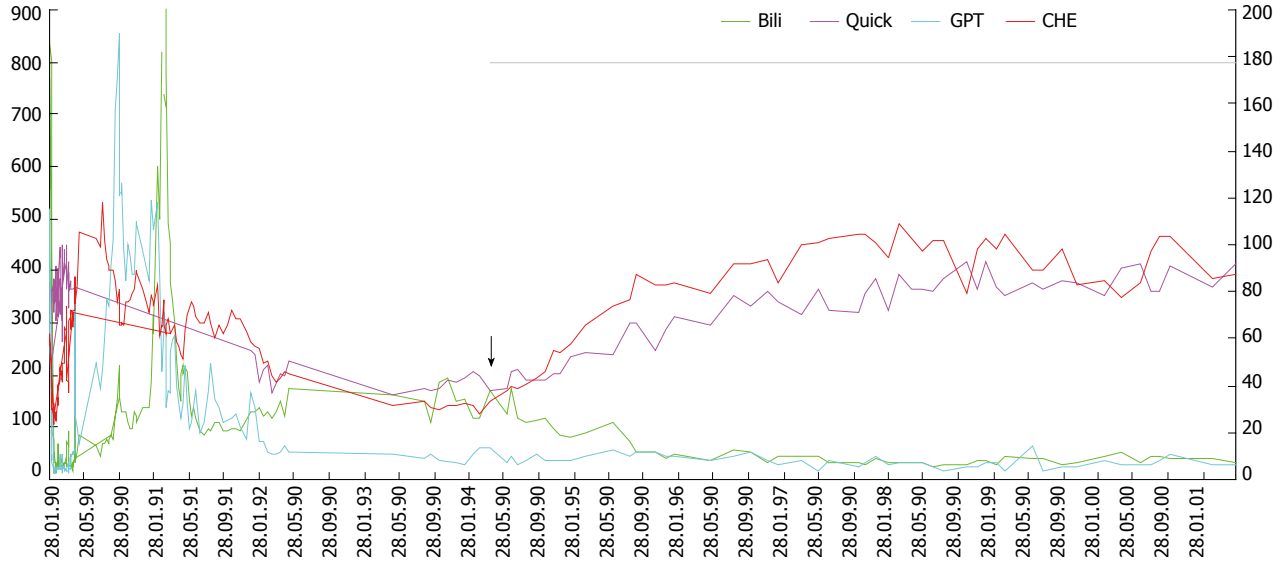

Figure 5 Improvement on famciclovir in a patient with continuous deterioration prior to initiation of famciclovir therapy. Arrow indicates start of famciclovir, where after Bilirubin slowly normalised, and both Quick test (Marker for impaired clotting function) and cholinesterase (CHE) stabilised indicating stabilisation of liver function. (unpulished).

profile, a rapid antiviral effect, and a relatively low cost of therapy. Viral load declines by 3-5 $\log_{10}$ copies/mL after a year of therapy compared to baseline values. The antiviral effect is accompanied by a significant decrease in ALT levels, and an improvement in the histology activity index. An improvement of liver fibrosis has also been observed during lamivudine therapy[41]. However, the primary goal of therapy, i.e. HBe seroconversion, is obtained only in approximately 20% of patients after 1 year of treatment, which was nevertheless significantly higher than in patients receiving placebo (5%-10%). Continuous lamivudine therapy is indicated in patients who do not seroconvert. It avoids a rebound of viral replication and exacerbations of liver disease. Continuing lamivudine therapy is associated with a progressive increase in the number of patients who undergo HBe seroconversion, reaching approximately 50% after 4 years of therapy[42]. A factor influencing the durability of HBe seroconversion is the duration of lamivudine therapy after seroconversion. In HBeAg negative patients, long-term lamivudine treatment is required because rebound is immediate after cessation[37].

Emtricitabine

Emtricitabine (FTC) is a L-deoxycytidine analogue as is lamivudine. Emtricitabine was also developed for HIV therapy, where it is often used in a fixed combination with tenofovir. Emtricitabine was evaluated in phase Ⅱ and phase Ⅲ trials. In a study randomising 98 patients to receive emtricitabine at 25, 100, or 200 mg daily for 48 wk and then 200 mg until wk 96, the dose of 200 mg daily provided the best results. After 2 years, 53% of the patients had serum HBV DNA below 4700 copies/mL, 33% seroconverted to anti-HBe and 85% had normal ALT levels. Resistance mutations were observed in 18% of patients after 96 wk of therapy[43].

A 200 mg dose of emtricitabine has been shown to be superior to placebo for histologic improvement (103 of 167 (62%) patients receiving FTC *vs* 20 of 81 (25%) receiving placebo; $P < 0.001$). Serum HBV DNA less than 400 copies/mL was achieved in 91 of 167 (54%) patients in the FTC group *vs* 2 of 81 (2%) in the placebo group ($P < 0.001$). Resistance towards FTC was detected in 20 of 159 FTC treated patients (13%, with a 95% confidence interval of 8%-18%). The safety profile of emtricitabine was found to be similar to that of placebo during treatment[44]. Being an L-nucleoside, FTC shows cross resistance to Lamivudine[45].

Telbivudine

Telbivudine is also an L-analogue, such as lamivudine, and it shares a similar resistance profile to lamivudine. However, resistance to telbivudine is associated with the YIDD mutation, leaving entecavir fully active. The safety, antiviral activity, and pharmacokinetics of telbivudine have been assessed in 43 adults with hepatitis B and antigen-positive chronic hepatitis B[46]. This placebo-controlled dose-escalation trial investigated six telbivudine daily dosing levels (25, 50, 100, 200, 400, and 800 mg/d); treatment was given for 4 wk. There was more than a 2 log reduction in all dose groups within one week, with disclosing higher potency of the > 400 mg dose only in the second phase. Telbivudine was well tolerated at all dosing levels, with no dose-related or treatment-related clinical or laboratory adverse events. Antiviral activity was dose-dependent, with a maximum at doses of 400 mg/d and or more. In the 800 mg/d cohort, the mean HBV DNA reduction was 3.75 $\log_{10}$ copies/mL at wk 4, comprising a 99.98% reduction in serum viral load. Subsequently, large phase Ⅲ studies have shown the superiority of telbivudine compared to lamivudine in the suppression of viral load (by 6.5 $\log_{10}$ versus 5.5 $\log_{10}$) and improvement of liver histology[47]. A 24 wk study also showed telbivudine to be more active than adefovir with a 6.3 *vs* 4.97 log reduction of HBV-DNA[48]. Telbivudine resistance was observed in

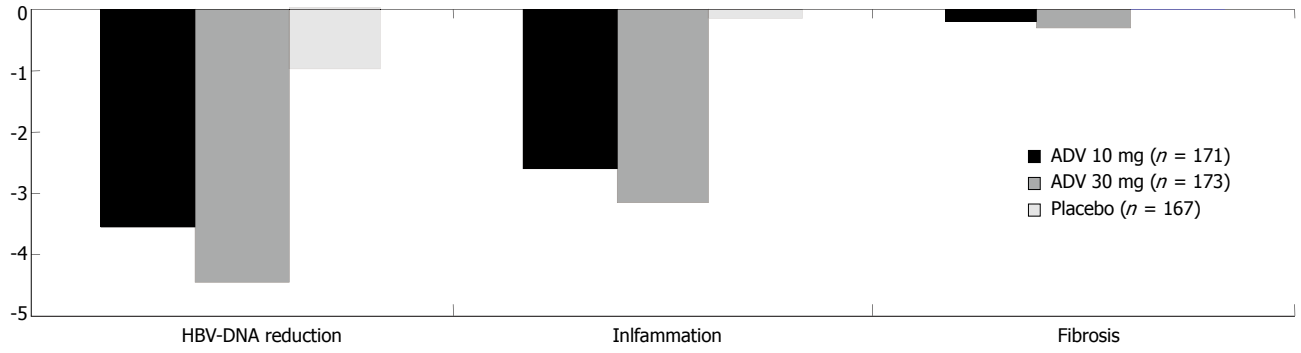

Figure 6 Reduction in HBV-DNA, as well as histological improvement in inflammation and fibrosis according to the Knodell score after 48 wk therapy with 10, 30 mg ADV. Adapted from Marcellin P, *et al*. *N Engl J Med* 2003.

approximately 5% of patients after 1 year of therapy and associated with a M204I mutation, as expected, within the "YMDD"-motif in the viral polymerase[49]. However, the M204V mutation, which is frequently associated with additional mutations at 180 and 173, has not been detected with telbivudine[50]. This might be another advantage in addition to its higher antiviral activity. Importantly, pharmacokinetics indicate no alteration with impaired hepatic function[51].

Adefovir

In the early 1990s, adefovir was shown to inhibit HBV and HIV in cell cultures[52,53]. Its development for HIV was halted because the dose required for HIV inhibition was associated with significant nephrotoxicity beyond 24 wk of treatment[54]. However, HBV was inhibited with lower doses of adefovir and it could even be used safely in renal impaired patients[55]. It was shown that a 10 mg dose provided a smaller decrease in viral load than a 30 mg dose (Figure 6) but there was a higher creatinine increase with the 30 mg dose and therefore only the 10 mg dose was developed further[56].

In a large phase Ⅲ trial, 515 patients with HBeAg positive chronic hepatitis B were treated with adefovir 10 mg (n = 171), adefovir 30 mg (n = 173) or placebo (n = 167) for 48 wk. HBe seroconversion was achieved only in a minority of patients, i.e. 14% in the 30 mg daily and 12% in the 10 mg daily dosing group of patients receiving adefovir dipivoxil versus 6% in the placebo group. ALT levels normalized in 48% and 55% of patients receiving adefovir 10 and 30 mg adefovir respectively, versus 16% in the placebo group. Reduction of HBV-DNA and liver inflammation and fibrosis improved significantly in patients given adefovir (Figure 6)[57]. Tolerance for the daily dose of 10 mg adefovir was comparable to placebo. Extended administration of adefovir dipivoxil showed an increased rate of HBe seroconversion over time: 14% of 296 patients, 33% of 231 patients, and 46% of 84 patients after 1, 2, and 3 years of therapy, respectively[57,58].

Similar to HBeAg positive patients, adefovir administration for 48 wk in HBeAg negative patients induced histologic improvement more frequently in adefovir treated (64%) *vs* placebo treated patients (33%, $P < 0.001$), and reduced serum HBV DNA below < 400 copies/mL [51% (63 of 123) *vs* 0%; $P < 0.001$][59]. HBV DNA was below 1000 copies/mL in 51%, 71% and 79% patients after 48, 96 and 144 wk, respectively[59-60]. Interestingly, in the majority of patients who were switched from adefovir to placebo, the benefit of treatment was lost, indicating that antiviral therapy with nucleoside analogs must be prolonged in this patient population to avoid viral reactivation and ALT flares. Side effects after 144 wk were similar to those observed at wk 48. It has been presented recently that 22/33 anti-HBeAg negative patients showed sustained response when adefovir was stopped after 4 to 5 years of continues adefovir therapy[122].

Entecavir

Entecavir was developed as an anti-herpes drug, but proved to display only moderate activity, which eventually led to discontinuation of development for this indication. However, Bristol-Myers Squibb discovered that entecavir was extremely potent against HBV through inhibition of HBV-DNA polymerase, with relatively low toxicity. Entecavir is the first HBV-specific antiviral to be licensed that seems to lack both HIV and herpesvirus cross-reactivity[61], which is especially attractive for HIV-HBV co-infected patients not yet requiring HIV-treatment. Entecavir has been evaluated for naïve patients in two controlled phase Ⅲ trials involving 715 HBeAg positive and 648 HBeAg-negative patients with chronic HBV infection, detectable HBV DNA, persistently elevated ALT levels and chronic inflammation on liver biopsy. Entecavir administered 0.5 mg orally once daily for 52 wk was shown to be superior to lamivudine (100 mg orally once daily for 52 wk) for the primary efficacy endpoint of histological improvement and for secondary endpoints, such as the reduction in viral load (6.9log *vs* 5.4log, $P < 0.001$ for HBeAg+; 5.0 *vs* 4.5log, $P < 0.001$ for HBeAg-) and normalization of ALT (68 *vs* 60%, $P = 0.02$ for HBeAg+; 78 *vs* 71%; $P = 0.045$ for HBeAg-)[62,63]. After 2 years of treatment, 81% of patients receiving entecavir had a viral load below 300 copies/mL versus only 39% of patients receiving lamivudine, 31% seronconverted to anti-HBe versus 26% in the lamivudine group, and 5% showed a clearance of HBsAg versus 3% in lamivudine treated patients[64]. The second year, however, was limited to 307 of the initial 709 patients. In lamivudine refractory

patients, entecavir administered at 1 mg once daily induced a significant viral load reduction and histological improvement, by comparison with the control group treated with lamivudine[65]. Entecavir was approved in 2005 by the US FDA for the treatment of chronic HBV infection in adults with evidence of active viral replication and either evidence of persistent elevation in serum ALT or histologically active disease. Entecavir resistant mutants have been described mainly in patients with lamivudine resistance[66]. Approximately 9% of lamivudine resistant patients treated with entecavir develop resistance to entecavir after 2 years of therapy. The resistant mutants are then resistant to both lamivudine and entecavir.

Tenofovir

Tenofovir is licensed for the treatment of HIV infection but has known activity against HBV as well. It is less nephrotoxic and therefore it can be used in a higher dose (300 mg) unlike adefovir, which is licensed for a 10 mg dose.

Tenofovir's anti-HBV activity has been studied *in vitro* and *in vivo* mostly in HIV infected patients coinfected with HBV. In this patient population, tenofovir administration decreased HBV load significantly both in lamivudine naïve and lamivudine resistant patients[67-69]. There is good evidence from non-randomized[70], but also a small randomised study, that tenofovir is more potent than adefovir in reducing HBV load[71]. Phase Ⅲ trials are ongoing to compare the anti-HBV activities of tenofovir and adefovir in HBV mono-infected patients and in HIV-HBV co-infected patients. Currently, even though it has higher potency and lower cost compared to adefovir, tenofovir cannot be prescribed. This can be considered as a drawback of modern bureaucratic medicine, which prohibits using a drug that has a better safety profile and higher activity at lower costs, but has not been specifically evaluated for that indication.

Clevudine

Clevudine is an artificial beta-L nucleoside analogue that shows cross-resistance to lamivudine[45]. It seems to have an advantage in that viral load rebound after therapy cessation is not immediate[72]. A specific attractive aspect of clevudine is it's activity against delta virus infection, at least in the woodchuck model[73].

Pradefovir (Remofovir)

There is evidence that the safety of ADV could be improved if liver-specific targeting could be achieved, thereby allowing higher liver-associated concentration without increase of systemic exposure with nephrotoxic consequences. One such prodrug is pradefovir, formerly remofovir[74], which is under clinical development. 10, 20 and 30 mg of pradefovir seem to be more potent than 10 mg of adefovir (-4.22, -4.33 , -5.06log *vs* -3.66) [75]. However, it needs to be determined whether it is more effective than tenofovir.

ANA380

ANA380 is a prodrug of ANA317, another recently reported substance with activity against lamivudine resistant HBV. Patients treated with ANA 380 at 30 mg, 60 mg, 90 mg, 150 mg and 240 mg dose levels experienced reduction in plasma HBV viral DNA at 12 wk of 2.8 log. 3.2 log, 3.9 log10, 3.9 log10 and 4.1 log10 units, respectively[76].

Myrcludex B: an acylated PreS1 peptide

It was found that the preS1 amino acids 2-48 mediate attachment of the virus to its target cells. Furthermore amino-terminally acylated peptides containing amino acids 2-18, and even more efficiently with 2-48 of the PreS1 domain, can be used to block hepatitis B virus infection[77]. Using this concept, Urban *et al,* developed a peptide that was shown to inhibit HBV-infection *in vitro* and in animal models and is currently being developed as an antiviral approach. It is currently not clear whether it will inhibit infection in a post exposure approach, i.e. after needle stick injury or liver transplantation of HBV-positive patients, to prevent re-infection or whether it might have antiviral activity in chronic hepatitis B.

COMBINATION THERAPY

Several studies have evaluated the efficacy of a combination of interferon alpha 2a or 2b with lamivudine and more recently a combination of Peg-IFN alpha 2a or 2b with lamivudine in comparison with pegIFN alone and/or lamivudine alone[11,27]. It was concluded that the efficacy of combined Peg-IFN plus lamivudine is not different from Peg-IFN alone if both are given for 48 wk. However, this depends on what you are observing. HBeAg seroconversion actually was even lower, though not significantly different, 24 wk post-treatment. Similarly the viral load reduction and normalisation of transaminases was similar between Peg-IFN plus lamivudine *vs* Peg-IFN monotherapy 24 wk after the end of therapy[78].

The decline of viral load was higher, however, in the combination group than in the single treatment group during therapy (Figure 3). The rate of lamivudine resistance was lower in patients who received a combination of lamivudine with pegIFN compared to lamivudine monotherapy, and following the state of art, one would not have stopped lamivudine therapy at 48 wk. Thus, it may be premature to state that Peg-IFN should not be combined with lamivudine, but this certainly would need further study.

Likewise, a very small study suggested that ccc-DNA reduction was augmented when adefovir is combined with Peg-IFN *vs* adefovir alone[79]. Whether this can eventually lead to higher HBsAg seroconversion rates needs to be determined in future studies.

A combination therapy approach is also suggested with use of some of the more recently developed antivirals. It had been shown that adefovir plus emtricitabin is superior to adefovir alone[80]. Given the similarity but superiority of tenofovir versus adefovir, the combination of tenofovir with emtricitabine appears especially promising, and since this combination is one of the backbones of HIV-antiretroviral therapy and there is already an excellent track record.

Recently, emtricitabine was also combined with 10 mg clevudine (1.8 to 2.3 log reduction) and results showed a superiority for the combination versus emtricitabine alone

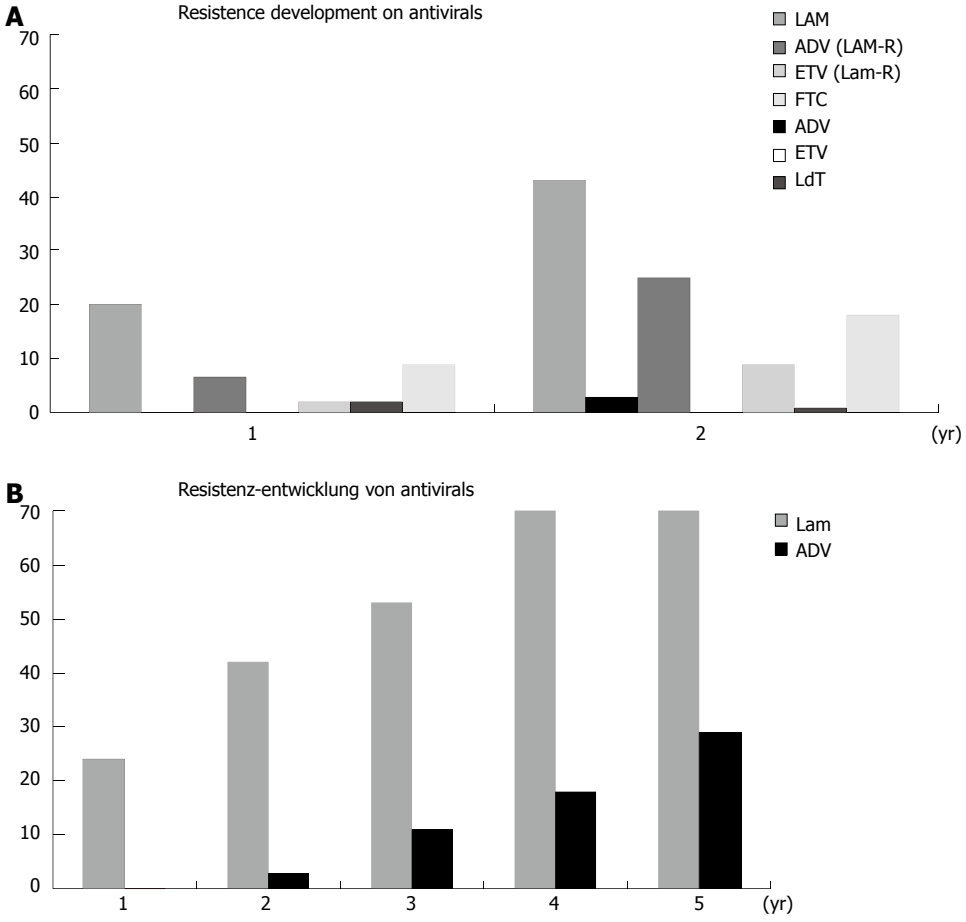

Figure 7 Prevalence of resistance on different antivirals, up to 2 (**A**) and up to 5 (**B**) year data.

(1.4 to 2.0 log reduction)[81]. These viral load reductions, however, were still lower than those reported on 50 mg clevudine monotherapy (s. clevudine above). Thus, in the combination trials each drug should also be tested as monotherapy to exclude the "combination effect" of higher potency for one of the drugs.

DRUG RESISTANCE

HBV replicates *via* an error prone viral reverse transcriptase resulting in a large pool of quasispecies with mutations interspersed throughout the genome. During antiviral drug selection pressure (e.g., lamivudine, adefovir, or entecavir), HBV mutants are selected from the preexisting pool of quasispecies and over time become the dominant species.

Drug resistant mutants emerge as a function of at least six factors: (1) the viral mutation frequency (annual error rate), (2) the intrinsic mutability of the antiviral target site (some mutants are lethal and cannot replicate), (3) the selective pressure exerted by the drug (the stronger the more likely a resistance emerges), (4) the magnitude and rate of virus replication (the higher the viral load, the more likely resistance emerges), (5) the overall replication fitness of the mutant (some mutants are replicating very poorly and some require addition compensatory mutations), and (6) the availability of replication space (the amount of cccDNA harboured in a cell is limited; if there is no space for new cccDNA the likelihood of resistance is reduced).

HBV resistance to antivirals can be defined at different levels, which usually develop sequentially: (1) genotypic resistance is the detection of polymerase gene mutations known to confer resistance to the drug, (2) virologic breakthrough has been defined as an increase of at least one $\log_{10}$ copies/mL compared to the lowest value during treatment, associated with the presence of resistance mutations following genotypic resistance, (3) clinical failure is defined as viral breakthrough and increase in ALT levels and subsequently progression of liver disease usually following the virological breakthrough. Very rarely increased replication of viruses can be observed after emergence of resistance[82], which was first described 40 years ago for enteroviruses[83], and some years ago for HIV[84,85], which has, however, minor clinical relevance because of the multiple drug approach in HIV.

One of the clear advantages of interferons is their inability to significantly induce mutations, which would subsequently abolish interferon activity. In contrast, all nucleos(t)ide given for more than 48 wk have been shown to induce mutations with various frequencies after 1 to 2 years and during longer treatment (Figure 7A and B), which leads to impaired sensitivity towards the appropriate antiviral. The first antiviral leading to some clinical improvement but also to mutations was famciclovir. It's signature mutation was L528M[32] (now corresponding to rtL180M, as numbering was changed to start at the start of the reverse transcriptase of HBV-DNA polymerase with the highly conserved EDWGPCDEHG motif[86]) thereby eliminating different numbering for different HBV

genotypes. Patients with such a L528M/rtL180M mutation were shown to be sensitive to lamivudine, at least until YMDD mutations due to lamivudine became known as well[32].

New drugs have become available and knowledge of the *in vitro* cross-resistance profile has provided the rationale for their use in patients with treatment failure. The rescue treatment of patients with drug resistance has improved significantly in recent years.

The major problem of long-term lamivudine therapy is the occurrence of drug resistance. The spontaneous variability of the HBV genome and the slow kinetics of viral clearance, are the biological basis for the selection of drug resistant mutants. The results of phase III clinical trials and of cohort studies have shown an incidence of lamivudine resistance of approximately 20% per year[87]. Lamivudine resistance develops in up to 70% of patients after 4 years of therapy[88,89], leading to an increase in viral load (viral breakthrough) that is followed by an increase in ALT levels (biochemical breakthrough), a reduced HBe seroconversion rate in HBeAg positive patients, and a progression of liver disease[87]. In some patients, especially those with liver cirrhosis or severe fibrosis, the biochemical breakthrough that follows lamivudine resistance may cause a severe and acute exacerbation of liver disease that may precipitate liver failure[88,90-92].

Long-term studies have shown that antiviral efficacy and histological improvement is progressively lost with time because the prevalence of resistance mutations increases as liver disease continues. This was observed in some patients with YMDD mutations but none without those mutations[93]. ALT levels increase progressively with the duration of infection with the YMDD mutants and it was reported that no patient who developed lamivudine resistance mutation for 24 mo had normal ALT levels[94]. It is therefore necessary to make an early diagnosis of drug resistance to adapt rescue antiviral therapy prior to the degradation of liver functions[92,95].

In a retrospective nationwide analysis of lamivudine therapy in Italy, the development of clinically important events after virological breakthroughs depended on the severity of the underlying liver disease; severe hepatitis flares at the emergence of YMDD were noted in patients with child B and C cirrhosis but not in patients with non-cirrhotic chronic hepatitis[96], which is in agreement with previous studies[91,92]. Interestingly, the rate of HCC was diminished even in multivariate analysis in patients with maintained response *vs* those with breakthrough[96].

Mutations conferring resistance to lamivudine are mainly located in the C domain of the reverse transcriptase within the YMDD motif, i.e. M204V or M204I, and may be associated with compensatory mutations in the C domain, i.e. V173L or L180M. After 1 year of treatment, lamivudine resistant mutants emerged in 22% of patients, increasing to 38% after 2 years, 53% after 3 years, 66% after 4 years, and 69% after 5 years[87,89,97]. However, this also means that approximately 30% of patients seem to never develop resistance against lamivudine. *In vitro* and *in vivo* studies showed that the main lamivudine resistant mutants remain sensitive to adefovir[98,99], tenofovir[70], and entecavir[62,100], even though susceptibility to entecavir was reduced *in vitro*[101].

Comparing the addition of adefovir to ongoing lamivudine and the switch from lamivudine to adefovir did not reveal any difference in viral load decline in these two treatment groups. However, recently Lampertico *et al*[102] presented data showing very pronounced viral load reduction if adefovir was added when viral resistance emerged instead of when clinical resistance with elevated liver enzymes was evident. In addition, the risk of resistance to adefovir was significantly less frequent in patients receiving adefovir in addition rather than as a substitute for lamivudine[103]. Thus, because of the lack of cross-resistance between the two drugs, there is now a consensus among experts that adefovir should be added to lamivudine in patients with lamivudine failure to prevent or delay the subsequent selection of new resistant mutants.

Because of the reduced susceptibility of the lamivudine resistance mutant to entecavir *in vitro*, entecavir was given to patients with lamivudine failure at a dose of 1 mg daily instead of 0.5 mg, which was given to naïve patients. Entecavir induced a significant decline in viral load in these lamivudine refractory patients[65]. Noteworthy, cases of entecavir resistance were described so far only in lamivudine resistant patients, suggesting that some level of cross-resistance between these two drugs is responsible for the selection of mutants resistant to both drugs. Based on these findings, follow-up studies are required to better determine the indication of entecavir in patients with prior lamivudine resistance.

Telbivudine and emtricitabine share the same resistance mutations as lamivudine except that telbivudine seems to not induce mutations at L180M and 173 as frequently. The year one resistance data within the GLOBE-study indicate that the telbivudine resistance is associated with a M250I mutation and not with a M250V mutation.

In patients treated continuously with adefovir 10 mg/d as a monotherapy, drug-resistant mutants emerged in 2%, 5.9%, 18%, and 29% of patients after 2-5 years, respectively. Resistance to adefovir is most frequently conferred by the selection of a rtN236T mutation in the D domain of the HBV polymerase or a rtA181V mutation in the B domain of the polymerase[104-106]. This may be accompanied by liver failure[107]. *In vitro*, the rtN236T mutation is sensitive to both lamivudine and entecavir and the rtA181V showed a decreased susceptibility to lamivudine, which can be confirmed *in vivo*[106,107]. Adefovir resistance can probably be significantly reduced if treatment is combined with lamivudine. In addition, it has been suggested that resistance to adefovir is more likely to develop in lamivudine resistant patients with 10% *vs* 0% after one year adefovir [108], which is in agreement with another Korean study reporting a resistance rate of 6.4% and 25.4% after 1 and 2 years adefovir therapy, respectively[109]. Mutant HBV with resistance against both adefovir and lamivudine can emerge[106].

Recently, it was suggested that a mutant/variant rtI233V is naturally occurring even before therapy in some HBV patients[110] and might be associated with reduced susceptibility to adefovir. Resistance was proven for that

mutation *in vitro* after it had been observed in three patients not responding to adefovir[111]. Surprisingly, this mutation has not been observed in patients developing virological breakthrough. This mutation has not, however, been seen in any of the 20 patients with insufficient response to adefovir from another institution[112]. Since 10% of patients with normal rt sequence have an insufficient response to adefovir, this may be more related to drug transporter polymorphisms, since they have been related to nephrotoxicity, but could also account for the insufficient response.

Entecavir resistance was observed mainly in the therapy of lamivudine refractory patients. The resistance rate appears to be approximately 10% after 2 years and 25% after 3 years in patients with lamivudine failure and 0.8% in naïve patients over 3 years[123]. The main resistance mutations are rtT184G, rtS202I, rtM250V on a background of lamivudine resistance mutations[113]. These mutants are resistant to lamivudine but appear to be susceptible to adefovir *in vitro*[114]. Clinical data are awaited to provide recommendation for the treatment of entecavir resistant patients. The emergence of entecavir resistance seems to be bound to the presence of a M250V mutation, thus leaving entecavir as a full option in case of telbivudine resistance.

Monitoring of antiviral therapy

Monitoring during antiviral therapy could serve different purposes: (1) estimation of the response based on early viral kinetics; and (2) early recognition of the development of viral resistance with an increase in the viral load after initial reduction or by mutation monitoring.

It was initially shown by Puchhammer-Stockl *et al*[115] that patients showing an early viral response are less likely to develop resistance with lamivudine, which was recently confirmed prospectively for telbivudine[116]. Nevertheless monitoring viral resistance by observing the emergence of mutations known to confer resistance would be the most sensitive way to monitor patients who remain viraemic on current treatments. Based on experience, it is not recommended to wait until an increase in viral load associated with ALT-elevation is evident, since these patients are less likely to respond as well as those placed on an alternative additional antiviral therapy earlier. In addition, this approach harbours the risk of hepatic decompensation. With any nucleos(t)ide there will always be a risk for the emergence of drug-resistance, which mandates monitoring patients on antiviral therapy. The rationale for the timing of monitoring derives from the consideration that the biochemical breakthrough usually occurs with a delay of several weeks after the virological breakthrough and that the clinical impact is usually different in non-cirrhotic than in cirrhotic disease. In the former, the ALT breakthrough most often has no major clinical consequences and in the latter it may precipitate liver failure and death. Monitoring should be performed by measuring the viral load with quantitative HBV DNA testing and certainly transaminases. If the residual viraemia remains high (see below) treatment should be switched to alternative therapy, if possible.

The antiviral response at wk 24 of therapy was found to be a predictor of subsequent efficacy (HBeAg loss, HBV DNA < 200 copies/mL, ALT normalization, and viral breakthrough) in patients treated with lamivudine or telbivudine[117]. In the 5-year study of adefovir administration in HBeAg negative chronic hepatitis, patients with a viral load lower than 3 $\log_{10}$ copies/mL after 1 year of therapy had a significantly lower risk of developing resistance by year 3 of treatment (< 3%) compared to a risk of 26% and 66% for those having a viral load between 3 and 6 $\log_{10}$ copies, and > 6 $\log_{10}$ copies/mL, respectively[118]. On the other hand, this suggests that those who do not achieve a viral load reduction should be given rescue therapy before the development of true resistance.

During long-term treatment, a 3 or 6 monthly assessment of viral load and serological markers is required to monitor antiviral treatment efficacy and determine whether the response is maintained or whether drug resistance is developing. Certainly drug compliance is important, as any drug interruption may lead to a rebound of viral replication and ALT flares. The detection of polymerase mutations can be performed by sequencing, line probe assay, and DNA chip technologies. Detection may become more complex when additional treatment options become available, since there is emerging evidence that the cross-resistance profile is different from one mutant to another[119,120]. The line probe assay is more sensitive than sequencing of PCR products but cannot detect new mutations.

New tools may become available in the future to monitor the efficacy of antiviral therapy, such as the quantification of intrahepatic cccDNA or the quantification of serum HBsAg as a surrogate marker. Furthermore, with the development of new drugs and the increasing complexity of the resistance profile, phenotypic assays to determine drug susceptibility of the clinical isolates may prove useful in tailoring antiviral therapy to the virological situation of the patient, as already shown in HIV.

CONCLUSIONS

Patients with minimal disease, whether in the immuntolerant phase or with inactive infection, should not be treated. However, if it is confirmed that the risk of HCC is 10% within 10 years for patients with more than 10^6 viral load, these patients should receive antiviral treatment irrespective of the activity of their liver disease. In patients with chronic hepatitis proven by ALT elevation and abnormal liver histology, antiviral therapy is indicated because all studies have shown that antiviral therapy decreases the risk of liver disease progression compared to the natural history of the disease. In patients who are HBeAg positive, the primary goal of antiviral therapy is to obtain HBe seroconversion. If the patient is young and has predictive factors of favourable response, a finite course of pegylated interferon should be tried as a first line option in genotype A and B patients. In other cases (including non-responders to IFN, patients intolerant to interferon and those with factors of poor response to interferon), long-term therapy

Table 2 Treatment options for chronic hepatitis B and their profile

	Standard Interferon PegIFN	Lamivudine	Adefovir	Entecavir
Viral suppression	4.5 log10 copies/mL	5-6 log10 copies/mL	3-4 log10 copies/mL	6-7 log10 copies/mL
Long term therapy	(6 to) 12 mo in HBe pos. Patients 24 mo in HBeAg neg. patients	+ (continuous)	+ (continuous)	+ (continuous)
Side effects	+	- to very low	- to very low	- to very low
HBe seroconversion	30%	15%-20% at 1 yr, 25%-30% at 2 yr	10%-15% at 1 yr	20% at 1 yr, 30% at 2 yr
Predictive factors for seroconversion	High ALT, low HBV DNA levels	High ALT	High ALT	?
Clearance of HBsAg	+	-	-	?
Cost	++ per months	+	++	(++)
Sustained response	< 30% HBeAg - ca. 30% in HBeAg +	Maintained response 30%-35% (3 yr)	Maintained response ⩾ 70% (5 yr)	Maintained response?
Maintained response	Not applicable	Maintained response 30%-35% (3 yr)	Maintained response ⩾ 70% (5 yr)	Maintained response?
Clearance of HBsAg	+ (Genotype dependent)	low	low	low
Resistance	No resistance but non-response	20% per year	0% at 1 yr up to 29% at yr 5	0% at 1 & 2 yr (2% at 1 and 10% at 2 yr in lam resistant patients)

with nucleos(t)ide analogues is usually needed.

Long-term therapy is probably required in patients who are HBeAg negative. Nucleoside analogues are better tolerated than pegylated interferon, but the therapeutic choice must take into account the risk of drug resistance (Table 2).

Likely future therapy is to begin with an inexpensive antiviral and then adding or switching to another in the case of insufficient response. In patients with severe liver disease, i.e. decompensated liver cirrhosis or HBV recurrence on the liver graft, one might consider combining nucleoside analogues lacking cross-resistance from the start to provide the best chance of long-term control of viral replication and disease progression.

Finally, it is recommended that physicians should be brought back into the position of prescribing licensed drugs, even if they are only licensed for another treatment, when there is evidence for superiority of such an approach. One such example is tenofovir, which has been licensed for HIV and displays higher efficacy and a better safety profile than adefovir.

REFERENCES

1 **World Health Organization**. Available from: URL: http://www.who.int/csr/disease/hepatitis/HepatitisB_whocdscsrlyo2002_2.pdf
2 **Chen CJ**, Yang HI, Su J, Jen CL, You SL, Lu SN, Huang GT, Iloeje UH. Risk of hepatocellular carcinoma across a biological gradient of serum hepatitis B virus DNA level. *JAMA* 2006; **295**: 65-73
3 **Weller IV**, Carreno V, Fowler MJ, Monjardino J, Makinen D, Thomas HC, Sherlock S. Acyclovir inhibits hepatitis B virus replication in man. *Lancet* 1982; **1**: 273
4 **Schalm SW**. Treatment of chronic hepatitis type virus B. *Hepatogastroenterology* 1984; **31**: 12-16
5 **Sherlock S**, Thomas HC. Treatment of chronic hepatitis due to hepatitis B virus. *Lancet* 1985; **2**: 1343-1346
6 **Trépo C**, Ouzan D, Fontanges T, Chevallier M, Chossegros P, Degos F, Chevallier P, Hantz O. Therapeutic activity of vidarabine in symptomatic chronic active hepatitis related to HBV. *J Hepatol* 1986; **3** Suppl 2: S97-S105
7 **Alexander GJ**, Fagan EA, Hegarty JE, Rolando N, Guarner P, Eddleston AL, Williams R. A controlled trial of acyclovir in stable chronic HBsAg, HBeAg-positive carriers. *J Hepatol* 1986; **3** Suppl 2: S123-S127
8 **Schalm SW**. Treatment of chronic hepatitis B. *Neth J Med* 1994; **44**: 103-109
9 **Hadziyannis SJ**, Manesis EK, Papakonstantinou A. Oral ganciclovir treatment in chronic hepatitis B virus infection: a pilot study. *J Hepatol* 1999; **31**: 210-214
10 **Niederau C**, Heintges T, Lange S, Goldmann G, Niederau CM, Mohr L, Häussinger D. Long-term follow-up of HBeAg-positive patients treated with interferon alfa for chronic hepatitis B. *N Engl J Med* 1996; **334**: 1422-1427
11 **Lau GK**, Piratvisuth T, Luo KX, Marcellin P, Thongsawat S, Cooksley G, Gane E, Fried MW, Chow WC, Paik SW, Chang WY, Berg T, Flisiak R, McCloud P, Pluck N. Peginterferon Alfa-2a, lamivudine, and the combination for HBeAg-positive chronic hepatitis B. *N Engl J Med* 2005; **352**: 2682-2695
12 **de Franchis R**, Hadengue A, Lau G, Lavanchy D, Lok A, McIntyre N, Mele A, Paumgartner G, Pietrangelo A, Rodés J, Rosenberg W, Valla D. EASL International Consensus Conference on Hepatitis B. 13-14 September, 2002 Geneva, Switzerland. Consensus statement (long version). *J Hepatol* 2003; **39** Suppl 1: S3-S25
13 **Yang HI**, Lu SN, Liaw YF, You SL, Sun CA, Wang LY, Hsiao CK, Chen PJ, Chen DS, Chen CJ. Hepatitis B e antigen and the risk of hepatocellular carcinoma. *N Engl J Med* 2002; **347**: 168-174
14 **Manno M**, Cammà C, Schepis F, Bassi F, Gelmini R, Giannini F, Miselli F, Grottola A, Ferretti I, Vecchi C, De Palma M, Villa E. Natural history of chronic HBV carriers in northern Italy: morbidity and mortality after 30 years. *Gastroenterology* 2004; **127**: 756-763
15 **Yuen MF**, Yuan HJ, Wong DK, Yuen JC, Wong WM, Chan AO, Wong BC, Lai KC, Lai CL. Prognostic determinants for chronic hepatitis B in Asians: therapeutic implications. *Gut* 2005; **54**: 1610-1614
16 **Realdi G**, Fattovich G, Hadziyannis S, Schalm SW, Almasio P, Sanchez-Tapias J, Christensen E, Giustina G, Noventa F. Survival and prognostic factors in 366 patients with compensated cirrhosis type B: a multicenter study. The Investigators of the European Concerted Action on Viral Hepatitis (EUROHEP). *J Hepatol* 1994; **21**: 656-666
17 **Li YH**, He YF, Jiang WQ, Wang FH, Lin XB, Zhang L, Xia ZJ, Sun XF, Huang HQ, Lin TY, He YJ, Guan ZZ. Lamivudine prophylaxis reduces the incidence and severity of hepatitis in hepatitis B virus carriers who receive chemotherapy for lymphoma. *Cancer* 2006; **106**: 1320-1325
18 **van Zonneveld M**, van Nunen AB, Niesters HG, de Man RA,

Schalm SW, Janssen HL. Lamivudine treatment during pregnancy to prevent perinatal transmission of hepatitis B virus infection. *J Viral Hepat* 2003; **10**: 294-297

19 **Li XM**, Yang YB, Hou HY, Shi ZJ, Shen HM, Teng BQ, Li AM, Shi MF, Zou L. Interruption of HBV intrauterine transmission: a clinical study. *World J Gastroenterol* 2003; **9**: 1501-1503

20 **Wiegand J**, Hasenclever D, Tillmann HL. Should treatment of hepatitis B depend on HBV genotypes? - A hypothesis generated from an explorative analysis of published evidence. Manuscript submitted

21 **Perrillo RP**, Schiff ER, Davis GL, Bodenheimer HC, Lindsay K, Payne J, Dienstag JL, O'Brien C, Tamburro C, Jacobson IM. A randomized, controlled trial of interferon alfa-2b alone and after prednisone withdrawal for the treatment of chronic hepatitis B. The Hepatitis Interventional Therapy Group. *N Engl J Med* 1990; **323**: 295-301

22 **Wong DK**, Cheung AM, O'Rourke K, Naylor CD, Detsky AS, Heathcote J. Effect of alpha-interferon treatment in patients with hepatitis B e antigen-positive chronic hepatitis B. A meta-analysis. *Ann Intern Med* 1993; **119**: 312-323

23 **Lok AS**, Chung HT, Liu VW, Ma OC. Long-term follow-up of chronic hepatitis B patients treated with interferon alfa. *Gastroenterology* 1993; **105**: 1833-1838

24 **Korenman J**, Baker B, Waggoner J, Everhart JE, Di Bisceglie AM, Hoofnagle JH. Long-term remission of chronic hepatitis B after alpha-interferon therapy. *Ann Intern Med* 1991; **114**: 629-634

25 **Lampertico P**, Del Ninno E, Manzin A, Donato MF, Rumi MG, Lunghi G, Morabito A, Clementi M, Colombo M. A randomized, controlled trial of a 24-month course of interferon alfa 2b in patients with chronic hepatitis B who had hepatitis B virus DNA without hepatitis B e antigen in serum. *Hepatology* 1997; **26**: 1621-1625

26 **Cooksley WG**, Piratvisuth T, Lee SD, Mahachai V, Chao YC, Tanwandee T, Chutaputti A, Chang WY, Zahm FE, Pluck N. Peginterferon alpha-2a (40 kDa): an advance in the treatment of hepatitis B e antigen-positive chronic hepatitis B. *J Viral Hepat* 2003; **10**: 298-305

27 **Janssen HL**, van Zonneveld M, Senturk H, Zeuzem S, Akarca US, Cakaloglu Y, Simon C, So TM, Gerken G, de Man RA, Niesters HG, Zondervan P, Hansen B, Schalm SW. Pegylated interferon alfa-2b alone or in combination with lamivudine for HBeAg-positive chronic hepatitis B: a randomised trial. *Lancet* 2005; **365**: 123-129

28 **Krüger M**, Tillmann HL, Trautwein C, Bode U, Oldhafer K, Maschek H, Böker KH, Broelsch CE, Pichlmayr R, Manns MP. Famciclovir treatment of hepatitis B virus recurrence after liver transplantation: a pilot study. *Liver Transpl Surg* 1996; **2**: 253-262

29 **Flemming P**, Tillmann HL, Barg-Hock H, Kleeberger W, Manns MP, Klempnauer J, Kreipe HH. Donor origin of de novo hepatocellular carcinoma in hepatic allografts. *Transplantation* 2003; **76**: 1625-1627

30 **Wedemeyer H**, Böker KH, Pethig K, Petzold DR, Flemming P, Tillmann HL, Vollmar J, Bastürk M, Goldmann E, Griffin KE, Haverich A, Manns MP. Famciclovir treatment of chronic hepatitis B in heart transplant recipients: a prospective trial. *Transplantation* 1999; **68**: 1503-1511

31 **Trépo C**, Jezek P, Atkinson G, Boon R, Young C. Famciclovir in chronic hepatitis B: results of a dose-finding study. *J Hepatol* 2000; **32**: 1011-1018

32 **Tillmann HL**, Trautwein C, Bock T, Böker KH, Jäckel E, Glowienka M, Oldhafer K, Bruns I, Gauthier J, Condreay LD, Raab HR, Manns MP. Mutational pattern of hepatitis B virus on sequential therapy with famciclovir and lamivudine in patients with hepatitis B virus reinfection occurring under HBIg immunoglobulin after liver transplantation. *Hepatology* 1999; **30**: 244-256

33 **van Leeuwen R**, Lange JM, Hussey EK, Donn KH, Hall ST, Harker AJ, Jonker P, Danner SA. The safety and pharmacokinetics of a reverse transcriptase inhibitor, 3TC, in patients with HIV infection: a phase I study. *AIDS* 1992; **6**: 1471-1475

34 **Xie H**, Voronkov M, Liotta DC, Korba BA, Schinazi RF, Richman DD, Hostetler KY. Phosphatidyl-2',3'-dideoxy-3'-thiacytidine: synthesis and antiviral activity in hepatitis B-and HIV-1-infected cells. *Antiviral Res* 1995; **28**: 113-120

35 **Dienstag JL**, Schiff ER, Wright TL, Perrillo RP, Hann HW, Goodman Z, Crowther L, Condreay LD, Woessner M, Rubin M, Brown NA. Lamivudine as initial treatment for chronic hepatitis B in the United States. *N Engl J Med* 1999; **341**: 1256-1263

36 **Lai CL**, Chien RN, Leung NW, Chang TT, Guan R, Tai DI, Ng KY, Wu PC, Dent JC, Barber J, Stephenson SL, Gray DF. A one-year trial of lamivudine for chronic hepatitis B. Asia Hepatitis Lamivudine Study Group. *N Engl J Med* 1998; **339**: 61-68

37 **Tassopoulos NC**, Volpes R, Pastore G, Heathcote J, Buti M, Goldin RD, Hawley S, Barber J, Condreay L, Gray DF. Efficacy of lamivudine in patients with hepatitis B e antigen-negative/hepatitis B virus DNA-positive (precore mutant) chronic hepatitis B.Lamivudine Precore Mutant Study Group. *Hepatology* 1999; **29**: 889-896

38 **Dienstag JL**, Perrillo RP, Schiff ER, Bartholomew M, Vicary C, Rubin M. A preliminary trial of lamivudine for chronic hepatitis B infection. *N Engl J Med* 1995; **333**: 1657-1661

39 **Nevens F**, Main J, Honkoop P, Tyrrell DL, Barber J, Sullivan MT, Fevery J, De Man RA, Thomas HC. Lamivudine therapy for chronic hepatitis B: a six-month randomized dose-ranging study. *Gastroenterology* 1997; **113**: 1258-1263

40 **Lai CL**, Ching CK, Tung AK, Li E, Young J, Hill A, Wong BC, Dent J, Wu PC. Lamivudine is effective in suppressing hepatitis B virus DNA in Chinese hepatitis B surface antigen carriers: a placebo-controlled trial. *Hepatology* 1997; **25**: 241-244

41 **Dienstag JL**, Goldin RD, Heathcote EJ, Hann HW, Woessner M, Stephenson SL, Gardner S, Gray DF, Schiff ER. Histological outcome during long-term lamivudine therapy. *Gastroenterology* 2003; **124**: 105-117

42 **Leung NW**, Lai CL, Chang TT, Guan R, Lee CM, Ng KY, Lim SG, Wu PC, Dent JC, Edmundson S, Condreay LD, Chien RN. Extended lamivudine treatment in patients with chronic hepatitis B enhances hepatitis B e antigen seroconversion rates: results after 3 years of therapy. *Hepatology* 2001; **33**: 1527-1532

43 **Gish RG**, Trinh H, Leung N, Chan FK, Fried MW, Wright TL, Wang C, Anderson J, Mondou E, Snow A, Sorbel J, Rousseau F, Corey L. Safety and antiviral activity of emtricitabine (FTC) for the treatment of chronic hepatitis B infection: a two-year study. *J Hepatol* 2005; **43**: 60-66

44 **Lim SG**, Ng TM, Kung N, Krastev Z, Volfova M, Husa P, Lee SS, Chan S, Shiffman ML, Washington MK, Rigney A, Anderson J, Mondou E, Snow A, Sorbel J, Guan R, Rousseau F. A double-blind placebo-controlled study of emtricitabine in chronic hepatitis B. *Arch Intern Med* 2006; **166**: 49-56

45 **Yang H**, Qi X, Sabogal A, Miller M, Xiong S, Delaney WE. Cross-resistance testing of next-generation nucleoside and nucleotide analogues against lamivudine-resistant HBV. *Antivir Ther* 2005; **10**: 625-633

46 **Lai CL**, Lim SG, Brown NA, Zhou XJ, Lloyd DM, Lee YM, Yuen MF, Chao GC, Myers MW. A dose-finding study of once-daily oral telbivudine in HBeAg-positive patients with chronic hepatitis B virus infection. *Hepatology* 2004; **40**: 719-726

47 **Lai C**, Gane E, Liaw YF. Telbivudine versus lamivudine for chronic hepatitis B: first year results from the interantional phase III globe trial. *Hepatology* 2005; **42** (Suppl 1): LB01, 748A

48 **Heathcote E**, Chan HL, Cho M, Lai C, Moon Y, Chao Y, Myers R, Minuk G, Marcellin P, Jeffers L, Sievert W, Kaiser R, Chao G, Brown N, 018 Study Group. A Randomized Trial of Telbivudine (LdT) *vs* Adefovir for HBeAg-Positive Chronic Hepatitis B: Results of the Primary Week 24 Analysis. *Gastroenterology* 2006; **130**: A476

49 **Lai CL**, Leung N, Teo EK, Tong M, Wong F, Hann HW, Han S, Poynard T, Myers M, Chao G, Lloyd D, Brown NA. A 1-year trial of telbivudine, lamivudine, and the combination in patients with hepatitis B e antigen-positive chronic hepatitis B. *Gastroenterology* 2005; **129**: 528-536

50 **Standring DN**, Seifer M, Patty A, Chapron C, Van Doorn LJ, Chao G, Brown N, Lai CL. HBV Resistance Determination From the Telbivudine GLOBE Registration Trial. *J Hepatol* 2006; **44** (Suppl 2): S191

51 **Zhou XJ**, Marbury TC, Alcorn HW, Smith WB, Dubuc Patrick G, Chao GC, Brown NA. Pharmacokinetics of telbivudine in subjects with various degrees of hepatic impairment. *Antimicrob Agents Chemother* 2006; **50**: 1721-1726

52 **Yokota T**, Mochizuki S, Konno K, Mori S, Shigeta S, De Clercq E. Phosphonylmethoxyalkyl derivatives of purine as inhibitors of human hepatitis B virus DNA synthesis. *Nucleic Acids Symp Ser* 1990;**(22)**: 17-18

53 **De Clercq E**. Chemotherapy of the acquired immune deficiency syndrome (AIDS): acyclic nucleoside phosphonate analogues. *Int J Immunopharmacol* 1991; **13** Suppl 1: 91-98

54 **Kahn J**, Lagakos S, Wulfsohn M, Cherng D, Miller M, Cherrington J, Hardy D, Beall G, Cooper R, Murphy R, Basgoz N, Ng E, Deeks S, Winslow D, Toole JJ, Coakley D. Efficacy and safety of adefovir dipivoxil with antiretroviral therapy: a randomized controlled trial. *JAMA* 1999; **282**: 2305-2312

55 **Fontaine H**, Vallet-Pichard A, Chaix ML, Currie G, Serpaggi J, Verkarre V, Varaut A, Morales E, Nalpas B, Brosgart C, Pol S. Efficacy and safety of adefovir dipivoxil in kidney recipients, hemodialysis patients, and patients with renal insufficiency. *Transplantation* 2005; **80**: 1086-1092

56 **Izzedine H**, Hulot JS, Launay-Vacher V, Marcellini P, Hadziyannis SJ, Currie G, Brosgart CL, Westland C, Arterbrun S, Deray G. Renal safety of adefovir dipivoxil in patients with chronic hepatitis B: two double-blind, randomized, placebo-controlled studies. *Kidney Int* 2004; **66**: 1153-1158

57 **Marcellin P**, Chang TT, Lim SG, Tong MJ, Sievert W, Shiffman ML, Jeffers L, Goodman Z, Wulfsohn MS, Xiong S, Fry J, Brosgart CL. Adefovir dipivoxil for the treatment of hepatitis B e antigen-positive chronic hepatitis B. *N Engl J Med* 2003; **348**: 808-816

58 **Marcellin P**, Chang T, Lim S, Sievert W, Tong M, Arterburm S, Xiong S, Brosgart CL, Currie G. Increasing serologic, virologic and biochemical response over time to adefovir dipivoxil (ADV) 10 Mg in HBeAg plus chronic hepatitis B (CHB) patients. *Gastroenterology* 2005; **128** Suppl 2: A741-A742

59 **Hadziyannis SJ**, Tassopoulos NC, Heathcote EJ, Chang TT, Kitis G, Rizzetto M, Marcellin P, Lim SG, Goodman Z, Wulfsohn MS, Xiong S, Fry J, Brosgart CL. Adefovir dipivoxil for the treatment of hepatitis B e antigen-negative chronic hepatitis B. *N Engl J Med* 2003; **348**: 800-807

60 **Hadziyannis SJ**, Tassopoulos NC, Heathcote EJ, Chang TT, Kitis G, Rizzetto M, Marcellin P, Lim SG, Goodman Z, Ma J, Arterburn S, Xiong S, Currie G, Brosgart CL. Long-term therapy with adefovir dipivoxil for HBeAg-negative chronic hepatitis B. *N Engl J Med* 2005; **352**: 2673-2681

61 **Billich A**. Entecavir (Bristol-Myers Squibb). *Curr Opin Investig Drugs* 2001; **2**: 617-621

62 **Chang TT**, Gish RG, de Man R, Gadano A, Sollano J, Chao YC, Lok AS, Han KH, Goodman Z, Zhu J, Cross A, DeHertogh D, Wilber R, Colonno R, Apelian D. A comparison of entecavir and lamivudine for HBeAg-positive chronic hepatitis B. *N Engl J Med* 2006; **354**: 1001-1010

63 **Lai CL**, Shouval D, Lok AS, Chang TT, Cheinquer H, Goodman Z, DeHertogh D, Wilber R, Zink RC, Cross A, Colonno R, Fernandes L. Entecavir versus lamivudine for patients with HBeAg-negative chronic hepatitis B. *N Engl J Med* 2006; **354**: 1011-1020

64 **Gish R**, Chang TT, De Man RA. Entecavir results in substantial virologic and biochemical improvement and HBeAg seroconversion through 96 weeks of treatment in HBeAg(+) chronic hepatitis B patients. *Hepatology* 2005; **41** (Suppl 1): A181, A267

65 **Chang TT**, Gish RG, Hadziyannis SJ, Cianciara J, Rizzetto M, Schiff ER, Pastore G, Bacon BR, Poynard T, Joshi S, Klesczewski KS, Thiry A, Rose RE, Colonno RJ, Hindes RG. A dose-ranging study of the efficacy and tolerability of entecavir in Lamivudine-refractory chronic hepatitis B patients. *Gastroenterology* 2005; **129**: 1198-1209

66 **Colonno RJ**, Rose R, Levine S, Baldick J, Pokornowski K, Plym M, Yu CF, Mazzucco C, Fang J, Hsu MJ, Walsh AW, Eggers B, Thiry A, Tenney DJ. Entecavir two year resistance update: no resistance observed in nucleoside naive patients and low frequency resistance emergence in lamivudine refractory patients. *Hepatology* 2005; **42** (Suppl 1): A962, 573A

67 **Lacombe K**, Gozlan J, Boelle PY, Serfaty L, Zoulim F, Valleron AJ, Girard PM. Long-term hepatitis B virus dynamics in HIV-hepatitis B virus-co-infected patients treated with tenofovir disoproxil fumarate. *AIDS* 2005; **19**: 907-915

68 **Benhamou Y**, Fleury H, Trimoulet P, Pellegrin I, Urbinelli R, Katlama C, Rozenbaum W, Le Teuff G, Trylesinski A, Piketty C. Anti-hepatitis B virus efficacy of tenofovir disoproxil fumarate in HIV-infected patients. *Hepatology* 2006; **43**: 548-555

69 **de Vries-Sluijs TE**, van der Eijk AA, Hansen BE, Osterhaus AD, de Man RA, van der Ende ME. Wild type and YMDD variant of hepatitis B virus: no difference in viral kinetics on lamivudine/tenofovir therapy in HIV-HBV co-infected patients. *J Clin Virol* 2006; **36**: 60-63

70 **van Bömmel F**, Wünsche T, Mauss S, Reinke P, Bergk A, Schürmann D, Wiedenmann B, Berg T. Comparison of adefovir and tenofovir in the treatment of lamivudine-resistant hepatitis B virus infection. *Hepatology* 2004; **40**: 1421-1425

71 **Peters M,** Anderson J, Lynch P, Jacobson J, Sherman K, Alston Smith B, Swindells S, Liu T, Johnson V, Pollard R, Rooney J, Polsky B, and AACTG team. Tenofivir disoproxil fumarate is not inferior to adefovir dipivoxil for the treatment of hepatitis B virus in subjects who are co-infected with HIV: Results of ATCG A5127. Boston: 12th CROI, 22-25th February 2005 Abstract 124

72 **Lee HS**, Chung YH, Lee K, Byun KS, Paik SW, Han JY, Yoo K, Yoo HW, Lee JH, Yoo BC. A 12-week clevudine therapy showed potent and durable antiviral activity in HBeAg-positive chronic hepatitis B. *Hepatology* 2006; **43**: 982-988

73 **Casey J**, Cote PJ, Toshkov IA, Chu CK, Gerin JL, Hornbuckle WE, Tennant BC, Korba BE. Clevudine inhibits hepatitis delta virus viremia: a pilot study of chronically infected woodchucks. *Antimicrob Agents Chem*other 2005; **49**: 4396-4399

74 **Lin CC**, Xu C, Teng A, Yeh LT, Peterson J. Pharmacokinetics of pradefovir and PMEA in healthy volunteers after oral dosing of pradefovir. *J Clin Pharmacol* 2005; **45**: 1250-1258

75 **Lin C**, Xu C, Yeh LT, Sullivan-Bolyai J, Xu Y. Pharmacokinetics and Pharmacodynamics of Pradefovir Mesylate, a Liver-Targeting Pro-Drug of PMEA, in HBV Patients. *J Hepatol* 2006; **44** (Suppl 2): S16

76 **Lai CL**, Han KH, Yoon SK, Um SH, Yuen MF, Kim HS, Lim HR, Chung HC, Lim CR, Hsyu P, Averett D, Worland S, Kim J. Phase II, mutli-centre, dose-escalating study of LB80380 (ANA380) in Hepatitis B patients with lamivudine-resistant YMDD mutant HBV. *J Hepatol* 2006; **44** (Suppl 2): S5

77 **Glebe D**, Urban S, Knoop EV, Cag N, Krass P, Grün S, Bulavaite A, Sasnauskas K, Gerlich WH. Mapping of the hepatitis B virus attachment site by use of infection-inhibiting preS1 lipopeptides and tupaia hepatocytes. *Gastroenterology* 2005; **129**: 234-245

78 **Marcellin P**, Lau GK, Bonino F, Farci P, Hadziyannis S, Jin R, Lu ZM, Piratvisuth T, Germanidis G, Yurdaydin C, Diago M, Gurel S, Lai MY, Button P, Pluck N. Peginterferon alfa-2a alone, lamivudine alone, and the two in combination in patients with HBeAg-negative chronic hepatitis B. *N Engl J Med* 2004; **351**: 1206-1217

79 **Wursthorn K**, Buggisch P, Zöllner B, Zankel M, Fischer C, Xiong S, Brosgart C, Currie G, Petersen J. Combination Therapy of PegInterferon -2b and adefovirdipivoxil in chronic hepatitis-B leads to a strong suppression of cccDNA and high rates of HBe and HBs seroconversion. *J Hepatol* 2005; **42** (Suppl 2): S32

80 **Lau G**, Cooksley H, Ribeiro RM, Powers KA, Bowden S, Mommeja-Marin H, Mondou E, Lewin S, Rousseau F, Perelson AS, Locarnini S, Naoumov NV. Randomized, double-blind study comparing adefovir dipivoxil (ADV) plus emtricitabine (FTC) combination therapy versus ADV alone in HBEAG(+) chronic hepatitis B: Efficacy and mechanisms of treatment response. *Hepatology* 2004; **40**: 272A

81 **Lim SG**, Krastev Z, Ng TM, Mechkov G, Kotzev IA, Chan S, Mondou E, Snow A, Sorbel J, Rousseau F. Randomized, double-blind study of emtricitabine (FTC) plus clevudine ver-

sus FTC alone in treatment of chronic hepatitis B. *Antimicrob Agents Chemother* 2006; **50**: 1642-1648
82 **Bock CT**, Tillmann HL, Torresi J, Klempnauer J, Locarnini S, Manns MP, Trautwein C. Selection of hepatitis B virus polymerase mutants with enhanced replication by lamivudine treatment after liver transplantation. *Gastroenterology* 2002; **122**: 264-273
83 **Eggers HJ**, Reich E, Tamm I. The drug-requiring phase in the growth of drug-dependent enteroviruses. *Proc Natl Acad Sci USA* 1963; **50**: 183-190
84 **Huang W**, Gamarnik A, Wrin T, Parkin NT, Hellmann NS, Deeks SG, Liegler T, Grant RM, Petropoulos CJ, Whitcomb JM. HIV-1 isolates that exhibit dose-dependent NNRTI stimulation of reverse transcripatase activity and viral replication. *Antiviral Therapy* 2000; **5** (Suppl 3): 23-24
85 **Huang W**, Parkin NT, Lie YS, Wrin T, Haubrich R, Deeks SG, Hellmann NS, Petropoulos CJ, Whitcomb JM. A novel HIV-1 RT mutations (M230L) confers NNRTI resistance and dose-dependent stimulation of replication. *Antiviral Therapy* 2000; **5** (Suppl 3): 24-25
86 **Stuyver LJ**, Locarnini SA, Lok A, Richman DD, Carman WF, Dienstag JL, Schinazi RF. Nomenclature for antiviral-resistant human hepatitis B virus mutations in the polymerase region. *Hepatology* 2001; **33**: 751-757
87 **Liaw YF**, Sung JJ, Chow WC, Farrell G, Lee CZ, Yuen H, Tanwandee T, Tao QM, Shue K, Keene ON, Dixon JS, Gray DF, Sabbat J. Lamivudine for patients with chronic hepatitis B and advanced liver disease. *N Engl J Med* 2004; **351**: 1521-1531
88 **Lai CL**, Dienstag J, Schiff E, Leung NW, Atkins M, Hunt C, Brown N, Woessner M, Boehme R, Condreay L. Prevalence and clinical correlates of YMDD variants during lamivudine therapy for patients with chronic hepatitis B. *Clin Infect Dis* 2003; **36**: 687-696
89 **Lok AS**, Lai CL, Leung N, Yao GB, Cui ZY, Schiff ER, Dienstag JL, Heathcote EJ, Little NR, Griffiths DA, Gardner SD,Castiglia M. Long-term safety of lamivudine treatment in patients with chronic hepatitis B. *Gastroenterology* 2003 ; **125**: 1714-1722
90 **Tillmann HL**, Trautwein C, Bock CT, Glomb I, Krüger M, Böker KH, Klempnauer J, Flemming P, Manns MP. Lamivudine transiently reduces viral load and improves liver function in liver transplant recipients with fibrosing cholestatic hepatitis. *Am J Gastroenterol* 2002; **97**: 777-778
91 **Hadziyannis SJ**, Papatheodoridis GV, Dimou E, Laras A, Papaioannou C. Efficacy of long-term lamivudine monotherapy in patients with hepatitis B e antigen-negative chronic hepatitis B. *Hepatology* 2000; **32**: 847-851
92 **Nafa S**, Ahmed S, Tavan D, Pichoud C, Berby F, Stuyver L, Johnson M, Merle P, Abidi H, Trépo C, Zoulim F. Early detection of viral resistance by determination of hepatitis B virus polymerase mutations in patients treated by lamivudine for chronic hepatitis B. *Hepatology* 2000; **32**: 1078-1088
93 **Rizzetto M**, Tassopoulos NC, Goldin RD, Esteban R, Santantonio T, Heathcote EJ, Lagget M, Taak NK, Woessner MA, Gardner SD. Extended lamivudine treatment in patients with HBeAg-negative chronic hepatitis B. *J Hepatol* 2005; **42**: 173-179
94 **Papatheodoridis GV**, Dimou E, Laras A, Papadimitropoulos V, Hadziyannis SJ. Course of virologic breakthroughs under long-term lamivudine in HBeAg-negative precore mutant HBV liver disease. *Hepatology* 2002; **36**: 219-226
95 **Lampertico P**, Viganò M, Manenti E, Iavarone M, Lunghi G, Colombo M. Adefovir rapidly suppresses hepatitis B in HBeAg-negative patients developing genotypic resistance to lamivudine. *Hepatology* 2005; **42**: 1414-1419
96 **Di Marco V**, Marzano A, Lampertico P, Andreone P, Santantonio T, Almasio PL, Rizzetto M, Craxì A. Clinical outcome of HBeAg-negative chronic hepatitis B in relation to virological response to lamivudine. *Hepatology* 2004; **40**: 883-891
97 **Liaw YF**, Leung NW, Chang TT, Guan R, Tai DI, Ng KY, Chien RN, Dent J, Roman L, Edmundson S, Lai CL. Effects of extended lamivudine therapy in Asian patients with chronic hepatitis B. Asia Hepatitis Lamivudine Study Group. *Gastroenterology* 2000; **119**: 172-180
98 **Peters MG**, Hann Hw Hw, Martin P, Heathcote EJ, Buggisch P, Rubin R, Bourliere M, Kowdley K, Trepo C, Gray Df Df, Sullivan M, Kleber K, Ebrahimi R, Xiong S, Brosgart CL. Adefovir dipivoxil alone or in combination with lamivudine in patients with lamivudine-resistant chronic hepatitis B. *Gastroenterology* 2004; **126**: 91-101
99 **Benhamou Y**, Bochet M, Thibault V, Calvez V, Fievet MH, Vig P, Gibbs CS, Brosgart C, Fry J, Namini H, Katlama C, Poynard T. Safety and efficacy of adefovir dipivoxil in patients co-infected with HIV-1 and lamivudine-resistant hepatitis B virus: an open-label pilot study. *Lancet* 2001; **358**: 718-723
100 **Sherman M**, Yurdaydin C, Sollano J, Silva M, Liaw YF, Cianciara J, Boron-Kaczmarska A, Martin P, Goodman Z, Colonno R, Cross A, Denisky G, Kreter B, Hindes R. Entecavir for treatment of lamivudine-refractory, HBeAg-positive chronic hepatitis B. *Gastroenterology* 2006; **130**: 2039-2049
101 **Levine S**, Hernandez D, Yamanaka G, Zhang S, Rose R, Weinheimer S, Colonno RJ. Efficacies of entecavir against lamivudine-resistant hepatitis B virus replication and recombinant polymerases *in vitro*. *Antimicrob Agents Chemother* 2002; **46**: 2525-2532
102 **Lampertico P**, Marzano A, Levrero M, Santantonio T, Andreone P, Brunetto M, Di Marco V, Fagioli S, Mazzalla, Raimondo G. A mutlicenter Italian study of rescue Adeovir dipivoxil therapy in Lamivudine resistant patients: A 2-year analysis of 650 patients. *J Hepatol* 2006; **44** (Suppl 2): S51
103 **Lampertico P**, Vigano M, Manenti E, Iavarone M, Lunghi G, Colombo M. Five years of sequential LAM to LAM+ADV therapy suppresses HBV replication in most HbeAg-negative cirrhotics, preventing decompensation but not hepatocellular carcinoma. *J Hepatol* 2006; **44** (Suppl 2): S38
104 **Angus P**, Vaughan R, Xiong S, Yang H, Delaney W, Gibbs C, Brosgart C, Colledge D, Edwards R, Ayres A, Bartholomeusz A, Locarnini S. Resistance to adefovir dipivoxil therapy associated with the selection of a novel mutation in the HBV polymerase. *Gastroenterology* 2003; **125**: 292-297
105 **Brunelle MN**, Jacquard AC, Pichoud C, Durantel D, Carrouée-Durantel S, Villeneuve JP, Trépo C, Zoulim F. Susceptibility to antivirals of a human HBV strain with mutations conferring resistance to both lamivudine and adefovir. *Hepatology* 2005; **41**: 1391-1398
106 **Villeneuve JP**, Durantel D, Durantel S, Westland C, Xiong S, Brosgart CL, Gibbs CS, Parvaz P, Werle B, Trépo C, Zoulim F. Selection of a hepatitis B virus strain resistant to adefovir in a liver transplantation patient. *J Hepatol* 2003; **39**: 1085-1089
107 **Fung SK**, Andreone P, Han SH, Rajender Reddy K, Regev A, Keeffe EB, Hussain M, Cursaro C, Richtmyer P, Marrero JA, Lok AS. Adefovir-resistant hepatitis B can be associated with viral rebound and hepatic decompensation. *J Hepatol* 2005; **43**: 937-943
108 **Lee YS**, Suh DJ, Lim YS, Jung SW, Kim KM, Lee HC, Chung YH, Lee YS, Yoo W, Kim SO. Increased risk of adefovir resistance in patients with lamivudine-resistant chronic hepatitis B after 48 weeks of adefovir dipivoxil monotherapy. *Hepatology* 2006; **43**: 1385-1391
109 **Yeon JE**, Yoo W, Hong SP, Chang YJ, Yu SK, Kim JH, Seo YS, Chung HJ, Moon MS, Kim SO, Byun KS, Lee CH. Resistance to adefovir dipivoxil in lamivudine resistant chronic hepatitis B patients treated with adefovir dipivoxil. *Gut* 2006; **55**: 1488-1495
110 **Chang TT**, Lai CL. Hepatitis B virus with primary resistance to adefovir. *N Engl J Med* 2006; **355**: 322-323; author reply 323
111 **Schildgen O**, Sirma H, Funk A, Olotu C, Wend UC, Hartmann H, Helm M, Rockstroh JK, Willems WR, Will H, Gerlich WH. Variant of hepatitis B virus with primary resistance to adefovir. *N Engl J Med* 2006; **354**: 1807-1812
112 **van Bömmel F**, Zöllner B, Sarrazin C, Spengler U, Hüppe D, Möller B, Feucht HH, Wiedenmann B, Berg T. Tenofovir for patients with lamivudine-resistant hepatitis B virus (HBV) infection and high HBV DNA level during adefovir therapy. *Hepatology* 2006; **44**: 318-325
113 **Tenney DJ**, Levine SM, Rose RE, Walsh AW, Weinheimer SP, Discotto L, Plym M, Pokornowski K, Yu CF, Angus P, Ayres A, Bartholomeusz A, Sievert W, Thompson G, Warner N, Lo-

carnini S, Colonno RJ. Clinical emergence of entecavir-resistant hepatitis B virus requires additional substitutions in virus already resistant to Lamivudine. *Antimicrob Agents Chemother* 2004; **48**: 3498-3507

114 **Villet S**, Pichoud C, Ollivet A, Villeneuve JP, Trepo C, Zoulim F. Sequential antiviral therapy leads to the emergence of multiple drug resistant hepatitis B virus. *Hepatology* 2005; **42** (Suppl 1): A981, 581A

115 **Puchhammer-Stöckl E**, Mandl CW, Kletzmayr J, Holzmann H, Hofmann A, Aberle SW, Heinz FX, Watschinger B, Hofmann H. Monitoring the virus load can predict the emergence of drug-resistant hepatitis B virus strains in renal transplantation patients during lamivudine therapy. *J Infect Dis* 2000; **181**: 2063-2066

116 **Zeuzem S**, Lai CL, Gane E, Liaw YF, Thongsawat S, Wang Y, Chen Y, Heathcote J, Rasenack J, Bzowej N, Naoumov N, Chao G, Fielman B, Brown N. Optimal virologic and clinical efficacy at one year is associated with maximal early HBV suppression in nucleoside-treated hepatitis B patients. *J Hepatol* 2006; **44** (Suppl 2): S24

117 **Lai C**, Gane E, Liaw YF. Telbivudine versus lamivudine for chronic hepatitis B: first year results from the interantional phase III globe trial. *Hepatology* 2005; **42** (Suppl 1): LB01, 748A

118 **Hadziyannis S**, Tassopoulos N, Chang T. Long-term adefovir dipivoxil treatment induces regression of liver fibrosis in patients with HBeAg-negative chronic hepatitis B: results after 5 years of therapy. *Hepatology* 2005; **42** (Suppl 1): LB14, 745A

119 **Durantel D**, Carrouée-Durantel S, Werle-Lapostolle B, Brunelle MN, Pichoud C, Trépo C, Zoulim F. A new strategy for studying in vitro the drug susceptibility of clinical isolates of human hepatitis B virus. *Hepatology* 2004; **40**: 855-864

120 **Yang H**, Westland C, Xiong S, Delaney WE. In vitro antiviral susceptibility of full-length clinical hepatitis B virus isolates cloned with a novel expression vector. *Antiviral Res* 2004; **61**: 27-36

121 **Iloeje UH**, Yang HI, Su J, Jen CL, You SL, Chen CJ. Predicting cirrhosis risk based on the level of circulating hepatitis B viral load. *Gastroenterology* 2006; **130**: 678-686

122 **Hadziyannis SJ**, Sevastinos V, Rapti IN, Tassopoulos. Sustained biochemical and virological remission after discontinuation of 4 to 5 years of adefovir dpivoxil (ADV) treatment in HBeAg-negative chronic hepatitis B. *AASLD* 2006: Abstract 114

123 **Colonno RJ**, Rose RE, Pokornowski K, Baldick CJ, Klesczewski K, Tenney D. Assessment at three years shows high barrier to resistance is maintained in entecavir-treated nucleoside naïve patients while resistance emergence increase over time in lamivudine refractory patients. *AASLD* 2006; Abstract 110

S- Editor Liu Y **L- Editor** Lutze M **E- Editor** Bi L

PO Box 2345, Beijing 100023, China
www.wjgnet.com
wjg@wjgnet.com

World J Gastroenterol 2007 January 7; 13(1): 141-145
World Journal of Gastroenterology ISSN 1007-9327

BASIC RESEARCH

Effects of nociceptin/orphanin FQ on rats with cathartic colon

Hai-Yan Li, Xiang Yan, Quan-Lai Xue, Yong-Ning Zhou, Yan Gao, Rui Wang, Yong-Ming Liu, Jun-Tao Ran

Hai-Yan Li, Quan-Lai Xue, Yan Gao, Department of Gastroenterology, the Affiliated Hospital of Jinchuan Corporation Company, Jinchang 737100, Gansu Province, China
Xiang Yan, Yong-Ning Zhou, Yong-Ming Liu, Jun-Tao Ran, Department of Geriatrics, 1st Affiliated Hospital of Lanzhou Univercity, Lanzhou 730000, Gansu Province, China
Rui Wang, Department of Life Science, Lanzhou University, Lanzhou 730000 , Gansu Province, China
Correspondence to: Professor Xiang Yan, Department of Geriatrics, 1st Affiliated Hospital of Lanzhou University, Lanzhou 730000, Gansu Province, China. lihaiyan99@tom.com
Telephone: +86-935-3628668 Fax: +86-935-8811453
Received: 2006-03-13 Accepted: 2006-07-10

Abstract

AIM: To demonstrate the change and effect of nociceptin/orphanin FQ in the colon of rats with cathartic colon.

METHODS: The cathartic colon model was established by feeding rats rhubarb for 3 mo, the changes of colonic electromyography were investigated by both suspension muscle strips test and serosal recordings of colonic myoelectrical activity. Immunohistochemical staining (S-P methods) and image analysis were used to determine the changes of nociceptin/orphanin FQ in the proximal colon and distal colon of rats with cathartic colon.

RESULTS: Suspension muscle strips test *in vitro* showed OFQ (10^{-9}-10^{-6} mol/L) concentration dependently caused an immediate tonic contraction in the isolated colon. But the increase of tension in cathartic colon was less than control groups ($P < 0.01$). Intravenous administration of OFQ (1 μg/kg) caused phasic contractions in the proximal colon, while the amplitude of phasic contractions caused by OFQ in cathartic colon was much lower than that in the control groups (2.58 ± 0.41 *vs* 4.16 ± 0.53, $t = -2.6$, $P = 0.012$). OFQ was highly expressed in the myenteric plexus of the rat colon but not in the muscle cells. The immunoreactivity of OFQ in the proximal colon in cathartic colon rats decreased significantly compared with the control group ($P = 0.001$).

CONCLUSION: Colonic smooth muscle of cathartic colon showed low sensitivity to the stimulation of OFQ, suggesting that it might be caused by the abnormal distribution of OFQ or the abnormalities of receptors, leading to the disorganization of dynamic and incoordinated contractions.

Key words: Nociceptin/Orphanin FQ; Opioid; Muscle tension; Colonic motility; Enteric nervous system; Cathartic colon

Li HY, Yan X, Xue QL, Zhou YN, Gao Y, Wang R, Liu YM, Ran JT. Effects of nociceptin/orphanin FQ on rats with cathartic colon. *World J Gastroenterol* 2007; 13(1): 141-145

http://www.wjgnet.com/1007-9327/13/141.asp

INTRODUCTION

Slow transit constipation (STC) is a common syndrome in idiopathic constipation. It is a severe disorder of colonic motility. Because of lack of understanding of the etiology, current medical treatments for STC are often ineffective[1]. It has been shown that predominant symptoms in STC correlate with the enteric nervous system (ENS) abnormalities[2]. Animal experiments have shown that stimulant laxatives can damage the ENS and cause changes of some enteric neurotransmitters and thus slow gastrointestinal tract transit occurs[3].

The peptide nociceptin, also called orphanin-FQ (N/OFQ), is a 17-amino-acid peptide and was identified in 1995[4]. Because it binds an opioid receptor like 1 (ORL1)receptor with a high affinity, it has been reported to be an endogeneous agonist for ORL1 receptor. *In situ* hybridization studies have revealed the wide distribution of the ORL1 receptor mRNA in the central nervous system of rats[5], especially in the coli involved in pain control, so most of the researches focused on the role of N/OFQ in analgesics. However, by the activation of the ORL1 receptor, N/OFQ can also influence reward, anxiety, feeding and memory processes[6,7], cardiovascular and renal functions[8,9], gastric and intestinal motility[10,11] and secretions[12,13].

The gastrointestinal tract is an important model system for the research of pharmocological characterization of opioid receptors. Therefore, if N/OFQ can also act as a brain-bowel peptide like classical opioid, it may play a role in the regulation of gastrointestinal tract functions. In this study, with a rat model of cathartic colon, we determined the effects of OFQ on mechanical activity of the rat colon and conducted immunohistochemical studies on rat colon to assess the changes of OFQ.

MATERIALS AND METHODS

Experimental animals

Fifty Wistar rats of either sex, obtained from the

Experimental Animal Center, Lanzhou University (Lanzhou, China), weighing 290 ± 50 g, were divided randomly into control group (n = 25) and cathartic colon group treated with rhubarb (n = 25). Rats were housed in cage, one per cage under standard laboratory conditions (room temperature, 18-28℃, relative humility, 40%-80%). Control rats were given soft chows, while the rats in rhubarb group were given chows premixed with rhubarb powder. The initial rhubarb dosage was 200 mg/kg·d, and another 200 mg/kg was added every day until it reached 1000 mg/kg·d for several days until loose stool disappeared. Then, rhubarb was added at 200 mg/kg·d again to 3600 mg/kg·d for 3 mo.

Materials

Tetrodotoxin (TTX) and naloxone were obtained from Sigma Co. USA. OFQ (1-17) was obtained from Physical Laboratories, School of Life Science, Lanzhou University (Lanzhou, China). Rabbit antinociceptin antiserum (Chemicon Pharmaceuticals Inc, 1:500. Goat anti-rabbit biotinylated secondary antibody (Rocland Laboratories, USA, 1:15000).

Motility studies

Wistar rats (body weight, 290 ± 50 g) were starved overnight and killed by head-strike, longitudinal muscle strips were isolated from proximal colon, muscle strips (10 mm in length and 3 mm in width) were suspended between 2 platinum electrodes in a 30 mL organ bath filled with Krebs-Henseleit buffer containing 118 mmol/L NaCl, 4.8 mmol/L KCl, 2.5 mmol/L $CaCl_2$, 25 mmol/L $NaHCO_3$, 1.2 mmol/L KH_2PO_4, 1.2 mmol/L $MgSO_4$, 11 mmol/L glucose and 0.1% bovine serum albumin. Krebs-Henseleit buffer solution was continuously gassed with 95%O_2-5%CO_2 and maintained at 37℃ and pH 7.4. Mechanical activity was recorded on a polygraph through isometric transducers. Muscle strips were stretched in 1-mm increments and repeatedly exposed to 10^{-6} mmol/L carbachol to determine L_0, the length at which the maximal active tension response developed. The resting of tension was kept constant during the equilibration period, dose-response curves were constructed after applying OFQ (10^{-9}-10^{-6} mol/L) to longitudinal muscle stripes from proximal colon. Doses of OFQ were administered at 20-min intervals. To investigate the neural pathways responsible for the contractile action of OFQ, we examined the effects of TTX and naloxone on OFQ-induced contractions. Muscle strips were preincubated with each antagonist for 10 min followed by incubation with OFQ (n = 8).

Response of colon in anesthetized rats

Colonic motility studies in anesthetized rats were carried out according to the procedures described previously (Nagasaki *et al*, 1989.) In brief, rats were fasted for 20 h and anesthetized with urethane (1.2 g/kg s.c.). After midline laparotomy, a strain gauge force transducer (F-081S, Star Medical, Japan) was sutured on the serosal surface of the proximal colon to record the circular muscle contraction. For intravenous administration of drugs, the right femoral vein was cannulated. After the contractile response to bethanechol (30 mg/kg i.v) became stable, OFQ (1 μg/kg) was administered intravenously (n = 7).

Immunohistochemistry

The animals were deeply anaesthetized with 5% isoflurane and perfused transcardially with aerated calcium-free Tyrode's solution, followed by a fixative containing 4% paraformaldehyde and 0.2% picric acid in 0.1 mol/L phosphate buffer (pH 7.2-7.4). The proximal and distal colons were removed immediately after perfusion, post-fixed in the same fixative for 4h and then cryoprotected in 10% sucrose in phosphate-buffered saline (PBS, pH 7.4) overnight.

A series of sections were cut and mounted on gelatin-subbed slides. Elimination of endogeneous peroxidase activity was performed with 0.3% hydrogen peroxide in PBS at room temperature for 30 min. The sections were pre-blocked with 3% normal goat serum, 0.5% triton X-100, and 1% bovine serum albumin in PBS for 30 min. Then incubated in rabbit antinociceptin antiserum (Chemicon Pharmaceuticals Inc, 1:500) at 4℃ overnight. The sections were rinsed with PBS and incubated for 1h with goat anti-rabbit biotinylated secondary antibody (Rocland Laboratories, USA, 1:15000). Then they were incubated in an avidin-biotin complex coupled to horseradish peroxidase for 10 min at room temperature. Finally, after rinsing with PBS, the nociceptin-positive neurons and nerve fibers were visualized using 3, 3' -diaminobenzidine (DAB, Maixin Chemical Co. Fuzhou, China). The slides were then dried, dehydrated in ethanol (70%-100% gradually), cleared in xylene, and coverslipped with mounting solution. Immunohistochemical image analysis was made to assess the changes of OFQ both in proximal and distal colons in two group rats (n = 10).

All animal experiments were carried out in accordance with the National Institutes of Health Guide for the Care and Use of Laboratory Animals.

Statistical analysis

Results were expressed as mean ± SE. Data were analyzed by SPSS10.0. Differences were analyzed by one-way analysis of variance ANOVA and independent t test. Probabilities of $P < 0.05$ were considered significant.

RESULTS

Motility studies

In vitro studies using longitudinal muscle revealed that OFQ (10^{-9}-10^{-6} mol/L) induced contractions in the colon. The threshold concentration of OFQ to induce contractions was 10^{-9} mol/L. In the proximal colon of two group rats, OFQ (10^{-9} to 10^{-6} mol/L) induced contractions in a dose-dependent manner (Figure1A), but the increase of tension in cathartic colon was lower than in the control groups (Figure1B). To determine if OFQ activity was mediated by neural pathways or if it was a direct myogenic effect, OFQ-induced contractions were examined in the presence of TTX. In the presence of TTX, OFQ failed to elicit additional contractions (Figure 1C). The contractions

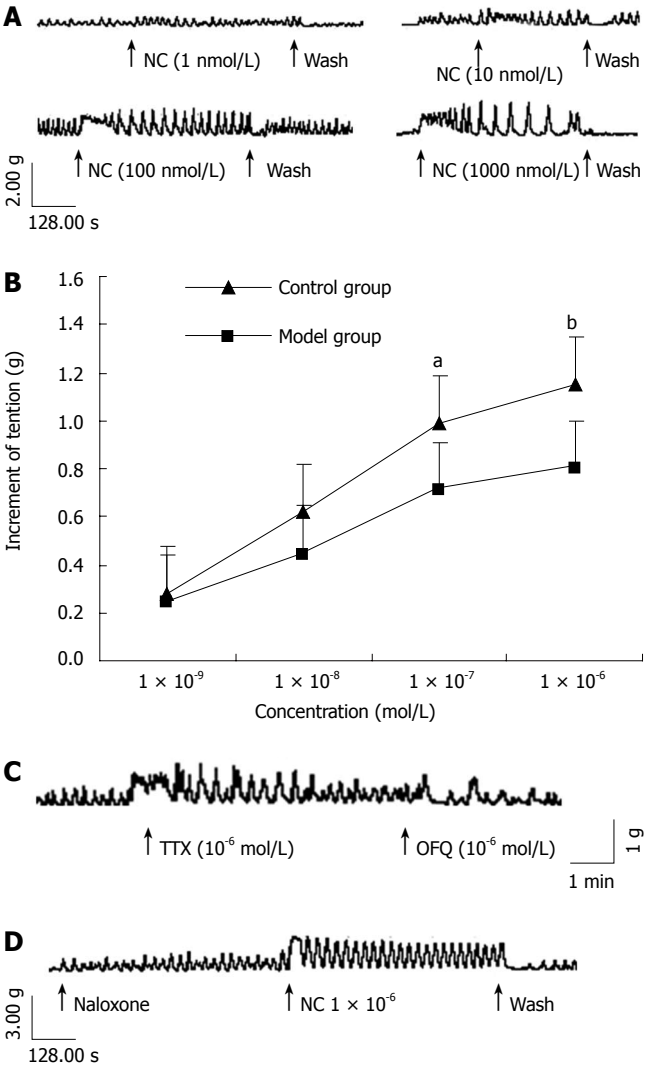

Figure 1 Effects of OFQ (10^{-9}-10^{-6}mol/L) on colon of rats *in vitro*. **A**: Effects of OFQ on the contractile activity of longitudinal muscle strips obtained from the rat proximal colon; **B**: Different effects of OFQ (10^{-9}-10^{-6} mol/L) on increment of tension in two groups of rats. $^{a}P < 0.05$ *vs* 1 × 10^{-9} mol/L; $^{b}P < 0.01$ *vs* 1 × 10^{-9} mol/L; **C**: In the presence of TTX (10^{-6} mol/L), OFQ (10^{-6} mol/L) failed to evoke additional contractions; **D**: The response to OFQ (1 × 10^{-6} mol/L) was not affected by naloxone (1 × 10^{-6} mol/L).

induced by OFQ (1 × 10^{-6} mol/L) were not affected by classical opioid antagonist, naloxone (1 × 10^{-6} mol/L) (Figure1D).

Intravenous administration of OFQ caused phasic contractions in the proximal colon (Figure 2A), it was not affected by classical opioid antagonist, naloxone (1 × 10^{-6} mol/L) (Figure 2B), but the amplitude of phasic contractions caused by OFQ in cathartic colon was much lower than control groups (Figure 2C, 2.58 ± 0.41 *vs* 4.16 ± 0.53, $t = -2.6$, $P = 0.012$).

Immunohistochemistry

Immunohistochemistry of OFQ in the rat gastrointestinal tract showed that Orphain FQ immunoreactive (OFQ-IR) neurons and nerve fibers were visualized in the myenteric plexus of the rat colon (Figure 3A). The immunoreactivity of OFQ in the myenteric plexus in the proximal cathartic colon of rats decreased significantly as compared with

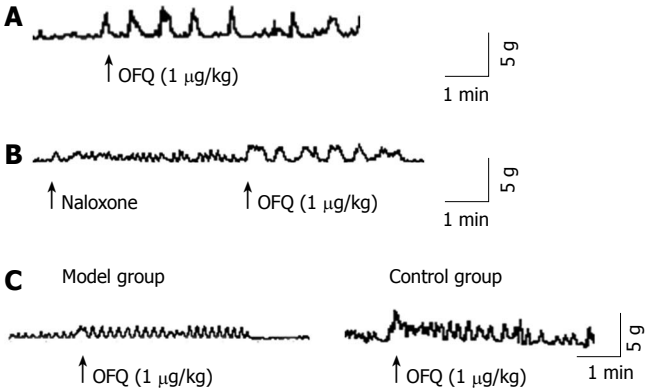

Figure 2 Effects of OFQ on colon of rats *in vivo*. **A**: Intravenous administration of OFQ (1 μg/kg) caused phasic contractions in the colon. **B**: Naloxone (300 μg/kg) has no effects on phasic contractions caused by intravenous administration of OFQ (1 μg/kg)in the proximal colon. **C**: Intravenous administration of OFQ (1 μg/kg) caused phasic contractions in the proximal colon in two groups.

the control group. (176.42 ± 5.792 *vs* 137.367 ± 25.508. $P = 0.001$) (Figure 3B, 3C). The negative control showed no staining of OFQ-IR in the myenteric plexus of the gastrointestinal tract.

DISCUSSION

Due to the diet and social-psychological changes, constipation has become an important factor affecting the quality of human life in modern society, therefore the morbidity is getting higher and higher. STC is a common syndrome in idiopathic constipation. It is a severe disorder of colonic motility characterized by a reduction in the frequency, amplitude and duration of propulsive contractions in the large bowel. Because of lack of understanding of the etiology, current medical treatments on STC are often ineffective. Animal experiments have shown that stimulant laxatives can damage ENS and cause the changes of some enteric neurotransmitters and thus the slow gastrointestinal tract transit occurs.

The innervation of the gastrointestinal tract is unique among the visceral organs. Neurons originating in the enteric ganglionated plexuses within the gut wall coordinate intrinsic reflexes associated with intestinal motility, epithelial secretion, and mucosal blood flow[14]. The myenteric plexus lies between the longitudinal and circular smooth muscle layers and regulates intestinal motor function. Bowel motility is controlled by a local network of intramural nerves[15]. Effects of opioid peptides on GI motility have been studied. Morphine can cause constipation due in part to slowing of GI transit and inhibition of active intestinal secretion, which was the normal side effect in clinical practice[16].

Despite its being homologous to classical opioids, dynorphin A, the OFQ/ORL1 system represents a new peptide-based signaling pathway, which is pharmacologically distinct from the opioid system[17]. Probing into the distribution and function of N/OFQ and ORL1 receptor in the gastrointestinal tract of the animal model will contribute to the overall understanding of the characteristics of this neuronic system, accelerating

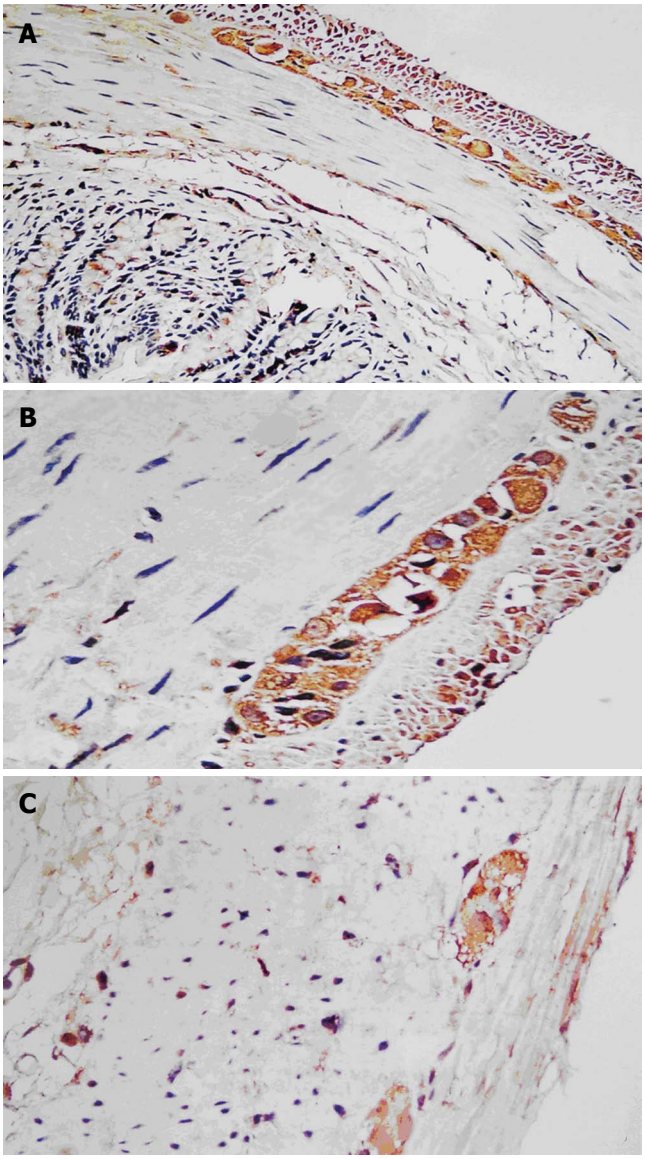

Figure 3 **A**: Expression of OFQ in the myenteric plexus of colon in control group. SP × 200; **B**: Strong positive expression of OFQ in colon of control group. SP × 400; **C**: Weaker positive expression of OFQ in colon of model group. SP × 400.

related researches of the gastrointestinal motility regulated by OFQ/ORL1 receptor system and promote the general comprehensivness of the opioid system. Thus, the model of rats with cathartic colon was established by feeding the rats with rhubarb for 3 months so as to illustrate the etiology of STC.

Our *in vitro* studies showed that OFQ induced contractions of colonic longitudinal muscle strips. In the proximal colon, OFQ (10^{-9}-10^{-6} mol/L) induced contractions in a dose-dependent manner (Figure 1). But the increase of tension in cathartic colon was lower than the control groups (Figure 2). The mechanisms underlying OFQ-induced contractions were further investigated in the proximal colon. To determine if OFQ activity was mediated by neural pathways or if it was a direct myogenic action, OFQ induced contractions were examined in the presence of TTX, it has been supposed that TTX can abolish neuronal transmitter transition[18]. In the presence of TTX, OFQ failed to evoke additional contractions, suggesting that action of OFQ is mediated by neural pathways. It was coincidental with the present study that OFQ was highly expressed in the myenteric plexus of the rat colon, but not in the muscle cells. The *in vitro*, inhibitory effects of OFQ on EFS-evoked muscle contractions has been reported for mouse vas deferens and guinea pig ileum[19]. EFS-evoked muscular contractions were significantly reduced by 50% in guinea pig ileum by OFQ (10^{-7} mol/L) and was significantly reduced in mouse vas deferens by OFQ. Thus, the mechanisms and sites of action of OFQ may differ among different regions of gastrointestinal tract and different species.

Our study *in vivo* showed that intravenous administration of OFQ (1 μg/kg) significantly increased muscle contractions in the proximal colon. These observations indicate that OFQ also stimulates colonic motility *in vivo*. The effects cannot be affected by classical antagonist, naloxone, but can be abolished in the presence of TTX, suggesting that the action of OFQ is nerve mediated. Currently, the physiological role of OFQ in colonic motility is unknown. However, Takahashi *et al*[20] in an *in vivo* study showed that intravenous administration of OFQ (3 pmol/kg to 3 nmol/L) significantly increased muscle contractions in the proximal colon. Furthermore, OFQ (1 nmol/L, subcutaneously) accelerated the colonic transit by promoting migrating colonic contractions in rats[21]. These observations also indicate that OFQ can stimulate colonic motility *in vivo*.

The immunoreactivity of OFQ in the myenteric plexus in the proximal region of the cathartic colon of rats decreased significantly compared with the control group. It has been suggested that OFQ prefered to be located in the stimulating motor neuron[22]. Colonic smooth muscle of cathartic colon showed low sensitivity to the stimulation of OFQ and this suggested it might becaused by the abnormal distribution of OFQ or the abnormalities of receptors, leading to the disorganization of dynamic and uncoordinated contractions.

In conclusion, OFQ seems to modulate the colonic transit independently from the classical opioid peptides[23]. We confirmed that OFQ is present in the gastrointestinal tract and has an effect on colonic motility. The physiological role of the nociceptin-QRL1 system in the colon is not clear but it may be significant to pathophysiological processes that underlie motor dysfunction of the bowel[24]. These findings indicate that OFQ is a brain-gut peptide and plays a role in the control of gastrointestinal functions[25]. The abnormalities of enteric nervous system are responsible for slow transit constipation. It also indicates that chronic application of stimulant laxatives can induce disorganization and damage the enteric nervous system[26,27] and accelerate the pathological changes of STC. But the pathophysiology of STC is complex and not easily approached through the data from animals alone. Further studies according to the clinical characteristics of STC patients could provide additional insight into this issue. It is necessary to investigate the mechanism underlying the biological actions of N/OFQ on GI. Because OFQ seems to exert

its stimulatory action in the colon[28,29], in the future, synthesized analogues of OFQ may be used to treat constipation secondary to colonic inertia[30].

REFERENCES

1 **Krammer H**, Schlieger F, Singer MV. [Therapeutic options of chronic constipation]. *Internist* (Berl) 2005; **46**: 1331-1338
2 **Bassotti G**, Villanacci V. Slow transit constipation: a functional disorder becomes an enteric neuropathy. *World J Gastroenterol* 2006; **12**: 4609-4613
3 **Liu BH**, Mo P, Zhang SB. Effects of mu and kappa opioid receptor agonists and antagonists on contraction of isolated colon strips of rats with cathartic colon. *World J Gastroenterol* 2004; **10**: 1672-1674
4 **Meunier JC**, Mollereau C, Toll L, Suaudeau C, Moisand C, Alvinerie P, Butour JL, Guillemot JC, Ferrara P, Monsarrat B. Isolation and structure of the endogenous agonist of opioid receptor-like ORL1 receptor. *Nature* 1995; **377**: 532-535
5 **Mollereau C**, Mouledous L. Tissue distribution of the opioid receptor-like (ORL1) receptor. *Peptides* 2000; **21**: 907-917
6 **Ciccocioppo R**, Economidou D, Fedeli A, Massi M. The nociceptin/orphanin FQ/NOP receptor system as a target for treatment of alcohol abuse: a review of recent work in alcohol-preferring rats. *Physiol Behav* 2003; **79**: 121-128
7 **Mamiya T**, Yamada K, Miyamoto Y, König N, Watanabe Y, Noda Y, Nabeshima T. Neuronal mechanism of nociceptin-induced modulation of learning and memory: involvement of N-methyl-D-aspartate receptors. *Mol Psychiatry* 2003; **8**: 752-765
8 **Mao L**, Wang JQ. Cardiovascular responses to microinjection of nociceptin and endomorphin-1 into the nucleus tractus solitarii in conscious rats. *Neuroscience* 2005; **132**: 1009-1015
9 **Mogil JS**, Pasternak GW. The molecular and behavioral pharmacology of the orphanin FQ/nociceptin peptide and receptor family. *Pharmacol Rev* 2001; **53**: 381-415
10 **Krowicki ZK**, Kapusta DR, Hornby PJ. Orphanin FQ/nociceptin and [Phe(1)Psi(CH(2)-NH)Gly(2)] nociceptin(1-13)-NH(2) stimulate gastric motor function in anaesthetized rats. *Br J Pharmacol* 2000; **130**: 1639-1645
11 **Broccardo M**, Guerrini R, Petrella C, Improta G. Gastrointestinal effects of intracerebroventricularly injected nociceptin/orphaninFQ in rats. *Peptides* 2004; **25**: 1013-1020
12 **Ishihara S**, Minowa S, Tsuchiya S, Horie S, Watanabe K, Murayama T. Gastric acid secretion stimulated by centrally injected nociceptin in urethane-anesthetized rats. *Eur J Pharmacol* 2002; **441**: 105-114
13 **Lippl F**, Schusdziarra V, Huepgens K, Allescher HD. Inhibitory effect of nociceptin on somatostatin secretion of the isolated perfused rat stomach. *Regul Pept* 2002; **107**: 37-42
14 **D'Agostino B**, Marrocco G, De Nardo M, Calò G, Guerrini R, Gallelli L, Advenier C, Rossi F. Activation of the nociceptin/orphanin FQ receptor reduces bronchoconstriction and microvascular leakage in a rabbit model of gastroesophageal reflux. *Br J Pharmacol* 2005; **144**: 813-820
15 **Bassotti G**, Villanacci V, Maurer CA, Fisogni S, Di Fabio F, Cadei M, Morelli A, Panagiotis T, Cathomas G, Salerni B. The role of glial cells and apoptosis of enteric neurones in the neuropathology of intractable slow transit constipation. *Gut* 2006; **55**: 41-46
16 **Mehendale SR**, Yuan CS. Opioid-induced gastrointestinal dysfunction. *Dig Dis* 2006; **24**: 105-112
17 **Grond S**, Meuser T, Pietruck C, Sablotzki A. [Nociceptin and the ORL1 receptor: pharmacology of a new opioid receptor]. *Anaesthesist* 2002; **51**: 996-1005
18 **Sakaba T**. Roles of the fast-releasing and the slowly releasing vesicles in synaptic transmission at the calyx of held. *J Neurosci* 2006; **26**: 5863-5871
19 **Zhang G**, Murray TF, Grandy DK. Orphanin FQ has an inhibitory effect on the guinea pig ileum and the mouse vas deferens. *Brain Res* 1997; **772**: 102-106
20 **Takahashi T**, Bagnol D, Schneider D, Mizuta Y, Ishiguchi T, LePard K, Galligan JJ, Watson SJ, Owyang C. Orphanin FQ causes contractions via inhibiting purinergic pathway in the rat colon. *Gastroenterology* 2000; **119**: 1054-1063
21 **Takahashi T**, Mizuta Y, Owyang C. Orphanin FQ, but not dynorphin A, accelerates colonic transit in rats. *Gastroenterology* 2000; **119**: 71-79
22 **O'Donnell AM**, Ellis LM, Riedl MS, Elde RP, Mawe GM. Distribution and chemical coding of orphanin FQ/nociceptin-immunoreactive neurons in the myenteric plexus of guinea pig intestines and sphincter of Oddi. *J Comp Neurol* 2001; **430**: 1-11
23 **Calo' G**, Guerrini R, Rizzi A, Salvadori S, Regoli D. Pharmacology of nociceptin and its receptor: a novel therapeutic target. *Br J Pharmacol* 2000; **129**: 1261-1283
24 **Osinski MA**, Brown DR. Orphanin FQ/nociceptin: a novel neuromodulator of gastrointestinal function? *Peptides* 2000; **21**: 999-1005
25 **Yazdani A**, Takahashi T, Bagnol D, Watson SJ, Owyang C. Functional significance of a newly discovered neuropeptide, orphanin FQ, in rat gastrointestinal motility. *Gastroenterology* 1999; **116**: 108-117
26 **Nadal SR**, Calore EE, Manzione CR, Puga FR, Perez NM. Effects of long-term administration of Senna occidentalis seeds in the large bowel of rats. *Pathol Res Pract* 2003; **199**: 733-737
27 **Kapur RP**. Neuropathology of paediatric chronic intestinal pseudo-obstruction and related animal models. *J Pathol* 2001; **194**: 277-288
28 **Abdelrahman AM**, Pang CC. Regional hemodynamic effects of nociceptin/orphanin FQ in the anesthetized rat. *Eur J Pharmacol* 2002; **450**: 263-266
29 **Tada H**, Nakagawa K, Yamamura T, Takahashi T. Antagonistic effects of CompB on orphanin FQ-induced colonic contractions in rats. *Eur J Pharmacol* 2002; **454**: 53-58
30 **Broccardo M**, Linari G, Guerrini R, Agostini S, Petrella C, Improta G. The effects of [Arg14, Lys15] nociceptin/orphanin FQ, a highly potent agonist of the NOP receptor, on *in vitro* and *in vivo* gastrointestinal functions. *Peptides* 2005; **26**: 1590-1597

S- Editor Liu Y **L- Editor** Ma JY **E- Editor** Ma WH

PO Box 2345, Beijing 100023, China
www.wjgnet.com
wjg@wjgnet.com

World J Gastroenterol 2007 January 7; 13(1): 146-151
World Journal of Gastroenterology ISSN 1007-9327

CLINICAL RESEARCH

Malignancy and mortality in a population-based cohort of patients with coeliac disease or 'gluten sensitivity'

LA Anderson, SA McMillan, RGP Watson, P Monaghan, AT Gavin, C Fox, LJ Murray

LA Anderson, P Monaghan, LJ Murray, Queen's University Belfast, Centre for Clinical and Population Sciences, Belfast, United Kingdom
SA McMillan, Royal Group of Hospitals, Regional Immunology Service, Belfast, United Kingdom
RGP Watson, Royal Group of Hospitals, Institute of Clinical Science, Belfast, United Kingdom.
AT Gavin, C Fox, Queen's University Belfast, Northern Ireland Cancer Registry, Belfast, United Kingdom
Supported by the Research and Development Office, Northern Ireland who funded Dr. Anderson to undertake the research through the Ireland-Northern Ireland-National Cancer Institute Cancer Consortium Cancer Prevention Fellowship Programme. The Northern Ireland Cancer Registry is funded by the Department of Health, Social Services & Public Safety Northern Ireland
Correspondence to: Dr. Lesley A Anderson, Centre for Clinical and Population Sciences, Mulhouse Building, Grosvenor Road, Belfast, BT12 6BJ, United Kingdom, l.anderson@qub.ac.uk
Telephone: +44-28-90632602 Fax: +44-28-90231907
Received: 2006-09-09 Accepted: 2006-10-23

Abstract

AIM: To determine the risk of malignancy and mortality in patients with a positive endomysial or anti-gliadin antibody test in Northern Ireland.

METHODS: A population-based retrospective cohort study design was used. Laboratory test results used in the diagnosis of coeliac disease were obtained from the Regional Immunology Laboratory, cancer statistics from the Northern Ireland Cancer Registry and mortality statistics from the General Registrar Office, Northern Ireland. Age standardized incidence ratios of malignant neoplasms and standardized mortality ratios of all-cause and cause-specific mortality were calculated.

RESULTS: A total of 13 338 people had an endomysial antibody and/or an anti-gliadin antibody test in Northern Ireland between 1993 and 1996. There were 490 patients who tested positive for endomysial antibodies and they were assumed to have coeliac disease. There were 1133 patients who tested positive for anti-gliadin antibodies and they were defined as gluten sensitive. Malignant neoplasms were not significantly associated with coeliac disease; however, all-cause mortality was significantly increased following diagnosis. The standardized incidence and mortality ratios for non-Hodgkin's lymphoma were increased in coeliac disease patients but did not reach statistical significance. Lung and breast cancer incidence were significantly lower and all-cause mortality, mortality from malignant neoplasms, non-Hodgkin's lymphoma and digestive system disorders were significantly higher in gluten sensitive patients compared to the Northern Ireland population.

CONCLUSION: Patients with coeliac disease or gluten sensitivity had higher mortality rates than the Northern Ireland population. This association persists more than one year after diagnosis in patients testing positive for anti-gliadin antibodies. Breast cancer is significantly reduced in the cohort of patients with gluten sensitivity.

Key words: Coeliac disease; Cancer; Mortality; Gluten sensitivity

Anderson LA, McMillan SA, Watson RGP, Monaghan P, Gavin AT, Fox C, Murray LJ. Malignancy and mortality in a population-based cohort of patients with coeliac disease or 'gluten sensitivity'. *World J Gastroenterol* 2007; 13(1): 146-151

http://www.wjgnet.com/1007-9327/13/146.asp

INTRODUCTION

Coeliac disease (CD) is an autoimmune disorder characterised by inflammation and villous atrophy of the small intestine, resulting in the malabsorption of vitamins and nutrients. It is caused by an immune response to wheat gluten (gliadin). Ireland is thought to have one of the highest incidences of CD in the world with a prevalence in Northern Ireland of at least 1 person per 122 in the population[1]. Diagnosis is normally confirmed by duodenal biopsy; however, highly sensitive and specific blood tests for CD are available including the transglutaminase antibody test (93% sensitive, > 99% specific) and the endomysial antibody (EMA) test (93% sensitive, > 98% specific)[2]. Another test the anti-gliadin antibody (AGA) test is not as sensitive or specific for CD. It is a measure of the immune response to gliadin and may detect people with gluten sensitivity who don't have clinically detectable CD. Patients testing positive for CD are advised to adhere to a strict gluten free diet for life[3,4] to avoid symptoms such as diarrhoea, anaemia and weight loss associated with this condition.

In addition to the significant morbidity that can be associated with this condition, CD is thought to be associated with an increased risk of malignancy and mortality. A recent European multi-centre study reported more than

a three-fold increased risk of non-Hodgkin's Lymphoma (NHL) in patients with clinically diagnosed CD[5]. Other studies have also reported an increased incidence and/or mortality of NHL in patients with CD[4,6-12]. Estimates of the standardised incidence ratio range from 3.3[5] to 18.0[10], although Card *et al*[7] suggest that the risk of NHL is at the lower end of these estimates.

CD has been associated with an increased risk of other cancers including cancers of the gastrointestinal tract[7-9,11], in particular cancers of the small intestine[7,9-11]. However, West *et al*[8] in a recent study including 4732 people with CD found that most cancers, except NHL, were reported within one year of diagnosis of CD.

Studies have also reported that CD may be associated with reduced risks of some cancers including breast cancer[8,11,13] although the reason for this association remains unknown. West *et al*[8] reported that lung cancer was less common in patients with CD with one possible explanation of the proposed protective effect of cigarette smoking[14].

Overall, mortality was higher in patients with CD compared to the population[8,10,15]. Metzger *et al*[15] reported a standardised mortality ratio (SMR) of all-cause mortality of 2.53 (95% CI 1.50-4.25) with an increased mortality from malignant neoplasms. West *et al*[8] observed that the association between all-cause mortality and CD remained significant more than one year after diagnosis.

The aim of this study was to identify the incidence of malignancy and mortality in patients with CD (positive EMA test) or patients with gluten sensitivity (positive AGA test) in a retrospective cohort study in Northern Ireland.

MATERIALS AND METHODS

Exposure measurement

A serological dataset of all patients investigated for suspected coeliac disease tested for IgA EMA and/or IgA AGA between 1993 and 1996 was obtained from the Regional Immunology Laboratory, Royal Group of Hospitals, Belfast. If patients had EMA/AGA tests on more than one occasion their date of inclusion in the study was the date of the first positive EMA or AGA result. Duplicates were removed and records with no date of birth excluded. Cases were defined as patients with 'coeliac disease' (positive EMA result) or 'patients with an intolerance to gliadin in the diet' (positive AGA, result more than 100×10^3 EU/L). No information was available on the EMA test results for 4585 patients who had an AGA test. These patients were excluded from the AGA positive, EMA negative analysis.

Outcome measurement - incidence

Researchers within the Northern Ireland Cancer Registry (NICR)-LAA, LJM, CF; who are experienced in the procedures involved in linking datasets, used forename, surname, date of birth and when available hospital number or General Practitioner name to match patients in the serological database to patients within the NICR database. EMA and AGA positive patients were followed-up for between 7 and 11 years until the end of December 2003. Exact and "fuzzy" matching algorithms were used to link patients in the two databases. "Fuzzy" matching used phonetic codes for the forename and surname to match similar sounding names which had different spellings (i.e. Smyth and Smith). If dates of birth were similar (i.e. 01/03/1975 and 03/01/1975) they were considered as potential matches. All "fuzzy" and potential matches were checked manually using all available information before being included in the study.

The main outcome measures were classified according to the International Classification of diseases (ICD) 9 before 2002 and ICD 10 thereafter: (1) Any malignant neoplasm (ICD 9: 140-208, 230-234; ICD 10: C00-C97); (2) NHL (ICD 9: 200, 202; ICD 10: C82-C85); (3) Gastrointestinal tract cancer (ICD 9: 150-154; ICD 10: C15-C21); (4) Small bowel cancer (ICD 9: 152; ICD 10: C17); (5) Lung cancer (ICD 9: 162-163; ICD 10: C34); (6) Breast cancer (ICD 9: 174-175; ICD 10: C50); (7) Prostate cancer (ICD 9: 185; ICD 10: C61); (8) Liver cancer (ICD 9: 155; ICD 10: C22).

Outcome measurement - mortality

The serological database was also linked by forename, surname and date of birth to death records held by the Registrar General's Office (GRO), Northern Ireland until the end of December 2003. These files contain cause-specific mortality data on all deaths occurring within Northern Ireland. Exact matching and "fuzzy" matching algorithms were used and potential matches were checked manually. Outcome measures included all-cause and cause-specific mortality. Ethical committee approval for this study was obtained from the Research Ethics Committee of the Queen's University Belfast to match the databases.

Statistical analysis

Total person-years of follow-up for the cohort of patients with a positive EMA test and for the cohort of patients with a positive AGA test were calculated by collating the person-years of follow-up for each patient from the date of entry into the cohort (1993 to 1996) until the date of death or 31st December 2003, whichever was earlier.

Indirect standardization was used to calculate standardised incidence ratios (SIRs) for all malignant neoplasms and for each cancer type (including NHL, gastrointestinal cancers, small bowel, breast, prostate, liver and lung cancer) for patients with a positive EMA test, for patients with a positive AGA test and for patients with a positive AGA test but a negative EMA test. The SIRs were calculated by taking the total number of observed cancers within the cohort of patients with a positive EMA or AGA test and dividing this by the expected number of cancers, calculated by applying age and sex-specific incidence rates within the Northern Ireland population to each cohort. CIs were estimated using the Poisson distribution. Standardised mortality ratios were calculated in a similar manner to the SIRs using all and cause-specific mortality figures obtained from the General Registrar Office, Northern Ireland.

RESULTS

Of the 13 338 patients in Northern Ireland who under-

Table 1 Number of EMA and AGA positive and negative patients

AGA	+ve EMA	-ve EMA	Not recorded	Total
+ve	275	456	402	1133
-ve	215	7807	4183	12 205
Total	490	8263	4585	13 338

Table 2 Standardised incidence ratio (SIR) of malignancies

	EMA +ve			AGA +ve			AGA +ve, EMA -ve		
	n	Expected *n*	SIR (95% CI)	*n*	Expected *n*	SIR (95% CI)	*n*	Expected *n*	SIR (95% CI)
All malignancies	24	25.41	0.94 (0.57-1.32)	96	86.13	1.11 (0.89-1.34)	68	37.28	1.82 (1.39-2.26)
All malignancies (> 6 mo after diagnosis)	20	24.26	0.82 (0.46-1.19)	75	86.05	0.87 (0.67-1.07)	52	39.84	1.31 (0.95-1.66)
All malignancies (> 12 mo after diagnosis)	18	24.24	0.74 (0.40-1.09)	67	85.94	0.78 (0.59-0.97)	44	37.15	1.18 (0.83-1.53)
Non-Hodgkin's lymphoma	2	0.27	7.47 (0.00-17.83)	6	2.59	2.32 (0.46-4.17)	3	0.52	5.76 (0.00-12.28)
Gastrointestinal cancer	4	2.97	1.35 (0.03-2.67)	14	11.70	1.20 (0.57-1.82)	9	5.24	1.72 (0.60-2.84)
Small intestine	1	0.04	23.33 (0.00-69.07)	1	0.14	7.28 (0.00-21.54)	1	0.06	15.51 (0.00-45.90)
Lung cancer	1	2.60	0.39 (0-1.14)	5	9.98	0.50 (0.06-0.94)	4	4.51	0.89 (0.02-1.76)
Breast cancer	4	3.92	1.02 (0.02-2.02)	5	10.53	0.47 (0.06-0.89)	1	4.09	0.24 (0.00-0.72)
Prostate cancer	2	1.12	1.78 (0.00-4.24)	8	6.30	1.27 (0.39-2.15)	3	3.13	0.96 (0.00-2.04)
Liver cancer	2	0.06	31.62 (0.00-75.45)	3	0.60	5.01 (0.00-10.69)	2	0.27	7.48 (0.00-17.86)

went EMA and/or AGA tests between 1993 and 1996 490 were EMA positive (5.6% of EMA tests), 1,133 AGA positive (8.5% of all AGA tests) and 456 patients were AGA positive and EMA negative (5.2% of those tested for both EMA and AGA) (Table 1).

The average age (age range) of patients with a positive EMA or AGA test were 45 (0-88) years and 50 (0-91) years respectively. Included in the database were 46 children (< 18 years) with a positive EMA test (9.2% of cohort) and 71 children with a positive AGA test (6.3% of cohort). In total 68.2% of EMA positives and 63.2% of AGA positives were male. The average AGA score in those testing positive was 215.4 × 10^3 EU/L (range 100-1163 × 10^3 EU/L).

Standardised incidence ratios-EMA

In total 24 (4.90%) of the EMA positive patients developed a malignant neoplasm during the follow-up period, 6 of which were diagnosed within 12 mo of the test. There were no significant associations between a positive EMA test and developing a malignant neoplasm (Table 2). Due to the small number of EMA positive patients developing malignancy the confidence intervals for the site specific cancers are large resulting in no significant associations despite a raised SIR being found for NHL [SIR 7.47 (95% CI 0.00-17.83)], small bowel cancer [SIR 23.33 (95% CI 0.00-69.07)] and primary liver cancer [SIR 31.62 (95% CI 0.00-75.45)]. Lung cancer appeared to be less common in EMA positive patients than in the Northern Ireland population [SIR 0.39 (95% CI 0-1.14)].

Standardised incidence ratios - AGA

In total 96 (8.47%) of the AGA positive population developed a malignant neoplasm. There were no significant associations between a positive AGA result and the development of malignant neoplasms (Table 2). However, malignancy was significantly raised in the AGA positive, EMA negative group [SIR 1.82 (95% CI 1.39-2.26)] (Table 2). This association was confined to males, SIR 2.90 (95% CI 2.11-3.69), and remained significant 6 and 12 mo after the AGA test, SIR 2.16 (95% CI 1.48-2.84) and SIR 1.91 (95% CI 1.27-2.55), respectively. Overall incidence of malignant neoplasms occurring 6 and 12 mo after the AGA test were significantly reduced in females SIR 0.60 (95% CI 0.27-0.92) and SIR 0.51 (95% CI 0.19-0.83) respectively. There was a significant inverse relationship between lung and breast cancer and a positive AGA result; however, only breast cancer was significantly reduced in the AGA positive EMA negative group. The SIR was raised for both small bowel and liver cancer but the results were not statistically significant.

Standardised mortality ratios - EMA

Overall mortality was significantly higher in the EMA positive population compared to the Northern Ireland population (Table 3). However, the statistically significant association did not remain when deaths within 6 mo or 1 year of the EMA test were excluded from the analysis. Although there were no other statistically significant association's mortality from NHL, endocrine deaths and urinary deaths appeared increased.

Standardised mortality ratios - AGA

Overall, mortality was higher in the AGA positive and in the AGA positive/EMA negative populations than in the Northern Ireland population (Table 3). This association

Table 3 Standardised mortality ratios (SMR) of all cause and cause-specific mortality

	EMA +ve			AGA +ve			AGA +ve, EMA -ve		
	n	Expected *n*	SMR (95% CI)	*n*	Expected *n*	SMR (95% CI)	*n*	Expected *n*	SMR (95% CI)
All cause mortality	46	26.01	1.77 (1.26-2.28)	234	101.25	2.31 (2.01-2.61)	114	47.25	2.41 (1.97-2.86)
All cause mortality (> 6 mo after diagnosis)	35	25.9	1.35 (0.90-1.80)	184	100.79	1.83 (1.56-2.09)	85	46.91	1.81 (1.43-2.20)
All cause mortality (> 12 mo after diagnosis)	32	25.91	1.24 (0.81-1.66)	165	100.09	1.65 (1.40-1.90)	75	46.59	1.61 (1.25-1.97)
Malignant neoplasms	9	7.05	1.28 (0.44-2.11)	52	32.28	1.61 (1.17-2.05)	27	14.55	1.86 (1.16-2.56)
NHL deaths	2	0.29	6.89 (0.00-16.44)	8	1.12	7.12 (2.18-12.05)	3	0.51	5.88 (0.00-12.53)
Endocrine deaths	1	0.16	6.10 (0.00-18.07)	2	0.24	8.19 (0.00-19.53)	1	0.58	1.73 (0.00-5.14)
Nervous system	1	0.25	3.96 (0.00-11.72)	2	2.92	0.69 (0.00-1.63)	1	2.92	0.34 (0.00-1.01)
Circulatory system	9	12.11	0.74 (0.26-1.23)	42	59.95	0.70 (0.49-0.91)	22	28.65	0.77 (0.45-1.09)
Respiratory system	3	2.67	1.12 (0.00-2.40)	35	25.18	1.39 (0.93-1.85)	2	1.45	1.38 (0.00-3.29)
Digestive system disorders	2	0.58	3.42 (0.00-8.17)	19	4.12	4.61 (2.54-6.68)	10	1.90	5.26 (2.00-8.52)

remained significant even when deaths occurring within 6 mo and one year of the test were excluded. Mortality caused by malignant neoplasms was also significantly raised in both groups as was mortality from digestive system disorders. Mortality from NHL was significantly higher and mortality from circulatory system disease was significantly lower in the AGA positive group but not in the AGA positive/EMA negative group.

DISCUSSION

In this retrospective cohort study the incidence of malignant neoplasms in patients with CD (positive EMA test) was similar to that of the Northern Ireland population. However, patients with gluten sensitivity (positive AGA test) had an increased incidence of malignant neoplasms within six months of diagnosis. In keeping with the findings of other studies all cause mortality was significantly raised in patients with CD; however, this was limited to the six month period following diagnosis. Patients with gluten sensitivity had a significantly raised SMR; this association remained significant more than 12 mo after diagnosis. Compared to the general population breast and lung cancer incidence were significantly lower in patients with gluten sensitivity. Mortality from malignant neoplasms, NHL and digestive system disorders was significantly increased.

The main strength of this study is its population-based design. All patients within Northern Ireland with clinical symptoms suspicious of CD and who also had a positive EMA and/or AGA test during the study period (1993 to 1996) were included. Since a wide spectrum of patients were included in the study the results should be more generalisable to patients with gluten sensitivity than the results of studies where CD was diagnosed in hospital or at referral centres[9-11,16,17]. It is likely that cases diagnosed as hospital in-patients or at referral centres have more severe disease and therefore cancer incidence and mortality may be higher in this group of patients than in all CD patients. CD may go undetected in the population and without screening it is difficult to generalise any of the results to all patients with CD within the population.

Population-based registers of cancer incidence and cause-specific mortality facilitated the matching process. Incomplete matching of patients on the serological database to the NICR and/or GRO database may result in an underestimation of the risk of malignancy and/or mortality compared to the general population. To minimize the possibility of observer bias the staff was blinded to the positive/negative result status of the patients during the matching process. Cancer incidence and mortality in EMA positive, AGA positive and AGA positive/EMA negative patients were compared to the rates in the Northern Ireland population. Other studies have used population-based controls[8] or population rates for comparison[7,10-12]; however, the study by Collin *et al*[17] used hospital outpatients undergoing upper gastrointestinal endoscopy as controls. These patients are likely to have been under investigation because of upper gastrointestinal symptoms and are unlikely to be representative of the general population. One of the proposed explanations for previous reports of increased gastrointestinal cancer incidence in CD patients[7-9,11] is that CD was diagnosed coincidentally when the patients were under investigation for tumour related symptoms. Several studies have reported cancer incidence and/or mortality rates with lag periods of between 1 and 5 years[7,10-12,16] after diagnosis of CD. We, therefore, included SIRs and SMRs excluding patients with an event in the 6-or 12-mo period post diagnosis.

There were 3908 person years of follow-up for malignancy and 3718 person years of follow-up for mortality in the cohort of patients with CD. Bias may have been introduced by loss to follow-up although emigration rates are low in Northern Ireland; data from the GRO (Northern Ireland) estimates that less than 0.1% of the population migrated from the province per year during the 1990s[18]. One of the potential weaknesses of this study was the lack of histological confirmation of CD. Although it is likely that jejunal biopsies were taken from patients with a positive EMA test gaining access to these records without patient consent would have required further ethical considerations. However, the sensitivity and specificity of the EMA test are high[2] and it is, therefore, likely to give a relatively accurate measure of the incidence of CD in the

cohort. The EMA test detects antibodies to an antigen (tissue transglutaminase) present in the endomysial lining of smooth muscle cells. The AGA test measures antibodies to gliadin which do not remain in patients who adhere to a strict gluten free diet. The assay will become negative if the patient is compliant with a gluten free diet. Therefore some patients with CD may not be detected within the cohort. The study by Logan *et al*[13] showed that cancer incidence was decreased in those who were diagnosed early and placed on a gluten-free diet. If this is the case then the incidence of malignancy in CD patients may be lower than reported. However, we had no way to determine whether or not the patients included in the study adhered to a strict gluten-free diet.

Another issue is that multiple comparisons may inflate the possibility of a Type 1 error occurring (i.e. the apparent association resulting by chance). However, only malignant neoplasms/causes of mortality where there had been a previous association or where there was an a priori hypothesis were investigated.

One issue with using these datasets and using a retrospective cohort design is that potential confounding variables were not collected at the time the cohort was established and therefore these could not be adjusted for in the analyses. Potential confounding variables could include co-existing medical conditions, smoking, body mass index, diet, age, sex, *etc*. For example, diabetes is associated with CD and possibly with endocrine deaths which were non-significantly raised and smoking which is less common in patients with CD[14] is associated with lung cancer incidence. There was a significantly reduced risk of lung cancer in patients with a positive AGA test and a non-significant reduced risk in patients with a positive EMA test. West *et al*[8] was the only study to attempt to adjust for potential confounding variables. Adjusting for BMI and smoking did not dramatically alter the observed associations; however, the authors suggest that data on potential confounders may be incomplete as it was obtained from routinely collected information.

Although some AGA positive/EMA negative patients may have CD there were a larger number that were AGA positive than expected according to the sensitivity of the EMA test. Therefore, some of these patients may be gluten sensitive but as yet have no damage to the endomycial muscle. If this is the case then this is the first study to investigate the risk of malignancy and mortality in this group of patients, who were excluded from the recent large study by West *et al*[8]. Mortality was significantly increased in this group of patients and remained elevated more than one year after the positive AGA test. Mortality from digestive system disorders was increased which was not surprising as a positive AGA test may be a marker for other gastrointestinal disorders. Interestingly, it is in this group of patients that breast cancer appears to be reduced. Other studies have reported reduced risks of breast cancer in patients with CD[8,11,13] although there were no significant associations between breast cancer and a positive EMA test in this study. Although the reason(s) for this association remain unknown Askling *et al*[11] suggest that the reduced risk of breast cancer may be a consequence of immune system dysfunction.

The size of the current study is smaller than the more recently published studies e.g. the study by West *et al*[8] who used the General Practice Research Database which had 4,732 CD patients. Malignancy was increased in patients in the first year after diagnosis but not beyond one year of follow-up. In the current study malignancy was not increased in patients with a positive EMA test but was in patients with a positive AGA test. Other studies have also reported no overall increased risk of malignancy in CD patients[7,16]. The size of the current study meant that there was insufficient power to detect any associations between cancer type and CD. However, the risk of NHL appeared to be increased which is in keeping with the results of other studies[3-5,7-12]. There was a significant increased risk of NHL deaths in patients with a positive AGA test. This group of patients is likely to include some patients with CD as there were a number of patients that had no EMA record in the database.

Malignancy and mortality were not significantly increased in patients with CD more than one year after diagnosis; however, overall mortality and mortality from malignant neoplasms were increased in patients who were gluten sensitive with a negative EMA test. If these patients do not have the histological characteristics of CD then it is important to determine the cause of the increased mortality. If this is limited to other digestive system disorders then patients with a negative EMA test but with symptoms should be further investigated for other digestive system disorders. Further investigations into this area are warranted to determine if it is gluten sensitivity that is associated with increased mortality and malignancy or to determine if it is just a marker for other gastrointestinal conditions.

In addition, it is important to determine the risk of malignancy and mortality in patients with a histological confirmation of CD. This study could be extended further by collecting pathology reports on all patients within the study and looking for evidence of villous atrophy. Information on confounding variables such as smoking status could also be collected. However, it is unlikely that patients could be approached because of data confidentiality issues. It is possible that cancer incidence and mortality change depending on the length of time since diagnosis. Therefore, an extension to this study would be to follow-up the patients for a longer period of time. The association with reduced breast cancer incidence is interesting and further studies to investigate this association may identify factors that are associated with reduced breast cancer incidence.

REFERENCES

1 **Johnston SD**, Watson RG, McMillan SA, Sloan J, Love AH. Prevalence of coeliac disease in Northern Ireland. *Lancet* 1997; **350**: 1370

2 **Lewis NR**, Scott BB. Systematic review: the use of serology to exclude or diagnose coeliac disease (a comparison of the endomysial and tissue transglutaminase antibody tests). *Aliment Pharmacol Ther* 2006; **24**: 47-54

3 **Holmes GK**, Prior P, Lane MR, Pope D, Allan RN. Malignancy in coeliac disease--effect of a gluten free diet. *Gut* 1989; **30**: 333-338

4 **Loftus CG**, Loftus EV. Cancer risk in celiac disease. *Gastroenterology* 2002; **123**: 1726-1729
5 **Mearin ML**, Catassi C, Brousse N, Brand R, Collin P, Fabiani E, Schweizer JJ, Abuzakouk M, Szajewska H, Hallert C, Farré Masip C, Holmes GK. European multi-centre study on coeliac disease and non-Hodgkin lymphoma. *Eur J Gastroenterol Hepatol* 2006; **18**: 187-194
6 **Smedby KE**, Akerman M, Hildebrand H, Glimelius B, Ekbom A, Askling J. Malignant lymphomas in coeliac disease: evidence of increased risks for lymphoma types other than enteropathy-type T cell lymphoma. *Gut* 2005; **54**: 54-59
7 **Card TR**, West J, Holmes GK. Risk of malignancy in diagnosed coeliac disease: a 24-year prospective, population-based, cohort study. *Aliment Pharmacol Ther* 2004; **20**: 769-775
8 **West J**, Logan RF, Smith CJ, Hubbard RB, Card TR. Malignancy and mortality in people with coeliac disease: population based cohort study. *BMJ* 2004; **329**: 716-719
9 **Green PH**, Fleischauer AT, Bhagat G, Goyal R, Jabri B, Neugut AI. Risk of malignancy in patients with celiac disease. *Am J Med* 2003; **115**: 191-195
10 **Peters U**, Askling J, Gridley G, Ekbom A, Linet M. Causes of death in patients with celiac disease in a population-based Swedish cohort. *Arch Intern Med* 2003; **163**: 1566-1572
11 **Askling J**, Linet M, Gridley G, Halstensen TS, Ekström K, Ekbom A. Cancer incidence in a population-based cohort of individuals hospitalized with celiac disease or dermatitis herpetiformis. *Gastroenterology* 2002; **123**: 1428-1435
12 **Corrao G**, Corazza GR, Bagnardi V, Brusco G, Ciacci C, Cottone M, Sategna Guidetti C, Usai P, Cesari P, Pelli MA, Loperfido S, Volta U, Calabró A, Certo M. Mortality in patients with coeliac disease and their relatives: a cohort study. *Lancet* 2001; **358**: 356-361
13 **Logan RF**, Rifkind EA, Turner ID, Ferguson A. Mortality in celiac disease. *Gastroenterology* 1989; **97**: 265-271
14 **Suman S**, Williams EJ, Thomas PW, Surgenor SL, Snook JA. Is the risk of adult coeliac disease causally related to cigarette exposure? *Eur J Gastroenterol Hepatol* 2003; **15**: 995-1000
15 **Metzger MH**, Heier M, Mäki M, Bravi E, Schneider A, Löwel H, Illig T, Schuppan D, Wichmann HE. Mortality excess in individuals with elevated IgA anti-transglutaminase antibodies: the KORA/MONICA Augsburg cohort study 1989-1998. *Eur J Epidemiol* 2006; **21**: 359-365
16 **Viljamaa M**, Kaukinen K, Pukkala E, Hervonen K, Reunala T, Collin P. Malignancies and mortality in patients with coeliac disease and dermatitis herpetiformis: 30-year population-based study. *Dig Liver Dis* 2006; **38**: 374-380
17 **Collin P**, Reunala T, Pukkala E, Laippala P, Keyriläinen O, Pasternack A. Coeliac disease--associated disorders and survival. *Gut* 1994; **35**: 1215-1218
18 **Northern Ireland Statistics and Research Agency**. Northern Ireland Migration Flows 1991-2005. Population statistics online, cited 2006-18-08. Available from: URL: http://www.nisra.gov.uk/archive/demography/population/net_migration_by_ageandsex05.xls

S- Editor Yang XX **L- Editor** Rippe RA **E- Editor** Liu WF

PO Box 2345, Beijing 100023, China
www.wjgnet.com
wjg@wjgnet.com

World J Gastroenterol 2007 January 7; 13(1): 152-157
World Journal of Gastroenterology ISSN 1007-9327

RAPID COMMUNICATION

Age-related histomorphologic changes in the canine gastrointestinal tract: A histologic and immunohistologic study

Berit Baum, Felix Meneses, Sven Kleinschmidt, Ingo Nolte, Marion Hewicker-Trautwein

Berit Baum, Sven Kleinschmidt, Marion Hewicker-Trautwein, Department of Pathology, University of Veterinary Medicine, Hannover, Germany
Felix Meneses, Ingo Nolte, Clinic for Small Animals, University of Veterinary Medicine, Hannover, Germany
Supported by the German Research Council (He 1548/4-2)
Correspondence to: Dr. Marion Hewicker-Trautwein, Professor, Department of Pathology, University of Veterinary Medicine, Buenteweg 17, Hannover D-30559, Germany. marion.hewicker-trautwein@tiho-hannover.de
Telephone: +49-511-9538630 Fax: +49-511-9538675
Received: 2006-09-06 Accepted: 2006-12-07

Abstract

AIM: To examine the changes in the histomorphology of the gastric, jejunal and colonic wall of dogs due to physiological aging.

METHODS: Full thickness biopsies were taken from the gastrointestinal tracts of 28 dogs of different ages. The thickness of the different layers of the wall was measured and the numbers of proliferating cells as indicated by immunohistochemical detection of Ki67 were counted.

RESULTS: In the three excision sites, the thickness of all subepithelial layers increased with rising age. The strongest correlation between age and thickness of the intestinal wall was found in the first 10 years of life and in the jejunum (r = 0.6-0.71 for the deep lamina propria mucosa, the muscularis mucosa, and the circular layer of the tunica muscularis). The number of proliferating cells decreased during aging, with the strongest correlation in the lamina propria mucosa and lamina muscularis mucosa of the jejunum and in the colonic submucosa (r = -0.61 to -0.71). Epithelial proliferation was only weakly correlated to the age.

CONCLUSION: The morphology of the deeper layers and the proliferation of mesenchymal cells of the intestinal wall of healthy dogs are correlated with age. Gastrointestinal epithelial proliferation is only weakly age-correlated.

Key words: Age; Canine; Intestine; Ki67; Stomach

Baum B, Meneses F, Kleinschmidt S, Nolte I, Hewicker-Trautwein M. Age-related histomorphologic changes in the canine gastrointestinal tract: A histologic and immunohistologic study. *World J Gastroenterol* 2007; 13(1): 152-157

http://www.wjgnet.com/1007-9327/13/152.asp

INTRODUCTION

Canine models are well known in the development of gastrointestinal drugs. On the other hand, an increasing number of biopsy samples are taken from the intestines of pet dogs with gastrointestinal symptoms and delivered to pathological diagnostic institutions for evaluation. Lesions, usually found in those specimens, however, are in most cases quantitative aberrations of normal morphology and cellular distribution rather than of a distinct qualitative kind. So a correct diagnosis is largely dependent on the experience of the examiner and the differentiation between physiological and pathological influences on the morphology. Data on the histological changes in the intestinal morphology in dependence on physiological processes, however, are very sparse. Suckling puppies exhibit rapid changes in the mucosal morphology that reach a comparatively stable state by the 42nd d of life[1]. In old dogs, Lafora body-like polyglucosan bodies have been described in the smooth musculature[2] and amyloid in the vessel walls of the large and small intestine without functional or neurological abnormalities[3]. Because of the usage of endoscopic biopsies, however, most examinations are limited to the mucosa[4]. The aim of this study was to characterize morphological alterations during the physiological course of aging including the different layers of the intestinal and gastric wall of dogs.

MATERIALS AND METHODS

Subjects

Tissue samples were obtained from 28 dogs of different age and breed (Table 1), which were patients of the Small Animal Clinic and were euthanatized for diseases unrelated to the gastrointestinal tract. Under general anesthesia, full thickness biopsies of the gastric, jejunal and colonic wall were surgically excised and immediately fixed in 100 mL/L

Table 1 Distribution of age, gender and breed

Age (yr)	Gender	Breed
0.25	M	Collie
0.5	M	Boxer
0.75	F	Rottweiler
0.75	M	West Highland White Terrier
2	F	Newfoundland
3	M	American Canadian White Shepard
3	M	Doberman-Pinscher
5	M	Fox Terrier
5	M	Mongrel
6	M	Pommeranian
6	F	German Shepherd Dog
7	M	Bernese Mountain Dog
7	F	Schnauzer
7	F	Caucasian Shepherd
7	F	Rottweiler
8	M	Mongrel
8	M	German Shorthaired Pointer
8.5	F	Mongrel
9	F	Mongrel
10	M	Mongrel
12	F	English Setter
12	M	Mongrel
12	M	Gordon Setter
13	F	Hovawart
13	F	Mongrel
14	F	Mongrel
14	F	Rottweiler
17	F	Mongrel

M: Male; F: Female.

neutral formalin. After fixation, the samples were routinely embedded in paraffin, cut, and stained with hematoxylin and eosin.

Evaluation of slides

All measurements were performed in a blind fashion, i.e., without knowledge of the animals' age. Distances and structural measurements were performed using a computer sustained manual system (ASM 68k), in which a line was projected into the microscopic ocular, that could be manually adjusted to the outlines of the respective structure to be determined. The resulting length of the line was calculated by the supporting computer system.

The following parameters were determined: in the stomach, depth of foveolae (epithelial length from the surface to the isthmus), length of whole gastric glands (epithelial length from the surface to the base of the gland), estimated percentage of chief cells and parietal cells in the pars principalis, number of fiber layers between the gland base and the lamina muscularis mucosa, thickness of the lamina muscularis mucosa, submucosa, and, because of the inconsistent orientation and borders of the single muscle layers in the stomach, of the tunica muscularis as a whole (Table 2); in the jejunum, villus length (length from the tip following the central lymphatic vessel to the crypt mouth), villus mid and base width (shortest distance from epithelial surface to epithelial surface in the middle of the villus and at the crypt mouth, respectively), crypt depth (length from the crypt mouth to the crypt base following the crypt lumen), thickness of the stratum compactum (distance between crypt base and lamina muscularis mucosa), lamina muscularis mucosa, submucosa, circular and longitudinal layer of the tunica muscularis mucosae (Table 3); in the colon, crypt depth, thickness of the lamina muscularis mucosa, submucosa, circular and longitudinal layer of the tunica muscularis mucosa (Table 4). All measurements were performed at four points of a well oriented section, which were equally distributed over its total length.

Table 2 Absolute values in the stomach

Age (yr)	Depth of foveolae (μm)	Glandular length (μm)	Chief cells (%)	Fibre layers (*n*)	Muscularis mucosa (μm)	Submucosa (μm)	Tunica muscularis (μm)
0.5	210	952	40	6	89.8	60	2076
0.75	226	1073	40	3	99.3	1157	2341
0.75	146	1076	60	4	146.8	365	1746
2	152	1249	70	6	133.0	866	2526
3	155	795	50	11	96.8		
3	228	1052	0	4	212.5	341	1600
5	169	942	70	4	142.3	867	2221
5	198	1013	60	5	96.5	972	1652
7	139	1012	40	3	140.0	869	3140
8	204	927	70	2	192.8	524	1488
8	141	774	30	7	136.8	653	2684
8	219	1074	30	4	154.8	169	968
9	167	986	60	4	249.0	551	2974
10	220	1146	40	6	122.8	1075	2337
12	245	1017	50	9	178.8	3501	2875
12	166	1165	40	5	112.8		
12	230	1059	70	6	121.3	1102	2191
14	189	795	20	12	154.5	1250	1205
17	294	815	20	6	120.5	694	2038

Immunohistochemical assay

In the jejunum and colon, where the most obvious changes in the thickness of wall layers were found, immunohistochemical detection of Ki67 was carried out to determine the proliferative index. The immunohistochemical reaction was performed as follows: Paraffin-embedded sections were dewaxed and treated with 50 mL/L H_2O_2 in ethanol for 30 min to inhibit endogenous peroxidase, followed by rinsing three times in phosphate-buffered saline (PBS). Antigen-retrieval was achieved by microwave treatment (20 min, 0.01 mol/L citrate buffer, pH 6). After demasking, the slides were incubated overnight with the first antibody (MIB-1, DAKOCytomation, Glostrup, Denmark) diluted 1:100 in PBS with 10 g/L bovine serum albumin. Binding of primary antibody was detected with a biotinylated second antibody (goat anti-mouse, diluted 1:200 in PBS) and the ABC-reagent (both Vector Laboratories, Burlingame, USA) according to the manufacturer's instructions using diaminobenzidine as chromogen. Finally, the slides were counterstained with hematoxylin. Negative control was performed with an identical procedure without the first antibody in the PBS/serum incubation step. An internal

Table 3 Absolute values in the jejunum (μm)

Age (yr)	Villus length	Crypt depth	Stratum compactum	Muscularis mucosa	Submucosa	Circular tunica muscularis	Longitudinal tunica muscularis
0.25	572	448	17	58	92	443	254
0.5	622	354	30.75	52	327	573	387
0.75	981	1051	24.25	82	273	729	478
0.75	570	269	35	56	193	519	304
2	536	435	39.75	88	161	542	182
5	894	412	67.25	67	229	764	368
5	882	303	37.75	62	183	658	338
6	867	406	62.75	68	217	585	249
7	589	623	45	73	176	602	346
7	906	466	32.25	99	228	766	454
7	630	381	56.25	106	292	639	418
8	596	333	87.25	162	232	802	285
12	647	314	108.25	150	294	1152	446
12	653	426	46.75	59	161	579	334
13	703	506	73	112	364	1047	217
13	709	344	53.4	146	339	672	290
14	726	475	44.75	89	267	793	370
14	700	514	104.2	136	233	971	535
17	695	403	40.5	75	309	693	304

Table 4 Absolute values in the colon (μm)

Age (yr)	Crypt length	Muscularis mucosa	Submucosa	Circular tunica muscularis	Longitudinal tunica muscularis
0.25	520	41.3	122	387	1235
0.5	530	40.3	165	454	707
0.75	488	60.0	203	338	537
0.75	515	52.8	133	540	530
2	515	56.3	362	541	562
5	609	54.0	388	557	968
5	577	82.3	349	792	682
6	533	48.3	531	728	701
6	363	51.0	375	449	855
7	716	77.7	299	617	1307
7	443	63.0	165	534	586
7	404	38.1	146	519	553
8.5	343	73.0	162	812	787
10	567	44.5	223	734	1034
12	485	40.5	462	510	568
12	460	59.5	372	641	810
13	399	45.5	191	776	1780
13	612	72.5	201	810	981
14	481	37.8	1397	784	575
17	607	48	315	607	359

positive control for the proliferation marker was present in all sections in the epithelial renewal zone of crypts and gastric pits.

Evaluation of Ki67-positive cells

In the jejunum and colon, the number of Ki67-positive cells (i.e. proliferating cells) was examined for the epithelia. Myocytes, myofibrocytes and fibrocytes could not be properly differentiated by morphological means in the immunohistochemically stained slides. For this reason, the number of proliferating cells per area comprises all cells of the lamina propria mucosa, lamina muscularis mucosa, submucosa, circular and longitudinal layer of the tunica muscularis, except round cells, especially leucocytes. All epithelial cells of approximately the lower 40% of the crypts stained positive for Ki67. Hence, comparison was made between the relative and absolute length of this compartment of the crypts. For the other layers, the absolute numbers of positive cells were counted in one whole section and set in relation to the total area of this layer in the respective section (Tables 5 and 6).

Statistical analysis

Values were checked for normal distribution. r is the Pearson product moment correlation coefficient as calculated by OpenOffice.org Calc.

RESULTS

General considerations

In the examined sections, no qualitative changes, such as scars or amyloid deposits, were found irrespective of the age of the dogs.

Stomach: In the fundic mucosa, only minor changes could be noted with increasing age. A tendency towards a relatively increased depth of foveolae could be noted and the lamina muscularis mucosa became thicker (Table 7). The relationship between age and lamina muscularis mucosa thickness was highest in dogs younger than 10 years (n = 14).

Jejunum: The mean thickness of all layers of the jejunum increased in size during aging (data not shown). The most significant changes were detected in the deeper layers of the intestinal wall during the first 10 years of life (n = 12), most obviously in the deepest part of the mucosal lamina propria in the jejunum. The distance between the crypt base and the lamina muscularis mucosa showed a strong correlation with the age of the examined dogs (Table 8). While villus length and crypt depth did not show any clear relationship with the age, the whole mucosal thickness increased with aging, mainly in the first 10 years of life. In the lamina muscularis mucosa, submucosa and circular layer of the tunica muscularis, the thickness also increased with age. In addition, in the lamina muscularis mucosa and circular layer, these changes displayed a stronger relationship in dogs less than 10 years. The longitudinal layer of the tunica muscularis did not show age-related changes.

Colon: The circular layer of the tunica muscularis displayed an age-related increase (Table 9). In contrast to the findings in the jejunum, only weak correlations between age and the thickness of the other mucosal or submucosal layers could be found.

Immunohistochemistry

Jejunum: In all layers of the intestinal wall, the numbers of proliferating cells were highest in young dogs, particularly those less than 3 years (data not shown). A

Table 5 Proliferation in the jejunum

Age (yr)	Proliferative length epithelium		Proliferating cells (*n*)					
	Absolute (μm)	Relative (%)	Villous lamina propria (/villus)	Intercrypt lamina propria (/intercrypt space)	Lamina propria below crypts	Muscularis mucosa (/mm length)	Submucosa (/mm length)	Tunica muscularis (/mm length)
0.25	296.4	69.3	4.57	0.77	22.62	8.25	6.25	1.28
0.5	179.2	75.2	25.21	2.16	35.50	10.50	1.34	0.37
0.75	278.4	61.5	3.79	1.22	14.39	5.19	2.99	0.58
0.75	1006.4	77.0	1.23	0.43	31.07	0.00	0.00	0.06
2	151.2	47.6	1.11	0.29	2.89	0.00	0.00	0.00
5	277.6	70.3	7.48	1.16	5.56	4.17	1.64	0.33
5	314.4	73.1	9.53	0.68	17.84	1.66	1.14	0.21
6	243.8	76.8	3.24	0.00	1.06	0.98	0.00	0.24
7	378.6	71.6	2.25	0.24	8.82	0.96	0.00	0.00
7	388.0	73.2	1.61	0.47	4.66	1.49	0.18	0.00
7	412.4	70.3	7.81	0.00	4.04	0.00	1.04	0.20
8	219.6	57.7	2.89	0.00	2.86	0.39	0.00	0.00
12	139.0	60.8	4.43	0.31	13.20	0.00	0.00	0.00
12	358.0	77.6	6.78	1.33	15.14	0.00	1.65	0.20
13	231.6	77.4	16.18	1.03	19.14	0.91	0.26	0.93
13	291.4	66.8	1.38	0.00	0.00	0.00	0.00	0.00
14	335.2	73.0	2.42	0.29	1.67	0.64	1.12	0.31
14	369.4	77.1	15.55	0.75	15.04	2.70	0.18	0.09
17	248.0	65.8	0.81	0.23	2.65	0.00	0.00	0.00

Table 6 Proliferation in the colon

Age (yr)	Proliferative length epithelium		Proliferating cells (*n*)				
	Absolute (μm)	Relative (%)	Intercrypt lamina propria (/intercrypt space)	Lamina propria below crypts	Muscularis mucosa (/mm length)	Submucosa (/mm length)	Tunica muscularis (/mm length)
0.25	147.4	28.8	2.117	1.59	32.07	5.21	1.33
0.5	179.0	32.2	0.943	1.67	9.20	2.63	0.12
0.75	90.2	20.3	0.388	0.36	0.98	0.78	0.04
0.75	217.8	39.4	2.048	0.79	1.64	1.21	0.09
2	129.8	27.8	0.194	0.28	0.00	0.39	0.00
5	192.0	32.9	2.251	0.89	3.02	1.14	0.17
5	219.5	36.9	0.657	0.71	2.63	0.37	0.11
6	189.2	56.4	0.276	0.11	1.05	0.43	0.59
6	194.4	37.4	0.563	0.33	1.35	0.62	0.10
7	118.4	29.8	0.248	0.00	0.00	0.40	0.00
7	158.0	31.8	0.226	0.18	0.00	1.12	0.05
7	215.8	33.3	0.838	0.63	2.01	0.52	0.00
8.5	150.0	37.1	0.583	0.24	1.12	0.00	0.05
10	132.8	26.1	1.059	1.60	3.18	0.21	0.04
12	151.8	32.8	1.031	1.49	6.13	0.27	0.16
12	173.4	33.9	0.6519	0.55	1.84	0.29	0.00
13	132.8	26.1	0.000	0.33	1.79	0.85	0.20
13	163.6	25.5	0.817	0.29	0.66	0.24	0.02
14	138.2	30.9	0.831	0.37	3.27	0.00	0.00
17	234.0	39.4	0.329	0.40	0.00	0.18	0.00

marked correlation between age and number of Ki67-positive cells could be found in dogs younger than 10 years (n = 12) for the lamina propria between crypts and between lamina muscularis mucosa and crypt base, for the lamina muscularis mucosa, for the submucosa and for the tunica muscularis (Table 9). Including the older dogs (> 10 years), correlation between age and thickness of the lamina muscularis mucosa remained strong. In contrast to the mesenchymal tissues, no clear correlation could be detected between age and epithelial proliferation.

Colon: As in the jejunum, the number of proliferating cells decreased with age. The strongest correlations were found, again, until the age of 10 (n = 13). In particular, the thickness of the lamina propria between crypt base and lamina muscularis mucosa, of the lamina muscularis mucosa and of the submucosa revealed a strong age-

Table 7 Strength of correlation between age and diameter of different layers in the stomach wall of dogs

	All ages	< 10 yr
Absolute foveolar depth	0.44	0.05
Relative foveolar depth	0.54	0.11
Lamina muscularis mucosa	0.17	0.58
Submucosa	0.35	0.17
Tunica muscularis	-0.04	0.01

Table 8 Strength of correlation between age and diameter of different layers in the jejunal wall of dogs

	All ages	< 10 yr
Villus length	-0.01	0.17
Crypt depth	-0.15	-0.2
Whole mucosa	0.5	0.1
Lamina propria	0.54	0.72
Lamina muscularis mucosa	0.51	0.61
Submucosa	0.46	0.13
Circular muscle layer	0.59	0.6
Longitudinal muscle layer	0.12	0.12

Table 9 Strength of correlation between age and diameter of different layers in the colonic wall of dogs

	All ages	< 10 yr
Crypt depth	0.01	-0.21
Lamina muscularis mucosa	-0.05	0.42
Submucosa	0.38	0.27
Circular muscle layer	0.61	0.63
Longitudinal muscle layer	0.2	0.17

Table 10 Strength of correlation between age and number of proliferating cells in the different wall layers of the jejunum and colon

	Jejunum		Colon	
	All ages	< 10 yr	All ages	< 10 yr
Absolute length of proliferating epithelium	-0.21	-0.16	0.07	0.17
Relative length of proliferating epithelium	0.15	0.07	0.02	0.37
Lamina propria of villi	-0.07	-0.28		
Lamina propria between crypts	-0.32	-0.62	-0.36	-0.43
Lamina propria below crypts	-0.46	-0.74	-0.24	-0.65
Lamina muscularis mucosa	-0.56	-0.61	-0.36	-0.5
Submucosa	-0.45	-0.54	-0.57	-0.61
Tunica muscularis	-0.29	-0.56	-0.36	-0.34

dependency in the number of proliferating cells (Table 10). In the submucosa, the correlation remained strong throughout the lifetime. The tunica muscularis and lamina propria between crypts showed only moderately age-related proliferation (r = -0.34 and -0.43, respectively).

DISCUSSION

The layers of the gastrointestinal wall beneath the mucosa comprise the major part of intestinal tissue. However, apart from pathological conditions, these tissues are thought to remain unchanged throughout lifetime. This study revealed that in dogs without gastrointestinal diseases, a continuous thickening of the deeper intestinal layers occurs, mainly during the first 10 years of life. In dogs, this period is regarded as young to middle-aged. Hence senile change in nutritional behavior and metabolism is unlikely to be the primary driving force in this development.

The strongest correlation between age and morphology could be detected in the jejunal lamina propria mucosa between crypt base and lamina muscularis mucosa. In textbooks of veterinary histology, this site is often referred to as stratum compactum[5], when it is easily discernable from the overlying lamina propria, as in the proximal small intestine. In the examined sections, no morphologically distinct stratum compactum could be detected, even in those dogs that presented with a very large distance between the crypt base and the lamina muscularis mucosa. This might be due to the more distally located excision site. This layer is thought to prevent perforation of the intestinal wall by food containing bones[4]. Similarly, the observed proliferation of this zone during lifetime in this study might have been stimulated by mucosal distension and alteration by sharp bone fragments. However, detailed anamnestic data about the diet fed to these dogs during their whole lifetime were not available.

Observations of alterations in the size of the lamina muscularis mucosa are restricted to experimental conditions, e.g. an increase in thickness after partial jejunectomy[6] in rats. The observed increase in the thickness of the muscular layer during lifetime is paralleled by observations in the jejuna of rats[7,8]. A possible explanation might be an increased workload for the musculature caused by a decrease in neuronal coordination as a result of the neuronal cell loss during aging, which has been described in humans[9] and rats[10]. If the increased muscular thickness is the result of a hypertrophy of muscle fibers or of the proliferation of connective tissue between fibers needs further, preferentially electron microscopic investigations.

In rats, epithelial cell proliferation increased in the first postnatal week and decreased or remained unaltered in the following months[7,11,12]. Differentiation of the brush border enzymes follows a similar course with a maximal development in young adulthood[13]. Examination of the mechanisms involved pointed to involvement of proliferation, apoptosis and crypt fission in the development of the intestinal mucosal epithelium[14,15], but delivered contradictory results in particular with regard to alteration of the apoptotic rate in aging rats[14,16-18]. In contrast to these findings, the epithelial proliferation in the canine tissues in this study and a study of the jejunal mucosal morphology in dogs of different weights and ages[19] remained stable throughout lifetime. This observation was also made in mice[20]. The discrepancy in the proliferative rate might be explained by different methods applied. While bromodeoxyuridine[16] and Ki-67

(this investigation) cover a small time span of the cycling process, proliferating cell nuclear antigen is expressed during a long period exceeding mitosis. The increased number of proliferative cells in aging rats found in the study using the latter method[18] might indicate rather decreased degradation of the detected enzyme than increased number of cycling cells. The deeper layers of the present study, however, contained a decreasing number of proliferating cells with rising age. This reduced speed of cellular turn-over might lead to a lower adaptability towards a changed digestibility of diet and a slower healing after damage in older dogs.

In conclusion, all layers of the canine jejunal and colonic wall, except for the epithelial monolayer, increase in thickness during aging, while the number of proliferating cells decreases. The underlying mechanisms and possible functional consequences need further investigation.

ACKNOWLEDGMENTS

We would like to thank Dr. K Rohn, Department of Biometry, Epidemiology and Information Processing, University of Veterinary Medicine Hannover, for assistance with the statistical analyses.

REFERENCES

1 **Paulsen DB**, Buddington KK, Buddington RK. Dimensions and histologic characteristics of the small intestine of dogs during postnatal development. *Am J Vet Res* 2003; **64**: 618-626
2 **Kamiya S**, Suzuki Y, Sugimura M. Polyglucosan bodies in the digestive tract of the aged dog. *Acta Neuropathol* 1983; **60**: 297-300
3 **Tani Y**, Uchida K, Uetsuka K, Nakamura S, Nakayama H, Goto N, Doi K. Amyloid deposits in the gastrointestinal tract of aging dogs. *Vet Pathol* 1997; **34**: 415-420
4 **van der Gaag I**, Happé RP. The histological appearance of peroral small intestinal biopsies in clinically healthy dogs and dogs with chronic diarrhea. *Zentralbl Veterinarmed A* 1990; **37**: 401-416
5 **Dellmann HD**. Textbook of Veterinary Histology. 5th ed. Baltimore: Lippincott Williams & Wilkins, 1998: 180
6 **Hanson WR**. Proliferative and morphological adaptation of the intestine to experimental resection. *Scand J Gastroenterol* Suppl 1982; **74**: 11-20
7 **Wang L**, Li J, Li Q, Zhang J, Duan XL. Morphological changes of cell proliferation and apoptosis in rat jejunal mucosa at different ages. *World J Gastroenterol* 2003; **9**: 2060-2064
8 **Schäfer KH**, Hänsgen A, Mestres P. Morphological changes of the myenteric plexus during early postnatal development of the rat. *Anat Rec* 1999; **256**: 20-28
9 **de Souza RR**, Moratelli HB, Borges N, Liberti EA. Age-induced nerve cell loss in the myenteric plexus of the small intestine in man. *Gerontology* 1993; **39**: 183-188
10 **Baker DM**, Santer RM. A quantitative study of the effects of age on the noradrenergic innervation of Auerbach's plexus in the rat. *Mech Ageing Dev* 1988; **42**: 147-158
11 **Viguera RM**, Rojas-Castañeda J, Hernández R, Reyes G, Alvarez C. Histological characteristics of the intestinal mucosa of the rat during the first year of life. *Lab Anim* 1999; **33**: 393-400
12 **Goodlad RA**, Wright NA. Changes in intestinal cell proliferation, absorptive capacity and structure in young, adult and old rats. *J Anat* 1990; **173**: 109-118
13 **Jang I**, Jung K, Cho J. Influence of age on duodenal brush border membrane and specific activities of brush border membrane enzymes in Wistar rats. *Exp Anim* 2000; **49**: 281-287
14 **Mandir N**, FitzGerald AJ, Goodlad RA. Differences in the effects of age on intestinal proliferation, crypt fission and apoptosis on the small intestine and the colon of the rat. *Int J Exp Pathol* 2005; **86**: 125-130
15 **Cummins AG**, Jones BJ, Thompson FM. Postnatal epithelial growth of the small intestine in the rat occurs by both crypt fission and crypt hyperplasia. *Dig Dis Sci* 2006; **51**: 718-723
16 **Lee HM**, Greeley GH, Englander EW. Effects of aging on expression of genes involved in regulation of proliferation and apoptosis in the colonic epithelium. *Mech Ageing Dev* 2000; **115**: 139-155
17 **Martin K**, Kirkwood TB, Potten CS. Age changes in stem cells of murine small intestinal crypts. *Exp Cell Res* 1998; **241**: 316-323
18 **Xiao ZQ**, Moragoda L, Jaszewski R, Hatfield JA, Fligiel SE, Majumdar AP. Aging is associated with increased proliferation and decreased apoptosis in the colonic mucosa. *Mech Ageing Dev* 2001; **122**: 1849-1864
19 **Hart IR**, Kidder DE. The quantitative assessment of normal canine small intestinal mucosa. *Res Vet Sci* 1978; **25**: 157-162
20 **Ferraris RP**, Vinnakota RR. The time course of adaptation of intestinal nutrient uptake in mice is independent of age. *J Nutr* 1995; **125**: 2172-2182

S- Editor Wang GP **L- Editor** Kumar M **E- Editor** Bai SH

PO Box 2345, Beijing 100023, China
www.wjgnet.com
wjg@wjgnet.com

World J Gastroenterol 2007 January 7; 13(1): 158
World Journal of Gastroenterology ISSN 1007-9327

AUTHOR'S FEEDBACK

Congratulation on *World Journal of Gastroenterology*

Frank Ivor Tovey

Frank Ivor Tovey, Honorary Research Felllow, Department of Surgery, University College London, London, United Kingdom
Correspondence to: Frank Ivor Tovey, OBE, ChM, FRCS, Honorary Research Felllow, Department of Surgery, University College London, London,
United Kingdom. frank@tovey.fsnet.co.uk
Telephone: +44-1256-461521 Fax: +44-1256-323696
Received: 2006-12-05 Accepted: 2006-12-06

Tovey FI. Congratulation on *World Journal of Gastroenterology*. *World J Gastroenterol* 2007; 13(1): 158

http://www.wjgnet.com/1007-9327/13/158.asp

Dear Professor Lian-Sheng Ma,
Professor Michael Hobsley and I have greatly enjoyed reading the account of all you have done towards the development of "The *World Journal of Gastroenterology*", as described in the article by Zhen-Xi Li in the November 21st. issue of the Journal. It is an amazing achievement! Yours is the only international gastroenterological journal to come out weekly! The standard of the articles is extremely high and the Journal is equal in size to "Gut" (Leaderette: 2005 Impact Factor-Gastroenterology & Hepatology list:1 GASTROENTEROLOGY 12.386; 2 HEPATOLOGY 9.792; GUT 7.692), which comes out only monthly. You have achieved all this in a matter of only 10 years-truly a wonderful achievement. We do congratulate you.

REFERENCE

1 **Li ZX**. How to establish a first-class international scientific journal in China? *World J Gastroenterol* 2006; **12**: 6905-6908

S- Editor Liu Y **E- Editor** Ma WH

PO Box 2345, Beijing 100023, China
www.wjgnet.com
wjg@wjgnet.com

World J Gastroenterol 2007 January 7; 13(1): 159
World Journal of Gastroenterology ISSN 1007-9327

PHOTO NEWS

President Lian-Sheng Ma met with Dr. Parimal Chowdhury, Professor of University of Arkansas for Medical Sciences

Ye Liu

Ye Liu, The WJG Press, Beijing 100023, China
Correspondence to: Ye Liu, Science Editor, The WJG Press, Room 1066, Yishou Garden, No. 58, North Langxinzhuang Road, PO Box 2345, Beijing 100023, China. y.liu@wjgnet.com
Telephone: +86-10-85381901-1006 Fax: +86-10-85381893
Received: 2006-11-29 Accepted: 2006-12-06

Liu Y. President Lian-Sheng Ma met with Dr. Parimal Chowdhury, Professor of University of Arkansas for Medical Sciences. *World J Gastroenterol* 2007; 13(1): 159

http://www.wjgnet.com/1007-9327/13/159.asp

Parimal Chowdhury (middle of front seat), Professor of University of Arkansas for Medical Sciences, and his wife (left of front seat) met with Lian-Sheng Ma (right of front seat), President of *WJG*, in Beijing, China, on November 29, 2006. The other in turn (from right of rear seat) are Jing Wang, Ye Liu, Yan Jiang, Jing-Yun Ma, Gai-Ping Wang, who are editors of *WJG*. (*WJG* Photo).

President Lian-Sheng Ma, Editor-in-Chief of *World Journal of Gastroenterology* (*WJG*), met with Dr. Parimal Chowdhury, from the University of Arkansas for Medical Sciences, member of *WJG* Editorial Board, and his wife in Beijing on November 29, 2006. The two sides held cordial and friendly talks.

President Ma extended his warm welcome to Mrs. Chowdhury. He firstly introduced to the guests the development of the journal. Currently, the editorial board of the *WJG* consists of 903 members from 52 countries, there are 5 science editors, 27 language editors located in 16 countries, 22 copy editors from 8 countries and 5 electronic editors. Totally 1223 articles were published in *WJG* from issue No.1 to issue No.42 in 2006, with authors distributed in 58 countries and regions, articles coming from outside China accounted for 77.35%, and the rejection rate was 46.44%. *WJG* is the only weekly journal in the fields of gastroenterology and liver diseases among SCI journals in the world. *WJG* was hit 13090137 times and downloaded 1313719 times online from April 15th, 2003 to November 1st, 2006. WJG was cited 2595 times in 2005 by 765 SCI journals, including 412 (15.87%) self-citations. *WJG* is an international academic journal of its kind published in English in China. Based on rapid development of basic research both in basic and clinical gastroenterology as well as growth of international exchange in science and technology, *WJG* converted to a weekly journal from 2005. PubMed and *WJG* electronic version of the text became available beginning from 1998 (ASP, PDF), and readers have free access to read the full texts of *WJG*. In this point, authors can make a timely and broad dissemination of their work to the world, and this has greatly expanded the international influence of the journal and attracted more high-quality manuscripts from different parts of the world.

Dr. Chowdhury was grateful for the hospitality given by President Ma and his staff and expressed his appreciation for the achievements and development of *WJG*. He mentioned that *WJG* is an open journal wide-ranging in contents and timely publication. Furthermore, it has the potential capacity of competing with similar international journals. Dr. Chowdhury also mentioned that Dr. Mark Donowitz, President of the American Gastroenterological Association (AGA), visited Hong Kong recently, is also very concerned about the development of *WJG*. He had a great admiration for the rich content, high quality of editing and printing and fast publishing frequency of *WJG*. It was his pleasure to work with *WJG*, said Dr. Chowdhury, adding that as one of the editorial board members of *WJG*, he will continue to contribute to *WJG* development.

Finally, President Ma expressed his gratitude to Dr. Chowdhury for his support and for his comments on *WJG*, for writing reviews, and organizing a series of articles as topic highlights in the past. Ma also expressed that *WJG* will continue to follow international standards and improve the academic quality in all aspects including peer review, copy editing, printing, *etc.* *WJG* will target to be the most outstanding international journals with respect to academic level be quality of editing from a scientific perspective and to be one of the top academic international journals in the next 3 to 5 years with the strong support of our country, the authors, readers, all editorial members and the international community.

E- Editor Ma WH

PO Box 2345, Beijing 100023, China
www.wjgnet.com
wjg@wjgnet.com

World J Gastroenterol 2007 January 7; 13(1): 160
World Journal of Gastroenterology ISSN 1007-9327

ACKNOWLEDGMENTS

Acknowledgments to Reviewers of *World Journal of Gastroenterology*

Many reviewers have contributed their expertise and time to the peer review, a critical process to ensure the quality of *World Journal of Gastroenterology*. The editors and authors of the articles submitted to the journal are grateful to the following reviewers for evaluating the articles (including those published in this issue and those rejected for this issue) during the last editing time period.

Kyoichi Adachi, MD
Department of Gastroenterology and Hepatology, Shimane University, School of Medicine Shimane, 89-1 Enya-cho, Izumo-shi Shimane 693-8501, Japan

Raul J Andrade, Associate Professor
Department of Medicine, University of Malaga, Boulevar louis pasteur 32, málaga 29010, Spain

Thomas F Baumert, Dr
Department of Medicine II, University of Freiburg, Hugstetter Strasse 55, D-79106 Freiburg, Germany

Reinhard Buettner, Professor
Institute of Pathology, University Hospital Bonn, Sigmund-Freud-Str. 25, D-53127 Bonn, Germany

Paolo Del Poggio, Dr
Hepatology Unit, Department of Internal Medicine, Treviglio Hospital, Piazza Ospedale 1, Treviglio Bg 24047, Italy

Olivier Detry, Dr
Department of Abdominal Surgery and Transplantation, University of Liège, CHU Sart Tilman B35, B-4000 Liège, Belgium

Curt Einarsson, Professor
Department of Medicine, Karolinska institute, Karolinska University Hospital Huddinge, Dept of Gastroenterology and Hepatology, K 63, Huddinge SE-141 86, Sweden

Xue-Gong Fan, Professor
Department of Infectious Diseases, Xiangya Hospital, Central South University, Changsha 410008, China

Mark A Feitelson, Dr
Pathology, Anatomy and Cell Biology of Thomas Jefferson University, Philadelphia 19107, United States

Valentin Fuhrmann, MD
Department of Internal Medicine 4, Intensive Care Unit, Medical University Vienna, Waehringer Guertel 18-20, A-1090 Vienna, Austria

Takahiro Fujimori, MD, PhD, Professor
Department of Surgical and Molecular Pathology, Dokkyo Univesity School of Medicine, 880 Kitakobayashi, Mibu, Shimotsuga, Tochigi 321-0293, Japan

Kazuhiro Hanazaki, MD
Department of Surgery, Shinonoi General Hospital, 666-1 Ai, Shinonoi, Nagano 388-8004, Japan

Eberhard Hildt, Dr
Molecular Virology-NG1, Robert Koch InstituteNordufer 20,D-13353 Berlin, Germany

Keiji Hirata, MD
Surgery 1, University of Occupational and Environmental Health, 1-1 Iseigaoka, Yahatanishi-ku, Kitakyushu 807-8555, Japan

Ton Lisman, PhD
Thrombosis and Haemostasis Laboratory, Department of Gastroenterology-Hepatology, University of Connecticut Health Center, 263 Farmington Ave, Farmington, CT 06030, United States

María Isabel Torres López, Professor
Experimental Biology, University of Jaen, araje de las Lagunillas s/n, Jaén 23071, Spain

Ran Oren, Professor
The Liver Unit, Department of Gastroenterology, Tel Aviv Sourasky Medical Center, Tel Aviv, Israel

Thierry Piche , MD, PhD
Department of Gastroenterology, Archet 2 Hospital, 151 RTE ST Antoine de Ginestiere 06202, Nice CEDEX 3, France

D Mark Pritchard, PhD
FRCP, Gastroenterology of University of Liverpool, 5th Floor UCD Building, Daulby St, Liverpool L69 3GA

Ian C Roberts-Thomson, Professor
Department of Gastroenterology and Hepatology, The Queen Elizabeth Hospital, 28 Woodville Road, Woodville South 5011, Australia

Luis Rodrigo, Professor
Gastroenterology Service, Hospital Central de Asturias, c/ Celestino Villamil, s.n., Oviedo 33.006, Spain

Spiros Sgouros
Naypaktias 5, Agia Paraskevi, Athens 15341, Greece

Seyed Alireza Taghavi, Associate Professor
Department of Internal Medicine, Nemazee Hospital, No.23, 59th Alley, Ghasrodasht St., Shiraz 71838-95453, Iran

Nick Paul Thompson, MD
Department of Medicine, Freeman Hospital, Newcastle Upon Tyne, NE7 7DN, Unite Kingdom

Nick Paul Thompson, MD
Department of Medicine, Freeman Hospital, Newcastle Upon Tyne, NE7 7DN, Unite Kingdom

Saúl Villa-Treviño, MD, PhD
Departamento de Biología Celular, Centro de Investigación y de Estudios Avanzados del IPN (Cinvestav), Ave. IPN No. 2508. Col. San Pedro, Zacatenco, C.P. 07360, México, DF, Mexico

HP Wang, Professor
Department of Emergency Medicine, National Taiwan University Hospital, No 7, Chung-Shan South Rd, Taipei 10016, Taiwan

Daniel Lindsay Worthley, Dr
Department of Gastroenterology and Hepatology, Flinders Medical Centre, Room 3D230, Bedford Park, SA 5042, Australia

Jia-Yu Xu, Professor
Shanghai Second Medical University, Rui Jin Hospital, 197 Rui Jin Er Road, Shanghai 200025, China

Takayuki Yamamoto, MD
Inflammatory Bowel Disease Center, Yokkaichi Social Insurance Hospital, 10-8 Hazuyamacho, Yokkaichi 510-0016, Japan

Eric M Yoshida, MD
Department of Medicine, University of British Columbia, 100-2647 Willow Street, Vancouver V5Z 3P1, Canada

Yuan Yuan, Professor
Cancer Institute of China Medical University, 155 North Nanjing Street, Heping District, Shenyang 110001, Liaoning Province, China

Xin-Xin Zhang, Professor
Department of Infectious Disease, Rui Jin Hospital, 197, Rui Jin Er Road, Shanghai 200025, China

PO Box 2345, Beijing 100023, China
www.wjgnet.com
wjg@wjgnet.com

World J Gastroenterol 2007 January 7; 13(1): 161
World Journal of Gastroenterology ISSN 1007-9327

Meetings

MAJOR MEETINGS COMING UP

Digestive Disease Week
19-24 May 2007
Washington Convention Center,
Washington DC

American College of
Gastroenterology Annual Scientific
Meeting
12-17 October 2007
Pennsylvania Convention Center
Philadelphia, PA

15th United European
Gastroenterology Week, UEGW
27-31 October 2007
Le Palais des Congrès de Paris,
Paris, France

NEXT 6 MONTHS

Meeting ILTS 13th Annual
International Congress
20-23 June 2007
Rio De Janeiro
www.ilts.org

Meeting Canadian Digestive Diseases
Week (CDDW)
16-20 February 2007
Banff - AB
cagoffice@cag-acg.org
www.cag-acg.org/cddw/cddw2007.
htm

Meeting Falk Research Workshop:
Morphogenesis and Cancerogenesis
of the Liver
25-26 January 2007
Goettingen
symposia@falkfoundation.de

Meeting ESGAR 2007 18th Annual
Meeting and Postgraduate Course
12-15 June 2007
Lisbon
fca@netvisao.pt

Meeting Falk Symposium 160:
Pathogenesis and Clinical Practice
in Gastroenterology
15-16 June 2007
Portoroz
symposia@falkfoundation.de

Meeting Falk Symposium 158:
Intestinal Inflammation and
Colorectal Cancer
23-24 March 2007
Sevilla
symposia@falkfoundation.de

Meeting 42nd Annual Meeting of
the European Association for
the Study of the Liver
11-15 April 2007
Barcelona
easl2007@easl.ch
www.easl.ch/liver-meeting/

Meeting European Society for
Paediatric Gastroenterology,
Hepatology and Nutrition
Congress 2007
9-12 May 2007
Barcelona
espghan2007@colloquium.fr

Meeting 9th World Congress
on Gastrointestinal Cancer
27-30 June 2007
Barcelona
meetings@imedex.com

Meeting Falk Symposium 159: IBD
2007-Achievements in Research
and Clinical Practice
4-5 May 2007
Istanbul
symposia@falkfoundation.de

Meeting BSG Annual Meeting
26-29 March 2007
Glasgow
www.bsg.org.uk/

Meeting Gastrointestinal Endoscopy
Best Practices: Today and Tomorrow,
ASGE Annual Postgraduate
Course at DDW
23-24 May 2007
Washington - DC
tkoral@asge.org

EVENTS AND MEETINGS IN 2007

Meeting ILTS 13th Annual
International Congress
20-23 June 2007
Rio De Janeiro
www.ilts.org

Meeting Canadian Digestive Diseases
Week (CDDW)
16-20 February 2007
Banff - AB
cagoffice@cag-acg.org
www.cag-acg.org/cddw/cddw2007.
htm

Meeting Falk Research Workshop:
Morphogenesis and Cancerogenesis
of the Liver
25-26 January 2007
Goettingen
symposia@falkfoundation.de

Meeting Falk Workshop: Mechanisms
of Intestinal Inflammation
10 October 2007
Dresden
symposia@falkfoundation.de

Meeting Falk Symposium 161: Future
Perspectives in Gastroenterology
11-12 October 2007
Dresden
symposia@falkfoundation.de

Meeting Falk Symposium 162: Liver
Cirrhosis-From Pathophysiology
to Disease Management
13-14 October 2007
Dresden
symposia@falkfoundation.de

Meeting 15th International Congress
of the European Association
for Endoscopic Surgery
4-7 July 2007
Athens
info@eaes-eur.org
congresses.eaes-eur.org/

Meeting APDW 2007-Asian Pacific
Digestive Disease Week 2007
15-18 October 2007
Kobe
apdw@convention.co.jp
www.apdw2007.org

Meeting ESGAR 2007 18th Annual
Meeting and Postgraduate Course
12-15 June 2007
Lisbon
fca@netvisao.pt

Meeting Falk Symposium 160:
Pathogenesis and Clinical Practice
in Gastroenterology
15-16 June 2007
Portoroz
symposia@falkfoundation.de

Meeting Falk Symposium 158:
Intestinal Inflammation
and Colorectal Cancer
23-24 March 2007
Sevilla
symposia@falkfoundation.de

Meeting 42nd Annual Meeting of
the European Association for
the Study of the Liver
11-15 April 2007
Barcelona
easl2007@easl.ch
www.easl.ch/liver-meeting/

Meeting European Society
for Paediatric Gastroenterology,
Hepatology and Nutrition Congress
2007
9-12 May 2007
Barcelona
espghan2007@colloquium.fr

Meeting 9th World Congress
on Gastrointestinal Cancer
27-30 June 2007
Barcelona
meetings@imedex.com

Meeting Falk Symposium 159:
IBD 2007 - Achievements in Research
and Clinical Practice
4-5 May 2007
Istanbul
symposia@falkfoundation.de

Meeting XXth International
Workshop on Heliobacter
and related bacteria in
cronic degistive inflammation
20-22 September 2007
Istanbul
www.heliobacter.org

Meeting BSG Annual Meeting
26-29 March 2007
Glasgow
www.bsg.org.uk/

Meeting 39th Meeting of
the European Pancreatic Club
4-7 July 2007
Newcastle
www.e-p-c2007.com

Meeting Gastrointestinal Endoscopy
Best Practices: Today and Tomorrow,
ASGE Annual Postgraduate Course
at DDW
23-24 May 2007
Washington - DC
tkoral@asge.org

Meeting The Liver Meeting® 2007-
57th Annual Meeting of the American
Association for the Study of Liver
Diseases
2-6 November 2007
Boston - MA
www.aasld.org

Gastro 2009, World Congress of Gastroenterology and Endoscopy London, United Kingdom 2009

PO Box 2345, Beijing 100023, China
www.wjgnet.com
wjg@wjgnet.com

World J Gastroenterol 2007 January 7; 13(1): 162-164
World Journal of Gastroenterology ISSN 1007-9327

Instructions to authors

GENERAL INFORMATION

World Journal of Gastroenterology (*WJG, World J Gastroenterol* ISSN 1007-9327 CN 14-1219/R) is a weekly journal of more than 48 000 circulation, published on the 7th, 14th, 21st and 28th of every month.

Original Research, Clinical Trials, Reviews, Comments, and Case Reports in esophageal cancer, gastric cancer, colon cancer, liver cancer, viral liver diseases, *etc.*, from all over the world are welcome on the condition that they have not been published previously and have not been submitted simultaneously elsewhere.

Indexed and abstracted in

Current Contents®/Clinical Medicine, Science Citation Index Expanded (also known as SciSearch®) and Journal Citation Reports/Science Edition, *Index Medicus*, MEDLINE and PubMed, Chemical Abstracts, EMBASE/Excerpta Medica, Abstracts Journals, *Nature Clinical Practice Gastroenterology and Hepatology*, CAB Abstracts and Global Health. ISI JCR 2003-2000 IF: 3.318, 2.532, 1.445 and 0.993.

Published by

The WJG Press

SUBMISSION OF MANUSCRIPTS

Manuscripts should be typed double-spaced on A4 (297 mm × 210 mm) white paper with outer margins of 2.5 cm. Number all pages consecutively, and start each of the following sections on a new page: Title Page , Abstract, Introduction, Materials and Methods, Results, Discussion, acknowledgements, References, Tables, Figures and Figure Legends. Neither the editors nor the Publisher is responsible for the opinions expressed by contributors. Manuscripts formally accepted for publication become the permanent property of The WJG Press, and may not be reproduced by any means, in whole or in part without the written permission of both the authors and the Publisher. We reserve the right to put onto our website and copy-edit accepted manuscripts. Authors should also follow the guidelines for the care and use of laboratory animals of their institution or national animal welfare committee.

Authors should retain one copy of the text, tables, photographs and illustrations, as rejected manuscripts will not be returned to the author(s) and the editors will not be responsible for the loss or damage to photographs and illustrations in mailing process.

Online submission

Online submission is strongly advised. Manuscripts should be submitted through the Online Submission System at: http://www.wjgnet.com/index.jsp. Authors are highly recommended to consult the ONLINE INSTRUCTIONS TO AUTHORS (http://www.wjgnet.com/wjg/help/instructions.jsp) before attempting to submit online. Authors encountering problems with the Online Submission System may send an email you describing the problem to wjg@wjgnet.com for assistance. If you submit your manuscript online, do not make a postal contribution. A repeated online submission for the same manuscript is strictly prohibited.

Postal submission

Send 3 duplicate hard copies of the full-text manuscript typed double-spaced on A4 (297 mm × 210 mm) white paper together with any original photographs or illustrations and a 3.5 inch computer diskette or CD-ROM containing an electronic copy of the manuscript including all the figures, graphs and tables in native Microsoft Word format or *.rtf format to:

Editorial Office

World Journal of Gastroenterology
Editorial Department: Apartment 1066, Yishou Garden,
58 North Langxinzhuang Road,
PO Box 2345, Beijing 100023, China
E-mail: wjg@wjgnet.com
http: //www.wjgnet.com
Telephone: +86-10-85381892
Fax: +86-10-85381893

MANUSCRIPT PREPARATION

All contributions should be written in English. All articles must be submitted using a word-processing software. All submissions must be typed in 1.5 line spacing and in word size 12 with ample margins. The letter font is Tahoma. For authors from China, one copy of the Chinese translation of the manuscript is also required (excluding references). Style should conform to our house format. Required information for each of the manuscript sections is as follows:

Title page

Full manuscript title, running title, all author(s) name(s), affiliations, institution(s) and/or department(s) where the work was accomplished, disclosure of any financial support for the research, and the name, full address, telephone and fax numbers and email address of the corresponding author should be included. Titles should be concise and informative (removing all unnecessary words), emphasize what is new, and avoid abbreviations. A short running title of less than 40 letters should be provided. List the author(s)' name(s) as follows: initial and/or first name, middle name or initial(s) and full family name.

Abstract

An informative, structured abstract of no more than 250 words should accompany each manuscript. Abstracts for original contributions should be structured into the following sections: AIM: Only the purpose should be included. METHODS: The materials, techniques, instruments and equipments, and the experimental procedures should be included. RESULTS: The observatory and experimental results, including data, effects, outcome, *etc.* should be included. Authors should present *P* value where necessary, and the significant data should accompany. CONCLUSION: Accurate view and the value of the results should be included.

The format of structured abstracts is at: http://www.wjgnet.com/wjg/help/11.doc

Key words

Please list 5-10 key words that could reflect content of the study mainly from *Index Medicus*.

Text

For most article types, the main text should be structured into the following sections: INTRODUCTION, MATERIALS AND METHODS, RESULTS and DISCUSSION, and should include in appropriate Figures and Tables. Data should be presented in the body text or in Figures and Tables, but not in both.

Illustrations

Figures should be numbered as 1, 2, 3 and so on, and mentioned clearly in the main text. Provide a brief title for each figure on a separate page. No detailed legend should be involved under the figures. This part should be added into the text where the figures are applicable. Digital images: black and white photographs should be scanned and saved in TIFF format at a resolution of 300 dpi; color images should be saved as CMYK (print files) but not as RGB (screen-viewing files). Place each photograph in a separate file. Print images: supply images of size no smaller than 126 mm × 85 mm printed on smooth surface paper; label the image by writing the Figure number and orientation using an arrow. Photomicrographs: indicate the original magnification and stain in the legend. Digital Drawings: supply files in EPS if created by freehand and illustrator, or TIFF from photoshops. EPS files must be accompanied by a version in native file format for editing purposes. Existing line drawings should be scanned at a resolution of 1200 dpi and as close as possible to the size where they will appear when printed. Please use uniform legends for the same subjects. For example: Figure 1 Pathological changes of atrophic gastritis after treatment. A: ...; B: ...; C: ...; D: ...; E: ...; F: ...; G: ...

Tables

Three-line tables should be numbered as 1, 2, 3 and so on, and mentioned clearly in the main text. Provide a brief title for each table. No detailed legend should be included under the tables. This part should be added into the text where the tables are applicable. The information should complement but not duplicate that contained in the text. Use one horizontal line under the title, a second under the column heads, and a third below the Table, above any footnotes. Vertical and italic lines should be omitted.

Notes in tables and illustrations

Data that are not statistically significant should not be noted. $^{a}P<0.05$, $^{b}P<0.01$ should be noted ($P>0.05$ should not be noted). If there are other series of *P* values, $^{c}P<0.05$ and $^{d}P<0.01$ are used. Third series of *P* values can be expressed as $^{e}P<0.05$ and $^{f}P<0.01$. Other notes in tables or under

illustrations should be expressed as ^1F, ^2F, ^3F; or some other symbols with a superscript (Arabic numerals) in the upper left corner. In a multi-curve illustration, each curve should be labeled with ●, ○, ■, □, ▲, △, *etc.* in a certain sequence.

Acknowledgments

Brief acknowledgments of persons who have made genuine contributions to the manuscripts and who endorse the data and conclusions are included. Authors are responsible for obtaining written permission to use any copyrighted text and/or illustrations.

REFERENCES

Coding system

The author should code the references according the citation order in text in Arabic numerals, put references codes in square brackets, superscript it at the end of citation content or the author name of the citation. For those citation content as the narrate part, the coding number and square brackets should be typeset normally. For example, Crohn's disease (CD) is associated with increased intestinal permeability[1,2]. If references are directly cited in the text, they would be put together with the text, for example, from references [19,22-24], we know that...

When the authors code the references, please ensure that the order in text is the same as in reference part and also insure the spelling accuracy of the first author's name. Do not code the same citation twice.

PMID requirement

PMID roots in the abstract serial number indexed by PubMed (http://www.ncbi.nlm.nih.gov/entrez/query.fcgi?db=PubMed). The author should supply the PMID for journal citation. For those references that have not been indexed by PubMed, a printed copy of the first page of the full reference should be submitted.

The accuracy of the information of the journal citations is very important. Through reference testing system, the authors and editor could check the authors name, title, journal title, publication date, volume number, start page, and end page. We will interlink all references with PubMed in ASP file so that the readers can read the abstract of the citations online immediately.

Style for journal references

Authors: the first author should be typed in bold-faced letter. The surname of all authors should be typed with the initial letter capitalized and followed by their name in abbreviation (For example, Lian-Sheng Ma is abbreviated as Ma LS, Bo-Rong Pan as Pan BR). Title of the cited article and italicized journal title (Journal title should be in its abbreviation form as shown in PubMed), publication date, volume number (in black), start page, and end page [PMID: 11819634]

Note: The author should test the references through reference testing system (http://www.wjgnet.com/cgi-bin/index.pl)

Style for book references

Authors: the first author should be typed in bold-faced letter. The surname of all authors should be typed with the initial letter capitalized and followed by their name in abbreviation (For example, Lian-Sheng Ma is abbreviated as Ma LS, Bo-Rong Pan as Pan BR) Book title. Publication number. Publication place: Publication press, Year: start page and end page.

Format

Journals

English journal article (list all authors and include the PMID where applicable)

1 **Grover VP**, Dresner MA, Forton DM, Counsell S, Larkman DJ, Patel N, Thomas HC, Taylor-Robinson SD. Current and future applications of magnetic resonance imaging and spectroscopy of the brain in hepatic encephalopathy. *World J Gastroenterol* 2006; **12**: 2969-2978 [PMID: 16718775]

Chinese journal article (list all authors and include the PMID where applicable)

2 **Lin GZ**, Wang XZ, Wang P, Lin J, Yang FD. Immunologic effect of Jianpi Yishen decoction in treatment of Pixu-diarrhoea. *Shijie Huaren Xiaohua Zazhi* 1999; **7**: 285-287

In press

3 **Tian D**, Araki H, Stahl E, Bergelson J, Kreitman M. Signature of balancing selection in Arabidopsis. *Proc Natl Acad Sci U S A* 2006; In press

Organization as author

4 **Diabetes Prevention Program Research Group**. Hypertension, insulin, and proinsulin in participants with impaired glucose tolerance. *Hypertension* 2002; **40**: 679-686 [PMID: 12411462]

Both personal authors and an organization as author

5 **Vallancien G**, Emberton M, Harving N, van Moorselaar RJ; Alf-One Study Group. Sexual dysfunction in 1, 274 European men suffering from lower urinary tract symptoms. *J Urol* 2003; **169**: 2257-2261 [PMID: 12771764]

No author given

6 21st century heart solution may have a sting in the tail. *BMJ* 2002; **325**: 184 [PMID: 12142303]

Volume with supplement

7 **Geraud G**, Spierings EL, Keywood C. Tolerability and safety of frovatriptan with short- and long-term use for treatment of migraine and in comparison with sumatriptan. *Headache* 2002; **42** Suppl 2: S93-99 [PMID: 12028325]

Issue with no volume

8 **Banit DM**, Kaufer H, Hartford JM. Intraoperative frozen section analysis in revision total joint arthroplasty. *Clin Orthop Relat Res* 2002; (**401**): 230-238 [PMID: 12151900]

No volume or issue

9 Outreach: bringing HIV-positive individuals into care. *HRSA Careaction* 2002; 1-6 [PMID: 12154804]

Books

Personal author(s)

10 **Sherlock S**, Dooley J. Diseases of the liver and billiary system. 9th ed. Oxford: Blackwell Sci Pub, 1993: 258-296

Chapter in a book (list all authors)

11 **Lam SK**. Academic investigator's perspectives of medical treatment for peptic ulcer. In: Swabb EA, Azabo S. Ulcer disease: investigation and basis for therapy. New York: Marcel Dekker, 1991: 431-450

Author(s) and editor(s)

12 **Breedlove GK**, Schorfheide AM. Adolescent pregnancy. 2nd ed. Wieczorek RR, editor. White Plains (NY): March of Dimes Education Services, 2001: 20-34

Conference proceedings

13 **Harnden P**, Joffe JK, Jones WG, editors. Germ cell tumours V. Proceedings of the 5th Germ Cell Tumour Conference; 2001 Sep 13-15; Leeds, UK. New York: Springer, 2002: 30-56

Conference paper

14 **Christensen S**, Oppacher F. An analysis of Koza's computational effort statistic for genetic programming. In: Foster JA, Lutton E, Miller J, Ryan C, Tettamanzi AG, editors. Genetic programming. EuroGP 2002: Proceedings of the 5th European Conference on Genetic Programming; 2002 Apr 3-5; Kinsdale, Ireland. Berlin: Springer, 2002: 182-191

Electronic journal (list all authors)

Morse SS. Factors in the emergence of infectious diseases. Emerg Infect Dis serial online, 1995-01-03, cited 1996-06-05; 1(1): 24 screens. Available from: URL: http//www.cdc.gov/ncidod/EID/eid.htm

Patent (list all authors)

16 **Pagedas AC**, inventor; Ancel Surgical R&D Inc., assignee. Flexible endoscopic grasping and cutting device and positioning tool assembly. United States patent US 20020103498. 2002 Aug 1

Inappropriate references

Authors should always cite references that are relevant to their article, and avoid any inappropriate references. Inappropriate references include those that are linked with a hyphen and the difference between the two numbers at two sides of the hyphen is more than 5. For example, [1-6], [2-14] and [1, 3, 4-10, 22] are all considered as inappropriate references. Authors should not cite their own unrelated published articles.

Statistical data

Present as mean ± SD or mean ± SE.

Statistical expression

Express t test as t (in italics), F test as F (in italics), chi square test as χ^2 (in Greek), related coefficient as r (in italics), degree of freedom as γ (in Greek), sample number as n (in italics), and probability as P (in italics).

Units

Use SI units. For example: body mass, m (B) = 78 kg; blood pressure, p(B) = 16.2/12.3 kPa; incubation time, t (incubation) = 96 h, blood glucose concentration, c (glucose) 6.4 ± 2.1 mmol/L; blood CEA mass concentration, p (CEA) = 8.6 24.5 μg/L; CO_2 volume fraction, 50 mL/L CO_2 not 5% CO_2; likewise for 40 g/L formaldehyde, not 10% formalin; and mass fraction, 8 ng/g, *etc.* Arabic numerals such as 23, 243, 641 should be read 23 243 641.

The format about how to accurately write common units and quantum is at: http://www.wjgnet.com/wjg/help/15.doc

Abbreviations

Standard abbreviations should be defined in the abstract and on first mention in the text. In general, terms should not be abbreviated unless they are used repeatedly and the abbreviation is helpful to the reader. Permissible abbreviations are listed in Units, Symbols and Abbreviations: A Guide for Biological and Medical Editors and Authors (Ed. Baron DN, 1988) published by The Royal Society of Medicine, London. Certain commonly used abbreviations, such as DNA, RNA, HIV, LD50, PCR, HBV, ECG, WBC, RBC, CT, ESR, CSF, IgG, ELISA, PBS, ATP, EDTA, mAb, can be used directly without further mention.

Italics

Quantities: *t* time or temperature, *c* concentration, *A* area, *l* length, *m* mass, *V* volume.
Genotypes: *gyr*A, *arg* 1, *c myc*, *c fos*, *etc.*
Restriction enzymes: *Eco*RI, *Hin*dI, *Bam*HI, *Kbo* I, *Kpn* I, *etc.*
Biology: *H pylori, E coli, etc.*

SUBMISSION OF THE REVISED MANUSCRIPTS AFTER ACCEPTED

Please revise your article according to the revision policies of *WJG*. The revised version including manuscript and high-resolution image figures (if any) should be copied on a floppy or compact disk. Author should send the revised manuscript, along with printed high-resolution color or black and white photos, copyright transfer letter, the final check list for authors, and responses to reviewers by a courier (such as EMS) (submission of revised manuscript by e-mail or on the *WJG* Editorial Office Online System is NOT available at present).

Language evaluation

The language of a manuscript will be graded before sending for revision. (1) Grade A: priority publishing; (2) Grade B: minor language polishing; (3) Grade C: a great deal of language polishing; (4) Grade D: rejected. The revised articles should be in grade B or grade A.

Copyright assignment form

Please downloaded CAF from http://www.wjgnet.com/wjg/help/9.doc.

We certify that the material contained in this manuscript:

Ms:

Title:

is original, except when appropriately referenced to other sources, and that written permission has been granted by any existing copyright holders. We agree to transfer to WJG all rights of our manuscript, including: (1) all copyright ownership in all print and electronic formats; (2) the right to grant permission to republish or reprint the stated material in whole or in part, with or without a fee; (3) the right to print copies for free distribution or sale; (4) the right to republish the stated material in a collection of articles or in any other format. We also agree that our article be put on the Internet.

Criteria for authorship: The WJG requests and publishes information about contributions of each author named to the submitted study. Authorship credit should be based on (1)direct participation in the study, including substantial contributions to conception and design of study, or acquisition of data, or analysis and interpretation of data; (2) manuscript writing, including drafting the article, or revising it critically for important intellectual content; (3)supportive work, including statistical analysis of data, or acquisition of funding, or administration, technology and materials support, or supervision, or supportive contributions. Authors should meet at least one of the three conditions. The WJG does not publish co-first authors and co-corresponding authors.

We hereby assign copyright transfer to WJG if this paper is accepted.

Author Name in full (Full names should be provided, with first name first, followed by middle names and family name at the last, eg, Eamonn MM Quigley). Handwritten names are not accepted.

Author Name in abbreviation (Family name is put first in full, followed by middle names and first name in abbreviation with first letter in capital, eg, Quigley EMM). Handwritten names are not accepted.

1 Full Name: _____
Abbreviation Name: _____
Signed: _____
Date: _____

2 Full Name: _____
Abbreviation Name: _____
Signed: _____
Date: _____

3 Full Name: _____
Abbreviation Name: _____
Signed: _____
Date: _____

4 Full Name: _____
Abbreviation Name: _____
Signed: _____
Date: _____

5 Full Name: _____
Abbreviation Name: _____
Signed: _____
Date: _____

6 Full Name: _____
Abbreviation Name: _____
Signed: _____
Date: _____

7 Full Name: _____
Abbreviation Name: _____
Signed: _____
Date: _____

8 Full Name: _____
Abbreviation Name: _____
Signed: _____
Date: _____

9 Full Name: _____
Abbreviation Name: _____
Signed: _____
Date: _____

10 Full Name: _____
Abbreviation Name: _____
Signed: _____
Date: _____

Final check list for authors

The format is at: http://www.wjgnet.com/wjg/help/13.doc

Responses to reviewers

Please revise your article according to the comments/suggestions of reviewers. The format for responses to the reviewers' comments is at: http://www.wjgnet.com/wjg/help/10.doc

Proof of financial support

For paper supported by a foundation, authors should provide a copy of the document and serial number of the foundation.

Publication fee

Authors of accepted articles must pay publication fee.
EDITORIAL and LETTERS TO THE EDITOR are free of change.

ISI journal citation reports
2003 – GASTROENTEROLOGY AND HEPATOLOGY

Rank	Abbreviated journal title	ISSN	2003 Total cites	Impact factor	Immediacy index	2003 Articles	Cited Half-life
1	GASTROENTEROLOGY	0016-5085	46 174	12.718	2.810	316	6.9
2	HEPATOLOGY	0270-9139	30 844	9.503	1.574	296	5.5
3	SEMIN LIVER DIS	0272-8087	2 524	6.524	0.810	42	4.7
4	GUT	0017-5749	20 612	5.883	1.147	307	6.5
5	J HEPATOL	0168-8278	11 111	5.283	0.879	281	5.0
6	LIVER TRANSPLANT	1527-6465	2 944	4.242	0.621	211	2.9
7	AM J GASTROENTEROL	0002-9270	17 923	4.172	0.678	391	5.1
8	ALIMENT PHARM THERAP	0269-2813	60 32	3.529	0.573	372	3.9
9	AM J PHYSIOL-GASTR L	0193-1857	11 047	3.421	0.634	268	5.9
10	GASTROINTEST ENDOSC	0016-5107	10 047	3.328	1.798	331	4.8
11	**WORLD J GASTROENTERO**	**1007-9327**	**2 387**	**3.318**	**0.345**	**632**	**2.4**
12	J VIRAL HEPATITIS	1352-0504	1 320	3.258	0.386	70	4.0
13	ENDOSCOPY	0013-726X	4 238	3.227	0.349	152	5.5
14	INFLAMM BOWEL DIS	1078-0998	1 278	3.023	0.625	40	3.8
15	HELICOBACTER	1083-4389	798	2.624	0.426	68	3.6
16	NEUROGASTROENT MOTIL	1350-1925	848	2.500	0.333	66	3.7
17	DIS COLON RECTUM	0012-3706	8 130	2.343	0.191	256	7.6
18	SCAND J GASTROENTERO	0036-5521	7 271	2.140	0.118	238	7.6
19	LIVER	0106-9543	1 337	2.076		0	5.4
20	J GASTROINTEST SURG	1091-255X	1 236	1.881	0.430	142	3.6
21	PANCREAS	0885-3177	2 271	1.855	0.364	140	5.8
22	INT J COLORECTAL DIS	0179-1958	1 167	1.848	0.373	83	6.4
23	GASTROENTEROL CLIN N	0889-8553	1 517	1.684	0.019	54	6.7
24	PANCREATOLOGY	1424-3903	240	1.596	0.115	52	2.2
25	EUR J GASTROEN HEPAT	0954-691X	3 163	1.578	0.367	177	4.6
26	J CLIN GASTROENTEROL	0192-0790	3 215	1.564	0.484	155	7.2
27	J GASTROEN HEPATOL	0815-9319	3 171	1.530	0.254	193	4.5
28	DIGEST LIVER DIS	1590-8658	637	1.463	0.151	159	2.5
29	J PEDIATR GASTR NUTR	0277-2116	3 963	1.402	0.257	183	6.1
30	DIGESTION	0012-2823	2 193	1.399	0.091	55	7.7
31	DIGEST DIS SCI	0163-2116	9 149	1.387	0.144	347	7.9
32	CAN J GASTROENTEROL	0835-7900	813	1.265	0.134	82	3.9
33	J GASTROENTEROL	0944-1174	1 625	1.179	0.319	191	4.5
34	DIGEST DIS	0257-2753	534	1.151	0.031	32	5.7
35	Z GASTROENTEROL	0044-2771	918	1.076	0.112	116	5.4
36	ABDOM IMAGING	0942-8925	1 190	0.996	0.194	124	5.0
37	BEST PRACT RES CL GA	1521-6918	342	0.992	0.000	66	3.4
38	HEPATOL RES	1386-6346	406	0.991	0.168	155	2.6
39	GASTROEN CLIN BIOL	0399-8320	1 497	0.884	0.235	153	6.3
40	HEPATO-GASTROENTEROL	0172-6390	3 886	0.837	0.044	544	5.0
41	DIS ESOPHAGUS	1120-8694	354	0.809	0.027	75	4.7
42	ACTA GASTRO-ENT BELG	0001-5644	345	0.670	0.065	31	5.2
43	DIGEST SURG	0253-4886	548	0.619	0.114	79	4.2
44	CURR OPIN GASTROEN	0267-1379	300	0.598	0.050	60	3.9
45	REV ESP ENFERM DIG	1130-0108	255	0.348	0.211	57	6.0
46	CHIR GASTROENTEROL	0177-9990	74	0.157	0.039	76	
47	LIVER INT	1478-3231	4		0.053	75	

World Journal of Gastroenterology®

Volume 13 Number 2
January 14, 2007

National Journal Award
2005

The WJG Press

The WJG Press, Apartment 1066 Yishou Garden, 58 North Langxinzhuang Road, PO Box 2345, Beijing 100023, China
Telephone: +86-10-85381892
Fax: +86-10-85381893
E-mail: wjg@wjgnet.com
http: //www.wjgnet.com

ISSN 1007-9327 CN 14-1219/R Local Post Offices Code No. 82-261

World Journal of Gastroenterology www.wjgnet.com Volume 13 Number 2 Jan 14 2007

ISSN 1007-9327
CN 14-1219/R

World Journal of Gastroenterology®

Indexed and Abstracted in:

Current Contents®/Clinical Medicine, Science Citation Index Expanded (also known as SciSearch®) and Journal Citation Reports/Science Edition, *Index Medicus*, MEDLINE and PubMed, Chemical Abstracts, EMBASE/Excerpta Medica, Abstracts Journals, *Nature Clinical Practice Gastroenterology and Hepatology*, CAB Abstracts and Global Health.
ISI JCR 2003-2000 IF: 3.318, 2.532, 1.445 and 0.993.

Volume 13 Number 2
January 14, 2007

World J Gastroenterol
2007 January 14; 13(2): 165-328
Online Submissions
www.wjgnet.com/wjg/index.jsp
www.wjgnet.com
Printed on Acid-free Paper

A Weekly Journal of Gastroenterology and Hepatology

National Journal Award
2005

World Journal of Gastroenterology®

Volume 13 Number 2
January 14, 2007

The WJG Press

Contents

World Journal of Gastroenterology
Volume 13 **Number** 2 **January** 14, 2007

Contents

World Journal of Gastroenterology
Volume 13 **Number** 2 **January** 14, 2007

Contents

Responsible E-Editor for this issue: Shao-Hua Bai

C-Editor for this issue: Gianfranco D Alpini, PhD, Professor

Responsible S-Editor for this issue: Xing-Xia Yang

World Journal of Gastroenterology (*World J Gastroenterol , WJG*), a leading international journal in gastroenterology and hepatology, has an established reputation for publishing first class research on esophageal cancer, gastric cancer, liver cancer, viral hepatitis, colorectal cancer, and *H pylori* infection, providing a forum for both clinicians and scientists, and has been indexed and abstracted in Current Contents®/Clinical Medicine, Science Citation Index Expanded (also known as SciSearch®) and Journal Citation Reports/Science Edition, *Index Medicus*, MEDLINE and PubMed, Chemical Abstracts, EMBASE/Excerpta Medica, Abstracts Journals, *Nature Clinical Practice Gastroenterology and Hepatology*, CAB Abstracts and Global Health. ISI JCR 2003-2000 IF: 3.318, 2.532, 1.445 and 0.993. *WJG* is a weekly journal published by The WJG Press. The publication date is on 7th, 14th, 21st, and 28th every month. The *WJG* is supported by The National Natural Science Foundation of China, No. 30224801 and No.30424812, which was founded with a name of *China National Journal of New Gastroenterology* on October 1,1995, and renamed as *WJG* on January 25, 1998.

PUBLISHED BY
The WJG Press

PRINTED BY
Printed in Beijing on acid-free paper by Beijing Kexin Printing House

 Print ISSN 1007-9327
CN 14-1219/R.

EDITORIAL OFFICE
World Journal of Gastroenterology,
The WJG Press, Apartment 1066 Yishou Garden, 58 North Langxinzhuang Road, PO Box 2345, Beijing 100023, China
Telephone: +86-10-85381892
Fax: +86-10-85381893
E-mail: wjg@wjgnet.com
http://www.wjgnet.com

SUBSCRIPTION AND AUTHOR REPRINTS
Jing Wang
The WJG Press, Apartment 1066 Yishou Garden, 58 North Langxinzhuang Road, PO Box 2345, Beijing 100023, China
Telephone: +86-10-85381892
Fax: +86-10-85381893
E-mail: j.wang@wjgnet.com
http://www.wjgnet.com

SUBSCRIPTION INFORMATION
Institutional Price 2007: USD 1500.00
Personal Price 2007: USD 700.00

INSTRUCTIONS TO AUTHORS
Full instructions are available online at http://www.wjgnet.com/wjg/help/instructions.jsp. If you do not have web access please contact the editorial office.

PO Box 2345, Beijing 100023, China
www.wjgnet.com
wjg@wjgnet.com

World J Gastroenterol 2007 January 14; 13(2): 165-169
World Journal of Gastroenterology ISSN 1007-9327

EDITORIAL

Role of endosonography in non-malignant pancreatic diseases

Kyung W Noh, Surakit Pungpapong, Massimo Raimondo

Kyung W Noh, Surakit Pungpapong, Massimo Raimondo, Division of Gastroenterology and Hepatology, Mayo Clinic College of Medicine, Jacksonville, FL, United States
Correspondence to: Massimo Raimondo, MD, FACG, Associate Professor of Medicine, Mayo Clinic College of Medicine, 4500 San Pablo Road, Jacksonville, FL 32224, United States. raimondo.massimo@mayo.edu
Telephone: +1-904-9536982 Fax: +1-904-9537260
Received: 2006-07-25 Accepted: 2006-10-05

Abstract

Endoscopic ultrasound (EUS) has emerged as a valuable tool in the evaluation of benign and malignant pancreatic diseases. The ability to obtain high quality images and perform fine-needle aspiration (FNA) has led EUS to become the diagnostic test of choice when evaluating the pancreas. This article will review the role of EUS in benign pancreatic diseases.

Key words: Endosonography; Chronic pancreatitis; Pancreatic cyst

Noh KW, Pungpapong S, Raimondo M. Role of endosonography in non-malignant pancreatic diseases. *World J Gastroenterol* 2007; 13(2): 165-169

http://www.wjgnet.com/1007-9327/13/165.asp

INTRODUCTION

Endoscopic ultrasound (EUS) was developed in part to better evaluate the pancreas. As the ultrasound probe lies in close proximity of the pancreas, high quality images can be obtained and FNA can be performed under ultrasound guidance. EUS is considered safer and less invasive than endoscopic retrograde pancreatography (ERP). Thus, EUS is an important diagnostic test when evaluating the pancreas, especially in the setting of benign pancreatic diseases.

CHRONIC PANCREATITIS

EUS appearance

The diagnosis of chronic pancreatitis *via* EUS is based on parenchymal and ductal criteria on examination of the pancreas. The presence of 5 or more criteria is generally considered highly suggestive or diagnostic of chronic pancreatitis and the presence of 2 or less criteria generally rules out the diagnosis of chronic pancreatitis.

To make the EUS diagnosis of chronic pancreatitis, one must understand the "normal" sonographic features of the pancreas. Several features were initially established by standard transabdominal ultrasound examinations of the pancreas. A "normal pancreas" was determined through studies such as that of Ikeda *et al*[1] who reported features of the pancreas in a large screening program in Japan. The pancreatic parenchyma in the absence of disease should appear homogeneous and have a "salt and pepper" appearance (Figure 1). The pancreatic duct should be seen as a smooth tubular structure coursing through the center of the pancreas. Side branches should not be visible.

The features of chronic pancreatitis can be divided into those that pertain to the parenchyma and the duct. These have been previously described by Lees[2,3] and Wiersema[4]. The parenchymal features include: hyperechogenic foci, hyperechogenic strands, lobulation, cysts, and calcifications; the ductal features include: main duct dilation, main duct irregularity, hyperechogenic main duct margins, and visible side branch ducts (Table 1).

Hyperechogenic foci and strands are bright echoes or string-like structures that may correlate histologically with thickened fibrous deposits[5]. These findings can be seen in patients with a normal pancreas, especially in older individuals. When hyperechogenic strands form a distinct "lobule", this is called lobulation (Figure 2). The pancreas thus appears inhomogeneous. This feature is more strongly associated with chronic pancreatitis as compared to hyperechogenic foci and strands alone. Calcifications of the pancreas are seen as hyperechoic or bright areas with acoustic shadowing. This feature is almost pathognomonic of chronic pancreatitis. Cysts are anechoic round or oval structures. Pancreatic cysts will be discussed further in the later sections of this article.

The size of a normal pancreatic duct is considered to be less than 3 mm in the head, 2 mm in the body and 1 mm in the tail of the pancreas. A larger duct is considered to be abnormal except in older patients when found as an isolated finding. An irregular duct correlates with focal dilation and narrowing of the main pancreatic duct. If a side branch is visible, this is considered a feature of chronic pancreatitis.

The threshold for EUS diagnosis of chronic pancreatitis can be varied. A lower threshold such as greater than 3 criteria will produce a high sensitivity, but a low specificity. By contrast, using a higher threshold such as greater than 5 criteria will produce a low sensitivity and a high specificity. Thus, if the purpose of the examination

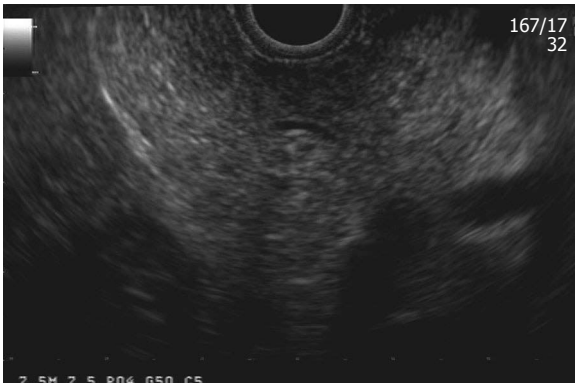

Figure 1 Normal pancreas.

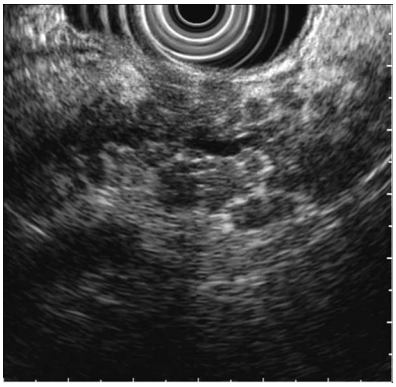

Figure 2 Lobular pancreas.

Table 1 Features of chronic pancreatitis

EUS criteria	Appearance	Histological correlate
Hyperechoic foci	Small distinct focus of bright echo	Focal fibrosis
Hyperechoic strands	Small string like bright echo	Bridging fibrosis
Lobularity	Rounded homogenous areas separated by hyperechoic strands	Fibrosis, glandular atrophy
Cyst	Abnormal anechoic round or oval structure	Cysts, pseudocyst
Calcification	Hyperechoic lesion with acoustic shadowing	Parenchymal calcification
Ductal dilation	> 3 mm in head, > 2 mm in body, > 1 mm in tail	Duct dilation
Side branch dilation	Small anechoic structure outside the main pancreatic duct	Side branch dilation
Duct irregularity	Coarse uneven outline of the duct	Focal dilation, narrowing
Hyperechoic duct margins	Hyperechoic margins of the main pancreatic duct	Periductal fibrosis

is to exclude disease, a low threshold should be used. However, if the purpose is to establish the diagnosis chronic pancreatitis, a higher threshold should be used.

Another important fact is that not all factors are equal when diagnosing chronic pancreatitis. The features of lobulation and calcification are suggestive of chronic pancreatitis even in the absence of other criteria. As mentioned earlier, some features such as a dilated duct can be a "normal" finding in older individuals[1]. Currently, there is no accepted scoring system to take these factors into consideration.

Recent experimental evidence suggests the complementary role of increased levels of an inflammatory mediator such as the interleukin 8 (IL-8) in pancreatic juice and EUS to diagnose chronic pancreatitis[6]. In this study, the specificity of the combination of tests (both increased pancreatic juice levels of IL-8 and abnormal EUS) reached 100%. Until these data are confirmed in larger studies, clinical judgment must be used to make a diagnosis of chronic pancreatitis.

The lack of a gold standard for diagnosis other than histology has pressed some investigators to explore the role of EUS-FNA in chronic pancreatitis. Hollerbach *et al*[7] performed EUS-FNA in 27 patients with different degrees of severity (as measured by ERP criteria). EUS was 97% sensitive but only 60% specific for the diagnosis of chronic pancreatitis. The only advantage of EUS-FNA in this study was represented by an increased negative predictive value. Few patients developed self-limited abdominal pain after the procedure, but no major complications were observed.

More recently, DeWitt *et al*[8] published their experience with EUS-FNA using the trucut needle which provides a core biopsy of the pancreas for histology. The results were compared with EUS and ERP. The authors observed poor agreement between EUS and EUS with trucut biopsy and only fair agreement between ERP and EUS with trucut biopsy. Therefore, the results of these studies induce caution when considering EUS-FNA (including the trucut needle) to diagnose chronic pancreatitis.

Conversely, EUS with trucut biopsy may have a significant role when considering the diagnosis of autoimmune chronic pancreatitis. Though the most characteristic endosonographic finding of this condition is diffuse pancreatic parenchyma enlargement (so-called sausage shape), there may be overlap with the non-autoimmune form of the disease or with cases of a pseudotumorous pancreatitis. Levy *et al*[9] reported their experience on 19 patients with autoimmune pancreatitis. In 10 patients who had EUS-FNA, the material retrieved was not adequate for the cytopathologist to make the diagnosis. However, the combination of the trucut needle and the immunohistochemistry staining for IgG 4 allowed the Authors to reach the correct final diagnosis of chronic autoimmune pancreatitis in virtually all patients. The authors concluded that though the EUS with trucut helps to make the diagnosis of autoimmune pancreatitis, this condition has still a low prevalence and a high suspicion of the disease with appropriate clinical presentation is necessary.

PANCREATIC CYSTS

EUS appearance

Improved imaging techniques and more frequent imaging of the abdomen has led to increased discovery of pancreatic cysts. These cysts pose a diagnostic and therapeutic challenge as the pathology ranges from benign pseudocysts to malignant cystic neoplasms. EUS plays an important role in the diagnosis and management of pancreatic cysts as allows for high quality images and the ability to perform fine needle aspiration.

Pseudocysts account for approximately 90% of pancreatic cystic lesions. Serous cystadenomas (SCA), mucinous cystadenomas (MCA) and intraductal papillary mucinous neoplasms (IPMN) account for the majority of the remaining 10% of cysts. Pseudocysts and SCA have little or no malignant potential as opposed to MCA and IPMN which are potentially malignant or malignant. Thus, it is important to identify mucinous cystic lesions.

Pseudocysts are inflammatory fluid collections that arise in the setting of acute or chronic pancreatitis. These cysts are anechoic, thick walled structures. Septations are rare and regional inflammatory lymph nodes may be seen. Aspiration of cyst fluid will reveal dark, thin fluid containing inflammatory cells and high levels of amylase.

SCA are benign cystic lesions of the pancreas[10] with the exception of a few case reports[11-13]. They have a female predilection and are most commonly discovered in the 7th decade of life[10,14,15]. These cysts are generally microcystic, but solid and macrocystic variants have been described[16-19]. This leads to a honeycomb appearance in cross-section. Central or "sunburst" calcification is considered pathognomonic, but is found in less than 20% of cases[15,20]. Cytology obtained from EUS guided FNA of these cysts is often non-diagnostic[21]. However, when an adequate sample is obtained, this will reveal cuboidal cells without the presence of mucin.

MCA are generally macrocystic, composed of a small number of discrete compartments greater than 2 cm in size[15]. The septations are thick, irregular and occasionally a peripheral area of calcification is present[22]. It has a female predilection, mostly present in the body-tail region of the pancreas and occur most commonly in the 5th to 7th decade of life[15,20,23]. The presence of mural nodules is suggestive of invasive carcinoma. The cyst fluid of MCA is viscous and clear. Cytology will reveal mucin rich fluid with columnar mucinous cells[15].

The EUS appearance of IPMN includes segmental or diffuse dilation of the main pancreatic duct or multiple pancreatic cysts that arise from the branch ducts of the main pancreatic duct. There is an equal or slightly higher incidence of IPMNs among males than in females. The peak incidence is in the 6th and 7th decade of life[15,24]. Like MCA, the cyst fluid is viscous, clear and will contain mucinous epithelial cells[15].

Cyst fluid analysis

Cyst fluid analysis of tumor markers has been studied to differentiate among benign and pre-malignant pancreatic cysts. In the Cooperative Pancreatic Cyst Study, the authors compared the findings of pancreatic cyst fluid of one hundred twelve patients obtained *via* EUS-FNA to surgical histology. EUS morphology, fluid cytology and cystic fluid tumor markers were evaluated. The results demonstrated that cyst fluid CEA levels (optimal cut-off 192 ng/mL) provided the greatest accuracy in differentiating mucinous versus non-mucinous pancreatic cysts. In addition, the accuracy of cyst fluid CEA was higher than that of EUS morphology, cyst fluid cytology or any combination of tests[25]. However, cyst fluid tumor marker values alone cannot definitively discriminate between mucinous and non-mucinous pancreatic cysts as there is overlap of CEA levels in these cysts[25,26].

New techniques

Trucut biopsy of the pancreatic cyst wall has been investigated as a possible method of diagnosing pancreatic cysts. Levy *et al*[27] performed EUS guided trucut biopsies (EUS-TCB) in ten patients. In seven patients, a diagnosis was established and no complications were reported. Although promising, EUS-TCB can be difficult to perform in the head of the pancreas given the risk of puncturing surrounding vasculature. In addition, the curvature of the scope may not allow for effective firing of the biopsy needle.

The role of pancreatic cyst fluid molecular analysis in predicting the pathology of the pancreatic cysts has been investigated. Khalid *et al*[28] analyzed pancreatic cystic fluid obtained *via* EUS-FNA in thirty-six patients with confirmed surgical histology. The authors hypothesized that polymerase chain reaction (PCR) amplification of DNA from whole or lysed cells shed into the cyst fluid may be predictive of cyst pathology. A high level of mutational damage would predict an underlying malignancy. In addition, as malignant cysts would have high cell turnover, cyst fluid DNA content may be higher in malignant cysts. Ten of the eleven malignant cysts carried multiple mutations as compared to no mutations in all ten benign cysts. The total amount of DNA in the malignant cysts was significantly higher than in the benign cysts.

INTERVENTIONAL EUS

Celiac plexus block

Pain associated with chronic pancreatitis can be difficult to control[29]. Often narcotic pain medications are required, but these are associated with significant adverse effects including constipation, nausea, vomiting and dependence. As pancreatic pain is mainly transmitted through the celiac plexus, celiac plexus neurolysis or block has been employed to manage pain related to pancreatic cancer or chronic pancreatitis. Initially, this was performed surgically or percutaneously. EUS-guided celiac plexus neurolysis was introduced by Wiersema *et al*[30] which was found to be as effective as the surgical or percutaneous approaches for the management of pancreatic cancer related pain. This technique was applied to manage pain from chronic pancreatitis[31,32]. Gress *et al*[31] reported a series of ninety patients with chronic pancreatitis who underwent EUS-guided celiac plexus block using Bupivacaine and Triamcinolone. Fifty-five percent of patients reported

a decrease in pain symptoms at 4 and 8 wk. A smaller percentage of patients experienced pain relief at 12 and 24 wk. The study was limited by a lack of a placebo arm which allows for potential bias. The use of celiac plexus block for the management of chronic pancreatitis pain remains uncertain and further studies are necessary.

Drainage of pseudocyst

Pancreatic pseudocysts may develop as sequela of acute or chronic pancreatitis. They can be asymptomatic and often resolve with time. However, when they become symptomatic or enlarge to greater than 6 cm in size, drainage is indicated. Traditionally, drainage of pseudocysts was performed surgically. However, percutaneous and endoscopic techniques have gained favor given the mortality and morbidity of surgery. The location of puncture for transgastric and transduodenal drainage of pseudocysts was determined by the bulge caused by the pseudocyst into the lumen. In the absence of a bulge, puncture of the cyst was a "blind" process increasing the risk of perforation and hemorrhage[33,34]. EUS allows for transgastric or transduodenal drainage of the pseudocyst under real time ultrasound guidance and thus minimizes the risk of complications. Various techniques have been described in the literature[34-42].

CONCLUSIONS

EUS is an essential tool in evaluating benign pancreatic diseases. Chronic pancreatitis and cystic lesions of the pancreas pose a diagnostic challenge. EUS carries an advantage over CT scans and endoscopic retrograde pancreatography in the diagnosis of chronic pancreatitis as it has the ability to detect parenchymal changes evident in early chronic pancreatitis. In the cases of pancreatic cysts, EUS allows for direct sampling of cyst fluid under ultrasound guidance to differentiate between cystic lesions of the pancreas. Overall, the ability to obtain important information regarding the pancreas through high quality images and FNA in a relatively safe manner is the main advantage of EUS.

REFERENCES

1 **Ikeda M**, Sato T, Morozumi A, Fujino MA, Yoda Y, Ochiai M, Kobayashi K. Morphologic changes in the pancreas detected by screening ultrasonography in a mass survey, with special reference to main duct dilatation, cyst formation, and calcification. *Pancreas* 1994; **9**: 508-512

2 **Lees WR**. Endoscopic ultrasonography of chronic pancreatitis and pancreatic pseudocysts. *Scand J Gastroenterol Suppl* 1986; **123**: 123-129

3 **Lees WR**, Vallon AG, Denyer ME, Vahl SP, Cotton PB. Prospective study of ultrasonography in chronic pancreatic disease. *Br Med J* 1979; **1**: 162-164

4 **Wiersema MJ**, Hawes RH, Lehman GA, Kochman ML, Sherman S, Kopecky KK. Prospective evaluation of endoscopic ultrasonography and endoscopic retrograde cholangiopancreatography in patients with chronic abdominal pain of suspected pancreatic origin. *Endoscopy* 1993; **25**: 555-564

5 **Sahai AV**. EUS and chronic pancreatitis. *Gastrointest Endosc* 2002; **56**: S76-S81

6 **Pungpapong S**, Noh KW, Al-Haddad M, Wallace MB, Woodward TA, Raimondo M. Combined pancreatic juice IL-8 concentration and EUS are highly predictive to diagnosis chronic pancreatitis. *Gastroenterology* 2006; **130**: A-13

7 **Hollerbach S**, Klamann A, Topalidis T, Schmiegel WH. Endoscopic ultrasonography (EUS) and fine-needle aspiration (FNA) cytology for diagnosis of chronic pancreatitis. *Endoscopy* 2001; **33**: 824-831

8 **DeWitt J**, McGreevy K, LeBlanc J, McHenry L, Cummings O, Sherman S. EUS-guided Trucut biopsy of suspected nonfocal chronic pancreatitis. *Gastrointest Endosc* 2005; **62**: 76-84

9 **Levy MJ**, Reddy RP, Wiersema MJ, Smyrk TC, Clain JE, Harewood GC, Pearson RK, Rajan E, Topazian MD, Yusuf TE, Chari ST, Petersen BT. EUS-guided trucut biopsy in establishing autoimmune pancreatitis as the cause of obstructive jaundice. *Gastrointest Endosc* 2005; **61**: 467-472

10 **Pyke CM**, van Heerden JA, Colby TV, Sarr MG, Weaver AL. The spectrum of serous cystadenoma of the pancreas. Clinical, pathologic, and surgical aspects. *Ann Surg* 1992; **215**: 132-139

11 **Abe H**, Kubota K, Mori M, Miki K, Minagawa M, Noie T, Kimura W, Makuuchi M. Serous cystadenoma of the pancreas with invasive growth: benign or malignant? *Am J Gastroenterol* 1998; **93**: 1963-1966

12 **Fujii H**, Kubo S, Hirohashi K, Kinoshita H, Yamamoto T, Wakasa K. Serous cystadenoma of the pancreas with atypical cells. Case report. *Int J Pancreatol* 1998; **23**: 165-169

13 **Ohta T**, Nagakawa T, Itoh H, Fonseca L, Miyazaki I, Terada T. A case of serous cystadenoma of the pancreas with focal malignant changes. *Int J Pancreatol* 1993; **14**: 283-289

14 **Fernández-del** Castillo C, Warshaw AL. Cystic tumors of the pancreas. *Surg Clin North Am* 1995; **75**: 1001-1016

15 **Brugge WR**, Lauwers GY, Sahani D, Fernandez-del Castillo C, Warshaw AL. Cystic neoplasms of the pancreas. *N Engl J Med* 2004; **351**: 1218-1226

16 **Hashimoto M**, Watanabe G, Miura Y, Matsuda M, Takeuchi K, Mori M. Macrocystic type of serous cystadenoma with a communication between the cyst and pancreatic duct. *J Gastroenterol Hepatol* 2001; **16**: 836-838

17 **Lewandrowski K**, Warshaw A, Compton C. Macrocystic serous cystadenoma of the pancreas: a morphologic variant differing from microcystic adenoma. *Hum Pathol* 1992; **23**: 871-875

18 **Sperti C**, Pasquali C, Perasole A, Liessi G, Pedrazzoli S. Macrocystic serous cystadenoma of the pancreas: clinicopathologic features in seven cases. *Int J Pancreatol* 2000; **28**: 1-7

19 **Brugge WR**. Evaluation of pancreatic cystic lesions with EUS. *Gastrointest Endosc* 2004; **59**: 698-707

20 **Warshaw AL**, Compton CC, Lewandrowski K, Cardenosa G, Mueller PR. Cystic tumors of the pancreas. New clinical, radiologic, and pathologic observations in 67 patients. *Ann Surg* 1990; **212**: 432-443; discussion 444-445

21 **Brugge WR**. The role of EUS in the diagnosis of cystic lesions of the pancreas. *Gastrointest Endosc* 2000; **52**: S18-S22

22 **Balci NC**, Semelka RC. Radiologic features of cystic, endocrine and other pancreatic neoplasms. *Eur J Radiol* 2001; **38**: 113-119

23 **Sarr MG**, Carpenter HA, Prabhakar LP, Orchard TF, Hughes S, van Heerden JA, DiMagno EP. Clinical and pathologic correlation of 84 mucinous cystic neoplasms of the pancreas: can one reliably differentiate benign from malignant (or premalignant) neoplasms? *Ann Surg* 2000; **231**: 205-212

24 **Kimura W**, Sasahira N, Yoshikawa T, Muto T, Makuuchi M. Duct-ectatic type of mucin producing tumor of the pancreas-new concept of pancreatic neoplasia. *Hepatogastroenterology* 1996; **43**: 692-709

25 **Brugge WR**, Lewandrowski K, Lee-Lewandrowski E, Centeno BA, Szydlo T, Regan S, del Castillo CF, Warshaw AL. Diagnosis of pancreatic cystic neoplasms: a report of the cooperative pancreatic cyst study. *Gastroenterology* 2004; **126**: 1330-1336

26 **Frossard JL**, Amouyal P, Amouyal G, Palazzo L, Amaris J, Soldan M, Giostra E, Spahr L, Hadengue A, Fabre M. Performance of endosonography-guided fine needle aspiration and biopsy in the diagnosis of pancreatic cystic lesions. *Am J Gastroenterol* 2003; **98**: 1516-1524

27 **Levy MJ**, Smyrk TC, Reddy RP, Clain JE, Harewood GC, Kendrick ML, Pearson RK, Petersen BT, Rajan E, Topazian MD, Wang KK, Wiersema MJ, Yusuf TE, Chari ST. Endoscopic ultrasound-guided trucut biopsy of the cyst wall for diagnosing cystic pancreatic tumors. *Clin Gastroenterol Hepatol* 2005; **3**: 974-979
28 **Khalid A**, McGrath KM, Zahid M, Wilson M, Brody D, Swalsky P, Moser AJ, Lee KK, Slivka A, Whitcomb DC, Finkelstein S. The role of pancreatic cyst fluid molecular analysis in predicting cyst pathology. *Clin Gastroenterol Hepatol* 2005; **3**: 967-973
29 **Lankisch PG**. Natural course of chronic pancreatitis. *Pancreatology* 2001; **1**: 3-14
30 **Wiersema MJ**, Wiersema LM. Endosonography-guided celiac plexus neurolysis. *Gastrointest Endosc* 1996; **44**: 656-662
31 **Gress F**, Schmitt C, Sherman S, Ciaccia D, Ikenberry S, Lehman G. Endoscopic ultrasound-guided celiac plexus block for managing abdominal pain associated with chronic pancreatitis: a prospective single center experience. *Am J Gastroenterol* 2001; **96**: 409-416
32 **Gress F**, Schmitt C, Sherman S, Ikenberry S, Lehman G. A prospective randomized comparison of endoscopic ultrasound- and computed tomography-guided celiac plexus block for managing chronic pancreatitis pain. *Am J Gastroenterol* 1999; **94**: 900-905
33 **Cremer M**, Deviere J, Engelholm L. Endoscopic management of cysts and pseudocysts in chronic pancreatitis: long-term follow-up after 7 years of experience. *Gastrointest Endosc* 1989; **35**: 1-9
34 **Sahel J**, Bastid C, Pellat B, Schurgers P, Sarles H. Endoscopic cystoduodenostomy of cysts of chronic calcifying pancreatitis: a report of 20 cases. *Pancreas* 1987; **2**: 447-453
35 **Binmoeller KF**, Seifert H, Soehendra N. Endoscopic pseudocyst drainage: a new instrument for simplified cystoenterostomy. *Gastrointest Endosc* 1994; **40**: 112
36 **Gerolami R**, Giovannini M, Laugier R. Endoscopic drainage of pancreatic pseudocysts guided by endosonography. *Endoscopy* 1997; **29**: 106-108
37 **Giovannini M**, Bernardini D, Seitz JF. Cystogastrotomy entirely performed under endosonography guidance for pancreatic pseudocyst: results in six patients. *Gastrointest Endosc* 1998; **48**: 200-203
38 **Giovannini M**, Pesenti C, Rolland AL, Moutardier V, Delpero JR. Endoscopic ultrasound-guided drainage of pancreatic pseudocysts or pancreatic abscesses using a therapeutic echo endoscope. *Endoscopy* 2001; **33**: 473-477
39 **Grimm H**, Binmoeller KF, Soehendra N. Endosonography-guided drainage of a pancreatic pseudocyst. *Gastrointest Endosc* 1992; **38**: 170-171
40 **Seifert H**, Dietrich C, Schmitt T, Caspary W, Wehrmann T. Endoscopic ultrasound-guided one-step transmural drainage of cystic abdominal lesions with a large-channel echo endoscope. *Endoscopy* 2000; **32**: 255-259
41 **Seifert H**, Faust D, Schmitt T, Dietrich C, Caspary W, Wehrmann T. Transmural drainage of cystic peripancreatic lesions with a new large-channel echo endoscope. *Endoscopy* 2001; **33**: 1022-1026
42 **Wiersema MJ**. Endosonography-guided cystoduodenostomy with a therapeutic ultrasound endoscope. *Gastrointest Endosc* 1996; **44**: 614-617

S- Editor Liu Y **L- Editor** Alpini GD **E- Editor** Lu W

PO Box 2345, Beijing 100023, China
www.wjgnet.com
wjg@wjgnet.com

World J Gastroenterol 2007 January 14; 13(2): 170-174
World Journal of Gastroenterology ISSN 1007-9327

EDITORIAL

Pancreatitis-associated protein: From a lectin to an anti-inflammatory cytokine

Daniel Closa, Yoshiharu Motoo, Juan L Iovanna

Daniel Closa, Department of Experimental Pathology, IIBB-CSIC, IDIBAPS, Barcelona, Spain
Yoshiharu Motoo, Department of Medical Oncology, Kanazawa Medical University, Ishikawa, Japan
Juan L Iovanna, INSERM U.624, Stress Cellulaire, Marseille, France
Correspondence to: Dr. Daniel Closa, Experimental Pathology Dept., IIBB-CSIC, c/ Rosselló 161, 7º, Barcelona 08036, Spain. dcabam@iibb.csic.es
Telephone: +34-93-3638307 Fax: +34-93-3638301
Received: 2006-07-07 Accepted: 2006-10-12

Abstract

Pancreatitis-associated protein (PAP) was discovered in the pancreatic juice of rats with acute pancreatitis. PAP is a 16 kDa secretory protein structurally related to the C-type lectins although classical lectin-related function has not been reported yet. Then, it was demonstrated that PAP expression may be activated in some tissues in a constitutive or injury- and inflammation-induced manner. More recently, it has been found that PAP acts as an anti-inflammatory factor *in vitro* and *in vivo*. PAP expression can be induced by several pro- and anti-inflammatory cytokines and by itself through a JAK/STAT3-dependent pathway. PAP is able to activate the expression of the anti-inflammatory factor SOCS3 through the JAK/STAT3-dependent pathway. The JAK/STAT3/SOCS3 pathway seems to be a common point between PAP and several cytokines. Therefore, it is reasonable to propose that PAP is a new anti-inflammatory cytokine.

Key words: Pancreatitis-associated protein; Pancreatitis; Janus kinases; STAT3; SOCS3; Anti-inflammatory; Lectin

Closa D, Motoo Y, Iovanna JL. Pancreatitis-associated protein: From a lectin to an anti-inflammatory cytokine. *World J Gastroenterol* 2007; 13(2): 170-174

http://www.wjgnet.com/1007-9327/13/170.asp

INTRODUCTION

In 1984, Keim and co-workers reported the presence of a new protein in pancreatic juice of rats after induction of acute pancreatitis[1]. This secretory protein was absent in control rats but appeared early after induction of pancreatitis and remained over-expressed for the following 3-4 d. The protein was detected also in pancreas homogenate and in zymogen granules. Due to the relationship with the induction of pancreatitis, the protein was denominated "pancreatitis associated protein" or PAP. Four years later, Tachibana and colleagues described the peptide 23 as a protein from the rat pituitary gland, which synthesis was stimulated by the growth hormone-releasing hormone and inhibited by somatostatin[2] but its primary structure remained unresolved at the time. The sequence of PAP was deduced after cloning the corresponding mRNA from rat[3] and human pancreas[4]. Only four years later Katsumata and co-workers reported that in fact, peptide 23, identified in 1988, was identical to PAP[5]. Finally, Lasserre and colleagues found that the PAP mRNA was overexpressed in 7 of 29 hepatocellular carcinomas[6] and named the encoded protein HIP. Therefore, peptide 23, HIP and PAP are three names for the same protein. In this review we will call it PAP because it is the first name adopted for this protein.

In healthy pancreas, PAP is constitutively expressed in the α-cells of Langerhans islets[7]. By contrast, in the exocrine pancreas, PAP is only expressed when the acinar cells are harmed[4]. In fact, PAP expression is activated in pancreatic acinar cells in response to many injuries such as acute and chronic pancreatitis[4], hypoxia[8], toxins[9], diabetes[10], lipopolysaccharides[11], hypotransferrinaemia[12], and in the transplanted tissue[13]. However, its expression is not restricted to pancreatic tissue, and could be observed in several organs. This includes the intestine during chronic inflammatory diseases such as Crohn's disease and ulcerative colitis[14,15] and in animal models of inflammatory bowel disease (IBD)[16]. PAP is also expressed in the brain tissue of Alzheimer patients[17,18], in the luminal epithelial cells of the uterus[19] and in a sub-population of developing motoneurons and, after peripheral injury, in sensory neurons and motoneurons[20,21]. Moreover, PAP mRNA expression was found activated in about 80% of the pancreatic adenocarcinomas of ductal origin and in 30% of mucinous cystadenomas[22]. The levels of PAP mRNA expression correlated with nodal invasion, presence of distant metastases and short survival. Also, in some cases peritumoral regions overexpressed PAP[23], indicating that both tumor and peritumoral cells contribute to the high PAP serum level observed in patients with pancreatic cancer. In the liver, PAP was found strongly activated in about 30% of the primary hepatocarcinomas,

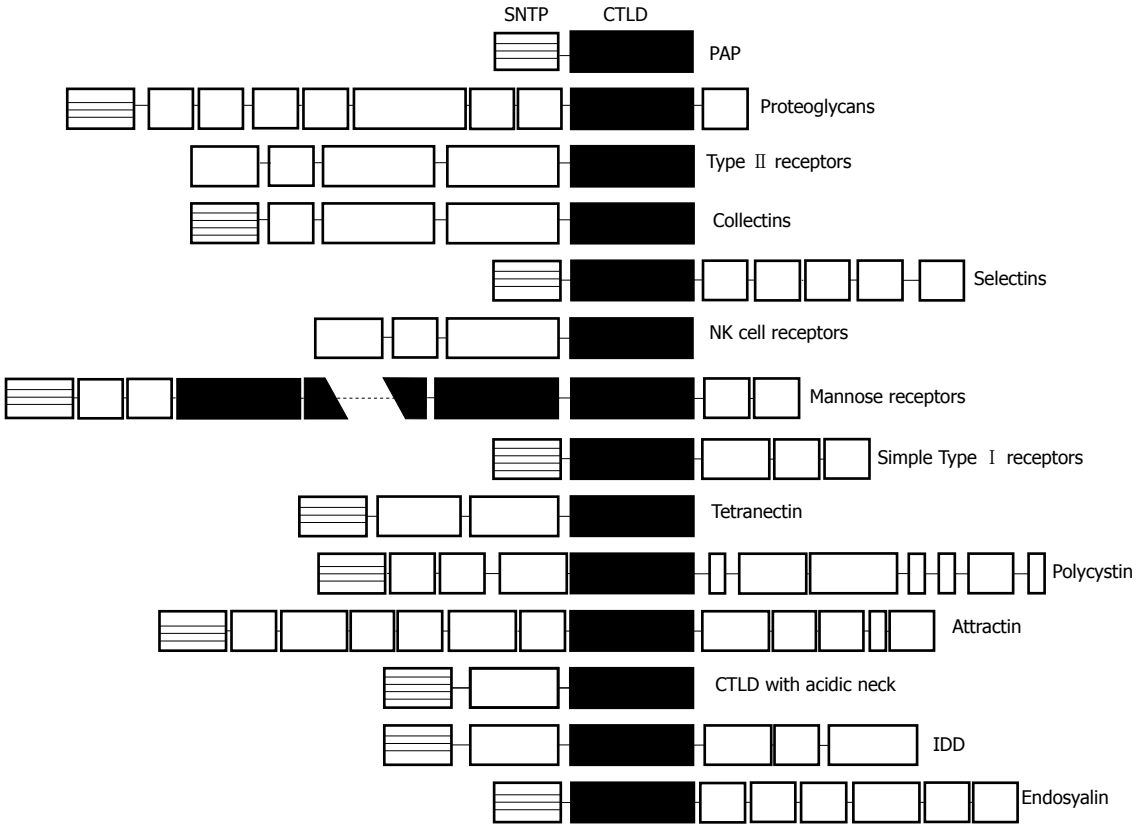

Figure 1 Schematic protein domains in the different C-type lectins. Sequences are aligned on the C-type lectin-like domain (CTLD). Note that PAP is the smallest protein member, containing only the CTLD linked to a short N-terminal peptide (SNTP).

but the forced expression of PAP in this organ does not induce tumor development[24].

PAP IS A LECTIN-RELATED PROTEIN

Computer analysis of the PAP sequence suggests a structural relationship with lectins[3]. Identities between PAP and the other animal and human lectins range from 16% to 26%. Homologous domain includes the conserved amino acids of the consensus carbohydrate binding domain of the Ca^{2+}-dependent lectins (C-type lectins) (Figure 1). However, initial attempts to characterize a carbohydrate binding activity, including erythrocyte agglutination or adsorption to affinity columns specific for different carbohydrates, failed[3]. The structural organization of the PAP gene reveals new clues to the evolutionary development of the lectin genes. The PAP coding sequence spans over six exons and the putative carbohydrate-recognition domain is encoded by exons Ⅳ, Ⅴ and Ⅵ. This gene organization suggests that PAP belongs to a new group of lectins which have evolved from the same carbohydrate-recognition domain ancestral precursor through a different process[25]. It is interesting to note that PAP is the smallest protein reported among the C-type lectins. In fact, it comprises a single carbohydrate-recognition domain linked to a signal peptide[26] whereas other C-type lectins contain the sugar-binding consensus combined with a variety of other protein domains which confer specific functions of lectins. In contrast, PAP does not have additional functional domains.

PAP IN PANCREATIC DISEASES

Early after its discovery it becomes clear that acinar cells of the pancreas are the main source of PAP in pathological situations. Using an experimental model of acute pancreatitis in rat, Morisset and co-workers found the induction of PAP and its localization in zymogen granules[27]. Bodeker and co-workers described the pattern of PAP up-regulation in exocrine pancreas during the progression of the disease[28]. The profiles obtained by Northern blot analysis with pancreatic RNAs, Western blot in pancreatic protein extracts and immunodetection are equivalent to that observed in human disease and in animal models. The absence of PAP in healthy pancreas and its strong induction observed during the early phase of the disease suggest that PAP could be a stress protein or an acute phase protein induced upon cell insult. This is of interest since pancreatic acute phase response, characterized by sudden changes in protein expression is a clear indicator of injury or infections in the pancreatic gland. Since PAP is overexpressed by pancreatic cells in response to cellular stress, it has been evaluated whether serum PAP could be an indicator of different pancreatic diseases. In an initial retrospective study[29], it has been suggested that PAP might be a useful serum marker in the following of acute pancreatitis. In particular, a continuous elevation of serum PAP concentrations indicates that pancreatitis is still in progress. Nevertheless, other studies revealed that despite severity of pancreatitis correlated with serum levels of PAP, the sensitivity of PAP did not allow distinguishing severe from mild acute pancreatitis, better than C reactive protein[30]. In the case of pancreatic cancer, PAP was also overexpressed and could be observed in malignant ductular structures in pancreatic carcinomas[22]. Other reports revealed that PAP was strongly expressed in acini adjacent to the invasive adenocarcinoma, suggesting that the main source of PAP release in the pancreatic

juice is acini[23]. Since overexpression of PAP significantly correlated with nodal involvement, distant metastasis, and short survival, it has been suggested that its expression in human pancreatic ductal adenocarcinoma could be an indicator of tumor aggressiveness[22].

PHYSIOLOGICAL FUNCTIONS OF PAP

The fact that PAP is secreted by pancreatic acinar cells into the pancreatic juice initially suggested a role for this protein in pancreatic juice homeostasis. Several data are in line with this. Pancreatic juice is supersaturated in $CaCO_3$ and, in the absence of physiological inhibitors, this salt will precipitate in crystal formation. Interestingly, lithostathine, another member of the PAP protein family, inhibits $CaCO_3$ crystal growth *in vitro*[31]. On the other hand, it has been shown that PAP can bind and aggregate several bacterial strains from the intestinal flora including Gram positive and Gram negative, aerobic and anaerobic bacteria, although without inhibiting their growth[3]. This fact suggests that PAP could act as an endogenous anti-bacterial agent that could play a protective role preventing infectious complications in acute pancreatitis. Another suggested function for PAP is related to the fact that PAP conferred significant resistance to apoptosis induced by TNFα[32] or by low doses of H_2O_2[33], indicating that during acute pancreatitis PAP generation could be part of a mechanism of pancreatic cell protection against apoptosis. This anti-apoptotic effect of PAP was also observed in liver in which PAP protects hepatocytes against TNFα-induced apoptosis[24]. An interesting role for PAP has also been observed in motoneurons. It has been reported that PAP expression is activated in developing and regenerating motoneurons[20]. This effect is related to ciliary neurotrophic factor (CNTF), which is an important survival factor for motoneurons. In cultured motoneurons, CNTF induces PAP expression which acts as an autocrine/paracrine neurotrophic factor in a subpopulation of motoneurons, by stimulating a survival pathway involving PI3 kinase, Akt kinase and NFκB[34]. Despite the obvious interest of these observations, it is difficult to link these effects with the enormous amount of PAP released by pancreas during acute pancreatitis or cellular stress. Consequently, other physiological functions, more closely related with pancreatic diseases, have been investigated.

PAP AS AN ANTI-INFLAMMATORY MEDIATOR

The initial indication that PAP could act as a modulat or of the inflammatory response has been provided by Heller and co-workers[35]. Using an *ex-vivo* model of lung perfusion, these authors observed that PAP reduces the severity of some features associated with N-formyl-methionyl-leucyl-phenyl-alanine (FMLP)-induced activation of leukocytes. This includes the generation of thromboxane B_2 and the tissue edema formation in the lung. Since PAP generation has been observed in diseases related with inflammatory processes (pancreatitis, Crohn's disease, etc.), it was speculated that PAP could act as a cell response to the inflammatory stress. This is in line with the fact that induction in the pancreas of an acute-phase response, in which PAP expression was activated, prior to triggering necrotizing pancreatitis, significantly improved the survival of the animals[36]. Studies demonstrated that the administration of anti-PAP antibodies in an experimental model of taurocholate-induced acute pancreatitis in rats was associated with increased inflammation in the pancreas, evidenced by more abundant necrosis, increased pancreatic myeloperoxidase (MPO) levels and more prominent neutrophil infiltration[37]. Similar results were observed in another study using PAP antisense oligodeoxyribonucle otides to block the expression of PAP prior to induction of pancreatitis. With this approach, pancreatitis-induced PAP expression was reduced by 55% and markers of inflammatory cell damage were increased. These include serum amylase activity, pancreas edema, serum C-reactive protein, leukocyte infiltration and fat necrosis. In addition, the expression of *IL-1α, IL-1β* and *IL-4* was increased in peripheral blood mononuclear cells[38]. Pre-treatment with PAP of the *in vitro* TNFα-stimulated macrophages results in a dose-dependent inhibition of *IL-6* and *TNFα* mRNA expression[37]. The inhibitory effect of PAP has been observed in different cell lines, including rat pancreatic acinar AR42J cells and human HT29 colon derived cells[39]. In these models, PAP prevented NFκB translocation/activation in response to TNFα, indicating that inhibition by PAP occurs, at least in part, upstream of NFκB pathway. It is of clinical interest that the anti-inflammatory effect of PAP could be observed in other organs than pancreas. For example, increased serum levels of PAP expression has been observed in IBD-affected patients and these levels correlated with clinical and endoscopic parameters. In addition, *ex vivo* experiments showed that intestinal PAP synthesis and secretion was increased in active IBD and correlated with endoscopic and histological severity of inflammatory lesions. Remarkably, PAP reduced the proinflammatory cytokines secretion of the incubation of intestinal mucosa from active Crohn's disease in a dose dependent manner[39]. Consequently, it could be suggested that the anti-inflammatory role of PAP is not restricted to the pancreas and could be a more general response of the epithelial cells against the inflammatory processes.

ANTI-INFLAMMATORY ACTIVITY OF PAP IS MEDIATED BY STAT3 ACTIVATION

The inhibitory effect of PAP on the pro-inflammatory NFκB pathway seems to be dependent on protein synthesis. This has been demonstrated in AR42J cells by using cycloheximide into the culture medium to prevent *de novo* protein synthesis[40]. As indicated above, TNFα induces overexpression of the *TNFα* gene itself and this autocrine loop could be blocked by PAP. However, PAP lost its ability when protein synthesis was inhibited by cycloheximide. This protein synthesis dependence to act as an anti-inflammatory factor shows similarities to IL-10 and IL-6, which depend in part on the synthesis of suppressor of cytokine signalling (SOCS) proteins[41,42]. Both IL-10 and IL-6 receptors are related to the JAK/STAT signal

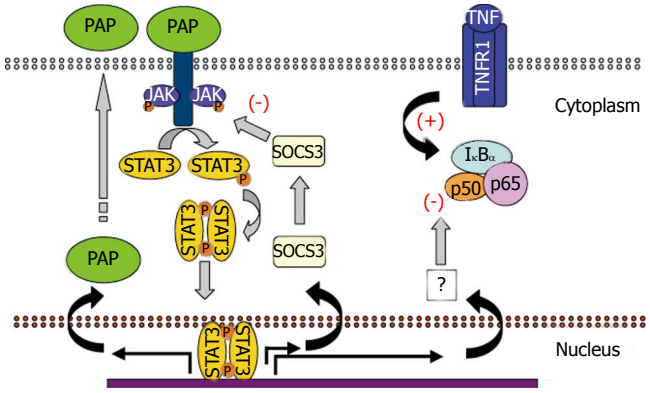

Figure 2 Anti-inflammatory pathway activated by PAP.

transduction pathways. Therefore, the relationship between PAP and JAK/STAT has also been evaluated. In a recent paper, it has been reported that PAP treatment of the AR42J cells results in a rapid and transient phosphorylation and nuclear translocation of STAT3 protein[40]. In addition, pre-treatment with JAK-specific inhibitors results in the blockage of the inhibitory effects induced by PAP. Finally, the PAP-dependent activation of STAT3 results in a strong activation of its gene target SOCS3 that in turn could be the mediator of the PAP anti-inflammatory effect. Altogether, these results indicate that PAP exerts their effects through the synthesis of a protein induced by the activation of the JAK/STAT signalling pathway. SOCS3 will be the best candidate.

PAP can be strongly induced by IL-6 and IL-10 and IL-10-related cytokines through a STAT3-mediated pathway. Interestingly, expression of PAP itself appears to be induced in pancreatic acinar cells by the presence of PAP in the medium. This is also related to the activation of STAT3 pathway since at least two functional STAT-responsible elements have been reported in the promoter of the PAP gene[43]. This self-induction suggests the existence of a positive feedback mechanism in pancreatic acinar cells *via* a PAP receptor and a cross-talk with other cytokines (Figure 2).

CONCLUDING REMARKS

PAP has been found as a 16 kDa secretory protein specifically induced in pancreas with acute pancreatitis. It has been demonstrated that PAP is activated in some tissues in a constitutive or injury- and inflammation-induced manner. PAP is structurally related to the C-type lectins although not classical lectin-related function has been reported. More recently, it has been found that PAP acts as an anti-inflammatory factor *in vitro* and *in vivo*. PAP expression can be induced by several pro- and anti-inflammatory cytokines and by itself through a JAK/STAT3-dependent pathway. PAP is able to activate the expression of the anti-inflammatory factor SOCS3 through the JAK/STAT3-dependent pathway. JAK/STAT3/SOCS3 pathway seems to be a common point between PAP and several cytokines. Therefore, it is reasonable to believe that PAP is a new anti-inflammatory cytokine.

REFERENCES

1 **Keim V**, Rohr G, Stöckert HG, Haberich FJ. An additional secretory protein in the rat pancreas. *Digestion* 1984; **29**: 242-249
2 **Tachibana K**, Marquardt H, Yokoya S, Friesen HG. Growth hormone-releasing hormone stimulates and somatostatin inhibits the release of a novel protein by cultured rat pituitary cells. *Mol Endocrinol* 1988; **2**: 973-978
3 **Iovanna J**, Orelle B, Keim V, Dagorn JC. Messenger RNA sequence and expression of rat pancreatitis-associated protein, a lectin-related protein overexpressed during acute experimental pancreatitis. *J Biol Chem* 1991; **266**: 24664-24669
4 **Orelle B**, Keim V, Masciotra L, Dagorn JC, Iovanna JL. Human pancreatitis-associated protein. Messenger RNA cloning and expression in pancreatic diseases. *J Clin Invest* 1992; **90**: 2284-2291
5 **Katsumata N**, Chakraborty C, Myal Y, Schroedter IC, Murphy LJ, Shiu RP, Friesen HG. Molecular cloning and expression of peptide 23, a growth hormone-releasing hormone-inducible pituitary protein. *Endocrinology* 1995; **136**: 1332-1339
6 **Lasserre C**, Christa L, Simon MT, Vernier P, Bréchot C. A novel gene (HIP) activated in human primary liver cancer. *Cancer Res* 1992; **52**: 5089-5095
7 **Christa L**, Carnot F, Simon MT, Levavasseur F, Stinnakre MG, Lasserre C, Thepot D, Clement B, Devinoy E, Brechot C. HIP/PAP is an adhesive protein expressed in hepatocarcinoma, normal Paneth, and pancreatic cells. *Am J Physiol* 1996; **271**: G993-G1002
8 **McKie AT**, Simpson RJ, Ghosh S, Peters TJ, Farzaneh F. Regulation of pancreatitis-associated protein (HIP/PAP) mRNA levels in mouse pancreas and small intestine. *Clin Sci (Lond)* 1996; **91**: 213-218
9 **Chen P**, Arias AE, Morisset J, Calvo E, Dagorn JC, Iovanna J, Bendayan M. Presence of pancreatitis-associated protein in pancreatic acinar cells of rats treated with chlorophenylalanine methyl ester. *Pancreas* 1996; **13**: 147-153
10 **Baeza N**, Sanchez D, Christa L, Guy-Crotte O, Vialettes B, Figarella C. Pancreatitis-associated protein (HIP/PAP) gene expression is upregulated in NOD mice pancreas and localized in exocrine tissue during diabetes. *Digestion* 2001; **64**: 233-239
11 **Vaccaro MI**, Calvo EL, Suburo AM, Sordelli DO, Lanosa G, Iovanna JL. Lipopolysaccharide directly affects pancreatic acinar cells: implications on acute pancreatitis pathophysiology. *Dig Dis Sci* 2000; **45**: 915-926
12 **Simpson RJ**, Deenmamode J, McKie AT, Raja KB, Salisbury JR, Iancu TC, Peters TJ. Time-course of iron overload and biochemical, histopathological and ultrastructural evidence of pancreatic damage in hypotransferrinaemic mice. *Clin Sci (Lond)* 1997; **93**: 453-462
13 **van der Pijl JW**, Boonstra JG, Barthellemy S, Smets YF, Hermans J, Bruijn JA, de Fijter JW, Daha MR, Dagorn JC. Pancreatitis-associated protein: a putative marker for pancreas graft rejection. *Transplantation* 1997; **63**: 995-1003
14 **Masciotra L**, Lechêne de la Porte P, Frigerio JM, Dusetti NJ, Dagorn JC, Iovanna JL. Immunocytochemical localization of pancreatitis-associated protein in human small intestine. *Dig Dis Sci* 1995; **40**: 519-524
15 **Dieckgraefe BK**, Stenson WF, Korzenik JR, Swanson PE, Harrington CA. Analysis of mucosal gene expression in inflammatory bowel disease by parallel oligonucleotide arrays. *Physiol Genomics* 2000; **4**: 1-11
16 **Lawrance IC**, Fiocchi C, Chakravarti S. Ulcerative colitis and Crohn's disease: distinctive gene expression profiles and novel susceptibility candidate genes. *Hum Mol Genet* 2001; **10**: 445-456
17 **Ozturk M**, de la Monte SM, Gross J, Wands JR. Elevated levels of an exocrine pancreatic secretory protein in Alzheimer disease brain. *Proc Natl Acad Sci USA* 1989; **86**: 419-423
18 **Duplan L**, Michel B, Boucraut J, Barthellémy S, Desplat-Jego S, Marin V, Gambarelli D, Bernard D, Berthézène P, Alescio-Lautier B, Verdier JM. Lithostathine and pancreatitis-

associated protein are involved in the very early stages of Alzheimer's disease. *Neurobiol Aging* 2001; **22**: 79-88

19 **Chakraborty C**, Vrontakis M, Molnar P, Schroedter IC, Katsumata N, Murphy LJ, Shiu RP, Friesen HG. Expression of pituitary peptide 23 in the rat uterus: regulation by estradiol. *Mol Cell Endocrinol* 1995; **108**: 149-154

20 **Livesey FJ**, O'Brien JA, Li M, Smith AG, Murphy LJ, Hunt SP. A Schwann cell mitogen accompanying regeneration of motor neurons. *Nature* 1997; **390**: 614-618

21 **Averill S**, Davis DR, Shortland PJ, Priestley JV, Hunt SP. Dynamic pattern of reg-2 expression in rat sensory neurons after peripheral nerve injury. *J Neurosci* 2002; **22**: 7493-7501

22 **Xie MJ**, Motoo Y, Iovanna JL, Su SB, Ohtsubo K, Matsubara F, Sawabu N. Overexpression of pancreatitis-associated protein (PAP) in human pancreatic ductal adenocarcinoma. *Dig Dis Sci* 2003; **48**: 459-464

23 **Rosty C**, Christa L, Kuzdzal S, Baldwin WM, Zahurak ML, Carnot F, Chan DW, Canto M, Lillemoe KD, Cameron JL, Yeo CJ, Hruban RH, Goggins M. Identification of hepatocarcinoma-intestine-pancreas/pancreatitis-associated protein I as a biomarker for pancreatic ductal adenocarcinoma by protein biochip technology. *Cancer Res* 2002; **62**: 1868-1875

24 **Simon MT**, Pauloin A, Normand G, Lieu HT, Mouly H, Pivert G, Carnot F, Tralhao JG, Brechot C, Christa L. HIP/PAP stimulates liver regeneration after partial hepatectomy and combines mitogenic and anti-apoptotic functions through the PKA signaling pathway. *FASEB J* 2003; **17**: 1441-1450

25 **Dusetti NJ**, Frigerio JM, Keim V, Dagorn JC, Iovanna JL. Structural organization of the gene encoding the rat pancreatitis-associated protein. Analysis of its evolutionary history reveals an ancient divergence from the other carbohydrate-recognition domain-containing genes. *J Biol Chem* 1993; **268**: 14470-14475

26 **Christa L**, Felin M, Morali O, Simon MT, Lasserre C, Brechot C, Sève AP. The human HIP gene, overexpressed in primary liver cancer encodes for a C-type carbohydrate binding protein with lactose binding activity. *FEBS Lett* 1994; **337**: 114-118

27 **Morisset J**, Iovanna J, Grondin G. Localization of rat pancreatitis-associated protein during bile salt-induced pancreatitis. *Gastroenterology* 1997; **112**: 543-550

28 **Bödeker H**, Fiedler F, Keim V, Dagorn JC, Iovanna JL. Pancreatitis-associated protein is upregulated in mouse pancreas during acute pancreatitis. *Digestion* 1998; **59**: 186-191

29 **Iovanna JL**, Keim V, Nordback I, Montalto G, Camarena J, Letoublon C, Lévy P, Berthézène P, Dagorn JC. Serum levels of pancreatitis-associated protein as indicators of the course of acute pancreatitis. Multicentric Study Group on Acute Pancreatitis. *Gastroenterology* 1994; **106**: 728-734

30 **Kemppainen E**, Sand J, Puolakkainen P, Laine S, Hedström J, Sainio V, Haapiainen R, Nordback I. Pancreatitis associated protein as an early marker of acute pancreatitis. *Gut* 1996; **39**: 675-678

31 **Multigner L**, Sarles H, Lombardo D, De Caro A. Pancreatic stone protein. II. Implication in stone formation during the course of chronic calcifying pancreatitis. *Gastroenterology* 1985; **89**: 387-391

32 **Malka D**, Vasseur S, Bödeker H, Ortiz EM, Dusetti NJ, Verrando P, Dagorn JC, Iovanna JL. Tumor necrosis factor alpha triggers antiapoptotic mechanisms in rat pancreatic cells through pancreatitis-associated protein I activation. *Gastroenterology* 2000; **119**: 816-828

33 **Ortiz EM**, Dusetti NJ, Vasseur S, Malka D, Bödeker H, Dagorn JC, Iovanna JL. The pancreatitis-associated protein is induced by free radicals in AR4-2J cells and confers cell resistance to apoptosis. *Gastroenterology* 1998; **114**: 808-816

34 **Nishimune H**, Vasseur S, Wiese S, Birling MC, Holtmann B, Sendtner M, Iovanna JL, Henderson CE. Reg-2 is a motoneuron neurotrophic factor and a signalling intermediate in the CNTF survival pathway. *Nat Cell Biol* 2000; **2**: 906-914

35 **Heller A**, Fiedler F, Schmeck J, Lück V, Iovanna JL, Koch T. Pancreatitis-associated protein protects the lung from leukocyte-induced injury. *Anesthesiology* 1999; **91**: 1408-1414

36 **Fiedler F**, Croissant N, Rehbein C, Iovanna JL, Dagorn JC, van Ackern K, Keim V. Acute-phase response of the rat pancreas protects against further aggression with severe necrotizing pancreatitis. *Crit Care Med* 1998; **26**: 887-894

37 **Vasseur S**, Folch-Puy E, Hlouschek V, Garcia S, Fiedler F, Lerch MM, Dagorn JC, Closa D, Iovanna JL. p8 improves pancreatic response to acute pancreatitis by enhancing the expression of the anti-inflammatory protein pancreatitis-associated protein I. *J Biol Chem* 2004; **279**: 7199-7207

38 **Zhang H**, Kandil E, Lin YY, Levi G, Zenilman ME. Targeted inhibition of gene expression of pancreatitis-associated proteins exacerbates the severity of acute pancreatitis in rats. *Scand J Gastroenterol* 2004; **39**: 870-881

39 **Gironella M**, Iovanna JL, Sans M, Gil F, Peñalva M, Closa D, Miquel R, Piqué JM, Panés J. Anti-inflammatory effects of pancreatitis associated protein in inflammatory bowel disease. *Gut* 2005; **54**: 1244-1253

40 **Folch-Puy E**, Granell S, Dagorn JC, Iovanna JL, Closa D. Pancreatitis-associated protein I suppresses NF-kappa B activation through a JAK/STAT-mediated mechanism in epithelial cells. *J Immunol* 2006; **176**: 3774-3779

41 **Berlato C**, Cassatella MA, Kinjyo I, Gatto L, Yoshimura A, Bazzoni F. Involvement of suppressor of cytokine signaling-3 as a mediator of the inhibitory effects of IL-10 on lipopolysaccharide-induced macrophage activation. *J Immunol* 2002; **168**: 6404-6411

42 **Croker BA**, Krebs DL, Zhang JG, Wormald S, Willson TA, Stanley EG, Robb L, Greenhalgh CJ, Förster I, Clausen BE, Nicola NA, Metcalf D, Hilton DJ, Roberts AW, Alexander WS. SOCS3 negatively regulates IL-6 signaling *in vivo*. *Nat Immunol* 2003; **4**: 540-545

43 **Dusetti NJ**, Ortiz EM, Mallo GV, Dagorn JC, Iovanna JL. Pancreatitis-associated protein I (PAP I), an acute phase protein induced by cytokines. Identification of two functional interleukin-6 response elements in the rat PAP I promoter region. *J Biol Chem* 1995; **270**: 22417-22421

S- Editor Liu Y **L- Editor** Zhu LH **E- Editor** Lu W

PO Box 2345, Beijing 100023, China
www.wjgnet.com
wjg@wjgnet.com

World J Gastroenterol 2007 January 14; 13(2): 175-191
World Journal of Gastroenterology ISSN 1007-9327

TOPIC HIGHLIGHT

Early diabetic neuropathy: Triggers and mechanisms

Maxim Dobretsov, Dmitry Romanovsky, Joseph R Stimers

Maxim Dobretsov, Departments of Anesthesiology, Neurobiology and Developmental Sciences, University of Arkansas for Medical Sciences, 4301 West Markham Street, Little Rock, AR 72205, United States
Dmitry Romanovsky, Department of Anesthesiology, University of Arkansas for Medical Sciences, 4301 West Markham Street, Little Rock, AR 72205, United States
Joseph R Stimers, Department of Pharmacology and Toxicology, University of Arkansas for Medical Sciences, 4301 West Markham Street, Little Rock, AR 72205, United States
Supported by NIH National Institute of Diabetes and Digestive and Kidney Diseases, No. DK067248
Correspondence to: Maxim Dobretsov, Department of Anesthesiology, Slot 515, University of Arkansas for Medical Sciences, 4301 West Markham Street, Little Rock, AR 72205, United States. dobretsovmaxim@uams.edu
Telephone: +1-501-6031936 Fax: +1-501-6031951
Received: 2006-08-17 Accepted: 2006-09-26

Abstract

Peripheral neuropathy, and specifically distal peripheral neuropathy (DPN), is one of the most frequent and troublesome complications of diabetes mellitus. It is the major reason for morbidity and mortality among diabetic patients. It is also frequently associated with debilitating pain. Unfortunately, our knowledge of the natural history and pathogenesis of this disease remains limited. For a long time hyperglycemia was viewed as a major, if not the sole factor, responsible for all symptomatic presentations of DPN. Multiple clinical observations and animal studies supported this view. The control of blood glucose as an obligatory step of therapy to delay or reverse DPN is no longer an arguable issue. However, while supporting evidence for the glycemic hypothesis has accumulated, multiple controversies accumulated as well. It is obvious now that DPN cannot be fully understood without considering factors besides hyperglycemia. Some symptoms of DPN may develop with little, if any, correlation with the glycemic status of a patient. It is also clear that identification of these putative non-glycemic mechanisms of DPN is of utmost importance for our understanding of failures with existing treatments and for the development of new approaches for diagnosis and therapy of DPN. In this work we will review the strengths and weaknesses of the glycemic hypothesis, focusing on clinical and animal data and on the pathogenesis of early stages and triggers of DPN other than hyperglycemia.

Key words: Diabetes; Pre-diabetes; Neuropathy; Impaired glucose tolerance; Hyperglycemia; Insulinopenia; Insulin-resistance

Dobretsov M, Romanovsky D, Stimers JR. Early diabetic neuropathy: Triggers and mechanisms. *World J Gastroenterol* 2007; 13(2): 175-191

http://www.wjgnet.com/1007-9327/13/175.asp

INTRODUCTION

Diabetes mellitus is a complex of metabolic disorders associated with insufficiency of insulin secretion, insulin action or both, and is manifested by hyperglycemia[1-3]. Diabetes is diagnosed when fasting blood glucose exceeds 6.9 mmol/L, or casual or 2-h glucose in a glucose tolerance test exceeds 11 mmol/L[4]. Control of blood glucose in vertebrate organisms is accomplished essentially by the action of two pancreatic hormones, i.e., insulin and glucagon, with the participation of epinephrine, ACTH, growth hormone and glucocorticoids occurring under special circumstances, such as stress. Insulin is released by islet beta cells in response to an increase of blood glucose (usually after a meal). It suppresses glucose production and stimulates the uptake and storage of glucose in skeletal muscle and liver (Figure 1). It also suppresses lipogenesis in the fat tissue and stimulates amino-acid synthesis in skeletal muscle. During a fasting state, when blood glucose is low or during stress requiring mobilization of energy, insulin secretion is suppressed and glucagon is released into the circulation by pancreatic α cells, opposing the action of insulin to increase the release of stored energy resources for use by the organism (Figure 1)[5,6].

The metabolic effects of insulin are mediated by activation of its cognate receptors that are expressed in target tissues (skeletal muscle, liver, fat) in large excess compared to the amount needed for normal regulation of glucose metabolism (spare receptors[7-10]). This lays a background for and signifies the paramount importance of the glucose control mechanisms. Indeed, in type 1 diabetes, which is usually associated with idiopathic autoimmune attack and destruction of islet beta cells, more than 90% of islet cells need to be destroyed or less than 10% of insulin production should remain for overt hyperglycemia to manifest[11]. Similarly, in type 2 diabetes, associated in its early stages with decreased sensitivity of insulin-responsive

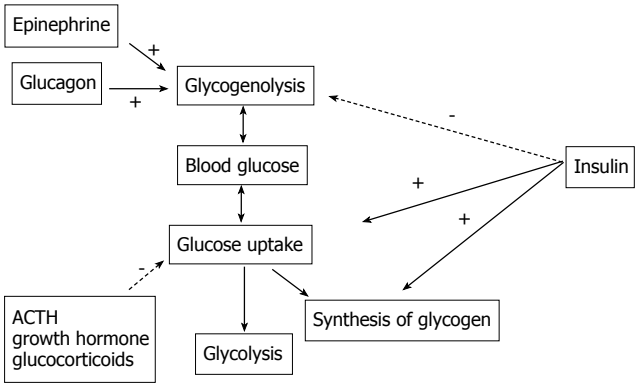

Figure 1 Hormonal regulation of systemic blood glucose.

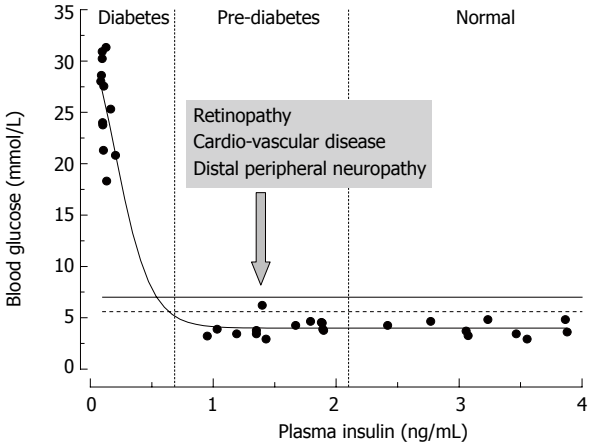

Figure 2 Relationships between rat plasma insulin and fasting blood glucose concentrations. Data are from normal and streptozotocin-injected adult Sprague-Dawley rats (the authors' unpublished observations). STZ-rats having moderate pancreatic impairment and moderately decreased plasma insulin (vertical dashed lines) do not develop overt hyperglycemia.

tissues to the action of the hormone (insulin resistance) and compensatory hyperinsulinemia, no clinical diabetes develops before muscle and fat tissue sensitivity to insulin is decreased below 50%-35% of normal[9]. In rats, and similarly in humans, plasma insulin may vary over the range of 1 to 4 ng/mL with fasting blood glucose exceeding the diabetic threshold of 6.9 mmol/L (solid line in Figure 2)[12-17] only in rare cases. In most cases, insulin must decrease to less than 0.5 ng/mL level (15% of control, 3.5 ng/mL level) in order to manifest overt hyperglycemia and diabetes.

Such a large safety factor for glucose control is of critical biological importance; however, clinically the impairment of insulin signaling in this disease process starts long before it manifests in overt hyperglycemia. With the discovery of insulin and improvement in techniques for blood glucose measurement, diabetes is not a life threatening disease by itself[18]. Therefore the long pre-clinical progression of diabetes could be a relatively minor issue; however, diabetes is associated with a variety of life threatening complications, among which distal peripheral neuropathy (DPN), cardio-vascular disease (CVD), retinopathy and renal disease are most frequent[2]. The problem is signs of these complications are frequently present prior to overt hyperglycemia and diabetes (Figure 2). Realization of this fact led to the definition of pre-diabetes as a state with moderate impairment of blood glucose control and high risk of development of overt diabetes, retinopathy and CVD[3,19]. Pre-diabetes is diagnosed when fasting blood glucose exceeds 5.6 mmol/L and/or 2-h glucose in a glucose tolerance test (GTT) exceeds 6.9 mM (impaired fasting glucose (IFG) and impaired glucose tolerance (IGT) dashed and solid horizontal lines in Figure 2, respectively)[4].

Establishing the correct lower limit for diagnosis of pre-diabetes is important because it determines whether clinical tests for complications should be performed and recommendations in life style and diet modifications should be presented to patients. In a recent study of young adult men, it was shown that fasting glucose exceeding 4.82 mmol/L constitutes an independent risk factor for developing type 2 diabetes in otherwise healthy subjects[20]. In another study of adult healthy men without diabetes or pre-diabetes, progressive loss of β-cell function and decrease in the first-phase of insulin secretion were detected at fasting glucose between 5.0 and 5.4 mmol/L[21]. Another clinically important issue is to understand the pathogenesis of diabetic complications, starting with pre-diabetic patients. This knowledge is required for early detection, prognosis and treatment of diabetic complications. Here we will discuss data and hypotheses for the triggers and progression of one such complication, which is distal peripheral neuropathy.

DISTAL PERIPHERAL NEUROPATHY

The prevalence of peripheral neuropathy in diabetic subjects approaches 70% and about 50% of these are cases of DPN[22-24]. The disease usually progresses to involve cardiac autonomic nerves, and as a result it is a major factor in mortality of diabetic subjects. DPN is also the major reason for loss of protective limb mechanical sensations, traumatic ulceration injures and therefore amputations[23,24]. Finally, about 11% of DPN cases are associated with chronic pain symptoms that severely diminish the quality of life and are frequently associated with depression[22,23]. The etiology of DPN is unknown and prediction of progression and treatments of the symptoms of DPN are limited[22,25-27].

Perhaps the largest problem associated with DPN, complicating its classification and treatment, is the variety of clinical presentations of this disease (Figure 3)[28-30]. Aside from a generally bilateral manifestation, distal to proximal advance and prevalence of sensory over motor impairment signs and symptoms, any two randomly selected cases of DPN may have nothing in common at the time of diagnosis and, to the extent it is known, their history and the pattern of their future progression may be very different. There are two broad categories of sensory symptoms of DPN, positive and negative[26,29]. Positive symptoms include pain, paresthesias and aberrant, exaggerated sensitivity to normally painless or moderately painful stimuli (allodynia and hyperalgesia). Negative

Positive sensory symptoms:
Chronic or Acute/Remitting:
Spontaneous:
Painless paresthesias:
numbness, tingling, pricking, burning, or creeping
Pain/dysesthesia: burning, electric, sharp, or dull/aching
Evoked pain/dysesthesia: allodynia or hyperalgesia, mechanical/tactile or thermal

Negative sensory signs/symptoms:
Decrease in sensory nerve amplitude/conduction velocity
Decrease or loss of perception:
Vibratory stimuli
Thermal stimuli (warming or cooling)
Tactile perception (light touch)
Nociception (hypoalgesia):
Thermal (heat or cold)
Mechanical (pin-prick)
Loss of tendon reflexes

Motor signs/symptoms
Decrease in motor nerve amplitude/conduction velocity
Muscle wasting

Figure 3 Signs and symptoms of distal peripheral neuropathy. Categories of symptoms most frequently manifested in humans with diabetes are given in bold.

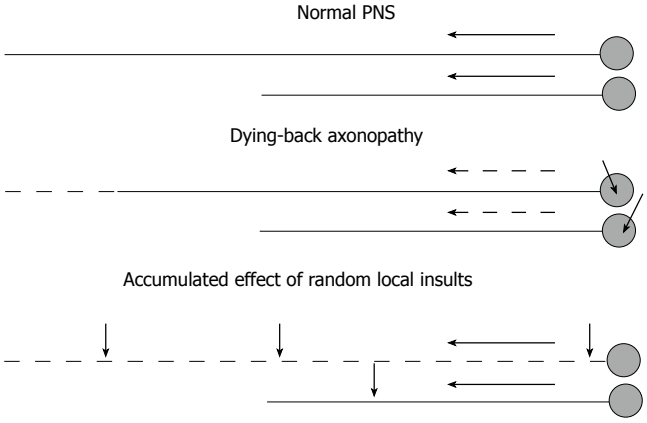

Figure 4 Hypotheses on distal-to-proximal progression of DPN. In normal PNS (top), neurons synthesize proteins in the cell body and transport them down the axon at the rate determined by axonal structural and functional needs. Impairment of synthesis or axonal transport of proteins will result in dying-back neuropathy, in which neurons with longest processes are affected first (middle). Alternatively, the neuropathy may result from effect of random local insults to the axon, with probability of accumulation of a critical number of such insults being higher for neurons having longer axons (bottom). Short arrows indicate non-specified axonal or neuronal injuries. Long solid or dashed arrows indicate normal or compromised axonal transport (respectively).

symptoms consist of loss of sensory perception in one or several modalities. Motor symptoms, if present, manifest as muscle weakness, and thus they are also negative. Finally, a classical electrophysiological, and also negative, sign of DPN is a decrease in nerve conduction velocity (NCV) and amplitude of compound action potentials (APs) in peripheral sensory and motor nerves[23,24,26,27,31]. Furthermore, three categories of DPN, acute painful remitting neuropathy, chronic painful neuropathy and painless neuropathy with ulcer can be outlined as separate clinical entities[24,32,33]. The relationships among these entities, however, if any exist, are not known. Within each of these groups, signs of demyelination of large peripheral fibers (decrease in NCV) may or may not co-exist with signs and symptoms of large fiber axonopathy (decrease in amplitude of compound APs, loss of vibration sensation and/or loss of stretch reflexes). Loss of warm and cold perception, impairment of unmyelinated and small myelinated fibers, may or may not co-exist with signs of large fiber abnormalities[24,31,32,34-36]. Furthermore, the pain normally conducted by small unmyelinated peripheral axons may or may not be present at the same time with any of the above mentioned symptoms[22-24,26,36,37]. Finally, the modalities of pain and the degree of involvement of autonomic nervous system impairment constitute another large set of variables[22,24,33,38-40].

From experiments in animals, and by analogy with other neuropathies, it can be suggested that the pathogenesis of negative symptoms and signs of DPN is likely to be associated with demyelination and axonal atrophy and degeneration[41,42]. Failure of re-innervation will make these symptoms essentially irreversible[42-44]. Mechanisms of neuropathic pain, paresthesias and hyperalgesia are less understood[27,40]. However, it is generally accepted that abnormally intense spontaneous input from primary afferent fibers to the spinal cord is a primary trigger of these symptoms[24,27,45,46]. At least three usually overlapping conditions, resulting in such abnormal activity of peripheral axons, are well established. First is impairment of endoneurial circulation and following it ischemia[47,48]. Second is impairment of axon-glia relationships and segmental or paranodal demyelination[49,50]. The third condition is an axonal injury and following it Wallerian degeneration and neuroma[51,52]. In addition, increased excitability of regenerating, and therefore not yet properly myelinated, nerve fibers may add to the generation of aberrant peripheral discharge and pain[53,54]. At least at advanced stages, evidence for axonal, glial and vascular injuries are detectable in most cases of DPN[41,55].

Further insight into the pathogenesis of DPN is provided by its diffuse, bilateral presentation and distal to proximal progression. The former suggests that systemic rather then local conditions underlie the clinical pathology, while the latter could indicate two possibilities (Figure 4). First, DPN may be a manifestation of dying back degeneration, with the primary insult consisting of the impairment of synthesis or efferent axonal transport of proteins, therefore affecting the function of the longest axons in the body that are most dependent on these mechanisms[42]. Failure of protein synthesis, including synthesis of some important neurotrophic molecules, in diabetes could result in impaired nerve regeneration and dying back axonopathy[43,44,55,56]. Alternatively, accumulation of the effects of multiple injuries randomly located along the axon, for example demyelinating injures, may result in a clinical picture that is practically indistinguishable from dying back neuropathy[41,42,57]. The longest axons in the body will most likely be hit by a critical number of such local insults and their function will fail first.

Micro-vascular disease followed by local impairment of blood supply to the nerve fascicules may be a basis for random demyelinating insults progressing later to axonal degeneration[58-60]. It is also conceivable that both mechanisms are operating at the same time. Both demyelination and axonal degeneration were detected in human DPN by electrophysiological tests and biopsy studies[24,41,61]. Peripheral axons are the longest in the human body, and this might be an important factor explaining PNS involvement superseding the CNS complications. Another potentially important reason for the high vulnerability of PNS to diabetic injury is the relatively weak anti-oxidative defenses of peripheral neurons (see Section 3).

While the discussion above appears to encompass all the major features of DPN, multiple questions related to the pathogenesis of DPN remain unresolved. Thus whether or not dying back axonopathy or multiple local injuries or both mechanisms lead to the disease, it is not clear why, in most cases of neuropathy, sensory symptoms prevail over signs of impairment to motor axons innervating the same distal areas of the human body. Furthermore, neither of these mechanisms explains a variety of clinical presentations of DPN nor answers the question of why some diabetic patients live without any symptoms of DPN for years[62]. Finally, major questions that remain to be answered include identifying pathogenic triggers of DPN, pathogenesis of individual symptoms, and relationships among different symptoms and signs of the disease[22,24].

To illustrate the importance of the latter question, two hypothetical scenarios of DPN are shown in Figure 5. In the first scenario (Figure 5, top), there is a single pathogenic process triggering and maintaining the disease. The course of the disease and its clinical manifestations at the time of diagnosis and neurological evaluation (ovals in the Figure 5) will be determined by the duration of DPN and individual differences in the genetic backgrounds of patients. From the point of view of the symptoms revealed by a neurological exam, the second scenario (Figure 5, bottom) is identical to the first one; the critically important difference, however, is that different sets of symptoms in this scenario are triggered and driven by entirely independent pathogenic mechanisms (symptoms "a", "c", and "d" *vs* symptom "b"). Some of the branches of the pathogenic process ("b" in the first scenario) may enter an irreversible stage. Therefore, the early detection of DPN is an obligatory condition for the successful treatment of this disease. The cartoons demonstrate also that identification of all participating triggering mechanisms and symptoms associated with them is another critical step for the efficient treatment of DPN.

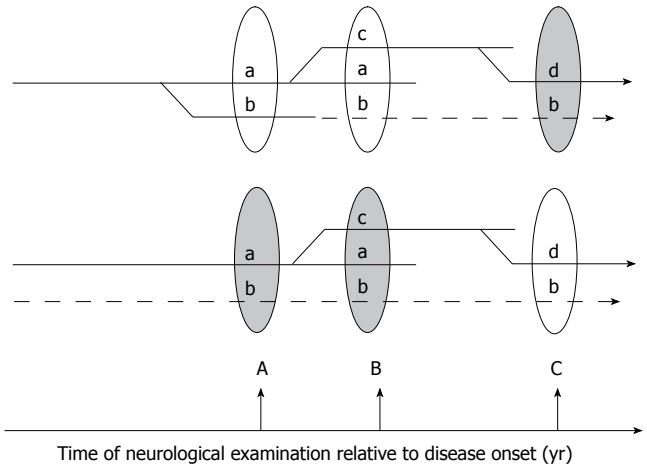

Figure 5 Hypothetical branching (top) and multi-trigger (bottom) pathogenesis of DPN. In the first scenario (top) all manifestations of the disease result from the unique branching pathogenic process, and symptom "b" discovered at the time of neurological exam B is not corrected by treatment because it has already progressed to an irreversible stage (dashed lines). Earlier diagnosis and institution of treatment (at time A) may critically change the outcome of therapy in this scenario. Alternatively (lower scenario), several independent factors may trigger and maintain the progression of DPN. In this case the therapy may fail to treat symptoms not because they are irreversible, but because the correct cause of the pathology is not identified and is not treated (dashed lines).

CHRONIC HYPERGLYCEMIA AND PATHOGENESIS OF DPN

DPN follows both type 1 and type 2 diabetes, and systemic hyperglycemia is the most obvious symptom that these types of the disease have in common[24,63,64], suggesting hyperglycemia as a universal trigger for DPN. Indeed, insulin treatment or treatment with insulin-sensitizing drugs to control hyperglycemia reverses some symptoms of DPN and delays its progression in general[65,66]. The Diabetes Control and Complications Trial (DCCT) data show that strict control of hyperglycemia in type 1 diabetes patients without clinical neuropathy decreased development of DPN in 60% of cases over 5 years of follow up study[67,68]. Well within the framework of the glycemic hypothesis, the failure to prevent all cases of DPN could be explained by the fact that glucose control can never be perfect. Type 1 and 2 patients are, on average, euglycemic for only about 62% of the day, while during the remaining 30% and 8% of the day they have various degrees of hyperglycemia and hypoglycemia, respectively[69]. Therefore, to avoid hypoglycemic crisis, the acceptable target value for blood glucose in controlled subjects is usually set to values above normal (6.7 to 10 mmol/L in DCCT and 6 mmol/L in U.K. Prospective Diabetes Study; of type 2 diabetic patients[65,68]). Another explanation for incomplete efficacy of glucose control is that, after long-standing diabetes, some neuropathic mechanisms may enter either an irreversible stage or a stage of progression that is already independent of the original trigger. With the limitations imposed by generally late diagnosis of diabetes and DPN[24,70,71], slowing of NCV, paraesthesia and painful symptoms appear to be the earliest (closest to the initiating pathogenic insult) manifestations of DPN. Therefore, it appears to be in good agreement with the glycemic hypothesis that in patients with newly diagnosed diabetes, NCV slowing and paresthesias (hyperglycemic neuropathy) can be frequently completely recovered with the establishment of euglycemia[31,42].

Further support for the glycemic hypothesis comes from research in animals, specifically rat models of type

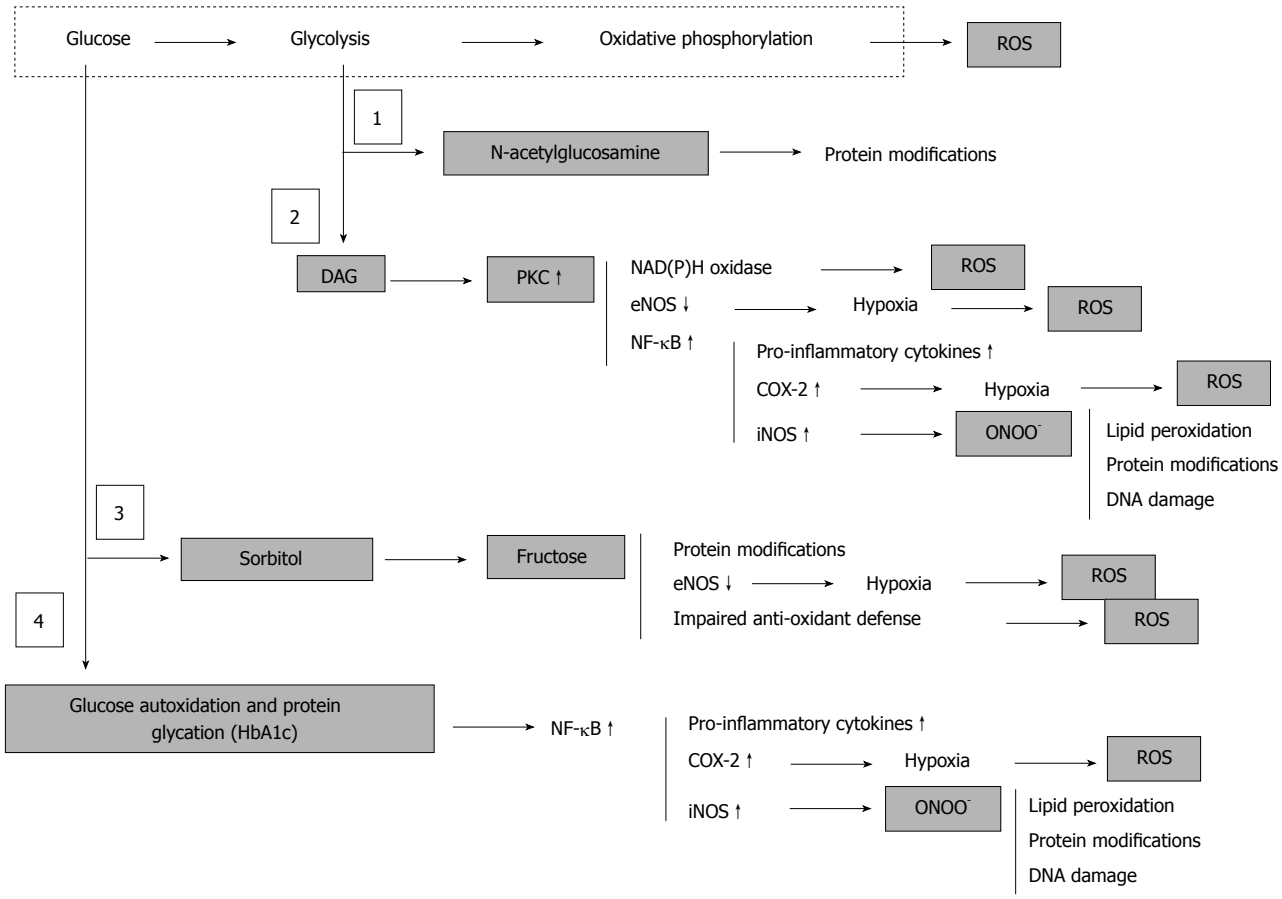

Figure 6 Hyperglycemia, derangement of cell metabolism and oxidative/nitrosative stress. Hyperglycemia associates with accumulation of fructose-6-phosphate and hexosamine pathway (1) to N-acetylglucosamine, accumulation of dihydroxyacetone phosphate and associated activation of PKC (2), activation of polyol sugar pathway (3), and glucose autoxidation and non-enzymatic protein glycation (4). These metabolic events are either regular physiologically important components cell metabolism (1, 2 and 3) or are normally under strict control of intrinsic intracellular defense mechanisms (4). However, under conditions of chronic hyperglycemia activation of these pathways leads to a global derangement of the cell and tissue homeostasis, which culminates in an uncontrolled cascade of abnormal protein modifications, oxidative/nitrosative stress and pro-inflammatory conditions.

1 diabetes (STZ-induced or spontaneous in BB-rats) and spontaneous type 2 diabetes in Zucker fatty rats[66,72] that appear to be the best studied animal models with regard to neuropathy. The short life span of rodents severely limits evaluation of chronic human diseases in these animals. Another limitation is that in behavioral tests, evoked pain manifested by limb withdrawal can be tested, but neither spontaneous pain nor changes in non-nociceptive sensory thresholds can be reliably measured in animals. Nonetheless, in general agreement with both clinical data on the earliest signs and symptoms of human DPN and the glycemic hypothesis, slowing of sensory[73-76] and motor[74,75,77-83] NCV and manifestations of evoked pain (hyperalgesia[75,84-87] and allodynia[85]) were shown to develop within the first month of onset of hyperglycemia in diabetic rats. With a longer time allowed (six to twelve months of diabetes) signs of axonopathy, demyelination and nerve degeneration can also be detected in diabetic animals[56,74,80,82,88-90]. Finally, early in the course of diabetes in rat models impairment of endoneurial blood flow and micro- and macrovascular reactivity are reported by many investigators[75,91-94]. Skin and arterial blood flow is abnormal early in diabetic patients[95-98], but no reduction in sural nerve blood flow was detected in humans with diabetes and mild DPN[99]. Thus, it is not clear whether impaired endoneurial blood flow represents a rat-specific component of DPN or if it is missed in humans because of its transient character and usually late detection of DPN in diabetic patients. In agreement with the glycemic hypothesis, all abnormalities found in rat models are reversible with normalization of blood glucose in insulin replacement experiments, and some of them (decreased pain pressure threshold) can be induced in normal rats by chronic *in vivo* perfusion of a DRG, or a segment of sciatic nerve with hyperglycemic solution[100,101].

Finally, support for the glycemic hypothesis is provided also by studies of cellular pathology associated with experimental diabetes. These studies show that practically all signs and symptoms of DPN observed in animal models may be linked to hyperglycemia-induced metabolic impairment of nerve, glial and endothelial cells in PNS. A detailed description of these studies is beyond the scope of the present work and can be found in a number of recent reviews[94,102-109]. The purpose of Figure 6 is only to provide a brief outline of cell metabolic abnormalities associated with diabetes and emphasize the findings directly relevant to the following discussion of triggers of early DPN.

Although the scheme in Figure 6 is simplified and omits many essential steps for the cascade of events [the poly (ADP-ribose) polymerase (PARP)[108]; activation and consequences of lipid peroxidation[110] are not shown], it clearly demonstrates the complexity of this cascade. Some events appear to be more specific to one type of cell than to another, and there is as yet no agreement on which events (for example activation of polyol pathway[111] or abnormally intensified oxidative phosphorylation[106]) plays a leading role in cellular impairment. Nonetheless, most of the data available indicate that all the various pathways activated by hyperglycemia converge in generation of excess reactive oxygen species (ROS). This process eventually overwhelms the intrinsic anti-oxidant mechanisms of the cell and ends in oxidative/nitrosative stress and pro-inflammatory conditions in the tissues[112-115]. The efficacy of treatment with anti-oxidants in correction of DPN in animals and humans supports this view[116-119].

In diabetic animals, oxidative stress injury develops in parallel in all major cellular elements of PNS. Injury to glial cells is responsible for the demyelination component of DPN, which may explain the decrease in NCV and painful manifestations of the disease. Oxidative stress in neurons might be responsible for axonopathy, impaired regenerative capacity of axons and negative symptoms of DPN. Glial cell injury will affect the nerve neurotrophism adding to the progression of neuronal defects. Finally, oxidative stress and impairment of nitric oxide (NO) production in the endothelium of epi- and endoneurial blood vessels results in impairment of endoneurial circulation and endoneurial hypoxia, exaggerating and speeding up the direct effect of hyperglycemic conditions on glial cells and neurons. Oxidative stress is pro-inflammatory, which affects the production of cytokines by glial cells, and provokes the recruitment of immune response cells into the affected tissue. This might be another important component of the pathogenesis and progression of DPN. Thus, combining these data and observations lays the foundation for a view of the natural history of DPN similar to that depicted in Figure 7 according to an expanded view of the glycemic hypothesis.

Perhaps the most attractive aspect of such a view of the pathogenesis of DPN is that while it suggests a unifying trigger and mechanism (hyperglycemia and oxidative stress) for all symptoms of DPN, it nevertheless remains flexible enough to leave room for individual variability in the rates of progression and spectrum of manifestations of the disease. Indeed, the actual effects of uniform pro-oxidative and pro-inflammatory conditions may differ sharply depending on differences of individual cells and tissues in their intrinsic anti-oxidant defenses and individual organisms in their immune defenses. The injuries to a single myelinating or non-myelinating Schwann cell, endothelial cell or neuron will unlikely have even subclinical significance. The death of several myelinating cells will result in a decrease of NCV in a given axon and injury to several endothelial cells may cause the closure of a given capillary. Yet there are many axons and there is regeneration of damaged axons, and there are many capillaries and regeneration of damaged and collateral capillaries. It is only after cellular defenses against the oxidative stress are overwhelmed in many cells that the sub-clinical signs of the disease may be expected to appear, and it is anticipated to take an even longer time before clinical manifestations will themselves appear. In agreement with this, *en mass* CNS cells appear to have a much higher capacity for anti-oxidative mechanisms than do PNS cells and this might be one of the reasons why diabetic neuropathy affects the CNS much later than it affects peripheral nervous functions[90,113,120].

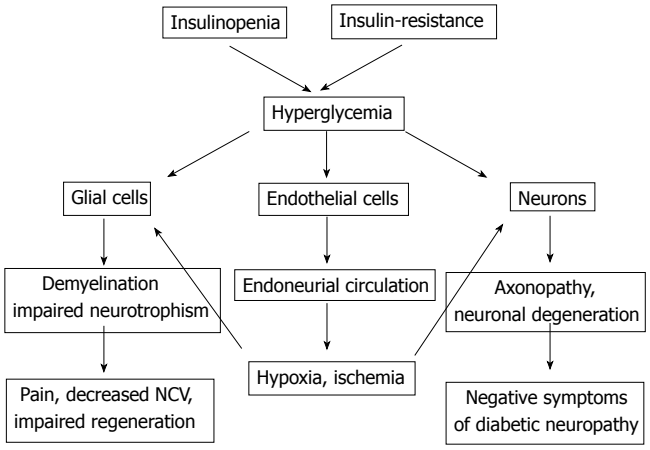

Figure 7 Pathogenesis of DPN with hyperglycemia as a major trigger of PNS injury.

DIFFICULTIES OF THE GLYCEMIC HYPOTHESIS

While apparently logical and consistent with many clinical observations and the results of animal studies, the glycemic hypothesis cannot completely explain all the data. Thus, experiments in rodents consistently demonstrate that the polyol pathway (conversion of glucose to sorbitol by aldose reductase and then to fructose by sorbitol dehydrogenase; pathway 3 in Figure 6) is an important source of reactive oxygen species, and inhibition of aldose reductase prevents or reverses many signs of DPN seen in diabetic animals[121]. The same treatment in humans, however, has shown questionable efficacy so far[27,53,122,123]. Other problems include the failure of a pre-clinical slowing of NCV[24,124] or increase in glycosylated hemoglobin[22] (HA1c, integral measure of persistent hyperglycemia; pathway 4 in Figure 6) to predict development or severity of symptoms of DPN. Also, the finding of an inverse correlation between hyperglycemia and pain severity in diabetic patients with remitting painful neuropathy at presentation[33] is inconsistent with the glycemic hypothesis. These and other similar inconsistencies certainly could be attributed to the complexity of the disease, differences in studied patient populations, or inadequate design of drug trials in terms of timing, duration or dose[121]. Similarly, the lack of absolute efficacy in glucose control in preventing DPN in humans with diabetes[68] could also be explained within the framework of the glycemic hypothesis considering the difficulty of maintaining blood glucose concentrations within the relatively narrow range of normal values, which suggests that the actual threshold for neuropathic effects of hyperglycemia is lower than was

previously thought. Therefore, recent findings of increased incidence of DPN in patients with pre-diabetes, many of whom have an impaired glucose tolerance (IGT) but not fasting hyperglycemia[22,25,70,71,125-127], appear to present the most serious challenge for the glycemic hypothesis.

The possibility that PNS injury may be triggered by exaggerated and prolonged postprandial hyperglycemic episodes, without necessarily requiring chronic hyperglycemia, should be considered to reconcile the glycemic hypothesis with observations of DPN in glucose intolerant patients[70,128-130]. Indeed, indices of large fiber function (ankle and knee reflexes and vibratory perception thresholds) were shown to decay with impairment of glucose tolerance in humans without diabetes and neuropathy[131]. Furthermore, pain is a frequent symptom of pre-diabetic DPN. An acute glucose infusion, which could be considered as an analog to a postprandial glucose surge, decreased thresholds to electrical stimulation in healthy adult volunteers[132] and decreased pain pressure thresholds in type 1 diabetic patients without clinical neuropathy[133]. In the latter study, however, no association between acute hyperglycemia and heat pain, warmth/cooling or vibration perception thresholds, was found[133]. Inconsistent with the idea that postprandial glucose changes have a neuropathic effect, no correlation was detected between short-term fluctuations in blood glucose and pain scores or heat pain thresholds in the study of type 1 and type 2 diabetic subjects with painful neuropathy[134]. Furthermore, no correlation between the number of glycemic excursions and the number of painful episodes was found in the study of type 1 patients with painless neuropathy[135].

Difficulties with the glycemic hypothesis are not unique to the human clinic. Thus in the STZ-rat model of diabetes, NCV could be corrected by a low level of insulin therapy below that required to correct hyperglycemia[89,136]. Pain pressure and von Frey filament thresholds studied in the same model demonstrate no correlation with the degree of hyperglycemia[84,101,137]. Furthermore, aldose reductase inhibitors (blockers of the polyol sugar pathway; Figure 6), given at doses sufficient to correct nerve sorbitol and fructose and heat pain thresholds, do not correct von Frey filament threshold in STZ-hyperglycemic rats[138,139]. As another example, pain pressure thresholds in type 2 diabetic Zucker rats could be corrected with insulin-like-growth factor Ⅱ (IGF-Ⅱ) that has no effect on blood glucose[86]. All these examples are taken from experiments in overtly diabetic and hyperglycemic animals. Therefore, formally the possibility remains that hyperglycemia was the triggering event for the observed abnormalities, but it is not required for the progression and maintenance of these pathologies. Whether DPN develops in pre-diabetic rats as it does in humans has not yet been studied. Since previous work has focused on diabetes, little attention has been devoted to the development of pre-diabetic animal models and studies of DPN in these models. Nonetheless, neuropathic decreases of mechanical and thermal nociceptive thresholds[140] and slowing of motor NCV[141] were observed in studies in Zucker-fatty rats. Since these are insulin-resistant but normoglycemic animals (type 2 pre-diabetes) the impaired glucose tolerance could be responsible for DPN in these animals. Recently, we described decreased pain pressure threshold in rats that were injected with STZ but remained normoglycemic[84]. These rats also had normal glucose tolerance, maintained normal levels of HbA1c, and normal concentrations of sorbitol in the nerve, suggesting that not only fasting but casual glucose also was maintained within physiological limits (Figure 8).

Thus there is solid evidence that hyperglycemia is an important factor of DPN. However, there are also both clinical and animal studies indicating that in addition to chronic and/or postprandial hyperglycemia, other pathogenic mechanisms must exist that trigger and maintain at least some of the symptoms of DPN. Identification of these factors is of critical importance for our understanding of both the natural history of pre-diabetic DPN and the pathogenesis of diabetic DPN in general[27,88].

INSULIN SIGNALING AND DPN

In the search for triggers of DPN other than hyperglycemia, it is important to note that successful reversion or postponing of DPN in clinical glucose control trials does not necessarily prove the glucose hypothesis[142]. Glucose metabolism is regulated by insulin *via* type B receptors (IR-B) abundantly expressed by liver, skeletal muscle and fat cells. Insulin receptors, however, are also expressed in central and peripheral nervous systems[143,144]. Furthermore, in PNS the highest densities of IRs are located on endothelial cells, paranodal loops of Schwann cells and medium and small size primary sensory neurons[143,144]. All these locations are strategically critical points of PNS function considering what is known about the pathogenic mechanisms of DPN. While the nervous system has mostly type A receptors (IR-A), the insulin affinities of these and IR-B receptors are similar ($K_{0.5}$ is 3 to 6 ng/mL[145]) and well within the range of circulating concentrations of insulin (1 to 6 ng/mL[12-17]). Thus, it is very possible that correction of insulin levels in treatments for Type 1 diabetes or insulin-sensitizing therapy in cases of type 2 diabetes not only corrects glucose metabolism, but also has independent effects on the function of PNS. Serious consideration of this hypothesis is warranted, first because it provides an explanation for at least some failures of glycemic controls to reverse DPN, and second because it may explain the development of DPN in pre-diabetic patients.

Insulinopenia (Type 1 diabetes and pre-diabetes)

As described in the Introduction, overt type 1 diabetes is preceded by a state of partial pancreatic damage and moderate insulinopenia in which insulin production is still satisfactory for blood glucose control[11]. The type 1 pre-diabetic state is probably short and little is known about neuropathy in these patients. The results of a recently completed follow-up to DCCT study of type 1 diabetic patients, however, has shown that regardless of the level of glycemic control, neuropathy is less prevalent in the group of patients that maintained intensive vs. conventional insulin therapy[146]. Further support for the

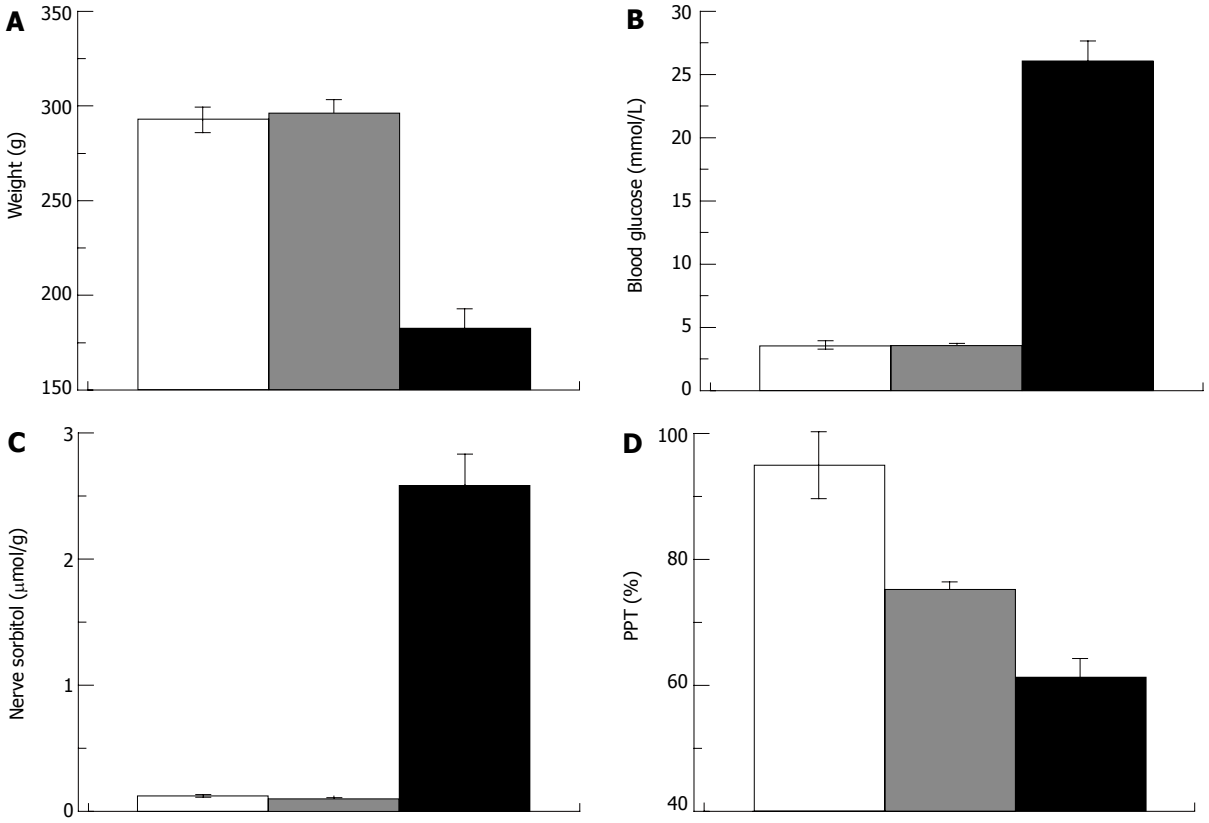

Figure 8 Pain pressure thresholds are not correlated with hyperglycemia. Weight (**A**), blood glucose (**B**), nerve sorbitol (**C**) and pain pressure thresholds (**D**) in control, STZ-normoglycemic and hyperglycemic rats (white, grey and black columns respectively; 2 wk after injection of 65 mg/kg STZ).

possibility of a direct role of insulinopenia in DPN comes from experiments in the STZ-rat model of type 1 diabetes. It was demonstrated that local insulin application to the nerve prevents motor NCV slowing in STZ-hyperglycemic rats[147]. Similarly, systemic[136] or intrathecal[89] application of insulin can correct sensory and motor NCV in STZ-treated rats without having an effect on hyperglycemia. Finally, in our experiments in rats that were injected with STZ and developed moderate insulinopenia but not fasting hyperglycemia (Figure 8), pressure pain thresholds were decreased in proportion to the degree of insulinopenia, and low dose insulin-replacement therapy corrected this defect without changes in the systemic blood glucose level (Figure 9). Taken together these data suggest that at least some signs of neuropathy (slowing of NCV, pressure-evoked pain in rats) may indeed be triggered by insulinopenia with no relevance to the blood glucose level. Another notable aspect of these experiments is that correction of nerve conduction[89,136,147] and pain pressure thresholds (Figure 9) with insulin treatment could be achieved without changes in systemic blood glucose levels, leading to an important implication that the thresholds of "metabolic" and "neuropathic" effects of insulinopenia may differ.

To date, detailed information on the relation between insulin and nerve conduction is not available. However, comparison of better studied "dose-response" relationships between insulin, blood glucose and pain pressure thresholds (Figure 10A) allows speculation that in the rat, control of glucose metabolism may tolerate at least five times lower insulin levels than does nerve function. Given that this difference was confirmed in both animals and humans, the outcome of these studies is of a great importance. This finding may explain the development of neuropathy in pre-diabetes and also suggests that neuropathy may start at stages preceding pre-diabetes, and some therapeutic interventions to correct insulin levels or insulin resistance (see next section) are warranted in pre-diabetic patients.

Differences in threshold concentrations of a ligand are usually determined by the differences in receptor properties. However, insulin affinities of IR-B and IR-A isoforms of the insulin receptor expressed in cells of organs responsible for glucose metabolism and in nerve tissue are too close to account for apparent differences in the concentrations of hormone required for maintaining normal blood glucose concentrations and normal pain pressure thresholds[145]. On the other hand, strong correlative relationships between insulin and pain pressure thresholds (Figure 9A) suggest a nearly direct link between insulin regulation and pressure pain mechanisms. The hypothesis of spare receptors[7,8,10] is the easiest way to explain this discrepancy. Thus as shown in Figure 10A, both metabolic and neuropathic effects of insulin may be described adequately within the concept of insulin binding with the same affinity ($K_{0.5}$ = 1 ng/mL) in nerve and in glucose controlling organs, if 65% of the receptor occupancy is needed to control nerve function, and only 10% of occupancy is required for glucose metabolism. Hill equations were used in this simulation; however, since the

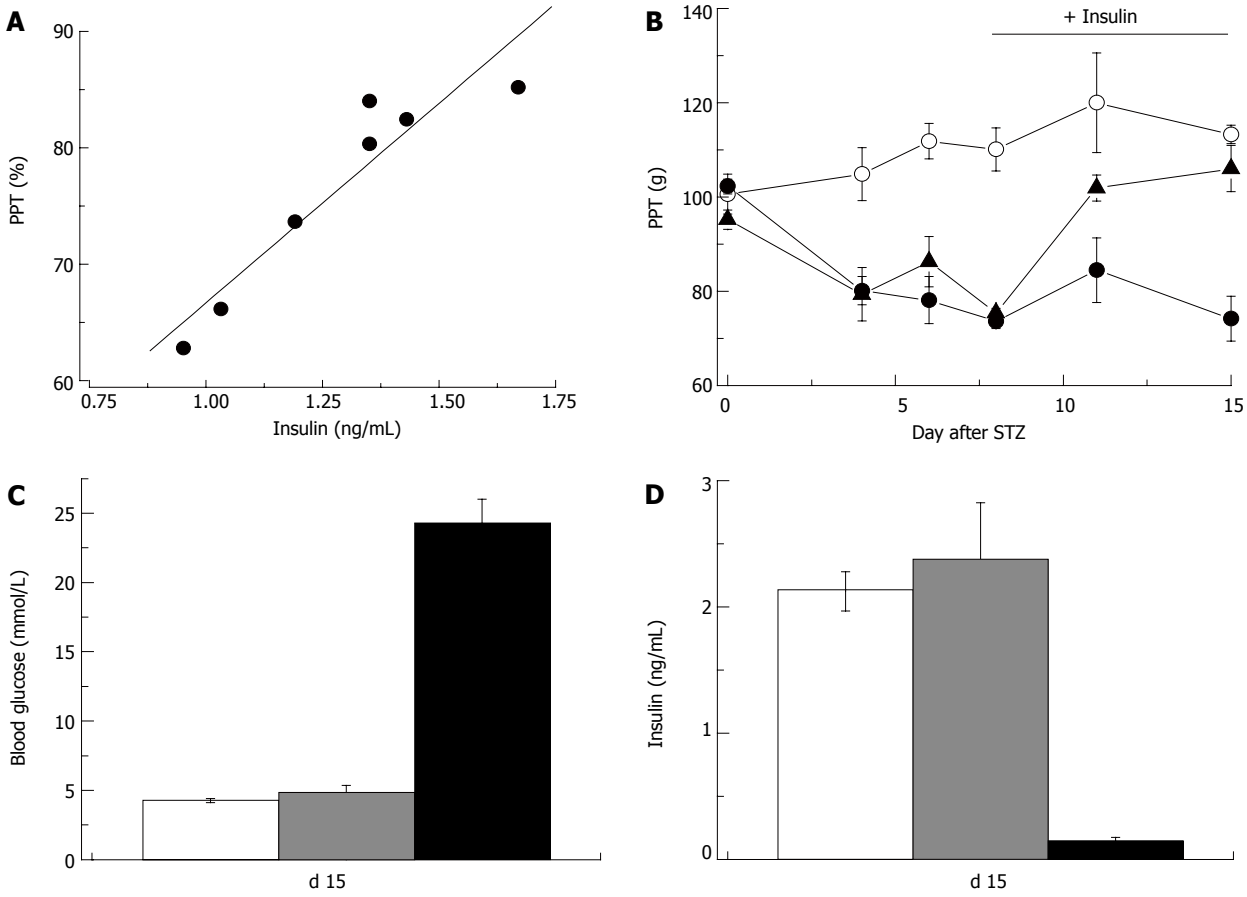

Figure 9 Insulin-dependence of pain pressure threshold in STZ-normoglycemic rats. Two weeks after injection of STZ pain pressure threshold of STZ-NG rats is decreased in proportion to the plasma insulin level (R = 0.97; **A**). Insulin replacement initiated one week after STZ injection (horizontal bar in panel **B**) does not change PPT of control or hyperglycemic rats, but corrects it in STZ-normoglycemic animals (empty and filled circles, and filled triangles, respectively). Insulin replacement, does not affect blood glucose (**C**), but normalizes plasma insulin level (**D**) in STZ-NG rats. In **C** and **D** white, grey and black columns represent control, STZ-NG and STZ-HG rats, respectively.

purpose was merely to illustrate the potential possibility of the given scenario, parameters of the equations were adjusted by a trial and error approach and no attempt was made to optimize the parameters. Some alternatives to this scenario will be discussed in section 6.1 of this review.

Insulin resistance

Prevalence of type 2 to type 1 diabetes is about 9 to 1 and most of the cases of human pre-diabetes are type 2 pre-diabetes or metabolic syndrome cases[24,125]. Over the long-term, insulin production is impaired in type 2 diabetes further increasing the incidence of DPN in this population by mechanisms described above. In a ten-year study of the natural history of type 2 diabetic patients, it was found that decreased serum insulin and increased blood glucose concentrations are independent predictors of DPN[148]. However, in early type 2 diabetes and pre-diabetes there is a compensatory hyperinsulinemia. Because of this hyperinsulinemia type 2 pre-diabetes usually spans a much longer period of time than does type 1 pre-diabetes. Thus, after 5 years only 20% to 35% of patients with impaired fasting glucose or impaired glucose tolerance develop overt hyperglycemia (see[70]). Despite this compensatory hyperinsulinemia, however, many type 2 pre-diabetic patients do develop DPN[125,126]. This latter observation suggests that in terms of neuropathic outcome, insulin resistance and insulinopenia may be equivalent states. It also suggests that increased production of insulin may fail to compensate for decreased sensitivity of PNS to regulation by insulin.

Not much experimental data exists to verify the validity of either of these suggestions. In studies in normal human volunteers, warmth detection threshold correlated with insulin but not fasting or 2-h GTT glucose, leading the authors to suggest that insulin resistance may determine some sensory functions of PNS[149]. This is also supported by observations of decreased NCV[141] and pressure pain thresholds[86] and the authors' unpublished observations in the Zucker fatty rat model of type 2 pre-diabetes. However, whether it is possible that hyperinsulinemia is effective in regulating glucose metabolism but fails to compensate for nerve insulin resistance is at this time absolutely not known. Furthermore, it is unknown if this mechanism plays a role in DPN associated with type 2 diabetes. In theory such a possibility does exist, and Figure 10B illustrates the scenario that we believe provides a useful working hypothesis for future experiments. Using "dose-response" relations as a starting point, shown in Figure 10A, the insulin resistant state that leads to type 2 diabetes may be modeled as a decrease in affinity of

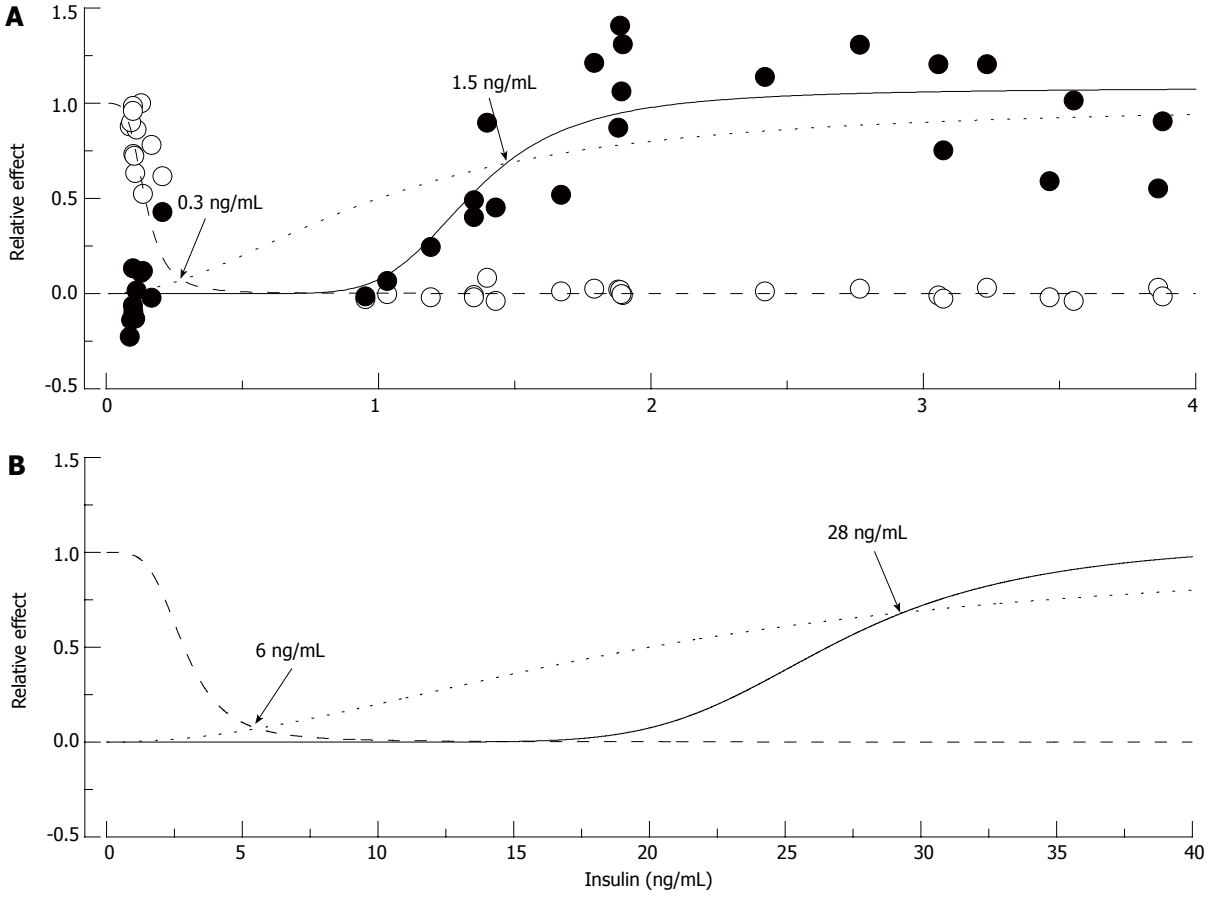

Figure 10 Putative "insulin-glucose metabolism" and "insulin-nerve function" relationships in normal and insulin-resistant rats. In **A**: Normal rats: Empty circles represent fasting glucose and filled circles pain pressure thresholds measured in control, STZ-NG and STZ-HG rats, pooled together and normalized to show relative changes of these parameter between control and diabetic animals. The data were fitted by Hill curves calculated based on the assumption that insulin binds to the receptor with an affinity of 1 ng/mL (dotted curve) and 10% and 65% occupancy of these receptors is required for maximum metabolic (intersection with dashed curve) and nerve (intersection with solid curve) effect of the hormone, respectively. In **B**: Insulin-Resistant Rats: Insulin resistant state was simulated by increasing $K_{0.5}$ of insulin binding to the receptor to 20 ng/mL. Points of intersections of the dotted curve with the dashed and solid curves recalculated with the new $K_{0.5}$ parameter show (arrows and labels) that maintaining glucose metabolism now requires about 6 ng/mL of plasma insulin, and nerve function requires at least 28 ng/mL of the hormone.

IR from 1 to 20 ng/mL, which leads to proportional rightward shifts of insulin-glucose metabolism and insulin-nerve function relationships. If the requirements of 10% and 65% occupancy of IR remain unchanged, maintenance of normal glucose metabolism under these new conditions will need about 6 ng/mL of circulating insulin and nearly 30 ng/mL insulin concentration will be the minimum needed to maintain normal PNS function. The calculated 6 ng/mL insulin concentration is in the range of insulin concentrations measured in Zucker fatty rats (5.1 to 11.7 ng/mL; model of compensated insulin resistance[150-152]). These latter numbers are, however, significantly lower than predicted by the model insulin concentration needed to maintain nerve function. Therefore, it may be speculated that the "set-point" or natural goal of compensatory hyperinsulinemia is merely to correct glucose metabolism, which is vitally important for the organism, with no concern about the less significant problem of nerve function.

Cellular mechanisms

Thus, while the connection remains speculative, the data above suggest that impairment of insulin signaling in PNS (because of decreased insulin production, insulin resistance or both) may be an important factor in the pathogenesis of DPN. Further studies are needed to confirm this hypothesis and further studies are also needed to understand the cellular mechanisms of insulin action in PNS.

Glucose is a major fuel for neurons of peripheral and central nervous systems. However, unlike that in major target tissues of insulin regulation, uptake of glucose in nervous tissue is an insulin-independent process. Therefore, the simple explanation of the neural effects of insulin to regulate the energy supply does not appear to be applicable. There should be some other role of IR in the nervous system. In the CNS, these receptors are involved in the insulin control of feeding behavior, reproductive and cognitive functions and neuromodulation[27,153]. Insulin also clearly has neurotrophic functions. It stimulates neurite outgrowth, is involved in peripheral nerve regeneration and is required for survival of sympathetic neurons (see[27]). These effects are likely very important for regeneration, which is suppressed in long-term DPN. For short term diabetes, the possibility of insulin regulation of axon-glia relationships, vascular permeability, and function of nociceptive primary afferent neurons[143,144] may be of importance. The possibility of a selective acute effect of

insulin on endoneurial blood flow (decrease) was also demonstrated by experiments in normal rats[154].

Note also that the negative cellular effects of hyperglycemia and insufficiency of insulin signaling seem to converge at some point. Pain pressure thresholds are decreased in rat models of local hyperglycemia with a time course and to a degree that is very similar to those in STZ-normoglycemic rats[101]. Since many studies support oxidative/nitrosative stress as a central event of hyperglycemic impairment, it is reasonable to suggest that oxidative/nitrosative stress can interfere with insulin regulation in some or all of the hyperglycemia-induced steps of the pathogenic cascade depicted in Figure 6. Insulin directly regulates inner mitochondrial membrane potentials and may affect oxidative phosphorylation[136]. Insulin also suppresses expression of NADPH oxidase[155] and controls expression of Nf-κB and associated inflammatory reactions[155,156]. In fact, the anti-inflammatory effects of insulin have been known since the discovery of the benefits of insulin therapy in systemic inflammatory responses to trauma or bacterial infection[157]. Insulin signaling also was shown to be linked to the regulation of Na, K-ATPase[158,159] and endothelial NO production[158,160]. These data suggest that insulinopenia does have the potential to produce the same or very similar neuropathic effects as were attributed previously solely to hyperglycemia.

OTHER FACTORS OF SIGNIFICANCE

While the above outlined insulin-signaling hypothesis of DPN appears compelling, it will certainly be corrected and modified in many of its segments to conform to the results of future studies. It can also be stated here, without reservation, that no complete picture of the pathogenesis of DPN will be created unless the roles of insulin-like growth factors and C-peptide are considered in addition to hyperglycemia and insulin signaling in PNS[142].

Insulin-like growth factors (IGFs)

IGFs are produced in the kidney, spinal cord, skeletal muscle and peripheral glia. IGFs possess multiple neurotrophic functions, including control of neuronal survival, neurite outgrowth and regeneration, and expression of genes encoding axonal cytoskeletal proteins (tubulins and neurofilaments)[142,161-166]. Interestingly, IGF-1 appears to be involved in the regulation of resistance to oxidative stress[167]. IGFs primarily act *via* specific receptors, but since IGFs are present in the circulation in a 100-fold excess compared to insulin, they may also bind to and activate IR, mimicking some but not all affects of insulin[168,145,165]. It might be important in this regard that, in peripheral nerve, IGF-I receptors are co-localized with IR in sensory neurons[169,170] and Schwann cells[171] and a large fraction of them are likely hybrids composed of protein subunits of both IR-A and IGF-I receptors[143,169]. These hybrid IR/IGF receptors have substantially higher affinity to IGF-I than to insulin[172,173]. However, even when present in physiological concentrations, insulin may still bind to and activate some portion of hybrid as well as homomeric IGF-I receptors[161,174]. In addition, IGF-I may act by suppressing growth hormone and improving insulin sensitivity and insulin production in type 1 and type 2 diabetic subjects[174-178]. Insulin on the other hand, may modify kidney production of IGFs, and *via* regulation of IGF binding proteins, it may control the activity of circulating IGFs[161,175,176]. Whether, any of these multiple mechanisms participate in the apparent dissociation of the metabolic and neuropathic effects of insulinopenia remains to be determined.

Abnormal expression and levels of circulating IGFs and/or changes in expression of receptors for IGF were measured in diabetic human subjects[174], in STZ-rats (see[179-181]), and in the type 2 diabetes Zucker diabetic fatty (ZDF) rat model[86]. Furthermore, in obese Zucker rats, both insulin- and IGF-I resistances were shown to develop and mediate impaired glucose tolerance in this model of pre-diabetes[182]. Thus potentially, *via* impairment of protein synthesis, insufficiency of IGFs may add to the pathogenesis of regenerative capacity, neurodegeneration and irreversible stages of DPN[142]. This suggestion is supported by observations of recovery of NCV and reversion of atrophy of myelinated sensory axons in the sural nerve of STZ rats treated with intrathecal IGF-I[89]. In addition, the defect in IGFs or IGF-receptor expression could also add to the pathogenesis of early symptoms of DPN either directly or through modulation of insulin production or nerve sensitivity to insulin. Indeed, down-regulation of IGF-I receptors, which is observed in nerves of STZ-diabetic rats, occurs comparatively early, within 1 week after the onset of hyperglycemia[181]. Furthermore, continuous subcutaneous infusion of IGF-Ⅱ was shown to recover pain pressure thresholds to a normal level after 6 wk of diabetes in the ZDF rat model[86]. The latter observation is interesting because, in STZ-diabetic rats, a similar magnitude and early decrease in pain pressure thresholds seems to result from insulinopenia (see previous section). Affinity of IGF-Ⅱ binding to brain type insulin receptors or to IGF-I-R is two-three times lower than that of respective natural ligands[145]. Therefore, the effect of IGF-Ⅱ on mechanical hyperalgesia may still be explained within the framework of our insulin signaling hypothesis of early neuropathy. However, the possibility of a more complex regulation of pain pressure thresholds cannot be excluded. It is important also that in all the examples above the effects of treatments with IGFs occurred with no measurable changes in the glycemic status of studied animals; once again suggesting that the pathogenesis of DPN is multifactorial.

C-peptide

C-peptide is a segment of the proinsulin molecule sliced off to form insulin. Acting through both its own receptors and modulating activity of insulin receptors, C-peptide produces multiple insulin and IGF-like effects[27,183,184]. C-peptide also enhances autophosphorylation of IR and effects of insulin, and treatment with C-peptide reverses decreased expression of IGF-I, NGF and neurotrophin-3 receptors in type 1 spontaneously diabetic rats[27,183,185]. Considering these effects and the fact that

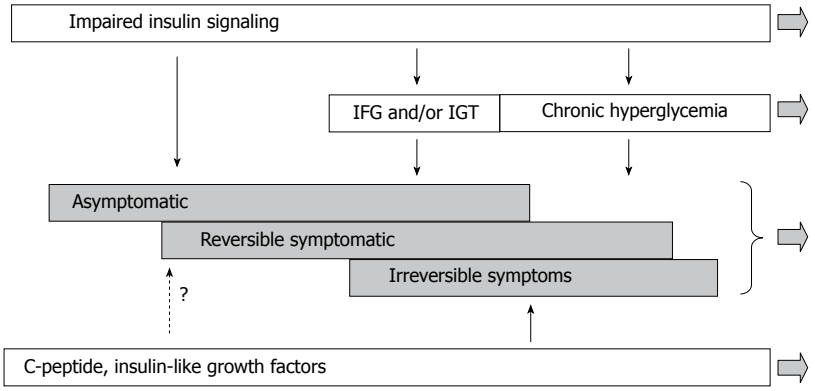

Figure 11 Modified scheme of pathogenesis of diffuse diabetic neuropathy with inclusion of insulin signaling. According to this view, the disease process starts before impairment of glucose metabolism becomes apparent. Derangement of insulin signaling in PNS triggers and maintains the neuropathy at this stage. Postprandial and chronic hyperglycemia is not the least important factor of DPN, but they become involved at relatively advanced stages of DPN. C-peptide and IGFs insufficiencies represent another important set of pathogenic mechanisms; however, the role of these mechanisms in early DPN remains undetermined.

C-peptide is secreted in equimolar concentrations with insulin, it can be concluded that C-peptide insufficiency may have an important role in the pathogenesis of type 1 diabetes[75,183,184]. In agreement with this implication, in patients with recently diagnosed type 1 diabetes, C-peptide treatment was shown to correct sensory NCV and vibration perception[186]. C-peptide treatment also corrects skin microcirculation in diabetic patients[187] and endoneurial blood flow and NCV slowing[75], thermal hyperalgesia, atrophy and degeneration of C-fibers[185] in BB/Wor type 1 diabetes rat model.

As expected, no differences in plasma C-peptide levels were found in pre-diabetic patients and patients with type 2 diabetes of short duration (less than 5 years from diagnosis), even though the number and severity of the signs and symptoms of DPN differed substantially between these groups[128]. What is less clear in the same study is a lack of detectable deficiency of C-peptide in advanced type 2 diabetes patients (more than 5 years) who could have been expected to start developing insulinopenia. In general, however, multiple questions remain to be resolved in relation to C-peptide and its role and mechanisms of action in DPN. Similar to conditions of chronic or postprandial hyperglycemia or impaired insulin- or IGF-signaling, C-peptide deficiency appears to affect activity of Na,K-ATPase, NO production and neurotrophism, but the C-peptide mediated regulation does not appear to depend on oxidative stress, which is apparently important in the pathogenesis of these conditions[75,188]. It is also not clear whether any of the symptoms may be directly attributed to C-peptide insufficiency in DPN. Endoneurial blood flow, NCV and heat nociception appear to be the foremost candidates[186,187], but antioxidant treatments and insulin replacement correct these abnormalities in STZ rats at least as efficiently as does C-peptide replacement in the BB/Wor rat model of type 1 diabetes.

CONCLUSION

DPN is a frequent and troublesome complication of diabetes mellitus. Diabetes manifests in a case-specific variety of signs and symptoms, and associates with complex biochemical, functional and structural abnormalities of the peripheral nervous system. While the obvious hyperglycemia present in diabetes can explain the development of these abnormalities, data suggest that other factors may also contribute. We have discussed the evidence for insulinopenia in type 1 diabetes or insulin resistance in type 2 diabetes as causal factors in the development of DPN. We have suggested that these two cases actually represent a single cause of impaired insulin signaling. Considering the role of insulin signaling in DPN more completely explains the changes in nerve function in pre-diabetic or early diabetic patients and animal models. This does not preclude hyperglycemia also as a factor in DPN, but allows a more complete picture of the disease process (Figure 11). In addition to insulin signaling, some evidence also exists for a role of IGF and C-peptide in mediating DPN. The pathogenesis of DPN is obviously multifactorial, and despite long-standing efforts, remains poorly understood. This work has also suggested that insulin signaling has effects that occur with different levels of receptor occupancy. Thus insulin action on nerve function requires a higher level of receptor occupancy than does insulin action on glycemic control. This could be explained by different levels of receptor coupling to second messenger signaling pathways in nerve versus liver or muscle. Future studies should elucidate these mechanisms so that a clearer picture of DPN can be obtained, especially in pre-diabetes where early detection could improve therapeutic outcomes.

REFERENCES

1 **American Diabetes Association**. Diagnosis and classification of diabetes mellitus. *Diabetes Care* 2006; **29** Suppl 1: S43-S48
2 **Diabetes in America**. Bethesda MR: National Diabetes Data Group, NIH, 1995: 1-733
3 **American Diabetes Association**. Report of the Expert Committee on the Diagnosis and Classification of Diabetes Mellitus. *Diabetes Care* 1997; **20**: 1183-1197
4 **American Diabetes Association**. Standards of medical care in diabetes--2006. *Diabetes Care* 2006; **29** Suppl 1: S4-S42
5 **Stryer L**. Biochemistry. New York: W.H. Freeman and Company, 1988: 1-1089
6 **Zierler K**. Whole body glucose metabolism. *Am J Physiol* 1999; **276**: E409-E426
7 **Kono T**, Barham FW. The relationship between the insulin-binding capacity of fat cells and the cellular response to insulin. Studies with intact and trypsin-treated fat cells. *J Biol Chem* 1971; **246**: 6210-6216
8 **Gliemann J**, Gammeltoft S, Vinten J. Time course of insulin-receptor binding and insulin-induced lipogenesis in isolated rat fat cells. *J Biol Chem* 1975; **250**: 3368-3374
9 **Kahn BB**, Rossetti L. Type 2 diabetes--who is conducting the orchestra? *Nat Genet* 1998; **20**: 223-225
10 **Olefsky JM**. Insensitivity of large rat adipocytes to the antilipolytic effects of insulin. *J Lipid Res* 1977; **18**: 459-464

11 **Eisenbarth GS**. Type I diabetes mellitus. A chronic autoimmune disease. *N Engl J Med* 1986; **314**: 1360-1368
12 **Kobayashi T**, Kamata K. Effect of insulin treatment on smooth muscle contractility and endothelium-dependent relaxation in rat aortae from established STZ-induced diabetes. *Br J Pharmacol* 1999; **127**: 835-842
13 **Burcelin R**, Eddouks M, Kande J, Assan R, Girard J. Evidence that GLUT-2 mRNA and protein concentrations are decreased by hyperinsulinaemia and increased by hyperglycaemia in liver of diabetic rats. *Biochem J* 1992; **288** (Pt 2): 675-679
14 **Rossetti L**, Giaccari A. Relative contribution of glycogen synthesis and glycolysis to insulin-mediated glucose uptake. A dose-response euglycemic clamp study in normal and diabetic rats. *J Clin Invest* 1990; **85**: 1785-1792
15 **Rossetti L**, Shulman GI, Zawalich W, DeFronzo RA. Effect of chronic hyperglycemia on in vivo insulin secretion in partially pancreatectomized rats. *J Clin Invest* 1987; **80**: 1037-1044
16 **Russell JW**, Golovoy D, Vincent AM, Mahendru P, Olzmann JA, Mentzer A, Feldman EL. High glucose-induced oxidative stress and mitochondrial dysfunction in neurons. *FASEB J* 2002; **16**: 1738-1748
17 **Lin CY**, Higginbotham DA, Judd RL, White BD. Central leptin increases insulin sensitivity in streptozotocin-induced diabetic rats. *Am J Physiol Endocrinol Metab* 2002; **282**: E1084-E1091
18 **Patlak M**. New weapons to combat an ancient disease: treating diabetes. *FASEB J* 2002; **16**: 1853
19 **Genuth S**, Alberti KG, Bennett P, Buse J, Defronzo R, Kahn R, Kitzmiller J, Knowler WC, Lebovitz H, Lernmark A, Nathan D, Palmer J, Rizza R, Saudek C, Shaw J, Steffes M, Stern M, Tuomilehto J, Zimmet P. Follow-up report on the diagnosis of diabetes mellitus. *Diabetes Care* 2003; **26**: 3160-3167
20 **Tirosh A**, Shai I, Tekes-Manova D, Israeli E, Pereg D, Shochat T, Kochba I, Rudich A. Normal fasting plasma glucose levels and type 2 diabetes in young men. *N Engl J Med* 2005; **353**: 1454-1462
21 **Godsland IF**, Jeffs JA, Johnston DG. Loss of beta cell function as fasting glucose increases in the non-diabetic range. *Diabetologia* 2004; **47**: 1157-1166
22 **Argoff CE**, Cole BE, Fishbain DA, Irving GA. Diabetic peripheral neuropathic pain: clinical and quality-of-life issues. *Mayo Clin Proc* 2006; **81**: S3-11
23 **Vinik AI**, Newlon P, Milicevic Z, McNitt P, Stansberry KB. Diabetic neuropathies: an overview of clinical aspects. In: LeRoith D, Taylor SI, Olefsky JM, editors. Diabetes Mellitus. Philadelphia, New-York: Lippincott-Raven Publishers, 1996: 737-751
24 **Vinik AI**, Mehrabyan A. Diabetic neuropathies. *Med Clin North Am* 2004; **88**: 947-999, xi
25 **Polydefkis M**, Griffin JW, McArthur J. New insights into diabetic polyneuropathy. *JAMA* 2003; **290**: 1371-1376
26 **Horowitz SH**. Diabetic neuropathy. *Clin Orthop Relat Res* 1993; **296**: 78-85
27 **Sugimoto K**, Murakawa Y, Sima AA. Diabetic neuropathy--a continuing enigma. *Diabetes Metab Res Rev* 2000; **16**: 408-433
28 **Bastyr EJ**, Price KL, Bril V. Development and validity testing of the neuropathy total symptom score-6: questionnaire for the study of sensory symptoms of diabetic peripheral neuropathy. *Clin Ther* 2005; **27**: 1278-1294
29 **Dyck PJ.** Detection, characterization, and staging of polyneuropathy: assessed in diabetics. *Muscle Nerve* 1988; **11**: 21-32
30 **Boulton AJ**, Vinik AI, Arezzo JC, Bril V, Feldman EL, Freeman R, Malik RA, Maser RE, Sosenko JM, Ziegler D. Diabetic neuropathies: a statement by the American Diabetes Association. *Diabetes Care* 2005; **28**: 956-962
31 **Thomas PK**. Classification, differential diagnosis, and staging of diabetic peripheral neuropathy. *Diabetes* 1997; **46** Suppl 2: S54-S57
32 **Young RJ**, Zhou YQ, Rodriguez E, Prescott RJ, Ewing DJ, Clarke BF. Variable relationship between peripheral somatic and autonomic neuropathy in patients with different syndromes of diabetic polyneuropathy. *Diabetes* 1986; **35**: 192-197
33 **Young RJ,** Ewing DJ, Clarke BF. Chronic and remitting painful diabetic polyneuropathy. Correlations with clinical features and subsequent changes in neurophysiology. *Diabetes Care* 1988; **11**: 34-40
34 **Maser RE**, Nielsen VK, Bass EB, Manjoo Q, Dorman JS, Kelsey SF, Becker DJ, Orchard TJ. Measuring diabetic neuropathy. Assessment and comparison of clinical examination and quantitative sensory testing. *Diabetes Care* 1989; **12**: 270-275
35 **Navarro X**, Kennedy WR, Fries TJ. Small nerve fiber dysfunction in diabetic neuropathy. *Muscle Nerve* 1989; **12**: 498-507
36 **Ellenberg M**. Diabetic neuropathy: clinical aspects. *Metabolism* 1976; **25**: 1627-1655
37 **Boulton AJ**. Management of diabetic peripheral neuropathy. *Clinical Diabetes* 2005; **23**: 9-15
38 **Belgrade MJ**, Cole BE, McCarberg BH, McLean MJ. Diabetic peripheral neuropathic pain: case studies. *Mayo Clin Proc* 2006; **81**: S26-S32
39 **Pfeifer MA**, Ross DR, Schrage JP, Gelber DA, Schumer MP, Crain GM, Markwell SJ, Jung S. A highly successful and novel model for treatment of chronic painful diabetic peripheral neuropathy. *Diabetes Care* 1993; **16**: 1103-1115
40 **Benbow SJ**, MacFarlane IA. Painful diabetic neuropathy. *Baillieres Best Pract Res Clin Endocrinol Metab* 1999; **13**: 295-308
41 **Dyck PJ**, Giannini C. Pathologic alterations in the diabetic neuropathies of humans: a review. *J Neuropathol Exp Neurol* 1996; **55**: 1181-1193
42 **Thomas PK**. Diabetic neuropathy: mechanisms and future treatment options. *J Neurol Neurosurg Psychiatry* 1999; **67**: 277-279
43 **Zochodne DW**. Neurotrophins and other growth factors in diabetic neuropathy. *Semin Neurol* 1996; **16**: 153-161
44 **Liuzzi FJ**, Bufton SM, Vinik AI. Streptozotocin-induced diabetes mellitus causes changes in primary sensory neuronal cytoskeletal mRNA levels that mimic those caused by axotomy. *Exp Neurol* 1998; **154**: 381-388
45 **Koltzenburg M**, Scadding J. Neuropathic pain. *Curr Opin Neurol* 2001; **14**: 641-647
46 **Torebjörk HE**, Lundberg LE, LaMotte RH. Central changes in processing of mechanoreceptive input in capsaicin-induced secondary hyperalgesia in humans. *J Physiol* 1992; **448**: 765-780
47 **Ochoa JL**, Torebjörk HE. Paraesthesiae from ectopic impulse generation in human sensory nerves. *Brain* 1980; **103**: 835-853
48 **Mogyoros I**, Bostock H, Burke D. Mechanisms of paresthesias arising from healthy axons. *Muscle Nerve* 2000; **23**: 310-320
49 **Wallace VC**, Cottrell DF, Brophy PJ, Fleetwood-Walker SM. Focal lysolecithin-induced demyelination of peripheral afferents results in neuropathic pain behavior that is attenuated by cannabinoids. *J Neurosci* 2003; **23**: 3221-3233
50 **Sima AA**, Nathaniel V, Bril V, McEwen TA, Greene DA. Histopathological heterogeneity of neuropathy in insulin - dependent and non-insulin-dependent diabetes, and demonstration of axo- glial dysjunction in human diabetic neuropathy. *J Clin Invest* 1988; **81**: 349-364
51 **Dyck PJ**, Lambert EH, O'Brien PC. Pain in peripheral neuropathy related to rate and kind of fiber degeneration. *Neurology* 1976; **26**: 466-471
52 **Bonica JJ**. The Managment of Pain. In: Loeser JD, Chapman CR, Fordyce WE. Philadelphia, London: Lea & Febiger, 1990: 1-958
53 **Hotta N**, Toyota T, Matsuoka K, Shigeta Y, Kikkawa R, Kaneko T, Takahashi A, Sugimura K, Koike Y, Ishii J, Sakamoto N. Clinical efficacy of fidarestat, a novel aldose reductase inhibitor, for diabetic peripheral neuropathy: a 52-week multicenter placebo- controlled double-blind parallel group study. *Diabetes Care* 2001; **24**: 1776-1782
54 **Brown MJ**, Martin JR, Asbury AK. Painful diabetic neuropathy. A morphometric study. *Arch Neurol* 1976; **33**: 164-171
55 **Britland ST**, Young RJ, Sharma AK, Clarke BF. Association of painful and painless diabetic polyneuropathy with different patterns of nerve fiber degeneration and regeneration. *Diabetes* 1990; **39**: 898-908
56 **Sima AA**. Peripheral neuropathy in the spontaneously diabetic BB-Wistar-rat. An ultrastructural study. *Acta Neuropathol* 1980; **51**: 223-227
57 **Waxman SG**. Pathophysiology of nerve conduction: relation to diabetic neuropathy. *Ann Intern Med* 1980; **92**: 297-301

58 **Johnson PC**, Doll SC, Cromey DW. Pathogenesis of diabetic neuropathy. *Ann Neurol* 1986; **19**: 450-457
59 **Dyck PJ**, Karnes JL, O'Brien P, Okazaki H, Lais A, Engelstad J. The spatial distribution of fiber loss in diabetic polyneuropathy suggests ischemia. *Ann Neurol* 1986; **19**: 440-449
60 **Dyck PJ**, Lais A, Karnes JL, O'Brien P, Rizza R. Fiber loss is primary and multifocal in sural nerves in diabetic polyneuropathy. *Ann Neurol* 1986; **19:** 425-439
61 **Dyck PJ**, Gutrecht JA, Bastron JA, Karnes WE, Dale AJ. Histologic and teased-fiber measurements of sural nerve in disorders of lower motor and primary sensory neurons. *Mayo Clin Proc* 1968; **43**: 81-123
62 **Malik RA**. The pathology of human diabetic neuropathy. *Diabetes* 1997; **46** Suppl 2: S50-S53
63 **Nathan DM**. The pathophysiology of diabetic complications: how much does the glucose hypothesis explain? *Ann Intern Med* 1996; **124**: 86-89
64 **Vinik AI**. Advances in diabetes for the millennium: new treatments for diabetic neuropathies. *MedGenMed* 2004; **6**: 13
65 **Skyler JS**. Effect of glycemic control on diabetes complications and on the prevention of diabetes. *Clinical Diabetes* 2004; **22**: 162-166
66 **Chronic Complications in Diabetes**. Ed: Sima AA. Animal Models and Chronic Complications. Amsterdam: Harwood Academic Publishers, 2000: 1-277
67 **Lasker RD**. The diabetes control and complications trial. Implications for policy and practice. *N Engl J Med* 1993; **329**: 1035-1036
68 **DCCT**. The effect of intensive treatment of diabetes on the development and progression of long-term complications in insulin-dependent diabetes mellitus. The Diabetes Control and Complications Trial Research Group. *N Engl J Med* 1993; **329**: 977-986
69 **Bode BW**, Schwartz S, Stubbs HA, Block JE. Glycemic characteristics in continuously monitored patients with type 1 and type 2 diabetes: normative values. *Diabetes Care* 2005; **28**: 2361-2366
70 **Singleton JR**, Smith AG, Bromberg MB. Increased prevalence of impaired glucose tolerance in patients with painful sensory neuropathy. *Diabetes Care* 2001; **24**: 1448-1453
71 **Novella SP**, Inzucchi SE, Goldstein JM. The frequency of undiagnosed diabetes and impaired glucose tolerance in patients with idiopathic sensory neuropathy. *Muscle Nerve* 2001; **24**: 1229-1231
72 **Animal Models of Diabetes**. Sima AA, Shafrir E, editors. A Primer. Amsterdam: Harwood Academic Publishers, 2001: 1-364
73 **Moore SA**, Peterson RG, Felten DL, O'Connor BL. A quantitative comparison of motor and sensory conduction velocities in short- and long-term streptozotocin- and alloxan-diabetic rats. *J Neurol Sci* 1980; **48**: 133-152
74 **Weis J**, Dimpfel W, Schröder JM. Nerve conduction changes and fine structural alterations of extra- and intrafusal muscle and nerve fibers in streptozotocin diabetic rats. *Muscle Nerve* 1995; **18:** 175-184
75 **Stevens MJ**, Zhang W, Li F, Sima AA. C-peptide corrects endoneurial blood flow but not oxidative stress in type 1 BB/Wor rats. *Am J Physiol Endocrinol Metab* 2004; **287**: E497-E505
76 **Zochodne DW**, Ho LT, Allison JA. Dorsal root ganglia microenvironment of female BB Wistar diabetic rats with mild neuropathy. *J Neurol Sci* 1994; **127**: 36-42
77 **Ferreira LD**, Huey PU, Pulford BE, Ishii DN, Eckel RH. Sciatic nerve lipoprotein lipase is reduced in streptozotocin-induced diabetes and corrected by insulin. *Endocrinology* 2002; **143**: 1213-1217
78 **Coppey LJ,** Davidson EP, Dunlap JA, Lund DD, Yorek MA. Slowing of motor nerve conduction velocity in streptozotocin-induced diabetic rats is preceded by impaired vasodilation in arterioles that overlie the sciatic nerve. *Int J Exp Diabetes Res* 2000; **1**: 131-143
79 **Qiang X**, Satoh J, Sagara M, Fukuzawa M, Masuda T, Sakata Y, Muto G, Muto Y, Takahashi K, Toyota T. Inhibitory effect of troglitazone on diabetic neuropathy in streptozotocin-induced diabetic rats. *Diabetologia* 1998; **41**: 1321-1326
80 **Sima AA**, Brismar T. Reversible diabetic nerve dysfunction: structural correlates to electrophysiological abnormalities. *Ann Neurol* 1985; **18**: 21-29
81 **Sima AA**, Lattimer SA, Yagihashi S, Greene DA. Axo-glial dysjunction. A novel structural lesion that accounts for poorly reversible slowing of nerve conduction in the spontaneously diabetic bio-breeding rat. *J Clin Invest* 1986; **77**: 474-484
82 **Greene DA**, Chakrabarti S, Lattimer SA, Sima AA. Role of sorbitol accumulation and myo-inositol depletion in paranodal swelling of large myelinated nerve fibers in the insulin-deficient spontaneously diabetic bio-breeding rat. Reversal by insulin replacement, an aldose reductase inhibitor, and myo-inositol. *J Clin Invest* 1987; **79**: 1479-1485
83 **Shimoshige Y**, Ikuma K, Yamamoto T, Takakura S, Kawamura I, Seki J, Mutoh S, Goto T. The effects of zenarestat, an aldose reductase inhibitor, on peripheral neuropathy in Zucker diabetic fatty rats. *Metabolism* 2000; **49**: 1395-1399
84 **Romanovsky D**, Hastings SL, Stimers JR, Dobretsov M. Relevance of hyperglycemia to early mechanical hyperalgesia in streptozotocin-induced diabetes. *J Peripher Nerv Syst* 2004; **9**: 62-69
85 **Chen SR**, Pan HL. Hypersensitivity of spinothalamic tract neurons associated with diabetic neuropathic pain in rats. *J Neurophysiol* 2002; **87:** 2726-2733
86 **Zhuang HX**, Wuarin L, Fei ZJ, Ishii DN. Insulin-like growth factor (IGF) gene expression is reduced in neural tissues and liver from rats with non-insulin-dependent diabetes mellitus, and IGF treatment ameliorates diabetic neuropathy. *J Pharmacol Exp Ther* 1997; **283**: 366-374
87 **Piercy V**, Banner SE, Bhattacharyya A, Parsons AA, Sanger GJ, Smith SA, Bingham S. Thermal, but not mechanical, nociceptive behavior is altered in the Zucker Diabetic Fatty rat and is independent of glycemic status. *J Diabetes Complications* 1999; **13**: 163-169
88 **Schmidt RE**, Dorsey DA, Beaudet LN, Parvin CA, Zhang W, Sima AA. Experimental rat models of types 1 and 2 diabetes differ in sympathetic neuroaxonal dystrophy. *J Neuropathol Exp Neurol* 2004; **63**: 450-460
89 **Brussee V,** Cunningham FA, Zochodne DW. Direct insulin signaling of neurons reverses diabetic neuropathy. *Diabetes* 2004; **53**: 1824-1830
90 **Schmeichel AM**, Schmelzer JD, Low PA. Oxidative injury and apoptosis of dorsal root ganglion neurons in chronic experimental diabetic neuropathy. *Diabetes* 2003; **52**: 165-171
91 **Cameron NE,** Cotter MA, Low PA. Nerve blood flow in early experimental diabetes in rats: relation to conduction deficits. *Am J Physiol* 1991; **261**: E1-E8
92 **Nagamatsu M**, Nickander KK, Schmelzer JD, Raya A, Wittrock DA, Tritschler H, Low PA. Lipoic acid improves nerve blood flow, reduces oxidative stress, and improves distal nerve conduction in experimental diabetic neuropathy. *Diabetes Care* 1995; **18**: 1160-1167
93 **Cameron NE**, Cotter MA, Jack AM, Basso MD, Hohman TC. Protein kinase C effects on nerve function, perfusion, Na(+), K(+)-ATPase activity and glutathione content in diabetic rats. *Diabetologia* 1999; **42**: 1120-1130
94 **Way KJ**, Katai N, King GL. Protein kinase C and the development of diabetic vascular complications. *Diabet Med* 2001; **18**: 945-959
95 **Hamdy O**, Ledbury S, Mullooly C, Jarema C, Porter S, Ovalle K, Moussa A, Caselli A, Caballero AE, Economides PA, Veves A, Horton ES. Lifestyle modification improves endothelial function in obese subjects with the insulin resistance syndrome. *Diabetes Care* 2003; **26**: 2119-2125
96 **Huvers FC**, De Leeuw PW, Houben AJ, De Haan CH, Hamulyak K, Schouten H, Wolffenbuttel BH, Schaper NC. Endothelium-dependent vasodilatation, plasma markers of endothelial function, and adrenergic vasoconstrictor responses in type 1 diabetes under near-normoglycemic conditions. *Diabetes* 1999; **48**: 1300-1307
97 **Khan F**, Elhadd TA, Greene SA, Belch JJ. Impaired skin microvascular function in children, adolescents, and young

adults with type 1 diabetes. *Diabetes Care* 2000; **23**: 215-220
98 **Caballero AE**, Arora S, Saouaf R, Lim SC, Smakowski P, Park JY, King GL, LoGerfo FW, Horton ES, Veves A. Microvascular and macrovascular reactivity is reduced in subjects at risk for type 2 diabetes. *Diabetes* 1999; **48**: 1856-1862
99 **Theriault M**, Dort J, Sutherland G, Zochodne DW. Local human sural nerve blood flow in diabetic and other polyneuropathies. *Brain* 1997; **120** (Pt 7): 1131-1138
100 **Dobretsov M**, Hastings SL, Stimers JR, Zhang JM. Mechanical hyperalgesia in rats with chronic perfusion of lumbar dorsal root ganglion with hyperglycemic solution. *J Neurosci Methods* 2001; **110**: 9-15
101 **Dobretsov M**, Hastings SL, Romanovsky D, Stimers JR, Zhang JM. Mechanical hyperalgesia in rat models of systemic and local hyperglycemia. *Brain Res* 2003; **960**: 174-183
102 **King RH**. The role of glycation in the pathogenesis of diabetic polyneuropathy. *Mol Pathol* 2001; **54**: 400-408
103 **Srivastava SK**, Ramana KV, Bhatnagar A. Role of aldose reductase and oxidative damage in diabetes and the consequent potential for therapeutic options. *Endocr Rev* 2005; **26**: 380-392
104 **Yabe-Nishimura C**. Aldose reductase in glucose toxicity: a potential target for the prevention of diabetic complications. *Pharmacol Rev* 1998; **50**: 21-33
105 **Reusch JE**. Diabetes, microvascular complications, and cardiovascular complications: what is it about glucose? *J Clin Invest* 2003; **112**: 986-988
106 **Brownlee M**. The pathobiology of diabetic complications: a unifying mechanism. *Diabetes* 2005; **54**: 1615-1625
107 **Pieper GM.** Review of alterations in endothelial nitric oxide production in diabetes: protective role of arginine on endothelial dysfunction. *Hypertension* 1998; **31**: 1047-1060
108 **Pacher P**, Szabó C. Role of poly(ADP-ribose) polymerase-1 activation in the pathogenesis of diabetic complications: endothelial dysfunction, as a common underlying theme. *Antioxid Redox Signal* 2005; **7**: 1568-1580
109 **Wang Y**, Schmeichel AM, Iida H, Schmelzer JD, Low PA. Ischemia-reperfusion injury causes oxidative stress and apoptosis of Schwann cell in acute and chronic experimental diabetic neuropathy. *Antioxid Redox Signal* 2005; **7**: 1513-1520
110 **Chait A**, Brunzell JD. Diabetes, lipids, and atherosclerosis. In: LeRoith D, Taylor SI, Olefsky JM. Diabetes Mellitus. Philadelphia, New York: Lippincott-Raven Publishers, 1996: 772-777
111 **Obrosova IG**. Increased sorbitol pathway activity generates oxidative stress in tissue sites for diabetic complications. *Antioxid Redox Signal* 2005; **7**: 1543-1552
112 **Kellogg AP**, Pop-Busui R. Peripheral nerve dysfunction in experimental diabetes is mediated by cyclooxygenase-2 and oxidative stress. *Antioxid Redox Signal* 2005; **7**: 1521-1529
113 **Greene DA**, Stevens MJ, Obrosova I, Feldman EL. Glucose-induced oxidative stress and programmed cell death in diabetic neuropathy. *Eur J Pharmacol* 1999; **375**: 217-223
114 **Feldman EL**. Oxidative stress and diabetic neuropathy: a new understanding of an old problem. *J Clin Invest* 2003; **111**: 431-433
115 **Ceriello A**, Motz E. Is oxidative stress the pathogenic mechanism underlying insulin resistance, diabetes, and cardiovascular disease? The common soil hypothesis revisited. *Arterioscler Thromb Vasc Biol* 2004; **24**: 816-823
116 **Kishi Y**, Schmelzer JD, Yao JK, Zollman PJ, Nickander KK, Tritschler HJ, Low PA. Alpha-lipoic acid: effect on glucose uptake, sorbitol pathway, and energy metabolism in experimental diabetic neuropathy. *Diabetes* 1999; **48**: 2045-2051
117 **Ametov AS**, Barinov A, Dyck PJ, Hermann R, Kozlova N, Litchy WJ, Low PA, Nehrdich D, Novosadova M, O'Brien PC, Reljanovic M, Samigullin R, Schuette K, Strokov I, Tritschler HJ, Wessel K, Yakhno N, Ziegler D. The sensory symptoms of diabetic polyneuropathy are improved with alpha-lipoic acid: the SYDNEY trial. *Diabetes Care* 2003; **26**: 770-776
118 **Maritim AC**, Sanders RA, Watkins JB. Diabetes, oxidative stress, and antioxidants: a review. *J Biochem Mol Toxicol* 2003; **17**: 24-38
119 **Johansen JS**, Harris AK, Rychly DJ, Ergul A. Oxidative stress and the use of antioxidants in diabetes: linking basic science to clinical practice. *Cardiovasc Diabetol* 2005; **4**: 5-25
120 **Petersen M**, LaMotte RH. Relationships between capsaicin sensitivity of mammalian sensory neurons, cell size and type of voltage gated Ca-currents. *Brain Res* 1991; **561**: 20-26
121 **Obrosova IG,** Van Huysen C, Fathallah L, Cao XC, Greene DA, Stevens MJ. An aldose reductase inhibitor reverses early diabetes-induced changes in peripheral nerve function, metabolism, and antioxidative defense. *FASEB J* 2002; **16**: 123-125
122 **Young RJ**, Ewing DJ, Clarke BF. A controlled trial of sorbinil, an aldose reductase inhibitor, in chronic painful diabetic neuropathy. *Diabetes* 1983; **32**: 938-942
123 **Martyn CN**, Reid W, Young RJ, Ewing DJ, Clarke BF. Six-month treatment with sorbinil in asymptomatic diabetic neuropathy. Failure to improve abnormal nerve function. *Diabetes* 1987; **36**: 987-990
124 **Boulton AJ**, Malik RA, Arezzo JC, Sosenko JM. Diabetic somatic neuropathies. *Diabetes Care* 2004; **27**: 1458-1486
125 **Singleton JR**, Smith AG, Russell J, Feldman EL. Polyneuropathy with Impaired Glucose Tolerance: Implications for Diagnosis and Therapy. *Curr Treat Options Neurol* 2005; **7**: 33-42
126 **Russell JW**, Feldman EL. Impaired glucose tolerance--does it cause neuropathy? *Muscle Nerve* 2001; **24**: 1109-1112
127 **Singleton JR**, Smith AG, Bromberg MB. Painful sensory polyneuropathy associated with impaired glucose tolerance. *Muscle Nerve* 2001; **24**: 1225-1228
128 **Pittenger GL**, Mehrabyan A, Simmons K, Amandarice C, Barlow P, Vinik AI. Small fiber neuropathy is associated with the metabolic syndrome. *Metab Syndr Relat Disord* 2005; **3**: 113-121
129 **Sumner CJ**, Sheth S, Griffin JW, Cornblath DR, Polydefkis M. The spectrum of neuropathy in diabetes and impaired glucose tolerance. *Neurology* 2003; **60**: 108-111
130 **Monnier L**, Mas E, Ginet C, Michel F, Villon L, Cristol JP, Colette C. Activation of oxidative stress by acute glucose fluctuations compared with sustained chronic hyperglycemia in patients with type 2 diabetes. *JAMA* 2006; **295**: 1681-1687
131 **de Neeling JN**, Beks PJ, Bertelsmann FW, Heine RJ, Bouter LM. Peripheral somatic nerve function in relation to glucose tolerance in an elderly Caucasian population: the Hoorn study. *Diabet Med* 1996; **13**: 960-966
132 **Morley GK**, Mooradian AD, Levine AS, Morley JE. Mechanism of pain in diabetic peripheral neuropathy. Effect of glucose on pain perception in humans. *Am J Med* 1984; **77**: 79-82
133 **Thye-Rønn P**, Sindrup SH, Arendt-Nielsen L, Brennum J, Hother-Nielsen O, Beck-Nielsen H. Effect of short-term hyperglycemia per se on nociceptive and non-nociceptive thresholds. *Pain* 1994; **56**: 43-49
134 **Chan AW**, MacFarlane IA, Bowsher D. Short term fluctuations in blood glucose concentrations do not alter pain perception in diabetic-patients with and without painful peripheral neuropathy. *Diabetes Res* 1990; **14**: 15-19
135 **Oyibo SO**, Prasad YD, Jackson NJ, Jude EB, Boulton AJ. The relationship between blood glucose excursions and painful diabetic peripheral neuropathy: a pilot study. *Diabet Med* 2002; **19**: 870-873
136 **Huang TJ**, Price SA, Chilton L, Calcutt NA, Tomlinson DR, Verkhratsky A, Fernyhough P. Insulin prevents depolarization of the mitochondrial inner membrane in sensory neurons of type 1 diabetic rats in the presence of sustained hyperglycemia. *Diabetes* 2003; **52**: 2129-2136
137 **Maneuf YP**, Blake R, Andrews NA, McKnight AT. Reduction by gabapentin of K+-evoked release of [3H]-glutamate from the caudal trigeminal nucleus of the streptozotocin-treated rat. *Br J Pharmacol* 2004; **141**: 574-579
138 **Calcutt NA**, Jorge MC, Yaksh TL, Chaplan SR. Tactile allodynia and formalin hyperalgesia in streptozotocin-diabetic rats: effects of insulin, aldose reductase inhibition and lidocaine. *Pain* 1996; **68**: 293-299

139 **Calcutt NA**, Freshwater JD, Mizisin AP. Prevention of sensory disorders in diabetic Sprague-Dawley rats by aldose reductase inhibition or treatment with ciliary neurotrophic factor. *Diabetologia* 2004; **47**: 718-724

140 **Roane DS**, Porter JR. Nociception and opioid-induced analgesia in lean (Fa/-) and obese (fa/fa) Zucker rats. *Physiol Behav* 1986; **38**: 215-218

141 **Oltman CL**, Coppey LJ, Gellett JS, Davidson EP, Lund DD, Yorek MA. Progression of vascular and neural dysfunction in sciatic nerves of Zucker diabetic fatty and Zucker rats. *Am J Physiol Endocrinol Metab* 2005; **289**: E113-E122

142 **Ishii DN**. Implication of insulin-like growth factors in the pathogenesis of diabetic neuropathy. *Brain Res Brain Res Rev* 1995; **20**: 47-67

143 **Sugimoto K**, Murakawa Y, Zhang W, Xu G, Sima AA. Insulin receptor in rat peripheral nerve: its localization and alternatively spliced isoforms. *Diabetes Metab Res Rev* 2000; **16**: 354-363

144 **Sugimoto K,** Murakawa Y, Sima AA. Expression and localization of insulin receptor in rat dorsal root ganglion and spinal cord. *J Peripher Nerv Syst* 2002; **7**: 44-53

145 **Frasca F**, Pandini G, Scalia P, Sciacca L, Mineo R, Costantino A, Goldfine ID, Belfiore A, Vigneri R. Insulin receptor isoform A, a newly recognized, high-affinity insulin-like growth factor II receptor in fetal and cancer cells. *Mol Cell Biol* 1999; **19**: 3278-3288

146 **Martin CL**, Albers J, Herman WH, Cleary P, Waberski B, Greene DA, Stevens MJ, Feldman EL. Neuropathy among the diabetes control and complications trial cohort 8 years after trial completion. *Diabetes Care* 2006; **29**: 340-344

147 **Singhal A**, Cheng C, Sun H, Zochodne DW. Near nerve local insulin prevents conduction slowing in experimental diabetes. *Brain Res* 1997; **763**: 209-214

148 **Partanen J**, Niskanen L, Lehtinen J, Mervaala E, Siitonen O, Uusitupa M. Natural history of peripheral neuropathy in patients with non-insulin-dependent diabetes mellitus. *N Engl J Med* 1995; **333**: 89-94

149 **Delaney CA**, Mouser JV, Westerman RA. Insulin sensitivity and sensory nerve function in non-diabetic human subjects. *Neurosci Lett* 1994; **180**: 277-280

150 **Jacob S**, Streeper RS, Fogt DL, Hokama JY, Tritschler HJ, Dietze GJ, Henriksen EJ. The antioxidant alpha-lipoic acid enhances insulin-stimulated glucose metabolism in insulin-resistant rat skeletal muscle. *Diabetes* 1996; **45**: 1024-1029

151 **Broca C**, Breil V, Cruciani-Guglielmacci C, Manteghetti M, Rouault C, Derouet M, Rizkalla S, Pau B, Petit P, Ribes G, Ktorza A, Gross R, Reach G, Taouis M. Insulinotropic agent ID-1101 (4-hydroxyisoleucine) activates insulin signaling in rat. *Am J Physiol Endocrinol Metab* 2004; **287**: E463-E471

152 **Wong V**, Stavar L, Szeto L, Uffelman K, Wang CH, Fantus IG, Lewis GF. Atorvastatin induces insulin sensitization in Zucker lean and fatty rats. *Atherosclerosis* 2006; **184**: 348-355

153 **Freychet P**. Insulin receptors and insulin actions in the nervous system. *Diabetes Metab Res Rev* 2000; **16**: 390-392

154 **Kihara M**, Zollman PJ, Smithson IL, Lagerlund TD, Low PA. Hypoxic effect of exogenous insulin on normal and diabetic peripheral nerve. *Am J Physiol* 1994; **266**: E980-E985

155 **Dandona P,** Mohanty P, Chaudhuri A, Garg R, Aljada A. Insulin infusion in acute illness. *J Clin Invest* 2005; **115**: 2069-2072

156 **Nedrebø T**, Karlsen TV, Salvesen GS, Reed RK. A novel function of insulin in rat dermis. *J Physiol* 2004; **559**: 583-591

157 **Jeschke MG**, Einspanier R, Klein D, Jauch KW. Insulin attenuates the systemic inflammatory response to thermal trauma. *Mol Med* 2002; **8**: 443-450

158 **Davel AP**, Rossoni LV, Vassallo DV. Effects of ouabain on the pressor response to phenylephrine and on the sodium pump activity in diabetic rats. *Eur J Pharmacol* 2000; **406**: 419-427

159 **Sweeney G**, Klip A. Regulation of the Na+/K+-ATPase by insulin: why and how? *Mol Cell Biochem* 1998; **182**: 121-133

160 **Steinberg HO,** Brechtel G, Johnson A, Fineberg N, Baron AD. Insulin-mediated skeletal muscle vasodilation is nitric oxide dependent. A novel action of insulin to increase nitric oxide release. *J Clin Invest* 1994; **94**: 1172-1179

161 **Ranke MB**. Insulin-like growth factor-I treatment of growth disorders, diabetes mellitus and insulin resistance. *Trends Endocrinol Metab* 2005; **16:** 190-197

162 **Recio-Pinto E**, Rechler MM, Ishii DN. Effects of insulin, insulin-like growth factor-II, and nerve growth factor on neurite formation and survival in cultured sympathetic and sensory neurons. *J Neurosci* 1986; **6:** 1211-1219

163 **Mill JF**, Chao MV, Ishii DN. Insulin, insulin-like growth factor II, and nerve growth factor effects on tubulin mRNA levels and neurite formation. *Proc Natl Acad Sci U S A* 1985; **82**: 7126-7130

164 **Near SL**, Whalen LR, Miller JA, Ishii DN. Insulin-like growth factor II stimulates motor nerve regeneration. *Proc Natl Acad Sci U S A* 1992; **89**: 11716-11720

165 **Dupont J,** Khan J, Qu BH, Metzler P, Helman L, LeRoith D. Insulin and IGF-1 induce different patterns of gene expression in mouse fibroblast NIH-3T3 cells: identification by cDNA microarray analysis. *Endocrinology* 2001; **142**: 4969-4975

166 **Meier C**, Parmantier E, Brennan A, Mirsky R, Jessen KR. Developing Schwann cells acquire the ability to survive without axons by establishing an autocrine circuit involving insulin-like growth factor, neurotrophin-3, and platelet-derived growth factor-BB. *J Neurosci* 1999; **19:** 3847-3859

167 **Holzenberger M**, Dupont J, Ducos B, Leneuve P, Géloën A, Even PC, Cervera P, Le Bouc Y. IGF-1 receptor regulates lifespan and resistance to oxidative stress in mice. *Nature* 2003; **421**: 182-187

168 **Rajkumar K**, Krsek M, Dheen ST, Murphy LJ. Impaired glucose homeostasis in insulin-like growth factor binding protein-1 transgenic mice. *J Clin Invest* 1996; **98**: 1818-1825

169 **Karagiannis SN**, King RH, Thomas PK. Colocalisation of insulin and IGF-1 receptors in cultured rat sensory and sympathetic ganglion cells. *J Anat* 1997; **191** (Pt 3): 431-440

170 **Craner MJ**, Klein JP, Black JA, Waxman SG. Preferential expression of IGF-I in small DRG neurons and down-regulation following injury. *Neuroreport* 2002; **13**: 1649-1652

171 **Cheng HL**, Randolph A, Yee D, Delafontaine P, Tennekoon G, Feldman EL. Characterization of insulin-like growth factor-I and its receptor and binding proteins in transected nerves and cultured Schwann cells. *J Neurochem* 1996; **66**: 525-536

172 **Jonas HA**, Harrison LC. The human placenta contains two distinct binding and immunoreactive species of insulin-like growth factor-I receptors. *J Biol Chem* 1985; **260**: 2288-2294

173 **Moxham CP**, Duronio V, Jacobs S. Insulin-like growth factor I receptor beta-subunit heterogeneity. Evidence for hybrid tetramers composed of insulin-like growth factor I and insulin receptor heterodimers. *J Biol Chem* 1989; **264**: 13238-13244

174 **Bondy CA**, Underwood LE, Clemmons DR, Guler HP, Bach MA, Skarulis M. Clinical uses of insulin-like growth factor I. *Ann Intern Med* 1994; **120**: 593-601

175 **Saukkonen T**, Amin R, Williams RM, Fox C, Yuen KC, White MA, Umpleby AM, Acerini CL, Dunger DB. Dose-dependent effects of recombinant human insulin-like growth factor (IGF)-I/IGF binding protein-3 complex on overnight growth hormone secretion and insulin sensitivity in type 1 diabetes. *J Clin Endocrinol Metab* 2004; **89**: 4634-4641

176 **Clemmons DR**, Moses AC, McKay MJ, Sommer A, Rosen DM, Ruckle J. The combination of insulin-like growth factor I and insulin-like growth factor-binding protein-3 reduces insulin requirements in insulin-dependent type 1 diabetes: evidence for in vivo biological activity. *J Clin Endocrinol Metab* 2000; **85**: 1518-1524

177 **Thrailkill KM**, Quattrin T, Baker L, Kuntze JE, Compton PG, Martha PM. Cotherapy with recombinant human insulin-like growth factor I and insulin improves glycemic control in type 1 diabetes. RhIGF-I in IDDM Study Group. *Diabetes Care* 1999; **22**: 585-592

178 **Cusi K**, DeFronzo R. Recombinant human insulin-like growth factor I treatment for 1 week improves metabolic control in type 2 diabetes by ameliorating hepatic and muscle insulin resistance. *J Clin Endocrinol Metab* 2000; **85**: 3077-3084

179 **Schmidt RE**, Dorsey DA, Beaudet LN, Peterson RG. Analysis of the Zucker Diabetic Fatty (ZDF) type 2 diabetic rat model suggests a neurotrophic role for insulin/IGF-I in diabetic

autonomic neuropathy. *Am J Pathol* 2003; **163**: 21-28
180 **Busiguina S**, Fernandez AM, Barrios V, Clark R, Tolbert DL, Berciano J, Torres-Aleman I. Neurodegeneration is associated to changes in serum insulin-like growth factors. *Neurobiol Dis* 2000; **7**: 657-665
181 **Chen HS**, Shan YX, Yang TL, Lin HD, Chen JW, Lin SJ, Wang PH. Insulin deficiency downregulated heat shock protein 60 and IGF-1 receptor signaling in diabetic myocardium. *Diabetes* 2005; **54**: 175-181
182 **Jacob RJ**, Sherwin RS, Greenawalt K, Shulman GI. Simultaneous insulinlike growth factor I and insulin resistance in obese Zucker rats. *Diabetes* 1992; **41**: 691-697
183 **Sima AA**. Diabetic neuropathy in type 1 and type 2 diabetes and the effects of C-peptide. *J Neurol Sci* 2004; **220**: 133-136
184 **Sima AA**, Zhang W, Grunberger G. Type 1 diabetic neuropathy and C-peptide. *Exp Diabesity Res* 2004; **5:** 65-77
185 **Kamiya H**, Zhang W, Sima AA. C-peptide prevents nociceptive sensory neuropathy in type 1 diabetes. *Ann Neurol* 2004; **56**: 827-835
186 **Ekberg K**, Brismar T, Johansson BL, Jonsson B, Lindström P, Wahren J. Amelioration of sensory nerve dysfunction by C-Peptide in patients with type 1 diabetes. *Diabetes* 2003; **52**: 536-541
187 **Forst T**, Kunt T, Pohlmann T, Goitom K, Engelbach M, Beyer J, Pfützner A. Biological activity of C-peptide on the skin microcirculation in patients with insulin-dependent diabetes mellitus. *J Clin Invest* 1998; **101**: 2036-2041
188 **Rola R**, Szulczyk P. Quantitative differences between kinetic properties of Na(+) currents in postganglionic sympathetic neurones projecting to muscular and cutaneous effectors. *Brain Res* 2000; **857**: 327-336

S- Editor Liu Y **L- Editor** Lutze M **E- Editor** Bi L

PO Box 2345, Beijing 100023, China
www.wjgnet.com
wjg@wjgnet.com

World J Gastroenterol 2007 January 14; 13(2): 192-218
World Journal of Gastroenterology ISSN 1007-9327

TOPIC HIGHLIGHT

Parimal Chowdhury, Professor, *Series Editors*

Advances in small animal mesentery models for *in vivo* flow cytometry, dynamic microscopy, and drug screening

Ekaterina I Galanzha, Valery V Tuchin, Vladimir P Zharov

Ekaterina I Galanzha, Vladimir P Zharov, Philips Classic Laser Laboratories, University of Arkansas for Medical Sciences (UAMS), Little Rock, AR, United States
Ekaterina I Galanzha, Valery V Tuchin, Department of Optics and Biomedical Physics, Research-Educational Institute of Optics and Biophotonics, Saratov State University, Saratov, Russia
Supported by NIH/NIBIB; No. EB001858, EB-000873, EB005123
Correspondence to: Ekaterina I Galanzha, MD, PhD, DSc, Philips Classic Laser Laboratories, University of Arkansas for Medical Sciences (UAMS), 4301 W. Markham St., Little Rock, AR 72205-7199, United States. egalanzha@uams.edu
Telephone: +1-501-5267620 Fax: +1-501-6868029
Received: 2006-10-10 Accepted: 2006-11-30

Key words: Lymph microcirculation; Transmission digital microscopy; Rat mesentery; Flow cytometry; Photothermal technique

Galanzha EI, Tuchin VV, Zharov VP. Advances in small animal mesentery models for *in vivo* flow cytometry, dynamic microscopy, and drug screening. *World J Gastroenterol* 2007; 13(2): 192-218

http://www.wjgnet.com/1007-9327/13/192.asp

Abstract

Using animal mesentery with intravital optical microscopy is a well-established experimental model for studying blood and lymph microcirculation *in vivo*. Recent advances in cell biology and optical techniques provide the basis for extending this model for new applications, which should generate significantly improved experimental data. This review summarizes the achievements in this specific area, including *in vivo* label-free blood and lymph photothermal flow cytometry, super-sensitive fluorescence image cytometry, light scattering and speckle flow cytometry, microvessel dynamic microscopy, infrared (IR) angiography, and high-speed imaging of individual cells in fast flow. The capabilities of these techniques, using the rat mesentery model, were demonstrated in various studies; e.g., real-time quantitative detection of circulating and migrating individual blood and cancer cells, studies on vascular dynamics with a focus on lymphatics under normal conditions and under different interventions (e.g. lasers, drugs, nicotine), assessment of lymphatic disturbances from experimental lymphedema, monitoring cell traffic between blood and lymph systems, and high-speed imaging of cell transient deformability in flow. In particular, the obtained results demonstrated that individual cell transportation in living organisms depends on cell type (e.g., normal blood or leukemic cells), the cell's functional state (e.g., live, apoptotic, or necrotic), and the functional status of the organism. Possible future applications, including *in vivo* early diagnosis and prevention of disease, monitoring immune response and apoptosis, chemo- and radio-sensitivity tests, and drug screening, are also discussed.

INTRODUCTION

It is difficult to access the gastrointestinal tract with powerful intravital high-resolution optical microscopy. One unique exception is the mesentery, which has as its main functions maintaining digestive organs in their proper positions while simultaneously providing routes for nerves and for blood and lymph vessels. To date, small animal mesentery is a well-established experimental model for studying blood and lymph microcirculation *in vivo*.

Historically, the first microscopic observation of the mesenteric lymph microvessels of a guinea pig was performed by Arnold Heller in 1869[1]. During the first 30-50 years of the 20th century, extensive *in vivo* studies of mesenteric microcirculation were undertaken[2-4]. In particular, the basics of capillary circulation were first studied in rat mesentery[3]. Later, this model was successfully used to study the fundamentals of the microvascular physiology of blood (i.e., microvascular rheology, hemodynamics, vasomotion, hematocrit, permeability of the vascular wall, flow velocity) and lymph (i.e., phasic contractile activity, flow velocity, and the diameter of small lymphatics) systems[5-26]. Using rat mesentery, Sekizuka *et al*[24] performed real-time videoanalysis of contractile lymphatic motion in rat mesentery and determined quantitatively the dynamics of the frequency of these contractions. Benoit *et al*[22] and Dixon *et al*[26] obtained basic data about relationships among lymphatic contractile activity, vessel diameter, and lymph flow velocity[23]. In particular, they established the correlation between cyclic fluctuations of lymph velocity

and vessel wall motion during the phasic contraction. Most of the results related to microvessel diameter and contractile activity were obtained with conventional transmission optical microscopy alone.

The mesentery model has also been used to study the effects of various hormones, mediators, drugs, and other environmental impacts on microcirculation, including the influence of histamine, norepinephrine, dopamine, dobutamine, PO_2, substance P, L-NAME, methylene blue, leukotrienes, histamine, platelet activating factor, temperature, low-power laser radiation, X-radiation, and others[3,20,27-34]. In particular, this model was used in the first study of the effects of nitric oxide (NO) on lymph microvessels *in vivo*: Shirasawa *et al*[35] showed the influence of a NO synthase inhibitor on lymphatic diameter and contractile activity, which was reversed after applying an endogenous NO donor (L-arginine). This model has also been employed to study microcirculation disturbances in experimental models of diseases such as diabetes, ischemia, hemorrhage, shock, inflammation, tumor, edema, and others[2,4,13,21,22,36,37].

Recent discoveries in cell biology (e.g., identification of the genes, such as VEGF-C and VEGF-D, expressed by endothelium or endothelial growth factors for lymphatics), along with advances in optical techniques (e.g., lasers, high-speed digital cameras, powerful software) have increased interest in this model and its capabilities for studying the fundamentals of blood and lymph microcirculation, including its potential for the molecular imaging of individual cells *in vivo*[38-40]. Nevertheless, some methods used in most experiments have limitations. For example, the majority of the results about platelets [e.g., platelet thrombosis, or their interaction with white blood cells (WBCs) or vessel walls], red blood cells (RBCs), and tumor cells were obtained with what are currently the most powerful techniques, such as fluorescent labe ling[12,13,21,41-43]. However, despite significant progress in the development of new labels[44-46] (e.g., quantum dots, fluorescent-specific antibodies[47]), these techniques *in vivo* (as in many other experiments *in vitro*) are potentially subject to photobleaching (despite the short exposure time), or cytotoxicity. Moreover, growing evidence shows that fluorescence labeling may seriously distort genuine cell properties, even without evident toxicity, and cellular physiologic functions. For example, acridine orange and Rhodamine 6G, traditional fluorescent dyes for leukocytes, have been demonstrated to be mutagenic and carcinogenic, and possibly cause phototoxic effects[48-51]. Fluorescence imaging of lymphatics by injecting fluorescein isothiocyanate (FITC)-dextran into the interstitial space led to elevated interstitial pressure and altered lymph viscosity[52]. These findings may raise some concern about the kinetics of labeled cells in flow, particularly about the main cause and the real rate of cell elimination from circulation, the actual properties of apoptotic or cancer cells, or the strong influence of the tags due to phagocytosis, or the interaction of tags with other cells[53-55]. All these concerns gain importance in *in vivo* studies in humans, and add to interest in developing label-free imaging. The mesentery model with advanced optical technique can provide a good quality of label-free imaging of moving cells.

In mesenteric microvessels, the imaging of flowing cells *in vivo* without any staining or labeling was realized mainly with transmission microscopy for slow moving, rolling (30-70 μm/s), and adhesive WBCs[10,12,14,15,17]. The monitoring of single RBCs and their small aggregates has usually been performed in two modes: 1) in selected microvessels (small venules or capillaries) with slow flow using a frame rate of 20-30 frames per second (fps), or 2) using a short time-exposure mode (~0.1-1 ms) by which only single images of fast-moving cells can be captured[56-58]. Only a few studies demonstrated relatively high-speed imaging for measuring flow velocity in the range of 750-2500 fps in blood flow, and approximately 500 fps in lymph flow[19,26,59]. Due to motion distortion, these speeds are not quite fast enough to image shape and subcellular structures of individual fast-moving cells. For example, imaging in blood microvessels, with typical flow velocities of 5-10 mm/s, requires imaging speed ranges of 5000-10 000 fps[58]. Additionally, simultaneous high-speed imaging with high optical resolution of individual moving cells has not yet been developed *in vivo*. This is crucial for *in vivo* flow cytometry (FC).

In this review, which is based on our 15 years of experience in this area, we summarize both our previous data, which are scattered or presented in difficult-to-access publications, as well as our latest achievements in *in vivo* label-free FC, high-speed imaging, and vessel dynamics, focusing on real-time monitoring of circulating and migrating blood and cancer cells in blood and lymph systems, and especially on our studies of microlymphatic function in normal and pathological states and under the impact of different therapeutic interventions.

FEATURES OF THE LYMPHATIC SYSTEM

Unlike the circular blood network, the lymphatic vasculature is an open-ended system that transports lymph from tissue to the blood system[60,61]. The initial lymphatics collect fluid and cells from the interstitial space of tissue and form the afferent (prenodal) lymph, which is transported through valvular prenodal lymphatics to the lymph nodes. In the lymph nodes, some fluid, debris, and pathogens are removed from lymph, while cells (mainly lymphocytes) are added to lymph. Lymph leaves the lymph node by efferent collecting lymphatics, and passes through the thoracic duct and enters into the inferior vena cava. During this process, some cells and proteins can re-circulate in the blood system-tissue-lymph system-blood system pathway. In contrast to blood, which is moved by one motor, the heart, the motion of lymph is primarily maintained by rhythmic contractions of vessel walls, called phasic contractions. Such contractions are initiated by pacemakers along vessels. Additionally, lymph vessels have well-developed bicuspid funnel-shaped valves (collagen sheets with filaments covered on both sides by endothelium), which are dispersed at regular intervals along the vessel and divide it into functional units-lymphangions (the fragment of the lymph vessel between input and output valves). The valves can block lymphatic lumen to prevent (at least partially) backflow and contribute to a

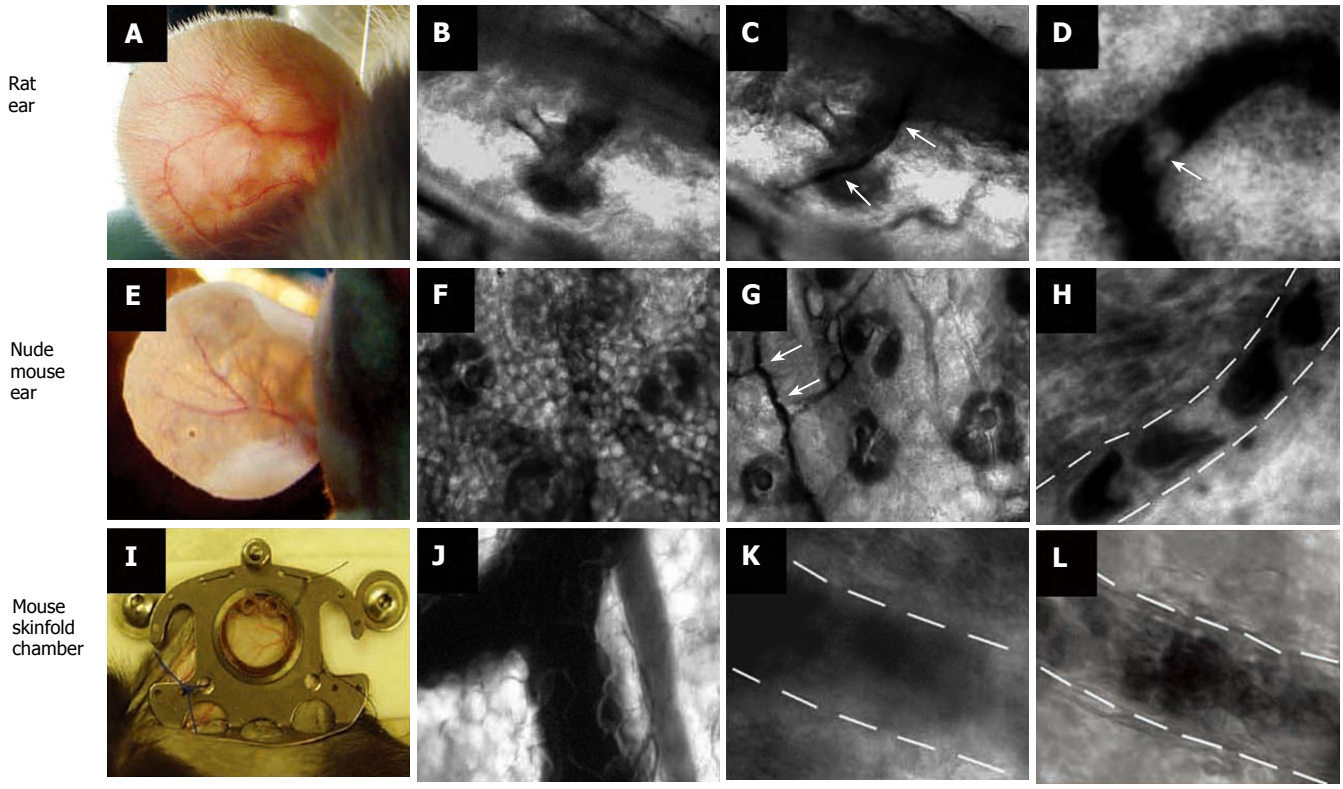

Figure 1 Label-free imaging of blood vessels in different animal models. Rat ear (with hair): **A**: External view of large vessel; **B**, **C**: transmission images of microvessel at low magnification (4 ×) before (**B**) and after (**C**) topical administration of an optical clearing agent such as glycerol (arrows show microvessel); **D**: high-resolution image of rolling WBC (arrow) in a venula (magnification 40 ×). Ear of nude mouse: **E**: external view of large vessels; **F**, **G**: transmission images of microvessels at low magnification (10 ×) before (**F**) and after (**G**) topical administration of glycerol (arrows show microvessel); **H**: high-resolution image of individual RBCs in a capillary (magnification 100 ×); **I**: large vessels in skinfold chamber of a mouse; **J**: transmission image of blood microvessel at low magnification (10 ×); **K**, **I**: high-resolution image of a venula before (**K**) and after (**I**) topical administration of glycerol (40 ×).

unidirectional flow. Some external forces, such as muscle contractions, respiratory movements, and intestinal peristalsis, can also maintain lymph motion. In general, lymph flow is turbulent, has an oscillating character, and is slower than blood motion. The lymphatics in an entire living organism have multi-level regulation, including the central nervous system, hormones, and local substances such as mediators, pH, and Ca ions[1,24,26,29,60-69].

Compared to the well-studied blood system, our understanding of lymph function is limited; however, rat mesentery, with its unique structure that we describe here, may help to fill knowledge gaps in this under-explored system. Below, we present a brief comparison of different animal models emphasizing the advantage of rat mesentery for monitoring single-cell transport under normal and pathologic conditions.

ANIMAL MODELS

Microcirculation has been successfully studied using optical microscopy in various animal models (e.g., rabbit or mouse ear, hamster or mouse dorsal skin-flap window or skin-fold chamber, or open cremaster muscle)[52-55,59,63,70-73]. The use of these models for high-resolution imaging of individual flowing or static cells may be somewhat limited because of significant light scattering from surrounding tissue (e.g., skin or muscles) and/or the relatively deep location of vessels below the skin. Image quality in these particular models can be improved in two ways: (1) by using thin hairless skin (e.g. ear of nude mouse ~270 μm thick), or (2) by decreasing light scattering using a recently developed optical clearing method combined with spectral selection (e.g. use a "green" filter to increase blood vessel contrast)[74-77].

Figure 1 illustrates our few attempts using these models and transmission microscopy to obtain high-resolution images of individual cells in blood flow without staining. In particular, we compared images of blood microvessels of ordinary (i.e. with hair, Figure 1A-D) and nude (i.e., hairless, Figure 1E-H) ear skin of rats and mice, and with mouse dorsal skin-fold chamber (Figure 1I-L). The best results were obtained with the nude mouse ear model in combination with optical clearing and a spectral filter in the range of the maximum absorption of hemoglobin, around 570-580 nm (Figure 1F-H). The dorsal skin-fold model provided a poorer quality image of an individual cell as compared with the RBC images of the skin-fold chamber (Figure 1L) and with RBC images of nude mouse ear (Figure 1H), and required an invasive procedure. In general, even after many improvements, all of these models provide monitoring of individual cells only in selected capillaries with single-file flow (RBCs travel in one line with the same velocity). In addition, the images of colorless lymphatics in skin can be obtained mainly with additional labeling with fluorescent or absorbing contrast agents (e.g. FITC-dextran and dyes such as isosulfan blue,

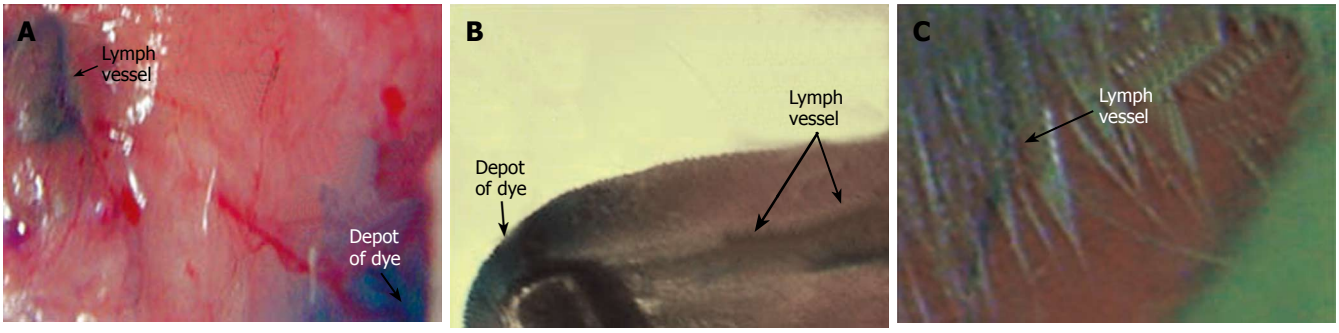

Figure 2 Imaging of lymph vessels using contrast agents in different rat models. Lymphatics labeled by a 1% solution of lymphazurin in muscles of (**A**) abdomen wall, (**B**) tongue, and (**C**) pad.

lymphazurin, and others; Figure 2)[52,78-80]. However, these procedures do not provide information on cell dynamics in flow or valve functioning.

In general, the best targets for conventional transmission microscopy are relatively transparent animal structures such as zebrafish, and vascular nets of the hamster cheek pouch[63,81-84]; however, these models are not ideal for studying lymph or blood vessels. The zebrafish (tropical fish) model is very different from human anatomy and physiology, and while the hamster cheek pouch model is good for visualizing blood microvessels, the lymphatics in the hamster cheek pouch are not well developed, preventing us from simultaneously studying blood and lymph systems, if desired.

To date, the best optical images of both lymph and blood microvessels have been obtained in the mesentery of small cold-blooded (frog) and mammalian (mouse, cat, rabbit, guinea pig, and rat) animals. However, the capillaries of frog mesenteric microvessels are relatively larger in diameter and their sensitivity to environmental impacts is markedly less than that of mammals[3]. Of the mammalian models, the rat is an excellent model in terms of size, physiology, and pharmacokinetics for broadening medical applications, including single-cell diagnostics[85-88]. Additionally, some rat models are able to mimic select human diseases. This is particularly important for understanding common mechanisms of microvessel physiology and pathology (edema, inflammation, tumor), as well as for studying specific features of mesenteric microvasculature under normal conditions (to maintain homeostasis in the abdominal space) and in mesentery-related diseases (e.g. mesothelioma, sclerosing mesenteritis, panniculitis, acute mesenteric vein thrombosis, tumor metastasis).

Mesentery consists of thin (8-15 μm), relatively transparent, duplex connective tissue, which is divided into triangular, relatively transparent windows by arteries (400-500 μm in diameter) and veins (600-700 μm in diameter) obscured by adipose tissue (Figure 3D)[3,89-91]. The smaller branches of these vessels leave the adipose regions and pass into the microvascular net (Figure 3E), which spreads out into transparent areas. On the venous side of the capillaries, there is an accumulation of initial lymphatics (Figure 3E-G). These initial lymphatics then pass into larger valvular lymphatics, which are located parallel with and very close to the venules (Figure 3E, H).

Thus, rat mesentery triangulars contains all the typical components of a microvascular net: a blood microvessel network including arterioles (diameter, 7-60 μm; velocity, 5-10 mm/s), venules (10-70 μm; 0.5-3 mm/s), and capillaries (5-9 μm; 0.1-1.4 mm/s), as well as well-developed microlymphatic vessels (diameter, 50-250 μm; velocity 0-7 mm/s) and clearly distinguishable initial lymphatics with migrating cells[3,24,26,58,66,92-94]. Figure 3 shows typical images obtained with the optical schematics portrayed in Figure 4.

The specific functional features of mesenteric vasculature involve a considerable gradient of venular permeability, a preponderance of fluid filtration, and a relatively low proportion (~15%) of re-absorption of interstitial fluid by capillaries[95,96]. Additionally, rat mesenteric blood microvascular is characterized by many communications between the capillary loops arising from neighboring arterioles with well-developed arterio-venous anastomoses, which shunt blood from arteriola to venula[3]. This structure can facilitate adaptation and maintenance of blood flow under different conditions.

For medical imaging, the main advantage of mesenteric microcirculation is that a single layer of blood and well-developed lymph microvessels lies in one plane (Figure 4B), which facilitates continuous observation of all components of the microvascular network (from arteriola to venula, together with lymph microvessels, Figure 3H), as well as label-free, high-resolution imaging of individual cells with almost ideal optical conditions (Figure 3I-N). Light is slightly attenuated, mainly in the relatively thin vessel wall, without any influence from other tissues, as it is in other models. The refractive indexes in the typical spectral range of 400-700 nm used for studies are lower for rat mesenteric tissue (n = 1.38) than for rat skin (n = 1.40-1.42) and, especially, for the epidermis (n = 1.55) for humans; thus, it is close to that of water (n = 1.33)[97]. As a result, these optical and geometric features significantly reduce unwanted scattered light, allowing the use of a microscopic objective with a high numerical aperture (up to 1.4) and high magnification (60× - 100×). Optical reflectance spectra from lymph vessels obtained *in vivo* with a fiber optic spectrometer (Model 1000, Ocean Optics, Inc., USA) demonstrated slight spectral features and time-dependence within 1-2 s (Figure 5), which can

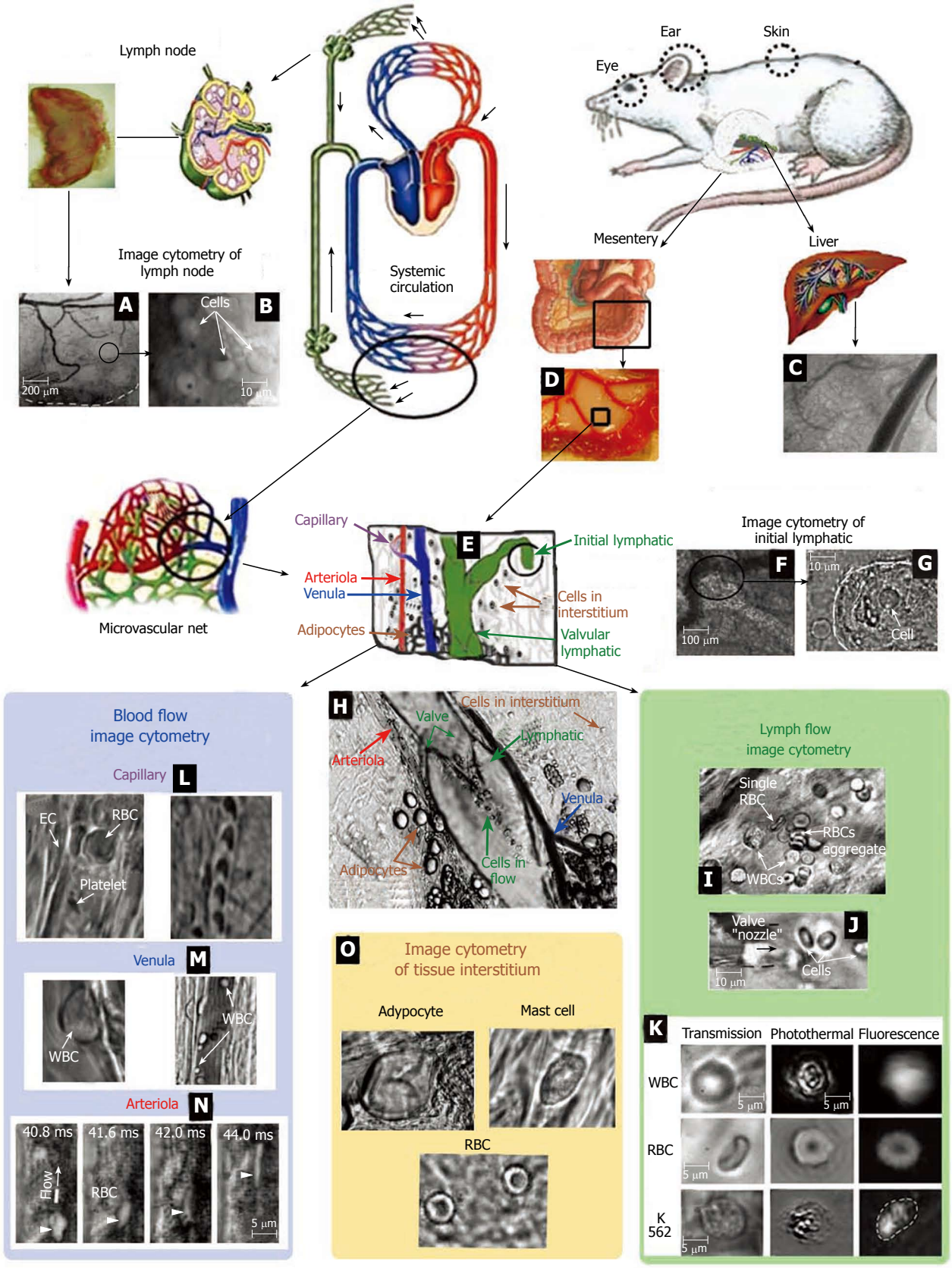

Figure 3 *In vivo* monitoring of microcirculation using rat mesentery. **A**, **B**: Sections of a single lymph node at different magnifications (4 × and 100 ×, respectively); **C**: liver section (10 ×); **D**: section of intestine with mesentery; **E**: schematic of typical tissue microvascular unit; **F**, **G**: initial lymphatic (4 × and 100 ×); **H**: section of mesenteric tissue with valvular lymph vessel and surrounding blood vessels (10 ×); **I**: high-resolution imaging of single WBCs and RBCs, as well as their aggregates in lymph flow (100 ×); **J**: valve tip with fast-flowing cells (100 ×); **K**: transmission, photothermal, and fluorescence images of individual WBC, RBC, and K562 leukemic cell in lymph flow; **L**: capillary at different magnifications, (left) high-resolution images of RBCs, platelets, and endothelial cells (EC) in capillary wall (100 ×) and (right) parachute-like RBCs at low magnification (10 ×); **M**: rolling WBC in venula (100 ×, 10 ×); **N**: four sequential high-resolution images of RBC shapes in fast arteriolar flow (velocity of 5 mm/s; 40 ×); **O**: high-resolution images of adipocyte, mast cell, and RBCs in the interstitial space (100 ×).

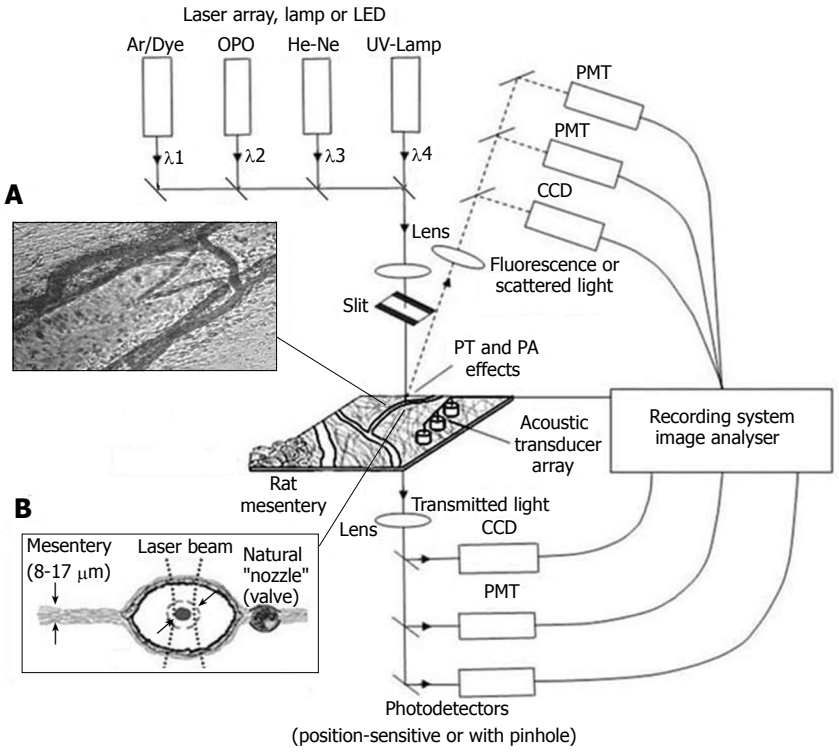

Figure 4 Integrated, multispectral FC *in vivo*. **A**: Typical transmission image of rat mesentery segment with lymph and blood microvessels; **B**: Schematic of the mesentery cross-section.

be explained by specific lymph flow oscillations[98]. An additional advantage of the mesenteric model is the good penetration of the reagents into the mesenteric lining. Thus, the responses of the microvascular network to different environmental impacts can be studied relatively easily using a simple topical application.

The well-developed procedure for preparing rat mesentery for studying microcirculation include anesthetizing the rat (ketamine/xylazine, 50/10 mg/kg, i.m.), followed by a laparotomy by mid-abdominal incision (~1 cm), gently exteriorizing the intestinal loop with mesentery from the abdomen and positioning it on a customized thermostabilizing microscope stage, which maintains the body temperature at approximately 37.7℃ [2,3,22-28,35,58,66,94]. The mesentery is bathed with a constant diffusion of warm Ringer's solution with a phosphate buffer and 1% bovine serum albumin (37℃, pH 7.4). In principle, these procedures may introduce some limitations and artifacts related to the anesthesia, the minimal but invasive surgical intervention, and periodic small vibrations of the mesentery due to intestinal motion[19,99]. However, according to experimental data gathered during at least 2-3 h of acute observation after microsurgery, these procedures do not produce marked changes in microvessel function (diameter, phasic activity, valve function, lymph flow) or in metabolic or respiratory parameters. Furthermore, the short timeframe during which the rapidly circulating cells are in the microvessels of the exposed mesenteric area significantly reduces the influence of this exposure on the properties of the flowing cells. Additionally, to decrease the effects of the surgical manipulations and to stabilize the microvascular parameters, the monitoring of cells in blood and lymph flow begins approximately 15 min after the laparotomy[93]. Coating the intestinal loop with oxygen-impermeable plastic foil helps maintain stable physiological

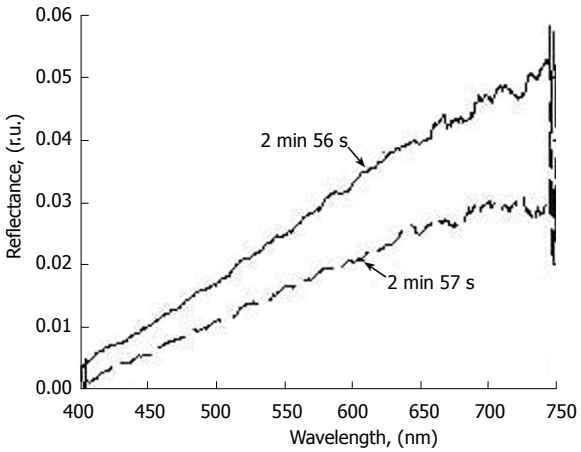

Figure 5 Time-resolved reflection spectra from the same point on the lymphatic vessel (D = 128 μm) at different times.

parameters for up to 5 h[100]. Our data also demonstrate that it is possible to repeat the surgical procedure to periodically monitor the same microcirculation area during the development of chronic pathology, even over a 2-mo timeframe[101]. To exclude the influence of microsurgery itself on the microcirculation, the data from experimental groups were usually compared with those from the corresponding control group, which undergo a mid-abdominal microincision without any other interventions.

In general, based upon our experience and the experiences of other groups, this easy-to-access mesentery microvessel model, which has significant features and advantages (see above) with only a few minor limitations, is a very promising vehicle for real-time monitoring, with the highest optical resolution, of individual static, migrating, and circulating cells (e.g. WBCs, RBCs, cancer cells, and

many others). Such a model is essential for studying immune function and the transport of proteins, cells, and liquid between the blood and lymph systems under normal and pathologic (lymphedema, metastasis, and many other lymph-related diseases) states.

INTEGRATED IMAGING SYSTEM

Recent progress in optical techniques enabled the development of a multi-module, multi-functional experimental system that integrates transmission digital microscopy (TDM), a photothermal (PT) method, a highly sensitive fluorescent and speckle technique with advanced charge-coupled device (CCD) or complementary metal oxide semiconductor (CMOS) cameras (Figure 4). The primary application of this system was for *in vivo* FC. Indeed, although *in vitro* FC is a powerful, established diagnostic method[102], only an *in vivo* study can assess physiologic and pathologic processes involving cell metabolism and cell-cell interactions (e.g., adhesion, aggregation, rolling effects, migration through vessel walls) in the real, complex environment of living organisms[53-55,84,99,103]. Further, invasive isolation of cells from their native environment and their processing may not only introduce artifacts, but also make it impossible to examine the same cell population over long time periods. Adaptation of FC for *in vivo* studies required overcoming problems related to light scattering by vessel walls and surrounding tissues, fluctuation of cell velocity, cell position in a vessel, and precautions with labeling procedures[53,54].

TDM module

TDM was built on the technical platform of an upright Olympus BX-51 microscope and provides the following functions: (1) imaging of relatively large structures such as lymph and blood microvessels with relatively low magnification (4 × -10 ×, Figure 3H); (2) quantitative dynamic evaluation of blood and lymph microvessel diameter, parameters of lymphatic phasic contractions and valve activity, and cell concentration in flow; (3) determination of cell velocity in lymph flow by video-recording cell movement [so-called particle image velocimetry (PIV)];[18,19] (4) navigation of the pulse laser beams on the desired area of the mesentery in other optical methods; and (5) single-cell identification at high magnification (40 ×, 60 ×, and 100 ×, water immersion)[58,94,104]. In particular, the mesentery model provides a unique opportunity to simultaneously image *in vivo*, with the highest optical resolution (~300 nm), individual cells in blood microvessels (Figure 3L and M) and small lymphatics (Figure 3F, G, I-K), tissue interstitium (Figure 3O), and lymph nodes (Figure 3A and B) located in the root of the mesentery and even in the liver.

The images were recorded with several digital cameras: a black-and-white Cohu 2122 and a color Nicon DXM1200, with speeds up to 25 fps and a minimal exposure time of 0.04 s. These speeds were sufficient to image relatively slow-moving individual cells, such as rolling leukocytes (30-70 μm/s), in blood flow (Figure 3M). We also used a highly sensitive CCD camera (Cascade 650, Photometrics) with speed of up to 500 fps and with a minimal exposure time of 0.1 ms. A high-speed CMOS camera (model MV-D1024-160-CL8; Photonfocus, Switzerland), with speeds of 10 000 fps for an area of 128 × 128 pixels and 39 000 fps for an area of 128 × 16 pixels, provided high-resolution imaging of fast-moving RBCs in blood flow (2-10 mm/s in arterioles and large venules, Figure 3N) and WBCs in valvular lymphatics (ranging from 0 to 7 mm/s). Scion Image (Scion Corp.), Nicon software (ACT-1), and WinX/32 V2.5.18.1 (Roper Scientific) were used for processing, capturing, measuring, and editing images of the moving cells.

Using TDM in the bright-field mode, the combination of light absorption and scattering effects on cells made it possible to visualize and identify most blood cells without conventional labeling and vital staining. In particular, due to relatively strong light absorption by RBCs, these single cells in flow appeared mostly as dark objects in the trans-illumination mode, while weakly absorbing WBCs and platelets appeared either as light objects (e.g., in the presence of many more strongly absorbing RBCs in blood flow or with dominant scattering effects) or, in contrast, as slightly dark objects (e.g., in the transparent plasma without RBCs). In the "packed" flow, RBCs sometimes exhibited bright margins or were seen as light objects due to multiple scattering effects. This is because the light, during propagation through many other RBCs and before reaching the plane of focus, was significantly scattered and attenuated through absorption, resulting in dominant scattering light around imaged cells.

The integration of high-resolution and high-speed monitoring improves PIV in the dynamic range and enhances spatial resolution and measurement accuracy. In particular, our technique enables us to measure the velocity of individual cells up to 10 mm/s without marked optical distortion of cell images in packed multi-file blood flow[104]. However, the low absorption sensitivity of TDM makes it impossible to differentiate individual cells with slight differences in absorption in fast flow *in vivo* (e.g. different WBCs or cancer cells).

PT module

To detect low-absorbing cells, PT methods were used with no cell labeling and inherence to scattered light. With these methods, absorption by non-fluorescent cellular components (most of which are naturally weakly fluorescent) is measured by monitoring thermal (due to picosecond-scale non-radiative relaxation of the absorbed energy) and accompanying effects directly in cells[105-109]. For non-fluorescent samples, PT methods currently offer the highest sensitivity for the absorption coefficient, on the order of 10^{-5}-10^{-6} cm^{-1}, which makes it possible to non-invasively (a short-term temperature elevation ⩽ 1-5℃) detect a single, unlabeled biomolecule with a sensitivity comparable to that of laser-fluorescence methods (i.e. with labeling)[109-111]. This absorption sensitivity threshold of the PT technique is at least four to five orders of magnitude better (e.g., 10^{-2}-10^{-3} cm^{-1} for single cells) than that of TDM, with the capability to measure absorption spectra at the subcellular level in weakly absorbing cells (e.g. WBCs

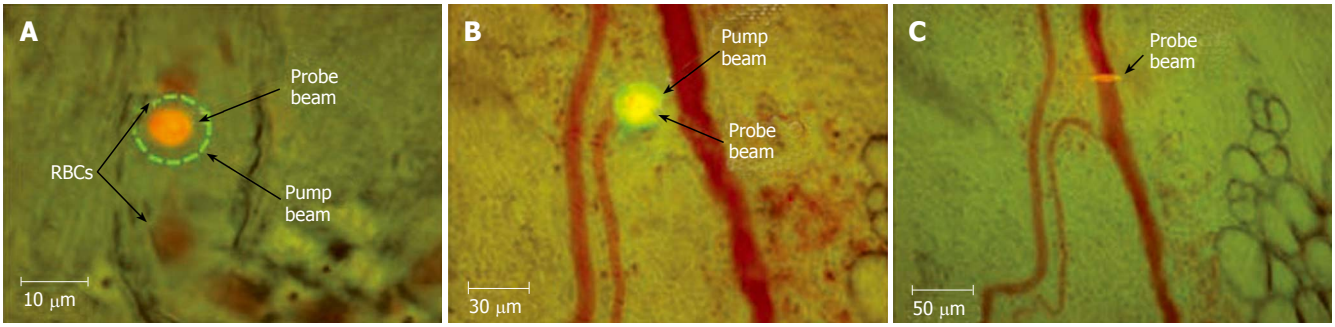

Figure 6 Typical positions of probe (red) and pump (green) laser beams during PT imaging. **A**: Circular beams in a blood capillary (cell velocity, ~0.5 mm/s; magnification, 100 ×); **B**: Overlapping pump and probe pulses in an artery (cell velocity, ~2 mm/s; magnification, 10 ×); **C**: an ellipsoidal beam geometry in a blood vessel (cell velocity, ~5 mm/s; magnification, 10 ×).

or cancer cells).

Briefly, in the first PT imaging (PTI) mode, individual cells were irradiated with a short, focused pump laser pulse of a tunable optical parametric oscillator (OPO) laser (wavelength, 420-2300 nm; pulse width, 8 ns; pulse energy, 0.1-10^3 μJ; Lotis Ltd., Minsk, Belarus; Figure 6)[109,112,113]. Time-resolved monitoring of temperature-dependent variations of the refractive index around the absorbing cellular structures or whole cells was accomplished with thermal-lens (thermolens) or phase-contrast imaging (Olympus BX51 microscope with a CCD camera; AE-260E, Apogee Inc.) using a second, collinear laser pulse of a Raman shifter (wavelength, 639 nm; pulse width, 13 ns; pulse energy, 10 nJ). In particular, in the phase contrast mode, a customized phase-contrast microobjective (20 ×) with a Zernike coaxial quarter-wave filter was used to image the probe laser beam. The diameters of the pump- and probe-beam spots were varied 20-40 μm and 15-25 μm, respectively.

A second thermolens mode made it possible to record a whole cell's time-resolved integral PT response *via* the defocusing effects of a collinear, intensity-stabilized He-Ne laser probe beam (wavelength, 633 nm; diameter, 15 μm; energy, 2 mW) as detected with a photodiode through a pinhole (0.5 mm). The PT response was recorded with a Tektronix TDS 3032B oscilloscope. In the presence of gaps between neighboring cells in lymph and blood flow (typical for small lymphatics and blood capillaries), we used a circular laser-beam geometry (Figure 6A). At short distances, selected experiments were performed with an elliptical beam shape (Figure 6C).

In contrast to TDM, the PT technique was able to identify low-absorbing cells (e.g. normal and apoptotic WBCs or cancer cells) in blood and lymph flow *in vivo* on the basis of their differences in integral and local absorption associated with specific heme proteins[58,77,94,114-118].

Laser speckle microscopy (LSM) module

Because of the varying velocities and trajectories of cell motion in cross-sections of vessels, time-consuming TDM is not well suited for rapidly estimating mean cell velocity in the presense of many cells in flow. The limitations of TDM were partially solved using the LSM technique (Figure 7)[66,68,98,119-122]. Laser radiation from a focused He-Ne laser beam (633 nm) scattered by a diffusely scattering object has a specific, speckle structure (Figure 7A and B), resulting from the interference of independent contributions from a large number of randomly distributed scattering centers. Detection of the speckle fluctuation' s intensity (Figure 7C) with a photodetector provides information of flow velocity estimated through the width of the power spectrum of these fluctuations or from the width of their autocorrelation function (Figure 7D and E). Figure 7D illustrates the spectrum recorded for the central part of a vessel (axial lymph flow), while Figure 7E demonstrates spectra obtained at points placed near the vessel wall. Such changes indicate that velocity decreases from a vessel's center to its periphery, which enables monitoring of the profile patterns of lymph-flow velocity for microlymphatics.

To increase its ability to measure the absolute value and direction of flow, we also used the speckle-correlation mode, which uses two photodetectors to record the intensity in fluctuations of the speckle field at two points[123,124]. The described algorithm was verified *in vivo* by measuring lymph flow in a lymphatic vessel with LSM (Figure 7F curve 1) and TDM (Figure 7F curve 2). There was relatively good correlation (coefficient of linear regression = 0.72) between the two methods; however, the LSM mode had advantages, such as rapid calculation of lymph-flow velocity (compared to TDM). On the other hand, combining LSM with TDM allowed us to: (1) monitor the quantitative dynamics of cell velocity in lymph or blood flow; (2) verify data from the speckle method; (3) obtain a profile of lymph velocity through the changing shapes of the speckle signal from the center region to the near-wall region; and (4) determine the dynamic relationships among changes in lymph flow velocity and other functional activities of lymphatics. This integrated schematic also has the potential for speckle-imaging of mesenteric structures at cellular and subcellular levels, including detection of individual cell rotation and functional state (e.g., live, apoptotic, and necrotic) in flow[118].

Fluorescent module

A fluorescence module was added to the integrated system to verify PT data and for independent applications using specific fluorescent tags to identify different cells with similar shapes and sizes (e.g. lymphocytes and leukemia

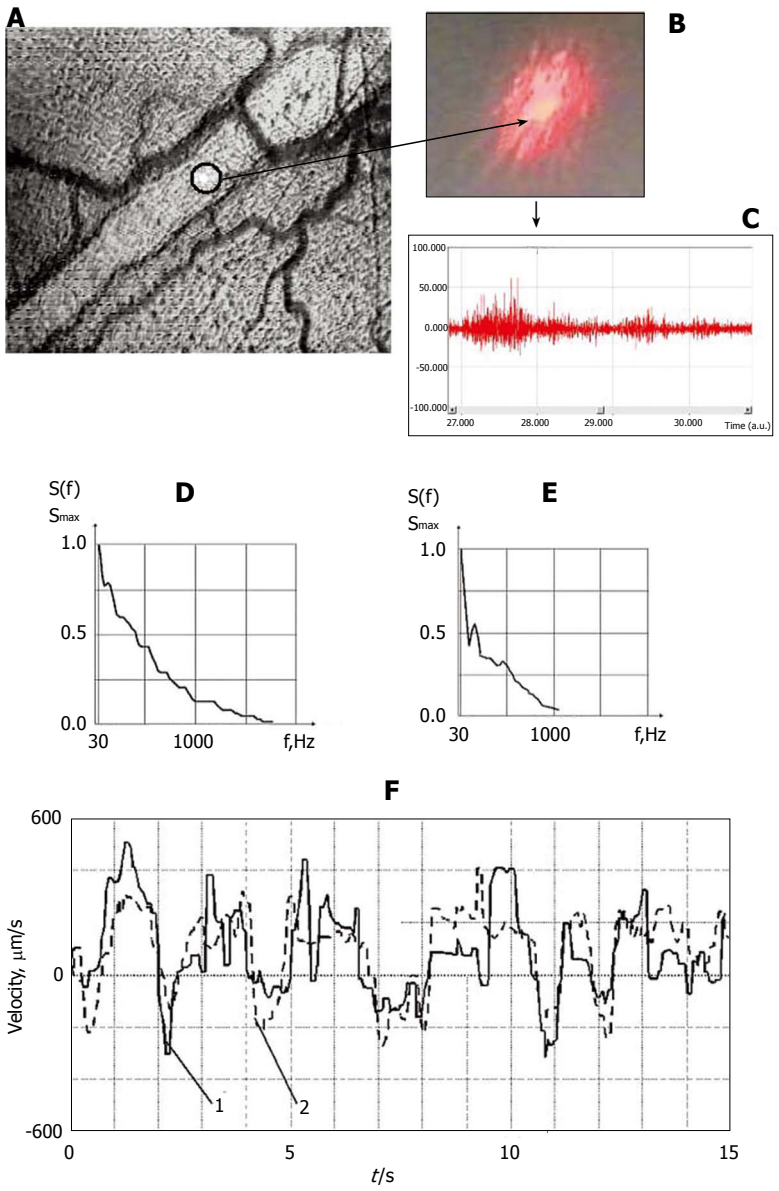

Figure 7 Integration of laser speckle and transmission microscopies for studying lymph flow dynamics. **A**: A laser beam was focused into a small-diameter spot (~5 μm) on axial lymph flow (microvessel diameter 55 μm); **B**: Lymph flow randomly modulated the focused Gaussian beam to provide scattered dynamic speckles images; **C**: Scattered intensity fluctuations were detected by a photodetector and transformed into an electrical output signal. **D** and **E**: Spectral shapes from scanning the lymphatic cross-section: (**D**) the spectrum when the laser beam was focused in axial flow and (**E**) when the laser beam was focused in flow near the lymphatic wall; **F**: Real-time dynamics of lymph-flow velocity in a lymph microvessel, recorded with a laser speckle technique (curve 1) and by processing the video recording (curve 2).

cells)[116,94]. Fluorescent imaging was performed with CCD cameras (Cascade 650, Photometrics, color Nicon DXM1200) and a super-sensitive PentaMAX camera with an intensifier (Princeton Instruments, Inc.).

STUDY OF MICROLYMPHATIC DYNAMICS

Label-free time-resolved lymphography

An essential ingredient in studying the functional activity of lymph microvessels is to know when the observed functions approximate normal conditions. The previously described imaging system allowed us to obtain such basic information on intact lymph microcirculation, including quantitative measurements such as indices of phasic contraction and valve function, the numbers of microvessels with lymph flow, the numbers of cells in lymph, and lymph flow velocity[58,66,101,125].

TDM images of rat mesentery at two relatively small magnifications (4 ×, field of view 250 × 350 μm and 10 ×, field of view 125 × 175 μm) allowed us to visualize the initial (Figure 3F) and valvular lymphatics (Figure 3H), the vessel wall, lymphatic valves, and cells in lymph flow, as well as neighboring blood microvessels. In particular, we studied small valvular lymphatics with mean diameters of 147 ± 3 μm. Half of these lymphatics in a normal state had spontaneous phasic contractions[101].

The rate (frequency) of contractions and contraction amplitude (the percentage difference between maximum and minimum diameters during contraction) vary significantly[66]. Benoit *et al*[22] found that the lymphangions with phasic contractions have mean end diastolic diameters of 69.2 ± 6.5 μm and systolic diameters of 39.4 ± 5.6 μm (i.e. an amplitude of 43%). In another paper, the same authors showed that lymphatics with mean end diastolic diameters of 106.9 ± 13.7 μm have a systolic diameter of 69.8 ± 8.8 μm (i.e. amplitude of 35%)[30]. From our data, lymphangions had mean diastolic diameters of 147 ± 3 μm and amplitudes of 29% ± 9%[58]. Thus summarized, these data indicate that the larger lymphatics have smaller amplitudes of phasic contractions. Our detailed analysis of relationships between diameter and amplitude revealed that the lymphangion with larger diameters have less amplitude

(Figure 8, unpublished), which is in line with the results presented above. In addition, we believe that the amplitude of phasic contractions should be analyzed in relation to valve activity; indeed, the amplitude of phasic contractions in lymphangions with active valves was 31% ± 4%, while in lymphangions with non-active valves it was only 6% ± 2%[66].

The majority of lymphatics with phasic contractions (78%) have active valves, which periodically open and close. An average activity rate (frequency of closing-opening cycles per minute) was 9-12/min[58,66,101,125].

Cells are moved in 85% of lymphangions and they are not found in 15% of lymphangions[66,125]. It is well known that some parts of blood capillaries do not work normally[61]. We speculate that the same situation may occur in lymphatics, in which activity can start under some specific circumstances, for example during disease development (e.g., lymphedema).

Lymph flow velocity is usually estimated by measuring cell velocity. Our measurements with a conventional video camera (25-30 fps) revealed that mean cell velocity in an axial flow in the non-valvular central part of mesenteric lymphangions (i.e. approximately equal distance between input and output valves) is 211-262 μm/s on average, with a maximum of 1-2 mm/s)[58,66,101,125]. When lymph flow goes through the valve, the phase contraction leads to acceleration of flow because of the narrow valve nozzle. In turn, this leads to significantly increased cell velocity.

Lymph usually moves in the forward direction for a short period of time; then, the motion is interrupted and the lymph stops for up to 1-1.5 s. After that, the lymph flow starts in the reverse direction. Usually, cells oscillate at a rate of 50-70 oscillations per minute[126]. Figure 9 shows oscillations during 15 s in a non-valvular part of an individual lymphangion (mean diameter in the investigated site = 170 ± 5 μm; mean cell velocity during the investigated time = 168 ± 6 μm/s)[126]. In some rare microvessels, the time-averaged velocity of lymph flow equaled zero. In this case, lymphocytes only oscillated relative to a position without the leak-back of lymph. Using a high-speed videotape recorder (2000 fps), Sekizuka *et al*[24] demonstrated that maximum cell velocity in rat mesenteric lymphatics was 2-3 mm/s. Later, using a relatively high-speed camera (500 fps), Zaviewa *et al* determined that maximum cell velocity in some mesenteric lymphatics may reach 7 mm/s and their oscillations correlate with phasic contractions[26]. Probably, such variability of cell velocity may result from different experimental conditions.

It is important that the analysis of lymph flow requires that we estimate both cellular and plasma velocities (analogous to blood flow). In fact, Starr *et al*[8] found that the blood flow in cat mesenteric microvessels *in vivo* is characterized by a discrepancy between RBC and plasma velocities. This discrepancy is dependent on the elastic properties of RBCs and flow dynamics, including plasma shear and pressure field. We expect a similar phenomenon in lymph flow, especially due to its oscillating character; however, these effects require further quantitative verification.

Depending on lymph flow velocity and vessel structure, cell distribution in the cross-section of the lymphangion varies[58,66,125]. Most often, at relatively low velocities and/or in the non-active valves (80% of cases), cell distribution was relatively uniform. However, at high velocities and/or in functioning valves (20% of cases), most cells were concentrated near the vessel axis.

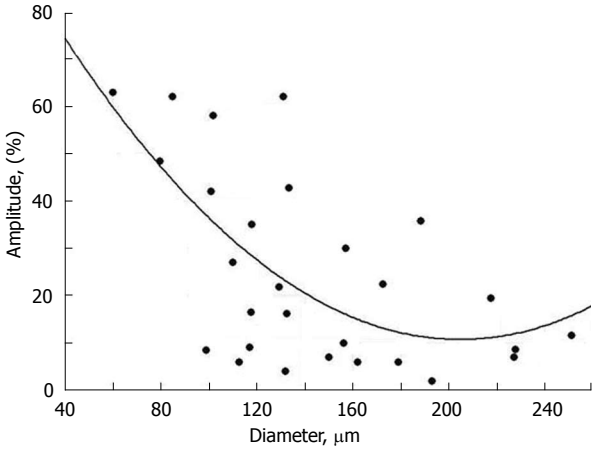

Figure 8 Diameter-amplitude relationship in rat mesenteric lymphangion. Cycles-experimental data, solid curve-approximation (A = 109.3-0.96 × D + 0.0024 × D^2, where A: amplitude and D: diameter).

It is well known that lymph has markedly lower concentrations of cells than blood. However, there is relatively little data about cell concentration in prenodal lymph. In particular, cell concentrations range from 200 to 1000 cells/μL in prenodal sheep's lymph and 100 cells/μL in prenodal rabbit's lymph[127,128]. It was found that approximately 1 × 10^6 cells/h (1.7 × 10^4 cells/min) go through a single prenodal (afferent) sheep's lymphatic[129,130].

According to our data, the cell concentration in rat mesenteric prenodal lymphatics is larger. Specifically, we measured the number of cells in a 50 μm × 50 μm square in the central part of a lymphangion from a rat mesenteric microvessel using 2D-imaging[66]. Because the depth of field was approximately 28 μm, the number of cells was determined in a 50 μm × 50 μm × 28 μm volume (i.e., 7 × 10^{-5} μL of lymph). Data is summarized in Table 1 (taking into account distribution of cells in a cross-section of a lymphangion, see above). Finally, the mean concentration of cells in the lymph flow of intact mesenteric microvessels was estimated as approximately 0.5-1 × 10^5 cells/μL. From these data, the average percent of cell fraction in lymphatics was 5.5%. This parameter is analogous to hematocrit in the blood system, and may be called lymphocrit. It is interesting that a 5%-6% level of hematocrit can be found only in blood capillaries, as compared to that in arterioles with diameters from 60-70 μm, in which the hematocrit achieved 20%-30%. Cell flux in the prenodal lymph was estimated to be 10-50 cells/s. The cell concentration in flow is usually higher in vessels with higher lymph flow velocities, and is somewhat correlated with the amplitude of phase contractions and rate of valve activity[66]. Recent data obtained by Dixon *et al*[131] with a high-speed video system and by capturing multiple contraction cycles in rat mesenteric lymphatic preparations with smaller diameters (91 ± 9 μm) revealed that lymphocyte densities were 12 000 ± 5200 cells/μL

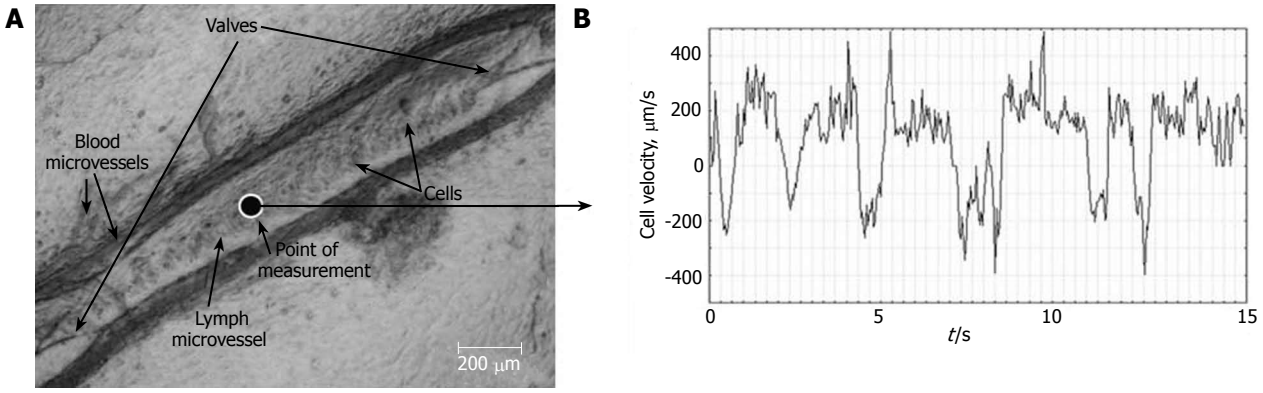

Figure 9 Real-time dynamics of cell velocity in axial lymph flow within the non-valvular segment of a lymphangion (mean diameter of 170 ± 5 μm) without phasic contractions and valve activities, measured by processing the video recording (μm/s) for 15 s.

Table 1 Relationship between lymphocrit and other parameters of microlymphatic function

	Cell concentration, cells/μL	Lymphocrit %	Proportion of Lymphangions %	Diameter μm	Parameters of phasic contractions		Valve activity per minute	Cell velocity (μm/s)
					Amplitude (%)	Count of contractions per minute		
Group 1	$< 3.75 \times 10^4$	< 2	22	$106 \pm 9^{a,b}$	$50 \pm 15^{a,b}$	12 ± 2	8 ± 0.5^{b}	161 ± 191
Group 2	3.75×10^4-12.2×10^4	2-6	45	141 ± 8^{a}	$28 \pm 7^{a,c}$	12 ± 1	11 ± 1	254 ± 151
Group 3	$> 12.2 \times 10^4$	> 6	33	165 ± 9^{b}	$14 \pm 5^{b,c}$	15 ± 1	16 ± 2.5^{b}	214 ± 19

$^{a}P < 0.05$, *vs* Group 2; $^{b}P < 0.05$, *vs* Group 3; $^{c}P < 0.05$, *vs* Group 3.

and cell flux was 990 ± 260 cells/min.

The relationship between lymphocrit and pathologies is still unknown. There are indications that the leg massage of healthy rabbits stimulates lymph flow and increases cell concentration, while leg edema due to venous pressure rising is not accompanied by an elevation in cell concentration[128].

Data about cell composition in afferent lymph are very limited and have been obtained in *in vitro* tests. In particular, 80%-90% of cells in normal prenodal lymph are related to mature lymphocytes, 5%-20% to macrophages and dendritic cells, and 0%-10% to other cells (e.g. basophilic blast cells, RBCs)[127]. The composition of WBC types changes based upon the pathology. For example, it is estimated that there is a significanct appearance of neutrophils in experimental peritonitis in sheep. Other important problems are the mechanisms by which different cells (e.g. metastatic tumor cells) enter into peripheral lymphatics. Recently, Azzali studied tumor-associated absorbing lymphatics in the peritumor area of fixed tissue specimens (adenocarcinoma, melanoma, colorectal cancer) using light microscopy, transmission electron microscopy, and histochemistry with 3-D image reconstruction[132]. He found that cancer cells can enter into lymphatics through intraendothelial channels (1.8-2.1 μm in diameter and 6.8-7.2 μm in length). These results are very promising, but such a mechanism remains to be proven in living cells *in vivo*.

Lymph and blood flow cytometry in vivo

We demonstrated the first application of the PT techniques for lymph and blood PT flow cytometry (PTFC) *in vivo* integrated with TDM[94,115,116,133]. To minimize cell image distortion due to spatial cell-radial fluctuations in lymph flow (up to 50 μm in 150-μm-diameter lymph vessels), cells were imaged immediately after passing through a lymphatic valve, which played the role of a natural nozzle, focusing the cells near the vessel axis (Figure 3J). Thus, lymphatic valves provided a natural type of "hydrodynamic focusing" (a term used in *in vitro* FC involving an artificial nozzle) to limit lateral fluctuation of cells up to a few micrometers.

High-resolution and high-speed TDM imaging provides a real-time monitoring of individual cells in blood (Figure 3L-N) and lymph flow (Figure 3I-K), as well as static and migrating cells in the interstitium (Figure 3O), lymph nodes (Figure 3A and B), and even in liver (Figure 3C)[58,94]. The high spatial resolution offered by TDM (300-500 nm at 40× - 100× magnification with water immersion) makes it possible to identify some types of moving cells based upon their sizes and shapes (e.g. WBCs and RBCs; Figure 3K). We can even monitor the rotation of a single RBC (Figure 10A-C) and visualize intralymphatic cell aggregates of different sizes in intact microlymphatics (Figure 10D-F).

PT module in integrated FC allows us to obtain PT images of flowing cells (e.g., lymphocytes, RBCs, and leukemic cells) with an absorption sensitivity approximately four orders of magnitude greater than the sensitivity of transmittance microscopy (Figure 3K, left and middle columns)[94]. In particular, PT images revealed the subcellular structures of these cells (Figure 3K, middle column) associated with the spatial distribution of cytochromes in lymphocytes and cancer cells and of hemoglobin in RBCs, which were not clearly visible with

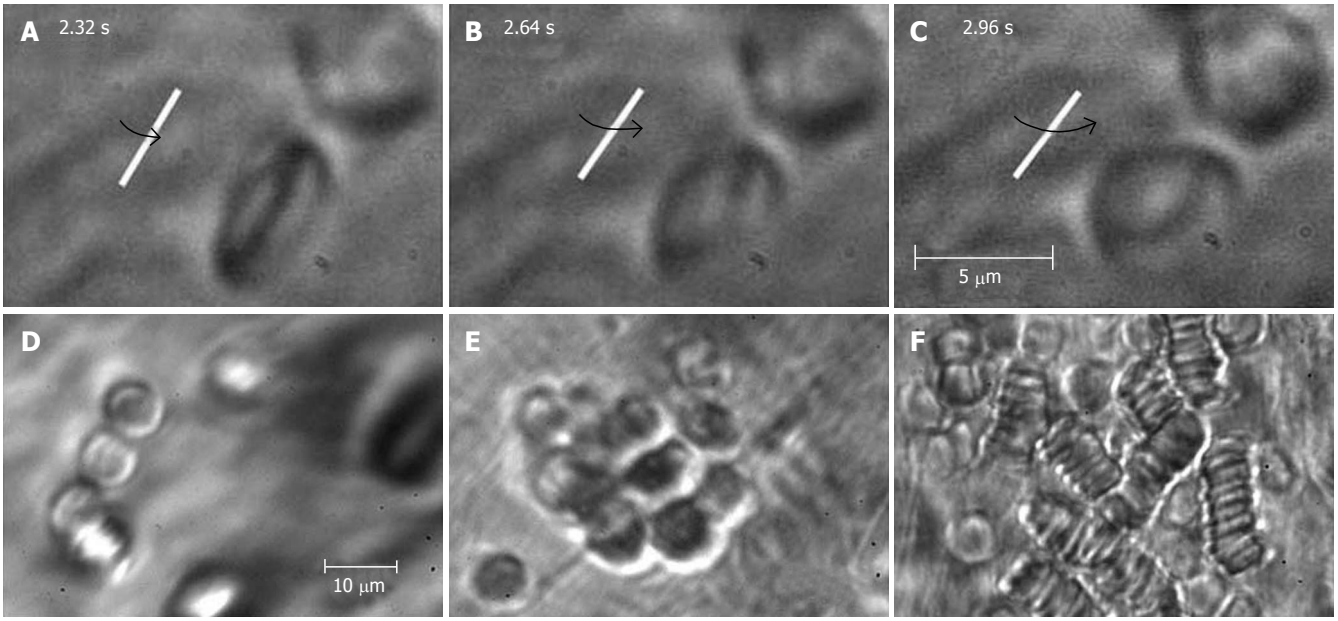

Figure 10 High-resolution monitoring of cell behavior in lymph flow. Top row (**A**-**C**): three sequential images of an individual RBC's rotation in lymph flow (lymphatic diameter 185 μm, mean cell velocity 220 μm/s, magnification 100 ×). Bottom row: moving aggregates of different sizes in lymph flow; **D**: Unstable aggregate of a few cells in intact lymphatic; **E**: large aggregate of RBCs in lymph flow resulting from venous insufficiency; **F**: rouleaux formation when numerous RBCs appeared in lymph flow due to laser-induced hemorrhage (magnification 100 ×).

TDM (Figure 3K, left column). Fluorescence images, obtained with a high-sensitivity CCD camera with an intensifier (PentaMAX, Princeton Instruments, Inc.), showed high image contrast (Figure 3K, right column) similar to that of PT images, although inconvenient staining procedures were required. Specifically, leukocytes were labeled with Rhodamine 6G. RBCs and K562 cells were labeled with FITC and MitoTracker Red, respectively. Because of differences in the optical properties of normal and cancerous cells, especially mitochondrial distribution[134,135], which can be visualized with the PT technique, we can assume that PTFC has the potential to distinguish these cells after further improvements.

PT-signal tracings from flowing cells in blood (Figure 11A) and lymph (Figure 11B-E) microvessels were obtained as a function of time[116,94] . Due to their different absorption properties, the significant (40-60-fold) differences in the integral PT amplitudes from RBCs and WBCs (lymphocytes) allowed us to distinguish cells using only the thermolens mode (i.e. even without imaging). Cells were also identified through differences in cooling times (6-10 μs for RBCs, and 20-25 μs for lymphocytes). PT signals from RBCs in blood flow showing a purely positive component indicate a linear positive PT response from the cells at a low laser energy level with no cell damage (temperature increase is usually 5-10℃, Figure 11A). The amplitude differences indicate differences in average absorption and reflect the natural heterogeneity of RBCs. The negative signal component from cells in lymph flow presented in Figure 11D is related to laser-induced photodamage through bubble formation around strongly absorbing cellular zones that have been overheated. The presence of both positive and negative components in the PT-signal amplitude tracing (Figure 11E) indicated a noninvasive condition for lymphocytes (which have a high photodamage threshold) and an invasive condition for RBCs (which have a low photodamage threshold) at the same energy level. Decreasing the laser energy level

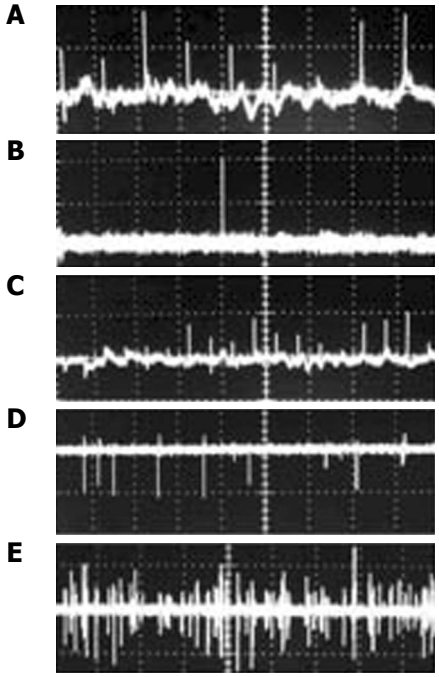

Figure 11 Typical PT-signal tracings from blood cells in blood and lymph flow: **A**: RBCs in blood flow; **B**: rare RBC in lymph flow; **C**: growing number of RBCs in lymph flow during laser-induced hemorrhage; **D**: laser-induced damage of RBCs in lymph flow and lymphocytes in lymph flow in linear and nonlinear PT modes; and **E**: lymphocytes and RBCs in lymph flow. Laser parameters: wavelength, 525 nm; energy/amplitude/time scale/division: (**A**), 0.3 μJ/50 mV/100 ms; (**B**), 0.5 μJ/20 mV/1 s/div; (**C**) 0.6 μJ/100 mV/200 ms/div, (**D**) 5 μJ/500 mV/4 s/div; and (**E**) 145 μJ/100 mV/10 s, respectively.

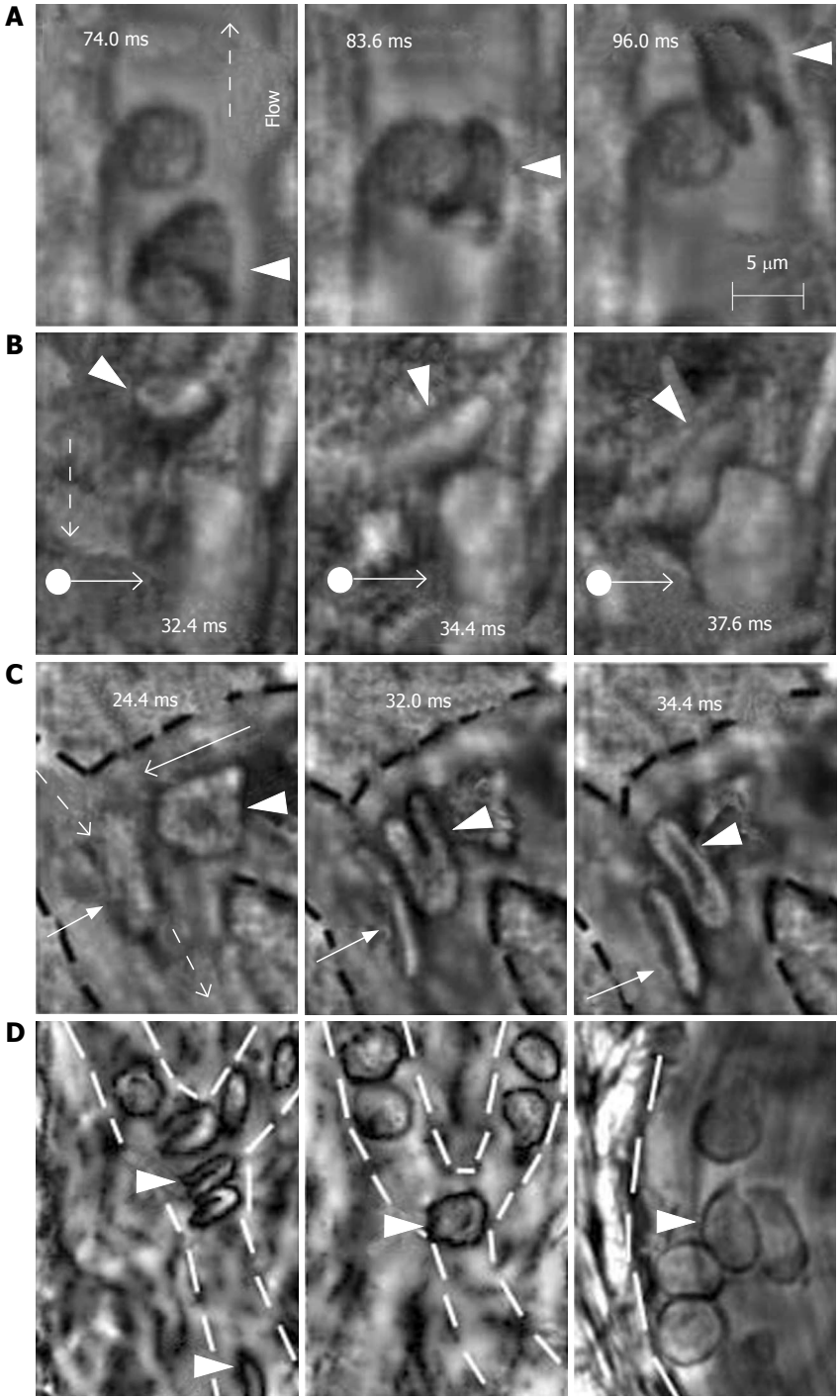

Figure 12 High-resolution, high-speed monitoring of cells in blood flow. RBCs are indicated by conventional arrows and triangle; rolling WBCs by arrows originating from filled circles; and direction of flow by dashed lines. **A**-**C**: behavior of normal RBCs and WBCs in flow (1250-2500 fps; 40 ×); **D**: The shapes of normal (left) and diamide-treated (middle) RBCs in single-file flow of small venula (diameter ~10 μm), and (right) adhesion of diamide-treated RBCs to wall of the relatively large venula (diameter -40 μm).

allows us to selectively identify rare RBCs in lymph flow. For example, Figure 11B shows the detection of single RBCs at a low laser energy level. This level did not produce notable PT signals from the many lymphocytes in lymph flow because of their low absorption. Laser-induced vessel injury led to a fast-growing number of RBCs in lymph flow (Figure 11C). The next tracing shows that the PT signals from RBCs at a relatively high laser energy level led to cell damage (Figure 11D).

HIGH-SPEED IMAGING OF INDIVIDUAL CELLS IN FAST BLOOD FLOW

This technique, using an advanced high-speed CMOS camera, reveals the high deformability of parachute-like RBCs as they are squeezed at 0.6 mm/s through a narrow gap between the vessel wall and rigid adherent cells on the opposite wall (Figure 12A)[104]. It also shows how quickly the relatively fast-flowing RBCs (~1 mm/s) change shape as they interact with the much more slowly moving (so-called rolling) leukocytes (~0.1 mm/s; Figure 12B). We also observed significant dynamic deformation of two RBCs in merging flow streams in a bifurcation zone (Figure 12C), and extremely fast stretching (0.4 ms at 2500 fps) of initially discoid RBCs to ~0.7-0.9 μm (Figure 3N). Our technique has provided relatively good contrast images of both slow- (20 μm/s, Figure 3L, left) and fast-flowing (2.5 mm/s) single platelets in blood microvessels. The best-quality images of platelets were obtained in the RBC-free

space of the microvessel lumen.

We also performed time-resolved monitoring of cell deformability. In particular, diamide (20 mg/kg) was injected in a rat's tail vein to increase the rigidity of RBCs *in vivo*. We observed a drug-induced decrease in the deformability of RBCs in fast blood flow (up to 5 mm/s) compared to RBCs in normal conditions, with maximum centrifugal forces acting on cells in curved capillaries (Figure 12D, left and middle). In addition, diamide led to adhesion of abnormal RBCs to vessel walls (Figure 12D, right). To our knowledge, this was the first time that these phenomena have been observed with high-speed, high-resolution imaging *in vivo*. After additional study, potential applications of this technique may include fundamental studies of dynamic cell-cell interactions in native flow or the identification of abnormal cells (e.g., cancerous cells or sickle RBCs) using their different dynamic deformability as new biological markers that are sensitive to disease development or to different interventions.

IMAGE CYTOMETRY OF STATIC CELLS AND TISSUE STRUCTURES

Interstitium

Figure 3O shows typical high-resolution TDM images of mast cells, adipocytes, and slow-moving RBCs in mesenteric interstitium[58,101]. This technique also provides distinct images of fibrils, as well as other static and migrating cells. In some cases, the phase-contrast images demonstrated better contrast of margins and sub-cellular structures for selected single cells in interstitium than does non phase-contrast at high magnification (100 ×, with water immersion), which prevents overlapping refractive heterogeneities of connective tissue (see images of mast cell and adipocytes in Figure 3O).

Lymph and blood microvessel walls

With TDM, we obtained high-resolution images of (1) distinct individual blood endotheliocytes (EC) of the capillary wall (Figure 3L, left); (2) the initial lymphatic wall with cells (e.g. leukocytes) migrated from interstitium (Figure 3G); and (3) lymphatic wall and valvular cusp structures of larger vessels[58].

Lymph node

Using a minimally invasive procedure, we demonstrated real-time, *in vivo* monitoring of individual cells in different domains of mesenteric lymph nodes (e.g., medullary sinus, light and marginal zones of marginal sinus) in their native state (unpublished data, Figure 3B)[94].

STUDY OF ENVIRONMENTAL IMPACTS ON LYMPHATICS

To date, the effects of environmental and therapeutic interventions on blood microcirculation have been studied in appropriate detail in humans and in different animal models, including the rat mesentery; however, the lymphatic system has received much less attention in spite of the many biological and medical problems associated with microlymphatic functioning and its disturbance in different diseases, including cancer metastasis, venous insufficiency, infections, inflammation, lymphatic malformations, and especially lymphedema[29,40,62]. To partially fill this knowledge gap, we used a rat model with an integrated optical technique to quantitatively study lymph and blood dynamics under different impacts, including chemical, drug, and physical interventions. In our study, we chose interventions that have effects on lymphatics that are unknown (dimethyl sulfoxide); incompletely known (β-adrenoceptor agonist and β_1- and β_2-adrenoceptor antagonists, donors of NO, low-power laser radiation); or controversial (inhibitors of NO-synthase). These effects were studied by real-time monitoring of the diameters and parameters of phasic contractions, and changes in lymph flow velocity, valve activity, and cell behavior in microvasculature.

Effects of adrenergic agonists and antagonists

One of the most important regulators of the vasculature is adrenergic regulation through α- and β-adrenoreceptors[61]. The effects of adrenergic agonists and antagonists on diameter and phasic contractions of microlymphatics have been described in *in vitro* or *in vivo* tests[22,29,30]. It is known that norepinephrine applied topically or injected intravenously instantly reduces the diameter and increases the contraction frequency of rat mesenteric lymphatics, while isoproterinol has opposite effects[29]. Moreover, the attempts to study the effects of α-adrenoagonists and antagonists on lymph flow in microvessels were made using calculated parameters of lymph outflow (as calculated with the following assumptions: strongly cylindrical, unchanging geometry of lymph vessel with unidirectional lymph flow)[22,30]. It was shown that α-adrenergic regulation of lymph outflow in mesenteric lymphatics is through α_1-receptors[30].

In our tests, we clarified the effects of a β-adrenoceptor agonist and antagonist (and their subtypes) on cell flow velocity *via* the direct monitoring of lymph flow, and determined the relationships between cell velocity and other parameters of microlymphatic function (diameter, amplitude and rate of phasic contractions, rate of valve activity) (Table 2). Isoprenaline, a β-adrenoceptor agonist, (10^{-5} mol/L, 15 min of topical application) caused dose- and time-dependent responses: 5 min following topical application, the percentage of contracting lymphangions was decreased from 60% to 33% and lymph flow velocity was inhibited from 134 ± 13 μm/s to 82 ± 19 μm/s ($P < 0.05$). Then, at 15 min, 40% of lymphangions exhibited lymphostasis accompanied by vessel constriction and depression of phasic activity. The adrenoceptor antagonists metoprolol (β_1) and butoxamin (β_2) were also applied topically at the same parameters (10^{-5} mol/L, 15 min). Both antagonists stimulated phasic contractions in non-active lymphangions. However, the effect of metoprolol was more marked, increasing the proportion of microlymphatics with contractile activity to 66%, while butoxamin stimulated phasic activity in only 32% of non-active lymphangions. As a result, metoprolol's action significantly increased lymph flow velocity (from 136 ± 14 μm/s to 198 ± 24 μm/s, $P < 0.02$), while it did not change with butoxamin. Based upon this data, we assume

Table 2 Effects of 15-min topical application of different vasoactive drugs on lymph microvessel functions

Drug	Diameter	Phasic activity	Lymph flow velocity
Sodium Nitroprusside (10^{-5} mol/L)	Dilation	Slight short-time inhibition	Unchanged
N-Nitro-L-Arginine (10^{-4} mol/L)	Unchanged	Stimulation	Stimulation
Isoprenaline (10^{-5} mol/L)	Constriction	Inhibition	Inhibition up to stasis
Metoprolol (10^{-5} mol/L)	Unchanged	Stimulation	Stimulation
Butoxamin (10^{-5} mol/L)	Unchanged	Slight stimulation	Unchanged
Dymethyl Sulfoxide, (30%)	Constriction	Stimulation	Stimulation in 50% of lymphangions
			Inhibition in 39% of lymphangions (without phasic contractions)

Table 3 Effects of 30% DMSO at the topical application on blood microvessel diameter

	Arterioles			Venules	
Before application	16.5 ± 0.49	25.3 ± 0.69	16.1 ± 0.79	24.9 ± 0.74	34.8 ± 0.66
After DMSO application					
1 min	17.4 ± 0.67	25.8 ± 1.09	18.6 ± 0.98[a]	29.6 ± 1.29[a]	39.0 ± 2.25
2 min	16.9 ± 0.83	28.1 ± 0.80[a]	19.2 ± 1.11[a]	28.9 ± 1.33[a]	38.8 ± 1.53[a]

Significant differences from state before application, [a]$P < 0.05$.

that lymph microvessels (and probably similar large lymph vessels), have β_1- and β_2- adrenoceptors.

No effects

Another essential regulative substance of lymph mesenteric microvessel function *in vivo* is nitric oxide (NO)[35,66,136,137]. According to our data, intravenous injection of an NO donor (sodium nitroprusside, 100 μg/kg, i.e. drug concentration in blood is 5×10^{-5} mol/L) caused slight dilation of lymphatics within 30 min[136]. However, sodium nitroprusside does not affect lymph flow. The response of lymphatics to direct topical application of sodium nitroprusside (10^{-5} mol/L, 30 min) was similar but more intense: dilation of lymphangions for 25 ± 2.5 μm was accompanied by slight transient inhibition of the proportion of lymphatics with phasic contractions and active valves[137].

While the hyper-production of NO does not change lymph flow, the inhibition of NO synthesis stimulated lymph motion (Table 2). Topical application of N-nitro-L-arginine, a known inhibitor of NO (10^{-4} mol/L, 30 min), first caused (fifth minute of application) a short-term decrease in the amplitude of phasic contractions (from 23% ± 3% to 11% ± 1%, $P < 0.001$) and stimulation of valve activity (rate of valve activity increased from 6 ± 1 to 11 ± 2 per min, $P < 0.05$)[66,137]. Then, from the tenth minute, we observed permanent stimulation of phasic activity and lymph flow. Shirasawa and coauthors concluded that a 15-min application of an NO donor and an inhibitor of NO synthase portray the direct effects of NO on microvessel walls[35]. Therefore, we speculate that NO can regulate lymph flow in microvessels due to (at least, partly) the direct action of NO on the endothelium and the smooth muscles of lymph microvessel walls.

Pharmacological effects of dimethyl sulfoxide (DMSO)

DMSO has a wide spectrum of biological activities, including high penetrating activity and significant vasoactive effects on blood vessels[138,139]. It is used for local treatment of trauma, arthrosis, and rheumatoid arthritis[140,141]. The effects of DMSO on the microlymphatic system are unknown. Experimental studies have revealed that a 30-min topical application of 30% DMSO caused specific, dynamic microvascular changes in blood and lymph[66,142]. Immediately after application (within the first minute), there was stasis within 100% of venules and 85%-95% of arterioles, with significant dilation (dilation began earlier and the diameter increased more in venules than in arterioles) and hemorrhaging around venules (Table 3). The marked responses of lymphatics started later (15 min of DMSO application), and appeared as a significant increase in lymph-flow velocity from 190 ± 12 μm/s (before DMSO application) to 233 ± 20 μm/s ($P < 0.05$) accompanied by stimulation of phasic contractions in 21% of lymphangion and decreasing of diameter. In parallel, the 39% of lymphatics is characterized by lymphostasis development (Table 2). Obtained on DMSO' s impacts on lymph and blood microvascular function can be used for assessment the possible side effects of this drug.

Effect of low-power laser irradiation

Publication of the positive clinical effects of low-power laser therapy, including lymphedema treatment, stimulated our interest in studying lymphatic response to this radiation[143-145]. The effects of low-power laser radiation (He-Ne laser) on intact lymph microvessels were studied at three radiation intensities-450 mW/cm^2, 45 mW/cm^2, and 14 mW/cm^2-each with an exposure time of 15 min[66,136,146]. Laser power of 14 mW/cm^2 did not have a significant effect on lymph microvessel function. After 5 min of irradiation at 45 mW/cm^2, 70% of lymphatics were dilated an average of 8 ± 1 μm ($P < 0.01$). After 15 min, the proportion of microvessels

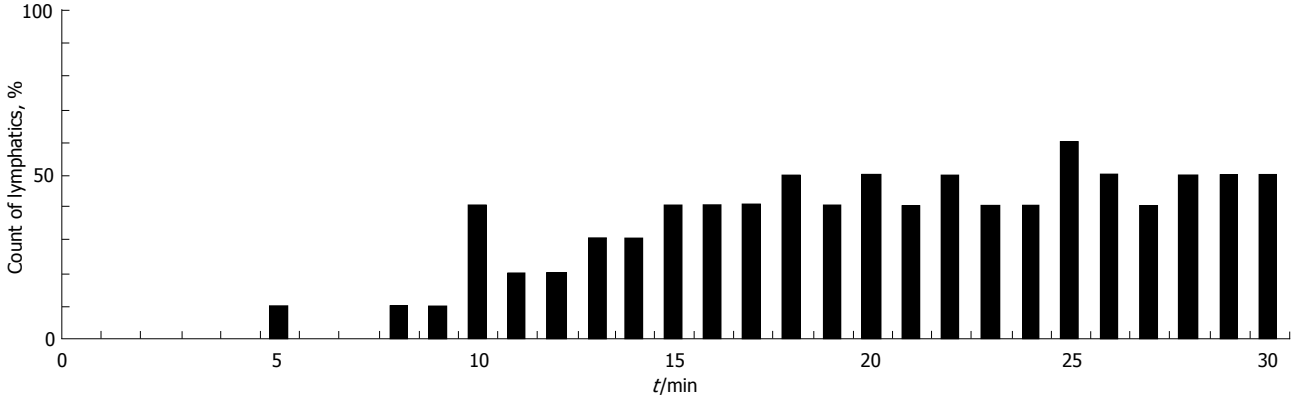

Figure 13 The percentage of lymphangions exhibiting phasic contractions during 30 min of irradiation with a He-Ne laser (450 mW/cm^2).

that were dilated (60%-70%) did not change, and phasic contractions appeared in 21% of lymphatics. When the lymphatics were irradiated at the highest laser power (450 mW/cm^2), similar dilation of the majority of microvessels was observed. Simultaneously, 15 min of laser radiation at 450 mW/cm^2 significantly stimulated contractions within a larger number of vessels (45%) than did irradiation at 45 mW/cm^2. The mean contractile amplitude of irradiated vessels was 1.5-fold greater than that of intact lymphatics (44% ± 5% compared to the amplitude of spontaneous contractions of 29% ± 9%). Increasing the irradiating time up to 30 min at 450 mW/cm^2 did not change the degree of lymphatic dilation and just slightly increased the proportion of lymphatics with phasic contractions (Figure 13). These laser effects were maintained up to 30 min after irradiation. None of the doses of laser radiation affected how the valve functioned. Thus, our data is in line with the results of Carati *et al*[32] in that low-power laser radiation may improve lymph drainage by stimulating phasic contractions and by dilation of microvessels.

High-power laser treatment of vascular abnormalities

Rat mesentery microvasculature is very useful as a model for laser treatment of port-wine stains and other vascular abnormalities. In particular, in one study, rat mesenteric blood vessels were irradiated with a laser pulse (585 nm, 0.2-0.6 ms pulse duration, 0.5-30 J/cm^2 radiant exposure)[147]. Video microscopy was used to assess vessel dilation, formation of intravascular thrombi, bubble formation, and vessel rupture. Changes in reflection during a laser pulse were measured by simultaneously recording the temporal behavior of the incident and reflected light. A threshold radiant exposure of approximately 3 J/cm^2 was found to produce changes in the optical properties of blood *in vivo*, confirming previous *in vitro* results. Often, laser exposure induced a significant increase in vessel diameter, up to three-four times the initial diameter within 200 ms after laser exposure. Sometimes, immediately after the pulse, round structures, interpreted as being gas bubbles, were seen within the vessel lumen.

We obtained similar results in our study with a 10 ms laser pulse (585 nm, 0.5-30 J/cm^2 radiant exposure). In addition, local hemorrhaging around venules with rupture of venular walls occurred at lower radiant exposures than in arterioles with smaller diameters (due to the more effective cooling effects in smaller vessels; Figure 14A and B). For the first time, significant constriction of neighboring lymphatics was observed, up to obliteration of lumina and lymph stasis (Figure 14C and D). Additionally, hemorrhage in the interstitium led to the entry of many RBCs (visualized as distinct red points by TDM) into the lymph flow. The PT mode of integrated PTFC proved this fact. In particular, PT-signal tracing specific for RBC laser energy levels showed a growing number of RBCs in lymph flow during laser-induced hemorrhage (Figure 11C).

Preliminary data from intravenous injection of 100-nm gold nanoparticles followed by laser irradiation of the mesentery demonstrate a decrease in the blood vessel damage threshold (approximately 3-5 times) compared to the damage induced without nanoparticles, despite the sub-optimal parameters of the laser used [wavelength was outside the maximum absorption of the nanoparticles (~525 nm), and of relatively long pulse duration]. Nevertheless, to our knowledge, this was the first demonstration of the application of nanotechnology to treat blood vessels with laser-activaded gold nanoparticles and their nanoclusters[148-154].

Combined action of laser and drugs

Sodium nitroprusside increased the sensitivity of lymph microvessels to low-power He-Ne laser radiation[136]. After intravenous injection of sodium nitroprusside (100 μg/kg), application of He-Ne laser radiation at the lowest power (14 mW/cm^2 for 15 min) stimulated phasic contractions in 44% of lymph microvessels against a background of stable dilation caused by the drug. Contractions occurred at a rate of 6-25/min and had amplitudes of 8-22 μm. In comparison, this dose of laser radiation alone had no notable effect on the phasic contractions of intact microvessels. Such an approach could have great potential for developing innovative therapies for some diseases (e.g., lymphedema).

Nicotine intoxication

Nicotine, an important component of cigarette smoke, was shown to be indirectly responsible for inducing

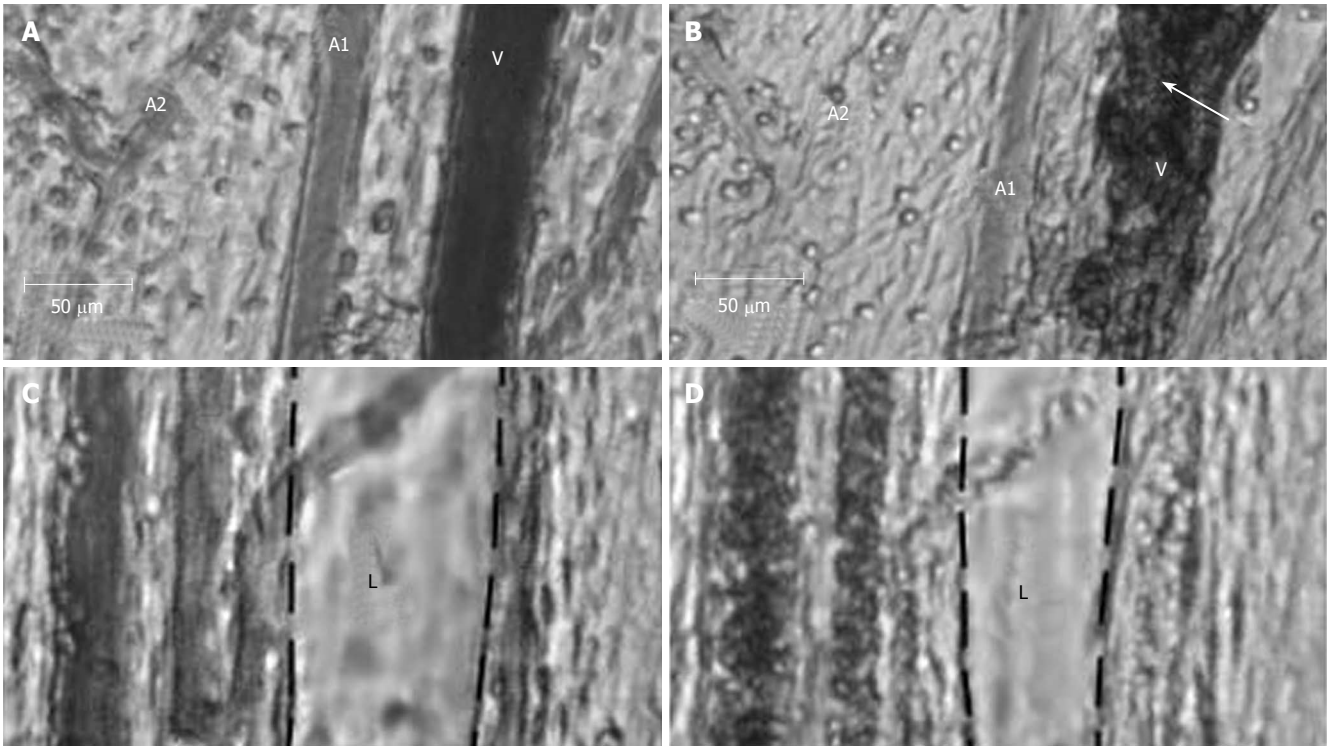

Figure 14 Effect of a laser pulse (585 nm, 10-ms pulse duration, 0.5-30 J/cm^2 radiant exposure) on blood and lymph microvessels *in vivo*. **A**: Intact venule (V) and arterioles (A1 and A2) with good blood flow; **B**: Damage to these microvessels immediately after laser pulse: local hemorrhage (arrow) around the venule (V) and stasis in a small arteriole (A2); **C**: Intact lymphatic (L) before laser pulse (black dash line shows internal margin of lymphatic wall); **D**: Laser-induced constriction of the lymphatic, which coincided with stasis in neighboring venules.

pathology in many tissues, both human and animal[155-157]. Exposure to cigarette smoke increases the nicotine level in the blood to a maximum in less than 10 s. Therefore, the immediate responses of the vascular network to the action of nicotine appear to be important in the development of acute pathology. The pathological effects of nicotine on blood microcirculation have been reported in sufficient detail, but its impact on the lymphatic system remains obscure.

We uncovered the first experimental evidence of potential active participation of lymph microvessels in the mechanisms of nicotine's effects *in vivo*[158]. The influence of nicotine on microlymphatics was determined using three routes of nicotine administration: (1) direct topical application in various concentrations (0.001 mmol/L, 10 mmol/L, and 100 mmol/L solutions) for 15 min; (2) acute injection of nicotine solution (10 mmol/L) through a cannulated vein; and (3) chronic administration for 14 d *via* subcutaneous injection from a mini-osmotic pump (10 mmol/L solution; 0.5 μL/h delivery rate).

The topical application showed that the most significant responses of microlymphatics to nicotine's impact were at 10 mmol/L and 100 mmol/L doses. In particular, the concentration of 10 mmol/L caused a significant, immediate short-term (12-40 s) constriction of 100% of the lymphangions. The effect started within 3-5 s of application (67% of cases) or after ~3 min of nicotine exposure (33% of cases). The lymphatic diameter was decreased by 34% ± 7% (more than ~2 times the amplitude of spontaneous phasic contractions before nicotine application). In all cases with the highest concentration of nicotine (100 mmol/L), the same immediate constrictions were associated with the slowing of lymph flow, local stable constriction of lymph microvessels, asynchronous motion of the lymphatic wall, stasis in blood microvessels, and disturbances of respiration. Thus, under the direct impact of nicotine, there were significant changes in small lymphatic function *in vivo*, which were dose and time dependent. We hypothesize that the obtained effects were the result of the direct action of nicotine on lymph microvessels and probably reflect specific endothelial dysfunction and/or injury of the contractile ability of the lymphatic wall.

Acute nicotine intoxication delivered intravenously slightly relaxed the lymphatics and was sometimes accompanied by slowing of lymph flow and short-term stasis in blood microvessels. Chronic intoxication using a 10 mmol/L concentration (effective at the topical application) did not markedly change the function of lymphatic and blood microvessels and did not differ markedly from that in the intact state. The absence of effects may be the result of adaptation of the microcirculation to the action of nicotine.

Thus, nicotine induces marked changes in small lymphatic function *via* its acute, direct impact *in vivo*. The observed microlymphatic disturbances due to the action of nicotine may be an important mechanism in the complex, immediate reaction of a healthy organism to cigarette smoke. The acute lymphatic damage caused by nicotine could be more crucial in some pathologies or treatments, and suggests that nicotine may contribute to vascular abnormalities and tissue edema.

EXPERIMENTAL MODELING OF DIFFERENT PATHOLOGIES

Damage to lymph microcirculation is an important mechanism underlying the development of many diseases (e.g., tumor, inflammation, infections, intoxications, lymphedema, lymphatic malformation) and often determines their severity[29,40,62,159]. Because rat mesentery is a highly informative *in vivo* model for functional analysis of lymph microdynamics, this animal model was used by us to study the mechanisms of microlymphatic disturbances resulting from different pathologies, such as models of staphylococcal intoxication, pathological stress, lymphedema, and venous insufficiency.

Staphylococcal intoxication

It is well known that α-toxin (α-hemolysin) is the protein produced by *Staphylococcus aureus* and causes serious blood circulatory disturbances with its appearance in blood during staphylococcal diseases; however, its effect on lymph microcirculation is still poorly understood[160-162]. In our study, we used an exotoxic complex (ETC) produced by culture *Staphylococcus aureus* O-15[66,142,163-166]. The main component of this complex is α-toxin (titer ~ 1:640); additionally, it contains a small amount of δ-toxin (titer ~ 1:64). Endotoxins, enterotoxins, and protein A are completely absent.

The staphylococcal intoxication was introduced by intravenous injection of ETC (0.2 mg/100 g) into the tail vein, after which we monitored microcirculation for 30 min. This dose caused serious intoxication. Animals with acute exotoxic shock (those dying within 30 min of ETC introduction) were excluded from the analysis. Disturbances of lymph microcirculation began immediately; after 1 min, the diameters of 75% of the lymphatics were slightly decreased (by 7 ± 2 μm). Between the fifth and tenth minutes of observation, in parallel with vasoconstriction, ETC induced pathologic phasic contractions, characterized by asynchronous wall motion, in half of the lymphatics. After 30 min, lymphatic disturbances were expanded by the development of lymphostasis in 53% of cases.

The resulting effects were due primarily to the direct action of the toxic complex on the lymphatics, as the topical application of ETC in the investigated microlymphatics caused similar microvascular disturbances during a 60-min period. In particular, after a short latent period (58 ± 9 s), ETC induced marked decreasing of lymphangion diameters (36 ± 11 μm from the initial diameter) and stimulated pathologic phasic contractions in 60% of cases. Pathologic phasic activity is characterized by irregular motion of lymphatic walls and defective relaxation (after contraction, the diastolic diameter is sometimes less than it was before). We observed simultaneous abnormalities in blood microvasculature (slowing down of blood flow in venules; increasing migration of leukocytes through venular walls into tissue; and local accumulation of leukocytes around blood microvessels and, as a result, compression of venules into irregular shapes). From the thirtieth to the sixtieth minute of observation, the pathologic constriction of lymph microvessels progressed to complete obliteration of the lymphatic lumen, inhibition of phasic contractions, and gradual development of lymphostasis in 90%-98% of lymphatics. In parallel, we observed blood flow slowing up to stasis and small hemorrhages around venules.

The underlying mechanisms of microlymphatic disturbances include the well-known ability of α-toxin to form the specific Ca^{2+} channels in cell membranes and, correspondingly, to disturb the transport Ca^{2+} in the smooth muscles of the vascular wall and, probably, in the pacemaker cells[167,168]. Thus, these data revealed that an important mechanism of staphylococcal vascular disturbances is damage to the lymph microcirculation. Therefore, therapies for staphylococcal pathology require the correction of microlymphatic dysfunction.

Pathologic effects on lymph microvessels are partially reversible by He-Ne laser radiation and some vasoactive drugs (Euphyllin, Verapamil, DMSO)[66,142,165,166]. In particular, irradiation of the mesentery (450 mW/cm^2 during the first 15 min following ETC application) attenuates typical toxin constriction. In contrast, preliminarily irradiating *in vitro* ETC (20 mW/cm^2, 60 min) attenuates development of lymphostasis: a 60-min application of non-irradiated ETC causes lymphostasis in 88% of lymphangia, while irradiated ETC led to lymphostasis in 57% of lymph microvessels. Thus, low-power laser radiation can attenuate lymphotoxic action *via* its effect on microlymphatic walls, as well as on the properties of ETC itself[166].

However, the most effective corrections of microlymphatic disturbances can be achieved by DMSO. It has been noted above that the effects of DMSO after ETC application (dilation of lymphatics, inhibition of pathologic phasic activity, restoration of lymph flow) are different from the effects on intact lymphatics. Moreover, these local, positive effects are associated with an increase in the duration of animal life, which has been demonstrated in experiments on mice injected with lethal doses of ETC[66,142,165].

Study of experimental lymphedema

Lymphedema is a complication of lymphatic drainage decompensation that may happen during congenital lymphatic dysplasia, hepatic cirrhosis, venous insufficiency, obstruction or surgical extirpation of lymph nodes[159,169,170]. In particular, post-mastectomy lymphedema (PML) develops in 25%-50% of cases after breast cancer treatment[171]. Generally, lymphedema damages the local lymphovascular network (e.g. in affected extremities) causing insufficient and abnormal lymph transport and, correspondingly, accumulation of protein-rich fluid in the interstitial space (tissue edema)[159,169,172]. Because the microvascular network is the principal site for fluid exchange between blood, lymph, and interstitial space, detailed studies of lymph microvessel disturbances during lymphedema have great importance. The efficacy of existing therapeutic treatments for PML is controversial, and clear scientific data have not emerged on the mechanisms of lymphedema development[143,170,171].

Obtaining data from human subjects involves many difficulties (e.g., unpredictability of the time of clinical

onset of PML, limitations of diagnostic methods, *etc.*)[170,173]. In experimental studies in rat, dog, and rabbit extremities, the multi-layers of lymph vascular networks, the rapid development of a good collateral network, and sufficient angiogenesis permit quick restoration of lymph pathways and drainage function, leading to prompt resolution of even acute edema without the appearance of long-term or chronic edema[174-177]. This precludes an informed study of chronic or long-term edema.

In light of these facts, the development of lymphedema in rat mesentery may make the detailed study of lymph and blood microvessel function in acute and chronic edema, because the single layer of vessels in this animal model reduces the opportunity for rapid development of collateral lymph flow. In our study, experimental lymphedema was created by microsurgical removal of regional lymph nodes (lymphadenectomy) or ligation of the collecting vein[101,126,178,179]. Then, the direct quantitative measurement of tissue water was performed in parallel to monitoring blood and lymph vessel activity, including mapping individual cell transport in microvessels and tissue.

After lymphadenectomy, dynamic observation of amounts of water revealed increasing edema from 30 min to 1 wk; the greatest degree of edema occurred at 1 wk with a gradual decrease in edema from 1 to 11 wk[101]. At the thirtieth minute post lymphadenectomy, these effects were accompanied by acute constriction of lymph vessels and slowing of lymph flow velocity from 302 ± 41 μm/s before extirpation to 155 ± 30 μm/s after extirpation ($P < 0.01$). After 1 wk of lymphedema, the lymphatics were overloaded (diameter increased from 133 ± 6 μm in their intact state to 147 ± 4 μm after lymphadenectomy, $P < 0.05$) with slowing lymph flow. Four weeks after lymphadenectomy, the amount of water in tissue included a range from significant compensation to progressive development of edema. In spite of this, lymph microvessels of all experimental animals (with compensation or with decompensation of edema) revealed significant dysfunction and structure damage (dilation, slowing of lymph flow, degenerative changes in the microlymphatic wall). Eleven weeks after lymphedema, we observed various microvascular disturbances, including lymphatic fibrosis at edema decompensation and significant dilation of lymph microvessels or lymphangiogenesis at edema compensation.

We obtained experimental evidence of the significant role of blood microvessels during lymphedema development after lymphadenectomy, which before was either not clear or was controversial. Marked changes in blood microvessels started at the stage of well-developed tissue edema and marked lymphatic disturbances. We observed dilation of blood microvessels, venules, and expansion of the microvascular network without significant hemorrhage in the interstitium[101].

Acute venous insufficiency (30 min after vein ligation) led to significant edema[101,126,178,179]. The comparison of acute lymphedema after lymphadenectomy and venous insufficiency revealed several similar changes, including inhibition of lymph flow and phasic activity. The specific disturbances after vein ligation included marked dilation of the blood vascular network; slowing (up to stasis) of blood flow in venules; and multiple hemorrhages adjacent to the venules and, as a result, the presence of many RBCs in the lymph.

Thus, unknown mechanisms of microvascular damage as well as the correlation between the functions of lymph microvessels, blood microvessels, and tissue edema in dynamic lymphedema development *in vivo* was established, which is important both for understanding mechanisms of lymphedema and for developing new treatment strategies.

Experimental model of sound-related stress

Experimental pathologic stress (2 h of immobilization and interrupted sound, 120 dB, 150-500 Hz) on rats led to significant (20%) increase in microlymphatic diameters ($P < 0.01$); intensification of lymph flow (mean cell velocity increased from 227 ± 8 μm/s in intact rats to 295 ± 12 μm/s in the stressed animals, $P < 0.001$), and stimulation of phasic contractions in 75% of lymphatics[179-181]. The resulting changes in lymph microvessel function probably stimulate lymph drainage and, therefore, play an adaptive role in this pathology.

REAL-TIME QUANTITATIVE MONITORING OF INDIVIDUAL CELL TRANSPORT *IN VIVO*

Normal rat lymphocytes, rat basophilic leukemia (RBL-1) cells, K562 human leukemia cells, and rat RBCs (for each cell type, 10^7-10^8 cells/mL) were labeled with FITC and introduced separately by bolus injection (100 μL) into the tail vein of rats with normal blood circulation or with acute venous insufficiency (ligation of collecting mesenteric vein). Over the next 30-60 min, we monitored in real-time the fluorescently labeled circulating, rolling, and adhesive cells in mesenteric blood vessels (diameter, 30-50 μm) and lymph microvessels (diameter, 120-180 μm), as well as visualized the distribution of the cells in mesenteric interstitial space. Simultaneous fluorescence and transmission imaging allowed us to distinguish the position of a single labeled cell. Accumulation of cells in mesenteric lymph nodes and the right lobe of the liver was monitored *in vivo* 60-90 min after the injections; each organ had been carefully exposed through a mid-abdominal incision and placed on a thermostabilizing microscope stage. To minimize light scattering by tissue and obtain deep, clear images of lymph nodes, we applied optical immersion technology (optical clearing method) using glycerol, which is an osmotic chemical[182,183]. In addition, the concentration of labeled cells in the systemic blood circulation was estimated by sampling blood through a catheter.

Normal and leukemic cell transport: a comparative analysis

We observed a significant number of rat RBCs, WBCs (lymphocytes), and leukemic cells in blood microvessels immediately after injection; 85%-95% of the cells were cleared from the microcirculation within the first 30 min (Figure 15A and B). In comparison, only a few human leukemia cells were found in the blood circulation within

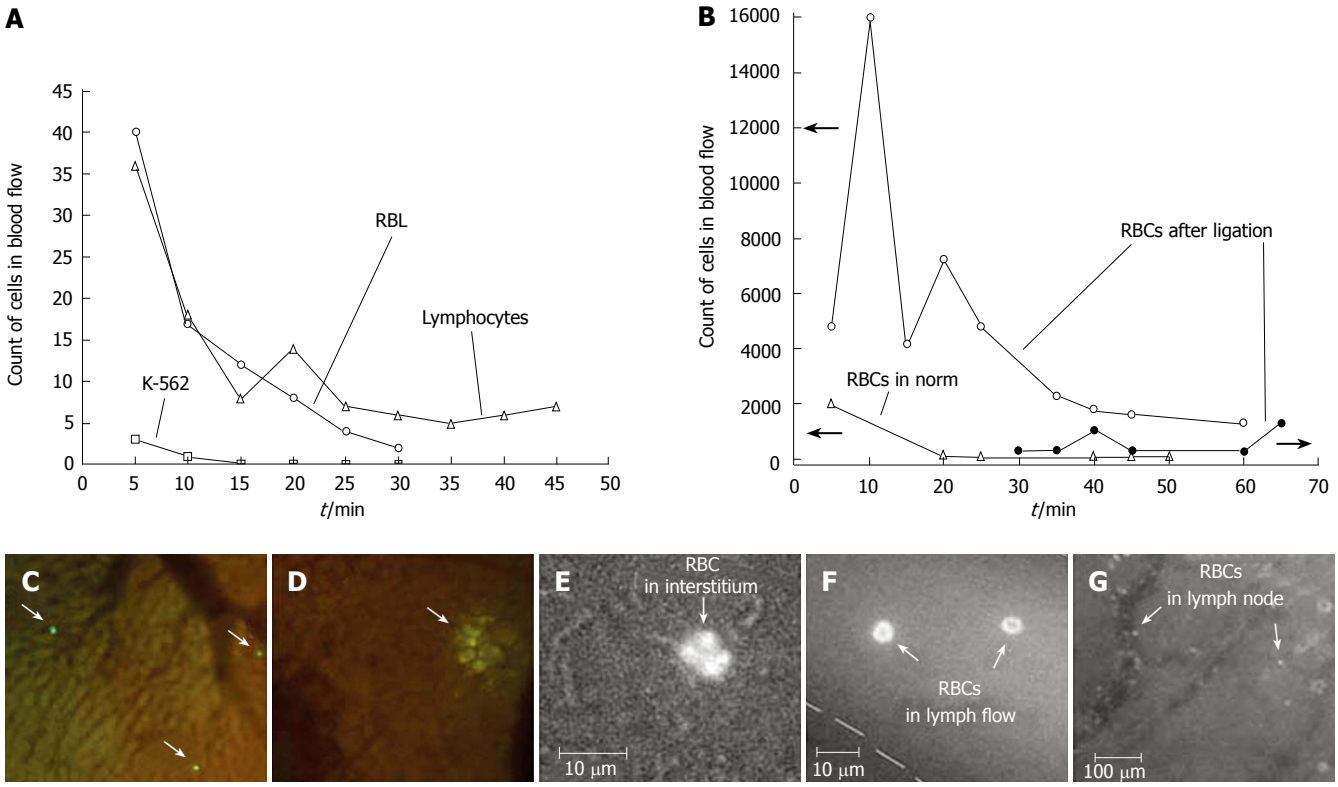

Figure 15 **A**: Monitoring of labeled rat lymphocytes, and rat (RBL) and human (K562) leukemia cells in blood vessels of rat mesentery; **B**: Simultaneous monitoring of RBCs in blood and lymph systems under normal conditions and with venous insufficiency; **C**, **D**: *In vivo* imaging of liver with (**C**) lymphocytes and (**D**) RBL leukemia cells. Monitoring RBC migration from blood vessel (**E**) through interstitium to (**F**) lymph vessel and (**G**) lymph node.

the first 5-10 min (Figure 15A), probably because 95% of the cells were cleared by a strong immune response immediately after injection. These cells then migrated into the interstitial space and were quickly destroyed. No cells appeared in lymphatic vessels during the first 60 min of observation.

In the first 5 min after bolus injections of WBCs or RBCs labeled with FITC (10^6 cells of each type in bolus), 50 times more RBCs were present in the circulation than were normal WBCs. Normal WBCs were detected in blood flow more often than rat leukemia cells (RBL-1 cells). RBL-1 cells, being ~1.5-2 times larger than normal WBCs, probably plugged small microvessels, thus decreasing the number of cells detected. In particular, Figure 15A shows that the number of WBCs was slightly higher than that of RBL-1 cells, although fewer WBCs (10^6 cells in bolus) than RBL-1 cells (10^7 cells in bolus) were injected. At 60-90 min of observation, both types of cells had accumulated mainly in the liver (Figure 15C and D). WBCs were visualized in liver as clearly distinguishable individual cells (Figure 15C), whereas RBL-1 cells appeared as a fluorescent spot (Figure 15D), probably because cells were destroyed in the liver, and only the rest of the dye was visible. However, both types of cells were identified after 3 h of observation in blood samples from large vessels; there were more WBCs than RBL-1 cells (10^3 *vs* 10^2). Thus, although the migrations of leukemic cells and normal cells in the same living organism represent some shared properties, they also display significantly distinct features. In the future, these distinct features may be used as diagnostic criteria for leukemia. Since the presented approach is able to analyze the transport of lymphocyte (important participants of immune response) it offers the potential to study *in vivo* immune responses at cellular and molecular levels.

Cell transport dynamic from blood to lymph during edema

The modeling of acute venous insufficiency and tissue edema caused marked changes in normal cell migration[101]. In particular, after injection of labeled RBCs, we observed a 5-min increase in the absolute number of labeled cells in the slowing blood flow of edematous tissue compared with normal blood flow (Figure 15B). Then, the slow-down of blood flow at the edema led to the output of many RBCs (10-15 min of observation) from blood vessels in mesenteric interstitium, where the trajectory of their motion is represented as episodic zigzag lines with mean velocities of 10-20 μm/s. As a result, RBCs moved through the interstitium to the lymphatics. After 30 min of monitoring, RBCs were identified in lymph flow (Figure 15F), and then in mesenteric lymph nodes (40-60 min of observation; Figure 15G). Thus, our integrated optical technique demonstrates unique capabilities for real-time monitoring of labeled cells in blood and lymph flow, as well as the migration of these cells into tissue interstitium and regional lymph nodes.

In vivo detection of flowing apoptotic cells

Apoptosis is referred to as programmed physiological cell death. *In vivo* study of apoptosis is crucial for understanding the fundamentals of cell biology; optimization of

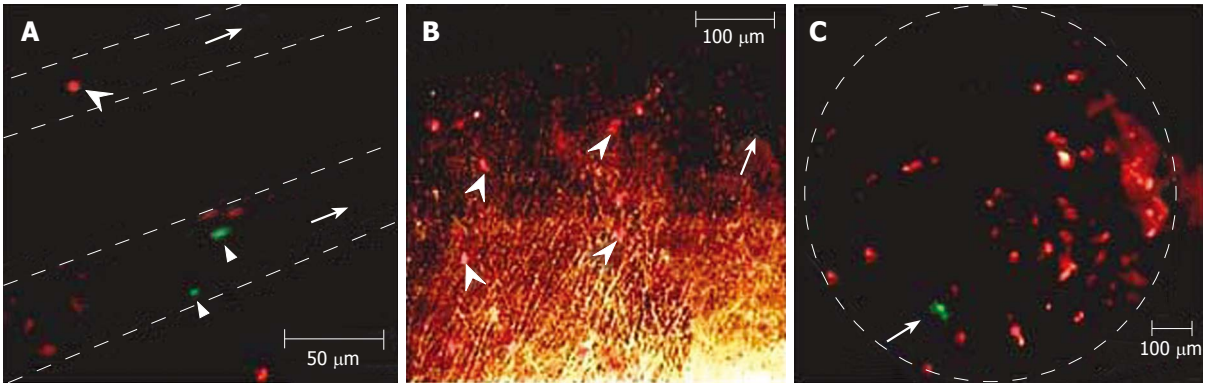

Figure 16 **A**: Apoptotic (arrowhead, red) and normal (two arrow triangles, green) cells in two blood vessels (dashed lines); **B**: Apoptotic cells (arrowhead, red) in interstitium (arrow shows one vessel); **C**: Normal (arrow, green) and apoptotic (red) cells in a lymph node (dashed line).

radiation therapy and chemotherapy; diagnosis of many diseases (e.g., metastasis development, cardiovascular diseases, hematological diseases, autoimmune diseases, neurodegenerative diseases, Alzheimer's disease); and assessment of acute organ transplant rejection or the effect of immunosuppressive drugs[134,184-195]. Despite significant progress in studying apoptosis *in vitro* with many powerful assays, adapting these assays to *in vivo* study of apoptosis is extremely difficult[184,185].

In our experiments, WBCs extracted from a rat underwent apoptosis after exposure to dexamethasone. They were then labeled with rhodamine 6G (red fluorescent emission). In addition, normal WBCs were labeled with FITC (green emission). A 50/50 mixture of labeled apoptotic and normal WBCs was injected into a rat's tail vein, and the appearance of the WBCs was monitored in rat mesentery venules with integrated PTFC. The fluorescence measurements (obtained by counting the number of cells in images) demonstrated the appearance of both normal and apoptotic cells in blood microvessel flow during the first minute (Figure 16A), and rapid clearing of apoptotic cells from circulation, with a half-life of ~8 min. We also observed: (1) rolling apoptotic cells in small venules within 10 min after the injections, (2) the appearance of apoptotic cells in the interstitium after 15 min (Figure 16B), and (3) significant accumulation of apoptotic cells in mesenteric lymph nodes (Figure 16C) after 30 min (see details of node location in Figure 3A and B).

Thus, the obtained results demonstrate that individual cell migration in living organisms depends on: (1) the morphological type of normal and abnormal cells (e.g. WBCs versus RBCs, WBCs versus leukemic cells), (2) the functional state of the cell (e.g. living versus apoptotic cells), and (3) the functional status of the entire organism (e.g. in norm versus in acute venous insufficiency at tissue edema). The high sensitivity of the PT technique to nanoscale morphologic events during apoptosis demonstrated *in vitro*[112-113], in combination with conventional fluorescent assays, makes it possible to apply this technique for detection of apoptotic cells *in vivo*.

IR ANGIOGRAPHY AND LYMPHGRAPHY

Indocianine green (ICG) is a well-known, relatively harmless dye for IR blood angiography and IR imaging of lymph nodes in human and animals[196-201]. Within the first seconds after intravenous injection, there is a shift in the absorption spectrum of ICG from 780 nm to 805 nm (spectral stabilization) due to two processes: polymerization of ICG molecules and their binding to plasma proteins and lipoproteins[196]. Plasma clearance of ICG is biphasic, showing a rapid first phase with a half-life of 4-6 min and a secondary phase with a half-life of more than 1 h[197]. ICG is eliminated from an organism by the enterohepatic route[197].

The imaging of blood vasculature by ICG is a well-known conventional approach; however, identification of the lymph microvascular network with ICG has not been previously studied. Recently, we performed first experiments with microlymphatics. Using TDM and fluorescent microscopy, we monitored typical microvascular units (venula, arteriola, and lymph microvessel of rat mesentery; Figure 17) after intravenous ICG injection (0.2 mL/100 g in rat's tail vein). Excitation at a wavelength of 805 nm, 0.25 mW/cm^2, was provided by continuous diode laser, and the re-emitted fluorescence was filtered at 830 nm and then detected using an intensified highly sensitive camera (PentoMAX, Roper Scientific). Our preliminary studies demonstrated that the first IR image of the venula appears 70-80 s after injection; then, in a short period of time (first 2 min after injection), dye appeared in the arteriola (Figure 17B). Forty to fifty minutes after injection, ICG accumulated (at least partly) in lymph microvessels (Figure 17C). Thus, ICG may potentially be used for study of blood and lymph microcirculation (IR angiography and lymphography), including a monitoring traffic dye in blood and lymph vascular nets.

CONCLUSIONS

As demonstrated in this paper, rat mesentery, in combination with advanced optical techniques, is an attractive animal model for *in vivo* lymph- and blood flow cytometry, high-resolution high speed cell imaging, IR time-resolved angiography and lymphography, real-time monitoring of cells traffic through tissue in norm, during diseases or in response to therapy.

Specifically, the capabilities of this model may include:

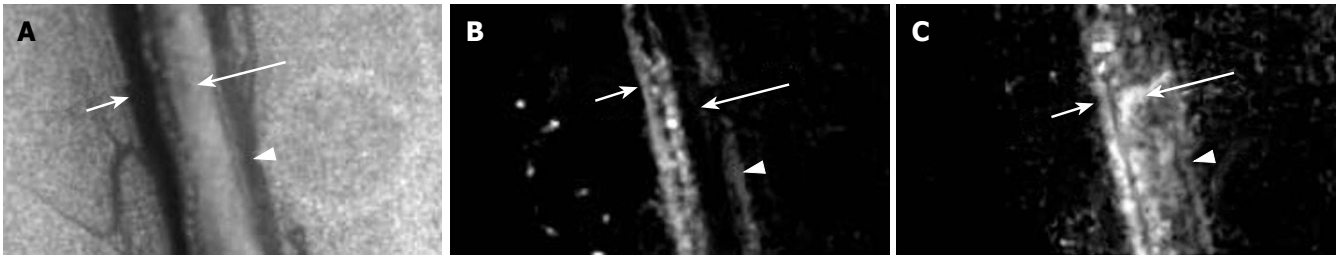

Figure 17 ICG IR blood and lymph microangiography. Transmission image before ICG injection (venula: short arrow, arteriola: triangle, lymph microvessel: long arrow) (**A**). Fluorescence images (excitation 805 nm; emission 830 nm) at the (**B**) 15th and (**C**) 45th min after ICG injection.

(1) analysis of cell pathways in tissue (blood microvessel, interstitium, afferent lymphatics) with migration through microvessel walls and accumulation in lymph nodes and liver; (2) quantitative monitoring of changes in the number of normal or abnormal cells in blood and lymph flow (blood and lymph FC); (3) identification of moving and static cells, including rare abnormal cells and apoptotic cells, through their size, shape, and specific sub-cellular structures; (4) high-resolution, high-speed monitoring of lymph and blood microrheology (e.g. transient deformability, cell aggregation), and interactions between different moving cells and between moving cells and endothelial cells of the vessel wall; (5) quantitative assessment of the clearance rate of circulating cells in lymph and blood flow; (6) analysis of *in vivo* immune responses at cellular and molecular levels; (7) *in vivo* monitoring of the circulation and migration of chylomicrons, bacteria, and viruses; (8) monitoring of dynamic thrombus and blood clot formation (with and without platelet participation); (9) label-free IR microvessel angiography and lymphography.

These advantages are crucial, both for understanding basic cell biology (e.g. metabolism and apoptosis), cell flow dynamics, and for conducting clinical studies of early disease diagnoses (e.g., cancer, sickle diseases, leukemia, edema, inflammation, infections) or assessment of innovative therapeutic interventions (pharmaceuticals, nicotine, lasers, or γ-radiation). Other potential applications may include radio and drug screening *in vivo* based on the previously described, promising *in vitro* techniques.

It is hoped that this review will serve not only as a helpful progress report and to provide certain leads for further research, but will also help attract the scientific interest and support that are required to solve these problems.

ACKNOWLEDGMENTS

The authors thank Grigory E Brill, PhD, DSc (Saratov Medical State University, Russia); Sergey S Ulianov, PhD, DSc (Saratov State University, Russia); Qingming Luo, PhD (Institute for Biomedical Photonics, Huazhong University of Science and Technology, China); Ivan V Fedosov, PhD (Saratov State University, Russia); Anastasia V Solovieva, PhD (Saratov Medical State University, Russia). We thank Tatiana V Stepanova for assisting with animal experiments, Dmitri O Lapotko, PhD for his significant contribution in the development of the PT setup, and Scott Ferguson, for assisting with laser measurements. We also thank the Office of Grants and Scientific Publications at the University of Arkansas for Medical Sciences for editorial assistance during the preparation of this manuscript.

REFERENCES

1 **Aukland K**. Arnold Heller and the lymph pump. *Acta Physiol Scand* 2005; **185**: 171-180
2 **Zweifach BW**, Lowenstein B, Chambers R. Response of blood capillaries to acute hemorrhage in the rat. *Am J Physiol* 1944; **142**: 80-93
3 **Chambers R**, Zweifach BW. Topography and function of the mesenteric capillary circulation. *Am J Anat* 1944; **75**: 173-205
4 **Wiggers CJ**. Peripheral circulation. *Annu Rev Physiol* 1947; **9**: 255-300
5 **Gaehtgens P**, Meiselman HJ, Wayland H. Erythrocyte flow velocities in mesenteric microvessels of the cat. *Microvasc Res* 1970; **2**: 151-162
6 **Johnson PC**. Red cell separation in the mesenteric capillary network. *Am J Physiol* 1971; **221**: 99-104
7 **Zweifach BW**, Prather JW. Micromanipulation of pressure in terminal lymphatics in the mesentery. *Am J Physiol* 1975; **228**: 1326-1335
8 **Starr MC**, Frasher WG. In vivo cellular and plasma velocities in microvessels of the cat mesentery. *Microvasc Res* 1975; **10**: 102-106
9 **Lipowsky HH**, Usami S, Chien S. In vivo measurements of "apparent viscosity" and microvessel hematocrit in the mesentery of the cat. *Microvasc Res* 1980; **19**: 297-319
10 **Firrell JC**, Lipowsky HH. Leukocyte margination and deformation in mesenteric venules of rat. *Am J Physiol* 1989; **256**: H1667-H1674
11 **Seki J**. Flow pulsation and network structure in mesenteric microvasculature of rats. *Am J Physiol* 1994; **266**: H811-H821
12 **Yamaki K**, Lindbom L, Thorlacius H, Hedqvist P, Raud J. An approach for studies of mediator-induced leukocyte rolling in the undisturbed microcirculation of the rat mesentery. *Br J Pharmacol* 1998; **123**: 381-389
13 **Frenette PS**, Moyna C, Hartwell DW, Lowe JB, Hynes RO, Wagner DD. Platelet-endothelial interactions in inflamed mesenteric venules. *Blood* 1998; **91**: 1318-1324
14 **Jiang Y**, Liu AH, Zhao KS. Studies on the flow and distribution of leukocytes in mesentery microcirculation of rats. *World J Gastroenterol* 1999; **5**: 231-234
15 **Pearson MJ**, Lipowsky HH. Influence of erythrocyte aggregation on leukocyte margination in postcapillary venules of rat mesentery. *Am J Physiol Heart Circ Physiol* 2000; **279**: H1460-H1471
16 **Osterloh K**, Gaehtgens P, Pries AR. Determination of microvascular flow pattern formation in vivo. *Am J Physiol Heart Circ Physiol* 2000; **278**: H1142-H1152
17 **He P**, Wang J, Zeng M. Leukocyte adhesion and microves-

sel permeability. *Am J Physiol Heart Circ Physiol* 2000; **278**: H1686-H1694
18 **Sugii Y**, Nishio S, Okamoto K. In vivo PIV measurement of red blood cell velocity field in microvessels considering mesentery motion. *Physiol Meas* 2002; **23**: 403-416
19 **Sugii Y**, Nishio S, Okamoto K. Measurement of a velocity field in microvessels using a high resolution PIV technique. *Ann N Y Acad Sci* 2002; **972**: 331-336
20 **Golub AS**, Pittman RN. Erythrocyte-associated transients in PO2 revealed in capillaries of rat mesentery. *Am J Physiol Heart Circ Physiol* 2005; **288**: H2735-H2743
21 **Ohshima N**. Engineering approaches to the microcirculation studies. *Clin Hemorheol Microcirc* 2006; **34**: 27-34
22 **Benoit JN**, Zawieja DC, Goodman AH, Granger HJ. Characterization of intact mesenteric lymphatic pump and its responsiveness to acute edemagenic stress. *Am J Physiol* 1989; **257**: H2059-H2069
23 **Benoit JN**. Relationships between lymphatic pump flow and total lymph flow in the small intestine. *Am J Physiol* 1991; **261**: H1970-H1978
24 **Sekizuka E**, Ohshio C, Minamitani H. Automatic analysis of moving images for the lymphocyte velocity measurement. *Microcirculation annual* 1995; **11**: 107-108
25 **Takahashi T**, Shibata M, Kamiya A. Mechanism of macromolecule concentration in collecting lymphatics in rat mesentery. *Microvasc Res* 1997; **54**: 193-205
26 **Dixon JB**, Zawieja DC, Gashev AA, Coté GL. Measuring microlymphatic flow using fast video microscopy. *J Biomed Opt* 2005; **10**: 064016
27 **Zweifach BW**, Kivy-Rosenberg E. Microcirculatory effects of whole-body X-irradiation and radiomimetic procedures. *Am J Physiol* 1965; **208**: 492-498
28 **Ferguson MK**, Shahinian HK, Michelassi F. Lymphatic smooth muscle responses to leukotrienes, histamine and platelet activating factor. *J Surg Res* 1988; **44**: 172-177
29 **Aukland K**, Reed RK. Interstitial-lymphatic mechanisms in the control of extracellular fluid volume. *Physiol Rev* 1993; **73**: 1-78
30 **Benoit JN**. Effects of alpha-adrenergic stimuli on mesenteric collecting lymphatics in the rat. *Am J Physiol* 1997; **273**: R331-R336
31 **Kimura M**, Mitani H, Bandoh T, Totsuka T, Hayashi S. Mast cell degranulation in rat mesenteric venule: effects of L-NAME, methylene blue and ketotifen. *Pharmacol Res* 1999; **39**: 397-402
32 **Carati CJ**, **Jobling J**, Fouyaxis J and **Gannon BJ.** Effect of low level laser on mesenteric lymphatics and blood vessels in-vivo. *Progress in Microcirculation Research* 1999; **10**: 77-80
33 **Torres LN**, Torres Filho IP. Determination of macromolecular exchange and PO2 in the microcirculation: a simple system for in vivo fluorescence and phosphorescence videomicroscopy. *Braz J Med Biol Res* 2001; **34**: 129-135
34 **Amerini S**, Ziche M, Greiner ST, Zawieja DC. Effects of substance P on mesenteric lymphatic contractility in the rat. *Lymphat Res Biol* 2004; **2**: 2-10
35 **Shirasawa Y**, Ikomi F, Ohhashi T. Physiological roles of endogenous nitric oxide in lymphatic pump activity of rat mesentery in vivo. *Am J Physiol Gastrointest Liver Physiol* 2000; **278**: G551-G556
36 **Arshi K**, Bendayan M, Ghitescu LD. Alterations of the rat mesentery vasculature in experimental diabetes. *Lab Invest* 2000; **80**: 1171-1184
37 **Yanagi K**, Ohshima N. Angiogenic vascular growth in the rat peritoneal disseminated tumor model. *Microvasc Res* 1996; **51**: 15-28
38 **Hayes H**, Kossmann E, Wilson E, Meininger C, Zawieja D. Development and characterization of endothelial cells from rat microlymphatics. *Lymphat Res Biol* 2003; **1**: 101-119
39 **Ji RC**. Characteristics of lymphatic endothelial cells in physiological and pathological conditions. *Histol Histopathol* 2005; **20**: 155-175
40 **Witte MH**, Jones K, Wilting J, Dictor M, Selg M, McHale N, Gershenwald JE, Jackson DG. Structure function relationships in the lymphatic system and implications for cancer biology. *Cancer Metastasis Rev* 2006; **25**: 159-184
41 **Morisaki H**, Katayama T, Kotake Y, Ito M, Handa M, Ikeda Y, Takeda J, Suematsu M. Carbon monoxide modulates endotoxin-induced microvascular leukocyte adhesion through platelet-dependent mechanisms. *Anesthesiology* 2002; **97**: 701-709
42 **Mouthon MA**, Vereycken-Holler V, Van der Meeren A, Gaugler MH. Irradiation increases the interactions of platelets with the endothelium in vivo: analysis by intravital microscopy. *Radiat Res* 2003; **160**: 593-599
43 **Yamagata K**, Kumagai K. Experimental study of lymphogenous peritoneal cancer dissemination: migration of fluorescent-labelled tumor cells in a rat model of mesenteric lymph vessel obstruction. *J Exp Clin Cancer Res* 2000; **19**: 211-217
44 **Bornhop DJ**, Contag CH, Licha K, Murphy CJ. Advance in contrast agents, reporters, and detection. *J Biomed Opt* 2001; **6**: 106-110
45 **Contag PR**, Olomu IN, Stevenson DK, Contag CH. Bioluminescent indicators in living mammals. *Nat Med* 1998; **4**: 245-247
46 **Ebert B**, Sukowski U, Grosenick D, Wabnitz H, Moesta KT, Licha K, Becker A, Semmler W, Schlag PM, Rinneberg H. Near-infrared fluorescent dyes for enhanced contrast in optical mammography: phantom experiments. *J Biomed Opt* 2001; **6**: 134-140
47 **Becker MD**, Planck SR, Crespo S, Garman K, Fleischman RJ, Dullforce P, Seitz GW, Martin TM, Parker DC, Rosenbaum JT. Immunohistology of antigen-presenting cells in vivo: a novel method for serial observation of fluorescently labeled cells. *Invest Ophthalmol Vis Sci* 2003; **44**: 2004-2009
48 **Nestmann ER**, Douglas GR, Matula TI, Grant CE, Kowbel DJ. Mutagenic activity of rhodamine dyes and their impurities as detected by mutation induction in Salmonella and DNA damage in Chinese hamster ovary cells. *Cancer Res* 1979; **39**: 4412-4417
49 **Saetzler RK**, Jallo J, Lehr HA, Philips CM, Vasthare U, Arfors KE, Tuma RF. Intravital fluorescence microscopy: impact of light-induced phototoxicity on adhesion of fluorescently labeled leukocytes. *J Histochem Cytochem* 1997; **45**: 505-513
50 **Zdolsek JM**. Acridine orange-mediated photodamage to cultured cells. *APMIS* 1993; **101**: 127-132
51 **Abbitt KB**, Rainger GE, Nash GB. Effects of fluorescent dyes on selectin and integrin-mediated stages of adhesion and migration of flowing leukocytes. *J Immunol Methods* 2000; **239**: 109-119
52 **Berk DA**, Swartz MA, Leu AJ, Jain RK. Transport in lymphatic capillaries. II. Microscopic velocity measurement with fluorescence photobleaching. *Am J Physiol* 1996; **270**: H330-H337
53 **Novak J**, Georgakoudi I, Wei X, Prossin A, Lin CP. In vivo flow cytometer for real-time detection and quantification of circulating cells. *Opt Lett* 2004; **29**: 77-79
54 **Georgakoudi I**, Solban N, Novak J, Rice WL, Wei X, Hasan T, Lin CP. In vivo flow cytometry: a new method for enumerating circulating cancer cells. *Cancer Res* 2004; **64**: 5044-5047
55 **Wei X**, Sipkins DA, Pitsillides CM, Novak J, Georgakoudi I, Lin CP. Real-time detection of circulating apoptotic cells by in vivo flow cytometry. *Mol Imaging* 2005; **4**: 415-416
56 **Pries AR**, Eriksson SE, Jepsen H. Real-time oriented image analysis in microcirculatory research. *Proc SPIE* 1989; **1357**: 257-263
57 **Skalak R**, Branemark PI. Deformation of red blood cells in capillaries. *Science* 1969; **164**: 717-719
58 **Galanzha EI**, Tuchin VV, Zharov VP. In vivo integrated flow image cytometry and lymph/blood vessels dynamic microscopy. *J Biomed Opt* 2005; **10**: 054018
59 **Kim S**, Popel AS, Intaglietta M, Johnson PC. Aggregate formation of erythrocytes in postcapillary venules. *Am J Physiol Heart Circ Physiol* 2005; **288**: H584-H590
60 **Rusznyak I**, Foldi M, Szabo G. Lymphatics and Lymph Circulation. 2nd ed. London: Pergamon, 1967
61 **Human Physiology**, Schmidt RF, Thews G, editors. Berlin

Heidelberg: Springer-Verlag, 1989
62 **Brown P**. Lymphatic system: unlocking the drains. *Nature* 2005; **436**: 456-458
63 **Schmid-Schönbein GW**. Microlymphatics and lymph flow. *Physiol Rev* 1990; **70**: 987-1028
64 **McHale NG**. Role of the lymph pump and its control. *NIPS* 1995; **10**: 112-117
65 **Vajda J**, Tomcsik M. The structure of the valves of the lymphatic vessels. *Acta Anat* (Basel) 1971; **78**: 521-531
66 **Galanzha EI**, Brill GE, Aizu Y, Ulyanov SS, Tuchin VV. Speckle and Doppler Methods of Blood and Lymph Flow Monitoring. In: Handbook of Optical Biomedical Diagnostics, Bellingham: SPIE Press, 2002: 875-937
67 **Galanzha EI**, Tuchin VV, Zharov VP, Solovieva AV, Stepanova TV, Brill GE. The diagnosis of lymph microcirculation on rat mesentery in vivo. *Proc SPIE* 2003; **4965**: 325- 333
68 **Galanzha EI**, Ulyanov SS, Tuchin VV, Brill GE, Solov`eva AV, Sedykh AV. Comparison of lymph and blood flow in microvessels: coherent optical measurements. *Proc SPIE* 2000; **4163**: 94-98
69 **Johnston MG**. The intrinsic lymph pump: progress and problems. *Lymphology* 1989; **22**: 116-122
70 **Mordon S**, Begu S, Buys B, Tourne-Peteilh C, Devoisselle JM. Study of platelet behavior in vivo after endothelial stimulation with laser irradiation using fluorescence intravital videomicroscopy and PEGylated liposome staining. *Microvasc Res* 2002; **64**: 316-325
71 **Baez S**. An open cremaster muscle preparation for the study of blood vessels by in vivo microscopy. *Microvasc Res* 1973; **5**: 384-394
72 **Haier J**, Korb T, Hotz B, Spiegel HU, Senninger N. An intravital model to monitor steps of metastatic tumor cell adhesion within the hepatic microcirculation. *J Gastrointest Surg* 2003; **7**: 507-514; discussion 514-515
73 **Schacht V**, Berens von Rautenfeld D, Abels C. The lymphatic system in the dorsal skinfold chamber of the Syrian golden hamster in vivo. *Arch Dermatol Res* 2004; **295**: 542-548
74 **Vargas G**, Readinger A, Dozier SS, Welch AJ. Morphological changes in blood vessels produced by hyperosmotic agents and measured by optical coherence tomography. *Photochem Photobiol* 2003; **77**: 541-549
75 **Galanzha EI**, Tuchin VV, Solov`eva AV, Stepanova TV, Luo Q, Cheng H. Skin backreflectance and microvascular system functioning at the action of osmotic agents. *J Phys D: Appl Phys* 2003; **36**: 1-8
76 **Zharov V**, Galanzha E, Shashkov E, Khlebtsov N, Tuchin V. *In vivo* photoacoustic flow cytometry for real-time monitoring of circulating cells and nanoparticles. *SPIE News room* 2006
77 **Zharov V**, Galanzha E, Shashkov E, Khlebtsov N, Tuchin V. *In vivo* integrated photoacoustic flow cytometry: Application for monitoring circulating cancer cells labeled with gold nanorods. Fifth Workshop on Optical Imaging from Bench to Bedside at the national Institutes of Health 2006: 126
78 **Kalchenko V**, Plaks V. Intravital Video Microscopy – From Simple Solutions to a Multiuser Core Facility. *Proc RMS* 2005; **40**: 221-226
79 **Kersey TW**, Van Eyk J, Lannin DR, Chua AN, Tafra L. Comparison of intradermal and subcutaneous injections in lymphatic mapping. *J Surg Res* 2001; **96**: 255-259
80 **Hirsch JI**, Tisnado J, Cho SR, Beachley MC. Use of isosulfan blue for identification of lymphatic vessels: experimental and clinical evaluation. *AJR Am J Roentgenol* 1982; **139**: 1061-1064
81 **Bowen CH**, Albertine KH. Initial lymphatics are present in the loose areolar connective tissue of the golden hamster's cheek pouch. *Microvasc Res* 1988; **35**: 236-241
82 **Schwerte T**, Pelster B. Digital motion analysis as a tool for analysing the shape and performance of the circulatory system in transparent animals. *J Exp Biol* 2000; **203**: 1659-1669
83 **Yaniv K**, Isogai S, Castranova D, Dye L, Hitomi J, Weinstein BM. Live imaging of lymphatic development in the zebrafish. *Nat Med* 2006; **12**: 711-716
84 **Weinstein B**. Vascular cell biology in vivo: a new piscine paradigm? *Trends Cell Biol* 2002; **12**: 439-445
85 **Baker HJ**, Lindsey JR, Weisbroth SH. The Laboratory Rat. New York: Academic, 1979
86 **Gill TJ**. The rat in biomedical research. *Physiologist* 1985; **28**: 9-17
87 **Gill TJ**, Smith GJ, Wissler RW, Kunz HW. The rat as an experimental animal. *Science* 1989; **245**: 269-276
88 **Murakami T**, Kobayashi E. Color-engineered rats and luminescent LacZ imaging: a new platform to visualize biological processes. *J Biomed Opt* 2005; **10**: 41204
89 **Gahm T**, Witte S. Measurement of the optical thickness of transparent tissue layers. *J Microsc* 1986; **141**: 101-110
90 **Barber BJ**, Oppenheimer J, Zawieja DC, Zimmermann HA. Variations in rat mesenteric tissue thickness due to microvasculature. *Am J Physiol* 1987; **253**: G549-G556
91 **Ghassemifar R**, Franzén L. A double-embedding technique for thin tissue membranes. *Biotech Histochem* 1992; **67**: 363-366
92 **Physiology of Blood Circulation: Physiology of vascular system**. Tkachenko BI, editor. Leningrad: Nauka, 1984 (in Russian)
93 **Chernuh AM**, Alexandrov PN, Alexeev OV. Microcirculation. Moscow: Medicine, 1984 (in Russian)
94 **Zharov VP**, Galanzha EI, Tuchin VV. In vivo photothermal flow cytometry: imaging and detection of individual cells in blood and lymph flow. *J Cell Biochem* 2006; **97**: 916-932
95 **Hauck G**. Functional aspects of the topical relationship between blood capillaries and lymphatics of the mesentery. *Pflugers Arch* 1973; **339**: 251-256
96 **Hauck G**. Origin of the mesenteric lymphatics and their topical relationship to the blood capillaries. *Bibl Anat* 1973; **12**: 356-360
97 **Tuchin VV**. The lasers and fiber optic in biomedical research. Saratov: Saratov State University Press, 1998 (In Russian)
98 **Galanzha EI**, Tuchin VV, Ulyanov SS, Solov'eva AV, Luo Q, Cheng H. Optical properties of lymph flow in single microvessels: biomicroscopic, speckle-interferometric, and spectroscopic measurements. *Proc SPIE* 2001; **4434**: 197-203
99 **Scheinecker C**. Application of in vivo microscopy: evaluating the immune response in living animals. *Arthritis Res Ther* 2005; **7**: 246-252
100 **Horstick G**, Kempf T, Lauterbach M, Ossendorf M, Kopacz L, Heimann A, Lehr HA, Bhakdi S, Meyer J, Kempski O. Plastic foil technique attenuates inflammation in mesenteric intravital microscopy. *J Surg Res* 2000; **94**: 28-34
101 **Galanzha EI**, Tuchin VV, Zharov VP. Optical monitoring of microlympatic disturbances during experimental lymphedema, *Lymphat Res Biol*, 2007: In press
102 **Givan AL**. Principles of flow cytometry: an overview. *Methods Cell Biol* 2001; **63**: 19-50
103 **Chung A**, Karlan S, Lindsley E, Wachsmann-Hogiu S, Farkas DL. In vivo cytometry: a spectrum of possibilities. *Cytometry A* 2006; **69**: 142-146
104 **Zharov VP**, Galanzha EI, Menyaev Y, Tuchin VV. In vivo high-speed imaging of individual cells in fast blood flow. *J Biomed Opt* 2006; **11**: 054034
105 **Zharov VP**, Letokhov VS. Laser Optoacoustic Spectroscopy. Berlin Heidelberg, New York: Springer-Verlag, 1986
106 **Zharov VP**. Laser optoacoustic spectroscopy in chromatography. In: Laser Analytical Spectrochemistry. Letokhov VS, editor. Boston, Mass: Bristol, 1986: 229-271
107 **Lapotko D**, Kuchinsky G, Potapnev M, Pechkovsky D. Photothermal image cytometry of human neutrophils. *Cytometry* 1996; **24**: 198-203
108 **Lapotko D**, Romanovskaya T, Kutchinsky G, Zharov V. Photothermal studies of modulating effect of photoactivated chlorin on interaction of blood cells with bacteria. *Cytometry* 1999; **37**: 320-326
109 **Zharov VP** and Lapotko DO. Photothermal imaging of nanoparticles and cells (review). *IEEE J Sel Topics Quant Electron* 2005; **11**: 733-751
110 **Tokeshi M**, Uchida M, Hibara A, Sawada T, Kitamori T. Determination of subyoctomole amounts of nonfluorescent

molecules using a thermal lens microscope: subsingle-molecule determination. *Anal Chem* 2001; **73**: 2112-2116
111 **Tamaki E**, Sato K, Tokeshi M, Sato K, Aihara M, Kitamori T. Single-cell analysis by a scanning thermal lens microscope with a microchip: direct monitoring of cytochrome c distribution during apoptosis process. *Anal Chem* 2002; **74**: 1560-1564
112 **Zharov VP**, Galitovsky V, Chowdhury P. Nanocluster model of photothermal assay: application for high-sensitive monitoring of nicotine-induced changes in metabolism, apoptosis, and necrosis at a cellular level. *J Biomed Opt* 2005; **10**: 44011
113 **Zharov VP**, Galitovskiy V, Lyle CS, Chambers TC. Superhigh-sensitivity photothermal monitoring of individual cell response to antitumor drug. *J Biomed Opt* 2006; 11: 064034
114 **Zharov VP**, Galanzha EI, Shashkov EV, Khlebtsov NG, Tuchin VV. In vivo photoacoustic flow cytometry for monitoring of circulating single cancer cells and contrast agents. *Opt Lett* 2006; **31:** 3623-3625
115 **Zharov VP**, Galanzha EI, Tuchin VV. Photothermal image flow cytometry in vivo. *Opt Lett* 2005; **30**: 628-630
116 **Zharov VP**, Galanzha EI, Tuchin VV. Integrated photothermal flow cytometry in vivo. *J Biomed Opt* 2005; **10**: 051502
117 **Zharov VP**, Galanzha EI, Tuchin VV. Confocal photothermal flow cytometry in vivo. *Proc SPIE* 2005; **5697**: 167-176
118 **Zharov V**, Menyaev Y, Shashkov E, Galanzha E, Khlebtsov B, Scheludko A, Zimnyakov D, and Tuchin V. Fluctuation of probe beam in thermolens schematics as potential indicator of cell metabolism, apoptosis, necrosis and laser impact. *Proc SPIE* 2006; **6085**: 10-21
119 **Bednov AA**, Ul'yanov SS, Tuchin VV, Brill GE, Zakharova (Galanzha) EI. Investigation of lymph dynamics by speckle-interferometry method. *Applied Nonlinear Dynamics* 1996; **4**: 45-54
120 **Bednov AA**, Brill GE, Tuchin VV, Ul`yanov SS, Zakharova (Galanzha) EI. Blood flow measurements in microvessels using focused laser beam diffraction phenomenon. *Proc SPIE* 1994; **2370**: 379-383
121 **Starukhin P**, Ulyanov S, Galanzha E, Tuchin V. Blood-flow measurements with a small number of scattering events. *Appl Opt* 2000; **39**: 2823-2830
122 **Ul`yanov SS**, Tuchin VV, Bednov AA, Zakharova (Galanzha) EI, Brill GE. The application of Speckle Interferometry for the Monitoring of Blood and Lymph Flow in Microvessels. *Lasers in Med Sci* 1997; **12**: 31-41
123 **Fedosov IV**, Ulianov SS, Galanzha EI, Galanzha VA, Tuchin VV. Laser Doppler and Speckle techniques for bioflow measurements. In: Handbook of Coherent Domain Optical Methods. *Springer*, 2004; XLII, **1**: 397-437
124 **Fedosov IV**, Tuchin VV, Galanzha EI, Solov'eva AV, Stepanova TV. Recording of lymph flow dynamics in microvessels using correlation properties of scattered coherent radiation. *Quantum Electronics* 2002; **32**: 970-974
125 **Brill' GE**, Galanzha EI, Ul'ianov SS, Tuchin VV, Stepanova TV, Solov'eva AV. [Functional organization of lymphatic microvessels of the rat mesentery]. *Ross Fiziol Zh Im I M Sechenova* 2001; **87**: 600-607
126 **Galanzha EI**, Tuchin VV, Solovieva AV, Zharov VP. Experimental evaluation on the transmission optical microscopy for the diagnosis of lymphedema. J Xray Sci Technol 2002; **10**: 215-223
127 **Smith JB**, McIntosh GH, Morris B. The traffic of cells through tissues: a study of peripheral lymph in sheep. *J Anat* 1970; **107**: 87-100
128 **Ikomi F**, Hunt J, Hanna G, Schmid-Schönbein GW. Interstitial fluid, plasma protein, colloid, and leukocyte uptake into initial lymphatics. *J Appl Physiol(1985)* 1996; **81**: 2060-2067
129 **Young AJ**. The physiology of lymphocyte migration through the single lymph node in vivo. *Semin Immunol* 1999; **11**: 73-83
130 **Hall JG**, Morris B. The origin of the cells in the efferent lymph from a single lymph node. *J Exp Med* 1965; **121**: 901-910
131 **Dixon JB**, Greiner ST, Gashev AA, Cote GL, Moore JE, Zawieja DC. Lymph flow, shear stress, and lymphocyte velocity in rat mesenteric prenodal lymphatics. *Microcirculation* 2006; **13**: 597-610
132 **Azzali G**. On the transendothelial passage of tumor cell from extravasal matrix into the lumen of absorbing lymphatic vessel. *Microvasc Res* 2006; **72**: 74-85
133 **Zharov V**, Galanzha E and Tuchin V. Photothermal imaging of moving cells in lymph and blood flow in vivo. *Proc SPIE* 2004; **5320**: 256-263
134 **Gourley PL**, Hendricks JK, McDonald AE, Copeland RG, Barrett KE, Gourley CR, Singh KK, Naviaux RK. Mitochondrial correlation microscopy and nanolaser spectroscopy - new tools for biophotonic detection of cancer in single cells. *Technol Cancer Res Treat* 2005; **4**: 585-592
135 **Gourley PL**, Hendricks JK, McDonald AE, Copeland RG, Barrett KE, Gourley CR, Naviaux RK. Ultrafast nanolaser flow device for detecting cancer in single cells. *Biomed Microdevices* 2005; **7**: 331-339
136 **Brill GE**, Tuchin VV, Zakharova (Galanzha) EI, Ul`yanov SS. Influence of low power laser irradiation on lymph microcirculation at the increasing of NO production. *Proc SPIE* 1999; **3726**: 157-162
137 **Galanzha EI**, Brill' GE, Solov'eva AV, Stepanova TV. [Nitric oxide in the lymphatic microvessel regulation]. *Ross Fiziol Zh Im I M Sechenova* 2002; **88**: 983-989
138 **Pitts LH**, Young AR, McCulloch J, MacKenzie E. Vasomotor effects of dimethyl sulfoxide on cat cerebral arteries in vitro and in vivo. *Stroke* 1986; **17**: 483-487
139 **Jacob SW**, Herschler R. Pharmacology of DMSO. *Cryobiology* 1986; **23**: 14-27
140 **Lockie LM**, Norcross BM. A clinical study on the effects of dimethyl sulfoxide in 103 patients with acute and chronic musculoskeletal injuries and inflammations. *Ann N Y Acad Sci* 1967; **141**: 599-602
141 **Spruance SL**, McKeough MB, Cardinal JR. Dimethyl sulfoxide as a vehicle for topical antiviral chemotherapy. *Ann N Y Acad Sci* 1983; **411**: 28-33
142 **Brill' GE**, Zakharova EI. [The effect of dimethyl sulfoxide on the changes in the lymph microcirculation induced by staphylococcal toxin]. *Eksp Klin Farmakol* 1998; **61**: 54-56
143 **Piller NB**, Thelander A. Treatment of chronic postmastectomy lymphedema with low level laser therapy: a 2.5 year follow-up. *Lymphology* 1998; **31**: 74-86
144 **Carati CJ**, Anderson SN, Gannon BJ, Piller NB. Treatment of postmastectomy lymphedema with low-level laser therapy: a double blind, placebo-controlled trial. *Cancer* 2003; **98**: 1114-1122
145 **Kaviani A**, Yousefi R, Mortaz HS and Ghodsi M. Postmastectomy lymphedema; application of low-level laser therapy. *Laser Sur Med* 2003; **S15**: 66-68
146 **Brill GE**, Zakharova (Galanzha) EI. Influence of low power laser radiation on lymphatic microvessels. Abstract book of the 5th Congress of the Asian-Pacific Association for Laser Medicine and Surgery; 1994 Nov. 20-25; Tel Aviv, Israel. Israel, 1994: 17
147 **Verkruysse W**, Beek JF, VanBavel E, van Gemert MJ, Spaan JA. Laser pulse impact on rat mesenteric blood vessels in relation to laser treatment of port wine stain. *Lasers Surg Med* 2001; **28**: 461-468
148 **Zharov VP**, Galitovsky V and Viegas M. Photothermal detection of local thermal effects during selective nanophotothermolysis. *Appl Phys Lett* 2003; **83**: 4897-4899
149 **Zharov VP**, Galitovskaya EN, Johnson C, Kelly T. Synergistic enhancement of selective nanophotothermolysis with gold nanoclusters: potential for cancer therapy. *Lasers Surg Med* 2005; **37**: 219-226
150 **Zharov VP**, Letfullin RR, and Galitovskaya EN. Microbubbles-overlapping mode for laser killing of cancer cells with absorbing nanoparticle clusters. *J Physics D: Appl Phys* 2005; **38**: 2571-2581
151 **Zharov VP**, Kim JW,Curiel DT, Everts M. Self-assembling nanoclusters in living systems: application for integrated

photothermal nanodiagnostics and nanotherapy. *J Nanomedicine* 2005; **1**: 326-345
152 **Zharov VP**, Mercer KE, Galitovskaya EN, Smeltzer MS. Photothermal nanotherapeutics and nanodiagnostics for selective killing of bacteria targeted with gold nanoparticles. *Biophys J* 2006; **90**: 619-627
153 **Everts M**, Saini V, Leddon JL, Kok RJ, Stoff-Khalili M, Preuss MA, Millican CL, Perkins G, Brown JM, Bagaria H, Nikles DE, Johnson DT, Zharov VP, Curiel DT. Covalently linked Au nanoparticles to a viral vector: potential for combined photothermal and gene cancer therapy. *Nano Lett* 2006; **6**: 587-591
154 **Saini V**, Zharov VP, Brazel CS, Nikles DE, Johnson DT, Everts M. Combination of viral biology and nanotechnology: new applications in nanomedicine. *Nanomedicine* 2006; **2**: 200-206
155 **Chowdhury P**, MacLeod S, Udupa KB, Rayford PL. Pathophysiological effects of nicotine on the pancreas: an update. *Exp Biol Med* (Maywood) 2002; **227**: 445-454
156 **A report of Surgeon General: The Health Consequences of Smoking**. Department of Health & Human Services, Public Health Services, Centers for Disease Control & Prevention, National Center for chronic disease prevention and health promotion, office of smoking & health, Washington, D.C. 2004
157 **Armitage AK**, Dollery CT, George CF, Houseman TH, Lewis PJ, Turner DM. Absorption and metabolism of nicotine from cigarettes. *Br Med J* 1975; **4**: 313-316
158 **Galanzha EL**, Chowhury P, Tuchim VV, Zharov VP. Monitoring of nicotine impact in microlymphatics of rat mesentery with time-resolved microscopy. *Lymphology* 2005; **38**: 181-192
159 **Jeltsch M**, Tammela T, Alitalo K, Wilting J. Genesis and pathogenesis of lymphatic vessels. *Cell Tissue Res* 2003; **314**: 69-84
160 **Arbuthnott JP**. Staphylococcal α-toxin. In: Microbiological toxins. New York, 1970: 189-236
161 **Brown DA**. Some effects of staphylococcal alpha-toxin on the cardiovascular system. *Br J Pharmacol Chemother* 1966; **26**: 580-590
162 **Thelestam M**, Blomqvist L. Staphylococcal alpha toxin--recent advances. *Toxicon* 1988; **26**: 55-65
163 **Brill GE**, Sergeev IP, Glazkova EI, Morokhovets NV. [Effect of staphylococcal toxin on the microcirculatory system]. *Patol Fiziol Eksp Ter* 1992; (**1**): 21-23
164 **Brill GE**, Zakharova (Galanzha) EI. The lymphatic microvessels disfunction under the influence of staphylococcal toxin. Proceedings of the 6th World Congress for Microcirculation; 1996 Aug 25-30; Munich, Germany. Messmer K, Kubler WM, editors. International Proceedings Division: Monduzzi Editore, 1996: 179-182
165 **Brill GE**, Zakharova (Galanzha) EI. Pharmacological correction of lymph microcirculation disorders induced by staphylococcal toxin. Proceedings of the 6th World Congress for Microcirculation; 1996 Aug 25-30; Munich, Germany. Messmer K, Kubler WM, editors. International Proceedings Division: Monduzzi Editore, 1996: 175-177
166 **Brill GE**, Zakharova (Galanzha) EI. Modification of lymphoconstriction action of staphylococcal toxin by laser radiation. *Laser Tech Optoelectronics* 1992; **1-2**: 36-39
167 **Harshman S**, Boquet P, Duflot E, Alouf JE, Montecucco C, Papini E. Staphylococcal alpha-toxin: a study of membrane penetration and pore formation. *J Biol Chem* 1989; **264**: 14978-14984
168 **Ward RJ**, Leonard K. The Staphylococcus aureus alpha-toxin channel complex and the effect of Ca^{2+} ions on its interaction with lipid layers. *J Struct Biol* 1992; **109**: 129-141
169 **Browse NL**, Stewart G. Lymphoedema: pathophysiology and classification. *J Cardiovasc Surg* (Torino) 1985; **26**: 91-106
170 **The diagnosis and treatment of peripheral lymphedema**. Consensus document of the International Society of Lymphology. *Lymphology* 2003; **36**: 84-91
171 **Bruns F**, Schueller P. Novel Treatment Options in Secondary Lymphedema. *AAHPM Bulletin* 2005; 5-7
172 **Szuba A**, Rockson SG. Lymphedema: anatomy, physiology and pathogenesis. *Vasc Med* 1997; **2**: 321-326
173 **Witte CL**, Witte MH, Unger EC, Williams WH, Bernas MJ, McNeill GC, Stazzone AM. Advances in imaging of lymph flow disorders. *Radiographics* 2000; **20**: 1697-1719
174 **Földi E**, Földi M, Clodius L. The lymphedema chaos: a lancet. *Ann Plast Surg* 1989; **22**: 505-515
175 **Gregl A**. [Secondary leg edema--experimental study]. *Z Lymphol* 1988; **12**: 48-53
176 **Pflug JJ**, Calnan JS. The experimental production of chronic lymphoedema. *Br J Plast Surg* 1971; **24**: 1-9
177 **Kinjo O**, Kusaba A. Lymphatic vessel-to-isolated-vein anastomosis for secondary lymphedema in a canine model. *Surg Today* 1995; **25**: 633-639
178 **Galanzha EI**, Tuchin VV, Solov'eva AV, Stepanova TV, Brill GE and Zharov VP. Development imaging and experimental model for studying pathogenesis and treatment efficacy of postmastectomy lymphedema. *Proc SPIE* 2002; **4624**: 123-129
179 **Galanzha EI**, Solov'eva AV, Stepanova TV, Tuchin VV, Brill GE and Zharov VP. Analysis of lymph microcirculation in norm, at the experimental lymphedema and pathological stress on animal model. Abstracts of the 22nd Meeting of the European Society for Microcirculation. Exeter, Devon, United Kingdom. August 28-30, 2002. *J Vasc Res* 2002; **39** Suppl 1**:** 9-99
180 **Solov'eva AV**, Brill GE, Galanzha EI, Stepanova TV. Stress-induced changes in lymph microcirculation. *Proc SPIE* 2004; **4241**: 309-311
181 **Solov'eva AV**, Galanzha EI, Stepanova TV, Brill' GE. Changes in lymph microcirculation during pathological stress. *Bull Exp Biol Med* 2002; **134**: 241-243
182 **Tuchin VV**. Optical clearing of tissue and blood using the immersion method. *J Phys D: Appl Phys* 2005; **38**: 2497-2518
183 **Tuchin VV**. Optical immersion as a new tool for controlling the optical properties of tissues and blood. *Laser Physics* 2005; **15**: 1109-1136
184 **Columbano A**. Cell death: current difficulties in discriminating apoptosis from necrosis in the context of pathological processes in vivo. *J Cell Biochem* 1995; **58**: 181-190
185 **Brauer M**. In vivo monitoring of apoptosis. *Prog Neuropsychopharmacol Biol Psychiatry* 2003; **27**: 323-331
186 **Darzynkiewicz Z**, Bedner E, Traganos F. Difficulties and pitfalls in analysis of apoptosis. *Methods Cell Biol* 2001; **63**: 527-546
187 **Alenzi FQ**, Wyse RK, Altamimi WG. Apoptosis as a tool for therapeutic agents in haematological diseases. *Expert Opin Biol Ther* 2004; **4**: 407-420
188 **Haas RL**, de Jong D, Valdés Olmos RA, Hoefnagel CA, van den Heuvel I, Zerp SF, Bartelink H, Verheij M. In vivo imaging of radiation-induced apoptosis in follicular lymphoma patients. *Int J Radiat Oncol Biol Phys* 2004; **59**: 782-787
189 **Yan SD**, Stern DM. Mitochondrial dysfunction and Alzheimer's disease: role of amyloid-beta peptide alcohol dehydrogenase (ABAD). *Int J Exp Pathol* 2005; **86**: 161-171
190 **Gradl G**, Gaida S, Gierer P, Mittlmeier T, Vollmar B. In vivo evidence for apoptosis, but not inflammation in the hindlimb muscle of neuropathic rats. *Pain* 2004; **112**: 121-130
191 **Al-Gubory KH**. Fibered confocal fluorescence microscopy for imaging apoptotic DNA fragmentation at the single-cell level in vivo. *Exp Cell Res* 2005; **310**: 474-481
192 **Chan K**, Truong D, Shangari N, O'Brien PJ. Drug-induced mitochondrial toxicity. *Expert Opin Drug Metab Toxicol* 2005; **1**: 655-669
193 **Alenzi FQ**. Apoptosis and diseases: regulation and clinical relevance. *Saudi Med J* 2005; **26**: 1679-1690
194 **Hunter AL**, Choy JC, Granville DJ. Detection of apoptosis in cardiovascular diseases. *Methods Mol Med* 2005; **112**: 277-289
195 **Nagata S**. Apoptosis and autoimmune diseases. *IUBMB Life* 2006; **58**: 358-362
196 **Desmettre T**, Devoisselle JM, Mordon S. Fluorescence properties and metabolic features of indocyanine green (ICG) as related to angiography. *Surv Ophthalmol* 2000; **45**: 15-27
197 **Bollinger A**, Saesseli B, Hoffmann U, Franzeck UK. Intravital detection of skin capillary aneurysms by videomicroscopy with indocyanine green in patients with progressive systemic sclerosis and related disorders. *Circulation* 1991; **83**: 546-551

198 **Borotto E**, Englender J, Pourny JC, Naveau S, Chaput JC, Lecarpentier Y. Detection of the fluorescence of GI vessels in rats using a CCD camera or a near-infrared video endoscope. *Gastrointest Endosc* 1999; **50**: 684-688

199 **Wei X**, Runnels JM, Lin CP. Selective uptake of indocyanine green by reticulocytes in circulation. *Invest Ophthalmol Vis Sci* 2003; **44**: 4489-4496

200 **Kitai T**, Inomoto T, Miwa M, Shikayama T. Fluorescence navigation with indocyanine green for detecting sentinel lymph nodes in breast cancer. *Breast Cancer* 2005; **12**: 211-215

201 **Moneta G**, Brülisauer M, Jäger K, Bollinger A. Infrared fluorescence videomicroscopy of skin capillaries with indocyanine green. *Int J Microcirc Clin Exp* 1987; **6**: 25-34

S- Editor Liu Y **L- Editor** Lutze M **E- Editor** Bai SH

PO Box 2345, Beijing 100023, China
www.wjgnet.com
wjg@wjgnet.com

World J Gastroenterol 2007 January 14; 13(2): 219-223
World Journal of Gastroenterology ISSN 1007-9327

REVIEW

Differential diagnosis between functional and organic intestinal disorders: Is there a role for non-invasive tests?

Francesco Costa, Maria Gloria Mumolo, Santino Marchi, Massimo Bellini

Francesco Costa, Maria Gloria Mumolo, Santino Marchi, Massimo Bellini, Section of Gastroenterology, Department of Internal Medicine,University of Pisa, Pisa, Italy
Correspondence to: Francesco Costa, MD, PhD, Dipartimento di Medicina Interna - S.O. di Gastroenterologia, Universita' di Pisa, Ospedale S. Chiara, Via Roma, PISA 67-56122, Italy. fcosta@med.unipi.it
Telephone: +39-50-993485-918720 Fax: +39-50-993050
Received: 2006-08-11 Accepted: 2006-11-11

Abstract

Abdominal pain and bowel habits alterations are common symptoms in the general population. The investigation to differentiate organic from functional bowel disorders represents a considerable burden both for patients and public health service. The selection of patients who should undergo endoscopic and/or radiological procedures is one of the key points of the diagnostic process, which should avoid the abuse of invasive and expensive tests as well as the underestimation of potentially harmful diseases. Over the coming years, clinicians and researchers will be challenged to develop strategies to increase the patient's compliance and to reduce the economic and social costs of the intestinal diseases.

Key words: Intestinal diseases; Intestinal inflammation; Functional bowel disorders; Faecal markers

Costa F, Mumolo MG, Marchi S, Bellini M. Differential diagnosis between functional and organic intestinal disorders: Is there a role for non-invasive tests? *World J Gastroenterol* 2007; 13(2): 219-223

http://www.wjgnet.com/1007-9327/13/219.asp

INTRODUCTION

For the sake of simplicity, bowel diseases have been divided into organic (OBD) and functional (FBD) disorders. In the past, FBD was merely considered an "umbrella" for many clinical pictures where the term functional reflected an unknown etiology and/or pathogenesis and their existence was even denied by some physicians[1,2]. In the last years, the fast-growing insight into the pathogenesis of intestinal diseases has been narrowing the field of disturbances "not explained by structural or biochemical abnormalities", in parallel with the progress of diagnostic tools and the development of novel technologies. Recent evidences, such as the role of serotonin in visceral functions[3-5], the post-infective onset of irritable bowel syndrome (IBS)[6] or data about potential neuroendocrine dysfunctions[7] shed light on the phenomena underlying FBD. The "biopsychosocial model" focused on the complex interplay among genetics, environment, psychosocial and physiological factors, significantly contributed to clarify the true genesis of "functional" symptoms and to modify both treatment and clinical outcome[8]. However, while the new scenario of pathogenesis suggests an overlapping between morphologic and functional abnormalities, in clinical practice the distinction is maintained in prognostic terms, as "functional" identifies scarcely evolutive and virtually harmless conditions.

As the intestine reacts to different stimuli with a limited array of symptoms, the investigation to differentiate OBD and FBD represents a considerable burden for both the patients and public health service.

The selection of patients who should undergo endoscopic and/or radiological procedures is one of the key points of the diagnostic process, which should avoid the abuse of invasive and expensive tests as well as the underestimation of potentially dangerous diseases. In particular, we should take into account the high prevalence and increasing incidence of colo-rectal cancer which, at an early stage, can be successfully treated by endoscopic resection. Nevertheless, colonoscopy is not advisable in all patients with abdominal complaints in the absence of "red flag" features (age > 45 years, anaemia, bleeding, fever, weight loss, etc.) (Figure 1). Chronic or recurrent abdominal pain and bowel habit alterations are common symptoms in the general population. Because a wide range of etiologies may underlie these symptoms, they do not allow a differential diagnosis between OBD (neoplasm, infectious enteritis, Crohn's disease, celiac disease, etc.) and FBD. Moreover, patients may present overlapping syndromes as OBD and FBD , are not mutually exclusive and can be present in the same patient. FBD, mainly IBS, which affect 5%-20% of general population, are the most common intestinal disorders in both primary and secondary care[9-11]. Most patients are diagnosed and treated by general practitioners (GPs) and only those unresponsive to conventional treatment[10,12] are eventually referred to a gastroenterologist[9,13].

In order to improve the positive identification of

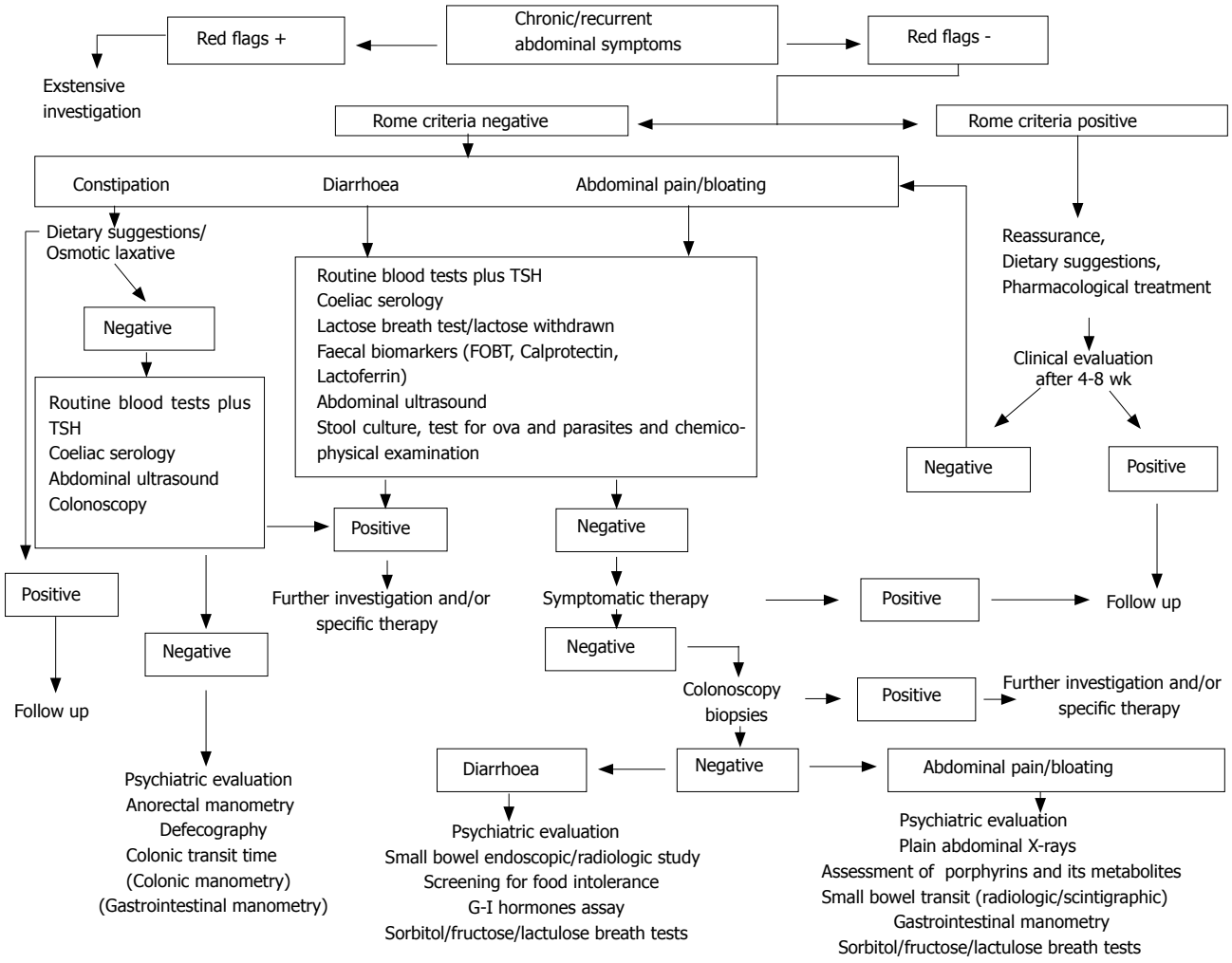

Figure 1 Suggested approach to the diagnosis of chronic abdominal symptoms.

patients affected with FBD, the Rome classification system has been developed. Although these guidelines have raised controversies about duration, frequency, severity and terminology itself of symptoms, they have created a common language for FBD and are now considered the gold standard. Unfortunately, Rome criteria have been developed by and for specialists working in the secondary care setting; they are ignored by many GPs and considered by others, as well as by many specialists, too complex and time-consuming and/or restrictive, suitable only for the tertiary care setting and for research purposes[14]. Therefore, many GPs and gastroenterologists are confident of making a correct diagnosis based on their personal criteria[14,15] and, in the absence of any biological or instrumental marker, FBD is still an exclusive diagnosis which often require extensive investigation. The recent Rome Ⅲ criteria appear to be simpler and less restrictive and hopefully will help the diagnosis of FBD on clinical basis[16].

When FBD is suspected, the clinical criteria can be combined with a number of non-invasive diagnostic tools. Unfortunately serological biomarkers of inflammation such as erythrocyte sedimentation rate, C-reactive protein, white cell count, platelet count, are not sufficiently sensitive or sufficiently specific because they do not directly reflect the level of local inflammation[17-19]. The faecal occult blood test is of little use in detecting inflammatory bowel diseases (IBD) and has a low sensitivity for the diagnosis of colon cancer, especially at an early stage[20,21]. Therefore, in recent years considerable effort has been devoted to find alternative solutions. The latest knowledge about the pathogenesis of FBD (infection, food allergy or intolerance)[22-24], have focused attention on the role of microscopic inflammation, bacterial overgrowth, altered immunity and even more subtle alterations, whose effects are detectable in non-invasive manner, by analysing stools, breath samples and blood.

FAECAL MARKERS

Neutrophil-derived proteins

Faecal neutrophil-derived proteins (mainly calprotectin and lactoferrin) assessment is receiving increasing attention as promising tools to differentiate OBD and FBD; although their clinical use needs definitive confirmation especially in the work-up of FBD, they could be the putative ideal test for non-invasive assessment of intestinal inflammation[25-27].

Calprotectin is a 36-kDa calcium and zinc binding protein that accounts for about 60% of total proteins in the cytosol fraction of neutrophil granulocytes[28,29]. An

increase in faecal calprotectin levels in IBD, colorectal cancer and non-steroidal anti-inflammatory drugs enteropathy has been reported[30-33]. In a study of Dolwani, faecal calprotectin was superior to small bowel barium follow-up in identifying patients with organic diseases[34]. In Crohn's disease (CD) and ulcerative colitis (UC), its levels closely correlated with the faecal excretion of ^{111}In-labelled leukocytes, which is considered to be the gold standard for measuring intestinal inflammation[35] and recently it has been reported that a high faecal calprotectin concentration may identify those IBD patients in remission who are at risk of early relapse[36,37]. Calprotectin has a high negative predictive value for intestinal inflammation. It has low specificity for intestinal pathology but, at a cut-off of 30 mg/L (150 μg/g of faeces by the new method), it showed a sensitivity of 100% in discriminating between active Crohn's disease and IBS[27]. The combined use of presence/absence of alarm features, Rome criteria and calprotectin test proved to be a non-invasive, effective mean of screening patients for organic intestinal disease[38].

Lactoferrin is an iron-binding protein contained in organic fluid, intestinal mucus and in neutrophils. Similarly to calprotectin, faecal lactoferrin proved to be a simple, sensitive marker of intestinal inflammation[25,39,40].

DNA

The molecular genetics of colorectal cancer provided the basis for the analysis of faecal DNA[41]. Colonoscopy is the best tool for the diagnosis of colorectal cancer but it cannot be proposed for a systematic screening of the entire population > 50 years of age. The recent availability of faecal-based, multi-target DNA panel has allowed a better sensitivity than faecal occult blood test for the detection of colorectal cancer[21]. This panel consists of different mutations (*K-ras* gene, *APC* gene, *p53* gene), markers of microsatellite-instability and markers of disordered apoptosis, clearly involved in the progression of colorectal cancer. Although the performance of faecal DNA testing is not comparable to colonoscopy, it is simple and non-invasive, therefore its use at frequent intervals might compensate for the lower diagnostic accuracy[21].

Pancreatic elastase

Chronic pancreatitis is a frequent cause of abdominal pain and diarrhoea whose diagnosis often requires complex and expensive procedures. The assessment of pancreatic elastase on stools seems to offer a better performance than previous non-invasive tests (i.e. serology, Pancreolauryl test, faecal tests for pancreatic enzyme) with a high sensitivity for moderate and severe pancreatic insufficiency[42,43]; this faecal test, like faecal neutrophil-derived protein assessment, is easy to perform, requires a single stool sample and offers a great advantage in terms of patient's compliance. Although most authors reported poor sensitivity for mild disease, its use has been recommended as a first choice test in patients with chronic diarrhoea of putative pancreatic origin[44].

If these experimental data are confirmed in large controlled studies, the routine use of faecal tests might contribute to the selection of patients with abdominal complaints both in the first diagnosis and in the follow-up avoiding invasive and expensive procedures.

BREATH TESTS

Breath analysis is a simple and safe alternative to invasive tests to investigate digestive functions. Exhaled hydrogen (H_2) and carbon (C) can be employed to assess malabsorption, gastrointestinal motility and *H pylori* infection. H_2 in humans is produced only by bacterial fermentation of carbohydrates[45]. This process has been related to the onset of symptoms such as diarrhoea, bloating and abdominal pain[46,47]. Different hydrogen breath tests are currently used to detect carbohydrate malabsorption. Lactose, fructose, sorbitol are the most commonly tested carbohydrates, although their role in symptoms of FBD is controversial, and the prevalence of lactose, fructose and sorbitol malabsorption in IBS patients is not different from healthy subjects[48].

Small intestinal bacterial overgrowth (SIBO) is a malabsorption syndrome characterized by more than 105 colonic type bacterial/mL of jejunal juice described in case of structural bowel alterations (surgical blind loop, stenosis, etc), motility disturbances (pseudo-obstruction, diabetic autonomic neuropathy, sclerodermia) and also present in chronic diseases (liver cirrhosis, chronic pancreatitis, chronic renal failure)[49]. Recent data also indicate that an altered gut flora may play a pathogenic role both in IBS and IBD[50,51]. It has been shown that eradication of SIBO eliminates IBS symptoms in 48% of patients[52]. Although jejunal culture is considered the gold standard for the diagnosis of SIBO, some drawbacks limit its widespread use; thus, glucose and lactulose breath tests are commonly employed. Breath tests based on the excretion of CO_2 subsequently measured by a mass spectrometer have been developed; they employ a variety of ^{13}C substrates to investigate the exocrine pancreatic function (^{13}C triolein, ^{13}C mixed chain triglyceride)[53], gastric emptying (^{13}C octanoate)[54], as well as in the diagnosis of *H pylori* infection (^{13}C urea)[55].

The simplicity and the safety of breath tests encouraged a widespread use, but the data on their low diagnostic accuracy should be taken into account and their use on regular basis cannot be recommended in clinical practice[56].

SERUM

Recent literature highlighted that approximately 4% of patients diagnosed as IBS are affected with celiac disease[57]. Altered bowel habits and abdominal pain, the clinical hallmark of IBS, are common in celiac patients, and serological assessment for anti-endomysial and anti-transglutaminase antibodies should be performed as a first level test when IBS is suspected. Many patients suffering from abdominal pain and/or bowel habit changes perceive their symptoms as related to some form of dietary intolerance and show a good response to an exclusive diet. Nevertheless, any attempt to correlate food-specific IgE production and chronic abdominal symptoms has been disappointing[24,58]. Although it has been reported

that sometimes IgE-mediated reactivity can present with chronic abdominal complaints, the measurement of food-specific IgE antibody concentrations to ascertain food intolerance in FBD is not justified and should be discouraged[59]. Preliminary data showed that high titres of food-specific IgG4 antibodies are present in IBS patients suggesting a diagnostic role in those cases of IBS who could benefit mostly by an exclusive diet[60]. Their clinical follow-up and further research are needed to clarify the importance of these findings and their role in clinical practice.

CONCLUSION

Likely the near future will lead to a deep revision of the concept of "functional disorder". The striking progress in our knowledge of the molecular basis of diseases is identifying new models for FBD pathogenesis, which tend to be less "functional" and more "organic".

These new evidences will have a relevant effect on the clinical management of intestinal diseases. We are not far from the time when the development of minimally or non-invasive techniques will allow an accurate diagnosis, a serial monitoring and a "real time" adjustment of therapy.

REFERENCES

1 **Drossman DA**. Functional GI disorders: what's in a name? *Gastroenterology* 2005; **128**: 1771-1772
2 **Christensen J**. Heraclides or the physician. *Gastroenterol Int* 1990; **3**: 45-48
3 **Gershon MD**. Review article: roles played by 5-hydroxytryptamine in the physiology of the bowel. *Aliment Pharmacol Ther* 1999; **13** Suppl 2: 15-30
4 **Camilleri M**. Pharmacogenomics and functional gastrointestinal disorders. *Pharmacogenomics* 2005; **6**: 491-501
5 **Bellini M**, Rappelli L, Blandizzi C, Costa F, Stasi C, Colucci R, Giannaccini G, Marazziti D, Betti L, Baroni S, Mumolo MG, Marchi S, Del Tacca M. Platelet serotonin transporter in patients with diarrhea-predominant irritable bowel syndrome both before and after treatment with alosetron. *Am J Gastroenterol* 2003; **98**: 2705-2711
6 **Drossman DA**. Mind over matter in the postinfective irritable bowel. *Gut* 1999; **44**: 306-307
7 **Dinan TG**, Quigley EM, Ahmed SM, Scully P, O'Brien S, O'Mahony L, O'Mahony S, Shanahan F, Keeling PW. Hypothalamic-pituitary-gut axis dysregulation in irritable bowel syndrome: plasma cytokines as a potential biomarker? *Gastroenterology* 2006; **130**: 304-311
8 **Drossman DA**. The functional gastrointestinal disorders and the Rome II process. *Gut* 1999; **45** Suppl 2: II1-II5
9 **Jones R**, Lydeard S. Irritable bowel syndrome in the general population. *BMJ* 1992; **304**: 87-90
10 **Thompson WG**, Heaton KW, Smyth GT, Smyth C. Irritable bowel syndrome in general practice: prevalence, characteristics, and referral. *Gut* 2000; **46**: 78-82
11 **Drossman DA**, Camilleri M, Mayer EA, Whitehead WE. AGA technical review on irritable bowel syndrome. *Gastroenterology* 2002; **123**: 2108-2131
12 **Gladman LM**, Gorard DA. General practitioner and hospital specialist attitudes to functional gastrointestinal disorders. *Aliment Pharmacol Ther* 2003; **17**: 651-654
13 **Heaton KW**, O'Donnell LJ, Braddon FE, Mountford RA, Hughes AO, Cripps PJ. Symptoms of irritable bowel syndrome in a British urban community: consulters and nonconsulters. *Gastroenterology* 1992; **102**: 1962-1967
14 **Bellini M**, Tosetti C, Costa F, Biagi S, Stasi C, Del Punta A, Monicelli P, Mumolo MG, Ricchiuti A, Bruzzi P, Marchi S. The general practitioner's approach to irritable bowel syndrome: from intention to practice. *Dig Liver Dis* 2005; **37**: 934-939
15 **Vandvik PO**, Aabakken L, Farup PG. Diagnosing irritable bowel syndrome: poor agreement between general practitioners and the Rome II criteria. *Scand J Gastroenterol* 2004; **39**: 448-453
16 **Longstreth GF**, Thompson WG, Chey WD, Houghton LA, Mearin F, Spiller RC. Functional bowel disorders. *Gastroenterology* 2006; **130**: 1480-1491
17 **Cronin CC**, Shanahan F. Immunological tests to monitor inflammatory bowel disease--have they delivered yet? *Am J Gastroenterol* 1998; **93**: 295-297
18 **Gabay C**, Kushner I. Acute-phase proteins and other systemic responses to inflammation. *N Engl J Med* 1999; **340**: 448-454
19 **Suffredini AF**, Fantuzzi G, Badolato R, Oppenheim JJ, O'Grady NP. New insights into the biology of the acute phase response. *J Clin Immunol* 1999; **19**: 203-214
20 **Tibble J**, Sigthorsson G, Foster R, Sherwood R, Fagerhol M, Bjarnason I. Faecal calprotectin and faecal occult blood tests in the diagnosis of colorectal carcinoma and adenoma. *Gut* 2001; **49**: 402-408
21 **Imperiale TF**, Ransohoff DF, Itzkowitz SH, Turnbull BA, Ross ME. Fecal DNA versus fecal occult blood for colorectal-cancer screening in an average-risk population. *N Engl J Med* 2004; **351**: 2704-2714
22 **Barbara G**, Stanghellini V, De Giorgio R, Cremon C, Cottrell GS, Santini D, Pasquinelli G, Morselli-Labate AM, Grady EF, Bunnett NW, Collins SM, Corinaldesi R. Activated mast cells in proximity to colonic nerves correlate with abdominal pain in irritable bowel syndrome. *Gastroenterology* 2004; **126**: 693-702
23 **Gonsalkorale WM**, Perrey C, Pravica V, Whorwell PJ, Hutchinson IV. Interleukin 10 genotypes in irritable bowel syndrome: evidence for an inflammatory component? *Gut* 2003; **52**: 91-93
24 **Atkinson W**, Sheldon TA, Shaath N, Whorwell PJ. Food elimination based on IgG antibodies in irritable bowel syndrome: a randomised controlled trial. *Gut* 2004; **53**: 1459-1464
25 **Kane SV**, Sandborn WJ, Rufo PA, Zholudev A, Boone J, Lyerly D, Camilleri M, Hanauer SB. Fecal lactoferrin is a sensitive and specific marker in identifying intestinal inflammation. *Am J Gastroenterol* 2003; **98**: 1309-1314
26 **Limburg PJ**, Ahlquist DA, Sandborn WJ, Mahoney DW, Devens ME, Harrington JJ, Zinsmeister AR. Fecal calprotectin levels predict colorectal inflammation among patients with chronic diarrhea referred for colonoscopy. *Am J Gastroenterol* 2000; **95**: 2831-2837
27 **Tibble J**, Teahon K, Thjodleifsson B, Roseth A, Sigthorsson G, Bridger S, Foster R, Sherwood R, Fagerhol M, Bjarnason I. A simple method for assessing intestinal inflammation in Crohn's disease. *Gut* 2000; **47**: 506-513
28 **Dale I**, Fagerhol MK, Naesgaard I. Purification and partial characterization of a highly immunogenic human leukocyte protein, the L1 antigen. *Eur J Biochem* 1983; **134**: 1-6
29 **Fagerhol MK**, Andersson KB, Naess-Andresen CF, Brandtzaeg P, Dale I. Calprotectin (the LI leukocyte protein). In: Smith V, Dedman JR, editors. Stimulus Response Coupling: the role of intracellular calcium-binding proteins. Boca Raton FL: CRC Press Inc, 1990: 187-210
30 **Røseth AG**, Aadland E, Jahnsen J, Raknerud N. Assessment of disease activity in ulcerative colitis by faecal calprotectin, a novel granulocyte marker protein. *Digestion* 1997; **58**: 176-180
31 **Costa F**, Mumolo MG, Bellini M, Romano MR, Ceccarelli L, Arpe P, Sterpi C, Marchi S, Maltinti G. Role of faecal calprotectin as non-invasive marker of intestinal inflammation. *Dig Liver Dis* 2003; **35**: 642-647
32 **Kronborg O**, Ugstad M, Fuglerud P, Johne B, Hardcastle J, Scholefield JH, Vellacott K, Moshakis V, Reynolds JR. Faecal calprotectin levels in a high risk population for colorectal neoplasia. *Gut* 2000; **46**: 795-800
33 **Tibble JA**, Sigthorsson G, Foster R, Scott D, Fagerhol MK,

Roseth A, Bjarnason I. High prevalence of NSAID enteropathy as shown by a simple faecal test. *Gut* 1999; **45**: 362-366
34 **Dolwani S**, Metzner M, Wassell JJ, Yong A, Hawthorne AB. Diagnostic accuracy of faecal calprotectin estimation in prediction of abnormal small bowel radiology. *Aliment Pharmacol Ther* 2004; **20**: 615-621
35 **Røseth AG**, Schmidt PN, Fagerhol MK. Correlation between faecal excretion of indium-111-labelled granulocytes and calprotectin, a granulocyte marker protein, in patients with inflammatory bowel disease. *Scand J Gastroenterol* 1999; **34**: 50-54
36 **Tibble JA**, Sigthorsson G, Bridger S, Fagerhol MK, Bjarnason I. Surrogate markers of intestinal inflammation are predictive of relapse in patients with inflammatory bowel disease. *Gastroenterology* 2000; **119**: 15-22
37 **Costa F**, Mumolo MG, Ceccarelli L, Bellini M, Romano MR, Sterpi C, Ricchiuti A, Marchi S, Bottai M. Calprotectin is a stronger predictive marker of relapse in ulcerative colitis than in Crohn's disease. *Gut* 2005; **54**: 364-368
38 **Tibble JA**, Sigthorsson G, Foster R, Forgacs I, Bjarnason I. Use of surrogate markers of inflammation and Rome criteria to distinguish organic from nonorganic intestinal disease. *Gastroenterology* 2002; **123**: 450-460
39 **Sugi K**, Saitoh O, Hirata I, Katsu K. Fecal lactoferrin as a marker for disease activity in inflammatory bowel disease: comparison with other neutrophil-derived proteins. *Am J Gastroenterol* 1996; **91**: 927-934
40 **Parsi MA**, Shen B, Achkar JP, Remzi FF, Goldblum JR, Boone J, Lin D, Connor JT, Fazio VW, Lashner BA. Fecal lactoferrin for diagnosis of symptomatic patients with ileal pouch-anal anastomosis. *Gastroenterology* 2004; **126**: 1280-1286
41 **Sidransky D**, Tokino T, Hamilton SR, Kinzler KW, Levin B, Frost P, Vogelstein B. Identification of ras oncogene mutations in the stool of patients with curable colorectal tumors. *Science* 1992; **256**: 102-105
42 **Löser C**, Möllgaard A, Fölsch UR. Faecal elastase 1: a novel, highly sensitive, and specific tubeless pancreatic function test. *Gut* 1996; **39**: 580-586
43 **Glasbrenner B**, Schön A, Klatt S, Beckh K, Adler G. Clinical evaluation of the faecal elastase test in the diagnosis and staging of chronic pancreatitis. *Eur J Gastroenterol Hepatol* 1996; **8**: 1117-1120
44 **Thomas PD**, Forbes A, Green J, Howdle P, Long R, Playford R, Sheridan M, Stevens R, Valori R, Walters J, Addison GM, Hill P, Brydon G. Guidelines for the investigation of chronic diarrhoea, 2nd edition. *Gut* 2003; **52** Suppl 5: v1-v15
45 **Levitt MD**. Production and excretion of hydrogen gas in man. *N Engl J Med* 1969; **281**: 122-127
46 **Böhmer CJ**, Tuynman HA. The effect of a lactose-restricted diet in patients with a positive lactose tolerance test, earlier diagnosed as irritable bowel syndrome: a 5-year follow-up study. *Eur J Gastroenterol Hepatol* 2001; **13**: 941-944
47 **Farup PG**, Monsbakken KW, Vandvik PO. Lactose malabsorption in a population with irritable bowel syndrome: prevalence and symptoms. A case-control study. *Scand J Gastroenterol* 2004; **39**: 645-649
48 **Nelis GF**, Vermeeren MA, Jansen W. Role of fructose-sorbitol malabsorption in the irritable bowel syndrome. *Gastroenterology* 1990; **99**: 1016-1020
49 **Teo M**, Chung S, Chitti L, Tran C, Kritas S, Butler R, Cummins A. Small bowel bacterial overgrowth is a common cause of chronic diarrhea. *J Gastroenterol Hepatol* 2004; **19**: 904-909
50 **Franchimont D**, Vermeire S, El Housni H, Pierik M, Van Steen K, Gustot T, Quertinmont E, Abramowicz M, Van Gossum A, Devière J, Rutgeerts P. Deficient host-bacteria interactions in inflammatory bowel disease? The toll-like receptor (TLR)-4 Asp299gly polymorphism is associated with Crohn's disease and ulcerative colitis. *Gut* 2004; **53**: 987-992
51 **Quigley EM**. Irritable bowel syndrome and inflammatory bowel disease: interrelated diseases? *Chin J Dig Dis* 2005; **6**: 122-132
52 **Pimentel M**, Chow EJ, Lin HC. Eradication of small intestinal bacterial overgrowth reduces symptoms of irritable bowel syndrome. *Am J Gastroenterol* 2000; **95**: 3503-3506
53 **Vantrappen GR**, Rutgeerts PJ, Ghoos YF, Hiele MI. Mixed triglyceride breath test: a noninvasive test of pancreatic lipase activity in the duodenum. *Gastroenterology* 1989; **96**: 1126-1134
54 **Ghoos YF**, Maes BD, Geypens BJ, Mys G, Hiele MI, Rutgeerts PJ, Vantrappen G. Measurement of gastric emptying rate of solids by means of a carbon-labeled octanoic acid breath test. *Gastroenterology* 1993; **104**: 1640-1647
55 **Soll AH**. Consensus conference. Medical treatment of peptic ulcer disease. Practice guidelines. Practice Parameters Committee of the American College of Gastroenterology. *JAMA* 1996; **275**: 622-629
56 **Simrén M**, Stotzer PO. Use and abuse of hydrogen breath tests. *Gut* 2006; **55**: 297-303
57 **Spiegel BM**, DeRosa VP, Gralnek IM, Wang V, Dulai GS. Testing for celiac sprue in irritable bowel syndrome with predominant diarrhea: a cost-effectiveness analysis. *Gastroenterology* 2004; **126**: 1721-1732
58 **Monsbakken KW**, Vandvik PO, Farup PG. Perceived food intolerance in subjects with irritable bowel syndrome--etiology, prevalence and consequences. *Eur J Clin Nutr* 2006; **60**: 667-672
59 **Sampson HA**, Sicherer SH, Birnbaum AH. AGA technical review on the evaluation of food allergy in gastrointestinal disorders. American Gastroenterological Association. *Gastroenterology* 2001; **120**: 1026-1040
60 **Zar S**, Benson MJ, Kumar D. Food-specific serum IgG4 and IgE titers to common food antigens in irritable bowel syndrome. *Am J Gastroenterol* 2005; **100**: 1550-1557

S- Editor Wang GP **L- Editor** Ma JY **E- Editor** Lu W

PO Box 2345, Beijing 100023, China
www.wjgnet.com
wjg@wjgnet.com

World J Gastroenterol 2007 January 14; 13(2): 224-227
World Journal of Gastroenterology ISSN 1007-9327

REVIEW

Importance of performance status for treatment outcome in advanced pancreatic cancer

Stefan Boeck, Axel Hinke, Ralf Wilkowski, Volker Heinemann

Stefan Boeck, Volker Heinemann, Department of Internal Medicine Ⅲ, Klinikum Grosshadern, Ludwig-Maximilians-University of Munich, Marchioninistrasse 15, 81377 Munich, Germany
Axel Hinke, WISP Research Institute, Karl-Benz-Str. 1, 40764 Langenfeld, Germany
Ralf Wilkowski, Department of Radiooncology, Klinikum Grosshadern, Ludwig-Maximilians-University of Munich, Marchioninistrasse 15, Munich 81377, Germany
Correspondence to: Professor Volker Heinemann, Department of Internal Medicine Ⅲ, Klinikum Grosshadern, Ludwig-Maximilians-University of Munich, Marchioninistrasse 15, Munich 81377,
Germany. volker.heinemann@med.uni-muenchen.de
Telephone: +49-89-70950 Fax: +49-89-70955256
Received: 2006-10-31 Accepted: 2006-12-11

Abstract

Despite progress in the treatment of advanced and metastatic pancreatic cancer (PC), the outcome of this disease remains dismal for the majority of patients. Given the moderate efficacy of treatment, prognostic factors may help to guide treatment decisions. Several trials identified baseline performance status as an important prognostic factor for survival. Unfit patients with a Karnofsky performance status (KPS) below 70% only have a marginal benefit from chemotherapy with gemcitabine (Gem) and may often benefit more from optimal supportive care. Once, however, the decision is taken to apply chemotherapy, KPS may be used to select either mono- or combination chemotherapy. Patients with a good performance status (KPS = 90%-100%) may have a significant and clinically relevant survival benefit from combination chemotherapy. By contrast, patients with a poor performance status (KPS $\leqslant$ 80%) have no advantage from intensified therapy and should rather receive single-agent treatment.

Key words: Chemotherapy; Gemcitabine; Pancreatic cancer; Performance status; Prognostic factor

Boeck S, Hinke A, Wilkowski R, Heinemann V. Importance of performance status for treatment outcome in advanced pancreatic cancer. *World J Gastroenterol* 2007; 13(2): 224-227

http://www.wjgnet.com/1007-9327/13/224.asp

INTRODUCTION

Advanced pancreatic cancer (PC) is an incurable disease and without appropriate treatment survival is limited to 3-4 mo. Since Burris *et al*[1] demonstrated the superiority of gemcitabine (Gem) over bolus 5-fluorouracil (5-FU), single-agent Gem has evolved as a standard of care. Numerous trials consistently support the notion that Gem alone may induce a median overall survival (OS) of 5-7 mo and a 1-year-survival of 11%-25%[2]. A great effort has been undertaken to improve these results by use of combination chemotherapy. Up to now, only two combinations, Gem plus erlotinib[3] and Gem plus capecitabine[4] have provided a significant prolongation of survival when compared to Gem alone.

Due to the moderate progress derived from chemotherapy, the question arises if subgroups of patients can be identified who benefit most from specific treatment strategies. Previous studies already tried to identify prognostic factors such as pre-treatment CA 19-9 levels[5,6], inflammatory response markers like C-reactive protein (CRP) or cytokines[7,8], serum-albumin levels[9] or pre-treatment performance status[10-12]. In this overview we analysed Karnofsky performance status (KPS) as a prognostic factor to define a patient group which may benefit from more intensive therapy as opposed to those patients who should rather receive single-agent treatment.

CLINICAL TRIALS

Single-agent therapy

The clinical importance of the KPS for the outcome of PC patients treated with Gem was first elucidated by Storniolo and co-workers[13]. Within an investigational new drug treatment program 3023 patients were evaluated. The analysis of baseline efficacy factors indicated that patients with a KPS $\geqslant$ 70% had a median survival of 5.5 mo as compared to only 2.4 mo observed in patients with a KPS < 70%. Also median time to disease progression (TTP) was greater in the good performance group (2.9 *vs* 1.7 mo, respectively). Interestingly, best tumor response was comparable between the two groups (12% *vs* 10%) supporting the notion that in PC response to therapy is only a poor surrogate endpoint for survival. In view of this analysis, it appears unlikely that patients with a KPS < 70% actually benefit from therapy and the conclusion may be drawn that chemotherapy with Gem should rather be withheld in patients with a very poor performance status.

Table 1 Influence of performance status on median survival in randomized phase Ⅲ trials

	Overall Survival (mo)		
	KPS 60-80	KPS 90-100	Reference
Gemcitabine + Cisplatin	4.9[1]	10.7	Heinemann *et al*
Gemcitabine	4.8[1]	6.9	
Statistical significance	$P = 0.64$	$P = 0.051$	
Gemcitabine + 5-FU/FA	3.4	8.5	Riess *et al*
Gemcitabine	4.9	6.2	
Statistical significance	$P = 0.62$	$P = 0.172$	
Gemcitabine + Capecitabine	5.3	10.1	Herrmann *et al*
Gemcitabine	7.0	7.5	
Statistical significance	$P = 0.22$	$P = 0.024$	

KPS = Karnofsky performance status, [1]subgroup with poor performance status defined as KPS 70%-80%.

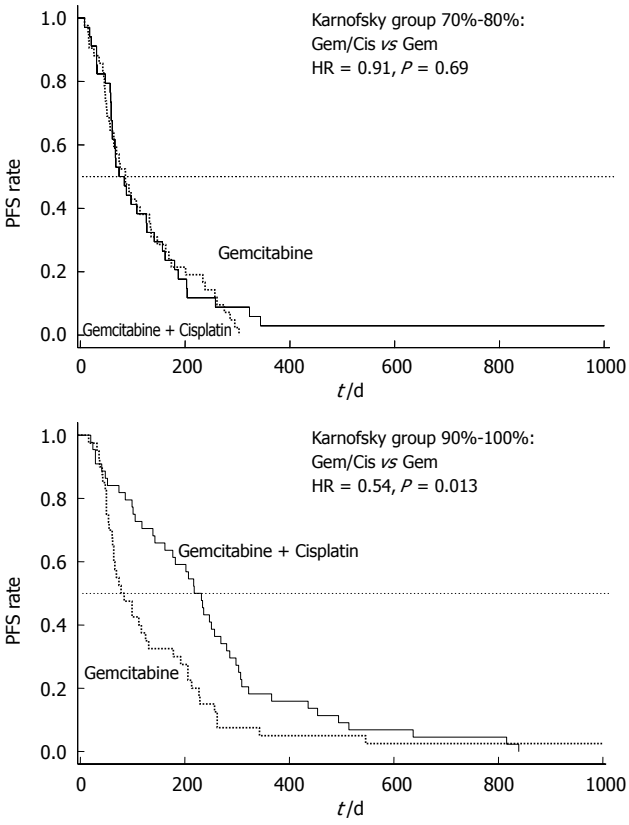

Figure 1 Randomized phase Ⅲ trial comparing gemcitabine (Gem) *vs* gemcitabine plus cisplatin (Cis): Subgroups KPS 70%-80% and KPS 90%-100%; Progression-free survival (PFS) by treatment arm (HR = hazard ratio).

Gemcitabine plus Cisplatin

The combination of Gem and cisplatin is based on a synergistic cytotoxic interaction of the two agents, namely the propensity of Gem to inhibit repair of cisplatin-induced DNA damage. In a randomized phase Ⅲ trial Gem plus cisplatin was compared to single-agent Gem[14]. In the combination arm, Gem (1000 mg/m^2) and cisplatin (50 mg/m^2) were both applied in a biweekly fashion, while in the single-agent arm Gem was given at a dose of 1000 mg/m^2 weekly times three in a 4-wk regimen. One hundred ninety-five patients with histologically confirmed advanced PC (KPS > 70%) were randomized and survival was evaluated as the primary end-point.

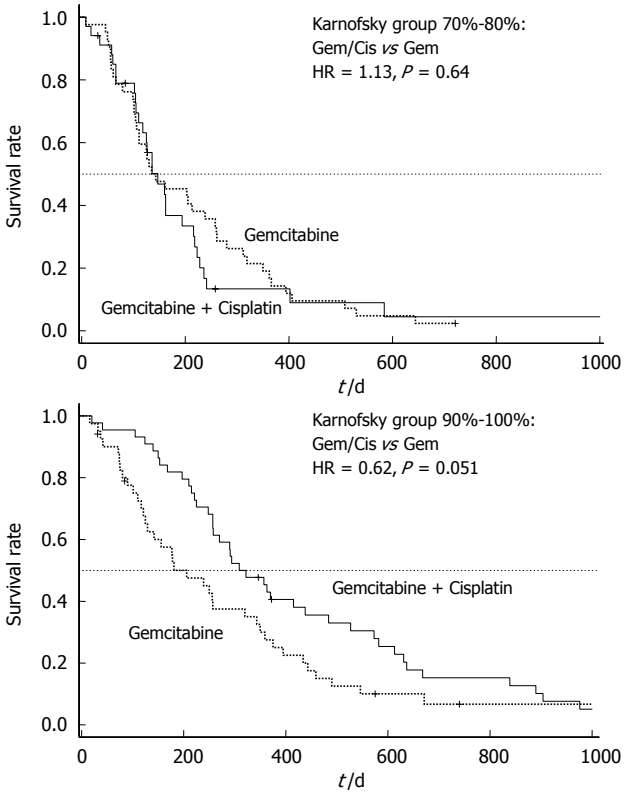

Figure 2 Randomized phase Ⅲ trial comparing gemcitabine (Gem) *vs* gemcitabine plus cisplatin (Cis): Subgroups KPS 70%-80% and KPS 90%-100%; Overall survival (OS) by treatment arm (HR = hazard ratio).

In a post-hoc analysis of this trial, patients were divided into groups with good (KPS = 90%-100%) and poor performance status (KPS = 70%-80%). Patients with a poor performance status at base-line (KPS 70%-80%) had no benefit from combination therapy as compared to Gem alone and comparably disappointing results were obtained for progression free survival (PFS: 2.8 *vs* 2.9 mo, $P = 0.69$) and OS (4.9 *vs* 4.8 mo, $P = 0.64$) (Table 1). By contrast, patients with a good KPS (90%-100%) who underwent treatment with Gem/cisplatin had a significantly longer PFS compared to patients treated with single-agent Gem (7.7 *vs* 2.8 mo, $P = 0.013$) (Figure 1). This prolongation of PFS also translated into a prolonged median OS (10.7 *vs* 6.9 mo), that reached a borderline level of statistical significance ($P = 0.051$) (Figure 2).

In the univariate analysis for prognostic factors, KPS (HR = 0.52, $P = 0.006$) and stage of disease (HR = 1.55, $P = 0.0048$) had a significant impact on survival, while age, gender, tumor grading and treatment arm did not. These data were confirmed in a multivariate analysis which identified KPS (HR = 0.59, $P = 0.0051$) and stage of disease (HR = 1.65, $P = 0.022$) as independent determinants of overall survival[14].

Gemcitabine plus 5-FU

The CONKO-002 trial compared the combination of Gem plus folinic acid (FA) and 5-FU to single-agent Gem[15]. In this randomized phase Ⅲ trial Gem was given at a dose of 1000 mg/m^2 together with FA 200 mg/m^2 and 5-FU 750 mg/m^2 weekly times four every six weeks. In the comparator arm, single-agent Gem was applied ac-

cording to the Burris regimen (1000 mg/m^2 weekly × 7 followed by two weeks rest and a subsequent application on d 1, 8, and 15 every four weeks[11]). Both treatment arms induced nearly identical results for tumor response rates (Gem/FA/5-FU *vs* Gem: RR = 4.8% *vs* 7.2%), median time to tumor progression (TTP = 3.5 *vs* 3.5 mo), and median survival time (OS = 5.9 *vs* 6.2 mo). Also in this trial, the subgroup analysis indicated that patients with a poor performance status (KPS = 60%-80%) responded in a different way compared to the good performance group (KPS = 90%-100%). In patients with a poor performance status, combination treatment induced a worse survival than gemcitabine alone (3.4 *vs* 4.9 mo). By contrast, a strong trend towards an improved survival was observed in the good performance group treated within the combination arm (8.5 *vs* 6.2 mo, $P = 0.172$) (Table 1).

Gemcitabine plus Capecitabine

Herrmann and co-workers performed a randomized trial comparing Gem (1000 mg/m^2, d 1 + 8, q 3 wk) plus capecitabine (650 mg/m^2 po bid d 1-14 q 3 wk) to Gem given according to the Burris-regimen[16]. While the combination induced a higher median PFS than Gem alone (4.8 *vs* 4.0 mo) and a longer median OS (8.4 mo *vs* 7.3 mo), these results failed to reach the level of statistical significance. In the unfavorable KPS group (60%-80%), survival with Gem/capecitabine was inferior to Gem alone (5.3 *vs* 7.0 mo), while in the good performance group the combination induced a significantly superior survival time (10.1 *vs* 7.5 mo, $P = 0.024$) (Table 1).

CONCLUSION

Despite recent advances in systemic treatment of patients with advanced PC, the prognosis still remains poor. Thus, pre-treatment patient selection, based on prognostic factors, for different therapeutic options (e.g. supportive care only, single-agent chemotherapy, combination chemotherapy) may turn out to gain clinical importance. Additionally, these prognostic factors may also be a useful for the design of future trials in advanced PC.

In the present review, we summarized the clinical importance of performance status as a prognostic factor for OS. In a randomized trial comparing Gem plus cisplatin to Gem alone potential prognostic factors such as stage of disease, KPS, treatment arm, age, sex, and pathological tumor grade were evaluated in a univariate analysis. Only pre-treatment KPS and distant metastasis could be identified as significant prognostic factors for OS. In a multivariate analysis, both could be confirmed as independent prognostic factors for PFS and OS[14]. The importance of performance status has already been observed by Louvet and co-workers who compared the Gem plus oxaliplatin combination to single-agent Gem[12]. He reported that distant metastasis and a poor PS (ECOG 2) at baseline were independent negative prognostic factors. These data were further supported by van Cutsem *et al*[9] who investigated the efficacy of Gem plus tipifarnib in a large randomized phase Ⅲ trial. ECOG performance status and stage of disease (locally advanced *vs* metastatic) were, besides tumor differentiation and albumin levels, highly significant prognostic factors for survival in a univariate analysis.

Once performance status is defined as a clinically relevant prognosticator for patient outcome, the question needs to be asked if performance status can also be used to guide adequate treatment selection. Storniolo *et al*[13] clearly demonstrated that the benefit from single-agent Gem is very low if patients with a KPS < 70% are treated. More often than not these patients will rather benefit from optimal supportive care.

Once, however, the decision is taken that a patient should receive chemotherapy it needs to be clarified if combination or single-agent chemotherapy is likely to provide an optimal therapeutic result. The relevance of KPS in this particular question was investigated based on a randomized trial comparing the Gem/cisplatin combination to Gem alone. In a retrospective subgroup analysis, patients with a good KPS (90%-100%) had a clear benefit from the Gem/cisplatin combination with regard to PFS (7.7 *vs* 2.8 mo, $P = 0.013$) and OS (10.7 *vs* 6.9 mo, $P = 0.051$). Outcome of patients with a poor KPS (70%-80%) was, however, not affected by the choice of treatment. Similar observations were also reported in two further phase Ⅲ trials[15,16]. While none of them demonstrated a significant superiority of combination chemotherapy for the whole study population, both trials could show a clinical relevant benefit for patients with a good performance status.

In conclusion, Gem-based combination regimens have the potential to prolong survival in patients with a good KPS, whereas patients with a poor KPS have no advantage and may as well receive single-agent Gem. Consideration of the performance status may, therefore, help to select adequate treatment strategies and thus may provide a reasonable step towards individualized therapy. Individualization of treatment becomes necessary since the benefit from more intensive combination chemotherapy can only be expected in defined subgroups of PC patients.

REFERENCES

1 **Burris HA**, Moore MJ, Andersen J, Green MR, Rothenberg ML, Modiano MR, Cripps MC, Portenoy RK, Storniolo AM, Tarassoff P, Nelson R, Dorr FA, Stephens CD, Von Hoff DD. Improvements in survival and clinical benefit with gemcitabine as first-line therapy for patients with advanced pancreas cancer: a randomized trial. *J Clin Oncol* 1997; **15**: 2403-2413

2 **Heinemann V**. Gemcitabine in the treatment of advanced pancreatic cancer: a comparative analysis of randomized trials. *Semin Oncol* 2002; **29**: 9-16

3 **Moore MJ**, Goldstein D, Hamm J, Finger A, Hecht J, Gallinger S, Au H, Ding K, Christy-Bittel J, Parulekar W. Erlotinib plus gemcitabine compared to gemcitabine alone in patients with advanced pancreatic cancer. A phase III trial of the National Cancer Institute of Canada Clinicals trials group [NCIC-CTG]. *Proc Am Soc Clin Oncol* 2005; **23**: 1

4 **Cunningham D**, Chau I, Stocken D, Davies C, Dunn J, Valle J, Smith D, Steward W, Harper P, Neoptolemos J. Phase III randomised comparison of gemcitabine (GEM) versus gemcitabine plus capecitabine (GEM-CAP) in patients with advanced pancreatic cancer. *Eur J Cancer Suppl* 2005; **3**: 11

5 **Saad ED**, Machado MC, Wajsbrot D, Abramoff R, Hoff PM, Tabacof J, Katz A, Simon SD, Gansl RC. Pretreatment CA 19-9 level as a prognostic factor in patients with advanced pancreatic cancer treated with gemcitabine. *Int J Gastrointest*

Cancer 2002; **32**: 35-41
6 **Maisey NR**, Norman AR, Hill A, Massey A, Oates J, Cunningham D. CA19-9 as a prognostic factor in inoperable pancreatic cancer: the implication for clinical trials. *Br J Cancer* 2005; **93**: 740-743
7 **Sawaki A**, Kanemitsu Y, Mizuno N, Takahashi K, Nakamura T, Ioka T, Tanaka S, Nakaizumi A, Salem AA, Ueda R, Yamao K. Practical prognostic index for patients with metastatic pancreatic cancer treated with gemcitabine. *J Gastroenterol Hepatol* 2008; **23**: 1292-1297
8 **Ebrahimi B**, Tucker SL, Li D, Abbruzzese JL, Kurzrock R. Cytokines in pancreatic carcinoma: correlation with phenotypic characteristics and prognosis. *Cancer* 2004; **101**: 2727-2736
9 **Van Cutsem E**, van de Velde H, Karasek P, Oettle H, Vervenne WL, Szawlowski A, Schoffski P, Post S, Verslype C, Neumann H, Safran H, Humblet Y, Perez Ruixo J, Ma Y, Von Hoff D. Phase III trial of gemcitabine plus tipifarnib compared with gemcitabine plus placebo in advanced pancreatic cancer. *J Clin Oncol* 2004; **22**: 1430-1438
10 **Ishii H**, Okada S, Nose H, Yoshimori M, Aoki K, Okusaka T. Prognostic factors in patients with advanced pancreatic cancer treated with systemic chemotherapy. *Pancreas* 1996; **12**: 267-271
11 **Ueno H**, Okada S, Okusaka T, Ikeda M. Prognostic factors in patients with metastatic pancreatic adenocarcinoma receiving systemic chemotherapy. *Oncology* 2000; **59**: 296-301
12 **Louvet C**, Labianca R, Hammel P, Lledo G, Zampino MG, André T, Zaniboni A, Ducreux M, Aitini E, Taïeb J, Faroux R, Lepere C, de Gramont A. Gemcitabine in combination with oxaliplatin compared with gemcitabine alone in locally advanced or metastatic pancreatic cancer: results of a GERCOR and GISCAD phase III trial. *J Clin Oncol* 2005; **23**: 3509-3516
13 **Storniolo AM**, Enas NH, Brown CA, Voi M, Rothenberg ML, Schilsky R. An investigational new drug treatment program for patients with gemcitabine: results for over 3000 patients with pancreatic carcinoma. *Cancer* 1999; **85**: 1261-1268
14 **Heinemann V**, Quietzsch D, Gieseler F, Gonnermann M, Schönekäs H, Rost A, Neuhaus H, Haag C, Clemens M, Heinrich B, Vehling-Kaiser U, Fuchs M, Fleckenstein D, Gesierich W, Uthgenannt D, Einsele H, Holstege A, Hinke A, Schalhorn A, Wilkowski R. Randomized phase III trial of gemcitabine plus cisplatin compared with gemcitabine alone in advanced pancreatic cancer. *J Clin Oncol* 2006; **24**: 3946-3952
15 **Riess H**, Helm A, Niedergethmann M, Schmidt-Wolf I, Moik M, Hammer C, Zippel K, Weigang-Köhler K, Stauch M, Oettle H. A randomised, prospective, multicenter phase III trial of gemcitabine, 5-fluorouracil (5-FU), folinic acid vs gemcitabine alone in patients with advanced pancreatic cancer. *Proc Am Soc Clin Oncol* 2005; **23**: 4009
16 **Herrmann R**, Bodoky G, Ruhstaller T, Glimelius B, Saletti P, Bajetta E, Schueller J, Bernhard J, Dietrich D, Scheithauer W. Gemcitabine (G) plus Capecitabine (C) versus G alone in locally advanced or metastatic pancreatic cancer: A randomized phase III study of the Swiss Group for Clinical Cancer Research (SAKK) and the Central European Cooperative Oncology Group (CECOG). *Proc Am Soc Clin Oncol* 2005; **23**: 4010

S- Editor Liu Y **L- Editor** Rippe RA **E- Editor** Liu WF

PO Box 2345, Beijing 100023, China
www.wjgnet.com
wjg@wjgnet.com

World J Gastroenterol 2007 January 14; 13(2): 228-235
World Journal of Gastroenterology ISSN 1007-9327

LIVER CANCER

Interferon-α response in chronic hepatitis B-transfected HepG2.2.15 cells is partially restored by lamivudine treatment

Shi-He Guan, Mengji Lu, Petra Grünewald, Michael Roggendorf, Guido Gerken, Jörg F Schlaak

Shi-He Guan, Petra Grünewald, Guido Gerken, Jörg F Schlaak, Department of Gastroenterology and Hepatology, University Hospital of Essen, Essen, Germany
Shi-He Guan, Mengji Lu, Michael Roggendorf, Institute of Virology, University Hospital of Essen, Essen, Germany
Shi-He Guan, Department of Laboratory Medicine, the first Affiliated Hospital of Anhui Medical University, China
Supported by grants from the Deutsche Forschungsgemeinschaft (DFG SCHL 377/2-2, LU 669/2-1 and GRK 1045/1)
Correspondence to: Jörg F Schlaak, MD, Professor of Medicine, Department of Gastroenterology and Hepatology, University Hospital of Essen, Hufelandstr. 55, Essen 45122, Germany. joerg.schlaak@uni-essen.de
Telephone: +49-201-7232518 Fax: +49-201-7235749
Received: 2006-08-08 Accepted: 2006-09-20

Abstract

AIM: To characterize the IFN-response and its modulation by the antiviral compound lamivudine in HBV-transfected HepG2.2.15 cells.

METHODS: HepG2.2.15 and HepG2 cells were stimulated with various concentrations of IFN-α2a in the presence or absence of lamivudine. Then, total RNA was extracted and analysed by customised cDNA arrays and northern blot for interferon-inducible genes (ISGs). In addition, cellular proteins were extracted for EMSA and western blot. HBV replication was assessed by southern blot or ELISAs for HBsAg and HBeAg.

RESULTS: Two genes (MxA, Cig5) with completely abolished and 4 genes (IFITM1, -2, -3, and 6-16) with partially reduced IFN-responses were identified in HepG2.2.15 cells. In 2 genes (IFITM1, 6-16), the response to IFN-α could be restored by treatment with lamivudine. This effect could not be explained by a direct modulation of the Jak/Stat signalling pathway since EMSA and western blot experiments revealed no suppression of Stat1 activation and ISGF3 formation after stimulation with IFN-α in HepG2.2.15 compared to HepG2 cells.

CONCLUSION: These results are consistent with the assumption that chronic hepatitis B may specifically modulate the cellular response to IFN by a selective blockage of some ISGs. Antiviral treatment with lamivudine may partially restore ISG expression by reducing HBV gene expression and replication.

Key words: Hepatitis B; IFN-α; Gene expression; Lamivudine

Guan SH, Lu M, Grünewald P, Roggendorf M, Gerken G, Schlaak JF. Interferon-α response in chronic hepatitis B-transfected HepG2.2.15 cells is partially restored by lamivudine treatment. *World J Gastroenterol* 2007; 13(2): 228-235

http://www.wjgnet.com/1007-9327/13/228.asp

INTRODUCTION

Hepatitis B (HBV) is a hepatotropic DNA virus capable of causing both acute and chronic hepatitis in humans. It is estimated that over 350 million people are chronically infected with HBV worldwide. Currently approved therapeutic strategies for treatment of HBV include interferon-alpha (IFN-α), the nucleoside analogue lamivudine and the nucleotide analogue adefovir[1,2]. However, only a minority of patients treated with IFN-α has a long-term sustained response with 'eradication' of the virus. Patients with a high viral load, in particular, rarely respond to IFN therapy. Treatment with lamivudine, on the other hand, is complicated by a high rate of viral resistance and a high relapse rate after cessation of therapy, respectively[3]. Both the emergence of viral resistance and relapse after therapy are often associated with a hepatitis flare, which can sometimes be fatal. Thus, novel strategies are needed to improve treatment for this disease.

To develop new regimens it is necessary to gain further insights into the interactions between HBV and the main antiviral system of the host, the IFN-system. It has been shown that type I and type II interferons are able to suppress HBV-replication in livers from HBV-transgenic mice[4-6]. This could also be demonstrated *in vitro* by using immortalized hepatocyte cell lines from these animals[7] and involves elimination of pregenomic RNA-containing capsids, inhibition of DNA replication and reduction of steady-state levels of HBV transcripts. The effector mechanisms that have been associated with IFN-induced suppression of HBV-replication include MxA[8] and proteasome mediated activities[9,10]. Additional data suggest a role for GTP-binding proteins, signalling and various other molecules in the control of HBV replication[11]. HBV can

counteract these antiviral effector mechanisms by inhibiting proteasome activities in an HBX-dependent manner[12] and by suppressing MxA expression at the promoter level[13]. Furthermore, it has been shown that HBV replicated at higher levels in HBV-transgenic mice crossed with IRF-1 or PKR deficient mice while replication was unchanged in transgenic mice crossed with RNase L deficient mice[14].

Assuming that HBV may interfere with the expression of ISGs, one would predict that the ISG expression in cell lines with and without HBV may be different and this would be modulated by inhibition of HBV gene expression and replication. The present study was performed to test this hypothesis. Using customized cDNA arrays for ISGs, we could identify 2 ISGs (MxA and Cig5) that are completely abolished in HBV-transfected HepG2.2.15 cells and 4 genes (IFITM1, -2, -3 and 6-16) with partially reduced responses. This suppression could partially be restored in 2 genes (IFITM1, 6-16) by treatment with the nucleoside analogue lamivudine suggesting an additional therapeutic mechanism for this drug.

MATERIALS AND METHODS

Cell culture

HepG2.2.15 cells were kindly provided by G. Acs (Mount Sinai Medical Cancer, New York, NY) and maintained in Dulbecco's Modified Eagle's Medium, supplemented with 2 mmol/L L-glutamine 50 IU/mL of penicillin, 50 mg/L of streptomycin, 500 mg/L of G418, 5% (vol/vol) fetal bovine serum, at 37℃ in humidified incubators at 5% CO_2. The cells were seeded at a density of 8×10^5 cells and maintained in a confluent state for 2 to 3 d before being treated with antiviral compounds. At first, various concentrations from 0.04 μmol/L to 100 μmol/L of lamivudine were used to reach the suitable drug concentration, which profoundly suppressed HBV replication without cytotoxicity. At the same time, a time course of drug action also was evaluated. Over a period of 10 d lamivudine was added to the medium daily, then the cells were stimulated by addition of IFN-α for 6 h. Thereafter, the media were collected and DNA or RNA was extracted for further analysis.

Analysis of secreted HBV particles

Detection of HBsAg and HBeAg was carried out by using a commercially available kit (Dade Behring) according to the manufacturer's instructions. Medium samples collected from HepG2.2.15 cells were centrifuged at 1200 rpm for 10 min to remove cellular debris, transferred to clean tubes and stored at -20℃ until analysed. HBsAg and HBeAg amounts were evaluated from absorbance reading values (450 nm) compared to the constructed controls.

HBV DNA analysis

Extracellular virion HBV-DNA analysis: Medium of HepG2.2.15 cells was collected and centrifuged (10 min, 2000 × g), and polyethylene glycol (M_r, 8000) was added to the supernatant at a concentration of 10% (wt/vol) followed by overnight precipitation at 4℃. The virions were pelletted (30 min, 10 000 × g), and the pellet was resuspended in lysis buffer (10 mmol/L Tris-Cl, 5 mmol/L EDTA, 150 mmol/L NaCl, 1% SDS) at room temperature for 15 min. Proteinase K was added at a concentration of 500 μg/mL and the suspension incubated for 2 h at 56℃. The digest was extracted with phenol/chloroform, 1:1 (vol/vol) or chloroform, respectively, and the DNA was precipitated with 2.5 vol. of ethanol. The DNA pellet was dissolved in TE solution and then spotted onto Hybond-N+ membranes. Alternatively, the DNA was electrophoresed in 1.2% agarose gel followed by blotting onto Hybond-N+ membranes. The bolt was hybridized with a ^{32}P-labeled HBV DNA probe (digested by Nsi I from plasmids that contained the full length HBV genome sequence dimer and labelled with a RediprimeTM Ⅱ Random prime labelling system), washed with 2 × SSC/0.1% SDS at room temperature for 20 min, twice, and 0.1 × SSC/0.1% SDS at 60℃ for 45 min, and then autoradiographed. The intensity of the autoradiographic dots or bands was quantitated using the Cyclone Storage Phosphor System (Packard Instrument Company, Median, Conn.). All drug concentrations were tested in duplicate or triplicate, with antiviral effects being scored as the amount of HBV DNA present in the media relative to that in untreated controls.

Intracellular HBV replicative intermediates (RI) analysis: HepG2.2.15 cells were consecutively treated with various concentrations of lamivudine for 10 d. The cytoplasmic preparations containing HBV core particles were isolated from the treated cells. Cells were lysed with lysis buffer (50 mmol/L Tris-Cl, PH 7.4, 150 mmol/L NaCl, 5 mmol/L $MgCl_2$, 0.5% NP-40) at room temperature for 5-10 min. The cytoplasmic fraction was separated from the nuclear fraction by centrifugation. Unprotected DNA was removed by adjusting cytoplasmic preparations so that they contained 10 mmol/L $MgCl_2$ and 500 μg/mL of DNase I (Roche, Germany) followed by a 1 h incubation at 37℃. To extract replicative intermediates (RI), EDTA, sodium dodecyl sulfate (SDS), NaCl and proteinase K (QIAGEN) were added separately and sequentially to final concentrations of 10 mmol/L EDTA, 1% SDS, 100 mmol/L NaCl and 500 mg/L of proteinase K. The sample was incubated for 1.5 h at 56℃ and then subjected to sequential phenol and chloroform extraction and isopropanol precipitation. Precipitated nucleic acids were resuspended in a small volume of TE solution and digested with 100 mg/L of RNase (Roche, Germany) for 1 h at 37℃. Twenty micrograms of cytoplasmic preparations containing HBV replicative intermediates DNA (RI) were then analysed by electrophoresis in 1.2% agarose gels, followed by blotting onto Hybond-N+ membranes. The bolt was hybridized with a 32P-labeled HBV DNA probe (digested by Nsi I from plasmids which contain full length HBV genome sequence dimer, and labelled with a RediprimeTM Ⅱ Random prime labelling system), washed with 2 × SSC/0.1% SDS at room temperature for 20 min, twice, and 0.1 × SSC/0.1% SDS at 60℃ for 45 min, and then autoradiographed as described above.

RNA extraction

Total RNA was isolated from cells using Trizol according

to the manufacturer's instructions. RNA quantity and quality was assessed by determination of the optical density at 260 and 280 nm using spectrophotometry and additional visualisation by agarose gel electrophoresis.

Gene expression profiling by customized cDNA macroarrays

Radiolabelled cDNA was generated from 20 μg total RNA by reverse transcription with Superscript Ⅱ (Gibco, MD) in the presence of ^{32}P-dCTP. Residual RNA was hydrolysed by alkaline treatment at 70℃ for 20 min and the cDNA was purified using G-50 columns (Amersham Pharmacia, UK). Before hybridisation to the macroarrays the labelled cDNA was mixed with 50 μg COT-DNA (Gibco) and 10 μg Poly-A DNA (Sigma), denatured at 95℃ for 5 min and hybridised for 1h to minimise non-specific binding. Preparation of the macroarrays (representing 150 known ISGs), hybridisation of the radioactive cDNAs and scanning and analysis of the macroarrays were carried out as described previously[15].

Northern blot analysis

5 μg of total RNA was electrophoresed through a 1.2% agarose gel containing formaldehyde and then transferred to Hybond-N+ membranes. The immobilized RNA was hybridized with a ^{32}P-labeled DNA probe (IMAGE clones PCR products, purified with Gel Extract kit, QIAGEN).

Electrophoretic Mobility Shift Assay

At 80% to 90% confluence, cells were stimulated with IFN-α for 6 h. Preparations of nuclear extracts were performed according to the instruction of the manufacturer (PIERCE, NE-PERTM Nuclear Extraction Reagent). Nuclear extracts/DNA binding reactions were performed in 20 μL containing 15 μg nuclear extract protein and 4 μL Gel Shift Binding 5 × Buffer (20% glycerol, 5 mmol/L $MgCl_2$, 2.5 mmol/L EDTA, 2.5 mmol/L DTT, 250 mmol/L Tris-Cl, PH 7.5, 0.25 mg/mL Poly (dI-dC) ·Poly (dI-dC)). ISRE/GAS consensus oligonucleotides (5'-AAG TAC TTT CAG TTT CAT ATT ACT CTA-3') from the promoter region of the IFN-α responsive genes were used. Mutant oligonucleotides (5'-AAG TAC TTT CAG TGG TCT ATT ACT CTA-3') were used as control. The probes were end-labeled with γ-^{32}P-ATP (U K, 3000 Ci/mol) at room temperature for 20 min. Complexes were separated from the probe in 4% naive poly-acrylamide gel in 0.5 × TBE buffer. The gels were subsequently dried and autoradiographed.

Western blot analysis

After interferon treatment, cells were washed once with ice-cold phosphate-buffered saline. Cells were lysed on ice for 30 min in 0.5 mL lysis buffer containing 50 mmol/L Tris, pH 8.0, 10% Glycerol, 0.5% NP40, 150 mmol/L NaCl, 1 mmol/L DTT, 1 mmol/L EDTA, 1 mmol/L Sodiumorthovanadate, 170 mg/L phenylmethylsulfonyl fluoride, 2 mg/L Aprotinin, 1 mg/L Leupeptin. Lysates were cleared by centrifugation in a microcentrifuge at high speed for 30 min at 4℃. Protein concentration of the supernatant was measured with Bradford reagent. Equal amounts (100 μg) of proteins were suspended in sodium-dodecyl sulphate (SDS)-sample buffer, boiled for 5 min and separated by electrophoresis (NuPAGE 4%-12% Bis-Tris Gel, Invitogen). The separated proteins were transferred to a polyvinylidene difluoride membrane (Hybond-P^{TM}, Amersham Biosciences). After blocking for 1 h at room temperature in 10% non-fat dry milk in Tris-buffered saline with 0.1% Tween-20 (TBST) or 1% BSA for antibodies specific for phosphorylated epitopes, membranes were incubated with anti-p38, anti-pp38 (Santa Cruz), anti-Stat1, anti-Stat1(pY701) and anti-ERK1, anti-ERK1/2(pT202/pY204) (BD Biosciences) overnight at 4℃, and thereafter with horseradish peroxidase-conjugated anti-rabbit or anti-Mouse IgG (1:5000) (Amersham Biosciences) for 1 h at room temperature. The proteins were detected with enhanced chemiluminescence reagent (ECL, Amersham).

Southern blot analysis

Twenty micrograms of cytoplasmic preparations containing HBV replicative intermediates (RI) DNA were analysed by Southern blotting as above.

RESULTS

Differential expression of ISGs in HepG2.2.15 and HepG2 upon stimulation with IFN-α

Type 1 IFNs are known to induce an intracellular antiviral state against many viruses. Therefore, we developed a customized cDNA array methodology to study the expression of IFN stimulated genes (ISGs). At present, this system permits the analysis of several hundred genes of interest. A substantial spectrum of known ISGs is analysed with this macroarray (Table 1). The sensitivity of this method has also been assessed previously[15]. Conventionally, in most micro- and macroarray systems a 2-fold change in the expression level is regarded as being significant.

In the established hepatoma cell line, hepG2.2.15 with stably transfected HBV genomes[16], ISG expression was examined using the cDNA macroarrays (Table 2). While many ISGs, e.g., 2-5 OAS, IFI 17, and RING4, were normally stimulated by IFN-α, several other ISGs were expressed at a lower level compared with the ISG expression in HepG2 cells. The induction of 2 ISGs, MxA and Cig5, was completely inhibited in HepG2.2.15 cells, while a partial inhibition was observed for 4 ISGs, IFITM1, IFITM2, IFITM3, and 6-16 (Table 1, Figure 1). Thus, only a subgroup of ISGs was down regulated in HepG2.2.15.

Analysis of the IFN response in HepG2.2.15 and HepG2 cells

The results above suggested that the IFN-signalling pathway is only partially inhibited in HepG2.2.15. Western blotting and EMSA and were carried out to analyse Stat1 activation and ISGF3 formation in HepG2 and HepG2.2.15 cells. The phosphorylated form of Stat1 was detected by western blot in IFN-α treated cells (Figure 2). The phosphorylation of Stat1 was enhanced in HepG2.2.15, compared with HepG2. Furthermore, Figure 3 showed that the formation of ISGF3 in HepG2.2.15 cells occurred after IFN-α stimulation, as occured in HepG2 cells.

Table 1 Complete list of genes investigated in this study

Gene Name	Acc. No.	Gene Name	Acc. No.	Gene Name	Acc. No.
101F6	AA544950	IFI 16	M63838	Mdm2	Z12020
2-5 OAS	X02875	IFI 41	L22342	MEN1	U93237
2-5 OAS	D00068	IFI 44	D28915	Met	AA410591
5' nucleotidase	X55740	IFI 6-16	BC015603	Mig	X72755
60S Ribosomal protein L11	U43522	IFI27	X67325	MIP-1b/CCL4	NM_002984
72 kDa type IV collagenase	J03210	IFI4	X79448	MLK 2	X90846
9-27	J04164	IFIT 1	M24594	MMP-1	M13509
ADAM-10	AF009615	IFIT4	U72882	MxA	M33882
ADAM-17	U69611	IFIT4	AF083470	MxA	M33882
akt-1	NM_005163	IFITM2	X57351	MxB	M30818
akt-2	M77198	IFITM3	X57352	MxB	M30818
Alpha-1-antiproteinase	K01396	IFN omega 1	X58822	NCAM	M74387
Alpha-crystallin	U05569	IFN-AR1	J03171	NF-IL-6	X52560
ATF-2	X15875	IFN-AR2	L42243	NFkB	M58603
Auto Ag SS-A/Ro	NM_003141	IFN-g	M29383	NKC-4	M59807
bad	U66879	IFN-GR1	J03143	n-myc	Y00664
BAK1	X84213	IFN-GR2	U05875	p19	U40343
BAX	U19599	IFI 17	J04164	p48/ISGF3g	M87503
Bax	L22474	IFP 35	U72882	p53	M14694
bcl-2	M14745	IFP-53	X62570	p57Kip2	U22398
BRCA1	U14680	IFRG28	AJ251832	p70 S6 kinase	M60724
BST2	D28137	ikBa	M69043	PAI-1	M16006
BTG1	X61123	IL-1 α	M28983	PCBP	M80563
Calcyclin	J02763	IL-10	M57627	PDGF-alpha	X06374
Calretiulin	M84739	IL-10 R α	U00672	PDK1	Y15056
CASP	AJ006470	IL-10 R β	Z17227	PDK2	NM_002611
Caspase 7	U67319	IL-12R β	U64198	Phosph. Scram. 1	AF098642
Caspase 8	X98172	IL13RA	U81379	Phosph.glycerate kin.	V00572
Caspase-1	M87507	IL13RA 2	U70981	Pi3-kinase	NM_006219
Caspase-9	U60521	IL-15	U14407	PIAS x-beta	AF077954
Cat. o-methyltransferase	M58525	IL-15RA	U31628	pig7	AF010312
CBFA	NM_004349	IL-18	D49950	pim-1	M16750
CBP	U85962	IL-18 bprot	AB019504	PK R	AF072860
CCR1	L09230	IL2	U25676	PKR	U50648
CCR5	U54994	IL-2R α	K03122	plectin (PLEC1)	U53204
CD5	X04391	IL2RG	D11086	PLOD2	U84573
cdk inhibitor p27KIP1	U10909	IL6	X04602	PML-1	M79462
C-fox	NM_005252	IL-8	M28130	PPP3CA	L14778
CG12-1	AF070675	IL8RB	L19593	Pro. 4-hydroxyl.	M24486
C-jun	J04111	iNOS	L09210	Prot.-ATPase-like pr.	D89052
C-myc	L00058	Int-6	U62962	PTEN	U96180
C-myc	V00568	Integrin β 7	M62880	pyridoxal kinase	U89606
Collagen α1 (I)	Z74615	integrin-β-6	NM_000888	raf (c-raf-1)	X03484
Collagen α2 (I)	J03464	IP-10	X02530	RAP46/Bag-1	Z35491
Collagen, type XVI, alpha 1	M92642	IP-30	J03909	RbAp48	X74262
Complement compound C1r	J04080	IRF 1	X14454	Reticulocalbin	D42073
COX17	L77701	IRF 4	U52682	RGS2	NM_002923
Cpp32	NM_004346	IRF 5	U51127	RHO	NM_000539
CREB	NM_004379	IRF-1	L05072	RHO GDP-dis.inh. 2	L20688
CTRL-1	X71877	IRF-2	X15949	RING 10	NM_004159
CXCR4	AF005058	Irf-7	U73036	RING4	X57522
Cyclin D1	M64349	ISG15	AA406020	Smad1	U59423
Cyp19 (aromata)	M28420	ISG15	M13755	Smad2	AF027964
Cys-X-Cys,member 11	AF030514	ISG-56K	M24594	Smad4	U44378
DEAD box binding protein 1	AF077951	KIAA0129	D50919	Smad5	U73825
DEAD-box protein p72	U59321	KIAA0235	D87078	Smad7	AF015261
Destrin	S65738	KIAA0284	AB006622	SnoN	X15219
DP (β1)	M83664	LIPA	U04285	SOCS 3/ssi-3	AB004904
DR-α	J00194	LMP-2	X66401	SOCS 4/CIS 4	AB006968
E2F-1	U47677	L-selectin	M25280	SOCS1	N91935

Gene Name	Acc. No.	Gene Name	Acc. No.	Gene Name	Acc. No.
egr-1	X52541	Mad 4	X03541	SOCS-1	NM_003745
Elastase 2	M34379	MAP2K1	NM_002755	SOCS2	AF020590
ERM	X76184	MAP2K1IP1	NM_021970	SOCS-3	NM_003955
F-actin capping protein	U56637	MAP2K2	L11285	Stannin	NM_003498
Farn. pyro. syn.	J05262	MAP2K3	NM_002756	STAT 6	U16031
FAS/Apo-1	M67454	MAP2K4	L36870	STAT1 (91kDa)	M97935
fas-ligand	U08137	MAP2K5	NM_002757	STAT1 (91kDa)	M97935
Fibronectin-1	X02761	MAP2K6	U39657	STAT2	M97934
FK506 binding protein 6	AF038847	MAP2K7	AF022805	STAT4	L78440
FKHRL1	AF041336	MAP3K1	AF042838	STAT5A	L41142
Folate receptor	X62753	MAP3K11	NM_002419	STAT5B	U47686
gadd45	M60974	MAP3K14	NM_003954	Succinyl CoA Ligase	AF058953
Galectin-1	J04456	MAP3K2	NM_006609	TAP1 (Ring4)	L21204
Gamma actin	X04098	MAP3K3	U78876	TFE3	X96717
Gamma2-adaptin (G2AD)	AF068706	MAP3K4	NM_005922	TGF-bR1	L11695
GAPDH	X01677	MAP3K5	NM_005923	TGF-bR2	D50683
GATA 3	X58072	MAP3K7	NM_003188	TGF-bR3	L07594
GBP-1	M55542	MAP4K1	NM_007181	TGIF	X89750
GBP-2	M55543	MAP4K3	NM_003618	TIMP-1	M59906
Granzyme B	M17016	MAPK10	NM_002753	TIMP-2	J05593
GSK3	NM_002093	MAPK11	NM_002751	TIMP-3	U14394
HCV-ass. p44	D28915	MAPK12	NM_002969	TIMP-4	U76456
HLA-A (MHCI Ag B27)	NM_002116	MAPK13	AF004709	TNF-alpha	X01394
HLA-E	X56841	MAPK14	NM_001315	TRAF6	U78798
Homo sapins STAT	M97936	MAPK3	X60188	Transferrin	M12530
Hou	U32849	MAPK6	NM_002748	Transthyretin	D00096
HPAST protein	AF001434	MAPK7	NM_002749	TRIP14	L40387
hsf1 (tcf5)	M64673	MAPK8	NM_002750	trk oncogene	X03541
hsp90 (CDw52)	X15183	MAPK8IP2	NM_012324	TTF-2	AF073771
Hypoxia-ind. Factor-1	U22431	MAPK9	U35003	UBE2L6	AA292074
ICAM-1	M24283	MAPKAPK2	NM_004759	VCAM -1	M30257
ICSB 1	M91196	MAPKAPK3	NM_004635	VEGF-C	U43142
IDO	M34455	MCP-1/CCL2	X14768	Virpirin (Cig5)	AF026941

Genes of interest were selected from the UniGene database. These genes comprise known ISGs and genes of intrinsic interest which might or might not be induced by IFNs in different cell systems. They include genes involved in cell proliferation, immune responses and the responses to a variety of cytokines. 5′ IMAGE clones with 0.5-0.8 kb length were chosen and obtained from RZPD, Berlin, Germany.

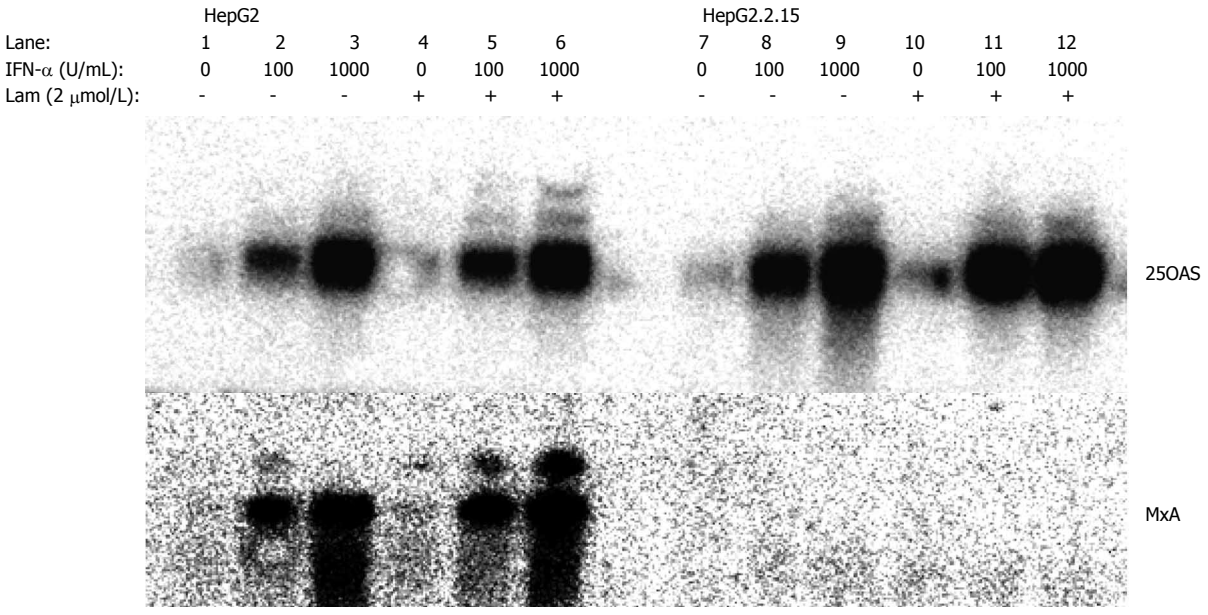

Figure 1 Northern blot analysis of ISG expression and its modulation by lamivudine in HepG2 and HepG2.2.15 cells. HepG2 and HepG2.2.15 cells were cultured in the absence or presence of 2 μmol/L of lamivudine for 10 d. Then, the cells were stimulated with 100 or 1000 IU/mL of IFN-α for 6 h. Total cellular RNAs were isolated for Northern blotting hybridization. Lam: lamivudine.

Table 2 Suppression of ISG induction in HepG2.2.15 cells, effect of lamivudine treatment

Gene	Acc. No.	HepG2	2.2.15	HepG2 /lam	2.2.15 /lam
Ⅰ complete inhibition					
MxA	M33882	5.9	0.6	4.0	0.8
cig5	AF026941	2.2	0.9	2.1	1.2
Ⅱ partial inhibition					
IFITM3	X57352	3.4	1.6	3.4	1.8
IFITM2	X57351	2.7	1.6	2.2	1.8
Ⅲ reversible inhibition					
IFI 6-16	BC015603	7.9	4.4	7.2	6.5
IFITM1	M24594	4.9	2.5	4.8	4.6
Ⅳ no inhibition					
2-5OAS	D00068	3.8	4.0	4.4	5.8
MxB	M30818	1.4	2.0	1.4	1.9
Caspase 7	U67319	2.3	2.4	2.2	2.1
IFI 17	J04164	3.3	2.9	2.8	2.7
IFI 27	X67325	1.9	2.1	1.8	2.2
IFI T4	U72882	2.7	1.9	2.6	1.8
RING4	X57522	2.4	2.3	2.5	3.5

Cells were stimulated with 100 U/mL IFN-α for 6 h with or without pretreatment with 2 μmol/L lamivudine for 10 d. Then, RNA was isolated and assayed by cDNA macroarray. Data are shown as fold induction compared to the untreated control. Lam: Lamivudine.

These data clearly show that the IFN-signalling pathway is generally not blocked in HepG2.2.15 cells. The results consistently show that both steps were evenly enhanced in HepG2.2.15. In addition, activation of ERK and p38 MAPKinase was not altered in HepG2.2.15 cells (data not shown).

Reduction of the production of HBV proteins and the HBV replication by lamivudine treatment

The difference in ISG expression in HepG2 and HepG2.2.15 cell lines may be partly due to the presence of HBV replication in the later one. Consequently, the ISG expression in HepG2.2.15 would change if the HBV gene expression or replication is suppressed. To test this hypothesis, we determined the optimal condition to reduce HBV gene expression and replication using the nucleoside analogue lamivudine. HepG2.2.15 cells were treated with lamivudine at various concentrations from 0.04 μmol/L to 100 μmol/L. The antiviral activity was determined by quantitation of secreted HBsAg and HBeAg particles, extracellular virions and intracellular HBV replicative intermediates (RI). Figure 4A shows that treatment with lamivudine led to a significant reduction of secreted HBsAg and HBeAg in the supernatant of HepG2.2.15 cells. Parallel to the reduction of HBsAg and HBeAg production, the extracellular virion DNA in the culture supernatant of HepG2.2.15 cells and intracellular HBV replicative intermediates (RI) decreased after treatment with 2 μmol/L or 20 μmol/L of lamivudine for 10 d (Figure 4B and C). Maximal levels of suppression of HBV were observed after 10 d of lamivudine treatment. At that time, levels of RI were not more than 1.5% of controls in cultures of the 2 μmol/L treatment group. Based on these results, we chose

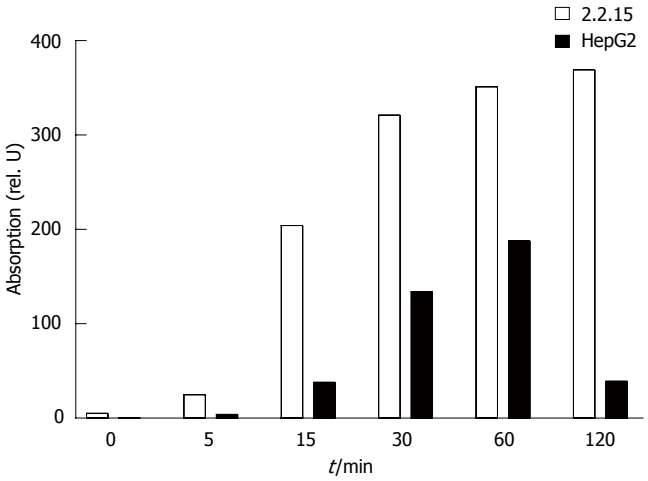

Figure 2 Analysis of Stat1 phosphorylation after IFN-α stimulation in HepG2 and HepG2.2.15 cells. Cells were stimulated with 100 U/mL of IFN-α for the indicated time points. Then, nuclear proteins were extracted and analysed by western blot. Data were quantified using Imagequant and are shown as relative units.

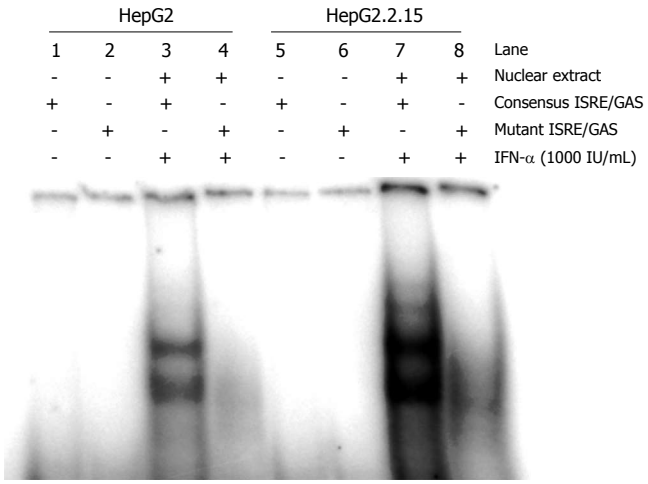

Figure 3 Analysis of ISGF3 formation after IFN-α stimulation in HepG2 and HepG2.2.15 cells. HepG2 and HepG2.2.15 cells were stimulated with 1000 IU/mL of IFN-α for 6 h followed by isolation of nuclear extracts (NE-PER™ reagent kits) for EMSA analysis.

a concentration of 2 μmol/L and duration of 10 d to suppress HBV replication in our system to study the modulatory effects of lamivudine on the IFN-response.

The IFN response in HepG2.2.15 and HepG2 cells after lamivudine treatment

The effect of lamivudine on ISG expression in HepG2.2.15 and HepG2 was investigated by using gene macroarrays. No effect was observed for the stimulation of MxA and Cig5 expression by lamivudine treatment (Table 2). Both genes did not respond with an increased expression upon IFN-α stimulation. An increase of the IFN-α concentration to 1000 units per mL or a prolonged incubation with IFN-α did not change the expression of MxA and cig5. The reduced induction of IFITM 2 and IFITM 3 expression could not be enhanced by lamivudine treatment. In contrast, IFITM1 and 6-16 expression could

be restored by lamivudine treatment of HepG2.2.15 cells (Table 1, Figure 1). This indicates that lamivudine can only partially normalize the IFN-response in HBV-transfected HepG2.2.15 cells at concentrations that profoundly inhibit viral replication and secretion of viral particles. Lamivudine had no effect on ISG expression in HepG2 cells and did not enhance the induction of many other ISGs, such as 2.5 OAS and MxB.

DISCUSSION

In the present work, we found that HepG2.2.15 and HepG2 respond differently to IFN-α. Several ISGs were not induced in HepG2.2.15 while they were expressed in HepG2 cells after IFN-α. There may be multiple reasons for the different ISG expression profiles in these cell lines, though HepG2.2.15 was derived from HepG2[16]. Previous data indicated that the expression of the IFN-inducible gene MxA was specifically inhibited by HBV proteins in HBV-transfected HepG2 or HuH7 cells[13], and this was accompanied by diminished antiviral activity of IFN[17]. In our study, we confirmed this finding with MxA expression being completely diminished in HBV-transfected HepG2.2.15 cells. In addition, we showed that additional ISG (Cig5, IFITM1, -2, -3 and 6-16) expression was completely abolished or partially reduced by HBV. The majority of ISGs, however, are expressed and inducible in both HepG2 and HepG2.2.15 cells, indicating that the HBV gene expression and replication had no effect on these ISGs. Consistently, Rosmorduc *et al*[17] demonstrated that 2´5OAS expression is not affected by HBV. Our results support the view that the HBV-mediated inhibition of the IFN-response, if any, represents a specific rather than global effect. The Stat1 activation or ISGF3 formation in HepG2.2.15 cells appeared to be normal, indicating that the Jak/Stat signalling pathway is intact and functional. These findings are corroborated by the data from Fernandez *et al*[13] who demonstrated that the inhibition of MxA induction in HepG2 cells occurs at the promoter level.

We then asked the question whether the HBV-mediated suppressive effect on the IFN-response could be reverted by treatment with the nucleoside analogue lamivudine, which is an effective inhibitor of HBV replication *in vitro*[18] and *in vivo*[19,20]. Lamivudine is phosphorylated within the cell and then incorporated into nascent viral DNA by the HBV polymerase during replication[21] resulting in the termination of HBV DNA elongation. Lamivudine also inhibits reverse transcriptase activity directly through competitive inhibition. Although some reports indicate that lamivudine exerts synergistic effects with IFN, the underlying mechanisms are not clear[22,23]. To answer this question we first established the optimal conditions for *in vitro* treatment of HepG2.2.15 cells with lamivudine. The results indicated that lamivudine exerted potent antiviral activities in our system as it strongly suppressed the formation of HBV replicative intermediates and extracellular HBV DNA at concentrations that correspond well to plasma levels found in patients that are treated with this drug. However, HBsAg and HBeAg secretion was only down regulated and not completely blocked. After treatment with lamivudine for 10 d, the induction of IFITM1 and 6-16 expression could be enhanced while MxA, Cig5, IFITM2 and IFITM3 induction remained unchanged. This indicates that lamivudine can at least partially improve the impaired IFN response in HBV-transfected cells. IFITM 1 to 3 and 6-16 belong to a family called small ISGs[24]. IFITM 1 to 3 are classified as members of the 1-8 group while 6-16 is a member of the ISG12 group. These genes were under the control of multiple elements responding to IFN-α stimulation including ISGF3 and interferon. It is likely that the lamivudine treatment partially reduces HBV gene expression and therefore contributes to the improved

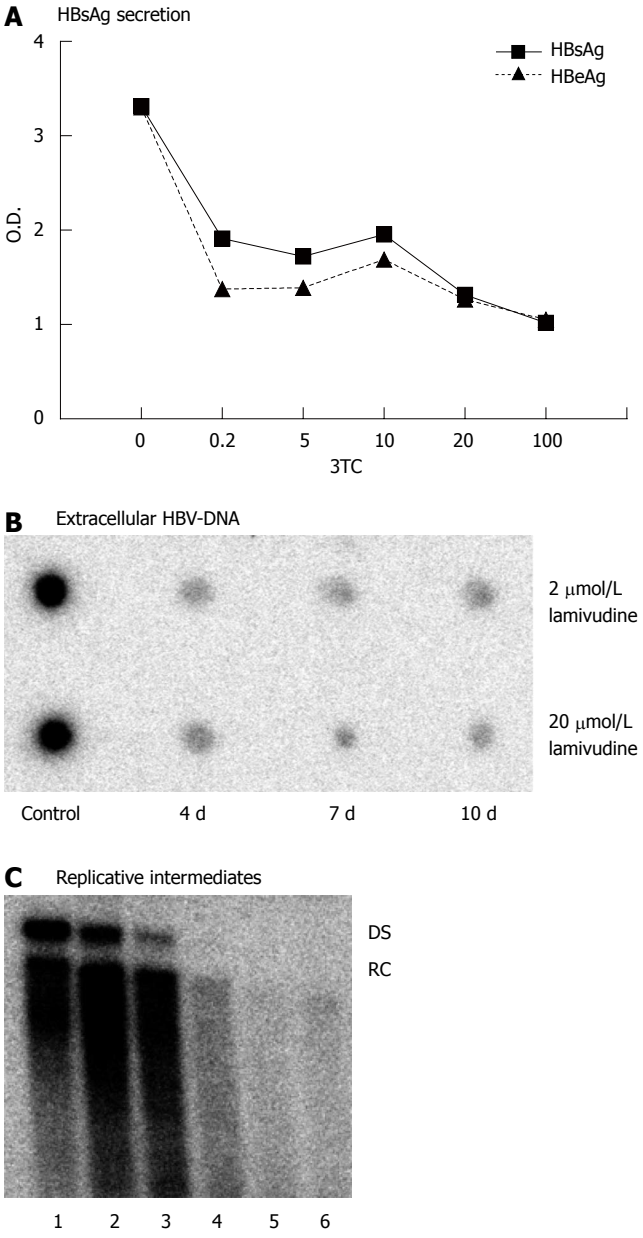

Figure 4 Antiviral effects of lamivudine in HepG2.2.15 cells. **A**: HepG2.2.15 cells were cultivated with various concentrations (0 to 100 μmol/L) of 3 TC for 10 d. Then, supernatants were harvested and assayed for the presence of HBsAg and HBeAg by ELISA; **B**: HepG2.2.15 cells were treated with 2 or 20 μmol/L of lamivudine for 4, 7 and 10 d, respectively. Then, supernatants were collected and extracellular HBV-DNA was analyzed by dot blot hybridization; **C**: HepG2.2.15 cells were treated with various concentrations of lamivudine for 10 d. Then, intracellular HBV replicative intermediates were isolated for southern blotting. Lane 1: control, lane 2: 0.04 μmol/L, lane 3: 0.2 μmol/L, lane 4: 5 μmol/L, lane 5: 25 μmol/L, lane 6: 125 μmol/L, RC, relaxed circular HBV-DNA; DS, double stranded linear HBV-DNA.

ISG expression. On the other hand, the continuing HBV protein production may still dominantly interfere with the expression of many ISGs, such as cig5 and IFITM3.

These findings are corroborated by our study that shows an improved IFN response of PBMC from HBV patients after treatment with adefovir. Some reports have also suggested a restoration of weak T helper cell and CTL responses after initiation of lamivudine therapy[25,26]. Although it is certainly a possibility, it still remains to be determined whether this effect can be explained by an enhanced responsiveness to IFNs.

In conclusion, our results suggest that HBV specifically modulates the IFN response in HepG2 cells by a selective suppression of certain ISGs. This suppression is at least partially reversible by antiviral treatment with the nucleoside analogue lamivudine.

REFERENCES

1 **Hadziyannis SJ**, Papatheodoridis GV, Vassilopoulos D. Treatment of HBeAg-negative chronic hepatitis B. *Semin Liver Dis* 2003; **23**: 81-88
2 **Heathcote J**. Treatment of HBe antigen-positive chronic hepatitis B. *Semin Liver Dis* 2003; **23**: 69-80
3 **Lok AS**, Lai CL, Leung N, Yao GB, Cui ZY, Schiff ER, Dienstag JL, Heathcote EJ, Little NR, Griffiths DA, Gardner SD, Castiglia M. Long-term safety of lamivudine treatment in patients with chronic hepatitis B. *Gastroenterology* 2003; **125**: 1714-1722
4 **Guidotti LG**, Ando K, Hobbs MV, Ishikawa T, Runkel L, Schreiber RD, Chisari FV. Cytotoxic T lymphocytes inhibit hepatitis B virus gene expression by a noncytolytic mechanism in transgenic mice. *Proc Natl Acad Sci USA* 1994; **91**: 3764-3768
5 **Guidotti LG**, Guilhot S, Chisari FV. Interleukin-2 and alpha/beta interferon down-regulate hepatitis B virus gene expression in vivo by tumor necrosis factor-dependent and -independent pathways. *J Virol* 1994; **68**: 1265-1270
6 **Wieland SF**, Guidotti LG, Chisari FV. Intrahepatic induction of alpha/beta interferon eliminates viral RNA-containing capsids in hepatitis B virus transgenic mice. *J Virol* 2000; **74**: 4165-4173
7 **Pasquetto V**, Wieland SF, Uprichard SL, Tripodi M, Chisari FV. Cytokine-sensitive replication of hepatitis B virus in immortalized mouse hepatocyte cultures. *J Virol* 2002; **76**: 5646-5653
8 **Gordien E**, Rosmorduc O, Peltekian C, Garreau F, Bréchot C, Kremsdorf D. Inhibition of hepatitis B virus replication by the interferon-inducible MxA protein. *J Virol* 2001; **75**: 2684-2691
9 **Robek MD**, Boyd BS, Wieland SF, Chisari FV. Signal transduction pathways that inhibit hepatitis B virus replication. *Proc Natl Acad Sci USA* 2004; **101**: 1743-1747
10 **Robek MD**, Wieland SF, Chisari FV. Inhibition of hepatitis B virus replication by interferon requires proteasome activity. *J Virol* 2002; **76**: 3570-3574
11 **Wieland SF**, Vega RG, Müller R, Evans CF, Hilbush B, Guidotti LG, Sutcliffe JG, Schultz PG, Chisari FV. Searching for interferon-induced genes that inhibit hepatitis B virus replication in transgenic mouse hepatocytes. *J Virol* 2003; **77**: 1227-1236
12 **Zhang Z**, Protzer U, Hu Z, Jacob J, Liang TJ. Inhibition of cellular proteasome activities enhances hepadnavirus replication in an HBX-dependent manner. *J Virol* 2004; **78**: 4566-4572
13 **Fernández M**, Quiroga JA, Carreño V. Hepatitis B virus downregulates the human interferon-inducible MxA promoter through direct interaction of precore/core proteins. *J Gen Virol* 2003; **84**: 2073-2082
14 **Guidotti LG**, Morris A, Mendez H, Koch R, Silverman RH, Williams BR, Chisari FV. Interferon-regulated pathways that control hepatitis B virus replication in transgenic mice. *J Virol* 2002; **76**: 2617-2621
15 **Schlaak JF**, Hilkens CM, Costa-Pereira AP, Strobl B, Aberger F, Frischauf AM, Kerr IM. Cell-type and donor-specific transcriptional responses to interferon-alpha. Use of customized gene arrays. *J Biol Chem* 2002; **277**: 49428-49437
16 **Sells MA**, Chen ML, Acs G. Production of hepatitis B virus particles in Hep G2 cells transfected with cloned hepatitis B virus DNA. *Proc Natl Acad Sci USA* 1987; **84**: 1005-1009
17 **Rosmorduc O**, Sirma H, Soussan P, Gordien E, Lebon P, Horisberger M, Bréchot C, Kremsdorf D. Inhibition of interferon-inducible MxA protein expression by hepatitis B virus capsid protein. *J Gen Virol* 1999; **80** (Pt 5): 1253-1262
18 **Doong SL**, Tsai CH, Schinazi RF, Liotta DC, Cheng YC. Inhibition of the replication of hepatitis B virus in vitro by 2',3'-dideoxy-3'-thiacytidine and related analogues. *Proc Natl Acad Sci USA* 1991; **88**: 8495-8499
19 **Nevens F**, Main J, Honkoop P, Tyrrell DL, Barber J, Sullivan MT, Fevery J, De Man RA, Thomas HC. Lamivudine therapy for chronic hepatitis B: a six-month randomized dose-ranging study. *Gastroenterology* 1997; **113**: 1258-1263
20 **Honkoop P**, de Man RA, Zondervan PE, Schalm SW. Histological improvement in patients with chronic hepatitis B virus infection treated with lamivudine. *Liver* 1997; **17**: 103-106
21 **Cammack N**, Rouse P, Marr CL, Reid PJ, Boehme RE, Coates JA, Penn CR, Cameron JM. Cellular metabolism of (-) enantiomeric 2'-deoxy-3'-thiacytidine. *Biochem Pharmacol* 1992; **43**: 2059-2064
22 **Korba BE**, Cote P, Hornbuckle W, Schinazi R, Gangemi JD, Tennant BC, Gerin JL. Enhanced antiviral benefit of combination therapy with lamivudine and alpha interferon against WHV replication in chronic carrier woodchucks. *Antivir Ther* 2000; **5**: 95-104
23 **Janssen HL**, van Zonneveld M, Senturk H, Zeuzem S, Akarca US, Cakaloglu Y, Simon C, So TM, Gerken G, de Man RA, Niesters HG, Zondervan P, Hansen B, Schalm SW. Pegylated interferon alfa-2b alone or in combination with lamivudine for HBeAg-positive chronic hepatitis B: a randomised trial. *Lancet* 2005; **365**: 123-129
24 **Martensen PM**, Justesen J. Small ISGs coming forward. *J Interferon Cytokine Res* 2004; **24**: 1-19
25 **Boni C**, Bertoletti A, Penna A, Cavalli A, Pilli M, Urbani S, Scognamiglio P, Boehme R, Panebianco R, Fiaccadori F, Ferrari C. Lamivudine treatment can restore T cell responsiveness in chronic hepatitis B. *J Clin Invest* 1998; **102**: 968-975
26 **Boni C**, Penna A, Ogg GS, Bertoletti A, Pilli M, Cavallo C, Cavalli A, Urbani S, Boehme R, Panebianco R, Fiaccadori F, Ferrari C. Lamivudine treatment can overcome cytotoxic T-cell hyporesponsiveness in chronic hepatitis B: new perspectives for immune therapy. *Hepatology* 2001; **33**: 963-971

S- Editor Wang J **L- Editor** Lutze M **E- Editor** Bai SH

PO Box 2345, Beijing 100023, China
www.wjgnet.com
wjg@wjgnet.com

World J Gastroenterol 2007 January 14; 13(2): 236-243
World Journal of Gastroenterology ISSN 1007-9327

BASIC RESEARCH

Correlation between *in vitro* and *in vivo* immunomodulatory properties of lactic acid bacteria

Benoit Foligne, Sophie Nutten, Corinne Grangette, Véronique Dennin, Denise Goudercourt, Sabine Poiret, Joelle Dewulf, Dominique Brassart, Annick Mercenier, Bruno Pot

Benoit Foligne, Sophie Nutten, Corinne Grangette, Véronique Dennin, Denise Goudercourt, Sabine Poiret, Joelle Dewulf, Annick Mercenier, Bruno Pot, Bactéries Lactiques et Immunité des Muqueuses, Institut Pasteur de Lille, France
Dominique Brassart, Danisco France, Culture Division, France; present address: Nestlé Nutrition, Vevey, Switzerland
Sophie Nutten, Annick Mercenier, Nestlé Research Center, Nutrition and Health Department, Lausanne, Switzerland
Supported by the EU granted QLK1-2000-00146 DEPROHEALTH research program, Institut Pasteur de Lille funding and funds from DANISCO France
Correspondence to: Dr. Bruno Pot, Bactéries Lactiques et Immunité des Muqueuses, Institut Pasteur de Lille, 1 Rue du Professeur Calmette, BP 245, Lille cedex F-59019, France. bruno.pot@ibl.fr
Telephone: +33-3-20871191 Fax: +33-3-20871192
Received: 2006-09-09 Accepted: 2006-12-07

Abstract

AIM: To investigate the correlation between the *in vitro* immune profile of probiotic strains and their ability to prevent experimental colitis in mice.

METHODS: *In vitro* immunomodulation was assessed by measuring interleukin (IL)-12p70, IL-10, tumor necrosis factor alpha (TNFα) and interferon γ (IFNγ) release by human peripheral blood mononuclear cells (PBMCs) after 24 h stimulation with 13 live bacterial strains. A murine model of acute TNBS-colitis was next used to evaluate the prophylactic protective capacity of the same set of strains.

RESULTS: A strain-specific *in vivo* protection was observed. The strains displaying an *in vitro* capacity to induce higher levels of the anti-inflammatory cytokine IL-10 and lower levels of the inflammatory cytokine IL-12, offered the best protection in the *in vivo* colitis model. In contrast, strains leading to a low IL-10/IL-12 cytokine ratio could not significantly attenuate colitis symptoms.

CONCLUSION: These results show that we could predict the *in vivo* protective capacity of the studied lactic acid bacteria (LAB) based on the cytokine profile we established *in vitro*. The PBMC-based assay we used may thus serve as a useful primary indicator to narrow down the number of candidate strains to be tested in murine models for their anti-inflammatory potential.

Key words: Inflammatory bowel disease; Probiotics; Cytokines; Peripheral blood mononuclear cells; Trinitrobenzene sulfonate-induced colitis

Foligne B, Nutten S, Grangette C, Dennin V, Goudercourt D, Poiret S, Dewulf J, Brassart D, Mercenier A, Pot B. Correlation between *in vitro* and *in vivo* immunomodulatory properties of lactic acid bacteria. *World J Gastroenterol* 2007; 13(2): 236-243

http://www.wjgnet.com/1007-9327/13/236.asp

INTRODUCTION

Probiotic lactobacilli and bifidobacteria are increasingly recognized as a way to prevent and/or treat intestinal disorders[1]. Probiotic treatment has been successful in a limited number of clinical inflammatory bowel disease (IBD) trials[2,3], as well as in various experimental rodent models for acute and chronic intestinal inflammation[4]. Cytokines are key regulators of inflammation in IBD, and several pro-inflammatory and immune regulatory cytokines are dysregulated in the mucosa of IBD patients. Probiotic–mediated immunomodulation represents an interesting option in the management of IBD[5] and it was shown that both the systemic and mucosal immune systems can be modulated by orally delivered bacteria[6-8]. However, not all candidate probiotics have been proven equally efficient due to the differences in survival and persistence of the strain in the gastro-intestinal tract, and/or to strain-specific interactions of the probiotic with the host immune system[9-11]. The selection of a successful protective strain may therefore rely on the proper screening of a large number of candidate strains for their technological and immunomodulatory performance.

However, it remains challenging to set up *in vitro* tests with a fair predictive value that would allow us to narrow down the number of candidate strains to be tested in animal models. Until now, results of *in vitro* studies have rarely been linked to *in vivo* effects[12,13]. This could possibly be explained by the variety of parameters that may interfere in the systematic comparison of strains such as the bacterial preparations used (viability, growth phase, dose and timing of administration), possible time effects (early *versus* late

immune responses), or physiological status and type of eukaryotic cells used. When testing human peripheral blood mononuclear cells (PBMCs), the *in vitro* experiment may also be influenced by the method of PBMC preparation as well as the variable responsiveness of the donors[10,14,15]. Once identified, however, these parameters/factors can be controlled by using standardized methodologies[16], allowing, on the one hand, to classify strains according to the *in vitro* differences in their interaction with human immunocompetent cells and, on the other hand, to confirm *in vivo* the "protective capacity" of the best candidate strains (showing between 30% and 70% reduction of the inflammatory score)[16,17]. In this paper we addressed the question whether prophylaxis by oral consumption of live non-pathogenic lactic acid bacteria (LAB) in experimental colitis actually matches their *in vitro* stimulation profile on human PBMCs. Cytokine profiles released *in vitro* by human PBMC stimulated with 13 bacterial strains were compared with the protection they offered in a murine trinitrobenzene sulfonate (TNBS) model of acute colitis. The results of this study demonstrate that the *in vitro* immune profiling of the strains is indeed predictive of their *in vivo* protective effect in a mouse colitis model. These findings support the idea that promising LAB strains for IBD alleviation may be discriminated from non-protective ones using *in vitro* and *in vivo* assays.

MATERIALS AND METHODS

Bacterial strains and growth conditions

Bacterial strains and their origin are shown in Table 1. *Lactobacillus* strains were grown under limited aeration at 37℃ in MRS medium (Difco) and *Bifidobacterium* strains were grown anaerobically in MRS supplemented with 0.05% L-cysteine-hydrochloride (Sigma). *Lactococcus lactis* MG1363 was grown at 30℃ in M17 medium supplemented with 0.5% glucose. *E. coli* and *S. gordonii* were grown at 37℃ in LB and BHI medium (Difco), respectively. The number of live bacteria (CFU) was deduced from the absorbance at 600 nm (A_{600}), using a calibration curve for each strain. For immune cell stimulation, bacterial cells were grown till stationary phase, washed and resuspended at 1×10^9 CFU/mL in phosphate buffered saline (PBS) containing 20% glycerol and stored at -80℃ until used for assays. For *in vivo* experiments, bacteria were grown for 18 h, washed twice in sterile PBS (pH 7.2) and resuspended at 1×10^9 CFU/mL in 0.2 mol/L $NaHCO_3$ buffer (pH 8.8) containing 2% glucose.

PBMC isolation

PBMCs were isolated from peripheral blood of healthy donors as previously described[18]. Briefly, after a Ficoll gradient centrifugation (Pharmacia, Uppsala, Sweden), mononuclear cells were collected, washed in RPMI 1640 medium (Live technologies, Paisley, Scotland) and adjusted to 2×10^6 cells/mL in RPMI 1640 supplemented with gentamicin (150 μg/mL), L-glutamine (2 mmol/L), and 10% foetal calf serum (FCS) (Gibco-BRL).

Induction of cytokine release

PBMCs (2×10^6 cells/mL) were seeded in 24-well tissue culture plates (Corning, NY). Twenty microliters of a thawed bacterial suspension at 10^9 CFU/mL were added (bacteria:cell ratio of 10:1). PBS containing 20% glycerol was used as a negative (non-stimulated) control. On the basis of preliminary time-course studies, 24 h stimulation corresponded to the best time point for cytokine responses of bacteria stimulated-PBMCs. After 24 h stimulation at 37℃ in an atmosphere of air with 5% CO_2, culture supernatants were collected, clarified by centrifugation and stored at -20℃ until cytokine analysis. Neither medium acidification nor bacterial proliferation was observed. Cytokines were measured by ELISA using BD pharmingen antibody pairs (BD Biosciences, San Jose, Ca, USA) for tumor necrosis factor alpha (TNFα), interleukin (IL)-10, interferon γ (IFNγ) and IL-12p70, according to the manufacturer's recommendations.

Table 1 Strains used with their origin

Bacterial species /subspecies	Strain designation	Type of isolate, source and/or reference
Lactobacillus salivarius subsp salivarius	Ls33	Commercial strain
Lactobacillus rhamnosus	Lr32	Commercial strain
Lactobacillus casei	Bl23	ATCC[1] 393, plasmid-cured
Lactobacillus acidophilus	NCFM	Human, commercial strain
Lactobacillus acidophilus	IPL[3] 908	Commercial isolate
Lactobacillus plantarum	NCIMB 8826	Human, NCIMB[2] collection
Lactobacillus plantarum	Lp115	Commercial strain
Bifidobacterium animalis subsp *lactis*	BL04	Commercial strain
Bifidobacterium animalis subsp *lactis*	BI07	Commercial strain
Bifidobacterium bifidum	BB02	Commercial strain
Lactococcus lactis	MG1363	Cheese starter derivative[42]
Streptococcus gordonii	V288 (Challis)	ATCC[1] 35105
Escherichia coli (non-pathogenic)	TG1	Cloning strain[43]

[1]ATCC: American type culture collection, Manassas, (VA), USA; [2]NCIMB: National collection of industrial and marine bacteria, Terry Research Station, Aberdeen, Scotland; [3]Institut Pasteur Lille, Lille, France.

Induction of colitis and inflammation scoring

Animal experiments were performed in an accredited establishment (number 59-35009; Institut Pasteur de Lille, France) and approved guidelines, according to French Ethical Committee and European Union Normatives (number 86/609/CEE). BALB/c and C57/Bl6 mice (female, 8 wk) were obtained from Charles River (St Germain sur l'Arbresle, France). A standardized murine TNBS colitis model was used in which sublethal levels of inflammation were induced[16]. Briefly, a 50 μL solution of 100 mg/kg (BALB/c mice) or 180 mg/kg (C57Bl6 mice) TNBS (Sigma) in 50% ethanol was slowly administered in the colon *via* a 3.5 F catheter. Bacterial suspensions (100 μL), containing 1×10^9 CFU/mL in $NaHCO_3$ buffer (or buffer alone for controls) were administered intragastrically to mice each day, starting 5 d before until d 1 after TNBS administration. The mice were weighed and killed 48 h after TNBS administration. Colons were removed, washed and opened. Inflammation grading was performed by two

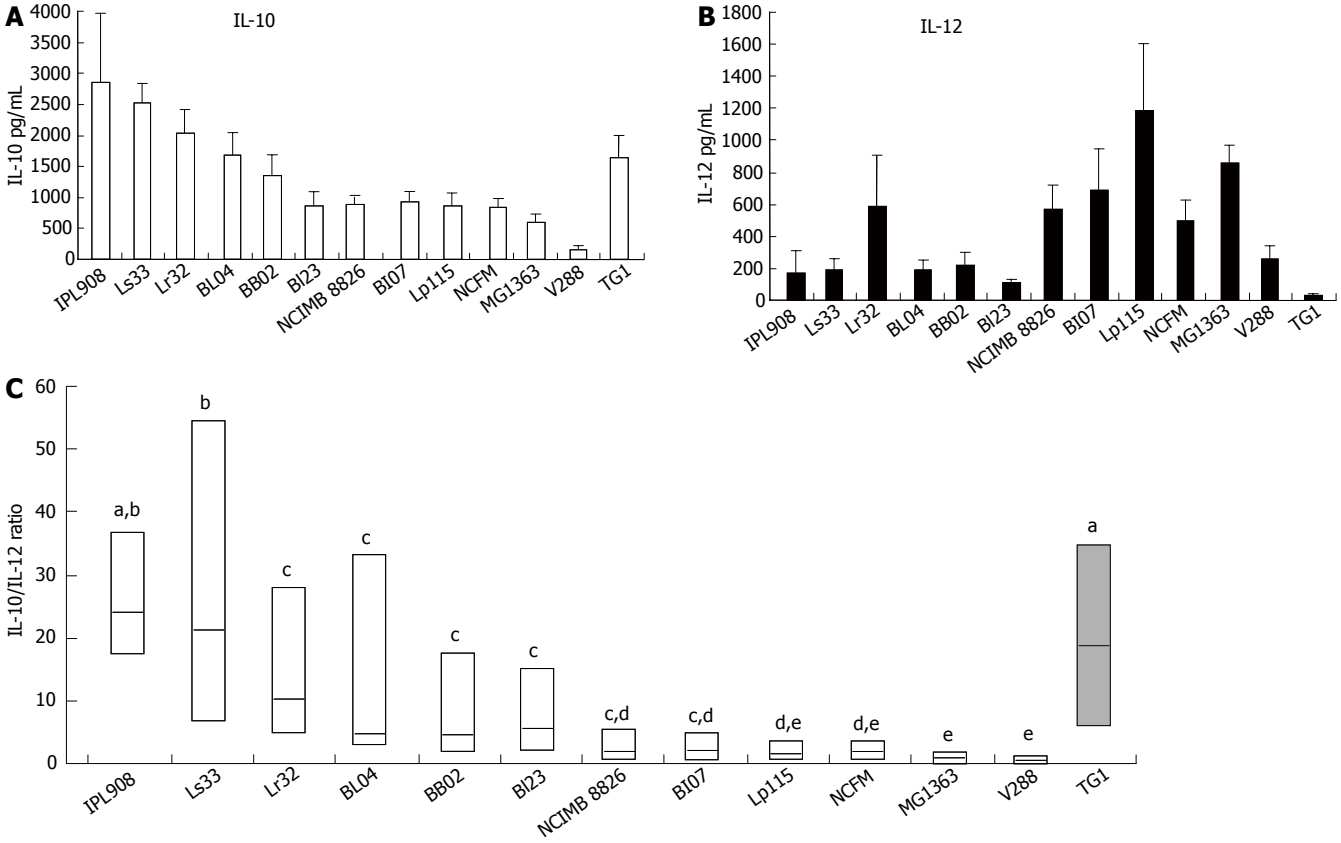

Figure 1 Strain-specific patterns of IL-10 (**A**) and IL-12p70 (**B**) release for various bacterial strains and IL-10/IL-12 ratios (**C**) for 6 to 12 independent healthy donors. Bars represent the mean ± SE values in pg/mL for 6 to 12 independent healthy donors. Ranked box and whisker plots show the median values and first to third quartiles in boxes. Different letters indicate significant differences according to Mann-Whitney *U* test ($P < 0.05$).

blinded observers, using the Wallace scoring method[19]. Results are expressed as % protection, corresponding to the reduction of the mean macroscopic inflammation score of bacteria-treated mice ($n = 10$) in comparison to the mean score of TNBS-treated control mice ($NaHCO_3$ buffer-treated mice, $n = 10$)[16]. Histological analysis was performed on hematoxylin/eosin-stained 5 μm tissue sections from colon samples fixed in 10% formalin and embedded in paraffin.

Statistical analysis

Results were analyzed by the non-parametric one-way analysis of variance and Mann-Whitney *U* test. Differences were judged to be statistically significant when the *P* value was < 0.05. For *in vivo* experiments, only protection levels exceeding 30% (positive and negative) were considered to be relevant, as previously described[16]. For the calculation of the IL-10/IL-12 ratio, all undetectable IL-12 values (below 50 pg/mL) were arbitrarily set at 50 pg/mL level to normalize aberrant quotients. Association of variables was analyzed by the *P* value-assigned Spearman rank correlation coefficient.

RESULTS

Cytokine release by PBMCs is strain specific

The *in vitro* immunostimulation by 13 live bacterial strains (Table 1) of PBMCs collected from 6 to 12 independent donors, revealed distinct and typical patterns of cytokine release. TNFα release was quite uniform for the different LAB investigated, while IFNγ showed variations tending to parallel IL-12 profiles (data not shown). IL-10 and IL-12 levels displayed a strain-specific pattern (Figure 1A and B). Variations in IL-10 concentrations were substantial with values ranging between 200 and 3000 pg/mL depending on the bacterial strain. For IL-12, we also observed significant variations between strains, covering a range of cytokine levels of 50 to 1200 pg/mL. As IL-10 and IL-12 appeared to be the most discriminative cytokines, we used the IL-10/IL-12 ratio (Figure 1C) to distinguish between strains exhibiting a "pro-" *versus* "anti-inflammatory" profile (low *versus* high IL-10/IL-12 ratio, respectively). This approach was found to be useful to identify strains with marked opposite profiles, but did not allow discrimination of strains with median cytokine ratios.

The variation in absolute cytokine concentrations released by PBMCs derived from different donors was examined by conducting successive experiments with a limited set of 6 strains (*E. coli* TG1, *L. salivarius* Ls33, *L. casei* Bl23, *L. plantarum* NCIMB 8826, *Lc. lactis* MG1363 and *L. acidophilus* NCFM). In general, for a variety of individual donors, the ranking of strains was quite reproducible: the most potent "anti-inflammatory" strains induced the highest IL-10 responses in all donors, while other strains were stronger IL-12 inducers in most donors. As an example, Figure 2A and B shows the IL-10 and IL-12 expression profiles for four donors in response to the six "reference" strains used. Relative differences

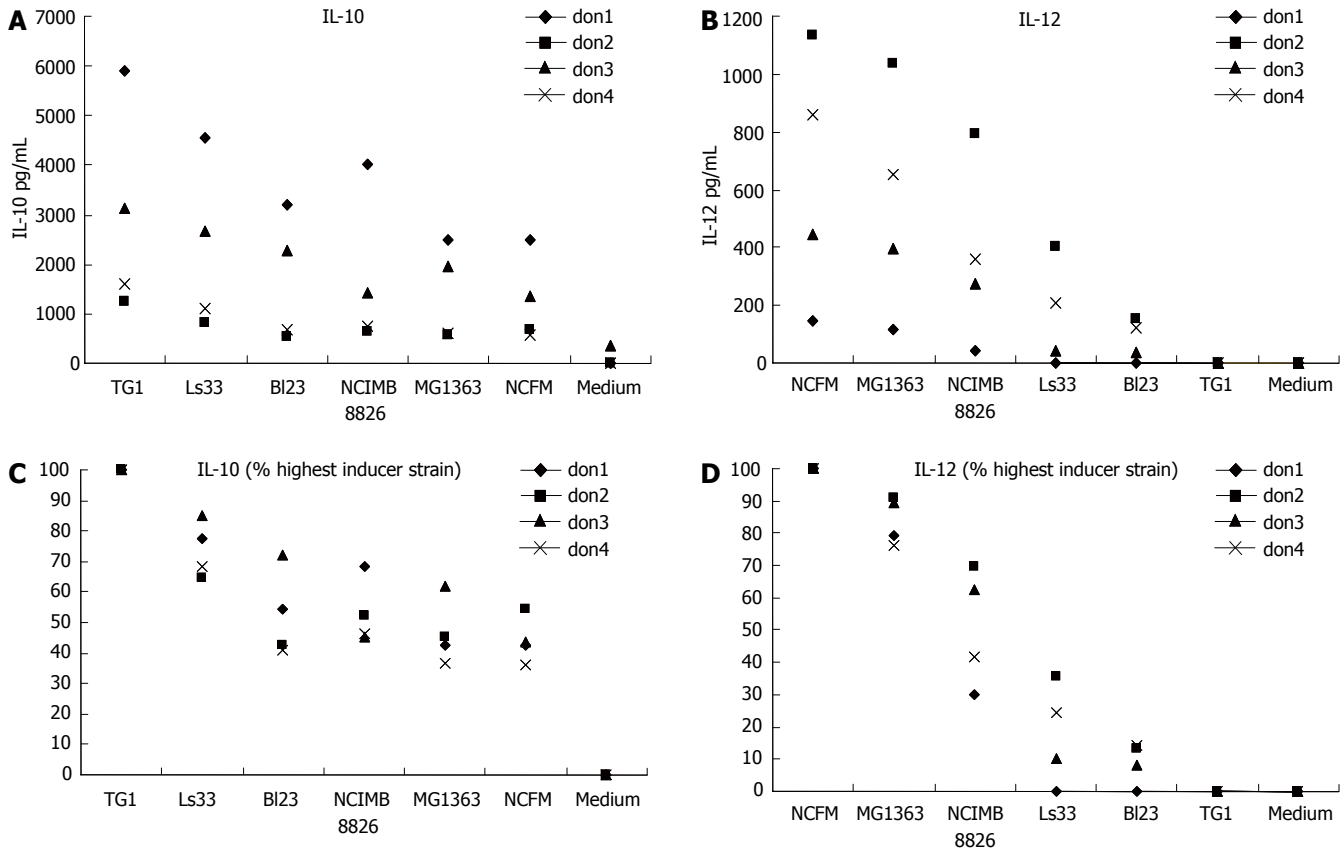

Figure 2 IL-10 (**A**) and IL-12p70 (**B**) release in 4 distinct individual human PBMC donors and the expression level of IL-10 (**C**) and IL-12p70 (**D**). Individual values are represented in pg/mL while IL-10 and IL-12p70 levels are expressed as % of the highest inducer strain. [a]$P < 0.05$.

between two strains, expressed as a percentage of the highest inducer, taken as internal control, were quite constant for all donors (Figures 2C and D). For example, we consistently found 35% and 82% difference ($P < 0.05$) between the strains *L. salivarius* Ls33 and *L. acidophilus* NCFM, for IL-10 and IL-12 induction, respectively. Based on these observations, both strains could be compared in a semi-quantitative way, using their average IL-10 and IL-12 release patterns upon stimulation of PBMCs from four different donors. To that extent we calculated a full matrix of *P*-values for the IL-10/IL-12 ratios obtained from several overlapping studies with reference strains as well as new isolates, for at least 4 PBMC donors, which allowed us to rank strains from an "anti-inflammatory" to a "pro-inflammatory" profile.

When applied to the 13 strains used in this study, this methodology established a semi-quantitative ranking, which could classify strains *L. salivarius* Ls33*, L. casei* Bl23*, L. rhamnosus* Lr32*, L. acidophilus* IPL908 as more anti-inflammatory than the three bifidobacteria and the two *L. plantarum* strains. *Lc. lactis* MG1363*, S. gordonii* V288 and *L. acidophilus* NCFM® strains showed a slightly pro-inflammatory profile with a very low IL-10/IL-12 ratio.

Protection of TNBS-induced colitis was strain-specific

We investigated the protective effect of the 13 strains studied *in vitro* against TNBS-induced colitis in mice (Figure 3). Ls33, Lr32, Bl23, IPL908 and BL04 strains consistently led to a considerable attenuation of colitis (data represent the result of usually 2 to 4 distinct experiments), with reduced weight loss, improved clinical parameters (rectal bleeding, stool consistency, *i.e.* liquid pasty stool and diarrhoea, lethargy; data not shown) and reduced macroscopic inflammation scores. Considering the % protection as the reduction of the mean macroscopic inflammation score of bacteria-treated mice ($n = 10$) in comparison to the mean score of TNBS-treated control mice, the *Lactobacillus plantarum* strains and the BB02 and Bl07 bifiidobacterial strains induced moderate but significant levels of protection. In contrast, no improvement in colitis was observed for the strains *L. acidophilus* NCFM*, Lc. lactis* MG1363 or *S. gordonii* V288 and for the non-pathogenic *E. coli* TG1. None of these strains, however, aggravated the symptoms of colitis. Histological analysis corroborated these findings, showing dramatic improvement in epithelial lesions of the animals receiving protective strains, with a significant decrease in goblet cells and crypt loss (data not shown), and reduced inflammatory infiltrates (mainly neutrophils) accompanied with a reduction of the colon wall thickness to almost normal levels (Figure 4).

Additional experiments confirmed this strain-specific protection in mice with a different genetic background (C57/Bl6 mice). The protection observed in BALB/c mice with *L. salivarius* Ls33 (56.5% ± 7.2%, $P < 0.01$) was confirmed in C57/Bl6 mice (47%, $P < 0.01$), whereas the *L. acidophilus* NCFM® and *E. coli* strains alleviated colitis neither in BALB/c mice (-12.5% ± 2.7%, NS; and +19.4% ± 3.7%, NS, respectively) nor in C57/Bl6 (+26%, NS; and -6.4%, NS, respectively).

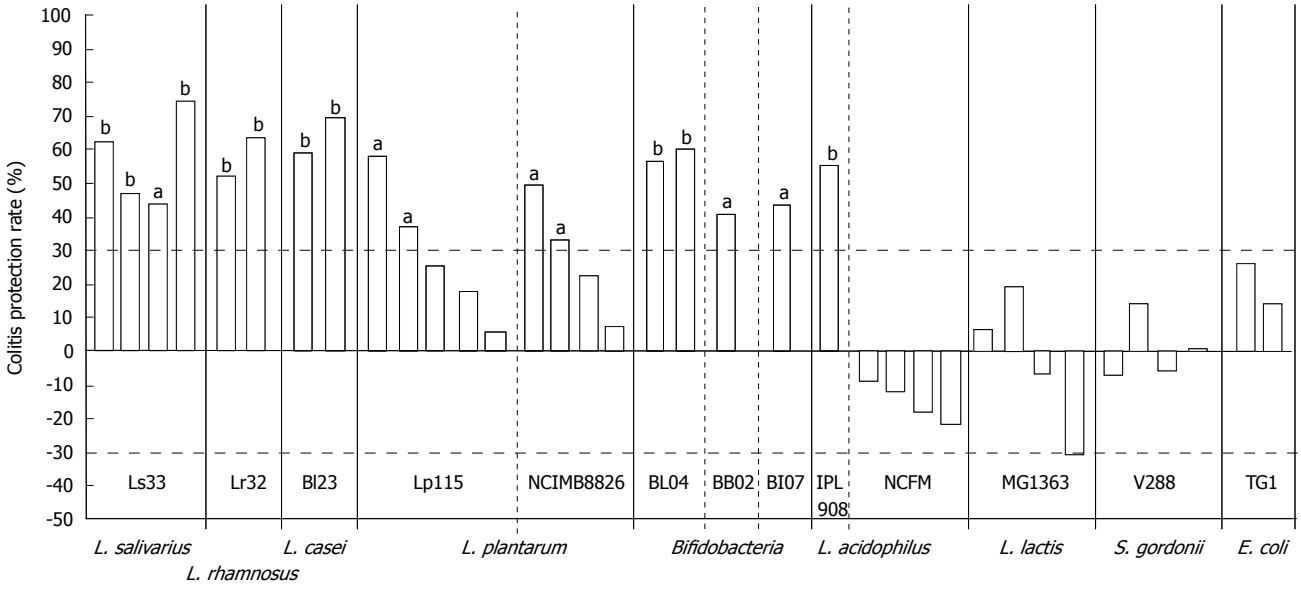

Figure 3 Protective effect of LAB strains against TNBS-induced colitis in BALB/c mice. Results are expressed as a % reduction of the mean macroscopic inflammation of mice treated with LAB as compared to the mean score of non-treated mice. Colitis index was assessed 48 h after TNBS administration. Each bar represents an independent experiment and corresponds to the ratio of control and LAB-treated mice groups (n = 10). $^{a}P < 0.05$, $^{b}P < 0.01$ *vs* TNBS-control group. The horizontal dashed lines indicate the 30% threshold of the uncertain statistical significance.

In vivo / In vitro correlation

Considering both *in vitro* and *in vivo* results, it was evident that strains displaying the highest *in vitro* anti-inflammatory profile (a high IL-10/IL-12 ratio) were the most protective in the *in vivo* colitis model, while those leading to intermediary *in vitro* IL-10/IL-12 ratios showed limited protection. In contrast, bacteria characterized by a low anti-inflammatory potential (low IL-10/IL-12 ratio) did not improve inflammation at all. As a result, with the exception of the Gram-negative *E. coli*, the ranking of all Gram-positive bacteria investigated, based on the *in vitro* cytokine profiling, closely matched the ranking based on the improvement of colitis symptoms. Although this link could not be expressed as an "exact linear" association between % protection and IL-10/IL-12 ratio, it was found to be highly significant using the Spearman rank correlation coefficient (r_s = 0.825, P <0.001) (Figure 5).

DISCUSSION

Immunomodulation through probiotics represents one of the current treatment options for IBD[5,20] and specific strains may stimulate immunomodulatory mediators, inhibit pro-inflammatory cytokines and influence the phenotypes of immunocompetent cells with subsequent events such as migration of dendritic cells and induction of regulatory T cells[15,21]. The mechanisms of action of probiotics are most probably multi-factorial, involving a variety of effector signals, cell types and receptors[22], and strains may differ in their respective ability to trigger these signals considering both immunocompetent and intestinal epithelial cells[23]. It has been proposed that some probiotics are able to prevent or restore intestinal homeostasis after an immune dysregulation, improving mucosal barrier functions as well as down-regulating inflammatory responses[24,25].

In this study, we aimed at developing a simple and standardized *in vitro* test allowing preliminary classification of candidate probiotic strains according to their immune modulation capacity that would be predictive of their *in vivo* effect. To this end, we ranked 13 LAB strains with reference to the IL10/IL12 cytokine ratio induced on human PBMCs and further assessed their protective effect against TNBS-induced colitis in mice.

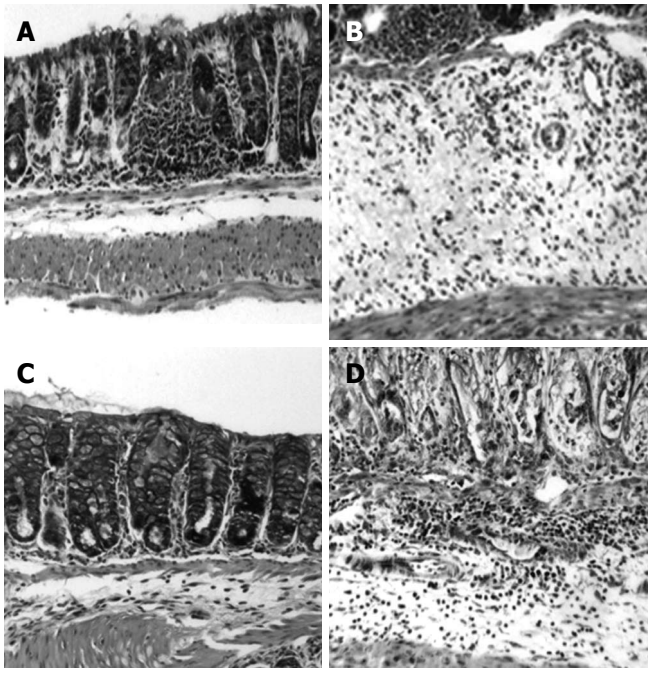

Figure 4 Hematoxylin/eosin staining of representative cross-sections of murine (BALB/c) distal colon (HE, x 20). **A**: Normal appearance of the colon from a negative control mice; **B**: Thickening of the colon wall accompanied with massive inflammatory infiltrate and muscular necrosis 2 d after TNBS-induction of colitis; **C**: Reduction of histological damage in *L. salivarius* Ls33-treated mice after TNBS administration; **D**: Lack of histological improvement of colitis in *L. acidophilus* NCFM-treated mice after TNBS administration.

We observed strong strain-specific variations of the *in vitro* cytokine induction profiles after stimulation of immunocompetent cells, which confirms the results reported in previous studies[9-11,15,26]. We also noted that differences between blood donors did not prevent us ranking the strains based on their cytokine responses as the relative responses of PBMCs to various LAB were consistent from one donor to another. PBMCs from healthy donors can thus be used to screen the immunomodulatory activity of candidate probiotic strains and this test/assay appears to be a good indicator of *in vivo* anti-inflammatory strains. Despite the fact that this assay does not clarify the physiological mechanism(s) involved, it seems to mimic how the immune system may sense the bacterial strains and consequently polarise the immune response. Strains leading to a high IL-10/IL-12 ratio would more easily slow down an early Th1 response.

In accordance with this hypothesis, we found differences in the *in vivo* protective capacity of the 13 studied strains against TNBS-induced inflammation[27]. This strain-specificity has already been described in other experimental models of colitis[28-31]. The variations we observed between different LAB strains in this respect cannot simply be explained by differences in persistence, especially when daily administrations maintain the level of bacteria in the gastro-intestinal tract. Of note, we have previously verified whether the anti-inflammatory profiles could in any way be linked to *in vitro* properties such as gastric juice (pepsin/pancreatin) and bile salt resistance, epithelial cell adhesion and *in vivo* intestinal persistence (unpublished data). However, no link was found between them.

Above all, we have demonstrated in this study that the ranking of strains obtained on the basis of an *in vitro* IL-10/IL-12 cytokine induction ratio closely matches the ranking of the *in vivo* ability of the strains to attenuate experimental colitis. The concordance between the *in vitro* and *in vivo* assays has been illustrated in the case of a cell-wall mutant of *L. plantarum*[18]. The importance of the IL-10/IL-12 ratio has also recently been highlighted by Peran *et al*[32] who showed that administration of a specific strain of *Lactobacillus salivarius* subsp. *salivarius* could improve the recovery of inflamed tissue in a TNBS model of rat colitis. This strain was selected among 30 LAB strains for eliciting the best IL-10/IL-12 and IL-10/TNFα ratios. Unfortunately, no strains exhibiting a moderate or low IL-10/IL-12 profile were included in the *in vivo* study, which could have validated the proposed screening strategy. Similarly, *in vitro* tests on immunocompetent cells have been used successfully to study the effect of distinct bacterial fractions (intact cell walls, protoplast and polysaccharide-peptidoglycans) of the strain *Lactobacillus casei* Shirota[33]. Using the ability of this strain to inhibit the LPS-induced IL-6 in mice bone marrow derived-DCs and PBMCs isolated from ulcerative colitis patients, the authors could establish that the polysaccharide-peptidoglycan complex was the most efficient compound to improve chronic colitis and ileitis in their mice model. Another example attesting similar links between *in vitro* macrophage stimulation and related protection in a murine TNBS model of colitis was reported for the anti-inflammatory drug "catapolside"[34], leading to clinical trials in IBD patients in Korea.

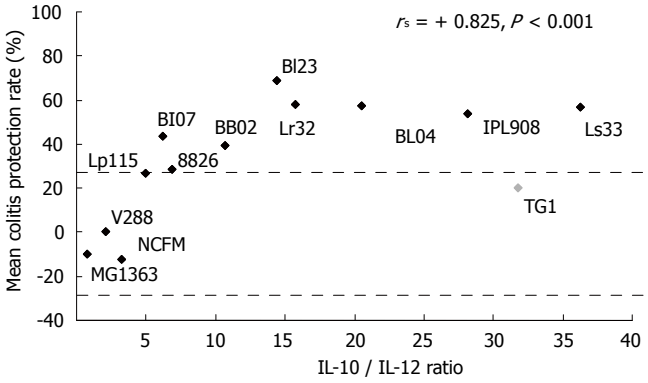

Figure 5 Correlation between the average protection against experimental colitis and the mean IL-10/IL-12 ratios obtained *in vitro*, for all investigated strains. Spearman coefficient (r_s = 0.825, P < 0.001). The horizontal dashed lines indicate the 30% threshold of unprotectiveness.

Recently, the PBMC IL-10/IL-12 ratio has also been used to follow the immunomodulatory properties of probiotics in a clinical study on irritable bowel syndrome (IBS)[31]. Despite different aetiology and characteristics, IBD and IBS share some aspects of immune dysregulation, and IBS has been documented to be associated with low-grade inflammation. Concomitantly to alleviation of the main IBS symptoms, the authors showed normalization of the PBMC IL-10/IL-12 ratio in patients receiving probiotics *versus* placebo, showing that *in vivo* probiotic efficiency can be correlated to specific *in vitro* assays.

Despite the positive correlation observed between *in vivo* protection and *in vitro* cytokine ratio, some restrictions are clear. First of all, the link is not valid for Gram-negative bacteria. Gram-negative bacteria, including both non-pathogenic and pathogenic strains, are well known to be potent inducers of monocytic IL-10, while Gram-positive species preferentially stimulate IL-12 [10]. These observations do not exclude Gram-negative strains from being anti-inflammatory. For example, bacteria such as the *E. coli* strain Nissle[35] or virulence-attenuated *Yersinia pseudotuberculosis* mutants[36] have been shown to be able to reduce colonic lesions and inflammatory mediators in murine models of experimental colitis. Secondly, it is not excluded that *Lactobacillus* strains may moderate colitis by non immune-related modes of action, as for example by acting on barrier integrity or influencing the oxidative pathway[37]. Alternatively, LAB strains with a rather pro-inflammatory profile may have other health benefits which substantiate their probiotic status[38,39].

The methods described in this paper can be used to screen a larger set of potential probiotic strains for their immunomodulatory properties, since they are relatively simple and quite reproducible. We are currently building a reference database including both *in vitro* cytokine profiles, as well as protection levels measured in the TNBS mice model for selected reference strains. This database encompasses strains and blends used in former clinical trials in IBD (i.e. *L. rhamnosus* GG, VSL#3 and *E. coli* strain Nissle[2,3,40,41]), which could further support

and validate the predictive value of the screening strategy presented in this paper.

In conclusion, our results linked *in vitro* and *in vivo* anti-inflammatory properties of a series of LAB and confirm that potential probiotic strains can be pre-screened *in vitro* for their immunomodulating potential, before animal and clinical investigations. This allows pre-selection of probiotics able to modulate the host immune system in a specific way while reducing considerably the use of animals for screening purposes. Besides these ethical considerations, the comparative study of strains carefully selected for either pro- or anti-inflammatory properties will assist further investigation of the mechanism(s) by which specific probiotics signal to the host.

COMMENTS

Background

Evidence exists for the protective role of selected probiotic strains in inflammatory bowel disease. Probiotic strains have clearly been shown to differ in their *in vitro* interaction with immunocompetent cells, especially in terms of cytokine responses. No clear link has been established so far between the *in vitro* immunomodulation potential (e.g. on PBMC's) of the probiotic strain and its ability to prevent experimental colitis in mice (e.g. in TNBS- induced colitis). The use of simple *in vitro* methods to select the most efficient strains for possible clinical trials will improve the quality and reduce the costs of this type of research.

Research frontiers

Improving gastrointestinal function is important for IBD patients and fundamental research is needed to develop new treatments for such pathogenesis. Probiotics are generally accepted to be one of these alternative methods. Few original research papers, however, have evaluated the potential of this approach by focusing on the level of the bacterial strain or strains used.

Probiotic-mediated immunomodulation represents an interesting option in the management of IBD and there is evidence that the immune system can be modulated by orally delivered bacteria. However, in some animal and clinical studies, probiotics did not show the expected beneficial effect. The selection of a successful protective strain may rely on a proper screening of a large number of candidate strains for their technological and immunomodulatory performance, as recently published in *WJG*. Together with proper *in vitro* analytical methods, the use of a reliable animal model is therefore indispensable. Using a well-standardized animal model, we have demonstrated that consistent differences in anti-inflammatory potential of several orally administered lactic acid bacteria could be observed in TNBS-induced colitis.

In the present study we linked for the first time the results of *in vitro* and *in vivo* anti-inflammatory readouts for 13 selected LAB, and confirmed herewith the strain-specific nature of the potential of probiotics to modulate the host's immune system and in assisting in the alleviation of intestinal disorders, IBD in particular.

Innovations and breakthroughs

Linking *in vitro* and *in vivo* anti-inflammatory properties of a series of LAB can confirm the interest of screening potential probiotic strains using *in vitro* assays, before launching animal and clinical investigations. This allows not only the pre-selection of probiotics able to modulate the host's immune system in a specific way while reducing considerably the use of animals for screening purposes, but also results in a classification of microorganisms that could be useful for the study or comparison of other probiotic properties. So, besides ethical considerations, the comparative study of strains carefully selected for either pro- or anti-inflammatory properties will assist further investigation of the mechanism(s) by which specific probiotics signal to the host.

Applications

The use of probiotic strains in IBD treatment has been controversial, because of some major drawbacks. The first is the type of inflammatory disease targeted (Crohn's disease on the one hand, with low success levels, *versus* ulcerative colitis and pouchitis where treatment was more successful). The second is that a comparison between a therapeutic preventive application in combination with or without traditional medication, is not always clear. The third is that the choice of strains or the mixture thereof is often made rather artificially and driven by available commercial preparations which are not necessarily developed or suitable for this type of medical application. Using the described selection procedure, the influence of well-selected strains (e.g. with expected positive and negative performance as anti-inflammatory agent) in different conditions (with or without traditional medication) of a selected animal model (prophylactic or therapeutic) can be evaluated unequivocally. The results should not only allow to select the best possible conditions for the follow-up clinical study but will also help to understand the underlying mechanisms and factors that influence the efficiency of the application.

Terminology

The TNBS mouse model of colitis is a hapten-induced experimental model (TNBS = 2, 4, 6-trinitrobenzene sulfonic acid), which has proven to be a very useful model for studying certain forms of human inflammatory bowel disease. This model has e.g. been used to show that an IL-12-driven, Th1 T cell-mediated inflammation of the colon is not only prevented by systemic administration of anti-IL-12 antibody, but can also be treated this way. Consequently anti-IL-12 is currently used in the treatment of Crohn's disease. Other studies with this model have established that mucosal inflammation and/or its prevention depend partially on a balance between pro-inflammatory Th1 T cell responses and anti-inflammatory TGF-β and IL-10 responses.

Peer review

This is an interesting study showing that *in vitro* assays using human PBMCs can partially translate to murine models of colitis giving an indication of the level of expected protection of this particular model of colitis using IL-10/IL-12 ratios. It would be interesting to discover whether this held out if colitis was induced before administration of the probiotic (perhaps a more physiological approach for therapy). However, this does offer some insight into prophylactic approaches for managing patients in remission.

REFERENCES

1 **Bergonzelli GE**, Blum S, Brussow H, Corthésy-Theulaz I. Probiotics as a treatment strategy for gastrointestinal diseases? *Digestion* 2005; **72**: 57-68

2 **Kruis W**, Fric P, Pokrotnieks J, Lukás M, Fixa B, Kascák M, Kamm MA, Weismueller J, Beglinger C, Stolte M, Wolff C, Schulze J. Maintaining remission of ulcerative colitis with the probiotic *Escherichia coli* Nissle 1917 is as effective as with standard mesalazine. *Gut* 2004; **53**: 1617-1623

3 **Gionchetti P**, Rizzello F, Helwig U, Venturi A, Lammers KM, Brigidi P, Vitali B, Poggioli G, Miglioli M, Campieri M. Prophylaxis of pouchitis onset with probiotic therapy: a double-blind, placebo-controlled trial. *Gastroenterology* 2003; **124**: 1202-1209

4 **Mahida YR**, Rolfe VE. Host-bacterial interactions in inflammatory bowel disease. *Clin Sci* (Lond) 2004; **107**: 331-341

5 **Hart AL**, Stagg AJ, Kamm MA. Use of probiotics in the treatment of inflammatory bowel disease. *J Clin Gastroenterol* 2003; **36**: 111-119

6 **Chapat L**, Chemin K, Dubois B, Bourdet-Sicard R, Kaiserlian D. *Lactobacillus casei* reduces CD8+ T cell-mediated skin inflammation. *Eur J Immunol* 2004; **34**: 2520-2528

7 **Maassen CB**, van Holten-Neelen C, Balk F, den Bak-Glashouwer MJ, Leer RJ, Laman JD, Boersma WJ, Claassen E. Strain-dependent induction of cytokine profiles in the gut by orally administered Lactobacillus strains. *Vaccine* 2000; **18**: 2613-2623

8 **McCarthy J**, O'Mahony L, O'Callaghan L, Sheil B, Vaughan EE, Fitzsimons N, Fitzgibbon J, O'Sullivan GC, Kiely B, Collins JK, Shanahan F. Double blind, placebo controlled trial of two probiotic strains in interleukin 10 knockout mice and mechanistic link with cytokine balance. *Gut* 2003; **52**: 975-980

9 **Fujiwara D**, Inoue S, Wakabayashi H, Fujii T. The anti-allergic effects of lactic acid bacteria are strain dependent and mediated by effects on both Th1/Th2 cytokine expression and balance. *Int Arch Allergy Immunol* 2004; **135**: 205-215

10 **Hessle C**, Andersson B, Wold AE. Gram-positive bacteria are potent inducers of monocytic interleukin-12 (IL-12) while gram-negative bacteria preferentially stimulate IL-10 produc-

tion. *Infect Immun* 2000; **68**: 3581-3586
11 **Kimoto H**, Mizumachi K, Okamoto T, Kurisaki J. New *Lactococcus* strain with immunomodulatory activity: enhancement of Th1-type immune response. *Microbiol Immunol* 2004; **48**: 75-82
12 **O'Mahony L**, O'Callaghan L, McCarthy J, Shilling D, Scully P, Sibartie S, Kavanagh E, Kirwan WO, Redmond HP, Collins JK, Shanahan F. Differential cytokine response from dendritic cells to commensal and pathogenic bacteria in different lymphoid compartments in humans. *Am J Physiol Gastrointest Liver Physiol* 2006; **290**: G839-G845
13 **Peña JA**, Rogers AB, Ge Z, Ng V, Li SY, Fox JG, Versalovic J. Probiotic *Lactobacillus* spp. diminish *Helicobacter hepaticus*-induced inflammatory bowel disease in interleukin-10-deficient mice. *Infect Immun* 2005; **73**: 912-920
14 **Christensen HR**, Frøkiaer H, Pestka JJ. Lactobacilli differentially modulate expression of cytokines and maturation surface markers in murine dendritic cells. *J Immunol* 2002; **168**: 171-178
15 **Hart AL**, Lammers K, Brigidi P, Vitali B, Rizzello F, Gionchetti P, Campieri M, Kamm MA, Knight SC, Stagg AJ. Modulation of human dendritic cell phenotype and function by probiotic bacteria. *Gut* 2004; **53**: 1602-1609
16 **Foligné B**, Nutten S, Steidler L, Dennin V, Goudercourt D, Mercenier A, Pot B. Recommendations for improved use of the murine TNBS-induced colitis model in evaluating anti-inflammatory properties of lactic acid bacteria: technical and microbiological aspects. *Dig Dis Sci* 2006; **51**: 390-400
17 **Foligné B**, Grangette C, Pot B. Probiotics in IBD: mucosal and systemic routes of administration may promote similar effects. *Gut* 2005; **54**: 727-728
18 **Grangette C**, Nutten S, Palumbo E, Morath S, Hermann C, Dewulf J, Pot B, Hartung T, Hols P, Mercenier A. Enhanced antiinflammatory capacity of a *Lactobacillus plantarum* mutant synthesizing modified teichoic acids. *Proc Natl Acad Sci USA* 2005; **102**: 10321-10326
19 **Wallace JL**, MacNaughton WK, Morris GP, Beck PL. Inhibition of leukotriene synthesis markedly accelerates healing in a rat model of inflammatory bowel disease. *Gastroenterology* 1989; **96**: 29-36
20 **Fedorak RN**, Madsen KL. Probiotics and the management of inflammatory bowel disease. *Inflamm Bowel Dis* 2004; **10**: 286-299
21 **Braat H**, van den Brande J, van Tol E, Hommes D, Peppelenbosch M, van Deventer S. *Lactobacillus rhamnosus* induces peripheral hyporesponsiveness in stimulated CD4+ T cells via modulation of dendritic cell function. *Am J Clin Nutr* 2004; **80**: 1618-1625
22 **Servin AL**. Antagonistic activities of lactobacilli and bifidobacteria against microbial pathogens. *FEMS Microbiol Rev* 2004; **28**: 405-440
23 **Riedel CU**, Foata F, Philippe D, Adolfsson O, Eikmanns BJ, Blum S. Anti-inflammatory effects of bifidobacteria by inhibition of LPS-induced NF-kappaB activation. *World J Gastroenterol* 2006; **12**: 3729-3735
24 **Llopis M**, Antolín M, Guarner F, Salas A, Malagelada JR. Mucosal colonisation with *Lactobacillus casei* mitigates barrier injury induced by exposure to trinitronbenzene sulphonic acid. *Gut* 2005; **54**: 955-959
25 **Oshima T**, Laroux FS, Coe LL, Morise Z, Kawachi S, Bauer P, Grisham MB, Specian RD, Carter P, Jennings S, Granger DN, Joh T, Alexander JS. Interferon-gamma and interleukin-10 reciprocally regulate endothelial junction integrity and barrier function. *Microvasc Res* 2001; **61**: 130-143
26 **He F**, Morita H, Ouwehand AC, Hosoda M, Hiramatsu M, Kurisaki J, Isolauri E, Benno Y, Salminen S. Stimulation of the secretion of pro-inflammatory cytokines by *Bifidobacterium* strains. *Microbiol Immunol* 2002; **46**: 781-785
27 **Sheil B**, McCarthy J, O'Mahony L, Bennett MW, Ryan P, Fitzgibbon JJ, Kiely B, Collins JK, Shanahan F. Is the mucosal route of administration essential for probiotic function? Subcutaneous administration is associated with attenuation of murine colitis and arthritis. *Gut* 2004; **53**: 694-700
28 **Cross ML**, Gill HS. Can immunoregulatory lactic acid bacteria be used as dietary supplements to limit allergies? *Int Arch Allergy Immunol* 2001; **125**: 112-119
29 **Osman N**, Adawi D, Ahrne S, Jeppsson B, Molin G. Modulation of the effect of dextran sulfate sodium-induced acute colitis by the administration of different probiotic strains of *Lactobacillus* and *Bifidobacterium*. *Dig Dis Sci* 2004; **49**: 320-327
30 **Shibolet O**, Karmeli F, Eliakim R, Swennen E, Brigidi P, Gionchetti P, Campieri M, Morgenstern S, Rachmilewitz D. Variable response to probiotics in two models of experimental colitis in rats. *Inflamm Bowel Dis* 2002; **8**: 399-406
31 **O'Mahony L**, McCarthy J, Kelly P, Hurley G, Luo F, Chen K, O'Sullivan GC, Kiely B, Collins JK, Shanahan F, Quigley EM. Lactobacillus and bifidobacterium in irritable bowel syndrome: symptom responses and relationship to cytokine profiles. *Gastroenterology* 2005; **128**: 541-551
32 **Peran L**, Camuesco D, Comalada M, Nieto A, Concha A, Diaz-Ropero MP, Olivares M, Xaus J, Zarzuelo A, Galvez J. Preventative effects of a probiotic, *Lactobacillus salivarius* ssp. *salivarius*, in the TNBS model of rat colitis. *World J Gastroenterol* 2005; **11**: 5185-5192
33 **Matsumoto S**, Hara T, Hori T, Mitsuyama K, Nagaoka M, Tomiyasu N, Suzuki A, Sata M. Probiotic *Lactobacillus*-induced improvement in murine chronic inflammatory bowel disease is associated with the down-regulation of pro-inflammatory cytokines in lamina propria mononuclear cells. *Clin Exp Immunol* 2005; **140**: 417-426
34 **Kim SW**, Choi SC, Choi EY, Kim KS, Oh JM, Lee HJ, Oh HM, Kim S, Oh BS, Kimm KC, Lee MH, Seo GS, Kim TH, Oh HC, Woo WH, Kim YS, Pae HO, Park DS, Chung HT, Jun CD. Catalposide, a compound isolated from catalpa ovata, attenuates induction of intestinal epithelial proinflammatory gene expression and reduces the severity of trinitrobenzene sulfonic Acid-induced colitis in mice. *Inflamm Bowel Dis* 2004; **10**: 564-572
35 **Schultz M**, Strauch UG, Linde HJ, Watzl S, Obermeier F, Göttl C, Dunger N, Grunwald N, Schölmerich J, Rath HC. Preventive effects of Escherichia coli strain Nissle 1917 on acute and chronic intestinal inflammation in two different murine models of colitis. *Clin Diagn Lab Immunol* 2004; **11**: 372-378
36 **Marceau M**, Dubuquoy L, Caucheteux-Rousseaux C, Foligne B, Desreumaux P, Simonet M. Yersinia pseudotuberculosis anti-inflammatory components reduce trinitrobenzene sulfonic acid-induced colitis in the mouse. *Infect Immun* 2004; **72**: 2438-2441
37 **Lamine F**, Eutamène H, Fioramonti J, Buéno L, Théodorou V. Colonic responses to *Lactobacillus farciminis* treatment in trinitrobenzene sulphonic acid-induced colitis in rats. *Scand J Gastroenterol* 2004; **39**: 1250-1258
38 **Varcoe JJ**, Krejcarek G, Busta F, Brady L. Prophylactic feeding of *Lactobacillus acidophilus* NCFM to mice attenuates overt colonic hyperplasia. *J Food Prot* 2003; **66**: 457-465
39 **Sanders ME**, Klaenhammer TR. Invited review: the scientific basis of *Lactobacillus acidophilus* NCFM functionality as a probiotic. *J Dairy Sci* 2001; **84**: 319-331
40 **Mimura T**, Rizzello F, Helwig U, Poggioli G, Schreiber S, Talbot IC, Nicholls RJ, Gionchetti P, Campieri M, Kamm MA. Once daily high dose probiotic therapy (VSL#3) for maintaining remission in recurrent or refractory pouchitis. *Gut* 2004; **53**: 108-114
41 **Prantera C**, Scribano ML, Falasco G, Andreoli A, Luzi C. Ineffectiveness of probiotics in preventing recurrence after curative resection for Crohn's disease: a randomised controlled trial with *Lactobacillus* GG. *Gut* 2002; **51**: 405-409
42 **Gasson MJ**. Plasmid complements of *Streptococcus lactis* NCDO 712 and other lactic streptococci after protoplast-induced curing. *J Bacteriol* 1983; **154**: 1-9
43 **Sambrook J**, Fritsch EF, Maniatis T. Molecular cloning: a laboratory manual, 2nd ed. New York: Cold Spring Harbor Laboratory, 1989

S- Editor Liu Y **L- Editor** Wang XL **E- Editor** Bai SH

PO Box 2345, Beijing 100023, China
www.wjgnet.com
wjg@wjgnet.com

World J Gastroenterol 2007 January 14; 13(2): 244-249
World Journal of Gastroenterology ISSN 1007-9327

BASIC RESEARCH

Rescue of the albino phenotype by introducing a functional tyrosinase minigene into Kunming albino mice

Dong Xiao, Ying Yue, Xin-Yan Deng, Bing Huang, Zhong-Min Guo, Yun Ma, Yi-Li Lin, Xun Hong, Huan Tang, Kang Xu, Xi-Gu Chen

Dong Xiao, Ying Yue, Xin-Yan Deng, Bing Huang, Zhong-Min Guo, Yun Ma, Yi-Li Lin, Xun Hong, Kang Xu, Xi-Gu Chen, Center of Experimental Animals, Sun Yat-sen University, Guangzhou 510080, Guangdong Province, China
Dong Xiao, Institute of Comparative Medicine and Center of Experimental Animals, Southern Medical University, Guangzhou 510515, Guangdong Province, China
Huan Tang, Department of Animal Science, College of Basic Medicine, the Third Military Medical University, Chongqing 400038, China
Supported by the National Natural Science Foundation of China, No. 30271177 and No. 39870676; National 9th Five-year Program, No. 101033; Major Science and Technology Projects of Guangdong Province, No. B602; Natural Science Foundation of Guangdong Province, No. 021903; Postdoctoral Fellowship Foundation of China (Series 29); Special Fund of Scientific Instrument Collaborative Share-net in Guangzhou. No. 2006176
Correspondence to: Xi-Gu Chen, Professor, Center of Experimental Animals, Sun Yat-Sen University, Guangzhou 510080, Guangdong Province, China. xiguchen@163.com
Telephone: +86-20-33151566 Fax: +86-20-87331230
Received: 2006-09-20 Accepted: 2006-11-24

Abstract

AIM: To use the tyrosinase minigene as a visual marker to perform microinjection training and improve the techniques related with transgene to greatly elevate the efficiency of gene transfer.

METHODS: A mouse tyrosinase minigene, i.e., TyBS, in which the 2.25-kb authentic genomic 5′ non-coding flanking sequence of mouse tyrosinase was fused to a mouse tyrosinase cDNA, was introduced into the fertilized eggs of outbred Kunming albino mice.

RESULTS: Of the 11 animals that developed from the injected eggs, two mice (P1 and #8) exhibited pigmented hair (P1) and eyes (P1 and #8), as confirmed by PCR analysis for the tyrosinase minigene integrated into the genome. When founder P1 was bred to Kunming male mouse, six progeny out of 11 offspring inherited the transgene and the pigmented-eye phenotype.

CONCLUSION: Taken together, these results suggest that this minigene encodes the active tyrosinase protein and that its 5′ flanking region contains the sequences regulating the expression of mouse tyrosinase gene as expected. We have rescued the albino phenotype by introduction and expression of a functional tyrosinase minigene in the Kunming albino mouse and the transgene can be passed to subsequent generation. These findings also indicate that TyBS can be a useful visual marker gene in the co-transgenic experiments.

Key words: Kunming mouse; Albino; Tyrosinase minigene; Transgenic mice; Melanization; Phenotypic rescue

Xiao D, Yue Y, Deng XY, Huang B, Guo ZM, Ma Y, Lin YL, Hong X, Tang H, Xu K, Chen XG. Rescue of the albino phenotype by introducing a functional tyrosinase minigene into Kunming albino mice. *World J Gastroenterol* 2007; 13(2): 244-249

http://www.wjgnet.com/1007-9327/13/244.asp

INTRODUCTION

Visible pigmentation in the mammals results from the synthesis and distribution of melanin in skin, hair bulbs and eyes[1-3]. Tyrosinase is the first and rate-limiting enzyme in the pathway for melanin production in melanocytes of the skin and eyes[1-3]. Mutation of the tyrosinase gene is a common cause of a similar phenotype in all vertebrates, known as albinism, due to a lack of melanin pigment[1,3]. In mouse, the albino phenotype is characterized by a total absence of pigmentation due to a mutation in the tyrosinase gene; several point mutations within the tyrosinase gene have been found, which can inactivate its function to result in oculocutaneous albinism (OCA)[1,3]. In mouse, the classical albino (*c*) mutation corresponds to a single-point mutation in the first exon of the tyrosinase gene, which brings about an amino acid mutation Cys103Ser, leading to the accumulation of a non-functional protein[4,5]. When mice are homozygous (*c*/*c*) for mutations that inactivate the tyrosinase gene, mice are albino regardless of the genotype at the other loci[1,3]. The entire common albino inbred strains of laboratory mice, such as FVB/N, BALB/c, *etc*, belonging to OCA, have the same point mutation in the tyrosinase gene, indicating that these strains are derived from a common ancestor[5]. The albino phenotype has been successfully corrected through the tyrosinase transgene, which can express the active tyrosinase in transgenic mice[5-18], rabbits[19], fish[20-22] and other vertebrates

expressing tyrosinase functional transgenes[23].

The Human and Model Organism Genome Projects have revealed the sequence information of many genes. A significant challenge for scientists over the next few decades is to annotate the human and model organism genomes with functional information. Genetically engineered mice will play a vital role in the study of the functional genome.

The production of transgenic mice, involving an intensive sequence of procedures in genetics, molecular biology, embryology and animal science, is usually time-consuming and labor-consuming. One problem with learning to do microinjections is that it can be a long wait between the time the microinjections are done and the time that the results are known, particularly if one waits until the microinjected embryos have developed into weaning age mice before screening. How to easily and rapidly assay for a successful pronuclear? There are a number of constructs that are particularly useful when learning to do microinjections. Among them, tyrosinase can be used to allow the visual identification of transgenic mice at birth in the first and all subsequent generations. Microinjection of a tyrosinase minigene into embryos from an albino mouse strain can result in gene cure of the albino defect and the pigment synthesis[5,6,18]. Pigmented mice with dark eyes can be easily identified by simply visible inspection at birth. In fact, the pigment epithelial cells of the retina begin to synthesize melanin by P10.5 of embryonic development[8,26] so that transgenic mice can be typically identified by visual inspection of the fetuses 2 wk after microinjection. The microinjection can be done using albino inbred strains (such as FVB/N and BALB/c) and inexpensive outbred albino strains (such as ICR and Kunming mice). Another advantage of the tyrosinase minigene is the fact that it is not detrimental to the health of the transgenic animals.

Therefore, we decided to use the tyrosinase minigene as a visual marker to perform microinjection training and improve the techniques related with transgene to greatly elevate the efficiency of gene transfer in our center.

MATERIALS AND METHODS

Production of the tyrosinase minigene transgenic mice

The tyrosinase minigene TyBS[5] used for microinjection was generously provided by Dr. P.A. Overbeek (Howard Hughes Medical Institute, Department of Cell Biology, Baylor College of Medicine, Houston, TX, USA) and Dr. F Beermann (Swiss Institute for Experimental Cancer Research, Switzerland).

Transgenic mice were generated by microinjection of single cell embryos using standard techniques[27]. The Kunming mouse strain, supplied by Center of Experimental Animals, Sun Yat-Sen University, was used as the source of embryos for the micromanipulation and for the subsequent breeding trials. For microinjection, the 4.1-kb fragment of tyrosinase minigene (Figure 1) was released free from the vector backbone of pTyBS[5] via digestion with *Eco*R I and *Kpn* I, thereafter isolated and purified using the QIA quick gel extraction kit (Qiagen, Hilden, Germany), diluted to a final concentration of 2

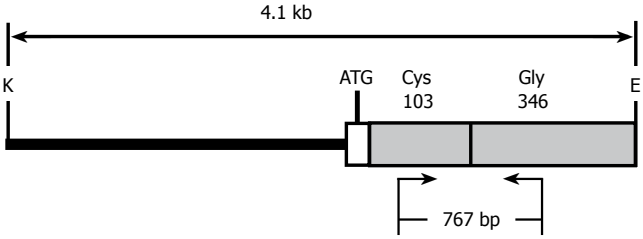

Figure 1 The structure of tyrosinase minigene construct TyBS used for microinjection. The construct contains a 2.25-kb tyrosinase promoter, i.e., 5' non-coding flanking sequence of mouse tyrosinase, as a single thick line plus 65 bp of tyrosinase exon I (to the *Xho* I site) and 1.785-kb *Xho* I-*Eco*R I fragment (shaded) (derived from Tyrs-J) containing tyrosinase cDNA and 3' non-coding flanking sequence. TyBS encodes cysteine at amino acid 103 and glycine at amino acid 346. The 4.1-kb injected fragment was obtained by pTyBS digestion with *Kpn* I and *Eco*R I. The restriction sites are: E, *Eco*R I; K, *Kpn* I. The primers specific for TyBS used in PCR reaction (small arrows) and the expected size of PCR products are indicated.

μg/mL DNA in injection buffer (10 mmol/L Tris/0.1 mmol/L EDTA, pH 7.4), and then microinjected into the pronuclear of one cell-stage fertilized embryos [Kunming mouse (♀) × Kunming mouse (♂)]. About 20-25 DNA-injected fertilized eggs that survived microinjection were implanted into the oviducts of one recipient pseudopregnant Kunming mouse 2-3 h after injection or the next day as previously described[27]. Potential transgenic founders were weaned at 3 wk of age. The offsprings were firstly screened for the presence of the transgene via pigmentation phenotypes derived from the existence of the functional tyrosinase minigene, followed by PCR analysis performed on the tail genomic DNA prepared with standard protocols[28]. All animal care and experimentation were performed according to the Study and Ethical Guidelines for Animal Care, handling and termination established by the Subcommittee of Sun Yat-Sen University on laboratory animal care. The presented work was approved by the ethical committee of Sun Yat-sen University and is covered by Chinese animal husbandary legislation.

Genotype analysis by PCR

PCR was performed on tail genomic DNA to further identify which mice have tyrosinase minigene integrated into their genome. The sequences of the forward primer (FP) within exon 1 and reverse primer (RP) within exon 4 used to amplify a 767-bp fragment of the tyrosinase minigene were: 5'-GGTTTCAACTGCGGAAACTG-3' (forward) and 5'-TGTGAGTGGACTGGCAAATC-3' (reverse) (Figure 1). PCR conditions were as follows: pre-denaturation at 94℃ for 7 min, followed by 30 amplification cycles of denaturation at 94℃ for 1 min, primer annealing at 58℃ for 1 min, and extension at 72℃ for 1 min 30 s, and finally an additional extension at 72℃ for 10 min. TyBS construct DNA was used as the positive control for each PCR reaction, and genomic DNA from normal Kunming mice was employed as a negative control for each PCR test. DNA samples were considered positive for a particular transgene if a band of the predicted size in the test samples was present with no amplification occurring in the control sample. Endogenous genomic

tyrosinase sequence was not amplified under this PCR conditions chosen here.

Mouse propagation and transmission

At 6-8 wk of age, founders shown to be transgenic for the tyrosinase minigene were mated with normal Kunming mice to generate F1. Pigmented F1 animals derived from founder, as well as albino non-transgenic littermates were further analyzed for the inheritance of the tyrosinase transgene by PCR using tyrosinase-FP/RP primers. PCR protocols for TyBS were noted above.

RESULTS

Rescue of the albino phenotype by tyrosinase transgene

Within the coding sequences of the tyrosinase gene, a G to C transversion at nucleotide 308, leading to a cysteine (Cys) to serine (Ser) mutation at amino acid 103, is sufficient to abrogate pigment production in mice[5]. This same base pair change is fully conserved in the classical albino strains of laboratory mice, such as FVB/N and BALB/c[5]. Albino Kunming mice are an outbred mouse strain that is homozygous mutant at the albino (*c*) locus. An albino mutation carried in the Kunming mouse strain should be also the result of a base substitution from G to C in exon I. It is, therefore, reasonable to expect that the albino phenotype can be rescued by introducing a functional tyrosinase minigene, such as TyBS, into albino embryos.

The tyrosinase minigene TyBS construct[5] used for microinjection is illustrated in Figure 1. As the expression of the tyrosinase minigene is easily detected by the pigmented phenotype, this gene can be used as a visual marker for the production of transgenic animals.

Of the 45 embryos transferred to the recipient females, 11 embryos developed to term. Two individuals of 11 siblings were transgenic, as demonstrated by pigmentation phenotype in the eyes (Figure 2A-D, F and G) and coat (Figure 2C, D and F), and PCR analyses (Figures 3A and B).

Furthermore, two TyBS transgenic mice, i.e. P1 (Figure 2A and B) and #8 (Figure 2G) which died 48 h after birth, had dark eyes at birth, and were immediately identifiable as transgenic mice. Although the extent of the coat pigmentation was non-standard like the wild-type phenotype, founder P1 exhibited the partially pigmented phenotype (Figure 2C, D and F). Over time, the coat of P1 with nearly black eyes (Figure 2A-D, F) became more heavily pigmented (light grey to dark grey) (Figure 2C, D and F), while the eye and fur phenotypes of non-transgenic littermate controls remained pink and albino throughout life (Figure 2C-E), respectively.

Transmissibility of the foreign transgene

To determine whether the TyBS transgene was transmitted to the next generation, at 6 wk of age female P1 was back-crossed to the parental mouse strain to give F1 generation. The progeny of P1 was analyzed for the inheritance of the transgene by eye phenotype, coat pigmentation and PCR.

From the cross between P1 and normal Kunming mouse, 11 offspring were obtained. Although all of littermates from P1 died immediately at birth, it was found that six out of the 11 siblings exhibited the pigmented eyes at birth (Figure 2H), as verified by PCR (Figure 3C).

Non-mosaic transgenic mice with one site of integration should transmit the transgenic DNA in a Mendelian fashion to about 50% of their offspring, whereas mosaic mice generally show a frequency of transmission of 25% or less. Note that founder mice that have more than one site of integration can produce litters where 75% or more of the offspring are transgenic, although the percent transmission for any one site of integration is expected to be average 50% or less[29,30]. It was concluded that founder P1, successfully transmitting the transgene in a Mendelian fashion to about 55% (6/11) of its progeny, is non-mosaic transgenic mouse.

Taken together, these data demonstrate that founder P1 can transmit the transgene to subsequent generation and its progeny show an inherited characteristic phenotype of pigmented eyes.

DISCUSSION

Coat color of the tyrosinase transgenic mice

Pigmentary genes are the first mammalian genes to be studied, mostly because of the obvious phenotypes associated with their mutations[23]. In this study, founder P1, harboring the tyrosinase minigene TyBS, exhibited light pigmentation, but non-standard wild-type coat color in the skin, although over time, P1 coat became more heavily pigmented. Similarly, the transgenic mice carrying TyBS construct showed considerable variation in the intensity of pigmentation, the coat colors were found to range from grayish to brownish, and none of the mice were black[5].

Actually, all these standard tyrosinase constructs, including TyBS, driven by the limited amount of 5' tyrosinase upstream regulatory sequences (ranging from 270- to 5500-bp promoter sequences) displayed a high degree of variability in coat pigmentation between independent lines[14,30-34], and the coat pigmentation did not reach the normal levels observed in the wild-type phenotype[6,18,30-32,35,36]. For example, in an evaluation of 39 transgenic founder animals and 44 transgenic lines, 5 phenotypic patterns of pigmentation were consistently observed, including albino, dark, light, mottled and Himalayan[32]. In fact, the tyrosinase minigene which is sufficient to produce normal levels of both eumelanin and phaeomelanin can give normal black or brown pigmentation on the appropriate non-agouti genetic backgrounds[5,32]. These abnormally expressional patterns might have been explained by position effects. In summary, these findings demonstrate that other regulatory regions within the tyrosinase gene are required to sustain the faithful expression of tyrosinase transgene, independent of integration site.

By flanking a tyrosinase minigene with tandem copies of the chicken β-globin 5' HS4 insulator, there is a significant reduction in variability among transgenic lines, with the resulting mice exhibiting the similar levels of coat pigmentation, which, in turn, improves the yield of phenotypically expected transgenic founders resulting from each microinjection session, and consequently reduces

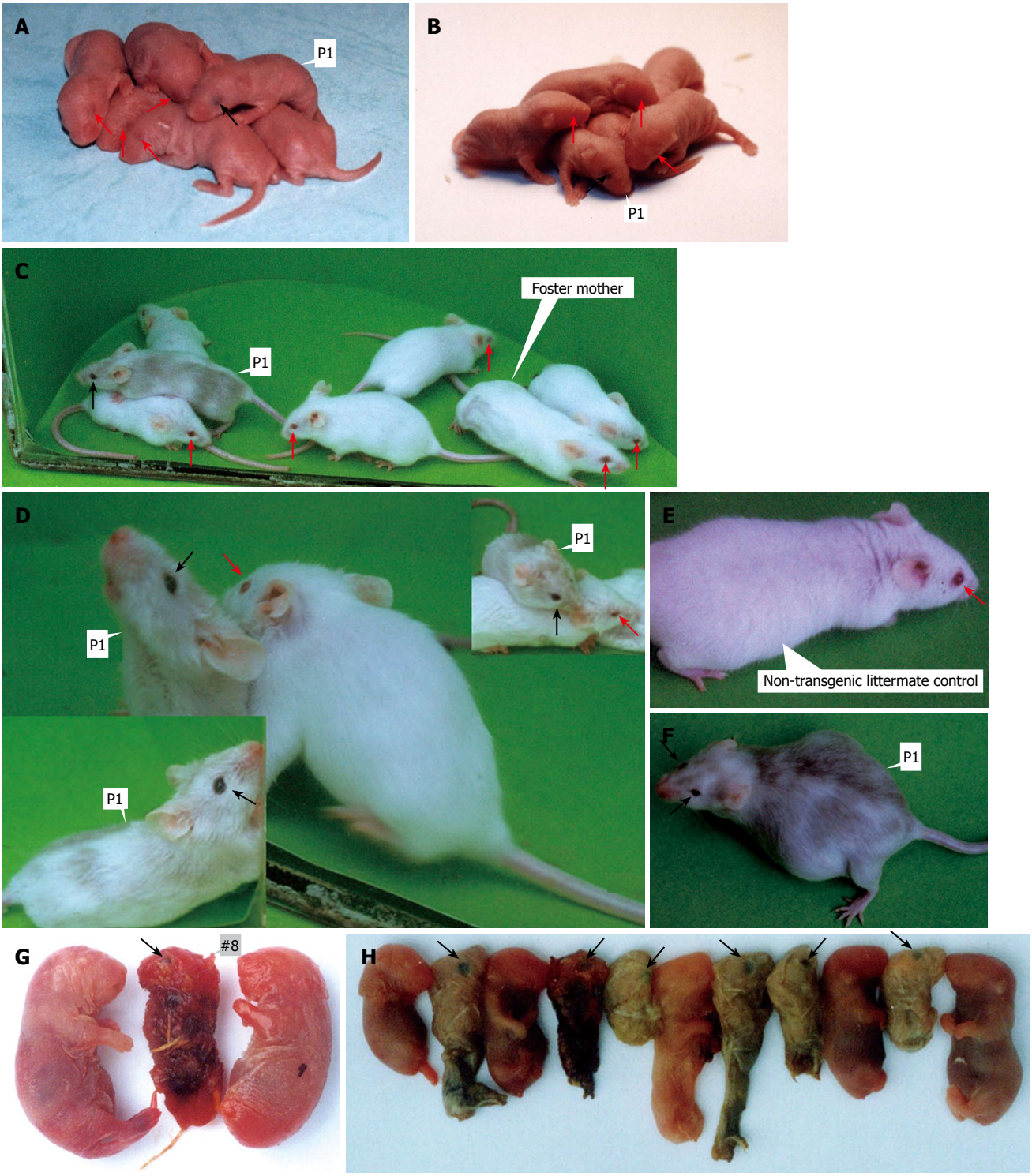

Figure 2 Eye and coat colors of tyrosinase minigene transgenic Kunming albino mice. One foster mother gave birth to six F0 pups (**A**-**F**); among the littermates, only one mouse (referred to as P1) had the pigmented eyes at birth. On July 15, another foster mother produced three F0 pups (**G**); of three siblings, only one mouse (referred to as #8) indicated the pigmented eyes at birth. P1 (♀) was crossed with normal Kunming albino mouse to give birth to 11 F1 offspring (**H**). All of the common albino strains of laboratory mice, such as FVB/N, BALB/c, and Kunming mouse (in China), have pink eyes and albino skin. (**A** and **B**) The **2**-d-old littermates. At birth, one pigmented mouse (P1) with dark eyes could be easily and immediately identified as a transgenic mouse by simple visual inspection. (**C**) The 4-wk-old littermates and Kunming albino foster mother. Founder P1 exhibited black eyes and light grey fur when compared to the non-transgenic littermate controls and Kunming albino foster mother with pink eyes and albino skin. No differences in phenotypes between transgenic mouse and the controls and foster mother except for melanization in eyes and hairs. Actually, the Kunming albino mouse was also used as a recipient strain for TyBS transgene in this project. (**D**) Eye color of the 4-wk-old P1 mouse compared with one of the non-transgenic littermates. One of the non-transgenic littermates (right of the middle map) had pink eyes, while at this age the heterozygote P1 (left of the middle map, upper and lower) had nearly black eyes. (**E** and **F**) The 8-wk-old non-transgenic littermate control and the adult P1 mouse (8-wk old), respectively. The non-transgenic littermate control (**E**, left) had pink eyes and albino coat, while at this age the heterozygote P1 mouse (**F**, right) had nearly black eyes and dark grey coat. Over time, the coat of P1 mouse became more heavily pigmented, while the eye and fur phenotypes of non-transgenic littermate control remained pink and albino throughout the life, respectively. (**G**) Eye color of the 1.5-d old #8 compared with its littermates. At birth, #8 with dark eyes could be easily and immediately identified as transgenic mice by simple visual inspection. Unfortunately, #8 as well as non-transgenic littermates without dark eyes were killed by foster mother 1.5 d after birth. **(H)** Eye color of F1 offspring (11) developed from mating of P1 and normal Kunming albino mouse. Founder P1 (♀) was back-crossed to normal Kunming albino mouse to produce eleven F1 generation. Unluckily, all of F1 offspring (11), born on September 8, died immediately at birth. P1 also deceased one month after delivery as it did not recover from giving birth to pubs. Of the 11 animals that developed from the mating aforementioned, six mice exhibited pigmented eyes. → and → indicate the pigmented eyes and non-pigmented eyes (pink), respectively.

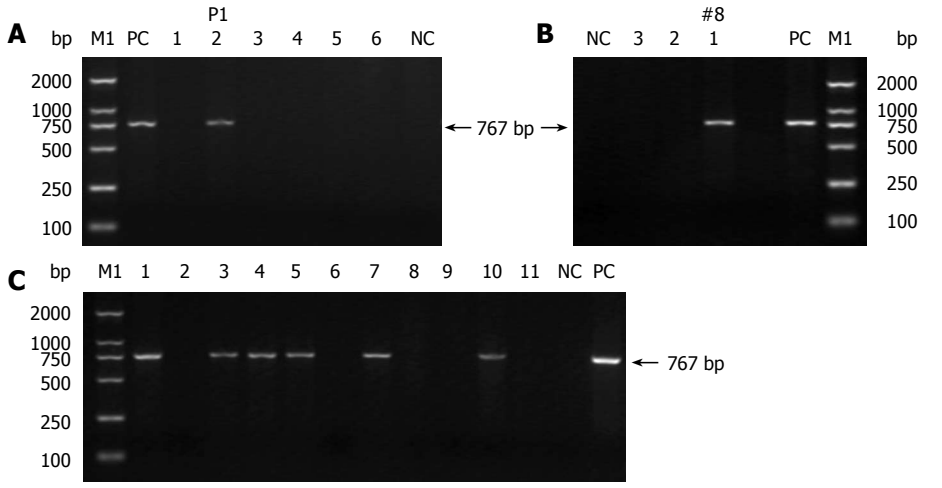

Figure 3 PCR detection of TyBS gene from genomic DNA of the potential transgenic founders (**A** and **B**) and subsequent generation(s) (**C**). Lane M1: DL 2000 DNA Marker (TaKaRa); lane PC: positive control (TyBS as template); lane NC: negative control using genomic DNA from normal Kunming mice as template. The arrows indicate the positions of PCR products amplified by the primers shown in Figure 1. (**A**) Littermates (F0, six mice) were verified for the transgene presence by PCR analysis. Lanes 1-6: genomic DNA from the potential founder(s) of 6 littermates; Lane 2: 767-bp band amplified from genomic DNA of P1 with pigmentation in the eyes. (**B**) Littermates (F0, three mice) were confirmed for the transgene presence by PCR analysis. Lanes 1-3: genomic DNA from the potential founder(s) of three siblings. Lane 1: 767-bp band amplified from genomic DNA of #8 with pigmentation in the eyes. Other details are as in Figure 2G. (**C**) Littermates (F1, 11 mice) were examined for the transgene presence by PCR analysis. The founder P1 (♀) was crossed with normal Kunming mouse to produce 11 littermates (F1) with six mice with pigmented eyes. Lanes 1-11: genomic DNA from F1 offspring derived from P1; Lanes 1, 3-5, 7, 10: 767-bp specific band amplified from genomic DNA of F1 offspring exhibiting pigmented eyes.

animal requirements for transgenic production[37].

Co-injection strategy for visually identifying the transgenic mice

Screening transgenic animals is usually time-consuming and labor-consuming. It would be very helpful if the transgenic animals could be identified by the visible inspection at birth. The functional tyrosinase gene introduced into an albino mouse strain leads to pigmentation in eyes and skin with high penetrance, and pigmented mice with dark eyes can be immediately identified by simply visible inspection at birth[23], as further confirmed by this study.

When two or several transgenic constructs are co-injected into single-cell fertilized embryos, the co-injected constructs typically co-integrate into the genome, where the transgene can independently express[38]. Theoretically, co-injection of tyrosinase transgenic construct with any other construct(s) should result in a certain percentage of transgenic mice carrying both transgenes at a single chromosomal site[23]. Additionally, co-injection experiments with the agouti transgenes and other transgenes demonstrated co-integration of the two constructs at the same chromosomal site in approximately 95% of F1 progeny, allowing transgene inheritance to be visibly detected[39]. The direct and visual detection of pigmentation in tyrosinase transgenic animals generated in the albino genetic backgrounds was repeatedly proposed by independent teams as a visual marker in co-injection strategies for the rapid detection of the successful tran sgenesis[12,30-33,35] and by our practices (data not shown). The utility of tyrosinase minigene co-injection with other construct(s) of interest is a useful adjunct to allow rapidly visual identification of transgenic mice at birth.

Moreover, another advantage of co-injection strategy is the fact that homozygous mice in most families can be identified by simply visual inspection, since the homozygous mice have darker coat colors, reflecting the increased gene dosage[32].

The co-injection strategy improves the yield of phenotypically desirable transgenic founder mice resulting from each microinjection session, and consequently reduces animal requirements for the transgenic production and routine genetic validation of transgenic lines.

In summary, we have successfully rescued the albino phenotype by introducing a functional tyrosinase gene into Kunming albino mouse. It should be pointed out here that TyBS and other tyrosinase transgenic constructs can be fused with any of the other genes and microinjected into fertilized eggs from albino murine strains in order to produce melanin pigments as an excellently visible marker for the generation and breeding of transgenic mice.

ACKNOWLEDGMENTS

We thank Dr. CY Fan (Department of Pathology and Otolaryngology, University of Arkansas for Medical Sciences, USA) for his unstinting advices and technical guidance in making transgenic mice, for his supportive and friendly attitude toward our projects. We thank Dr. F Beermann (Swiss Institute for Experimental Cancer Research, Switzerland) for kindly gifting the plasmids of ptrTyr5 and pTyBS, Dr. PA Overbeek (Howard Hughes Medical Institute, Department of Cell Biology, Baylor College of Medicine, Houston, TX, USA) for providing the vectors (e.g., pTyBS and pTy811C), and Professor G Schutz [Deutsches Krebsforschungszentrum (DKFZ), Heidelberg, Germany] for providing the plasmid ptrTyr5. We are also indebted to the expert technical assistance of JY Han, HH Zhang, GG Qiu, WG Huang, FY Chen, FR Ni, JY Xie and JH Wang, Center of Experimental Animals, Sun Yat-Sen University.

REFERENCES

1 **del Marmol V**, Beermann F. Tyrosinase and related proteins in mammalian pigmentation. *FEBS Lett* 1996; **381**: 165-168
2 **Nadeau JH**. Modifier genes in mice and humans. *Nat Rev Genet* 2001; **2**: 165-174
3 **Oetting WS**. The tyrosinase gene and oculocutaneous albinism type 1 (OCA1): A model for understanding the molecular biology of melanin formation. *Pigment Cell Res* 2000; **13**: 320-325
4 **Jackson IJ**. Molecular and developmental genetics of mouse coat color. *Annu Rev Genet* 1994; **28**: 189-217
5 **Yokoyama T**, Silversides DW, Waymire KG, Kwon BS, Takeuchi T, Overbeek PA. Conserved cysteine to serine mutation in tyrosinase is responsible for the classical albino mutation in laboratory mice. *Nucleic Acids Res* 1990; **18**: 7293-7298
6 **Beermann F**, Ruppert S, Hummler E, Bosch FX, Müller G, Rüther U, Schütz G. Rescue of the albino phenotype by introduction of a functional tyrosinase gene into mice. *EMBO J* 1990; **9**: 2819-2826
7 **Beermann F**, Schmid E, Ganss R, Schütz G, Ruppert S. Molecular characterization of the mouse tyrosinase gene: pigment cell-specific expression in transgenic mice. *Pigment Cell Res* 1992; **5**: 295-299
8 **Beermann F**, Schmid E, Schütz G. Expression of the mouse tyrosinase gene during embryonic development: recapitulation of the temporal regulation in transgenic mice. *Proc Natl Acad Sci USA* 1992; **89**: 2809-2813
9 **Ganss R**, Montoliu L, Monaghan AP, Schütz G. A cell-specific enhancer far upstream of the mouse tyrosinase gene confers high level and copy number-related expression in transgenic mice. *EMBO J* 1994; **13**: 3083-3093
10 **Jeffery G**, Brem G, Montoliu L. Correction of retinal abnormalities found in albinism by introduction of a functional tyrosinase gene in transgenic mice and rabbits. *Brain Res Dev Brain Res* 1997; **99**: 95-102
11 **Jeffery G**, Schütz G, Montoliu L. Correction of abnormal retinal pathways found with albinism by introduction of a functional tyrosinase gene in transgenic mice. *Dev Biol* 1994; **166**: 460-464
12 **Kang JK**, Kim JH, Lee SH, Kim DH, Kim HS, Lee JE, Seo JS. Development of spontaneous hyperplastic skin lesions and chemically induced skin papillomas in transgenic mice expressing human papillomavirus type 16 E6/E7 genes. *Cancer Lett* 2000; **160**: 177-183
13 Klüppel **M**, Beermann F, Ruppert S, Schmid E, Hummler E, Schütz G. The mouse tyrosinase promoter is sufficient for expression in melanocytes and in the pigmented epithelium of the retina. *Proc Natl Acad Sci USA* 1991; **88**: 3777-3781
14 **Porter SD**, Hu J, Gilks CB. Distal upstream tyrosinase S/MAR-containing sequence has regulatory properties specific to subsets of melanocytes. *Dev Genet* 1999; **25**: 40-48
15 **Schedl A**, Beermann F, Thies E, Montoliu L, Kelsey G, Schütz G. Transgenic mice generated by pronuclear injection of a yeast artificial chromosome. *Nucleic Acids Res* 1992; **20**: 3073-3077
16 **Takeuchi T**, Tanaka S, Tanaka M. Expression of tyrosinase gene in transgenic mice: programmed versus non-programmed expression. *J Invest Dermatol* 1993; **100**: 141S-145S
17 **Tanaka S**, Takeuchi T. Expression of tyrosinase gene in transgenic albino mice: the heritable patterned coat colors. *Pigment Cell Res* 1992; **5**: 300-303
18 **Tanaka S**, Yamamoto H, Takeuchi S, Takeuchi T. Melanization in albino mice transformed by introducing cloned mouse tyrosinase gene. *Development* 1990; **108**: 223-227
19 **Aigner B**, Brem G. Tyrosinase as a marker gene and model for screening transgenes in mice and rabbits. *Theriogenology* 1993; **39**: 177
20 **Hyodo-Taguchi Y**, Winkler C, Kurihara Y, Schartl A, Schartl M. Phenotypic rescue of the albino mutation in the medakafish (Oryzias latipes) by a mouse tyrosinase transgene. *Mech Dev* 1997; **68**: 27-35
21 **Fu L**, Mambrini M, Perrot E, Chourrout D. Stable and full rescue of the pigmentation in a medaka albino mutant by transfer of a 17 kb genomic clone containing the medaka tyrosinase gene. *Gene* 2000; **241**: 205-211
22 **Tseng FS**, Liao IC, Tsai HJ. Transient expression of mouse tyrosinase gene in albino walking catfish Clarias fuscus by subcutaneous microinjection. *Fish Sci* 1995; **61**: 163
23 **Giraldo P**, Montoliu L. Artificial chromosome transgenesis in pigmentary research. *Pigment Cell Res* 2002; **15**: 258-264
24 **Bockamp E**, Maringer M, Spangenberg C, Fees S, Fraser S, Eshkind L, Oesch F, Zabel B. Of mice and models: improved animal models for biomedical research. *Physiol Genomics* 2002; **11**: 115-132
25 **van der Weyden L**, Adams DJ, Bradley A. Tools for targeted manipulation of the mouse genome. *Physiol Genomics* 2002; **11**: 133-164
26 **Le Douarin N**. The Neural Crest. Cambridge: Cambridge University Press, 1997: 1-600
27 **Nagy A**, Gertsensten M, Vintersten K, Behringer R. Manipulating the Mouse Embryo: A Laboratory Manual. 3rd ed. New York: Cold Spring Harbor Press, 2003: 1-600
28 **Sambrook JE**, Fritsch F, Maniatis T. Molecular Cloning: A Laboratory Manual. 3rd ed. New York: Cold Spring Harbor Laboratory Press, 2001: 1-800
29 **Tymms MJ**, Kola I. Gene knockout protocols. Totowa: Humana Press Inc, 2001: 1-370
30 **Overbeek PA**. Factors affecting transgenic animal production. In: Pinkert CA. Transgenic Animal Technology: A Laboratory Handbook. San Diego: Academic Press Inc, 1994: 69-114
31 **Aigner B**, Brem G. Tyrosinase as a marker gene for studying transmission and expression of transgenes in mice. *Transgenics* 1994; **1**: 417-429
32 **Methot D**, Reudelhuber TL, Silversides DW. Evaluation of tyrosinase minigene co-injection as a marker for genetic manipulations in transgenic mice. *Nucleic Acids Res* 1995; **23**: 4551-4556
33 **Overbeek PA**, Aguilar-Cordova E, Hanten G, Schaffner DL, Patel P, Lebovitz RM, Lieberman MW. Coinjection strategy for visual identification of transgenic mice. *Transgenic Res* 1991; **1**: 31-37
34 **Porter SD**, Meyer CJ. A distal tyrosinase upstream element stimulates gene expression in neural-crest-derived melanocytes of transgenic mice: position-independent and mosaic expression. *Development* 1994; **120**: 2103-2111
35 **Beermann F**, Ruppert S, Hummler E, Schütz G. Tyrosinase as a marker for transgenic mice. *Nucleic Acids Res* 1991; **19**: 958
36 **Montoliu L**, Schedl A, Kelsey G, Lichter P, Larin Z, Lehrach H, Schütz G. Generation of transgenic mice with yeast artificial chromosomes. *Cold Spring Harb Symp Quant Biol* 1993; **58**: 55-62
37 **Potts W**, Tucker D, Wood H, Martin C. Chicken beta-globin 5'HS4 insulators function to reduce variability in transgenic founder mice. *Biochem Biophys Res Commun* 2000; **273**: 1015-1018
38 **Behringer RR**, Ryan TM, Palmiter RD, Brinster RL, Townes TM. Human gamma- to beta-globin gene switching in transgenic mice. *Genes Dev* 1990; **4**: 380-389
39 **Kucera GT**, Bortner DM, Rosenberg MP. Overexpression of an Agouti cDNA in the skin of transgenic mice recapitulates dominant coat color phenotypes of spontaneous mutants. *Dev Biol* 1996; **173**: 162-173

S- Editor Liu Y **L- Editor** Kumar M **E- Editor** Liu WF

PO Box 2345, Beijing 100023, China
www.wjgnet.com
wjg@wjgnet.com

World J Gastroenterol 2007 January 14; 13(2): 250-256
World Journal of Gastroenterology ISSN 1007-9327

BASIC RESEARCH

Antiproliferation and apoptosis induction of paeonol in HepG2 cells

Shu-Ping Xu , Guo-Ping Sun, Yu-Xian Shen, Wei Wei, Wan-Ren Peng, Hua Wang

Shu-Ping Xu, Yu-Xian Shen, Wei Wei, Institute of Clinical Pharmacology of Anhui Medical University, Key Laboratory of Antiinflammatory and Immunological Pharmacology in Anhui Province, Key Laboratory of Research and Development of Chinese Medicine of Anhui province, Hefei 230032, Anhui Province, China
Guo-Ping Sun, Wan-Ren Peng, Department of Oncology, The First Affiliated Hospital of Anhui Medical University, Hefei 230022, Anhui Province, China
Hua Wang, Department of Oncology, Provincial Hospital of Anhui, Hefei 230001, Anhui Province, China
Supported by the Natural Science Foundation of Anhui Province, No. 00044414, No. 050430901; the Key Project of the Natural Science Foundation of the Department of Education, Anhui Province, No. 2003Kj037zd and the Natural Science Foundation of the Department of Health, Anhui Province, No. 2002A025
Correspondence to: Dr. Guo-Ping Sun, Department of Oncology, The First Affiliated Hospital of Anhui Medical University, No. 210, Ji Xi Road, Hefei 230022, Anhui Province, China. sunguoping@ahmu.edu.cn
Telephone: +86-551-2922354
Received: 2006-09-09 Accepted: 2006-11-20

Abstract

AIM: To investigate the antiproliferative effect of paeonol (Pae) used alone or in combination with chemotherapeutic agents [cisplatin (CDDP), doxorubicin (DOX) and 5-fluorouracil (5-FU)] on human hepatoma cell line HepG2 and the possible mechanisms.

METHODS: The cytotoxic effect of drugs on HepG2 cells was measured by 3-(4, 5-dimethylthiazol-2-yl)-2, 5-diphenyltetra-zolium bromide (MTT) assay. Morphologic changes were observed by acridine orange (AO) fluorescence staining. Cell cycle and apoptosis rate were detected by flow cytometry (FCM). Drug-drug interactions were analyzed by the coefficient of drug interaction (CDI).

RESULTS: Pae (7.81-250 mg/L) had an inhibitory effect on the proliferation of HepG2 cells in a dose-dependent manner, with the IC_{50} value of (104.77 ± 7.28) mg/L. AO fluorescence staining and FCM assays showed that Pae induced apoptosis and arrested cell cycle at S phase in HepG2 cells. Further, different extent synergisms were observed when Pae (15.63, 31.25, 62.5 mg/L) was combined with CDDP (0.31-2.5 mg/L), DOX (0.16-1.25 mg/L), or 5-FU (12.5-100 mg/L) at appropriate concentrations. The IC_{50} value of the three drugs decreased dramatically when combined with Pae ($P < 0.01$). Of the three different combinations, the sensitivity of cells to drugs was considerably different.

CONCLUSION: Pae had a significant growth-inhibitory effect on the human hepatoma cell line HepG2, which may be related to apoptosis induction and cell cycle arrest. It also can enhance the cytotoxicity of chemotherapeutic agents on HepG2 cells, and the S phase arrest induced by Pae may be one of the mechanisms of these interactions.

Key words: Paeonol; Hepatocellular carcinoma; Apoptosis; Cell cycle; Cisplatin; Doxorubicin; 5-fluorouracil; Synergistic effect

Xu SP, Sun GP, Shen YX, Wei W, Peng WR, Wang H. Antiproliferation and apoptosis induction of paeonol in HepG2 cells. *World J Gastroenterol* 2007; 13(2): 250-256

http://www.wjgnet.com/1007-9327/13/250.asp

INTRODUCTION

Hepatocellular carcinoma (HCC) is the fifth most common cancer and the third leading cause of cancer-related death worldwide[1]. Eighty percent of the burden is borne by countries in Asia and Sub-Saharan Africa[2]. Although recent advances in management with a multidisciplinary approach results in improved local and regional disease control, the 5-year survival rate is still less than 10%[3]. Thus it is imperative to develop more effective and low-toxic chemotherapy agents.

Chinese herbal medicines are now attracting great attention in the world, which also show promising effects in treatment of cancers, including HCC[4]. Paeonol (Pae, 2-hydroxy-4-methoxyacetophenone, Figure 1), is a natural product extracted from the root of Paeonia Suffruticosa Andrew[5]. In our previous study, the antineoplastic activity of Pae has been demonstrated both in various cell lines[6] and in animal models[7,8]. The present study was designed to investigate the antiproliferative effect of Pae used alone or in combination with chemotherapeutic drugs [cisplatin (CDDP), doxorubicin (DOX) and 5-fluorouracil (5-FU)] on human hepatoma cell line HepG2 and the possible mechanisms.

MATERIALS AND METHODS

Cells and culture conditions

Human hepatocellular carcinoma cell line HepG2 was

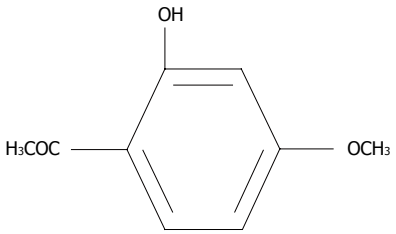

Figure 1 Structure of Pae (2-hydroxy-4-methoxyacetophenone).

purchased from Shanghai Institute of Hepatocarcinoma. HepG2 cells were cultured in Dulbecco's modified Eagle's medium (DMEM) supplemented with 10% fetal bovine serum (FBS) and incubated at 37℃ in a humidified atmosphere with 5% CO_2.

Drugs and reagents

Pae Injection was purchased from the First Pharmaceutical Factory of Shanghai, China (Cat. No. 990402, 10 mg/2 mL); CDDP Injection was purchased from Nanjing Pharmaceutical Co. Ltd, China (Cat. No. 20050602, 20 mg/20 mL); DOX was provided by Wanle Pharmaceutical Inc., Shenzhen, China (Cat. No. 0407E1, 10 mg/ampoule); 5-FU Injection was supplied by Shanghai Haipu Pharmaceutical Factory, China (Cat. No. 031109, 0.25 g/10 mL); DMEM was purchased from GIBCO BRL, Life Technologies Inc. (New York, USA); 3-[4, 5-dimethylthiazol-2-yl]-2, 5-diphenyltetra-zolium bromide (MTT) and acridine orange (AO) were from Sigma Co., USA. DNA-Prep-Reagents Kit was provided by Beckman Coulter Co. USA(Cat. No. 760279K).

In vitro cytotoxicity assay

HepG2 cells were seeded in 96-well plates at a density of 1-5 × 10^3 cells/well in 100 μL DMEM containing 10% FBS overnight. Nonadherent cells were removed by gentle washing. Then cells were treated with various concentrations of the drugs. After 44 h of drug exposure, 20 μL MTT solution (5 g/L) was added to each well for another 4 h at 37℃. The formazine was solved in 150 μL/well dimethyl sulfoxide (DMSO) and the absorbance was detected at 490 nm using ELx800 Strip reader (Bio-Tek, USA). The percentage of cytotoxicity was calculated as follows: Cytotoxicity (%) = (1-A_{490} of experimental well)/A_{490} of control well. The median inhibitory concentration (IC_{50}) (defined as the drug concentration at which cell growth was inhibited by 50%) was assessed from the dose-response curves.

Analysis of in vitro drug interaction

The coefficient of drug interaction (CDI) was used to analyze the synergistically inhibitory effect of drug combinations[9]. CDI is calculated as follows: CDI = AB/(A × B). According to the absorbance of each group, AB is the ratio of the combination groups to control group; A or B is the ratio of the single agent groups to control group. Thus CDI value less than, equal to or greater than 1 indicates that the drugs are synergistic, additive or antagonistic, respectively. CDI less than 0.7 indicates that the drugs are significantly synergistic.

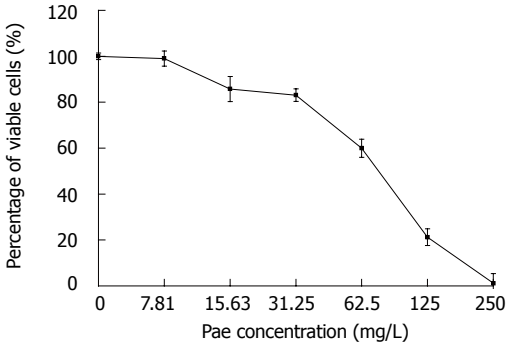

Figure 2 Dose-dependent cytotoxicity of Pae in HepG2 cells. Data are presented as mean ± SE (error bar) of triplicate experiments.

AO fluorescence staining

Cells were cultured in 6-well plates containing cover slips overnight. After incubation with Pae for 24 h, the cover slips were washed twice with PBS, fixed with 95% ethanol for 15 min, acidified with 1% acetic acid for 30 s, dyed with 0.1 g/L AO for 10 min, differentiated with 0.1 mol/L $CaCl_2$ for 2 min, and then washed with PBS 3 times. The cover slips were sealed and observed under a fluorescence microscope (OLYMPUS, Japan).

Flow cytometry assay

Cells were cultured in 6-well plates and allowed to grow to 75%-80% confluency. Nonadherent cells were removed by gentle washing, and the media were removed and replaced with fresh medium containing Pae at the desired concentrations. After exposure to drugs for 24 h, cells were collected and centrifuged at 1500 r/min in a 15 mL tube for 10 min. The cells were washed twice with PBS and resuspended in 50 μL fixing buffer at a room temperature for 20 s, then 500 μL propidium iodide (PI) staining buffer was added in the dark at room temperature for 30 min (according to the procedure program of the DNA-Prep Coulter reagents kit). A minimum of 1 × 10^5 cells for each group was analyzed using an EPICS XL-MCL model Coulter counter. Cell cycle distribution was analyzed using Mcycle software.

Statistical analysis

Biostatistical analyses were done using the SPSS 11.5 software package. All experiments were repeated at least three times. Results of multiple experiments are given as the mean ± SE. Non-parametric Kruskal-Wallis test was used to detect differences among the different experimental groups. Mann-Whitney *U* test was subsequently used for statistical evaluation in two-group comparisons. Pearson correlation coefficients were used for continuous independent and dependent variables. A level of $P < 0.05$ was accepted as statistically significant.

RESULTS

Effect of pae on the proliferation of HepG2 cells

We first examined the effect of Pae on the proliferation of HepG2 cells. As shown in Figure 2, a dramatic dose-

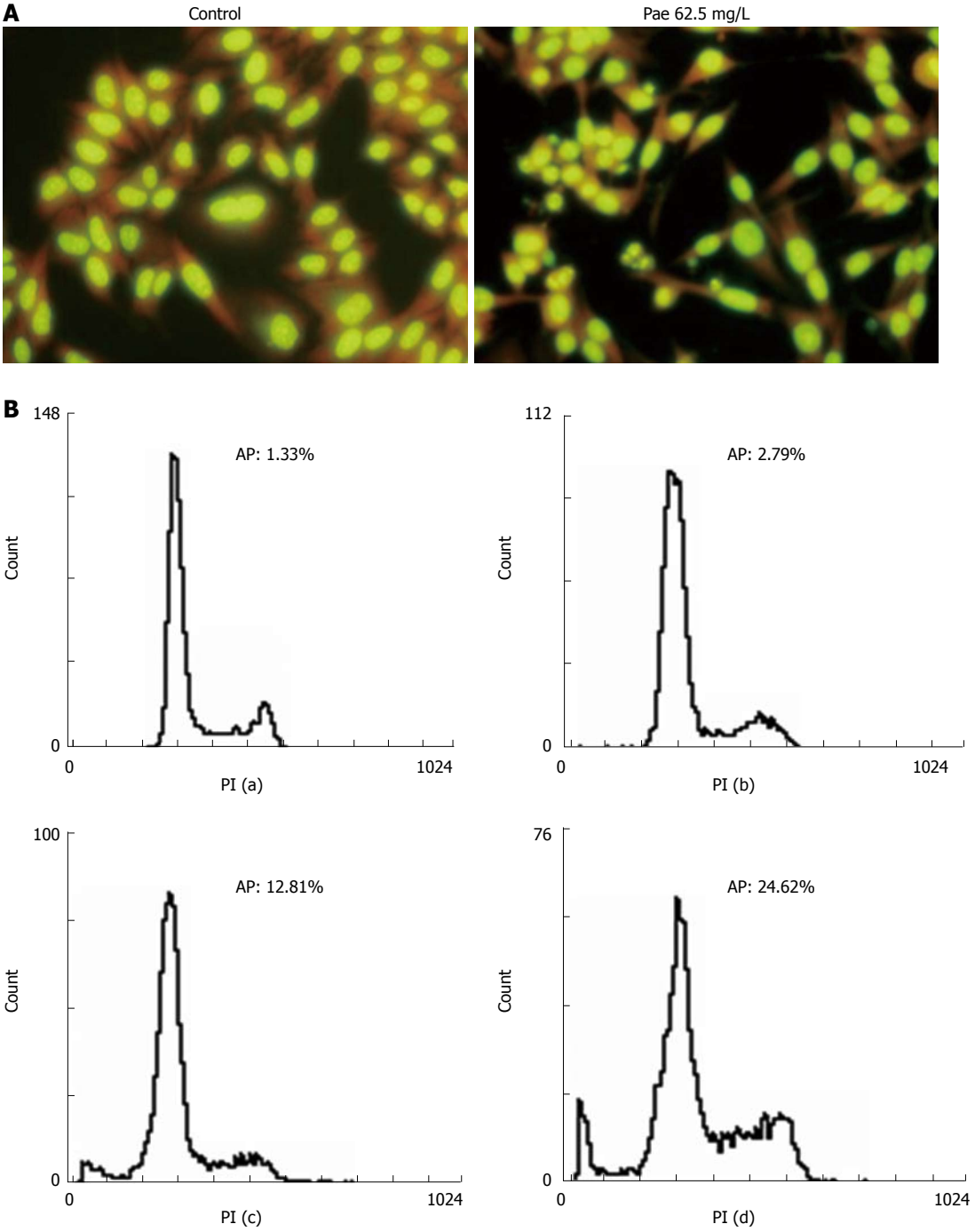

Figure 3 Effect of Pae on apoptosis in $HepG_2$ cells. **A**: Morphological changes of $HepG_2$ cells treated with Pae 62.5 mg/L (× 320); **B**: Flow cytometry analysis of $HepG_2$ cells treated with Pae for 24 h. (a). Control; (b).Pae 31.25 mg/L; (c).Pae 62.5 mg/L; (d).Pae 125 mg/L.

dependent reduction of cell viability was seen in cells incubated with Pae at concentrations of 7.81-250 mg/L for 48 h. The *r* value of dose-effect curves was 0.959 ($P < 0.01$) and the IC_{50} value of Pae was (104.77 ± 7.28) mg/L ($P < 0.01$).

Effects of Pae on apoptosis in $HepG_2$ cells

Morphological evidence of apoptosis was demonstrated by AO fluorescence staining. AO could be seen in all cells and the nuclei appeared green and chromatin was stained yellow (Figure 3A). Cells treated with Pae showed typically apoptotic changes, such as chromatin condensation, membrane blebing, deformed and fragmented nuclei.

FCM assay was performed to analyze apoptosis in $HepG_2$ cells treated with various concentrations of Pae for 24 h. It was found that the sub-G_1 peak appeared before G_1 phase, which represents apoptotic cell population (Figure 3B), in a dose- and time-dependent manner (Figure 4).

Effects of Pae on cell cycle in $HepG_2$ cells

Mcycle software was used to analyze the kinetic changes of cell cycle distribution. In untreated $HepG_2$ controls, cells were present in G_0/G_1 (71.79% ± 2.76%), S (20.31%

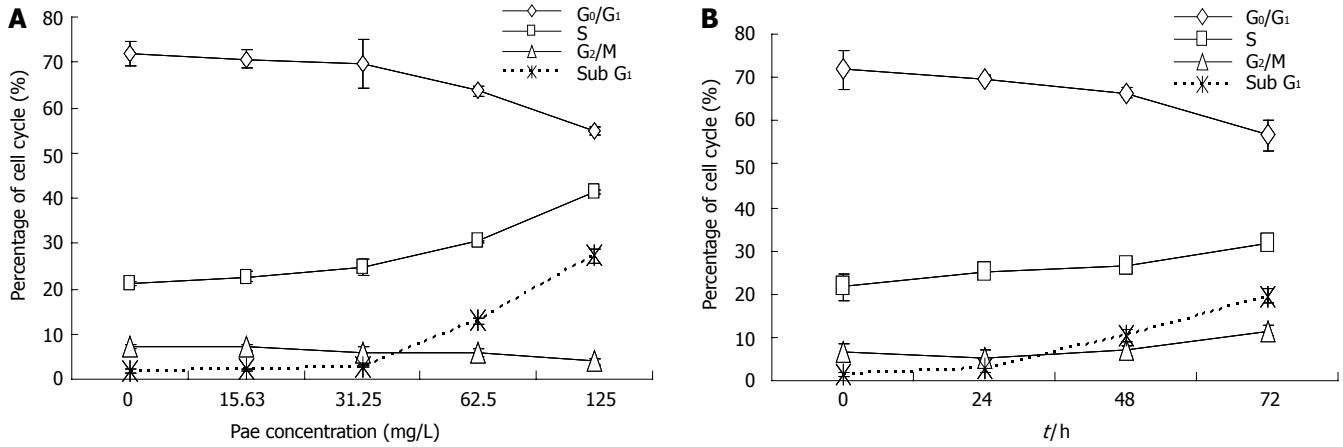

Figure 4 Effect of Pae on cell cycle in HepG2 cells. The distribution of cells in the sub-G1, G0/G1, S, and G2/M phases of the cell cycle were calculated and plotted. (**A**): Dose-dependent curve of cell cycle distribution induced by Pae. (**B**): Time-dependent curve of cell cycle distribution induced by Pae 31.25 mg/L. Each point represents triplicate experiments. Bars ± SE.

± 0.58%), and G2/M (7.16% ± 0.57%) phases. For HepG2 cells exposed to various concentrations of Pae, the S-phase fraction increased while G0/G1 fraction decreased in a dose-dependent manner (Figure 4A). And the percentages of cells in S phase increased to 24.98% ± 1.63%, 26.54% ± 1.53%, 31.72% ± 4.85% after 24, 48, and 72 h, respectively, when compared with untreated control cells, which was accompanied by a concomitant decrease of cells in the G0/G1 phase of the cell cycle (Figure 4B). It indicated that Pae might arrest the cell cycle at the S phase, and this blockage of cell cycle may prevent cells from entering M phase.

Pae enhancing the cytotoxicity of chemotherapeutic drugs on HepG2 cells

Growth-inhibition assays were performed to investigate whether Pae can enhance the antiproliferative effects of chemotherapeutic agents on HepG2 cells. Three doses of Pae (15.63, 31.25 and 62.5 mg/L) were combined with different concentrations of CDDP, DOX, and 5-FU, respectively. For each experiment, a dose-response curve of each single chemotherapeutic agent and its combination with Pae was drawn, which showed that Pae increased the cytotoxicity of CDDP, DOX, and 5-FU on HepG2 cells. The IC_{50} value of the three drugs decreased dramatically at different extents when combined with Pae. For example, in the presence of 15.63, 31.25 and 62.5 mg/L Pae, the IC_{50} of CDDP reduced from 0.591 ± 0.053 mg/L to 0.366 ± 0.011, 0.161 ± 0.018, 0.007 ± 0.002 mg/L, respectively. That of DOX reduced from 0.489 ± 0.124 mg/L to 0.175 ± 0.043, 0.037 ± 0.012, 0.032 ± 0.005 mg/L. And that of 5-FU reduced from 310.783 ± 13.094 mg/L to 161.759 ± 9.507, 8.646 ± 2.331, 5.021 ± 0.962 mg/L, respectively ($P < 0.01$, Figure 5A-C).

We analyzed the nature of the interaction between Pae and the three drugs using CDI, which quantitatively measures the interaction of two drugs. As shown in Figure 5D, Pae and CDDP yielded synergistic interactions across a wide concentration range. The synergistic effect was most prominent when 15.63 mg/L Pae was combined with 1.25 mg/L CDDP (CDI < 0.7). While a significant synergistic effect was only obtained when Pae concentration reached 31.25 and 62.5 mg/L in combination with 0.16 mg/L and 0.31 mg/L DOX, respectively. When DOX reached 1.25 mg/L, the interaction was antagonistic (Figure 5E). Pae had a relatively weak activity to enhance the antiproliferative effect of 5-FU in HepG2 cells. If the concentrations of drugs were too high or too low, the synergistic cytotoxic effects could not be achieved. The combinations of Pae at 31.25 mg/L and 5-FU at 12.5 and 25 mg/L exhibited significantly synergistic activity against HepG2 cells, while an antagonistic effect was observed at 62.5 mg/L of Pae in combination with 25-100 mg/L of 5-FU (Figure 5F).

DISCUSSION

Currently, a variety of cytotoxic and antiproliferative agents have been tested in HCC treatment, which are used alone, or in combination with other drugs or other treatment modalities[10]. Agents with partial response rates near or above 10% include DOX, CDDP and 5-FU[11-13]. However, high doses of these drugs lead to severe toxicities, which have a negative effect on patients' survival. The use of less toxic doses in combination with other anti-proliferative agents would be desirable[14-17].

Pae is isolated from the herb *Pycnostelma paniculatum* (Bunge) K.S., and the root of the plant *Paeonia Suffruticosa* Andrew[5]. It is a white needle crystal with a relatively low-melting point of 51℃-52℃. The molecular weight of Pae is 166.18 ku and the molecular formula is $C_9H_{10}O_3$[18]. Pae possesses extensive pharmacological activities such as sedation, hypnosis, antipyresis, analgesic, antioxidation, antiinflammation, and immunoregulation[19]. Additionally, Pae had minimal systemic toxicity (LD_{50} 3430 mg/kg) when it was orally administrated to mice[20]. In our previous study, the antineoplastic activity of Pae has been demonstrated both in cell lines, such as human erythromyeloid cell line K562, breast cancer gene cell line T6-17, human hepatoma cell line Bel-7404, and cervical

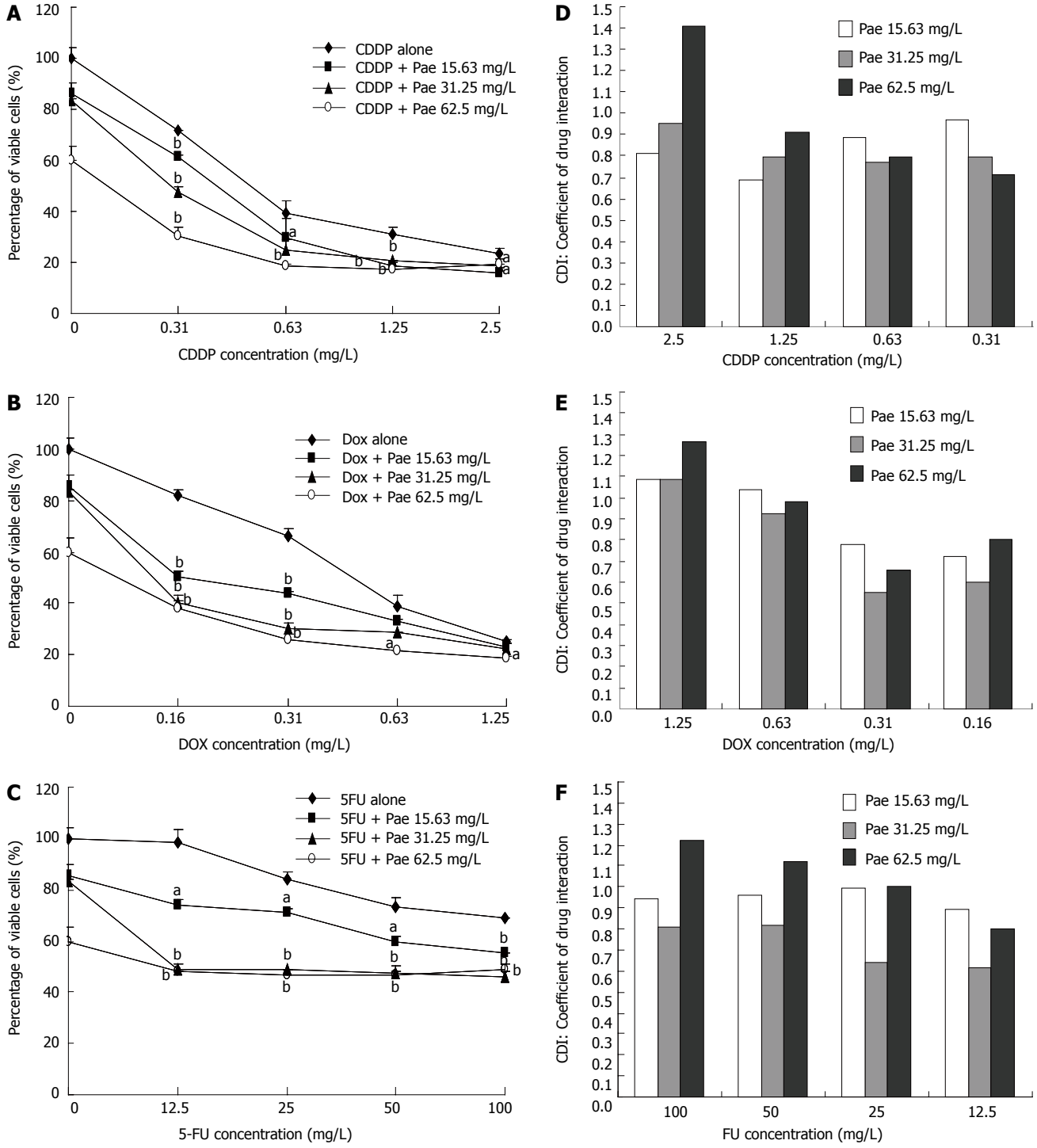

Figure 5 The synergistically antiproliferative effect of Pae combined with CDDP (**A**), DOX (**B**), or 5-FU (**C**) on HepG2 cells. The dots represent the concentrations of chemotherapeutic drugs as 0 on the dose-response curves which means treatment with Pae alone. Data are presented as mean ± SE of triplicate experiments. $^{a}P < 0.05$, $^{b}P < 0.01$, *vs* chemotherapeutic drugs alone. And CDI for the combination treatment of Pae with CDDP (**D**), DOX (**E**), or 5-FU (**F**) on HepG2 cells.

cancer cell line Hela[6], and in animal models bearing HepA hepatocarcinoma[7,8]. Ji *et al*[21] demonstrated that Pae at a low concentration had synergetic effects with 5-FU, MMC and CDDP on inhibiting the proliferation of human colorectal cancer cell line HT-29.

In the present study, Pae exhibited growth inhibition to HepG2 cells in a dose-dependent manner, with the IC_{50} value of 104.77 (± 7.28 mg/L) mg/L. Although the exact mechanism of the cytotoxicity of Pae against HepG2 cells is not entirely clear, many potential mechanisms have been proposed for the growth inhibition of Pae in cultured cells and animal models. These mechanisms include induction of apoptosis[22-23] and immunoregulation such as promoted lymphocyte proliferation, IL-2 production by splenocytes, and TNF-α production by PMφ from the model mice[7,8]. Apoptosis is a mechanism by which cells undergo death to control cell proliferation or in response to DNA damage. A tumor occurs when the balance of

cell proliferation and cell death is broken[24]. Induction of apoptosis is an effective strategy for cancer therapy[25]. In the present study, the cells treated with Pae showed typical characteristics of apoptosis. Similarly, apoptotic peak appeared before G_1 phase after treatment with Pae, which resulted from the internucleosomal degradation of DNA, in a dose- and time-dependent manner. Moreover, the $HepG_2$ cells exposed to Pae for 24 h showed depletion of the G_0/G_1 fraction and accumulation in S-phase. Accumulation in S-phase has also been reported by Liu *et al*[22], in which Pae could induce cell cycle disturbance and S phase of the HT-29 cells was increased, while G_0/G_1 and G_2/M phase of the cells were decreased. The S phase arrest and apoptosis induction of Pae on $HepG_2$ cells might be its main mechanism.

Meanwhile, $HepG_2$ cells were treated with the combinations of Pae and different chemotherapeutic agents. The results indicated that the growth inhibitory effect of CDDP, DOX, or 5-FU, respectively, was enhanced significantly by Pae at appropriate concentrations. Among the three agents examined, CDDP showed the most wide synergistic effect with Pae. The synergistic effect was most prominent (CDI < 0.7 =) when 15.63 mg/L Pae was combined with 1.25 mg/L CDDP. This indicated that the combination of Pae and CDDP at certain concentrations might help reduce nausea, vomiting and serious kidney toxicity of CDDP. Similar results that Pae in combination with anticancer drugs had synergistic effects at lower concentrations and had antagonistic effects at higher concentrations were observed in DOX and 5-FU, but with different sensitivities. The S phase arrest of Pae may be one of the mechanisms related with these interactions. 5-FU belongs to cell cycle specific agents, which acts specifically on cells in S phase[26]. The cytotoxic effects of CDDP and DOX are generally considered to be non-cell-cycle specific[27-28]. Nevertheless, DOX has the most killing effect on S phase cells[28]. CDDP is most specific to G_1 phase cells, while it also has strong effects on cells in S phase[29]. Further studies are needed to investigate the mechanisms of these synergisms, which favor the reasonable application of Pae to HCC treatment.

ACKNOWLEDGMENTS

We thank Dr. Zhimin Zhai and Qing Li for FACS analysis, the Central Laboratory of the Provincial Hospital of Anhui.

COMMENTS

Background

Hepatocellular carcinoma (HCC) is a major contributor to cancer incidence and mortality in the world. No effective treatment is available by now. Therefore, there is a critical need to develop more strategies for chemotherapy of hepatoma.

Research frontiers

Currently, a variety of cytotoxic and antiproliferative agents have been tested in HCC treatment, which are used alone, or in combination with other drugs or with different modalities of treatment. Chinese herbal medicines are now attracting great attention in the world, which also show promising effects in HCC therapy. Paeonol, a natural product extracted from the root of Paeonia Suffruticosa Andrew, has shown antineoplastic activities both in cell lines and in animal models.

Innovations and breakthroughs

This is the first report on the antiproliferation, induction of apoptosis and cell cycle arrest by Pae in $HepG_2$ cells.

Applications

Pae may be expected to be effective and useful as a new agent in hepatoma chemotherapy.

Peer review

The authors examine the cytotoxic effect of Pae only in $HepG_2$ cells. It remains unclear whether the effect of Pae in $HepG_2$ cells can be generalized to other hepatoma cells. The authors should examine the effect of Pae using a panel of hepatoma cell lines; The data in Figure 4 suggested that Pae induces S-phase arrest in $HepG_2$ cells. However, the molecular basis for S-phase arrest is not clearly shown. The authors should examine whether Pae has an effect in cells arrested at G_1/S phase using pre-treatment of cells such as hydroxyurea. It would be important to examine the expression of p21, p27 CDK1 and cyclinA after treatment with Pae.

REFERENCES

1 **Parkin DM**, Bray F, Ferlay J, Pisani P. Estimating the world cancer burden: Globocan 2000. *Int J Cancer* 2001; **94**: 153-156
2 **McGlynn KA**, London WT. Epidemiology and natural history of hepatocellular carcinoma. *Best Pract Res Clin Gastroenterol* 2005; **19**: 3-23
3 **Johnson PJ**. Hepatocellular carcinoma: is current therapy really altering outcome? *Gut* 2002; **51**: 459-462
4 **Shu X**, McCulloch M, Xiao H, Broffman M, Gao J. Chinese herbal medicine and chemotherapy in the treatment of hepatocellular carcinoma: a meta-analysis of randomized controlled trials. *Integr Cancer Ther* 2005; **4**: 219-229
5 **Riley CM**, Ren TC. Simple method for the determination of paeonol in human and rabbit plasma by high-performance liquid chromatography using solid-phase extraction and ultraviolet detection. *J Chromatogr* 1989; **489**: 432-437
6 **Sun GP**, Wang H, Shen YX, Xu SY. Inhibitory effects of paeonol on the proliferation on four tumor cell lines. *Anhui Yiyao* 2004; **8**: 85-87
7 **Sun GP**, Shen YX, Zhang LL, Zhou AW, Wei W, Xu SY. Study on immunomodulation and antitumor activity of paeonol in HepA tumor mice. *Zhongguo Yaolixie Tongbao* 2003; **19**:160-162
8 **Sun GP**, Shen YX, Zhang LL, Wang H, Wei W, Xu SY. Antitumor effect of paeonol in vitro and in vivo. *Anhui Keji Xueyuan Xuebao* 2002; **37**: 183-185
9 **Cao SS**, Zhen YS. Potentiation of antimetabolite antitumor activity in vivo by dipyridamole and amphotericin B. *Cancer Chemother Pharmacol* 1989; **24**: 181-186
10 **Zhu AX**. Systemic therapy of advanced hepatocellular carcinoma: how hopeful should we be? *Oncologist* 2006; **11**: 790-800
11 **Okada S**, Okazaki N, Nose H, Shimada Y, Yoshimori M, Aoki K. A phase 2 study of cisplatin in patients with hepatocellular carcinoma. *Oncology* 1993; **50**: 22-26
12 **Lai CL**, Wu PC, Chan GC, Lok AS, Lin HJ. Doxorubicin versus no antitumor therapy in inoperable hepatocellular carcinoma. A prospective randomized trial. *Cancer* 1988; **62**: 479-483
13 **Lin DY**, Lin SM, Liaw YF. Non-surgical treatment of hepatocellular carcinoma. *J Gastroenterol Hepatol* 1997; **12**: S319-S328
14 **Leung TW,** Patt YZ, Lau WY, Ho SK, Yu SC, Chan AT, Mok TS, Yeo W, Liew CT, Leung NW, Tang AM, Johnson PJ**.** Complete pathological remission is possible with systemic combination chemotherapy for inoperable hepatocellular carcinoma. *Clin Cancer Res* 1999; **5**: 1676-1681
15 **Yeo W**, Mok TS, Zee B, Leung TW, Lai PB, Lau WY, Koh J, Mo FK, Yu SC, Chan AT, Hui P, Ma B, Lam KC, Ho WM, Wong HT, Tang A, Johnson PJ. A randomized phase III study of doxorubicin versus cisplatin/interferon alpha-2b/doxorubicin/fluorouracil (PIAF) combination chemotherapy

for unresectable hepatocellular carcinoma. *J Natl Cancer Inst* 2005; **97**: 1532-1538

16 **Lee J,** Park JO, Kim WS, Park SH, Park KW, Choi MS, Lee JH, Koh KC, Paik SW, Yoo BC, Joh J, Kim K, Jung CW, Park YS, Im YH, Kang WK, Lee MH, Park K. Phase II study of doxorubicin and cisplatin in patients with metastatic hepatocellular carcinoma. *Cancer Chemother Pharmacol* 2004; **54**: 385-390

17 **Yin XY**, Lü MD, Liang LJ, Lai JM, Li DM, Kuang M. Systemic chemo-immunotherapy for advanced-stage hepatocellular carcinoma. *World J Gastroenterol* 2005; **11**: 2526-2529

18 **Mimura K**, Baba S. Determination of paeonol metabolites in man by the use of stable isotopes. *Chem Pharm Bull (Tokyo)* 1981; **29**: 2043-2050

19 **Sun YC**, Shen YX, Sun GP. Advances in the studies of major pharmacological activity of paeonol. *Zhongchengyao Zazhi* 2004; **26**: 579-582

20 **Jiang SP**, Chen YX. Advances in the research and its clinical application of Cynanchum paniculatum (Bge.) Kitag. Zhongguo Zhongyao Zazhi 1994; **19**: 311-314

21 **Ji CY**, Tan SY, Liu CQ. Inhibitory effect of paeonol on the proliferation of human colorectal cancer cell line HT-29 and its synergistic effect with chemotherapy agents. *Zhongguo Zhongyao Zazhi* 2005; **17**: 122-124

22 **Liu CQ**, Tan SY, Ji CY, Luo HS, Yu JP. The effects of paeonol on inhibiting the proliferation of human colorectal cancer cell line HT-29 and its molecule mechanism. *Zhongguo Yaolixie Tongbao* 2005; **21**: 1251-1254

23 **Sun GP**, Wang H, Shen YX, Zhai ZM, Wei W, Xu SY. Study on effects of paeonol in inhibiting growth of K562 and inducing its apoptosis. *Zhongguo Yaolixie Tongbao* 2004; **20**: 550-552

24 **Evan GI**, Vousden KH. Proliferation, cell cycle and apoptosis in cancer. *Nature* 2001; **411**: 342-348

25 **Kerr JF**, Winterford CM, Harmon BV. Apoptosis. Its significance in cancer and cancer therapy. *Cancer* 1994; **73**: 2013-2026

26 **Petru E,** Sevin BU, Haas J, Ramos R, Perras J. A correlation of cell cycle perturbations with chemosensitivity in human ovarian cancer cells exposed to cytotoxic drugs in vitro. *Gynecol Oncol* 1995; **58**: 48-57

27 **Bergerat JP**, Barlogie B, Göhde W, Johnston DA, Drewinko B. In vitro cytokinetic response of human colon cancer cells to cis-dichlorodiammineplatinum(II). *Cancer Res* 1979; **39**: 4356-4363

28 **Takahashi K**, Ebihara K, Honda Y, Nishikawa K, Kita M, Oomura M, Shibasaki C. Antitumor activity of cis-dichlorodiammineplatinum(II) and its effect on cell cycle progression. *Gan To Kagaku Ryoho* 1982; **9**: 624-631

29 **Potter AJ**, Rabinovitch PS. The cell cycle phases of DNA damage and repair initiated by topoisomerase II-targeting chemotherapeutic drugs. *Mutat Res* 2005; **572**: 27-44

S- Editor Liu Y **L- Editor** Zhu LH **E- Editor** Ma WH

PO Box 2345, Beijing 100023, China
www.wjgnet.com
wjg@wjgnet.com

World J Gastroenterol 2007 January 14; 13(2): 257-263
World Journal of Gastroenterology ISSN 1007-9327

CLINICAL RESEARCH

Detection of disseminated pancreatic cells by amplification of cytokeratin-19 with quantitative RT-PCR in blood, bone marrow and peritoneal lavage of pancreatic carcinoma patients

Katrin Hoffmann, Christiane Kerner, Wolfgang Wilfert, Marc Mueller, Joachim Thiery, Johann Hauss, Helmut Witzigmann

Katrin Hoffmann, Christiane Kerner, Johann Hauss, Helmut Witzigmann, Department of Visceral, Transplantation, Thoracic and Vascular Surgery, University of Leipzig, Germany
Wolfgang Wilfert, Marc Mueller, Joachim Thiery, Institute of Laboratory Medicine, Clinical Chemistry and Molecular Diagnostics, University of Leipzig, Germany
Correspondence to: Dr. Katrin Hoffmann, Department of General Surgery, Ruprecht Karls University of Heidelberg, Im Neuenheimer Feld 110, Heidelberg 69120, Germany. katrin.hoffmann@med.uni-heidelberg.de
Telephone: +49-6221-566110 Fax: +49-6221-564215
Received: 2006-09-05 Accepted: 2006-11-28

Abstract

AIM: To evaluate the diagnostic potential of cytokeratin-19 (CK-19) mRNA for the detection of disseminated tumor cells in blood, bone marrow and peritoneal lavage in patients with ductal adenocarcinoma of the pancreas.

METHODS: Sixty-eight patients with pancreatic cancer (n = 37), chronic pancreatitis (n = 16), and non-pancreatic benign surgical diseases (n = 15, control group) were included in the study. Venous blood was taken preoperatively, intraoperatively and at postoperative d 1 and 10. Preoperative bone marrow aspirates and peritoneal lavage taken before mobilization of the tumor were analyzed. All samples were evaluated for disseminated tumor cells by CK-19-specific nested-PCR and quantitative fluorogenic RT-PCR.

RESULTS: CK-19 mRNA expression was increased in 24 (64%) blood samples and 11 (30%) of the peritoneal lavage samples in the patients with pancreatic cancer. In 15 (40%) of the patients with pancreatic cancer, disseminated tumor cells were detected in venous blood and bone marrow and/or peritoneal lavage. In the peritoneal lavage, the detection rates were correlated with the tumor size and the tumor differentiation. CK-19 levels were increased in pT3/T4 and moderately/poorly differentiated tumors (G2/G3). Pancreatic cancer patients with at least one CK-19 mRNA-positive sample showed a trend towards shorter survival. Pancreatic cancer patients showed significantly increased detection rates of disseminated tumor cells in blood and peritoneal lavage compared to the controls and the patients with chronic pancreatitis.

CONCLUSION: Disseminated tumor cells can be detected in patients with pancreatic ductal adenocarcinoma by CK-19 fluorogenic RT-PCR. In peritoneal lavage, detection rate is correlated with tumor stage and differentiation. In the clinical use, CK-19 is suitable for the distinction between malignant and benign pancreatic disease in combination with other tumor-specific markers.

Key words: Tumor cell dissemination; Pancreatic cancer; Cytokeratin-19

Hoffmann K, Kerner C, Wilfert W, Mueller M, Thiery J, Hauss J, Witzigmann H. Detection of disseminated pancreatic cells by amplification of cytokeratin-19 with quantitative RT-PCR in blood, bone marrow and peritoneal lavage of pancreatic carcinoma patients. *World J Gastroenterol* 2007; 13(2): 257-263

http://www.wjgnet.com/1007-9327/13/257.asp

INTRODUCTION

Pancreatic cancer is one of the top five causes of cancer death in the Western world. The 5-year survival rates are around 4%[1,2]. Tumor resection is associated with prolonged survival and postoperative adjuvant chemotherapy may further improve long-term results[3,4]. However, curative treatment of most patients fails due to local recurrence and hepatic metastases occurring within two years after surgery[5,6]. Occult micro-metastases caused by disseminated tumor cells are the most limiting factor for the improvement of mortality rates. Their influence on prognosis and development of new therapeutic strategies has not yet been completely elucidated.

Disseminated tumor cells are not ascertainable with current staging methods. Additional to cytology, immunohistochemical analysis is the standard for identification of tumor cells. Despite improvement of detection rates by conventional cytology, conflicting result regarding the prognostic relevance have been reported[7]. Several studies focused on molecular biological approaches for the qualitative or semi-quantitative verification of tumor cell dissemination in pancreatic cancer[8-12]. Reverse transcriptase polymerase chain reaction (RT-PCR) has a high sensitivity and allows the identification of approximately 1 tumor cell in 10^7 normal peripheral mononuclear blood cells[13]. Using qualitative PCR methods, varying frequency of gene transcripts and false positive results have been reported[14-16]. Therefore, tumor cell detection in patients with ductal adenocarcinoma of the pancreas is still a matter of debate.

Nowadays CEA and CA 19-9 are established as clinical markers for pancreatic cancer. However, expressions of these antigens have also been reported in cholangitis, chronic pancreatitis and various gastrointestinal tumors[17]. Various studies used cytokeratin-19 (CK-19) for pancreatic cell detection. CK-19 has been identified as a reliable marker for epithelial cell differentiation[18]. It is specific for undifferentiated pancreatic ductal cells and homogenously expressed at high levels in primary pancreatic adenocarcinoma and pancreatic carcinoma metastases[19,20]. CK-19 is not expressed in hematopoetic cells and therefore suited for detection of disseminated pancreatic cells in the peripheral blood[19,21].

Here, we report on the expression of CK-19 mRNA in blood, bone marrow and peritoneal lavage in 68 patients. Nested-PCR and quantitative fluorogenic RT-PCR were used to detect dissemination of pancreatic cells in patients with pancreatic cancer, chronic pancreatitis and non-pancreatic benign surgical diseases. The purpose of this study was to evaluate the potential of qualitative nested-PCR and quantitative RT-PCR for the detection of disseminated pancreatic cells and the differentiation between chronic pancreatitis and pancreatic cancer.

MATERIALS AND METHODS

Patients

This prospective study was approved by the Ethical Commission of the University of Leipzig and informed written consent was obtained from each patient. Peripheral blood samples, bone marrow aspirations and peritoneal lavage of 68 patients were analyzed. Thirty-seven patients with histologically confirmed primary pancreatic cancer, 16 patients with chronic pancreatitis and 15 controls with non-pancreatic benign surgical diseases participated in the study. In all patients, diagnosis was confirmed by the resected specimen or tumor biopsy for non-resectable cancers (n = 11). Patients with pancreatic cancer were staged according to the UICC guidelines 2005[22]. According to the UICC stage, 4 (10%) patients had stage Ⅰ, 3 (8%) stage Ⅱ, 19 (51%) stage Ⅲ, and 11 (29%) stage Ⅳ pancreatic cancer. The survival time of the patients ranged between 3 and 48 mo (median survival: 12 mo). Patients with cancer of the common bile duct, the ampulla of Vater or the duodenum were excluded from the study.

Samples

Four blood samples were obtained from each patient through central venous catheter 30 min preoperatively, intraoperatively after mobilization of the pancreas and 24 h as well as 10 d after the operation. Bone marrow samples were obtained after induction of general anesthesia by aspiration from the iliac crest and heparinized. Peritoneal lavage was performed immediately after exploration of the abdominal cavity. About 500 mL of sterile isotonic sodium chloride solution was instilled, removed after irrigation and then EDTA buffer was added.

RNA extraction and cDNA synthesis

All samples were diluted and washed with 10 mL of erythrocyte lysis buffer. The mononuclear cell fraction was isolated by Ficoll-Isopaque (Amersham, Braunschweig, Germany). Total RNA was extracted using guanidinium-isothiocyanate-phenol-chloroform-based method (Trizol, Gibco BRL, Life Technologies, Gaithersburg, USA). RNA integrity was checked electrophoretically and quantified spectrophotometrically. First strand cDNA was generated from 3 μg of total RNA diluted with 10 μL of RNase-free water using 1 μL of Random Hexamer Primer (Roche Diagnostics, Basel, Switzerland) and incubated for 10 min at 68℃. After chilling on ice, 7 μL of master mixture, according to Superscript Ⅱ kit (Invitrogen, Carlsbad, USA), was added and after 60 min of incubation at 42℃, the reaction was inactivated for 10 min at 80℃.

Qualitative nested-PCR

Qualitative analysis of CK-19 expression was carried out using nested-PCR. Two different pairs of primer (n-PCR1/n-PCR2) were designed. The second set of primers amplifies inside the amplification sites of n-PCR1 primers to improve the specificity of PCR. Then 5 μL of cDNA was diluted with 45 μL of mixture containing 1 μL of each n-PCR1 primer, 10 × PCR buffer, dNTP PCR, AmpliTaq polymerase (Perkin Elmer Life and Analytical Sciences, Boston, USA) and DNase-free water for first round PCR. The conditions for PCR step one and two were one cycle at 95℃ for 3 min, followed by 40 cycles at 57℃ for 20 s, 72℃ for 50 s and a final extension at 72℃ for 10 min. For second round PCR, 1 μL of aliquot of the first round PCR product was added to 49 μL of master mixture containing 1 μL of each n-PCR2 primer. Two negative controls were included per run. Ten microliters of all PCR products were electrophoresed on 20 g/L agarose gels and visualized after ethidium bromide staining (Table 1).

Quantitative RT-PCR

CK-19 and housekeeping genes beta-actin primers and fluorogenic probes were designed using Primer Express software (Primerexpress Version 2.0, Perkin Elmer) (Table 1). PCR primers and probes have been positioned to span exon-intron boundaries. Amplification and detection of CK-19 a and b pseudogen are unlikely because probe and

Table 1 Sequences for quantitative RT-PCR and nested-PCR primers and flourescent probes

	Forward primer	Reverse primer	Length (bp)
TaqMan primer CK-19	5'-GAAGGCCTGAAGGAAGAGCTG-3'	5'-CCTCCCACTTGGCCCCT-3'	80
TaqMan primer beta-actin	5'-TCCAGAGGCGCTCTTCCA-3'	5'-CGCACTTCATGATCGAGTTGA-3'	86
Vector primer CK-19	5'-AACTCCAGGATTGTCCTGCAG-3'	5'-TCCCGGTTCAATTCTTCAGTC-3'	401
Vector primer beta-actin	5'-GCACCACTGGCATTGTCATG-3'	5'-CCACACGGAGTACTTGCGC-3'	581
Nested-PCR primer CK-19	5'-AACTCCAGGATTGTCCTGCAG-3'	5'-TCCCGGTTCAATTCTTCAGTC-3'	401
Nested-PCR primer CK-19	5'-GAAGGCCTGAAGGAAGAGCTG-3'	5'-CCTCCCACTTGGCCCCT-3'	80
Probe CK-19	5'-CCTACCTGAAGAAGAACCATGAGGAGGAAATCAGTA-3'		
Probe beta-actin	5′-CCTCCTTCCTGGGCATGGAGTCCTG-3′		

primer contain several mismatches. mRNA quantification was carried out using the one tube, one enzyme fluorogenic RT-PCR protocol[23]. Ten microliters of cDNA was diluted with 40 μL of master mixture containing TaqPolymerase, dNTP mixture and 10 × AmpliTaq buffer A, 200 nmol/L probe, 900 nmol/L primer and 25 mmol/L $MgCl_2$. After 10 min of denaturation at 95℃, PCR was carried out for 40 cycles at 95℃ for 15 s and extension at 60℃ for 60 s in the presence of the probe. RT-PCR monitoring was achieved by measuring the fluorescent signal of the probe at the end of the annealing phase of each cycle. mRNA quantification was recorded and analyzed with the ABI 7700 Prism Sequence detection system (Perkin Elmer Applied Biosystems, Foster City, CA, USA). Two no-template controls were used to monitor contamination in every run. Accurate quantification was achieved through generation of standard curves by serial dilution of CK-19 and beta-actin RNA transcribed by RNA polymerase. The sensitivity of the technique was evaluated by serial control analysis obtained in dilution experiments with CK-19-expressing cancer cell lines (CaPan2, PANC1). It was possible to detect the CK-19 mRNA expression of one cell of the cell lines in 1 mL of normal peripheral blood.

Evaluation criteria

For nested-PCR, the samples were tested twice. If a CK-19 signal was detected, the sample was judged positive. The fluorogenic RT-PCR assay was done twice for each sample. The average value of both duplicates for each sample was used as quantitative value. Samples were excluded from the investigation if the expression of the house-keeping gene beta-actin was below 10^6 copies. The ratio of copies of CK 19 mRNA per 10^6 copies of beta-actin mRNA was used for further analysis. The introduction of a cut-off was required, due to high illegitimate background transcription in the control group. The samples which exceeded the maximum value of the CK-19 mRNA expression in the control group were defined as CK-19 mRNA-positive.

Statistical analysis

Mann-Whitney rank sum test was used for quantitative analysis to asses the differences in the means. Fisher's exact test was used for qualitative analysis. Two-tailed *P* value less than 0.05 was considered statistically significant. Kaplan-Meier and log-rank test were used for analysis of survival. Statistical analysis was carried out using SigmaStat 1.0 software (Jandel Scientific Corp., Erkrath, Germany).

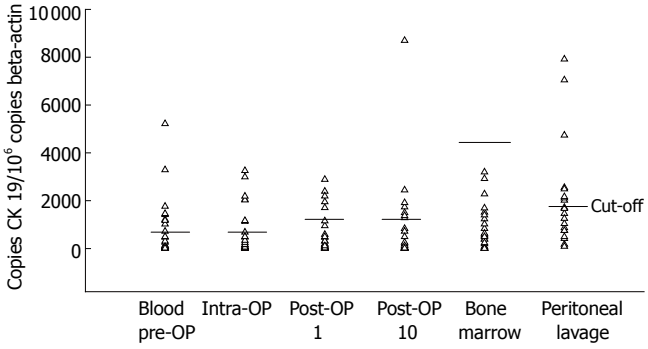

Figure 1 Quantitative values of cytokeratin-19 transcription in blood, bone marrow and peritoneal lavage of the patients with pancreatic cancer. [1]Cut-off: Maximal expression of CK-19 mRNA in healthy control patients.

RESULTS

Qualitative nested-PCR

CK-19 mRNA expression was detectable in the blood in 65% (24/37) of the patients with pancreatic cancer, 53% (8/16) of the patients with chronic pancreatitis and 18% (3/15) of the control group. The analysis of the bone marrow samples revealed detectable CK-19 mRNA in 56% (21/37) of pancreatic cancer patients, 46% (7/16) of chronic pancreatitis patients and 66% (10/15) of the control group. In 51% (19/37) of the patients with pancreatic cancer and 46% (7/16) of the patients with chronic pancreatitis and 46% (7/15) of the control group, CK-19 mRNA was detectable in the peritoneal lavage. There was no statistically significant difference between the groups.

Quantitative real-time RT-PCR

Blood, bone marrow and peritoneal lavage samples of 37 patients with pancreatic cancer were analyzed by CK-19 fluorogenic RT-PCR. CK-19 mRNA transcripts were detected in 70% (26/37) of blood samples, 67% (25/37) of bone marrow aspirates and 54% (20/37) of peritoneal lavage samples. In 40% (15/37) of the patients, PCR result was obtained from at least two compartments. We found that 64% (24/37) of the blood samples and 30% (11/37) of the peritoneal lavage samples showed CK-19 mRNA expression above the cut-off value and were defined as CK-19 mRNA-positive (Figure 1).

The CK-19 signal exceeded the cut-off value in 21% (8/37) of the pre-operatively and 19% (7/37) of the

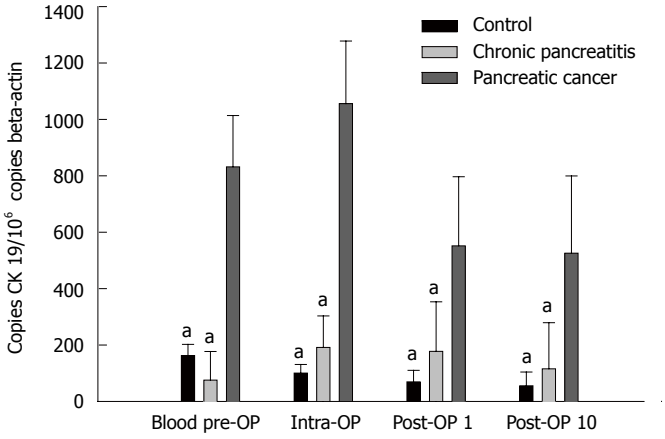

Figure 2 Quantitative analysis of CK-19 expression in blood (mean ± SD). $^{a}P < 0.05$ *vs* pancreatic cancer.

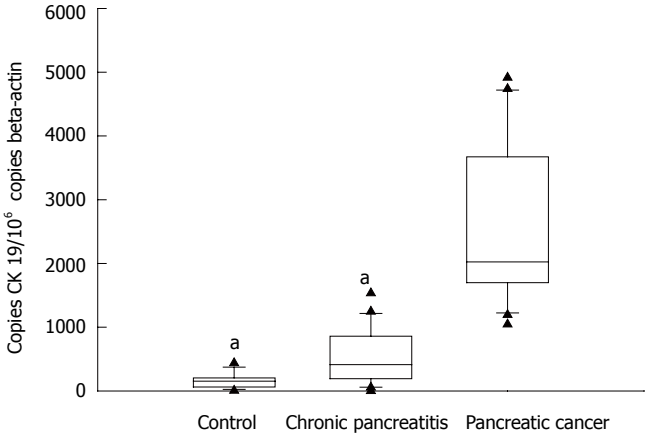

Figure 3 Quantitative CK-19 expression in peritoneal lavage of the patients with pancreatic cancer (mean ± SD, $^{a}P < 0.05$ *vs* pancreatic cancer).

intraoperatively taken blood samples. Likewise, 13% (5/37) of the samples taken at the first postoperative day and 10% (4/37) of the samples taken at the 10th postoperative day showed expression of CK-19 mRNA. The median mRNA expression was significantly increased in the patients compared to the control group at the four time points ($P < 0.05$) (Figure 2). The CK-19 levels showed a trend to increase intraoperatively and decrease at the 1st and 10th postoperative days below the pre-operative level ($P = 0.07$). We found 64% (24/37) of the bone marrow samples exhibited detectable CK-19 mRNA expression. None of the samples exceeded the CK-19 mRNA expression of the control group. The detection rate was not statistically different. In the peritoneal lavage, CK-19 signal was detected in 54% (20/37); 30% (11/37) of these samples exceeded the maximum level of the control group and were found to be CK-19 mRNA-positive. Compared to the control group, the median CK-19 mRNA expression was at least 10-fold increased (533 ± 121 copies CK-19/10^6 copies beta-actin *vs* 6262 ± 557 copies CK 19/10^6 copies beta-actin, $P < 0.01$) (Figure 3) .

The correlation analysis of marker detection and stage of disease was performed for blood, bone marrow and peritoneal lavage. In peritoneal lavage, CK-19 mRNA levels correlated with the tumor size and were increased 3 times in the patients with a pT3/pT4 tumor compared to the patients with pT1/pT2 tumors (874 ± 87 copies/10^6 copies beta-actin *vs* 2884 ± 473 copies/10^6 copies beta-actin ($P < 0.05$). Detection rates were increased for the patients with moderate or poorly differentiated tumors (pG2/pG3) compared to the patients with well differentiated tumors (pG1) (3560 ± 302 copies CK-19/10^6 copies beta-actin *vs* 1055 ± 88 copies CK-19/10^6 copies beta-actin, $P < 0.05$) (Figure 4). The detection rates were not significantly different regarding the N stage or in blood and bone marrow samples. At the endpoint of the study, 14 patients had died of metastasized disease or tumor recurrence; 57% (8/14) of these patients had at least one CK-19 positive sample. No significant difference in the median survival was observed between the patients with positive CK-19 mRNA expression and negative CK-19 mRNA expression (10 mo *vs* 15 mo, $P = 0.15$).

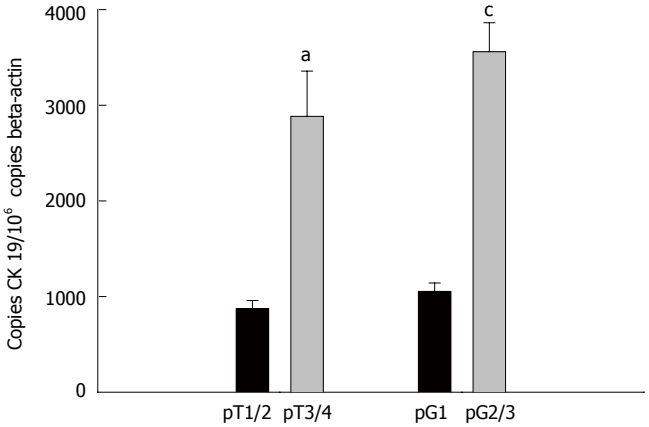

Figure 4 Quantitative CK-19 expression in peritoneal lavage of the patients with tumors (mean ± SD). $^{a}P < 0.05$ *vs* pT1/2; $^{c}P < 0.05$ *vs* pG1.

Blood, bone marrow and peritoneal lavage samples of 31 patients without malignancies (15 patients of the control group and 16 patients with chronic pancreatitis) were evaluated. CK-19 expression was detectable in 80% (12/15) of the samples taken from the control group. The highest detectable CK-19 signal was used as the base line for the cut-off values which were as follows: blood preoperatively 1064 copies CK-19 per 10^6 copies beta-actin, intraoperatively 984 copies CK-19 per 10^6 copies beta-actin, 1st and 10th postoperative days 1179 copies CK-19 per 10^6 copies beta-actin; bone marrow 4200 copies CK-19 per 10^6 copies beta-actin; and peritoneal lavage 1600 copies CK-19 per 10^6 copies beta-actin.

CK-19 mRNA could be detected in 80% (12/16) of the blood samples, 53% (8/16) of the bone marrow aspirates and 60% (9/16) of peritoneal lavage of the patients with chronic pancreatitis. No analyzed sample exceeded the maximal CK-19 mRNA expression of the control group. We observed a five-fold lower CK-19 signal in the peripheral blood compared to the patients with pancreatic cancer (142 ± 138 copies/10^6 copies beta-actin *vs* 741 ± 278 copies/10^6 copies beta-actin). The gene expression was significantly different at the four investigated time points ($P < 0.01$) (Figure 2). Analysis

of the bone marrow samples did not reveal any obvious difference in the CK-19 mRNA expression between the investigated groups. Compared to the patients with pancreatic cancer, the median CK-19 mRNA expression in the peritoneal lavage was 10-fold lower in the patients with chronic pancreatitis (261 ± 134 copies/10^6 copies beta-actin *vs* 3319 ± 484 copies/10^6 copies beta-actin, $P < 0.01$).

DISCUSSION

The long-term survival rates for patients with pancreatic cancer remain low. Without treatment, the 5-year survival rates are 0.4% to 4%[1,24]. Up to 80% of patients develop recurrent disease within 2 years after tumor resection[5]. Despite progress in adjuvant therapy and application of new chemo-radio-immunotherapy protocols, the high recurrence rate is the most limiting factor for the improvement of the patients prognosis[3,25]. Therefore, more sensitive staging methods are needed for this kind of tumor. Minimal residual disease caused by the spread of tumor cells into the circulation either before or during surgery is discussed as a main reason for early metastases and local recurrence in pancreatic cancer[26,27]. To detect tumor cells in the circulation, several studies have focused on cytokeratins and their potential role as tumor-specific markers[11,12,20,28-32]. However, conventional cytology, immunohistochemistry and molecular biological approaches reported conflicting results regarding the prevalence of CK-19 positive disseminated tumor cells and the impact on the prognosis of patients[12,33]. A reason for this is the target gene expression by non-neoplastic cells. False-positive results caused by illegitimate background transcription of CK-19 as seen in this study pose a major problem for qualitative PCR analysis. Gene transcription of CK-19 in healthy control groups and patients with benign disease has been reported in up to 80% of the analyzed samples[14,16]. In order to prevent false-positive results and increase the specificity, samples in this study were analyzed by quantitative RT-PCR. This approach facilitated the definition of cut-off values representing the maximal target gene expression in the control group. Regarding the results of nested-PCR in our study group, the qualitative PCR analysis of CK-19 expression can not be recommended for the detection of disseminated pancreatic cells.

Despite detection rates between 4%-100% using K-ras, CEA and cytokeratines as markers, up to now, tumor cell dissemination in the blood is not identified as an independent prognostic marker in pancreatic cancer[12,34-39]. In our sample series, 64% of peripheral blood samples taken from the patients with pancreatic cancer were detected to be CK-19-positive by quantitative fluorogenic RT-PCR. To reflect the dynamics of tumor cell dissemination during surgical intervention, blood samples were analyzed at four different time points showing target gene detection rates significantly higher compared to the control group. As described for K-ras and CEA mRNA, the amount of detectable CK-19 transcripts showed a trend to increase intraoperatively and decrease postoperatively below the preoperative level[26,36,37]. In consistent with Aihara *et al*[29], the CK-19 mRNA expression in the peripheral blood in our study showed higher levels.

Various studies have focused on the detection of disseminated pancreatic tumor cells in the bone marrow. Though positive detection rates have been reported between 24% and 58% for different markers, the tumor cell detection in the bone marrow does not correlate with tumor stage and is not an independent prognostic marker[11,12,34,35]. There is only one study by Soeth *et al*[36] demonstrating a benefit in survival in patients with CK-20-negative bone marrow aspirates. The data obtained in our study confirm the results of Dimmler *et al*[14], who dissuade from use of CK-19 for analysis of bone marrow due to high levels of illegitimate background expression in healthy controls. In contrast, peritoneal lavage was identified to be suitable to represent the actual state of tumor dissemination. The immunohistochemical analysis of the peritoneal lavage reported detection rates between 20% and 58% for marker-positive pancreatic cells[34,35,37-39]. Compared to the analysis by Inoue *et al*[40] who reported 10% of K-ras mRNA-positive cells, our detection rate of CK-19 positive cells was 30%. To the best of our knowledge, this sample series is the first report that shows a correlation between the CK-19 mRNA expression in the peritoneal lavage and the tumor size and tumor differentiation. A correlation between positive tumor cell detection and impaired patient survival as reported for cytological analysis by Yachida *et al*[37] and Makary *et al*[41] could not be detected.

Besides the detection of dissemination of neoplastic cells, the differentiation between malignant and benign pancreatic disease is of major interest for clinicians. Up to now, several markers such as K-ras, p53 and CEA failed as serum marker for a differential diagnosis[17,42]. CK 19-9 is the best characterized serum marker but has no absolute specificity. This is the first study that evaluates CK-19 mRNA expression in different compartments for the potential to differentiate between pancreatic cancer and chronic pancreatitis. In our study, the patients with pancreatic cancer showed an unequivocally increased CK-19 expression compared to the patients with chronic pancreatitis. Ten-fold higher expression levels in the peripheral blood as well as in the peritoneal lavage from the pancreatic cancer patients compared to the chronic pancreatitis patients indicated that quantitative fluorogenic RT-PCR is suited for the distinction between malignant and benign pancreatic disease.

In conclusion, our data suggest that CK-19-positive tumor cells can be detected in patients with pancreatic carcinoma in venous blood and peritoneal lavage by using fluorogenic RT-PCR. The prevalence of isolated tumor cells in peritoneal lavage increases significantly with the tumor stage and differentiation. The application of highly sensitive RT-PCR technique may improve the staging of patients and the monitoring of the residual tumor cell burden within the context of adjuvant systemic therapies. For the clinical use, the combination of tumor-specific markers is indispensable to increase the specificity of this test.

COMMENTS

Background

Pancreatic cancer is one of the top five causes of cancer death in the Western world. Occult micro-metastases caused by disseminated tumor cells are the most limiting factor for the improvement of mortality rates.

Research frontiers

Additional to cytology, immunohistochemical analysis is the standard for identification of disseminated tumor cells. Nevertheless, conflicting results regarding the prognostic relevance have been reported. Molecular biological approaches, such as reverse transcriptase polymerase chain reaction (RT-PCR), have a high sensitivity and specificity and might be more suitable for the analysis of disseminated tumor cells.

Innovations and breakthroughs

Various studies used cytokeratin-19 (CK-19) for pancreatic cell detection that has been identified as a reliable marker for epithelial cell differentiation and is homogenously expressed at high levels in primary pancreatic adenocarcinoma and pancreatic carcinoma metastases. Until now, CK-19 mRNA expression has not been identified as an independent prognostic indicator in pancreatic cancer.

Applications

Our data suggest that CK-19-positive tumor cells can be detected in patients with pancreatic carcinoma in venous blood and peritoneal lavage by using fluorogenic RT-PCR. The prevalence of isolated tumor cells in peritoneal lavage increases significantly with the tumor stage and differentiation. The application of highly sensitive RT-PCR technique may improve the staging of patients and the monitoring of the residual tumor cell burden within the context of adjuvant systemic therapies. For the clinical use, the combination of tumor-specific markers is indispensable to increase the specificity of this test.

Peer review

The authors demonstrate that quantification of CK-19 seems to be a reliable marker for the differential diagnosis of ductal pancreatic cancer and for staging. The Material and Methods, Results and Discussion are adequate and the paper provides new information for the investigators in this field.

REFERENCES

1 **Jemal A**, Murray T, Samuels A, Ghafoor A, Ward E, Thun MJ. Cancer statistics 2003. *CA Cancer J Clin* 2003; **53**: 5-26
2 **Parkin DM**, Bray FI, Devesa SS. Cancer burden in the year 2000. The global picture. *Eur J Cancer* 2001; **37** Suppl 8: S4-S66
3 **Neoptolemos JP**, Stocken DD, Friess H, Bassi C, Dunn JA, Hickey H, Beger H, Fernandez-Cruz L, Dervenis C, Lacaine F, Falconi M, Pederzoli P, Pap A, Spooner D, Kerr DJ, Büchler MW. A randomized trial of chemoradiotherapy and chemotherapy after resection of pancreatic cancer. *N Engl J Med* 2004; **350**: 1200-1210
4 **Wagner M**, Redaelli C, Lietz M, Seiler CA, Friess H, Büchler MW. Curative resection is the single most important factor determining outcome in patients with pancreatic adenocarcinoma. *Br J Surg* 2004; **91**: 586-594
5 **Griffin JF**, Smalley SR, Jewell W, Paradelo JC, Reymond RD, Hassanein RE, Evans RG. Patterns of failure after curative resection of pancreatic carcinoma. *Cancer* 1990; **66**: 56-61
6 **Westerdahl J**, Andrén-Sandberg A, Ihse I. Recurrence of exocrine pancreatic cancer-local or hepatic? *Hepatogastroenterology* 1993; **40**: 384-387
7 **Vogel I**, Kalthoff H, Henne-Bruns D, Kremer B. Detection and prognostic impact of disseminated tumor cells in pancreatic carcinoma. *Pancreatology* 2002; **2**: 79-88
8 **Bilchik A**, Miyashiro M, Kelley M, Kuo C, Fujiwara Y, Nakamori S, Monden M, Hoon DS. Molecular detection of metastatic pancreatic carcinoma cells using a multimarker reverse transcriptase-polymerase chain reaction assay. *Cancer* 2000; **88**: 1037-1044
9 **Leach SD**, Rose JA, Lowy AM, Lee JE, Charnsangavej C, Abbruzzese JL, Katz RL, Evans DB. Significance of peritoneal cytology in patients with potentially resectable adenocarcinoma of the pancreatic head. *Surgery* 1995; **118**: 472-478
10 **Meszoely IM**, Lee JS, Watson JC, Meyers M, Wang H, Hoffman JP. Peritoneal cytology in patients with potentially resectable adenocarcinoma of the pancreas. *Am Surg* 2004; **70**: 208-213; discussion 213-214
11 **Thorban S**, Roder JD, Siewert JR. Detection of micrometastasis in bone marrow of pancreatic cancer patients. *Ann Oncol* 1999; **10** Suppl 4: 111-113
12 **Z'graggen K**, Centeno BA, Fernandez-del Castillo C, Jimenez RE, Werner J, Warshaw AL. Biological implications of tumor cells in blood and bone marrow of pancreatic cancer patients. *Surgery* 2001; **129**: 537-546
13 **Pantel K**, von Knebel Doeberitz M. Detection and clinical relevance of micrometastatic cancer cells. *Curr Opin Oncol* 2000; **12**: 95-101
14 **Dimmler A**, Gerhards R, Betz C, Günther K, Reingruber B, Horbach T, Baumann I, Kirchner T, Hohenberger W, Papadopoulos T. Transcription of cytokeratins 8, 18, and 19 in bone marrow and limited expression of cytokeratins 7 and 20 by carcinoma cells: inherent limitations for RT-PCR in the detection of isolated tumor cells. *Lab Invest* 2001; **81**: 1351-1361
15 **Dingemans AM**, Brakenhoff RH, Postmus PE, Giaccone G. Detection of cytokeratin-19 transcripts by reverse transcriptase-polymerase chain reaction in lung cancer cell lines and blood of lung cancer patients. *Lab Invest* 1997; **77**: 213-220
16 **Van Trappen PO**, Gyselman VG, Lowe DG, Ryan A, Oram DH, Bosze P, Weekes AR, Shepherd JH, Dorudi S, Bustin SA, Jacobs IJ. Molecular quantification and mapping of lymph-node micrometastases in cervical cancer. *Lancet* 2001; **357**: 15-20
17 **Sawabu N**, Watanabe H, Yamaguchi Y, Ohtsubo K, Motoo Y. Serum tumor markers and molecular biological diagnosis in pancreatic cancer. *Pancreas* 2004; **28**: 263-267
18 **Moll R**. Cytokeratins as markers of differentiation. Expression profiles in epithelia and epithelial tumors. *Veroff Pathol* 1993; **142**: 1-197
19 **Bouwens L**. Cytokeratins and cell differentiation in the pancreas. *J Pathol* 1998; **184**: 234-239
20 **Schüssler MH**, Skoudy A, Ramaekers F, Real FX. Intermediate filaments as differentiation markers of normal pancreas and pancreas cancer. *Am J Pathol* 1992; **140**: 559-568
21 **Ruud P**, Fodstad O, Hovig E. Identification of a novel cytokeratin 19 pseudogene that may interfere with reverse transcriptase-polymerase chain reaction assays used to detect micrometastatic tumor cells. *Int J Cancer* 1999; **80**: 119-125
22 **Wittekind C**, Compton CC, Greene FL, Sobin LH. TNM residual tumor classification revisited. *Cancer* 2002; **94**: 2511-2516
23 **Bustin SA**, Gyselman VG, Williams NS, Dorudi S. Detection of cytokeratins 19/20 and guanylyl cyclase C in peripheral blood of colorectal cancer patients. *Br J Cancer* 1999; **79**: 1813-1820
24 **Bramhall SR**, Allum WH, Jones AG, Allwood A, Cummins C, Neoptolemos JP. Treatment and survival in 13,560 patients with pancreatic cancer, and incidence of the disease, in the West Midlands: an epidemiological study. *Br J Surg* 1995; **82**: 111-115
25 **Picozzi VJ**, Traverso LW. The Virginia Mason approach to localized pancreatic cancer. *Surg Oncol Clin N Am* 2004; **13**: 663-674, ix
26 **Romsdahl MM**, Valaitis J, McGrath RG, McGrew EA. Circulating tumor cells in patients with carcinoma. Method and recent studies. *JAMA* 1965; **193**: 1087-1090
27 **Pantel K**, Schlimok G, Braun S, Kutter D, Lindemann F, Schaller G, Funke I, Izbicki JR, Riethmüller G. Differential expression of proliferation-associated molecules in individual micrometastatic carcinoma cells. *J Natl Cancer Inst* 1993; **85**: 1419-1424
28 **Vogel I**, Kalthoff H. Disseminated tumour cells. Their detection and significance for prognosis of gastrointestinal and pancreatic carcinomas. *Virchows Arch* 2001; **439**: 109-117

29 **Aihara T**, Noguchi S, Ishikawa O, Furukawa H, Hiratsuka M, Ohigashi H, Nakamori S, Monden M, Imaoka S. Detection of pancreatic and gastric cancer cells in peripheral and portal blood by amplification of keratin 19 mRNA with reverse transcriptase-polymerase chain reaction. *Int J Cancer* 1997; **72**: 408-411

30 **van Heek NT**, Tascilar M, van Beekveld JL, Drillenburg P, Offerhaus GJ, Gouma DJ. Micrometastases in bone marrow of patients with suspected pancreatic and ampullary cancer. *Eur J Surg Oncol* 2001; **27**: 740-745

31 **Wildi S**, Kleeff J, Maruyama H, Maurer CA, Friess H, Büchler MW, Lander AD, Korc M. Characterization of cytokeratin 20 expression in pancreatic and colorectal cancer. *Clin Cancer Res* 1999; **5**: 2840-2847

32 **Goldstein NS**, Bassi D. Cytokeratins 7, 17, and 20 reactivity in pancreatic and ampulla of vater adenocarcinomas. Percentage of positivity and distribution is affected by the cut-point threshold. *Am J Clin Pathol* 2001; **115**: 695-702

33 **Roder JD**, Thorban S, Pantel K, Siewert JR. Micrometastases in bone marrow: prognostic indicators for pancreatic cancer. *World J Surg* 1999; **23**: 888-891

34 **Juhl H**, Stritzel M, Wroblewski A, Henne-Bruns D, Kremer B, Schmiegel W, Neumaier M, Wagener C, Schreiber HW, Kalthoff H. Immunocytological detection of micrometastatic cells: comparative evaluation of findings in the peritoneal cavity and the bone marrow of gastric, colorectal and pancreatic cancer patients. *Int J Cancer* 1994; **57**: 330-335

35 **Vogel I**, Krüger U, Marxsen J, Soeth E, Kalthoff H, Henne-Bruns D, Kremer B, Juhl H. Disseminated tumor cells in pancreatic cancer patients detected by immunocytology: a new prognostic factor. *Clin Cancer Res* 1999; **5**: 593-599

36 **Soeth E**, Grigoleit U, Moellmann B, Röder C, Schniewind B, Kremer B, Kalthoff H, Vogel I. Detection of tumor cell dissemination in pancreatic ductal carcinoma patients by CK 20 RT-PCR indicates poor survival. *J Cancer Res Clin Oncol* 2005; **131**: 669-676

37 **Makary MA**, Warshaw AL, Centeno BA, Willet CG, Rattner DW, Fernández-del Castillo C. Implications of peritoneal cytology for pancreatic cancer management. *Arch Surg* 1998; **133**: 361-365

38 **Nakao A**, Oshima K, Takeda S, Kaneko T, Kanazumi N, Inoue S, Nomoto S, Kawase Y, Kasuya H. Peritoneal washings cytology combined with immunocytochemical staining in pancreatic cancer. *Hepatogastroenterology* 1999; **46**: 2974-2977

39 **Nomoto S**, Nakao A, Kasai Y, Inoue S, Harada A, Nonami T, Takagi H. Peritoneal washing cytology combined with immunocytochemical staining and detecting mutant K-ras in pancreatic cancer: comparison of the sensitivity and availability of various methods. *Pancreas* 1997; **14**: 126-132

40 **Inoue S**, Nakao A, Kasai Y, Harada A, Nonami T, Takagi H. Detection of hepatic micrometastasis in pancreatic adenocarcinoma patients by two-stage polymerase chain reaction/restriction fragment length polymorphism analysis. *Jpn J Cancer Res* 1995; **86**: 626-630

41 **Yachida S**, Fukushima N, Sakamoto M, Matsuno Y, Kosuge T, Hirohashi S. Implications of peritoneal washing cytology in patients with potentially resectable pancreatic cancer. *Br J Surg* 2002; **89**: 573-578

42 **Kimura W**, Zhao B, Futakawa N, Muto T, Makuuchi M. Significance of K-ras codon 12 point mutation in pancreatic juice in the diagnosis of carcinoma of the pancreas. *Hepatogastroenterology* 1999; **46**: 532-539

S- Editor Wang GP **L- Editor** Kumar M **E- Editor** Ma WH

PO Box 2345, Beijing 100023, China
www.wjgnet.com
wjg@wjgnet.com

World J Gastroenterol 2007 January 14; 13(2): 264-269
World Journal of Gastroenterology ISSN 1007-9327

CLINICAL RESEARCH

Efficacy of long term cyclic administration of the poorly absorbed antibiotic Rifaximin in symptomatic, uncomplicated colonic diverticular disease

Antonio Colecchia, Amanda Vestito, Francesca Pasqui, Giuseppe Mazzella, Enrico Roda, Francesca Pistoia, Giovanni Brandimarte, Davide Festi

Antonio Colecchia, Amanda Vestito, Francesca Pasqui, Giuseppe Mazzella, Enrico Roda, Davide Festi, Department of Internal Medicine and Gastroenterology, University of Bologna, Cristo Re Hospital, Rome, Italy
Francesca Pistoia, Department of Surgery, University of L'Aquila, Cristo Re Hospital, Rome, Italy
Giovanni Brandimarte, Department of Internal Medicine, Cristo Re Hospital, Rome, Italy
Correspondence to: Davide Festi, MD, Dipartimento di Medicina Interna e Gastroenterologia Policlinico S.Orsola, Via Massarenti 9, Bologna 40138, Italy. davide.festi@unibo.it
Telephone: +39-51-6364123 Fax: +39-51-6364123
Received: 2006-08-30 Accepted: 2006-10-20

Abstract

AIM: To comparatively evaluate the long term efficacy of Rifaximin and dietary fibers in reducing symptoms and/or complication frequency in symptomatic, uncomplicated diverticular disease.

METHODS: 307 patients (118 males, 189 females, age range: 40-80 years) were enrolled in the study and randomly assigned to: Rifaximin (400 mg bid for 7 d every month) plus dietary fiber supplementation (at least 20 gr/d) or dietary fiber supplementation alone. The study duration was 24 mo; both clinical examination and symptoms' questionnaire were performed every two months.

RESULTS: Both treatments reduced symptom frequency, but Rifaximin at a greater extent, when compared to basal values. Symptomatic score declined during both treatments, but a greater reduction was evident in the Rifaximin group (6.4 ± 2.8 and 6.2 ± 2.6 at enrollment, P = NS, 1.0 ± 0.7 and 2.4 ± 1.7 after 24 mo, $P < 0.001$, respectively). Probability of symptom reduction was higher and complication frequency lower (Kaplan-Meyer method) in the Rifaximin group ($P < 0.0001$ and 0.028, respectively).

CONCLUSION: In patients with symptomatic, uncomplicated diverticular disease, cyclic administration of Rifaximin plus dietary fiber supplementation is more effective in reducing both symptom and complication frequency than simple dietary fiber supplementation. Long term administration of the poorly absorbed antibiotic Rifaximin is safe and well tolerated by the patients, confirming the usefulness of this therapeutic strategy in the overall management of diverticular disease.

Key words: Dietary fiber; Antibiotics; Abdominal symptoms; Diverticulitis

Colecchia A, Vestito A, Pasqui F, Mazzella G, Roda E, Pistoia F, Brandimarte G, Festi D. Efficacy of long term cyclic administration of the poorly absorbed antibiotic Rifaximin in symptomatic, uncomplicated colonic diverticular disease. *World J Gastroenterol* 2007; 13(2): 264-269

http://www.wjgnet.com/1007-9327/13/264.asp

INTRODUCTION

Diverticular disease of the colon represents the most common disease affecting the large bowel in the Western world[1]; the disease is more frequent in USA than in Europe and it represents a rare clinical condition in Africa[2]. Prevalence of diverticular disease is largely age-dependent and is uncommon, with a rate less than 5%, in subjects under 40 years of age, increasing up to 65% in those aged 65 years or more[3]. Diverticular disease and its clinical consequences have recently become increasingly prevalent, paralleling western patterns of living and eating, the ageing population, and economic and industrial development[4]. Although a large majority of patients with diverticular disease will remain entirely asymptomatic for their entire life, 20% of them may manifest clinical illness[4,5] and a worse quality of life[6]. Furthermore, since available data[2,3] suggest that the incidence of diverticular disease is increasing and that its prevalence increases with age, the identification of a management strategy for the disease represents an healthy priority. Several guidelines are actually available to manage diverticular disease[7,8]; there is a consensus that conservative treatment is indicated in patients with a first attack of uncomplicated diverticulitis, since about 70% of patients treated for a first episode recover and have no further problems[9]. However, a 60% risk of developing complications has been reported in patients with recurrent attacks[2]. Conservative treatment is aimed at the relief of symptoms and at preventing

major complications[8,9]. Available evidence[10] suggests that antibiotics, and namely topical antibiotics, and dietary fibers represent useful treatments for uncomplicated diverticular disease and for preventing disease complications. Different antibiotics have been tested, but the possibility of side effect development due to their long-term use have discouraged their employment[10].

Rifaximin is a rifamycin analogue with a broad spectrum of activity similar to that of rifampicin and it is poorly absorbed in the gastrointestinal tract[11], thus conferring to this drug a high safety profile. Due to these properties, Rifaximin has been tested in different gastrointestinal diseases, and in diverticular disease too[12,13]. Two randomized clinical trials[14,15] performed in patients with uncomplicated diverticular disease showed that Rifaximin plus dietary fiber supplementation was more effective in improving symptoms than dietary fibre supplementation alone after 12 mo of treatment.

Since the uncertainties regarding the natural history of the disease, and in particular the predictors for the progression from uncomplicated to complicated disease, and the lack of a definite indication for long term management of uncomplicated disease, data on long-term treatment with topical antibiotics and dietary fibers would be necessary.

Therefore, the aim of the present study was to evaluate the long-term efficacy of cyclic administration of Rifaximin plus fiber supplementation versus fiber supplementation alone on symptoms and clinical manifestations in patients with symptomatic, but uncomplicted, diverticular disease.

MATERIALS AND METHODS

Study design

This was a multicenter, open, prospective, randomized, controlled study. Patients were randomly assigned to one of the two treatment regimens: one group received Rifaximin (400 mg bid for 7 d every month) plus dietary fiber supplementation (at least 20 gr/d) (Rifaximin group) and the other group simple dietary fiber supplementation (at least 20 gr/d) (fiber group). The study duration was 24 mo.

Patients were consecutively assigned to one group or to the other by a computer-generated randomization scheme. Informed consent was obtained from each patient and the study protocol was approved by the local Ethis Committee.

Patients

Consecutive patients with symptomatic, uncomplicated diverticular disease were enrolled. Inclusion criteria for the study were: age between 40 and 80 years, endoscopic or radiological evidence of diverticular disease of the sigmoid and/or descending colon, presence of symptoms attributable to the diverticular disease of the colon such as lower abdominal pain/discomfort, bloating, tenesmus, diarrhea and abdominal tenderness. Patients who referred the continuous presence of three, or more, of these symptoms for at least 1 mo before the enrolment entered in the study.

Exclusion criteria were represented by the presence of a solitary diverticulum of the right colon, signs of complicated diverticular disease, previous colonic surgery, neoplastic or haematological diseases, immunodeficiency, pregnancy and questionable ability to cooperate. Patients who assumed antibiotics in the previous 4 wk were also excluded.

Clinical evaluation

At enrolment and every 2 mo until the 24 mo patients underwent clinical examination; a questionnaire inquiring about the presence and severity of abdominal symptoms was also performed. Five clinical variables (lower abdominal pain/discomfort, bloating, tenesmus, diarrhea and abdominal tenderness) were graded according to the following scale: 0 = no symptoms; 1 = mild symptoms, easily tolerated; 2 = moderate symptoms, sufficient to cause interference with normal daily activities; 3 = severe, incapacitating symptoms, with inability to perform normal daily activities. Consequently the global score could range from 0 (absence of symptoms) to 15 (presence of all symptoms with the higher degree of severity).

Biochemical tests were performed at enrolment, and after 12 and 24 mo of treatment .

Statistical methods

On the presumption of a 40% reduction at 24 mo in the frequency of symptoms with dietary fiber and a 65% reduction with Rifaximin plus fiber treatment, and considering the delta between the frequencies to be either equal to or at least 25%, a two-tail significance test, a significance level of $\alpha = 0.05$, a 99% power and a 3:2 allocation ratio (in order to better satisfy the secondary end-point), the number of patients to be enrolled was 177 patients for the Rifaximin group and 110 for the fibers group. Presuming a 10% of drop-out, it was necessary to enrol 307 patients (185 for the active group and 122 for the control group)[16].

χ^2 test or Fisher's exact test were used to compare the distribution of categorical or absolute variables within the studied groups. Parametric tests (Levene's test, *t* test, one- and two-way analysis of variance and repeated-measure ANOVA) were used to analyze continuous parameters. Non-parametric tests, one-way analysis of variance (Friedman's test) and Wilcoxon test were applied to analyze the same parameters in subgroups of patients in whom a distribution normality of character being studied could not be presumed[17].

Kaplan Meier curves were used to estimate the probability of a reduction in symptom score and of complication development in the two groups of patients; differences between the two branches were evaluated by means of Log-rank test. Results were expressed as mean ± SD and a *P* value less than 0.05 was considered as statistically significant. Data analysis was performed using SPSS version 13.0.

RESULTS

Patients

Three-hundred and seven (307) patients were enrolled, 118 males and 189 females.

Table 1 shows demographic and clinical characteristics

Table 1 Demographic and clinical characteristics of study patients

	Rifaximin plus fibers (n = 184)	Fibers (n = 123)	P
Gender			
Males	68 (37.0%)	50 (40.7%)	[1]NS
Females	116 (63.0%)	73 (59.3%)	
Age (yr)	63.6 ± 11.7	60.7 ± 12.5	[2]NS
Site of diverticula			
Left colon	47 (25.5%)	26 (21.1%)	
Colon-sigma	59 (32.1%)	38 (30.9%)	[3]NS
Sigma	73 (39.7%)	56 (45.5%)	
Sigma-rectum	5 (2.7%)	3 (2.4%)	
Symptoms (%)			
Lower abdominal pain	87.5%	90.2%	[1]NS
Bloating	85.9%	78.0%	[1]NS
Tenesmus	35.3%	29.3%	[1]NS
Diarrhoea	35.9%	32.5%	[1]NS
Abdominal tenderness	71.2%	69.1%	[1]NS
Symptoms score	6.4 ± 2.8	6.2 ± 2.6	[1]NS

[1]χ^2 test with continuity correction; [2]t test; [3]χ^2 test.

Table 2 Mean baseline values of biochemical parameters

	Rifaximin plus fibers	Fibers	P
ESR (mm/h)	24.9 ± 17.7	22.8 ± 17.8	NS
Leukocytes (mm^3)	8128.1 ± 2377.7	7836.9 ± 2019.6	NS
Neutrophils (mm^3)	68.3 ± 12.1	68.7 ± 9.6	NS
Ht (%)	41.9 ± 5.3	42.2 ± 4.0	NS
Creatininemia (mg/dL)	0.97 ± 0.25	0.98 ± 0.19	NS
Blood nitrogen (mg/dL)	38.3 ± 12.7	36.5 ± 11.2	NS
Blood sodium (nmol/L)	138.8 ± 4.9	139.4 ± 17.8	NS
Potassemia (nmol/L)	4.23 ± 0.46	4.15 ± 0.35	NS
AST (IU/L)	23.9 ± 17.2	21.8 ± 10.8	NS
ALT (IU/L)	25.0 ± 23.1	22.1 ± 14.1	NS
AP (IU/L)	151.7 ± 65.4	142.4 ± 65.6	NS
γGT (IU/L)	34.8 ± 33.4	33.7 ± 26.1	NS
Total proteins (g/dL)	6.85 ± 0.58	6.90 ± 0.42	NS

t-test for corrected for multiple comparison.

Table 3 Symptom frequency (%) at baseline, after 12 and 24 mo of treatment

	Rifaximin plus fibers			Fibers			P
Mo	0	12th	24th	0	12th	24th	at 24th
Lower abdominal pain	87.5	17.2	12.9	90.2	28.8	19.2	0.05[1]
Bloating	85.9	35.0	21.9	78.0	43.3	40.3	< 0.002[1]
Tenesmus	35.3	3.2	3.9	29.3	2.9	9.6	= 0.05[1]
Diarrhoea	35.9	7.0	3.9	32.5	1.0	2.9	NS[2]
Abdominal tenderness	71.2	19.0	6.5	69.1	35.6	21.2	< 0.001[1]

[1]χ^2 test; [2]Fisher's Exact test.

of the enrolled patients: no difference was found between the two groups of patients in terms of gender, age and colonic distribution of the disease as well as frequency of abdominal symptoms and global symptom score. Diagnosis of diverticular disease was performed by colonoscopy in 46.2% of patients treated with Rifaximin and in 53.7% of patients treated with fibers, and by barium enema in 60.9% and 48.8% of patients, respectively (P = NS). Again, no difference was present at baseline between the two groups of treatment as far as biochemical parameters are concerned (Table 2).

Fourty-eight (48) patients did not complete the study, 25 patients of the Rifaximin group and 23 patients of the fibers group; 28 patients (17 of the Rifaximin group and 11 of the fibers group, P = NS, Fisher's exact test) were drop-outs: in the Rifaximin group 14 patients refused to continue the study, 2 patients died for cardiovascular disease and 1 patient for causes unrelated to diverticular disease, while in the fibers group 10 patients refused to continue the study and 1 patient underwent surgery for gallstone disease. Side effects (mainly represented by nausea, headache and weakness) occurred in 4 patients of the Rifaximin group and in 3 patients of the fibers group (P = NS). Frequency of complications was significantly different (P = 0.041) between the two groups: in fact complications occurred in 4 patients of the Rifaximin group (2 cases of rectal bleeding, and 2 of diverticulitis) and in 9 of the fiber group (4 cases of intestinal infections, 1 of rectal bleeding and 4 of diverticulitis).

The effect of treatments on clinical signs and symptoms is illustrated in Table 3: both treatments induced a significant reduction in symptom frequency in all patients after 12 mo. After 24 mo of treatment, Rifaximin was able to further reduce symptoms as lower abdominal pain, bloating, tenesmus and abdominal tenderness while no difference was observed in patients treated with fibers alone between the results observed at the 12th and the 24th mo.

The effect of treatments on the symptomatic score is shown in Figure 1: although both treatments were able to significantly reduce the symptom score, this result was differently reached: at baseline the symptom score was similar, while at the end of the study period a significant difference ($P < 0.01$) was present between the Rifaximin treated group and the fiber group (1.0 ± 0.7 and 2.4 ± 1.7, respectively).

The clinical effect of the two treatments evaluated according to the Kaplan-Meier method is shown in Figure 2: the probability of symptom remission in symptomatic patients was significantly higher ($P < 0.0001$) in the Rifaximin group than in the control group. Although the overall clinical efficacy of the two regimens is different, a similar behaviour can be observed: the cumulative survival progressively declined during the first 12 mo of treatment, remaining constant during the following 12 mo. Rifaximin treatment was also able to induce a lower frequency of recurrence of symptoms: six (3.2%) Rifaximin treated patients had a further episode of abdominal symptoms, while in the fibers group the corresponding figure was three (9.6%) patients ($P < 0.03$).

No significant alterations in biochemical tests were observed in the two groups of patients (Table 4). The probability of developing complications during the study in the two groups of patients evaluated according to the

Table 4 Mean value of biochemical parameters before and at the end of treatment period

	Rifaximin plus fibers		*P*	Fibers		*P*
	Baseline	at 24 mo		Baseline	at 24 mo	
ESR (mm/h)	24.8 ± 18.2	15.2 ± 14.4	< 0.001	23.2 ± 18.6	17.8 ± 15.3	< 0.05
Leukocytes (mm^3)	8330.3 ± 2554.4	6515.8 ± 1393.9	< 0.001	7944.9 ± 2091.4	6918.5 ± 1719.8	< 0.01
Neutrophils (mm^3)	67.8 ± 12.3	62.0 ± 10.9	< 0.005	68.9 ± 9.9	65.5 ± 8.7	< 0.03
Creatininemia (mg/dL)	0.98 ± 0.25	0.96 ± 0.21	NS	0.98 ± 0.19	0.94 ± 0.17	NS
Blood nitrogen (mg/dL)	39.4 ± 13.0	37.7 ± 10.6	NS	37.1 ± 11.3	33.7 ± 9.9	< 0.05
Blood sodium (nmol/L)	138.8 ± 5.0	140.0 ± 5.1	< 0.05	139.2 ± 5.2	139.1 ± 6.5	NS
Potassemia (nmol/L)	4.22 ± 0.45	4.21 ± 0.46	NS	4.20 ± 0.37	4.18 ± 0.30	NS
AST (IU/L)	23.2 ± 15.1	21.3 ± 12.7	NS	22.5 ± 11.1	20.8 ± 10.5	NS
ALT (U/L)	23.9 ± 14.6	21.8 ± 11.6	NS	22.7 ± 14.4	19.1 ± 8.8	< 0.05
AP (U/L)	147.3 ± 63.2	164.3 ± 65.6	< 0.05	140.6 ± 69.3	149.1 ± 62.4	NS
γGT (U/L)	33.0 ± 24.1	36.6 ± 24.3	NS	35.4 ± 27.3	30.2 ± 18.4	NS
Total proteins (g/dL)	6.85 ± 0.57	6.89 ± 0.58	NS	6.90 ± 0.44	6.78 ± 0.89	NS

t test for paired data, corrected for multiple comparison.

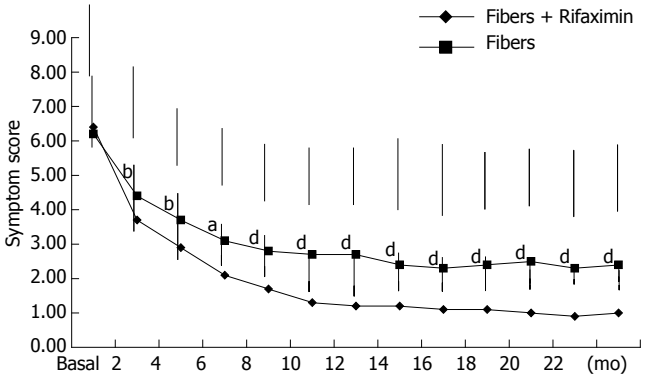

Figure 1 Changes in symptoms score after Rifaximin plus fiber supplementation and fiber supplementation alone (mean ± SD). *t* test for independent samples corrected for multiple comparison: $^{a}P < 0.05$; $^{b}P < 0.01$; $^{d}P < 0.001$.

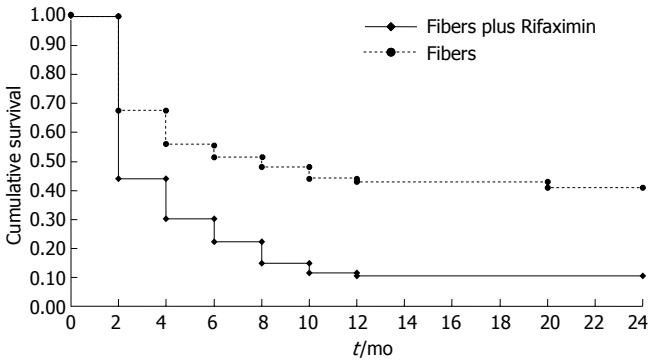

Figure 2 Probability of symptom reduction in patients treated with Rifaximin plus fibers or with fiber supplementation alone. Kaplan-Meier method: Test Log Rank: $P < 0.0001$.

Kaplan-Meier method is illustrated in Figure 3: as observed for symptoms, Rifaximin administration documented a more favourable effect, being significantly lower ($P < 0.028$) the probability of developing complications with respect to fiber supplementation. Although with a different rate of probability, both treatments induced a progressively reduced frequency of complications during the whole study period.

DISCUSSION

The present study suggest that the cyclic, long term administration of the non-absorbable antibiotic Rifaximin associated with dietary fiber supplementation is more effective than dietary fiber supplementation alone in reducing the clinical manifestations of patients with symptomatic, uncomplicated diverticular disease. Furthermore, Rifaximin treatment is more effective than fiber administration influencing the clinical course of the disease, since both probability of symptom recurrence and development of disease complications are significantly reduced.

Diverticular disease of the colon is common in developed countries and its prevalence is correlated with advancing age[1-4]. Studies on the natural history of the disease[3,5,9] have indicated that most patients with colonic diverticula remain entirely asymptomatic for their lifetime. Actually there are no definitive data to support any therapeutic recommendation, or routine follow-up regimen, for asymptomatic subjects, although it is reasonable to recommend a life-style characterized by regular physical activity and a diet high in fruit and vegetable fibers[18]. According to available guidelines[7,8] in symptomatic, but uncomplicated, diverticular disease treatment is aimed at symptom-relief and at prevention of complications (diverticulitis, hemorrage). Different agents have been proposed, such as bulking agents, antispasmodics, topical antibiotics, on the basis of different potential pathophysiological mechanism/s, i.e. abnormal colonic motility, inadequate intake of dietary fibers, intestinal bacterial overgrowth and mucosal inflammation[10,19-23].

The efficacy of fiber supplementation in the treatment of symptomatic diverticular disease remains controversial, although it is considered a mainstay for treatment[10]. The efficacy of dietary fibers in reducing symptoms and in improving intestinal function is probably related to its ability to hold water, to increase luminal intestinal mass,

to relax the intestinal wall and to lower the intraluminal pressure[24,25].

Antibiotics are routinely used in the treatment of inflammatory complications of diverticular disease. In symptomatic, but uncomplicated diverticular disease, the use of antibiotics seems without a rationale. However, recent studies have suggested the presence, at least in a sub-group of patients, of an intestinal bacterial overgrowth[21], a condition that may allow an excessive production of bowel gas with secondary development of abdominal pain, bloating and tenderness. Furthermore, intestinal bacterial overgrowth may contribute to maintain a chronic, low-grade mucosal inflammation, as suggested in irritable bowel syndrome[26], which could be responsible for symptom development[19].

Rifaximin has been tested in both uncontrolled[12,13] and controlled[14,15] clinical studies to treat symptomatic, uncomplicated diverticular disease, with encouraging results.

The mechanism by which Rifaximin improves symptoms in uncomplicated diverticular disease is unclear. It has been suggested a synergistic effect of Rifaximin and high fiber diet in reducing proliferation of gut microflora, with a consequent decrease in bacterial hydrogen and methane production and/or in expanding faecal mass, due to a decrease in bacterial degradation of fibers[15,27].

Furthermore, Rifaximin may improve symptoms and lower the frequency of disease complications reducing intestinal bacterial overgrowth[19,21]. Rifaximin may also enhance faecal bulking and faecal weight, as shown for other antibiotics[28], and decrease the intraluminal colonic pressure, one of the pathogenetic mechanisms for diverticula development[20]. Due to the therapeutic uncertainties of both Rifaximin and fiber supplementation, in the present study we decided to comparatively evaluate these two agents. The results we obtained confirm and extend to a longer period previous observations by Papi *et al*[14] and Latella *et al*[15], who found that administration for 12 mo of Rifaximin plus dietary fiber supplementation was more effective in improving symptoms than dietary fibre supplementation alone. The present study documents that the efficacy of Rifaximin plus fiber supplementation is not only maintained, but it is more evident after 24 mo of treatment than fibers alone. According to the probability curves, the beneficial clinical effect of Rifaximin treatment is more pronounced during the first 12 mo, but it may last up to 24 mo. This observation is important, since it suggests a positive effect of Rifaximin treatment on the natural history of diverticular disease. Up to now, no definitive data are available regarding the way to prevent the development/maintenance of disease symptoms and complications. As far as the last point is concerned, the present study indicates that Rifaximin treatment significantly reduces the probability of complication development and that this effect is constant during the whole study period.

In conclusion the present study documents that in patients with symptomatic, uncomplicated diverticular disease, cyclic administration of Rifaximin plus fiber supplementation is more effective in reducing symptom persistence/recurrence and complication development than dietary fiber alone. Cyclic, long term administration of this non-absorbable antibiotic is safe and well tolerated by the patients, confirming the clinical usefulness of this therapeutic strategy in the overall management of diverticular disease. Further studies are needed to better identify the mechanism/s of action of both Rifaximin and of its association with dietary fibers.

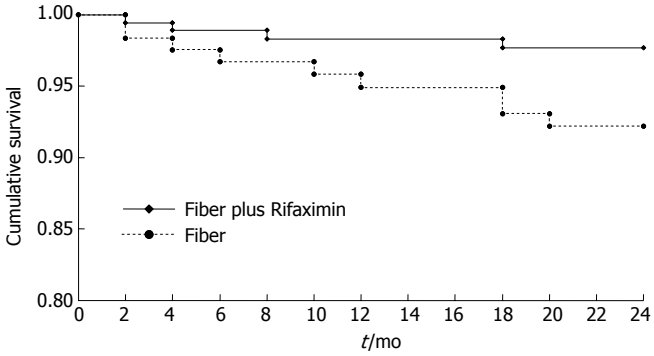

Figure 3 Probability of complication development in patients treated with Rifaximin plus fibers or with fibers supplementation alone. Kaplan-Meier method. Test Log Rank: $P = 0.028$.

REFERENCES

1 **Stollman N**, Raskin JB. Diverticular disease of the colon. *Lancet* 2004; **363**: 631-639

2 **Delvaux M**. Diverticular disease of the colon in Europe: epidemiology, impact on citizen health and prevention. *Aliment Pharmacol Ther* 2003; **18** Suppl 3: 71-74

3 **Parks TG**. Natural history of diverticular disease of the colon. *Clin Gastroenterol* 1975; **4**: 53-69

4 **Kang JY**, Melville D, Maxwell JD. Epidemiology and management of diverticular disease of the colon. *Drugs Aging* 2004; **21**: 211-228

5 **Farmakis N**, Tudor RG, Keighley MR. The 5-year natural history of complicated diverticular disease. *Br J Surg* 1994; **81**: 733-735

6 **Bolster LT**, Papagrigoriadis S. Diverticular disease has an impact on quality of life -- results of a preliminary study. *Colorectal Dis* 2003; **5**: 320-323

7 **Köhler L**, Sauerland S, Neugebauer E. Diagnosis and treatment of diverticular disease: results of a consensus development conference. The Scientific Committee of the European Association for Endoscopic Surgery. *Surg Endosc* 1999; **13**: 430-436

8 **Stollman NH**, Raskin JB. Diagnosis and management of diverticular disease of the colon in adults. Ad Hoc Practice Parameters Committee of the American College of Gastroenterology. *Am J Gastroenterol* 1999; **94**: 3110-3121

9 **Mizuki A**, Nagata H, Tatemichi M, Kaneda S, Tsukada N, Ishii H, Hibi T. The out-patient management of patients with acute mild-to-moderate colonic diverticulitis. *Aliment Pharmacol Ther* 2005; **21**: 889-897

10 **Simpson J**, Spiller R. Colonic diverticular disease. *Clin Evid* 2004; (**12**): 599-609

11 **Gillis JC**, Brogden RN. Rifaximin. A review of its antibacterial activity, pharmacokinetic properties and therapeutic potential in conditions mediated by gastrointestinal bacteria. *Drugs* 1995; **49**: 467-484

12 **Papi C**, Ciaco A, Koch M, Capurso L. Efficacy of rifaximin on symptoms of uncomplicated diverticular disease of the colon. A pilot multicentre open trial. Diverticular Disease Study Group. *Ital J Gastroenterol* 1992; **24**: 452-456

13 **Ventrucci M**, Ferrieri A, Bergami R, Roda E. Evaluation of the effect of rifaximin in colon diverticular disease by means

of lactulose hydrogen breath test. *Curr Med Res Opin* 1994; **13**: 202-206
14 **Papi C**, Ciaco A, Koch M, Capurso L. Efficacy of rifaximin in the treatment of symptomatic diverticular disease of the colon. A multicentre double-blind placebo-controlled trial. *Aliment Pharmacol Ther* 1995; **9**: 33-39
15 **Latella G**, Pimpo MT, Sottili S, Zippi M, Viscido A, Chiaramonte M, Frieri G. Rifaximin improves symptoms of acquired uncomplicated diverticular disease of the colon. *Int J Colorectal Dis* 2003; **18**: 55-62
16 **Casagrande JT**, Pike MC. An improved approximate formula for calculating sample sizes for comparing two binomial distributions. *Biometrics* 1978; **34**: 483-486
17 **Armitage P**, Berry G. Statistical methods in medical research. UK: Black-Well Scientific Publication Limited, Oxford, 1994
18 **Aldoori WH**, Giovannucci EL, Rimm EB, Wing AL, Trichopoulos DV, Willett WC. A prospective study of diet and the risk of symptomatic diverticular disease in men. Am J Clin Nutr 1994; **60**: 757-764
19 **Colecchia A**, Sandri L, Capodicasa S, Vestito A, Mazzella G, Staniscia T, Roda E, Festi D. Diverticular disease of the colon: new perspectives in symptom development and treatment. *World J Gastroenterol* 2003; **9**: 1385-1389
20 **Bassotti G**, Battaglia E, De Roberto G, Morelli A, Tonini M, Villanacci V. Alterations in colonic motility and relationship to pain in colonic diverticulosis. *Clin Gastroenterol Hepatol* 2005; **3**: 248-253
21 **Tursi A**, Brandimarte G, Giorgetti GM, Elisei W. Assessment of small intestinal bacterial overgrowth in uncomplicated acute diverticulitis of the colon. *World J Gastroenterol* 2005; **11**: 2773-2776
22 **Simpson JK**, Metcalfe DD. Mastocytosis and disorders of mast cell proliferation. *Clin Rev Allergy Immunol* 2002; **22**: 175-188
23 **Petruzziello L**, Iacopini F, Bulajic M, Shah S, Costamagna G. Review article: uncomplicated diverticular disease of the colon. *Aliment Pharmacol Ther* 2006; **23**: 1379-1391
24 **Lupton JR**, Turner ND. Potential protective mechanisms of wheat bran fiber. *Am J Med* 1999; **106**: 24S-27S
25 **Brodribb AJ**. Treatment of symptomatic diverticular disease with a high-fibre diet. *Lancet* 1977; **1**: 664-666
26 **Barbara G**, De Giorgio R, Stanghellini V, Cremon C, Corinaldesi R. A role for inflammation in irritable bowel syndrome? *Gut* 2002; **51** Suppl 1: i41-i44
27 **Papi C**, Koch M, Capurso L. Management of diverticular disease: is there room for rifaximin? *Chemotherapy* 2005; **51** Suppl 1: 110-114
28 **Kurpad AV**, Shetty PS. Effects of antimicrobial therapy on faecal bulking. *Gut* 1986; **27**: 55-58

S- Editor Liu Y **L- Editor** Alpini GD **E- Editor** Bi L

PO Box 2345, Beijing 100023, China
www.wjgnet.com
wjg@wjgnet.com

World J Gastroenterol 2007 January 14; 13(2): 270-275
World Journal of Gastroenterology ISSN 1007-9327

CLINICAL RESEARCH

Proximal gastric motility in critically ill patients with type 2 diabetes mellitus

Nam Q Nguyen, Robert J Fraser, Laura K Bryant, Marianne Chapman, Richard H Holloway

Nam Q Nguyen, Richard H Holloway, Department of Gastroenterology, Hepatology and General Medicine, Royal Adelaide Hospital, South Australia
Robert J Fraser, Laura K Bryant, Investigation and Procedures Unit, Repatriation General Hospital; South Australia
Marianne Chapman, Anaesthesia and Intensive Care, Royal Adelaide Hospital, South Australia
Supported by a project grant from the National Health and Medical Research Council of Australia.
Correspondence to: Dr Nam Q Nguyen, Department of Gastroenterology, Royal Adelaide Hospital, North Terrace, Adelaide, SA 5000, Australia. qnguyen@mail.rah.sa.gov.au
Telephone: + 61-8-82225207 Fax: + 61-8-82225885
Received: 2006-10-25 Accepted: 2006-12-12

Abstract

AIM: To investigate the proximal gastric motor response to duodenal nutrients in critically ill patients with long-standing type 2 diabetes mellitus.

METHODS: Proximal gastric motility was assessed (using a barostat) in 10 critically ill patients with type 2 diabetes mellitus (59 ± 3 years) during two 60-min duodenal infusions of Ensure® (1 and 2 kcal/min), in random order, separated by 2 h fasting. Data were compared with 15 non-diabetic critically ill patients (48 ± 5 years) and 10 healthy volunteers (28 ± 3 years).

RESULTS: Baseline proximal gastric volumes were similar between the three groups. In diabetic patients, proximal gastric relaxation during 1 kcal/min nutrient infusion was similar to non-diabetic patients and healthy controls. In contrast, relaxation during 2 kcal/min infusion was initially reduced in diabetic patients ($P < 0.05$) but increased to a level similar to healthy humans, unlike non-diabetic patients where relaxation was impaired throughout the infusion. Duodenal nutrient stimulation reduced the fundic wave frequency in a dose-dependent fashion in both the critically ill diabetic patients and healthy subjects, but not in critically ill patients without diabetes. Fundic wave frequency in diabetic patients and healthy subjects was greater than in non-diabetic patients.

CONCLUSION: In patients with diabetes mellitus, proximal gastric motility is less disturbed than non-diabetic patients during critical illness, suggesting that these patients may not be at greater risk of delayed gastric emptying.

Key words: Proximal gastric function; Diabetes mellitus type 2; Critical illness; Enteral nutrition

Nguyen NQ, Fraser RJ, Bryant LK, Chapman M, Holloway RH. Proximal gastric motility in critically ill patients with type 2 diabetes mellitus. *World J Gastroenterol* 2007; 13(2): 270-275

http://www.wjgnet.com/1007-9327/13/270.asp

INTRODUCTION

In the community, approximately 50% of patients with type 1 or 2 diabetes mellitus (DM) have gastroparesis[1]. Although gastric emptying of either a solid or semi-solid meal is consistently slow in these patients, gastric emptying of liquid meals is variable[1-4]. The aetiology of slow gastric emptying and the variable rate of liquid emptying are unclear, but may be related to hyperglycemia or autonomic neuropathy[1,5-7], factors that result in motor dysfunction of both the proximal and distal stomach[1,7,8].

Delayed gastric emptying is also common in critically ill patients[9-11] and is associated with disturbed motility of both the proximal and distal stomach[10,12,13]. In health, the proximal stomach is a major determinant of liquid gastric emptying and is regulated by feedback from the small intestine. In health, the fundus relaxes in response to the presence of nutrient in the duodenum[14]. Critically ill patients without DM have been reported to have impaired proximal gastric relaxation, reduced fundic wave activity and a failed recovery of proximal gastric volume to pre-stimulation level[12]. Currently, there are no data on the impact of DM on gastric motor function or emptying during critical illness, despite the fact that one-third of patients admitted to critical care units have DM[15]. Given that both DM and critical illness are risk factors for disturbed gastric motility, we hypothesized that critically ill patients with DM would have abnormal proximal gastric motor activity during fasting and in response to duodenal nutrient infusion, compared to non-diabetic critically ill patients and healthy humans.

MATERIALS AND METHODS

Subjects

Studies were performed in 25 sedated and mechanically ventilated critically ill patients, who were admitted to a level-3 mixed intensive care unit between January and September 2004. All patients required enteral nutrition. Ten

patients had documented type 2 DM with a mean duration of 7.9 ± 1.8 years. Seven of the diabetic patients had required insulin therapy prior to ICU admission. Formal testing for the presence of autonomic neuropathy was not performed. Fifteen critically ill patients without diabetes mellitus served as patient controls. Exclusion criteria for all patients were (1) recent major abdominal surgery, (2) any contra-indication to passage of an enteral tube, (3) administration of opioid analgesia, benzodiazepines or prokinetic therapy within the previous 24 h, and (4) previous gastric, oesophageal or intestinal surgery. All patients received an insulin infusion for blood glucose control according to a standardized protocol that started on admission and aimed to maintain blood glucose concentrations between 5.0 and 7.9 mmol/L. Data from both patient groups were compared to 10 healthy volunteers, who had no history of systemic or gastrointestinal disease and were not taking any medication. Healthy volunteers were instructed to refrain from smoking for 24 h prior to the study.

Written informed consent was obtained from healthy subjects and the next of kin of patients prior to enrolment into the study. The protocol was approved by the Human Research Ethics Committee of the Royal Adelaide Hospital.

Measurement of proximal gastric motility

Proximal gastric motility was measured using an electronic gastric barostat[16] (Distender Series Ⅱ; G&J Electronics, Ontario, Canada). A thin flaccid-walled bag with a maximum capacity of 1000 mL was attached to the distal end of the assembly, which was connected to the system *via* pressure and volume ports. Changes in proximal gastric volume were measured indirectly by changes in the volume of the polyethylene bag.

Data were stored onto a Powermac 7100 computer (Apple Computer, Cupertino, CA), using custom-written data-acquisition software (Labview: National Instruments, Austin, TX). This software was also used to program the barostat to perform distensions in stepwise increments. Recorded data were imported into a display and analysis program (Acqknowledge, Biopac System, Goleta, CA) for manual analysis.

Blood glucose concentrations

Marked hyperglycaemia may alter small intestinal feedback and adversely affect gastric motility[5-7]. Blood glucose concentrations were measured using a portable glucometer (Precision Plus, Abbott Laboratories, Bedford, USA) immediately before and every 20 min during nutrient infusion.

Protocol

All subjects were studied after at least 6 h fasting and in a 30 degree recumbent position. To standardise the sedative regimen in patients, propofol alone was used, and opioids, benzodiazepines or prokinetic agents were not administered for 24 h prior to and during the study. In patients, placement of both the barostat catheter and post-pyloric feeding tube were performed at the bedside with endoscopic assistance, without additional sedation to that required for ventilation. A 12 French × 114 cm naso-duodenal feeding tube (Flexiflo, Abbott, Ireland) was inserted into the duodenum over a guidewire (THSF-35-260, Cook, Australia). The barostat catheter was then guided through the mouth into the stomach by the endoscope. The barostat bag was inflated with 400 mL of air and gently retracted into the fundus under direct vision. Gastric contents (air and fluid) were aspirated completely prior to withdrawal of the endoscope. Correct placement of the feeding tube was confirmed by measurement of the duodenal trans-mucosal potential difference (TMPD)[16] and subsequently by radiography[13].

In healthy subjects, the barostat assembly and feeding tube were swallowed and allowed to pass into the correct position spontaneously, without the assistance of endoscopy. Duodenal nutrient infusion was achieved by inserting a silicon-rubber catheter (Dentsleeve, Adelaide, Australia) with a central feeding lumen and lead-weighted tip into the stomach. The tube passed spontaneously into the duodenum using phase 2 and 3 of the migrating motor complex. Movement of the catheter into the correct position was monitored continuously by measurement of the antro-duodenal TMPD gradient[16]. Radiological confirmation was not performed in healthy subjects. The barostat catheter was then inserted to a depth of 55 cm, the bag inflated with 400 mL of air and the assembly pulled back until resistance was felt[17].

Following confirmation that both assemblies were positioned correctly, air in the barostat bag was aspirated manually and the catheter was connected to the barostat pump. The minimum distending pressure (MDP), defined as the first pressure level that provided an intragastric bag volume of more than 30 mL, was determined[17]. The intra-bag pressure for the study was set at MDP + 2 mmHg[17]. All studies began with a 15-min baseline recording, during which normal saline (0.9% NaCl) was infused into the duodenum at a rate of 240 mL/h (baseline 1). Each subject then received two 60 minute duodenal infusions of Ensure® (Abbott Laboratories, Ohio, USA; nutrient content: 13% protein, 64% carbohydrate, 21% fat; energy density: 1 kcal/mL) at 1 and 2 kcal/min, in a randomised order. Ensure® was diluted with normal saline to 1:4 for the 1 kcal/min infusion and to 1:2 for 2 kcal/min infusion, and infused at a rate of 240 mL/h. The nutrient infusions were separated by a 2 h 'washout period', consisting of 90 min of no infusion, followed by 30 min of intraduodenal saline infusion (baseline 2). Blood samples for the measurement of blood glucose concentration were collected at baseline and every 20 min during nutrient infusion. Barostat recordings were performed continuously over 4 h. The study protocol is outlined in Figure 1.

Data analysis

Intra-bag volumes were determined at 2-min intervals and the mean baseline volume was measured over 10 min before each infusion. Changes in intra-bag volume during nutrient infusion were calculated as the difference between the actual volume and the mean baseline volume. The serial changes in bag volume during the infusions were plotted and compared. Proximal gastric relaxation was indirectly inferred by an increase in bag volume[17]. The time course for the proximal stomach to return to baseline volume af-

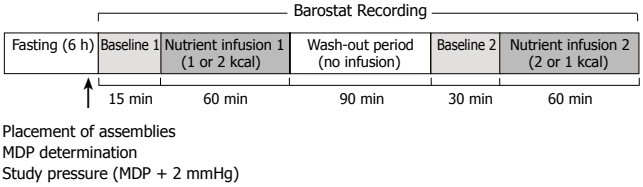

Figure 1 Schematic outline of study protocol.

ter nutrient stimulation was assessed by analysis of the 2 h "no-infusion" period; and was defined as the time taken for the relaxed fundus to return to pre-stimulation level for > 5 min. Assessment of fundic slow volume waves (FW) was also performed. These were defined as changes in proximal gastric volume of greater than 30 mL that reverted in less than 2 min to a volume within 50% of the previous level[17]. The number and amplitude of FWs (per 10 min) was determined during fasting and in response to duodenal nutrient infusion.

Statistical analysis

Data are expressed as mean ± SE. Differences in demographic characteristics, baseline volumes, MDP, FW frequency, peak volume response and the time required for the proximal stomach to return to baseline volume, were compared between the three groups using Student's unpaired *t*-test. ANOVA was used to compare the proximal gastric volume, fundic wave and blood glucose responses to nutrient infusion between the groups, with time and treatment as the factors. A P value < 0.05 was considered statistically significant.

RESULTS

Oral intubation of the assembly was tolerated well by all subjects and no complications occurred in any group. Demographic characteristics of the study groups are summarized in Table 1. The MDP was higher in both patient groups compared to healthy subjects ($P < 0.05$), but was similar between diabetic and non-diabetic patients (Table 2). Baseline proximal gastric volumes were similar between the three groups.

Proximal gastric volume response to duodenal nutrients

In response to duodenal nutrients, healthy volunteers demonstrated a "biphasic" proximal gastric volume response. Following an initial rapid relaxation, the fundus partially contracted and then exhibited a sustained relaxation throughout the remainder of the infusion (Figure 2). In non-diabetic critically ill patients, there was an overall impairment of both the initial and later phase of the response. In diabetic patients, however, there was an absence of the initial response in the first 20 min during both 1 and 2 kcal/min infusions. Thereafter, the proximal gastric volume increased to the level observed in healthy volunteers.

During the 1 kcal/min infusion there was no difference in the proximal gastric volume response between diabetic critically ill patients and the other two groups. However, during the first 20 min of the 2 kcal/min infusion, the proximal gastric volume was significantly smaller in diabetic critically ill patients than in non-diabetic critically ill patients and healthy subjects. Thereafter, the proximal gastric volume of diabetic patients was greater than that of non-diabetic patients and similar to healthy subjects (Figure 2).

Table 1 Demographic characteristics of the critically ill patients and healthy subjects

	Diabetic ICU patients (n = 10)	Non-diabetic ICU patients (n = 15)	Healthy subjects (n = 10)
Age (yr)	59 ± 3[a]	48 ± 5[a]	28 ± 3
Gender (M:F)	5:5	12:3	7:3
BMI (kg/m^2)	35 ± 3[c]	27 ± 1	25 ± 1
APACHE II score			
On admission	28.6 ± 1.5	23.2 ± 0.8	N/A
On study day	24.7 ± 1.5	21.1 ± 1.3	
Diagnoses	Sepsis (3)	Sepsis (3)	N/A
	Pneumonia (3)	Pancreatitis (2)	
	Severe asthma (1)	Head trauma (2)	
	MVA (1)	MVA (3)	
	Angioedema (1)	Cardiac failure (2)	
	Sub-arachnoid haemorrhage (1)	Burn (1)	
		Lung abscess (1)	
		Meningitis (1)	

MVA: Motor Vehicle Accident. [a]$P < 0.05$ *vs* healthy subjects; [c]$P < 0.05$ *vs* healthy subjects and non-diabetic critically ill patients.

Table 2 Comparison of proximal gastric motor activity between critically ill patients and healthy subjects

	Diabetic ICU patients (n = 10)	Non-diabetic ICU patients (n = 15)	Healthy subjects (n = 10)
MDP (mmHg)	11.9 ± 1.0[a]	11.3 ± 1.2[a]	7.1 ± 0.6
Baseline intra-gastric volume (mL)	187 ± 43	197 ± 22	182 ± 19
Time to recovery of baseline volume following infusion (min)	41 ± 15[a]	83 ± 11[c]	15 ± 4

[a]$P < 0.05$ *vs* healthy subjects; [c]$P < 0.05$ *vs* diabetic patients and healthy subjects.

Recovery of proximal gastric volume after nutrient stimulation

The proximal gastric volume returned to baseline level within 60 min following cessation of nutrient stimulation in all diabetic patients and healthy subjects, but in only 2 of the 15 non-diabetic patients. In diabetic patients, the time taken for the proximal gastric volume to return to baseline level was significantly shorter than in non-diabetic patients and longer than healthy subjects (Table 2).

Fundic volume wave frequency

At baseline, the mean frequency of FWs in diabetic patients (10.2 ± 1.7 waves/10 min) was similar to that of healthy subjects (11.8 ± 0.9 waves/10 min; $P = 0.38$), but was higher than non-diabetic patients (7.0 ± 0.8 waves/10 min; $P < 0.05$; Figure 3).

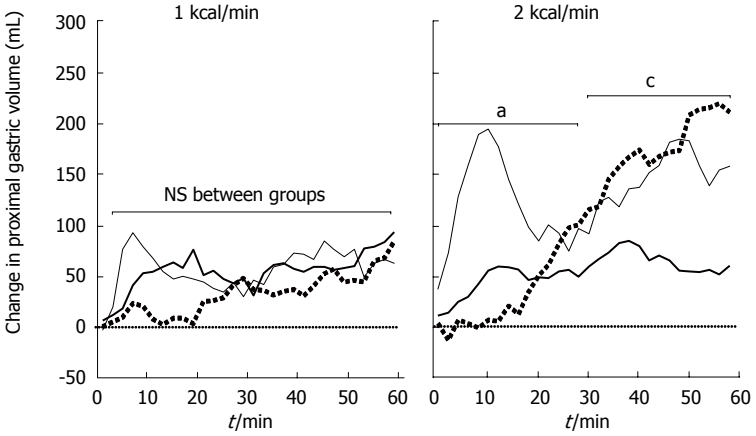

Figure 2 Changes in proximal gastric volume during duodenal nutrient stimulation (1 and 2 kcal/min) in critically ill patients and healthy subjects. $^{a}P < 0.05$, ICU patients *vs* healthy subjects during 0-30 min; $^{c}P < 0.05$, non-DM patients *vs* diabetic patients and healthy subjects during 30- 60 min.

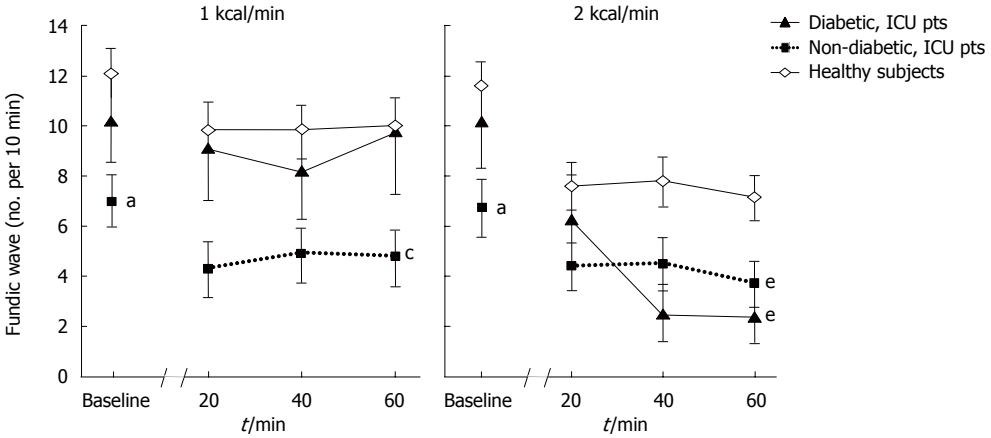

Figure 3 Frequency of fundic slow wave contractions at baseline and during duodenal nutrient infusion (1 and 2 kcal/min) in critically ill patients and healthy subjects. $^{a}P < 0.05$ *vs* healthy subjects and diabetic patients at baseline; $^{c}P < 0.05$ *vs* healthy subjects and diabetic patients during 1 kcal infusion; $^{e}P < 0.05$ *vs* healthy subjects during 2 kcal infusion.

The impact of duodenal nutrient stimulation on the frequency of FWs in diabetic patients was similar to that of healthy subjects but differed from non-diabetic patients (Figure 3). Nutrient stimulation with 1 kcal/min infusion did not reduce the mean frequency of FWs in either diabetic patients (9.0 ± 2.0 waves/10 min) or healthy subjects (9.9 ± 1.0 waves/10 min), in contrast to non-diabetic patients (4.4 ± 0.9 waves/10 min; $P < 0.05$). However, in all 3 groups the 2 kcal/min nutrient infusion significantly reduced the mean frequency of FWs compared to baseline (diabetic: 3.9 ± 1.1 waves/10 min, $P < 0.05$; healthy: 7.6 ± 0.8 waves/10 min, $P < 0.001$; non-diabetic: 4.2 ± 0.9 waves/10 min, $P < 0.05$). The magnitude of reduction in FW frequency during 2 kcal/min was greatest in diabetic patients (-6.6 ± 1.7 waves/10 min), compared to healthy subjects (-4.0 ± 0.7 waves/10 min, $P < 0.05$) and non-diabetic patients (-1.9 ± 0.6, $P < 0.001$; Figure 3).

Overall, the frequency of FWs in diabetic patients during 1 kcal/min infusion was similar to that of healthy subjects, but was higher than non-diabetic patients. In contrast, due to the greater magnitude of reduction in FW frequency by a higher nutrient load, fundic wave activity during 2 kcal/min infusion in diabetic patients was similar to that of non-diabetic patients, but less than that of healthy subjects (Figure 3).

Blood glucose concentrations

Overall, both fasting and nutrient-stimulated blood glucose concentrations were higher in critically ill patients than in healthy subjects (Figure 4). There were no significant differences in blood glucose concentrations between diabetic and non-diabetic patients, reflecting the use of an insulin infusion protocol in all patients.

DISCUSSION

This is the first study to examine proximal gastric motor activity in critically ill patients with type 2 diabetes mellitus. The results show that the response to intestinal nutrient feedback is characterized by an initial absence of proximal gastric relaxation, after which the volume increased to a level similar to that seen in healthy volunteers. Furthermore, the delayed volume response was associated with a nutrient load-dependent reduction in fundic wave activity and a slightly impaired recovery of the proximal gastric volume to baseline level. This is in contrast to non-diabetic critically ill patients, who demonstrated a sustained impairment of proximal gastric relaxation, a reduction in fundic wave activity even during 1 kcal/min infusion and a failure of the fundus to recover to baseline volume. These findings support a recent retrospective study, which suggested that type 2 diabetes mellitus may not be a risk factor for delayed gastric emptying in critical illness[18].

A notable feature of the proximal gastric response to nutrient stimulation in diabetic patients was the complete absence of proximal gastric relaxation during the first 20 min of nutrient infusion, however the reason for this re-

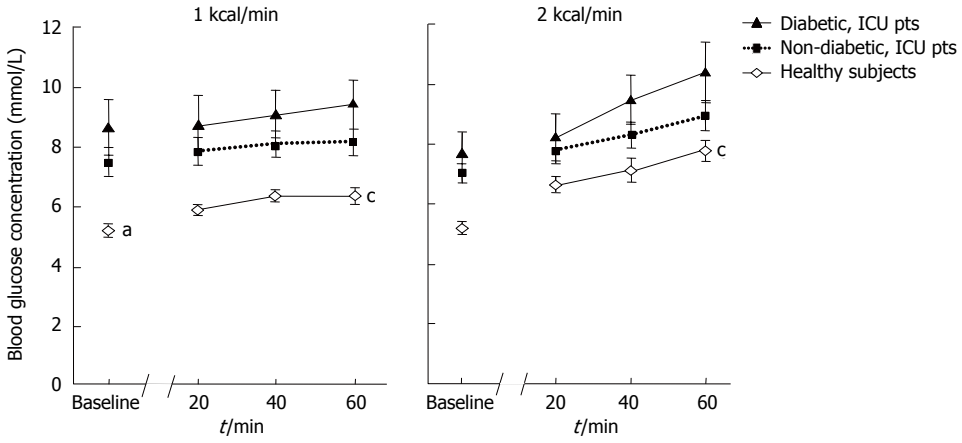

Figure 4 Blood glucose concentration at baseline and during nutrient infusion in critically ill patients and healthy subjects. $^{a}P < 0.05$ *vs* critically ill patients at baseline; $^{c}P < 0.05$ *vs* critically ill patients during nutrient infusion.

sponse remains unclear. In health, gastro-enteric feedback is regulated by neuro-hormonal pathways[14,16-19], and proximal gastric tone is modulated by a balance between the excitatory cholinergic nerves and the inhibitory nitrergic neural inputs from the vagus[20]. As autonomic dysfunction is common in patients with diabetic autonomic neuropathy[8] and during critical illness[21] the greater degree of impaired relaxation in our diabetic patients may relate to an adverse 'additive-effect' of both factors on the autonomic nervous system[20-22]. Formal testing for autonomic neuropathy was not performed in the current study as this was not feasible in the acute critical care setting. A prevalence of autonomic neuropathy of more than 50% would be expected, based on a previous study in diabetic patients with a similar mean duration of disease[23]. Furthermore, disturbances in the metabolism of nitric oxide, a key transmitter in the regulation of gastrointestinal motor function, may also be important[22]. Impaired proximal gastric relaxation is associated with altered levels of nitric oxide[1,8], and has been reported in both patients with diabetes mellitus[1] and critical illness[24]. Whilst increased cytokine production[25] and drug usage[26] can also contribute to impaired relaxation, the impact of these factors are likely to be similar between diabetic and non-DM critically ill patients and probably do not account for the differences in gastric motility seen between the groups.

Following the initial impairment of relaxation, the proximal gastric volume in diabetic critically ill patients increased to a level comparable to that of healthy subjects. This finding has not been previously reported in either patients with critical illness or diabetes mellitus alone. In the later, proximal gastric motor responses to gastric but not duodenal nutrients have been evaluated and further studies to assess this may provide useful information. The mechanisms underlying this normalization of proximal gastric motility are unknown. Despite the use of a standardized insulin protocol in all patients during the study, a small degree of hyperglycaemia occurred in diabetic patients during the latter half of the 2 kcal/min infusion (Figure 4). Although hyperglycaemia has been shown to induce proximal gastric relaxation[7], the absolute increase in blood glucose level was small and therefore unlikely to have contributed significantly to the subsequent response. The diabetic patients had a higher BMI than the healthy volunteers, however no differences in either proximal gastric volume or compliance have been reported between obese and lean subjects[27,28]. Thus, a higher BMI in diabetic patients seems unlikely to have contributed to the differences in proximal gastric motility. Opiate drugs such as morphine were excluded 24 h prior to the study, hence are unlikely to explain our findings[29].

To standardize the nutrient stimulation and enable a reliable assessment of the entero-gastric feedback response, feeds were delivered directly into the duodenum at a rate consistent with normal gastric emptying. Intra-gastric delivery of nutrients was not used in the current study because gastric emptying is frequently impaired in the critically ill. Furthermore, both gastric motility and emptying of a liquid meal may be altered by the presence of a barostat balloon[30]. In addition, intra-duodenal nutrient stimulation with 1 and 2 kcal/min nutrient loads enabled examination of the dose-dependency of the proximal gastric motor response[16,17,19].

Previous studies in critically ill patients have suggested enhanced entero-gastric feedback in response to duodenal nutrient stimulation[12]. In contrast to the non-diabetic patients, diabetic critically ill patients had a dose-dependent reduction in fundic wave activity, similar to the healthy subjects. The different responses in fundic wave activity during the 1 and 2 kcal/min nutrient loads between the diabetic and non-diabetic patients suggest that entero-gastric feedback is not increased in diabetic patients. Furthermore, apart from an initial delay in relaxation, the overall proximal gastric motor responses to nutrients in diabetic critically ill patients were similar to those of healthy subjects. As the proximal stomach is a major determinant of liquid gastric emptying[16,17,19], these findings may explain the relatively normal gastric emptying observed in this group of patients[14].

Whether differences in the 'accommodative' response to nutrients between the two patient groups affect their ability to tolerate bolus or continuous gastric feeds remains to be determined and requires further study. It is conceivable that slow continuous feeds may be better tolerated in non-diabetic critically ill patients as proximal gastric relaxation is small and slow during nutrient stimulation[9,11]. In contrast, the relatively normal 'biphasic' proximal gastric response in the diabetic critically ill patients may allow better tolerance to bolus gastric feeds.

In conclusion, proximal gastric motor responses to

duodenal nutrient are relatively normal in type 2 diabetic patients during critical illness. These motor findings support data which suggests these patients may have normal gastric emptying[18] and may be less prone to developing naso-gastric feed intolerance than non-diabetic, critically ill patients.

REFERENCES

1 **Horowitz M**, Wishart JM, Jones KL, Hebbard GS. Gastric emptying in diabetes: an overview. *Diabet Med* 1996; **13**: S16-S22

2 **Weytjens C**, Keymeulen B, Van Haleweyn C, Somers G, Bossuyt A. Rapid gastric emptying of a liquid meal in long-term Type 2 diabetes mellitus. *Diabet Med* 1998; **15**: 1022-1027

3 **Bertin E**, Schneider N, Abdelli N, Wampach H, Cadiot G, Loboguerrero A, Leutenegger M, Liehn JC, Thiefin G. Gastric emptying is accelerated in obese type 2 diabetic patients without autonomic neuropathy. *Diabetes Metab* 2001; **27**: 357-364

4 **Phillips WT**, Schwartz JG, McMahan CA. Rapid gastric emptying in patients with early non-insulin-dependent diabetes mellitus. *N Engl J Med* 1991; **324**: 130-131

5 **Rayner CK**, Samsom M, Jones KL, Horowitz M. Relationships of upper gastrointestinal motor and sensory function with glycemic control. *Diabetes Care* 2001; **24**: 371-381

6 **Fraser RJ**, Horowitz M, Maddox AF, Harding PE, Chatterton BE, Dent J. Hyperglycaemia slows gastric emptying in type 1 (insulin-dependent) diabetes mellitus. *Diabetologia* 1990; **33**: 675-680

7 **Hebbard GS**, Sun WM, Dent J, Horowitz M. Hyperglycaemia affects proximal gastric motor and sensory function in normal subjects. *Eur J Gastroenterol Hepatol* 1996; **8**: 211-217

8 **Samsom M**, Roelofs JM, Akkermans LM, van Berge Henegouwen GP, Smout AJ. Proximal gastric motor activity in response to a liquid meal in type I diabetes mellitus with autonomic neuropathy. *Dig Dis Sci* 1998; **43**: 491-496

9 **Heyland DK**, Tougas G, King D, Cook DJ. Impaired gastric emptying in mechanically ventilated, critically ill patients. *Intensive Care Med* 1996; **22**: 1339-1344

10 **Dive A**, Moulart M, Jonard P, Jamart J, Mahieu P. Gastroduodenal motility in mechanically ventilated critically ill patients: a manometric study. *Crit Care Med* 1994; **22**: 441-447

11 **Mutlu GM**, Mutlu EA, Factor P. GI complications in patients receiving mechanical ventilation. *Chest* 2001; **119**: 1222-1241

12 **Nguyen NQ**, Fraser RJ, Chapman M, Bryant LK, Holloway RH, Vozzo R, Feinle-Bisset C. Proximal gastric response to small intestinal nutrients is abnormal in mechanically ventilated critically ill patients. *World J Gastroenterol* 2006; **12**: 4383-4388

13 **Chapman M**, Fraser R, Vozzo R, Bryant L, Tam W, Nguyen N, Zacharakis B, Butler R, Davidson G, Horowitz M. Antro-pyloro-duodenal motor responses to gastric and duodenal nutrient in critically ill patients. *Gut* 2005; **54**: 1384-1390

14 **Lin HC**, Doty JE, Reedy TJ, Meyer JH. Inhibition of gastric emptying by glucose depends on length of intestine exposed to nutrient. *Am J Physiol* 1989; **256**: G404-G411

15 **Umpierrez GE**, Isaacs SD, Bazargan N, You X, Thaler LM, Kitabchi AE. Hyperglycemia: an independent marker of in-hospital mortality in patients with undiagnosed diabetes. *J Clin Endocrinol Metab* 2002; **87**: 978-982

16 **Heddle R**, Collins PJ, Dent J, Horowitz M, Read NW, Chatterton B, Houghton LA. Motor mechanisms associated with slowing of the gastric emptying of a solid meal by an intraduodenal lipid infusion. *J Gastroenterol Hepatol* 1989; **4**: 437-447

17 **Azpiroz F**, Malagelada JR. Intestinal control of gastric tone. *Am J Physiol* 1985; **249**: G501-G509

18 **Nguyen NQ**, Chapman M, Fraser RJ, Ritz M, Bryant LK, Butler R, Davidson G, Zacharakis B, Holloway RH. Long-standing type II diabetes mellitus is not a risk factor for slow gastric emptying in critically ill patients. *Intensive Care Med* 2006; **32**: 1365-1370

19 **Kelly KA**. Gastric emptying of liquids and solids: roles of proximal and distal stomach. *Am J Physiol* 1980; **239**: G71-G76

20 **Paterson CA**, Anvari M, Tougas G, Huizinga JD. Nitrergic and cholinergic vagal pathways involved in the regulation of canine proximal gastric tone: an in vivo study. *Neurogastroenterol Motil* 2000; **12**: 301-306

21 **Schmidt HB**, Werdan K, Müller-Werdan U. Autonomic dysfunction in the ICU patient. *Curr Opin Crit Care* 2001; **7**: 314-322

22 **Kellow JE**, Delvaux M, Azpiroz F, Camilleri M, Quigley EM, Thompson DG. Principles of applied neurogastroenterology: physiology/motility-sensation. *Gut* 1999; **45** Suppl 2: II17-II24

23 **Valensi P,** Pariès J, Attali JR. Cardiac autonomic neuropathy in diabetic patients: influence of diabetes duration, obesity, and microangiopathic complications--the French multicenter study. *Metabolism* 2003; **52**: 815-820

24 **Argaman Z**, Young VR, Noviski N, Castillo-Rosas L, Lu XM, Zurakowski D, Cooper M, Davison C, Tharakan JF, Ajami A, Castillo L. Arginine and nitric oxide metabolism in critically ill septic pediatric patients. *Crit Care Med* 2003; **31**: 591-597

25 **Emch GS**, Hermann GE, Rogers RC. TNF-alpha activates solitary nucleus neurons responsive to gastric distension. *Am J Physiol Gastrointest Liver Physiol* 2000; **279**: G582-G586

26 **Lee TL**, Ang SB, Dambisya YM, Adaikan GP, Lau LC. The effect of propofol on human gastric and colonic muscle contractions. *Anesth Analg* 1999; **89**: 1246-1249

27 **Park MI**, Camilleri M. Gastric motor and sensory functions in obesity. *Obes Res* 2005; **13**: 491-500

28 **Kim DY**, Camilleri M, Murray JA, Stephens DA, Levine JA, Burton DD. Is there a role for gastric accommodation and satiety in asymptomatic obese people? *Obes Res* 2001; **9**: 655-661

29 **Lefebvre RA**, Willems JL, Bogaert MG. Gastric relaxation and vomiting by apomorphine, morphine and fentanyl in the conscious dog. *Eur J Pharmacol* 1981; **69**: 139-145

30 **Ropert A**, des Varannes SB, Bizais Y, Rozé C, Galmiche JP. Simultaneous assessment of liquid emptying and proximal gastric tone in humans. *Gastroenterology* 1993; **105**: 667-674

S- Editor Liu Y **L- Editor** Iqbal A **E- Editor** Liu WF

PO Box 2345, Beijing 100023, China
www.wjgnet.com
wjg@wjgnet.com

World J Gastroenterol 2007 January 14; 13(2): 276-279
World Journal of Gastroenterology ISSN 1007-9327

CLINICAL RESEARCH

Role of ciprofloxacin in patients with cholestasis after endoscopic retrograde cholangiopancreatography

Thawee Ratanachu-ek, Pitchaya Prajanphanit, Kawin Leelawat, Suchart Chantawibul, Sukij Panpimanmas, Somboon Subwongcharoen, Jerasak Wannaprasert

Thawee Ratanachu-ek, Pitchaya Prajanphanit, Kawin Leelawat, Suchart Chantawibul, Sukij Panpimanmas, Somboon Subwongcharoen, Jerasak Wannaprasert, Department of Surgery, Rajavithi Hospital, Bangkok 10400, Thailand
Correspondence to: Thawee Ratanachu-ek, Department of Surgery, Rajavithi Hospital, Rajavithi Rd, Rajathevi, Bangkok 10400, Thailand. Thawee1958@hotmail.com
Telephone: +66-2-3548080 Fax: +66-2-3548080
Received: 2006-09-13 Accepted: 2006-11-14

Key words: Antibiotic; Cholestasis; Cholangitis; Endoscopic retrograde cholangiopancreatography; Biliary drainage

Ratanachu-ek T, Prajanphanit P, Leelawat K, Chantawibul S, Panpimanmas S, Subwongcharoen S, Wannaprasert J. Role of ciprofloxacin in patients with cholestasis after endoscopic retrograde cholangiopancreatography. *World J Gastroenterol* 2007; 13(2): 276-279

http://www.wjgnet.com/1007-9327/13/276.asp

Abstract

AIM: To determine the role of ciprofloxacin in reducing cholangitis in cholestatic patients with adequate biliary drainage after endoscopic retrograde cholangiopancreatography (ERCP).

METHODS: A randomized, controlled trial was performed in 48 cholestatic patients at Rajavithi Hospital (Tertiary Referral Center for ERCP: 600 cases per year). All the 48 patients received 200 mg ciprofloxacin intravenous injection for 30 min before starting any procedures, and then were randomly divided in two groups. Twenty-two patients in study group continually received ciprofloxacin until 48 h after ERCP. Causes of biliary obstruction, bacteriology of bile and blood (in cholangitis) and clinical cholangitis were recorded.

RESULTS: Forty-eight patients were enrolled and divided into continuous ciprofloxacin treatment group (n = 22) and discontinuous ciprofloxacin treatment group (n = 26). During ERCP, stones were found in 22 patients, malignant diseases in 24 patients and other pathologic lesions in 5 patients. One (4.5%) of the 22 patients who received ciprofloxacin and 2 (6.3%) of the 26 patients who discontinued ciprofloxacin after ERCP developed cholangitis (relative risk = 0.71; 95% CI = 0.14-3.65; P = 0.88). Bacterobilia was found in 27 (56.3%) out of 48 patients. *E. coli* and *Streptococcus viridans* were the most common organisms.

CONCLUSION: Continual use of ciprofloxacin in patients with cholestasis after adequate biliary drainage procedures plays no role in reducing cholangitis.

INTRODUCTION

Endoscopic retrograde cholangiopancreatography (ERCP) is widely used in diagnosis and treatment of biliary and pancreatic diseases[1,2]. Acute cholangitis and septicemia remain serious complications related to this technique[3]. The incidence of cholangitis is 0.8%-19%, and its mortality rate is 10%[4].

The role of prophylactic antibiotics after ERCP has been recently assessed in several placebo-controlled randomized trials[5-9]. This procedure plays an essential part in high risk patients with prosthetic valve and history of endocarditis, obstructed bile duct, pancreatic cystic lesion and inadequate common bile duct drainage[3,10]. To date, no antibiotic regimen has emerged. Most of the bacterial florae in bile of patients with cholangitis and asymptomatic bacterobilia are Gram-negative organisms such as *E. coli, Klebsella spp.* and Gram-positive organisms such as *Enterococcus fecalis*[5-6,11-13]. The choice of an antibiotic regimen should be able to cover the Gram-negative bacteria and effectively penetrates the obstructed biliary tree. Ciprofloxacin attains a concentration in bile of approximately 20% of the mean peak level in serum, even in an obstructed biliary system. This drug level is still 10 times higher than MIC of the Gram-negative bacteria and is the most effective antibiotic against the Gram-negative bacteria, as indicated in the standard guidelines[3,5,7,10,12-13].

Ciprofloxacin is highly effective against cholestasis. However, no previous clinical study has reported the role of continuous use of ciprofloxacin in cholestatic patients after ERCP. Although many professional gastrointestinal societies recommend prophylactic use of antibiotics in the treatment of obstructive jaundice patients after ERCP, no guideline has been established after adequate biliary drainage.

The aim of this study was to evaluate the effect of

ciprofloxacin in reducing the incidence of cholangitis after adequate endoscopic biliary drainage.

MATERIALS AND METHODS

Subjects

This study was a randomized, controlled trial approved by the Ethics Committee of Rajavithi Hospital. Cholestatic patients in Rajavithi Hospital (Tertiary Referral Center for ERCP), Bangkok, Thailand, admitted between June 2005 and May 2006 were included in this study. Inclusion criteria included age of 18 years or older, cholestasis (at least two from 4 criteria of total bilirubin > 2 mg/dL, serum alkaline phosphatase more than twice of normal value, alanine transaminase > 40 mmol/L and ultrasound or CT-scan showing dilated bile duct). All the patients underwent ERCP and gave their written informed consent to participate in the study. Patients were excluded from the study if they refused to participate in the study, or had endocarditis or vulvular heart disease, history of allergy to fluoroquinolone group, cholangitis or sepsis, use of antibiotics within 7 d before ERCP.

Methods

All cholestatic patients received 200 mg ciprofloxacin intravenous injection about 30 min before ERCP. Bile was aspirated before contrast medium was injected and sent to cultivation. Those who did not have biliary drainage after ERCP were excluded from this study, and ciprofloxacin was given until infection subsided. All patients who had adequate biliary drainage (defined as total relief of bile duct obstruction by stone extraction, sphincterotomy or stent replacement), were randomly divided into two groups: continuous ciprofloxacin treatment group and discontinuous ciprofloxacin treatment group. Ciprofloxacin (200 mg) intravenous injection every 12 h was given to the continuous ciprofloxacin treatment group for 48 h after ERCP, and discontinued if no infection signs and symptoms were found. The discontinuous ciprofloxacin treatment group was not given any ciprofloxacin after an adequate biliary drainage. If cholangitis occurred in any group, 200 mg ciprofloxacin intravenous injection every 12 h or other proper antibiotics (following blood or bile culture and sensitivity) were given until the infection subsided (no fever and WBC < $10 \times 10^9/m^3$) (Figure 1).

Vital signs were monitored every 8 h, liver function test and CBC count were performed once a day. Hemoculture was done if body temperature was above 38℃. Monitoring was continued until the doctor decided to discontinue it based on the following criteria, including stable vital signs, body temperature below 38℃, improvement in cholestasis and jaundice, and absence of abdominal pain.

ERCP was performed in all patients by the same endoscopist (Dr. Thawee Ratanachu-ek) under TJF-160 endoscope. After successful cannulation of the common bile duct, bile samples were obtained for bacteriological culture, and the definitive treatment for obstruction was performed. After each endoscopic procedure, endoscopes were manually washed by trained nurses according to the manufacturer's instructions.

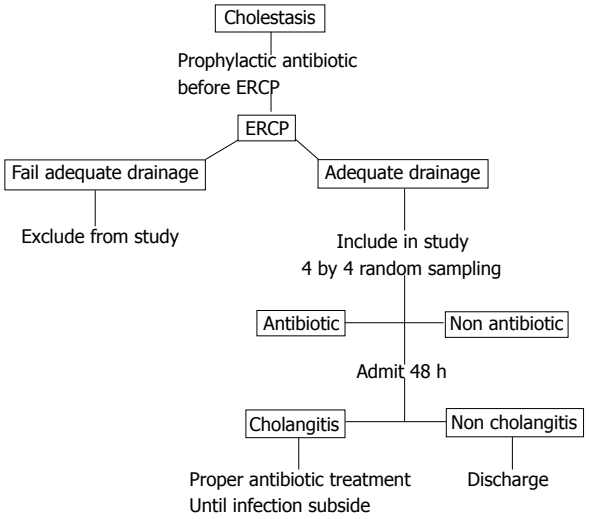

Figure 1 Flow chart of cholestasis management.

Statistical analysis

All statiscal analyses were performed using the Yates' modified chi-square test and Student's *t* test, and expressed as mean ± SD.

RESULTS

During June 2005 and May 2006, 48 patients after ERCP were enrolled in the study. All the patients received prophylactic ciprofloxacin, and divided into two groups: continuous ciprofloxacin treatment group (n = 22) and discontinuous ciprofloxacin treatment group (n = 26). The clinical characteristics and demographics in both groups were similar (Table 1). Stones were the most common cause of cholestasis in both groups. Diagnosis and intervention during ERCP are presented in Table 1.

Cholangitis was found in one (4.5%) out of 22 patients in the continuous ciprofloxacin treatment group and 2 (7.7%) out of 26 patients in the discontinuous ciprofloxacin treatment group. No sepsis and death occurred in this study.

The incidence of cholangitis was also similar in ciprofloxacin-treated patients after ERCP and controls (the relative risk = 0.71, 95% CI = 0.14 to 3.65). The total incidence of bacterobilia was 56.3% (27/48). The incidence of bacterobilia was 59.1% (13/22) in the continuous ciprofloxacin treatment group and 53.8% (14/26) in the control group (relative risk = 1.12, 95% CI = 0.60 to 2.11) (Table 2).

Gram-negative organisms were the most commonly found in the bile cultures. The bacteriology of bile cultures from both groups is illustrated in Table 3.

Three (11.1%) out of 27 patients with bacterobilia who developed cholangitis were found to have Gram-negative organisms in their blood culture. One female patient in the continuous ciprofloxacin treatment group had hepatocellular cancer, and a stent was inserted to the right anterior segment of the liver. She was febrile on the second day after ERCP, indicating that she had

Table 1 Clinical characteristics of 48 patients undergoing ERCP

Characteristic	Ciprofloxacin (*n* = 22)		None-ciprofloxacin (*n* = 26)	
	n	%	*n*	%
Sex (M:F)	13:9	59.1:40.9	11:15	42.3:57.7
Age (mean ± SD yr)	58.68 ± 13.7		61.08 ± 11.9	
Causes				
Bile duct stone	7	31.8	15	57.7
Cancer	13	59.1	11	42.3
Cholangiocarcinoma	6	27.3	6	23.1
Periampullary cancer	6	27.3	5	19.2
Hepatocellular cancer	1	4.5	0	0
Others	2	9.1	3	11.54
Bile duct stricture	1	4.5	1	3.8
Pseudocyst	1	4.5	0	0
Choledochal cyst	0	0	1	3.8
Chronicpancreatitis	0	0	1	3.8
Interventions				
Stone extraction	5	22.7	13	50
Sphincterotomy	13	59.1	14	53.8
Stent placement	16	72.7	14	53.8

Table 2 Incidence of cholangitis and bacteremia in two study groups

Complication	Ciprofloxacin post-ERCP		Relative risk	95% CI
	Yes (*n* = 22)	No (*n* = 26)		
Cholangitis	1 (4.5%)	2 (7.7%)	0.71	0.14-3.65
Bacteremia	13 (59.1%)	14 (53.8%)	1.12	0.60-2.11

Table 3 Bacterial species in cultures of bile from 48 patients

Bacterial culture	Antibiotic (22) *n* (%)	No antibiotic (26) *n* (%)	*P*
Negative	9 (40.9)	12 (46.2)	0.72
Positive	13 (59.1)	14 (53.8)	0.72
Gram negative			
E. coli	4 (30.8)	3 (21.4)	0.81
Klebsella spp.	2 (15.4)	2 (14.3)	0.73
Pseudomonas spp.	2 (15.4)	1 (7.1)	0.88
Gram positive	3 (13.6)	9 (34.6)	0.09
Streptococcus viridans	3	4 (28.6)	
Streptococcus bovis	0	1 (7.1)	
Enterococcus fecalis	0	3 (21.4)	
Staphylococcus spp.	0	1 (7.1)	
Non *C. albican*	1 (7.7)	0	

Table 4 Bile and hemoculture in three cholangitis patients

Group	Bacteriology	
	Bile culture	Hemoculture
Antibiotic group	*Streptococcus-viridans*	Negative
No antibiotic group		
First patient	*E. coli*	Negative
Second patient	*Pseudomonas spp.*	Negative

leukocytosis (WBC count was $10.8 \times 10^9/m^3$). She received 2 g ceftriazone intravenous injection daily for 11 d until infection subsided.

Two patients developed cholangitis in the discontinuous ciprofloxacin treatment group. Both received proper antibiotics until infection subsided. The results of bile cultures and hemocultures are shown in Table 4.

DISCUSSION

Bacteremia and cholangitis are the important complications of ERCP, and their incidence varies from 0.8%-19%[4]. It is known that prophylactic antibiotic treatment before ERCP plays a crucial role in the treatment of high risk patients with bile duct obstruction, pancreatic pseudocyst and inadequate cholestatic drainage[3,10-11]. However, the efficacy of such extensive use of antibiotics after ERCP has not been previously demonstrated, thus leading to the design of our study.

All the patients had mild or moderate cholangitis. This might be due to a benefit of the routine use of prophylactic ciprofloxacin in cholestatic patients before ERCP. Loperfido *et al*[14] found that small center, jaundice and male sex were risk factors for developing cholangitis after ERCP. We had only one male patient out of 3 cholangitis patients who had obstructive jaundice in our hospital (Tertiary Referral Center for ERCP: 600 cases per year).

In our study, cholangitis incidence after ERCP was lower than that in previous studies[8,9,15]. This might be attributed to the low natural incidence of the disease[4], standard sterile technique used in our hospital, and all procedures done by the same endoscopist, and our technique in collecting the bile before injecting contrast media. All these suggest that bacteriologic study and release of biliary tract pressure can reduce the incidence of pressure-induced sepsis.

E. coli, Streptococcus viridans and *Klebsiella spp.* are the most frequently isolated organisms from bile. Rung R *et al*[13] have found a similar incidence of bacterobilia (56.3%). Ciprofloxacin was chosen in our study because of its efficacy against most Gram-negative organisms (*E. coli* and *Klebsiella spp.*) which are the pathogens most frequently found in biliary tract infection[5-6,12-13,16-17] and its penetration into the obstructive biliary tree[6].

We found 12 Gram-positive bacteria in bile cultures (*Streptococcus viridans* and *Enterococcus spp.*) of the 27 bacterobilia specimens (56.3%), which is consistent with previous studies on bacteriology of bile in patients with obstructive jaundice, showing that *Streptococcus viridans* and *Enterococcus spp.* are the most common Gram-positive bacteria in bile cultures[18-23]. Clark *et al*[24] have found the same results and recommended ampicillin/sulbactam for all biliary obstructions with positive bile *Enterococci*. We conclude that once Gram positive bacteria are detected, perioperative use of appropriate antibiotics is mandatory to reduce postoperative septic complications.

The results of our trial showed no difference in the incidences of cholangitis between the two groups (4.5% in the continuous ciprofloxacin treatment group and 7.7% in discontinuous ciprofloxacin treatment group, relative risk = 0.71, 95% CI = 0.14 to 3.65, $P = 0.88$).

Alveyn CG *et al*[25] used 750 mg of ciprofloxacin taken

orally in 47 jaundice patients about 90 min before ERCP to prevent sepsis and we used the same sample size (48 patients). Our suggestion is that if a larger sample size is employed, this outcome may be strongly enforced.

In conclusion, extensive use of antibiotics after adequate drainage by ERCP in cholestatic patients does not substantially reduce the incidence of cholangitis. Continuous use of antibiotics is unnecessary in these patients. The results of this study may contribute to decreasing the drawbacks of the widespread use of antibiotics including cost, adverse effects, and emergency of resistant strains of bacteria.

REFERENCES

1 **Carr-Locke DL**. Overview of the role of ERCP in the management of diseases of the biliary tract and the pancreas**.** *Gastrointest Endosc* 2002; **56**: :S157-S160

2 **ASGE guidelines for clinical application**. The role of ERCP in diseases of the biliary tract and pancreas. American Society for Gastrointestinal Endoscopy. *Gastrointest Endosc* 1999; **50**: 915-920

3 **Rey JR**, Axon A, Budzynska A, Kruse A, Nowak A. Guidelines of the European Society of Gastrointestinal Endoscopy (E.S.G.E.) antibiotic prophylaxis for gastrointestinal endoscopy. European Society of Gastrointestinal Endoscopy. *Endoscopy* 1998; **30**: 318-324

4 **Bilbao MK**, Dotter CT, Lee TG, Katon RM. Complications of endoscopic retrograde cholangiopancreatography (ERCP). A study of 10,000 cases. *Gastroenterology* 1976; **70**: 314-320

5 **Sung JJ**, Lyon DJ, Suen R, Chung SC, Co AL, Cheng AF, Leung JW, Li AK. Intravenous ciprofloxacin as treatment for patients with acute suppurative cholangitis: a randomized, controlled clinical trial. *J Antimicrob Chemother* 1995; **35**: 855-864

6 **van den Hazel SJ**, Speelman P, Tytgat GN, Dankert J, van Leeuwen DJ. Role of antibiotics in the treatment and prevention of acute and recurrent cholangitis. *Clin Infect Dis* 1994; **19**: 279-286

7 **Mehal WZ**, Culshaw KD, Tillotson GS, Chapman RW. Antibiotic prophylaxis for ERCP: a randomized clinical trial comparing ciprofloxacin and cefuroxime in 200 patients at high risk of cholangitis. *Eur J Gastroenterol Hepatol* 1995; **7**: 841-845

8 **Niederau C**, Pohlmann U, Lübke H, Thomas L. Prophylactic antibiotic treatment in therapeutic or complicated diagnostic ERCP: results of a randomized controlled clinical study. *Gastrointest Endosc* 1994; **40**: 533-537

9 **Byl B**, Devière J, Struelens MJ, Roucloux I, De Coninck A, Thys JP, Cremer M. Antibiotic prophylaxis for infectious complications after therapeutic endoscopic retrograde cholangiopancreatography: a randomized, double-blind, placebo-controlled study. *Clin Infect Dis* 1995; **20**: 1236-1240

10 **Hirota WK**, Petersen K, Baron TH, Goldstein JL, Jacobson BC, Leighton JA, Mallery JS, Waring JP, Fanelli RD, Wheeler-Harbough J, Faigel DO. Guidelines for antibiotic prophylaxis for GI endoscopy. *Gastrointest Endosc* 2003; **58**: 475-482

11 **American Society for Gastrointestinal Endoscopy**. Antibiotic prophylaxis for gastrointestinal endoscopy. *Gastrointest Endosc* 1995; **42**: 630-635

12 **McGrath K**, Baillie J. Cholangitis. Current treatment options in gastroenterology. *Gastroenterology* 1999; **2**: 323-336

13 **Rerknimitr R**, Fogel EL, Kalayci C, Esber E, Lehman GA, Sherman S. Microbiology of bile in patients with cholangitis or cholestasis with and without plastic biliary endoprosthesis. *Gastrointest Endosc* 2002; **56**: 885-889

14 **Loperfido S**, Angelini G, Benedetti G, Chilovi F, Costan F, De Berardinis F, De Bernardin M, Ederle A, Fina P, Fratton A. Major early complications from diagnostic and therapeutic ERCP: a prospective multicenter study. *Gastrointest Endosc* 1998; **48**: 1-10

15 **Leung JW**, Venezuela RR. Cholangiosepsis: endoscopic drainage and antibiotic therapy. *Endoscopy* 1991; **23**: 220-223

16 **Brandes JW**, Scheffer B, Lorenz-Meyer H, Körst HA, Littmann KP. ERCP: Complications and prophylaxis a controlled study. *Endoscopy* 1981; **13**: 27-30

17 **Finkelstein R**, Yassin K, Suissa A, Lavy A, Eidelman S. Failure of cefonicid prophylaxis for infectious complications related to endoscopic retrograde cholangiopancreatography. *Clin Infect Dis* 1996; **23**: 378-379

18 **Siegman-Igra Y**, Schwartz D, Konforti N. Polymicrobial bacteremia. *Med Microbiol Immunol* 1988; **177**: 169-179

19 **Hochwald SN**, Burke EC, Jarnagin WR, Fong Y, Blumgart LH. Association of preoperative biliary stenting with increased postoperative infectious complications in proximal cholangiocarcinoma. *Arch Surg* 1999; **134**: 261-266

20 **Nomura T**, Shirai Y, Hatakeyama K. Enterococcal bactibilia in patients with malignant biliary obstruction. *Dig Dis Sci* 2000; **45**: 2183-2186

21 **Sheen-Chen S**, Chen W, Eng H, Sheen C, Chou F, Cheng Y, Lee T. Bacteriology and antimicrobial choice in hepatolithiasis. *Am J Infect Control* 2000; **28**: 298-301

22 **Flores C**, Maguilnik I, Hadlich E, Goldani LZ. Microbiology of choledochal bile in patients with choledocholithiasis admitted to a tertiary hospital. *J Gastroenterol Hepatol* 2003; **18**: 333-336

23 **Ryan JM**, Ryan BM, Smith TP. Antibiotic prophylaxis in interventional radiology. *J Vasc Interv Radiol* 2004; **15**: 547-556

24 **Clark CD**, Picus D, Dunagan WC. Bloodstream infections after interventional procedures in the biliary tract. *Radiology* 1994; **191**: 495-499

25 **Alveyn CG**, Robertson DA, Wright R, Lowes JA, Tillotson G. Prevention of sepsis following endoscopic retrograde cholangi opancreatography. *J Hosp Infect* 1991; **19** Suppl C: 65-70

S- Editor Wang GP **L- Editor** Wang XL **E- Editor** Bai SH

PO Box 2345, Beijing 100023, China
www.wjgnet.com
wjg@wjgnet.com

World J Gastroenterol 2007 January 14; 13(2): 280-284
World Journal of Gastroenterology ISSN 1007-9327

RAPID COMMUNICATION

Twenty-four hour intra-arterial infusion of 5-fluorouracil, cisplatin, and leucovorin is more effective than 6-hour infusion for advanced hepatocellular carcinoma

Hidenari Nagai, Masahiro Kanayama, Katsuya Higami, Kouichi Momiyama, Akiko Ikoma, Naoki Okano, Katsuhiko Matsumaru, Manabu Watanabe, Koji Ishii, Yasukiyo Sumino, Kazumasa Miki

Hidenari Nagai, Masahiro Kanayama, Katsuya Higami, Kouichi Momiyama, Akiko Ikoma, Naoki Okano, Katsuhiko Matsumaru, Manabu Watanabe, Koji Ishii, Yasukiyo Sumino, Kazumasa Miki, Division of Gastroenterology and Hepatology, Toho University Medical Center, Omori Hospital, 6-11-1, Omorinishi, Ota-ku, Tokyo 143-8541, Japan
Correspondence to: Hidenari Nagai, Division of Gastroenterology and Hepatology, Toho University Medical Center, Omori Hospital, 6-11-1, Omorinishi, Ota-ku, Tokyo 143-8541, Japan. hidenari@aol.com
Telephone: +81-3-37624151 Fax: +81-3-37638542
Received: 2006-06-19 Accepted: 2006-08-22

Key words: 5-fluorouracil; Cisplatin; Advanced hepatocellular carcinoma; Liver cirrhosis; Intra-arterial chemotherapy

Nagai H, Kanayama M, Higami K, Momiyama K, Ikoma A, Okano N, Matsumaru K, Watanabe M, Ishii K, Sumino Y, Miki K. Twenty-four hour intra-arterial infusion of 5-fluorouracil, cisplatin, and leucovorin is more effective than 6-hour infusion for advanced hepatocellular carcinoma. *World J Gastroenterol* 2007; 13(2): 280-284

http://www.wjgnet.com/1007-9327/13/280.asp

Abstract

AIM: To evaluate the time dependence of intra-arterial 5-fluorouracil (5-FU) therapy for advanced hepatocellular carcinoma (aHCC).

METHODS: Thirty-seven adult Japanese patients who had aHCC and liver cirrhosis were treated with combined intra-arterial 5-FU, cisplatin (CDDP), and leucovorin (LV). The Japan Integrated Staging score (JIS score) of each patient was 3 or more. The patients were divided into two groups, after which the 15 patients in group S were treated with 6-h infusion chemotherapy (LV at 12 mg/h, CDDP at 10 mg/h, and 5-FU at 250 mg/m^2 per 4 h) and the 22 patients in group L were treated with 24-h infusion chemotherapy (LV at 12 mg/h, CDDP at 10 mg/h, and 5-FU at 250 mg/m^2 per 22 h). Continuous infusion chemotherapy was performed *via* the proper hepatic artery every 5 d for 4 wk using an implanted drug reservoir.

RESULTS: The percentages of patients with a partial response after 4 wk of chemotherapy were 6.7% in group S and 31.8% in group L. The survival of group L was significantly better than that of group S, with the median survival time being 496 d in group L and 226 d in group S ($P < 0.05$).

CONCLUSION: Continuous 24-h intra-arterial infusion is more effective for aHCC and can markedly prolong survival time as compared to 6-h infusion.

INTRODUCTION

The majority of patients with advanced hepatocellular carcinoma (aHCC) survive no longer than 6 mo from the day of initial diagnosis[1]. It was reported that improvement of implanted drug delivery systems has made it possible to administer repeated hepatic arterial infusion of anticancer agents to patients with aHCC and that hepatic arterial infusion therapy not only improved survival but also the quality of life (QOL)[2]. Continuous local arterial infusion of 5-fluorouracil (5-FU) and cisplatin (CDDP) using an infuser pump and an implanted reservoir has been shown to prolong the survival of patients with severe advanced HCC[2-4]. Leucovorin is a biochemical modulator of 5-FU[5-7]. A randomized study showed that the regimen using CDDP, 5-FU, and leucovorin (LV) was significantly better than that of the low-dose CDDP and 5-FU alone[8]. However, there were differences of the response rate and the regimen used in these studies, such as 250 mg of 5-FU for 5 or 24 h. For staging of HCC, Cancer of the Liver Italian Program (CLIP) score[9] has been reported to be very useful[10-12]. However, it was also reported that the stratification ability and prognostic power of the Japan Integrated Staging (JIS) score[13] were superior to those of the CLIP score for staging of HCC[14]. Accordingly, this study was performed to evaluate the time dependence of intra-arterial 5-FU therapy for aHCC by using the JIS score.

MATERIALS AND METHODS

Patients

Thirty-seven adult Japanese patients who had aHCC and

Table 1 Clinical characteristic of the 37 patients with advanced HCC and HCV cirrhosis

Mean age	Group S: 68.3 yr
	Group L: 66.6 yr
Gender	Group S: 10 males, 15 females
	Group L: 15 males, 7 females
Child-Pugh classification	Group S A: 6, B: 7, C: 2
	Group L A: 11, B: 9, C: 2
Stage	Group S Ⅲ: 2, IVA: 12, IVB: 1 (Vp3: 4, Vp4: 1, vv2: 0)
	Group L Ⅲ: 1, IVA: 14, IVB: 7 (Vp3: 3, Vp4: 0, vv2: 1)
JIS score	Group S 3: 7, 4: 7, 5: 1
	Group L 3: 12, 4: 8, 5: 2

liver cirrhosis due to HCV infection (C-LC) were treated with combined intra-arterial 5-FU, CDDP, and LV at Omori Hospital, Japan between 2000 and 2005. According to the computed tomography (CT) findings, the tumors were inoperable, with a JIS score of 3 or more in all patients.

Chemotherapy regimen

The patients were divided into two groups. Group S comprised 15 patients (10 men and 5 women) who were treated with 6-h infusion chemotherapy (LV at 12 mg/h, CDDP at 10 mg/h, and 5-FU at 250 mg/m^2 per 4 h), while group L included 22 patients (15 men and 7 women) who were treated with 24-h infusion chemotherapy (LV at 12 mg/h, CDDP at 10 mg/h, and 5-FU at 250 mg/m^2 per 22 h). Doses of the chemotherapy were according to a previous report[8]. Continuous infusion chemotherapy was performed *via* the proper hepatic artery every 5 d for 4 wk using a catheter connected to a subcutaneously implanted drug delivery system. Subsequently, the same chemotherapy was continued for as long as possible.

System placement technique

In all patients, an intra-arterial catheter was inserted *via* the femoral artery and was attached to a subcutaneously implanted reservoir[15]. In principle, the gastroduodenal artery and the right gastric artery were occluded with steel coils to prevent gastroduodenal injury from anticancer agents. Written informed consent was obtained from each patient or family members after the possible complications of reservoir implantation and arterial infusion chemotherapy had been fully explained.

Evaluation of therapeutic effect

On CT scans obtained after 4 wk of treatment, the size of the intrahepatic tumors was measured as the product of the two longest perpendicular diameters of the largest tumor. CT images were acquired according to the same method as performed for pretreatment workup. The response criteria defined by the Liver Cancer Study Group of Japan were used. A complete response (CR) was defined as disappearance of the tumor and no evidence of new lesions for at least 4 wk, while a partial response (PR) was defined as reduction of the product of the two longest diameters by more than 50%. An increase of the product by more than 25% was defined as progressive disease (PD), and the changes in between PD and PR were defined as stable disease (SD). The response was also evaluated by measuring serum alpha-fetoprotein (AFP), AFP-L3, and PIVKA-Ⅱ levels in the patients with elevated levels of these markers. The survival period was defined as the interval between the start of treatment and death.

Table 2 Objective response and survival in the both group (%)

		JIS score		
	Group	3	4	5
1-yr	Group S	14.3	0.0	0.0
	Group L	50.0	16.7	16.7
2-yr	Group S	0.0	0.0	0.0
	Group L	16.7	0.0	0.0
3-yr	Group S	0.0	0.0	0.0
	Group L	16.7	0.0	0.0

Objective response rate: Group S 6.7% (1/15 cases) CR: PR: SD: PD = 0: 1: 3: 11; Group L 31.8% (7/22 cases) CR: PR: SD: PD = 0: 7: 9: 6.

Statistical analysis

The Mann-Whitney test was used to compare the patient characteristics between the two groups. Survival was evaluated by the Kaplan-Meier method, and the significance of differences in survival was determined by the log rank test. *P* value less than 0.05 was considered statistically significant.

RESULTS

The group S comprised a total of 10 men and 5 women aged 54 to 79 years (mean ± SD, 68.3 ± 7.4 years), while the group L comprised 15 men and 7 women aged 52 to 76 years old (mean ± SD, 66.6 ± 7.8 years). There was no significant difference between the both groups. The Child-Pugh class was A for 6 patients in group S and 11 patients in group L, while it was B for 7 and 9 patients, respectively, and C for 2 patients in each group. Two patients had stage Ⅲ, 12 stage ⅣA, and one patient stage ⅣB disease in group S, while the respective numbers were 1, 14, and 7 in group L. Seven patients had a JIS score of 3, seven patients had a JIS score of 4, and one patient had a JIS score of 5 in group S, while the respective numbers were 12, 8, and 2 in group L. In group S, one patient had tumor thrombi in major branches of the portal vein and four patients had tumor thrombi in the first portal branch. In group L, there was also one patient with tumor invasion into the right hepatic vein and four patients with tumor thrombi in the first portal branch (Table 1).

Response

Table 2 summarizes the response to treatment and the survival of the aHCC patients, all of whom had a JIS score ⩾ 3. In group S, one of the 15 (6.7%) patients achieved PR, but no patient achieved CR. Also, 11 of the 15 (73.3%)

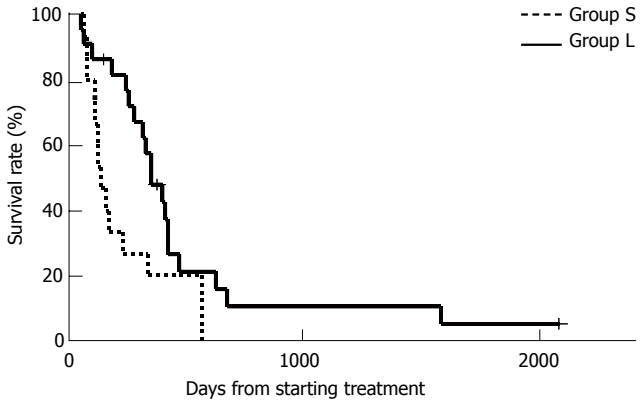

Figure 1 Survival curves plotted by the Kaplan-Meier method. The survival of group L was significantly better than that of group S. The median survival time was 496 d in group L *versus* 226 d in group S ($^aP < 0.05$, Kaplan-Meier method and log-rank test).

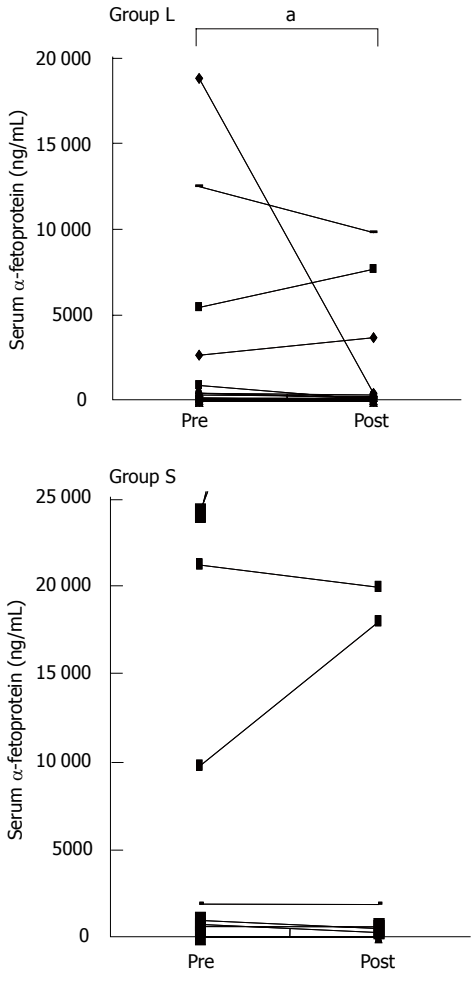

Figure 2 Changes of serum AFP following treatment in the both groups. In group L, the serum AFP level decreased significantly after treatment compared with before treatment ($^aP < 0.05$, Mann-Whitney test).

patients showed PD and 3 (20.0%) patients had SD. In group L, seven of the 22 (31.8%) patients achieved PR, although none of the patients achieved CR. Six of the 22 (27.3%) patients showed PD, but 9 (40.9%) patients had SD. The response rate in group L was significantly better than that in group S ($P < 0.05$, Mann-Whitney test).

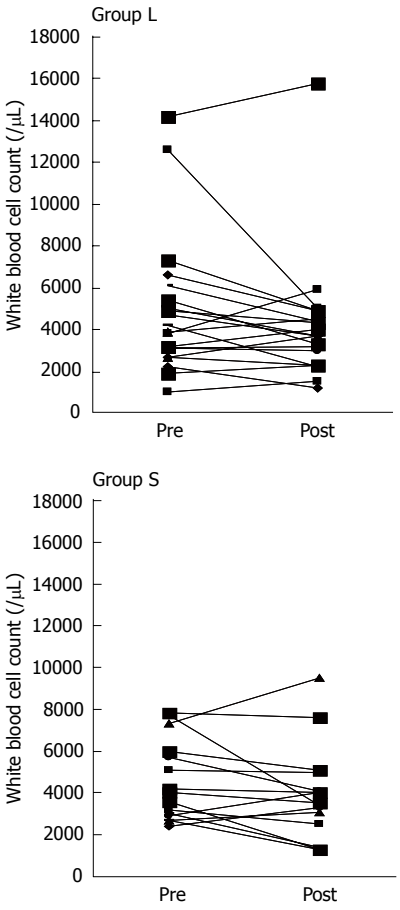

Figure 3 Changes of the white blood cell count following treatment in the both groups. There were no significant differences in either group.

Survival

In group S, the 1-year survival rates for the patients with a JIS score of 3, 4, and 5 were 14.3%, 0.0%, and 0.0%, respectively. There were no survivors for 2 years or more. In group L, the 1-year survival rates for the patients with a JIS score of 3, 4, and 5 were 50.0%, 16.7%, and 16.7%, respectively, while the 2-year survival rates for those patients were 16.7%, 0%, and 0%, respectively. None of the patients in either group survived for 3 years (Table 2). The survival of group L was significantly better than that of group S, with the median survival time being 496 d in group L and 226 d in group S ($P < 0.05$) (Figure 1).

Tumor markers

Figure 2 summarizes the changes of serum AFP following treatments in both groups. In group L, the serum AFP level decreased significantly after treatment compared with that before treatment. However, there was no significant change of the serum AFP level in group S. Moreover, there were no significant changes of the serum AFP-L3 and PIVKA-Ⅱ levels in both groups (data not shown).

Hematologic toxicity

Figure 3 summarizes the changes of the white blood cell count following treatment in both groups, showing that there were no significant differences in either of the groups. Similarly, there were no significant changes of

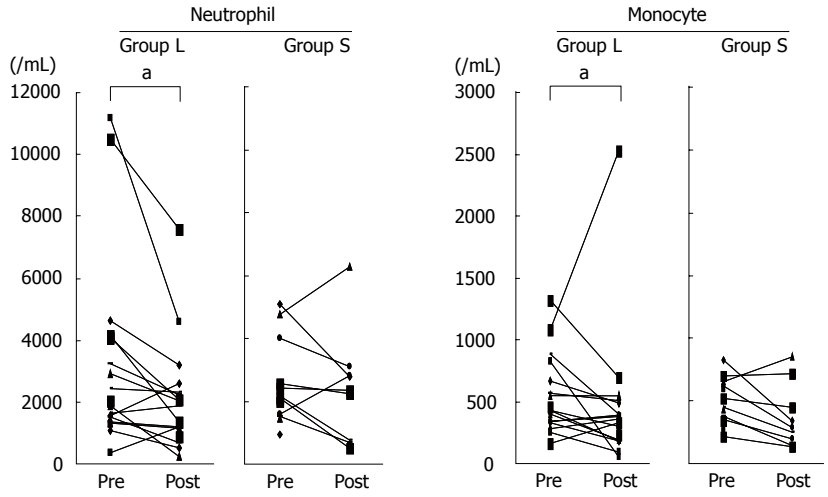

Figure 4 Changes of neutrophil and monocyte counts following treatment in the both groups. In group L, the neutrophil and monocyte counts were significantly decreased after treatment as compared with before treatment ($^aP < 0.05$, Mann-Whitney test).

lymphocyte or platelet count before and after treatment in either group (data not shown). However, the neutrophil and monocyte counts were significantly decreased after treatments in group L compared to group S (Figure 4).

DISCUSSION

The majority of patients with advanced hepatocellular carcinoma (aHCC) live no longer than 6 mo from the day of diagnosis[1]. It was also reported that the average survival of patients with aHCC was 4 mo from the onset of symptoms and 2 mo from the time of admission[16]. In the present study, one of 15 (6.7%) patients in group S achieved PR, while seven of 22 (31.8%) patients in group L reached a state of PR. The survival of group L was significantly better than that of group S, with the median survival time being 496 d in group L *versus* 226 d in group S. Moreover, the serum AFP level decreased significantly after treatment in group L, although this change was not observed in group S. Regarding hematologic toxicity, the neutrophil and monocyte counts were significantly decreased after treatment in group L, while these changes were not observed in group S. In the present study, the severity of disease was assessed by the JIS score, making it possible to observe effect of continuous intra-arterial infusion for 6 and 24 h in C-LC patients with aHCC of similar severity. It was demonstrated that the method of continuous intra-arterial infusion for 24 h was more effective and could prolong survival compared to 6-h infusion. Both treatments were effective for aHCC in the patients with C-LC, when we excluded the patients with a JIS score $\leqslant 2$ in this study. However, 24-h infusion caused a greater decrease of the neutrophil and monocyte counts compared to 6-h infusion.

5-FU and CDDP have been the most commonly used drugs in combination regimens because CDDP amplifies the effect of 5-FU by biochemical modulation in addition to its own action[6,17,18]. Moreover, LV has a synergistic effect in promoting the biochemical modulation of 5-FU. It has been reported that chemotherapy using 5-FU, CDDP, and LV is superior to other treatments (5-FU alone, CDDP alone, and 5-FU plus LV) with respect to controlling tumor growth, even if the concentrations of 5-FU and LV are reduced by half[8]. Therefore, we selected the combination of 5-FU, CDDP, and LV for intra-arterial infusion to treat aHCC, based on the employment of CDDP and LV as modulators of 5-FU. 5-FU has been reported to exhibit its anticancer effects *via* the following mechanisms: (1) Inhibition of deoxyribonucleic acid (DNA) synthesis through inactivation of thymidylate synthase (TS) by formation of a complex between methyle netetrahydrofolate (CH_2FH_4) and 5-fluoro-2'-deoxyuridine 5'-monophosphate (FdUMP), which is synthesized from 5-FU. (2) Interference with ribonucleic acid (RNA) metabolism by the uptake of phosphated 5-fluorouridine 5'-triphosphate into RNA[19]. It was also reported that a single dose of 5-FU is more effective for causing RNA dysfunction, while continuous infusion causes more DNA damage[20]. Another study showed that 5-FU was almost undetectable in the peripheral blood when 5-FU and low-dose CDDP were continuously infused *via* a central vein or *via* the hepatic artery in patients with adavanced or metastatic HCC[21]. These reports indicate that the method of continuous intra-arterial infusion for 24 h would cause more damage to tumor DNA in our C-LC patients with aHCC compared with 6-h infusion, although 24-h infusion had stronger hematologic toxicity than 6-h infusion. Our results might also be supported by the report that 5-FU has a time-dependent anticancer effect and shows stronger cell-killing activity *in vitro* when exposure is continued for a longer period[22].

In conclusion, continuous 24-h intra-arterial infusion is more effective and can prolong survival as compared with 6-h infusion in C-LC patients with aHCC, although 24-h infusion is associated with stronger hematologic toxicity.

REFERENCES

1 **Okuda K**, Ohtsuki T, Obata H, Tomimatsu M, Okazaki N, Hasegawa H, Nakajima Y, Ohnishi K. Natural history of hepatocellular carcinoma and prognosis in relation to treatment. Study of 850 patients. *Cancer* 1985; **56**: 918-928

2 **Toyoda H**, Nakano S, Kumada T, Takeda I, Sugiyama K, Osada T, Kiriyama S, Suga T, Takahashi M. The efficacy of continuous local arterial infusion of 5-fluorouracil and cisplatin through an implanted reservoir for severe advanced hepatocellular carcinoma. *Oncology* 1995; **52**: 295-299

3 **Murata K**, Shiraki K, Kawakita T, Yamamoto N, Okano H, Nakamura M, Sakai T, Deguchi M, Ohmori S, Nakano T. Low-

dose chemotherapy of cisplatin and 5-fluorouracil or doxorubicin via implanted fusion port for unresectable hepatocellular carcinoma. *Anticancer Res* 2003; **23**: 1719-1722

4 **Okuda K**, Tanaka M, Shibata J, Ando E, Ogata T, Kinoshita H, Eriguchi N, Aoyagi S, Tanikawa K. Hepatic arterial infusion chemotherapy with continuous low dose administration of cisplatin and 5-fluorouracil for multiple recurrence of hepatocellular carcinoma after surgical treatment. *Oncol Rep* 1999; **6**: 587-591

5 **O'Connell MJ**. A phase III trial of 5-fluorouracil and leucovorin in the treatment of advanced colorectal cancer. A Mayo Clinic/North Central Cancer Treatment Group study. *Cancer* 1989; **63**: 1026-1030

6 **Poon MA**, O'Connell MJ, Moertel CG, Wieand HS, Cullinan SA, Everson LK, Krook JE, Mailliard JA, Laurie JA, Tschetter LK. Biochemical modulation of fluorouracil: evidence of significant improvement of survival and quality of life in patients with advanced colorectal carcinoma. *J Clin Oncol* 1989; **7**: 1407-1418

7 **Buroker TR**, O'Connell MJ, Wieand HS, Krook JE, Gerstner JB, Mailliard JA, Schaefer PL, Levitt R, Kardinal CG, Gesme DH. Randomized comparison of two schedules of fluorouracil and leucovorin in the treatment of advanced colorectal cancer. *J Clin Oncol* 1994; **12**: 14-20

8 **Yamasaki T**, Kurokawa F, Shirahashi H, Kusano N, Hironaka K, Masuhara M, Okita K. Novel arterial infusion chemotherapy using cisplatin, 5-fluorouracil, and leucovorin for patients with advanced hepatocellular carcinoma. *Hepatol Res* 2002; **23**: 7-17

9 A new prognostic system for hepatocellular carcinoma: a retrospective study of 435 patients: the Cancer of the Liver Italian Program (CLIP) investigators. *Hepatology* 1998; **28**: 751-755

10 **Farinati F**, Rinaldi M, Gianni S, Naccarato R. How should patients with hepatocellular carcinoma be staged? Validation of a new prognostic system. *Cancer* 2000; **89**: 2266-2273

11 **Levy I**, Sherman M. Staging of hepatocellular carcinoma: assessment of the CLIP, Okuda, and Child-Pugh staging systems in a cohort of 257 patients in Toronto. *Gut* 2002; **50**: 881-885

12 **Ueno S**, Tanabe G, Sako K, Hiwaki T, Hokotate H, Fukukura Y, Baba Y, Imamura Y, Aikou T. Discrimination value of the new western prognostic system (CLIP score) for hepatocellular carcinoma in 662 Japanese patients. Cancer of the Liver Italian Program. *Hepatology* 2001; **34**: 529-534

13 **Kudo M**, Chung H, Osaki Y. Prognostic staging system for hepatocellular carcinoma (CLIP score): its value and limitations, and a proposal for a new staging system, the Japan Integrated Staging Score (JIS score). *J Gastroenterol* 2003; **38**: 207-215

14 **Kudo M**, Chung H, Haji S, Osaki Y, Oka H, Seki T, Kasugai H, Sasaki Y, Matsunaga T. Validation of a new prognostic staging system for hepatocellular carcinoma: the JIS score compared with the CLIP score. *Hepatology* 2004; **40**: 1396-1405

15 **Iwamiya T**, Sawada S, Ohta Y. Repeated arterial infusion chemotherapy for inoperable hepatocellular carcinoma using an implantable drug delivery system. *Cancer Chemother Pharmacol* 1994; **33** Suppl: S134-S138

16 **Nagasue N**, Yukaya H, Hamada T, Hirose S, Kanashima R, Inokuchi K. The natural history of hepatocellular carcinoma. A study of 100 untreated cases. *Cancer* 1984; **54**: 1461-1465

17 **LoRusso P**, Pazdur R, Redman BG, Kinzie J, Vaitkevicius V. Low-dose continuous infusion 5-fluorouracil and cisplatin: phase II evaluation in advanced colorectal carcinoma. *Am J Clin Oncol* 1989; **12**: 486-490

18 **Scanlon KJ**, Newman EM, Lu Y, Priest DG. Biochemical basis for cisplatin and 5-fluorouracil synergism in human ovarian carcinoma cells. *Proc Natl Acad Sci USA* 1986; **83**: 8923-8925

19 **Harbers E,** Chaudhuri NK, Heidelberger C. Studies on fluorinated pyrimidines. VIII. Further biochemical and metabolic investigations. *J Biol Chem* 1959; **234**: 1255-1262

20 **Iba T**, Kidokoro A, Fukunaga M, Sugiyama K, Fukunaga T, Aihara N. Effect and mechanism of orally administered leucovorin/5-fluorouracil on colon cancer. *Gan To Kagaku Ryoho* 2003; **30**: 2077-2081

21 **Tanioka H**, Tsuji A, Morita S, Horimi T, Takamatsu M, Shirasaka T, Mizushima T, Ochi K, Kiura K, Tanimoto M. Combination chemotherapy with continuous 5-fluorouracil and low-dose cisplatin infusion for advanced hepatocellular carcinoma. *Anticancer Res* 2003; **23**: 1891-1897

22 **Drewinko B**, Yang LY. Cellular basis for the inefficacy of 5-FU in human colon carcinoma. *Cancer Treat Rep* 1985; **69**: 1391-1398

S- Editor Wang J **L- Editor** Kumar M **E- Editor** Bai SH

PO Box 2345, Beijing 100023, China
www.wjgnet.com
wjg@wjgnet.com

World J Gastroenterol 2007 January 14; 13(2): 285-288
World Journal of Gastroenterology ISSN 1007-9327

RAPID COMMUNICATION

Totally laparoscopic trans-hiatal gastroesophagectomy for benign diseases of the esophago-gastric junction

Jean-Louis Dulucq, Pascal Wintringer, Ahmad Mahajna

Jean-Louis Dulucq, Pascal Wintringer, Ahmad Mahajna, Department of Abdominal Surgery, Institute of Laparoscopic Surgery, Maison de Santé Protestante, Bagatelle Hospital, Route de Toulouse 203, Talence-Bordeaux 33401, France
Correspondence to: Jean-Louis Dulucq, Department of Abdominal Surgery, Institute of Laparoscopic Surgery, Maison de Santé Protestante, Bagatelle Hospital, Route de Toulouse 203, Talence-Bordeaux 33401, France. info@ils-chirurgie.com
Telephone: +33-557-123521 Fax: +33-557-123420
Received: 2006-09-24 Accepted: 2006-12-09

13(2): 285-288

http://www.wjgnet.com/1007-9327/13/285.asp

Abstract

AIM: To prospectively present our initial experience with totally laparoscopic transhiatal esophagogastrectomies for benign diseases of the cardia and distal esophagus.

METHODS: Laparoscopic gastric mobilization and tubularization combined with transhiatal esophageal dissection and intrathoracic esophagogastric anastomosis accomplished by a circular stapler was done in 3 patients. There were 2 females and 1 male patient with a mean age of 73 ± 5 years.

RESULTS: Two patients were operated on due to benign stromal tumor of the cardia and one patient had severe oesophageal peptic stenosis. Mean blood loss was 47 ± 15 mL and mean operating time was 130 ± 10 min. There were no cases that required conversion to laparotomy. All patients were extubated immediately after surgery. Soft diet intake and ambulation times were 5.1 ± 0.4 d and 2.6 ± 0.6 d, respectively. There were no intraoperative and postoperative complications and there were no perioperative deaths. The average length of hospital stay was 9.3 ± 3 d. All procedures were curative and all resected margins were tumor free. The mean number of retrieved lymph nodes was 18 ± 8.

CONCLUSION: Laparoscopic transhiatal esophagogastrectomy for benign lesions has good effects and proves feasible and safe.

Key words: Esophagogastrectomy; Transhiatal resection; Cardial tumor; Laparoscopy; Stromal tumor

Dulucq JL, Wintringer P, Mahajna A. Totally laparoscopic trans-hiatal gastroesophagectomy for benign diseases of the esophago-gastric junction. *World J Gastroenterol* 2007;

INTRODUCTION

In recent years, the incidence of adenocarcinoma of the lower esophagus and cardia has increased[1]. Surgery remains the treatment of choice for these cancers, since it provides definitive treatment and long-term survival for some patients and offers splendid palliation for many others. The most common surgeries for resectable lesions are total gastrectomy with distal esophagectomy, Ivor Lewis esophagectomy and the blunt transhiatal procedure[2,3]. These traditional approaches are frequently associated with significant morbidity and mortality rates ranging from 5% to 10%[4-6]. With the development of minimally invasive surgery during the last decade, attempts were made to use alternative minimally invasive methods for esophageal dissection, which avoid an open thoracotomy incision and therefore reduce the associated morbidity[7-11]. However, combined methods using thoracoscopic dissection with conventional abdominal approaches have not achieved a significant reduction in respiratory morbidity, mostly due to the upper midline abdominal incision[12,13]. Better outcomes were achieved by the use of laparoscopic gastric mobilization combined with transhiatal or thoracoscopic esophageal mobilization and cervical or thoracic anastomoses[14,15].

The present study reports on our initial experience with laparoscopic gastric mobilization and transhiatal oesophageal dissection with intrathoracic esophagogastric anastomosis without abdominal, cervical or thoracic incisions for benign diseases of the cardia and distal esophagus prospectively.

MATERIALS AND METHODS

Patients

The clinical records of patients who underwent laparoscopic gastroesophagectomy in the Department of Abdominal Surgery of the Institute of Laparoscopic Surgery (ILS, Bordeaux) were collected prospectively. All patients underwent preoperative workup including upper gastrointestinal barium swallow, endoscopy with biopsies, endoscopic ultrasonography and dynamic CT scanning

of the chest, abdomen and pelvis, in order to establish the diagnosis and determine the extent and staging of the disease. Twenty-eight patients with a malignancy underwent combined laparoscopic and thoracoscopic Ivor Lewis esophagectomy and were excluded from this study. For precise laparoscopic resection in one case of a small intraluminal lesion, we used preoperative endoscopic location and applied metal clips identified by intraoperative X-ray control. Prior to the operations, all cases were reviewed at a meeting attended by staff surgeons, oncologists, gastroenterologists and pathologists. Patients were informed which procedure was expected and the possibility of conversion was discussed. All patients were put on antithrombotic prophylaxis by low-weight heparin and given elastic stockings. Postoperatively, all patients were given total parenteral nutrition for the first 5 d. A hydrosoluble contrast swallow was performed on the 5th postoperative day and if normal, enteral feeding was started.

Studied data

The patients' demographic data, surgeries, postoperative courses and outpatient follow-up were studied. The following data were collected prospectively: age, sex, preoperative work-up, types and locations of the tumor, duration of surgery, blood loss, intraoperative complications, pathological findings and nodal status, postoperative complications, hospital stay, recurrence and distant events. Variables are presented as mean and standard deviation.

Surgical techniques

The patient was placed in a 25° reverse-Trendelenburg position with split legs; the operating surgeon stood between the legs, the assistant surgeon stood on the left side of the patient and the camera holding assistant was on the right side. A total of five operating trocars were used: a 0° videoscope was introduced through a 10 mm supraumbilical trocar, two 12 mm working ports were placed to the right and left of the midline, and two 5 mm exposure trocars were in sub-xiphoid and left lateral position (Figure 1). Laparoscopic explorations were done by creating a pneumoperitoneum with CO_2 to a maximum pressure of 12 mmHg. After exploration of the peritoneal cavity the greater curvature was mobilized by dissection of the greater omentum from the transverse colon using scissors and Ligasure® (Valleylab, Tyco Healthcare Group Lp, Boulder, CO 80 301-3299, UK) or harmonic scalpel (Ethicon Endo-surgery, Cincinnati, OH. USA). The left gastric vessels were exposed and clipped and divided at their roots while the lymph nodes were dissected. The greater curvature mobilization was continued in a distal to proximal direction while the right gastric and gastroepiploic arteries were preserved. A Kocher maneuver was performed followed by gastric tubularization: After definition of the distal margin of the specimen, an endoscopic linear stapler (Ethicon Endo-surgery, Cincinnati, OH. USA) was used to divide the small curvature and create a tube of the greater curvature that would later allow anastomosis with the esophagus. The right diaphragmatic crus was dissected to expose the lower mediastinum. The fundus and abdominal esophagus were mobilized by division of the gastrophrenic peritoneal reflection and separation of the gastroesophageal junction from the left and right crus. The hiatus was entered and the mediastinal esophagus was dissected. The dissection limits were between the left and right parietal pleuras, the pericardium and left pulmonary vein anteriorly and the aorta posteriorly. The anterior and posterior vagal nerves were identified and divided and finally the esophagus was transected 2 to 3 cm above the lesion with free margins.

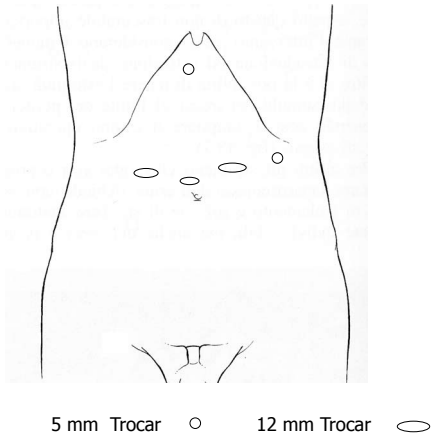

Figure 1 Trocar placement for transhiatal esophagogastrectomy.

For reconstruction a 25 mm circular stapler (Ethicon Endo-surgery, Cincinnati, OH, USA) was used to perform intracorporeal esophagogastric anastomosis. The anvil was prepared by tying a thread with a needle to the tip and then inserted into the peritoneal cavity through a port-site. The anvil was introduced through the lateral esophageal wall 1.5 cm proximal to the transection line, the needle exited through the esophageal wall and then the esophageal stump was closed by a linear endo GIA stapler. The circular stapler was introduced by enlarging one of the left sided trocar sites, entered into the still attached lesser curvature, then passed into the gastric tube. After the stapler was connected to the anvil, the esogastric anastomosis was created, and the stapler removed. The tissue doughnuts were carefully checked. The gastric tube was transected with a linear stapler proximal to the anastomosis, making sure to leave at least 1 cm of tissue so as not to create ischemia. The resected specimen was placed inside a bag (Endo Catch II, Auto Suture European Services Center, S.A., 78990 Elancourt, France) and was removed through enlargement of one of the port wounds.

RESULTS

Patients' characteristics

Between April 2002 and January 2005, we performed laparoscopic gastroesophagectomy in 3 patients. There were 2 female and 1 male patients with a mean age of 73 ± 5 years. The presenting syndromes were abdominal pain and dyspepsia in the first patient, upper gastrointestinal bleeding in the second patient, and dysphagia and weight loss in the last patient. Patients' preoperative risk was evaluated

Table 1 Patient demographics and presenting symptoms

No.	Age (yr)	Gender	ASA	Symptoms	Pathologic site	Pathology
1	67	M	1	Abdominal pain and dyspepsia	Gastroesophageal junction	Gastrointestinal stromal tumor
2	79	F	2	Upper gastrointestinal bleeding	Gastroesophageal junction	Gastrointestinal stromal tumor
3	73	F	2	Dysphagia and weight loss	Distal esophagus	Severe fibrosis

ASA: American Society of Anesthesiologists physical status score.

according to the American Society of Anesthesiologists physical status score (ASA) (Table 1).

Perioperative data

The perioperative data were as follows: Mean blood loss was 47 ± 15 mL and mean operating time was 130 ± 10 min. There were no cases that required conversion to laparotomy. All patients had their tracheal tube removed immediately after surgery. Mean stay time in Intensive Care Unit was 2.3 ± 0.5 d. Resumation of soft diet intake and ambulation times were 5.1 ± 0.4 d and 2.6 ± 0.6 d, respectively. There were no intraoperative or postoperative complications and there were no perioperative deaths. The average length of hospital stay was 9.3 ± 3 d.

Pathologic findings

Two patients were operated on for benign lesions, which were gastrointestinal stromal tumors of the gastroesophageal junction. One patient had severe fibrosis causing severe stenosis of the distal esophagus due to prolonged gastroesophageal reflux.

All procedures were curative and all resected margins were disease or tumor free. The mean tumor size of the surgical specimens was 3.1 ± 1 cm and the mean number of retrieved lymph nodes was 18 ± 8. The patients were cured of lesions and symptoms during a follow-up of 25 ± 12 mo.

DISCUSSION

In spite of modern surgical techniques and improved perioperative care, conventional surgical approaches for benign and malignant lesions of the esophagus and cardia have not significantly lowered the postoperative morbidity and mortality rates. The mortality rates from esophagectomy ranged from 8% in high volume-centers to as high as 23% in low-volume centers[16]. Respiratory complications associated with thoracotomy and prolonged deflation of the right lung during the operation, as well as infections due to anastomotic leaks are the major causes of perioperative morbidity in these surgeries. The high morbidity rates lead to increased cost, prolonged hospital stay, and occasionally, to mortality. Therefore, patients with esophageal cancer, in particular, older patients and those with co-morbid conditions may not be referred for operation at all.

During the 1970s Orringer introduced the technique of transhiatal esophagectomy, which avoids thoracotomy[3]. However, the use of an open approach has not clearly demonstrated reduction of the risk of postoperative respiratory complications or postoperative mortality. In addition, part of the dissection is "blind" with the consequent risk of bleeding, particularly from the azygus vein, and damage to the trachea and bronchi.

With the advent of minimally invasive surgical techniques, various minimally invasive surgical approaches to esophagectomy were introduced. The initial one was thoracoscopic esophagectomy combined with a laparotomy[13,17-19]. In contrast to expectations, no clear benefits were shown and in some of the early series it was clear that postoperative pulmonary complications were common following this approach[13]. Many other groups who performed thoracoscopic esophagectomy noted respiratory complications. Cuschieri noted pulmonary consolidation in 12% of 26 patients[7]. Gossot and colleagues had a 17% incidence of atelectasis requiring prolonged ventilation[20], Collard and co-workers described a 17% incidence of pneumonitis[21], and Dexter and associates reported that 3 of 13 respiratory complications were fatal[9]. A study from Hong Kong comparing thoracoscopy and open thoracotomy found no significant difference in cardiopulmonary complications[17].

Considering that postoperative pulmonary complications are mainly caused by the prolonged deflation of the right lung during the operation and that midline abdominal and thoracic incisions compromise respiratory ability, we tried to avoid laparotomy and thoracotomy using the laparoscopic transhiatal approach. This approach could reduce postoperative morbidities and speed recovery. We performed laparoscopic gastric mobilization and transhiatal esophageal dissection with intrathoracic esophagogastric anastomosis to treat benign cardial and distal esophageal tumors. Laparoscopic transhiatal esophagogastrectomy was described recently by Costi and colleagues[22], who found that this approach minimizes postoperative complications and gives good results. The technique described by Costi *et al* is quite similar to ours while the main difference is the esophago-gastric anastomosis: Costi *et al* tied the stapler's anvil to the end of an oro-gastric tube which was inserted orally down to the esophageal stump.

Our preliminary results showed that laparoscopic transhiatal esophagogastrectomy without abdominal or thoracic incisions were feasible and safe. There was no need to convert to open surgery, the estimated blood loss was minimal and there were no intraoperative complications. The operative time was shorter than in the other approaches, which necessitated patient's position change and two working fields. There were no intraoperative ventilation difficulties, all patients were extubated immediately after surgery and there were no postoperative pulmonary complications. The patients were ambulated early and the postoperative course

was uneventful in all cases. The mean hospital stay was 11 d (Hospital stay in France, unlike US or other countries, is influenced not only by medical, but also cultural and patient related factors.). We used a narrow gastric tube without pyloroplasty, to avoid the potential problems associated with dumping as supported by previous studies[23]. One concern usually raised regarding the treatment of malignant diseases by minimally invasive approaches is whether these approaches provide an adequate cancer resection, allowing free tumor margins and extensive lymph node dissection, while being minimally invasive. Previous studies concluded that the use of laparoscopic assisted transhiatal dissection for distal esophageal cancer allows enhanced tumor and nodal clearance compared with the standard transhiatal approach[24]. A randomized study comparing an extended thoracic approach and transhiatal approach in 220 patients with adenocarcinoma of the esophagus found no significant difference in survival between the 2 groups[25]. There are no randomized studies comparing the laparoscopic and open transhiatal approach for malignant lesions. Despite that all resected margins in our study were tumor free and the mean number of retrieved lymph nodes was 18 ± 8, which is comparable with the thoracoscopic and open surgery series, our strategy for malignant lesions of the cardia and distal esophagus is to perform combined laparoscopic and thoracoscopic Ivor Lewis esophagectomy with en bloc mediastinal lymhadenectomy.

In conclusion, our preliminary results demonstrate that laparoscopic transhiatal esophagogastrectomy for benign lesions of the cardia and distal esophagus has good effects and is feasible and safe. Further studies with a larger number of patients and longer follow up are needed to establish this approach.

ACKNOWLEDGMENTS

We thank Dr. Mitkal Sharon for valuable help in proofreading this paper.

REFERENCES

1 **Pera M**, Cameron AJ, Trastek VF, Carpenter HA, Zinsmeister AR. Increasing incidence of adenocarcinoma of the esophagus and esophagogastric junction. *Gastroenterology* 1993; **104**: 510-513
2 **Lewis I**. The surgical treatment of carcinoma of the oesophagus; with special reference to a new operation for growths of the middle third. *Br J Surg* 1946; **34**: 18-31
3 **Orringer MB**. Transhiatal esophagectomy without thoracotomy for carcinoma of the thoracic esophagus. *Ann Surg* 1984; **200**: 282-288
4 **Bosset JF**, Gignoux M, Triboulet JP, Tiret E, Mantion G, Elias D, Lozach P, Ollier JC, Pavy JJ, Mercier M, Sahmoud T. Chemoradiotherapy followed by surgery compared with surgery alone in squamous-cell cancer of the esophagus. *N Engl J Med* 1997; **337**: 161-167
5 **Earlam R**, Cunha-Melo JR. Oesophageal squamous cell carcinoma: I. A critical review of surgery. *Br J Surg* 1980; **67**: 381-390
6 **Watson A**. Operable esophageal cancer: current results from the West. *World J Surg* 1994; **18**: 361-366
7 **Cuschieri A**. Thoracoscopic subtotal oesophagectomy. *Endosc Surg Allied Technol* 1994; **2**: 21-25
8 **Cuschieri A**, Shimi S, Banting S. Endoscopic oesophagectomy through a right thoracoscopic approach. *J R Coll Surg Edinb* 1992; **37**: 7-11
9 **Dexter SP**, Martin IG, McMahon MJ. Radical thoracoscopic esophagectomy for cancer. *Surg Endosc* 1996; **10**: 147-151
10 **Lloyd DM**, Vipond M, Robertson GS, Hanning C, Veitch PS. Thoracoscopic oesophago-gastrectomy--a new technique for intra-thoracic stapling. *Endosc Surg Allied Technol* 1994; **2**: 26-31
11 **Watson DI**, Davies N, Jamieson GG. Totally endoscopic Ivor Lewis esophagectomy. *Surg Endosc* 1999; **13**: 293-297
12 **Gossot D**, Cattan P, Fritsch S, Halimi B, Sarfati E, Celerier M. Can the morbidity of esophagectomy be reduced by the thoracoscopic approach? *Surg Endosc* 1995; **9**: 1113-1115
13 **McAnena OJ**, Rogers J, Williams NS. Right thoracoscopically assisted oesophagectomy for cancer. *Br J Surg* 1994; **81**: 236-238
14 **DePaula AL**, Hashiba K, Ferreira EA, de Paula RA, Grecco E. Laparoscopic transhiatal esophagectomy with esophagogastroplasty. *Surg Laparosc Endosc* 1995; **5**: 1-5
15 **Jagot P**, Sauvanet A, Berthoux L, Belghiti J. Laparoscopic mobilization of the stomach for oesophageal replacement. *Br J Surg* 1996; **83**: 540-542
16 **Birkmeyer JD**, Siewers AE, Finlayson EV, Stukel TA, Lucas FL, Batista I, Welch HG, Wennberg DE. Hospital volume and surgical mortality in the United States. *N Engl J Med* 2002; **346**: 1128-1137
17 **Law S**, Fok M, Chu KM, Wong J. Thoracoscopic esophagectomy for esophageal cancer. *Surgery* 1997; **122**: 8-14
18 **Peracchia A**, Rosati R, Fumagalli U, Bona S, Chella B. Thoracoscopic esophagectomy: are there benefits? *Semin Surg Oncol* 1997; **13**: 259-262
19 **Kawahara K**, Maekawa T, Okabayashi K, Hideshima T, Shiraishi T, Yoshinaga Y, Shirakusa T. Video-assisted thoracoscopic esophagectomy for esophageal cancer. *Surg Endosc* 1999; **13**: 218-223
20 **Gossot D**, Fourquier P, Celerier M. Thoracoscopic esophagectomy: technique and initial results. *Ann Thorac Surg* 1993; **56**: 667-670
21 **Collard JM**, Lengele B, Otte JB, Kestens PJ. En bloc and standard esophagectomies by thoracoscopy. *Ann Thorac Surg* 1993; **56**: 675-679
22 **Costi R**, Himpens J, Bruyns J, Cadière GB. Totally laparoscopic transhiatal esophago-gastrectomy without thoracic or cervical access. The least invasive surgery for adenocarcinoma of the cardia? *Surg Endosc* 2004; **18**: 629-632
23 **Bemelman WA**, Taat CW, Slors JF, van Lanschot JJ, Obertop H. Delayed postoperative emptying after esophageal resection is dependent on the size of the gastric substitute. *J Am Coll Surg* 1995; **180**: 461- 464
24 **Sadanaga N**, Kuwano H, Watanabe M, Ikebe M, Mori M, Maekawa S, Hashizume M, Kitano S, Sugimachi K. Laparoscopy-assisted surgery: a new technique for transhiatal esophageal dissection. *Am J Surg* 1994; **168**: 355-357
25 **Hulscher JB**, van Sandick JW, de Boer AG, Wijnhoven BP, Tijssen JG, Fockens P, Stalmeier PF, ten Kate FJ, van Dekken H, Obertop H, Tilanus HW, van Lanschot JJ. Extended transthoracic resection compared with limited transhiatal resection for adenocarcinoma of the esophagus. *N Engl J Med* 2002; **347**: 1662-1669

S- Editor Wang GP **L- Editor** Zhu LH **E- Editor** Bai SH

PO Box 2345, Beijing 100023, China
www.wjgnet.com
wjg@wjgnet.com

World J Gastroenterol 2007 January 14; 13(2): 289-293
World Journal of Gastroenterology ISSN 1007-9327

RAPID COMMUNICATION

Impact of endoscopic ultrasound-guided fine needle biopsy for diagnosis of pancreatic masses

Julio Iglesias-Garcia, Enrique Dominguez-Munoz, Antonio Lozano-Leon, Ihab Abdulkader, Jose Larino-Noia, Jose Antunez, Jeronimo Forteza

Julio Iglesias-Garcia, Enrique Dominguez-Munoz, Jose Larino-Noia, Gastroenterology Department, University Hospital, Santiago de Compostela, Spain
Julio Iglesias-Garcia, Enrique Dominguez-Munoz, Antonio Lozano-Leon, Jose Larino-Noia, Foundation for Research in Digestive Diseases, Santiago de Compostela, Spain
Ihab Abdulkader, Jose Antunez, Jeronimo Forteza, Pathology Department, University Hospital, Santiago de Compostela, Spain
Correspondence to: Julio Iglesias-García, Gastroenterology Department, University Hospital, c/Choupana s/n 15706 Santiago de Compostela, Spain. jiglesiasg@fienad.com
Telephone: +34-981-951364 Fax: +34-981-951365
Received: 2006-09-20 Accepted: 2006-12-06

Abstract

AIM: To evaluate the diagnostic accuracy of histological evaluation of pancreatic tissue samples obtained by a modified method for recovering and processing the endoscopic ultrasound (EUS)-guided fine needle aspiration (FNA) material in the differential diagnosis of pancreatic solid masses.

METHODS: Sixty-two consecutive patients with pancreatic masses were prospectively studied. EUS was performed by the linear scanning Pentax FG-38UX echoendoscope. Three FNAs (22G needle) were carried out during each procedure. The materials obtained with first and second punctures were processed for cytological study. Materials of the third puncture were recovered into 10% formol solution by careful injection of saline solution through the needle, and processed for histological study.

RESULTS: Length of the core specimen obtained for histological analysis was 6.5 ± 5.3 mm (range 1-22 mm). Cytological and histological samples were considered as adequate in 51 (82.3%) and 52 cases (83.9%), respectively. Overall sensitivity of both pancreatic cytology and histology for diagnosis of malignancy was 68.4%. Contrary to cytology, histology was able to diagnose tumours other than adenocarcinomas, and all cases of inflammatory masses. Combination of cytology and histology allowed obtaining an adequate sample in 56 cases (90.3%), with a global sensitivity of 84.21%, specificity of 100% and an overall accuracy of 90.32%. The complication rate was 1.6%.

CONCLUSION: Adequate pancreatic core specimens for histological examination can be obtained by EUS-guided FNA. This technique is mainly useful for the diagnosis of different types of pancreatic tumours and evaluation of benign diseases.

Key words: Endoscopic ultrasound; Fine needle aspiration; Cytology; Biopsy; Pancreatic cancer

Iglesias-Garcia J, Dominguez-Munoz E, Lozano-Leon A, Abdulkader I, Larino-Noia J, Antunez J, Forteza J. Impact of endoscopic ultrasound-guided fine needle biopsy for diagnosis of pancreatic masses. *World J Gastroenterol* 2007; 13(2): 289-293

http://www.wjgnet.com/1007-9327/13/289.asp

INTRODUCTION

Differential diagnosis of pancreatic masses is a frequent clinical challenge. Therapeutic decision in this context is mainly based on the ability to establish or exclude malignancy[1]. Although ductal adenocarcinoma is the most frequent cause of pancreatic masses, other neoplasms (e.g. lymphoma, cystic tumours) and benign conditions (e.g. chronic pancreatitis) with different prognoses and treatment options can arise within the pancreas. A histological diagnosis becomes therefore highly relevant for an optimal therapeutic decision[2].

Endoscopic ultrasound (EUS)-guided fine needle aspiration (FNA) has been proved to be a safe and useful method for tissue sampling of intramural and extramural gastrointestinal lesions including the pancreas[3,4]. Cytological study of the materials obtained by FNA allows the evaluation of cellular findings suggestive of malignancy, such as anisonucleosis, nuclear membrane irregularity and nuclear enlargement. Unfortunately, inflammation causes a reactive and regenerative process leading to cellular changes that can be difficult to distinguish from well-differentiated neoplasias. Histological study of tissue samples allows the assessment of tissue architecture and cell morphology, as well as the performance of immunohistochemical analysis[5,6], thus usually providing with a higher diagnostic accuracy than cytology.

Retrieving pancreatic tissue fragments with different EUS-guided techniques has been explored. In this context,

needles of different diameters and trucut needles have been used with variable success and complication rates[7-11].

The aim of the present study was to evaluate the diagnostic accuracy of the histological evaluation of pancreatic tissue samples obtained by a modified method for recovering and processing the EUS-guided FNA material in the differential diagnosis of pancreatic solid masses.

MATERIALS AND METHODS

Subjects

Sixty-two consecutive patients (mean age 57 years, range 20 to 83 years, 35 males and 27 females), who underwent an EUS-guided FNA for the evaluation of solid pancreatic masses were prospectively included in the study over a two-years period.

Methods

In addition to abdominal ultrasound, all patients had a previous evaluation of the pancreatic mass by CT scan. Lesions were located in the head of the pancreas in 45 cases, in the body in 15 cases, and in the tail in two cases. Once the corresponding signed informed consent was obtained, EUS was performed under conscious sedation by a single operator (JIG). A standard blood coagulation analysis was performed before EUS-guided FNA, and an uncorrectable coagulation profile (prothrombin time < 60%) was considered as a contraindication for the procedure.

EUS was performed using a convex array echoendoscope (Pentax FG-38UX®), connected to an ultrasound equipment Hitachi-E6000®. FNA was performed with a standard 22-gauge needle (Sonotip Ⅱ®, Mediglobe, Germany). This needle is equipped with a round nitinol stylet covered by a 118 cm protective metal spiral coil sheath. The needle can be advanced up to 8.5 cm from the spiral sheath. The target lesion was endosonographically visualized and the region was scanned for vessels using colour and pulsed Doppler. FNA was performed from the duodenum or the stomach according to the location of the lesion in the head or the body/tail of the pancreas, respectively. Before puncture, the stylet was withdrawn several millimeters, thereby exposing the sharp needle tip. The needle was then advanced into the target tissue under endosonographic guidance (Figure 1). Once the lesion was penetrated, the stylet was advanced to the original position to "unplug" the needle, and to push out any potentially needle-clogging tissue or body fluids. The stylet was then removed and suction was applied using a 5 mL syringe while moving the needle to and fro within the lesion. Suction was released before removing the needle. This procedure was repeated three times and the material obtained was recovered as follows: (1) The samples obtained after the first and second punctures were expelled on microscope slides by pushing the needle stylet and injecting air through the needle. The material was then spread on the slides, fixed in 96% ethanol and processed for cytological study by Papanicolau staining (Figure 2). Cytology samples were evaluated for cellular preservation, background substance, cellularity, architectural integrity, and cytoplasmic and nuclear details. Cytology diagnoses were categorized into non-diagnostic,

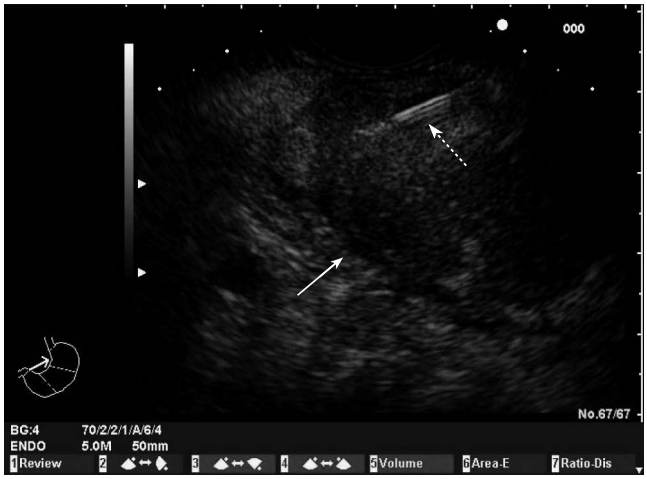

Figure 1 Endoscopic ultrasound image of a mass in the body of the pancreas. Fine needle aspiration of the mass (White arrow: pancreatic mass; Dotted arrow: FNA needle).

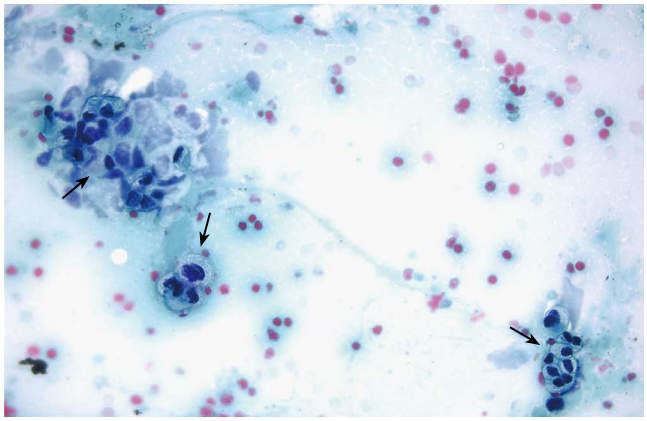

Figure 2 Cytological evaluation of a pancreatic sample obtained by EUS-guided FNA. The presence of marked cellular atypia (arrows) supports the diagnosis of adenocarcinoma of the pancreas (Papanicolau staining × 40).

negative for malignancy, and positive for malignancy, based on published criteria[12]. (2) Samples obtained after the third puncture were recovered into a tube containing a 10% formol solution by injecting 2 ml of saline solution through the needle (Figure 3). Samples were then embedded in paraffin. Tissue sections of 3 to 4 μm were stained by the classical haematoxylin-eosin technique for morphological evaluation. The sample was considered adequate if a coherent core tissue specimen from the target lesion was obtained (Figure 4).

No pathologist was present in the endoscopy room during the procedure. Samples were initially processed by the endoscopist, who was specifically trained with this aim by pathologists. Thus, no microscopic evaluation of sample adequacy was performed at that time. Two experienced pathologists examined both cytological smears and histological specimens. Cytological and histological findings were compared with the surgical specimen as gold standards in patients who were further operated upon. In non-operated patients, a clinical, morphological (EUS and CT scan) and biochemical evaluation (including serum levels of Ca 19.9) over a minimum follow-up

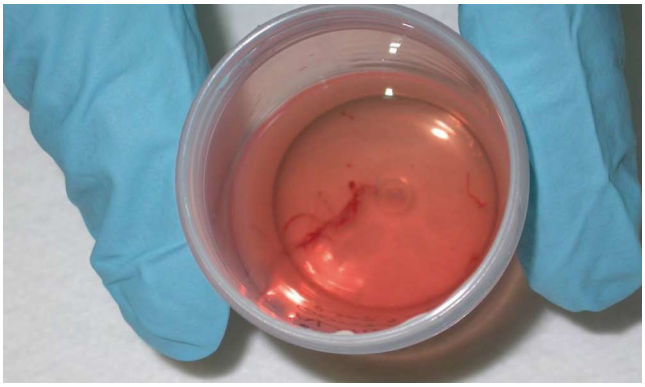

Figure 3 Core of pancreatic tissue obtained by expelling the content of the needle into a tube with 10% formol solution by careful injection of saline solution after EUS-guided FNA.

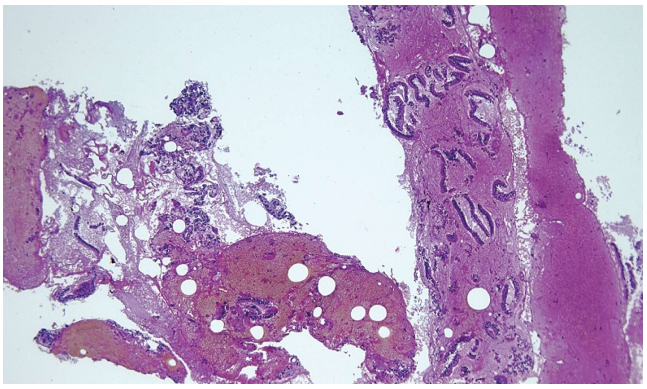

Figure 4 Adenocarcinoma of the pancreas. Histological study of the tissue sample obtained by EUS-guided FNA (HE × 5).

of at least 6 mo was considered as gold standards. The criteria for establishing a benign course of disease were thus a subjective well-being, absence of weight loss, no progression of the disease on imaging studies and no elevation of serum tumour markers.

Statistical analysis

Sensitivity, specificity, overall accuracy and positive and negative predictive values for malignancy were calculated. Data from histology and cytology are shown as percentages and 95% confidence intervals and compared by the Fisher's exact test. $P < 0.05$ was considered as significant.

RESULTS

Pancreatic masses were secondary to a malignant condition in 38 cases (61.3%), and to benign diseases in 24 cases (38.7%). Distribution of patients according to the final diagnosis based on the gold standards is shown in Table 1. A total of 27 patients underwent surgery, including 20 pancreatic adenocarcinomas, one patient with an endocrine tumour, and 6 patients with an inflammatory mass related to a chronic pancreatitis. The remaining 35 patients were followed up for a median of 10 mo (range 6-20 mo).

The length of the core specimen obtained for histological analysis was 6.5 ± 5.3 mm (range 1-22 mm). Cytological and histological samples were considered as adequate in 51 (82.3%, 95% CI, 71.0%-89.8%) and 52 cases (83.9%, 95% CI, 72.8%-91.0%), respectively (not significant). Global sensitivity of both pancreatic cytology and histology for diagnosis of malignancy was 68.4% (52.5%-80.9%).

Table 1 Distribution of patients according to the final diagnosis and number of patients correctly diagnosed by cytological and histological evaluation of samples obtained by EUS-guided FNA

Final diagnosis	*n*	Correct diagnosis by cytology	Correct diagnosis by histology	Correct diagnosis by both cytology and histology
Adenocarcinoma	33	24	21	27
Anaplastic carcinoma	1	1	1	1
Small cell lung cancer	1	0	1	1
Squamous cell carcinoma	1	1	1	1
B cell lymphoma	1	0	1	1
Endocrine carcinoma	1	0	1	1
Inflammatory process	24	17	24	24
Total	62	42	55	56

Table 2 Accuracy of EUS-guided FNA for detection of malignancy in pancreatic solid masses in cases of adequate FNA sampling (95% CI)

	Cytology	Histology	*P*
Sensitivity	76.5% (60.0-87.6)	92.85% (77.3-98.0)	0.097
Specificity	100% (81.6-100)	100% (86.2-100)	NS
Negative predictive value	68.0% (48.4-82.8)	92.3% (75.9-97.9)[a]	< 0.05
Positive predictive value	100% (87.1-100)	100% (87.1-100)	NS
Overall accuracy	84.3% (72.0-91.8)	96.1% (87.0-98.9)	0.05

NS: not significant. [a]$P < 0.05$ *vs* cytology.

Diagnostic accuracy of both techniques in cases of adequate sample is shown in Table 2. In this context, histology tended to be more sensitive and accurate, and showed a significantly higher negative predictive value for malignancy than cytology.

Histological evaluation provided a correct diagnosis in all 24 cases of inflammatory masses, compared with 17 cases correctly classified by cytology (Table 1). Although both techniques were similarly sensitive for the diagnosis of pancreatic adenocarcinomas, histology was the only one able to diagnose other tumours like lymphomas, endocrine tumours and small cell lung cancer metastasis (Table 1). The combination of cytology and histology allowed obtaining an adequate sample in 56 cases (90.3%, 95% CI, 80.4%-95.5%), and a correct diagnosis in all 24 cases of inflammatory masses and 32 cases of pancreatic malignancy (Table 1). Thus, the global sensitivity of EUS-guided FNA was 84.21% (95% CI, 69.6%-92.6%), specificity of 100% (95% CI, 86.2%-100%), and overall accuracy of 90.32% (95% CI, 80.4%-95.5%).

The complication rate of the procedure was 1.6%, and only one case of mild acute pancreatitis that resolved within three days of conservative treatment was observed. No patient died because of the procedure.

DISCUSSION

Recovery of pancreatic EUS-guided FNA specimen into a 10% formol solution by careful injection of saline through the needle allows obtaining an adequate tissue sample for histological diagnosis of pancreatic masses in most cases. Compared to cytology, histology provides a significantly higher negative predictive value for malignancy, and tends to be more accurate. In addition, tumours other than adenocarcinomas are more easily diagnosed by histology.

Several studies have evaluated the accuracy of cytology after EUS-guided FNA for the diagnostic assessment of pancreatic masses. According to those reports, an adequate cytological specimen can be obtained in 82% to 91% of cases, with a sensitivity for malignancy ranging from 64% to 96%[13-25]. In our series, the sensitivity of cytology for the diagnosis of malignancy was 68.4%, which improved up to 76.5% when only adequate samples were considered, similar to the previous report.

In previous studies showing high diagnostic yields of cytology, 3 to 6 needle passes through the lesion[16-23,26] and on-site evaluation of the FNA sample adequacy by a cytopathologist[10,27-29] was considered essential. We were able to obtain an adequate sample in 90% of cases by performing three passes, two for cytological evaluation and one for histological evaluation.

Compared to cytology, histological evaluation of a tissue sample seems to have several advantages, such as a better distinction between well-differentiated adenocarcinoma and chronic pancreatitis, an appropriate cellular subtyping and architectural analysis for the diagnosis of tumours (i.e. lymphoma), as well as the possibility of using special stains[5,6]. In our series, obtaining a core specimen for histological evaluation allowed us to categorize malignant lesions that, although rare, were impossible to be diagnosed by cytology (i.e., pancreatic lymphomas, small cell lung cancer metastasis and endocrine carcinomas). Histological analyses were also able to properly diagnose benign pancreatic lesions in all patients. However, we had difficulties in acquisition of adequate samples from pancreatic adenocarcinomas, which might be explained by the tissue features of this solid tumour, characterized by infiltrating duct-like and tubular structures embedded in a highly desmoplastic stroma[30].

Different needles and different needle diameters have been evaluated to obtain core tissue specimens for histopathological analysis[7-11]. Binmoeller *et al*[7] were able to obtain adequate tissue core specimens in 40 out of 45 patients with pancreatic masses using an 18-gauge needle. Despite that, the sensitivity for detection of a malignancy was only 53%[7]. In a more recent retrospective study, Levy *et al*[9] reported an accuracy of 85% for the diagnosis of different pancreatic and non-pancreatic lesions using a 19-gauge trucut needle, compared to a 60% accuracy achieved by the standard fine needle aspiration technique. Varadarajulu *et al*[10] compared a 19-gauge trucut needle with the standard 22-gauge needle with fine needle aspiration, and no difference in the diagnostic accuracy between both techniques was found (78% *vs* 89%). The diagnostic yield of the trucut needle biopsy is strongly limited to lesions located in the head of the pancreas[11]. This is due to the impossibility to reach within the duodenum the degree of deflection of the echoendoscope tip required to bring the target lesion to an adequate position for puncture. Larghi *et al*[11], despite performing trucut needle biopsy only in lesions accessible for the transgastric approach, were able to obtain materials in only 74% of cases, with an overall diagnostic accuracy of 61%. Contrary to these, the method described in the present study allowed us to achieve a high diagnostic accuracy for pancreatic masses located both in the head and in the body and tail of the pancreas.

Despite the advantages of obtaining tissue core specimens for histological analysis, two cases in our series of malignant pancreatic masses were only detected by cytology. This strongly argues in favour of obtaining specimens for both cytological and histological evaluation. Similar data were reported by other authors[7,9]. In fact, this approach allowed obtaining an adequate sample (either for histology and/or cytology) in 90.3% of cases, with an overall diagnostic accuracy for a malignancy as high as of 90.3%.

EUS-guided biopsy of the pancreas is a safe technique[31,32], with a slightly higher complication rate related to the use of trucut needles[10]. In fact, the risk of pancreatitis and bleeding has been reported to be higher with trucut needles than with the standard FNA needles[10], even though this was not confirmed by other authors[7,11]. A case of mild acute pancreatitis was the only complication observed in the present series after EUS-guided FNA of the pancreas. This low complication rate is similar to that reported previously using a standard 22G needle[21-25].

In conclusion, pancreatic core specimens for histological examination can be obtained by EUS-guided FNA with a 22-gauge needle by careful injection of saline through the needle and by expelling the tissue samples into a tube containing 10% formol solution. The samples obtained by this procedure are highly adequate for histological analyses allowing an appropriate evaluation of pancreatic solid masses. This technique is mainly useful for the diagnosis of different types of pancreatic tumours as well as for the evaluation of benign diseases. Combination with cytology tends to increase the sensitivity of histology for the diagnosis of pancreatic adenocarcinomas.

COMMENTS

Background

Differential diagnosis of pancreatic masses is a frequent clinical challenge. Endoscopic ultrasound (EUS)-guided fine needle aspiration (FNA) has been proved to be a safe and useful method for tissue sampling of pancreatic solid masses. Histological study of tissue samples allows the assessment of tissue architecture and cell morphology, as well as the performance of immunohistochemical analysis, thus usually providing with a higher diagnostic accuracy than cytology.

Research frontiers

Further research is needed in order to improve the diagnostic yield of EUS-guided biopsy, and to provide with better material from pancreatic lesions. Availability of adequate pancreatic tissue samples may allow performing immunohistochemical studies, molecular analysis, and evaluation of genetic mutations, thus providing the basis for a better knowledge of pancreatic diseases.

Innovations and breakthroughs

Our study demonstrates that a core specimen from pancreatic solid masses can

be obtained using a standard 22 gauge needle, thus allowing the histological evaluation of pancreatic lesions. Retrieving pancreatic tissue fragments has been explored using different types of needles (e.g., trucut needles) and different ways of sample processing. In contrast to trucut needles, our technique allows access to lesions located at the head of the pancreas with a low complication rate.

Applications

Obtaining samples of pancreatic tissue allows the histological evaluation of pancreatic solid masses, which may be of help for the diagnosis of different pancreatic tumours as well as for the evaluation of benign diseases like chronic pancreatitis.

Peer review

This paper provides support for the use of this modified method when performing fine needle biopsy of solid pancreatic masses.

REFERENCES

1 **Tamm E**, Charnsangavej C. Pancreatic cancer: current concepts in imaging for diagnosis and staging. *Cancer J* 2001; **7**: 298-311
2 **Cohen SJ**, Pinover WH, Watson JC, Meropol NJ. Pancreatic cancer. *Curr Treat Options Oncol* 2000; **1**: 375-386
3 **Rösch T**. Endoscopic ultrasonography. *Br J Surg* 1997; **84**: 1329-1331
4 **Hawes RH**. Endoscopic ultrasound. *Gastrointest Endosc Clin N Am* 2000; **10**: 161-174, viii
5 **Ribeiro A**, Vazquez-Sequeiros E, Wiersema LM, Wang KK, Clain JE, Wiersema MJ. EUS-guided fine-needle aspiration combined with flow cytometry and immunocytochemistry in the diagnosis of lymphoma. *Gastrointest Endosc* 2001; **53**: 485-491
6 **Mesa H**, Stelow EB, Stanley MW, Mallery S, Lai R, Bardales RH. Diagnosis of nonprimary pancreatic neoplasms by endoscopic ultrasound-guided fine-needle aspiration. *Diagn Cytopathol* 2004; **31**: 313-318
7 **Binmoeller KF**, Thul R, Rathod V, Henke P, Brand B, Jabusch HC, Soehendra N. Endoscopic ultrasound-guided, 18-gauge, fine needle aspiration biopsy of the pancreas using a 2.8 mm channel convex array echoendoscope. *Gastrointest Endosc* 1998; **47**: 121-127
8 **Harada N**, Kouzu T, Arima M, Isono K. Endoscopic ultrasound-guided histologic needle biopsy: preliminary results using a newly developed endoscopic ultrasound transducer. *Gastrointest Endosc* 1996; **44**: 327-330
9 **Levy MJ**, Jondal ML, Clain J, Wiersema MJ. Preliminary experience with an EUS-guided trucut biopsy needle compared with EUS-guided FNA. *Gastrointest Endosc* 2003; **57**: 101-106
10 **Varadarajulu S**, Fraig M, Schmulewitz N, Roberts S, Wildi S, Hawes RH, Hoffman BJ, Wallace MB. Comparison of EUS-guided 19-gauge Trucut needle biopsy with EUS-guided fine-needle aspiration. *Endoscopy* 2004; **36**: 397-401
11 **Larghi A**, Verna EC, Stavropoulos SN, Rotterdam H, Lightdale CJ, Stevens PD. EUS-guided trucut needle biopsies in patients with solid pancreatic masses: a prospective study. *Gastrointest Endosc* 2004; **59**: 185-190
12 **Robins DB**, Katz RL, Evans DB, Atkinson EN, Green L. Fine needle aspiration of the pancreas. In quest of accuracy. *Acta Cytol* 1995; **39**: 1-10
13 **Voss M**, Hammel P, Molas G, Palazzo L, Dancour A, O'Toole D, Terris B, Degott C, Bernades P, Ruszniewski P. Value of endoscopic ultrasound guided fine needle aspiration biopsy in the diagnosis of solid pancreatic masses. *Gut* 2000; **46**: 244-249
14 **Wiersema MJ**, Kochman ML, Cramer HM, Tao LC, Wiersema LM. Endosonography-guided real-time fine-needle aspiration biopsy. *Gastrointest Endosc* 1994; **40**: 700-707
15 **Chang KJ**, Katz KD, Durbin TE, Erickson RA, Butler JA, Lin F, Wuerker RB. Endoscopic ultrasound-guided fine-needle aspiration. *Gastrointest Endosc* 1994; **40**: 694-699
16 **Erickson RA**, Sayage-Rabie L, Beissner RS. Factors predicting the number of EUS-guided fine-needle passes for diagnosis of pancreatic malignancies. *Gastrointest Endosc* 2000; **51**: 184-190
17 **Binmoeller KF**, Rathod VD. Difficult pancreatic mass FNA: tips for success. *Gastrointest Endosc* 2002; **56**: S86-S91
18 **Bhutani MS**, Hawes RH, Baron PL, Sanders-Cliette A, van Velse A, Osborne JF, Hoffman BJ. Endoscopic ultrasound guided fine needle aspiration of malignant pancreatic lesions. *Endoscopy* 1997; **29**: 854-858
19 **Harewood GC**, Wiersema MJ. Endosonography-guided fine needle aspiration biopsy in the evaluation of pancreatic masses. *Am J Gastroenterol* 2002; **97**: 1386-1391
20 **Giovannini M**, Seitz JF, Monges G, Perrier H, Rabbia I. Fine-needle aspiration cytology guided by endoscopic ultrasonography: results in 141 patients. *Endoscopy* 1995; **27**: 171-177
21 **Gress FG**, Hawes RH, Savides TJ, Ikenberry SO, Lehman GA. Endoscopic ultrasound-guided fine-needle aspiration biopsy using linear array and radial scanning endosonography. *Gastrointest Endosc* 1997; **45**: 243-250
22 **Raut CP**, Grau AM, Staerkel GA, Kaw M, Tamm EP, Wolff RA, Vauthey JN, Lee JE, Pisters PW, Evans DB. Diagnostic accuracy of endoscopic ultrasound-guided fine-needle aspiration in patients with presumed pancreatic cancer. *J Gastrointest Surg* 2003; **7**: 118-126; discussion 127-128
23 **Wiersema MJ**, Vilmann P, Giovannini M, Chang KJ, Wiersema LM. Endosonography-guided fine-needle aspiration biopsy: diagnostic accuracy and complication assessment. *Gastroenterology* 1997; **112**: 1087-1095
24 **Chhieng DC**, Jhala D, Jhala N, Eltoum I, Chen VK, Vickers S, Heslin MJ, Wilcox CM, Eloubeidi MA. Endoscopic ultrasound-guided fine-needle aspiration biopsy: a study of 103 cases. *Cancer* 2002; **96**: 232-239
25 **Williams DB**, Sahai AV, Aabakken L, Penman ID, van Velse A, Webb J, Wilson M, Hoffman BJ, Hawes RH. Endoscopic ultrasound guided fine needle aspiration biopsy: a large single centre experience. *Gut* 1999; **44**: 720-726
26 **Erickson RA**. EUS-guided FNA. *Gastrointest Endosc* 2004; **60**: 267-279
27 **Klapman JB**, Logrono R, Dye CE, Waxman I. Clinical impact of on-site cytopathology interpretation on endoscopic ultrasound-guided fine needle aspiration. *Am J Gastroenterol* 2003; **98**: 1289-1294
28 **Jhala NC**, Jhala DN, Chhieng DC, Eloubeidi MA, Eltoum IA. Endoscopic ultrasound-guided fine-needle aspiration. A cytopathologist's perspective. *Am J Clin Pathol* 2003; **120**: 351-367
29 **Chang KJ**, Nguyen P, Erickson RA, Durbin TE, Katz KD. The clinical utility of endoscopic ultrasound-guided fine-needle aspiration in the diagnosis and staging of pancreatic carcinoma. *Gastrointest Endosc* 1997; **45**: 387-393
30 **Klöppel G**, Hruban RH, Longnecker DS, Adler G, Kern SE, Partanen TJ. Ductal adenocarcinoma of the pancreas. In: Hamilton SR, Aaltonen LA, editors. Pathology and Genetics of Tumours of the Digestive System. WHO Classification of Tumours. Lyon: IARC Press, 2000: 221-230
31 **O'Toole D**, Palazzo L, Arotçarena R, Dancour A, Aubert A, Hammel P, Amaris J, Ruszniewski P. Assessment of complications of EUS-guided fine-needle aspiration. *Gastrointest Endosc* 2001; **53**: 470-474
32 **Micames C**, Jowell PS, White R, Paulson E, Nelson R, Morse M, Hurwitz H, Pappas T, Tyler D, McGrath K. Lower frequency of peritoneal carcinomatosis in patients with pancreatic cancer diagnosed by EUS-guided FNA vs. percutaneous FNA. *Gastrointest Endosc* 2003; **58**: 690-695

S- Editor Wang GP **L- Editor** Zhu LH **E- Editor** Liu WF

PO Box 2345, Beijing 100023, China
www.wjgnet.com
wjg@wjgnet.com

World J Gastroenterol 2007 January 14; 13(2): 294-298
World Journal of Gastroenterology ISSN 1007-9327

RAPID COMMUNICATION

Immunogenicity of recombinant hepatitis B virus vaccine in patients with and without chronic hepatitis C virus infection: A case-control study

Naser Ebrahimi Daryani, Mohsen Nassiri-Toosi, Armin Rashidi, Iman Khodarahmi

Naser Ebrahimi Daryani, Mohsen Nassiri-Toosi, Armin Rashidi, Iman Khodarahmi, Department of Gastroenterology, Medical School, Tehran University of Medical Sciences, Tehran, Iran
Correspondence to: Iman Khodarahmi, Department of Gastroenterology, Medical School, Tehran University of Medical Sciences, Unit 9, No. 41 Kashani St., Dabestan Ave., Seyed Khandan, Tehran, Iran. ikhodarahm@student.tums.ac.ir
Telephone: +98-21-88468178 Fax: +98-21-22646984
Received: 2006-09-06 Accepted: 2006-12-05

Abstract

AIM: To compare the response of standard hepatitis B virus (HBV) vaccination between patients with chronic hepatitis C virus (HCV) infection and healthy individuals.

METHODS: This is a prospective case-control study. A total of 38 patients with chronic HCV infection and 40 healthy controls were included. Vaccination was performed by injection of 20 μg recombinant HBsAg into the deltoid muscle at mo 0, 1 and 6. Anti-HBs concentration was determined 3 mo after the last dose and compared between the two groups. The response pattern was characterized as (1) high-response when the anti-HBs antibody titer was > 100 IU/L, (2) low-response when the titer was 10-100 IU/L and (3) no-response when the titer was < 10 IU/L.

RESULTS: In the patient group, there were 10/38 (26.3%) non-responders, 8/38 (21.1%) low-responders and 20/38 (52.6%) high-responders. The corresponding values in the control group were 2/40 (5.0%), 7/40 (17.5%) and 31/40 (77.5%), respectively. The response pattern was statistically different between the two groups. In multivariate analysis, smoking was a significant confounder, while HCV infection lost its significant correlation with lower antibody response.

CONCLUSION: Patients with chronic HCV infection tend to respond weakly to HBV vaccination compared to healthy individuals, though this correlation is not independent according to multivariate analysis.

Key words: Immunogenicity; Hepatitis B; Vaccine; Hepatitis C; Antibody response

Daryani NE, Nassiri-Toosi M, Rashidi A, Khodarahmi I. Immunogenicity of recombinant hepatitis B virus vaccine in patients with and without chronic hepatitis C virus infection: A case-control study. *World J Gastroenterol* 2007; 13(2): 294-298

http://www.wjgnet.com/1007-9327/13/294.asp

INTRODUCTION

One major transmission route for both hepatitis C virus (HCV) and hepatitis B virus (HBV) is the parenteral route, and the sources of infection include administration of blood or blood products[1,2], intravenous drug use[3,4] and needle-stick accidents[5,6]. According to the analysis of the Third National Health and Nutrition Survey, more than 25% of HCV-positive patients in the United States had hepatitis B markers, a proportion nearly six times that in the HCV-negative group[3]. However, the actual prevalence of HBV infection in patients with HCV infection is probably underestimated[7,8]. Although it has been shown that superinfection of either HBV or HCV may suppress the other's replicative levels, coinfection with both viruses has synergistic effects with regard to histological lesions, progression to cirrhosis and cancer development[9-13]. As such it has been recommended by the National Institutes of Health (NIH) that individuals with HCV be vaccinated against HBV infection to prevent such an outcome[14].

HBV vaccination at standard doses (20 μg for adults at mo 0, 1, and 6) results in an effective antibody response in 90% to 98% of healthy individuals[15,16]. However, reduced immunogenicity of the vaccine has been established in persons with chronic liver disease, patients receiving hemodialysis, patients with HIV infection and those awaiting transplantation[17-21]. To the best of our knowledge, only a few studies, with inconsistent results, have compared the immunogenicity of standard HBV vaccination in chronic hepatitis C patients with that in healthy individuals through a case-control study[22-24]. Therefore, we found it valuable to compare the response of standard HBV vaccination between patients with chronic HCV infection and healthy individuals in a prospective case-control study.

MATERIALS AND METHODS

Subjects

Between April 2005 and August 2006, 38 patients with

chronic hepatitis C infection (patients group) and 40 healthy individuals (control group) referred to our clinic were enrolled in this case-control study. Totally there were 50 males and 28 females with a mean age of 37.6 ± 12.8 years. All participants gave written informed consent and the study protocol was approved by the Ethical Committee of Tehran University of Medical Sciences. Inclusion criteria for the patient group were: age > 18 years, HCV infection diagnosed by positive HCV serological markers assessed by ELISA (Abbott Laboratories, North Chicago, IL, USA) and confirmed by the presence of serum HCV RNA detected by PCR, chronic infection diagnosed by serum alanine aminotransferase (ALT) levels of at least twice the upper normal values (> 90 IU/L) for at least two times within a period longer than 6 mo and/or a liver biopsy showing evidence of chronic hepatitis. The control group was selected from healthy adults older than 18 years. Exclusion criteria were: pregnancy, lactation, known bleeding diathesis, current intravenous drug use, alcohol consumption > 30 g/d, history of cancer or transplantation, receiving immunosuppressive medications (excluding interferon), previous hepatitis B vaccination, history of allergy to vaccine components, current or previous hepatitis B infection (positive HBs Ag, anti-HBc Ab/anti-HBs Ab by ELISA), laboratory or clinical evidence of other chronic liver diseases including cirrhosis of any etiology, presence of HIV infection, chronic renal failure (serum creatinine > 2.5) or hemodialysis.

The following variables were recorded for all participants: age (year), sex, body mass (kg), height (m), smoking, alcohol use, history of intravenous drug use. Body mass index (BMI) was calculated by dividing mass (kg) by squared height (m^2). Liver biopsy during two years before vaccination showing the stage and grade of liver involvement according to Ishak *et al*[25] and HCV genotype (determined by PCR-RFLP) was available for 31 and 34 patients, respectively. Baseline ALT (IU/L) was determined by commercial kits for all patients.

Methods

Vaccination was performed by injection of 20 μg recombinant HBsAg (Euvax B, LG Chem, Korea) into the deltoid muscle at mo 0, 1 and 6. Anti-HBs concentration was determined 3 mo after the last dose and expressed as IU/L. The response pattern was characterized as (1) high-response when anti-HBs antibody titer was > 100 IU/L, (2) low-response when the titer was 10-100 IU/L and (3) no-response when the titer was < 10 IU/L. Patients were monitored after each vaccine dose for the occurrences of local (pain, induration, flush) and general (headache, fatigue, fever) side effects.

Statistical analysis

The results are presented as mean ± SD. χ^2 test with Fisher's exact test was used to compare qualitative variables between the groups. Student's *t* test and analysis of variance (ANOVA) were used to compare the quantitative variables between two and multiple groups, respectively. The independent predictive factors of vaccine response were identified by multivariate analysis using multiple logistic regression. Statistical analysis was conducted with SPSS 11.5 software (SPSS Inc., Chicago, IL, USA). Throughout analysis, $P < 0.05$ was considered statistically significant.

Table 1 Characteristics of patients and controls (mean ± SD)

Characteristic	Patient group (n = 38)	Control group (n = 40)	P
Age (yr)	41.1 ± 10.3[a]	34.2 ± 14.2	0.017
Male/Female	30/8[b]	20/20	0.010
BMI (kg/m^2)	24.8 ± 4.7	24.3 ± 4.9	0.691
Smoking *n* (%)	25 (65.8)[b]	3 (7.5)	< 0.001
Alcohol *n* (%)	6 (15.8)	1 (2.5)	0.054
History of iv drug use *n* (%)	9 (23.7)[b]	0 (0)	0.001

[a]$P < 0.05$, [b]$P < 0.01$ *vs* control group.

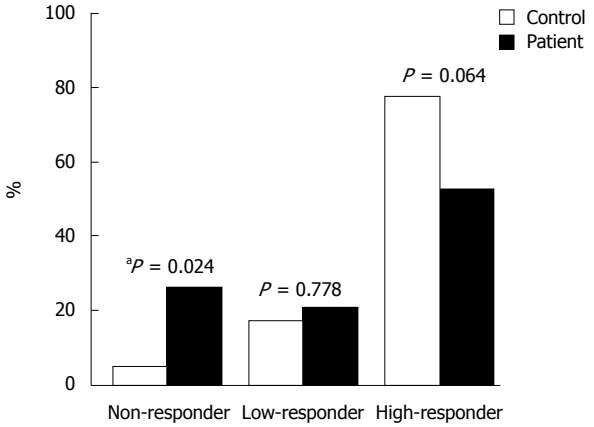

Figure 1 Response to HBV vaccination in patient and control groups. Non-responder (anti-HBs < 10 IU/L); Low-responder (10 IU/L < anti-HBs < 100 IU/L); High-responder (anti-HBs > 100 IU/L). [a]$P < 0.05$ *vs* control group.

RESULTS

Characteristics of patients and controls

Patients were significantly older than healthy subjects ($P = 0.017$). Also, patients were more frequently males ($P = 0.010$), smokers ($P < 0.001$) and previous intravenous drug users ($P = 0.001$) (Table 1).

Antibody response

A total of 28/38 (73.7%) chronic hepatitis C patients responded to the vaccination course (anti-HBs > 10 IU/L) compared with 38/40 (95.0%) controls ($P = 0.012$). In the patient group, there were 10/38 (26.3%) non-responders, 8/38 (21.1%) low-responders and 20/38 (52.6%) high-responders. The corresponding values in the control group were 2/40 (5.0%), 7/40 (17.5%) and 31/40 (77.5%), respectively (Figure 1). The response pattern was statistically different between the two groups ($P = 0.021$). The frequency of non-responders was significantly higher in the patient group ($P = 0.024$ after Bonferroni's correction). However, the frequency of low-responders ($P = 0.778$) and high-responders ($P = 0.064$) was not significantly different between the two groups. Since

Table 2 Characteristics of hepatitis C patients according to vaccine response (mean ± SD)

Characteristics	Non-responder (n = 10)	Responder (n =28)	P
Age (yr)	41.5 ± 11.3	41.0 ± 10.2	0.897
Male/Female	8/2	22/6	1.000
BMI (kg/m^2)	26.6 ± 6.0	24.2 ± 4.1	0.192
Smoking n (%)	9 (90.0)	16 (57.1)	0.118
Alcohol n (%)	2 (20.0)	4 (14.3)	0.644
Hx of iv drug use n (%)	2 (20.0)	7 (25.0)	1.000
ALT (IU/L)	177.1 ± 293.9	78.3 ± 165.3	0.199
Liver disease			
HAI grade (0-18)[1]	5.4 ± 2.1	5.6 ± 1.9	0.773
HAI stage (0-6)[1]	2.3 ± 1.1	2.6 ± 1.6	0.669
HCV genotype n (%)	8	26	
1a	6 (75.0)	14 (53.8)	0.422
Other than 1a	2 (25.0)	12 (46.2)	

[1]According to Knodell's histological activity index (HAI) as modified by Ishak *et al*[25].Non-responder (anti-HBs < 10 IU/L); Responder (anti-HBs > 10 IU/L). Hx:history.

Table 3 Characteristics of hepatitis C patients according to vaccine response

Characteristic	Non-responder (n = 10)	Low-responder (n = 8)	High-responder (n = 20)	P
Age (yr)	41.5 ± 11.3	46.1 ± 9.0	39.0 ± 10.1	0.394
Male/Female	8/2	5/3	17/3	0.417
BMI (kg/m^2)	26.6 ± 6.0	24.9 ± 3.0	23.8 ± 4.6	0.903
Smoking n (%)	9 (90.0)	4 (50.0)	12 (60.0)	0.150
Alcohol n (%)	2 (20.0)	0 (0)	4 (20.0)	0.387
Hx of iv drug use n (%)	2 (20.0)	2 (25.0)	5 (25.0)	0.950
ALT (IU/L)	177.1 ± 293.9	149.8 ± 304.6	49.8 ± 40.3	0.711
Liver disease				
HAI grade (0-18)	5.4 ± 2.1	5.4 ± 2.8	5.7 ± 1.3	0.607
HAI stage (0-6)	2.3 ± 1.1	2.4 ± 1.8	2.7 ± 1.5	0.986
HCV genotype n (%)	8	8	18	
1a	6 (75.0)[a]	7 (87.5)[a]	7 (38.9)[a]	0.038
Other than 1a	2 (25.0)	1 (12.5)	11 (61.1)	

Non-responder (anti-HBs < 10 IU/L); Low-responder (10 IU/L < anti-HBs < 100 IU/L); High-responder (anti-HBs > 100 IU/L). [a]P < 0.05 comparison between three groups.

the patient and control groups were not matched in age, sex, smoking and history of iv drug use, binary logistic regression was performed to adjust for these parameters. Response (anti-HBs > 10 IU/L) was considered as the dependent variable, while hepatitis C infection, age, sex, smoking and history of iv drug use were included as covariates. None of hepatitis C infection (P = 0.448), age (P = 0.078), sex (P = 0.480) and history of iv drug use (P = 0.127) were independently correlated with lower antibody response in the patient group. However, smoking was a significant confounder (P = 0.024; odds ratio: 25.64; 95% confidence interval: 1.54-500).

Characteristics of hepatitis C patients according to vaccine response

The comparison of characteristics of patients between responders and non-responders to HBV vaccine showed no significant difference regarding age, sex ratio, BMI, smoking, alcohol use, history of iv drug use, baseline ALT level, stage and grade of liver disease and genotype (1a *vs* others, Table 2). When patients were categorized into three groups of non-, low- and high-responders, none of the variables except genotype (P = 0.038) had a significant correlation with response category anymore (Table 3). Genotype 1a was more frequently observed in non-responders. However, when Bonferroni's correction was applied for subgroup analysis, this correlation was no longer significant. In summary, no correlation was found between the variables studied and response in either type of analysis.

Side effects

No severe side effects following vaccination were observed in chronic hepatitis C patients. Local adverse effects (erythema, pain at injection point, induration) following vaccination were observed in 4/38 (10.5%) patients. Systemic side effects such as flulike syndrome, headache, fever and fatigue occurred several days following vaccine injections in 1/38 (2.6%) patients.

DISCUSSION

In the present study, the antibody response to standard HBV vaccination with a dose of 20 μg at mo 0, 1 and 6 in individuals with non-cirrhotic chronic hepatitis C infection was evaluated and compared with healthy controls. The frequency of high-responders, low-responders and non-responders in the patient and control groups was 52.6%, 21.1%, 26.3% and 77.5%, 17.5%, 5.0%, respectively (P = 0.021). Non-responders were significantly more common in the patient group (P = 0.024). However, this correlation was not significant in multivariate analysis anymore when age, sex, smoking and history of iv drug use were controlled as potential confounders. In our patient group, there was no correlation between antibody response and variables such as age, sex, BMI, smoking, alcohol use, history of iv drug use, baseline ALT levels, stage and grade of liver disease and genotype.

Several studies have compared the immunogenicity of hepatitis B vaccination with different protocols between healthy individuals and hepatitis C patients. Some of them, like our study, have failed to demonstrate a significant correlation between chronic hepatitis C and antibody response[22,26-28]. However, some authors have shown that responses were weaker in patients than in controls[23,24,29,30]. Hence the results still remain controversial. Among the above mentioned studies, only three have used the same vaccination protocol as ours[22-24]. Lee *et al*[22] compared the immunogenicity of HBV vaccination between 26 hepatitis C patients and 35 controls. The groups were similar in age, but the control group was significantly younger than the patient group. One month after the last dose, 88.5% of patients and 91.4% of controls responded to vaccination with anti-HBs > 10 IU/L. The difference was not statistically significant[22].

In another study of 48 patients and 11 controls, Chlabicz *et al*[23] showed that 72.9% of patients and 90.9% of controls responded (anti-HBs > 10 IU/L) to HBV vaccination one month after the last dose. The groups

were similar in age, sex, BMI and smoking frequency but the difference in antibody response was not significant either. One year after the last dose, there was a significant reduction in antibody response among patients so that only 34.1% of them remained responders. The corresponding value in the control group was 90% at the same time ($P < 0.05$).

Finally, Mattos *et al*[24] reported in their study of 85 patients and 46 healthy adults that 55.3% of patients and 97.8% of controls responded (anti-HBs > 10 IU/L) to HBV vaccination one month after the third vaccine dose. Non-responders were significantly more common in the patient group ($P < 0.001$). The patient and control groups were matched in sex, BMI, alcohol use and smoking, but the patient group was significantly older than the control group. In multivariate regression to control for age as a potential confounder, HCV positivity remained significantly correlated with the lower antibody response ($P = 0.0013$). The patient group in this study included both cirrhotic and non-cirrhotic individuals. Considering that cirrhosis is associated with a lower antibody response[26,31], inhomogeneity of the patient group might have had a role in the significant correlation in this study[24].

We only considered non-cirrhotic patients in our study. The results of multivariate regression showed that hepatitis C infection did not play an independent role in decreasing antibody response. Rather, smoking was a significant confounder ($P = 0.024$; odds ratio: 25.64; 95% confidence interval: 1.54-500). This finding is in agreement with previous studies[32,33]. When patients were categorized into two (responder and non-responder) or three groups (non-, low- and high-responder), no variables studied had a significant correlation with antibody response. Previous studies, as well as ours, failed to show a significant correlation between antibody response and age, sex, BMI, smoking, alcohol use, iv drug use, baseline ALT level or liver histology (grade, stage)[24,29,30]. Mattos *et al*[24] showed that the percentage of non-responders was significantly higher in patients with genotype 1 ($P = 0.04$). Considering that they had three subgroups of patients according to their response, subgroup analysis with a Bonferroni's correction (which changes the P value to $P_c = 0.08$) seemed to be necessary to make a justifiable conclusion. We did not achieve a significant correlation, which was supported by Leroy *et al*[29].

No clinically significant adverse effect was seen in our patients. Local side effects following vaccination were observed in 10.5%, while systemic side effects such as flulike syndrome, headache, fever and fatigue occurred in 2.6% of patients. These rates are almost similar to those reported in other studies[22,26,30]. In conclusion, patients with chronic hepatitis C infection tend to respond weakly to HBV vaccination compared to healthy individuals, though this correlation is not independent according to multivariate analysis.

COMMENTS

Background

Several studies have compared the immunogenicity of hepatitis B vaccination between healthy individuals and hepatitis C patients. Some of them have failed to demonstrate a significant correlation between chronic hepatitis C and antibody response. However, some authors have shown that responses were weaker in patients than in controls.

Research frontiers

Coinfection with both hepatitis B and C viruses has synergistic effects with regard to histological lesions, progression to cirrhosis and cancer development. Therefore, it may be very beneficial to prevent HBV superinfection in hepatitis C patients.

Innovations and breakthroughs

Considering the various vaccination protocols used in HCV patients and also controversial results, we found it valuable to compare the response of standard HBV vaccination between patients with chronic HCV infection and healthy individuals in a prospective case-control study. The results showed that hepatitis C infection does not decrease the immune response to HBV vaccination.

Applications

Based on the results of this study, in the absence of factors known to weaken the immune response, hepatitis C patients do not seem to need additional doses of HBV vaccine or antibody titration after standard HBV vaccination. However, these considerations should be taken into account when vaccinating a hepatitis C patient in general, i.e. one with commonly coexisting immunity-related risk factors.

Terminology

Multivariate analysis: When compared groups are not similar in some possibly important features such as sex or age, performing a multivariate analysis using multiple logistic regression can adjust groups for such potential confounders.

Bonferroni's correction: A method to adjust the level of significance when multiple comparisons are made.

Peer review

If we accept that HBV vaccine may be useful in HCV patients, the basic steps of research should be: to evaluate the rate of response in HCV carriers and to verify whether this rate is acceptable in terms of cost benefit. The patients and controls were significantly different in age, sex, smoking frequency and intravenous drug use.

REFERENCES

1 **Alter MJ**. Epidemiology of hepatitis C. *Hepatology* 1997; **26**: 62S-65S

2 Recommendations for prevention and control of hepatitis C virus (HCV) infection and HCV-related chronic disease. Centers for Disease Control and Prevention. *MMWR Recomm Rep* 1998; **47**: 1-39

3 **Alter MJ**, Kruszon-Moran D, Nainan OV, McQuillan GM, Gao F, Moyer LA, Kaslow RA, Margolis HS. The prevalence of hepatitis C virus infection in the United States, 1988 through 1994. *N Engl J Med* 1999; **341**: 556-562

4 **Murphy EL**, Bryzman SM, Glynn SA, Ameti DI, Thomson RA, Williams AE, Nass CC, Ownby HE, Schreiber GB, Kong F, Neal KR, Nemo GJ. Risk factors for hepatitis C virus infection in United States blood donors. NHLBI Retrovirus Epidemiology Donor Study (REDS) *Hepatology* 2000; **31**: 756-762

5 **Balasekaran R**, Bulterys M, Jamal MM, Quinn PG, Johnston DE, Skipper B, Chaturvedi S, Arora S. A case-control study of risk factors for sporadic hepatitis C virus infection in the southwestern United States. *Am J Gastroenterol* 1999; **94**: 1341-1346

6 **Kiyosawa K**, Sodeyama T, Tanaka E, Nakano Y, Furuta S, Nishioka K, Purcell RH, Alter HJ. Hepatitis C in hospital employees with needlestick injuries. *Ann Intern Med* 1991; **115**: 367-369

7 **Cacciola I**, Pollicino T, Squadrito G, Cerenzia G, Orlando ME, Raimondo G. Occult hepatitis B virus infection in patients with chronic hepatitis C liver disease. *N Engl J Med* 1999; **341**: 22-26

8 **Villa E**, Grottola A, Buttafoco P, Trande P, Merighi A, Fratti N, Seium Y, Cioni G, Manenti F. Evidence for hepatitis B virus infection in patients with chronic hepatitis C with and without serological markers of hepatitis B. *Dig Dis Sci* 1995; **40**: 8-13
9 **Crespo J**, Lozano JL, Carte B, de las Heras B, de la Cruz F, Pons-Romero F. Viral replication in patients with concomitant hepatitis B and C virus infections. *Eur J Clin Microbiol Infect Dis* 1997; **16**: 445-451
10 **Ohkawa K**, Hayashi N, Yuki N, Masuzawa M, Kato M, Yamamoto K, Hosotsubo H, Deguchi M, Katayama K, Kasahara A. Long-term follow-up of hepatitis B virus and hepatitis C virus replicative levels in chronic hepatitis patients coinfected with both viruses. *J Med Virol* 1995; **46**: 258-264
11 **Zarski JP**, Bohn B, Bastie A, Pawlotsky JM, Baud M, Bost-Bezeaux F, Tran van Nhieu J, Seigneurin JM, Buffet C, Dhumeaux D. Characteristics of patients with dual infection by hepatitis B and C viruses. *J Hepatol* 1998; **28**: 27-33
12 **Liaw YF**, Yeh CT, Tsai SL. Impact of acute hepatitis B virus superinfection on chronic hepatitis C virus infection. *Am J Gastroenterol* 2000; **95**: 2978-2980
13 **Kaklamani E**, Trichopoulos D, Tzonou A, Zavitsanos X, Koumantaki Y, Hatzakis A, Hsieh CC, Hatziyannis S. Hepatitis B and C viruses and their interaction in the origin of hepatocellular carcinoma. *JAMA* 1991; **265**: 1974-1976
14 **NIH consensus development conference targets prevention and management of hepatitis C**. *Am Fam Physician* 1997; **56**: 959-961
15 **Dienstag JL**, Werner BG, Polk BF, Snydman DR, Craven DE, Platt R, Crumpacker CS, Ouellet-Hellstrom R, Grady GF. Hepatitis B vaccine in health care personnel: safety, immunogenicity, and indicators of efficacy. *Ann Intern Med* 1984; **101**: 34-40
16 **Rahman F**, Dahmen A, Herzog-Hauff S, Böcher WO, Galle PR, Löhr HF. Cellular and humoral immune responses induced by intradermal or intramuscular vaccination with the major hepatitis B surface antigen. *Hepatology* 2000; **31**: 521-527
17 **Keeffe EB**, Krause DS. Hepatitis B vaccination of patients with chronic liver disease. *Liver Transpl Surg* 1998; **4**: 437-439
18 **Stevens CE**, Szmuness W, Goodman AI, Weseley SA, Fotino M. Hepatitis B vaccine: immune responses in haemodialysis patients. *Lancet* 1980; **2**: 1211-1213
19 **Collier AC**, Corey L, Murphy VL, Handsfield HH. Antibody to human immunodeficiency virus (HIV) and suboptimal response to hepatitis B vaccination. *Ann Intern Med* 1988; **109**: 101-105
20 **Jacobson IM**, Jaffers G, Dienstag JL, Tolkoff-Rubin NE, Cosimi AB, Delmonico F, Watkins E, Hinkle C, O'Rourke S, Russell PS. Immunogenicity of hepatitis B vaccine in renal transplant recipients. *Transplantation* 1985; **39**: 393-395
21 **Van Thiel DH**, el-Ashmawy L, Love K, Gavaler JS, Starzl TE. Response to hepatitis B vaccination by liver transplant candidates. *Dig Dis Sci* 1992; **37**: 1245-1249
22 **Lee SD**, Chan CY, Yu MI, Lu RH, Chang FY, Lo KJ. Hepatitis B vaccination in patients with chronic hepatitis C. *J Med Virol* 1999; **59**: 463-468
23 **Chlabicz S**, Grzeszczuk A, Łapiński TW. Hepatitis B vaccine immunogenicity in patients with chronic HCV infection at one year follow-up: the effect of interferon-alpha therapy. *Med Sci Monit* 2002; **8**: CR379-CR383
24 **Mattos AA**, Gomes EB, Tovo CV, Alexandre CO, Remião JO. Hepatitis B vaccine efficacy in patients with chronic liver disease by hepatitis C virus. *Arq Gastroenterol* 2004; **41**: 180-184
25 **Ishak K**, Baptista A, Bianchi L, Callea F, De Groote J, Gudat F, Denk H, Desmet V, Korb G, MacSween RN. Histological grading and staging of chronic hepatitis. *J Hepatol* 1995; **22**: 696-699
26 **De Maria N**, Idilman R, Colantoni A, Van Thiel DH. Increased effective immunogenicity to high-dose and short-interval hepatitis B virus vaccination in individuals with chronic hepatitis without cirrhosis. *J Viral Hepat* 2001; **8**: 372-376
27 **De Maria N**, Idilman R, Colantoni A, Harig JM, Van Thiel DH. Antibody response to hepatitis B virus vaccination in individuals with hepatitis C virus infection. *Hepatology* 2000; **32**: 444-445
28 **Kamel M**, el Manialawi M, Miller FD. Recombinant hepatitis B vaccine immunogenicity in presence of hepatitis C virus seropositivity. *Lancet* 1994; **343**: 552
29 **Leroy V**, Bourliere M, Durand M, Abergel A, Tran A, Baud M, Botta-Fridlund D, Gerolami A, Ouzan D, Halfon P, Zarski JP. The antibody response to hepatitis B virus vaccination is negatively influenced by the hepatitis C virus viral load in patients with chronic hepatitis C: a case-control study. *Eur J Gastroenterol Hepatol* 2002; **14**: 485-489
30 **Wiedmann M**, Liebert UG, Oesen U, Porst H, Wiese M, Schroeder S, Halm U, Mössner J, Berr F. Decreased immunogenicity of recombinant hepatitis B vaccine in chronic hepatitis C. *Hepatology* 2000; **31**: 230-234
31 **Domínguez M**, Bárcena R, García M, López-Sanroman A, Nuño J. Vaccination against hepatitis B virus in cirrhotic patients on liver transplant waiting list. *Liver Transpl* 2000; **6**: 440-442
32 **Hollinger FB**. Factors influencing the immune response to hepatitis B vaccine, booster dose guidelines, and vaccine protocol recommendations. *Am J Med* 1989; **87**: 36S-40S
33 **Lemon SM**, Thomas DL. Vaccines to prevent viral hepatitis. *N Engl J Med* 1997; **336**: 196-204

S- Editor Wang GP **L- Editor** Zhu LH **E- Editor** Liu WF

PO Box 2345, Beijing 100023, China
www.wjgnet.com
wjg@wjgnet.com

World J Gastroenterol 2007 January 14; 13(2): 299-305
World Journal of Gastroenterology ISSN 1007-9327

RAPID COMMUNICATION

Ginkgo biloba extract (EGb 761) attenuates lung injury induced by intestinal ischemia/reperfusion in rats: Roles of oxidative stress and nitric oxide

Ke-Xuan Liu, Wei-Kang Wu, Wei He, Chui-Liang Liu

Ke-Xuan Liu, Department of Anesthesiology, The First Affiliated Hospital, Sun Yat-Sen University, Guangzhou 510080, Guangdong Province, China
Wei-Kang Wu, The Institute of Integrated Traditional Chinese Medicine and Western Medicine, Sun Yat-Sen University, Guangzhou 510080, Guangdong Province, China
Wei He, Department of Anesthesiology, Guangdong Provincial People's Hospital, Guangzhou 510080, Guangdong Province, China
Chui-Liang Liu, Department of Anesthesiology, Guangdong Provincial Hospital of Traditional Chinese Medicine, Guangzhou 510120, Guangdong Province, China
Supported by grants from the Administration of Traditional Chinese Medicine of Guangdong Province, China, No. 1040066; Natural Science Foundation of Guangdong Province, China, No. 05300758; National Natural Science Foundation of China, No. 30672021
Correspondence to: Dr. Ke-Xuan Liu, Department of Anesthesiology, the First Affiliated Hospital, Sun Yat-Sen University, Guangzhou 510080, Guangdong Province, China. liukexuan807@yahoo.com.cn
Telephone: +86-20-87755766-8273
Received: 2006-10-12 Accepted: 2006-11-23

Abstract

AIM: To investigate the effect of ginkgo biloba extract (EGb 761) on lung injury induced by intestinal ischemia/reperfusion (Ⅱ/R).

METHODS: The rat model of Ⅱ/R injury was produced by clamping the superior mesenteric artery for 60 min followed by reperfusion for 180 min. The rats were randomly allocated into sham, Ⅱ/R, and EGb + Ⅱ/R groups. In EGb + Ⅱ/R group, EGb 761 (100 mg/kg per day) was given *via* a gastric tube for 7 consecutive days prior to surgery. Rats in Ⅱ/R and sham groups were treated with equal volumes of the vehicle of EGb 761. Lung injury was assessed by light microscopy, wet-to-dry lung weight ratio (W/D) and pulmonary permeability index (PPI). The levels of malondialdehyde (MDA) and nitrite/nitrate (NO_2^-/NO_3^-), as well as the activities of superoxide dismutase (SOD) and myeloperoxidase (MPO) were examined. Western blot was used to determine the expression of inducible nitric oxide synthase (iNOS).

RESULTS: EGb 761 markedly improved mean arterial pressure and attenuated lung injury, manifested by the improvement of histological changes and significant decreases of pulmonary W/D and PPI ($P < 0.05$ or 0.01). Moreover, EGb 761 markedly increased SOD activity, reduced MDA levels and MPO activity, and suppressed NO generation accompanied by down-regulation of iNOS expression ($P < 0.05$ or 0.01).

CONCLUSION: The results indicate that EGb 761 has a protective effect on lung injury induced by Ⅱ/R, which may be related to its antioxidant property and suppressions of neutrophil accumulation and iNOS-induced NO generation. EGb 761 seems to be an effective therapeutic agent for critically ill patients with respiratory failure related to Ⅱ/R.

Key words: Ginkgo biloba Extract; Intestine; Reperfusion injury; Lung; Adult respiratory distress syndrome; Vascular permeability; Nitric oxide; Lipid peroxidation

Liu KX, Wu WK, He W, Liu CL. Ginkgo biloba extract (EGb 761) attenuates lung injury induced by intestinal ischemia/reperfusion in rats: Roles of oxidative stress and nitric oxide. *World J Gastroenterol* 2007; 13(2): 299-305

http://www.wjgnet.com/1007-9327/13/299.asp

INTRODUCTION

Intestinal ischemia/reperfusion (Ⅱ/R) injury is a grave condition resulting from acute mesenteric ischemia, hemorrhagic, traumatic or septic shock, or severe burns and some surgical procedures including small bowel transplantation and abdominal aortic surgery[1]. It is well-known that Ⅱ/R not only causes injury of the intestine itself, but also involves severe destruction of remote organs and even multiple organ dysfunction[2,3]. Of these remote organ injuries, lung injury has been well-characterized as an acute inflammation with sequestration of leukocytes and their enzymatic products in lung tissue, increased microvascular permeability, perivascular and interstitial edema, and pulmonary edema[4]. These pulmonary processes incited by remote Ⅱ/R injury frequently lead to the clinical picture of acute respiratory distress syndrome[5].

The mechanisms of lung injury induced by Ⅱ/R are very complex. It is well-established that lipid peroxidation is one of the major factors causing lung injury[6,7]. In

addition, evidence showed that overproduction of nitric oxide (NO) generated by inducible nitric oxide synthase (iNOS) not only aggravates oxidative damage[8,9], but leads to pulmonary microvascular dysfunction as well[10]. Thus, the therapeutical strategy by removing free radicals and reducing NO overproduction should be potential effective strategies for the protection against lung injury following Ⅱ/R.

Extracts from the leaves of ginkgo biloba have been widely used therapeutically in China and Western countries for years. Standard ginkgo biloba extract, EGb 761, contains 22%-27% flavonoids and 5%-7% terpenoids, which are the most important active substances in the extract[11]. Today, EGb 761 is widely prescribed for treatment of disorders such as Alzheimer's disease and neuronal hypoxia, both of which have etiologies associated with oxidative stress[11-13]. In the cardiovascular system, it can protect the heart against ischaemia/reperfusion damage[14] and alleviate vascular endothelial cell injury[15]. Thus, currently, EGb 761 is also widely used in treating cardiovascular diseases[16].

EGB 761 has a broad spectrum of pharmacological activities. However, most of the investigations were focused on cardio-cerebral vascular diseases. Recently, several studies showed that EGb 761 decreases malondialdehyde (MDA) and myeloperoxidase (MPO, an indicator of tissue neutrophil accumulation) levels[17] and protects against histological damage in intestinal mucosa after Ⅱ/R[18]. However, there is no report about the effect of EGb 761 on lung injury induced by Ⅱ/R.

Based on the above findings, we postulate that EGb 761 can exert a protective effect on Ⅱ/R-induced lung injury. Thus, the present study was undertaken to confirm the above hypothesis and elucidate the mechanisms related to pulmonary lipid peroxidation, neutrophil sequestration and nitric oxide (NO) production regulated by induced nitric oxide synthase (iNOS) expression.

MATERIALS AND METHODS

Animal preparation

The current study was approved by the Animal Care Committee of Sun Yat-sen University and performed in accordance with the guidelines for the use of experimental animals by the Ministry of Health. Twenty-four adult pathogen-free male Wistar rats weighing between 230-302 g were housed in individual cages in a cohorted temperature-controlled room with alternating 12 h light/dark cycles, and acclimated for a week before the study. Food was removed 8 h prior to the study, and all rats had free access to water.

Establishment of intestinal ischemia/reperfusion rat models

All rats were anesthetized with pentobarbital (30 mg/kg body weight, intraperitoneally). A polyethylene catheter (PE-10) was inserted into the left carotid artery. The catheter was connected to MacLab digital data acquisition system (PowerLab/4SP ADI Instruments, Ugo Basile Comerio, VA, Italy) *via* a pressure transducer (TSD104A Biopac Systems, 2 Biological Instruments, Besozzo, VA, Italy) for monitoring mean arterial pressure (MAP). Periodically, the cannula was flushed with normal saline (100 μL) to maintain recording fidelity. The rat model was established according to our previous method[19]. The small intestine was exteriorized by midline laparotomy and the superior mesenteric artery (SMA) was occluded by microvascular clip. After 60 min of ischemia, the SMA was reperfused for 180 min. Ischemia was determined by the existence of pulseless or pale color of the small intestine. The return of pulse and restoration of pink color were assumed to be due to the reperfusion of the intestine.

Experimental protocol

The rats were randomly allocated into one of 3 equal groups (n = 8): Sham, Ⅱ/R and EGb + Ⅱ/R. The surgical sham group underwent full surgical preparation including the isolation of SMA without the occlusion. In EGb + Ⅱ/R group, EGb 761 (100 mg/kg per day) was given *via* gastric tube for 7 consecutive days prior to surgery. EGb 761 was dissolved in normal saline at the concentration of 100 mg/mL. Rats in Ⅱ/R group and sham group were treated with equal volumes of the vehicle (normal saline solution) of EGb 761. EGb 761 was supplied by Zhejiang Kangenbei Pharmaceutical Company, China (No. 21003). It contains 24% ginkgo-flavonole glycosides and 6% terpenoids.

Sample collection of blood and lung tissues

After 3-h reperfusion, blood samples were taken from carotid artery. A median sternotomy was performed, and the left main bronchus and right lower lobe bronchus were clamped. The trachea was cannulated and the right upper and middle lobes were lavaged three times with 2 mL of saline containing 0.07 mmol/L EDTA. The collected blood and bronchoalveolar lavage (BAL) fluids were centrifuged at 3000 r/min for 15 min, and the supernatant was stored at -80℃ for subsequent measurement of protein content. The right lower lung lobe was divided into two parts for histology examination and the assessment of pulmonary edema. The left upper and lower lung lobes were used for biochemical and Western blotting analyses, respectively.

Lung histology examination

Part of the right lower lung lobe was harvested and fixed in 10% formalin. After embedded in paraffin, sections of 8 mm were stained with hematoxylin and eosin for light microscopy.

Assessment of pulmonary vascular permeability and pulmonary edema

Pulmonary permeability index (PPI) served as indicators of high pulmonary vascular permeability. PPI was assessed by the ratio of protein concentration in BAL fluid to that in plasma. The protein concentrations of blood and BAL fluid were detected by Coomassie brilliant blue method according to the manufacturer's instructions (Nanjing Jiancheng Corp., China). The severity of pulmonary edema was estimated by wet-to-dry lung weight ratio (W/D). After the wet weight of the lungs was measured, the lungs

were completely dried in a vacuum oven (DP22; Yamato Scientific, Tokyo, Japan) at 95℃ for 48 h to remove any gravimetrically detectable water.

Detection of myeloperoxidase activity in lung tissue

Myeloperoxidase (MPO) activity was detected according to the method described by Barry *et al*[20]. After weighing, the lung assay sample was homogenised in 5 mL of 0.5% hexadecyltrimethyl ammonium bromide (Sigma, U.K.) in 50 mmol potassium phosphate buffer (pH 6). The homogenate was freeze-thawed twice, and then centrifuged at 13000 *g* for 5 min. The resulting supernatant was assayed spectrophotometrically for MPO activity by incubating 0.1 mL of the supernatant with 2.9 mL of solution B. Solution B was prepared by dissolving 2.9 mL of O-dionisidine hydrochloride (Sigma, U.K.) in 90 mL of distilled water and addition of 10 mL of 50 mmol potassium phosphate buffer (pH 6) and hydrogen peroxide (final concentration 0.0005%). The change in absorbance with time at 460 nm was then recorded continuously (Philips PU/VIS specvasculature trophotometer). One unit of MPO was defined as that degrading 1 μmol peroxide per minute at 25℃. Results were expressed as units per gram of lung tissue.

Detection of oxidative stress in lung tissue

Lung tissues were homogenized on ice in normal saline. The homogenates were centrifuged at 4000 r/min at 4℃ for 10 min. MDA levels in the supernatants were determined by measurement of thiobarbituric acid-reactive substance levels using MDA assay kit (Nanjing Jiancheng Corp., China) according to the manufacturer's instructions. The results were calculated as nmol per 100 mg of protein (nmol/100 mg). SOD activity in the supernatants was evaluated by inhibition of nitroblue tetrazolium (NBT) reduction by O_2^- generated by the xanthine/xanthine oxidase system in accordance with the manufacturer's instructions (Nanjing Jiancheng Corp., China). The results were expressed as U/100 mg protein.

Detection of nitrite/nitrate in lung tissue

Lung tissues (100 mg) were weighed and made into 10% homogenates with 0.9 mL normal saline. After centrifugation for 10 min at 10000 r/min, the supernatant was placed in boiling water for 3 min and then centrifuged for 5 min at 10000 g. The supernatant (0.1 mL) was taken for the detection of nitrite/nitrate (NO_2^-/NO_3^-) production, an indicator of NO synthesis, with an NO assay kit (Nanjing Jiancheng Corp., China) following the manufacturer's instructions. Results were calculated as micromoles per 100 grams of protein (μmol/100 mg protein).

Western blotting analysis for inducible nitric oxide synthase in lung tissue

The left lower lung lobe was homogenized with PBS (pH 7.2) and centrifuged at 4℃, 18 000 r/min for 10 min. After precipitation, the unsolubilized fraction was discarded. The protein concentration in the supernatant was determined by Coomassie blue dyebinding assay (Nanjing Jiancheng Corp. China). Aliquots (30 mg) of proteins from each sample were electrophoresed on a 120 g/L SDS-polyacrylamide gel for 4 h at 100 V. The protein samples were transferred onto a nitrocellulose membrane (Amersham, USA). The membrane was then probed with polyclonal rabbit anti-rat inducible nitric oxide synthase (iNOS) antibody (1:50 dilution, Santa Cruz Co., USA) for 2 h at 37℃. After 3 washes with TPBS, blots were visualized with the use of an amplified HRP kit (Wuhan Boshide Corp, China). The presence of iNOS was indicated by the presence of brown color.

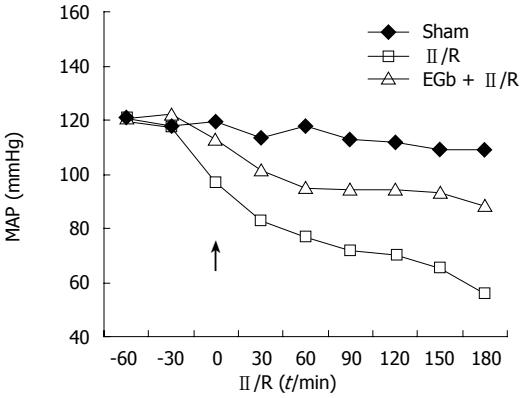

Figure 1 Effects of EGb 761 (arrow indicates the starting point of reperfusion) on mean arterial pressure (MAP) after Ⅱ/R in anaesthetized rats. A rapid drop in MAP was recorded immediately after the beginning of reperfusion of the ischemic bowel. Data are the means of 8 rats (SD not shown). EGb 761 markedly increased MAP. There were significant differences in MAP at all time points after reperfusion between Ⅱ/R and EGb + Ⅱ/R groups ($P < 0.01$).

Statistical analysis

Statistical analysis was performed using SPSS (version 10.1; SPSS for Windows, Chicago, IL) software. Data were expressed as mean ± SD. One-way analysis of variance was used for multiple comparisons and least significant difference test (LSD-t) was used for intra-group comparison. $P < 0.05$ was considered statistically significant.

RESULTS

Changes in MAP

There was no death of any rats during the experiment. There were no significant differences in the weight of the rats and the temperature in the laboratory among the groups. Figure 1 illustrates the time course of MAP in the three experimental groups. A rapid drop in MAP was recorded immediately after the release of the arterial occlusion and the beginning of reperfusion of the ischemic bowel. EGb 761 significantly improved MAP. There was a significant difference in MAP at all time points after reperfusion between Ⅱ/R and EGb + Ⅱ/R groups ($P < 0.01$).

Pathological changes of lung tissue

The histological structure of alveolar and mesenchymal cells was normal in the lungs of sham group (Figure 2A), while the lung tissues from Ⅱ/R group were significantly damaged with pulmonary edema, hemorrhage and

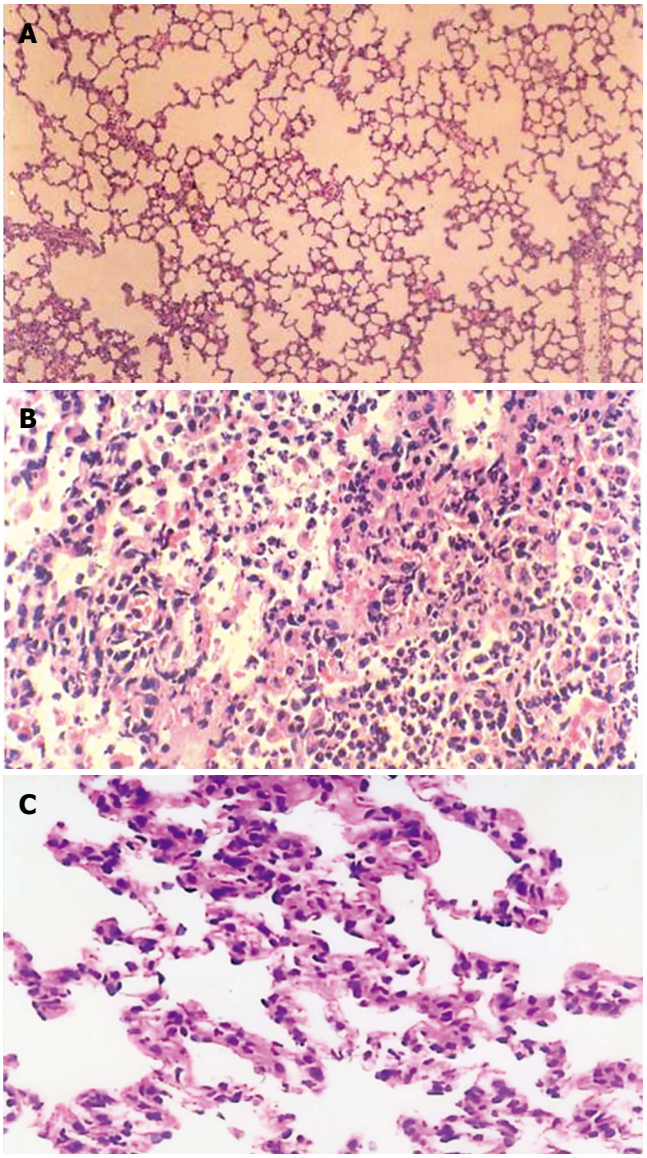

Figure 2 Light microscopic observation of the lung tissues after Ⅱ/R with pretreatment of EGb 761 in rats. **A**: The normal lung tissue structure was found in sham group (× 100); **B:** Lung edema, hemorrhage and inflammatory cell sequestration were found in Ⅱ/R group (× 200); **C**: Decreased morphological changes induced by Ⅱ/R were found in EGb + Ⅱ/R group (× 200).

inflammatory cell infiltration (Figure 2B). Pretreatment with EGb 761 could attenuate significantly the lung injury as shown by light microscopy (Figure 2C).

Changes in W/D and PPI in lung tissues

Compared with the sham group, the lung W/D and PPI in Ⅱ/R group were increased significantly ($P < 0.05$, $P < 0.01$). Compared with the Ⅱ/R group, the lung W/D and PPI in EGb + Ⅱ/R group were significantly decreased ($P < 0.05$ or 0.01) (Table 1).

Changes in MPO activity in lung tissues

MPO activity in Ⅱ/R group was significantly higher than that in the sham group ($P < 0.01$). Compared with Ⅱ/R group, MPO activity in EGb + Ⅱ/R group was markedly reduced ($P < 0.01$), but still higher than that in the sham group ($P < 0.05$) (Table 2).

Table 1 Changes in W/D and PPI in lung tissues (mean ± SD)

	n	Sham	Ⅱ/R	EGb + Ⅱ/R
PPI ($\times 10^{-3}$)	8	1.08 ± 0.42	4.02 ± 0.82[b]	2.23 ± 0.45[a,c]
W/D (%)	8	13.75 ± 5.18	29.62 ± 3.39[a]	16.34 ± 6.45[d]

[a]$P < 0.05$, [b]$P < 0.01$ *vs* sham group; [c]$P < 0.05$, [d]$P < 0.01$ *vs* Ⅱ/R group. W/D: Wet-to-dry lung weight ratio, PPI: pulmonary permeability index.

Table 2 Changes in the activities of SOD and MPO, the levels of MDA and NO_2^-/NO_3^- in lung tissues (mean ± SD)

	n	Sham	Ⅱ/R	EGb + Ⅱ/R
MDA (nmol/100 mg)	8	41.34 ± 6.45	68.52 ± 8.69[b]	44.56 ± 6.13[d]
SOD activity (U/100 mg)	8	101.8 ± 10.32	61.09 ± 6.52[b]	84.36 ± 8.25[a,c]
NO_2^-/NO_3^- (μmol/100 mg)	8	40.36 ± 9.68	78.54 ± 12.36[b]	44.13 ± 8.56[d]
MPO activity (U/g)	8	3.26 ± 0.78	6.93 ± 0.79[b]	4.14 ± 0.76[a,d]

[a]$P < 0.05$, [b]$P < 0.01$ *vs* sham group; [c]$P < 0.05$, [d]$P < 0.01$ *vs* Ⅱ/R group. MPO: Myeloperoxidase; NO_2^-/NO_3^-: nitrite/nitrate; MDA: malondialdehyde; SOD: superoxide dismutase.

Changes in lung MDA levels and SOD activity in lung tissues

MDA levels in Ⅱ/R group were significantly higher than that in the sham group ($P < 0.01$). Compared with Ⅱ/R group, MDA levels in EGb+ Ⅱ/R group were markedly decreased ($P < 0.01$). SOD activity in Ⅱ/R group was markedly lower than that of the sham group ($P < 0.01$). It was increased significantly in EGb + Ⅱ/R group ($P < 0.01$), but still lower than that of the sham group ($P < 0.05$) (Table 2).

Changes in lung NO_2^-/NO_3^- levels in lung tissues

Compared with the sham group, lung NO_2^-/NO_3^- levels in Ⅱ/R group were increased significantly ($P < 0.01$). Compared with the Ⅱ/R group, NO_2^-/NO_3^- levels in EGb + Ⅱ/R group were decreased significantly ($P < 0.01$) (Table 2).

Changes in iNOS expression in lung tissues

Western blotting showed that very weak positive signals were found in the lung tissues of the sham group. Significant increases of iNOS protein expression were seen in the Ⅱ/R group. There were still notable positive signals in EGb + Ⅱ/R group, but it was weaker for the Ⅱ/R group (Figure 3).

DISCUSSION

Currently, EGb 761 is commonly used in treating cardiovascular diseases and cerebral vascular diseases in many countries. As far as we know, the present study is the first to investigate its effects on Ⅱ/R-induced lung injury. The results showed that EGb 761 can markedly improve MAP and attenuate lung injury, manifested by the improvement of the histological damage and significant decreases of pulmonary W/D and PPI (variables related to lung injury). These findings suggest that the administration

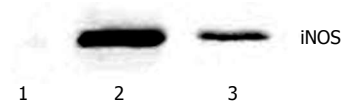

Figure 3 Western blotting analysis of iNOS in rat lung. 1. Sham group; 2. Ⅱ/R group; 3. EGb + Ⅱ/R group. The intensity of the bands was greater in Ⅱ/R group compared with EGb + Ⅱ/R group. A prominent band of iNOS protein was demonstrated at approximately 70 Kd.

of EGb 761 may be a potential effective therapeutical approach for the prevention from Ⅱ/R-induced lung injury.

The mechanisms of lung injury after Ⅱ/R are complex and poorly understood. It is thought that the damage of intestinal mucosal barrier following Ⅱ/R causes the dislocation of bacteria or endogenous endotoxins, leading to systemic inflammatory reactions[20-22]. The neutrophil and their enzymatic products are sequestrated in lung tissues, which causes increased microvascular permeability, perivascular and interstitial edema, and pulmonary edema[4,22,23].

MPO is a haem-containing enzyme located within the azurophil granules of neutrophils, and its activity is known as an indicator of tissue neutrophil accumulation[24]. The present study showed that EGb 761 markedly reduced MPO activity, suggesting that its protective effect on Ⅱ/R-induced lung injury might be related to the suppression of neutrophil accumulation. Our findings are well supported by previous studies, in which EGb 761 suppressed neutrophil sequestration in hepatic and renal tissues evidenced by decreased MPO activity[25,26]. Previous studies also demonstrated that EGb 761 increases peripheral and cerebral blood flow and improves microcirculation, and reduces capillary permeability[27,28], indicating the effect of EGb 761 on neutrophil accumulation. However, the related mechanisms need further investigation.

It is well documented that lipid peroxidation due to Ⅱ/R is one of the main causes for lung injury[6,7]. MDA is the direct product of lipid peroxidation. Therefore, the extent of lipid peroxidation can be assessed by measuring MDA levels in tissues[29]. SOD is the major enzyme for scavenging oxygen free radicals, and its activity can reflect its functional status[30]. Previous studies have shown that EGb 761 can interact as a free radical scavenger and an inhibitor of lipid peroxidation with all, or nearly all, reactive oxygen species[27]. In the present study, EGb 761 was demonstrated to inhibit MDA production and increase SOD activity, suggesting that the inhibition of lipid peroxidation may be one of the mechanisms attributable to the protective effects of EGb 761 on Ⅱ/R-induced lung injury.

Several recent observations implicate that NO may be an important participant in the pulmonary response to Ⅱ/R[31]. It has been suggested that NO, produced from endothelial constitutive nitric oxide synthase (ecNOS), may be an important protective molecule at the onset of Ⅱ/R. In this regard, inhibitors of endogenous NO production greatly exacerbate the increase in epithelial permeability and cardiovascular dysfunction in the reperfused post-ischemia intestine[31,32]. Excessive NO production has been attributed to the second NOS (inducible NOS, iNOS) that is not present under normal conditions but can be induced in response to systemic inflammatory states, including Ⅱ/R. The induction of iNOS has been implicated in the pathogenesis of Ⅱ/R and it was reported that the inhibitions of iNOS activity and NO production could attenuate Ⅱ/R injury[10,33]. In the present study, we further studied the contribution of iNOS to Ⅱ/R-induced lung injury. The results showed that 60 min of intestinal ischemia followed by 180 min of reperfusion significantly upregulated the lung iNOS expression, accompanied by marked elevation of pulmonary nitrate/nitrite (stable metabolites of NO) levels. This is consistent with the findings of Virlos *et al*[10], who demonstrated that pulmonary iNOS activity in rats subjected to Ⅱ/R was significantly increased and of Zhou *et al*[8], who showed that systemic inflammatory response and lung injury occur following Ⅱ/R with an overproduction of NO accompanied by the increases of iNOS expression and the formation of peroxynitrite in the lungs. The mechanisms of the cytotoxic actions of excessive NO production have not been fully understood. It has been suggested that the superoxide ions react with NO to produce peroxynitrite, which then causes accentuated lipid peroxidation, proteic and DNA modifications resulting in cellular damages[34]. Taken together, the iNOS-NO-peroxynitrite dependent pathway may be one of the mechanisms of Ⅱ/R-induced lung injury.

The effect of EGb 761 on NO generation in lung tissue following Ⅱ/R was studied for the first time in the present study. The results showed that EGb 761 significantly reduced the generation of NO accompanied by the down-regulation of iNOS expression. Varga *et al* showed that EGb 761 directly acts as an NO scavenger and concomitantly inhibits the expression of iNOS mRNA in myocardial tissues, thus improving the recovery of postischemic cardiac function after myocardial ischemia/reperfusion[35]. In addition, EGb 761 inhibits NO production in lipopolysaccharide/gamma interferon (LPS/IFN-γ)-activated macrophages by concomitantly scavenging NO and inhibiting iNOS mRNA and enzyme activity[36,37]. Although the experimental models employed in previous studies are different from the present study, these findings can, at least in part, support our current conclusion that the protective effect of EGb 761 on lung injury may be attributable to its suppression on the iNOS-NO dependent pathway.

There is little information on the mechanisms of the effect of EGb 761 on the iNOS-NO dependent pathway. A most recent study showed the preventive effect of EGb on the lipopolysaccharide-induced expressions of iNOS *via* the suppression of nuclear factor-kappaB (NF-κB) in RAW 264.7 cells. Thus, the suppression of NF-κB might be the potential mechanism underlying the findings that EGb 761 reduces NO production and concomitantly inhibits iNOS expression in lung tissues following Ⅱ/R[38].

There are some limitations in the present study. First, EGb 761 is a specific and complex product prepared from ginkgo leaves. EGb 761 used in this study contained 24% ginkgo-flavonole glycosides and 6% terpenoids. Which

components produce the protective effect or work more in protecting against Ⅱ/R-induced lung injury in the present study remains to be elucidated. Second, we did not employ selective inhibitor of iNOS to strengthen the present conclusion, because we focused on investigating the protective effect of EGb 761 on lung injury and thus only preliminarily studied the related mechanisms.

In conclusion, the present study indicates that EGb 761 has a protective effect on lung injury induced by Ⅱ/R, which may be related to its antioxidative property and the suppressions of neutrophil accumulation and iNOS-induced NO generation. EGb 761 appears to be an effective therapeutic agent for some critically ill patients with respiratory failure related to Ⅱ/R, although its mechanisms remain to be elucidated.

ACKNOWLEDGMENTS

We thank Dr. You-Kai Zhu and Dr. Ming-Qi Zhao for their help with experimental techniques.

COMMENTS

Background

EGb 761 is widely used in treating cardio-cerebral vascular diseases mainly due to its action of anti-oxidative damage; however, there is no report about its effect on lung injury induced by intestinal ischemia/reperfusion. The present study was undertaken to confirm the above hypothesis and elucidate the mechanisms related to pulmonary lipid peroxidation, neutrophil sequestration and nitric oxide (NO) production regulated by induced nitric oxide synthase (iNOS) expression.

Research frontiers

EGb 761 has been reported to be effective for the disorders such as Alzheimer's disease and neuronal hypoxia and to protect the heart against ischaemia/reperfusion damage and to alleviate vascular endothelial cell injury, which all have etiologies associated with oxidative stress.

Innovations and breakthroughs

Previous studies showed the protective effect of EGb 761 on cardio-cerebral ischemia/reperfusion injury and intestinal mucosa injury following intestinal ischemia/reperfusion (II/R). The present study indicates that EGb 761 has a protective effect on lung injury induced by II/R and the mechanism may be related to its antioxidative property and the suppressions of neutrophil accumulation and iNOS-induced NO generation.

Applications

Remote lung injury induced by intestinal ischemia reperfusion (II/R) due to acute mesenteric ischemia, hemorrhagic, traumatic or septic shock, or severe burns and some surgical procedures including small bowel transplantation and abdominal aortic surgery often leads to the clinical picture of acute respiratory distress syndrome. EGb 761 has been demonstrated to have the protective effect on lung injury and thus appears to be an effective therapeutic agent for some critically ill patients with respiratory failure related to II/R.

Terminology

Excessive production of nitric oxide (NO) is attributed to the upregulation of inducible nitric oxide synthase (iNOS) expression that is not present under normal conditions, but can be induced in response to systemic inflammatory states, including II/R. NO can react with superoxide ions to produce peroxynitrite, which then causes accentuated lipid peroxidation, proteic and DNA modifications, resulting in cellular damages. This is described as an iNOS-NO-peroxynitrite dependent pathway.

Peer review

This manuscript is very interesting. The title accurately reflects the major contents of the article. The results provide sufficient experimental evidences from which conclusions are drawn. The conclusions are scientifically reliable and valuable.

REFERENCES

1 **Homer-Vanniasinkam S**, Crinnion JN, Gough MJ. Post-ischaemic organ dysfunction: a review. *Eur J Vasc Endovasc Surg* 1997; **14**: 195-203
2 **Deitch EA**. Role of the gut lymphatic system in multiple organ failure. *Curr Opin Crit Care* 2001; **7**: 92-98
3 **Mitsuoka H**, Kistler EB, Schmid-Schönbein GW. Protease inhibition in the intestinal lumen: attenuation of systemic inflammation and early indicators of multiple organ failure in shock. *Shock* 2002; **17**: 205-209
4 **Turnage RH**, Guice KS, Oldham KT. Pulmonary microvascular injury following intestinal reperfusion. *New Horiz* 1994; **2**: 463-475
5 **Ware LB**, Matthay MA. The acute respiratory distress syndrome. *N Engl J Med* 2000; **342**: 1334-1349
6 **Rossman JE**, Caty MG, Zheng S, Karamanoukian HL, Thusu K, Azizkhan RG, Dandona P. Mucosal protection from intestinal ischemia-reperfusion reduces oxidant injury to the lung. *J Surg Res* 1997; **73**: 41-46
7 **Giakoustidis AE**, Giakoustidis DE, Iliadis S, Papageorgiou G, Koliakou K, Kontos N, Taitzoglou I, Botsoglou E, Papanikolaou V, Atmatzidis K, Takoudas D, Antoniadis A. Attenuation of intestinal ischemia/reperfusion induced liver and lung injury by intraperitoneal administration of (-)-epigallocatechin-3-gallate. *Free Radic Res* 2006; **40**: 103-110
8 **Zhou JL**, Jin GH, Yi YL, Zhang JL, Huang XL. Role of nitric oxide and peroxynitrite anion in lung injury induced by intestinal ischemia-reperfusion in rats. *World J Gastroenterol* 2003; **9**: 1318-1322
9 **Pararajasingam R**, Weight SC, Bell PR, Nicholson ML, Sayers RD. Pulmonary nitric oxide metabolism following infrarenal aortic cross-clamp-induced ischaemia-reperfusion injury. *Eur J Vasc Endovasc Surg* 2000; **19**: 47-51
10 **Turnage RH**, Wright JK, Iglesias J, LaNoue JL, Nguyen H, Kim L, Myers S. Intestinal reperfusion-induced pulmonary edema is related to increased pulmonary inducible nitric oxide synthase activity. *Surgery* 1998; **124**: 457-462; discussion 462-463
11 **Kleijnen J**, Knipschild P. Ginkgo biloba. *Lancet* 1992; **340**: 1136-1139
12 **Luo Y**. Alzheimer's disease, the nematode Caenorhabditis elegans, and ginkgo biloba leaf extract. *Life Sci* 2006; **78**: 2066-2072
13 **Chandrasekaran K**, Mehrabian Z, Spinnewyn B, Drieu K, Fiskum G. Neuroprotective effects of bilobalide, a component of the Ginkgo biloba extract (EGb 761), in gerbil global brain ischemia. *Brain Res* 2001; **922**: 282-292
14 **Yuan LP**, Chen ZW, Li F, Dong LY, Chen FH. Protective effect of total flavones of rhododendra on ischemic myocardial injury in rabbits. *Am J Chin Med* 2006; **34**: 483-492
15 **Cheung F**, Siow YL, Chen WZ, O K. Inhibitory effect of Ginkgo biloba extract on the expression of inducible nitric oxide synthase in endothelial cells. *Biochem Pharmacol* 1999; **58**: 1665-1673
16 **Diamond BJ**, Shiflett SC, Feiwel N, Matheis RJ, Noskin O, Richards JA, Schoenberger NE. Ginkgo biloba extract: mechanisms and clinical indications. *Arch Phys Med Rehabil* 2000; **81**: 668-678
17 **Pehlivan M**, Dalbeler Y, Hazinedaroglu S, Arikan Y, Erkek AB, Günal O, Türkçapar N, Türkçapar AG. An assessment of the effect of Ginkgo Biloba EGb 761 on ischemia reperfusion injury of intestine. *Hepatogastroenterology* 2002; **49**: 201-204
18 **Onen A**, Deveci E, Inalöz SS, Isik B, Kilinc M. Histopathological assessment of the prophylactic effect of gingko-biloba extract on intestinal ischemia-reperfusion injury. *Acta Gastroenterol Belg* 1999; **62**: 386-389
19 **Liu KX**, Wu WK, He W, Sun HL. Study on sini decoction in treatment of intestinal ischemia-reperfusion injury in rats: mechanism relating to oxygen radical and bcl-2 protein.

Zhongguo Zhongyao Zazhi 2006; **31**: 329-332, 348
20 **Turnage RH**, Guice KS, Oldham KT. Endotoxemia and remote organ injury following intestinal reperfusion. *J Surg Res* 1994; **56**: 571-578
21 **Yao Y**, Yu Y, Chen J. The effect of intestinal ischemia/reperfusion on increased sensitivity to endotoxin and its potential mechanism. *Zhonghua Zhengxing Shaoshang Waike Zazhi* 1999; **15**: 301-304
22 **Olanders K**, Sun Z, Börjesson A, Dib M, Andersson E, Lasson A, Ohlsson T, Andersson R. The effect of intestinal ischemia and reperfusion injury on ICAM-1 expression, endothelial barrier function, neutrophil tissue influx, and protease inhibitor levels in rats. *Shock* 2002; **18**: 86-92
23 **Ishii H**, Ishibashi M, Takayama M, Nishida T, Yoshida M. The role of cytokine-induced neutrophil chemoattractant-1 in neutrophil mediated remote lung injury after intestinal ischaemia/reperfusion in rats. *Respirology* 2000; **5**: 325-331
24 **Winterbourn CC**, Kettle AJ. Biomarkers of myeloperoxidase-derived hypochlorous acid. *Free Radic Biol Med* 2000; **29**: 403-409
25 **Sener G**, Kabasakal L, Yüksel M, Gedik N, Alican Y. Hepatic fibrosis in biliary-obstructed rats is prevented by Ginkgo biloba treatment. *World J Gastroenterol* 2005; **11**: 5444-5449
26 **Gulec M**, Iraz M, Yilmaz HR, Ozyurt H, Temel I. The effects of ginkgo biloba extract on tissue adenosine deaminase, xanthine oxidase, myeloperoxidase, malondialdehyde, and nitric oxide in cisplatin-induced nephrotoxicity. *Toxicol Ind Health* 2006; **22**: 125-130
27 **Clostre F**. Ginkgo biloba extract (EGb 761). State of knowledge in the dawn of the year 2000. *Ann Pharm Fr* 1999; **57** Suppl 1: S18-S88
28 **Lagrue G**, Behar A, Kazandjian M, Rahbar K. Idiopathic cyclic edema. The role of capillary hyperpermeability and its correction by Ginkgo biloba extract. *Presse Med* 1986; **15**: 1550-1553
29 **Requena JR**, Fu MX, Ahmed MU, Jenkins AJ, Lyons TJ, Thorpe SR. Lipoxidation products as biomarkers of oxidative damage to proteins during lipid peroxidation reactions. *Nephrol Dial Transplant* 1996; **11** Suppl 5: 48-53
30 **Cuzzocrea S**, Mazzon E, Dugo L, Caputi AP, Aston K, Riley DP, Salvemini D. Protective effects of a new stable, highly active SOD mimetic, M40401 in splanchnic artery occlusion and reperfusion. *Br J Pharmacol* 2001; **132**: 19-29
31 **Khanna A**, Rossman JE, Fung HL, Caty MG. Attenuated nitric oxide synthase activity and protein expression accompany intestinal ischemia/reperfusion injury in rats. *Biochem Biophys Res Commun* 2000; **269**: 160-164
32 **Virlos IT**, Inglott FS, Williamson RC, Mathie RT. Differential expression of pulmonary nitric oxide synthase isoforms after intestinal ischemia-reperfusion. *Hepatogastroenterology* 2003; **50**: 31-36
33 **Suzuki Y**, Deitch EA, Mishima S, Lu Q, Xu D. Inducible nitric oxide synthase gene knockout mice have increased resistance to gut injury and bacterial translocation after an intestinal ischemia-reperfusion injury. *Crit Care Med* 2000; **28**: 3692-3696
34 **Pryor WA**, Squadrito GL. The chemistry of peroxynitrite: a product from the reaction of nitric oxide with superoxide. *Am J Physiol* 1995; **268**: L699-L722
35 **Varga E**, Bodi A, Ferdinandy P, Droy-Lefaix MT, Blasig IE, Tosaki A. The protective effect of EGb 761 in isolated ischemic/reperfused rat hearts: a link between cardiac function and nitric oxide production. *J Cardiovasc Pharmacol* 1999; **34**: 711-717
36 **Kobuchi H**, Packer L. Bio-normalizer modulates interferon-gamma-induced nitric oxide production in the mouse macrophage cell line RAW 264.7. *Biochem Mol Biol Int* 1997; **43**: 141-152
37 **Marcocci L**, Maguire JJ, Droy-Lefaix MT, Packer L. The nitric oxide-scavenging properties of Ginkgo biloba extract EGb 761. *Biochem Biophys Res Commun* 1994; **201**: 748-755
38 **Park YM**, Won JH, Yun KJ, Ryu JH, Han YN, Choi SK, Lee KT. Preventive effect of Ginkgo biloba extract (GBB) on the lipopolysaccharide-induced expressions of inducible nitric oxide synthase and cyclooxygenase-2 via suppression of nuclear factor-kappaB in RAW 264.7 cells. *Biol Pharm Bull* 2006; **29**: 985-990

S- Editor Liu Y **L- Editor** Zhu LH **E- Editor** Liu WF

PO Box 2345, Beijing 100023, China
www.wjgnet.com
wjg@wjgnet.com

World J Gastroenterol 2007 January 14; 13(2): 306-309
World Journal of Gastroenterology ISSN 1007-9327

CASE REPORT

Are heat stroke and physical exhaustion underestimated causes of acute hepatic failure?

Kilian Weigand, Carina Riediger, Wolfgang Stremmel, Christa Flechtenmacher, Jens Encke

Kilian Weigand, Carina Riediger, Wolfgang Stremmel, Jens Encke, Department of Gastroenterology and Hepatology, Medicine Ⅳ, University of Heidelberg, 69120 Heidelberg, Germany
Christa Flechtenmacher, Department of Pathology, University of Heidelberg, 69120 Heidelberg, Germany
Correspondence to: Kilian Weigand, Universitaetsklinikum Heidelberg, Medizin Ⅳ, Abteilung fuer Gastroenterologie, Im Neuenheimer Feld 410, Heidelberg D-69120, Germany. kilian.weigand@med.uni-heidelberg.de
Telephone: +49-6221-5638747 Fax: +49-6221-565361
Received: 2006-04-28 Accepted: 2006-10-27

Abstract

While cardiopulmonary symptoms are common in patients undergoing classical or, due to physical exercise, exertional heat stroke, the failure of other organs is a rarely described phenomenon. Here we present two cases of acute hepatic failure, one due to classic heat shock, while the other occurred while the patient was doing a marathon-type running. Both cases presented with very high transaminases and significantly elevated international normalized ratio (INR). No other causes for liver failure could be identified but physical exhaustion and hyperthermia.

Key words: Heat stroke; Acute hepatic failure; Heat shock; Liver failure; Hyperthermia

Weigand K, Riediger C, Stremmel W, Flechtenmacher C, Encke J. Are heat stroke and physical exhaustion underestimated causes of acute hepatic failure? *World J Gastroenterol* 2007; 13(2): 306-309

http://www.wjgnet.com/1007-9327/13/306.asp

INTRODUCTION

Heat stroke is a life-threatening condition that can be fatal if proper assessment and treatment are not initiated rapidely[1,2]. A variable degree of organ involvement is present in heat stroke[3]. At the beginning, there is heat exhaustion, characterized by nonspecific symptoms such as malaise, headache and nausea. Untreated this illness results in heat stroke, a serious disease possibly involving central nervous system dysfunction, rhabdomyolysis, arrhythmias, disseminated intravascular coagulation and hepatic failure, not uncommon followed by death[4].

The current model of heat stroke favors hyperthermia as trigger, while endotoxaemia drives the disease. However, the pathology is not fully understood[2]. In athletes undergoing intense training a variety of immune and gastrointestinal disturbances can occur. We here describe two completely different causes of heat stroke resulting in acute and severe liver failure as leading symptom.

CASE REPORTS

Case one

A 23-year old male was delivered to our intensive care unit (ICU) after he collapsed running a half-marathon. He had no former medical history and was in good physical shape. He took no medication and was negative for an obtained drug screening. By admission he felt fatigue and complained about nausea and vomiting. The laboratory results showed elevated levels of 12427 U/L creatinine kinase (CK) (normal < 145 U/L), 5821 U/L lactate dehydrogenase (LDH) (normal < 248 U/L), 8378 U/L aspartate aminotransferase (AST) (normal < 31 U/L), 9765 U/L alanine aminotransferase (ALT) (normal < 34 U/L), 40 mg/dL bilirubin (normal < 1.0 mg/dL) and 2.8 international normalized ratio (INR) (normal < 1.2) (Figure 1). The other basic laboratory parameters were within normal range. The patient was monitored and treated with intravenous fluid (5 to 6 liters per 24 h).

To exclude other causes for acute hepatic failure, virus serologies were obtained. Besides positive IgG of hepatitis A and B due to immunization, there were no serological findings for acute or chronic hepatitis A, B, C or human immunodeficiency virus (HIV). Also acute infection with cytomegaly virus (CMV), herpes simplex virus (HSV) or epstein-barr virus (EBV) was ruled out. The autoimmune antibodies (ANA, ANCA, SMA, LKM, mitochondrial antibodies) were also negative. In addition, protein electrophoresis gave no pathologic findings. Serum levels for alpha-1-antitrypsin, iron and transferrin were within normal range. Ferritin was raised to 29490 μg/L (normal 30-300 μg/L), probably due to destruction of hepatocytes. Because of lowered caeruloplasmin (serum) and copper (serum and 24-h urine) levels, a liver biopsy was performed. The histology showed intact architecture of the lobules. Portal fields showed no signs of fibrosis or inflammatory infiltration. Accentuated centrolobular

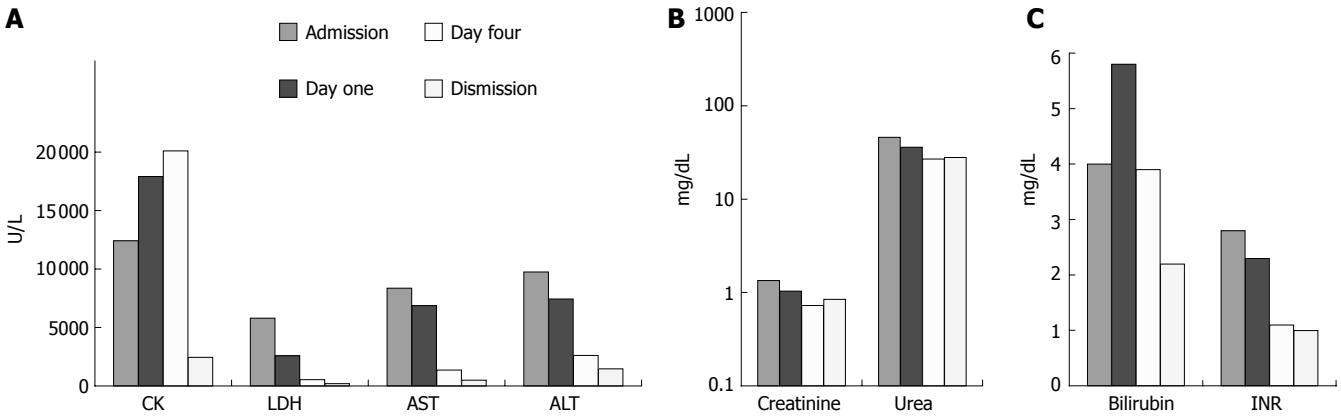

Figure 1 Basic laboratory parameters of a 23-yr-old male patient presenting with liver failure after exertional heat stroke. **A**: Creatinine kinase (CK), lactate dehydrogenase (LDH), aspartate aminotransferase (AST) and alanine amino-transferase (ALT) at admission and during progression in a linear scale; **B**: Creatinine and urea in a logarithmic scale; **C**: Bilirubin and international normalized ratio (INR) in a linear scale.

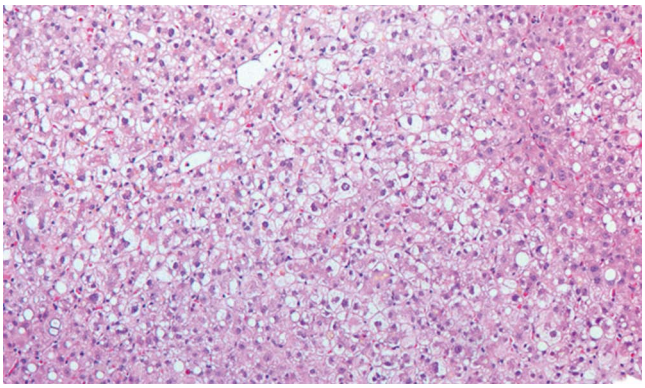

Figure 2 HE-staining of a liver biopsy derived from a 23-yr-old male presenting with liver failure after exertional heat stroke. Microscopy showed liver tissue with intact architecture of the lobules. Portal fields showed no signs of fibrosis or inflammatory infiltration. Accentuated centrolobular necrosis was accompanied with fatty degeneration of hepatocytes. Additionally, focal bile inclusions were found without Mallory bodies, iron debris and atypical cellular proliferation. Altogether, the morphological picture does not fit acute Wilson's disease, hemochromatosis or infection, but ischemic liver disease.

necrosis and fatty degeneration of hepatocytes were seen. Additionally, focal bile inclusions were found. Altogether, the morphological picture did not fit acute Wilson's disease, hemochromatosis or infection, but ischemic liver disease (Figure 2).

Abdominal ultrasound including duplex sonography, besides a slight hepatosplenomegaly, demonstrated no abnormal findings. To exclude a cardiac reason for the patient's collapse, both a 24-h electrocardiogram and an echocardiogram showed normal heart function and structure.

The patient stayed in the ICU for 5 d, while the laboratory results were declining (Figure 1) (208 U/L LDH, 676 U/L AST, 1438 U/L ALT, 2.2 mg/dL bilirubin, 1.1 INR). Initially, the CK did rise to levels higher than 30000 U/L, but on d 5 after admission it dropped to 4948 U/L. Renal function was normal at all times due to high fluid application and keeping the urine-pH above 7.5. On d 6, the patient was transferred from ICU to a regular ward in good health and mostly recompensated laboratory parameters for further monitoring. At follow-up one week later the patient was in good health and showed normal laboratory parameters.

Case two

A 46-year old male was delivered to our ICU after he had collapsed due to heat shock. His working place was below a roof window and it was a very hot day. In the after-noon, after working all day, he finally suffered from a seizure and was found cardiorespiratory stable but unconscious with his temperature of 42℃.

By admission laboratory findings demonstrated a clinical picture of acute hepatic failure with very high levels of transaminases (15929 U/L AST, 10050 U/L ALT), bilirubin (1.9 mg/dL) and malfunction in liver synthesis (1.9 INR) (Figure 3). Further laboratory parameters showed an elevated LDH (15831 U/L), CK (6452 U/L), Troponin T (1.18 μg/L, normal < 0.03 μg/L), creatinine (1.78 mg/dL, normal < 1.3 mg/dL) and urea (50 mg/dL, normal < 45 mg/dL). All other basic parameters were within normal range.

Besides a seizure in 1989 due to an intra-cerebral bleeding, the patient had no past medical history. We started to treat him with intravenous fluid (5 to 6 liters per 24 h). Because of acute renal dysfunction he was treated two times with hemodialysis.

To exclude other reasons for acute hepatic failure he received further examinations. An abdominal ultrasound including duplex sonography showed no alterations. No pathologic serum markers for alpha1-antitrypsin, caeruloplasmin, copper, iron, ferritin, AFP or autoimmune antibodies (ANA, ds-DNA, ANCA, LKM, SMA, mitochondrial antibodies) were observed. Virus serologies were positive for HSV-IgG, VZV-IgG, EBV-IgG, but negative for IgM, as a parameter for acute infection. Hepatitis A was IgG positive due to immunization. All other infectious causes tested, like CMV, influenza A and B, hanta virus, hepatitis B and C, HIV and leptospirosis, were negative. Additionally, an obtained drug screening was negative.

The patient was further monitored in our ICU and received treatment of cooling and intravenous fluid. The

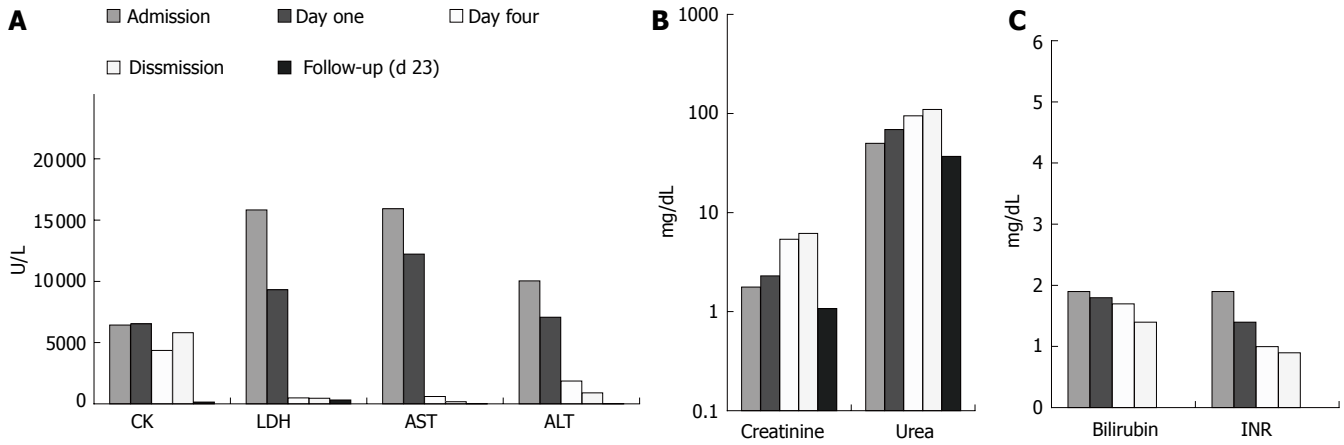

Figure 3 Basic laboratory parameters of a 46-year old male presenting with liver failure due to classic heat stroke. **A**: Creatinine kinase (CK), lactate dehydrogenase (LDH), aspartate aminotransferase (AST) and alanine amino-transferase (ALT) at admission and during progression in a linear scale; **B**: Creatinine and urea in a logarithmic scale; **C**: Bilirubin and international normalized ratio (INR) in a linear scale.

patient regained consciousness within 36 h after therapy was started and the abnormal laboratory parameters excluding creatinine and urea, returned slowly to normal within a few days. Because of the elevated myocardial enzymes at admission, an echocardiogram and an electro cardiogram (ECG) were obtained. While the ECG was normal, the echocardiogram showed a very mild hypertrophic obstructive cardiomyopathy (HOCM), unknown so far, but a good right and left ventricular function and no contraction disorders of the myocardium. Also, the patient did not suffer from chest pain or dyspnoea at all times.

Six days after admission the patient had lowered laboratory parameters (Figure 3) (512 U/L LDH, 620 U/L AST, 1889 U/L ALT, 1.7 mg/dL bilirubin, 4376 U/L CK, 0.35 μg/L TNT, 1.0 INR), but still high urea and creatinine levels. He was transferred to a nephrology ward where he continued to get hemodialysis, until the kidney function was resolved. Twenty-three days later he presented again at the outpatient clinic with almost normalized laboratory parameters (Figure 3).

DISCUSSION

Described in this paper are two cases of acute hepatic failure due to physical exhaustion/heat shock. While the first patient had no other organ disorders, the second suffered from multi-organ failure including heart, kidneys and brain, and mainly liver malfunction.

It has been rarely reported that physical exhaustion can lead to hyperthermia, coma, rhabdomyolysis and organ failure[5,6]. Classic heat stroke however, is a more common disease with the life-threatening core body temperature higher than 40.5℃. Its associated clinical manifestations are exsiccosis, fatigue, nausea, vomiting, disorientation and coma[7]. Possible complications are cardiopulmonary dysfunction, acid-base or electrolyte disorders, as well as failure of other organs. Recently, a study demonstrated that 21 of 28 patients with heat stroke developed organ dysfunctions. Acute respiratory distress syndrome is the frequently encountered complication[8], while liver malfunction has not been reported. Our two cases indicate that liver failure may be more often than expected. Liver failure due to heat stroke begins with the same common symptoms, like nausea and exhaustion. When collapse, hyperthermia and multi-organ failure occur, it may be diagnosed[9], indicating that a rise in liver enzymes is an important predictive factor[8]. In our cases, liver failure was the leading symptom, causing cerebral disorders and renal dysfunction. Liver transplantation is the only possible treatment for severe hepatic damage. Recently, the first long-term follow-up of liver transplantation for hepatic failure due to heat stroke has been reported[10].

The recommended treatment for such severe cases is fluid application and rebalancing acid-base and electrolyte disorders as well as close monitoring, except for liver transplantation. Other treatments, like application of human umbilical cord blood cells as described in rats, to lower intracerebral changes due to heat stroke, remain speculative and under experiment at present[11].

The mechanism underlying liver failure in heath shock patients is not totally understood. An earlier study showed that systemic or intrahepatic circulatory disturbance as seen in disseminated intravascular coagulation (DIC), may be the cause[12]. In one case, a portal vein thrombosis has been found[9], which could result in liver and other organ failure. However, in our cases, the duplex sonography showed no big vessel thrombosis, whereas DIC could not be excluded. Although DIC could explain the raised liver enzymes in our second case, the cardiac problems due to HOCM contributing to the liver failure could not be ruled out. Nevertheless, we think that a cardiac reason is unlikely, because the right and left ventricular function of the patients was excellent at all times.

It has been reported that the intracranial pressure rises and cerebral ischemia occurs due to lower arterial pressure during heat stroke, resulting in lower blood flow and intracranial pO_2[11]. It remains for further study if the same mechanism is responsible for liver damage. If so, this could result in a therapeutic application of vasoactive substances to increase intrahepatic blood flow in patients with severe liver damage after heat stroke.

Another review published in 2004 has discussed a possible function of immune response in organ failure

of patients suffering from hyperthermia during physical exercise[13]. Since a reduced splanchnic blood flow which can result in gastrointestinal barrier dysfunction and increased permeability can be measured, endotoxin causing immune reactions could enter internal organs and drive organ damage. This may lead to the assumption that application of immune suppressive medication could be tested.

Besides liver malfunction, renal problems were the leading cause of liver failure in our cases. This is most likely explained by exsiccosis. Nevertheless, it is also possible that the high CK is an additionally cause of renal disorder.

In conclusion, patients with hepatic failure due to physical exhaustion or heat stroke should be closely monitored and severe problems like bleeding, hepatic coma and acute renal malfunction should be recognized as early as possible.

REFERENCES

1 **Casa DJ**, Armstrong LE, Ganio MS, Yeargin SW. Exertional heat stroke in competitive athletes. *Curr Sports Med Rep* 2005; **4**: 309-317

2 **Lim CL**, Mackinnon LT. The roles of exercise-induced immune system disturbances in the pathology of heat stroke: the dual pathway model of heat stroke. *Sports Med* 2006; **36**: 39-64

3 **Sucholeiki R**. Heatstroke. *Semin Neurol* 2005; **25**: 307-314

4 **Glazer JL**. Management of heatstroke and heat exhaustion. *Am Fam Physician* 2005; **71**: 2133-2140

5 **Lepape A**, Sarron C, Grozel JM, Perdrix JP, Banssillon V. A severe form of heat stroke in a long-distance runner. *Ann Fr Anesth Reanim* 1986; **5**: 441-444

6 **Bruguera M**. Liver and sports. *Med Clin* (Barc) 2004; **122**: 111-114

7 **Yeo TP**. Heat stroke: a comprehensive review. *AACN Clin Issues* 2004; **15**: 280-293

8 **Varghese GM**, John G, Thomas K, Abraham OC, Mathai D. Predictors of multi-organ dysfunction in heatstroke. *Emerg Med J* 2005; **22**: 185-187

9 **Scobie BA**. Gastrointestinal emergencies with marathon-type running: omental infarction with pancreatitis and liver failure with portal vein thrombosis. *N Z Med J* 1998; **111**: 211-212

10 **Takahashi K**, Chin K, Ogawa K, Kasahara M, Sakaguchi T, Hasegawa S, Sumi K, Nakamura T, Tamaki A, Mishima M, Nakamura T, Tanaka K. Living donor liver transplantation with noninvasive ventilation for exertional heat stroke and severe rhabdomyolysis. *Liver Transpl* 2005; **11**: 570-572

11 **Chen SH**, Chang FM, Tsai YC, Huang KF, Lin MT. Resuscitation from experimental heatstroke by transplantation of human umbilical cord blood cells. *Crit Care Med* 2005; **33**: 1377-1383

12 **Irie H**, Mori W. Fatal hepatic necrosis after shock. *Acta Pathol Jpn* 1986; **36**: 363-374

13 **Lambert GP**. Role of gastrointestinal permeability in exertional heatstroke. *Exerc Sport Sci Rev* 2004; **32**: 185-190

S- Editor Wang GP **L- Editor** Wang XL **E- Editor** Ma WH

PO Box 2345, Beijing 100023, China
www.wjgnet.com
wjg@wjgnet.com

World J Gastroenterol 2007 January 14; 13(2): 310-312
World Journal of Gastroenterology ISSN 1007-9327

CASE REPORT

Jejuno-jejunal invagination due to intestinal melanoma

Giuseppe Resta, Gabriele Anania, Federico Messina, Damiano de Tullio, Gloria Ferrocci, Federico Zanzi, Davide Pellegrini, Rocco Stano, Giorgio Cavallesco, Gianfranco Azzena, Savino Occhionorelli

Giuseppe Resta, Gabriele Anania, Federico Messina, Damiano de Tullio, Gloria Ferrocci, Federico Zanzi, Davide Pellegrini, Rocco Stano, Giorgio Cavallesco, Gianfranco Azzena, Savino Occhionorelli, Università degli Studi di Ferrara, Dipartimento di Scienze Chirurgiche Anestesiologiche e Radiologiche, Istituto di Clinica Chirurgica, Arcispedale "S. Anna", Ferrara, Italy

Correspondence to: Dr. Federico Messina, Università degli Studi di Ferrara, Dipartimento di Scienze Chirurgiche Anestesiologiche e Radiologiche, Istituto di Clinica Chirurgica. Arcispedale "S. Anna", Corso Giovecca, Ferrara 203-44100, Italy. f.messina@email.it
Telephone: +39-532-236316 **Fax:** +39-532-209819
Received: 2006-10-22 **Accepted:** 2006-12-07

Abstract

Cutaneous melanoma is one of the most studied neoplastic lesions in biology and clinical oncology. It has been well documented that this type of neoplasm presents a high metastatic rate, and is able to involve nearly every tissue. Non-cutaneous melanoma represents an unusual pattern of melanoma, and the small intestine is an uncommon anatomic localization. Herein we report an extremely rare clinical case of a young woman affected by a bleeding jejunal melanoma, whose early clinical presentation was an intestinal invagination.

Key words: Cutaneous melanoma; Intestinal obstruction; Intestinal melanoma; Invagination

Resta G, Anania G, Messina F, de Tullio D, Ferrocci G, Zanzi F, Pellegrini D, Stano R, Cavallesco G, Azzena G, Occhionorelli S. Jejuno-jejunal invagination due to intestinal melanoma. *World J Gastroenterol* 2007; 13(2): 310-312

http://www.wjgnet.com/1007-9327/13/310.asp

INTRODUCTION

Cutaneous melanoma is a malignancy characterized by a high mortality rate. It can metastasize to all organs, although the gastrointestinal tract is an unusual metastatic localization. In 50% of cutaneous melanomas, in fact, metastases in the gastroenteric tract are diagnosed upon autopsy, and only in 5% of cases, they are diagnosed clinically[1,2]. Intestinal metastases of cutaneous melanomas are linked to a baleful prognosis, with a survival average of 6-10 mo after surgery[3,4].

Many studies have demonstrated that only surgery can lead to a control of chronic anemia related to intestinal melanoma bleeding and resolution of the episodes of intestinal sub-occlusion. Surgery on melanoma metastases moreover, can guarantee an increase of survival, in addition to an excellent improvement in quality of life[5-7]. Intestinal metastases represent the occurrence of an occult skin melanoma in only 3%-5% of cases, in which a spontaneous regression of the cutaneous lesion happens[8]. Intestinal metastasis bleeding is extremely rare[9,10].

In order to add more information about surgical presentation of intestinal occult melanoma herein we describe a case of a young woman affected by bloody jejunal metastasis of occult cutaneous melanoma, complicated by intestinal invagination-an extremely rare case in the adult population.

CASE REPORT

A 45-year old woman complained of continual nausea and biliary vomiting, associated with a weight loss of 5 kg. Due to localized abdominal pain, mainly in the right hypochondrium and episodes of hematemesis, the patient was admitted to our hospital. Blood tests revealed sideropenic anemia with 81 g/L haemoglobin, serum iron 100 pg/L, ferritin 23 μg/L, and fecal occult blood test (FOBT) positive in three fecal samples. A gastroscopy was performed, which showed the presence of grade I esophagitis, moderate hiatal hernia and chronic erosive gastritis. The colonoscopy was incomplete due to the presence of colic stools. Abdominal ultrasonography highlighted a distension of the intestinal loops without signs of parenchymatous organ pathology. The patient therefore received an abdominal CT, which suggested the presence of a gastric distension with duodenum-jejunal distension and the presence of a jejunal loop with thickened walls. A second hyperdense image inside the intestinal lumen, forming a target-shaped image was also present: typical feature of intestinal invagination (Figure 1). We therefore decided to proceed to urgent surgical operation after blood transfusion. During surgery, intra-peritoneal fluid was found and samples were removed for cytological testing. Invagination at the third jejunal loop (Figure 2) was evidenced. The presence of hypertrophic lymphatic tissue with intestinal mesenteric lymphoadenomegalia was also present. Manual resolution of the invagination was carried out. This procedure highlighted the presence of a hyperchromic ulcerated neo-

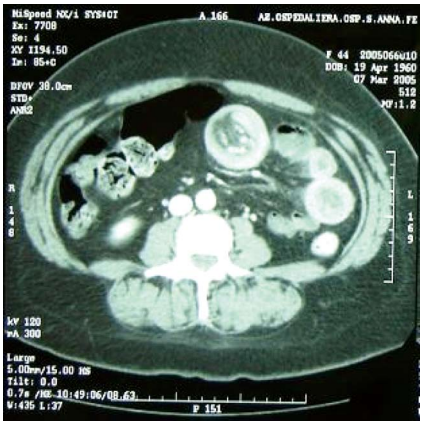

Figure 1 Duodenum-jejunal distension and the presence of a jejunal loop with thickened walls, with a second hyper-dense image inside the same lumen, forming a target-shaped aspect characteristic of intestinal invagination.

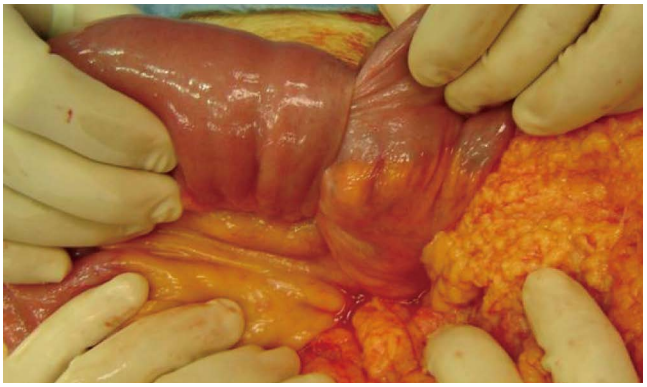

Figure 2 Invagination at the third jejunal loop.

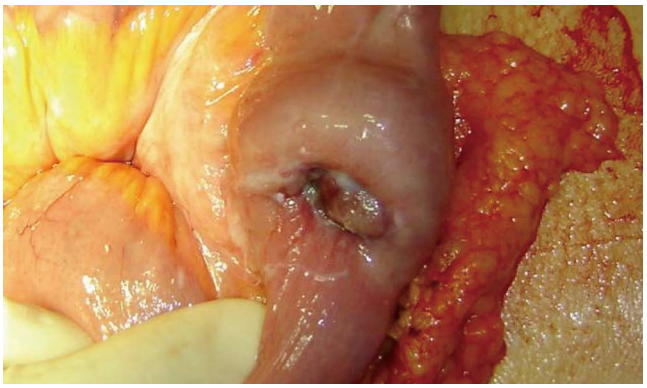

Figure 3 Presence of a hyperchromic ulcerated neoformation, with signs of recent bleeding of the serosa.

formation, with obvious signs of recent bleeding coming from the serosa (Figure 3).

Thorough exploration of the abdominal cavity did not detect further replicative lesions. Resection of the third jejunal loop containing the neoformations and the whole underlying mesentery with its lymph nodes, was performed. The intestinal continuity was restored through a latero-lateral jejuno-jejunal anastomosis.

The post-operative course was uneventful and the patient was discharged after 10 postoperative days. The definitive histological examination showed the presence of an intestinal metastasis of cutaneous melanoma of unknown origin (Figures 4 and 5). The patient was then referred to an oncologic centre for the search of the primary melanoma localization. At three, six months and a year follow-up, the patient is alive and no signs of skin melanoma have been detected.

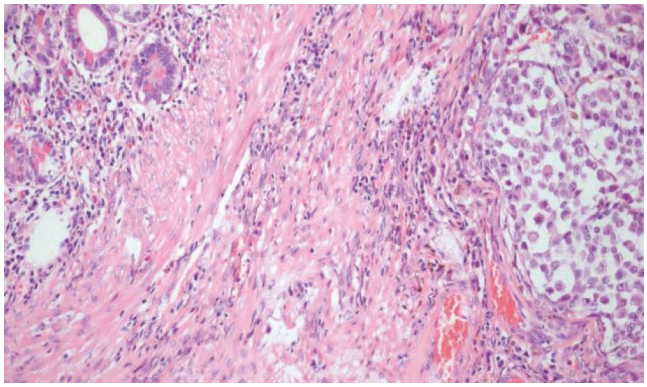

Figure 4 Ileal wall infiltrated with metastatic melanomatous cells with nuclear pseudoinclusions and nucleoli, in nest and trabecular arrangement (HE x 10).

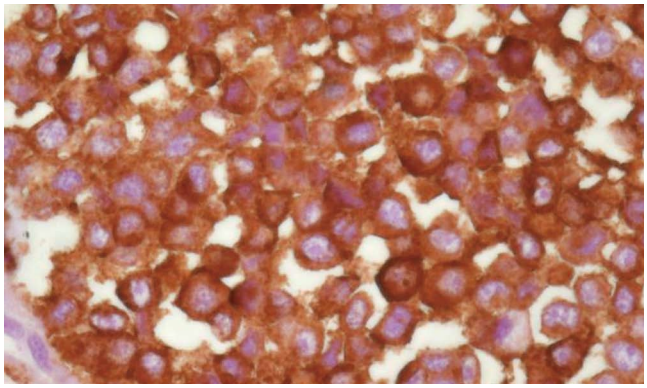

Figure 5 Strong positivity at immunohistochemical assay for HMB45.

DISCUSSION

The peculiar rarity of this clinical case represents the principal reason for our interest. In spite of the clinical manifestation and the diagnostic-therapeutic approach adopted, this case presents many conditions that have been previously poorly documented in international literature.

Our patient presented a chronic anemia and repeated biliary vomiting that were related to the erosive gastritis and esophagitis identified by the gastroscopy, even if this did not necessarily exclude chronic bleeding from neoplastic lesions. The pre-operative CT scan of parajejunal lymphoadenomegalia prompted us to suspect the presence of a neoplastic lesion causing the jejunal invagination. Jejunal invagination in an adult, in fact, can cause 1%-3% of surgically treated intestinal occlusion but is mainly due to peritoneal adhesion or to the presence of intestinal anastomosis[11] and less frequently to a neoplasm. Melanoma intestinal metastasis is clinically diagnosed only in 3%-5% of cases, and is usually found to affect the stomach or the colon. Jejunal location is much less frequent[12] and, if present, does not show clinical signs till diagnosed at autopsy. A diagnosis based on the finding of metastatic

lesions, without identification of the primary cutaneous source, as described in our report, is carried out in only 3% of melanomas. Even if the etiology of primary gastrointestinal melanomas remain undefined, some authors suggest that primary gastrointestinal melanomas are derived from melanoblastic cells of the neural crest which, migrating through the omphalomesenteric canal or APUD cells, reach the intestinal tract, undergoing neoplastic transformation[13]. Non-cutaneous melanomas represent a rare form of melanoma. In a review of 84 836 cases of melanoma, 91.2% were cutaneous, 5.2% ocular, 2.2% of unknown primary site and only 1.3% of gastrointestinal mucosa[14]. Melanomas that arise on mucosal surfaces appear to be more aggressive and are associated with worse prognosis than cutaneous melanomas. The poorer prognosis may be related to the delay in diagnosis, to their more aggressive behaviour, or to earlier dissemination because of the rich lymphatic and vascular supply of the gastrointestinal mucosa[15,16].

Our case shows that the presence of an early complication due to intestinal occlusion, through a sequential and appropriate instrumental diagnostic evaluation, gave us the opportunity to identify a rare melanotic lesion. Moreover, the right surgical approach has given us the opportunity to improve the length and quality of the life of this unlucky patient.

REFERENCES

1 **Reintgen DS**, Thompson W, Garbutt J, Seigler HF. Radiologic, endoscopic, and surgical considerations of melanoma metastatic to the gastrointestinal tract. *Surgery* 1984; **95**: 635-639

2 **de la Monte SM**, Moore GW, Hutchins GM. Patterned distribution of metastases from malignant melanoma in humans. *Cancer Res* 1983; **43**: 3427-3433

3 **Ihde JK**, Coit DG. Melanoma metastatic to stomach, small bowel, or colon. *Am J Surg* 1991; **162**: 208-211

4 **Caputy GG**, Donohue JH, Goellner JR, Weaver AL. Metastatic melanoma of the gastrointestinal tract. Results of surgical management. *Arch Surg* 1991; **126**: 1353-1358

5 **Khadra MH**, Thompson JF, Milton GW, McCarthy WH. The justification for surgical treatment of metastatic melanoma of the gastrointestinal tract. *Surg Gynecol Obstet* 1990; **171**: 413-416

6 **Agrawal S**, Yao TJ, Coit DG. Surgery for melanoma metastatic to the gastrointestinal tract. *Ann Surg Oncol* 1999; **6**: 336-344

7 **Ollila DW**, Essner R, Wanek LA, Morton DL. Surgical resection for melanoma metastatic to the gastrointestinal tract. *Arch Surg* 1996; **131**: 975-979; 979-980

8 **Reintgen DS**, McCarty KS, Woodard B, Cox E, Seigler HF. Metastatic malignant melanoma with an unknown primary. *Surg Gynecol Obstet* 1983; **156**: 335-340

9 **Loualidi A**, Spooren PF, Grubben MJ, Blomjous CE, Goey SH. Duodenal metastasis: an uncommon cause of occult small intestinal bleeding. *Neth J Med* 2004; **62**: 201-205

10 **Wulf V**, Schröder HJ. Metastasis to the small intestine of malignant melanoma as a rare cause of intestinal hemorrhage. *Zentralbl Chir* 1994; **119**: 515-516

11 **Begos DG**, Sandor A, Modlin IM. The diagnosis and management of adult intussusception. *Am J Surg* 1997; **173**: 88-94

12 **Pacovský Z**, Fait V. Distant metastasis of malignant melanoma in the small intestine. *Rozhl Chir* 1992; **71**: 424-428

13 **Elsayed AM**, Albahra M, Nzeako UC, Sobin LH. Malignant melanomas in the small intestine: a study of 103 patients. *Am J Gastroenterol* 1996; **91**: 1001-1006

14 **Chang AE**, Karnell LH, Menck HR. The National Cancer Data Base report on cutaneous and noncutaneous melanoma: a summary of 84,836 cases from the past decade. The American College of Surgeons Commission on Cancer and the American Cancer Society. *Cancer* 1998; **83**: 1664-1678

15 **Sachs DL**, Lowe L, Chang AE, Carson E, Johnson TM. Do primary small intestinal melanomas exist? Report of a case. *J Am Acad Dermatol* 1999; **41**: 1042-1044

16 **Lagoudianakis EE**, Genetzakis M, Tsekouras DK, Papadima A, Kafiri G, Toutouzas K, Katergiannakis V, Manouras A. Primary gastric melanoma: a case report. *World J Gastroenterol* 2006; **12**: 4425-4427

S- Editor Wang GP **L- Editor** Zhu LH **E- Editor** Liu WF

PO Box 2345, Beijing 100023, China
www.wjgnet.com
wjg@wjgnet.com

World J Gastroenterol 2007 January 14; 13(2): 313-315
World Journal of Gastroenterology ISSN 1007-9327

CASE REPORT

An unusual cause of cholecystitis: Heterotopic pancreatic tissue in the gallbladder

Gülsüm Özlem Elpek, Sevgi Bozova, Gökben Yıldırım Küpesiz, Mehmet Öğüş

Gülsüm Özlem Elpek, Sevgi Bozova, Gökben Yıldırım Küpesiz, Akdeniz University, Medical School, Department of Pathology, Yeni Tıp, Dekanlık, 07070, Antalya, Turkey
Mehmet Öğüş, Akdeniz University, Medical School, Department of General Surgery, Yeni Tıp, Dekanlık, 07070, Antalya, Turkey
Correspondence to: Gülsüm Özlem Elpek, Akdeniz University, Medical School, Yeni Tıp, Dekanlık, 07070, Antalya, Turkey. elpek@akdeniz.edu.tr
Telephone: +90-242-2274488 Fax: +90-242-2274488
Received: 2006-09-29 Accepted: 2006-12-05

Abstract

Gallbladder localization of heterotopic pancreas (HP) is uncommon and very rarely gives rise to symptoms. Herein we report a case of HP found in the gallbladder neck presented with signs and symptoms of cholecystitis. The patient was a 40-year old male, suffering from epigastric pain, abdominal fullness and fever. On physical examination, the right upper abdomen was tender with a positive Murphy's sign. Ultrasonographic examination showed a hydropic gallbladder without stones and he underwent a cholecystectomy. Pathological examination revealed an intramural nodule (9 mm) in the neck region which is consisted of acini, ducts and islet cells of an aberrant pancreatic tissue. Although HP is encountered rarely in the gallbladder and is found incidentally during pathological studies, this case emphasizes that HP might cause symptoms and present clinically as cholecystitis. For this reason, in patients presenting with symptomatic gallbladder diseases, including cholecystitis without any other pathology, HP should be taken into consideration before it is diagnosed as "idiopathic".

Key words: Heterotopic tissues; Pancreas; Acalculous cholecystitis; Gallbladder

Elpek GÖ, Bozova S, Küpesiz GY, Öğüş M. An unusual cause of cholecystitis: Heterotopic pancreatic tissue in the gallbladder. *World J Gastroenterol* 2007; 13(2): 313-315

http://www.wjgnet.com/1007-9327/13/313.asp

INTRODUCTION

Heterotopic pancreas (HP) is defined as the presence of pancreatic tissue lying outside its normal location and lacking anatomical or vascular continuity with the pancreas proper[1]. In 85% to 90% of reported cases, HP has been found in stomach, duodenum, upper jejunum, whereas its presence in the gallbladder is very rare[1-3]. Similar to HP of other organs, HP of the gallbladder itself has no clinical importance and is found incidentally in most cases. However, there have been some reports of symptomatic gallbladder disease[4-7]. Herein we report a case of HP in the neck of the gallbladder who presented with clinical findings of cholecystitis.

CASE REPORT

A 40-year old male presented to the hospital with epigastric pain, abdominal fullness and fever three days ago. On physical examination, the right upper abdomen was tender with a positive Murphy's sign. His laboratory data revealed total bilirubin = 1.5 mg/dL, direct bilirubin = 0.8 mg/dL, ALP = 398 U/dL, SGOT = 70 U/dL, SGPT = 60 U/dL, GGT = 90U/dL. Ultrasonographic (US) examination showed a hydropic gallbladder without stones. A cholecystectomy was performed. The macroscopic findings were as follows: gallbladder measuring 80 mm × 50 mm × 40 mm, wall thickness 3-12 mm. In the neck region, a yellowish-white intramural nodule measuring 9 mm × 8 mm × 8 mm was observed. Microscopic examination revealed aberrant pancreatic tissue consisting of acini, ducts and chromogranin A expressing islet cells. No direct connection with the gallbladder lumen was observed (Figure 1). The whole specimen was embedded stepwise for further microscopic evaluation, but any other pancreatic tissue was not detected. The diagnosis was thereby established as chronic cholecystitis with heterotopic pancreas. All symptoms disappeared following cholecystectomy and the patient recovered completely.

DISCUSSION

Although HP is the second most prevalent pancreatic anomaly, the incidence in gastrointestinal tract is estimated to be from 0.55% to 13.7% on autopsy, and 0.2% in laparatomy[6]. Despite the frequent occurrence of HP in the stomach, duodenum and upper jejunum, the gallbladder localization is extremely rare. Since the first publication by Poppi in 1916, only 29 more cases of HP worldwide in the gallbladder have been reported in a review of the literature up to the present[8]. In these cases there is a higher incidence of female patients between 40 and 50 years of age[9]. However, similar to our case, its

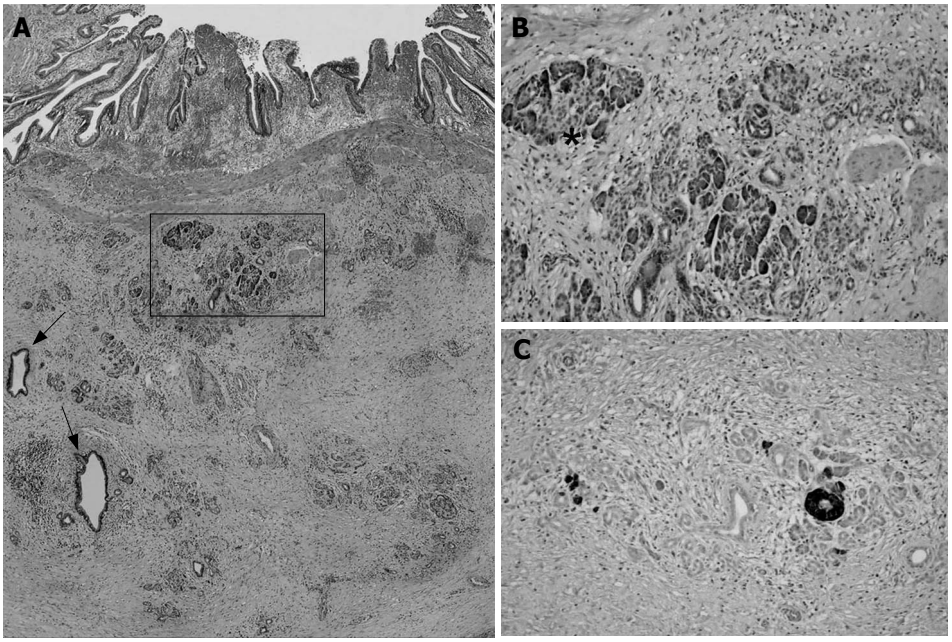

Figure 1 Histological sections of HP showing dilated ducts (arrows, H&E x 100) and acini (**A**), acinar and islet cells (asterisk, H&E x 250) (**B**), and chromogranin A expressing islet cells (Mayer's haematoxylin x 250) (**C**) in submucosa of gallbladder neck.

occurrences have been reported in men. In half of the reported cases, HP is preferentially localized close to the neck of the gallbladder[9]. Parallel to this observation, in our patient HP was located in the neck region.

HP in the gallbladder is very rarely symptomatic. In most reported cases, it is an incidental pathological findings and coexists with gallstones[9,10]. However, there have been some reported symptomatic gallbladder diseases due to HP[4-7]. In one case HP has been found to cause perforation of the gallbladder and lead to peritonitis[5]. Similar to our case, in two cases HP has been found to stimulate cholecystopathy with all symptoms disappearing following cholecystectomy[4,7]. Inceoglu *et al*[6] have reported a case of HP in the cystic duct with hydrops of the gallbladder and chronic pancreatitis of the ectopic tissue. In all cases including the case presented here, because of its rare occurrence as a symptomatic lesion, HP is not taken into consideration in the clinical differential diagnosis. Indeed, as in other organs, the preoperative diagnosis of HP in gallbladder is difficult[10,11]. Symptomatology and clinical findings in most cases suggest gallbladder disease, mainly lithiasis and cholecystitis[9]. It was pointed out that HP located especially in the neck region might prevent bile flow like a stone and cause hydrops of the gallbladder mimicking the clinical findings of these diseases[6]. From this point of view, in our case localization of HP in the neck region might explain the clinical findings of cholecystitis related to hydrops of the gallbladder without cholelithiasis. Recently it was indicated that, despite its high resolution, US is not specific for HP and impossible to distinguish HP from other lesions such as cholesterol polyps, adenoma and carcinoma[9,11]. Parallel to these observations, in our case while US examination revealed a hydropic gallbladder without stones, it failed to detect HP. For these reasons, we suggest that the rare occurrence of HP in the gallbladder and its presence as an incidental finding in cholecystectomy materials do not exclude its consideration in the differential diagnosis of symptomatic gallbladder diseases.

Our histopathological examination revealed a HP constituted of acini, ducts and islet cells, corresponding to the total heterotopia[8]. Although panreatitis may occur in HP, the present case had no histopathological findings of pancreatitis[6].

The origin of heterotopic pancreatic tissue is controversial but two theories have been proposed. One suggests that pancreatic tissue is separated from the main pancreas during embryonic rotation[5,6], the other is that during the growth of the ventral pancreatic bud a proportion is transported by the longitudinal growth of the intestines[5,6]. Therefore its presence in the gallbladder might indicate derivation from the ventral diverticulum. On the other hand, the site of organ/tissue formation is also determined by strictly coordinated developmental programs involving interplay between extracellular signaling and intracellular transcriptional factor networks. It has been demonstrated that in mammals the developmental decisions according to the state of the immediate neighbors are controlled through the Notch signaling system[12]. Several studies indicate that this system also plays an essential role in the precise orchestration of cell-fate decisions in the developing pancreas[13]. Hes-1 (Hairy enhancer of split), a main effector of Notch signaling is required for region-appropriate specification of the pancreas in the developing foregut endoderm[14]. In experimental studies, ectopic pancreas formation has been observed in Hes-1 knockout mice and the plasticity of endodermal progenitors of the gut, bile duct, and pancreas has been suggested[14,15]. In light of these observations, we consider that besides two proposed theories, abnormalities in the Notch signaling system, especially in Hes-1 expression during embryogenesis may also contribute to the formation of HP of the gallbladder.

In conclusion, HP of the gallbladder is a very rare condition which is diagnosed incidentally, but may cause clinical symptoms such as cholecystitis and should be taken into consideration in patients with symptomatic

gallbladder disease without any other specific clinical and laboratory findings before it is diagnosed as idiopathic.

REFERENCES

1 **Armstrong CP**, King PM, Dixon JM, Macleod IB. The clinical significance of heterotopic pancreas in the gastrointestinal tract. *Br J Surg* 1981; **68**: 384-387

2 **Dolan RV**, ReMine WH, Dockerty MB. The fate of heterotopic pancreatic tissue. A study of 212 cases. *Arch Surg* 1974; **109**: 762-765

3 **Rosai JR**. Pancreas and periampullary region: heterotopic pancreas In: Rosai JR, editor. Ackerman's Surgical Pathology. *St Louis: Mosby*, 2004: 10063.

4 **Brown HW**, Tabbah I. Aberrant pancreatic tissue in the wall of the gallbladder: report of a case simulating gallstone disease. *Int Surg* 1979; **64**: 43-44

5 **Ben-Baruch D**, Sandbank Y, Wolloch Y. Heterotopic pancreatic tissue in the gallbladder. *Acta Chir Scand* 1986; **152**: 557-558

6 **Inceoglu R**, Dosluoglu HH, Kullu S, Ahiskali R, Doslu FA. An unusual cause of hydropic gallbladder and biliary colic--heterotopic pancreatic tissue in the cystic duct: report of a case and review of the literature. *Surg Today* 1993; **23**: 532-534

7 **Bhana BD**, Chetty R. Heterotopic pancreas--an unusual cause of cholecystitis. *S Afr J Surg* 1999; **37**: 105-107

8 **Neupert G**, Appel P, Braun S, Tonus C. Heterotopic pancreas in the gallbladder. Diagnosis, therapy, and course of a rare developmental anomaly of the pancreas. *Chirurg* 2007; **78**: 261-264

9 **Kondi-Paphiti A**, Antoniou AG, Kotsis T, Polimeneas G. Aberrant pancreas in the gallbladder wall. *Eur Radiol* 1997; **7**: 1064-1066

10 **Mboti F**, Maassarani F, De Keuleneer R. Cholecystitis associated with heterotopic pancreas. *Acta Chir Belg* 2003; **103**: 110-112

11 **Mönig SP**, Selzner M, Raab M, Eidt S. Heterotopic pancreas. A difficult diagnosis. *Dig Dis Sci* 1996; **41**: 1238-1240

12 **Artavanis-Tsakonas S**, Rand MD, Lake RJ. Notch signaling: cell fate control and signal integration in development. *Science* 1999; **284**: 770-776

13 **Murtaugh LC**, Stanger BZ, Kwan KM, Melton DA. Notch signaling controls multiple steps of pancreatic differentiation. *Proc Natl Acad Sci USA* 2003; **100**: 14920-14925

14 **Sumazaki R**, Shiojiri N, Isoyama S, Masu M, Keino-Masu K, Osawa M, Nakauchi H, Kageyama R, Matsui A. Conversion of biliary system to pancreatic tissue in Hes1-deficient mice. *Nat Genet* 2004; **36**: 83-87

15 **Fukuda A**, Kawaguchi Y, Furuyama K, Kodama S, Horiguchi M, Kuhara T, Koizumi M, Boyer DF, Fujimoto K, Doi R, Kageyama R, Wright CV, Chiba T. Ectopic pancreas formation in Hes1 -knockout mice reveals plasticity of endodermal progenitors of the gut, bile duct, and pancreas. *J Clin Invest* 2006; **116**: 1484-1493

S- Editor Liu Y **L- Editor** Wang XL **E- Editor** Lu W

PO Box 2345, Beijing 100023, China
www.wjgnet.com
wjg@wjgnet.com

World J Gastroenterol 2007 January 14; 13(2): 316-319
World Journal of Gastroenterology ISSN 1007-9327

CASE REPORT

A case of interstitial pneumonitis in a patient with ulcerative colitis treated with azathioprine

Ferenc Nagy, Tamas Molnar, Eva Makula, Ildiko Kiss, Peter Milassin, Eva Zollei, Laszlo Tiszlavicz, Janos Lonovics

Ferenc Nagy, Tamas Molnar, Janos Lonovics, First Department of Medicine, University of Szeged, Faculty of Medicine, Szeged, Hungary
Eva Makula, Ildiko Kiss, Peter Milassin, Department of Radiology, University of Szeged, Faculty of Medicine, Szeged, Hungary
Eva Zollei, Medical Intensive Care Unit, University of Szeged, Faculty of Medicine, Szeged, Hungary
Laszlo Tiszlavicz, Institute of Pathology, University of Szeged, Faculty of Medicine, Szeged, Hungary
Correspondence to: Ferenc Nagy MD, PhD. First Department of Medicine, Faculty of Medicine, University of Szeged, Koranyi fasor 8, H-6701, Szeged, POB 427, Hungary. agyferi@in1st.szote.u-szeged.hu
Telephone: +36-62-545189 Fax: +36-62-545185
Received: 2006-09-20 Accepted: 2006-10-25

Abstract

The early hypersensitivity reaction and late bone marrow depression are well-known side-effects of azathioprine, whereas interstitial pneumonia is a rare complication. A 40-year old male patient had been treated with azathioprine in consequence of extensive ulcerative colitis for 10 years. He then complained of 7 d of fever, cough and catarrhal signs, without symptoms of active colitis. Opportunistic infections were ruled out. The chest X-ray, CT and lung biopsy demonstrated the presence of interstitial inflammation. Azathioprine therapy was discontinued as a potential source of the pulmonary infiltrate. In response to steroid therapy, and intensive care, the pulmonary infiltrate gradually decreased within 4 wk. Three months later, his ulcerative colitis relapsed, and ileo-anal pouch surgery was performed. In cases of atypical pneumonia, without a proven infection, azathioprine-associated interstitial pneumonitis may be present, which heals after withdrawal of the drug.

Key words: Inflammatory bowel disease; Ulcerative colitis; Azathioprine; Interstitial pneumonitis

Nagy F, Molnar T, Makula E, Kiss I, Milassin P, Zollei E, Tiszlavicz L, Lonovics J. A case of interstitial pneumonitis in a patient with ulcerative colitis treated with azathioprine. *World J Gastroenterol* 2007; 13(2): 316-319

http://www.wjgnet.com/1007-9327/13/316.asp

INTRODUCTION

Azathioprine (Imuran® Glaxo-SmithKline) (AZA), one of the most commonly prescribed immunosuppressive drugs, is mainly administered in the treatment of immune-mediated diseases. AZA has been used to combat inflammatory bowel diseases (IBD) such as ulcerative colitis and Crohn's disease since the 1960s[1]. It has been shown to reduce the number of lamina propria plasma cells, to alter the function of lymphocytes and natural killer cells and to exert an anti-inflammatory effect[2]. In IBD, azathioprine is used in both steroid-dependent and steroid-resistant cases. The clinical efficacy starts within 3-6 mo after the initiation of therapy. It is effective in more than half of the patients[3]. The early hypersensitivity reaction (nausea, fever, hepatitis and pancreatitis) and late bone marrow depression (leukopenia and macrocytosis) are relatively common side-effects[4], but interstitial pneumonitis is rare.

CASE REPORT

A 41-year old male patient with known ulcerative colitis since 1988 was referred to the Department of Medicine by his GP in June 2003 with symptoms and signs of relapse. His pancolitis had been treated with AZA (1.8 mg/kg per day) since 1993 because of frequent relapses. During the therapy only mild (1-2 blood-streaked stools) and rare (for 1-2 wk periods, once or twice yearly) relapses occurred. The patient was in good physical condition for his age and he was able to work. Six weeks before his admission, there was a severe relapse. He complained of anorexia, a weight loss (15 kg) and frequent bowel movements (10-12 times/d), accompanied with colicky pain and blood in the stools. Fever, dyspnoea and cardiac symptoms were not present. His treatment on admission was: 1 g olsalazine, 150 mg azathioprine, 12 mg methylprednisolone daily. Physical examination of the cardiorespiratory system was negative and diffuse abdominal tenderness was detected. His weight was 91 kg, his height was 182 cm, and his temperature was normal. The blood chemistry at the time of admission was as follows: ESR = 76 mm/h, serum sodium = 132 mmol/L, potassium = 3.7 mmol/L, haematocrit = 32%, hb = 111 g/L, TIBC = 55 μmol/L, white blood cell count = 4.400 G/L, and platelets = 368.000 G/L. Liver function tests were normal. Colonoscopy revealed severe active extensive ulcerative colitis involving the whole transversal colon. In response to parenteral corticosteroid treatment, his condition improved. He was discharged in good condition after

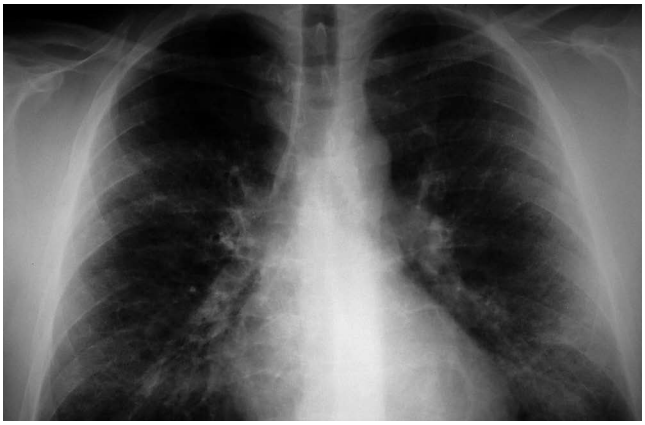

Figure 1 Chest X-ray (2003-09-09) showing moderate reticular enhancement with ring-like consolidation in both lungs (but predominantly the right), without cardiac or aortic abnormalities.

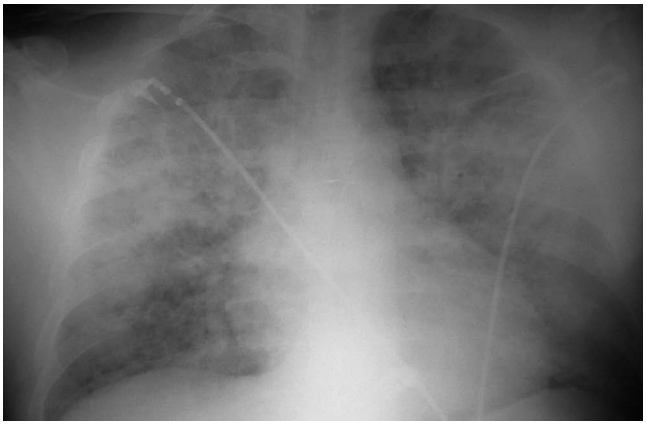

Figure 2 Chest X-ray (2003-09-14) showing significant progression and volume loss in both lungs. A palm-sized homogeneous consolidation developed in the central part of the lung, a marked interstitial enhancement was seen in other parts of the lung. The radiological image suggested ARDS. The heart was enlarged.

11 d on 48 mg/d oral methylprednisolone and 150 mg/d AZA.

After a remission period, which lasted throughout the summer, he presented to the Department of Medicine in September 2003 with complaints of weakness, weight loss, coughing and fever, the latter appearing every evening for a week. He did not cough up blood. He had 2-4 stools daily, without blood. He had no abdominal symptoms. His daily treatment on admission was 150 mg AZA, 16 mg methylprednisolone and doxycycline (prescribed by his GP). The results of physical examinations (cardiovascular and respiratory systems and abdomen) were normal. Septic fever was present. Blood chemistry values were as follows: ESR = 125 mm/h, haematocrit = 31%, hb = 10.7 g/L, white blood cell count = 4.100 G/L, platelets = 325.000 G/L, CRP = 351 mg/L, and uric acid = 471 μmol/L. The haemoculture was negative and procalcitonin was 0.07 ng/mL. The bacteriology (pharynx, sputum and urine) and virology (CMV, EBV, Coxackie and adenovirus) tests were negative.

The chest X-ray (2003-09-09) revealed moderately increased interstitial shadowing with a ring-like consolidation in both lungs (predominantly in the right), without cardiac or aortic abnormalities. The follow-up chest X-ray revealed progression (Figure 1). Despite the discontinuation of AZA, progressive interstitial inflammation was detected in both lungs. The patient was treated with 1 g/d clarithromycin intravenously and 12 mg methylprednisolone orally. He was transferred to the intensive care unit because of the possibility of a severe opportunistic infection or an autoimmune disease. AZA-associated pneumonitis was also suspected.

His respiratory failure was treated in the intensive care unit. Dyspnoea occurred on minor exertion, the patient had orthostatic hypotension, and he was weak. On physical examination, the liver was palpable 2 cm beyond the costal margin. Except for dyspnoea nothing abnormal was detected. Blood chemistry showed ESR = 120 mm/h, haematocrit = 26%, hb = 90 g/L, white blood cell count = 2.970-3.200 G/L, platelets = 426.000 G/L, SGOT = 246 U/L, SGPT = 91 U/L, gamma GT = 600 U/L, LDH = 1125 U/L, and procalcitonin = 0.07 ng/L. Nasal oxygen supplementation was initiated, and a bronchial lavage sample was collected from the lower respiratory tract under anaesthesia. Arterial blood gas analyses displayed pH = 7.455, pCO_2 = 33.0, pO_2 = 50.9 mmHg, and sO_2 = 86.2%. Two days later the corresponding values of pH, pCO_2, pO_2, and sO_2 were: 7.394%, 41.7%, 75.1% and 94.0%, respectively. Neither typical nor atypical pathogens were detected in bacteriology samples. CMV PCR and Legionella IgM-IgG were also negative.

The follow-up chest X-ray examination (Figure 2), revealed a significant progression of the interstitial shadowing in both lungs. A palm-sized homogeneous consolidation was seen in the hilar area and marked interstitial shadowing in the remaining parts of the lungs. The radiological appearance was suggestive of acute respiratory distress syndrome (ARDS). Cardiac enlargement was demonstrated.

The chest CT examination revealed a 2-cm wide pleural effusion with increased alveolar/air-space shadowing bilaterally. The X-ray and CT examinations suggested ARDS. A needle biopsy was performed from the apex of the right lung. The histology showed intraluminal myxoid polyps (Masson bodies) in the alveoli (Figures 3,4,5). Vasculitis and *Pneumocystis carinii* infection were excluded. The results of the histology and immuno-histochemistry suggested a diagnosis of bronchiolitis obliterans organizing pneumonia (BOOP), but hypersensitivity pneumonitis was also regarded as a possibility. After sulphametoxasol/trimetroprim and methylprednisolone therapy, his condition gradually improved (Figure 6), and his liver and renal functions became normal. At the time of discharge, he was treated with 3 g sulphasalazine, 1 g sulphamethoxazole/trimethroprim and 8 mg methylprednisolone daily.

Three months later (2004-09-01) only mild dyspnoea occurred on exertion, but he had 8-10 liquid stools daily, occasionally with some blood on the surface of faeces. He had neither fever nor extraintestinal symptoms. The results of chest and heart examination were normal, but the sigma was tender. Corticosteroid therapy was restarted with 64 mg/d methylprednisolone. Blood chemistry

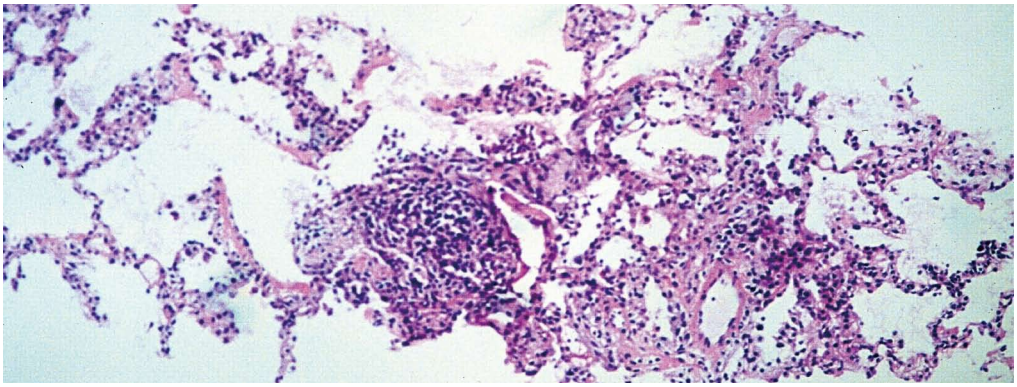

Figure 3 Histology of lung needle biopsy (HE, 112 ×).

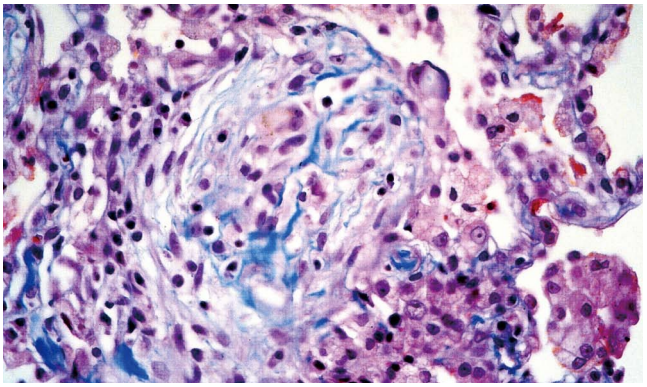

Figure 4 Histology showing the pathognomic Masson bodies for BOOP and polypous proliferation of new connective tissue in the alveolus (trichrome, 224 ×).

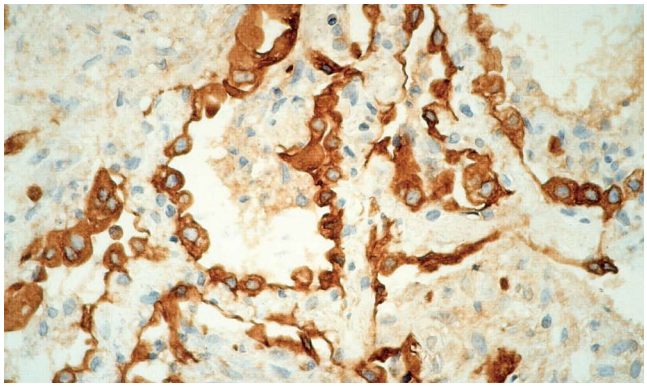

Figure 5 Immunohistochemistry for the expression of CK 7. Interstitial fibrosis and proliferation of type II pneumocytes are apparent (224 ×).

showed serum Fe = 21.3 μmol/L, uric acid = 461 μmol/L, gamma GT = 121 U/L, cholesterol = 7.75 mmol/L, triglyceride = 2.3 mmol/L, white blood cell count = 7. 870 G/L and platelets = 223. 000 G/L. Pulmonary functions were VC = 110%, RV = 109%, spirometry FVC = 104%, FEV_1 = 112%. The diffusion capacity values (DLCO = 74%, DLCO/VA = 60%) suggested a slightly decreased diffusion capacity. The chest X-ray revealed a further improvement of the lung volume. Interstitial shadowing was still present in the perihilar region of the lungs. Colonoscopy could only be carried out to 20 cm because of the pain and active colitis. The surface of mucosa was reddish, vulnerable and ulcerated, corresponding to active ulcerative colitis. In view of his previous history, proctocolectomy had to be considered. The first surgical intervention was carried out a month later and, after the ileal-pouch anal anastomosis (IPAA), the temporary anus prae was closed in August 2004. He had no complaints after the operation, produced 4-5 stools daily and was not on any medication.

DISCUSSION

In IBD patients, AZA treatment is worth starting if the patient is steroid-refractory (the effective dose does not lead to remission) or steroid dependent (discontinuation of the steroid causes a relapse)[5]. The first clinical results were inhomogeneous as concerns efficacy, because of the long time until the onset of action. Hawthorne *et al*[6] have proven the beneficial effect of the medication on the maintenance of remission in ulcerative colitis. In their study, seventy-nine patients who had been taking AZA for 6 mo were then divided into two groups. One of the groups continued to receive the therapy while placebo was administered to the patients in the other. The relapse rate was 36% in the AZA-treated group and 59% in the placebo group.

The mechanism of action of AZA is unknown. In IBD, the drug decreases the number of lamina propria plasma cells and alters the functions of lymphocytes and natural killer cells.

The therapeutic effect has been explained by the apoptosis-inducing behaviour of the drug. Tiede *et al*[7] considered that 6-thioGTP, a metabolite of AZA, could alter the apoptosis of T cells. The metabolite inhibits the activation of certain genes inside the cells, and induces apoptosis via a mitochondrial path.

Bedrossian *et al*[8] have noted bilateral lung infiltration with a reduced pO_2 in 7 kidney-transplanted patients treated with AZA, which was not cured by antibiotic therapy. In their study, lung biopsy revealed an abnormal histology, which varied from diffuse alveolar damage to interstitial pneumonia and pulmonary fibrosis. No immune deposition, eosinophilia, vasculitis or granuloma could be detected, and the bacteriologyical findings were negative. When AZA was withdrawn from the treatment, the infiltration was significantly diminished in 2 patients who exhibited diffuse alveolar damage, but 4 patients diagnosed as interstitial pneumonitis, died of ARDS. The biopsies revealed hyaline membranes, intraalveolar oedema and damage to

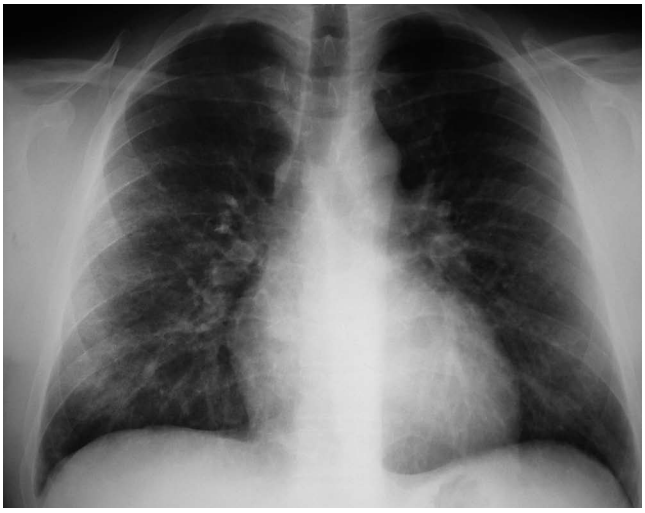

Figure 6 Chest X-ray (2003-10-15) showing improvement of lung volumes. Reticular enhancement of the middle part of the lungs is still present.

the alveolar epithelium in those who received low doses of AZA, and atypical epithelial hyperplasia, reorganization of the distal air spaces and fibrosis in the cases treated with high doses of AZA. Histologically the changes observed could not be distinguished from the characteristic changes caused by other pulmonary toxic drugs.

In our case, AZA treatment, initiated because of the common and serious relapses of extensive ulcerative colitis, ensured a good condition for almost 10 years. The patient was hospitalized because of a severe relapse in June 2003, but at that time no pulmonary abnormality was found. Remission was achieved with intravenous corticosteroid therapy. Three months later (2003-09-09), the patient presented with cough, catarrhal signs and pulmonary infiltration. We initially thought of concomitant infection, which may be expected during immunosuppressive treatment. In consequence of earlier therapy the pancolitis was in remission. After admission, the dose of AZA was reduced, and doxycycline was changed to chlarythromycin. However, despite his good general condition and the conventional treatment, the pulmonary infiltration rapidly deteriorated. Dyspnoea developed, which necessitated intensive care. Concomitant infection was not confirmed by the diagnostic examinations, and broad-spectrum antibiotics were proven ineffective. The lung biopsy results and the clinical features strongly suggested that he had AZA-associated interstitial pneumonia. Other causes of BOOP, such as eosinophilic pneumonia, vasculitis, irradiation, nitrofurantoin, gold, amiodarone and methotrexate, were excluded. In view of the results, AZA treatment was discontinued, oral corticosteroid medication was continued and the patient's condition gradually improved. Three months later (December 2003), ulcerative colitis relapsed. In view of the clinical course of ulcerative colitis (frequent recurrences and AZA-induced interstitial pneumonitis), proctocolectomy was recommended. After surgery, the patient's condition normalized without any further treatment.

In summary, in cases of atypical pneumonia without a proven opportunistic infection, AZA-associated interstitial pneumonitis may be present, which heals after withdrawal of the drug.

REFERENCES

1 **Dubinsky MC**. Azathioprine, 6-mercaptopurine in inflammatory bowel disease: pharmacology, efficacy, and safety. *Clin Gastroenterol Hepatol* 2004; **2**: 731-743

2 **Siegel CA**, Sands BE. Review article: practical management of inflammatory bowel disease patients taking immunomodulators. *Aliment Pharmacol Ther* 2005; **22**: 1-16

3 **Carter MJ**, Lobo AJ, Travis SP. Guidelines for the management of inflammatory bowel disease in adults. *Gut* 2004; **53** Suppl 5: V1-V16

4 **Domènech E**. Inflammatory bowel disease: current therapeutic options. *Digestion* 2006; **73** Suppl 1: 67-76

5 **Nagy F**. Conservative therapy of inflammatory bowel diseases. *Orv Hetil* 2002; **143**: 2763-2768

6 **Hawthorne AB**, Logan RF, Hawkey CJ, Foster PN, Axon AT, Swarbrick ET, Scott BB, Lennard-Jones JE. Randomised controlled trial of azathioprine withdrawal in ulcerative colitis. *BMJ* 1992; **305**: 20-22

7 **Tiede I**, Fritz G, Strand S, Poppe D, Dvorsky R, Strand D, Lehr HA, Wirtz S, Becker C, Atreya R, Mudter J, Hildner K, Bartsch B, Holtmann M, Blumberg R, Walczak H, Iven H, Galle PR, Ahmadian MR, Neurath MF. CD28-dependent Rac1 activation is the molecular target of azathioprine in primary human CD4+ T lymphocytes. *J Clin Invest* 2003; **111**: 1133-1145

8 **Bedrossian CW**, Sussman J, Conklin RH, Kahan B. Azathioprine-associated interstitial pneumonitis. *Am J Clin Pathol* 1984; **82**: 148-154

S- Editor Wang J **L- Editor** Wang XL **E- Editor** Liu WF

PO Box 2345, Beijing 100023, China
www.wjgnet.com
wjg@wjgnet.com

World J Gastroenterol 2007 January 14; 13(2): 320-323
World Journal of Gastroenterology ISSN 1007-9327

CASE REPORT

Gallbladder lymphangioma: A case report and review of the literature

Jwa-Kyung Kim, Kyo-Sang Yoo, Joon Ho Moon, Kwang Hyuk Park, Yong Woo Chung, Kyoung Oh Kim, Cheol Hee Park, Taeho Hahn, Sang Hoon Park, Jong Hyeok Kim, Jang Yeong Jeon, Min Jung Kim, Kwang Seon Min, Choong Kee Park

Jwa-Kyung Kim, Kyo-Sang Yoo, Joon Ho Moon, Kwang Hyuk Park, Yong Woo Chung, Kyoung Oh Kim, Cheol Hee Park, Taeho Hahn, Sang Hoon Park, Jong Hyeok Kim, Choong Kee Park, Department of Gastroenterology and Hepatology, Hallym University College of Medicine, Anyang, Korea
Jang Yeong Jeon, Department of Surgery, Hallym University College of Medicine, Anyang, Korea
Min Jung Kim, Department of Diagnostic Radiology, Hallym University College of Medicine, Anyang, Korea
Kwang Seon Min, Department of Pathology, Hallym University College of Medicine, Anyang, Korea
Correspondence to: Kyo-Sang Yoo, MD, PhD, Department of Gastroenterology and Hepatology, Hallym University Sacred Heart Hospital, 896 Pyeongchon-dong, Dongan-gu, Anyang, Gyeonggi 431-070, Korea. stanyoo@hallym.ac.kr
Telephone: +82-31-380-6065 Fax: +82-31-386-2269
Received: 2006-11-08 Accepted: 2006-12-06

Abstract

Lymphangiomas are rare, benign tumors of the lymphatic system, usually present in children aged 5 years and younger. Because they are asymptomatic until the mass enlarges to cause symptoms, most lymphangiomas are diagnosed at adulthood incidentally. We experienced a case of a 60-year-old man diagnosed with a cystic lymphangioma of the gallbladder, which was successfully resected without any complication. Magnetic resonance imaging and magnetic resonance cholangiopancreatography were very helpful for the diagnosis of the cystic lesion around the gallbladder as were ultrasonography and computed tomography scan. These showed a multi-lobulated cystic mass with intact cystic duct and bile duct in the gallbladder fossa. The patient underwent an open cholecystectomy and the histological findings were consistent with a cystic lymphangioma of the gallbladder. We here report the case of cystic lymphangioma of the gallbladder with a review of the literature.

Key words: Lymphangioma; Gallbladder; Cholecystectomy

Kim JK, Yoo KS, Moon JH, Park KH, Chung YW, Kim KO, Park CH, Hahn T, Park SH, Kim JH, Jeon JY, Kim MJ, Min KS, Park CK. Gallbladder lymphangioma: A case report and review of the literature. *World J Gastroenterol* 2007; 13(2): 320-323

http://www.wjgnet.com/1007-9327/13/320.asp

INTRODUCTION

Lymphangiomas are uncommon benign congenital malformations of the lymphatic system[1-3]. About 95% lymphangiomas occur in the skin and the subcutaneous tissues of the head, neck and axillary region and the remaining 5% appear in other parts of the body such as lungs, pleura, pericardium, esophagus, stomach, jejunum, colon, pancreas, liver, gallbladder, kidney, and the mesentery[3-5]. Because most lymphangiomas are multicystic, lobulated lesions, they may be confused with other lesions, such as intrahepatic simple cysts, ductal ectasia, liver hemangiomas, pericholecystic cystic tumors or angiosarcomas. Various imaging studies are often required for accurate diagnosis and to differentiate gallbladder lymphangiomas from other lesions[3,6,7]. Recently, magnetic resonance imaging (MRI) and magnetic resonance cholangiopancreatography (MRCP) have been shown to be helpful for the characterization of the lesions as well as an evaluation of the relation to the adjacent organs. Complete surgical resection is the treatment of choice for gallbladder lymphangioma, and recently successful laparoscopic resection also has been reported[8].

CASE REPORT

A 60-year-old man was admitted to Hallym University Sacred Heart Hospital for treatment of aspiration pneumonia. He presented a high fever, chills and coughing, and had no abdominal pain or discomfort. Chest computed tomography (CT) scan for evaluation of the pneumonia unexpectedly showed a large lobulating low density lesion in the liver near the gallbladder in addition to pneumonic infiltration of the lungs. The patient was referred to our department for evaluation of the large cystic lesion. Abdominal ultrasonography (US) showed a hypoechoic mass encircling the gallbladder lumen in the liver (Figure 1). Abdominal CT showed an approximately 5.2 cm-sized multi-lobulated cystic mass, insinuating gallbladder lymphangioma, between the liver and the gallbladder bed (Figure 2). Abdominal MRI was performed for the characterization and anatomical evaluation of the lesion. Axial T2-weighted image showed an intact lumen

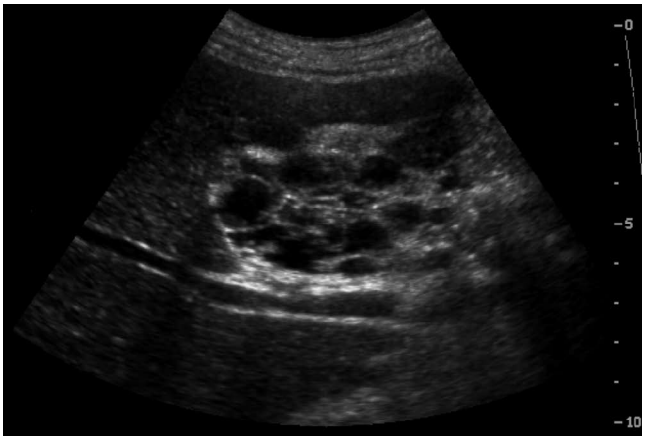

Figure 1 Abdominal ultrasonography showing multi-loculated cystic mass and intact gallbladder lumen.

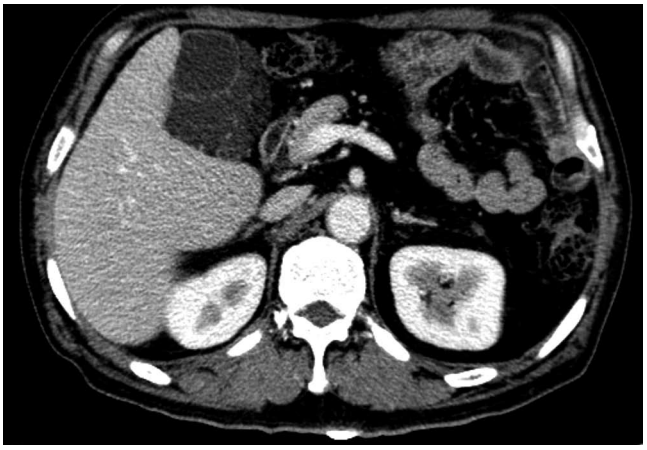

Figure 2 Abdominal computed tomography (CT) image showing a low-density multilocular cystic lesion with septation originated from the gallbladder fossa.

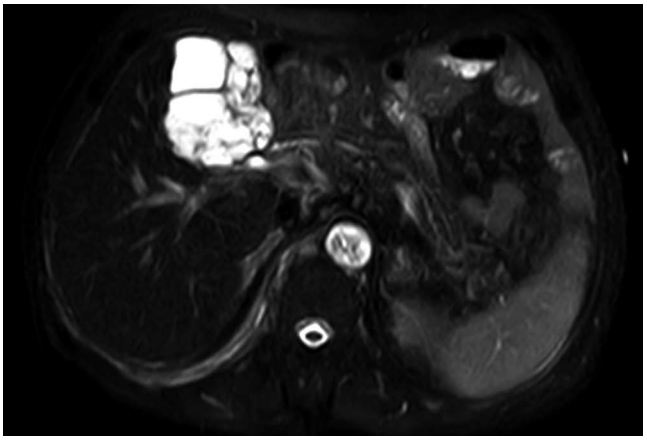

Figure 3 Axial T2-weighted magnetic resonance (MR) image showing a thin multi-septated cystic mass (high-signal intensity) with scalloping margin.

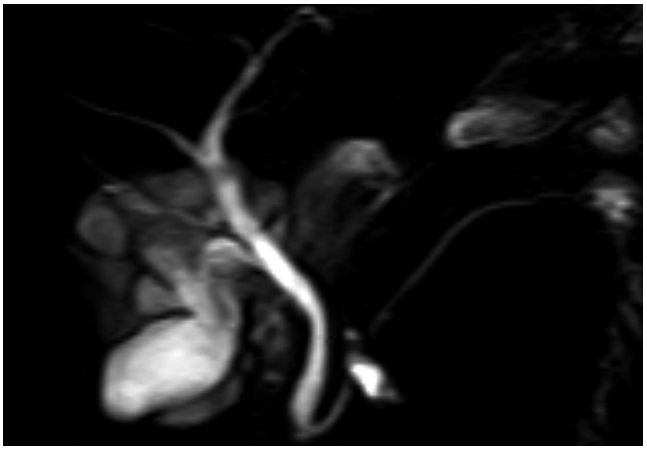

Figure 4 Magnetic resonance cholangiopancreatography (MRCP) image showing gallbladder encapsulated by variable sized multi-cystic lesions, which have no communication with biliary system.

of the gallbladder (low-signal intensity) surrounded by a thin multi-septated cystic mass (high-signal intensity) with scalloping margin (Figure 3). This finding strongly suggested a lymphangioma arising from the lymphatic tissue of the gallbladder wall. MRCP also clearly showed a large multi-cystic gallbladder lymphangioma in the gallbladder fossa (Figure 4). Characteristically, the cystic duct and bile duct were completely separated from the lymphangioma, and were well preserved. Additionally, the gallbladder was obviously visualized and its contraction was grossly normal (ejection fraction = 89%) on hepatobiliary DISIDA scan.

An open cholecystectomy was performed after resolution of the pneumonia. At surgical exploration, a well-defined multi-lobular cystic tumor encapsulating the gallbladder was observed. Grossly the tumor was measured 5.5 cm × 4.3 cm × 3.5 cm in size and was clearly separated from the liver. When the tumor was cut off from the surface, the gallbladder mucosa was intact and various-sized multiple cysts were shown. Each cyst was filled with serous or hemorrhagic lymphatic fluid. Histological evaluation revealed a flat endothelial lining encircling each cyst and multiple lymphocyte aggregations beside the cyst (Figure 5). This demonstrated that the cyst was a lymphatic space. The lesion was diagnosed as a cystic lymphangioma of the gallbladder because it had no connection with adjacent normal lymphatics. CT at 12 mo following the surgical resection showed no evidence of recurrence.

DISCUSSION

Lymphangiomas are benign tumors that may appear in any organ of the body except the brain. It more commonly involves the skin and soft tissue of the head and neck (95%), and lymphangioma occurring in the gastrointestinal tract is rare. A lymphangioma arising from the gallbladder is extremely rare, representing only 0.8%-1% of all intra-abdominal lymphangiomas[1-5], and only a few cases have been reported. Lymphangiomas are classified as simple, cavernous, and cystic types based on their histological findings[3,6,9-11]. The simple type is usually situated superficially in the skin and is composed of small thin-walled lymphatic vessels. The cavernous type is composed of dilated lymphatic vessels and lymphoid stroma, and has a connection with spaces of various normal adjacent lymphatics. The cystic type consists of lymphatic spaces

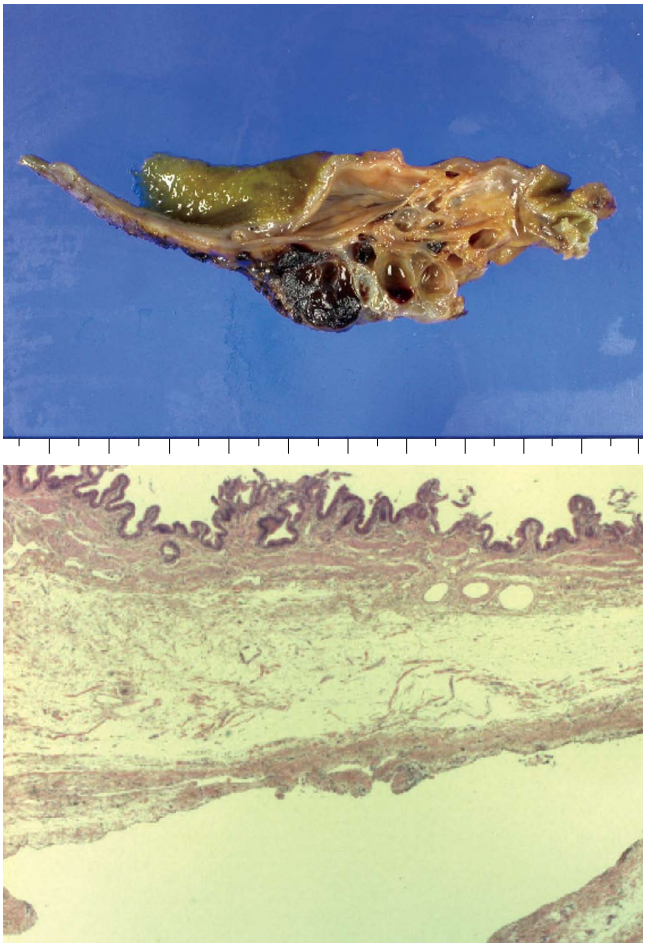

Figure 5 Gross appearance of resected specimen showing a well-marginated multi cystic lesion filled with yellowish fluid, and microphotograph from the cholecystectomy specimen showing a lymphatic space lined with flat endothelium (hematoxylin and eosin staining, × 12.5).

of various sizes that contain fascicles of smooth muscle and collagen bundles, but has no connection with adjacent normal lymphatics[11,12].

The etiology of lymphangiomas could be explained by several theories[1,6]. The most powerful one is that it is a congenital abnormality of the lymphatic system. Failure to establish connection with the normal drainage vessel causes sequestration of lymphatic tissue during embryogenesis. This theory would explain why lymphangioma occurs primarily in children. However, other views suggest that secondary causes such as abdominal trauma, lymphatic obstruction, inflammatory processes, surgery, or radiation therapy may lead to the formation of lymphangiomas[1,6].

Clinical presentations of these tumors are variable. Most cases are asymptomatic or have non-specific symptoms, such as nausea, vomiting, dyspepsia, abdominal discomfort or a palpable mass. In the past it was somewhat difficult to diagnose a lymphangioma before surgical or histological identification. Preoperative diagnosis of gallbladder lymphangioma remains difficult because it is very rare, and sometimes imaging studies such as US and CT cannot distinguish it from other lesions. The findings of US and CT show a large cystic lesion, but it is difficult to find where the lesion originates from and to understand its relation to surrounding organs.

However recently, various advanced imaging studies, especially MRI and MRCP, can support the diagnosis of lymphangiomas more easily before exploration[1,6,7]. US seems to be useful in defining the mass as a multilocular cystic lesion, but often does not distinguish between a hepatic lesion and a pericholecystic lesion. CT shows a simple or multilocular cystic lesion with the density of water. The septa of the cysts are of uniform thickness. Administering contrast agents intravenously can enhance the wall of the cysts[6]. However, the findings of CT of previous reports only showed cystic lesion in the gallbladder fossa or inferior to the liver, but could not show that the lesion was arising from the gallbladder. Moreover, the gallbladder was not visible due to cystic lesions in most of them, as was evident in the present case. Although hemorrhage within the lymphangioma was readily noted on follow-up CT, it might have been difficult to differentiate it from an intracystic solid lesion if the case was initially presented after hemorrhage[6].

In our study, MRI and MRCP are very helpful for making the correct diagnosis. One recent report described the MR findings of gallbladder lymphangiomas based on the findings of splenic cystic lymphangiomas[6]. This report suggested that characteristic MR findings would be very helpful for the differential diagnosis of gallbladder lymphangioma, and characterizing the mass even if the cystic lesion was complicated by intracystic hemorrhage. Axial T1- and T2-weighted and coronal MR images clearly depicted the lumen of the gallbladder and the multiseptated cystic mass originating in the gallbladder wall. MR imaging, including MRCP, clearly defined the mass and its relation to the gallbladder. The characteristic thin-walled multilocular cystic appearance was clearly depicted on MR imaging and was helpful for making the correct diagnosis[1,3,6,7]. MRCP characteristically showed that the cystic duct and bile duct were well preserved and were completely separated from the lymphangioma, as the finding of the present case. This was the typical feature of such lymphangiomas that had no communication between the mass and the biliary system. Therefore, if a gallbladder lymphangioma is suspected, MRI and MRCP should be recommended.

For the management of lymphangiomas, complete total surgical excision is known to be the standard treatment. If the mass grows large to compress surrounding structures and vessels, it can cause significant symptoms and morbidities. Furthermore, if it progresses to be complicated, intra-abdominal infection, rupture, torsion or hemorrhage can occur. A recent report suggested that two cases of gallbladder lymphangiomas were successfully treated by laparoscopic cholecystectomy, even though their size was more than 15 cm in diameter[8]. While we did not perform laparoscopic cholecystectomy, laparoscopic resection was possible because the lesion was relatively small compared to the previous report and was easily separated from the adjacent organs at surgical exploration. However, in a recent case, *en bloc* resection of the extrahepatic bile duct including the gallbladder was necessary because a huge cystic lesion adhered to the entire extrahepatic bile duct anteriorly and posteriorly, and part of the cyst also adhered to the right hepatic artery[1]. Therefore, laparoscopic resection was preferably

performed after evaluation of the extent of the cystic mass and its relation to adjacent organs. Recurrence has been reported with incomplete resection, but if the lesion is completely resected, long-term prognosis is excellent[12].

REFERENCES

1 **Noh KW**, Bouras EP, Bridges MD, Nakhleh RE, Nguyen JH. Gallbladder lymphangioma: a case report and review of the literature. *J Hepatobiliary Pancreat Surg* 2005; **12**: 405-408

2 **Ohba K**, Sugauchi F, Orito E, Suzuki K, Ohno T, Mizoguchi N, Koide T, Terashima H, Nakano T, Mizokami M. Cystic lymphangioma of the gall-bladder: a case report. *J Gastroenterol Hepatol* 1995; **10**: 693-696

3 **Lörken M**, Marnitz U, Manegold E, Schumpelick V. Intra-abdominal lymphangioma. *Chirurg* 2001; **72**: 72-77

4 **Bishop MD**, Steer M. Pancreatic cystic lymphangioma in an adult. *Pancreas* 2001; **22**: 101-102

5 **Takiff H**, Calabria R, Yin L, Stabile BE. Mesenteric cysts and intra-abdominal cystic lymphangiomas. *Arch Surg* 1985; **120**: 1266-1269

6 **Choi JY**, Kim MJ, Chung JJ, Park SI, Lee JT, Yoo HS, Kim L, Choi JS. Gallbladder lymphangioma: MR findings. *Abdom Imaging* 2002; **27**: 54-57

7 **Vargas-Serrano B**, Alegre-Bernal N, Cortina-Moreno B, Rodriguez-Romero R, Sanchez-Ortega F. Abdominal cystic lymphangiomas: US and CT findings. *Eur J Radiol* 1995; **19**: 183-187

8 **Yang HR**, Jan YY, Huang SF, Yeh TS, Tseng JH, Chen MF. Laparoscopic cholecystectomy for gallbladder lymphangiomas. *Surg Endosc* 2003; **17**: 1676

9 **Yoshida Y**, Okamura T, Ezaki T, Yano K, Kodate M, Murata I, Kaido M. Lymphangioma of the oesophagus: a case report an d review of the literature. *Thorax* 1994; **49**: 1267-1268

10 **Roisman I**, Manny J, Fields S, Shiloni E. Intra-abdominal lymphangioma. *Br J Surg* 1989; **76**: 485-489

11 **Chung JH**, Suh YL, Park IA, Jang JJ, Chi JG, Kim YI, Kim WH. A pathologic study of abdominal lymphangiomas. *J Korean Med Sci* 1999; **14**: 257-262

12 **Amadori G**, Micciolo R, Poletti A. A case of intra-abdominal multiple lymphangiomas in an adult in whom the immunological evaluation supported the diagnosis. *Eur J Gastroenterol Hepatol* 1999; **11**: 347-351

S- Editor Liu Y **L- Editor** Zhu LH **E- Editor** Liu WF

PO Box 2345, Beijing 100023, China
www.wjgnet.com
wjg@wjgnet.com

World J Gastroenterol 2007 January 14; 13(2): 324
World Journal of Gastroenterology ISSN 1007-9327

ACKNOWLEDGMENTS

Acknowledgments to Reviewers of *World Journal of Gastroenterology*

Many reviewers have contributed their expertise and time to the peer review, a critical process to ensure the quality of *World Journal of Gastroenterology*. The editors and authors of the articles submitted to the journal are grateful to the following reviewers for evaluating the articles (including those were published and those were rejected in this issue) during the last editing period of time.

Gary A Abrams, Associate Professor
Department of Medicine, University of Alabama at Birmingham, 1530 3rd Ave South, Birmingham 35294, United States

Agustin Albillos, Associate Professor
Departamento de Medicina, Facultad de Medicina-Campus Universitario, Universidad de Alcalá, Carretera Madrid-Barcelona km.33.600, Alcalá de Henares, Madrid 28871, Spain

Masahiro Arai, MD, PhD
Department of Gastroenterology, Toshiba General Hospital, 6-3-22 Higashi-ooi, Shinagawa-ku,Tokyo 140-8522, Japan

Olivier Barbier
CHUQ-CHUL Research Center, 2705 Laurier Boulevard, Québec G1V 4G2, Canada

Gabrio Bassotti, MD
Department of Clinical and Experimental Medicine, University of Perugia, Via Enrico dal Pozzo, Padiglione W, Perugia 06100, Italy

Edmund J Bini, Professor
VA New York Harbor Healthcare System, Division of Gastroenterology (111D), 423 East 23rd Street, New York, NY 10010, United States

Luigi Bonavina, Professor
Department of Surgery, Policlinico San Donato, University of Milano, via Morandi 30, Milano 20097, Italy

Josep M Bordas, MD
Department of Gastroenterology IMD, Hospital Clinic", Llusanes 11-13 at, Barcelona 08022, Spain

Joseph Daoud Boujaoude, Assistant Professor
Department of Gastroenterology, Hotel-Dieu de FranceHospital, aint-Joseph University, Beirut 961, Lebanon

Michele Cicala, Professor
Ipartimento di Malattie dell'Apparato Digerente, Università Campus Bio-Medico, Via Longoni, 83-00155 Rome, Italy

Andrew D Clouston, Associate Professor
Histopath Laboratories, Suite 4, Level 9, Strathfield Plaza, Strathfield, Sydney, 2135, Australia

Zong-Jie Cui, PhD, Professor
Institute of Cell Biology, Beijing Normal University, 19 XinJieKouWaiDaJie, Beijing 100875, China

Paolo Del Poggio, Dr.
Hepatology Unit, Department of Internal Medicine, Treviglio Hospital, Piazza Ospedale 1, Treviglio Bg 24047, Italy

Olivier Detry, Dr.
Department of Abdominal Surgery and Transplantation, University of Liège, CHU Sart Tilman B35, B-4000 Liège, Belgium

John Frank Di Mari, Assistant Professor
Internal Medicine, Gastroenterology ,9.138 MRB 301 University Blvd. Galveston, Texas 77555-1064, United States

Michael Anthony Fink
MBBS FRACS, Department of Surgery, The University of Melbourne, Austin Hospital, Melbourne, Victoria 3084, Australia

Kazuma Fujimoto, Professor
Department of Internal Medicine, Saga Medical School, Nabeshima, Saga, Saga 849-8501, Japan

Kazuma Fujimoto, Professor
Department of Internal Medicine, Saga Medical School, Nabeshima, Saga, Saga 849-8501, Japan

Mitsuhiro Fujishiro, Dr.
Department of Gastroenterology, Faculty of Medicine, University of Tokyo, 7-3-1 Hongo, Bunkyo-ku, Tokyo, Japan

Elizabeth Furrie, PhD
Department of Immunology, Ninewells hospital and Medical School, Dundee DD1 9SY, United Kingdom

Florian Graepler, Dr.
Department of Gastroenterology, Hepatology and Infectious Diseases, University Hospital Tuebingen, Otfried-Mueller-Str. 10, D-72076 Tuebingen, Germany

Khek-Yu Ho, Professor
Department of Medicine, National University Hospital, 119074, Singapore

Yik-Hong Ho, Professor
Department of Surgery, School of Medicine, James Cook University, Townsville 4811, Australia

Myung-Hwan Kim, Professor
Department of Internal Medicine, University of Ulsan College of Medicine, Asan Medical Center, 388-1 Pungnap-dong, Songpa-gu, Seoul 138-736, South Korea

Elias A Kouroumalis, Professor
Department of Gastroenterology, University of Crete, Medical School, Department of Gastroenterology, University Hospital, PO Box 1352, Heraklion, Crete 71110, Greece

Peter Laszlo Lakatos, MD, PhD, Assistant Professor
1st Department of Medicine, Semmelweis University, Koranyi S 2A, Budapest H1083, Hungary

Kurt Lenz, Professor
Department of Internal Medicine, Konventhospital Barmherzige Brueder, A-4020 Linz, Austria

María Isabel Torres López, Professor
Experimental Biology, University of Jaen, araje de las Lagunillas s/n, Jaén 23071, Spain

Giulio Marchesini, Professor
Department of Internal Medicine and Gastroenterology, "Alma Mater Studiorum" University of Bologna, Policlinico S. Orsola, Via Massarenti 9, Bologna 40138, Italy

Giulio Marchesini, Professor
Department of Internal Medicine and Gastroenterology, "Alma Mater Studiorum" University of Bologna, Policlinico S. Orsola, Via Massarenti 9, Bologna 40138, Italy

George Michalopoulos, MD, PhD
Department of Pathology, University of Pittsburgh, School of Medicine, S-410 Biomedical Science Tower, Pittsburgh, PA 15261, United States

Gerald Y Minuk, Dr.
Section of Hepatology, University of Manitoba, Room 803E-715 McDermot Avenue, Winnipeg, Manitoba R3E 3P4, Canada

Thierry Piche, MD, PhD
Department of Gastroenterology, Archet 2 Hospital, 151 RTE ST Antoine de Ginestiere 06202, Nice CEDEX 3, France

Eamonn M Quigley, Professor
Department of Medicine National University of Ireland, Cork, Cork University Hospital Clinical Sciences Building Wilton, Cork, Ireland

Luis Rodrigo, Professor
Gastroenterology Service, Hospital Central de Asturias, c/ Celestino Villamil, s.n., Oviedo 33.006, Spain

Yoshio Shirai, Associate Professor
Division of Digestive and General Surgery, Niigata University Graduate School of Medical and Dental Sciences, 1-757 Asahimachi-dori, Niigata City 951-8510, Japan

Qin Su, Professor
Department of Pathology, Cancer Hospital and Cancer Institute, Chinese Academy of Medical Sciences and Peking Medical College, PO Box 2258, Beijing 100021, China

Tadashi Takeda, MD
Department of Hepatology, Osaka City University, 1-4-3 Asahimachi, Abeno-ku, Osaka 545-8585, Japan

Kiichi Tamada, MD
Department of Gastroenterology, Jichi Medical Shool, 3311-1 Yakushiji,Minamikawa chi,Kawachigun, Tochigi 329-0498, Japan

Minoru Toyota, Dr.
First Department of Internal Medicine, Sapporo Medical University, South-1, West-16, Sapporo 060-8543, Japan

Yvan Vandenplas, Professor
Department of Pediatrics, AZ-VUB, Laarbeeklaan 101, Brussels 1090, Belgium

Takayuki Yamamoto, MD
Inflammatory Bowel Disease Center, Yokkaichi Social Insurance Hospital, 10-8 Hazuyamacho, Yokkaichi 510-0016, Japan

PO Box 2345, Beijing 100023, China
www.wjgnet.com
wjg@wjgnet.com

World J Gastroenterol 2007 January 14; 13(2): 325
World Journal of Gastroenterology ISSN 1007-9327

Meetings

MAJOR MEETINGS COMING UP

Meeting Falk Research Workshop: Morphogenesis and Cancerogenesis of the Liver
25-26 January 2007
Goettingen
symposia@falkfoundation.de

Meeting Canadian Digestive Diseases Week (CDDW)
16-20 February 2007
Banff-AB
cagoffice@cag-acg.org
www.cag-acg.org/cddw/cddw2007.htm

Meeting Falk Symposium 158: Intestinal Inflammation and Colorectal Cancer
23-24 March 2007
Sevilla
symposia@falkfoundation.de

Meeting BSG Annual Meeting
26-29 March 2007
Glasgow
www.bsg.org.uk/

NEXT 6 MONTHS

Meeting 42nd Annual Meeting of the European Association for the Study of the Liver
11-15 April 2007
Barcelona
easl2007@easl.ch
www.easl.ch/liver-meeting/

Meeting Falk Symposium 159: IBD 2007 - Achievements in Research and Clinical Practice
4-5 May 2007
Istanbul
symposia@falkfoundation.de

Meeting European Society for Paediatric Gastroenterology, Hepatology and Nutrition Congress 2007
9-12 May 2007
Barcelona
espghan2007@colloquium.fr

Digestive Disease Week
19-24 May 2007
Washington Convention Center, Washington DC

Meeting Gastrointestinal Endoscopy Best Practices: Today and Tomorrow, ASGE Annual Postgraduate Course at DDW
23-24 May 2007
Washington-DC
tkoral@asge.org

Meeting ESGAR 2007 18th Annual Meeting and Postgraduate Course
12-15 June 2007
Lisbon
fca@netvisao.pt

Meeting Falk Symposium 160: Pathogenesis and Clinical Practice in Gastroenterology
15-16 June 2007
Portoroz
symposia@falkfoundation.de

Meeting ILTS 13th Annual International Congress
20-23 June 2007
Rio De Janeiro
www.ilts.org

Meeting 9th World Congress on Gastrointestinal Cancer
27-30 June 2007
Barcelona
meetings@imedex.com

EVENTS AND MEETINGS IN 2007

Meeting Falk Research Workshop: Morphogenesis and Cancerogenesis of the Liver
25-26 January 2007
Goettingen
symposia@falkfoundation.de

Meeting Canadian Digestive Diseases Week (CDDW)
16-20 February 2007
Banff-AB
cagoffice@cag-acg.org
www.cag-acg.org/cddw/cddw2007.htm

Meeting Falk Symposium 158: Intestinal Inflammation and Colorectal Cancer
23-24 March 2007
Sevilla
symposia@falkfoundation.de

Meeting BSG Annual Meeting
26-29 March 2007
Glasgow
www.bsg.org.uk/

Meeting 42nd Annual Meeting of the European Association for the Study of the Liver
11-15 April 2007
Barcelona
easl2007@easl.ch
www.easl.ch/liver-meeting/

Meeting Falk Symposium 159: IBD 2007 - Achievements in Research and Clinical Practice
4-5 May 2007
Istanbul
symposia@falkfoundation.de

Meeting European Society for Paediatric Gastroenterology, Hepatology and Nutrition Congress 2007
9-12 May 2007
Barcelona
espghan2007@colloquium.fr

Meeting Gastrointestinal Endoscopy Best Practices: Today and Tomorrow, ASGE Annual Postgraduate Course at DDW
23-24 May 2007
Washington-DC
tkoral@asge.org

Meeting ESGAR 2007 18th Annual Meeting and Postgraduate Course
12-15 June 2007
Lisbon
fca@netvisao.pt

Meeting Falk Symposium 160: Pathogenesis and Clinical Practice in Gastroenterology
15-16 June 2007
Portoroz
symposia@falkfoundation.de

Meeting ILTS 13th Annual International Congress
20-23 June 2007
Rio De Janeiro
www.ilts.org

Meeting 9th World Congress on Gastrointestinal Cancer
27-30 June 2007
Barcelona
meetings@imedex.com

Meeting 15th International Congress of the European Association for Endoscopic Surgery
4-7 July 2007
Athens
info@eaes-eur.org
congresses.eaes-eur.org/

Meeting 39th Meeting of the European Pancreatic Club
4-7 July 2007
Newcastle
www.e-p-c2007.com

Meeting XXth International Workshop on Heliobacter and related bacteria in cronic degistive inflammation
20-22 September 2007
Istanbul
www.heliobacter.org

Meeting Falk Workshop: Mechanisms of Intestinal Inflammation
10 October 2007
Dresden
symposia@falkfoundation.de

Meeting Falk Symposium 161: Future Perspectives in Gastroenterology
11-12 October 2007
Dresden
symposia@falkfoundation.de

Meeting Falk Symposium 162: Liver Cirrhosis - From Pathophysiology to Disease Management
13-14 October 2007
Dresden
symposia@falkfoundation.de

American College of Gastroenterology Annual Scientific Meeting
12-17 October 2007
Pennsylvania Convention Center
Philadelphia, PA

Meeting APDW 2007 - Asian Pacific Digestive Disease Week 2007
15-18 October 2007
Kobe
apdw@convention.co.jp
www.apdw2007.org

15th United European Gastroenterology Week, UEGW
27-31 October 2007
Le Palais des Congrès de Paris, Paris, France

Meeting The Liver Meeting® 2007 - 57th Annual Meeting of the American Association for the Study of Liver Diseases
2-6 November 2007
Boston-MA
www.aasld.org

Gastro 2009, World Congress of Gastroenterology and Endoscopy London, United Kingdom 2009

PO Box 2345, Beijing 100023, China
www.wjgnet.com
wjg@wjgnet.com

World J Gastroenterol 2007 January 14; 13(2): 326-328
World Journal of Gastroenterology ISSN 1007-9327

Instructions to authors

GENERAL INFORMATION

World Journal of Gastroenterology (*WJG, World J Gastroenterol* ISSN 1007-9327 CN 14-1219/R) is a weekly journal of more than 48 000 circulation, published on the 7th, 14th, 21st and 28th of every month.

Original Research, Clinical Trials, Reviews, Comments, and Case Reports in esophageal cancer, gastric cancer, colon cancer, liver cancer, viral liver diseases, *etc.*, from all over the world are welcome on the condition that they have not been published previously and have not been submitted simultaneously elsewhere.

Indexed and abstracted in

Current Contents®/Clinical Medicine, Science Citation Index Expanded (also known as SciSearch®) and Journal Citation Reports/Science Edition, *Index Medicus*, MEDLINE and PubMed, Chemical Abstracts, EMBASE/Excerpta Medica, Abstracts Journals, *Nature Clinical Practice Gastroenterology and Hepatology*, CAB Abstracts and Global Health. ISI JCR 2003-2000 IF: 3.318, 2.532, 1.445 and 0.993.

Published by

The WJG Press

SUBMISSION OF MANUSCRIPTS

Manuscripts should be typed double-spaced on A4 (297 mm × 210 mm) white paper with outer margins of 2.5 cm. Number all pages consecutively, and start each of the following sections on a new page: Title Page , Abstract, Introduction, Materials and Methods, Results, Discussion, acknowledgements, References, Tables, Figures and Figure Legends. Neither the editors nor the Publisher is responsible for the opinions expressed by contributors. Manuscripts formally accepted for publication become the permanent property of The WJG Press, and may not be reproduced by any means, in whole or in part without the written permission of both the authors and the Publisher. We reserve the right to put onto our website and copy-edit accepted manuscripts. Authors should also follow the guidelines for the care and use of laboratory animals of their institution or national animal welfare committee.

Authors should retain one copy of the text, tables, photographs and illustrations, as rejected manuscripts will not be returned to the author(s) and the editors will not be responsible for the loss or damage to photographs and illustrations in mailing process.

Online submission

Online submission is strongly advised. Manuscripts should be submitted through the Online Submission System at: http://www.wjgnet.com/index.jsp. Authors are highly recommended to consult the ONLINE INSTRUCTIONS TO AUTHORS (http://www.wjgnet.com/wjg/help/instructions.jsp) before attempting to submit online. Authors encountering problems with the Online Submission System may send an email you describing the problem to wjg@wjgnet.com for assistance. If you submit your manuscript online, do not make a postal contribution. A repeated online submission for the same manuscript is strictly prohibited.

Postal submission

Send 3 duplicate hard copies of the full-text manuscript typed double-spaced on A4 (297 mm × 210 mm) white paper together with any original photographs or illustrations and a 3.5 inch computer diskette or CD-ROM containing an electronic copy of the manuscript including all the figures, graphs and tables in native Microsoft Word format or *.rtf format to:

Editorial Office

World Journal of Gastroenterology
Editorial Department: Apartment 1066, Yishou Garden,
58 North Langxinzhuang Road,
PO Box 2345, Beijing 100023, China
E-mail: wjg@wjgnet.com
http: //www.wjgnet.com
Telephone: +86-10-85381892
Fax: +86-10-85381893

MANUSCRIPT PREPARATION

All contributions should be written in English. All articles must be submitted using a word-processing software. All submissions must be typed in 1.5 line spacing and in word size 12 with ample margins. The letter font is Tahoma. For authors from China, one copy of the Chinese translation of the manuscript is also required (excluding references). Style should conform to our house format. Required information for each of the manuscript sections is as follows:

Title page

Full manuscript title, running title, all author(s) name(s), affiliations, institution(s) and/or department(s) where the work was accomplished, disclosure of any financial support for the research, and the name, full address, telephone and fax numbers and email address of the corresponding author should be included. Titles should be concise and informative (removing all unnecessary words), emphasize what is new, and avoid abbreviations. A short running title of less than 40 letters should be provided. List the author(s)' name(s) as follows: initial and/or first name, middle name or initial(s) and full family name.

Abstract

An informative, structured abstract of no more than 250 words should accompany each manuscript. Abstracts for original contributions should be structured into the following sections: AIM: Only the purpose should be included. METHODS: The materials, techniques, instruments and equipments, and the experimental procedures should be included. RESULTS: The observatory and experimental results, including data, effects, outcome, *etc.* should be included. Authors should present *P* value where necessary, and the significant data should accompany. CONCLUSION: Accurate view and the value of the results should be included.

The format of structured abstracts is at: http://www.wjgnet.com/wjg/help/11.doc

Key words

Please list 5-10 key words that could reflect content of the study mainly from *Index Medicus*.

Text

For most article types, the main text should be structured into the following sections: INTRODUCTION, MATERIALS AND METHODS, RESULTS and DISCUSSION, and should include in appropriate Figures and Tables. Data should be presented in the body text or in Figures and Tables, but not in both.

Illustrations

Figures should be numbered as 1, 2, 3 and so on, and mentioned clearly in the main text. Provide a brief title for each figure on a separate page. No detailed legend should be involved under the figures. This part should be added into the text where the figures are applicable. Digital images: black and white photographs should be scanned and saved in TIFF format at a resolution of 300 dpi; color images should be saved as CMYK (print files) but not as RGB (screen-viewing files). Place each photograph in a separate file. Print images: supply images of size no smaller than 126 mm × 85 mm printed on smooth surface paper; label the image by writing the Figure number and orientation using an arrow. Photomicrographs: indicate the original magnification and stain in the legend. Digital Drawings: supply files in EPS if created by freehand and illustrator, or TIFF from photoshops. EPS files must be accompanied by a version in native file format for editing purposes. Existing line drawings should be scanned at a resolution of 1200 dpi and as close as possible to the size where they will appear when printed. Please use uniform legends for the same subjects. For example: Figure 1 Pathological changes of atrophic gastritis after treatment. A: ...; B: ...; C: ...; D: ...; E: ...; F: ...; G: ...

Tables

Three-line tables should be numbered as 1, 2, 3 and so on, and mentioned clearly in the main text. Provide a brief title for each table. No detailed legend should be included under the tables. This part should be added into the text where the tables are applicable. The information should complement but not duplicate that contained in the text. Use one horizontal line under the title, a second under the column heads, and a third below the Table, above any footnotes. Vertical and italic lines should be omitted.

Notes in tables and illustrations

Data that are not statistically significant should not be noted. $^{a}P<0.05$, $^{b}P<0.01$ should be noted ($P>0.05$ should not be noted). If there are other series of *P* values, $^{c}P<0.05$ and $^{d}P<0.01$ are used. Third series of *P* values can be expressed as $^{e}P<0.05$ and $^{f}P<0.01$. Other notes in tables or under

illustrations should be expressed as ^{1}F, ^{2}F, ^{3}F; or some other symbols with a superscript (Arabic numerals) in the upper left corner. In a multi-curve illustration, each curve should be labeled with ●, ○, ■, □, ▲, △, *etc.* in a certain sequence.

Acknowledgments

Brief acknowledgments of persons who have made genuine contributions to the manuscripts and who endorse the data and conclusions are included. Authors are responsible for obtaining written permission to use any copyrighted text and/or illustrations.

REFERENCES

Coding system

The author should code the references according the citation order in text in Arabic numerals, put references codes in square brackets, superscript it at the end of citation content or the author name of the citation. For those citation content as the narrate part, the coding number and square brackets should be typeset normally. For example, Crohn's disease (CD) is associated with increased intestinal permeability[1,2]. If references are directly cited in the text, they would be put together with the text, for example, from references [19,22-24], we know that...

When the authors code the references, please ensure that the order in text is the same as in reference part and also insure the spelling accuracy of the first author's name. Do not code the same citation twice.

PMID requirement

PMID roots in the abstract serial number indexed by PubMed (http://www.ncbi.nlm.nih.gov/entrez/query.fcgi?db=PubMed). The author should supply the PMID for journal citation. For those references that have not been indexed by PubMed, a printed copy of the first page of the full reference should be submitted.

The accuracy of the information of the journal citations is very important. Through reference testing system, the authors and editor could check the authors name, title, journal title, publication date, volume number, start page, and end page. We will interlink all references with PubMed in ASP file so that the readers can read the abstract of the citations online immediately.

Style for journal references

Authors: the first author should be typed in bold-faced letter. The surname of all authors should be typed with the initial letter capitalized and followed by their name in abbreviation (For example, Lian-Sheng Ma is abbreviated as Ma LS, Bo-Rong Pan as Pan BR). Title of the cited article and italicized journal title (Journal title should be in its abbreviation form as shown in PubMed), publication date, volume number (in black), start page, and end page [PMID: 11819634]

Note: The author should test the references through reference testing system (http://www.wjgnet.com/cgi-bin/index.pl)

Style for book references

Authors: the first author should be typed in bold-faced letter. The surname of all authors should be typed with the initial letter capitalized and followed by their name in abbreviation (For example, Lian-Sheng Ma is abbreviated as Ma LS, Bo-Rong Pan as Pan BR) Book title. Publication number. Publication place: Publication press, Year: start page and end page.

Format

Journals

English journal article (list all authors and include the PMID where applicable)

1 **Grover VP**, Dresner MA, Forton DM, Counsell S, Larkman DJ, Patel N, Thomas HC, Taylor-Robinson SD. Current and future applications of magnetic resonance imaging and spectroscopy of the brain in hepatic encephalopathy. *World J Gastroenterol* 2006; **12**: 2969-2978 [PMID: 16718775]

Chinese journal article (list all authors and include the PMID where applicable)

2 **Lin GZ**, Wang XZ, Wang P, Lin J, Yang FD. Immunologic effect of Jianpi Yishen decoction in treatment of Pixu-diarrhoea. *Shijie Huaren Xiaohua Zazhi* 1999; **7**: 285-287

In press

3 **Tian D**, Araki H, Stahl E, Bergelson J, Kreitman M. Signature of balancing selection in Arabidopsis. *Proc Natl Acad Sci U S A* 2006; In press

Organization as author

4 **Diabetes Prevention Program Research Group**. Hypertension, insulin, and proinsulin in participants with impaired glucose tolerance. *Hypertension* 2002; **40**: 679-686 [PMID: 12411462]

Both personal authors and an organization as author

5 **Vallancien G**, Emberton M, Harving N, van Moorselaar RJ; Alf-One Study Group. Sexual dysfunction in 1, 274 European men suffering from lower urinary tract symptoms. *J Urol* 2003; **169**: 2257-2261 [PMID: 12771764]

No author given

6 21st century heart solution may have a sting in the tail. *BMJ* 2002; **325**: 184 [PMID: 12142303]

Volume with supplement

7 **Geraud G**, Spierings EL, Keywood C. Tolerability and safety of frovatriptan with short- and long-term use for treatment of migraine and in comparison with sumatriptan. *Headache* 2002; **42** Suppl 2: S93-99 [PMID: 12028325]

Issue with no volume

8 **Banit DM**, Kaufer H, Hartford JM. Intraoperative frozen section analysis in revision total joint arthroplasty. *Clin Orthop Relat Res* 2002; (**401**): 230-238 [PMID: 12151900]

No volume or issue

9 Outreach: bringing HIV-positive individuals into care. *HRSA Careaction* 2002; 1-6 [PMID: 12154804]

Books

Personal author(s)

10 **Sherlock S**, Dooley J. Diseases of the liver and billiary system. 9th ed. Oxford: Blackwell Sci Pub, 1993: 258-296

Chapter in a book (list all authors)

11 **Lam SK**. Academic investigator's perspectives of medical treatment for peptic ulcer. In: Swabb EA, Azabo S. Ulcer disease: investigation and basis for therapy. New York: Marcel Dekker, 1991: 431-450

Author(s) and editor(s)

12 **Breedlove GK**, Schorfheide AM. Adolescent pregnancy. 2nd ed. Wieczorek RR, editor. White Plains (NY): March of Dimes Education Services, 2001: 20-34

Conference proceedings

13 **Harnden P**, Joffe JK, Jones WG, editors. Germ cell tumours V. Proceedings of the 5th Germ Cell Tumour Conference; 2001 Sep 13-15; Leeds, UK. New York: Springer, 2002: 30-56

Conference paper

14 **Christensen S**, Oppacher F. An analysis of Koza's computational effort statistic for genetic programming. In: Foster JA, Lutton E, Miller J, Ryan C, Tettamanzi AG, editors. Genetic programming. EuroGP 2002: Proceedings of the 5th European Conference on Genetic Programming; 2002 Apr 3-5; Kinsdale, Ireland. Berlin: Springer, 2002: 182-191

Electronic journal (list all authors)

Morse SS. Factors in the emergence of infectious diseases. Emerg Infect Dis serial online, 1995-01-03, cited 1996-06-05; 1(1): 24 screens. Available from: URL: http//www.cdc.gov/ncidod/EID/eid.htm

Patent (list all authors)

16 **Pagedas AC**, inventor; Ancel Surgical R&D Inc., assignee. Flexible endoscopic grasping and cutting device and positioning tool assembly. United States patent US 20020103498. 2002 Aug 1

Inappropriate references

Authors should always cite references that are relevant to their article, and avoid any inappropriate references. Inappropriate references include those that are linked with a hyphen and the difference between the two numbers at two sides of the hyphen is more than 5. For example, [1-6], [2-14] and [1, 3, 4-10, 22] are all considered as inappropriate references. Authors should not cite their own unrelated published articles.

Statistical data

Present as mean ± SD or mean ± SE.

Statistical expression

Express t test as t (in italics), F test as F (in italics), chi square test as χ^2 (in Greek), related coefficient as r (in italics), degree of freedom as γ (in Greek), sample number as n (in italics), and probability as P (in italics).

Units

Use SI units. For example: body mass, m (B) = 78 kg; blood pressure, p(B) = 16.2/12.3 kPa; incubation time, t (incubation) = 96 h, blood glucose concentration, c (glucose) 6.4 ± 2.1 mmol/L; blood CEA mass concentration, p (CEA) = 8.6 24.5 μg/L; CO_2 volume fraction, 50 mL/L CO_2 not 5% CO_2; likewise for 40 g/L formaldehyde, not 10% formalin; and mass fraction, 8 ng/g, *etc.* Arabic numerals such as 23, 243, 641 should be read 23 243 641.

The format about how to accurately write common units and quantum is at: http://www.wjgnet.com/wjg/help/15.doc

Abbreviations
Standard abbreviations should be defined in the abstract and on first mention in the text. In general, terms should not be abbreviated unless they are used repeatedly and the abbreviation is helpful to the reader. Permissible abbreviations are listed in Units, Symbols and Abbreviations: A Guide for Biological and Medical Editors and Authors (Ed. Baron DN, 1988) published by The Royal Society of Medicine, London. Certain commonly used abbreviations, such as DNA, RNA, HIV, LD50, PCR, HBV, ECG, WBC, RBC, CT, ESR, CSF, IgG, ELISA, PBS, ATP, EDTA, mAb, can be used directly without further mention.

Italics
Quantities: *t* time or temperature, *c* concentration, *A* area, *l* length, *m* mass, *V* volume.
Genotypes: *gyr*A, *arg* 1, *c myc*, *c fos*, *etc.*
Restriction enzymes: *Eco*RI, *Hin*dI, *Bam*HI, *Kbo* I, *Kpn* I, *etc.*
Biology: *H pylori, E coli, etc.*

SUBMISSION OF THE REVISED MANUSCRIPTS AFTER ACCEPTED

Please revise your article according to the revision policies of *WJG*. The revised version including manuscript and high-resolution image figures (if any) should be copied on a floppy or compact disk. Author should send the revised manuscript, along with printed high-resolution color or black and white photos, copyright transfer letter, the final check list for authors, and responses to reviewers by a courier (such as EMS) (submission of revised manuscript by e-mail or on the *WJG* Editorial Office Online System is NOT available at present).

Language evaluation
The language of a manuscript will be graded before sending for revision. (1) Grade A: priority publishing; (2) Grade B: minor language polishing; (3) Grade C: a great deal of language polishing; (4) Grade D: rejected. The revised articles should be in grade B or grade A.

Copyright assignment form
Please downloaded CAF from http://www.wjgnet.com/wjg/help/9.doc.

We certify that the material contained in this manuscript:

Ms:

Title:

is original, except when appropriately referenced to other sources, and that written permission has been granted by any existing copyright holders. We agree to transfer to WJG all rights of our manuscript, including: (1) all copyright ownership in all print and electronic formats; (2) the right to grant permission to republish or reprint the stated material in whole or in part, with or without a fee; (3) the right to print copies for free distribution or sale; (4) the right to republish the stated material in a collection of articles or in any other format. We also agree that our article be put on the Internet.

Criteria for authorship: The WJG requests and publishes information about contributions of each author named to the submitted study. Authorship credit should be based on (1)direct participation in the study, including substantial contributions to conception and design of study, or acquisition of data, or analysis and interpretation of data; (2) manuscript writing, including drafting the article, or revising it critically for important intellectual content; (3)supportive work, including statistical analysis of data, or acquisition of funding, or administration, technology and materials support, or supervision, or supportive contributions. Authors should meet at least one of the three conditions. The WJG does not publish co-first authors and co-corresponding authors.

We hereby assign copyright transfer to WJG if this paper is accepted.

Author Name in full (Full names should be provided, with first name first, followed by middle names and family name at the last, eg, Eamonn MM Quigley). Handwritten names are not accepted.

Author Name in abbreviation (Family name is put first in full, followed by middle names and first name in abbreviation with first letter in capital, eg, Quigley EMM). Handwritten names are not accepted.

1 Full Name: _____
Abbreviation Name: _____
Signed: _____
Date: _____

2 Full Name: _____
Abbreviation Name: _____
Signed: _____
Date: _____

3 Full Name: _____
Abbreviation Name: _____
Signed: _____
Date: _____

4 Full Name: _____
Abbreviation Name: _____
Signed: _____
Date: _____

5 Full Name: _____
Abbreviation Name: _____
Signed: _____
Date: _____

6 Full Name: _____
Abbreviation Name: _____
Signed: _____
Date: _____

7 Full Name: _____
Abbreviation Name: _____
Signed: _____
Date: _____

8 Full Name: _____
Abbreviation Name: _____
Signed: _____
Date: _____

9 Full Name: _____
Abbreviation Name: _____
Signed: _____
Date: _____

10 Full Name: _____
Abbreviation Name: _____
Signed: _____
Date: _____

Final check list for authors
The format is at: http://www.wjgnet.com/wjg/help/13.doc

Responses to reviewers
Please revise your article according to the comments/suggestions of reviewers. The format for responses to the reviewers' comments is at: http://www.wjgnet.com/wjg/help/10.doc

Proof of financial support
For paper supported by a foundation, authors should provide a copy of the document and serial number of the foundation.

Publication fee
Authors of accepted articles must pay publication fee.
EDITORIAL and LETTERS TO THE EDITOR are free of change.

World Journal of
Gastroenterology®
Volume 13 Number 3
January 21, 2007

National Journal Award
2005

The WJG Press

The WJG Press, Apartment 1066 Yishou Garden, 58 North
Langxinzhuang Road, PO Box 2345, Beijing 100023, China
Telephone: +86-10-85381901
Fax: +86-10-85381893
E-mail: wjg@wjgnet.com
http: //www.wjgnet.com

ISSN 1007-9327 CN 14-1219/R Local Post Offices Code No. 82-261

World Journal of Gastroenterology www.wjgnet.com Volume 13 Number 03 Jan 21 2007

ISSN 1007-9327
CN 14-1219/R

World Journal of
Gastroenterology®

Indexed and Abstracted in:

Current Contents®/Clinical Medicine, Science Citation Index Expanded (also known as SciSearch®) and Journal Citation Reports/Science Edition, *Index Medicus*, MEDLINE and PubMed, Chemical Abstracts, EMBASE/Excerpta Medica, Abstracts Journals, *Nature Clinical Practice Gastroenterology and Hepatology*, CAB Abstracts and Global Health.
ISI JCR 2003-2000 IF: 3.318, 2.532, 1.445 and 0.993.

Volume 13 Number 3
January 21, 2007

World J Gastroenterol
2007 January 21; 13(3): 329-492
Online Submissions
www.wjgnet.com/wjg/index.jsp
www.wjgnet.com
Printed on Acid-free Paper

A Weekly Journal of Gastroenterology and Hepatology

National Journal Award
2005

World Journal of Gastroenterology®

Volume 13 Number 3
January 21, 2007

The WJG Press

Contents

World Journal of Gastroenterology
Volume 13 **Number** 3 **January** 21, 2007

Contents

World Journal of Gastroenterology
Volume 13 **Number** 3 **January** 21, 2007

Contents

Responsible E-Editor for this issue: Ling Bi

C-Editor for this issue: Thierry Piche, MD, PhD

Responsible S-Editor for this issue: Jing Wang

World Journal of Gastroenterology (*World J Gastroenterol , WJG*), a leading international journal in gastroenterology and hepatology, has an established reputation for publishing first class research on esophageal cancer, gastric cancer, liver cancer, viral hepatitis, colorectal cancer, and *H pylori* infection, providing a forum for both clinicians and scientists, and has been indexed and abstracted in Current Contents®/Clinical Medicine, Science Citation Index Expanded (also known as SciSearch®) and Journal Citation Reports/Science Edition, *Index Medicus*, MEDLINE and PubMed, Chemical Abstracts, EMBASE/Excerpta Medica, Abstracts Journals, *Nature Clinical Practice Gastroenterology and Hepatology*, CAB Abstracts and Global Health. ISI JCR 2003-2000 IF: 3.318, 2.532, 1.445 and 0.993. *WJG* is a weekly journal published by The WJG Press. The publication date is on 7th, 14th, 21st, and 28th every month. The *WJG* is supported by The National Natural Science Foundation of China, No. 30224801 and No.30424812, which was founded with a name of *China National Journal of New Gastroenterology* on October 1,1995, and renamed as *WJG* on January 25, 1998.

PUBLISHED BY
The WJG Press

PRINTED BY
Printed in Beijing on acid-free paper by Beijing Kexin Printing House

 Print ISSN 1007-9327
CN 14-1219/R.

EDITORIAL OFFICE
World Journal of Gastroenterology,
The WJG Press, Apartment 1066 Yishou Garden, 58 North Langxinzhuang Road, PO Box 2345, Beijing 100023, China
Telephone: +86-10-85381892
Fax: +86-10-85381893
E-mail: wjg@wjgnet.com
http://www.wjgnet.com

SUBSCRIPTION AND AUTHOR REPRINTS
Jing Wang
The WJG Press, Apartment 1066 Yishou Garden, 58 North Langxinzhuang Road, PO Box 2345, Beijing 100023, China
Telephone: +86-10-85381892
Fax: +86-10-85381893
E-mail: j.wang@wjgnet.com
http://www.wjgnet.com

SUBSCRIPTION INFORMATION
Institutional Price 2007: USD 1500.00
Personal Price 2007: USD 700.00

INSTRUCTIONS TO AUTHORS
Full instructions are available online at http://www.wjgnet.com/wjg/help/instructions.jsp. If you do not have web access please contact the editorial office.

PO Box 2345, Beijing 100023, China
www.wjgnet.com
wjg@wjgnet.com

World J Gastroenterol 2007 January 21; 13(3): 329-340
World Journal of Gastroenterology ISSN 1007-9327

EDITORIAL

Assessment of drug-induced hepatotoxicity in clinical practice: A challenge for gastroenterologists

Raúl J Andrade, Mercedes Robles, Alejandra Fernández-Castañer, Susana López-Ortega, M Carmen López-Vega, M Isabel Lucena

Raúl J Andrade, Mercedes Robles, Alejandra Fernández-Castañer, Susana López-Ortega, M Carmen López-Vega, Liver Unit, Gastroenterology Service, "Virgen de la Victoria" University Hospital and School of Medicine, Málaga, Spain
M Isabel Lucena, Clinical Pharmacology Service, "Virgen de la Victoria" University Hospital and School of Medicine, Málaga, Spain
Supported partly by research grants from the Agencia Española del Medicamento and from the Fondo de Investigación Sanitaria (FIS 04-1688 and FIS 04-1759)
Correspondence to: Professor Raúl J Andrade, MD, PhD, Unidad de Hepatología, Departamento de Medicina, Facultad de Medicina, Boulevard Louis Pasteur 32, Málaga 29071, Spain. andrade@uma.es
Telephone: +34-952-134242 Fax: +34-952-131511
Received: 2006-08-24 Accepted: 2006-11-29

Abstract

Currently, pharmaceutical preparations are serious contributors to liver disease; hepatotoxicity ranking as the most frequent cause for acute liver failure and post-commercialization regulatory decisions. The diagnosis of hepatotoxicity remains a difficult task because of the lack of reliable markers for use in general clinical practice. To incriminate any given drug in an episode of liver dysfunction is a step-by-step process that requires a high degree of suspicion, compatible chronology, awareness of the drug's hepatotoxic potential, the exclusion of alternative causes of liver damage and the ability to detect the presence of subtle data that favors a toxic etiology. This process is time-consuming and the final result is frequently inaccurate. Diagnostic algorithms may add consistency to the diagnostic process by translating the suspicion into a quantitative score. Such scales are useful since they provide a framework that emphasizes the features that merit attention in cases of suspected hepatic adverse reaction as well. Current efforts in collecting bona fide cases of drug-induced hepatotoxicity will make refinements of existing scales feasible. It is now relatively easy to accommodate relevant data within the scoring system and to delete low-impact items. Efforts should also be directed toward the development of an abridged instrument for use in evaluating suspected drug-induced hepatotoxicity at the very beginning of the diagnosis and treatment process when clinical decisions need to be made. The instrument chosen would enable a confident diagnosis to be made on admission of the patient and treatment to be fine-tuned as further information is collected.

Key words: Drug-induced hepatotoxicity; Causality assessment; Diagnostic algorithms; Clinical scales

Andrade RJ, Robles M, Fernández-Castañer A, López-Ortega S, López-Vega MC, Lucena MI. Assessment of drug-induced hepatotoxicity in clinical practice: A challenge for gastroenterologists. *World J Gastroenterol* 2007; 13(3): 329-340

http://www.wjgnet.com/1007-9327/13/329.asp

INTRODUCTION

Idiosyncratic liver disease caused by drugs or toxins is a major challenge of modern hepatology, and is a somewhat neglected field as well. The reasons for this are varied. Firstly, hepatotoxicity is rarely encountered in standard clinical practice because of its relatively low incidence compared to other hepatic diseases and the difficulties in confidently diagnosing the condition. Secondly, there have not been substantial advances in recent decades in the understanding of its pathogenesis, which is mostly due to the lack of validated animal models for investigating idiosyncratic hepatotoxicity. As such, susceptibility factors that can predispose individuals to adverse hepatic reactions to drugs have not been conclusively identified, nor has there been any development of reliable and standardized markers for the identification and measurement of toxic liver damage[1]. Co-operative efforts are being encouraged so as to prospectively collect bona fide cases from which quality data and biological samples could be obtained for genome-wide studies[2,3].

Hepatotoxicity has a considerable impact on health because many of the hepatic reactions induced by pharmaceutical preparations can be very severe. A survey from the Acute Liver Failure Study Group (ALFSG) of the patients admitted in 17 US hospitals showed that prescribed drugs (including acetaminophen) accounted for > 50% of cases of acute liver failure[4]. Indeed, drug-induced hepatotoxicity is still the main reason for cessation of further drug development and, as well, for post-approval drug regulatory decisions including removal of several culprit drugs from the market[5]. Recent examples

in the USA and Europe are troglitazone, bromfenac, trovafloxacin, ebrotidine, nimesulide, nefazodone and ximelagatran[6-8].

CLINICAL PRESENTATION OF DRUG-INDUCED HEPATOTOXICITY

In standard clinical practice, drug-induced hepatotoxicity may present in several ways (clinical and pathological) that simulate known forms of acute and chronic liver diseases; the severity ranging from sub-clinical elevations in liver enzyme concentrations to acute liver failure. Gastroenterologists need to bear hepatotoxicity in mind when conducting a differential diagnosis in every patient who presents with liver dysfunction. Mainly, drugs tend to induce acute hepatitis, cholestasis or a mixed condition. A clinical picture resembling acute viral hepatitis with jaundice, malaise, anorexia, nausea and abdominal pain is the principal presentation but, because every liver cell may be the target of drug-induced toxicity, many other expressions of hepatotoxicity may be evident including chronic hepatitis, cirrhosis, sinusoidal obstruction syndrome or neoplasm[9].

Liver histology (although not very specific and at best resulting in "compatible with") is the ideal tool to date for defining the pattern of hepatotoxicity. However, since a liver biopsy specimen is often not available, the pattern of drug-related liver injury is, from a practical standpoint, classified according to laboratory data. This mainly includes the activity of serum alanine aminotransferase (ALT) and alkaline phosphatase (AP) with the increase in activity being expressed with respect to the upper limit of normal (ULN) and the ratio of the measured activities[10]. This classification is somewhat arbitrary and insufficient in classifying all types of drug-induced liver damage (e.g. vascular lesions and chronic damage, in general), however, the system does have some prognostic value.

Acute hepatocellular (e.g., cytotoxic, cytolytic) liver injury is defined by ALT > 2-fold that of ULN (2N) or an ALT/AP ratio $\geqslant 5$[10]. Patients with this particular type of liver damage have non-specific clinical features, and jaundice is not always evident. Sometimes there are clues of drug allergy, such as fever, rash or peripheral eosinophilia. Serum levels of aminotransferase are markedly increased. Liver histology shows variable degrees of cell necrosis and inflammation, mainly in zone 3 of the hepatic accini together with an abundance of eosinophils in the infiltrate, which is consistent with a toxic etiology[9,11-14]. These expressions of hepatotoxicity are observed with many drugs (Table 1). Patients with acute hepatocellular injury related to drugs are at risk of acute liver failure. The observation by Hyman Zimmerman, known as "Hy's rule"[9], predicts a mean mortality (or its surrogate marker, liver transplantation) of 10% for jaundiced patients with acute toxic hepatocellular damage (providing total bilirubin is not elevated as a result of other causes such as biliary obstruction or Gilbert syndrome). Two recent studies[3,15] have validated this observation using multivariate analysis, and they indicated that, apart from total bilirubin and the hepatocellular-type of injury, other variables such older age, female gender and AST levels were independently associated with a poor outcome[3,15].

Acute cholestatic injury, defined as an increase in serum AP > 2N or by an ALT/AP $\leqslant 2$ is classified into two subtypes: pure, "bland" or canalicular cholestasis; and acute cholestatic or hepatocanalicular hepatitis. Patients with acute cholestasis usually present with jaundice and itching. The canalicular pattern is characterized by an increase in conjugated bilirubin, AP and γ-glutamyl transpeptidase (γ-GT) with minimal, if any, impairment in serum transaminases. Liver biopsy shows hepatocyte cholestasis and dilated biliary canaliculi with bile plugs, but with little or no inflammation and necrosis[14]. Anabolic and contraceptive steroids typically produce this expression of hepatotoxicity.

Symptoms in the hepatocanalicular type of damage include abdominal pain and fever and, as such, resemble acute biliary obstruction. However, the associated hypersensitivity features that sometimes occur are an important clue toward the diagnosis of hepatotoxicity. Liver biopsy reveals variable degrees of portal inflammation and hepatocyte necrosis, in addition to marked cholestasis of centrilobular predominance[9,11,14]. Older age has been found to increase the likelihood of drug-induced hepatotoxicity being expressed as cholestatic damage[3,16]. Typical examples of drugs that cause this variety of liver damage are amoxicillin-clavulanate, macrolide antibiotics and phenothiazine neuroleptics, but many others have a similar capacity (Table 2).

In mixed hepatic injury the clinical and biological picture is intermediate between the hepatocellular and cholestatic patterns, and features of either type may predominate. By definition, the ALT/AP ratio is between 2 and 5. Allergy reactions are often present, as well as a granulomatous reaction in the liver biopsy specimen. When faced with a mixed hepatitis clinical picture, the gastroenterologists should always seek a culprit medication since this type of injury is far more characteristic of drug-induced hepatotoxicity than of viral hepatitis[9]. Almost all drugs that produce cholestatic injury are also capable of inducing a mixed pattern.

Although drug-induced cholestatic and mixed lesions progress to acute liver failure less frequently than hepatocellular types, their resolution is generally slower. For example, a long-term follow-up of a large cohort in a Registry demonstrated a significantly higher trend towards becoming chronic in cholestatic/mixed cases compared to hepatocelullar-type disease[17].

DIAGNOSIS IN THE CLINICAL SETTING

A straightforward diagnosis of hepatotoxicity in clinical practice is seldom possible. An exception is when symptoms of hepatitis rapidly ensue following the obvious exposure to an over-dosage of intrinsic hepatotoxins, such as acetaminophen. In these circumstances, blood concentrations of the compound could be used to confirm the suspicion. In a few other instances the diagnosis can be easily established if liver damage becomes apparent after re-exposure to a drug that had been suspected as being the cause of previous hepatitis. This topic of re-challenge is discussed in more detail later.

Table 1 Medications, herbal products and illicit drugs related to the hepatocellular-type of damage

Compound	Other injury	Comments
Acarbose		FHF
Allopurinol	Granuloma	Hypersensitivity
Amiodarone	Phospholipidosis, cirrhosis	
Amoxicillin, Ampicillin		
Anti-HIV: (Didanosine, Zidovudine, protease inhibitors)		
NSAIDs (AAS, Ibuprofen, Diclofenac, Piroxicam, Indometacin)		Nimesulide; withdrawn
Asparaginase	Steatosis	
Bentazepam	Chronic hepatitis	
Chlormethizole	Cholestatic hepatitis	FHF
Cocaine, Ecstasy and amphetamine derivatives		FHF
Diphenytoin		Hypersensitivity
Disulfiram		FHF
Ebrotidine	Cirrhosis	FHF
Fluoxetine, Paroxetine	Chronic hepatitis	
Flutamide		FHF
Halothane		
Hypolipemics; Lovastatin, Pravastatin, Simvastatin, Atorvastatin		
Isoniazid	Granuloma, chronic hepatitis	FHF
Ketoconazole, Mebendazole, Albendazole, Pentamidine		FHF
Mesalazine	Chronic hepatitis	Autoimmune features
Methotrexate	Steatosis, fibrosis, cirrhosis	
Minocycline	Chronic hepatitis, steatosis	Autoimmune features
Nitrofurantoin	Chronic hepatitis	
Nefazodone		FHF, withdrawn
Omeprazole		
Penicillin G	Prolonged cholestasis	
Pyrazinamide		
Herbal remedies		FHF
Germander (Teucrium chamaedrys), senna		
Pennyroyal oil, kava-kava		
Camellia sinnensis (green tea); Chinese herbal medicines		
Risperidone		
Ritodrine		
Sulfasalazine		Hypersensitivity
Telithromycin		
Terbinafine	Cholestatic hepatitis	FHF
Tetracycline	Micro-steatosis	FHF
Tolcapone		FHF, withdrawn
Topiramate		
Trazodone	Chronic hepatitis	
Trovafloxacin		FHF, withdrawn in Europe
Valproic acid	Micro-steatosis	
Venlafaxine		
Verapamil	Granuloma	
Vitamin A	Fibrosis, cirrhosis	
Ximelagatran		FHF, discontinued

Features of hypersensitivity include fever, rash and eosinophilia; FHF: Fulminant hepatic failure.

Direct evidence for idiosyncratic hepatotoxicity is rarely available. This includes, for a few drugs, the detection of serum circulating autoantibodies to specific forms of cythocrome P450 (Table 3). Most of these drugs have been withdrawn from the market. This circumstance, in addition to uncertainty regarding sensitivity and specificity of the autoantibody test, makes such a situation irrelevant in current clinical practice[18].

Another tool that has been used in the search for evidence of drug allergy is the lymphocyte-stimulation test. This comprises counting of lymphocyte proliferation following exposure of peripheral blood mononuclear cells (monocytes) from the patient to the suspected drug *in vitro*. Using radiolabel led thymidine incorporation in the presence of a prostaglandin inhibitor (such as indometacin), prevents the suppressive influence of activated monocytes on T-cells[19,20]. However, a positive response merely indicates sensitization towards a certain drug and cannot actually be related to effector mechanisms (symptoms) while, on the contrary, a negative test does

Table 2 Medications associated with the cholestatic-type damage

Compound	Other injury	Comment
Cholestasis without hepatitis (canalicular/bland/pure jaundice)		
Estrogens, contraceptive steroids and anabolic-steroids (Budd-Chiari, adenoma, carcinoma, peliosis hepatitis, adenoma, carcinoma)		
Cholestatis with hepatitis (hepatocanalicular jaundice)		
Amoxicillin-clavulanic acid	Chronic cholestasis	VBDS
Atorvastatin	Chronic cholestasis	
Azathioprine	Chronic cholestasis	
Benoxaprofen (withdrawn)		
Bupropion	Chronic cholestasis	
Captopril, enalapril, fosinopril		
Carbamazepine	Chronic cholestasis	VBDS
Carbimazole		
Cloxacillin, dicloxacillin, flucloxacillin		
Clindamycin	Chronic cholestasis	
Ciprofloxacin, norfloxacin		
Cyproheptadine	Chronic cholestasis	VBDS
Diazepam, nitrazepam		
Erythromycins	Chronic cholestasis	VBDS
Gold compounds, penicillamine		
Herbal remedies:		
Chaparral leaf (Larrea tridentate); Glycyrrhizin, greater celandine (Chelidonium majus)		
Irbesartan	Chronic cholestasis	
Lipid lowering agents ("statins")		
Macrolide antibiotics		
Mianserin		
Mirtazapine	Chronic cholestasis	
Phenotiazines (chlorpromazine)	Chronic cholestasis	
Robecoxib, celecoxib		
Rosiglitazone, oioglitazone		
Roxithromycin	Chronic cholestasis	
Sulfamethoxazole-trimethoprim	Chronic cholestasis	VBDS
Sulfonamides	Chronic cholestasis	
Sulfonylureas (Glibenclamide, Chlorpropamide)		
Sulindac, piroxicam, diclofenac, ibuprofen		
Terbinafine	Chronic cholestasis	VBDS
Tamoxifen	Hepatocellular, peliosis Chronic cholestasis	
Tetracycline	Chronic cholestasis	
Ticlopidine & Clopidogrel	Chronic cholestasis	
Thiabendazole		VBDS
Tricyclic antidepressants (Amitriptyline, Imipramine)	Chronic cholestasis	VBDS
Sclerosing cholangitis-like	Floxuridine (intra-arterial)	
Cholangiodestructive (primary biliary cirrhosis)	Chlorpromazine, ajmaline	

VBDS: Vanishing bile duct syndrome.

Table 3 Autoantibodies specific to drug-induced hepatotoxicity

Autoantibody	Example
Anti-mitochondrial (anti-M6) autoantibody	Iproniazid
Anti-liver kidney microsomal 2 antibody (anti-LKM2)	Tienilic acid
Anti CYP 1A2	Dihydralazine
Anti CYP 2E1	Halothane
Anti-liver microsomal autoantibody	Carbamazepine
Anti-microsomal epoxide hydrolase	Germander

CYP: Cytochrome P450.

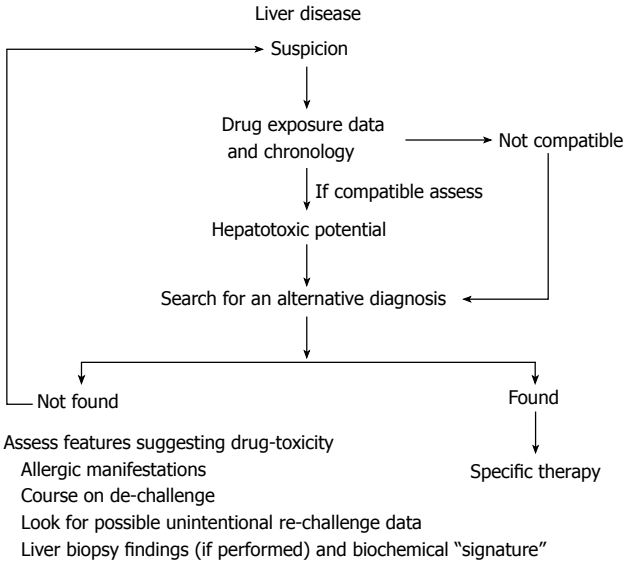

Figure 1 Approaching a suspicion of drug-induced hepatotoxicity.

not exclude drug allergy[21]. Finally, these *in vitro* tests are difficult to standardize, are poorly reproducible between laboratories, and have not gained general clinical acceptance[20,21].

Hence, in the absence of an acceptable and convenient gold standard, the diagnosis is subjective and is made with varying levels of confidence based on a combination of factors including temporal associations and with respect to latency, the rate of improvement after cessation of the drug, and the definitive exclusion of alternative possible causes[22]. Confounding features include multiple drugs prescribed for many patients, lack of information on doses consumed as well as stop and start dates[23]. A careful "step-by-step" approach should proceed according to the outline in Figure 1[24].

Screening for drug exposure and assessment of its hepatotoxic potential

A thorough drug and chemical history is essential, including prescribed and over-the-counter medications as well as consumption of illicit (recreational) drugs. Soliciting medication containers or a written medication plan, when available, assists the patient's recall and reduces errors[3]. In unconscious or confused patients or in those who are able to collaborate with the physician, the relatives or care-givers should be consulted.

The question that needs to be addressed is whether the treatment had commenced well before symptom presentation or in the early phase of hepatitis. This is because the suspected drug could actually have been prescribed to alleviate the first symptoms of hepatitis, such as gastrointestinal complaints or malaise. If this is not the case, duration of therapy with the suspected drug must be screened. Liver tests, if performed before starting the drug, can be very valuable in the patient's assessment. The latency period of different drugs varies widely. However, there is a relatively consistent "signature" for each drug

which is linked to the mechanism of damage involved. Details can usually be elicited from the patient. For instance, intrinsic hepatotoxins induce overt liver damage within a few hours of exposure. In most idiosyncratic cases, the latency period is roughly between 1 wk and 3 mo. In general, allergic hepatic reactions are likely to occur within 1 to 5 wk of taking the drug.

A delay of > 3 mo is typically seen with compounds that act by non-allergic mechanisms; i.e. "metabolic idiosyncrasy". While drug-induced acute hepatitis seldom occurs after > 12 mo of exposure, these long latency-periods are still possible in unusual forms of chronic liver damage (such as steato-hepatitis, fibrosis and chronic hepatitis) in which the expression of hepatotoxicity is symptom-less and which allows the contra-indicated treatment to continue[25-31], or simply because the type of lesion requires prolonged exposure to become manifest (e.g. vascular lesions and tumors)[32,33].

In some instances the role of a drug is difficult to recognize because of a considerable delay (up to 3 or 4 wk) between the interruption of therapy and clinical presentation of the condition. Examples include amoxicillin-clavulanate[34], midecamycin[35] and trovafloxacin[36]. The reasons for this are unclear and could be that such an unusual time-course might combine a late immune response to the drug if its retention in the body is protracted[37].

There is no clear rule in identifying the culprit drug if the patient is taking various medications simultaneously. Attention should be paid to the latest drug introduced into the patient's regimen since this is the one that is likely to have stimulated the reaction. However, when a known hepatotoxic drug antedates the latest medication introduced then it seems reasonable to ascribe the clinical picture to the combination of the drugs because of the possibility of pharmaco-kinetic interaction[3,38].

With respect to the hepatotoxic potential of screened drugs, their potentials for causing liver damage are not the same, and almost all marketed medications have been incriminated in incidences of hepatotoxicity[39]. For instance, some drugs like isoniazid, diclofenac, and amoxicillin-clavulanate are well-known hepatotoxic agents[3] while others such as digoxin rank very low on the list of hepatotoxins[9]. The main causative group of drugs, in a large cohort of hepatotoxicity cases collected in the Spanish Registry, was antibiotics followed by non-steroidal anti-inflammatory drugs (NSAIDs)[3]. Further, among the drugs most-frequently associated with idiosyncratic acute liver failure reported by the ALFSG, were antibiotics (particularly isoniazid), non-steroidal analgesics, anti-seizure medications and herbal preparations[40].

Valuable information can be accessed from databases of hepatotoxic drugs, such as HEPATOX from France[39], lists in reference textbooks[9,11,41] or more up-to-date resources such as MEDLINE-PubMed database of the National Library of Medicine where MESHing the name of the drug together with the terms "hepatotoxicity," "hepatitis," "drug-induced hepatotoxicity," or simply "liver" can provide useful details.

If the patient has been taking a newly marketed drug, the data on its hepatotoxic potential, if known, would only be available in pre-approval clinical trials (usually involving 1500-2500 patients). This size of trial would not have the power to detect significant (clinically overt) liver disease since finding hepatotoxicity with an incidence of 1:10 000 (the approximate incidence of most idiosyncratic reactions) would require 30 000 patients to be treated in the trial ("rule of threes")[42]. Nevertheless, the appearance of less prominent signals of liver damage in pre-approval studies should be carefully noted. These include the incidence of asymptomatic ALT and bilirubin elevations. An ALT $\geqslant$ 8N or a $\geqslant$ 1.5 fold increase in direct bilirubin, especially if it is accompanied by a raised ALT, deserves special attention since this rarely occurs in ostensibly normal populations.

Exclusion of other causes of liver damage

Diagnostic evaluation of any patient with acute liver disease of unknown origin should comprise a careful history to exclude alcohol abuse, recent episodes of hypotension, epidemiological risk factors of infectious hepatitis, specific serology and molecular biology studies for common viruses involved in viral hepatitis, as well as screening for autoimmune hepatitis. All patients should also have an abdominal ultrasound examination to exclude mechanical biliary obstruction.

The appropriateness of additional investigation would depend on the presence of particular symptoms or analytical features (Table 4). Patients with the cholestatic or mixed pattern of hepatic injury may require complementary imaging by magnetic resonance cholangiography or endoscopic retrograde cholangiography, despite normal abdominal ultrasound findings, so as to exclude benign or malignant obstruction of the biliary tract.

Features suggesting toxic liver damage

Once alternative causes of liver damage have been ruled out, the suspicion of drug-induced hepatotoxicity can be confirmed by a careful scrutiny of co-existing features of drug-allergy, by noting the course following drug cessation and following a re-challenge dose, as well as through biopsy findings or biochemical patterns compatible with toxic liver damage[24]. Drug-allergy manifestations are associated with widely variable hepatotoxicity rates depending, mainly, on the drug class. Features that suggest drug-allergy include, skin rash, fever, peripheral eosinophilia, short latency period (1 mo or less) and rapid symptoms recurrence on re-challenge. Hematological features including granulocytopenia, thrombopenia or hemolytic anemia as well as renal and pancreatic involvement may also accompany some instances of drug-induced immuno-allergic hepatic injury[43,44]. In rare cases the extreme skin involvement of Steven-Johnson syndrome or the Lyell syndrome are strong clues to drug hypersensitivity[9]. However, because these manifestations occur in a minority of cases of hepatotoxicity, their absence is not necessarily a helpful sign. In our Spanish Registry[3], some of the hallmarks of hypersensitivity (e.g., fever, rash, eosinophilia, cytopenia) were present only in 106 of 446 cases (23%) with idiosyncratic hepatotoxicity.

In some instances, typical hypersensitivity symptoms

Table 4 Clinical work-up to identify other possible causes of liver disease

Test	Condition	Commentary
Viral serology IgM anti-HAV IgM anti-HBc Anti-HCV, RNA-HCV (RT-PCR) IgM-CMV IgM-EBV Herpes virus	Viral hepatitis	Less frequent in older patients, especially Hepatitis A, search for epidemiologic risk factors, outcome may be similar to that of DILI following de-challenge.
Bacterial serology: Salmonella, Campylobacter, Listeria, Coxiella	Bacterial hepatitis	If persistent fever and/or diarrhea
Serology for syphilis	Secondary syphilis	Multiple sexual partners. Disproportionately high serum AP levels.
Autoimmunity (ANA, ANCA, AMA, ASMA, anti-LKM-1)	Autoimmune hepatitis, Primary biliary cirrhosis	Women, ambiguous course following de-challenge. Other autoimmunity features.
AST/ALT ratio > 2	Alcoholic hepatitis	Alcohol abuse. Moderate increase in transaminases despite severity at presentation
Ceruloplasmine, urine cooper	Wilson's disease	Patients < 40 yr
Alfa-1 antitrypsin	Deficit of α-1 antitrypsin	Pulmonary disease
Transferrin saturation	Hemochromatosis	In anicteric hepatocellular damage. Middle-aged men and older women.
Brilliant eco texture of the Liver.	Non-alcoholic steatohepatitis	In anicteric hepatocellular damage. Obesity, Metabolic syndrome.
Transaminase levels markedly high	Ischemic hepatitis	Disproportionately high AST levels. Hypotension, shock, recent surgery, heart failure, antecedent vascular disease, elderly
Dilated bile ducts by image procedures (AU, CT, MRCP and ERCP)	Biliary obstruction	Colic abdominal pain, cholestatic/mixed pattern.

ALT: alanine aminotransferase; AP: alkaline phosphatase; AST: aspartate aminotransferase; AU: abdominal ultrasound examination; Anti-HAV: Hepatitis A antibody; Anti-HBc: Hepatitis B core antibody; Anti-HCV: Hepatitis C antibody; anti-LKM-1: Liver-kidney microsomal antibody type 1; AMA: antimitochondrial antibody; ANA: antinuclear antibody; ANCA: perinuclear antineutrophil cytoplasmic antibody; ASMA: antismooth muscle antibody; BPC: Biliary primary cirrhosis; CMV: cytomegalovirus; CT: computed tomography; EBV: Epstein-Barr virus; ERCP: Endoscopic retrograde cholangiography; MRCP: Magnetic resonance cholangiography.

are absent. However, clues pointing toward an immuno-allergic reaction might come from the presence of more subtle features, such as detectable serum autoantibodies and antinuclear and anti-smooth-muscle antibodies[12,31]. It is very likely that immunologic and metabolic idiosyncrasies operate concurrently in many cases of drug-induced hepatic injury[9,18].

The value of hypersensitivity features as indirect evidence of drug-allergy is currently under debate. In a large cohort of patients with drug-induced idiosyncratic liver disease, a link between HLA-DRB1*15 and-DQB1*06 alleles and the cholestatic/mixed injury (but not hepatocellular injury) was established. The frequency of DRB1*07 and DQB1*02 alleles was also reduced in the cholestatic/mixed injury group[45]. Conversely, there were no differences in HLA-class II allele distributions between hepatotoxicity patients who had and those who had not any hypersensitivity features. This would suggest that the majority of cholestatic/mixed cases might have an allergy pre-disposition that was genetic, irrespective of whether they have accompanying signs of drug-allergy. This is less certain in hepatocellular cases with hypersensitivity features[46].

Rapid improvements in biochemical values following withdrawal of drug therapy raises the possibility of a toxic etiology, even though this outcome may be seen in viral hepatitis as well. For hepatocellular injury, the involvement of a drug has been defined as being "highly likely" if there is a decrease of at least 50% in the levels of liver enzymes in the first 8 d following cessation of the therapy[9]. Although less conclusive, expert consensus still considers drug involvement "suggestive" (and positively weighted on the clinical scale) if such a decrease occurs within 30 d following cessation of the therapy[10].

Gastroenterologists assessing suspected drug hepatotoxicity should be aware that other atypical outcomes make laboratory scrutiny following drug withdrawal less categorical. In general, cholestatic reactions subside more slowly, with abnormal enzyme levels persisting for long periods of more than one year in some instances[47,48].

Particularly confusing is the clinical evolution of some severe cases in which the injury may progress over several days despite drug cessation, or even progressing to fulminant hepatic failure[49,50]. Conversely, the phenomenon of "adaptation" to injury can occur with some drugs (e.g. statins). This can be responsible for the spontaneous improvement in liver function tests, despite the drug treatment being continued[42].

Currently, the only way to confidently confirm idiosyncratic drug-induced hepatotoxicity is by demonstrating a recrudescence of liver injury following re-challenge with the suspected agent. Strictly, a positive response following re-exposure can be defined as a doubling of ALT and AP values for hepatocellular and cholestatic reactions, respectively. From a practical standpoint, however, it is hard to demonstrate this in most circumstances in which unintentional re-exposure occurs. Conversely, with careful inquiry a history of inadvertent re-challenge may be sometimes elicited because jaundice

Table 5 Rationale for performing liver biopsy in a case suspected of having drug-induced hepatotoxicity

Clinical setting	Presentation
Any clinical context	Putative drugs not previously incriminated in liver toxicity
Acute or chronic liver disease	Female, autoantibody sero-positive
	High serum gammaglobulin and immunoglobulin G levels at presentation
	Incomplete or ambiguous de-challenge
Chronic alcoholism	Acute deterioration during aversive therapy (disulfiram, carbimide calcium)
Any acute liver deterioration in a patient with cirrhosis or chronic hepatitis C.	e.g. worsening of liver function in a patient with primary biliary cirrhosis receiving rifampicin or a chronic hepatitis C patient receiving ibuprofen
Chronic impairment in liver tests in non-jaundiced patients.	Especially if constitutional symptoms and/or clinical signs of portal hypertension are disclosed.
Young patients with sero-negative acute hepatitis or chronic liver disease.	Moderate decrease in ceruloplasmin levels or slight increases in urinary copper excretion.

had not accompanied the index episode and the symptoms were non-specific at the time (e.g., malaise, gastrointestinal complaints) and were thus easily overlooked. In such cases, what was believed to be the first instance of hepatitis was, in reality, a re-challenge episode[24].

Intentional re-challenge implies several practical problems. Firstly, re-challenge is strictly contra-indicated in drug-induced hepatocellular hepatitis with associated hypersensitivity features because there is the risk of inducing a more severe, or even fulminant, clinical picture. Secondly, the amount of drug required to provoke the reaction is not known. Arbitrarily, a single dose needs to be chosen. Arguably, however, several doses may be necessary to reproduce liver damage in "metabolic" (non-allergic) drug-induced hepatotoxicity. This false negative response to re-challenge has been demonstrated for isoniazid[9] and, probably, applies to many other drugs operating under similar mechanisms. Finally, and most importantly, re-exposure of the patient to the suspected drug cannot be ethically supported purely for diagnostic purposes. Re-exposure should be attempted only when the drug being used is deemed essential for disease treatment, such as in the treatment of tuberculosis with isoniazid. Written informed consent needs to be obtained from the patient. Nevertheless, taking into consideration the consequences of misdiagnosing hepatotoxicity in pre-approval clinical trials[12], we believe that testing clinical or sub-clinical hepatitis in the trial setting might be an additional indication for re-challenge[24].

A common misconception among clinical gastroenterologists is the need to have a liver biopsy specimen to establish a diagnosis of drug-induced hepatotoxicity with confidence. Rather, since there are no histological findings specific for toxic damage, liver biopsy should not be performed routinely for this indication[14,51]. Indeed, a liver biopsy specimen, which is often taken several days after the clinical presentation of the symptoms when the pathological features are beginning to wane, may generate perplexity and confusion in cases in which chronological sequence criteria are critical and when exclusion of alternative causes appear to incriminate the drug.

Currently, a reasonable approach for performing a liver biopsy in patients with suspected drug-induced hepatotoxicity is restricted[13] to when the patient may have an underlying liver disease and, hence, it is difficult to ascribe the picture to the candidate drug or to a recrudescence of the disease (Table 5) or, alternatively, to characterize the pattern of injury with those drugs that had not been previously incriminated in hepatotoxicity[12,30,36]. We believe that a liver biopsy is also justified for identifying more severe or residual lesions (e.g. fibrosis), which could have prognostic significance. For instance, in some chronic variants of hepatotoxicity, clinical and laboratory features reflect the severity of the liver injury[30,31] poorly and a liver biopsy may clarify its true magnitude. Further, severe bile duct injury during cholestatic hepatitis has been shown to be predictive of clinical evolution into chronic cholestasis[52], and, in a retrospective study, the presence of fibrosis in the index liver biopsy had been related to the development of chronic liver disease[53].

Since a liver biopsy is not available in most cases, focus on the biochemical expression of hepatic damage may help in incriminating a specific medication. Each drug appears to have its own "signature" in relation to a more-or-less specific pattern of liver injury[7,42]. Although this is true for some drugs (e.g., estrogens induce cholestatic injury and seldom any present with any other pattern of damage), for most other drugs such consistency is not so clear. For instance, amoxicillin-clavulanate tends to produce cholestatic or mixed damage, although hepatocellular damage has been reported frequently as well[16,54]. Hepatocellular and cholestatic or mixed injury have been noted with nimesulide[55] or troglitazone[56,57], among others. Hence it is important for gastroenterologists to view a suspicion of drug-induced hepatotoxicity with caution and with awareness that any given drug can produce diverse types of injury[58].

CAUSALITY ASSESSMENT METHODS: IN SEARCH OF GREATER OBJECTIVITY

Clinical judgment is a necessary first step in the identification of any hepatic disease suspected of being caused by a drug or toxin. Diagnostic precision and objectivity are essential from the perspective of the practicing clinician who must decide whether to continue, or to stop, a therapy even though it may be the most appropriate for the disease under treatment and which might induce new events in the future if not correctly

identified. Except for the very rare circumstances in which an unintentional positive re-challenge may confirm the putative involvement of a drug, the evidence that is usually collected is often circumstantial, based on subjective impressions from previous experiences, and can lead to inaccurate diagnosis[59]. The process is time-consuming and delays clinical judgment; at least until other possible causes of liver disease have been excluded.

An approach that does not follow objective guidelines that complement standard clinical practice, results in causation categories that may be defined as drug-related (e.g. acetaminophen overdose, instances of positive re-challenge), not drug related (an alternative explanation found) or when the role of a medication may appear conditional[22]. This last judgment in which subjectivity prevails does, indeed, represent the bulk of situations in standard clinical practice. In addition, this judgment depends closely on the attending physician's skill and attitude towards the disease under consideration. Hence, agreement among physicians who evaluate a given case of drug-suspected hepatotoxicity may differ considerably. Variations in data consistency, completeness, and subjective weighting of causality arguments would, presumably, contribute to these differences.

Algorithms or clinical scales

Over the last three decades, several groups have developed methods to improve the consistency, accuracy and objectiveness in causality assessment of adverse drug reactions. The qualities required for any scoring system are, usually, reproducibility and validity[60]. Reproducibility ensures an identical result when the scales are applied irrespective of the user. Validity refers to the capacity to distinguish between cases when the drug is responsible, and cases when the drug it is not responsible.

There are two possible categories of approach: the probabilistic approach[61] based on Bayesian statistics, which is rarely used in routine clinical practice because the approach requires precisely-quantified data to model the probability distributions for each parameter. The alternative approach is the widely used algorithm or clinical scale[62]. The key features of an adverse reaction are identified and integrated into an objective rating scale based on the sum of weighted numerical values assigned to individual axes of a decision strategy. The scores are translated into categories of suspicion. The different causality assessment methods developed can produce different numerical scales that may or may not be super-imposable and with non-identical categories of suspicion. This complicates any comparisons among the different scales[62].

The Naranjo Adverse Drug Reaction Probability Scale (1981) proposed for adverse reactions to drugs (not restricted to hepatotoxicity) offers the advantage of simplicity and wide applicability[63]. This scale involves ten "yes", "no" or "not known or inapplicable" answers to questions concerning several disease-related areas: temporal relationship, competing causes, de-challenge/re-challenge results, and knowledge of the drug's reactions. In addition, universally-accepted criteria are introduced: placebo challenge, drug concentrations and objective measurement of adverse drug reaction. An adverse drug reaction is described as a probability category based on the total score. The categories are: definite ($\geqslant$ 9 points scored), likely (5 to 8 points), possible (1 to 4 points), and doubtful ($\leqslant$ 0 points). The scale has been validated and has resulted in improved reproducibility of patient evaluations. The main source of inter-observer disagreement has been the question of alternative causes and reflects, perhaps, the complexity of the clinical situation and differences in clinical training among observers. Despite the lack of specificity with respect to hepatotoxicity, use of the Naranjo scale is a requirement by some journals when adverse drug-related events are reported[63,64] and, as well, in reporting to national drug monitoring bodies.

In 1992, under the auspices of the Council for International Organizations of Medical Sciences, a working group developed and implemented a standardized method for drug causality assessment and the scales are named after the organizers of the consensus meeting: CIOMS or RUCAM (Roussel Uclaf Causality Assessment Method)[65,66]. This method provides a standardized scoring system in which the limits and contents of most criteria were decided by consensus among experts on the basis of organ-oriented characteristics. The time-to-onset and duration are evaluated separately for hepatocellular versus cholestatic/mixed reactions since the latter can occur long after the cessation and may be resolved much more slowly (Table 6). The CIOMS/RUCAM scale provides a scoring system for 6 axes in the decision strategy. The categories of suspicion are "definite or highly probable" (score > 8), "probable" (score 6-8), "possible" (score 3-5), "unlikely" (score 1-2) and "excluded" (score $\leqslant$ 0). One of the advantages of this system that is of note is that there are very few questions that require a subjective response. The scale can assign a definitive diagnosis of drug-induced hepatotoxicity in patients even without re-challenge. Also, it performs well with newly-marketed drugs or for a previously-unreported liver injury associated with an older drug. The major drawback is its complexity. It requires training in its administration and is less efficient when a user is unfamiliar with the format. The scale may seem cumbersome and while reading across the page, care needs to be taken to not misunderstand the questions; otherwise careless errors can be made. Recently, experts have criticized the weighting attributed to certain of the risk factors (e.g., age of the patient > 55 years, alcohol consumption, pregnancy) which, at best, would be significant only for a limited number of drugs[23,42].

More recently, Maria and Victorino from Portugal developed a simplified scoring system to overcome the above-mentioned problems. Called the Clinical Diagnostic Scale[67] (also termed the M&V scale) it uses several features of the CIOMS/RUCAM scale while omitting and adding others (Table 6). Five components were selected for inclusion in the scale: temporal relationship between drug intake and the onset of clinical symptoms, exclusion of alternative causes, presence of extra-hepatic manifestations (e.g., rash, fever, arthralgia, eosinophilia > 6% and cytopenia), intentional or accidental re-exposure to the drug, and previous reports in the literature. The sum of the points for each parameter can vary from -6

Table 6 Comparison of the scores for individual axes of the CIOMS and Maria & Victorino diagnostic scales

CIOMS criteria	Score	Maria & Victorino criteria	Score
Chronology criterion		Chronology criterion	
From drug intake until event onset	+2 to +1	From drug intake until event onset	+1 to +3
From drug withdrawal until event onset	+1 to 0	From drug withdrawal until event onset	-3 to +3
Time-course of the reaction	-2 to +3	Time-course of the reaction	0 to +3
Risk factors		Exclusion of alternative causes	-3 to +3
Age	+1 to 0		
Alcohol	+1 to 0	Extra-hepatic manifestations	0 to +3
Concomitant therapy	-3 to 0	Literature data	-3 to +2
Exclusion of non-drug-related causes	-3 to +2	Re-challenge	0 to +3
Literature data	0 to +2		
Re-challenge	-2 to +3		

to +20. Concordance with the five classic degrees of probability of adverse drug reactions is established on the basis of the tabulated score as follows: "definite" (score > 17), "probable" (score 14-17), "possible" (score 10-13), "unlikely" (score 6-9) and "excluded" (score < 6). The authors highlighted some limitations of the scale: The instrument performs poorly in atypical cases of drugs with unusually-long latency periods or chronic outcome. There is room for improvement in the exclusion of alternative causes of liver injury by more clearly specifying the clinical conditions to be excluded, as well as including detailed criteria for exclusion. The main advantage of the M&V scale is its ease of application in standard clinical practice.

Comparison of assessment methods in hepatotoxicity

The merits of the CIOMS and the M&V scales and their degree of concordance were compared in a population of 215 patients included in a registry of hepatotoxicity[68]. Causality in this population had been verified previously by 3 experts as being drug-induced (185) or as non-drug (30 cases). Complete agreement between the M&V scale and the CIOMS scale was obtained in only 42 cases (18%). Discrepancies in the assessment of causality occurred in 186 ratings; in each of these cases the CIOMS scale ascribed a higher level of certainty than the M&V scale. The M&V system classified only about one third of the cases as "probable" or "definite", and tended to underestimate the probability of causality. Indeed, the performance of the M&V scale was poor in reactions with long latency periods (more than 15 d; for example amoxicillin/clavulanic acid), clinical progression to chronic status following withdrawal (cholestatic pattern), or death.

The concordance of assessment was low because the two methods assigned different weightings to the assessment criteria and, as such, the reasons for discordance could be clearly identified. For example, a time-lapse of > 15 d between drug withdrawal and event onset can be rectified by subtracting 3 points from the score on the M&V scale. A time-lapse of > 6 mo between drug withdrawal and normalization of laboratory values (in cholestatic or mixed type of injury) or 2 mo (in hepatocellular damage) precluded a "definite" or "probable" diagnosis being reached. Unknown reactions to drugs marketed for > 5 years preclude a "certainty" diagnosis. Conversely, the best correlation between the two scales was found for drug-induced liver injury that included a probable immuno-allergic mechanism. This is because the M&V scale includes questions that apply only to cases with extra-hepatic features. It would appear, therefore, that the CIOMS instrument shows better agreement with "common sense" clinical judgment. Aside from its clinical validity, the usefulness of the CIOMS scale is that it provides a framework that emphasizes topics that need to be addressed in cases of suspected hepatic adverse reaction in order to improve the consistency of judgment[68].

The Clinical Diagnostic Scale (CDS or M&V) was further evaluated in the causality assessment of 135 hepatotoxic adverse drug reaction reports[69]. Initially, the CIOMS criteria were used to classify reactions as "drug-related", "drug-unrelated" and "indeterminate." Reports classified as drug-related (49 reactions) scored higher on the clinical scale, with a median score of 12 (range 8-15). Of those, no reactions were classified as "definite", 20 were classified as "probable" and 23 as "possible". It is important to note that 6 patients were classified as "unlikely". The authors suggested that a cut-off score > 9 (falling into the category of "possible") be used in clinical decision-making. It is of further note that "possible" is a fairly low category adjacent to "unlikely" and this makes the cut-off score somewhat unreliable for decision-making. In addition, the authors did not assess or compare the merits of the two systems in any detail[70]. Six patients whose hepatotoxicity was considered drug-related on the basis of the consensus classification (four of these patients having a positive re-challenge) scored < 10 ("unlikely"). Two patients had flucloxacillin-induced cholestasis that first appeared > 15 d following drug withdrawal, and in two other patients the reactions were fatal and therefore precluded an accurate assignment of cause. Two other patients with a long latency period scored only 1 point each for the onset-of-reaction score. These examples confirm the limitations of the clinical scale, as highlighted by the authors themselves and which are in accordance with the conclusions reached by Lucena *et al*[68].

These comparative studies clearly show that the CIOMS scale, although far from being a perfect instrument, provides a uniform basis from which to develop a more precise approach in determining the causes of drug-induced hepatotoxicity. Indeed, medical

journals should insist on the application of the scale as a quality control prior to accepting reports of hepatotoxicity. Nevertheless, rules for assigning causality in drug-induced liver injury are no substitute for clinical judgment. For instance, when more than one drug could be the culprit, a "blind" application of the scale can lead to a somewhat misleading causality assessment if only chronological criteria are taken into account[38]. To avoid this, attention should be paid to major drug metabolic mechanisms in relation to potential pharmacokinetic interactions with the drug[71].

FUTURE DIRECTIONS

Apart from the development of unequivocal diagnostic biomarkers in the near future, it would be feasible in the short term to develop some refinements to make the CIOM scale more realistic; more relevant data can be incorporated and low-impact items need to be deleted from the scoring system. This task will be helped by using large databases of *bona fide* cases of hepatotoxicity. The DILIN network is developing and testing such a causality assessment method by a complex computer-based process for gathering and distributing relevant information[72]. This analysis would useful to confirm or discard alcohol, age >55 years and pregnancy as general risk factors for hepatotoxicity, while evaluating the roles of other candidate susceptibility factors such as obesity (a condition that is associated with an increased expression of CYP2E1)[1]. Further, the age cut-off point does not consider the pediatric age range as a risk factor for toxicity of some drugs. Other known risk factors for individual drugs when present in the appropriate setting should be incorporated (e.g. HIV infection in sulfonamide use, co-infection with hepatitis B/hepatitis C virus and antiretroviral drugs, female gender for diclofenac).

In real practice, to make a definite diagnosis of drug-induced hepatotoxicity, clinicians pay much attention in assigning causality to a concordance between the actual biochemical profile of the patient and that which is provided by consensus guidelines relating to the suspected drug (for instance, cholestatic damage with amoxicillin-clavulanate use). As well, the presence of hypersensitivity features is considered by practicing physicians of crucial value in the attribution of culpability to a specific drug. Neither biochemical "signature" nor hypersensitivity features are weighted in the CIOMS scale[73] and these discrepancies await resolution.

Apart from these important questions, there is the need to validate a new instrument with an abridged scale that would provide a better approximation to the truth; i.e., the likelihood that a given case of hepatitis is due to a specific drug, at the very beginning of the patient evaluation process when key clinical decisions need to be made. The diagnosis needs to be made with confidence on admission of the patient and maintained while further confirmatory information is gathered. This would be the goal of a clinical assessment tool for the evaluation of drug-induced hepatotoxicity.

REFERENCES

1 **Bissell DM**, Gores GJ, Laskin DL, Hoofnagle JH. Drug-induced liver injury: mechanisms and test systems. *Hepatology* 2001; **33**: 1009-1013
2 **Hoofnagle JH**. Drug-induced liver injury network (DILIN). *Hepatology* 2004; **40**: 773
3 **Andrade RJ**, Lucena MI, Fernández MC, Pelaez G, Pachkoria K, García-Ruiz E, García-Muñoz B, González-Grande R, Pizarro A, Durán JA, Jiménez M, Rodrigo L, Romero-Gomez M, Navarro JM, Planas R, Costa J, Borras A, Soler A, Salmerón J, Martin-Vivaldi R. Drug-induced liver injury: an analysis of 461 incidences submitted to the Spanish registry over a 10-year period. *Gastroenterology* 2005; **129**: 512-521
4 **Ostapowicz G**, Fontana RJ, Schiødt FV, Larson A, Davern TJ, Han SH, McCashland TM, Shakil AO, Hay JE, Hynan L, Crippin JS, Blei AT, Samuel G, Reisch J, Lee WM. Results of a prospective study of acute liver failure at 17 tertiary care centers in the United States. *Ann Intern Med* 2002; **137**: 947-954
5 **Bakke OM**, Manocchia M, de Abajo F, Kaitin KI, Lasagna L. Drug safety discontinuations in the United Kingdom, the United States, and Spain from 1974 through 1993: a regulatory perspective. *Clin Pharmacol Ther* 1995; **58**: 108-117
6 **Shah RR**. Drug-induced hepatotoxicity: pharmacokinetic perspectives and strategies for risk reduction. *Adverse Drug React Toxicol Rev* 1999; **18**: 181-233
7 **Lee WM**. Drug-induced hepatotoxicity. *N Engl J Med* 2003; **349**: 474-485
8 **Mohapatra R**, Tran M, Gore JM, Spencer FA. A review of the oral direct thrombin inhibitor ximelagatran: not yet the end of the warfarin era. *Am Heart J* 2005; **150**: 19-26
9 **Zimmerman HJ**. Hepatotoxicity. The adverse effects of Drugs and Other Chemicals on the Liver. 2nd ed. Philadelphia: Lippincott Williams & Wilkins, 1999
10 **Bénichou C**. Criteria of drug-induced liver disorders. Report of an international consensus meeting. *J Hepatol* 1990; **11**: 272-276
11 **Farrell GC**. Drug Induced Liver Disease. London: Churchill-Livingstone, 1994
12 **Andrade RJ**, Lucena MI, Martin-Vivaldi R, Fernandez MC, Nogueras F, Pelaez G, Gomez-Outes A, Garcia-Escaño MD, Bellot V, Hervás A, Cárdenas F, Bermudez F, Romero M, Salmerón J. Acute liver injury associated with the use of ebrotidine, a new H_2-receptor antagonist. *J Hepatol* 1999; **31**: 641-646
13 **Larrey D**. Drug-induced liver diseases. *J Hepatol* 2000; **32**: 77-88
14 **Goodman ZD**. Drug hepatotoxicity. *Clin Liver Dis* 2002; **6**: 381-397
15 **Björnsson E**, Olsson R. Outcome and prognostic markers in severe drug-induced liver disease. *Hepatology* 2005; **42**: 481-489
16 **Lucena MI**, Andrade RJ, Fernández MC, Pachkoria K, Pelaez G, Durán JA, Villar M, Rodrigo L, Romero-Gomez M, Planas R, Barriocanal A, Costa J, Guarner C, Blanco S, Navarro JM, Pons F, Castiella A, Avila S. Determinants of the clinical expression of amoxicillin-clavulanate hepatotoxicity: a prospective series from Spain. *Hepatology* 2006; **44**: 850-856
17 **Andrade RJ**, Lucena MI, Kaplowitz N, García-Muñoz B, Borraz Y, Pachkoria K, García-Cortés M, Fernández MC, Pelaez G, Rodrigo L, Durán JA, Costa J, Planas R, Barriocanal A, Guarner C, Romero-Gomez M, Muñoz-Yagüe T, Salmerón J, Hidalgo R. Outcome of acute idiosyncratic drug-induced liver injury: Long-term follow-up in a hepatotoxicity registry. *Hepatology* 2006; **44**: 1581-1588
18 **Kaplowitz N**. Drug-induced liver disorders: introduction and overview. In: Kaplowitz N, Deleve LD, editors. Drug-induced liver disease. New York: Marcel Dekker Inc., 2003: 1-14
19 **Maria VA**, Victorino RM. Diagnostic value of specific T-cell reactivity to drugs in 95 cases of drug induced liver injury. *Gut* 1997; **41**: 534-540
20 **Maria VA**, Victorino RM. Immunological investigation in hepatic drug reactions. *Clin Exp Allergy* 1998; **28** Suppl 4: 71-77

21 **Berg PA**, Becker EW. The lymphocyte transformation test-a debated method for the evaluation of drug allergic hepatic injury. *J Hepatol* 1995; **22**: 115-118
22 **Kaplowitz N**. Causality assessment versus guilt-by-association in drug hepatotoxicity. *Hepatology* 2001; **33**: 308-310
23 **Lee WM**, Senior JR. Recognizing drug-induced liver injury: current problems, possible solutions. *Toxicol Pathol* 2005; **33**: 155-164
24 **Andrade RJ**, Camargo R, Lucena MI, González-Grande R. Causality assessment in drug-induced hepatotoxicity. *Expert Opin Drug Saf* 2004; **3**: 329-344
25 **Lewis JH**, Ranard RC, Caruso A, Jackson LK, Mullick F, Ishak KG, Seeff LB, Zimmerman HJ. Amiodarone hepatotoxicity: prevalence and clinicopathologic correlations among 104 patients. *Hepatology* 1989; **9**: 679-685
26 **Oien KA**, Moffat D, Curry GW, Dickson J, Habeshaw T, Mills PR, MacSween RN. Cirrhosis with steatohepatitis after adjuvant tamoxifen. *Lancet* 1999; **353**: 36-37
27 **Lewis JH**, Schiff E. Methotrexate-induced chronic liver injury: guidelines for detection and prevention. The ACG Committee on FDA-related matters. American College of Gastroenterology. *Am J Gastroenterol* 1988; **83**: 1337-1345
28 **Sharp JR**, Ishak KG, Zimmerman HJ. Chronic active hepatitis and severe hepatic necrosis associated with nitrofurantoin. *Ann Intern Med* 1980; **92**: 14-19
29 **Sturkenboom MC**, Meier CR, Jick H, Stricker BH. Minocycline and lupuslike syndrome in acne patients. *Arch Intern Med* 1999; **159**: 493-497
30 **Andrade RJ**, Lucena MI, Alcantara R, Fraile JM. Bentazepam-associated chronic liver disease. *Lancet* 1994; **343**: 860
31 **Andrade RJ**, Lucena MI, Aguilar J, Lazo MD, Camargo R, Moreno P, García-Escaño MD, Marquez A, Alcántara R, Alcáin G. Chronic liver injury related to use of bentazepam: an unusual instance of benzodiazepine hepatotoxicity. *Dig Dis Sci* 2000; **45**: 1400-1404
32 **Ishak KG**, Zimmerman HJ. Hepatotoxic effects of the anabolic/androgenic steroids. *Semin Liver Dis* 1987; **7**: 230-236
33 **Ishak KG**, Zimmerman HJ. Morphologic spectrum of drug-induced hepatic disease. *Gastroenterol Clin North Am* 1995; **24**: 759-786
34 **Andrade RJ**, Lucena MI, Fernández MC, Vega JL, Camargo R. Hepatotoxicity in patients with cirrhosis, an often unrecognized problem: lessons from a fatal case related to amoxicillin/clavulanic acid. *Dig Dis Sci* 2001; **46**: 1416-1419
35 **Pérez Moreno JM**, Saldaña González FJ, Puertas Montenegro M, Báez Perea J. Cholestatic hepatitis caused by midecamycin. *Gastroenterol Hepatol* 1996; **19**: 459-461
36 **Lucena MI**, Andrade RJ, Rodrigo L, Salmerón J, Alvarez A, Lopez-Garrido MJ, Camargo R, Alcantára R. Trovafloxacin-induced acute hepatitis. *Clin Infect Dis* 2000; **30**: 400-401
37 **Kaplowitz N**. Drug-induced liver injury. *Clin Infect Dis* 2004; **38** Suppl 2: S44-S48
38 **Lucena MI**, Andrade RJ, Vicioso L, González FJ, Pachkoria K, García-Muñoz B. Prolonged cholestasis after raloxifene and fenofibrate interaction: A case report. *World J Gastroenterol* 2006; **12**: 5244-5246
39 **Biour M**, Poupon R, Grangé JD, Chazouillères O. Drug-induced hepatotoxicity. The 13th updated edition of the bibliographic database of drug-related liver injuries and responsible drugs. *Gastroenterol Clin Biol* 2000; **24**: 1052-1091
40 **Lee WM**. Acute liver failure in the United States. *Semin Liver Dis* 2003; **23**: 217-226
41 **Stricker BHCH**. Drug-induced Hepatic Injury, 2nd ed. Amsterdam: Elsevier, 1992
42 **Kaplowitz N**. Drug-induced liver disorders: implications for drug development and regulation. *Drug Saf* 2001; **24**: 483-490
43 **Carrillo-Jimenez R**, Nurnberger M. Celecoxib-induced acute pancreatitis and hepatitis: a case report. *Arch Intern Med* 2000; **160**: 553-554
44 **Schattner A**, Sokolovskaya N, Cohen J. Fatal hepatitis and renal failure during treatment with nimesulide. *J Intern Med* 2000; **247**: 153-155
45 **Andrade RJ**, Lucena MI, Alonso A, García-Cortes M, García-Ruiz E, Benitez R, Fernández MC, Pelaez G, Romero M, Corpas R, Durán JA, Jiménez M, Rodrigo L, Nogueras F, Martín-Vivaldi R, Navarro JM, Salmerón J, de la Cuesta FS, Hidalgo R. HLA class II genotype influences the type of liver injury in drug-induced idiosyncratic liver disease. *Hepatology* 2004; **39**: 1603-1612
46 **Velayudham LS**, Farrell GC. Drug-induced cholestasis. Expert *Opin Drug Saf* 2003; **2**: 287-304
47 **Andrade RJ**, Guilarte J, Salmerón FJ, Lucena MI, Bellot V. Benzylpenicillin-induced prolonged cholestasis. *Ann Pharmacother* 2001; **35**: 783-784
48 **Andrade RJ**, Lucena MI, Fernández MC, Vega JL, García-Cortés M, Casado M, Guerrero-Sanchez E, Pulido-Fernandez F. Cholestatic hepatitis related to use of irbesartan: a case report and a literature review of angiotensin II antagonist-associated hepatotoxicity. *Eur J Gastroenterol Hepatol* 2002; **14**: 887-890
49 **Andrade RJ**, Lucena MI, Fernández MC, González M. Fatal hepatitis associated with nimesulide. *J Hepatol* 2000; **32**: 174
50 **Lucena MI**, Andrade RJ, Gomez-Outes A, Rubio M, Cabello MR. Acute liver failure after treatment with nefazodone. *Dig Dis Sci* 1999; **44**: 2577-2579
51 **Bianchi L**. Liver biopsy in elevated liver functions tests? An old question revisited. *J Hepatol* 2001; **35**: 290-294
52 **Degott C**, Feldmann G, Larrey D, Durand-Schneider AM, Grange D, Machayekhi JP, Moreau A, Potet F, Benhamou JP. Drug-induced prolonged cholestasis in adults: a histological semiquantitative study demonstrating progressive ductopenia. *Hepatology* 1992; **15**: 244-251
53 **Aithal PG**, Day CP. The natural history of histologically proved drug induced liver disease. *Gut* 1999; **44**: 731-735
54 **Brown SJ**, Desmond PV. Hepatotoxicity of antimicrobial agents. *Semin Liver Dis* 2002; **22**: 157-167
55 **Van Steenbergen W**, Peeters P, De Bondt J, Staessen D, Büscher H, Laporta T, Roskams T, Desmet V. Nimesulide-induced acute hepatitis: evidence from six cases. *J Hepatol* 1998; **29**: 135-141
56 **Herrine SK**, Choudhary C. Severe hepatotoxicity associated with troglitazone. *Ann Intern Med* 1999; **130**: 163-164
57 **Bonkovsky HL**, Azar R, Bird S, Szabo G, Banner B. Severe cholestatic hepatitis caused by thiazolidinediones: risks associated with substituting rosiglitazone for troglitazone. *Dig Dis Sc*i 2002; **47**: 1632-1637
58 **Andrade RJ**, Lucena MI. Drug-induced hepatotoxicity. *N Engl J Med* 2003; **349**: 1974-1976; author reply 1974-1976
59 **Aithal GP**, Rawlins MD, Day CP. Accuracy of hepatic adverse drug reaction reporting in one English health region. *BMJ* 1999; **319**: 1541
60 **Hutchinson TA**, Lane DA. Assessing methods for causality assessment of suspected adverse drug reactions. *J Clin Epidemiol* 1989; **42**: 5-16
61 **Bate A**, Lindquist M, Edwards IR, Olsson S, Orre R, Lansner A, De Freitas RM. A Bayesian neural network method for adverse drug reaction signal generation. *Eur J Clin Pharmacol* 1998; **54**: 315-321
62 **Pere JC**, Begaud B, Haramburu F, Albin H. Computerized comparison of six adverse drug reaction assessment procedures. *Clin Pharmacol Ther* 1986; **40**: 451-461
63 **Naranjo CA**, Busto U, Sellers EM, Sandor P, Ruiz I, Roberts EA, Janecek E, Domecq C, Greenblatt DJ. A method for estimating the probability of adverse drug reactions. *Clin Pharmacol Ther* 1981; **30**: 239-245
64 **García-Cortés M**, Lucena MI, Andrade RJ, Camargo R, Alcántara R. Is the Naranjo probability scale accurate enough to ascertain causality in drug-induced hepatotoxicity? *Ann Pharmacothe*r 2004; **38**: 1540-1541
65 **Danan G**, Benichou C. Causality assessment of adverse reactions to drugs--I. A novel method based on the conclusions of international consensus meetings: application to drug-induced liver injuries. *J Clin Epidemiol* 1993; **46**: 1323-1330
66 **Benichou C**, Danan G, Flahault A. Causality assessment of adverse reactions to drugs--II. An original model for validation of drug causality assessment methods: case reports with positive rechallenge. *J Clin Epidemiol* 1993; **46**: 1331-1336

67 **Maria VA**, Victorino RM. Development and validation of a clinical scale for the diagnosis of drug-induced hepatitis. *Hepatology* 1997; **26**: 664-669
68 **Lucena MI**, Camargo R, Andrade RJ, Perez-Sanchez CJ, Sanchez De La Cuesta F. Comparison of two clinical scales for causality assessment in hepatotoxicity. *Hepatology* 2001; **33**: 123-130
69 **Aithal GP**, Rawlins MD, Day CP. Clinical diagnostic scale: a useful tool in the evaluation of suspected hepatotoxic adverse drug reactions. *J Hepatol* 2000; **33**: 949-952
70 **Lee WM**. Assessing causality in drug-induced liver injury. *J Hepatol* 2000; **33**: 1003-1005
71 **Andrade RJ**, Lucena MI. Acute fulminant hepatitis after treatment with rabeprazole and terbinafine: is rabeprazole the culprit? *Arch Intern Med* 2002; **162**: 360-361
72 **Watkins PB**, Seeff LB. Drug-induced liver injury: summary of a single topic clinical research conference. *Hepatology* 2006; **43**: 618-631
73 **Takamori Y**, Takikawa H, Kumagi T, Oriyi M, Watanaba M, Shibuya A, Hisamochi A, Kumashiro R, Ito T, Mitsumoto Y, Nakamura A, Sakayuchi T. Assessment of the diagnostic scale for drug-induced liver injury by the international consensus meeting and a proposal of its modifications. *Hepatology* 2003; **38** Suppl 1: 703A

S- Editor Wang GP **L- Editor** Luzte M **E- Editor** Bi L

PO Box 2345, Beijing 100023, China
www.wjgnet.com
wjg@wjgnet.com

World J Gastroenterol 2007 January 21; 13(3): 341-348
World Journal of Gastroenterology ISSN 1007-9327

Identification of the differential expressive tumor associated genes in rectal cancers by cDNA microarray

Xue-Qin Gao, Jin-Xiang Han, Zhong-Fa Xu, Wei-Dong Zhang, Hua-Ning Zhang, Hai-Yan Huang

Xue-Qin Gao, Jin-Xiang Han, Hua-Ning Zhang, Hai-Yan Huang, Key Laboratory for Biotech-Drug, Ministry of Health, Key Laboratory of Modern Drugs and Technology of Shandong Province, Shandong Medical and Biotechnology Center, Shandong Academy of Medical Sciences, Jinan 250062, Shandong Province, China
Zhong-Fa Xu, Department of Surgery, Shandong Tumor Hospital, Shandong Academy of Medical Sciences, Jinan 250117, Shandong Province, China
Wei-Dong Zhang, Department of Experimental Pathology, Institute of Basic Medicine, Shandong Academy of Medical Sciences, Jinan 250062, Shandong Province, China
Supported by Major Project of Shandong Provincial Science and Technology, No.011100105, and Shandong Natural Sciences Funding Committee, No. Y2003C03
Correspondence to: Jin-Xiang Han, Shandong Medical and Biotechnology Center, Shandong Academy of Medical Sciences; Key Laboratory for Biotech Drugs, Ministry of Health; Key Laboratory of Modern Drugs and Technology of Shandong Province; 89 Jingshi Road, Jinan 250062, Shandong Province, China. samshjx@sina.com
Telephone: +86-531-82919888 Fax: +86-531-82951586
Received: 2006-07-27 Accepted: 2006-09-26

Abstract

AIM: To identify tumor associated genes of rectal cancer and to probe the application possibility of gene expression profiles for the classification of tumors.

METHODS: Rectal cancer tissues and their paired normal mucosa were obtained from patients undergoing surgical resection of rectal cancer. Total RNA was extracted using Trizol reagents. First strand cDNA synthesis was indirectly labeled with aminoallyl-dUTP and coupled with Cy3 or Cy5 dye NHS mono-functional ester. After normalization to total spots, the genes which background subtracted intensity did not exceed 2 SD above the mean blank were excluded. The data were then sorted to obtain genes differentially expressed by $\geqslant$ 2 fold up or down in at least 5 of the 21 patients.

RESULTS: In the 21 rectal cancer patients, 23 genes were up-regulated in at least 5 samples and 15 genes were down-regulated in at least 5 patients. Hierachical cluster analysis classified the patients into two groups according to the clinicopathological stage, with one group being all above stage Ⅱ and one group all below stage Ⅱ.

CONCLUSION: The up-regulated genes and down-regulated genes may be molecular markers of rectal cancer. The expression profiles can be used for classification of rectal cancer.

Key words: Rectal cancer; Tumor associated genes; cDNA microarray; Differential expression genes

Gao XQ, Han JX, Xu ZF, Zhang WD, Zhang HN, Huang HY. Identification of the differential expressive tumor associated genes in rectal cancers by cDNA microarray. *World J Gastroenterol* 2007; 13(3): 341-348

http://www.wjgnet.com/1007-9327/13/341.asp

INTRODUCTION

Colorectal cancer (CRC) is one of the most common causes of cancer related deaths, the majority of which are secondary to liver metastasis. Whereas significant improvements have been made in patient survival, the mortality is still quite high in patients with metastatic cancer[1]. Clinical trials of new therapeutic agents are constantly ongoing and drug effectiveness is improving. However, a complete cure for patients with advanced colorectal cancer awaits new targets and strategies. To achieve this goal, a comprehensive understanding of the mechanisms of colorectal carcinogenesis is essential. In the last two decades these mechanisms have been intensively studied. At the molecular level, activation of oncogenes[2] and inactivation of tumor suppressor genes are processes known to be involved in colorectal cancer[3,4]. CRC typically develops over decades and involves multiple genetic events. This has led to the development of a multi-step model of colorectal tumorigenesis[5]. It is generally accepted that one of the initiating steps in colorectal carcinogenesis is mutation in APC tumor suppressor gene[6].

APC is known to bind to a cell signaling/transcription factor β catenin. Activation of the Wnt pathway normally signals the association of β-catenin with members of the T-cek factor/lymphocyte-enhancer factor family and translocation to nucleous[7,8]. This complex can activate the transcription of a variety of target genes including c-Myc[9] and cyclin D1[10,11]. Loss of APC function leads to an abnormal accumulation of β-catenin and dys-regulates Wnt signaling[12]. Traditional methods of identifying novel targets that are involved in colon cancer progression are based on the studies of individual

genes. The developments of oligonucleotide or cDNA microarrays have made it possible to permit the expression levels of tens of thousands of genes to be monitored simultaneously and rapidly. These new methods have been used to identify the genes involved in colorectal cancer development. By using cDNA microarray with different number of elements, many genes have been identified. Kitahara[13] identified 235 genes of differential expression in 9216 human genes by using laser-capture micro-dissection. These differentially expressed genes include those associated with signal transduction, metabolic enzymes, production of reactive oxygen species, cell cycle, transcription, mitosis and apoptosis[13]. In another study, Williams identified 2632 genes (574 up-regulated and 2058 down-regulated) of totally 9592 genes microarray were consistently expressed in one-third patients[14]. In an effort to use gene expression profiles to find the molecular marker of rectal cancer, we constructed cDNA microarray with 373 known genes and 73 expressed sequence tags (ESTs) that are related to the pathogenesis of tumor.

MATERIALS AND METHODS

Fabrication of tumor associated genes cDNA microarray. Totally 447 cDNA clones were obtained from the Research Genetics (Invitrogen, life Technologies, USA). *E. coli* with cDNA clones were cultured with LB supplemented with ampicillin (50 mg/L) or chloramphenicol (170 mg/L). Clone plasmids were extracted with Edge BioSystems plasmid extraction kit. Clone inserts were PCR amplified from the plasmids with M13 vector specific universal primer (M13F: 5'-GGT GTA AAA CGA CGG CCA GTG-3'; M13R: 5'-CAC ACA GGA AAC AGC TAT G-3') in 96-well PCR microtiters. The PCR products were purified according to protocols published previously, and resuspended in Arrayit Spot solution [DNA precipitations. http://cmgm.stanford.edu/pbrown/protocols/2_DNA.html[15]. The re-suspended PCR products were printed in duplicate on silianated glass slides (Cel associated) with Cartisan Spot machines and UV-cross-linked at 3500 mJ using Stratagene cross-linker. Printed slides were post-processed using an online method[16].

Tissue samples

Rectal cancer tissues and their corresponding normal rectal tissues were obtained with informed consent from 21 patients who underwent surgical resection of their tumor in Shandong Tumor Hospital. The tissues were stored at -80℃. Tissues were homogenized with Trizol (Life Technologies) in homogenizer of IKA. Total RNA was extracted according to the manufacturer's protocols. The $A_{(260/280)}$ of total RNA was between 1.8-2.0.

Probe preparation and hybridization and data analysis

Twenty microgram of total RNA from matched tumor/normal sample was reverse transcribed into cDNA using Superscript Ⅱ (Invitrogen, Carlsbad CA) with random hexamers (Invitrogen, Carlsbad CA). Probe preparation was done based on online protocols and as described by Yang[17] and slightly modified by our laboratory[18]. First strand cDNA synthesis was primed with 6 μg random hexamers (Life Technologies) by heating at 70℃ for 10 min, snap-cooling on ice for 30 s and incubated at room temperature for an additional 5-10 min. Reverse transcription was performed in the presence of 500 μmol/L each of dATP, dCTP and dGTP, 200 μmol/L aminoalyl-dUTP (Sigma), 300 μmol/L dTTP, 1 × first strand buffer, 10 μmol/L dithiolhreitol, and 400 U superscript Ⅱ (Life Technologies, Carlsbad, CA) in 30 μL reaction at 42℃ overnight. Reactions were quenched with 0.5 mol/L EDTA and RNA template was hydrolyzed by addition of 10 μL of 1 mol/L NaOH followed by heating at 70℃ for 10 min. Reactions were neutralized with 10 μL 1 mol/L HCl and cDNA was purified with Amicon Microcon YM100 according to the manufacturer's protocol. cDNA was lyophilized in speed vaccum Centrifuger (Eppendorf 5301) and resuspended in 4.5 μL of 0.1 mol/L sodium carbonate(pH 9.0) buffer. NHS ester (4.5 μL) Cy3 or Cy5 dye (Amersham Pharmacia, GE Healthcare) in DMSO [dye from one tube (1 mg) was dissolved in 73 μL of DMSO] was added and reactions were incubated at room temperature in the dark for 1 h. Coupling reactions were quenched by addition of 41 μL of 0.1 mol/L sodium acetate, pH 5.2, and unincorporated dye was removed using QiaQuick PCR purification kits according to the manufacturer's instruction.

Hybridization and image processing

Each slide was printed with duplicate microarrays. Slides were prehybridized in 1% BSA, 5 × SSC, 0.1% SDS for 45 min, washed by dipping in double distilled deionized H_2O and 2-propanol twice and air dried and used in 1 h. Fluorescent cDNA probes were lyophylized to dryness and resuspended in 10 μL hybridization buffer (formamide 5 μL, 20 × SSC 2.5 μL, RGDDH 201 μL, 2% SDS 0.5 μL and 1 μL human cot-1 DNA). Combined Cy dye labeled probes were denatured at 100℃ water bath for 2 min and cooled at room temperature for 5 min. Room temperature probes were applied to the pre-hybridized microarray and covered with hybridized coverslip (Sigma) and placed in the hybridization chamber (Corning). Hybridizations were carried out at 42℃ water bath for 20-22 h followed by washing in 2 × SSC and 0.1% SDS for 3 min, 1 × SSC for 2 min and 0.2 × SSC for 1 min and 0.05 × SSC for 10 s, and dried by spinning in plate centrifuge at 800 rotation/min for 4 min. Arrays were scanned using a Scan-array 4000 dual color confocal laser scanner (Packard Bioscience). Data were saved as paired TIFF images. Paired images were analyzed with Quantarray 3.0 provided by the Scanner. After normalized to the total, genes of which the background subtracted intensity did not exceed 2 SD above the mean blank were excluded. The data were then sorted to obtain genes differentially expressed by $\geqslant$ 2 fold or $\leqslant$ 0.5 in at least 5 of the patients.

Semi-quantitative RT-PCR

Some of the differentially expressed genes were selected for validation of the microarray results with semi-quantitative RT-PCR. The sequences of the primers were designed with online primer design software (Primer 3 old

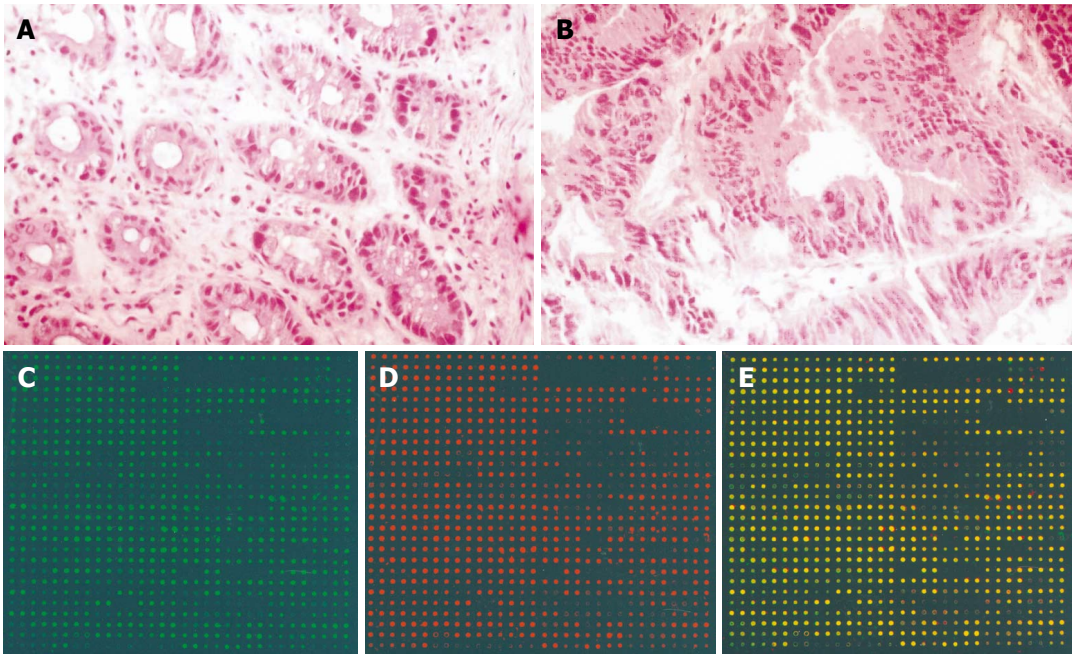

Figure 1 Histopathological examination of the tumor tissues of rectal cancer. **A**: Normal rectal mucosa tissue; **B**: Adenocarcinoma of rectal tissues; **C**, **D** and **E**: images of normal tissue, tumor tissues and overlay image of the tumor to normal of patient No.19 respectively. The density of the spot reflects the fluorescent intensity of the genes. In the overlay images, the yellow spots represent the expression of the genes in tumor tissues and normal tissues were not significant. The red spots represent the up-regulated genes in rectal cancer tissues. The green spots represent the down-regulated genes in rectal cancer tissues.

Version http://www.genome.wi.mit.edu/cgi-bin/primer/primer3.cgi#PRIMER_self_any[19]. The sequences of primers used for RT-PCR are as follows: MTA1 forward, 5'-AGCTACGAGCAGCACAACGGGGT-3', reverse, 5'-CACGCTTGGTTTCCGAGGAT-3'; β-actin forward, 5'-GTGGGGCGCCCCAGGCACCA-3', reverse, 5'-CTCCTTAATGTCACGCACGATTTC-3'[12]. RT-PCRs were performed with TAKARA version 2.1 RT-PCR kit using random primers in 25 μL volume. The PCR reaction was performed at 94℃ for 2 min, followed by 30 cycles at 94℃ for 30 s, 56℃ for 30 s and 72℃ for 30 s and a final extension at 72℃ for 5 min. β-actin was used as internal control. The products were electrophoresed in 1% agarose (Spanish).

Immunohistochemistry analysis of the BCL-2 protein expression in all patients

All the samples of rectal cancer and paired normal tissues were subject to immunohistochemistry examination for the expression of BCL-2 to validate the results of microarray. The primary antibody of BCL-2 was a product of Santa Cruz (1:100 dilution). The expressions of BCL-2 in tumor and normal tissues were read by two pathologists blindly. The image was captured with NIKON H600L microscope with digital camera.

Cluster analysis and principal component analysis

The normalized ratios of all pairs of samples of rectal cancer were put into an Excel-sheet. And every ratio was log2 transformed and saved as a tab-delimited Txt. file that was ready to be analyzed with Version 5.0 kindly provided online free of charge by Professor Leif E Peterson (http://mbcr.bcm.tmc.edu/genepi)[20].

RESULTS

Totally 21 pairs of rectal samples were analyzed. Their pathological and clinical characteristics are shown in Table 1. The tissue samples were all confirmed to be rectal cancer and normal paired tissues (Figure 1A and B). The differential expression genes were identified by a tumor associated genes microarray fabricated in our laboratory. The representative scan images are shown in Figure 1C, D and E which represented the image of normal tissue, rectal cancer and the overlay of the image respectively. In the overlay images of microarray, red color spots represented genes that were up-regulated in rectal cancer tissues, green color spots represented down-regulated genes and yellow color spots represented the expression of genes in cancer

Table 1 Clinical data of the rectal cancer patients

Patient No.	Age (yr)	Sex	TNM	Clinical stage
1	31	Male	T4N2M0	Ⅲ
2	51	Female	T3N1M0	Ⅲ
3	47	Male	T3N1M0	Ⅲ
4	67	Female	T3N0M0	Ⅱ
6	49	Male	T2N2M0	Ⅲ
7	38	Male	T3N0M0	Ⅱ
8	59	Female	T3N0M0	Ⅱ
9	53	Male	T3N0M0	Ⅱ
10	62	Male	T2N0M0	Ⅰ
11	62	Male	T3N1M0	Ⅲ
12	41	Male	T3N1M0	Ⅲ
13	33	Male	T4N0M0	Ⅱ
14	76	Male	T3N1M0	Ⅲ
15	75	Female	T2N0M0	Ⅰ
16	32	Female	T3N1Mo	Ⅲ
17	65	Female	T3N1Mo	Ⅱ
18	48	Female	T3N0Mo	Ⅱ
19	32	Male	T3N2M0	Ⅲ
20	68	Male	T2N0M0	Ⅰ
21	76	Male	T3N0M0	Ⅱ
22	76	Male	T3N0M0	Ⅱ

T1-4 represent the size of the tumor; N0-4 represent the level of node metastasis; M1-4 represent the level of metastasis.

Table 2 Commonly up-regulated genes in rectal cancer patients showing ≥ 2 fold over expression

Accession No.	Gene description	Patients (*n*)
NM_000184	Hs.23763, hemoglobin, gamma G (186624)	8
NM_000633	B-cell CLL/lymphoma 2 (BCL2), nuclear gene encoding mitochondrial protein, transcript variant alpha (3950016)	6
Not found	Hs.77579, ESTs (2811005)	6
Not found	Hs.87497, ESTs (1216395)	5
BB366468	Hs.126701, ESTs, Weakly similar to homolog of the Aspergillus nidulans sudD gene product [H.sapiens] (1082187)	5
NM_000600	Interleukin 6 (interferon, beta 2) (IL6) (3876176)	5
NM_004469	c-fos induced growth factor (vascular endothelial growth factor D) (FIGF) (160946)	5
BM440387	KIAA0712 gene product (539641)	5
BB217505	Hs.106513, Homo sapiens mRNA; cDNA DKFZp586I1518 (from clone DKFZp586I1518) (585388)	5
NM_002210	Integrin, alpha V (vitronectin receptor, alpha polypeptide, antigen CD51) (ITGAV) (3878920)	5
L12168	Adenylyl cyclase-associated protein (2217802)	5
NM_007047	Hs.19301, butyrophilin, subfamily 3, member A2 (1070574)	5
NM_018844	b-cell receptor associated protein (2746778)	5
U41371	Spliceosome associated protein 145 (1964680)	5
NM_001022	Hs.5621, ribosomal protein S19 (728984)	5
NM_002506	Nerve growth factor, beta polypeptide (NGFB) (72869)	5
NM_000121	Erythropoietin receptor (EPOR) (114048)	5
NM_003371	Vav 2 oncogene (VAV2) (3861692)	5
NM_000267	Neurofibromin 1 (neurofibromatosis, von Recklinghausen disease, Watson disease) (NF1) (3868563)	5
AF071400	Plasminogen activator inhibitor, type Ⅱ (arginine-serpin) (PAI2) (323255)	5
NM_006059	Laminin, gamma 3 (LAMC3) (2497685)	5
NM_002865	Hs.234726, RAB2, member RAS oncogene family (728947)	5
NM_013230	Hs.180414, CD24 antigen (small cell lung carcinoma cluster 4 antigen) (115306)	5

The number in the brackets represents IMAGE clone number.

Table 3 Commonly down-regulated genes in rectal cancers showing < 0.5 under expression

Accession No.	Gene description	Patients (*n*)
Not found	Hs.170311, EST (126182)	5
NM_004689	Metastasis associated 1 (MTA1) (4054392)	5
BC001766	S100 calcium-binding protein, beta (neural) (S100B) (759948)	5
NM_005246	Fer (fps/fes related) tyrosine kinase (phosphoprotein NCP94) (FER) (3886018)	5
NM_001920	Decorin (DCN) (274397)	5
NM_001951	E2F transcription factor 5, p130-binding (E2F5) (701492)	5
NM_002211	Homo sapiens integrin, beta 1 (fibronectin receptor, beta polypeptide, antigen CD29 includes MDF2, MSK12) (ITGB1) (531839)	5
Not found	Hs.23954, ESTs (132543)	5
Not found	Hs.5621, ESTs (2947053)	5
NM_007191	Wnt inhibitory factor-1 (WIF-1) (40908)	5
NM_021785	Retinoic acid induced 2 (RAI2) (501868)	5
Not found	Tachykinin, precursor 1 (substance K, substance P, neurokinin 1, neurokinin 2, neuromedin L, neurokinin alpha, neuropeptide K, neuropeptide gamma) (TAC1), transcript variant beta (784179)	5
NM_004345	Cathelicidin antimicrobial peptide (CAMP) (3057931)	5
AF385430	Rho GTPase activating protein 1 (ARHGAP1) (3896574)	5
NM_005252	v-fos FBJ murine osteosarcoma viral oncogene homolog (FOS) (755279)	5

The numbers in the brackets represent IMAGE clone number.

tissue, which were between 0.5-2.0. If the ratio of the duplicate spots was the same, we defined it the significantly differentially expressed gene. The expression ratios of tumor associated genes in tumor and paired normal rectal tissues were analyzed with QuantaArray 3.0 and normalized to the total. The 2-fold up- or down-regulated genes were defined as differential expression genes.

The results showed that 23 genes were up-regulated in at least 5 samples (Table 2) and 15 genes were down regulated at least in 5 samples (Table 3). The up-regulated genes included growth factors, growth factor receptor, nuclear transcription factor, oncogenes, adhesion molecules, and some metabolic enzymes.

To validate the results of microarray examination, the expression of MTA1 mRNA was measured with semi-quantitative RT-PCR using β-actin as internal control. The results showed that the MTA1 expression was down-regulated (Figure 2). The up-regulation of BCL-2 was also validated by immunohistochemistry and significant expression of BCL-2 was shown in tumor tissues and less expression in normal rectal mucosa (Figure 3A-D).

For the cluster analysis, the Claufavor version 6.0 supplied kindly by Professor Leif Peterson was used to classify the patients or genes by gene expression profiles. As a result, the patients were classified into two groups, with patients No 22, 13, 12, 1, 11, 21, 19, 2, 6, 16, 15, 3 into one group which were all above grade Ⅱ except patient No 15 and the other patients into another group. The top 100 genes that were related with rectal cancer are shown in Figure 4A and B. Principal component analysis showed that all the genes were belonged to 7 factors, in which 17 genes were positively correlated with factor 1 ($r > 0.45$). They are as follows: apoptosis associated protein, xeroderma pigmentosum, complementation group A (XPA), early endosome antigen 1162 kDa (EEA), lactate dehydrogenase A, spectrin, alpha non-erythrocytic 1 (alpha-fodrin), small nuclear ribonucleoprotein associated protein n (human), phorbol-12-myristate-13-acetate-induced protein 1 (PMAIP1) , RAS p21 protein activator (GTPase activating protein) 1 (RASA1), cathepsin D (lysosomal aspartyl protease) (CTSD), v-ski avian sarcoma viral oncogene homolog (SKI), Hs.271616, ESTs, small nuclear ribonucleoprotein associated proteins b and b' (human); contains mer22.

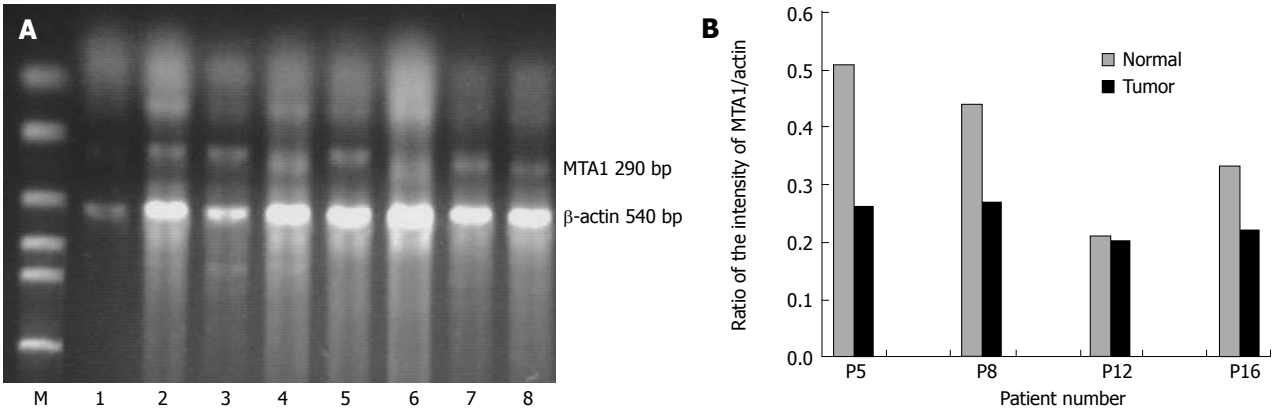

Figure 2 Semi-quantitative RT-PCR of MTA1 mRNA. **A**: Electrophoresis image of MTA1 expression, lanes 1-8 represent the mRNA expression of MTA1 in 4 pairs of rectal cancer patients, respectively. Lanes 1, 3, 5, 7 were normal tissues and 2, 3, 6, 8 were tumor tissues. **B**: The semi-quantitative analysis results with spot intensity software. The ratios of MTA1 in tumor tissues were lower than that of paired normal tissues.

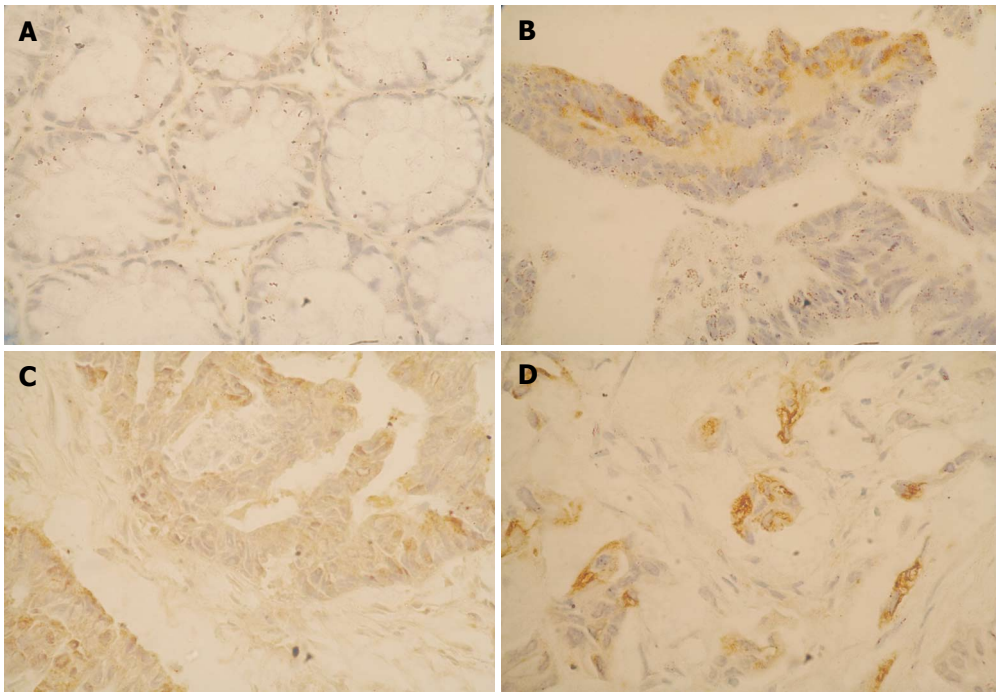

Figure 3 Validation of the expression of BCL-2 with immunohistochemistry method. **A**: The normal rectal mucosa. There was no expression of BCL-2 in all the cells; **B**: The expression of BCL-2 in well differentiated rectal cancer. The tumor cells were stained yellow-brown by DAB; **C**: The expression of BCL-2 in another intermediately differentiated rectal cancer. The expression of BCL-2 was also significant in tumor cells; **D**: The expression of BCL-2 in poorly differentiated rectal tissues.

t1 mer22 repetitive element, CD83 antigen (activated B lymphocytes, immunoglobulin superfamily) (CD83), bone marrow stromal cell antigen 1 (BST1), Wnt inhibitory factor-1 (WIF-1), histone deacetylase 1 (HDAC1), microvascular endothelial differentiation gene 1 (MDG1).

Nine genes were negatively correlated with factor 3 ($r < -0.45$) (Figure 4B); they are as follows: apoptosis associated protein, phospholipase C, delta 1 (PLCD1), small nuclear ribonucleoprotein associated protein n (human), RAS p21 protein activator (GTPase activating protein) 1 (RASA1), cathepsin D (lysosomal aspartyl protease) (CTSD), met proto-oncogene (hepatocyte growth factor receptor) (MET), 65 KDa yes-associated protein; contains Alu repetitive element; contains element MER31 repetitive element, KIAA0712 gene product, ESTs (Weakly similar to homolog of the Aspergillus nidulans sudD gene product). These results showed that microarray expression profiles may be used for the classification of rectal cancer.

DISCUSSION

Differential gene expression can be detected in several ways, including differential screening of cDNA libraries[21], subtraction hybridization[22] differential display of RNA[23], serial analysis of gene expression (SAGE)[24] and cDNA microarray[25]. Among these cDNA microarray is the most commonly used technique now for surveying many samples with thousands of genes[26]. By using cDNA microarray methods and laser capture microdissection, 235 differential expression genes were identified from colorectal cancers[14]. A colonchip has been constructed for the identification of genes that are related to colorectal cancer tumorigenesis, 59 genes showing two-fold increase of altered expression with 23 genes commonly up-regulated and 36 genes commonly down-regulated in colorectal cancer[27]. All these studies were about colorectal carcinoma, while few were concerned with rectal cancer. Moreover, rectal cancer has the tendency to occur in young

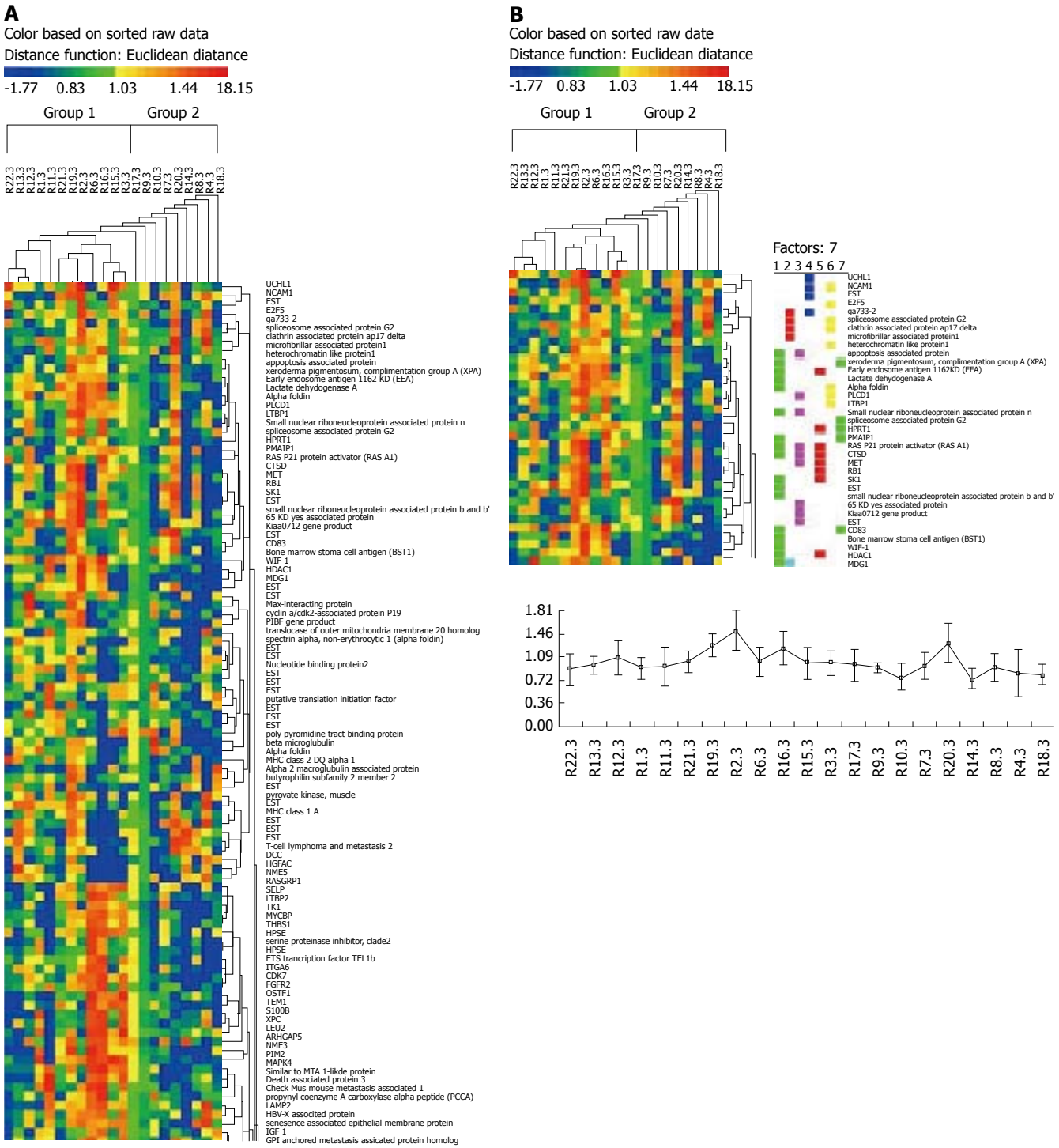

Figure 4 Hierarchial cluster analysis and principal component analysis results. **A**: Hierachial cluster analysis of patients and genes. The patients could be classified into two groups: one group of clinicopathological stage above grade Ⅱ and one group below grade Ⅱ. **B**: Principal component analysis of the genes related to rectal cancer.

age. To identify the molecular markers of rectal cancer we constructed a tumor associated genes cDNA microarray for the evaluation of the predisposition to metastasis with gene expression profiles. All the tumor associated genes were selected from literatures that are related with the growth, invasion and metastasis process of tumor and some ESTs. We used this cDNA microarray to detect the differential expression genes that play important roles in the pathogenesis of rectal cancer. We found that 23 genes were up-regulated in rectal cancers compared with their paired normal tissues. The most commonly expressed gene in rectal cancers was BCL-2. It was validated by immunohistochemistry. We also found that oncogene vav-2 was up-regulated in 5 of the 21 patients. Vav-2 acts as a guanosine nucleotide exchange factor (GEF) for RhoG and RhoA-like GTPases in a phosphotyrosine-dependent manner. Vav-2 oncogenic activation correlates with the acquisition of phosphorylation-independent exchange activity. *In vivo*, wild-type Vav-2 is activated oncogenically by tyrosine kinases, an effect enhanced further by co-expression of RhoA. Likewise, the Vav-2 oncoprotein synergizes with RhoA and RhoB proteins in cellular

transformation. Transient transfection assays in NIH-3T3 cells show that phosphorylated wild-type Vav-2 and the Vav-2 oncoprotein induce cytoskeletal changes resembling those observed by the activation of the RhoG pathway. In contrast, the constitutive expression of the Vav-2 oncoprotein in rodent fibroblasts leads to major alterations in cell morphology and to highly enlarged cells in which karyokinesis and cytokinesis frequently are uncoupled[28].

There were 15 down-regulated genes including PIGF gene products, MTA1, WIF-1 ras-guanine releasing protein and all pre-mRNA cleavage factor Im. There was a controversial report that MTA1 are down-regulated in rectal cancer and it has been validated by RT-PCR. Toh *et al*[29] reported a relative over-expression of MTA1 mRNA (tumor/normal ratio $\geqslant$ 2) was observed in 14 of 36 (38.9%) colorectal carcinomas. Tumors over-expressing MTA1 mRNA exhibited a significantly deeper wall invasion and a higher rate of metastasis to lymph nodes, and tended to be at an advanced Dukes' stage with frequent lymphatic involvement[29].

In addition, Nicolson has reported the over-expression of MTA1 in several cell lines (the breast, ovarian, lung, gastric and colorectal cancer but not melanoma or sarcoma) and cancerous tissues (breast, esophageal, colorectal, gastric and pancreatic cancer)[30]. Giannini *et al*[31] have reported that MTA1 increased in tumor tissues than in normal tissues by real-time PCR. This difference may be attributed to the different function MTA1 exerts in different tumor stage. Further studies are needed at protein levels.

To investigate the possibility of classification of tumor with gene expression profiles, hierarchical cluster analysis was done and the results showed that the patients could be divided into two groups: clinicopathological grade higher than grade Ⅱ and the other below grade Ⅱ.

Many studies have done to uncover mechanisms underlying progression of colorectal carcinogenesis and to identify genes associated with the liver metastasis. Li *et al*[32] analyzed expression profiles of 14 primary colorectal cancers with liver metastases, and compared them with profiles of 11 non-metastatic carcinomas and those of 9 adenomas of the colon. A hierarchical cluster analysis using data from a cDNA microarray containing 23040 genes indicated that the cancers with metastasis had different expression profiles from those without metastasis although a number of genes were commonly up-regulated in primary cancers of both categories. They found that 54 genes were frequently up-regulated and 375 genes were frequently down-regulated in primary tumors with metastases to liver, but not in tumors without metastasis. Subsequent quantitative PCR experiments confirmed that PRDX4, CKS2, MAGED2, and an EST (GenBank accession number BF696304) were expressed at significantly higher levels in tumors with metastasis[32]. Koehler has studied the expression profiles of 25 colorectal carcinomas (CRCs, pT1-4), corresponding normal colonic mucosa, and 14 liver metastases using cDNA arrays containing 1176 cancer-related genes (Clontech). They found no specific expression signature in matching metastases, but a set of 23 classifier genes with statistically significant expression patterns in high- and low-stage tumors was identified[33].

Komori *et al*[34] constructed the gene expression profiles of 50 colorectal cancers (CRCs) and 12 normal colorectal epithelia using a cDNA microarray specially constructed for CRC. Hierarchical clustering analysis and principal component analysis could clearly distinguish the gene profiles of cancer tissues from those of normal tissues. They identified 22 up-regulated genes and 32 down-regulated genes in CRC. Many of these genes have been previously identified in association with human carcinogenesis, being 68% and 78%, respectively[34].

Moreover, D'Arrigo *et al*[35] compared the transcriptional profiles of 10 radically resected primary CRCs from patients who did not develop distant metastases within a 5-year follow-up period with those of 10 primary/metastatic tumor pairs from patients with synchronous liver metastases. Arrays of 7864 human cDNAs were utilized using laser-microdissected bioptic tissues. Of 37 gene expression differences found between the 2 groups of primary tumors, 29 were also different between non-metastasizing tumors from metastases. The gene encoding mannosyl (alpha-1, 3-)-glycoprotein beta-1, 4-N-acetyl-glucosaminyl-transferase (GnT-Ⅳ) became significantly up-regulated in primary/metastatic tumor pairs ($P < 0.001$)[35]. All these results were obtained from colorectal cancer. However, colon cancer and rectal cancer may have different molecular markers. Our methods have similar ability in classifying tumor with gene expression profiles.

In conclusion, we have screened 23 up-regulated genes and 15 down-regulated genes from 21 rectal cancers. Hierarchical cluster analysis divided the patients into one group with clinicopathological stage above Ⅱ, and one group below stage Ⅱ. These genes may be the molecular markers of rectal cancer. In addition, we have also found gene expression profiles in different stage of rectal cancers and to further screen the molecular markers in each stage of the cancer larger samples are needed.

ACKNOWLEDGMENTS

We thank Professor Leaf Peterson at Baylor College of Medicine for his free CLUSFAVOR 5.0 software and his instruction for the study. We also thank Dr Feng-Wei Wang in Medical College of Wisconsin for the language correction.

REFERENCES

1 **Gutman M**, Fidler IJ. Biology of human colon cancer metastasis. *World J Surg* 1995; **19**: 226-234
2 **Forrester K**, Almoguera C, Han K, Grizzle WE, Perucho M. Detection of high incidence of K-ras oncogenes during human colon tumorigenesis. *Nature* 1987; **327**: 298-303
3 **Baker SJ**, Fearon ER, Nigro JM, Hamilton SR, Preisinger AC, Jessup JM, vanTuinen P, Ledbetter DH, Barker DF, Nakamura Y, White R, Vogelstein B. Chromosome 17 deletions and p53 gene mutations in colorectal carcinomas. *Science* 1989; **244**: 217-221
4 **Fearon ER**, Cho KR, Nigro JM, Kern SE, Simons JW, Ruppert JM, Hamilton SR, Preisinger AC, Thomas G, Kinzler KW. Identification of a chromosome 18q gene that is altered in colorectal cancers. *Science* 1990; **247**: 49-56
5 **Kinzler KW**, Vogelstein B. Lessons from hereditary colorectal

cancer. *Cell* 1996; **87**: 159-170
6 **Groden J**, Thliveris A, Samowitz W, Carlson M, Gelbert L, Albertsen H, Joslyn G, Stevens J, Spirio L, Robertson M. Identification and characterization of the familial adenomatous polyposis coli gene. *Cell* 1991; **66**: 589-600
7 **Powell SM**, Zilz N, Beazer-Barclay Y, Bryan TM, Hamilton SR, Thibodeau SN, Vogelstein B, Kinzler KW. APC mutations occur early during colorectal tumorigenesis. *Nature* 1992; **359**: 235-237
8 **Behrens J**, von Kries JP, Kühl M, Bruhn L, Wedlich D, Grosschedl R, Birchmeier W. Functional interaction of beta-catenin with the transcription factor LEF-1. *Nature* 1996; **382**: 638-642
9 **He TC**, Sparks AB, Rago C, Hermeking H, Zawel L, da Costa LT, Morin PJ, Vogelstein B, Kinzler KW. Identification of c-MYC as a target of the APC pathway. *Science* 1998; **281**: 1509-1512
10 **Shtutman M**, Zhurinsky J, Simcha I, Albanese C, D'Amico M, Pestell R, Ben-Ze'ev A. The cyclin D1 gene is a target of the beta-catenin/LEF-1 pathway. *Proc Natl Acad Sci USA* 1999; **96**: 5522-5527
11 **Tetsu O**, McCormick F. Beta-catenin regulates expression of cyclin D1 in colon carcinoma cells. *Nature* 1999; **398**: 422-426
12 **Sparks AB**, Morin PJ, Vogelstein B, Kinzler KW. Mutational analysis of the APC/beta-catenin/Tcf pathway in colorectal cancer. *Cancer Res* 1998; **58**: 1130-1134
13 **Kitahara O**, Furukawa Y, Tanaka T, Kihara C, Ono K, Yanagawa R, Nita ME, Takagi T, Nakamura Y, Tsunoda T. Alterations of gene expression during colorectal carcinogenesis revealed by cDNA microarrays after laser-capture microdissection of tumor tissues and normal epithelia. *Cancer Res* 2001; **61**: 3544-3549
14 **Williams NS**, Gaynor RB, Scoggin S, Verma U, Gokaslan T, Simmang C, Fleming J, Tavana D, Frenkel E, Becerra C. Identification and validation of genes involved in the pathogenesis of colorectal cancer using cDNA microarrays and RNA interference. *Clin Cancer Res* 2003; **9**: 931-946
15 **DNA precipitations**. Available from: http://cmgm.stanford.edu/pbrown/protocols/2_DNA.html
16 **Post processing of microarrays**. Available from: http://www.umbi.umd.edu/~cbr/postprocessing601.html
17 **Yang IV**, Chen E, Hasseman JP, Liang W, Frank BC, Wang S, Sharov V, Saeed AI, White J, Li J, Lee NH, Yeatman TJ, Quackenbush J. Within the fold: assessing differential expression measures and reproducibility in microarray assays. *Genome Biol* 2002; **3**: research0062
18 **Gao XQ**, Han JX, Huang HY, Yan S, Song CZ, Huang HN. Effects of aspirin on metastasis-associated gene expression detected by cDNA microarray. *Acta Pharmacol Sin* 2004; **25**: 1327-1333
19 **Online primer design software**.Available from: http://www.genome.wi.mit.edu/cgi-bin/primer/primer3.cgi#PRIMER_self_any
20 **Peterson LE**. CLUSFAVOR 5.0: hierarchical cluster and principal-component analysis of microarray-based transcriptional profiles. *Genome Biol* 2002; **3**: SOFTWARE0002
21 **Höög C**. Isolation of a large number of novel mammalian genes by a differential cDNA library screening strategy. *Nucleic Acids Res* 1991; **19**: 6123-6127
22 **Sagerström CG**, Sun BI, Sive HL. Subtractive cloning: past, present, and future. *Annu Rev Biochem* 1997; **66**: 751-783
23 **Liang P**, Pardee AB. Differential display of eukaryotic messenger RNA by means of the polymerase chain reaction. *Science* 1992; **257**: 967-971
24 **Velculescu VE**, Zhang L, Vogelstein B, Kinzler KW. Serial analysis of gene expression. *Science* 1995; **270**: 484-487
25 **Schena M**, Shalon D, Davis RW, Brown PO. Quantitative monitoring of gene expression patterns with a complementary DNA microarray. *Science* 1995; **270**: 467-470
26 **DeRisi J**, Penland L, Brown PO, Bittner ML, Meltzer PS, Ray M, Chen Y, Su YA, Trent JM. Use of a cDNA microarray to analyse gene expression patterns in human cancer. *Nat Genet* 1996; **14**: 457-460
27 **Takemasa I**, Higuchi H, Yamamoto H, Sekimoto M, Tomita N, Nakamori S, Matoba R, Monden M, Matsubara K. Construction of preferential cDNA microarray specialized for human colorectal carcinoma: molecular sketch of colorectal cancer. *Biochem Biophys Res Commun* 2001; **285**: 1244-1249
28 **Schuebel KE**, Movilla N, Rosa JL, Bustelo XR. Phosphorylation-dependent and constitutive activation of Rho proteins by wild-type and oncogenic Vav-2. *EMBO J* 1998; **17**: 6608-6621
29 **Toh Y**, Oki E, Oda S, Tokunaga E, Ohno S, Maehara Y, Nicolson GL, Sugimachi K. Overexpression of the MTA1 gene in gastrointestinal carcinomas: correlation with invasion and metastasis. *Int J Cancer* 1997; **74**: 459-463
30 **Nicolson GL**, Nawa A, Toh Y, Taniguchi S, Nishimori K, Moustafa A. Tumor metastasis-associated human MTA1 gene and its MTA1 protein product: role in epithelial cancer cell invasion, proliferation and nuclear regulation. *Clin Exp Metastasis* 2003; **20**: 19-24
31 **Giannini R**, Cavallini A. Expression analysis of a subset of coregulators and three nuclear receptors in human colorectal carcinoma. *Anticancer Res* 2005; **25**: 4287-4292
32 **Li M**, Lin YM, Hasegawa S, Shimokawa T, Murata K, Kameyama M, Ishikawa O, Katagiri T, Tsunoda T, Nakamura Y, Furukawa Y. Genes associated with liver metastasis of colon cancer, identified by genome-wide cDNA microarray. *Int J Oncol* 2004; **24**: 305-312
33 **Koehler A**, Bataille F, Schmid C, Ruemmele P, Waldeck A, Blaszyk H, Hartmann A, Hofstaedter F, Dietmaier W. Gene expression profiling of colorectal cancer and metastases divides tumours according to their clinicopathological stage. *J Pathol* 2004; **204**: 65-74
34 **Komori T**, Takemasa I, Higuchi H, Yamasaki M, Ikeda M, Yamamoto H, Ohue M, Nakamori S, Sekimoto M, Matsubara K, Monden M. Identification of differentially expressed genes involved in colorectal carcinogenesis using a cDNA microarray. *J Exp Clin Cancer Res* 2004; **23**: 521-527
35 **D'Arrigo A**, Belluco C, Ambrosi A, Digito M, Esposito G, Bertola A, Fabris M, Nofrate V, Mammano E, Leon A, Nitti D, Lise M. Metastatic transcriptional pattern revealed by gene expression profiling in primary colorectal carcinoma. *Int J Cancer* 2005; **115**: 256-262

S- Editor Wang GP **L- Editor** Zhu LH **E- Editor** Bi L

PO Box 2345, Beijing 100023, China
www.wjgnet.com
wjg@wjgnet.com

World J Gastroenterol 2007 January 21; 13(3): 349-354
World Journal of Gastroenterology ISSN 1007-9327

Red wine and green tea reduce *H pylori*- or VacA-induced gastritis in a mouse model

Paolo Ruggiero, Giacomo Rossi, Francesco Tombola, Laura Pancotto, Laura Lauretti, Giuseppe Del Giudice, Mario Zoratti

Paolo Ruggiero, Laura Pancotto, Laura Lauretti, Giuseppe Del Giudice, Novartis Vaccines & Diagnostics s.r.l., Research Center, Siena, Italy
Giacomo Rossi, Department of Veterinary Science, University of Camerino, Matelica, Italy
Francesco Tombola, Department of Biomedical Sciences, University of Padova, Italy
Francesco Tombola, Mario Zoratti, CNR Institute of Neuroscience, Section for Biomembranes, Padova, Italy
Supported partly by a CNR Target Project Biotechnology grant and a University of Padova Young Investigator grant
Correspondence to: Paolo Ruggiero, Novartis Vaccines & Diagnostics s.r.l., Research Center, Via Fiorentina 1, Siena I-53100, Italy. paolo.ruggiero@novartis.com
Telephone: +39-577-243111 Fax: +39-577-243564
Received: 2006-10-09 Accepted: 2006-12-01

Abstract

AIM: To investigate whether red wine and green tea could exert anti-*H pylori* or anti-VacA activity *in vivo* in a mouse model of experimental infection.

METHODS: Ethanol-free red wine and green tea concentrates were administered orally as a mixture of the two beverages to *H pylori* infected mice, or separately to VacA-treated mice. Gastric colonization and gastric inflammation were quantified by microbiological, histopathological, and immunohistochemical analyses.

RESULTS: In *H pylori*-infected mice, the red wine and green tea mixture significantly prevented gastritis and limited the localization of bacteria and VacA to the surface of the gastric epithelium. Similarly, both beverages significantly prevented gastric epithelium damage in VacA-treated mice; green tea, but not red wine, also altered the VacA localization in the gastric epithelium.

CONCLUSION: Red wine and green tea are able to prevent *H pylori*-induced gastric epithelium damage, possibly involving VacA inhibition. This observation supports the possible relevance of diet on the pathological outcome of *H pylori* infection.

Key words: VacA; *H pylori*; Gastritis; Wine; Tea; Polyphenols

Ruggiero P, Rossi G, Tombola F, Pancotto L, Lauretti L, Del Giudice G, Zoratti M. Red wine and green tea reduce *H pylori*- or VacA-induced gastritis in a mouse model. *World J Gastroenterol* 2007; 13(3): 349-354

http://www.wjgnet.com/1007-9327/13/349.asp

INTRODUCTION

H pylori chronically infects human stomach, causing atrophic gastritis. The majority of infections are asymptomatic; nevertheless, infected individuals can incur severe gastroduodenal diseases such as peptic ulcer[1] and gastric mucosa-associated lymphoid tissue (MALT) lymphoma[2]. *H pylori* infection plays a relevant role in gastric carcinogenesis, which was also shown in animals[3]. The current antibiotic-based therapies against *H pylori* are generally effective, but can fail due to antibiotic resistance or lack of patient compliance. To colonize the host stomach, *H pylori* expresses several factors that can play a role in pathogenesis. One that is most characterized is the vacuolating cytotoxin VacA, which induces cell vacuolation and rearrangements of late endosomes and lysosomes *in vitro*[4]. VacA forms anion-selective, urea-permeable channels in artificial and plasma membranes[5]. It promotes diffusion across the epithelium of urea[6], which is hydrolysed by *H pylori* urease, leading neutralisation of acidic gastric juice and thus favouring bacterial survival. *In vitro*, VacA exhibits several properties that suggest its role in disturbing the host immune system, although *in vivo* experimental proof of similar activity remains to be provided[7]. The most evident *in vivo* activity of VacA is to cause damage of gastric epithelium, as shown in murine models[8,9]. Plant-derived substances have been reported to limit *H pylori* gastric colonization in Mongolian gerbils[10,11]. We have previously found that polyphenols and polyphenol-rich beverages, such as tea and wine, inhibit VacA activity *in vitro*[12], and that some polyphenols can limit both *H pylori*- and VacA-induced gastric damage *in vivo*[13]. Also, it has been recently reported that hop bract extract exerts anti-VacA activity in vitro and *in vivo*[14]. In the present paper we investigated whether red wine and green tea concentrates could influence gastric colonization or gastric pathology in *H pylori*-infected or VacA-treated mice.

MATERIALS AND METHODS

Bacteria

SPM 326, a Type I *H pylor*i strain expressing s1/m1 VacA isoform, was used[15]. Bacteria were grown at 37℃ in Columbia Agar (Oxoid, Basingstoke, UK) plates containing 5% fresh defibrinated horse serum and Dent's supplement (Oxoid), under microaerophylic conditions, using CampyGen (Oxoid), and harvested in saline immediately before challenge.

Toxin

Native s1/m1-type VacA was produced and tested for vacuolating activity on HeLa cells as previously described[16,17]. Prior to use, it was activated at pH 2.0 for 10 min at R.T., then neutralized and diluted in saline.

Red wine and green tea concentrates

Red wine (RW) was produced on a local (Sarmede, Italy) family vineyard by the traditional spontaneous fermentation process, without additives. Green tea (GT) infusion was obtained by boiling 2 g of lyophilised and otherwise untreated leaves from Morocco in 1 L of distilled water for 5 min. GT and alcohol-free RW concentrates were obtained by vacuum distillation at 30℃, then stored in aliquots at -20℃. Prior to administration concentrates were thawed, diluted in water to reach 3-fold (RW) or 1.5-fold (GT) concentration in comparison with the original volume, and filtered at 0.2 μm. RW + GT mixture was prepared at the same final concentrations.

Mice and study design

Specific-pathogen-free mice (Charles River, Calco, Italy) were housed and treated in compliance with the current law. The schedule of the treatments is summarized in Table 1. Overnight starved 6-wk old CD1 mice (average body weight 22 g) were infected intragastrically by two administrations each other day of 10^8 CFU/mouse[15]. Alternatively, starved 6-wk old BALB/c mice (average body weight 18 g) received two intragastric administrations each other day of either 10 μg or 50 μg of VacA[8]. Controls received saline only. Starting 24 h before infection or VacA administration, the animals had free access to drinking water containing 1% glucose and RW + GT in the case of *H pylori* infection, RW or GT in the case of VacA administration. Controls drank a 1% glucose solution. The beverages were changed daily; their intake was about 5 mL/d per mouse, without appreciable differences among the different groups. Two weeks after infection, or 4 d after the first VacA treatment, the animals were euthanized, and each stomach immediately removed and cut along the greater and lesser curvature, obtaining two equivalent parts. One part was formalin fixed and paraffin embedded for further histopathological analysis. Gastric mucosa was scraped from the remaining half stomach and cultured on selective plates, prepared as described above with the addition of 0.2 mg/mL bacitracin (Sigma-Aldrich), to quantify *H pylori* colony forming units (CFU).

Table 1 Schedule of treatments

Group	*n*	D -1 to the D of sacrifice	D 0	D 2	D 4	D 14
RW + GT	6	RW + GT	Infection	Infection	-	Sacrifice
Infected	6	1% glucose	Infection	Infection	-	Sacrifice
Non infected	6	1% glucose	Saline	Saline	-	Sacrifice
RW	5	RW	VacA 10 μg	VacA 10 μg	Sacrifice	-
	5	RW	VacA 50 μg	VacA 50 μg	Sacrifice	-
GT	5	GT	VacA 10 μg	VacA 10 μg	Sacrifice	-
	5	GT	VacA 50 μg	VacA 50 μg	Sacrifice	-
VacA control	5	1% glucose	VacA 10 μg	VacA 10 μg	Sacrifice	-
	5	1% glucose	VacA 50 μg	VacA 50 μg	Sacrifice	-
Saline	5	1% glucose	Saline	Saline	Sacrifice	-

Histopathology

From paraffin-embedded stomachs 4 μm-thick sections were cut, dewaxed, and stained with haematoxylin-eosin (HE), then blindly examined. Gastritis was graded in antrum, corpus and fundus of each stomach according to the updated Sydney System[18], and scored from 0 to 3 corresponding to normal, mild, moderate and severe, respectively. Gastric sections were also subjected to immunohistochemical (IHC) staining using either an anti-*H pylori* polyclonal antibody (HistoLine) or an anti-VacA monoclonal antibody as already described[13,19].

Statistical analysis

Data were evaluated by one-tailed Mann-Whitney *U* test. Probability values less than 5% ($P < 0.05$) were considered and referred to as statistically significant.

RESULTS

Red wine and green tea alter the H pylori localization in gastric mucosa

H pylori SPM 326 colonized stomachs of both control and RW + GT-treated mice, giving geometric means of 1.6×10^3 and 2.6×10^3 CFU/stomach respectively, lacking significant difference ($P = 0.22$). While in RW + GT-treated animals *H pylori* was detectable by IHC mainly on the surface of the gastric mucosa (Figure 1A), in the infected control both superficial and deep staining was observed (Figure 1C). In adjacent sections, VacA localization by IHC resulted very similar to that of *H pylori*, with the difference that VacA staining appeared slightly weaker in RW + GT-treated animals (Figure 1B) and slightly stronger in the infected controls (Figure 1D) as compared with the corresponding *H pylori* staining.

Red wine and green tea prevent H pylori-induced gastritis

The observation of HE-stained sections of gastric mucosa of *H pylori*-infected controls revealed gastric inflammation of normal/mild grade in antrum, and mild/moderate in corpus and fundus. Gastritis scores were assigned to antrum, corpus and fundus of each mouse stomach and the mean of the three gastric sites was calculated. RW + GT-treated mice showed gastritis scores significantly lower than those of the corresponding infected, untreated controls ($P < 0.05$) (Figure 2A).

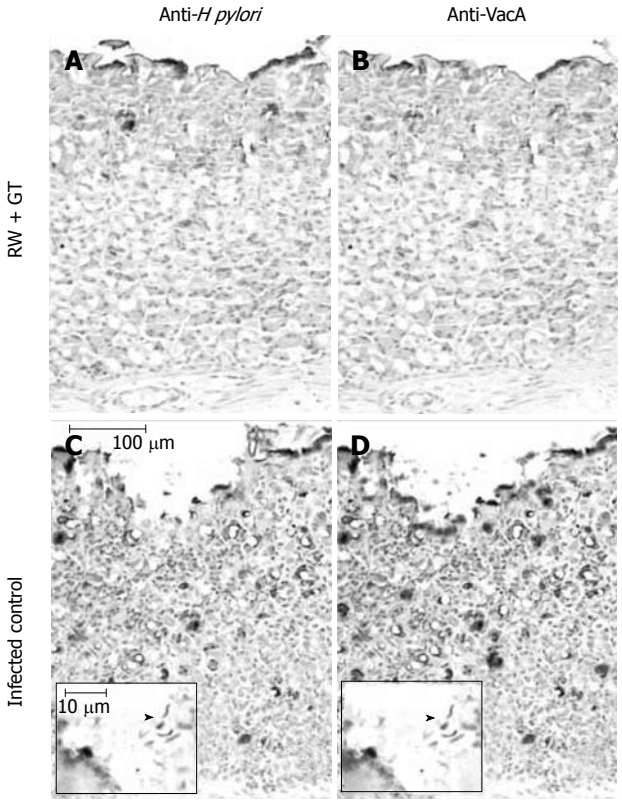

Figure 1 Representative images of IHC detection of *H pylori* (**A** and **C**) or VacA (**B** and **D**) in gastric mucosa sections from *H pylori*-infected mice in the presence (**A** and **B**) or in the absence (**C** and **D**) of RW + GT treatment. In the gastric epithelium of infected controls (**C** and **D**, adjacent sections) *H pylori* and VacA are detectable with a similar pattern, both superficially and deeply, while upon RW + GT treatment (**A** and **B**, adjacent sections) the immunostaining is mainly confined to the surface of the epithelium. Inserts at larger magnification show typical *H pylori* morphology (arrowheads).

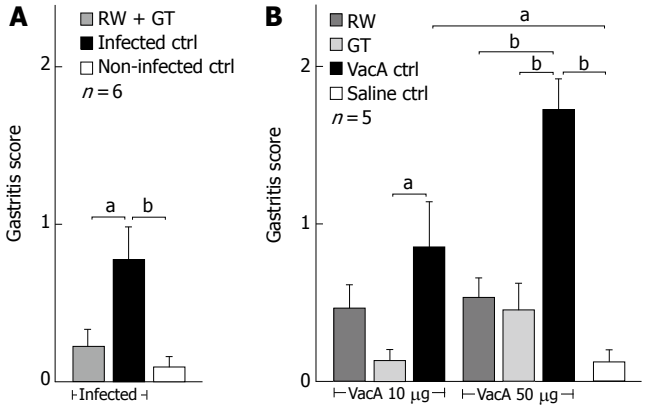

Figure 2 Gastritis score of *H pylori*-infected (**A**) or VacA-treated (**B**) mice in the presence or in the absence of RW and/or GT as indicated. Mean of antrum, corpus and fundus scores of each group. Bars = SE. $^{a}P < 0.05$, $^{b}P < 0.01$ comparison between the indicated groups.

Red wine and green tea prevent VacA-induced gastritis

Administration of 10 μg of VacA induced significant gastritis as compared with saline treatment ($P < 0.05$), although epithelial damage was little or absent in the antrum, and very mild in corpus and fundus. With this dose of VacA, reduction of gastritis scores was significant upon administration of GT ($P < 0.05$), but not of RW. Treatment with 50 μg of VacA induced significant ($P < 0.01$) and more evident gastritis (Figure 2B). The mucosal alterations were significantly milder in mice receiving RW or GT (Figures 2B, 3A and C) than those observed in VacA controls (Figures 2B and 3E). VacA controls presented mild epithelial damage in the antrum, and moderate/severe in corpus and fundus, where alteration of mucosal architecture was observed, with epithelial vacuolisation, diffuse mucosal erosion, and some ulcerations (Figure 3E). Gastric mucosa from saline controls did not show appreciable alterations as expected (Figures 2B and 3G).

Green tea alters VacA localization in gastric mucosa

The presence and distribution of VacA was examined by IHC in RW- and GT-treated gastric mucosa (Figure 3B and D), in comparison with VacA and saline controls (Figure 3F and H). VacA was detected both superficially and deeply in the gastric mucosa of mice that received either 10 μg (data not shown) or 50 μg of VacA (Figure 3F), the higher VacA dose producing a qualitatively similar but more intense staining than the lower dose. RW-treated mice showed similar staining as compared with VacA-treated controls (Figure 3B and F, respectively). In contrast, gastric mucosa of GT-treated mice showed only superficial staining of VacA, which was undetectable in the gland crypts (Figure 3D). Saline controls were completely negative as expected (Figure 3H).

DISCUSSION

Upon experimental infection, CD1 mice are stably colonized by *H pylori* and develop gastric inflammation reproducing several of the aspects of the gastric pathology observed in infected humans[15]. We chose to test in this model RW and GT on the basis of their previously demonstrated anti-VacA activity[12], and also because they are very common beverages, whose activity against *H pylori* has been already proposed in other models[20,21]. In our model, upon *H pylori* infection, RW + GT did not induce significant variation of gastric colonization levels in terms of CFU count, although qualitatively altering the distribution of bacteria that were localized more superficially in the gastric epithelium. We cannot exclude that such a difference of bacterial localization could have affected the quantification of colonization. However, if on one hand the action of RW + GT on *H pylori* infection level was difficult to quantify, on the other hand we observed a measurable and significant reduction of gastric inflammation. This result could be due to the observed restriction of the infection to the surface of gastric epithelium, but also to the possible inhibition of VacA exerted by RW + GT *in vivo*. In fact, VacA-deficient strains are able to infect mice, even though VacA can confer an advantage at early stages of the infection[22]. Thus, *in vivo* inhibition of VacA could be reasonably expected to limit gastric damage, but not necessarily to produce a significant and stable decrease of *H pylori* colonization. Therefore, we evaluated the ability of GT and RW to prevent gastric epithelium damage induced by administration of purified native VacA to BALB/c mice. This mouse strain does not allow stable colonization by SPM326[23], whereas it

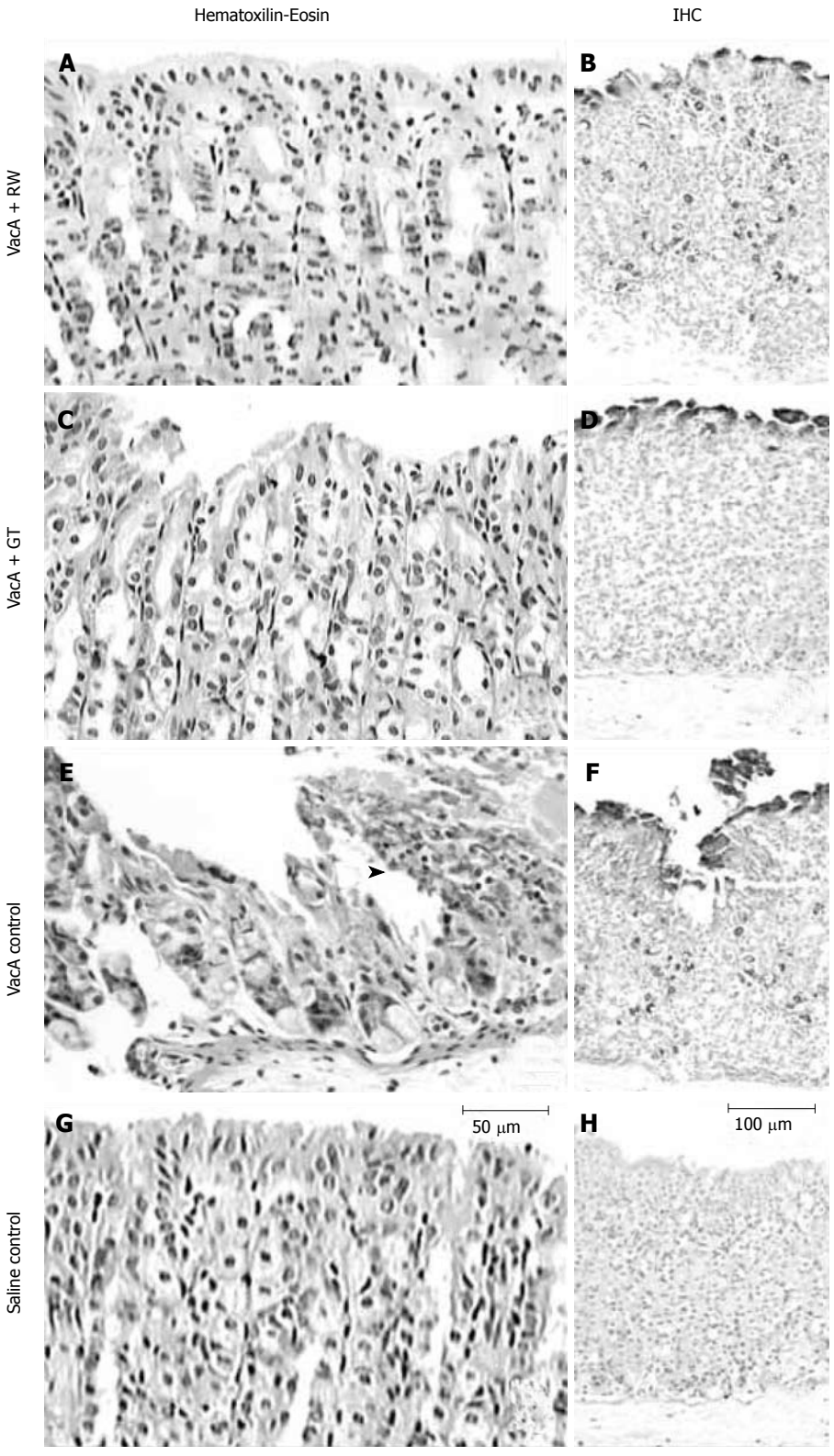

Figure 3 Representative images of sections of gastric corpus mucosa of mice treated with 50 μg of VacA in the presence (**A**-**D**) or in the absence (**E** and **F**) of RW or GT as indicated, in comparison with saline-treated control (**G** and **H**). HE staining (**A**, **C**, **E** and **G**): VacA control (**E**) shows a typical loss of mucosal architecture, with areas of cellular debris and inflammatory cells admixture (arrowhead), almost undetectable in the presence of RW (**A**) or GT (**C**). IHC detection of VacA (**B**, **D**, **F** and **H**): distribution of VacA upon RW treatment (**B**) is both superficial and deep, similarly to that of VacA-treated control (**F**), while upon GT treatment (**D**) VacA is detectable only on the surface of gastric epithelium.

is sensitive to VacA[8]. In this model both GT and RW were able to significantly prevent VacA-induced gastric inflammation. Moreover, GT treatment resulted in VacA to be localized only on the surface of the gastric epithelium, and not in the gland crypts, similarly to the results observed in *H pylori*-infected mice subjected to RW + GT treatment, and also similarly to that reported for hop bracts extract administration to VacA-treated mice[14]. Thus, under our experimental conditions, different actions on VacA appear to be exerted by RW and GT, the former preventing gastric epithelium damage without altering the toxin localization, the latter also limiting its penetration in the gastric epithelium. It must be remarked that VacA is not the only actor on the scene of the pathological outcome of *H pylori* infection, whose mechanisms are only partially known, and that the identification of *H pylori* virulence factors still requires investigation[24]. Both in humans and animals, the disease outcome depends on the virulence of the infecting

strain and on the host's genetic background and immune response[25-27]. Also, the development of gastric pathology in humans can be influenced by lifestyle[28,29], and more generally by environmental factors. However, due to the evidence of the direct role of VacA in determining gastric damage[8,30,31], its inhibition can be reasonably considered relevant to limit *H pylori*-induced gastric pathology. In conclusion, we have shown that green tea and red wine can prevent the deterioration of gastric mucosa induced by *H pylori* infection or VacA administration in mice, possibly involving inhibition of VacA toxin. The potential relevance in humans of this protective activity deserves further investigation.

ACKNOWLEDGMENTS

We are indebted with G Matteucci and R Sabato for managing animal resources, and with S Torricelli and M Tortoli for animal handling.

COMMENTS

Background

H pylori infection of human stomach causes atrophic gastritis, peptic ulcer and gastric mucosa-associated lymphoid tissue (MALT) lymphoma, and plays a relevant role in gastric carcinogenesis. The current antibiotic-based therapy faces problems of antibiotic resistance or lack of patient compliance. No vaccines are presently licensed. Current research focuses on both antimicrobials and vaccines.

Research frontiers

Several plant extracts or plant-derived substances, including polyphenols, have been reported to exert anti-*H pylori* activity *in vitro* and/or, more importantly, *in vivo*. This research field could lead not only to discover new antimicrobials, but also to clarify the possible relevance of diet in the complex mechanism of host-pathogen interaction and in the pathological outcome of *H pylori* infection.

Innovations and breakthroughs

We report for the first time the ability of the mixture of red wine (RW) and green tea (GT) to restrict to the mucosal surface the *H pylori* gastric colonization, which otherwise was both superficial and deep. The altered colonization in RW + GT-treated mice was accompanied by the prevention of gastritis, similarly to that reported by Matsubara et al with GT extracts in Mongolian gerbils. In mice administered with VacA toxin, GT treatment both prevented gastric inflammation and limited VacA penetration into the gastric mucosa, while RW was able to prevent gastric inflammation only; the effect of both substances can be at least in part related to VacA inhibition, which we have previously observed *in vitro* with these substances. The results obtained with GT in VacA-treated mice are similar to those reported by Yahiro et al with hop bracts extract.

Peer review

The authors described the effects of red wine and green tea against gastritis by infection of *H pylori* or VacA in mice. It was interesting that the combination red wine and green tea prevented induction of damage of gastric mucosa in the animal model. However, it is not clear whether red wine and green tea could prevent the damage, respectively.

Because the authors treated the animals before administration of the microorganism (or VacA), it was not clear if the combined treatment could inhibit the established gastritis either. Further work could better clarify this point.

REFERENCES

1 **Sontag SJ**. Guilty as charged: bugs and drugs in gastric ulcer. *Am J Gastroenterol* 1997; **92**: 1255-1261
2 **Du MQ**, Isaccson PG. Gastric MALT lymphoma: from aetiology to treatment. *Lancet Oncol* 2002; **3**: 97-104
3 **Sepulveda AR**, Graham DY. Role of *Helicobacter pylori* in gastric carcinogenesis. *Gastroenterol Clin North Am* 2002; **31**: 517-535, x
4 **Reyrat JM**, Pelicic V, Papini E, Montecucco C, Rappuoli R, Telford JL. Towards deciphering the Helicobacter pylori cytotoxin. *Mol Microbiol* 1999; **34**: 197-204
5 **Montecucco C**, de Bernard M. Molecular and cellular mechanisms of action of the vacuolating cytotoxin (VacA) and neutrophil-activating protein (HP-NAP) virulence factors of *Helicobacter pylori*. *Microbes Infect* 2003; **5**: 715-721
6 **Tombola F**, Morbiato L, Del Giudice G, Rappuoli R, Zoratti M, Papini E. The *Helicobacter pylori* VacA toxin is a urea permease that promotes urea diffusion across epithelia. *J Clin Invest* 2001; **108**: 929-937
7 **Schmees C**, Gerhard M, Treptau T, Voland P, Schwendy S, Rad R, Prinz C. VacA-associated inhibition of T-cell function: reviewed and reconsidered. *Helicobacter* 2006; **11**: 144-146
8 **Telford JL**, Ghiara P, Dell'Orco M, Comanducci M, Burroni D, Bugnoli M, Tecce MF, Censini S, Covacci A, Xiang Z. Gene structure of the *Helicobacter pylori* cytotoxin and evidence of its key role in gastric disease. *J Exp Med* 1994; **179**: 1653-1658
9 **Fujikawa A**, Shirasaka D, Yamamoto S, Ota H, Yahiro K, Fukada M, Shintani T, Wada A, Aoyama N, Hirayama T, Fukamachi H, Noda M. Mice deficient in protein tyrosine phosphatase receptor type Z are resistant to gastric ulcer induction by VacA of *Helicobacter pylori*. *Nat Genet* 2003; **33**: 375-381
10 **Kataoka M**, Hirata K, Kunikata T, Ushio S, Iwaki K, Ohashi K, Ikeda M, Kurimoto M. Antibacterial action of tryptanthrin and kaempferol, isolated from the indigo plant (Polygonum tinctorium Lour.), against *Helicobacter pylori*-infected Mongolian gerbils. *J Gastroenterol* 2001; **36**: 5-9
11 **Takabayashi F**, Harada N, Yamada M, Murohisa B, Oguni I. Inhibitory effect of green tea catechins in combination with sucralfate on *Helicobacter pylori* infection in Mongolian gerbils. *J Gastroenterol* 2004; **39**: 61-63
12 **Tombola F**, Campello S, De Luca L, Ruggiero P, Del Giudice G, Papini E, Zoratti M. Plant polyphenols inhibit VacA, a toxin secreted by the gastric pathogen *Helicobacter pylori*. *FEBS Lett* 2003; **543**: 184-189
13 **Ruggiero P**, Tombola F, Rossi G, Pancotto L, Lauretti L, Del Giudice G, Zoratti M. Polyphenols reduce gastritis induced by *Helicobacter pylori* infection or VacA toxin administration in mice. *Antimicrob Agents Chemother* 2006; **50**: 2550-2552
14 **Yahiro K**, Shirasaka D, Tagashira M, Wada A, Morinaga N, Kuroda F, Choi O, Inoue M, Aoyama N, Ikeda M, Hirayama T, Moss J, Noda M. Inhibitory effects of polyphenols on gastric injury by *Helicobacter pylori* VacA toxin. *Helicobacter* 2005; **10**: 231-239
15 **Marchetti M**, Aricò B, Burroni D, Figura N, Rappuoli R, Ghiara P. Development of a mouse model of *Helicobacter pylori* infection that mimics human disease. *Science* 1995; **267**: 1655-1658
16 **Manetti R**, Massari P, Burroni D, de Bernard M, Marchini A, Olivieri R, Papini E, Montecucco C, Rappuoli R, Telford JL. *Helicobacter pylori* cytotoxin: importance of native conformation for induction of neutralizing antibodies. *Infect Immun* 1995; **63**: 4476-4480
17 **Papini E**, de Bernard M, Milia E, Bugnoli M, Zerial M, Rappuoli R, Montecucco C. Cellular vacuoles induced by *Helicobacter pylori* originate from late endosomal compartments. *Proc Natl Acad Sci USA* 1994; **91**: 9720-9724
18 **Dixon MF**, Genta RM, Yardley JH, Correa P. Classification and grading of gastritis. The updated Sydney System. International Workshop on the Histopathology of Gastritis, Houston 1994. *Am J Surg Pathol* 1996; **20**: 1161-1181
19 **Rossi G**, Ruggiero P, Peppoloni S, Pancotto L, Fortuna D, Lauretti L, Volpini G, Mancianti S, Corazza M, Taccini E, Di Pisa F, Rappuoli R, Del Giudice G. Therapeutic vaccination against *Helicobacter pylori* in the beagle dog experimental model: safety, immunogenicity, and efficacy. *Infect Immun* 2004; **72**: 3252-3259
20 **Mahady GB**, Pendland SL, Chadwick LR. Resveratrol and red wine extracts inhibit the growth of CagA+ strains of *Helicobacter pylori in vitro*. *Am J Gastroenterol* 2003; **98**: 1440-1441
21 **Matsubara S**, Shibata H, Ishikawa F, Yokokura T, Takahashi M, Sugimura T, Wakabayashi K. Suppression of *Helicobacter*

pylori-induced gastritis by green tea extract in Mongolian gerbils. *Biochem Biophys Res Commun* 2003; **310**: 715-719

22 **Salama NR**, Otto G, Tompkins L, Falkow S. Vacuolating cytotoxin of *Helicobacter pylori* plays a role during colonization in a mouse model of infection. *Infect Immun* 2001; **69**: 730-736

23 **van Doorn NE**, Namavar F, Sparrius M, Stoof J, van Rees EP, van Doorn LJ, Vandenbroucke-Grauls CM. *Helicobacter pylori*-associated gastritis in mice is host and strain specific. *Infect Immun* 1999; **67**: 3040-3046

24 **Lu H**, Yamaoka Y, Graham DY. *Helicobacter pylori* virulence factors: facts and fantasies. *Curr Opin Gastroenterol* 2005; **21**: 653-659

25 **Del Giudice G**, Covacci A, Telford JL, Montecucco C, Rappuoli R. The design of vaccines against *Helicobacter pylori* and their development. *Annu Rev Immunol* 2001; **19**: 523-563

26 **Rad R**, Dossumbekova A, Neu B, Lang R, Bauer S, Saur D, Gerhard M, Prinz C. Cytokine gene polymorphisms influence mucosal cytokine expression, gastric inflammation, and host specific colonisation during *Helicobacter pylori* infection. *Gut* 2004; **53**: 1082-1089

27 **Hwang IR**, Kodama T, Kikuchi S, Sakai K, Peterson LE, Graham DY, Yamaoka Y. Effect of interleukin 1 polymorphisms on gastric mucosal interleukin 1beta production in *Helicobacter pylori* infection. *Gastroenterology* 2002; **123**: 1793-1803

28 **Kelley JR**, Duggan JM. Gastric cancer epidemiology and risk factors. *J Clin Epidemiol* 2003; **56**: 1-9

29 **Simán JH**, Forsgren A, Berglund G, Florén CH. Tobacco smoking increases the risk for gastric adenocarcinoma among *Helicobacter pylori*-infected individuals. *Scand J Gastroenterol* 2001; **36**: 208-213

30 **de Bernard M**, Cappon A, Del Giudice G, Rappuoli R, Montecucco C. The multiple cellular activities of the VacA cytotoxin of *Helicobacter pylori*. *Int J Med Microbiol* 2004; **293**: 589-597

31 **Wada A**, Yamasaki E, Hirayama T. *Helicobacter pylori* vacuolating cytotoxin, VacA, is responsible for gastric ulceration. *J Biochem* 2004; **136**: 741-746

S- Editor Wang GP **L- Editor** Luzte M **E- Editor** Bi L

PO Box 2345, Beijing 100023, China
www.wjgnet.com
wjg@wjgnet.com

World J Gastroenterol 2007 January 21; 13(3): 355-360
World Journal of Gastroenterology ISSN 1007-9327

Hepatitis C virus genotypes in Serbia and Montenegro: The prevalence and clinical significance

Neda Svirtlih, Dragan Delic, Jasmina Simonovic, Djordje Jevtovic, Ljubisa Dokic, Eleonora Gvozdenovic, Ivan Boricic, Dragica Terzic, Sladjana Pavic, Gorana Neskovic, Sonja Zerjav, Vladimir Urban

Neda Svirtlih, Dragan Delic, Jasmina Simonovic, Djordje Jevtovic, Ljubisa Dokic, Eleonora Gvozdenovic, Sonja Zerjav, Institute for Infectious Diseases, Clinical Centre of Serbia, Belgrade, Serbia
Ivan Boricic, Institute for Pathology Medical Faculty University of Belgrade, Serbia
Dragica Terzic, Clinical Centre of Podgorica, Montenegro
Sladjana Pavic, General Hospital, Uzice, Serbia
Gorana Neskovic, Institute for Nuclear Sciences, Vinca, Serbia
Vladimir Urban, Medical Faculty University of Belgrade, Serbia
Correspondence to: Professor Neda Svirtlih, MD, PhD, Institute for Infectious Diseases, Clinical Centre of Serbia, Bul Oslobodjenja 16, Belgrade 11000, Serbia. laslo@bitsyu.net
Telephone: +381-11-2683366 Fax: +381-11-684272
Received: 2006-09-22 Accepted: 2006-10-16

Abstract

AIM: To investigate the prevalence of hepatitis C virus (HCV) genotypes in Serbia and Montenegro and their influence on some clinical characteristics in patients with chronic HCV infection.

METHODS: A total of 164 patients was investigated. Complete history, route of infection, assessment of alcohol consumption, an abdominal ultrasound, standard biochemical tests and liver biopsy were done. Gene sequencing of 5′ NTR type-specific PCR or commercial kits was performed for HCV genotyping and subtyping. The SPSS for Windows (version 10.0) was used for univariate regression analysis with further multivariate analysis.

RESULTS: The genotypes 1, 2, 3, 4, 1b3a and 1b4 were present in 57.9%, 3.7%, 23.2%, 6.7%, 6.7% and 1.8% of the patients, respectively. The genotype 1 (mainly the subtype 1b) was found to be independent of age in subjects older than 40 years, high viral load, more severe necro-inflammatory activity, advanced stage of fibrosis, and absence of intravenous drug abuse. The genotype 3a was associated with intravenous drug abuse and the age below 40. Multivariate analysis demonstrated age over 40 and intravenous drug abuse as the positive predictive factors for the genotypes 1b and 3a, respectively.

CONCLUSION: In Serbia and Montenegro, the genotypes 1b and 3a predominate in patients with chronic HCV infection. The subtype 1b is characteristic of older patients, while the genotype 3a is common in drug abusers. Association of the subtype 1b with advanced liver disease, higher viral load and histological activity suggests earlier infection with this genotype and eventually its increased pathogenicity.

Key words: Hepatitis C virus; Genotypes; Prevalence; Serbia; Montenegro

Svirtlih N, Delic D, Simonovic J, Jevtovic D, Dokic L, Gvozdenovic E, Boricic I, Terzic D, Pavic S, Neskovic G, Zerjav S, Urban V. Hepatitis C virus genotypes in Serbia and Montenegro: The prevalence and clinical significance. *World J Gastroenterol* 2007; 13(3): 355-360

http://www.wjgnet.com/1007-9327/13/355.asp

INTRODUCTION

Analysis of genome of hepatitis C virus (HCV) isolates from around the world has shown substantial heterogeneity of nucleotide sequences and has identified at least six genotypes[1,2]. The prevalence of HCV genotypes mostly depends on geographic location and for that reason, the genotype identification is crucially important in epidemiological investigation[3]. However, it is thought that HCV genotypes may influence some diversity in liver disease presentation, its outcome and response to antiviral treatment[4].

The aim of our study was to determine the HCV genotype prevalence in this area of the Southeast part of the Balkan and to evaluate the genotype distribution and its association with some clinical characteristics in patients with chronic HCV infection.

MATERIALS AND METHODS

Subjects

We retrospectively studied 164 patients with chronic HCV infection that had been selected for antiviral treatment. Patients were hospitalized in the Institute for Infectious and Tropical Diseases, Department for Viral Hepatitis, from January 1, 2005 to March 31, 2006. Patients with decompensated liver cirrhosis, hepatocellular carcinoma (HCC), co-infection with hepatitis B virus (HBV) and human immunodeficiency virus (HIV) were excluded

Table 1 Age of patients with chronic hepatitis C infection according to genotypes

Genotype	*n*	Mean ± SD (yr)	Range (yr)
1[1]	95	44 ± 12	21-65
2	6	36 ± 13	22-51
3	38	37 ± 10	23-62
4	11	32 ± 13	16-55
1b3a	11	31 ± 9	18-48
1b4	3	42 ± 11	33-54
Total	164	41 ± 12	16-65

[1]Including 1b, 1a, 1ab and two non-determined subtypes.

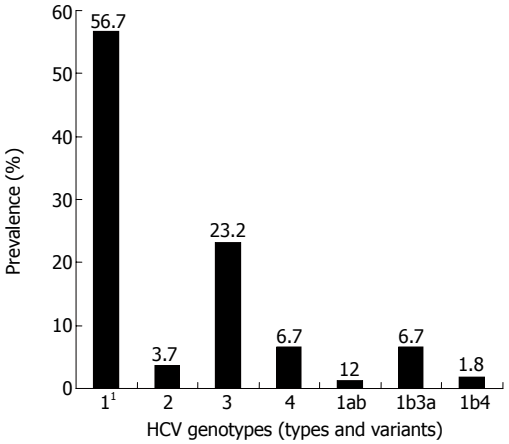

Figure 1 Distribution of HCV genotypes in patients with chronic HCV infection. 1[1]: 96.7% subtype 1b, 1.1% subtype 1a, 2.2% non-determined subtypes.

from the study. Complete history with possible route of infection, physical examination, assessment of alcohol consumption, an abdominal ultrasound and standard biochemical liver functional tests were taken in investigated patients. Alanine aminotransferase (ALT) values were measured at presentation. Percutaneous liver biopsy was performed in all patients. The hepatic pathology expert assessed histological grades (activity) and stages (fibrosis) with Masson's trichrome stained tissue specimens, using the Ischak scoring system[5]. In the whole cohort of patients, there were 98 males and 66 females, aged from 16-65 years (mean, 41 ± 12).

Viral investigations

For detection of sera specific antibodies to HCV and HIV (anti-HCV, anti-HIV) and surface HBV antigen (HBsAg), commercial kits were used (Ortho EIA; BioRad, ELISA). Quantification of the viral genome (HCV RNA) in sera was done by the amplification method (Amplicor Roche Monitor) and expressed in copies/mL (dividing factor in IU/mL is 2.7). Gene sequencing of 5' NTR type-specific PCR or commercial kits (InnoLipa, Innogenetics, Genotyping Linear Array hepatitis C virus test, Roche Diagnostics) was performed for HCV genotyping and subtyping.

All tests of association between the genotypes and other parameters were based preferentially on data for the genotypes 1, 3 and 1b3a because only a few patients (less than 5%) had the genotypes 2 and 1b4. Histological scores of activity and fibrosis, viral load, and ALT values were separately divided into two categorical groups in order to evaluate the possible difference in pathogenicity of the genotypes. Activity scores combined necro-inflammatory lesions, periportal necrosis and lobular necrosis were graded as scores $\leqslant$ 2 (absent-mild) and scores $\geqslant$ 3 (moderate-severe). Fibrosis scores were divided into scores $\leqslant$ 3 (absent-moderate) and $\geqslant$ 4-6 (severe -cirrhosis). Viral load of HCV RNA was determined as high $\geqslant 2 \times 10^6$ copies/mL. Values of ALT were determined high if they were 2.5 × and 5 × higher than normal values ($\leqslant$ 41 IU/mL).

Statistical analysis

The electronic database organized in the Statistical Package for Social Science (SPSS) for Windows (version 10.0) was used. The results are expressed as means ± SD or as percentages. Parametric (Mann-Whitney test, Kruskal-Wallis test) and non-parametric tests (chi-square test, Fisher's exact test) and the Spearman correlation test were performed to identify significantly different variables that entered into univariate logistical regression analysis with further multivariate analysis. The level of significance was set at $P < 0.05$ and in the case of multiple testing at $P < 0.01$. Data is presented with 95% confidence levels.

RESULTS

Genotype distribution

The most commonly detected genotype in the whole cohort was genotype 1 (57.9%), with the predominant subtype 1b (54.9%). The subtype 1a was detected in one patient (0.6%) only. Genotype 3 was comprised exclusively of the subtype 3a, while genotype 2 comprised the subtypes a, b and c. Mixed inter- genotype infection, such as 1b3a and 1b4 were detected in 13 (8.54%) patients, while mixed intra-genotype infection (1ab) was detected in two (1.2%) patients (Figure 1).

Association of the genotypes and demographic and behavioral data

Statistical analysis did not show a difference in the frequency distribution of genotypes according to gender of the patients. The age of the patients was analyzed as a continuous and a categorical variable (< 40 and $\geqslant$ 40 years). Result of ages of the patients in detail is presented in Table 1. Significant statistical difference was found between ages of the patients depending on the genotypes ($\chi^2 = 23.474$; $r = 3$; $P < 0.001$). Patients with genotype 1 (44.31 ± 12) were older than patients with genotypes 3, 4 and 1b3a (37.18 ± 10.02 versus 32 ± 12.59 versus 31 ± 8.73, $P < 0.01$, $P < 0.01$ and $P < 0.001$, respectively). In the whole cohort, approximately a half of the patients (52%) were aged $\geqslant$ 40 years. Analyzing the genotypes according to ages over $\geqslant$ 40, differences in frequency distribution were found for genotypes 1, 3 and 1b3a (33 versus 25 versus 9, $P < 0.01$, $P < 0.05$ and $P < 0.05$, respectively).

Table 2 Univariate logistic regression analysis of HCV genotypes according to age equal/older than 40 years

Genotype	Significance	Exp (B)	Lower-Upper[1]
1[2]	0.000	3.757	1.952-7.232
3[3]	0.015	0.390	0.183-0.832
1b3a	0.036	0.187	0.039-0.896

[1]95.0% CI for EXP (B); [2]Including subtypes 1b (94.74%), 1a (1.05%), intra-genotype variant 1ab (2.1%), and non-determined subtypes (2.1%); [3]3b subtype.

Result of univariate logistic analysis of all three genotypes according to age ⩾ 40 years is presented in Table 2. Univariate analysis demonstrated independent association of age ⩾ 40 years and all three genotypes: 1 (mainly subtype 1b), 3a and 1b3a. Further multivariate analysis revealed only the age ⩾ 40 years as the positive predictive factor for the genotype 1 [$P < 0.001$, Exp (B) = 3.757; 1.952-7.232].

Data about alcohol consumption were available from 161 patients, 30 of them admitted moderate or heavy alcohol abuse (30 g/d or more). There was no statistically significant difference of the frequency distribution of the genotypes according to moderate and/or heavy alcohol consumption.

Genotypes and route of infection

The possible route of infection was recognized in 98 (59.7%) patients. Among these patients, patients who had a history of intravenous drug use (IVDU), received blood transfusion, had accidental inoculation and/or were undergoing chronic hemodialysis, and healthcare workers, were found in 45.9%, 32.6%, 15.3% and 6.1%, respectively. Statistical analysis showed significant differences in frequency of genotypes 1 and genotype 3 and IVDU (19/95 *vs* 17/38, $P < 0.05$ and $P < 0.05$, respectively). Result of univariate logistic analysis of the genotypes 1 and genotype 3a and IVDU is presented in Table 3. Univariate analysis demonstrated independent association of the IVDU and the genotypes 1 (96.7% subtype 1b) and 3a. Further multivariate analysis revealed IVDU as the positive predictive factor for the genotype 3a [$P < 0.01$, Exp (B) = 2.833; 318-6.089].

Genotypes and histological findings

Fibrosis score was assessed in all patients. Score from ⩽ 3 and ⩾ 4 had 60% and 40% of the patients, respectively. Significant difference was found in the distribution of genotype 1 and fibrosis score ⩾ 4 (45 *vs* 21, $P < 0.05$). Further univariate logistic analysis showed a fibrosis score ⩾ 4 being independent of genotype 1 [$P < 0.05$, Exp (B) = 2.056; 1.072-3.938]. Histological activity was assessed in 161 patients and scores of ⩽ 2, and ⩾ 3 were established in 93.1% and 6.8% of patients, respectively. Statistical analysis of frequency in HCV genotype distribution according to activity score ⩾ 3 showed a significant difference in frequency of genotype 1 and other genotypes and histological activity (92 *vs* 69, $P < 0.05$), and also the positive correlation between these two variables ($P < 0.05$). But further univariate logistic analysis did not show independent association of genotype 1 and histological activity score ⩾ 3.

Table 3 Univariate logistic regression analysis of HCV genotypes according to patients with a history of intravenous drug abuse

Genotype	Significance	Exp (B)	Lower-Upper[1]
1[2]	0.013	0.413	0.205-0.833
3[3]	0.008	2.833	1.318-6.089

[1]95.0% CI for EXP (B); [2]Including subtypes 1b (96.7%), 1a (1.1%), intra-genotype variant 1ab (1.2%), and non-determined subtypes (2.2%); [3]3b subtype.

Table 4 Multivariate logistic analysis of HCV genotype 1 according to age, high HCV RNA, fibrosis score and intravenous drug use (IVDU)

Variable	Significance	EXP (B)	Lower-Upper[1]
⩾ 40 yr	0.000	3.747	1.952-7.232
High RNA	0.012	3.819	1.339-10.89
Fibrosis score ⩾ 4	0.030	2.413	1.072-3.938
IVDU	0.013	0.413	0.205-0.833

[1]95.0% CI for EXP (B).

Genotypes and biochemical activity

Values of ALT varied from 11 IU/L to 292 IU/L (mean, 80 ± 53). ALT values 2.5 × and 5 × higher than normal value (102.5 IU/mL; 205 IU/mL) had 22.6% and 3.6% of the patients, respectively. No significant difference was found in the frequency of genotype distribution and the value of ALT 2.5 × higher than normal value.

Genotypes and viral load

Viral load was quantified in 126 sera samples. The level of HCV RNA varied from 2000 copies/mL to 31 333 575 copies/mL (mean, 1 694 690 ± 3 284 562). Out of all patients, 27 (21%) had a high level of HCV RNA. Statistically significant difference in frequency of high HCV RNA was found for genotype 1 (96.7% subtype 1b) and other genotypes (23/57 *vs* 4/42, $P < 0.05$). A positive correlation was found between genotype 1 and high viral load ($P < 0.05$), as the univariate logistic analysis also revealed genotype 1 in independent association with high level of HCV RNA [$P< 0.05$, Exp (B) = 3.819, 1.339-10.89].

Finally, multivariate logistic regression analysis was calculated for genotypes 1 and 3a resulting in significance using univariate analysis. The result of multivariate logistic analysis for genotype 1 is presented in Table 4. The result of multivariate logistic analysis for genotype 3a is presented in Table 5. Accordingly, genotype 1 was demonstrated as significant for the age ⩾ 40 years [$P=$ 0.000, Exp (B) = 3.747, 1.952-7.232] whilst the genotype 3a was demonstrated as significant for IVDU [$P=$ 0.008, Exp (B) = 2.833, 1.318-6.089].

DISCUSSION

The predominating genotype in our study is the genotype 1 (57.9%), mostly the subtype 1b. The genotype 3a is the second most common genotype encountered in 23.2%. The prevalence of HCV genotypes in our investigation is mainly similar to reports of the HCV genotype distribution in other parts of Europe[6-10]. Our current results also confirm findings from Serbia previously published[11,12]. The difference between our result and results from some other European investigators suggests the lower prevalence of the subtype 1a in our cohort that we detected only in one patient. Also, the reported prevalence by other investigators of the genotype 2 particularly in advanced liver disease was more common than we found in our study[13,14]. However, comparison of the prevalence of genotypes between our results and results of other reports also depends on the time of these investigations. In the last decade, a shift in genotype distribution is obvious in many countries, mostly comprising an increase of the prevalence of the genotypes 3a, 1a and 4, and a decrease of the prevalence of genotypes 1b and 2[8,10,14]. The route of HCV transmission mainly causes this epidemiological change in genotype distribution whereas the intravenous drug abuse associated with genotype 3a and 1a has become nowadays the major risk factor of HCV infection[9,10,14-17]. In our investigation, only one patient with genotype 1a cannot confirm this epidemiological shift in IVDU patients of this genotype.

Evaluating the association of the genotypes and demographic data of the patients, we did not find differences in genotype distribution and gender of the patients or alcohol abuse. According to these results, we cannot point out female hormones or moderate to heavy alcohol abuse as participating factors in different disease presentation in association with the genotypes. Conversely, investigation of ages of the patients indicates that older age is strongly associated with the distribution of the genotypes. We found that the genotype 1 was the most common genotype in older patients, while the genotypes 3a, 4 and 1b3a characterized younger patients. Although all three genotypes are independent risk factors for ages over 40, genotype 1 for the age over 40 and genotypes 3a and 1b3a for the patients younger than 40, only the genotype 1 has the predictive importance. According to this finding, we can assume that infection with genotype 1 in this part of Balkan occurred earlier in the past than infection with other genotypes, subtypes and mixed inter-genotype infections, e.g., 4, 3a and 1b3a.

Early investigations from the USA did not find an association between HCV genotypes and mode of transmission[18]. However, the investigators from Europe reported that patients with a history of blood transfusion were mostly infected with genotype 1b while intravenous drug abusers were infected with genotype 3a[7,9,10,15-17,19,20]. Our results show that the genotype 3a is the most important predictive factor for IVDU that is in concordance with these reports. Although we did not confirm correlation of genotype 1b with a mode of HCV transmission, the presence of this genotype as the independent negative risk factor for IVDU may suggest other routes of infection. Additionally, it is possible that relatively high prevalence of mixed inter-genotype infection of 1b3a and 1b4 (8.5%) in our patients can suggest repeated infection in the same persons, although we did not find any association between these genotypes and mode of HCV transmission. Moreover, according to our study, genotype 1 (mostly subtype 1b) is the most common genotype in patients with advanced HCV-related liver disease (fibrosis score equal/higher than 4). We can assume that this association between subtype 1b and more progressive disease is paradigmatic for earlier infection with this subtype in comparison with the subtype 3a and mixed infection with 1b3a. Some previous reports also suggested that subtype 1b is associated with a more advanced stage of liver disease[19,21,22]. Concerning this problem, we must underscore that our cohort was a select group of patients preparing for antiviral treatment. Because of that, patients with end stage liver disease and HCC were excluded from the study. There is a probability that inclusion of these patients may give a more convincing association between the genotypes and the stage of the HCV-related disease.

Table 5 Multivariate logistic regression analysis of HCV genotype 3 according to age and intravenous drug use (IVDU)

Variable	Significance	Exp (B)	Lower-Upper[1]
Age ⩾ 40 yr	0.015	0.390	0.183-0.832
IVDU	0.008	2.833	1.318-6.089

[1]95.0% CI for EXP (B).

However, our result of the association of the HCV genotype 1 with a high level of HCV RNA and higher histological activity suggests possible increased pathogenicity of this particular genotype. Although many authors did not confirm this association, some of them suggested similar findings as we did[13,18,19,23]. We must remember again that our study was a cross-sectional and retrospective investigation, and that the factor of time was not taken into account. In any case, our findings that genotype 1b is characterized with a higher level of RNA; in correlation with increased necro-inflammatory changes in the liver than other genotypes, although lack of an increase in biochemical activity could not be ignored as a possible indicator for increased pathogenicity of subtype 1b. Certainly, association between genotypes and the level of HCV RNA and necro-inflammatory activity may need to be investigated in future studies.

Finally, we can conclude that genotype 1, particularly the subtype 1b in older patients with chronic HCV infection, predominates in this geographic Southeast part of the Balkan. The second common prevalence of genotype 3, subtype 3a in younger patients, suggests the increased number of IVDU as the main mode of HCV transmission. The role of subtype 1b that correlates with high viral load and higher histological activity could indicate potentially more pathogenicity of this subtype with consequences such as longer persistence and more aggressive influence in disease outcome that requires careful analysis in prospective setting.

COMMENTS

Background

Hepatitis C virus (HCV) represents a cause of chronic liver disease that may progress to cirrhosis with serious consequences. Analysis of the HCV genome demonstrated its high heterogeneity and identified at least six different genotypes divided into several subtypes that have epidemiological and clinical importance.

Research frontiers

Important areas in investigation of HCV-related chronic liver diseases are identifying infected persons, recognize the route of its transmission, evaluation of the stage of the disease, use of antiviral therapy and prevention measures.

Innovations and breakthroughs

Prevalence of different HCV genotypes and subtypes and their influence on some clinical characteristics in the Southern part of the Balkan was investigated in 164 patients with chronic hepatitis C. The most common genotype is 1 (57.9%), mainly subtype 1b. Genotype 3 (3a) is the second most common genotype, whilst genotypes 1a and 2 are less common than in other European countries. Genotypes 1 and 3a were found as predicting factors for older age and IVDU, respectively.

Application

Actual epidemiologic study of HCV genotypes in specific areas is present in the article. Additionally, different genotypes were related to age, gender, alcohol abuse, route of transmission, biochemical activity, histological findings and viral load. Eventual shifts in the correlation data will be recognized in the future.

Terminology

HCV is a distinct member of the family *Flaviviridae* and placed into a separate genus, named *Hepacivirus*. Genotypes and subtypes of HCV represent its extensive genetic heterogeneity. Genotypes depend mainly on the geographic location and are classified into six main groups, designated as genotypes 1 to 6, with further subdivision within each genotype (a, b, c, *etc*.). It has been reported that genotypes differ in the severity of the liver disease they cause, baseline of serum RNA levels, response to antiviral treatment and route of transmission.

Peer review

This article is an essentially confirmatory paper of the previously published observation on the genotype distribution in Serbia, particularly the confirmation of an unusual high prevalence of mixed genotype infection (about 8%-9% in the two papers). The finding of higher HCV RNA levels in genotype 1b is contradicted in most literature and the claim that genotype 1b had higher pathogenicity cannot be substantiated, unless in a prospective setting.

REFERENCES

1 **Choo QL,** Richman KH, Han JH, Berger K, Lee C, Dong C, Gallegos C, Coit D, Medina-Selby R, Barr PJ. Genetic organization and diversity of the hepatitis C virus. *Proc Natl Acad Sci USA* 1991; **88:** 2451-2455

2 **Simmonds P,** Smith DB, McOmish F, Yap PL, Kolberg J, Urdea MS, Holmes EC. Identification of genotypes of hepatitis C virus by sequence comparisons in the core, E1 and NS-5 regions. *J Gen Virol* 1994; **75** (Pt 5)**:** 1053-1061

3 **Simmonds P.** Genetic diversity and evolution of hepatitis C virus-15 years on. *J Gen Virol* 2004; **85**: 3173-3188

4 **Zein NN.** Clinical significance of hepatitis C virus genotypes. *Clin Microbiol Rev* 2000; **13:** 223-235

5 **Ishak K,** Baptista A, Bianchi L, Callea F, De Groote J, Gudat F, Denk H, Desmet V, Korb G, MacSween RN. Histological grading and staging of chronic hepatitis. *J Hepatol* 1995; **22:** 696-699

6 **Pawlotsky JM**, Tsakiris L, Roudot-Thoraval F, Pellet C, Stuyver L, Duval J, Dhumeaux D. Relationship between hepatitis C virus genotypes and sources of infection in patients with chronic hepatitis C. *J Infect Dis* 1995; **171**: 1607-1610

7 **Kleter B,** Brouwer JT, Nevens F, van Doorn LJ, Elewaut A, Versieck J, Michielsen PP, Hautekeete ML, Chamuleau RA, Brénard R, Bourgeois N, Adler M, Quint WG, Bronkhorst CM, Heijtink RA, Hop WJ, Fevery J, Schalm SW. Hepatitis C virus genotypes: epidemiological and clinical associations. Benelux Study Group on Treatment of Chronic Hepatitis C. *Liver* 1998; **18:** 32-38

8 **Ross RS,** Viazov S, Renzing-Köhler K, Roggendorf M. Changes in the epidemiology of hepatitis C infection in Germany: shift in the predominance of hepatitis C subtypes. *J Med Virol* 2000; **60:** 122-125

9 **Elghouzzi MH,** Bouchardeau F, Pillonel J, Boiret E, Tirtaine C, Barlet V, Moncharmont P, Maisonneuve P, du Puy-Montbrun MC, Lyon-Caen D, Couroucé AM. Hepatitis C virus: routes of infection and genotypes in a cohort of anti-HCV-positive French blood donors. *Vox Sang* 2000; **79:** 138-144

10 **Savvas SP,** Koskinas J, Sinani C, Hadziyannis A, Spanou F, Hadziyannis SJ. Changes in epidemiological patterns of HCV infection and their impact on liver disease over the last 20 years in Greece. *J Viral Hepat* 2005; **12:** 551-557

11 **Stamenkovic G,** Zerjav S, Velickovic ZM, Krtolica K, Samardzija VL, Jemuovic L, Nozic D, Dimitrijevic B. Distribution of HCV genotypes among risk groups in Serbia. *Eur J Epidemiol* 2000; **16:** 949-954

12 **Hozić D,** Stamenković G, Bojić I, Dimitrijević J, Krstić L. Role of various virus genotypes in progression of chronic hepatitis C. *Vojnosanit Pregl* 2002; **59:** 141-145

13 **Fattovich G**, Ribero ML, Pantalena M, Diodati G, Almasio P, Nevens F, Tremolada F, Degos F, Rai J, Solinas A, Mura D, Tocco A, Zagni I, Fabris F, Lomonaco L, Noventa F, Realdi G, Schalm SW, Tagger A. Hepatitis C virus genotypes: distribution and clinical significance in patients with cirrhosis type C seen at tertiary referral centres in Europe. *J Viral Hepat* 2001; **8**: 206-216

14 **Payan C**, Roudot-Thoraval F, Marcellin P, Bled N, Duverlie G, Fouchard-Hubert I, Trimoulet P, Couzigou P, Cointe D, Chaput C, Henquell C, Abergel A, Pawlotsky JM, Hezode C, Coudé M, Blanchi A, Alain S, Loustaud-Ratti V, Chevallier P, Trepo C, Gerolami V, Portal I, Halfon P, Bourlière M, Bogard M, Plouvier E, Laffont C, Agius G, Silvain C, Brodard V, Thiefin G, Buffet-Janvresse C, Riachi G, Grattard F, Bourlet T, Stoll-Keller F, Doffoel M, Izopet J, Barange K, Martinot-Peignoux M, Branger M, Rosenberg A, Sogni P, Chaix ML, Pol S, Thibault V, Opolon P, Charrois A, Serfaty L, Fouqueray B, Grange JD, Lefrère JJ, Lunel-Fabiani F. Changing of hepatitis C virus genotype patterns in France at the beginning of the third millenium: The GEMHEP GenoCII Study. *J Viral Hepat* 2005; **12**: 405-413

15 **Dal Molin G,** Ansaldi F, Biagi C, D'Agaro P, Comar M, Crocè L, Tiribelli C, Campello C. Changing molecular epidemiology of hepatitis C virus infection in Northeast Italy. *J Med Virol* 2002; **68:** 352-356

16 **Kalinina O,** Norder H, Vetrov T, Zhdanov K, Barzunova M, Plotnikova V, Mukomolov S, Magnius LO. Shift in predominating subtype of HCV from 1b to 3a in St. Petersburg mediated by increase in injecting drug use. *J Med Virol* 2001; **65:** 517-524

17 **Balogun MA,** Laurichesse H, Ramsay ME, Sellwood J, Westmoreland D, Paver WK, Pugh SF, Zuckerman M, Pillay D, Wreghitt T. Risk factors, clinical features and genotype distribution of diagnosed hepatitis C virus infections: a pilot for a sentinel laboratory-based surveillance. *Commun Dis Public Health* 2003; **6:** 34-39

18 **Zein NN,** Rakela J, Krawitt EL, Reddy KR, Tominaga T, Persing DH. Hepatitis C virus genotypes in the United States: epidemiology, pathogenicity, and response to interferon therapy. Collaborative Study Group. *Ann Intern Med* 1996; **125:** 634-639

19 **Vince A,** Palmović D, Kutela N, Sonicky Z, Jeren T, Radovani M. HCV genotypes in patients with chronic hepatitis C in Croatia. *Infection* 1998; **26:** 173-177

20 **Serra MA**, Rodríguez F, del Olmo JA, Escudero A, Rodrigo JM. Influence of age and date of infection on distribution of hepatitis C virus genotypes and fibrosis stage. *J Viral Hepat* 2003; **10**: 183-188

21 **Cathomas G,** McGandy CE, Terracciano LM, Gudat F, Bianchi L. Detection and typing of hepatitis C RNA in liver biopsies

and its relation to histopathology. *Virchows Arch* 1996; **429:** 353-358

22 **Pozzato G**, Kaneko S, Moretti M, Crocè LS, Franzin F, Unoura M, Bercich L, Tiribelli C, Crovatto M, Santini G. Different genotypes of hepatitis C virus are associated with different severity of chronic liver disease. *J Med Virol* 1994; **43**: 291-296

23 **Sagnelli E,** Coppola N, Scolastico C, Mogavero AR, Filippini P, Piccinino F. HCV genotype and "silent" HBV coinfection: two main risk factors for a more severe liver disease. *J Med Virol* 2001; **64:** 350-355

S- Editor Pan BR **L- Editor** Alpini GD **E- Editor** Bi L

PO Box 2345, Beijing 100023, China
www.wjgnet.com
wjg@wjgnet.com

World J Gastroenterol 2007 January 21; 13(3): 361-368
World Journal of Gastroenterology ISSN 1007-9327

BASIC RESEARCH

Monounsaturated fat decreases hepatic lipid content in non-alcoholic fatty liver disease in rats

Osamah Hussein, Masha Grosovski, Etti Lasri, Sergio Svalb, Uzi Ravid, Nimer Assy

Osamah Hussein, Etti Lasri, Nimer Assy, Internal Medicine A, Sieff Government Hospital, Safed, Israel
Nimer Assy, Liver Unit, Sieff Government Hospital, Safed, Israel
Sergio Svalb, Department of Pathology, Sieff Government Hospital, Safed, Israel
Nimer Assy, Faculty of Medicine, Technion Israel Institute of Technology, Haifa, Israel
Masha Grosovski, Etti Lasri, Ort Braude College of Engineering, Karmiel, Israel
Uzi Ravid, Newe Ya'ar Research Center, Ministry of Agriculture, Ramat Yeshai, Israel
Correspondence to: Nimer Assy, Liver Unit, Department of Internal Medicine "A" Sieff Government Hospital, PO Box 1008, Safed 13100, Israel. assy.n@ziv.health.gov.il
Telephone: +972-46828581 Fax: +972-46828944
Received: 2006-07-03 Accepted: 2006-12-11

Abstract

AIM: To evaluate the effects of different types of dietary fats on the hepatic lipid content and oxidative stress parameters in rat liver with experimental non-alcoholic fatty liver disease (NAFLD).

METHODS: A total of 32 Sprague-Dawley rats were randomly divided into five groups. The rats in the control group (n = 8) were on chow diet (Group 1), rats (n = 6) on methionine choline-deficient diet (MCDD) (Group 2), rats (n = 6) on MCDD enriched with olive oil (Group 3), rats (n = 6) on MCDD with fish oil (Group 4) and rats (n = 6) on MCDD with butter fat (Group 5). After 2 mo, blood and liver sections were examined for lipids composition and oxidative stress parameters.

RESULTS: The liver weight/rat weight ratio increased in all treatment groups as compared with the control group. Severe fatty liver was seen in MCDD + fish oil and in MCDD + butter fat groups, but not in MCDD and MCDD + olive oil groups. The increase in hepatic triglycerides (TG) levels was blunted by 30% in MCDD + olive oil group (0.59 ± 0.09) compared with MCDD group (0.85 ± 0.04, P < 0.004), by 37% compared with MCDD + fish oil group (0.95 ± 0.07, P < 0.001), and by 33% compared with MCDD + butter group (0.09 ± 0.1, P < 0.01). The increase in serum TG was lowered by 10% in MCDD + olive oil group (0.9 ± 0.07) compared with MCDD group (1.05 ± 0.06). Hepatic cholesterol increased by 15-fold in MCDD group [(0.08 ± 0.02, this increment was blunted by 21% in MCDD + fish oil group (0.09 ± 0.02)]. In comparison with the control group, ratio of long-chain polyunsaturated fatty acids omega-6/omega-3 increased in MCDD + olive oil, MCDD + fish oil and MCDD + butter fat groups by 345-, 30- and 397-fold, respectively. In comparison to MCDD group (1.58 ± 0.08), hepatic MDA contents in MCDD + olive oil (3.3 ± 0.6), MCDD + fish oil (3.0 ± 0.4), and MCDD + butter group (2.9 ± 0.36) were increased by 108%, 91% and 87%, respectively (P < 0.004). Hepatic paraoxonase activity decreased significantly in all treatment groups, mostly with MCDD + olive oil group (-68%).

CONCLUSION: Olive oil decreases the accumulation of triglyceride in the liver of rats with NAFLD, but does not provide the greatest antioxidant activity.

Key words: Fatty liver; Non-alcoholic steatohepatitis; Dietary fat; Fatty acids; Methionine choline-deficient diet; Insulin resistance; Olive oil; Oxidative stress; Paraoxonase

Hussein O, Grosovski M, Lasri E, Svalb S, Ravid U, Assy N. Monounsaturated fat decreases hepatic lipid content in non-alcoholic fatty liver disease in rats. *World J Gastroenterol* 2007; 13(3): 361-368

http://www.wjgnet.com/1007-9327/13/361.asp

INTRODUCTION

Non-alcoholic steatohepatitis (NASH) pathogenesis includes insulin resistance, increased exposure of the hepatocytes to TNF-α and increased oxidative stress[1]. The development of hepatic steatosis results from an imbalance in the rate of entry, synthesis, or clearance of fat from the liver. More specifically, the increased influx of free fatty acids to the liver, reduced free fatty acid β-oxidation, a reduced hepatic secretion of triglyceride-rich lipoproteins and increased lipid peroxidation may be altered[1].

Hepatic triglycerides are derived from different sources. First, from endogenous fatty acids which are synthesized in the liver. Second, from dietary triglycerides that enter the liver *via* the chylomicron remnant pathway and finally from free fatty acids that are released from adipose tissues during periods of fasting. An impaired postprandial triglyceride response has been reported in patients with NASH[2]. This may promote fatty liver in several ways, such as increasing

hepatic uptake of triglyceride-rich lipoproteins and their remnants in the postprandial period[2,3]. The contribution of hepatic lipogenesis to triglyceride secretion was 3 times higher in the patients as compared with the controls while that of non-esterified fatty acids (NEFA) re-esterification was reduced by 52%. Thus, enhanced lipogenesis appears as a prominent abnormality of hepatic fatty metabolism in the subjects with NASH[4].

Several studies have emphasized the importance of dietary composition in the treatment of fatty liver. However, the optimal diet for prevention of NASH is unknown. NASH patients had significantly higher overnight fasting blood concentration of total and free fatty acids than controls, and higher total saturated and monounsaturated levels of lipid fractions, mainly due to increase of palmitate, palmitoleate and oleate acids[5,6]. Low-calorie diet for 2 wk in Sprague-Dawley rats exerted no significant effects on either serum lipid disorders or hepatic inflammatory changes[7]. Dietary omega-3 and omega-6 polyunsaturated fatty acids (PUFA), present in fish oil, can regulate hepatic lipogenesis by reducing sterol-regulatory element-binding protein-1 in the liver[8]. Moreover, PUFA administration decreased fatty acids, such as oleate (C18:1 n-9), palmitate (C16:0) and palmitoleate (C16:1 n-7)[9]. Diet of NASH patients who were free of hyperlipidemia, diabetes and obesity was richer in saturated fat and poorer in PUFA[10]. PUFA may act as "fuel partitioners", directing fatty acids away from triglyceride storage and toward oxidation[11]. A recent clinical study that compared 19 patients who had non-alcoholic fatty liver disease (NAFLD) with 11 normal control subjects revealed that patients with NAFLD had a higher ratio of long-chain polyunsaturated fatty acids omega-6/omega-3 in their livers than did control subjects[6]. When dietary monounsaturated fatty acids, mainly oleic acid present in olive oil, replace high-carbohydrate diets, plasma triglycerides concentration decrease, both in patients without diabetes and in those with type 2 diabetes[12]. These findings provide the rational for undertaking the experiment to test the hypothesis that supplementation of different oils to methionine choline-deficient diet could attenuate fatty liver changes in a novel model of hepatic steatosis.

The aim of the current study was to evaluate the effects of different types of dietary fats (monosaturated fatty acids present in olive oil; polyunsaturated fatty acids present in fish oil, and saturated fatty acids present in butter) on the hepatic lipid content and oxidative stress in rat liver with experimental NAFLD.

MATERIALS AND METHODS

Animals and protocol

Methionine choline-deficient diet (MCDD) is the most widely used model for NASH in rats[13]. The development of steatosis is caused by impaired very low-density lipoprotein (VLDL) secretion. Unlike animals fed a choline-sufficient diet which developed only steatosis but not inflammation and fibrosis, animals fed an MCDD diet showed fibrosing steatohepatitis[13]. Thirty-two Sprague-Dawley rats were randomly divided into five groups. The animals in the control group (n = 8) were on chow diet (Group 1). In group 2, there were six rats on methionine choline-deficient diet (MCDD). In group 3, there were six rats on MCDD supplemented with olive oil (0.45 mg/g rat weight). In group 4, six rats were on MCDD with fish oil (0.45 mg/g rat weight) and in group 5, 6 rats were on MCDD with butter-fat (0.45 mg/g rat weight). In all treatment groups, the MCDD diet was supplemented simply with the different oils and not as a semi-purified diet. The dietary fat was monitored daily and was supplied by the local pharmacy of the Sieff Hospital, Safed, Israel, and not by commercial sources. After two months, the rats were generally anesthetized and blood was sampled by heart puncture. Rats were sacrificed and the liver sections were examined. All animals were treated humanely and in accordance with the guidelines of the institution. The composition of the experimental diets and the levels of lipid fractions are shown in Table 1.

Table 1 Lipid composition of dietary fats (g/100 g total lipids)

Lipid	Olive oil	Fish oil	Butter
Energy (kcal)	884	902	717
Fatty acid, total saturated	13.8	29.89	51.36
16:0 palmitic	11.29	16.64	21.69
Fatty acid, total monounsaturated	72.96	33.84	21.02
18:1 undifferentiated	71.26	14.75	19.96
Fatty acid, total polyunsaturated	10.52	31.86	3.04
18:2 undifferentiated	9.76	2.01	2.72

Biochemistry

Determination of hepatic lipids composition: Rat liver lipid was extracted using the homogenate according to Folch *et al*[14]. Triglyceride concentration was determined according to the method of Gottfried and Rosenberg[15]. Total cholesterol concentration was determined as previously described[16]. Total lipid concentrations were determined using sulphophosphovaniline[17]. Phospholipids concentrations were determined by lipid phosphorus assay[18]. Phospholipids were separated into component species by thin layer chromatography (TLC) using silica gel G plates and chloroform: methanol: water (65:25:4, v/v) as the solvent system. The position of individual phospholipids was determined using the respective standards. The results were reported as percentage of total phospholipids content[19].

Determination of hepatic pro-oxidant and anti-oxidants: Paraoxonase activity was measured according to the method described elsewhere[20] using 1.0 mmol/L phenyl acetate as substrate. α-tocopherol was estimated sp ectrophotometrically[21]. Hepatic maleic dialdehyde (MDA) was estimated spectrophotometrically using thiobarbituric acid assay[22].

Fatty acids composition: Rat liver cytosol was prepared by differential centrifugation. Approximately 0.5 g of the liver was homogenized in 5 mL of ice-cold 50 mmol/L phosphate buffer solution (pH 7.4). The liver homogenate was centrifuged for 10 min at 5000 r/min at 4℃, and the pellet was discarded. The supernatant was further centrifuged for 30 min at 8000 r/min at 4℃. Fatty acid methyl esters were analyzed by gas chromatography using

Table 2 Effect of MCDD alone or enriched with different fats on rat body or liver weight (mean ± SD, *n* = 6)

Group	Diet	Baseline rats weight (g)	Final rats weight (g)	Final liver weight (g)	Liver weight/rat weight ratio
1	Control	246 ± 6	367 ± 3	8.8 ± 0.3	0.023
2	MCDD	249 ± 6	184 ± 8	6.8 ± 0.6	0.037[a]
3	MCDD + olive oil	247 ± 6	177 ± 7	6.6 ± 0.6	0.037[a]
4	MCDD + fish oil	246 ± 7	176 ± 6	5.8 ± 0.6	0.033[a]
5	MCDD + butter	242 ± 5	178 ± 6	6.6 ± 0.5	0.037[a]

[a]$P < 0.05$ *vs* control group.

palmitic acid as the marker of fatty acids[23].

Histology

The specimens were fixed in buffered formalin and embedded in paraffin. Hematoxylin and eosin (H&E) sections, periodic acid Schiff with diastase stain for inflammatory grading as well as Mason's trichrome and reticulin stains were reviewed for fibrosis and architectural changes. The necroinflammatory grade and stage of fibrosis were assessed according the method of Brunt *et al*[24]. Steatosis was graded by semi-quantitative analysis as follows: mild = 5%-30%; moderate = 30%-60%; and severe = more than 60% of hepatocytes affected. Each biopsy was analyzed and graded by the same pathologist who was blinded to the rats group.

Statistical analysis

Results were expressed as mean ± SD. Analysis of variance was used to compare multiple group means, followed by the Newman-Keuls test to determine statistical significance between two groups. When the data were not normally distributed, the Kruskal-Wallis test was performed to compare multiple group means, followed by Mann-Whitney test. Correlation analysis was performed using Spearman rank correlation. The statistical comparisons were performed using the unit values rather than percentages. $P < 0.05$ was considered statistically significant. The statistical analysis was performed using the Winstat program for windows (Kalmia, MA).

RESULTS

Liver weight/rat weight ratio

Rat weights significantly increased in the control group by 49% and decreased in MCDD, MCDD + olive oil, MCDD + fish oil, and MCDD + butter group by 35%, 40%, 40%, and 37%, respectively ($P < 0.05$). Rat liver weights decreased relatively to the control group in MCDD, MCDD + olive oil, MCDD + fish oil, and MCDD + butter group by 22%, 25%, 34%, and 25%, respectively ($P < 0.05$, Table 2). Rat liver weight: rat weight ratios were markedly increased in MCDD, MCDD + olive oil, MCDD + fish oil, and MCDD + butter group by 54%, 54%, 38%, and 54%, respectively ($P < 0.05$).

Extent of fatty infiltration

There was a significant increase in the extent of fatty liver in MCDD, MCDD + olive oil, MCDD + fish oil, and MCDD + butter groups as compared to the control group ($P < 0.001$). While no severe fatty (> 60%) infiltration was observed in MCDD + olive oil group, severe hepatic fatty infiltration was observed in 33% of rats in MCDD + fish oil group and in 83% of rats in MCDD + butter group ($P < 0.01$, Figure 1A). Mild to moderate fatty infiltration was similar in MCDD and MCDD + olive oil groups but significantly lower in MCDD + fish oil (67% of rats) and MCDD +butter group (17% of rats) ($P < 0.01$, Figure 1B). No inflammation was detected in the livers of the control group. Mild inflammatory changes were observed in all rats in MCDD, and MCDD + olive oil groups. While 66% of the rats in MCDD + butter group were without hepatic inflammatory changes, 50% of the rats in MCDD + fish oil group had moderate inflammatory changes (Table 3).

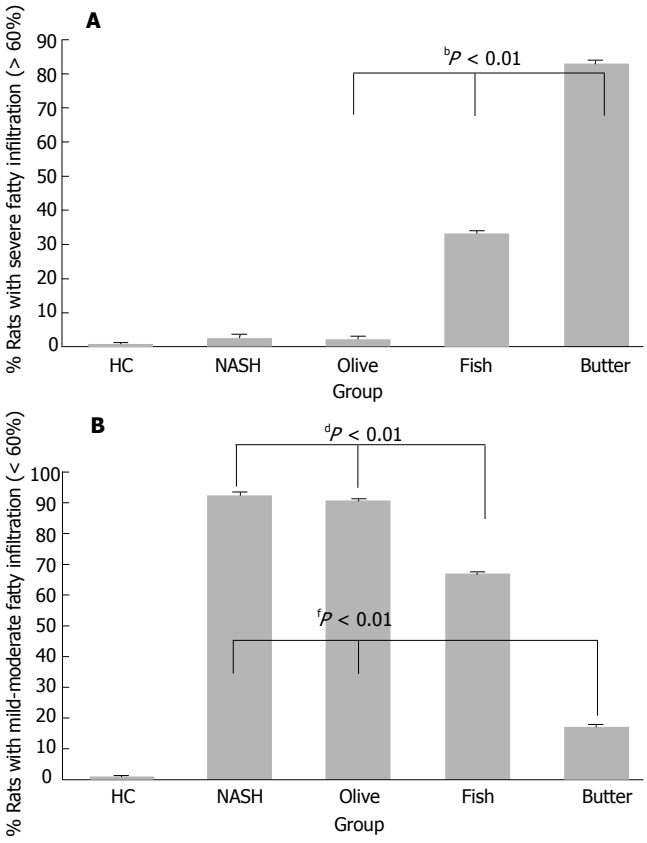

Figure 1 Extent of hepatic fatty infiltration (**A**: severe; **B**: mild) in the different treatment groups. [b]$P < 0.01$, comparison among olive oil, fish oil and butter fat groups; [d]$P < 0.01$, comparison among fish oil, NASH and olive oil groups; [f]$P < 0.01$, comparison among butter fat, NASH and olive oil groups.

Hepatic lipids

Hepatic triglyceride content (mol/g liver) increased by 43-, 30-, 48- and 45-fold in MCDD (0.85 ± 0.04), MCDD + olive oil (0.59 ± 0.09), MCDD + fish oil (0.95 ± 0.07), and MCDD + butter (0.09 ± 0.1) groups, respectively, as compared to the control group (0.024 ± 0.007, $P < 0.001$). Most importantly, this increase was blunted by 30% in MCDD + olive oil group compared with MCDD group only ($P < 0.004$), by 37% in MCDD + olive oil group compared with MCDD + fish oil group ($P < 0.001$), and by 33% in MCDD + olive oil group compared with MCDD + butter group ($P < 0.001$, Figure 2). Hepatic

Table 3 Effect of MCDD alone or enriched with different fats on hepatic fat infiltration and inflammation

Group	Diet	Fatty liver		Inflammation		
		< 60% (%)	> 60% (%)	Absent (%)	Mild (%)	Moderate (%)
1	Control (n = 8)	0	0	0	0	0
2	MCDD (n = 5)	100[a]	0	0	100[a]	0
3	MCDD + olive oil (n = 6)	100[a]	0	0	100[a]	0
4	MCDD + fish oil (n = 6)	67[a]	33.3[a]	17	33.3[a]	50[ac]
5	MCDD + butter (n = 6)	17	83[a]	66[ac]	17	17

[a]$P < 0.05$ *vs* control group; [c]$P < 0.05$ *vs* group 3.

cholesterol content increased by 15-fold in MCDD group (0.08 ± 0.02) compared with the control group (0.03 ± 0.01). In MCDD + fish oil group, this increment was blunted by 21% compared with MCDD group. There was a significant increase in lipid content in the liver of MCDD (1.9 ± 0.14), MCDD + olive oil (2.06 ± 0.4), MCDD + fish oil (1.9 ± 0.35), and MCDD + butter (1.98 ± 0.39) groups by 6.8-, 7.1-, 6.6- and 6.8-fold, respectively, as compared to the control group (0.28 ± 0.03, $P < 0.01$). Phospholipids content in the liver decreased in MCDD group (0.21 ± 0.04) by 2.6-fold compared with the control group (0.55 ± 0.04, $P < 0.05$). All phospholipids fractions (lysolecithin, sphingomyelin, lecithin, phosphatidyl inositol and phosphatidyl ethanolamine) were reduced in the liver of all treatment groups.

Plasma lipids

Serum triglyceride levels (mmol/L) increased significantly in MCDD (1.05 ± 0.06), MCDD + olive oil (0.9 ± 0.07), MCDD + fish oil (1.02 ± 0.08), and MCDD + butter (0.97 ± 0.4) groups by 98%, 79%, 94%, and 85%, respectively, as compared to the control group (0.53 ± 0.09), ($P <$ 0.05). This increment was significantly lowered (by -10%) in MCDD + olive oil group as compared with MCDD group ($P < 0.02$). Serum cholesterol levels (mmol/L) were not significantly different among the control (1.2 ± 0.37), MCDD (1.0 ± 0.1), and MCDD + olive oil (0.87 ± 0.2) groups, but increased by 33% and 22% in MCDD + fish oil (1.4 ± 0.2), and MCDD + butter (1.27 ± 0.2) groups, respectively, when compared with MCDD group. Plasma lipid content (3.4 ± 1.0) did not change in any treatment group. Phospholipids levels in serum decreased in MCDD group (0.63 ± 0.1) by 5.4-fold compared with the control group (3.4 ± 0.4), but no significant difference in phospholipids level was observed between among the treatment groups. All phospholipids fractions (lysolecithin, sphingomyelin, lecithin, phosphatidyl inositol and phosphatidyl ethanolamine) were reduced in plasma.

Hepatic pro-oxidant and anti-oxidants

MDA hepatic content (mol/g liver) increased significantly in MCDD (1.58 ± 0.8), MCDD + olive oil (3.3 ± 0.6), MCDD + fish oil (3.0 ± 0.4), and MCDD + butter (2.9 ± 0.36) groups in comparison to the control group (0.2 ± 0.1) by 7.4-, 15.3-, 14 and 13.7-fold, respectively ($P <$ 0.05). Moreover, MDA hepatic contents in MCDD + olive oil, MCDD + fish oil, and MCDD + butter groups were higher in comparison to MCDD group by 108%, 91% and 87%, respectively ($P < 0.004$). Paraoxonase activity decreased significantly in the livers of all treatment groups. The most prominent decrease in paraoxonase activity was observed in MCDD + olive oil group (1.36 ± 0.28, -68%, $P < 0.01$, Figure 3). α-tocopherol content in the liver (mg/g liver) decreased in MCDD + olive oil group (0.26 ± 0.09) by 63% compared with the control group (0.7 ± 0.05, $P < 0.01$), by 61% in comparison with MCDD + fish oil (0.66 ± 0.1) group ($P < 0.003$) and by 64% compared with MCDD + butter group (0.7 ± 0.09, $P < 0.002$). However, no significant differences were found among the other groups.

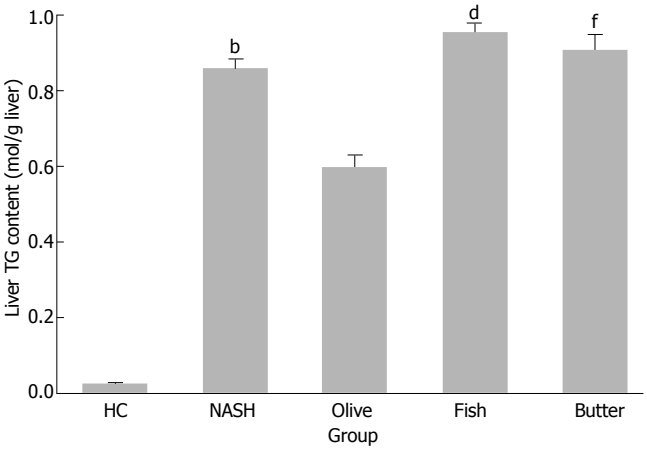

Figure 2 Hepatic triglycerides content (mol/g liver) in the different treatment groups. [b]$P < 0.004$, [d]$P < 0.001$, [f]$P < 0.001$ *vs* olive oil group.

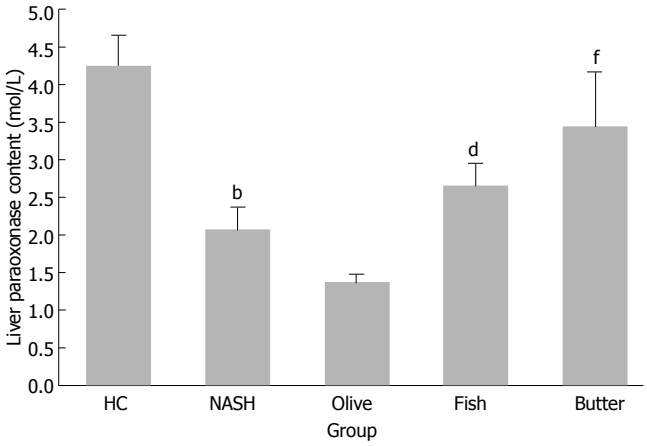

Figure 3 Hepatic paraoxonase contents (mol/L) in the different treatment groups. [b]$P < 0.01$, [d]$P < 0.01$, [f]$P < 0.01$ *vs* olive oil group.

Plasma pro-oxidant and anti-oxidants

There was no obvious difference between the control group (8.8 ± 1.6) and MCDD group (7.5 ± 1.5) in plasma concentrations of MDA. MCDD + olive oil (11.9 ± 3.2), MCDD + fish oil (11.3 ± 5.1) and MCDD + butter (10.1 ± 6.3) groups had significantly higher plasma

Table 4 Effect of MCDD alone or enriched with different fats on fatty acids percentage in the liver

Fatty acids components	Control	MCDD	MCDD + olive oil	MCDD + fish oil	MCDD + butter	[1]*P*	[2]*P* (Friedman test)
C14:0 Myristic	0.2 ± 0.2	0.5 ± 0.1	0.3 ± 0.2	0.4 ± 0.2	0.4 ± 0.2	0.003	0.002
C16:0 Palmitic	19 ± 1	17 ± 1.1	15.3 ± 1.4[ac]	15.5 ± 1.1	15.7 ± 2.3	0.001	0.006
C16:1 Palmitoleic	0.1 ± 0.2	0.7 ± 0.1	0.4 ± 0.2	0.7 ± 0.1	0.4 ± 0.2	0.007	0.02
C18:0 Stearic	21.8 ± 1.6	5.8 ± 0.6	5.7 ± 0.7[ac]	6.2 ± 0.5	6.1 ± 0.9	0.002	0.01
C18:1n9t Elaidic	2.1 ± 0.1	1.5 ± 1.3	22.8 ± 1.3	17.8 ± 1.1	21.3 ± 1.1	0.001	0.006
C18:1n9c Oleic	4.9 ± 0.8	20.7 ± 0.7	25.9 ± 3.3[ac]	2.0 ± 0.1	5.3 ± 8.7	0.001	0.006
C18:2n6c Linolelaidic	18.6 ± 1.8	32.4 ± 0.7	30.5 ± 1.7[ac]	29.5 ± 2.1	31.5 ± 2.1	0.001	0.006
C18:3n3 Linolenic	0.5 ± 0.3	0.3 ± 0.1	0.2 ± 0.2[c]	0.2 ± 0.2	0.3 ± 0.2	0.007	0.02
C23:0 Tricosanoic	22.0 ± 2.4	10.0 ± 1.1	7.8 ± 2.1[ac]	0	0	0.003	0.02
C20:4n6 Arachidonic	0.1 ± 0.2	0	9.2 ± 0.6[ac]	6.5 ± 0.6	9.7 ± 1.2	0.002	0.006
C22:6n3 Docosahexaenoic	4.5 ± 0.9	1.3 ± 0.5	1.2 ± 0.4	9.0 ± 1.2	1.1 ± 0.6	0.006	0.01
C20:5n3 Eicosapentaenoic	0	0.1 ± 0.1	0	0.9 ± 0.1	0	0.003	0.002

[1]Comparison between MCDD and treatment groups; [2]comparison between the three treatment groups. [a]$P < 0.02$ *vs* MCDD + fish oil; [c]$P < 0.02$ *vs* MCDD + butter group.

concentration of MDA in comparison with MCDD group by 59%, 51% and 35%, respectively ($P < 0.05$). Plasma α-tocopherol level decreased in MCDD group (2.5 ± 0.87) by 57% in comparison with the control group (5.7 ± 0.78, $P < 0.001$). Plasma α-tocopherol levels were increased by 70% in MCDD + olive oil group (4.2 ± 0.5, $P = 0.003$), by 87.3% in MCDD + fish oil group (4.6 ± 0.56) and by 45% in MCDD + butter group (3.6 ± 0.5) as comparison to MCDD group ($P < 0.05$).

Hepatic composition of fatty acids

MCCD diet did not increase palmitic acid percentage in the livers of the rats, but did increase significantly the oleic acid percentage by 4.2-fold. MCDD enrichment by olive oil further increased the oleic acid percentage by 25% ($P < 0.05$). Palmitoleic acid had small contribution to fatty acid liver content and increased in all other treated rat groups on MCDD by 4-7-fold. Fish oil did not alter either the palmitic or palmitoleic acid percentages in the livers of MCDD + fish oil group as compared with MCDD group (Table 4).

Long-chain polyunsaturated fatty acids (PUFA) n6:n3 ratio increased in MCDD + olive oil, MCDD + fish oil and MCDD + butter fat groups by 345-, 30- and 397-fold, respectively in comparison with the control group. MCDD enriched with olive or fish oil or butter fat increased arachidonic acid percentages in the rat livers. This increment was 29% less in MCDD + fish oil group when compared with MCDD + olive oil ($P < 0.05$). C20:4n6/C18:2n6 ratios increased in MCDD + olive fat, MCDD + fish oil and MCDD + butter fat groups by 56-, 41- and 57-fold, respectively, in comparison with the control group (Table 4). C22:6n3 percentage in the rat livers decreased by 3.5-fold in MCDD group in comparison with the control group. This decrease was also noted in the rat groups on MCDD enriched with olive oil or with butter fats. On the contrary, C22:6n3 percentage in the liver increased by 2-fold in MCDD + fish oil group in comparison with the control group (Table 4). Enrichment of MCDD by olive oil, fish oil and butter fat increased elaidic acid percentage by 15.2-, 11.9- and 14.2-fold, respectively, compared to MCDD group. Fish oil blunted elaidic acid percentage increase in the rat livers by 22% in comparison with olive oil. C18:1n9c/C18:0 ratios increased in MCDD, MCDD + olive oil, MCDD + fish oil and MCDD + butter fat groups by 16-, 20-, 1-, and 4-fold, respectively, when compared to the control group (Table 4). Correlations between the levels of various fats, triglycerides, cholesterol, phospholipids, saturated and unsaturated fatty acids in the MCDD + olive oil group and the oxidant-antioxidant status are shown in Table 5. A strong correlation was noted between hepatic MDA levels and hepatic cholesterol ($r = -0.8$), phospholipids ($r = -0.6$), and palmitic acid ($r = 0.6$), as well as between hepatic alpha-tocopherol and linolelaidic acid ($r = 0.97$), elaidic acid ($r = 0.9$), oleic acid ($r = -0.7$), and arachidonic acid ($r = -0.7$). Hepatic paroxonase correlated well with tricosanoic acid ($r = 0.9$), stearic acid ($r = -0.9$), oleic acid ($r = -0.8$), and arachidonic acid ($r = -0.7$) (Table 5).

Table 5 Correlations between hepatic lipid fractions and parameters of oxidant-antioxidant status in the MCDD + olive oil group

Parameter	Malonyl dialdehyde (MDA)	Alpha-tocopherol	Paraoxonase
Triglycerides	$r = -0.4$	$r = 0.45$	$r = -0.004$
Cholesterol	$r = -0.8$	$r = 0.05$	$r = 0.3$
Phospholipids	$r = -0.6$	$r = -0.4$	$r = -0.6$
Lipids	$r = -0.2$	$r = -0.4$	$r = -0.2$
Palmitic	$r = 0.6$	$r = 0.1$	$r = 0.1$
Stearic	$r = -0.5$	$r = -0.4$	$r = -0.9$
Elaidic	$r = 0.1$	$r = 0.9$	$r = 0.6$
Oleic	$r = -0.2$	$r = -0.7$	$r = -0.8$
Linolelaidic	$r = 0.2$	$r = 0.97$	$r = 0.66$
Tricosanoic	$r = 0.5$	$r = 0.4$	$r = 0.9$
Arachidonic	$r = -0.3$	$r = -0.7$	$r = -0.7$

DISCUSSION

The results of this study clearly indicate that rats on MCDD diet supplemented with olive oil, but not fish oil or butter fat, store less triglycerides in their liver and prevent the occurrence of dietary-induced severe

hepatic steatosis. Moreover, the results indicate also that olive oil diet provides the least antioxidant capability, whereas the fish oil and butter fat diets behave similarly with regard to antioxidant activities. As expected, these rats lost about 40% of body weight[25]. This weight loss is not in accordance with the clinical picture of NASH found in humans and may then results from the loss of subcutaneous fat[26]. Hepatic insulin resistance in the MCDD model of fatty liver is most likely caused by CYP2E1-induced oxidative stress and by elevated serum triglyceride levels[1]. In the current study, serum triglyceride levels were higher in all groups on MCDD (alone or enriched with fat) than in the control group, a finding which is also in accordance with the clinical NASH profile. Triglyceride content in the livers of the MCDD + olive oil group was lower than other groups on MCDD or MCDD enriched with saturated or polyunsaturated fatty acids. This may have been due to the inhibition of hepatic triacylglycerol synthesis[27], and stimulation of hepatic peroxisomal beta-oxidation produced by the olive oil diet[28]. Decrease in lipoprotein lipase and triacylglycerol lipase in the liver after olive and fish oil consumption has also been described and this may be an adaptive response to the low concentration of substrates (triacylglycerol) for these enzymes. The low levels of triglycerides in the liver after olive oil consumption may also be related to the reduced levels of plasma triglycerides found in our study. Moreover, monounsaturated fatty acids, present in olive oil, may improve insulin resistance, and enhance the release of triglyceride from the liver. This also decreases leak of free fatty acids from peripheral adipose tissue back to the liver and may explain the difference between the olive oil and butter groups.

In animal studies, saturated fat, present in butter, significantly increased insulin resistance, whereas long- and short-chain omega-3 fatty acids improved it, and the effects of monounsaturated and omega-6 polyunsaturated fatty acids ranged somewhere in between the two. In humans, shifting from a diet rich in saturated to one rich in monounsaturated fatty acid improved insulin sensitivity in healthy people[28]. Saturated fat [(myristic acid (14:0) and di-homo-γ-linolenic acid (18:3 n-6)] and the percentage of body fat had the strongest correlation with fasting insulin[29]. In normal subjects, consuming diet enriched with 10% elaidic (18:1 trans) acid induced insulin resistance acutely. In the present study, polyunsaturated fatty acids, present in fish oil failed to blunt the triglyceride accumulation in the liver. Fifty-nine percent of fatty acids stored in the liver of NASH patients arises from serum non-esterified fatty acids (NEFA), 26% from *de novo* lipogenesis and 15% from the diet[30]. Thus, the contribution of dietary olive oil to the fatty acid content in the liver appears small, suggesting the presence of other mechanisms preventing the accumulation of fatty acids in the liver under diet enrichment with olive oil. Eicosapentaenoic fatty acid administration decreased hepatic triglyceride content in ob/ob mice[31]. Polyunsaturated fatty acids can shift the energy balance from storage to consumption. Polyunsaturated fatty acids, particularly those of the n-3 family, play pivotal roles as "fuel partitioners" in that they direct fatty acids away from triglyceride storage and toward oxidation and they enhance glucose flux to glycogen[31]. In the present study, the MCDD model of NASH did not show the protective effect of polyunsaturated fatty acids on triglyceride accumulation in the liver. Whether this is due to enhanced hepatic lipogenesis or decreased β-oxidation remains unclear.

The rates of oxidation for the same amount of fatty acids differed among healthy persons, e.g., more than 37% of the dose of lauric acid (12:0) was oxidized compared with less than 15% of the dose of stearic acid (18:0)[32]. In dietary fat-enriched diets, the increased free fatty acids influx into the hepatocytes exceeds the liver capacity to assemble or/and export triglyceride-rich VLDL particles, causing hepatic steatosis. This increases the substrate for lipid peroxidation in the liver[33-35]. Polyunsaturated fatty acids are prone to spontaneous peroxidation, thus forming lipid hydroperoxides and reactive aldehydes[33,34]. At the same time, free fatty acid content in the hepatocytes up-regulates PPAR-α. This enhances mitochondrial long-chain fatty acid β-oxidation, initiation of omega-oxidation of fatty acids in the microsomes[36,37] and peroxisomal β-oxidation[38] resulting in generation of reactive oxygen species accumulation[39]. MCDD diet increased oxidative stress in the liver, but not in the plasma. Fat enrichment with olive oil, fish oil or butter fat added more oxidative stress in the liver and in the plasma. This increased oxidative stress in the liver did not impoverish α-tocopherol hepatic content in the rat groups fed diets enriched with fish oil or with butter. This, presumably, is due to the high content of α-tocopherol in these two food resources. Hepatic paraoxonase activity decreased in all rat groups on MCDD. This decreased activity may be the result of hepatic injury secondary to fat accumulation and increased oxidative stress. Plasma paraoxonase 1 activity is decreased in chronic liver disease in correlation with the degree of hepatic dysfunction[40]. Paraoxonase gene expression has been observed only in the liver[41]. This decrease in paraoxonase activity was more pronounced in the rats fed MCDD enriched with olive oil. The oxidative stress in the liver of this group was also higher than other groups on MCDD. The reasons for that are unclear. It appears that changes in the liver fatty acid composition, due mainly to n-3 lipids, may increase the activity of some anti-oxidant enzymes. A potential mechanism for the induction of hepatic anti-oxidants following butter feeding might be an increase in the expression of their genes; induction of the expression of anti-oxidant enzymes has been reported in circumstances where an increase in free radicals is produced, such as ageing[42].

Analysis of the fatty acid composition in the rat liver showed that MCDD increased palmitoleic and oleic acids percentage in the liver, but not palmitic acid. NASH patients showed increased overnight fasting serum levels of palmitic, palmitoleic and oleic acids[5], suggesting that the source of these fatty acids in the liver is from blood circulation and not from gastrointestinal tract. Hepatic long-chain PUFA n6/n3 ratios increased in MCDD + olive oil, MCDD + fish oil and MCDD + butter fat groups in comparison with the control group. Increased long-chain PUFA n-6/n-3 ratio in the liver of NASH patients

may favor lipid synthesis over oxidation and secretion, thereby leading to steatosis[6]. This ratio increased less in MCDD + fish oil group, yet the MCDD + olive oil group had a lower fat content in the liver, making this ratio less effective in determining fatty acid content in the fatty liver in the MCDD rat model.

MCDD alone or enriched with olive, butter or fish fat increased arachidonic acid percentage in the rat livers, a possible marker of increased inflammatory state in the liver. Fish oil increased arachidonic acid less than olive or butter-supplemented groups, because PUFA can confer anti-inflammatory effect.

In the MCDD model, there was no reduction in C20:2n6/C18:2n6 ratio. In a previous study, NASH patients showed depletion of long-chain PUFA of the n-6 and n-3 series in the liver triacylglycerols[6]. In the present study, C22:6n3 was depleted in MCDD, MCDD + olive oil and MCDD + butter fat, but not in MCDD + fish oil due to dietary addition to the MCDD. MCDD enriched with olive oil, fish oil and butter fat increased hepatic elaidic acid percentage. Elaidic acid leads to defective PUFA desaturation by inhibiting desaturase and subsequently to depletion of hepatic long-chain PUFA[6], but in the present study, C22:6n3 was depleted in MCDD group without a change in hepatic content percentage of elaidic acid. C22:6n3 depletion in MCDD, MCDD + olive oil and MCDD + butter fat may be due to inadequate intake of precursors, such as 18:3 n-3 and a higher peroxidation of long-chain PUFA due to oxidative stress[6].

Although the MCDD model of fatty liver is the most commonly used in experimental studies, one limitation of our study is that MCDD model is not the ideal model for studying insulin resistance in humans and an extensive number of additional experiments would be required to be performed in order to derive definitive data in insulin-resistant models[26]. Another concern is that the rats fed MCDD for nine weeks did not develop the same phenotype as previous reports of MCDD-induced NASH in mice (as short as 10 d of MCDD). The phenotype described here largely consisted of marked steatosis with mild inflammation and mild fibrosis[43].

Increased MDA level, and reduced serum paraoxonase 1 (PON1) activity reflect increased oxidative damage in rats with steatohepatitis. Reactive oxygen species, which are formed due to increased microsomal, peroxisomal and mitochondrial oxidation, trigger lipid peroxidation; this in turn causes cell death and release of MDA[1]. It also has been shown that TNF-α down-regulates mRNA expression of paraoxonase in Hep G2 cells[44]. This cytokine-mediated reduction of paraoxonase production by the liver might be responsible for the decreased paraoxonase activity in steatohepatitis. On the other hand, decreased paraoxonase activity could be accepted as another evidence of increased lipid peroxidation, since it was shown that a decrease in liver microsomal paraoxonase activity is an early biochemical change related to lipid peroxidation and liver injury observed in the rats with CCl4-induced cirrhosis[45].

In conclusion, olive oil decreases the accumulation of triglycerides in the liver of rats with NASH, thereby suggesting that olive oil should be included in the diet of patients with NASH and NAFLD.

REFERENCES

1 **Day CP**. Pathogenesis of steatohepatitis. *Best Pract Res Clin Gastroenterol* 2002; **16**: 663-678
2 **Cassader M**, Gambino R, Musso G, Depetris N, Mecca F, Cavallo-Perin P, Pacini G, Rizzetto M, Pagano G. Postprandial triglyceride-rich lipoprotein metabolism and insulin sensitivity in nonalcoholic steatohepatitis patients. *Lipids* 2001; **36**: 1117-1124
3 **Cooper AD**. Hepatic uptake of chylomicron remnants. *J Lipid Res* 1997; **38**: 2173-2192
4 **Diraison F**, Moulin P, Beylot M. Contribution of hepatic de novo lipogenesis and reesterification of plasma non esterified fatty acids to plasma triglyceride synthesis during non-alcoholic fatty liver disease. *Diabetes Metab* 2003; **29**: 478-485
5 **de Almeida IT**, Cortez-Pinto H, Fidalgo G, Rodrigues D, Camilo ME. Plasma total and free fatty acids composition in human non-alcoholic steatohepatitis. *Clin Nutr* 2002; **21**: 219-223
6 **Araya J**, Rodrigo R, Videla LA, Thielemann L, Orellana M, Pettinelli P, Poniachik J. Increase in long-chain polyunsaturated fatty acid n - 6/n - 3 ratio in relation to hepatic steatosis in patients with non-alcoholic fatty liver disease. *Clin Sci (Lond)* 2004; **106**: 635-643
7 **Fan JG**, Zhong L, Xu ZJ, Tia LY, Ding XD, Li MS, Wang GL. Effects of low-calorie diet on steatohepatitis in rats with obesity and hyperlipidemia. *World J Gastroenterol* 2003; **9**: 2045-2049
8 **Clarke SD**, Jump DB. Dietary polyunsaturated fatty acid regulation of gene transcription. *Annu Rev Nutr* 1994; **14**: 83-98
9 **Sekiya M**, Yahagi N, Matsuzaka T, Najima Y, Nakakuki M, Nagai R, Ishibashi S, Osuga J, Yamada N, Shimano H. Polyunsaturated fatty acids ameliorate hepatic steatosis in obese mice by SREBP-1 suppression. *Hepatology* 2003; **38**: 1529-1539
10 **Musso G**, Gambino R, De Michieli F, Cassader M, Rizzetto M, Durazzo M, Fagà E, Silli B, Pagano G. Dietary habits and their relations to insulin resistance and postprandial lipemia in nonalcoholic steatohepatitis. *Hepatology* 2003; **37**: 909-916
11 **Kliewer SA**, Sundseth SS, Jones SA, Brown PJ, Wisely GB, Koble CS, Devchand P, Wahli W, Willson TM, Lenhard JM, Lehmann JM. Fatty acids and eicosanoids regulate gene expression through direct interactions with peroxisome proliferator-activated receptors alpha and gamma. *Proc Natl Acad Sci USA* 1997; **94**: 4318-4323
12 **Grundy SM**. Comparison of monounsaturated fatty acids and carbohydrates for lowering plasma cholesterol. *N Engl J Med* 1986; **314**: 745-748
13 **Koteish A**, Diehl AM. Animal models of steatosis. *Semin Liver Dis* 2001; **21**: 89-104
14 **Folch J**, Lees M, Sloane Stanley GH. A simple method for the isolation and purification of total lipides from animal tissues. *J Biol Chem* 1957; **226**: 497-509
15 **Gottfried SP**, Rosenberg B. Improved manual spectrophotometric procedure for determination of serum triglycerides. *Clin Chem* 1973; **19**: 1077-1078
16 **Taylor RP**, Broccoli AV, Grisham CM. Enzymatic and colorimetric determination of total serum cholesterol. An undergraduate biochemistry laboratory experiment. *J Chem Educ* 1978; **55**: 63-64
17 **Barnes H**, Blackstock J. Estimation of lipids in marine animals and tissues: detailed investigation of the sulfophosphovanillin method for 'total' lipid. *J exp Mar Biol Ecol* 1973; **12**: 103-118
18 **Bartlett GR**. Phosphorus assay in column chromatography. *J Biol Chem* 1959; **234**: 466-468
19 **Kupke IR**, Zeugner S. Quantitative high-performance thin-layer chromatography of lipids in plasma and liver homogenates after direct application of 0.5-microliter samples to the silica-gel layer. *J Chromatogr* 1978; **146**: 261-271

20 **Gan KN**, Smolen A, Eckerson HW, La Du BN. Purification of human serum paraoxonase/arylesterase. Evidence for one esterase catalyzing both activities. *Drug Metab Dispos* 1991; **19**: 100-106

21 **Gowenlock HA**, McMurray JR.Vitamins. In: Gowenlock HA, McMurray JR, McLauchlan DM, editors. Varley's Practical Clinical Biochemistry. 6th ed. London: Heinmann Medical Books 1988: 894-930

22 **Yagi K**. Lipid peroxides and human diseases. *Chem Phys Lipids* 1987; **45**: 337-351

23 **Parks EJ**, Krauss RM, Christiansen MP, Neese RA, Hellerstein MK. Effects of a low-fat, high-carbohydrate diet on VLDL-triglyceride assembly, production, and clearance. *J Clin Invest* 1999; **104**: 1087-1096

24 **Brunt EM**, Janney CG, Di Bisceglie AM, Neuschwander-Tetri BA, Bacon BR. Nonalcoholic steatohepatitis: a proposal for grading and staging the histological lesions. *Am J Gastroenterol* 1999; **94**: 2467-2474

25 **Farrell G**. Animal models of steatohepatitis. In: Farrell G, George J, de la M Hall P, McCullough AJ, editors. Fatty liver disease: NASH and related disorders. Massachusetts: Blackwell, 2005: 91-108

26 **Rinella ME**, Green RM. The methionine-choline deficient dietary model of steatohepatitis does not exhibit insulin resistance. *J Hepatol* 2004; **40**: 47-51

27 **Wong SH**, Nestel PJ, Trimble RP, Storer GB, Illman RJ, Topping DL. The adaptive effects of dietary fish and safflower oil on lipid and lipoprotein metabolism in perfused rat liver. *Biochim Biophys Acta* 1984; **792**: 103-109

28 **Rivellese AA**, De Natale C, Lilli S. Type of dietary fat and insulin resistance. *Ann N Y Acad Sci* 2002; **967**: 329-335

29 **Lovejoy JC**, Champagne CM, Smith SR, DeLany JP, Bray GA, Lefevre M, Denkins YM, Rood JC. Relationship of dietary fat and serum cholesterol ester and phospholipid fatty acids to markers of insulin resistance in men and women with a range of glucose tolerance. *Metabolism* 2001; **50**: 86-92

30 **Donnelly KL**, Smith CI, Schwarzenberg SJ, Jessurun J, Boldt MD, Parks EJ. Sources of fatty acids stored in liver and secreted via lipoproteins in patients with nonalcoholic fatty liver disease. *J Clin Invest* 2005; **115**: 1343-1351

31 **Clarke SD**. Nonalcoholic steatosis and steatohepatitis. I. Molecular mechanism for polyunsaturated fatty acid regulation of gene transcription. *Am J Physiol Gastrointest Liver Physiol* 2001; **281**: G865-G869

32 **DeLany JP**, Windhauser MM, Champagne CM, Bray GA. Differential oxidation of individual dietary fatty acids in humans. *Am J Clin Nutr* 2000; **72**: 905-911

33 **Mylonas C**, Kouretas D. Lipid peroxidation and tissue damage. *In Vivo* 1999; **13**: 295-309

34 **Jaeschke H**, Gores GJ, Cederbaum AI, Hinson JA, Pessayre D, Lemasters JJ. Mechanisms of hepatotoxicity. *Toxicol Sci* 2002; **65**: 166-176

35 **Tang DG**, La E, Kern J, Kehrer JP. Fatty acid oxidation and signaling in apoptosis. *Biol Chem* 2002; **383**: 425-442

36 **Mortensen PB**. Formation and degradation of dicarboxylic acids in relation to alterations in fatty acid oxidation in rats. *Biochim Biophys Acta* 1992; **1124**: 71-79

37 **Kaikaus RM**, Chan WK, Lysenko N, Ray R, Ortiz de Montellano PR, Bass NM. Induction of peroxisomal fatty acid beta-oxidation and liver fatty acid-binding protein by peroxisome proliferators. Mediation via the cytochrome P-450IVA1 omega-hydroxylase pathway. *J Biol Chem* 1993; **268**: 9593-9603

38 **Kliewer SA**, Xu HE, Lambert MH, Willson TM. Peroxisome proliferator-activated receptors: from genes to physiology. *Recent Prog Horm Res* 2001; **56**: 239-263

39 **Bocher V**, Pineda-Torra I, Fruchart JC, Staels B. PPARs: transcription factors controlling lipid and lipoprotein metabolism. *Ann N Y Acad Sci* 2002; **967**: 7-18

40 **Ferré N**, Camps J, Prats E, Vilella E, Paul A, Figuera L, Joven J. Serum paraoxonase activity: a new additional test for the improved evaluation of chronic liver damage. *Clin Chem* 2002; **48**: 261-268

41 **Leviev I**, Negro F, James RW. Two alleles of the human paraoxonase gene produce different amounts of mRNA. An explanation for differences in serum concentrations of paraoxonase associated with the (Leu-Met54) polymorphism. *Arterioscler Thromb Vasc Biol* 1997; **17**: 2935-2939

42 **de Haan JB**, Newman JD, Kola I. Cu/Zn superoxide dismutase mRNA and enzyme activity, and susceptibility to lipid peroxidation, increases with aging in murine brains. *Brain Res Mol Brain Res* 1992; **13**: 179-187

43 **George J**, Pera N, Phung N, Leclercq I, Yun Hou J, Farrell G. Lipid peroxidation, stellate cell activation and hepatic fibrogenesis in a rat model of chronic steatohepatitis. *J Hepatol* 2003; **39**: 756-764

44 **Kumon Y**, Nakauchi Y, Suehiro T, Shiinoki T, Tanimoto N, Inoue M, Nakamura T, Hashimoto K, Sipe JD. Proinflammatory cytokines but not acute phase serum amyloid A or C-reactive protein, downregulate paraoxonase 1 (PON1) expression by HepG2 cells. *Amyloid* 2002; **9**: 160-164

45 **Ferré N**, Camps J, Cabré M, Paul A, Joven J. Hepatic paraoxonase activity alterations and free radical production in rats with experimental cirrhosis. *Metabolism* 2001; **50**: 997-1000

S- Editor Wang GP **L- Editor** Kumar M **E- Editor** Lu W

PO Box 2345, Beijing 100023, China
www.wjgnet.com
wjg@wjgnet.com

World J Gastroenterol 2007 January 21; 13(3): 369-377
World Journal of Gastroenterology ISSN 1007-9327

BASIC RESEARCH

Expression patterns and action analysis of genes associated with inflammatory responses during rat liver regeneration

Heng-Yi Shao, Li-Feng Zhao, Cun-Shuan Xu

Heng-Yi Shao, Cun-Shuan Xu, College of Life Science, Henan Normal University, Xinxiang 453007, Henan Province, China
Li-Feng Zhao, Key Laboratory for Cell Differentiation Regulation, Xinxiang 453007, Henan Province, China
Supported by the National Natural Science Foundation of China, No. 30270673
Correspondence to: Professor Cun-Shuan Xu, College of Life Science, Henan Normal University, Xinxiang 453007, Henan Province, China. xucs@x263.net
Telephone: +86-373-3326001 Fax: +86-373-3326524
Received: 2006-08-25 Accepted: 2006-10-06

Abstract

AIM: To study the relationship between inflammatory response and liver regeneration (LR) at transcriptional level.

METHODS: After partial hepatectomy (PH) of rats, the genes associated with inflammatory response were obtained according to the databases, and the gene expression changes during LR were checked by the Rat Genome 230 2.0 array.

RESULTS: Two hundred and thirty-nine genes were associated with liver regeneration. The initial and total expressing gene numbers found in initiation phase (0.5-4 h after PH), G_0/G_1 transition (4-6 h after PH), cell proliferation (6-66 h after PH), cell differentiation and structure-function reconstruction (66-168 h after PH) of liver regeneration were 107, 34, 126, 6 and 107, 92, 233, 145 respectively, showing that the associated genes were mainly triggered at the beginning of liver regeneration, and worked at different phases. According to their expression similarity, these genes were classified into 5 groups: only up-regulated, predominantly up-, only down-, predominantly down-, up- and down-, involving 92, 25, 77, 14 and 31 genes, respectively. The total times of their up- and down-regulated expression were 975 and 494, respectively, demonstrating that the expressions of the majority of genes were increased, and that of a few genes were decreased. Their time relevance was classified into 13 groups, showing that the cellular physiological and biochemical activities were staggered during liver regeneration. According to gene expression patterns, they were classified into 33 types, suggesting that the activities were diverse and complex during liver regeneration.

CONCLUSION: Inflammatory response is closely associated with liver regeneration, in which 239 LR-associated genes play an important role.

Key words: Partial hepatectomy; Rat Genome 230 2.0 array; Inflammatory response; Genes associated with liver regeneration

Shao HY, Zhao LF, Xu CS. Expression patterns and action analysis of genes associated with inflammatory responses during rat liver regeneration. *World J Gastroenterol* 2007; 13(3): 369-377

http://www.wjgnet.com/1007-9327/13/369.asp

INTRODUCTION

Partial hepatectomy (PH)[1], being severely harmful to the body, can cause inflammatory response[2]. Furthermore, it also activates the remaining liver cells to enter into cell cycle to replenish the lost livers, which is called liver regeneration (LR)[3,4]. Generally, an inflammatory response goes through the following processes: the change of vascular permeability[5] as a result of the tissue injury[6], leukocytes' escape from blood vessel, activation and proliferation of target cells induced by released cytokines, elimination of foreign materials, wound repair and so on[6]. It is a defense mechanism developed during the long-term evolutionary process, being closely linked to survival of living organisms[7].

Usually, the process of LR is classified based on the cellular physiological activities into 4 phases consisting of the initiation (0.5-4 h after PH), the G_0/G_1 transition (4-6 h after PH), the cell proliferation (6-66 h after PH), the cell differentiation and structure-function reorganization (66-168 h after PH)[8], or divided according to time course into 4 phases including forepart (0.5-4 h after PH), prophase (6-12 h after PH), metaphase (16-66 h after PH), and anaphase (72-168 h after PH)[9], in which a variety of physiological and biochemical events including cell activation, de-differentiation, proliferation and its regulation, re-differentiation, reorganization of structure-function[10] are involved. The process is regulated by many factors including inflammation[11]. Studying the relationship between inflammatory response and liver regeneration at transcriptional level is helpful to clarify the molecular mechanism of liver regeneration[9,12]. In the current study,

the expression changes of genes in regenerating liver were detected by Rat Genome 230 2.0 array[13,14] containing 409 genes associated with inflammatory response. Two hundred and thirty-nine genes were found associated with liver regeneration[15], and their expression changes, patterns and roles in LR were preliminarily analyzed.

MATERIALS AND METHODS

Regenerating liver preparation

Healthy SD rats weighing 200-250 g were obtained from the Animal Center of Henan Normal University. The rats were separated into groups at random and each group included 6 rats (Male:Female = 1:1). PH was performed according to Higgins and Anderson[3]: the left and middle lobes of the liver were removed. Rats were killed by cervical vertebra dislocation at 0.5, 1, 2, 4, 6, 8, 12, 24, 36, 54, 66, 72, 120, 144 and 168 h after partial hepatectomy and the regenerating livers were examined at corresponding time points. The livers were rinsed three times in PBS at 4℃. Then 100-200 mg liver tissues from middle parts of the right lobe, six samples of each group were gathered and mixed together to a total of 1-2 g (0.1-0.2 g × 6) of liver tissue, and stored at -80℃. The sham-operation (SO) groups were treated the same way with partial hepatectomy ones except that the liver lobes were unremoved. The laws of animal protection of China were followed strictly.

RNA isolation and purification

Total RNA was isolated from frozen livers according to the manual of Trizol kit (Invitrogen)[16] and then purified based on the guide of RNeasy mini kit (Qiagen)[17]. Total RNA samples were examined and exhibited a 2:1 ratio of 28S to 18S rRNA intensities by agarose electrophoresis (180 V, 0.5 h). Total RNA concentration and purity were estimated by optical density measurements at 260/280 nm[18].

cDNA, cRNA synthesis and purification

As template, 1-8 μg total RNA was used for cDNA synthesis. cDNA and cRNA synthesis were proceeded according to the methods established by Affymetrix[13]. cRNA labeled with biotin was synthesized using 12 μL of the above synthesized cDNA as the template, and cDNA and cRNA were purified[13]. Measurement of concentration, purity and quality of cDNA and cRNA was the same as above.

cRNA fragmentation and microarray detection

Fifteen microliters (1 μg/μL) cRNA incubated with 5 × fragmentation buffer at 94℃ for 35 min was digested into 35-200 bp fragments. Rat Genome 230 2.0 microarray produced by Affymetrix was prehybridized, then the hybridization buffer was added at 45℃, and spun at 60 rotations per min for 16 h. The microarray was washed and stained by GeneChip fluidics station 450 (Affymetrix Inc., USA). The chips were scanned by GeneChip Scan 3000 (Affymetrix Inc., USA), and the signal values of gene expression were observed[14].

Microarray data analysis

The normalized signal values, signal detections (P, A, M) and experiment/control (Ri) were obtained by quantifying and normalizing the signal values using GCOS1.2[14].

Normalization of microarray data

To minimize error in the microarray analysis, each analysis was performed three times by Rat Genome 230 2.0 microarray. Result with a total ratio was maximal (R^m) and that of which the average of three housekeeping genes (β-actin, hexokinase and glyseraldehyde-3-phosphate dehydrogenase) approached 1.0 (R^h) were taken as a reference. The modified data were generated using a correction factor (R^m/R^h) multiplying the ratio of every gene in R^h at each time point. To remove spurious gene expression changes resulting from errors in the microarray analysis, the gene expression profiles at 0-4 h, 6-12 h and 12-24 h after PH were reorganized by NAP software (normalization analysis program) according to the cell cycle progression of the regenerating hepatocytes. Data statistics and cluster analysis were done using GeneMath, GeneSpring, and Microsoft Excel software[14,19,20].

Identification of genes associated with liver regeneration

Firstly, the nomenclature of inflammatory response was adopted from the GENEONTOLOGY database (www.geneontology.org), and than input into NCBI (www.ncbi.nlm.nih.gov) and RGD (rgd.mcw.edu) to identify the rat, mouse and human genes associated with the inflammatory response. According to maps of biological pathways embodied by GENMAPP (www.genmapp.org), KEGG (www.genome.jp/kegg/pathway.html#amino) and BIOCARTA (www.biocarta.com/genes/index.asp), the genes associated with inflammatory response were collated. The results of this analysis were coded, and compared with the results from human and mouse studies in order to identify human and mouse genes which are different from those of rat. In comparison of these genes with the analysis output of the Rat Genome 230 2.0 array, those genes that showed a greater than twofold change in expression level, regarded as meaningful expression changes[15], were referred to as rat homologous genes or rat specific genes associated with inflammatory response. Genes that displayed reproducible results with three independent analyses with the chip and showed a greater than twofold change in expression level at least at one time point during liver regeneration with significant difference ($0.01 \leqslant P < 0.05$) or extremely significant difference ($P \leqslant 0.01$) between PH and sham operation (SO), were referred to as associated with liver regeneration.

RESULTS

Expression changes of genes associated with inflammatory response during liver regeneration

According to the databases at NCBI, GENMAPP, KEGG, BIOCARTA and RGD, 661 genes were involved in inflammatory response, in which, 405 genes were contained in the Rat Genome 230 2.0 array. Among them, the expression of 239 genes displayed meaningful changes at least at one time point after PH, showed significant or extremely significant differences in expression when compared between PH and SO, and displayed reproducible

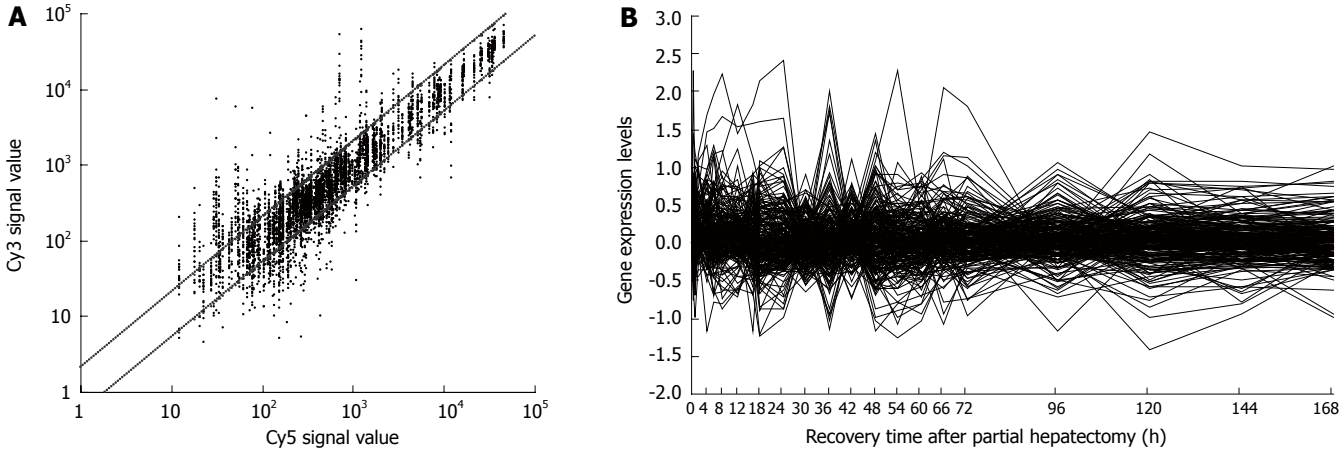

Figure 1 Expression frequency, abundance and changes of 239 inflammatory response-associated genes during rat liver regeneration. Detection data of Rat Genome 230 2.0 array were analyzed and graphed by Microsoft Excel. **A**: Gene expression frequency. The dots above bias represent the genes up-regulated more than two fold, and total times of up-regulation were 975; those below bias down-regulated more than two fold, and times of down-regulation were 494; and the ones between biases no-sense alteration; **B**: Gene expression abundance and changes. One hundred and sixty-two genes were 2-257 fold up-regulated, and 147 genes 2-25 fold down-regulated.

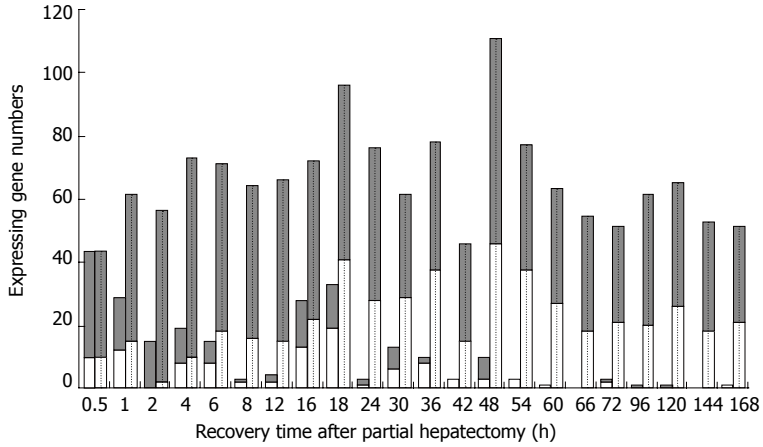

Figure 2 The initial and total expression profiles of 239 inflammatory response-associated genes at each time point of liver regeneration. Grey bars: Up-regulated gene; White bars: Down-regulated. Blank bars represent initial expressing genes, in which up-regulated genes were predominant in the forepart, and the down-regulated in the prophase and metaphase, whereas very few in the anaphase. Dotted bars represent the total expressing genes, in which some genes were up-regulated, and the others down-regulated during the whole LR.

results by three detections with Rat Genome 230 2.0 array, suggesting that the genes were associated with LR. Change in up-regulation ranged from 2 to 257 times higher than control, and down-regulation ranged from 2 to 25 times lower than control (Table 1). The data indicated that 92 genes were up-regulated, 77 genes down-, and 70 genes up/down-during liver regeneration. The total up- and down-regulated times were 975 and 494, respectively (Figure 1A). At the initiation phase (0.5-4 h after PH), 77 genes displayed up-regulation, 27 genes down, 3 genes up/down; at the G0/G1 transition (4-6 h after PH), 70 genes up-regulated, 20 genes down-, and 2 genes up/down-; at the cell proliferation phase (6-66 h after PH), 102 genes up- regulated, 84 genes down-, and 47 genes up/down-; at cell differentiation and structure-function reorganization phase (66-168 h after PH), 82 genes up- regulated, 44 genes down-, and 19 genes up/down- (Figure 1B).

Initial expression time of genes associated with inflammatory response during liver regeneration

At each time point of liver regeneration, the numbers of initial up-, down-regulated and total up-, down-regulated genes are as followings: both 34 and 10 at 0.5 h; 17, 12 and 47, 15 at 1 h; 15, 0 and 55, 2 at 2 h; 11, 8 and 64, 10 at 4 h; 7, 8 and 54, 18 at 6 h; 1, 2 and 49, 16 at 8 h; 2, 2 and 52, 15 at 12 h; 15, 13 and 51, 22 at 16 h; 14, 19 and 56, 41 at 18 h; 2, 1 and 49, 28 at 24 h; 7, 6 and 33, 29 at 30 h; 2, 8 and 41, 38 at 36 h; 0, 3 and 31, 15 at 42 h; 7, 3 and 66, 46 at 48 h; 0, 3 and 40, 38 at 54 h; 0, 1 and 37, 27 at 60 h; 0, 0 and 37, 18 at 66 h; 1, 2 and 31, 21 at 72 h; 1, 0 and 42, 20 at 96 h; 1, 0 and 40, 26 at 120 h; 0, 0 and 35, 18 at 144 h; 0, 1 and 31, 21 at 168 h (Figure 2). Generally, gene expression changes occurred during the whole liver regeneration, and the up- and down-regulations were 975 and 494 times, respectively. There were predominantly initial up-regulated genes in the forepart, and the down- regulated genes in the prophase and metaphase, whereas only a few in the anaphase.

Expression similarity and time relevance of genes associated with inflammatory response during liver regeneration

Two hundred and thirty-nine genes could be characterized based on their similarity in expression as following: only up-, predominantly up-, only down-, predominantly down-, up/down-regulated, involving 92, 25, 77, 14 and 31 genes, respectively (Figure 3). According to time relevance, they were classified into 13 groups, including 0.5 and 1 h, 2 h, 4 and 6 h, 8 and 12, 16 and 96 h, 18 and 24 h, 30 and 42 h, 36 h, 48 h, 54 and 60 h, 66 and 72 h, 120 and 144 h,

Table 1 Expression abundance of 239 inflammatory response-associated genes during rat liver regeneration

Gene abbr.	Associated with others	Fold difference	Gene abbr.	Associated with others	Fold difference	Gene abbr.	Associated with others	Fold difference	Gene abbr.	Associated with others	Fold difference
1 Vascular reaction			S100a9		4.9	[1]Serpine1		16.7	Ndst1		0.5, 2.1
Adcyap1		3.5	Scube1	2[b]	3.2	Socs1		0.5, 2.4	Nfatc4		0.5
Alox5		0.2, 2.5	[1]Socs3		0.1, 2.5	Tgfb2		0.5, 2.9	Nfkb1		0.4, 2.3
Alox5ap		4.9	Stab1		0.4	Tnfrsf11b		0.3, 8.7	Nrf1		0.2, 2.4
Aoc3		6.1	Tac1		0.2	Tp53		2.9	Pap		68.6
Bdkrb2		0.4	Tlr2		10.6	Traf1		0.4	Pecam1		3.5
Cr2		6.0	Tlr4		0.5	**3 Cell activation, proliferation and**			Prdx5		0.5
Crp		0.5	Vps45		12.6	**differentiation**			Prg2		0.3
Ctsb		3.6	Zap70		0.4	**a Cell activation**			Prg3		0.2
Ctsc		0.4	Zfp36		0.1, 4.6	Acadm		6.9	Prkca		0.5, 4.6
Cysltr1		0.1, 2.1	**b Cytokine**			Adprtl1		0.5	Proc		0.3
Edg3		4.0	[1]A2m		0.4, 46.2	Ager	4	0.4	Procr		6.5
F2	2[b]	0.3	Abcb1		4.6	Ambp		5.1	Prok2		8.6
F3	2[b]	0.1, 2.0	Agtr1a		0.4	Aox1		0.3	Pten		0.5
Ggtla1		4.0	Atrn		4.4	Baat		0.2	Rage		0.4
Itga1		2.9	Bcl2a1		0.3, 5.3	C3		0.2	Rela	2[a]	0.5
Klkb1		0.4	Bdnf		0.4, 2.6	C3ar1		0.3, 2.3	Ripk2		0.4
Kng1		2.1	Casp1		3.0	C4a		0.5	Sele	3[b]	12.9
Ltb4r	3[a]	0.5, 8.7	Ccl17		0.1	C5r1		0.4, 2.6	Slpi		2.1
Nos3	2[b]	0.3, 2.1	Ccl19		3.9	Casp8		10.6	Sod2		5.6
Oldlr1		0.3, 6.5	Ccl2		18.5	Cd80		0.3, 3.0	Spn		0.2, 4.0
Ptafr		7.1	Ccl20		8.0	Cd86		2.6	Tgfb1		4.0
Ptger3	2[a]	0.2	Ccl21b		0.1, 2.0	Chuk		0.3	Tmem23		0.2, 4.3
Ptges		4.5	Ccl24		4.0	Cnr2		0.5, 2.6	[1]Tnf		3.2
Ptgs2		0.1, 2.1	Ccl27		0.3	Crcp		0.3	Tnfaip6		0.2, 2.1
Reg3g		0.3, 7.5	Ccl4		0.2, 3.0	Crebbp		0.1	Tnfrsf4		0.3, 2.3
Spin2a		0.2, 4.3	Ccl7		22.6	Csf2		0.3	Tnfsf11		2.3
Spink5		0.1	Ccr1		0.4, 27.9	[1]Ctgf		13.9	Tnfsf4		0.2, 2.3
2 Release cytokine			Cd274		0.3	Cybb	4	2.5	**b Cell proliferation**		
a Process of release			Cklf1		8.3	Dusp1		0.4, 6.0	Akt1		3.9
Abcf1		2.1	Clec7a		0.2	Dysf		0.5, 4.9	B7h3		3.5
Abcf2		0.4	Ctla4		0.3	Fabp4		29.9	Bcl6		8.6
Abcf3		0.5, 2.3	Cxcl10		0.3, 9.2	Fos		28.4	Cd22		0.4
Adm		8.0	Cxcl12		0.2	[1]Foxm1		13.9	Hdac7a		0.5, 4.3
Adora2a		0.5	Cxcl16		0.3	Gal		11.3	Igh-1a		0.3
[1]Anxa1		4.3	Ddt		4.4	[1]Hgf		0.4	Il15	3[a]	0.4
Apoa2		2.9	Dfy		0.4, 8.5	Hmox2		0.4	Il2		0.3, 3.5
Apol3		2.6	Dmd		0.3	[1]Hpse		0.3, 6.3	Il4	3[a,c]	0.1, 2.6
App		6.4	Ebi3		0.2	Icam1		3.0	Il5	3c	3.5
Blvra		3.5	Ela2		0.5, 52.0	Ighe		0.2, 2.5	Il7	3[c]	2.8
C1qr1	4	5.5	F2	1	0.3	Ikbkb		0.3	Indo		0.4, 2.3
Cd163		0.2	F3	1	0.1, 2.0	Ikbkg		0.4	Odc1		3.3
Cd74		0.4	Gif		0.1	Il15	3[b]	0.4	Plp		0.1
Chst1		0.0	Gsk3b		0.4	Il16		0.4, 3.1	Ppara		0.3
Chst2		4.4	Hrh1		0.5, 9.9	[1]Il1B		0.4	Sele	3[a]	12.9
Col1a2		3.0	Hrh4		7.5	Il1f5		0.4, 2.8	Spp1	3[c]	0.5, 2.7
Col3a1		0.3, 6.5	[1]Ifng		6.5	Il1f8		0.5	**c Cell differentiation**		
Crbpb		3.1	Igfbp4		0.5	Il1r1		0.5	Il12rb2		2.8
Esrra		0.2	Il17f		0.1	Il1rn		16.3	Il4	3[a,b]	0.1, 2.6
Fcgr1		2.6	Il6		0.3, 6.1	Il22ra2		0.1	Il5	3[b]	3.5
Itgb2		0.5	Il6r		3.0	IL2ra		0.3, 4.3	Il7	3[b]	2.8
Klrg1		0.4	Ins1		2.1	Il2rg		0.2, 5.1	Spp1	3[b]	0.5, 2.7
Lcn2		0.5, 257.2	Jak2		6.5	Il4	3[b,c]	0.1, 2.6	Stat5a		0.2
Map2k3		0.4	Jun		1.0, 6.9	Il5ra		7.0	Stat5b		0.3
Mapk1		2.7	Lif		0.4, 3.0	Itgam	4	3.4	Tslp		0.5, 6.1
Mbp		0.4	Loc297568		0.4	Lama5		3.8	**4 Phagocytosis**		
Ms4a1	3[a]	0.1	Mapk8		0.5, 19.7	Lamc1		0.4, 2.5	Ager	3[a]	0.4
Ncf1		0.2, 3.7	[1]Mmp9		0.5, 9.5	Ltb4r	1	0.5, 8.7	C1qr1	2[a]	5.5
Nfkbiz		6.6	Nos3	1	0.3, 2.1	Mbl2		0.2	Cybb	3[a]	2.5
Nostrin		8.0	P2rx7		0.4, 2.5	Mcpt6		0.2	Itgam	3[a]	3.4
Orm1		2.8	Pbef1		8.1	Mif		3.2	Itih4		0.3
Parg		4.8	Pik3cd		0.3	Mob		7.0	Lyz		0.4, 3.7
Pla2g4b		2.0	Plaur		13.9	Ms4a1	2[a]	0.1	Nox1		0.3, 8.6
Psen2		0.2	Ppbp		0.1, 2.1	Ms4a2		0.4, 5.3	Nox4		0.1, 3.0
Ptger3	1	0.2	Ptgs1		0.7, 3.4	Mug1		0.1, 3.5			
Reg3a		0.1, 64.0	Rgs16		0.1, 8.6	Myd88		2.1			
Rela	3[a]	0.5	Serpinb5		0.5, 12.1	Ncr3		0.3			

[1]Indicates the reported genes associated with liver regeneration; the letters "a" and "b" at the top right corner of the number "2" respectively indicate "Process of release" and "Cytokine" during the process of release cytokine, the letters "a", "b" and "c" at the top right corner of the number "3" respectively refer to "Cell activation", "Cell proliferation" and "Cell differentiation" in the process of cell activation, proliferation and differentiation.

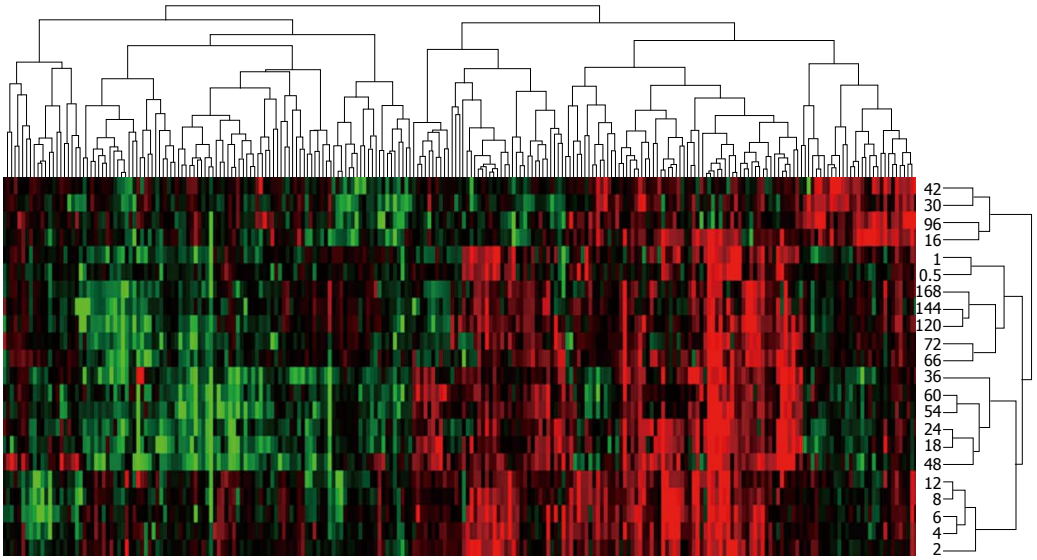

Figure 3 Expression similarity and time relevance clusters of 239 inflammatory response-associated genes during liver regeneration. Detection data of Rat Genome 230 2.0 array were analyzed by H-clustering. Red represents up-regulated genes chiefly associated with promotion of inflammatory response; Green represents down-regulation ones mainly associated with suppression of inflammatory response; Black: No-sense in expression change. The upper and right trees respectively show expression similarity and time series clusters, by which the above genes were classified into 5 and 13 groups separately.

168 h and the up- and down-regulated times were 81 and 25, 55 and 2, 118 and 28, 101 and 31, 93 and 42, 105 and 69, 64 and 44, 41 and 38, 66 and 46, 77 and 65, 68 and 39, 75 and 44, 31 and 21 respectively (Figure 3). The up-regulated genes were chiefly ones promoting inflammatory response, and the down-regulated genes were mostly ones suppressing inflammatory response.

Expression patterns of genes associated with inflammatory response during liver regeneration

Two hundred and thirty-nine genes were categorized into 33 patterns, according to the changes in their expression. (1) up-regulation at one time point, i.e. 4, 6, 16, 18, 30, 48, 96, 120 h after partial hepatectomy (Figure 4A), 11 genes involved; (2) up at two time points, i.e. 6 and 66 h, 12 and 60 h, 16 and 42 h, 16 and 96 h, 24 and 48 h, 30 and 42 h, 36 and 66 h, 48 and 120 h, 72 and 120 h (Figure 4B), 13 genes involved; (3) up at three time points (Figure 4C), 5 genes involved; (4) up at multiple time points (Figure 4D), 6 genes involved; (5) up at one time phase, i.e. 0.5-6 h, 0.5-8 h, 1-48 h, 6-12 h (Figure 4E), 4 genes involved; (6) up at two time phases, i.e. 16-24 h and 42-48 h (Figure 4E), 1 gene involved; (7) up at three time phases (Figure 4E), 1 gene involved; (8) up at multiple time phases (Figure 4E), 1 gene involved; (9) up at one time point/phase, i.e. 0.5 and 4-12 h, 18 and 48-60 h, 48 and 2-24 h, 54 and 6-24 h, 66 and 6-24 h, 96 and 1-24 h, 120 and 2-72 h, 120 and 0.5-8 h (Figure 4F), 8 genes involved; (10) up at one time point/two phases (Figure 4G), 5 genes involved; (11) up at one time point/three phases (Figure 4G), 3 genes involved; (12) up at two time points/one phase (Figure 4H), 7 genes involved; (13) up at two time points/phases (Figure 4I), 6 genes involved; (14) up at two time points/three phases (Figure 4J), 8 genes involved; (15) up at three time points/one phase (Figure 4K), 1 gene involved; (16) up at three time points/two phases (Figure 4K), 6 genes involved; (17) up at multiple time points/phases (Figure 4L), 6 genes involved; (18) down at one time point, i.e. 4, 6, 16, 18, 30, 36, 42, 48, 54, 60, 72, 168 h (Figure 4M, 4N), 28 genes involved; (19) down at two time points, i.e. 0.5 and 48 h, 1 and 72 h, 16 and 42 h, 16 and 30 h, 18 and 54 h, 18 and 168 h, 30 and 42 h, 30 and 96 h, 42 and 66 h (Figure 4O), 11 genes involved; (20) down at three time points (Figure 4O), 2 genes involved; (21) down at multiple time points (Figure 4O), 1 gene involved; (22) down at one phase i.e. 4-8 h, 4-6 h, 4-12 h, 6-12 h (Figure 4P), 4 genes involved; (23) down at two phases, i.e. 18-24 and 48-54 h (Figure 4P), 1 gene involved; (24) down at one time point/phase, i.e. 36 and 48-60 h, 48 and 12-30 h, 48 and 18-24 h, 54 and 18-24 h, 72 and 120-144 h (Figure 4Q), 5 genes involved; (25) down at one time point/two phases (Figure 4Q), 4 genes involved; (26) down at one time point/three phases (Figure 4Q), 2 genes involved; (27) down at two time points/one phase (Figure 4R), 6 genes involved; (28) down at two time points/phases (Figure 4R), 6 genes involved; (29) down at three time points/one phase (Figure 4S), 2 genes involved; (30) down at multiple time points/phases (Figure 4S), 5 genes involved; (31) predominantly up (Figure 4T and U), 25 genes involved; (32) predominantly down (Figure 4V), 14 genes involved; (33) similarly up/down (Figure 4W and X), 31 genes involved.

DISCUSSION

Inflammatory response is a self-protection mechanism formed during the long evolution, closely bound up with higher animal survival. In the process, six proteins including leukotriene B4 receptor (LTB4R), are associated with vascular reactions, through enhancing vascular permeability[21]. In addition, seven other proteins including platelet-activating factor receptor (PTAFR) have a role in increasing vasodilatation and permeability[22]. Four proteins including oxidized low density lipoprotein receptor 1 (OLDLR1) promote leukocytes and proteins to exude from vessels[23]. Four proteins including regenerating islet derived 3 gamma (REG3G) accelerate vasodilatation[24]. Four proteins including amine oxidase copper containing 3 (AOC3) restrain leucocytes to migrate to sites of inflammation[25]. The meaningful expression profiles of the genes encoding the above proteins were the same or similar at some points while different at others, indicating that they may co-regulate vascular reaction. Among them,

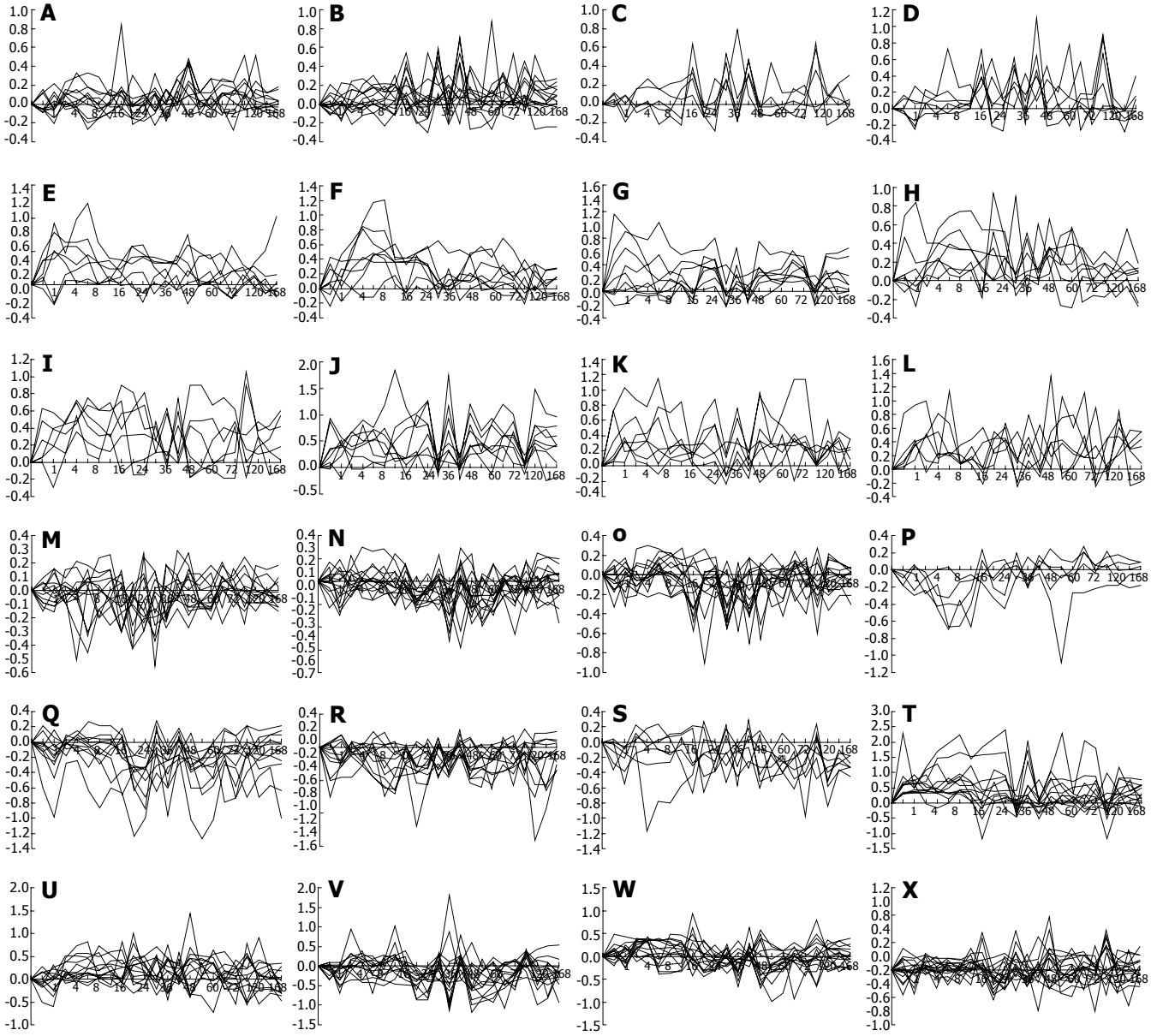

Figure 4 Thirty-three gene expression patterns of 239 inflammatory response-associated genes during liver regeneration. Expression patterns were obtained by the analysis of detection results of Rat Genome 230 2.0 array with Microsoft Excel. **A**-**L**: 92 up-regulated genes; **M**-**S**: 77 down-regulated genes; **T**-**X**: 70 up/down-regulated genes. X-axis represents recovery time after partial hepatectomy (h); Y-axis shows logarithm ratio of the signal values of genes at each time point to control.

aoc3 was up-regulated at 36, 54 and 168 h after PH, and reached a peak at 36 h, which was 6.1 fold of control. *ltb4r* was up- at 6, 18, 36, 48 and 60 h after PH, and reached a peak at 60 h, which was 6 fold of control. *oldlr1* was up- at 2-6, 18-24 and 48-66 h after PH, and reached a peak at 6 h, which was 6.5 fold of control. *ptafr* was up- at 16, 30, 42 and 96 h after PH, and reached a peak at 96 h, which was 7.1 fold of control. *reg3g* was up- at 12 and 36 h after PH, and reached a peak at 36 h, which was 7.5 fold of control. It is assumed that the above genes play a key role in vascular reaction during liver regeneration.

Ten proteins including lipocalin 2 (LCN2), associated with cytokine release, are activated by interleukins to promote inflammation[26]. Integrin beta 2 (ITGB2) stimulates leucocytes to secrete IL-12[27]. Nine proteins including regenerating islet-derived 3 alpha (REG3A) accelerate cytokines synthesis[28]. Fourteen proteins including toll-like receptor 2 (TLR2) increase activation of macrophages[29]. Nine proteins including vacuolar protein sorting 45 (VPS45) stimulate the release of inflammatory factors, such as histamine, bradykinin[30]. The meaningful expression profiles of the genes encoding these proteins, being the same or similar at some points while different at others, indicate that they may co-regulate cytokine release. Among them, *lcn2* was up-regulated at 0.5-24, 36, 48-72 and 120-168 h after partial hepatectomy, and reached a peak at 24 h, which was 257 fold of control. *reg3a* was up- at 12, 36 and 96 h after PH, and reached a peak at 36 h, which was 64 fold of control. *tlr2* was up- at 0.5-8, 18-66 and 120-168 h after PH, and reached a peak at 168 h, which was 10.6 fold of control. *vps45* was up- at 16, 30, 42 and 96 h after PH, and reached a peak at 42 h, which was 12.6 fold of control. It is suggested that the above genes play a key role in cytokine release during liver regeneration.

Twelve proteins including chemokine C-C motif ligand 7 (CCL7), associated with inflammatory response, accelerate T cell migration to sites of inflammation[31]. Nine proteins including plasminogen activator urokinase receptor (PLAUR) promote leukocyte adhesion[32]. Eight proteins including serine or cysteine peptidase inhibitor clade E member 1(SERPINE1) promote inflammatory cell migration[33]. Ten proteins including mitogen-activated protein kinase 8 (MAPK8) promote neutrophils, macrophages and T cells to ooze from blood vessel[34]. ATP-binding cassette sub-family B member 1 (ABCB1) enhances the transduction of inflammatory signaling[35]. Three proteins including alpha-2-macroglobulin (A2M) restrain the activities of various proteases including trypsin, thrombin and collagenase[36]. Twelve proteins including chemokine C-C motif receptor 1 (CCR1) inhibit the activities of leukocyte and inflammatory protein (MIP)-1 by enhancing the chemotaxis of neutrophils, monocytes, lymphocytes and eosinophils[37]. The meaningful expression profiles of these genes showed the sameness or similarity at some points while exhibited difference at others, suggesting that they may regulate the cytokine-mediated inflammation together. Among them, *a2m* was up- at 0.5-24, 36 and 48-54 h, and reached a peak at 8 h, which was 46.2 fold of control. This is generally consistent with the result reported by Scotte *et al*[38]. *serpine1* was up- at 1-48 h, and reached a peak at 6 h, which was 16.7 fold of control. This is in conformity with the result reported by Mueller *et al*[39]. *ccl7* was up- at 1-4, 12, 24, 48, 66 and 144-168 h, and reached a peak at 48 h, which was 22.6 fold of control. *ccr1* was up- at 8-36, 48 and 120 h, and reached a peak at 48 h, which was 27.9 fold of control. *mapk8* was up- at 0.5-24, 48-60, 72 and 144 h, having a peak at 4 h, which was 12 fold of control. *plaur* was up- at 1, 6, 18-24, 48, 72 and 120 h, and had the highest abundance of 13.9 fold at 6 h. It indicates that these genes play a key role in inflammation during liver regeneration.

Among the proteins associated with the inflammatory cell activation, connective tissue growth factor (CTGF) enhances macrophage activity via M-CSF (macrophage colony-stimulating factor)[40]. Eight proteins including cysteine aspartate-specific protease 8 (CASP8) lead inflammatory response by accelerating neutrophil apoptosis[41]. Ten proteins including v-fos FBJ murine osteosarcoma viral oncogene homolog (FOS) accelerate inflammatory response by activating MAPK[42]. Six proteins including forkhead box M1 (FOXM1) induce inflammatory response when they are over expressed[43]. Seven proteins including pancreatitis-associated protein (PAP) inhibit inflammatory response by suppressing the activity of NFκB[44]. Six proteins including fatty acid binding protein 4 (FABP4) inhibit inflammatory response by reducing the activities of NFκB and IκB of macrophages[45]. Eight proteins including interleukin 1 receptor antagonist (IL1RN) decrease inflammatory response by inhibiting the activities of IL1A and IL1B[46]. Four proteins including galanin (GAL) suppress inflammatory response by inhibiting proliferation of thymus cells and macrophages[47]. The meaningful expression profiles of the genes encoding the proteins mentioned above showed the sameness or similarity at some point while exhibited difference at others, implying that they may co-regulate the activity of inflammatory cell. Among them, *ctgf* was up- at 0.5-8, 18-24, 36, 54 and 72 h after PH, and reached a peak at 6 h, which was 13.9 fold of control. This is consistent with the results reported by Pi *et al*[48]. *foxm1* was up- at 1, 18-24, 36, 48-72 and 120 h after PH, and reached a peak at 66 h, which was 13.9 fold of control. This is in line with the results reported by Wang *et al*[43]. *casp8* was up- at 1, 18-24, 36, 48-72 and 120-168 h, and reached a peak at 48 h, which was 10.6 fold of control. *fabp4* was up- at 4, 12-24, 36, 48-72 and 120-168 h, and reached a peak at 120 h, which was 29.9 fold of control. *fos* was up- at 0.5-30, 42-48 and 120 h after PH, and reached a peak at 0.5 h, which was 28.4 fold of control. *gal* was up- at 1-16, 30, 42 and 96-120 h after PH, and reached a peak at 96 h, which was 11.3 fold of control. *il1rn* was up- at 2-24 and 48 h after PH, and reached a peak at 8 h, which was 16.3 fold of control. *pap* was up- at 1-24, 36, 48-54, 66 and 120-144 h after PH, and reached a peak at 12 h, which was 68.6 fold of control. It is assumed that these genes play vital roles in inflammatory cell activation during LR.

Nine proteins including B-cell CLL/lymphoma 6 (BCL6), associated with inflammatory cell proliferation, promote the proliferation of T cells and B cells[49]. Five proteins including selectin E (SELE) promote recruitment of white blood cells to inflammation sites by activating neutrophils[50]. Three proteins including cluster of differentiation 276 (CD276) induced by LPS inhibit T cell proliferation[51]. The meaningful expression profiles of the genes encoding these proteins showed the sameness or similarity at some points while difference at others, indicating that they may modulate inflammatory cell proliferation together. Remarkably, *sele* showed up-regulation at 0.5-2, 16-24, 36, 54-66 and 96-120 h with the highest abundance of 12.9 fold of control at 66 h after PH. *bcl6* was up- at 0.5-12, 24, 48-54, 72 and 120-168 h, and reached a peak at 0.5 h, which was 8.6 times higher than the control. It is supposed that they are important in inflammatory cell proliferation during liver regeneration.

Interleukin 12 receptor beta 2 (IL12RB2), associated with inflammatory cells differentiation, promotes Th1 cells differentiation[52]. Three proteins including thymic stromal lymphopoietin (TSLP) facilitate the differentiation of CD4(+)T cells to Th2 cells[53]. The meaningful expression profiles of the genes encoding these proteins exhibited the sameness or similarity at some points while difference at others, indicating that they may co-regulate inflammatory cell differentiation. Remarkably, *tslp* displayed up-regulation at 18-24, 36, 48-60, 72 and 120-144 h with the highest abundance of 6.1 fold at 18 h after PH, indicating that it is essential to inflammatory cell differentiation during liver regeneration.

Five proteins including complement component 1 q subcomponent receptor 1 (C1QR1), associated with inflammation elimination, can clear dead cells by promoting monocytes, neutrophils and epithelial cells to secrete inflammatory factors[54]. Lysozyme(LYZ) promotes bacterialepicyte dissolution[55]. NADPH oxidase 1, 4 (NOX1, NOX4) accelerate cell aging by catalyzing production of active oxygen[56]. The meaningful expression changes of these genes displaying sameness or similarity at some

points while difference at others indicate that they may co-regulate subsidence of inflammation. Especially, *lyz* was up-regulated at 1-4, 48 and 96 h, and reached a peak at 48 h, which was 3.7 times higher than the control. *nox1* was up- at 0.5-8, 18 and 120 h, and had a peak expression at 2 h, which was 8.6 times higher than the control. *c1qr1* was up- at 0.5-12, 24, 36, 60-72 and 120-168 h, reaching a peak at 8 h, which was 5.5-fold of control. It is supposed that the three genes are of importance in eliminating inflammation during liver regeneration.

In conclusion, the expression changes of the inflammatory response-associated genes after partial hepatectomy in rats have been investigated with high-throughput gene expression analysis. It is preliminarily confirmed that inflammatory response is enhanced during liver regeneration; that Rat Genome 230 2.0 array is a useful tool for analysis of the inflammatory response at the transcriptional level. However, the process of DNA→ mRNA→ protein→ function is influenced by many factors including protein interaction. Therefore, further analyses of our results using techniques, such as Northern blotting, protein chip, RNA interference, protein-interaction are needed.

REFERENCES

1 **Terui K**, Ozaki M. The role of STAT3 in liver regeneration. *Drugs Today (Barc)* 2005; **41**: 461-469
2 **Ogoke BA**. The management of the atlanto-occipital and atlanto-axial joint pain. *Pain Physician* 2000; **3**: 289-293
3 **Higgins GM**, Anderson R M. Experimental pathology of the liver: restoration of the liver of the white rat following partial surgical removal. *J Arch Pathol* 1931; **12**: 186-222
4 **Michalopoulos GK**, DeFrances M. Liver regeneration. *Adv Biochem Eng Biotechnol* 2005; **93**: 101-134
5 **Yamayoshi Y**, Watanabe T, Tanabe M, Hoshino K, Matsumoto K, Morikawa Y, Shimadzu M, Kitajima M, Tanigawara Y. Novel application of ProteinChip technology exploring acute rejection markers of rat small bowel transplantation. *Transplantation* 2006; **82**: 320-326
6 **Nanobashvili KV**, Okropiridze TV, Kapanadze RV. Cytological issues of Curiosin's influence on the inflammatory processes in parodontal tissues. *Georgian Med News* 2006; **135**: 57-60
7 **Hirsch IB**. Inpatient diabetes: review of data from the cardiac care unit. *Endocr Pract* 2006; **12** Suppl 3: 27-34
8 **Taub R**. Liver regeneration: from myth to mechanism. *Nat Rev Mol Cell Biol* 2004; **5**: 836-847
9 **Fausto N**, Campbell JS, Riehle KJ. Liver regeneration. *Hepatology* 2006; **43**: S45-S53
10 **Xu CS**, Zhao LF, Yang KJ, Zhang JB. The origination and action of the hepatic stems cells. *ShiYan ShengWu XueBao* 2004; **37**: 72-77
11 **Sonesson B**, Rosengren E, Hansson AS, Hansson C. UVB-induced inflammation gives increased d-dopachrome tautomerase activity in blister fluid which correlates with macrophage migration inhibitory factor. *Exp Dermatol* 2003; **12**: 278-282
12 **Dransfeld O**, Gehrmann T, Köhrer K, Kircheis G, Holneicher C, Häussinger D, Wettstein M. Oligonucleotide microarray analysis of differential transporter regulation in the regenerating rat liver. *Liver Int* 2005; **25**: 1243-1258
13 **Li L**, Roden J, Shapiro BE, Wold BJ, Bhatia S, Forman SJ, Bhatia R. Reproducibility, fidelity, and discriminant validity of mRNA amplification for microarray analysis from primary hematopoietic cells. *J Mol Diagn* 2005; **7**: 48-56
14 **Hood L**. Leroy Hood expounds the principles, practice and future of systems biology. *Drug Discov Today* 2003; **8**: 436-438
15 **Yue H,** Eastman PS, Wang BB, Minor J, Doctolero MH, Nuttall RL, Stack R, Becker JW, Montgomery JR, Vainer M, Johnston R. An evaluation of the performance of cDNA microarrays for detecting changes in global mRNA expression. *Nucleic Acids Res* 2001; **29**: E41-E41
16 **Knepp JH**, Geahr MA, Forman MS, Valsamakis A. Comparison of automated and manual nucleic acid extraction methods for detection of enterovirus RNA. *J Clin Microbiol* 2003; **41**: 3532-3536
17 **Nuyts S**, Van Mellaert L, Lambin P, Anné J. Efficient isolation of total RNA from Clostridium without DNA contamination. *J Microbiol Methods* 2001; **44:** 235-238
18 **Arkin A**, Ross J, McAdams HH. Stochastic kinetic analysis of developmental pathway bifurcation in phage lambda-infected Escherichia coli cells. *Genetics* 1998; **149**: 1633-1648
19 **Eisen MB**, Spellman PT, Brown PO, Botstein D. Cluster analysis and display of genome-wide expression patterns. *Proc Natl Acad Sci USA* 1998; **95**: 14863-14868
20 **Werner T**. Cluster analysis and promoter modelling as bioinformatics tools for the identification of target genes from expression array data. *Pharmacogenomics* 2001; **2**: 25-36
21 **Toda A**, Yokomizo T, Masuda K, Nakao A, Izumi T, Shimizu T. Cloning and characterization of rat leukotriene B(4) receptor. *Biochem Biophys Res Commun* 1999; **262**: 806-812
22 **Negrão-Corrêa D**, Souza DG, Pinho V, Barsante MM, Souza AL, Teixeira MM. Platelet-activating factor receptor deficiency delays elimination of adult worms but reduces fecundity in Strongyloides venezuelensis-infected mice. *Infect Immun* 2004; **72**: 1135-1142
23 **Honjo M**, Nakamura K, Yamashiro K, Kiryu J, Tanihara H, McEvoy LM, Honda Y, Butcher EC, Masaki T, Sawamura T. Lectin-like oxidized LDL receptor-1 is a cell-adhesion molecule involved in endotoxin-induced inflammation. *Proc Natl Acad Sci USA* 2003; **100**: 1274-1279
24 **Keilbaugh SA**, Shin ME, Banchereau RF, McVay LD, Boyko N, Artis D, Cebra JJ, Wu GD. Activation of RegIIIbeta/gamma and interferon gamma expression in the intestinal tract of SCID mice: an innate response to bacterial colonisation of the gut. *Gut* 2005; **54:** 623-629
25 **Merinen M**, Irjala H, Salmi M, Jaakkola I, Hänninen A, Jalkanen S. Vascular adhesion protein-1 is involved in both acute and chronic inflammation in the mouse. *Am J Pathol* 2005; **166**: 793-800
26 **Cowland JB**, Sørensen OE, Sehested M, Borregaard N. Neutrophil gelatinase-associated lipocalin is up-regulated in human epithelial cells by IL-1 beta, but not by TNF-alpha. *J Immunol* 2003; **171**: 6630-6639
27 **Emoto M**, Miyamoto M, Emoto Y, Yoshizawa I, Brinkmann V, van Rooijen N, Kaufmann SH. Highly biased type 1 immune responses in mice deficient in LFA-1 in Listeria monocytogenes infection are caused by elevated IL-12 production by granulocytes. *J Immunol* 2003; **171**: 3970-3976
28 **Drognitz O**, Michel P, Koczan D, Neeff H, Mikami Y, Obermaier R, Thiesen HJ, Hopt UT, Loebler M. Characterization of ischemia/reperfusion-induced gene expression in experimental pancreas transplantation. *Transplantation* 2006; **81**: 1428-1434
29 **Arbour NC**, Lorenz E, Schutte BC, Zabner J, Kline JN, Jones M, Frees K, Watt JL, Schwartz DA. TLR4 mutations are associated with endotoxin hyporesponsiveness in humans. *Nat Genet* 2000; **25**: 187-191
30 **Rajasekariah P**, Eyre HJ, Stanley KK, Walls RS, Sutherland GR. Molecular cloning and characterization of a cDNA encoding the human leucocyte vacuolar protein sorting (h1Vps45). *Int J Biochem Cell Biol* 1999; **31**: 683-694
31 **Michalec L**, Choudhury BK, Postlethwait E, Wild JS, Alam R, Lett-Brown M, Sur S. CCL7 and CXCL10 orchestrate oxidative stress-induced neutrophilic lung inflammation. *J Immunol* 2002; **168**: 846-852
32 **Shushakova N**, Eden G, Dangers M, Menne J, Gueler F, Luft FC, Haller H, Dumler I. The urokinase/urokinase receptor system mediates the IgG immune complex-induced inflammation in lung. *J Immunol* 2005; **175**: 4060-4068
33 **Aso Y**, Wakabayashi S, Yamamoto R, Matsutomo R, Takebayashi K, Inukai T. Metabolic syndrome accompanied by

hypercholesterolemia is strongly associated with proinflammatory state and impairment of fibrinolysis in patients with type 2 diabetes: synergistic effects of plasminogen activator inhibitor-1 and thrombin-activatable fibrinolysis inhibitor. *Diabetes Care* 2005; **28**: 2211-2216

34 **Stambe C**, Atkins RC, Hill PA, Nikolic-Paterson DJ. Activation and cellular localization of the p38 and JNK MAPK pathways in rat crescentic glomerulonephritis. *Kidney Int* 2003; **64:** 2121-2132

35 **Jansen G**, Scheper RJ, Dijkmans BA. Multidrug resistance proteins in rheumatoid arthritis, role in disease-modifying antirheumatic drug efficacy and inflammatory processes: an overview. *Scand J Rheumatol* 2003; **32**: 325-336

36 **Milosavljevic TS**, Petrovic MV, Cvetkovic ID, Grigorov II. DNA binding activity of C/EBPbeta and C/EBPdelta for the rat alpha2-macroglobulin gene promoter is regulated in an acute-phase dependent manner. *Biochemistry (Mosc)* 2002; **67**: 918-926

37 **Gao JL**, Wynn TA, Chang Y, Lee EJ, Broxmeyer HE, Cooper S, Tiffany HL, Westphal H, Kwon-Chung J, Murphy PM. Impaired host defense, hematopoiesis, granulomatous inflammation and type 1-type 2 cytokine balance in mice lacking CC chemokine receptor 1. *J Exp Med* 1997; **185**: 1959-1968

38 **Scotté M**, Masson S, Lyoumi S, Hiron M, Ténière P, Lebreton JP, Daveau M. Cytokine gene expression in liver following minor or major hepatectomy in rat. *Cytokine* 1997; **9**: 859-867

39 **Mueller L**, Broering DC, Meyer J, Vashist Y, Goettsche J, Wilms C, Rogiers X. The induction of the immediate-early-genes Egr-1, PAI-1 and PRL-1 during liver regeneration in surgical models is related to increased portal flow. *J Hepatol* 2002; **37**: 606-612

40 **Nakao K**, Kubota S, Doi H, Eguchi T, Oka M, Fujisawa T, Nishida T, Takigawa M. Collaborative action of M-CSF and CTGF/CCN2 in articular chondrocytes: possible regenerative roles in articular cartilage metabolism. *Bone* 2005; **36**: 884-892

41 **Alvarado-Kristensson M**, Melander F, Leandersson K, Rönnstrand L, Wernstedt C, Andersson T. p38-MAPK signals survival by phosphorylation of caspase-8 and caspase-3 in human neutrophils. *J Exp Med* 2004; **199**: 449-458

42 **Mahimainathan L**, Ghosh-Choudhury N, Venkatesan BA, Danda RS, Choudhury GG. EGF stimulates mesangial cell mitogenesis via PI3-kinase-mediated MAPK-dependent and AKT kinase-independent manner: involvement of c-fos and p27Kip1. *Am J Physiol Renal Physiol* 2005; **289**: F72-F82

43 **Wang X**, Bhattacharyya D, Dennewitz MB, Kalinichenko VV, Zhou Y, Lepe R, Costa RH. Rapid hepatocyte nuclear translocation of the Forkhead Box M1B (FoxM1B) transcription factor caused a transient increase in size of regenerating transgenic hepatocytes. *Gene Expr* 2003; **11**: 149-162

44 **Vasseur S**, Folch-Puy E, Hlouschek V, Garcia S, Fiedler F, Lerch MM, Dagorn JC, Closa D, Iovanna JL. p8 improves pancreatic response to acute pancreatitis by enhancing the expression of the anti-inflammatory protein pancreatitis-associated protein I. *J Biol Chem* 2004; **279**: 7199-7207

45 **Makowski L**, Brittingham KC, Reynolds JM, Suttles J, Hotamisligil GS. The fatty acid-binding protein, aP2, coordinates macrophage cholesterol trafficking and inflammatory activity. Macrophage expression of aP2 impacts peroxisome proliferator-activated receptor gamma and IkappaB kinase activities. *J Biol Chem* 2005; **280**: 12888-12895

46 **Pastor IJ**, Laso FJ, Romero A, González-Sarmiento R. Interleukin-1 gene cluster polymorphisms and alcoholism in Spanish men. *Alcohol Alcohol* 2005; **40**: 181-186

47 **Qinyang W**, Hultenby K, Adlan E, Lindgren JU. Galanin in adjuvant arthritis in the rat. *J Rheumatol* 2004; **31**: 302-307

48 **Pi L**, Oh SH, Shupe T, Petersen BE. Role of connective tissue growth factor in oval cell response during liver regeneration after 2-AAF/PHx in rats. *Gastroenterology* 2005; **128**: 2077-2088

49 **Dogan A**, Burke JS, Goteri G, Stitson RN, Wotherspoon AC, Isaacson PG. Micronodular T-cell/histiocyte-rich large B-cell lymphoma of the spleen: histology, immunophenotype, and differential diagnosis. *Am J Surg Pathol* 2003; **27**: 903-911

50 **Bevilacqua MP**, Stengelin S, Gimbrone MA, Seed B. Endothelial leukocyte adhesion molecule 1: an inducible receptor for neutrophils related to complement regulatory proteins and lectins. *Science* 1989; **243**: 1160-1165

51 **Prasad DV**, Nguyen T, Li Z, Yang Y, Duong J, Wang Y, Dong C. Murine B7-H3 is a negative regulator of T cells. *J Immunol* 2004; **173**: 2500-2506

52 **Akahoshi M**, Ishihara M, Remus N, Uno K, Miyake K, Hirota T, Nakashima K, Matsuda A, Kanda M, Enomoto T, Ohno S, Nakashima H, Casanova JL, Hopkin JM, Tamari M, Mao XQ, Shirakawa T. Association between IFNA genotype and the risk of sarcoidosis. *Hum Genet* 2004; **114**: 503-509

53 **Ito T**, Wang YH, Duramad O, Hori T, Delespesse GJ, Watanabe N, Qin FX, Yao Z, Cao W, Liu YJ. TSLP-activated dendritic cells induce an inflammatory T helper type 2 cell response through OX40 ligand. *J Exp Med* 2005; **202**: 1213-1223

54 **Bohlson SS**, Silva R, Fonseca MI, Tenner AJ. CD93 is rapidly shed from the surface of human myeloid cells and the soluble form is detected in human plasma. *J Immunol* 2005; **175**: 1239-1247

55 **Kaur G**, Sarwar Alam M, Athar M. Nimbidin suppresses functions of macrophages and neutrophils: relevance to its antiinflammatory mechanisms. *Phytother Res* 2004; **18**: 419-424

56 **Plesková M**, Beck KF, Behrens MH, Huwiler A, Fichtlscherer B, Wingerter O, Brandes RP, Mülsch A, Pfeilschifter J. Nitric oxide down-regulates the expression of the catalytic NADPH oxidase subunit Nox1 in rat renal mesangial cells. *FASEB J* 2006; **20**: 139-141

S- Editor Liu Y **L- Editor** Zhu LH **E- Editor** Bi L

PO Box 2345, Beijing 100023, China
www.wjgnet.com
wjg@wjgnet.com

World J Gastroenterol 2007 January 21; 13(3): 378-382
World Journal of Gastroenterology ISSN 1007-9327

BASIC RESEARCH

Effect of emodin on pancreatic fibrosis in rats

Cai-Hua Wang, Zhi-Qiang Gao, Bing Ye, Jian-Ting Cai, Chuan-Gao Xie, Ke-Da Qian, Qin Du

Cai-Hua Wang, Zhi-Qiang Gao, Bing Ye, Jian-Ting Cai, Chuan-Gao Xie, Ke-Da Qian, Qin Du, Department of Gastroenterology, 2nd Affiliated Hosipital, School of Medicine, Zhejiang University, Hangzhou 310009, Zhejiang Province, China
Supported by a grant from Science and Technology Bureau of Zhejiang Province, No. J30448
Correspondence to: Dr. Cai-Hua Wang, Department of Gastroenterology, 2nd Affiliated Hosipital, School of Medicine, Zhejiang University, Hangzhou 310009, Zhejiang Province, China. wangcaihua66@163.com
Telephone: +86-571-87783564 Fax: +86-571-87068001
Received: 2006-10-19 Accepted: 2006-11-06

Abstract

AIM: To establish the rats model of chronic fibrosing pancreatitis and to prove the anti-fibrotic effect of emodin in chronic pancreatitis with fibrosis.

METHODS: Fifty rats were randomly divided into five groups, 10 rats in each group. Trinitrobenzene sulfonic acid (TNBS) was infused into the pancreatic duct to induce chronic pancreatitis in rats (except for normal group). Emodin-treated rats were fed with different doses of emodin (20, 40 and 80 mg/kg body weight) for 28 d, while normal group and control group received 0.9% sodium chloride solution. Serum levels of hyaluronic acid (HA) and laminin (LN) were determined by radioimmunoassay. Histopathological alterations were studied by optical microscopy. Expression of collagen was also examined while transforming growth factor-beta-1 (TGF-β_1) was localized by immunochemistry.

RESULTS: In emodin-treated rats, the serum levels of HA and LN were decreased significantly (HA, 62.2 ± 19.3 μg/L *vs* 112.7 ± 26.5 μg/L, $P < 0.05$; LN 44.3 ± 10.4 μg/L *vs* 86.2 ± 16.5 μg/L, $P < 0.05$); the degree of fibrosis was ameliorated observably; the expression of collagen in pancreatic tissue was reduced especially in high-dose emodin-treated group (36% ± 5% *vs* 42% ± 6%, $P < 0.05$); with the increased doses of emodin, the expression of TGF-β_1 was declined, compared with those in control group.

CONCLUSION: Emodin has an anti-fibrotic effect on pancreatic fibrosis in rats. Because of its anti-fibrotic effect, it could be a potential herb for the treatment of chronic pancreatitis.

Key words: Emodin; Fibrosis; Chronic pancreatitis; Animal model

Wang CH, Gao ZQ, Ye B, Cai JT, Xie CG, Qian KD, Du Q. Effect of emodin on pancreatic fibrosis in rats. *World J Gastroenterol* 2007; 13(3): 378-382

http://www.wjgnet.com/1007-9327/13/378.asp

INTRODUCTION

Chronic pancreatitis is characterized morphologically by a progressive pancreatic fibrotic process[1]. Extracellular matrix (ECM) components are distributed in both healthy and diseased pancreas, and there is an increased deposition of disorganized ECM components in chronic pancreatitis[2]. However, the mechanism of the fibrotic process is not fully understood. Progressive fibrosis is a characteristic feature of chronic pancreatitis of various etiologies, thus anti-fibrosis is the key to the therapy of chronic pancreatitis. However, no ideal treatment is available yet. Could traditional Chinese herbs be effective? Emodin (1, 3, 8-trihydroxy-6-methylanthraquinone) isolated from a great deal of herbs is an effective constituent with many effects. Lots of pharmaceutical studies have demonstrated that emodin has many biological effects[3-5], such as anticancer, antimicrobial, and anti-inflammatory effects, *etc*. Moreover, several studies[6,7] have revealed that emodin is efficacious in the management of acute pancreatitis and hepato-cirrhosis, but studies on chronic pancreatitis are rare. We designed this experiment to investigate the effect of emodin on pancreatic fibrosis in rats, and elucidate its potential therapeutic mechnisms.

MATERIALS AND METHODS

Materials

Male Sprague-Dawley rats weighing 200-250 g were provided by the Animal Center of Zhejiang University. Trinitrobeneze sulfonic acid (TNBS) was obtained from Sigma Chemical Company. Radioimmunoassay kits of rat hyaluronic acid (HA) and laminin (LN) were purchased from Shanghai Tiancheng Science and Technology Ltd. Emodin was offered by Hunan Huaguang Chemical Company. TGF-β_1 polyclonal antiboby was provided by Santa Cruz Company. Immunochemistry kits (Envision TM) were offered by DAKO, Denmark.

Grouping and animal model

Fifty male Sprague-Dawley rats were randomly divided into five groups, 10 rats in each group. A chronic pancreatitis model was induced in rats by infusion of TNBS into the pancreatic duct with a modification of the method

Table 1 Grading of pancreatic fibrosis

Grade	Duct dilation	Periductal fibrosis	Intralobular fibrosis	Glandular atrophy
F0	-	-	-	-
F1	+	-	-	-
F2	+	+	-	-
F3	+	+	+	-
F4	+	+	+	+

described by Puig-Divi *et al*[8] (except for normal group). After fasted for 3 d, the rats in group 1 (normal group, nonoperation) and group 2 (control group, nontreating) received oral 0.9% sodium chloride solution. Emodin-treated rats in groups 3-5 were fed with different doses of emodin (20, 40 and 80 mg/kg body mass). Twenty-eight days after treatment, all rats were killed. Pancreatic tissues and blood samples were collected and kept for further study.

Measurement of serum HA and LN

Blood samples were obtained 28 d after treatment, and serum levels of HA and LN were determined by radioimmunoassay.

Histological examination

Paraffin sections of rat pancreatic tissue were stained with hematoxylin and eosin. We evaluated the morphologic changes by light-microscopy. Grading of pancreatic fibrosis was carried out as previously described[9] (Table 1).

Mesurement of collagen expression

Pancreatic fibrosis was observed by the Van Gieson staining, semi-quantitative analysis of collagen fibres was carried out by the KS400 imaging analysis system (KS400 ver. 2.0).

Immunochemistry

Paraffin-embedded tissue sections were subjected to immunostaining using the DAKO EnVisin two-step procedure. Tissue sections were submerged for 10 min in Tris buffered saline (TBS) (10 mmol/L Tris-HCl, 0.85% NaCl, pH 7.4) containing 3% hydrogen peroxide in order to quench the endogenous peroxidase activity. Following washing with distilled water, the sections were incubated in TBS with polyclonal antibodies against TGF-β_1 diluted at 1:200 for 30 min. After 10-min washing with TBS, the sections were incubated with Envision TM for another 30 min. After washing with TBS for 10 min, the sections were incubated with diaminobenzidine (DAB) as a substrate and counterstained. The results were evaluated by microscopy. All samples were classified according to the percentage of TGF-β_1 positive cells (brown colour reaction). We defined 0 as no, + as 0%-25%, +2 as 25%-50%, +3 as 50%-75%, +4 as > 75%.

Statistical analysis

Serum levels of HA and LN and pancreatic collagen content were expressed as mean ± SE. Student's *t* test was used for statistical analysis. Chi square test was used for the ranked data statistical analysis. If the expected cell count was less than or equal to 5, Fisher's exact test was used. SPSS 11.0 was used for statistical analysis, and $P < 0.05$ was considered statistically significant.

Table 2 Effect of emodin on serum hyaluronic acid (HA) and laminin (LN) (mean ± SE)

Group	*n*	HA (μg/L)	LN (μg/L)
1 (Normal)	10	55.2 ± 23.7	40.5 ± 12.2
2 (Control)	8	112.7 ± 26.5[b]	86.2 ± 16.5[b]
3 (emodin, 20 mg/kg)	8	86.6 ± 22.1[a]	66.8 ± 14.4[a]
4 (emodin, 40 mg/kg)	8	78.0 ± 24.5[d]	56.7 ± 12.3[a]
5 (emodin, 80 mg/kg)	9	62.2 ± 19.3[d]	44.3 ± 10.4[d]

[b]$P < 0.01$ *vs* group 1; [a]$P < 0.05$, [d]$P < 0.01$ *vs* group 2.

RESULTS

Survival rate of rats

The survival rate was 83.3% in emodin-treated groups (25/30) and 80.0% (8/10) in control group. However, no significant difference was found between these groups.

Serum HA and LN

The mean serum level of HA and LN was the lowest in normal group (group 1, $P < 0.05$), and the levels of HA and LN were significantly lower in emodin-treated groups (groups 3-5) than in control group (group 2, $P < 0.05$). With the increased doses of emodin, the serum levels of HA and LN were decreased in emodin-treated groups, but there was no statistically significant difference between them (Table 2).

Histopathological examination

Pancreatic fibrosis was evaluated according to the criteria described above (Table 1), and the results are shown in Figure 1. The extent of fibrosis was much milder in emodin-treated groups than in control group. Structural changes such as periductal fibrosis, intralobular fibrosis and glandular atrophy were ameliorated. With the increased doses of emodin, the changes were significantly improved.

Pancreatic collagen content

Pancreatic collagen was detected by Van Gieson staining. An extensive accumulation of collagen and glandular atrophy were found in control group, while the accumulation of collagen was decreased and no glandular atrophy was found in emodin-treated groups. We obtained the positive proportions of Van Gieson staining by the imaging analysis system. The positive proportions in each group are shown in Table 3. With the increased doses of emodin, the changes were improved obviously. Only a significant difference was found between group 5 and group 2 ($P < 0.05$).

Immunochemistry

Four groups (except for normal group) showed TGF-β_1 expression (brown colour reaction) (Figure 2). The

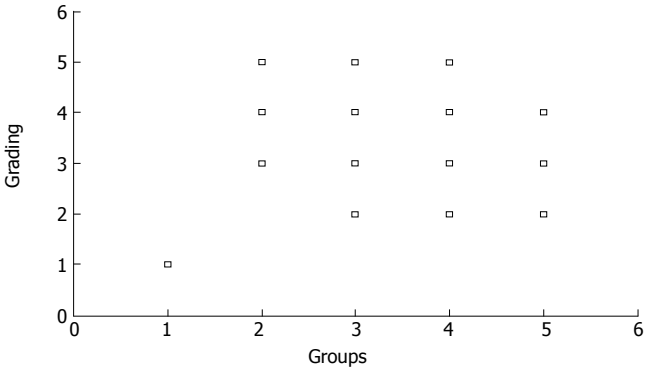

Figure 1 Effect of emodin on histopathological alterations in rats. Grading: 1 = F0, 2 = F1, 3 = F2, 4 = F3, 5 = F4, 6 = F5.

results are shown in Table 4. With the increased doses of emodin, the changes were improved obviously, similar to the above results. For the sake of statistical analysis, we divied all samples into two large groups: low expression of TGF-β_1 (0, +1, +2) and high expression of TGF-β_1 (+3, +4). Fisher's exact test was used for statistical analysis. Compared with group 2 (0 rat in low expression group and 8 rats in high expression group), a significant difference was found between group 4 (7 rats in low expression group and 1 rat in high expression group) and group 5 (9 rats in low expression group and 0 rat in high expression group) ($P < 0.05$). Compared with group 3 (4 rats in low expression group and 4 rats in high expression group), only group 5 had a significant difference ($P < 0.05$). There was no statistically significant difference between any other two groups.

Table 3 Pancreatic collagen content in different groups (mean ± SE, %)

Group	*n*	Positive proportion
2 (Control)	8	42 ± 6
3 (emodin, 20 mg/kg)	8	39 ± 7
4 (emodin, 40 mg/kg)	8	38 ± 4
5 (emodin, 80 mg/kg)	9	36 ± 5[a]

[a]$P < 0.05$ *vs* group 2.

Table 4 Immunochemistry results in different groups (percentage of TGF-β_1 positive cells)

Group	*n*	0	+	+2	+3	+4
1 (Normal)	10	9	1	0	0	0
2 (Control)	8	0	0	0	4	4
3 (emodin, 20 mg/kg)	8	0	0	4	4	0
4 (emodin, 40 mg/kg)	8	0	4	3	1	0
5 (emodin, 80 mg/kg)	9	4	5	0	0	0

0: No; +: 0%-25%; + 2: 25%-50%; + 3: 50%-75%; + 4: > 75%.

DISCUSSION

The incidence of chronic pancreatitis is increasing, and the most important etiological factor is alcohol. The pathogenesis of chronic pancreatitis has not been completely understood. Nevertheless, it was reported that various factors such as TGF-β_1, ECM, oxidative stress *etc,* are involved in the progression of pancreatic fibrosis[10,11]. Since pancreatic fibrosis is the characteristic feature of chronic pancreatitis, preventing and inverting pancreatic fibrosis is the key to therapy of chronic pancreatitis and amelioration of its prognosis.

Drugs which could prevent or invert pancreatic fibrosis might be developed and interventioned for the treatment of chronic pancreatitis with fibrosis. Emodin isolated from a great deal of herbs is an effective constituent with many effects[3-5]. It was reported that emodin could inhibit the expression of α-smooth muscle actin (α-SMA) and reduce the transformation and synthesis of TGF-β_1[6]. Some researchers observed that emodin could inhibit transformation of hepatic stellate cells (HSCs) from G_1 phase to S phase and S phase to G_2 phase that could prevent HSC proliferation. It also has been reported that emodin could inhibit lipid peroxidation[12]. However, previous studies of emodin mainly focused on how to inhibit liver fibrosis, while studies on pancreatic fibrosis are rare. The aim of this research was to study the effect of emodin on pancreatic fibrosis, and the results of our study indicate that emodin has an anti-fibrotic effect on pancreatic fibrosis in rats.

Cells similar to HSCs have been identified and isolated from the pancreas, known as pancreatic stellate cells (PSCs)[13,14]. It was reported that PSCs are activated in both experimental and human pancreatic fibrosis and these activated PSCs are the main cellular source of collagen in chronic pancreatitis[15], suggesting that pathological alteration of pancteatic fibrosis is similar to liver fibrosis, and may share the same mechanism of fibrosis and anti-fibrosis.

The potential mechanisms of emodin include the following aspects. The first is cell protection. As we know, tissue injury is the first step of fibrosis. Apte *et al*[16] showed that activated PSCs around the pancreatic micrangium express α-SMA, which could aggravate fibrosis of the pancreas, because of vasoconstriction and pancreatic ischemia caused by α-SMA. Emodin could protect pancreatic cells and organs from impairment. In our study, the extent of fibrosis was much milder in emodin-treated groups than in control group. This may be the first mechanism of emodin's anti-fibrotic effect. The second is the effect of emodin on cytokines. PSCs produce ECM after stimulation with TGF-β_1, platelet-derived growth factor (PDGF), *etc*[17]. It was reported that TGF is the key regulating factor of fibrosis. Modulation of TGF-β signaling may be the therapeutic target for the prevention of chronic pancreatitis[18]. It was reported that emodin could inhibit the expression of TGF-β_1 in liver fibrosis model of rats[6]. Imanishi *et al*[19] found that emodin could modulate the effect of PDGF, which could slow down the progression of fibrosis. In our study, emodin-treated groups showed low expression of TGF-β_1, especially in high-dose emodin-treated group. Emodin could counteract cytokines and their receptors, which are

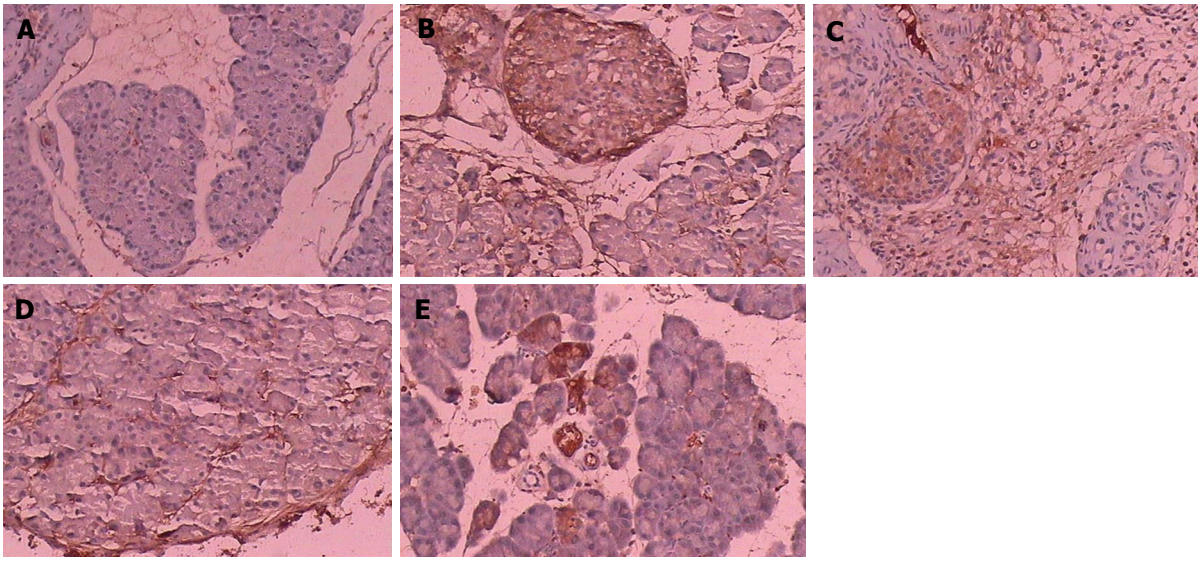

Figure 2 Pancreatic immunochemistry changes in normal group (**A**), control group (**B**) and 20 mg/kg (**C**), 40 mg/kg (**D**) and 80 mg/kg (**E**) emodin-treated groups (× 100). Normal group had no TGF-β_1 expression (brown color reaction), control group had the highest expression of TGF-β_1 while 20, 40 and 80 mg/kg emodin-treated groups had different levels of TGF-β_1 expression.

relevant to the progression of fibrosis, and then brings its anti-fibrotic effect into play. The third is the regulatory effect of emodin on ECM metabolism. Disbalance in ECM metabolism is the common way of fibrosis. Chronic pancreatitis is due to the cumulative intrapancreatic ECM deposition. ECM is consisted of collagens and noncollagenous glycoproteins (fibronectin, laminin). It was reported that serum HA and LN are two important markers responsible for the degrees of fibrosis[20]. Our study revealed that the serum levels of HA and LN were significantly lower in emodin-treated groups than in control group, suggesting that emodin can affect the metabolism of ECM. However, the exact mechanism by which emodin regulates the content of ECM still needs further investigation. The fourth is the effect of emodin on ECM-producing cells. PSCs rapidly proliferate following injury and are the major source of pancreatic ECM component during pancreatic fibrogenesis, and accumulating evidence has placed PSCs at the center of pancreatic fibrosis[15]. Emodin not only inhibits proliferation and activation of PSCs, but also induces their apoptosis. This is another mechanism underlying the anti-fibrotic effect of emodin. The fifth is the antioxidizing effect of emodin. Yoo and co-workers[11] reported that oxidative stress is principally involved in the pathogenesis of chronic pancreatitis with fibrosis and antioxidants could prevent and ameliorate the extent of pancreatic fibrosis, suggesting that antioxidants can be considered in preventing and treating chronic pancreatitis. Eomdin could inhibit lipid peroxidation[12], and antioxidization maybe another mechanism underlying the anti-fibrotic effect of emodin.

Chronic pancreatitis is a progressive pancreatic fibrotic process, and anti-fibrosis is the key therapy for liver fibrosis. However, previous studies on the effect of emodin on chronic pancreatitis in rats are not available. Our study showed that emodin had an effect on pancreatic fibrosis in rats.

The results of this study indicate that emodin can significantly affect the development of pancreatic fibrosis by reducing the serum levels of HA and LN, ameliorating the degrees of fibrosis, diminishing the content of collagen, inhibiting TGF-β_1 expression. Therefore emodin has an excellent prospect in the development of some new praeparatum for the management of chronic pancreatits. However, there are still some questions we need to answer, such as whether emodin can be used in patients with chronic pancreatitis, whether it is safe, since few previous data are available so far. Further detailed experiments and clinical trails are required to prove the potential clinical application. As a traditional herb, emodin also has a long long way to go.

COMMENTS

Background

Chronic pancreatitis is characterized by a progressive pancreatic fibrotic process. However, the mechanism of fibrotic process is not fully understood. Thus anti-fibrosis is the key to the therapy of chronic pancreatitis.

Research frontiers

Emodin has many biological effects, but studies about its application in chronic pancreatitis are rare.

Innovations and breakthroughs

There are few studies on the application of emodin in chronic pancreatitis. We designed this experiment to investigate the effect of emodin on pancreatic fibrosis.

Applications

No ideal therapy is available so far for the treatment of chronic pancreatitis. Emodin may be efficacious in the management of chronic pancreatitis in rats.

Terminology

Emodin (1, 3, 8-trihydroxy-6-methylanthraquinone), isolated from a great deal of herbs, is an effective constituent with many effects, such as anticancer, antimicrobial, and anti-inflammatory effects, *etc*.

Peer review

The topic is of interest because up to now no antifibrotic treatment option is

available in patients with chronic pancreatitis. The positive effect of emodin on development of pancreatic fibrosis described in this paper shows that emodin may be a potential treatment option.

REFERENCES

1 **Keith RG**. Definition and classification of chronic pancreatitis. *World J Surg* 2003; **27**: 1172-1174
2 **Kennedy RH**, Bockman DE, Uscanga L, Choux R, Grimaud JA, Sarles H. Pancreatic extracellular matrix alterations in chronic pancreatitis. *Pancreas* 1987; **2**: 61-72
3 **Zhang L**, Chang CJ, Bacus SS, Hung MC. Suppressed transformation and induced differentiation of HER-2/neu-overexpressing breast cancer cells by emodin. *Cancer Res* 1995; **55**: 3890-3896
4 **Chang CH**, Lin CC, Yang JJ, Namba T, Hattori M. Anti-inflammatory effects of emodin from ventilago leiocarpa. *Am J Chin Med* 1996; **24**: 139-142
5 **Kuo YC**, Meng HC, Tsai WJ. Regulation of cell proliferation, inflammatory cytokine production and calcium mobilization in primary human T lymphocytes by emodin from Polygonum hypoleucum Ohwi. *Inflamm Res* 2001; **50**: 73-82
6 **Zhan YT**, Liu B, Li DG, Bi CS. Mechanism of emodin for antifibrosis of liver. *Zhonghua Ganzangbing Zazhi* 2004; **12**: 245-246
7 **Lou KX**, Gong ZH, Yuan YZ. Study on effect of emodin on TGF beta 1 expression in pancreatic tissue of rats suffering from acute pancreatitis. *Zhongguo Zhongxiyi Jiehe Zazhi* 2001; **21**: 433-436
8 **Puig-Diví V**, Molero X, Salas A, Guarner F, Guarner L, Malagelada JR. Induction of chronic pancreatic disease by trinitrobenzene sulfonic acid infusion into rat pancreatic ducts. *Pancreas* 1996; **13**: 417-424
9 **Chinese Medical Association**. Prevention and treatment of Viral Hepatitis. *Zhonghua Neike Zazhi* 2001; **40**: 62-68
10 **Yoshikawa H**, Kihara Y, Taguchi M, Yamaguchi T, Nakamura H, Otsuki M. Role of TGF-beta1 in the development of pancreatic fibrosis in Otsuka Long-Evans Tokushima Fatty rats. *Am J Physiol Gastrointest Liver Physiol* 2002; **282**: G549-G558
11 **Yoo BM**, Oh TY, Kim YB, Yeo M, Lee JS, Surh YJ, Ahn BO, Kim WH, Sohn S, Kim JH, Hahm KB. Novel antioxidant ameliorates the fibrosis and inflammation of cerulein-induced chronic pancreatitis in a mouse model. *Pancreatology* 2005; **5**: 165-176
12 **Huang SS**, Yeh SF, Hong CY. Effect of anthraquinone derivatives on lipid peroxidation in rat heart mitochondria: structure-activity relationship. *J Nat Prod* 1995; **58**: 1365-1371
13 **Apte MV**, Haber PS, Applegate TL, Norton ID, McCaughan GW, Korsten MA, Pirola RC, Wilson JS. Periacinar stellate shaped cells in rat pancreas: identification, isolation, and culture. *Gut* 1998; **43**: 128-133
14 **Bachem MG**, Schneider E, Gross H, Weidenbach H, Schmid RM, Menke A, Siech M, Beger H, Grünert A, Adler G. Identification, culture, and characterization of pancreatic stellate cells in rats and humans. *Gastroenterology* 1998; **115**: 421-432
15 **Apte MV**, Haber PS, Darby SJ, Rodgers SC, McCaughan GW, Korsten MA, Pirola RC, Wilson JS. Pancreatic stellate cells are activated by proinflammatory cytokines: implications for pancreatic fibrogenesis. *Gut* 1999; **44**: 534-541
16 **Apte MV**, Phillips PA, Fahmy RG, Darby SJ, Rodgers SC, McCaughan GW, Korsten MA, Pirola RC, Naidoo D, Wilson JS. Does alcohol directly stimulate pancreatic fibrogenesis? Studies with rat pancreatic stellate cells. *Gastroenterology* 2000; **118**: 780-794
17 **Schneider E**, Schmid-Kotsas A, Zhao J, Weidenbach H, Schmid RM, Menke A, Adler G, Waltenberger J, Grünert A, Bachem MG. Identification of mediators stimulating proliferation and matrix synthesis of rat pancreatic stellate cells. *Am J Physiol Cell Physiol* 2001; **281**: C532-C543
18 **Yoo BM**, Yeo M, Oh TY, Choi JH, Kim WW, Kim JH, Cho SW, Kim SJ, Hahm KB. Amelioration of pancreatic fibrosis in mice with defective TGF-beta signaling. *Pancreas* 2005; **30**: e71-e79
19 **Imanishi Y**, Maeda N, Otogawa K, Seki S, Matsui H, Kawada N, Arakawa T. Herb medicine Inchin-ko-to (TJ-135) regulates PDGF-BB-dependent signaling pathways of hepatic stellate cells in primary culture and attenuates development of liver fibrosis induced by thioacetamide administration in rats. *J Hepatol* 2004; **41**: 242-250
20 **Zheng M**, Cai W, Weng H, Liu R. Determination of serum fibrosis indexes in patients with chronic hepatitis and its significance. *Chin Med J* (Engl) 2003; **116**: 346-349

S- Editor Wang GP **L- Editor** Wang XL **E- Editor** Bi L

PO Box 2345, Beijing 100023, China
www.wjgnet.com
wjg@wjgnet.com

World J Gastroenterol 2007 January 21; 13(3): 383-390
World Journal of Gastroenterology ISSN 1007-9327

CLINICAL RESEARCH

A specific gene-expression signature quantifies the degree of hepatic fibrosis in patients with chronic liver disease

Tohru Utsunomiya, Masahiro Okamoto, Shigeki Wakiyama, Masaji Hashimoto, Kengo Fukuzawa, Takahiro Ezaki, Shinichi Aishima, Yasuji Yoshikawa, Taizo Hanai, Hiroshi Inoue, Graham F Barnard, Masaki Mori

Tohru Utsunomiya, Masahiro Okamoto, Hiroshi Inoue, Masaki Mori, Department of Molecular and Surgical Oncology, Medical Institute of Bioregulation, Kyushu University, Beppu, Japan
Yasuji Yoshikawa, Department of Pathology, Medical Institute of Bioregulation, Kyushu University, Beppu, Japan
Shigeki Wakiyama, Department of Surgery, Iizuka Hospital, Iizuka, Japan
Masaji Hashimoto, Department of Digestive Surgery, Toranomon Hospital and Okinaka Memorial Institute for Medical Research, Tokyo, Japan
Kengo Fukuzawa, Department of Surgery, Oita Red Cross Hospital, Oita, Japan
Takahiro Ezaki, Department of Surgery, Hiroshima Red Cross Hospital and Atomic Bomb Survivors Hospital, Hiroshima, Japan
Shinichi Aishima, Department of Anatomic pathology, Graduate School of Medical Sciences, Kyushu University, Fukuoka, Japan
Taizo Hanai, Laboratory for Bioinformatics, Graduate School of Systems Life Sciences, Kyushu University, Fukuoka, Japan
Graham F Barnard, Division of Gastroenterology, University of Massachusetts Medical School, Worcester, MA, United States
Supported partly by Grants-in-Aid for Scientific Research (S) (17109013) and for Scientific Research (C) (17591411 and 15591411), a Health and Labor Sciences Research Grant on Hepatitis and BSE (14230801), the Uehara Memorial Foundation, Yasuda Medical Research Foundation, Japanese Foundation for Multidisciplinary Treatment of Cancer, and Princes Takamatsu Cancer research Fund
Correspondence to: Dr. Masaki Mori, Department of Molecular and Surgical Oncology, Medical Institute of Bioregulation, Kyushu University, Tsurumihara 4546, Beppu 874-0838, Japan. mmori@tsurumi.beppu.kyushu-u.ac.jp
Telephone: +81-977-271650 Fax: +81-977-271651
Received: 2006-08-05 Accepted: 2006-09-22

Abstract

AIM: To study a more accurate quantification of hepatic fibrosis which would provide clinically useful information for monitoring the progression of chronic liver disease.

METHODS: Using a cDNA microarray containing over 22000 clones, we analyzed the gene-expression profiles of non-cancerous liver in 74 patients who underwent hepatic resection. We calculated the ratio of azan-stained: total area, and determined the morphologic fibrosis index (MFI), as a mean of 9 section-images. We used the MFI as a reference standard to evaluate our method for assessing liver fibrosis.

RESULTS: We identified 39 genes that collectively showed a good correlation (r > 0.50) between gene-expression and the severity of liver fibrosis. Many of the identified genes were involved in immune responses and cell signaling. To quantify the extent of liver fibrosis, we developed a new genetic fibrosis index (GFI) based on gene-expression profiling of 4 clones using a linear support vector regression analysis. This technique, based on a supervised learning analysis, correctly quantified the various degrees of fibrosis in both 74 training samples (r = 0.76, 2.2% *vs* 2.8%, P < 0.0001) and 12 independent additional test samples (r = 0.75, 9.8% *vs* 8.6%, P < 0.005). It was far better in assessing liver fibrosis than blood markers such as prothrombin time (r = -0.53), type Ⅳ collagen 7s (r = 0.48), hyaluronic acid (r = 0.41), and aspartate aminotransferase to platelets ratio index (APRI) (r = 0.38).

CONCLUSION: Our cDNA microarray-based strategy may help clinicians to precisely and objectively monitor the severity of liver fibrosis.

Key words: Liver fibrosis; Hepatitis virus; DNA microarray; Supervised learning analysis; Scoring system

Utsunomiya T, Okamoto M, Wakiyama S, Hashimoto M, Fukuzawa K, Ezaki T, Aishima S, Yoshikawa Y, Hanai T, Inoue H, Barnard GF, Mori M. A specific gene-expression signature quantifies the degree of hepatic fibrosis in patients with chronic liver disease. *World J Gastroenterol* 2007; 13(3): 383-390

http://www.wjgnet.com/1007-9327/13/383.asp

INTRODUCTION

The prognosis and management of chronic liver diseases often depends heavily on the degree of liver fibrosis. This is particularly true of viral hepatitis, where chronic hepatitis B and C infections affect as many as 370 and 130 million persons respectively worldwide[1,2]. Liver histology has been the gold standard for monitoring hepatic fibrosis. In response to a need for critical evaluation of fibrosis in controlled therapeutic trials, a variety of staging systems have been developed[3,4]. However, intra- and inter-observer variability has resulted in discrepant staging, even in studies involving expert hepatopathologists[5]. Alternatively, several serum markers, such as alpha2 macroglobulin

and hyaluronic acid, have substantial predictive value for the diagnosis of cirrhosis, but not the important earlier stages of liver fibrosis[6]. Therefore development of a new comprehensive and objective evaluation system to quantify the extent of liver fibrosis is important. More recently, the value of noninvasive assessments of liver fibrosis, such as liver stiffness (Fibroscan) and METAVIR fibrosis score have been studied[7-10]. However, no standard diagnostic modality is currently established for assessing liver fibrosis.

To date, there are a few DNA microarray studies investigating gene-expression patterns of non-cancerous liver from patients with chronic liver disease[11-15]. These studies successfully identified differentially regulated genes in liver fibrosis, but none investigated any correlation between gene-expression profiles and the extent of liver fibrosis. In our recent report[16], we demonstrated that a specific gene-expression signature can objectively and accurately quantify the variable degrees of hepatic fibrosis in a rat model. Here, we focused on identifying whether our molecular based strategy precisely quantifies the severities of liver fibrosis in humans as well.

MATERIALS AND METHODS

Liver samples

Seventy-four patients, including 67 with hepatocellular carcinoma (HCC) and 7 with colorectal liver metastasis who had undergone an initial hepatectomy at our institute and affiliated hospitals were entered in this study. The 67 included 11 positive for hepatitis B surface antigen (HBsAg), 47 positive for hepatitis C virus (HCV) antibody, and 9 negative for either HBsAg or HCV antibody. The 7 metastatic patients were seronegative for either HBsAg or HCV antibody, and they all had liver function values within the normal limits and histologically normal liver was analyzed. The resected non-cancerous liver specimens were meticulously taken as far from the tumor as possible, and were immediately frozen in liquid nitrogen and kept at -80℃ until subsequent RNA preparation. Remaining liver was soaked in 10% formaldehyde then embedded in paraffin for azan staining. Written informed consent was obtained from all patients according to the guidelines approved by the Institutional Research Board at each hospital.

Preparation of sections and measurement of the area of liver fibrosis

Five thick fixed sections were stained with azan for collagen fibers as described previously[16]. The section images (× 40) were randomly selected and captured using the Sony DXC S500/OL digital camera. These captured images were entered into a personal computer as PICT files (Adobe Photoshop version 7.0). To determine the morphologic fibrosis index (MFI), the ratio of azan-stained:total area was calculated as described[16]. We examined how many or few section-images would be sufficient to determine the MFI as a reference for the degree of liver fibrosis (Figure 1). The fluctuation rate of the MFI in each liver specimen was calculated as follows:

Fluctuation rate (%) = $(n - n\text{-}1)/n\text{-}1 \times 100$

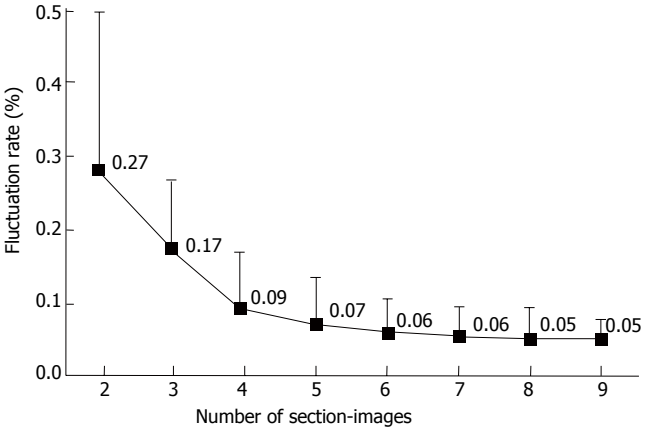

Figure 1 The number of section-images used to calculate the morphological fibrosis index (MFI) and the fluctuation rates of the MFI in the 12 randomly selected liver samples (mean ± SD).

where, n represents the mean MFI value for n section-images. We calculated the fluctuation rates in 12 randomly selected liver tissue specimens and plotted the mean of these 12 samples according to the number of section-images. As expected, when the number of images was small, the mean MFI value fluctuated markedly. As the number of section-images increased, the fluctuation attenuated and a plateau was subsequently reached at 9 images. In this study, we thus determined the MFI value as a mean of 9 section-images. The mean MFI value (1.13%) of the 7 patients with colorectal liver metastasis but normal liver histology was considered as background and subtracted to determine the MFI values for the 67 patients with HCC.

All non-cancerous liver specimens were independently examined by 2 experienced hepatopathologists (A.S. and Y.Y.) blinded to the results of the DNA microarray analysis, MFI values, and clinical data. The severity of liver fibrosis (0-4) was evaluated semi-quantitatively according to the METAVIR scoring system[5]: F0, no fibrosis; F1, portal fibrosis without septa; F2, portal fibrosis and few septa; F3, numerous septa without cirrhosis; and F4, cirrhosis. Quadratic weighted kappa was calculated to estimate the reproducibility of the staging between the 2 pathologists.

Liver function tests

We calculated the Pearson correlation coefficient between MFI values and 10 preoperative clinical parameters that have been associated with liver function or disease: indocyanine green dye retention at 15 min, prothrombin time (as a% of normal time), hepaplastin, platelet count, albumin, total bilirubin, aspartate aminotransferase, alanine aminotransferase, type Ⅳ collagen 7 s and hyaluronic acid. The correlation coefficient between the MFI and aspartate aminotransferase to platelets ratio index (APRI)[17] was also calculated.

RNA preparation

Total liver RNA was isolated from frozen tissue by a guanidium/cesium trifluoroacetate extraction method

using a Quick Prep total RNA extraction kit (Amersham Pharmacia Biotech, Little Chalfont, England)[18]. To ensure the use of only high quality RNA, the concentration and purity were determined by an Agilent 2100 bioanalyzer (Agilent Technologies, Palo Alto, CA)[19].

Oligonucleotide microarray

We used the commercially available Human 1A Oligo Microarray (Agilent) containing over 22 000 unique 60-mer oligonucleotides representing over 17 000 unique human genes, listed http://www.chem.agilent.com/scripts/generic.asp?lpage=5175&indcol=Y&prodcol = Y. Cyanine-labeled cRNA was prepared using a T7 linear amplification as described in the Agilent Low RNA Input Fluorescent Linear Amplification Kit Manual (Agilent). Briefly, 50 ng of purified total RNA was reverse transcribed to generate double-stranded cDNA using an oligo dT T7 promoter primer and MMLV reverse transcriptase. Next, cRNA was synthesized using T7 RNA polymerase, which simultaneously incorporated Cy3 or Cy5 labeled CTP. During this process, experimental samples from potentially fibrotic liver specimens were labeled with Cy5 whereas a control sample from a mixture of the 7 normal liver specimens was labeled with Cy3. The quality of the cRNA was again checked using the Agilent 2100 Bioanalyzer. One microgram aliquots each of Cy3 and Cy5 labeled cRNA were combined, and fragmented in a hybridization cocktail (Agilent). The labeled cRNAs were then hybridized to 60-mer probe oligonucleotide microarrays and incubated for 17 h at 60℃. The fluorescent intensities were determined by an Agilent DNA Microarray Scanner and were analyzed using G2567AA Feature Extraction Software Version A.7.5.1 (Agilent), which used the LOWESS (locally weighted linear regression curve fit) normalization method. The gene-expression values were calculated as the log ratio of the Cy5 to Cy3 channel signals. All calculated data were imported into the Rosetta Luminator system v2.0. (Rosetta Biosoftware, Kirkland, WA) and all intensity data were plotted as log ratios. The original data will be available at URL supplemental website at http://www.mib-beppu.kyushu-u.ac.jp/MIB_res/clin_surg/MA/MA_data.html. This microarray study followed MIAME guidelines issued by the Microarray Gene Expression Data group[20].

Identification of genes associated with liver fibrosis

We first excluded genes which had missing values in > 20% of samples. We thus analyzed 16 990 genes, missing values in each sample were estimated using the 10-nearest neighbors' method based on the Euclid distance[21]. The 67 samples whose MFI values were measured, and the 7 normal liver samples (MFI = 0%), were used for this analysis. The correlation coefficient between MFI values and the expression of each gene in the 74 samples was calculated.

Development of quantification scores for liver fibrosis: Genetic fibrosis index

Next, we determined the parameters in the estimation equation using a linear support vector regression (L-SVR) analysis[22]. The estimation equation based on the L-SVR was expressed in linear equation form, namely "the estimated MFI value = parameter 1 × the expression value of gene a1 + parameter 2 × the expression value of gene a2 + … + constant b". These parameters and the constant were determined according to Cherkassky's method[23]. Here, we define the estimated MFI value based on the gene-expression values as the genetic fibrosis index (GFI)[16]. To select the optimal set of marker genes that best correlate GFI to MFI, we used a forward-backward stepwise selection method. In this method, the correlation coefficient between the expression value of each gene listed in Table 1 and the MFI value for the 74 samples was calculated and genes with the highest correlation coefficients were selected. Using these selected genes, the estimation equation parameters and constant were determined, and the correlation coefficient between the GFI and MFI values was calculated one at a time by the L-SVR based system. We repeated these steps with the addition or elimination of genes to improve the correlation coefficient, and we subsequently determined the 4 optimized marker clones. For independent validation, the GFI of 12 additional test samples (one normal and 11 chronically damaged livers) was calculated using these 4 marker clones.

RESULTS

MFI and the histological stage of liver fibrosis

The MFI of the 67 patients with HCC ranged from 0.2% to 18.8% (6.8% ± 3.5%). To understand the distribution of MFI values in a clinical setting, we first examined the correlation between the MFI and the stage of liver fibrosis in the METAVIR scoring system (Figure 2). The correlation coefficients between the MFI and the stages of liver fibrosis by Pathologists A and B were $r = 0.62$ and $r = 0.61$, respectively. The reproducibility of the METAVIR scoring between the 2 pathologists was good (quadratic weighted kappa = 0.86). The mean MFI value for liver cirrhosis, stage F4, was approximately 10%.

MFI and liver function tests

We next determined the correlation between the MFI and the results of so-called liver function tests in the 74 samples. The best correlation coefficient ($r = -0.53$) was observed between the MFI and the prothrombin time. The platelet count ($r = -0.52$), indocyanine green dye retention test at 15 min ($r = 0.49$), and type IV collagen 7s ($r = 0.48$) also had good correlation coefficients (Figure 3). Conversely, APRI did not correlate well with the MFI ($r = 0.38$).

Identification of differentially regulated genes during liver fibrogenesis

We identified differentially regulated genes associated with the degree of liver fibrosis in the 74 samples. Thirty-nine genes showed a good correlation ($r > 0.50$) between gene-expression and MFI (Table 1). There were no genes with a correlation coefficient more negative than -0.5. The 39 genes included 24 named genes 18 of which (75%) were associated with immune functions. Specifically, 9 genes

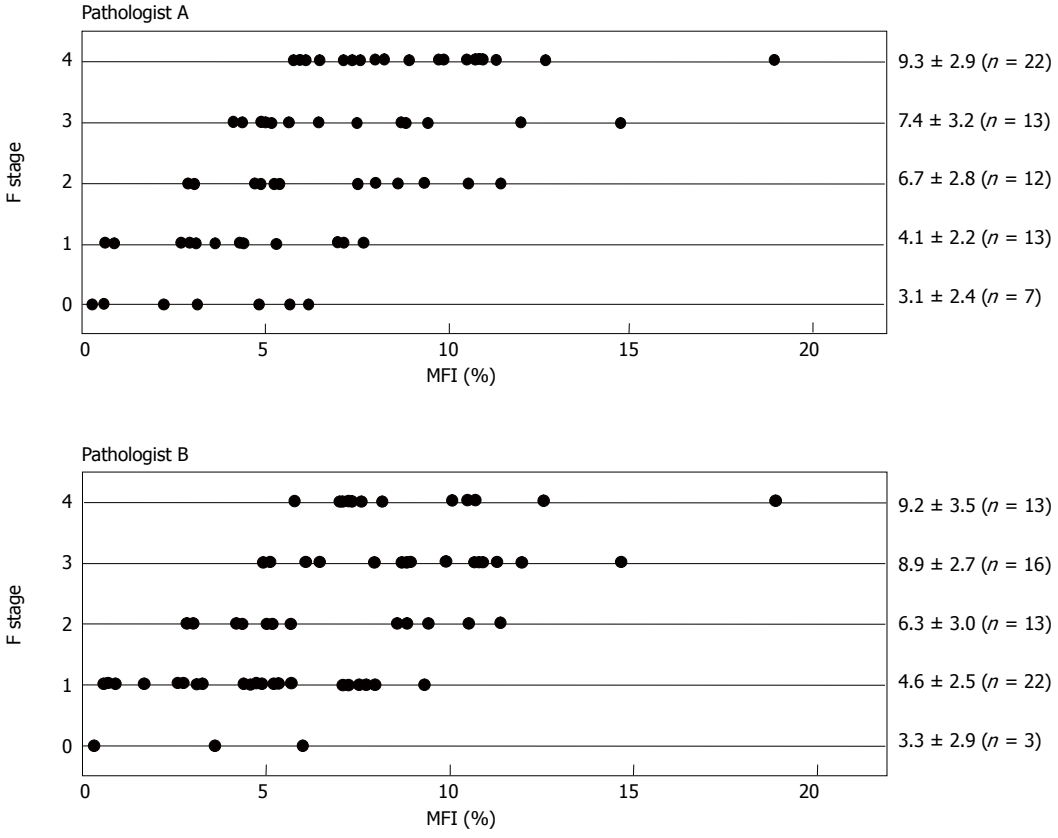

Figure 2 Relationship between the morphological fibrosis index (MFI) and the histological stage of liver fibrosis. METAVIR scores were independently determined by two experienced pathologists.

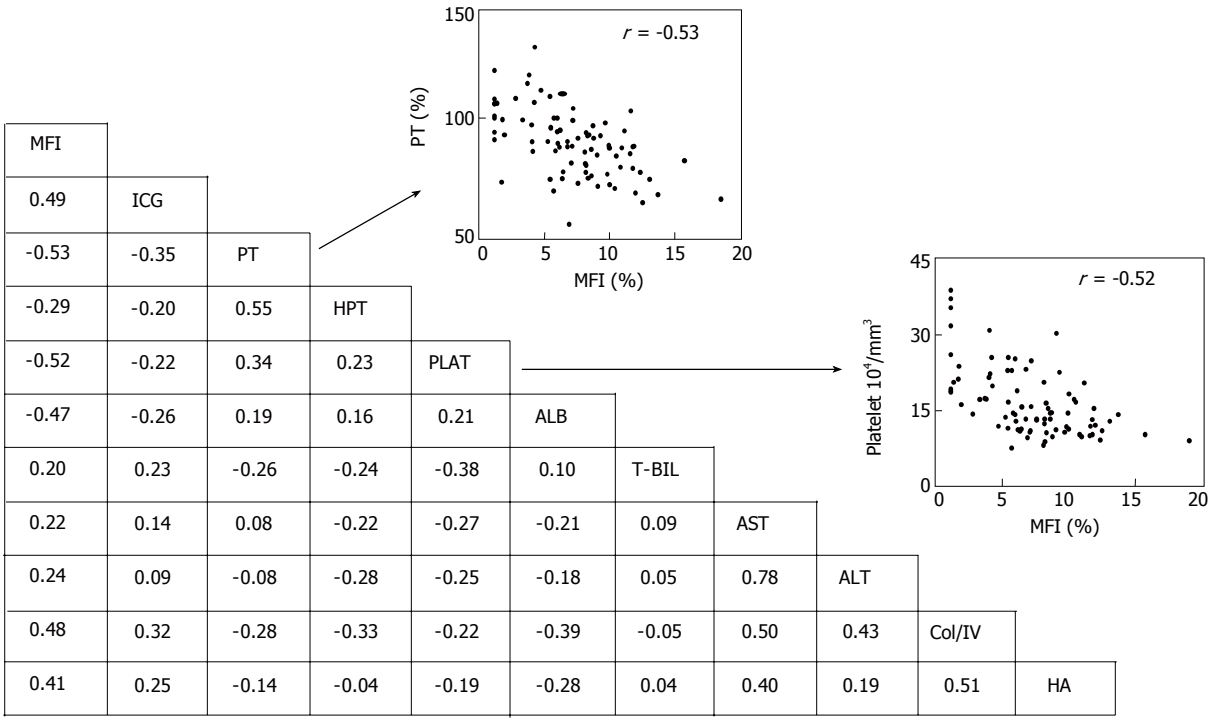

MFI										
0.49	ICG									
-0.53	-0.35	PT								
-0.29	-0.20	0.55	HPT							
-0.52	-0.22	0.34	0.23	PLAT						
-0.47	-0.26	0.19	0.16	0.21	ALB					
0.20	0.23	-0.26	-0.24	-0.38	0.10	T-BIL				
0.22	0.14	0.08	-0.22	-0.27	-0.21	0.09	AST			
0.24	0.09	-0.08	-0.28	-0.25	-0.18	0.05	0.78	ALT		
0.48	0.32	-0.28	-0.33	-0.22	-0.39	-0.05	0.50	0.43	Col/IV	
0.41	0.25	-0.14	-0.04	-0.19	-0.28	0.04	0.40	0.19	0.51	HA

Figure 3 Correlation coefficient among parameters for the assessment of liver damage. The left column represents the correlation coefficient between the morphological fibrosis index (MFI) values and clinical parameters of liver function tests. ICG: Indocyanine green dye retention test at 15 min; PT: Prothrombin time (as a % of normal); HPT: Hepaplastin test; PLAT: Platelet count; ALB: Albumin; T-Bil: Total bilirubin; AST: Aspartate aminotransferase; ALT: Alanine aminotransferase; Col/IV: Type Ⅳ collagen 7s; HA: Hyaluronic acid.

encoded major histocompatibility complex (MHC) class Ⅱ molecules, such as *HLA-DR4* and *HLA-DRB5*. The most highly correlated gene was *PIK3C2B*, involved in intracellular signaling pathways. *PRKCB1*, *PTPRC*, *UNC5B*, and *ARHGDIB* are also associated with intracellular signaling pathways.

Table 1 Thirty-nine genes associated ($r > 0.50$) with the degree of liver fibrosis (MFI value)

Accession No.	Gene Name	Description	CC[1]
NM_002646	PIK3C2B[2]	Phosphoinositide-3-kinase, class 2, beta polypeptide	0.60
NM_152270	NM_152270[2]	Hypothetical protein FLJ34922 (FLJ34922)	0.59
NP113470	NP113470	Unknown	0.58
AK024488	AK024488	FLJ00087 protein	0.57
AB064167	AB064167	IGL mRNA for immunoglobulin lambda light chain VLJ region	0.57
BC015833	BC015833	cDNA clone MGC:27152 IMAGE:4691630	0.57
A_23_P32661	A_23_P32661	Unknown	0.57
M35730	M35730	MHC class Ⅱ DQ3.1ER (DR4)	0.56
NP077661	NP077661	Unknown	0.56
D29642	D29642	KIAA0053	0.56
NM_001778	CD48	CD48 antigen (B-cell membrane protein)	0.56
NM_006144	GZMA	Granzyme A (granzyme 1, cytotoxic) T-lymphocyte-associated serine esterase 3)	0.56
NM_002125	HLA-DRB5	MHC class Ⅱ, DR beta 5	0.55
NM_001803	CDW52	CDW52 antigen (CAMPATH-1 antigen)	0.55
NP649772	NP649772	Unknown	0.54
THC1889877	THC1889877	Unknown	0.54
AX721203	AX721203	Sequence 163 from Patent WO0220754	0.54
BC036926	BC0369262	cDNA clone MGC:46491 IMAGE:5225843	0.54
M13975	M13975	Protein kinase C beta-Ⅱ type (PRKCB1)	0.53
AF035024	AF035024	MCE11H myosin-reactive immunoglobulin heavy chain variable region	0.53
NM_033503	BMF	Bcl2 modifying factor (BMF), mRNA	0.53
A_23_P124264	A_23_P124264	Unknown	0.53
U96396	U96396	Anti-streptococcal/anti-myosin immunoglobulin kappa light chain variable region	0.53
A_23_P435390	A_23_P435390	Unknown	0.53
A_23_P9854	A_23_P9854	Unknown	0.52
AF490771	AF490771	MHC class Ⅱ antigen (HLA-DRB1) mRNA, HLA-DRB1*1401 allele	0.52
NM_002121	HLA-DPB1	MHC class Ⅱ, DP beta 1	0.52
L03178	L03178	Cell-type T-cell immunoglobulin gamma chain, V region (IGHV@)	0.52
NM_170744	UNC5B	Unc-5 homolog B (C. elegans)	0.51
S65186	S65186[2]	EMT=T-cell-specific tyrosine kinase	0.51
NM_022555	HLA-DRB3	MHC class Ⅱ, DR beta 3	0.51
NM_001175	ARHGDIB	Rho GDP dissociation inhibitor (GDI) beta	0.51
NM_002118	HLA-DMB	MHC class Ⅱ, DM beta	0.51
NM_002838	PTPRC	Protein tyrosine phosphatase, receptor type, C	0.51
L34102	L34102	MHC class Ⅱ HLA-DQB1*0502	0.51
AB020689	AB020689	KIAA0882 protein	0.51
NM_002341	LTB	Lymphotoxin beta (TNF superfamily, member 3)	0.50
AJ297586	AJ297586	MHC class Ⅱ antigen (HLA-DRB1 gene), DRB1*0402 allele	0.50
NM_033554	HLA-DPA1	MHC class Ⅱ, DP alpha 1	0.50

[1]For each clone, the correlation coefficient (CC) between the gene expression level and the morphological fibrosis index (MFI) was determined; [2]These 4 clones were used to calculate the genetic fibrosis index (GFI).

Development of a genetic fibrotic index to quantify the degree of liver fibrosis

We selected 4 clones, namely *PIK3C2B*, *NM_152270*, *BC036926*, and *S65186*, as the optimal marker set using the supervised learning method, L-SVR analysis. Based on the expression profiles of only these 4 clones, the GFI of each sample was then calculated, and the correlation between the GFI and the MFI was determined (Figure 4A). Our method correctly quantified the degree of liver fibrosis in the 74 training samples (Figure 4A, $r = 0.76$, $P < 0.0001$). Furthermore, an almost identical quantification was successfully achieved in the 12 additional independent test samples (one normal and 11 chronically damaged livers) (Figure 4B, $r = 0.75$, $P < 0.005$), supporting the usefulness of our quantifying system for liver fibrosis. Two representative azan-stained images of test samples with a good correlation between GFI and MFI are shown in Figure 4C. In addition, we showed that good correlations were obtained both in livers positive for HBsAg and those positive for HCV antibody (Figure 5).

DISCUSSION

To assess the severity of hepatic fibrosis using newer methods, such as Fibroscan and Fibrotest[7-10], most recent studies use the liver biopsy as a reference standard. However, studies using the Fibrotest have suggested that most errors are due to the histological staging itself[24], particularly, the difficulty in distinguishing F2 from F1 or F3 seems to be the main cause of misclassification. Histological scoring system, such as the METAVIR fibrosis score, is a categorical assessment and not a numerical

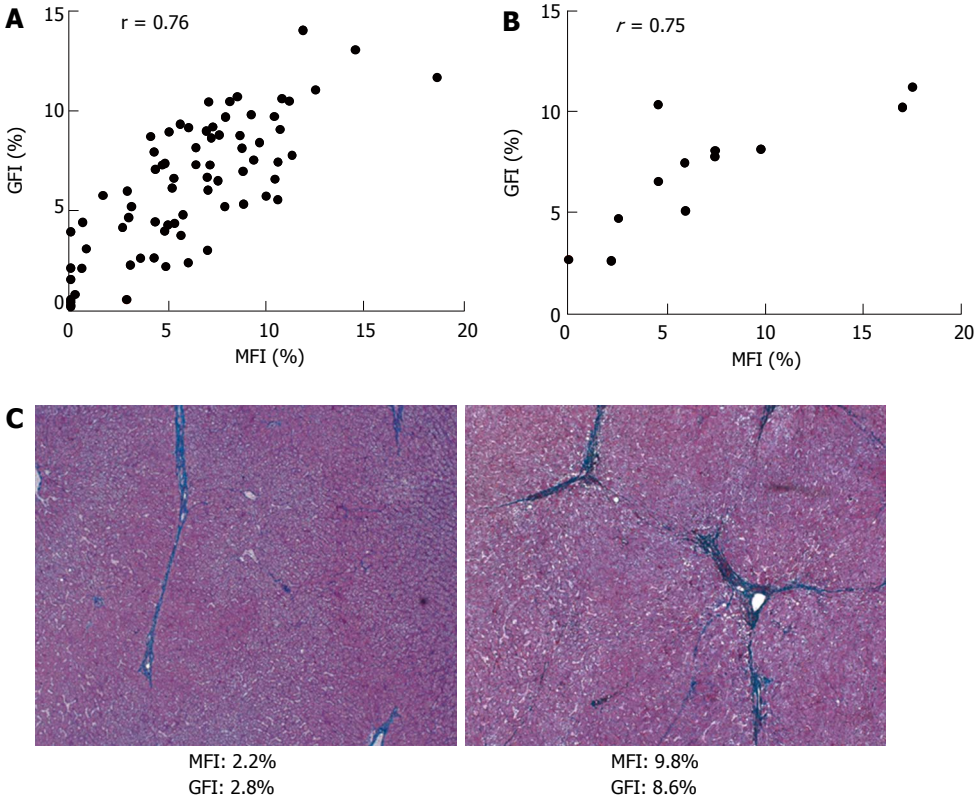

Figure 4 Correlation between the morphologic MFI values and the genetic GFI values in the 74 training samples (**A**) and the 12 test samples (**B**). (**C**) Two representative sections after azan staining (× 40) and their corresponding MFI and the GFI values.

measurement along a continuum in a mathematical sense[25]. In the current study, we therefore used as our reference the MFI, which is a mean of 9 surgical section-images, and subsequently investigated the value of our cDNA microarray-based strategy for the assessment of liver fibrosis. Although the MFI correlates well with the METAVIR scoring system (Figure 2), there was overlap among the different stages, indicating a limitation of such a histological staging system. The MFI can represent a linear score from mild fibrosis to overt cirrhotic livers. It has been reported that the area of fibrosis determined by image analysis is a reliable morphological method and was superior to histological staging, even if only small pieces of liver biopsy specimens were examined[26,27]. To the best of our knowledge, this is the first study to use the area of fibrosis (MFI) of human surgical specimens, which provide relatively large amounts of liver tissue, as a reference standard to evaluate new strategies for assessing hepatic fibrosis.

Using a cDNA microarray containing over 22000 clones, we analyzed the gene-expression profiles of liver tissue specimens and correlated them to the MFI values. We identified 39 differentially regulated genes, including 24 named genes, associated with the degree of liver fibrosis in 74 liver samples. Both the number of genes and the number of patients examined in this study were larger than those of previous reports investigating gene expression profiles of human livers with fibrosis[11-15]. Many of the genes we identified are involved in immune responses and cell signaling, which is consistent with a previous report investigating HCV-infected livers[14,15]. Among these, genes encoding MHC class II molecules were correlated most predominantly to the severity of liver fibrosis. Because MHC gene products are critical in regulating antiviral

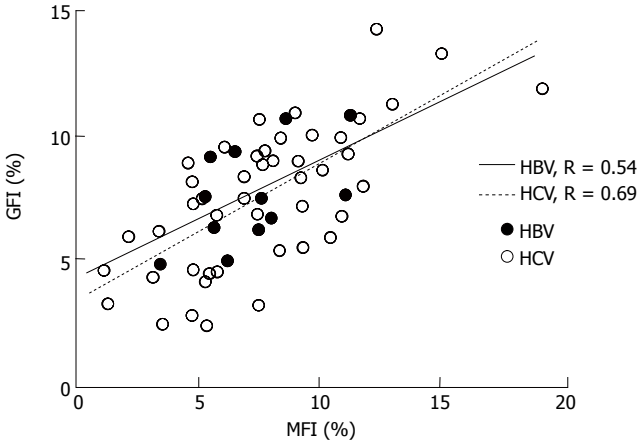

Figure 5 Correlation between the morphologic MFI values and the genetic GFI values in livers infected with hepatitis B virus (HBV) and hepatitis C virus (HCV).

immune reactions against both HBV and HCV, genetic factors controlling the host's immune response might also play an important role in determining the disease severity in patients with viral hepatitis[28-30]. In addition, we identified several genes, such as *PIK3C2B* and *ARHGDIB*, which regulate the activation of hepatic stellate cells[31,32], which might contribute to the molecular pathogenesis of liver fibrosis.

To examine possible advantages of our method over the use of blood markers of liver damage, we calculated the correlation coefficient between the MFI and 10 clinical parameters of so-called "liver function tests" (Figure 3) to include some of the large number of promising serum markers of hepatic fibrosis, e.g. collagen IV and hyaluronic acid. Prothrombin time correlated best with the MFI (r = 0.53). The correlation

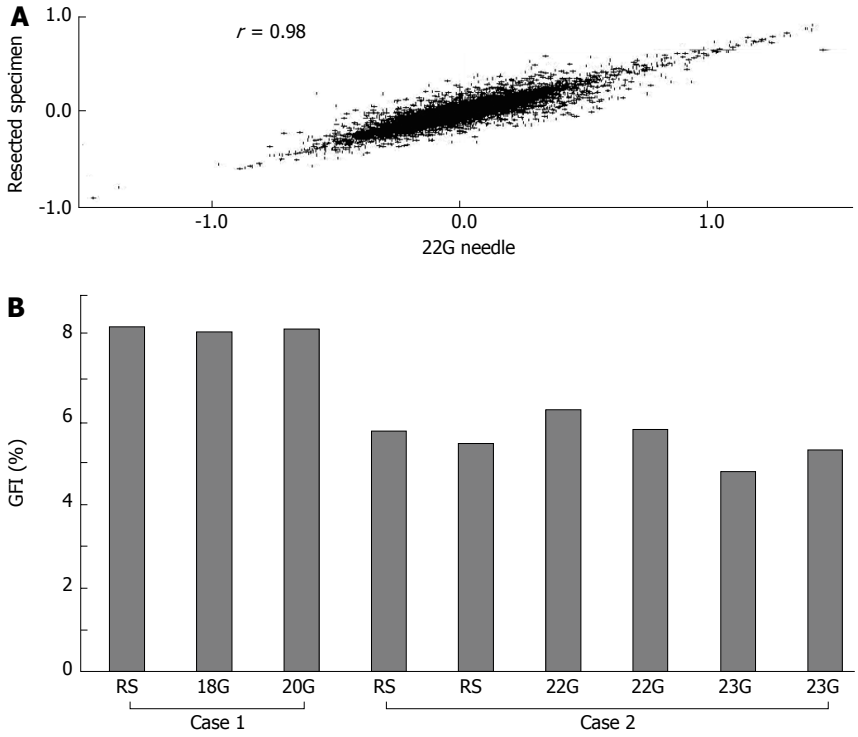

Figure 6 Gene-expression correlation between surgical resection and 22-guage needle liver biopsy specimens from the same patient. Intensity data were plotted and the correlation coefficient calculated by the Rosetta Luminator system v2.0 (**A**). The GFI values of resected and biopsy specimens were determined using the same formula based on the 4 marker clones (**B**). RS: Resected specimen.

coefficient (r = 0.38) between the MFI and the APRI[17] was inferior to that of the prothrombin time alone. It may well be that a panel of serum markers may prove more accurate than any individual marker. We next developed quantified scores for human liver fibrosis based on a specific gene-expression signature or index (GFI), which was validated by a supervised learning analysis. Our data showed that the GFI in the 74 training samples correlated with the MFI markedly better (r = 0.76) than any biochemical or hematological markers examined in this study. Furthermore, a similar correlation (r = 0.75) was confirmed in the 12 test samples as well. Therefore, our current study demonstrates for the first time that a single test based on gene-expression profiling accurately quantifies the variable extent of liver fibrosis in a clinical setting.

Marker genes involved in the pathogenesis of liver fibrosis might differ depending upon the etiology of the chronic liver damage. We therefore examined whether a different correlation with the MFI was observed between different etiologies (Figure 5). The correlation between MFI and GFI did not apparently differ markedly between HBV and HCV infected livers. This is reasonable because we selected our marker genes that were correlated to the degree of liver fibrosis regardless of etiology. One might expect a better performance if we analyzed samples with a single cause of liver fibrosis. However, we did not obtain better results even when we examined only livers infected with HCV (n = 54) using the same statistical method (data not shown).

Although the MFI may reliably determine the extent of fibrosis, a distinct advantage of the GFI is the potential for measuring a fibrosis index using very small liver biopsies. For example, in preliminary studies there was a very high correlation (r = 0.98, P < 0.01) between the levels of gene expression comparing genetic profiles of resected liver tissue and very small 22-guage liver biopsy specimens from the same patient (Figure 6A). Regardless of the sample size, the GFI values were quite reproducible from the same patient (Figure 6B). We extracted on average 3.4 ± 0.5 g of high quality total RNA using the 23-guage Surecut needle (TSK Laboratories), while only 0.2 g total RNA is sufficient for microarray analysis in our system. This will need to be validated with a larger number of patients, and might even include sampling more than two liver areas to reduce sampling error with minimal risk using the 23-guage needle.

Finally, we successfully created a scoring system to accurately and objectively quantify the degree of liver fibrosis in humans, based on the gene-expression signatures. This genome-wide information contributes to an improved understanding of molecular alterations during the development of liver cirrhosis, and could potentially become a powerful tool for monitoring the stage of liver fibrosis before and after treatment, such as with interferon/ribavirin therapy. This may be particularly important given recent exciting evidence on the potential reversibility of hepatic fibrosis in some patients[33]. Although our method still relies on invasively obtained liver tissue, however small, our data does draw attention to potentially helpful novel diagnostic and therapeutic targets, some of which may even have serum-measurable correlates based on future research.

REFERENCES

1 **Alter MJ**. Epidemiology of viral hepatitis and HIV co-infection. *J Hepatol* 2006; **44**: S6-S9
2 **Williams R**. Global challenges in liver disease. *Hepatology* 2006; **44**: 521-526
3 **Knodell RG**, Ishak KG, Black WC, Chen TS, Craig R, Kaplowitz N, Kiernan TW, Wollman J. Formulation and application of a numerical scoring system for assessing histological activity

in asymptomatic chronic active hepatitis. *Hepatology* 1981; **1**: 431-435
4 **Desmet VJ**, Gerber M, Hoofnagle JH, Manns M, Scheuer PJ. Classification of chronic hepatitis: diagnosis, grading and staging. *Hepatology* 1994; **19**: 1513-1520
5 **The French METAVIR Cooperative STUDT Group**. Intraobserver and interobserver variations in liver biopsy interpretation in patients with chronic hepatitis C. The French METAVIR Cooperative Study Group. *Hepatology* 1994; **20**: 15-20
6 **Imbert-Bismut F**, Ratziu V, Pieroni L, Charlotte F, Benhamou Y, Poynard T. Biochemical markers of liver fibrosis in patients with hepatitis C virus infection: a prospective study. *Lancet* 2001; **357**: 1069-1075
7 **Castéra L**, Vergniol J, Foucher J, Le Bail B, Chanteloup E, Haaser M, Darriet M, Couzigou P, De Lédinghen V. Prospective comparison of transient elastography, Fibrotest, APRI, and liver biopsy for the assessment of fibrosis in chronic hepatitis C. *Gastroenterology* 2005; **128**: 343-350
8 **Lackner C**, Struber G, Liegl B, Leibl S, Ofner P, Bankuti C, Bauer B, Stauber RE. Comparison and validation of simple noninvasive tests for prediction of fibrosis in chronic hepatitis C. *Hepatology* 2005; **41**: 1376-1382
9 **Colletta C**, Smirne C, Fabris C, Toniutto P, Rapetti R, Minisini R, Pirisi M. Value of two noninvasive methods to detect progression of fibrosis among HCV carriers with normal aminotransferases. *Hepatology* 2005; **42**: 838-845
10 **Foucher J**, Chanteloup E, Vergniol J, Castéra L, Le Bail B, Adhoute X, Bertet J, Couzigou P, de Lédinghen V. Diagnosis of cirrhosis by transient elastography (FibroScan): a prospective study. *Gut* 2006; **55**: 403-408
11 **Honda M**, Kaneko S, Kawai H, Shirota Y, Kobayashi K. Differential gene expression between chronic hepatitis B and C hepatic lesion. *Gastroenterology* 2001; **120**: 955-966
12 **Smith MW**, Yue ZN, Korth MJ, Do HA, Boix L, Fausto N, Bruix J, Carithers RL, Katze MG. Hepatitis C virus and liver disease: global transcriptional profiling and identification of potential markers. *Hepatology* 2003; **38**: 1458-1467
13 **Kim JW**, Ye Q, Forgues M, Chen Y, Budhu A, Sime J, Hofseth LJ, Kaul R, Wang XW. Cancer-associated molecular signature in the tissue samples of patients with cirrhosis. *Hepatology* 2004; **39**: 518-527
14 **Shao RX**, Hoshida Y, Otsuka M, Kato N, Tateishi R, Teratani T, Shiina S, Taniguchi H, Moriyama M, Kawabe T, Omata M. Hepatic gene expression profiles associated with fibrosis progression and hepatocarcinogenesis in hepatitis C patients. *World J Gastroenterol* 2005; **11**: 1995-1999
15 **Smith MW**, Walters KA, Korth MJ, Fitzgibbon M, Proll S, Thompson JC, Yeh MM, Shuhart MC, Furlong JC, Cox PP, Thomas DL, Phillips JD, Kushner JP, Fausto N, Carithers RL, Katze MG. Gene expression patterns that correlate with hepatitis C and early progression to fibrosis in liver transplant recipients. *Gastroenterology* 2006; **130**: 179-187
16 **Utsunomiya T**, Okamoto M, Hashimoto M, Yoshinaga K, Shiraishi T, Tanaka F, Mimori K, Inoue H, Watanabe G, Barnard GF, Mori M. A gene-expression signature can quantify the degree of hepatic fibrosis in the rat. *J Hepatol* 2004; **41**: 399-406
17 **Wai CT**, Greenson JK, Fontana RJ, Kalbfleisch JD, Marrero JA, Conjeevaram HS, Lok AS. A simple noninvasive index can predict both significant fibrosis and cirrhosis in patients with chronic hepatitis C. *Hepatology* 2003; **38**: 518-526
18 **Utsunomiya T**, Hara Y, Kataoka A, Morita M, Arakawa H, Mori M, Nishimura S. Cystatin-like metastasis-associated protein mRNA expression in human colorectal cancer is associated with both liver metastasis and patient survival. *Clin Cancer Res* 2002; **8**: 2591-2594
19 **Nishida K**, Mine S, Utsunomiya T, Inoue H, Okamoto M, Udagawa H, Hanai T, Mori M. Global analysis of altered gene expressions during the process of esophageal squamous cell carcinogenesis in the rat: a study combined with a laser microdissection and a cDNA microarray. *Cancer Res* 2005; **65**: 401-409
20 **Brazma A**, Hingamp P, Quackenbush J, Sherlock G, Spellman P, Stoeckert C, Aach J, Ansorge W, Ball CA, Causton HC, Gaasterland T, Glenisson P, Holstege FC, Kim IF, Markowitz V, Matese JC, Parkinson H, Robinson A, Sarkans U, Schulze-Kremer S, Stewart J, Taylor R, Vilo J, Vingron M. Minimum information about a microarray experiment (MIAME)-toward standards for microarray data. *Nat Genet* 2001; **29**: 365-371
21 **Troyanskaya O**, Cantor M, Sherlock G, Brown P, Hastie T, Tibshirani R, Botstein D, Altman RB. Missing value estimation methods for DNA microarrays. *Bioinformatics* 2001; **17**: 520-525
22 **Brown MP**, Grundy WN, Lin D, Cristianini N, Sugnet CW, Furey TS, Ares M, Haussler D. Knowledge-based analysis of microarray gene expression data by using support vector machines. *Proc Natl Acad Sci USA* 2000; **97**: 262-267
23 **Cherkassky V**, Ma Y. Practical selection of SVM parameters and noise estimation for SVM regression. *Neural Netw* 2004; **17**: 113-126
24 **Poynard T**, Munteanu M, Imbert-Bismut F, Charlotte F, Thabut D, Le Calvez S, Messous D, Thibault V, Benhamou Y, Moussalli J, Ratziu V. Prospective analysis of discordant results between biochemical markers and biopsy in patients with chronic hepatitis C. *Clin Chem* 2004; **50**: 1344-1355
25 **Standish RA**, Cholongitas E, Dhillon A, Burroughs AK, Dhillon AP. An appraisal of the histopathological assessment of liver fibrosis. *Gut* 2006; **55**: 569-578
26 **Pilette C**, Rousselet MC, Bedossa P, Chappard D, Oberti F, Rifflet H, Maïga MY, Gallois Y, Calès P. Histopathological evaluation of liver fibrosis: quantitative image analysis vs semi-quantitative scores. Comparison with serum markers. *J Hepatol* 1998; **28**: 439-446
27 **Calès P**, Oberti F, Michalak S, Hubert-Fouchard I, Rousselet MC, Konaté A, Gallois Y, Ternisien C, Chevailler A, Lunel F. A novel panel of blood markers to assess the degree of liver fibrosis. *Hepatology* 2005; **42**: 1373-1381
28 **Thursz MR**, Kwiatkowski D, Allsopp CE, Greenwood BM, Thomas HC, Hill AV. Association between an MHC class II allele and clearance of hepatitis B virus in the Gambia. *N Engl J Med* 1995; **332**: 1065-1069
29 **Alric L**, Fort M, Izopet J, Vinel JP, Charlet JP, Selves J, Puel J, Pascal JP, Duffaut M, Abbal M. Genes of the major histocompatibility complex class II influence the outcome of hepatitis C virus infection. *Gastroenterology* 1997; **113**: 1675-1681
30 **Asti M**, Martinetti M, Zavaglia C, Cuccia MC, Gusberti L, Tinelli C, Cividini A, Bruno S, Salvaneschi L, Ideo G, Mondelli MU, Silini EM. Human leukocyte antigen class II and III alleles and severity of hepatitis C virus-related chronic liver disease. *Hepatology* 1999; **29**: 1272-1279
31 **Bataller R**, Paik YH, Lindquist JN, Lemasters JJ, Brenner DA. Hepatitis C virus core and nonstructural proteins induce fibrogenic effects in hepatic stellate cells. *Gastroenterology* 2004; **126**: 529-540
32 **Kato M**, Iwamoto H, Higashi N, Sugimoto R, Uchimura K, Tada S, Sakai H, Nakamuta M, Nawata H. Role of Rho small GTP binding protein in the regulation of actin cytoskeleton in hepatic stellate cells. *J Hepatol* 1999; **31**: 91-99
33 **Poynard T**, McHutchison J, Manns M, Trepo C, Lindsay K, Goodman Z, Ling MH, Albrecht J. Impact of pegylated interferon alfa-2b and ribavirin on liver fibrosis in patients with chronic hepatitis C. *Gastroenterology* 2002; **122**: 1303-1313

S- Editor Wang GP **L- Editor** Alpini GD **E- Editor** Bi L

PO Box 2345, Beijing 100023, China
www.wjgnet.com
wjg@wjgnet.com

World J Gastroenterol 2007 January 21; 13(3): 391-397
World Journal of Gastroenterology ISSN 1007-9327

CLINICAL RESEARCH

Yoga: A tool for improving the quality of life in chronic pancreatitis

Surinder Sareen, Vinita Kumari, Karaminder Singh Gajebasia, Nimanpreet Kaur Gajebasia

Surinder Sareen, Vinita Kumari, Grantham and District Hospital, United Lincolnshire Hospitals NHS Trust, Grantham NG31 8DG, United Kingdom
Karaminder Singh Gajebasia, Nimanpreet Kaur Gajebasia, Government Medical College, Patiala, India
Correspondence to: Surinder Sareen, Grantham and District Hospital, United Lincolnshire Hospitals NHS Trust, Grantham NG318DG, 6, Norton Street, Grantham, NG31 6BY, United Kingdom. surinder_sareen@yahoo.com
Telephone: +1-476-591515
Received: 2006-09-01 Accepted: 2006-09-19

Abstract

AIM: To determine the effectiveness of yoga on improving the quality of life in patients of chronic pancreatitis.

METHODS: The patients were randomized to two groups. The control group continued their usual care as directed by their physicians. Patients in the yoga group, in addition, received biweekly yoga sessions for 12 wk. The patients' demographic and health behaviour variables were assessed before and after the yoga programme using Medical Outcomes Short Form (SF-36) for quality of life, Profile of Mood States for assessing mood and Symptoms of Stress Inventory for measuring stress.

RESULTS: A total of 60 patients were enrolled, with 8 drop-outs.Thirty patients were randomized to the yoga group and 30 to the control group. Significant improvements were seen in overall quality of life, symptoms of stress, mood changes, alcohol dependence and appetite after the 12 wk period apart from the general feeling of well-being and desire to continue with the programme in future in the yoga group, while there was no difference in the control group.

CONCLUSION: Yoga is effective on improving the quality of life in patients of chronic pancreatitis.

Key words: Yoga; Chronic pancreatitis; Quality of life

Sareen S, Kumari V, Gajebasia KS, Gajebasia NK. Yoga: A tool for improving the quality of life in chronic pancreatitis. *World J Gastroenterol* 2007; 13(3): 391-397

http://www.wjgnet.com/1007-9327/13/391.asp

INTRODUCTION

The pain that develops in chronic pancreatitis is often severe, chronic, aggravated by meals and may be present continuously including at night. In some patients the pain is so severe that they develop a fear for eating and, as a consequence, they lose significant amounts of weight. The pain may begin gradually; however, in many patients over time they develop into continuous pain. The pain is usually worse in the back rather than in the front of the abdomen. The severity of the pain makes many patients into pain cripples. The worsening of the pain with meals may lead to avoidance of foods, causing severe weight loss and malnutrition of the patient.

Treatment of the pain requires familiarity with the patient's disease, an understanding of wide variations in presentation and manifestations of chronic pancreatitis and knowledge of the different treatment options available, their advantages and disadvantages. Treatment is best provided in a centre where experienced physicians from different specialties provide comprehensive approaches to the care of the patient and there is coordination of care between the different specialties.

At our center, we offer a comprehensive approach to pain from pancreatic diseases with clinical evaluation by a pain management specialist, pancreatic surgeon, gastroenterologist and psychologist as indicated. Many patients may also require treatment in a rehabilitation program prior to or after the surgery for drug dependency. The drug dependency develops on narcotic drugs due to years of over usage prior to a surgical consultation in many patients. Yoga was introduced as a tool for rehabilitation programme and to supplement the other pain relief measures being taken by the patients.

Therapy of chronic pancreatitis rests on five arms: Avoidance of alcohol, treatment of pain, replacement therapy for exocrine and endocrine insufficiency and adequate nutrition. Alcohol withdrawal improves pain and the patient's compliance. It also seems to retard the chronic inflammatory process. Therapy of pain depends on the pathomechanism of pain. There is a lack of prospective, controlled studies comparing various treatment regimens. Thus, treatment options are partly dependent on the experience of the physician taking care of the patient. Thanks to improved substitution with acid resistant porcine pancreatic extracts with high lipase activity, fat restriction is no longer of paramount importance. However, supply with sufficient calories is still difficult due

to pain and inadequate compliance[1].

It was reported that the use of alternative therapies in the United States increased from 33.8% in 1990 to 42.1% in 1997[2]. Therapeutic recreation (TR) has traditionally provided many of approaches in their work with clients. Typically embedded in the rubric of stress management, TR professionals teach and provide complementary alimentary medicine (CAM) techniques such as aromatherapy, massage, yoga, and tai chi to clients[3]. Yoga as a clinical intervention has been associated with a variety of physical and psychological health outcomes such as improved mood and reduced symptoms of anxiety and depression[4].

Stress reduction and anxiety management programs could be useful for any disease because they help to create a supportive environment, in which the individual may have reduced anxiety. Caroleo identified several programs that reduce stress and anxiety among AIDS patients, including "yoga, massage, acupuncture, acupressure, chiropractic services, meditation, reiki, physical and breathing exercises and visualization"[5].

Despite yoga's wide popularity, there are limited numbers of randomized, controlled yoga studies using objective quantitative outcome measures, and these studies often have small numbers of subjects[6-9].

MATERIALS AND METHODS

A computer-generated random allocation sequence was prepared. The assignments were placed in serially numbered, sealed, opaque envelopes. Patients were randomized after enrolment. The study enroller screened the patient and, if the patient was qualified, obtained informed consent and completed the baseline measurement. Then the next envelope was opened and the treatment allocation discussed. No assignment was reused with another patient once the envelope had been opened. Patients completed their own assessments, and blinding was not possible.

Both treatment groups continued the standard therapy as directed by their primary physician during the 12 wk intervention period. Patients were asked to remain on the same medications and not to start new ones. A medication diary was provided to document medications for pain, and their dosages, frequencies and side effects.

Data collection

Demographic data and patients' history were obtained using a checklist and short answer questionnaire. Demographic variables included age, ethnic background, marital status, education, employment status, and occupation.

The SF-36 questionnaire was used to assess the quality of life. SF-36 is a generic health outcome measure that is designed for use across varied populations[10]. It is comprised of 36 items across eight scales: physical functioning, role function-physical, bodily pain, general health, vitality, social functioning, role function-emotional, and mental health. Each scale is scored from 0 to 100, with higher values indicating more favourable health status. The SF-36 has been used in numerous studies of cancer patients and has evidence of validity in both cancer and pain patient groups[11,12].

The Profile of Mood States (POMS)[13] is a 65-item scale, which assesses six affective dimensions. It has been widely used in the assessment of mood changes resulting from a variety of interventions due to its responsiveness and has been used extensively in various populations[14].

The Symptoms of Stress Inventory (SOSI) is designed to measure physical, psychological, and behavioural responses to stressful situations. Respondents are instructed to rate the frequency with which they experience various stress-related symptoms on a five-point scale, ranging from "never" to "frequently," during a designated time frame selected by the investigator (in this case, the past week). The SOSI overcomes the limitations of checklist measures, which assume universally valid weightings of stressful events based on normative data, by focusing on manifest symptoms of stress and obviates the need for patients to identify and rate all relevant stressful events occurring in their lives. Both predictive and concurrent validities have been demonstrated, and, in a mixed chronic-illness sample of patients with malignant melanoma and myocardial infarction, manifest symptom distress as measured by the SOSI was directly related to functional alterations due to disease and inversely related to cognitive adaptation and perceived quality of life[15].

The yoga program was designed to complement the management of pain and anxiety based on a sequence of yoga poses by B.K.S. Iyengar[16]. Iyengar is one of the world's foremost exponents of yoga and is recognized by the medical community in India as an expert in treating medical problems with yoga. Iyengar has evolved the therapeutic application of yoga postures. Iyengar's yoga is particularly beneficial for people with chronic pain because he has researched and understood the therapeutic benefits of the poses[17]. In consultation with a certified yoga instructor, the psychiatrist, members of the interdisciplinary team and the literature on lyengar's sequence of poses, a yoga program was designed for participants.

The yoga program was implemented, directed and evaluated by the authors. Yoga sessions were planned for thrice a week over a 12 wk period. Each session lasted approximately one hour. The sessions were held in early morning in an open park. This area provided ample space for participants to practice yoga without feeling confined.

Prior to the start of the yoga intervention, the authors consulted with the nurse manager, attending physician and psychiatrist, and reviewed the medical records to authenticate the diagnosis of chronic pancreatitis for each participant. Prior to the start of the yoga program, each participant was interviewed to determine his or her willingness to participate in the study and signed informed consent for involvement in the study.

At this time, each participant was given a brief definition of yoga and particularly a description of the sequence of poses that were to be used. Preparation and guidelines for the yoga classes were reviewed, such as to come empty stomach, not to eat anything for one hour before the session, and wearing loose and comfortable clothing. Finally, participants were told of the duration and frequency of the yoga program and that if they wish, they

Table 1 Demographic profile of the participants, (mean ± SD)

Variable	Yoga group	Control group	*P*
Age (yr)	50 ± 5.2	50 ± 6.3	0.712
Body mass (kg)	55.4 ± 17.6	56.1 ± 16.4	0.801
Education (yr)	16.0 ± 2.4	15.8 ± 3.2	0.72
Marital status (% married)	73	74	0.865
Employment (% employed)	56	57	0.928

could discontinue participation at any time.

As the participants entered the session, initial evaluation data were collected including the recording of each participant's pain levels, weight, average diet, pain relief medications.

As in many classical yoga classes, the class started with 15 min of meditation. During the meditation, the participants were instructed to breathe diaphragmatically. This breathing technique 'pranayama' allowed the participants to slow down their breathing and at the same time begin to slow down their body and mind. Further instructions were given to clear the mind of any unwanted thoughts and as the thoughts came into their mind, to allow them to flow freely out. During the meditation, the participants were instructed to concentrate on their breathing and follow each breath. After meditation, the participants completed a 10-min warm-up of various yoga arm stretches and movements to relax their muscles and circulate their blood and oxygen throughout their body. Once warm-ups were completed, each participant attempted to remain in each pose for 1 to 3 min or as tolerated. Modifications were necessary for several of the participants when the poses became too uncomfortable.

At the end of the last pose, the relaxation pose (Savasana), participants were instructed to slowly awaken the body by opening their eyes and begin to gently stretch various parts of the body such as neck, hands, and feet. Participants then completed a seated cross-leg pose with their palms together at the heart.

Suitable alterations were made in yoga programme for the participants finding some difficulty in doing the various poses (asanas).

Analysis and observations

Out of 30 patients randomised to yoga group, 26 completed the full 12 weeks course. They ranged in age from 41 to 69 years (mean, 50). All participants were diagnosed with chronic pancreatitis and were taking pain and anxiety medications. 86% of the patients were males and 90% of them were alcoholic at some stage of their life.

Statistical analysis

All data were analysed using the SPSS version 12 statistical software package. Descriptive statistics (frequencies, means, standard deviations, and percentages) were used to characterize the sample. An alpha level for a significant difference was set at 0.01 because of the number of variables.

Table 2 Comparison of SF-36 score in yoga and control groups, (mean ± SD)

SF-36 subscale	Yoga group			Control group		
	0 wk	12 wk	*P*	0 wk	12 wk	*P*
Physical functioning	62.9 ± 0.6	74.1 ± 0.5	0.0001	63.8 ± 0.8	63.6 ± 0.6	0.08
General health	66.8 ± 0.4	74.8 ± 0.3	0.001	67.7 ± 11.3	69.6 ± 12.4	0.10
Role-physical	57.9 ± 21.4	63.1 ± 19.3	< 0.01	56.3 ± 18.6	54.6 ± 16.7	0.12
Bodily pain	41.4 ± 14.1	60.4 ± 14.4	< 0.01	45.5 ± 17.4	48.0 ± 15.9	0.05
Vitality	32.1 ± 14.2	45.2 ± 16.3	< 0.01	33.2 ± 13.9	33.0 ± 12.6	0.61
Social functioning	61.4 ± 22.3	78.4 ± 20.2	< 0.01	63.8 ± 18.1	70.5 ± 15.7	0.22
Role-emotional	47.2 ± 38.8	77.7 ± 30.1	< 0.01	47.8 ± 29.7	48.6 ± 31.1	0.55
Mental health	41.3 ± 14.3	61.3 ± 13.9	< 0.01	45.9 ± 12.6	46.3 ± 15.9	0.33

Data were analysed using the intention-to-treat approach. The last-observation-carried-forward procedure was used for participants who did not complete the trial. No transformations were required for statistical analyses. Baseline comparisons between the two groups were made using independent-sample *t*-tests for continuous data and Pearson's χ^2 tests for categorical data. This adjusted statistical analysis was performed to reduce the impact of baseline differences on study outcomes (given the relatively small sample size of the trial). A two-sided *P* value of < 0.05 indicated statistical significance. No adjustments were made for multiple comparisons. Data are presented as the means ± SD with 95% confidence intervals. As a check for the validity of the parametric test, we also made a nonparametric analysis for 2 independent groups (Mann Whitney *U*) and found the same variables to be significant as by the *t*-test. Formal directional hypotheses were not made a priori. However, we expected to find improvement in quality of life in participants in the yoga programme.

RESULTS

There was no statistical difference between the demographic profile of the patients in yoga group and control group (Table 1), indicating that the participants were properly randomised and matched.

Quality of life scores

The SF-36 results shown in Table 2 revealed a statistically significant improvement in all components of the scoring system in the participants of the yoga group, while there was no marked difference after 12 wk in the control group. Only scores of those who completed the program ($n = 52$) were included because 12 wk scores were not available for dropouts. Dropouts were eliminated from all subsequent analyses. The scores before the start of yoga programme in both groups were comparable, indicating the appropriate matching of the participants.

Mood scores

POMS change scores for all patients (yoga and control)

Table 3 Comparison of POMS score between yoga and control groups, (mean ± SD)

Variable	Yoga group		Control group	
	0 wk	12 wk	0 wk	12 wk
Anxiety	11.7 ± 6.5	9.1 ± 5.4[a]	11.5 ± 4.6	11.7 ± 5.3
Depression	9.7 ± 6.6	5.4 ± 5.8[d]	9.6 ± 4.7	9.4 ± 6.3
Anger	9.8 ± 5.6	5.9 ± 6.6[b]	9.6 ± 6.1	9.2 ± 2.6
Vigour	12.8 ± 3.8	17.1 ± 5.2[b]	12.9 ± 2.6	13.6 ± 6.0
Fatigue	14.1 ± 3.4	8.6 ± 3.8[b]	13.9 ± 4.1	14.2 ± 4.3
Confusion	5.5 ± 4.9	3.2 ± 2.8[b]	5.7 ± 1.8	5.6 ± 2.3

[a]$P < 0.05$; [b]$P < 0.01$; [d]$P < 0.001$.

who completed the study are presented in Table 3. At 12 wk (after the yoga group had completed the program), POMS scores were significantly higher in the yoga group, indicating less mood disturbance. When change scores were calculated and assessed with independent-samples *t* tests, the difference between the two groups was even clearer, with significantly more change in the direction of reduced mood disturbance in the yoga group. The treatment program resulted in a 40% reduction in Total Mood Disturbance as measured by the POMS; while the reduction in the control group was only 2%.

Stress scores

SOSI scores for the yoga and control groups before and after the yoga programme are presented in Table 4. There were no differences between the two groups before the start of yoga programme, again indicating that the groups were initially matched in stress symptoms. There was a statistically significant decline in stress scores in the patients of yoga group after 12 wk, while there was no difference in the scores in control group. Using independent-samples *t* test, there was a greater decrease in yoga group in the subscales of depression, gastrointestinal, habitual patterns and anxiety scores.

General well being

Interviews were conducted with participants at the end of the 12-wk yoga intervention to help determine its effectiveness. Each participant's thoughts regarding the yoga intervention were noted and all candidates claimed some benefits from the yoga programme. While each individual reported gains as a result of the yoga intervention, perhaps the best indicator of its effectiveness was found in the participant's request to continue the program. After the conclusion of the 12-wk yoga intervention, all participants expressed an interest in continuing the yoga.

DISCUSSION

These results provided evidence that a relatively brief mindfulness meditation and exercise based stress reduction programme could effectively improve the quality of life, mood disturbance and stress related symptoms in patients with chronic pancreatitis, consistent with other investigations of similar interventions in different

Table 4 Comparison of SOSI score between yoga and control groups, (mean ± SD)

Variable	Yoga group		Control group	
	0 wk	12 wk	0 wk	12 wk
Peripheral manifestations	5.3 ± 3.6	3.6 ± 3.3[b]	5.4 ± 4.1	5.2 ± 3.8
Cardiopulmonary	5.4 ± 5.1	4.2 ± 4.3[a]	5.7 ± 4.8	5.9 ± 3.4
Central-neurological	2.1 ± 1.8	1.9 ± 1.4	2.2 ± 1.4	1.8 ± 1.7
Gastrointestinal	9.5 ± 4.6	5.3 ± 5.8[b]	9.1 ± 4.3	8.9 ± 5.4
Muscle tension	11.4 ± 4.9	7.8 ± 3.4[a]	12.1 ± 4.5	11.7 ± 4.4
Habitual patterns	19.2 ± 6.8	13.8 ± 7.1[b]	20.1 ± 7.8	19.9 ± 6.6
Depression	9.9 ± 4.2	4.9 ± 4.7[b]	10.2 ± 3.9	9.8 ± 5.2
Anxiety/fear	12.4 ± 2.7	6.5 ± 4.9[b]	11.7 ± 3.1	11.9 ± 4.2
Emotional irritability	9.7 ± 6.1	6.0 ± 5.4[a]	9.3 ± 5.8	9.5 ± 4.4
Cognitive disorganization	7.5 ± 5.9	5.7 ± 7.1[a]	7.8 ± 6.2	7.9 ± 5.7
Total stress scores	92.4 ± 45.7	59.7 ± 47.4	93.6 ± 45.9	92.4 ± 44.8

[a]$P < 0.05$; [b]$P < 0.01$ *vs* control.

populations[18-20]. It is reasonable to conclude that even greater benefits may be obtained by participants who continue to practice over time and adopt yoga as part of their daily life. The current study was a pragmatic one, intending to study yoga as it is commonly practiced, i.e. as an adjunctive therapy to the standard therapy. The clinical question the study sought to answer was: does yoga add any benefit to patients with chronic pancreatitis in addition to the standard therapy? Our data indicate that yoga plus the standard therapy does increase quality of life in these patients compared with the standard therapy alone, in a clinically and statistically significant manner. Our protocol does not require a standardized regimen for the standard therapy, which makes it possible for baseline differences between the two treatment groups to occur. In addition, every patient followed the standard therapy protocol within defined parameters. The data from this pragmatic study also more closely resembles the clinical setting in which yoga is actually used, i.e. an adjunctive therapy to a variety of standard therapies.

It is commonly held that patients choose to use CAM because they are dissatisfied with conventional treatments that are perceived to be ineffective or have unpleasant side effects, or to be impersonal or too costly[21]. It has, however, been pointed out that disenchantment with conventional medicine is not necessarily the reason why patients turn to CAM[22]. This appears to be supported by a US study that reported users of alternative health care are no more dissatisfied with or distrustful of conventional care than non-users are[23].

In addition, an extensive review of meta-analyses and recently published studies of mind–body therapies concluded that there is strong evidence for the efficacy of mind-body therapies for coronary artery disease, headaches, insomnia, incontinence, chronic low back pain, disease and treatment-related symptoms of cancer, and improving post-surgical outcomes[24].

Most standard therapies for chronic pancreatitis frequently carry adverse effects, particularly in older patients, further compromising their quality of

life. NSAIDs carry a 2- to 5-fold increased risk of gastrointestinal bleeding, which increases with age[25]. NSAID-induced renal, cardiovascular, central nervous system (CNS) and hematological side effects are also more common in older individuals. Use of narcotic analgesic agents results in an increased risk of falls in patients aged 60 yr and over (odds ratio of 1.54)[26], as does polypharmacy with CNS active medications (odds ratio of 2.37)[27]. Bed rest leads to de-conditioning and osteoporosis, especially in the elderly, who often are already at risk for these conditions[28]. The literature has shown yoga to be a safe treatment. Our study, likewise, documents its safety. When yoga was added to the standard therapy, patients tended to take fewer medications.

There has been little research on the mechanisms by which yoga practice might relieve back pain. Although Westerners often think of yoga as a form of exercise, the practice of yoga places as much emphasis on mental focus as on physical movement[29]. and considers the breath, which links the mind and the body, as the key to achieving both physical and psychological benefits[17].

Several large follow-up studies in the past decade suggest that recurrent acute exacerbations dominate the clinical picture in the first few years after onset of symptoms, and progressive pancreatic insufficiency is the predominant feature in the late stages of the disease[30].

Chronic pain is complex physiologically and there are many influencing factors on the pain experience. The approach to treatment therefore needs to be multimodal, often with a number of different interventions, both physical and psychological, delivered in parallel. Chronic pain differs from acute pain in that management follows a rehabilitative rather than a treatment model, though these are not mutually exclusive. Full assessment of the patient, preferably multi-disciplinarily, will improve his or her outlook. Management should be holistic, rigorous in the application of conventional therapies (including analgesics and physical therapy) and ready to admit an improved understanding of psychological and social techniques[31-33].

Patients appreciate their surgeon's continued interest and involvement in their disease and management, and the surgeon can overcome a sense of abandonment that may accompany the discharge of a patient who is not fully healed. Patients who have chronic pain often understand that their pain will not disappear. That their surgeon will not disappear can help them to accept and live with their pain[34,35].

Chronic pain can trigger a cycle of disabilities. Those who suffer from it often retreat into themselves, becoming inactive and minimizing contact with other people. This lack of social interaction often contributes to feelings of depression and isolation. These individuals traditionally rely on pain medications to get through the day and then to sleep, and those medications may cause side effects including dizziness, nausea, and drowsiness that immobilize them further. In addition, the severe pain commonly leads to inactivity that weakens or de-conditions muscles to make them feel even more infirm. Over time, despair may set in, and pain may seem even worse. Chronic pain is pervasive and often limits participation in desired activities.

Because pain is such a complicated problem, managing it requires a multidimensional approach. Some patients seek alternative solutions such as yoga to relieve their pain. Because yoga is multifaceted physical exercise, breathing, relaxation and meditation is integrated into one's being when it is practiced. Such integration has a strengthening effect on the whole self, and fortifies resistance to pain. Yoga offers a very distinct approach to pain. It brings awareness to the body, especially to the parts that are in pain. Yoga helps individuals become more accepting of their body and less judgmental and reactive to pain. With time, an individual with pain will know what makes them feel worse and how to coax their body into balance. Additionally, as individuals practice various yoga poses, their attention is gently directed to other parts of the body at any given moment. In other words, attention is diverted from pain areas and focused on yoga poses. Finally, the poses themselves can ease pain. They can increase muscle strength and flexibility, improve circulation in the joints and muscles, and stimulate the brain to produce painkilling chemicals.

Studies indicate that yoga was beneficial in reducing anxiety and depression in older adults who attended a geriatric clinic and presented with a wide range of affective symptoms related to anxiety and depression[36].

Yoga lowers heart rate, promotes deeper breathing, and induces brain wave patterns that are associated with relaxation and optimism. These effects are much like those of meditation, and it is appropriate to think of yoga as a kind of meditation to the body. A study of 22 medical patients with a defined anxiety disorder showed clinical and statistically significant improvements in objective symptoms of anxiety and panic following an eight-week outpatient physician-referred group stress reduction intervention based on mindfulness meditation and yoga stretches[37].

Regular practice of the classical yoga postures can be quite helpful in producing a healthy immune system and proper environment for its functioning. Many of the Iyengar yoga poses are extremely effective in producing the "relaxation response" and in counteracting the negative effects of the "stress response" on the immune system[38]. These poses are useful for calming and nurturing and are especially valuable when one is too sick or too weak to perform the more vigorous, classical poses[39].

Yoga helps lower stress hormones that compromise the immune system, while also conditioning the lungs and respiratory tract, stimulating the lymphatic system to oust toxins from the body, and bringing oxygenated blood to various organs to ensure their optimal function. The practice of specific asanas can help balance the immune system and help support the thymus and blood to the sinus.

This brief review of the literature provides preliminary support for considering yoga as a CAM intervention in patients who are experiencing pain and anxiety. The literature, while limited, indicates that yoga has been shown to be effective in minimizing pain and anxiety in some populations, specifically the elderly and individuals with behavioural health diagnoses, and that it is effective in minimizing stress in cancer patients. The literature also indicates that pain and anxiety are frequent and distressing

co-occurring disorders in patients of chronic pancreatitis that significantly detract from their health and well-being. Based on this review, yoga may be a beneficial intervention for managing patients with chronic pancreatitis.

Future yoga intervention studies will be needed to carefully control for the class aspect that may be beneficial to everyone, especially seniors. There is also likely some placebo effect related to the yoga intervention. One group has already shown that psychological benefits of an aerobic exercise intervention in a group of healthy young adults could be increased simply by telling subjects that the exercise program was specifically designed to improve psychological well being[40].

Further studies should be emphasized to examine the long-term effects of yoga in terms of management for patients of chronic pancreatitis. In our study, the participants self-reported a decrease in pain and anxiety frequently after each yoga session; however, this study did not examine how long these reductions were maintained. Besides, we did not compare the biochemical data of the patients before and after the yoga programme, which can be researched in future studies. While findings from the current study provide preliminary results, indicating that yoga can be used as an intervention to reduce stress and anxiety in patients of chronic pancreatitis, proper training and knowledge of the principles that guide the practice of yoga must be thoroughly understood and demonstrated by any recreation therapist who would like to use this intervention with clients.

As the use of CAM techniques continues to become more common in many health care facilities, it will only benefit recreation therapists to take advantage of a modality such as yoga to assist in the self-management of illness and disease. Nonetheless, there is room for more education of patients and professionals, and for more research in order to establish the effectiveness of the wide range of management options available.

REFERENCES

1 **Mössner J**. Chronic pancreatitis: nutrition and pain therapy. *Praxis (Bern 1994)* 1998; **87**: 1548-1557
2 **Eisenberg DM**, Davis RB, Ettner SL, Appel S, Wilkey S, Van Rompay M, Kessler RC. Trends in alternative medicine use in the United States, 1990-1997: results of a follow-up national survey. *JAMA* 1998; **280**: 1569-1575
3 **Pirotta MV**, Cohen MM, Kotsirilos V, Farish SJ. Complementary therapies: have they become accepted in general practice? *Med J Aust* 2000; **172**: 105-109
4 **Lewith GT**. Complementary and alternative medicine: an educational, attitudinal and research challenge. *Med J Aust* 2000; **172**: 102-103
5 **Caroleo OO**. AIDS: meeting the needs through therapeutic recreation. *Ther Recreation J* 1988; **22**: 71-78
6 **Garfinkel MS**, Singhal A, Katz WA, Allan DA, Reshetar R, Schumacher HR. Yoga-based intervention for carpal tunnel syndrome: a randomized trial. *JAMA* 1998; **280**: 1601-1603
7 **Cohen L**, Warneke C, Fouladi RT, Rodriguez MA, Chaoul-Reich A. Psychological adjustment and sleep quality in a randomized trial of the effects of a Tibetan yoga intervention in patients with lymphoma. *Cancer* 2004; **100**: 2253-2260
8 **Oken BS**, Kishiyama S, Zajdel D, Bourdette D, Carlsen J, Haas M, Hugos C, Kraemer DF, Lawrence J, Mass M. Randomized controlled trial of yoga and exercise in multiple sclerosis. *Neurology* 2004; **62**: 2058-2064
9 **Bausell RB**, Lee WL, Berman BM. Demographic and health-related correlates to visits to complementary and alternative medical providers. *Med Care* 2001; **39**: 190-196
10 **McHorney CA**, Ware JE, Lu JF, Sherbourne CD. The MOS 36-item Short-Form Health Survey (SF-36): III. Tests of data quality, scaling assumptions, and reliability across diverse patient groups. *Med Care* 1994; **32**: 40-66
11 **Fiebiger W**, Mitterbauer C, Oberbauer R. Health-related quality of life outcomes after kidney transplantation. *Health Qual Life Outcomes* 2004; **2**: 2
12 **Neumann L**, Berzak A, Buskila D. Measuring health status in Israeli patients with fibromyalgia syndrome and widespread pain and healthy individuals: utility of the short form 36-item health survey (SF-36). *Semin Arthritis Rheum* 2000; **29**: 400-408
13 **Albani C**, Blaser G, Geyer M, Schmutzer G, Brähler E, Bailer H, Grulke N. The German short version of "Profile of Mood States" (POMS): psychometric evaluation in a representative sample. *Psychother Psychosom Med Psycho*l 2005; **55**: 324-330
14 **Cassileth BR**, Lusk EJ, Strouse TB, Miller DS, Brown LL, Cross PA. A psychological analysis of cancer patients and their next-of-kin. *Cancer* 1985; **55**: 72-76
15 **Carlson LE**, Ursuliak Z, Goodey E, Angen M, Speca M. The effects of a mindfulness meditation-based stress reduction program on mood and symptoms of stress in cancer outpatients: 6-month follow-up. *Support Care Cancer* 2001; **9**: 112-123
16 **Williams KA**, Petronis J, Smith D, Goodrich D, Wu J, Ravi N, Doyle EJ, Gregory Juckett R, Munoz Kolar M, Gross R, Steinberg L. Effect of Iyengar yoga therapy for chronic low back pain. *Pain* 2005; **115**: 107-117
17 **Sovik R**. The science of breathing--the yogic view. *Prog Brain Res* 2000; **122**: 491-505
18 **Kabat-Zinn J**, Massion AO, Kristeller J, Peterson LG, Fletcher KE, Pbert L, Lenderking WR, Santorelli SF. Effectiveness of a meditation-based stress reduction program in the treatment of anxiety disorders. *Am J Psychiatry* 1992; **149**: 936-943
19 **Kaplan KH**, Goldenberg DL, Galvin-Nadeau M. The impact of a meditation-based stress reduction program on fibromyalgia. *Gen Hosp Psychiatry* 1993; **15**: 284-289
20 **Kabat-Zinn J**, Wheeler E, Light T, Skillings A, Scharf MJ, Cropley TG, Hosmer D, Bernhard JD. Influence of a mindfulness meditation-based stress reduction intervention on rates of skin clearing in patients with moderate to severe psoriasis undergoing phototherapy (UVB) and photochemotherapy (PUVA). *Psychosom Med* 1998; **60**: 625-632
21 **Menniti-Ippolito F**, Gargiulo L, Bologna E, Forcella E, Raschetti R. Use of unconventional medicine in Italy: a nationwide survey. *Eur J Clin Pharmacol* 2002; **58**: 61-64
22 **Bensoussan A**. Complementary medicine--where lies its appeal? *Med J Aust* 1999; **170**: 247-248
23 **Astin JA**. Why patients use alternative medicine: results of a national study. *JAMA* 1998; **279**: 1548-1553
24 **Astin JA**, Shapiro SL, Eisenberg DM, Forys KL. Mind-body medicine: state of the science, implications for practice. *J Am Board Fam Pract* 2003; **16**: 131-147
25 **Johnson AG**, Day RO. The problems and pitfalls of NSAID therapy in the elderly (Part I). *Drugs Aging* 1991; **1**: 130-143
26 **Leipzig RM**, Cumming RG, Tinetti ME. Drugs and falls in older people: a systematic review and meta-analysis: I. Psychotropic drugs. *J Am Geriatr Soc* 1999; **47**: 30-39
27 **Weiner DK**, Hanlon JT, Studenski SA. Effects of central nervous system polypharmacy on falls liability in community-dwelling elderly. *Gerontology* 1998; **44**: 217-221
28 **Bloomfield SA**. Changes in musculoskeletal structure and function with prolonged bed rest. *Med Sci Sports Exerc* 1997; **29**: 197-206
29 **Carlson LE**, Speca M, Patel KD, Goodey E. Mindfulness-based stress reduction in relation to quality of life, mood, symptoms of stress and levels of cortisol, dehydroepiandrosterone sulfate (DHEAS) and melatonin in breast and prostate cancer outpatients. *Psychoneuroendocrinology* 2004; **29**: 448-474
30 **Chari ST**, Singer MV. The problem of classification and staging of chronic pancreatitis. Proposals based on current knowledge of its natural history. *Scand J Gastroenterol* 1994; **29**: 949-960

31 **Smith BH**, Hopton JL, Chambers WA. Chronic pain in primary care. *Fam Pract* 1999; **16**: 475-482
32 **Glasbrenner B**, Adler G. Evaluating pain and the quality of life in chronic pancreatitis. *Int J Pancreatol* 1997; **22**: 163-170
33 **Assan R**, Alexandre JH, Tiengo A, Marre M, Costamailleres L, Lhomme C. Survival and rehabilitation after total pancreatectomy. A follow-up of 36 patients. *Diabete Metab* 1985; **11**: 303-309
34 **Thompson AR**, Wolfe JJ. Chronic pain management in the surgical patient. *Surg Clin North Am* 2005; **85**: 209-224
35 **Sakorafas GH**, Farnell MB, Farley DR, Rowland CM, Sarr MG. Long-term results after surgery for chronic pancreatitis. *Int J Pancreatol* 2000; **27**: 131-142
36 **DiBenedetto M**, Innes KE, Taylor AG, Rodeheaver PF, Boxer JA, Wright HJ, Kerrigan DC. Effect of a gentle Iyengar yoga program on gait in the elderly: an exploratory study. *Arch Phys Med Rehabil* 2005; **86**: 1830-1837
37 **Miller JJ**, Fletcher K, Kabat-Zinn J. Three-year follow-up and clinical implications of a mindfulness meditation-based stress reduction intervention in the treatment of anxiety disorders. *Gen Hosp Psychiatry* 1995; **17**: 192-200
38 **Woolery A**, Myers H, Sternlieb B, Zeltzer L. A yoga intervention for young adults with elevated symptoms of depression. *Altern Ther Health Med* 2004; **10**: 60-63
39 **Garfinkel M**, Schumacher HR. Yoga. *Rheum Dis Clin North Am* 2000; **26**: 125-132,x
40 **Desharnais R**, Jobin J, Côté C, Lévesque L, Godin G. Aerobic exercise and the placebo effect: a controlled study. *Psychosom Med* 1993; **55**: 149-154

S- Editor Pan BR **L- Editor** Zhu LH **E- Editor** Bi L

PO Box 2345, Beijing 100023, China
www.wjgnet.com
wjg@wjgnet.com

World J Gastroenterol 2007 January 21; 13(3): 398-402
World Journal of Gastroenterology ISSN 1007-9327

CLINICAL RESEARCH

Leptin levels in the differential diagnosis between benign and malignant ascites

Mehmet Buyukberber, Mehmet Koruk, M Cemil Savas, Murat T Gulsen, Yavuz Pehlivan, Rukiye Deveci, Alper Sevinc, Serdar Gergerlioglu

Mehmet Buyukberber, Mehmet Koruk, M Cemil Savas, Murat T Gulsen, Department of Gastroenterology, Gaziantep University, School of Medicine, 27310 Gaziantep, Turkey
Yavuz Pehlivan, Department of Internal Medicine, Gaziantep University, School of Medicine, 27310 Gaziantep, Turkey
Rukiye Deveci, Department of Biochemistry, Gaziantep University, School of Medicine, 27310 Gaziantep, Turkey
Alper Sevinc, Department of Medical Oncology, Gaziantep University, School of Medicine, Gaziantep Oncology Hospital, 27310 Gaziantep, Turkey
Serdar Gergerlioglu, Department of Physiology, Gaziantep University, School of Medicine, 27310 Gaziantep, Turkey
Correspondence to: Dr. Alper Sevinc, Gaziantep University, School of Medicine, Department of Medical Oncology, Gaziantep Oncology Hospital, TR-27310 Gaziantep, Turkey. sevinc@gantep.edu.tr
Telephone: +90-342-4720711 Fax: +90-342-4720718
Received: 2006-08-24 Accepted: 2006-12-04

Abstract

AIM: To evaluate the role of leptin levels in the differential diagnosis of ascites.

METHODS: Ascitic leptin, TNFα and serum leptin levels were measured in 77 patients with ascites (35 with malignancies, 30 cirrhosis and 12 tuberculosis). Control serum samples were obtained from 20 healthy subjects. Leptin and TNFα levels were measured by ELISA. Body mass index (BMI) and percentage of body fat (BFM) by skin fold measurement were calculated for all patients and control groups. Peritoneal biopsy, ascites cytology and cultures or biochemical values were used for the diagnosis of patients.

RESULTS: In patients with malignancies, the mean serum and ascites leptin levels and their ratios were significantly decreased compared to the other patient groups and controls. In tuberculosis peritonitis, ascitic fluid TNFα levels were significantly higher than malignant ascites and cirrhotic sterile ascites. BMI and BFM values did not distinguish between patients and controls.

CONCLUSION: In patients with malignant ascites, levels of leptin and TNFα were significantly lower than in patients with tuberculous ascites.

Key words: Leptin; Benign ascites; Malignant ascites; Tuberculosis; Cirrhosis

Buyukberber M, Koruk M, Savas MC, Gulsen MT, Pehlivan Y, Deveci R, Sevinc A, Gergerlioglu S. Leptin levels in the differential diagnosis between benign and malignant ascites. *World J Gastroenterol* 2007; 13(3): 398-402

http://www.wjgnet.com/1007-9327/13/398.asp

INTRODUCTION

Leptin, a product of the obese gene, is a multifunctional hormone secreted predominantly by adipocytes. It was discovered in 1994 by Friedman *et al*[1]. The importance of leptin in the regulation of energy balance, food intake and body composition through a central feedback mechanism has been demonstrated in both animal and human studies[2-5]. In humans, circulating leptin levels exhibit a particularly strong positive correlation with the body fat mass (BFM), body mass index (BMI) and sex. Serum leptin concentration is higher in obese than in lean subjects and in females than in males[6]. On the other hand, leptin serum levels can be altered in various diseases[7].

Liver cirrhosis is associated with hypercatabolism and malnutrition that leads to increased energy expenditure[8]. Previous studies have shown that circulating leptin levels are modestly elevated in patients with alcoholic and posthepatic cirrhosis[9-12]. Another study reported that the ascitic fluid leptin levels of cirrhotic patients with sterile ascites are on average two times higher than circulating levels of this hormone[13]. Serum leptin levels have been reported to be reduced in cancer patients[14,15]. Abramov *et al*[16] found low leptin levels in serum, pleural, peritoneal fluids and in Meigs' syndrome as well. In the literature, there is no study about leptin levels in malignant ascites. In patients with active pulmonary tuberculosis, a previous study found increased leptin concentrations and a correlation with increased concentrations of tumor necrosis factor than control groups. After antituberculosis therapy, leptin levels of these patients were elevated, but this increase was not statistically significant[17]. However, in a recent study in patients with active pulmonary tuberculosis, leptin levels were determined to be decreased. Reduced body fat content secondary to anorexia and cachexia during the active disease period was claimed as a reason for this[18]. To our knowledge, there is no study

about this subject in either ascites or serum of patients with tuberculosis peritonitis.

There are problems in the differential diagnosis of ascites. Especially diagnosis of exudative ascites (including lymphoma, various forms of peritonitis, peritoneal carcinomatosis, and peritoneal tuberculosis) is a dilemma. Non-invasive tests such as laboratory tests, acid-fast stain and culture of the ascitic fluid, ADA levels are usually insufficient for the differential diagnosis of ascites[19,20]. Therefore laparoscopy with directed biopsy is necessary for the diagnosis of ascites. In the light of these findings of our prospective study, leptin may be accepted as a new criterion for the differential diagnosis of malignant and benign ascites.

MATERIALS AND METHODS

Materials

The study population consisted of 77 patients with ascites and 20 healthy people who were recruited from the Department of Gastroenterology, Gaziantep University Hospital, Gaziantep, Turkey. The patients were divided into three groups. Group Ⅰ consisted of 35 patients with various types of malignant diseases (seven ovarian adenocarcinoma, ten adenocarcinoma of the colon, five lymphoma, seven pancreatic adenocarcinoma, six gastric adenocarcinoma). Mean age was 56.2 ± 17.4 years (20 men and 15 women). Group Ⅱ included 30 cirrhotic patients (mean age 55.05 ± 13.26 years, 15 men and 15 women). The diagnosis of cirrhosis was based on the typical findings of hepatic cirrhotic appearance, splenomegaly, esophageal varices and ascites (by ultrasonography and upper gastrointestinal endoscopical examinations), with biochemical data. Etiology of cirrhosis was hepatitis C virus in fifteen patients, hepatitis B virus in thirteen patients and cryptogenic in two patients. The severity of cirrhosis was graded according to the Child-Pugh classification[21]. All of the patients were Child C. Group Ⅲ consisted of 12 patients with tuberculous peritonitis (these patients were diagnosed with laparoscopic peritoneal biopsy, mean age 51.9 ± 15.3 years, 5 men and 7 women). The control groups included 20 healthy volunteers (mean age 52.9 ± 13.3 years, 10 men and 10 women). Exclusion criteria were diabetes mellitus, existence of pleural effusion, gastrointestinal bleeding, spontaneous bacterial peritonitis and renal failure, treatment with corticosteroids, immunosuppressive agents and oral contraceptive agents within the last 6 mo. Control group consisted of healthy individuals with normal medical history, physical examination and blood biochemistry. None of them have had a restriction of diet for loosing weight during the last three months. The local ethics committee approved the study and written consents were received from all participants.

Methods

Blood samples were obtained in the early morning after an overnight fasting (12 h). The blood was centrifuged at 3000 rpm for 20 min at 4℃ and serums were was stored at -80℃ until analysis of leptin concentrations. Biochemical analyses were done during the same day. After paracentesis of peritoneal fluid, ascitic fluid was collected under sterile conditions and seeded in both aerobic and anaerobic cultures. It was immediately centrifuged at 3000 rpm for 20 min at 4℃ and stored at -80℃ in tubes for assessment of leptin levels. Ascitic fluid was also obtained for routine biochemical analysis, cytologic exam and white blood cell counts.

Body composition such as BMI, skin fold thickness, body fat percentage (BFP), and BFM analysis was performed in patients and controls. BMI was defined for study populations as weight divided by height squared (kg/m^2). Skinfold thickness was measured at four different sites on the left side of the body (triceps, biceps, subscapular and supra-iliac) using a Holtain skinfold caliper. Percent body fat (%BF) was calculated using the Jacksons' formula[22], BFM was calculated using BFP and body weight as in kilograms, and triceps skinfold thickness less than a 10^{th} of a percentile[23] was excluded. Serum and ascitic fluid leptin and serum TNFα levels were measured by a commercially available ELISA kit (Quantikine Human Leptin Immunoassay; RD Systems). The lower limit of detection was 0.05 μg/L. The intra-assay and interassay coefficients of variation was below 12%.

Statistical analysis

Results were given as mean ± SE. Comparisons between and among the groups were made using a non-parametric test (Mann-Whitney *U* test) and one way ANOVA variant analyses. Statistical analysis for the comparison of serum and ascitic fluid analyses was carried out by means of Wilcoxon matched pairs signed rank test. The correlation among numerical data was analyzed by the Pearson correlation coefficient (*r*). Spearman's rank correlation test was used for estimation of the level of the association between two variables. Data were statistically evaluated using the SPSS v10.0 (Statistical Program for Social Science, version 10.0, Chicago, IL, USA) software packages. $P < 0.05$ was taken as significant.

RESULTS

Patients' demographic data

The demographic, anthropometrical characteristics of all patients and control groups are showed in Table 1. There were no statistically significant differences between three patients groups and the controls regarding BMI, BFP and BFM ($P > 0.05$).

Serum and ascitic fluid leptin and TNFα levels

The main biochemical analyses, leptin, and TNFα levels of the ascitic fluid of the patients and serum leptin levels are shown in Table 2. None of the patients had spontaneous bacterial peritonitis. Serum concentrations of leptin were significantly elevated in tuberculosis and cirrhotic patients compared with serum levels in control and malignant patients groups ($P = 0.0001$). There were no statistically significant differences in serum leptin levels between cirrhosis and tuberculosis patient groups ($P > 0.05$). In addition serum leptin levels of malignant patients were

Table 1 Demographic and anthropometrical characteristics of all subjects

Characteristic	Mean age ± SD (yr)	BMI (kg/m^2)	BFP (%)	BFM (kg)
Cirrhotic patients (n = 30)	55.05 ± 13.26	22.1	26.4	17.3
Male (n = 15)	57.2 ± 12.3	21.5	23.8	16.6
Female (n = 15)	53.3 ± 13.05	22.6	28.8	17.9
Malignant ascites (n = 35)	56.2 ± 17.4	22.4	26.8	17.4
Male (n = 20)	58.2 ± 15.3	22.1	24.2	17.1
Female (n = 15)	54.1 ± 14.2	22.8	29.4	17.9
Tuberculous peritonitis (n = 12)	51.9 ± 15.3	22.6	26.9	17.6
Male (n = 5)	53.8 ± 13.2	22.2	24.6	17.2
Female (n = 7)	50.1 ± 12.4	23	29.4	18.1
Control (n = 20)	52.9 ± 13.3	22.7	27	17.7
Male (n = 10)	54.6 ± 11.8	22.5	24.8	17.3
Female (n = 10)	51.6 ± 10.9	22.9	29.2	18.2

Table 2 Ascitic leptin, TNFα and serum leptin levels in study population (mean ± SD)

	Control subjects	Cirrhotic patients	Malignant ascites	Tuberculous peritonitis
Leptin (ascites) (μg/L)	-	7.19 ± 3.43	2.45 ± 1.25	5.59 ± 1.08
Leptin (serum) (μg/L)	2.93 ± 0.32	3.77 ± 2.04	1.30 ± 0.63	3.72 ± 0.64
TNFα (ascites) (ng/L)	-	30.36 ± 6.37	29.65 ± 7.08	65.5 ± 18.4
Total proteins (ascites) (g/L)	-	15.4 ± 6.3	26.1 ± 11.5	28.2 ± 21.9
Albumin (ascites) (g/L)	-	7.1 ± 4.0	14.3 ± 7.2	13 ± 11.6
LDH (ascites) (U/L)	-	142.97 ± 93.99	546.5 ± 473.8	351.40 ± 378.82
Glucose (ascites) (mg/L)	-	1253.6 ± 348.1	1057.2 ± 443.8	1176 ± 482.3
Total leukocyte (ascites) (× 10^6/L)	-	0.43 ± 0.46	976 ± 608.4	1.16 ± 1.17
Neutrophils (ascites) (× 10^6/L)	-	0.22 ± 0.31	668.19 ± 416.3	0.44 ± 0.63
Lymphocytes (ascites) (× 10^6/L)	-	0.12 ± 0.01	223.34 ± 102.3	0.75 ± 0.32

significantly lower than control groups ($P < 0.001$, Table 2).

On the other hand, the levels of leptin in ascitic fluid were significantly higher in tuberculosis and cirrhotic patients than in patients with malignant effusions ($P < 0.001$). In cirrhotic patients, ascitic fluid levels of leptin were higher than in patients with tuberculosis peritonitis, but the difference was not statistically statistically significant ($P > 0.05$, Table 2). Leptin levels were significantly higher in ascitic fluid than in serum ($P < 0.01$ Wilcoxon test), with a mean ascites/serum ratio of approximately 2.0 in all patient groups (Table 2). Serum and ascitic fluid leptin levels showed significant positive correlation in all patient groups (Malignant group: $r = 0.979$, $P = 0.0001$; Cirrhotic group: $r = 0.999$, $P = 0.0001$; Tuberculosis group: $r = 0.995$, $P = 0.0001$).

Ascites TNFα levels were significantly increased in patients with tuberculosis peritonitis, when compared to the other patient groups. Ascites TNFα levels were not statistically significant between cirrhosis and malignant ascites groups ($P < 0.001$, Table 2). We observed that ascitic fluid TNFα levels were significantly positively correlated with ascitic leptin levels in the tuberculosis peritonitis group ($r = 0.979$, $P = 0.0001$). However, this correlation was not observed in the other patient groups.

DISCUSSION

Recently, several studies have suggested that serum levels of leptin are significantly elevated in patients with chronic liver disease. The relation between serum levels of leptin, TNFα, and associated liver fibrosis have been investigated in patients with chronic hepatitis C by Piche *et al*[24]. Serum fasting levels of leptin were significantly more elevated than the control group and a significant correlation has been demonstrated between serum levels of leptin, TNFα and severity of liver fibrosis in those patients[24]. Several studies found higher leptin levels among female alcoholic cirrhotic patients than the control group[10,11] and Henriksen *et al*[11] suggested that the elevated circulating leptin in patients with alcoholic cirrhosis was most likely caused by a combination of decreased renal extraction and increased release from fat tissue areas. However, in an animal study with chronic ethanol consumption rats, it has been shown that serum concentrations of tumor necrosis factor were increased and leptin was induced in the liver and peripheral adipose tissues by TNFα[25]. In addition, experimental and animal studies have shown that TNFα is one of the major leptin producer and regulators in anorexia and inflammation[26-28]. It has also been suggested that leptin mediates anorexia in chronic inflammatory states[29]. Anorexia and increased energy expenditure usually accompanies cirrhosis[30]. In previous studies, association between the severity of posthepatitis cirrhosis and serum leptin levels is controversial[12,30,31]. In cirrhotic patients, a significant negative correlation was found between serum levels of leptin and Child-Pugh score[31]. On the contrary, a significant elevation in leptin levels was observed as the Child-Pugh score worsened independently of gender and BMI in cirrhotic patients. Anorexia and hypermetabolism in cirrhosis are held responsible for this[12]. In our study, we also observed that circulating leptin levels were increased in the non-alcoholic cirrhosis group caused by viral hepatitis and not in the control group.

Previous studies have demonstrated that TNFα levels are elevated in the ascitic fluid of cirrhotic patients with spontaneous bacterial peritonitis[32]. Nevertheless Giannini *et al*[13] found that serum and ascitic TNFα levels are significantly elevated but serum and ascites TNFα levels were not correlated and the ascitic fluid leptin levels were either twice as high as serum levels or positively correlated in cirrhotic patients with sterile ascites. High leptin levels in ascites were explained as a result of TNFα stimulation and production of intra-abdominal leptin. The results of our study support the hypothesis of Giannini *et al*[13]. In 30 patients with active pulmonary tuberculosis in Turkey, a recent study found increased leptin concentrations and a correlation with TNFα[17]. Similar results were reported in another study from Turkey involving 25 patients with tuberculosis[33]. After antituberculosis therapy in two studies, leptin levels were more elevated. One study from

Indonesia found lower leptin concentrations in 60 HIV-negative patients with active tuberculosis compared to 30 healthy control[18]. In another study performed in with patients with tuberculous pleural effusions, it has been demonstrated that serum and pleural fluid levels of tumor necrosis factor were significantly elevated compared with transudative pleural effusion[34]. For the time, no study dealing with leptin concentrations in tuberculosis peritonitis has been reported in the literature to our knowledge. In this study, we found that ascitic fluid TNFα levels in tuberculosis peritonitis are significantly elevated when compared to the other patients groups, serum and ascitic leptin levels were significantly higher than in malignant patients. In addition, we observed that ascitic fluid TNFα levels were significantly positively correlated with ascitic leptin levels in the tuberculosis peritonitis group. Our findings support that in tuberculosis peritonitis, TNFα may be a major stimulating factor of leptin secretion.

Low serum leptin levels have been observed in patients with malignancy[14,15]. It has been shown that serum leptin levels of prostate cancer are lower than benign prostatic hyperplasia[14]. On the other hand, it has recently been demonstrated that in patients with pre-menopausal carcinoma in situ of the breast cancer, serum leptin levels were decreased compared with the control group[15]. In a case report, while levels of leptin in the serum, peritoneal and pleural fluids were lower in patient Meigs' syndrome, serum levels were increased following surgical therapy of the tumor along with the resolution of ascites and pleural fluids. Abramov and coworkers suggested that mediators of the tumoral tissue inhibit leptin secretion and excision of the tumoral tissue increased leptin levels[16]. In patients with malignant pleural effusions, levels of TNFα were significantly lower than in patients with tuberculous effusions[34]. In a recent study, we investigated the importance of ascitic fluid LDH level and LDH isoenzyme activities in patients with malignant and nonmalignant ascites. LDH level, LDH-4 activity and LDH-5 activity were found to be significantly higher, and LDH-1 activity was found to be lower in malignant ascites when compared with nonmalignant ascites. We conclude that ascitic LDH and its isoenzyme pattern may be helpful for the differential diagnosis of ascites[35].

According to our knowledge, there is no study about leptin levels in malignant ascites in the literature. In the present study, we observed that ascitic fluid TNFα levels, serum and ascitic fluid leptin levels of malignant patients are significantly lower than tuberculosis patients. Is the reason for low leptin levels that some mediators released by the tumor which inhibit leptin secretion? Or does decreased body fat, secondary to malnutrition and cachexia caused by tumor, results in decreased levels of leptin? More studies are necessary to explain these. In summary, our study has demonstrated that serum and ascitic fluid leptin levels of malignant patients are significantly lower than tuberculosis peritonitis and cirrhotic patients with sterile ascites. These findings suggest that leptin may be an important marker in the malignant ascitic fluid. Especially, leptin as a tumour marker may be useful in differential diagnosis of benign and malignant ascites.

REFERENCES

1 **Friedman JM**, Halaas JL. Leptin and the regulation of body weight in mammals. *Nature* 1998; **395**: 763-770
2 **Friedman JM**. Leptin, leptin receptors and the control of body weight. *Eur J Med Res* 1997; **2**: 7-13
3 **Tartaglia LA**. The leptin receptor. *J Biol Chem* 1997; **272**: 6093-6096
4 **Kennedy A**, Gettys TW, Watson P, Wallace P, Ganaway E, Pan Q, Garvey WT. The metabolic significance of leptin in humans: gender-based differences in relationship to adiposity, insulin sensitivity, and energy expenditure. *J Clin Endocrinol Metab* 1997; **82**: 1293-1300
5 **Considine RV**, Sinha MK, Heiman ML, Kriauciunas A, Stephens TW, Nyce MR, Ohannesian JP, Marco CC, McKee LJ, Bauer TL. Serum immunoreactive-leptin concentrations in normal-weight and obese humans. *N Engl J Med* 1996; **334**: 292-295
6 **Van Gaal LF**, Wauters MA, Mertens IL, Considine RV, De Leeuw IH. Clinical endocrinology of human leptin. *Int J Obes Relat Metab Disord* 1999; **23** Suppl 1: 29-36
7 **Mantzoros CS**. The role of leptin in human obesity and disease: a review of current evidence. *Ann Intern Med* 1999; **130**: 671-680
8 **Greco AV**, Mingrone G, Benedetti G, Capristo E, Tataranni PA, Gasbarrini G. Daily energy and substrate metabolism in patients with cirrhosis. *Hepatology* 1998; **27**: 346-350
9 **Shimizu H**, Kakizaki S, Tsuchiya T, Nagamine T, Takagi H, Takayama H, Kobayashi I, Mori M. An increase of circulating leptin in patients with liver cirrhosis. *Int J Obes Relat Metab Disord* 1998; **22**: 1234-1238
10 **McCullough AJ**, Bugianesi E, Marchesini G, Kalhan SC. Gender-dependent alterations in serum leptin in alcoholic cirrhosis. *Gastroenterology* 1998; **115**: 947-953
11 **Henriksen JH**, Holst JJ, Møller S, Brinch K, Bendtsen F. Increased circulating leptin in alcoholic cirrhosis: relation to release and disposal. *Hepatology* 1999; **29**: 1818-1824
12 **Bolukbas FF**, Bolukbas C, Horoz M, Gumus M, Erdogan M, Zeyrek F, Yayla A, Ovunc O. Child-Pugh classification dependent alterations in serum leptin levels among cirrhotic patients: a case controlled study. *BMC Gastroenterol* 2004; **4**: 23
13 **Giannini E**, Romagnoli P, Tenconi GL, Botta F, Malfatti F, Chiarbonello B, Mamone M, Barreca T, Testa R. High ascitic fluid leptin levels in patients with decompensated liver cirrhosis and sterile ascites: relationship with TNF-alpha levels. *Dig Dis Sci* 2004; **49**: 275-280
14 **Lagiou P**, Signorello LB, Trichopoulos D, Tzonou A, Trichopoulou A, Mantzoros CS. Leptin in relation to prostate cancer and benign prostatic hyperplasia. *Int J Cancer* 1998; **76**: 25-28
15 **Mantzoros CS**, Bolhke K, Moschos S, Cramer DW. Leptin in relation to carcinoma in situ of the breast: a study of pre-menopausal cases and controls. *Int J Cancer* 1999; **80**: 523-526
16 **Abramov Y**, Anteby SO, Fatum M, Fasouliotis SJ, Barak V. The kinetics of leptin in Meigs' syndrome. *Gynecol Oncol* 2001; **83**: 316-318
17 **Cakir B**, Yönem A, Güler S, Odabaşi E, Demirbaş B, Gürsoy G, Aral Y. Relation of leptin and tumor necrosis factor alpha to body weight changes in patients with pulmonary tuberculosis. *Horm Res* 1999; **52**: 279-283
18 **van Crevel R**, Karyadi E, Netea MG, Verhoef H, Nelwan RH, West CE, van der Meer JW. Decreased plasma leptin concentrations in tuberculosis patients are associated with wasting and inflammation. *J Clin Endocrinol Metab* 2002; **87**: 758-763
19 **Demir K**, Okten A, Kaymakoglu S, Dincer D, Besisik F, Cevikbas U, Ozdil S, Bostas G, Mungan Z, Cakaloglu Y. Tuberculous peritonitis--reports of 26 cases, detailing diagnostic and therapeutic problems. *Eur J Gastroenterol Hepatol* 2001; **13**: 581-585
20 **Buyukberber M**, Sevinc A, Cagliyan CE, Gulsen MT, Sari I, Camci C. Non-Hodgkin lymphoma with high adenosine deaminase levels mimicking peritoneal tuberculosis: an

unusual presentation. *Leuk Lymphoma* 2006; **47**: 565-568
21 **Pugh RN**, Murray-Lyon IM, Dawson JL, Pietroni MC, Williams R. Transection of the oesophagus for bleeding oesophageal varices. *Br J Surg* 1973; **60**: 646-649
22 **Jackson AS**, Pollock ML, Ward A. Generalized equations for predicting body density of women. *Med Sci Sports Exerc* 1980; **12**: 175-181
23 **Heymsfield SB**, Williams PJ. Nutritional assessment by clinical and biochemical methods. In: Shils ME, Young VR. Modern nutrition in health and disease. 7th ed. Philadelphia: Lea & Febiger, 1988: 817-860
24 **Piche T**, Vandenbos F, Abakar-Mahamat A, Vanbiervliet G, Barjoan EM, Calle G, Giudicelli J, Ferrua B, Laffont C, Benzaken S, Tran A. The severity of liver fibrosis is associated with high leptin levels in chronic hepatitis C. *J Viral Hepat* 2004; **11**: 91-96
25 **Lin HZ**, Yang SQ, Zeldin G, Diehl AM. Chronic ethanol consumption induces the production of tumor necrosis factor-alpha and related cytokines in liver and adipose tissue. *Alcohol Clin Exp Res* 1998; **22**: 231S-237S
26 **Grunfeld C**, Zhao C, Fuller J, Pollack A, Moser A, Friedman J, Feingold KR. Endotoxin and cytokines induce expression of leptin, the ob gene product, in hamsters. *J Clin Invest* 1996; **97**: 2152-2157
27 **Zumbach MS**, Boehme MW, Wahl P, Stremmel W, Ziegler R, Nawroth PP. Tumor necrosis factor increases serum leptin levels in humans. *J Clin Endocrinol Metab* 1997; **82**: 4080-4082
28 **Kirchgessner TG**, Uysal KT, Wiesbrock SM, Marino MW, Hotamisligil GS. Tumor necrosis factor-alpha contributes to obesity-related hyperleptinemia by regulating leptin release from adipocytes. *J Clin Invest* 1997; **100**: 2777-2782
29 **Sarraf P**, Frederich RC, Turner EM, Ma G, Jaskowiak NT, Rivet DJ, Flier JS, Lowell BB, Fraker DL, Alexander HR. Multiple cytokines and acute inflammation raise mouse leptin levels: potential role in inflammatory anorexia. *J Exp Med* 1997; **185**: 171-175
30 **Müller MJ**, Lautz HU, Plogmann B, Bürger M, Körber J, Schmidt FW. Energy expenditure and substrate oxidation in patients with cirrhosis: the impact of cause, clinical staging and nutritional state. *Hepatology* 1992; **15**: 782-794
31 **Testa R**, Franceschini R, Giannini E, Cataldi A, Botta F, Fasoli A, Tenerelli P, Rolandi E, Barreca T. Serum leptin levels in patients with viral chronic hepatitis or liver cirrhosis. *J Hepatol* 2000; **33**: 33-37
32 **Greco AV**, Mingrone G, Favuzzi A, Capristo E, Gniuli D, Addolorato G, Brunani A, Cavagnin F, Gasbarrini G. Serum leptin levels in post-hepatitis liver cirrhosis. *J Hepatol* 2000; **33**: 38-42
33 **Navasa M**, Follo A, Filella X, Jiménez W, Francitorra A, Planas R, Rimola A, Arroyo V, Rodés J. Tumor necrosis factor and interleukin-6 in spontaneous bacterial peritonitis in cirrhosis: relationship with the development of renal impairment and mortality. *Hepatology* 1998; **27**: 1227-1232
34 **Yüksel I**, Sencan M, Dökmetaş HS, Dökmetaş I, Ataseven H, Yönem O. The relation between serum leptin levels and body fat mass in patients with active lung tuberculosis. *Endocr Res* 2003; **29**: 257-264
35 **Hamed EA**, El-Noweihi AM, Mohamed AZ, Mahmoud A. Vasoactive mediators (VEGF and TNF-alpha) in patients with malignant and tuberculous pleural effusions. *Respirology* 2004; **9**: 81-86
36 **Sevinc A**, Sari R, Fadillioglu E. The utility of lactate dehydrogenase isoenzyme pattern in the diagnostic evaluation of malignant and nonmalignant ascites. *J Natl Med Assoc* 2005; **97**: 79-84

S- Editor Wang GP **L- Editor** Alpini GD **E- Editor** Lu W

PO Box 2345, Beijing 100023, China
www.wjgnet.com
wjg@wjgnet.com

World J Gastroenterol 2007 January 21; 13(3): 403-407
World Journal of Gastroenterology ISSN 1007-9327

RAPID COMMUNICATION

Environmental noise alters gastric myoelectrical activity: Effect of age

James S Castle, Jin-Hong Xing, Mark R Warner, Mark A Korsten

James S Castle, Jin-Hong Xing, Mark R Warner, Mark A Korsten, Medical Program and Audiology Service, James J Peters VA Medical Center, Bronx, NY and Mount Sinai School of Medicine, New York, United States
Correspondence to: Mark A Korsten, MD, James J Peters VA Medical Center, 130 W. Kingsbridge Road, Bronx, New York 10468, United States. mark.korsten@med.va.gov
Telephone: +1-718-5849000-6753 Fax: +1-718-7414233
Received: 2006-10-20 Accepted: 2006-12-11

Abstract

AIM: To evaluate the effect of age and acoustic stress on gastric myoelectrical activity (GMA) and autonomic nervous system function.

METHODS: Twenty-one male subjects (age range 22-71 years, mean 44 years) were recruited and exposed, in random order, to three auditory stimuli (Hospital noise, conversation babble and traffic noise) after a 20-min baseline. All periods lasted 20 min and were interspersed with a 10 min of recovery. GMA was obtained using a Synectics Microdigitrapper. Autonomic nerve function was assessed by monitoring blood pressure and heart rate using an automatic recording device.

RESULTS: Dominant power tended to decrease with increase of age ($P < 0.05$). The overall percentage of three cycle per minute (CPM) activity decreased during exposure to hospital noise (12.0%, $P < 0.05$), traffic noise (13.9%, $P < 0.05$), and conversation babble (7.1%). The subjects in the younger group (< 50 years) showed a consistent reduction in the percentage of 3 CPM activity during hospital noise (22.9%, $P < 0.05$), traffic noise (19.0%, $P < 0.05$), and conversation babble (15.5%). These observations were accompanied by a significant increase in bradygastria: hospital noise ($P < 0.05$) and traffic noise ($P < 0.05$). In contrast, the subjects over 50 years of age did not exhibit a significant decrease in 3 CPM activity. Regardless of age, noise did not alter blood pressure or heart rate.

CONCLUSION: GMA changes with age. Loud noise can alter GMA, especially in younger individuals. Our data indicate that even short-term exposure to noise may alter the contractility of the stomach.

Key words: Noise; Acoustic stress; Gastric myoelectrical activity; Electrogastrogram; Autonomic nervous system

Castle JS, Xing JH, Warner MR, Korsten MA. Environmental noise alters gastric myoelectrical activity: Effect of age. *World J Gastroenterol* 2007; 13(3): 403-407

http://www.wjgnet.com/1007-9327/13/403.asp

INTRODUCTION

Excessive noise has been linked to a variety of health issues, including hearing loss[1] mental illness[2,3], sleep disturbance[4], hypertension[5,6] and cardiovascular diseases[7-9]. In terms of gastrointestinal tract, non-specific abdominal complaints[10,11], gastritis and peptic ulcers[12,13] have been noted in populations, including workers, that are exposed to high levels of environmental noise. Despite this relationship with gastric disorders, little is known regarding the effects of loud sounds on gastrointestinal function. On theoretical grounds, however, an interaction between noise and gastrointestinal function would seem likely given the abundant neural connections between the human auditory system, the autonomic nervous system and the gastrointestinal tract[1]. To the extent that noise has an influence on the autonomic nervous system, an effect on many digestive functions, including peristalsis and acid secretion, would be expected. In this respect, Tomei *et al*[13] observed that noise increased gastric acid production in humans with normal baseline levels of gastric acid, and Gue *et al*[14] have shown that noises slows the emptying of food from canine stomach.

The motility of the stomach is controlled by gastric myoelectrical activity (GMA) that results in contractions of its muscular component. GMA is measured and recorded using surface electrodes. The information so obtained is termed an electrogastrogram (EGG). The EGG is obtained using standard EKG electrodes placed on the skin of the upper abdominal wall. These signals are amplified and filtered prior to computer analysis. The validity of such cutaneous measurements has been validated by simultaneously obtaining direct measurements form the wall of the stomach[15,16]. In humans, the normal GMA is an approximately 3 cycles per minute (CPM) sinusoidal wave, and these waves may result in gastric contractions at a similar frequency. Additionally, under normal conditions, most of the voltage (termed "power") measured during EGG is concentrated around the 3 CPM activity.

From a clinical standpoint, EGG recordings have been employed to investigate patients with dyspepsia whose complaints cannot be defined by routine tests, such as barium X-rays and endoscopy. In this respect, a dominant frequency of GMA greater or less than 3 CPM or a shift in the relative distribution of power away from 3 CPM activity are associated with abnormalities of gastric motor activity[17]. These alterations are thought to be the basis of many stomach complaints collectively referred to as "indigestion" or "dyspepsia".

In light of above observations, the hypothesis evolved that loud noise might alter the EGG, perhaps by a mechanism involving the autonomic nervous system. To test this possibility, we exposed healthy volunteers to a variety of noises while recording the myoelectrical activity of their stomachs and monitoring their blood pressure and heart rate. A secondary hypothesis of this study was that advancing age would attenuate the effects of noise inasmuch as the reactivity of the autonomic nervous system declines with age.

Under the conditions employed in our study, we found that noise was capable of decreasing the percentage of normal 3 CPM activity and these changes were less pronounced in older individuals.

MATERIALS AND METHODS

Subjects

This investigation was approved by the Human Studies Subcommittee (IRB) of the James J. Peters VA Medical Center and informed consent was obtained prior to initiating the studies herein described. A screening hearing test was performed several days prior to the study which assessed the ability to identify sounds at a volume equal or less that 25 dB hearing level at 500, 1000, and 2000 Hz in the both ears and a sound at a volume equal to or less than 45 dB at 4000 Hz in the both ears. If the subjects could not correctly identify each sound, they were excluded from the study and were referred for further workup to the audiology service. All subjects were considered healthy and had no underlying medical problems. Volunteers were excluded from the study if detailed questioning revealed a previous history of chronic gastrointestinal discomforts including heartburn, abdominal pain, constipation or diarrhea. In addition, entry into the study required a normal baseline EGG with a dominant frequency between 2.4-3.7 CPM. Of the 26 screened candidates, 21 male subjects (age range 22-71 years, mean 44 years) met the criteria for inclusion into the study.

Experimental protocol

All subjects were requested not to eat or drink within 4 h prior to the start of the study. They were seated in a special sound room in a reclining chair and instructed not to move or talk for the remainder of the study. The sound room was double walled and approximately thirty-five square feet in area. The ambient noise levels were well within the standards of the American National Standards Institute. The subjects were observed through a one-way viewing window so as to discourage any movement during the study. The subjects were fitted with both an automatic blood pressure recording device and three electrodes that measured GMA.

The duration of the study was 110 min. During this period, the subjects wore stereophonic headphones continuously and were exposed in a random pattern to three periods of different types of auditory stimuli. A twenty-minute baseline period of silence preceded the auditory stimuli. Each stimulus lasted 20 min and was interspersed with a 10 min of silence as a recovery period to minimize potential carry-over effect from previous period. The 10-min recovery time was assumed to be adequate as our preliminary study had shown the effect of noise on GMA did not go beyond this period of time. The three auditory stimuli were as follows: (1) unedited hospital noise recorded during the afternoon of a weekday in the Intensive Care Unit of the James J. Peters Veterans Affairs Medical Center and played back at a level of 87.4 dBA (SPL), a level comparable to that of actual ambient level meter; (2) conversation babble (Auditec, St. Louis, MO) played back at a sound level of 91.3 dBA (SPL); and (3) traffic noise in New York City played back at a sound level of 85.6 dBA. All sound pressure levels were measured with a Lason-Davis 800 B precision sound level meter.

Since GMA may change with age, and many responses to auditory stimuli are believed to decline with age, we further divided subjects into two groups, those under 50 years of age (age range 22-47 years, mean 34 years, n = 12), and those over 50 years of age (age range 51-71 years, mean 56 years, n = 9). The baseline characteristics of GMA of these two age groups were compared and the effect of noise on these two particular age groups was analyzed.

Electrogastrogram

Gastric myoelectrical activity was recorded using a Microdigitrapper (Medtronic-Synectics, Shoreview, Minnesota). Three surface electrodes were placed on the anterior wall of the abdomen. The first electrode was placed midway between the xiphoid and the umbilicus. The second electrode was placed 5 cm to the right of the first electrode. The third electrode was placed five centimeters to the left and thirty degrees above the first electrode. Excess hair was shaved from the immediate area, the skin was gently abraded with an alcohol swab, and conducting gel was applied. All recordings were made at a sampling frequency of 4 Hz, with a cutoff frequency of 15 Hz. The recorded data were uploaded into a computer, transformed (fast-Fourier) and analyzed using a dedicated software (Multigram Version 6.31, Medtronic's-Synectics, Shoreview, Minnesota). Visual inspection of the raw data was performed to detect motion artifacts prior to analysis. Several quantitative parameters were derived including the percentage of 3 CPM activity (defined as normal myoelectrical activity in the range of 2.4-3.7 CPM), bradygastria (< 2.4 CPM) and tachygastria (> 3.7 CPM), dominant frequency (DF) and dominant power (DP). DF refers to the frequency at which the EGG power spectrum has a peak power in the range of 0.5-9.0 CPM, which equals to the frequency of the gastric slow wave measured

Table 1 Characteristics of baseline gastric myoelectrical activity over age

	Dominant frequency	Dominant power	3 CPM activity (%)
Age < 50 yr (n = 12)	3.0 ± 0.1	401.4 ± 103.8	87.9 ± 5.1
Age > 50 yr (n = 9)	3.1 ± 0.3	115.1 ± 45.7	77.7 ± 7.6
P value	P = 0.724	P < 0.05	P = 0.259

from the implanted serosal electrodes[15,16]. The power at the DF in the power spectrum of the EGG was defined as the DP. The relative change of the EGG dominant power may reflect gastric contractility[16,18].

Blood pressure and heart rate monitoring

An automatic blood pressure recording device was applied *via* an arm cuff placed around the upper arm of each participant. Recordings were made automatically every 5 min during the whole course of study. Systolic pressure, diastolic pressure and heart rate were analyzed to see whether noise affected autonomic nerve activity.

Statistical analysis

Data were presented either as percent change relative to baseline (percentage of 3 CPM activity, bradygastria and tachygastria) or means ± SE (DF and DP). Student's t test or one way RM ANOVA was used for comparison wherever appropriate. A P value less than 0.05 was considered statistically significant.

RESULTS

Effect of age on GMA

We subjectively divided participants into two age groups, using age 50 as a cutoff line. Percentage of 3 CPM activity, DF and DP were derived from the twenty-minute baseline period and comparisons were made between these two age groups. Detailed data are presented in Table 1. In brief, though no significant difference was observed in DF and percentage of 3 CPM activity during the baseline, younger people tended to have obviously higher dominant power (401.4 ± 03.8) than those above age 50 (115.1 ± 45.7, P < 0.05).

Effect of noise on percentage of 3 CPM activity

During exposure to hospital noise and traffic noise, the percentage of 3 CPM activity (range 2.4-3.7 CPM) was decreased by 12.0% (P < 0.05) and 13.9% (P < 0.05), respectively, in our overall population (n = 21). Reduction in percentage of 3 CPM activity was also observed during exposure to conversation babble (7.1%), but was not statistically significant.

In the younger group (n = 12; age range 22-47 years, mean 34 years), the percentage of 3 CPM activity decreased to a greater degree during exposure to hospital noise (22.9%, P < 0.05) and traffic noise (19.0%, P < 0.05). A non-significant decrease was also seen during conversation noise (15.5%). In the older group (n = 9; age range 51-71 years, mean 56 years) showed no such a trend. In fact, during exposure to hospital noise and conversation babble, their percent activity of 3 CPM actually increased by 2.5% and 4%, respectively. During exposure to traffic noise, the percent activity of 3 CPM fell in this group by 7.1%.

Decreases in 3 CPM activity were accompanied mainly by rises in bradygastria activity. In the younger group, bradygastria activity rose during hospital and traffic noise by 16.3% (P < 0.05) and 13.4% (P < 0.05), respectively.

Table 2 Effect of various types of noise on blood pressure and heart rate

		Baseline	ICU	Babble	Traffic
Age < 50 yr (n = 12)	Systolic	122.2 ± 11.3	122.1 ± 19.3	119.3 ± 13.2	122.2 ± 12.6
	Diastolic	78.1 ± 11.5	76.1 ± 14.8	74.3 ± 12.9	79.2 ± 12.6
	Pulse	73.6 ± 9.5	75.6 ± 10.2	76.4 ± 14.8	75.5 ± 9.8
Age > 50 yr (n = 9)	Systolic	132.9 ± 18.8	136.5 ± 15.6	135.1 ± 19.3	136.0 ± 14.8
	Diastolic	85.4 ± 11.4	85.7 ± 11.3	86.3 ± 13.1	83.6 ± 12.3
	Pulse	70.7 ± 16.5	75.4 ± 14.8	72.9 ± 15.1	71.7 ± 15.0

No significant change was observed in these parameters during exposure to auditory stimuli.

Effect of noise on dominant frequency and dominant power

Trends toward a decrease in DF (Figure 1) and an elevation in DP (Figure 2) were consistently observed in the both age groups (> 50 years and < 50 years), but none of them reached statistical significance.

Effect of noise on autonomic nerve activity

No effect of noise was seen either on diastolic, systolic pressure or on heart rate (Table 2). For the total population in the study, systolic pressure changed by 1.6 mmHg, -0.5 mmHg, and 1.4 mmHg for hospital, conversation, and traffic noise, respectively. Diastolic pressure changed by -0.9 mmHg, -1.6 mmHg, and -0.2 mmHg, respectively (Table 1). Finally, heart rate changed by 3.2 beats per minute (bpm), 2.5 bpm, and 1.5 bpm, respectively.

DISCUSSION

Our results indicate that GMA may change with advancing age, manifested mainly by a decline in dominant power. In addition, the average percentage of 3 CPM activity declined during exposure to noise in the younger subjects. Together with these decreases in 3 CPM activity, bradygastria became more prominent. A trend toward a decrease in DF and an elevation in DP was consistently observed during exposure to noises in both age groups. None of the noises employed in this study had a significant effect on autonomic nerve function reflected by blood pressure and heart rate.

Many non-auditory effects of noise have been described and have been reviewed in detail elsewhere[1]. In general terms, these non-auditory responses can be considered reflexive in nature and tend to increase the level of alertness and arousal. These reflexes included a focused posture directed to the source of noise, a shunting blood away from vegetative regions like the stomach, a rise in adrenalin, noradrenalin, and 17-hydroxycorticosteroids,

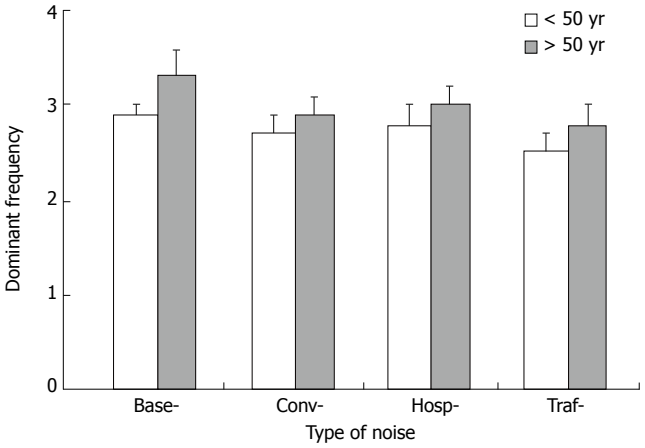

Figure 1 Effect of various types of noises on dominant frequency in the subjects of age below 50 (n = 12) and above 50 (n = 9). Base-, baseline; Conv-, conversation babble; Hosp-, hospital noise; Traf-, traffic noise. One-way RM ANOVA *vs* individual baseline, no statistical significance was observed.

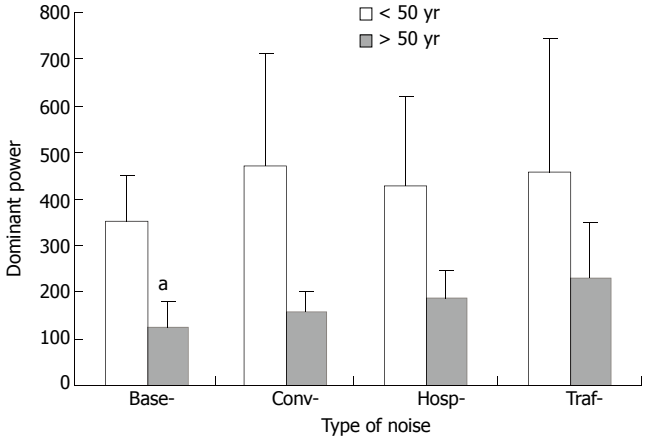

Figure 2 Effect of various types of noises on dominant power (DP) in the subjects of age below 50 (n = 12) and above 50 (n = 9). Base-, baseline; Conv-, conversation babble; Hosp-, hospital noise; Traf-, traffic noise. One-way RM ANOVA *vs* individual baseline, no significance was observed. The baseline DP of the older group (age > 50 yr) was significantly lower than that of the younger group (age < 50 yr): $^{a}P < 0.05$, Student's t test.

a release of glucose into the blood stream, and an increase in blood pressure[19,20].

Many non-auditory responses to noise have been linked to activation of the autonomic nervous system. However, in the present study, noise did not alter blood pressure or heart rate. These are parameters that one would have expected to reflect enhancement of the autonomic nervous system and which have previously been shown to be affected by loud noise[5,6,11]. Our negative results in this regard suggest that, under the present conditions, alterations in GMA may occur at levels of autonomic stimulation less intense than that required to alter the circulatory system.

Our findings that exposure to noise decreases the percentage of normal 3 CPM activity is consistent with a recent report[21] in which the authors found that loud music and household noise all tended to alter the rhythmicity of gastric slow waves by an increase in bradygastria and a concurrent reduction in the normal 2-4 CPM activity. As in the present study, there were no signs of autonomic activation.

Workers in noisy jobs commonly report nausea and are known to have an increased incidence of digestive disorders including gastritis and ulcers[10,13]. As noted before, acoustic stress has been linked to increased gastric acid secretion[13]. An additional mechanism is suggested by the present study. Our finding that the percentage of normal 3 CPM activity decreased in younger subjects after exposure to noises raised the possibility that digestive problems, at least in part, might reflect alterations in contractile activity of the stomach. In this respect, it has been demonstrated that reduction in the normal GMA, the presence of bradygastria or arrhythmias is associated with reduced or absent gastric contractions[22]. Decreased movement of gastrointestinal tract has long been considered *a sine qua non* of the "fight or flight" response and, as noted above, probably arises from autonomic (specifically, sympathetic) stimulation. Our findings are consistent with studies by Gue *et al*[14], showing that the noise slowed the emptying of food by the canine stomach.

The relationship between age and characteristics of GMA has been investigated. It is clear that gastric slow waves are absent at birth and go through periods of maturation after birth[23]. Whether GMA changes with the advancement of age at adulthood is still inconclusive but studies have reported that aging increases the instability of electrical frequency[24], or the frequencies of the rhythm of surface EGG[25]. In our study, it is interesting to note that the dominant power was significantly lower in the older subjects than those of younger group. Although the significance of this phenomenon is unclear, it is possible that the aging stomach might be less active in motility and strength.

Advancing age is accompanied by a deterioration of autonomic nervous function[26]. This may, in part, explain why GMA of older individuals is diminished during exposure to stimuli such as meal[27], or head out of water immersion[28]. Finally, in an animal study by Pharm and Willott[29], it was determined that the "threshold" auditory stimulus required to initiate an acoustic startle response grew with age. These studies may clarify why older subjects in our study showed a diminished gastric electrical response to noise that did the younger subjects.

In previous studies, noise has been observed to both increase[5,19,30] and have no effect[31,32] on blood pressure and heart rate. Our own negative results in this respect are consistent with the latter findings. However, the duration, intensity and quality of the noise undoubtedly determine whether and to what extent an effect on blood pressure and heart rate will be observed.

COMMENTS

Background

To understand the influence of environmental noises on GI physiological functions.

Research frontiers

Environmental noises have been linked to cardiovascular and neurological disorders. However, the effect of noise on the GI system has been minimally explored.

Innovations and breakthroughs

This is the first study that to show that noise can affect physiological gastric electrical activity in healthy subjects and that the degree of this effect seems to be age-related.

Applications

Prevention of over-exposure to environmental noises may prevent some negative health issues.

Terminology

Electrogastrogram: Gastric myoelectrical activity is recorded using a portable device *via* surface electrodes placed on the anterior wall of the abdomen.

Peer review

It is a well-written study. Electrogastrography is an evolving field, and worth of further investigation.

REFERENCES

1 **Kryter K**. The handbook of hearing and the effects of noise. New York: Academic Press, 1994
2 **Abey-Wickrama I**, A'Brook MF, Gattoni FE, Herridge CF. Mental-hospital admissions and aircraft noise. *Lancet* 1969; **2**: 1275-1277
3 **Meecham WC**, Smith HG. Effects of jet aircraft noise on mental hospital admissions. *Br J Audiol* 1977; **11**: 81-85
4 **Ohrström E**. Sleep disturbances caused by road traffic noise-Studies in laboratory and field. *Noise Health* 2000; **2**: 71-78
5 **Andrén L**, Hansson L, Björkman M, Jonsson A. Noise as a contributory factor in the development of elevated arterial pressure. A study of the mechanisms by which noise may raise blood pressure in man. *Acta Med Scand* 1980; **207**: 493-498
6 **Belli S**, Sani L, Scarficcia G, Sorrentino R. Arterial hypertension and noise: a cross-sectional study. *Am J Ind Med* 1984; **6**: 59-65
7 **Cohen S**, Krantz DS, Evans GW, Stokols D. Cardiovascular and behavioral effects of community noise. *Am Sci* 1981; **69**: 528-535
8 **Knipschild P. VIII**. Medical effects of aircraft noise: review and literature. *Int Arch Occup Environ Health* 1977; **40**: 201-204
9 **Tomei F**, Tomao E, Papaleo B, Baccolo TP, Alfì P. Study of some cardiovascular parameters after chronic exposure to noise. *Int J Cardiol* 1991; **33**: 393-399
10 **Berland T**. The fight for quiet. Englewood Cliffs, New Jersey: Prentice-Hall, 1970
11 **Falk SA**, Woods NF. Hospital noise--levels and potential health hazards. *N Engl J Med* 1973; **289**: 774-781
12 **Karagodina L**. Effect of aircraft noise on the population near airports. *Hyg Sanit* (USSR) 1969; **34**: 182-187
13 **Tomei F**, Papaleo B, Baccolo TP, Persechino B, Spanò G, Rosati MV. Noise and gastric secretion. *Am J Ind Med* 1994; **26**: 367-372
14 **Gué M**, Peeters T, Depoortere I, Vantrappen G, Buéno L. Stress-induced changes in gastric emptying, postprandial motility, and plasma gut hormone levels in dogs. *Gastroenterology* 1989; **97**: 1101-1107
15 **Hamilton JW**, Bellahsene BE, Reichelderfer M, Webster JG, Bass P. Human electrogastrograms. Comparison of surface and mucosal recordings. *Dig Dis Sci* 1986; **31**: 33-39
16 **Chen JD**, Schirmer BD, McCallum RW. Serosal and cutaneous recordings of gastric myoelectrical activity in patients with gastroparesis. *Am J Physiol* 1994; **266**: G90-G98
17 **Telander RL**, Morgan KG, Kreulen DL, Schmalz PF, Kelly KA, Szurszewski JH. Human gastric atony with tachygastria and gastric retention. *Gastroenterology* 1978; **75**: 497-501
18 **Smout AJ**, van der Schee EJ, Grashuis JL. What is measured in electrogastrography? *Dig Dis Sci* 1980; **25**: 179-187
19 **Andrén L**, Hansson L, Eggertsen R, Hedner T, Karlberg BE. Circulatory effects of noise. *Acta Med Scand* 1983; **213**: 31-35
20 **Arguelles AE**, Ibeas D, Ottone JP, Chekherdemian M. Pituitary-adrenal stimulation by sound of different frequencies. *J Clin Endocrinol Metab* 1962; **22**: 846-852
21 **Chen DD**, Xu X, Wang Z, Chen JD. Alteration of gastric myoelectrical and autonomic activities with audio stimulation in healthy humans. *Scand J Gastroenterol* 2005; **40**: 814-821
22 **Xing J**, Qian L, Chen J. Experimental gastric dysrhythmias and its correlation with in vivo gastric muscle contractions. *World J Gastroenterol* 2006; **12**: 3994-3998
23 **Chen JD**, Co E, Liang J, Pan J, Sutphen J, Torres-Pinedo RB, Orr WC. Patterns of gastric myoelectrical activity in human subjects of different ages. *Am J Physiol* 1997; **272**: G1022-G1027
24 **Pfaffenbach B**, Adamek RJ, Kuhn K, Wegener M. Electrogastrography in healthy subjects. Evaluation of normal values, influence of age and gender. *Dig Dis Sci* 1995; **40**: 1445-1450
25 **Nishimura N**, Hongo M, Yamada M, Kawakami H, Toyota T. Gastric myoelectrical activities in elderly human subjects--surface electrogastrographic observations. *J Smooth Muscle Res* 1995; **31**: 43-49
26 **Stansberry KB**, Hill MA, Shapiro SA, McNitt PM, Bhatt BA, Vinik AI. Impairment of peripheral blood flow responses in diabetes resembles an enhanced aging effect. *Diabetes Care* 1997; **20**: 1711-1716
27 **Parkman HP**, Harris AD, Miller MA, Fisher RS. Influence of age, gender, and menstrual cycle on the normal electrogastrogram. *Am J Gastroenterol* 1996; **91**: 127-133
28 **Miwa C**, Mano T, Saito M, Iwase S, Matsukawa T, Sugiyama Y, Koga K. Ageing reduces sympatho-suppressive response to head-out water immersion in humans. *Acta Physiol Scand* 1996; **158**: 15-20
29 **Parham K**, Willott JF. Acoustic startle response in young and aging C57BL/6J and CBA/J mice. *Behav Neurosci* 1988; **102**: 881-886
30 **Eggertsen R**, Svensson A, Magnusson M, Andrén L. Hemodynamic effects of loud noise before and after central sympathetic nervous stimulation. *Acta Med Scand* 1987; **221**: 159-164
31 **Malchaire JB**, Mullier M. Occupational exposure to noise and hypertension: a retrospective study. *Ann Occup Hyg* 1979; **22**: 63-66
32 **Santana VS**, Barberino JL. Occupational noise exposure and hypertension. *Rev Saude Publica* 1995; **29**: 478-487

S- Editor Liu Y **L- Editor** Kumar M **E- Editor** Bi L

PO Box 2345, Beijing 100023, China
www.wjgnet.com
wjg@wjgnet.com

World J Gastroenterol 2007 January 21; 13(3): 408-413
World Journal of Gastroenterology ISSN 1007-9327

RAPID COMMUNICATION

Extrahepatic collaterals and liver damage in embolotherapy for ruptured hepatic artery pseudoaneurysm following hepatobiliary pancreatic surgery

Yoshitsugu Tajima, Tamotsu Kuroki, Ryuji Tsutsumi, Ichiro Sakamoto, Masataka Uetani, Takashi Kanematsu

Yoshitsugu Tajima, Tamotsu Kuroki, Ryuji Tsutsumi, Takashi Kanematsu, Department of Surgery, Nagasaki University Graduate School of Biomedical Sciences, 1-7-1 Sakamoto, Nagasaki 852-8501, Japan
Ichiro Sakamoto, Masataka Uetani, Department of Radiology and Radiation Biology, Nagasaki University Graduate School of Biomedical Sciences, 1-7-1 Sakamoto, Nagasaki 852-8501, Japan
Correspondence to: Yoshitsugu Tajima, MD, Department of Surgery, Nagasaki University Graduate School of Biomedical Sciences, 1-7-1 Sakamoto, Nagasaki 852-8501, Japan. ytajima@net.nagasaki-u.ac.jp
Telephone: +81-958-497316 Fax: +81-958-497319
Received: 2006-09-25 Accepted: 2006-10-17

Abstract

AIM: To evaluate the effects of extrahepatic collaterals to the liver on liver damage and patient outcome after embolotherapy for the ruptured hepatic artery pseudoaneurysm following hepatobiliary pancreatic surgery.

METHODS: We reviewed 9 patients who underwent transcatheter arterial embolization (TAE) for the ruptured hepatic artery pseudoaneurysm following major hepatobiliary pancreatic surgery between June 1992 and April 2006. We paid special attention to the extrahepatic arterial collaterals to the liver which may affect post-TAE liver damage and patient outcome.

RESULTS: The underlying diseases were all malignancies, and the surgical procedures included hepatopancreatoduodenectomy in 2 patients, hepatic resection with removal of the bile duct in 5, and pancreaticoduodenectomy in 2. A total of 11 pseudoaneurysm developed: 4 in the common hepatic artery, 4 in the proper hepatic artery, and 3 in the right hepatic artery. Successful hemostasis was accomplished with the initial TAE in all patients, except for 1. Extrahepatic arterial pathways to the liver, including the right inferior phrenic artery, the jejunal branches, and the aberrant left hepatic artery, were identified in 8 of the 9 patients after the completion of TAE. The development of collaterals depended on the extent of liver mobilization during the hepatic resection, the postoperative period, the presence or absence of an aberrant left hepatic artery, and the concomitant arterial stenosis adjacent to the pseudoaneurysm. The liver tolerated TAE without significant consequences when at least one of the collaterals from the inferior phrenic artery or the aberrant left hepatic artery was present. One patient, however, with no extrahepatic collaterals died of liver failure due to total liver necrosis 9 d after TAE.

CONCLUSION: When TAE is performed on ruptured hepatic artery pseudoaneurysm, reduced collateral pathways to the liver created by the primary surgical procedure and a short postoperative interval may lead to an unfavorable outcome.

Key words: Hepatic artery pseudoaneurysm; Transcatheter arterial embolization; Extrahepatic collateral pathways; Liver damage; Hepatobiliary pancreatic surgery

Tajima Y, Kuroki T, Tsutsumi R, Sakamoto I, Uetani M, Kanematsu T. Extrahepatic collaterals and liver damage in embolotherapy for ruptured hepatic artery pseudoaneurysm following hepatobiliary pancreatic surgery. *World J Gastroenterol* 2007; 13(3): 408-413

http://www.wjgnet.com/1007-9327/13/408.asp

INTRODUCTION

Delayed massive arterial bleeding in the postoperative period is a rare complication for patients with hepatobiliary pancreatic diseases, but often results in a lethal outcome due to the abrupt onset of massive hemorrhage. Bleeding occurs mainly from erosion or pseudoaneurysm of major visceral arteries as a result of an adjacent septic condition or an intraoperative arterial injury[1-3].

Transcatheter arterial embolization (TAE) has been proposed as the first-line treatment to control massive bleeding associated with a ruptured hepatic artery pseudoaneurysm after hepatobiliary pancreatic surgery because of its advantages over surgery. Such advantages include an easier approach, precise localization of the pseudoaneurysm, assessment of collateral pathways to the liver, less chance of re-bleeding, and low mortality rates[1-7]. Meanwhile, TAE on the hepatic artery may lead to liver abscesses, gallbladder necrosis, biliary stricture, intrahepatic biloma, and embolization of normal vessels[8-10]. Furthermore, hepatic TAE may cause a total interruption of the arterial blood supply to the liver, thus

presenting a risk for liver infarction, especially in patients after right or left hepatic lobectomy[11-14].

In this study, we retrospectively reviewed the patients who underwent TAE for a ruptured hepatic artery pseudoaneurysm following major hepatobiliary pancreatic surgery, paying special attention to the extrahepatic collateral pathways which may be associated with post-TAE liver damage and a negative patient outcome.

MATERIALS AND METHODS

Between June 1992 and April 2006, 10 patients developed a rupture of the hepatic artery pseudoaneurysm following major hepatobiliary pancreatic surgery in our department. This included 1 patient who suddenly died due to abrupt massive hemorrhaging. The remaining 9 patients who underwent a diagnostic angiography and subsequent transcatheter hemostasis treatment were reviewed in this study. The clinical characteristics of these 9 patients are summarized in Table 1. These patients included 6 men and 3 women with a mean age of 70 years (range 63-75). A total of 11 pseudoaneurysms developed: 4 in the common hepatic artery, 4 in the proper hepatic artery, and 3 in the right hepatic artery. Subsequent ruptures of the portal vein were seen in 2 patients. The underlying diseases included hilar bile duct carcinoma, ampullary carcinoma, gallbladder carcinoma, intrahepatic cholangiocarcinoma, and metastatic liver cancer from colon cancer.

The surgical procedures performed were hepatopancreatoduodenectomy in 2 patients, left hepatic lobectomy with a resection of the caudate lobe and bile duct in 4, a segmental resection of the liver with removal of the bile duct in 1, and pylorus-preserving or conventional pancreaticoduodenectomy in 2. All patients received lymphadenectomy around the hepatic artery. During the hepatic resection, the whole liver was mobilized from the diaphragm for the surgical procedure in 2 patients, and a unilateral mobilization of the liver was done in 4 patients. The postoperative complications included hepaticojejunal or pancreaticojejunal anastomotic leakage in 6 patients. The bleeding from ruptured pseudoaneurysm occurred 12-256 d following the primary operation. During the follow-up, 2 patients (cases no.1 and 2) had melena or hematemesis. Of the remaining 7 patients, 6 presented bleeding from the drain in the abdominal cavity, which was preceded by an intermittent minor hemorrhage or "sentinel bleed" in 5 of the cases. A contrast-enhanced abdominal CT scan was carried out immediately after the initial "sentinel bleed" in 2 patients, and both depicted pseudoaneurysm in the hepatic artery (Figure 1). In addition, hemorrhagic shock (systolic blood pressure < 90 mmHg, pulse rate > 100/min) was presented in 6 of the patients.

The diagnostic angiography was performed using a 4-Fr or 5-Fr angiographic catheter (Clinical Supply, Tokyo, Japan) through a transfemoral approach. In all cases, celiac, common hepatic, and superior mesenteric angiographies and arterial portographies, were routinely taken to detect the bleeding points. Immediately after identifying pseudoaneurysms, with or without extravasation of the contrast madia, TAE was performed with distal and proximal placement of embolic coils to the pseudoaneurysm for the hemostasis. The embolic coils used were 0.035-inch stainless-steel coils, 3-8 mm in diameter, or 0.018-inch platinum coils, and 3-6 mm in diameter (Cook, Bloomington, IN).

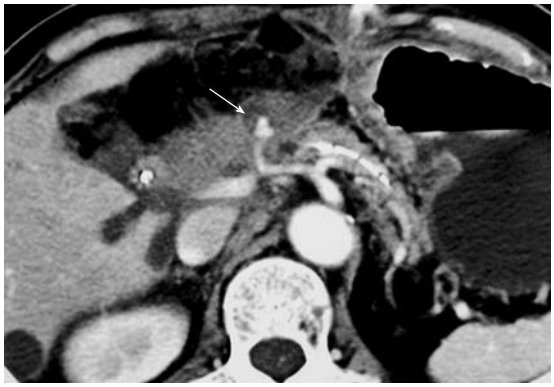

Figure 1 A 66-year-old female with pylorus-preserving pancreaticoduodenectomy (12 d after surgery). A contrast-enhanced CT scan presents a pseudoaneurysm on the distal side of the common hepatic artery (arrow).

The procedural success of TAE and the presence of collateral arterial blood flow to the liver were confirmed at the end of the procedure by performing angiographies of the celiac, superior mesenteric, and inferior phrenic arteries. The hepatic function tests evaluated before and after TAE included total bilirubin (T-Bil), aspartate aminotransferase (AST), and alanine aminotranferease (ALT). We retrospectively reviewed the 9 patients with special attention paid to the impact of collateral pathways to the liver on post-TAE complications and patient outcome.

RESULTS

Embolization of the hepatic artery was done in the extrahepatic level in all patients (Table 2). However, the embolic coils migrated to the intrahepatic level of the left hepatic artery in 2 patients. An immediate successful hemostasis was accomplished during the initial TAE in all cases, except for 1 patient (case no. 3) who required a second TAE because of re-bleeding 1 hour after the first procedure. The first TAE was performed at the proximal side of the right hepatic artery where pseudoaneurysm and extravasation were observed. The second TAE was performed by adding the coils distally and proximally.

Angiographies after the completion of the TAE showed extrahepatic collateral pathways to the liver in 8 of 9 patients. This consisted of the right inferior phrenic artery in 6 cases (Figure 2), the jejunal branches in 2 (Figure 3), and the aberrant left hepatic artery branched from the left gastric artery in the other 2. These collateral pathways supply the arterial flow throughout the hepatic lobes via intrahepatic communicating branches (Figure 4). Among these extrahepatic collaterals, the main collateral pathways to the liver were either the right inferior phrenic artery or the aberrant left hepatic artery. In 5 patients who underwent a hepatic resection without whole liver mobilization, the collateral pathways from the right inferior phrenic artery were well developed. In 2

Table 1 Clinical characteristics of patients with ruptured hepatic artery pseudoaneurysms after hepatobiliary pancreatic surgery

Case no.	Age/ sex	Underlying diseases	Surgical procedures	Hepatic lobes mobilized	Postoperative complications	Postoperative interval (d)	Clinical presentation	Sentinel bleed	Pseudoaneurysm		
									Location	size (cm)	Extra-vasation
1	75/M	Metastatic liver cancer	HTX (S7 + 8), BDR	R	None	256	Melena	No	PHA	2.7	Yes
2	74/M	Intrahepatic cholangiocarcinoma	HTX (S1 + 2 + 3 + 4), BDR	R&L	HJ leak	105	Hematemesis, shock	No	PHA	0.7	Yes
3	66/M	Hilar bile duct carcinoma	HTX (S1 + 2 + 3 + 4), PD	R&L	HJ leak	28	BFD, shock	Yes	PHA, RHA	2.2, 3.1	Yes
4	71/M	Hilar bile duct carcinoma	HTX (S1 + 2 + 3 + 4), BDR	L	HJ leak	19	BFD, shock	Yes	RHA	2.8	Yes
5	76/F	Intrahepatic cholangiocarcinoma	HTX (S1 + 2 + 3 + 4), BDR	L	None	17	Hematemesis, shock	No	PHA	1.5	Yes
6	72/M	Hilar bile duct carcinoma	HTX (S1 + 2 + 3 + 4), BDR	L	HJ leak	15	BFD	Yes	CHA	1.3	No
7	67/F	Gallbladder carcinoma	HTX (S4a + 5), PD	None	PJ leak	35	BFD	No	CHA	1.2	Yes
8	63/M	Ampullary carcinoma	PD	None	PJ leak	23	BFD, shock	Yes	CHA, RHA	1.5, 2.3	Yes
9	66/F	Ampullary carcinoma	PPPD	None	None	12	BFD, shock	Yes	CHA	0.8	No

HTX: hepatectomy; BDR: bile duct resection; S7 + 8: hepatic posterior inferior and superior segments; S1 + 2 + 3 + 4: caudate lobe and hepatic lateral and medial segments; S4a + 5: hepatic medial inferior and anteror inferior segments; PD: pancreaticoduodenectomy; PPPD: pylorus-preserving pancreaticoduodenectomy; R: right; L: left; HJ: hepaticojejunal anastomosis; PJ: pancreaticojejunal anastomosis; BFD: bleeding from drain; PHA: proper hepatic artery; RHA: right hepatic artery; CHA: common hepatic artery.

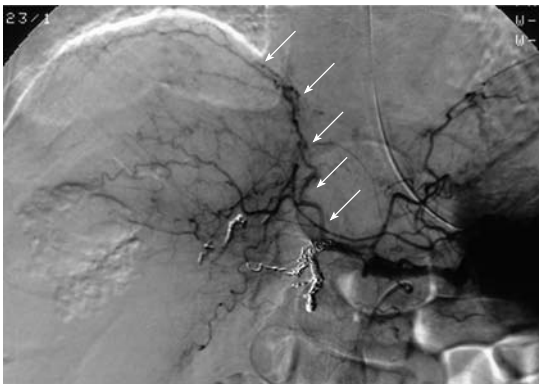

Figure 2 A 74-year-old male with left hepatic lobectomy (105 d after surgery). The right inferior phrenic artery (arrows) is presented as a collateral pathway to the liver on an angiography after TAE for the proper hepatic and gastroduodenal arteries.

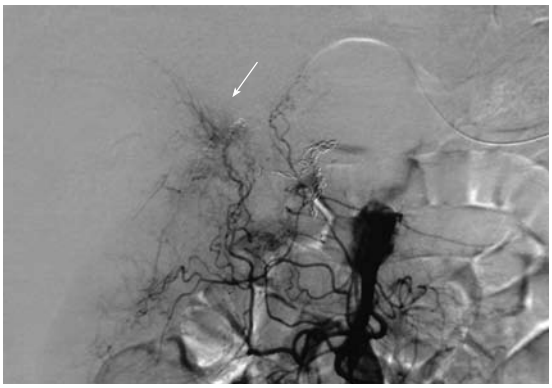

Figure 3 The jejunal branches (arrow) are seen as a collateral pathway to the liver in the same patient as in Figure 2.

patients who received whole liver mobilization from the diaphragm during the hepatic resection, 1 patient (case no. 2) presented a well-developed collateral pathway from the right inferior phrenic artery, but the other (case no. 3) demonstrated no collateral pathways. The postoperative interval was 105 d and 28 d, respectively. Collateral pathways from the jejunal branches were seen in 2 patients who had a long postoperative course (cases no. 1 and 2), meanwhile, arterial stenosis or spasm adjacent to the pseudoaneurysm were identified in 6 patients. The extra- and intrahepatic arterial pathways to the liver developed in accordance with the degree of arterial stenosis (Figure 5).

One patient with no extrahepatic collateral pathways to the liver died of liver failure due to total liver necrosis 9 d after TAE. However, 8 patients with extrahepatic collateral pathways tolerated TAE. Six of these 8 patients showed mild to moderate elevations of T-Bil, AST, and ALT after TAE, and liver functions returned to normal within 10 d without any complication. The remaining 2 patients (cases no. 7 and 8) showed a considerable liver dysfunction likely due to a chance migration of embolic coils to the left hepatic artery during TAE. They were subsequently cured with a conservative treatment, although 1 patient developed a liver abscess in the left hepatic lobe.

Two patients who developed a rupture of the portal vein after TAE were managed with re-laparotomy (case no. 2) and interventional radiologic technique (case no. 6), respectively. In the former, the rupture of the portal vein occurred 37 d after TAE, in which the embolic coils in the proper hepatic artery migrated to the adjacent portal vein, resulting in disruption of the vein. Although this patient underwent re-laparotomy, the ruptured portal vein could not be repaired due to huge adhesions around the portal system and the fragility of the portal vein. He died of multiple organ failure (MOF) 14 d after re-laparotomy. In the latter patient, the bleeding from the portal vein

Table 2 Results of embolotherapy for ruptured hepatic artery pseudoaneurysms after hepatobiliary pancreatic surgery

Case no.	Arteries embolized	No.of coils placed	Migration of coils	TAE success	Collateral pathways				Hepatic arterial stenosis	Changes in liver function tests: pre-TAE→post-TAE (days after TAE)			Follow-up interval after TAE	Outcome
					RIPA	Jejunal branches	aberrant LHA	intrahepatic branches		T-Bil (mg/dL)	AST (IU/L)	ALT (IU/L)		
1	PHA	17	No	Complete	Good	Good	None	Fair	Yes	1.2→3.2 (3)	29→131 (3)	22→112 (3)	34 mo	Alive
2	PHA, GDA	18	No	Complete	Good	Good	None	Good	Yes	1.1→1.3 (5)	26→41 (1)	12→16 (1)	52 d	Died of MOF
3	PHA, RHA	13	No	Complete	Poor	Poor	None	?	No	1.3→19.4 (3)	65→9750 (2)	79→7865 (3)	9 d	Died of liver failure
4	RHA	10	No	Complete	Good	Poor	None	Good	Yes	1.7→5.6 (1)	46→214 (1)	34→132 (1)	7 mo	Died of local recurrence
5	PHA	9	No	Complete	Fair	Poor	None	Fair	No	0.9→2.5 (5)	20→141 (4)	24→289 (4)	6 mo	Alive
6	CHA	12	No	Complete	Good	Poor	None	Good	Yes	1.6→6.2 (3)	22→118 (3)	21→95 (4)	54 d	Died of MOF
7	CHA	6	Yes	Complete	Fair	Poor	None	Fair	No	1.2→3.2 (3)	29→965 (3)	22→947 (3)	9 mo	Died of liver metastasis
8	CHA, RHA	13	Yes	Complete	Poor	Poor	Good	Good	Yes	0.6→1.1 (5)	38→439 (1)	57→700 (2)	48 mo	Alive
9	CHA	22	No	Complete	Poor	Poor	Good	Good	Yes	0.5→2.2 (3)	20→144 (1)	48→241 (1)	58 mo	Alive

PHA: proper hepatic artery; DGA: gastroduodenal artery; RHA: right hepatic artery; CHA: common hepatic artery; RIPA: right inferior phrenic artery; LHA: left hepatic artery; T-Bil: total bilirubin; AST: aspartate aminotransferase; ALT: alanine aminotranferease; MOF: multiple organ failure.

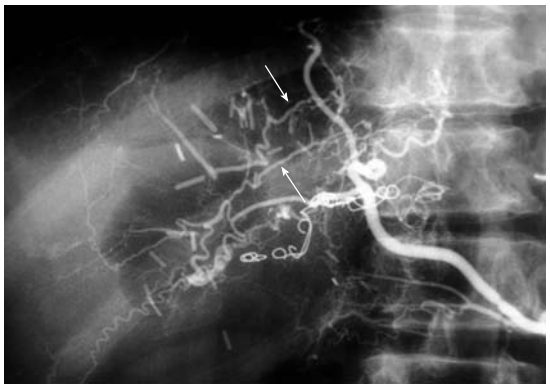

Figure 4 A 71-year-old male with left hepatic lobectomy (41 d after surgery). The intrahepatic communicating branches (arrows) are visualized via the branches of the right inferior phrenic artery on an angiography after TAE for the right hepatic artery.

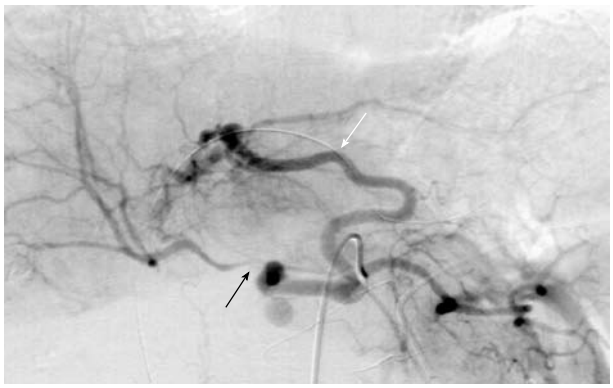

Figure 5 A diagnostic celiac angiography showing a stenosis of the right hepatic artery (black arrow) distal to the ruptured hepatic artery pseudoaneurysm in the same patient as in Figure 1. The aberrant left hepatic artery (white arrow) originating from the left gastric artery was dilated and supplied arterial blood flow to the right hepatic artery through the intrahepatic communicating branches before TAE.

occurred 3 d after TAE. A Gianturco expandable metallic stent (Z-stent; Cook, Bloomington, IN) was placed in the portal vein to bridge the site of venous disruption via a peripheral branch of the ileocecal vein under a small laparotomy in the right lower quadrant of the abdomen. The extra-portal cavity was then packed with 30 microcoils through a slit in the Z-stent. This patient died of MOF induced by sepsis originating from the abscess around the microcoils packed in the extra-portal cavity 51 d after placement of the stent.

DISCUSSION

Massive arterial bleeding can occur early or late in the postoperative course of patients undergoing hepatobiliary pancreatic surgery. Early bleeding within 24 h after operation usually originates from vessels at the anastomotic suture-line or in the intra-abdominal cavity due to inadequate hemostasis[15,16]. On the other hand, delayed bleeding occurs mainly due to erosion or pseudoaneurysm of major visceral arteries and has a higher mortality rate than those with suture-line bleeding[16].

Three major predisposing factors for delayed arterial bleeding after hepatobiliary pancreatic surgery have been suggested: (1) digestion of arterial walls due to activated pancreatic juice or infectious bile from anastomotic insufficiency, (2) arterial irritation by localized abscess in the intra-abdominal space, and (3) a mechanical injury of the artery during operation, particularly due to lymph node dissection for malignancy[1-3,14,17,18]. In the present study, lymphadenectomy around the hepatic artery was performed on all 9 patients. In addition, postoperative hepaticojejunal or pancreaticojejunal anastomotic leakage was identified in 6 cases. Although the rupture of visceral arteries after surgery may be a complex process and actual pathogenesis remains obscure, histopathology of autopsy

of our case no. 3 demonstrated that infectious bile invaded the hepatic arterial wall and completely destroyed the media consisting of elastic fibers[11].

The compensatory arterial circulation to the liver after TAE for the treatment of ruptured hepatic artery pseudoaneurysm was recognized in 8 of the 9 patients who underwent major hepatobiliary pancreatic surgery in this study. Michels has described the details of extrahepatic arterial collaterals to the liver after ligation of the hepatic artery in a series of 200 cases of hepatic resection, in which at least 26 possible routes of collateral arterial blood supply to the liver from the common hepatic trunk were noted[19]. Among them, the following are clinically important: (1) the subphrenic branch of the phrenic artery or internal mammary artery, (2) the aberrant hepatic artery, (3) the periductal arterial plexus, (4) other collaterals into the hepatic hilum from the superior mesenteric artery, and (5) the intrahepatic branches[19,20]. Although the significance of extrahepatic collateral pathways in association with liver damage after hepatic TAE has been reported[2,21-23], the relationship between the primary surgical procedure and the development of extrahepatic collaterals following hepatobiliary pancreatic surgery has not been described in detail.

In this study, the main collateral pathways to the liver after TAE in patients with major hepatobiliary pancreatic surgery included the right inferior phrenic artery, the aberrant left hepatic artery, and the intrahepatic communicating branches. The development of these collaterals depended on the primary operative procedure, postoperative duration, and concurrent arterial stenosis adjacent to the pseudoaneurysm. They subsequently affected post-TAE liver damage and patient outcome. Following TAE, total liver necrosis occurred in 1 patient who had no extrahepatic collateral pathways. This was probably due to whole liver mobilization during hepat opancreatoduodenectomy 28 d prior to TAE. Another patient received whole liver mobilization along with left hepatic lobectomy 105 d prior to TAE, and showed a well-developed collateral pathway from the right inferior phrenic artery. Conversely, the inferior phrenic artery was maintained in 5 patients who underwent a hepatic resection without whole liver mobilization. The hepatic arterial stenosis adjacent to the pseudoaneurysm was also associated with the development of extra- and intrahepatic collateral pathways. As a result, the liver tolerated TAE without significant consequences when one of the collaterals from the inferior phrenic artery or the aberrant left hepatic artery was present. Therefore, when performing hepatic TAE, all the information mentioned above should be considered in individual patients who have undergone hepatobiliary pancreatic surgery. TAE on the hepatic artery has generally been considered to be relatively safe if the portal blood flow is maintained[12,13,24]. However, it could result in an unfavorable outcome when the development of extrahepatic pathways to the liver is poor. In such cases, endovascular repair of hepatic artery pseudoaneurysms using a stent-graft with preservation of the arterial blood flow to the liver[25], may be an alternative treatment to TAE.

Brodsky and Turnbull[26] emphasize a "sentinel bleeding" as a precursor of vessel erosion after pancreatic surgery. In our series, episodes of sentinel bleeding from the drainage tube prior to massive hemorrhage were recognized in 5 patients. Interestingly, an urgent contrast-enhanced CT scan successfully depicted hepatic artery pseudoaneurysm in 2 patients when the abdominal CT scan was carried out immediately after the initial sentinel bleeding. The significance of a CT scan in the detection of visceral pseudoaneurysm following pancreaticoduodenectomy has previously been reported[1,27]. Moreover, a dilated right inferior phrenic artery representing an extrahepatic collateral after TAE for hepatocellular carcinoma has been demonstrated by using biphasic helical CT scans[28]. Early diagnosis and management of an arterial pseudoaneurysm before it ruptures is essential to improve the prognosis of this condition. Accordingly, early CT scan should be required in patients associated with postoperative leakage of enteric anastomosis or intra-abdominal abscess, as well as in cases with a sentinel bleeding after surgery.

Subsequent ruptures of the portal vein were seen in 2 patients. Although the Z-stent placement in the portal vein was effective in the hemostasis of 1 case, the patient finally died of MOF induced by sepsis originating from abscess around the microcoils packed in the extra-portal cavity. In such a case, a "second-look" operation for the abscess should be performed after the hemodynamic condition of the patient becomes stable.

In conclusion, TAE should be the first choice of treatment for ruptured hepatic artery pseudoaneurysms after hepatobiliary pancreatic surgery. In performing hepatic TAE, however, information on liver mobilization, the postoperative period, the presence or absence of an aberrant left hepatic artery, and concomitant arterial stenosis adjacent to the pseudoaneurysm is of prime importance due to these factors affecting the development of extrahepatic collateral pathways to the liver and the post-TAE patient outcome.

REFERENCES

1 **Reber PU**, Baer HU, Patel AG, Triller J, Büchler MW. Life-threatening upper gastrointestinal tract bleeding caused by ruptured extrahepatic pseudoaneurysm after pancreatoduodenectomy. *Surgery* 1998; **124**: 114-115

2 **Yoshida T**, Matsumoto T, Morii Y, Aramaki M, Bandoh T, Kawano K, Kitano S. Delayed massive intraperitoneal hemorrhage after pancreatoduodenectomy. *Int Surg* 1998; **83**: 131-135

3 **Okuno A**, Miyazaki M, Ito H, Ambiru S, Yoshidome H, Shimizu H, Nakagawa K, Shimizu Y, Nukui Y, Nakajima N. Nonsurgical management of ruptured pseudoaneurysm in patients with hepatobiliary pancreatic diseases. *Am J Gastroenterol* 2001; **96**: 1067-1071

4 **Aranha GV**, O'Neil S, Borge MA. Successful nonoperative management of bleeding hepatic artery pseudoaneurysm following pancreaticoduodenectomy. *Dig Surg* 1999; **16**: 528-530

5 **Salam TA**, Lumsden AB, Martin LG, Smith RB. Nonoperative management of visceral aneurysms and pseudoaneurysms. *Am J Surg* 1992; **164**: 215-219

6 Sohn TA, Yeo CJ, Cameron JL, Geschwind JF, Mitchell SE, Venbrux AC, Lillemoe KD. Pancreaticoduodenectomy: role of interventional radiologists in managing patients and complications. *J Gastrointest Surg* 2003; **7**: 209-219

7 **de Perrot M**, Berney T, Deléaval J, Bühler L, Mentha G, Morel P. Management of true aneurysms of the pancreaticoduodenal

arteries. *Ann Surg* 1999; **229**: 416-420
8 **Kadir S**, Athanasoulis CA, Ring EJ, Greenfield A. Transcatheter embolization of intrahepatic arterial aneurysms. *Radiology* 1980; **134**: 335-339
9 **Rivitz S**M, Waltman AC, Kelsey PB. Embolization of an hepatic artery pseudoaneurysm following laparoscopic cholecystectomy. *Cardiovasc Intervent Radiol* 1996; **19**: 43-46
10 **Sakamoto I**, Iwanaga S, Nagaoki K, Matsuoka Y, Ashizawa K, Uetani M, Fukuda T, Okimoto T, Okudaira S, Omagari K, Hayashi K, Matsunaga N. Intrahepatic biloma formation (bile duct necrosis) after transcatheter arterial chemoembolization. *AJR Am J Roentgenol* 2003; **181**: 79-87
11 **Sasaki M**, Tomioka T, Kanematsu T, Ashizawa K, Sakamoto I, Matsunaga N. Ruputure of the right hepatic artery after left lobectomy of the liver in patients with bile duct carcinoma. *ActaMed Nagasaki* 1997; **42**; 54-57
12 **Reber PU**, Baer HU, Patel AG, Wildi S, Triller J, Büchler MW. Superselective microcoil embolization: treatment of choice in high-risk patients with extrahepatic pseudoaneurysms of the hepatic arteries. *J Am Coll Surg* 1998; **186**: 325-330
13 **Sato N**, Yamaguchi K, Shimizu S, Morisaki T, Yokohata K, Chijiiwa K, Tanaka M. Coil embolization of bleeding visceral pseudoaneurysms following pancreatectomy: the importance of early angiography. *Arch Surg* 1998; **133**: 1099-1102
14 **Choi SH**, Moon HJ, Heo JS, Joh JW, Kim YI. Delayed hemorrhage after pancreaticoduodenectomy. *J Am Coll Surg* 2004; **199**: 186-191
15 **van Berge Henegouwen MI**, Allema JH, van Gulik TM, Verbeek PC, Obertop H, Gouma DJ. Delayed massive haemorrhage after pancreatic and biliary surgery. *Br J Surg* 1995; **82**: 1527-1531
16 **Miedema BW**, Sarr MG, van Heerden JA, Nagorney DM, McIlrath DC, Ilstrup D. Complications following pancreaticoduodenectomy. Current management. *Arch Surg* 1992; **127**: 945-949; discussion 949-950
17 **Tien YW**, Lee PH, Yang CY, Ho MC, Chiu YF. Risk factors of massive bleeding related to pancreatic leak after pancreaticoduodenectomy. *J Am Coll Surg* 2005; **201**: 554-559
18 **Rumstadt B**, Schwab M, Korth P, Samman M, Trede M. Hemorrhage after pancreatoduodenectomy. *Ann Surg* 1998; **227**: 236-241
19 **Michels NA**. Collateral arterial pathways to the liver after ligation of the hepatic artery and removal of the celiac axis. *Cancer* 1953; **6**: 708-724
20 **Charnsangavej C**, Chuang VP, Wallace S, Soo CS, Bowers T. Angiographic classification of hepatic arterial collaterals. *Radiology* 1982; **144**: 485-494
21 **Siablis D**, Tepetes K, Vasiou K, Karnabatidis D, Perifanos S, Tzorakoleftherakis E. Hepatic artery pseudoaneurysm following laparoscopic cholecystectomy: transcatheter intraarterial embolization. *Hepatogastroenterology* 1996; **43**: 1343-1346
22 **Takeuchi Y**, Arai Y, Inaba Y, Ohno K, Maeda T, Itai Y. Extrahepatic arterial supply to the liver: observation with a unified CT and angiography system during temporary balloon occlusion of the proper hepatic artery. *Radiology* 1998; **209**: 121-128
23 **Miyamoto N**, Kodama Y, Endo H, Shimizu T, Miyasaka K. Hepatic artery embolization for postoperative hemorrhage in upper abdominal surgery. *Abdom Imaging* 2003; **28**: 347-353
24 **Doppman JL**, Girton M, Kahn R. Proximal versus peripheral hepatic artery embolization experimental study in monkeys. *Radiology* 1978; **128**: 577-588
25 **Venturini M**, Angeli E, Salvioni M, De Cobelli F, Trentin C, Carlucci M, Staudacher C, Del Maschio A. Hemorrhage from a right hepatic artery pseudoaneurysm: endovascular treatment with a coronary stent-graft. *J Endovasc Ther* 2002; **9**: 221-224
26 **Brodsky JT**, Turnbull AD. Arterial hemorrhage after pancreatoduodenectomy. The 'sentinel bleed'. *Arch Surg* 1991; **126**: 1037-1040
27 **Santoro R**, Carlini M, Carboni F, Nicolas C, Santoro E. Delayed massive arterial hemorrhage after pancreaticoduodenectomy for cancer. Management of a life-threatening complication. *Hepatogastroenterology* 2003; **50**: 2199-2204
28 **Gokan T**, Hashimoto T, Matsui S, Kushihashi T, Nobusawa H, Munechika H. Helical CT demonstration of dilated right inferior phrenic arteries as extrahepatic collateral arteries of hepatocellular carcinomas. *J Comput Assist Tomogr* 2001; **25**: 68-73

S- Editor Wang J **L- Editor** Ma JY **E- Editor** Bi L

PO Box 2345, Beijing 100023, China
www.wjgnet.com
wjg@wjgnet.com

World J Gastroenterol 2007 January 21; 13(3): 414-420
World Journal of Gastroenterology ISSN 1007-9327

RAPID COMMUNICATION

Clinical features and prognosis of patients with extrahepatic metastases from hepatocellular carcinoma

Kiminori Uka, Hiroshi Aikata, Shintaro Takaki, Hiroo Shirakawa, Soo Cheol Jeong, Keitaro Yamashina, Akira Hiramatsu, Hideaki Kodama, Shoichi Takahashi, Kazuaki Chayama

Kiminori Uka, Hiroshi Aikata, Shintaro Takaki, Hiroo Shirakawa, Soo Cheol Jeong, Keitaro Yamashina, Akira Hiramatsu, Hideaki Kodama, Shoichi Takahashi, Kazuaki Chayama, Department of Medicine and Molecular Science, Division of Frontier Medical Science, Programs for Biomedical Research, Graduate School of Biomedical Sciences, Hiroshima University, Hiroshima, Japan
Correspondence to: Kiminori Uka, MD, Department of Medicine and Molecular Science, Division of Frontier Medical Science, Programs for Biomedical Research, Graduate School of Biomedical Sciences, Hiroshima University, 1-2-3 Kasumi, Minami-ku, Hiroshima 734-8551, Japan. kiminori@hiroshima-u.ac.jp
Fax: +81-82-2575194
Received: 2006-10-29 Accepted: 2006-12-08

Abstract

AIM: To assess the clinical features and prognosis of 151 patients with extrahepatic metastases from primary hepatocellular carcinoma (HCC), and describe the treatment strategy for such patients.

METHODS: After the diagnosis of HCC, all 995 consecutive HCC patients were followed up at regular intervals and 151 (15.2%) patients were found to have extrahepatic metastases at the initial diagnosis of primary HCC or developed such tumors during the follow-up period. We assessed their clinical features, prognosis, and treatment strategies.

RESULTS: The most frequent site of extrahepatic metastases was the lungs (47%), followed by lymph nodes (45%), bones (37%), and adrenal glands (12%). The cumulative survival rates after the initial diagnosis of extrahepatic metastases at 6, 12, 24, and 36 mo were 44.1%, 21.7%, 14.2%, 7.1%, respectively. The median survival time was 4.9 mo (range, 0-37 mo). Fourteen patients (11%) died of extrahepatic HCC, others died of primary HCC or liver failure.

CONCLUSION: The prognosis of HCC patients with extrahepatic metastases is poor. With regard to the cause of death, many patients would die of intrahepatic HCC and few of extrahepatic metastases. Although most of HCC patients with extrahepatic metastases should undergo treatment for the primary HCC mainly, treatment of extrahepatic metastases in selected HCC patients who have good hepatic reserve, intrahepatic tumor stage (T0-T2), and are free of portal venous invasion may improve survival.

Key words: Hepatocellular carcinoma; Extrahepatic metastases; Prognosis; Causes of death

Uka K, Aikata H, Takaki S, Shirakawa H, Jeong SC, Yamashina K, Hiramatsu A, Kodama H, Takahashi S, Chayama K. Clinical features and prognosis of patients with extrahepatic metastases from hepatocellular carcinoma. *World J Gastroenterol* 2007; 13(3): 414-420

http://www.wjgnet.com/1007-9327/13/414.asp

INTRODUCTION

Hepatocellular carcinoma (HCC) is a highly malignant tumor with frequent intrahepatic metastasis. The prognosis of HCC patients has improved because of progress in therapeutic procedures, such as surgical resection, radiofrequency ablation (RFA), percutaneous ethanol injection (PEI), and transcatheter arterial chemoembolization (TACE)[1-3]. Moreover, progress in diagnostic modalities, such as ultrasonography (US), computed tomography (CT), magnetic resonance imaging (MRI), and digital subtraction angiography (AG) has led to a better detection of patients with early and small HCC or asymptomatic extrahepatic metastases.

The above improvements in survival and diagnostic modalities have resulted in increased detection of extrahepatic metastases from primary HCC and further increases are anticipated in the future. Several groups have investigated extrahepatic metastases from HCC, but many of such cases were in autopsy cases, in a small number of cases or case reports[4-15]. At present, the prognosis of patients with extrahepatic metastases from primary HCC is poor[16,17]. In this regard, there is only little information about the causes of death of such patients[18], and there is no consensus on the treatment strategy for extrahepatic metastases from HCC. For example, what treatment strategy should be used to treat intrahepatic HCC or extrahepatic metastases? Among patients with extrahepatic metastases from primary HCC, which patients should be treated? To our knowledge, there are no reports that

deal directly with these questions. In this relatively large study, we retrospectively assessed the clinical features and prognosis of 151 patients with extrahepatic metastases from primary HCCs, and described the treatment strategy for such patients.

MATERIALS AND METHODS

Patients

From June 1990 to December 2005, 995 consecutive patients with HCC were admitted to our hospital. Among these patients, 880 were initially diagnosed with HCC in our hospital while the others were treated previously for HCC in other hospitals. Extrahepatic metastases from primary HCC were detected in 151 (15.2%) of 995 patients. None of the patients was treated for extrahepatic metastases. All the 151 HCC patients with extrahepatic metastases (117 men and 34 women, median age: 64 years, range: 21-82 years) were enrolled in the present study.

Table 1 summarizes the clinical profile of the 151 patients at the initial diagnosis of extrahepatic metastases. These 151 patients were divided into groups A and B. Group A was consisted of 68 patients presented with extrahepatic metastases together with primary HCC at the initial diagnosis of HCC, group B was composed of 83 patients who received treatment for intrahepatic HCC, and developed extrahepatic metastases during the follow-up period. Among them, 37 (25%) patients were treated previously for primary HCC in other hospitals, 90 patients were of performance status (PS) of 0, 43 patients of 1, 9 patients of 2, 6 patients of 3, and 3 patients of 4[19]. The etiology of the background liver disease was hepatitis B virus (HBV) in 33 patients, hepatitis C virus (HCV) in 89 patients, HBV and HCV in 5 patients, and non-B non-C in 24 patients. The hepatic reserve was Child-Pugh grade A in 88 patients, grade B in 48 patients, and grade C in 15 patients. We evaluated the primary tumor stage according to the Liver Cancer Study Group of Japan criteria[20], based on the following three conditions (T factor): solitary, < 2 cm in diameter, and no vessel invasion. T1 was defined as fulfilling the three conditions, T2 as fulfilling two of the three conditions, T3 as fulfilling one of the three conditions, T4 as fulfilling none of the three conditions. The primary HCC tumor stage at the first diagnosis of extrahepatic metastases was T0 (no intrahepatic HCC) in 11 (7%) patients, T1 in 4 (3%) patients, T2 in 13 (9%) patients, T3 in 43 (28%) patients, and T4 in 80 (53%) patients. Twenty seven of 28 patients with intrahepatic tumor stage T0-T2 were treated previously for intrahepatic HCC. The median size of the main intrahepatic primary tumor was 48 mm (range, 0-160 mm). Intrahepatic tumor morphology was nodular type in 83 (55%) patients, non-nodular type in 57 (38%) patients, and no intrahepatic HCC in 11 (7%) patients. Table 1 lists the sites of extrahepatic metastases at enrollment. Among the 151 patients with extrahepatic metastases, the sites of metastases were the lungs in 63 patients, lymph nodes in 60 patients, bones in 51 patients, adrenal glands in 16 patients and other locations (e.g., peritoneum, pancreas and nasal passages). In some patients, two or more distant metastatic tumors were found in one or more organs.

Table 1 Clinical profile of 151 HCC patients with extrahepatic metastases at the initial diagnosis of extrahepatic metastases

Age (yr)	64 (21-82)
Sex (male/female)	117/34
Etiology (HBV/HCV/HBV + HCV/others)	33/89/5/24
PS (0/1/2/3/4)	90/43/9/6/3
Intrahepatic tumor stage (T0/1/2/3/4)	11/4/13/43/80
Intrahepatic main tumor size (mm)	48 (0-160)
Intrahepatic tumor volume (< 50%/≥ 50%)	103/48
Intrahepatic tumor morphology (nodular type/non nodular type/no intrahepatic HCC)	83/57/11
Grade of portal vein invasion (Vp 0/1/2/3/4)	74/0/26/28/23
Child-Pugh grade (A/B/C)	88/48/15
AFP (ng/mL)	741.8 (< 5-861 600)
DCP (mAU/mL)	1300 (< 10-391 400)
Site of extrahepatic metastases, *n* (%)	
Lung	63 (42)
Lymph nodes	60 (40)
Bone	51 (34)
Adrenal	16 (11)
Peritoneum	1 (0.7)
Pancreas	1 (0.7)
Nasal passages	1 (0.7)

Data are expressed as medians and ranges unless indicated otherwise. HBV: hepatitis B virus; HCV: hepatitis C virus; PS: Eastern Cooperative Oncology Group performance status; T0: no intrahepatic HCC; Portal invasion assessed Vp1: tumor thrombus in a third or more of the peripheral branches; Vp2: in the second branch; Vp3: in the first branch; Vp4: in the trunk; AFP: alpha-fetoprotein; DCP: Des-γ-carboxy prothrombin.

Hepatocellular carcinoma

A definitive diagnosis of HCC was based on the finding of typical hypervascular radiological features or histopathological examination of needle biopsy specimen. HCC was also assessed by US, CT, and/or AG. Furthermore, CT was obtained during arterial portography and computerized tomographic hepatic arteriography. Further assessment of HCC was conducted by measuring α-fetoprotein (AFP) and des-γ-carboxy prothrombin (DCP).

Extrahepatic metastases were diagnosed by CT, MRI, bone scintigraphy, X-ray, and/or positron emission tomography (PET) with ^{18}F-fluorodeoxyglucose (FDG), or diagnosed by histopathological examination of surgically resected specimen or biopsy. When we suspected extrahepatic metastases with HCC, we always ruled out other malignancies (such as gastric cancer, colon cancer and lung cancer) by several imaging modalities, serological tumor markers and/or pathological examination.

Follow- up

All the 151 HCC patients with extrahepatic metastases were followed up during the observation period and no one was lost to follow-up. The median follow-up period was 4.9 mo (range, 1-37 mo). After the diagnosis of HCC, all patients were screened at regular intervals for the development of intra/extra hepatic metastases by clinical examination, AFP, DCP, and/or various imaging modalities. Serological tumor markers were measured once every month. US, CT or MRI was performed once every three to six months.

Statistical analysis and ethical considerations

Differences between groups were examined for statistical significance using the Mann-Whitney test (*U*-test) and χ^2 test where appropriate. Cumulative survival rate was assessed by the Kaplan-Meier life-table method and the differences were evaluated by the log rank test. The following 15 potential predictors were assessed in this study: PS (0 *vs* 1-4), age (≤ 65 *vs* > 65 years), sex (M *vs* F), Child-Pugh stage (A *vs* B, C), intrahepatic tumor stage (T0-T2 *vs* T3, T4), main intrahepatic tumor size (≤ 50 *vs* > 50 mm), intrahepatic tumor volume (≤ 50% *vs* > 50%), intrahepatic tumor morphology (nodular type *vs* non nodular type), portal venous invasion (Vp 0-2 *vs* > Vp 3, 4), AFP (≤ 400 ng/mL *vs* > 400 ng/mL), DCP (≤ 1000 mAU/mL *vs* > 1000 mAU/mL), site of extrahepatic metastases (lung *vs* others, bone *vs* others, only lymph node *vs* others), and treatment for extrahepatic metastases (performed *vs* not performed). All factors that were at least marginally associated with the survival after diagnosis of extrahepatic metastases ($P < 0.05$) were entered into a multivariate analysis. The hazard ratio and 95% confidence interval (95% CI) were calculated to assess the relative risk confidence. All analyses described above were performed using the SPSS program (version 11.0, SPSS Inc., Chicago, IL).

The study protocol was approved by the Human Ethics Review Committee of Graduate School of Biomedical Sciences, Hiroshima University and a signed consent form was obtained from each patient.

RESULTS

Site of extrahepatic metastases

Table 2 lists the sites of extrahepatic metastases identified throughout the follow-up period. The most frequent site of metastases that were identified throughout the follow-up period was the lung (n = 71 patients, 47%), followed by lymph nodes (n = 68 patients, 45%), bone (n = 56 patients, 37%), and adrenal glands (n = 18 patients, 12%). Brain metastases were identified in 2 (1%) patients. One (0.7%) patient each had metastases in the peritoneum, pancreas, nasal passages, muscle, skin, diaphragm, and colon. Autopsy was performed in 14 cases with metastases. Despite the detection of extrahepatic metastases in these 14 patients before autopsy, additional extrahepatic metastases were detected on postmortem examination (lymph nodes, diaphragm, and colon). At the first diagnosis of extrahepatic metastases, 109 (72%) patients had single-organ metastases, while the others had multiple organ metastases.

Among the 71 patients with lung metastases, 23 patients had bilateral lung metastases, 14 had additional extrapulmonary site of metastatic disease. The size of pulmonary nodules ranged from 9 to 30 mm at initial diagnosis of extrahepatic HCC. Few patients had symptoms (cough, dyspnea, and pleural effusion) related to lung metastases, and 8 patients who had severe symptoms died subsequently of respiratory failure. The median survival period of these 8 patients was 4.3 mo (range, 2.5-14.4 mo).

Table 2 Sites of extrahepatic HCC detected throughout the entire follow-up period

Site	Patients (n = 151), n (%)
Lung	71 (47)
Lymph nodes	68 (45)
Bone	56 (37)
Adrenal	18 (12)
Brain	2 (1)
Peritoneum	1 (0.7)
Pancreas	1 (0.7)
Nasal	1 (0.7)
Muscle	1 (0.7)
Skin	1 (0.7)
Diaphragm	1 (0.7)
Colon	1 (0.7)

Among the 68 patients with lymph node metastases, metastases were identified in 64 regional lymph nodes. The most common site was in the paraaortic nodes (31/64), followed by portohepatic nodes (21/64), periceliac nodes (6/64) and peripancreatic nodes (6/64). The majority of patients with regional lymph nodes metastases were asymptomatic, but few regional lymph nodes (portohepatic nodes) caused obstructive jaundice. Distant nodal metastases were found at 17 sites. The most common site was the mediastinum nodes (10/17), followed by subclavicular nodes (3/17), iliac nodes (2/17), cardiophrenic node (1/17), and retrocrural node (1/17). All distant lymph node metastases were not associated with clinical symptoms in this study.

Fifteen of 56 patients with bone metastases had multiple bone metastases at the initial diagnosis of bone metastases. The total number of bone metastatic sites was 88. The most frequent site was the vertebra (63/88; cervical vertebrae = 9, thoracic vertebrae = 38, and lumbar vertebrae = 16), followed by the ribs (8/88). Bone metastases were diagnosed by CT, MRI, bone scintigraphy, and/or PET with FDG.

Of the 18 patients with adrenal gland metastases, 13 had right adrenal gland metastases, 4 had left adrenal gland metastases and only one patient had bilateral metastases. These metastases were not associated with symptoms.

Treatments of extrahepatic metastases

All patients with Child-Pugh grade other than C or PS other than 2-4 were treated for intrahepatic HCC, and many of them were continuously treated after the diagnosis of extrahepatic metastases. On the other hand, HCC patients with Child-Pugh grade C or PS of 2-4 received supportive care. Forty-nine (32%) of 151 patients were treated for extrahepatic metastases by surgical resection, TACE, systemic chemotherapy, and/or radiotherapy. The 49 patients had extrahepatic metastases that were considered to worsen prognosis.

Surgical resection was performed in three (2%) patients (with regional lymph node, adrenal gland and lung metastases). The survival periods after surgical resection of extrahepatic metastases were 7 mo (in patients with lymph node metastases), 23 mo (in patients adrenal gland metastases), and 37 mo (in patients with lung metastases).

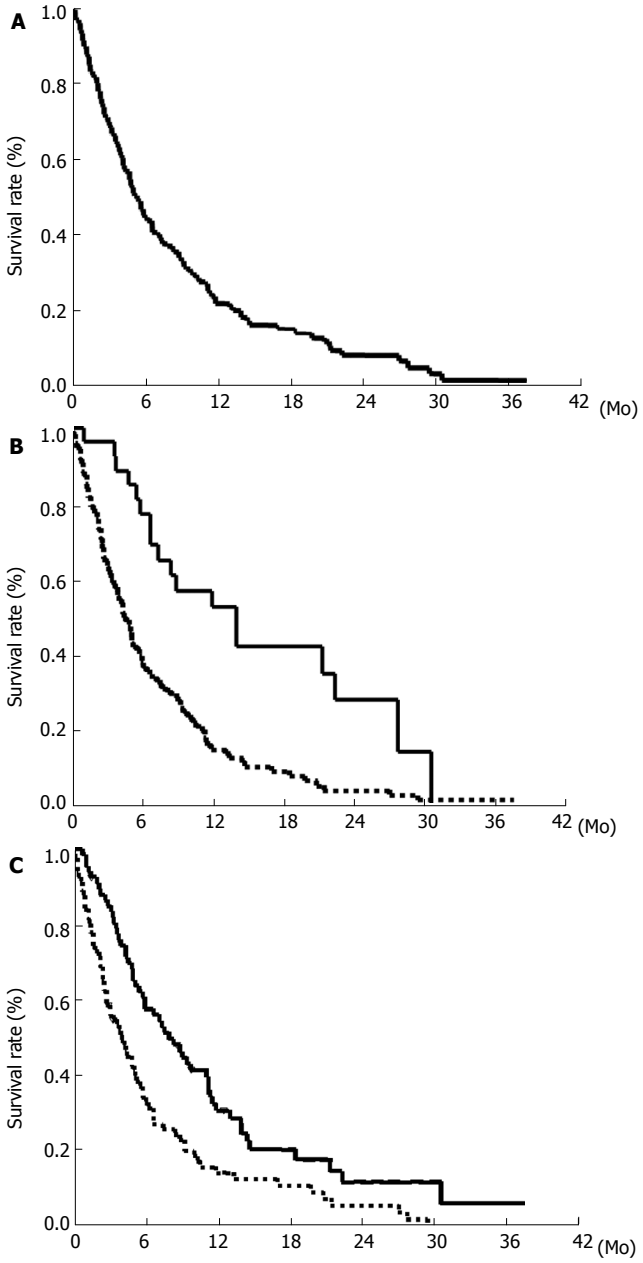

Figure 1 Survival rate of 151 HCC patients with extrahepatic metastases (**A**), intrahepatic tumor stage (**B**) [solid line: T0-T2, dashed line: T3, T4 (log-rank test: $P < 0.001$)], and after treatment of extrahepatic metastases (**C**) [solid line: treatment group, dashed line: no treatment group (log-rank test: $P < 0.001$)].

These three were all alive without recurrence of extrahepatic metastases during the observation period. In each of these 3 patients, hepatic reserve was Child-Pugh stage A, no intrahepatic HCC was not detected, and PS was 0.

TACE was performed in 8 (5%) patients (7 patients with adrenal gland metastases, and one patient with paraaortic lymph node metastases). Systemic chemotherapy was used in 39 (26%) patients. Chemotherapy included 5-fluorouracil, carboplatin, cisplatin. Twenty-five of the 39 patients had lung metastases, 10 had lymph node metastases, 2 had bone metastases, one had lung and lymph node metastases, and one had lung, adrenal gland and lymph node metastases.

Radiotherapy was performed in 36 (24%) patients.

Table 3 Univariate analysis of predictors of survival after initial diagnosis of extrahepatic metastases in 151 patients

Variable	Hazard Ratio	95% CI	*P*
PS (0 *vs* 1-4)	2.181	1.50-3.17	< 0.001
Age (≤ 65 *vs* > 65 yr)	0.988	0.97-1.0	0.18
Sex (M *vs* F)	0.889	0.57-1.38	0.601
Child Pugh stage (A *vs* B, C)	2.323	1.73-3.12	< 0.001
Intrahepatic main tumor size (≤ 50 *vs* > 50 mm)	2.321	1.52-3.54	< 0.001
Intrahepatic tumor volume (≤ 50 *vs* > 50%)	2.523	1.71-3.72	< 0.001
Intrahepatic tumor morphology (nodular *vs* non nodular)	1.506	1.04-2.18	0.03
Vp (0-2 *vs* 3, 4)	2.247	1.53-3.29	< 0.001
AFP (≤ 400 *vs* > 400 ng/mL)	1.158	0.80-1.68	0.439
DCP (≤ 1000 *vs* > 1000 mAU/mL)	1.584	1.08-2.33	0.02
Treatment (performed *vs* not performed)[1]	2.385	1.51-3.77	< 0.001
Site (lung *vs* others)[2]	1.065	0.74-1.52	0.731
Site (bone *vs* others)	1.61	1.11-2.33	0.012
Site (only lymph node *vs* others)	1.133	0.74-1.74	0.567

[1]Treatments: various treatments for extrahepatic metastases (surgical resection, TACE, systemic chemotherapy and/or radiotherapy); [2]Site: site of extrahepatic metastases.

Curative therapy was performed in 10 patients (6 patients with lymph node metastases and 4 patients with adrenal gland metastases). Palliative therapy was performed in the remaining 26 patients who had severe pain due to bone metastases. Furthermore, 9 patients with painful bone metastases were treated with RFA therapy combined with cementoplasty[21]. Nonsteroidal anti-inflammatory drugs or opioids were used in patients with bone metastases due to severe pain.

Survival data

The cumulative survival rates of the 151 HCC patients with extrahepatic metastases after initial diagnosis of extrahepatic metastases at 6, 12, 24, and 36 mo were 44.1%, 21.7%, 14.2%, and 7.1%, respectively (Figure 1A). The median survival period was 4.9 mo (range, 1-37 mo). Survival was compared among patients with intrahepatic tumor stage T0-T2 and T3, T4 (Figure 1B). The rate was significantly higher in the intrahepatic tumor stage T0-T2 groups than in the T3, T4 groups ($P < 0.001$). We investigated the determinants of survival after initial diagnosis of extrahepatic metastases. Univariate analysis identified the following 9 factors significantly influencing survival: PS, 0 ($P < 0.001$); Child-Pugh grade, A ($P < 0.001$); intrahepatic main tumor size, < 50 mm ($P < 0.001$); intrahepatic tumor volume, < 50% ($P < 0.001$); portal venous invasion, Vp 0-2 ($P < 0.001$); use of treatment for extrahepatic metastases ($P < 0.001$, Figure 1C); bone metastasis ($P = 0.012$); DCP < 1000 mAU/mL ($P = 0.02$); and nodular type intrahepatic tumor ($P = 0.03$) (Table 3). Since the variables could be mutually correlated, multivariate analysis was performed. The analysis identified the following four variables as significant and independent determinants of survival after initial diagnosis of extrahepatic metastases: PS ($P < 0.001$), portal venous invasion ($P < 0.001$), treatment of extrahepatic metastases ($P = 0.003$), and Child-Pugh grade ($P = 0.009$) (Table 4).

Table 4 Multivariate analysis of predictors of survival after initial diagnosis of extrahepatic metastases among 151 patients

Variable	Hazard ratio	95% CI	*P*
PS (0 *vs* 1-4)	5.576	2.431-12.152	< 0.001
Vp (0-2 *vs* 3, 4)	4.792	2.137-10.712	< 0.001
Treatment (performed *vs* not performed)	4.134	1.539-11.011	0.003
Child pugh stage (A *vs* B, C)	2.372	1.247-4.914	0.008

Causes of death

Twenty-five patients were still alive at the end of this study while 126 patients died. Of the latter group, intrahepatic tumor stages at the first diagnosis of extrahepatic metastases were T0-2 in 17 patients and T3-4 in 109 patients. One hundred and twelve (89%) patients died of intrahepatic HCC or liver failure. Fourteen (11%) patients died of extrahepatic HCC (Table 5). Eight patients died of respiratory failure due to lung metastases. Four patients died of bone metastases-related disease. Two patients died of obstructive jaundice due to portohepatic node metastasis.

Of the 4 patients who died of bone metastases-related disease, 3 died of intracranial hypertension due to skull metastasis. Another patient died of vertebra metastasis-related disease. He was 69-year old at first diagnosis of bone metastases. He suffered from complete spinal cord injury due to vertebral metastasis with gradual worsening of PS. Finally, PS changed to 4 and the patient died of aspiration-related pneumonia. The survival period after first diagnosis of extrahepatic metastases was 11.5 mo.

Among the 14 patients who died of extrahepatic HCC, 3 had chronic hepatitis, 7 had cirrhosis of Child-Pugh grade A, 3 had cirrhosis of Child-Pugh grade B, and 1 had cirrhosis of Child-Pugh grade C. All patients who died of extrahepatic HCC with the exception of that with Child-Pugh grade C had some hepatic reserve until death. Intrahepatic tumor stage at first diagnosis of extrahepatic metastases was T0 (3 patients), T1 (4 patients), T2 (1 patient), T3 (5 patients), and T4 (1 patient). All 8 patients with intrahepatic tumor stage T0-T2 were treated previously for intrahepatic HCC. Eight of 17 (47%) patients with intrahepatic tumor stage T0-T2 died of extrahepatic metastases. On the other hand, 6 of 109 (6%) patients with intrahepatic tumor stages T3 and T4 died of extrahepatic metastases. The mortality rate of patients with intrahepatic tumor stage T0-T2 was significantly higher than that of patients with intrahepatic tumor stages T3 and T4 ($P = 0.001$) (Table 6).

Table 5 Clinical profile of 14 patients who died of extrahepatic metastases during the follow-up period

Case	Presentation	Site	Intrahepatic HCC stage	Sex	Age (yr)	Child-Pugh stage	Etiology
1	R	Lung	T3	M	65	A	HCV
2	R	Lung	T4	M	35	CH	HBV
3	R	Lung	T3	M	56	A	HBV
4	R	Lung, vertebra	T0	M	40	CH	HBV
5	R	Lung, vertebra	T1	M	69	A	HBV
6	R	Lung, LN	T0	M	63	B	HBV
7	R	Lung, vertebra, nasal	T0	M	50	A	HBV
8	R	Lung	T3	M	73	A	NBNC
9	I	Skull	T1	M	57	A	HCV
10	I	Skull	T2	F	72	C	HCV
11	I	Skull	T3	M	56	B	HCV
12	A	Vertebra	T3	M	69	A	HCV
13	O	Lung, rib, LN	T1	M	74	A	HCV
14	O	Vertebra, LN	T1	M	70	B	HCV

All patients with intrahepatic tumor stage T0-T2 were treated previously for intrahepatic HCC. R: respiratory failure; CH: chronic hepatitis; LN: lymph node; NBNC: no hepatitis B virus or hepatitis C virus; I: intracranial hypertension symptom; A: aspiration-related pneumonia; O: obstructive jaundice.

Table 6 Causes of death of 126 HCC patients with extrahepatic metastases

Intrahepatic tumor stage	Intrahepatic HCC or liver failure	Extrahepatic HCC
T0-2 (*n* = 17)	53% (9/17)	47% (8/17)
T3-4 (*n* = 109)	94% (103/109)	6% (6/109)

DISCUSSION

The prognosis of HCC patients with extrahepatic metastases is unsatisfactory[16,17] and often not well known[18]. In the present study, we assessed the clinical features and prognosis of 151 consecutive HCC patients with extrahepatic metastases. The incidence of extrahepatic metastases from HCC was 15.2%. The most frequent metastatic sites were the lung, lymph nodes, bone, and adrenal gland. The cumulative survival rates of the 151 patients after the initial diagnosis of extrahepatic metastases at 6, 12, 24, and 36 mo were 44.1%, 21.7%, 14.2%, 7.1%, respectively. The median survival period was 4.9 mo (range, 1-37 mo). The mortality rate due to extrahepatic metastases from HCC was 11% (14/126).

Extrahepatic metastases have been reported to occur in 13.5%-42% of HCC patients[22-24]. In this study, the prevalence of extrahepatic metastases was 15.2%. Though we screened all HCC patients at regular intervals for intra/extra hepatic metastases, not all patients received a full metastatic follow up based on the use of several diagnostic techniques. Since the majority of HCC patients with extrahepatic metastases were asymptomatic, it is possible to miss asymptomatic metastases such as those in the lungs, distant lymph nodes, muscles and rectum.

Based on the initial diagnosis of intrahepatic HCC, Natsuizaka *et al*[16] reported that patients with advanced HCC develop extrahepatic metastases significantly more frequently than those with less advanced HCC. At the initial diagnosis of extrahepatic metastases, many HCC patients with extrahepatic metastases have been reported

to have advanced intrahepatic stage[16,22]. In our study, 123 (81%) patients with extrahepatic metastases had intrahepatic tumor stages T3 (28%) and T4 (53%), at the initial diagnosis of extrahepatic metastases, suggesting that HCC patients with advanced intrahepatic tumor stage (T3, T4) are at risk of developong extrahepatic metastases, and that such patients should be followed up carefully.

On the other hand, our study identified 28 (19%) patients with early intrahepatic tumor stage (T0-T2) at the initial diagnosis of extrahepatic HCC. Eight of the 17 (47%) patients later died of extrahepatic metastases. With regard to previous treatment, 27 of 28 patients with early intrahepatic tumor stage were treated previously for intrahepatic HCC. Considering the possibility of extrahepatic metastases, HCC patients with early intrahepatic tumor stage should be followed up carefully, particurally those who have been treated previously for intrahepatic HCC. This also includes HCC patients who have received complete resection or ablation.

In this study, the most frequent metastatic sites were the lungs, lymph nodes, bones, and adrenal glands. Other studies have reported similar findings[16,22]. HCC is thought to spread mainly *via* the hematogenous route, thus causing intra/extra hepatic metastases. Most of HCCs are hypervascular tumors. Moreover, HCC tends to invade vessels, such as portal and hepatic veins. Therefore, HCC could spread through the lung and systemic circulation via the hepatic or portal vein. This could explain why the lung is the most frequent site of metastases in HCC. Most of HCC patients with lung metastases are asymptomatic. To detect lung metastases from HCC, chest CT should be performed at regular intervals during routine metastasis follow-up.

Though there is no standard treatment for extrahepatic metastases of primary HCC, several authors have reported the use of various treatment modalities for extrahepatic metastases[5,7,15,23,25-28]. Some reports have described successful treatment of extrahepatic metastases with no or few intrahepatic HCC[5,7,25,26]. However, only few HCC patients can undergo surgical resection of extrahepatic metastases because of hepatic reserve or intraheatic tumor stage. In this study, the prognosis of 3 patients after surgical resection of extrahepatic metastases seemed good. These 3 patients had good hepatic reserve, no intrahepatic HCC (PS = 0) and no intra/extra hepatic HCC and are expected to have good prognosis. The clinical features of HCC patients with extrahepatic metastases varied widely. All patients were not symptomatic and thus not necessary to receive treatment of extrahepatic metastases. Thus, treatment of extrahepatic metastases from primary HCC must be performed carefully taking into consideration the clinical features.

Multivariate analysis in our study identified PS, portal venous invasion, treatment for extrahepatic metastases, and Child-Pugh grade as important determinants of survival after the initial diagnosis of extrahepatic metastases. Ishii *et al*[17] reported that brain metastases, number of metastatic tumors and primary tumor status are important factors for survival. In our study, only two patients had brain metastases. With regard to the number of metastatic tumors, we might miss asymptomatic metastases. Thus, we did not include brain metastasis and number of metastatic tumors in this multivariate analysis. Treatment of extrahepatic metastases was an important determinant of survival in our study. There might be selection bias of patients treated for extrahepatic metastases because many of them had good hepatic reserve. HCC patients with poor hepatic reserve did not receive treatment for extrahepatic metastases in this study. Regardless of such bias, treatment of extrahepatic metastases might be important for improvement of prognosis.

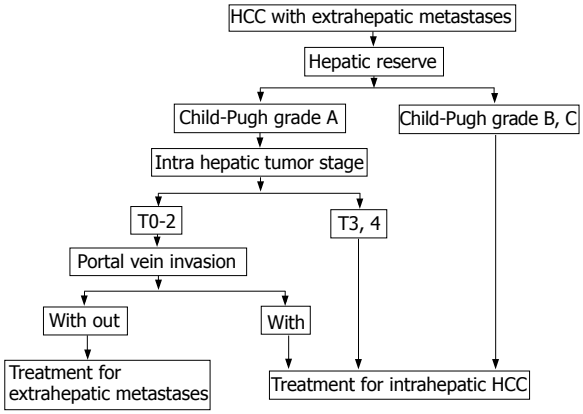

Figure 2 Initial sites to be treated.

With regard to the cause of death, many HCC patients with extrahepatic metastases died of intrahepatic HCC or liver failure and few (11%) died of extrahepatic HCC. Of the 14 patients who died of extrahepatic metastases, 10 had good hepatic reserve and 8 had early intrahepatic tumor stage, at the initial diagnosis of extrahepatic metastases. Usually, HCC patients with good hepatic reserve, no or few intrahepatic HCCs, and those without portal venous invasion show relatively good prognosis. According to the univariate analysis of HCC patients with extrahepatic metastases, patients with early intrahepatic tumor stage have a significantly better prognosis than those with advanced intrahepatic tumor stage. In our study, the mortality rate due to extrahepatic metastases with early intrahepatic tumor stage was significantly higher than that due to those with advanced intrahepatic tumor stage. This might be explained by the differences in survival periods between these intrahepatic tumor stage groups. Extrahepatic metastases with early intrahepatic tumor stage can spread during the relatively long survival period, and few patients die of extrahepatic metastases. Extrahepatic metastasis with early intrahepatic tumor stage is a very important cause of death of HCC patients. Successful treatment of extrahepatic metastases in HCC patients with early intrahepatic tumor stage might improve the prognosis.

In conclusion, the majority of HCC patients with extrahepatic metastases should undergo treatment for intrahepatic HCC. Selected HCC patients with critical extrahepatic metastases could undergo treatment for extrahepatic metastases. However, these selected patients must have good hepatic reserve, intrahepatic tumor stage: T0-T2, and are free of portal venous invasion (Figure 2). The important sites of critical metastases from primary

HCC are the lungs, bones and the portohepatic node. Further studies are needed for the improvement of the prognosis of HCC patients with extrahepatic metastases.

REFERENCES

1 **Poon RT**, Fan ST, Lo CM, Ng IO, Liu CL, Lam CM, Wong J. Improving survival results after resection of hepatocellular carcinoma: a prospective study of 377 patients over 10 years. *Ann Surg* 2001; **234**: 63-70
2 **Wu MC**, Shen F. Progress in research of liver surgery in China. *World J Gastroenterol* 2000; **6**: 773-776
3 **Tang Z**. Recent advances in clinical research of hepatocellular carcinoma in China. *Chin Med J (Engl)* 1995; **108**: 568-570
4 **Lo CM**, Lai EC, Fan ST, Choi TK, Wong J. Resection for extrahepatic recurrence of hepatocellular carcinoma. *Br J Surg* 1994; **81**: 1019-1021
5 **Lam CM**, Lo CM, Yuen WK, Liu CL, Fan ST. Prolonged survival in selected patients following surgical resection for pulmonary metastasis from hepatocellular carcinoma. *Br J Surg* 1998; **85**: 1198-1200
6 **Kuromatsu R**, Hirai K, Majima Y, Fujimoto T, Shimauchi Y, Tsukiyama Y, Aoki E, Saitsu H, Nakashima O, Kojiro M. A patient with hepatocellular carcinoma who underwent resection of the primary lesion 10 years ago and resection of a giant adrenal metastasis 8 and a half years later. *Gastroenterol Jpn* 1993; **28**: 312-316
7 **Inagaki Y**, Unoura M, Urabe T, Ogino H, Terasaki S, Matsushita E, Kaneko S, Morioka T, Furusawa A, Wakabayashi T. Distant metastasis of hepatocellular carcinoma after successful treatment of the primary lesion. *Hepatogastroenterology* 1993; **40**: 316-319
8 **Okazaki N**, Yoshino M, Yoshida T, Hirohashi S, Kishi K, Shimosato Y. Bone metastasis in hepatocellular carcinoma. *Cancer* 1985; **55**: 1991-1994
9 **Kay RM**, Eckardt JJ, Goldstein LI, Busuttil RW. Metastatic hepatocellular carcinoma to bone in a liver transplant patient. A case report. *Clin Orthop Relat Res* 1994; (303): 237-241
10 **Knight TE**, Woo AS, Blaisdell JM. Hepatocellular carcinoma invasive to chest wall. *Int J Dermatol* 1992; **31**: 273-276
11 **Kim PN**, Kim IY, Lee KS. Intraperitoneal seeding from hepatoma. *Abdom Imaging* 1994; **19**: 309-312
12 **Barasch E**, Frazier OH, Silberman H, Shannon RL, Wilansky S. Left atrial metastasis from hepatocellular carcinoma: a case report. *J Am Soc Echocardiogr* 1994; **7**: 547-549
13 **Fujimoto H**, Murakami K, Nosaka K, Arimizu N. Splenic metastasis of hepatocellular carcinoma. Accumulation of Tc-99m HDP. *Clin Nucl Med* 1992; **17**: 99-100
14 **Kim HS**, Shin JW, Kim GY, Kim YM, Cha HJ, Jeong YK, Jeong ID, Bang SJ, Kim do H, Park NH. Metastasis of hepatocellular carcinoma to the small bowel manifested by intussusception. *World J Gastroenterol* 2006; **12**: 1969-1971
15 **Zeng ZC**, Tang ZY, Fan J, Zhou J, Qin LX, Ye SL, Sun HC, Wang BL, Zhang JY, Yu Y, Cheng JM, Wang XL, Guo W. Radiation therapy for adrenal gland metastases from hepatocellular carcinoma. *Jpn J Clin Oncol* 2005; **35**: 61-67
16 **Natsuizaka M**, Omura T, Akaike T, Kuwata Y, Yamazaki K, Sato T, Karino Y, Toyota J, Suga T, Asaka M. Clinical features of hepatocellular carcinoma with extrahepatic metastases. *J Gastroenterol Hepatol* 2005; **20**: 1781-1787
17 **Ishii H**, Furuse J, Kinoshita T, Konishi M, Nakagohri T, Takahashi S, Gotohda N, Nakachi K, Yoshino M. Extrahepatic spread from hepatocellular carcinoma: who are candidates for aggressive anti-cancer treatment? *Jpn J Clin Oncol* 2004; **34**: 733-739
18 **Okusaka T**, Okada S, Ishii H, Nose H, Nagahama H, Nakasuka H, Ikeda K, Yoshimori M. Prognosis of hepatocellular carcinoma patients with extrahepatic metastases. *Hepatogastroenterology* 1997; **44**: 251-257
19 **Oken MM**, Creech RH, Tormey DC, Horton J, Davis TE, McFadden ET, Carbone PP. Toxicity and response criteria of the Eastern Cooperative Oncology Group. *Am J Clin Oncol* 1982; **5**: 649-655
20 Liver Cancer Study Group of Japan. The general rules for the clinical and pathological study of primary liver cancer (in Japanese). 4th ed. Tokyo: Kanehara, 2000: 19
21 **Toyota N**, Naito A, Kakizawa H, Hieda M, Hirai N, Tachikake T, Kimura T, Fukuda H, Ito K. Radiofrequency ablation therapy combined with cementoplasty for painful bone metastases: initial experience. *Cardiovasc Intervent Radiol* 2005; **28**: 578-583
22 **Katyal S**, Oliver JH, Peterson MS, Ferris JV, Carr BS, Baron RL. Extrahepatic metastases of hepatocellular carcinoma. *Radiology* 2000; **216**: 698-703
23 **Shuto T**, Hirohashi K, Kubo S, Tanaka H, Yamamoto T, Higaki I, Takemura S, Kinoshita H. Treatment of adrenal metastases after hepatic resection of a hepatocellular carcinoma. *Dig Surg* 2001; **18**: 294-297
24 **Si MS**, Amersi F, Golish SR, Ortiz JA, Zaky J, Finklestein D, Busuttil RW, Imagawa DK. Prevalence of metastases in hepatocellular carcinoma: risk factors and impact on survival. *Am Surg* 2003; **69**: 879-885
25 **Nakayama H**, Takayama T, Makuuchi M, Yamasaki S, Kosuge T, Shimada K, Yamamoto J. Resection of peritoneal metastases from hepatocellular carcinoma. *Hepatogastroenterology* 1999; **46**: 1049-1052
26 **Kurachi K**, Suzuki S, Yokoi Y, Okumura T, Inaba K, Igarashi T, Takehara Y, Konno H, Baba S, Nakamura S. A 5-year survivor after resection of peritoneal metastases from pedunculated-type hepatocellular carcinoma. *J Gastroenterol* 2002; **37**: 571-574
27 **Momoi H**, Shimahara Y, Terajima H, Iimuro Y, Yamamoto N, Yamamoto Y, Ikai I, Yamaoka Y. Management of adrenal metastasis from hepatocellular carcinoma. *Surg Today* 2002; **32**: 1035-1041
28 **Zeng ZC**, Tang ZY, Fan J, Qin LX, Ye SL, Zhou J, Sun HC, Wang BL, Wang JH. Consideration of role of radiotherapy for lymph node metastases in patients with HCC: retrospective analysis for prognostic factors from 125 patients. *Int J Radiat Oncol Biol Phys* 2005; **63**: 1067-1076

S- Editor Liu Y **L- Editor** Wang XL **E- Editor** Lu W

PO Box 2345, Beijing 100023, China
www.wjgnet.com
wjg@wjgnet.com

World J Gastroenterol 2007 January 21; 13(3): 421-425
World Journal of Gastroenterology ISSN 1007-9327

RAPID COMMUNICATION

Serum levels of soluble Fas, nitric oxide and cytokines in acute decompensated cirrhotic patients

Christoph Elsing, Sabine Harenberg, Wolfgang Stremmel, Thomas Herrmann

Christoph Elsing, Sabine Harenberg, Department of Gastroenterology, St. Elisabeth Hospital, Dorsten, Germany
Wolfgang Stremmel, Thomas Herrmann, Department of Gastroenterology, University of Heidelberg, Germany
Correspondence to: Christoph Elsing, MD, Gastroenterology, Department of Medicine, St. Elisabeth-Hospital, PO Box 580, Dorsten 46225, Germany. c.elsing@krankenhaus-dorsten.de
Telephone: +49-236-2292744 Fax: +49-236-29217044
Received: 2006-08-09 Accepted: 2006-11-04

Abstract

AIM: To evaluate plasma levels of nitrite/nitrate (NOx), soluble Fas (sFas) antigen, tumor necrosis factor alpha (TNF-α) and interleukin-6 (IL-6) in patients with compensated and acute decompensated cirrhosis and to evaluate mediators causing acute decompensation in liver cirrhosis.

METHODS: This prospective study was conducted in the medical intensive care unit of an academic tertiary center. Fifty-five patients with acute decompensation (gastrointestinal hemorrhage, encephalopathy, hydropic decompensation) and twenty-five patients with compensated liver cirrhosis were included. Blood samples were taken for analyses of sFas, Nox, IL-6, TNF-α. Liver enzymes and kidney functions were also tested.

RESULTS: In patients with acute decompensation, plasma sFas levels were higher than in non-decompensated patients (15305 ± 4646 *vs* 12458 ± 4322 pg/mL, $P < 0.05$). This was also true for the subgroup of patients with alcoholic liver cirrhosis ($P < 0.05$). The other mediators were not different and none of the parameters predicted survival, except for ALT (alanine-aminotransferase). In patients with portal-hypertension-induced acute hemorrhage, NOx levels were significantly lower than in patients with other forms of decompensation (70.8 ± 48.3 *vs* 112.9 ± 74.9 pg/mL, $P < 0.05$). When NOx levels were normalized to creatinine levels, the difference disappeared. IL-6, TNF-α and sFas were not different between bleeders and non-bleeders. In decompensated patients sFas, IL-6 and NOx levels correlated positively with creatinine levels, while IL-6 levels were dependent on Child class.

CONCLUSION: In acute decompensated cirrhotic patients sFas is increased, suggesting a role of apoptosis in this process and patients with acute bleeding have lower NOx levels. However, in this acute complex clinical situation, kidney function seems to have a predominant influence on mediator levels.

Key words: Variceal hemorrhage; Liver cirrhosis; Cytokine; Nitrite/nitrate; Soluble Fas

Elsing C, Harenberg S, Stremmel W, Herrmann T. Serum levels of soluble Fas, nitric oxide and cytokines in acute decompensated cirrhotic patients. *World J Gastroenterol* 2007; 13(3): 421-425

http://www.wjgnet.com/1007-9327/13/421.asp

INTRODUCTION

Liver cirrhosis with portal hypertension is characterized by several systemic and splanchnic hemodynamic changes, such as splanchnic and systemic vasodilation, with increased cardiac output and a compensatory renal vasoconstriction[1]. A high level of nitric oxide (NOx), a short-lived soluble vasodilating molecule, has been proposed as one of the major endogenous vasodilators in portal hypertension[2,3]. Increased serum NOx levels in patients with cirrhosis have been reported repeatedly[4-10]. It is also thought to be the cause of some of the complications associated with end stage liver disease. Certain complications of cirrhosis such as the hepatopulmonary syndrome may be in part mediated by local overproduction of nitric oxide[11]. In contrast, exogenous application of nitrates is helpful in primary prophylaxis of variceal hemorrhage[12] and the endothelial dysfunction in cirrhosis results in impaired release of endothelial relaxing factors including NO[13]. Therefore, we speculated that changes in NOx levels could lead to acute decompensation of liver cirrhosis. In addition to NOx, other mediators such as tumor necrosis factor-α (TNF-α) and interleukin-6 (IL-6) have also been associated with the hemodynamic alterations in liver cirrhosis[14-18] and might therefore influence events of acute decompensation.

Experimental studies have also suggested that apoptosis *via* the soluble Fas (sFas)/Fas-ligand (FasL) signalling system may play an important role in the development of liver failure[19]. High levels of sFas have also been described in certain chronic liver diseases[20,21]. However, the effects on acute decompensation of chronic liver diseases are not yet known. The aim of our study was to evaluate serum

levels of NOx, cytokines and sFas in patients with portal-hypertension-associated gastrointestinal hemorrhage and to compare these with levels in patients with other forms of acute decompensation or compensated cirrhosis.

MATERIALS AND METHODS

Patients

A total of 80 consecutive patients with liver cirrhosis with (n = 55) and without (n = 25) decompensation entered this prospective study at the Department of Medicine, University Hospital Heidelberg between October 1999 and June 2000. Patients with decompensation had to be admitted immediately to the Intensive Care Unit of the medical department. Patients with additional signs of infection were excluded from this study to eliminate the influence of the infection *per se* on serum levels of NOx, cytokines and sFas[22]. The study was approved by the ethical committee of the University of Heidelberg. After signing informed consent patients were enrolled.

Criteria for decompensation in patients with histologically proven cirrhosis were: hydropic decompensation with ascites and peripheral edema (hydropic decompensation), encephalopathy or portal-hypertension-associated gastrointestinal hemorrhage. Patients were categorized according to their initial symptoms, and no patient was in more than one category. The severity of liver disease was evaluated according to Pugh's modification of Child's criteria.

Since cytokine levels are influenced by accompanying infections, patients with additional signs of infection were excluded. Spontaneous bacterial peritonitis (SBP) was defined as infection of the ascetic fluid, in the absence of any intra-abdominal source of infection, with a neutrophil count higher than 250 cells/mm^3 ascitic fluid and/or a positive culture. Urinary tract infection was considered when the polymorphonuclear cell count was higher than 10^5/mm^3 and/or a positive culture of urine. Systemic infection was diagnosed when two positive blood cultures were found. A pneumonia was diagnosed based on a positive sputum culture and/or typical chest X-ray.

On admission blood samples for cytokines, NOx and soluble Fas were taken. These parameters were measured together with routine laboratory tests on admission so as to exclude influences of therapies and disease outcomes on cytokine levels. The clinical and biochemical features of the patients are shown in Table 1. Five ml blood was obtained on admission in S-monovettes (Sarstedt, Germany). Serum was immediately separated by centrifugation (3000 r/min), divided into aliquot portions and stored at -25℃ until assayed (within 2 mo of sampling).

Table 1 Patient characteristics on admission

Characteristics	Decompensated cirrhosis (n = 55)	Compensated cirrhosis (n = 25)
Age (yr)	56.1 ± 14.2	55.6 ± 13.7
Gender (M/F)	34/21	15/10
Etiology of cirrhosis		
Alcoholic	31 (56%)	14 (56%)
Viral	8 (15%)	2 (8%)
Others	16 (29%)	9 (36%)
Child Pugh class		
A/B/C	7/24/24	19/6/0

Methods

IL-6 and TNF-α were measured in duplicates using commercially available EIA assays (CYTImmune Sciences Inc. College Park, MD USA). TNF-α assay sensitivity was 4.8 pg/mL, the intra-assay coefficient of variation was ± 8.3%, and the inter-assay coefficient of variation was ± 10.8%. For IL-6 the assay sensitivity was 3.4 pg/mL, the intra-assay coefficient of variation was ± 8.1%, and the inter-assay coefficient of variation was ± 10.4%.

SFas in serum was quantified by a colorimetric ELISA kit (Quantikine, R&D Systems GmbH Wiesbaden, Germany) according to the manufacturers' instructions. Serum samples (100 μL) were poured into antibody-coated wells using multichannel pipettes, then incubated for 2 h at room temperatures. After washing four times 200 μL peroxidase-conjugated-polyclonal antibody solution was added to each well and incubated for 2 h at a room temperature. After washing, the substrate solution (200 μL) was added to each well and incubated for 30 min. The stop solution (50 μL) was then added to the wells and the absorbance of each well was measured at a wavelength of 450 nm (Anthos AR 2001). SFas concentrations were calculated by comparison of the optical densities (mean of duplicate patient samples) to those of the standard run on the same plate. For sFas the assay sensitivity was 3.4 pg/mL, the intra-assay coefficient of variation was ± 3.8%, and the inter-ssay coefficient of variation was ± 4.5%.

NOx was determined from total nitrite levels. Total nitrite measurements were performed on stored samples from all patients, using commercially available kits (Nitric Oxide Assay, R&D Systems GmbH Wiesbaden, Germany). The assay involved the conversion of nitrate to nitrite by nitrate reductase. The detection of nitrite is determined as a colored azo-dye product of the Griess reaction that absorbs visible light. The concentration of NO was indirectly measured by determining both nitrate and nitrite levels in the same sample. Before analyses samples were thawed at a room temperature and ultrafiltered through a 10000 Molecular Weight cutoff filter (Microcon YM-10, Millipore Corporation, USA) to eliminate proteins. Supernatants were placed in microtiter plates in duplicates. The steps used in the assay followed manufacturers' guidelines. After development, plates were read on a microtiter plate scanner (Anthos AR 2001 [550 nm]) and the endogenous nitrite and total nitrite concentrations were calculated by normalization of the optical densities (mean of duplicate samples) of patient samples to those of the standard on the same plate.

The nitrate concentration was determined by subtracting the endogenous nitrite concentration from the total nitrite concentration. The analytic sensitivity of the nitrite assay is typically less than 0.22 μmol/L and of the nitrate reduction assay 0.54 μmol/L. Liver enzymes and creatinine levels were measured using standard commercial

photometric assays. Because NOx levels correlate with kidney function (serum creatinine), they were divided by creatinine levels[16].

Statistical analysis

The data were evaluated using descriptive statistical methods (mean ± SD, ranges). For comparison of two independent variables the non-parametric Mann-Whitney U-test was used. $P < 0.05$ was considered significant. Correlations were assessed by Spearman's test. Statistical calculations were performed using SPSS Version 10.0 for Windows (SPSS Inc. Chicago, USA).

RESULTS

A total of 80 patients were consecutively analyzed. There were more men than women (Table 1). Alcohol was the predominant reason for cirrhosis in both groups (56%). Liver cirrhosis, as assessed by the Child-Pugh score, showed higher stages in the decompensated group.

Decompensated vs compensated cirrhosis

Serum levels of soluble Fas, NOx, TNF-α and IL-6 of patients with and without hepatic decompensation are summarized in Table 2. Among these only sFas was different ($P < 0.05$) between the groups with greater values in patients with decompensation. Further differences between the groups were aspartate-aminotransferase (AST) and alanine-aminotransferase (ALT) levels. In decompensated patients the values averaged 99.7 ± 273.1 U/L and 46.3 ± 153.8 U/L, respectively. The corresponding values in compensated patients were 25.2 ± 15.6 and 20.5 ± 13.9 U/L ($P < 0.05$). Kidney function, as determined by serum levels of creatinine, was impaired in patients with decompensation (1.3 ± 0.9 *vs* 0.8 ± 0.2 mg/dL, $P < 0.01$).

Survival

Within the follow up period of two months, 7 patients with decompensated livers died, while none of the compensated patients died. In comparison to the decompensated survivors, neither sFas, NOx, and TNF-α nor IL-6 levels were different. Kidney function was also comparable. However, ALT levels were significantly higher in patients who died during the observation period (73.6 ± 74.8 *vs* 42.0 ± 162.8 U/L, $P < 0.01$).

Comparison of decompensated patients with and without bleeding

Portal hypertension related gastrointestinal hemorrhage was the reason for admission in 21 patients. IL-6, TNF-α and sFas levels were not significantly different between patients with and without bleeding. However, NOx levels were significantly lower in patients with bleeding (70.8 ± 48.3 *vs* 112.9 ± 74.9 pg/mL, $P < 0.05$). At the beginning kidney function, as assessed by creatinine levels, was poorer in patients with bleeding compared to patients without bleeding (0.9 ± 0.4 *vs* 1.5 ± 1.0 mg/dL, $P < 0.05$). NOx levels are dependent on kidney function and were therefore normalized to creatinine levels. This eliminated the difference. In the bleeding group, the ratio was 0.88 ± 0.62 *vs* 1.13 ± 0.95 in decompensated patients without bleeding (P = NS). In addition, transaminase levels were not different between the patient groups.

Table 2 Serum levels of soluble Fas (sFas), nitrite/nitrate (NOx), tumor necrosis factor alpha (TNF-α) and interleukin-6 (IL-6) in patients with acute decompensation (hemorrhage, encephalopathy, and hydropic decompensation) of liver cirrhosis (mean ± SD)

	Decompensated cirrhosis (n = 55)	Compensated cirrhosis (n = 25)
SFas (pg/mL)	15305 ± 4646	12458 ± 4322[a]
NOx (μmol/L)	96.9 ± 68.7	64.2 ± 40.2
TNF-α (pg/mL)	90.9 ± 65.2	73.5 ± 46.5
IL-6 (pg/mL)	84.8 ± 154.3	180.9 ± 662.2

[a]$P < 0.05$ *vs* decompensated cirrhosis.

Correlation between mediators, transaminases (ALT, AST) and creatinine levels in patients with decompensated cirrhosis

Serum sFas levels and NOx correlated positively with creatinine levels ($P < 0.05$). Serum TNF-α and IL-6 levels showed no correlations and none of the mediators correlated with each other, whereas ALT correlated with AST ($P < 0.001$).

Etiology of cirrhosis

In patients with decompensated livers, alcohol was the reason for cirrhosis in 31 cases and viral infection was the cause in 8 patients. In alcoholic cirrhosis NOx levels were higher (104.2 ± 57.5 μmol/L), while in viral hepatitis NOx levels were significantly lower (63.9 ± 60.7 μmol/L, $P < 0.05$). In patients with alcoholic decompensated cirrhosis sFas levels were higher (15711 ± 4406 pg/mL) than in patients with compensated alcoholic cirrhosis (14882 + 4588 pg/mL, $P < 0.05$). This again indicates a potential role of apoptosis in deteriorating liver function in these patients. The TNF-α and IL-6 levels were similar in both groups.

Dependency on liver function

Several reports have found a correlation between liver function, as assessed by the Child-Pugh score, and cytokine levels. For sFas, TNF-α and NOx no dependency on liver function was observed. However, there was a clear dependency of IL-6 levels on liver function. With deteriorating liver function, IL-6 levels increased significantly ($P < 0.05$) (Figure 1).

DISCUSSION

Acute decompensation of liver cirrhosis is a life threatening complication of a chronic disease. The reasons why acute decompensation occurs are not well understood, but bacterial infections are thought to be involved in some patients[23]. To exclude this possibility and to evaluate the role of different mediators only patients without any signs

of infection were enrolled in this study. Our results showed that in a large cohort of decompensated cirrhotic patients decompensation was accompanied by increased sFas levels. This was independent of the kind of decompensation, i.e., bleeding or hydropic decompensation and was also independent of Child stage. SFas had no relation to outcomes or transaminase levels, but correlated with kidney function.

The data showed that clinical progression and decompensation of liver disease was accompanied by an increase in sFas levels. These results are consistent with other studies demonstrating that the clinical progression of HBV from acute to chronic to malignancy is reflected by a profile of steadily increasing sFas levels[21]. Similar results were reported in patients with chronic hepatitis C[24]. We first describe such a correlation in patients with acute decompensation of chronic liver disease, especially in patients with alcoholic cirrhosis. Evidence from *in vitro* studies suggests that sFas can interfere with immune cell-mediated Fas/FasL apoptosis induction[25,26]. The results therefore indicate that such interference plays a progressively enhanced role during the evolution of the disease and the occurrence of acute decompensation.

In accordance with other studies we also found a dependency of sFas levels on kidney function[27]. In patients with chronic renal failure and in patients undergoing dialysis elevated sFas levels have been described. Therefore, the elevation of sFas levels in our patients might also be mediated by the degree of kidney failure. This additional factor was not mentioned in several other studies where kidney function was not evaluated.

Among many potential mediators, NOx has emerged as the main candidate implicated in the pathogenesis of the hemodynamic alterations in liver cirrhosis. In chronic liver diseases NOx is either produced as a result of high systemic endotoxin levels or shares stress of endothelial cells. In our study, NOx levels tended to be greater in patients with decompensated liver cirrhosis, however, this did not reach statistical significance. Among the decompensated patients, those with portal hypertension associated bleeding (i.e., variceal bleeding, portal hypertensive gastropathy and colonopathy) had significantly lower NOx levels than patients with other forms of decompensation (i. e., encephalopathy, hydropic decompensation).

NOx levels are determined not only by NO production but also by the degree of kidney dysfunction, the fasting state and exogenous nitrate sources[28]. There is an inverse correlation of kidney function and NOx serum levels[16]. In our cirrhotic patients with bleeding, kidney function at entry was better, as assessed by measuring serum creatinine levels, than in patients with other forms of decompensation. We therefore normalized NOx levels to serum creatinine levels and found no difference in NOx levels in decompensated patients with and without bleeding[16], thus changes in NOx levels were not responsible for the acute bleeding episode. Kidney function was evaluated by creatinine levels. This is sufficient, since alterations in kidney functions reflected by changes of creatinine concentrations are accompanied by changes in NOx levels[29]. NOx levels were determined within 24 h after admission of the patients. Since NOx serum levels have a half-life period of 5 h and serum samples from all patients were obtained in similar fashion, this should not have influenced our results[30].

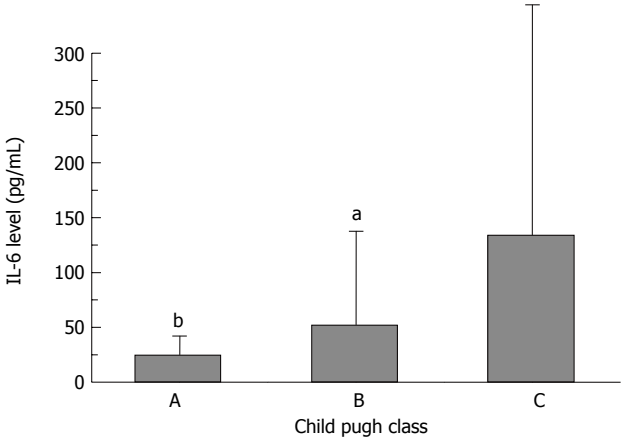

Figure 1 Dependency of IL-6 on Child Pugh class in patients with acutely decompensated liver cirrhosis (mean ± SD). $^{a}P < 0.05$, $^{b}P < 0.01$ *vs* class C.

In our study NOx levels were determined regardless of the fasting state. However, it has to be kept in mind that a gastrointestinal bleeding leads to a high intestinal protein load and induces encephalopathy in severe cirrhotic patients. Thus, our bleeding patients had an endogenous protein load, which could have even higher plasma NOx levels.

NOx is not the only mediator involved in the hyperdynamic circulation in cirrhosis. IL-6 and TNF-α are also thought to be involved[14,31,32] and both are able to increase NOx levels. In our study there were no differences at all between the groups and also patients with bleeding had no difference in these cytokine levels compared to patients with other forms of decompensation. Moreover, we could not find a dependency of TNF-α, sFas and NOx levels on liver function as assessed by the Child classification. Only IL-6 levels showed a dependency on liver function. This is in contrast to some studies, where such a relation could be observed[10]. Other studies were inconsistent[16]. However, serum levels were not corrected for kidney function[10]. It has been suggested that some of the elevations seen in these mediators are a consequence of liver cirrhosis and its hemodynamic alterations, rather than the cause of them. In fact, IL-6 is cleared mainly in the liver[33], and consequently the elevated IL-6 levels might be secondary to liver dysfunction.

In summary, we show that IL-6 and TNF-α are not altered in acute decompensated patients. SFas and NOx levels are different, but dependent of and correlated with kidney function. None of the mediators alone is able to induce acute decompensation. However, in this acute complex clinical situation, kidney function seems to have predominant influence on mediator levels.

REFERENCES

1 **Liu H**, Gaskari SA, Lee SS. Cardiac and vascular changes in cirrhosis: pathogenic mechanisms. *World J Gastroenterol* 2006; **12**: 837-842

2 **Vallance P**, Moncada S. Hyperdynamic circulation in cirrhosis: a role for nitric oxide? *Lancet* 1991; **337**: 776-778
3 **Sogni P**, Moreau R, Gadano A, Lebrec D. The role of nitric oxide in the hyperdynamic circulatory syndrome associated with portal hypertension. *J Hepatol* 1995; **23**: 218-224
4 **Moriyama A**, Masumoto A, Nanri H, Tabaru A, Unoki H, Imoto I, Ikeda M, Otsuki M. High plasma concentrations of nitrite/nitrate in patients with hepatocellular carcinoma. *Am J Gastroenterol* 1997; **92**: 1520-1523
5 **Guarner C**, Soriano G, Tomas A, Bulbena O, Novella MT, Balanzo J, Vilardell F, Mourelle M, Moncada S. Increased serum nitrite and nitrate levels in patients with cirrhosis: relationship to endotoxemia. *Hepatology* 1993; **18**: 1139-1143
6 **Yokoyama M**, Shijo H, Ota K, Kubara K, Kokawa H, Kim T, Akiyoshi N, Okumura M, Inoue K. Systemic hemodynamics and serum nitrate levels in patients undergoing endoscopic variceal ligation. *Hepatology* 1996; **24**: 47-52
7 **Bories PN**, Campillo B, Azaou L, Scherman E. Long-lasting NO overproduction in cirrhotic patients with spontaneous bacterial peritonitis. *Hepatology* 1997; **25**: 1328-1333
8 **Genesca J**, Segura R, Gonzalez A, Catalan R, Marti R, Torregrosa M, Cereto F, Martinez M, Esteban R, Guardia J. Nitric oxide may contribute to nocturnal hemodynamic changes in cirrhotic patients. *Am J Gastroenterol* 2000; **95**: 1539-1544
9 **Barak N**, Zemel R, Ben-Ari Z, Braun M, Tur-Kaspa R. Nitric oxide metabolites in decompensated liver cirrhosis. *Dig Dis Sci* 1999; **44**: 1338-1341
10 **Arkenau HT**, Stichtenoth DO, Frölich JC, Manns MP, Böker KH. Elevated nitric oxide levels in patients with chronic liver disease and cirrhosis correlate with disease stage and parameters of hyperdynamic circulation. *Z Gastroenterol* 2002; **40**: 907-913
11 **Gschossmann JM**, Essig M, Reichen J, Scheurer U, Gerken G. The hepato-pulmonary syndrome--where do we stand in the year 2006?. *Z Gastroenterol* 2006; **44**: 249-256
12 **Lowe RC**, Grace ND. Primary prophylaxis of variceal hemorrhage. *Clin Liver Dis* 2001; **5**: 665-676
13 **Gupta TK**, Toruner M, Chung MK, Groszmann RJ. Endothelial dysfunction and decreased production of nitric oxide in the intrahepatic microcirculation of cirrhotic rats. *Hepatology* 1998; **28**: 926-931
14 **Byl B**, Roucloux I, Crusiaux A, Dupont E, Devière J. Tumor necrosis factor alpha and interleukin 6 plasma levels in infected cirrhotic patients. *Gastroenterology* 1993; **104**: 1492-1497
15 **Tilg H**, Wilmer A, Vogel W, Herold M, Nölchen B, Judmaier G, Huber C. Serum levels of cytokines in chronic liver diseases. *Gastroenterology* 1992; **103**: 264-274
16 **Genesca J**, Gonzalez A, Segura R, Catalan R, Marti R, Varela E, Cadelina G, Martinez M, Lopez-Talavera JC, Esteban R, Groszmann RJ, Guardia J. Interleukin-6, nitric oxide, and the clinical and hemodynamic alterations of patients with liver cirrhosis. *Am J Gastroenterol* 1999; **94**: 169-177
17 **Lopez-Talavera JC**, Merrill WW, Groszmann RJ. Tumor necrosis factor alpha: a major contributor to the hyperdynamic circulation in prehepatic portal-hypertensive rats. *Gastroenterology* 1995; **108**: 761-767
18 **Lee FY**, Lu RH, Tsai YT, Lin HC, Hou MC, Li CP, Liao TM, Lin LF, Wang SS, Lee SD. Plasma interleukin-6 levels in patients with cirrhosis. Relationship to endotoxemia, tumor necrosis factor-alpha, and hyperdynamic circulation. *Scand J Gastroenterol* 1996; **31**: 500-505
19 **Nakae H**, Narita K, Endo S. Soluble Fas and soluble Fas ligand levels in patients with acute hepatic failure. *J Crit Care* 2001; **16**: 59-63
20 **Jodo S**, Kobayashi S, Nakajima Y, Matsunaga T, Nakayama N, Ogura N, Kayagaki N, Okumura K, Koike T. Elevated serum levels of soluble Fas/APO-1 (CD95) in patients with hepatocellular carcinoma. *Clin Exp Immunol* 1998; **112**: 166-171
21 **Song le H**, Binh VQ, Duy DN, Bock TC, Kremsner PG, Luty AJ, Mavoungou E. Variations in the serum concentrations of soluble Fas and soluble Fas ligand in Vietnamese patients infected with hepatitis B virus. *J Med Virol* 2004; **73**: 244-249
22 **Connert S**, Stremmel W, Elsing C. Procalcitonin is a valid marker of infection in decompensated cirrhosis. *Z Gastroenterol* 2003; **41**: 165-170
23 **Goulis J**, Patch D, Burroughs AK. Bacterial infection in the pathogenesis of variceal bleeding. *Lancet* 1999; **353**: 139-142
24 **Raghuraman S**, Abraham P, Daniel HD, Ramakrishna BS, Sridharan G. Characterization of soluble FAS, FAS ligand and tumour necrosis factor-alpha in patients with chronic HCV infection. *J Clin Virol* 2005; **34**: 63-70
25 **Cheng J**, Zhou T, Liu C, Shapiro JP, Brauer MJ, Kiefer MC, Barr PJ, Mountz JD. Protection from Fas-mediated apoptosis by a soluble form of the Fas molecule. *Science* 1994; **263**: 1759-1762
26 **Suda T**, Hashimoto H, Tanaka M, Ochi T, Nagata S. Membrane Fas ligand kills human peripheral blood T lymphocytes, and soluble Fas ligand blocks the killing. *J Exp Med* 1997; **186**: 2045-2050
27 **Perianayagam MC**, Murray SL, Balakrishnan VS, Guo D, King AJ, Pereira BJ, Jaber BL. Serum soluble Fas (CD95) and Fas ligand profiles in chronic kidney failure. *J Lab Clin Med* 2000; **136**: 320-327
28 **Heller J**, Kristeleit H, Brensing KA, Woitas RP, Spengler U, Sauerbruch T. Nitrite and nitrate levels in patients with cirrhosis of the liver: influence of kidney function and fasting state. *Scand J Gastroenterol* 1999; **34**: 297-302
29 **Mackenzie IM**, Ekangaki A, Young JD, Garrard CS. Effect of renal function on serum nitrogen oxide concentrations. *Clin Chem* 1996; **42**: 440-444
30 **Ward FW**, Coates ME, Walker R. Influence of dietary protein and gut microflora on endogenous synthesis of nitrate and N-nitrosamines in the rat. *Food Chem Toxicol* 1989; **27**: 445-449
31 **Odeh M**, Sabo E, Srugo I, Oliven A. Serum levels of tumor necrosis factor-alpha correlate with severity of hepatic encephalopathy due to chronic liver failure. *Liver Int* 2004; **24**: 110-116
32 **Nagano T**, Yamamoto K, Matsumoto S, Okamoto R, Tagashira M, Ibuki N, Matsumura S, Yabushita K, Okano N, Tsuji T. Cytokine profile in the liver of primary biliary cirrhosis. *J Clin Immunol* 1999; **19**: 422-427
33 **Castell JV**, Geiger T, Gross V, Andus T, Walter E, Hirano T, Kishimoto T, Heinrich PC. Plasma clearance, organ distribution and target cells of interleukin-6/hepatocyte-stimulating factor in the rat. *Eur J Biochem* 1988; **177**: 357-361

S- Editor Wang GP **L- Editor** Zhu LH **E- Editor** Bi L

PO Box 2345, Beijing 100023, China
www.wjgnet.com
wjg@wjgnet.com

World J Gastroenterol 2007 January 21; 13(3): 426-431
World Journal of Gastroenterology ISSN 1007-9327

RAPID COMMUNICATION

Expression of COX-2, PCNA, Ki-67 and p53 in gastrointestinal stromal tumors and its relationship with histopathological parameters

Derya Gumurdulu, Seyda Erdogan, Fazilet Kayaselcuk, Gulsah Seydaoglu, Cem K Parsak, Orhan Demircan, Ilhan Tuncer

Derya Gumurdulu, Seyda Erdogan, Ilhan Tuncer, Department of Pathology of Affiliated Hospital, Faculty of Medicine, Cukurova University, Adana 01330, Turkey
Fazilet Kayaselcuk, Department of Pathology of Affiliated Hospital, Baskent University Adana Resarch and Practice Center, Adana 01330, Turkey
Gulsah Seydaoglu, Department of Biostatistics of Affiliated Hospital, Faculty of Medicine, Cukurova University, Adana 01330, Turkey
Cem K Parsak, Orhan Demircan, Department of Surgery of Affiliated Hospital, Faculty of Medicine, Cukurova University, Adana 01330, Turkey
Correspondence to: Dr. Derya Gumurdulu, Department of Pathology, Faculty of Medicine, Cukurova University, Adana 01330, Turkey. gumurdulu@yahoo.com
Telephone: +90-322-3386060 Fax: +90-322-3386956
Received: 2006-09-30 Accepted: 2006-11-21

Abstract

AIM: To investigate the expression of Cyclooxygenase-2 (COX-2), proliferating cell nuclear antigen (PCNA), Ki-67 and p53 in gastrointestinal stromal tumors (GISTs) and its relationship with histopathological parameters.

METHODS: Twenty-five GISTs were examined by light microscopy and immunohistochemistry. c-kit, CD34, SMA, S-100 protein, COX-2, PCNA, Ki-67 and p53 were detected immunohistochemically and the relationship was evaluated among histopathologic parameters such as mitotic index (MI), tumor grade, tumor size, COX-2, PCNA, Ki-67 and p53.

RESULTS: COX-2 protein expression was found in 19 of 25 (76%) of the tumors, and expression was noted in the cytoplasm of the tumor cells. p53 was significantly related to MI and tumor grade but no relationship was found between COX-2, proliferation markers and MI, tumor grade and tumor size.

CONCLUSION: COX-2 is expressed in most GISTs and it may play an important role in the proliferation and progression of these tumors or a useful marker to identify GIST. Although immunohistochemical assessment of p53 can be used for distinguishing the risk groups of GISTs, tumor size and mitotic rate should be considered at the same time.

Key words: Gastrointestinal stromal tumor; Cyclooxygenase-2; Proliferating cell nuclear antigen; Ki-67; p53; Immunohistochemistry

Gumurdulu D, Erdogan S, Kayaselcuk F, Seydaoglu G, Parsak CK, Demircan O, Tuncer I. Expression of COX-2, PCNA, Ki-67 and p53 in gastrointestinal stromal tumors and its relationship with histopathological parameters. *World J Gastroenterol* 2007; 13(3): 426-431

http://www.wjgnet.com/1007-9327/13/426.asp

INTRODUCTION

Gastrointestinal stromal tumors (GISTs) are specific mesenchymal tumors of gastrointestinal tract (GI) that may occur in the entire length of GI tract from the esophagus to the anus[1]. Its histopathological origin has recently been suggested to be the intertistial cells of Cajal (ICC)[2]. For the majority of GISTs, it may be very difficult or impossible to determine the presence of any specific line of differentiation histologically. Tumors showing partial or incomplete myogenic, neural or myenteric ganglionic features may present virtually identical features under light microscopy[3].

However, immunohistochemistry of GISTs yields a diverse and confusing array of data, the antibodies most commonly used to characterize GISTs are those direct against vimentin, desmin, muscle spesific actin (MSA), smooth muscle actin (SMA), S-100 protein, neurofilament (NF), neurone spesific enolase (NSE), PGP9.5, CD34 and CD117 (c-kit). The myogenic markers MSA and SMA are variably expressed, whereas desmin is almost never present. Furthermore, MSA and SMA are generally only focally present or completely absent, indicating that most smooth muscle differentiation is incomplete. A possible schwannian/neural differentiation (S-100 protein, PGP9.5 and NSE positivity) may be present in a proportion of SMA and MSA negative tumors, both myogenic and schwannian/neural differentiation in a small proportion of tumors, whereas a small number of GISTs were positive for vimentin only and exhibited no detectable

differentiation immunohistochemically[1-4].

The results of recent molecular pathologic studies that most GISTs are immunoreactive for CD34, a hematopoietic progenitor cell antigen, and CD117, c-kit proto-oncogen protein, as well as the gain of function c-kit gene mutations cause pathologic activation of the tyrosine kinase of c-kit in GISTs, seem to support the concept of GISTs as a biologically distinct entity[5,6].

The cyclooxygenase (COX) isoenzymes, COX-1 and COX-2 catalyze in the oxidation of arachidonic acid to prostaglandins, prostacyclin and tromboxanes and are inhibited by aspirin and non-steroidal anti-inflammatory drugs (NSAIDs)[7]. COX-1 is constitutively expressed in most normal tissues; COX-2 is induced by cytokines, mitogenic agents, and growth factors, and it produces inflammation and cell growth. Up-regulation of this enzyme *in vitro* has several tumorigenic effects such as induction of cell cycle arrest, resistance to apoptosis, increased cell growth, and stimulation of mitogenesis[7-8]. Recent studies have shown that COX-2 expression is elevated in gastrointestinal carcinomas but little is known about COX-2 expression in GISTs[9-11].

Multiple histological parameters such as mitosis, tumor size, cellularity, necrosis and pleomorphism have been used to predict the biological behavior of GISTs with limited success[2,12]. The proliferation markers Ki-67 and PCNA and tumor suppressor gene p53 have been reported as prognostic markers in many tumors, but only a few such studies have been reported in GISTs[2].

In this study, we used CD34, SMA and S-100 for differentiation of GISTs and investigated the expression of COX-2 in an attempt to correlate histopathologic parameters such as mitotic index (MI), tumor grade and tumor size and COX-2, proliferating cell nuclear antigen (PCNA), Ki-67 and p53.

MATERIALS AND METHODS

Formalin-fixed, paraffin-embedded tissue sections from 25 primary GISTs were obtained from the files of the Faculty of Medicine, Cukurova University, and Department of Pathology, Baskent University Adana Resarch and Practice Hospital. The material consisted of 11 gastric, 11 small intestinal, and 3 large intestinal tumors. The GIST cases were re-evaluated to confirm the diagnosis, and choose appropriate blocks of paraffin-embedded tissue for immunohistochemical analysis. Clinical information, including tumor size, was obtained from the surgical and pathological records. The tumors were reclassified as very low risk, low risk, intermediate risk and high risk according to MI (mitotic figures per 50 high-power fields; HPF) and tumor size (Table 1)[13].

Table 1 Risk categories in GISTs

	Size	Mitotic count
Very low risk	< 2 cm	< 5/50 HPF
Low risk	2-5 cm	< 5/50 HPF
Intermediate risk	< 5 cm	6-10/50 HPF
	5-10 cm	< 5/50 HPF
High risk	> 5 cm	> 5/50 HPF
	> 10 cm	Any mitotic rate
	Any size	> 10/50 HPF

Immunohistochemical analysis

Immunohistochemistry was performed using a strept avidin-biotin-peroxidese technique with antibodies to c-kit (CD117, monoclonal mouse antibody, Novacastra-dilution 1:30), CD34 (monoclonal mouse antibody, Dako-dilution 1:40), vimentin (monoclonal mouse antibody, Biogenex-dilution 1:100), SMA (monoclonal mouse antibody, Novacastra-dilution 1:50), S-100 protein (polyclonal rabbit antibody, Novacastra-dilution 1:200), COX-2 (polyclonal goat antibody, Santa Cruz-dilution 1:100), Ki-67 (polyclonal rabbit antibody, Dako-dilution 1:50), PCNA (monoclonal mouse antibody, Biogenex-dilution 1:25), p53 (monoclonal mouse antibody, Dako-dilution 1:60). A 5-μm thick sections of formalin-fixed, paraffin-embedded tissue samples were deparaffinized and rehydrated through a series of graded alcohols. Endogenous peroxidase activity was blocked by a 30-min incubation in 3% hydrogen peroxide-methanol solution and washed in phosphate-buffered saline (PBS). The slides were kept in citrate buffer for 5-10 min in a microwave oven, rinsed in PBS at room temperature and incubated for 20-30 min with A2 blocking serum (citrate buffer incubation was not performed for vimentin, and the sections were incubated with 0.1% trypsin for 30 min). After washing, the sections were incubated for 60-120 min with primary antibodies and incubated for 30 min with biotinylated horse anti-mouse IgG immunglobulin (Dako, K0675). The sections were incubated for 30 min with strept avidin peroxidase reagent and washed again. The immunoperoxidase was visualized with AEC (3 amino 9 ethyl carbazole), (Dako, AEC substrate K0696). The sections were counterstained with Mayer's hematoxylin and then coverslipped.

Assessment of staining reactions

The cytoplasmic immunostaining for c-kit, vimentin, CD34, SMA, S-100 and COX-2, and nuclear staining for Ki-67, PCNA and p53 were considered as positive reaction. The following scoring system was used for Ki-67 and PCNA: score 0, not positive; score 1, positively stained nuclei in < 10% of the tumor cells; score 2, 10-50% positive; and score 3, > 50% positive. The following scoring system was used for p53 evaluation: 0, not positive; 1+, 1-25% positive; 2+, 25-50% positive; 3+, 50-75% positive and 4+, > 75% positive.

Statistical analysis

Chi-square test was used to analyse the relation between MI, tumor grade, tumor size and COX-2, Ki-67, PCNA and p53. A P value of < 0.05 was considered significant in difference. Statistical analyses were performed with SPSS version 10.0 (Chicago, USA).

RESULTS

Sixteen (64%) of 25 GIST cases were male and 9 (36%) were female. Their ages ranged from 38 to 81 with a mean age of 62.30 ± 11.18 years (male: 62.86 ± 10.97, female:

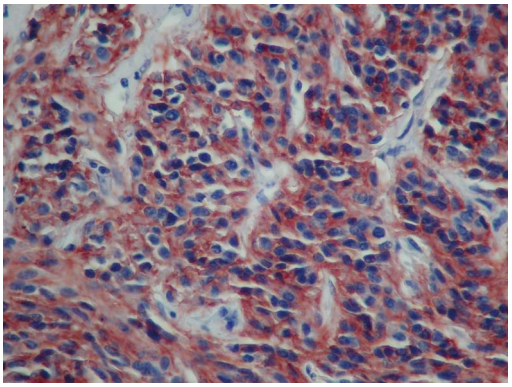

Figure 1 Diffuse cytoplasmic staining of COX-2 in the tumor cells of GIST.

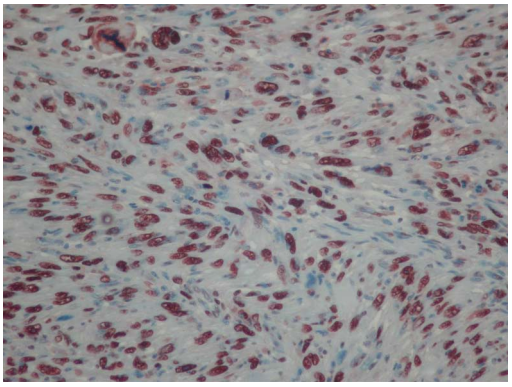

Figure 2 High PCNA immunoreactivity in GIST with more than 50% of nuclear positivity.

61.44 ± 12.12). Eleven (44%) of the tumors originated from stomach, 11 (44%) from small intestine and 3 (12%) from large intestine. The mean size of the tumor was 7.70 ± 3.62 cm, 10.0 ± 4.43 cm and 5.0 ± 1.73 cm and the mean mitotic index of the tumor was 5.60 ± 5.10, 11.0 ± 10.76 and 16.0 ± 7.21 in stomach, small intestine and large intestine, respectively. The tumors were classified as low risk (n = 3), intermediate risk (n = 6) and high risk (n = 16). Two of the low risk tumors were gastric and one was small intestinal. Four of the intermediate risk tumors were gastric and two were small intestinal tumors. Five of the high risk tumors were gastric, eight were small intestinal and three were large intestinal tumors. The clinicopathological data of the 25 patients with GIST are summarized in Table 2. The immunostaining results are listed in Table 3.

All 25 cases of GIST were positive for vimentin. Twenty-three (92%) tumors were positive for c-kit. Only one small intestinal and one large intestinal tumors were negative for c-kit but these tumors showed positive reactivity with CD34. There was diffuse cytoplasmic staining for both c-kit and CD34. CD34 reactivity was found in 21(84%) tumors. Two gastric and two small intestinal tumors were negative for CD34. Ten (40%) tumors were positive for SMA. There was focal cytoplasmic staining for SMA. The frequency of SMA reactivity was higher in the nonstomach tumors (6 in small intestine and 2 in large intestine). S-100 reactivity was found in 16 tumors (6 in stomach, 8 in small intestine and 2 in large intestine). There was focal staining for S-100. Both SMA and S-100 reactivity were found in 5 intestinal tumors while they were found only in 2 gastric tumors. In contrast, 5 gastric tumors were negative for SMA and S-100 while only one intestinal tumor was negative.

COX-2 immunostaining was found in 19 of 25 (76%) of the tumors (Figure 1). Three gastric and three small intestinal tumors were negative for COX-2. In the stomach, two high risk and only one low risk tumor were negative. In the small intestine, two high risk and one intermediate risk tumors showed negative staining with COX-2 (Table 3).

PCNA index was high in most cases; score 3 was found in 18 (72%) tumors; and score 2 in 5 (20%) (Figure 2). Only one case was negative for PCNA. Based on Ki-67 index, score 0 was assigned to 9 (36%) tumors; score 1, to

Table 2 Clinicopathological features of 25 patients with GISTs

Variables	Cases n (%)
Sex	
Male	16 (64)
Female	9 (36)
Site	
Stomach	11 (44)
Small intestine	11 (44)
Large intestine	3 (12)
Tumor size (cm)	
< 2 cm	0 (0)
2-5 cm	4 (16)
5-10 cm	16 (64)
> 10 cm	5 (20)
Mitosis	
< 5	11 (44)
⩾ 5	14 (56)
Diagnosis	
Very low risk	0 (0)
Low risk	3 (12)
Intermediate risk	6 (24)
High risk	16 (64)

Table 3 Immunostaining results of 25 cases of GISTs

Site of origin	c-kit +	COX-2 +	CD34 +	SMA + S-100 +	SMA + S-100 -	SMA - S-100 +	SMA - S-100 -
Stomach (n = 11)							
Low risk	2	1	2	-	-	1	1
Intermediate risk	4	4	3	-	-	2	2
High risk	5	3	4	2	-	1	2
Small intestine (n = 11)							
Low risk	1	1	1	-	1	-	-
Intermediate risk	2	1	2	1	-	1	-
High risk	7	6	6	2	2	4	-
Large intestine (n = 3)							
High risk	2	3	3	2	-	-	1
Total n (%)	23 (92)	19 (76)	21 (84)	7 (28)	3 (12)	9 (36)	6 (24)

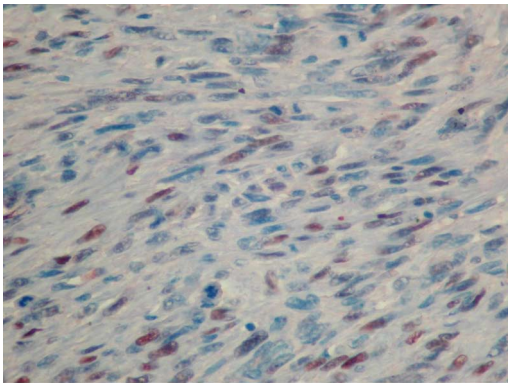

Figure 3 Low Ki-67 immunoreactivity in GIST with less than 50% of nuclear positivity.

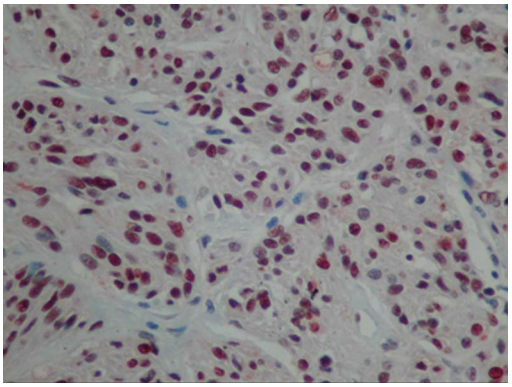

Figure 4 High p53 immunoreactivity in GIST with more than 75% of nuclear positivity.

10 (40%); score 2, to 5 (20%); and score 3, to only one (4%) (Figure 3).

p53 was positive in 18 (72%) tumors whereas it was negative in 7 (28%) (Figure 4). Immunostaining results for p53 are shown in Table 4.

Follow-up information was available in 13 cases. Four patients died in early postoperative period (4-21 d). Two patients died 18-24 mo after diagnosis. Seven patients are alive 36-12 mo after diagnosis.

Statistically, p53 was related to MI and tumor risk groups ($P < 0.05$). Although p53 score was markedly high in cases with tumor size > 5 cm in diameter, it was statistically insignificant ($P = 0.05$). There was no relationship between COX-2, proliferation markers (PCNA, Ki-67) and MI, tumor risk groups and tumor size ($P > 0.05$).

Table 4 The results of immunohistochemical staining for p53

p53 index	0	1	2	3	4
Low risk	1	1	1	0	0
Intermediate risk	0	2	1	1	2
High risk	6	6	2	2	0
Total	7	9	4	3	2

DISCUSSION

GISTs differ from true leiomyomas, leiomyosarcomas and schwannomas, and their histological origin has recently been suggested to be the ICC. These cells are located between the muscular layers of gastric and intestinal wall associated with the myenteric plexus which are thought to play a role incoordinating intestinal motility. Ultrastructurally, they show both incomplete myogenic and neural differentiation and characterized by dual immunopositivity for CD34 and CD117[4,13]. It is also accepted that the term "GIST" should apply only to neoplasms expressing CD117 with only very rare exceptions. The majority of studies have demonstrated that immunoreactivity for CD34 is seen in 60%-80% of cases[6,13,14].

Beside consistent positivity for CD117 and CD34, 30%-40% of GISTs show immunopositivity for SMA and usually 5%-10% and rarely up to 40% show immunopositivity for S-100 protein[3,13,15].

In our study, SMA positivity was seen most often in bowel tumors with a ratio of 40%. Some studies have showed a reciprocal relationship with CD34 expression and SMA positivity. Similarly, SMA negative tumors were often CD34 positive in our cases. Additionally, the percentage of S-100 protein reactivity was higher than most of the previous studies. Beside conflicting results in the literature this finding may represent autonomic nerve-like differentiation in a proportion of GISTs so that the relationship between GAN and GISTs can not be ignored. Also, a significant number of gastric tumors were negative for SMA and S-100 protein while most of bowel tumors had showed S-100 protein and/or SMA positivity.

Overexpression of COX-2 has been reported in various types of gastrointestinal carcinomas[9-11]. COX-2 is located in tumor-derived epithelial cells of colonic adenocarcinomas, whereas it is found in stroma cells in tissues of colonic adenoma and colorectal carcinoma[9,16]. In addition, COX-2 is also located in interstitial cells of colonic adenomatous polyps[17-19]. These discrepant findings should be sorted out to determine the role of COX-2 in not only carcinogenesis but also tumor growth and progression of human carcinomas in terms of epithelial-stromal interactions[8]. Asano *et al*[8] showed that the expression of COX-2 in gallbladder carcinoma was increased in parallel to the depth of invasion. Sheehan *et al*[7] described for the first time the expression of COX-2 in GISTs, and demonstrated COX-2 protein expression in 12 of 15 (80%) of the tumors. Stewart *et al*[20] showed COX-2 protein expression in 35 of 38 (92%) GISTs and indicated that COX-2 may be useful as an additional molecular marker to aid in the identification of GIST, particularly in those cases with epithelioid histology or where KIT is only weakly or focally positive. Epidemiologic data suggest that the treatment with aspirin and NSAIDs prevents colorectal cancer and reduces the size and number of corectal polyps[21,22]. There is no evidence of inhibitory effect of aspirin or NSAIDs in GISTs but treatment with COX inhibitors as adjuvant therapy may be beneficial.

There are many parameters for distinguishing benign from malignant GISTs such as MI, tumor size, cellularity, necrosis, mucosal invasion. MI and tumor size are the most reasonable and replicable parameters[13,23].

Other parameters have been studied to evaluate GISTs behaviors, including immunohistochemical markers of cell proliferation (e.g., Ki-67, MIB-1, PCNA), flow cytometry, image analysis, telomerase activity and assessment of nucleolar organizer regions[13,24].

There are controversies about prognostic impact of PCNA[25-28]. Ray and *et al*[25] demonstrated that PCNA index was correlated with necrosis, high grade atypia, cellularity and mitotic rate. In contrast, Sbasching *et al*[27] did not find a correlation of PCNA expression with survival in GIST. More recently, Ki-67 analogues have replaced PCNA because PCNA index is instable due to variations in antigen preservation and recovery[29]. Seidal *et al*[30] studied 31 cases of GIST and found a correlation with Ki-67 and outcome of patients. Wang *et al*[2] showed that expression of Ki-67 was more frequently seen in malignant GISTs than in benign GISTs. Regarding p53 expression in GIST, only a few studies have been carried out, with conflicting results. Al-Bozom[23] evaluated p53 expression in 15 cases and concluded that p53 is usefull in distinguishing between benign and malignant GIST. In contrast, Lopes *et al*[31] studied 33 cases and did not find any correlation between p53 and behavior.

In our study, p53 was found to be related to MI and tumor grade ($P < 0.05$). Although p53 score was markedly high in the cases with tumor size > 5 cm in diameter, it was statistically insignificant ($P = 0.05$). We could not find any significant relationshiop between proliferation markers (PCNA, Ki-67), MI, tumor grade and tumor size ($P > 0.05$).

In conclusion, COX-2 is expressed in most GISTs and may play an important role in the proliferation and progression of these tumors or a useful marker to help identify GIST. Immunohistochemical assessment of p53 can be used for distinguishing the risk groups of GISTs but the best way to distinguish the risk groups of these tumors is thought to be the tumor size and mitotic rate. We found out that PCNA and Ki-67 are independent factors from MI, tumor grade and tumor size. Further studies to find additional prognostic parameters will provide valuable insights into the behavior of GISTs.

REFERENCES

1 **Miettinen M**, Lasota J. Gastrointestinal stromal tumors--definition, clinical, histological, immunohistochemical, and molecular genetic features and differential diagnosis. *Virchows Arch* 2001; **438**: 1-12

2 **Wang X**, Mori I, Tang W, Utsunomiya H, Nakamura M, Nakamura Y, Zhou G, Kakudo K. Gastrointestinal stromal tumors: clinicopathological study of Chinese cases. *Pathol Int* 2001; **51**: 701-706

3 **Suster S**. Gastrointestinal stromal tumors. *Semin Diagn Pathol* 1996; **13**: 297-313

4 **Graadt van Roggen JF**, van Velthuysen ML, Hogendoorn PC. The histopathological differential diagnosis of gastrointestinal stromal tumours. *J Clin Pathol* 2001; **54**: 96-102

5 **Hasegawa T**, Matsuno Y, Shimoda T, Hirohashi S. Gastrointestinal stromal tumor: consistent CD117 immunostaining for diagnosis, and prognostic classification based on tumor size and MIB-1 grade. *Hum Pathol* 2002; **33**: 669-676

6 **Miettinen M**, Sarlomo-Rikala M, Lasota J. Gastrointestinal stromal tumors: recent advances in understanding of their biology. *Hum Pathol* 1999; **30**: 1213-1220

7 **Sheehan KM**, Sabah M, Cummins RJ, O'Grady A, Murray FE, Leader MB, Kay EW. Cyclooxygenase-2 expression in stromal tumors of the gastrointestinal tract. *Hum Pathol* 2003; **34**: 1242-1246

8 **Asano T**, Shoda J, Ueda T, Kawamoto T, Todoroki T, Shimonishi M, Tanabe T, Sugimoto Y, Ichikawa A, Mutoh M, Tanaka N, Miwa M. Expressions of cyclooxygenase-2 and prostaglandin E-receptors in carcinoma of the gallbladder: crucial role of arachidonate metabolism in tumor growth and progression. *Clin Cancer Res* 2002; **8**: 1157-1167

9 **Sano H**, Kawahito Y, Wilder RL, Hashiramoto A, Mukai S, Asai K, Kimura S, Kato H, Kondo M, Hla T. Expression of cyclooxygenase-1 and -2 in human colorectal cancer. *Cancer Res* 1995; **55**: 3785-3789

10 **Tsujii M**, Kawano S, DuBois RN. Cyclooxygenase-2 expression in human colon cancer cells increases metastatic potential. *Proc Natl Acad Sci USA* 1997; **94**: 3336-3340

11 **Fujita T**, Matsui M, Takaku K, Uetake H, Ichikawa W, Taketo MM, Sugihara K. Size- and invasion-dependent increase in cyclooxygenase 2 levels in human colorectal carcinomas. *Cancer Res* 1998; **58**: 4823-4826

12 **Basson MD**, Modlin IM, Flynn SD. Current clinical and pathologic perspectives on gastric stromal tumors. *Surg Gynecol Obstet* 1992; **175**: 477-489

13 **Fletcher CD**, Berman JJ, Corless C, Gorstein F, Lasota J, Longley BJ, Miettinen M, O'Leary TJ, Remotti H, Rubin BP, Shmookler B, Sobin LH, Weiss SW. Diagnosis of gastrointestinal stromal tumors: A consensus approach. *Hum Pathol* 2002; **33**: 459-465

14 **Berman J**, O'Leary TJ. Gastrointestinal stromal tumor workshop. *Hum Pathol* 2001; **32**: 578-582

15 **Miettinen M**. Gastrointestinal stromal tumors. An immunohistochemical study of cellular differentiation. *Am J Clin Pathol* 1988; **89**: 601-610

16 **Bamba H**, Ota S, Kato A, Adachi A, Itoyama S, Matsuzaki F. High expression of cyclooxygenase-2 in macrophages of human colonic adenoma. *Int J Cancer* 1999; **83**: 470-475

17 **Oshima M**, Dinchuk JE, Kargman SL, Oshima H, Hancock B, Kwong E, Trzaskos JM, Evans JF, Taketo MM. Suppression of intestinal polyposis in Apc delta716 knockout mice by inhibition of cyclooxygenase 2 (COX-2). *Cell* 1996; **87**: 803-809

18 **Hull MA**, Booth JK, Tisbury A, Scott N, Bonifer C, Markham AF, Coletta PL. Cyclooxygenase 2 is up-regulated and localized to macrophages in the intestine of Min mice. *Br J Cancer* 1999; **79**: 1399-1405

19 **Shattuck-Brandt RL**, Varilek GW, Radhika A, Yang F, Washington MK, DuBois RN. Cyclooxygenase 2 expression is increased in the stroma of colon carcinomas from IL-10(-/-) mice. *Gastroenterology* 2000; **118**: 337-345

20 **Stewart AE**, Heslin MH, Arch J, Jhala N, Ragland B, Gomez F, Bland KI, Arnoletti JP. Cyclooxygenase-2 expression and clinical outcome in gastrointestinal stromal tumors. *J Gastrointest Surg* 2006; **10**: 315-319

21 **Thun MJ**, Namboodiri MM, Calle EE, Flanders WD, Heath CW. Aspirin use and risk of fatal cancer. *Cancer Res* 1993; **53**: 1322-1327

22 **Steinbach G**, Lynch PM, Phillips RK, Wallace MH, Hawk E, Gordon GB, Wakabayashi N, Saunders B, Shen Y, Fujimura T, Su LK, Levin B, Godio L, Patterson S, Rodriguez-Bigas MA, Jester SL, King KL, Schumacher M, Abbruzzese J, DuBois RN, Hittelman WN, Zimmerman S, Sherman JW, Kelloff G. The effect of celecoxib, a cyclooxygenase-2 inhibitor, in familial adenomatous polyposis. *N Engl J Med* 2000; **342**: 1946-1952

23 **Al-Bozom IA**. p53 expression in gastrointestinal stromal tumors. *Pathol Int* 2001; **51**: 519-523

24 **Sakurai S**, Fukayama M, Kaizaki Y, Saito K, Kanazawa K, Kitamura M, Iwasaki Y, Hishima T, Hayashi Y, Koike M. Telomerase activity in gastrointestinal stromal tumors. *Cancer* 1998; **83**: 2060-2066

25 **Ray R**, Tahan SR, Andrews C, Goldman H. Stromal tumors of the stomach: prognostic value of the PCNA index. *Mod Pathol* 1994; **7**: 26-30

26 **Amin MB**, Ma CK, Linden MD, Kubus JJ, Zarbo RJ. Prognostic value of proliferating cell nuclear antigen index in gastric stromal tumors. Correlation with mitotic count and clinical outcome. *Am J Clin Pathol* 1993; **100**: 428-432

27 **Sbaschnig RJ**, Cunningham RE, Sobin LH, O'Leary TJ. Proliferating-cell nuclear antigen immunocytochemistry in the evaluation of gastrointestinal smooth-muscle tumors. *Mod Pathol* 1994; **7**: 780-783
28 **Shirai H**, Takeuchi T, Naka T, Minaghi S, Kimura A, Hamazaki S, Ito H. Gastrointestinal stromal tumor of the stomach: report of a case. *Surg Today* 2001; **31**: 346-349
29 **Carrillo R**, Candia A, Rodriguez-Peralto JL, Caz V. Prognostic significance of DNA ploidy and proliferative index (MIB-1 index) in gastrointestinal stromal tumors. *Hum Pathol* 1997; **28**: 160-165
30 **Seidal T**, Edvardsson H. Expression of c-kit (CD117) and Ki67 provides information about the possible cell of origin and clinical course of gastrointestinal stromal tumours. *Histopathology* 1999; **34**: 416-424
31 **Lopes JM**, Silva P, Seixas M, Cirnes L, Seruca R. Microsatellite instability is not associated with degree of malignancy and p53 expression of gastrointestinal stromal tumours. *Histopathology* 1998; **33**: 579-581

S- Editor Liu Y **L- Editor** Ma JY **E- Editor** Lu W

PO Box 2345, Beijing 100023, China
www.wjgnet.com
wjg@wjgnet.com

World J Gastroenterol 2007 January 21; 13(3): 432-437
World Journal of Gastroenterology ISSN 1007-9327

RAPID COMMUNICATION

Acute mechanical bowel obstruction: Clinical presentation, etiology, management and outcome

Haridimos Markogiannakis, Evangelos Messaris, Dimitrios Dardamanis, Nikolaos Pararas, Dimitrios Tzertzemelis, Panagiotis Giannopoulos, Andreas Larentzakis, Emmanuel Lagoudianakis, Andreas Manouras, Ioannis Bramis

Haridimos Markogiannakis, Evangelos Messaris, Dimitrios Dardamanis, Nikolaos Pararas, Dimitrios Tzertzemelis, Panagiotis Giannopoulos, Andreas Larentzakis, Emmanuel Lagoudianakis, Andreas Manouras, Ioannis Bramis, 1st Department of Propaedeutic Surgery, Hippokration Hospital, Athens Medical School, University of Athens, Vasilissis Sofias 114 Avenue, Athens 11527, Greece
Correspondence to: Dr. Haridimos Markogiannakis, MD, Kerasoudos 54 street, 15771 Zografou, Athens, Greece. hmarkogiannakis@mycosmos.gr
Telephone: +30-697-6788806 Fax: +30-210-7707574
Received: 2006-11-12 Accepted: 2006-12-12

Abstract

AIM: To identify and analyze the clinical presentation, management and outcome of patients with acute mechanical bowel obstruction along with the etiology of obstruction and the incidence and causes of bowel ischemia, necrosis, and perforation.

METHODS: This is a prospective observational study of all adult patients admitted with acute mechanical bowel obstruction between 2001 and 2002.

RESULTS: Of the 150 consecutive patients included in the study, 114 (76%) presented with small bowel and 36 (24%) with large bowel obstruction. Absence of passage of flatus (90%) and/or feces (80.6%) and abdominal distension (65.3%) were the most common symptoms and physical finding, respectively. Adhesions (64.8%), incarcerated hernias (14.8%), and large bowel cancer (13.4%) were the most frequent causes of obstruction. Eighty-eight patients (58.7%) were treated conservatively and 62 (41.3%) were operated (29 on the first day). Bowel ischemia was found in 21 cases (14%), necrosis in 14 (9.3%), and perforation in 8 (5.3%). Hernias, large bowel cancer, and adhesions were the most frequent causes of bowel ischemia (57.2%, 19.1%, 14.3%), necrosis (42.8%, 21.4%, 21.4%), and perforation (50%, 25%, 25%). A significantly higher risk of strangulation was noticed in incarcerated hernias than all the other obstruction causes.

CONCLUSION: Absence of passage of flatus and/or feces and abdominal distension are the most common symptoms and physical finding of patients with acute mechanical bowel obstruction, respectively. Adhesions, hernias, and large bowel cancer are the most common causes of obstruction, as well as of bowel ischemia, necrosis, and perforation. Although an important proportion of these patients can be nonoperatively treated, a substantial portion requires immediate operation. Great caution should be taken for the treatment of these patients since the incidence of bowel ischemia, necrosis, and perforation is significantly high.

Key words: Acute mechanical bowel obstruction; Clinical presentation; Etiology; Management; Outcome

Markogiannakis H, Messaris E, Dardamanis D, Pararas N, Tzertzemelis D, Giannopoulos P, Larentzakis A, Lagoudianakis E, Manouras A, Bramis I. Acute mechanical bowel obstruction: Clinical presentation, etiology, management and outcome. *World J Gastroenterol* 2007; 13(3): 432-437

http://www.wjgnet.com/1007-9327/13/432.asp

INTRODUCTION

Acute mechanical bowel obstruction is a common surgical emergency and a frequently encountered problem in abdominal surgery[1,2]. It constitutes a major cause of morbidity and financial expenditure in hospitals around the world[3] and a significant cause of admissions to emergency surgical departments[2,4]. Intestinal obstruction belongs to highly severe conditions, requiring a quick and correct diagnosis as well as immediate, rational and effective therapy[5,6].

Surgeons are concerned about bowel obstruction cases because strangulation, causing bowel ischemia, necrosis and perforation might be involved, and it is often difficult to distinguish simple obstruction from strangulation. Accurate early recognition of intestinal strangulation in patients with mechanical bowel obstruction is important to decide on emergency surgery or to allow safe nonoperative management of carefully selected patients[1,2,7,8]. Although close and careful clinical evaluation, in conjunction with laboratory and radiologic studies, is essential for the decision of proper management of patients with acute mechanical bowel obstruction[1], a preoperative diagnosis of bowel strangulation cannot be made or excluded reliably by any known parameter, combinations of parameters, or

by experienced clinical judgement[7-9].

Mechanical bowel obstruction is an old and common surgical emergency[1,2]. Immediate and correct diagnosis of this condition and its etiology is essential[5,6,9-11], and appropriate treatment is of utmost importance[5,6,9-11]. The clinical picture, however, of these patients[6,12,13] along with the etiology of obstruction[1,3,11,14-16] and strangulation prevalence are variable[8,17,18], while appropriate management remains controversial[1-3,10,17,19]. We, therefore, conducted this prospective study to identify and analyze the clinical presentation of patients with acute mechanical bowel obstruction in our department, the etiology of obstruction as well as management and outcome of these patients. Moreover, we evaluated the incidence and causes of bowel ischemia, necrosis, and perforation.

MATERIALS AND METHODS

This is a prospective observational study of all adult (over 14 years old) patients admitted to the 1st Department of Propaedeutic Surgery, Hippokration Hospital, Athens Medical School, University of Athens with a diagnosis of acute mechanical bowel obstruction between January 2001 and December 2002. The enrollment of the patients in the study was approved by the ethics committee of the University of Athens and written informed consent was obtained from all patients. Patients with paralytic ileus were excluded from our study while, since our hospital does not have a Pediatric Surgery Department, patients under 14 years of age are not referred to our hospital. Consequently, all adult patients with clinical and radiological evidence of acute mechanical bowel obstruction were included in the study.

Data collection (including pre-hospital, emergency department and in-hospital information) was started immediately after patients' arrival at the Surgical Emergency Department and continued on a daily basis. Recorded variables were: age, gender, time between the onset of symptoms and arrival at the emergency department, vital signs (systolic and diastolic arterial blood pressures, heart rate, breathing rate, and body temperature), symptoms and physical examination findings, white blood cell (WBC) counts, imaging features, types of management, time between arrival and operation, operative findings, etiology of obstruction, incidence and causes of bowel ischemia, necrosis, and perforation, complications, admission in the Intensive Care Unit (ICU), length of ICU and hospital stay, and the final outcome of the patients.

Vital signs were non-invasively measured every 3 h apart from the patients who were admitted to the ICU and had continuous invasive monitoring. Serial clinical examinations every 6 h by the same attending surgical team were performed in all patients to evaluate the patients' symptoms and signs. All patients underwent WBC count testing as well as plain abdominal X-ray every 24 h. Abdominal ultrasound (US) was performed in all patients on arrival at the Surgical Emergency Department while an abdominal computed tomography (CT) scan and colonoscopy were performed in a portion of the patients based on the clinical judgement of the attending surgical team.

Table 1 Demographic, clinical, and laboratory data of the total study group on arrival at the Emergency Department (n = 150)

Value	Variable
Age (yr)[1]	63.8 ± 1.3 (65.0) (range: 16-98)
Sex (Male/Female)[2]	M: 60 (40%)/F: 90 (60%)
Time between onset of symptoms and arrival (h)[1]	33.5 ± 2.3 (24.0) (range: 2-120)
Systolic arterial blood pressure (mmHg)[1]	121.2 ± 1.7 (120.0) (range: 80-170)
Diastolic arterial blood pressure (mmHg)[1]	62.1 ± 0.9 (65.0) (range: 40-90)
Heart rate (/min)[1]	80.4 ± 0.8 (79.5) (range: 60-130)
Breathing rate (/min)[1]	15.4 ± 0.1 (15.0) (range:11-22)
Body temperature (℃)[1]	36.4 ± 0.03 (36.4) (range: 35.5-37.4)
Fever (temperature > 38.0℃)[2]	0 (0%)
Absence of passage of flatus[2]	135 (90%)
Absence of passage of feces[2]	121 (80.6%)
Vomiting[2]	118 (78.6%)
Nausea[2]	89 (59.3%)
Abdominal discomfort[2]	99 (66%)
Abdominal distension[2]	98 (65.3%)
Colicky abdominal pain[2]	111 (74%)
Continuous abdominal pain[2]	22 (14.6%)
Abdominal muscle guarding[2]	56 (37.3%)
Rebound tenderness[2]	7 (4.6%)
Small bowel obstruction[2]	114 (76%)
Large bowel obstruction[2]	36 (24%)
White blood cell (WBC) count (10^9/L)[1]	9.93 ± 0.29 (8.90) [range: 3.58-24.4]
Leukocytosis[2] (WBC count > 10.8 × 10^9/L)[2]	55 (36.6%)

[1]Values are expressed as mean ± SE and median (parenthesis); [2]Values are expressed as number of patients and percentage (parenthesis).

Criteria for operative management of the patients were hemodynamic instability despite fluid resuscitation with crystalloid solution or recurrence of instability after initial stabilization, peritoneal signs on physical examination, identification by imaging studies (X-ray, US, or CT scan) of bowel ischemia, necrosis, and/or perforation, and failure of nonoperative management on the 4th post-admission day.

Intraoperative findings were also recorded with great emphasis on the etiology of obstruction as well as the incidence and causes of bowel ischemia, necrosis, and perforation.

RESULTS

During the two years study period, 150 consecutive adult patients with acute mechanical bowel obstruction were admitted and composed our study group. Mean age of the patients was 63.8 ± 1.3 years while women comprised 60% of the group. The majority of the patients (76%) presented with small bowel obstruction. Demographic, clinical, and laboratory data of the study group on arrival at the Emergency Department are presented in Table 1. Regarding clinical presentation of the patients, absence of passage of flatus (90%) and/or feces (80.6%) were the most common presenting symptoms and abdominal distension (65.3%) was the most frequent physical finding on clinical examination.

Table 2 Etiology of acute mechanical bowel obstruction *n* (%)

Cause	Small bowel obstruction group (*n* = 114)	Large bowel obstruction group (*n* = 36)	Total study group (*n* = 150)
Adhesions	84 (73.8%)	13 (36.3%)	97 (64.8%)
Hernia	21 (18.5%)	1 (2.7%)	22 (14.8%)
Large bowel cancer	3 (2.6%)	17 (47.4%)	20 (13.4%)
Small bowel tumor	3 (2.6%)	0 (0%)	3 (2.0%)
Retroperitoneal tumor	0 (0%)	2 (5.5%)	2 (1.3%)
Crohn's disease	2 (1.7%)	0 (0%)	2 (1.3%)
Small bowel volvulus	1 (0.8%)	0 (0%)	1 (0.6%)
Ovarian cystadenocarcinoma	0 (0%)	1 (2.7%)	1 (0.6%)
Acute diverticulitis	0 (0%)	1 (2.7%)	1 (0.6%)
Sigmoid volvulus	0 (0%)	1 (2.7%)	1 (0.6%)

Table 4 Incidence of bowel ischemia, necrosis, and perforation *n* (%)

Value	Small bowel obstruction group (*n* = 114)	Large bowel obstruction group (*n* = 36)	Total study group (*n* = 150)
Ischemia	15 (13.2%)	6 (16.6%)	21 (14%)
Necrosis	8 (7%)	6 (16.6%)	14 (9.3%)
Perforation	4 (3.5%)	4 (11.1%)	8 (5.3%)

Table 3 Management and outcome of the patients

Value	Small bowel obstruction group (*n* = 114)	Large bowel obstruction group (*n* = 36)	Total study group (*n* = 150)
Operative treatment[1]	35 (30.7%)	27 (75%)	62 (41.3%)
Nonoperative treatment[1]	79 (69.3%)	9 (25%)	88 (58.7%)
Time between arrival and operation (h)[2]	30.2 ± 4.1 (10.0) [range: 2-96]	71.2 ± 3.2 (78.0) [range: 4-164]	48.1 ± 4.2 (26.0) [range: 2-164]
Operation on the 1st day[1]	22 (19.3%)	7 (19.4%)	29 (19.3%)
Operation on the 2nd day[1]	4 (3.5%)	2 (5.5%)	6 (4%)
Operation on the 3rd day[1]	5 (4.3%)	3 (8.3%)	8 (5.3%)
Complication[1]	4 (3.5%)	2 (5.5%)	6 (4%)
Intensive Care Unit (ICU) admission[1]	6 (5.2%)	3 (8.3%)	9 (6%)
ICU length of stay (d)[2]	6.3 ± 0.5 (2.0) [range: 1-25]	4.0 ± 0.7 (5.0) [range: 2-5]	5.5 ± 2.4 (3.0) [range: 1-25]
Hospital length of stay (d)[2]	6.0 ± 0.6 (5.0) [range: 2-32]	9.8 ± 1.1 (11.0) [range: 3-20]	6.9 ± 0.3 (6.0) [range: 2-32]
Mortality[1]	1 (0.8%)	1 (2.7%)	2 (1.3%)

[1]Values are expressed as number of patients and percentage (parenthesis); [2]Values are expressed as mean ± SE and median (parenthesis).

The etiology of obstruction is shown in Table 2. Regarding patients with small bowel obstruction, adhesions, incarcerated hernias, large bowel cancer, and small bowel tumors were the most frequent causes of obstruction (73.8%, 18.5%, 2.6%, and 2.6%, respectively). Large bowel cancer, adhesions, retroperitoneal tumors, and hernias were the most common causes in large intestinal obstruction group (47.4%, 36.3%, 5.5%, and 2.7%, respectively). Finally, in the total study group of patients with small or large bowel obstruction, adhesions, incarcerated hernias, and large bowel cancer constituted the most frequent causes (64.8%, 14.8%, and 13.4%, respectively). Moreover, all patients with adhesive obstruction had previously undergone abdominal operations; the vast majority of these cases had undergone one operation (*n* = 70, 72.1%), 18 (18.6%) had two, and 9 (9.3%) had three operations. In terms of the types of previous operations, 34 patients (25.6%) had undergone an appendectomy, 31 (23.3%) gynecological procedures, 21 (15.8%) had a cholecystectomy, 15 (11.2%) had large bowel cancer resection, 13 (9.8%) had adhesiolysis in previous mechanical bowel obstruction episodes, 8 (6.0%) had abdominal wall hernia repair surgical procedures, and 11 (8.3%) had other surgical procedures. It is of note that, except for 3 patients with a laparoscopic cholecystectomy in the group of two previous abdominal operations, all patients had undergone open surgical procedures. Furthermore, regarding the types of incarcerated hernias, 9 patients (40.9%) presented with an inguinal hernia, 4 (18.2%) with an umbilical hernia, 3 (13.6%) with an incisional hernia, and 2 (9.1%) with a femoral hernia, while in 4 patients (18.2%) an internal hernia was intraoperatively identified. Sigmoid cancer was overrepresented accounting for 15 (75%) of the 20 patients with obstruction due to a large bowel cancer, whereas two (10%) patients had an ascending colon cancer, one (5%) had a transverse colon cancer, one (5%) had a descending colon cancer, and one (5%) had a rectum cancer.

Data regarding management and outcome of the patients are described in Table 3. Eighty-eight patients (58.7%) of the total study group were safely and effectively treated conservatively. Nonoperatively treated patients composed the highest proportion (69.3%) of the patients with acute mechanical small bowel obstruction, while they only accounted for the minority (25%) in the large intestinal obstruction group. Of the 62 patients (41.3% of the total study group) who were operatively treated, a substantial portion (19.3%) required surgical intervention on the first day. Six cases (4%) sustained complications; two suffered from septic shock along with acute respiratory and renal failure, one suffered from pneumonia, one suffered from myocardial infarction, one had urinary tract infection, and one was reoperated because of an anastomotic leakage. Two patients died, resulting in a mortality rate of 1.3%; one died due to multiple organ failure attributable to sepsis and one died owing to myocardial infarction.

As it is shown in Table 4, the rate of bowel ischemia, necrosis, and perforation in the total study group were significantly high (14%, 9.3%, and 5.3%, respectively). In the small bowel obstruction group, ischemia was intraoperatively reversible in 7 out of 15 patients, whereas the remaining 8 patients had bowel necrosis. In contrast, no reversible ischemia was observed in the large bowel obstruction group. Therefore, although patients with small bowel obstruction and those with large bowel obstruction presented similar ischemia rate, the incidence of necrosis

Table 5 Etiology of small bowel ischemia, necrosis, and perforation (small bowel obstruction group, *n* = 114) *n* (%)

Cause	Ischemia (*n* = 15)	Necrosis (*n* = 8)	Perforation (*n* = 4)
Hernia	11 (73.3%)	5 (62.5%)	3 (75%)
Adhesions	2 (13.3%)	2 (25%)	1 (25%)
Small bowel volvulus	1 (6.7%)	1 (12.5%)	0 (0%)
Large bowel cancer	1 (6.7%)	0 (0%)	0 (0%)
Small bowel tumor	0 (0%)	0 (0%)	0 (0%)

Table 6 Etiology of large bowel ischemia, necrosis, and perforation (large bowel obstruction group, *n* = 36) *n* (%)

Cause	Ischemia (*n* = 6)	Necrosis (*n* = 6)	Perforation (*n* = 4)
Large bowel cancer	3 (50%)	3 (50%)	2 (50%)
Adhesions	1 (16.6%)	1 (16.6%)	1 (25%)
Hernia	1 (16.6%)	1 (16.6%)	1 (25%)
Sigmoid volvulus	1 (16.6%)	1 (16.6%)	0 (0%)
Retroperitoneal tumor	0 (0%)	0 (0%)	0 (0%)
Ovarian cystadenocarcinoma	0 (0%)	0 (0%)	0 (0%)

and perforation was much higher in the large intestine group.

Etiology of bowel ischemia, necrosis, and perforation in the small bowel obstruction group, the large bowel obstruction group, and the total study group is presented in Table 5, Table 6 and Table 7, respectively. Incarcerated hernias were the cause in the vast majority of the small bowel obstruction group, that presented ischemia, necrosis, and perforation, while adhesions were the second most frequent cause. Regarding the large bowel obstruction group, large bowel cancer, adhesions, and hernias constituted the most common causes. Finally, in the total group, hernias, large bowel cancer, and adhesions were the most frequent causes of bowel ischemia, necrosis, and perforation. It was notable that bowel ischemia was reversible in half of the cases with obstruction due to incarcerated hernias justifying, thus, immediate operative intervention in these patients.

With regard to the risk of strangulation, a significantly much higher risk was noticed in incarcerated hernias than all the other obstruction causes. Of the 22 patients with acute mechanical bowel obstruction caused by incarcerated hernias, 12 (54.6%) had bowel ischemia, 6 (27.3%) had necrosis, and 4 (18.2%) had sustained perforation. On the contrary, only 3 (3.1%) of the 97 cases with adhesive obstruction presented ischemia and necrosis, and 2 (2.1%) had perforation. Additionally, out of 20 patients with obstruction due to large bowel cancer, 4 (20%) had ischemia, 3 (15%) had necrosis, and 2 (10%) had perforation.

Table 7 Etiology of bowel ischemia, necrosis, and perforation (total study group, *n* = 150) *n* (%)

Cause	Ischemia (*n* = 21)	Necrosis (*n* = 14)	Perforation (*n* = 8)
Hernia	12 (57.2%)	6 (42.8%)	4 (50%)
Large bowel cancer	4 (19.1%)	3 (21.4%)	2 (25%)
Adhesions	3 (14.3%)	3 (21.4%)	2 (25%)
Small bowel volvulus	1 (4.7%)	1 (7.2%)	0 (0%)
Sigmoid volvulus	1 (4.7%)	1 (7.2%)	0 (0%)
Small bowel tumor	0 (0%)	0 (0%)	0 (0%)
Retroperitoneal tumor	0 (0%)	0 (0%)	0 (0%)
Ovarian cystadenocarcinoma	0 (0%)	0 (0%)	0 (0%)

DISCUSSION

Acute mechanical bowel obstruction remains a frequently encountered problem in abdominal surgery and a common surgical emergency[1,2], which is a frequent cause of admissions to hospital emergency surgical departments[2,4].

The majority of our study group presented with acute mechanical small bowel obstruction. This has also been found in other studies with small bowel obstruction accounting for about 80% of total obstruction cases[9,20,21]. Regarding clinical presentation of our patients, absence of passage of flatus and/or feces were the most frequent presenting symptoms and abdominal distension was the most common physical finding on clinical examination. Additionally, vomiting, nausea, colicky abdominal pain, and abdominal discomfort were frequent symptoms on arrival. Our results, even though some differences are noticed, are in accordance with the literature[6,12,13,22,23]. Particularly, Cheadle *et al*[6] reported abdominal pain (92%), vomiting (82%), abdominal tenderness (64%), and distention (59%) as the most frequent symptoms and signs, whereas abdominal distension, bilious vomiting, absolute constipation and abdominal pain were the main signs and symptoms in another series[12]. Perea *et al*[13] prospectively studied 100 patients with adhesive small bowel obstruction and found that the presenting symptoms were vomiting (77%), colicky abdominal pain (68%), absence of passage of flatus and/or feces (52%), and constant pain (12%), whereas abdominal distension constituted the most frequent clinical sign with a prevalence of 56%. In a study of patients with bowel obstruction due to large bowel volvulus, the most common sign of sigmoid volvulus was distension (79%) and the most frequent symptoms were pain (58%) and obstipation (55%), whereas most patients with cecal volvulus presented with pain (89%)[22]. Furthermore, in a review of cases with obstruction because of small and large bowel intussusception, abdominal pain, nausea, vomiting, and abdominal distension were the commonest symptoms and signs, respectively[23].

Adhesions, incarcerated hernias, and large bowel cancer constitute the most frequent causes of obstruction[3,4,9,11,14,16,17,20,21,24-30]. This finding was also noticed in our study. Moreover, adhesions were the most prevalent etiology of obstruction in the small bowel obstruction group and the total study group and the second most common etiology in the large bowel group. Several studies postulate that adhesions are responsible for 32%-74% of bowel obstruction and are the leading cause of small intestinal obstruction representing 45%-80% of it[1-4,7,9,14,17,20,24-26,28-30]. The vast majority (65%-90%) of the patients with adhesive obstruction have undergone previous abdominal operations[6,13,14,18,19,26,28,29]. In the present study,

this was observed in all such patients. As for the types of previous operations in our study patients, appendectomies, gynecological operations, cholecystectomies, and large bowel cancer resections were more prevalent. This is also in accordance with the literature[2,18,19,28,29]. Even though the appropriate management of adhesive obstruction is still controversial, a substantial share of these patients, ranging from 35% to 75% in several studies, can safely and effectively be treated with nonoperative management as it was also shown in our patients[2,3,9,12,16-19,24,28-30]. The increasing role of adhesions as a cause of acute intestinal obstruction demands greater need for routine preventive measures against adhesion formation[14]. A number of intraoperative measures are now encouraged during elective abdominal surgery to reduce the incidence of adhesions that might subsequently produce intestinal obstruction[1].

As it was also observed in our study, large bowel cancer, particularly sigmoid cancer, is the most common etiology of obstruction in patients with large intestinal obstruction with a prevalence of 40%-90%[9,10,14,21]. The majority of such patients in our study were operatively treated. Moreover, incarcerated hernias were the second most common etiology of obstruction as well as the predominant cause of bowel ischemia, necrosis, and perforation. It should also be emphasized that bowel ischemia was reversible in half of our cases with obstruction due to incarcerated hernias justifying, thus, immediate surgery in these patients. Since abdominal hernias continue to account for 8%-25% of all cases of intestinal obstruction[1,4,14,17,20,24,26,30], while in a few series represent the most common cause of intestinal obstruction accounting for 30%-55%[11,16,21,27], and, moreover, they still remain the most common cause of strangulation[1,4,11,17,21,24,27], surgeons should continue their aggressive attitude towards elective repair of all abdominal hernias as well as towards immediate operative intervention in patients with acute mechanical bowel obstruction secondary to incarcerated hernias.

Other less common causes of obstruction reported in the literature are Crohn's disease[3,17,20] and gallstones[21], accounting for 3%-7% and 2% of small bowel obstruction cases, respectively, and bowel volvulus[14,15,20,24] and intussus ception[14,20,25], accounting for 4%-15% and 4%-8% of total obstruction cases, respectively. In our series, the prevalence of Crohn's disease and bowel volvulus was much lower, whereas no case of obstruction due to gallstone or intussusception was observed.

An important share of our patients was successfully nonoperatively treated. This was more prevalent regarding adhesive small bowel obstruction. This has also been noticed in other studies[2,3,9,12,16-19,24,28-30]. Similar to other studies[12,24], of those patients that were operated, a substantial proportion required immediate operation.

Much attention should be paid to the treatment of these patients since the incidence of bowel ischemia, necrosis, and perforation is significantly high. Strangulation rate in the literature ranges from 7% to 42%[4,8,12,17,24,26,28]. In addition, Kossi *et al*[18] reported an incidence of ischemia of 20%, of necrosis of 8%, and of perforation of 2%. In regard to the risk of strangulation in the present study, a significantly much higher risk was noticed in incarcerated hernias in comparison to all the other obstruction causes. Moreover, the incidence of bowel ischemia, necrosis, and perforation in adhesive obstruction was very low. These results have been also described in other studies[1,4,11,17,21,24,27].

In our study, complication and mortality rate were relatively low. In the literature, complication rate ranges from 6% to 47%[6,20,25,27,31,32] whereas mortality ranges from 2% to 19%[4,6,11,14,17-20,24-27,31,32].

In general, appropriate treatment of acute mechanical bowel obstruction as well as timing of surgery for patients selected to undergo operative intervention still remain controversial[1-3,10,17,19]. Management of this condition requires careful assessment and awareness while the appropriate treatment needs to be tailored to the individual situation[10,19]. Furthermore, no specific factors that may predict success of conservative or surgical management have been identified[19]. Although modern surgical management continues to focus appropriately on avoiding operative delay whenever surgery is indicated, not every patient is always best served by immediate operation. As it was also proved in the present study, certain entities, such as bowel obstruction secondary to incarcerated abdominal wall hernia, and patients with clinical signs and symptoms suggestive of strangulation do require prompt operative intervention[1,3,16,17]. Other conditions, however, such as postoperative adhesions, particularly in patients with numerous previous abdominal procedures or concomitant medical problems, often justifiably benefit from a trial of nonoperative management[1-3,9,16-18,28-30]. A substantial portion of these patients was successfully conservatively treated in our study. As it was also shown in this study, the risk of strangulation with adhesive bowel obstruction is significantly lower as compared to incarcerated hernia[1,4,17,24].

Strangulated obstruction requires emergency surgery, and early recognition is often life-saving since delay in treatment is an independent predictive factor of mortality and, in addition, bowel strangulation is an independent predictor of complication and, even more, of mortality while the mortality rates of patients with strangulated obstruction are two to 10 times higher than those of patients with non-strangulated obstructi on[4,6,10,11,12,14,16,17,31]. Moreover, accurate early recognition of intestinal strangulation in patients with mechanical bowel obstruction is important to allow safe nonoperative management of carefully selected patients[1,2,7,8]. Traditionally, such recognition is based on the presence of one or more of the classical signs: vascular compromise, continuous abdominal pain, fever, tachycardia, peritoneal signs on physical examination, leukocytosis, and metabolic acidosis[7,8]. Close and careful clinical evaluation, in conjunction with laboratory and radiologic studies, is essential for the decision of proper management of patients with acute mechanical bowel obstruction; if any uncertainty exists, prompt operative intervention is indicated[1]. It should be emphasized, though, that great caution should be taken for the management of these patients since studies have shown that preoperative diagnosis of bowel strangulation cannot be made or excluded reliably by any known clinical, laboratory, or

radiologic parameter, combinations of parameters, or by experienced clinical judgement[7-9].

In conclusion, absence of passage of flatus and/or feces and abdominal distension are the most common symptoms and physical finding of patients with acute mechanical bowel obstruction, respectively. Adhesions, hernias, and large bowel cancer are the most common causes of obstruction as well as of bowel ischemia, necrosis, and perforation. Although an important share of these patients can be safely and effectively nonoperatively treated, particularly those with adhesive obstruction, a substantial portion requires immediate operation. Moreover, the risk of strangulation is significantly higher in incarcerated hernias than other obstruction causes. Great caution should be taken for the treatment of patients with acute mechanical bowel obstruction since the incidence of bowel ischemia, necrosis, and perforation is significantly high. Further studies are necessary in order to determine appropriate management for treatment of these patients as well as to identify accurate early predictors of success of conservative or operative treatment and, particularly, of intestinal strangulation giving the greatest attention to reversible ischemia.

REFERENCES

1 **Mucha P**. Small intestinal obstruction. *Surg Clin North Am* 1987; **67**: 597-620
2 **Miller G**, Boman J, Shrier I, Gordon PH. Natural history of patients with adhesive small bowel obstruction. *Br J Surg* 2000; **87**: 1240-1247
3 **Miller G**, Boman J, Shrier I, Gordon PH. Etiology of small bowel obstruction. *Am J Surg* 2000; **180**: 33-36
4 **Ihedioha U**, Alani A, Modak P, Chong P, O'Dwyer PJ. Hernias are the most common cause of strangulation in patients presenting with small bowel obstruction. *Hernia* 2006; **10**: 338-340
5 **Díte P**, Lata J, Novotný I. Intestinal obstruction and perforation--the role of the gastroenterologist. *Dig Dis* 2003; **21**: 63-67
6 **Cheadle WG**, Garr EE, Richardson JD. The importance of early diagnosis of small bowel obstruction. *Am Surg* 1988; **54**: 565-569
7 **Richards WO**, Williams LF. Obstruction of the large and small intestine. *Surg Clin North Am* 1988; **68**: 355-376
8 **Sarr MG**, Bulkley GB, Zuidema GD. Preoperative recognition of intestinal strangulation obstruction. Prospective evaluation of diagnostic capability. *Am J Surg* 1983; **145**: 176-182
9 **Renzulli P**, Krähenbühl L, Sadowski C, al-Adili F, Maurer CA, Büchler MW. Modern diagnostic strategy in ileus. *Zentralbl Chir* 1998; **123**: 1334-1339
10 **Lopez-Kostner F**, Hool GR, Lavery IC. Management and causes of acute large-bowel obstruction. *Surg Clin North Am* 1997; **77**: 1265-1290
11 **Chiedozi LC**, Aboh IO, Piserchia NE. Mechanical bowel obstruction. Review of 316 cases in Benin City. *Am J Surg* 1980; **139**: 389-393
12 **Kuremu RT**, Jumbi G. Adhesive intestinal obstruction. *East Afr Med J* 2006; **83**: 333-336
13 **Perea García J**, Turégano Fuentes T, Quijada García B, Trujillo A, Cereceda P, Díaz Zorita B, Pérez Díaz D, Sanz Sánchez M. Adhesive small bowel obstruction: predictive value of oral contrast administration on the need for surgery. *Rev Esp Enferm Dig* 2004; **96**: 191-200
14 **Lawal OO**, Olayinka OS, Bankole JO. Spectrum of causes of intestinal obstruction in adult Nigerian patients. *S Afr J Surg* 2005; **43**: 34-36
15 **Gürleyik E**, Gürleyik G. Small bowel volvulus: a common cause of mechanical intestinal obstruction in our region. *Eur J Surg* 1998; **164**: 51-55
16 **Tamijmarane A**, Chandra S, Smile SR. Clinical aspects of adhesive intestinal obstruction. *Trop Gastroenterol* 2000; **21**: 141-143
17 **Bizer LS**, Liebling RW, Delany HM, Gliedman ML. Small bowel obstruction: the role of nonoperative treatment in simple intestinal obstruction and predictive criteria for strangulation obstruction. *Surgery* 1981; **89**: 407-413
18 **Kössi J**, Salminen P, Laato M. The epidemiology and treatment patterns of postoperative adhesion induced intestinal obstruction in Varsinais-Suomi Hospital District. *Scand J Surg* 2004; **93**: 68-72
19 **Williams SB**, Greenspon J, Young HA, Orkin BA. Small bowel obstruction: conservative vs. surgical management. *Dis Colon Rectum* 2005; **48**: 1140-1146
20 **Mohamed AY**, al-Ghaithi A, Langevin JM, Nassar AH. Causes and management of intestinal obstruction in a Saudi Arabian hospital. *J R Coll Surg Edinb* 1997; **42**: 21-23
21 **Wysocki A**, Krzywoń J. Causes of intestinal obstruction. *Przegl Lek* 2001; **58**: 507-508
22 **Lau KC**, Miller BJ, Schache DJ, Cohen JR. A study of large-bowel volvulus in urban Australia. *Can J Surg* 2006; **49**: 203-207
23 **Zubaidi A**, Al-Saif F, Silverman R. Adult intussusception: a retrospective review. *Dis Colon Rectum* 2006; **49**: 1546-1551
24 **McEntee G**, Pender D, Mulvin D, McCullough M, Naeeder S, Farah S, Badurdeen MS, Ferraro V, Cham C, Gillham N. Current spectrum of intestinal obstruction. *Br J Surg* 1987; **74**: 976-980
25 **Kirshtein B**, Roy-Shapira A, Lantsberg L, Avinoach E, Mizrahi S. Laparoscopic management of acute small bowel obstruction. *Surg Endosc* 2005; **19**: 464-467
26 **Roscher R**, Frank R, Baumann A, Beger HG. Results of surgical treatment of mechanical ileus of the small intestine. *Chirurg* 1991; **62**: 614-619
27 **Akçakaya A**, Alimoğlu O, Hevenk T, Baş G, Sahin M. Mechanical intestinal obstruction caused by abdominal wall hernias. *Ulus Travma Derg* 2000; **6**: 260-265
28 **Cox MR**, Gunn IF, Eastman MC, Hunt RF, Heinz AW. The operative aetiology and types of adhesions causing small bowel obstruction. *Aust N Z J Surg* 1993; **63**: 848-852
29 **Stricker B**, Blanco J, Fox HE. The gynecologic contribution to intestinal obstruction in females. *J Am Coll Surg* 1994; **178**: 617-620
30 **Foster NM**, McGory ML, Zingmond DS, Ko CY. Small bowel obstruction: a population-based appraisal. *J Am Coll Surg* 2006; **203**: 170-176
31 **Uludağ M**, Akgün I, Yetkin G, Kebudi A, Işgör A, Sener A. Factors affecting morbidity and mortality in mechanical intestinal obstruction. *Ulus Travma Derg* 2004; **10**: 177-184
32 **Biondo S**, Parés D, Frago R, Martí-Ragué J, Kreisler E, De Oca J, Jaurrieta E. Large bowel obstruction: predictive factors for postoperative mortality. *Dis Colon Rectum* 2004; **47**: 1889-1897

S- Editor Liu Y **L- Editor** Zhu LH **E- Editor** Lu W

PO Box 2345, Beijing 100023, China
www.wjgnet.com
wjg@wjgnet.com

World J Gastroenterol 2007 January 21; 13(3): 438-443
World Journal of Gastroenterology ISSN 1007-9327

RAPID COMMUNICATION

Depression and anxiety levels in therapy-naïve patients with inflammatory bowel disease and cancer of the colon

Branislav R Filipović, Branka F Filipović, Mirko Kerkez, Nikola Milinić, Tomislav Ranđelović

Branislav R Filipović, Institute of Anatomy, School of Medicine, Belgrade, Serbia
Branka F Filipović, Nikola Milinić, Clinical and Hospital Center "Bežanijska Kosa", Department of Gastroenterology, Belgrade, Serbia
Mirko Kerkez, Department of Gastrointestinal Surgery, Clinical Center of Serbia, Serbia
Tomislav Ranđelović, Department of Gastrointestinal Surgery, Clinical and Hospital Center "Bežanijska Kosa", Belgrade, Serbia
Correspondence to: Professor Branislav Filipović, MD, DSc, Institute of Anatomy, School of Medicine, 4/2 Dr Subotića, Belgrade 11000, Serbia. filipbr@bitsyu.net
Telephone: +38-11-2685846 Fax: +38-11-2686172
Received: 2006-10-15 Accepted: 2006-12-07

Abstract

AIM: To assess whether depression and anxiety are more expressed in patients with the first episode of inflammatory bowel disease (IBD) than in individuals with newly discovered cancer of the colon (CCa).

METHODS: A total of 32 patients with IBD including 13 males and 19 females, aged 27 to 74, and 30 patients with CCa including 20 males and 10 females, aged 39-78, underwent a structured interview, which comprised Hamilton's Depression Rating Inventory, Hamilton's Anxiety Rating Inventory and Paykel's Stressful Events Rating Scale.

RESULTS: Patients of the IBD group expressed both depression and anxiety. Depressive mood, sense of guilt, psychomotor retardation and somatic anxiety were also more pronounced in IBD patients. The discriminant function analysis revealed the total depressive score was of high importance for the classification of a newly diagnosed patient into one of the groups.

CONCLUSION: Newly diagnosed patients with IBD have higher levels of depression and anxiety. Moreover, a psychiatrist in the treatment team is advisable from the beginning.

Key words: Crohn's disease; Ulcerative colitis; Colon cancer; Mood disorder

Filipović BR, Filipović BF, Kerkez M, Milinić N, Randelović T. Depression and anxiety levels in therapy-naïve patients with inflammatory bowel disease and cancer of the colon. *World J Gastroenterol* 2007; 13(3): 438-443

http://www.wjgnet.com/1007-9327/13/438.asp

INTRODUCTION

Patients with inflammatory bowel disease (IBD-the common term which comprises Crohn's disease and ulcerative colitis) and cancer of the colon often report serious psychological and emotional morbidities[1,2]. Though specific pathophysiological links between psychiatric disorders such as depression or anxiety and inflammatory bowel disease have largely been discredited[3,4], little is known about the influences of depression and anxiety on the ongoing adaptation that these patients make to the aversive symptoms of their chronic disease[5]. It is almost impossible to tell whether the psychiatric discomfort influences the severity of the gastrointestinal symptoms or, conversely, could gastrointestinal symptoms aggravate the psychiatric status. Stressful life events and psychological distress have been shown in patients without IBD to be associated with common bowel symptoms such as irregularity, gas and bloating, and abdominal pain, often labeled as irritable bowel syndrome or functional bowel diseases[6,7].

This study presents pilot data in which we sought to investigate the effects of common psychiatric illnesses (i.e., anxiety and depression episodes) on the appearance and functional disability in 32 first episode, therapy-naïve patients with IBD, and 30 patients with newly diagnosed cancer of the colon. We hypothesized that the presence and intensiveness of one or both current psychiatric disorders (depression and anxiety) have a higher impact on the appearance of one of the diseases of interest. Also, we attempted to estimate the eventual difference of the initial levels of the psychological suffers, and which one, if not both, of the two groups of patients requires the routine preliminary psychiatric evaluation prior to the beginning of gastroenterological treatment.

MATERIALS AND METHODS

Setting

This study is a subset of a larger investigation of 71 patients with the first episode of IBD and 40 patients with newly diagnosed cancer of the colon (CCa), out of which

32 patients with IBD (21 with ulcerative colitis [UC] and 11 with Crohn's disease [CD]), 13 (8 with UC and 5 with CD) males and 19 females (13 with UC and 6 with CD), aged 27 to 74 years (49.16 ± 16.58) and 30 patients with CCa, 20 males and 10 females, aged 39-78 years (63.47 ± 9.14) met with the recruiting criteria and were included in the study. The study was conducted at the Department of Gastrointestinal Surgery, Clinical Center of Serbia, and Department of Gastroenterohepatology, Clinical and Hospital Center "Bezhanijska Kosa". All patients of 18 years old or over attending the Gastroenterology Clinics and Gastrointestinal Surgery Department from March to October 2003 who presented symptoms common for IBD and CCa: blunt abdominal pain, rectorrhagia and diarrhea syndrome on the first visit, were eligible for the study. The participating gastroenterologist or gastrointestinal surgeon (M.K. T.R., and B.F.F.) screened the clinic appointment schedule each morning and directly communicated with the other staff gastroenterologists or surgeons on a daily basis to recruit their patients into the study. Patients were interviewed at the end of their medical appointments or at a more convenient time, no later than 2 d from their medical visits or admission to hospitals. Only patients who satisfied all the recruiting criteria were selected for the study. The results of the interviews were matched with the final diagnosis, but no matched pair procedure between groups was used. The entire testing was designed and supervised by the psychiatrist (BRF). The study was approved by the Ethical Committee of the School of Medicine, Belgrade.

Recruiting criteria

The patients included in the study met the following criteria: No previous treatment for one of the diseases of interest; a negative family history of IBD and CCa; no previous treatment for any psychiatric illness or disorder; no self-medications for any kind of gastrointestinal or psychiatric illnesses; weight loss not surpassing 5 kg in the last month and they were not under weight loss regimes; radiographs of the lungs and ultrasonographic examination (N.M. M.K. and B.F.F.) of the abdominal and pelvic cavities free of metastasis and anatomical abnormalities; no surgical intervention in past three years; no abdominal or any kind of mutilating surgical intervention; not treated for any kind of malignancy; not suffering from an immunodeficiency disease, especially human immunodeficiency virus infection or systemic lupus; a negative history of bowel inflammation caused by infectious agents in last one year; and hepatitis B (HBs) or hepatitis C negativity. The definitive diagnosis was confirmed after immediate endoscopy-guided biopsy and subsequent histopathological examination. During the interview, 39 IBD patients were found to be unsuitable while 10 patients with colorectal cancer were omitted from further investigation. The difference was caused by more pronounced sincerity in answers during the admittance and higher motivation to be part of the study among patients with CCa.

Structured interview

All the patients, after being informed in detail about the study and signing a written consent, underwent the structured psychiatric interview, which involved Hamilton's depression inventory consisting of 21 items[8] and Hamilton's anxiety inventory consisting of 14 items[9]. Results were interpreted using Hamilton's depression and anxiety rating scales. All the items were rated in 5 grades: 0, absent; 1, mild; 2, moderate; 3, severe; 4, incapacitating (some items, like insomnia, hypochondriasis, diurnal mood variations, insight into the illness and obsessive-compulsive symptomatology are only graded in three levels: 0, absent; 1, doubtful or trivial; 2, present). Usually, Hamilton depression and anxiety inventories contain items related to gastrointestinal symptoms and weight loss. This time they were omitted because the mentioned symptomatology is part of the illness. Interpretation of the total score of Hamilton's depression rating scale is: less than 8, without depression; 9-17, mild depression; 18-24, moderate depression; higher than 24, severe depression requiring hospitalization. According to the Hamilton's anxiety rating scale, persons with generalized anxiety disorder and panic disorder tended to have a total anxiety score of above 20. The 61 item-Paykel's scale for stressful events[10] was used to evaluate the possible influence of different life events in the past one-year period on the appearance of the diseases of interest. The interview was performed by three previously trained interns in psychiatry as part of their professional educations in liaison psychiatry. All the testing was conducted in Serbian language, and priory to the final diagnosis was reported to the patient. To the moment, the definitive diagnosis was available only to the relevant intern and surgery specialists (B.F.F., M.K., N.M. T.R.).

Clinical evaluation

Index of the activity for patients of the IBD group was computed according to the standard procedures for patients with newly diagnosed CD and UC. For patients with CD, a routine Crohn's disease activity index (CDAI)[11] comprising eight items was categorized as follows: (1) Number of liquid or very soft stools in one week × 2; (2) Sum of seven daily abdominal pain ratings (0: none; 1: mild; 2: moderate; 3: severe) × 5; (3) Sum of seven daily ratings of general well-being (0: well; 1: slightly below par; 2: poor; 3: very poor; 4: terrible) × 7; (3) Symptoms or findings probably related to CA (arthritis or arthralgia, iritis or uveitis, erythema nodosum, pyoderma gangrenosum, aphthous stomatitis, anal fissure, fistula or perirectal abscess, other bowel-related fistula, febrile episodes over 37.8℃ during the past week) × 20; (4) Taking Lomotil® or opiates for diarrhea (yes or no) × 30; (5) Abnormal mass (0: none; 0.4: questionable; 1: present) × 10; (6) Hematocrit (normal average: male, 47, female, 42), obtained values should be subtracted from the average. Score is multiplied with 6; (7) Body weight: 100 × [1 - actual body weight/ standard weight], where standard weight is computed from the tables using the body height and age of the patients; (8) Active phase of CD takes values between 220 and 450. Average index in our group was 289.84 ± 45.37 (221-375). For UD activity index, a modified Ulcerative Disease Scoring System[12] was used: (1) Stool frequency (0: normal number; 1: 1-2 stools more than normal; 2: 3-4 stools

Table 1 Expression of the depression symptoms according to the results from Hamilton's Depression Inventory (IBD/CCa)

Symptom	0	1	2	3	4	Statistical analysis
Depressive mood	2/9	3/8	7/8	6/3	14/2	$\chi^2 = 16.75$, DF = 4, $P = 0.002$
Guilty feelings	15/23	0/4	5/3	6/0	6/0	$\chi^2 = 18.14$, DF = 4, $P = 0.001$
Suicide	28/29	-	2/0	-	2/1	$\chi^2 = 2.28$, DF = 2, $P > 0.05$
Early insomnia	17/10	2/10	13/10			$\chi^2 = 4.48$, DF = 2, $P = 0.024$
Transitory insomnia	15/11	3/11	14/8			$\chi^2 = 6.77$, DF = 2, $P = 0.034$
Late insomnia	18/12	3/7	11/11			$\chi^2 = 2.74$, DF = 2, $P > 0.05$
Work and life activities	13/17	5/7	5/3	7/3	2/0	$\chi^2 = 4.91$, DF = 4, $P > 0.05$
Retardation psychomotor	17/21	4/9	7/0	2/0	2/0	$\chi^2 = 13.29$, DF = 4, $P = 0.01$
Agitation	6/13	4/9	4/6	9/2	9/0	$\chi^2 = 18.31$, DF = 4, $P = 0.01$
Anxiety-psychological	5/14	5/8	1/4	12/4	9/0	$\chi^2 = 19.71$, DF = 4, $P = 0.01$
Anxiety-somatic	14/10	7/8	2/10	6/2	3/0	$\chi^2 = 11.04$, DF = 4, $P < 0.05$
Hypochondriasis	28/28	4/1	0/1			$\chi^2 = 2.738$, DF = 2, $P > 0.05$
Insight into the presence of the illness	13/8	17/6	2/16			$\chi^2 = 17.29$, DF = 4, $P < 0.001$
Diurnal variations of the mood	13/15	9/13	10/2			$\chi^2 = 2.738$, DF = 2, $P > 0.05$
Depersonalization and derealization, presence of the nihilistic ideas	24/29	5/1	1/0	2/0	-	$\chi^2 = 6.08$, DF = 3, $P > 0.05$
Paranoid ideas	30/29	0/1	2/0	-	-	$\chi^2 = 2.96$, DF = 2, $P > 0.05$
Obsessive-compulsive symptomatology	29/29	1/1	2/0			$\chi^2 = 1.94$, DF = 2, $P > 0.05$
Mean score ± SD						18.56 ± 877/10.83 ± 5.26; $t = 4.17$, DF = 60, $P < 0.001$
Centroids: IBD = 0.513, CCa = - 0.547						Equation for the selection: -2.033 + 0.137 × total depressive score
Section point (average of the centroids) = -0017						

more than normal; 3: 5 or more stools than normal). Each subject reported his/her degree of abnormality of the stool frequency. (2) Rectal bleeding (0: no blood; 1: streaks of blood with stools less than half the time; 2: obvious blood with stools most of the time; 3: blood alone passed). The daily bleeding score represents the most severe bleeding of the day. (3) Modified Baron Score for findings of endoscopy (0: normal or non-inflamed mucosa; 1: mild disease-erythema, decrease vascular pattern, mild friability; 2: moderate-marked erythema, absent vascular pattern, friability, erosions; 3: Severe-spontaneous bleeding, ulcerations). (4) Physician's global assessment: 0: normal; 1: mild disease; 2: moderate; 3: severe. The physicians' global assessment acknowledges three other criteria, the subject's daily record of abdominal discomfort and general sense of well-being, and other observations, such as physical findings and subject's performance status. Rating of the severity: 1-5, mild; 6-10, moderate; 11, severe. Average UC activity index in our study group was 8 ± 2 (range, 5-12). Clinical evaluation of cancers was performed by TNM classification as follows: Stage Ⅰ (T2 N0 M0), 18 cases; Stage Ⅱ (T3 N0 M0), 10 cases; Stage Ⅲ (T3 N1 M0), 1 case and T3 N2 M0, 1 case. Indices were compared to the total scores of depression and anxiety rating scales in order to investigate the eventual correlation between them.

Statistical analysis

After coding, all the answers were systematized in the common database, and the following statistical analyses were performed: The Kolmogorov-Smirnoff *Z* test was used to evaluate distribution of the data. The results were satisfactory: all the values belonged to normal distribution, which made them adequate for the subsequent statistical testing. Besides usual parameters of central tendency (descriptive statistics: mean, standard deviation [SD], extreme values); Pearson's Chi-square test and Fisher's exact probability test were used to reveal the differences in attributive values. Student's *t* test for independent samples was applied to evaluate possible differences in parametric data. The Pearson's bivariate correlation was used to investigate the interconnection between the depression and anxiety scores and in-group's life span. This test was enforced by the difference in average life span between groups, mostly dependent on the nature of the very illness: 49.16 ± 16.58 for persons in IBD groups and 63.47 ± 9.14 for persons with CCa (*t*-test = -5.094, degrees of freedom [DF] = 30, $P < 0.01$). No correlation was obtained whatsoever $r = -0.225$, N = 62, $P > 0.05$, for the depression score, and $r = -0.149$, N = 62, $P > 0.05$, for the anxiety score. The same test was used to correlate the IBD activity indices with total scores of depression and anxiety questionnaires. Discriminant function analysis (DFA) was used to determine which variable(s) discriminate between two groups: IBD and CCa. Centroids are mathematically derived grouping values whereas the section point between groups used the average of the centroids. The entire testing was performed at 95% level of confidence.

RESULTS

Depression levels

Differences in the levels of the depression symptoms are shown in Table 1. The main difference was found in the intense of the depressive mood and in the sense of guilt, which were significantly higher in the group with IBD. Also, IBD patients expressed problems with early and transitory insomnia and had a poorer ability to focus their attention on various activities and manual or intellectual work, which resulted in slow down in everyday activities. Agitation, anxiousness, early and transitory insomnia and somatic symptoms were more pronounced in the IBD group, likewise. On the other hand, awareness that something is going wrong with them was expressed in CCa patients. Twenty-two out of 32 patients with IBD and

Table 2 Expression of the anxiousness symptoms according to the Hamilton's Anxiety Rating Inventory (IBD/CCa)

Symptom	0	1	2	3	4	Statistical analysis
Anxious mood-greed, hopelessness	4/9	1/8	6/5	10/5	11/3	$\chi^2 = 13.55$, DF = 4, $P = 0.009$
Tension	4/7	1/8	6/5	10/9	11/1	$\chi^2 = 14.69$, DF = 4, $P = 0.005$
Fears: dark, loneliness, animals	19/26	2/1	4/2	7/0	0/1	$\chi^2 = 10.03$, DF = 4, $P = 0.04$
Intellectual impairments-memory problems, difficulties in communication	18/22	6/4	5/4	3/0	-	$\chi^2 = 3.85$, DF = 3, $P > 0.05$
Depressive aspect	5/15	3/4	4/8	6/1	2/14	$\chi^2 = 19.003$, DF = 4, $P = 0.002$
Somatic symptoms: muscular symptoms, sensory symptoms-tinnitus, blurred vision, attacks of heath, itching, etc., cardiovascular symptoms-tachycardia, palpitations, sense of pulsing, irregularities in heart actions, respiratory symptoms, urogenital symptoms	16/9	3/3	7/10	2/7	4/1	$\chi^2 = 7.01$, DF = 4, $P > 0.05$
Neurovegetative symptoms-face blushing, mouth dryness, vertigo, sweating	20/18	1/6	7/6	4/0	-	$\chi^2 = 7.7$, DF = 4, $P > 0.05$
Behavior during the interview-restlessness, agitation, walking around, frowned face, tense, sobbing, accelerated breathing, pallor, gulping and belching, vivid muscular reflexes, jerks, dilated pupillae, exophthalmus	4/10	0/5	8/13	10/0	10/0	$\chi^2 = 24.06$, DF = 4, $P < 0.001$
Mean score ± SD	16.22 ± 7.42/9.73 ± 6.03; $t = 3.76$, DF = 60, $P < 0.01$					

5 CCa patients could be considered seriously depressive because their total score surpassed the accepted limit of 16 points (*F*-test: $P = 4.02 \times 10\text{-}5$). A correlation between IBD activity indices and the depression total score was not revealed: For CD, $r = 0.39$, df = 17, $P > 0.05$; for UC, $r = 0.004$, df = 10, $P > 0.05$. The TNM system for cancer staging was not adequate for any kind of correlation testing.

Anxiousness levels

The trend disclosed in the depression evaluation remained when the anxiousness level was analyzed (Table 2): Patients with IBD expressed higher levels of anxiousness, nervous tension and susceptibilities to different kinds of fears. Despite the absence of significant differences in neurovegetative symptom intensity, the behavior of IBD patients exhibited more pronounced neurotic components: vivid facial mimics and gesticulation, gulping and belching during the conversation, with occasional staring into the examiner, associated with intermittent jerks of facial muscles and musculature of the extremities (not the ticks). The total anxiousness score did not correlate with IBD activity indices: for CD, $F = 0.06$, df = 17, $P > 0.05$; for UC, $F = 0.013$, df = 10, $P > 0.05$.

Paykel's scale for stressful events

Evaluation of the impacts of events, mostly stressful ones, on the appearance of either IBD or CCa showed no significant differences between the groups (Table 3). Financial difficulties, major or minor, dominated among stressors. The necessities for hospitalization of one of the family members seemed to bother more people who had cancer than those with IBD, while separation from a close person seemed to influence more IBD patients. On the other hand, only three patients of the IBD group and six from CCa group had no stress events at all in the past one year.

Discriminant function analysis (DFA)

This analysis was used to investigate whether one of the obtained parametric values (total scores of depression and/or anxiety) possessed a predictive potential, i.e. could it be used for classification of a newly discovered case into one of the groups of interest. This analysis delineated total depressive score as such a parameter that an equation for an a priori selection was computed (Table 1). Application of this equation to our samples showed 79.04% of accuracy (13 out of 62 cases were inadequately classified). The main problem was represented by the patients with IBD and low depressive scores and, *vice versa*, CCa patients with high depressive scores. Nonetheless, almost 80% of correctly classified patients were quite satisfactory for the accuracy of the DFA equation.

Finally, no gender-based and in-group differences between patients with UC and CD were obtained.

Table 3 Major stressful events (revealed in five or more persons in at least one of the groups) in IBD and CCa suffering patients according to the Paykel's scale

Event	IBD group (*n*)	CCa group (*n*)
Death of family members	8	7
Major financial difficulties	12	10
Business failure	5	2
Hospitalization of the family member due to serious illnesses	4	8
Frequent argues with parents	5	0
Separation from close person	7	2
Death of close friend	3	5
Minor financial difficulties	9	8
Mild organic illness	4	7
No stressful events at all	3	6

$\chi^2 = 12.83$, DF = 9, $P > 0.05$.

DISCUSSION

In this interview-based case-control study we intended to investigate how great the impact of anxiety and depression was on patients with IBD and cancer of the colon. The results suggested that psychological conditions influenced the pathogenesis of IBD. The uncontrolled trial, relatively

restrictive criteria and not very large sample limited the interpretation of the results. Nevertheless, proclaimed criteria were necessary to eliminate the influence of the genetic factors, major surgery consequences and other impacts on the appearance of IBD or CCa. The difference in life span and gender between our groups could be interpreted by the nature of the illnesses: IBD has already been reported as an illness with slight female predominance[13], while, according to epidemiological studies, males have higher mortality rate of cancer of the colon (8.4: 6.0/100 000 inhabitants)[14]. Surprisingly, women smokers have milder forms of IBD and less need for hemicolectomy[15]. Moreover, ethnic-based differences in the prevalence of IBD exist as well, and it is higher in Caucasians than in the Hispanic population of North America[16].

Still, there are some dilemmas about emotional status in IBD and CCa: one of the most frequent is: Could the depression be of the reactive type and could the symptoms of the gastrointestinal disease influence the presence of emotional instability? Moreover, patients are required to observe his/her own blood in the stool, in addition to suffering the abdominal pain and tenderness. Results of several studies have suggested that IBD patients more frequently suffer from psychiatric illnesses, particularly depression and anxiety at a triple higher rate than either the general population or patients with other kinds of chronic illnesses[17-19]. Individuals with IBD and similar bowel disorders experience a frequency of depression that is triple those of the general population. It is important for clinicians to assess depression and suicidal ideation among their patients with active IBD symptoms, particularly among those reporting moderate to severe pain[20]. The results of some studies suggested that psychoimmunological components might be involved in the etiology of IBD[21,22], but such a possibility is relatively uncertain due to the small relative risk for persons with depression affected by IBD[21]. Some authors tried to link the IBD occurrence with some personality traits[19,23], such as neuroticism or introversion, but we did not examine personality traits or disorders, thus we remained limited to depression and anxiety as ICD-10 recognized diagnoses. Nonetheless, emotional abuse, depression, self-accusing and the sense of guilt, have already been reported to be more common in women with irritable bowel syndrome[24], and, according to our results, sense of guilt, which involves self-blame as well, were emphasized in persons with IBD[21]. On the other hand, judging from the data obtained in this study, CCa patients had better insight into the illness and this could be the reason why patients with IBD, to our highly empiric observation, more frequently abandon the therapy as soon as they get better, without the permit of their gastroenterologists.

Recent studies showed that depression occurring with the recurrence of IBD in chronic patients and with anxiety and poor quality of health condition may exert a negative influence on the course of IBD[25]. Furthermore, some investigators reported simultaneous rise of CDAI and depression rate, estimated by Beck's depression self rating scale during disease progression, an evaluation independently confirms the lack of correlation between the clinical activity of the illness and the level of anxiety and depression revealed by Hamilton's rating scale, considering the high correlation between two mentioned scales in sensitivity for mood changes[26]. Also, antidepressants in the therapy of IBD is suggested for two reasons: first, the reduction of the depression and anxiety and, second, but not less important, the pain relief[20,27]. Recent studies, however, warn that the treatment with Selective seritonin reuptake inhibitors (SSRIs) could increase the bleeding risk in patients with IBD[28].

No difference in the impact of stressful events was found in our study. According to the investigation using Paykel's scale published elsewhere, stressful events are correlated with the major depression and generalized anxiety disorder, but no specificities in life events could be delineated[29]. We can speculate that stressful events could indirectly influence the IBD occurrence, worsening the depressive and anxiety symptoms that are undeniably related to the presence of IBD. For CCa, genetic, nutritional or environmental factors seem to be decisive, while circumstances play an ambiguous and, probably, less relevant role in its pathogenesis[30-32].

In conclusion, patients with newly obtained inflammatory bowel disease have higher levels of depression and anxiety, compared with individuals with newly diagnosed colon cancer. The discriminant function analysis reveals the total depression score as a parameter of importance for the classification of a newly diagnosed patient into one of the groups of interest. Our analysis indicates that the psychiatrist should take part in the treatment of IBD, although, according to our results, the initial IBD activity indices show no correlation with the depression or anxiety scores. On the other hand, events in the past one year do not have a particular influence on the occurrence of either inflammatory bowel disease or colon cancer.

COMMENTS

Background

It has already been reported that the level of depression and anxiety is augmented in patients with inflammatory bowel disease (IBD) and cancer of the colon (CCa). The present study compares the level of anxiety and depression in therapy-naïve, first episode IBD patients to those suffering from newly discovered CCa, using Hamilton's Depression Scale and Hamilton's Anxiety Scale.

Research frontiers

Both IBD and CCa should be recognized as complex illnesses, especially IBD and it is advisable that psychiatrists should be included in the team for the treatment.

Innovations and breakthroughs

No comparison has been made between emotional states in IBD and CCa suffering patients so far. The current study emphasizes the impact of depression and anxiety on the appearance of IBD, rather than the formation of CCa.

Applications

Continual psychiatric evaluation is recommended in IBD suffering patients and psychiatric treatment is necessary, parallel to the IBD medication in order to restrict the depression and to improve the pain in IBD suffering individuals.

Peer review

This study compares anxiety and depression levels in patients with IBD and patients with CCa. It is understandably written and discriminates certain reasons of

depression and anxiety in patients with IBD. The study is well designed and results are convincing. The presentation and readability of the manuscript is satisfactory.

REFERENCES

1 **Ashbury FD**, Madlensky L, Raich P, Thompson M, Whitney G, Hotz K, Kralj B, Edell WS. Antidepressant prescribing in community cancer care. *Support Care Cancer* 2003; **11**: 278-285
2 **Meyer TJ**, Mark MM. Effects of psychosocial interventions with adult cancer patients: a meta-analysis of randomized experiments. *Health Psychol* 1995; **14**: 101-108
3 **Aronowitz R**, Spiro HM. The rise and fall of the psychosomatic hypothesis in ulcerative colitis. *J Clin Gastroenterol* 1988; **10**: 298-305
4 **North CS**, Clouse RE, Spitznagel EL, Alpers DH. The relation of ulcerative colitis to psychiatric factors: a review of findings and methods. *Am J Psychiatry* 1990; **147**: 974-981
5 **Walker EA**, Gelfand MD, Gelfand AN, Creed F, Katon WJ. The relationship of current psychiatric disorder to functional disability and distress in patients with inflammatory bowel disease. *Gen Hosp Psychiatry* 1996; **18**: 220-229
6 **Lydiard RB**, Fossey MD, Marsh W, Ballenger JC. Prevalence of psychiatric disorders in patients with irritable bowel syndrome. *Psychosomatics* 1993; **34**: 229-234
7 **Walker EA**, Roy-Byrne PP, Katon WJ. Irritable bowel syndrome and psychiatric illness. *Am J Psychiatry* 1990; **147**: 565-572
8 **Hamilton M**. A rating scale for depression. *J Neurol Neurosurg Psychiatry* 1960; **23**: 56-62
9 **Gjerris A**, Bech P, Bøjholm S, Bolwig TG, Kramp P, Clemmesen L, Andersen J, Jensen E, Rafaelsen OJ. The Hamilton Anxiety Scale. Evaluation of homogeneity and inter-observer reliability in patients with depressive disorders. *J Affect Disord* 1983; **5**: 163-170
10 **Paykel ES**. Methodological aspects of life events research. *J Psychosom Res* 1983; **27**: 341-352
11 **Best WR**, Becktel JM, Singleton JW, Kern F. Development of a Crohn's disease activity index. National Cooperative Crohn's Disease Study. *Gastroenterology* 1976; **70**: 439-444
12 **Schroeder KW**, Tremaine WJ, Ilstrup DM. Coated oral 5-aminosalicylic acid therapy for mildly to moderately active ulcerative colitis. A randomized study. *N Engl J Med* 1987; **317**: 1625-1629
13 **Loftus EV**, Schoenfeld P, Sandborn WJ. The epidemiology and natural history of Crohn's disease in population-based patient cohorts from North America: a systematic review. *Aliment Pharmacol Ther* 2002; **16**: 51-60
14 **Adanja B**, Gledovic Z, Pekmezovic T, Vlajinac H, Jarebinski M, Zivaljevic V, Pavlovic M. Mortality trends of malignant tumours of digestive organs in Belgrade, Yugoslavia, 1975-1997. *Dig Liver Dis* 2000; **32**: 386-391
15 **Cosnes J**. Tobacco and IBD: relevance in the understanding of disease mechanisms and clinical practice. *Best Pract Res Clin Gastroenterol* 2004; **18**: 481-496
16 **Kurata JH**, Kantor-Fish S, Frankl H, Godby P, Vadheim CM. Crohn's disease among ethnic groups in a large health maintenance organization. *Gastroenterology* 1992; **102**: 1940-1948
17 **Addolorato G**, Capristo E, Stefanini GF, Gasbarrini G. Inflammatory bowel disease: a study of the association between anxiety and depression, physical morbidity, and nutritional status. *Scand J Gastroenterol* 1997; **32**: 1013-1021
18 **Magni G**, Bernasconi G, Mauro P, D'Odorico A, Sturniolo GC, Canton G, Martin A. Psychiatric diagnoses in ulcerative colitis. A controlled study. *Br J Psychiatry* 1991; **158**: 413-415
19 **Robertson DA**, Ray J, Diamond I, Edwards JG. Personality profile and affective state of patients with inflammatory bowel disease. *Gut* 1989; **30**: 623-626
20 **Fuller-Thomson E**, Sulman J. Depression and inflammatory bowel disease: findings from two nationally representative Canadian surveys. *Inflamm Bowel Dis* 2006; **12**: 697-707
21 **Kurina LM**, Goldacre MJ, Yeates D, Gill LE. Depression and anxiety in people with inflammatory bowel disease. *J Epidemiol Community Health* 2001; **55**: 716-720
22 **Stein M**. Stress, depression, and the immune system. *J Clin Psychiatry* 1989; **50** Suppl: 35-40; discussion 41-42
23 **Tocchi A**, Lepre L, Liotta G, Mazzoni G, Costa G, Taborra L, Miccini M. Familial and psychological risk factors of ulcerative colitis. *Ital J Gastroenterol Hepatol* 1997; **29**: 395-398
24 **Ali A**, Toner BB, Stuckless N, Gallop R, Diamant NE, Gould MI, Vidins EI. Emotional abuse, self-blame, and self-silencing in women with irritable bowel syndrome. *Psychosom Med* 2000; **62**: 76-82
25 **Mittermaier C**, Dejaco C, Waldhoer T, Oefferlbauer-Ernst A, Miehsler W, Beier M, Tillinger W, Gangl A, Moser G. Impact of depressive mood on relapse in patients with inflammatory bowel disease: a prospective 18-month follow-up study. *Psychosom Med* 2004; **66**: 79-84
26 **Bech P**. Depression: influence on time estimation and time experiments. *Acta Psychiatr Scand* 1975; **51**: 42-50
27 **Clary G**, Onken J. What are the current recommendations for diagnosing and treating depression in Crohn's disease? Available from: URL: http://dukemedmag.duke.edu/assets/articles/5475/Clinician_Q&A.pdf
28 **de Jong JC**, van den Berg PB, Tobi H, de Jong-van den Berg LT. Combined use of SSRIs and NSAIDs increases the risk of gastrointestinal adverse effects. *Br J Clin Pharmacol* 2003; **55**: 591-595
29 **Newman SC**, Bland RC. Life events and the 1-year prevalence of major depressive episode, generalized anxiety disorder, and panic disorder in a community sample. *Compr Psychiatry* 1994; **35**: 76-82
30 **Kemp Z**, Thirlwell C, Sieber O, Silver A, Tomlinson I. An update on the genetics of colorectal cancer. *Hum Mol Genet* 2004; **13** Spec No 2: R177-R185
31 **Pritchard DM**, Watson AJ. Apoptosis and gastrointestinal pharmacology. *Pharmacol Ther* 1996; **72**: 149-169
32 **Satia-Abouta J**, Galanko JA, Martin CF, Ammerman A, Sandler RS. Food groups and colon cancer risk in African-Americans and Caucasians. *Int J Cancer* 2004; **109**: 728-736

S- Editor Wang GP **L- Editor** Zhu LH **E- Editor** Lu W

PO Box 2345, Beijing 100023, China
www.wjgnet.com
wjg@wjgnet.com

World J Gastroenterol 2007 January 21; 13(3): 444-447
World Journal of Gastroenterology ISSN 1007-9327

RAPID COMMUNICATION

Premedication with pronase or N-acetylcysteine improves visibility during gastroendoscopy: An endoscopist-blinded, prospective, randomized study

Chun-Chao Chang, Sheng-Hsuan Chen, Chih-Ping Lin, Ching-Ruey Hsieh, Horng-Yuan Lou, Fat-Moon Suk, Shiann Pan, Ming-Shun Wu, Jun-Nan Chen, Yung-Fa Chen

Chun-Chao Chang, Sheng-Hsuan Chen, Ching-Ruey Hsieh, Horng-Yuan Lou, Fat-Moon Suk, Shiann Pan, Division of Gastroenterology, Department of Internal Medicine, Taipei Medical University Hospital; Digestive Disease Research Center, Taipei Medical University; Taipei, Taiwan, China
Ming-Shun Wu, Jun-Nan Chen, Yung-Fa Chen, Taipei Medical University-Municipal Wan-Fang Hospital, Taipei, Taiwan, China
Chih-Ping Lin, Department of Internal Medicine, Min-Sheng General Hospital, Taoyuan, Taiwan, China
Supported by a grant of TMU93-AE1-B-07 and 93 MSH-TMU-09 of Taipei Medical University
Correspondence to: Dr. Chun-Chao Chang, Division of Gastroenterology, Department of Internal Medicine, Taipei Medical University Hospital, 252 Wu-Hsing Street, Taipei 110, Taiwan, China. chunchao@tmu.edu.tw
Telephone: +886-2-27372181-3903 Fax: +886-2-27363051
Received: 2006-03-13 Accepted: 2006-12-11

Abstract

AIM: To assess the efficacy of premedicaton with pronase or N-acetylcysteine (NAC) at 20 min before upper gastrointestinal (UGI) endoscopy and to determine whether pronase or NAC pretreatment influences the reliability of the rapid urease test.

METHODS: A total of 146 patients were prospectively and randomly assigned into the study groups according to different premedications before endoscopy. One endoscopist assessed mucosal visibility (MV) with scores ranged from 1 to 4 at four sites in the stomach. The sum of the MV scores from these four locations was defined as the total mucosal visibility (TMV) score. Identification of *H pylori* was performed using CLO test, histology, and serology.

RESULTS: The Group with pronase premedication had a significantly lower TMV score than did the groups with gascon and gascon water ($P < 0.001$ and $P < 0.01$, respectively). The group with NAC had a significantly lower TMV score than the group with gascon ($P < 0.01$) and a trend of a lower MV score than the group with gascon water ($P = 0.06$). The TMV score did not significantly differ between the group with pronase and the group with NAC ($P = 0.39$ and $P = 0.14$, respectively). The sensitivity and specificity of the CLO test were 92.5% and 93.9%, respectively, in groups premedicated with pronase and NAC together.

CONCLUSION: Premedication with pronase or NAC at 20 min before UGI endoscopy improves the mucosal visibility of the stomach. Neither pronase nor NAC produces any obvious interference with the CLO test for the identification of *H pylori* infection.

Key words: Pronase; N-acetylcysteine; *H pylori;* Gastrointestinal endoscopy

Chang CC, Chen SH, Lin CP, Hsieh CR, Lou HY, Suk FM, Pan S, Wu MS, Chen JN, Chen YF. Premedication with pronase or N-acetylcysteine improves visibility during gastroendoscopy: An endoscopist-blinded, prospective, randomized study. *World J Gastroenterol* 2007; 13(3): 444-447

http://www.wjgnet.com/1007-9327/13/444.asp

INTRODUCTION

The 5-year survival rate for early gastric cancer exceeds 90%[1,2]. Western endoscopists are less successful than Japanese endoscopists in the detection of gastric cancers at an early stage. This is not because the Japanese endoscopists detect the cancers by screening the asymptomatic population. Even in Japan, most cases are incidental findings of opportunistic screening at endoscopy, and only 10% of gastric cancers are picked up by screening program[3,4]. More than 50% of all gastric cancers in Japan were found in an early stage but probably fewer than 5% are in the West[5,6]. A single-center study in the UK reported that 13.5% patients (11 of 81 patients presenting with advanced gastric cancer) supposed to be missed of early gastric cancer those who had undergone endoscopy within the previous 2 years[7]. A diagnosis of early gastric cancer can be improved by effective premedication with a defoaming agent during upper gastrointestinal endoscopy. Dimethylpolysiloxane (DMPS) is commonly used at most endoscopic centers to eliminate bubbles and foam[8-10]. However, a lot of mucus and bubbles can still be encountered with premedication of DMPS during gastroendoscopy. Pronase is a proteolytic enzyme isolated in 1962 from the culture filtrate of Septomyces griseus which has already been used as a

raw material to prepare anti-inflammatory and digestive enzymes. In 1964, Koga and Arakawa used this enzyme as a premedication for roentgenographic examinations to remove gastric mucus[11]. Since then, Ida *et al*[12] applied this enzyme to gastroendoscopy. Fujii *et al*[13] also concluded that premedication with pronase improved endoscopic visualization during conventional endoscopy and chromoendoscopy. They recommended routinely use of pronase for endoscopy is helpful. N-acetylcysteine (NAC) is both a mucolytic agent and a thiol-containing antioxidant. NAC, unlike some other bronchial mucolytics such as carbocysteine and bromhexine, has been shown in *in vitro* studies to change the viscoelastic properties of gastric mucin[14]. In this study, we investigated the effectiveness of premedications with DMPS only, DMPS with water, DMPS with pronase, and DMPS with NAC on the visibility during UGI endoscopy.

Pronase and NAC are both mycolytic agents. There are two studies discussing about *H pylori* detection after treatment with pronase and NAC[15,16]. Rapid urease testing is most commonly used to identify *H pylori* during the examination of UGI endoscopy. Therefore, we also attempted to determine whether pronase or NAC pretreatment influences the reliability of identifying *H pylori* infection by the rapid urease test.

MATERIALS AND METHODS

Patients

From January to July 2005, 146 consecutive patients were referred to our department for upper gastrointestinal (UGI) endoscopy. We excluded those patients with previous gastric surgery, gastric malignancy, corrosive gastric injury, or gastrointestinal bleeding.

UGI endoscopic procedures were performed by a single experienced endoscopist (Chang CC) between 9:00 am and 1:00 pm in the endoscopic room of Taipei Medical University Hospital. Patients who consented to participate in the study were randomly assigned to four different oral liquid solutions for premedication before endoscopy. All oral solutions were given around 20 min before UGI endoscopy. The endoscope used was a GIF-Q240X video endoscope (Olympus, Tokyo, Japan).

The patients were randomly divided into four groups according to the treatment with oral liquid solutions. Group A: 100 mg, 5 mL of DMPS (Gascon, Kisssi Corp., Matsumoto, Japan); Group B: 100 mg, 5 mL of DMPS plus water up to 100 mL; Group C: 20 000 U pronase (Pronase MS, Kaken Corp., Tokyo, Japan), 1.2 g sodium bicarbonate, 100 mg, 5 mL of DMPS plus water up 100 mL water; and Group D: 400 mg N-acetylcysteine (Acetin, Synmosa Corp., Taipei, Taiwan), 5 mL of DMPS plus water up 100 mL.

The endoscopist was unaware of the kind of oral liquid solution used for premedication for each patient before UGI endoscopy. UGI endoscopy was performed to check the mucosal visibility of the gastric antrum, the greater curvature of the gastric lower body, the greater curvature of the gastric upper body, and the gastric fundus. The scores of mucosal visibility were classified from 1 to 4 and this score was modified from Kuo *et al*[15] (Figure 1A-D).

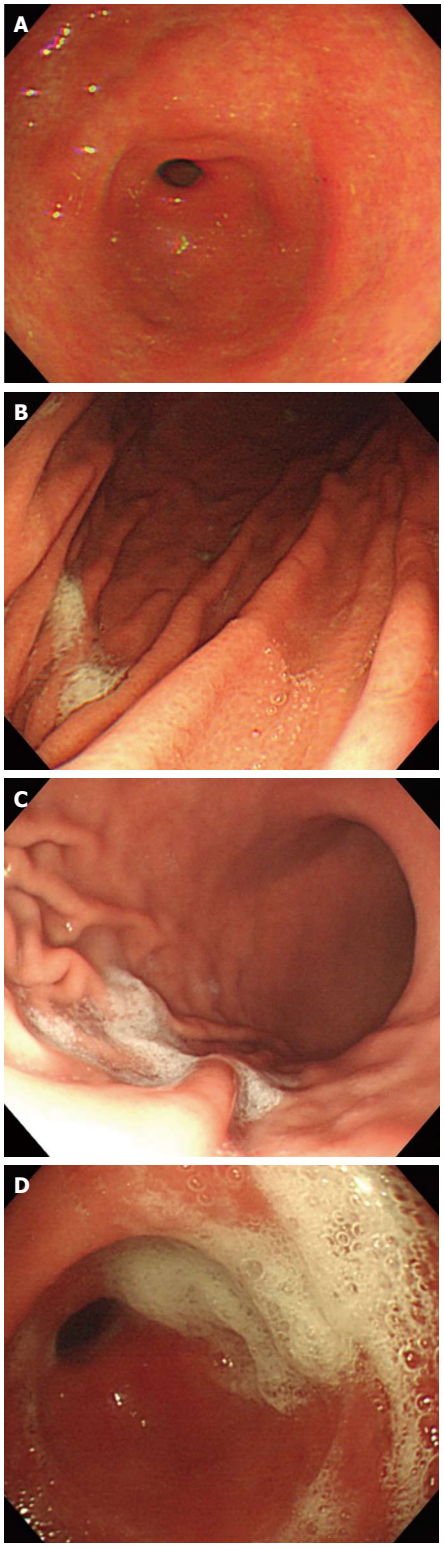

Figure 1 Mucosal visibility scores evaluated during UGI endoscopy. (**A**) Score 1: No adherent mucus on the gastric mucosa; (**B**) Score 2: a small amount of mucus on the gastric mucosa without obscuring the vision; (**C**) Score 3: a large amount of mucus on the gastric mucosa, which took less than 50 mL of water to clear; and (**D**) Score 4: a large amount of mucus on the gastric mucosa, which took more than 50 mL of water to clear.

Score 1: No adherent mucus on the gastric mucosa; Score 2: little amount of mucus on the gastric mucosa but no obscuring vision; Score 3: large amount of mucus on the gastric mucosa, with less than 50 mL of water to clear; Score 4: large amount of mucus on the gastric mucosa, with more than 50 mL of water to clear. The sum of the scores from the four locations was defined as the total mucosal visibility score (TMVS).

The rapid urease test using the Campylobacter-like organism test (CLO test; Delta West, Perth, Australia), the

Table 1 Demographic characteristics of patients

Category	Group A	Group B	Group C	Group D
Number (*n*)	39	35	34	39
Age (yr)	44.4 ± 14.2	44.1 ± 14.4	47.8 ± 13.9	48.7 ± 16.5
Gender (M:F)	18:21	18:17	16:18	18:21
Indication				
Cancer screening	9	9	7	10
Dyspepsia	20	17	18	22
Acid regurgitation	10	9	9	7

No significant difference between each two groups. Group A received dimethylpolysiloxane, group B received dimethylpolysiloxane plus water, group C received pronase, sodium bicarbonate, and dimethylpolysiloxane plus water, and group D received N-acetylcysteine and dimethylpolysiloxane plus water.

Table 2 Mucosal visibility scores at different locations of the stomach (mean ± SD)

	Antrum	Greater curvature of the lower gastric body	Greater curvature of the upper gastric body	Fundus
Group A	$1.74 \pm 0.91^{e,g}$	$2.18 \pm 1.14^{e,g}$	$2.92 \pm 1.06^{c,e,g}$	$1.38 \pm 0.67^{c,e,g}$
Group B	$1.49 \pm 0.82^{e,g}$	$1.89 \pm 0.87^{e,g}$	$2.49 \pm 0.82^{a,e}$	$1.80 \pm 0.80^{a,e}$
Group C	$1.18 \pm 0.63^{a,c}$	$1.38 \pm 0.78^{a,c}$	$2.06 \pm 0.89^{a,c}$	$1.21 \pm 0.41^{a,c}$
Group D	$1.21 \pm 0.52^{a,c}$	$1.77 \pm 0.90^{a,c}$	2.33 ± 0.79^{a}	$1.28 \pm 0.67^{a,c}$
Total	1.41 ± 0.77	1.82 ± 0.95	2.46 ± 0.94	1.41 ± 0.69

There were significant differences in mucosal visibility scores in the upper gastric body when compared to the antrum, lower gastric body, and fundus. $^{a}P < 0.05$ *vs* group A; $^{c}P < 0.05$ *vs* group B; $^{e}P < 0.05$ *vs* group C; $^{g}P < 0.05$ *vs* group D. (a, c, e, g: one-way analysis of variance and Tukey's multiple comparison).

Table 3 CLO test for *H pylor* detection in groups C and D

Category	*H pylori*-positive	*H pylori*-negative
Positive CLO test	37	2
Negative CLO test	3	31

$P < 0.05$ by Chi-square test.

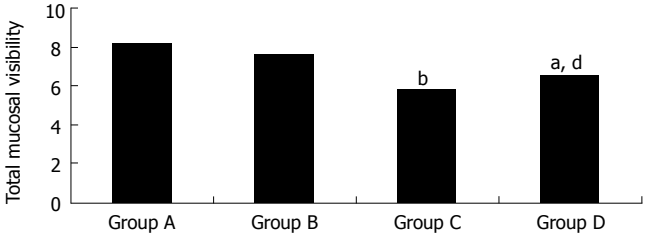

Figure 2 Total mucosal visibility score of each group. $^{b}P < 0.01$ *vs* groups A and B; $^{d}P < 0.01$ *vs* group A, $^{a}P = 0.06$ *vs* group B.

histologic examination for *H pylori* using hematoxylin-eosin staining during the UGI endoscopy and serum anti-*H pylori* IgG were carried out to determine the presence of infection by *H pylori*. *H pylori* infection was considered when two of the three tests were positive.

Statistical analysis

The demographic characteristics were assessed using a chi-square test or one-way analysis of variance. The visibility scores for the four groups were assessed using one-way analysis of variance with Tukey's multiple comparisons. The correlation of the results of the CLO test was analyzed using a chi-square test. The results were expressed as mean ± SD. $P < 0.05$ was considered statistically significant.

RESULTS

Of 147 patients (70 men and 77 women), 39, 35, 34, and 39 patients were randomly placed in groups A, B, C, and D, respectively. The demographic data of patients are shown in Table 1. The mean (± SD) ages of groups A, B, C, and D were 44.4 ± 14.2, 44.1 ± 14.4, 47.8 ± 13.9, and 48.7 ± 16.5 years, respectively. The ratios of males to females among groups A, B, C, and D were 1:1.1, 1:0.9, 0.9:1 and 1:1.1, respectively. There was no significant statistical difference between any pair of groups for age or the gender ratio.

The means of the TMV score among groups A, B, C, and D were 8.2 ± 3.1, 7.6 ± 2.6, 5.8 ± 2.3, and 6.5 ± 2.2, respectively. Group C had a significantly lower TMV score than groups A and B ($P < 0.001$ and $P < 0.01$, respectively). Group D also had a significantly lower TMV score than group A ($P < 0.01$) and a trend of a lower TMV score than group B ($P = 0.06$) (Figure 2). The TMV score did not significantly differ between groups A and B or between groups C and D ($P = 0.39$ and $P = 0.14$, respectively). The visibility score of each location of the stomach and TMV score for each group are shown in Table 2.

The scores of mucosal visibility at different locations in all patients were 1.4 ± 0.7 at the gastric fundus, 2.5 ± 0.9 at the greater curvature of the upper gastric body, 1.8 ± 0.9 at the greater curvature of the lower gastric body, and 1.4 ± 0.7 at the gastric antrum. A significantly poorer visibility score of the greater curvature of the upper gastric body compared to that of the gastric fundus, the greater curvature of the lower gastric body, and the gastric antrum was noted (all $P < 0.05$). In addition, the greater curvature of the lower gastric body had a significantly poor visibility score than did the gastric fundus and the gastric antrum (both $P < 0.05$). There was no significant difference of mucosal visibility score between the gastric antrum and the gastric fundus.

According to the effect of pronase and NAC on the reliability of the CLO test for identifying *H pylori* infection (Table 3), 68 of 73 patients had matching results between the CLO test and *H pylori* infection ($P < 0.05$). The sensitivity and specificity were 92.5 % and 93.9%, respectively.

DISCUSSION

For better visualization of the gastric mucosa, decreasing the amount of mucus and bubbles is very important during UGI endoscopy. Adequate premedication can eliminate

the need to carry out flushing during the procedure. In Japan, pronase is widely used as a mucolytic agent before gastrointestinal endoscopy. A randomized study by Fujii *et al*[13] showed that premedication with pronase significantly improved visibility before and after methylene blue spraying and also significantly shortened the time for the chromoendoscopic examination. Kuo *et al*[15] also concluded that premedicaiton with 2000 U pronase, 1.2 g of sodium bicarbonate, 100 mg of DMPS plus up to 100 mL of warm water provided the clearest endoscopic visibility. Without the application of DMPS, pronase alone could not improve endoscopic visibility[15]. Similarly, in our study, we found that group C (premedication with 20 000 U pronase, 1.2 g of sodium bicarbonate, 100 mg of DMPS plus up to 100 mL of warm water) had better TMV scores than those in groups A and B. In comparison to the study by Kuo *et al*[15], we used 20 000 U pronase rather than 2000 U pronase. In addition to the different doses of pronase, we gave all premedications around 20 min before UGI endoscopy, and we did not ask patients to change position before UGI endoscopy. Because the fluid ingested by those patients flowed into the gastric fundus, then gradually into the gastric antrum by the way of the gastric body, we thought it was not necessary to change the position before UGI endoscopy. Moreover, there can still be a lot of bubbles in the stomach 10 min after administering DMPS prior to UGI endoscopy in our previous experience.

NAC is a mucolytic agent which is commonly used for digestion of the esophageal mucus for the detection of Barrett's esophageal cancer prior to chromoendoscopy with methylene blue[17,18]. Its effectiveness in improving the mucosal visibility of the stomach during UGI endoscopy is not known. In our study, NAC also provided better TMV scores in the stomach as did pronase. Premedication with NAC can achieve good mucosal visibility during gastrointestinal endoscopy if pronase is not available.

In our study, we found the greater curvature of the upper gastric body had the poorest mucosal visibility among all locations evaluated, suggesting that this area needs to be observed with caution during UGI endoscopy.

Pronase and NAC can disrupt the gastric mucus by a mucolytic effect. It is not well known whether pronase or NAC interferes with the accuracy of the CLO test for identifying *H pylori* infection. Our study showed greater than 90% sensitivity and specificity for the CLO test with premedication with pronase or NAC, which is consistent with the study by Kuo *et al*[15] based on the urea breath test. In conclusion, in order to improve the mucosal visibility of the stomach, premedication with pronase or NAC at 20 min before UGI endoscopy is feasible. It is not necessary to change the position of the patient from supine, left or right lateral to prone before UGI endoscopy. The greater curvature of the upper gastric body needs to be cautiously observed, for it had the poorest mucosal visibility among all locations evaluated. Neither pronase nor NAC produce any obvious interference with the CLO test for identifying *H pylori* infection.

REFERENCES

1 **Everett SM**, Axon AT. Early gastric cancer: disease or pseudo-disease? *Lancet* 1998; **351**: 1350-1352
2 **Sue-Ling HM**, Martin I, Griffith J, Ward DC, Quirke P, Dixon MF, Axon AT, McMahon MJ, Johnston D. Early gastric cancer: 46 cases treated in one surgical department. *Gut* 1992; **33**: 1318-1322
3 Medical Examinations for Digestive Cancer in 1995 Group. National Report. *J Gastroenterol Mass Surv* 1998; **130**: 251-269
4 **Rembacken BJ**, Gotoda T, Fujii T, Axon AT. Endoscopic mucosal resection. *Endoscopy* 2001; **33**: 709-718
5 **Shimizu S**, Tada M, Kawai K. Endoscopic ultrasonography in inflammatory bowel diseases. *Gastrointest Endosc Clin N Am* 1995; **5**: 851-859
6 **Ballantyne KC**, Morris DL, Jones JA, Gregson RH, Hardcastle JD. Accuracy of identification of early gastric cancer. *Br J Surg* 1987; **74**: 618-619
7 **Suvakovic Z**, Bramble MG, Jones R, Wilson C, Idle N, Ryott J. Improving the detection rate of early gastric cancer requires more than open access gastroscopy: a five year study. *Gut* 1997; **41**: 308-313
8 **Banerjee B**, Parker J, Waits W, Davis B. Effectiveness of preprocedure simethicone drink in improving visibility during esophagogastroduodenoscopy: a double-blind, randomized study. *J Clin Gastroenterol* 1992; **15**: 264-265
9 **McDonald GB**, O'Leary R, Stratton C. Pre-endoscopic use of oral simethicone. *Gastrointest Endosc* 1978; **24**: 283
10 **Waye JD**, Pitman E, Weiss A, Krueger K. The bubble problem in endoscopy. An evaluation of a new aid in endoscopy. A double blind study. *Gastrointest Endosc* 1967; **14**: 34-35
11 **Koga M**, Arakawa K. On the application of enzymatic mucinolysis in x-ray diagnosis of the stomach. *Nihon Igaku Hoshasen Gakkai Zasshi* 1964; **24**: 1011-1031
12 **Ida K,** Okuda J, Nakazawa S, Yoshino J. Clinical evaluation of premedication with KPD (pronase) in gastroendoscopy-placbo-contolled double blind study in dye scattering endoscopy. *Clin Rep* 1991; **25**: 1793-1804
13 **Fujii T**, Iishi H, Tatsuta M, Hirasawa R, Uedo N, Hifumi K, Omori M. Effectiveness of premedication with pronase for improving visibility during gastroendoscopy: a randomized controlled trial. *Gastrointest Endosc* 1998; **47**: 382-387
14 **Misawa M**, Imamura N. In vitro evaluation of mucolytic activities of some expectorants using porcine gastric mucin *Nihon Yakurigaku Zasshi* 1988; **92**: 263-270
15 **Kuo CH**, Sheu BS, Kao AW, Wu CH, Chuang CH. A defoaming agent should be used with pronase premedication to improve visibility in upper gastrointestinal endoscopy. *Endoscopy* 2002; **34**: 531-534
16 **Huynh HQ**, Couper RT, Tran CD, Moore L, Kelso R, Butler RN. N-acetylcysteine, a novel treatment for Helicobacter pylori infection. *Dig Dis Sci* 2004; **49**: 1853-1861
17 **Wo JM**, Ray MB, Mayfield-Stokes S, Al-Sabbagh G, Gebrail F, Slone SP, Wilson MA. Comparison of methylene blue-directed biopsies and conventional biopsies in the detection of intestinal metaplasia and dysplasia in Barrett's esophagus: a preliminary study. *Gastrointest Endosc* 2001; **54**: 294-301
18 **Dave U**, Shousha S, Westaby D. Methylene blue staining: is it really useful in Barrett's esophagus? *Gastrointest Endosc* 2001; **53**: 333-335

S- Editor Liu Y **L- Editor** Kumar M **E- Editor** Lu W

PO Box 2345, Beijing 100023, China
www.wjgnet.com
wjg@wjgnet.com

World J Gastroenterol 2007 January 21; 13(3): 448-451
World Journal of Gastroenterology ISSN 1007-9327

RAPID COMMUNICATION

Liu-stain quick cytodiagnosis of ultrasound-guided fine needle aspiration in diagnosis of liver tumors

Chi-Sin Changchien, Jing-Houng Wang, Sheng-Nan Lu, Chao-Hung Hung, Chien-Hung Chen, Chuan-Mo Lee

Chi-Sin Changchien, Jing-Houng Wang, Sheng-Nan Lu, Chao-Hung Hung, Chien-Hung Chen, Chuan-Mo Lee, Division of Hepato-Gastroenterology, Department of Internal Medicine, Chang-Gung Memorial Hospital, Kaohsiung Medical Center, Chang Gung University, College of Medicine, Taiwan, China
Correspondence to: Dr. Chi-Sin Changchien, Division of Hepato-Gastroenterology, Department of Internal Medicine, Chang-Gung Memorial Hospital, Kaohsiung Medical Center, Chang Gung University, College of Medicine, 123, Ta-Pei road, Niao Sung Hsiang, Kaohsiung Hsien, Taiwan, China. cschangchien@adm.cgmh.org.tw
Telephone: +886-7-7317123 Fax: +886-7-7322402
Received: 2006-10-11 Accepted: 2006-12-04

Key words: Liver tumor; Cytology; Ultrasound guided FNA; Liu stain

Changchien CS, Wang JH, Lu SN, Hung CH, Chen CH, Lee CM. Liu-stain quick cytodiagnosis of ultrasound-guided fine needle aspiration in diagnosis of liver tumors. *World J Gastroenterol* 2007; 13(3): 448-451

http://www.wjgnet.com/1007-9327/13/448.asp

Abstract

AIM: To combine ultrasound-guided fine-needle aspiration (US-FNA) and Liu (Riu) stain to make a quick study on liver tumor lesions.

METHODS: Two hundred and twenty-eight aspirations from 232 patients were completely studied. The operator himself made the quick cytodiagnosis of US-FNA smear stained by Liu method within thirty minutes. The US-FNA specimen was also sent to the pathological department for cytological study and cellblock histology. The result of our Liu-stain quick cytodiagnosis in each patient was confirmed by the final cytopathological diagnosis from pathological report.

RESULTS: Among 228 samples, the quick cytodiagnosis revealed 146 malignancies, 81 benign lesions and one inadequate specimen. Cytopathological diagnosis from the pathological department revealed 150 malignancies, and 78 benign lesions. Four well-differentiated hepatocellular carcinomas (HCCs) were under-diagnosed by quick cytodiagnosis as benign and 3 benign lesions were over-diagnosed as well-differentiated HCCs. Compared with cytopathological diagnosis, quick cytodiagnosis correctly diagnosed 143 malignancies and 77 benign lesions. Except for the one inadequate specimen in quick cytodiagnosis, the accuracy of quick cytodiagnosis was 96.9% (220/227), and its sensitivity, specificity and positive and negative predictive values were 97.9%, 95.1%, 97.3% and 96.3%, respectively.

CONCLUSION: Liu-stain quick cytodiagnosis is a fast, convenient, safe and effective method for hepatologists in clinic practice to diagnose liver tumor. In few cases of well-differentiated HCC, Liu-stain quick cytodiagnosis has its limitation.

INTRODUCTION

Abdominal ultrasonography now is the first line to find liver tumor. Fine needle aspiration (FNA) is able to get tumor specimens for cytological interpretation[1]. Ultrasound-guided FNA (US-FNA) can get a correct specimen and provide a good diagnosis of liver tumor[2-4]. US-FNA is a safe and effective method for cytodiagnosis of liver tumor[2-4]. Tsou *et al*[5] reported that fine needle aspiration cytodiagnosis with Riu's stain has its value in diagnosing liver tumors. The procedure of Liu (Riu) stain takes about two minutes. So, Liu stain for FNA smear is a quick method in cytological study. We tried to combine the ultrasound-guided FNA and Liu stain to shorten the time of cytodiagnosis of liver tumors.

MATERIALS AND METHODS

Case selection

From June 2004 to May 2005, 232 patients (128 males, 104 females) underwent US-FNA for liver nodular lesions with a diameter > 1 cm detected by abdominal sonography. US-FNA was done from one lesion in each patient who signed the informed consent. The diameter of lesions ranged 1-16 cm. The mean age of 232 patients was 56.9 (range 25-96) years. A total of 232 aspirations were done. The patients who had positive malignant result from the pathological department underwent tumor treatment modalities (such as pure ethanol injection or radiofrequency ablation for small tumors, or surgical resection of operable tumors, or transhepatic arterial embolization of larger tumors). The patients who had benign result from the pathological report were followed up for six to twelve months with no change in alpha-fetal protein level, ultrasound examination, and clinic course.

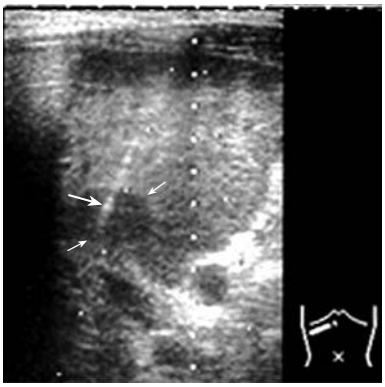

Figure 1 Needle aspiration under real-time ultrasound guidance. The needle (larger arrow) is advanced into the liver nodular lesion (small arrows) through the abdominal wall and liver parenchyma under the direct guidance of US.

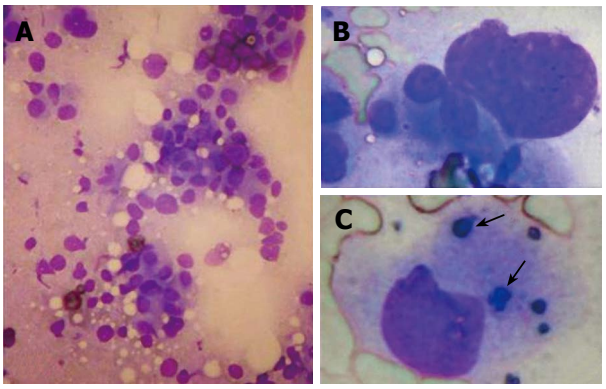

Figure 2 Cytodiagnosis of hepatocellular carcinoma by quick Liu stain showing scattered distribution of malignant cells bearing atypical naked (**A**) and large nuclei (**B**) with scanty cytoplasm but without trabecular structure and sinusoids (**A**: 100 x, **B**: 400 x) and bile pigmentation (arrows) in cytoplasma (**C**) (400 x).

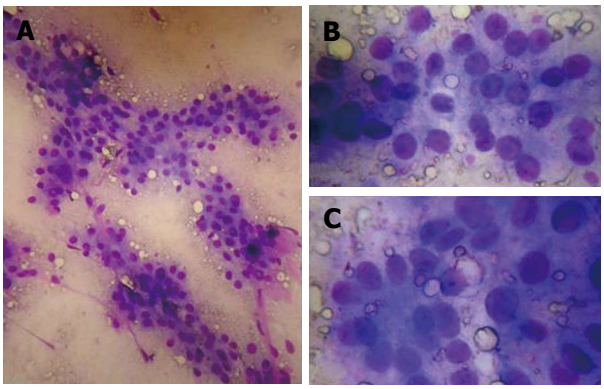

Figure 3 Cytodiagnosis of well-differentiated hepatocellular carcinoma by quick Liu stain showing cytological features of well-differentiated HCC with thicked trabecular structure (**A**) and polygonal tumor cells bearing centrally placed nuclei with a mild degree of pleomorphism and enlargement (**B**) (**A**: 100 x, **B**: 400 x) and cellular monomorphism and mildly increased nuclear/cytoplasmic ratio (**C**). Glandular structure was present, but the reticular pattern was not shown in Liu stain.

Specimen preparation

All US-FNAs were performed with Aloka SSD-680 or 2000 machine (Aloka Corp. Tokyo, Japan) using a 3.75-MHz lineal puncture probe or convex probe with a puncture adaptor. Needle aspiration was done under real-time US guidance with a 15-cm long 22-gauge Chiba needle (Hakko-Shoji, Tokyo) attached to a 20-mL syringe. The needle was advanced into the liver nodular lesion through the abdominal wall and liver parenchyma under the direct guidance of US (Figure 1). The piston of the syringe was pulled back and maintained in a maximal aspiration position to obtain the maximal negative pressure. The needle was quickly moved back and forth several times (about 3-5 passes) in the lesion under US observation. After this, the piston of the syringe was released and the pressure returned to normal, and the needle was withdrawn. The aspiration material was ejected and smeared onto glass slides (average 3-5 slides). One to two slides were stained by Liu stain solution and cytological reading was immediately done by the operator himself and Dr. Wang, and had cytological training at the Department of Pathology, Kurume University School of Medicine. The Liu stain solution for blood smear containing 2 kinds of solution, Liu A and B was used. The cytological smear for quick cytodiagnosis was directly (without dry-up) stained with Liu A for 30 s and then with Liu B for 1 min. After the stain solution was washed softly with water and the slide was dried by tissue paper, cytological reading was done, it took about 10 min. The cytological reader had the clinical data as assistant information. The total time of quick cytodiagnosis of US-FNA with Liu stain was within thirty minutes (including US-FNA procedure).

The remaining 2-3 slides were fixed in 95% ethanol and sent to the pathological department for hematoxylin and eosin (H & E) and/or papanicolaou staining. The remaining small, cohesive tissue fragments were also collected into a tube containing 10% neutral buffered formalin and processed for cell block histology study. The tissue was held using 2% agarose and paraffin-embeded. The pathologists studied the ethanol-fixed cytology and cellblock histology. The smear for quick cytodiagnosis was not sent for pathological study.

The quick cytodiagnosis was made depending on the findings on any slides. The cytological results were categorized into four groups: benign, suspicious for malignancy, positive for malignancy, and inadequate specimen. The positive malignancy encompassed both primary (hepatocellular carcinoma and cholangocarcinoma) and metastatic malignancies. The diagnosis of hepatocellular carcinoma (HCC) by quick cytology depended on the high cellularity with high nuclear/cytoplasmic ratios, polygonal outlines, dense granular cytoplasm, central nuclei and obvious morphologic kinship of tumor cells similar to ordinary hepatocytes. The characteristic findings in trabecular pattern and/or bile production (Figures 2 and 3) were also a clue to HCCs. The result of our Liu-stain quick cytodiagnosis in each patient was confirmed by the final cytopathological diagnosis from the pathological report. The diagnostic accuracy of quick cytodiagnosis was compared with that of cytopathological diagnosis. Sensitivity and specificity were calculated using conventional methods. Diagnostic accuracy was calculated as follows: (TP+TN)/(TP + TN+FP + FN), where TP = true positive, TN = true negative, FP = true positive and FN = false negative.

RESULTS

Four patients were excluded due to inadequate specimens

for both quick Liu-stain cytodiagnosis and cytopathological diagnosis. Among the 228 patients enrolled, the quick cytodiagnosis revealed 142 malignancies (Figure 2), 4 suspicious malignancies, 81 benign lesions and one inadequate specimen. Cytopathological diagnosis from the pathological department revealed 150 malignancies, and 78 benign lesions. Four suspicious malignancies by quick cytodiagnosis were 2 suspicious HCCs and 2 necrotic tissues with ghost cells. The former two were finally diagnosed as HCC and the latter two as metastatic adenocarcinoma and lymphoma respectively. One inadequate specimen by quick cytodiagnosis was proved to be adenocarcinoma by cytopathological diagnosis.

A total of 146 cases were diagnosed as malignancy by quick cytodiagnosis. Among them, 115 cases were diagnosed as HCC (1.2 cm-over 10 cm in diameter). For the 115 HCCs by quick cytodiagnosis, 14 were initially diagnosed as well-differentiated HCCs (Figure 3). Among them, 5 were well-differentiated, 6 moderately-differentiated and 3 non-malignancies by cytopathological diagnosis. The diameter of these three non-malignancies ranged 1.2 cm-1.6 cm. Of the 81 benign lesions by quick cytodiagnosis, four were proved to be well-differentiated HCCs and one to be adenomyolipoma with fat by cytopathological diagnosis. The overall quick cytodiagnosis rate was 96.5% (143 + 77/228). Except for one inadequate specimen in quick cytodiagnosis, the accuracy of quick cytodiagnosis was 96.9% (220/227), and the sensitivity, specificity, positive and negative predictive values were 97.9%, 95.1%, 97.3% and 96.3%, respectively.

Among the 143 malignancies, 13 cases of malignancy by quick cytodiagnosis did not match the final cytopathological diagnosis. Four HCCs became adenocarcinoma, 3 adenocarcinomas became HCC, and 6 malignancies without identification of cell nature became three adenocarcinomas, two HCCs and one transitional cell carcinoma.

The final diagnosis of 150 cytopathological malignancies revealed 126 HCCs, 18 adenocarcinomas (including 3 cholangiocarcinomas), 2 lymphomas, 2 unidentified malignancies, one squamous cell carcinoma, and one transitional cell carcinoma. The 78 benign lesions included fibroconnective tissue (regeneration nodule), focal nodular hyperplasia (6 cases), abscess (8 cases), hemangioma (2 cases), and others (leiomyoma, adenomyolipoma). No complication in relation with quick cytodiagnosis was found in the study.

DISCUSSION

The specimen was sent to our pathological department, and cytopathological diagnosis was made by hematoxylin and eosin (H & E) and/or Papanicolaou staining and cell block histology. Special staining (in some cases) was also done to identify the nature of malignancy. It was reported that cytodiagnosis of liver tumors has good sensitivity and specificity[4], suggesting that our final results based on the cytopathological diagnosis from our pathological department are reliable.

In this study, the overall quick cytodiagnosis rate was 96.5% (143+77/228). The accuracy of quick cytodiagnosis in 227 cases of liver tumor was 96.9% (220/227), and its sensitivity, specificity, positive and negative predictive values were 97.9%, 95.1%, 97.3% and 96.3%, respectively. The results of Liu-stain quick cytodiagnosis were acceptable, compared with the reported sensitivity of 67%-100% and specificity of 80%-100%[1], and 93.3 % sensitivity and 100% specificity by Riu's stain study[5]. The process of Liu stain on smears takes about 2 min. Including FNA aspiration procedure and cytological reading, the quick cytodiagnosis in this study took about thirty minutes to make a diagnosis. The procedure of cytodiagnosis was fast and effective in diagnosing liver tumors. It is very convenient for a hepatologist to diagnose liver tumors.

In most of our cases, Liu stain provided sufficient diagnostic elements, such as nuclear/cytoplasmic ratio, nuclear pattern, hyperchromatin, *etc*, to make a correct diagnosis of malignant or benign tumors. However, the nature of malignancy in quick cytodiagnosis was hard to identify in 13 cases, because special staining and cellblock histology were not available. This is the limitation of quick Liu stain cytodiagnosis. Although some limitations in diagnosing the nature of malignancies, quick cytodiagnosis can identify malignant from benign tumors except in some conditions such as well-differentiated HCCs.

In this series, incorrect diagnosis was made in 7 cases by quick cytodiagnosis. Four well-differentiated HCCs were under-diagnosed as benign tumors and 3 benign lesions were over-diagnosed as well-differentiated HCC. The mistake always occurs in the cases of well-differentiated HCC. Through the under-diagnosed cases of well-differentiated HCC in this study, we have got experience and increased our ability to diagnose well-differentiated HCC. Although the improvement in diagnosing well-differentiated HCC, we are still not able to make a perfect diagnosis of well-differentiated HCC, because the Liu stain alone cannot provide the complete information on the diagnosis of well-differentiated HCC. Boer *et al*[6] suggested that FNA cytodiagnosis of well-differentiated HCC should pay close attention to the architectural features and reticulin stain in both smears and cell blocks. The reticular pattern is an important criterion in diagnosing malignancy[7,8]. Without cell block and reticulin stain, the reticular pattern in aspiration cytological smear is hard to identify. Since the architecture features in Liu stain cytology show a poor reticular pattern, it was difficult to make a differentiation between the well-differentiated HCC and benign lesion in our 7 cases. In this study, although we made a correct diagnosis of 11 well-differentiated HCCs by quick cytodiagnosis, Liu-stain quick cytodiagnosis is not sufficient in diagnosing well-differentiated HCC.

Under ultrasound-guidance, FNA may correctly get specimens from small lesions less than 1 cm in diameter (Figure 1). FNA is also safer than core biopsy in getting specimens from liver to which it is difficult to approach. The Liu stain is a very simple and quick method in cytological study. In practice, we usually achieve one-shot aspiration to get specimens[5]. The quick Liu-stain is done immediately and the operator reads the cytological findings. If the specimen is inadequate or not informative, a second or third shot of aspiration should be done. The

conventional cytopathology preparation cannot provide the opportunity to do a second aspiration. Liu-stain quick cytodiagnosis can minimize the failure of FNA aspiration. In this study, it was as lower as 2.2% (5/232). Therefore, Liu-stain quick cytodiagnosis may avoid inadequate specimens and improve cytodiagnosis. The process of Liu stain needs no air-drying of smears, the biosafety is stable, even in infective cases.

In conclusion, Liu-stain quick cytodiagnosis is a fast, safe, convenient and effective method for hepatologists to diagnose liver tumors and may provide a quick decision in HCC treatment. However, Liu-stain quick cytodiagnosis had its limitation in diagnosing well-differentiated HCC.

APPENDIX

Liu stain solution (Figure 4).

COMMENTS

Innovations and breakthroughs

US-FNA cytodiagnosis of liver tumors has been confirmed, US-FNA Liu-stain cytodiagnosis makes a correct and quick cytodiagnosis of liver tumors.

Applications

Diagnosis of liver malignancy by quick cytodiagnosis should be performed as early as possible. When the specimen is inadequate or not informative, subsequent US-FNA aspiration should be performed to avoid the failure of cytodiagnosis.

Peer review

The manuscript is interesting and could help obtain more informative histological data without loosing time and significant impact in clinical hepatology.

REFERENCES

1 **Hertz G**, Reddy VB, Green L, Spitz D, Massarani-Wafai R, Selvaggi SM, Kluskens L, Gattuso P. Fine-needle aspiration biopsy of the liver: a multicenter study of 602 radiologically guided FNA. *Diagn Cytopathol* 2000; **23**: 326-328

2 **Chiu KW**, Chang-Chien CS, Chen L, Liaw YF. Ultrasonically-guided needle aspiration with preparation of cell blocks in the diagnosis of liver tumors. *Hepatogastroenterology* 1994; **41**: 30-33

3 **Tsai YY**, Lu SN, Changchien CS, Wang JH, Lee CM, Eng HL, Chang WC. Combined cytologic and histologic diagnosis of liver tumors via one-shot aspiration. *Hepatogastroenterology* 2002; **49**: 644-647

4 **Kuo FY**, Chen WJ, Lu SN, Wang JH, Eng HL. Fine needle aspiration cytodiagnosis of liver tumors. *Acta Cytol* 2004; **48**: 142-148

5 **Tsou MH**, Lin YM, Lin KJ, Ko JS, Wu ML. Fine needle aspiration cytodiagnosis of liver tumors. Results obtained with Riu's stain. *Acta Cytol* 1998; **42**: 1359-1364

6 **de Boer WB**, Segal A, Frost FA, Sterrett GF. Cytodiagnosis of well differentiated hepatocellular carcinoma: can indeterminate diagnoses be reduced? *Cancer* 1999; **87**: 270-277

7 **Zainol H**, Sumithran E. Combined cytological and histological diagnosis of hepatocellular carcinoma in ultrasonically guided fine needle biopsy specimens. *Histopathology* 1993; **22**: 581-586

8 **Rapaccini GL**, Pompili M, Caturelli E, Fusilli S, Trombino C, Gomes V, Squillante MM, Castelvetere M, Aliotta A, Grattagliano A. Ultrasound-guided fine-needle biopsy of hepatocellular carcinoma: comparison between smear cytology and microhistology. *Am J Gastroenterol* 1994; **89**: 898-902

S- Editor Liu Y **L- Editor** Wang XL **E- Editor** Bi L

PO Box 2345, Beijing 100023, China
www.wjgnet.com
wjg@wjgnet.com

World J Gastroenterol 2007 January 21; 13(3): 452-456
World Journal of Gastroenterology ISSN 1007-9327

RAPID COMMUNICATION

Short-term application of low-dose growth hormone in surgical patients: Effects on nitrogen balance and blood glucose

Ming-Ming Zhang, Xiao-Ting Wu, Yong Zhou, Kun Qian, Ya-Min Zheng

Ming-Ming Zhang, Xiao-Ting Wu, Yong Zhou, Kun Qian, Department of General Surgery, West China Hospital, Sichuan University, Chengdu 610041, Sichuan Province, China
Ya-Min Zheng, Department of General Surgery, Xuanwu Hospital, Capital University of Medical Sciences, Beijing 100053, China
Correspondence to: Professor Xiao-Ting Wu, Department of General Surgery, West China Hospital, Sichuan University, 37 Guo Xue Rd., Chengdu 610041, Sichuan Province, China. wawjwj_100@163.com
Telephone: +86-28-66839171 Fax: +86-28-85422483
Received: 2006-10-14 Accepted: 2006-12-09

Abstract

AIM: To investigate the effectiveness and safety of recombinant human growth hormone (rhGH) in postoperative patients.

METHODS: A total of 48 consecutive patients undergoing abdominal operations were randomized to receive either subcutaneous rhGH (0.15 IU/kg) or placebo (menstruum) injections daily for 7 d after surgery. The two groups had similar nutritional intake. Blood samples for serum fibronectin, albumin, prealbumin, transferrin and the total lymphocyte count, as well as glucose levels were collected to study the rhGH effect. Basal laboratory evaluation, and nutritional status were estimated on d 1 before as baseline and d 3 and 10 after operation using standard laboratory techniques. Nitrogen balance was measured from d 3 to 9 after operation.

RESULTS: The cumulative nitrogen balance was significantly improved in rhGH group compared with the placebo group (11.37 ± 16.82 *vs* -9.11 ± 17.52, $P = 0.0003$). Serum fibronectin was also significantly higher in the rhGH group than in the placebo group (104.77 ± 19.94 *vs* 93.03 ± 16.03, $P < 0.05$), whereas changes in serum albumin, prealbumin, transferrin and total lymphocyte counts were not statistically significant. Mean blood glucose levels were significantly higher in the rhGH group from d 3 to 6 after operation.

CONCLUSION: If blood glucose can be controlled, low-dose growth hormone together with hypocaloric nutrition is effective on improving positive nitrogen balance and protein conservation and safe is in postoperative patients.

Key words: Growth hormone; Nutritional support; Abdominal surgery; Hyperglycemia; Nitrogen balance

Zhang MM, Wu XT, Zhou Y, Qian K, Zheng YM. Short-term application of low-dose growth hormone in surgical patients: Effects on nitrogen balance and blood glucose. *World J Gastroenterol* 2007; 13(3): 452-456

http://www.wjgnet.com/1007-9327/13/452.asp

INTRODUCTION

Patients undergoing abdominal surgery often suffer severe trauma or infections associated with the catabolic responses[1], which cannot be prevented with conventional parenteral or enteral nutritional formulas[2,3]. Administration of recombinant human growth hormone (rhGH) has been shown to significantly maintain the nitrogen balance in surgery patients receiving either parenteral or enteral nutrition[4-7]. However, it is still uncertain whether short-term treatment with low-dose rhGH is effective as well and whether its effect on blood glucose will lead to more severe outcomes. Furthermore, there is a lack of well-controlled prospective clinical studies investigating the clinical value of serum proteins as nutritional assessment indexes in GH-treated patients. The objective of the present study was to evaluate the relative nitrogen and protein conservation effects associated with administration of rhGH together with hypocaloric nutritional support after elective abdominal surgery. In addition, we measured the changes in blood glucose levels, the effects of hyperglycemia caused by rhGH administration on postoperative convalescence and other adverse events during GH treatment period.

MATERIALS AND METHODS

Patients

The study was conducted in accordance with the guidelines for Good Clinical Practice and the provisions of the Declaration of Helsinki in 1995 as revised in Edinburgh 2000, and approved by the Ethical Review Committee of West China Hospital. Only those who consented to participate after explanation of the objectives and the protocol were included in the study. Signed, informed consent was obtained from all patients and their close relatives.

Forty-eight adult patients were enrolled in the study, and all met the following criteria: undergoing an elective

abdominal operation; aged 18-75 years; willing and able to comprehend the protocol and give written informed consent. Exclusion criteria were as follows: severe bacterial infection, liver and renal dysfunction, previous or current treatment with corticosteroids, diabetic mellitus or fasting glucose levels greater than or equal to 7.0 mmol/L, metabolic diseases, gestation, severe malnutrition (serum albumin < 21 g/L), tumor recrudescence or metastasis.

Study design

The study was a randomized**,** prospective, double-blind, placebo-controlled clinical trial. Eligible patients were arranged randomly as follows: rhGH or placebo group with each group including 24 patients. The randomization codes were prepared with the random number table according to the design of a computer. Patients, surgeons and nursing staff members remained blind to the allocation status of the study drugs throughout the experimentation.

After the operation, all patients received continuous combined intravenous or/and enteral nutrition. The daily total caloric requirement was 20 kcal/kg and total nitrogen requirement was 140 mg of nitrogen/kg. Parenteral nutrition (PN) solution was prepared aseptically using commercially available products, including vitamins, trace elements and electrolytes (Addamel, Vitalipid, Soluvit and Glycophos; Fresenius Kabi Deutschiand GmbH, Bad Homberg, Germany). Amino acid injections were provided as Novamin 8.5% and 11.4% (Fresenius Kabi Deutschiand GmbH). Energy calories were provided with glucose and fat emulsion injections (glucose 50% and Lipovenos® MCT 20%; Fresenius Kabi Deutschiand GmbH). All the nutrients were given in an all-in-one bag. Enteral nutrition (EN) emulsion (Fresubin®, Fresenius Kabi Deutschiand GmbH) was provided orally or *via* a nasogastric tube with a continuous perfusion pump.

Postoperatively, patients received general intravenous infusions with only glucose on d 1; PN provided only half of total caloric and nitrogen requirement on d 2 and all of total requirement on d 3; on d 4, PN provided 2/3 of total requirement and EN provided another 1/3; on d 5, PN provided 1/3 of total requirement and EN provided 2/3; only EN emulsion was given from d 6 to 9.

From d 3 to 10 post operation, patients were randomly assigned to receive identical-looking treatments consisting of either rhGH (JINTROPIN®, 0.15 IU/kg) or menstruum injections (1 mL, consisting of glycin, mannitol, lactose and sodium bicarbonate) subcutaneously once daily. rhGH and placebo were provided by GeneScience Pharmaceuticals Co. Ltd, Changchun, China.

Laboratory and nutritional condition measurements

Blood samples were drawn from each patient before operation to measure baseline values and on d 3 and 10 after operation to study the rhGH effect. Complete blood counts were estimated by the XE-2100 (Sysmex, Kobe, Japan). Plasma glucose, serum urea nitrogen, creatinine, bilirubin, alanine aminotransferase, alkaline phosphatase, total protein, albumin and electrolytes were estimated by an Olympus AU5400 Autoanalyser (Olympus, Tokyo, Japan). Serum fibronectin, prealbumin and transferrin were estimated by immunoturbidimetry and radioimmunoassay methods, respectively. Body weight were confirmed using qualified body weight scales before operation and on postoperative d 3 and 10.

Table 1 Baseline characteristics of patients (mean ± SD)

Variable	Placebo (n = 24)	rhGH (n = 24)	P
Age (yr)	58.50 ± 9.35	59.08 ± 10.93	0.789
Range	39-75	35-74	
Sex (female/male)	11/13	9/15	0.558
Weight (kg)	57.90 ± 8.42	56.19 ± 11.83	0.567
Height (cm)	162.42 ± 6.92	162.88 ± 7.16	0.823
Sepsis score	0.79 ± 0.98	0.67 ± 0.87	0.742
Operation position, n (%)			
Resection of stomach	6 (25)	5 (20.8)	0.297
Resection of colon	5 (20.8)	7 (29.2)	
Resection of rectum	12 (50)	9 (37.5)	
Others	1 (4.2)	3 (12.5)	

Nitrogen balance

Daily nitrogen input was assumed to be the nitrogen contents of PN and/or EN solution given. Daily nitrogen loss was assessed by collecting 24-h output and measuring the nitrogen content in feces, urine and gastric juice. Nitrogen loss through the surgical drains was also included. Daily nitrogen balance was calculated by subtracting daily nitrogen output from daily nitrogen input. Accumulated nitrogen balance was calculated by subtracting 7 d nitrogen output from 7 d nitrogen input. Nitrogen contents of samples were determined by the micro-Kjeldahl procedure[8].

Monitoring of adverse effects

All outcome and adverse effect parameters were monitored, especially GH-related adverse effects such as hyperglycemia, hypertension, edema, tetter, arthritis, and hand stiffness. Routine clinical evaluation included breath rate, pulse rate, temperatures and blood pressures. All infection, sepsis and deaths and their causes were recorded.

Statistical analysis

All data were assessed for normality of distribution and equality of variance. Student's t test and ANOVA were used to compare normally distributed data. Data are presented throughout as means and standard deviations (SD). Categorical data were compared using the Pearson χ^2 test or Fisher exact test. All data analysis was performed using the program SPSS 11.5 for Windows. $P < 0.05$ was considered statistically significant.

RESULTS

Patient characteristics

There were no differences between the two groups in baseline characteristics (Table 1).

Daily and accumulated nitrogen balance

Changes in daily nitrogen balance are shown in Table 2. Patients given rhGH showed decreased nitrogen excretion and increased nitrogen retention compared with patients

Table 2 Daily and accumulated nitrogen balance after operation (g)

Time after operation	rhGH (n = 24)	Placebo (n = 24)	P
D 3	0.29 ± 3.31	-0.86 ± 5.81	0.405
D 4	0.87 ± 3.23	-2.43 ± 5.60	0.016
D 5	0.87 ± 3.85	-0.94 ± 5.93	0.217
D 6	1.71 ± 3.56	-1.03 ± 3.47	0.010
D 7	2.76 ± 2.91	-1.35 ± 3.13	< 0.001
D 8	2.69 ± 2.89	-1.08 ± 3.48	< 0.001
D 9	2.18 ± 4.27	-1.36 ± 6.16	0.025
Accumulated NB (7 d)	11.37 ± 16.82	-9.11 ± 17.52	0.0003

Data presented as mean ± SD. NB: Nitrogen balance.

given the placebo during the study period. Postoperatively, daily nitrogen balance in the rhGH group was increased significantly compared with the placebo group on d 4 and from d 6 to 9 ($P < 0.05$). On d 9, the accumulated nitrogen balance in the rhGH group was significantly improved compared with the placebo group.

Nutritional condition measurement

On d 1 before and d 3 after operation, there were no significant differences between the two groups in serum albumin, transferrin, prealbumin, fibronectin and total lymphocyte counts. On postoperative d 10, mean serum fibronectin levels were significantly higher in thr rhGH group than in the placebo group. While mean serum albumin, transferrin, prealbumin levels and total lymphocyte counts were not significantly different between the two groups (Table 3). The weight change was also not significantly different between the two groups.

Adverse events

The main adverse effects seen during the study are summarized in Tables 4 and 5. Mean blood glucose levels were significantly higher in the rhGH group from d 3 to d 6 after operation (Table 4). Twenty-three patients in the rhGH group experienced hyperglycemia and 5 of these required insulin treatment (Table 5). Furthermore, 3 patients had other mild adverse events including 1 patient with edema, 1 with tetter and 1 with a fever. In the placebo group, 3 of 4 patients presenting hyperglycemia required insulin treatment. Concerning adverse events not related to the trial drug, 5 placebo-treated patients experienced mild electrolytes imbalance. There were no significant differences between the two groups in complete blood counts, liver and renal functions, body weights and the daily clinical parameters such as temperatures, blood pressures, and pulses.

Table 3 Nutritional condition measurement of two group patients

Test	D 1	D 3	D 10
Albumin (g/L)			
rhGH	40.85 ± 3.09	33.26 ± 3.82	35.16 ± 4.21
Placebo	41.19 ± 4.17	33.95 ± 3.68	35.57 ± 3.84
Transferrin (g/L)			
rhGH	2.41 ± 0.45	1.75 ± 0.44	2.15 ± 0.66
Placebo	2.51 ± 0.45	1.79 ± 0.42	2.11 ± 0.44
Prealbumin (mg/L)			
rhGH	133.90 ± 83.95	71.44 ± 46.54	105.51 ± 69.30
Placebo	164.03 ± 88.16	85.55 ± 57.87	109.99 ± 97.37
Fibronectin (mg/L)			
rhGH	97.40 ± 11.74	80.85 ± 8.13	104.77 ± 19.94[a]
Placebo	98.70 ± 20.17	83.69 ± 10.50	93.03 ± 16.03
TLC (10^9/L)			
rhGH	1.64 ± 0.60	1.03 ± 0.33	1.36 ± 0.54
Placebo	1.59 ± 0.52	1.15 ± 0.59	1.38 ± 0.46

Values are mean ± SD. TLC: Total lymphocyte count. [a]$P < 0.05$ *vs* placebo group.

DISCUSSION

Many attempts have been made to reverse the catabolic changes that occur in postoperative patients. Conventional nutrition support is unable to provide adequate nutritional supplements to increase or even maintain body proteins in hypercatabolic response conditions[9-11]. Recent studies indicated that rhGH had beneficial effects on stimulating body protein syntheses and producing nitrogen-spacing effects[6,12-14].

However, the impact of rhGH on body proteins and the change in blood glucose levels have not been previously investigated in patients receiving PN or EN following elective gastrointestinal surgeries[15-17]. In the present experiment, we observed the effect of rhGH on nitrogen balance, plasma proteins and blood glucose levels. The number of patients enrolled in the study is based on previous publications and the dosage of rhGH used is small considering its efficacy and safety[7,18,19]. rhGH treatment significantly increased the nitrogen retention of postoperative patients compared with the placebo group. Nitrogen balance began to improve from postoperative d 3 in the rhGH group, and 15 of 24 patients showed positive nitrogen balance on d 4. On d 9, 21 of 24 patients showed positive nitrogen balance in the rhGH group and the accumulated nitrogen balance was positive nitrogen balance, which was significantly different compared with the placebo group. Patients receiving only standard nutrition support were in a state of negative nitrogen balance during the whole period of the study. Our results demonstrated that administration of rhGH could result in significant anabolic effects on nitrogen balance and improve the efficiency of nutrition support.

In fact, changes of nitrogen balance may be associated with protein synthesis and breakdown[12,13,16]. The alteration in concentrations of plasma proteins reflects the metabolic responses to surgical traumas[20]. We found that serum fibronectin levels were higher in the rhGH group than in the control group after termination of treatment. This reflects a beneficial effect of rhGH on protein synthesis. However, serum transferrin, albumin, and prealbumin levels were not significantly different between the two groups. The potential reason might be that these protein levels are markedly affected by the acute-phase responses, thus they are not sufficiently sensitive and reliable in

Table 4 Comparison of blood glucose levels

Test	D 1	D 3	D 4	D 5	D 6	D 7	D 8	D 9
Glucose (mmol/L)								
rhGH	5.14 ± 0.64	6.71 ± 1.93[a]	7.17 ± 1.86[a]	8.28 ± 2.30[a]	7.68 ± 2.15[a]	7.29 ± 2.93	6.40 ± 2.00	6.20 ± 2.13
Placebo	5.26 ± 1.09	5.68 ± 1.33	5.81 ± 1.56	5.84 ± 1.48	5.95 ± 2.34	6.01 ± 2.64	5.66 ± 2.03	5.70 ± 1.89

Values are mean ± SD. [a]$P < 0.05$ *vs* placebo group.

Table 5 Main adverse events

Event	rhGH group	Placebo group
Hyperglycemia	23[a]	4
Tetter	1	0
Sepsis	0	0
Infection	2	3
Death	0	0

[a]$P < 0.05$ *vs* placebo group.

nutritional assessment[21-23].

GH given during sepsis has been thought to impair immune function and result in hyperglycemia, which may explain why acute critically ill patients do not benefit from GH treatment[24,25]. However, GH can be administrated safely after acute inflammatory response stage for elective surgery patients, especially with a low dose and temporary duration of treatment. rhGH treatment was generally well tolerated with no serious adverse events in our trial. The mortality rate in the GH-treated group was zero, confirming its safety. These results are contrary to the increase in mortality among critically ill patients treated with GH reported in two large clinical trials by Takala *et al*[24]. We hypothesize that this discrepancy might be due to the difference in study patients. In our study, the patient populations were elective surgery subjects. Moreover, rhGH given during the response to stress leads to uncontrolled systemic inflammation in Takala's study. The main adverse events of the rhGH treatment were hyperglycemia. Insulin resistance caused by rhGH plays an important role in the rise of blood glucose. Other reasons may include nutritional support and systemic inflammation syndrome[26,27]. In our test, the hyperglycemia caused by rhGH administration was mild, for which low-dose rhGH and hypocaloric nutrition may be the reason. Furthermore, the hyperglycemia could be controlled easily by insulin. Considering the difference between critically ill patients and elective surgery patients, rhGH seems to be well tolerated after operation.

Our study included 14 cancer patients in the rhGH group, so the potential tumor-promoting effect of GH must be addressed. In animal models, whether rhGH administration promotes tumor recurrence is controversial[28-30]. Several authors even concluded that GH could promote host growth selectively and inhibit tumor metastasis[31,32]. Only two trials assessed the impact of GH on tumor recurrence in humans. Based on 2632 adverse events reports, the National Cooperative Growth Study analyzed the recurrence of brain tumors in patients receiving long-term GH replacement. It was concluded that there was no evidence of increased tumor recurrence[33]. Only one study investigated the impact of short-term treatment with three different doses of GH on long-term tumor recurrence in postoperative cancer patients[34]. Thirty-five percent of rhGH-treated patients showed tumor recurrences in comparison to 44% of patients given placebo. Based on the above two studies, we believe that when complete resection and appropriate antineoplastic treatment is administered, short-term GH treatment can be given safely to cancer patients.

In conclusion, our results indicate that postoperative rhGH treatment for 7 d improves nitrogen retention and protein conservation, enhances the efficiency of nutrition support in adult patients undergoing major abdominal surgeries. rhGH also is well tolerated without clinically significant adverse effects and the blood glucose level can be well controlled. A larger trial is required to measure clinical endpoints such as infection, morbidities, mortalities and tumor recurrences.

COMMENTS

Background

Administration of recombinant human growth hormone has been shown to significantly maintain the nitrogen balance in surgery patients receiving nutritional support. However, it is still uncertain whether short-term treatment of low-dose recombinant human growth hormone (rhGH) is effective as well and whether its effect on blood glucose will lead to higher risk.

Research frontiers

Conventional nutrition support is unable to provide adequate nutritional supplements to increase or even maintain body protein under hypercatabolic response conditions. Recent studies indicated that rhGH had beneficial effects on stimulating body protein and producing nitrogen-spacing effects.

Innovations and breakthroughs

The present study confirmed that administration of rhGH together with hypocaloric nutrition support produced nitrogen conservation and protein synthesis effects after elective abdominal surgery. In addition, the changes in blood glucose levels, especially the hyperglycemia caused by rhGH administration was slight and could be controlled in GH treatment period.

Applications

Our results indicate that postoperative rhGH treatment improves nitrogen retention and protein conservation, enhances the efficiency of nutrition support in adult patients undergoing major abdominal surgery. rhGH also is well tolerated without clinically significant adverse effects and the blood glucose level can be well controlled.

Peer review

The authors assess the role of a low dose of growth hormone in postoperative nitrogen balance in patients undergoing gastrointestinal operations who also received a "hypocaloric" feeding. They also discuss the adverse effects and potential disadvantage of rhGH administration and monitor the change of blood

glucose levels. The study demonstrates that the appropriate application of rhGH is well tolerated and of great benefit to postoperative patients.

REFERENCES

1 **Hill GL**, Douglas RG, Schroeder D. Metabolic basis for the management of patients undergoing major surgery. *World J Surg* 1993; **17**: 146-153
2 **Petersson B**, Wernerman J, Waller SO, von der Decken A, Vinnars E. Elective abdominal surgery depresses muscle protein synthesis and increases subjective fatigue: effects lasting more than 30 days. *Br J Surg* 1990; **77**: 796-800
3 Perioperative total parenteral nutrition in surgical patients. The Veterans Affairs Total Parenteral Nutrition Cooperative Study Group. *N Engl J Med* 1991; **325**: 525-532
4 **Losada F**, García-Luna PP, Gómez-Cía T, Garrido M, Pereira JL, Marín F, Astorga R. Effects of human recombinant growth hormone on donor-site healing in burned adults. *World J Surg* 2002; **26**: 2-8
5 **Hammarqvist F**, Sandgren A, Andersson K, Essén P, McNurlan MA, Garlick PJ, Wernerman J. Growth hormone together with glutamine-containing total parenteral nutrition maintains muscle glutamine levels and results in a less negative nitrogen balance after surgical trauma. *Surgery* 2001; **129**: 576-586
6 **Ziegler TR**, Rombeau JL, Young LS, Fong Y, Marano M, Lowry SF, Wilmore DW. Recombinant human growth hormone enhances the metabolic efficacy of parenteral nutrition: a double-blind, randomized controlled study. *J Clin Endocrinol Metab* 1992; **74**: 865-873
7 **Jensen MB**, Kissmeyer-Nielsen P, Laurberg S. Perioperative growth hormone treatment increases nitrogen and fluid balance and results in short-term and long-term conservation of lean tissue mass. *Am J Clin Nutr* 1998; **68**: 840-846
8 **Concon JM**, Soltess D. Rapid micro Kjeldahl digestion of cereal grains and other biological materials. *Anal Biochem* 1973; **53**: 35-41
9 **Byrne TA**, Morrissey TB, Gatzen C, Benfell K, Nattakom TV, Scheltinga MR, LeBoff MS, Ziegler TR, Wilmore DW. Anabolic therapy with growth hormone accelerates protein gain in surgical patients requiring nutritional rehabilitation. *Ann Surg* 1993; **218**: 400-416; discussion 416-418
10 **Vara-Thorbeck R**, Guerrero JA, Ruiz-Requena ME, Capitán J, Rodriguez M, Rosell J, Mekinassi K, Maldonado M, Martin R. Effects of growth hormone in patients receiving total parenteral nutrition following major gastrointestinal surgery. *Hepatogastroenterology* 1992; **39**: 270-272
11 **Kolstad O**, Jenssen TG, Ingebretsen OC, Vinnars E, Revhaug A. Combination of recombinant human growth hormone and glutamine-enriched total parenteral nutrition to surgical patients: effects on circulating amino acids. *Clin Nutr* 2001; **20**: 503-510
12 **Nørrelund H**, Nair KS, Jørgensen JO, Christiansen JS, Møller N. The protein-retaining effects of growth hormone during fasting involve inhibition of muscle-protein breakdown. *Diabetes* 2001; **50**: 96-104
13 **Nørrelund H**, Møller N, Nair KS, Christiansen JS, Jørgensen JO. Continuation of growth hormone (GH) substitution during fasting in GH-deficient patients decreases urea excretion and conserves protein synthesis. *J Clin Endocrinol Metab* 2001; **86**: 3120-3129
14 **Carrel AL**, Allen DB. Effects of growth hormone on adipose tissue. *J Pediatr Endocrinol Metab* 2000; **13** Suppl 2: 1003-1009
15 **Kissmeyer-Nielsen P**, Jensen MB, Laurberg S. Perioperative growth hormone treatment and functional outcome after major abdominal surgery: a randomized, double-blind, controlled study. *Ann Surg* 1999; **229**: 298-302
16 **Petersen SR**, Holaday NJ, Jeevanandam M. Enhancement of protein synthesis efficiency in parenterally fed trauma victims by adjuvant recombinant human growth hormone. *J Trauma* 1994; **36**: 726-733
17 **Biolo G**, Iscra F, Bosutti A, Toigo G, Ciocchi B, Geatti O, Gullo A, Guarnieri G. Growth hormone decreases muscle glutamine production and stimulates protein synthesis in hypercatabolic patients. *Am J Physiol Endocrinol Metab* 2000; **279**: E323-E332
18 **Vara-Thorbeck R**, Guerrero JA, Rosell J, Ruiz-Requena E, Capitán JM. Exogenous growth hormone: effects on the catabolic response to surgically produced acute stress and on postoperative immune function. *World J Surg* 1993; **17**: 530-537; discussion 537-538
19 **Chu LW**, Lam KS, Tam SC, Hu WJ, Hui SL, Chiu A, Chiu KC, Ng P. A randomized controlled trial of low-dose recombinant human growth hormone in the treatment of malnourished elderly medical patients. *J Clin Endocrinol Metab* 2001; **86**: 1913-1920
20 **Petersen SR**, Jeevanandam M, Shahbazian LM, Holaday NJ. Reprioritization of liver protein synthesis resulting from recombinant human growth hormone supplementation in parenterally fed trauma patients: the effect of growth hormone on the acute-phase response. *J Trauma* 1997; **42**: 987-995; discussion 995-996
21 **Muscaritoli M**, Conversano L, Cangiano C, Capria S, Laviano A, Arcese W, Rossi Fanelli F. Biochemical indices may not accurately reflect changes in nutritional status after allogeneic bone marrow transplantation. *Nutrition* 1995; **11**: 433-436
22 **Phang PT**, Aeberhardt LE. Effect of nutritional support on routine nutrition assessment parameters and body composition in intensive care unit patients. *Can J Surg* 1996; **39**: 212-219
23 **Jones CH**, Newstead CG, Will EJ, Smye SW, Davison AM. Assessment of nutritional status in CAPD patients: serum albumin is not a useful measure. *Nephrol Dial Transplant* 1997; **12**: 1406-1413
24 **Takala J**, Ruokonen E, Webster NR, Nielsen MS, Zandstra DF, Vundelinckx G, Hinds CJ. Increased mortality associated with growth hormone treatment in critically ill adults. *N Engl J Med* 1999; **341**: 785-792
25 **van den Berghe G**, Wouters P, Weekers F, Verwaest C, Bruyninckx F, Schetz M, Vlasselaers D, Ferdinande P, Lauwers P, Bouillon R. Intensive insulin therapy in critically ill patients. *N Engl J Med* 2001; **345**: 1359-1367
26 **Valera A**, Rodriguez-Gil JE, Yun JS, McGrane MM, Hanson RW, Bosch F. Glucose metabolism in transgenic mice containing a chimeric P-enolpyruvate carboxykinase/bovine growth hormone gene. *FASEB J* 1993; **7**: 791-800
27 **Ikeda A**, Chang KT, Matsumoto Y, Furuhata Y, Nishihara M, Sasaki F, Takahashi M. Obesity and insulin resistance in human growth hormone transgenic rats. *Endocrinology* 1998; **139**: 3057-3063
28 **Ng EH**, Rock CS, Lazarus D, Staiano-Coico L, Fischer E, Moldawer LL, Lowry SF. Impact of exogenous growth hormone on host preservation and tumor cell-cycle distribution in a rat sarcoma model. *J Surg Res* 1991; **51**: 99-105
29 **Wolf RF**, Ng B, Weksler B, Burt M, Brennan MF. Effect of growth hormone on tumor and host in an animal model. *Ann Surg Oncol* 1994; **1**: 314-320
30 **Akaza H**, Matsuki K, Matsushima H, Koiso K, Aso Y. Stimulatory effects of growth hormone on rat bladder carcinogenesis. *Cancer* 1991; **68**: 2418-2421
31 **Torosian MH**. Growth hormone and prostate cancer growth and metastasis in tumor-bearing animals. *J Pediatr Endocrinol* 1993; **6**: 93-97
32 **Bartlett DL**, Charland S, Torosian MH. Growth hormone, insulin, and somatostatin therapy of cancer cachexia. *Cancer* 1994; **73**: 1499-1504
33 **Maneatis T**, Baptista J, Connelly K, Blethen S. Growth hormone safety update from the National Cooperative Growth Study. *J Pediatr Endocrinol Metab* 2000; **13** Suppl 2: 1035-1044
34 **Tacke J**, Bolder U, Herrmann A, Berger G, Jauch KW. Long-term risk of gastrointestinal tumor recurrence after postoperative treatment with recombinant human growth hormone. *JPEN J Parenter Enteral Nutr* 2000; **24**: 140-144

S- Editor Wang GP **L- Editor** Zhu LH **E- Editor** Bi L

PO Box 2345, Beijing 100023, China
www.wjgnet.com
wjg@wjgnet.com

World J Gastroenterol 2007 January 21; 13(3): 457-461
World Journal of Gastroenterology ISSN 1007-9327

RAPID COMMUNICATION

Effect of non-anticoagulant N-desulfated heparin on expression of vascular endothelial growth factor, angiogenesis and metastasis of orthotopic implantation of human gastric carcinoma

Jin-Lian Chen, Jing Hong, Jin-Lai Lu, Ming-Xiang Chen, Wei-Xiong Chen, Jin-Shui Zhu, Ni-Wei Chen, Guo-Qiang Chen, Jian-Guo Geng

Jin-Lian Chen, Jing Hong, Jin-Lai Lu, Ming-Xiang Chen, Wei-Xiong Chen, Jin-Shui Zhu, Ni-Wei Chen, Department of Gastroenterology, Shanghai Sixth People's Hospital, Shanghai Jiaotong University, Shanghai 200233, China
Guo-Qiang Chen, Shanghai Laboratory Animal Center, Chinese Academy of Sciences, Shanghai 200031, China
Jian-Guo Geng, Shanghai Institute of Cell Biology, Chinese Academy of Sciences, Shanghai 200031, China
Supported by the Scientific Foundation of Shanghai Public Health Administration, No. 034045
Correspondence to: Jin-Lian Chen, Department of Gastroenterology, Shanghai Sixth People's Hospital, Shanghai Jiaotong University, Shanghai 200233, China. wqq-021002@163.com
Telephone: +86-21-64369181 Fax: +86-21-64369181
Received: 2006-10-13 Accepted: 2006-12-04

Abstract

AIM: To investigate the effect of N-desulfated heparin on tumor metastasis and angiogenesis, and expression of vascular endothelial growth factor (VEGF) of orthotopic implantation of human gastric carcinoma in male severe combined immune deficiency (SCID) mice.

METHODS: Human gastric cancer SGC-7901 cells were orthotopically implanted into the stomach of SCID mice. The mice were randomly divided into normal saline group and N-desulfated heparin group. One week after operation, the mice in N-desulfated heparin group received i.v. injections of N-desulfated heparin (Shanghai Institute of Cell Biology, Chinese Academy of Sciences, 10 mg/kg.d) twice weekly for 3 wk. The mice in normal saline group received i.v. injections of normal saline (100 μL) twice weekly for 3 wk. The mice were sacrificed six weeks after implantation. Tumor metastasis was evaluated histologically for metastasis under microscope. Intratumoral microvessel density (MVD) and VEGF expression were evaluated immuohistochemically. VEGF mRNA expression in gastric tissue of SCID mice was detected by real time PCR.

RESULTS: The tumor metastasis rate was 80% in normal saline group and 20% in N-desulfated heparin group ($P < 0.05$). MVD was 8.0 ± 3.1 in normal saline group and 4.3 ± 1.8 in N-desulfated heparin group ($P < 0.05$). VEGF positive immunostaining was found in cytoplasm of cancer cells. The rate of VEGF positive expression was higher in normal saline group than in N-desulfated heparin treated group (90% *vs* 20%, $P < 0.05$). VEGF mRNA expression was significantly inhibited by N-desulfated heparin and was higher in normal saline group than in N-desulfated heparin group (Ct value 19.51 ± 1.01 *vs* 22.55 ± 1.36, $P < 0.05$). N-desulfated heparin significantly inhibited the expression of VEGF mRNA in cancer cells. No bleeding occurred in N-desulfated heparin group.

CONCLUSION: N-desulfated heparin can inhibit metastasis of gastric cancer by suppressing tumor VEGF expression and tumor angiogenesis, but has no obvious anticoagulant activity.

Key words: N-desulfated heparin; Gastric carcinoma; Metastasis; Tumor angiogenesis; Vascular endothelial growth factor

Chen JL, Hong J, Lu JL, Chen MX, Chen WX, Zhu JS, Chen NW, Chen GQ, Geng JG. Effect of non-anticoagulant N-desulfated heparin on expression of vascular endothelial growth factor, angiogenesis and metastasis of orthotopic implantation of human gastric carcinoma. *World J Gastroenterol* 2007; 13(3): 457-461

http://www.wjgnet.com/1007-9327/13/457.asp

INTRODUCTION

Gastric carcinoma is one of the most frequent malignancies and is the leading cause of cancer deaths in China. Up to now, there is no effective treatment for metastasis of tumor. Recent studies showed that angiogenesis plays a crucial role in tumor growth and metastasis. The regulation of angiogenesis is balanced by proangiogenic and antiangiogenic factors and is associated with prognosis of patients with tumors. Inhibition of angiogenesis can control tumor metastasis and improve the prognosis[1-4]. Vascular endothelial growth factor (VEGF) and fibroblast growth factor-2 (FGF-2) are the main

factors promoting angiogenesis, and anti-VEGF therapy is effective in inhibiting angiogenesis and metastasis of tumor[5-7].

Heparin, a highly sulfated proteoglan, has been extensively used as an anticoagulant drug for a long time. Aside from its anticoagulant action, heparin binds to various growth factors, cytokines, and extracellular proteins and consequently is able to affect migration of cancer cells and angiogenesis in tumors. *In vitro* study[8] indicates that heparin can inhibit VEGF and FGF-2-induced proliferation of vascular endothelial cells and vascular formation, while *in vivo* study[9] has demonstrated that heparin has antimetastatic activity. However, clinical use of heparin in treatment of tumor is limited by its strong anticoagulant activity, which may cause severe bleeding complications. Chemically modified heparin shows a significantly reduced anticoagulant activity and enhanced ability to interact with FGF, VEGF and hepatocyte growth factor, which are known to stimulate angiogenesis[10]. In this study, we investigated the effect of N-desulfated heparin on tumor metastasis in mouse models of human gastric cancer constructed by orthotopic implantation of histologically intact tumor tissue.

MATERIALS AND METHODS

Materials

Goat anti-human CD34 antibody and goat anti-human VEGF antibody were obtained from Santa Cruz Biotechnical Company. VEGF probe for real time PCR was provided by Daan Gene Company of Zhongshan University.

Animal model

Male severe combined immune deficiency (SCID) mice were obtained from Shanghai Experimental Animal Center of Chinese Academy of Sciences. Animals used were 6 wk old and weighed 20-25 g. Human gastric cancer SGC-7901 (Shanghai Cancer Institute), a poorly-differentiated adenocarcinoma line, was originally derived from a primary tumor and maintained by passage in the subcutis of nude mice. Animal models were made using orthotopic implantation of histologically intact tissue of human gastric carcinoma[11]. Tumors were resected aseptically. Necrotic tissues were cut and the remaining healthy tumor tissues were scissor minced into pieces (about 5 mm × 7 mm in diameter) in Hank's balanced salt solution. Each tumor piece was weighed and adjusted to be 150 mg. Mice were anesthetized with 4.3% trichloraldehyde hydrate. An incision was made through the left upper abdominal pararectal line. Then peritoneal cavity was carefully exposed and a part of serosal membrane in the middle of the greater curvature of stomach was mechanically injured using scissors. A tumor piece of 150 mg was fixed on each injured site of the serosal surface. The stomach was returned to the peritoneal cavity, and the abdominal wall and skin were closed.

After metastatic models were made, the mice were randomly divided into N-desulfated heparin group (n = 10) and normal saline group (n = 10). One week after operation, the mice in N-desulfated heparin group received i.v. injections of N-desulfated heparin (Shanghai Institute of Cell Biology, Chinese Academy of Sciences, 10 mg/kg.d) twice weekly for 3 wk. The mice in normal saline group received i.v. injections of normal saline (100 μL) twice weekly for 3 wk. The mice were weighed twice weekly.

Sample collection and pathological examination

All animals were sacrificed 6 wk after implantation. An incision was made through the abdominal wall, and then peritoneal cavity was carefully exposed. Tumors growing on the stomach wall were removed and fixed in 10% formalin, and processed for routine paraffin embedding. Tissues from all organs and lymph nodes were collected and fixed in 10% formalin, and processed for routine paraffin embedding after careful macroscopic examination. Four-micron-thick sections were stained with hematoxylin and eosin, and evaluated histologically for liver metastasis or lymph node metastasis or other organ metastasis under microscope.

Mean microvascular density of tumor (MVD)

Immunostaining was performed using a labeled streptavidin biotin method. Four-micron-thick sections were deparaffined in xylene and rehydrated with graded alcohol. Immunohistochemical staining was carried out to detect CD34 expression following the manufacturer's protocol. The concentration of anti-CD34 antibody was 1:300. MVD (CD34-positive microvessels) was calculated under 200 fold microscope. The modified Weidner's method was used for the evaluation of MVD according to CD34 endothelial cell immunostaining. For the microvessel counting, positive stainings for MVD in 5 most highly vascularized areas in each section were counted in 200 × fields. MVD was expressed as average of the microvessel count in the areas.

Detection of VEGF protein expression

Immunostaining was performed using a labeled streptavidin biotin method. Four-micron-thick sections were deparaffined in xylene and rehydrated with graded alcohol. Immunohistochemical staining was carried out to detect VEGF expression following the manufacturer's protocol. The concentration of anti-VEGF antibody was 1:60. Positive cells under 10% were defined as positive +, over 10% as positive ++. Positive expression was defined as positive + or positive ++. VEGF primers and probe used are VEGF f: GTTCGAGGAAAGGGAAAGGGTC, VEGF r: GCGAGTCTGTGTTTTTGCAGGA, VEGF probe: AGCGCAAGAAATCCCGGTTTAAATC.

Detection of VEGF mRNA expression

VEGF RNA was isolated by method of Trizol. Synthesis of the first strand cDNA was performed according to the instructions delivered with reverse transcription kit, using human VEGF antisense strand primers and reverse transcriptase. After 1 h incubation at 37℃, samples were heat inactivated for 3 min at 95℃ and kept at -80℃ until use.

Aliquots of 5 μL of cDNA were amplified in a final

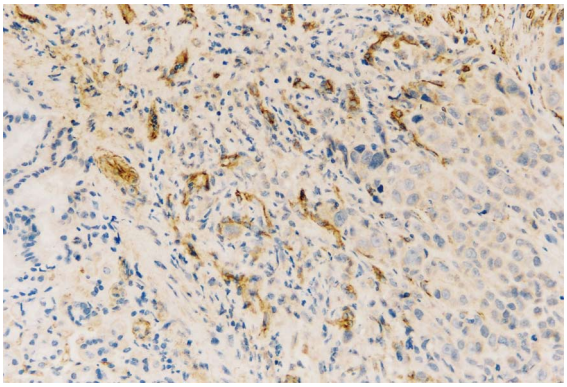

Figure 1 CD34 expression in intratumoral endothelium of gastric cancer × 200.

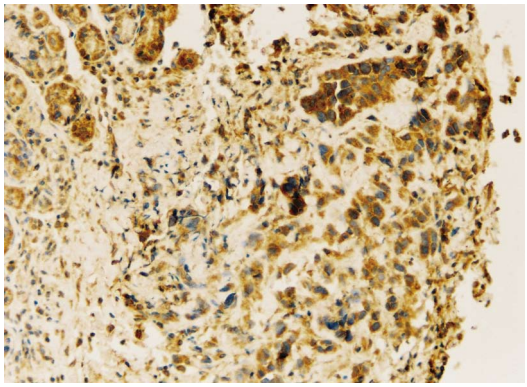

Figure 2 VEGF positive immunostaining in cytoplasm of gastric cancer cells × 200.

Table 1 Effect of N-desulfated heparin on VEGF expression in gastric cancer (mean ± SD)

Groups	*n*	-	+	++	Positive rate (%)
Normal saline group	10	1	2	7	90
N-desulfated heparin group	10	8	1	1	20[a]

[a]$P < 0.05$ *vs* normal salt group.

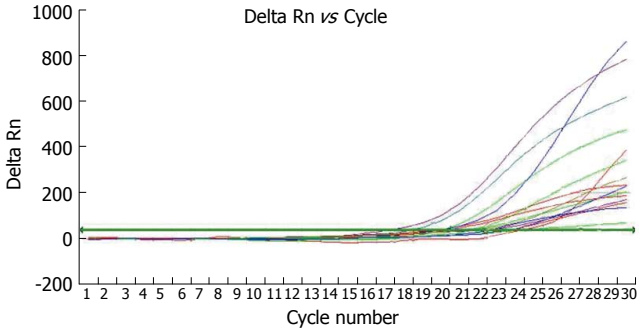

Figure 3 VEGF mRNA expression in normal saline and N-desulfated heparin treated mice.

volume of 50 μL using PCR buffer at the presence of 1 μL of Taq DNA polymerase and 0.5 μL of VEGF probe. Samples were amplified at 93℃ for 2 min, at 93℃ for 0.5 min and at 55℃ for 1min followed by 40 cycles. Real time PCR was carried out in an automated real time PCR cycler (American ABI 7000).

Statistical analysis

All data were expressed as mean ± SD. Student's *t* test and χ^2 precise method were used to determine changes in different groups. $P < 0.05$ was considered statistically significant.

RESULTS

Inhibition of N-desulfated heparin on metastasis of human gastric cancer

All mice developed localized tumors at the implanted site which were poorly-differentiated adenocarcinomas under microscope. Tumor growth did not differ significantly between the animals treated with normal saline or with N-desulfated heparin. Of the 10 animals treated with normal saline, 8 developed metastatic tumors in regional lymph nodes, 6 in liver, and 6 in other organs. However, after the mice were treated with N-desulfated heparin for 3 wk, metastasis of tumor was inhibited significantly. Of the 10 animals treated with N-desulfated heparin, 2 developed metastatic tumors in liver. The metastatic rate was higher in mice treated with normal saline than in those treated with N-desulfated heparin (80% *vs* 20%, $P < 0.05$).

N-desulfated heparin had no significant effect on body changes in SCID mice. No bleeding complications were found in N-desulfated heparin group.

Effect of N-desulfated heparin on MVD

In normal saline-treated mice, many CD34 positively stained vessels were diffusely located and formed tube-like structures in tumor (Figure 1). However, they were almost absent in N-desulfated heparin- treated mice. The MVD was significantly lower in N-desulfated heparin-treated mice than in normal saline-treated mice (4.3 ± 1.8 *vs* 8.0 ± 3.1, $P < 0.05$).

Effect of N-desulfated heparin on VEGF protein expression

Under microscope, VEGF positive immunostaining was found in cytoplasm of cancer cells (Figure 2). The rate of VEGF positive expression was higher in normal saline group than in N-desulfated heparin group ($P < 0.05$, Table 1).

Effect of N-desulfated heparin on VEGF mRNA expression

VEGF mRNA expression in gastric tissue of SCID mice detected by real time PCR was higher in normal saline group than in N-desulfated heparin group (Ct value 19.51 ± 1.01 *vs* 22.55 ± 1.36, $P < 0.05$) (Figure 3).

DISCUSSION

Recent studies showed that angiogenesis is a critical determinant of solid tumor metastasis, and antiangiogenic therapy plays an important role in improving prognosis of patients with gastric carcinoma[12-14]. It was reported that low molecular weight heparin has significantly-

reduced anticoagulant activity and enhanced ability to bind to FGF-2 and VEGF, thus inhibiting angiogenesis of tumor[15].

N-desulfated heparin, a modified heparin, is known to have more significantly-reduced anticoagulant activity (1/76 of heparin) than O-desulfated heparin (5%-30% of heparin) or N-acetylated heparin (10% of heparin)[16]. There is no report so far on the effect of N-desulfated heparin on tumor metastasis. Therefore, the effect of N-desulfated heparin on tumor metastasis, angiogenesis and VEGF expression was observed in mouse model of orthotopic implantation of human gastric carcinoma tissue.

In the present study, tumor metastasis was inhibited significantly by N-desulfated heparin. Szende *et al*[17] found that fraxiparine has a significant effect on lung metastases, while heparin does not influence metastasis. These data suggest that low molecular heparin may be of antimetastatic activity[18]. Kragh *et al*[19] reported that non-anticoagulant heparin can inhibit tumor metastasis.

To evaluate the effect of N-desulfated heparin on angiogenesis, immunohistochemical staining of CD34 in tumors was carried out. The results showed that N-desulfated heparin significantly inhibited angiogenesis in these tumors. Mousa *et al*[20] have demonstrated anti-angiogenic activity of the low molecular weight heparin, tinzaparin. Naggi *et al*[10] reported that N-acetylatedand and glycol-split heparins are potential antiangiogenic and antimetastatic agents which are more effective than unmodified heparin, suggesting that N-desulfated heparin can inhibit tumor metastasis by inhibiting angiogenesis.

In the present study, the rate of VEGF positive expression was higher in normal saline group than in N-desulfated heparin group and VEGF mRNA expression was higher in normal saline group than in N-desulfated heparin group, demonstrating that N-desulfated heparin can significantly inhibit the expression of VEGF in cancer cells. Kakeji *et al*[21] showed that VEGF is expressed in early and advanced gastric cancer. Multivariate analysis has revealed that VEGF is an independent prognostic factor and an independent risk factor for liver metastasis. Fondevila *et al*[22] demonstrated that VEGF expression is an independent predictor of tumor recurrence and survival following curative resection of gastric cancer. Pisano *et al*[23] showed that undersulfated, low-molecular-weight glycol-split heparin may be an antiangiogenic VEGF antagonist. In the present study, hemorrhage was never observed in N-desulfated heparin treated mice, suggesting that N-desulfated heparin has no obvious anticoagulant activity.

In conclusion, VEGF produced by cancer cells is an angiogenic factor in human cancer tissue and plays an important role in tumor metastasis. N-desulfated heparin inhibits tumor metastasis by inhibiting expression of VEGF and angiogenesis and can be used in the treatment of tumor metastasis.

REFERENCES

1 **Klerk CP**, Smorenburg SM, Otten HM, Lensing AW, Prins MH, Piovella F, Prandoni P, Bos MM, Richel DJ, van Tienhoven G, Büller HR. The effect of low molecular weight heparin on survival in patients with advanced malignancy. *J Clin Oncol* 2005; **23**: 2130-2135

2 **Castelli R**, Porro F, Tarsia P. The heparins and cancer: review of clinical trials and biological properties. *Vasc Med* 2004; **9**: 205-213

3 **Shinkaruk S**, Bayle M, Laïn G, Déléris G. Vascular endothelial cell growth factor (VEGF), an emerging target for cancer chemotherapy. *Curr Med Chem Anticancer Agents* 2003; **3**: 95-117

4 **Tsujitani S**, Saito H, Maeta Y, Yamaguchi K, Tatebe S, Kondo A, Kaibara N. Neoangiogenesis in patients with gastric carcinoma in relation to the expression of vascular endothelial growth factor and thymidine phosphorylase. *Anticancer Res* 2004; **24**: 1853-1859

5 **Reinmuth N**, Parikh AA, Ahmad SA, Liu W, Stoeltzing O, Fan F, Takeda A, Akagi M, Ellis LM. Biology of angiogenesis in tumors of the gastrointestinal tract. *Microsc Res Tech* 2003; **60**: 199-207

6 **Petralia GA**, Lemoine NR, Kakkar AK. Mechanisms of disease: the impact of antithrombotic therapy in cancer patients. *Nat Clin Pract Oncol* 2005; **2**: 356-363

7 **Jung YD**, Mansfield PF, Akagi M, Takeda A, Liu W, Bucana CD, Hicklin DJ, Ellis LM. Effects of combination anti-vascular endothelial growth factor receptor and anti-epidermal growth factor receptor therapies on the growth of gastric cancer in a nude mouse model. *Eur J Cancer* 2002; **38**: 1133-1140

8 **Tóvári J**, Bereczky B, Gilly R, Skopál J, Vágó A, Tímár J. Heparin inhibits metastatization of experimental melanoma. *Magy Onkol* 2004; **48**: 235-241

9 **Bobek V**, Kovarík J. Antitumor and antimetastatic effect of warfarin and heparins. *Biomed Pharmacother* 2004; **58**: 213-219

10 **Naggi A**, Casu B, Perez M, Torri G, Cassinelli G, Penco S, Pisano C, Giannini G, Ishai-Michaeli R, Vlodavsky I. Modulation of the heparanase-inhibiting activity of heparin through selective desulfation, graded N-acetylation, and glycol splitting. *J Biol Chem* 2005; **280**: 12103-12113

11 **Chen JL**, Chen WX, Zhu JS, Chen NW, Zhou T, Yao M, Zhang DQ, Wu YL. Effect of P-selectin monoclonal antibody on metastasis of gastric cancer and immune function. *World J Gastroenterol* 2003; **9**: 1607-1610

12 **Mousa SA**. Low-molecular-weight heparin in thrombosis and cancer. *Semin Thromb Hemost* 2004; **30** Suppl 1: 25-30

13 **Zacharski LR**. Anticoagulants in cancer treatment: malignancy as a solid phase coagulopathy. *Cancer Lett* 2002; **186**: 1-9

14 **Ranieri G**, Coviello M, Chiriatti A, Stea B, Montemurro S, Quaranta M, Dittadi R, Paradiso A. Vascular endothelial growth factor assessment in different blood fractions of gastrointestinal cancer patients and healthy controls. *Oncol Rep* 2004; **11**: 435-439

15 **Ono K**, Ishihara M, Ishikawa K, Ozeki Y, Deguchi H, Sato M, Hashimoto H, Saito Y, Yura H, Kurita A, Maehara T. Periodate-treated, non-anticoagulant heparin-carrying polystyrene (NAC-HCPS) affects angiogenesis and inhibits subcutaneous induced tumour growth and metastasis to the lung. *Br J Cancer* 2002; **86**: 1803-1812

16 **Zhou T**, Chen JL, Song W, Wang F, Zhang MJ, Ni PH, Geng JG. Effect of N-desulfated heparin on hepatic/renal ischemia reperfusion injury in rats. *World J Gastroenterol* 2002; **8**: 897-900

17 **Szende B**, Paku S, Rácz G, Kopper L. Effect of Fraxiparine and heparin on experimental tumor metastasis in mice. *Anticancer Res* 2005; **25**: 2869-2872

18 **Amirkhosravi A**, Mousa SA, Amaya M, Francis JL. Antimetastatic effect of tinzaparin, a low-molecular-weight heparin. *J Thromb Haemost* 2003; **1**: 1972-1976

19 **Kragh M**, Binderup L, Vig Hjarnaa PJ, Bramm E, Johansen KB, Frimundt Petersen C. Non-anti-coagulant heparin inhibits metastasis but not primary tumor growth. *Oncol Rep* 2005; **14**: 99-104

20 **Mousa SA**, Mohamed S. Anti-angiogenic mechanisms and efficacy of the low molecular weight heparin, tinzaparin: anti-cancer efficacy. *Oncol Rep* 2004; **12**: 683-688

21 **Kakeji Y**, Koga T, Sumiyoshi Y, Shibahara K, Oda S, Maehara Y, Sugimachi K. Clinical significance of vascular endothelial

growth factor expression in gastric cancer. *J Exp Clin Cancer Res* 2002; **21**: 125-129

22 **Fondevila C**, Metges JP, Fuster J, Grau JJ, Palacín A, Castells A, Volant A, Pera M. p53 and VEGF expression are independent predictors of tumour recurrence and survival following curative resection of gastric cancer. *Br J Cancer* 2004; **90**: 206-215

23 **Pisano C**, Aulicino C, Vesci L, Casu B, Naggi A, Torri G, Ribatti D, Belleri M, Rusnati M, Presta M. Undersulfated, low-molecular-weight glycol-split heparin as an antiangiogenic VEGF antagonist. *Glycobiology* 2005; **15**: 1C-6C

S- Editor Liu Y **L- Editor** Wang XL **E- Editor** Bi L

PO Box 2345, Beijing 100023, China
www.wjgnet.com
wjg@wjgnet.com

World J Gastroenterol 2007 January 21; 13(3): 462-466
World Journal of Gastroenterology ISSN 1007-9327

RAPID COMMUNICATION

Protective effect and mechanism of stronger neo-minophagen C against fulminant hepatic failure

Bao-Shan Yang, Ying-Ji Ma, Yan Wang, Li-Yan Chen, Man-Ru Bi, Bing-Zhu Yan, Lu Bai, Hui Zhou, Fu-Xiang Wang

Bao-Shan Yang, Ying-Ji Ma, Yan Wang, Li-Yan Chen, Man-Ru Bi, Bing-Zhu Yan, Lu Bai, Hui Zhou, Fu-Xiang Wang, Department of Infectious Diseases, the First Clinical Hospital of Harbin Medical University, Harbin 150001, Heilongjiang Province, China
Supported by the Key Program During the Tenth Five-Year Plan of HeilongJiang Province, No. 200101031-00
Correspondence to: Yan Wang, Department of Infectious Diseases, the First Clinical Hospital of Harbin Medical University, Harbin 150001, Heilongjiang Province, China. wangyanzzz@hotmail.com
Telephone: +86-451-53601175 Fax: +86-451-53621909
Received: 2006-10-19 Accepted: 2006-11-27

Abstract

AIM: To investigate the protective effect of stronger neo-minophafen C (SNMC) on fulminant hepatic failure (FHF) and its underlying mechanism.

METHODS: A mouse model of FHF was established by intraperitoneal injection of galactosamine (D-Gal N) and lipopolysaccharide (LPS). The survival rate, liver function, inflammatory factor and liver pathological change were obtained with and without SNMC treatment. Hepatocyte survival was estimated by observing the stained mitochondria structure with terminal deoxynucleotidyl transferase-mediated deoxyuridine triphosphate fluorescence nick end labeling (TUNEL) method and antibodies against cytochrome C (Cyt-C) and caspase-3.

RESULTS: The levels of plasma tumor necrosis factor alpha (TNF-α), nitric oxide (NO), ET-1, interleukin-6 (IL-6), and the degree of hepatic tissue injury were decreased in the SNMC-treated groups compared with those in the model group ($P < 0.01$). However, there were no differences after different dosages administered at different time points. There was a significant difference in survival rates between the SNMC-treated groups and the model group ($P < 0.01$). The apoptosis index was 32.3% at 6 h after a low dose of SNMC, which was considerably decreased from 32.3% ± 4.7% *vs* 5% ± 2.83% ($P < 0.05$) to 5% on d 7. The expression of Cyt-C and caspase-3 decreased with the prolongation of therapeutic time. Typical hepatocyte apoptosis was obviously ameliorated under electron microscope with the prolongation of therapeutic time.

CONCLUSION: SNMC can effectively protect liver against FHF induced by LPS/D-Gal N. SNMC can prevent hepatocyte apoptosis by inhibiting inflammatory reaction and stabilizing mitochondria membrane to suppress the release of Cyt-C and sequent activation of caspase-3.

Key words: Stronger neo-minophagen C; Fulminant hepatic failure; Cytochrome C; Caspase-3

Yang BS, Ma YJ, Wang Y, Chen LY, Bi MR, Yan BZ, Bai L, Zhou H, Wang FX. Protective effect and mechanism of stronger neo-minophagen C against fulminant hepatic failure. *World J Gastroenterol* 2007; 13(3): 462-466

http://www.wjgnet.com/1007-9327/13/462.asp

INTRODUCTION

Fulminant hepatic failure (FHF) is clinically characterized by prolonged prothrombin time and hepatic encephalopathy. It has been known that the onset of acute and chronic hepatitis is related to the inflammatory necrosis resulting from cell immunity and abnormal hepatocyte apoptosis caused by injury in mitochondria[1,2]. Stronger neo-minophagen C (SNMC), a compound mainly composed of glycyrrhizic acid, has anti-inflammatory and anti-allergic effects. However, it is not clear whether this compound protects liver against FHF[3]. The present study was to clarify the effect of SNMC on immune-mediated injury and hepatic cell apoptosis and its mechanism underlying liver failure induced by endotoxin.

MATERIALS AND METHODS

Kunming mice weighing 18-20 g at the age of 6-7 wk were provided by the Center of Experimental Animals of Harbin Medical University. Female mice were never impregnated and reproduced. SNMC was obtained from Minofayan Pharmaceutical Co, Ltd, Japan. Galactosamine (D-Gal N) and lipopolysaccharide (LPS) were purchased from Sigma. Nitric oxide (NO) fluorescein reagent kit was obtained from Jian Cheng Bio-Engineering Research Institute (Nanjing, China). Tumor necrosis factor alpha (TNF-α), ET-1, interleukin-6 (IL-6) radioimmunoassay reagent kits were bought from Radioimmunoassay Institute, General Hospital of Chinese PLA. Caspase-3 monoclonal antibody was from Sigma. Anti cytochrome C (Cyt-C) antibody immunohistochemistry staining reagent kit and terminal deoxynucleotidyl transferase-mediated

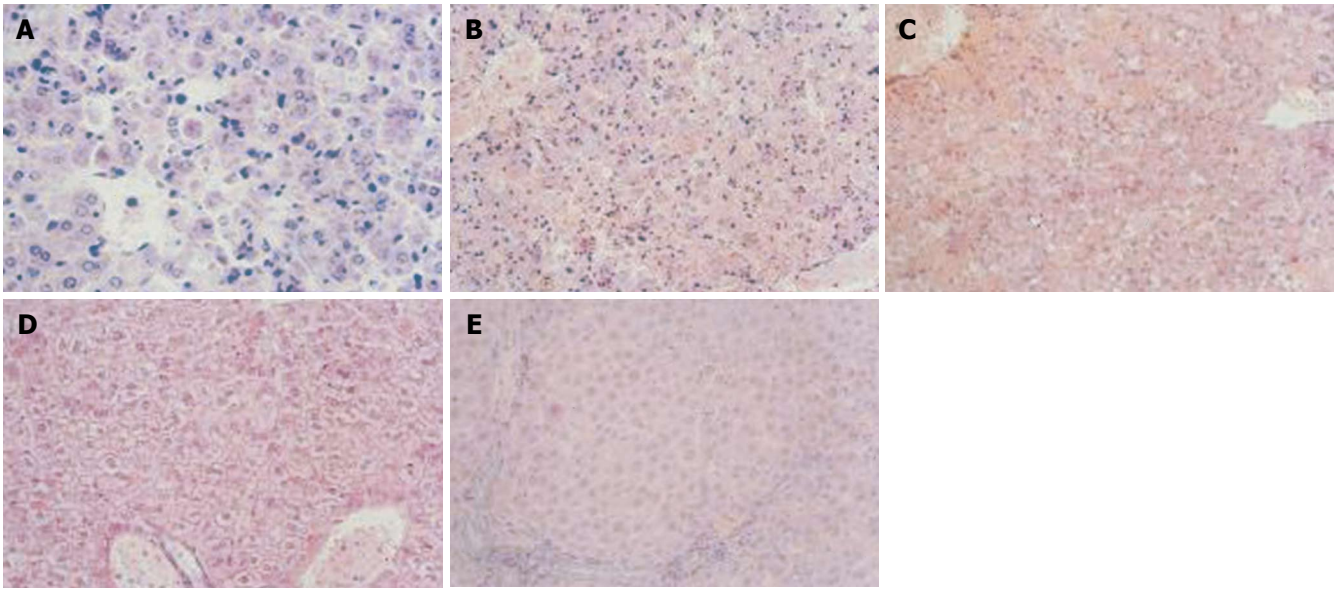

Figure 1 Optical microscopy showing liver cell apoptosis and necrosis (**A**) and liver cell necrosis (**B**) 24 h (**C**), 36 h (**D**), 72 h (**E**) after given SNMC (HE, × 20).

deoxyuridine triphosphate fluorescence nick end labeling (TUNEL) reagent kit were purchased from Zhongshan Biotechnology Co, Ltd (Beijing, China).

Preparation

D-Gal N (1000 mg/kg) and LPS (100 μg/kg) were injected into the abdominal cavity of mice to induce FHF. Pathological changes in liver tissues corresponded to the FHF pathological features (Figure 1A and B). One hundred and ten mice were randomly divied into control group, model group and treatment group. Mice in the control group were administered SNMC for a week before LPS/D-Gal N treatment. Mice in the model group were given SNMC and LPS/D-Gal N at the same time. Mice in the treatment group were injected with LPS/D-Gal N 8 h after SNMC was given. The results showed that 280 mL, 200 mL and 140 mL SNMC had the most significant protective effect. The survival rate of mice in the model group after injected 140 mL SNMC was the highest. Then 60 mice were given 140 mL SNMC and 5 mice in each group were sacrificed 6 h, 1 d, 3 d and 7 d after LPS/D-Gal N injection. Liver tissue was collected for immunohistochemical analysis. Pyrogen free blood sample was obtained from eyeball and centrifuged for 10 min at 3000 r/min to get serum/plasma. Serum and plasma were stored at -20℃.

Experiment

TNF-α, ET-1, IL-6 were determined by radioimmunoassay (RIA). The nitrate reductase method was employed to analyze NO. Alanine aminotransferase (ALT), total bilirubin (TBIL) and albumin (ALB) were analyzed with fully automatic biochemical instruments.

Four pieces of the left lobe of liver were taken. One was fixed in 2.5% glutaraldehyde for electron microscopy (EM), 2 were fixed in 4% paraformaldehyde and embedded in paraffin for immunohistochemical analysis, and 1 was fixed in 10% formalin and embedded in paraffin for histological examination.

Routinely deparaffinaged and rehydrated sections were stained with cell apoptosis detection kit according to the manufacturer's instructions. The sections were visualized with diaminobenzidine (DAB). The apoptosis index was calculated and the degree of hepatocyte apoptosis was determined. The cells with brown nuclei and cytoplasm were regarded as apoptotic cells, whereas the cells with blue nuclei were considered normal cells. The sections were incubated with monoclonal antibodies against caspase-3 (1:100) and Cyt-C antibody (1:100) after routine deparaffinage and rehydration, and stained with DAB and counterstained with hematoxylin.

Statistical analysis

The data were expressed as mean ± SD. All statistical analyses were performed using the Statistical Program for Social Sciences (SPSS 10.0 for Windows). F test was used for comparing variables. The 95% confidence interval for all estimates was provided when appropriate. $P < 0.05$ was considered statistically.

RESULTS

Ssurvival rate within 24 h

All the mice of the control group were alive at the end of experiments. Death occurred in the model group at 6 h after LPS/D-Gal N treatment and all mice died within 21 h. Death occurred in the SNMC-treated group at 8 h and all the survivors lived for more than 24 h. The survival rate for the model group was 60% after 140 mL SNMC was given.

Liver tissue histophysiological response

In the control group, the structure of hepatic lobules was intact, and the hepatocytes were radially arranged around the central vein. In the model group, histological hepatocyte damage with slight hydropic degeneration

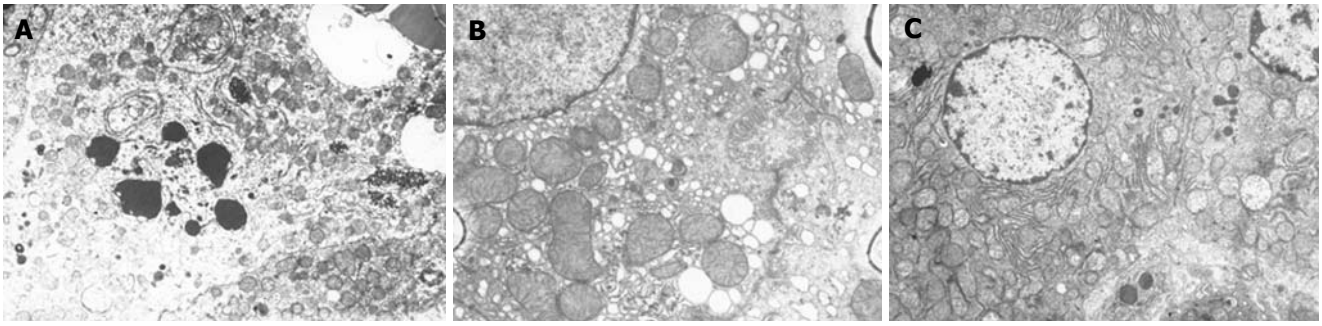

Figure 2 Electron microscopy showing results in model group (**A**) (× 6000), 3 d (**B**) (× 10 000) and 7 d (**C**) after given SNMC (× 6000).

Table 1 Levels of NO, TNF-α, ET-1, IL-6, ALT, ALB, and TBIL in control, model and treatment groups (mean ± SD)

Groups	Mice (*n*)	NO (μmol/L)	TNF-α (ng/mL)	ET-1 (pg/mL)	IL-6 (pg/mL)	ALT (u/L)	ALB (g/L)	TBIL (u/L)
Control group	6	45.1 ± 14.01	0.77 ± 0.08	50.8 ± 7.58	57.07 ± 12.67	67.17 ± 12.62	32.18 ± 4.16	9.2 ± 8.75
Model group	6	725.94 ± 156.94	3.75 ± 0.50	309.41 ± 38.45	413.56 ± 69.02	1406.33 ± 47.42	21.13 ± 3.66	70.03 ± 17.22
Treatment group	6	199.42 ± 85.98	1.34 ± 0.31	129.11 ± 17.97	155.22 ± 59.37	799.33 ± 171.19	20.03 ± 3.01	8.87 ± 0.85
140 mL group	6	215.01 ± 28.72	1.35 ± 0.17	183.07 ± 75.93	149.81 ± 44.69	25.96 ± 6.35	26.10 ± 1.97	59 ± 29.31
200 mL group	6	87.88 ± 12.46	1.34 ± 0.31	157.41 ± 35.64	133.89 ± 30.48	1169 ± 149.92	20.9 ± 1.28	27.33 ± 2.94
280 mL group	6	184.54 ± 19.84	1.27 ± 0.27	216.15 ± 24.47	179.97 ± 65.09	24.33 ± 8.02	21.37 ± 5.44	51.5 ± 14.94

$F_{(4,29)} = 2.70$.

could be seen 3-5 h after the administration of D-Gal N and LPS. Furthermore, pronounced hydropic degeneration, slight spotty necrosis and apoptotic bodies (Figure 1A) could be observed 6 after administration of D-Gal N and LPS. Widespread necrosis (exceeding 2/3 of the whole slide), dissociated hepatocytes with loss of the normal structure of liver, hemorrhage and neutrophil and lymphocyte infiltration were seen mainly in necrosis area and periportal zone 12 h after administration of D-Gal N and LPS (Figure 1B). However, various degrees of hydropic and vacuolar degeneration were found in the model group 24 h after administration of 140 mL SNMC (Figure 1C). In the model group, marked cytoplasm rarefaction was found 36-48 h after administration of D-Gal N and LPS (Figure 1D), while sporadic and focal necrosis (Figure 1E) as well as inflammatory cell infiltration were found 72 h after administration of D-Gal N and LPS.

Levels of TNF-α, ET-1, IL-6, ALT, ALB, and TBIL in control, model and treatment groups

The F values were determined in the control, model and treatment groups. The results were as follows: F (NO) = 58.328, F (TNF-α) = 69.489, F (ET-1) = 57.328, F (IL-6) = 46.914, F (ALT) = 3.257, F (TBIL) = 7.477, [$F_{(4,25)0.05}$ = 2.76, $P < 0.05$]. F (ALB) = 1.204, NS. The F values in the treatment group were as follows: F (NO) = 2.676, F (TNF-α) = 2.043, F (ET-1) = 3.347, F (IL-6) = 2.676, F (ALT) = 0.452, F (ALB) = 1.535, F (TBIL) = 0.020, [$F_{(2,12)0.05}$ = 3.68, NS]. The F values in different groups injected with different dosages of SNMC were as follows: F (NO) = 84.907, F (TNF-α) = 44.519, F (ET-1) = 13.236, F (IL-6) = 37.760, F (ALT) = 2.904, F (TBIL) = 7.681, [$F_{(4,25)0.05}$ = 2.76, $P <$ 0.05), F (ALB) = 1.004, NS. The results of different dosages were: F (NO) = 3.351, F (TBIL) = 2.756, [$F_{(2,12)0.05}$ = 3.68, NS], with no significant differences (Table 1).

Results of electron microscopy (EM)

In the control group, the hepatocytes with prominent nuclei were well arranged in plates and abundant in structure of intracellular membrane. However, the model group showed condensed nuclei, chromatin margination, enlarged mitochondria, and derangement of plasmalemma and inner cytomembrane (Figure 2A). Condensed nuclei, chromatin margination, and enlarged rough endoplasmic reticulum (RER) showing degranulation were present in the 140 mL SNMC group. Normal bilayer nuclear membrane, abundant crista mitochondria, moderate density of matrix, tight cholangiole junctions and intact endothelium of the hepatic sinusoid were observed 3 d after administration of SNMC (Figure 2B). After 7 d, the structure of liver cell membranes was intact, the cell organs were rich, the crista mitochondria were dense, the matrix density was moderate, and the structure of hepatic sinusoid endothelia was intact. We could see the penetration of liver cell microvilli inside the Disse interspace (Figure 2C).

Detection of hepatocyte apoptosis

Two sections from each group were observed at each indicated time. Five visual fields of each section were analyzed, and 100 cell nuclei were counted in each visual field. The average percentage of hepatocyte apoptosis was considered the index of apoptosis[4] (Table 2). The apoptotic cells were characterized by intact bilayered cytomembrane and condensed nuclei. Nuclei and/or cytoplasm with brown staining (leakage of nuclear DNA) were assessed as positive staining. Besides, the apoptotic bodies were also positively stained. No apoptotic cells were

found in the control group. More apoptotic liver cells were found mainly in the necrosis area of the model group with the prolongation of time.

Detection of cytosol cytochrome C (Cyt-C) and caspase-3

Cytoplasm with brown staining was assessed as positive. Three fields randomly selected from each section were chosen to detect Cyt-C and caspase-3 positive cells under optical microscope at a magnification of 400. The mean value was considered the positive cell number of each group (Table 2). In the control group, hepatocytes were normal in size and shape and well arranged. Cyt-C and caspase-3 were expressed only in a few scattered cells. In the model group, liver cells were mainly expressed in the inflammation necrosis area and portal area, and showed positive Cyt-C and caspase-3 staining. In the treatment group, the expression of Cyt-C and caspase-3 was gradually decreased and the structure of liver cells was gradually recovered with the prolongation of time.

Table 2 Hepatocyte apoptosis index and number of cells expressing Cyt-C and caspase-3 (mean ± SD, number/HP)

Groups	Number	Apoptosis index	Cyt-C	Caspase-3
Control group	5	0	1.67 ± 0.90	3.87 ± 2.42
Model group	5	33.2 ± 4.37	59.47 ± 3.79	85.6 ± 6.25
After therapy 6 h	5	32.3 ± 4.7	58.47 ± 3.83	84.00 ± 5.54
After therapy 1 d	5	26.6 ± 4.67[b]	46.33 ± 5.51[b]	72.3 ± 5.21[b]
After therapy 3 d	5	19.9 ± 3.54[b]	31.53 ± 2.83[b]	56.13 ± 6.87[b]
After therapy 5 d	5	11.1 ± 2.77[b]	25.47 ± 3.94[b]	34.1 ± 4.87[b]
After therapy 7 d	5	5 ± 2.83[b]	15.00 ± 4.11[b]	17 ± 4.5[b]

[b]$P < 0.01$ *vs* the model group. Apoptosis index: $t_{6h} = 0.56$, $t_{1d} = 4.10$, $t_{3d} = 8.26$, $t_{5d} = 13.73$, $t_{7d} = 17.52$. Cyt-c: $t_{6h} = 0.72$, $t_{1d} = 9.45$, $t_{3d} = 20.1$, $t_{5d} = 24.46$, $t_{7d} = 31.99$. Caspase-3: $t_{6h} = 1.09$, $t_{1d} = 12.2$, $t_{3d} = 26.9$, $t_{5d} = 47.2$, $t_{7d} = 62.9$.

DISCUSSION

It is well-known that virus infection results in primary liver injury and endotoxin, by which inflammatory mediator-induced secondary liver injury is caused, leading to hepatocyte apoptosis and necrosis[5]. TNF-α, one of the most important inflammatory mediators, induces hepatocyte apoptosis and necrosis through the activation of caspase-3, leading to liver cell DNA shift[6]. In the present study, SNMC reduced serum level of ALT, ALB and total bilirubin, and attenuated hepatocyte apoptosis, leading to the secondary liver injury induced by LPS. Its related mechanisms such as reducing the release of NO and ET-1, restraining the formation of hepatic sinusoid microthrombi and microcirculation dysfunction, inhibiting immunologic injury caused by cytokines especially TNF-α, and suppressing the formation of endotoxin, may contribute to the protective effect against FHF[7]. However, in the present study, SNMC failed to raise the albumin levels during FHF, probably due to the longer half life of albumin.

Most researchers believe that abnormal hepatocyte apoptosis contributes significantly to the occurrence of FHF[8]. The crucial role of mitochondria and Cyt-C in hepatocyte survival and death has caused more and more attention. Some mediators in the mitochondria are closely associated with cell apoptosis, including Cyt-C, apoptosis inducing factor (AIF) and reactive oxygen species (ROS). Under the stimulation of apoptosis signals, augmented mitochondrial membrane permeability initiates a series of key changes including release of Cyt-C, decrease in mitochondrial transmembrane potential, alteration of the oxidation-reduction system inside the cells and intervention with the Bc1 gene family, thus finally leading to hepatocyte apoptosis[9].

TUNEL staining results indicated that the apoptosis index in the treatment group decreased from 32.3% at 6 h to 5% on d 7 after LPS/D-Gal N injection ($P < 0.05$). Typical morphological changes during apoptosis, including nucleus shrinkage and chromatin margination *etc*, were observed under electron microscope (EM) in the model group. The treatment group improved proportionately with the prolongation of therapeutic time. The results suggest that SNMC can effectively attenuate hepatocyte apoptosis.

The release of Cyt-C is a key event in the apoptosis process[10]. Cyt-C has a duplex function as an initiator to activate cell apoptosis and participate in electron transfer. Cyt-C shifting to the cytoplasm could bring about a cascade of reactions of caspases, finally activate caspase-3 and result in hepatocyte apoptosis. Immunohistochemistry staining demonstrated that Cyt-C and caspase-3 expression was significantly reduced in treatment group with the prolongation of therapeutic time when compared with the model group ($P < 0.01$), suggesting that the expression of caspase-3 is closely related with Cyt-C and possibly regulated by releasing Cyt-C. Meanwhile, we speculated that SNMC inhibited the progression of hepatocyte apoptosis mainly by stabilizing the mitochondrial membrane and inhibiting the release of Cyt-C and subsequent caspase-3 activations.

The present study demonstrated that SNMC not only reduced serum aminotransferase and bilirubin, but also attenuated the hepatocyte apoptosis. SNMC reduced the necrotic area and increased the survival rate of mice by promoting hepatocyte regeneration and recovery of denatured cells, and protecting the undamaged cells. However, the dosages of SNMC in the treatment of FHF and the therapeutic time have not yet been firmly established. The low dose administered in this experiment corresponds to ordinary clinical dosages. Whether high dose would bring about toxic effects or other side effects awaits future study.

In summary, the results of the present study support SNMC treatment for FHF, but the precise mechanism should be further studied.

COMMENTS

Background

It is well-known that virus infection results in primary liver injury and endotoxin, by which inflammatory mediator-induced secondary liver injury is caused, thus finally leading to hepatocyte apoptosis and necrosis. Most researchers believe that abnormal hepatocyte apoptosis contributes significantly to the occurrence of FHF.

Research frontiers

SNMC, a compound mainly composed of glycyrrhizic acid, has anti-inflammatory and anti-allergic effects. However, it is not clear whether this compound protects liver against FHF. The present study was to clarify the effects of SNMC on immune-mediated injury and hepatic cell apoptosis and its related mechanisms underlying liver failure induced by endotoxin.

Innovations and breakthroughs

SNMC can effectively protect liver against FHF induced by LPS/D-Gal N. SNMC prevents hepatocyte apoptosis by inhibiting inflammatory reaction and stabilizing mitochondria membrane to suppress the release of Cyt-C and sequent activation of caspase-3.

Applications

SNMC can not only reduce serum aminotransferase and bilirubin, but also the mortality of patients with FHF.

Terminology

SNMC, a compound mainly composed of glycyrrhizic acid, has anti-inflammatory and anti-allergic effects.

REFERENCES

1 **Ogasawara J**, Watanabe-Fukunaga R, Adachi M, Matsuzawa A, Kasugai T, Kitamura Y, Itoh N, Suda T, Nagata S. Lethal effect of the anti-Fas antibody in mice. *Nature* 1993; **364**: 806-809
2 **Ryo K**, Kamogawa Y, Ikeda I, Yamauchi K, Yonehara S, Nagata S, Hayashi N. Significance of Fas antigen-mediated apoptosis in human fulminant hepatic failure. *Am J Gastroenterol* 2000; **95**: 2047-2055
3 **Song FW**, Li XJ. The research of the protective effect of SNMC on histopathology of Liver. *Zhonghua Xiandai Yixue Zazhi* 2001; **11**: 24-25
4 **Kondo T**, Suda T, Fukuyama H, Adachi M, Nagata S. Essential roles of the Fas ligand in the development of hepatitis. *Nat Med* 1997; **3**: 409-413
5 **Zhang YS**, Tu ZG. Regulation of alpha 1-adrenoceptor on rat hepatocyte apoptosis induced by D-galactosamine and lipopolysaccharide. *Acta Pharmacol Sin* 2000; **21**: 627-632
6 **Hoofnagle JH**, Carithers RL, Shapiro C, Ascher N. Fulminant hepatic failure: summary of a workshop. *Hepatology* 1995; **21**: 240-252
7 **Alison MR**, Sarraf CE. Liver cell death: patterns and mechanisms. *Gut* 1994; **35**: 577-581
8 **Wang YM**, Feng GH, Li Y. Relationship of Tumor Necrosis Factor-α and hepatocytes apoptosis in fulminant hepatic failure. *Zhonghua Neike Zazhi* 2002; **31**: 410-412
9 **Xiang XX**, Wang GJ, Cai X. Research of the therapy to prevent hepatocytes apoptosis on Fulminant liver failure. *Linchuang Ganzangbing Zazhi* 2001; **6**: 64-65
10 **Finkel E**. The mitochondrion: is it central to apoptosis? *Science* 2001; **292**: 624-626

S- Editor Liu Y **L- Editor** Wang XL **E- Editor** Bi L

PO Box 2345, Beijing 100023, China
www.wjgnet.com
wjg@wjgnet.com

World J Gastroenterol 2007 January 21; 13(3): 467-469
World Journal of Gastroenterology ISSN 1007-9327

CASE REPORT

Rectal angiolipoma diagnosed after surgical resection: A case report

Mitsuru Ishizuka, Hitoshi Nagata, Kazutoshi Takagi, Toru Horie, Akihito Abe, Keiichi Kubota

Mitsuru Ishizuka, Hitoshi Nagata, Kazutoshi Takagi, Toru Horie, Akihito Abe, Keiichi Kubota, Department of Gastroenterological Surgery, Dokkyo University School of Medicine, Tochigi, Japan
Correspondence to: Mitsuru Ishizuka, MD, Department of Gastroenterological Surgery, Dokkyo University School of Medicine, 880 Kitakobayashi, Mibu, Tochigi 321-0293, Japan. mm-ishizuka@umin.ac.jp
Telephone: +81-282-872158 Fax: +81-282-866317
Received: 2006-09-28 Accepted: 2006-12-11

Abstract

Angiolipoma is a common benign tumor with a characteristic vascular component that usually occurs in subcutaneous tissue. Although lipomas are frequently encountered at colonoscopy as submucosal tumors, angiolipomas are rarely found in the gastrointestinal tract including the large intestine. Here we report a 77-year old Japanese man who underwent transanal resection of a tumor that was diagnosed tentatively as a leiomyoma. Histologically, the tumor consisted of mature fat cells and blood vessels. Immunohistochemically, the tumor cells were negative for c-kit and HMB-45, which are consistently expressed in tumors such as gastrointestinal stromal tumor and angiomyolipoma. The tumor was therefore diagnosed as an angiolipoma. This is thought to be the first case report of a surgically resected angiolipoma of the rectum.

Key words: Angiolipoma; Angiomyolipoma; Gastrointestinal stromal tumor

Ishizuka M, Nagata H, Takagi K, Horie T, Abe A, Kubota K. Rectal angiolipoma diagnosed after surgical resection: A case report. *World J Gastroenterol* 2007; 13(3): 467-469

http://www.wjgnet.com/1007-9327/13/467.asp

INTRODUCTION

Angiolipomas are subcutaneous tumors made up of mature fat and prominent blood vessels, and usually occur in young adults and older teenagers. They are rarely larger than 2 cm in diameter, frequently multiple, and characteristically tender or painful[1]. The most common locations are the forearm, trunk, and upper arm, and they rarely occur in the gastrointestinal tract. Grossly, angiolipomas are well circumscribed and yellow with varying amounts of red surface. A characteristic feature is fibrin thrombi within the vessels. The proportion of adipose and vascular tissue varies from predominantly lipomatous to predominantly angiomatous. Here we describe the first case of rectal angiolipoma diagnosed postoperatively.

CASE REPORT

A 77-year old Japanese man was admitted to our hospital with a 1-year history of anal bleeding. The patient lacked any findings suggestive of tuberous sclerosis. He had no cutaneous or retinal lesions, neurologic symptoms, or evidence of mental retardation. The family history and past medical history were unremarkable. All routine laboratory parameters, including carcinoembryonic antigen, were within normal limits. A double-contrast barium enema revealed a sessile lesion in the periproctic area measuring 20 mm × 15 mm (Figure 1). A subsequent colonofiberscopy disclosed a sessile-type submucosal tumor with internal hemorrhoids, and the tumor had no reddish depression or ulceration at its top (Figure 2). The other parts of the colon and rectum appeared normal. A biopsy specimen revealed proliferation of the muscle component with no atypical cells. A tentative diagnosis of leiomyoma was therefore made. Enhanced CT of the abdomen demonstrated a partially enhanced mass lesion with fat component which was not suspected of having infiltrated the proper muscle layer, on the right wall of the lower rectum (Figure 3). Trans-anal endoscopic ultrasonography revealed that the tumor was located in the submucosal layer. Because the tumor was considered to be benign, and difficult to resect by endoscopic surgery, we elected to perform trans-anal tumor resection with an ultrasonically activated device (Harmonic Scalpel®) to prevent bleeding from the internal hemorrhoids. Under general anesthesia, with the patient in the lithotomy position, we were able to approach the anal side of the tumor easily and resect it without massive oozing. Complete resection was performed with a sufficient surgical margin from the submucosal tumor. The total operation time was 42 min and bleeding was only slight. The postoperative course was uncomplicated, and the patient was discharged five days later. He was followed up for 12 mo at the outpatient clinic and no tumor recurrence was observed during that time. Macroscopic observation revealed that the sessile tumor, measuring 2

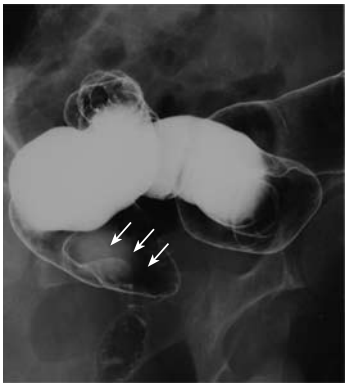

Figure 1 Double-contrast barium enema revealing a 20 mm × 15 mm sessile lesion in the periproctic area (arrows).

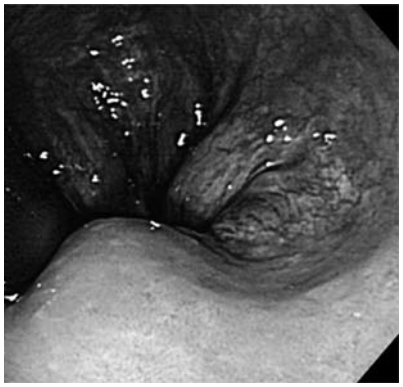

Figure 2 Colonoscopy disclosing a sessile lesion with a smooth surface.

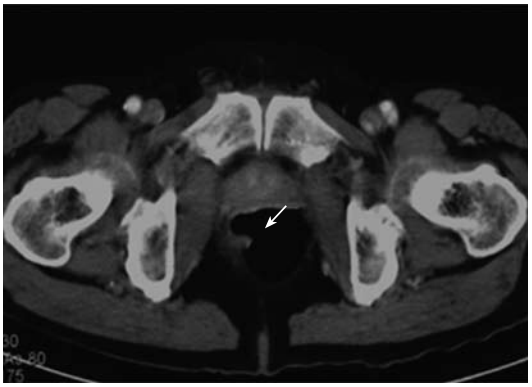

Figure 3 Enhanced CT of the lower abdomen demonstrating a fat-containing and slightly enhanced mass at a slice level corresponding to the right side of the lower rectum (arrow).

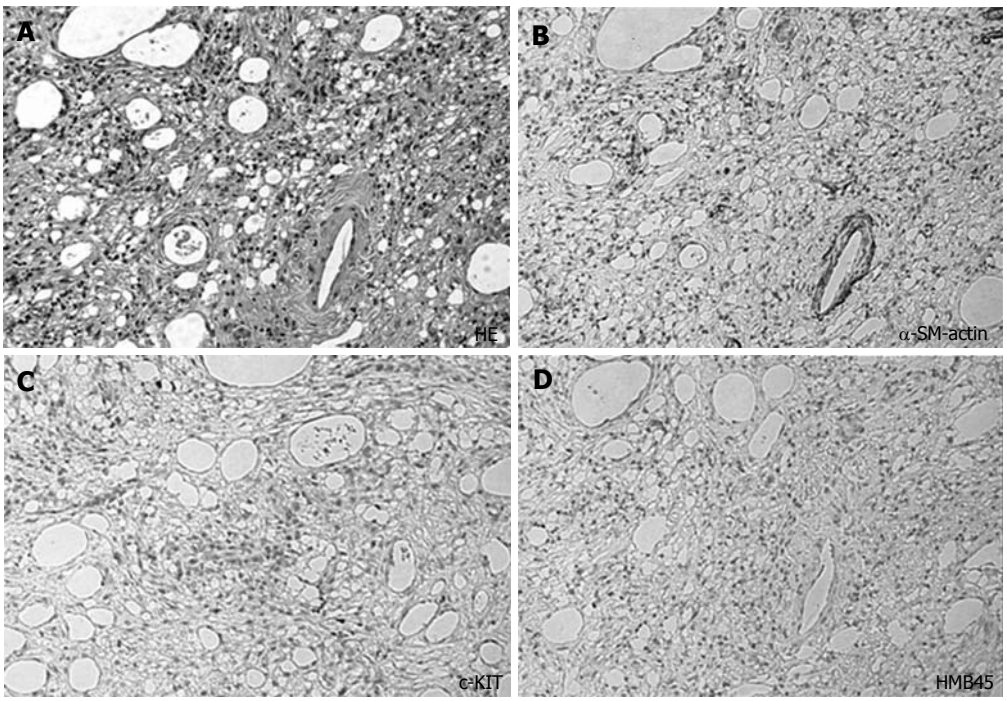

Figure 4 The tumor composed of a mixture of fat cells, proliferated blood vessels, spindle cells and immature mesenchymal cells (**A**), smooth muscle of a blood vessel demonstrating staining for alpha-smooth muscle actin but not for spindle cells (**B**), no tumor cells but only a few histiocytes displaying staining for c-kit (**C**), and no cells showing positive staining for HBM-45 (**D**).

cm × 1.5 cm × 1 cm, was yellowish in color, located in the submucosal layer and covered with normal mucosa. A cross-section of the formalin-fixed tumor revealed massive growth without a capsule. The proper muscle layer was not infiltrated by the tumor. The tumor consisted of mature fat cells and blood vessels of various sizes. No mitoses or cytological atypia were found in the cells. Immunohistochemical staining for alpha-smooth muscle actin, S-100 protein, HMB-45 and c-kit was performed. Only the blood vessels were positive for alpha-smooth muscle actin, and the tumor cells were negative for HMB-45, c-kit and S-100 (Figure 4).

DISCUSSION

Angiolipoma was first described in 1912 by Bowen[2]. In 1960, Howard and Helwig[3] demonstrated that the clinicopathologic features of angiolipomas differ from those of lipomas, thereby delineating angiolipoma as a new entity. Angiolipomas usually develop as encapsulated subcutaneous tumors, most commonly on the arms and trunk in young adults. Only 15 cases of angiolipoma occurring in the gastrointestinal tract were found in a MEDLINE search. These angiolipomas were located in the esophagus in one case[4], the stomach in 4 cases[5-8], the small intestine in 5 cases[9-13] and the colon in 5 cases[14-18]. The search revealed no reported cases of rectal angiolipoma. There are clinical differences between angiolipomas located in the gastrointestinal tract and those commonly occurring in subcutaneous tissue. The 15 reported gastrointestinal lesions were all solitary, and 4 showed bleeding from the tumor[5,8,9,13], all except one[7] occurring in elderly patients. In the bleeding cases, the tumor was over 2 cm in diameter and the bleeding point was located on the top of the tumor[14,16], which had a pumpkin-like shape[16]. In the present case, the tumor was less than 2 cm in diameter and its surface was covered with smooth and normal mucosa. It was thought that the tumor was too small to show a bleed-

ing tendency. The differential diagnosis of angiolipoma includes angiomyolipoma[19], which is composed of smooth muscle, fatty tissue and blood vessels. Because a minor smooth muscle component was recognized in this case, the initial pathological diagnosis was angiomyolipoma. However, examination in detail showed that proliferation of the lamina muscularis mucosae might have caused physical irritation, especially during defecation, and that the smooth muscle component was not a dominant component of the tumor. Additionally, immunohistochemical staining for HMB-45 was effective for differential diagnosis between angiolipoma and angiomyolipoma. In this case, HMB45 staining was negative. However, there is a case report of angiomyolipoma that was immunohistochemically negative for HMB45[15]. In addition, pathologically, angiomyolipoma is common in the kidney and is often associated with dermatomyositis.

Angiomyolipoma is difficult to diagnose preoperatively and is usually diagnosed as lipoma.

Surgical excision is the treatment of choice. The recurrence rate is high in cases that are inadequately resected, but when the tumor can be removed completely, the prognosis is excellent. In this case, we selected transanal tumor resection because of the difficulty to obtain a good field for performing endoscopic resection[20] or transanal endoscopic microsurgery for this periproctic tumor with internal hemorrhoids that would bleed easily. Transanal tumor resection allowed us to obtain a good field and we were able to minimize bleeding from the internal hemorrhoids by removing the tumor with a Harmonic Scalpel® with a sufficient surgical margin.

REFERENCES

1 **Rogy MA**, Mirza D, Berlakovich G, Winkelbauer F, Rauhs R. Submucous large-bowel lipomas--presentation and management. An 18-year study. *Eur J Surg* 1991; **157**: 51-55

2 **Bowen JT**. Multiple subcutaneous hemangiomas, together with multiple lipomas, occurring in enormous numbers in anotherwise healthy, muscular subject. *Am J Med Sci* 1912; **144**: 189-192

3 **Howard WR**, Helwig EB. Angiolipoma. *Arch Dermatol* 1960; **82**: 924-931

4 **Kline ME**, Patel BU, Agosti SJ. Noninfiltrating angiolipoma of the mediastinum. *Radiology* 1990; **175**: 737-738

5 **DeRidder PH**, Levine AJ, Katta JJ, Catto JA. Angiolipoma of the stomach as a cause of chronic upper gastrointestinal bleeding. *Surg Endosc* 1989; **3**: 106-108

6 **Ferrozzi F**, Tognini G, Marchesi G, Spaggiari E, Pavone P. Gastric tumors with fatty components. CT findings and differential diagnosis. *Radiol Med* 2000; **100**: 343-347

7 **Hunt J**, Tindal D. Solitary gastric Peutz-Jeghers polyp and angiolipoma presenting as acute haemorrhage. *Aust N Z J Surg* 1996; **66**: 713-715

8 **McGregor DH**, Kerley SW, McGregor MS. Case report: gastric angiolipoma with chronic hemorrhage and severe anemia. *Am J Med Sci* 1993; **305**: 229-235

9 **Aouad K**, Texier P, Bloch F, De Labriolle-Vaylet C, Bouillot JL. Benign angiolipoma of the Bauhin valve causing severe digestive tract bleeding. *Gastroenterol Clin Biol* 2000; **24**: 686-688

10 **Jung IS**, Jang JY, Ryu CB, Hong SJ, Kim JO, Cho JY, Lee JS, Lee MS, Jin SY, Shim CS, Kim BS. Angiolipoma of the duodenum diagnosed after endoscopic resection. *Endoscopy* 2004; **36**: 375

11 **Kaneko T**, Karasawa Y, Inada H, Tamura Y, Yamamura N, Iijima Y, Nagata A, Oohata T, Shirota H, Nakamura T, Hara E. An adult case of intussusception due to inverted Meckel's diverticulum accompanied by angiolipoma. *Nihon Shokakibyo Gakkai Zasshi* 1996; **93**: 260-265

12 **Kwak HS**, Kim CS, Lee JM. Small intestinal angiolipoma: MR imaging appearance. *Abdom Imaging* 2003; **28**: 515-517

13 **Manner M**, Scholz E, Wehrmann M, Stickel W. Invagination caused by angiolipoma of the small intestine: a rare cause of occult gastrointestinal hemorrhage. *Chirurg* 2001; **72**: 305-307

14 **Kato K**, Matsuda M, Onodera K, Sakata H, Kobayashi T, Kasai S. Angiolipoma of the colon with right lower quadrant abdominal pain. *Dig Surg* 1999; **16**: 441-444

15 **Maesawa C**, Tamura G, Sawada H, Kamioki S, Nakajima Y, Satodate R. Angiomyolipoma arising in the colon. *Am J Gastroenterol* 1996; **91**: 1852-1854

16 **Okuyama T**, Yoshida M, Watanabe M, Kinoshita Y, Harada Y. Angiolipoma of the colon diagnosed after endoscopic resection. *Gastrointest Endosc* 2002; **55**: 748-750

17 **Saroglia G**, Coverlizza S, Roatta L, Leli R, Fontana D. Angiolipoma of the cecum. *Minerva Chir* 1996; **51**: 59-62

18 **Vandamme J**. Angiolipoma of the colon. *Acta Gastroenterol Belg* 1964; **27**: 750-757

19 **Chen JS**, Kuo LJ, Lin PY , Changchien CR. Angiomyolipoma of the colon: report of a case and review of the literature. *Dis Colon Rectum* 2003; **46**: 547-549

20 **Pfeil SA**, Weaver MG, Abdul-Karim FW, Yang P. Colonic lipomas: outcome of endoscopic removal. *Gastrointest Endosc* 1990; **36**: 435-438

S- Editor Liu Y **L- Editor** Wang XL **E- Editor** Bi L

PO Box 2345, Beijing 100023, China
www.wjgnet.com
wjg@wjgnet.com

World J Gastroenterol 2007 January 21; 13(3): 470-473
World Journal of Gastroenterology ISSN 1007-9327

CASE REPORT

A case of scirrhous gastric cancer with peritonitis carcinomatosa controlled by TS-1® + paclitaxel for 36 mo after diagnosis

Yusuke Koizumi, Hirozumi Obata, Akinori Hara, Takashi Nishimura, Kenichiro Sakamoto, Yoshihide Fujiyama

Yusuke Koizumi, Takashi Nishimura, Yoshihide Fujiyama, Department of Gastroenterology and Hematology, Shiga University of Medical Science, Otsu, Japan
Hirozumi Obata, Kenichiro Sakamoto, Department of Medicine, Saiseikai Suita Hospital, Suita, Japan
Akinori Hara, Department of Surgery, Saiseikai Suita Hopspital, Suita, Japan
Correspondence to: Dr. Yusuke Koizumi, Department of Gastroenterology and Hematology, Shiga University of Medical Science, Seta-Tsukinowa-cho, Otsu, Shiga 520-2192, Japan. yjkoizumi-1975@s9.dion.ne.jp
Telephone: +81-77-5482217 Fax: +81-77-5482219
Received: 2006-11-11 Accepted: 2006-12-12

Abstract

A 34-year-old female complaining of abdominal fullness was diagnosed as scirrhous gastric cancer (type 4') with peritonitis carcinomatosa in July 2002. A combined chemotherapy regimen was selected to control massive ascites; TS-1® 80 mg/m^2 was given orally on d 1-14, 22-35, and paclitaxel 50 mg/m^2 was administered intravenously on d 1, 8, 22 and 29. After 2 courses of this regimen, the primary tumor was markedly reduced, and ascites completely vanished. Alopecia (grade 1, since d 30), leukocytopenia (grade 2, on d 34) and anemia (grade 2, on d 34) were the only adverse events throughout the following courses. The chemotherapy was effective for 28 mo, and then it was discontinued upon the patient's own request, and she survived for 36 mo after diagnosis.

Key words: TS-1®; Paclitaxel; Scirrhous gastric cancer; Peritonitis carcinomatosa

Koizumi Y, Obata H, Hara A, Nishimura T, Sakamoto K, Fujiyama Y. A case of scirrhous gastric cancer with peritonitis carcinomatosa controlled by TS-1® + paclitaxel for 36 mo after diagnosis. *World J Gastroenterol* 2007; 13(3): 470-473

http://www.wjgnet.com/1007-9327/13/470.asp

INTRODUCTION

Scirrhous gastric cancer has long been, and still is a devastating disease, especially when it is complicated with peritonitis carcinomatosa, which has no effective treatment at all up to date. On the other hand, the introduction of novel antineoplastic agents and protocols has led to certain improvement in the treatment of gastric cancer, including distant metastasis and/or malignant ascites. Here we report a case of scirrhous gastric cancer with peritonitis carcinomatosa, treated with repetitive courses of TS-1® (Tegafur-Gimeracil-Oteracil potassium) plus paclitaxel, which resulted in partial remission with disappearance of malignant ascites for over 28 mo, and survival of the patient for 36 mo after diagnosis.

CASE REPORT

A 34-year-old female, complaining of abdominal fullness, visited our hospital on 15th July, 2002. She has been disturbed by epigastric discomfort, increasing abdominal fullness and severe constipation for about a month. And she gained weight by 5-6 kg within 2 mo. Physical examinations showed obvious abdominal distension with an abdominal circumference of 80.0 cm, and body weight of 60 kg for a height of 167.5 cm. A low grade fever (37.2℃) was the only abnormal finding in vital signs. Laboratory data revealed no major abnormalities other than hypercholesterolemia. CEA and CA19-9 were within normal range, while CA125 was slightly elevated (Table 1). A paracentesis was performed to examine the ascites, and the findings were as follows: turbid and yellow colored, specific gradient = 1.034, with 1070 cells/mm^3 including many clusters of adenocarcinoma cells. A gastroscopy revealed conspicuous swelling of gastric fold with multiple erosions, and poor wall expansion exclusively at the body. The antral mucosa seemed almost intact except one submucosal tumor (SMT) like lesion at the greater curvature. Expandability at the antrum was fair (Figure 1A-C). A biopsy examination confirmed poorly differentiated adenocarcinoma and signet ring cell carcinoma. In upper GI series, the wall expansion was poor at the body (Figure 2A). Local and distant lymph node metastases were unlikely on CT scan images; yet massive ascites were detected, extending from the liver surface to the pelvic cavity (Figure 3A and B). A barium enema revealed severe stenosis of the rectosigmoid colon, probably caused by the extrinsic compression due to peritonitis carcinomatosa (Figure 4A). We therefore diagnosed this case as "scirrhous gastric cancer (type 4') with peritonitis carcinomatosa".

We selected TS-1® and paclitaxel as a combined

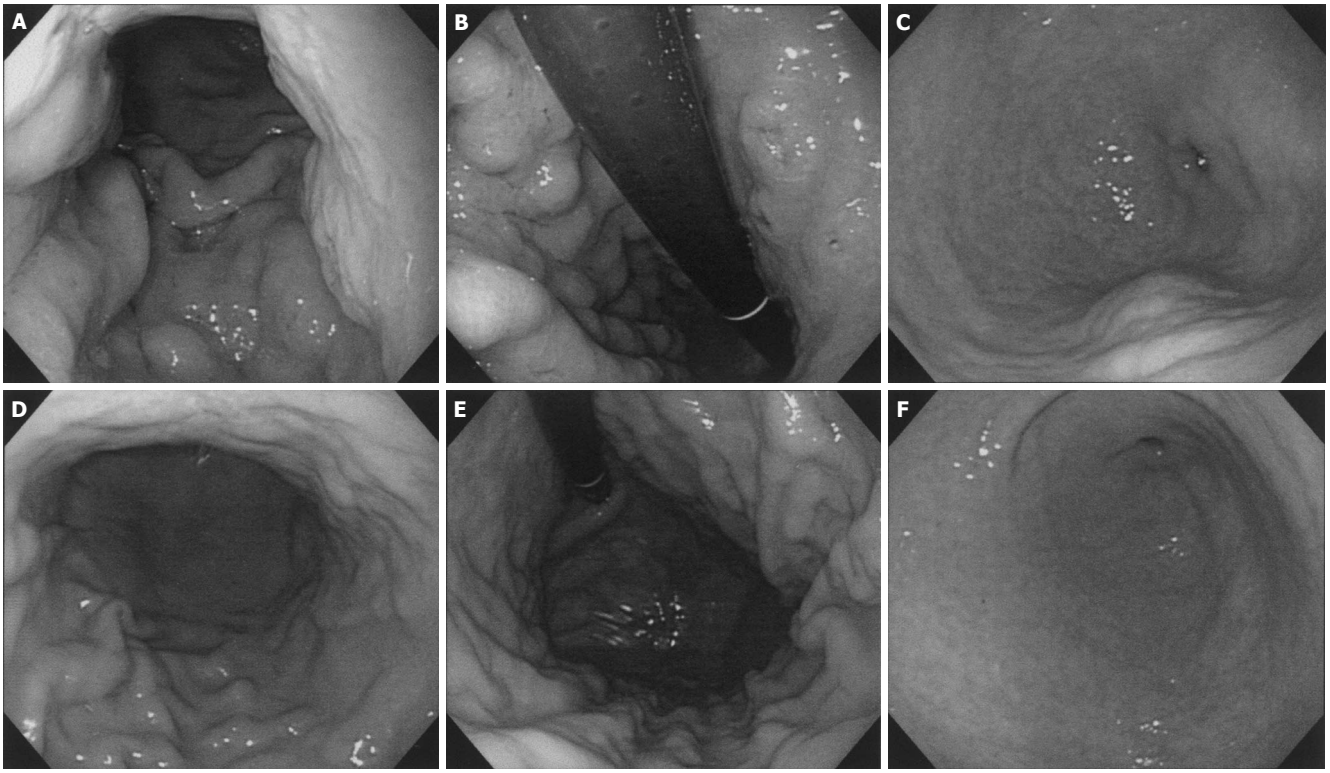

Figure 1 Gastroscopic findings at diagnosis (upper lane, **A**-**C**) and after 4 courses of chemotherapy (lower lane, **D**-**F**). **A**: Lower body: Wall thickening and erosions can be observed; **B**: Mid body: Wall expandability is extremely poor in this part; **C**: Antrum: An SMT like lesion at the greater curvature suggests submucosal invasion of the cancer; **D**: Lower body: Wall thickening is less prominent; **E**: Mid body: Wall expandability has drastically improved; **F**: Antrum: the SMT like lesion has disappeared.

chemotherapy regimen. TS-1® 80 mg/m^2 was given orally on d 1-14 and 22-35, and paclitaxel 50 mg/m^2 was administered intravenously on d 1, 8, 22 and 29. One course consisted of 35 d, and the following 2 wk were spent as a drug-free period. After 2 courses, the primary tumor was markedly reduced, and the gastric wall expandability improved (Figure 1D-F) (Figure 2C). Ascites have completely vanished (Figure 3C and D), and wall expandability of the sigmoid colon was also improved (Figure 4B).

Adverse effects were carefully monitored and evaluated according to the NCI-CTC criteria. Transient leukocytopenia (grade 2, WBC 2700/μL) and anemia (grade 2, Hb 93 g/L) were observed on d 34, however, both improved during the late courses. Alopecia (grade 1, since d 30) was the only adverse event throughout the following courses.

Since the 1st of August 2002, this regimen was performed predominantly at home, except during the days of paclitaxel infusion (2 days' admission for each), and 27 courses have been completed with the patient in partial remission state, with neither ascites progression nor impairment of activity of daily living. In November 2004, the patient requested to stop further treatment, and the chemotherapy was disrupted in the 28th month since the initial diagnosis. After a 2 mo interval, the patient was, again, hospitalized for the recurrence of massive ascites in January 2005. TS-1® + paclitaxel regimen was resumed immediately; yet the control of ascites was difficult. Despite following several months of treatment, the patient died of peritonitis carcinomatosa in July 2005, 36 mo after the diagnosis. The primary tumor in the stomach has been reduced in size, and no metastases other than in peritoneum were detected.

Table 1 Laboratory findings on admission

WBC	5.3 × 10^9/L	ALP	142 IU/L
Neutrophil	75.4%	Total bilirubin	5 mg/L
Eosinophil	1.9%	Glucose	830 mg/L
Basophil	0.8%	Total cholesterol	3210 mg/L
Monocyte	3.9%	Triglyceride	770 mg/L
Lymphocyte	18%	Na	143 mEq
RBC	4.12 × 10^{12}/L	Cl	107 mEq
Hematocrit	38.1%	K	3.7 mEq
Hemoglobin	126 g/L	BUN	153 mg/L
MCV	92.5 fL	Creatinine	8 mg/L
MCH	30.6 pg	CRP	1 mg/L
MCHC	331 g/L	CEA	< 0.2 μg/L
Platelet	2.6 × 10^{11}/L	CA19-9	9.7 kU/L
Total protein	67 g/L	CA125	44 kU/L
Albumin	37 g/L	PT	10.6 s (99%)
GOT	23 IU/L	APTT	29 s
GPT	21 IU/L	Fbg	2600 mg/L
LDH	275 IU/L		

Hypercholesterolemia and mild elevation of CA125 were the only abnormal findings. WBC: White blood cells; RBC: Red blood cells; MCV: Mean corpuscular volume; MCH: Mean corpuscular hemoglobin; MCHC: Mean corpuscular hemoglobin concentration; GOT: Glutamic oxaloacetic transaminase; GPT: Glutamic pyruvic transaminase; LDH: Lactate dehydrogenase; ALP: Alkaline phosphatase; BUN: Blood urea nitrogen; CRP: C-reactive protein; CEA: Carcinoembryonic antigen; CA19-9: Carbohydrate antigen 19-9; CA125: Carbohydrate antigen 125; PT: Prothrombin time; APTT: Activated partial thromboplastin time; Fbg: Fibrinogen.

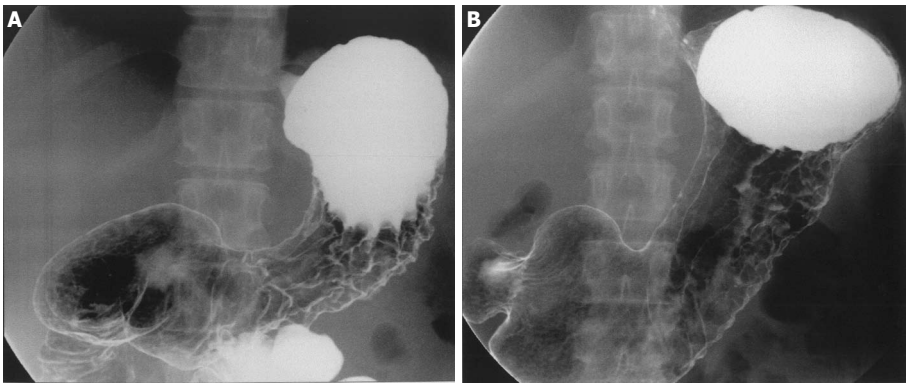

Figure 2 Upper gastrointestinal series before (**A**) and after treatment (**B**). **A**: At diagnosis, wall thickening and loss of expandability is prominent at the body, while normal mucosa is relatively spared at the antrum; **B**: After 6 courses of chemotherapy, the expandability at the body has restored.

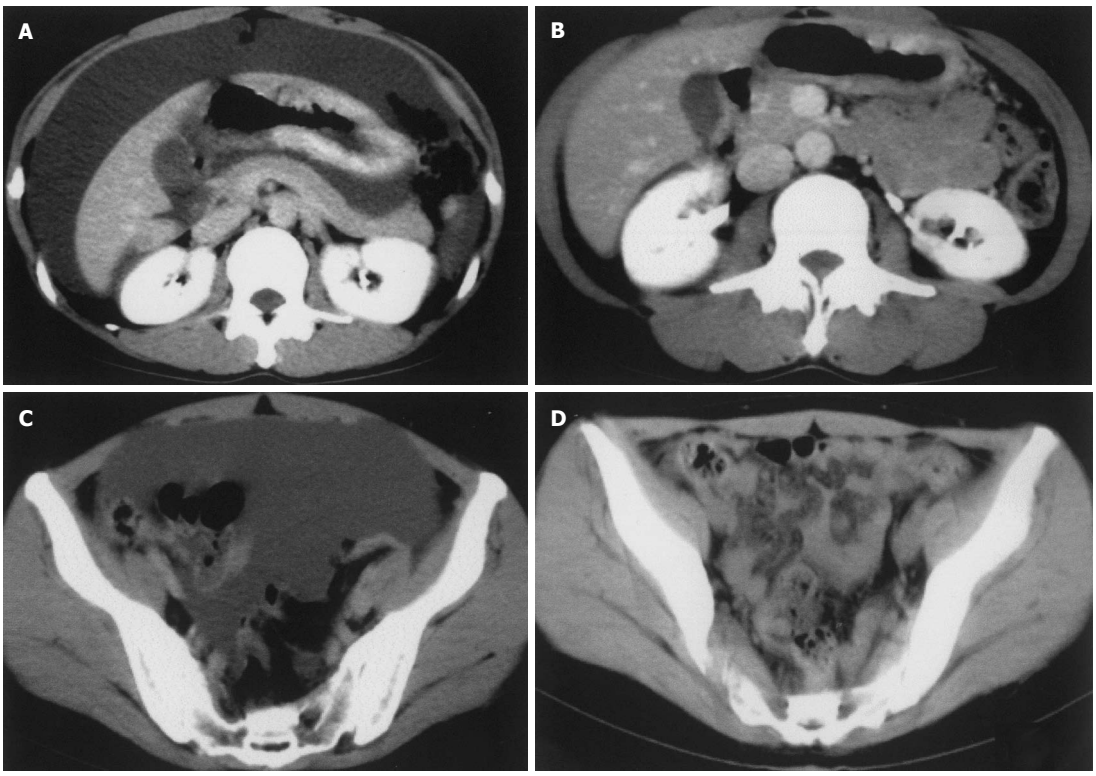

Figure 3 CT scan findings before (Left, **A** and **C**) and after 6 courses of chemotherapy (Right, **B** and **D**). **A**: Antral level: Wall thickening at the body and massive ascites are detected; **B**: Antral level: Wall thickening at the body is less prominent and no ascites can be observed; **C**: Pelvic level: Massive ascites extend to pelvic level; **D**: Pelvic level: Ascites have completely vanished.

DISCUSSION

The prognosis of scirrhous gastric cancer (type 4') is extremely poor, and the 5-year survival rate is reported to be 8.7%-11.3%[1,2]. According to Green *et al*[3], the median survival time (MST) is estimated to be 5.4 mo with chemotherapy, and 1.1 mo with best supportive care. Peritoneal invasion is found in many advanced cases, and even after treatment most of them recur with peritonitis carcinomatosa. Many attempts have been made to treat these cases, for example, systemic/intraperitoneal administration of antineoplastic agents, immunomodulative therapy or hyperthermia, yet none of them have proved prominent efficacy.

On the other hand, TS-1®, both in monotherapy and combined chemotherapy, has shown superior results in the treatment of gastric cancer. In a phase Ⅱ trial in Japan, single administration of TS-1® yielded a higher efficacy (46.5%, 60/129 cases), longer MST (8.1 mo), with a lower incidence of adverse events than historical controls (5-FU, DXR, MTX + LV, CDDP). It proved to be one of the most promising antineoplastic agents[4]. However, against poorly differentiated gastric cancer, the agents above are effective in only a certain proportion of patients. Peritonitis carcinomatosa is especially difficult to treat and is critical to the prognosis. There are several case reports demonstrating the effect of TS-1®, as a monotherapy, against malignant ascites, but evidences from clinical trials are yet to come. To achieve a higher response rate in treating peritonitis carcinomatosa, local concentrations of the agents in ascites are an important factor, and the agents should have different pharmacological effects from TS-1®. Taking these into consideration, we selected paclitaxel as the counterpart of TS-1®, based on the evidence that paclitaxel is highly infiltrative into ascites[5].

Paclitaxel is a novel antimitotic agent, which promotes tubulin polymerization and stabilizes microtubules, resulting in inhibition of mitosis. Besides, it is said to induce tumor apoptosis and inhibit tumor angiogenesis[6]. This agent has been selected as one of the second-line drugs against gastric cancer, especially for cases refractory to first-line drugs (i.e., CDDP, 5-FU) or recurrent cases

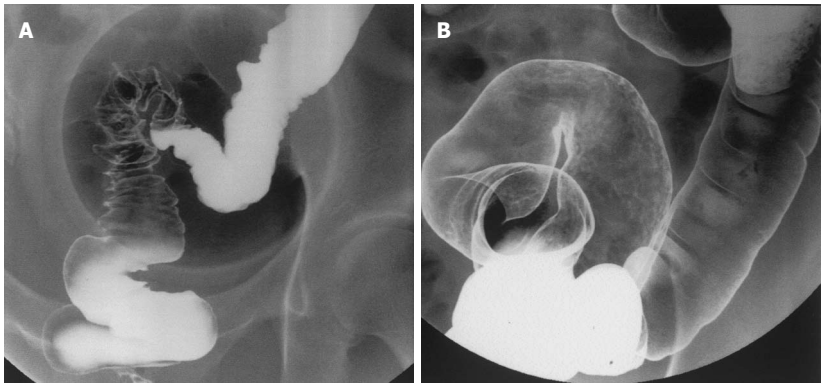

Figure 4 Barium enema before (**A**) and after treatment (**B**). **A**: At diagnosis, poorly expandable segments within the rectosigmoid suggest severe malignant ascites; **B**: After 6 courses of chemotherapy, the rectosigmoidal colon can fully expand with air enema.

after surgery. As a monotherapy, the response rate was 26% in previously treated gastric cancer and 21% in those with prior chemotherapy. And it is remarkable that paclitaxel is the only drug, used in uncombined regimens, that increased over 300 d of MST against advanced and recurrent gastric cancer, regardless of prior treatment history[7]. The administration of paclitaxel against previously untreated gastric cancer has seldom been reported, and the evaluation of combined regimens with TS-1® is still ongoing in phase Ⅰ/Ⅱ studies. At present, the safety of the regimen has been reported in phase Ⅰ study[8], but the efficacy is yet to be proved.

In this aspect, our report suggested important findings; the combined regimen of paclitaxel + TS-1® was safely administered for previously untreated gastric cancer patient, and it was remarkably effective against massive invasion of the cancer, peritonitis carcinomatosa. With the development of many other combined regimens, the treatment against gastric cancer would have various choices. At least, TS-1® + paclitaxel could be one of the first-line regimens against far advanced gastric cancer, especially poorly differentiated adenocarcinoma complicated with peritonitis carcinomatosa.

REFERENCES

1 **Kim DY**, Kim HR, Kim YJ, Kim S. Clinicopathological features of patients with Borrmann type IV gastric carcinoma. *ANZ J Surg* 2002; **72**: 739-742
2 **Chen CY**, Wu CW, Lo SS, Hsieh MC, Lui WY, Shen KH. Peritoneal carcinomatosis and lymph node metastasis are prognostic indicators in patients with Borrmann type IV gastric carcinoma. *Hepatogastroenterology* 2002; **49**: 874-877
3 **Green D**, Ponce de Leon S, Leon-Rodriguez E, Sosa-Sanchez R. Adenocarcinoma of the stomach: univariate and multivariate analysis of factors associated with survival. *Am J Clin Oncol* 2002; **25**: 84-89
4 **Sakata Y**, Ohtsu A, Horikoshi N, Sugimachi K, Mitachi Y, Taguchi T. Late phase II study of novel oral fluoropyrimidine anticancer drug S-1 (1 M tegafur-0.4 M gimestat-1 M otastat potassium) in advanced gastric cancer patients. *Eur J Cancer* 1998; **34**: 1715-1720
5 **Huizing MT**, Rosing H, Huinink WWB. Increased Paclitaxel (P) levels in patients (PTS) with ovary cancer and ascitic (AS) fluid. *Proc ASCO* 1996; **15**: 180
6 **Horwitz SB**. Taxol (paclitaxel): mechanisms of action. *Ann Oncol* 1994; **5** Suppl 6: S3-S6
7 **Yamada Y**, Shirao K, Ohtsu A, Boku N, Hyodo I, Saitoh H, Miyata Y, Taguchi T. Phase II trial of paclitaxel by three-hour infusion for advanced gastric cancer with short premedication for prophylaxis against paclitaxel-associated hypersensitivity reactions. *Ann Oncol* 2001; **12**: 1133-1137
8 **Ueda Y**, Yamagishi H, Ichikawa D, Morii J, Koizumi K, Kakihara N, Shimotsuma M, Takenaka A, Yamashita T, Kurioka H, Nishiyama M, Morita S, Nakamura K, Sakamoto J. Phase I study of a combination of s-1 and weekly paclitaxel in patients with advanced or recurrent gastric cancer. *Oncology* 2005; **69**: 261-268

S- Editor Wang GP **L- Editor** Zhu LH **E- Editor** Lu W

PO Box 2345, Beijing 100023, China
www.wjgnet.com
wjg@wjgnet.com

World J Gastroenterol 2007 January 21; 13(3): 474-477
World Journal of Gastroenterology ISSN 1007-9327

CASE REPORT

Diagnosis by endoscopic ultrasound guided fine needle aspiration of tuberculous lymphadenitis involving the peripancreatic lymph nodes: A case report

Joseph D Boujaoude, Khalil Honein, Cesar Yaghi, Claude Ghora, Gerard Abadjian, Raymond Sayegh

Joseph D Boujaoude, Khalil Honein, Cesar Yaghi, Raymond Sayegh, Department of Gastroenterology, Hotel-Dieu de France hospital, Saint-Joseph University, Beirut, Lebanon
Claude Ghora, Gerard Abadjian, Department of Pathology, Hotel-Dieu de France hospital, Saint-Joseph University, Beirut, Lebanon
Correspondence to: Joseph D Boujaoude, MD, Department of Gastroenterology, Hotel-Dieu de France Hospital, Saint-Joseph University, Beirut, Lebanon. jbouj@hotmail.com
Telephone: +961-3-704890 Fax: +961-1-615295
Received: 2006-02-07 Accepted: 2006-07-07

Abstract

Pancreatic tuberculosis is an extremely rare form of extrapulmonary disease. The diagnosis preoperatively is difficult because clinical, laboratory and radiologic findings are nonspecific. Published data indicate that these lesions mimic cystic neoplasms of the pancreas and the confirmation of clinical suspicion could only be obtained by an open surgical biopsy. Recently, fine needle aspiration cytology has been shown to be a safe, reliable and cost-effective alternative. We report a new case of a peripancreatic tuberculosis in a 52 year old woman and review the relevant literature, paying special attention to the usefulness of endoscopic ultrasound guided-fine needle aspiration in the diagnosis of abdominal tuberculosis.

Key words: EUS guided-FNA; Pancreatic; Tuberculosis

Boujaoude JD, Honein K, Yaghi C, Ghora C, Abadjian G, Sayegh R. Diagnosis by endoscopic ultrasound guided fine needle aspiration of tuberculous lymphadenitis involving the peripancreatic lymph nodes: A case report. *World J Gastroenterol* 2007; 13(3): 474-477

http://www.wjgnet.com/1007-9327/13/474.asp

INTRODUCTION

Tuberculosis is a potentially systemic disease that can affect any organ[1]. Extra-pulmonary organ involvement of tuberculosis is estimated to occur in 10% to 15% of the patients noninfected by HIV. With the increasing use of immunosuppressants and the emergence of AIDS, there has been a resurgence of tuberculosis and the frequency is about 50% to 70% in patients infected by HIV[2]. Abdominal tuberculosis is one of the most prevalent forms of extra-pulmonary diseases. Abdominal infection with tuberculosis commonly affects the spleen, liver and ileo-cecal region. Pancreatic tuberculosis is an extremely rare disease, especially when it is isolated in the pancreas[3]. The abdominal form of tuberculosis has an insidious course without any specific clinical, laboratory or radiological findings[4]. As a result, the diagnosis of abdominal tuberculosis is correct in only 35%-50% of cases and a diagnostic delay is not unusual[5]. Most cases are not diagnosed preoperatively because special staining of biopsy specimens is necessary and cultures of the aspirate require prolonged incubation[6].

A case is presented that highlights the benefit of endoscopic ultrasound (EUS) for evaluation of pancreatic and peri-pancreatic lymphadenopathy tuberculosis. In particular, this case demonstrates the value to obtain suitable tissue samples by EUS fine needle aspiration, thus avoiding unnecessary surgical explorations.

CASE REPORT

A 52-year-old woman, native of a small city in Lebanon, was admitted to the hospital for abdominal pain and fever. She was a cigarette smoker (60 pq/year) without excessive alcohol consumption and had a history of pulmonary embolism. She had been well until one month earlier, when mild epigastric pain developed. Four days before admission, the abdominal pain became constant and severe and nausea developed. She had also chills without frank rigors and a weight loss of 8 kg. The temperature was 38.5℃, the pulse was 100 beats/min, and the respiratory rate was 20 breaths/min. The blood pressure was 130/85 mmHg. On physical examination, the patient did not appear to be severely suffered and there was no jaundice. The lungs and heart sounds were normal. The abdomen was flat, and bowel sounds were present. There was a diffuse abdominal tenderness without rebound tenderness. No mass or hernia was detected. The arms and legs were well perfused. No abnormalities were found on rectal examination. The WBC was normal. C reactive protein (CRP) was moderately elevated (40 UI, normal < 6). The plasma levels of urea nitrogen, creatinine, glucose, electrolytes,

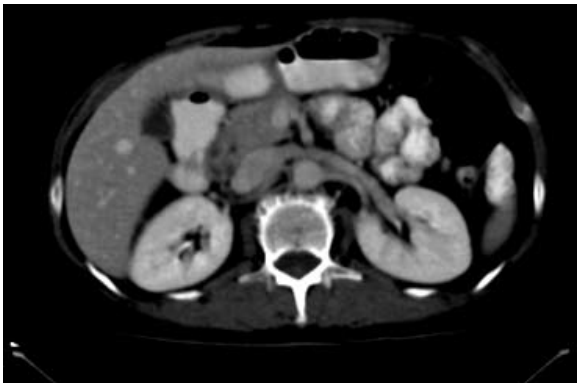

Figure 1 Abdominal computed tomograph revealed a heterogeneously enhanced, multicystic structure, 3 cm in diameter, cephalad to the pancreatic head.

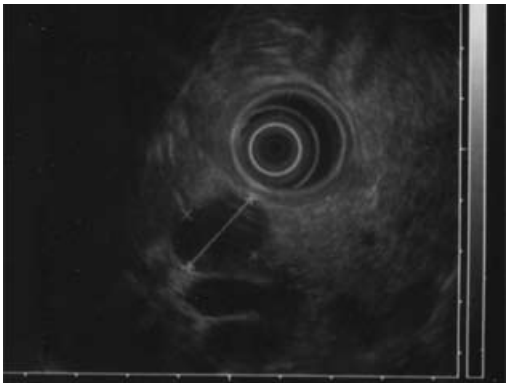

Figure 2 EUS with a radial echoendoscope revealed a large, 2-2.5 cm anoechoic, homogenous, well-defined mass which lay adjacent to the neck of the pancreas.

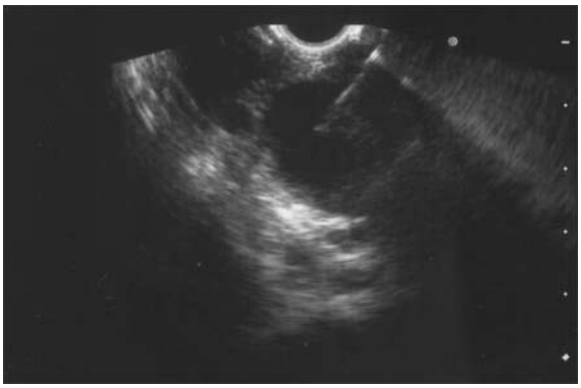

Figure 3 EUS-guided FNA of the peripancreatic lesion was performed using a linear-array echoendoscope.

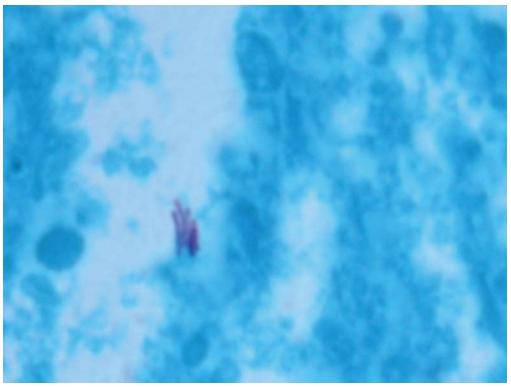

Figure 4 Staining with Ziel Nielson within 30 min yielded a positive result for acid-fast bacilli.

bilirubin, amylase and lipase were normal. Activities of aspartate aminotransferase, alanine aminotransferase and alkaline phosphatase were normal. The total protein level was 75 g/L. A stool specimen was negative for occult blood. The urinalysis was normal. Serologic tests of wright and widal were normal. Radiographs of the abdomen in the supine and upright positions showed air-filled loops of the small bowel, without dilatation or air-fluid levels. No abnormal calcifications were identified. Abdominal and pelvic computed tomographic (CT) studies, performed after the oral and intravenous administration of contrast material, revealed a heterogeneously enhanced, multicystic structure, 3 cm in diameter, cephalad to the pancreatic head (Figure 1). The remainder of the pancreas was unremarkable. The liver, spleen, gallbladder, adrenal glands, kidneys, distal small bowel, colon, urinary bladder, and imaged bones were unremarkable, and no retroperitoneal lymphadenopathy was evident. EUS with a radial echoendoscope (GF-UM160; Olympus [key med], UK) revealed a large, 2-2.5 cm anoechoic, homogenous, well-defined mass, which lay adjacent to the neck of the pancreas (Figure 2). Another homogeneous tumor, 1 to 1.3 cm in diameter, was detected between splenic vessels. EUS-guided FNA (EUS FNA) of the peripancreatic lesion was performed using a linear-array echoendoscope (GF-UC 160P, Olympus) (Figure 3). Blood-stained cellular aspirates were obtained in a total of 2 passes with a 22-gauge needle (Echotip; Wilson Cook). An initial examination of the specimen was not diagnostic (squamous cells, macrophages, and inflammatory cells with no malignant tumor cells). Staining with Ziel Nielson within 30 min yielded a positive result for acid-fast bacilli (Figure 4). Although the patient had no personal or familial history of tuberculosis, the tuberculin test result was positive. The diagnosis of tuberculosis was adopted, and we initiated a four-drug regimen. She was treated with that regimen for 2 months and tolerated it well.

DISCUSSION

Tuberculosis of the pancreas and peripancreatic lymph nodes in immunocompetent patients is rare and could present a diagnostic challenge[1]. The main symptoms are non-specific: epigastric pain, fever, anorexia and weight loss. The duration of symptoms prior to presentation ranges from 5 d to 5 mo[7]. This rare infection usually starts in the peripancreatic lymph nodes and initially spares the pancreas[8]. Tuberculosis can affect the pancreas either by contiguous spread from the peripancreatic lymph nodes or by hematogenous spread[9].

The diagnosis remains difficult and it is especially difficult to differentiate pancreatic tuberculosis from a

pancreatic tumor[1]. Lesions resulting from mycobacterial infection of the pancreas are often complex and cystic and they mimic cystic neoplasms of the pancreas[10-11]. Their cystic nature and the finding of rim enhancement on CT studies probably reflect the presence of central necrosis[12]. The diagnosis of abdominal tuberculosis classically requires microbiological and culture confirmation of mycobacterium tuberculosis[13]. In the past, histopathological and/or bacteriological confirmation of the clinical suspicion of abdominal tuberculosis could only be obtained by an open surgical biopsy[14]. During recent years, fine needle aspiration cytology (FNAC) has been shown to be a safe, quick, reliable and cost-effective alternative for obtaining tissue for cytopathological and bacteriological examination[15]. US guided FNAC is widely accepted as an accurate and safe technique for obtaining tissue from lesions located in virtually any region of the body[16]. In a study by Das *et al*[17], US guidance helped in obtaining an adequate sample in a significantly higher percentage of cases (84.6%) compared with non-guided FNAC (61.5%). On the basis of cytomorphological analysis, results were classified into four groups as follows: (1) definite evidence of tuberculosis: epithelioid granulomas or necrotic material positive for acid-fast bacilli (AFB); (2) presumptive evidence of tuberculosis: epithelioid granulomas with or without necrosis but negative for AFB; (3) suggestive of tuberculosis, presence of necrotic material only with AFB negativity, but in an appropriate clinical setting and with characteristic radiological findings; (4) negative for tuberculosis, presence of atypical inflammation or inadequate material or non representative samples[14].

EUS has been shown to have a high sensitivity for detecting pancreatic masses, although its ability to distinguish a malignancy from an inflammatory disease may be limited[18]. EUS guided-FNA may detect a variety of pathologic processes in the pancreas, including malignant or benign neoplasms, pseudocysts, and reactive changes. Pancreatic EUS guided-FNA allows an accurate and safe diagnosis without the risk, the cost, and the time expenditure of an open biopsy or laparotomy. A review of the literature about image-guided FNA biopsy of the pancreas reveals a relatively high overall sensitivity (64%-98%), specificity (80%-100%), and positive predictive value (98.4%-100%)[19]. Recent technologic advances have made EUS-guided FNA of pancreatic lesions practical. In a study by Volmar *et al*[20], a logistic regression analysis showed that for lesions < 3 cm, the EUS-guided FNA method had higher accuracy than US or CT guided-FNA and no statistically significant difference was seen for larger lesions or for the number of FNA passes. Tumor seeding along a needle tract is an established complication of percutaneous sampling of pancreatic masses under CT or transcutaneous US guidance. The risk of peritoneal carcinomatosis appears to be lower with EUS-guided FNA compared with transcutaneous sampling methods[21]. This is a potential advantage often cited for EUS-FNA. For these reasons, EUS-guided FNA is the method of choice to obtain a tissue sample from the pancreas.

The present case illustrates the usefulness of EUS guided-FNA in the diagnosis of tuberculous lymphadenitis involving peripancreatic lymph nodes.

In conclusion, EUS guided FNA offers a safe and accurate method of achieving a diagnosis in patients with suspected abdominal tuberculosis who present with radiologically demonstrable lesions, especially involving the lymph nodes. EUS guided-FNA should be used as a first step in the diagnosis of abdominal tuberculosis. A laparotomy should be performed only when complications develop or the diagnosis remains unclear in spite of these diagnostic modalities.

REFERENCES

1 **Xia F**, Poon RT, Wang SG, Bie P, Huang XQ, Dong JH. Tuberculosis of pancreas and peripancreatic lymph nodes in immunocompetent patients: experience from China. *World J Gastroenterol* 2003; **9**: 1361-1364

2 **Runyon BA**. Textbook of Gastroenterology. 2nd ed. Philadelphia: *Lippincott* 1995: 928

3 **Sanabe N**, Ikematsu Y, Nishiwaki Y, Kida H, Murohisa G, Ozawa T, Hasegawa S, Okawada T, Toritsuka T, Waki S. Pancreatic tuberculosis. *J Hepatobiliary Pancreat Surg* 2002; **9**: 515-518

4 **Uygur-Bayramicli O**, Dabak G, Dabak R. A clinical dilemma: abdominal tuberculosis. *World J Gastroenterol* 2003; **9**: 1098-1101

5 **al-Hadeedi S**, Walia HS, al-Sayer HM. Abdominal tuberculosis. *Can J Surg* 1990; **33**: 233-237

6 **Riaz AA**, Singh A, Robshaw P, Isla AM. Tuberculosis of the pancreas diagnosed with needle aspiration. *Scand J Infect Dis* 2002; **34**: 303-304

7 **Zhao JP**, Chen ZX. The diagnosis and treatment of tuberculosis of pancreas and peripancreatic lymph nodes. *Zhongguo Jijiu Yixue* 1999; **19**: 737-737

8 **Muneef MA**, Memish Z, Mahmoud SA, Sadoon SA, Bannatyne R, Khan Y. Tuberculosis in the belly: a review of forty-six cases involving the gastrointestinal tract and peritoneum. *Scand J Gastroenterol* 2001; **36**: 528-532

9 **Franco-Paredes C**, Leonard M, Jurado R, Blumberg HM, Smith RM. Tuberculosis of the pancreas: report of two cases and review of the literature. *Am J Med Sci* 2002; **323**: 54-58

10 **Liu Q**, He Z, Bie P. Solitary pancreatic tuberculous abscess mimicking prancreatic cystadenocarcinoma: a case report. *BMC Gastroenterol* 2003; **3**: 1

11 **Kouraklis** G, Glinavou A, Karayiannakis A, Karatzas G. Primary Tuberculosis of the Pancreas Mimicking a Pancreatic Tumor. *Int J Gastrointest Cancer* 2001; **29**: 151-154

12 **Nataraj G**, Kurup S, Pandit A, Mehta P. Correlation of fine needle aspiration cytology, smear and culture in tuberculous lymphadenitis: a prospective study. *J Postgrad Med* 2002; **48**: 113-116

13 **al-Quorain AA**, Facharzt MB, al-Freihi HM, al-Gindan YM, al-Awad N. Abdominal tuberculosis in Saudi Arabia: a clinicopathological study of 65 cases. *Am J Gastroenterol* 1993; **88**: 75-79

14 **Suri R**, Gupta S, Gupta SK, Singh K, Suri S. Ultrasound guided fine needle aspiration cytology in abdominal tuberculosis. *Br J Radiol* 1998; **71**: 723-727

15 **Radhika S**, Rajwanshi A, Kochhar R, Kochhar S, Dey P, Roy P. Abdominal tuberculosis. Diagnosis by fine needle aspiration cytology. *Acta Cytol* 1993; **37**: 673-678

16 **al-Mofleh IA**. Ultrasound-guided fine needle aspiration of retroperitoneal, abdominal and pelvic lymph nodes. Diagnostic reliability. *Acta Cytol* 1992; **36**: 413-415

17 **Das DK**, Pant CS. Fine needle aspiration cytologic diagnosis of gastrointestinal tract lesions. A study of 78 cases. *Acta Cytol* 1994; **38**: 723-729

18 **Brand B**, Pfaff T, Binmoeller KF, Sriram PV, Fritscher-Ravens A, Knöfel WT, Jäckle S, Soehendra N. Endoscopic ultrasound for differential diagnosis of focal pancreatic lesions, confirmed by surgery. *Scand J Gastroenterol* 2000; **35**: 1221-1228

19 **Antillon MR**, Chang KJ. Endoscopic and endosonography

guided fine-needle aspiration. *Gastrointest Endosc Clin N Am* 2000; **10**: 619-636, vi

20 **Volmar KE**, Vollmer RT, Jowell PS, Nelson RC, Xie HB. Pancreatic FNA in 1000 cases: a comparison of imaging modalities. *Gastrointest Endosc* 2005; **61**: 854-861

21 **Micames C**, Jowell PS, White R, Paulson E, Nelson R, Morse M, Hurwitz H, Pappas T, Tyler D, McGrath K. Lower frequency of peritoneal carcinomatosis in patients with pancreatic cancer diagnosed by EUS-guided FNA vs. percutaneous FNA. *Gastrointest Endosc* 2003; **58**: 690-695

S- Editor Yang XX **L- Editor** Zhu LH **E- Editor** Bi L

PO Box 2345, Beijing 100023, China
www.wjgnet.com
wjg@wjgnet.com

World J Gastroenterol 2007 January 21; 13(3): 478-479
World Journal of Gastroenterology ISSN 1007-9327

CASE REPORT

Pancreatic tuberculosis-abdominal tuberculosis presenting as pancreatic abscesses and colonic perforation

Premanayagam Veerabadran, Prasad Sasnur, Sankar Subramanian, Subramanian Marappagounder

Premanayagam Veerabadran, Prasad Sasnur, Department of Surgical Gastroenterology, Sri Ramachandra Medical College and Research Institute, Porur, Chennai, Tamilnadu, India
Sankar Subramanian, Department of Surgical Gastroenterology, Sri Ramachandra Medical College and Research Institute, Porur, Chennai, Tamilnadu, India
Subramanian Marappagounder, Department of Surgical Gastroenterology, Sri Ramachandra Medical College and Research Institute, Porur, Chennai, Tamilnadu, India
Correspondence to: Premanayagam Veerabadran, MS, Department of Surgical Gastroenterology, Sri Ramachandra Medical College and Research Institute, 67, Ramasamy salai, K K Nagar, Chennai 600078, Tamilnadu, India. premnayagam@lycos.com
Telephone: +91-44-24838292 Fax: +91-44-24767008
Received: 2006-08-18 Accepted: 2006-12-07

Abstract

Isolated pancreatic tuberculosis is an extremely rare condition, more so in an immunocompetent individual. Its presentation as pancreatic abscesses with colonic perforation has not been reported so far. This condition poses difficulties in clinical diagnoses. Herein we report a case who was operated in another hospital for pancreatic abscesses, and referred to our institution later when he developed fecal peritonitis due to colonic perforation. Re-laparotomy, resection and exteriorisation of the colon were done. Acid fast bacilli was seen in the histopathological examination of the resected colon. The patient responded remarkably to anti-tuberculous therapy and two sittings of debridement. Post procedure the patient developed pancreatic fistula, which was managed successfully with stenting. Pancreatic tuberculosis should be considered as a differential diagnosis when pancreatitis is atypical.

Key words: Pancreas; Tuberculosis; Acute pancreatitis; Pancreatic abscess; Colonic perforation

Veerabadran P, Sasnur P, Subramanian S, Marappagounder S. Pancreatic tuberculosis-abdominal tuberculosis presenting as pancreatic abscesses and colonic perforation. *World J Gastroenterol* 2007; 13(3): 478-479

http://www.wjgnet.com/1007-9327/13/478.asp

INTRODUCTION

Tuberculosis (TB) of the abdomen is seen in 12% of patients with miliary TB[1]. Isolated involvement of the pancreas without military TB or immunocompromised status is extremely rare. In view of the non-specific clinical presentation, the disease can elude a diagnosis, but once diagnosed it responds favourably to anti-tuberculous therapies (ATT).

CASE REPORT

A 28-year-old male patient was admitted to the casualty department with suspected fecal peritonitis 10 d after having undergone a laparotomy and drainage for pancreatic abscesses at another hospital. He was put on continuous peritoneal lavage. The patient had a history of vague back pain for the past 6 mo. The diagnosis was based on a CT scan as he presented with an unexplained and non-responding fever. CT showed multiple hypodense well defined lesions behind the pancreas (Figure 1).

On admission to our institution, the patient was in a state of severe sepsis with ventilator and hemodynamic support. His abdomen was distended and there was feculent discharge from the main wound and drain. The patient underwent an exploratory laparotomy, which revealed 1 L of purulent fluid and two perforations in the transverse colon. The pancreas appeared edematous and collections of pus were found behind the head of the pancreas. Limited segmental excision of the colon, peritoneal lavage, proximal colostomy and end mucous fistula were done. The patient was managed in the intensive care unit (ICU) in the post-operative period. The patient continued to be in sepsis and was performed a re-exploration, lavage, and laparotomy.

Histopathological examinations (HPE) revealed acid fast bacilli (AFB) (Figure 2) in the specimen of the serosal side of the colon and hence the patient was started on streptomycin/izoniazid/rifampicin/ethambutol. The patient recovered well in the post operative period except for increased pancreatic fluid in the drain tube (71 318 IU/L). The ERCP showed pancreatic ductal disruption and a normal biliary tree. Pancreatic stenting was done. Two days later he was operated for the wound closure. The patient improved with ATT/antibiotics/octreotide/ionotropes and nutritional support and was discharged after two

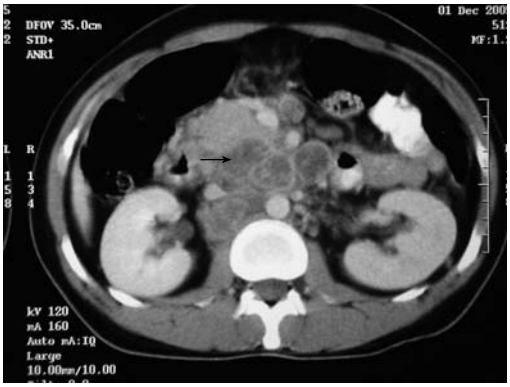

Figure 1 Low density area within lymph node.

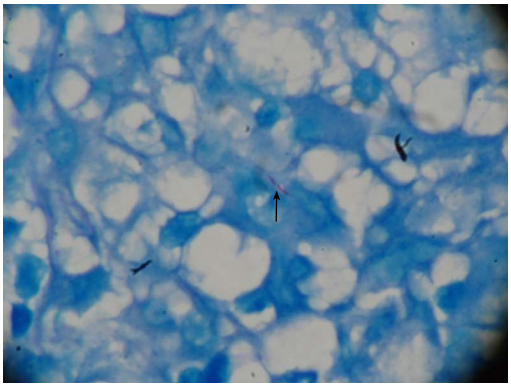

Figure 2 Acid fast bacilli.

weeks. He has improved and gained weight on follow up. A colostomy closure is planned as he has recovered completely.

DISCUSSION

TB of the pancreas is a rare disease and the incidence has been reported to be around 0%-4.7%[2,3]. So far 38 cases of TB of the pancreas were reviewed in a report published in 2000[4] and many more case reports have been published. Various modes of presentation have been reported including pancreatic abscesses[5], acute or chronic pancreatitis, gastrointestinal (GI) bleeding, obstructive jaundice, portal vein obstruction and pancreatic mass mimicking malignancy. Our case is an extremely rare presentation with pancreatic abscesses and colonic perforation. The patient did not have a personal or family history of TB and was immunocompetent with no evidence of any other foci of TB.

Infection is said to involve the pancreas by direct extension, lymphohematogenous dissemination or following reactivation of previous abdominal TB[5,6]. Contrast enhanced CT (CECT) scans may demonstrate a focal hypodense mass, diffuse enlargement of the pancreas, but none of the signs are pathognomonic. Ring enhancement or low-density areas within enlarged lymph nodes should make one suspect tuberculous lymph nodes[7].

In the case we have reported the diagnosis of TB was a surprise and was revealed on HPE of the biopsy specimen obtained at a laparotomy[5], the demonstration of AFB is even more rare as most of the abdominal tuberculosis are paucibacillary. Percutaneous image guided fine needle aspiration of suspicious lesions might suggest the diagnosis of tuberculosis, thereby obviating the need for a diagnostic laparotomy[5].

The presence of caseating granulomatous inflammation is the commonest finding on HPE. In almost half of the patients with extra pulmonary TB, Ziehl Neelson staining for AFB and prolonged culture for mycobacterium tuberculosis has been found negative[8]. Very few are diagnosed by FNA/BIOPSY[5-10]. Once the diagnosis has been established, the majority of patients with tuberculosis respond favourably to ATT[5].

In view of the nonspecific clinical presentation and absence of pathognomonic features on imaging studies, the physician should be alert and have a high index of suspicion, particularly when dealing with young patients, coming from endemic areas with a short duration of symptoms of common pancreatic diseases.

REFERENCES

1 **Haddad FS**, Ghossain A, Sawaya E, Nelson AR. Abdominal tuberculosis. *Dis Colon Rectum* 1987; **30**: 724-735
2 **Bhansali SK**. Abdominal tuberculosis. Experiences with 300 cases. *Am J Gastroenterol* 1977; **67**: 324-337
3 **Auerbach O**. Acute Generalized Miliary Tuberculosis. *Am J Pathol* 1944; **20**: 121-136
4 **Evans JD**, Hamanaka Y, Olliff SP, Neoptolemos JP. Tuberculosis of the pancreas presenting as metastatic pancreatic carcinoma. A case report and review of the literature. *Dig Surg* 2000; **17**: 183-187
5 **Stambler JB**, Klibaner MI, Bliss CM, LaMont JT. Tuberculous abscess of the pancreas. *Gastroenterology* 1982; **83**: 922-925
6 **Stock KP**, Riemann JF, Stadler W, Rösch W. Tuberculosis of the pancreas. *Endoscopy* 1981; **13**: 178-180
7 **Hulnick DH**, Megibow AJ, Naidich DP, Hilton S, Cho KC, Balthazar EJ. Abdominal tuberculosis: CT evaluation. *Radiology* 1985; **157**: 199-204
8 **Farer LS**, Lowell AM, Meador MP. Extrapulmonary tuberculosis in the United States. *Am J Epidemiol* 1979; **109**: 205-217
9 **Addison NV**. Abdominal tuberculosis--a disease revived. *Ann R Coll Surg Engl* 1983; **65**: 105-111
10 **Khoury GA**, Payne CR, Harvey DR. Tuberculosis of the peritoneal cavity. *Br J Surg* 1978; **65**: 808-811

S- Editor Wang GP **L- Editor** Zhu LH **E- Editor** Bi L

PO Box 2345, Beijing 100023, China
www.wjgnet.com
wjg@wjgnet.com

World J Gastroenterol 2007 January 21; 13(3): 480-482
World Journal of Gastroenterology ISSN 1007-9327

CASE REPORT

Chylous ascites secondary to hyperlipidemic pancreatitis with normal serum amylase and lipase

Fahmi Yousef Khan, Issa Matar

Fahmi Yousef Khan, Issa Matar, Department of Medicine, Hamad Medical Corporation, Doha, Qatar
Correspondence to: Dr. Fahmi Yousef Khan, MD, Senior specialist, Department of Medicine, Hamad Medical Corporation, Doha, Qatar. fakhanqal@yahoo.co.uk
Telephone: +974-5275989 Fax: +974-4392273
Received: 2006-09-15 Accepted: 2006-12-02

Abstract

A 54-year old man with a family history of hyperlipidemia was admitted with a 12 h history of severe generalized abdominal pain associated with nausea, vomiting and abdominal distension. Examination of the abdomen revealed tenderness in the periumblical area with shifting dullness. Serum pancreatic amylase was 29 IU/L and lipase 44 IU/L, triglyceride 36.28 mmol/L. Ultrasound showed ascites. CT of the abdomen with contrast showed inflammatory changes surrounding the pancreas consistent with acute pancreatitis. Ultrasound (US) guided abdomen paracentesis yielded a milky fluid with high triglyceride content consistent with chylous ascites. The patient was kept fasting and intravenous fluid hydration was provided. Meperidine was administered for pain relief. On the following days the patient's condition improved and he was gradually restarted on a low-fat diet, and fat lowering agent (gemfibrozil) was begun, 600 mg twice a day. On d 14, abdomen US was repeated and showed fluid free peritoneal cavity. The patient was discharged after 18 d of hospitalization with 600 mg gemfibrozil twice a day. At the time of discharge, the fasting triglyceride was 4.2 mmol/L. After four weeks the patient was seen in the clinic, he was well.

Key words: Amylase; Chylous ascites; Hyperlipidemic pancreatitis

Khan FY, Matar I. Chylous ascites secondary to hyperlipidemic pancreatitis with normal serum amylase and lipase. *World J Gastroenterol* 2007; 13(3): 480-482

http://www.wjgnet.com/1007-9327/13/480.asp

INTRODUCTION

There are many etiologic factors leading to pancreatitis. Hypertriglyceridemia (HTG) is seldom diagnosed as one of these factors. Pancreatitis secondary to HTG, presents typically as an episode of acute pancreatitis (AP) or recurrent AP, rarely as chronic pancreatitis. Although AP often requires clinicians to rely on laboratory tests, such as serum amylase and lipase, as diagnostic aids, patients with acute pancreatitis secondary to HTG can have normal amylase[1] and lipase levels. Furthermore, acute pancreatitis is a recognized cause of chylous ascites[2]. Association of normal amylase and lipase acute pancreatitis secondary to HTG with chylous ascites is extremely rare. A PubMed search of the literature revealed no cases with such association. We report here an exceptionally rare case of a 54-year old man with chylous ascites secondary to hyperlipidemic pancreatitis with normal serum amylase and lipase.

CASE REPORT

A 54-year old man was admitted with a 12 h history of severe generalized abdominal pain associated with nausea, vomiting and abdominal distension. His history was negative for weight loss, malignancy, recent abdominal surgery, travel abroad, abdominal trauma, and underlying liver or kidney diseases. He had a positive family history of hyperlipidemia. Initial examination was notable for a temperature of 37℃, pulse 113 beats/min, respiratory rate 16/min, and blood pressure 130/85 mmHg. The patient appeared ill and examination of the abdomen revealed tenderness in the periumblical area with shifting dullness but without organomegaly. Rectal examination was normal. The remainder of the examination was unremarkable.

Initial investigations showed hemoglobin level of 150 g/L, total leucocyte count 12 × 10^9/L (60% neutrophils, 31% lymphocytes) and adequate number of platelets. Blood chemistry, liver function test and coagulation profile were normal. Serum pancreatic amylase was 29 IU/L (normal, 15-55 IU/L) and lipase 44 IU/L (normal, 13-60 IU/L), triglyceride 36.28 mmol/L, total cholesterol 5.2 mmol/L. On the next day serum pancreatic amylase was 45 IU/L, lipase 50.2 IU/L, and fasting triglyceride 25 mmol/L. An antibody to human immunodeficiency virus was negative.

Ultrasound showed fluid collection (ascites) but could not visualize the pancrease. CT of the abdomen and pelvis with contrast showed pelvic ascites (Figure 1A) and inflammatory changes surrounding the pancreas consistent with acute pancreatitis (Figure 1B). The pancreas was well demarcated and homogenous with no focal lesions. No

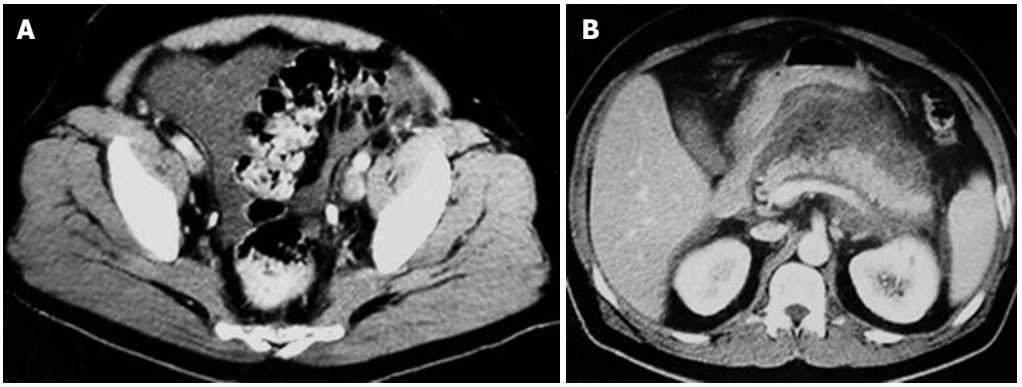

Figure 1 CT of the abdomen with contrast showing pelvic ascites (**A**) and inflammatory changes surrounding the pancreas (**B**). The pancreas is well demarcated and homogenous with no focal lesions.

abnormal masses or enlarged lymph nodes were found.

Acute pancreatitis secondary to hypertriglyceridaemia was diagnosed despite normal plasma amylase and lipase concentrations. Ultrasound-guided abdomen paracentesis yielded a milky fluid with the following biochemical composition: 3.2 g/L triglycerides, 0.85 g/L cholesterol, 49 g/L total protein, 30 g/L albumin, 0.72 g/L glucose and 121 U/L LDH. Cell count of the fluid was 230×10^6/L and no acid-fast bacilli (AFB) were present in smear. This high triglyceride ascites was consistent with chylous ascites.

The patient was kept fasting from the first hospital day, and intravenous fluid hydration was provided. Meperidine was administered for pain relief. On the 5th hospital day the pain reduced and the serum pancreatic amylase was 48 IU/L, lipase 55 IU/L, and triglyceride 16.2 mmol/L. On the 6th d a low fat diet was resumed and fat lowering agent (gemfibrozil) was initiated, 600 mg, twice a day. On 14th d abdomen ultrasound (US) was repeated and showed fluid free peritoneal cavity. Workup for lymphoma and malignancy including chest CT, colonoscopy and upper endoscopy were negative. A culture of ascitic fluid for TB infection was negative. The patient was discharged after 18 d of hospitalization with gemfibrozil 600 mg twice a day. At the time of discharge, the serum pancreatic amylase was 15 IU/L, lipase 33 IU/L, and triglyceride 4.2 mmol/L.

On follow-up evaluation approximately 4 wk after the patient was discharged from the hospital, the patient was symptom free. Repeat physical examination was unremarkable. Laboratory evaluation yielded serum pancreatic amylase of 8 IU/L and lipase of 20 IU/L, triglyceride of 3.2 mmol/L. Abdomen ultrasound and CT showed fluid free peritoneal cavity with normal pancreas.

DISCUSSION

Acute pancreatitis is an important cause of acute upper abdominal pain. Because its clinical features are similar to a number of other acute illnesses, it is difficult to make a diagnosis only on the basis of symptoms and signs. Acute pancreatitis can be suspected clinically, but requires biochemical and radiologic and sometimes histologic evidence to confirm the diagnosis.

The diagnosis is most often confirmed by evaluation of serum amylase and lipase levels. The diagnosis of acute pancreatitis is made by a serum amylase activity four times above normal (or by a lipase activity greater than twice the upper limit of normal)[3].

The sensitivity and specificity of amylase and lipase are reported to be considerably dependent on the detection method used, ranging from 70% to 100% and 33% to 89% for serum amylase, and from 74% to 100% and 34% to 100% for serum lipase, respectively[4]. Recognizing factors that reduce the sensitivity and specificity of serum amylase and lipase can help prevent misdiagnosis and allow for appropriate treatment. Factors that can lead to normal amylase and lipase values are hypertriglyceridemia (as in this patient) and extensive pancreatic necrosis (acute fulminant or acute chronic pancreatitis)[5].

In such patients (as in this patient) CT scanning provides an accurate confirmation of clinical and laboratory findings and offers excellent anatomic and morphologic representation of the pancreas and peripancreatic tissue.

It was observed that plasma triglyceride levels higher than 500 mg/dL interfere with *in vitro* determination of the actual amylase level by preventing the calorimetric reading of the assay end point[4]. However, the reasons for normal serum amylase and lipase level in patients with hypertriglyceridemia-associated pancreatitis are still a dilemma. We reviewed the files of the patients admitted to our hospital with acute pancreatitis, from January 2004 to December 2005. The number of patients labeled as hypertriglyceridemia-associated pancreatitis was 18, of which only one patient (5.5%) had normal serum amylase and lipase level. Serial dilutions of the patient' s sample with the assay buffer to reduce interference of light transmission by hyperlipidemic serum can reveal an abnormal amylase value that was previously masked by the lactescent plasma[1].

Overall, although pancreatitis caused by hypertriglyceridemia has the same prognosis as other causes of the acute episode[6], early recognition and treatment have been shown to hasten clinical recovery[7,8].

True chylous ascites is defined as the presence of ascitic fluid with high fat (triglyceride) content, usually higher than 2 g/L, although some authors use a cutoff value of 1.1 g/L[9-12]. True chylous ascites must be distinguished from chyliform and pseudochylous effusions, in which the turbid, milky appearance is due to cellular degeneration caused by bacterial peritonitis or malignancy. A low triglyceride level is characteristic of these effusions.

There are multiple causes of chylous ascites. The

most common causes in Western countries are abdominal malignancy and cirrhosis, which account for over two-thirds of all cases. In contrast, infectious etiologies (i.e., tuberculosis and filariasis) are responsible for the majority of cases in developing countries. Other causes include congenital, inflammatory (e.g., acute and chronic pancreatitis), post-operative, traumatic, and miscellaneous disorders.

Kelley and Butt of the Mayo Clinic[13] reported that 62 (87%) of 71 cases of chylous ascites, were secondary to malignancy.

Chylous ascites might occur due to different mechanisms[14]: (1) obstruction of the lymph flow caused by external pressure (mass) causing leakage from dilated subserosal lymphatics into the peritoneal cavity; (2) exudation of lymph through the walls of dilated retroperitoneal vessels lacking valves, which leak fluid through a fistula into the peritoneal cavity as in congenital lymphangiectasia; and (3) traumatic thoracic duct obstruction causing direct leakage of chyle through a lymphoperitoneal fistula.

Basically, acute or chronic pancreatitis, can cause compression of adjacent lymphatic channels resulting in chylous ascites[15].

Conservative medical treatment should be the first step in managing all patients with chylous ascites. The treatment should be directed at the underlying disorder. In this patient, cure of acute pancreatitis and reduction in triglyceride level led to resolution of chylous ascites. General measures include withholding oral feedings and starting total parenteral nutrition to minimize pancreatic exocrine secretion[16]. One-third of patients can improve on conservative management and do not require any further intervention[17]. Treatment with somatostatin or octreotide together with diuretics and repeated paracentesis may be beneficial for some patients[18,19]. Some patients fail medical therapy, ultimately requiring surgery[20].

In conclusion, relying solely on high serum amylase and/or lipase level to establish the diagnosis of acute pancreatitis is unjustified and should be abandoned, because hypertriglyceridemia can cause spuriously normal amylase and lipase levels. Consequently, abdominal computer tomography scan might be useful in establishing the diagnosis of acute pancreatitis when hypertriglyceridemia interferes with the evaluation of pancreatic enzyme activities and ultrasound examination provides poor pancreatic visualization.

REFERENCES

1 **Fallat RW**, Vester JW, Glueck CJ. Suppression of amylase activity by hypertriglyceridemia. *JAMA* 1973; **225**: 1331-1334
2 **Ben-Ami H**, Nagachandran P, Assalia A, Edoute Y. Acute transient chylous ascites associated with acute biliary pancreatitis. *Am J Med Sci* 1999; **318**: 122-123
3 **Steinberg W**, Goldstein S, Davis N. Diagnostic assays in acute pancreatitis. *Ann Intern Med* 1985; **103**: 475-476
4 **Wong EC**, Butch AW, Rosenblum JL. The clinical chemistry laboratory and acute pancreatitis. *Clin Chem* 1993; **39**: 234-243
5 **Greenberger NJ**, Toskes PP. Approach to the patient with pancreatic disease. In: Braunwald E, Isselbacher KJ, Petersdorf RG, Wilson JD, Martin JB, Fauci AS, editors. Harrison's principles of internal medicine. New York: McGraw Hill, 1987: 1368-1372
6 **Fortson MR**, Freedman SN, Webster PD. Clinical assessment of hyperlipidemic pancreatitis. *Am J Gastroenterol* 1995; **90**: 2134-2139
7 **Piolot A**, Nadler F, Cavallero E, Coquard JL, Jacotot B. Prevention of recurrent acute pancreatitis in patients with severe hypertriglyceridemia: value of regular plasmapheresis. *Pancreas* 1996; **13**: 96-99
8 **Tenner S**, Banks PA. Acute pancreatitis: nonsurgical management. *World J Surg* 1997; **21**: 143-148
9 **Cárdenas A**, Chopra S. Chylous ascites. *Am J Gastroenterol* 2002; **97**: 1896-1900
10 **Press OW**, Press NO, Kaufman SD. Evaluation and management of chylous ascites. *Ann Intern Med* 1982; **96**: 358-364
11 **Runyon BA**, Akriviadis EA, Keyser AJ. The opacity of portal hypertension-related ascites correlates with the fluid's triglyceride concentration. *Am J Clin Pathol* 1991; **96**: 142-143
12 **Jüngst D**, Gerbes AL, Martin R, Paumgartner G. Value of ascitic lipids in the differentiation between cirrhotic and malignant ascites. *Hepatology* 1986; **6**: 239-243
13 **Kelley ML**, Butt HR. Chylous ascites: an analysis of its etiology. *Gastroenterology* 1960; **39**: 161-170
14 **Browse NL**, Wilson NM, Russo F, al-Hassan H, Allen DR. Aetiology and treatment of chylous ascites. *Br J Surg* 1992; **79**: 1145-1150
15 **Goldfarb JP**. Chylous effusions secondary to pancreatitis: case report and review of the literature. *Am J Gastroenterol* 1984; **79**: 133-135
16 **Variyam EP**. Central vein hyperalimentation in pancreatic ascites. *Am J Gastroenterol* 1983; **78**: 178-181
17 **Stone LD**. Pancreatic ascites. *Br J Hosp Med* 1986; **35**: 252-253
18 **Oktedalen O**, Nygaard K, Osnes M. Somatostatin in the treatment of pancreatic ascites. *Gastroenterology* 1990; **99**: 1520-1521
19 **Uhl W**, Anghelacopoulos SE, Friess H, Büchler MW. The role of octreotide and somatostatin in acute and chronic pancreatitis. *Digestion* 1999; **60** Suppl 2: 23-31
20 **Gómez-Cerezo J**, Barbado Cano A, Suárez I, Soto A, Ríos JJ, Vázquez JJ. Pancreatic ascites: study of therapeutic options by analysis of case reports and case series between the years 1975 and 2000. *Am J Gastroenterol* 2003; **98**: 568-577

S- Editor Pan BR **L- Editor** Wang XL **E- Editor** Bi L

PO Box 2345, Beijing 100023, China
www.wjgnet.com
wjg@wjgnet.com

World J Gastroenterol 2007 January 21; 13(3): 483-485
World Journal of Gastroenterology ISSN 1007-9327

CASE REPORT

Spontaneous gastrojejunal fistula is a complication of gastric ulcer

Đorđe M Ćulafić, Olivera D Matejić, Vladimir S Đukić, Miodrag D Vukčević, Mirko D Kerkez

Đorđe M Ćulafić, Olivera D Matejić, Clinic of Gastroenterology and Hepatology, Institute of Digestive Diseases, Clinical Center of Serbia, Medical Faculty, Belgrade, Serbia
Vladimir S Đukić, Mirko D Kerkez, Clinic of Surgery, Institute of Digestive Diseases, Clinical Center of Serbia, Medical Faculty, Belgrade, Serbia
Miodrag D Vukčević, Institute of Pulmonary Diseases, Clinical Center of Serbia, Medical Faculty, Belgrade, Serbia
Correspondence to: Assistant Professor Đorđe Ćulafić, Institute of Digestive Diseases, Clinical Center of Serbia, Koste Todorovića 6, Belgrade 11000, Serbia. dculafic@eunet.yu
Telephone: +387-11-2629811 Fax: +387-11-2629811
Received: 2006-10-19 Accepted: 2006-12-07

Abstract

Spontaneous gastrojejunal fistula formation is an extremely rare complication of gastric ulcer disease. We report a 77-year old woman who presented with diffuse abdominal pain, weight loss, malaise, nausea, and occasional dark stools. Laboratory tests showed extreme hyposideremic anemia with inflammatory syndrome. In addition, biochemical parameters of malnourishment were presented. Upper endoscopy revealed the patent esophagus along the full length without any pathological changes. Large and deep ulceration with perforation in the small intestine was detected in the posterior gastric wall. The small intestine loop was reached by endoscope through spontaneously developed gastrojejunal fistula. Polytopic biopsies of described ulcerative change were carried out. Histopathologically reepithelialized ulcerous zone was seen in the gastric mucosa. Also, gastrojejunal fistula was visualized after wide opening of hepatogastric and gastrocolic ligament. Jejunal loop 25 cm from ligament of Treitz was attached to mesocolon and posterior gastric wall because of ulcer penetration. Postoperative course was uneventful. Per oral intake started on the 4th postoperative day, and the patient was discharged on the 8th postoperative day. In summary, this case indicates that persistent symptoms of peptic ulcer disease associated with nutritional disturbances may be caused by gastrojejunal fistula.

Key words: Gastric ulcer; Spontaneous; Gastrojejunal fistula

Ćulafić ĐM, Matejić OD, Đukić VS, Vukčević MD, Kerkez MD. Spontaneous gastrojejunal fistula is a complication of gastric ulcer. *World J Gastroenterol* 2007; 13(3): 483-485

http://www.wjgnet.com/1007-9327/13/483.asp

INTRODUCTION

The inflammatory response to deeply penetrating peptic ulcer can lead to formation of a fistula between the stomach and duodenum or any structure nearby. Fistulae to the pancreatic duct, biliary tract, and colon have been described more commonly. Fistula arising between the stomach and duodenum called "double pylorus" is also a well-recognized complication of peptic ulcer disease[1,2]. Rarely, duodenal ulcer can penetrate to adjoin vascular structures and induce aorto-enteric or cavo-enteric fistula[3,4]. Such fistulae are usually characterized by less acute symptoms and in some instances represent a very challenging problem. In each case in which fistula is identified, cancer must be considered in differential diagnosis. In general, the small intestine is not found in proximity to the stomach or duodenum, protected as it is by the transverse colon and mesocolon. However, fistula to the small intestine has been reported to occur with typical ulcer symptoms[5]. We present a case of gastric ulcer disease complicated by gastrojejunal fistula.

CASE REPORT

A 77-year old woman was admitted for diffuse abdominal pain, weight loss, malaise, nausea, and occasional dark stools. Physical examination revealed malnourished, pale skin and apparent mucosa. The abdomen was soft (no local or rebound tenderness), diffusely painful, mostly in epigastrium. Laboratory test showed extreme hyposideremic anemia (HGB = 39 g/L, RBC=2.38 × 10^{12}/L, HCT = 13.4%, MCV = 5.64 × 10^{-14} L, and serum Fe = 5.6 μmol/L) and inflammatory syndrome (ESR = 44 mm/h, fibrinogen = 7.4 g/L, C-reactive protein = 38.0 mg/L, and PLT = 813 × 10^{9}/L). In addition, biochemical parameters of malnourishment were presented (such as cholesterol level = 3.0 mmol/L, triglycerides = 0.6 mmol/L, total proteins = 55.5 g/L, and serum albumins = 29 g/L). Upper endoscopy revealed the patent esophagus along the full length without any pathological changes. Large and deep ulceration with perforation in the small intestine was detected in the posterior gastric wall (Figure 1). The small intestine loop was reached by endoscope through spontaneously developed gastrojejunal fistula (Figure 2). Antrum, pylorus, bulbus and postbulbar duodenum were

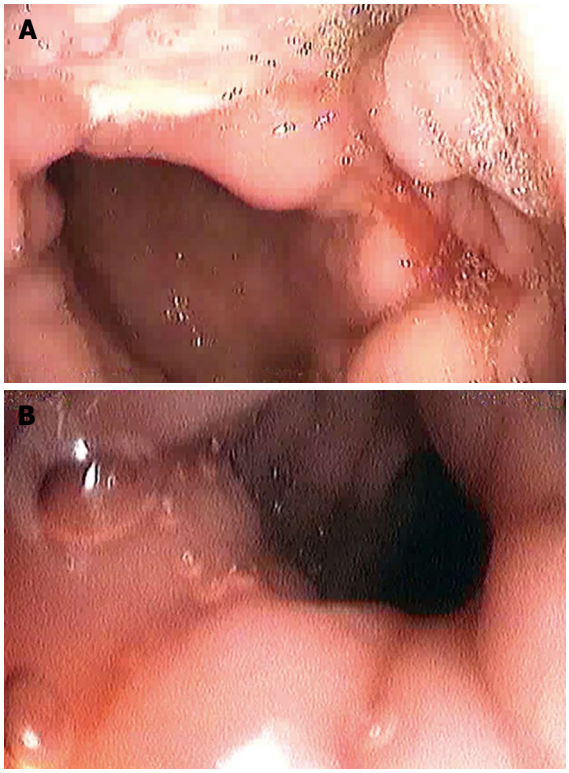

Figure 1 Upper endoscopy showing large and deep ulceration in the posterior gastric wall (**A**) and ulceration with perforation in the small intestine (**B**).

normal in appearance. Polytopic biopsies of described ulcerative change were carried out. A histopathologically reepithelialized ulcerous zone was seen in the gastric mucosa. The signs of chronic antral atrophic inflammation were noted around the ulcerous mucosal parts, with strong activity, and hypersecretory and partially regenerative foveolar hyperplasia. *H pylori* test result was negative. The signs of non-specific active non-homogenous inflammatory infiltration with occasional sero-hemorrhagic superficial exudation were present in the mucosa of the small intestine. Real-time abdominal ultrasonography and computerized tomography findings were normal.

Upper central laparotomy was performed. A gastrojejunal fistula was visualized after wide opening of hepatogastric and gastrocolic ligament. The jejunal loop 25 cm from ligament of Treitz was attached to mesocolon and posterior gastric wall because of ulcer penetration (Figure 3A). After careful division of the jejunal loop from duodenojejunal reflection, the fistula was resected (Figure 3B). The jejunal loop defect was closed after wedge excision (histopathological verification ex tempore confirmed benign finding), with two-layer 4.0 vicryl (Ethicon) stitches. Subsequently, subtotal mastectomy was performed because of another giant gastric ulcer proximal to fistula. Gastrojejunostomy was created in the usual fashion (two layers of 4.0 vicryl) continuously with retro colic position of anatomists. After lavage and drainage of the right sub hepatic space, the abdominal wound was closed with Maxon-loop2 (Davis-Gecko). Postoperative course was uneventful**.** Per oral intake started on the 4th postoperative day, and the patient was discharged on the 8th postoperative day.

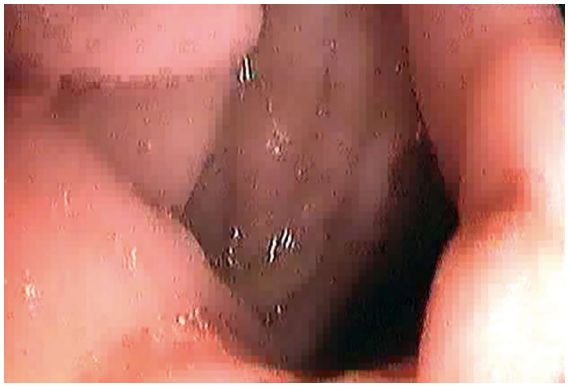

Figure 2 Small intestine loop reached by endoscope through spontaneously eloped gastrojejunal fistula.

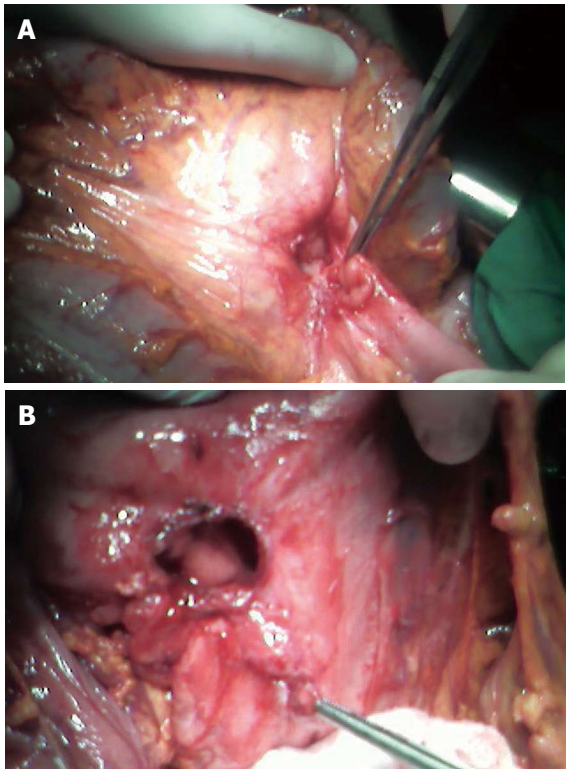

Figure 3 Hole in mescaline with gastrojejunal fistula (**A**) and defect in posterior gastric wall after resection of fistula and deep gastric ulcer (**B**).

DISCUSSION

Spontaneous gastrojejunal fistula formation is rare and its differential diagnosis is multifactorial. Malignancy should be ruled out by careful endoscopic evaluation and appropriate imaging studies. Precise etiologic determination is necessary for proper management. In contrast to gastrocolic fistula, symptoms of the gastrojejunal fistula are those of the ulcer diathesis itself. However, if the target region of the fistula is very proximal, there is no short-circuiting of gastric contents; but if the target site is distal, the symptoms and nutritional disturbances may be similar to those observed with gastrocolic fistula[6].

Our patient manifested the symptoms of nutritional disturbances other than symptoms of ulceration, abdominal pains and recurring hemorrhage. Matsuoka *et al*[7]

have described an 81-year old woman who had multiple recurrences of gastric ulcer after the left femoral head fracture, necessitating the mechanical bone head exchange operation. Gastro-endoscopic examination revealed a giant ulcer with long-axis diameter of more than 5 cm in the lesser curvature of stomach. Two weeks later, a fistula was formed between the stomach and jejunum. It was successfully managed by intravenous H_2-antagonist and oral intake was restricted. Operative stress and application of ipriflavone appeared to have induced gastric ulcer recurrence. However, malnourishment of the patient contributed to the development of fistula between the stomach and jejunum which was very lean and had minimal mesenteric adipose tissue. Our patient was also lean with minimal mesenteric adipose tissue. However, risk factors, *H pylori* infection, nonsteroidal anti-inflammatory drug ingestion, and operative stress were absent. Indications for surgery are other complications such as free perforation, obstruction, refractory bleeding, or failure to heal with maximum medical therapy and persistent symptoms, rather than the fistula *per se*.

In case of our patient, surgical intervention was definitely indicated due to recurrent bleeding and symptoms of nutritional disturbances. In addition, gastrojejunal fistula secondary to gastric cancer is extremely rare. Choi *et al*[8] have described a 56-year-old man who was diagnosed with advanced gastric cancer. Fluoroscopic examination visualized two abnormal passages of contrast medium from the stomach: one to the colon, and the other to the jejunum. Fiber gastroscopy revealed a tumor in the greater curvature of stomach which appeared to penetrate in the colon, and a tumor in the antrum directly which invaded the jejunum. Souma *et al*[9] have described a 55-year old man seen for epigastralgia and weight loss. Barium radiography and endoscopic study revealed a gastric cancer associated with gastrojejunal fistula. At laparotomy, they found that the gastric tumor had extended to the transverse mesocolon, jejunum and pancreas, although no liver metastasis or peritoneal dissemination was seen. In addition, this patient, to their knowledge, is the fifth reported case in the world. In summary, this case indicates that persistent symptoms of peptic ulcer disease associated with nutritional disturbances may be caused by gastrojejunal fistula.

REFERENCES

1 **Einhorn RI**, Grace ND, Banks PA. The clinical significance and natural history of the double pylorus. *Dig Dis Sci* 1984; **29**: 213-218

2 **Hu TH**, Tai DI, Changchien CS, Chen TY, Chang WC. Double pylorus: report of a longitudinal follow-up in two refractory cases with underlying diseases. *Am J Gastroenterol* 1995; **90**: 815-818

3 **Odze RD**, Bégin LR. Peptic-ulcer-induced aortoenteric fistula. Report of a case and review of the literature. *J Clin Gastroenterol* 1991; **13**: 682-686

4 **Godwin TA**, Mercer G, Holodny AI. Fatal embolization of intestinal contents through a duodenocaval fistula. *Arch Pathol Lab Med* 1991; **115**: 93-95

5 **Phifer TJ**, Gladney JD, McDonald JC. Gastrojejunal fistula: a complication of peptic ulcer disease. *South Med J* 1986; **79**: 1015-1017

6 **Tavenor T**, Smith S, Sullivan S. Gastrocolic fistula. A review of 15 cases and an update of the literature. *J Clin Gastroenterol* 1993; **16**: 189-191

7 **Matsuoka M**, Yoshida Y, Hayakawa K, Fukuchi S. Gastrojejunal fistula caused by gastric ulcer. *J Gastroenterol* 1998; **33**: 267-271

8 **Choi SW**, Yang JM, Kim SS, Kang SH, Ro HJ, Song KS, Ha HK, Lim KW, Kim JS. A case of combined gastrojejunal and gastrocolic fistula secondary to gastric cancer. *J Korean Med* Sci 1996; **11**: 437-439

9 **Souma S**, Ishimoto K, Ohyanagi H. A case of extended operation for gastric cancer accompanied with gastrojejunal fistula and pancreas invasion. *Jpn J Gastroentrol Surg* 2004; **37**: 1639-1643

S- Editor Wang GP **L- Editor** Wang XL **E- Editor** Bi L

PO Box 2345, Beijing 100023, China
www.wjgnet.com
wjg@wjgnet.com

World J Gastroenterol 2007 January 21; 13(3): 486-487
World Journal of Gastroenterology ISSN 1007-9327

LETTERS TO THE EDITOR

Does type of instrument influence colonoscopy performance and sedation practice?

Ramesh P Arasaradnam, Paul D Hurlstone

Ramesh P Arasaradnam, School of Clinical Medical Sciences, Newcastle University, Newcastle, United Kingdom
Paul D Hurlstone, Academic Department of Gastroenterology, Sheffield Teaching Hospitals, Sheffield, United kingdom
Correspondence to: Ramesh P Arasaradnam, M2020, Cookson Building, School of Clinical Medical Sciences, Newcastle University, Newcastle NE2 4HH, United Kingdom. r.p.arasaradnam@ncl.ac.uk
Telephone: +44-191-2225951 Fax: +44-191-2226720
Received: 2006-10-04 Accepted: 2006-11-11

Key words: Colonoscopic performance; Sedation; Olympus; Fujinon

Arasaradnam RP, Hurlstone PD. Does type of instrument influence colonoscopy performance and sedation practice? *World J Gastroenterol* 2007; 13(3): 486-487

http://www.wjgnet.com/1007-9327/13/486.asp

TO THE EDITOR

In the UK, clear guidelines exist as to the expected level of competence an individual endoscopist should achieve. This is of utmost importance given the variance in practice among endoscopic departments as highlighted by the National Colonoscopy audit in 2002[1]. The audited variables included sedation practice, caecal completion and complication rates, but not the type of instrument used.

The type of instrument used has been shown by some groups to influence colonoscopy performance; for example paediatric colonoscopies are thought to aid intubation in patients with fixed angulation of the colon whilst variable stiffness colonoscopes are useful to negotiate tortuous recto-sigmoid junctions. Several studies have attempted to determine if different instruments have effects either on caecal intubation or time to caecal intubation. The findings however are conflicting, with some studies showing a benefit[2-3] and others none[4-6]. Most of these studies made comparisons between different types of Olympus colonoscopes, i.e. single manufacturer rather than an alternative (Fujinon/Pentax). Furthermore, only one study[2] assessed the dose and type of sedation used whilst in two studies[4,5], assessments were by a single experienced endoscopist. Thus, it is difficult to conclude definitively if a different make of colonoscope in less experienced hands influences not only colonoscopic performance but also sedation practice. The aim of this study was to determine if the type of colonoscope used could influence not only caecal intubation rates but also sedation practice.

Table 1 Subject characteristics and summary of results

Total (n = 199)	M:F	Age (SD) (yr)	Mean dose of Mdz/mg (SD)	No sedation	CIR	TIR
Olympus CF 240 (n = 105)	1:1.3	65 (± 14)	2.7 (± 1.4)	31 (30%)	102 (97%)	73 (70%)
Fujinon EC-450 (n = 94)	1:2.1	64 (± 11)	3.7[b] (± 1.4)	0	84[d] (89%)	46 (49%)

SD: Standard Deviation; Mdz: Midazolam; CIR: Caecal intubation rates; TIR: Terminal ileal intubation rate. [b]$P < 0.001$, [d]$P < 0.001$ comparison between Fujinon EC-450 and Olympus CF 240 on mean dose of Mdz and CIR.

We studied 199 consecutive procedures on two sites performed by a single endoscopist prospectively. The first 105 procedures were performed using the Olympus EVIS CF 240 variable stiffness scope whilst the subsequent 94 were performed using a Fujinon EC-450 WL scope. Demographic data, dose and type of sedation used as well as caecal and terminal ileal intubation rates were recorded. Results are shown in Table 1.

Indications for colonoscopy were similar in both groups as were hysterectomy rates (5%). Mean list size was 5 (range 4-6) patients and the number of therapeutic procedures was 8 (8%) in the first 105 procedures and 20 (21%) in the subsequent 94. Adjusted completion rates were superior with the Olympus colonoscope (97% *vs* 89%; $P < 0.001$) compared to the Fujinon colonosocpe. Similarly, adjusted analgesic dose was also significant with patients endoscoped with the Olympus colonoscope requiring less Midazolam (2.7 mg *vs* 3.7 mg; $P < 0.001$) whilst none required any opioid analgesics. Moreover, 30% endoscoped with the Olympus colonoscope required no sedation at all. Individual departmental caecal completion rates were similar to those of the endoscopist in this study, thereby precluding a learning curve phenomenon with the different make of colonoscopes. Although this study was not randomised and for obvious reasons cannot be blinded, operator bias was reduced as the operator had near equal experience with both types of scopes. This is the first study to our knowledge that has compared two different makes of instruments and shown that it influences not only caecal intubation rates but also sedation practice.

The optical performance of the Fujinon system is deemed superior than that of the Olympus system[7] with better resolution at target distances of less than 1 cm. A 'back to back' randomised study design, using the two

different systems to determine rates of early mucosal changes, would be required to determine if this was clinically significant. The implications of colonoscopic performance and sedation practice being influenced by different makes of instrument are far reaching. It has implications not only in training endoscopists but also in assessing individual performance, particularly those undertaking colon cancer screening.

ACKNOWLEDGMENTS

The authors would like to thank all Endoscopic Unit staff at Wansbeck General Hospital, Ashington and Northern General Hospital, Sheffield, United Kingdom.

REFERENCES

1 **Bowles CJ**, Leicester R, Romaya C, Swarbrick E, Williams CB, Epstein O. A prospective study of colonoscopy practice in the UK today: are we adequately prepared for national colorectal cancer screening tomorrow? *Gut* 2004; **53**: 277-283

2 **Saifuddin T**, Trivedi M, King PD, Madsen R, Marshall JB. Usefulness of a pediatric colonoscope for colonoscopy in adults. *Gastrointest Endosc* 2000; **51**: 314-317

3 **Kaffes AJ**, Mishra A, Ding SL, Hope R, Williams SJ, Gillespie PE, Bourke MJ. A prospective trial of variable stiffness pediatric vs. standard instrument colonoscopy. *Gastrointest Endosc* 2003; **58**: 685-689

4 **Waye JD**, Bashkoff E. Total colonoscopy: is it always possible? *Gastrointest Endosc* 1991; **37**: 152-154

5 **Rex DK**. Effect of variable stiffness colonoscopes on cecal intubation times for routine colonoscopy by an experienced examiner in sedated patients. *Endoscopy* 2001; **33**: 60-64

6 **Okamoto M**, Kawabe T, Kato J, Yamaji Y, Ikenoue T, Omata M. Ultrathin colonoscope with a diameter of 9.8 mm for total colonoscopy. *J Clin Gastroenterol* 2005; **39**: 679-683

7 **Knyrim K**, Seidlitz H, Vakil N, Hagenmüller F, Classen M. Optical performance of electronic imaging systems for the colon. *Gastroenterology* 1989; **96**: 776-782

S- Editor Wang GP **L- Editor** Ma JY **E- Editor** Lu W

PO Box 2345, Beijing 100023, China
www.wjgnet.com
wjg@wjgnet.com

World J Gastroenterol 2007 January 21; 13(3): 488
World Journal of Gastroenterology ISSN 1007-9327

ACKNOWLEDGMENTS

Acknowledgments to Reviewers of *World Journal of Gastroenterology*

Many reviewers have contributed their expertise and time to the peer review, a critical process to ensure the quality of *World Journal of Gastroenterology*. The editors and authors of the articles submitted to the journal are grateful to the following reviewers for evaluating the articles (including those published in this issue and those rejected for this issue) during the last editing time period.

Takafumi Ando, MD
Nagoya University Graduate School of Medicine, Therapeutic Medicine, 65 Tsurumai-cho, Showa-ku, Nagoya 466-8550, Japan

Josep M Bordas, MD
Department of Gastroenterology IMD, Hospital Clinic", Llusanes 11-13 at, Barcelona 08022, Spain

Giuseppe Chiarioni, Dr
Gastroenterological Rehabilitation Division of the University of Verona, Valeggio sul Mincio Hospital, Azienda Ospedale di Valeggio s/M, Valeggio s/M 37067, Italy

Julio Horacio Carri, Professor
Internal Medicine-Gastroenterology, Universidad Nacional de Córdoba, Av.Estrada 160-P 5-Department D, Córdoba 5000, Argentina

Christoph F Dietrich, MD
Innere Medizin 2, Caritas-Krankenhaus, Uhlandstr. 7, Bad Mergentheim97980, Germany

Da-Jun Deng, Professor
Department of Cancer Etiology, Peking University School of Oncology, 1 Da-Hong-Luo-Chang Street, Western District, Beijing 100034, China

Marko Duvnjak, MD
Department of Gastroenterology and Hepatology, Sestre milosrdnice University Hospital, Vinogradska cesta 29, 10000 Zagreb, Croatia

Miguel Carneiro De Moura, Professor
Department of Gastroenterology, Medical School of Lisbon, Av Prof Egas Moniz,1649-028 Lisboa, Portugal

Nageshwar Duvvuru Reddy, Professor
Asian Institute of Gastroenterology, 6-3-652, Somajiguda, Hyderabad-500 082, India

Chris E Forsmark, Professor
Division of Gastroenterology, Hepatology, and Nutrition , University of Florida , Box 100214, Room HD-602 1600 SW Archer Road Gainesville, FL, 32610-0214, United States

Mark D Gorrell, PhD
Centenary Institute of Cancer Medicine and Cell Biology, Locked bag No. 6, Newtown, NSW 2042, Australia

Xupeng Ge, MD, PhD
Division of Transplantation Surgery, CLINTEC, Karolinska Institute, Karolinska University Hospital-Huddinge, Stockholm 14186, Sweden

Guang-Cun Huang, PhD
Department of Pathology, Shanghai Medical College, Fudan University, 138 Yixueyuan Road, Shanghai 200032, China

Kazuhiro Hanazaki, MD
Department of Surgery, Shinonoi General Hospital, 666-1 Ai, Shinonoi, Nagano 388-8004, Japan

Ai-Ping Lu, Professor
China Academy of Traditional Chinese Medicine, Dongzhimen Nei, 18 Beixincang, Beijing 100700, China

Masatoshi Makuuchi, Professor
Department of Surgery, Graduate School of Medicine University of Tokyo, T Hepato-Biliary-Pancreatic Surgery Division Tokyo 113-8655, Japan

Yoshiharu Motoo, Professor
Department of Medical Oncology, Kanazawa Medical University, 1-1 Daigaku, Uchinada, Ishikawa 920-0293, Japan

Francesco Negro, MD
Divisions of Gastroenterology and Hepatology and of Clinical Pathology, Hôpital Cantonal Universitaire, 24 rue Micheli-du-Crest, CH-1211 Genève 14, Switzerland

Yaron Niv, Professor
Department of Gastroenterology, Rabin Medical Center, Beilinson Campus, Tel Aviv University, 2 Hadekel St., Pardesia 42815, Israel

Johann Ockenga, Dr
Gastroenterology, Hepatology and Endocrinology, Charite-Universitatsmedizin Berlin, Schumannstrasse 20/21, 10117 Berlin, Germany

Osman Cavit Ozdogan, Associate Professor
Department of Gastroenterology, Liver Unit, Marmara University School of Medicine, Istanbul 34662, Turkey

Bo-Rong Pan, Professor
Departmant of Oncology, Xijing Hospital, Fourth Military Medical University, No.1, F. 8, Bldg 10, 97 Changying East Road, Xi'an 710032, Shaanxi Province, China

CS Pitchumoni, Professor
Robert Wood Johnson School of Medicine, Robert Wood Johnson School of Medicine, New Brunswiuc NJ D8903, United States

Markus Peck-Radosavljevic, Professor
Department of Internal Medicine IV, Division of Gastroenterology and Hepatology, University of Vienna, W?hringergürtel 18-20, A-1090 Vienna, Austria

Bernardino Rampone, Dr
Department of General Surgery and Surgical Oncology, University of Siena, viale Bracci, Siena 53100, Italy

Francis Seow-Choen, Professor
Seow-Choen Colorectal Centre, Mt Elizabeth Medical Centre, Singapore, 3 Mt Elizabeth Medical Centre #09-10, 228510, Singapore

Hitoshi Togashi, Associate Professor
Department of Gastroenterology, Course of Internal Medicine and Therapeutics, Yamagata University School of Medicine, 2-2-2 Iida-Nishi, Yamagata 990-9585, Japan

Kiichi Tamada, MD
Department of Gastroenterology, Jichi Medical Shool, 3311-1 Yakushiji,Minamika wachi,Kawachigun, Tochigi 329-0498, Japan

Seyed Alireza Taghavi, Associate Professor
Department of Internal Medicine, Nemazee Hospital, No.23, 59th Alley, Ghasrodasht St., Shiraz 71838-95453, Iran

Simon D Taylor-Robinson, MD
Department of Medicine A, Imperial College London, Hammersmith Hospital, Du Cane Road, London W12 0HS, United Kingdom

Seng-Lai Tan, Principal Scientist
Eli Lilly and Company, Indianapolis 46285, United States

Ian David Wallace, MD
Shakespeare Specialist Group, 181 Shakesperare Rd, Milford, Auckland 1309, New Zealand

Yuan Yuan, Professor
Cancer Institute of China Medical University, 155 North Nanjing Street, Heping District, Shenyang 110001, Liaoning Province, China

Michael E Zenilman, MD
Clarence and Mary Dennis Professor and Chairman, Department of Surgery, SUNY Downstate Medical Center, Box 40, 450 Clarkson Avenue, Brooklyn, NY 11202, United States

Shu Zheng, Professor
Scientific Director of Cancer Institute, Zhejiang University, Secondary Affiliated Hospital, Zhejiang University, 88# Jiefang Road, Hangzhou 310009, Zhejiang Province, China

PO Box 2345, Beijing 100023, China
www.wjgnet.com
wjg@wjgnet.com

World J Gastroenterol 2007 January 21; 13(3): 489
World Journal of Gastroenterology ISSN 1007-9327

Meetings

MAJOR MEETINGS COMING UP

Meeting Falk Research Workshop: Morphogenesis and Cancerogenesis of the Liver
25-26 January 2007
Goettingen
symposia@falkfoundation.de

Meeting Canadian Digestive Diseases Week (CDDW)
16-20 February 2007
Banff-AB
cagoffice@cag-acg.org
www.cag-acg.org/cddw/cddw2007.htm

Meeting Falk Symposium 158: Intestinal Inflammation and Colorectal Cancer
23-24 March 2007
Sevilla
symposia@falkfoundation.de

Meeting BSG Annual Meeting
26-29 March 2007
Glasgow
www.bsg.org.uk/

NEXT 6 MONTHS

Meeting 42nd Annual Meeting of the European Association for the Study of the Liver
11-15 April 2007
Barcelona
easl2007@easl.ch
www.easl.ch/liver-meeting/

Meeting Falk Symposium 159: IBD 2007 - Achievements in Research and Clinical Practice
4-5 May 2007
Istanbul
symposia@falkfoundation.de

Meeting European Society for Paediatric Gastroenterology, Hepatology and Nutrition Congress 2007
9-12 May 2007
Barcelona
espghan2007@colloquium.fr

Digestive Disease Week
19-24 May 2007
Washington Convention Center, Washington DC

Meeting Gastrointestinal Endoscopy Best Practices: Today and Tomorrow, ASGE Annual Postgraduate Course at DDW
23-24 May 2007
Washington-DC
tkoral@asge.org

Meeting ESGAR 2007 18th Annual Meeting and Postgraduate Course
12-15 June 2007
Lisbon
fca@netvisao.pt

Meeting Falk Symposium 160: Pathogenesis and Clinical Practice in Gastroenterology
15-16 June 2007
Portoroz
symposia@falkfoundation.de

Meeting ILTS 13th Annual International Congress
20-23 June 2007
Rio De Janeiro
www.ilts.org

Meeting 9th World Congress on Gastrointestinal Cancer
27-30 June 2007
Barcelona
meetings@imedex.com

EVENTS AND MEETINGS IN 2007

Meeting Falk Research Workshop: Morphogenesis and Cancerogenesis of the Liver
25-26 January 2007
Goettingen
symposia@falkfoundation.de

Meeting Canadian Digestive Diseases Week (CDDW)
16-20 February 2007
Banff-AB
cagoffice@cag-acg.org
www.cag-acg.org/cddw/cddw2007.htm

Meeting Falk Symposium 158: Intestinal Inflammation and Colorectal Cancer
23-24 March 2007
Sevilla
symposia@falkfoundation.de

Meeting BSG Annual Meeting
26-29 March 2007
Glasgow
www.bsg.org.uk/

Meeting 42nd Annual Meeting of the European Association for the Study of the Liver
11-15 April 2007
Barcelona
easl2007@easl.ch
www.easl.ch/liver-meeting/

Meeting Falk Symposium 159: IBD 2007 - Achievements in Research and Clinical Practice
4-5 May 2007
Istanbul
symposia@falkfoundation.de

Meeting European Society for Paediatric Gastroenterology, Hepatology and Nutrition Congress 2007
9-12 May 2007
Barcelona
espghan2007@colloquium.fr

Meeting Gastrointestinal Endoscopy Best Practices: Today and Tomorrow, ASGE Annual Postgraduate Course at DDW
23-24 May 2007
Washington-DC
tkoral@asge.org

Meeting ESGAR 2007 18th Annual Meeting and Postgraduate Course
12-15 June 2007
Lisbon
fca@netvisao.pt

Meeting Falk Symposium 160: Pathogenesis and Clinical Practice in Gastroenterology
15-16 June 2007
Portoroz
symposia@falkfoundation.de

Meeting ILTS 13th Annual International Congress
20-23 June 2007
Rio De Janeiro
www.ilts.org

Meeting 9th World Congress on Gastrointestinal Cancer
27-30 June 2007
Barcelona
meetings@imedex.com

Meeting 15th International Congress of the European Association for Endoscopic Surgery
4-7 July 2007
Athens
info@eaes-eur.org
congresses.eaes-eur.org/

Meeting 39th Meeting of the European Pancreatic Club
4-7 July 2007
Newcastle
www.e-p-c2007.com

Meeting XXth International Workshop on Heliobacter and related bacteria in cronic degistive inflammation
20-22 September 2007
Istanbul
www.heliobacter.org

Meeting Falk Workshop: Mechanisms of Intestinal Inflammation
10 October 2007
Dresden
symposia@falkfoundation.de

Meeting Falk Symposium 161: Future Perspectives in Gastroenterology
11-12 October 2007
Dresden
symposia@falkfoundation.de

Meeting Falk Symposium 162: Liver Cirrhosis - From Pathophysiology to Disease Management
13-14 October 2007
Dresden
symposia@falkfoundation.de

American College of Gastroenterology Annual Scientific Meeting
12-17 October 2007
Pennsylvania Convention Center
Philadelphia, PA

Meeting APDW 2007 - Asian Pacific Digestive Disease Week 2007
15-18 October 2007
Kobe
apdw@convention.co.jp
www.apdw2007.org

15th United European Gastroenterology Week, UEGW
27-31 October 2007
Le Palais des Congrès de Paris, Paris, France

Meeting The Liver Meeting® 2007 - 57th Annual Meeting of the American Association for the Study of Liver Diseases
2-6 November 2007
Boston-MA
www.aasld.org

Gastro 2009, World Congress of Gastroenterology and Endoscopy London, United Kingdom 2009

PO Box 2345, Beijing 100023, China
www.wjgnet.com
wjg@wjgnet.com

World J Gastroenterol 2007 January 21; 13(3): 490-492
World Journal of Gastroenterology ISSN 1007-9327

Instructions to authors

GENERAL INFORMATION

World Journal of Gastroenterology (*WJG, World J Gastroenterol* ISSN 1007-9327 CN 14-1219/R) is a weekly journal of more than 48 000 circulation, published on the 7th, 14th, 21st and 28th of every month.

Original Research, Clinical Trials, Reviews, Comments, and Case Reports in esophageal cancer, gastric cancer, colon cancer, liver cancer, viral liver diseases, *etc.*, from all over the world are welcome on the condition that they have not been published previously and have not been submitted simultaneously elsewhere.

Indexed and abstracted in

Current Contents®/Clinical Medicine, Science Citation Index Expanded (also known as SciSearch®) and Journal Citation Reports/Science Edition, *Index Medicus*, MEDLINE and PubMed, Chemical Abstracts, EMBASE/Excerpta Medica, Abstracts Journals, *Nature Clinical Practice Gastroenterology and Hepatology*, CAB Abstracts and Global Health. ISI JCR 2003-2000 IF: 3.318, 2.532, 1.445 and 0.993.

Published by

The WJG Press

SUBMISSION OF MANUSCRIPTS

Manuscripts should be typed double-spaced on A4 (297 mm × 210 mm) white paper with outer margins of 2.5 cm. Number all pages consecutively, and start each of the following sections on a new page: Title Page , Abstract, Introduction, Materials and Methods, Results, Discussion, acknowledgements, References, Tables, Figures and Figure Legends. Neither the editors nor the Publisher is responsible for the opinions expressed by contributors. Manuscripts formally accepted for publication become the permanent property of The WJG Press, and may not be reproduced by any means, in whole or in part without the written permission of both the authors and the Publisher. We reserve the right to put onto our website and copy-edit accepted manuscripts. Authors should also follow the guidelines for the care and use of laboratory animals of their institution or national animal welfare committee.

Authors should retain one copy of the text, tables, photographs and illustrations, as rejected manuscripts will not be returned to the author(s) and the editors will not be responsible for the loss or damage to photographs and illustrations in mailing process.

Online submission

Online submission is strongly advised. Manuscripts should be submitted through the Online Submission System at: http://www.wjgnet.com/index.jsp. Authors are highly recommended to consult the ONLINE INSTRUCTIONS TO AUTHORS (http://www.wjgnet.com/wjg/help/instructions.jsp) before attempting to submit online. Authors encountering problems with the Online Submission System may send an email you describing the problem to wjg@wjgnet.com for assistance. If you submit your manuscript online, do not make a postal contribution. A repeated online submission for the same manuscript is strictly prohibited.

Postal submission

Send 3 duplicate hard copies of the full-text manuscript typed double-spaced on A4 (297 mm × 210 mm) white paper together with any original photographs or illustrations and a 3.5 inch computer diskette or CD-ROM containing an electronic copy of the manuscript including all the figures, graphs and tables in native Microsoft Word format or *.rtf format to:

Editorial Office

World Journal of Gastroenterology
Editorial Department: Apartment 1066, Yishou Garden,
58 North Langxinzhuang Road,
PO Box 2345, Beijing 100023, China
E-mail: wjg@wjgnet.com
http: //www.wjgnet.com
Telephone: +86-10-85381892
Fax: +86-10-85381893

MANUSCRIPT PREPARATION

All contributions should be written in English. All articles must be submitted using a word-processing software. All submissions must be typed in 1.5 line spacing and in word size 12 with ample margins. The letter font is Tahoma. For authors from China, one copy of the Chinese translation of the manuscript is also required (excluding references). Style should conform to our house format. Required information for each of the manuscript sections is as follows:

Title page

Full manuscript title, running title, all author(s) name(s), affiliations, institution(s) and/or department(s) where the work was accomplished, disclosure of any financial support for the research, and the name, full address, telephone and fax numbers and email address of the corresponding author should be included. Titles should be concise and informative (removing all unnecessary words), emphasize what is new, and avoid abbreviations. A short running title of less than 40 letters should be provided. List the author(s)' name(s) as follows: initial and/or first name, middle name or initial(s) and full family name.

Abstract

An informative, structured abstract of no more than 250 words should accompany each manuscript. Abstracts for original contributions should be structured into the following sections: AIM: Only the purpose should be included. METHODS: The materials, techniques, instruments and equipments, and the experimental procedures should be included. RESULTS: The observatory and experimental results, including data, effects, outcome, *etc.* should be included. Authors should present *P* value where necessary, and the significant data should accompany. CONCLUSION: Accurate view and the value of the results should be included.

The format of structured abstracts is at: http://www.wjgnet.com/wjg/help/11.doc

Key words

Please list 5-10 key words that could reflect content of the study mainly from *Index Medicus*.

Text

For most article types, the main text should be structured into the following sections: INTRODUCTION, MATERIALS AND METHODS, RESULTS and DISCUSSION, and should include in appropriate Figures and Tables. Data should be presented in the body text or in Figures and Tables, but not in both.

Illustrations

Figures should be numbered as 1, 2, 3 and so on, and mentioned clearly in the main text. Provide a brief title for each figure on a separate page. No detailed legend should be involved under the figures. This part should be added into the text where the figures are applicable. Digital images: black and white photographs should be scanned and saved in TIFF format at a resolution of 300 dpi; color images should be saved as CMYK (print files) but not as RGB (screen-viewing files). Place each photograph in a separate file. Print images: supply images of size no smaller than 126 mm × 85 mm printed on smooth surface paper; label the image by writing the Figure number and orientation using an arrow. Photomicrographs: indicate the original magnification and stain in the legend. Digital Drawings: supply files in EPS if created by freehand and illustrator, or TIFF from photoshops. EPS files must be accompanied by a version in native file format for editing purposes. Existing line drawings should be scanned at a resolution of 1200 dpi and as close as possible to the size where they will appear when printed. Please use uniform legends for the same subjects. For example: Figure 1 Pathological changes of atrophic gastritis after treatment. A: ...; B: ...; C: ...; D: ...; E: ...; F: ...; G: ...

Tables

Three-line tables should be numbered as 1, 2, 3 and so on, and mentioned clearly in the main text. Provide a brief title for each table. No detailed legend should be included under the tables. This part should be added into the text where the tables are applicable. The information should complement but not duplicate that contained in the text. Use one horizontal line under the title, a second under the column heads, and a third below the Table, above any footnotes. Vertical and italic lines should be omitted.

Notes in tables and illustrations

Data that are not statistically significant should not be noted. $^{a}P<0.05$, $^{b}P<0.01$ should be noted ($P>0.05$ should not be noted). If there are other series of *P* values, $^{c}P<0.05$ and $^{d}P<0.01$ are used. Third series of *P* values can be expressed as $^{e}P<0.05$ and $^{f}P<0.01$. Other notes in tables or under

illustrations should be expressed as ^1F, ^2F, ^3F; or some other symbols with a superscript (Arabic numerals) in the upper left corner. In a multi-curve illustration, each curve should be labeled with ●, ○, ■, □, ▲, △, *etc.* in a certain sequence.

Acknowledgments

Brief acknowledgments of persons who have made genuine contributions to the manuscripts and who endorse the data and conclusions are included. Authors are responsible for obtaining written permission to use any copyrighted text and/or illustrations.

REFERENCES

Coding system

The author should code the references according the citation order in text in Arabic numerals, put references codes in square brackets, superscript it at the end of citation content or the author name of the citation. For those citation content as the narrate part, the coding number and square brackets should be typeset normally. For example, Crohn's disease (CD) is associated with increased intestinal permeability[1,2]. If references are directly cited in the text, they would be put together with the text, for example, from references [19,22-24], we know that...

When the authors code the references, please ensure that the order in text is the same as in reference part and also insure the spelling accuracy of the first author's name. Do not code the same citation twice.

PMID requirement

PMID roots in the abstract serial number indexed by PubMed (http://www.ncbi.nlm.nih.gov/entrez/query.fcgi?db=PubMed). The author should supply the PMID for journal citation. For those references that have not been indexed by PubMed, a printed copy of the first page of the full reference should be submitted.

The accuracy of the information of the journal citations is very important. Through reference testing system, the authors and editor could check the authors name, title, journal title, publication date, volume number, start page, and end page. We will interlink all references with PubMed in ASP file so that the readers can read the abstract of the citations online immediately.

Style for journal references

Authors: the first author should be typed in bold-faced letter. The surname of all authors should be typed with the initial letter capitalized and followed by their name in abbreviation (For example, Lian-Sheng Ma is abbreviated as Ma LS, Bo-Rong Pan as Pan BR). Title of the cited article and italicized journal title (Journal title should be in its abbreviation form as shown in PubMed), publication date, volume number (in black), start page, and end page [PMID: 11819634]

Note: The author should test the references through reference testing system (http://www.wjgnet.com/cgi-bin/index.pl)

Style for book references

Authors: the first author should be typed in bold-faced letter. The surname of all authors should be typed with the initial letter capitalized and followed by their name in abbreviation (For example, Lian-Sheng Ma is abbreviated as Ma LS, Bo-Rong Pan as Pan BR) Book title. Publication number. Publication place: Publication press, Year: start page and end page.

Format

Journals

English journal article (list all authors and include the PMID where applicable)

1 **Grover VP**, Dresner MA, Forton DM, Counsell S, Larkman DJ, Patel N, Thomas HC, Taylor-Robinson SD. Current and future applications of magnetic resonance imaging and spectroscopy of the brain in hepatic encephalopathy. *World J Gastroenterol* 2006; **12**: 2969-2978 [PMID: 16718775]

Chinese journal article (list all authors and include the PMID where applicable)

2 **Lin GZ**, Wang XZ, Wang P, Lin J, Yang FD. Immunologic effect of Jianpi Yishen decoction in treatment of Pixu-diarrhoea. *Shijie Huaren Xiaohua Zazhi* 1999; **7**: 285-287

In press

3 **Tian D**, Araki H, Stahl E, Bergelson J, Kreitman M. Signature of balancing selection in Arabidopsis. *Proc Natl Acad Sci U S A* 2006; In press

Organization as author

4 **Diabetes Prevention Program Research Group**. Hypertension, insulin, and proinsulin in participants with impaired glucose tolerance. *Hypertension* 2002; **40**: 679-686 [PMID: 12411462]

Both personal authors and an organization as author

5 **Vallancien G**, Emberton M, Harving N, van Moorselaar RJ; Alf-One Study Group. Sexual dysfunction in 1, 274 European men suffering from lower urinary tract symptoms. *J Urol* 2003; **169**: 2257-2261 [PMID: 12771764]

No author given

6 21st century heart solution may have a sting in the tail. *BMJ* 2002; **325**: 184 [PMID: 12142303]

Volume with supplement

7 **Geraud G**, Spierings EL, Keywood C. Tolerability and safety of frovatriptan with short- and long-term use for treatment of migraine and in comparison with sumatriptan. *Headache* 2002; **42** Suppl 2: S93-99 [PMID: 12028325]

Issue with no volume

8 **Banit DM**, Kaufer H, Hartford JM. Intraoperative frozen section analysis in revision total joint arthroplasty. *Clin Orthop Relat Res* 2002; (**401**): 230-238 [PMID: 12151900]

No volume or issue

9 Outreach: bringing HIV-positive individuals into care. *HRSA Careaction* 2002; 1-6 [PMID: 12154804]

Books

Personal author(s)

10 **Sherlock S**, Dooley J. Diseases of the liver and billiary system. 9th ed. Oxford: Blackwell Sci Pub, 1993: 258-296

Chapter in a book (list all authors)

11 **Lam SK**. Academic investigator's perspectives of medical treatment for peptic ulcer. In: Swabb EA, Azabo S. Ulcer disease: investigation and basis for therapy. New York: Marcel Dekker, 1991: 431-450

Author(s) and editor(s)

12 **Breedlove GK**, Schorfheide AM. Adolescent pregnancy. 2nd ed. Wieczorek RR, editor. White Plains (NY): March of Dimes Education Services, 2001: 20-34

Conference proceedings

13 **Harnden P**, Joffe JK, Jones WG, editors. Germ cell tumours V. Proceedings of the 5th Germ Cell Tumour Conference; 2001 Sep 13-15; Leeds, UK. New York: Springer, 2002: 30-56

Conference paper

14 **Christensen S**, Oppacher F. An analysis of Koza's computational effort statistic for genetic programming. In: Foster JA, Lutton E, Miller J, Ryan C, Tettamanzi AG, editors. Genetic programming. EuroGP 2002: Proceedings of the 5th European Conference on Genetic Programming; 2002 Apr 3-5; Kinsdale, Ireland. Berlin: Springer, 2002: 182-191

Electronic journal (list all authors)

Morse SS. Factors in the emergence of infectious diseases. Emerg Infect Dis serial online, 1995-01-03, cited 1996-06-05; 1(1): 24 screens. Available from: URL: http//www.cdc.gov/ncidod/EID/eid.htm

Patent (list all authors)

16 **Pagedas AC**, inventor; Ancel Surgical R&D Inc., assignee. Flexible endoscopic grasping and cutting device and positioning tool assembly. United States patent US 20020103498. 2002 Aug 1

Inappropriate references

Authors should always cite references that are relevant to their article, and avoid any inappropriate references. Inappropriate references include those that are linked with a hyphen and the difference between the two numbers at two sides of the hyphen is more than 5. For example, [1-6], [2-14] and [1, 3, 4-10, 22] are all considered as inappropriate references. Authors should not cite their own unrelated published articles.

Statistical data

Present as mean ± SD or mean ± SE.

Statistical expression

Express t test as t (in italics), F test as F (in italics), chi square test as χ^2 (in Greek), related coefficient as r (in italics), degree of freedom as γ (in Greek), sample number as n (in italics), and probability as P (in italics).

Units

Use SI units. For example: body mass, m (B) = 78 kg; blood pressure, p(B) = 16.2/12.3 kPa; incubation time, t (incubation) = 96 h, blood glucose concentration, c (glucose) 6.4 ± 2.1 mmol/L; blood CEA mass concentration, p (CEA) = 8.6 24.5 μg/L; CO_2 volume fraction, 50 mL/L CO_2 not 5% CO_2; likewise for 40 g/L formaldehyde, not 10% formalin; and mass fraction, 8 ng/g, *etc.* Arabic numerals such as 23, 243, 641 should be read 23 243 641.

The format about how to accurately write common units and quantum is at: http://www.wjgnet.com/wjg/help/15.doc

Abbreviations

Standard abbreviations should be defined in the abstract and on first mention in the text. In general, terms should not be abbreviated unless they are used repeatedly and the abbreviation is helpful to the reader. Permissible abbreviations are listed in Units, Symbols and Abbreviations: A Guide for Biological and Medical Editors and Authors (Ed. Baron DN, 1988) published by The Royal Society of Medicine, London. Certain commonly used abbreviations, such as DNA, RNA, HIV, LD50, PCR, HBV, ECG, WBC, RBC, CT, ESR, CSF, IgG, ELISA, PBS, ATP, EDTA, mAb, can be used directly without further mention.

Italics

Quantities: *t* time or temperature, *c* concentration, *A* area, *l* length, *m* mass, *V* volume.
Genotypes: *gyr*A, *arg* 1, *c myc*, *c fos*, *etc.*
Restriction enzymes: *Eco*RI, *Hin*dI, *Bam*HI, *Kbo* I, *Kpn* I, *etc.*
Biology: *H pylori, E coli, etc.*

SUBMISSION OF THE REVISED MANUSCRIPTS AFTER ACCEPTED

Please revise your article according to the revision policies of *WJG*. The revised version including manuscript and high-resolution image figures (if any) should be copied on a floppy or compact disk. Author should send the revised manuscript, along with printed high-resolution color or black and white photos, copyright transfer letter, the final check list for authors, and responses to reviewers by a courier (such as EMS) (submission of revised manuscript by e-mail or on the *WJG* Editorial Office Online System is NOT available at present).

Language evaluation

The language of a manuscript will be graded before sending for revision. (1) Grade A: priority publishing; (2) Grade B: minor language polishing; (3) Grade C: a great deal of language polishing; (4) Grade D: rejected. The revised articles should be in grade B or grade A.

Copyright assignment form

Please downloaded CAF from http://www.wjgnet.com/wjg/help/9.doc.

We certify that the material contained in this manuscript:

Ms:

Title:

is original, except when appropriately referenced to other sources, and that written permission has been granted by any existing copyright holders. We agree to transfer to WJG all rights of our manuscript, including: (1) all copyright ownership in all print and electronic formats; (2) the right to grant permission to republish or reprint the stated material in whole or in part, with or without a fee; (3) the right to print copies for free distribution or sale; (4) the right to republish the stated material in a collection of articles or in any other format. We also agree that our article be put on the Internet.

Criteria for authorship: The WJG requests and publishes information about contributions of each author named to the submitted study. Authorship credit should be based on (1)direct participation in the study, including substantial contributions to conception and design of study, or acquisition of data, or analysis and interpretation of data; (2) manuscript writing, including drafting the article, or revising it critically for important intellectual content; (3)supportive work, including statistical analysis of data, or acquisition of funding, or administration, technology and materials support, or supervision, or supportive contributions. Authors should meet at least one of the three conditions. The WJG does not publish co-first authors and co-corresponding authors.

We hereby assign copyright transfer to WJG if this paper is accepted.

Author Name in full (Full names should be provided, with first name first, followed by middle names and family name at the last, eg, Eamonn MM Quigley). Handwritten names are not accepted.

Author Name in abbreviation (Family name is put first in full, followed by middle names and first name in abbreviation with first letter in capital, eg, Quigley EMM). Handwritten names are not accepted.

1 Full Name: _____
Abbreviation Name: _____
Signed: _____
Date: _____

2 Full Name: _____
Abbreviation Name: _____
Signed: _____
Date: _____

3 Full Name: _____
Abbreviation Name: _____
Signed: _____
Date: _____

4 Full Name: _____
Abbreviation Name: _____
Signed: _____
Date: _____

5 Full Name: _____
Abbreviation Name: _____
Signed: _____
Date: _____

6 Full Name: _____
Abbreviation Name: _____
Signed: _____
Date: _____

7 Full Name: _____
Abbreviation Name: _____
Signed: _____
Date: _____

8 Full Name: _____
Abbreviation Name: _____
Signed: _____
Date: _____

9 Full Name: _____
Abbreviation Name: _____
Signed: _____
Date: _____

10 Full Name: _____
Abbreviation Name: _____
Signed: _____
Date: _____

Final check list for authors

The format is at: http://www.wjgnet.com/wjg/help/13.doc

Responses to reviewers

Please revise your article according to the comments/suggestions of reviewers. The format for responses to the reviewers' comments is at: http://www.wjgnet.com/wjg/help/10.doc

Proof of financial support

For paper supported by a foundation, authors should provide a copy of the document and serial number of the foundation.

Publication fee

Authors of accepted articles must pay publication fee.
EDITORIAL and LETTERS TO THE EDITOR are free of change.

ISSN 1007-9327
CN 14-1219/R

World Journal of Gastroenterology®

Volume 13 Number 4
January 28, 2007

National Journal Award
2005

The WJG Press

The WJG Press, Apartment 1066 Yishou Garden, 58 North Langxinzhuang Road, PO Box 2345, Beijing 100023, China
Telephone: +86-10-85381901
Fax: +86-10-85381893
E-mail: wjg@wjgnet.com
http: //www.wjgnet.com

ISSN 1007-9327 CN 14-1219/R Local Post Offices Code No. 82-261

World Journal of Gastroenterology

www.wjgnet.com

Volume 13 Number 4 Jan 28 2007

WJG

World Journal of Gastroenterology®

Indexed and Abstracted in:

Current Contents®/Clinical Medicine, Science Citation Index Expanded (also known as SciSearch®) and Journal Citation Reports/Science Edition, *Index Medicus*, MEDLINE and PubMed, Chemical Abstracts, EMBASE/Excerpta Medica, Abstracts Journals, *Nature Clinical Practice Gastroenterology and Hepatology*, CAB Abstracts and Global Health.
ISI JCR 2003-2000 IF: 3.318, 2.532, 1.445 and 0.993.

Volume 13 Number 4
January 28, 2007

World J Gastroenterol
2007 January 28; 13(4): 493-656
Online Submissions
www.wjgnet.com/wjg/index.jsp
www.wjgnet.com
Printed on Acid-free Paper

A Weekly Journal of Gastroenterology and Hepatology

National Journal Award
2005

World Journal of Gastroenterology®

Volume 13 Number 4
January 28, 2007

The WJG Press

Contents

World Journal of Gastroenterology
Volume 13 **Number** 4 **January** 28, 2007

Contents

World Journal of Gastroenterology
Volume 13 **Number** 4 **January** 28, 2007

Contents

Responsible E-Editor for this issue: Wei Lu

C-Editor for this issue: Kirsteen N Browning, PhD

Responsible S-Editor for this issue: Jing Wang

World Journal of Gastroenterology (*World J Gastroenterol , WJG*), a leading international journal in gastroenterology and hepatology, has an established reputation for publishing first class research on esophageal cancer, gastric cancer, liver cancer, viral hepatitis, colorectal cancer, and *H pylori* infection, providing a forum for both clinicians and scientists, and has been indexed and abstracted in Current Contents®/Clinical Medicine, Science Citation Index Expanded (also known as SciSearch®) and Journal Citation Reports/Science Edition, *Index Medicus*, MEDLINE and PubMed, Chemical Abstracts, EMBASE/Excerpta Medica, Abstracts Journals, *Nature Clinical Practice Gastroenterology and Hepatology*, CAB Abstracts and Global Health. ISI JCR 2003-2000 IF: 3.318, 2.532, 1.445 and 0.993. *WJG* is a weekly journal published by The WJG Press. The publication date is on 7th, 14th, 21st, and 28th every month. The *WJG* is supported by The National Natural Science Foundation of China, No. 30224801 and No.30424812, which was founded with a name of *China National Journal of New Gastroenterology* on October 1,1995, and renamed as *WJG* on January 25, 1998.

PUBLISHED BY
The WJG Press

PRINTED BY
Printed in Beijing on acid-free paper by Beijing Kexin Printing House

 Print ISSN 1007-9327
CN 14-1219/R.

EDITORIAL OFFICE
World Journal of Gastroenterology,
The WJG Press, Apartment 1066 Yishou Garden, 58 North Langxinzhuang Road, PO Box 2345, Beijing 100023, China
Telephone: +86-10-85381892
Fax: +86-10-85381893
E-mail: wjg@wjgnet.com
http://www.wjgnet.com

SUBSCRIPTION AND AUTHOR REPRINTS
Jing Wang
The WJG Press, Apartment 1066 Yishou Garden, 58 North Langxinzhuang Road, PO Box 2345, Beijing 100023, China
Telephone: +86-10-85381892
Fax: +86-10-85381893
E-mail: j.wang@wjgnet.com
http://www.wjgnet.com

SUBSCRIPTION INFORMATION
Institutional Price 2007: USD 1500.00
Personal Price 2007: USD 700.00

INSTRUCTIONS TO AUTHORS
Full instructions are available online at http://www.wjgnet.com/wjg/help/instructions.jsp. If you do not have web access please contact the editorial office.

PO Box 2345, Beijing 100023, China
www.wjgnet.com
wjg@wjgnet.com

World J Gastroenterol 2007 January 28; 13(4): 493-496
World Journal of Gastroenterology ISSN 1007-9327

REVIEW

Physiological and clinical significance of enterochromaffin-like cell activation in the regulation of gastric acid secretion

Guanglin Cui, Helge L Waldum

Guanglin Cui, Laboratory of Gastroenterology, Institute of Clinical Medicine, Faculty of Medicine, University of Tromsø, Tromsø, Norway
Helge L Waldum, Department of Gastroenterology and Hepatology, University Hospital of Trondheim, Norwegian University of Science and Technology, Trondheim, Norway
Co-correspondence: Helge L Waldum
Correspondence to: Dr. Guanglin Cui, Laboratory of Gastroenterology, Institute of Clinical Medicine, Faculty of Medicine, University of Tromsø, Tromsø N-9037, Norway. guanglin.cui@fagmed.uit.no
Telephone: +47-7764-4847 Fax: +47-7764-4650
Received: 2006-10-17 Accepted: 2006-12-05

Abstract

Gastric acid plays an important role in digesting food (especially protein), iron absorption, and destroying swallowed micro-organisms. H+ is secreted by the oxyntic parietal cells and its secretion is regulated by endocrine, neurocrine and paracrine mechanisms. Gastrin released from the antral G cell is the principal physiological stimulus of gastric acid secretion. Activation of the enterochromaffin-like (ECL) cell is accepted as the main source of histamine participating in the regulation of acid secretion and is functionally and trophically controlled by gastrin, which is mediated by gastrin/CCK-2 receptors expressed on the ECL cell. However, long-term hypergastrinemia will induce ECL cell hyperplasia and probably carcinoids. Clinically, potent inhibitors of acid secretion have been prescribed widely to patients with acid-related disorders. Long-term potent acid inhibition evokes a marked increase in plasma gastrin levels, leading to enlargement of oxyntic mucosa with ECL cell hyperplasia. Accordingly, the induction of ECL cell hyperplasia and carcinoids remains a topic of considerable concern, especially in long-term use. In addition, the activation of ECL cells also induces another clinical concern, i.e., rebound acid hypersecretion after acid inhibition. Recent experimental and clinical findings indicate that the activation of ECL cells plays a critical role both physiologically and clinically in the regulation of gastric acid secretion.

Key words: Enterochromaffin-like cell; Gastrin; Gastric acid; Gastric carcinoid; Rebound acid hypersecretion

Cui G, Waldum HL. Physiological and clinical significance of enterochromaffin-like cell activation in the regulation of gastric acid secretion. *World J Gastroenterol* 2007; 13(4): 493-496

http://www.wjgnet.com/1007-9327/13/493.asp

INTRODUCTION

One of the main functions of the stomach is to produce hydrochloric acid, which plays an important role in protein digestion, iron absorption and particularly in destroying swallowed micro-organisms[1,2]. The stomach is rich in neuroendocrine cells[3-5]. At present, at least six endocrine cells have been described in the stomach: G cells, D cells, enterochromaffin-like (ECL) cells, A-like cells, D1/P cells, and enterochromaffin (EC) cells. In the stomach, G cells are found only in the antral mucosa, while A-like and ECL cells are confined to the oxyntic mucosa[4]. D and D1/P cells are found in both the antral and oxyntic mucosa. These endocrine cells constitute approximately 2% of the oxyntic mucosal cells in rodents. The ECL cell was originally described by Hakanson *et al*[6] and Capella *et al*[7] respectively. However, its physiological function was also long disputed, except for in rat where it was initially recognised as the major histamine producing cell of the stomach[8]. It is now recognized that the ECL cell is the dominant endocrine cell in the oxyntic mucosa of all mammals studied so far. Localization within the glands differs from one species to another. In rodents, they are mainly located in the basal third of the oxyntic mucosa. Gastric acid is produced by the parietal cell in the oxyntic mucosa[9], and the production of acid is regulated by neurons, hormones and paracrine substances[10,11].

Gastrin released from the antral G cells, histamine from the oxyntic ECL cells and acetylcholine (Ach) from postganglionic cholinergic neurons are the main stimuli of acid secretion[9]. The ECL cell is under the control of gastrin. Gastrin-ECL cell axis activation has been found to be important physiologically and pathophysiologically. In this mini-review, we will summarize the physiological and clinical significance of ECL cell activation in regulating gastric acid secretion.

THE PHYSIOLOGICAL SIGNIFICANCE OF ECL CELL ACTIVATION IN REGULATING GASTRIC ACID SECRETION

Gastrin is a potent stimulus of gastric acid secretion by stimulating the release of histamine from ECL cells[12-16]. The gastrin-ECL cell axis plays a critical role in regulating acid secretion from parietal cells. In the totally isolated vascularly perfused rat stomach model, gastrin induces an immediate and concentration-dependent histamine release from the ECL cell[12]. With concomitant administration of the histamine-2 (H2) receptor antagonist, ranitidine, together with gastrin, the acid secretion in the isolated stomach model is reduced to baseline level. Thus, the stimulation of acid secretion by gastrin occurs most likely *via* histamine release from the ECL cells *via* gastrin/CCK-2 receptors[17-20]. This finding was supported by studies using isolated ECL cells *in vivo*[21-23]. Not only histamine release but also the synthesis of histamine in the ECL cell is regulated by gastrin[24-26]. Administration of exogenous gastrin, at a dose giving concentration in the physiological range, can evoke a significant increase in histidine decarboxylase (HDC) activity[13], as well as an increase in HDC mRNA abundance[24-26]. HDC catalyses the formation of histamine from histidine. Endogeneous hypergastrinemia after potent acid inhibition can induce a similar increase in HDC activity[13,27]. Histamine release from ECL cells is considered to be a limiting step in gastrin-stimulated maximal gastric acid secretion[12,28]. Now it is generally accepted that the gastrin-histamine sequence is the main pathway for gastrin stimulation of gastric acid secretion. Recently, the role of gastrin precursors (glycine-extended gastrin and progastrin) in stimulating acid secretion was also postulated[29,30]. It was found that a high dose infusion of glycine-extended gastrin into isolated stomach can activate histamine release from ECL cells and acid secretion, which could be blocked by antagonists of H2 receptors and gastrin/CCK-2 receptors[31,32]. This supported the activation of ECL cells as mediating the main pathway of glycine-extended gastrin acid secretion stimulation. Moreover, the role of glycine-extended gastrin in preserving parietal cell density was found. Coexpression of glycine-extended gastrin with gastrin in transgenic mice reduced long-term hypergastrinemia induced parietal cell loss. Thus, an important physiological role of gastrin precursors was postulated[30].

Furthermore, the stomach is innervated by different nerves[33] and peptides produced by intrinsic neurons influence stomach functions, including acid secretion[34]. The vagal efferent fibers are preganglionic, and do not directly innervate stomach endocrine or exocrine cells[33]. The targets of these vagal preganglionic neurons are the intrinsic neurons that are located in the myenteric ganglion cells. The intrinsic neurons contain Ach and different peptides[33], such as GRP, VIP, galanin, and PACAP. They innervate the G, D, ECL and parietal cells. The effect of vagal nerves on gastric acid secretion is complex. Ach mainly has a direct effect on acid secretion by acting on a M3 receptor on the parietal cell. *In vivo*, galanin and PYY, for example, have been shown to inhibit histamine release from ECL cells *via* their own receptors[35-39]. VIP induces somatostatin release from D cells, but stimulates histamine release from ECL cells probably *via* a PACAP receptor[35,36,39,40]. PACAP is a potent stimulus of histamine release from ECL cells *via* PACAP-1 receptors[36,39,41,42]. Gastric acid secretion, besides being regulated by the hormonal and neural routes, is also regulated by paracrine factors[11]. Somatostatin, which is a principal paracrine inhibitory factor, can exert its inhibitory effect on gastric acid secretion[17]. The reciprocal paracrine pathway between D and G cells is well known[43], and ECL cells are also in close contact with oxyntic D cells[4]. The antral somatostatin acts on the antral G cells, while the oxyntic somatostatin affects both ECL cells and parietal cells. Thus, somatostatin inhibits acid secretion *via* actions on different cells of the gastrin-ECL cell axis.

THE CLINICAL SIGNIFICANCE OF ECL CELL ACTIVATION IN LONG-TERM GASTRIC ACID INHIBITION

Potent acid inhibitors, such as proton pump inhibitors (PPIs), are highly effective gastric antisecretory agents with long duration[44]. They are intensively used to treat acid related disorders, and are nowadays prescribed even for children[45]. ECL cells are activated during the use of potent acid inhibitors. From a clinical viewpoint, safety concerns for such long-term activation by acid inhibitors have to be considered.

Rebound acid hypersecretion was first described in rats more than 20 years ago after treatment with omeprazole[46]. In humans, rebound acid hypersecretion was found in patients who received long-term acid inhibitors, such as H2 receptor antagonists and PPIs[47-51]. It has been observed that a 3-mo omeprazole treatment, at a dose of 40 mg daily in patients with reflux esophagitis, resulted in a significant (over 50%) increased maximal acid secretion accompanied by remarkable elevated gastrin and histamine levels[48]. This finding was confirmed in our subsequent studies[52,53] and others[50,51], and is due to the fact that gastrin is the most important trophic factor for ECL cell self-replication and that histamine released from ECLs cell is the main stimulator for gastric acid secretion. Long-term acid inhibition induces hypergastrinemia and ECL cell hyperplasia in patients treated with PPIs for various diseases with dyspepsia. The mechanism of rebound acid hypersecretion is likely related to the activation of the gastrin-ECL cell axis caused by drug-induced hypoacidity.

Apart from a stimulatory action on gastric acid secretion, gastrin also has a trophic effect on the oxyntic mucosa[54-56], particularly on ECL cells, which are stimulated to replicate *via* gastrin/CCK-2 receptors expressed in ECL cells[13,19,20]. It has become apparent that rat ECL cells, in response to hypergastrinemia, whether endogenous or exogenous, show hypertrophy within days, hyperplasia within weeks and carcinoids after months through a sequence of diffuse-linear-micronodular hyperplasia to ECL carcinoids[13]. Therefore, there is a causal connection between hypergastrinemia and ECL cell carcinogenesis[13,57-59]. Thus, in patients received long-term

acid inhibiton treatment, another concern is the increased gastric carcinoid risk. In fact, sporadic gastric carcinoid cases have been reported in patients exposed to long-term PPI treatments[60,61]. Long-term safety is still of high concern.

Finally, gastrin was also connected with other types of human cancers; i.e. gastric and colonic adenocarcinoma, and more recently, studying the important role of precursors for gastrin progastrin and glycine-extended gastrin in the carcinogeneiss of gastrointestinal mucosa has been one of the developing research fields. Several outstanding reviews have summarised this topic[62-65]. Thus, whether long-term activation of ECL cells by potent acid inhibition can contribute to increased risk of gastrointestinal adenocarcinoma in humans is still unknown and needs to be studied in the future. In addition, one of the growth factors that regenerates gene proteins, i.e., (Reg)-1, that is mainly released from ECL cells has been found to be a unique growth factor of gastric mucosal cells[66] and may play an important trophic role in the development of gastric cancer[67].

CONCLUSION

It is now generally accepted that ECL cell activation is the most important physiological pathway in the regulation of gastric acid secretion, which is being influenced by both activating and inhibiting stimuli. Furthermore, it has become apparent that the gastrin-ECL cell axis also plays a role in gastric acid disorder, such as rebound acid hypersecretion, and increased risk for gastric tumorigenesis, especially in chronic hypergastrinemic conditions. Therefore, clinicians should be aware that there are important clinical safety issues related to the dose and duration of potent inhibitors of acid secretion.

REFERENCES

1 **Håkanson R**, Alumets J, Ekelund M, Hedenbro J, Liedberg G, Lorén I, Sundler F, Vallgren S. Stimulation of gastric acid secretion. *Scand J Gastroenterol Suppl* 1979; **55**: 21-28
2 **Martinsen TC**, Bergh K, Waldum HL. Gastric juice: a barrier against infectious diseases. *Basic Clin Pharmacol Toxicol* 2005; **96**: 94-102
3 **Fujita T**, Kobayashi S. Structure and function of gut endocrine cells. *Int Rev Cytol Suppl* 1977; **6**: 187-233
4 **Solcia E**, Rindi G, Buffa R, Fiocca R, Capella C. Gastric endocrine cells: types, function and growth. *Regul Pept* 2000; **93**: 31-35
5 **Sundler F**, Böttcher G, Ekblad E, Håkanson R. The neuroendocrine system of the gut. *Acta Oncol* 1989; **28**: 303-314
6 **Håkanson R**, Owman C, Sporrong B, Sundler F. Electron microscopic identification of the histamine-storing argyrophil (enterochromaffin-like) cells in the rat stomach. *Z Zellforsch Mikrosk Anat* 1971; **122**: 460-466
7 **Capella C**, Vassallo G, Solcia E. Light and electron microscopic identification of the histamine-storing argyrophil (ECL) cell in murine stomach and of its equivalent in other mammals. *Z Zellforsch Mikrosk Anat* 1971; **118**: 68-84
8 **Håkanson R**, Böttcher G, Ekblad E, Panula P, Simonsson M, Dohlsten M, Hallberg T, Sundler F. Histamine in endocrine cells in the stomach. A survey of several species using a panel of histamine antibodies. *Histochemistry* 1986; **86**: 5-17
9 **Hersey SJ**, Sachs G. Gastric acid secretion. *Physiol Rev* 1995; **75**: 155-189
10 **Geibel JP**, Wagner C. An update on acid secretion. *Rev Physiol Biochem Pharmacol* 2006; **156**: 45-60
11 **Schubert ML**. Gastric secretion. *Curr Opin Gastroenterol* 2005; **21**: 636-643
12 **Sandvik AK**, Waldum HL, Kleveland PM, Schulze Søgnen B. Gastrin produces an immediate and dose-dependent histamine release preceding acid secretion in the totally isolated, vascularly perfused rat stomach. *Scand J Gastroenterol* 1987; **22**: 803-808
13 **Håkanson R**, Chen D, Tielemans Y, Andersson K, Ryberg B, Sundler F, Mattsson H. ECL cells: biology and pathobiology. *Digestion* 1994; **55** Suppl 3: 38-45
14 **Waldum HL**, Sandvik AK, Brenna E, Petersen H. Gastrin-histamine sequence in the regulation of gastric acid secretion. *Gut* 1991; **32**: 698-701
15 **Sawada M**, Dickinson CJ. The G cell. *Annu Rev Physiol* 1997; **59**: 273-298
16 **Mulholland MW**, Debas HT. Physiology and pathophysiology of gastrin: a review. *Surgery* 1988; **103**: 135-147
17 **Sandvik AK**, Waldum HL. Aspects of the regulation of gastric histamine release. *Scand J Gastroenterol Suppl* 1991; **180**: 108-112
18 **Waldum HL**, Sandvik AK, Brenna E, Kleveland PM. The gastrin-histamine sequence. *Gastroenterology* 1996; **111**: 838-839
19 **Sandvik AK**, Waldum HL. CCK-B (gastrin) receptor regulates gastric histamine release and acid secretion. *Am J Physiol* 1991; **260**: G925-G928
20 **Ding XQ**, Lindström E, Håkanson R. Time-course of deactivation of rat stomach ECL cells following cholecystokinin B/gastrin receptor blockade. *Br J Pharmacol* 1997; **122**: 1-6
21 **Brenna E**, Waldum HL. Studies of isolated parietal and enterochromaffin-like cells from the rat. *Scand J Gastroenterol* 1991; **26**: 1295-1306
22 **Chuang CN**, Tanner M, Chen MC, Davidson S, Soll AH. Gastrin induction of histamine release from primary cultures of canine oxyntic mucosal cells. *Am J Physiol* 1992; **263**: G460-G465
23 **Prinz C**, Scott DR, Hurwitz D, Helander HF, Sachs G. Gastrin effects on isolated rat enterochromaffin-like cells in primary culture. *Am J Physiol* 1994; **267**: G663-G675
24 **Sandvik AK**, Dimaline R, Mårvik R, Brenna E, Waldum HL. Gastrin regulates histidine decarboxylase activity and mRNA abundance in rat oxyntic mucosa. *Am J Physiol* 1994; **267**: G254-G258
25 **Höcker M**, Zhang Z, Koh TJ, Wang TC. The regulation of histidine decarboxylase gene expression. *Yale J Biol Med* 1996; **69**: 21-33
26 **Dimaline R**, Sandvik AK. Histidine decarboxylase gene expression in rat fundus is regulated by gastrin. *FEBS Lett* 1991; **281**: 20-22
27 **Brenna E**, Håkanson R, Sundler F, Sandvik AK, Waldum HL. The effect of omeprazole-induced hypergastrinemia on the oxyntic mucosa of mastomys. *Scand J Gastroenterol* 1991; **26**: 667-672
28 **Kleveland PM**, Waldum HL, Larsson H. Gastric acid secretion in the totally isolated, vascularly perfused rat stomach. A selective muscarinic-1 agent does, whereas gastrin does not, augment maximal histamine-stimulated acid secretion. *Scand J Gastroenterol* 1987; **22**: 705-713
29 **Chen D**, Zhao CM, Dockray GJ, Varro A, Van Hoek A, Sinclair NF, Wang TC, Koh TJ. Glycine-extended gastrin synergizes with gastrin 17 to stimulate acid secretion in gastrin-deficient mice. *Gastroenterology* 2000; **119**: 756-765
30 **Cui G**, Koh TJ, Chen D, Zhao CM, Takaishi S, Dockray GJ, Varro A, Rogers AB, Fox JG, Wang TC. Overexpression of glycine-extended gastrin inhibits parietal cell loss and atrophy in the mouse stomach. *Cancer Res* 2004; **64**: 8160-8166
31 **Sandvik AK**, Dockray GJ. Biological activity of carboxy-terminal gastrin analogs. *Eur J Pharmacol* 1999; **364**: 199-203
32 **Cui GL**, Sandvik AK, Munkvold B, Waldum HL. Glycine-extended gastrin-17 stimulates acid secretion only via CCK-2 receptor-induced histamine release in the totally isolated vascularly perfused rat stomach. *Acta Physiol Scand* 2002; **174**: 125-130

33 **Ekblad E**, Mei Q, Sundler F. Innervation of the gastric mucosa. *Microsc Res Tech* 2000; **48**: 241-257
34 **Walsh JH**. Peptides as regulators of gastric acid secretion. *Annu Rev Physiol* 1988; **50**: 41-63
35 **Sandor A**, Kidd M, Lawton GP, Miu K, Tang LH, Modlin IM. Neurohormonal modulation of rat enterochromaffin-like cell histamine secretion. *Gastroenterology* 1996; **110**: 1084-1092
36 **Pisegna JR**, Ohning GV, Athmann C, Zeng N, Walsh JH, Sachs G. Role of PACAP1 receptor in regulation of ECL cells and gastric acid secretion by pituitary adenylate cyclase activating peptide. *Ann N Y Acad Sci* 2000; **921**: 233-241
37 **Zeng N**, Walsh JH, Kang T, Wu SV, Sachs G. Peptide YY inhibition of rat gastric enterochromaffin-like cell function. *Gastroenterology* 1997; **112**: 127-135
38 **Zeng N**, Kang T, Wen Y, Wong H, Walsh J, Sachs G. Galanin inhibition of enterochromaffin-like cell function. *Gastroenterology* 1998; **115**: 330-339
39 **Zeng N**, Athmann C, Kang T, Lyu RM, Walsh JH, Ohning GV, Sachs G, Pisegna JR. PACAP type I receptor activation regulates ECL cells and gastric acid secretion. *J Clin Invest* 1999; **104**: 1383-1391
40 **Lindström E**, Eliasson L, Björkqvist M, Håkanson R. Gastrin and the neuropeptide PACAP evoke secretion from rat stomach histamine-containing (ECL) cells by stimulating influx of Ca2+ through different Ca2+ channels. *J Physiol* 2001; **535**: 663-677
41 **Läuff JM**, Modlin IM, Tang LH. Biological relevance of pituitary adenylate cyclase-activating polypeptide (PACAP) in the gastrointestinal tract. *Regul Pept* 1999; **84**: 1-12
42 **Sandvik AK**, Cui G, Bakke I, Munkvold B, Waldum HL. PACAP stimulates gastric acid secretion in the rat by inducing histamine release. *Am J Physiol Gastrointest Liver Physiol* 2001; **281**: G997-G1003
43 **Larsson LI**, Goltermann N, de Magistris L, Rehfeld JF, Schwartz TW. Somatostatin cell processes as pathways for paracrine secretion. *Science* 1979; **205**: 1393-1395
44 **Shin JM**, Cho YM, Sachs G. Chemistry of covalent inhibition of the gastric (H+, K+)-ATPase by proton pump inhibitors. *J Am Chem Soc* 2004; **126**: 7800-7811
45 **Israel DM**, Hassall E. Omerprazole and other proton pump inhibitors: pharmacology, efficacy, and safety, with special reference to use in children. *J Pediatr Gastroenterol Nutr* 1998; **27**: 568-579
46 **Larsson H**, Carlsson E, Ryberg B, Fryklund J, Wallmark B. Rat parietal cell function after prolonged inhibition of gastric acid secretion. *Am J Physiol* 1988; **254**: G33-G39
47 **Fullarton GM**, McLauchlan G, Macdonald A, Crean GP, McColl KE. Rebound nocturnal hypersecretion after four weeks treatment with an H2 receptor antagonist. *Gut* 1989; **30**: 449-454
48 **Waldum HL**, Arnestad JS, Brenna E, Eide I, Syversen U, Sandvik AK. Marked increase in gastric acid secretory capacity after omeprazole treatment. *Gut* 1996; **39**: 649-653
49 **el-Omar E**, Banerjee S, Wirz A, Penman I, Ardill JE, McColl KE. Marked rebound acid hypersecretion after treatment with ranitidine. *Am J Gastroenterol* 1996; **91**: 355-359
50 **Gillen D**, Wirz AA, Ardill JE, McColl KE. Rebound hypersecretion after omeprazole and its relation to on-treatment acid suppression and *Helicobacter pylori* status. *Gastroenterology* 1999; **116**: 239-247
51 **Kuipers EJ**, Klinkenberg-Knol EC. *Helicobacter pylori*, acid, and omeprazole revisited: bacterial eradication and rebound hypersecretion. *Gastroenterology* 1999; **116**: 479-483
52 **Qvigstad G**, Waldum H. Rebound hypersecretion after inhibition of gastric acid secretion. *Basic Clin Pharmacol Toxicol* 2004; **94**: 202-208
53 **Fossmark R**, Johnsen G, Johanessen E, Waldum HL. Rebound acid hypersecretion after long-term inhibition of gastric acid secretion. *Aliment Pharmacol Ther* 2005; **21**: 149-154
54 **Dockray GJ**. Topical review. Gastrin and gastric epithelial physiology. *J Physiol* 1999; **518** (Pt 2): 315-324
55 **Håkanson R**, Oscarson J, Sundler F. Gastrin and the trophic control of gastric mucosa. *Scand J Gastroenterol Suppl* 1986; **118**: 18-30
56 **Koh TJ**, Chen D. Gastrin as a growth factor in the gastrointestinal tract. *Regul Pept* 2000; **93**: 37-44
57 **Waldum HL**, Brenna E, Sandvik AK. Relationship of ECL cells and gastric neoplasia. *Yale J Biol Med* 1998; **71**: 325-335.
58 **Waldum HL**, Sandvik AK, Idle JR. Gastrin is the most important factor in ECL tumorigenesis. *Gastroenterology* 1998; **114**: 1113-1115
59 **Cui G**, Qvigstad G, Falkmer S, Sandvik AK, Kawase S, Waldum HL. Spontaneous ECLomas in cotton rats (Sigmodon hispidus): tumours occurring in hypoacidic/hypergastrinaemic animals with normal parietal cells. *Carcinogenesis* 2000; **21**: 23-27
60 **Dawson R**, Manson JM. Omeprazole in oesophageal reflux disease. *Lancet* 2000; **356**: 1770-1771
61 **Attila T**, Santharam R, Blom D, Komorowski R, Koch TR. Multifocal gastric carcinoid tumor in a patient with pernicious anemia receiving lansoprazole. *Dig Dis Sci* 2005; **50**: 509-513
62 **Ferrand A**, Wang TC. Gastrin and cancer: a review. *Cancer Lett* 2006; **238**: 15-29
63 **Aly A**, Shulkes A, Baldwin GS. Gastrins, cholecystokinins and gastrointestinal cancer. *Biochim Biophys Acta* 2004; **1704**: 1-10
64 **Takhar AS**, Eremin O, Watson SA. The role of gastrin in colorectal carcinogenesis. *Surgeon* 2004; **2**: 251-257
65 **Rengifo-Cam W**, Singh P. Role of progastrins and gastrins and their receptors in GI and pancreatic cancers: targets for treatment. *Curr Pharm Des* 2004; **10**: 2345-2358
66 **Kinoshita Y**, Ishihara S, Kadowaki Y, Fukui H, Chiba T. Reg protein is a unique growth factor of gastric mucosal cells. *J Gastroenterol* 2004; **39**: 507-513
67 **Sekikawa A**, Fukui H, Fujii S, Takeda J, Nanakin A, Hisatsune H, Seno H, Takasawa S, Okamoto H, Fujimori T, Chiba T. REG Ialpha protein may function as a trophic and/or anti-apoptotic factor in the development of gastric cancer. *Gastroenterology* 2005; **128**: 642-653

S- Editor Liu Y **L- Editor** Lutze M **E- Editor** Liu WF

PO Box 2345, Beijing 100023, China
www.wjgnet.com
wjg@wjgnet.com

World J Gastroenterol 2007 January 28; 13(4): 497-502
World Journal of Gastroenterology ISSN 1007-9327

REVIEW

Impact of tiny miRNAs on cancers

Wei Liu, Sheng-Yong Mao, Wei-Yun Zhu

Wei Liu, Sheng-Yong Mao, Wei-Yun Zhu, Laboratory of Gastrointestinal Microbiology, College of Animal Science and Technology, Nanjing Agricultural University, Nanjing 210095, Zhejiang Province, China
Supported by the National Basic Research Program of China (2004CB1175004) and the National Natural Science of Foundation of China, No. 30025034
Correspondence to: Wei-Yun Zhu, Laboratory of Gastrointestinal Microbiology, College of Animal Science and Technology, Nanjing Agricultural University, Nanjing 210095, Zhejiang Province, China. zhuweiyunnjau@hotmail.com
Telephone: +86-25-84395523 Fax: +86-25-84395314
Received: 2006-09-16 Accepted: 2006-11-27

Abstract

miRNAs are a class of small, ~22nt, non-coding RNAs that negatively regulate gene expression at the post-transcriptional level. They play profound and pervasive roles in manipulating gene expression involved in cell development, proliferation and apoptosis in various eukaryotes, which, in theory, could provide an access to many human diseases in theory. Recent evidence demonstrates that aberrant miRNA expression is a hallmark of tumor development, revealing that miRNA genes could function as potential oncogenes and repressors in the human body. miRNAs can affect tumorigenesis mainly by interrupting the cell cycle at the cellular level and by interacting with signaling, oncogenes and with the response to environmental factors at the molecular level. The established miRNA expression signature could be a potent tool to diagnose and treat human cancers in the future.

Key words: miRNAs; Cancers; Oncogenes and repressors; Tumorigenesis; miRNA expression signature

Liu W, Mao SY, Zhu WY. Impact of tiny miRNAs on cancers. *World J Gastroenterol* 2007; 13(4): 497-502

http://www.wjgnet.com/1007-9327/13/497.asp

INTRODUCTION

miRNAs (microRNAs) are a subset of small, typically 21-23 nt in length, non-coding RNAs evolutionarily conserved in many organisms as disparate as yeast, fruit flies, human and plants[1]. This growing family of small RNAs was first discovered in *Caenorhabditis elegans* in 1993[2] and newly honored as a milestone in the process of the gene concept[3]. Until now hundreds of miRNAs have been identified in many organisms by using experimental and bioinformatic prediction approaches. It is well known that, unlike its cousin signal interfering RNAs (siRNAs), miRNAs have the unique ability to negatively regulate gene expression involved in cell development, proliferation, apoptosis and the stress response[4]. Consequently, it is proposed that these biological properties of miRNAs could offer an access to many human diseases including cancers[5]. Recent findings have demonstrated that miRNAs play critical roles in human cancer, revealing that miRNAs could act as potential oncogenes and repressors[6,7]. Thus, this class of miRNAs are now dubbed 'oncomirs'-miRNAs which is closely related to tumor[8].

Cancer is characterized by uncontrolled proliferation and the inappropriate survival of damaged cells. Although cells have evolutionarily developed several safeguards to prevent malignant transformation during development and adulthood, this normal process can be disrupted in cancer cells. Cancer cells can take advantage of their unique strategy to escape scrutiny during cell division. The oncogenesis conventionally refers to tumor suppressors and oncogenes, such as APC, κ-RAS, Myc, P53 and P21. Although these regulatory molecules do play critical roles in tumor development, recent intense interest is being attached to miRNAs.

We are just beginning to appreciate the novel involvement of miRNAs in human cancers but much more remain obscure. Few investigations to date have converged to support the concrete links between miRNAs and each cancer species. However, most cancer species share the same mechanisms that give rise to tumorigenesis even in different tissues, so the general mechanism may be applied extensively to each cancer species. The potential link between miRNAs and tumors discussed in this review will be limited to only a few of the elucidated cancers.

miRNA BIOGENESIS AND MECHANISMS OF GENE EXPRESSION CONTROL

The biogenesis of miRNAs has recently been elucidated (Figure 1)[1]. RNA Pol Ⅱ generally transcribes miRNA genes in the nucleus and gives rise to large primary miRNA (pri-miRNA) transcripts that, like mRNA, are capped at 5' terminus and polyadenylated at 3' terminus. The initial pri-miRNAs are then processed by RNase Ⅲ,

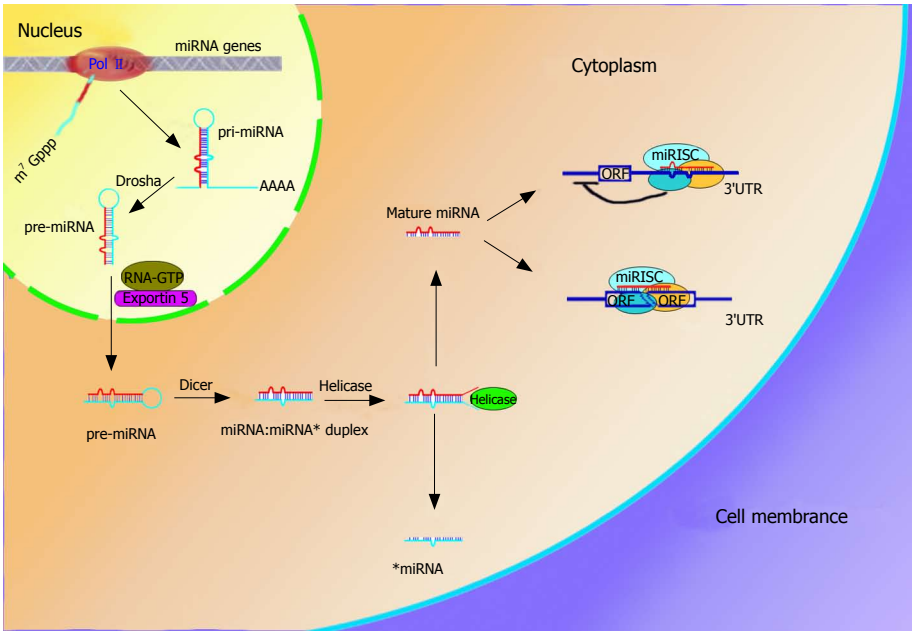

Figure 1 miRNAs biogenesis and two mechanisms involved in gene expression. MiRNAs genes often cluster on the chromosome and are transcribed by RNA Pol Ⅱ to form pri-miRNAs in the nucleus. The pri-miRNAs then undergo procession by RNase Ⅲ, Drasha, and are exported to cytoplasm by Exportin 5. Another RNase Ⅲ, Dicer, further processes the pre-miRNA to generate a ~22nt miRNA:miRNA* duplex, where miRNA* is complementary to miRNA. Helicase can divide the duplex into two separate ones. Whereas miRNA* is degraded, mature miRNA can enter the the miRNA-induced silence complex (miRISC). The miRISC complex block protein synthesis by imperfectly binding to the 3'UTR of the mRNA (upper right), the other one is to endonucleolytically cleave the target mRNA by perfect or nearly perfect base pairing (lower right).

Drasha, to form 70-bp pre-miRNAs in the nucleus. The pre-miRNAs are exported into the cytoplasm by the RNA GTP-dependent transporter Exportin 5 and undergo an additional processing step to produce a miRNA:miRNA* duplex with the aid of another RNase Ⅲ, Dicer. The RNA duplex is subsequently unwound by Helicase and the mature miRNA finally enter the RNA-induced silence complex (RISC)[9,10].

Two mechanisms of miRNA repression have been suggested depending on the degree of complementarities between the miRNAs and the target mRNAs (Figure 1)[4]. First, is interference with protein synthesis by binding to imperfect complementary sites within the 3' untranslated region of the target mRNA. The 3'UTR of target mRNA usually contains multiple complementary sites for distinct miRNAs, but the precise mechanism is still poorly understood. Second, is endonucleolytic cleavage of the target mRNA by perfect base pairing. The latter was previously thought to function solely in flowering plants, but the paradigm that animal miRNAs do not affect th stability of imperfectly base-paired miRNA has been challenged recently. Lim *et al*[11] used microarray analysis to investigate changes in global mRNA level in HeLa cells in response to miRNAs that are normally undetectable in those malignant cells and observed the reduction of 100-200 genes at the mRNA level. This observed reduction in mRNA level was attributed to AU-rich elements (AREs) that induced mRNA turnover by degrading mRNAs in exosome[12]. AREs are often found in transcripts that encode cell proliferation factors (e.g., TNF-α, GM-CSF, c-Fos, IL-6 and IL-8), and therefore stability of these transcripts in the absence of specific miRNAs contributes to the cell proliferation that accelerate tumor formation and development[13]. Nevertheless, one recent finding indicated that the reverse step also exists in the latter mechanism, where the mRNA can be relieved from the miRNA-induced inhibition in cells subject to different stress conditions[14]. This repression and derepression of mRNA expression cooperatively contribute to the dynamic balance of mRNA in cells, but the detailed mechanism is still not clear.

miRNAs could provide a convenient and efficient pathway to manipulate gene expression at posttranscriptional level. Natural miRNAs exert their effects by base pairing with the target mRNAs in a much more compact and energy-efficient manner than protein encoding regulatory molecules like enzymes and hormones, which show a necessary adaptation to regulate gene expression in eukaryotes[15].

miRNA GENE CLUSTERS AND LOCI

The human genome contains up to 1000 miRNA genes, which constitute approximately 1-5% of the expressed genes[16]. miRNAs are endogenetically conserved with evolutionary plasticity in eukaryotic genomes and are often organized in tandem and closely clustered on the chromosome[17]. This arrangement can have particular significance in the control of gene expression. When clustered miRNAs have a similar sequence, miRNAs gene products may synchronize to regulate a set of mRNA targets. However, clusters can also contain miRNAs with different sequences that extensively deploy toward their specific targets. These closely related characteristics may allow miRNAs to function as pleiotropic regulators at the cellular level in many organisms.

Over half of miRNA genes (52.5%) are located in or near fragile sites or cancer-associated genomic regions[18]. These sites are preferential sites of sister chromatin exchange, translocation, deletion, amplification or integration of plasmid DNA and tumor-associated virus, which frequently cause the aberrant miRNA expression during pathogenesis. For instance, *miR-15a* and *miR-16a* genes, frequently deleted and/or underexpressed in patients with B cell chronic lymphocytic leukemia, map to 13q14 that is deleted in many cases[19]. This result highlights that aberrant miRNA expression is possibly geared towards the intrinsic defect that gives rise to tumors.

miRNA IN CANCER STEM CELLS

Most tissues contain rare cells that follow the norm of stem cell biology to tissue self-renewal and repair[20]. The unprecedented self-renewal rate of robust tissues (like intestine, skin, blood and breast) often parallels a high susceptibility to malignant transformation, because the molecular mechanisms that control homeostatic self-renewal and those underlie tumors are evidently symmetric[21]. Currently the emerging notion is that tumor might contain stem cell-like 'cancer stem cells'-rare cells with indefinite proliferative potential that trigger tumor formation and growth, and with the presumed ability to transport new tumor seeds to distant sites[22]. Despite this controversial notion, one cancer (leukaemias) of the haematopoietic system provides the strong evidence that cancer cell proliferation is driven by cancer stem cells[23]. Given that cancer cells and normal stem cells share the similar potential to indefinite self-renew, it seems reasonable to propose that newly arising cancer cells appropriate the machinery for self-renewing cell division which is normally used in stem cells[24].

It is well known that miRNAs function as critical regulators of gene expression in the control of stem cells during development[5]. If miRNAs play a similar role in cancer stem cells then, in theory, it is possible support the hypothesis that several miRNAs appropriate the miRNA-mediated machinery for self-renewal in stem cells to develop tumors. Indeed, it has been validated that tumor tissues are constantly characterized with altered miRNA expressions.

A HALLMARK OF TUMOR

Currently the potential connection between miRNAs and cancers is just beginning to be appreciated. Cancer cells tend to undergo the distinct expression of miRNA, distinguishing them from the normal ones. Calin *et al*[25] first found that specific miRNA expression is abnormal in B-leukemia, suggesting that altered miRNA expression correlate with specific tumor development. In accordance with this, Michael *et al*[26] investigated possible changes at the miRNA level during tumorigenesis and showed the reduced accumulation of two specific miRNAs: miR-143 and miR-145, but consistent levels of the 70-bp precursor pre-miRNA in colorectal neoplasia as well as breast carcinoma, prostate carcinoma, chronic myelogenous leukemia and cervical carcinoma, implying that many tumors share aberrant specific miRNA expression. Recently Lu *et al*[27] found that cancer cell lines showed low miRNA expression profile when they used a new, bead-based flow cytometric miRNA expression profiling method to analyze a large-scale expression of 217 mammalian miRNA from 334 samples including multiple human cancers. Their study further demonstrated that tumors originating from tissue with a common embryonic source share the similar miRNA, but not mRNA, expression signature, and that distinct patterns of miRNA expression are consistent with the developmental history of human cancer, revealing that miRNAs could be used to classify different cancers and validate the developmental history of cancer. Volinia *et al*[7] further found that global miRNA expression signatures from solid tumors show a good separation between the different tissues, but not all miRNA expressions are underexpressed compared with their respective normal tissues. The studies support the hypothesis that the global change in miRNA expression is a hallmark of all human cancers, providing a hint that miRNAs correlate with various tumor development.

Moreover, impaired components of machinery mediating miRNA processing and miRNA-mediating gene repression give rise to tumorigenesis[28,29], demonstrating that altered specific miRNAs expression might play a causal role in the generation or/and maintenance of tumors. This description of cancers in molecular terms is likely to improve the way in which human cancers are diagnosed, classified, monitored, and (specially) treated, which will promise the emergency of the new era in cancer research in the future[30].

miRNA AND CELL CYCLE

Normal cells can tightly control cell proliferation and death by means of the cell cycle, thereby preventing malignant transformation during development and adulthood. The 3'UTR of mRNAs encoding many cell cycle-associated cytokines often contain binding sites to miRNAs, indicating that normal miRNAs are essential for cell cycle control. Hatfield *et al*[31] reported that *Drosophila melanogaster* germline stem cells subject to constitutively eliminated miRNA expression exhibited normal identity but were defective in cell cycle control, showing that miRNAs are essential in the control of cell cycle. Thus constitutive miRNAs are necessary to control cell cycle and maintain the balance of cell proliferation, differentiation and apoptosis, which play essential roles in preventing normal tissues from malignancy[32,33].

However, cancer cells are insensitive to cell division stop signals in an environment where most of the cells are quiescent. It is tempting to speculate that miRNAs could have a similar role in cancer cells and particularly rare cancer stem cells, where the disrupted miRNAs expression makes cells insensitive to environmental signals that normally stop the cell cycle. Brennecke *et al*[34] assigned a novel role to miRNA encoded by the *bantam* gene in control of cell proliferation and apoptosis during Drosophila development. *Bantam* miRNA could stimulate cell proliferation and simultaneously suppress apoptosis by manipulating the proapoptosis gene *hid* expression. It controls both cell growth and cycle progression in a coordinated manner, revealing that the putative vertebrate homologs of *bantam* miRNA genes may be oncogenes, whereas there are no homologues of *bantam* in human, other oncogenic miRNAs could play a similar role in control of cell proliferation and apoptosis. When the miRNA expression is impaired, normal tissues could have a high risk to develop tumor.

miRNA AND CANCER-ASSOCIATED SIGNALING PATHWAYS

The signaling transductions (Wnt, Notch, SHH and BMP) play essential roles in the processes of cell life at the

molecular level, but these pathways controlling cell growth and differentiation in normal cell are almost invariably changed in cancer. Consistent with the altered miRNA expression in cancer cells, it is reasonable that the two can work together to control cell fate.

Several cancer-associated signaling pathways directly regulate expression of specific miRNA genes. Yoo *et al*[35] found that LIN-12/Notch signaling pathway directly binds to one miRNA gene, *mir-61*, and promote its expression in vulval precursor cells during *C. elegans* development. Stimulated expression of *mir-61* gene subsequently represses the translation of Vav-1, the ortholog of the vav oncogene, who negatively regulates the *lin-2* gene activity. These cyclic regulations form a positive feedback loop that helps maximize *lin-12* activity and continually stimulate Notch signaling pathway (Figure 2). It has been known that Notch signaling pathway plays an important role in many cancer species. If the similar mechanisms exist in cancer cell, this positive loop could trigger and accelerate tumorigenesis.

miRNAs can influence the signaling pathway by repressing several secreted signaling proteins. RAS is a signaling protein in many significant signaling pathways and its overexpression usually results in oncogenic transformation. The 3'UTL of the human RAS genes contains multiple *let-7* complementary sites, allowing *let-7* to regulate RAS expression. Johnson *et al*[36] found that *let*-7 expression is lower in lung tumors than in the normal lung tissue, providing a possible strategy to treat lung cancer by repairing mutated *let-7* gene. It was reported that miR-143 and miR-145, lower in colorectal cancer than in normal tissues, are predicted to regulate several target mRNAs encoding components of signal transduction pathway (Raf, Rho, GTPase activating protein, G-protein γ, NF-κB and HGK)[26]. Hence, the direct and indirect interaction between miRNAs and secreted signaling protein can influence tumorigenesis.

Thus, it is supposed that miRNAs and signal as well as other regulatory molecules constitute a network where normal cells follow a rule to divide, differentiate, and die. When the regulatory network is impaired, cell cycle will be out of control, giving rise to tumor development. However, the networks of miRNAs and signals are largely elusive to date.

INTERACTION BETWEEN miRNA AND ONCOGENES

Due to mutation, many human proto-oncogenes can convert to oncogenes. These oncogenes often encode common regulatory molecules that can stimulate the tumor development in the body. For example, the proto-oncogene *C-MYC* encodes a helix-loop-helix leucine zipper transcriptional factor that regulates cell proliferation, growth and apoptosis. Recent findings revealed that c-Myc directly binds to the locus of a cluster of six miRNAs and stimulates their expression[37]. Overexpression of *miR-17-5p* and *miR-20a*, two miRNAs in this cluster, reduced the expression of E2F1 (one transcriptional factor). c-Myc and E2F1 are reciprocally induced in normal cell to form a putative positive feedback loop, like the one between *mir-16* and LIN-12. So these two miRNAs provide a potent tool to dampen this reciprocal activation and tightly regulate c-Myc-mediated cellular proliferation in normal cells. When this cluster of miRNA genes is deleted or underexpressed, the cell cycle would be out of control and have a risk of tumorigenesis.

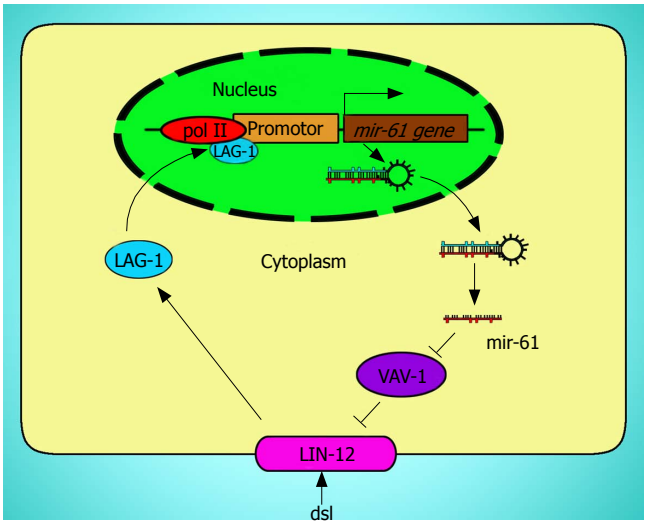

Figure 2 The positive loop between *mir-16* and LIN-12. Exogenous signal activates LIN-12/Notch signaling pathway, which promotes the transcription of *mir-61*. Overexpression of *mir-61* inhibits the activity of VAV-1 (purple) that reduces the activity of LIN-12 (pink), where LIN-12, mir-61, and VAV-1 form a feedback loop that helps maximize LIN-12 activity.

Notably, not all miRNAs function as tumor repressors in the body. For example, enforced expression of the *mir-17-92* cluster positively cooperates with c-Myc expression to accelerate tumor development in a mouse B-cell lymphoma model, implicating that the *mir-17-92* cluster as a potential oncogene[2]. The oncogenic miRNAs can be upregulated in cancer cells, which are consistent with the conclusion drawn by Volinia that not all miRNAs are underexpressed in cancer cells[7]. In fact, specific miRNA expression influencing cell fate is dependant on the milieu of miRNAs and their target mRNAs expressed in individual cell.

RULERS OF miRNA

As the pleiotropic regulators in cells, who regulate the expression of miRNA genes? As LIN-12/Notch signaling pathway directly regulates the expression of *mir-16* gene discussed above[35], it seems that the regulation of miRNA expression follows the classic model widely used to control the mRNA expression. Taganov *et al*[38] recently reported that three putative NF-κB consensus binding sites locate upstream of the predicted *miRNA-146* gene, so *miRNA-146* is a NF-κB-dependent gene. Is this general model the common one or just an exceptional one with respect to diverse miRNAs and cytokines in cells? Our understanding of this knowledge awaits further investigations.

NOT THE END OF STORY

We have discussed the potential roles of miRNAs in cancers by means of cell cycle, signaling and oncogene, but they are just the tip of emerging iceberg, because exploding data show that miRNAs have a potentially much more widely influence over diverse developmental and physiological pathways than imagined. Recent evidence revealed that miRNAs could participate in genomic stability and epigenetic modification[2,39], in metabolic changes compatible with tumor formation, growth and metastasis[40], and in the immune response to virus-mediated infection[41-45]. Many more aspects of miRNAs are available for exploration, so this is not the whole story.

More intriguingly, the other cousin of miRNAs, piwi-interacting RNAs (piRNAs), have just been discovered in rat germline cells and are also shown to control gene expression involved in sperm development at posttranscriptional level[46]. The world of three small RNAs (siRNAs, miRNAs, and piRNAs) is undoubtedly yielding newly provocative insights and revolutionizing our thinking about genome control[47]. Although transcriptional control is the most prevalent form of gene expression control, it is by no means the only way in complex eukaryotes. For example, it is important for mature blood red cells to control the stability of expressed mRNAs accounting for no extra mRNA transcription any more or is for immune cells to make a rapid response to stress without mRNAs transcription initiation. Posttranscriptional control has been ignored, but many novel small RNAs are changing our thinking.

PROSPEROUS OUTLOOK IN miRNA

Evaluating the novel roles of miRNAs as repressors and oncogenes enriches our knowledge, which addresses the precise mechanism leading to tumorigenesis. The investigation will certainly bring about a potent tool to diagnose and treat human cancers, but a detailed, mechanistic understanding of miRNAs functions as oncogenes and tumor repressors is now retarded by lacking a valid and efficient biochemical technique to precisely identify miRNAs and their corresponding targets. It is estimated that many more miRNAs are still waiting to be discovered in the human genome and functions of most known miRNAs have not been elucidated. The other challenge is to accurately identify targets that are manipulated by miRNAs, because miRNAs can bind to their imperfect targets, even with no canonical complementarities that allow short stretch of mismatched base-pairs and G-U base pair. Other outstanding questions about miRNAs remain unresolved. What regulates the expression of miRNAs? Do distinct miRNAs have a direct function in cancer progression, or just simply differentially modulate in tumor? Who determines the opposite roles of miRNAs as both oncogenes and repressors? Do miRNAs act mainly to 'fine-tune' gene expression or more often as binary on/off switch? What factors affect the accessibility and efficacy of a miRNA at a 3'UTR? Another key one is how to apply this novel technique to cancer therapy. However, more sophisticated experimental approaches, in combination with computational prediction strategies, will shed light on these challenges.

It has been shown that miRNA expression profile is a more accurate signature than protein expression one, and several patients got better prognosis after repairing the abrogated miRNAs. We enthusiastically expect that traditional and bioinformatics technique will generate a tremendous amount of excitement and inspiration about miRNAs in future.

REFERENCES

1 **Bartel DP**. MicroRNAs: genomics, biogenesis, mechanism, and function. *Cell* 2004; **116**: 281-297
2 **Lee RC**, Feinbaum RL, Ambros V. The C. elegans heterochronic gene lin-4 encodes small RNAs with antisense complementarity to lin-14. *Cell* 1993; **75**: 843-854
3 **Pearson H**. Genetics: what is a gene? *Nature* 2006; **441**: 398-401
4 **Ambros V**. The functions of animal microRNAs. *Nature* 2004; **431**: 350-355
5 **Alvarez-Garcia I**, Miska EA. MicroRNA functions in animal development and human disease. *Development* 2005; **132**: 4653-4662
6 **He L**, Thomson JM, Hemann MT, Hernando-Monge E, Mu D, Goodson S, Powers S, Cordon-Cardo C, Lowe SW, Hannon GJ, Hammond SM. A microRNA polycistron as a potential human oncogene. *Nature* 2005; **435**: 828-833
7 **Volinia S**, Calin GA, Liu CG, Ambs S, Cimmino A, Petrocca F, Visone R, Iorio M, Roldo C, Ferracin M, Prueitt RL, Yanaihara N, Lanza G, Scarpa A, Vecchione A, Negrini M, Harris CC, Croce CM. A microRNA expression signature of human solid tumors defines cancer gene targets. *Proc Natl Acad Sci USA* 2006; **103**: 2257-2261
8 **Esquela-Kerscher A**, Slack FJ. Oncomirs - microRNAs with a role in cancer. *Nat Rev Cancer* 2006; **6**: 259-269
9 **Denli AM**, Tops BB, Plasterk RH, Ketting RF, Hannon GJ. Processing of primary microRNAs by the Microprocessor complex. *Nature* 2004; **432**: 231-235
10 **Gregory RI**, Yan KP, Amuthan G, Chendrimada T, Doratotaj B, Cooch N, Shiekhattar R. The Microprocessor complex mediates the genesis of microRNAs. *Nature* 2004; **432**: 235-240
11 **Lim LP**, Lau NC, Garrett-Engele P, Grimson A, Schelter JM, Castle J, Bartel DP, Linsley PS, Johnson JM. Microarray analysis shows that some microRNAs downregulate large numbers of target mRNAs. *Nature* 2005; **433**: 769-773
12 **Jing Q**, Huang S, Guth S, Zarubin T, Motoyama A, Chen J, Di Padova F, Lin SC, Gram H, Han J. Involvement of microRNA in AU-rich element-mediated mRNA instability. *Cell* 2005; **120**: 623-634
13 **Sontheimer EJ**, Carthew RW. Silence from within: endogenous siRNAs and miRNAs. *Cell* 2005; **122**: 9-12
14 **Bhattacharyya SN**, Habermacher R, Martine U, Closs EI, Filipowicz W. Relief of microRNA-mediated translational repression in human cells subjected to stress. *Cell* 2006; **125**: 1111-1124
15 **Mattick JS**, Makunin IV. Small regulatory RNAs in mammals. *Hum Mol Genet* 2005; **14** Spec No 1: R121-R132
16 **Berezikov E**, Guryev V, van de Belt J, Wienholds E, Plasterk RH, Cuppen E. Phylogenetic shadowing and computational identification of human microRNA genes. *Cell* 2005; **120**: 21-24
17 **Lau NC**, Lim LP, Weinstein EG, Bartel DP. An abundant class of tiny RNAs with probable regulatory roles in Caenorhabditis elegans. *Science* 2001; **294**: 858-862
18 **Calin GA**, Sevignani C, Dumitru CD, Hyslop T, Noch E, Yendamuri S, Shimizu M, Rattan S, Bullrich F, Negrini M, Croce CM. Human microRNA genes are frequently located at fragile sites and genomic regions involved in cancers. *Proc Natl Acad Sci USA* 2004; **101**: 2999-3004
19 **Calin GA**, Ferracin M, Cimmino A, Di Leva G, Shimizu M, Wojcik SE, Iorio MV, Visone R, Sever NI, Fabbri M, Iuliano

R, Palumbo T, Pichiorri F, Roldo C, Garzon R, Sevignani C, Rassenti L, Alder H, Volinia S, Liu CG, Kipps TJ, Negrini M, Croce CM. A MicroRNA signature associated with prognosis and progression in chronic lymphocytic leukemia. *N Engl J Med* 2005; **353**: 1793-1801

20 **Morrison SJ**, Kimble J. Asymmetric and symmetric stem-cell divisions in development and cancer. *Nature* 2006; **441**: 1068-1074

21 **Radtke F**, Clevers H. Self-renewal and cancer of the gut: two sides of a coin. *Science* 2005; **307**: 1904-1909

22 **Reya T**, Morrison SJ, Clarke MF, Weissman IL. Stem cells, cancer, and cancer stem cells. *Nature* 2001; **414**: 105-111

23 **Grandics P**. The cancer stem cell: evidence for its origin as an injured autoreactive T cell. *Mol Cancer* 2006; **5**: 6

24 **Clarke MF**, Fuller M. Stem cells and cancer: two faces of eve. *Cell* 2006; **124**: 1111-1115

25 **Calin GA**, Dumitru CD, Shimizu M, Bichi R, Zupo S, Noch E, Aldler H, Rattan S, Keating M, Rai K, Rassenti L, Kipps T, Negrini M, Bullrich F, Croce CM. Frequent deletions and down-regulation of micro- RNA genes miR15 and miR16 at 13q14 in chronic lymphocytic leukemia. *Proc Natl Acad Sci USA* 2002; **99**: 15524-15529

26 **Michael MZ**, O' Connor SM, van Holst Pellekaan NG, Young GP, James RJ. Reduced accumulation of specific microRNAs in colorectal neoplasia. *Mol Cancer Res* 2003; **1**: 882-891

27 **Lu J**, Getz G, Miska EA, Alvarez-Saavedra E, Lamb J, Peck D, Sweet-Cordero A, Ebert BL, Mak RH, Ferrando AA, Downing JR, Jacks T, Horvitz HR, Golub TR. MicroRNA expression profiles classify human cancers. *Nature* 2005; **435**: 834-838

28 **Karube Y**, Tanaka H, Osada H, Tomida S, Tatematsu Y, Yanagisawa K, Yatabe Y, Takamizawa J, Miyoshi S, Mitsudomi T, Takahashi T. Reduced expression of Dicer associated with poor prognosis in lung cancer patients. *Cancer Sci* 2005; **96**: 111-115

29 **Liu J**, Carmell MA, Rivas FV, Marsden CG, Thomson JM, Song JJ, Hammond SM, Joshua-Tor L, Hannon GJ. Argonaute2 is the catalytic engine of mammalian RNAi. *Science* 2004; **305**: 1437-1441

30 **Varmus H**. The new era in cancer research. *Science* 2006; **312**: 1162-1165

31 **Hatfield SD**, Shcherbata HR, Fischer KA, Nakahara K, Carthew RW, Ruohola-Baker H. Stem cell division is regulated by the microRNA pathway. *Nature* 2005; **435**: 974-978

32 **Xu P**, Vernooy SY, Guo M, Hay BA. The Drosophila microRNA Mir-14 suppresses cell death and is required for normal fat metabolism. *Curr Biol* 2003; **13**: 790-795

33 **Xu P**, Guo M, Hay BA. MicroRNAs and the regulation of cell death. *Trends Genet* 2004; **20**: 617-624

34 **Brennecke J**, Hipfner DR, Stark A, Russell RB, Cohen SM. *bantam* encodes a developmentally regulated microRNA that controls cell proliferation and regulates the proapoptotic gene hid in Drosophila. *Cell* 2003; **113**: 25-36

35 **Yoo AS**, Greenwald I. LIN-12/Notch activation leads to microRNA-mediated down-regulation of Vav in C. elegans. *Science* 2005; **310**: 1330-1333

36 **Johnson SM**, Grosshans H, Shingara J, Byrom M, Jarvis R, Cheng A, Labourier E, Reinert KL, Brown D, Slack FJ. RAS is regulated by the let-7 microRNA family. *Cell* 2005; **120**: 635-647

37 **O'Donnell KA**, Wentzel EA, Zeller KI, Dang CV, Mendell JT. c-Myc-regulated microRNAs modulate E2F1 expression. *Nature* 2005; **435**: 839-843

38 **Taganov KD**, Boldin MP, Chang KJ, Baltimore D. NF-kappaB-dependent induction of microRNA miR-146, an inhibitor targeted to signaling proteins of innate immune responses. *Proc Natl Acad Sci USA* 2006; **103**: 12481-12486

39 **Zhang L**, Huang J, Yang N, Greshock J, Megraw MS, Giannakakis A, Liang S, Naylor TL, Barchetti A, Ward MR, Yao G, Medina A, O'brien-Jenkins A, Katsaros D, Hatzigeorgiou A, Gimotty PA, Weber BL, Coukos G. microRNAs exhibit high frequency genomic alterations in human cancer. *Proc Natl Acad Sci USA* 2006; **103**: 9136-9141

40 **Vella MC**, Choi EY, Lin SY, Reinert K, Slack FJ. The C. elegans microRNA let-7 binds to imperfect let-7 complementary sites from the lin-41 3'UTR. *Genes Dev* 2004; **18**: 132-137

41 **Sullivan CS**, Ganem D. MicroRNAs and viral infection. *Mol Cell* 2005; **20**: 3-7

42 **Sullivan CS**, Grundhoff AT, Tevethia S, Pipas JM, Ganem D. SV40-encoded microRNAs regulate viral gene expression and reduce susceptibility to cytotoxic T cells. *Nature* 2005; **435**: 682-686

43 **Nair V**, Zavolan M. Virus-encoded microRNAs: novel regulators of gene expression. *Trends Microbiol* 2006; **14**: 169-175

44 **Pfeffer S**, Zavolan M, Grässer FA, Chien M, Russo JJ, Ju J, John B, Enright AJ, Marks D, Sander C, Tuschl T. Identification of virus-encoded microRNAs. *Science* 2004; **304**: 734-736

45 **Lecellier CH**, Dunoyer P, Arar K, Lehmann-Che J, Eyquem S, Himber C, Saïb A, Voinnet O. A cellular microRNA mediates antiviral defense in human cells. *Science* 2005; **308**: 557-560

46 **Lau NC**, Seto AG, Kim J, Kuramochi-Miyagawa S, Nakano T, Bartel DP, Kingston RE. Characterization of the piRNA complex from rat testes. *Science* 2006; **313**: 363-367

47 **Carthew RW**. Molecular biology. A new RNA dimension to genome control. *Science* 2006; **313**: 305-306

S- Editor Liu Y **L- Editor** Ma JY **E- Editor** Bai SH

PO Box 2345, Beijing 100023, China
www.wjgnet.com
wjg@wjgnet.com

World J Gastroenterol 2007 January 28; 13(4): 503-508
World Journal of Gastroenterology ISSN 1007-9327

Chromosome 11 aneusomy in esophageal cancers and precancerous lesions- an early event in neoplastic transformation: An interphase fluorescence *in situ* hybridization study from south India

Vasavi Mohan, Shivani Ponnala, Hemakumar M Reddy, Radha Sistla, Rachel A Jesudasan, Yog Raj Ahuja, Qurratulain Hasan

Vasavi Mohan, Shivani Ponnala, Qurratulain Hasan, Department of Genetics & Molecular Medicine, Kamineni Hospitals, LB Nagar, Hyderabad, AP, India
Hemakumar M Reddy, Rachel A Jesudasan, Department of Molecular Biology, Center for Cellular and Molecular Biology, Uppal Road, Hyderabad, AP, India
Radha Sistla, Department of Pathology, Kamineni Hospitals, Hyderabad, AP, India
Yog Raj Ahuja, Department of Genetics, Vasavi Hospital and Research Center, Lakdi-ka-pul, Hyderabad, AP, India
Qurratulain Hasan, Department of Genetics, Bhagwan Mahavir Medical Research Center, AC Guards, Hyderabad, AP, India
Correspondence to: Dr. Vasavi Mohan, Department of Genetics & Molecular Medicine, Kamineni Hospitals, LB Nagar, Hyderabad 500068, Andhra Pradesh, India. greenpastures@gmail.com
Telephone: +91-98840-02982 Fax: +91-40-24022277
Received: 2006-10-06 Accepted: 2006-11-27

Abstract

AIM: To detect aneusomic changes with respect to chromosome 11 copy number in esophageal precancers and cancers wherein the generation of cancer-specific phenotypes is believed to be associated with specific chromosomal aneuploidies.

METHODS: We performed fluorescence *in situ* hybridization (FISH) on esophageal tissue paraffin sections to analyze changes in chromosome 11 copy number using apotome-generated images by optical sectioning microscopy. Sections were prepared from esophageal tumor tissue, tissues showing preneoplastic changes and histologically normal tissues (control) obtained from patients referred to the clinic for endoscopic evaluation.

RESULTS: Our results demonstrated that aneusomy was seen in all the cancers and preneoplastic tissues, while none of the controls showed aneusomic cells. There was no increase in aneusomy from precancers to cancers.

CONCLUSION: Our results suggest that evaluation of chromosome 11 aneusomy in esophageal tissue using FISH with an appropriate signal capture-analysis system, can be used as an ancillary molecular marker predictive of early neoplastic changes. Future studies can be directed towards the genes on chromosome 11, which may play a role in the neoplastic transformation of esophageal precancerous lesions to cancers.

Key words: Esophageal cancer; Aneusomy; Chromosome 11; Fluorescence *in situ* hybridization; Early detection

Vasavi M, Ponnala S, Reddy HM, Sistla R, Jesudasan RA, Ahuja YR, Hasan Q. Chromosome 11 aneusomy in esophageal cancers and precancerous lesions- an early event in neoplastic transformation: An interphase fluorescence *in situ* hybridization study from south India. *World J Gastroenterol* 2007; 13(4): 503-508

http://www.wjgnet.com/1007-9327/13/503.asp

INTRODUCTION

More than 30% of the adult population exhibits upper gastrointestinal tract disorders associated with symptoms such as regurgitation, heartburn and dysphagia, warranting an endoscopic evaluation. Some of these esophageal pathologies require medication while others can be managed by altering life-style and dietary habits. A certain percentage of these, however, progress into esophageal malignancies. In India, esophageal cancer is the second leading cancer in men and fourth leading cancer in women[1].

Epithelial tumors of the esophagus [squamous cell carcinoma (SCC) and adenocarcinoma (ADC)] are responsible for more than 95% of all esophageal carcinomas. This malignancy presents generally as a locally advanced disease, hence leading to poor prognosis with an average 5-year survival of < 12% in India[2]. Abnormal proliferation of the esophageal epithelial cells with hyperplasia and dysplasia in the normal squamous lining are regarded as premalignant lesions[3,4]. Another common premalignant condition is Barrett's esophagus (BE), where patients have a forty-fold increased risk for developing adenocarcinoma as compared to normal individuals. Although significant advances have been made in the diagnosis and treatment of esophageal carcinomas, not many studies have evaluated markers in the target tissue, in association with increased risk for malignant

transformation. Hence, there is a need to identify the genetic and molecular factors responsible for the progression of these esophageal lesions into malignancy.

Neoplastic progression is a complex multistep process associated with gross chromosomal alterations and mutations in regulatory genes, culminating in tumorigenesis. Genomic instability is a prominent feature of most cancers, wherein aneuploidy, a change in chromosomal number caused by unequal partitioning of chromosomes during cell division, occurs frequently in many solid tumors[5,6]. Aneuploidy then generates specific aneusomies autocatalytically, due to errors in chromosome segregation and repair processes[7]. Aneusomies have been reported in non-cancerous conditions such as Down's syndrome, wherein the extra chromosome 21 is considered to be associated with an increased risk for leukemias. The study of human cancers shows evidence for cancer-specific aneusomies, despite a plethora of unspecific aneuploidies[8,9]. Recently, it has been demonstrated cytogenetically that chromosome 11 may be important in the etiology of SCC of the esophagus[10,11].

The present study was a hospital-based, unmatched, case-control study in 25 cases referred to our clinic from different hospitals in Hyderabad, South India. Chromosome 11 aneusomy was investigated in esophageal biopsies taken from controls, premalignant and malignant lesions, using fluorescence *in situ* hybridisation (FISH). Our results demonstrated that aneusomy was seen in all the cancers and preneoplastic tissues, while none of the controls showed aneusomic cells. There was no increase in aneusomy from precancers to cancers. Evaluation of chromosome 11 aneusomy in esophageal tissue can be used as an ancillary molecular marker predictive of early neoplastic changes.

MATERIALS AND METHODS

Tissue specimens

Esophageal biopsy specimens were endoscopically resected from patients referred for histopathological evaluation by a qualified gastroenterologist. The control samples were taken from those patients undergoing an endoscopy, which showed normal tissue histology. All samples were included in the study after informed consent was obtained from the patients. The study was approved by our Institutional Ethical Committee. Formalin-fixed, paraffin-embedded tissue sections from 25 selected cases were subjected to FISH analysis subsequent to confirmation by histology.

Histopathological analysis

Paraffin-embedded tissue sections (4 μm thick) were first subject to deparaffinization. Slides were placed in xylene (3 min × 3 min), 100% alcohol (3 min × 3 min), rinsed in running water and stained with haematoxylin (Harries, Merck) for 5-10 min. They were then placed in running water, dipped in 1% hydrochloric acid and subsequently transferred to Eosin yellow staining (Merck) for 30 s. After that the slides were passed through graded alcohol series for dehydration, placed in xylene and mounted in DPX (Ref: Histopathology Laboratory, Armed Forces Institute of Pathology, Washington DC, 20 305, USA). Suitable images of the required areas from representative tissue sections were taken using a CCD camera (Figure 1).

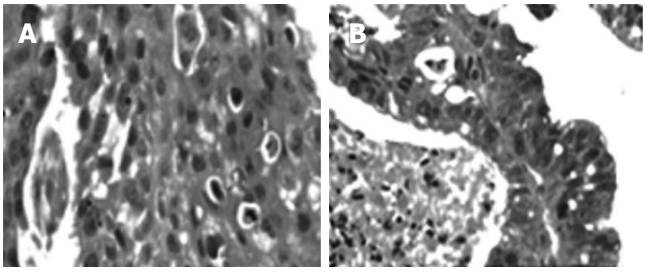

Figure 1 Representative HE stained sections at × 400 magnification selected for FISH analysis. **A**: Neoplastic streaks with eosin stained keratin pearls indicating a well-differentiated squamous cell carcinoma; **B**: Adenocarcinomatous tissue showing columnar epithelial replacement of the normal squamous lining.

Based on the endoscopic and histopathological evaluation, 25 tissue biopsies were selected for FISH analysis using a Spectrum Green labeled, centromere enumeration probe (CEP) for chromosome 11 [Vysis India Ltd] (This was used instead of the LSI probes that would help evaluate gene amplification).

FISH on esophageal tissue sections

Paraffin sections of 4 μm thick were deparaffinized in an oven at 95℃ for 20 min, then immediately placed in xylene (3 min × 3 min) and transferred into 100% ethanol (3 min × 5 min). Dried slides were incubated in 2 × SSC solution at 75℃ for 10 min followed by treatment with proteinase K solution (2 mg/mL) at 37℃ for 15 min. The slides were rinsed in 2 × SSC solution at room temperature. They were then immersed in a 75℃ denaturant bath (70% formamide/2 × SSC) for 5 min and dehydrated in gradient ethanol. Dry slides were placed on a 45-50℃ slide warmer. Probe mixture was simultaneously prepared at room temperature (7 μL of hybridization buffer + 1 μL Spectrum Green labeled CEP 11 DNA probe + 2 μL purified double distilled H_2O) and then denatured at 95℃. Ten microliters of the probe mix were applied to the slide, and a coverslip was placed on it immediately. The slides were hybridized in a pre-warmed humidified chamber overnight (12-16 h) at 37℃. Post-hybridization washes were done with freshly prepared 0.4 × SSC/0.3% NP-40 solution at 55℃ followed by 2 × SSC/0.1% NP-40 at room temperature. The slides were then air-dried in the dark. Ten microliter DAPI counterstain was applied to the target area and a coverslip was placed on it carefully to avoid formation of air bubbles.

The slides were viewed under a fluorescence microscope (Olympus, Optical sectioning microscope attached to an Axioplan imaging Apotome apparatus, Zeiss, Germany) using a suitable filter set (DAPI Exc: 367nm; Emi: 452 nm and Spectrum Green Exc: 509 nm; Emi: 538 nm). The optical sectioning microscope provided a high-quality image enhancement required for proper signal visualization. The sections were visualized through Optical sectioning mode using the Apotome for the best probe signals in a 3D mode. Ten to fifteen areas per slide were taken for analysis based on the density of the nuclei. Each area allowed optical sectioning of about

Table 1 Details of cases analyzed for chromosome 11 aneusomy using FISH in different esophageal pathologies and controls

Case, No.	Case type	Details	Chromosome 11 % aneusomy		
			Trisomy (%)	Tetrasomy (%)	Pentasomy (%)
1	Controls	Normal	-	-	-
2		Normal	-	-	-
3		Normal	-	-	-
4		Normal	-	-	-
5		Normal	-	-	-
6	Precancers	Sq. dysplasia (High grade)	4.0	-	-
7		Sq. dysplasia (High grade)	10.0	0.4	-
8		Barrett's dysplasia (High grade)	15.2	2.4	0.8
9		Barrett's dysplasia (High grade)	5.6	-	-
10	Cancers	ADC	12.8	2.0	-
11		ADC	10.0	2.0	-
12		WDSCC	11.2	-	-
13		WDSCC	12.8	0.4	-
14		WDSCC	8.8	2.4	-
15		MDSCC	10.0	0.8	-
16		MDSCC	12.8	0.4	0.4
17		MDSCC	5.2	0.8	-
18		PDSCC	1.6	-	-
19		PDSCC	6.0	-	-
20		PDSCC	3.2	-	-

Percentage of aneusomy in different cases from the first 250 cells scored. (Monosomies and normal disomies are not shown in the table). ADC: Adenocarcinoma; WDSCC: Well differentiated SCC; MDSCC: Moderately differentiated SCC; PDSCC: Poorly differentiated SCC; Sq. : Squamous.

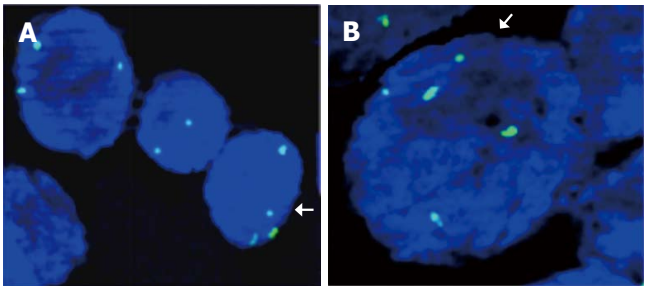

Figure 2 Images showing aneusomy with regard to chromosome 11 in esophageal cancer cells. **A**: Trisomy and tetrasomy chromosome 11 in the same area; **B**: Pentasomy chromosome 11 with normal disomy.

8-10 consecutive sections using the apotome. The images were captured at 1500 × magnification with oil immersion. Analysis was done using the 3D analysis of the Axiovision Apotome 1 imaging and Adobe Photoshop 7.0 version softwares.

Criteria for evaluating FISH signals

Data were scored from areas showing uniform fluorescence intensity. We screened a large number of nuclei per sample in order that we did not miss any aneusomic cells, especially with respect to precancer tissues. In each case, clear, distinct FISH signals were evaluated by counting 250 non-overlapping nuclei. Only those samples in which the artifactual nullisomy (negative nuclei) did not exceed the prescribed 25% were chosen for evaluation. A baseline frequency of monosomic population was established to control 'truncation' artifacts resulting from cut nuclei during microtomy.

RESULTS

From the patients with upper GI tract disorders referred for endoscopic evaluation, 25 cases were selected into the FISH study based on endoscopic and histopathological categorization. Of these 25 cases, 20 gave analyzable results; they included five normal tissues, four precancers (two squamous dysplasias and two BE with high-grade dysplasia) and eleven esophageal cancers as shown in Table 1.

FISH was performed on a few metaphase cells and, in conjunction with G-banded chromosome analysis, we confirmed the probe hybridization. Subsequently the method was applied to esophageal tissue sections obtained from paraffin blocks. Optical sectioning generated 3D images were evaluated and screened for chromosome 11 probe signals (Figure 2).

The results in each sample were tabulated as nullisomy (absence of signals), monosomy (single signal), normal disomic condition (two signals), trisomy (three signals), tetrasomy (four signals) and pentasomy (five signals). Esophageal tumor cells with trisomic, tetrasomic and pentasomic signals indicating the presence of extra chromosome 11 are shown in Figure 3.

Artifactual nullisomy was found to be less than 15% in all 20 cases studied. Monosomy was seen in < 35% of the cells in all three groups of controls, precancers and cancers; this was not included in the analysis as it was considered as a technical artifact. The controls showed normal disomy in all the remaining cells analyzed. Premalignant tissues showed an increase in the copy number of chromosome 11; all the four precancer cases showed trisomy of chromosome 11 (4%, 10%, 15.2%, 5.6%); of these, one case with severe squamous dysplasia exhibited tetrasomy (0.4%), and a case of BE with high

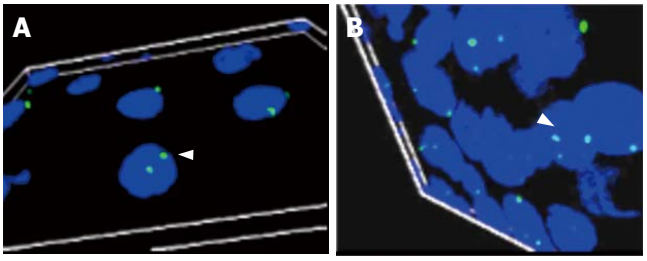

Figure 3 Axiovision Apotome software generated 3D-image from overlay of 10 consecutive images captured by the Optical sectioning microscopy. **A**: A portion of the esophageal tissue section from the control showing normal disomy of chromosome 11 (indicated by an arrow); **B**: Tissues from patients with well-differentiated squamous cell carcinoma (arrow indicating cell with trisomy for chromosome 11).

grade dysplasia showed tetrasomy and pentasomy of chromosome 11 (2.4% and 0.8%), respectively (Table 1).

All eleven cancer cases showed varying degrees of aneusomy of chromosome 11 in the affected tissues. Both cases of adenocarcinoma showed trisomy and tetrasomy. Of the remaining SCC cases, 4/9 showed only trisomy, 5/9 also showed tetrasomy and 1/9 also exhibited pentasomy of chromosome 11 (Table 1).

DISCUSSION

Chromosomal instability leading to aneuploidy and subsequently, specific aneusomies is characteristic of cancers[7,12]. In spite of the somatic gene-mutation hypothesis supporting the role of oncogenes and tumor suppressor genes in carcinogenesis, it has not been possible to disprove the century-old aneuploidy hypothesis even today. Cancer independent evidence suggests that specific aneusomies encode the phenotypes of irreversible precancerous lesions and are sufficient to alter the phenotype of eukaryotic cells to trigger cellular transformation[13-16]. Given this, it follows that chromosome number mutation, not gene mutation alone, is a probable cause of many dominant cancer cell phenotypes. Aneusomy can alter the dosage and thus the relevant activities of thousands of genes on the chromosome involved. Dividing aneuploid cells become increasingly unstable and most of these cells die eventually; rarely, these generate a specific aneusomy which then promotes the cell toward neoplastic transformation.

Specific chromosomal aneuploidies are characteristic of solid tumors unlike the random aneuploidies exhibited in hematological malignancies[9,17]. Chromosome 11 has a number of oncogenes and tumor suppressors including Cyclin D1, which is overexpressed in a wide variety of human neoplasms[18,19]. Reports suggest that overexpression of cyclin D1 is not due to gene amplification but due to chromosome number changes[5]. Other studies show the partial segmental aneusomy involving chromosome 11 in esophageal cancers, indicating its probable role in the disease etiology[10,11]. In the present work, FISH was used to assess change in chromosome 11 copy number in esophageal tumors using centromeric DNA probes.

Interestingly, our results showed that 100% of the cancerous lesions of the esophagus were aneusomic for chromosome 11. These ranged from trisomies to pentasomies in the same sample, indicating heterogeneity in the tumor tissue (Table 1). The baseline monosomy established (due to experimental artifacts) was similar in all controls, precancers and cancers. This is the first study to report that chromosome 11 copy number is altered in both esophageal SCC and ADC tumors. Because the number of ADC cases was small, there was no significant difference in the levels of aneusomy between SCC and ADC tumors. None of the controls showed any aneusomy suggesting that this chromosomal alteration is associated only with the neoplastic changes.

In addition, we also made a detailed investigation regarding the esophageal pathologies in each sub-group (though small in number) and the aneusomy in them.

There have been very few reports of specific aneusomies in esophageal premalignant lesions; using FISH, some studies showed hyperdiploidy involving chromosomes 4 and 8 in BE, aneuploidy in chromosome 11 in esophageal tumors and Barrett's dysplasias[20-23]. In the present work, all the precancerous lesions including BE with high-grade dysplasia exhibited aneusomy of chromosome 11. Our data indicate that levels of aneusomy of chromosome 11 seemed to occur increasingly in preneoplastic tissues suggesting that there may be genes on chromosome 11 that have a role in the initiation and neoplastic transformation of esophageal lesions.

Cytogenetic analysis by conventional chromosomal banding is labor-intensive and time-consuming. Besides, it is difficult to analyze some of the complex karyotypes characteristic of many human tumors. On the other hand, FISH is a relatively more convenient and quick method for evaluating tissue cell chromosomal changes[24,25]. Moreover, we have observed that by using adequate fluorescent signal capture (optical sectioning microscopic method) and analysis systems, an accurate estimate of the changes in chromosome copy number could be obtained from tumor tissues, based on which we could make satisfactory interpretations. Our study supports the finding that solid tumor cancers are often aneuploid for specific chromosomes and this may be used as an ancillary marker for detecting early changes associated with cancer.

Epigenetic changes like DNA methylation may lead to chromosomal instability, activation of endogenous parasitic sequences and mutations[26]. Cancer cells undergo methylation changes resulting in overexpression/silencing of several genes that are responsible for maintaining chromosomal integrity. Our study also revealed that 4/11 cancers and 2/5 precancers with increased copies of chromosome 11 had a hypermethylated hMLH1 repair gene promoter known to be responsible for altered repair efficiency (data not shown).

We did not perform any studies to assess whether this aneusomy correlates with the DNA content aneuploidy (i.e. gross chromosomal instability) of the tissues. The sample number (with a mix of ADCs and SCCs, which might have different etiologies), though, was not sufficient to make conclusions about predictive values, the results showed the differences in the frequencies of aneusomy in the two types of tumor. The present work clearly indicates that aneusomy is observed in early esophageal

lesions and may be involved in neoplastic transformation. Aneusomy of other chromosomes cannot be ruled out, however here, chromosome 11 is clearly demonstrated in all the esophageal pathologies studied. This marker merits investigation in a larger number of cases to determine its potential as a predictive molecular marker for an increased risk for malignant transformation.

ACKNOWLEDGMENTS

We acknowledge help from Gastroenterology Units of Bhagwan Mahavir Medical Research Center, AC Guards, Hyderabad, Osmania General Hospital, Afzalgunj, Hyderabad and Kamineni Hospitals, LB Nagar, Hyderabad. We thank Mr. Srinivas and Mr.Mallesh, technicians of the Department of Pathology for their assistance with histopathology.

COMMENTS

Background

More than 30% of the adult population exhibits esophageal tract disorders, where a certain proportion of chronic cases even develop malignancy. Markers for early detection, which will help improve survival and treatment response are still lacking. This study investigates specific aneusomies which are believed to be associated with solid cancer phenotypes.

Research frontiers

Current biopsy surveillance programs are based on histopathological assessment of the tissue. However, molecular changes precede visible histopathological changes in cancer. FISH-based assay using brush cytology specimens (more easily accessible than biopsy) are increasingly used for investigation of chromosomal alterations and after validation these molecular markers can be used for routine surveillance in order to aid in early detection.

Innovations and breakthroughs

FISH, when compared to conventional cytogenetic analysis, is a more convenient and quick method for evaluating tissue cell chromosomal changes. An apotome-attached optical sectioning microscope to capture fluorescent probe signals has shown maximum efficiency for signal analysis in tissue FISH. This will aid in satisfactory data collection and interpretation.

Applications

Chromosome 11 aneusomy has been demonstrated in all the cases of cancer and precancer studied by us indicating its potential as an early marker for neoplastic transformation. Our results call for evaluating this marker in a larger cohort of patients.

Terminology

Regurgitation: bringing back undigested food from the stomach; Dysphagia: difficulty in swallowing; Dysplasia: Nuclear atypia, loss of normal cell polarity, and abnormal tissue maturation.

REFERENCES

1 **Gajalakshmi V**, Swaminathan R, Shanta V. An Independent Survey to Assess Completeness of Registration: Population Based Cancer Registry, Chennai, India. *Asian Pac J Cancer Prev* 2001; **2**: 179-183
2 **Gupta NM**, Jindal R, Prakash O, Gupta R, Bhasin DK. Comparison of the clinical profile and outcome for squamous cell carcinoma and adenocarcinoma of the distal esophagus and cardia in India. *Surg Today* 2001; **31**: 400-404
3 **Kagawa Y**, Yoshida K, Hirai T, Toge T, Yokozaki H, Yasui W, Tahara E. Microsatellite instability in squamous cell carcinomas and dysplasias of the esophagus. *Anticancer Res* 2000; **20**: 213-217
4 **Lehrbach DM**, Nita ME, Cecconello I. Molecular aspects of esophageal squamous cell carcinoma carcinogenesis. *Arq Gastroenterol* 2003; **40**: 256-261
5 **Lung JC**, Chu JS, Yu JC, Yue CT, Lo YL, Shen CY, Wu CW. Aberrant expression of cell-cycle regulator cyclin D1 in breast cancer is related to chromosomal genomic instability. *Genes Chromosomes Cancer* 2002; **34**: 276-284
6 **Kops GJ**, Weaver BA, Cleveland DW. On the road to cancer: aneuploidy and the mitotic checkpoint. *Nat Rev Cancer* 2005; **5**: 773-785
7 **Fabarius A**, Willer A, Yerganian G, Hehlmann R, Duesberg P. Specific aneusomies in Chinese hamster cells at different stages of neoplastic transformation, initiated by nitrosomethylurea. *Proc Natl Acad Sci USA* 2002; **99**: 6778-6783
8 **Wolf NG**, Abdul-Karim FW, Schork NJ, Schwartz S. Origins of heterogeneous ovarian carcinomas. A molecular cytogenetic analysis of histologically benign, low malignant potential, and fully malignant components. *Am J Pathol* 1996; **149**: 511-520
9 **Alcaraz A**, Takahashi S, Brown JA, Herath JF, Bergstralh EJ, Larson-Keller JJ, Lieber MM, Jenkins RB. Aneuploidy and aneusomy of chromosome 7 detected by fluorescence in situ hybridization are markers of poor prognosis in prostate cancer. *Cancer Res* 1994; **54**: 3998-4002
10 **Yen CC**, Chen YJ, Lu KH, Hsia JY, Chen JT, Hu CP, Chen PM, Liu JH, Chiou TJ, Wang WS, Yang MH, Chao TC, Lin CH. Genotypic analysis of esophageal squamous cell carcinoma by molecular cytogenetics and real-time quantitative polymerase chain reaction. *Int J Oncol* 2003; **23**: 871-881
11 **Jin Y**, Jin C, Law S, Chu KM, Zhang H, Strombeck B, Yuen AP, Kwong YL. Cytogenetic and fluorescence in situ hybridization characterization of clonal chromosomal aberrations and CCND1 amplification in esophageal carcinomas. *Cancer Genet Cytogenet* 2004; **148**: 21-28
12 **Jallepalli PV**, Lengauer C. Chromosome segregation and cancer: cutting through the mystery. *Nat Rev Cancer* 2001; **1**: 109-117
13 **Duesberg P**, Rasnick D, Li R, Winters L, Rausch C, Hehlmann R. How aneuploidy may cause cancer and genetic instability. *Anticancer Res* 1999; **19**: 4887-4906
14 **Duesberg P**, Li R, Rasnick D, Rausch C, Willer A, Kraemer A, Yerganian G, Hehlmann R. Aneuploidy precedes and segregates with chemical carcinogenesis. *Cancer Genet Cytogenet* 2000; **119**: 83-93
15 **Lindsley DL**, Sandler L, Baker BS, Carpenter AT, Denell RE, Hall JC, Jacobs PA, Miklos GL, Davis BK, Gethmann RC, Hardy RW, Steven AH, Miller M, Nozawa H, Parry DM, Gould-Somero M, Gould-Somero M. Segmental aneuploidy and the genetic gross structure of the Drosophila genome. *Genetics* 1972; **71**: 157-184
16 **Webb T**. When theories collide: experts develop different models for carcinogenesis. *J Natl Cancer Inst* 2001; **93**: 92-94
17 **Mitelman F**. Catalogue of chromosome aberrations in cancer. *Cytogenet Cell Genet* 1983; **36**: 1-515
18 **Hui AB**, Or YY, Takano H, Tsang RK, To KF, Guan XY, Sham JS, Hung KW, Lam CN, van Hasselt CA, Kuo WL, Gray JW, Huang DP, Lo KW. Array-based comparative genomic hybridization analysis identified cyclin D1 as a target oncogene at 11q13.3 in nasopharyngeal carcinoma. *Cancer Res* 2005; **65**: 8125-8133
19 **Segas JV**, Lazaris AC, Nikolopoulos TP, Kavantzas NG, Lendari IE, Tzagkaroulakis AM, Patsouris ES, Ferekidis EA. Cyclin D1 protein tissue detection in laryngeal cancer. *ORL J Otorhinolaryngol Relat Spec* 2005; **67**: 319-325
20 **Fahmy M**, Skacel M, Gramlich TL, Brainard JA, Rice TW, Goldblum JR, Connor JT, Casey G, Legator MS, Tubbs RR, Falk GW. Chromosomal gains and genomic loss of p53 and p16 genes in Barrett's esophagus detected by fluorescence in situ hybridization of cytology specimens. *Mod Pathol* 2004; **17**: 588-596
21 **Doak SH**, Saidely D, Jenkins GJ, Parry EM, Griffiths AP, Baxter JN, Parry JM. Generation of locus-specific probes for interphase fluorescence in situ hybridisation--application in

Barrett's esophagus. *Exp Mol Pathol* 2004; **77**: 26-33
22 **Manoel-Caetano Fda S**, Borim AA, Caetano A, Cury PM, Silva AE. Cytogenetic alterations in chagasic achalasia compared to esophageal carcinoma. *Cancer Genet Cytogenet* 2004; **149**: 17-22
23 **Finley JC**, Reid BJ, Odze RD, Sanchez CA, Galipeau P, Li X, Self SG, Gollahon KA, Blount PL, Rabinovitch PS. Chromosomal instability in Barrett's esophagus is related to telomere shortening. *Cancer Epidemiol Biomarkers Prev* 2006; **15**: 1451-1457
24 **Cortés-Gutiérrez EI**, Dávila-Rodríguez MI, Muraira-Rodríguez M, Said-Fernández S, Cerda-Flores RM. Association between the stages of cervical cancer and chromosome 1 aneusomy. *Cancer Genet Cytogenet* 2005; **159**: 44-47
25 **Watters AD**, Going JJ, Cooke TG, Bartlett JM. Chromosome 17 aneusomy is associated with poor prognostic factors in invasive breast carcinoma. *Breast Cancer Res Treat* 2003; **77**: 109-114
26 **Esteller M**, Herman JG. Cancer as an epigenetic disease: DNA methylation and chromatin alterations in human tumours. *J Pathol* 2002; **196**: 1-7

S- Editor Liu Y **L- Editor** Zhu LH **E- Editor** Liu WF

PO Box 2345, Beijing 100023, China
www.wjgnet.com
wjg@wjgnet.com

World J Gastroenterol 2007 January 28; 13(4): 509-514
World Journal of Gastroenterology ISSN 1007-9327

Effect of 2-(8-hydroxy-6-methoxy-1-oxo-1H-2-benzopyran-3-yl) propionic acid in combination with carboplatin on gastric carcinoma growth *in vivo*

Jin-Lian Chen, Jin-Shui Zhu, Jing Hong, Ming-Xiang Chen, Jin-Lai Lu, Wei-Xiong Chen, Bo Shen, Zu-Ming Zhu, Ni-Wei Chen

Jin-Lian Chen, Jin-Shui Zhu, Jing Hong, Ming-Xiang Chen, Jin-Lai Lu, Wei-Xiong Chen, Bo Shen, Zu-Ming Zhu, Ni-Wei Chen, Department of Gastroenterology, Shanghai Sixth People's Hospital, Shanghai Jiaotong University, Shanghai 200233, China
Supported by the Science foundation of Shanghai Public Health Administration, No.034045
Correspondence to: Jin-Lian Chen, Department of Gastroenterology, Shanghai Sixth People's Hospital, Shanghai Jiaotong University, Shanghai 200233, China. wqq_021002@163.com
Telephone: +86-21-64369181 Fax: +86-21-64369181
Received: 2006-10-11 Accepted: 2006-12-07

Abstract

AIM: To investigate the effects of 2-(8-hydroxy-6-methoxy-1-oxo-1H-2-benzopyran-3-yl) propionic acid (NM-3) alone and in combination with carboplatin on tumor growth and apoptosis in mouse models of human gastric cancer constructed by subcutaneous implantation of histologically intact tumor tissue.

METHODS: Human gastric cancer SGC-7901 tissues were implanted into the dorsal subcutis of nude mice. One week after tumors reached to a volume of 50-100 mm^3 for around 1 wk, these mice were randomly divided into 8 groups (n = 10). NM-3 was injected peritoneally at the dose of 10 mg/kg, 20 mg/kg or 40 mg/kg every other day for 5 wk, combined with carboplatin (5 mg/kg) every third day for 4 wk. As controls of combined treatment, another 4 groups of mice were injected with either NM-3 at 10 mg/kg, 20 mg/kg or 40 mg/kg, or with carboplatin alone (5 mg/kg). The control mice received normal saline. Tumor weight, tumor growth inhibition (TGI), and intratumoral microvessel density (MVD) were evaluated. Apoptosis of human gastric cancer was detected by TUNEL method and flow cytometry analysis, respectively.

RESULTS: The mean tumor volume (692.40 ± 58.43 mm^3, 548.30 ± 66.02 mm^3, 382.13 ± 43.52 mm^3) after treatment with carboplatin combined NM-3 at the dose of 10 mg/kg, 20 mg/kg or 40 mg/kg was lower than that after treatment with either NM-3 at the dose of 10 mg/kg, 20 mg/kg or 40 mg/kg or with carboplatin alone. Compared with the normal saline group, NM-3 administered at 10 mg/kg, 20 mg/kg or 40 mg/kg significantly reduced the tumor weight in these groups (P < 0.05). Carboplatin used alone at 5 mg/kg showed minimal effects. But NM-3 in combination with carboplatin had greater effects of tumor weight than either NM-3 or carboplatin alone. NM-3 alone at the dose 10 mg/kg or in combination with carboplatin had no obvious effects on body changes. Two mice died of diarrhea in each of the two groups treated with 40 mg/kg NM-3 or with 40 mg/kg NM-3 in combination with carboplatin. A significant increase in apoptosis was observed in the NM-3 treated groups, and the effect was more significant in the groups treated with carboplatin in combination with NM-3 at 10 mg/kg, 20 mg/kg and 40 mg/kg, than in the control group. The induction of apoptosis was positively associated with the dose of NM-3. NM-3 significantly reduced the neo-microvascular formation of gastric cancer. The MVD was lower in the groups treated with NM-3 or with NM-3 in combination with carboplatin than in the group treated with carboplatin or in the normal saline group (P < 0.05).

CONCLUSION: The results suggest that the inhibitory effect of NM-3 on gastric cancer growth is mediated through decreased angiogenesis and the increased induction of apoptosis. Furthermore, NM-3 alone at the dose of 10 mg/kg or in combination with carboplatin has no obvious effects on body changes, indicating that NM-3 in combination with carboplatin may be effective in the treatment of gastric cancer. The toxicity of NM-3 needs further studies.

Key words: NM-3; Carboplatin; Gastric carcinoma; Angiogenesis; Apoptosis

Chen JL, Zhu JS, Hong J, Chen MX, Lu JL, Chen WX, Shen B, Zhu ZM, Chen NW. Effect of 2-(8-hydroxy-6-methoxy-1-oxo-1H-2-benzopyran-3-yl) propionic acid in combination with carboplatin on gastric carcinoma growth *in vivo*. *World J Gastroenterol* 2007; 13(4): 509-514

http://www.wjgnet.com/1007-9327/13/509.asp

INTRODUCTION

Gastric carcinoma is one of the most frequent malignancies and one of the major causes of cancer deaths

in China[1]. Up to now, the prognosis of patients with gastric cancer is very poor because gastric cancer is usually diagnosed at its advanced stage throughout the world. Even after curative resection, it remains at a high risk of relapse. Chemotherapy is one of the most important treatment modalities for gastric cancer. However, its effect is limited due to its adverse reactions and resistance of tumor cells to chemotherapeutic agents[2].

Apoptosis plays an important role in the growth of malignant tumor cells. It has been shown that apoptosis can be induced in gastric cancer by some chemotherapeutic drugs, such as 5-fluorouracil, cisplatin and paclitaxel[3]. Recent studies have demonstrated that angiogenesis plays a crucial role in tumor growth and metastasis. Vascular endothelial growth factor (VEGF) and fibroblast growth factor-2 (FGF-2) are the main factors promoting angiogenesis[4-6]. It has been shown that radiation-induced tumor regression is enhanced by angiogenesis inhibitors. Angiostatin or antibody to VEGF in combination with chemotherapy produces greater antitumor effects than either treatment alone[7,8].

Recently, induction of apoptosis by antiangiogenic therapy has been suggested as a new anticancer strategy[9]. 2- (8-hydroxy-6-methoxy-1-oxo-1H-2-benzopyran-3-yl) propionic acid (NM-3), is a synthetic derivative of cytogenin. *In vitro* studies have demonstrated that the inhibitory effects of NM-3 at lower concentrations are stronger on the growth of human umbilical vein endothelial cells than on the growth of normal fibroblasts or tumor cells[10]. NM-3 alone inhibits endothelial sprouting and tube formation *in vitro*. It has been shown that NM-3 can enhance 5-fluorouracil-induced tumor growth inhibition in breast carcinoma xenografts with no effects on body changes[11]. In this study, we investigated the effects of NM-3 alone or in combination with carboplatin on tumor growth and apoptosis in mouse models of human gastric cancer constructed by subcutaneous implantation of histologically intact tumor tissue.

MATERIALS AND METHODS

Materials

Male BALB/c/nu/nu nude mice were obtained from Shanghai Experimental Animal Center of the Chinese Academy of Sciences. Animals used were 6-wk old and weighed 20-25 g. Human gastric cancer SGC-7901 was obtained from Shanghai Cancer Institute. NM-3 was provided by professor Robert (National Cancer Research Center of America), concentration of NM-3 was 20 mg/mL.

Animal experimental method

Animal models were made using subcutaneous implantation of histologically intact tissue of human gastric carcinoma. Tumors were resected aseptically. Necrotic tissue was removed and the remaining tumor tissues were minced into pieces about 2 mm in diameter and implanted into the dorsal subcutis of mice.

One week after tumors reached a volume of 50-100 mm^3 for around 1 wk, these mice were randomly divided into 8 groups (n = 10). NM-3 was injected peritoneally at the dose of 10 mg/kg, 20 mg/kg or 40 mg/kg every other day for 5 wk, in combination with carboplatin (5 mg/kg) every third day for 4 wk. As controls of combined treatment, another four groups of mice were injected NM-3 or carboplatin alone. The control mice received normal saline as indicated. The mice were weighed twice weekly, and tumor measurements were taken by calipers twice weekly. Tumor volume was measured using the formula ($V = ab^2/2$), where a is the largest diameter and b the smallest diameter. Tumor growth inhibition (TGI) in each group was (mean control tumor weight - mean treated tumor weight)/mean control tumor weight × 100%.

Sample collection and pathological examination

All animals were sacrificed 7 wk after the implantation. Tumors were biopsied, fixed in 10% formalin, and processed for routine paraffin embedding. Tumors were evaluated histologically under microscope.

Mean microvascular density (MVD of tumor)

Four-micron-thick sections were deparaffined in xylene and rehydrated in graded alcohol. Immunostaining was performed using a labeled streptavidin biotin method. Immunohistochemical staining was carried out to detect CD34 expression following the manufacturer's protocol (Santa Cruz Biotech Company). The modified Weidner's method was used for the evaluation of MVD according to CD34 endothelial cell immunostaining. For microvessel counting, positive staining for MVD in five most highly vascularized areas in each section was counted in 200 × fields. MVD was expressed as the average of the microvessel count in the 5 areas. Any endothelial cell or endothelial cluster positive for CD34 (brown-yellow staining) was a single countable microvessel.

Detection of cell apoptosis idex (AI)

Apoptosis of human gastric cancer was detected by terminal deoxynuclotidyl transferase- mediated deoxyuridine triphosphate-fluorescene nick end labeling (TUNEL) method and flow cytometry analysis, respectively. TUNEL method was performed as indicated. Flow cytometry analysis was conducted as follows. In brief, propidium iodide (PI) staining was used for flow cytometric detection of apoptosis, 1×10^6 cells from each of the samples were treated with RNase and stained with PI. DNA strand-labeled apoptotic cells were calculated with a flow cytometer (FACS Calibur, Becton Dickinson, USA.). Data were collected from 1×10^6 cells/sample, stored and analyzed using CELLQUES'T and MODFITLT for macV 1.01 software.

Statistical analysis

All data were expressed as mean ± SD. Student's t test was used to determine changes in different groups. $P < 0.05$ was considered statistically significant.

RESULTS

Inhibitory effect of NM-3 on growth of xenografted human gastric cancer in nude mice

The mean tumor volume (MTV) in the groups treated

Table 1 Inhibitory effect of NM-3 on gastric cancer growth (mean ± SD)

Groups	*n*	MTV (mm^3)	Body weight (g)	Tumor weight (mg)	TGI (%)
Normal saline	10	81.24 ± 12.63	25.8 ± 1.04	1754.0 ± 144.2	
NM-3 (10 mg/kg)	10	79.68 ± 13.72	24.4 ± 0.76	1351.0 ± 116.9	23.0[a]
NM-3 (20 mg/kg)	10	81.08 ± 12.90	23.1 ± 0.82	1041.1 ± 143.5	40.6[a]
NM-3 (40 mg/kg)	8	81.36 ± 11.20	22.9 ± 1.06	765.5 ± 140.1	56.2[a,c]
NM-3 (10 mg/kg) + carplatin	10	80.29 ± 14.26	24.2 ± 0.88	1002.0 ± 101.4	42.7[a,c]
NM-3 (20 mg/kg) + carplatin	10	82.30 ± 14.53	24.4 ± 0.78	919.0 ± 149.8	47.6[a,c]
NM-3 (40 mg/kg) + carplatin	8	81.97 ± 12.77	22.5 ± 1.13	645.7 ± 135.1	63.2[a,c]
Carplatin	10	80.01 ± 13.67	23.0 ± 1.03	1655.0 ± 157.4	5.6

[a]$P < 0.05$ *vs* normal saline control group and carboplatin group, [c]$P < 0.05$ *vs* NM-3 (10 mg/kg) group.

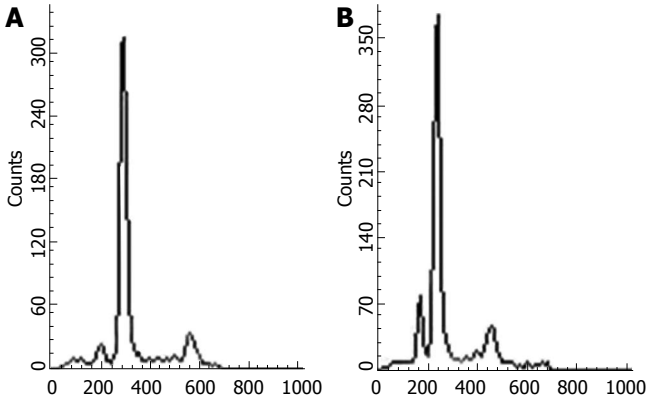

Figure 1 Propidium iodide (PI) staining for flow cytometric detection of apoptosis in control group (**A**) and NM-3- treated group (**B**).

with 10 mg/kg, 20 mg/kg or 40 mg/kg NM-3 was 989.50 ± 102.17 mm^3, 826.20 ± 76.52 mm^3, and 709.75 ± 89.30 mm^3, respectively, which was significantly smaller than that in the control group receiving normal saline (1609.60 ± 122.11 mm^3, $P < 0.05$). Carboplatin at the dose of 5 mg/kg had no significant inhibitory action on gastric carcinoma with MTV being 1532.14 ± 110.12 mm^3. However, the mean tumor volume in groups treated with carboplatin in combination with NM-3 was 692.40 ± 58.43 mm^3, 548.30 ± 66.02 mm^3, and 382.13 ± 43.52 mm^3, respectively, which was lower than that in the groups treated either with NM-3 or with carboplatin alone. Compared with the normal saline group, NM-3 administered at 10 mg/kg, 20 mg/kg or 40 mg/kg significantly reduced the tumor weight in these groups, and the effect was more significant when NM-3 was given at a dose of 40 mg/kg ($P < 0.05$). Carboplatin used alone at the dose of 5 mg/kg showed minimal effects. But NM-3 in combination with carboplatin, however, had a more significant effect on tumor weight than NM-3 or carboplatin alone (Table 1).The mean tumor volume did not differ among groups before treatment (Table 1).

During the experiment, diarrhea occurred in some mice when NM-3 was given at the dose of 20 mg/kg or 40 mg/kg. Two mice died of diarrhea in each of the two groups treated with 40 mg/kg NM-3 or with 40 mg/kg NM-3 in combination with carboplatin. The remaining mice recovered at the latter stage of the experiment. NM-3 alone at the dose of 10 mg/kg or in combination with carboplatin had no obvious effects on body changes.

Table 2 Effect of NM-3 on cell apoptosis of gastric cancer (mean ± SD, %)

Groups	*n*	AI (TUNEL)	AI (FAScan)
Normal saline	10	2.12 ± 2.19	1.59 ± 0.24
NM-3 (10 mg/kg)	10	6.02 ± 1.63[a]	3.84 ± 0.68[a]
NM-3 (20 mg/kg)	10	10.43 ± 3.15[a,c]	8.21 ± 1.01[a,c]
NM-3 (40 mg/kg)	8	22.06 ± 5.68[a,c]	18.26 ± 4.46[a,c]
NM-3 (10 mg/kg) + carplatin	10	8.66 ± 2.35[a,c]	6.96 ± 0.65[a,c]
NM-3 (20 mg/kg) + carplatin	10	12.63 ± 3.75[a,c]	10.65 ± 1.43[a,c]
NM-3 (40 mg/kg) + carplatin	8	24.63 ± 3.67[a,c]	21.66 ± 2.96[a,c]
Carplatin	10	2.47 ± 0.31	1.85 ± 0.34

[a]$P < 0.05$ *vs* normal saline control group and carboplatin group, [c]$P < 0.05$ *vs* NM-3 (10 mg/kg) group.

Effect of NM-3 on cell apoptosis of human gastric cancer cells

Apoptosis of gastric cancer cells was observed microscopically. Manifestations of apoptosis could be found more frequently in NM-3-treated groups, such as cell shrinkage, nuclear condensation, DNA fragmentation and formation of apoptotic bodies. Apoptosis was detected with flow cytometry (Figure 1).

The apoptosis index of tumors treated with carboplatin alone was not significantly different from that of the control group ($P > 0.05$). However, a significant increase in apoptosis was observed in the NM-3-treated groups, and the effect was more significant in the groups treated with carplatin in combination with NM-3 at 10 mg/kg, 20 mg/kg and 40 mg/kg than in the control group (Table 2). The induction of apoptosis was positively associated with the dose of NM-3.

Effect of NM-3 on MVD

NM-3 significantly reduced the neo-microvascular formation of gastric cancer implanted into nude mice. The MVD was lower in groups treated with NM-3 or with NM-3 in combination with carboplatin than in carboplatin group or normal saline group ($P < 0.05$). More significant inhibitory effects on MVD of tumor were observed in NM-3-treated groups at the dose of 40 mg/kg or in combination with carboplatin than in control group ($P < 0.05$, Table 3, Figure 2A-H).

DISCUSSION

Recent studies have shown that angiogenesis plays a

Table 3 Effect of NM-3 on MVD (mean ± SD)

Groups	*n*	MVD
Normal saline	10	7.30 ± 0.53
NM-3 (10 mg/kg)	10	5.10 ± 0.40[a]
NM-3 (20 mg/kg)	10	4.72 ± 0.51[a]
NM-3 (40 mg/kg)	8	2.02 ± 0.50[a,c]
NM-3 (10 mg/kg) + carplatin	10	4.96 ± 0.37[a]
NM-3 (20 mg/kg) + carplatin	10	4.80 ± 0.39[a]
NM-3 (40 mg/kg) + carplatin	8	1.78 ± 0.42[a,c]
Carplatin	10	6.98 ± 0.45

[a]$P < 0.05$ *vs* normal saline control group and carboplatin group, [c]$P < 0.05$ *vs* NM-3 (10 mg/kg) group.

critical role in solid tumor growth and its development[8]. Antiangiogenic agents inhibit tumor growth by preventing proliferation, migration and sprouting of tumor endothelial cells and formation of new blood vessels. Antiangiogenic therapy plays an important role in improving prognosis of patients with gastric carcinoma[12-15]. NM-3, a small molecule isocoumarin, is a recently discovered angiogenesis inhibitor. It has been shown that NM-3 enhances the antitumor effects of some chemotherapeutic drugs in breast and prostate tumor models[11]. The increased antitumor effects of chemotherapy in combination with NM-3 can be achieved without any apparent increase in toxicity. To date, the effect of antitumor and induction of cell apoptosis of NM-3 on human gastric cancer have not been reported. It is worthwhile, therefore, to further research its antitumor mechanisms underlying gastric cancer.

In the present study, NM-3 significantly inhibited the growth of human gastric cancer in mice. Compared with the controls, growth of the tumor implanted subcutaneously was remarkably reduced in size and weight in the mice treated with NM-3 at the doses of 10 mg/kg, 20 mg/kg, 40 mg/kg. These doses of NM-3 in combination with carboplatin delayed the growth of SGC-7901 human gastric cancer in mice, compared with NM-3 or carboplatin alone. NM-3 alone at the dose of 10 mg/kg or in combination with carboplatin had no obvious effects on body changes. However, two mice died of diarrhea in each of the two groups treated with 40 mg/kg NM-3 or with 40 mg/kg NM-3 in combination with carboplatin, suggesting that the toxicity and doses of NM-3 used in patients need further studies. Although tumor growth was inhibited by NM-3 in combination with carboplatin as compared with normal saline group, tumor weight increased. This may be due to the lower dose of carboplatin used. In our study, carboplatin at the dose of 5 mg/kg showed minimal effects on tumor growth. Previous studies have demonstrated that chemotherapy in combination with an angiogenesis inhibitor can enhance tumor growth inhibition. Reimer *et al*[11] demonstrated that NM-3 can significantly enhance tumor growth inhibition in breast and prostate carcinoma xenografts at nontoxic doses in combination with 5-fluorouoacil, paclitaxel or cyclophosphamide given at subtherapeutic doses. These effects were particularly marked when NM-3 was combined with cyclophosphamide. Vinblastine in combination with

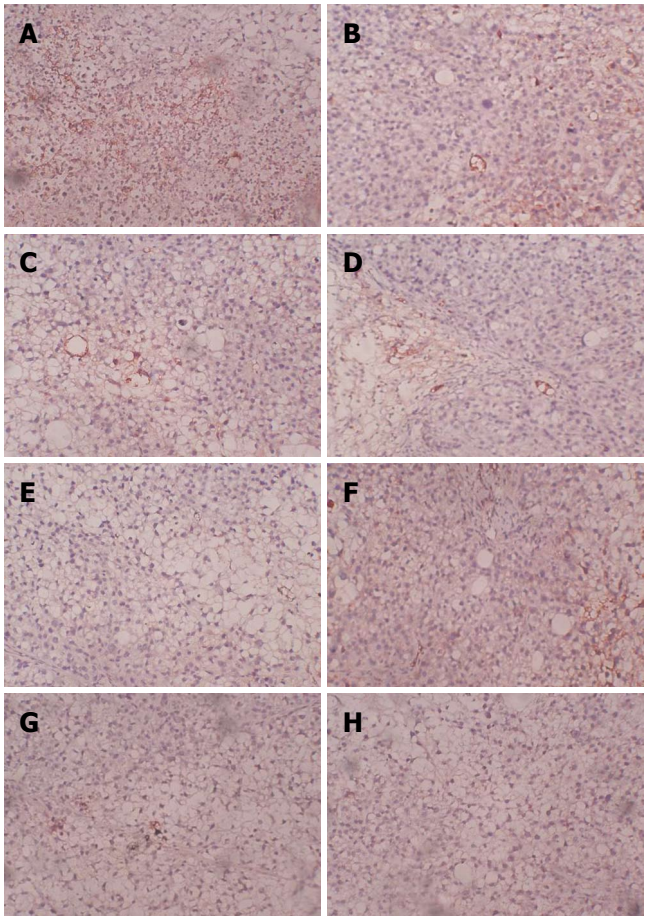

Figure 2 Immunohistochemical method for detection of microvessel density in mice injected with normal saline (**A**); carboplatin alone (**B**); 10 mg/kg NM-3 (**C**); 20 mg/kg NM-3 (**D**); 40 mg/kg NM-3 (**E**); 10 mg/kg NM-3 in combination with 5 mg/kg carboplatin (**F**); 20 mg/kg NM-3 in combination with 5 mg/kg carboplatin (**G**); 40 mg/kg NM-3 in combination with 5 mg/kg carboplatin (**H**); × 200.

VEGF receptor-2 antibody could cause sustained tumor regression. Salloum *et al*[10] studied the antitumor effects of NM-3 in combination with radiotherapy, and found that the tumor is significantly regressed after combined treatment compared with radiotherapy alone with no increase in systemic or local tissue toxicity, suggesting that NM-3 in combination with chemotherapy or radiotherapy can increase the efficacy of cancer treatment.

Cell apoptosis is an active death process of cells, its imbalance or changes are related to the occurrence of many diseases. Gastric cancer is not only a disease with abnormal cell proliferation and differentiation, but also a disease with abnormal apoptosis[16,17]. Increased apoptosis in human gastric cancer cells could be observed after treatment with 5-fluorouracil, cisplatin, *etc*. The results suggest that these drugs can be used in the treatment of patients with gastric cancer by inducing apoptosis of cancer cells. The results obtained by TUNEL method and cytometry analysis indicate that apoptosis is induced by NM-3. Matsuhashi *et al*[18] investigated the relationship between p53 expression and apoptosis induction of 5-fluorouracil and cisplatin on gastric cancer cells, and found that combined administration of 5-fluorouracil and cisplatin does not induce apoptosis of MKN-28 (mutant-type p53), while apoptotic cells can be observed in the case

of MKN-45 (wild-type p53). Browder *et al*[19] demonstrated that TNP-470 at a low dose in combination with cyclophosphamide can eradicate drug-resistant Lewis lung carcinoma. Agata *et al*[20] revealed that NM-3 potentiates dexamethasone-induced apoptosis of human multiple myeloma cells. Moreover, NM-3 is effective against dexamethasone-resistant RPMI8226 and U266 multiple myeloma cells. NM-3 enhances dexamethasone-induced release of mitochondrial apoptogenic factors (cytochrome c and smac/DIABLO) and dexamethasone-induced activation of intrinsic caspase-9→caspase-3 apoptotic pathway. These results suggest that NM-3 inhibits the growth of gastric cancer by enhancing apoptosis of cancer cells.

Angiogenesis has been implicated in the growth and metastasis of gastric cancer. MaCarty *et al*[21] reported that ZD6474, a vascular endothelial growth factor receptor (tyrosine kinase inhibitor) inhibits orthotopic growth and angiogenesis of gastric cancer and increases tumor cell apoptosis. Stoeltzing *et al*[22] demonstrated that inhibition of hypoxia-inducible factor 1 activity can inhibit gastric cancer growth and angiogenesis. Kamiya *et al*[23] showed that the antitumor effect of VEGF Ab on gastric cancer is exerted by inducing mild hypoxia and apoptosis. Reimer *et al*[11] reported that the antitumor effects of NM-3 in combination with chemotherapeutic agents are mediated through decreased proliferation of endothelial cells. The present study indicated that NM-3 significantly inhibited angiogenesis in gastric cancer, suggesting that apoptosis of gastric cancer is mediated by NM-3 through decreased angiogenesis and that the inhibitory effect of NM-3 on gastric cancer growth is related to the induction of apoptosis.

In conclusion, NM-3 in combination with carboplatin is effective against gastric cancer. The toxicity and mechanism of NM-3 underlying apoptosis of gastric cancer need further studies.

COMMENTS

Background

Gastric carcinoma is one of the most frequent malignancies in China. Angiogenesis plays a crucial role in tumor growth and metastasis. Recently, induction of apoptosis by antiangiogenic therapy has been suggested as a new anticancer strategy.

Research frontiers

2-(8-hydroxy-6-methoxy-1-oxo-1H-2-benzopyran-3-yl) propionic acid (NM-3) is a synthetic derivative of cytogenin. In vitro studies have demonstrated that the inhibitory effects of NM-3 at lower concentrations are stronger on human umbilical vein endothelial cells than on normal fibroblasts or tumor cells. NM-3 alone inhibits endothelial sprouting and tube formation *in vitro*.

Innovations and breakthroughs

There is some experience of NM-3 as an apoptotic and antiangiogenic inducer in other types of tumors such as lung and prostatic cancers, but not in gastric cancer which is associated with high chemotherapy resistance. Inhibitory effects of NM-3 on gastric cancer growth are mediated through decreased angiogenesis and the increased induction of apoptosis. NM-3 at the dose of 10 mg/kg alone or in combination with carboplatin has no obvious effects on body changes.

Applications

NM-3 in combination with carboplatin may be effective against gastric cancer.

Peer review

This is a well designed experimental study of apoptosis and effects of NM-3 and carboplatin on gastric cancer model (SGC-7901). There is some experience in NM-3 as an apoptotic and antiangiogenic inducer in other types of tumors such as lung and prostatic cancers, but not in gastric cancer which is associated with high chemotherapy resistance. The paper is interesting.

REFERENCES

1 **Chen JL**, Chen WX, Zhu JS, Chen NW, Zhou T, Yao M, Zhang DQ, Wu YL. Effect of P-selectin monoclonal antibody on metastasis of gastric cancer and immune function. *World J Gastroenterol* 2003; **9**: 1607-1610

2 **Lim L**, Michael M, Mann GB, Leong T. Adjuvant therapy in gastric cancer. *J Clin Oncol* 2005; **23**: 6220-6232

3 **Matsuhashi N**, Saio M, Matsuo A, Sugiyama Y, Saji S. Apoptosis induced by 5-fluorouracil, cisplatin and paclitaxel are associated with p53 gene status in gastric cancer cell lines. *Int J Oncol* 2005; **26**: 1563-1567

4 **Huang SP**, Wu MS, Shun CT, Wang HP, Lin MT, Kuo ML, Lin JT. Interleukin-6 increases vascular endothelial growth factor and angiogenesis in gastric carcinoma. *J Biomed Sci* 2004; **11**: 517-527

5 **Sun J**, Blaskovich MA, Jain RK, Delarue F, Paris D, Brem S, Wotoczek-Obadia M, Lin Q, Coppola D, Choi K, Mullan M, Hamilton AD, Sebti SM. Blocking angiogenesis and tumorigenesis with GFA-116, a synthetic molecule that inhibits binding of vascular endothelial growth factor to its receptor. *Cancer Res* 2004; **64**: 3586-3592

6 **Levin EG**, Sikora L, Ding L, Rao SP, Sriramarao P. Suppression of tumor growth and angiogenesis in vivo by a truncated form of 24-kd fibroblast growth factor (FGF)-2. *Am J Pathol* 2004; **164**: 1183-1190

7 **Atiqur Rahman M**, Toi M. Anti-angiogenic therapy in breast cancer. *Biomed Pharmacother* 2003; **57**: 463-470

8 **Wahl ML**, Moser TL, Pizzo SV. Angiostatin and anti-angiogenic therapy in human disease. *Recent Prog Horm Res* 2004; **59**: 73-104

9 **Hinoda Y**, Sasaki S, Ishida T, Imai K. Monoclonal antibodies as effective therapeutic agents for solid tumors. *Cancer Sci* 2004; **95**: 621-625

10 **Salloum RM**, Jaskowiak NT, Mauceri HJ, Seetharam S, Beckett MA, Koons AM, Hari DM, Gupta VK, Reimer C, Kalluri R, Posner MC, Hellman S, Kufe DW, Weichselbaum RR. NM-3, an isocoumarin, increases the antitumor effects of radiotherapy without toxicity. *Cancer Res* 2000; **60**: 6958-6963

11 **Reimer CL**, Agata N, Tammam JG, Bamberg M, Dickerson WM, Kamphaus GD, Rook SL, Milhollen M, Fram R, Kalluri R, Kufe D, Kharbanda S. Antineoplastic effects of chemotherapeutic agents are potentiated by NM-3, an inhibitor of angiogenesis. *Cancer Res* 2002; **62**: 789-795

12 **Hohenberger P**, Gretschel S. Gastric cancer. *Lancet* 2003; **362**: 305-315

13 **Reinmuth N**, Parikh AA, Ahmad SA, Liu W, Stoeltzing O, Fan F, Takeda A, Akagi M, Ellis LM. Biology of angiogenesis in tumors of the gastrointestinal tract. *Microsc Res Tech* 2003; **60**: 199-207

14 **Saito H**, Tsujitani S. Angiogenesis, angiogenic factor expression and prognosis of gastric carcinoma. *Anticancer Res* 2001; **21**: 4365-4372

15 **Tenderenda M**, Rutkowski P, Jesionek-Kupnicka D, Kubiak R. Expression of CD34 in gastric cancer and its correlation with histology, stage, proliferation activity, p53 expression and apoptotic index. *Pathol Oncol Res* 2001; **7**: 129-134

16 **Furuya D**, Tsuji N, Yagihashi A, Watanabe N. Beclin 1 augmented cis-diamminedichloroplatinum induced apoptosis via enhancing caspase-9 activity. *Exp Cell Res* 2005; **307**: 26-40

17 **Forones NM**, Carvalho AP, Giannotti-Filho O, Lourenço LG, Oshima CT. Cell proliferation and apoptosis in gastric cancer and intestinal metaplasia. *Arq Gastroenterol* 2005; **42**: 30-34

18 **Matsuhashi N**, Saio M, Matsuo A, Sugiyama Y, Saji S. The

evaluation of gastric cancer sensitivity to 5-FU/CDDP in terms of induction of apoptosis: time- and p53 expression-dependency of anti-cancer drugs. *Oncol Rep* 2005; **14**: 609-615

19 **Browder T**, Butterfield CE, Kräling BM, Shi B, Marshall B, O'Reilly MS, Folkman J. Antiangiogenic scheduling of chemotherapy improves efficacy against experimental drug-resistant cancer. *Cancer Res* 2000; **60**: 1878-1886

20 **Agata N**, Nogi H, Milhollen M, Kharbanda S, Kufe D. 2-(8-Hydroxy-6-methoxy-1-oxo-1H-2-benzopyran-3-yl)propionic acid, a small molecule isocoumarin, potentiates dexamethasone-induced apoptosis of human multiple myeloma cells. *Cancer Res* 2004; **64**: 8512-8516

21 **McCarty MF**, Wey J, Stoeltzing O, Liu W, Fan F, Bucana C, Mansfield PF, Ryan AJ, Ellis LM. ZD6474, a vascular endothelial growth factor receptor tyrosine kinase inhibitor with additional activity against epidermal growth factor receptor tyrosine kinase, inhibits orthotopic growth and angiogenesis of gastric cancer. *Mol Cancer Ther* 2004; **3**: 1041-1048

22 **Stoeltzing O**, McCarty MF, Wey JS, Fan F, Liu W, Belcheva A, Bucana CD, Semenza GL, Ellis LM. Role of hypoxia-inducible factor 1alpha in gastric cancer cell growth, angiogenesis, and vessel maturation. *J Natl Cancer Inst* 2004; **96**: 946-956

23 **Kamiya K**, Konno H, Tanaka T, Baba M, Matsumoto K, Sakaguchi T, Yukita A, Asano M, Suzuki H, Arai T, Nakamura S. Antitumor effect on human gastric cancer and induction of apoptosis by vascular endothelial growth factor neutralizing antibody. *Jpn J Cancer Res* 1999; **90**: 794-800

S- Editor Liu Y **L- Editor** Wang XL **E- Editor** Ma WH

PO Box 2345, Beijing 100023, China
www.wjgnet.com
wjg@wjgnet.com

World J Gastroenterol 2007 January 28; 13(4): 515-524
World Journal of Gastroenterology ISSN 1007-9327

Usefulness of two independent histopathological classifications of tumor regression in patients with rectal cancer submitted to hyperfractionated pre-operative radiotherapy

Łukasz Liszka, Ewa Zielińska-Pająk, Jacek Pająk, Dariusz Gołka, Jacek Starzewski, Zbigniew Lorenc

Łukasz Liszka, Ewa Zielińska-Pająk, Jacek Pająk, Department of Pathology, Medical University of Silesia, ul. Medyków 14, Katowice 40-754, Poland
Dariusz Gołka, Department of Pathology, Victoria Hospital, Whinney Heys Road, Blackpool FY3 8NR, United Kingdom
Jacek Starzewski, Zbigniew Lorenc, Department of General and Colorectal Surgery, Medical University of Silesia, Plac Medyków 1, Sosnowiec 41-200, Poland
Correspondence to: Jacek Pająk, Department of Pathology, Medical University of Silesia, ul. Medyków 14, Katowice 40-754, Poland. makpaj@o2.pl
Telephone: +48-32-2525080 Fax: +48-32-2525080
Received: 2006-10-03 Accepted: 2006-12-11

Abstract

AIM: To assess the usefulness of two independent histopathological classifications of rectal cancer regression following neo-adjuvant therapy.

METHODS: Forty patients at the initial stage cT3NxM0 submitted to preoperative radiotherapy (42 Gy during 18 d) and then to radical surgical treatment. The relationship between "T-downstaging" versus regressive changes expressed by tumor regression grade (TRG 1-5) and Nasierowska-Guttmejer classification (NG 1-3) was studied as well as the relationship between TRG and NG versus local tumor stage ypT and lymph nodes status, ypN.

RESULTS: Complete regression (ypT0, TRG 1) was found in one patient. "T-downstaging" was observed in 11 (27.5%) patients. There was a weak statistical significance of the relationship between "T-downstaging" and TRG staging and NG stage. Patients with ypT1 were diagnosed as TRG 2-3 while those with ypT3 as TRG5. No lymph node metastases were found in patients with TRG 1-2. None of the patients without lymph node metastases were diagnosed as TRG 5. Patients in the ypT1 stage were NG 1-2. No lymph node metastases were found in NG 1. There was a significant correlation between TRG and NG.

CONCLUSION: Histopathological classifications may be useful in the monitoring of the effects of hyperfractionated preoperative radiotherapy in patients with rectal cancer at the stage of cT3NxM0. There is no unequivocal relationship between "T-downstaging" and TRG and NG. There is some concordance in the assessment of lymph node status with ypT, TRG and NG. TRG and NG are of limited value for the risk assessment of the lymph node involvement.

Key words: Rectal cancer; Adenocarcinoma; Neoadjuvant therapy; Preoperative radiotherapy; Neoplasm staging

Liszka Ł, Zielińska-Pająk E, Pająk J, Gołka D, Starzewski J, Lorenc Z. Usefulness of two independent histopathological classifications of tumor regression in patients with rectal cancer submitted to hyperfractionated pre-operative radiotherapy. *World J Gastroenterol* 2007; 13(4): 515-524

http://www.wjgnet.com/1007-9327/13/515.asp

INTRODUCTION

Colorectal cancer is the third most common malignancy diagnosed in the USA[1]. The estimated colorectal cancer mortality in the USA in 2006 is 55170[2]. The primary treatment method for rectal cancer is surgery, namely anterior rectal resection, abdomino-perineal resection or local excision[3-6]. Preoperative radiotherapy and radiochemotherapy play an increasing role in the treatment of rectal cancer[7-13]. The effectiveness of neo-adjuvant therapy may be assessed and monitored by means of long-term survival follow up, incidence of local recurrence, estimation of the percentage of patients with primary high stage tumor suitable for radical surgery, estimation of the percentage of patients suitable for sphincter-saving surgery or by monitoring the tumor stage using visualizing diagnostic methods[14,15]. Transrectal ultrasound (TRUS) is a useful method for the assessment of the local tumor stage and the regional lymph node status prior to neo-adjuvant therapy[3,4,6,16]. Basing on TRUS and histopathological examination one can define the tumor regression parameter "T-downstaging". Lower ypT parameter value (local tumor stage assessed by the pathologist in surgical specimen following neo-adjuvant therapy) than uT (local

tumor stage assessed by surgeon with use of TRUS prior to neo-adjuvant therapy) is considered an evidence of tumor regression. The value of ypT parameter equal or higher than uT indicates lack of tumor regression[11,14,17-21].

This parameter may also be applied to the regression of metastatic regional lymph nodes in rectal cancer, "N-downstaging"[17,20,22-26].

Preoperative radiotherapy and radiochemotherapy evokes a range of morphological changes in the microscopic picture of rectal cancer including increased tumor necrosis, cellular and nuclear atypia, endocrine differentiation of tumor cells, increased stromal fibrosis, quantitative and qualitative changes of the stromal inflammatory exudates, formation of mucin pools, surface ulceration, peritumoral eosinophilic infiltrate, dysplastic and adenomatous changes (high-grade dysplasia, and low-grade adenoma component in the intestinal mucosa)[5,27,28]. Several histopathological classifications of rectal carcinoma response to neo-adjuvant therapy have been proposed[5,20,29-33]. However, none of these classifications is used in routine histopathological diagnostics. This results from the fact that macro- and microscopic changes within the tumor structure and surrounding tissues are not a specific response to ionizing radiation but also may result from the non-specific inflammation, hormonal therapy and local immune reaction[5,7]. Tumor regression grade (TRG) is a semi-quantitative parameter describing a relative proportion of residual tumor and stromal fibrosis. It is regarded a useful parameter for the assessment of histopathological changes in tumor following neo-adjuvant therapy[14,18,19,21,22,29,34-38]. There are five grades of cancer response to treatment in TRG staging, ranging from TRG 1-no residual cancer cells in the intestinal wall, replaced by fibrous tissue, through TRG 2-presence of occasional residual cancer cells, scattered in fibrous stroma, TRG 3-fibrosis dominating over residual cancer, TRG 4-residual cancer outgrowing fibrosis, to TRG 5-no tumor response or regression, no fibrosis with extensive residual cancer[29]. Another classification, proposed by Nasierowska-Guttmejer (NG) distinguishes three degrees of cancer response to neo-adjuvant therapy depending on the intensity of the morphological changes. At present one should assess cancer cell degeneration (no cancer cells, high, moderate and low-grade degeneration), mucus pools (present or absent) and necrosis (absent, $\leqslant$ 50% cancer tissue, > 50% cancer tissue). Point scores are designated to each parameter of tumor response to neo-adjuvant therapy and then are summarized[5].

Some authors believe that "T-downstaging" does not precisely reflect cancer regression following neo-adjuvant therapy. They state that residual cancer has a form of rather small foci surrounded by fibrous tissue and they are localized in all layers of the rectal wall. Such a deep localization results in diagnosis of high tumor stage despite a good response to radiotherapy. This phenomenon justifies the search for the histopathological tumor regression grading systems[14,20,35,39]. Rodel *et al*[40] suggest that tumor regression following radiotherapy reflects its less aggressive potential resulting from the molecular profile. Particular biological properties of a tumor influencing its chemo-radiosensitivity may also prove to be of long-term prognostic significance, especially in cases submitted to neo-adjuvant therapy.

TRG classification is probably superior versus "T-downstaging" in terms of the evaluation of neo-adjuvant therapeutic effects[14]. Reports on the relationship between "T-downstaging" or ypT and TRG are not numerous, and are with regard to preoperative long-term radiotherapy and chemoradiotherapy[21,22,35,36]. The relationship between TRG and the probability of lymph nodes involvement has been described in detail only in patients with rectal cancer submitted to long-term radio-chemotherapy[22,41]. So far, no results have been published comparing the NG with other rectal cancer regression assessment systems following neo-adjuvant therapy.

The aim of the present study is to evaluate if two independent histopathological classifications based on semiquantitative assessment of regressive changes may prove useful for the monitoring of patients with rectal adenocarcinoma, initial stage cT3NxM0 submitted to preoperative hyperfractionated radiotherapy.

Our particular aim was to assess whether there is any relationship between: (1) "T-downstaging" and histopathological staging systems of cancer response to neo-adjuvant treatment (TRG and NG systems); (2) "T-downstaging" and local tumor stage and lymph node status; (3) TRG and NG classification and local tumor stage and lymph node status; (4) mutual relationships between TRG and NG systems.

MATERIALS AND METHODS

Patients

The study encompassed patients with rectal adenocarcinoma submitted to hyperfractionated preoperative radiotherapy, with perirectal tissue invasion assessed with ultrasound examination prior to neo-adjuvant treatment (TRUS: uT3). Patients' general performance status according to the Eastern Cooperative Oncology Group classification ranged from 0 to 2 points. Patients with distant metastases found on chest X-ray, and abdominal and pelvis CT examination were excluded from the study. Also, patients formerly submitted to radiotherapy due to present disease or another neoplasm were not included into the study. None of the patients had a history of inflammatory bowel disease.

Forty patients were included into the study. Median age was 64 (range 45-75) years. Ultrasound examination protocol has been described previously[6]. All patients were submitted to preoperative hyperfractionated radiotherapy. A total dose of 42 Gy in 28 fractions during 18 d (twice a day, 1.8 Gy, 5 d/wk, and with a minimum 6 h interval between doses) using a three-field isocentric technique-one posterior and two lateral portals. Photon rays of 20 (10-23) MV were used. The edge of the posterior field was situated 5 cm below the lower tumor margin. The lateral margins of the lateral fields extended beyond the pelvic inlet. The upper edge was at the top of the fifth lumbar vertebra. The target volume included the tumor and regional lymph nodes. The standard size of the posterior

Table 1 Clinicopathological characteristics of study patients

Median age (mean ± SD) (yr)	64 (61.75 ± 10.0)	
M:F	1:1	
Lymph node involvement prior to radiotherapy (cN)		
cN0	25	62.5%
cN+	15	37.5%
Tumor stage		
ypT0	1	2.5%
ypT1	4	10%
ypT2	6	15%
ypT3	29	72.5%
Lymph node status		
ypN0	26	65%
ypN1	8	20%
ypN2	6	15%
Number of lymph node assessed-median (mean ± SD)	16 (18 ± 11.5)	
Number of affected lymph nodes-median (mean ± SD)	0 (2.6 ± 6.9)	
Tumor histological grade (G)[1]		
G1	5	12.8%
G2	32	82.1%
G3	2	5.1%
Median tumor diameter[1] (mean ± SD) (mm)	33.5 (33.7 ± 16.1)	

[1]One case ypT0 (2.5%) had not been taken into account.

field was 12 cm × 15 cm and 10 cm × 15 cm for the lateral fields. Surgery was performed 1-7 d (mean, 5 d) following radiotherapy. Thirty one (77.5%) anterior resections, 8 (20.0%) abdomino-perineal resections and 1 (2.5%) Hartmann's operation, were performed.

Pathological examination

Surgical specimens were submitted to histopathological examination according to standard protocol[42]. Special attention was paid to definite, probable and potential prognostic factors[43]. The following pathological parameters were evaluated: local tumor stage (ypT), regional lymph node status (ypN), tumor grade (G1, G2, G3), number of metastatic lymph nodes, and parameters of the tumor response to radiotherapy. The latter included: cancer cell degeneration (severe, moderate, mild), mucin pools (absent, present), tumor necrosis (absent, $\leqslant$ 50%, > 50% of the tumor), tumor response to radiotherapy according to NG (1-3)[5], and TRG (1-5)[29] classification. In cases with non-homogeneous tumor response pattern to radiotherapy, the area of the weakest response was taken into account[38]. Routine surgical specimens submitted for histopathological examination were evaluated retrospectively. Concerning radiotherapy and surgery, the nature of the study was observatory and not experimental.

Statistical analysis

A study population was divided into 2 groups upon the "T-downstaging" tumor regression parameter. A group with features of cancer regression, ypT < uT (R group) and with no regression, ypT $\geqslant$ uT (NR group) were distinguished. The differences between groups in parameters studied were tested using Pearson's χ^2 test, Fisher's exact test, and Mann-Whitney's *U* test. Correlation was assessed with Spearman's rank correlation. $P < 0.05$ was considered statistically significant.

Table 2 Relationship between "T-downstaging" and prognostic parameters

Feature	Group R (n = 11)	Group NR (n = 29)	P
Median age (range) (mean ± SD) (yr)	70 (55-77) (67.7 ± 7.2)	61 (45-70) (59.4 ± 9.9)	< 0.05
Tumor stage			< 0.000
ypT0	1 (9.1%)	0	
ypT1	4 (36.4%)	0	
ypT2	6 (54.6%)	0	
ypT3	0	29 (100.0%)	
TRG			< 0.08
1	1 (9.1%)	0	
2	2 (18.2%)	1 (3.5%)	
3	6 (54.6%)	11 (37.9%)	
4	2 (18.2%)	14 (48.3%)	
5	0	3 (10.3%)	
NG			< 0.08
1	5 (45.5%)	4 (13.8%)	
2	2 (18.2%)	4 (13.8%)	
3	4 (36.4%)	21 (72.4%)	

RESULTS

Demographic data and staging parameters are presented in Table 1. Local tumor stage, ypT3 was found in 29 (72.5%) patients. "T-downstaging" was observed in 11 out of 40 (27.5%) patients. Six (15.0%) of them showed downstaging to ypT2, and 4 (10.0%) to ypT1. In one case, histopathological examination has shown no evidence of carcinoma in the intestinal wall (ypT0, TRG 1). Also, no lymph node involvement was found in this patient (ypT0N0). TRUS examination showed features of lymph node involvement in 15 (37.5%) patients. In 8 (20%) of 15 patients in whom TRUS examination showed lymph node involvement, microscopic examination revealed stage ypN0. In 7 (17.5%) out of 25 patients with no evidence of lymph node involvement in TRUS examination, histopathological examination showed presence of metastases. TRG grades 2, 3 and 4 were diagnosed in 3 (7.5%), 17 (42.5%) and 16 (40.0%) patients, respectively. No tumor regression (TRG 5) was found in 3 (7.5%) patients. Features of moderate or severe cancer cell degeneration were observed in 17 (42.5%) patients. Mucus lakes were seen in 22 (55.0%) cases. Necrosis was present in 27 (67.5%) of cases including 1 case with more than 50% of tumor involvement. Stage 1, 2, and 3 of NG classification was reported in 9 (22.5%), 6 (15.0%), and 25 (62.5%) patients, respectively.

Median age (range) in the group with tumor regression was higher than those of patients with no evidence of regression (Table 2). Groups R and NR included 5 (45.5%) and 15 (51.7%) men (NS), respectively. TRUS examination performed prior to neo-adjuvant therapy revealed lymph node involvement in groups R and NR in 4 (36.36%) and 11 (37.93%) patients (NS), respectively. Stage ypN0, ypN1 and ypN2 was found in 9 (81.8%), 2 (18.2%), and

Table 3 Relationship between tumor stage and TRG

	TRG 1	TRG 2	TRG 3	TRG 4	TRG 5
Local tumor stage[1,a]					
ypT0	1	-	-	-	-
ypT1	-	2	2	-	-
ypT2	-	-	4	2	-
ypT3	-	1	11	14	3
Lymph nodes involvement[2,c]					
ypN0	1	3	14	8	-
ypN1	-	-	1	5	2
ypN2	-	-	2	3	1

[1]Spearman R correlation $r = 0.47$; [a]$P < 0.005$, comparison between different local tumor stages. [2]Spearman R correlation $r = 0.47$; [c]$P < 0.005$, comparison between different lymph nodes involvements.

Table 4 Relationship between tumor stage and NG

	NG 1	NG 2	NG 3
Local tumor stage[1,b]			
ypT0	1	-	-
ypT1	3	1	-
ypT2	1	1	4
ypT3	4	4	21
Lymph node involvement[2,a]			
ypN0	9	5	12
ypN1	-	-	8
ypN2	-	1	5

[1]Spearman R correlation $r = 0.42$; [b]$P < 0.01$, comparison between different local tumor stages. [2]Spearman R correlation $r = 0.45$; [a]$P < 0.005$, comparison of lymph node involvement.

0 patients in group R and 17 (58.6%), 6 (20.7%) and 6 (20.7%) in group NR (NS). A trend ($P < 0.12$) indicating a relationship between the number of lymph nodes assessed and "T-downstaging" was found. Median (range) number of lymph nodes in group R was 11 (3-35), and 17 (3-41) in group NR. The number of involved lymph nodes in the group R (median, range) did not differ from the number of nodes in group NR, 0 (0-1) and 0 (0-35) (NS), respectively. Tumor grade G1 was found in 2 (20.0%) patients, G2 in 7 (70.0%), and G3 in 1 (10.0%) patient in the R group, and in 3 (10.3%), 25 (86.2%), and 1 (3.5%) patients in the NR group (NS); one (2.5%) case at the ypT0 stage had not been taken into account. Median (range) tumor diameter in groups R and NR was 26 (10-65) mm and 35 (10-70) mm, respectively (NS). The relationship between "T-downstaging" and TRG staging as well as the NG stage was at the borderline of statistical significance. The relationship between TRG and NG *vs.* local tumor stage and lymph node status is shown in Tables 3 and 4. Patients with ypT1 were diagnosed as TRG 2-3. Patients with TRG5 were classified as ypT3. No lymph node metastases were found in patients with TRG 1-2 (ypN0). None of the patients without lymph nodes metastases were diagnosed as TRG 5. Patients in the ypT1 stage were diagnosed as NG 1-2. No lymph node metastases were found in NG 1. There was a relationship between TRG and NG (correlation $R = 0.58$, $P < 0.01$). Patients with TRG 1-2 were classified as NG 1. Patients with TRG 5 were diagnosed as NG 3.

DISCUSSION

Ultrasound-histopathological tumor regression parameter, "T-downstaging" represents a simple marker of rectal cancer radiosensitivity both in patients submitted to short-term preoperative radiotherapy[11,18,19,44,45] as well as in patients with surgery delayed by 1 to 8 wk following irradiation[17,20,21,23,25-28,34-36,39,46-49]. Reports have been published showing the prognostic value of "T-downstaging" for overall survival[17,28,34], cancer-specific survival[48], recurrence-free survival[48] , disease-free survival[25,28], local recurrence risk[26,34,48], and the risk of distant metastases[48]. Read *et al*[50] showed that the local staging following neo-adjuvant therapy enables the risk assessment of lymph node metastases. This finding may prove to be of significance during planning of surgical treatment. The percentage of patients with "T-downstaging" in the group submitted to long-term radiotherapy and radiochemotherapy ranged from 23/88 (26.0%) to 15/20 (75.0%)[14,17,20-24,27,34-36,39,46-49,51,52]. Among patients submitted to short-term preoperative radiotherapy "T-downstaging" ranged between 10/28 (35.7%) and 44/104 (43%)[11,14,18,19]. An alternative way for the assessment of local tumor stage decrease is comparison of ypT in patients from study groups and control groups in randomized trials on the effects of neo-adjuvant therapy[53]. Results of randomized studies on effects of short-term preoperative radiotherapy with a dose of 25 Gy on local tumor stage were discrepant[8,44]. In the presented material, "T-downstaging" was achieved in 11/40 (27.5%) patients. No correlation between "T-downstaging" and lymph node involvement, tumor grade and its diameter were found. In patients submitted to neo-adjuvant therapy the number of assessed lymph nodes is usually lower than in patients treated with surgery only [54]. In the present study, a tendency towards statistical significance ($P < 0.12$) of the correlation between "T-downstaging" and the number of evaluated lymph nodes was observed. More lymph nodes were found in patients with local stage ypT3 (group NR) than in those with ypT0-2 stage. Joseph *et al*[55] showed that in patients with colon cancer at T1/T2 stage more lymph nodes must be studied than in patients with T3/T4 in order to reliably define stage pN0. However, frequently the surgical approach is completely different in patients with lower local stage a limited lymph node resection is performed[57].

In the presented study, "downstaging" parameter was evaluated exclusively in order to show cancer regression within the rectal wall ("T-downstaging"). This results from the fact that the sensitivity of ultrasound evaluation of affected lymph nodes prior to radiotherapy is probably not sufficient to make a reference point for other, strictly histopathological tumor regression classifications. The accuracy of ultrasound examination in the evaluation of lymph node involvement is 65%-81% and the accuracy of the local tumor stage assessment is 82% to 93%[3]. Another argument against uN parameter in the evaluation of rectal cancer regression is that uN is of

no prognostic significance[17,49]. Some authors studied "N-downstaging" parameter[17,20,22-26,36,47] and showed its prognostic value[17]. The percentage of patients submitted to radiochemotherapy or radiotherapy with long time intervals between neo-adjuvant treatment and surgery, in which "N-downstaging" was noted, ranged from 13/26 (50.0%) to 38/42 (90.4%)[17,20,22-26,36,47]. Tumor size decrease, 'sterilization' and lymph node atrophy are the classic effects of radiotherapy[20,44,45]. Graf *et al*[53] showed that short-term preoperative radiotherapy results in decreased risk of lymph node involvement.

TRG 1 indicates that no cancer cells have been identified in the rectal wall[18,19,21,29]. Some researchers refer TRG 1 to patients with no cancer cells in the entire post-surgical specimen[37]. The term-pathological complete response (pCR) of rectal cancer to preoperative radiotherapy regards the situation in which histopathological examination does not show the neoplasm in the rectal wall, lymph nodes and mesorectum[25,26,35-38,46,48-50,57-61]. This is in accordance with the definition developed by the WHO initiative[62]. A stage of pCR is sometimes identified with ypT0N0 - the situation in which there is no evidence of neoplastic tissue in the rectal wall and in the lymph nodes[17,23]. Cases with only a few residual cells or small clusters of cells detected in histopathological examination of surgical specimens are by some authors classified as pCR[63]. In the presented study, the authors have assumed that the term pCR represents the situation in which no cancer cells were found in the surgical specimen. There is no absolute concordance between pCR and clinical complete response (assessed by per rectum digital examination and in proctoscopy): pCR may regard barely 25.0% of patients submitted to long-term preoperative chemoradiotherapy with clinical complete response[61]. A complete response to radiotherapy in comparison with the presence of residual cancer tissue is associated with better overall survival rate[46], longer disease-free survival[25], and lower risk of local recurrence[46]. However, some authors claim that complete regression is of no prognostic significance[37]. Guillem *et al*[59] did not show any differences in long-term prognosis among patients with complete cancer regression in comparison with almost complete response ($\geqslant$ 95.0% regression) to neo-adjuvant therapy.

Demonstrating a complete remission is important not only because of its prognostic value but also because of the need of assessment of indications for the postoperative chemotherapy or radiotherapy, for the decision about the appropriate method of surgery[20,37,45,46,49,57,58,63,64] or to compare the effects of different treatment methods[45]. Zmora *et al*[58] showed that metastases to regional lymph nodes and cancer cells in the mesorectal tissue may be present in patients with complete tumor regression within the rectal wall (TRG 1, ypT0)[58]. However, neo-adjuvant therapy makes it possible to reduce the percentage of patients submitted to abdomino-perineal resection and, in some cases, to perform local tumor excision[15,25,41,49,64-67]. Randomized study conducted by Polish researchers on a group of 316 patients treated with long-term radiochemotherapy or short-term preoperative radiotherapy did not show differences in terms of sphincter preservation rate (58% *vs* 61%, P = 0.57)[67]. Appropriate selection of the study patients treated with local excision is a very important issue[41,64-66,68]. The local tumor stage seems to be a reliable predictor of lymph node regression in these patients[41,64]. The assessment of eventual residual cancer, local stage (ypT), surgical clearance in the resection margins in patients submitted to local resection may reveal the necessity of immediate radical resection (performed within 30 d after the primary surgery)[65,66,68]. Also, intraoperative frozen section may prove useful for the assessment of tumor stage and margins' status. In cases in which a more advanced stage (pT2 or pT3) is likely to be found at the time of surgery or where the surgical clearance could be doubtful, the patient should be prepared for the possibility of wide excision at the same operation[66].

Another interesting issue is the assessment of cancer regression following neo-adjuvant therapy with use of TRG classification on intraoperational microscopic examination. In particular, this regards patients with an evident but incomplete regression. One could expect that the lacking concordance between local tumor stage ypT and TRG in post-operative histopathological examination, as mentioned above, apply also to intra-operation evaluation[20,35,39]. Considering the fact, that local excision following neo-adjuvant treatment is a therapeutic option for carefully selected patients, it could be eventually considered in patients with an evident but incomplete tumor regression. These patients are characterized by a low risk of local recurrence[18,22]. In the present study we have observed 1 case of coincidence of ypT3 and TRG 2. In the absence of reliable alternative methods, microscopic examination plays an important role in the evaluation of cancer regression following neo-adjuvant treatment. Digital rectal examination, computerized tomography, transrectal ultrasound examination and magnetic resonance are of limited value in terms of assessment of residual cancer following long-term pre-operative radio- and radiochemotherapy, especially to demonstrate pCR[61,69]. However, Gavioli *et al*[70] believe that TRUS is a very useful tool, when the same experienced operator performs it before and after neo-adjuvant treatment since it leads to demonstrate tumor regression in a qualitative and quantitative way. Moreover, they proposed that TRUS performed 6-8 wk following irradiation makes it possible to visualize fibrous changes only, which does not, however, disqualify this diagnostic method. The extent of fibrosis indicates the possible depth of residual cancer infiltration-cancer cells are believed to be present within fibrous areas only[70]. The use of magnetic resonance volumetry may also be useful in quantitative assessment of cancer regression following neo-adjuvant treatment[71]. The difficulties in achieving high level of reliability of visualizing diagnostic methods result from similar signal intensity (echogenity) between residual cancer, fibrous tissue, mucus pools and peritumoral inflammatory infiltration[71]. The use of 18-fluorodeoxyglucose positron emission tomography may prove effective in assessment of tumor response to neo-adjuvant therapy[33]. Full thickness local excision still

remains an experimental treatment method[64].

The significance of pCR following radiotherapy has not been ultimately confirmed. It is possible that better long-term survival in patients with pCR results from different biological properties of the tumor. Also, interesting reports have been presented, showing that patients submitted to neo-adjuvant chemotherapy and receiving statins showed higher a pCR rate[72]. The percentage of patients with complete regression following long-term radiochemotherapy and radiotherapy ranged from 1/43 (2.3%) to 7/20 (35.0%)[5,17,20-21,23-27,35-37,47-52,57-61,67,73]. The percentage of patients presenting complete cancer regression following short-term radiotherapy ranges between 0% and 10/191 (5.2%)[10,11,18,19,50]. In the present study we have observed 1 case (2.5%) with complete tumor regression.

The period between the termination of neo-adjuvant therapy and surgery in long-term radiochemotherapy and radiotherapy schemes is a few days and a few weeks, respectively. One may assume that short-term radiotherapy will result in relatively lesser tumor regression[10,23,63]. The results obtained in large study groups indicate that the short-term radiotherapy results not only in a decrease of the tumor diameter[44,45,53], but also in decreased number of affected lymph nodes[53]. A decrease in tumor diameter is not, however, equivalent with the decrease in local extent of tumor. Some authors believe that the period shorter than 10 d is insufficient to achieve tumor regression following radiotherapy with a dose of 25 Gy[45]. The proposition of the role of the time period between neo-adjuvant treatment and the percentage of pCR has its supporters[26,63] and opponents[24,73]. It was, however, shown that the period of a few days between the termination of neo-adjuvant therapy and surgery is sufficient enough for the development of morphological changes within the tumor and in its gene expression profile[44,74].

It was demonstrated that there is a relationship between TRG and overall survival, disease-free survival, and the risk of local tumor recurrence[18,22]. Other authors suggest that TRG estimation does not enable long-term prognosis in patients with rectal cancer[37]. There are some doubts regarding the reliability of this classification due to its subjective nature[20]. Interobserver variability of the TRG system was found to be satisfactory (kappa 0.64) or mediocre (kappa 0.44). It is higher when a 5-point system is simplified to 3-point[21,38]. For the reliability assessment it is important that significant fibrosis may accompany neoplastic tissue even when no neo-adjuvant therapy had been administered[38]. In the presented study, we have not shown unequivocal correlation between "T-downstaging" and TRG. We have found a correlation of TRG and ypT parameters. The reliability of TRG as a lymph node predictor is not unequivocal. Veccio *et al*[22] showed that lymph node involvement is not observed in 41/45 (91.0%) patients submitted to long-term preoperative chemoradiotherapy at TRG 1-2 stage. Kim *et al*[41] showed that histopathological assessment of tumor response to preoperative long-term radiochemotherapy (performed with use of the method described by Dworak *et al*[32], similar to the TRG system) is, along with ypT, an independent predictor of lymph node involvement. In the present study, ypN0 stage was observed in all patients with TRG 1-2. We have not found any definite relationship between "T-downstaging" and the NG stage. The results indicate the correlation between TRG and NG. However, these classifications are based on the evaluation of different morphological parameters. Rectal Cancer Regression Grade (RCRG) classification proposed by Wheeler *et al*[20,39] is next to the TRG system and Dworak *et al*[32] classification, one of the most widely used in studies documenting rectal cancer regression following neo-adjuvant therapy. It defines 3 degrees of tumor regression: 1, no cancer nests or microscopic collections of cancer cells embedded in fibrous stroma; 2, residual neoplasm seen grossly but with evident fibrosis; 3, carcinoma seen grossly with discreet or absent fibrosis. According to some researchers, such distinguishing of neoplastic tissue and fibrosis is not reliable[38,58]. Due to these reservations and the retrospective nature of the study, this grading system had not been taken into consideration in the present study.

At present, there is no uniform, widely accepted histopathological classification used for the evaluation of rectal cancer regression following preoperative radiotherapy. As far as the need for evaluation of residual cancer raises no objections, its interpretation and clinical consequences of radiation-induced changes in the rectal wall and within the tumor are not clear[5,27,44,74]. It is also unclear to what extent the presence of necrosis one may assign to its radiotherapeutic effect and to what extent it is a result of ischemic changes due to local perfusion disturbance. Fibrosis that accompanies neoplastic tumor may reflect both natural protective body mechanisms as well as being a result of chronic inflammation[7]. Mucin pools in tissues previously occupied by neoplastic tissue are qualitatively different from changes described as colitis cystica profunda, which may develop within the normal intestinal wall following radiotherapy[20]. The presence of mucin pools (induced mucinous carcinoma, colloid response) should be taken into account in the differential diagnosis of mucus-secreting adenocarcinoma[28,74]. The prognostic value of other morphological changes observed within the residual neoplastic tissue (the intensity and the nature of inflammatory infiltrations accompanying fibrous tissue and cancer cell clusters, cancer cell nuclear pleomorphism and hyperchromasia, mucinous cancer component, low tumor histological grade) and in the intestinal wall (surface ulceration, dysplastic changes, low-grade adenoma component) has not been unequivocally established[27,44,74]. Figures 1-6 show examples of neo-adjuvant therapy induced changes.

The retrospective nature of the presented study and the relatively small group of study patients impose careful interpretation of the presented results. Few reports on "T-downgrading", TRG and NG in patients submitted to short-term radiotherapy according to the regimen presented make the presented results suitable for further prospective studies on a larger population.

In conclusion, histopathological classifications based on the assessment of regressive changes may be useful in the

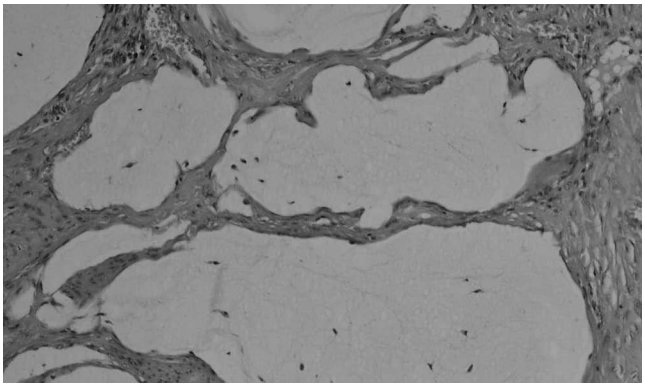

Figure 1 Acellular mucin pools in the intestinal wall (HE x 200).

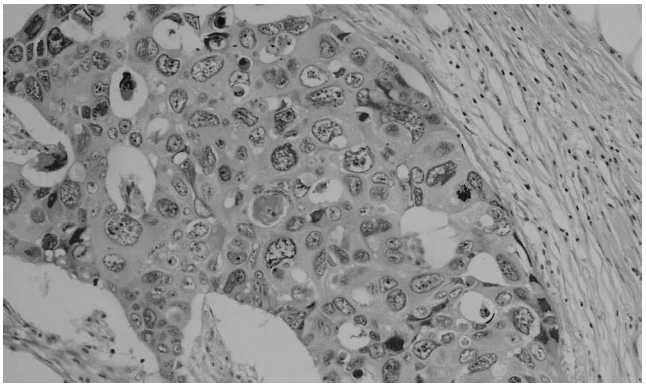

Figure 4 Degenerated adenocarcinoma cells following radiotherapy (HE x 125).

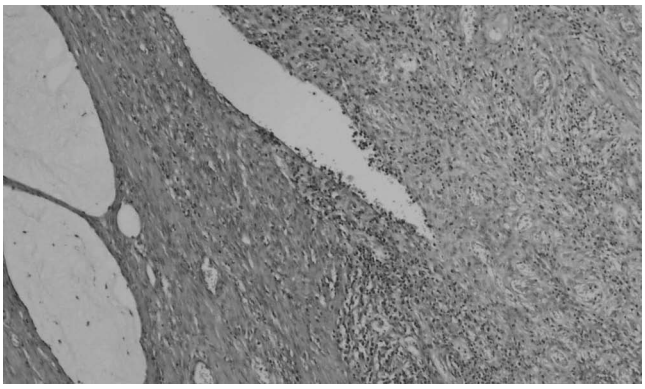

Figure 2 Complete tumor regression following radiotherapy. Inflammatory infiltrations, mucin pool and focal fibrosis in the stroma (HE x 64).

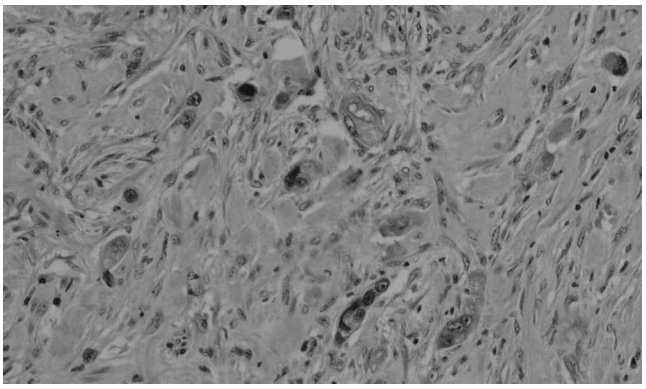

Figure 5 Dispersed degenerated adenocarcinoma cells following radiotherapy (HE x 125).

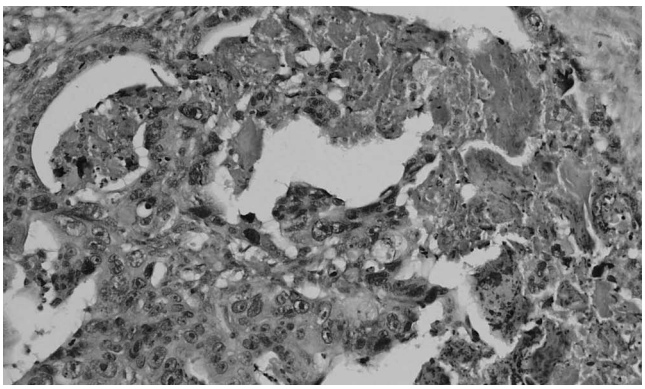

Figure 3 Degeneration and necrosis of tumor cells following radiotherapy (HE x 250).

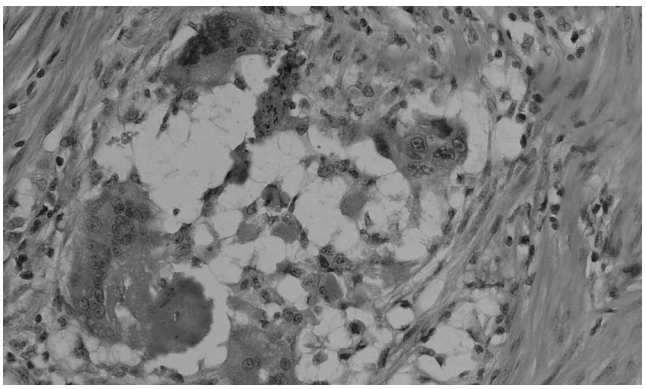

Figure 6 Macrophages and multinucleated (giant) cells close to necrotic tumor areas (HE x 200).

monitoring of effects of hyperfractionated preoperative radiotherapy in patients with rectal cancer at the initial stage of cT3NxM0. There is no unequivocal relationship between "T-dowstaging" and the tumor regression assessed with TRG and Nasierowska-Guttmejer classification. Poor tumor regression was seen more frequently in patients with no evident "T-downstaging". No relationships have been found between "T-downstaging" and lymph node involvement, tumor histological grade or tumor diameter. There is a clear but limited concordance in the assessment of regressive changes with ypT and TRG or NG. TRG and NG classifications are probably of limited predictive value in terms of lymph node involvement. There is a non-coincidental relationship between the assessment of radiation-induced regressive changes with use of TRG and NG classifications.

It is possible that immunohistochemical evaluation or molecular biology techniques applied to pre-operative biopsy samples may prove to be of predictive value in the future[21,34,52,75]. Undoubtedly, histopathological evaluation of the neoplastic tissue regression following preoperative radiotherapy is very important and necessary,

since ultrasound examination here is of limited reliability. Histopathological evaluation of rectal cancer regression may also prove to be useful for the evaluation of the effectiveness of future radio- and radio-chemotherapeutic treatment methods. It might also enable to isolate the population of rectal cancer patients in whom the adjuvant treatment would be especially justified.

REFERENCES

1 **National Comprehensive Cancer Network**. Rectal Cancer. Clinical Practice Guidelines in Oncology. Version 2.2006; cited 2006-04-24. Available from: URL: http://www.nccn.org/professionals/physician_gls/PDF/rectal.pdf
2 **Jemal A**, Siegel R, Ward E, Murray T, Xu J, Smigal C, Thun MJ. Cancer statistics, 2006. *CA Cancer J Clin* 2006; **56**: 106-130
3 **Church JM**, Gibbs P, Chao MW, Tjandra JJ. Optimizing the outcome for patients with rectal cancer. *Dis Colon Rectum* 2003; **46**: 389-402
4 **Tjandra JJ**, Kilkenny JW, Buie WD, Hyman N, Simmang C, Anthony T, Orsay C, Church J, Otchy D, Cohen J, Place R, Denstman F, Rakinic J, Moore R, Whiteford M. Practice parameters for the management of rectal cancer (revised). *Dis Colon Rectum* 2005; **48**: 411-423
5 **Nasierowska-Guttmejer A**. Histopathological and immunohistochemical markers in rectal cancer after preoperative radiochemotherapy. *J Oncol* 2001; **51** Suppl 3: 1-57 (in Polish, with English abstract)
6 **Pawelczyk I**, Pajak J, Wydmanski J, Kozera J, Dyczkowski K, Lorek A. The usefulness of transrectal ultrasound for assessment of local progression of rectal cancer after hyperfractionated preoperative radiotherapy. *Chir Pol* 2001; **4**: 163-170. Available from: URL: http://www.chirurgia.med.pl/en/darmowy_pdf.phtml?indeks=4&indeks_art=
7 **Wheeler JM**, Warren BF, Jones AC, Mortensen NJ. Preoperative radiotherapy for rectal cancer: implications for surgeons, pathologists and radiologists. *Br J Surg* 1999; **86**: 1108-1120
8 Improved survival with preoperative radiotherapy in resectable rectal cancer. Swedish Rectal Cancer Trial. *N Engl J Med* 1997; **336**: 980-987
9 **Folkesson J**, Birgisson H, Pahlman L, Cedermark B, Glimelius B, Gunnarsson U. Swedish Rectal Cancer Trial: long lasting benefits from radiotherapy on survival and local recurrence rate. *J Clin Oncol* 2005; **23**: 5644-5650
10 **Nasierowska-Guttmejer A**. The comparison of immunohistochemical proliferation and apoptosis markers in rectal carcinoma treated surgically or by preoperative radiochemotherapy. *Pol J Pathol* 2001; **52**: 53-61
11 **Voelter V**, Stupp R, Matter M, Gillet M, Bouzourene H, Leyvraz S, Coucke P. Preoperative hyperfractionated accelerated radiotherapy (HART) and concomitant CPT-11 in locally advanced rectal carcinoma: a phase I study. *Int J Radiat Oncol Biol Phys* 2003; **56**: 1288-1294
12 **Coucke PA**, Sartorelli B, Cuttat JF, Jeanneret W, Gillet M, Mirimanoff RO. The rationale to switch from postoperative hyperfractionated accelerated radiotherapy to preoperative hyperfractionated accelerated radiotherapy in rectal cancer. *Int J Radiat Oncol Biol Phys* 1995; **32**: 181-188
13 **Camma C**, Giunta M, Fiorica F, Pagliaro L, Craxi A, Cottone M. Preoperative radiotherapy for resectable rectal cancer: A meta-analysis. *JAMA* 2000; **284**: 1008-1015
14 **Vironen J**, Juhola M, Kairaluoma M, Jantunen I, Kellokumpu I. Tumour regression grading in the evaluation of tumour response after different preoperative radiotherapy treatments for rectal carcinoma. *Int J Colorectal Dis* 2005; **20**: 440-445
15 **Rengan R**, Paty P, Wong WD, Guillem J, Weiser M, Temple L, Saltz L, Minsky BD. Distal cT2N0 rectal cancer: is there an alternative to abdominoperineal resection? *J Clin Oncol* 2005; **23**: 4905-4912
16 **Heimann TM**, Szporn AH. Color atlas of preoperative staging and surgical treatment options in rectal cancer. 1st ed. Baltimore: Williams and Wilkins, 1998: 40-49
17 **Roman S**, Cenni JC, Roy P, Pujol B, Napoleon B, Keriven-Souquet O, Souquet JC. Value of rectal ultrasound in predicting staging and outcome in patients with rectal adenocarcinoma. *Dis Colon Rectum* 2004; **47**: 1323-1330
18 **Bouzourene H**, Bosman FT, Matter M, Coucke P. Predictive factors in locally advanced rectal cancer treated with preoperative hyperfractionated and accelerated radiotherapy. *Hum Pathol* 2003; **34**: 541-548
19 **Bouzourene H**, Bosman FT, Seelentag W, Matter M, Coucke P. Importance of tumor regression assessment in predicting the outcome in patients with locally advanced rectal carcinoma who are treated with preoperative radiotherapy. *Cancer* 2002; **94**: 1121-1130
20 **Wheeler JM**, Warren BF, Mortensen NJ, Ekanyaka N, Kulacoglu H, Jones AC, George BD, Kettlewell MG. Quantification of histologic regression of rectal cancer after irradiation: a proposal for a modified staging system. *Dis Colon Rectum* 2002; **45**: 1051-1056
21 **Morgan MJ**, Koorey DJ, Painter D, Findlay M, Tran K, Stevens G, Solomon MJ. Histological tumour response to pre-operative combined modality therapy in locally advanced rectal cancer. *Colorectal Dis* 2002; **4**: 177-183
22 **Vecchio FM**, Valentini V, Minsky BD, Padula GD, Venkatraman ES, Balducci M, Micciche F, Ricci R, Morganti AG, Gambacorta MA, Maurizi F, Coco C. The relationship of pathologic tumor regression grade (TRG) and outcomes after preoperative therapy in rectal cancer. *Int J Radiat Oncol Biol Phys* 2005; **62**: 752-760
23 **Moore HG**, Gittleman AE, Minsky BD, Wong D, Paty PB, Weiser M, Temple L, Saltz L, Shia J, Guillem JG. Rate of pathologic complete response with increased interval between preoperative combined modality therapy and rectal cancer resection. *Dis Colon Rectum* 2004; **47**: 279-286
24 **Stein DE**, Mahmoud NN, Anne PR, Rose DG, Isenberg GA, Goldstein SD, Mitchell E, Fry RD. Longer time interval between completion of neoadjuvant chemoradiation and surgical resection does not improve downstaging of rectal carcinoma. *Dis Colon Rectum* 2003; **46**: 448-453
25 **Theodoropoulos G**, Wise WE, Padmanabhan A, Kerner BA, Taylor CW, Aguilar PS, Khanduja KS. T-level downstaging and complete pathologic response after preoperative chemoradiation for advanced rectal cancer result in decreased recurrence and improved disease-free survival. *Dis Colon Rectum* 2002; **45**: 895-903
26 **Ratto C**, Valentini V, Morganti AG, Barbaro B, Coco C, Sofo L, Balducci M, Gentile PC, Pacelli F, Doglietto GB, Picciocchi A, Cellini N. Combined-modality therapy in locally advanced primary rectal cancer. *Dis Colon Rectum* 2003; 46: 59-67
27 **Shia J**, Guillem JG, Moore HG, Tickoo SK, Qin J, Ruo L, Suriawinata A, Paty PB, Minsky BD, Weiser MR, Temple LK, Wong WD, Klimstra DS. Patterns of morphologic alteration in residual rectal carcinoma following preoperative chemoradiation and their association with long-term outcome. *Am J Surg Pathol* 2004; **28**: 215-223
28 **Rullier A**, Laurent C, Vendrely V, Le Bail B, Bioulac-Sage P, Rullier E. Impact of colloid response on survival after preoperative radiotherapy in locally advanced rectal carcinoma. *Am J Surg Pathol* 2005; **29**: 602-606
29 **Mandard AM**, Dalibard F, Mandard JC, Marnay J, Henry-Amar M, Petiot JF, Roussel A, Jacob JH, Segol P, Samama G. Pathologic assessment of tumor regression after preoperative chemoradiotherapy of esophageal carcinoma. Clinicopathologic correlations. *Cancer* 1994; **73**: 2680-2686
30 **Spitz FR**, Giacco GG, Hess K, Larry L, Rich TA, Janjan N, Cleary KR, Skibber JM. p53 immunohistochemical staining predicts residual disease after chemoradiation in patients with high-risk rectal cancer. *Clin Cancer Res* 1997; **3**: 1685-1690
31 **Berger C**, de Muret A, Garaud P, Chapet S, Bourlier P, Reynaud-Bougnoux A, Dorval E, de Calan L, Huten N, le Folch O, Calais G. Preoperative radiotherapy (RT) for rectal cancer: predictive factors of tumor downstaging and residual tumor cell density (RTCD): prognostic implications. *Int J Radiat Oncol*

Biol Phys 1997; **37**: 619-627
32 **Dworak O**, Keilholz L, Hoffmann A. Pathological features of rectal cancer after preoperative radiochemotherapy. *Int J Colorectal Dis* 1997; **12**: 19-23
33 **Guillem JG**, Puig-La Calle J Jr, Akhurst T, Tickoo S, Ruo L, Minsky BD, Gollub MJ, Klimstra DS, Mazumdar M, Paty PB, Macapinlac H, Yeung H, Saltz L, Finn RD, Erdi Y, Humm J, Cohen AM, Larson S. Prospective assessment of primary rectal cancer response to preoperative radiation and chemotherapy using 18-fluorodeoxyglucose positron emission tomography. *Dis Colon Rectum* 2000; **43**: 18-24
34 **Saw RP**, Morgan M, Koorey D, Painter D, Findlay M, Stevens G, Clarke S, Chapuis P, Solomon MJ. p53, deleted in colorectal cancer gene, and thymidylate synthase as predictors of histopathologic response and survival in low, locally advanced rectal cancer treated with preoperative adjuvant therapy. *Dis Colon Rectum* 2003; **46**: 192-202
35 **Gambacorta MA**, Valentini V, Morganti AG, Mantini G, Micciche F, Ratto C, Di Miceli D, Rotondi F, Alfieri S, Doglietto GB, Vargas JG, De Paoli A, Rossi C, Cellini N. Chemoradiation with raltitrexed (Tomudex) in preoperative treatment of stage II-III resectable rectal cancer: a phase II study. *Int J Radiat Oncol Biol Phys* 2004; **60**: 130-138
36 **Valentini V**, Coco C, Cellini N, Picciocchi A, Fares MC, Rosetto ME, Mantini G, Morganti AG, Barbaro B, Cogliandolo S, Nuzzo G, Tedesco M, Ambesi-Impiombato F, Cosimelli M, Rotman M. Ten years of preoperative chemoradiation for extraperitoneal T3 rectal cancer: acute toxicity, tumor response, and sphincter preservation in three consecutive studies. *Int J Radiat Oncol Biol Phys* 2001; **51**: 371-383
37 **Pucciarelli S**, Toppan P, Friso ML, Russo V, Pasetto L, Urso E, Marino F, Ambrosi A, Lise M. Complete pathologic response following preoperative chemoradiation therapy for middle to lower rectal cancer is not a prognostic factor for a better outcome. *Dis Colon Rectum* 2004; **47**: 1798-1807
38 **Ryan R**, Gibbons D, Hyland JM, Treanor D, White A, Mulcahy HE, O'Donoghue DP, Moriarty M, Fennelly D, Sheahan K. Pathological response following long-course neoadjuvant chemoradiotherapy for locally advanced rectal cancer. *Histopathology* 2005; **47**: 141-146
39 **Wheeler JM**, Dodds E, Warren BF, Cunningham C, George BD, Jones AC, Mortensen NJ. Preoperative chemoradiotherapy and total mesorectal excision surgery for locally advanced rectal cancer: correlation with rectal cancer regression grade. *Dis Colon Rectum* 2004; **47**: 2025-2031
40 **Rodel C**, Martus P, Papadoupolos T, Fuzesi L, Klimpfinger M, Fietkau R, Liersch T, Hohenberger W, Raab R, Sauer R, Wittekind C. Prognostic significance of tumor regression after preoperative chemoradiotherapy for rectal cancer. *J Clin Oncol* 2005; **23**: 8688-8696
41 **Kim DW**, Kim DY, Kim TH, Jung KH, Chang HJ, Sohn DK, Lim SB, Choi HS, Jeong SY, Park JG. Is T classification still correlated with lymph node status after preoperative chemoradiotherapy for rectal cancer? *Cancer* 2006; **106**: 1694-1700
42 **Compton CC**. Updated protocol for the examination of specimens from patients with carcinomas of the colon and rectum, excluding carcinoid tumors, lymphomas, sarcomas, and tumors of the vermiform appendix: a basis for checklists. Cancer Committee. *Arch Pathol Lab Med* 2000; **124**: 1016-1025
43 **Compton CC**, Fielding LP, Burgart LJ, Conley B, Cooper HS, Hamilton SR, Hammond ME, Henson DE, Hutter RV, Nagle RB, Nielsen ML, Sargent DJ, Taylor CR, Welton M, Willett C. Prognostic factors in colorectal cancer. College of American Pathologists Consensus Statement 1999. *Arch Pathol Lab Med* 2000; **124**: 979-994
44 **Nagtegaal ID**, Marijnen CA, Kranenbarg EK, Mulder-Stapel A, Hermans J, van de Velde CJ, van Krieken JH. Short-term preoperative radiotherapy interferes with the determination of pathological parameters in rectal cancer. *J Pathol* 2002; **197**: 20-27
45 **Marijnen CA**, Nagtegaal ID, Klein Kranenbarg E, Hermans J, van de Velde CJ, Leer JW, van Krieken JH. No downstaging after short-term preoperative radiotherapy in rectal cancer patients. *J Clin Oncol* 2001; **19**: 1976-1984
46 **Garcia-Aguilar J**, Hernandez de Anda E, Sirivongs P, Lee SH, Madoff RD, Rothenberger DA. A pathologic complete response to preoperative chemoradiation is associated with lower local recurrence and improved survival in rectal cancer patients treated by mesorectal excision. *Dis Colon Rectum* 2003; **46**: 298-304
47 **Meade PG**, Blatchford GJ, Thorson AG, Christensen MA, Ternent CA. Preoperative chemoradiation downstages locally advanced ultrasound-staged rectal cancer. *Am J Surg* 1995; **170**: 609-612; discussion 612-613
48 **Kaminsky-Forrett MC**, Conroy T, Luporsi E, Peiffert D, Lapeyre M, Boissel P, Guillemin F, Bey P. Prognostic implications of downstaging following preoperative radiation therapy for operable T3-T4 rectal cancer. *Int J Radiat Oncol Biol Phys* 1998; **42**: 935-941
49 **Janjan NA**, Khoo VS, Abbruzzese J, Pazdur R, Dubrow R, Cleary KR, Allen PK, Lynch PM, Glober G, Wolff R, Rich TA, Skibber J. Tumor downstaging and sphincter preservation with preoperative chemoradiation in locally advanced rectal cancer: the M. D. Anderson Cancer Center experience. *Int J Radiat Oncol Biol Phys* 1999; **44**: 1027-1038
50 **Read TE**, Andujar JE, Caushaj PF, Johnston DR, Dietz DW, Myerson RJ, Fleshman JW, Birnbaum EH, Mutch MG, Kodner IJ. Neoadjuvant therapy for rectal cancer: histologic response of the primary tumor predicts nodal status. *Dis Colon Rectum* 2004; **47**: 825-831
51 **Moutardier V**, Tardat E, Giovannini M, Lelong B, Guiramand J, Magnin V, Houvenaeghel G, Delpero JR. Long-term results of preoperative radiotherapy for 113 cases of UT3 and UT4 rectal cancer: a need for long-term follow-up. *Dis Colon Rectum* 2003; **46**: 1194-1199
52 **Lopez-Crapez E**, Bibeau F, Thezenas S, Ychou M, Simony-Lafontaine J, Thirion A, Azria D, Grenier J, Senesse P. p53 status and response to radiotherapy in rectal cancer: a prospective multilevel analysis. *Br J Cancer* 2005; **92**: 2114-2121
53 **Graf W**, Dahlberg M, Osman MM, Holmberg L, Pahlman L, Glimelius B. Short-term preoperative radiotherapy results in down-staging of rectal cancer: a study of 1316 patients. *Radiother Oncol* 1997; **43**: 133-137
54 **Wijesuriya RE**, Deen KI, Hewavisenthi J, Balawardana J, Perera M. Neoadjuvant therapy for rectal cancer down-stages the tumor but reduces lymph node harvest significantly. *Surg Today* 2005; **35**: 442-445
55 **Joseph NE**, Sigurdson ER, Hanlon AL, Wang H, Mayer RJ, MacDonald JS, Catalano PJ, Haller DG. Accuracy of determining nodal negativity in colorectal cancer on the basis of the number of nodes retrieved on resection. *Ann Surg Oncol* 2003; **10**: 213-218
56 **Bilchik A**. More (nodes) + more (analysis) = less (mortality): challenging the therapeutic equation for early-stage colon cancer. *Ann Surg Oncol* 2003; **10**: 203-205
57 **Brown CL**, Ternent CA, Thorson AG, Christensen MA, Blatchford GJ, Shashidharan M, Haynatzki GR. Response to preoperative chemoradiation in stage II and III rectal cancer. *Dis Colon Rectum* 2003; **46**: 1189-1193
58 **Zmora O**, Dasilva GM, Gurland B, Pfeffer R, Koller M, Nogueras JJ, Wexner SD. Does rectal wall tumor eradication with preoperative chemoradiation permit a change in the operative strategy? *Dis Colon Rectum* 2004; **47**: 1607-1612
59 **Guillem JG**, Chessin DB, Cohen AM, Shia J, Mazumdar M, Enker W, Paty PB, Weiser MR, Klimstra D, Saltz L, Minsky BD, Wong WD. Long-term oncologic outcome following preoperative combined modality therapy and total mesorectal excision of locally advanced rectal cancer. *Ann Surg* 2005; **241**: 829-836; discussion 836-838
60 **Mohiuddin M**, Regine WF, John WJ, Hagihara PF, McGrath PC, Kenady DE, Marks G. Preoperative chemoradiation in fixed distal rectal cancer: dose time factors for pathological complete response. *Int J Radiat Oncol Biol Phys* 2000; **46**: 883-888
61 **Hiotis SP**, Weber SM, Cohen AM, Minsky BD, Paty PB, Guillem JG, Wagman R, Saltz LB, Wong WD. Assessing the

predictive value of clinical complete response to neoadjuvant therapy for rectal cancer: an analysis of 488 patients. *J Am Coll Surg* 2002; **194**: 131-135; discussion 135-136

62 **Miller AB**, Hoogstraten B, Staquet M, Winkler A. Reporting results of cancer treatment. *Cancer* 1981; **47**: 207-214

63 **Francois Y**, Nemoz CJ, Baulieux J, Vignal J, Grandjean JP, Partensky C, Souquet JC, Adeleine P, Gerard JP. Influence of the interval between preoperative radiation therapy and surgery on downstaging and on the rate of sphincter-sparing surgery for rectal cancer: the Lyon R90-01 randomized trial. *J Clin Oncol* 1999; **17**: 2396

64 **Bujko K**, Nowacki MP, Nasierowska-Guttmejer A, Kepca L, Winkler-Spytkowska B, Suwinski R, Oledzki J, Stryczynska G, Weiczorak A, Serkies K, Rogowska D, Tokar P. Prediction of mesorectal nodal metastases after chemoradiation for rectal cancer: results of a randomised trial: implication for subsequent local excision. *Radiother Oncol* 2005; **76**: 234-240

65 **Kim CJ**, Yeatman TJ, Coppola D, Trotti A, Williams B, Barthel JS, Dinwoodie W, Karl RC, Marcet J. Local excision of T2 and T3 rectal cancers after downstaging chemoradiation. *Ann Surg* 2001; **234**: 352-358; discussion 358-359

66 **Schell SR**, Zlotecki RA, Mendenhall WM, Marsh RW, Vauthey JN, Copeland EM 3rd. Transanal excision of locally advanced rectal cancers downstaged using neoadjuvant chemoradiotherapy. *J Am Coll Surg* 2002; **194**: 584-590; discussion 590-591

67 **Bujko K**, Nowacki MP, Nasierowska-Guttmejer A, Michalski W, Bebenek M, Pudelko M, Kryj M, Oledzki J, Szmeja J, Sluszniak J, Serkies K, Kladny J, Pamucka M, Kukolowicz P. Sphincter preservation following preoperative radiotherapy for rectal cancer: report of a randomised trial comparing short-term radiotherapy vs. conventionally fractionated radiochemotherapy. *Radiother Oncol* 2004; **72**: 15-24

68 **Hahnloser D**, Wolff BG, Larson DW, Ping J, Nivatvongs S. Immediate radical resection after local excision of rectal cancer: an oncologic compromise? *Dis Colon Rectum* 2005; **48**: 429-437

69 **Kahn H**, Alexander A, Rakinic J, Nagle D, Fry R. Preoperative staging of irradiated rectal cancers using digital rectal examination, computed tomography, endorectal ultrasound, and magnetic resonance imaging does not accurately predict T0,N0 pathology. *Dis Colon Rectum* 1997; **40**: 140-144

70 **Gavioli M**, Bagni A, Piccagli I, Fundaro S, Natalini G. Usefulness of endorectal ultrasound after preoperative radiotherapy in rectal cancer: comparison between sonographic and histopathologic changes. *Dis Colon Rectum* 2000; **43**: 1075-1083

71 **Kim YH**, Kim DY, Kim TH, Jung KH, Chang HJ, Jeong SY, Sohn DK, Choi HS, Ahn JB, Kim DH, Lim SB, Lee JS, Park JG. Usefulness of magnetic resonance volumetric evaluation in predicting response to preoperative concurrent chemoradiotherapy in patients with resectable rectal cancer. *Int J Radiat Oncol Biol Phys* 2005; **62**: 761-768

72 **Katz MS**, Minsky BD, Saltz LB, Riedel E, Chessin DB, Guillem JG. Association of statin use with a pathologic complete response to neoadjuvant chemoradiation for rectal cancer. *Int J Radiat Oncol Biol Phys* 2005; **62**: 1363-1370

73 **Henri M**, Latulippe JF, Heyen F, Dube S. Complete pathologic response after chemoradiation for rectal cancer. *Dis Colon Rectum* 2005; **48**: 1097-1098 ; author reply 1098

74 **Nagtegaal I**, Gaspar C, Marijnen C, Van De Velde C, Fodde R, Van Krieken H. Morphological changes in tumour type after radiotherapy are accompanied by changes in gene expression profile but not in clinical behaviour. *J Pathol* 2004; **204**: 183-192

75 **Suzuki T**, Sadahiro S, Fukasawa M, Ishikawa K, Kamijo A, Yasuda S, Makuuchi H, Ohizumi Y, Murayama C. Predictive factors of tumor shrinkage and histological regression in patients who received preoperative radiotherapy for rectal cancer. *Jpn J Clin Oncol* 2004; **34**: 740-746

S- Editor Wang GP **L- Editor** Alpini GD **E- Editor** Ma WH

PO Box 2345, Beijing 100023, China
www.wjgnet.com
wjg@wjgnet.com

World J Gastroenterol 2007 January 28; 13(4): 525-531
World Journal of Gastroenterology ISSN 1007-9327

Sequential algorithms combining non-invasive markers and biopsy for the assessment of liver fibrosis in chronic hepatitis B

Giada Sebastiani, Alessandro Vario, Maria Guido, Alfredo Alberti

Giada Sebastiani, Alessandro Vario, Alfredo Alberti, Department of Clinical and Experimental Medicine, University of Padova, Padova, Italy
Maria Guido, Department of Oncological and Surgical Sciences, University of Padova, Padova, Italy
Correspondence to: Professor Alfredo Alberti, Department of Clinical and Experimental Medicine, Via Giustiniani 2, University of Padova, Padova 35100, Italy. alfredo_alberti@tin.it
Telephone: +39-49-8212294 Fax: +39-49-8211826
Received: 2006-10-01 Accepted: 2006-12-11

Key words: Chronic hepatitis B; Hepatic fibrosis; Liver biopsy; Non-invasive markers; Stepwise combination algorithms

Sebastiani G, Vario A, Guido M, Alberti A. Sequential algorithms combining non-invasive markers and biopsy for the assessment of liver fibrosis in chronic hepatitis B. *World J Gastroenterol* 2007; 13(4): 525-531

http://www.wjgnet.com/1007-9327/13/525.asp

Abstract

AIM: To assess the performance of several non-invasive markers and of our recently proposed stepwise combination algorithms to diagnose significant fibrosis (F $\geqslant$ 2 by METAVIR) and cirrhosis (F4 by METAVIR) in chronic hepatitis B (CHB).

METHODS: One hundred and ten consecutive patients (80 males, 30 females, mean age: 42.6 ± 11.3) with CHB undergoing diagnostic liver biopsy were included. AST-to-Platelet ratio (APRI), Forns' index, AST-to-ALT Ratio, Goteborg University Cirrhosis Index (GUCI), Hui's model and Fibrotest were measured on the day of liver biopsy. The performance of these methods and of sequential algorithms combining Fibrotest, APRI and biopsy was defined by positive (PPV) and negative (NPV) predictive values, accuracy and area under the curve (AUC).

RESULTS: PPV for significant fibrosis was excellent (100%) with Forns and high (> 92%) with APRI, GUCI, Fibrotest and Hui. However, significant fibrosis could not be excluded by any marker (NPV < 65%). Fibrotest had the best PPV and NPV for cirrhosis (87% and 90%, respectively). Fibrotest showed the best AUC for both significant fibrosis and cirrhosis (0.85 and 0.76, respectively). Stepwise combination algorithms of APRI, Fibrotest and biopsy showed excellent performance (0.96 AUC, 100% NPV) for significant fibrosis and 0.95 AUC, 98% NPV for cirrhosis, with 50%-80% reduced need for liver biopsy.

CONCLUSION: In CHB sequential combination of APRI, Fibrotest and liver biopsy greatly improves the diagnostic performance of the single non-invasive markers. Need for liver biopsy is reduced by 50%-80% but cannot be completely avoided. Non-invasive markers and biopsy should be considered as agonists and not antagonists towards the common goal of estimating liver fibrosis.

INTRODUCTION

Chronic hepatitis B (CHB) remains a serious global health concern. Approximately 350 million people are chronically infected, and 500 000 to 1.2 million deaths per year are attributed to HBV-associated complications[1]. Among patients with active viral replication, cirrhosis will develop in 15 to 20 percent within five years[2]. For patients with cirrhosis, acute exacerbation can occur and the disease may progress to end stage complications[2]. The histopathological pathway of progressive liver disease is characterised by the formation and accumulation of fibrosis, leading to increasing distortion of the hepatic architecture, that is the hallmark of evolution to cirrhosis. Liver fibrosis is the result of chronic injury and plays a direct role in the pathogenesis of hepatocellular dysfunction and portal hypertension. Current guidelines recommend that patients with HBV-DNA > 10^5 copies/mL and persistent or intermittent elevation in aminotrasferase levels should be evaluated further with liver biopsy, that is the gold standard for the assessment of fibrosis[3]. This procedure provides information on the severity of necroinflammatory activity and on the stage of fibrosis, features which are essential for estimating prognosis and the need for antiviral therapy[2,4,5]. However, biopsy is a costly procedure associated with side effects and some risks[6-8]. It also has limitations in underestimating liver fibrosis with small samples and is prone to intra- and inter-observer variation[9-12]. Moreover, several studies suggested that liver biopsy is far away from being a perfect gold standard since its performance is size-dependent[9,13-14]. Some studies would suggest that an adequate liver biopsy sample should contain more than 5 portal tracts and be at least 15 mm in length[11,15,16]. In a critical review of the literature concerning the use of liver biopsy in chronic viral hepatitis,

Guido and Rugge suggest that in an era of evidence-based medicine the use and interpretation of liver biopsy is very often flawed by unacceptable methodological limits and that a biopsy sample of 20 mm or more containing at least 11 complete portal tracts should be considered reliable for adequate grading and staging[14]. Other authors have recommended even bigger samples[17]. The pathologist need for obtaining a liver sample of adequate size is in contrast with the patient's need of a procedure causing limited pain and with the clinician's need of a safe procedure. A French survey which interviewed 1177 general practitioners concluded that liver biopsy may be refused by up to 59% of patients with chronic hepatitis C and that 22% of the physicians share the same concern regarding this invasive procedure[18]. In this regard, a recent survey assessing the consensus among Italian hepatologists on when and how to take a liver biopsy in chronic hepatitis C showed great divergence in the management of the same subgroup of patients[19]. Considering these limitations and patient reluctance to undergo liver biopsy, a great interest and many studies have been recently dedicated to the development of non-invasive markers as surrogates of liver biopsy. Most of the studies on non-invasive markers of liver fibrosis have been conducted in chronic hepatitis C and few data are available on the applicability of this approach to patients with CHB. Several markers have been described with variable diagnostic accuracy in hepatitis C, but the expected rate of misdiagnosis for each single test is still around 20%[11,20]. To overcome this limitation, recently we have developed and validated sequential algorithms that combine non-invasive markers with liver biopsy[21]. This approach allowed us to reach excellent diagnostic accuracy (> 95%) for both significant fibrosis and cirrhosis in patients with chronic hepatitis C with around 50%-70% reduced need of taking a liver biopsy. We have now assessed the performance of several non-invasive markers and of our stepwise algorithms in patients with CHB.

MATERIALS AND METHODS

Patients

This study included 110 consecutive patients with a diagnosis of chronic HBV infection, as defined by positive hepatitis B surface (HBsAg) for at least 6 mo, who underwent a diagnostic percutaneous liver biopsy at the Department of Clinical and Experimental Medicine at the University of Padova between March 2003 and June 2005. All patients were positive for serum HBV-DNA by polymerase chain reaction (PCR) and had compensated chronic HBV infection. The exclusion criteria were any other cause of chronic liver disease, and clinical signs of liver cirrhosis, co-infection with HCV or HIV and co-morbidities that could confound the results of the non-invasive markers adopted, clinical signs of liver cirrhosis. These included current alcohol intake (> 20 g/die), haemolysis, Gilbert's syndrome, and hematologic causes of thrombocytopenia. All biopsies were obtained with the 16G Menghini type needle. To limit the risk of fibrosis underestimation, patients with biopsy samples shorter than 1.5 cm or containing less than 7 portal tracts were excluded[11,15,16,22]. Informed consent was obtained from all patients participating in the study that was conducted according to the rules of the Declaration of Helsinki.

Virologic assays

HBsAg, hepatitis Be antigen (HBeAg), and antibodies to HBeAg and HDV were determined using commercial assays (Roche Diagnostics, Basel, Switzerland). HBV DNA level was measured by real-time PCR and expressed as $\log_{10}$ copies/mL.

Histological assessment

Liver biopsies were fixed in formalin and embedded in paraffin. The slides were stained with hematoxylin-eosin, van Gieson stain for collagen, PAS after diastase digestion and Perls' Prussian blue method. The slides were evaluated by a single Pathologist (MG) who was unaware of the clinical data. Fibrosis was scored according to the METAVIR system, which was previously applied in other reports on CHB[23-25]. Fibrosis was staged from F0 to F4: F0, no fibrosis; F1, portal fibrosis without septa; F2, portal fibrosis with few septa; F3, numerous septa without cirrhosis; and F4, cirrhosis. Significant fibrosis was defined as a METAVIR score of F2 or more ($F \geqslant 2$), cirrhosis was defined as a METAVIR score of F4.

Non-invasive markers of liver fibrosis

All patients were evaluated for AST-to-Platelet Ratio Index (APRI), Forns' index, AST-to-ALT ratio (AAR), Hui's model, Goteborg University Cirrhosis Index (GUCI), Fibrotest. The rationale for the choice of the non-invasive markers was their simplicity together with a reported good performance for APRI, Forns' index, AAR and GUCI, and the high number of validation studies reported together with a good performance for Fibrotest[26-30]. Hui's model, based on a combination of body mass index, total bilirubin, platelets and albumin, was chosen since it is the only non-invasive marker developed in patients with hepatitis B[31]. The markers were all calculated using fasting serum samples obtained on the same day of liver biopsy. For this purpose platelet count, aspartate aminotransferase (AST), alanine aminotransferase (ALT), gamma-glutamiltranspeptidase (γGT), cholesterol levels, haptoglobin, apolipoprotein A1, alpha-2-macroglobulin, total bilirubin, prothrombin time (international normalised ratio, INR), albumin were routinely determined using validated methods. Fibrotest results were kindly provided by T. Poynard, Universite Paris VI, Paris, France. For all the non invasive methods the cut-off values indicated in the original reports were applied[26-31].

Stepwise combination algorithms for liver fibrosis

The algorithms recently developed by us for patient with chronic hepatitis C were applied to this cohort of hepatitis B patients. The diagnostic algorithms were developed by modelling the best algorithm for liver fibrosis in different clinical scenarios, as described in a previous study[21]. Algorithm A (for significant fibrosis, $F \geqslant 2$ by METAVIR) and algorithm B (for cirrhosis, F4 by METAVIR) are described in Figure 1A and B.

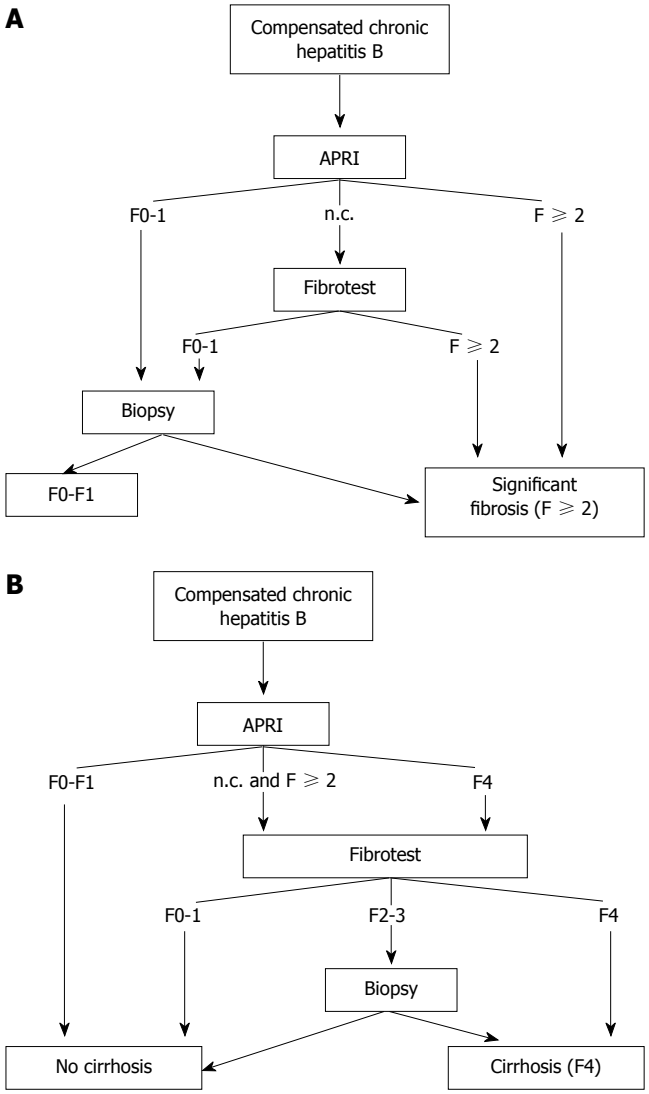

Figure 1 **A**: Algorithm A for detection of significant fibrosis (F ⩾ 2 by METAVIR) in HBV patients. F0-1 by APRI is intended as APRI < 0.5. F ⩾ 2 by APRI is intended as APRI > 1.5. n.c. by APRI is intended as APRI > 0.5 and < 1.5; **B**: Algorithm B for detection of cirrhosis (F4 by METAVIR) in HBV patients. F0-1 by APRI is intended as APRI < 0.5. F ⩾ 2 by APRI is intended as APRI > 1.5. F4 by APRI is intended as APRI ⩾ 2. n.c. by APRI is intended as APRI > 0.5 and < 1.5.

Statistical analysis

The primary endpoints were the detection of significant fibrosis (F ⩾ 2) and cirrhosis (F4). These thresholds were selected since the first is generally considered an indication for antiviral therapy and the second requires a specific management and follow-up. Descriptive results were expressed as mean ± standard deviation (SD) or number (percentage) of patients with a condition. Kappa statistics was used to measure intra-observer variation in the histopathological evaluation of the degree of fibrosis. The performance of the non-invasive methods for liver fibrosis was measured as sensitivity, specificity, positive predictive value (PPV), negative predictive value (NPV), accuracy, and likelihood ratios (LR). Sensitivity, specificity, PPV, NPV and accuracy were expressed as percentage. The diagnostic value of the non-invasive methods was expressed using the Area Under the receiver operating characteristic Curve (AUC) and its corresponding 95% confidence intervals (CI).

Table 1 Demographic, laboratory and histological characteristics of the 110 patients with chronic hepatitis B

Males *n* (%)	80 (72.7)
Age (mean yr ± SD)	42.6 ± 11.3
BMI (kg/m^2)	24.2 ± 3.3
AST (mean IU/L ± SD)	73.4 ± 61.2
AST / ULN ratio (mean ± SD)	1.75 ± 1.47
ALT (mean IU/L ± SD)	144.5 ± 148.0
ALT / ULN ratio (mean ± SD)	3.14 ± 3.3
γGT (mean IU/L ± SD)	46.4 ± 49.1
γGT / ULN ratio (mean ± SD)	0.81 ± 0.84
Bilirubin (mean μmol/L ± SD)	13.9 ± 6.48
PLT (mean 10^9/L ± SD)	194.6 ± 56.9
Albumin (mean g/L ± SD)	42.7 ± 5
Cholesterol (mean mg/dL ± SD)	177.5 ± 32.9
INR (mean value ± SD)	1.12 ± 0.1
Haptoglobin (mean g/L ± SD)	1.05 ± 0.6
α_2M (mean g/L ± SD)	2.67 ± 0.84
ApoA1 (mean g/L ± SD)	1.48 ± 6.48
Viral load (mean log$_{10}$ cp/mL ± SD)	2.15 ± 1.18
HBeAg positive cases (%)	20 (18.2)
HDV co-infected cases (%)	8 (7.3)
Staging *n* (%)	
F0	15 (13.6)
F1	20 (18.2)
F2	40 (36.4)
F3	13 (11.8)
F4	22 (20.0)

SD: standard deviation; ULN: upper limits of normal;PLT: platelets; INR: international normalised ratio; α_2M: alpha-2-macroglobulin; ApoA1: apolipoprotein A1.

RESULTS

Demographic, laboratory and histological features of the 110 patients with CHB are described in Table 1. Mean age was 42.6 ± 11.3 years and 80 patients (72.7%) were males. Twenty cases (18.2%) were HBeAg positive and 8 cases (7.3%) were co-infected with HDV. Prevalence of significant fibrosis (F ⩾ 2) and cirrhosis was 68.2% and 20%, respectively. The mean length of liver specimens was 1.69 ± 0.29 cm and mean complete portal tracts number was 9.9 ± 3.6. Intra-observer agreement was assessed by re-evaluating a subset of 50 randomly chosen samples: k value was higher than 0.90.

Performance of non-invasive methods for the diagnosis of significant fibrosis (F ⩾ 2)

Seventy-five patients (68.2%) had significant fibrosis as defined by METAVIR fibrosis stage F ⩾ 2. The performance of the non-invasive markers in diagnosing significant fibrosis is shown in Table 2. AAR was not included here since it identifies cirrhosis but does not discriminate significant fibrosis. Fibrotest, GUCI and Hui' s model classified all cases while both APRI and Forns' index were unable to classify one third of the patients. All the methods showed high PPV (> 90%) for significant fibrosis. Forns' index had an excellent 100% PPV with a 6.9 cut-off but its diagnostic value was quite low, at 0.63 AUC (95% CI: 0.50-0.76). The NPV was quite low for all the non-invasive markers (always < 65%), so that significant fibrosis could not be reliably excluded by any of these markers. Fibrotest, APRI and GUCI showed good overall

Table 2 Performance of the non-invasive methods and of the algorithm A in detecting significant fibrosis (≥ F2 by METAVIR) in patients with CHB

	Fibrotest	Forns		APRI		GUCI	Hui's model	Algorithm A
Classified cases (%)	100	63.3		66.2		100	100	100
Cut-off	F2	4.2	6.9	0.5	1.5	0.2	0.15	na
Sensitivity (%)	80.8	58.3	14.6	70.8	27.1	66.7	50	100
Specificity (%)	90	78.3	100	87	95.7	95.7	90.9	91.3
PPV (%)	95.5	90.6	100	94.1	97.9	97.9	96.3	96
NPV (%)	64.3	53.5	35.9	62.2	39.7	58.9	45.8	100
LR +	8.1	2.69	0.146	5.45	6.3	15.5	5.49	11.49
LR -	0.21	0.53	0.85	0.36	0.76	0.35	0.55	0
Accuracy (%)	83.3	64.8	42.3	76.1	49.3	76.1	62.2	97.2
AUC (95% CI)	0.85 (0.75-0.95)	0.63 (0.50-0.76)		0.72 (0.58-0.86)		0.81 (0.70-0.92)	0.71 (0.56-0.86)	0.96 (0.92-1)

APRI: aspartate aminotransferase to platelets ratio; GUCI: Goteborg University Cirrhosis Index; na: not available; PPV: positive predictive value; NPV: negative predictive value; LR+: positive likelihood ratio; LR-: negative likelihood ratio; AUC: area under the curve; CI: confidence interval.

Table 3 Performance of the non-invasive methods and of the algorithm B in detecting cirrhosis (F4 by METAVIR) in patients with CHB

	Fibrotest	APRI	AAR	GUCI	Algorithm B
Classified cases (%)	100	66.2	100	100	100
Cut-off	F4	2	1	1	na
Sensitivity (%)	55.6	42.9	7.1	21.4	92.9
Specificity (%)	96.3	85.4	94.7	91.2	96.5
PPV (%)	90	53.8	82.4	73.7	87.5
NPV (%)	87.1	91.1	81.4	83.8	98.3
LR +	15	2.94	1.34	2.43	26.5
LR -	0.46	0.67	0.98	0.86	0.07
Accuracy (%)	86.1	79.2	77.5	77.5	95.8
AUC (95% CI)	0.76 (0.67-0.85)	0.64 (0.53-0.75)	0.51 (0.39-0.62)	0.56 (0.47-0.65)	0.95 (0.90-1)

accuracy (83.3%, 76.1% and 76.1% respectively). Among the non-invasive methods, Fibrotest showed the best diagnostic value as indicated by an AUC of 0.85 (95% CI: 0.75-0.95).

Performance of non-invasive methods for the diagnosis of cirrhosis (F4)

Twenty-two patients (20%) had cirrhosis as defined by METAVIR fibrosis stage F4. The performance of the non-invasive markers in diagnosing cirrhosis is shown in Table 3. Forns' index and Hui's model were not considered here since they do not discriminate between significant fibrosis and cirrhosis. Fibrotest had the best PPV (90%) and very good accuracy (86.1%). The overall diagnostic value of Fibrotest was quite good, with 0.76 AUC (95% CI: 0.67-0.85). APRI showed good NPV and accuracy but the diagnostic value, described by AUC, was rather low (0.64; 95% CI: 0.53-0.75). The other markers showed an even lower diagnostic value, with AUCs around 0.5.

Performance of stepwise algorithms for the diagnosis of significant fibrosis and cirrhosis

The performance of stepwise algorithms for the detection of significant fibrosis (algorithm A) and cirrhosis (algorithm B) is reported in Tables 2 and 3, respectively. Table 4 describes in details the number of tests and of liver biopsies needed when the two algorithms were applied to our cohort of patients with CHB. The stepwise algorithm for significant fibrosis (algorithm A) excluded the presence of F ≥ 2 by METAVIR with excellent 100% NPV. It also showed a very high accuracy, with excellent 97.2%, and it presented with an excellent diagnostic value, with 0.96 AUC (95% CI: 0.92-1). This algorithm permitted avoidance of liver biopsy in about half of the cases (Table 4). Algorithm B showed excellent 95.8% accuracy and 0.95 AUC (95% CI: 0.90-1) in the identification of cirrhosis. Furthermore, this algorithm reduced by more than 80% the need for liver biopsy (Table 4).

DISCUSSION

Several non-invasive markers of liver fibrosis have been recently described, mainly in patients with hepatitis C, but their implementation in clinical practice as a substitute for invasive liver biopsy has been delayed by lack of adequate accuracy in assessing individual patients. Indeed, according to the most recent International Guidelines and Recommendations, inter-laboratory variability, lack of reproducibility and, most important, an expected rate of misdiagnosis of at least 20% do not yet allow the use of these methods in clinical practice[11,32]. Since the diagnostic performance of described non-invasive markers is variable depending on the stage of fibrosis and other patient characteristics, they can be used to reduce rather than completely substitute the need for liver biopsy. Recently we have described stepwise combination algorithms based on

the use of two non-invasive markers (APRI and Fibrotest) and liver biopsy[16]. When applied to patients with chronic hepatitis C these algorithms were proven to correctly identify significant fibrosis and cirrhosis with high (> 95%) accuracy and 50%-70% reduction in liver biopsy. Very few studies have investigated the role of non-invasive markers of liver fibrosis in hepatitis B. Indeed, significant differences exist between CHB and chronic HCV infection in natural history, laboratory parameters, liver histology and associated comorbidities. For example, elevated ALT reflects accurately the necroinflammatory activity of CHB and is used as one of the criteria for antiviral therapy while the same could not be applied to hepatitis C[3]. Steatosis is an important feature of chronic HCV infection while its role in CHB is unclear[33]. The association of diabetes mellitus with chronic hepatitis C has not been found in CHB[34]. Since CHB has specific pathogenetic mechanisms and is associated strongly with liver disease, the results of the studies on hepatitis C cannot be directly transferred to hepatitis B and a dedicated validation of the markers should be provided. The latest AASLD guidelines on management of chronic hepatitis B recommend that patients with HBV-DNA > 10^5 copies/ml and persistent or intermittent elevation in transaminase levels should be evaluated further with liver biopsy[3]. Moreover, prior to consider of antiviral treatment, liver biopsy is still recommended. Assessment of the stage of liver disease is indeed fundamental for treatment decision in any patient presenting with compensated chronic HBV infection. The available evidences suggest that non-invasive markers of liver fibrosis in hepatitis B present with a similar accuracy to hepatitis C. Lebensztejn *et al*[35] assessed the value of some non-invasive markers of liver fibrosis in few children with chronic hepatitis B and found that a combination of hyaluronan and laminin had 0.84 AUC. Hui and colleagues developed a predictive model based on body mass index and three routine laboratory tests, which showed 0.79 AUC[31]. Two recent reports applied Fibrotest in CHB showing 0.77 and 0.78 AUC for detection of significant fibrosis and cirrhosis, respectively[24,25]. Our results, based on an independent application of Fibrotest to CHB patients, showed an accuracy that is similar to that reported by Poynard's group. A very recent study by Zeng *et al*[36] proposed a non-invasive combination model based on alpha-2-macroglobulin, hyaluronan, age and γGT and it showed an AUC between 0.77 and 0.84. For all these markers, the expected rate of misdiagnosis was around 20%, thus similar to that reported for hepatitis C which is considered not satisfactory by many clinicians. Very recently the use of "proteome" technology has been introduced in studying liver fibrosis. In 46 patients with chronic hepatitis B, 30 features predictive of significant fibrosis and cirrhosis were identified. The AUC for this analysis was very promising, being 0.906 and 0.921 for advanced fibrosis and cirrhosis, respectively[37]. However, this is a quite complicated method that might not be available for large scale testing. Moreover, the excellent performance reported in that preliminary study should be confirmed by others. In our study we found that Fibrotest had the best performance when compared to other non-invasive methods. However, none of the investigated non-invasive markers of liver fibrosis had adequate accuracy for universal use in substitution of liver biopsy, the expected rate of misdiagnosis being 15%-35% for significant fibrosis and 25%-45% for cirrhosis. On the other hand, when APRI and Fibrotest were combined with liver biopsy in sequential algorithms, we could reach > 95% accuracy for detecting significant fibrosis or cirrhosis, with a 50%-80% reduced need for liver biopsy, as already described previously in patients with compensated chronic hepatitis C. With this approach, the number of liver biopsies needed decreased especially for the patients at higher risk of cirrhosis and this appears particularly important since the risk of liver biopsy complications is increased in cirrhotic cases. The overall cost of these algorithms appears favourable compared to universal use of liver biopsy. Indeed, for a cohort of one hundred patients algorithm A requires 100 APRIs, 34 Fibrotests and 52 biopsies while algorithm B requires 100 APRIs, 52 Fibrotests and 19 biopsies (Table 4). A cost-benefit analysis indicates that in the US a liver biopsy costs 1032 USD, which increases to 2745 USD when a complication occurs[8]. Fibrotest-Fibrosure is a commercialised method with a cost of around 90 euros (Biopredictive, Houilles, France). According to these values, algorithm A and algorithm B would result in a 50% and 75% reduction in cost compared to liver biopsy, respectively.

Table 4 Features of clinical interest of stepwise algorithms in chronic hepatitis B

	Algorithm A	Algorithm B
Saved biopsies (%)	48	81
APRI performed (%)	100	100
Fibrotest performed (%)	34	52
Under-diagnosed and unclassified (%)	0	0
Over-diagnosed (%)	3	3

Algorithm A: algorithm for significant fibrosis (F ⩾ 2 by METAVIR); Algorithm B: algorithm for cirrhosis (F4 by METAVIR); APRI: aspartate aminotransferase to platelets ratio.

There are some limitations in our study. This was in fact a retrospective study, with a quite limited number of cases. Another limitation could be in the choice of the dimension of biopsy sample. We have here included specimens of at least 1.5 cm length and containing 7 portal tracts on the basis of the recommendations of some authors[11,15,16,22]. However, several observations from the pathologists would suggest even bigger samples for a correct staging of liver fibrosis[13,14,17]. Finally, recent criticisms suggested that liver biopsy is not a perfect gold standard for fibrosis evaluation due to its large variability (sampling error plus observer error). Indeed, Bedossa *et al*[13] indicated that biopsy is an estimate of liver fibrosis which, when compared with the whole liver, showed a coefficient of variation greater than 40% with length greater than 15 mm with 80% accuracy.

In conclusion, this study suggests that in hepatitis B currently available non-invasive tests do not show a diagnostic performance that would be considered adequate by many clinicians. However, their stepwise combined use can be most useful to reduce the need for liver biopsy

without loosing diagnostic accuracy. In this respect liver biopsy and non-invasive markers should be considered as agonists and not as antagonists towards the common goal of correctly classifying the stage of liver fibrosis. Priority should be given to large scale validation studies of these algorithms in different patient populations inclusive of all major etiologies of chronic liver disease and most frequent cofactors, which may affect the diagnostic performance of fibrosis markers.

COMMENTS

Background

Non-invasive markers of liver fibrosis have been recently proposed as substitutes for liver biopsy but their reported accuracy was around 80%. They have been mostly validated in hepatitis C while few studies have been conducted in hepatitis B. We have recently shown that stepwise combination of non-invasive markers and liver biopsy permitted to obtain excellent accuracy (> 95%) by saving 50%-70% liver biopsies in hepatitis C. We applied our method to a cohort of patients with chronic hepatitis B.

Research frontiers

Nowadays many clinicians show concerns about the role of liver biopsy in chronic viral hepatitis due to side effects, intra- and inter-observer variation and costs. Some non-invasive methods for liver fibrosis have been proposed but International Guidelines still do not recommend a routine use of the markers due to lack of reproducibility and an expected misdiagnosis rate of 20%. Thus, a trusted method that avoides a number of liver biopsies by maintaining excellent accuracy is urgently needed.

Innovations and breakthroughs

In this article we validated in hepatitis B a recently proposed method for the detection of liver fibrosis and cirrhosis in hepatitis C. This is the first sequential approach based on a first line assessment by non-invasive markers of liver fibrosis followed by liver biopsy in unclassified cases or cases in which non-invasive methods do not reach a satisfactory accuracy. The overall accuracy of this method is > 95% and it saved 50%-80% liver biopsies. This is a rational and practical way to apply non-invasive markers in hepatitis B and it introduces a new concept: non-invasive markers and liver biopsy are agonists and not antagonists towards the common goal of classifying liver fibrosis.

Applications

The most accurate non-invasive markers should be used as a first line assessment, limiting liver biopsy to the cases in whom they are unclassified or show low predictive value. For the future, priority should be given to large scale validation studies of these algorithms and the most promising non-invasive markers in different patient populations inclusive of all major etiologies of chronic liver disease and most frequent cofactors which may affect the diagnostic performance of fibrosis markers.

Terminology

(1) Fibrotest: a commercial panel of serum markers combining γGT, alpha-2-macroglobulin, haptoglobin, apolipoprotein A1, total bilirubin for the non invasive assessment of liver fibrosis. It has been extensively validated in hepatitis C. The overall accuracy of the panel is good but it combines also uncommon parameters. Only two, not independent, validation studies on hepatitis B have been so far conducted. (2) APRI: a simple test combining AST and platelet count group for the non-invasive prediction of significant fibrosis and cirrhosis in hepatitis C. It is a very simple and economic tool but it is somehow less accurate than fibrotest and it presents with a significant percentage of unclassified cases. To our knowledge, this is the first validation of APRI in an independent series of HBV patients. (3) Forns' index: an index combining, age, platelet, γGT, cholesterol for the non-invasive prediction of significant fibrosis in hepatitis C. It is a quite simple index, combining common parameters (except for cholesterol) but it showed a significant number of unclassified cases. To our knowledge, this is the first application of Forns' index to a cohort of patients with CHB. (4) GUCI: a simple index combining AST, platelets and INR. It showed good accuracy in hepatitis C for both significant fibrosis and cirrhosis. It has never been applied to HBV cases. (5) Hui's model: a panel combining albumin, BMI, total bilirubin and platelet count for the prediction of significant fibrosis. It has been developed for hepatitis B patients and no validation study has to date been conducted.

Peer review

Evaluate the applicability and prognostic value of a previously developed algorithm that includes a combination of two different serum marker tests for the detection of liver fibrosis to avoid liver biopsies in patients with chronic HBV infection. This is an excellent paper that investigates the performance of non-invasive tests for estimating liver fibrosis in patients with chronic hepatitis B. The study is timely and provides useful information.

REFERENCES

1 **Lavanchy D**. Hepatitis B virus epidemiology, disease burden, treatment, and current and emerging prevention and control measures. *J Viral Hepat* 2004; **11**: 97-107
2 **Fattovich G**, Brollo L, Giustina G, Noventa F, Pontisso P, Alberti A, Realdi G, Ruol A. Natural history and prognostic factors for chronic hepatitis type B. *Gut* 1991; **32**: 294-298
3 **Lok AS**, McMahon BJ. Chronic hepatitis B: update of recommendations. *Hepatology* 2004; **39**: 857-861
4 **Weissberg JI**, Andres LL, Smith CI, Weick S, Nichols JE, Garcia G, Robinson WS, Merigan TC, Gregory PB. Survival in chronic hepatitis B. An analysis of 379 patients. *Ann Intern Med* 1984; **101**: 613-616
5 **Lai CL**, Shouval D, Lok AS, Chang TT, Cheinquer H, Goodman Z, DeHertogh D, Wilber R, Zink RC, Cross A, Colonno R, Fernandes L. Entecavir versus lamivudine for patients with HBeAg-negative chronic hepatitis B. *N Engl J Med* 2006; **354**: 1011-1020
6 **Piccinino F**, Sagnelli E, Pasquale G, Giusti G. Complications following percutaneous liver biopsy. A multicentre retrospective study on 68,276 biopsies. *J Hepatol* 1986; **2**: 165-173
7 **Gunneson TJ**, Menon KV, Wiesner RH, Daniels JA, Hay JE, Charlton MR, Brandhagen DJ, Rosen CB, Porayko MK. Ultrasound-assisted percutaneous liver biopsy performed by a physician assistant. *Am J Gastroenterol* 2002; **97**: 1472-1475
8 **Wong JB**, Koff RS. Watchful waiting with periodic liver biopsy versus immediate empirical therapy for histologically mild chronic hepatitis C. A cost-effectiveness analysis. *Ann Intern Med* 2000; **133**: 665-675
9 **Colloredo G**, Guido M, Sonzogni A, Leandro G. Impact of liver biopsy size on histological evaluation of chronic viral hepatitis: the smaller the sample, the milder the disease. *J Hepatol* 2003; **39**: 239-244
10 **Regev A**, Berho M, Jeffers LJ, Milikowski C, Molina EG, Pyrsopoulos NT, Feng ZZ, Reddy KR, Schiff ER. Sampling error and intraobserver variation in liver biopsy in patients with chronic HCV infection. *Am J Gastroenterol* 2002; **97**: 2614-2618
11 **Afdhal NH**, Nunes D. Evaluation of liver fibrosis: a concise review. *Am J Gastroenterol* 2004; **99**: 1160-1174
12 **Rousselet MC**, Michalak S, Dupré F, Croué A, Bedossa P, Saint-André JP, Calès P. Sources of variability in histological scoring of chronic viral hepatitis. *Hepatology* 2005; **41**: 257-264
13 **Bedossa P**, Dargère D, Paradis V. Sampling variability of liver fibrosis in chronic hepatitis C. *Hepatology* 2003; **38**: 1449-1457
14 **Guido M**, Rugge M. Liver biopsy sampling in chronic viral hepatitis. *Semin Liver Dis* 2004; **24**: 89-97
15 **Hübscher SG**. Histological grading and staging in chronic hepatitis: clinical applications and problems. *J Hepatol* 1998; **29**: 1015-1022
16 **Schlichting P**, Hølund B, Poulsen H. Liver biopsy in chronic aggressive hepatitis. Diagnostic reproducibility in relation to size of specimen. *Scand J Gastroenterol* 1983; **18**: 27-32
17 **Scheuer PJ**. Liver biopsy size matters in chronic hepatitis: bigger is better. *Hepatology* 2003; **38**: 1356-1358
18 **Bonny C**, Rayssiguier R, Ughetto S, Aublet-Cuvelier B, Baranger J, Blanchet G, Delteil J, Hautefeuille P, Lapalus F, Montanier P, Bommelaer G, Abergel A. Medical practices and

expectations of general practitioners in relation to hepatitis C virus infection in the Auvergne region. *Gastroenterol Clin Biol* 2003; **27**: 1021-1025

19 **Almasio PL**, Niero M, Angioli D, Ascione A, Gullini S, Minoli G, Oprandi NC, Pinzello GB, Verme G, Andriulli A. Experts' opinions on the role of liver biopsy in HCV infection: a Delphi survey by the Italian Association of Hospital Gastroenterologists (A.I.G.O.). *J Hepatol* 2005; **43**: 381-387

20 **Sebastiani G**, Alberti A. Non invasive fibrosis biomarkers reduce but not substitute the need for liver biopsy. *World J Gastroenterol* 2006; **12**: 3682-3694

21 **Sebastiani G**, Vario A, Guido M, Noventa F, Plebani M, Pistis R, Ferrari A, Alberti A. Stepwise combination algorithms of non-invasive markers to diagnose significant fibrosis in chronic hepatitis C. *J Hepatol* 2006; **44**: 686-693

22 **Poynard T**, Munteanu M, Imbert-Bismut F, Charlotte F, Thabut D, Le Calvez S, Messous D, Thibault V, Benhamou Y, Moussalli J, Ratziu V. Prospective analysis of discordant results between biochemical markers and biopsy in patients with chronic hepatitis C. *Clin Chem* 2004; **50**: 1344-1355

23 **Intraobserver and interobserver variations in liver biopsy interpretation in patients with chronic hepatitis C**. The French METAVIR Cooperative Study Group. *Hepatology* 1994; **20**: 15-20

24 **Myers RP**, Tainturier MH, Ratziu V, Piton A, Thibault V, Imbert-Bismut F, Messous D, Charlotte F, Di Martino V, Benhamou Y, Poynard T. Prediction of liver histological lesions with biochemical markers in patients with chronic hepatitis B. *J Hepatol* 2003; **39**: 222-230

25 **Poynard T**, Zoulim F, Ratziu V, Degos F, Imbert-Bismut F, Deny P, Landais P, El Hasnaoui A, Slama A, Blin P, Thibault V, Parvaz P, Munteanu M, Trepo C. Longitudinal assessment of histology surrogate markers (FibroTest-ActiTest) during lamivudine therapy in patients with chronic hepatitis B infection. *Am J Gastroenterol* 2005; **100**: 1970-1980

26 **Wai CT**, Greenson JK, Fontana RJ, Kalbfleisch JD, Marrero JA, Conjeevaram HS, Lok AS. A simple noninvasive index can predict both significant fibrosis and cirrhosis in patients with chronic hepatitis C. *Hepatology* 2003; **38**: 518-526

27 **Forns X**, Ampurdanès S, Llovet JM, Aponte J, Quintó L, Martínez-Bauer E, Bruguera M, Sánchez-Tapias JM, Rodés J. Identification of chronic hepatitis C patients without hepatic fibrosis by a simple predictive model. *Hepatology* 2002; **36**: 986-992

28 **Imbert-Bismut F**, Ratziu V, Pieroni L, Charlotte F, Benhamou Y, Poynard T. Biochemical markers of liver fibrosis in patients with hepatitis C virus infection: a prospective study. *Lancet* 2001; **357**: 1069-1075

29 **Giannini E**, Risso D, Botta F, Chiarbonello B, Fasoli A, Malfatti F, Romagnoli P, Testa E, Ceppa P, Testa R. Validity and clinical utility of the aspartate aminotransferase-alanine aminotransferase ratio in assessing disease severity and prognosis in patients with hepatitis C virus-related chronic liver disease. *Arch Intern Med* 2003; **163**: 218-224

30 **Islam S**, Antonsson L, Westin J, Lagging M. Cirrhosis in hepatitis C virus-infected patients can be excluded using an index of standard biochemical serum markers. *Scand J Gastroenterol* 2005; **40**: 867-872

31 **Hui AY**, Chan HL, Wong VW, Liew CT, Chim AM, Chan FK, Sung JJ. Identification of chronic hepatitis B patients without significant liver fibrosis by a simple noninvasive predictive model. *Am J Gastroenterol* 2005; **100**: 616-623

32 **Strader DB**, Wright T, Thomas DL, Seeff LB. Diagnosis, management, and treatment of hepatitis C. *Hepatology* 2004; **39**: 1147-1171

33 **Lonardo A**, Adinolfi LE, Loria P, Carulli N, Ruggiero G, Day CP. Steatosis and hepatitis C virus: mechanisms and significance for hepatic and extrahepatic disease. *Gastroenterology* 2004; **126**: 586-597

34 **Lecube A, Hernández** C, Genescà J, Simó R. Glucose abnormalities in patients with hepatitis C virus infection: Epidemiology and pathogenesis. *Diabetes Care* 2006; **29**: 1140-1149

35 **Lebensztejn DM**, Kaczmarski M, Sobaniec-Łotowska M, Bauer M, Voelker M, Schuppan D. Serum laminin-2 and hyaluronan predict severe liver fibrosis in children with chronic hepatitis B. *Hepatology* 2004; **39**: 868-869

36 **Zeng MD**, Lu LG, Mao YM, Qiu DK, Li JQ, Wan MB, Chen CW, Wang JY, Cai X, Gao CF, Zhou XQ. Prediction of significant fibrosis in HBeAg-positive patients with chronic hepatitis B by a noninvasive model. *Hepatology* 2005; **42**: 1437-1445

37 **Poon TC**, Hui AY, Chan HL, Ang IL, Chow SM, Wong N, Sung JJ. Prediction of liver fibrosis and cirrhosis in chronic hepatitis B infection by serum proteomic fingerprinting: a pilot study. *Clin Chem* 2005; **51**: 328-335

S- Editor Liu Y **L- Editor** Alpini GD **E- Editor** Ma WH

PO Box 2345, Beijing 100023, China
www.wjgnet.com
wjg@wjgnet.com

World J Gastroenterol 2007 January 28; 13(4): 532-537
World Journal of Gastroenterology ISSN 1007-9327

Serum-free culture of *H pylori* intensifies cytotoxicity

Hiroyuki Ohno, Akiyuki Murano

Hiroyuki Ohno, Department of Medicine and Clinical Oncology, Graduate School of Medicine, Chiba University, Chiba 260-8670, Japan
Akiyuki Murano, Department of Clinical Molecular Biology, Graduate School of Medicine, Chiba University, Chiba 260-8670, Japan
Correspondence to: Hiroyuki Ohno, Department of Medicine and Clinical Oncology, Graduate School of Medicine, Chiba University, Chiba 260-8670, Japan. hiroohno-cib@umin.ac.jp
Telephone: +81-47-357-7090 Fax: +81-47-357-7309
Received: 2005-07-03 Accepted: 2005-10-10

Abstract

AIM: To perform a long culture passage of *H pylori* without serum, taking into account its cytotoxicity and the presence of the probable new cytotoxic factor.

METHODS: One sample of *H pylori* 60190 (ATCC 49503) was grown on Brain Heart Infusion (BHI) agar containing 0.5% 2,6-di-O-methyl-β-cyclodextrin without any serum, being passaged 70-100 times every 3-4 d for approximately 2 h, while another sample of *H pylori* contained 70 mL/L fetal calf serum without 2,6-di-O-methyl-β-cyclodextrin. Their supernatant and extract after 16 h in culture were evaluated for changes in cell morphology and for cell viability using HeLa cells. Furthermore, the characteristics of the probable cytotoxic factor in the extract were examined on partial purification studies and its cytotoxicity was evaluated in various human cells.

RESULTS: The supernatant and the extract of the bacterium grown on serum-free medium had strong cytotoxicity compared with those grown on serum-containing medium. They irreversibly damaged HeLa cells without vacuolation that was altogether different from that of the bacterium when grown with serum. Their cytotoxicity was easily measured by cell viability assay. The probable cytotoxic factor partially purified and detected by chromatography had characteristics difference from that of vacuolating toxin and a broad cytotoxicity toward various cell lines.

CONCLUSION: Serum-free long culture method of *H pylori* makes its supernatant and its extract cytotoxic enough to be easily measured by cell viability assay. The probable cytotoxic factor has a unique characteristic and might be a new cytotoxin.

Key words: *H pylori*; Cytotoxicity; Serum-free long culture

Ohno H, Murano A. Serum-free culture of *H pylori* intensifies cytotoxicity. *World J Gastroenterol* 2007; 13(4): 532-537

http://www.wjgnet.com/1007-9327/13/532.asp

INTRODUCTION

Irreversible degeneration and cell death were induced in gastric mucous epithelium infected with *H pylori* both in an *in vitro* and an *in vivo* study, including electron microscopic examination. These cells deteriorated without vacuolations, and biopsy specimens containing the organism obtained from gastric mucosa demonstrated a loss of microvilli and irreversible cell damage[1-4]. Even after eradication therapy of the bacterium, there were no significant differences in the histological scores and atrophic scores in the inflammation of the gastric body and the atrophy of the antrum[5-9]. However, the only known cytotoxic factor of *H pylori* is vacuolating toxin (Vac A), which causes vacuolations in assay cells 18-24 h after addition, but is a reversible and weak cytotoxin[10,11]. The clinical findings that the bacterium caused irreversible and severe destruction to the gastric lineage appear incompatible with the *in vitro* observations that *H pylori* produces only a reversible and comparatively weak cytotoxin that induces vacuolations. Whether there is any direct irreversible cytotoxic factor of *H pylori* remains to be determined. Although, so far, none of the studied factors met these requirements, there is some evidences that indicated cytoskeletal cell death or round-formed cell death differed from vacuolation-formed cell death[3,12,13].

To our best of knowledge, this is the first report about the cytotoxicity of *H pylori* after a long duration of culture without serum. We cultured *H pylori* 60190, plating many passages without serum for approximately two years, considering that the cell growth environments should be as near as possible to the actual intragastric ones. Here, we showed serum-free long period culture made the supernatant and the extract of *H pylori* dramatically cytotoxic such that it induced irreversible decayed cell death easily measurable with a cell viability assay. Cell death induced by these samples showed a rapid development of the cell death process and was rarely accompanied by vacuolation. These observations might explain clinical findings and develop into a new field of the bacterium's cytotoxicity.

MATERIALS AND METHODS

Materials

The *H pylori* strain 60190 was obtained from American Type Culture Collection. Brain Heart Infusion (BHI) was purchased from DIFCO Laboratories and 2,6-di-O-methyl-β-cyclodextrin was purchased from Wako Pure Chemical Industries Ltd.

Culture conditions and preparation of bacterial extract

H pylori 60190 (ATCC49503) was the source for purification. Bacterial cells were grown on Brain Heart Infusion (BHI) agar containing 5% fetal calf serum for 7-10 d, then transferred to BHI broth containing 2,6-di-O-methyl-β-cyclodextrin with gradual stepwise decreases, i.e., 5%, 2%, 1%, 0.5%, of the concentration for 2-4 d without serum and maintaining stable growth conditions, being passaged 100-120 times every 3-4 d. Then bacterial cells were scraped and cultured for 16 h at 37℃ in the liquid medium of BHI containing 0.5% 2,6-di-O-methyl-β-cyclodextrin without serum in an ambient atmosphere containing 50 mL/L CO_2, while agitating with a rotary shaker. Bacterial cells were collected by centrifugation at 12000 *g* for 20 min at 4℃ and suspended in 10 mmol/L Tris-HCl buffer (pH 7.7). The cells were washed once and sonicated at 54% effect for 30 s × 6 sets in Ultrasonic Disruptor (Tomy Seiko Co., Ltd.) and stored at -80℃ overnight. Sonically disrupted cells were thawed and sonicated again under the conditions previously described and centrifuged at 100000 *g* for 60 min at 4℃. The aliquots of the most upper layer were stored at -80℃ until use.

Cytotoxicity assay with cell viability

HeLa cells (Cell Resource Center for Biomedical Research, Tohoku University) cultured in Eagle's modified minimal essential medium containing 100 mL/L fetal bovine serum (MEM-FBS) were seeded into 96-well plates at a density of 10^4 cells per well. After 24 h, the cells were washed twice with PBS and challenged with 10 μL of aliquots of serial fraction or serial dilution of protein solution with 90 μL of MEM-FBS for a total volume of 100 μL per well. Cells were incubated at 37℃ for 24 h and cell viability was evaluated by WST-1 assay using Cell Counting kits (DOJINDO Laboratories). Each determination was performed in triple wells.

Purification of cytotoxic factor

Proteins in the bacterial extract were precipitated with a 700 g/L saturated solution of ammonium sulfate. After centrifugation at 12000 *g* for 20 min, the pellets were resuspended in 10 mmol/L Tris-HCl buffer (pH 7.7) and dialyzed against the same buffer.

The anion exchange chromatography was performed on DEAE Sephacel (Amersham Pharmacia Biotech UK Ltd.) with 10 mmol/L Tris-HCl buffer (pH 7.7). The cation exchange chromatography was CM Sepharose Fast Flow (Amersham Pharmacia Biotech UK Ltd.) with 10 mmol/L Tris-HCl buffer (pH 5.8). The proteins were eluted with the same buffer containing a linear gradient of 0-0.3 mol/L NaCl and 0-1.0 mol/L NaCl, respectively. Size exclusion chromatography was performed on a Superose 12 HR 10/30 column (Pharmacia) with buffer containing 10 mmol/L Tris-HCl (pH 7.7) and 0.15 mol/L NaCl at a flow rate of 0.25 mL/min.

RESULTS

Morphological change of HeLa cells

We cultured *H pylori* 60190 with or without serum for approximately two years. The serum-free culture method using 0.5% 2,6-di-O-methyl-β-cyclodextrin was less favorable for the bacterium and made it inclined to be easily autolysed in the culturing process. In this study, we defined the serum-free method to culture the bacterium using Brain Heart Infusion (DIFCO) and 0.5% 2,6-di-O-methyl-β-cyclodextrin without serum for approximately two years in semisolid medium, and the conventional method using Brain Heart Infusion and 70 mL/L serum without cyclodextrin in semisolid medium. After more than approximately 100 passages, both the supernatant and the extract of the bacterium cultured with the serum-free method induced characteristic morphological changes in HeLa cells, compared to the supernatant and the extract cultured using serum; the cells exposed to its supernatant showed a round-formed shape or small debris with a destroyed contour without vacuolation and the cells exposed to its extract showed an elongated or spindle-like shape with a decrease in cell number in 24 h, while the control cells exposed to the supernatant and the extract had scarcely changed, except for some vacuolations that were similar to the previously reported morphological change (Figure 1).

We observed that both HeLa cells exposed to the supernatant and the extract of the bacterium cultured without serum showed the round-formed change or round debris through the elongated and spindle-like shape without vacuolation. We examined whether HeLa cells exposed to the extract had undergone the same changes using a denser extract. We found that both of the HeLa cells exposed to the supernatant and the extract finally showed the round-formed or shrunken-formed change through the elongated or spindle-like form after 24 h. We compared the morphologic change of HeLa cells exposed to the extract cultured with serum and cultured for approximately one year without serum (Figure 2), and considered that both contained probably a similar cytotoxic factor.

The conventional search of cytotoxin in *H pylori* used the uptake of neutral red into the vacuole of sample-treated cells because the supernatant of the bacterium caused some vacuolations in cells[14], but scarcely any degeneration or remarkable decrease of the number of assay cells. No direct cell viability assay, therefore, was used in search of the cytotoxic factor of *H pylori*. However, we were able to successfully adopt this cell viability assay in place of the neutral red uptake method because of the radical cytotoxicity of the supernatant and the extract cultured without serum.

Cytotoxicity measured by cell viability assay

The cytotoxicity was determined with an assay using HeLa cell viability with WST-1 tetrazolium and a lactate

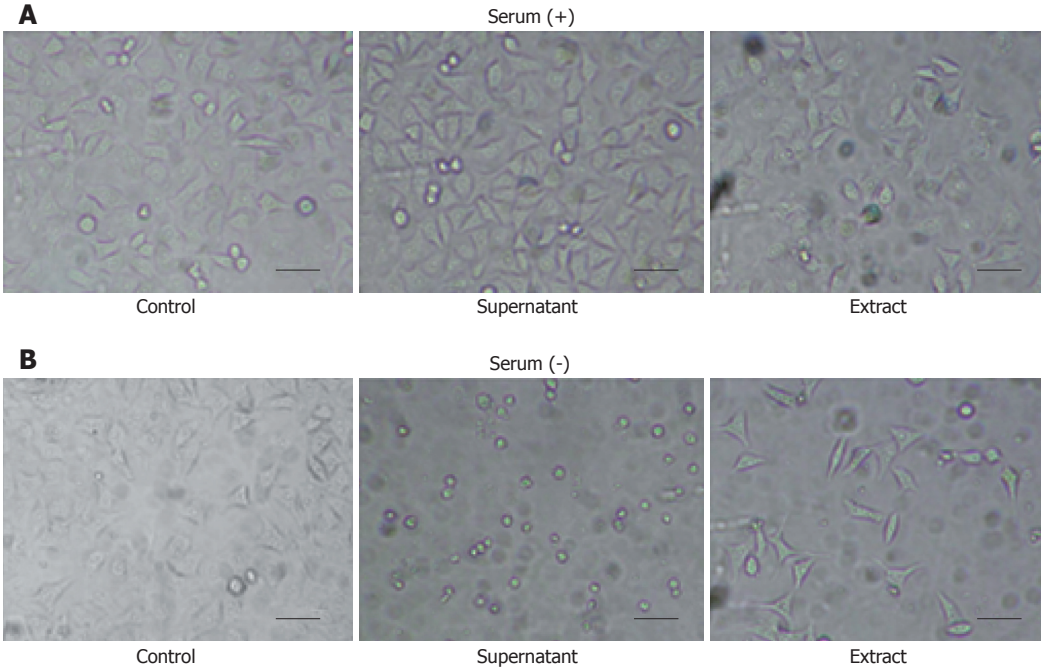

Figure 1 Morphologic change of HeLa cells caused by the supernatant and the extract of *H pylori* with or without serum after 24 h. HeLa cells were seeded at 5000 cells per well in every plate. The concentration of the supernatant cultured with or without serum was 2.1 mg/mL and the concentration of the respective extract was 0.5 mg/mL. **A**: HeLa cells exposed to the supernatant of the method using serum showed little change and the ones exposed to the extract also showed no remarkable changes but included a few minor vacuolations compared to the control; **B**: HeLa cells exposed to the supernatant of the method without serum showed a round-formed shape and a decayed contour with greatly decreased cell number, and those exposed to its extract showed an elongated or spindle-like shape with a decrease in cell number. Scale bar, 200 μm.

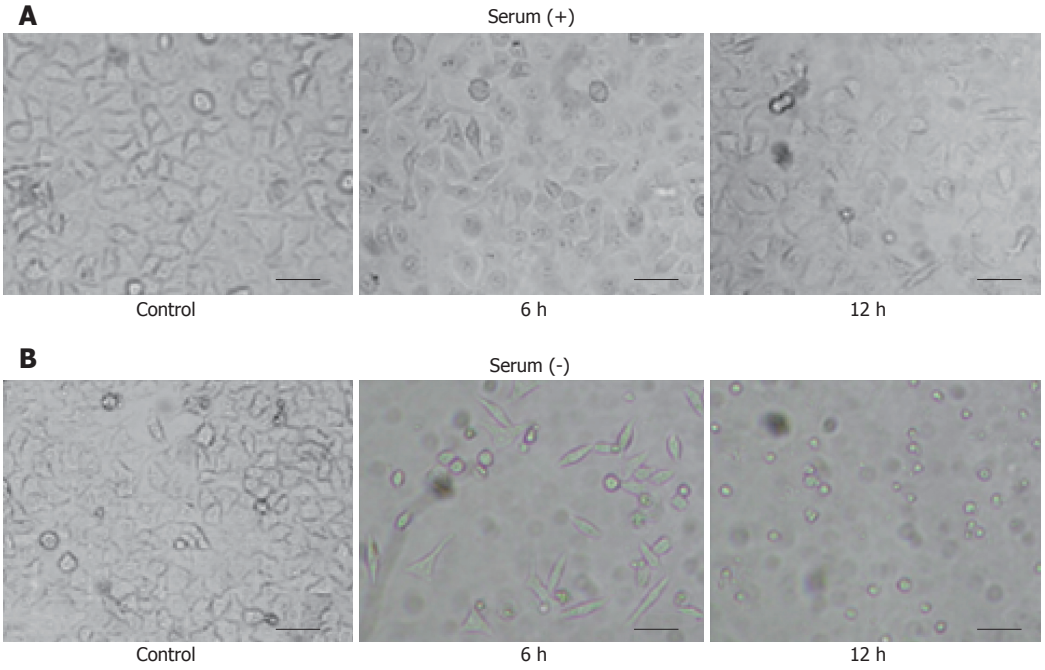

Figure 2 Morphologic change of HeLa cells caused by *H pylori* 1.0 mg/mL cell extract with or without serum. HeLa cells exposed to the extract cultured without serum showed the characteristic morphological changes in 12 h. **A**: HeLa cells exposed to the extract cultured with serum 6 h and 12 h after addition of the extract showed no remarkable changes but a small decrease in cell number; **B**: HeLa cells exposed to the extract cultured without serum 6 h and 12 h after addition of the extract showed the round-formed shape or round debris with a decayed contour through the elongated or spindle-like shape without vacuolations. Scale bar, 200 μm.

dehydrogenase release assay. This cell viability assay revealed the intense cytotoxicity toward HeLa cells, as we predicted. Both the supernatant and the extract cultured without serum had a greater cytotoxicity toward HeLa cells than the ones cultured with serum. The extract, especially of that cultured without serum, had a far greater cytotoxicity than that cultured with serum (Figure 3). This cytotoxicity was thought to be irreversible because the viability assay used measured the intracellular enzyme in the dead or destroyed cells. No cell reversibility could be ascertained for certain when we removed the supernatant and the extract from the cells at 6 h and 12 h after the addition and replaced it with the control lysate for a further 24 h observation (data not shown).

Purification in accordance to the passage time

We pursued the growing cytotoxicity of the extract using a cell viability assay and anion exchange chromatography in accordance to the passage time without serum. The extract at the onset of culturing without serum showed two minor dips of cell viability at approximately 0.1 mol/L NaCl and 0.2 mol/L NaCl with gradient elution, respectively. The extract after approximately 6 mo of culture (approximately 50 passages) from the onset indicated clearer minor dips at the same concentration of the NaCl linear gradient elution; while approximately one year (approximately 100 passages) from its onset without serum, the extract had a major dip at 0.2 mol/L NaCl and a minor dip at 0.1 mol/L NaCl with far less elution protein. We found that the putative cytotoxic

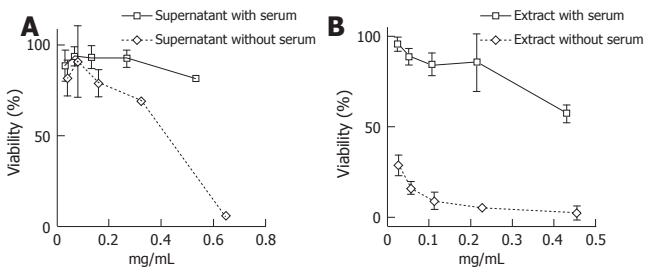

Figure 3 Cell viability assay of the supernatant and the extract of serum-free cultured *H pylori* at the onset of culturing and long cultured *H pylori*, approximately 100 passages after the onset of culturing. **A**: Long serum-free cultured supernatant showing dose-dependent decrease curves of cell viability; **B**: Long serum-free cultured extract showing further dose-dependent decrease curves of cell viability. Each point represents the mean ± SD from three separate experiments.

factor had an isoelectric point less than pH 7.7 due to the use of the buffer with pH 7.7 (Figure 4).

Purification on cation exchange chromatography and size exclusion chromatography

In addition, we examined the extract cultured approximately one year (approximately 100 passages) from its onset without serum using cation exchange chromatography and size exclusion chromatography. Cation exchange chromatography showed one clear dip at around 0.3 mol/L NaCl in the gradient elution that indicated that the putative cytotoxic factor had an isoelectric point of more than pH 5.8 due to the use of the buffer with pH 5.8. Size exclusion chromatography showed a sharp dip at around 37-45 ku, which was different from the molecular mass of the vacuolating toxin (87 ku) (Figure 5).

Cytotoxicity toward human cells

These extracts partially purified by anion exchange chromatography showed robust cytotoxicity toward HeLa cells and other human cells, including AZ521 (gastric carcinoma cells), HLF (hepatocellular carcinoma cells), Caco2 (colorectal carcinoma cells), and HL60 (promyeloblastic leukemia cells) (Figure 6).

DISCUSSION

This is probably the first report about serum-free long culture method of *H pylori*. We showed that the established strain, *H pylori* 60190, could be converted to a far more cytotoxic strain with a serum-free long culture method that was altogether different from that obtained using conventional culture methods including serum. This cytotoxicity was acquired by the long process of culturing it without serum. Both the supernatant and the extract cultured without serum caused cytotoxicity toward HeLa cells that was distinctly different from the cytotoxicity of H pylori cultured using serum of the conventional method to help the feeble growth of *H pylori*. The conventional method using serum certainly may ultimately help the growth state[15] but was considered to be very much unlike the actual growing environment. 2,6-Di-O-methyl-β-cyclodextrin (CD) is considered to reduce the toxic effect

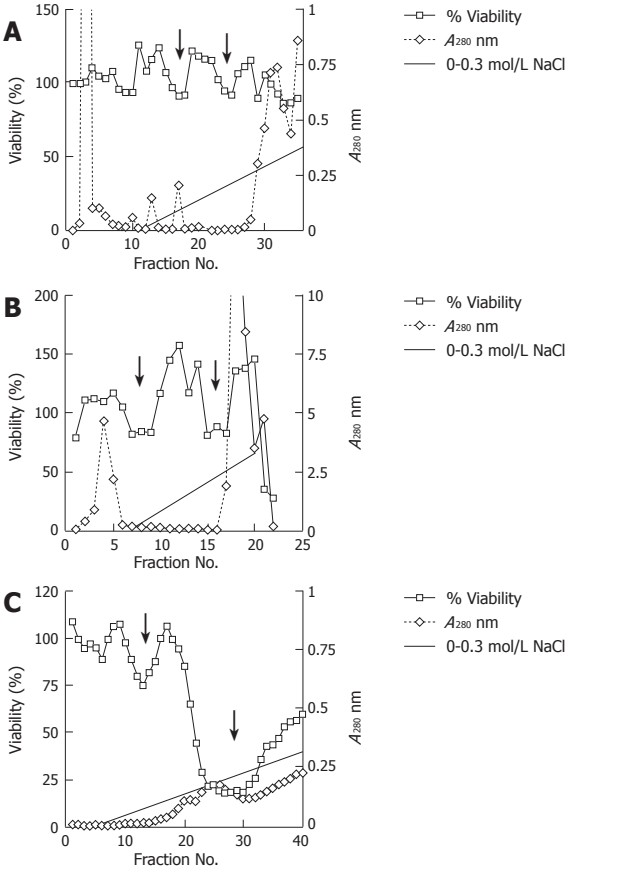

Figure 4 Analysis of the column anion exchange chromatography of the extract cultured without serum. Cell viability that represents the putative cytotoxic factor was measured for cell viability at A_{415} using the WST1 method. Column eluates that represent the protein densities were monitored at A_{280} for each of the filtrated fractions. Proteins were eluted with a linear gradient of 0-0.3 mol/L NaCl. **A**: Anion exchange chromatography of the cell extract protein at the onset of culturing without serum. Two minor dips of cell viability are indicated (arrows); **B**: Anion exchange chromatography of the cell extract protein approximately 50 passages (approximately 6 mo) after the onset of culturing without serum. Two clearer minor dips of cell viabilities are indicated (arrows); **C**: Anion exchange chromatography of the cell extract protein approximately 100 passages (approximately one year) after the onset of culturing without serum. One minor dip and one major dip are at 0.1 mol/L NaCl and 0.2 mol/L NaCl, respectively (arrows).

of fatty acids as well as bovine serum albumin (BSA)[16,17]. Although blood and serum may contain growth-stimulatory factors required by the organism[14], the strain 60190, we used, grew in media with CD without any serum, but did not grow in media without sera or CD as the other strains were reported[18].

The supernatant of the serum-free culture was reported to cause epithelial cytoskeletal disruption[13] after as little as 48 h culture, while 72 h culture decreased the apoptotic signaling of cells, as compared to serum-containing cultures[19]. Serum-free culture method may be less favorable to the organism but more useful with the research of its cytotoxic factors.

Most *in vitro* studies hitherto have used *H pylori* strains cultured using serum, and if any serum-free culture of the bacterium was used for a short time[10,14], it may have been that the supernatant caused the morphological cytotoxic change with vacuolations and without any remarkable cell viability loss or any decrease of assay cell number. However, we discovered the supernatant and the extract of the bacterium cultured for long periods of

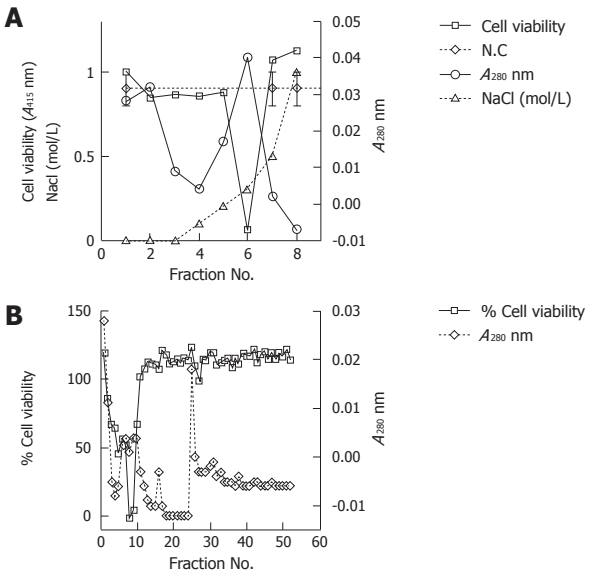

Figure 5 Analysis of the extract cultured without serum. Cell viability that represents the putative cytotoxic factor was measured for cell viability at A_{415} using the WST1 method. Column eluates that represent protein densities were monitored at A_{280} for each filtrated fraction. **A**: Cation exchange chromatography of the cell extract protein approximately 100 passages (approximately one year) after the onset of culturing without serum. The cell extract proteins were eluted with a stepwise gradient of 0-0.5 mol/L NaCl; **B**: Size exclusion chromatography of the cell extract protein approximately 100 passages (approximately one year) after the onset of culturing without serum.

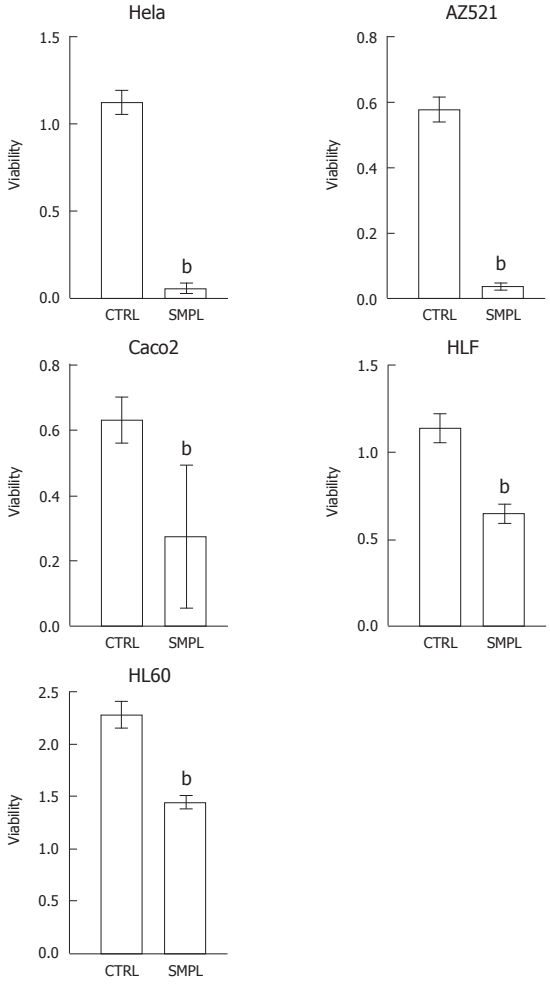

Figure 6 Cytotoxicity of the extract partially purified by anion exchange chromatography. Each bar represents mean + SE of three separate experiments. CTRL: control lysate; SMPL: sample lysate. $^{b}P < 0.01$ *vs* CTRL.

time without serum had a different cytotoxicity in both the cell morphology and the activity that scaled up with the passage duration for a year or more, Furthermore, the shape of the organism cultured in serum-free medium had seemed to be more cocoid form than that would be in serum-containing medium.

In addition, our chromatography study showed that putative cytotoxic factor had an isoelectric point between pH 5.8 to 7.7, with a molecular mass of approximately 37-45 ku, which was different from that of the vacuolating toxin (87 ku). The anion exchange chromatography study appeared to indicate two cell-viability dips, a minor dip and a major dip. Further investigation will be required to determine the number of possible factors involved.

This experimental method might represent a state closer to that of the actual intragastric state, rather than that obtained by using conventional serum-using studies. The experimental method reported herein may also produce results more closely related to clinical observations, which would redress the conventional concept that *H pylori* has only a weak and reversible cytotoxin. *H pylori* might, in fact, be more insidious and more fierce than the researchers had ever conceived.

Our result may provide a new approach to the cytotoxin research and elucidate a pathological mechanism in *H pylori* using this new method, which is different from that of the vacuolating toxin, the only presently known cytotoxin.

ACKNOWLEDGMENTS

We thank Ohno M and Tamanoi I for constructive comments.

REFERENCES

1 **Tricottet V,** Bruneval P, Vire O, Camilleri JP, Bloch F, Bonte N, Roge J. Campylobacter-like organisms and surface epithelium abnormalities in active, chronic gastritis in humans: an ultrastructural study. *Ultrastruct Pathol* 1986; **10**: 113-122

2 **Taniguchi Y,** Ido K, Kimura K, Satoh K, Yoshida Y, Takimoto T, Kihira K, Ookawara S, Mato M. Morphological aspects of the cytotoxic action of *Helicobacter pylori*. *Eur J Gastroenterol Hepatol* 1994; **6 Suppl 1**: S17-S21

3 **Wang XM,** Kojima T, Satoh K, Taniguchi Y, Tokumaru K, Saifuku K, Seki M, Kihira K, Ido K, Uchida JY, Ohmori C, Takaoka T, Kimura K. The value of LYM-1 cells for examining vacuole formation and loss of cell viability induced by culture supernates of *Helicobacter pylori*. *J Med Microbiol* 1997; **46**: 705-709

4 **Hessey SJ,** Spencer J, Wyatt JI, Sobala G, Rathbone BJ, Axon AT, Dixon MF. Bacterial adhesion and disease activity in Helicobacter associated chronic gastritis. *Gut* 1990; **31**: 134-138

5 **Yamada T,** Miwa H, Fujino T, Hirai S, Yokoyama T, Sato N. Improvement of gastric atrophy after *Helicobacter pylori* eradication therapy. *J Clin Gastroenterol* 2003; **36**: 405-410

6 **Tucci A,** Poli L, Tosetti C, Biasco G, Grigioni W, Varoli O, Mazzoni C, Paparo GF, Stanghellini V, Caletti G. Reversal of fundic atrophy after eradication of *Helicobacter pylori*. *Am J Gastroenterol* 1998; **93**: 1425-1431

7 **Forbes GM,** Warren JR, Glaser ME, Cullen DJ, Marshall BJ, Collins BJ. Long-term follow-up of gastric histology after *Helicobacter pylori* eradication. *J Gastroenterol Hepatol* 1996; **11**: 670-673

8 **Annibale B,** Aprile MR, D'ambra G, Caruana P, Bordi C,

Delle Fave G. Cure of *Helicobacter pylori* infection in atrophic body gastritis patients does not improve mucosal atrophy but reduces hypergastrinemia and its related effects on body ECL-cell hyperplasia. *Aliment Pharmacol Ther* 2000; **14**: 625-634

9 **Satoh K,** Kimura K, Takimoto T, Kihira K. A follow-up study of atrophic gastritis and intestinal metaplasia after eradication of *Helicobacter pylori*. *Helicobacter* 1998; **3**: 236-240

10 **Cover TL,** Halter SA, Blaser MJ. Characterization of HeLa cell vacuoles induced by *Helicobacter pylori* broth culture supernatant. *Hum Pathol* 1992; **23**: 1004-1010

11 **Yahiro K,** Niidome T, Hatakeyama T, Aoyagi H, Kurazono H, Padilla PI, Wada A, Hirayama T. *Helicobacter pylori* vacuolating cytotoxin binds to the 140-kDa protein in human gastric cancer cell lines, AZ-521 and AGS. *Biochem Biophys Res Commun* 1997; **238**: 629-632

12 **Guillemin K**, Salama NR, Tompkins LS, Falkow S. Cag pathogenicity island-specific responses of gastric epithelial cells to *Helicobacter pylori* infection. *Proc Natl Acad Sci USA* 2002; **99**: 15136-15141

13 **Bebb JR,** Letley DP, Rhead JL, Atherton JC. *Helicobacter pylori* supernatants cause epithelial cytoskeletal disruption that is bacterial strain and epithelial cell line dependent but not toxin VacA dependent. *Infect Immun* 2003; **71**: 3623-3627

14 **Cover TL,** Blaser MJ. Purification and characterization of the vacuolating toxin from *Helicobacter pylori*. *J Biol Chem* 1992; **267**: 10570-10575

15 **Shahamat M,** Mai UE, Paszko-Kolva C, Yamamoto H, Colwell RR. Evaluation of liquid media for growth of Helicobacter pylori. *J Clin Microbiol* 1991; **29**: 2835-2837

16 **Hazell SL,** Graham DY. Unsaturated fatty acids and viability of *Helicobacter* (*Campylobacter*) *pylori*. *J Clin Microbiol* 1990; **28**: 1060-1061

17 **Khulusi S,** Ahmed HA, Patel P, Mendall MA, Northfield TC. The effects of unsaturated fatty acids on *Helicobacter pylori in vitro*. *J Med Microbiol* 1995; **42**: 276-282

18 **Olivieri R,** Bugnoli M, Armellini D, Bianciardi S, Rappuoli R, Bayeli PF, Abate L, Esposito E, de Gregorio L, Aziz J. Growth of Helicobacter pylori in media containing cyclodextrins. *J Clin Microbiol* 1993; **31**: 160-162

19 **Shibayama K,** Doi Y, Shibata N, Yagi T, Nada T, Iinuma Y, Arakawa Y. Apoptotic signaling pathway activated by *Helicobacter pylori* infection and increase of apoptosis-inducing activity under serum-starved conditions. *Infect Immun* 2001; **69**: 3181-3189

S- Editor Wang J **L- Editor** Kumar M **E- Editor** Liu WF

PO Box 2345, Beijing 100023, China
www.wjgnet.com
wjg@wjgnet.com

World J Gastroenterol 2007 January 28; 13(4): 538-547
World Journal of Gastroenterology ISSN 1007-9327

BASIC RESEARCH

Pretreatment with adenosine and adenosine A1 receptor agonist protects against intestinal ischemia-reperfusion injury in rat

V Haktan Ozacmak, Hale Sayan

V Haktan Ozacmak, Hale Sayan, Department of Physiology, School of Medicine, Zonguldak Karaelmas University, Kozlu 67600, Zonguldak, Turkey
Supported by Zonguldak Karaelmas University Research Projects Fund, No. 2003-01-09
Correspondence to: Dr. VH Ozacmak, Department of Physiology, School of Medicine, Zonguldak Karaelmas University, Kozlu 67600, Zonguldak, Turkey. vhaktan@yahoo.com
Telephone: +90-372-2610243 Fax: +90-372-2610264
Received: 2006-07-07 Accepted: 2006-11-03

Abstract

AIM: To examine the effects of adenosine and A1 receptor activation on reperfusion-induced small intestinal injury.

METHODS: Rats were randomized into groups with sham operation, ischemia and reperfusion, and systemic treatments with either adenosine or 2-chloro-N^6-cyclopentyladenosine, A1 receptor agonist or 8-cyclopentyl-1,3-dipropylxanthine, A1 receptor antagonist, plus adenosine before ischemia. Following reperfusion, contractions of ileum segments in response to KCl, carbachol and substance P were recorded. Tissue myeloperoxidase, malondialdehyde, and reduced glutathione levels were measured.

RESULTS: Ischemia significantly decreased both contraction and reduced glutathione level which were ameliorated by adenosine and agonist administration. Treatment also decreased neutrophil infiltration and membrane lipid peroxidation. Beneficial effects of adenosine were abolished by pretreatment with A1 receptor antagonist.

CONCLUSION: The data suggest that adenosine and A1 receptor stimulation attenuate ischemic intestinal injury via decreasing oxidative stress, lowering neutrophil infiltration, and increasing reduced glutathione content.

Key words: Adenosine; Adenosine A1 receptor; Intestinal ischemia; Pharmacological preconditioning

Ozacmak VH, Sayan H. Pretreatment with adenosine and adenosine A1 receptor agonist protects against intestinal ischemia-reperfusion in rat. *World J Gastroenterol* 2007; 13(4): 538-547

http://www.wjgnet.com/1007-9327/13/538.asp

INTRODUCTION

Ischemia-reperfusion (I/R) injury of the intestine is a significant problem in a numerous situations such as abdominal aortic aneurysm surgery, small bowel transplantation, cardiopulmonary bypass, strangulated hernias, and neonatal necrotizing enterocolitis[1]. Decreased contractile activity, increased microvascular permeability, and dysfunction of mucosal barrier are all associated with intestinal I/R[2,3]. I/R injury of the intestine is an intricate and multifactorial pathophysiological process that involves the formation and action of oxygen free radicals (OFRs)[3-9], inflammatory cytokines, the complement system[1,3] and neutrophil infiltration[1-3,6,7,10] at the site of damage.

The purine nucleoside adenosine is one of the major local regulators of normal tissue function, acting in both an autocrine and paracrine fashion. Its regulatory function becomes pronounced especially when energy supply ceases abruptly as in the case of ischemia, and fails to meet cellular energy demand. Adenosine exerts its effects by interacting with its receptors, four of which have been cloned and characterized as adenosine A_1, A_{2a}, A_{2b}, and A_3[11-13]. The physiological role of adenosine in the gastrointestinal tract is still poorly understood, particularly with regard to colonic and ileal motor functions. It has been reported that A_1 adenosine receptor (A_1AR) antagonists increase defecation in rats[13] and that A_1AR agonists can inhibit intestinal fluid secretion and peristalsis *via* adenosine A_{2B} and A_1 receptors, respectively[14].

One of the cellular events observed during ischemia is the increased consumption of ATP, leading to accumulation of adenosine with thereby elevating extracellular adenosine. The accumulation of adenosine is believed to contribute to cytoprotection in the ischemic tissue[11,12]. Furthermore, adenosine which is released during short periods of ischemia followed by reperfusion, provides cytoprotection against a subsequent sustained ischemia in heart, resulting in reduced infarct size[15-20]. This is known as the preconditioning effect of adenosine, which is mediated mostly through the activation of cardiac A_1ARs before ischemia[11,12,18]. It is well documented that the early[19,20] and late[11,15,18] phases of ischemic tolerance are mediated by adenosine in myocardium. That adenosine exerts anti-ischemic actions is indicated by

a number of studies using adenosine receptor agonists and antagonists[15-18] as well as animals overexpressing or lacking A_1AR[21,22]. Administration of adenosine either prior to ischemia or during reperfusion has been shown to attenuate myocardial injury[23,24]. Treatment with adenosine A_1AR agonist initiates preconditioning not only in heart[15-18,25] but also in tissues such as kidney[26,27] and brain[28,29], resulting in attenuation of ischemic injury. One of the underlying mechanisms suggested for adenosine receptor-mediated preconditioning in the heard is through involvement of protein kinase C (PKC) in heart[11,12,30]. Activation of PKC induces opening of ATP-sensitive K^+ channels[11,12,31]. Among other effectors that most likely contribute to the cytoprotection by adenosine are mitogen activated protein (MAP) kinases[25,31-33], heat shock proteins (HSPs)[11-15,34], antioxidant enzymes[15,34] and inducible nitric oxide synthase (iNOS)[11,12]. Moreover, induction and activation of manganese superoxide dismutase (Mn-SOD) is also believed to be a significant factor in mediating myocardial adaptation in response to activation of A_1AR[15].

In the phenomenon of ischemic preconditioning (IPC), a short period of ischemia protects the organs (e.g. heart) against a subsequent more substantial ischemic injury[35]. In fact, IPC has been one of the most promising strategies against reperfusion injury during the last few years. It appears to elevate the tolerance of the intestine to I/R injury. A number of experimental studies have shown that reperfusion injury in small intestine is prevented by IPC[36-40]. IPC conducted in small intestine reduces postischemic leukocyte adhesion by maintaining the bioavailability of nitric oxide[41]. Moreover, it lowers the expression of P-selectin[38], which is a downstream effector target of the adenosine-initiated, PKC dependent, signalling pathway in intestine. Although activation of PKC triggered by adenosine has been a crucial factor for initiating the beneficial actions of IPC in most tissues, the effector of the preconditioning phenomenon appears to vary among tissues. Activated-K^+ channels[42], nitric oxide[39,41] and endogenous opioid peptides[43] have reported to be the other downstream effectors of IPC in intestine. Based primarily on animal experiments, the identification of the molecular mechanisms that are responsible for protection by IPC, has provided opportunities to consider several rational targets for pharmacological intervention. Consequently, a variety of drugs have been demonstrated to be able to mimic IPC when applied instead of ischemia. This is known as pharmacological preconditioning (PPC). Recently, various studies carried out in rat small intestine have demonstrated that establishing PPC by administration of either adenosine[37] or A_1AR agonist[38] mimics the protective effects of IPC. Intensive investigation has been focused on explaining how adenosine accomplishes the beneficial effect of preconditioning. For instance, currently published studies suggest important anti-ischemic roles of the A_1[18,25,30], A_3[17,21] or A_{2a}[44,45] adenosine receptors in heart. On the other hand, relatively little data are available on the role of the different adenosine receptors in mediating cytoprotection in intestinal tissue which is exposed to I/R. The majority of studies strongly suggest that adenosine can promote protection against I/R injury via activation of different adenosine receptors in various tissues. A substantial number of studies report that IPC has been beneficial in human heart and the liver. However, both prospective controlled studies in human and experimental studies in animals are lacking[1]. Furthermore, research based on administration of drugs that can mimic the effects of IPC is required further to explore the cellular events during I/R injury of the intestine. To date, there is no direct evidence showing possible effects of adenosine and A_1AR activation on reduced contractility of intestinal smooth muscle due to I/R injury. Therefore, the present study was constructed to explore the possible effects of adenosine and A_1AR activation on reperfusion injury of small intestinal tissue by evaluating contractile response and levels of thiobarbituric acid-reactive substances (TBARS, a marker of lipid peroxidation), reduced glutathione (GSH, an endogenous antioxidant), and myeloperoxidase (MPO an index of neutrophil infiltration), in terminal ileum subjected to I/R.

MATERIALS AND METHODS

Animals

Following Ethical Committee approval, forty adult male Wistar rats, weighing 200-230 g, were obtained from the Experimental Research Section of Zonguldak Karaelmas University, where animals have been reared and maintained under standard conditions, such as stable room temperature (23 ± 2℃), a 12 h light: 12 h dark cycle, and feeding with commercial rat chow and tap water *ad libitum*. Experimental manipulations and surgical operations were approved by the Animal Ethical Committee of the University. Maximum care and a humane approach to use of animals was of primary consideration.

Experimental groups and operative procedures

The surgical goal was to induce mesenteric ischemia in rats for 30 min followed by a 180 min reperfusion period. On the day before surgery, each animal was fasted overnight with unlimited access to water. Briefly, each animal was anesthetized by an intraperitoneal injection of 50 mg/kg sodium thiopenthal followed by a midline incision made into the peritoneal cavity. The small bowel was exteriorized gently to the left onto moist gauze, and then the superior mesenteric artery (SMA) was carefully exposed, isolated, and clamped using a microvascular clamp. Intestinal ischemia was confirmed by obvious lack of pulse in the SMA and paleness of the jejunum and ileum. The intestines were then meticulously placed back into the abdomen which was closed with two small clamps. Following 30 min of occlusion time, the clamping was gently released and the intestine inspected for proper reperfusion characterized by regular pulsation. Throughout the surgical procedure, each animal was placed under a heating lamp to maintain constant body temperature (e.g. 37℃). For the purpose of assessing the roles of adenosine and A_1AR agonist, animals were randomly divided into five groups: (1) Sham-operated group, subjected to laparatomy without performing the occlusion of the SMA; (2) I/R group, subjected to the occlusion of SMA followed by reperfusion; (3) CPA-treated group (0.1 mg/kg, 5 min prior to ischemia) + I/R; (4) Adenosine-treated group (10 mg/kg, 5 min prior

to ischemia) + I/R; (5) DPCPX pretreatment (1 mg/kg, 15 min prior to adenosine administration) + adenosine treatment (10 mg/kg, 5 min prior to ischemia) + I/R. In the last group, confirming the possible effect of selective A_1AR agonist CPA on reperfusion injury, the selective A_1AR antagonist DPCPX was administered 15 min prior to adenosine treatment. The route and volume for drug administration were the tail vein and 200 μL, respectively. To animals in both sham-control and I/R-control groups were given sterile serum physiological solution in the same volume instead. Choice of dose regimen for the drugs was based on published studies in the literature[22,37,38].

Preparation of terminal ileum

Upon completion of the I/R period, and whilst still unconcious, the animals were sacrificed by exsanguination of the abdominal aorta. Strips of terminal ileum of 10 mm length were immediately removed 10 cm oral to the ileocecal junction and transferred into a Petri dish containing Krebs solution (in mmol/L: NaCl 118, $NaHCO_3$ 24.88, KH_2PO_4 1.18, KCl 4.7, $MgSO_4$ 1.16, $CaCl_2$ 2.52 and glucose 11.1). Then, tissue was longitudinally suspended in a standard organ chamber, and continuously perfused with 20 mL of preoxygenated Krebs solution (pH 7.4), which was bubbled constantly with a mixture of 950 mL/L O_2 and 50 mL/L CO_2 gas and maintained at a temperature of 37℃. One end of the tissue strip was tied to a fixed post and the other attached to an isometric force transducer under a resting tension of 2 g. Isometric responses were monitored by external force displacement transducer (FDA-10A, Commat Iletisim Co., Ankara, Turkey) and recorded on the computer using MP 30 software (Biopac Systems Inc., Santa Barbara, CA, USA). In the organ bath, each strip was allowed to equilibrate for 1 h with intervening washes every 15 min before adding any compound. Tissue samples also obtained from small intestine approximately 10 cm proximal to the ileocecal area were frozen immediately and stored at -40℃ for biochemical measurements.

Concentration-response curves

At the beginning of each experiment to observe dose-contractile response relationship, KCl was added to the organ chamber to a final concentration of 30 mmol/L. For the preparation of high K^+ solutions, NaCl was exchanged for an equimolar amount of KCl to maintain the physiological osmolarity of the Krebs solution. The contraction recorded in response to KCl was considered as a reference response. Afterwards, the contractions in response to carbachol and substance P at various final concentrations ranging from 10^{-9} mol/L to 10^{-2} mol/L were recorded by pipetting these compounds into the organ bath in a cumulative fashion at equal intervals. At the end of the experiment, the response to 30 mmol/L KCl was measured again to confirm and evaluate the degree of tissue viability. The amplitude of all contractions was then normalized for each g of tissue and expressed as percentage of the initial KCl-reference response. The number of experiments, represented as "*n*", indicates that each experiment was performed with a tissue sample taken from one animal. All experiments were conducted in a paired way. For the purpose of evaluating the effects of ligand, agonist, and antagonist, the maximum response (E_{max}) and pD_2 values (e.g. the negative logarithm of the concentration for the half-maximal response, ED_{50}) were computed by using GraphPad Prism Software 3.02 (GraphPad Prism Inc., San Diego, CA, USA)[46]. The pD_2 values (apparent agonist affinity constants) were calculated from each agonist concentration–response curve by linear regression of the linear median part of the sigmoid curve and taken as a measure of the sensitivity of the tissues to each agonist.

Drugs

Adenosine, CPA, DPCPX, carbachol and substance P were purchased from Sigma (Sigma Chemical Co., St. Louis, MO, USA). They were dissolved in double distilled water, except for CPA and DPCPX which were initially prepared in dimethyl sulphoxide and then diluted in physiological saline. Adenosine, CPA, and DPCPX were prepared fresh just before usage. Carbachol and substance P were made up at different concentrations and kept frozen in aliquots. Compounds, which were used for preparing Krebs solution, were purchased from Merck (Merck KGaA, Darmstadt, Germany). All other reagents, including trichloroacetic acid (TCA), thiobarbituric acid (TBA), butylated hydroxy toluene (BHT), and dithiobisnitrobenzoate (DTNB) were obtained from Sigma.

Determination of tissue TBARS and GSH

Tissue TBARS content was measured in order to estimate the extent of lipid peroxidation in the injured terminal ileum. Samples obtained from each group were stored at -40℃ until assayed. Tissue samples were washed in ice-cold Krebs solution, blotted on absorbent paper and weighed. Afterwards, each sample was minced followed by homogenization with 10 mL of 100 g/L TCA per g of tissue, using a motor-driven homogenizer (Heidolph Diax 900, Heidolph Elektro GmbH&Co.KG, Kelheim, Germany). Then, the tissue TBARS levels were measured spectrophotometrically based on a method described by Casini *et al*[47] and expressed as nmol/g of tissue weight. Briefly, following two consecutive centrifugations at 3000 g for 15 min, 750 μL supernatant was added to equal volume of 6.7 g/L TBA and heated to 100℃ for 15 min. The absorbance of the samples was then measured spectrophotometrically at 535 nm (Smart Spectro, LaMotte Co., Chestertown, MD, USA).

The GSH content of the samples were measured by applying a modified Ellman method[48]. In brief, 2 mL of 0.3 mol/L Na_2HPO_4 solution was mixed with 0.5 mL of supernatant obtained by employing the homogenization procedure described above. Into the mixture, 0.2 mL of DTNB solution was added followed by reading absorbance at 412 nm. The tissue GSH levels were expressed as μmol/g of tissue weight.

Measurement of tissue MPO activity

The degree of neutrophil accumulation in the intestinal tissue samples was measured by assaying MPO activity as described by Bradley *et al*[49]. Briefly, upon thawing, each

Table 1 E_{max} and pD_2 values of carbachol and substance P (n = 8, means ± SE)

	Sham Control	I/R Control	CPA-I/R	ADO-I/R	DPCPX + ADO-I/R
Carbachol					
E_{max}	488.67 ± 47.01	157.05 ± 41.35[a]	395.05 ± 32.62[c]	372.21 ± 54.68[c]	212.35 ± 40.09[a]
pD_2	6.30 ± 0.19	7.02 ± 0.31	6.24 ± 0.40	6.94 ± 0.13	5.81 ± 0.18
Substance P					
E_{max}	255.94 ± 31.17	115.00 ± 13.36[a]	148.19 ± 13.80[a]	242.93 ± 46.55[c]	259.61 ± 24.62[c]
pD_2	6.51 ± 0.05	8.29 ± 1.08	7.00 ± 0.22	6.69 ± 0.28	6.51 ± 0.07

[a]P < 0.05 *vs* sham-operated control group, [c]P < 0.05 *vs* I/R control group.

sample was very finely minced with surgical blade in a petri dish containing 50 mmol/L potassium phosphate buffer (PB, pH 6.0) at a volume 20 times the tissue weight (e.g. 1 mL) followed by homogenization for 5 min in ice-cold PB by means of motor driven homogenizer. The homogenate was centrifuged at 40 000 g for 15 min at 4℃. The homogenized tissue pellet was suspended in 50 mmol/L PB containing 5 g/L hexadecyltrimethylammonium bromide (HETAB) and then homogenized again. Following three freeze and thaw cycles with sonication (Bandelin Sonopuls HD2070, Bandelin Electronic GmbH&CO.KG, Berlin, Germany) between cycles, the samples were centrifuged at 40 000 g for 10 min. Aliquots of supernatant (0.1 mL) were added to 2.9 mL of reaction mixture containing 0.167 mg/mL of *o*-dianisidine, and 20 mmol/L H_2O_2 solution, which were prepared in 50 mmol/L of PB. Immediately after adding the aliquot to the mixture, the change in absorbance at 460 nm was measured for 5 min. One unit of MPO activity was defined as that degrading 1 μmol of peroxide per min at 25℃. The activity was then normalized as unit per mg of tissue (U/mg).

Statistical analysis

Values for the experiments dealing with contractility were normalized for per g of tissue followed by expressing them as percentage of KCl response. Each data point represents mean ± SE. For statistical evaluation, SPSS 11.0 statistical software package programme was used (SPSS Inc., Chicago, IL, USA). One-way analysis of variance (ANOVA) was applied for statistical comparison of groups, followed by analysis with Tukey-Kramer test so as to determine differences between the groups. Probability value (P) of 0.05 or less was considered statistically meaningful.

RESULTS

Ileal longitudinal muscle contractility

For longitudinal ileum muscle collected from sham control, CPA-treated, adenosine-treated, and DPCPX-adenosine-treated animals, mean contraction responses to 30 mmol/L KCl were measured as 0.59 ± 0.01 g; 0.40 ± 0.09 g; 0.50 ± 0.22 g; and 0.44 ± 0.21 g, respectively, which were statistically indistinguishable (Figure 1). In I/R control group however, the contractile response (0.26 ± 0.08 g) was significantly reduced when compared to that in sham-operated control group (P = 0.012).

The addition of carbachol at concentrations from 10^{-9} mol/L to 10^{-2} mol/L into the organ bath resulted

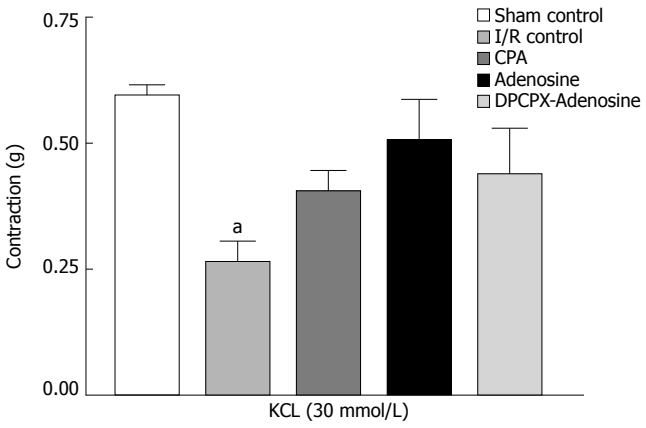

Figure 1 Mean contraction of longitudinal ileum muscle isolated from sham-operated control, I/R control, CPA-I/R, adenosine-I/R, and DPCPX-adenosine-I/R rats in response to 30 mmol/L KCl. Data are expressed as means ± SE (n = 8). [a]P < 0.05 *vs* sham-operated control group.

in a dose-dependent contractile effect on the terminal ileum segments from all groups (Figure 2), providing sigmoid curves with E_{max} and pD_2 values (Figure 3). E_{max} value for carbachol was significantly lower in the I/R control group than in the sham-operated control group (157.04% ± 41.35% *vs* 488.66% ± 47.01%, respectively). In other words, contraction in response to carbachol was significantly reduced by induction of I/R. Statistical difference between the groups appeared to be meaningful at 10^{-6} mol/L (P = 0.02), reaching a maximal level at 10^{-3} mol/L of carbachol (P = 0.0001). The I/R-induced reduction in contractility was significantly restored by treatments with both CPA and adenosine but not by pretreatment with DPCPX. Amelioration of reduced contractions with CPA and adenosine therapies became statistically significant at millimolar doses of carbachol (P = 0.03 at 10^{-3} mol/L and 10^{-2} mol/L).

Comparison of the E_{max} values showed that average contraction of ileum samples in I/R group was just 32% of that in sham-operated control group, while those in CPA- and adenosine-treated groups were approximately 81% and 76%, respectively (Table 1). In the group pretreated with DPCPX, E_{max} was found to be approximately 60% of that in sham control group, which was statistically significant (P < 0.05). On the other hand, no statistically significant change was detected in the corresponding pD_2 values in any group (Table 1).

In response to various concentrations of substance

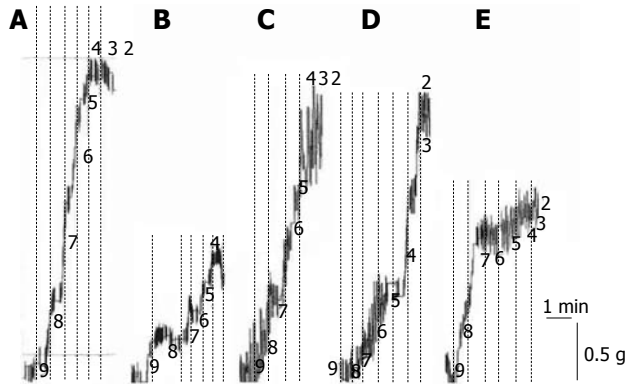

Figure 2 Representative traces showing responses generated by various concentrations of carbachol in longitudinal ileum muscle isolated from sham-operated control (**A**), I/R control (**B**), CPA–I/R (**C**), adenosine-I/R (**D**), and DPCPX-adenosine-I/R (**E**) rats.

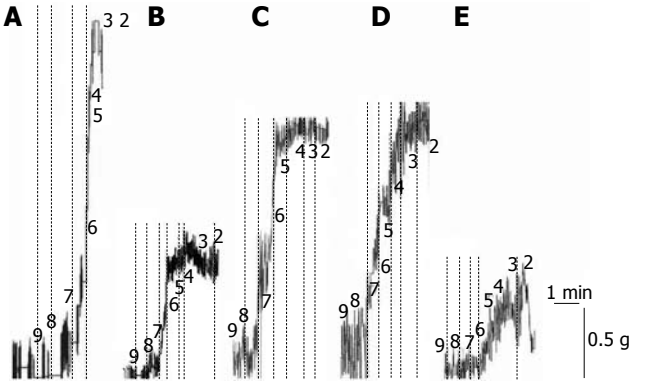

Figure 4 Representative traces showing responses generated by various concentrations of substance P in longitudinal ileum muscle isolated from sham-operated control (**A**), I/R control (**B**), CPA-I/R (**C**), adenosine-I/R (**D**), and DPCPX-adenosine-I/R (**E**) rats.

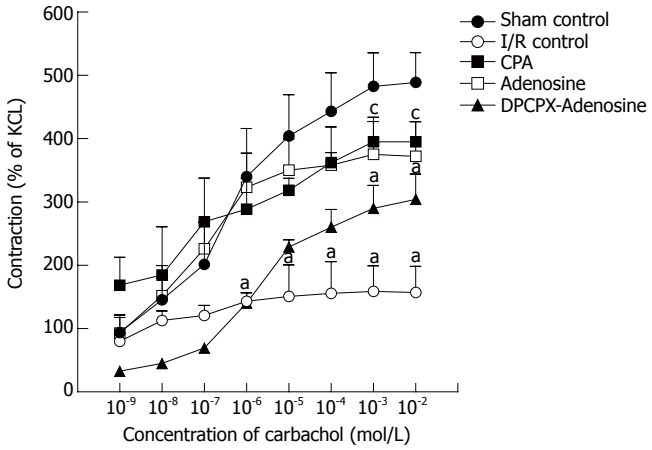

Figure 3 Dose-response curves of carbachol in longitudinal ileum muscle isolated from sham-operated control, I/R control, CPA-I/R, adenosine-I/R, and DPCPX-adenosine-I/R rats. Data are expressed as means ± SE (n = 8). $^{a}P < 0.05$ *vs* sham-operated control, $^{c}P < 0.05$ *vs* I/R control groups.

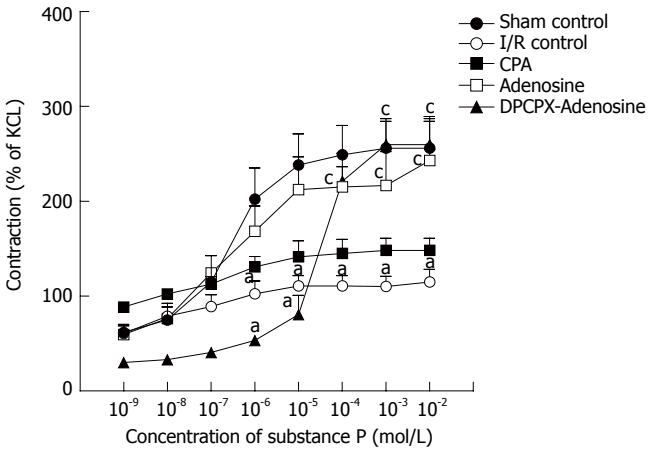

Figure 5 Dose-response curves of substance P in longitudinal ileum muscle isolated from sham-operated control, I/R control, CPA-I/R, adenosine-I/R, and DPCPX-adenosine-I/R rats. Data are expressed as means ± SE (n = 8). $^{a}P < 0.05$ *vs* sham-operated control, $^{c}P < 0.05$ *vs* I/R control groups.

P ranging from 10^{-9} mol/L to 10^{-2} mol/L, terminal ileum samples contracted in a dose-dependent fashion in all groups (Figure 4), rendering sigmoid curves with E_{max} and pD_2 values (Figure 5). The contractile response induced by substance P was significantly and dose-dependently inhibited by induction of I/R. Statistical difference between sham-operated control rats and I/R control animals was significant at 10^{-6} mol/L and over doses of substance P ($P < 0.05$). Reduced contractility due to I/R was alleviated significantly by adenosine treatment ($P < 0.05$). This effect of adenosine was completely lost once DPCPX was given prior to adenosine administration. However, the exacerbating effect of DPCPX was significantly evident in response to substance P at doses lower than 10^{-5} mol/L (Figure 5). Above this concentration, as shown in the ascending part of the curve, responses in both adenosine- and DPCPX-adenosine-treated groups were statistically indistinguishable. Accordingly, there was a statistically significant difference between I/R control group and DPCPX-adenosine-treated group in response to 10^{-4} mol/L ($P = 0.022$), 10^{-3} mol/L ($P = 0.004$), and 10^{-2} mol/L ($P = 0.011$) of substance P. Regarding the corresponding pD_2 values, no statistically significant change was detected in any group (Table 1).

TBARS level

Average TBARS content of intestinal samples from sham-operated animals was 54.18 ± 3.26 nmol/g tissue, while that from I/R control rats was 78.27 ± 7.60 nmol/g tissue (Figure 6). I/R caused approximately 1.45 fold increase in TBARS content of the tissue, which was significantly different from that measured in samples from sham-operated animals ($P = 0.002$). Administration of either CPA or adenosine prior to the induction of ischemia significantly reduced the elevated TBARS content to the levels observed in sham control rats. Mean values of the both groups (39.87 ± 11.02 nmol/g tissue and 56.49 ± 7.03 nmol/g tissue, respectively) were significantly different from that of the I/R control group ($P = 0.001$). On the other hand, in the case of DPCPX pretreatment before

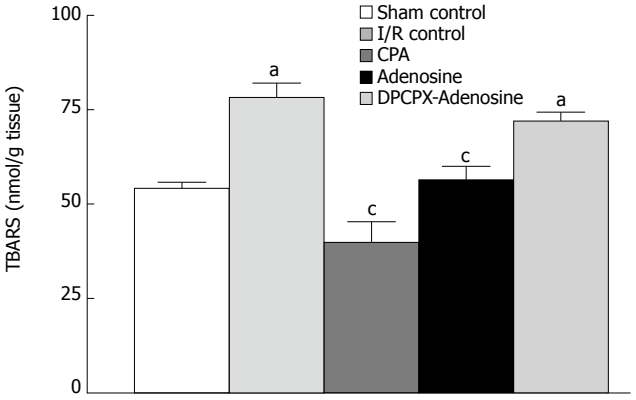

Figure 6 TBARS content of ileum samples from sham-operated control, I/R control, CPA-I/R, adenosine-I/R, and DPCPX-adenosine-I/R rats. Data are expressed as means ± SE (n = 8). $^{a}P < 0.05$ *vs* sham-operated control, $^{c}P < 0.05$ *vs* I/R control groups.

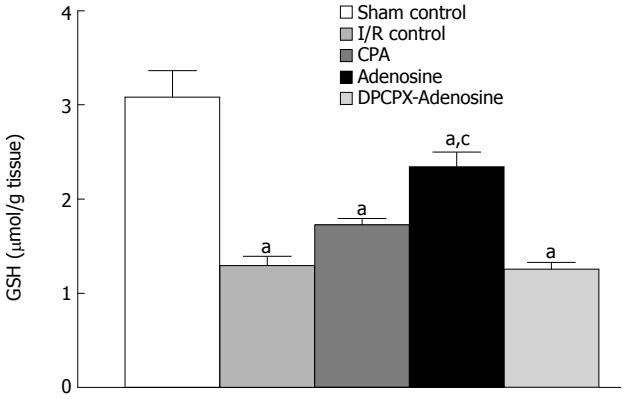

Figure 7 GSH content of ileum samples from sham-operated control, I/R control, CPA-I/R, adenosine-I/R, and DPCPX-adenosine-I/R rats. Data are expressed as means ± SE (n = 8). $^{a}P < 0.05$ *vs* sham-operated control, $^{c}P < 0.05$ *vs* I/R control groups.

adenosine administration followed by I/R, the average TBARS content was 72.02 ± 4.34 nmol/g tissue, which was not significantly different from that in the I/R control group.

GSH level

As shown in Figure 7, the amount of GSH measured in tissues subjected to I/R (1.29 ± 0.19 μmol/g tissue) decreased approximately 58% compared to that measured in the tissues from the sham-operated group (3.08 ± 0.27 μmol/g tissue) ($P < 0.001$). Levels of tissue GSH were statistically indistinguishable when comparing the samples from I/R control group with those from CPA-treated group. In contrast, treatment with adenosine significantly ameliorated the decreased amount of GSH. Mean GSH content was 2.34 ± 0.31 μmol/g tissue, which was significantly different from that measured in I/R control animals ($P = 0.002$). However, pretreatment with DPCPX prevented this effect of adenosine, reducing GSH content to the levels observed in I/R control animals.

MPO activity

MPO enzyme activities in the terminal ileum samples from animals subjected to sham operation, I/R, CPA treatment, adenosine treatment, and DPCPX-adenosine treatment averaged 6.09 ± 1.04 U/mg tissue, 18.19 ± 6.57 U/mg tissue, 10.80 ± 3.66 U/mg tissue, 5.58 ± 2.89 U/mg tissue, and 21.45 ± 9.61 U/mg tissue, respectively (Figure 8).

I/R caused approximately a 3 fold increase in MPO activity of terminal ileum tissue compared to the basal level of the activity ($P < 0.0001$), which was measured in tissues of sham control animals (Figure 8). As MPO activity of samples from animals treated with CPA or adenosine were significantly different from that in I/R group ($P = 0.056$ and $P = 0.0001$, respectively), it appeared that pretreatment with DPCPX completely abolished the reducing effect of adenosine on MPO activity. Clearly, no statistical difference was observed in MPO activity between I/R control animals and DPCPX-pretreated rats, while there was a significant difference between CPA-treated animals and DPCPX-pretreated animals ($P = 0.023$) as well as between adenosine-treated group and DPCPX-pretreated group ($P < 0.0001$).

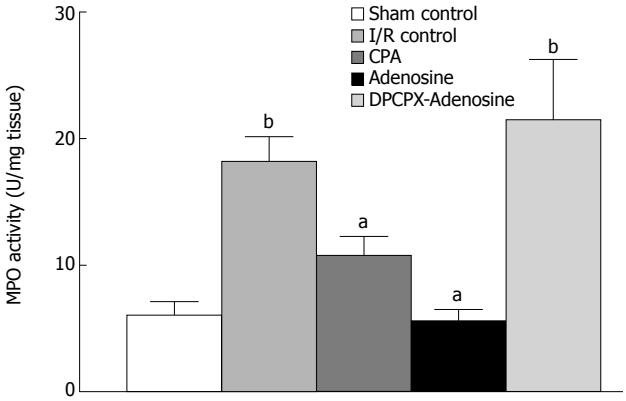

Figure 8 MPO level of ileum samples from sham-operated control, I/R control, CPA-I/R, adenosine-I/R, and DPCPX-adenosine-I/R animals. Results are the means ± SE of 6 to 8 animals in each group. $^{a}P < 0.05$ *vs* I/R control, $^{b}P < 0.001$ *vs* sham-operated control.

DISCUSSION

The major findings of the present study can be summarized as follows: (1) I/R resulted in reduced ileal contractility in response to KCl, carbachol, and substance P as well as elevating oxidative stress and neutrophil infiltration; (2) These disturbances were significantly ameliorated by either adenosine administration or A_1AR activation in the preischemic period; (3) Adenosine and A_1AR-mediated protection against I/R injury seemed to be associated with decreased oxidative stress and MPO activity; (4) A_1AR antagonist DPCPX diminished the injury-sparing effect of PPC with adenosine as observed in other tissues. Pharmacological blockade of A_1ARs exacerbated the contractile response of small intestinal smooth muscle.

I/R results in disrupted exogenous electrical activity and contractile response of ileum[8-10]. A substantial amount of evidence indicates that the pathogenesis of I/R and I/R-induced motor alterations have been related to OFRs[1-3,6,8] and activated neutrophils[1-3,10]. Intestinal I/R sets the groundwork for an inflammatory response in

the vicinity of muscularis cells, provoking the recruitment and extravasation of leukocytes into smooth muscle syncytium[2,10]. A number of experimental studies have been conducted in order to test various pharmacological agents that might reduce reperfusion injury of the intestinal mucosa[4,5,7,9,50,51] with the intention of improving life-span after acute mesenteric ischemia,.

Our results showed that intestinal I/R resulted in decreased ileal contractility in response to carbachol, subtance P, and KCl; therefore influencing both receptor-mediated induction and non-receptor-mediated induction. That the pD_2 values in all groups were statistically indifferent from each other however, suggest that I/R does not alter agonist-receptor interaction. Hence, the reduced E_{max} value in I/R group may be dependent partly on change in the regulation of postreceptor processes (e.g. excitation-contraction coupling)[9,46]. Furthermore, the decreased contraction response also observed in non-receptor-mediated induction strongly supports this possibility.

IPC makes reference to a phenomenon in which the harmful effects of prolonged ischemia is prevented by exposure of a tissue to brief periods of ischemia[35]. In spite of the fact that it is highly complicated in nature, IPC has been successfully applied to various animal models of intestinal I/R, resulting in attenuation of the reperfusion injury[37-40,52]. However, although IPC has been shown to be beneficial in the human heart and liver, prospectively controlled studies in both humans and animals involving IPC and PPC of the intestine are inadequate. More research focused on the application of drugs that can mimic the effects of IPC is needed to analyze the cellular and molecular events during I/R injury of the intestine so as to attenuate I/R injury[1]. Both animal and human studies have revealed that adenosine is one of the major triggers for IPC. A study done by Unal *et al*[37] has demonstrated that administration of adenosine prior to ischemia is as effective as IPC for inducing ischemic tolerance in rats. Data gathered in the present study confirms this finding and show that the treatment with adenosine significantly restored I/R-reduced contractile response. Furthermore, the treatment also provided such beneficial effects such as elevating GSH content, lowering lipid peroxidation, and reducing neutrophil infiltration. In addition, that the A_1AR antagonist DPCPX significantly blocked these protective effects of adenosine is consistent with the hypothesis that PPC with adenosine is primarily mediated via A_1ARs.

The findings of the present study revealed that non-receptor mediated (e.g. KCl-induced) and receptor mediated (e.g. carbacol- and substance P-induced) ileal contractions that were reduced significantly due to I/R, were improved remarkably and returned to sham-control levels by systemic administration of adenosine or CPA. During the process of preconditioning, adenosine is generated in the ischemic tissue. The endogenous adenosine or selective pharmacological agonists activate A_1ARs. Preischemic activation of A_1ARs has been demonstrated to prevent from I/R damage in various organs including heart[15-18,25], kidney[26,27] and brain[28,29]. In these studies, the activation of A_1ARs has been strongly implicated in the mediation of IPC. Adenosine therapy before induction of ischemia has been reported to attenuate ischemic injury in heart[23,24] and intestine[37]. Furthermore, pharmacological blockade of A_1AR during preconditioning eliminates the achivement of protection[15-18]. The protective effect of A_1AR activation is accomplished through the activation of PKC, leading to translocation of PKC to sarcolemmal and to mitochondrial membranes. Activated PKC then induces an increase in opening of ATP-sensitive K^+ channels in heart[11,12]. Stimulation of A_1ARs also precedes the early activation of some other kinases such as tyrosine kinases, p38, MAPK[11,19,25,31,33], ERK[32], and Akt[20]. Additionally, in protection obtained by agonist-induced stimulation of A_1AR, elevated content or activity of many proteins have been demonstrated such as HSP 27[11] and Mn-SOD[15]. Despite the existence and involvement of relatively large number of effector molecules, it appears that they vary among tissues. In small intestine, for instance, Davis *et al*[38] report that pharmacological modulation of A_1ARs is involved in reduced expression of P-selectin, which is a downstream effector target of the adenosine-initiated, PKC dependent, anti-inflammatory signaling pathway in preconditioning. In our study, I/R of small intestine elevated the tissue TBARS content, indicating enhanced generation of OFRs; therefore, inducing lipid peroxidation. Systemic administration of adenosine or CPA appeared to be protective against I/R-induced reduction of contractility via, at least, inhibiting lipid peroxidation and neutrophil infiltration as confirmed by reduction of TBARS and MPO levels, respectively. Another significant observation reported recently is that activation of A_1ARs *in vitro* prevents cellular functions from H_2O_2-induced injury through signaling pathways related to PKC in renal proximal tubular cells[53]. The same observation has been demonstrated in other studies on heart[54,55] and kidney[53]. In these studies, activation of A_1ARs *in vivo* and *in vitro* is reported to be associated with protection against H_2O_2-induced oxidative injury by modulation of the detrimental increases in intracellular calcium concentration and by means of activation of cardiomyocyte K^+ channels after H_2O_2 exposure.

GSH is an endogenous antioxidant and present in all animal cells. Reacting with free radicals, it can provide protection from singlet oxygen, hydroxyl radical and superoxide anion[31]. Many published studies indicate that tissue injury, induced by various stimuli (e.g. I/R), is coupled with glutathione depletion[9]. In the present study, we showed that depleted GSH content in ischemic ileal tissue was recovered by adenosine or CPA therapies. In other words, inducing PPC with these drugs maintained GSH content during reperfusion. This effect may be related to activation of PKC since adenosine has been reported to induce the activation of antioxidant enzymes *in vitro* and since it is suggested that the stimulatory action of adenosine is likely involved in PKC-mediated phosphorylation. Such a mechanism could serve to decrease the levels of OFRs, which would otherwise be harmful to the cell. This very effect of adenosine is also evident *in vivo*, and may account for adenosine-induced reduction of lipid peroxidation in cochlea[34]. Although the

present study has not examined antioxidant enzymes or PKC, the elevated level of GSH implicates the potential involvement of a cytoprotective mechanism related to adenosine and A1 receptor activation.

Modulation of the inflammatory response following I/R injury is an important component of tissue defense, mostly because inflammation is the major component of cell death and motor alteration in intestine subjected to intestinal injury. In the initial period of I/R, generation of OFRs occurs, which is the most likely the initial factor responsible for the induction of neutrophil chemotactic activity. Afterwards an influx of leukocytes during reperfusion triggers an intricate cascade of proinflammatory events associated with cytokine/chemokine release and free radical-mediated intestinal injury[1,3]. Upon attachment to endothelium, neutrophils cause the secretion of additional OFRs, contributing to the damage. At this point, the enzyme MPO, found largely in leukocytes particularly in neutrophils, provides an opportunity to check the tissue level of the cells since it is a marker of neutrophil infiltration and accumulation into tissues[27]. In the present study, we have demonstrated that the therapy with A_1AR agonist CPA prevented neutrophil infiltration into the reperfused-intestine as shown by the decrese in MPO content. This finding is in agreement with those of previous studies which reports that A_1AR stimulation is associated with decreased inflammation and MPO levels[22,27,38].

In the present study, we have demonstrated that administration of adenosine and the A_1AR agonist CPA ameliorated intestinal contractile dysfunction induced by I/R. The outcome of the study suggests that preischemic administration of adenosine or CPA may protect intestine, as indicated by recovery of contractile response, possibly through decreasing oxidative strees and reducing neutrophil infiltration. In conclusion, our findings suggest the cellular mechanism by which adenosine and pharmacological stimulation of A_1ARs attenuate intestinal injury, which may indicate the possible therapeutic usage of adenosine as an adjunct for ischemia and ischemia related small bowel diseases.

ACKNOWLEDGMENTS

We are greatful to Hasan Tahsin Yilmaz and Ramazan Temel for their unfailing assistance in animal care and maintaining standard conditions of animal research laboratory.

COMMENTS

Background

A number of experimental studies have shown that reperfusion injury in the small intestine is prevented by ischemic preconditioning (IPC). Moreover, various studies using rat small intestine have demonstrated that establishing pharmacological preconditioning (PPC) by administration of either adenosine or adenosine A1 receptor agonist mimic the protective effects of IPC. On the other hand, relatively little data is available on the role of the different adenosine receptors in mediating cytoprotection during intestinal I/R injury. There is no direct evidence which confirms the possible effects of adenosine and adenosine A1 receptor activation on I/R injury- related decreased in contractility of intestinal smooth muscle.

Research frontiers

That adenosine exerts anti-ischaemic actions is indicated by a number of studies using adenosine receptor agonists and antagonists as well as animals overexpressing or lacking the adenosine A1 receptor. Administration of adenosine either prior to ischemia or during reperfusion has been shown to attenuate myocardial injury. Treatment with adenosine A1 receptor agonist initiates preconditioning not only in heart but also in such tissues as kidney and brain, resulting in attenuation of ischemic injury.

Innovations and breakthroughs

IPC of the small intestine reduces postischemic leukocyte adhesion by maintaining the bioavailability of nitric oxide. Moreover, it lowers the expression of P-selectin, which is a downstream effector target of the adenosine-initiated, PKC dependent, signalling pathway in intestine. Although activation of PKC triggered by adenosine is a crucial factor for initiating the beneficial actions of IPC in most tissues, the effector of the preconditioning phenomenon appears to vary among tissues. Activated-K^+ channels, nitric oxide, and endogenous opioid peptides have reported to be the other downstream effectors of IPC in intestine. Furthermore, currently published studies suggest important anti-ischemic roles of the A_1, A_3 or A_{2a} adenosine receptors in heart.

Applications

The therapeutic efficacy of adenosine and the adenosine A1 agonist, 2-chloro-N^6-cyclopentyladenosine (CPA) should be examined for potential clinical application in the treatment of conditions related to intestinal ischemia-reperfusion injury, such as small bowel transplantation, strangulated hernias, and abdominal aortic aneurysm. In addition, it would be worthwhile to focus onthe possible effector molecules (e.g. involvement of PKC, opening of mitochondrial ATP-sensitive K^+ channels, or activation of Akt) which underlie the mechanism (s) responsible for the beneficial effects of adenosine and CPA observed in the present study.

Terminology

Ischemia: deficient supply of blood to a body part (e.g. any organ) that is due to obstruction of the inflow of arterial blood (for example, by narrowing of arteries as a result of spasm or disease); Ischemia-reperfusion: interruption of the blood flow to a tissue for a period of time followed by restoration of blood flow. During the ischaemic period , a sequence of events is initiated that may ultimately lead to cellular dysfunction or even cell death; Reperfusion injury: When ischemia is ended by restoration of blood flow, a second series of injurious events ensue producing additional damage. The injury produced by reperfusion is more severe that that induced by ischemia and is called reperfusion injury. The primary harmful events are the formation of cytotoxic oxidants (also commonly called oxygen free radicals) derived from molecular oxygen, oxygen free radical-mediated damage to cellular membranes via lipid peroxidation, loss of cellular calcium balance, and generation of inflammatory reaction at the site of damage; Oxidative stress: stress on the body or organism that results from the cumulative damage done by oxygen free radicals which are inadequately neutralized by antioxidants; Agonist: a chemical substance capable of combining with a receptor on a cell and initiating the same reaction or activity typically produced by the binding of an endogenous substance; Antagonist: a chemical substance that acts through receptor to reduce the physiological activity of another chemical or endogenous substance.

Peer review

The present study is interesting, well designed, and contained novel findings. The study is set up throughly and the paper is well written. The conclusions are well based and are of clinical value.

REFERENCES

1 **Mallick IH**, Yang W, Winslet MC, Seifalian AM. Ischemia-reperfusion injury of the intestine and protective strategies against injury. *Dig Dis Sci* 2004; **49**: 1359-1377
2 **Lodato RF**, Khan AR, Zembowicz MJ, Weisbrodt NW, Pressley TA, Li YF, Lodato JA, Zembowicz A, Moody FG. Roles of IL-1 and TNF in the decreased ileal muscle contractility induced by lipopolysaccharide. *Am J Physiol* 1999; **276**: G1356-G1362
3 **Carden DL**, Granger DN. Pathophysiology of ischaemia-reperfusion injury. *J Pathol* 2000; **190**: 255-266
4 **Arumugam TV**, Shiels IA, Woodruff TM, Reid RC, Fairlie DP, Taylor SM. Protective effect of a new C5a receptor antagonist against ischemia-reperfusion injury in the rat small intestine. *J Surg Res* 2002; **103**: 260-267

5 **Bielefeldt K**, Conklin JL. Intestinal motility during hypoxia and reoxygenation in vitro. *Dig Dis Sci* 1997; **42**: 878-884
6 **Khanna A**, Rossman JE, Fung HL, Caty MG. Attenuated nitric oxide synthase activity and protein expression accompany intestinal ischemia/reperfusion injury in rats. *Biochem Biophys Res Commun* 2000; **269**: 160-164
7 **Poussios D**, Andreadou I, Papalois A, Rekka E, Gavalakis N, Aroni K, Kourounakis PN, Fotiadis C, Sechas MN. Protective effect of a novel antioxidant non-steroidal anti-inflammatory agent (compound IA) on intestinal viability after acute mesenteric ischemia and reperfusion. *Eur J Pharmacol* 2003; **465**: 275-280
8 **Takahashi A**, Tomomasa T, Kaneko H, Watanabe T, Tabata M, Morikawa H, Tsuchida Y, Kuwano H. Intestinal motility in an in vivo rat model of intestinal ischemia-reperfusion with special reference to the effects of nitric oxide on the motility changes. *J Pediatr Gastroenterol Nutr* 2001; **33**: 283-288
9 **Ozacmak VH**, Sayan H, Arslan SO, Altaner S, Aktas RG. Protective effect of melatonin on contractile activity and oxidative injury induced by ischemia and reperfusion of rat ileum. *Life Sci* 2005; **76**: 1575-1588
10 **Hassoun HT**, Weisbrodt NW, Mercer DW, Kozar RA, Moody FG, Moore FA. Inducible nitric oxide synthase mediates gut ischemia/reperfusion-induced ileus only after severe insults. *J Surg Res* 2001; **97**: 150-154
11 **Baxter GF**. Role of adenosine in delayed preconditioning of myocardium. *Cardiovasc Res* 2002; **55**: 483-494
12 **Mubagwa K**, Flameng W. Adenosine, adenosine receptors and myocardial protection: an updated overview. *Cardiovasc Res* 2001; **52**: 25-39
13 **Kadowaki M**, Tokita K, Nagakura Y, Takeda M, Hanaoka K, Tomoi M. Adenosine A1 receptor blockade reverses dysmotility induced by ischemia-reperfusion in rat colon. *Eur J Pharmacol* 2000; **409**: 319-323
14 **Nicholls J**, Hourani SM. Characterization of adenosine receptors on rat ileum, ileal longitudinal muscle and muscularis mucosae. *Eur J Pharmacol* 1997; **338**: 143-150
15 **Dana A**, Jonassen AK, Yamashita N, Yellon DM. Adenosine A(1) receptor activation induces delayed preconditioning in rats mediated by manganese superoxide dismutase. *Circulation* 2000; **101**: 2841-2848
16 **Mozzicato S**, Joshi BV, Jacobson KA, Liang BT. Role of direct RhoA-phospholipase D1 interaction in mediating adenosine-induced protection from cardiac ischemia. *FASEB J* 2004; **18**: 406-408
17 **De Jonge R**, Out M, Maas WJ, De Jong JW. Preconditioning of rat hearts by adenosine A1 or A3 receptor activation. *Eur J Pharmacol* 2002; **441**: 165-172
18 **Kristo G**, Yoshimura Y, Keith BJ, Stevens RM, Jahania SA, Mentzer RM, Lasley RD. Adenosine A1/A2a receptor agonist AMP-579 induces acute and delayed preconditioning against in vivo myocardial stunning. *Am J Physiol Heart Circ Physiol* 2004; **287**: H2746-H2753
19 **Headrick JP**, Hack B, Ashton KJ. Acute adenosinergic cardioprotection in ischemic-reperfused hearts. *Am J Physiol Heart Circ Physiol* 2003; **285**: H1797-H1818
20 **Solenkova NV**, Solodushko V, Cohen MV, Downey JM. Endogenous adenosine protects preconditioned heart during early minutes of reperfusion by activating Akt. *Am J Physiol Heart Circ Physiol* 2006; **290**: H441-H449
21 **Maddock HL**, Mocanu MM, Yellon DM. Adenosine A(3) receptor activation protects the myocardium from reperfusion/reoxygenation injury. *Am J Physiol Heart Circ Physiol* 2002; **283**: H1307-H1313
22 **Lee HT**, Gallos G, Nasr SH, Emala CW. A_1 adenosine receptor activation inhibits inflammation, necrosis, and apoptosis after renal ischemia-reperfusion injury in mice. *J Am Soc Nephrol* 2004; **15**: 102-111
23 **Randhawa MP**, Lasley RD, Mentzer RM. Salutary effects of exogenous adenosine administration on in vivo myocardial stunning. *J Thorac Cardiovasc Surg* 1995; **110**: 63-74
24 **Sekili S**, Jeroudi MO, Tang XL, Zughaib M, Sun JZ, Bolli R. Effect of adenosine on myocardial 'stunning' in the dog. *Circ Res* 1995; **76**: 82-94
25 **Yoshimura Y**, Kristo G, Keith BJ, Jahania SA, Mentzer RM, Lasley RD. The p38 MAPK inhibitor SB203580 blocks adenosine A(1) receptor-induced attenuation of *in vivo* myocardial stunning. *Cardiovasc Drugs Ther* 2004; **18**: 433-440
26 **Sugino H**, Shimada H, Tsuchimoto K. Role of adenosine in renal protection induced by a brief episode of ischemic preconditioning in rats. *Jpn J Pharmacol* 2001; **87**: 134-142
27 **Lee HT**, Xu H, Nasr SH, Schnermann J, Emala CW. A1 adenosine receptor knockout mice exhibit increased renal injury following ischemia and reperfusion. *Am J Physiol Renal Physiol* 2004; **286**: F298-F306
28 **Nakamura M**, Nakakimura K, Matsumoto M, Sakabe T. Rapid tolerance to focal cerebral ischemia in rats is attenuated by adenosine A1 receptor antagonist. *J Cereb Blood Flow Metab* 2002; **22**: 161-170
29 **Hiraide T**, Katsura K, Muramatsu H, Asano G, Katayama Y. Adenosine receptor antagonists cancelled the ischemic tolerance phenomenon in gerbil. *Brain Res* 2001; **910**: 94-98
30 **Kudo M**, Wang Y, Xu M, Ayub A, Ashraf M. Adenosine A(1) receptor mediates late preconditioning via activation of PKC-delta signaling pathway. *Am J Physiol Heart Circ Physiol* 2002; **283**: H296-H301
31 **Zhao X**, Alexander JS, Zhang S, Zhu Y, Sieber NJ, Aw TY, Carden DL. Redox regulation of endothelial barrier integrity. *Am J Physiol Lung Cell Mol Physiol* 2001; **281**: L879-L886
32 **Reid EA**, Kristo G, Yoshimura Y, Ballard-Croft C, Keith BJ, Mentzer RM, Lasley RD. In vivo adenosine receptor preconditioning reduces myocardial infarct size via subcellular ERK signaling. *Am J Physiol Heart Circ Physiol* 2005; **288**: H2253-H2259
33 **Ballard-Croft C**, Kristo G, Yoshimura Y, Reid E, Keith BJ, Mentzer RM, Lasley RD. Acute adenosine preconditioning is mediated by p38 MAPK activation in discrete subcellular compartments. *Am J Physiol Heart Circ Physiol* 2005; **288**: H1359-H1366
34 **Ramkumar V**, Hallam DM, Nie Z. Adenosine, oxidative stress and cytoprotection. *Jpn J Pharmacol* 2001; **86**: 265-274
35 **Ishida T**, Yarimizu K, Gute DC, Korthuis RJ. Mechanisms of ischemic preconditioning. *Shock* 1997; **8**: 86-94
36 **Mallick IH**, Yang W, Winslet MC, Seifalian AM. Ischaemic preconditioning improves microvascular perfusion and oxygenation following reperfusion injury of the intestine. *Br J Surg* 2005; **92**: 1169-1176
37 **Unal S**, Demirkan F, Arslan E, Cin I, Cinel L, Eskandari G, Cinel I. Comparison of ischemic and chemical preconditioning in jejunal flaps in the rat. *Plast Reconstr Surg* 2003; **112**: 1024-1031
38 **Davis JM**, Gute DC, Jones S, Krsmanovic A, Korthuis RJ. Ischemic preconditioning prevents postischemic P-selectin expression in the rat small intestine. *Am J Physiol* 1999; **277**: H2476-H2481
39 **Vlasov TD**, Smirnov DA, Nutfullina GM. Preconditioning of the small intestine to ischemia in rats. *Neurosci Behav Physiol* 2002; **32**: 449-453
40 **Sola A**, De Oca J, González R, Prats N, Roselló-Catafau J, Gelpí E, Jaurrieta E, Hotter G. Protective effect of ischemic preconditioning on cold preservation and reperfusion injury associated with rat intestinal transplantation. *Ann Surg* 2001; **234**: 98-106
41 **Hotter G**, Closa D, Prados M, Fernández-Cruz L, Prats N, Gelpí E, Roselló-Catafau J. Intestinal preconditioning is mediated by a transient increase in nitric oxide. *Biochem Biophys Res Commun* 1996; **222**: 27-32
42 **Yang SP**, Hao YB, Wu YX, Dun W, Shen LH, Zhang Y. Ischemic preconditioning mediated by activation of KATP channels in rat small intestine. *Zhongguo Yao Li Xue Bao* 1999; **20**: 341-344
43 **Zhang Y**, Wu YX, Hao YB, Dun Y, Yang SP. Role of endogenous opioid peptides in protection of ischemic preconditioning in rat small intestine. *Life Sci* 2001; **68**: 1013-1019
44 **Boucher M**, Pesant S, Falcao S, de Montigny C, Schampaert E, Cardinal R, Rousseau G. Post-ischemic cardioprotection by A2A adenosine receptors: dependent of phosphatidylinositol 3-kinase pathway. *J Cardiovasc Pharmacol* 2004; **43**: 416-422
45 **Boucher M**, Wann BP, Kaloustian S, Massé R, Schampaert E, Cardinal R, Rousseau G. Sustained cardioprotection afforded

by A2A adenosine receptor stimulation after 72 hours of myocardial reperfusion. *J Cardiovasc Pharmacol* 2005; **45**: 439-446
46 **Kaya TT**, Koyluoglu G, Soydan AS, Arpacik M, Karadas B. Effects of nimesulide and pentoxifylline on decreased contractile responses in rat ileum with peritonitis. *Eur J Pharmacol* 2002; **442**: 147-153
47 **Casini AF**, Ferrali M, Pompella A, Maellaro E, Comporti M. Lipid peroxidation and cellular damage in extrahepatic tissues of bromobenzene-intoxicated mice. *Am J Pathol* 1986; **123**: 520-531
48 **Aykaç G**, Uysal M, Yalçin AS, Koçak-Toker N, Sivas A, Oz H. The effect of chronic ethanol ingestion on hepatic lipid peroxide, glutathione, glutathione peroxidase and glutathione transferase in rats. *Toxicology* 1985; **36**: 71-76
49 **Bradley PP**, Priebat DA, Christensen RD, Rothstein G. Measurement of cutaneous inflammation: estimation of neutrophil content with an enzyme marker. *J Invest Dermatol* 1982; **78**: 206-209
50 **Ferrer JV**, Ariceta J, Guerrero D, Gomis T, Larrea MM, Balén E, Lera JM. Allopurinol and N-acetylcysteine avoid 60% of intestinal necrosis in an ischemia-reperfusion experimental model. *Transplant Proc* 1998; **30**: 2672
51 **Jacob T,** Ascher E, Hingorani A, Kallakuri S. Glycine prevents the induction of apoptosis attributed to mesenteric ischemia/reperfusion injury in a rat model. *Surgery* 2003; **134**: 457-466
52 **Aban N**, Cinel L, Tamer L, Aktas A, Aban M. Ischemic preconditioning reduces caspase-related intestinal apoptosis. *Surg Today* 2005; **35:** 228-234
53 **Lee HT**, Emala CW. Adenosine attenuates oxidant injury in human proximal tubular cells via A(1) and A(2a) adenosine receptors. *Am J Physiol Renal Physiol* 2002; **282**: F844-F852
54 **Narayan P**, Mentzer RM, Lasley RD. Adenosine A1 receptor activation reduces reactive oxygen species and attenuates stunning in ventricular myocytes. *J Mol Cell Cardiol* 2001; **33**: 121-129
55 **Thomas GP**, Sims SM, Cook MA, Karmazyn M. Hydrogen peroxide-induced stimulation of L-type calcium current in guinea pig ventricular myocytes and its inhibition by adenosine A1 receptor activation. *J Pharmacol Exp Ther* 1998; **286:** 1208-1214

S- Editor Liu Y **L- Editor** Lalor PF **E- Editor** Bi L

PO Box 2345, Beijing 100023, China
www.wjgnet.com
wjg@wjgnet.com

World J Gastroenterol 2007 January 28; 13(4): 548-556
World Journal of Gastroenterology ISSN 1007-9327

BASIC RESEARCH

Influence of dexamethasone on inflammatory mediators and NF-κB expression in multiple organs of rats with severe acute pancreatitis

Xi-Ping Zhang, Ling Zhang, Lin-Jie Chen, Qi-Hui Cheng, Jian-Mei Wang, Wei Cai, Hai-Ping Shen, Jun Cai

Xi-Ping Zhang, Department of General Surgery, Hangzhou First People's Hospital, Hangzhou 310006, Zhejiang Province, China
Ling Zhang, Class s0201 of Seven Year's Clinical Medicine, Shanxi Medical University, Taiyuan 310001, Shanxi Province, China
Lin-Jie Chen, Zhejiang University of Traditional Chinese Medical, Hangzhou 310053, Zhejiang Province, China
Qi-Hui Cheng, Department of Gynaecology and Obstetrics, Hangzhou First People's Hospital, Hangzhou 310006, Zhejiang Province, China
Jian-Mei Wang, Supply Room, Hangzhou First People's Hospital, Hangzhou 310006, Zhejiang Province, China
Wei Cai, Hai-Ping Shen, Jun Cai, Operating Room, Hangzhou First People's Hospital, Hangzhou 310006, Zhejiang Province, China
Supported by Technological Foundation Project of Traditional Chinese Medicine Science of Zhejiang Province, NO. 2003C130 and NO. 2004C142; Foundation Project for Medical Science and Technology of Zhejiang province, No. 2003B134; Grave Foundation Project for Technological and Development of Hangzhou, No. 2003123B19; Intensive Foundation Project for Technology of Hangzhou, NO. 2004Z006; Foundation Project for Medical Science and Technology of Hangzhou, No. 2003A004; and Foundation Project for Technology of Hangzhou, No. 2005224
Correspondence to: Xi-Ping Zhang, MD, Department of General Surgery, Hangzhou First People's Hospital, 261 Huansha Road, Hangzhou 310006, Zhejiang Province,
China. zxp99688@vip.163.com
Telephone: +86-571-87065701 Fax: +86-571-87914773
Received: 2006-07-23 Accepted: 2006-12-12

Abstract

AIM: To observe the therapeutic effects of dexamethasone on rats with severe acute pancreatitis (SAP) and investigate the influences of dexamethasone on the inflammatory mediators and NF-κB expression in multiple organs of SAP rats as well as the mechanisms involved.

METHODS: Ninety Sprague-Dawley (SD) rats with SAP were randomly divided into the model group (n = 45) and dexamethasone treatment group (n = 45), and another 45 rats were selected for the sham operation group. All groups were randomly subdivided into the 3 h, 6 h and 12 h groups, each group containing 15 rats. The survival of all groups and pathological changes of multiple organs (liver, kidney and lung) were observed at different time points after the operation. The pathological score of multiple organs was carried out, followed by the determination of amylase, endotoxin and TNF-α contents in blood. The tissue microarray was used to detect the expression levels of NF-κB p65 protein in multiple organs.

RESULTS: There was no marked difference between the model group and treatment group in the survival rate. The amylase content of the treatment group was significantly lower compared to the model group at 12 h (P < 0.01, 7791.00 *vs* 9195.00). Moreover, the endotoxin and TNF-α levels of the treatment group were significantly lower than that of the model group at 6 h and 12 h (P < 0.01, 0.040 *vs* 0.055, 0.042 *vs* 0.059 and P < 0.05, 58.30 *vs* 77.54, 38.70 *vs* 67.30, respectively). Regarding the changes in liver NF-κB expression, the model group significantly exceeded the sham operation group at 3 h (P < 0.01, 1.00 *vs* 0.00), and the treatment group significantly exceeded the sham operation group at 12 h (P < 0.01, 1.00 *vs* 0.00), whereas no marked difference was observed between the model group and treatment group at all time points. The kidney NF-κB expression level in the treatment group significantly exceeded the model group (P < 0.05, 2.00 *vs* 0.00) and the sham operation group (P < 0.01, 2.00 *vs* 0.00) at 12 h. No NF-κB expression in the lung was found in any group.

CONCLUSION: Dexamethasone can lower the amylase, endotoxin and TNF-α levels as well as mortality of SAP rats. NF-κB plays an important role in multiple organ injury. Further studies should be conducted to determine whether dexamethasone can ameliorate the pathological changes of multiple organs by reducing the NF-κB expression in the liver and kidney. The advantages of tissue microarrays in pancreatitis pathological examination include time- and energy- saving, and are highly efficient and representative. The restriction of tissue microarrays on the representation of tissues to various extents due to small diameter may lead to the deviation of analysis.

Key words: Severe acute pancreatitis; Dexamethasone; NF-κB; Tissue microarrays; Mutiple organs

Zhang XP, Zhang L ,Chen LJ, Cheng QH, Wang JM, Cai W, Shen HP, Cai J. Influence of dexamethasone on inflammatory mediators and NF-κB expression in multiple

organs of rats with severe acute pancreatitis. *World J Gastroenterol* 2007; 13(4):548-556

http://www.wjgnet.com/1007-9327/13/548.asp

INTRODUCTION

Severe acute pancreatitis (SAP), as one of the common presentations of clinically acute abdomen is a systemic disease in which the local inflammatory pathological changes of pancreas involve multiple organs[1]. It is recently believed the systemic inflammatory response syndrome (SIRS) due to the excessive inflammatory reactions plays an extremely important role in SAP pathogenesis, which is relatively complicated[2,3]. Although the exact pathogenesis remains unclear[4]. Studies in recent years have found that NF-κB (nuclear factor kappa-B) which is a main factor in the genetic transcription of inflammation, presents high expression state in acute pancreatitis and plays an important role in the onset and turnover of acute pancreatitis together with other inflammatory cytokines[5-7]. Dexamethasone is the antagonist of a non-specific inflammatory mediator[8]. Studies have shown that dexamethasone can lower the expression level of NF-κB by inducing the release of NF-κB profilin (IκB)[9]. In this study, we prepared rat SAP models by using the improved Aho's method[10], and investigated the therapeutic effects of dexamethasone on the SAP rats and examined the influences of dexamethasone on the inflammatory mediators and NF-κB expression in multiple organs of the rats.

MATERIALS AND METHODS

Materials

Clean grade healthy male Sprague-Dawley (SD) rats weighing 250-300 g were purchased from the Experimental Animal Center of Medical School, Zhejiang University, China. Sodium taurocholate and sodium pentobarbital were purchased from Sigma Company, USA. Dexamethasone injection was purchased from Zhejiang Xinchang Pharmaceutical Company. NF-κB p65 antibody was purchased from Santa Cruz Company, USA. The full automatic biochemical analyzer was used to determine the plasma amylase level (U/L). Plasma endotoxin Tachypleus Amebocyte Lysate Kit was purchased from Shanghai Yihua Medical Science and Technology Corporation (Institute of Medical Analysis in Shanghai, China), the calculation unit for content is EU/mL. TNF-α ELISA kit was purchased from Jingmei Bioengineering Corporation, China, the calculation unit for content is pg/mL (ng/L).

Animal grouping

We adopted the improved Aho's method[10] to prepare 90 SAP rat models and randomly divided into the model group (45 rats) and treatment group (45 rats). Another 45 rats were selected as the sham operation group. All groups were randomly subdivided into the 3, 6 and 12 h groups, each group containing 15 rats. The dexamethasone treatment group was injected once with dexamethasone (1 mL = 5 mg) *via* the vena caudalis, 0.5 mg/100 g body weight 15 min after successful preparation of SAP model. During the laparotomy in the sham operation group, we performed pancreas and duodenum manipulation, observed pathological changes of multiple organs and finally closed the abdomen. The sham operation group and model group were injected with same amount of normal saline (0.1 mL/100 g body weight) *via* the vena caudalis 15 min after the operation.

Animal model preparation

Fasting and water restriction was imposed on all rat groups 12 h prior to the operation. The rats were anesthetized by intraperitoneal injection of 20 g/L sodium pentobarbital (0.25 mL/100 g body weight) and the operation was performed under aseptic conditions. Model group: After entering the abdomen *via* median epigastric incision, the bile-pancreatic duct, hepatic hilus and common hepatic duct were identified; the duodenal papilla inside the duodenum duct wall was identified, and then a No. 5 needle was used to drill a hole in the mesenteric avascular area. A segmental epidural catheter was inserted into the duodenum cavity *via* the hole, and then inserted into the bile-pancreatic duct toward the direction of papilla in a retrograde way, a microvascular clamp was used to nip the catheter head temporarily. Meanwhile, another microvascular clamp was used to temporarily occlude the common hepatic duct at the confluence of the hepatic duct. After connecting the epidural catheter end with the transfusion converter, 3.5% sodium taurocholate (0.1 mL/100 g) was transfused *via* the microinjection pump at a speed of 0.2 mL/min, stayed for 4 min after injection, and then the microvascular clamp and epidural catheter were removed. After checking for bile leakage, the hole in the lateral duodenal wall was sutured. A sterile cotton ball was used to absorb up the anaesthetic in the abdominal cavity and then the abdomen was closed.

Preparation of tissue microarrays of mutiple organs

We fixed the tissue sample with neutral formalin, prepared the routine paraffin block (named donor block), cut the donor block into 5-μm thick tissue section and carried out routine hematoxylin-eosin (HE) staining as well as microscopic morphological observation under microscope, and then selected the required representative area, marked the locations on the HE sections and also on the corresponding part of the donor block. We prepared the blank block as the recipient block in the size of 45 mm × 20 mm × 15 mm and drilled the recipient block with the tissue microarrays section (Beecher Instruments, USA), the diameter of the drilling needle is 2.0 mm. In obtaining of the donor block tissue microarrays, we used another drilling needle (its inner diameter is equal to the outer diameter of the former drilling needle) to drill the marked location of paraffin block and collected the tissue microarray. Its length was about 0.1 mm shorter than the depth of hole. The tissue microarrays collecting method was just the same as that of drilling the recipient block. After pushing out the tissue microarrays, we directly

inserted it or inserted it with forceps into the hole of recipient block. After pressing the tissue microarrays downwards with common glass slide, we used the distance adjuster to correctly move the drilling needle to a proper distance forward and back or right and left. This process was repeated and could insert tens of tissue microarrays into the recipient block in an orderly fashion. Finally, we piled up three glass slides to press all the tissue microarrays and thus the prepared tissue microarrays section block had flat and smooth surface. We put the prepared tissue microarrays section block into the paraffin block again to make the mold, and put it into a 60℃ oven for 1 h so that the paraffin of the tissue microarrays and recipient block could be melted together. We took the mold out of the oven gently, cooled the half melted paraffin at the room temperature (about 30 min) and then cooled it in a -20℃ refrigerator for 6 min. Later, we took the tissue microarrays section block out of the mold and stored it in a 4℃ refrigerator for later use. We took out the standby paraffin block and rapidly nipped it on the sectioning machine for correction till all the tissue microarrays were on the same plane, then stuck the ice block on the paraffin block for about 5 min and cut into 10-30 successive sections of 5-μm thickness and used the ice block to freeze the paraffin block. We repeated the above process until finishing sectioning of the tissue, floated the successive sections on the cool water and let it spread naturally. Then we used the ophthalmic elbowed forceps and glass slide to separate the sections during which the first section on the head part of the successive sections could be stuck to the glass slide, fixed and separated it with forceps to avoid loss of tissue microarrays sample due to the leakage of tissue section during separation. The sections were transferred into 45℃ warm water to spread for 1 min to ensure their full spreading without scattering. The sections were backed by the glass slide processed by 10% APES acetone solution for staining. We incubated the prepared tissue microarrays sections into a 60℃ oven for 1 h, took them out, cooled it at room temperature and put it into a -20℃ refrigerator for later use.

NF-κB p65 immunohistochemical staining (supersensitive S-P method)

We baked the section at 60℃ for 16 h and dewaxed in a routine fashion. We carried out antigen retrieval at high temperature and high pressure for 2 min, dropped reagent A to block the endogenous peroxidase, incubated at room temperature for 10 min, followed by washing with distilled water thrice, with biotin blocking reagent A at room temperature for 10 min, twice with PBS for 5 min each, with biotin blocking reagent B, at room temperature for 10 min, and twice with PBS for 5 min each. We added the normal goat serum-blocking liquid, incubated at room temperature for 20 min and removed the extra liquid, then added primary antibody (1:100 dilution), incubated over night at 4℃, washed thrice with PBS for 5 min each, and again incubated with secondary antibody at room temperature for 10 min, washed thrice with PBS for 5 min each. We added streptomycete antibiotin-peroxidase solution, put at room temperature for 10 min, washed four times with PBS for 5 min each, and then added freshly prepared DAB solution for coloration. The sections were observed under microscope and washed with distilled water.

Table 1 Comparison of plasma amylase [M (Q_R)]

Group (time/h)	3 h	6 h	12 h
Sham operation	2038.00 (346.00)	2117.00 (324.00)	1725.00 (434.00)
Model	7423.00 (2275.00)	8149.00 (1540.00)	9195.00 (1298.00)
Treatment	6739.00 (2310.00)	7839.00 (2258.00)	7791.00 (1863.00)

Observational index

Survival rate: The rat mortality observed at 3 h, 6 h, and 12 h after operation and the survival rate was calculated.

Pathological changes of mutiple organs: After mercy killing the rats anesthetized by sodium pentobarbital in batches, the gross samples of mutiple organs (liver, kidney, lung) were collected and observed for the pathological changes.

NF-κB p65 protein expression in the mutiple organs: We applied tissue microarrays to prepare microarray sections of the mutiple organs, and, using immunohistochemical S-P method, observed the NF-κB p65 protein expression and carried out the comprehensive assessment according to the positive cell percentage: < 10% (-); 10%-20% (+); 20%-50% (++); > 50% (+++).

Statistical analysis

The statistical analysis was conducted using the SPSS11.5 software. The Kruskal-Wallis test was applied for comparison of the three groups. The Bonferroni test was applied to the two-group comparison. The likelihood ratio Chi-square test was applied to compare the survival rate. $P < 0.05$ was considered statistically significant.

RESULTS

Survival rate

The 3 h, 6 h and 12 h mortality of the model group were 0% (0/15), 0% (0/15), 13.33% (2/15), respectively. The entire survival rate was 86.67%, while the survival rate of sham operation group and treatment group at all time points were 100%. But the survival rate at different time points was not significantly different between the model group and treatment group.

Comparison of plasma amylase content of all groups

Plasma amylase content was significantly increased in the model group and dexamethasone treatment group compared to the sham operation group at all time points ($P < 0.001$). No marked difference was observed in plasma amylase content between the dexamethasone treatment group and model group at 3 h and 6 h. However, plasma amylase content was found to be significantly less in the dexamethasone treatment group than the model group at 12 h ($P < 0.01$) (Table 1).

Comparison of plasma endotoxin content of all groups

Plasma endotoxin content was significantly increased in

Table 2 Comparison of plasma endotoxin [M (Q_R)]

Group (time/h)	3 h	6 h	12 h
Sham operation	0.015 (0.007)	0.015 (0.007)	0.016 (0.005)
Model	0.035 (0.0170)	0.055 (0.025)	0.059 (0.020)
Treatment	0.030 (0.0140)	0.040 (0.012)	0.042 (0.018)

Table 3 Comparison of serum TNF-α [M (Q_R)]

Group (time/h)	3 h	6 h	12 h
Sham operation	3.30 (3.60)	4.90 (2.60)	3.70 (2.30)
Model	46.13 (37.95)	77.54 (42.16)	67.30 (32.13)
Treatment	38.40 (26.60)	58.30 (26.40)	38.70 (28.50)

the model group and dexamethasone treatment group than the sham operation group at all time points ($P < 0.001$). No marked difference was observed in plasma endotoxin content between the dexamethasone treatment group and model group at 3 h. However, plasma endotoxin content was found to be significantly less in the dexamethasone treatment group compared to the model group at 6 h and 12 h ($P < 0.01$) (Table 2).

Comparison of serum TNF-α content of all groups

Serum TNF-α content was obviously increased in the model group and dexamethasone treatment group compared to the sham operation group at all time points ($P < 0.001$). No obvious difference was observed in serum TNF-α content between the dexamethasone treatment group and model group at 3 h. Serum TNF-α content was found to be significantly less in the dexamethasone treatment group compared to the model group at 6 h and 12 h ($P < 0.05$) (Table 3).

Macroscopic and microscopic changes of the liver

Sham operation group: Macroscopically, we observed normal color without obvious swelling of the liver in all groups. Microscopically, roughly normal hepatic tissue, slight inflammatory cell infiltration in the portal area, normal morphous of most liver cells, some with acidophilia apomorphosis or slight expansion and congestion of sinus hepaticus were observed.

Model group: Macroscopically, in the 3 h group, slight swelling of the liver was observed, and some rats had local grey plaques with unclear boundary, while in the 6 h and 12 h groups, pale, turbid color or congestion on the liver, and some with scattered grey plague in irregular shape or necrosis were observed. Microscopically, we observed swelling or acidophilia apomorphosis of the liver cells, inflammatory cell infiltration in the portal area, expansion and congestion of sinus hepaticus, and scattered spotty necrosis in the hepatic lobule in the 3 h group, obvious swelling of the liver cells, increased range and area of the liver cell necrosis, visible focal or massive hemorrhagic necrosis, inflammatory cell infiltration in necrosis focus, obvious congestion of partial sinus hepaticus, bile duct proliferation and scattered necrosis of single cell in the portal area (concentration and fragmentation of nucelus) in the 6 h group, obviously damaged structure of the hepatic lobule, further increased necrosis range and area of the liver cells, more inflammatory cell infiltration in the lobule and/or portal area, and obvious congestion of sinus hepaticus in the 12 h group.

Dexamethasone treatment group: Macroscopically, the gross liver pathological changes of the dexamethasone treatment group at 6 h and 12 h were milder than those of the model group, most significantly at 12 h. Microscopically, we observed slight swelling of the liver cells, slight expansion and congestion of the sinus hepaticus, scattered inflammatory cell infiltration but with significantly less scale in the portal area at all time points in the dexamethasone treatment group, while more limited necrosis range of the liver cells, no obvious lamellar necrosis at 6 h and 12 h groups. The gross pathological changes of the dexamethasone treatment group were milder than those of the model group at 6 h and 12 h, most significantly at 12 h.

Macroscopic and microscopic changes of the kidney

Sham operation group: Macroscopically, no swelling of the kidney with normal morphous, and no bleeding point on the renal cortex surface were observed. Microscopically, normal structures of renal glomerulus, renal tubule and renal interstitium without any obvious pathological changes were observed in most of the rats, while unclear boundary of the renal tubular epithelial cells (especially proximal tubule), stenosis and atresia of lumens, congestion of renal glomerulus and interstitial edema were observed in a small number of rats.

Model group: Macroscopically, in the 3 h group, no obvious gross changes in the kidney, while in the 6 h and 12 h groups, renal swelling, tension of the kidney envelope, scattered bleeding points on surface of the kidney envelope in some rats and slight hemorrhagic urine within the pelvis in severe cases were observed. Microscopically, in the 3 h group, congestion of glomerular capillary, swelling of the renal tubular epithelial cells, scattered necrosis, unclear cell boundary, stenosis or atresia of lumens, visible protein cast, interstitial edema and inflammatory cell infiltration, while in the 6 h and 12 h groups, obvious congestion of glomerular capillary, swelling of the renal tubular epithelial cells, scattered necrosis, interstitial edema, inflammatory cell infiltration were observed. Moreover, eosinophilic staining floss, red cells and eosinophilic staining homogen cast or red cell cast in the glomerular capsule were observed. There were expansion of renal tubule lumens in medulla, atrophia of endothelial cells and the pathological changes grew worse with time; lamellar necrosis of the renal tubular epithelial cells in a small number of rats.

Dexamethasone treatment group: Macroscopically, in the 6 h and 12 h groups, the gross pathological changes of the dexamethasone treatment group were milder than those of the model group. Microscopically, we observed milder congestion of glomerular capillary, swelling of the renal tubular epithelial cells as well as less eosinophilic staining floss and red cells in the renal capsule and less inflammatory cell infiltration than those of the model group; edema of renal interstitium and scattered necrosis

Table 4 The changes of expression level of NF-κB in the liver

Group	(Time/h)	Cases	Pathologic grade			
			-	+	++	+++
Sham operation	3	15	15	0	0	0
	6	15	15	0	0	0
	12	15	15	0	0	0
Model	3	15	7	4	4	0
	6	15	10	3	2	0
	12	13	11	1	1	0
Treatment	3	15	12	1	2	0
	6	15	11	1	3	0
	12	15	9	3	3	0

Table 5 Comparison of the expression level of NF-κB in the liver [M (Q_R)]

Group	3 h	6 h	12 h
Sham operation	0.00 (0.00)	0.00 (0.00)	0.00 (0.00)
Model	1.00 (2.00)	0.00 (1.00)	0.00 (0.00)
Treatment	0.00 (0.00)	0.00 (1.00)	0.00 (1.00)

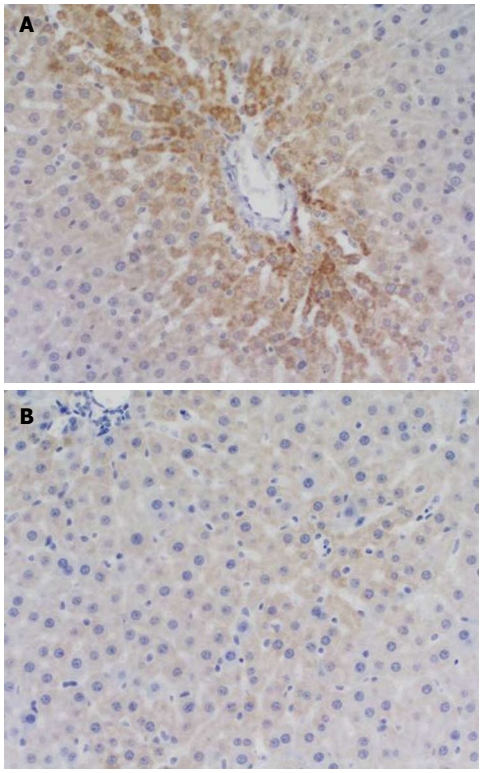

Figure 1 NF-κB expressions in the liver in the model group-3 h, (++) × 200 (**A**) and the treatment group-3 h, (-) × 200 (**B**).

in a small part of the renal tubular epithelial cells.

Macroscopic and microscopic changes of the lung

Sham operation group: Macroscopically, normal color and structure of the lung on both sides, no bleeding point on the surface and no effusion in the thoracic cavity were observed. Microscopically, normal function of the most lung tissues, but quite few with slight edema and inflammatory cell infiltration of interstitium were observed.

Model group: Macroscopically, in the 3 h group, obvious hyperemia and edema of the pulmonary lobes on both sides, dark red bleeding points on the local pulmonary lobe surface, small amount of amber and dilute effusion in the thoracic cavity, while in the 6 h and 12 h groups, aggravated pathological changes of the lung on both sides with prolonged time after modeling, lump-like pruinosus plaque on the lung surface, increased effusion in the thoracic cavity, and some hemorrhagic changes were observed. Microscopically, in the 3 h group, edema of the lung interstitium and alveolar space, widened interstitium of alveolar wall, visible inflammatory cell infiltration, telangiectasis and congestion of alveolar wall and widened alveolar septum, while in the 6 h and 12 h groups, further increased range of pathological changes of pulmonary lobes, obviously increased effusion in alveolar space, edema and bleeding of interstitium and alveolar space, obviously widened alveolar septum, more inflammatory cell infiltration and lucent kytoplasm of local tunica mucosa bronchiorum epithelium were observed.

Dexamethasone treatment group: Macroscopically, no obvious bleeding point on the pulmonary lobe surface, sound elasticity of pulmonary lobes, no obvious effusion in the thoracic cavity were observed; the gross lung pathological changes were milder than those of the model group at all time points, indicating obvious therapeutic effects. Microscopically, most lung tissue restored normal structures, and few with slight edema of interstitium and alveolar space were observed, indicating obvious therapeutic effects.

Changes of NF-κB expression levels in the liver of all groups

The positive NF-κB staining was located in the cytoplasm of the liver cells. The NF-κB expressions were all negative in the sham operation group at different time points, partly negative and partly + or ++ at 3 h in the model group. Most expressions of the model group were negative at 6 h and 12 h and a small part + or ++, while the negative rate of the model group at 12 h surpassed that at 6 h. There was no marked difference among all groups at 6 h. There was no marked difference between the model group and treatment group at all time points. However, the model group significantly exceeded the sham operation group at 3 h ($P < 0.01$) and the treatment group significantly exceeded the sham operation group at 12 h ($P < 0.01$) (Tables 4 and 5, Figure 1A and B).

Changes of NF-κB expression levels in the kidney of all groups

The positive NF-κB staining was located in the cytoplasm of renal tubular epithelial cells (Table 3). The expressions of the sham operation group were all negative at different time points. Most expressions of the model group were negative at 3 h and 6 h and a small part + or ++. The expressions of the model group were all negative at 12 h. Most expressions of the treatment group were negative at 3 h and a quite small part + or ++. Most expressions of the treatment group were negative at 6 h and a quite small part ++. The expressions of the treatment group were partly negative and partly + or ++ at 12 h. There were no marked differences between the model group and

Table 6 The changes of expression level of NF-κB in the kidney

Group	(Time/h)	Cases	Pathologic grade			
			-	+	++	+++
Sham operation	3	15	15	0	0	0
	6	15	15	0	0	0
	12	15	15	0	0	0
Model	3	15	13	1	1	0
	6	15	12	1	2	0
	12	13	13	0	0	0
Treatment	3	15	12	2	1	0
	6	15	13	0	2	0
	12	15	9	2	3	1

Table 7 Comparison of the expression level of NF-κB in the kidney [M (Q_R)]

Group	3 h	6 h	12 h
Sham operation	0.00 (0.00)	0.00 (0.00)	0.00 (0.00)
Model	0.00 (0.00)	0.00 (0.00)	0.00 (0.00)
Treatment	0.00 (0.00)	0.00 (0.00)	0.00 (2.00)

treatment group at all time points, moreover, no obvious differences among all groups at 3 h and 6 h. However, the treatment group significantly exceeded the model group ($P < 0.05$) and sham operation group ($P < 0.01$) at 12 h (Tables 6 and 7, Figure 2A, B and C).

Changes of NF-κB expression levels in the lung of all groups

NF-κB expressions in the lung of all groups were negative (Figure 3).

DISCUSSION

As one of the common clinical acute abdomen, severe acute pancreatitis (SAP) usually accompanied by the obvious inflammatory reactions besides local pathological injuries can lead to systemic inflammatory response syndrome (SIRS) or even the complication of multiple organ injury, further multiple organ dysfunction syndrome (MODS)[11], resulting in quite high mortality. Although people have conducted enormous studies on AP pathogenesis and brought forward many valuable theories such as the theory of oxygen-free radicals[12], the exact mechanism remains unclear. Studies in recent years have proven that the activation of NF-κB plays an extremely important role in the onset process of SAP[7,13,14].

NF-κB, a protein with multi-attribute transcription-regulating effect, consists of NF-κB/Rel protein family members. NF-κB is usually combined with NF-κB profilin (IκB) to form an inactive trimer that cannot enter the cell nucleus but exists in the cytoplasm[15,16]. A series of enzymes can be activated through signal transduction pathway after the stimulation of TNF-α, IL-1, LPS[17] to activate NF-κB and next IκB kinase to realize the phosphorylation of IκB. When IκB falls off the NF-κB complex, the activated NF-κB will move into the cell nucleus, bind to the κB structural domain of the promoter or enhancer of target gene and cause the transcription of many factors[18-20], including cytokines, chemotactic factor, macrophage chemotactic peptide, cellular adhesion molecule, growth factor, immune receptor and acute phase reactive protein.

The NF-κB p65 involved in this experiment is one of the important composing members of NF-κB/Rel family with 65 000 of relative molecular weight. Its most common

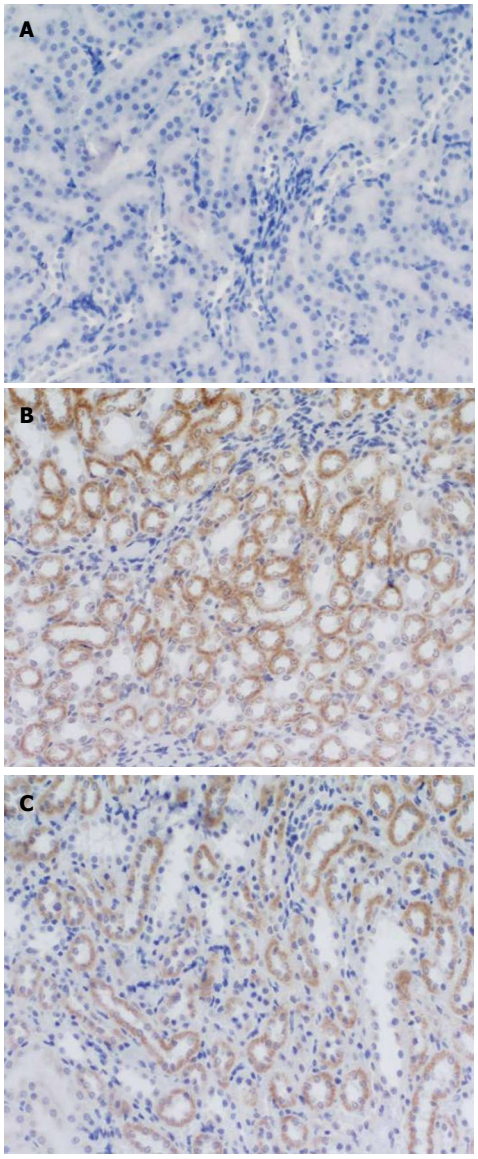

Figure 2 NF-κB expressions in the kidney in the sham operation group-12 h, (-) × 200 (**A**), model group-6 h, (++) × 200 (**B**) and model group-12 h, (++) × 200 (**C**).

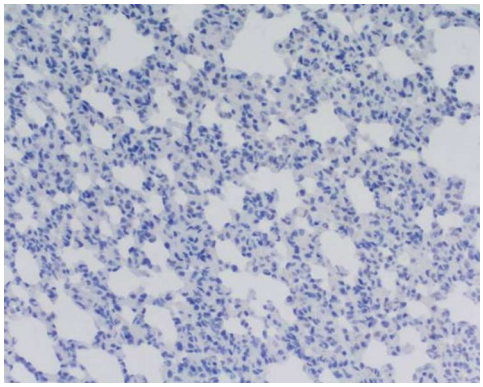

Figure 3 NF-κB expressions in the lung in the sham operation group-3 h, (-) × 200.

form in cell is the heterotic dimer of NF-κB consisting of p65 and p50. When resting, it is combined with its inhibitor IκB to exist in the cytoplasm. When stimulated, the NF-κB will be transferred into nucleus through IκB degradation to combine the κB sequence of the promoter and enhancer area of the regulated gene, promote the transcription of these genes[5] and participate in the tissue injury caused by manifold factors[21]. Tietz *et al*[22] respectively determined the serum concentration of TNF-α and IL-6 as well as their mRNA expression levels in mice with acute pancreatitis through ELISA and RT-PCR methods, and found that the genetic expression of inflammation promoting cytokines like TNF-α and IL-6 played an extremely important role in the progression of acute pancreatitis.

Dexamethasone, a kind of glucocorticoid, can inhibit the gene synthesis of manifold inflammatory mediators and inhibit inflammatory mediators by increasing the synthesis of anti-inflammatory protein[8]. The possible mechanism for dexamethasone inhibition of NF-κB activation could be: (1) As a hormone where the ligand binds to its corresponding receptor and activates it. The activated glucocorticoid receptor directly couples the RelA subunit of NF-κB in the cell nucleus to inhibit the functions of NF-κB. (2) The activated glucocorticoid receptor blocks the nucleus shifting of NF-κB and its combination with DNA by enhancing the genetic transcription of IκB and raising its level.

Acute liver injury is also a common complication of SAP. Studies found that NF-κB plays an important role in the liver injury process of SAP rats[23,24]. NF-κB after activation can promote liver injury by promoting the genetic transcription of TNF-α and IL-6[25]. NF-κB inhibitor can protect the liver by inhibiting the activation of NF-κB. Some studies believe liver cells are not only target cells of SAP liver injury but also could be the effector cells of inflammatory reactions secreting cytokines. They can act on the liver cells through autocrine or paracrine fashion to aggravate the liver injury[26]. In this experiment, we observed the rise of NF-κB p65- positive cell percentage and expression of manifold inflammation-inducing factors which participated in the liver injury complicated with SAP. The positive cell percentage of the dexamethasone treatment group dropped at 3 h and 6 h possibly because dexamethasone had inhibited the activation of NF-κB, reduced the expression of relevant cytokines and thereby alleviated the liver injury. It should be mentioned that the positive cell rate of the treatment group had risen compared with the model group at 12 h, while the statistical results showed no marked difference between the model group and treatment group at all time points. Theoretically, the positive cell rate should decline possibly due to the following factors: (1) With features like time- and energy- saving and high efficiency, the tissue microarray sections of 2.0 mm in diameter may not reflect the whole tissue picture and, to a certain extent, its representation is limited. (2) With different case numbers, the two groups cannot be compared directly. Statistical results showed no marked difference between the model group and treatment group at all time points; (3) There were also possible faults in reagent selection and staining.

Acute kidney injury is also one of the common complications of SAP with few relevant reports currently. In this experiment, the NF-κB expression level of the treatment group significantly exceeded that of the model group at 12 h after dexamethasone treatment, which is contradictory to the theory to certain extent and we can hardly understand. The reason could resemble that of the aforementioned liver. The main reason is still that the representation of tissue microarrays sections of 2.0 mm in diameter is doubtful and could lead to the deviation of the experimental results. We have planned to select three 2.0-mm points for each tissue in subsequent studies to ensure the representation of tissue. In common studies, the determination and analysis of a single index usually could pose many limitations. Therefore, we add the determination of multiple indexes into the experiment including the plasma amylase content, plasma endotoxin content and serum TNF-α content in order to completely evaluate the therapeutic effects and mechanism of dexamethasone.

Acute lung injury is one of the most common severe complications of SAP[27]. The mechanism responsible for acute lung injury caused by SAP is quite complicated and remains unclear till now. It is now believed that pancreatin, adhension molecule, neutrophil, various inflammatory mediators, etc play extremely important roles in the onset process[28-30]. It has been shown an increase in expression of manifold inflammation-inducing cytokines in the lung tissue at early injury stage, while the activation of transcription factor NF-κB can stimulate the expression of manifold cytokines. Studies show the selective use of NF-κB inhibitor can markedly lower the injury degree of the pancreas and lung, indicating the important role of NF-κB in SAP complicated with the lung injury[31-33]. This experiment has observed the NF-κB p65 expression in the lung tissue but the NF-κB expression levels in the lungs of all groups were negative, indicating that the non-expression of NF-κB p65 in the lung could be related to the reagents. The reagents used in this experiment did not stain in the lung.

In conclusion, NF-κB plays an important role in multiple organ injury. Further studies should be conducted to determine whether dexamethasone could alleviate the pathological changes of multiple organs by reducing the NF-κB expression of the liver and kidney. The advantages of tissue microarrays in pancreatitis pathological examination include saving time and energy, they are highly efficient and representative. The restriction on the representation of tissues to various extents due to small diameter may lead to the deviation of analysis.

Produced mainly by the pancreas, amylase (AMS) has an important effect on digestion of polysaccharide in food and acute pancreatitis is the most common cause of its rise. The rising degree of AMS activity is not certainly related to the injury degree of pancreatic tissue. But the more obviously AMS rises, the more severe the injury becomes. Our study showed that the amylase content of the model group increased with time and the amylase content in plasma dropped after treatment.

Endotoxin is a kind of compound of lipopolysaccharide (LPS) and small protein (Protein) on the cell wall of Gram-

negative bacteria. It is specific not because it is a bacteria or metabolite of bacteria but a substance with endotoxin bioactivity only released after death or disintegration of bacteria. Its chemical composition mainly consists of O-specific chain, core polysaccharide and lipoid A. Endotoxemia results when the endotoxin can be detected in the circulatory blood, which could cause a series of pathophysiological changes including sepsis, shock, and diffuse intravascular coagulation and multiple organ dysfunction syndrome (MODS). The role of endotoxin in onset of acute pancreatitis covers the following aspects: (1) Interfering the normal function of cell membrane by non-specific combination with it; (2) Directly destroying the lysosomal membrane within cells of mononuclear phagocytic system to cause cell damage; (3) Damaging mitochondria structure, affecting the coupling process of ATP enzyme and oxidative phosphorylation and causing disturbance in energy metabolism; (4) Changing the immune function of body; (5) Causing a series of pathological or pathophysiological changes of body, affecting the vasomotor function, activating vasoactive substance, reducing platelet and leukocyte, lowering blood pressure or even causing DIC, MOSF, etc.

Mainly generated from the activated mononuclear macrophage, TNF-α is a kind of polypeptide cytokine with extensive biologic activities. The secretion of appropriate amounts of TNF-α had protecting effects and can promote the chemotaxis and antimicrobial effects of PMN, macrophage and eosinophile granulocyte and is one of the defense mechanisms of the body. The excessive secretion of TNF-α could cause inflammatory reactions. High concentration of TNF-α entering the blood flow could also cause fever, drop of blood pressure and reduction of tissue perfusion through lowering myocardial contraction force and tension of vascular smooth muscle as well as metabolic disorder, organ injury and even multi-system damage. It has potentially lethal effects.

Our experiment found no marked difference in the plasma amylase content at 3 h and 6 h between the treatment group and model group, while the plasma amylase content of the treatment group was significantly lower than that of the model group at 12 h ($P < 0.01$). The plasma endotoxin content of the treatment group was significantly lower than that of the model group at 6 h and 12 h ($P < 0.01$). The serum TNF-α level of the treatment group was significantly lower than that of the model group at 6 h and 12 h ($P < 0.05$). Thus, it is concluded that dexamethasone can lower the plasma amylase, plasma endotoxin and serum TNF-α content of rats with SAP as well as their mortality.

The tissue microarrays (TMA) technology adopted by us in this study is exactly the new biochip technology currently extensively applied to basic and clinical applications as well as in other fields. The tissue microarray technology has exceeded the traditional histopathological section technology which is single in sample and low in efficiency[34]. The advantages of TMA are high-throughput, economic, time-saving, reliable result, convenient for experimental control, etc. Since the most distinguished feature of tissue microarrays is to combine the study of gene and its expression products with histomorphology, it possesses great potential in oncopathology studies[35,36], and current studies also mainly focus on this area[37-44]. The chip preparation, staining, examination, etc have restrained the application of this technology in non-tumor diseases. To the best of our knowledge, there was no study report in literature on applying tissue microarrays to pancreatitis pathological examination before our experiment was conducted. Thus this article has taken the lead.

We used the tissue microarray section maker (Beecher Instruments, USA) to drill a hole of 2.0 mm in diameter on recipient block and combined the immunohistochemical method to examine the NF-κB expression levels of the multiple organs. The experimental results are unsatisfactory mainly because the tissue representation has been restricted to different extents due to the small diameter. However, there are advantages of tissue microarrays shown in its application in the pathological examination of pancreatitis, including time- and energy-saving and high efficiency.

REFERENCES

1 **Renzulli P**, Jakob SM, Täuber M, Candinas D, Gloor B. Severe acute pancreatitis: case-oriented discussion of interdisciplinary management. *Pancreatology* 2005; **5**: 145-156
2 **Kim CD**. Pancreatitis-etiology and pathogenesis. *Korean J Gastroenterol* 2005; **46**: 321-332
3 **Hirota M**, Sugita H, Maeda K, Ichibara A, Ogawa M. Concept of SIRS and severe acute pancreatitis. *Nihon Rinsho* 2004; **62**: 2128-2136
4 **Weber CK**, Adler G. From acinar cell damage to systemic inflammatory response: current concepts in pancreatitis. *Pancreatology* 2001; **1**: 356-362
5 **Algül H**, Tando Y, Schneider G, Weidenbach H, Adler G, Schmid RM. Acute experimental pancreatitis and NF-kappaB/Rel activation. *Pancreatology* 2002; **2**: 503-509
6 **Satoh A**, Masamune A, Kimura K, Kaneko K, Sakai Y, Yamagiwa T, Satoh M, Kikuta K, Asakura T, Shimosegawa T. Nuclear factor kappa B expression in peripheral blood mononuclear cells of patients with acute pancreatitis. *Pancreas* 2003; **26**: 350-356
7 **O'Reilly DA**, Roberts JR, Cartmell MT, Demaine AG, Kingsnorth AN. Heat shock factor-1 and nuclear factor-kappaB are systemically activated in human acute pancreatitis. *JOP* 2006; **7**: 174-184
8 **Dong R**, Wang ZF, LV Y. Treatment of severe acute pancreatitis with large dosage of dexamethasone in rats. *Zhonghua Putong Waike Zazhi* 2001; **10**: 314-317
9 **Brummer E**, Choi JH, Stevens DA. Interaction between conidia, lung macrophages, immunosuppressants, proinflammatory cytokines and transcriptional regulation. *Med Mycol* 2005; **43** Suppl 1: S177-S179
10 **Zhang XP**, Zhou YF. An ideal rat model of acute necrosis pancreatitis. *Weichangbingxue yu Ganzangbingxue Zazhi* 2003; **12**: 530-531
11 **Shi C**, Zhao X, Lagergren A, Sigvardsson M, Wang X, Andersson R. Immune status and inflammatory response differ locally and systemically in severe acute pancreatitis. *Scand J Gastroenterol* 2006; **41**: 472-480
12 **Shi C**, Andersson R, Zhao X, Wang X. Potential role of reactive oxygen species in pancreatitis-associated multiple organ dysfunction. *Pancreatology* 2005; **5**: 492-500
13 **Chen X**, Ji B, Han B, Ernst SA, Simeone D, Logsdon CD. NF-kappaB activation in pancreas induces pancreatic and systemic inflammatory response. *Gastroenterology* 2002; **122**: 448-457
14 **Weber CK**, Adler G. Acute pancreatitis. *Curr Opin Gastroenterol* 2003; **19**: 447-450
15 **Pande V**, Ramos MJ. NF-kappaB in human disease: current inhibitors and prospects for de novo structure based design of inhibitors. *Curr Med Chem* 2005; **12**: 357-374
16 **Yamamoto Y**, Gaynor RB. IkappaB kinases: key regulators of

the NF-kappaB pathway. *Trends Biochem Sci* 2004; **29**: 72-79
17 **Shishodia S**, Aggarwal BB. Nuclear factor-kappaB activation: a question of life or death. *J Biochem Mol Biol* 2002; **35**: 28-40
18 **Choi EK**, Jang HC, Kim JH, Kim HJ, Kang HC, Paek YW, Lee HC, Lee SH, Oh WM, Kang IC. Enhancement of cytokine-mediated NF-kappaB activation by phosphatidylinositol 3-kinase inhibitors in monocytic cells. *Int Immunopharmacol* 2006; **6**: 908-915
19 **Su JR**, Zhao ZC, Chen WL, Wang X. The effect of activated nuclear factor-kappaB in pathogenesis of acute pancreatitis. *Zhonghua YiXue ZaZhi* 2003; **83**: 1497-1500
20 **Meng Y**, Ma QY, Kou XP, Xu J. Effect of resveratrol on activation of nuclear factor kappa-B and inflammatory factors in rat model of acute pancreatitis. *World J Gastroenterol* 2005; **11**: 525-528
21 **Xu X**, Sun SQ, Zhang ZY. Experimental Study on Intrapulmonary Expression of Nuclear Factor-κB, Inflammatory Mediators and Lung Injury in Rats With Severe Acute Pancreatitis. *Zhongguo Linchuang Yixue* 2003; **20**: 84-87
22 **Tietz AB**, Malo A, Diebold J, Kotlyarov A, Herbst A, Kolligs FT, Brandt-Nedelev B, Halangk W, Gaestel M, Göke B, Schäfer C. Gene deletion of MK2 inhibits TNF-alpha and IL-6 and protects against cerulein-induced pancreatitis. *Am J Physiol Gastrointest Liver Physiol* 2006; **290**: G1298-G1306
23 **Zhao YF**, Zhai WL, Zhang SJ, Chen XP. Protection effect of triptolide to liver injury in rats with severe acute pancreatitis. *Hepatobiliary Pancreat Dis Int* 2005; **4**: 604-608
24 **Jaffray C**, Yang J, Norman J. Elastase mimics pancreatitis-induced hepatic injury via inflammatory mediators. *J Surg Res* 2000; **90**: 95-101
25 **Murr MM**, Yang J, Fier A, Kaylor P, Mastorides S, Norman JG. Pancreatic elastase induces liver injury by activating cytokine production within Kupffer cells via nuclear factor-Kappa B. *J Gastrointest Surg* 2002; **6**: 474-480
26 **Yuan YZ**, Ji L, Zhu Y. The role of nuclear factor-κB in the pathogenesis of severe acute pancreatitis-associated hepatic injury. *Shanghai Yixue Zazhi* 2002; **25**: 172-175
27 **Liu XM**, Xu J, Wang ZF. Pathogenesis of acute lung injury in rats with severe acute pancreatitis. *Hepatobiliary Pancreat Dis Int* 2005; **4**: 614-617
28 **Surbatović M**, Jovanović K, Radaković S, Filipović N. Pathophysiological aspects of severe acute pancreatitis-associated lung injury. *Srp Arh Celok Lek* 2005; **133**: 76-81
29 **Zhao X**, Dib M, Andersson E, Shi C, Widegren B, Wang X, Andersson R. Alterations of adhesion molecule expression and inflammatory mediators in acute lung injury induced by septic and non-septic challenges. *Lung* 2005; **183**: 87-100
30 **Zhao QL**, Huang CY, Huang Y, Wang JF, Liu J. Study on acute pancreatitis-associated lung injury induced by L-arginine in mice. *Sichuan Daxue Xuebao Yixueban* 2004; **35**: 839-842
31 **Ethridge RT**, Hashimoto K, Chung DH, Ehlers RA, Rajaraman S, Evers BM. Selective inhibition of NF-kappaB attenuates the severity of cerulein-induced acute pancreatitis. *J Am Coll Surg* 2002; **195**: 497-505
32 **Virlos I**, Mazzon E, Serraino I, Genovese T, Di Paola R, Thiemerman C, Siriwardena A, Cuzzocrea S. Calpain I inhibitor ameliorates the indices of disease severity in a murine model of cerulein-induced acute pancreatitis. *Intensive Care Med* 2004; **30**: 1645-1651
33 **Virlos I**, Mazzon E, Serraino I, Di Paola R, Genovese T, Britti D, Thiemerman C, Siriwardena A, Cuzzocrea S. Pyrrolidine dithiocarbamate reduces the severity of cerulein-induced murine acute pancreatitis. *Shock* 2003; **20**: 544-550
34 **Kononen J**, Bubendorf L, Kallioniemi A, Bärlund M, Schraml P, Leighton S, Torhorst J, Mihatsch MJ, Sauter G, Kallioniemi OP. Tissue microarrays for high-throughput molecular profiling of tumor specimens. *Nat Med* 1998; **4**: 844-847
35 **Chen Q**, Shi QL. Application of tissue microarrays technique in lymphoma studies. *Zhenduan Binglixue Zazhi* 2003; **110**: 182-184
36 **Yan XC**, Duan GJ. Study on tumors by tissue microarrays (tissue chip). *Zhongguo Zhongliu Fangzhi Zazhi* 2003; **30**: 519-521
37 **Gaiser T**, Thorns C, Merz H, Noack F, Feller AC, Lange K. Gene profiling in anaplastic large-cell lymphoma-derived cell lines with cDNA expression arrays. *J Hematother Stem Cell Res* 2002; **11**: 423-428
38 **Husson H**, Carideo EG, Neuberg D, Schultze J, Munoz O, Marks PW, Donovan JW, Chillemi AC, O'Connell P, Freedman AS. Gene expression profiling of follicular lymphoma and normal germinal center B cells using cDNA arrays. *Blood* 2002; **99**: 282-289
39 **Oka T**, Yoshino T, Hayashi K, Ohara N, Nakanishi T, Yamaai Y, Hiraki A, Sogawa CA, Kondo E, Teramoto N, Takahashi K, Tsuchiyama J, Akagi T. Reduction of hematopoietic cell-specific tyrosine phosphatase SHP-1 gene expression in natural killer cell lymphoma and various types of lymphomas/leukemias : combination analysis with cDNA expression array and tissue microarray. *Am J Pathol* 2001; **159**: 1495-1505
40 **Natkunam Y**, Warnke RA, Montgomery K, Falini B, van De Rijn M. Analysis of MUM1/IRF4 protein expression using tissue microarrays and immunohistochemistry. *Mod Pathol* 2001; **14**: 686-694
41 **Florell SR**, Coffin CM, Holden JA, Zimmermann JW, Gerwels JW, Summers BK, Jones DA, Leachman SA. Preservation of RNA for functional genomic studies: a multidisciplinary tumor bank protocol. *Mod Pathol* 2001; **14**: 116-128
42 **Kipps TJ**. Advances in classification and therapy of indolent B-cell malignancies. *Semin Oncol* 2002; **29**: 98-104
43 **Manley S**, Mucci NR, De Marzo AM, Rubin MA. Relational database structure to manage high-density tissue microarray data and images for pathology studies focusing on clinical outcome: the prostate specialized program of research excellence model. *Am J Pathol* 2001; **159**: 837-843
44 **Parker RL**, Huntsman DG, Lesack DW, Cupples JB, Grant DR, Akbari M, Gilks CB. Assessment of interlaboratory variation in the immunohistochemical determination of estrogen receptor status using a breast cancer tissue microarray. *Am J Clin Pathol* 2002; **117**: 723-728

S- Editor Liu Y **L- Editor** Kumar M **E- Editor** Lu W

PO Box 2345, Beijing 100023, China
www.wjgnet.com
wjg@wjgnet.com

World J Gastroenterol 2007 January 28; 13(4): 557-563
World Journal of Gastroenterology ISSN 1007-9327

BASIC RESEARCH

Inhibitory effects of saikosaponin-d on CCl_4-induced hepatic fibrogenesis in rats

Shuang-Suo Dang, Bao-Feng Wang, Yan-An Cheng, Ping Song, Zhen-Guo Liu, Zong-Fang Li

Shuang-Suo Dang, Bao-Feng Wang, Yan-An Cheng, Ping Song, Zhen-Guo Liu, Department of Infectious Diseases, Second Hospital of Xi'an Jiaotong University, Xi'an 710004, Shaanxi Province, China
Zong-Fang Li, Department of Surgery, Second Hospital of Xi'an Jiaotong University, Xi'an 710004, Shaanxi Province, China
Supported by the National Natural Science Foundation of China, No. 30471982
Correspondence to: Shuang-Suo Dang, Department of Infectious Disease, Second Hospital of Xi'an Jiaotong University, Xi'an 710004, Shaanxi Province, China. shuangsuo640212@sohu.com
Telephone: +86-29-87679688 Fax: +86-29-87678599
Received: 2006-09-22 Accepted: 2006-10-16

Abstract

AIM: To investigate the suppressive effect of saikosaponin-d (SSd) on hepatic fibrosis in rats induced by CCl_4 injections in combination with alcohol and high fat, low protein feeding and its relationship with the expression of nuclear factor-κB (NF-κB), tumor necrosis factor-alpha (TNF-α) and interleukins-6 (IL-6).

METHODS: Hepatic fibrosis models were induced by subcutaneous injection of CCl_4 at a dosage of 3 mL/kg in rats. At the same time, rats in treatment groups were injected intraperitoneally with SSd at different doses (1.0, 1.5 and 2.0 mg/kg) once daily for 6 wk in combination with CCl_4, while the control group received olive oil instead of CCl_4. At the end of the experiment, rats were anesthetized and killed (except for 8 rats which died during the experiment; 2 from the model group, 3 in high-dose group, 1 in medium-dose group and 2 in low-dose group). Hematoxylin and eosin (HE) staining and Van Gieson staining were used to examine the changes in liver pathology. The levels of alanine aminotransferase (ALT), triglyeride (TG), albumin (ALB), globulin (GLB), hyaluronic acid (HA) and laminin (LN) in serum and the content of hydroxyproline (HYP) in liver were measured by biochemical examinations and radioimmuneoassay, respectively. In addition, the expression of TNF-α and IL-6 in liver homogenate was evaluated by enzyme-linked immunosorbent assay (ELISA) and the levels of NF-κBp65 and I-κBα in liver tissue were analyzed by Western blotting.

RESULTS: Both histological examination and Van Gieson staining demonstrated that SSd could attenuate the area and extent of necrosis and reduce the scores of liver fibrosis. Similarly, the levels of ALT, TG, GLB, HA, and LN in serum, and the contents of HYP, TNF-α and IL-6 in liver were all significantly increased in model group in comparison with those in control group. Whereas, the treatment with SSd markedly reduced all the above parameters compared with the model group, especially in the medium group (ALT: 412 ± 94.5 IU/L *vs* 113.76 ± 14.91 IU/L, TG: 0.95 ± 0.16 mmol/L *vs* 0.51 ± 0.06 mmol/L, GLB: 35.62 ± 3.28 g/L *vs* 24.82 ± 2.73 g/L, HA: 42.15 ± 8.25 ng/mL *vs* 19.83 ± 3.12 ng/mL, LN: 27.56 ± 4.21 ng/mL *vs* 13.78 ± 2.57 ng/mL, HYP: 27.32 ± 4.32 μg/mg *vs* 16.20 ± 3.12 μg/mg, TNF-α: 4.38 ± 0.76 ng/L *vs* 1.94 ± 0.27 ng/L, IL-6: 28.24 ± 6.37 pg/g *vs* 12.72 ± 5.26 pg/g, respectively, $P < 0.01$). SSd also decreased ALB in serum (28.49 ± 4.93 g/L *vs* 37.51 ± 3.17 g/L, $P < 0.05$). Moreover, the expression of NF-κB p65 in the liver of treated groups was lower than that in model groups while the expression of I-κBα was higher in treated group than in model group ($P < 0.01$). The expression of NF-κBp65 and TNF-α had a positive correlation with the level of HA in serum of rats after treatment with CCl_4 ($r = 0.862$, $P < 0.01$; $r = 0.928$, $P < 0.01$, respectively).

CONCLUSION: SSd attenuates CCl_4-induced hepatic fibrosis in rats, which may be related to its effects of hepato-protective and anti-inflammation properties, the down-regulation of liver TNF-α, IL-6 and NF-κBp65 expression and the increased I-κBα activity in liver.

Key words: Saikosaponin-d; Hepatic fibrosis; Tumor necrosis factor; Interleukins-6; Nuclear factor-κB; Inhibitory κB alpha

Dang SS, Wang BF, Cheng YA, Song P, Liu ZG, Li ZF. Inhibitory effects of saikosaponin-d on CCl_4-induced hepatic fibrogenesis in rats. *World J Gastroenterol* 2007; 13(4): 557-563

http://www.wjgnet.com/1007-9327/13/557.asp

INTRODUCTION

Hepatic fibrosis represents the wound healing response of the liver to repeated liver injuries, and is associated with increased inflammatory cell infiltration and may involve the interplay of different inflammatory mediators, which is a common stage in most chronic liver diseases[1-5]. If treated properly in this stage, hepatic fibrosis can be

reversed and its progression to irreversible cirrhosis often leading to lethal complications and high mortality may be prevented[6-9]. Nuclear factor-κB (NF-κB) as a critical component in inflammatory conditions can produce proinflammatory cytokines such as tumor necrosis factor-alpha (TNF-α) and interleukin-6 (IL-6), which are involved in the process of fibrogenesis[10-13]. Therefore, suppressing the inflammatory response and reducing the release of proinflammatory cytokines such as NF-κB, TNF-α and IL-6, may prevent and reverse hepatic fibrosis. Saikosaponin-d (SSd) is a major active component extracted from the root of Bupleurum falcatum. It has been demonstrated that SSd has a wide variety of pharmacological activities, such as liver-protective activity, and anti-hepatic fibrosis or anti-microbial or anti-tumor and anti-inflammatory activities[14-17]. However, its molecular mechanism involved in therapeutic effects of SSd on hepatic fibrosis has not been completely elucidated. Our present study was designed to further evaluate the effect of SSd on hepatic fibrosis in rats induced by CCl_4 and its relationship with the expression of NF-κB, TNF-α and IL-6.

MATERIALS AND METHODS

Reagents

SSd was purchased from Jiangxi Herbfine Hi-tech Co. Ltd. CCl_4 (Xi'an Chemical Factory) was diluted into 400 g/L in olive oil before it was used. Enzyme-linked immunosorbent assay (ELISA) kit for mouse TNF-α and IL-6 was purchased from R&D Systems Co. Ltd (USA). Hydroxyproline (HYP) assay kit was a product of Nanjing Jiancheng Bioengineering Institute. Kits for HA and LN were bought from Senxiong Company, Shanghai, China. Polyclonal rabbit anti-rat P65 and I-κBα were purchased from Santa Cruz Biotechnology (USA). HRP-labeled goat-anti-rabbit IgG was obtained from HuaMei Company, Shanghai, China.

Animals

Seventy-five adult male SD rats weighing 160-200 g were provided by the Laboratory Animal Center of Medical College, Xi'an Jiaotong University. The rats were randomly divided into 5 groups (n = 15): control group, model group, and three treatment groups. Except for the control rats, all rats were subcutaneously injected with 400 g/L CCl_4 (CCl_4: olive oil = 2:3), 3 mL/kg, b.w, at every 3 d for 6 wk, and fed with high fat, low protein diet (75% pure maize plus 20% lard and 0.5% cholesterol) and 300 mL/L alcohol in the drinking water. In the 3 treatment groups, SSd was administered daily, *via* intraperitoneal injection at a dosage of 2.0, 1.5 and 1.0 mg/kg for 6 wk, respectively. After 6 wk, all rats were anesthetized with 200 g/L urethane (5 mL/kg, abdominal injection). Blood was taken from the abdominal aorta. Serum was separated by centrifugation at 4℃ and kept at -20℃ for assay. Liver tissue was homogenized in cold saline for pathological diagnosis.

Light microscopic examination

Liver tissue was fixed in a 40 g/L solution of formaldehyde in 0.1 mol/L phosphate-buffed saline (pH 7.4), and embedded in paraffin. Five-micrometer thick sections were prepared. All the sections stained with HE and standard Van Gieson (VG) were coded and scored by blind reading. Van Gieson's method was used to detect collagen fibers[18]. Liver condition was classified according to the standard formulated by China Medical Association in 1995[19], and fibrosis was graded from 0 to 4 (0: no fibrosis; 1: portal area fibrosis; 2: fibrotic septa between portal tracts; 3: fibrosis septa and structure disturbance of hepatic lobule and 4: cirrhosis).

Biochemical determination

Serum levels of alanine transaminase (ALT), albumin (ALB), triglyeride (TG) and globulin (GLB) were measured by routine laboratory methods using a 7170-automatic biochemistry analyzer (Tokyo, Japan). Serum hyaluronic acid (HA) and laminin (LN) were detected by radioimmunoassay, and the content of hydroxyproline (HYP) in liver was determined according to the method described by Jamall *et al*[20]. The contents of TNF-α and IL-6 protein in liver homogenate were determined by ELISA according to the corresponding protocols of the kits.

Western blotting detection

Nuclear and cytosolic protein extracts were prepared according to manufacturer's instructions provided with the kits (Active Motif Corp, USA). Nuclear or cytosolic proteins (100 μg each) were run on a 10% SDS-PAGE gel and transferred electrophoretically onto a nitro-cellulose membrane respectively (Shanghai Huashun Corp, China). The membrane was blocked overnight with 10% nonfat milk prior to incubation with polyclonal rabbit anti-rat I-κBα antibody (1:800) or anti-NF-κBp65 antibody (1:1000) at room temperature for 2 h. After washed with PBS, the blots were incubated with HRP-labeled goat-anti-rabbit serum for 1 h and colored on X-ray film by ECL.

Statistical analysis

Quantitative data were analyzed using ANOVA by SPSS 13.0 statistic package and RIDIT test was used for statistical analysis of the qualitative data. All data were expressed as mean ± SD. The correlation was analyzed by Spearman's correlation analysis. All P values were two-tailed. $P < 0.05$ was considered statistically significant.

RESULTS

Pathological assay

At the end of the experiment, liver tissue samples from control rats showed normal lobular architecture with central veins and radiating hepatic cords (Figure 1A). Liver tissue samples from model group showed that more fibrous tissues were formed extending into the hepatic lobules to separate them completely. A large number of inflammatory cells infiltrated in the intralobular and interlobular regions. The liver structure was disordered and there were more necrotic and fatty degenerated liver cells compared with the controls (Figures 1B and 1D). In the 3 treatment groups, however, hepatocyte degeneration,

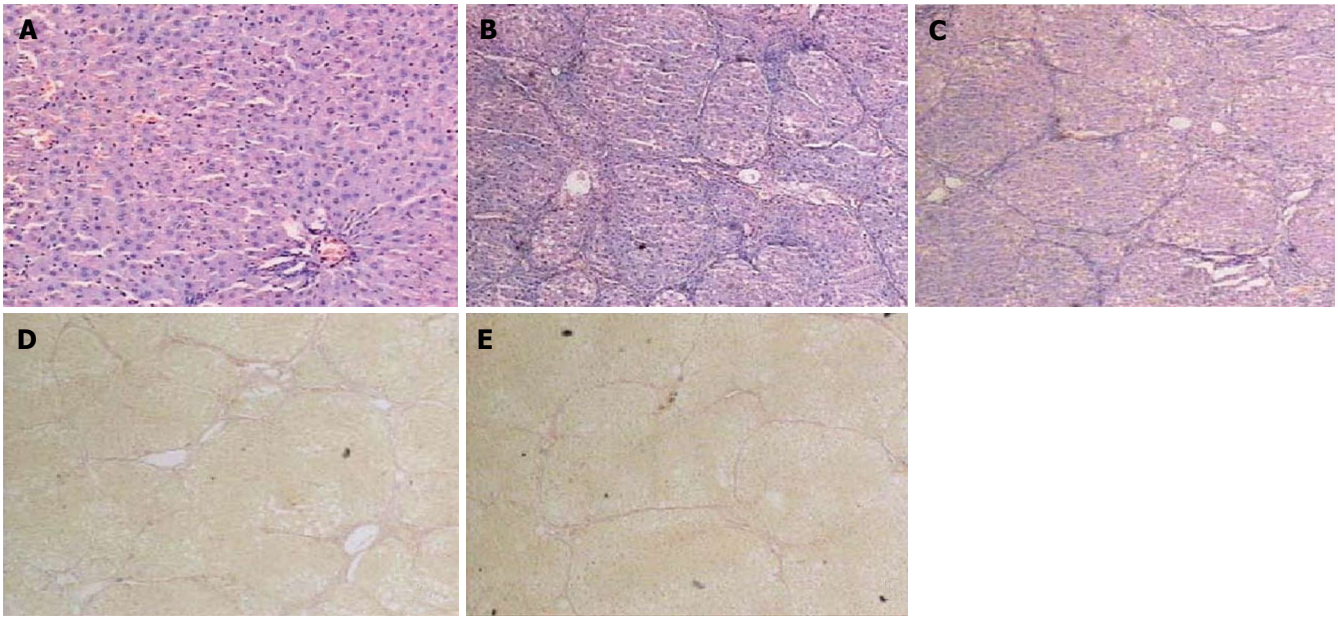

Figure 1 Light microscopy showing normal liver tissue in control group (**A**) (HE × 100), degenerated and necrotic liver cells associated with inflammatory cells in model group (**B**) (HE × 40), attenuated necrosis and infiltration of inflammatory cells after SSd treatment (**C**) (HE × 40), collagen fibers deposited in spaces of Disse and formation of pseudoloculi in model group (**D**) (Van Gieson × 40), and liver fibrosis tissue in SSd group (**E**). The pathological change of liver was much milder in SSd group than in model group (Van Gieson × 40).

necrosis and infiltration of inflammatory cells were all apparently ameliorated and collagen deposition was also markedly reduced (Figures 1C and 1E). Compared with model group, the liver condition of rats in SSd treatment groups was significantly improved (Table 1).

Detection of serum HA, LN and liver function

As is shown in Figure 2A, HA and LN levels in serum were significantly higher in model group than in the controls, but they were markedly decreased in 3 treatment groups compared with the model group. Compared with the controls, the serum ALT, TG and GLB levels in model group were all significantly increased while the level of ALB was decreased ($P < 0.001$, $P < 0.05$), respectively. However, the levels of ALT, TG and GLB were all in the 3 treatment groups, especially in the group receiving the middle dose of SSd, and the level of ALB was increased compared with the model group ($P < 0.05$) (Table 2).

TNF-α, IL-6 and HYP contents in liver tissue

The contents of TNF-α, IL-6 and HYP were all significantly lower in SSd treatment groups than in the model group (Figures 2B and 2C). Furthermore, among the 3 treatment groups the high-dose group showed the best effect. The liver HYP level in three SSd treatment groups and TNF-α, IL-6 content in high-dose group were higher than those in the controls, with no significant difference between them ($P > 0.05$). However, there was a significant difference in the contents of TNF-α, IL-6 between low- and medium-SSd treatment groups and control group ($P < 0.05$).

Western blot analysis

NF-κBp65 expression was increased significantly in model group compared with the control group, whereas it was markedly decreased in all SSd treatment groups ($P < 0.01$), especial in the high-dose group. There was no significant difference in the expression of NF-κBp65 between SSd treatment groups and control group ($P > 0.05$) (Figure 2D). On the contrary, its inhibitory IκBα was significantly decreased in model group while increased in SSd treatment group compared with the model group ($P < 0.01$) (Figures 3A and 3B). Therefore, SSd could significantly inhibit the activation of NF-κB, which might be associated with increased I-κBα degradation.

Table 1 Pathological observation of liver condition

Group	*n*	Liver condition					*U*
		0	Ⅰ	Ⅱ	Ⅲ	Ⅳ	
Model	13	0	0	0	4	9	
High-dose	12	0	5	3	2	2	3.26[a]
Medium-dose	14	0	6	4	3	1	4.17[b]
Low-dose	13	0	3	2	6	2	2.96[a]

U represents the RIDIT value of the two groups, $P < 0.05$ indicates $U > 1.96$, $P < 0.01$ indicates $U > 2.58$. [a]$P < 0.05$, [b]$P < 0.01$ *vs* model group.

Correlation analysis

Correlation analysis revealed that NF-κBp65 had a highly positive correlation with the expression of TNF-α protein ($r = 0.823$, $P < 0.01$). Both NF-κBp65 and TNF-α had a strong positive correlation with the levels of HA in serum of rats induced by CCl_4 ($r = 0.862$, $P < 0.01$; $r = 0.928$, $P < 0.01$, respectively).

DISCUSSION

Hepatic fibrosis is a chronic inflammation-associated

Table 2 Serum level of ALT, ALB, GLB, TG and liver HYP (mean ± SD)

Group	*n*	ALT (IU/L)	ALB (g/L)	GLB (g/L)	TG (mmol/L)	Liver HYP (μg/mg protein)
Control	15	67.58 ± 11.21	41.12 ± 2.54	21.48 ± 3.24	0.39 ± 0.08	9.80 ± 1.07
Model	13	412 ± 94.50	28.49 ± 4.93	35.62 ± 3.28	0.95 ± 0.16	27.54 ± 4.32
High-dose	12	173.09 ± 24.62[b,c]	35.73 ± 2.73[a]	25.59 ± 3.61[a]	0.61 ± 0.10[b]	12.83 ± 2.54[a,d]
Medium-dose	14	113.76 ± 14.91[a,d]	37.51 ± 3.17[a]	24.82 ± 2.73[a]	0.51 ± 0.06[a]	16.20 ± 3.12[b,d]
Low-dose	13	152.86 ± 19.19[b,c]	34.31 ± 4.52[b]	27.51 ± 2.41[b]	0.58 ± 0.07[b]	14.38 ± 2.18[b,d]

ALT: Alanine aminotransferase; ALB: Albumin; GLB: Globulin; TG: Triglyeride; HYP: Hydroxyproline. [a]$P < 0.05$, [b]$P < 0.01$ *vs* control group; [c]$P < 0.05$, [d]$P < 0.01$ *vs* model group.

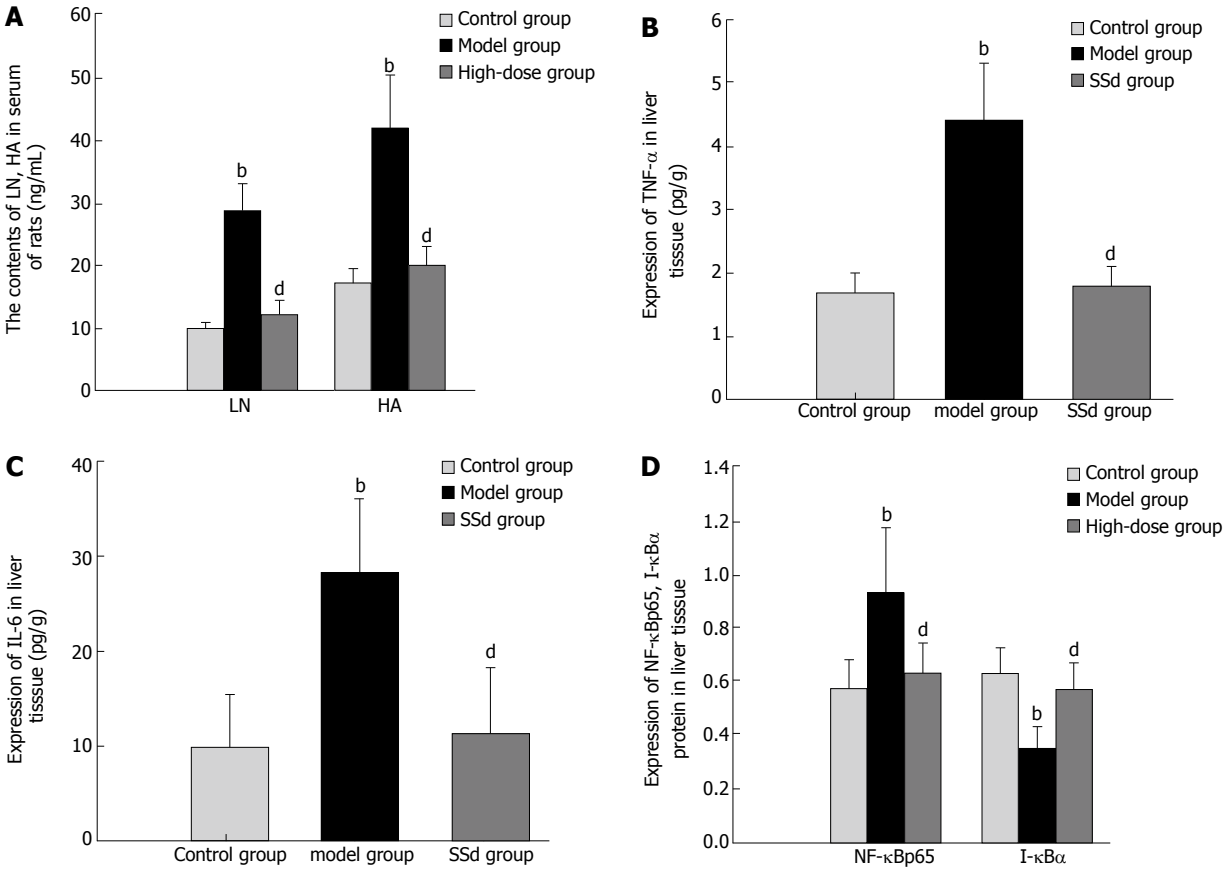

Figure 2 Analysis of serum LN and HA levels (**A**), expressions of TNF-α (**B**), IL-6 (**C**), and NF-κBp65 and I-κBα (**D**) in liver tissue after treatment with SSd. [b]$P < 0.01$ *vs* control group; [d]$P < 0.01$ *vs* model group.

disease, which is involved in the infiltration of inflammatory cells and releasing of proinflammatory cytokines, such as TNF-α and IL-6. As a result, hepatic stellate cells (HSCs) are transformed into myofibroblast cells to synthesize more collagen and proteoglycans, increasing deposition and altered composition of extracellular matrix (ECM) in liver[21-24]. Based on the current knowledge, a "three-step cascade theory of inflammation involving in liver fibrogenesis" including preinflammatory phases 1-3, has been proposed by Gressner[25], which implies that multiple inflammatory cell interactions with Kupffer cells, platelets, endothelial cells and hepatocytes mediated by various cytokines and growth factors (TNF-α, IL-6 and TGF-β) are involved in the mechanism of fibrogenesis. Therefore, suppressing the inflammatory response can prevent and reverse hepatic fibrosis. Our study showed that, 6 wk treatment with SSd, especially at the middle dose used, could decrease serum levels of ALT, TG, GLB and ALB in rats with hepatic injury caused by CCl_4. Histological examination also demonstrated that a large number of inflammatory cells infiltrated the intralobular and interlobular regions, more fibrous tissue was formed and the margin of liver was uneven in model group compared with the control group. In contrast, SSd especially its medium-dose could obviously attenuate the extent of necrosis and reduce the immigration of inflammatory cells compared with the model group, and no pseudoloculus could be observed. Moreover, SSd could decrease the scores of hepatic fibrosis grading (Table 1), indicating that SSd can significantly protect liver against fibrosis, which may be related to its inhibitory effects on inflammation. These findings are consistent with

previously reported results[26]. It has been demonstrated that SSd has marked inhibitory actions on the processes of inflammation, including capillary permeability, releasing of inflammation mediators, leukoplasia and desmoplasia[15,27,28]. In addition, SSd can increase serum concentrations of adrenocorticotropic hormone and corticosterone[29] as well as corticotropin-releasing factor (mRNA) level in the hypothalamus[16].

HA and LN levels in serum and HYP in liver are the important indices reflecting the degree of hepatic fibrosis[30-32]. In this study, the contents of HA and LN in serum and HYP in liver were much higher than those in the controls, but markedly lower in treatment groups ($P < 0.01$), indicating that SSd can prevent hepatic fibrosis due to chronic liver injury, thus delaying the development of cirrhosis.

Recent studies have identified NF-κB as a critical component to bridge inflammation by producing proinflammatory cytokines (such as TNF-α and IL-6) and more ECM in liver, thus further boosting inflammatory processes and activating HSCs[21-23,33-36]. It was also reported that TNF-α released from activating macrophages can turn up NF-κB activity both in target tissue cells and in macrophages themselves[37-40].

NF-κB is a transcription factor consisting of p65 and p50 subunits of the Rel protein family[41]. In most cells, it binds to its inhibitory counterpart I-κBα and other IκB proteins to form P65-P50-IκB trimer which is located in the cytoplasm as an inactive complex. Following I-κBα degradation by a complex signaling cascade initiated on the cell surface, the activated NF-κBp65 disassociates from I-κBα and shifts into nuclei where it binds to specific DNA motifs to regulate transcriptional activity of its target genes involved in HSC activation[42], releasing of proinflammatory cytokines including IL-6 and TNF-α. Thus, inhabiting IκBα phosphorylation is an indispensable step to activate the NF-κB signaling pathway[43-46]. In the present study, NF-κBp65 expression increased significantly in model group compared with normal control group, whereas it was markedly decreased in all SSd treatment groups, especial in the high-dose group. There was no difference in the expression of NF-κBp65 between SSd treatment groups and control group. On the contrary, its inhibitory I-κBα was significantly lower in model group but higher in SSd treatment group, suggesting that SSd can significantly inhibit the activation of NF-κBp65, which may be associated with a reduction in I-κBα degradation.

In addition, Spearman's correlation analysis showed that NF-κBp65 was highly correlated with the expression of TNF-α protein ($r = 0.823$, $P < 0.01$) and both of them had a strong positive correlation with the serum levels of HA induced by CCl_4 ($r = 0.862$, $P < 0.01$; $r = 0.928$, $P < 0.01$, respectively).

In conclusion, SSd has beneficial effects on hepatic fibrosis. Down-regulation of TNF-α, IL-6 and NF-κBp65 expression and increased I-κBα activity of SSd in rat liver may play an important role in the improvement of hepatic fibrosis induced by CCl_4. Since hepatic fibrogenesis is a very complicated process, the underlying mechanisms of SSd remain to be further explored.

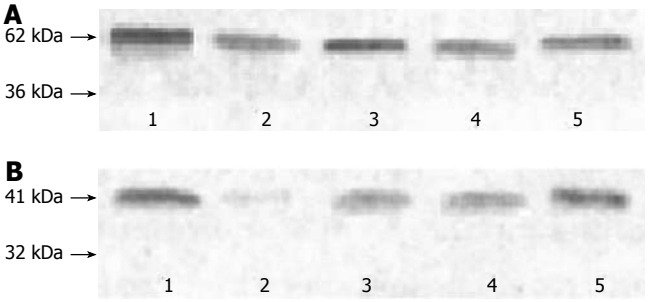

Figure 3 Images of Western blotting of NF-κBp65 (**A**) and I-κBα (**B**) in liver tissue of rats. Lane 1: NF-κBp65 and I-κBα protein in control group; lane 2: NF-κBp65 and I-κBα in model group; lanes 3-5: NF-κBp65 and I-κBα in SSd group (from low to high-dose group).

COMMENTS

Background

Hepatic fibrosis is a chronic inflammation-associated disease, which is involved in the infiltration of inflammatory cells and releasing of proinflammatory cytokines, such as NF-κB, TNF-α and IL-6. Recently, more and more clinical and experimental observations have demonstrated that SSd, a traditional Chinese medicine, is of some preventive and therapeutic values against liver fibrosis, whereas, the molecular mechanism involved in therapeutic effects of SSd on hepatic fibrosis has not been completely elucidated. Therefore, the aim of our study was to further evaluate the anti-hepatic fibrosis effect of SSd in rats and to study its relationship with the expression of NF-κBp65, TNF -α and IL-6.

Research frontiers

NF-κB as a critical component to bridge inflammation, can produce proinflammatory cytokines such as TNF-α and IL-6, which are involved in the process of fibrogenesis. Our study aimed at investigating the suppressive effect of SSd on hepatic fibrosis in rats induced by CCl_4 from the level of cytokine and its relationship with the expression of NF-κBp65, TNF-α and IL-6.

Innovations and breakthroughs

SSd has beneficial effects on hepatic fibrosis, and the down-regulation of TNF-α, IL-6 and NF-κBp65 expression and increased I-κBα activity of SSd in rat liver may play an important role in the improvement of hepatic fibrosis induced by CCl_4.

Applications

SSd may play a role in antifibrotic therapy. It protects liver cells against fibrosis and inhibits collagen fiber deposition in liver, and therefore can be used in the treatment of cirrhosis in clinic practice.

Terminology

Nuclear factor-κB (NF-κB) is a transcription factor consisting of p65 and p50 subunits of the Rel protein family. In most cells, it binds to its inhibitory counterpart I-κBα and other I-κB proteins to form P65-P50-IκB trimer that is located in the cytoplasm as an inactive complex. Following I-κBα degradation by a complex signaling cascade initiated at the cell surface, the activated NF-κBp65 disassociates from I-κBα and shifts into nuclei where it binds to specific DNA motifs to regulate transcriptional activity of its target genes involved in HSC activation, releasing of proinflammatory cytokines.

Peer review

In this study, rats with liver fibrosis were treated with CCl_4 in combination with ethanol, high fat and low protein diet. Rats receiving SSd in combination with CCl_4 injection developed less liver fibrosis. The effect was associated with less liver damage indicated by lower transaminase and higher albumin levels. Additionally, less activation of NF-κB was observed in the liver of treated rats, suggesting that SSd could attenuate CCl_4-induced liver fibrosis by down-regulating the inflammatory response in the liver. The study addresses an interesting issue, but the value of this study in its current form is limited. The data provided are preliminary but do not sufficiently support the conclusions drawn by the authors.

REFERENCES

1 **Gressner AM**. Cytokines and cellular crosstalk involved in the activation of fat-storing cells. *J Hepatol* 1995; **22**: 28-36
2 **Melgert BN**, Olinga P, Van Der Laan JM, Weert B, Cho J, Schuppan D, Groothuis GM, Meijer DK, Poelstra K. Targeting dexamethasone to Kupffer cells: effects on liver inflammation and fibrosis in rats. *Hepatology* 2001; **34**: 719-728
3 **Friedman SL**. Molecular regulation of hepatic fibrosis, an integrated cellular response to tissue injury. *J Biol Chem* 2000; **275**: 2247-2250
4 **Lamireau T**, Desmoulière A, Bioulac-Sage P, Rosenbaum J. Mechanisms of hepatic fibrogenesis. *Arch Pediatr* 2002; **9**: 392-405
5 **Zhang LJ**, Yu JP, Li D, Huang YH, Chen ZX, Wang XZ. Effects of cytokines on carbon tetrachloride-induced hepatic fibrogenesis in rats. *World J Gastroenterol* 2004; **10**: 77-81
6 **Okazaki I**, Watanabe T, Hozawa S, Niioka M, Arai M, Maruyama K. Reversibility of hepatic fibrosis: from the first report of collagenase in the liver to the possibility of gene therapy for recovery. *Keio J Med* 2001; **50**: 58-65
7 **Chen M**, Wang GJ, Diao Y, Xu RA, Xie HT, Li XY, Sun JG. Adeno-associated virus mediated interferon-gamma inhibits the progression of hepatic fibrosis in vitro and *in vivo*. *World J Gastroenterol* 2005; **11**: 4045-4051
8 **Okazaki I**, Watanabe T, Hozawa S, Arai M, Maruyama K. Molecular mechanism of the reversibility of hepatic fibrosis: with special reference to the role of matrix metalloproteinases. *J Gastroenterol Hepatol* 2000; **15** Suppl: D26-D32
9 **Croquet V**, Moal F, Veal N, Wang J, Oberti F, Roux J, Vuillemin E, Gallois Y, Douay O, Chappard D, Calès P. Hemodynamic and antifibrotic effects of losartan in rats with liver fibrosis and/or portal hypertension. *J Hepatol* 2002; **37**: 773-780
10 **Schwabe RF**, Schnabl B, Kweon YO, Brenner DA. CD40 activates NF-kappa B and c-Jun N-terminal kinase and enhances chemokine secretion on activated human hepatic stellate cells. *J Immunol* 2001; **166**: 6812-6819
11 **Sudo K**, Yamada Y, Moriwaki H, Saito K, Seishima M. Lack of tumor necrosis factor receptor type 1 inhibits liver fibrosis induced by carbon tetrachloride in mice. *Cytokine* 2005; **29**: 236-244
12 **Chong LW**, Hsu YC, Chiu YT, Yang KC, Huang YT. Anti-fibrotic effects of thalidomide on hepatic stellate cells and dimethylnitrosamine-intoxicated rats. *J Biomed Sci* 2006; **13**: 403-418
13 **Luedde T**, Beraza N, Trautwein C. Evaluation of the role of nuclear factor-kappaB signaling in liver injury using genetic animal models. *J Gastroenterol Hepatol* 2006; **21** Suppl 3: S43-S46
14 **Liang Y**, Cui R. Advances in the study of anti-inflammatory and immunoregulatory effects of saikosaponins and their similar substances. *Zhongguo Zhongxiyi Jiehe Zazhi* 1998; **18**: 446-448
15 **Bermejo Benito P**, Abad Martínez MJ, Silván Sen AM, Sanz Gómez A, Fernández Matellano L, Sánchez Contreras S, Díaz Lanza AM. In vivo and in vitro antiinflammatory activity of saikosaponins. *Life Sci* 1998; **63**: 1147-1156
16 **Dobashi I**, Tozawa F, Horiba N, Sakai Y, Sakai K, Suda T. Central administration of saikosaponin-d increases corticotropin-releasing factor mRNA levels in the rat hypothalamus. *Neurosci Lett* 1995; **197**: 235-238
17 **Chiang LC**, Ng LT, Liu LT, Shieh DE, Lin CC. Cytotoxicity and anti-hepatitis B virus activities of saikosaponins from Bupleurum species. *Planta Med* 2003; **69**: 705-709
18 **Wei HS**, Lu HM, Li DG, Zhan YT, Wang ZR, Huang X, Cheng JL, Xu QF. The regulatory role of AT 1 receptor on activated HSCs in hepatic fibrogenesis:effects of RAS inhibitors on hepatic fibrosis induced by CCl(4). *World J Gastroenterol* 2000; **6**: 824-828
19 **China Medical Association infectious branch**. The standard of grading and staging of viral hepatitis. *Zhonghua Chuanranbing Zazhi* 1995; **13**: 241-247
20 **Jamall IS**, Finelli VN, Que Hee SS. A simple method to determine nanogram levels of 4-hydroxyproline in biological tissues. *Anal Biochem* 1981; **112**: 70-75
21 **Tomita K**, Tamiya G, Ando S, Ohsumi K, Chiyo T, Mizutani A, Kitamura N, Toda K, Kaneko T, Horie Y, Han JY, Kato S, Shimoda M, Oike Y, Tomizawa M, Makino S, Ohkura T, Saito H, Kumagai N, Nagata H, Ishii H, Hibi T. Tumour necrosis factor alpha signalling through activation of Kupffer cells plays an essential role in liver fibrosis of non-alcoholic steatohepatitis in mice. *Gut* 2006; **55**: 415-424
22 **Luckey SW**, Taylor M, Sampey BP, Scheinman RI, Petersen DR. 4-hydroxynonenal decreases interleukin-6 expression and protein production in primary rat Kupffer cells by inhibiting nuclear factor-kappaB activation. *J Pharmacol Exp Ther* 2002; **302**: 296-303
23 **Sung CK**, She H, Xiong S, Tsukamoto H. Tumor necrosis factor-alpha inhibits peroxisome proliferator-activated receptor gamma activity at a posttranslational level in hepatic stellate cells. *Am J Physiol Gastrointest Liver Physiol* 2004; **286**: G722-G729
24 **Lee KS**, Lee SJ, Park HJ, Chung JP, Han KH, Chon CY, Lee SI, Moon YM. Oxidative stress effect on the activation of hepatic stellate cells. *Yonsei Med J* 2001; **42**: 1-8
25 **Gressner AM**. Mediators of hepatic fibrogenesis. *Hepatogastroenterology* 1996; **43**: 92-103
26 **Yamamoto M**, Kumagai A, Yamamura Y. Structure and action of saikosaponins isolated from Bupleurum falcatum L. II. Metabolic actions of saikosaponins, especially a plasma cholesterol-lowering action. *Arzneimittelforschung* 1975; **25**: 1240-1243
27 **Navarro P**, Giner RM, Recio MC, Máñez S, Cerdá -Nicolás M, Ríos JL. In vivo anti-inflammatory activity of saponins from Bupleurum rotundifolium. *Life Sci* 2001; **68**: 1199-1206
28 **Yamamoto M**, Kumagai A, Yamamura Y. Structure and actions of saikosaponins isolated from Bupleurum falcatum L. I. Anti-inflammatory action of saikosaponins. *Arzneimittelforschung* 1975; **25**: 1021-1023
29 **Hiai S**, Yokoyama H, Nagasawa T, Oura H. Stimulation of the pituitary-adrenocortical axis by saikosaponin of Bupleuri radix. *Chem Pharm Bull* (Tokyo) 1981; **29**: 495-499
30 **Hayasaka A**, Saisho H. Serum markers as tools to monitor liver fibrosis. *Digestion* 1998; **59**: 381-384
31 **Körner T**, Kropf J, Gressner AM. Serum laminin and hyaluronan in liver cirrhosis: markers of progression with high prognostic value. *J Hepatol* 1996; **25**: 684-688
32 **Murawaki Y**, Ikuta Y, Koda M, Nishimura Y, Kawasaki H. Clinical significance of serum hyaluronan in patients with chronic viral liver disease. *J Gastroenterol Hepatol* 1996; **11**: 459-465
33 **Tak P**P, Firestein GS. NF-kappaB: a key role in inflammatory diseases. *J Clin Invest* 2001; **107**: 7-11
34 **Chen K**, Long YM, Wang H, Lan L, Lin ZH. Activation of nuclear factor-kappa B and effects of pyrrolidine dithiocarbamate on TNBS-induced rat colitis. *World J Gastroenterol* 2005; **11**: 1508-1514
35 **Rahman I**, Marwick J, Kirkham P. Redox modulation of chromatin remodeling: impact on histone acetylation and deacetylation, NF-kappaB and pro-inflammatory gene expression. *Biochem Pharmacol* 2004; **68**: 1255-1267
36 **Luckey SW**, Petersen DR. Activation of Kupffer cells during the course of carbon tetrachloride-induced liver injury and fibrosis in rats. *Exp Mol Pathol* 2001; **71**: 226-240
37 **Sizemore N**, Leung S, Stark GR. Activation of phosphatidylinositol 3-kinase in response to interleukin-1 leads to phosphorylation and activation of the NF-kappaB p65/RelA subunit. *Mol Cell Biol* 1999; **19**: 4798-4805
38 **Baldwin AS**. The NF-kappa B and I kappa B proteins: new discoveries and insights. *Annu Rev Immunol* 1996; **14**: 649-683
39 **Yoshimura A**, Mori H, Ohishi M, Aki D, Hanada T. Negative regulation of cytokine signaling influences inflammation. *Curr Opin Immunol* 2003; **15**: 704-708
40 **Wang D**, Baldwin AS. Activation of nuclear factor-kappaB-dependent transcription by tumor necrosis factor-alpha is mediated through phosphorylation of RelA/p65 on serine 529. *J Biol Chem* 1998; **273**: 29411-29416
41 **Cowburn AS**, Deighton J, Walmsley SR, Chilvers ER. The

survival effect of TNF-alpha in human neutrophils is mediated via NF-kappa B-dependent IL-8 release. *Eur J Immunol* 2004; **34**: 1733-1743

42 **Karin M**, Ben-Neriah Y. Phosphorylation meets ubiquitination: the control of NF-[kappa]B activity. *Annu Rev Immunol* 2000; **18**: 621-663

43 **Hellerbrand C**, Jobin C, Iimuro Y, Licato L, Sartor RB, Brenner DA. Inhibition of NFkappaB in activated rat hepatic stellate cells by proteasome inhibitors and an IkappaB super-repressor. *Hepatology* 1998; **27**: 1285-1295

44 **Elsharkawy AM**, Wright MC, Hay RT, Arthur MJ, Hughes T, Bahr MJ, Degitz K, Mann DA. Persistent activation of nuclear factor-kappaB in cultured rat hepatic stellate cells involves the induction of potentially novel Rel-like factors and prolonged changes in the expression of IkappaB family proteins. *Hepatology* 1999; **30**: 761-769

45 **Karin M**. How NF-kappaB is activated: the role of the IkappaB kinase (IKK) complex. *Oncogene* 1999; **18**: 6867-6874

46 **Ghosh S**, Karin M. Missing pieces in the NF-kappaB puzzle. *Cell* 2002; **109** Suppl: S81-S96

S- Editor Wang GP **L- Editor** Wang XL **E- Editor** Bi L

PO Box 2345, Beijing 100023, China
www.wjgnet.com
wjg@wjgnet.com

World J Gastroenterol 2007 January 28; 13(4): 564-571
World Journal of Gastroenterology ISSN 1007-9327

BASIC RESEARCH

Protection of *Veratrum nigrum L. var. ussuriense Nakai alkaloids* against ischemia-reperfusion injury of the rat liver

Zhen-Zhen Wang, Wei-Jie Zhao, Xue-Song Zhang, Xiao-Feng Tian, Yu-Zhu Wang, Feng Zhang, Jin-Chan Yuan, Guo-Zhu Han, Ke-Xin Liu, Ji-Hong Yao

Zhen-Zhen Wang, Yu-Zhu Wang, Feng Zhang, Jin-Chan Yuan, Guo-Zhu Han, Ke-Xin Liu, Ji-Hong Yao, Department of Pharmacology, Dalian Medical University, Dalian 116027, Liaoning Province, China
Wei-Jie Zhao, Department of Chemical Pharmaceutics, Dalian University of Science and Technology, Dalian 116027, Liaoning Province, China
Xue-Song Zhang, Xiao-Feng Tian, Department of General Surgery, Second Affiliated Hospital of Dalian Medical University, Dalian 116023, Liaoning Province, China
Correspondence to: Professor Ji-Hong Yao, Department of Pharmacology, Dalian Medical University, Dalian 116027, Liaoning Province, China. yaojihong65@tom.com
Telephone: +86-411-84720229 Fax: +86-411-84720031
Received: 2006-09-25 Accepted: 2006-11-02

Abstract

AIM: To investigate the protective effects and possible mechanisms of *Veratrum nigrum L.var. ussuriense Nakai alkaloids* (VnA) on hepatic ischemia/reperfusion (I/R) injury in rats.

METHODS: Forty male Wistar rats were randomly divided into four experimental groups (n = 10 in each): (A) Control group (the sham operation group); (B) I/R group (pretreated with normal saline); (C) Small-dose (10 μg/kg) VnA pretreatment group; (D) Large-dose (20 μg/kg) VnA pretreatment group. Hepatic ischemia/reperfusion (Hepatic I/R) was induced by occlusion of the portal vein and the hepatic artery for 90 min, followed by reperfusion for 240 min. The pretreatment groups were administered with VnA intraperitoneally, 30 min before surgery, while the control group and I/R group were given equal volumes of normal saline. Superoxide dismutase (SOD) activity, myeloperoxidase (MPO) activity and nitric oxide (NO) content in the liver tissue at the end of reperfusion were determined and liver function was measured. The expression of intercellular adhesion molecule-1 (ICAM-1) and E-selectin (ES) were detected by immunohistochemical examinations and Western blot analyses.

RESULTS: The results showed that hepatic I/R elicited a significant increase in the plasma levels of alanine aminotransferase (ALT: 74.53 ± 2.58 IU/L *vs* 1512.54 ± 200.76 IU/L, $P < 0.01$) and lactic dehydrogenase (LDH: 473.48 ± 52.17 IU/L *vs* 5821.53 ± 163.69 IU/L, $P < 0.01$), as well as the levels of MPO (1.97 ± 0.11 U/g *vs* 2.57 ± 0.13 U/g, $P < 0.01$) and NO (69.37 ± 1.52 μmol/g protein *vs* 78.39 ± 2.28 μmol/g protein, $P < 0.01$) in the liver tissue, all of which were reduced by pretreatment with VnA, respectively (ALT: 1512.54 ± 200.76 IU/L *vs* 977.93 ± 89.62 IU/L, 909.81 ± 132.76 IU/L, $P < 0.01$, $P < 0.01$; LDH: 5821.53 ± 163.69 IU/L *vs* 3015.44 ± 253.01 IU/L, 2448.75 ± 169.4 IU/L, $P < 0.01$, $P < 0.01$; MPO: 2.57 ± 0.13 U/g *vs* 2.13 ± 0.13 U/g, 2.07 ± 0.05 U/g, $P < 0.01$, $P < 0.01$; NO: 78.39 ± 2.28 μmol/g protein *vs* 71.11 ± 1.73 μmol/g protein, 68.58 ± 1.95 μmol/g protein, $P < 0.05$, $P < 0.01$). The activity of SOD (361.75 ± 16.22 U/mg protein *vs* 263.19 ± 12.10 U/mg protein, $P < 0.01$) in the liver tissue was decreased after I/R, which was enhanced by VnA pretreatment (263.19 ± 12.10 U/mg protein *vs* 299.40 ± 10.80 U/mg protein, 302.09 ± 14.80 U/mg protein, $P < 0.05$, $P < 0.05$). Simultaneously, the histological evidence of liver hemorrhage, polymorphonuclear neutrophil infiltration and the overexpression of ICAM-1 and E-selectin in the liver tissue were observed, all of which were attenuated in the VnA pretreated groups.

CONCLUSION: The results demonstrate that VnA pretreatment exerts significant protection against hepatic I/R injury in rats. The protective effects are possibly associated with enhancement of antioxidant capacity, reduction of inflammatory responses and suppressed expression of ICAM-1 and E-selectin.

Key words: *Veratrum nigrum L.var. ussuriense Nakai alkaloids*; Hepatic Ischemia/Reperfusion Injury; Intracellular adhesion molecule-1; E-selectin

Wang ZZ, Zhao WJ, Zhang XS, Tian XF, Wang YZ, Zhang F, Yuan JC, Han GZ, Liu KX, Yao JH. Protection of *Veratrum nigrum L. var. ussuriense Nakai alkaloids* against ischemia-reperfusion injury of the rat liver. *World J Gastroenterol* 2007; 13(4): 564-571

http://www.wjgnet.com/1007-9327/13/564.asp

INTRODUCTION

Re-establishment of blood flow to the ischemic tissue is the therapeutic goal in the treatment of arterial occlusion.

However, surgically restoring the blood flow often leads to continued or accelerated local tissue injury and systemic toxicity[1]. Hepatic ischemia/reperfusion (Hepatic I/R) injury is an important non-immunologic problem and a limitating factor in liver transplantation and it may result in liver dysfunction, liver failure, and even death[2]. Hepatic I/R injury is one of the major complications of hepatic resection, hemorrhagic shock with fluid resuscitation, and liver transplantation, particularly with grafts from marginal donors[3]. The mechanisms underlying ischemia/reperfusion induced organ damage are likely multifactorial and interdependent. Previous studies have identified many mediators involved in the pathogenesis of hepatic I/R injury. Among them, reactive oxygen species (ROS)[4] released by active Kupffer cells, and proinflammatory cytokines[5-7] are central to this process. Expression of the adhesion molecules is up-regulated by cytokines and mediates the recruitment of neutrophils to the liver resulting in hepatic injury[8-9]. In addition, selectins are also up-regulated during this process[10].

It has been shown that short episodes of liver ischemia confer protection against longer ischemic insults and subsequent I/R injury. This phenomenon is called ischemic or mechanical preconditioning[11-12]. Pharmacological preconditioning can be an effective alternative to ischemic preconditioning. With pharmacological preconditioning, liver protection is achieved by the administration of substances before or at the early phase of the I/R process.

Veratrum nigrum L.var. ussuriense Nakai alkaloids (VnA) is the total alkaloid extracted from the root of *Veratrum nigrum L. var. ussuriense Nakai* of Mount Qian in Liaoning Province, China. VnA contains at least eleven alkaloids featuring an ester-type isosteroidal structure identified by modern analytical techniques such as HPLC-MS, NMR, *etc*. The principal components of VnA include verussurien, verabenzoamine, verazine, germidine, jervine, germerine, 15-O-(methylbuty-royl)-germine, verussurinine, neogermbudine, zygadenine and echinuline[13-15]. Some researchers have demonstrated that VnA has powerful inhibitory effects against both arterial and venous thrombosis, and it could produce beneficial effects on brain I/R injury[16-18]. In this study, we investigated whether VnA had a protective effect against liver injury induced by hepatic I/R and explored its putative protective mechanism.

MATERIALS AND METHODS

Reagents

The VnA hydrochloride injection (100 mg/L) was prepared by the Department of Pharmaceutical Engineering, Dalian University of Science and Technology. It was diluted to the required concentrations with sterile saline solution prior to use.

Animals

Male Wistar rats (Experimental Animal Center of Dalian Medical University, Dalian, China) weighing 220 ± 20 g were used in this study. All rats were fed with standard laboratory chow and water, and housed in accordance with institutional animal care guidelines.

Experimental design

Male Wistar rats were fasted overnight but had free access to tap water. The rats were assigned randomly into four experimental groups (n = 10 in each): (A) Control group (the sham operation group); (B) I/R group (pretreated with normal saline); (C) Small-dose (10 μg/kg) VnA pretreatment group; (D) Large-dose (20 μg/kg) VnA pretreatment group. The model of hepatic I/R injury was established by the clamping and unclamping of the vessels supplying the left lateral and median hepatic lobes, which account for 70% of the rat liver mass, according to the published method[12]. We reproduced a lobar rather than a total hepatic I/R injury model to induce a severe hepatic ischemic insult without mesenteric venous congestion to avoid the development of intestinal congestion and leakage of bacteria or bacterial products into the circulation[6,19]. Briefly, 30 min before operation, the rats received intraperitoneally VnA (10 μg/kg, 20 μg/kg) or equal volumes of normal saline solution. A midline laparotomy was performed and a microvascular clip was placed to interrupt the arterial and portal venous blood flow to the left and middle lobes of the liver. Reflow was initiated after 90 min of hepatic ischemia by removing the clamp. The doses of VnA administration were determined according to previous studies, combined with our preliminary experiments[17-18]. All rats were killed at 240 min of reperfusion, and blood and liver samples were obtained for the following analyses.

Histopathological assessment

Liver samples were fixed in 10% formalin and embedded in paraffin. Five-micrometer sections of liver tissue were stained with hematoxylin and eosin according to standard procedures. Light microscopy was used to assess the degree of liver damage.

Measurement of plasma alanine aminotransferase (ALT) and lactic dehydrogenase (LDH) level

The abdominal aorta was punctured and 5 mL of blood was taken and put into heparinized tubes. The blood sample was centrifuged at 3000 r/min for 15 min at a room temperature to separate plasma for analyses. The plasma concentrations of ALT (a specific marker for hepatic parenchymal injury), and LDH were measured with an OLYMPUS AU5400 automatic analyzer. Both values were expressed as U/L.

Liver superoxide dismutase (SOD), myeloperoxidase (MPO) and nitric oxide (NO) assay

Liver samples were homogenized on ice in 5 volumes of normal saline and centrifuged at 3000 r/min for 15 min. Liver SOD, MPO and NO levels were measured using an assay kit (Nanjing Jiancheng Bioengineering Institute, Nanjing, China) following the manufacturer's instructions. The levels of SOD, MPO and NO were expressed as U/mgprot, U/g and μmol/gprot, respectively.

Immunohistochemical analyses

Formalin-fixed, paraffin-embedded liver specimens were stained by streptavidin/peroxidase immunohistochemistry

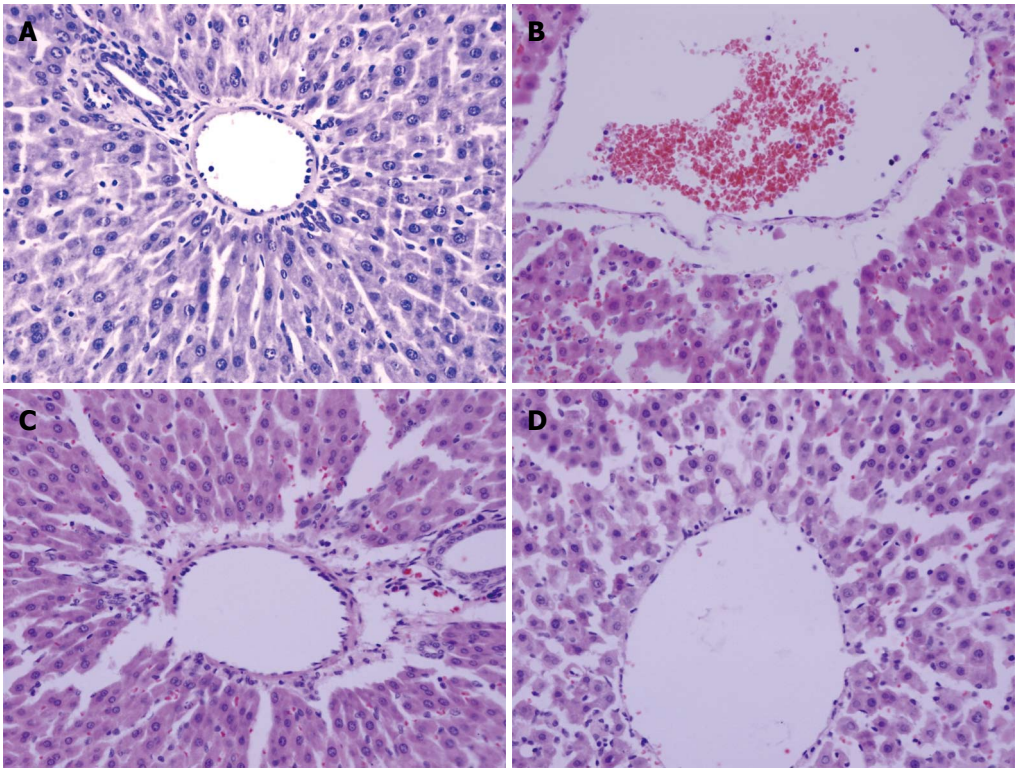

Figure 1 Changes of histology in the liver tissue 90 min after ischemia and 240 min after reperfusion in rats (× 400). Five μm sections of liver tissue were stained with hematoxylin and eosin according to standard procedures. For all groups, n = 10. **A**: Control group: Normal appearance of hepatocytes and sinusoids; **B**: I/R group: Histological edema, hemorrhage, partial exfoliation of blood vessel endothelium and infiltration with inflammatory cells; **C**: I/R + VnA (10 μg/kg) group: A significant amelioration of histological edema, hemorrhage, and exfoliation of blood vessel endothelium; **D**: I/R + VnA (20 μg/kg) group: Slight inflammatory cell infiltration with most hepatocytes in normal appearance.

technique for intercellular adhesion molecule-1 (ICAM-1) and E-selectin (ES) detection. Five-micrometer sections were treated with 0.3% H_2O_2 in methanol to block endogenous peroxide activity and then incubated with the polyclonal rabbit anti-rat ICAM-1 and E-selectin antibody (Wuhan Boster Biological Technology Co., Ltd, Wuhan, China, both 1:500 dilution). Biotinylated anti-rabbit immunoglobulin was added as a secondary antibody. The horseradish peroxidase labeled streptomycin-avidin complex was then used to detect the second antibody. Finally, slides were stained with 3,3'-diaminobenzidine, which was used as a chromagen, and the sections were counterstained with hematoxylin before being examined under a light microscope. The brown or dark brown stained cells were considered as positive. The results were evaluated semi-quantitatively according to the percentage of positive cells in 5 high power fields at 400 multiple signal magnification: 0, less than 5%; 1, from 6% to 25%; 2, from 26% to 50%; 3, from 51% to 75%; 4, more than 75%[20].

ICAM-1 and E-selectin Western blot analysis

Frozen liver tissue was homogenized with PBS (pH = 7.2) and centrifuged at 4℃, 10 000 g for 10 min. After precipitation the insoluble fraction was discarded, and the protein concentration in the supernatant was determined by a spectrophotometer. Aliquots (20 μg) of protein from each sample were loaded into each lane of 10% SDS-PAGE gel electrophoresis and then electroblotted onto nitrocellulose membranes (Millipore, Bedford, MA). The membranes were then probed with the rabbit antibody against rat ICAM-1(intercellular adhesion molecule-1) or E-selectin (Boster Biological Technology Co., Ltd, Wuhan, China, both 1:1000 dilution) and biotin-conjugated anti-rabbit IgG (Fuzhou Maixin Biological Technology Co., Ltd, Fuzhou, China) according to the manufacturer's recommendations. The signals were visualized by a DAB assay kit (Fuzhou Maixin Biological Technology Co., Ltd, Fuzhou, China) and analyzed with a gel imaging system (Kodak system EDAS120, Japan).

Statistical analyses

All data were presented as mean ± SD. Statistical analyses were performed using one-way analysis of variance (ANOVA) with the SPSS 11.5 statistical software package. The differences between means were analyzed using Student-Newman-Keuls (SNK) test for multiple comparisons. P values less than 0.05 were considered statistically significant.

RESULTS

Pathological alterations of liver tissue

The histological structure of cells was normal in the control group. After 90 min of hepatic ischemia followed by 240 min of reperfusion, the occluded liver tissue appeared as dark color with an obtuse fringe. Compared with the control group, the liver tissue from the I/R group was markedly damaged characterized by edema, hemorrhage, partial exfoliation of vascular endothelium and infiltration with inflammatory cells under the microscope. Pretreatment of rats with 10 or 20 μg/kg VnA resulted in a significant amelioration of hepatic injury (Figure 1).

Levels of plasma liver enzymes

Liver function was tested by measuring plasma levels of ALT and LDH. Hepatic I/R led to a marked elevation of plasma ALT and LDH activity (ALT: 74.53 ± 2.58 IU/L *vs* 1512.54 ± 200.76 IU/L, $P < 0.01$; LDH: 473.48 ± 52.17

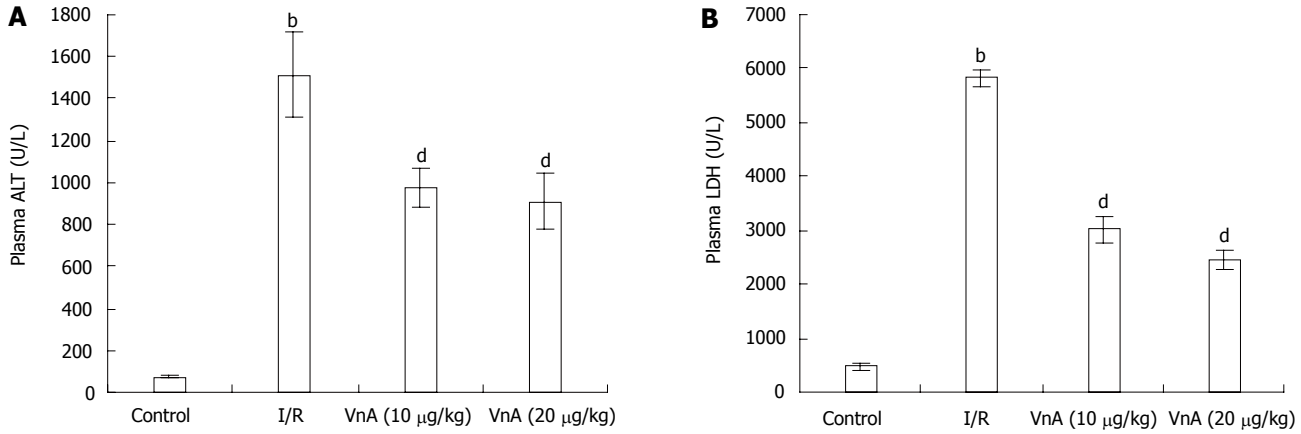

Figure 2 Plasma aminotransferase (ALT) (**A**) and acetic dehydrogenase (LDH) (**B**) levels in different groups (mean ± SD, $n = 10$). After 90 min of hepatic ischemia and 4 h of reperfusion, plasma levels of ALT and LDH were determined with an OLYMPUS AU5400 automatic analyzer. $^{b}P < 0.01$ *vs* control group; $^{d}P < 0.01$ *vs* I/R group.

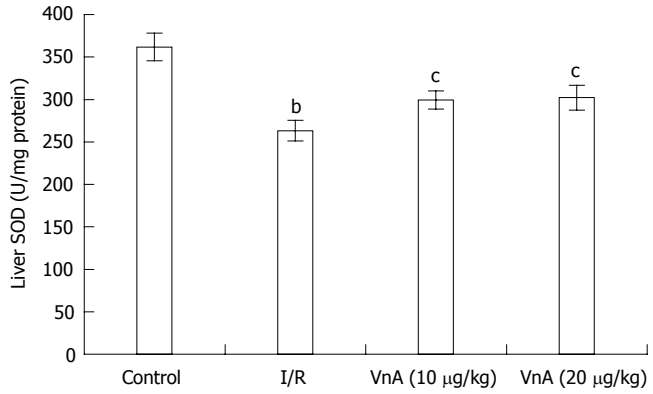

Figure 3 Activity of superoxide dismutase (SOD) in the liver tissue in different groups (mean ± SD, $n = 10$). After 90 min of ischemia and 4 h of reperfusion, the liver tissue was homogenized and assayed for SOD levels with an SOD assay kit as the index of hepatic oxidative stress. $^{b}P < 0.01$ *vs* control group; $^{c}P < 0.05$ *vs* I/R group.

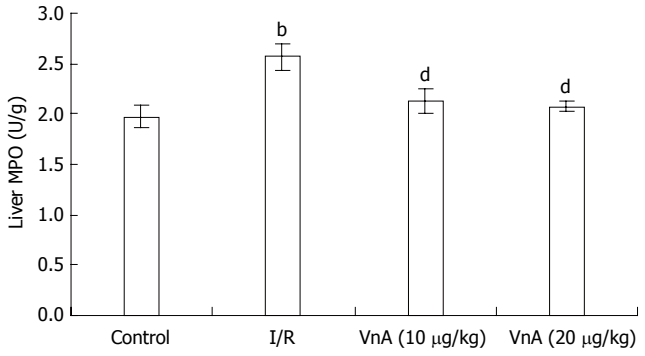

Figure 4 Activity of myeloperoxidase (MPO) in the liver tissue in different groups (mean ± SD, $n = 10$). MPO contents in liver tissue were analyzed with an MPO assay kit as the index of neutrophil recruitment. $^{b}P < 0.01$ *vs* control group; $^{d}P < 0.01$ *vs* I/R group.

IU/L *vs* 5821.53 ± 163.69 IU/L, $P < 0.01$, Figure 2). The increase in plasma ALT activity elicited by hepatic I/R was significantly attenuated by administration of VnA at doses of 10 and 20 μg/kg by about 35.35% and 39.85%, respectively (1512.54 ± 200.76 IU/L *vs* 977.93 ± 89.62 IU/L, 909.81 ± 132.76 IU/L, $P < 0.01$, $P < 0.01$); and the activity of LDH was reduced by administration of VnA at doses of 10 and 20 μg/kg by about 48.20% and 57.94%, respectively (5821.53 ± 163.69 IU/L *vs* 3015.44 ± 253.01 IU/L, 2448.75 ± 169.4 IU/L, $P < 0.01$, $P < 0.01$). This result demonstrated the dose-dependent protective effects of VnA on liver injury.

SOD activity in liver tissue

Compared with the control group, the level of liver SOD in the I/R group reduced significantly (361.75 ± 16.22 U/mg protein *vs* 263.19 ± 12.10 U/mg protein, $P < 0.01$). After administration of VnA at doses of 10 and 20 μg/kg, respectively, the liver SOD activity was elevated significantly (263.19 ± 12.10 U/mg protein *vs* 299.40 ± 10.80 U/mg protein, 302.09 ± 14.80 U/mg protein, $P < 0.05$, $P < 0.05$, Figure 3).

MPO activity in liver tissue

Hepatic neutrophil recruitment was determined by liver MPO content. Hepatic I/R caused a marked increase in liver MPO content compared with the control group (1.97 ± 0.11 U/g *vs* 2.57 ± 0.13 U/g, $P < 0.01$). Administration of VnA at doses of 10 and 20 μg/kg resulted in a marked reduction of MPO in a dose-dependent manner (2.57 ± 0.13 U/g *vs* 2.13 ± 0.13 U/g, 2.07 ± 0.05 U/g, $P < 0.01$, $P < 0.01$), suggesting that VnA prevents leukocyte recruitment to the liver tissue (Figure 4).

NO content in liver tissue

The level of NO in the liver tissue was significantly higher in the I/R group compared with the control group (69.37 ± 1.52 μmol/g protein *vs* 78.39 ± 2.28 μmol/g protein, $P < 0.01$). Pretreatment with VnA at both 10 and 20 μg/kg, however, caused an obvious reduction in a dose-dependent manner when compared with the I/R group (78.39 ± 2.28 μmol/g protein *vs* 71.11 ± 1.73 μmol/g protein, 68.58 ± 1.95 μmol/g protein, $P < 0.05$, $P < 0.01$, Figure 5).

Immunohistochemical analysis for liver ICAM-1 and E-selectin

The expression of ICAM-1 and E-selectin in the control

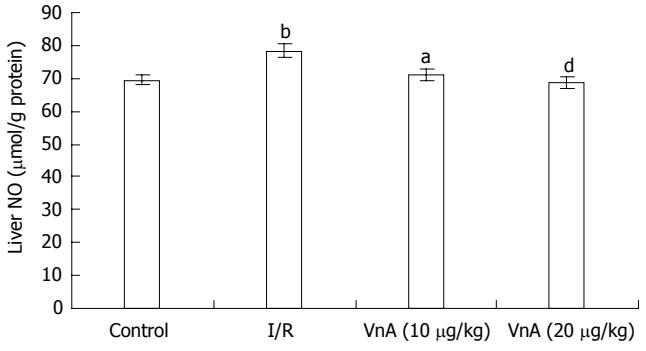

Figure 5 Content of nitric oxide (NO) in the liver tissue in different groups (mean ± SD, n = 10). After 90 min of ischemia and 4 h of reperfusion, the liver tissue was homogenized and assayed for NO levels with an NO assay kit as the index of hepatic oxidative stress. $^{b}P < 0.01$ *vs* control group. $^{a}P < 0.05$, $^{d}P < 0.01$ *vs* I/R group.

group showed as light brown immunostaining. However, their expression was highly up-regulated after 90 min of ischemia and 240 min of reperfusion ($P < 0.01$). Compared with the I/R group, the increase of ICAM-1 and E-selectin expression was significantly suppressed by VnA in a dose-dependent manner ($P < 0.05$, $P < 0.01$; $P < 0.05$, $P < 0.05$ respectively) (Figure 6, Figure 7 and Figure 8).

Western blot analysis for liver ICAM-1 and E-selectin

Western blot showed weak positive ICAM-1 and E-selectin signals in the control group. In contrast, a marked increase in ICAM-1 and E-selectin protein expression in the liver tissue was found in the I/R group. Compared with the I/R group, the signals were weakened obviously in the VnA pretreated group (Figure 9).

DISCUSSION

Liver I/R injury occurs in a number of clinical settings including liver surgery, transplantation, and hemorrhagic shock. A major disadvantage of this event is an acute inflammatory response that may cause significant organ damage or dysfunction. Experimental evidence demonstrates that kupffer cells play an important part in mediating hepatic I/R[21-22]. Kuppfer cell activation leads to structural changes, formation of vascular ROS and production of proinflammatory cytokines, which in turn induce the expression of adhesion molecules in vascular endothelial cells and stimulate the production and release of neutrophil-attracting chemokines. Neutrophil recruitment in the liver tissue causes direct hepatocellular damage through exhaustion of hepatic microcirculation by blocking the capillary perfusion and releasing ROS and proteases[23-24].

VnA is a well known herbal plant widely distributed in the northeast region of China and has various pharmacological effects including antithrombotic and antihypertensive properties[15,17]. Some researchers have also demonstrated that VnA exerted beneficial effects on brain I/R injury by inhibiting oxidation and leukocyte priming and expression of inflammatory mediators[18]. In the present study, we demonstrated that VnA pretreatment at doses of 10 and 20 μg/kg could attenuate hepatic I/R injury, indicated by improved alteration in liver tissue pathology and liver function, by an enhanced antioxidant capacity with augmentation of free radical scavengers and reduced polymorphonuclear neutrophil (PMN) infiltration, as well as by suppressed overexpression of adhesion molecules and selectins.

Reperfusion of the ischemic liver in rats resulted in hepatic damage with histological evidence of liver hemorrhage, edema, accumulation of adherent leukocytes in sinusoids and terminal hepatic vein (THV), as well as partial exfoliation of blood vessel endothelia. Furthermore, hepatic I/R caused the release of liver enzymes into the blood stream, thereby eliciting a significant increase in plasma levels of ALT and LDH. VnA pretreatment abated liver pathologic injury and reduced plasma ALT and LDH activity, thus liver function was ameliorated.

SOD catalyses the dismutation of the superoxide anion ($O_2^{\cdot}$) into H_2O_2, which can be transformed into H_2O and O_2 by catalase (CAT). In this study, we found that I/R impaired SOD activity, as indicated by the markedly lowered activity compared with the control group. But in the VnA pretreated group, the decrease of SOD activity was significantly counteracted. In addition, the hepatic I/R increased the levels of nitric oxide (NO), an important ROS product. This result is consistent with a previous report[25]. NO may combine with superoxide radicals to form peroxynitrite, a substance extremely toxic to cells[26]. VnA pretreatment significantly decreased liver NO content, resulting in a significant reduction in liver damage when compared with the control group. These data indicated that VnA might confer protection on the liver during I/R injury in part by improving activity of the endogenous antioxidant enzyme, which scavenges ROS and reduces their effects.

Because MPO is an enzyme restricted mainly to PMNs, the increase in MPO activity reflects neutrophil tissue infiltration. The significant increase in MPO activity in the liver tissue after hepatic I/R in the present study is consistent with another study[27]. However, VnA significantly blunted the increase of liver MPO activity compared with the I/R group. That is to say, VnA reduced infiltration of leukocytes into the inflammatory sites.

ICAM-1 is a member of the immunoglobulin superfamily that mediates firm adhesion and emigration of activated leukocytes in postcapillary venules, which process may be one of the important steps in the development of tissue injury and organ dysfunction[28]. Previous studies have shown an upregulation of ICAM-1 expression following endothelial cell activation with cytokines or LPS, accompanied by an increased binding of neutrophils and lymphocytes to endothelial cells. An anti-ICAM-1 monoclonal antibody inhibited neutrophil infiltration into pericentral sinusoids and improved and restored liver integrity in I/R injury[29]. In this study we detected overexpression of ICAM-1 after hepatic I/R, which was significantly decreased in the VnA pretreated groups. This indicated that VnA could suppress leukocyte adhesion to endothelia.

Murine E-selectin is a 110 kDa, type-1 transmembrane glycoprotein expressed only in endothelial cells after cytokine activation[30]. E-selectin participates in leukocyte

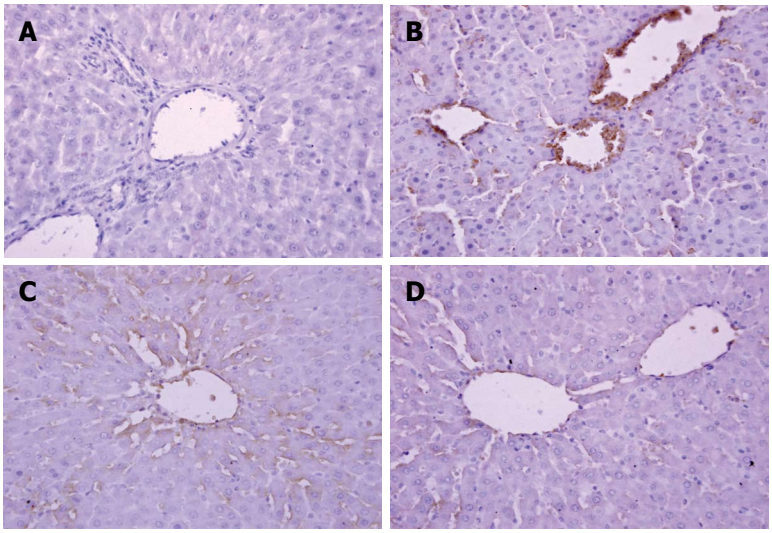

Figure 6 Immunohistochemical staining of adhesion molecule-1 (ICAM-1) expression in the liver tissue after 90 min of ischemia and reperfusion for 240 min in rats (× 400). Formalin-fixed, paraffin-embedded liver specimens were stained by streptavidin/peroxidase immunohistochemistry technique. For all groups, *n* = 10. **A**: Control group; **B**: I/R group; **C**: I/R + VnA (10 μg/kg) group; **D**: I/R + VnA (20 μg/kg) group.

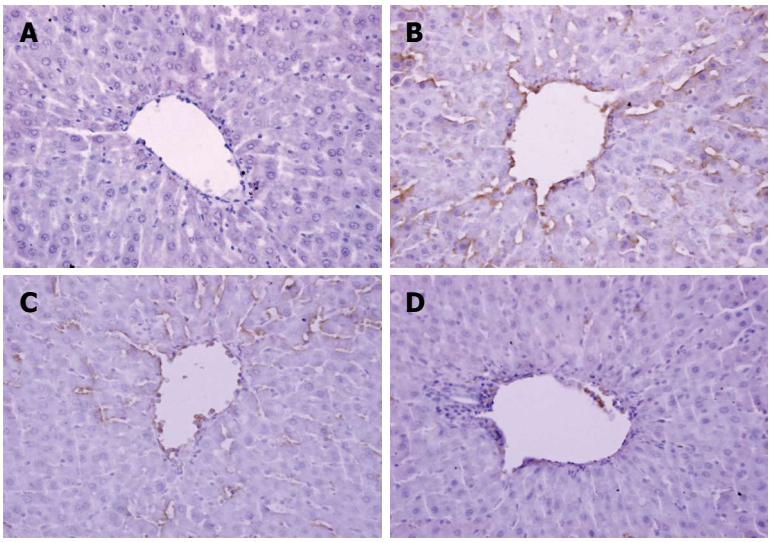

Figure 7 Immunohistochemical staining of E-selectin in liver tissue after ischemia for 90 min and reperfusion for 240 min in rats (× 400). Formalin-fixed, paraffin-embedded liver specimens were stained by the streptavidin/peroxidase immunohistochemistry technique. For all groups, *n* = 10. **A**: Control group; **B**: I/R group; **C**: I/R + VnA (10 μg/kg) group; **D**: I/R + VnA (20 μg/kg) group.

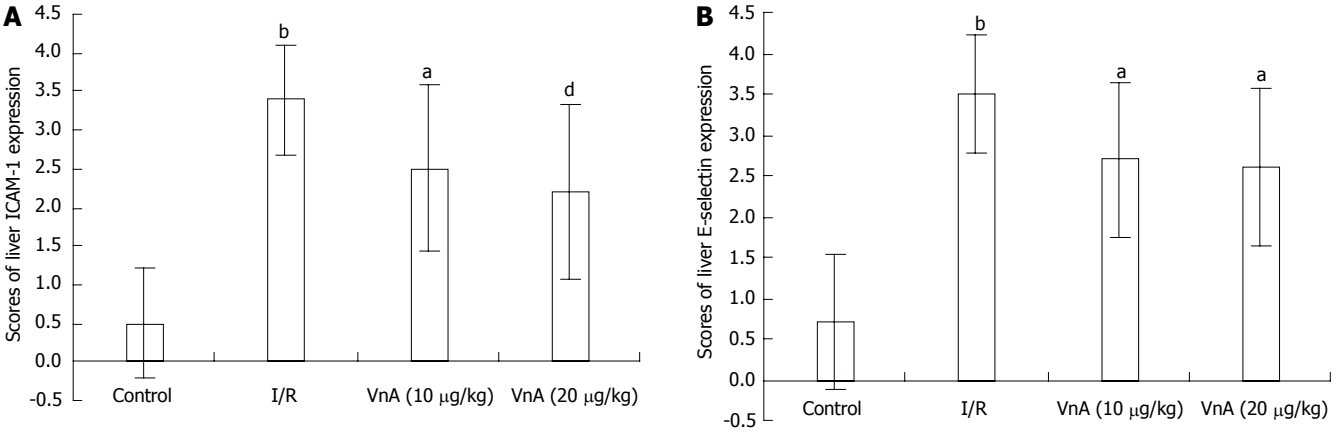

Figure 8 Immunohistochemical results (semi-quantitative analysis) of adhesion molecule-1 (ICAM-1) (**A**) and E-selectin (**B**) in liver tissue in different groups. Data were presented as mean ± SD. $^{b}P < 0.01$ *vs* Control group; $^{a}P < 0.05$, $^{d}P < 0.01$ *vs* I/R group.

rolling and firm adhesion *in vitro*[31] and *in vivo*[32]. It is down-regulated by re-internalization and by shedding from the endothelial surface into the plasma[33]. Previous studies revealed that blockade of E-selectin protected from severe acute renal failure induced by ischemia-reperfusion[34]. In our study, E-selectin was also found to be overexpressed after hepatic I/R, however, this was attenuated in the VnA pretreated groups as compared with the I/R group.

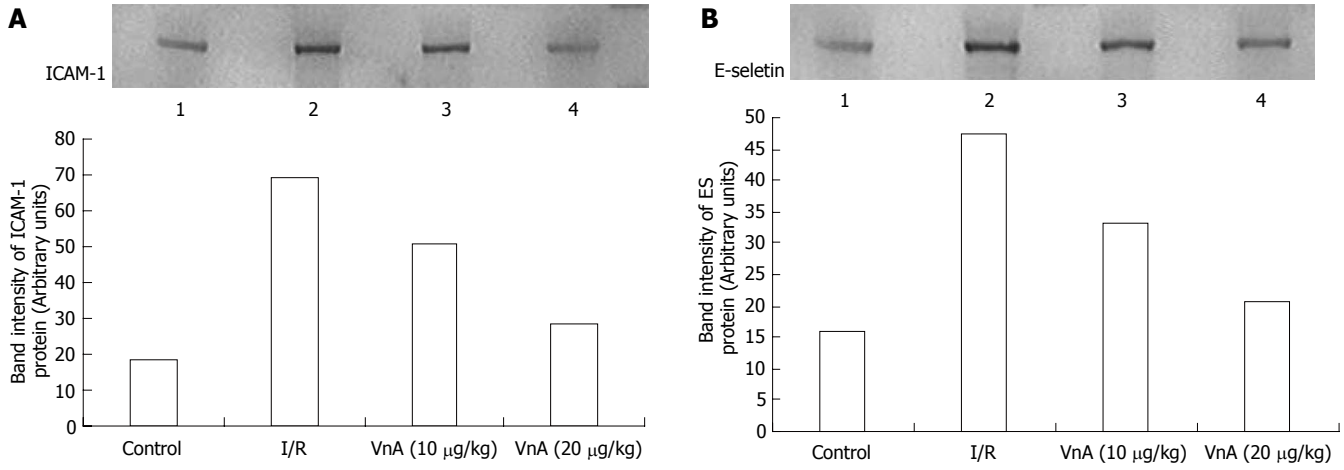

Figure 9 Liver adhesion molecule-1 (ICAM-1) (**A**) and E-selectin (ES) (**B**) protein signals of Western blot analyzed with a gel imaging system (Kodak system EDAS120, Japan). For all groups, *n* = 10. L1: Control group; L2: I/R group; L3: VnA (10 μg/kg) group; L4: VnA (20 μg/kg) group. Compared with the control group, the signals in I/R group increased and weakened in the VnA pretreated group in a dose-dependent manner.

The above results suggested that ICAM-1 and E-selectin dependent neutrophil recruitment into the liver tissue was responsible partially for hepatic I/R. The dose-dependent protective effects of VnA were likely related to the suppression of ICAM-1 and E-selectin expression. This suppression reduced the neutrophil recruitment associated with the hepatic I/R, and effectively protected the liver against ischemia/reperfusion.

In conclusion, VnA has protective effects against liver injury induced by hepatic I/R. The protective effects are probably associated with enhancement of antioxidant capacities, reduction of inflammatory responses and suppressed expression of ICAM-1 and E-selectin. These findings may be useful for clinical management to reduce I/R related hepatic damage. However, the precise mechanisms of VnA protecting against hepatic I/R still need to be clarified in further studies.

ACKNOWLEDGMENTS

The authors thank Professors Sen Lü and Min Liu, Laboratory of Molecular Biology (State Administration of Traditional Chinese Medicine), Second Affiliated Hospital of Dalian Medical University for their technical assistance. The excellent technical assistance of Dr. Yu-Zhong Li and Zhen-Guo Li (Department of Docimasiology, Second Affiliated Hospital of Dalian Medical University) are acknowledged.

REFERENCES

1 **Haimovici H**. Arterial embolism with acute massive ischemic myopathy and myoglobinuria: evaluation of a hitherto unreported syndrome with report of two cases. *Surgery* 1960; **47**: 739-747
2 **Cheng F**, Li YP, Cheng JQ, Feng L, Li SF. The protective mechanism of Yisheng Injection against hepatic ischemia reperfusion injury in mice. *World J Gastroenterol* 2004; **10**: 1198-1203
3 **Ozturk H**, Gezici A, Ozturk H. The effect of celecoxib, a selective COX-2 inhibitor, on liver ischemia/reperfusion-induced oxidative stress in rats. *Hepatol Res* 2006; **34**: 76-83
4 **Jaeschke H**, Farhood A. Neutrophil and Kupffer cell-induced oxidant stress and ischemia-reperfusion injury in rat liver. *Am J Physiol* 1991; **260**: G355-G362
5 **Jiang Y**, Gu XP, Qiu YD, Sun XM, Chen LL, Zhang LH, Ding YT. Ischemic preconditioning decreases C-X-C chemokine expression and neutrophil accumulation early after liver transplantation in rats. *World J Gastroenterol* 2003; **9**: 2025-2029
6 **Colletti LM**, Remick DG, Burtch GD, Kunkel SL, Strieter RM, Campbell DA. Role of tumor necrosis factor-alpha in the pathophysiologic alterations after hepatic ischemia/reperfusion injury in the rat. *J Clin Invest* 1990; **85**: 1936-1943
7 **Colletti LM**, Cortis A, Lukacs N, Kunkel SL, Green M, Strieter RM. Tumor necrosis factor up-regulates intercellular adhesion molecule 1, which is important in the neutrophil-dependent lung and liver injury associated with hepatic ischemia and reperfusion in the rat. *Shock* 1998; **10**: 182-191
8 **Farhood A**, McGuire GM, Manning AM, Miyasaka M, Smith CW, Jaeschke H. Intercellular adhesion molecule 1 (ICAM-1) expression and its role in neutrophil-induced ischemia-reperfusion injury in rat liver. *J Leukoc Biol* 1995; **57**: 368-374
9 **Gong JP**, Wu CX, Liu CA, Li SW, Shi YJ, Li XH, Peng Y. Liver sinusoidal endothelial cell injury by neutrophils in rats with acute obstructive cholangitis. *World J Gastroenterol* 2002; **8**: 342-345
10 **Vestweber D**, Blanks JE. Mechanisms that regulate the function of the selectins and their ligands. *Physiol Rev* 1999; **79**: 181-213
11 **Peralta C**, Hotter G, Closa D, Gelpí E, Bulbena O, Roselló-Catafau J. Protective effect of preconditioning on the injury associated to hepatic ischemia-reperfusion in the rat: role of nitric oxide and adenosine. *Hepatology* 1997; **25**: 934-937
12 **Yoshizumi T**, Yanaga K, Soejima Y, Maeda T, Uchiyama H, Sugimachi K. Amelioration of liver injury by ischaemic preconditioning. *Br J Surg* 1998; **85**: 1636-1640
13 **Tezuka Y**, Kikuchi T, Zhao W, Chen J, Guo Y. (+)-Verussurine, a new steroidal alkaloid from the roots and rhizomes of veratrum nigrum var. ussuriense and structure revision of (+)-verabenzoamine1. *J Nat Prod* 1998; **61**: 1397-1399
14 **Zhao WJ**, Meng QW, Wang SS. Studies on Chemical Constituents of Veratrum nigrum L. var. ussuriense Nakai. *Zhongguo Zhongyao Zazhi* 2003; **28**: 884-885
15 **Li H**, Gao GY, Li SY, Zhao WJ, Guo YT, Liang ZJ. Effects of Veratrum nigrum alkaloids on central catecholaminergic neurons of renal hypertensive rats. *Acta Pharmacol Sin* 2000; **21**: 23-28
16 **Li WP**, Gao DY, Zhou Q, Gao GY, Han GZ, Zhao WJ. Neuroprotective effects of VnA on rats with focal cerebral ischemia injury. *Zhongguo Yaoxue Zazhi* 2002; **37**: 624
17 **Han GZ**, Li XY, Lü L, Li WP, Zhao WJ. Antithrombotic effects of Veratrum nigrum var. ussuriense alkaloids. *Zhongcaoyao*

2003; **34**: 1107-1110
18 **You GX**, Zhou Q, Li WP, Han GZ, Zhao WJ. Neuroprotection of Veratrum nigrum var. ussurience alkaloids on focal cerebral ischemia-reperfusion injury in rats. *Zhongcaoyao* 2004; **35**: 908-911
19 **Kojima Y**, Suzuki S, Tsuchiya Y, Konno H, Baba S, Nakamura S. Regulation of pro-inflammatory and anti-inflammatory cytokine responses by Kupffer cells in endotoxin-enhanced reperfusion injury after total hepatic ischemia. *Transpl Int* 2003; **16**: 231-240
20 **Song M**, Xia B, Li J. Effects of topical treatment of sodium butyrate and 5-aminosalicylic acid on expression of trefoil factor 3, interleukin 1beta, and nuclear factor kappaB in trinitrobenzene sulphonic acid induced colitis in rats. *Postgrad Med J* 2006; **82**: 130-135
21 **Zhang JX**, Wu HS, Wang H, Zhang JH, Wang Y, Zheng QC. Protection against hepatic ischemia/reperfusion injury via downregulation of toll-like receptor 2 expression by inhibition of Kupffer cell function. *World J Gastroenterol* 2005; **11**: 4423-4426
22 **Schümann J**, Wolf D, Pahl A, Brune K, Papadopoulos T, van Rooijen N, Tiegs G. Importance of Kupffer cells for T-cell-dependent liver injury in mice. *Am J Pathol* 2000; **157**: 1671-1683
23 **Jaeschke H**. Reactive oxygen and mechanisms of inflammatory liver injury. *J Gastroenterol Hepatol* 2000; **15**: 718-724
24 **Weiss SJ**. Tissue destruction by neutrophils. *N Engl J Med* 1989; **320**: 365-376
25 **Beckman JS**, Beckman TW, Chen J, Marshall PA, Freeman BA. Apparent hydroxyl radical production by peroxynitrite: implications for endothelial injury from nitric oxide and superoxide. *Proc Natl Acad Sci USA* 1990; **87**: 1620-1624
26 **Karaman A**, Fadillioglu E, Turkmen E, Tas E, Yilmaz Z. Protective effects of leflunomide against ischemia-reperfusion injury of the rat liver. *Pediatr Surg Int* 2006; **22**: 428-434
27 **Yuan GJ**, Ma JC, Gong ZJ, Sun XM, Zheng SH, Li X. Modulation of liver oxidant-antioxidant system by ischemic preconditioning during ischemia/reperfusion injury in rats. *World J Gastroenterol* 2005; **11**: 1825-1828
28 **Olanders K**, Sun Z, Börjesson A, Dib M, Andersson E, Lasson A, Ohlsson T, Andersson R. The effect of intestinal ischemia and reperfusion injury on ICAM-1 expression, endothelial barrier function, neutrophil tissue influx, and protease inhibitor levels in rats. *Shock* 2002; **18**: 86-92
29 **Nakano H**, Nagasaki H, Yoshida K, Kigawa G, Fujiwara Y, Kitamura N, Kuzume M, Takeuchi S, Sasaki J, Shimura H, Yamaguchi M, Kumada K. N-acetylcysteine and anti-ICAM-1 monoclonal antibody reduce ischemia-reperfusion injury of the steatotic rat liver. *Transplant Proc* 1998; **30**: 3763
30 **Bevilacqua MP**, Pober JS, Mendrick DL, Cotran RS, Gimbrone MA. Identification of an inducible endothelial-leukocyte adhesion molecule. *Proc Natl Acad Sci USA* 1987; **84**: 9238-9242
31 **Lawrence MB**, Springer TA. Neutrophils roll on E-selectin. *J Immunol* 1993; **151**: 6338-6346
32 **Ley K**, Allietta M, Bullard DC, Morgan S. Importance of E-selectin for firm leukocyte adhesion in vivo. *Circ Res* 1998; **83**: 287-294
33 **Subramaniam M**, Koedam JA, Wagner DD. Divergent fates of P- and E-selectins after their expression on the plasma membrane. *Mol Biol Cell* 1993; **4**: 791-801
34 **Singbartl K**, Ley K. Protection from ischemia-reperfusion induced severe acute renal failure by blocking E-selectin. *Crit Care Med* 2000; **28**: 2507-2514

S- Editor Wang GP **L- Editor** Zhu LH **E- Editor** Bai SH

PO Box 2345, Beijing 100023, China
www.wjgnet.com
wjg@wjgnet.com

World J Gastroenterol 2007 January 28; 13(4): 572-578
World Journal of Gastroenterology ISSN 1007-9327

CLINICAL RESEARCH

Gastrointestinal symptoms in a Japanese population: A health diary study

Yasuharu Tokuda, Osamu Takahashi, Sachiko Ohde, Masaaki Shakudo, Haruo Yanai, Takuro Shimbo, Shunichi Fukuhara, Shigeaki Hinohara, Tsuguya Fukui

Yasuharu Tokuda, Osamu Takahashi, Sachiko Ohde, Shigeaki Hinohara, Tsuguya Fukui, Clinical Practice Evaluation and Research Center, St. Luke's Life Science Institute, St. Luke's International Hospital, Japan
Masaaki Shakudo, Intermedica, Co, Japan
Haruo Yanai, St. Luke's Graduate School of Nursing, Japan
Takuro Shimbo, Research Institute, International Medical Center, Japan
Shunichi Fukuhara, Department of Epidemiology and Healthcare Research, Kyoto University Graduate School of Medicine and Public Health, Japan
Supported by Clinical Research Grant from St. Luke's Life Science Institute
Correspondence to: Yasuharu Tokuda, MD, MPH; Clinical Practice Evaluation and Research Center, St. Luke's Life Science Institute, St Luke's International Hospital 9-1 Akashi-cho, Chuo-city, Tokyo 104-8560, Japan. tokuyasu@orange.ocn.ne.jp
Telephone: +81-3-5550-2426 Fax: +81-3-5550-2426
Received: 2006-10-20 Accepted: 2006-12-04

Abstract

AIM: To investigate the incidence of gastrointestinal symptoms and the nature of consequent utilization of health care services in a Japanese population.

METHODS: Using self-report, we conducted a prospective cohort study of a nationally representative sample of the Japanese population over a one-month period to determine the incidence of gastrointestinal symptoms of all kinds and resultant health care utilization. Both information on visits to physicians and use of complementary and alternative medicine therapies were collected.

RESULTS: From a total of 3568 in the recruitment sample, 3477 participants completed a health diary (response rate 97%). The data of 112 participants with baseline active gastrointestinal diseases were excluded from the analysis, leaving 3365 participants in the study. The incidence of gastrointestinal symptoms was 25% and the mean number of symptomatic episodes was 0.66 in a month. Abdominal pain, diarrhea, nausea, constipation and dyspepsia were the most frequent symptoms. Female gender, younger age, and low baseline quality of life were risk factors for developing these symptoms. The participants were more likely to treat themselves, using dietary, complementary or alternative medicines, than to visit physicians, except in the case of vomiting.

CONCLUSION: Gastrointestinal symptoms are common in the Japanese population, with an incidence of 25%. Abdominal pain, diarrhea, nausea, constipation and dyspepsia are the most frequent symptoms. Risk factors for developing these symptoms include female gender, younger age, and low baseline quality of life.

Key words: Gastrointestinal diseases; Abdominal Pain; Diarrhea; Nausea; Constipation; Dyspepsia

Tokuda Y, Takahashi O, Ohde S, Shakudo M, Yanai H, Shimbo T, Fukuhara S, Hinohara S, Fukui T. Gastrointestinal symptoms in a Japanese population: A health diary study. *World J Gastroenterol* 2007; 13(4): 572-578

http://www.wjgnet.com/1007-9327/13/572.asp

INTRODUCTION

Although the prevalence of gastrointestinal disease in the Japanese population is known to be high, its epidemiology, incidence, and the consequent utilization of health care services are not well described[1-3]. An accurate analysis of the incidence of the various symptoms and of the health care services utilized in relation to them would clarify the public health consequences of gastrointestinal symptoms and assist in the setting of priorities in the allocation of health care services and future research funding. There is also little information on the use of complementary and alternative medicine as compared with conventional medicine in the treatment of the various symptoms of gastrointestinal disease. This prospective cohort study was designed to ascertain the incidence of gastrointestinal symptoms in the Japanese general population and to document the subsequent use of health care, as recorded by the participants in a health diary.

MATERIALS AND METHODS

Participants

This analysis of the incidence of gastrointestinal symptoms and subsequent health care practices in Japan is drawn from a prospective cohort study, using participants' health diaries established for the ecological analysis of

medical care in Japanese communities[4]. A population-weighted random sample of households was selected by controlling for the size of cities, towns and villages. Participants who had baseline active gastrointestinal diseases were excluded from the analysis. Because of the national policy of universal health insurance coverage in Japan, all households sampled were covered by health insurance. Prior ethical approval from the Research Ethics Committee of Kyoto University Graduate School of Medicine was obtained.

There are advantages to using health diaries when investigating individual health and related behavior[4-8]. Health diaries can provide an immediate and continuous record of daily health events and behaviors, and minimize recall bias[4], without the intervention of direct observational measures[7,9]. The methodology of this health diary study is described in detail elsewhere[4].

Data collection

For the purposes of the study, the independent variables were baseline demographic and clinical data. The dependent variables were self-reported gastrointestinal symptoms, which were categorized and coded based on the ICPC-2 (International Classification of Primary Care second edition). They included diffuse abdominal pain, upper abdominal pain, diarrhea, nausea, constipation, dyspepsia, vomiting, abdominal fullness, heartburn, lower abdominal pain, hematemesis, and hematochezia.

The health diary procedure required the keeping of a daily record for one month, from October 1 to October 31, 2003, of all health-related events, including gastrointestinal symptoms, health care accessed, and anything else of relevance. The health diary format specifically sought responses to the following questions: (1) Did you have any pain or other health symptoms that caused you discomfort? (2) If so, what kind of symptoms did you have? (3) If the answer to the first question was yes, did you consult a physician? Did you use dietary supplements such as nutritional drinks, vitamins, and calcium? Did you undergo any physical remedy, such as acupressure, acupuncture, or massage? Subjects younger than 15 years old were also included in this study. The parents of these children were requested to ask the questionnaires and record them accordingly. We did not include the use of over-the-counter-medications as utilizations of health care services in this study.

Data was extracted on the number of days in which symptom-related visits to a physician occurred during the study period, whether to a primary care physician, a community hospital, a university hospital, or an emergency department. Data was also collected on the number of days complementary and alternative medicines were used, whether dietary supplements or physical remedies. The use of complementary and alternative medicine was divided into two categories: (1) Dietary complementary and alternative medicine, such as nutritional drinks, herbs, kampo, supplements, vitamins, minerals, and other dietary substances; (2) Physical complementary and alternative medicine, such as massage, acupuncture, acupressure, Judo-seifuku, moxibustion, chiropractic, and similar physical manipulations.

Baseline data, including demographic, health-related, and socioeconomic information, was also collected. The SF-8 instrument was used to measure baseline health-related quality of life. The SF-8 generates a health profile consisting of eight scales and two summary measures: a physical component summary (PCS8) and a mental component summary (MCS8)[10]. The SF-8 is scored by assigning the mean SF-36 scale score for the Japanese population as measured in 2002 to each response category of the SF-8 measuring the same concept. A higher or lower individual score indicates a better or worse health status than the mean, respectively[11]. We also included the baseline number for comorbidity as a covariate. The number of co-morbidities was calculated by counting the number of diseases present with no weights[12].

Data on a number of characteristics was collected as socioeconomic baseline measurements. Annual household income was divided into 6 categories. Employment status was recorded as one of 6 categories: student, homemaker, jobless or not able to work, retiree, part-time employee, and full-time employee or self-employed worker. Self-reported educational attainment was also classified at 6 levels: junior high school or below, high school graduate, vocational college, 1-2 years college, college degree, graduate school degree or higher.

Statistical analysis

The incidence (proportions) and the number of episodes (days with the symptom) of individual gastrointestinal symptoms were calculated during the one-month study period. Multivariable adjusted Poisson regression models were constructed to obtain adjusted rate ratios for the number of episodes of the various gastrointestinal symptoms in relation to baseline demographic and clinical factors. Health care utilization for one month of participants who developed gastrointestinal symptoms was also calculated. A two-tailed *P*-value of 0.05 was regarded as statistically significant. The STATA software version 8.2 (College Station, Texas, USA) was used for all statistical analyses.

RESULTS

From a total of 3568 in the study recruitment sample, 3477 participants completed the diary (97.4%). Of these, 112 with baseline active gastrointestinal diseases were excluded and the remaining 3365 participants were enrolled in the study (Table 1). 1573 (46%) were men. The mean age was 34 years (range 0-96 years). 17% of the 3365 participants lived in large cities, 24% in medium-sized cities, 38% in small cities, and 21% in rural areas. Table 1 shows the demographic, socioeconomic and clinical characteristics of the participants in two groups: those who developed any gastrointestinal symptom and those who recorded none. A univariate analysis showed no significant differences in socioeconomic characteristics between the two groups. A trend test yielded $P = 0.212$ for annual household income, $P = 0.143$ for occupational status, and $P = 0.719$ for educational attainment. Chi-square tests showed significant differences between the two groups on the variables of gender ($P < 0.001$), past history of gastrointestinal disease

Table 1 Demographic, socioeconomic and clinical characteristics of the participants

Variable	All participants (n = 3365)		Developed GI symptoms (n = 856)		No GI symptoms (n = 2509)	
	n	%	n	%	n	%
Demographics						
Gender						
Male	1573	45.7	328	38.3	1245	49.6
Female	1792	53.3	528	61.7	1264	50.4
Age (yr)						
0-9	651	19.3	155	18.1	496	19.8
10-19	431	12.8	104	12.1	327	13.0
20-29	416	12.4	133	15.5	283	11.3
30-39	476	14.1	139	16.2	337	13.4
40-49	490	14.6	134	15.7	356	14.2
50-59	345	10.3	76	8.9	269	10.7
60-69	331	9.8	61	7.1	270	10.8
70-79	188	5.6	45	5.3	143	5.7
⩾ 80	37	1.1	9	1.1	28	1.1
Socioeconomic characteristics						
Annual household income						
< 3 000 000 Japanese yen	424	12.6	112	13.1	312	12.4
3 000 000 to < 5 000 000	652	19.4	189	22.1	463	18.5
5 000 000 to < 7 000 000	522	15.5	127	14.8	395	15.7
7 000 000 to < 10 000 000	426	12.7	111	13.0	315	12.6
10 000 000 to < 12 000 000	167	5.0	42	4.9	125	5.0
⩾ 12 000 000	82	2.4	16	1.9	66	2.6
N/A	1092	32.5	259	30.3	833	33.2
Employment status						
Full-time employee/self-employed	1086	32.3	274	32.0	812	32.4
Part-time employee	374	11.1	100	11.7	274	10.9
Retiree	129	3.8	26	3.0	103	4.1
Jobless or unable to work	91	2.7	24	2.8	67	2.7
Homemaker	490	14.6	153	17.9	337	13.4
Student	89	2.6	18	2.1	71	2.8
N/A	1106	32.9	261	30.5	845	33.7
Educational attainment						
Junior high school or lower	84	2.5	16	1.9	68	2.7
High school graduate	471	14.0	122	14.3	349	13.9
Vocational college	135	4.0	38	4.4	97	3.9
1-3 yr of college	156	4.6	50	5.8	106	4.2
College degree	336	10.0	85	9.9	251	10.0
Graduate school degree	23	0.7	8	0.9	15	0.6
N/A	2160	64.2	537	62.7	1623	64.7
Baseline clinical characteristics						
Previous GI diseases						
Yes	326	9.7	117	13.7	209	8.3
No	2956	87.8	722	84.3	2234	89.0
N/A	83	2.5	17	2.0	66	2.6
No. of comorbidities						
None	2548	75.7	646	75.5	1902	75.8
One	578	17.2	157	18.3	421	16.8
Two or more	239	7.1	53	6.2	186	7.4
PCS8 score						
⩾ 50	1930	57.4	458	53.5	1472	58.7
< 50	1304	38.8	363	42.4	941	37.5
N/A	131	3.9	35	4.1	96	3.8
MCS8 score						
⩾ 50	1704	50.6	368	43.0	1336	53.2
< 50	1530	45.5	453	52.9	1077	42.9
N/A	131	3.9	35	4.1	96	3.8

N/A: indicates data not available; GI: gastrointestinal; PCS8: physical component of SF8; MCS8: mental component of SF8.

Table 2 Incidence and the number of episodes of gastrointestinal symptoms (n = 3365)

Symptom	Incidence per month		Episodes in a month	
	n	(% of total)	mean	SD
Any gastrointestinal symtoms	856	(25.44)	0.656	1.794
Diffuse abdominal pain	401	(11.92)	0.214	0.799
Upper abdominal pain	179	(5.32)	0.114	0.801
Diarrhea	169	(5.02)	0.095	0.651
Nausea	148	(4.40)	0.067	0.393
Constipation	70	(2.08)	0.064	0.689
Dyspepsia	86	(2.56)	0.051	0.423
Vomiting	44	(1.31)	0.016	0.164
Abdominal fullness	34	(1.01)	0.015	0.187
Heartburn	18	(0.53)	0.010	0.173
Lower abdominal pain	16	(0.48)	0.009	0.158
Hematemesis	1	(0.03)	0.000	0.017

SD: standard deviation. There were no participants with hematochezia.

($P < 0.001$), MCS8 ($P < 0.001$), and PCS8 ($P = 0.008$).

Table 2 shows the incidence per month for 3365 participants and the number of episodes of gastrointestinal symptoms of these participants during the one month study period. 856 (25%) developed one or more gastrointestinal symptoms. The symptoms of high incidence ($\geqslant$ 1%) were diffuse abdominal pain (12%), upper abdominal pain (5%), diarrhea (5%), nausea (4%), dyspepsia (3%), constipation (2%), vomiting (1%), and abdominal fullness (1%). The mean number of episodes of gastrointestinal symptoms of any kind was 0.66 in the one-month period. The symptoms with a high number of episodes were diffuse abdominal pain (0.21), upper abdominal pain (0.11), diarrhea (0.10), nausea (0.07), constipation (0.06), dyspepsia (0.05), vomiting (0.02), and abdominal fullness (0.01).

Table 3 shows rate ratios based on multivariable adjusted Poisson regression analyses. Age and the number of comorbidity are treated as continuous variables in this Table. Gastrointestinal symptoms were reported more commonly by women than men. Symptoms with a significantly higher number of episodes in women were diffuse abdominal pain, upper abdominal pain, nausea, and constipation, and symptoms with a significantly higher number of episodes in men were diarrhea and heartburn.

Gastrointestinal symptoms were reported more often in younger than in older age groups. Symptoms associated with older age were upper abdominal pain, dyspepsia, constipation, abdominal fullness, and heartburn, while symptoms associated with younger age were diffuse abdominal pain, diarrhea, nausea, and vomiting. The symptoms that featured in comorbidity were nausea and constipation.

Gastrointestinal symptoms were reported more often by participants with poor baseline quality of life scores. Diffuse abdominal pain, diarrhea and dyspepsia were symptoms associated with a poor baseline score on the physical component of the health-related quality of life test. Symptoms associated with a poor baseline score on the mental component of the health-related quality of life test were diffuse abdominal pain, upper abdominal pain, nausea, constipation, and abdominal fullness.

Table 4 shows the health care utilization characteristics of participants with one or more gastrointestinal symptoms in the survey month. Overall, use of dietary complementary and alternative medicine was more frequent than visiting a physician (Bonferroni pair-wise comparison, $P < 0.001$), but visiting a physician was more frequent than use of physical forms of complementary and alternative medicine (Bonferroni pair-wise comparison, $P < 0.001$). However, visiting a physician was more frequent than use of dietary complementary and alternative medicine in those whose symptom was vomiting. Among those with dyspepsia and heartburn, use of both dietary and physical complementary and alternative medicine was more frequent than visiting a physician.

DISCUSSION

Our results indicate that gastrointestinal symptoms are of common occurrence in the Japanese general population, with about a quarter developing a gastrointestinal symptom of some kind in a month. Abdominal pain, diarrhea, nausea, constipation and dyspepsia were the most frequent gastrointestinal symptoms in our sample. Risks for developing these symptoms differ in relation to the baseline factors of gender, age, and quality of life. Japanese who develop gastrointestinal symptoms are more likely to treat themselves with dietary forms of complementary and alternative medicine than to visit physicians, except in the case of vomiting.

Gastrointestinal symptoms with a high incidence were, in order, diffuse and upper abdominal pain, diarrhea, nausea, constipation, and dyspepsia. These findings are consistent with those of one previous study[2], while another found that diarrhea was more common than abdominal pain[3]. It may be that self-reporting of diarrhea underestimates its actual incidence[13]. A study that asks about diarrhea and loose stools separately obtains a lower incidence of diarrhea than one in which participants include loose stool in their definition of diarrhea[3]. Thus differences in participants' definitions could account for differences in the estimated incidence of diarrhea between previous studies[14].

Our study found that women were more likely to develop diffuse and upper abdominal pain, nausea, and constipation than men. Previous studies suggest that the incidence of many gastrointestinal symptoms is higher in women than in men[1,3,15-18], and many studies indicate that abdominal pain, specifically, is more common in women[1,3,15-18], although two studies have shown no gender difference[19,20]. Abdominal fullness, also, is more common in women than in men[21]. A higher prevalence of occult irritable bowel syndrome in women could account for the higher incidence and prevalence of such symptoms as abdominal pain, nausea, and constipation[3,22]. Alternatively, a higher sensitivity in the perception of such symptoms in women could also contribute to the difference[3].

Our study found that men were more likely to develop diarrhea and heartburn than women. This finding differs from a number of studies indicating no gender difference for diarrhea[3,16,18], while a recent international study found

Table 3 Rate ratios based on multivariable adjusted poisson regression analyses

Variable symptom	Female gender	Older age	Previous GI disease	No. of comorbidity	Better PCS8	Better MCS8
Any gastrointestinal symtoms	1.412	0.994	1.894	1.055	0.738	0.645
	(< 0.01)	(< 0.01)	(< 0.01)	NS	(< 0.01)	(< 0.01)
Diffuse abdominal pain	1.455	0.980	1.385	0.886	0.545	0.548
	(< 0.01)	(< 0.01)	(< 0.01)	NS	(< 0.01)	(< 0.01)
Upper abdominal pain	1.485	1.016	2.504	0.855	0.975	0.426
	(< 0.01)	(< 0.01)	(< 0.01)	(< 0.05)	NS	(< 0.01)
Diarrhea	0.765	0.972	1.485	0.981	0.636	0.986
	(< 0.05)	(< 0.01)	(< 0.05)	NS	(< 0.01)	NS
Nausea	2.828	0.983	2.364	1.259	1.032	0.575
	(< 0.01)	(< 0.01)	(< 0.01)	(< 0.01)	NS	(< 0.01)
Dyspepsia	1.171	1.033	4.035	0.888	0.462	1.068
	NS	(< 0.01)	(< 0.01)	NS	(< 0.01)	NS
Constipation	2.877	1.014	1.198	1.427	1.234	0.364
	(< 0.01)	(< 0.01)	NS	(< 0.01)	NS	(< 0.01)
Vomiting	0.847	0.940	1.617	1.141	0.903	1.421
	NS	(< 0.01)	NS	NS	NS	NS
Abdominal fullness	1.833	1.020	1.871	0.936	1.305	0.476
	NS	(< 0.05)	NS	NS	NS	(< 0.05)
Heartburn	0.286	1.053	2.653	1.027	1.324	1.227
	(< 0.01)	(< 0.01)	(< 0.05)	NS	NS	NS
Lower abdominal pain	1.555	1.005	0.844	1.023	0.699	0.515
	NS	NS	NS	NS	NS	NS

GI: gastrointestinal; PCS8: physical component of SF8; MCS8: mental component of SF8. Adjusted for all covariates shown above. The numbers of parehtheses indicate statistically significant *P*-values. Age and No. of comorbidity were treated as continuous variables. PCS8 and MCS8 were treated as binary variables with cutoff pint of 50. Hematemesis and hematochezia could not be analyzed becaused of few incidence.

Table 4 Health care utilization in a month among the participants with gastrointestinal symptoms

	Visits to a physician		Dietary CAM uses		Physical CAM uses	
Symptom	mean (d)	SD	mean (d)	SD	mean (d)	SD
Any gastrointestinal symptoms	0.67	1.502	1.82	5.614	0.12	0.891
Diffuse abdominal pain	0.58	1.518	1.48	5.075	0.10	1.133
Upper abdominal pain	0.45	1.040	2.76	6.823	0.32	1.791
Diarrhea	0.81	1.300	1.39	4.747	0.07	0.431
Nausea	0.76	1.274	1.70	4.738	0.25	1.851
Dyspepsia	0.50	1.344	4.47	8.023	0.52	2.533
Constipation	0.90	1.746	2.43	6.333	0.20	0.651
Vomiting	1.64	2.354	0.89	2.442	0.00	0.00
Abdominal fullness	0.32	0.638	2.91	6.440	0.06	0.343
Heartburn	0.44	0.784	2.11	3.692	0.50	1.465
Lower abdominal pain	0.63	1.628	2.06	7.206	0.19	0.750
Hematemesis	0.00	0.000	0.00	0.000	0.00	0.000

CAM: complementary and alternative medicine; SD: standard deviation. Hematochezia could not be analyzed becaused of few incidence.

that the incidence of diarrhea was higher in women in a number of countries, including Australia, Canada, Ireland, and the United States[23]. Gastroesophageal reflux disease symptoms, such as heartburn and acid regurgitation, showed no gender difference in an earlier Japanese study[24], and studies in Sweden and Belgium also found no gender difference in the prevalence of heartburn[1,25]. These conflicting results suggest the need for further investigation.

Overall, gastrointestinal symptoms were reported more commonly in younger than in older participants in the current study. Previous studies have shown a significantly higher prevalence of abdominal symptoms in young women, which decreases with age[1,3,26]. Nevertheless the current study found that older individuals are more likely to suffer upper abdominal pain, dyspepsia, constipation, abdominal fullness, and heartburn than the young. The young are more likely to report diffuse abdominal pain, diarrhea, nausea, and vomiting than the old. This difference between the old and the young in the incidence of many gastrointestinal symptoms may derive from an age-associated change in visceral sensitivity[3], but the

source of the difference has not yet been established.

Our study found that those with a poor baseline score on the physical component of quality of life had a higher likelihood than those with an average score of developing diffuse abdominal pain, diarrhea and dyspepsia, while those with a poor baseline score on the mental component of quality of life were more likely than those with an average score to report diffuse and upper abdominal pain, nausea, constipation, and abdominal fullness. To our knowledge, this study is the first prospective cohort study to analyze baseline quality of life scores as predictors of gastrointestinal symptoms. A possible higher prevalence of occult irritable bowel syndrome in those with a poor score on the mental component of the quality of life measure may explain their higher incidence and prevalence of such symptoms as abdominal pain, nausea, constipation, and abdominal fullness[3,22]. This finding requires further study for confirmation.

The current study may be the first prospective cohort study to describe health care utilization in individuals in response to gastrointestinal symptoms. Our results indicate that self-treatment with dietary complementary and alternative medicine is more frequent than visiting a physician regarding all symptoms except vomiting. Recourse to physical as well as dietary complementary and alternative therapies was more frequent than visiting a physician in the case of dyspepsia and heartburn.

Complementary and alternative therapies, some of which had their origins in Japan, are increasingly used by the general population in industrialized countries[27-29]. This is true of a substantial proportion of the Japanese population, who use them frequently at a high cost to personal income[30]. Patients with functional and general gastrointestinal disorders are likely to turn to complementary and alternative medicine when conventional therapies fail to relieve their symptoms[31]. Therefore physicians need to keep their knowledge up to date on the regulations, side effects, and possible benefits of specific herbal products used by patients[32]. Studies of the effectiveness of complementary and alternative therapies for functional gastrointestinal disorders have, however, often been limited by study designs[33].

It should be borne in mind that the health diaries in this study were self-reports and therefore subjective. A further limitation is that information on the severity of symptoms was not requested. As symptoms were not classified as less or more severe, there was no means of determining whether severity differentially influenced decisions to note them in the diaries or to seek different forms of treatment. This may have resulted in misclassification biases[14].

In summary, gastrointestinal symptoms are of common occurrence in the Japanese population. Overall, the mean number of episodes of gastrointestinal symptoms was 0.66 in a month. About a quarter of respondents developed at least one gastrointestinal symptom in the course of the month. Abdominal pain, diarrhea, nausea, constipation and dyspepsia were the most frequent gastrointestinal symptoms. Female gender, younger age, and low baseline quality of life are risk factors for developing gastrointestinal symptoms. Japanese with gastrointestinal symptoms other than vomiting are more likely to resort to dietary forms of complementary and alternative medicine than to visit physicians.

ACKNOWLEDGMENTS

We thank Kenji Sakurai MD FACS for his support of our research, and we thank Mikio Kumagai, Riki Tanaka, Yumiko Yotsumoto, Yuko Iwasawa, and Sayoko Yamauchi for their excellent secretarial assistance.

COMMENTS

Background

The incidence of gastrointestinal symptoms and the nature of consequent utilization of health care services in the Japanese population are not well documented. Our aim was to provide better description in this epidemiology of gastrointestinal symptoms.

Research frontiers

The prevalence of gastrointestinal disease in the Japanese population is known to be high. However, its epidemiology, its incidence, and the consequent utilization of health care services are not well described. There is also little information on the use of complementary and alternative medicine as compared with conventional medicine in the treatment of the various symptoms of gastrointestinal disease.

Innovations and breakthroughs

In this study of Japan, the incidence of gastrointestinal symptoms was 25% and the mean number of the symptomatic episodes was 0.66 in a month. Abdominal pain, diarrhea, nausea, constipation and dyspepsia were the most frequent symptoms. Female gender, younger age, and low baseline quality of life were risk factors for developing these symptoms. The participants were more likely to treat themselves, using dietary complementary or alternative medicines, than to visit physicians, except in the case of vomiting.

Applications

Gastrointestinal symptoms are very common in the Japanese general population. The most frequent symptoms include abdominal pain, diarrhea, nausea, constipation and dyspepsia. Risk factors for developing these symptoms are female gender, younger age, and low baseline quality of life. These results may help to understand the public health consequences of gastrointestinal symptoms and to assist in the setting of priorities in the allocation of health care services and of future research funding.

Terminology

Health diary: a daily record of daily health events and behaviors. This research methodology can provide an immediate and continuous record of daily health events and behaviors and minimize recall bias without the intervention of direct observational measures.

Peer review

This article documented about epidemiology of gastrointestinal symptom among Japanese. Study period is relatively short. Generally, it is well designed and clarified the incidence of gastrointestinal symptom among Japanese. The study also revealed Japanese actions to gastrointestinal symptoms.

REFERENCES

1 **Agréus L**, Svärdsudd K, Nyrén O, Tibblin G. The epidemiology of abdominal symptoms: prevalence and demographic characteristics in a Swedish adult population. A report from the Abdominal Symptom Study. *Scand J Gastroenterol* 1994; **29**: 102-109

2 **Ho KY**, Kang JY, Seow A. Prevalence of gastrointestinal symptoms in a multiracial Asian population, with particular reference to reflux-type symptoms. *Am J Gastroenterol* 1998; **93**: 1816-1822

3 **Sandler RS**, Stewart WF, Liberman JN, Ricci JA, Zorich NL. Abdominal pain, bloating, and diarrhea in the United States:

prevalence and impact. *Dig Dis Sci* 2000; **45**: 1166-1171
4 **Fukui T**, Rhaman M, Takahashi O, Saito M, Shimbo T, Endo H, Misao H, Fukuhara S, Hinohara S. The ecology of medical care in Japan. *JMAJ* 2005; **48**: 163-167
5 **White KL**, Williams TF, Greenberg BG. The ecology of medical care. *N Engl J Med* 1961; **265**: 885-892
6 **Green LA**, Fryer GE, Yawn BP, Lanier D, Dovey SM. The ecology of medical care revisited. *N Engl J Med* 2001; **344**: 2021-2025
7 **Gibson V**. An analysis of the use of diaries as a data collection method. *Nurse Researcher* 1995; **3**: 66-73
8 **Bruijnzeels MA**, van der Wouden JC, Foets M, Prins A, van den Heuvel WJ. Validity and accuracy of interview and diary data on children's medical utilisation in The Netherlands. *J Epidemiol Community Health* 1998; **52**: 65-69
9 **Anhøj J**, Møldrup C. Feasibility of collecting diary data from asthma patients through mobile phones and SMS (short message service): response rate analysis and focus group evaluation from a pilot study. *J Med Internet Res* 2004; **6**: e42
10 **Turner-Bowker DM**, Bayliss MS, Ware JE, Kosinski M. Usefulness of the SF-8 Health Survey for comparing the impact of migraine and other conditions. *Qual Life Res* 2003; **12**: 1003-1012
11 **Fukuhara S**, Suzukamo Y. Manual of the SF-8 Japanese version, (in Japanese). Kyoto: Institute for Health Outcomes and Process Evaluation Research, 2004
12 **de Groot V**, Beckerman H, Lankhorst GJ, Bouter LM. How to measure comorbidity. a critical review of available methods. *J Clin Epidemiol* 2003; **56**: 221-229
13 **Talley NJ**, Weaver AL, Zinsmeister AR, Melton LJ. Self-reported diarrhea: what does it mean? *Am J Gastroenterol* 1994; **89**: 1160-1164
14 **Sackett DL**. Bias in analytic research. *J Chronic Dis* 1979; **32**: 51-63
15 **Kay L**, Jørgensen T, Jensen KH. Epidemiology of abdominal symptoms in a random population: prevalence, incidence, and natural history. *Eur J Epidemiol* 1994; **10**: 559-566
16 **Hammond EC**. Some Preliminary Findings on Physical Complaints from a Prospective Study of 1,064,004 Men and Women. *Am J Public Health Nations Health* 1964; **54**: 11-23
17 **Talley NJ**, O'Keefe EA, Zinsmeister AR, Melton LJ. Prevalence of gastrointestinal symptoms in the elderly: a population-based study. *Gastroenterology* 1992; **102**: 895-901
18 **Hale WE**, Perkins LL, May FE, Marks RG, Stewart RB. Symptom prevalence in the elderly. An evaluation of age, sex, disease, and medication use. *J Am Geriatr Soc* 1986; **34**: 333-340
19 **Talley NJ**, Zinsmeister AR, Van Dyke C, Melton LJ. Epidemiology of colonic symptoms and the irritable bowel syndrome. *Gastroenterology* 1991; **101**: 927-934
20 **Halder SL**, McBeth J, Silman AJ, Thompson DG, Macfarlane GJ. Psychosocial risk factors for the onset of abdominal pain. Results from a large prospective population-based study. *Int J Epidemiol* 2002; **31**: 1219-1225; discussion 1225-1226
21 **Taub E**, Cuevas JL, Cook EW, Crowell M, Whitehead WE. Irritable bowel syndrome defined by factor analysis. Gender and race comparisons. *Dig Dis Sci* 1995; **40**: 2647-2655
22 **Kay L**, Jørgensen T. Redefining abdominal syndromes. Results of a population-based study. *Scand J Gastroenterol* 1996; **31**: 469-475
23 **Scallan E**, Majowicz SE, Hall G, Banerjee A, Bowman CL, Daly L, Jones T, Kirk MD, Fitzgerald M, Angulo FJ. Prevalence of diarrhoea in the community in Australia, Canada, Ireland, and the United States. *Int J Epidemiol* 2005; **34**: 454-460
24 **Fujiwara Y**, Higuchi K, Watanabe Y, Shiba M, Watanabe T, Tominaga K, Oshitani N, Matsumoto T, Nishikawa H, Arakawa T. Prevalence of gastroesophageal reflux disease and gastroesophageal reflux disease symptoms in Japan. *J Gastroenterol Hepatol* 2005; **20**: 26-29
25 **Louis E**, DeLooze D, Deprez P, Hiele M, Urbain D, Pelckmans P, Devière J, Deltenre M. Heartburn in Belgium: prevalence, impact on daily life, and utilization of medical resources. *Eur J Gastroenterol Hepatol* 2002; **14**: 279-284
26 **Thompson WG**, Heaton KW. Functional bowel disorders in apparently healthy people. *Gastroenterology* 1980; **79**: 283-288
27 **Eisenberg DM**, Davis RB, Ettner SL, Appel S, Wilkey S, Van Rompay M, Kessler RC. Trends in alternative medicine use in the United States, 1990-1997: results of a follow-up national survey. *JAMA* 1998; **280**: 1569-1575
28 **Ernst E**, White A. The BBC survey of complementary medicine use in the UK. *Complement Ther Med* 2000; **8**: 32-36
29 **Ernst E**. Prevalence of use of complementary/alternative medicine: a systematic review. *Bull World Health Organ* 2000; **78**: 252-257
30 **Yamashita H**, Tsukayama H, Sugishita C. Popularity of complementary and alternative medicine in Japan: a telephone survey. *Complement Ther Med* 2002; **10**: 84-93
31 **Kong SC**, Hurlstone DP, Pocock CY, Walkington LA, Farquharson NR, Bramble MG, McAlindon ME, Sanders DS. The Incidence of self-prescribed oral complementary and alternative medicine use by patients with gastrointestinal diseases. *J Clin Gastroenterol* 2005; **39**: 138-141
32 **Comar KM**, Kirby DF. Herbal remedies in gastroenterology. *J Clin Gastroenterol* 2005; **39**: 457-468
33 **Tillisch K**. Complementary and alternative medicine for functional gastrointestinal disorders. *Gut* 2006; **55**: 593-596

S- Editor Liu Y **L- Editor** Lutze M **E- Editor** Liu WF

PO Box 2345, Beijing 100023, China
www.wjgnet.com
wjg@wjgnet.com

World J Gastroenterol 2007 January 28; 13(4): 579-584
World Journal of Gastroenterology ISSN 1007-9327

RAPID COMMUNICATION

Recent Ⅳ-drug users with chronic hepatitis C can be efficiently treated with daily high dose induction therapy using consensus interferon: An open-label pilot study

Th Witthoeft, M Fuchs, D Ludwig

Th Witthoeft, D Ludwig, University Hospital Schleswig-Holstein Campus Luebeck, Department of Medicine I, Division of Gastroenterology, Luebeck, Germany
M Fuchs, University Hospital Ulm, Department of Medicine I, Ulm, Germany
Supported by Yamanouchi Pharma GmbH (now Astellas Pharma GmbH, Munich, Germany)
Correspondence to: Dr. Thomas Witthoeft, University Hospital Schleswig-Holstein Campus Luebeck, Dept. of Medicine I, Div. of Gastroenterology, Ratzeburger Allee 160, Luebeck 23538, Germany. witthoeft@uni-luebeck.de
Telephone: +49-451-5002351 Fax: +49-451-5003645
Received: 2006-10-24 Accepted: 2006-12-19

Key words: Consensus-interferon; Hepatitis C; Polymerase chain reaction; Sustained virological response

Witthoeft T, Fuchs M, Ludwig D. Recent Ⅳ-drug users with chronic hepatitis C can be efficiently treated with daily high dose induction therapy using consensus interferon: An open-label pilot study. *World J Gastroenterol* 2007; 13(4): 579-584

http://www.wjgnet.com/1007-9327/13/579.asp

Abstract

AIM: To investigate the use of high dose consensus-interferon in combination with ribavirin in former iv drug users infected with hepatitis C.

METHODS: We started, before pegylated (PEG)-interferons were available, an open-label study to investigate the efficacy and tolerability of high dose induction therapy with consensus interferon (CIFN) and ribavirin in treatment of naiive patients with chronic hepatitis C. Fifty-eight patients who were former iv drug users, were enrolled receiving 18 μg of CIFN daily for 8 wk, followed by 9 μg daily for up to wk 24 or 48 and 800 mg of ribavirin daily. End point of the study was tolerability and eradication of the virus at wk 48 and sustained virological response at wk 72.

RESULTS: More than 62% of patients responded to the treatment with CIFN at wk 24 or 48, respectively, showing a negative qualitative PCR [genotype 1 fourteen patients (56%), genotype 2 five (50%), genotype 3 thirteen (87%), genotype 4 four (50%)]. Forty-eight percent of genotype 1 patients showed sustained virological response (SVR) six months after the treatment.

CONCLUSION: CIFN on a daily basis is well tolerated and side effects like leuko- and thrombocytopenia are moderate. End of therapy (EOT) rates are slightly lower than the newer standard therapy with pegylated interferons. CIFN on a daily basis might be a favourable therapy regimen for patients with GT1 and high viral load or for non-responders after failure of standard therapy.

INTRODUCTION

Under physiological conditions, interferon-α (IFN-α) is a key cytokine produced by virtually all cells in the mammalian organism in response to a variety of bacterial and viral stimuli. In response to viral infection, IFN-α produced by the infected target cells induces a number of cellular genes involved in inhibition of viral replication. In addition, IFN-α is secreted by stimulated NK-cells and T-cells and exerts a multitude of immune stimulatory effects of innate and adaptive immunity[1].

The current standard of treating patients with chronic hepatitis C infection is using IFN-α with or without ribavirin and great advances have been achieved[2]. So far two allelic α-2 species, interferon α-2a and interferon α-2b, have been used. Introduction of pegylated IFN in 2001 showed a slight increase in the overall sustained virological response rates (approximately 55%) compared to conventional IFN-α[3,4]. However, recent studies showed that these response rates depend on several factors, including HCV genotype, baseline viral load, ethnicity, body weight and presence of advanced liver disease[3]. More than 75% of patients in western Europe are infected with genotype 1 often showing a high viral load and these patients are so called "difficult to treat" and therefore remain at risk not to respond to standard HCV treatments[5].

Before pegylated IFN was available, we introduced a study using IFN-alfacon-1, a second-generation cytokine that was engineered to contain the most frequently occurring amino acids among the non-allelic IFN-α subtypes in humans[6]. *In vitro* studies showed that IFN-alfacon-1 induces a more dramatic decrease of HCV-

RNA compared to IFN-2b[7] and shows a 10-time higher antiviral efficacy[6]. The rationale for daily dosing in our study was the fact that serum levels of IFN-α given three times a week were dropping almost below the detection limit every other day and therefore reducing the antiviral capability. High initial dosing would reduce the viral load even further and early virological response (EVR) would lead to a higher SVR than 9 μg daily[8]. Taking these results into account, the aim of this study was to look at the efficacy, tolerability and safety of high dose IFN-alfacon-1 plus ribavirin combination therapy in patients with chronic hepatitis C.

MATERIALS AND METHODS

Patient population

Patients aged 18 years and older with a serological and histological diagnosis of chronic HCV infection were asked to participate in the study. All patients were naïve to antiviral treatment and were recent iv drug users referred by a clinic with a detoxification program. Each individual had to be off drugs for at least 4 to 6 mo, and replacement medication (e.g. buprenorphine) was allowed. The local ethics committee approved the study and informed consent of patients was obtained prior to serological and histological testing and antiviral therapy. The study protocol was in accordance to the 1975 Declaration of Helsinki.

Inclusion criteria required that patients had detectable serum HCV-RNA and liver biopsy compatible with a diagnosis of chronic HCV infection. Exclusion criteria included decompensated liver disease, hemoglobin < 12 g/dL for men and women, white blood cell count < 3000/μL, neutrophil count < 1500/μL, and platelet count < 70 000/μL. Patients with hepatitis B virus (HBV) or HIV infection were excluded. Similarly, patients with antinuclear antibody ⩾ 160 or diagnosis of other chronic liver diseases (hemochromatosis, alpha1-antitrypsin deficiency, Wilson's disease, or other chronic liver diseases), or who had prior organ transplantation or hyper- or hypothyroidism were also excluded. A history of major depression or ongoing alcohol or drug abuse within the previous 6 mo, renal insufficiency, hemophilia, poorly controlled diabetes, cardiac disease, immunologically mediated diseases, active seizure disorders or brain injury requiring medication for stabilization and pregnancy were further criteria for not being included in the study. Eleven patients were on replacement medication including methadone and codeine.

Study design

The study was a mono-center clinical trial with consecutive and prospective enrolment. All patients were naïve to antiviral therapy including IFN and ribavirin. All patients received a high induction therapy with IFN-alfacon-1, 18 μg (Inferax®; Yamanouchi Pharma GmbH, Heidelberg, now Astellas Pharma GmbH, Munich) subcutaneously daily for eight weeks, followed by 9 μg subcutaneously daily until the end of treatment. Ribavirin (Meduna Pharma GmbH, Isernhagen, Germany), 800 mg daily, was administered bid over the whole treatment period. If HCV RNA levels were detectable after 24 wk, treatment was considered as failure and stopped; if HCV RNA was undetectable at wk 24, treatment was continued for a total of 48 wk in HCV genotypes 1 and 4. Treatment of genotypes 2 and 3 was stopped after 24 wk in general. After therapy was ended, patients were followed up for an additional 24 wk.

It was initially planned to treat 100 patients. However, after 58 subjects were enrolled, recruitment was suspended because of ethical concern following the release of pegylated IFN α-2b which became the standard of treatment.

Identification of genotype

HCV genotyping was performed using the INNO-LiPA HCV Ⅱ kit assay (Innogenetics, Gent, Belgium).

Serum HCV RNA

Reverse-transcription polymerase chain reaction was performed using the Cobas Amplicor hepatitis C monitor test (v2.0, Roche Diagnostics, Grenzach-Wyhlen, Germany). The results of HCV RNA are expressed as international units per millilitre based on published formulas where 2 000 000 copies are equivalent to 800.000 IU/mL[9].

Assessment of efficacy

The primary end point of the study was assessment of sustained virological response rate defined as loss of detectable HCV RNA by RT-PCR at wk 72 [24 wk after end of therapy (EOT)]. A secondary end point was assessment of the sustained biochemical response (SBR), defined as normalization of serum alanine aminotransferase (ALT) at wk 72. No second histological end point was sought. Early virological response (EVR) at wk 4 was not determined.

Assessment of safety and tolerability

Safety and tolerability assessments were performed at 0, 2, 4, 8, 12, 24, and 48 wk of therapy and then 12 and 24 wk post-treatment. All adverse events, laboratory test-results, discontinuation or withdrawal due to adverse events, and dose reduction were recorded and evaluated.

Statistical analysis

Analysis was based on the intent to treat 48 patients enrolled in the study. Data were described by rates, means with standard deviation, medians, and ranges. In addition, multivariate step-wise logistic regression was used to identify independent predictors from baseline characteristics which were associated with SVR in univariate analysis. All *P*-values reported were two-sided and *P*-values below 5% were considered statistically significant.

RESULTS

Patients

Between July 2000 and May 2003, 58 patients with chronic

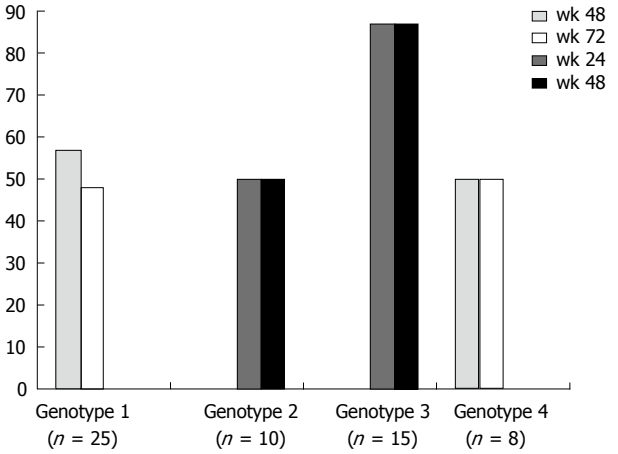

Figure 1 Response rates (in percent) after end of therapy (EOT) at wk 24 or 48 and sustained virological response (SVR) after 48 or 72 wk after beginning of antiviral therapy. Two patients with genotype 1 showed a relapse of the hepatitis C virus during 6 mo of follow at wk 72. In two patients genotype was not evaluated prior to therapy. Patients got antiviral treatment for 48 wk and both achieved SVR at wk 72.

Table 1 Demographic and clinical characteristics of 58 patients, *n* (%)

Characteristics	
Mean age, years, (range)	36 (22–62)
Sex	
Male	33
Female	25
Race	
Caucasian	48 (100)
ALT, IU/L (range)	57 (9-263)
HCV-RNA level, > 800.000 IU/mL	23 (40)
Mean level, IU/mL	615.000
HCV genotype	
1, 1a, 1b, 4	32 (55)
2a, 2b, 3	24 (42)
Not available	2 (3)
HCV genotype 1 and HCV-RNA > 800.000 IU/mL	19 (33)
Liver biopsy (available in 56 out of 58 patients)	
No chronic hepatitis	10 (17)
Chronic hepatitis	43 (74)
Cirrhosis	3 (5)
Co-medication	
Methadone	4 (7)
Codeine	7 (12)

Table 2 Sustained viralogical response by HCV genotype, gender and sex (wk 72), *n* (%)

All genotypes	
< 800.000 IU/mL	23/33 (70)
⩾ 800.000 IU/mL	13/25 (52)
Genotype 1	
< 800.000 IU/mL	5/6 (83)
⩾ 800.000 IU/mL	9/19 (47)
Non-genotype 1	
< 800.000 IU/mL	18/27 (67)
⩾ 800.000 IU/mL	4/6 (67)
Sex	
Male	16/33 (49)
Female	14/25 (56)

Sixteen patients who failed to follow up, dropped off the study due to side effects or died and were taken as non-responders, *n* = 58.

HCV infection were enrolled at our site in Luebeck. Of these patients, 57% were men and 43% women. All patients were of Caucasian origin and the mean age was 36 years. Ninety percent of the patients showed a histological diagnosis of chronic hepatitis and only 2% showed histologically cirrhosis that was deemed clinically compensated. The mean serum HCV RNA concentration was 617.000 IU/mL. Fifty-two percent of the patients were infected with genotype 1. Genotypes 2 and 3 were present in 39% of the patients and 4% of the patients showed genotype 4. The baseline characteristics are shown in Table 1.

Efficacy

Overall, 62% of the patients showed a sustained virological response (SVR) at the end of therapy, whereas 16 individuals did not respond to the therapy. ALT levels dropped significantly from initially elevated levels during the first 12 wk of therapy, whereas AST and bilirubin were stable in the normal laboratory range. Fifty-six percent and 50% of the patients with genotypes 1 and 4, respectively, showed a virological response at the end of treatment, while 48% and 48% respectively, reached a sustained virological response at wk 72. In the group of patients with easy to treat genotypes 2 and 3, 50% and 87% respectively, achieved a negative HCV-PCR at the end of treatment and no relapse occurred in these 19 patients until wk 48 (Figure 1). The patients with a low viral load (< 800.000 IU/mL) initially had a slightly greater chance of achieving SVR compared to those with a high viral load (48% *vs* 40%) irrespective of their genotype (Table 2). Women responded slightly better to therapy than men. The drop in viral load was accompanied with a significant decrease in ALT levels throughout the first three months of therapy (57 U/L to 22 U/L). AST levels were in their normal range at the beginning of treatment and there was only little if any further normalisation (25 U/L to 17 U/L). In some patients bilirubin was slightly elevated as well but showed normal levels at the end of therapy (data not shown). There was no positive correlation between either genotype or ALT or SVR (data not shown).

Neither consensus interferon (CIFN) nor ribavirin dosing had to be modified throughout the therapy in any patient.

Co-medication with either methadone or codeine did not play a role in treating patients with HCV. Neither dosage nor application of replacement medicine had to be adjusted. The patients on replacement medication did not succeed in regard to SVR compared to those without methadone or codeine (data not shown). Ninety-two percent of the patients, who did achieve sustained virological response, took more than 80% of medication throughout the whole treatment period, demonstrating a remarkably high adherence to antiviral therapy.

However, only 2 out of all patients (all genotype 1) with negative PCR at wk 48 (EOT) had a virological relapse during the follow-up period between wk 48 and 72.

Table 3 Frequency of laboratory abnormalities (n = 58)

Event	n
Neutropenia	
< 1500	21
< 1000	10
< 500	1
Anemia	
< 10.5 g	1
< 8.5 g	0
Platelets	
< 100.000	4
< 50.000	0

Tolerablity

Seven patients showed a relapse of their intravenous drug abuse prior to the end of therapy and one 28-year old male patient died due to a heroin overdose. Six patients stoped therapy due to treatment-related side-effects (bleeding due to low platelets). Two patients did not show up for follow-up visits during antiviral treatment. No patient showed evidence of hypocalcemia, previously reported for daily dosing of CIFN[10]. Liver function in all patients was stable as measured clinically and by testing of coagulation function and serum albumin (data not shown).

Safety and adverse events

There was one serious adverse event 8 wk after beginning of therapy, leading to a death due to an overdose of intravenous heroin abuse. Six patients showed a restart of their iv drug abuse while on combination therapy. One patient developed a major depression, one female patient showed a significant drop in platelets (43.000/μL), one showed recurrent epistaxis (89.000/μL) and one male patient showed a long- lasting episode of arthritis and suicidal thoughts. Otherwise dose modifications due to adverse events were not necessary in any patient.

The spectrum of side effects of daily high dose induction therapy with CIFN was similar to previous trials with IFN and ribavirin. All the 58 patients were included in safety analysis. All the patients experienced flu-like symptoms (100%). Most of them experienced fatigue (93%), headache (91%), cough (72%), and mood disorders (87%). Two patients experienced bleeding disorders due to low platelets [e.g. bleeding gingivitis (101/nL), epistaxis (89/nL)] and one patient was taken off antiviral medication due to a significant drop of WBC (Table 3). One patient did not receive further treatment at wk 8 due to impaired vision, myalgia, and suicidal thoughts. None of the patient experiencing mood disorders required any psychopharmacological co-medication.

In patients with significant neutropenia, this side effect occurred mostly during wk 6 and 8 of therapy, after being treated with high dose CIFN for the first 8 wk. GMCSF was not administered since low neutrophil count always returned to almost normal level in all patients by reducing daily CIFN dosing to 9 μg daily according to the study protocol. Neither platelets nor blood transfusion was given in patients with low platelets due to CIFN or anemia due to ribavirin.

One severe adverse event occurred due to the relapse of intravenous drug use followed by a lethal overdose injection. Five other patients took intravenous drugs as well and were immediately taken off the antiviral study drugs.

Table 4 Questionnaire (Int. Quality of Life Assessment SF-36). Listed are those answers presenting the majority of possible answers (%)

	wk 0	wk 12
Personal feeling	Very good (76)	Good (63)
Personal feeling compared to last week	Good (77)	Better (55)
Impaired physical activity	Never (90)	Slightly (77)
Impaired physical activity compared to last week	Never (88)	Slightly (73)
Emotional problems	Never (93)	Never (48)
Pain	None (90)	None (30)
Pain last week	None (83)	None (54)
Feeling depressed	Never (88)	Seldom (45)
Feeling happy	Often (85)	Sometimes (50)
Feeling tired	Seldom (77)	Sometimes (51)
Impaired personal contact to relatives and friends due to disease	Never (88)	Seldom (71)
"I'm feeling fit like others"	Mostly (94)	No (37)
"I'm feeling healthy"	Mostly (78)	No (65)
"I expect not to feel healthy"	Do not know (44)	No (32)

International quality of life assessment

Because personal mental and physical components of health of a patient undergoing such an antiviral therapy is important, each patient was requested to answer a widely accepted questionnaire (IQOLA SF-36, German Acute version 1.0) with respect to the quality of life at wk 0 and 12.

There was a decrease in well being after 12 wk of therapy, but a significant number felt better after finishing the high induction treatment period. The physical activity in most patients was slightly impaired 3 mo after therapy (Table 4). There was a significant increase in emotional distress at wk 12 compared to wk 0, possibly due to CIFN. More patients experienced physical pain (70%), depression (50%), unhappiness (50%) and tiredness (51%) at wk 12, while personal contact to friends and relatives was not influenced by therapy (29%). Due to the side effects, fewer people (35%) felt healthy three months after the beginning of treatment and 68% did not feel healthy during the upcoming treatment phase.

DISCUSSION

Chronic hepatitis C virus infection is responsible for an increase in morbidity and mortality. This is the first study on the treatment of naïve patients with chronic HCV infection with high-dosing of IFN-alfacon-1 in combination with ribavirin. Recent intravenous drug addicts can be successfully treated for HCV and the response rates are as good as in patients without iv drug history.

The goal of our study was to address the issue of efficacy, tolerability and safety of daily high dose induction therapy with consensus-interferon (CIFN) and ribavirin in naïve HCV-infected patients. However, the usually recommended dosing of CIFN is 9 μg, three times a week

at the beginning of the trial. Ribavirin was given on a daily basis at 800 mg, irrespective of the genotyping. Weight-based dosing of ribavirin for therapy in HCV genotypes 1 and 4 has been introduced after several studies were conducted in 2001[3].

All patients received a higher dosage of interferon (18 μg of CIFN subcutaneously daily for up to 8 wk followed by 9 μg daily) in combination with ribavirin for 24 or 48 wk. The patients were then carefully followed up for an additional 24 wk.

The overall response rate was 62 % showing a sustained virological response (SVR) 24 wk after the EOT. There was a slight difference ($P < 0.05$) in response rates in regard to the initial viral load. The patients with a low viral load (< 800.000 IU/mL) responded better (70% *vs* 52%) than those with a high viral load. These results are comparable to data (54%) obtained with pegylated α-2b/ribavirin[3].

There was a significant difference ($P < 0.01$) in response rates for the patients with a high viral load. With respect to genotyping, the patients with non-genotype 1 showed a SVR rate of 67% compared to 47% in the genotype 1 patients, even though the number of patients in the later group was quite small. In contrast, different response rates were obtained for HCV-infected patients presenting a low viral load initially. The non-genotype 1 patients showed a 64% SVR rate compared to 83% for the genotype 1-infected individuals. This fact might be explained by the small number of patients presenting genotype 1 and low-viral load. Overall, the patients with genotype 1 and high viral load showed an acceptable response rate, which is in accordance to Sjögren *et al*[11], showing a higher response rate for this population treated with CIFN and ribavirin instead of pegylated interferon α-2b and ribavirin (46% *vs* 14%).

In this treatment-naïve patient population, neither baseline ALT nor genotype was significantly associated with SVR, similar to other reports comparing treatment of non-responders with either CIFN or pegylated interferon α-2b in combination with ribavirin[15].

Adherence to therapy is another important issue for success of treatment[12]. Therapy with a wide range of side effects is less favourable and therefore less successful in achieving SVR. In our study, the overall adherence was good and comparable to previous studies[13]. It is known that HCV-1-infected patients maintained on > 80% of their interferon or peginterferon α-2b and ribavirin dosage for the duration of treatment have enhanced sustained response rates. In addition, some results suggest that adherence enhances the likelihood of achieving an initial virologic response[12].

However, the rate of reuse of intravenous drugs in almost 10% of patients (6 out of 58 patients) is substantial and accounts partly for the high drop-out rate in our study even though former iv drug users had to be off active drug use for at least 6 mo prior to study enrolment.

The increased side effects in patients treated with CIFN at a high induction rate (18 μg *vs* 9 μg daily) can result in a higher drop out rate[14,15]. The initial rapid decline in viral load at wk 4 is counteracted by increased side effects, resulting in a lesser SVR rate, at least in non responders[15].

In conclusion, the safety and tolerability profile of this treatment is reasonable in a certain subset of patients, but might be difficult to tolerate in some individuals, resulting in discontinuation of therapy. However, these data suggest that CIFN may be safely combined with ribavirin and enhance the sustained response rate when close monitoring of side-effects and laboratory results are obeyed[10]. Patients with chronic hepatitis C and genotype 2 or 3 should be treated with pegylated interferon α-2a or 2b in combination with ribavirin for up to 24 wk[16], respectively. In difficult-to-treat patients with genotype 1 and high viral load, a daily therapy regimen with consensus interferon in combination with ribavirin might be of choice as well as in non-responders to combination therapy[15,17].

This is the first study showing that recent iv drug users can be safely and successfully treated for HCV if they are closely monitored.

REFERENCES

1 **Pestka S**. The human interferon-alpha species and hybrid proteins. *Semin Oncol* 1997; **24**: S9-4-S9-17
2 **Cornberg M**, Wedemeyer H, Manns MP. Treatment of chronic hepatitis C with PEGylated interferon and ribavirin. *Curr Gastroenterol Rep* 2002; **4**: 23-30
3 **Manns MP**, McHutchison JG, Gordon SC, Rustgi VK, Shiffman M, Reindollar R, Goodman ZD, Koury K, Ling M, Albrecht JK. Peginterferon alfa-2b plus ribavirin compared with interferon alfa-2b plus ribavirin for initial treatment of chronic hepatitis C: a randomised trial. *Lancet* 2001; **358**: 958-965
4 **Fried MW**, Shiffman ML, Reddy KR, Smith C, Marinos G, Gonçales FL, Häussinger D, Diago M, Carosi G, Dhumeaux D, Craxi A, Lin A, Hoffman J, Yu J. Peginterferon alfa-2a plus ribavirin for chronic hepatitis C virus infection. *N Engl J Med* 2002; **347**: 975-982
5 **Di Bisceglie AM**, Hoofnagle JH. Optimal therapy of hepatitis C. *Hepatology* 2002; **36**: S121-S127
6 **Blatt LM**, Davis JM, Klein SB, Taylor MW. The biologic activity and molecular characterization of a novel synthetic interferon-alpha species, consensus interferon. *J Interferon Cytokine Res* 1996; **16**: 489-499
7 **Tong MJ**, Reddy KR, Lee WM, Pockros PJ, Hoefs JC, Keeffe EB, Hollinger FB, Hathcote EJ, White H, Foust RT, Jensen DM, Krawitt EL, Fromm H, Black M, Blatt LM, Klein M, Lubina J. Treatment of chronic hepatitis C with consensus interferon: a multicenter, randomized, controlled trial. Consensus Interferon Study Group. *Hepatology* 1997; **26**: 747-754
8 **Lam NP**, Neumann AU, Gretch DR, Wiley TE, Perelson AS, Layden TJ. Dose-dependent acute clearance of hepatitis C genotype 1 virus with interferon alfa. *Hepatology* 1997; **26**: 226-231
9 **Pawlotsky JM**, Bouvier-Alias M, Hezode C, Darthuy F, Remire J, Dhumeaux D. Standardization of hepatitis C virus RNA quantification. *Hepatology* 2000; **32**: 654-659
10 **Pockros PJ**, Reindollar R, McHutchinson J, Reddy R, Wright T, Boyd DG, Wilkes LB. The safety and tolerability of daily infergen plus ribavirin in the treatment of naïïve chronic hepatitis C patients. *J Viral Hepat* 2003; **10**: 55-60
11 **Sjogren MH**, Sjogren R, Holtzmuller K, Winston B, Butterfield B, Drake S, Watts A, Howard R, Smith M. Interferon alfacon-1 and ribavirin versus interferon alpha-2b and ribavirin in the treatment of chronic hepatitis C. *Dig Dis Sci* 2005; **50**: 727-732
12 **McHutchison JG**, Manns M, Patel K, Poynard T, Lindsay KL, Trepo C, Dienstag J, Lee WM, Mak C, Garaud JJ, Albrecht JK. Adherence to combination therapy enhances sustained response in genotype-1-infected patients with chronic hepatitis C. *Gastroenterology* 2002; **123**: 1061-1069
13 **Fattovich G**, Zagni I, Minola E, Felder M, Rovere P, Carlotto

A, Suppressa S, Miracolo A, Paternoster C, Rizzo C, Rossini A, Benedetti P, Capanni M, Ferrara C, Costa P, Bertin T, Pantalena M, Lomonaco L, Scattolini C, Mazzella G, Giusti M, Boccia S, Milani S, Marin R, Lisa Ribero M, Tagger A. A randomized trial of consensus interferon in combination with ribavirin as initial treatment for chronic hepatitis C. *J Hepatol* 2003; **39**: 843-849

14 **Moskovitz DN**, Manoharan P, Heathcote EJ. High dose consensus interferon in nonresponders to interferon alpha-2b and ribavirin with chronic hepatitis C. *Can J Gastroenterol* 2003; **17**: 479-482

15 **Cornberg M**, Hadem J, Herrmann E, Schuppert F, Schmidt HH, Reiser M, Marschal O, Steffen M, Manns MP, Wedemeyer H. Treatment with daily consensus interferon (CIFN) plus ribavirin in non-responder patients with chronic hepatitis C: a randomized open-label pilot study. *J Hepatol* 2006; **44**: 291-301

16 **von Wagner M**, Huber M, Berg T, Hinrichsen H, Rasenack J, Heintges T, Bergk A, Bernsmeier C, Häussinger D, Herrmann E, Zeuzem S. Peginterferon-alpha-2a (40KD) and ribavirin for 16 or 24 weeks in patients with genotype 2 or 3 chronic hepatitis C. *Gastroenterology* 2005; **129**: 522-527

17 **Böcher WO**, Schuchmann M, Link R, Hillenbrand H, Rahman F, Sprinzl M, Mudter J, Löhr HF, Galle PR. Consensus interferon and ribavirin for patients with chronic hepatitis C and failure of previous interferon-alpha therapy. *Liver Int* 2006; **26**: 319-325

S- Editor Liu Y **L- Editor** Wang XL **E- Editor** Lu W

PO Box 2345, Beijing 100023, China
www.wjgnet.com
wjg@wjgnet.com

World J Gastroenterol 2007 January 28; 13(4): 585-587
World Journal of Gastroenterology ISSN 1007-9327

RAPID COMMUNICATION

Elastic band ligation of hemorrhoids: Flexible gastroscope or rigid proctoscope?

M Cazemier, RJF Felt-Bersma, MA Cuesta, CJJ Mulder

M Cazemier, RJF Felt-Bersma, CJJ Mulder, Department of Gastroenterology and Hepatology, VU University Medical Center, Amsterdam, The Netherlands
MA Cuesta, Department of Gastrointestinal Surgery, VU University Medical Center, Amsterdam, The Netherlands
Correspondence to: M Cazemier, Department of Gastroenterology and Hepatology, VU University Medical Center, Amsterdam, VU Medical Center, PO Box 7057, 1007 MB Amsterdam, The Netherlands. marcel.cazemier@wanadoo.nl
Telephone: +31-204-440613 Fax: +31-204-440554
Received: 2006-10-31 Accepted: 2006-12-25

Key words: Hemorrhoids; Barron ligation; Rigid scope; Endoscope; Anal endosonography

Cazemier M, Felt-Bersma RJF, Cuesta MA, Mulder CJJ. Elastic band ligation of hemorrhoids: Flexible gastroscope or rigid proctoscope? *World J Gastroenterol* 2007; 13(4): 585-587

http://www.wjgnet.com/1007-9327/13/585.asp

Abstract

AIM: To compare rigid proctoscope and flexible endoscope for elastic band ligation of internal hemorrhoids.

METHODS: Patients between 18 and 80 years old, with chronic complaints (blood loss, pain, itching or prolapse) of internal hemorrhoids of grade I-Ⅲ, were randomized to elastic band ligation by rigid proctoscope or flexible endoscope (preloaded with 7 bands). Patients were re-treated every 6 wk until the cessation of complaints. Evaluation by three-dimensional anal endosonography was performed.

RESULTS: Forty-one patients were included (median age 52.0, range 27-79 years, 20 men). Nineteen patients were treated with a rigid proctoscope and twenty two with a flexible endoscope. Twenty-nine patients had grade Ⅰ hemorrhoids, 9 patients had grade Ⅱ hemorrhoids and 3 patients had grade Ⅲ hemorrhoids. All patients needed a minimum of 1 treatment and a maximum of 3 treatments. A median of 4.0 bands was used in the rigid proctoscope group and a median of 6.0 bands was used in the flexible endoscope group ($P < 0.05$). Pain after ligation tended to be more frequent in patients treated with the flexible endoscope (first treatment: 3 *vs* 10 patients, $P < 0.05$). Three-dimensional endosonography showed no sphincter defects or alterations in submucosal thickness.

CONCLUSION: Both techniques are easy to perform, well tolerated and have a good and fast effect. It is easier to perform more ligations with the flexible endoscope. Additional advantages of the flexible scope are the maneuverability and photographic documentation. However, treatment with the flexible endoscope might be more painful and is more expensive.

INTRODUCTION

The initial treatment of symptomatic internal hemorrhoids is conservative and consists of a fiber enriched diet, increased fluid intake, prevention of straining and local hygiene, which may be combined with local anesthetic and antiphlogistic medication[1,2]. Over 90% of patients with symptomatic hemorrhoids can be treated conservatively or by rubber band ligation. Infrared coagulation and cryotherapy are also options, but are no longer commonly applied[3]. Surgery is reserved for the most severe cases. Since the early sixties the treatment of choice for persisting internal hemorrhoids is elastic band ligation by means of a rigid proctoscope (Barron ligation)[4,5]. Wrobleski *et al*[6] reported results of long term follow up (mean of 60 mo) of 266 patients; 80% had fewer symptoms and 69% had no symptoms. The procedure is usually safe and can be easily repeated[7]. Some studies evaluated the use of a flexible endoscope equipped with a ligation cap, normally used for ligation of esophageal varices, in treating hemorrhoids[8-11]. A flexible endoscope could have some advantages such as more maneuverability, a wider view and photographic documentation. The present prospective randomized trial was performed to compare both techniques in effectiveness. Additionally we used a three-dimensional endosonography to evaluate changes in the submucosa and sphincter defects.

MATERIALS AND METHODS

Patients between 18 and 80 years old, with chronic complaints (blood loss, pain, itching or prolapse) of internal hemorrhoids grade I-Ⅲ, were randomized by computer software to elastic band ligation by rigid proctoscope or gastroscope (Olympus Excera®). Patients were re-treated every 6 wk till the cessation of complaints.

The rigid proctoscope was gently introduced and then

Table 1 Patient characteristics and results

	Proctoscope	Gastroscope
n	19	22
Age [median (range)]	53 (27-75)	50.5 (33-79)
Male/Female	7/12	13/9
Hemorrhoids grade I	15	14
Hemorrhoids grade Ⅱ	4	5
Hemorrhoids grade Ⅲ	0	3
No of treatments [median (range)]	1.0 (1-3)	1.0 (1-3)
No of total ligations [median (range)]	4.0 (2-10)	6.0 (1-15)[a]
Pain after treatment	3	10[a]
Cost	3 euro	150 euro

[a]$P < 0.05$ *vs* proctoscope.

elastic bands were applied using a standard elastic band applicator in anterograde fashion. For endoscopic ligation, a single-use multiband ligator device (Sevenshooter®, Boston Scientific, USA) was attached to the end of a gastroscope. The device can only be attached to a gastroscope. The Sevenshooter is provided with 7 bands. The hemorrhoids were suctioned into the ligation cap in either retrograde or antegrade fashion. The number of bands applied depended on the amount of hemorrhoidal tissue present. All treatments were performed in an outpatient setting.

A three-dimensional anal endosonography was made before the first treatment and 6 wk after the last treatment. Endosonography was performed, using a three dimensional diagnostic ultrasound system (Hawk type 2102, B-K Medical) with a 16 MHz rotating endoprobe (type 1850, focal range 2 to 4.5 cm) covered by a hard sonolucent cone (diameter 1.7 cm) filled with water, producing a 360° view. Three dimensional anal endosonography was performed according to a standard procedure. The endoprobe was covered with a lubricated condom which was filled with ultrasound gel. The probe was then introduced into the rectum and a recording was made of the distal part of the rectum, the puborectalis muscle and the anal canal. After the endosonography, images were reconstructed to three dimensional images by computer software. The Medical Ethical Committee granted approval for this study.

Statistical analysis

Data are presented as a median with range. Differences between groups were assessed with a Mann-Whitney test, Chi square test or Fischer's exact test when appropriate. $P < 0.05$ was taken as significant.

RESULTS

Detailed demographic and clinical data are shown in Table 1. Forty-one patients (median age 52, range 27-79 years, 20 men) with recurrent rectal bleeding, pain, itching or prolapse underwent ligation. Nobody had been treated previously. All procedures were easy to perform. Sometimes, in patients treated with the flexible endoscope, a rectal enema was needed when the rectum was not clean.

Nineteen patients were treated with a rigid proctoscope and twenty two with a flexible endoscope. Twenty-nine, 9, and 3 patients had grade Ⅰ, Ⅱ and Ⅲ hemorrhoids, respectively.

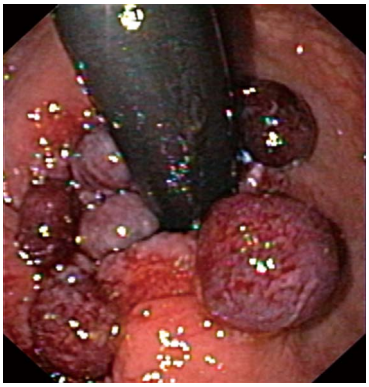

Figure 1 Picture showing the retroflexed endoscopic view after ligation.

Patients treated with a proctoscope needed a median of 1 treatment (range 1-3) and patients treated with an endoscope also needed a median of 1 treatment (range 1-3, $P = 0.664$).

A median of 4 bands (range 2-10) was used in the rigid proctoscope group and a median of 6 bands (range 1-15) was used in the flexible endoscope group ($P < 0.05$) (Figure 1).

In the group treated with a rigid proctoscope, 5 patients needed 1 re-treatment and 1 patient needed 2 re-treatments. In the group treated with a flexible endocope, 2 patients needed 1 re-treatment and 1 patient needed 2 re-treatments.

Two patients were excluded from follow up: One patient had a rupture of an abdominal aortic aneurysm and 1 patient developed an anal fissure.

Pain after ligation was more frequent in patients treated with the flexible endoscope (first treatment: 3 *vs* 10 patients, $P < 0.05$). The single-use ligation device (Sevenshooter®) costs approximately 150 euro for one set (2005). One elastic band for the rigid proctoscope costs approximately 0.50 euro. Further costs (cleaning of the gastroscope and proctoscope, personnel costs) did not substantially differ between both techniques.

With three-dimensional endosonography 30 patients were evaluated before and after treatment. Hemorrhoidal tissue was clearly visible in all patients. No sphincter defects were found before and after treatment and there was no significant change in submucosa thickness after endoscopic/proctoscopic treatment (Figure 2). After one year follow up, 5 patients needed re-treatment (2 proctoscope, 3 gastroscope).

DISCUSSION

Hemorrhoids are a major health problem; the community-wide prevalence in the Western World is reported to be around 4%. Adequate intake of fluids and fiber, use of suppositories, stool softeners and topical creams are important in the treatment of hemorrhoids, especially in grade I disease. When conservative treatment fails, there are still options, including surgical therapy.

Rubber band ligation with a proctoscope is very effective and inexpensive. Since 2005, it has been the treatment of choice. Studies have been undertaken investigating effectiveness and new techniques[12-14].

There have been 4 studies that analyzed the use of

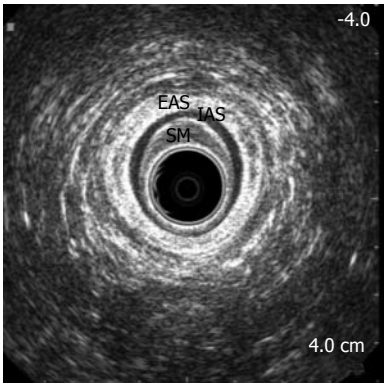

Figure 2 Endosonographic image showing thickening of the submucosa. IAS: Internal anal sphincter; EAS: External anal sphincter; SM: Submucosa (hypoechogenic area is hemorrhoidal).

a flexible endoscope for hemorrhoidal elastic band ligation[8-11]. These studies conclude that it is a safe and efficient method with some advantages, although costs are still a major drawback. Only one study compared endoscopic band ligation (reusable) with the conventional rubber band ligation through a rigid proctoscope[10].

In our pilot study we found that both techniques were easy to perform, well tolerated and had a good and fast effect. It was easier to perform more ligations with the flexible endoscope. No serious adverse events were reported. Additional advantages of the flexible scope were the maneuverability and photographic documentation.

However, treatment with the flexible endoscope seemed to be more painful and was more expensive. More pain sensation can be explained by the learning curve we had to deal with and that more bands could be applied. In contrast, Wehrmann *et al*[10] found no significant difference in pain and reported that the total number of bands applied was significantly lower in the group treated with the endoscope.

So far as we know, this is the first study that evaluated with three-dimensional endosonography the presence of possible sphincter defects and changes in the submucosa. Poen *et al*[15] already found, with two-dimensional endosonography, no difference in appearance of the anal configuration after treatment with either rubber band ligation or infrared coagulation. In our study no significant alterations or sphincter defects were found and these endosonographic findings confirmed that band ligation is a safe technique.

When costs can be reduced the endoscopic treatment of hemorrhoids can be a good alternative for ligation with the rigid proctoscope.

In summary, endoscopic ligation is an effective, safe treatment and is comparable with proctoscopic ligation. However, the treatment is more expensive.

REFERENCES

1 **Poen AC**, Felt-Bersma RJ, Cuesta MA, Devillé W, Meuwissen SG. A randomized controlled trial of rubber band ligation versus infra-red coagulation in the treatment of internal haemorrhoids. *Eur J Gastroenterol Hepatol* 2000; **12**: 535-539
2 **Johanson JF**, Sonnenberg A. The prevalence of hemorrhoids and chronic constipation. An epidemiologic study. *Gastroenterology* 1990; **98**: 380-386
3 **Madoff RD**, Fleshman JW. American Gastroenterological Association technical review on the diagnosis and treatment of hemorrhoids. *Gastroenterology* 2004; **126**: 1463-1473
4 **Blaisdell PC.** Office ligation of internal hemorrhoids. *Am J Surg* 1958; **96**: 401-404
5 **Barron J.** Office ligation of internal hemorrhoids. *Am J Surg* 1963; **105**: 563-570
6 **Wrobleski DE**, Corman ML, Veidenheimer MC, Coller JA. Long-term evaluation of rubber ring ligation in hemorrhoidal disease. *Dis Colon Rectum* 1980; **23**: 478-482
7 **Iyer VS**, Shrier I, Gordon PH. Long-term outcome of rubber band ligation for symptomatic primary and recurrent internal hemorrhoids. *Dis Colon Rectum* 2004; **47**: 1364-1370
8 **Trowers EA**, Ganga U, Rizk R, Ojo E, Hodges D. Endoscopic hemorrhoidal ligation: preliminary clinical experience. *Gastrointest Endosc* 1998; **48**: 49-52
9 **Dickey W**, Garrett D. Hemorrhoid banding using videoendoscopic anoscopy and a single-handed ligator: an effective, inexpensive alternative to endoscopic band ligation. *Am J Gastroenterol* 2000; **95**: 1714-1716
10 **Wehrmann T**, Riphaus A, Feinstein J, Stergiou N. Hemorrhoidal elastic band ligation with flexible videoendoscopes: a prospective, randomized comparison with the conventional technique that uses rigid proctoscopes. *Gastrointest Endosc* 2004; **60**: 191-195
11 **Fukuda A**, Kajiyama T, Arakawa H, Kishimoto H, Someda H, Sakai M, Tsunekawa S, Chiba T. Retroflexed endoscopic multiple band ligation of symptomatic internal hemorrhoids. *Gastrointest Endosc* 2004; **59**: 380-384
12 **Takano M**, Iwadare J, Ohba H, Takamura H, Masuda Y, Matsuo K, Kanai T, Ieda H, Hattori Y, Kurata S, Koganezawa S, Hamano K, Tsuchiya S. Sclerosing therapy of internal hemorrhoids with a novel sclerosing agent. Comparison with ligation and excision. *Int J Colorectal Dis* 2006; **21**: 44-51
13 **Kwok SY**, Chung CC, Tsui KK, Li MK. A double-blind, randomized trial comparing Ligasure and Harmonic Scalpel hemorrhoidectomy. *Dis Colon Rectum* 2005; **48**: 344-348
14 **Fukuda A**, Kajiyama T, Kishimoto H, Arakawa H, Someda H, Sakai M, Seno H, Chiba T. Colonoscopic classification of internal hemorrhoids: usefulness in endoscopic band ligation. *J Gastroenterol Hepatol* 2005; **20**: 46-50
15 **Poen AC**, Felt-Bersma RJF, Cuesta MA, Meuwissen SGM. Anal endosonography in haemorrhoidal disease: do anatomical changes have clinical implications? *Colorectal Dis* 1999; **1**: 146-150

S- Editor Liu Y **L- Editor** Zhu LH **E- Editor** Bi L

PO Box 2345, Beijing 100023, China
www.wjgnet.com
wjg@wjgnet.com

World J Gastroenterol 2007 January 28; 13(4): 588-593
World Journal of Gastroenterology ISSN 1007-9327

RAPID COMMUNICATION

Immunohistochemical analysis of p53, cyclinD1, RB1, c-fos and N-ras gene expression in hepatocellular carcinoma in Iran

SJ Moghaddam, EN Haghighi, S Samiee, N Shahid, AR Keramati, S Dadgar, MR Zali

SJ Moghaddam, EN Haghighi, S Samiee, N Shahid, AR Keramati, S Dadgar, MR Zali, Research Center for Gastroenterology and Liver Disease, Shaheed Beheshti University of Medical Sciences, and Academy of Medical Sciences, Iran
Supported by Academy of Medical Sciences, Iran
Correspondence to: Mohammad Reza Zali, MD, FACG, University Professor in Shahid Beheshti University of Medical Sciences, President of Research Center for Gastroenterology and Liver Disease, 7th floor, Taleghani Hospital Tabnak St., Evin,Tehran 19857, Iran. zali@rcgld.org
Telephone: +98-21-22418871 Fax: +98-21-22402639
Received: 2006-07-13 Accepted: 2006-11-27

Key words: Hepatocellular Carcinoma; Iran; Expression of p53, cyclinD1, RB1, c-fos and N-ras genes

Moghaddam SJ, Haghigh EN, Samiee S, Shahid N, Keramati AR, Dadgar S, Zali MR. Immunohistochemical analysis of p53, cyclinD1, RB1, c-fos and N-ras gene expression in hepatocellular carcinoma in Iran. *World J Gastroenterol* 2007; 13(4):588-593

http://www.wjgnet.com/1007-9327/13/588.asp

Abstract

AIM: To study the effect of some genes especially those involved in cell cycle regulation on hepatocellular carcinoma.

METHODS: Paraffin-embedded tissue samples of 25 patients (18 males and 7 females) with hepatocellular carcinoma were collected from 22 pathology centers in Tehran during 2000-2001, and stained using immunohistochemistry method (avidin-biotin-peroxidase) for detection of p53, cyclinD1, RB1, c-fos and N-ras proteins.

RESULTS: Six (24%), 5 (20%), 12 (48%) and 2 samples (8%) were positive for p53, cyclinD1, C-fos and N-ras expression, respectively. Twenty-two (88%) samples had alterations in the G1 cell-cycle checkpoint protein expression (RB1 or cyclinD1). P53 positive samples showed a higher (9 times) risk of being positive for RB1 protein than p53 negative samples. Loss of expression of RB1 in association with p53 over-expression was observed in 4 (66.7%) of 6 samples. Loss of expression of RB1 was seen in all cyclinD1 positive, 20 (90.9%) N-ras negative, and 11 (50%) C-fos positive samples, respectively. CyclinD1 positive samples showed a higher (2.85 and 4.75 times) risk of being positive for c-fos and N-ras expression than cyclinD1 negative samples.

CONCLUSION: The expression of p53, RB1 and c-fos genes appears to have a key role in the pathogenesis of hepatocellular carcinoma in Iran. Simultaneous overexpression of these genes is significantly associated with their loss of expression during development of hepatocellular carcinoma.

INTRODUCTION

Hepatocellular carcinoma (HCC) is the most common primary malignant tumor of the liver and the fourth most common cause of cancer-related death in the world[1]. Male predominance is, however, more obvious in populations at high risk of developing this tumor (mean ratio 3.7:1.0) than in those at low or intermediate risk (2.4:1.0)[2].

HCC has a heterogenous geographical distribution. Countries or regions with the highest incidence (50-120 cases per 100 000 population per year) include China, Taiwan, Korea and other Southeast Asian countries, as well as Sub-Saharan Africa. HCC is linked to environmental, dietary, and lifestyle factors, so that its incidence and distribution vary widely among ethnic groups, geographic regions, and the two sexes[3]. Tumor suppressor genes such as RB1 and p53 may play a significant part in hepatocarcinogensis[3]. As a favorable background for neoplastic transformation, cirrhosis is expected to harbor early genetic changes, but very few studies have been conducted thus far to address this issue. Ashida *et al*[4] have reported in both HCC and adjacent cirrhosis a 60% rate of loss of heterozygosity (LOH) at 13q, the site of the RB1 gene. The loss of heterozygosity and abnormalities in structure and function of the p53 gene are also frequently found in HCC patients[5]. A specific p53 mutation is found in more than 50% of HCC patients from India, China and South Africa, where dietary aflatoxins are suspected to be the major liver specific carcinogens[5-11]. However, it occurs less frequently in Western countries[3,5]. Activation of oncogenes of the "ras" family and others has been detected during chemically induced HCC in rodents, but there is little evidence of such activation in human tumors[12]. CyclinD1 over-expression may be an early event in hepatocarcinogenesis and plays a role in tumor differentiation[13]. Yuen *et al*[14] reported that the expression of c-fos is significantly higher in tumor tissue than in non-

tumor tissue. Specific mutations of the p53, cyclinD1, RB1, c-fos, and N-ras genes and their expression in HCC have been reported from several parts of the world, but to the authors' knowledge to date, the expression status of these genes has not been studied in HCC patients in Iran, where the frequency of chronic hepatitis B and C virus infection as well as exposure to dietary aflatoxin is very high[15].

MATERIALS AND METHODS

Sample collection

Formalin-fixed and paraffin-embedded tissue samples of 25 patients (18 males and 7 females) with documented HCC (surgically resected material or biopsy) were provided for analysis. The samples were collected from 22 pathology centers in Tehran during 2000-2001. The study was approved by the Medical Ethics Committee, Ministry of Health, Iran, as conforming to the ethical guidelines of the 1975 Declaration of Helsinki. Hospital records were used to verify age, sex and other demographic items.

Tissue preparation

These samples were sectioned and stained with hematoxylin and eosin (HE). Diagnosis of HCC was confirmed and the grade of tumor was determined according to the criteria proposed by the World Health Organization by the collaborating pathologist in Research Center for Gastroenterology and Liver Disease.

HCC was considered to be adequate for immunohistochemical study only if the block was of adequate size (surface area of section > 4 cm^2 and > 10% of the surface area of the block was occupied by the tumor).

Immunostaining

The technique was based on avidin-biotin-peroxidase method using 10% formaldehyde-fixed and paraffin-embedded sections. The selected paraffin blocks were cut into 5 μm-thick sections. The sections were applied to precoated glass slides to avoid becoming detached, then dried at 37℃ overnight followed by drying at 56℃ for 60 min, deparaffinized with xylene and rehydrated through graded concentrations of alcohol. Antigen retrieval was performed by 3 × 5-min cycles of microwave oven heating (750W) at 100℃ in 0.01 mol/L citrate buffer at pH 6. After washing and rinsing with Tris-buffered saline (TBS, 0.05 M, pH 7.2-7.6), endogenous-peroxidase activity was blocked with 3% hydrogen peroxide for 10 min at room temperature and then rinsed with distilled water. Subsequently, sections were treated for 10 min with 10% bovine serum albumin (BSA) at room temperature for blocking nonspecific background staining. Afterward, primary monoclonal mouse antihuman-p53 protein, clone DO-7, isotype IgG2bkappa (DAKO, Lot 108) at dilution 1:100, primary monoclonal mouse antihuman-RB1 gene product, clone RB1, isotype IgG1kappa (DAKO, Lot 019) at dilution 1:50, primary monoclonal mouse antihuman-cyclinD1, clone DCS-6, isotype IgG2a kappa (DAKO, Lot 012) at dilution 1:50, primary monoclonal mouse antihuman-c-fos, clone D-1, isotype IgG2b (Santa Cruz Biotechnology Inc., Lot J 251) at dilution 1:100 and primary monoclonal mouse antihuman-N-ras, clone F155, isotype IgG1 (Santa Cruz Biotechnology Inc., Lot I 251) at dilution 1:100 were added and incubated in a moist chamber overnight at 4℃. The sections were again washed three times in TBS for 5 min using the DAKO LSAB2 system (Universal, HRP, Lot 10106). Goat anti-mouse and anti-rabbit biotinylated IgG (diluted in PBS containing carrier protein and 0.015 mol/L sodium azide) and preincubated streptavidin conjugated to horseradish peroxidase (diluted in PBS containing carrier protein and anti-microbial agents) were added for 30 min at room temperature. The sections were washed in TBS as before and then developed in prepared 3-amino-9-ethylcarbazole substrate chromogen (AEC/H_2O_2) for p53 and RB1 and in prepared 3,3'-diaminobenzidine chromogen solution (DAB/H_2O_2) for cyclinD1, c-fos and N-ras for 10 min at room temperature. The sections were then washed in water, counterstained with Mayer's hematoxylin for 2-5 min at room temperature, dehydrated, cleared with 37 mmol/L ammonia water, rinsed in a bath of distilled water for 2-5 min, finally mounted and coverslipped with Faramount aqueous-based mounting medium (DAKO, Lot 00029). A section of the same tumor incubated in BSA instead of the primary antibody was included as the negative control. We used one standard p53 positive section of human SCC (DAKO, Lot 071-1), one known RB1 negative retinoblastoma section, one known cyclin D1 positive breast tumor section, one known c-fos positive astrocytoma section and one known N-ras positive lymphoma section as a positive control for each staining.

Assessment of immunostaining

Staining of p53, RB1, cyclinD1, c-fos and N-ras genes was examined at high power fields (× 400) under a standard light microscope. Nuclear staining was regarded as positive if there was homogeneous staining or > 10% of the cancer cells were heterogeneously stained.

Statistical analysis

The results were expressed as frequency for gene expression changes and odds ratio for association between expression changes of these five genes. All statistical tests were performed with the Program Statistical Package for the Social Sciences (SPSS version 11, Chicago, IL).

RESULTS

The mean ± SD age of our patients was 60.56 ± 12.52 years and the highest frequency (44%) was seen in the sixth decade of life. Male to female ratio was 2.57 (18 males and 7 females) and mean ± SD age of patients in each sex was 62.72 ± 10.43 years and 55 ± 16.4 years, respectively.

Histopathology

All the 25 samples were well differentiated (grade Ⅰ).

Accumulation of p53, RB1, cyclinD1, c-fos and N-ras proteins

Intense immunostaining of p53, RB1, cyclinD1, c-fos and

Table 1 Expression of p53 gene in relation to the expression of RB1, cyclinD1, c-fos and N-ras genes, *n* (%)

Gene expression	RB1		Cyclin-D1		c-fos		N-ras	
	Positive	Negative	Positive	Negative	Positive	Negative	Positive	Negative
P53 positive	2 (33.3)	4 (66.7)	2 (33.3)	4 (66.7)	4 (66.7)	2 (33.3)	1 (16.75)	5 (83.3)
P53 negative	1 (5.3)	18 (94.7)	3 (15.8)	16 (84.2)	8 (42.1)	11 (57.9)	1 (5.3)	18 (94.7)
	OR: 0.1, 95% CI: 0.0-1.5		OR: 2.6, 95% CI: 0.3-21.7		OR: 2.7, 95% CI: 0.4-18.8		OR: 3.6, 95% CI: 0.1-68.3	

Table 2 RB1 gene expression in relation to the expression of c-fos and N-ras genes, *n* (%)

Gene expression	c-fos		N-ras	
	Positive	Negative	Positive	Negative
RB1 positive	1 (33.3)	2 (66.7)	0	3 (100)
RB1 negative	11 (50)	11 (50)	2 (9.1)	20 (90.9)
	OR: 0.5, 95% CI: 0.0-6.3		OR: 1.1, 95% CI : 0.9-1.2	

Table 3 G1 checkpoint protein expression in relation to p53, *n* (%)

Expression pattern of G1 checkpoint proteins	P53 (+)	P53 (-)	*P*
Rb+/cyclinD1+	Zero	Zero	
Rb-/cyclinD1+	2 (40)	3 (60)	
Rb-/cyclinD1-	2 (11.8)	15 (88.2)	0.02
Subtotal	4 (66.6)	18 (94.7)	
Rb+/cyclin D1-	2 (66.7)	1 (33.3)	
Total	6 (24)	19 (76)	

N-ras proteins was observed in the cell nuclei of tissues. Overall, six (24%) samples showed nuclear accumulation of p53 protein in varying proportions of tumor cells, the rest of the samples (76%) were negative. Twenty-two (88%) samples showed complete loss of RB1 protein expression in the primary tumor, the rest of the tumors (12%) displayed variable proportions of RB1 protein positive tumor cells. The intensity and subcellular location of the staining in the tumor were similar to those observed in the normal epithelia. We detected high levels of cyclinD1 protein in 5 (20%) samples while 20 (80%) samples were negative for cyclinD1 expression. The frequency of c-fos and N-ras positive staining was 48% (12 samples) and 8% (2 samples), respectively. The expression of p53 gene in relation to the expression of RB1, cyclinD1, c-fos and N-ras genes is depicted in Table 1. The RB1 gene expression in relation to the expression of c-fos and N-ras genes is shown in Table 2. Of those samples positive for the c-fos gene, 1 (8.3%) was N-ras positive and 11 (91.7%) were N-ras negative. On the other hand, among the c-fos negative samples, 1 (7.7%) was N-ras positive and 12 (92.3%) were N-ras negative.

When overexpression of p53 was seen, loss of expression of RB1 was found in 4 (66.7%) samples. Loss of expression of RB1 was observed in all those with positive cyclinD1 (5 samples), while expression of RB1 was found in 17 (85%) with negative cyclinD1, and in 3 (15%) samples with positive RB1. CyclinD1 positive samples showed a higher risk of being positive for C-fos and N-ras (2.85 and 4.75 times, respectively) than cyclinD1 negative samples. Finally, loss of expression of RB1 was detected in 2 samples with overexpression of N-ras. On the other hand, among the samples with loss of expression of RB1, overexpression of c-fos was found in 11 (50%).

Overall, 22/25 (88%) samples had alterations in the G1 cell-cycle checkpoint proteins, as assessed by means of cyclinD1 and RB1 expression (Table 3). These occurred in 4 (66.6%) of 6 p53-positive samples and in 18 (94.7%) of 19 p53-negative samples. P53-negative samples showed absence of the RB1 protein more frequently. P53 positive samples showed a higher (9 times) risk of being positive for RB1 than p53 negative samples, being 3.6, 2.75, and 2.66 for N-ras, c-fos, and cyclinD1, respectively. In samples with cyclinD1 positive staining, the risk of being positive for N-ras was 4.75 times higher in samples with cyclinD1 positive staining than in samples with negative cyclinD1 staining for this protein.

DISCUSSION

Several oncogenic pathways have been implicated in malignant transformation of liver cells. Inactivation of the p53 tumor suppressor gene by mutations and allelic deletions in about 30% of HCC cases has been associated predominantly with exposure to aflatoxin B1 and hepatitis B virus infection[16]. Activation of cyclinD1, c-fos and N-ras and disruption of the RB1 pathway are also commonly involved in liver tumorigenesis. New major challenges include the identification of candidate genes located in frequently altered chromosomal regions and oncogenic pathways driven by different risk factors. Deranged expression of cell cycle modulators has been reported to contribute to the development and progression of HCC[17]. In human HCC, high frequencies of aberration have been detected in the p53 and RB1 genes[14]. Mutations of the p53 tumor suppressor gene have been reported to occur with varying frequency in different geographic regions, which might be a different etiology for HCC[18]. In our study, nuclear accumulation of p53 protein was seen in 24% of samples. Mutations of this gene have been identified in 30%-50% of HCC patients in some geographic areas[19]. An *et al*[20] reported that there is histological heterogeneity in established HCC, which is accompanied with increased proliferative activity and p53 overexpression. Overexpression of p53 has identified in 37.5% of Japanese HCC patients and 62.5% of Indonesian HCC patients[18]. Recently, Ming *et al*[21] also showed that the frequency of mutation of p53 gene is much higher in high prevalent HCC area than in the low-risk HCC area in China. More than 95% cancer specimens

exhibit strong intranuclear accumulation of p53 protein, which can be detected by immunohistology. However, Biersing *et al*[22] and Vesey[23] have found little or no point mutations of p53 gene in human hepatocarcinoma in Swedish and Australian patients. Therefore overexpression of p53 protein in hepatocarcinoma specimens can be used as the mutant p53 biopathological marker in tumor tissues. Qin *et al*[8] reported that accumulation of p53 is a valuable marker for predicting the prognosis of HCC patients. Lin GY *et al*[7] reported that inactivation of the tumor suppressor genes p53 and RB1 has been demonstrated in different forms, and implies the pathogenesis of human malignant diseases. The study of Kondoh *et al*[24] supports the idea that deletion or inactivation of tumor suppressors including RB1, p53 and other candidate genes seems to be common events in HCC development. Abnormalities of the RB1 tumor suppressor gene have been found in 20%-25% of HCCs, including 80%-86% of HCCs with p53 mutations[19]. Nishida *et al*[25] reported that RB1 protein is positive in 85.6% of HCC cases but is not related to any clinicopathological parameters. Positive immunostaining for RB1 and mutant p53 protein is detectable in 58% and 37% of HCCs, respectively[26]. Loss of expression of RB1 in HCC has been reported in several studies[21,27]. In this study, loss of expression of RB1 gene was found in 88% of samples. The proto-oncogene c-fos is involved in cell cycle progression and cellular proliferation[14]. Abuthnot *et al*[28] reported that c-myc and c-fos mRNA, as well as their protein products, are increased in human liver cancers. Wang *et al*[29] have also found an apparently higher expression of N-ras and c-fos in human hepatoma than in its adjacent liver tissue. Recently, Feng *et al*[30,31] reported that the positive rates and signal intensity of c-fos and some other proteins in HCC are significantly higher than those in pericarcinomatous tissues. Yuen *et al*[14] found that the expression of c-fos was significantly higher in tumor tissue than in nontumor tissue (91% *vs* 0%, $P < 0.0001$). C-fos primarily induces cyclinD1 up-regulation by a mediator called MAPK/ERK[32]. In our study, the expression of c-fos gene was detected in 48% of patients with documented HCC. There was no significant relationship between c-fos and Cyclin-D1 expressions. Aflatoxin B1 may evoke an intense and prolonged expression of c-fos, including persistent signals for regeneration, which in turn may activate the replication of immature cells[33]. CyclinD1 is frequently overexpressed in a variety of cancers, including HCC, as a result of gene amplification. Overexpression of cyclinD1 protein, through gene amplification, correlates with poor prognosis of several cancers, but its role in HCC is the subject of controversy. Increased expression of cyclinD1 may play an important role in the development of HCC owing to the perturbation of normal control of the cell cycle[34]. On the other hand, Azechi *et al*[35] reported that cyclinD1 is a known oncogene and a key regulator of cell cycle progression. Amplification of the cyclinD1 gene and its overexpression are associated with aggressive forms of HCC. Overexpression of cyclinD1 is sufficient to initiate hepatocellular carcinogenesis. Choi *et al*[17] and Deane *et al*[36] have found a positive relationship between cyclinD1 overexpression and advanced tumor stage and aberrant p53 expression in HCC ($P < 0.05$). Joo *et al*[13] reported that cyclinD1 overexpression may confer additional growth advantages to the tumor in addition to protein RB1 inactivation in HCC. On the contrary, Sato *et al*[37] have found no significant relationship between the expressions of cyclinD1 and p53. Ito *et al*[38] conducted a simultaneous immunohistochemical study with p53 and cyclinD1 antibody in the same series of HCC and revealed that 88% of the patients positive for cyclinD1 also expressed p53 and 91% of the patients negative for p53 did not express cyclinD1, suggesting that cyclinD1 is expressed later than the alteration of p53 in the progression of human HCC. In our study, cyclinD1 was positively related to aberrant p53 expression. In HCC, N-ras was first proved as one of the transforming genes[39], which belongs to the G protein family. When it is converted to an active oncogene by point mutation, chromosome rearrangement or gene amplification, the signal transmission of cell membranes may change, which drives cell division, leading to abnormal differentiation and formation of neoplasm. Cerruti[40] and Tada[41] reported that the mutagenesis of a proto-oncogene from "ras" family and p53 tumor suppressor gene might be the most important event in HCC. Tabor[19] reported that overexpression of oncogenes N-ras and c-fos has been found in high percentages of HCC patients. Imai *et al*[42] and Tamano *et al*[43] found that mutations of ras oncogene may be the early events, and the expression in tumor or non-tumor tissues can be detected with different rates. Luo *et al*[26] reported that N-ras and p53 genes might be involved in the carcinogenesis and development of HCC. They also showed that mutation of the tumor suppressor gene p53 can convert ras gene into oncogene. In their study, 38% of HCCs with N-ras gene mutation did not express p53 protein, indicating that some other genes or factors may participate in the carcinogenesis and development of HCC. In our study, 83% of p53 positive samples did not show N-ras mutation. Chao *et al*[9] suggested that activation of the ras gene might not be a major event in aflatoxin-related human hepatocarcinogenesis. This hypothesis is supported by another study[44] conducted in southern Africa on Blacks, where dietary exposure to aflatoxin is a risk factor.

In conclusion, as in other parts of the world, the change in expression pattern of these genes especially p53, RB1 and c-fos, appears to have a key role in the pathogenesis of HCC in Iran. There is likely a relation between the simultaneous changes in these genes during development of HCC. This research might shed some light on the carcinogenic role of the expression of p53, RB1, cyclinD1, c-fos and N-ras genes. Besides, in order to understand the exact role of these changes in development of HCC, further studies with a larger number of samples are essential.

ACKNOWLEDGMENTS

The authors thank Dr. Hamid Asadzadeh, Dr. Hamid Mohaghegh and Mrs. Fatemeh Solgi for their assistance in sample collection, Mrs. Soodabeh Ghasemi and Mrs. Shabnam Emami for tissue preparation. They also thank Mrs. Farnoosh Afshar Amin for data collection.

REFERENCES

1 **Roncalli M**, Bianchi P, Grimaldi GC, Ricci D, Laghi L, Maggioni M, Opocher E, Borzio M, Coggi G. Fractional allelic loss in non-end-stage cirrhosis: correlations with hepatocellular carcinoma development during follow-up. *Hepatology* 2000; **31**: 846-850
2 **Okuda K**. Epidemiology of primary liver cancer. In: Tobe T, editor. Primary liver cancer in Japan, Tokyo: Springer-Verlag, 1992: 3
3 **Colombo M**. Malignant neoplasms of the liver. In: Schiff ER, Sorrell MF, Maddrey WC, editors. Diseases of the liver. Philadelphia: Lippincott Williams & Wilkins, 2003: 1377
4 **Ashida K**, Kishimoto Y, Nakamoto K, Wada K, Shiota G, Hirooka Y, Kamisaki Y, Itoh T, Kawasaki H. Loss of heterozygosity of the retinoblastoma gene in liver cirrhosis accompanying hepatocellular carcinoma. *J Cancer Res Clin Oncol* 1997; **123**: 489-495
5 **Katiyar S**, Dash BC, Thakur V, Guptan RC, Sarin SK, Das BC. P53 tumor suppressor gene mutations in hepatocellular carcinoma patients in India. *Cancer* 2000; **88**: 1565-1573
6 **Lane DP**. Cancer. p53, guardian of the genome. *Nature* 1992; **358**: 15-16
7 **Lin GY**, Chen ZL, Lu CM, Li Y, Ping XJ, Huang R. Immunohistochemical study on p53, H-rasp21, c-erbB-2 protein and PCNA expression in HCC tissues of Han and minority ethnic patients. *World J Gastroenterol* 2000; **6**: 234-238
8 **Qin LX**, Tang ZY, Ma ZC, Wu ZQ, Zhou XD, Ye QH, Ji Y, Huang LW, Jia HL, Sun HC, Wang L. P53 immunohistochemical scoring: an independent prognostic marker for patients after hepatocellular carcinoma resection. *World J Gastroenterol* 2002; **8**: 459-463
9 **Chao HK**, Tsai TF, Lin CS, Su TS. Evidence that mutational activation of the ras genes may not be involved in aflatoxin B(1)-induced human hepatocarcinogenesis, based on sequence analysis of the ras and p53 genes. *Mol Carcinog* 1999; **26**: 69-73
10 **Murakami Y**, Hayashi K, Hirohashi S, Sekiya T. Aberrations of the tumor suppressor p53 and retinoblastoma genes in human hepatocellular carcinomas. *Cancer Res* 1991; **51**: 5520-5525
11 **Teramoto T**, Satonaka K, Kitazawa S, Fujimori T, Hayashi K, Maeda S. p53 gene abnormalities are closely related to hepatoviral infections and occur at a late stage of hepatocarcinogenesis. *Cancer Res* 1994; **54**: 231-235
12 **Dominguez-Malagón H**, Gaytan-Graham S. Hepatocellular carcinoma: an update. *Ultrastruct Pathol* 2001; **25**: 497-516
13 **Joo M**, Kang YK, Kim MR, Lee HK, Jang JJ. Cyclin D1 overexpression in hepatocellular carcinoma. *Liver* 2001; **21**: 89-95
14 **Yuen MF**, Wu PC, Lai VC, Lau JY, Lai CL. Expression of c-Myc, c-Fos, and c-jun in hepatocellular carcinoma. *Cancer* 2001; **91**: 106-112
15 **Adibi P**, Ghassemian R, Alavian SM, Ranjbar M, Mohammadalizadeh AH, Nematizadeh F, Mamani M, Rezazadeh M, Keramat F, Ardalan A, Esmaeili A, Zali MR. Effectiveness of hepatitis B vaccination in children of chronic hepatitis B mothers. *Saudi Med J* 2004; **25**: 1414-1418
16 **Lévy L**, Renard CA, Wei Y, Buendia MA. Genetic alterations and oncogenic pathways in hepatocellular carcinoma. *Ann N Y Acad Sci* 2002; **963**: 21-36
17 **Choi YL**, Park SH, Jang JJ, Park CK. Expression of the G1-S modulators in hepatitis B virus-related hepatocellular carcinoma and dysplastic nodule: association of cyclin D1 and p53 proteins with the progression of hepatocellular carcinoma. *J Korean Med Sci* 2001; **16**: 424-432
18 **Marwoto W**, Miskad UA, Siregar NC, Gani RA, Boedihusodo U, Nurdjanah S, Suwarso P, Hasan HA, Akbar N, Noer HM, Hayashi Y. Immunohistochemical study of P53, PCNA and AFP in hepatocellular carcinoma, a comparison between Indonesian and Japanese cases. *Kobe J Med Sci* 2000; **46**: 217-229
19 **Tabor E**. Tumor suppressor genes, growth factor genes, and oncogenes in hepatitis B virus-associated hepatocellular carcinoma. *J Med Virol* 1994; **42**: 357-365
20 **An FQ**, Matsuda M, Fujii H, Tang RF, Amemiya H, Dai YM, Matsumoto Y. Tumor heterogeneity in small hepatocellular carcinoma: analysis of tumor cell proliferation, expression and mutation of p53 AND beta-catenin. *Int J Cancer* 2001; **93**: 468-474
21 **Buendia MA**. Genetics of hepatocellular carcinoma. *Semin Cancer Biol* 2000; **10**: 185-200
22 **Bjersing L**, Andersson C, Lithner F. Hepatocellular carcinoma in patients from northern Sweden with acute intermittent porphyria: morphology and mutations. *Cancer Epidemiol Biomarkers Prev* 1996; **5**: 393-397
23 **Vesey DA**, Hayward NK, Cooksley WG. p53 gene in hepatocellular carcinomas from Australia. *Cancer Detect Prev* 1994; **18**: 123-130
24 **Kondoh N**, Wakatsuki T, Hada A, Shuda M, Tanaka K, Arai M, Yamamoto M. Genetic and epigenetic events in human hepatocarcinogenesis. *Int J Oncol* 2001; **18**: 1271-1278
25 **Nishida N**, Fukuda Y, Ishizaki K, Nakao K. Alteration of cell cycle-related genes in hepatocarcinogenesis. *Histol Histopathol* 1997; **12**: 1019-1025
26 **Luo D**, Liu QF, Gove C, Naomov N, Su JJ, Williams R. Analysis of N-ras gene mutation and p53 gene expression in human hepatocellular carcinomas. *World J Gastroenterol* 1998; **4**: 97-99
27 **Okamoto Y**. Dibutyryl cyclic AMP-induced enhancement of RB protein degradation in human hepatoma cells. *Anticancer Res* 1999; **19**: 5181-5185
28 **Arbuthnot P**, Kew M, Fitschen W. c-fos and c-myc oncoprotein expression in human hepatocellular carcinomas. *Anticancer Res* 1991; **11**: 921-924
29 **Wang Z**, Xiang Q, Li D, Li S. Correlation between gene expression and chromatin conformation of c-fos and N-ras in human liver and hepatoma. *Chin Med Sci J* 1991; **6**: 6-8
30 **Feng DY**, Zheng H, Jiang HY. Effects of Stat3 phosphorylation and expression of c-fos and c-jun proteins on hepatocarcinogenesis. *Hunan Yike Daxue Xuebao* 2001; **26**: 17-19
31 **Feng DY**, Zheng H, Tan Y, Cheng RX. Effect of phosphorylation of MAPK and Stat3 and expression of c-fos and c-jun proteins on hepatocarcinogenesis and their clinical significance. *World J Gastroenterol* 2001; **7**: 33-36
32 **Ito Y**, Sasaki Y, Horimoto M, Wada S, Tanaka Y, Kasahara A, Ueki T, Hirano T, Yamamoto H, Fujimoto J, Okamoto E, Hayashi N, Hori M. Activation of mitogen-activated protein kinases/extracellular signal-regulated kinases in human hepatocellular carcinoma. *Hepatology* 1998; **27**: 951-958
33 **Hong SW**, Park C. The effect of aflatoxin B1 on the expression of early response genes and transforming growth factor-alpha in CCl4 induced rat liver injury. *Yonsei Med J* 1997; **38**: 167-177
34 **Zhang YJ**, Chen SY, Chen CJ, Santella RM. Polymorphisms in cyclin D1 gene and hepatocellular carcinoma. *Mol Carcinog* 2002; **33**: 125-129
35 **Azechi H**, Nishida N, Fukuda Y, Nishimura T, Minata M, Katsuma H, Kuno M, Ito T, Komeda T, Kita R, Takahashi R, Nakao K. Disruption of the p16/cyclin D1/retinoblastoma protein pathway in the majority of human hepatocellular carcinomas. *Oncology* 2001; **60**: 346-354
36 **Deane NG**, Parker MA, Aramandla R, Diehl L, Lee WJ, Washington MK, Nanney LB, Shyr Y, Beauchamp RD. Hepatocellular carcinoma results from chronic cyclin D1 overexpression in transgenic mice. *Cancer Res* 2001; **61**: 5389-5395
37 **Sato Y**, Itoh F, Hareyama M, Satoh M, Hinoda Y, Seto M, Ueda R, Imai K. Association of cyclin D1 expression with factors correlated with tumor progression in human hepatocellular carcinoma. *J Gastroenterol* 1999; **34**: 486-493
38 **Ito Y**, Matsuura N, Sakon M, Miyoshi E, Noda K, Takeda T, Umeshita K, Nagano H, Nakamori S, Dono K, Tsujimoto M, Nakahara M, Nakao K, Taniguchi N, Monden M. Expression and prognostic roles of the G1-S modulators in hepatocellular carcinoma: p27 independently predicts the recurrence. *Hepatology* 1999; **30**: 90-99
39 **Farshid M**, Tabor E. Expression of oncogenes and tumor suppressor genes in human hepatocellular carcinoma and hepatoblastoma cell lines. *J Med Virol* 1992; **38**: 235-239
40 **Cerutti P**, Hussain P, Pourzand C, Aguilar F. Mutagenesis of

the H-ras protooncogene and the p53 tumor suppressor gene. *Cancer Res* 1994; **54**: 1934s-1938s

41 **Tada M**, Omata M, Ohto M. Analysis of ras gene mutations in human hepatic malignant tumors by polymerase chain reaction and direct sequencing. *Cancer Res* 1990; **50**: 1121-1124

42 **Imai Y**, Oda H, Arai M, Shimizu S, Nakatsuru Y, Inoue T, Ishikawa T. Mutational analysis of the p53 and K-ras genes and allelotype study of the Rb-1 gene for investigating the pathogenesis of combined hapatocellular-cholangiocellular carcinomas. *Jpn J Cancer Res* 1996; **87**: 1056-1062

43 **Tamano S**, Ward JM, Diwan BA, Keefer LK, Weghorst CM, Calvert RJ, Henneman JR, Ramljak D, Rice JM. Histogenesis and the role of p53 and K-ras mutations in hepatocarcinogenesis by glyceryl trinitrate (nitroglycerin) in male F344 rats. *Carcinogenesis* 1996; **17**: 2477-2486

44 **Leon M**, Kew MC. Analysis of ras gene mutations in hepatocellular carcinoma in southern African blacks. *Anticancer Res* 1995; **15**: 859-861

S- Editor Liu Y **L- Editor** Wang XL **E- Editor** Lu W

PO Box 2345, Beijing 100023, China
www.wjgnet.com
wjg@wjgnet.com

World J Gastroenterol 2007 January 28; 13(4): 594-599
World Journal of Gastroenterology ISSN 1007-9327

RAPID COMMUNICATION

Achalasia and thyroid disease

Mohammad Hassan Emami, Mostafa Raisi, Jaleh Amini, Hamed Daghaghzadeh

Mohammad Hassan Emami, Hamed Daghaghzadeh, Isfahan University of Medical Sciences and Poursina Hakim Research Institution, Isfahan, Iran
Mostafa Raisi, Jaleh Amini, Poursina Hakim Research Institution, Isfahan, Iran
Supported by Poursina Hakim Research Institution, Isfahan, Iran
Correspondence to: Mostafa Raisi, Poursina Hakim Research Institution, PO Box: 81465-1798, No9- Behesht building-Bozorgmehr Av. Isfahan, Iran. mostafaraisi@yahoo.com
Telephone: +98-913-3154000 Fax: +98-311-2667542
Received: 2006-11-12 Accepted: 2006-12-21

Abstract

AIM: To investigate some possible etiologies of achalasia by screening patients with achalasia for some autoimmune diseases such as thyroid disease.

METHODS: We examined 30 known cases of achalasia (20 females, 10 males). Their age ranged 15-70 years. All of them were referred to our institute for treatment. Their sera were evaluated to detect some possible associations with rheumatoid disease, thyroid disease, inflammatory process, anemia, *etc*.

RESULTS: Seven out of 30 patients (23%) had thyroid disease including four patients with hypothyroidism (13.3%), two patients with hyperthyroidism (6.6%), and one had only thyroid nodule but was in euthyroid state (3.3%). Two of these hypothyroid patients had no related clinical symptoms (subclinical) and two had clinical manifestations of hypothyroidism**.** There were no correlations between the intensity of thyroid diseases and the severity of achalasia symptoms.

CONCLUSION: The etiology of achalasia is unknown although autoimmunity has been implicated and is supported by several studies. Thyroid disease presents concomitantly with achalasia in about one fourth of our patients who may have a common etiology.

Key words: Achalasia; Thyroid disease; Hypothyroidism; Esophageal motility; Etiology

Emami MH, Raisi M, Amini J, Daghaghzadeh H. Achalasia and thyroid disease. *World J Gastroenterol* 2007; 13(4): 594-599

http://www.wjgnet.com/1007-9327/13/594.asp

INTRODUCTION

Achalasia is a common and well characterized primary motility disorder of the esophageal body and lower esophageal sphincter (LES), causing impaired progressive peristalsis in the esophageal body, incomplete relaxation of LES during swallowing, and sometimes increased abnormal relaxation of the LES pressure. Previous studies evaluating esophagomyotomy and esophageal resection specimens have shown that the presence of myenteric inflammation is a consistent and early pathologic change in patients with achalasia[1,2]. The disorder is observed in both genders primarily in the fifth and sixth decades of life, although achalasia can present at any age[3,4]. The cause of the degeneration of neurons in achalasia is not known. The observations that achalasia is associated with HLA-DQw1 and that affected patients often have circulating antibodies to enteric neurons suggest that achalasia may be an autoimmune disorder[5-7]. Nonspecific degeneration of smooth muscle cells and a loss of small nerve fibers have been reported[8-10]. Another controversial issue is the role of inflammatory infiltrates in the pathogenesis of the disease. A study has suggested that complement activation is involved in the autoimmune pathogenesis of achalasia[11]. Achalasia is associated with extra esophageal autonomic nervous dysfunction that involves cardiovascular and papillary function as well as regulation of mesenteric arterial blood flow[12]. Some investigators have proposed that achalasia may result from chronic infections with herpes zoster or measles viruses, but modern studies have not confirmed an association between achalasia and any recognized viral disease[13,14]. However, a recent study also showed that there is no association between the most common viruses and achalasia[14]. As myenteric neurons synthesizing nitric oxide are responsible for the inhibitory component of esophageal peristalsis and LES relaxation, it is considered likely that these neurons are involved in this disease[15,16].

Since there is no consistent single abnormality in achalasia, this study was designed to evaluate the relationship between achalasia and some of the commonest autoimmune diseases.

MATERIALS AND METHODS

Patients

All 42 newly diagnosed patients referred between 2001 and 2005 to our research center (Poursina Hakim Research Institution, Gastroenterology Division, Isfahan, Iran) were examined prospectively and enrolled in the study. Poursina

Hakim Institution is a reference tertiary care center that services a population of about 4 000 000 individuals in the central area of Iran. Of the 42 enrolled cases in the study based on clinical and radiological findings, 6 patients with pseudoachalasia but without endoscopic features of achalasia were excluded due to non-compliance (one case) or some other reasons such as loss of follow-up due to changing their address or phone number, immigration to other provinces and admission by other physicians far from our institution. Finally 30 cases were included. Their symptoms, laboratory results, and historical and functional data were recorded. Achalasia was defined by clinical criteria, namely prolonged (more than 1 year) intermittent or progressive dysphagia to liquids and solids in addition to some other minor symptoms such as regurgitation, chest pain and nocturnal cough plus barium swallow with a typical beak like appearance. We obtained posterior-anterior chest x ray radiographies at 1, 5, and 20 min after a single barium meal to assess barium column and measure its heights and widths as well as the delay time of esophageal clearance (timed barium swallow). Upper gastrointestinal endoscopy was done to confirm the diagnosis and to rule out secondary achalasia (such as esophageal tumors of cardia and fundus, submucosal tumor of distal esophagus, peptic stricture and other mucosal or infiltrative lesions of the esophagus or gastric cardia). Endoscopic findings suggestive of achalasia may be seen and are very helpful if endoscopy is done carefully by experts in this field. Some of the suggestive criteria for achalasia are as following: esophageal dilation, esophageal dysmotility or aperistalsis in response to air insufflations, abnormal LES opening and high pressure LES during scope passage. Manometery although very helpful especially in early stages of the disease, was not available in our province at the time of the study, so it was not done for most of them.

Exclusion criteria included those found to have an underlying malignancy during the study, any types of generalized neuropathies, diabetes mellitus, non-compliance or unwillingness of patients to continue the study, and finally those lost to follow up by any reason.

The patients' history was taken using a structured questionnaire. We interviewed, examined and completed a questionnaire designed to detect possibility of connective tissue and autoimmune diseases, other gastrointestinal motility disorders, diabetes mellitus, use of immunosuppressive medications, chronic viral illnesses, thyroid problems, usage of a regular immunosuppressive medication and also habits and addictions for all patients. Informed consent was obtained from all patients. None of the patients underwent surgical therapy.

Laboratory methods

After diagnosis of achalasia, all patients were screened for a set of selected autoimmune disease and other markers as shown in Table 1. Serum factors were evaluated by biochemical techniques. A double check of laboratory tests was conducted by a second laboratory to assure validity of abnormal results. Equivocal laboratory results were rechecked by a reference laboratory.

Symptoms

Clinical data regarding symptoms of dysphagia, regurgitation, and chest pain, nocturnal cough and pyrosis were collected by means of a validated questionnaire. Dysphagia was described as difficulty in swallowing, and regurgitation as the sensation of stomach contents going up the esophagus. The frequency of each symptom was graded on a scale ranging from 0 to 5 (0 = none, 1 = once per month or less, 2 = once per week up to three to four times a month, 3 = two to four times per week, 4 = once per day, 5 = several times per day). This scoring system is similar, but with some modifications, to that used by Eckardt *et al*[17] and modified by Vaezi *et al*[18].

Table 1 Test and methods used in this study

Test title	Kit	Manufactured country
Anti nuclear anti body (ANA)	Biostems	Spain
Antineutrophil cytoplasm antibody (c-ANCA)	Binding site	England
Calcium	Man	Iran
Phosphorus	Man	Iran
Alkaline phosphatase	Man	Iran
Thyroid stimulating hormone(TSH)	Isfahan pharmacology faculty	Iran
T3 Resin uptake	kavoshiar	Iran
T3, T4	Isfahan pharmacology faculty	Iran
Albumin	Man	Iran
Globulin	Man	Iran
Rapid plasmin reagin (RPR)	Anison	Iran
Urine analysis	Combi	Germany
Complete blood count	-	Germany

All tests except for urine analysis were performed on blood or serum samples.

Statistical analysis

For comparison between patients with achalasia and normal population, Student's *t*-test assuming equal variance was used. In addition, we analyzed the symptoms using the non-parametric Mann-Whitney test, because the data were not normally distributed.

RESULTS

Of the 42 newly suspected achalasia patients referred to our institution, 36 (11 men and 25 women) fulfilled the participating criteria in the study, but only 30 (20 females, 10 males) finished the study. The remaining six patients were statistically similar by age and gender to the 30 cases and they had no unusual reason for their loss of follow-up.

Thyroid disease

Of the 30 patients, 7 had thyroid disease (23.7%), 4 had hypothyroidism (13.3%), 2 had hyperthyroidism (6.7%) and one (3.3%) had only a thyroid nodule in euthyroid state. Two of these hypothyroidism patients had no related clinical symptoms (subclinical) and two had clinical manifestations of hypothyroidism. Both patients with subclinical hypothyroidism were diagnosed in our

Table 2 Average score of all patients and those suffering from thyroid disease respectively (mean ± SD)

	Patients with hypothyroidism	Patients with benign thyroid diseases[1]	Patients without thyroid problems	Mean score of all patients
Age	39.5 ± 14.3[a]	35.8[b] ± 11.9[b]	38.5 ± 18.1	37.9 ± 16.7
Dysphagia	5[c]	4.5 ± 1.1[d]	4.8 ± 0.45	4.8 ± 0.66
Regurgitation	5[e]	4.7 ± 0.75[f]	3.5 ± 1.9	3.8 ± 1.8
Nocturnal cough	2.5 ± 2.8[g]	2.5 ± 2.5[h]	2.5 ± 2.2	2.5 ± 2.2
Chest discomfort	3.75 ± 1.5[i]	2.2 ± 2.1[j]	1.86 ± 2.7	1.96 ± 2
Weight loss	0.5 ± 0.5[k]	0.4 ± 0.5[l]	0.65 ± 4.08	0.6 ± 0.49

Scoring system: 0 = none; 1 = once per month or less; 2 = three to four times a month; 3 = two to four times per week; 4 = once per day; 5 = several times per day, [1]Composed of thyroid nodules, hypothyroidism and hyperthyroidism. No significant differences between groups were found by independent *t*-test, Mann-Witney test and chi-square test. *P* values of differences between thyroid disease groups and other patients with achalasia: [a]: 0.7; [b]: 0.7; [c]: 0.5; [d]: 0.6; [e]: 0.09; [f]: 0.1; [g]: 1; [h]: 0.97; [i]: 0.08; [j]: 0.57; [k]: 0.6; [l]: 0.3. (the first and second columns were compared with the third column).

Table 3 Overall and specific ethnicity and gender of all patients and those suffering from thyroid disease respectively

	Hypothyroid patients		Benign thyroid diseases[1]		Without thyroid problems		Total	
	n	%	*n*	%	*n*	%	*n*	%
Number	4	13.3	7	23.7	23	76.6	30	100
Gender	♂1 ♀3	♂25 ♀75	♂2 ♀5	♂28 ♀72	♂8 ♀15	♂34 ♀66	♂10 ♀20	♂33 ♀67
Ethnicity[2]	F: 3	F: 75	F: 5	F: 71	F: 16	F: 69	F: 21	F: 70
	B: 1	B: 25	B: 2	B: 28	B: 5	B: 21	B: 7	B: 23

[1]Composed of thyroid nodules, hypothyroidism and hyperthyroidism. [2]Composed of the most common ethnicity in patients, F: Fars; B: Bakhtiari.

screening. One patient experienced hypothyroid shock after balloon dilation therapy (cool skin, hypothermia, hypotension and bradicardia not responsive to volume expansion and intravenous atropine injection). She had clinical symptoms of hypothyroidism which was not detected before balloon dilation therapy. The results of laboratory tests are listed in Table 2.

Patients' ethnicity

There were 21 (70%) Fars (the major Persian ethnicity), 7 Bakhtiari, an Iranian tribe, living in west of Isfahan Province) (23%), one Gilaki (another group of Iranians originating from northern Iran) (3.3%), and one patient was Turkish inhabitant in the central area of Iran (3.3. 0%).

Age and symptoms

The median age of onset of symptoms was 37 years (range 15-80 years). The mean age of patients with thyroid disease and other patients with achalasia was 35.8 and 38.5 years (*P*: 0.9). All patients complained of dysphagia to both liquids and solids. Regurgitation, weight loss, chest discomfort and heartburn were reported in 28 (93.3%), 18 (60%), 15 (50%) and 8 (26.6%) patients, respectively.

The symptoms of patients were compared (Table 2). Correlations between the intensity of thyroid disease and the severity of achalasia symptoms were statistically insignificant by Mann-Whitney test.

Prevalence and incidence of achalasia

In 2002 -2005, 42 cases of suspected achalasia were identified in or referred to our center. Of these, 19 were residents of Isfahan during the period of the study. The population of Isfahan was about 4 million in 2006. The overall ethnic- and gender-specific incidences of achalasia in our cases are shown in Table 3. No strong history of rheumatic disease or neuropathy in patients and their family was detected in our study.

Serological study

All serum samples were evaluated with sensitive tests for autoimmune diseases but we did not find any positive test except for 2 positive anti nuclear antibody tests (6.6%). Evaluation for vasculitis, some electrolyte disturbances, and anemia did not show any important finding (Table 4).

DISCUSSION

Although achalasia is a historically recognized clinical entity, its fundamental pathophysiology remains poorly understood. Primary achalasia accounts for the majority of cases. The etiology of primary achalasia is not entirely clear and probably multidimensional[19] including genetic predisposition (supported by the concordance for the disease in monozygotic twins[20] and associations with some HLA loci[7]), inflammation (myopathy of the smooth muscle cells[21], neuropathy[22,23] and inflammatory changes in esophageal specimens[24]), infections (virus[14], Chagas' disease, poliomyelitis[25,26], varicella zoster virus[27] and Helicobacter[28]), ischemia, toxicity and autoimmune disease[19]. Some other diseases postulate these etiologies such as concomitant appearance of achalasia and Guillain-Barré syndrome [29], Parkinson's disease[30], triple A syndrome[31], *etc.*

Table 4 Final result of laboratory evaluation in all patients

Test	Normal (%)	Abnormal (%)
Thyroid function tests	80	20
Calcium and phosphorus	100	-
Alkaline phosphatase	100	-
Albumin	100	-
Globulin	100	-
ANA	93.4	6.6
C_ANCA	100	-
RPR (VDRL)	100	-
Complete Blood Count	100	-
Urine analysis	100	-

All tests except for urine analysis were performed on blood or serum samples.

There are some reports about thyroid and esophageal problems in animals[32] but we have not found any reports about such problems in humans in English articles. Although it has been reported that there is a correlation between achalasia and autoimmune diseases, this is the first cross sectional study evaluating the relative prevalence of these problems (rheumatic disease, thyroid disease, inflammatory disease, *etc*) in a consecutive series of patients affected by achalasia which led us to a few interesting points. First, the results of serological tests obtained from this study confirmed some literature data that predict a potential autoimmune etiology of achalasia. Second, an association was found between thyroid problems and achalasia. Third, the frequency of thyroid disease was higher in patients with achalasia than in normal population.

It was reported that the prevalence of hypothyroidism is 4.6% (0.3% clinical and 4.3% subclinical) in the United States of America[33]. Whickham showed that the prevalence of spontaneous hypothyroidism in community is 1.5% in females and less than 0.1% in males [34]. These prevalence rates are similar to those reported in Finland[35], Japan[36], and in another US survey[37-39]. Heydarian and Azizi reported that the prevalence of hyperthyroidism, overt and subclinical hypothyroidism is 0.45%, 0.35% and 2.2% in Iran, respectively[40]. The prevalence of hypothyroidism and benign thyroid diseases (hypothyroidism, hyperthyroidism and thyroid nodules) in our patients was significantly higher than that reported in latter study (*P* value and confidence interval for each group were 0.025 and 0.000, 1.3-43.4 and 2.9-76.5 respectively).

The mean age of our patients is one -two decades lower than reported in other studies[3,4]. It may have a role in these findings. We found about a 5-fold rise in the prevalence of thyroid dysfunction in this study. Since our center is the only center offering balloon dilation therapy in Isfahan, we can assume that the overall population with achalasia in this area is very similar to that registered in our center and therefore these data are repeatable in our future study, but they may not be generalized in all cases of achalasia in other societies. Hence we suggest a similar study in all centers working in this subject. We should direct our future studies to find the possible genetic and environmental risk factors for earlier disease in this geographic area.

The reason why there is such a relatively strong association between these diseases can be explained by the literature describing most thyroid problems as probable autoimmune diseases[41-44]. Autoimmune etiology of achalasia is also supported by the presence of circulating autoantibodies against the myenteric plexus and inflammatory T-cell infiltrates in the myenteric plexus, as well as the increased prevalence of HLA class Ⅱ antigens. Possibly the initiating event may be an unknown environmental insult due to a viral infection resulting in inflammation of the myenteric plexus in susceptible patients. Not all affected individuals develop achalasia[45]. However, autommunity at least has a concomitant or susceptible role in pathogenesis.

Is there a symptomatic mimicry between achalasia and thyroid diseases? There is some evidence in animal model that a mega esophagus may occur in hypothyroidism which is a criterion of achalasia[32]. We had one clinical hypothyroid patient and one clinical hyperthyroid patient detected before balloon dilation therapy. We treated these two patients with levothyroxine and methimazole respectively for 6 mo after achievement of euthyroid state. No clinical or radiological improvements were obtained in symptomatology and radiological findings of achalasia after treatment, suggesting that what we found is actually a true association rather than a symptomatic mimicry or a transient neurological dysfunction. We also found a 6% positive ANA in this series which is similar to that in general population[46]. These findings may give some stronger evidence for certain autoimmune bases of achalasia. However, more and larger groups are necessary and a larger spectrum of autoimmune markers must be tested to make it possible to establish the utility of the issue in the early diagnosis of achalasia and identification of different etiologic mechanisms, which would allow us to think about novel outline of management since the existing treatments are only partially palliative.

We also found a hypothyroid shock after balloon dilation therapy which was fortunately well managed because we were alert to the problem. Therefore we recommend clinical evaluation of thyroid disease for all patients and thyroid function test for suspicious cases to control thyroid function before any invasive therapy. Clinical severity was statistically similar in both groups of patients with normal and abnormal thyroid function tests. Therefore we cannot predict the possibility of thyroid disease on the basis of severity indexes.

In conclusion, achalasia may be associated with thyroid diseases (hypothyroidism, hyperthyroidism and thyroid nodules), and this association should be kept in mind when a new case of achalasia is diagnosed. More accurate and extensive immunopathological studies should be performed to assess the possibility of a common immunopathogenesis or a cause and effect relationship in these diseases.

ACKNOWLEDGMENTS

The authors thank Ziba Farajzadegan MD, Hamid Tavakoli MD, Mehran Haghighi MD, Abbas Esmaeili MD, Peyman

Adibi MD, Ali Akbar Vosughi MD, Mandana Soleymani MS, and other Poursina Hakim colleagues for their superb assistance in executing, coordinating and analyzing this project.

REFERENCES

1 **Goldblum JR**, Rice TW, Richter JE. Histopathologic features in esophagomyotomy specimens from patients with achalasia. *Gastroenterology* 1996; **111**: 648-654
2 **Clark SB**, Rice TW, Tubbs RR, Richter JE, Goldblum JR. The nature of the myenteric infiltrate in achalasia: an immunohistochemical analysis. *Am J Surg Pathol* 2000; **24**: 1153-1158
3 **Paterson WG**. Etiology and pathogenesis of achalasia. *Gastrointest Endosc Clin N Am* 2001; **11**: 249-266, vi
4 **Vaezi MF**, Richter JE. Diagnosis and management of achalasia. American College of Gastroenterology Practice Parameter Committee. *Am J Gastroenterol* 1999; **94**: 3406-3412
5 **Wong RK**, Maydonovitch CL, Metz SJ, Baker JR. Significant DQw1 association in achalasia. *Dig Dis Sci* 1989; **34**: 349-352
6 **Verne GN**, Sallustio JE, Eaker EY. Anti-myenteric neuronal antibodies in patients with achalasia. A prospective study. *Dig Dis Sci* 1997; **42**: 307-313
7 **Verne GN**, Hahn AB, Pineau BC, Hoffman BJ, Wojciechowski BW, Wu WC. Association of HLA-DR and -DQ alleles with idiopathic achalasia. *Gastroenterology* 1999; **117**: 26-31
8 **Casella RR**, Ellis FH Jr, Brown AL. Fine structure changes in achalasia of the esophagus. II. Esophageal smooth muscle. *Am J Pathol* 1965; **46**: 467-475
9 **Friesen DL**, Henderson RD, Hanna W. Ultrastructure of the esophageal muscle in achalasia and diffuse esophageal spasm. *Am J Clin Pathol* 1983; **79**: 319-325
10 **Mosley RG**, Reichelderfer M, Sengupta A, Singaram C. Innervation of an esophageal ectatic submucosal blood vessel in achalasia and a comparison with normals. *Am J Gastroenterol* 1994; **89**: 1874-1879
11 **Storch WB**, Eckardt VF, Junginger T. Complement components and terminal complement complex in oesophageal smooth muscle of patients with achalasia. *Cell Mol Biol* (Noisy-le-grand) 2002; **48**: 247-252
12 **von Herbay A**, Heyer T, Olk W, Kiesewalter B, Auer P, Enck P, Häussinger D, Frieling T. Autonomic dysfunction in patients with achalasia of the oesophagus. *Neurogastroenterol Motil* 1998; **10**: 387-393
13 **Niwamoto H**, Okamoto E, Fujimoto J, Takeuchi M, Furuyama J, Yamamoto Y. Are human herpes viruses or measles virus associated with esophageal achalasia? *Dig Dis Sci* 1995; **40**: 859-864
14 **Birgisson S**, Galinski MS, Goldblum JR, Rice TW, Richter JE. Achalasia is not associated with measles or known herpes and human papilloma viruses. *Dig Dis Sci* 1997; **42**: 300-306
15 **De Giorgio R**, Di Simone MP, Stanghellini V, Barbara G, Tonini M, Salvioli B, Mattioli S, Corinaldesi R. Esophageal and gastric nitric oxide synthesizing innervation in primary achalasia. *Am J Gastroenterol* 1999; **94**: 2357-2362
16 **Mearin F**, Mourelle M, Guarner F, Salas A, Riveros-Moreno V, Moncada S, Malagelada JR. Patients with achalasia lack nitric oxide synthase in the gastro-oesophageal junction. *Eur J Clin Invest* 1993; **23**: 724-728
17 **Eckardt VF**, Aignherr C, Bernhard G. Predictors of outcome in patients with achalasia treated by pneumatic dilation. *Gastroenterology* 1992; **103**: 1732-1738
18 **Vaezi MF**, Richter JE, Wilcox CM, Schroeder PL, Birgisson S, Slaughter RL, Koehler RE, Baker ME. Botulinum toxin versus pneumatic dilatation in the treatment of achalasia: a randomised trial. *Gut* 1999; **44**: 231-239
19 **Podas T**, Eaden J, Mayberry M, Mayberry J. Achalasia: a critical review of epidemiological studies. *Am J Gastroenterol* 1998; **93**: 2345-2347
20 **Zilberstein B**, de Cleva R, Gabriel AG, Neto SG, Gama-Rodrigues JJ. Congenital achalasia: facts and fantasies. *Dis Esophagus* 2005; **18**: 335-337
21 **Gockel I**, Bohl JR, Junginger T. Achalasia: new insights in pathogenesis. *Am J Gastroenterol* 2006; **101**: 202-203
22 **Csendes A**, Smok G, Braghetto I, González P, Henríquez A, Csendes P, Pizurno D. Histological studies of Auerbach's plexuses of the oesophagus, stomach, jejunum, and colon in patients with achalasia of the oesophagus: correlation with gastric acid secretion, presence of parietal cells and gastric emptying of solids. *Gut* 1992; **33**: 150-154
23 **Storch WB**, Eckardt VF, Wienbeck M, Eberl T, Auer PG, Hecker A, Junginger T, Bosseckert H. Autoantibodies to Auerbach's plexus in achalasia. *Cell Mol Biol* (Noisy-le-grand) 1995; **41**: 1033-1038
24 **Raymond L**, Lach B, Shamji FM. Inflammatory aetiology of primary oesophageal achalasia: an immunohistochemical and ultrastructural study of Auerbach's plexus. *Histopathology* 1999; **35**: 445-453
25 **Dantas RO**, Meneghelli UG. Achalasia occurring years after acute poliomyelitis. *Arq Gastroenterol* 1993; **30**: 58-61
26 **Benini L**, Sembenini C, Bulighin GM, Polo A, Ederle A, Zambito A, Vantini I. Achalasia. A possible late cause of postpolio dysphagia. *Dig Dis Sci* 1996; **41**: 516-518
27 **Castex F**, Guillemot F, Talbodec N, Colombel JF, Paris JC, Cortot A. Association of an attack of varicella and an achalasia. *Am J Gastroenterol* 1995; **90**: 1188-1189
28 **Kountouras J**, Zavos C, Chatzopoulos D. Apoptosis and autoimmunity as proposed pathogenetic links between *Helicobacter pylori* infection and idiopathic achalasia. *Med Hypotheses* 2004; **63**: 624-629
29 **Firouzi M**, Keshavarzian A. Guillain-Barre syndrome and achalasia: two manifestations of a viral disease or coincidental association? *Am J Gastroenterol* 1994; **89**: 1585-1587
30 **Johnston BT**, Colcher A, Li Q, Gideon RM, Castell JA, Castell DO. Repetitive proximal esophageal contractions: a new manometric finding and a possible further link between Parkinson's disease and achalasia. *Dysphagia* 2001; **16**: 186-189
31 **Allgrove J**, Clayden GS, Grant DB, Macaulay JC. Familial glucocorticoid deficiency with achalasia of the cardia and deficient tear production. *Lancet* 1978; **1**: 1284-1286
32 **Jaggy A**, Oliver JE. Neurologic manifestations of thyroid disease. *Vet Clin North Am Small Anim Pract* 1994; **24**: 487-494
33 **Tunbridge WM**, Evered DC, Hall R, Appleton D, Brewis M, Clark F, Evans JG, Young E, Bird T, Smith PA. The spectrum of thyroid disease in a community: the Whickham survey. *Clin Endocrinol* (Oxf) 1977; **7**: 481-493
34 **Hollowell JG**, Staehling NW, Flanders WD, Hannon WH, Gunter EW, Spencer CA, Braverman LE. Serum TSH, T(4), and thyroid antibodies in the United States population (1988 to 1994): National Health and Nutrition Examination Survey (NHANES III). *J Clin Endocrinol Metab* 2002; **87**: 489-499
35 **Gordin A**, Heinonen OP, Saarinen P, Lamberg BA. Serum-thyrotrophin in symptomless autoimmune thyroiditis. *Lancet* 1972; **1**: 551-554
36 **Okamura K**, Ueda K, Sone H, Ikenoue H, Hasuo Y, Sato K, Yoshinari M, Fujishima M. A sensitive thyroid stimulating hormone assay for screening of thyroid functional disorder in elderly Japanese. *J Am Geriatr Soc* 1989; **37**: 317-322
37 **Jacobson DL**, Gange SJ, Rose NR, Graham NM. Epidemiology and estimated population burden of selected autoimmune diseases in the United States. *Clin Immunol Immunopathol* 1997; **84**: 223-243
38 **Canaris GJ**, Manowitz NR, Mayor G, Ridgway EC. The Colorado thyroid disease prevalence study. *Arch Intern Med* 2000; **160**: 526-534
39 **Sawin CT**, Castelli WP, Hershman JM, McNamara P, Bacharach P. The aging thyroid. Thyroid deficiency in the Framingham Study. *Arch Intern Med* 1985; **145**: 1386-1388
40 **Heydarian P**, Azizi F. Thyroid dysfunction and autoantibodies 10 years after implementation of universal salt iodization: Tehran Thyroid Study, *Irn J Endocrinol Metab* 2003; **4**: 229-241
41 **Dayan CM**, Daniels GH. Chronic autoimmune thyroiditis. *N*

Engl J Med 1996; **335**: 99-107
42 **Knobel M**, Barca MF, Pedrinola F, Medeiros-Neto G. Prevalence of anti-thyroid peroxidase antibodies in autoimmune and nonautoimmune thyroid disorders in a relatively low-iodine environment. *J Endocrinol Invest* 1994; **17**: 837-842
43 **Mariotti S**, Caturegli P, Piccolo P, Barbesino G, Pinchera A. Antithyroid peroxidase autoantibodies in thyroid diseases. *J Clin Endocrinol Metab* 1990; **71**: 661-669
44 **Feldt-Rasmussen U**. Analytical and clinical performance goals for testing autoantibodies to thyroperoxidase, thyroglobulin, and thyrotropin receptor. *Clin Chem* 1996; **42**: 160-163
45 **Park W**, Vaezi MF. Etiology and pathogenesis of achalasia: the current understanding. *Am J Gastroenterol* 2005; **100**: 1404-1414
46 **Azizah MR**, Azila MN, Zulkifli MN, Norita TY. The prevalence of antinuclear, anti-dsDNA, anti-Sm and anti-RNP antibodies in a group of healthy blood donors. *Asian Pac J Allergy Immunol* 1996; **14**: 125-128

S- Editor Liu Y **L- Editor** Wang XL **E- Editor** Liu WF

PO Box 2345, Beijing 100023, China
www.wjgnet.com
wjg@wjgnet.com

World J Gastroenterol 2007 January 28; 13(4): 600-606
World Journal of Gastroenterology ISSN 1007-9327

RAPID COMMUNICATION

Analysis of immune responses against *H pylori* in rabbits

Khademul Islam, Ibrahim Khalil, Chowdhury Rafiqul Ahsan, Mahmuda Yasmin, Jamalun Nessa

Khademul Islam, Department of Genetic Engineering and Biotechnology, University of Dhaka, Dhaka 1000, Bangladesh
Ibrahim Khalil, Chowdhury Rafiqul Ahsan, Mahmuda Yasmin, Jamalun Nessa, Department of Microbiology, University of Dhaka, Dhaka 1000, Bangladesh
Supported by Research Funds of Microbiology Department, Dhaka University
Correspondence to: Dr. Jamalun Nessa, Assistant Professor, Department of Microbiology, University of Dhaka, Dhaka 1000, Bangladesh. jamalun17@yahoo.com
Telephone: +880-2-966192073-7745 Fax: +880-2-8615583
Received: 2006-08-08 Accepted: 2006-11-21

Abstract

AIM: To investigate the immunogenicity of *H pylori* proteins, to evaluate the production rate of anti *H pylori* IgG antibodies in relation to time and to demonstrate the fidelity of newly optimized in-house enzyme-linked immunosorbent assay (ELISA) technique as an alternative for *H pylori* infection assay.

METHODS: In the present study, 100 μg of formalin-fixed *H pylori* whole cell antigens was injected into an experimental animal (New Zealand white female rabbit) intramuscularly on d 0, 16, 27 and 36. The first two doses were injected with adjuvants. On d 0, a serum sample was collected from the rabbit before immunization and this pre-immunized serum was used as a negative control for the whole study. To evaluate the immunogenic responses of the injected antigen, serum samples were collected from the rabbit at regular intervals up to d 42. The sera were analyzed using in-house ELISA and Western blot techniques.

RESULTS: The production of anti *H pylori* IgG antibodies in the rabbit in response to the injected antigen increased almost exponentially up to d 14 and after that it was maintained at the same level until the last day (d 42). By analyzing the immune profiles of immunized sera, 11 proteins were identified to be immunogenic, among them 2 (approximately 100 kDa and 85 kDa) were most prominent.

CONCLUSION: Analysis of the immune responses against pathogenic microorganisms like *H pylori* is necessary for the development of various diagnostic and preventive approaches. The results of this experiment reveal that the formalin-fixed *H pylori* whole cell antigens injected into the rabbit are highly immunogenic. These prominent proteins (approximately 100 kDa and 85 kDa) might have higher immunogenic effects among humans infected with *H pylori* and some of these immunogenic proteins can be included in diagnostic approaches based on serology and also for vaccine formulation. The in-house ELISA is a promising alternative compared to invasive techniques.

Key words: *H pylori*; Whole cell antigen; Immunogenicity; Rabbit; Serum antibody kinetics; In-house enzyme-linked immunosorbent assay

Islam K, Khalil I, Ahsan CR, Yasmin M, Nessa J. Analysis of immune responses against *H pylori* in rabbits. *World J Gastroenterol* 2007; 13(4): 600-606

http://www.wjgnet.com/1007-9327/13/600.asp

INTRODUCTION

In the early 1980's, Barry Marshall and Robin Warren of Australia discovered the bacterium *H pylori* in the stomach lining of patients with chronic gastritis and peptic ulcers[1]. The discovery of the infective organism *H pylori* and its involvement in these diseases has changed our views on how to diagnose and treat these diseases. Strains carrying the genes encoding the cytotoxin-associated protein (Cag-A) cause chronic active gastritis[2]. Gastric infection with *H pylori* is one of the common chronic infections in humans, causing substantial morbidity and some mortality[3]. Before an active protective response occurs, the gut must first be exposed to *H pylori*, which is a slowly growing microaerophilic, highly motile, Gram-negative spiral organism whose most striking biochemical characteristic is the abundant production of urease[4]. Colonization of *H pylori* in the gastric epithelium leads to a chronic inflammatory reaction[5-7]. Such a reaction may involve specific IgG and/or IgA antibody responses against the bacterium both in the peripheral blood and in the gastric mucosa. However, despite the production of such antibodies, the microorganism usually persists and gastritis progresses chronically through unknown mechanisms[8].

H pylori infection and peptic ulcer disease are more common in developing countries than in developed countries. Until the mid 1980s, it was felt that one or more of these factors working together could lead to the development of gastritis and ulcers. Since then, evidence has been mounting that *H pylori* has a major role in causing these diseases. Today the standard triple antibiotic

therapy is amoxicillin, clarithromycin and proton pump inhibitors such as omeprazole. Unfortunately, an increasing number of infected individuals are found to harbour bacteria resistant to first-line antibiotics. This results in initial treatment failure and requires additional rounds of antibiotic therapy[9]. One of the promising recent developments in medicine is the concept that chronic afflictions, such as peptic ulcer disease and cancer, can be controlled through immunization like classic infectious diseases. One approach has been the oral administration of purified recombinant subunit proteins of *H pylori* and a mucosal adjuvant, the labile toxin (LT) of Escherichia coli[10,11]. As a single-component vaccine, urease protein has shown some prophylactic and therapeutic activity in animal models and partial therapeutic activity in humans[12]. Another research was directed at the comparison of adjuvants and vaccine delivery systems and toward the immunologic mechanisms mediating protection[13].

Serological methods for detection of *H pylori* infection have reached sufficient accuracy and can be used as screening tests before endoscopy or for seroepidemiological surveys[4]. A number of different serological techniques have been used to detect antibodies, including haemagglutination, complement fixation, coagglutination, indirect immunofluorescence and latex agglutination[14]. Antibodies developed in rabbits against *H pylori* antigen can easily be detected by slide agglutination test. However, immunoblotting and enzyme-linked immunosorbent assay (ELISA) have emerged as the most frequently used techniques. A combination of immunoblotting and ELISA is the most efficient means of detecting serum antibodies to *H pylori* antigens and can be applied to the screening of rabbit sera for *H pylori*-specific antibodies[15]. These two techniques can be used in analysis of immune responses against *H pylori* in rabbits.

It is difficult to eradicate *H pylori* by antibiotic therapy and to date no vaccine is available for use in humans[16]. An effective vaccine would be a desirable way to control *H pylori*-induced gastric disease. Initial studies in animal models have demonstrated the feasibility of immunization, thus leading to high hopes for a human vaccine. In the mouse model, immunological approaches have to date not brought a satisfactory explanation for the mechanisms of protection against this largely luminal pathogen. In the present study, we used a rabbit model with whole cell extract from *H pylori* as antigen to analyze the immune responses.

MATERIALS AND METHODS

Animals

In this study, two healthy New Zealand white female rabbits aged 2 mo (weighing 2 kg) were used for serum antibody response. Although other strains of rabbits (e.g., Californian, Giant blank, Beveren etc) were available, this strain could easily adapt to the tropical area like Bangladesh (studied area). A great care was taken during the study with proper feeding and supplying adequate amount of fresh water daily. Rabbit house was cleaned daily. During the study, the climate was fine. Hygiene condition was maintained properly.

Preparation of whole cell antigen

Bacterial cells were grown and harvested from agar plates. Bacterial cells were suspended in phosphate buffered saline (PBS) containing 1% (w/v) formalin and kept at 4℃ for 1 h. The cells were then centrifuged at 12 500 × *g* for 5 min and the pellet was resuspended in 1 mL of PBS. The cells were washed 4 times in PBS to remove the formalin. Finally, a suspension of 1 mg/mL cells in PBS was made.

Preparation of antigen adjuvant mixture

H pylori antigens were administered in combination with incomplete Freund's adjuvant (which does not contain killed mycobacteria) to enhance the response to the first two doses. Freund's adjuvant is a water-in-oil emulsion consisting primarily of mineral oil. The oil acts as a repository, which releases the immunogen. The mixture was prepared by taking 250 μL of *H pylori* whole cell antigen (formalin fixed, 1 mg/mL, stored at -20℃) with 250 μL of incomplete Freund's adjuvant and then 200 μL of antigen-adjuvant mixture was injected intramuscularly.

Immunization of rabbits

Using a 22G needle, rabbits were immunized intramuscularly with whole cell antigen adjuvant mixture on d 0 and 16. Subsequent doses without adjuvant were administered on d 27 and 36. However, before immunization 1.5 mL blood was collected from the marginal vein of the ear for collecting pre-immunization sera. This was used as a negative control.

Blood collection

After immunization, rabbit blood were collected from marginal ear vein on d 0, 7, 17, 21, 27 and 35. Blood was also collected by cardiac puncture on d 42. Serum was separated from these blood samples and analyzed for antibody response by in-house ELISA and immunoblot techniques.

In-house ELISA

An aliquot of formalin-fixed bacteria was diluted in coating buffer to a final concentration of 1 μg/100 μL. One hundred μL of antigen preparation was added to all the wells except wells A1 and B1, which were used to calibrate the ELISA reader. The plates were covered with plate sealer and incubated at 4℃ overnight. On the following day, the plates were washed 3 times with PBS containing 0.05% Tween-20 (PBS-Tween 20). The wells were blocked with 200 μL of 1% (w/v) bovine serum albumin (BSA) in PBS, and then plates were incubated at 37℃ for 30 min. The PBS-BSA was discarded and the plates were washed 3 times with PBS-Tween 20. Then, 100 μL of diluted serum samples (neat, 1:50, 1:100, 1:200, 1:400 and 1:800 dilution in PBS) collected on d 7, 14, 21, 27, 35 and 42 was added into each of two consecutive wells, i.e. duplicate wells were used for each sample and each dilution. To the wells A1 and B1, 100 μL of PBS was added. The plate was covered with the plate sealer and incubated at room temperature for 2 h. The plate was

then washed three times as described above and 100 μL of diluted secondary antibody conjugate (1:3000 in PBS) was added (goat anti-rabbit polyvalent antibody conjugated with alkaline phosphatase; A-3937, Sigma Chemical Co, Ltd. UK), and incubated at room temperature for 2 h. The plate was again washed three times with PBS Tween-20 and 200 μL of 1 mg/mL substrate (p-nitrophenyl phosphate in diethanolamine buffer) was added to each well. The plate was placed in dark and an optical density (A_{405}) was measured after exactly 25 min. In this study, a sample was considered positive for antibodies to *H pylori* if the absorbance of the reaction was ⩾ 1. Any value < 1 was considered seronegative[17]. For the validation of the experiment, a positive serum sample from humans was tested by in-house ELISA using similar dilution (Neat, 1:50, 1:100, 1:200, 1:400, and 1:800). For ELISA, all the tests were done in duplicate well to minimize the handling error. The average of the two values from duplicate well was used for further data analysis.

Immunoblot

The 7 serum samples collected from rabbits on d 7, 14, 21, 35 and 42 were examined by immunoblot assay to check the immunological response of the pre-immunized polyclonal rabbit serum to the antigens from whole cell extract of *H pylori*.

Preparation of whole cell extracts for SDS-PAGE

After confluent growth, bacterial cells were harvested and taken into preweighed, screw-capped Eppendorf tubes. Bacteria were sedimented by centrifugation at 12500 × *g* for 2 min and suspended in sodium dodecyl sulphate-polyacrylamide gel electrophoresis (SDS-PAGE) solubilization buffer[18] to a cell concentration of 500 μg cells per 5 μL. The suspension was incubated at 100℃ for 5 min to denature bacterial proteins and DNA was disrupted by brief sonication (30 s). The suspension was reheated at 100℃ for 2 min and then diluted in SDS-PAGE solubilization buffer to produce a final concentration of 70 μg whole cell extract per 5 μL. The aliquots were stored at -20℃ for SDS-PAGE.

SDS-PAGE

The SDS-PAGE profile of whole cell extract was prepared as described previously[19]. Gels comprised a 4.5% (w/w) acrylamide stacking gel and a 12.5% (w/w) acrylamide separation gel. Samples were applied to gels alongside protein molecular weight standards (1610305; Bio-Rad, UK). Electrophoresis was performed using a minigel system (Consort, UK) with a constant current of 40 mA for 40 min. Gels were either stained with Coomassie blue[19] or used for immunoblotting.

Immunoblotting

H pylori serostatus in all serum samples was determined by immunoblot technique as described previously[20]. The SDS-PAGE protein profiles were transferred onto nitrocellulose sheets[21] using a semidry electrotransfer apparatus (Bio-Rad). Individual protein profiles were prepared by cutting nitrocellulose sheets into strips. Strips were incubated separately with different rabbit serum (1:200 dilution in 3% skimmed milk) samples (primary antibody). Antibody-antigen complexes were detected with a goat anti-rabbit polyvalent antibody conjugated with alkaline phosphatase, diluted 1:5000 in 3% skimmed milk. Color development was carried out in a polythene bag at 37℃ in the dark for 10 min. Individual serum antibodies binding to five or more protein bands were considered positive results and those binding to less than five protein bands were considered negative results[20].

Table 1 Serum antibody response in rabbit to *H pylori* whole cell antigen detected by in-house ELISA

		Dilution of sera				
Serum collection	Neat	1:50	1:100	1:200	1:400	1:800
d 0	0.998	0.847	0.620	0.063	0.024	Not done
d 7	2.777	2.562	2.029	1.835	1.245	1.028
d 14	2.003	3.136	2.792	2.241	0.408	1.404
d 21	3.004	3.267	2.857	3.303	2.973	1.974
d 27	2.805	2.894	2.021	2.074	2.323	1.004
d 35	2.62	2.958	3.128	2.947	3.112	2.857
d 42	3.002	2.945	2.763	2.719	2.999	3.303

RESULTS

The serum collected from two rabbits for six weeks was examined for antibodies specific for antigen using in-house ELISA. Absorbance values ⩾ 1 at 405 nm were considered seropositive (Table 1). The collected immunized sera from rabbits were evaluated and the result supported that the experimental animal (rabbit) was effectively immunized with *H pylori* whole cell antigen. For the validation of the experiment, a positive serum sample from humans was tested by using similar dilution (Neat, 1:50, 1:100, 1:200, 1:400, 1:800). The ELISA values (OD_{405}) from all dilutions showed presence of adequate amount of anti *H pylori* antibody. There was also a negative control serum collected from the rabbit on d 0 (before immunization with formalin-fixed *H pylori* whole cell antigen). The ELISA values from different dilutions showed that the negative control serum had no antibodies against *H pylori* antigen. Using ELISA values for 1:50 dilution on different days (0, 7, 14, 21, 27, 35, and 42) a plot of antibody titer versus time was drawn (Figure 1). Similar results were obtained from other dilutions (neat, 1:50, 1:100, 1:200, 1:400 and 1:800) (data not shown). The graph showed a significant increase in anti *H pylori* antibody production with time. After immunization, the production of anti *H pylori* antibody increased almost exponentially up to d 14 and after that, it maintained at the same level until the last day.

The serum samples collected from the rabbit were examined by immunoblot assay. A variable number of protein bands were observed among the immune profiles (Figure 2). Serum sample collected on d 0 represented pre-immunized serum and no visible protein band was observed, indicating absence of anti *H pylori* antibody. Several protein bands in other samples (collected on d 7, 14, 21, 27, 35 and 42) suggested that tested sera

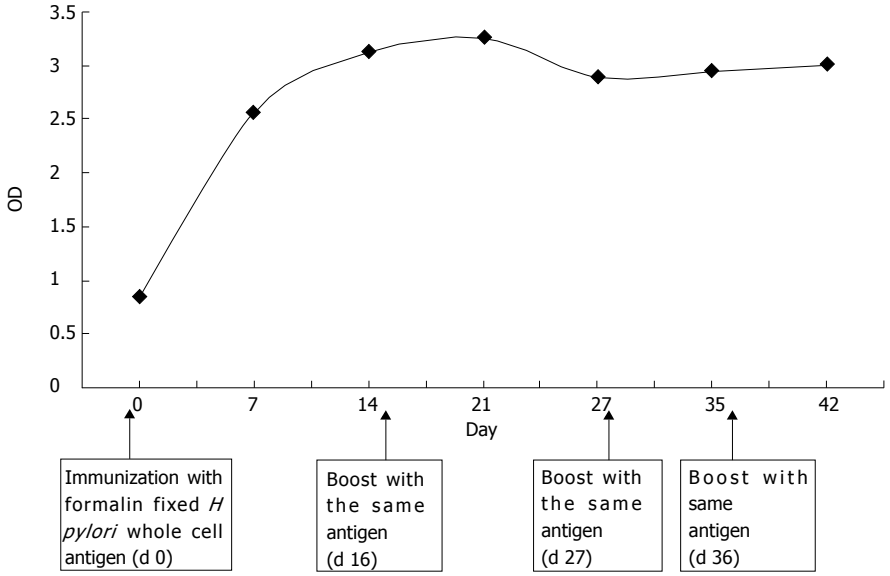

Figure 1 Kinetics of anti *H pylori* antibody responses in rabbits. Female rabbits were infected with formalin-fixed *H pylori* whole cell antigens and blood samples were collected at various time points after *H pylori* infection. Sera (1:50 dilution) were subjected to ELISA for antibody titer measurement (in terms of OD). The arrows indicate the time points when rabbits were challenged with antigens (booster dose).

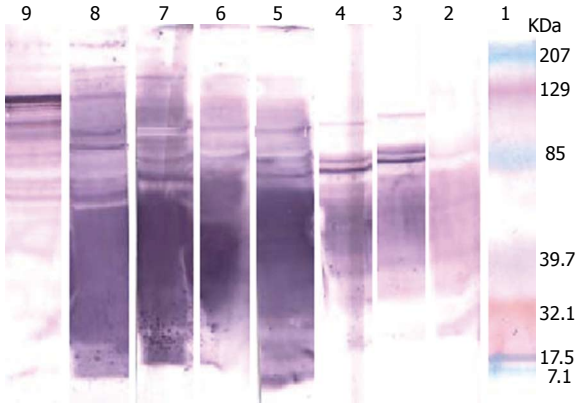

Figure 2 Western blot with whole cell extracts of *H pylori* against previously immunized rabbit sera and a human serum. Lane 1: molecular weight marker; lanes 2 to 8: serum collected on d 0, 7, 14, 21, 28, 35, and 42 respectively; lane 9: positive human serum.

had antibodies against *H pylori*. Immunoreactivity of the protein bands increased gradually from d 7 to d 42, suggesting that the production of antibody against *H pylori* increased with time in the rabbit. A positive serum sample from humans was also tested and found to have antibodies against that antigen.

The presence or absence of anti *H pylori* antibodies in pre-immunized and immunized rabbits was examined by in-house ELISA and immunoblotting. The findings from the two immunoassays showed a significant correlation ($P = 0.001$) (Table 2).

Table 2 Serum antibody responses of subjects to *H pylori* antigens detected by immunoblotting and in-house ELISA

Collection of serum samples	Sera with antibodies by immunoblotting[1]	Sera with antibodies by ELISA[2]
d 0	-	-
d 7	+	+
d 14	+	+
d 21	+	+
d 27	+	+
d 35	+	+
d 42	+	+

[1]In immunoblotting more than 4 protein bands indicated positive results; [2]When ELISA values were $\geqslant 1.0$, OD_{405} was considered positive results.

DISCUSSION

Current antibiotic regimens against *H pylori* infection may be effective, but complex dosing and development of resistance are always concerns. Animal studies and limited clinical trials of *H pylori* antigens have been conducted, with no final conclusive findings. A number of data now exist, supporting the potential for protection against *H pylori*. However, we are still at a preliminary stage in clinical development. The best immunogens, the best mode of presentation, the number of doses needed, optimal age at immunization, expected benefit, cost-effectiveness, and other factors involved in vaccine development require further study[13]. The present study employed rabbits to clarify the immunogenicity of *H pylori* proteins and to evaluate the production rate of anti *H pylori* IgG antibodies in relation to time.

For serological diagnosis of *H pylori* infection, immune responses against the relevant microorganism can be analyzed in experimental animal models. When endoscopy is not performed, the most commonly used diagnostic approach is the laboratory-based serological test. Enzyme-linked immunosorbent assay (ELISA) detects various classes of antibodies to *H pylori*, indicating current or past infection. Because *H pylori* infection is not known to spontaneously resolve, a positive serologic test suggests active infection in patients who have not undergone eradication therapy[22]. Although *H pylori* is not an invasive bacterium, it actively stimulates the immune system in its host by releasing lipopolysaccharides and immunogenic proteins. An immune response accompanies the presence of the bacterium in 98% of the cases[23]. The sensitivity and specificity of ELISA to identify infectious microorganisms are quite high. In the present study, since the antibody

response occurred a few days after a new infection or after a booster dose of antigen with or without adjuvant, the subject had to mount a strong immune response

IgG usually appears several days after *H pylori* infection in rabbits. But after eradication of *H pylori*, the drop in antibody titer is not significant until the 6th mo in humans[24]. In the present study, specific IgG antibodies to *H pylori* were detected in rabbit sera with the help of enzyme immunoassay. Analysis of serum samples by in-house ELISA technique is an alternative for *H pylori* infection assay. The present study evaluated the noninvasive methods to screen for *H pylori* infection in rabbits. The relationship between time course and magnitude of antibody response showed the kinetics of the development of specific antibody responses in the studied animals (Figure 1). A clear kinetics of the development of anti *H pylori* antibody response found in the rabbit showed a significant increase in anti *H pylori* IgG antibody production with time. After immunization, the production of anti *H pylori* antibody increased almost exponentially up to d 14 and after that, it maintained at the same level till the last day of serum collection. The ELISA values from different dilutions showed that the negative control serum had no antibodies against *H pylori* antigen. However, 1:400 dilution of serum (collected at d 14) showed a negative ELISA value, which could be due to the handling error.

A large number of different proteins present in single cells and may play a major antigenic role in infection. The complex pathogenesis of this infection[25,26], including the presence of antigens on *H pylori* in the host[27], demands better approaches to the identification of novel immunogens that would give substantial protection. The selection of defined and well-characterized antigens appears to be the most viable approach. The present in-house ELISA with formalin-fixed whole cell antigens had a high diagnostic value for studied animals. Antibody was raised against whole cell antigens which were at first confirmed by the slide agglutination test. The collected sera subjected to immunoblot analysis showed a number of antibody bands. Some bands were more prominent than others in relation to color intensity. Previous studies revealed that *H pylori* whole cell lysate contains protein bands like CagA (140-121 kDa), VacA (87 kDa), heat-shock protein (60 kDa), two urease subunits of 62 and 26 kDa and thiol peroxidase (18 kDa)[28], suggesting that the concentration of some proteins from the whole cells is high. These proteins might have immunogenic effects in the rabbit. By analyzing the immune profiles of immunized serum samples collected at regular intervals from the rabbit, 11 proteins were identified to be immunogenic, of which 2 were more prominent than others (approximately 100 kDa and 85 kDa). Haque *et al*[29] showed that approximately 61 kDa, 58 kDa and 24 kDa proteins from whole cell extract of *H pylori* are immunogenic. However, they could not prove it conclusively. The present study identified two such potential antigens which were proved most potent in eliciting protective immunity.

It is reasonable to assume that more than one protective component is needed in a vaccine[13]. Therefore the previously identified urease[8] or catalase[30] alone could not be used for final vaccine formulation. There is also concern about inducing an immune response to heat shock protein B (HspB) because this protein has homologies to the GroEL family of heat shock proteins[31]. In the present study, we demonstrated some potential immunogens which could give better protection and could be used for diagnosis purpose.

Adjuvant is an important component of any vaccine. It is responsible for stimulating immune system. In some previous trials[10,30], cholera toxin was used as adjuvant for immunization of mice. However this effort might raise multiple problems including safety. E. coli heat-labile toxin (LT) that was used as an oral adjuvant in humans does not show a significant decrease in gastric *H pylori* density but is associated with cramping and diarrhea[32]. Due to all these adverse effects, no suitable and safe adjuvants are currently available for use in humans[33]. However, in the present study an incomplete form of Freund's adjuvant not containing such a cytotoxic agent was used to enhance the immune response. Therefore, this adjuvant could be considered a substitute to cholera toxin or other toxic adjuvants.

The identified proteins might have higher immunogenic effects among humans infected with *H pylori* and some of these immunogenic proteins could be included in diagnostic approaches based on serology and also in vaccine preparation. However, further characterization of these antigens is required. Finally, in-house ELISA and immunoblot can be better applied in analysis of antigenic response in experimental animal model (rabbits).

COMMENTS

Background

Gastric infection with *H pylori* is one of the common chronic infections in humans, causing substantial morbidity and some mortality. Still there is still no effective vaccine against *H pylori,* a causative agent of gastric and peptic ulcer. We are still at a preliminary stage in clinical development. The best immunogens, the best mode of presentation, the number of doses needed, optimal age at immunization, expected benefit, cost-effectiveness, and other factors involved in vaccine development require further study. Initial studies in animal models have demonstrated the feasibility of immunization, thus leading to high hopes for a human vaccine. In the mouse model, immunological approaches have to date not brought a satisfactory explanation for the mechanisms of protection against this largely luminal pathogen. In the present study, we used a rabbit model with the whole cell extract antigens from *H pylori*.

Research frontiers

H pylori infection is a newly discovered stomach infection which was first reported by Barry Marshall and Robin Warren of Perth, Western Australia, in 1983, who were awarded the Nobel Prize in Medicine in 2005 for their work on *H pylori*. The Sydney gastroenterolgist Thomas Borody invented the first triple therapy in 1987. Such a therapy has revolutionized the treatment of gastric ulcer. Mode of infection, mechanism of pathogenesis, host immune response, chemotherapy and vaccine development are important areas of research.

Innovations and breakthroughs

Initial studies in animal models have demonstrated the feasibility of immunization, thus leading to high hopes for a human vaccine against *H pylori*. In the mouse model, immunological approaches have to date not brought a satisfactory explanation for the mechanisms of protection against this luminal pathogen. In the present study, we used a rabbit model with the whole cell extract from *H pylori* as antigen. The experiment identified two prominent proteins (approximately 100 kDa and 85 kDa) which have higher immunogenic effects among humans infected with

H pylori and some of these immunogenic proteins could be included in diagnostic approaches based on serology and also for vaccine formulation. Most of the previous studies used cholera toxin as adjuvants which have some side effects. In the present study, we used an incomplete form of Freund's adjuvant which does not contain cytotoxic agent. We established and optimized the low cost, non-invasive in-house ELISA technique for the detection of *H pylori* infection in Bangladeshi people.

Applications

Analysis of the immune responses against pathogenic microorganisms like *H pylori* is necessary for the development of various diagnostic and preventive approaches. The results of our experiment reveal that formalin-fixed *H pylori* whole cell antigens injected into the rabbit are highly immunogenic. These prominent proteins (approximately 100 kDa and 85 kDa) might have higher immunogenic effects among humans infected with *H pylori* and some of these immunogenic proteins could be included in diagnostic approaches based on serology. The in-house ELISA is a promising alternative in the developing countries compared to high cost invasive techniques.

Terminology

Freund's adjuvant is an antigen solution emulsified in mineral oil, and can be used as an immunopotentiator (booster of the immune system). The so-called complete form (FCA) is composed of inactivated and dried mycobacteria, usually Mycobacterium tuberculosis (the pathogenic agent of tuberculosis). The so-called incomplete form (FIA) is the same adjuvant without the mycobacterial components and is named after Jules T. Freund (1890-1960), a Hungarian-born American immunologist.

Peer review

It is an interesting study. The science seems good and the study is well performed. The results are also of interest.

REFERENCES

1 **Van den Bulck K**, Decostere A, Baele M, Marechal M, Ducatelle R, Haesebrouck F. Low frequency of Helicobacter species in the stomachs of experimental rabbits. *Lab Anim* 2006; **40**: 282-287

2 **Aucher P**, Petit ML, Mannant PR, Pezennec L, Babin P, Fauchere JL. Use of immunoblot assay to define serum antibody patterns associated with Helicobacter pylori infection and with H. pylori-related ulcers. *J Clin Microbiol* 1998; **36**: 931-936

3 **Lepper PM**, Möricke A, Vogt K, Bode G, Trautmann M. Comparison of different criteria for interpretation of immunoglobulin G immunoblotting results for diagnosis of Helicobacter pylori infection. *Clin Diagn Lab Immunol* 2004; **11**: 569-576

4 **Barrow GI** , Felthem RKA. Cown and Steel's Manual for the Identification of Medical Bacteria. 3rd editors. London: Cambrigde University Press, 2004: 121-130

5 **Berstad AE**, Brandtzaeg P, Stave R, Halstensen TS. Epithelium related deposition of activated complement in Helicobacter pylori associated gastritis. *Gut* 1997; **40**: 196-203

6 **Karttunen R**, Karttunen T, Ekre HP, MacDonald TT. Interferon gamma and interleukin 4 secreting cells in the gastric antrum in Helicobacter pylori positive and negative gastritis. *Gut* 1995; **36**: 341-345

7 **Mai UE**, Perez-Perez GI, Wahl LM, Wahl SM, Blaser MJ, Smith PD. Soluble surface proteins from Helicobacter pylori activate monocytes/macrophages by lipopolysaccharide-independent mechanism. *J Clin Invest* 1991; **87**: 894-900

8 **Futagami S**, Takahashi H, Norose Y, Kobayashi M. Systemic and local immune responses against Helicobacter pylori urease in patients with chronic gastritis: distinct IgA and IgG productive sites. *Gut* 1998; **43**: 168-175

9 **Mirbagheri SA**, Hasibi M, Abouzari M, Rashidi A. Triple, standard quadruple and ampicillin-sulbactam-based quadruple therapies for H. pylori eradication: a comparative three-armed randomized clinical trial. *World J Gastroenterol* 2006; **12**: 4888-4891

10 **Weltzin R**, Guy B, Thomas WD, Giannasca PJ, Monath TP. Parenteral adjuvant activities of Escherichia coli heat-labile toxin and its B subunit for immunization of mice against gastric Helicobacter pylori infection. *Infect Immun* 2000; **68**: 2775-2782

11 **Nyström J**, Raghavan S, Svennerholm AM. Mucosal immune responses are related to reduction of bacterial colonization in the stomach after therapeutic Helicobacter pylori immunization in mice. *Microbes Infect* 2006; **8**: 442-449

12 **Ermak TH**, Giannasca PJ, Nichols R, Myers GA, Nedrud J, Weltzin R, Lee CK, Kleanthous H, Monath TP. Immunization of mice with urease vaccine affords protection against Helicobacter pylori infection in the absence of antibodies and is mediated by MHC class II-restricted responses. *J Exp Med* 1998; **188**: 2277-2288

13 **Monath TP**, Lee CK, Ermak TH, Myers GA, Weltzin RA, Giannasca PJ, Thomas WD, Soman G, Bhagat H, Ackerman SA, Kleanthous HK. The Search for Vaccines Against Helicobacter pylori. *Infect in Med* 1998; **15**: 534-546

14 **Mayo K**, Pretolani S, Gasbarrini G, Ghironzi G, Megraud F. Heterogeneity of immunoglobulin G response to Helicobacter pylori measured by the unweighted pair group method with averages. *Clin Diagn Lab Immunol* 1998; **5**: 70-73

15 **Nessa J**, Chart H, Owen RJ, Drasar B. Human serum antibody response to Helicobacter pylori whole cell antigen in an institutionalized Bangladeshi population. *J Appl Microbiol* 2001; **90**: 68-72

16 **Axon AT**. Treatment of Helicobacter pylori: future therapeutic and prophylactic perspectives. *Gut* 1998; **43** Suppl 1: S70-S73

17 **Islam ABMMK**, Yasmin M, Ahasan R, Nessa J. Helicobacter pylori Infection in Bangladeshi Population: Serodiagnosis, Seroprevalence and Risk Factors. *Dhaka Univ J Biol Sci* 2005; **14**(1): 1-8

18 **Laemmli UK**. Cleavage of structural proteins during the assembly of the head of bacteriophage T4. *Nature* 1970; **227**: 680-685

19 **Chart H**, Jenkins C, Smith HR, Rowe B. Serum antibodies to secreted proteins in patients infected with Escherichia coli O157 and other VTEC. *Epidemiol Infect* 1998; **120**: 239-243

20 **Rahman F**, Islam ABMMK, Nessa J, Ahsan CR Yasmin M. Correlation in prevalence, risk factors and serological detection of Helicobacter pylori by different techniques. *Bangladesh J Microbiol* 2005; **22**: 152-157

21 **Towbin H**, Gordon J. Immunoblotting and dot immunobinding--current status and outlook. *J Immunol Methods* 1984; **72**: 313-340

22 **Feldman RA**, Eccersley AJ, Hardie JM. Epidemiology of Helicobacter pylori: acquisition, transmission, population prevalence and disease-to-infection ratio. *Br Med Bull* 1998; **54**: 39-53

23 **Tam YH**, Yeung CK, Lee KH. Seven-day is more effective than 4-day ranitidine bismuth citrate-based triple therapy in eradication of Helicobacter pylori in children: a prospective randomized study. *Aliment Pharmacol Ther* 2006; **24**: 81-86

24 **Kivi M**, Tindberg Y. Helicobacter pylori occurrence and transmission: a family affair? *Scand J Infect Dis* 2006; **38**: 407-417

25 **Blaser MJ**. Helicobacter pylori and the pathogenesis of gastroduodenal inflammation. *J Infect Dis* 1990; **161**: 626-633

26 **Labigne A**, de Reuse H. Determinants of Helicobacter pylori pathogenicity. *Infect Agents Dis* 1996; **5**: 191-202

27 **Appelmelk BJ**, Simoons-Smit I, Negrini R, Moran AP, Aspinall GO, Forte JG, De Vries T, Quan H, Verboom T, Maaskant JJ, Ghiara P, Kuipers EJ, Bloemena E, Tadema TM, Townsend RR, Tyagarajan K, Crothers JM, Monteiro MA, Savio A, De Graaff J. Potential role of molecular mimicry between Helicobacter pylori lipopolysaccharide and host Lewis blood group antigens in autoimmunity. *Infect Immun* 1996; **64**: 2031-2040

28 **Ji KY**, Hu FL. Interaction or relationship between Helicobacter pylori and non-steroidal anti-inflammatory drugs in upper gastrointestinal diseases. *World J Gastroenterol* 2006; **12**: 3789-3792

29 **Haque M**, Rahman KM, Khan AK, Hassan M, Miah MR, Qadri

F, Akhter Q. Antigen profile of Helicobacter pylori strains isolated from peptic ulcer patients in Dhaka, Bangladesh. *Bangladesh Med Res Counc Bull* 1993; **19**: 71-78

30 **Radcliff FJ**, Hazell SL, Kolesnikow T, Doidge C, Lee A. Catalase, a novel antigen for Helicobacter pylori vaccination. *Infect Immun* 1997; **65**: 4668-4674

31 **Ferrero RL**, Thiberge JM, Kansau I, Wuscher N, Huerre M, Labigne A. The GroES homolog of Helicobacter pylori confers protective immunity against mucosal infection in mice. *Proc Natl Acad Sci USA* 1995; **92**: 6499-6503

32 **Michetti P**, Kreiss C, Kotloff KL, Porta N, Blanco JL, Bachmann D, Herranz M, Saldinger PF, Corthésy-Theulaz I, Losonsky G, Nichols R, Simon J, Stolte M, Ackerman S, Monath TP, Blum AL. Oral immunization with urease and Escherichia coli heat-labile enterotoxin is safe and immunogenic in Helicobacter pylori-infected adults. *Gastroenterology* 1999; **116**: 804-812

33 **Arora S**, Czinn SJ. Vaccination as a method of preventing Helicobacter pylori-associated gastric cancer. *Cancer Epidemiol Biomarkers Prev* 2005; **14**: 1890-1891

S- Editor Liu Y **L- Editor** Wang XL **E- Editor** Lu W

PO Box 2345, Beijing 100023, China
www.wjgnet.com
wjg@wjgnet.com

World J Gastroenterol 2007 January 28; 13(4): 607-611
World Journal of Gastroenterology ISSN 1007-9327

RAPID COMMUNICATION

Beneficial effects of *Foeniculum vulgare* on ethanol-induced acute gastric mucosal injury in rats

Fatih Mehmet Birdane, Mustafa Cemek, Yavuz Osman Birdane, İlhami Gülçin, Mehmet Emin Büyükokuroğlu

Fatih Mehmet Birdane, Department of Internal Medicine, Faculty of Veterinary Medicine, Afyon Kocatepe University, Afyon, Turkey
Mustafa Cemek, Department of Chemistry (Biochemistry Division), Faculty of Science and Arts, Afyon Kocatepe University, Afyon, Turkey
Yavuz Osman Birdane, Department of Pharmacology and Toxicology, Faculty of Veterinary Medicine, Afyon Kocatepe University, Afyon, Turkey
İlhami Gülçin, Department of Chemistry, Faculty of Science and Arts, Atatürk University, Erzurum, Turkey
Mehmet Emin Büyükokuroğlu, Department of Pharmacology, Faculty of Medicine, Afyon Kocatepe University, Afyon, Turkey
Correspondence to: Mehmet Emin Büyükokuroğlu, Department of Pharmacology, Faculty of Medicine, Afyon Kocatepe University, Ali Çetinkaya Kampüsü, İzmir yolu 8. km TR-03200, Afyonkarahisar, Turkey. memin@aku.edu.tr
Telephone: +90-272- 2140152 Fax: +90-272-2142060
Received: 2006-05-25 Accepted: 2006-12-15

Abstract

AIM: To examine the anti-ulcerogenic and antioxidant effects of aqueous extracts of *Foeniculum vulgare* (FVE) on ethanol-induced gastric lesions in rats.

METHODS: FVE was administered by gavage at doses of 75, 150 and 300 mg/kg, and famotidine was used at the dose of 20 mg/kg. Following a 60 min period, all the rats were given 1 mL of ethanol (80%) by gavage. One hour after the administration of ethanol, all groups were sacrificed, and the gastric ulcer index was calculated; whole blood malondialdehyde (MDA) and reduced glutathione (GSH), serum nitrate, nitrite, ascorbic acid, retinol and β-carotene levels were measured in all the groups.

RESULTS: It was found that pretreatment with FVE significantly reduced ethanol-induced gastric damage. This effect of FVE was highest and statistically significant in 300 mg/kg group compared with the control (4.18 ± 2.81 *vs* 13.15 ± 4.08, $P < 0.001$). Also, pretreatment with FVE significantly reduced the MDA levels, while significantly increased GSH, nitrite, nitrate, ascorbic acid, retinol and β-carotene levels.

CONCLUSION: FVE has clearly a protective effect against ethanol-induced gastric mucosal lesion, and this effect, at least in part, depends upon the reduction in lipid peroxidation and augmentation in the antioxidant activity.

Key words: *Foeniculum vulgare*; Ethanol; Rat; Ulcer; Antioxidant

Birdane FM, Cemek M, Birdane YO, Gülçin İ, Büyükokuroğlu ME. Beneficial effects of *Foeniculum vulgare* on ethanol-induced acute gastric mucosal injury in rats. *World J Gastroenterol* 2007; 13(4): 607-611

http://www.wjgnet.com/1007-9327/13/607.asp

INTRODUCTION

Peptic ulcer is a common disorder of the gastrointestinal system and millions of people suffer from this disease in the world. The medical cost of treating peptic ulcer and its complications amounts to billions of dollars annually. The pathogenesis of peptic ulcer disease is multifactorial, including chronically using non-steroid anti- inflammatory drugs, cigarette smoking, alcohol, and reactive oxygen species (ROS). ROS are generated by cells in some physiological and pathological circumstances. Any derangement between pro-oxidants and antioxidants, in which pro-oxidants prevail is known as oxidative stress[1]. Insufficient antioxidant protection or excess production of ROS can result in this condition. ROS can react with all macromolecules, such as lipids, proteins, nucleic acids, and carbohydrates, particularly polyunsaturated fatty acids on cell membranes. After the beginning of an initial reaction with ROS, a continuing chain reaction is started and cell injury and, ultimately, cell death occur[2]. Peptic ulcer is produced by the imbalance between gastroduodenal mucosal defense mechanisms and offensive factors. Some studies have revealed that ROS and lipid peroxidation are implicated in the pathogenesis of ethanol-induced gastric lesions and gastrointestinal damage, and they attack and damage many biological molecules such as prostaglandins[3-5]. Therefore, treatment with antioxidants and free radical scavengers can decrease ethanol-induced gastric mucosal damage.

Foeniculum vulgare (FVE) is a well-known umbelliferous plant. For centuries, FVE fruits have been used as traditional herbal medicine in Europe and China. It is native to southern Europe and the Mediterranean area. The seeds of this plant have been known to be able to regulate menstruation, alleviate the symptoms of female climacteric syndrome, and increase libido[6]. FVE also

possesses emnenagague and galactagogue properties[7]. It has been reported that FVE could be used in the pediatric colic and some respiratory disorders due to its anti-spasmodic effects[8,9]. Seeds of it are used in folk remedies for treatment of dysmenorrhea. FVE (in Turkish "Rezene") is natively found in North and West regions of Turkey. It is cultivated for the herb as a spice (flavouring salads) and medicine in Turkey. Powders or tablets (0.5-1 g) of seeds, or its infusion forms (2%) are taken 2-3 times per day. As a medicinal plant, FVE has been used as an antispasmodic, carminative, diuretic, lactation stimulant, and as dressings for wounds in Turkish traditional medicine[10]. It contains 1%-3% of a volatile oil, which is composed of 50%-85% of anethole and about 20% of d-fenchone[11,12]. Other compunds present in FVE are d-a-pinene, d-a-phellandrene, dipentene, methyl chavicol, feniculun, anisaldehyde, and anisic acid[11,13].

The aim of this work was to assess the gastroprotective activity of FVE in rat models of experimentally ethanol-induced gastric lesions. In particular, we investigated the effects of aqueous extracts of FVE on gross mucosal lesions in the stomach, glutathione (GSH), nitrite, nitrate, ascorbic acid, retinol and β-carotene levels, and changes in lipid peroxidation determined by measuring malondialdehyde (MDA) levels in the blood.

MATERIALS AND METHODS

Plant material

The aerial parts of FVE were collected in June 2003 from Bursa. The plant was identified by the Department of Botany of Science and Arts Faculty, Atatürk University, Erzurum, Turkey, where a voucher specimen is kept.

Extraction and preparation of test samples

Air-dried FVE was pulverized with a blender. Obtained plant material (230 g) was mixed with boiling distilled water and stirred on the hot plate for 15 min. Subsequently, it was filtered over Whatman No.1 paper. Finally, the filtrate was frozen and lyophilized in a lyophilizator (Labconco, Freezone 1L, USA) at a 5 μmHg pressure and -50℃ (14.9 g).

Animals

Thirty-five Sprague-Dawley rats with a weight range of 190-225 g were used for the experimentation. The rats were fed with standard laboratory chow and water before the experiment. Rats were divided into 5 equal groups (n = 7) and housed in cages. Twenty-four hours before the experiment, the rats were fasted and allowed access to water *ad libitum*. The investigation was conducted in accordance with the Guide for the Care and Use of Laboratory Animals published by the US National Institutes of Health (NIH Publication no. 85-23, revised 1996) and approval has been received from our institutional Animal Ethics Committee.

Chemicals

Chemicals used in this investigation, GSH, thiobarbituric acid, phosphate buffer, butylated hydroxytoluene, trichloroacetic acid, EDTA, [5,5-dithiobis-(2-nitrobenzoic acid)], phenylendiamine, sodium azide, 2,4-dinitrophe nylhydrazine, ethanol, hexane, sodium nitrite, sodium nitrate, sulfanilamide, N-(1-Naphthyl) ethylenediamine dihydrochloride and vanadium (Ⅲ) chloride were purchased from Sigma. All the other chemicals and reagents used in this study were of analytical grade.

Ulcer study

The anti-ulcerogenic effect of FVE was investigated with the ethanol-induced ulcer model. On the first day of the experiment, groups 1, 2 and 3 were administered with 75, 150 and 300 mg/kg FVE, group 4 was administered with 20 mg/kg famotidine, and group 5 was administered with saline solution. All of drugs were administered by gavage at the same volume (0.5 mL). Following a 60 min period, all the rats were given 1 mL of ethanol (80%) by gavage. One hour after the administration of ethanol, rats were injected with a high dose of ketamine (100 mg/kg), blood samples were taken by cardiac punctures, and stomachs were removed and opened along the greater curvature and washed in physiological saline solution. For measurement of the gross gastric mucosal lesions, freshly excised stomachs were laid flat and the mucosal lesions were traced on clear acetate paper. Gross mucosal lesions were recognised as hemorrhage or linear breaks (erosions) with damage to the mucosal surface. The area of stomach tissue and gross lesions were approximately calculated by planimetry using a simple magnifier. The results were translated to the term of "total ulcer area/total gastric area" and these were expressed as an ulcer index (%).

Biochemical analysis

Fasting blood samples were drawn into heparin-free tubes during routine blood sampling for biochemical analysis. After immediate centrifugation (1000 g for 10 min at 4℃), the serum was stored in polystyrene plastic tubes at -70℃ until analysis. Whole blood was collected into heparinized tubes and whole blood MDA and GSH levels were studied on the same day of admission.

Whole blood MDA (as an important indicator of lipid peroxidation) levels were measured according to a method of Jain *et al*[14]. The principle of the method was based on the spectrophotometric measurement of the color developed during the reaction of thiobarbituric acid with MDA. Concentrations of thiobarbituric acid reactive substances (TBARS) were calculated by the absorbance coefficient of malondialdehyde–thiobarbituric acid complex and expressed as nmol/mL. Whole blood GSH concentrations were also measured by the spectrophotometric method[15]. The concentrations of nitric oxide (nitrate and nitrite) were detected by the methods of Miranda *et al*[16]. Nitrite and nitrate calibration standards were prepared by diluting sodium nitrite and sodium nitrate in pure water. After loading the plate with samples (100 μL), addition of vanadium (Ⅲ) chloride (100 μL) to each well was rapidly followed by addition of the Griess reagents, sulfanilamide (50 μL) and N-(1-Naphthyl) ethylenediamine dihydrochloride (50 μL). The Griess solutions may also be premixed immediately prior to application to the plate. Nitrite mixed with Griess

Table 1 Effects of aqueous extracts of *Foe* FVE and famotidine on ethanol-induced gastric mucosal injury in rats

Groups (n = 7)	Ulcer index (%) (mean ± SD)	Inhibition (%)
Control (ethanol)	13.15 ± 4.08	-
75 mg/kg FVE + Ethanol	8.18 ± 2.66	37.8
150 mg/kg FVE + Ethanol	9.48 ± 3.78	27.9
300 mg/kg FVE + Ethanol	4.18 ± 2.81[b]	68.2
20 mg/kg Famotidine + Ethanol	8.68 ± 2.63[a]	34

[a]$P < 0.05$, [b]$P < 0.001$, *vs* ethanol.

reagents forms a chromophore from the diazotization of sulfanilamide by acidic nitrite followed by coupling with bicyclic amines, such as N-1-(naphthyl) ethylenediamine. Sample blank values were obtained by substituting diluting medium for Griess reagent. Nitrite was measured in a similar manner except that samples and nitrite standards were only exposed to Griess reagents. The absorbance at 540 nm was read to assess the total level of nitrite and nitrate in all samples[16]. Serum vitamin C (ascorbic acid) level was determined after derivatization with 2,4-dinitr ophenylhydrazine[17]. The levels of β-carotene at 425 nm and vitamin A (retinol) at 325 nm were detected after the reaction of serum: ethanol: hexane at the ratio of 1:1:3, respectively[18].

Statistical analysis

All values were expressed as mean ± SD. Statistical analyses of data were performed using a one-way analysis of variance (ANOVA) and Tukey's posttest. A value of $P < 0.05$ was considered statistically significant.

RESULTS

Ulcer study

Ulcer indices (UI) are shown in Table 1. Per-oral administration of 80% ethanol produced multiple mucosal lesions in the rat stomach. Pre-treatment with FVE and famotidine were found to inhibit ethanol-induced gastric mucosal injury. This inhibitor effect of FVE was highest and statistically significant in the 300 mg/kg group and higher than that of famotidine group. In 75 mg/kg and 150 mg/kg of FVE groups, the inhibitor effects on ethanol-induced gastric mucosal injury were similar to famotidine group, which were not significant statistically. Famotidine also significantly inhibited ethanol-induced gastric lesions compared with the control.

Biochemical analysis

MDA levels of whole blood are shown in Table 2. The administration of ethanol increased the MDA level in whole blood. In contrast, pretreatment with FVE significantly decrased the MDA levels at doses of 150 and 300 mg/kg, compared with ethanol administered alone. Additionally, famotidine was found to prevent the rise in MDA level.

GSH level in whole blood was decreased in the ethanol-administered group. In contrast, GSH levels significantly increased at doses of 150 and 300 mg/kg FVE and in famotidine groups (Table 2). Nitrite and nitrate levels in serum were decreased in the ethanol administered group, while increased in the FVE groups. This increase was significant only in 75 and 150 mg/kg FVE groups, but not in 300 mg/kg FVE or famotidine groups (Table 2). All doses of FVE and famotidine increased the serum ascorbic acid levels, whereas only 300 mg/kg of FVE induced a significant increase (Table 3). On the other hand, serum β-carotene and retinol levels in FVE groups were higher than that of control, while the difference was significant only in the 150 mg/kg FVE group (Table 3).

Table 2 Effects of aqueous extracts of FVE and famotidine on whole blood MDA and GSH, and serum nitrite and nitrate levels (mean ± SD) in rats

Groups (n = 7)	MDA (nml/mL)	GSH (mg/dL)	Nitrite (mg/L)	Nitrate (mg/L)
Control (ethanol)	5.29 ± 0.6	44.46 ± 3.1	1.33 ± 0.7	4.55 ± 2.6
75 mg/kg FVE + Ethanol	4.51 ± 1.0	48.87 ± 2.5	2.56 ± 0.9[a]	8.81 ± 2.7[a]
150 mg/kg FVE +Ethanol	4.05 ± 0.3[a]	56.79 ± 3.3[d]	2.73 ± 0.5[a]	8.88 ± 1.9[a]
300 mg/kg FVE + Ethanol	4.12 ± 0.6[a]	51.34 ± 3.1[b]	1.64 ± 0.5	5.52 ± 1.7
20 mg/kg Famotidine + Ethanol	3.98 ± 0.7[a]	51.68 ± 3.2[b]	2.10 ± 0.8	6.82 ± 2.1

[a]$P < 0.05$, [b]$P < 0.01$, [d]$P < 0.001$, *vs* ethanol.

Table 3 Effects of aqueous extract of FVE and famotidine on serum antioxidant vitamins levels (mean ± SD) in rats

Groups (n = 7)	Ascorbic Acid (mg/dL)	β-Carotene (μg/dL)	Retinol (μg/dL)
Control (ethanol)	0.81 ± 0.2	26.09 ± 1.5	57.42 ± 3.4
75 mg/kg FVE + Ethanol	0.85 ± 0.2	27.48 ± 1.9	58.79 ± 4.6
150 mg/kg FVE + Ethanol	0.95 ± 0.2	31.13 ± 2.1[b]	68.45 ± 4.9[b]
300 mg/kg FVE + Ethanol	0.98 ± 0.2[a]	28.76 ± 1.8	63.61 ± 4.5
20 mg/kg Famotidine + Ethanol	0.97 ± 0.3	26.55 ± 1.6	58.57 ± 3.6

[a]$P < 0.05$, [b]$P < 0.01$, *vs* ethanol.

DISCUSSION

For a long time, peptic ulcer has been one of the important causes of morbidities and mortalities. Several factors such as increased vascular permeability, gastric motility and vagal activity, decreased gastric blood flow and protective prostaglandin levels play an important role in gastric ulcer pathogenesis. The treatment of peptic ulcers is still a big challenge and development of new drugs is urgent. There are a number of medicinal plants that have been shown to be effective against ulcer diseases in traditional medicine[19]. Because of the folkloric uses, these medicinal plants may be a good source for the development of potential drugs. In recent years, many efforts have been done to explore new anti-ulcer drugs from natural resources, and antiulcer activity of a variety of chemical compounds isolated from medicinal plants have been determined[20,21].

Ethanol is a commonly used ulcerogenic agent and when given by gavage to rats, it produces severe gastric hemorrhagic lesions. The mechanism of ethanol-induced gastric lesions is varied, including the depletion of gastric mucus content, damaged mucosal blood flow and mucosal cell injury. In addition, ethanol-induced gastric mucosal damage is associated with overproduction of free radicals, which lead to an increased lipid peroxidation[22]. Increase in lipid peroxide content and oxygen-derived free radicals results in marked changes in cellular levels and causes membrane damage, cell death, exfoliation and epithelial erosion. Accumulation of activated neutrophils in the gastric mucosa may be a source of free radicals. Several studies revealed that some antioxidant drugs such as melatonin and dantrolene have protective effects against ethanol-induced acute gastric injury in rats[23-25]. Results of the present study showed that all doses of FVE prevented gastric tissue damage against ethanol-induced stress, only significantly in the highest dose group. Furthermore, FVE decreased the lipid peroxidation and increased the non-enzymatic antioxidant. Antioxidative properties may, at least partially, be one of the possible mechanisms by which FVE ameliorated the ethanol-induced gastric lesions.

GSH is a well-known antioxidant, which is usually present as the most abundant low-molecular mass thiol in most organisms. It has various functions in the defense against oxidative stress and xenobiotic toxicity. It can act as an electron donor for glutathione peroxidase in animal cells, and also directly reacts with ROS. GSH is readily oxidized to glutathione disulfide (GSSG) by glutathione peroxidase, as well as by the reaction with ROS[26], which may subsequently cause the reduction in GSH levels.

Nitrate and nitrite [a marker of endogenous nitric oxide (NO) production], as a free radical, seems to be a potential antioxidant. It takes part in termination of lipid peroxidation (LPO) reactions. NO is an effective chain-breaking antioxidant in free radical-mediated LPO. It reacts rapidly with peroxyl radicals as a sacrificial chain-terminating antioxidant. The antioxidant effect of NO on LPO has been explained by terminating the radical chain reaction through the reaction of NO with lipid peroxy radical (ROO·) to form adducts by equation[27-29]. The protective effect of NO on LPO has also been shown[30,31].

$$4\ NO + 2\ ROO\cdot + H_2O \rightarrow 2\ ROONO + 2\ NO + H_2O \rightarrow RONO_2 + RONO + 2\ HNO_2$$

Aerobic organisms are protected against ROS by enzymatic antioxidant (superoxide dismutase, glutathione peroxidase and catalase) and non-enzymatic antioxidant (such as β-carotene, retinol, vitamin C and GSH) defense systems. Antioxidant vitamins, such as ascorbic acid, retinol and β-carotene play an important acute and chronic role in reducing or eliminating the oxidant damage produced by ROS[32]. In the present study, we also measured serum antioxidant vitamin capacity and, levels of all of the antioxidant vitamins were increased in FVE, but not in famotidine treated groups. Increase in vitamin levels in FVE groups may be related to vitamin content in FVE.

The preliminary phytochemical screening of FVE showed the presence of up to 8% volatile oil (including about 85% of anethole, up to 5% of estragole, and fenchone), flavonoids (rutin, quercetin and kaempferol glycosides), coumarins (bergapten, imperatorin, xanthotoxin and marmesin), sterols and sugars. These are also present in oil of FVE, d-a-pinene, d-a-phellandrene, dipentene, methyl chavicol, anisic acid, anisaldehyde and limonene[11-13,33]. Previous studies proved that anethole possesses significant antioxidant, anti-inflammatory and ulcer healing activity in experimental models[34]. Additionally, flavonoids, sterols, tannins and coumarins of some plants are also known to possess antiulcer activity[35-38]. Therefore, the presence of flavonoids content and other bioactive compounds in FVE may be associated with the ulcer preventing action.

In conclusion, our data show that FVE has an obvious gastroprotective effect and antioxidant properties. Although it is unclear about the exact mechanism underlying these actions, the effects on acute gastric lesions suggest a multifactorial mechanism, involving the antioxidant properties of FVE. FVE may be a new alternative for clinical management of gastric ulcer diseases and/or an antioxidant against oxidative stress. Further studies are required to clarify the anti-ulcer and antioxidant actions of FVE.

REFERENCES

1 **Halliwell B**, Gutteridge JMC. Free Radicals in Biology and Medicine. New York: Oxford University Press, 1989
2 **Kannan K**, Jain SK. Oxidative stress and apoptosis. *Pathophysiology* 2000; **7**: 153-163
3 **Cho CH**, Pfeiffer CJ, Misra HP. Ulcerogenic mechanism of ethanol and the action of sulphanilyl fluoride on the rat stomach in-vivo. *J Pharm Pharmacol* 1991; **43**: 495-498
4 **Lutnicki K**, Wróbel J, Ledwozyw A, Trebas-Pietraś E. The effect of calcium ions on the intensity of peroxidation processes and the severity of ethanol-induced injury to the rat' s gastric mucosa. *Arch Vet Pol* 1992; **32**: 125-132
5 **Bast A**, Haenen GR, Doelman CJ. Oxidants and antioxidants: state of the art. *Am J Med* 1991; **91**: 2S-13S
6 **Albert-Puleo M**. Fennel and anise as estrogenic agents. *J Ethnopharmacol* 1980; **2**: 337-344
7 **Ostad SN**, Soodi M, Shariffzadeh M, Khorshidi N, Marzban H. The effect of fennel essential oil on uterine contraction as a model for dysmenorrhea, pharmacology and toxicology study. *J Ethnopharmacol* 2001; **76**: 299-304
8 **Savino F**, Cresi F, Castagno E, Silvestro L, Oggero R. A randomized double-blind placebo-controlled trial of a standardized extract of Matricariae recutita, Foeniculum vulgare and Melissa officinalis (ColiMil) in the treatment of breastfed colicky infants. *Phytother Res* 2005; **19**: 335-340
9 **Ozbek H**, Uğraş S, Dülger H, Bayram I, Tuncer I, Oztürk G, Oztürk A. Hepatoprotective effect of Foeniculum vulgare essential oil. *Fitoterapia* 2003; **74**: 317-319
10 **Baytop T**. Therapy with Medicinal Plants in Turkey (Past and Present), vol. 3255. Istanbul: Publications of the Istanbul University, 1984: 359
11 **Mimica-Dukić N**, Kujundzić S, Soković M, Couladis M. Essential oil composition and antifungal activity of Foeniculum vulgare Mill obtained by different distillation conditions. *Phytother Res* 2003; **17**: 368-371
12 **Dadalioglu I**, Evrendilek GA. Chemical compositions and antibacterial effects of essential oils of Turkish oregano (Origanum minutiflorum), bay laurel (Laurus nobilis), Spanish lavender (Lavandula stoechas L.), and fennel (Foeniculum vulgare) on common foodborne pathogens. *J Agric Food Chem*

2004; **52**: 8255-8260
13 **Piccaglia R**, Marotti M. Characterization of some Italian types of wild fennel (Foeniculum vulgare Mill.). *J Agric Food Chem* 2001; **49**: 239-244
14 **Jain SK**, McVie R, Duett J, Herbst JJ. Erythrocyte membrane lipid peroxidation and glycosylated hemoglobin in diabetes. *Diabetes* 1989; **38**: 1539-1543
15 **Griffith OW**. Determination of glutathione and glutathione disulfide using glutathione reductase and 2-vinylpyridine. *Anal Biochem* 1980; **106**: 207-212
16 **Miranda KM**, Espey MG, Wink DA. A rapid, simple spectrophotometric method for simultaneous detection of nitrate and nitrite. *Nitric Oxide* 2001; **5**: 62-71
17 **Omaye ST**, Turnbul JD, Savberlich HE. Ascorbic acid analysis. II. Determination after derivatisation with 2.2. dinitrophenylhidrazine. Selected methods for determination of ascorbic acid in animal cells tissues and fluids, In: McCormick DB, Wright LD, editors. Methods in Enzymology. New York: Academic Press, 1979: 7-8
18 **Suzuki J**, Katoh N. A simple and cheap methods for measuring serum vitamin A in cattle using only a spectrophotometer. *Nihon Juigaku Zasshi* 1990; **52**: 1281-1283
19 **Schmeda-Hirschmann G**, Yesilada E. Traditional medicine and gastroprotective crude drugs. *J Ethnopharmacol* 2005; **100**: 61-66
20 **Süleyman H**, Demirezer LO, Büyükokuroglu ME, Akcay MF, Gepdiremen A, Banoglu ZN, Göçer F. Antiulcerogenic effect of Hippophae rhamnoides L. *Phytother Res* 2001; **15**: 625-627
21 **Odabasoglu F**, Cakir A, Suleyman H, Aslan A, Bayir Y, Halici M, Kazaz C. Gastroprotective and antioxidant effects of usnic acid on indomethacin-induced gastric ulcer in rats. *J Ethnopharmacol* 2006; **103**: 59-65
22 **Kahraman A**, Erkasap N, Köken T, Serteser M, Aktepe F, Erkasap S. The antioxidative and antihistaminic properties of quercetin in ethanol-induced gastric lesions. *Toxicology* 2003; **183**: 133-142
23 **Brzozowski T**, Konturek PC, Konturek SJ, Pajdo R, Bielanski W, Brzozowska I, Stachura J, Hahn EG. The role of melatonin and L-tryptophan in prevention of acute gastric lesions induced by stress, ethanol, ischemia, and aspirin. *J Pineal Res* 1997; **23**: 79-89
24 **Alarcón de la Lastra C**, Motilva V, Martín MJ, Nieto A, Barranco MD, Cabeza J, Herrerías JM. Protective effect of melatonin on indomethacin-induced gastric injury in rats. *J Pineal Res* 1999; **26**: 101-107
25 **Büyükokuroğlu ME**, Taysi S, Polat F, Göçer F. Mechanism of the beneficial effects of dantrolene sodium on ethanol-induced acute gastric mucosal injury in rats. *Pharmacol Res* 2002; **45**: 421-425
26 **Meister A**, Anderson ME. Glutathione. *Annu Rev Biochem* 1983; **52**: 711-760
27 **Hiramoto K**, Ohkawa T, Oikawa N, Kikugawa K. Is nitric oxide (NO) an antioxidant or a prooxidant for lipid peroxidation? *Chem Pharm Bull* (Tokyo) 2003; **51**: 1046-1050
28 **O'Donnell VB**, Chumley PH, Hogg N, Bloodsworth A, Darley-Usmar VM, Freeman BA. Nitric oxide inhibition of lipid peroxidation: kinetics of reaction with lipid peroxyl radicals and comparison with alpha-tocopherol. *Biochemistry* 1997; **36**: 15216-15223
29 **O'Donnell VB**, Eiserich JP, Bloodsworth A, Chumley PH, Kirk M, Barnes S, Darley-Usmar VM, Freeman BA. Nitration of unsaturated fatty acids by nitric oxide-derived reactive species. *Methods Enzymol* 1999; **301**: 454-470
30 **Jessup W**, Mohr D, Gieseg SP, Dean RT, Stocker R. The participation of nitric oxide in cell free- and its restriction of macrophage-mediated oxidation of low-density lipoprotein. *Biochim Biophys Acta* 1992; **1180**: 73-82
31 **Hayashi K**, Noguchi N, Niki E. Action of nitric oxide as an antioxidant against oxidation of soybean phosphatidylcholine liposomal membranes. *FEBS Lett* 1995; **370**: 37-40
32 **Halliwell B**. Antioxidants in human health and disease. *Annu Rev Nutr* 1996; **16**: 33-50
33 **Díaz-Maroto MC**, Díaz-Maroto Hidalgo IJ, Sánchez-Palomo E, Pérez-Coello MS. Volatile components and key odorants of fennel (Foeniculum vulgare Mill.) and thyme (Thymus vulgaris L.) oil extracts obtained by simultaneous distillation-extraction and supercritical fluid extraction. *J Agric Food Chem* 2005; **53**: 5385-5389
34 **Freire RS**, Morais SM, Catunda-Junior FE, Pinheiro DC. Synthesis and antioxidant, anti-inflammatory and gastroprotector activities of anethole and related compounds. *Bioorg Med Chem* 2005; **13**: 4353-4358
35 **Parejo I**, Jauregui O, Sánchez-Rabaneda F, Viladomat F, Bastida J, Codina C. Separation and characterization of phenolic compounds in fennel (Foeniculum vulgare) using liquid chromatography-negative electrospray ionization tandem mass spectrometry. *J Agric Food Chem* 2004; **52**: 3679-3687
36 **Al-Howiriny T**, Al-Sohaibani M, El-Tahir K, Rafatullah S. Prevention of experimentally-induced gastric ulcers in rats by an ethanolic extract of "Parsley" Petroselinum crispum. *Am J Chin Med* 2003; **31**: 699-711
37 **Khalil ML**. Biological activity of bee propolis in health and disease. *Asian Pac J Cancer Prev* 2006; **7**: 22-31
38 **Bighetti AE**, Antônio MA, Kohn LK, Rehder VL, Foglio MA, Possenti A, Vilela L, Carvalho JE. Antiulcerogenic activity of a crude hydroalcoholic extract and coumarin isolated from Mikania laevigata Schultz Bip. *Phytomedicine* 2005; **12**: 72-77

S- Editor Liu Y **L- Editor** Zhu LH **E- Editor** Lu W

PO Box 2345, Beijing 100023, China
www.wjgnet.com
wjg@wjgnet.com

World J Gastroenterol 2007 January 28; 13(4): 612-618
World Journal of Gastroenterology ISSN 1007-9327

RAPID COMMUNICATION

Distribution of trace metal concentrations in paired cancerous and non-cancerous human stomach tissues

Mehmet Yaman, Gokce Kaya, Hayrettin Yekeler

Mehmet Yaman, Gokce Kaya, Firat University, Sciences and Arts Faculty, Chemistry Department, Elazig, Turkey
Hayrettin Yekeler, Chief of Staff in State Hospital, Elazig, Turkey
Correspondence to: Professor Mehmet Yaman, Firat University, Sciences and Arts Faculty, Chemistry Department, Elazig 23119, Turkey. myaman@firat.edu.tr
Telephone: +90-424-2370000 Fax: +90-424-2330062
Received: 2006-08-23 Accepted: 2006-10-23

Abstract

AIM: To assess whether trace metal concentrations (which influence metabolism as both essential and non-essential elements) are increased or decreased in cancerous tissues and to understand the precise role of these metals in carcinogenesis.

METHODS: Concentrations of trace metals including Cd, Ni, Cu, Zn, Fe, Mg and Ca in both cancerous and non-cancerous stomach tissue samples were determined by atomic absorption spectrometry (AAS). Tissue samples were digested using microwave energy. Slotted tube atom trap was used to improve the sensitivity of copper and cadmium in flame AAS determinations.

RESULTS: From the obtained data in this study, the concentrations of nickel, copper and iron in the cancerous human stomach were found to be significantly higher than those in the non-cancerous tissues, by using *t*-test for the paired samples. Furthermore, the average calcium concentrations in the cancerous stomach tissue samples were found to be significantly lower than those in the non-cancerous stomach tissue samples by using *t*-test. Exceedingly high Zn concentrations (207-826 mg/kg) were found in two paired stomach tissue samples from both cancerous and non-cancerous parts.

CONCLUSION: In contrast to the literature data for Cu and Fe, the concentrations of copper, iron and nickel in cancerous tissue samples are higher than those in the non-cancerous samples. Furthermore, the Ca levels are lower in cancerous tissue samples than in non-cancerous tissue samples.

Key words: Cancer; Trace metals; Human stomach; Microwave energy; Atomic absorption

Yaman M, Kaya G, Yekeler H. Distribution of trace metal concentrations in paired cancerous and non-cancerous human stomach tissues. *World J Gastroenterol* 2007; 13(4): 612-618

http://www.wjgnet.com/1007-9327/13/612.asp

INTRODUCTION

The importance of essential trace metals in health and disease is indisputable because of their essential role in specific concentration ranges and toxic role at relatively high levels. Essential trace elements have four major functions as stabilizers, elements of structure, essential elements for hormonal function and cofactors in enzymes. As a result, the lack of essential trace elements influences structure alone or alters function of structure through the lack of stabilization, change of charge properties or allosteric configuration[1]. It may be expected that deficiency of essential trace elements as cofactors of enzymes could severely impair the host's resistance against carcinogenic stress[2]. Among these elements, zinc is a component of more than 3000 zinc-associated transcription factors including DNA-binding proteins with zinc fingers, and more than 300 enzymes including Cu/Zn superoxide dismutase (CuZnSOD) (SOD is an important antioxidant enzyme for cellular protection against reactive oxygen species (ROS) and several proteins involved in DNA repair[3-5]. Metallothioneins, being intracellular polypeptides have a remarkable ability to bind to metallic ions including both essential and also toxic metals such as cadmium or lead. Copper is a component of more than 30 enzymes including caeruloplasmine, cytochrome oxidase, lysine oxidase, dopamine-hydroxylase, ascorbate oxidase and tyrosinase in human body, some of which are involved in collagen synthesis, as well as being necessary for the healthy development of connective tissue, nerve coverings and bone[6,7].

The role of metals in the development and inhibition of cancer has a complex character and raises many questions. In the past 25 years, some metals including cadmium, nickel, arsenic, beryllium and chromium (VI), have been recognized as human or animal carcinogens in addition to primary carcinogens such as radiation, viruses and other chemicals[7,8]. Their carcinogenic potential depend largely on factors such as oxidation states and chemical species[9]. It is supposed that oxidative DNA lesions play an important role in various diseases including cancer and premature aging. The increase in oxidative

DNA lesions are frequently described as being attributable to metal exposure. Metal carcinogenesis is mediated either by the increased generation of highly ROS on the basis of ESR spin trapping studies[10] and/or by interference with DNA repair processes[11]. Almost all metals are able to generate ROS, which can explain a great part of both their carcinogenicity and their aptitude in the treatment of cancer. Induction of oxidative DNA damage and interaction with DNA repair processes can lead to an enhancement of genotoxicity in combination with a variety of DNA-damaging agents. Nucleotide excision repair (NER) which is the major repair system, is inhibited at low levels as well as at non-cytotoxic concentrations of Ni (Ⅱ), Cd (Ⅱ), Co (Ⅱ) and As (Ⅲ). The repair of oxidative DNA base modifications is disturbed by Ni (Ⅱ) and Cd (Ⅱ) ions. One reason for repair inhibition appears to be the displacement of Zn (Ⅱ) and Mg (Ⅱ)[12]. Magnesium and Zn, that are cofactors for DNA polymerase, are effective protectors against carcinogenesis *in vivo*. Although Zn and Cu concentrations in serum and tissues of cancer patients have been studied extensively, the precise role of these metals in carcinogenesis is not clearly understood. While a great depth of literature is available regarding the alterations in the levels of trace elements in serum, relatively few studies are available on trace element levels in cancerous and non-cancerous human stomach tissue. Reddy and coworkers reported that the concentrations of essential metals including Fe, Zn and Cu are significantly lower in cancerous stomach tissue than in normal tissues[13]. Similarly, the lower Fe and Zn levels in cancerous stomach tissues than in normal tissues are also supported by von Czarnowski and coworkers[14]. Few studies have simultaneously determined both toxic and essential trace elements in cancerous and non-cancerous stomach tissues. On the other hand, most studies have been performed on dried and occasionally homogenized samples, that disturb the tissue from its natural physiological state. Ng and coworkers[15] reported that the wet-to-dry ratio of tumor (malignant) breast tissues is higher (more 2-times) than that of the normal tissues. Therefore the elevation of elemental contents in tumors is significantly different from that in normal tissues when concentrations are adjusted by using the wet-to-dry ratio of the samples. The same study noted that the wet-to-dry ratio varies significantly amongst specimens, not only of different types but also between samples of the same group[15]. Therefore, evaluation of trace element levels in dried samples should be regarded as incomplete in the absence of wet-to-dry ratios for individual specimens. It would appear that study of fresh and unprocessed specimens is preferable. On the other hand, the ratio of Cu to Zn (Cu/Zn) intake is widely utilized to assist diagnosis of various cancers or tumors[16]. The usefulness of the tissue-metal determination in cancer prevention, detection, monitoring, treatment and prognosis requires further investigation.

In our laboratory, atomic absorption spectrometry (AAS) being the most common analytical technique has been successfully used for trace metal analysis in biological samples[17-20]. To improve the sensitivity of flame atomic absorption spectrometry (FAAS), a slotted tube atom trap (STAT) has been used for some metals such as Cd, Pb and Cu in biological matrices[19-22]. In the current study, the concentrations of various minor and trace metals, including Cd, Ni, Cu, Zn, Fe, Mg and Ca in cancerous and non-cancerous stomach tissues, were determined by atomic absorption spectrophotometry. For digestion of the tissues, a microwave oven was used.

MATERIALS AND METHODS

Apparatus and reagents

An ATI UNICAM 929 flame atomic absorption spectrophotometer (FAAS) equipped with ATI UNICAM and KOTTO hollow cathode lamps was used for metal determinations. The optimum conditions for FAAS are given in Table 1. A STAT was used to improve the Cd and Cu sensitivities by FAAS. A domestic microwave oven (Kenwood) was used for digestion of the tissues. Unless stated otherwise, all chemicals used were of analytical grade. Throughout the analysis, doubly distilled water was used. All glass apparatus (Pyrex) were kept permanently full of 1 mol/L nitric acid when they were not used. In the digestion procedures, concentrated nitric acid (65%, Merck) and hydrogen peroxide (35%, Merck) were used. Stock solutions of metals (1000 mg/L) were prepared by dissolving their salts (Merck) in 1.0 mol/L nitric acid.

Preparation of samples

Fresh stomach tissue samples were taken since fresh and formalin-fixed tissues have been demonstrated to yield virtually the same results for essential and toxic metals including Ca, Mg, Fe, Cu, Zn, As, Cd, Hg and Pb[23]. In the current study, the samples were obtained in the formaldehyde solution from private Pathology Laboratories and the pathology laboratories of Firat University in Elazig, Turkey, after surgery and histopathologic examination. A total of eighteen samples were taken, of which four cancerous (malign) stomach tissue samples were taken from patients of different sex, age and living conditions, described as independent samples in this study, the other fourteen samples were taken from both cancerous (malign) and non-cancerous (normal) stomach tissues, described as paired samples in this study. All the patients were diagnosed as grade Ⅱ-Ⅲ or Ⅲ-Ⅳ adenocarcinoma except that one patient at the age of 80 years had grade I and poorly differentiated adenocarcinoma. Furthermore, most patients had metastatic and differentiated adenocarcinoma. The tissue samples were cut into small pieces with a stainless steel knife and transferred to a beaker.

Digestion of tissue samples

Exactly 2.0 mL of the mixture of HNO_3/H_2O_2 (2:1) was added to 0.7 g of the tissue samples. The mixture was placed into the water bath at 70℃ for 30 min and stirred occasionally. Then, 1.0 mL of the same acid mixture was added, and the mixture was transferred into a Teflon vessel bomb for the microwave oven. The bomb was closed, and the solution was placed inside the microwave

Table 1 Operation parameters for flame atomic absorption spectrophotometer

Parameter	Cd	Ni	Cu	Zn	Fe	Mg	Ca
Wavelength (nm)	228.8	232	324.8	213.9	248.3	285.2	422.7
HCL current (mA)	4	7.5	3	9.5	15	15	6
Acetylene flow rate (L/min)	0.5	0.5	0.5	0.5	0.5	0.5	4.2
N_2O flow rate (L/min)	-	-	-	-	-	-	4.7
Air flow rate (L/min)	4	4	4	4	4	4	-
Slit (nm)	0.5	0.2	0.5	0.5	0.2	0.5	0.5

Table 2 Equations of the curves

Equation		
Y = 2.4972x + 1.12	$R^2 = 0.99$	For Cd (4-100 ng/mL by STAT-AAS)
Y = 0.3278x - 0.2083	$R^2 = 1$	For Cu (25-400 ng/mL by STAT-AAS)
Y = 85x + 0.5	$R^2 = 0.99$	For Ni (0.2-2.0 mg/L)
Y = 302x + 0.75	$R^2 = 0.99$	For Zn (0.1-1.0 mg/L)
Y = 64x + 0.43	$R^2 = 1$	For Fe (0.20-3.0 mg/L)
Y = 515x + 7.0	$R^2 = 0.99$	For Mg (0.25-2.0 mg/L)
Y = 305x + 39	$R^2 = 1$	For Ca (0.25-2.0 mg/L)

oven. Radiation was applied for 3 min at 450 W. After addition of 0.5 mL of the same acid mixture, radiation was repeated for 3 min. After cooling for 5 min, 2.0 mL of 0.1 mol/L HNO_3 was added, and the solution was transferred into a Pyrex tube. After centrifugation, the clear solution was measured by FAAS. Three different portions of each sample were digested and the average value was calculated for the same tissue. Blank digests were carried out in the same way.

RESULTS

Calibration curves were obtained by using solutions of the studied elements at different concentrations. The graphs obtained were linear in the concentration range and the equations of the curves are described in Table 2.

Analytical performance

The accuracy of the method was studied by examining the recovery of metals from stomach tissue samples fortified with various amounts of the studied metals. The following metal amounts were added: 30 ng/g of Cd, 200 ng/g of Ni, 0.3 mg/kg of Cu, 10 mg/kg of Zn, 10 mg/kg of Fe, 100 mg/kg of Mg and 300 mg/kg of Ca. After digestion in microwave oven, the recoveries were found to be at least 90% for all studied metals. Furthermore, the standard addition method was used to remove possible interferences caused by the matrix. The slopes of the calibration curves for all studied elements were compared with those obtained by the standard addition method. The slopes of the calibration curves were found to be the same as those obtained with the standard addition method. In other words, all of the standard addition curves were parallel to the calibration curves. These results indicated the absence of chemical interference.

Levels of the metals including Cd, Ni, Cu, Zn, Fe, Mg and Ca in the reagent blanks in the analytical steps were found to be 0.5, 25, 10, 50, 50, 105 and 190 ng/mL with the standard deviations being 0.1, 4.0, 1.5, 9.0, 8.0, 20 and 35, respectively. Therefore, the detection limits for these elements defined as three times the s values of blanks were calculated as 0.3, 12, 4.5, 27, 24, 60 and 105 ng/mL. The precision of the standard deviations for 10 samples of the same tissue was found to be less than 10% for all studied elements.

Comparison of metal levels in cancerous and non-cancerous tissues

Metals are considered to act not only as carcinogens but also as co-carcinogens that activate carcinogenic chemicals. In evaluating the differences in cancerous and non-cancerous tissue samples, two comparisons were conducted: one between paired cancerous and non-cancerous tissue samples, the other between total cancerous and non-cancerous samples. *P* values (obtained by using *t*-test) less than 0.05 were considered significantly different between the two groups. The samples with exceptionally high values were disregarded in calculating the average and range.

Data related with carcinogenic effects of cadmium are available from the literature[24]. Multiple studies have linked occupational exposure to Cd with pulmonary cancer in humans, whereas a few studies showed that Cd exposure is associated with cancers of stomach and other sites in humans[24]. As it can be seen from Table 3, there was no significant difference in Cd concentrations between cancerous and non-cancerous stomach tissue samples, in the present study.

Nickel: The International Agency for Research on Cancer (IARC) has classified the carcinogenic substances in two groups. Group 1 includes substances "known to be human carcinogens or sufficient evidence of carcinogenicity from studies in humans", group 2 includes substances "reasonably anticipated to be a human carcinogen". The chemicals in group 2 are classified in two subgroups by IARC. Group 2A includes substances "probably carcinogenic to humans", and group 2B includes substances "possibly carcinogenic to humans" [8]. Kasprazak and coworkers[25] have made an overall evaluation of the carcinogenicity of nickel and found that Ni compounds are carcinogenic to humans (group 1), and metallic nickel is possibly carcinogenic to humans (group 2B).

vonCzarnowski *et al*[14] showed that Ni levels are lower in cancerous (malign) stomach tissues than in normal stomach tissues, whereas Reddy *et al*[13] reported that nickel concentrations are 6-time higher in cancerous stomach tissues than in normal stomach tissues. In this study, the Ni levels in cancerous stomach tissue samples were significantly higher ($P < 0.05$ for the paired samples) than those in the non-cancerous stomach tissue samples (Tables

Table 3 Trace metal concentrations in cancerous and non-cancerous stomach tissues. Every single cancerous tissue belongs to a different patient (mean ± SD, *n* = 3)

Tissue	Cd (ng/g)		Ni (ng/g)		Cu (mg/kg)		Zn (mg/kg)		Fe (mg/kg)		Mg (mg/kg)		Ca (mg/kg)	
(Age)	Cancerous	non-can-cerous	Cancerous	non-cancerous	Cancer-ous	non-cancerous	Cancer-ous	non-cancerous	Cancerous	non-cancerous	Cancer-ous	non-cancerous	Cancer-ous	non-cancerous
Stomach (65)	30 ± 9		230 ± 55		0.6 ± 0.1		11 ± 1		24 ± 3		508 ± 75[2]		526 ± 85	
Stomach (62)	156 ± 16		260 ± 30		0.9 ± 0.1		26 ± 2		8 ± 1		203 ± 18		545 ± 90	
Stomach (80)	50 ± 9		740 ± 84		0.9 ± 0.2		23 ± 24		65 ± 30		44 ± 17[2]		1010 ± 930	
Stomach (66)	29 ± 16		820 ± 113		0.7 ± 0.1		7 ± 1		60 ± 17		112 ± 30		480 ± 130	
Stomach (58)[1]	10 ± 3	33 ± 6	905 ± 690	328 ± 55	1.2 ± 0.1	1.0 ± 0.3	11 ± 1	23 ± 0.1	25 ± 4	19 ± 8	80 ± 10	200 ± 14	390 ± 76	834 ± 155
Stomach (60)[1]	33 ± 10	42 ± 7	1120 ± 265	840 ± 93	1.8 ± 0.1	1.5 ± 0.2	12 ± 2	17 ± 1	16 ± 2	21 ± 2	150 ± 12	84 ± 10	335 ± 41	450 ± 86
Stomach (57)[1]	68 ± 26	130 ± 21	510 ± 80	439 ± 57	1.5 ± 0.2	1.2 ± 0.1	16 ± 2	21 ± 4	37 ± 9	18 ± 5	210 ± 23	190 ± 15	432 ± 96	1047 ± 120
Stomach (59)[1]	90 ± 15	63 ± 8	2010 ± 356	1240 ± 112	1.7 ± 0.2	0.9 ± 0.1	25 ± 3	19 ± 1	40 ± 5	23 ± 3	106 ± 11	45 ± 5[2]	235 ± 34	492 ± 75
Stomach (52)[1]	107 ± 19	55 ± 5	335 ± 164	321 ± 237	1.5 ± 0.6	1.1 ± 0.3	22 ± 2	19 ± 1	34 ± 14	36 ± 21	210 ± 15	300 ± 128	911 ± 215	1199 ± 53
Stomach (51)[1]	22 ± 9	58 ± 8	740 ± 145	720 ± 95	1.1 ± 0.2	0.6 ± 0.1	18 ± 2	16 ± 1	35 ± 4	34 ± 3	24 ± 3[2]	30 ± 5[2]	403 ± 55	523 ± 41
Stomach (66)[1]	31 ± 3	33 ± 6	527 ± 116	241 ± 32	2.8 ± 0.1	0.9 ± 0.5	41 ± 4	30 ± 15	20 ± 2	23 ± 7	270 ± 15	241 ± 30	530 ± 10	624 ± 78
Stomach (60)[1]	30 ± 6	55 ± 6	360 ± 92	270 ± 32	0.5 ± 0.07	0.7 ± 0.1	25 ± 2	30 ± 3	9 ± 2	10 ± 3	200 ± 28	215 ± 25	600 ± 110	615 ± 65
Stomach (49)[1]	10 ± 1	33 ± 3	182 ± 72	190 ± 5	4.3 ± 0.5	2.1 ± 1.6	19 ± 4	23 ± 2	17 ± 3	20 ± 4	130 ± 21	110 ± 17	460 ± 62	484 ± 56
Stomach (55)[1]	30 ± 5	32 ± 4	500 ± 98	240 ± 28	2.8 ± 0.1	1.2 ± 0.2	33 ± 3	35 ± 4	12 ± 3	18 ± 4	190 ± 20	135 ± 15	533 ± 67	624 ± 60
Stomach (50)[1]	65 ± 17	85 ± 10	700 ± 85	750 ± 103	1.7 ± 0.1	0.8 ± 0.1	207 ± 19[2]	826 ± 55[2]	25 ± 2	13 ± 2	314 ± 30	184 ± 22	746 ± 86	713 ± 66
Stomach (53)[1]	60 ± 12	80 ± 11	300 ± 45	130 ± 12	2.4 ± 0.3	0.8 ± 0.1	410 ± 28[2]	380 ± 36[2]	26 ± 3	15 ± 2	207 ± 31	275 ± 10	685 ± 74	715 ± 61
Stomach (40)[1]	70 ± 12	105 ± 10	730 ± 98	850 ± 120	2.2 ± 0.2	1.9 ± 0.1	15 ± 2	16 ± 2	42 ± 4	25 ± 3	215 ± 10	200 ± 40	375 ± 42	417 ± 36
Stomach (51)[1]	32 ± 5	100 ± 12	410 ± 65	800 ± 112	2.2 ± 0.2	1.3 ± 0.1	17 ± 1	16 ± 2	42 ± 5	24 ± 2	327 ± 30	210 ± 25	476 ± 26	508 ± 52
Average	51 ± 37	65 ± 31	632 ± 430	526 ± 335	1.7 ± 1	1.1 ± 0.4	20 ± 9	22 ± 6	30 ± 16	21 ± 7	195 ± 72	195 ± 63	537 ± 196	660 ± 230
Range	10-156	32-130	230-2010	130-1240	0.5-4.3	0.6-2.1	7-41	16-30	8-65	10-36	24-508	30-300	235-1010	417-1199

[1]Cancerous and non-cancerous tissues in lines belong to the same persons; [2]These values are not included in calculation of average and in range data.

Table 4 Significant and tendentious elements in cancerous human stomach tissue except for the last one

Status	Stomach	*P* (for paired samples)	*P* (for total samples)
Significant	Ca (-)	0.009	0.122
	Cu (+)	0.001	0.036
	Fe (+)	0.046	0.065
Tendentious	Ni (+)	0.092	0.409
		0.025	

3, 4 and Figure 1).

Copper: Although copper is an essential element for humans and animals, high concentrations of Cu (above normal) could induce growth proliferation and cancer by damaging DNA with toxic free hydroxyl radicals[26]. Conflicting results regarding Cu concentrations have been observed in cancerous and normal stomach tissues[13,14]. VonCzarnowski and coworkers[14] reported that there are no differences in Cu concentrations between cancerous (malign) and normal stomach tissue samples, whereas Reddy and coworkers[13] described that Cu levels in cancerous stomach tissue samples are 3-time lower than those in normal stomach tissue samples. In the present study, the Cu levels in cancerous stomach tissues were significantly higher ($P = 8.10^{-4}$ for the paired samples and $P < 0.05$ for total samples) than those in non-cancerous stomach samples (Tables 3, 4 and Figure 2). The mechanism of copper elevation in cancerous tissues may be explained by modifications in the relationships among trace elements with reduced catabolism or by increased neoplastic synthesis of ceruoplasmin. Metal carcinogenesis is mediated either by the increased generation of highly ROS (Fenton reaction) and/or by interference with DNA repair processes[11,26]. Since almost all metals are able to generate ROS, further studies on the determination of trace element levels together with ROS production

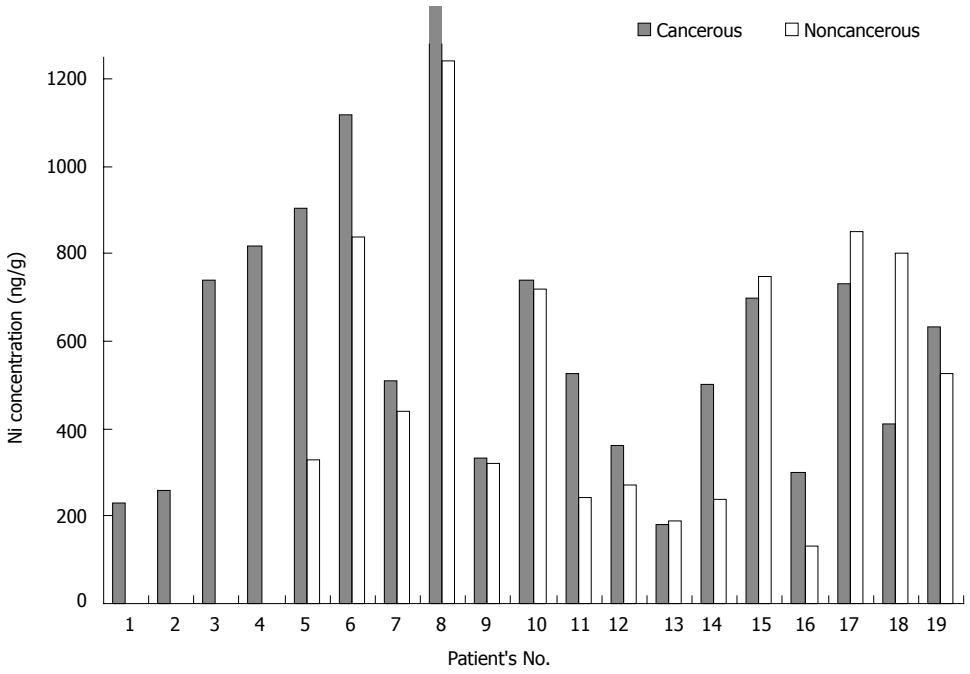

Figure 1 Comparison of Ni levels between cancerous and non-cancerous stomach tissue samples. The concentration of number 19 is average value.

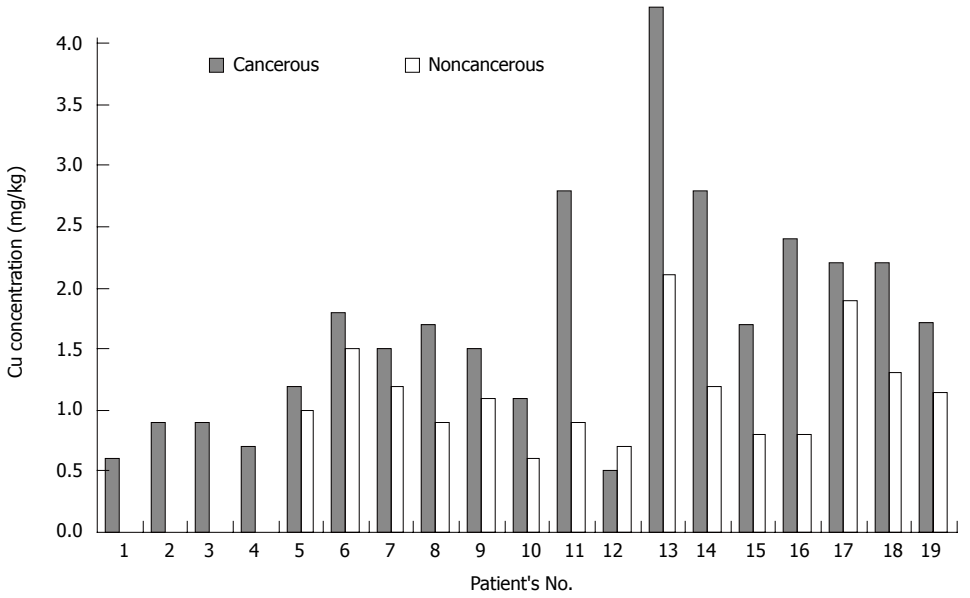

Figure 2 Comparison of Cu levels between cancerous and non-cancerous stomach tissue samples. The concentration of number 19 is average value.

are needed. Consequently, the physiological processes underlying tumor development can lead to uptake of trace elements by neoplastic cells because of the increased cellular and enzymatic activity.

Zinc: It was reported that Zn concentrations in cancerous stomach tissue are lower than those in normal tissues[13-14]. It can be seen from Table 3, there was no significant difference in Zn concentrations between cancerous and non-cancerous stomach tissue the paired samples. Excessive zinc concentrations were found in both cancerous and non-cancerous stomach tissues from two patients. Unfortunately, we could not explain these excessive Zn levels.

Iron: Although Fe is an essential nutritional element for all life forms, it is known that excess iron and iron deficiency also lead to oxidative DNA damage[27]. It was reported that iron levels are significantly decreased in cancerous stomach tissue in comparison with those in normal stomach tissue[13-14]. On the other hand, Hercberg and coworkers[28] reported that serum ferritin concentration >160 ng/mL is an increased risk of developing cancer in women but not in men. In this study, Fe levels in the cancerous stomach tissue samples were significantly higher ($P < 0.05$ for the paired samples and $P = 0.065$ for all samples) than those in the non-cancerous tissue samples (Tables 3, 4 and Figure 3). These findings can also be explained by the Fenton reaction described above.

Calcium: It was reported that calcium concentrations in cancerous stomach tissues are lower than those in the normal tissues[13], whereas steady Ca concentrations are observed in cancerous and normal stomach tissues[14]. In this study, Ca levels in the cancerous stomach tissue samples were significantly lower ($P < 0.01$ for the paired samples) than those in the non-cancerous tissue samples,

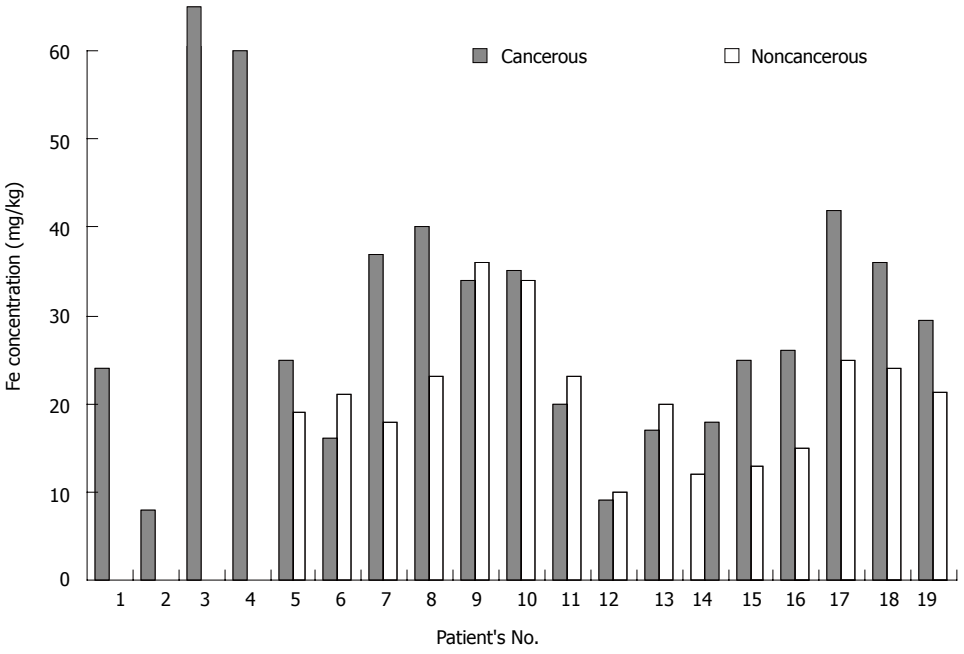

Figure 3 Comparison of Fe levels between cancerous and non-cancerous stomach tissue samples. The concentration of number 19 is average value.

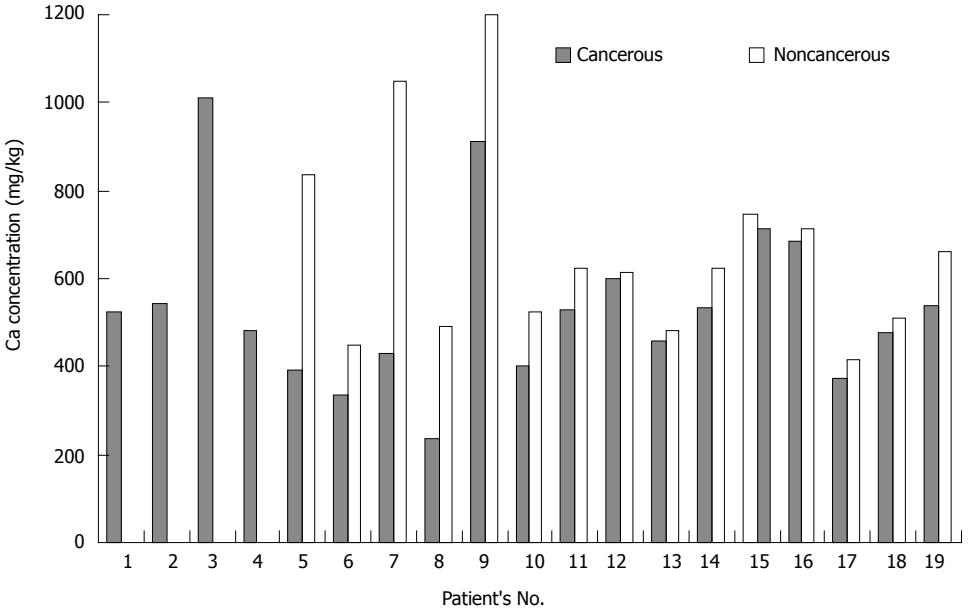

Figure 4 Comparison of Ca levels between cancerous and non-cancerous stomach tissue samples. The concentration of number 19 is average value.

similar to the results of Reddy coworkers (Tables 3, 4 and Figure 4). It was described that Ni^{+2} can block Ca^{+2} channels and hence, nickel releases the stored intracellular Ca^{+2} via a mechanism underlying the interaction between Ni^{+2} ions and the cell surface Ca^{+2} receptor[25]. The results of this study, involving the lower Ca concentrations in cancerous stomach tissue samples than in the non-cancerous tissue samples, agree with the observed higher Ni levels in cancerous tissues than in non-cancerous tissues.

Magnesium: There were no significant differences in the Mg concentrations between cancerous and non-cancerous stomach tissues (Table 3).

The significant and tendentious elements are listed in Table 4. The positive sign was used to illustrate accumulation of the elements in cancerous tissue, and the minus sign was used to indicate the depletion of elements in the cancerous stomach tissue samples in comparison to the non-cancerous tissue samples.

DISCUSSION

Reddy and coworkers[13] found that the concentrations of trace metals in normal/cancerous tissues (mg/kg) on dry weight basis are as follows: Fe = 2408/684, Cu = 63.5/21.2, Zn = 818/229, Ni = 10.5/60, Pb = 8.8/8.1 and Ca = 647/433. They described that the low iron level observed in carcinoma tissue of stomach might not initiate carcinoma in stomach, but the low absorption of iron may be due to the lack of HCl which in turn may be due to the carcinogenic nature of stomach. The lower iron levels observed in cancer tissue of stomach is supported by vonCzarnowski and coworkers[14]. In the present study, copper, iron and nickel concentrations in cancerous stomach tissue samples were higher than those in non-

cancerous stomach tissue samples. Although ROS were not measured in this study, these results are in agreement with the reported data[29]. Furthermore, we found that Ca levels in the cancerous stomach tissue samples were lower than those in the non-cancerous stomach tissue samples. It was reported that calcium and magnesium concentrations, similar to iron, nickel and zinc in cancerous prostate tissue are higher than those in non-cancerous prostate tissue[18]. The increase in calcium concentration and its heterogeneous distribution in malign prostate tissue in contrast to the data obtained in stomach tissue may be attributed to calcium functions and behaviors depending on the organ type. The organ-dependency on the changes in trace metal concentrations in cancerous and endometrial tissues[30] also supports these explanations. We think that the decreased Ca levels and the increased Ni concentrations in cancerous stomach tissues as well as its heterogeneous distribution in comparison to non-cancerous samples are very important for the investigation of cancer mechanism in this organ due to the displacement of Ni with Ca. The results in disagreement with the explanations above may be attributed to their subgroups of cancerous properties because the different mechanisms may be effective in such conditions.

In conclusion, STAT can be used to improve the sensitivity of copper and cadmium. In addition, the tissue digested in a microwave oven has very low blank values and can reduce the risk of metal loss or contaminations. The closed microwave digestion offers an easy and reliable method for the complete dissolution of tissues prior to the determination of trace metals.

REFERENCES

1 **Feinendegen LE**, Kasperek K. Medical aspects of trace element research. *Trace Elem Anal Chem Med Biol* 1980; 1-17
2 **Schrauzer GN**. The role of trace elements in the etiology of cancer. *Trace Elem Anal Chem Med Biol* 1980; 183-195
3 **Beyersmann D**. Homeostasis and cellular functions of zinc. *Materıalwıssenschaft und werkstofftechnık* 2002, **33**: 764-769
4 **Auld DS**. Zinc coordination sphere in biochemical zinc sites. *Biometals* 2001; **14**: 271-313
5 **Ho E**. Zinc deficiency, DNA damage and cancer risk. *J Nutr Biochem* 2004; **15**: 572-578
6 **Cai L**, Li XK, Song Y, Cherian MG. Essentiality, toxicology and chelation therapy of zinc and copper. *Curr Med Chem* 2005; **12**: 2753-2763
7 **Mertz W**. Trace elements in human and animal nutrition. 5th ed. San Diego, California: Academic Press, 1987: 1-2
8 **Tomatis L**. The identification of human carcinogens and primary prevention of cancer. *Mutat Res* 2000; **462**: 407-421
9 **Rojas E**, Herrera LA, Poirier LA, Ostrosky-Wegman P. Are metals dietary carcinogens? *Mutat Res* 1999; **443**: 157-181
10 **Wang Y**, Fang J, Leonard SS, Rao KM. Cadmium inhibits the electron transfer chain and induces reactive oxygen species. *Free Radic Biol Med* 2004; **36**: 1434-1443
11 **Merzenich H**, Hartwig A, Ahrens W, Beyersmann D, Schlepegrell R, Scholze M, Timm J, Jöckel KH. Biomonitoring on carcinogenic metals and oxidative DNA damage in a cross-sectional study. *Cancer Epidemiol Biomarkers Prev* 2001; **10**: 515-522
12 **Hartwig A**. Recent advances in metal carcinogenicity. *Pure Appl Chem* 2000; **72**: 1007-1014
13 **Reddy SB**, Charles AJ, Raju GJN, Vijayan V, Reddy BS, Kumar MR, Sundareswar B. Trace elemental analysis of carcinoma kidney and stomach by PIXE method. *Nucl Instr Meth Phys Res B* 2003; **207**: 345-355
14 **VonCzarnowski D**, Denkhaus E, Lemke K. Determination of trace element distribution in cancerous and normal human tissues by total X-ray fluorescence analysis. *Spectrochim Acta B* 1997; **52**: 1047-1052
15 **Ng KH**, Bradley DA, Looi LM. Elevated trace element concentrations in malignant breast tissues. *Br J Radiol* 1997; **70**: 375-382
16 **Zhai H**, Chen X, Hu Z. Study on the relationship between intake of trace elements and breast cancer mortality with chemometric methods. *Comput Biol Chem* 2003; **27**: 581-586
17 **Yaman M**. Nickel speciation in soil and the relationship with its concentration in fruits. *Bull Environ Contam Toxicol* 2000; **65**: 545-552
18 **Yaman M**, Atici D, Bakirdere S, Akdeniz I. Comparison of trace metal concentrations in malign and benign human prostate. *J Med Chem* 2005; **48**: 630-634
19 **Yaman M**. The improvement of sensitivity in lead and cadmium determinations using flame atomic absorption spectrometry. *Anal Biochem* 2005; **339**: 1-8
20 **Yaman M**, Akdeniz I. Sensitivity enhancement in flame atomic absorption spectrometry for determination of copper in human thyroid tissues. *Anal Sci* 2004; **20**: 1363-1366
21 **Yaman M**. Determination of Cd and Pb in Human Urine by STAT-FAAS after enrichment on Activated Carbon. *J Anal At Spectrom* 1999; **14**: 275-278
22 **Yaman M**, Dilgin Y. AAS Determination of Cadmium in Fruits and Soils. *At. Spectros* 2002; **23**: 59-64
23 **Bush VJ**, Moyer TP, Batts KP, Parisi JE. Essential and toxic element concentrations in fresh and formalin-fixed human autopsy tissues. *Clin Chem* 1995; **41**: 284-294
24 **Waisberg M**, Joseph P, Hale B, Beyersmann D. Molecular and cellular mechanisms of cadmium carcinogenesis. *Toxicology* 2003; **192**: 95-117
25 **Kasprzak KS**, Sunderman FW, Salnikow K. Nickel carcinogenesis. *Mutat Res* 2003; **533**: 67-97
26 **Theophanides T**, Anastassopoulou J. Copper and carcinogenesis. *Crit Rev Oncol Hematol* 2002; **42**: 57-64
27 **Ames BN**. DNA damage from micronutrient deficiencies is likely to be a major cause of cancer. *Mutat Res* 2001; **475**: 7-20
28 **Hercberg S**, Estaquio C, Czernichow S, Mennen L, Noisette N, Bertrais S, Renversez JC, Briançon S, Favier A, Galan P. Iron status and risk of cancers in the SU.VI.MAX cohort. *J Nutr* 2005; **135**: 2664-2668
29 **Yaman M**. Comprehensive comparison of trace metal concentrations in cancerous and non-cancerous human tissues. *Curr Med Chem* 2006; **13**: 2513-2525
30 **Yaman M**, Kaya G, Simsek M. Comparison of trace element concentrations in cancerous and noncancerous human endometrial and ovary tissues. *Int J Gynecol Cancer* 2007;**17**:220-228

S- Editor Wang GP **L- Editor** Wang XL **E- Editor** Ma WH

PO Box 2345, Beijing 100023, China
www.wjgnet.com
wjg@wjgnet.com

World J Gastroenterol 2007 January 28; 13(4): 619-622
World Journal of Gastroenterology ISSN 1007-9327

RAPID COMMUNICATION

Evaluation of the effect of partial splenic embolization on platelet values for liver cirrhosis patients with thrombocytopenia

Chi-Ming Lee, Ting-Kai Leung, Hung-Jung Wang, Wei-Hsing Lee, Li-Kuo Shen, Jean-Dean Liu, Chun-Chao Chang, Ya-Yen Chen

Chi-Ming Lee, Ting-Kai Leung, Hung-Jung Wang, Wei-Hsing Lee, Li-Kuo Shen, Ya-Yen Chen, Department of Diagnostic Radiology, Taipei Medical University Hospital, Taipei, Taiwan, China
Chi-Ming Lee, Ting-Kai Leung, Department of Medicine, Taipei Medical University, Taipei, Taiwan, China
Jean-Dean Liu, Chun-Chao Chang, Division of Gastroenterology, Department of Internal Medicine, Taipei Medical University Hospital, Taipei, Taiwan, China
Supported by the Min-Sheng Healthcare, No.93MSH-TMU-12
Correspondence to: Hung-Jung Wang, 252, Wu Hsing Street, 110, Taipei, Taiwan, China. yayen0220@yahoo.com.tw
Telephone: +886-2-27372181-1131 Fax: +886-2-23780943
Received: 2006-11-03 Accepted: 2006-12-25

Abstract

AIM: To investigate the effect of partial splenic embolization (PSE) on platelet values in liver cirrhosis patients with thrombocytopenia and to determine the effective embolization area for platelet values improvement.

METHODS: Blood parameters and liver function indicators were measured on 10 liver cirrhosis patients (6 in Child-Pugh grade A and 4 in grade B) with thrombocytopenia (platelet values < 80 × $10^3/\mu L$) before embolization. Computed tomography scan was also needed in advance to acquire the splenic baseline. After 2 to 3 d, angiography and splenic embolization were performed. A second computed tomography scan was made to confirm the embolization area after 2 to 3 wk of embolization. The blood parameters of patients were also examined biweekly during the 1 year follow-up period.

RESULTS: According to the computed tomography images after partial splenic embolization, we divided all patients into two groups: low (< 30%), and high (≥ 30%) embolization area groups. The platelet values were increased by 3 times compared to baseline levels after 2 wk of embolization in high embolization area group. In addition, there were significant differences in platelet values between low and high embolization area groups. GPT values decreased significantly in all patients after 2 wk of embolization. The improvement in platelet and GPT values still persisted until 1 year after PSE. In addition, 3 of 4 (75%) Child-Pugh grade B patients progressed to grade A after 2 mo of PSE. The complication rate in < 30% and ≥ 30% embolization area groups was 50% and 100%, respectively.

CONCLUSION: Partial splenic embolization is an effective method to improve platelet values and GPT values in liver cirrhosis patients with thrombocytopenia and the ≥ 30% embolization area is meaningful for platelet values improvement. The relationship between the complication rate and embolization area needs further studies.

Key words: Partial splenic embolization; Liver cirrhosis; Thrombocytopenia

Lee CM, Leung TK, Wang HJ, Lee WH, Shen LK, Liu JD, Chang CC, Chen YY. Evaluation of the effect of partial splenic embolization on platelet values for liver cirrhosis patients with thrombocytopenia. *World J Gastroenterol* 2007; 13(4): 619-622

http://www.wjgnet.com/1007-9327/13/619.asp

INTRODUCTION

The spleen is known to be involved in thrombocytopenia associated with liver cirrhosis[1]. Thrombocytopenia in patients with liver cirrhosis has been reported to be caused by an increased platelet pool in the enlarged spleen[2], impaired platelet production in the bone marrow[3], decreased platelet function[4], and abnormalities in the platelet membranes[5]. Recently, an article[6] reported that decreased production of thrombopoietin (TPO) might also promote the development of thrombocytopenia in liver cirrhosis. Partial embolization of the splenic vessels has been used to treat hypersplenism of thrombocytopenia in liver cirrhosis patients. Mozes *et al*[7] described the benefit of partial splenic embolization (PSE) in reducing the prevalence of complications from splenic artery embolization. Miyazaki *et al*[8] reported the effectiveness of PSE in thrombocytopenia. Their reports suggested that PSE might be a safe and effective alternative to splenectomy in the treatment of thrombocytopenia. The aim of the current study was to investigate the effect of partial splenic embolization on platelet values in liver cirrhosis patients with thrombocytopenia and to determine

the effective embolization area for platelet values improvement.

MATERIALS AND METHODS

Ten liver cirrhosis patients with thrombocytopenia (platelet value < $80 \times 10^3/\mu L$) were transferred to our department to receive partial splenic embolization at Taipei Medical University Hospital from January 2004 to September 2005. All patients gave informed consent before their participation, and the Ethics Committee of Taipei Medical University Hospital approved the study. The Child-Pugh classifications of these 10 patients were grade A in 6 and grade B in 4 patients. They had no other chronic diseases. Before partial splenic embolization, measurements were taken of platelet, white blood counts, hemoglobin, bilirubin, alkaline phosphatase, and liver function indicators [aspartate aminotransferase, ASAT (GOT), and alanine aminotransferase, ALAT(GPT)].

Before the PSE, they underwent computed tomography (CT, HiSpeed CT/I; GE Medical Systems, Milwaukee, WI, USA) to observe the basal status of the spleen and calculate the volume of the spleen using the software of CT. After 2 to 3 d, angiography and PSE were performed, respectively. A femoral artery approach was used for superselective catheterization of the splenic artery. The catheter tip was placed as distally as possible in either the hilus of the spleen or the intrasplenic artery. Embolization was done by injections of a gelatin sponge (Gelfoam cube, Upjohn, Kalamazoo, USA) cut into 1 to 2 mm cube and suspended in 1 g cefazolin-containing solution. When the blood flow in this artery stopped, we finished the embolization. After 2 to 3 wk of PSE, we did CT scan again to confirm the embolization area via calculating the volume of the spleen. In addition, these patients took antibiotics orally to prevent sepsis. During the one year follow up period, we measured the blood parameters mentioned above biweekly, and recorded the blood parameters at every time point.

Statistical analysis

Blood parameters were compared using paired *t* test. $P < 0.05$ means significant differences.

RESULTS

The mean age of our patients was 56 years (from 19 to 71). According to the embolization areas presented on CT, we divided all patients into two groups: low embolization group (< 30%): 2 patients, and high embolization group (≥ 30%): 8 patients. The average embolization areas in these two groups were 20% and 40%, respectively. The effect of PSE on platelet values is listed in Table 1. In high embolization area group, the platelet values after 2 wk and 1 year of embolization were 2 to 3 times the basal values. In addition, we also evaluated the effect of different embolization areas on platelet values. We observed a marked variation of platelet values between low and high embolization groups. We found that an embolization area equal to or higher than 30% is an effective embolization area for improvement of platelet values.

Table 1 Effects of partial splenic embolization on platelet values

Basal values ($\times 10^3/\mu L$)	Embolization area (%)	After 2 wk ($\times 10^3/\mu L$)	After 1 year ($\times 10^3/\mu L$)
Low embolization			
56	15	69	66
54	25	66	51
Average platelet value		67.5	58.5
High embolization			
60	35	175[1]	136[1]
40	45	203[1]	158[1]
67	35	258[1]	140[1]
61	30	212[1]	185[1]
58	30	207[1]	149[1]
64	30	71	59
48	50	250[1]	195[1]
51	65	159[1]	141[1]
Average platelet value		192[2]	145[2]

[1]Means significant differences in platelet values between basal values and post-embolization values; [2]Means significant differences in platelet values between low and high embolization areas groups.

Table 2 Effect of partial splenic embolization on GPT values

Basal values (IU/L)	Embolization area (%)	After 2 wk (IU/L)	After 1 year (IU/L)
Low embolization			
145	15	46[1]	45[1]
95	25	57[1]	51[1]
Average GPT value		51.5	48
High embolization			
87	35	47[1]	52[1]
76	45	50[1]	51[1]
102	35	54[1]	40[1]
98	30	44[1]	51[1]
87	30	56[1]	44[1]
116	30	58[1]	54[1]
79	50	59[1]	55[1]
66	65	45[1]	35[1]
Average GPT value		52	48

[1]Means significant differences in GPT values between basal values and post-embolization values.

PSE cannot improve the GOT values markedly; however, the GPT values of these 10 patients after 2 wk of PSE decreased baldly and the range of degradation was from 32% to 68% (Table 2). We also found that the improvement of platelet and GPT values still persisted until 1 year after PSE. In addition, 3 of 4 (75%) Child-Pugh grade B patients progressed to grade A after 2 mo of PSE. It suggested that the PSE may improve the liver function with a long-term efficiency. The PSE procedure did not affect other blood parameters.

Regarding complications, there were fever in 10 (100%), pain in 8 (80%) and ascites in 1 (10%) of patients. Ascites occurred in high embolization group. The complication rate in < 30% and in ≥ 30% groups were 50% and 100%, respectively.

DISCUSSION

In 1973 Maddison[9] reported the first case of splenic

artery embolization. In 1979, Spigos[10] cured 14 hypersplenism cases using PSE. Since then, PSE has become a major therapy clinically for hypersplenism. The spleen represents one fourth of the total lymphatic mass, serves as a biological filter for the clearance of bacteria and also is essential for rapid antibody production after challenge with blood-borne particulate antigens in the absence of preexisting antibodies[11]. In addition, the spleen appears to be the site of production of a nonspecific leukophilic immunoglobin, tuftsin, that increases the phagocytic activity of polymorphonuclear leucocytes. Thus, it is apparent that the spleen has important and critical functions and its removal is not to be taken lightly[12]. Partial splenic embolization represents a potential alternative method to splenectomy when ablation of the splenic parenchyma is desired, particularly in compromised patients, where splenectomy carries significant morbidity and mortality rates. Partial splenic embolization has been successfully used experimentally in the treatment of thrombocytopenia or splenic trauma. Hematologic changes after embolization have been observed, especially in platelet values. There have also been sporadic reports[13,14] of successful splenic embolization in humans with thrombocytopenia due to hypersplenism of portal hypertension. Several studies[15,16] demonstrated that PSE could not only improve the symptoms of hypersplenism but also could reserve the spleen for immune function maintenance.

A major finding in this study is the effectiveness of PSE in improving platelet values and the extent of embolization seems to be critical in the efficacy of PSE. According to Bruno's study[17], embolization of 50% or less of the splenic mass was almost invariably associated with an elevation of platelet values. In another study[18], the authors demonstrated that 65%-70% embolization area is effectiveness in platelet values improvement in liver cirrhosis patients with thrombocytopenia. In Kimuro's study[19], the platelet counts were improved from $5.6 \times 10^3/\mu L$ to $36 \times 10^3/\mu L$ in 80% embolization area group and from $6.2 \times 10^3/\mu L$ to $25 \times 10^3/\mu L$ in 70% embolization area group, which is significantly higher than the former. According to the studies mentioned above, it is suggested that the improved efficacy of PSE on platelet values relates closely to embolization area. In our study, we observed a marked variation of platelet value between low and high embolization groups. We assume that an embolization area equal to or higher than 30% is an effective embolization area for platelet values improvement. Our result is not similar to previous studies. We presume that the limited patient number results in the fact that we cannot differentiate the age, basal platelet values and Child-Pugh classification of patients. Compared to the Bruno and Miyazaki's large-scale studies, there are more variabilities in our study. The various results probably have multiple causes, but patient selection, with different degrees of hepatic insufficiency, is probably of greatest importance.

The complications after PSE include pneumonia, ascites, bleeding, peritonitis, etc. In our study, there were fever in 10 patients, pain in 8 (7 in high embolization and 1 in low embolization) and ascites in 1 (in high embolization). The complication rate in $< 30\%$ and in $\geqslant 30\%$ groups was 50% and 100%, respectively. In Mukaiya's study[20], they divided all patients into three groups: $< 50\%$, 50%-70% and $\geqslant 70\%$ according to the embolization area. The complication rate was 28%, 56% and 95%, respectively. In another study[18], the authors also demonstrated that the complication rate associated with the embolization area, which is similar to our study. However, in Hong's study[21], they conducted linear regression analysis between complication rate and embolization area and the correlation coefficient was 0.587. Hong considered that embolization area will affect the complication rate, however, it is not an absolute factor. The relationship between these two parameters needs further study.

Our results showed that the GPT values of these 10 patients after 2 wk of PSE decreased badly and the range of degradation was from 32% to 68%. We also found that the improvement in GPT values persisted until 1 year after PSE. As compared with GPT, GOT is not a specific indicator for liver function. Generally speaking, GOT and GPT values will increase when hepatitis occurs, however, GOT also exists in erythrocytes, cardiac muscles and skeletal muscles. Some extrahepatic diseases, such as myocardial infarction, myocardial necrosis, hemolysis and several muscle related diseases could result in GOT increase. On the contrary, almost all GPT exists in the liver, so that GPT is more specific than GOT for liver function. This is the reason why PSE improved GPT values markedly while there was no effect on GOT values. In addition, 3 of 4 (75%) Child-Pugh grade B patients progressed to grade A after 2 mo of PSE. We suppose that the PSE may be able to improve the liver function, with a long term efficiency. In Noguchi's study[22], 1 liver cirrhosis patient with Child-Pugh grade C progressed to grade B after 6 mo of PSE; 3 of 5 Child-Pugh grade B patients progressed to grade A. In Vujic's study[23], they found liver function improvement in 56 of 128 patients (43.8%) who underwent PSE and their clinical expression included albumin increase and prothrombin formation time abridgement. According to Wang[24], the mechanism by which PSE improves liver function may involve immunologic mechanisms and hemodynamic changes. Noguchi *et al*[22] reported that after PSE the changes in the platelet count as compared with the preoperative value negatively correlate with the change in the platelet-associated immunoglobulin G levels. That study suggested that PSE improves the thrombocytopenia induced by immunologic mechanisms in cirrhotic patients. As for hemodynamic mechanisms, Barcena *et al*[25] reported that PSE decreased blood flow in the splenic artery and increased blood flow in the hepatic artery and superior mesenteric artery. In addition, Kato *et al*[26] found that the decrease in total portal blood flow and the relative increase in the mesenteric blood flow after PSE may decrease liver congestion, enhance the blood supply, and increase the supply of cytokines derived from the digestive tract.

In conclusion, partial splenic embolization is an effective method to improve platelet values in liver cirrhosis patients with thrombocytopenia. We also find that the $\geqslant 30\%$ embolization area is meaningful for

platelet values improvement. The relationship between complication rate and embolization area needs further studies.

COMMENTS

Background

The spleen is known to be involved in thrombocytopenia associated with liver cirrhosis. Thrombocytopenia in patients with liver cirrhosis has been reported to be caused by an increased platelet pool in the enlarged spleen, impaired platelet production in the bone marrow, a decreased platelet function, and abnormalities in the platelets membranes. Partial embolization of the spleen vessels has been used to treat hypersplenism of thrombocytopenia in liver cirrhosis patients. Studies suggested that PSE might be a safe and effective alternative to splenectomy in the treatment of thrombocytopenia.

Innovations and breakthroughs

The focus of most previous studies is to evaluate the effectiveness of partial splenic embolization on blood parameters (especially platelets values). The breakthrough of our article is that we found out the efficient embolization area for platelet value improvement, and this provides a meaningful reference for clinic physicians in their therapy.

Applications

Clinical physicians should adopt the minimal partial splenic embolization area, which could improve the platelet value for treatment of the liver cirrhosis patients with thrombocytopenia. The major advantage is fewer complications after embolization. The $\geqslant$ 30% efficient embolization area shown in our article is multivariate depending on the techniques and patient status; however, we provide another meaningful cerebration for clinical treatment.

Terminology

PSE: Partial splenic embolization.

Peer review

This article evaluated the effect of the degree of partial splenic embolisation on platelet values in cirrhotic patients with hypersplenism. The data suggest that at least 30% of the spleen area must be embolisation area in order to increase platelet counts sufficiently.

REFERENCES

1 **Aster RH**. Immune thrombocytopenia caused by glycoprotein IIb/IIIa inhibitors. *Chest* 2005; **127**: 53S-59S
2 **Coons JC**, Barcelona RA, Freedy T, Hagerty MF. Eptifibatide-associated acute, profound thrombocytopenia. *Ann Pharmacother* 2005; **39**: 368-372
3 **Khaykin Y**, Paradiso-Hardy FL, Madan M. Acute thrombocytopenia associated with eptifibatide therapy. *Can J Cardiol* 2003; **19**: 797-801
4 **Ziporen L**, Li ZQ, Park KS, Sabnekar P, Liu WY, Arepally G, Shoenfeld Y, Kieber-Emmons T, Cines DB, Poncz M. Defining an antigenic epitope on platelet factor 4 associated with heparin-induced thrombocytopenia. *Blood* 1998; **92**: 3250-3259
5 **Curtis BR**, Swyers J, Divgi A, McFarland JG, Aster RH. Thrombocytopenia after second exposure to abciximab is caused by antibodies that recognize abciximab-coated platelets. *Blood* 2002; **99**: 2054-2059
6 **Xu RY**, Liu B, Lin N. Therapeutic effects of endoscopic variceal ligation combined with partial splenic embolization for portal hypertension. *World J Gastroenterol* 2004; **10**: 1072-1074
7 **Ando H**, Ito T, Nagaya M. Partial splenic embolization decreases the serum bilirubin level in patients with hypersplenism following the Kasai procedure for biliary atresia. *J Am Coll Surg* 1996; **182**: 206-210
8 **Miyazaki M**, Itoh H, Kaiho T, Ohtawa S, Ambiru S, Hayashi S, Nakajima N, Oh H, Asai T, Iseki T. Partial splenic embolization for the treatment of chronic idiopathic thrombocytopenic purpura. *AJR Am J Roentgenol* 1994; **163**: 123-126
9 **Maddison FE**. Embolic therapy of hypersplenism. *Invest Radiol* 1973; **8**: 280-281
10 **Spigos DG**, Jonasson O, Mozes M, Capek V. Partial splenic embolization in the treatment of hypersplenism. *AJR Am J Roentgenol* 1979; **132**: 777-782
11 **Stanisławska J**, Interewicz B, Maksymowicz M, Moscicka M, Olszewski WL. The response of spleen dendritic cell-enriched population to bacterial and allogeneic antigens. *Ann Transplant* 2005; **10**: 17-23
12 **Israel DM**, Hassall E, Culham JA, Phillips RR. Partial splenic embolization in children with hypersplenism. *J Pediatr* 1994; **124**: 95-100
13 **Ohmoto K**, Iguchi Y, Miyake I. Long-term evaluation of partial splenic embolization for liver cirrhosis and hepatocellular carcinoma accompanied by hypersplenism. *Hepatol Res* 1998; **11**: 73-83
14 **Mazzucconi MG**, Arista MC, Peraino M, Chistolini A, Felici C, Francavilla V, Macale E, Conti L, Gandolfo GM. Long-term follow-up of autoimmune thrombocytopenic purpura (ATP) patients submitted to splenectomy. *Eur J Haematol* 1999; **62**: 219-222
15 **Berchtold P**, McMillan R. Therapy of chronic idiopathic thrombocytopenic purpura in adults. *Blood* 1989; **74**: 2309-2317
16 **Tsiotos G**, Schlinkert RT. Laparoscopic splenectomy for immune thrombocytopenic purpura. *Arch Surg* 1997; **132**: 642-646
17 **Bruno S**. Partial splenic embolization for the treatment of hypersplenism in cirrhosis. *Hepatology* 1993; **18**: 309-314
18 **Ganesh A**, Rose JB, Maxwell LG. Protracted pain following partial splenic embolization in an adolescent female with hypersplenism. *Paediatr Anaesth* 2005; **15**: 1013-1015
19 **Kaushansky K**. Thrombopoietin: the primary regulator of platelet production. *Blood* 1995; **86**: 419-431
20 **Mukaiya M**, Hirata K, Yamashiro K, Katsuramaki T, Kimura H, Denno R. Changes in portal hemodynamics and hepatic function after partial splenic embolization (PSE) and percutaneous transhepatic obliteration (PTO). *Cancer Chemother Pharmacol* 1994; **33** Suppl: S37-S41
21 **Hong YC**, Wu HK, Yang AD. Evaluation of partial splenic embolization in patients with hypersplenism in cirrhosis. *Chin J Radiol* 1999; **24**: 233-237
22 **Noguchi H**, Hirai K, Aoki Y, Sakata K, Tanikawa K. Changes in platelet kinetics after a partial splenic arterial embolization in cirrhotic patients with hypersplenism. *Hepatology* 1995; **22**: 1682-1688
23 **Vujic I**, Lauver JW. Severe complications from partial splenic embolization in patients with liver failure. *Br J Radiol* 1981; **54**: 492-495
24 **Wang BH**, Zhou LQ. Partial splenic embolization therapy for chronic idiopathic thrombocytopenic purpura in children: a report of 2 cases. *Zhongguo DangDai ErKe ZaZhi* 2006; **8**: 2 p following 172
25 **Bárcena R**, Moreno A, Foruny JR, Moreno A, Sánchez J, Gil-Grande L, Blázquez J, Nuño J, Fortún J, Rodriguez-Gandía MA, Otón E. Improved graft function in liver-transplanted patients after partial splenic embolization: reversal of splenic artery steal syndrome? *Clin Transplant* 2006; **20**: 517-523
26 **Kato M**, Shimohashi N, Ouchi J, Yoshida K, Tanabe Y, Takenaka K, Nakamuta M. Partial splenic embolization facilitates completion of interferon therapy in patients with chronic HCV infection and hypersplenism. *J Gastroenterol* 2005; **40**: 1076-1077

S- Editor Liu Y **L- Editor** Zhu LH **E- Editor** Lu W

PO Box 2345, Beijing 100023, China
www.wjgnet.com
wjg@wjgnet.com

World J Gastroenterol 2007 January 28; 13(4): 623-627
World Journal of Gastroenterology ISSN 1007-9327

RAPID COMMUNICATION

Therapeutic effects of Caspase-1 inhibitors on acute lung injury in experimental severe acute pancreatitis

Xiao-Hua Zhang, Ren-Min Zhu, Wen-An Xu, Hai-Jun Wan, Heng Lu

Xiao-Hua Zhang, Ren-Min Zhu, Wen-An Xu, Hai-Jun Wan, Heng Lu, Department of Gastroenterology, Jinling Hospital, Nanjing 210002, Jiangsu Province, China
Correspondence to: Ren-Min Zhu, Department of Gastroenterology, Jinling Hospital, No.305, East Zhongshan Road, Nanjing 210002, Jiangsu Province,
China. jszhxh@sina.com
Telephone: +86-25-80860048 Fax: +86-25-80861126
Received: 2006-09-10 Accepted: 2006-12-11

Abstract

AIM: To assess the therapeutic effect of Caspase-1 inhibitors (ICE-I) on acute lung injury (ALI) in experimental severe acute pancreatitis (SAP).

METHODS: Forty-two SD rats were randomly divided into 3 groups: healthy controls (HC, n = 6); SAP-S group (n = 18); SAP-ICE-I group (n = 18). SAP was induced by retrograde infusion of 5% sodium taurocholate into the bile-pancreatic duct. HC rats underwent the same surgical procedures and duct cannulation without sodium taurocholate infusion. In SAP-S group, rats received the first intraperitoneal injection of isotonic saline 2 h after induction of acute pancreatitis and a repeated injection after 12 h. In SAP-ICE-I group, the rats were firstly given ICE inhibitors intraperitoneally 2 h after induction of pancreatitis. As in SAP-S group, the injection was repeated at 12 h. Serum IL-1β was measured by ELISA. Intrapulmonary expression of Caspase-1, IL-1β and IL-18 mRNA were detected by semi-quantitative RT-PCR. The wet/dry weight ratios and histopathological changes of the lungs were also evaluated.

RESULTS: Serum IL-1β levels in SAP-S group were 276.77 ± 44.92 pg/mL at 6 h, 308.99 ± 34.95 pg/mL at 12 h, and 311.60 ± 46.51 pg/mL at 18 h, which were increased significantly (P < 0.01, *vs* HC). In SAP-ICE-I group, those values were decreased significantly (P < 0.01, *vs* SAP-S). Intrapulmonary expression of Caspase-1, IL-1β and IL-18 mRNA were observed in the HC group, while they were increased significantly in the SAP-S group (P < 0.01, *vs* HC). The expression of IL-1β and IL-18 mRNA were decreased significantly in the SAP-ICE-I group (P < 0.01, *vs* SAP-S), whereas Caspase-1 mRNA expression had no significant difference (P > 0.05). The wet/dry weight ratios of the lungs in the SAP-S group were increased significantly (P < 0.05 at 6 h, P < 0.01 at 12 h and 18 h, *vs* HC) and they were decreased significantly in the SAP-ICE-I group (P < 0.05, *vs* SAP-S). Caspase-1 inhibitors ameliorated the severity of ALI in SAP.

CONCLUSION: Caspase-1 activation, and overproduction of IL-1β and IL-18 play an important role in the course of ALI, and Caspase-1 inhibition is effective for the treatment of ALI in experimental SAP.

Key words: Severe acute pancreatitis; Caspase-1; Interleukin-1β; Interleukin-18; Acute lung injury

Zhang XH, Zhu RM, Xu WA, Wan HJ, Lu H. Therapeutic effects of Caspase-1 inhibitors on acute lung injury in experimental severe acute pancreatitis. *World J Gastroenterol* 2007; 13(4): 623-627

http://www.wjgnet.com/1007-9327/13/623.asp

INTRODUCTION

Patients with severe acute pancreatitis (SAP) is often complicated with acute lung injury (ALI), which is difficult to deal with clinically. IL-1β and TNF-α are currently believed to play an important role in promoting local tissue destruction and remote organ failure in the course of SAP[1,2]. IL-18 is a novel proinflammatory cytokine, sharing striking structural and functional similarities to IL-1β. Caspase-1, also termed IL-1β-converting-enzyme (ICE), is the first member of the family of cysteine proteases called Caspases, with the functions of proteolytic cleavage of IL-1β and IL-18 precursors into their active forms. Suppression of IL-1β and IL-18 by inhibiting the function of ICE, subsequently alleviating cascade reactions, may have a therapeutic significance for SAP and systemic inflammatory response syndrome (SIRS).

In this study, an experimental model of SAP was induced in SD rats. Serum IL-1β levels, intrapulmonary expression of Caspase-1, IL-1β and IL-18 mRNA were measured respectively, and the wet/dry weight ratios and histopathological alterations in the lungs were observed to assess the therapeutic effect of Caspase-1 inhibitors on ALI in SAP.

MATERIALS AND METHODS

Experimental animal models and grouping

Healthy adult male Sprague-Dawley rats weighing 230-250

g were provided by the Experimental Animal Center of Jingling Hospital in Nanjing. All forty-two rats were randomly divided into 3 groups: healthy controls (HC, n = 6); SAP-S group (n = 18); SAP-ICE-I group (n = 18). The latter two groups were further divided into 6, 12, and 18 h time points, and each contained 6 rats. SAP was induced by retrograde infusion of 5% sodium taurocholate into the bile-pancreatic duct in SD rats[3-7]. HC rats underwent the same surgical procedures and duct cannulation without sodium taurocholate infusion. In the SAP-S group, the rats received the first intraperitoneal injection of isotonic saline 2 h after induction of acute pancreatitis and a second injection after 12 h. In the SAP-ICE-I group, the rats were firstly given 0.25 mg of an ICE inhibitor (Ac-Tyr-Val-Ala-Asp-2,6-dimethylbenzoyloxymethylketone) dissolved in 1 mL sterile phosphate-buffered saline intraperitoneally 2 h after induction of pancreatitis. As in the SAP-S group, this was repeated at 12 h. Surviving rats were killed at certain time points, and all samples were obtained for subsequent analysis.

Measurement of serum IL-1β levels

Serum IL-1β levels were measured using a commercial enzyme-linked immunosorbent assay (ELISA) according to the manufacturer's instructions (B&C Co.). All samples were tested in duplicate and expressed as the means.

RT-PCR examination of intrapulmonary Caspase-1, IL-1β and IL-18 mRNA

Reagents and primers: TRIZOL Reagent was purchased from Gibco BRL Life Technologies. One Step RNA PCR kit (AMV) was purchased from TaKaRa Biotechnology (Dalian) Co., Ltd. The sequences of IL-1β, IL-18 and β-actin primers (designed by Primer 3 software, synthesized by Sangon Biotechnology Co. Shanghai) were as follows: upstream and downstream primers, respectively: 5'-AAG GTC CTG AGG GCA AAG AG-3' and 5'-GTG TTG CAG ATA ATG AGG GC-3' for Caspase-1 (500 bp of amplification products); 5'-AGA AGC TGT GGC AGC TAC CT-3' and 5'-TTG GGA TCC ACA CTC TCC AG-3' for IL-1β (400 bp of amplification products); 5' -GCT GCA ATA CCA GAA GAA GG-3' and 5'-AGA TAG GGT CAC AGC CAG TC-3' for IL-18 (300 bp of amplification products); 5'-AGG GTG TGA TGG TGG GTA TG-3' and 5'-CAT AGC TCT TCT CCA GGG AG-3' for β-actin (600 bp of amplification products).

Total lung RNA extraction: Total RNA was extracted from the lung tissue by TRIZOL Reagent according to the manufacturer's protocol. One hundred mg of lung tissue was homogenized in 1 mL of TRIZOL Reagent. Following homogenization, insoluble material was removed from the homogenate by centrifugation at 12000 r/min for 10 min at 4℃ and the homogenized tissue was incubated for 5 min at a room temperature. Then 0.2 mL of chloroform was then added. The tube was shaken vigorously for 15 s and incubated at room temperature for 3 min. The sample was centrifuged at 12000 r/min for 15 min at 4℃ and the upper aqueous phase was transferred to another tube. After that 0.5 mL of isopropyl alcohol was added. The sample was incubated at room temperature for 10 min and centrifuged at 12000 r/min for 10 min at 4℃. The supernatant was discarded and the RNA pellets were washed with 1 mL of 75% ethanol. The samples were mixed by vortexing and centrifuged at 7000 r/min for 5 min at 4℃. At the end of the procedure, the RNA pellet was air-dried for 10 min, dissolved in 50 μL of DEPC water, and stored at -80℃. The A260/280 ratio was measured with an ultraviolet spectrophotometer and the RNA content was calculated (1A260 = 40 μg/mL).

RT-PCR was carried out using the One Step method. The total RT-PCR volume of each Eppendorf tube was 50 μL, including 5 μL of 10 × One Step RNA PCR buffer, 10 μL of $MgCl_2$ (25 mol/L), 5 μL of dNTPs (10 mol/L), 1 μL of RNase inhibitor (40 U/μL), 1 μL of AMV RTase XL (5 U/μL), 1 μL of AMV-Optimized Taq (5 U/μL), 1 μL of upstream specific primer, 1 μL of downstream specific primer, 1 μL of experimental sample(≤ 1 μg total RNA), 24 μL of RNase Free dH_2O. Each RT-PCR conditions were as follows: 30 min at 50℃ for RT reactions, 2 min at 94℃ for RTase inactivation, 30 s at 94℃, 30 s at 51℃, 90 s at 72℃ for 30 cycles (Caspase-1); 30 s at 94℃, 30 s at 53ºC, and 90 s at 72℃ for 30 cycles (IL-1β); 30 s at 94℃, 30 s at 55ºC, and 90 s at 72℃ for 30 cycles(IL-18); 30 s at 94℃, 30 s at 55℃, and 90 s at 72℃ for 35 cycles (β-actin). RT-PCR was terminated with an elongation step at 72℃ for 5 min, and PCR products were stored at 4℃. Five μL of the reaction products was visualized by electrophoresis in 2% agarose gels containing ethidium bromide. Ultraviolet illumination was used to visualize the DNA bands, and the gels were photographed digitally. Band intensity was determined by optical density with individual PCR product/β-actin cDNA ratios.

W/D ratio of the lung tissue

To assess tissue edema, the right lung was removed after the experiment, then weighed and dried in a 80℃ oven for 72 h until the weight was constant, and the ratio of wet weight to dry weight (W/D ratio) was then obtained.

Histologic examination

According to routine procedures, paraffin sections of the lung tissue samples were prepared by HE staining, and histologic alterations of lung tissue were observed by light microscopy.

Statistical analysis

All values were presented as mean ± SD. Statistical analysis was performed using SPSS 11.0 statistical software applying One-Way ANOVA. A value of $P < 0.05$ was regarded as statistically significant.

RESULTS

Serum IL-1β levels

In the SAP-S group and the SAP-ICE-I group, the serum IL-1β levels at all time points were significantly higher than those of HC ($P < 0.01$), whereas serum IL-1β levels were significantly decreased in the SAP-ICE-I group ($P < 0.01$) in comparison with the SAP-S group (Table 1).

Table 1 Serum IL-1β levels and W/D ratios of the lungs in rats with SAP (mean ± SD)

Group	*n*	IL-1β (pg/mL)	W/D ratio of lung (g/g)
HC	6	90.13 ± 21.13	4.32 ± 0.33
SAP-S			
6 h	6	276.77 ± 44.92[b]	4.85 ± 0.38[a]
12 h	6	308.99 ± 34.95[b]	4.97 ± 0.47[b]
18 h	5	311.60 ± 46.51[b]	5.03 ± 0.46[b]
SAP-ICE-I			
6 h	6	151.42 ± 27.26[b,d]	4.38 ± 0.36[c]
12 h	6	152.47 ± 29.60[b,d]	4.48 ± 0.37[c]
18 h	6	175.45 ± 29.72[b,d]	4.51 ± 0.36[c]

[a]$P < 0.05$, [b]$P < 0.01$ *vs* HC group; [c]$P < 0.05$, [d]$P < 0.01$ *vs* SAP-S group.

Table 2 Intrapulmonary expression of Caspase-1, IL-1β and IL-18 mRNA in rats with SAP (mean ± SD)

Group	*n*	Caspase-1 mRNA	IL-1β mRNA	IL-18 mRNA
HC	6	0.57 ± 0.06	0.42 ± 0.03	0.55 ± 0.05
SAP-S				
6 h	6	0.71 ± 0.04[b]	0.75 ± 0.05[b]	0.82 ± 0.05[b]
12 h	6	0.71 ± 0.05[b]	0.81 ± 0.06[b]	0.83 ± 0.06[b]
18 h	5	0.72 ± 0.04[b]	0.79 ± 0.07[b]	0.82 ± 0.07[b]
SAP-ICE-I				
6 h	6	0.72 ± 0.05[b]	0.52 ± 0.05[b,d]	0.58 ± 0.06[d]
12 h	6	0.72 ± 0.06[b]	0.50 ± 0.04[b,d]	0.55 ± 0.04[d]
18 h	6	0.69 ± 0.08[b]	0.49 ± 0.04[a,d]	0.57 ± 0.04[d]

[a]$P < 0.05$, [b]$P < 0.01$ *vs* HC group; [c]$P < 0.05$, [d]$P < 0.01$ *vs* SAP-S group.

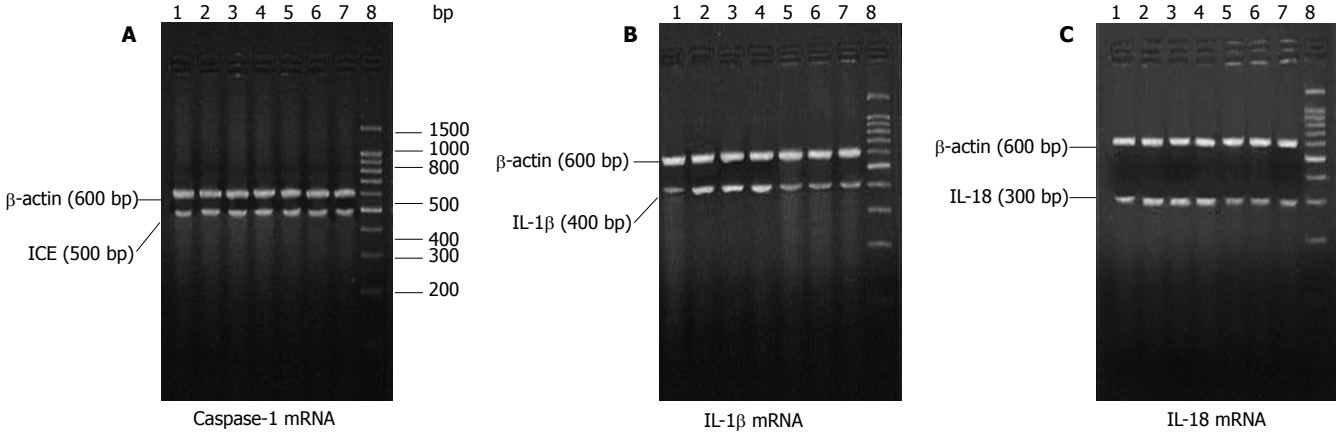

Figure 1 Intrapulmonary expression of Caspase-1, IL-1β and IL-18 mRNA in rats with SAP. Lane 1: HC; lanes 2-4: 6-18 h in SAP-S; lanes 5-7: 6-18 h in SAP-ICE-I; lane 8: Marker.

Intrapulmonary expression of Caspase-1, IL-1β and IL-18 mRNA

Intrapulmonary expression of Caspase-1, IL-1β and IL-18 mRNA were observed in the HC group, which were increased significantly in the SAP-S group ($P < 0.01$ *vs* HC). The expression of IL-1β and IL-18 mRNA were significantly decreased with ICE inhibition ($P < 0.01$), whereas Caspase-1 mRNA expression had no significant difference ($P > 0.05$) (Table 2, Figure 1 A-C).

W/D ratio of the lung tissue

In the SAP-S group, W/D ratios were increased significantly ($P < 0.05$ at 6 h, $P < 0.01$ at 12 h and 18 h, *vs* HC), and those were significantly attenuated with ICE inhibition ($P < 0.01$) (Table 1).

Pathologic alterations in lung tissue

Observed under a light microscope, the pulmonary structures of the HC group were basically normal. However, characteristics of typical lung injury could be seen in the SAP-S group, represented by marked congestion, edema and masses of inflammatory cell infiltration in pulmonary interstitium and aveoli, thickened alveolar septum, which became progressively severe after SAP induction. Compared with the SAP-S group, such pathologic changes were much less in the SAP-ICE-I group.

DISCUSSION

SAP is often complicated with multiple systemic organ failure (MSOF), which is the major cause of death in SAP. In extra-pancreatic organs, ALI is most prominent. About 20% of cases with SAP may develop adult respiratory distress syndrome (ARDS). One third of the patients die during the early stages of SAP, a half of which die as a result of ARDS[8,9]. At present, the role of cytokines in the pathogenesis of SAP has become a hot issue in the research field. Of the numerous cytokines, IL-1β and TNF-α have been confirmed to play an important role in the development of systemic complications of SAP. However, their roles in mediating ALI during SAP are not completely understood.

Caspase-1/ICE is one member of the family of cysteine proteases called Caspases. One of the major functions of ICE is the proteolytic cleavage of the 31 000 molecular weight IL-1β precursor into its biologically active 17 000 form. IL-1β is an inflammatory cytokine produced by activated lymphocytes and monocytes. IL-1β and TNF-α are primary inducers of IL-6 and IL-8 production, and are known to cause fever, hypoperfusion, circulatory collapse, shock, metabolic acidosis, cardiac dysfunction, and the occurrence of ARDS. Norman *et al*[10] showed that no IL-1β mRNA expression was found in the lungs of healthy mice, and that intrapulmonary IL-1β mRNA and protein expression were increased after SAP

induction. Paszkowski *et al*[11] demonstrated that IL-1β mRNA expression could be found in the lungs of healthy rats, and that intrapulmonary IL-1β mRNA expression was upregulated in SAP, in proportion to the severity of ALI, suggesting the existence of a significant correlation between overproduction of IL-1β in the lungs and ALI in SAP.

Ac-Tyr-Val-Ala-Asp-2,6-dimethylbenzoyloxymethylketone used in this study is a highly competitive and irreversible inhibitor of ICE. It inactivates the enzyme and is relatively inert toward other bionucleophiles such as glutathione. Previous studies showed changes in serum amylase and pancreas in SAP[12,13]. In this study, the ICE inhibitor was injected into rats intraperitoneally 2 h after SAP was induced by retrograde infusion of 5% sodium taurocholate into the bili-pancreatic duct. A remarkable elevation of serum IL-1β levels, an upregulation of intrapulmonary Caspase-1 and IL-1β mRNA expression, an increased W/D ratio of the lung and obvious pathological changes after induction of SAP were observed; serum and intrapulmonary IL-1β expression were decreased significantly, with an improvement of pathological changes in rats treated with ICE inhibitors. These suggest that the therapeutic effects of ICE inhibitors on ALI in SAP may be associated with a reduced IL-1β-mediated injury. Besides generating large numbers of active IL-1β, ICE is also known to process the inactive precursor of IL-18 into its bioactive forms[14-17]. IL-18, formerly called IFN-γ-inducing factor, is a novel proinflammatory cytokine with an 18000 molecular weight, sharing striking structural and functional similarities to IL-1β. In addition, the biological activity of IL-18 is closely related to that of IL-1β: IL-18 induces the gene expression and synthesis of IL-1, TNF, and several chemokines by means of a putative IL-18 receptor complex. Also, IL-18 plays an important role in the Th-1 response to the stimulation of virul antigens, primarily because of its ability to induce IFN-γ production in T cells and NK cells. Rau *et al*[18] reported that local and systemic IL-18 concentrations are significantly elevated in patients with AP, and that serum IL-18 concentrations closely correlate with the development of pancreatic necrosis and remote organ failure. In the current study, intrapulmonary IL-18 mRNA expression was measured by RT-PCR. Marked upregulation of IL-18 mRNA was observed in the lungs after induction of SAP, and intrapulmonary IL-18 expression was significantly decreased in rats treated with ICE inhibitors. In addition, it is well established that IL-1β, IL-18, and TNF-α share a close interrelationship by inducing the synthesis of each other[14,19,20]. Paszkowski *et al*[11] indicated that intrapulmonary TNF-α mRNA expression was uniformly downregulated in rats receiving the treatment of ICE inhibitors, suggesting that the therapeutic effects of ICE inhibitors on ALI in SAP may correlate with a decrease in TNF-α-mediated injury. Considering that the synthesis of IL-1β, IL-18, and TNF-α could be induced by each other, plus the alterations in W/D ratios of the lungs and histopathologic changes in SAP, we speculate that as with TNF-α and IL-1β, overproduction of IL-18 in the lungs plays an important role in the course of SAP complicated with ALI, and that therapeutic effects of ICE inhibitors on ALI in SAP may be associated with the inhibition of IL-18.

In summary, activation of Caspase-1/ICE, and overproduction of IL-1β and IL-18 in the lungs play an important role during the course of ALI and ARDS in SAP, and ICE inhibitors are effective against ALI in SAP. The mechanisms for ICE inhibition may be associated with decreased cytokine-mediated injury, such as IL-1β, IL-18 and TNF-α. Therefore, studies of the mechanism for ALI in SAP may shed new light on understanding of SIRS and MSOF, as well as the prevention and treatment for SAP.

ACKNOWLEDGMENTS

We thank Professor Zhao-Shen Li and Zhen-Xing Tu, Department of Gastroenterology, Changhai Hospital, Shanghai, for their expert assistance in this study.

REFERENCES

1 **Laveda R**, Martinez J, Munoz C, Penalva JC, Saez J, Belda G, Navarro S, Feu F, Mas A, Palazon JM, Sanchez-Paya J, Such J, Perez-Mateo M. Different profile of cytokine synthesis according to the severity of acute pancreatitis. *World J Gastroenterol* 2005; **11**: 5309-5313

2 **Granger J**, Remick D. Acute pancreatitis: models, markers, and mediators. *Shock* 2005; **24** Suppl 1: 45-51

3 **Aho HJ**, Koskensalo SM, Nevalainen TJ. Experimental pancreatitis in the rat. Sodium taurocholate-induced acute haemorrhagic pancreatitis. *Scand J Gastroenterol* 1980; **15**: 411-416

4 **Lange JF**, van Gool J, Tytgat GN. Experimental pancreatitis in the rat: role of bile reflux in sodium taurocholate-induced acute haemorrhagic pancreatitis. *Eur Surg Res* 1986; **18**: 369-374

5 **Rau B**, Paszkowski A, Lillich S, Baumgart K, Möller P, Beger HG. Differential effects of caspase-1/interleukin-1beta-converting enzyme on acinar cell necrosis and apoptosis in severe acute experimental pancreatitis. *Lab Invest* 2001; **81**: 1001-1013

6 **Nakamura H**, Honda H, Tashiro M, Taguchi M, Yoshikawa H, Otsuki M. Increased expression of 19-kD interacting protein-3-like protein and the relationship to apoptosis in the lung of rats with severe acute pancreatitis. *Crit Care Med* 2003; **31**: 2527-2534

7 **Meng Y**, Zhang M, Xu J, Liu XM, Ma QY. Effect of resveratrol on microcirculation disorder and lung injury following severe acute pancreatitis in rats. *World J Gastroenterol* 2005; **11**: 433-435

8 **Steer ML**. Relationship between pancreatitis and lung diseases. *Respir Physiol* 2001; **128**: 13-16

9 **Bhatia M**, Slavin J, Cao Y, Basbaum AI, Neoptolemos JP. Preprotachykinin-A gene deletion protects mice against acute pancreatitis and associated lung injury. *Am J Physiol Gastrointest Liver Physiol* 2003; **284**: G830-G836

10 **Norman JG**, Fink GW, Denham W, Yang J, Carter G, Sexton C, Falkner J, Gower WR, Franz MG. Tissue-specific cytokine production during experimental acute pancreatitis. A probable mechanism for distant organ dysfunction. *Dig Dis Sci* 1997; **42**: 1783-1788

11 **Paszkowski AS**, Rau B, Mayer JM, Möller P, Beger HG. Therapeutic application of caspase 1/interleukin-1beta-converting enzyme inhibitor decreases the death rate in severe acute experimental pancreatitis. *Ann Surg* 2002; **235**: 68-76

12 **Liu HB**, Cui NQ, Li DH, Chen C. Role of Kupffer cells in acute hemorrhagic necrotizing pancreatitis-associated lung injury of rats. *World J Gastroenterol* 2006; **12**: 403-407

13 **Mota RA**, Sánchez-Bueno F, Saenz L, Hernández-Espinosa D, Jimeno J, Tornel PL, Martínez-Torrano A, Ramírez P, Parrilla P, Yélamos J. Inhibition of poly(ADP-ribose) polymerase attenuates the severity of acute pancreatitis and associated

lung injury. *Lab Invest* 2005; **85**: 1250-1262
14 **Dinarello CA**. Interleukin-1 beta, interleukin-18, and the interleukin-1 beta converting enzyme. *Ann N Y Acad Sci* 1998; **856**: 1-11
15 **Fantuzzi G**, Dinarello CA. Interleukin-18 and interleukin-1 beta: two cytokine substrates for ICE (caspase-1). *J Clin Immunol* 1999; **19**: 1-11
16 **Cordoba-Rodriguez R**, Fang H, Lankford CS, Frucht DM. Anthrax lethal toxin rapidly activates caspase-1/ICE and induces extracellular release of interleukin (IL)-1beta and IL-18. *J Biol Chem* 2004; **279**: 20563-20566
17 **Coward WR**, Marei A, Yang A, Vasa-Nicotera MM, Chow SC. Statin-induced proinflammatory response in mitogen-activated peripheral blood mononuclear cells through the activation of caspase-1 and IL-18 secretion in monocytes. *J Immunol* 2006; **176**: 5284-5292
18 **Rau B**, Baumgart K, Paszkowski AS, Mayer JM, Beger HG. Clinical relevance of caspase-1 activated cytokines in acute pancreatitis: high correlation of serum interleukin-18 with pancreatic necrosis and systemic complications. *Crit Care Med* 2001; **29**: 1556-1562
19 **Norman J**. The role of cytokines in the pathogenesis of acute pancreatitis. *Am J Surg* 1998; **175**: 76-83
20 **Ogawa M**. Acute pancreatitis and cytokines: "second attack" by septic complication leads to organ failure. *Pancreas* 1998; **16**: 312-315

S- Editor Liu Y **L- Editor** Zhu LH **E- Editor** Lu W

PO Box 2345, Beijing 100023, China
www.wjgnet.com
wjg@wjgnet.com

World J Gastroenterol 2007 January 28; 13(4): 628-632
World Journal of Gastroenterology ISSN 1007-9327

RAPID COMMUNICATION

Evaluation of prognostic markers in severe drug-induced liver disease

Bo Li, Zhi Wang, Jian-Jiang Fang, Ci-Yi Xu,Wei-Xing Chen

Bo Li, Jian-jiang Fang, Department of Emergency, Lihuili Hospital of Ningbo Medical Center, Ningbo 315041, Zhejiang Province, China
Zhi Wang, Department of Pediatrics, Ningbo Women and Children's Hospital, Ningbo 315012, Zhejiang Province, China
Ci-Yi Xu, Department of ICU, Lihuili Hospital of Ningbo Medical Center, Ningbo 315041, Zhejiang Province, China
Wei-Xing Chen, Department of Gastroenterology, First Affiliated Hospital, Zhejiang University School of Medicine, Hangzhou 310003, Zhejiang Province, China
Correspondence to: Bo Li, Department of Emergency, Lihuili Hospital of Ningbo Medical Center, Ningbo, 315041, Zhejiang Province, China. libo19810427@163.com
Telephone: +86-574-87018638 Fax: +86-574-87392232
Received: 2006-10-27 Accepted: 2006-11-14

Abstract

AIM: To analyze the outcome of patients with severe drug-induced liver disease (DILD) associated with jaundice classified as hepatocellular, cholestatic or mixed liver injury and to evaluate the validity of Hy's rule and the most important predictors for outcome.

METHODS: The Adverse Drug Reaction Advisory Committee was set up in 1997 in our hospital to identify all suspicions of DILD following a structured prospective report form. Liver damage was divided into hepatocellular, cholestatic, and mixed types according to laboratory and histologic criteria when available. Further evaluation of causality assessment was performed.

RESULTS: From January 1997 to December 2004, 265 patients were diagnosed with DILD, and 140 (52.8%) of them were female. hepatocellular damage was the most common (72.1%), the incidence of death was 9.9% in patients with hepatocellular damage and 9.5% in patients with cholestatic/mixed damage ($P < 0.05$). There was no difference in age of dead and recovered patients. The proportion of females and males was similar in recovered and dead patients, no difference was observed in duration of treatment between the two groups. The serum total bilirubin ($P < 0.001$), direct bilirubin ($P < 0.001$) and aspartate transaminase (AST) ($P = 0.013$) values were higher in dead patients than in recovered patients. Chinese herbal medicine was the most frequently prescribed, accounting for 24.2% of the whole series. However, antitubercular drugs (3.4%) were found to be the primary etiological factor for fetal DILD. Factors associated with the development of fulminant hepatic failure were hepatic encephalopathy (OR = 43.66, 95% CI = 8.47-224.95, $P < 0.0001$), ascite (OR = 28.48, 95% CI = 9.26-87.58, $P < 0.0001$), jaundice (OR = 11.43, 95% CI = 1.52-85.96, $P = 0.003$), alcohol abuse (OR = 3.83, 95% CI = 1.26-11.67, $P = 0.035$) and direct bilirubin (OR = 1.93, 95% CI = 1.25-2.58, $P = 0.012$).

CONCLUSION: Death occurs in 9.8% of patients with DILD. Chinese herbal medicine stands out as the most common drug for DILD. While antitubercular drugs are found to be the primary etiological factor for fetal DILD, hepatic encephalopathy, ascites, jaundice, alcohol abuse and direct bilirubin levels are associated with the death of DILD patients.

Key words: Drug-induced liver disease; Prognosis; Prognostic marker; Mortality

Li B, Wang Z, Fang JJ, Xu CY, Chen WX. Evaluation of prognostic markers in severe drug-induced liver disease. *World J Gastroenterol* 2007; 13(4): 628-632

http://www.wjgnet.com/1007-9327/13/628.asp

INTRODUCTION

Drug-induced liver disease (DILD) is an adverse drug reaction-induced disease. Almost all drugs can elevate liver enzyme level and cause DILD. However, the majority of drugs exhibit low incidences of hepatic adverse reactions. Therefore, DILD is mostly identified only after broad clinical drug application (phase Ⅳ). Well-established causes of DILD include non-steroidal anti-inflammatory drugs (NSAIDs), antibiotics, antiepileptics, statins, tuberculostatics and herbal medicines[1,2].

High serum aminotransferase (hepatocellular injury) and jaundice levels induced by different drugs have been reported to result in a mortality of 10%-50%[3-5]. These observations have been named "Hy's rule" after Hyman Zimmerman, who first described them. The rule states that if both drug-induced hepatocellular injury and jaundice occur simultaneously without biliary obstruction, a mortality of at least 10% can be expected[3,5,6]. Hy's rule defined as DILD with serum alanine aminotransferase (ALT) levels 3 or more times the upper limit of normal

(ULN) + serum bilirubin levels 2 or more times the ULN level, has been advocated by the US Food and Drug Administration for use in the assessment of hepatotoxicity of newly developed drugs[5,7]. However, this rule has never been scientifically validated. The sensitivity and specificity of clinical jaundice for the outcome in patients with drug-induced hepatocellular (HC) injury are unknown. The most important predictors of outcome in DILD with HC injury have not been analyzed in a large number of patients. Furthermore, information about the prognosis in other forms of DILD (e.g., DILD with cholestatic or mixed damage) is limited.

In our hospital, a systematic monitoring system for DILD has been in use since 1997, with regular causality assessment offering the opportunity to evaluate a large number of patients with DILD. The aim of this study was to analyze the outcome of patients with severe DILD associated with jaundice classified as HC, cholestatic (CS), or mixed liver injury and to evaluate the validity of Hy's rule and the most important predictors for outcome.

MATERIALS AND METHODS

All reports of suspected drug-induced liver injury received by the Adverse Drug Reaction Advisory Committee (ADRAC) in our hospital between 1997 and 2004 have been computerized and are available for legally acceptable users with a password online. Our analysis was restricted to patients with serum bilirubin levels two-fold higher than the ULN level. Furthermore, in patients with HC injury, our analysis was restricted to those patients with ALT levels 3 or more times the ULN level as well as serum bilirubin levels 2 or more times the ULN level.

A total of 301 reports fulfilling these criteria were evaluated using international consensus criteria [RousselUclaf causality assessment method (RUCAM)][8,9] to assess the probability of a causal relationship between drug exposure and liver disease. Causality assessment was performed based on information about the onset time of reaction of the drug, the development of liver tests after cessation of the drug, the presence of risk factors, and known hepatotoxicity of the suspected drug and concomitant drug or drugs[8]. Furthermore, investigations were performed to exclude non-drug causes for the reaction. Thus, abnormal liver tests shortly after the use of a new drug, rapid decline of abnormal liver test values after stopping the drug, and exclusion of other causes gave high scores compatible with the drug as a possible, probable, or highly probable cause of the reaction[8]. If the report did not receive a high enough score to consider a causal relationship with the suspected drug, the reaction did not likely occur in accordance with the criteria or the relationship was excluded. Each author scored approximately one fifth of the cases. We all performed assessment of 100 cases independently and found very low intraobserver variability with no disagreement in the assessment of cases.

Because many patients had been exposed to several drugs at the time when liver injury occurred, it is not always possible to deduce which drug is most likely responsible for it. In such cases, the reaction was judged to bepotentially caused by more than one drug. On the other hand, if there was a close temporal relationship between the liver injury and treatment of patients with only one of many drugs, which was then considered to be the suspected drug.

The computerized reports include all relevant facts from medical records and the results of laboratory investigations. The following information was collected from the reports: duration of exposure, drug(s) suspected to be responsible, age and sex of the patients, duration of treatment, type of liver injury, results of AST and ALT as well as alkaline phosphatase (ALP) and bilirubin tests, nondrug causes, and outcome of the patients (recovery, death or liver transplantation).

The type of liver damage was classified according to the International Consensus Meeting criteria[8,9], using ALT and alkaline phosphatase activity, expressed as a multiple of the upper limit of normality, to determine the ratio (R) of ALT/AP. The type of liver damage was hepatocellular when $R > 5$, cholestatic when $R < 2$, and mixed when $R > 2$ but < 5. The liver tests used for the classification of liver damage were the first blood test available after liver injury.

Statistical analysis

For descriptive purposes, Fisher's exact test was used to test differences in dichotomous variables between groups. Mann-Whitney test was used for continuous variables. Stepwise logistic regression was performed for multivariate purposes to predict death. All tests were two-tailed and conducted at a 5% significance level.

RESULTS

During 1997-2004, ADRAC received 301 reports of suspected DILD. Of which 265 reports of DILD fulfilled the RUCAM criteria for at least a possible relationship. According to the RUCAM criteria, 22 reports (8.3%) had a possible relationship, 183 (69.1%) a probable relationship, and 60 (22.6%) a highly probable relationship. These 265 reports with a possible/probable/highly probable relationship to drug(s) included 191 with HC injury, 51 with CS injury, and 23 with mixed liver injury (Table 1).Table 1 shows the age and sex, duration of treatment, and peak liver test values in patients with different types of DILD.

There were no differences in the age of patients with HC or CS or mixed injury ($P = 0.127$). A higher proportion of females were observed in all different subgroups, in which females accounted for 53%. The total protein was different both in patients with HC and CS injury ($P = 0.003$) and in those with CS and mixed injury ($P = 0.041$).The difference in albumin between patients with HC and CS injury was significant ($P < 0.001$). Total and direct bilirubin levels were higher in patients with CS injury than in those with HC injury ($P = 0.043$ and $P < 0.001$ respectively) and mixed injury ($P < 0.001$ and $P = 0.01$ respectively). Obviously, the ALT, AST and ALP values were different in patients with mixed injury or with HC or CS injury.

Twenty-six (9.8%) of the 265 patients died of liver

Table 1 A age and sex, duration of treatment, and peak liver test values in patients with different types of DILD

	Total	Hepatocelluar	Cholestatic	Mixed
Number	265	191	51	23
Age ($\bar{x} \pm s$)	48.6 ± 13.7	47.8 ± 13.8	52.1 ± 13.0	47.3 ± 14.0
Sex (F/M)	140/125	100/91	27/24	13/10
Duration of	25.9	24.6	31.4	21.7
treatment (d)	(1-121)	(1-120)	(8-121)	(1-47)
Total bilirubin	95.7	67.5	236	105.5
(μmol/L)	(7-701)	(7-701)	(11-615)	(14-630)
Direct bilirubin	49.4	31.8	126.8	47.5
(μmol/L)	(2-461)	(2-338)	(3-461)	(3.3-281)
Total protein (g/L)	66.9 ± 9.4	67.7 ± 9.6	63.3 ± 8.8	68.1 ± 8.0
Albumin (g/L)	38.1 ± 7.3	39.1 ± 6.9	34.9 ± 8.3	36.4 ± 6.2
ALT (U/L)	351.5	313.8	123.4	557
	(13-2652)	(20-2652)	(13-1079)	(92-1600)
AST (U/L)	230.1	282.9	111.8	393
	(18-1925)	(19-1925)	(18-1165)	(48-1553)
ALP (U/L)	141.8	69.6	117.8	318.8
	(51-1165)	(51-370)	(70-1165)	(147-801)
GGT (U/L)	200.7	112.9	254	241
	(16-3102)	(17-788)	(16-3102)	(87-969)

The laboratory parameters are all peak values before treatment.

Table 2 Comparison between died and recovered patients with DILD

	Died	Recoverd	*P*
Age	52 ± 13.8	48 ± 13.7	0.187
Sex (F/M)	13/13	127/112	NS
Duration of treanment (d)	29 (1-79)	25.7 (1-121)	NS
Total bilirubin	333.3 (38-695)	82.7 (7-701)	< 0.001
Direct bilirubin	218.2 (11.5-330)	44.0 (2-461)	< 0.001
ALT	351 (78-1906)	341.8 (13-2652)	0.293
AST	339 (52-1700)	213.8 (18-1925)	0.013
ALP	139.1 (51-561)	144.4 (51-1165)	0.805
GGT	124.8 (44-1483)	203.8 (16-3102)	0.193

The laboratory parameters are all peak values. Results are expressed as mean ± SD or medians.

failure (Table 2).The following drugs were associated with death: antitubercular drugs (n = 9), medicinal herbs (n = 5), immunodepressants (n = 2), antimycotic drugs (n = 2), antiinfection drugs (n = 1), nonsteroidal anti-inflammatory drugs (n = 1), antidepressant drugs (n = 1), antithyroid drugs (n = 1), antigout preparation (n = 1), and other drugs (n = 3). There were no differences in age of the dead and recovered patients. The proportion of females and males was similar in recovered and dead patients, and no difference was observed in duration of treatment between them.

The levels of serum total bilirubin, direct bilirubin and AST were higher in dead patients than in recovered patients, whereas the levels of ALT, ALP and GGT were similar in the two groups.

A comparison between the dead and recovered patients in the HC group revealed no differences in age, sex, duration of treatment, ALT or ALP (Table 3). Total bilirubin and AST levels were higher in deceased patients with HC injury than in those with CS/mixed injury, while total bilirubin levels were significantly higher only in deceased patients (Table 3).

Table 3 Comparison between died and recovered patients with hepatocellular injury or with cholestatic/mixed liver injury

	Hepatocellular injury		Cholestatic/mixed injury	
	Died	Recovered	Died	Recovered
Number	19	172	7	67
Age	51.3 ± 13.4	47.5 ± 13.9	54.0 ± 15.7	50.3 ± 13.2
Sex, F/M (%)	11/8	89/83	2/5	38/29
Duration of	30.8	23.8	22	30
treatment	(1-79)	(1-120)	(13-40)	(1-121)
Total	330.5	67.6	169.6	83.8
bilirubin	(38-695)	(7-701)[b]	(50-630)	(11-615)[b]
ALT	488.5	414.5	230.5	192.5
	(106-2652)	(20-1906)	(78-692)	(13-1600)
AST	392.3	270.8	265.5	143.0
	(99-170)	(19-1925)[a]	(52-1272)	(18-1553)
ALP	133.7	130.1	268	310.1
	(51-370)	(51-266)	(70-561)	(72-1165)

The laboratory parameters are all peak values. Results are expressed as mean ± SD or medians. [a]$P < 0.05$, [b]$P < 0.001$ *vs* the control group.

Table 4 Factors associated with death of the patients with DILD

Independent variables	Coefficient	OR (95% CI)	*P*
HE	2.232	43.66 (8.47-224.95)	< 0.001
Ascite	2.883	28.48 (9.26-87.58)	< 0.001
Jaundice	1.124	11.43 (1.52-85.96)	0.003
Alcohol abuse	1.511	3.83 (1.26-11.67)	0.035
Direct bilirubin	-0.007	1.93 (1.25-2.58)	0.012

CI = confidence interval; OR = odds ratio, HE = hepatic encephalopathy, Constant = -15.37.

Logistic regression analysis showed that hepatic encephalopathy ($P < 0.001$), ascite ($P < 0.001$), jaundice ($P = 0.003$), alcohol abuse ($P = 0.035$) and direct bilirubin ($P = 0.012$) could independently predict death (Table 4).

The drugs associated with DILD are listed in Table 5. The largest number of reports on drug-induced fatal HC injury was related to antitubercular drugs (because only 2 DILDs were associated with antigout drug, we did not calculate the mortality induced by this drug). In this group, 7 out of the 20 patients died (35%).The second most commonly reported drug type associated with mortality was antifungal agents (33.3%). The mortality ranging from 35% of antitubercular drugs to 0% in reports is related to many other drugs. As in CS/mixed injury, the highest number of reports of death is related to immunosuppressive agent (28.6%). The mortality ranges from 0% with most of the drugs to 28.6%. Overall, antitubercular drugs (32.1%) are the primary etiological factor for fetal DILD.

DISCUSSION

Drug-induced hepatotoxicity remains a challenge to modern hepatology. Hepatotoxicity is typically detected when several thousands of patients are exposed to drugs, and regulatory authorities are often compelled to make dicisions based on scanty, fragmentary, and incomplete

Table 5 Patients with hepatocellular, cholestatic or mixed liver injury and their death due to different drugs

	Hepatocellular	Death	Cholestatic/mixed	Death	Total study group	Death
Antituberculous drugs	20	7	8	2	28	9
Immunodepressant	26	0	7	2	33	2
Antineoplastic agent	8	0	6	0	14	0
Antibiotics	17	1	8	0	25	4
Chinese herbal medicine	51	5	13	0	64	5
Antipyretic analgesic	8	1	2	0	10	1
Antidepressant drug	5	0	5	1	10	1
Cardiovascular drugs	10	0	1	0	11	0
Sedative hypnotics	1	0	0	0	1	0
Drugs for peptic ulcer	1	0	0	0	1	0
Antithyroid drugs	12	0	11	1	23	1
Antifungal agent	6	2	2	0	8	2
Hypoglycemic agent	5	0	2	0	7	0
Drugs for prostate	1	0	0	0	1	0
Antigout drug	2	1	0	0	2	1
Others	18	2	9	1	27	3

epidemiologic data. In addition, a major challenge is the ability to identify predisposed subjects before they receive drugs. The susceptibility of individuals to genetic and environmental factors is still poorly understood. In this study, we analyzed cases of toxic liver injury prospectively collected from our hospital during the past 8 years.

Hyman Zimmerman, the pioneer in the field of DILD, observed that combined HC injury (high aminotransferase) and jaundice induced by a drug is associated with the poor prognosis of patients, with a fatality rate of 10%-50% for different drugs involved (Hy's rule)[3-6]. It was reported that a new drug should be stopped in patients if their AST and ALT levels are 3-fold higher than ULN level, and bilirubin levels are 2-fold higher than ULN level[7]. Concomitant jaundice and hepatocellular injury observed in clinical trials of new drugs are considered to cause serious troubles concerning safety in the postmarketing phase, when a much larger number of patients are exposed to drugs[5].

Our analysis is unique because it was performed in a large cohort of patients with severe DILD, giving the opportunity to elucidate the most important predictors for outcome. Adverse drug reactions are significantly underreported. The true incidence of hepatic adverse drug reactions has been recently observed. However, a recent prospective survey of drug-induced liver injury in the general population in France suggests that at most, only 1 out of 16 cases of DILD in France is actually reported[10].

Heptatotoxicity was found in a higher proportion of females (53%) in our study, which is consistent with the reported epidemiologic data[10,11]. No difference was found in age of the deceased and recovered patients in our study. A recent study from Japan reported that there is also no difference in age of decreased and recovered patients with DILD[12]. The levels of serum total bilirubin and AST were higher in deceased patients than in recovered patients, whereas ALT, ALP and GGT levels were similar in the two groups in the current study, suggesting that hepatic encephalopathy, ascites, jaundice, alcohol abuse and direct bilirubin increase the risk of death in patients with DILD.

We found that the main causative drugs were Chinese herbal medicine (24.2%), followed by immunosuppressive agents (12.5%), antituberculous drugs (10.6%), antibiotics (9.4%), antithyroid drugs (8.7%). But antituberculous drugs (32.1%) were the leading cause of fatal DILD.

In summary, Chinese herbal medicine is the most common drug associated with liver injury, and the mortality rate is 9.8% in patients with DILD. Hepatic encephalopathy, ascites, jaundice, alcohol abuse and direct bilirubin are associated with the death of patients with DILD. Our ADRAC has proved to be an effective instrument in detecting cases of idiosyncratic liver disease and delineating a profile of risk factors for severity. Further efforts must be made to prevent hepatic adverse reactions to drugs.

REFERENCES

1 **Pratt DS**, Kaplan MM. Evaluation of abnormal liver-enzyme results in asymptomatic patients. *N Engl J Med* 2000; **342**: 1266-1271

2 **Lee WM**. Drug-induced hepatotoxicity. *N Engl J Med* 1995; **333**: 1118-1127

3 **Zimmerman HJ**. Drug-induced liver disease. *Clin Liver Dis* 2000; **4**: 73-96, vi

4 **Black M**, Mitchell JR, Zimmerman HJ, Ishak KG, Epler GR. Isoniazid-associated hepatitis in 114 patients. *Gastroenterology* 1975; **69**: 289-302

5 **Senior JR**. Regulatory perspectives. In: Kaplowitz N, DeLeve LD, editors. Drug-Induced Liver Disease. New York: Marcel Dekker, 2003: 739-754

6 **Zimmerman HJ**. Drug-induced liver disease. In: Sciff ER, Sorrell MF, Maddrey WC, editors. Sciff"s Diseases of the Liver. 8th ed. Philadelphia:Lippincott-Raven Publishers, 1999: 973-1064

7 **Davidson CS**, Leevy CM, Chamberlayne EC, editors. Guidelines for Detection of Hepatotoxicity Due to Drugs and Chemicals. Fogarthy Conference, 1978. NIH publication no. 79-313. Washington, DC: US Government Printing Office, 1979

8 **Danan G**, Benichou C. Causality assessment of adverse reactions to drugs--I. A novel method based on the conclusions of international consensus meetings: application to drug-induced liver injuries. *J Clin Epidemiol* 1993; **46**: 1323-1330

9 **Bénichou C**. Criteria of drug-induced liver disorders. Report of an international consensus meeting. *J Hepatol* 1990; **11**: 272-276

10 **Sgro C**, Clinard F, Ouazir K, Chanay H, Allard C, Guilleminet C, Lenoir C, Lemoine A, Hillon P. Incidence of drug-induced hepatic injuries: a French population-based study. *Hepatology*

2002; **36**: 451-455

11 **Friis H**, Andreasen PB. Drug-induced hepatic injury: an analysis of 1100 cases reported to the Danish Committee on Adverse Drug Reactions between 1978 and 1987. *J Intern Med* 1992; **232**: 133-138

12 **Ohmori S**, Shiraki K, Inoue H, Okano H, Yamanaka T, Deguchi M, Sakai T, Takase K, Nakano T, Tameda Y. Clinical characteristics and prognostic indicators of drug-induced fulminant hepatic failure. *Hepatogastroenterology* 2003; **50**: 1531-1534

S- Editor Liu Y **L- Editor** Wang XL **E- Editor** Lu W

PO Box 2345, Beijing 100023, China
www.wjgnet.com
wjg@wjgnet.com

World J Gastroenterol 2007 January 28; 13(4): 633-636
World Journal of Gastroenterology ISSN 1007-9327

RAPID COMMUNICATION

Diagnosis and management of colonic injuries following blunt trauma

Yi-Xiong Zheng, Li Chen, Si-Feng Tao, Ping Song, Shao-Ming Xu

Yi-Xiong Zheng, Li Chen, Si-Feng Tao, Ping Song, Shao-Ming Xu, Department of Surgery, Second Affiliated Hospital, School of Medicine, Zhejiang University, Hangzhou 310009, Zhejiang Province, China
Correspondence to: Dr. Yi-Xiong Zheng, Department of Surgery, Second Affiliated Hospital, School of Medicine, Zhejiang University, Hangzhou 310009, Zhejiang Province, China. zyx_xxn@hotmail.com
Telephone: +86-571-87783580
Received: 2006-10-11 Accepted: 2006-10-28

Abstract

AIM: To retrospectively evaluate the preoperative diagnostic approaches and management of colonic injuries following blunt abdominal trauma.

METHODS: A total of 82 patients with colonic injuries caused by blunt trauma between January 1992 and December 2005 were enrolled. Data were collected on clinical presentation, investigations, diagnostic methods, associated injuries, and operative management. Colonic injury-related mortality and abdominal complications were analyzed.

RESULTS: Colonic injuries were caused mainly by motor vehicle accidents. Of the 82 patients, 58 (70.3%) had other associated injuries. Laparotomy was performed within 6 h after injury in 69 cases (84.1%), laparoscopy in 3 because of haemodynamic instability. The most commonly injured site was located in the transverse colon. The mean colon injury scale score was 2.8. The degree of faecal contamination was classified as mild in 18 (22.0%), moderate in 42 (51.2%), severe in 14 (17.1%), and unknown in 8 (9.8%) cases. Sixty-seven patients (81.7%) were treated with primary repair or resection and anastomosis. Faecal stream diversion was performed in 15 cases (18.3%). The overall mortality rate was 6.1%. The incidence of colonic injury-related abdominal complications was 20.7%. The only independent predictor of complications was the degree of peritoneal faecal contamination (P = 0.02).

CONCLUSION: Colonic injuries following blunt trauma are especially important because of the severity and complexity of associated injuries. A thorough physical examination and a combination of tests can be used to evaluate the indications for laparotomy. One stage management at the time of initial exploration is most often used for colonic injuries.

Key words: Colonic injuries; Blunt trauma; Operation; Faecal stream diversion; Rretrospective study

Zheng YX, Chen L, Tao SF, Song P, Xu SM. Diagnosis and management of colonic injuries following blunt trauma. *World J Gastroenterol* 2007; 13(4): 633-636

http://www.wjgnet.com/1007-9327/13/633.asp

INTRODUCTION

Although the colon is often injured in case of penetrating abdominal trauma, a significant proportion of colonic injuries caused by road accidents is a grossly destructive blunt type associated with damage to multiple organs[1-3]. The diagnosis and management of blunt colon injuries are still debatable. The aim of this retrospective study was to evaluate the preoperative diagnostic methods and management of colonic injuries following blunt abdominal trauma.

MATERIALS AND METHODS

Subjects

All patients with colonic injuries caused by blunt trauma presenting to the Emergency Center of the Second Affiliated Hospital of School of Medicine of Zhejiang University between January 1992 and December 2005 were enrolled. The criterion for inclusion in the study was full thickness perforation of colon injuries requiring surgical repair. Data were collected on clinical presentation, investigations, diagnostic methods, associated injuries, operative management, morbidity and mortality.

Haemodynamic status was determined based on their heart rate and systolic blood pressure (BP) on admission. A systolic BP equal to or < 90 mmHg on admission was interpreted as haemodynamic instability or presence of shock. The time from injury to operation was recorded. The site of colon injury (right colon defined as the right of the middle colic vessels, left colon the left of the vessels) and major associated injuries of the head, thorax, pelvis, axial skeleton, major blood vessels and long bones were recorded.

The severity of colon injury was graded according to the colon injury scale (CIS) score[4]. CIS score was definited as follows: grade 1: contusion and serosal tear without devascularization, grade 2: laceration of less than 50% of the wall, grade 3: laceration of 50% or greater of the wall, grade 4: 100% transection of the wall, and grade 5: complete transection with tissue loss and devascularization, an advanced grade for multiple injuries to the colon. The degree of faecal spillage (the gross extent of intra-abdominal faecal contamination) was categorized as mild: stool contamination on local or one quadrant, moderate: stool contamination on 2 to 3 quadrants, and severe: stool contamination on all four quadrants[5].

Methods

All patients were resuscitated and received intravenous antibiotics in the emergency room. The discretion of operative options was based on Stone's exclusion factors for primary repair[6] and surgeons' experience. The outcome variables of the study included colonic injury-related mortality and abdominal complications (anastomotic leak, intra-abdominal abscess or peritonitis, and colon obstruction or necrosis, if it was judged to be directly related to the colonic trauma).

Statistical analysis

All analyses were carried out by SPSS 12.0 statistical software. Independent predictors for colostomy and post-operative complications were determined by entering potential confounders into a multivariate stepwise (backward elimination) logistic regression. Variables considered in the model for colostomy included age, mechanism of injury, shock on admission, CIS, degree of peritoneal faecal contamination, location of colon injury, and associated intra-abdominal injury. $P < 0.05$ was considered statistically significant.

RESULTS

Demographic data

A total of 82 patients were included in this study. There were 77 males (93.9%) and 5 females (6.1%). Their age ranged 15-67 years with a mean of 37.6 years. Colonic injury was found in 57 patients (69.5%) due to motor vehicle accidents, in 18 (22.0%) due to building accidents, in 6 (7.3%) due to criminal assault, and in 1 (1.2%) due to burst injury.

Clinical presentation

Abdominal signs could not be detected in 8 cases (9.8%) because of head injuries, intoxication or sedation. Seventy patients (94.6%) had moderate to severe abdominal tenderness, 18 (24.3%) had diffuse peritonism, 23 (28.0%) had shock on admission. In addition, hematuria was found in 12 patients (14.6%), paraplegia in 2 (2.4%), aerocele of scroticles in 2 (2.4%) patients. Plain abdominal radiograph was performed to find pneumoperitoneum and intestinal obstruction in 54 patients. Diagnostic peritoneal lavage (DPL) or paracentesis was performed in 65 cases, which was positive in 43 cases (noncongested blood in 20 cases, pus in 23 cases). Abdominal ultrasonography (US) and computed tomography (CT) were performed in 58 and 10 cases respectively. Among them, 12 were diagnosed as gastrointestinal injury with intraperitoneal free fluid.

Table 1 Associated injuries in 82 patients with blunt colonic injuries

	n
Intra-abdominal	
Small bowel	42
Spleen	11
Liver	9
Kidney	4
Urinary bladder	3
Pancreas	2
Ureter	2
Stomach	2
Duodenum	1
Diaphragm	1
Extra-abdominal	
Head	12
Chest	6
Vascular peripheral	5
Fracture vertebral lumbar	5
Fracture pelvis	2

Associated injuries

Fifty-eight patients (70.3%) were found to have one or more associated injuries (Table 1). The most commonly associated intra-abdominal injury occurred in the small bowel (51.2%), followed by in the speen, liver, and kidney. Multiple colonic wounds were observed in 4 cases (4.9%), Isolated colon injury in 20 cases (24.4%). The range of intra-abdominal organs injured was 1-4, with a mean of 2.3.

Timing and indications for laparotomy

Seven patients (8.5%) underwent immediate laparotomy (< 2 h after injury), 4 for severe peritonitis and 3 due to haemodynamic instability. Laparotomy was performed between 2 h and 6 h after injury in 62 cases (75.6%). Of them, 33 had a laparotomy because of abdominal signs with evidence of peritonitis at admission or during observation, 35 because of positive DPL or paracentesis. Eighteen (51.4%) of these patients had more than one significant intra-abdominal injury. An abdominal CT scan or US imaging with diagnostic or suspicious findings was the main reason for laparotomy in 15 cases (18.3%). Colonic injuries were found in 2 patients at diagnostic laparoscopy (Figure 1).

Site and nature of injuries

A total of 87 colonic injuries were found in 82 patients. The most often wounded site was located in the transverse colon (32 cases, 36.8%). The right colon injury was found in 21 cases, the descending colon injury in 16, the sigmoid colon injury in 13, and the intraperitoneal rectum injury in 5. The mean CIS score was 2.8 ± 1.2. The degree of faecal contamination was classified by the operating surgeon as mild in 18 cases (22.0%), moderate in 42 (51.2%), severe in 14 (17.1%), and unknown in 8 (9.8%).

Management and prognosis

Therapeutic options were considered: two-stage management for those with any type of faecal stream diversion, while one stage management for those undergoing primary repair of the injured colon with or without anastomosis. The successful rate for colonic wounds without diversion was 81.7% (67 cases). Primary repair was undertaken in 37 cases with resection and primary anastomosis in a further 30 cases. Two-stage operation was performed in 15 cases (18.3%): repair and protective ostomy in 11 cases, exteriorisation of the repaired bowel in 3 cases, Hartmann's operation in 1 case. The overall mortality rate was 6.1% (5/82). The overall incidence of colonic injury-related abdominal complications was 20.7% (17/82). The most common complications were anastomotic leak (12 cases), intra-abdominal abscess (10 cases), wound infection (12 cases) and colon obstruction or necrosis (4 cases). The only independent predictor of complications was the degree of peritoneal faecal contamination (P = 0.02). There was no significant correlation between age, mechanism of injury, shock on admission, location of colon injury, therapeutic options and outcome in terms of morbidity and mortality.

DISCUSSION

Injuries of the hollow viscera are far less common in blunt abdominal trauma than in penetrating abdominal trauma. Blunt abdominal trauma accounts for approximately 5% to 15% of all operative abdominal injuries[3,7]. The majority of colonic injuries caused by penetrating trauma are dominant[1-3,5]. Nevertheless, in our experience about 6.5% of patients with blunt trauma at admission had injuries to the colon and rectum, which is slightly higher than the reported 5%[8]. Despite their infrequence, traumatic blunt injuries to the colon are extremely destructive and generally associated with damage to multiple organ systems, making diagnosis and treatment difficult. It was reported that delayed management of colonic injuries results in a high incidence of morbidity[9]. Therefore, further researches on guidelines for the diagnosis and surgical management of colonic injuries following blunt trauma are especially important.

No clinical investigations are available to compare with gastrointestinal tract injuries. Moreover, clinical assessment can be unreliable in patients following blunt trauma due to distracting injuries, head and spinal cord injuries, and shock. Less than 50% of gastrointestinal tract injuries resulting from blunt trauma are reported to have sufficient clinical findings to indicate the need for laparotomy[10]. In this study, 3 patients with unstable haemodynamics undergoing immediate laparotomy (< 2 h) showed marked evidence for abdominal injury. The other 4 patients with gross abdominal distension and marked tenderness were also immediately operated. In 6 patients presented within two hours, abdominal signs were vague at initial evaluation but became marked over a few hours at a repeated examination. The finding of abdominal signs in the other 27 cases presented between two and six hours after trauma resulted in laparotomy. Tenderness or other abdominal findings were usually apparent within 24 h.

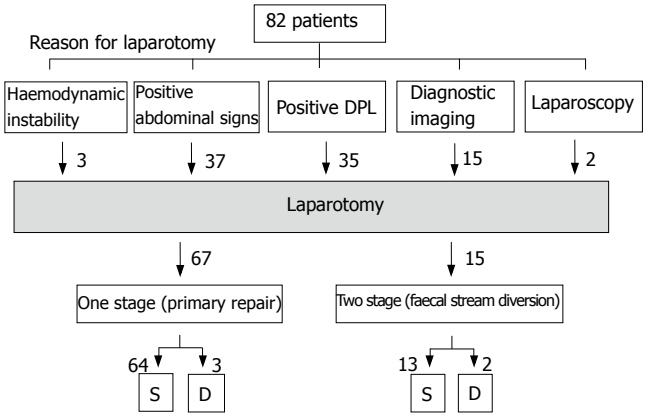

Figure 1 Outcome of 82 patients with colonic injuries. S = survived, D = died.

Physical examination and diagnostic tests can be used to evaluate patients with blunt abdominal trauma, including DPL, US, CT, and diagnostic laparoscopy. Speed and efficiency are important factors in the performing such tests[3]. It is reported that peritoneal lavage cell count may also be useful in early detection of hollow viscus injury[11,12]. Although DPL is sensitive in identifying haemoperitoneum and associated hollow viscus injury, it has been criticised for its higher rate of non-therapeutic laparotomy (NTL) and inconvenience in practice[12]. In this study, the presence of positive DPL or paracentesis was an important clinical finding. The routine use of diagnostic celiocentesis to detect possible intra-abdominal injuries in cardiovascularly stable patients has been used to differentiate between injuries that require a therapeutic laparotomy and those that do not[13]. Suspicious diagnosis of gastrointestinal tract injuries was indicated in 35 cases in this study. However, the diagnostic rate of colonic injuries by DPL or celiocentesis was decreased over the study period, which may be due to the increased use of imaging techniques to assess haemodynamically stable trauma patients.

US is convenient, cheap and noninvasive. A positive study is defined as evidence of free fluid or solid-organ parenchymal injury. Abdominal CT is also useful in the diagnosis of abdominal injuries as it accurately delineates solid organ injuries and retroperitoneal lesions. While some advocate limiting imaging tests to evaluation of patients with DPL-positive results and haemodynamic stability, US and CT remain the preferred tool in the evaluation of blunt abdominal trauma[3,14]. The accuracy of abdominal US for evaluating blunt abdominal trauma is comparable to the reported accuracy[15]. However, only 10 out of the 58 scans in our study could diagnose intra-abdominal gastrointestinal tract injuries with 5 being suspicious of a significant intra-abdominal injury. Some patients with free fluid but no evidence of a solid viscus injury might presumably be overlooked.

Although the role of laparoscopy in abdominal trauma is controversial[16], diagnostic laparoscopy has been introduced in our emergency center. Its indications have expanded from identifying the causative pathology of acute abdominal pain to avoidance of unnecessary laparotomies, treatment of intra-abdominal lesions, and

can be used as a resource for evaluating blunt abdominal trauma. Diagnostic laparoscopy was performed in 2 cases in our study and some direct indications for colonic injuries (such as faecal spillage, colon rupture) were found in both cases. Take together, the indications for laparotomy were determined according one of the following findings: haemodynamic instability with reasonable clinical suspicion of an intra-abdominal cause, positive abdominal signs, positive DPL, positive diagnostic imaging and abdominal finding by laparoscopy.

The management of colonic injuries has changed significantly from "faecal diversion dogma" to primary repair[2,3]. Although several studies showed that diversion is not mandatory, additional considerations in management should be taken into account regarding grossly destructive colon injuries. In our study, mild, moderate and severe faecal contamination was found in 22.0%, 51.2%, and 17.1% of patients, respectively at laparotomy. In 15 patients (18.3%), primary laparotomy was terminated before the completion of definitive surgery (abbreviated laparotomy or damage control).

It was reported that the mortality of colonic injuries have declined to 2%-12%[1,3,17]. Primary closure or resection and anastomosis can be used in patients with colonic injury. The results are generally favorable, due to the advances in intensive care techniques and antibiotic therapy. Primary repair reduces operation and postoperative complications, avoids a second operation, stoma complications, and the financial burden related to colostomy care. A number of factors have been traditionally accepted to be associated with higher mortality and morbidity of primary colonic repair. It was reported that patients should be excluded from primary repair in the presence of shock, major blood loss, > two organs injured, faecal contamination higher than 'mild', delay of repair > 8 h and destructive wounds of the colon or abdominal wall requiring resection[6]. The grade of colonic injuries trends to be independently associated with intra-abdominal complications. In our study, the overall mortality rate was 6.1%. Although neither grade of injury nor ostomy formation demonstrated a significant impact on morbidity, peritoneal faecal contamination has shown its significant predictive value for complications. We advocate that peritoneal faecal contamination should be thoroughly removed during operation to reduce postoperative abdominal septic morbidities. There was no difference between patients with primary repair and faecal stream diversion. However, other organ injuries must be kept in mind. Colostomy may be indicated due to unusual conditions, such as intramural hematomas causing compression ischemia and delayed perforation, mesenteric hematomas causing vascular compression with subsequent infarction, and perforations in omentum or other surrounding organs[3]. All together, the decision for a primary anastomosis, especially after segmental resection in the descending colon, should be individualized according to the injuries in different patients.

REFERENCES

1 **Tzovaras G**, Hatzitheofilou C. New trends in the management of colonic trauma. *Injury* 2005; **36**: 1011-1015
2 **Bowley DM**, Boffard KD, Goosen J, Bebington BD, Plani F. Evolving concepts in the management of colonic injury. *Injury* 2001; **32**: 435-439
3 **Cleary RK**, Pomerantz RA, Lampman RM. Colon and rectal injuries. *Dis Colon Rectum* 2006; **49**: 1203-1222
4 **Moore EE**, Cogbill TH, Malangoni MA, Jurkovich GJ, Champion HR, Gennarelli TA, McAninch JW, Pachter HL, Shackford SR, Trafton PG. Organ injury scaling, II: Pancreas, duodenum, small bowel, colon, and rectum. *J Trauma* 1990; **30**: 1427-1429
5 **Xu SM**, Zheng YX, Gong WH, Wang P. Management of colorectal injuries. *Zhonghua Putong Waike Zazhi* 2004; **19**: 337-339
6 **Stone HH**, Fabian TC. Management of perforating colon trauma: randomization between primary closure and exteriorization. *Ann Surg* 1979; **190**: 430-436
7 **Ricciardi R**, Paterson CA, Islam S, Sweeney WB, Baker SP, Counihan TC. Independent predictors of morbidity and mortality in blunt colon trauma. *Am Surg* 2004; **70**: 75-79
8 **Wisner DH**, Chun Y, Blaisdell FW. Blunt intestinal injury. Keys to diagnosis and management. *Arch Surg* 1990; **125**: 1319-1322; discussion 1322-1323
9 **Hoyt DB**, Coimbra R, Potenza B. Management of Acute Trauma. In: Townsend CM, Beauchamp RD, Evers BM, Mattox KL. Sabiston textbook of surgery. 17th ed. Amsterdam: Elsevier Science, 2004: 485-529
10 **Hughes TM**, Elton C, Hitos K, Perez JV, McDougall PA. Intra-abdominal gastrointestinal tract injuries following blunt trauma: the experience of an Australian trauma centre. *Injury* 2002; **33**: 617-626
11 **Olsen WR**, Hildreth DH. Abdominal paracentesis and peritoneal lavage in blunt abdominal trauma. *J Trauma* 1971; **11**: 824-829
12 **Nagy KK**, Roberts RR, Joseph KT, Smith RF, An GC, Bokhari F, Barrett J. Experience with over 2500 diagnostic peritoneal lavages. *Injury* 2000; **31**: 479-482
13 **Wang P**, Zheng YX, Xu SM, Cui L. Diagnosis and management of 96 cases with colorectal injuries. *Zhonghua Jizhen Yixue Zazhi* 2003; **12**: 487-489
14 **Marco GG**, Diego S, Giulio A, Luca S. Screening US and CT for blunt abdominal trauma: a retrospective study. *Eur J Radiol* 2005; **56**: 97-101
15 **Nural MS**, Yardan T, Güven H, Baydin A, Bayrak IK, Kati C. Diagnostic value of ultrasonography in the evaluation of blunt abdominal trauma. *Diagn Interv Radiol* 2005; **11**: 41-44
16 **Chelly MR**, Major K, Spivak J, Hui T, Hiatt JR, Margulies DR. The value of laparoscopy in management of abdominal trauma. *Am Surg* 2003; **69**: 957-960
17 **Burch JM**. Injury to the colon and rectum. In: Mattox KL, Feliciano DV, Moore EE. Trauma. 4th ed. New York: McGraw-Hill, 1999: 763-782

S- Editor Wang J **L- Editor** Wang XL **E- Editor** Lu W

PO Box 2345, Beijing 100023, China
www.wjgnet.com
wjg@wjgnet.com

World J Gastroenterol 2007 January 28; 13(4): 637-638
World Journal of Gastroenterology ISSN 1007-9327

CASE REPORT

A case of acute infectious mononucleosis presenting with very high ferritin

Muhammed Hameed Thoufeeq, Shahul Leyakath Ali Khan, Sanjiv Kumar Jain, Hasanain Al-Shakerchi, Munem Hussain

Muhammed Hameed Thoufeeq, Sanjiv Kumar Jain, Hasanain Al-Shakerchi, Munem Hussain, Department of Medicine, Pilgrim Hospital, Boston, United States
Shahul Leyakath Ali Khan, Department of Medicine, Bronglais Hospital, Aberystwyth, Wales, United Kingdom
Correspondence to: Muhammed H Thoufeeq, Department of Medicine, Pilgrim Hospital, Boston, PE21 9QS, United Kingdom. mo.thoufeeq@gmail.com
Telephone: +44-7154-830670
Received: 2006-11-10 Accepted: 2006-12-21

Abstract

Hepatitis is an important but uncommon manifestation of acute Epstein Barr infection. Infectious mononucleosis is usually a disease of young adults. We report a case of infectious mononucleosis in a 72-year old jaundiced gentleman with ferritin level of 2438 that normalised on clinical improvement.

Key words: Epstein Barr virus; Infectious mononucleosis; Ferritin; Jaundice; Liver function tests

Thoufeeq MH, Ali Khan SL, Jain SK, Al-Shakerchi H, Hussain M. A case of acute infectious mononucleosis presenting with very high ferritin. *World J Gastroenterol* 2007; 13(4): 637-638

http://www.wjgnet.com/1007-9327/13/637.asp

INTRODUCTION

Hepatitis is an important but uncommon manifestation of acute Epstein Barr infection. Infectious mononucleosis is usually a disease of young adults. We report a case of infectious mononucleosis in a 72-year old jaundiced gentleman with ferritin level of 2438 that normalised on clinical improvement.

CASE REPORT

A 72-year old retired farmer was admitted with a three-week history of feeling generally unwell. He gave a history of loss of appetite with stable weight. He denied any history of fever. Having a long history of prostatism, he was found to be in urinary retention at the same time for which he was catheterised. He was not started on any new medications and denied taking any over the counter medications. He said his urine was dark and sometimes had dysuria. He denied any gastro-intestinal symptoms.

His past history included osteoarthritis, previous myocardial infarction in 1993, gastro-oesophageal reflux disease and laparoscopic herniorrhaphy,

His medications were 75 mg aspirin, 10 mg atorvastatin, 300 mg quinine sulphate, 20 mg omeprazole and 5 mg amlodipine once daily. He said he was allergic to codeine phosphate. He was living on his own and his wife had recently passed away. His alcohol intake was negligible. There was no family history of any clinical significance.

On clinical examination he was noticed to be jaundiced, afebrile, haemodynamically stable. There were no stigmata of chronic liver disease. His abdomen was soft with mild tenderness elicited in the right hypochondrium. No organomegaly or masses were noted. Examinations of cardiovascular and respiratory systems were normal.

His blood tests were as follows: Hb = 14.7 g/dL (13.5-16.9), WBC = 6.1 (4.5-13.0), platelets = 161 (150-400), MCV = 92 fL (84-99.0), neutrophils = 1.65 (2.0-7.5), lymphocytes = 3.97 (1.5-4.0). A blood film showed a moderate number of atypical lymphocytes.

Serum ferritin was high at 2438 μg/L (25-400). Haemochromatosis screen was negative. PT, APTT and fibrinogen were normal. Sodium was 135 mmol/L (135-145), potassium 4.2 mmol/L (3.5-5.3), urea 6.1 mmol/L (3-7) and creatinine 102 μmol/L (53-115) (Table 1).

Bilirubin was 50 μmol/L (0-20), alanine aminotransferase (ALT) 254 U/L (0-37), alkaline phosphatase (ALP) 677 U/L (39-128), gamma glutamic transpeptidase(GT) 817, albumin 34 g/dL (35-52), calcium 2.18 mmol/L (2.1-2.6), C reactive protein (CRP) 21 mg/L (0-8), alfa- fetoprotein 3.5 (0-5.8), C3 and C4 (complements) were normal; IgM was 3.73 g/L (0.5-2).

Blood and urine cultures were negative. Hepatitis A, B, C and CMV serology were negative. Anti Epstein Barr virus (EBV) capsid antigens IgG and IgM were detected, Anti EBV nuclear antigen IgG was also detected.

Anti nuclear antibody (ANA) was negative. Anti neutrophil cytoplasmic antibody (ANCA), antimitochondrial, smooth muscle, liver kidney microsomal antibodies were all negative.

Chest and abdominal X-rays showed no radiological abnormalities. He had an abdominal CT showing moderate

Table 1 Abnormal blood tests in patient

1	Ferritin 2438 (25-400)
2	Bilirubin 50 (0-30)
3	ALT 254 (0-30)
4	ALP 677
5	Gamma GT 817
6	CRP 21 (0-8)
7	IgM 3.73 (0.5-2)
8	Anti EBV nuclear IgG detected
9	Anti EBV capsid antigen IgM and IgG detected
10	Atypical lymphocytes

splenomegaly and liver changes that were suggested as possibly secondary to hepatitis.

He was managed conservatively, his LFTs improved. He remained very well and was discharged after 2 wk of hospitalisation.

He was seen in Outpatient Follow-up Clinic after 4 mo, he was well and his weight was stable. His ferritin and LFT at that time became normal.

DISCUSSION

Infectious mononucleosis (IM) was first described in 1920. It was not until 1968 that EBV infection was described as a causative agent of IM. Incubation period is 25-50 d. It is usually a self-limiting disease.

There is a mortality rate of 0.1% associated with IM. Ninety percent of patients have asymptomatic deranged liver function tests, but jaundice is rare. EBV hepatitis is an important cause of viral hepatitis.

Fulminant hepatitis is rare but has been reported[1]. Severe hepatitis is rare, although it has been reported. Hepatomegaly is frequently present. Jaundice is rare. Occasionally, jaundice may be due to autoimmune haemolysis. Cholestasis can be noticed[2]. Splenomegaly is common and 50%-75% of patients develop it. Dommerby *et al*[3] reported that all patients have ultrasonic splenomegaly but that is palpable in only a few. Splenic rupture should be ruled out in patients who present with severe abdomen pain. Rupture can be precipitated by sports activity or can occur spontaneously and 0.1%- 0.5% of cases can result in rupture[4]. Spleen is most vulnerable to rupture in the 2nd and 3rd week of infection. Preparation with amoxicillin can result in rash frequently. Fever can be noted in 90 % of cases, usually low grade. Maculo- popular rash can be noticed in 5%-10% of cases, but is more common in children.

Malaise and fatigue may persist for weeks or months after IM. Persistent EBV infection is not a cause of chronic fatigue syndrome (CFS). High titres of antibodies to EBV may be noticed in patients with CFS that are identical to healthy EBV- sero positive adults.

Table 2 Gastrointestinal manifestations of EBV infection

1	Asymptomatic deranged LFTs
2	Viral hepatitis, usually self limiting
3	Fulminant hepatitis
4	Cholestasis
5	Auto-immune haemolysis causing jaundice
6	Splenomegaly
7	Splenic rupture (rare)

Duncan syndrome, a rare X linked recessive disorder, was reported by Purtilo *et al* in 1975 which is characterised by a defect in the immune response against EBV resulting failure to prevent EBV replication and hence leading to fatal complications[5]. Patients with combined immunodeficiency, Wiskott- Aldrich syndrome and Ataxia telangiectasia develop severe IM[6]. Likewise, patients with acquired immunodeficiency states like patients with AIDS or those receiving immunosuppressive agents develop severe IM and malignant lymphoma[7].

Treatment for IM is supportive with analgesic as required and rest. Due to the risk of splenic rupture physical activity in excess is to be avoided. There is no place for oral glucocorticoids in uncomplicated IM. In patients with severe tonsillar enlargement that might predispose to airway obstruction, severe thrombocytopenia or haemolytic anaemia, Prednisolone 40 to 60 mg once daily for 2-3 d with tapering over 3 wk is adviced.

In conclusion, acute EBV hepatitis should be ruled out in acutely jaundiced patients with high ferritin at any age group (Table 2).

REFERENCES

1 **Papatheodoridis GV**, Delladetsima JK, Kavallierou L, Kapranos N, Tassopoulos NC. Fulminant hepatitis due to Epstein-Barr virus infection. *J Hepatol* 1995; **23**: 348-350

2 **Shaukat A**, Tsai HT, Rutherford R, Anania FA. Epstein-Barr virus induced hepatitis: An important cause of cholestasis. *Hepatol Res* 2005; **33**: 24-26

3 **Dommerby H**, Stangerup SE, Stangerup M, Hancke S. Hepatosplenomegaly in infectious mononucleosis, assessed by ultrasonic scanning. *J Laryngol Otol* 1986; **100**: 573-579

4 **Stockinger ZT**. Infectious mononucleosis presenting as spontaneous splenic rupture without other symptoms. *Mil Med* 2003; **168**: 722-724

5 **Purtilo DT**, Cassel CK, Yang JP, Harper R. X-linked recessive progressive combined variable immunodeficiency (Duncan's disease). *Lancet* 1975; **1**: 935-940

6 **Joncas J**, Lapointe N, Gervais F, Leyritz M. Unusual prevalence of Epstein-Barr virus early antigen (EBV-EA) antibodies in ataxia telangiectasia. *J Immunol* 1977; **119**: 1857-1859

7 **Petersen JM**, Tubbs RR, Savage RA, Calabrese LC, Proffitt MR, Manolova Y, Manolov G, Shumaker A, Tatsumi E, McClain K. Small noncleaved B cell Burkitt-like lymphoma with chromosome t(8;14) translocation and Epstein-Barr virus nuclear-associated antigen in a homosexual man with acquired immune deficiency syndrome. *Am J Med* 1985; **78**: 141-148

S- Editor Liu Y **L- Editor** Wang XL **E- Editor** Liu WF

PO Box 2345, Beijing 100023, China
www.wjgnet.com
wjg@wjgnet.com

World J Gastroenterol 2007 January 28; 13(4): 639-642
World Journal of Gastroenterology ISSN 1007-9327

CASE REPORT

An autopsy case showing massive fibrinoid necrosis of the portal tracts of the liver with cholangiographic findings similar to those of primary sclerosing cholangitis

Hiroshi Hano, Ichiro Takagi, Keisuke Nagatsuma, Tomoe Lu, Chenxi Meng, Satoru Chiba

Hiroshi Hano, Keisuke Nagatsuma, Tomoe Lu, Chenxi Meng, Satoru Chiba, Department of Pathology, Jikei University School of Medicine, Tokyo, Japan
Ichiro Takagi, Department of Internal Medicine Division of Gastroenterology and Hepatology, Jikei University School of Medicine, Tokyo, Japan
Correspondence to: Dr. Hiroshi Hano, Department of Pathology, Jikei University School of Medicine, 3-25-8, Nishishinbashi, Minato-ku, Tokyo 105-8461, Japan. hhano@jikei.ac.jp
Telephone: +81-3-34331111-2230 Fax: +81-3-54720700
Received: 2006-10-13 Accepted: 2006-12-18

Abstract

An 81-year-old Japanese man with jaundice was strongly suspected clinically of having primary sclerosing cholangitis based on clinical examinations and later died of hepatic failure. The entire course of the disease lasted about 10 mo. The autopsy revealed extensive fibrinoid necrosis in the liver, kidney, spleen, pancreas, lung, lymph nodes, and pleura. Particularly extensive fibrinoid necrosis in the portal tracts of the liver induced severe stenoses of the intrahepatic bile ducts, resulting in cholestasis in association with prominent liver injury. There were no findings indicating primary sclerosing cholangitis. The hepatic lesions in this case did not coincide with any known disease including collagen diseases. To clarify the cause of irregular stenoses of the intrahepatic biliary trees on cholangiographic findings, we postulate that some form of immunological derangement might be involved in pathogenesis of fibrinoid necrosis. However, the true etiology remains unknown.

Key words: Jaundice; Fibrinoid necrosis; Cholangiography; Primary sclerosing cholangitis; Liver; Autopsy

Hano H, Takagi I, Nagatsuma K, Lu T, Meng C, Chiba S. An autopsy case showing massive fibrinoid necroses of the portal tracts of the liver with cholangiographic findings similar to those of primary sclerosing cholangitis. *World J Gastroenterol* 2007; 13(4): 639-642

http://www.wjgnet.com/1007-9327/13/639.asp

INTRODUCTION

We herein present an unusual autopsy case showing systemic fibrinoid necroses in various organs. The case was strongly suspected clinically of primary sclerosing cholangitis (PSC) based on the cholangiographic findings; however, the autopsy disclosed systemic fibrinoid necroses instead of histological features of PSC. Particularly noteworthy was the presence of fibrinoid necrosis in the portal tracts of the liver caused stenoses of the biliary trees in association with cholestasis. We could not find any similar case reported in the literature. Presently, the etiology remains unknown.

CASE REPORT

About 10 mo before admission to our hospital, an 81-year-old Japanese man was admitted to a local hospital because of jaundice. Laboratory examinations revealed elevated levels of serum total bilirubin and other serum enzymes such as alkaline phosphatase, γ-glutamyltranspeptidase, leucine aminopeptidase. Serum autoantibodies such as anti nuclear antibody, anti mitochondrial antibody and anti smooth muscle antibody were negative. Endoscopical retrograde cholangiogram showed characteristic irregularity and beading of the intrahepatic biliary tree (Figure 1). No extrahepatic involvement was found. The patient was strongly suspected clinically of PSC. The pathologic diagnosis of the liver biopsy specimen was liver damage with cholestasis. Concentric fibrosis around the bile ducts suggesting PSC was not found. The patient was transferred to our hospital 18 d before death because of aggravation of jaundice, anorexia and easy fatigability. Chronological laboratory data is shown in Table 1. Serum fibrinogen was within normal lower limit. Plasminogen and D-dimer in serum were not examined. Serologic markers for hepatits B and C viral hepatitis were negative. These findings indicated that the liver cell damage rapidly worsened with aggravation of cholestasis, especially in end stage. Despite symptomatic and supportive treatment, the jaundice became progressively worse, and ascites and hepatic encephalopathy developed. The patient eventually died of hepatic failure.

An autopsy was performed about two hours after his death. The diagnoses at autopsy except for systemic fibrinoid necrosis were cholestatic liver damage, acute

Table 1 Laboratory data

			d 1	d 38	d 48	d 54				
Peripheral blood							*Serological tests*			
WBC	/μL	(4500-8500)	8400	8800	9200	16900	IgG	mg/dL	(800-1800)	1629
Hemoglobin	g/dL	(13.5-16.5)	12.1	12.9	11.5	11.4	IgA	mg/dL	(130-290)	182
Platelet	$\times 10^4$/μL	(15.0-35.0)	26.8	26.6	20.8	18.6	IgM	mg/dL	(100-180)	68
							C_3	mg/dL	(70-100)	99
Coagulation tests							C_4	mg/dL	(11-44)	46.5
Prothrombin time	%	(> 70%)	55	37	52	26	CH_{50}	U/mL	(28-45)	44.6
Hepaplastin test	%	(> 70%)	90	44	57	38	Serum-Cu	μg/dL	(78-131)	247
Fibrinogen	mg/dL	(150-400)		158	176	160				
							Viral markers			
Blood chemistry							HBsAg			(-)
AST	IU/L	(10-30)	185	134	98	422	HCVAb			(-)
ALT	IU/L	(6-40)	126	91	59	174				
LDH	IU/L	(160-325)	450	646	439	812	*Auto antibodies*			
ALP	IU/L	(120-400)	1359	834	692	556	Anti nucleic antibody			(-)
LAP	IU/L	(105-235)		528	472	425	LE test			(-)
γ-GTP	IU/L	(4-70)	296	151	119	73	Anti DNA antibody			(-)
T-Bil	mg/dL	(0.1-0.8)	10.7	15.8	16.2	18.5	Anti SMA antibody			(-)
D-Bil	mg/dL	(0-0.3)	5		9.1	10.9	Anti mitochondrion antibody			(-)
TP	g/dL	(6.7-8.3)	6.4	6.3	5.2	4.9				
Alb	g/dL	(3.5-5.2)	3.3	2.8	2.8	2.6	*Tumor markers*			
TC	mg/dL	(120-220)	260	319	193	158	AFP	ng/mL	(1-15)	2
BUN	mg/dL	(8-20)		32	68	150	CEA	ng/mL	(5.8↓)	6.1
Cr	mg/dL	(0.5-1.1)	1.2	1.3	3.1	7.7	CA19-9	U/mL	(37↓)	2470
Serological test	mg/dL									
CRP		(0-0.5)	1.8	1.3	1.5	8.8				

D: hospital day; Underline: abnormal value.

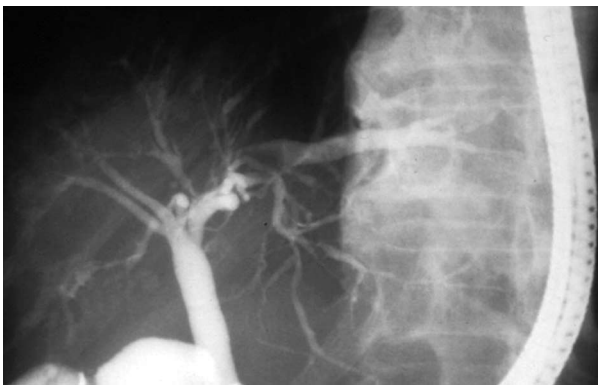

Figure 1 Endoscopic retrograde cholangiogram. Intrahepatic biliary branches showed irregularity and extensive beading (arrows). The long arrow indicates the dilatation of the bile duct due to stenosis caused by the pressure of cysts.

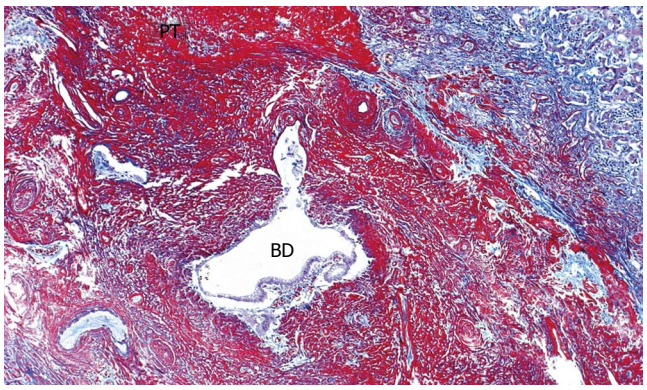

Figure 2 Extensive fibrinoid necrosis in large portal tract. Septal bile duct is buried in the fibrinoid material (Masson's trichrome x 1). PT: portal tract, BD: bile duct.

renal swelling, acute pancreatitis, mild cardiac hypertrophy (350 g) and latent adenocarcinoma of the prostate. Pathologic findings concerning fibrinoid necrosis are described as follows.

The liver (1380 g) showed a deeply yellow-brown cut-surface due to cholestasis with scattered simple small cysts. Gross examination could not detect remarkable changes of the common bile duct and bilateral hepatic ducts. Microscopically the most striking feature was a massive deposition of homogeneous material stained scarlet with Masson's trichrome in the portal tracts (Figure 2). Careful examinations disclosed that the material was deposited in the walls of arteries and portal veins as well as in the connective tissue (Figure 3). In the bile ducts the deposits circumscribed the lumen leaving the epithelial lining intact and caused marked stenosis. The area of the involved vessels and ducts extended from the distal interlobular portion to the proximal septal portion (Figures 2 and 3). The material was stained violet with PTAH and immunohistochemically was positive for fibrinogen and negative for immunoglobulins such as IgG, IgM, and IgA, C3 and C1q (Figure 4A). Electron microscopic findings of the liver were electron dense materials deposited in the involved tissue (Figure 4B). The results of these stainings and electronmicrogram suggested that the lesion with homogeneous material deposition was fibrinoid necrosis. In addition, the portal tracts were enlarged and

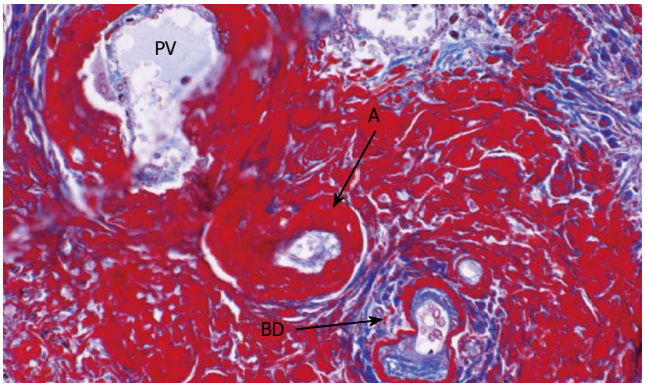

Figure 3 A smaller portal tract. Fibrinoid material is deposited in the connective tissue, walls of the arteries and periductular connective tissue (Masson's trichrome x 20). PV: portal vein, A: artery, BD: bile duct.

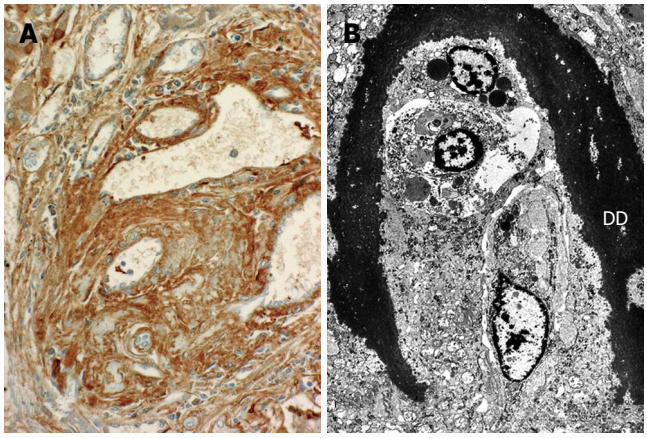

Figure 4 **A**: Immunohistochemical staining demonstrates the positivity of the fibrinoid material for fibrinogen; **B**: An electron micrograph shows dense deposit materials suggestive of fibrinoid necrosis around the small bile ducts in the portal tract of the liver (original magnification x 2000).

infiltrated with lymphocytes and plasma cells with an occasional intermingling of polymorphonuclear cells, ductular proliferation and fibrosis. The histologic features were biliary interface activity, resulting from cholestasis. However, it was noted that the lesion with fibrinoid necrosis was scarcely accompanied by inflammatory reactions. Cholestasis also caused conspicuous parenchymal damage including feathery degeneration or necrosis. Although the liver was extensively examined histologically, there were no detectable features of PSC.

The kidney (250 g, respectively) showed marked swelling. Histologically fresh fibrinoid necrosis was found in various degrees mainly in the wall of the interlobular arteries (Figure 5). However, it was not accompanied by any inflammatory reaction. Elastica-Van Gieson stain also demonstrated the destructive changes of the arterial walls suggestive of old vascular lesions. Occasionally, focal fibrinoid necrosis involved tubules and connective tissue.

Intensive fibrinoid necrosis was noticed in lymph nodes and the spleen. Old vascular lesions were also found frequently in the spleen. The pancreas, lung and pleura showed scattered foci of fresh fibrinoid change.

On re-examination of the liver biopsy specimen, the same fibrinoid necrosis as observed on autopsy materials was seen in the portal tracts.

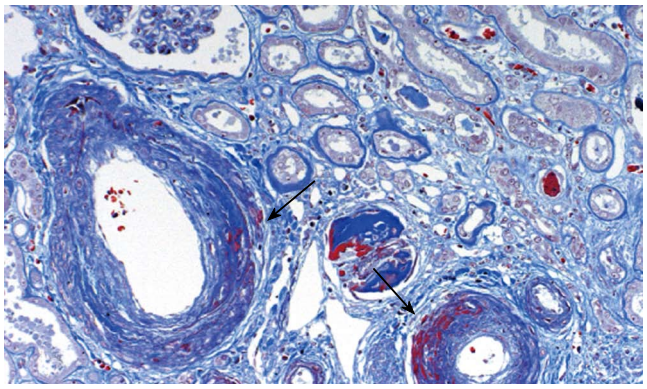

Figure 5 Kidney. Fibrinoid necroses were seen in the walls of the interlobular arteries (arrows) (Masson's trichrome x 10).

DISCUSSION

The case reported here is characterized with unusual systemic fibrinoid necroses in the walls of blood vessels and connective tissue in various organs, especially in the liver. It is clear that massive fibrinoid material around the bile ducts compressed the lumen and caused various degrees of stenoses. It was considered that such stenosis of the bile ducts resulted in the findings similar to those of PSC on the cholangiogram[1,2]. Obstructive jaundice over time aggravated and severely damaged the liver parenchyma. This was considered to reflect the progressive deposition of fibrinoid material in the portal tracts.

Klemperer proposed the term, collagen diseases, to describe systemic connective tissue disorders that are characterized histologically by fibrinoid necrosis of the connective tissue[3,4]. Thereafter many studies clarified that fibrinoid material is composed mainly of fibrins, while other minor components are immunoglobulins. Although the pathogenesis of fibrinoid necrosis has not yet been fully elucidated, it is assumed to result from the insudation of immunoglobulins into blood vessel walls, leading to activation of the coagulation cascade and deposition of fibrins[5]. Furthermore, fibrinoid necrosis of blood vessels is also known to develop in non-autoimmune diseases like malignant hypertension[6,7]. In our case laboratory findings or symptoms were not suggestive of any autoimmune disease or malignant hypertension. The liver pathology was also quite different from that of reported cases with collagen diseases[8-10]. On a search of the literature using key words such as fibrinoid necrosis, vasculitis, we could not find any case similar to ours.

It is well known that the main cholangiographic features of PSC are a beaded appearance, very short strictures, and diverticulum-like outpourchings[11]. Cholangiographic differential diagnosis of PSC involves cholangiocarcinoma, cirrhosis, acute cholangitis, and advanced primary biliary cirrhosis in general[12]. In addition, it might be necessary, in diagnosing PSC, to keep in mind that the lesions severely involving the portal tracts like our case also cause severe damage, besides stenosis of the biliary tracts.

REFERENCES

1 **Elias E**, Summerfield JA, Dick R, Sherlock S. Endoscopic retrograde cholangiopancreatography in the diagnosis of jaundice associated with ulcerative colitis. *Gastroenterology* 1974; **67**: 907-911

2 **Lindor KD**, Larusso NF. Primary sclerosing cholangitis. In: Schiff ER, Sorrell MF, Maddrey WC, editors. Schiff's Diseases of the liver 9th ed. Philadelphia: Liptoncott Williams & Wilkins, 2003: 673-684

3 **Klemperer P**, Pollack AD, Baehr G. Landmark article May 23, 1942: Diffuse collagen disease. Acute disseminated lupus erythematosus and diffuse scleroderma. By Paul Klemperer, Abou D. Pollack and George Baehr. *JAMA* 1984; **251**: 1593-1594

4 **Klemperer P**. The concept of collagen diseases. *Am J Pathol* 1950; **26**: 505-519

5 **Moor S**, Jennette JC, Rosen S. Vascular system. In Damjanov I, Linder J, editors. Anderson's pathology. 10th ed. St. Louis: Mosby, 1996: 1397-1445

6 **Heptinstall RH**. Malignant hypertension; a study of fifty-one cases. *J Pathol Bacteriol* 1953; **65**: 423-439

7 **Olson FG**. Hypertension: Essential and secondary forms. In:Jenett JC, Olson JL, Schwartz MM, Silva FG, editors. Heptinstall's pathology of the kidney. 5th ed. Philadelphia: Lippincott-Raven, 1998: 943-1002

8 **Matsumoto T**, Kobayashi S, Shimizu H, Nakajima M, Watanabe S, Kitami N, Sato N, Abe H, Aoki Y, Hoshi T, Hashimoto H. The liver in collagen diseases: pathologic study of 160 cases with particular reference to hepatic arteritis, primary biliary cirrhosis, autoimmune hepatitis and nodular regenerative hyperplasia of the liver. *Liver* 2000; **20**: 366-373

9 **Cowan RE**, Mallinson CN, Thomas GE, Thomson AD. Polyarteritis nodosa of the liver: a report of two cases. *Postgrad Med J* 1977; **53**: 89-93

10 **Burt AD**, Portmann BC, MacSween RNM. Liver pathology associated with disases of other organs or systems. In MacSween RNM, Burt AD, Portmann BC, Ishak KG, Scheuer PJ, Anthony PP, editors. Pathology of the liver. 4th ed. London: Churchill Livingstone, 2002: 827-883

11 **LaRusso NF**, Wiesner RH, Ludwig J, MacCarty RL. Current concepts. Primary sclerosing cholangitis. *N Engl J Med* 1984; **310**: 899-903

12 **Gulliver DJ**, Baker ME, Putnam W, Baillie J, Rice R, Cotton PB. Bile duct diverticula and webs: nonspecific cholangiographic features of primary sclerosing cholangitis. *AJR Am J Roentgenol* 1991; **157**: 281-285

S- Editor Liu Y **L- Editor** Zhu LH **E- Editor** Ma WH

PO Box 2345, Beijing 100023, China
www.wjgnet.com
wjg@wjgnet.com

World J Gastroenterol 2007 January 28; 13(4): 643-646
World Journal of Gastroenterology ISSN 1007-9327

CASE REPORT

Pouchitis and pre-pouch ileitis developed after restorative proctocolectomy for ulcerative colitis: A case report

Takashi Iwata, Takayuki Yamamoto, Satoru Umegae, Koichi Matsumoto

Takashi Iwata, Takayuki Yamamoto, Satoru Umegae, Koichi Matsumoto, Inflammatory Bowel Disease Center and Department of Surgery, Yokkaichi Social Insurance Hospital, 10-8 Hazuyamacho, Yokkaichi, Mie 510-0016, Japan
Correspondence to: Takayuki Yamamoto, Inflammatory Bowel Disease Center and Department of Surgery, Yokkaichi Social Insurance Hospital, 10-8 Hazuyamacho, Yokkaichi, Mie 510-0016, Japan. nao-taka@sannet.ne.jp
Telephone: +81-593-31-2000 Fax: +81-593-31-0354
Received: 2006-10-23 Accepted: 2006-12-14

Abstract

We report a case of pouchitis and pre-pouch ileitis, and inflammation in the neo-terminal ileum proximal to the pouch, developed after restorative proctocolectomy for ulcerative colitis. A 35-year old female presented with fever and abdominal pain five weeks after ileostomy closure following proctocolectomy. Computed tomography showed collection of feces in the pouch and proximal ileum. A drainage tube was placed in the pouch perianally, and purulent feces were discharged. With antibiotic treatment, her symptoms disappeared, but two weeks later, she repeatedly developed fever and abdominal pain along with anal bleeding. Pouchscopy showed mucosal inflammation in both the pouch and the pre-pouch ileum. The mucosal cytokine production was elevated in the pouch and pre-pouch ileum. With antibiotic and corticosteroid therapy, her symptoms were improved along with improvement of endoscopic inflammation and decrease of mucosal cytokine production. The fecal stasis with bacterial overgrowth is the major pathogenesis of pouchitis and pre-pouch ileitis in our case.

Key words: Mucosal cytokines; Pouchitis; Pre-pouch ileitis; Restorative proctocolectomy; Ulcerative colitis

Iwata T, Yamamoto T, Umegae S, Matsumoto K. Pouchitis and pre-pouch ileitis developed after restorative proctocolectomy for ulcerative colitis: A case report. *World J Gastroenterol* 2007; 13(4): 643-646

http://www.wjgnet.com/1007-9327/13/643.asp

INTRODUCTION

Restorative proctocolectomy with ileal pouch-anal anastomosis has become the surgical procedure of choice for patients with ulcerative colitis (UC)[1-3]. Pouchitis is the most common complication following restorative proctocolectomy for UC[1-5]. Patients with UC may develop inflammation in the neo-terminal ileum (pre-pouch ileum) proximal to the pouch, so called pre-pouch ileitis. So far, there has been only one study reporting the details of pre-pouch ileitis. Bell and colleagues[6] retrospectively investigated the clinicopathological characteristics of pre-pouch ileitis using their pouch database, however the pathogenesis of pre-pouch ileitis is unknown. We have recently experienced one patient in whom both pouchitis and pre-pouch ileitis developed after restorative proctocolectomy for UC. The purpose of this article is to report the case of our patient, and to discuss the pathogenesis of pre-pouch ileitis based on the clinicopathological and immunological findings.

CASE REPORT

Clinical presentations

In July 2005, we received a 35-year old female with a six-year history of UC requiring surgical treatment. Small bowel follow-through, barium enema and ileocolonoscopy with histological examinations confirmed UC but not Crohn's disease. She had a history of allergy to sulfasalazine and mesalazine. She was treated with long-term corticosteroid therapy, and the cumulative dose of prednisolone administered before operation was more than 20 g. Selective granulocyte and monocyte adsorption apheresis therapy was not effective. She had no history of extraintestinal manifestations. Endoscopically, the extent of disease was pancolitis without backwash ileitis. The indication for surgery was steroid-dependency and chronic continuous disease. A laparoscopic-assisted proctocolectomy with ileal pouch-anal canal anastomosis was performed. The J-shaped pouch (15 cm in length) was constructed using a linear stapler. A stapled ileo-anal canal anastomosis was performed at approximately 2 cm from the dentate line. There was no difficulty in mobilizing the ileal pouch sufficiently to achieve a tension-free anastomosis. The covering ileostomy was constructed to protect the anastomosis. After operation, she developed no serious complications, and was doing well with her ileostomy. Histological diagnosis of the colectomy specimen was UC, and there were no findings of inflammation in the terminal ileum.

Before ileostomy closure, a pouchgram, pouchscopy with biopsy, and manometric study were performed. The pouchgram showed no findings of anastomotic leak, fistulae and strictures, decreased pouch compliance, a long efferent loop, or decreased pouch emptying. Both

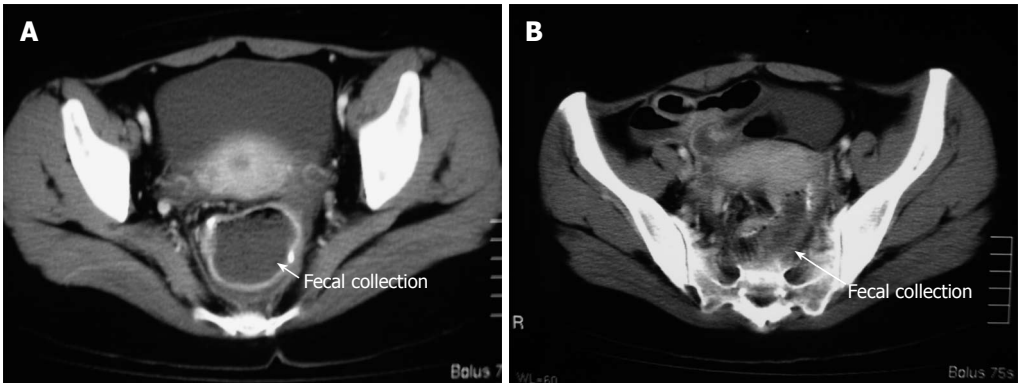

Figure 1 Abdominal computed tomography showing a massive collection of feces in the pouch (**A**) and proximal ileum (**B**).

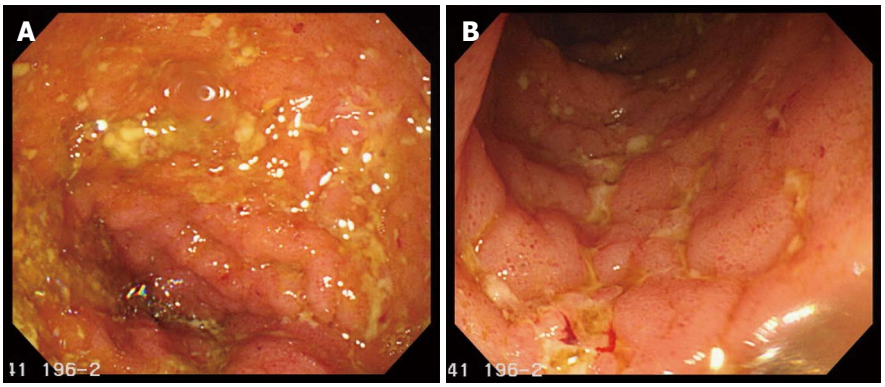

Figure 2 Pouchscopy showing inflammation conditions such as edema, granularity, friability, loss of vascular pattern, and erosions in both the pouch (**A**) and the pre-pouch ileum (continuous 30 cm proximal to the pouch) (**B**).

endoscopically and histologically, there were no findings of inflammation in the pouch and proximal ileum. In the manometric study, the resting anal pressure was 42 mmHg compared with 65 mmHg before pouch construction. The squeezing pressure was 110 mmHg compared with 128 mmHg before pouch construction. In March 2006, she had her ileostomy closed. Postoperatively, she was doing well, and on a normal diet. However, five weeks after operation, she developed high fever (40℃) and severe abdominal pain. Retrospectively, the number of defecations did not change (7-10 times/d), but the fecal volume on each defecation remarkably decreased for several days before her symptoms occurred. Abdominal computed tomography (CT) showed a massive collection of feces in the pouch and proximal ileum (Figure 1). A drainage tube was placed in the pouch perianally, and a large amount of purulent feces were discharged. In fecal culture, *Salmonella, Shigella, Campylobacter, Escherichia coli* O157, *Yersinia, Vibrio* and *Clostridium difficile* were negative, whereas *Escherichia coli* and *Staphylococcus aureu*s were positive. She was managed with total parenteral nutrition in combination with intravenous antibiotic administration (imipenem, 1.0 g/d for one week). Her symptoms disappeared after the five-day drainage of the feces, and she was back on a normal diet. However, two weeks later, she repeatedly presented with fever (40℃) and severe abdominal pain along with mild anal bleeding. Pouchscopy showed inflammatory conditions such as edema, granularity, friability, loss of vascular pattern, and erosions in both the pouch and the pre-pouch ileum (continuous 30 cm proximal to the pouch, Figure 2). The inflammation was milder more proximally. Biopsies were taken for histological examination and mucosal cytokine measurement. Histologically, moderate leukocyte infiltration without crypt abscess formation was observed in both the pouch and the pre-pouch ileum. According to the pouchitis disease activity index by Sandborn[5], her score was 12, and she was diagnosed as having pouchitis (≥ 7 points). Antibiotics (cefmetazone sodium, 2.0 g/d for one week), and prednisolone (30 mg/d for one week) were administered intravenously. Her symptoms were rapidly improved, and pouchscopy after the one-week treatment revealed improvement in mucosal inflammation. Thereafter, predonisolone was orally given (15 mg/d for two weeks, and then 10 mg/d for two weeks). Four months after ileostomy closure following pouch operation, she was doing well with normal bowel function (defecation, 5-7 times/d; soiling, 1 time/2 wk).

Laboratory data

Using the biopsy specimens obtained during pouchscopy, the mucosal cytokine (interleukin (IL)-1β, IL-6, IL-8, and tumor necrosis factor alpha (TNF-α) levels were measured by the enzyme-linked immunosorbent assay as previously reported (Table 1)[7]. In this patient, the mucosal cytokine levels were examined before ileostomy closure, at the time of diagnosis of pouchitis and pre-pouch ileitis, and one week after the treatment for inflammation, and compared with those in 28 patients without pouchitis or pre-pouch ileitis three months after ileostomy closure following ileal pouch construction for UC in our previous study[7]. At the diagnosis of pouchitis and pre-pouch ileitis, the mucosal cytokine levels were remarkably elevated in both the pouch and the pre-pouch ileum compared with those before ileostomy closure. White blood cell (WBC) count

Table 1 Change of mucosal cytokine production in the pouch and pre-pouch ileum

	Before ileostomy closure	At the diagnosis ofpouchitis and pre-pouch ileitis	After treatment	Patients without pouchitis or pre-pouch ileitis[1]
Pouch (pg/mg of tissue)				
IL-1β	25	730	98	34.5 (26-39)
IL-6	590	14000	2700	900 (580-1480)
IL-8	31	840	290	58 (34-76)
TNF-α	10	350	67	38.5 (27-60)
Pre-pouch ileum (pg/mg of tissue)				
IL-1β	17	560	91	10.5 (5-22)
IL-6	600	17000	3600	570 (420-720)
IL-8	22	710	190	19.5 (10-41)
TNF-α	13	270	82	12 (5-18)

IL: Interleukin; TNF: tumor necrosis factor. [1]Median values (interquartile range) for 24 patients without pouchitis or pre-pouch ileitis three months after ileostomy closure following restorative proctocolectomy for ulcerative colitis[7].

was 12300/mm^3, platelet cont was 443000/mm^3, and C-reactive protein (CRP) level was 19.34 mg/dL. After the one-week administration of antibiotics and prednisolone, the mucosal cytokine levels markedly decreased along with endoscopic improvement of mucosal inflammation. At that time, WBC count was 10800/mm^3, platelet count was 506000/mm^3, and CRP level was 0.09 mg/dL.

DISCUSSION

The etiology of pouchitis is still unknown. A variety of factors such as fecal stasis, bacterial overgrowth, immune alternation, bile acid toxicity, short-chain fatty acid deficiency, and ischemia may affect the development of pouchitis[4,8,9]. In our research[7], to examine the impact of the fecal stream and stasis on immunological reactions in the pouch and proximal ileum, mucosal cytokine production was measured before and after ileostomy closure following proctocolectomy for UC. No patients developed pouchitis or pre-pouch ileitis during the study period. We found that immunological reactions in the pouch occurred soon after ileostomy closure, and continued thereafter[7]. In contrast, cytokine production was not elevated in the proximal ileum, where the fecal stasis does not often occur. Thus, the fecal stasis may play an important part in the pathogenesis of immunological reactions in the pouch[7].

Bell and colleagues[6] reported that 15 (2.6%) of 571 inflammatory bowel disease patients undergoing restorative proctocolectomy developed pre-pouch ileitis. However, this incidence may be underestimated because their study was retrospective, and the pre-pouch ileum was not routinely examined. The median age of the 15 patients (eight females) was 36 years, and the median duration from pouch construction to diagnosis of pre-pouch ileitis was three years. The most common clinical presentations were frequency of defecation (40%) and bowel obstruction (40%). Preoperatively, backwash ileitis was observed in 18% of the patients, and 27% had a history of extraintestinal manifestations. All patients had continuous disease from the neo-terminal ileum-pouch junction for a distance of 1 cm to more than 50 cm proximally becoming milder more proximally. Concomitant pouchitis was observed in 47% of the patients. Nine patients had narrowing of the lumen in the pre-pouch ileum, and in two of these there was a severe stricture. One patient had a fistula from the pre-pouch ileum to the vagina. Eleven patients with symptoms were treated, of whom eight required surgery (resection in six, strictureplasty in one, defunctioning ileostomy in one).

In the study by Bell and colleagues[6], there were no statements about the pathogenesis of pre-pouch ileitis. Only half of their patients with pre-pouch ileitis had concomitant pouchitis. Several patients presented with tight stricture, deep ulcerations or fistula. We suspect that these patients may have Crohn's disease, although the histological diagnosis based on the colectomy specimen was confirmed as UC[6]. Wolf *et al*[10] reported that afferent limb ulcers predict Crohn's disease in patients with ileal pouch-anal anastomosis. In our case, findings suggesting Crohn's disease were not observed.

The pathogenesis of pre-pouch ileitis is also unknown. Our patient developed a massive collection of feces in the pouch and pre-pouch ileum in the early postoperative period after ileostomy closure, which was detected by CT. Before her symptoms (fever and abdominal pain) occurred, the fecal volume remarkably decreased, although the number of defecations did not change. The cause of fecal collection is unknown. Before ileostomy closure, pouchgram showed no evidence of anastomotic strictures, decreased pouch compliance, or decreased pouch emptying. The results in our manometric study were similar to those in patients with normal pouch function after restorative proctocolectomy in the previous study[11]. Although a longer follow-up was necessary, she had neither evacuation problems nor impaired pouch emptying at the time of our report (four months after ileostomy closure). If she had the similar symptoms such as fever and abdominal pain along with a decrease in volume of feces, further studies were needed to examine her pouch function.

In our case, endoscopic and histological features of mucosal inflammation were similar in the pouch and pre-pouch ileum, although the inflammation was milder more proximally. Bell and colleagues[6] also found that the histological findings of pouchitis and pre-pouch ileitis are similar. In our institution, mucosal cytokine production is routinely investigated before and after ileostomy closure following restorative proctocolectomy for UC[7]. In this report, at the diagnosis of pouchitis and pre-pouch ileitis, the mucosal IL-1β, IL-6, IL-8, and TNF-α levels were remarkably elevated in both the pouch and the pre-pouch ileum compared with those before ileostomy closure, which were much higher than those in patients without pouchitis or pre-pouch ileitis in our previous study (Table 1)[7], suggesting that both pouchitis and pre-pouch ileitis are associated with increased mucosal cytokine production. There seemed to be no significant difference in cytokine production between pouchitis and pre-pouch ileitis. These cytokine levels remarkably decreased after antibiotic and steroid medication. Purulent feces were discharged through a drainage tube placed in the pouch. In fecal culture, *E.*

coli and *Staphylococcus aureus* were detected, which may have caused severe clinical symptoms such as high fever and abdominal pain.

In conclusion, fecal stasis along with subsequent bacterial overgrowth is the major pathogenesis of both pouchitis and pre-pouch ileitis. The pathogenesis may be similar in pouchitis and pre-pouch ileitis due to the similar endoscopic, histological and immunological features. Further studies are needed to fully understand the pathogenesis of pouchitis and pre-pouch ileitis after restorative proctocolectomy for UC.

REFERENCES

1 **Bach SP,** Mortensen NJ. Revolution and evolution: 30 years of ileoanal pouch surgery. *Inflamm Bowel Dis* 2006; **12**: 131-145

2 **Michelassi F**, Lee J, Rubin M, Fichera A, Kasza K, Karrison T, Hurst RD. Long-term functional results after ileal pouch anal restorative proctocolectomy for ulcerative colitis: a prospective observational study. *Ann Surg* 2003; **238**: 433-441; discussion 442-445

3 **Delaney CP,** Fazio VW, Remzi FH, Hammel J, Church JM, Hull TL, Senagore AJ, Strong SA, Lavery IC. Prospective, age-related analysis of surgical results, functional outcome, and quality of life after ileal pouch-anal anastomosis. *Ann Surg* 2003; **238**: 221-228

4 **Pardi DS,** Sandborn WJ. Systematic review: the management of pouchitis. *Aliment Pharmacol Ther* 2006; **23**: 1087-1096

5 **Sandborn WJ,** Tremaine WJ, Batts KP, Pemberton JH, Phillips SF. Pouchitis after ileal pouch-anal anastomosis: a Pouchitis Disease Activity Index. *Mayo Clin Proc* 1994; **69**: 409-415

6 **Bell AJ,** Price AB, Forbes A, Ciclitira PJ, Groves C, Nicholls RJ. Pre-pouch ileitis: a disease of the ileum in ulcerative colitis after restorative proctocolectomy. *Colorectal Dis* 2006; **8**: 402-410

7 **Yamamoto T,** Umegae S, Kitagawa T, Matsumoto K. The impact of the fecal stream and stasis on immunologic reactions in ileal pouch after restorative proctocolectomy for ulcerative colitis: a prospective, pilot study. *Am J Gastroenterol* 2005; **100**: 2248-2253

8 **Sandborn WJ.** Pouchitis following ileal pouch-anal anastomosis: definition, pathogenesis, and treatment. *Gastroenterology* 1994; **107**: 1856-1860

9 **Yantiss RK,** Sapp HL, Farraye FA, El-Zammar O, O'Brien MJ, Fruin AB, Stucchi AF, Brien TP, Becker JM, Odze RD. Histologic predictors of pouchitis in patients with chronic ulcerative colitis. *Am J Surg Pathol* 2004; **28**: 999-1006

10 **Wolf JM,** Achkar JP, Lashner BA, Delaney CP, Petras RE, Goldblum JR, Connor JT, Remzi FH, Fazio VW. Afferent limb ulcers predict Crohn's disease in patients with ileal pouch-anal anastomosis. *Gastroenterology* 2004; **126**: 1686-1691

11 **Morgado PJ**, Wexner SD, James K, Nogueras JJ, Jagelman DG. Ileal pouch-anal anastomosis: is preoperative anal manometry predictive of postoperative functional outcome? *Dis Colon Rectum* 1994; **37**: 224-228

S- Editor Liu Y **L- Editor** Wang XL **E- Editor** Bai SH

PO Box 2345, Beijing 100023, China
www.wjgnet.com
wjg@wjgnet.com

World J Gastroenterol 2007 January 28; 13(4): 647-648
World Journal of Gastroenterology ISSN 1007-9327

CASE REPORT

Cytomegalovirus hepatitis and myopericarditis

Leire Zubiaurre, Eva Zapata, Luis Bujanda, María Castillo, Igor Oyarzabal, Maria A Gutiérrez-Stampa, Angel Cosme

Leire Zubiaurre, Eva Zapata, Luis Bujanda, Angel Cosme, Department of Digestive disease, Hospital Donostia, Spain
María Castillo, Department of Cardiology, Hospital Donostia, Spain
Igor Oyarzabal, Department of Urology. Hospital Donostia, Spain
Maria A Gutiérrez-Stampa, Department of General Medicine, Donostia, Spain
Correspondence to: Leire Zubiaurre, Department of Digestive disease, Hospital Donostia, Paseo Beguiristain S/N, 20014 San Sebastián (Gipúzcoa), Spain. leirezubi@yahoo.es
Telephone: +34-985-943007173 Fax: +34-985-943007065
Received: 2006-05-23 Accepted: 2006-06-15

Abstract

Cytomegalovirus (CMV) infection in inmunocompetent hosts generally is asymptomatic or may present as a mononucleosis syndrome but rarely can lead to severe organ complications. We report a case of simultaneous hepatic and pericardic CMV infection in a 36-year old immunocompetent man. He was admitted to coronary unit with fever, chest pain radiated to shoulders, changes on electrocardiogram with diffuse ST elevation and modest laboratory elevations in the MB fraction of creatine kinase (CK-MB) of 33.77 μg/L (0.1-6.73), serum cardiac troponin T of 0.904 ng/mL (0-0.4), creatine kinase of 454 U/L (20-195) and myoglobin of 480.4 μg/L (28-72). Routine laboratory test detected an elevation of aminotransferase level: alanine aminotransferase 1445 U/L, aspartate aminotransferase 601 U/L. We ruled out other causes of hepatitis with normal results except IgM CMV. The patient was diagnosed with myopericarditis and hepatitis caused by cytomegalovirus and started symptomatic treatment with salicylic acid. In few days the laboratory findings became normal and the patient was discharged.

Key words: Cytomegalovirus; Hepatitis; Myopericarditis; Pericarditis

Zubiaurre L, Zapata E, Bujanda L, Castillo M, Oyarzabal I, Gutiérrez-Stampa MA, Cosme A. Cytomegalovirus hepatitis and myopericarditis. *World J Gastroenterol* 2007; 13(4): 647-648

http://www.wjgnet.com/1007-9327/13/647.asp

INTRODUCTION

Cytomegalovirus (CMV) infection in an immunocompetent host, rarely can lead to severe organ specific complications[1,2]. A variety of presentations have been described, ranging from a common form of infectious mononucleosis to systemic disease (gastrointestinal, cardiovascular, hepatic, neurologic manifestations) with significant morbidity. We report a case of simultaneous hepatic and pericardic CMV infection in an immunocompetent host.

CASE REPORT

A 36-year old man was admitted to our hospital with fever and chest pain radiated to shoulders. He had no other relevant medical history and physical examination was normal. Electrocardiogram showed diffuse ST elevation and laboratory test displayed modest elevations in MB fraction of creatine kinase (CK-MB) of 33.77 μg/L (0.1-6.73), serum cardiac troponin T of 0.904 ng/mL (0-0.4), creatine kinase of 454 U/L (20-195) and myoglobin of 480.4 μg/L (28-72). The patient was diagnosed with myopericarditis and admitted to the coronary unit. Routine laboratory tests detected an elevation of aminotransferase level: alanine aminotransferase 1445 U/L (6-41), aspartate aminotransferase 601 U/L (6-38). Other laboratory parameters were normal including gamma glutamyl transpeptidase, alkaline phophatase, bilirubin, cholesterol, electrolytes, complete blood cell count and coagulation test. We ruled out other causes of hepatitis: medications, alcohol abuse, hepatitis B, hepatitis C, hereditary hemochromatosis, hepatic steatosis and steatohepatitis, thyroid disorders, celiac disease, autoimmune hepatitis, Wilson´s disease and alpha 1 antitrypsin deficiency. Finally we looked for a less common infection etiology (Epstein Barr virus, cytomegalovirus and atypical bacteria). The results were normal except for IgM CMV. The patient was diagnosed with myopericarditis and hepatitis caused by cytomegalovirus and started symptomatic treatment with salicylic acid. In few days the laboratory findings became normal and the patient was discharged.

DISCUSSION

CMV infection in immunocompetent patients is common with a substantial morbidity and mortality. It is generally asymptomatic in immunocompetent hosts or may present

as a mononucleosis syndrome. Occasionally primary CMV infection can lead to severe organ specific complications[1,2]. Although these cases are rare, gastrointestinal, cardiovascular, neurologic, hepatic disorders have been reported.

Liver function abnormalities are frequently encountered in patients with symptomatic CMV infection. Subclinical transaminitis is the most common finding in immunocompetent patients, and elevations of alkaline phosphatase and total bilirubin are less typical[1,3,4]. Pericarditis and myocarditis have been described in immunocompetent patients with acute CMV infection[5,6]. We have found only one case reporting simultaneous infection of liver and myopericardia with cytomegalovirus[7].

Since symptomatic CMV infection is generally self-limited with complete recovery over a period of days to weeks, it is difficult to prove whether antiviral therapy has a significant impact on the clinical outcome.

REFERENCES

1 **Cohen JI**, Corey GR. Cytomegalovirus infection in the normal host. *Medicine* (Baltimore) 1985; **64**: 100-114

2 **Horwitz CA**, Henle W, Henle G, Snover D, Rudnick H, Balfour HH, Mazur MH, Watson R, Schwartz B, Muller N. Clinical and laboratory evaluation of cytomegalovirus-induced mononucleosis in previously healthy individuals. Report of 82 cases. *Medicine* (Baltimore) 1986; **65**: 124-134

3 **Clarke J**, Craig RM, Saffro R, Murphy P, Yokoo H. Cytomegalovirus granulomatous hepatitis. *Am J Med* 1979; **66**: 264-269

4 **Bonkowsky HL**, Lee RV, Klatskin G. Acute granulomatous hepatitis. Occurrence in cytomegalovirus mononucleosis. *JAMA* 1975; **233**: 1284-1288

5 **Campbell PT**, Li JS, Wall TC, O'Connor CM, Van Trigt P, Kenney RT, Melhus O, Corey GR. Cytomegalovirus pericarditis: a case series and review of the literature. *Am J Med Sci* 1995; **309**: 229-234

6 **Schönian U**, Crombach M, Maser S, Maisch B. Cytomegalovirus-associated heart muscle disease. *Eur Heart J* 1995; **16** Suppl O: 46-49

7 **Räsänen V**, Saikku P. Cytomegalovirus hepatitis and pericarditis. *Duodecim* 1968; **84**: 270-273

S- Editor Wang J **L- Editor** Wang XL **E- Editor** Bai SH

PO Box 2345, Beijing 100023, China
www.wjgnet.com
wjg@wjgnet.com

World J Gastroenterol 2007 January 28; 13(4): 649-650
World Journal of Gastroenterology ISSN 1007-9327

Indian patients with nonalcoholic fatty liver disease presenting with raised transaminases are different at presentation

Ajay Duseja, Ashim Das, Radha Krishan Dhiman, Yogesh Kumar Chawla, Reena Das, Sanjay Bhadada, Ravinder Sialy, Kiran Kumar Thumburu, Anil Bhansali, Naveen Kalra

Ajay Duseja, Radha Krishan Dhiman, Yogesh Kumar Chawla, Kiran Kumar Thumburu, Department of Hepatology, Postgraduate Institute of Medical Education and Research, Chandigarh, India
Ashim Das, Department of Histopathology, Postgraduate Institute of Medical Education and Research, Chandigarh, India
Reena Das, Department of Hematology, Postgraduate Institute of Medical Education and Research, Chandigarh, India
Sanjay Bhadada, Ravinder Sialy, Anil Bhansali, Department of Endocrinology, Postgraduate Institute of Medical Education and Research, Chandigarh, India
Naveen Kalra, Department of Radiodiagnosis and Imaging, Postgraduate Institute of Medical Education and Research, Chandigarh, India
Correspondence to: Dr. Ajay Duseja, MD, DM, FACG, Assistant Professor, Department of Hepatology, PGIMER, Chandigarh, India. ajayduseja@yahoo.co.in
Telephone: +91-172-2756336 Fax: +91-172-2744401
Received: 2006-10-29 Accepted: 2006-12-13

Duseja A, Das A, Dhiman RK, Chawla YK, Das R, Bhadada S, Sialy R, Thumburu KK, Bhansali A, Kalra N. Indian patients with nonalcoholic fatty liver disease presenting with raised transaminases are different at presentation. *World J Gastroenterol* 2007; 13(4): 649-650

http://www.wjgnet.com/1007-9327/13/649.asp

TO THE EDITOR

We read with great interest the article, "Non-alcoholic fatty liver disease may not be a severe disease at presentation among Asian Indians" by Madan *et al*[1] in the recent issue of *WJG*. Twenty-eight (55%) out of 51 patients with non-alcoholic fatty liver disease (NAFLD) who presented with abnormal transaminases had histological evidence of nonalcoholic steatohepatitis (NASH). The majority of patients had grade 1 [32 (63%)] or grade 2 [16 (31%)] inflammation and either had no [23 (45%)] fibrosis or stage I [19 (37%)] fibrosis. None of the patients had cirrhosis[1]. We agree with Madan *et al*[1] that Asian Indians with NAFLD who present with unexplained increase in transaminases may have mild disease at presentation on the basis of similar observations made by us[2]. NAFLD has a spectrum which includes patients with only steatosis and NASH that can progress to cirrhotic and hepatocellular carcinoma[3]. Of the 127 NAFLD patients (July 2001-March 2006) who presented with raised transaminases for at least 6 mo with negative viral, autoimmune and metabolic workup analyzed in our study, 43 underwent liver biopsy (Table 1). Only half of them [22 (51%)] had histological evidence of NASH as defined by either class Ⅲ [8 (19%)] or class Ⅳ [14 (32%)] NAFLD according to Matteoni *et al*[4]. The other 21 (49%) patients either had class Ⅰ [2 (5%)] or class Ⅱ [19 (44%)] disease not amounting to histological NASH (Table 1). In the 22 patients with histological NASH evaluated as per Brunt *et al*[5], the majority had mild to moderate inflammation and either no fibrosis or stage Ⅰ to Ⅱ fibrosis. Only 18% patients had stage Ⅲ fibrosis and none of the patients had cirrhosis of the liver (Table 1).

The majority of patients studied by us were males with a mean age of 39.2 ± 10.7 years (Table 2), which is similar to data shown by Madan *et al*[1]. In addition to the mild histological disease at presentation, there are other differences in NAFLD patients from India and those from the West[2]. When we used the Asia Pacific criteria[6,7], even though most of our patients had central obesity [104 (82%)] and were either overweight [27 (21%)] or obese [86 (68%)] they did not have the kind of morbid obesity seen in patients from the West (Table 2). The mean body weight and body mass index (BMI) of our patients were 71 kg and 28.7 kg/m^2 respectively, much less than those reported from the West[8,9], but were similar to the data shown by Madan *et al*[1] who also found that the median BMI is 26.7 (range 21.3-32.5) kg/m^2 and the majority of them are obese (69%) according to the Asian Pacific criteria. When the ATP Ⅲ criteria with modified waist were used in 81 of our patients to define metabolic syndrome, around half of them [39 (48%)] had metabolic syndrome, also less than reported in patients from the West (Table 2)[10]. We attributed low prevalence of metabolic syndrome in our patients to the lower prevalence of diabetes mellitus [16 (13%)] and hypertension [13 (10%)] at presentation, which is similar to the data reported by Madan *et al*[1] (10% and 11.8% respectively) in their study. Furthermore, the low prevalence of metabolic syndrome (20.9%) in the study of Madan *et al*[1] could be due to their use of BMI as a surrogate marker for waist, which may not always be true. Indians may have a normal BMI with an abnormal waist which is related to more of central obesity rather than overall obesity. It is possible that diabetes mellitus occurs late in the course of this disease when the degree

Table 1 Liver histology in 43 patients with nonalcoholic fatty liver disease (NAFLD), *n* (%)

Class Ⅰ	2 (5)
Class Ⅱ	19 (44)
Class Ⅲ	8 (19)
Class Ⅳ	14 (32)
NASH (class Ⅲ + Ⅳ) on histology (*n* = 22)	
Grade 1	10 (45)
2	12 (55)
3	0
Stage 0	6 (27)
1	7 (32)
2	5 (23)
3	4 (18)
4	0
Perls' Prussian blue staining on liver biopsy (*n* = 30)	
0	20 (67)
1+	6 (20)
2+	4 (13)
3+	0
4+	0

Table 2 Clinical and laboratory parameters in 127 patients with nonalcoholic fatty liver disease (NAFLD)

mean age ± SD (yr)	39.2 ± 10.7
Males	84
Mean body weight (range) (kg)	71 (45-100)
Mean BMI (range) (kg/m^2)	28.7 (19-34)
Overweight	27 (21%)
Obesity	86 (68%)
Abnormal waist	104 (82%)
Insulin resistance	48/58 (83%)
Diabetes mellitus	16 (13%)
Hypertension	13 (10%)
Dyslipidemia	67 (53%)
Metabolic syndrome	39/81 (48%)

of insulin resistance increases and our patients could represent patients in the early spectrum of NAFLD with less severe disease and diabetes mellitus at presentation with raised transaminases. Diabetes mellitus is one of the risk factors for severe liver disease in NAFLD and absence of this risk factor in majority of our patients may explain the mild disease on liver biopsy.

Insulin resistance is very common in patients with NAFLD irrespective of the methodology used. Eighty percent of 51 patients in the study by Madan *et al*[1] had abnormal homeostasis model assessment for insulin resistance (HOMA-IR). We found insulin resistance in all of our 22 patients initially studied by insulin tolerance test (ITT) and later in 48 (83%) of 58 patients studied by HOMA-IR (Table 2)[2,11,12].

Though not studied by Madan *et al*[1], another difference in Indian patients and those from the West is the presence of serum and liver iron abnormalities and HFE gene mutations[2,13,14]. Only 4 (5%) of our 87 patients had abnormal serum ferritin or transferrin saturation and 4 (13%) of 30 patients studied were heterozygotes for H63D mutation. None of the patients had C282Y HFE gene mutation. The majority of our patients had negative Perls' staining for iron on liver biopsy (Table 1) and there was no correlation between the iron staining and degree of necro-inflammation and fibrosis, suggesting that serum and liver iron and HFE gene mutations play a very little role in Indian patients with NAFLD[2,13,14].

In conclusion, Indian patients with NAFLD who present with incidental detection of raised transaminases representing a part of spectrum of patients with NAFLD have a milder disease at presentation. Whether NAFLD in Indian patients is overall mild or overall different from other parts of the world requires analysis of full spectrum of NAFLD patients.

REFERENCES

1 **Madan K**, Batra Y, Gupta SD, Chander B, Rajan KD, Tewatia MS, Panda SK, Acharya SK. Non-alcoholic fatty liver disease may not be a severe disease at presentation among Asian Indians. *World J Gastroenterol* 2006; **12**: 3400-3405

2 **Duseja A,** Das A, Das R, Dhiman RK, Chawla Y, Bhansali A, Kalra N. Clinicopathological profile of Indian patients with nonalcoholic fatty liver disease is different from the west. *Dig Dis Sci* 2006; In press

3 **Duseja A**, Nanda M, Das A, Das R, Bhansali A, Chawla Y. Prevalence of obesity, diabetes mellitus and hyperlipidaemia in patients with cryptogenic liver cirrhosis. *Trop Gastroenterol* 2004; **25**: 15-17

4 **Matteoni CA,** Younossi ZM, Gramlich T, Boparai N, Liu YC, McCullough AJ. Nonalcoholic fatty liver disease: a spectrum of clinical and pathological severity. *Gastroenterology* 1999; **116**: 1413-1419

5 **Brunt EM**, Janney CG, Di Bisceglie AM, Neuschwander-Tetri BA, Bacon BR. Nonalcoholic steatohepatitis: a proposal for grading and staging the histological lesions. *Am J Gastroenterol* 1999; **94**: 2467-2474

6 **Steering Committee of the WHO Western Pacific Region, IASO & IOTF.** The Asia-Pacific perspective: redefining obesity and its treatment. Melbourne: Australia Pty Ltd, 2000: 8-56

7 **Dhiman RK**, Duseja A, Chawla Y. Asians need different criteria for defining overweight and obesity. *Arch Intern Med* 2005; **165**: 1069-1070

8 **Sanyal AJ**. AGA technical review on nonalcoholic fatty liver disease. *Gastroenterology* 2002; **123**: 1705-1725

9 **Angulo P**. Nonalcoholic fatty liver disease. *N Engl J Med* 2002; **346**: 1221-1231

10 **Marchesini G**, Bugianesi E, Forlani G, Cerrelli F, Lenzi M, Manini R, Natale S, Vanni E, Villanova N, Melchionda N, Rizzetto M. Nonalcoholic fatty liver, steatohepatitis, and the metabolic syndrome. *Hepatology* 2003; **37**: 917-923

11 **Duseja A**, Murlidharan R, Bhansali A, Sharma S, Das A, Das R, Chawla Y. Assessment of insulin resistance and effect of metformin in nonalcoholic steatohepatitis--a preliminary report. *Indian J Gastroenterol* 2004; **23**: 12-15

12 **Duseja A**, Sialy R, Kiran Kumar T, Das A, Dhiman RK, Bhansali A, Chawla YK. Insulin tolerance test is comparable to homeostasis model assessment for insulin resistance in patients with nonalcoholic fatty liver disease. *Gastroenterology* 2006; **130**: A-821 (suppl 2)

13 **Duseja A**, Das R, Das A, Dhiman RK, Chawla YK, Garewal G. Serum iron levels and hepatic iron overload in patients with nonalcoholic steatohepatitis. *Dig Dis Sci* 2006; 51: 1730-1731

14 **Duseja A**, Das R, Nanda M, Das A, Garewal G, Chawla Y. Nonalcoholic steatohepatitis in Asian Indians is neither associated with iron overload nor with HFE gene mutations. *World J Gastroenterol* 2005; **11**: 393-395

S- Editor Wang GP **L- Editor** Wang XL **E- Editor** Bai SH

PO Box 2345, Beijing 100023, China
www.wjgnet.com
wjg@wjgnet.com

World J Gastroenterol 2007 January 28; 13(4): 651
World Journal of Gastroenterology ISSN 1007-9327

Treatment regimen design in clinical radiotherapy for hepatoma

Jian-She Yang

Jian-She Yang, Life Science School of Northwest Normal University, Lanzhou 730070, Gansu Province, China
Jian-She Yang, Shanghai Institute of Applied Physics, Chinese Academy of Sciences, Shanghai 201800, China
Correspondence to: Jian-She Yang, PhD, Associate Professor, Northwest Normal University, No.967 Anning Road (East), Anning District, Lanzhou 730070, Gansu Province, China. yangjs@impcas.ac.cn
Telephone: +86-21-59554727 Fax: +86-931-7971564
Received: 2006-10-27 Accepted: 2006-12-14

Key words: Radiotherapy; Treatment regimen design; Treatment of hepatoma

Yang JS. Treatment regimen design in clinical radiotherapy for hepatoma. *World J Gastroenterol* 2007; 13(4): 651

http://www.wjgnet.com/1007-9327/13/651.asp

TO THE EDITOR

Recently, the paper by Wang *et al*[1] published in *World Journal of Gastroenterology* has given rise to great interest of many researchers. It is well known that hepatoma is one of the lethal diseases with a high incidence in the world, especially in Asia. Radiotherapy is the main treatment modality of hepatoma in clinical practice. Unfortunately, intrinsic radiosensitivity of cancer cells is not fully understood, though a large number of papers on it are now available. Yang and colleagues[2] have developed the premature chromosome condensation technique for clinical radiotherapy of hepatoma. A precise and quick measurement of cell radiosensitivity can detect the high-risk results after exposure to a large dose.

Premature chromosome condensation technique can quickly and precisely detect radiation-induced chromosome damage[3-5]. Chromatid breaks are regarded as a good radiodosimetry, which highly correlates with cell survival and radiosensitivity[6]. However, they are not a negative value as described by Wang *et al*[1]. I recommend her to further measure them in order to perfect this promising approach.

REFERENCES

1 **Wang ZZ**, Li WJ, Zhang H, Yang JS, Qiu R, Wang X. Comparison of clonogenic assay with premature chromosome condensation assay in prediction of human cell radiosensitivity. *World J Gastroenterol* 2006; **12**: 2601-2605
2 **Jianshe Y**, Xigang J, Wenjian L, Zhuanzi W, Guangming Z, Jufang W, Bingrong D, Qingxiang G, Linda W. Correlation between initial chromatid damage and survival of various cell lines exposed to heavy charged particles. *Radiat Environ Biophys* 2006; **45**: 261-266
3 **Yang JS**, Li WJ, Jin XD, Jing XG, Guo CL, Wei W, Gao QX. Radiobiological response of human hepatoma and normal liver cells exposed to carbon ions generated by Heavy Ion Research Facility in Lanzhou. *Sci China Ser G* 2006; **49**: 72-76
4 **Jianshe Y**, Wenjian L, Xiaodong J, Xigang J, Chuanling G, Wei W, Qingxiang G. Survival and initial chromatid breakage in normal and tumour cells exposed in vitro to gamma rays and carbon ions at the HIRFL. *Br J Radiol* 2006; **79**: 518-521
5 **Yang JS**, Jing XG, Wang ZZ, Li WJ. A correlation between radiation sensitivity and initial chromatid breaks in cancer cell lines revealed by Calyculin A-induced premature condensation. *J Cen Europe Bio* 2006; **1**: 451-462
6 **Yang JS**, Li WJ, Zhou GM, Jin XD, Xia JG, Wang JF, Wang ZZ, Guo CL, Gao QX. Comparative study on radiosensitivity of various tumor cells and human normal liver cells. *World J Gastroenterol* 2005; **11**: 4098-4101

S- Editor Liu Y **L- Editor** Wang XL **E- Editor** Ma WH

PO Box 2345, Beijing 100023, China
www.wjgnet.com
wjg@wjgnet.com

World J Gastroenterol 2007 January 28; 13(4): 652
World Journal of Gastroenterology ISSN 1007-9327

ACKNOWLEDGMENTS

Acknowledgments to Reviewers of *World Journal of Gastroenterology*

Many reviewers have contributed their expertise and time to the peer review, a critical process to ensure the quality of *World Journal of Gastroenterology*. The editors and authors of the articles submitted to the journal are grateful to the following reviewers for evaluating the articles (including those published in this issue and those rejected for this issue) during the last editing time period.

Katsunori Iijima, Dr
Division of Gastroenterology, Tohoku University Graduate School of Medicine, 1-1 Seiryo-machi, Aobaku., Sendai 980-8574, Japan

Juan Lucio Iovanna, Professor
Centre de Recherche INSERM, Unité 624, Stress Cellulaire, Parc Scientifique et Technologique de Luminy case 915, 13288 Cedex 9 Marseille, France

Ming Li, Associate Professor
Tulane University Health Sciences Center, 1430 Tulane Ave Sl-83, New Orleans 70112, United States

Luigi Bonavina, Professor
Department of Surgery, Policlinico San Donato, University of Milano, via Morandi 30, Milano 20097, Italy

Josep M Bordas, MD
Department of Gastroenterology IMD, Hospital Clinic", Llusanes 11-13 at, Barcelona 08022, Spain

Ming_shiang Wu, Dr, Associate Professor
Internal Medicine, National Taiwan University Hospital, No 7, Chung-Shan S. Rd., Taipei 100, Taiwan, China

Francis Seow-Choen, Professor
Seow-Choen Colorectal Centre, Mt Elizabeth Medical Centre, Singapore, 3 Mt Elizabeth Medical Centre #09-10, 228510, Singapore

Frank Lammert, Prof, Dr
Department of Internal Medicine I, University Hospital Bonn, University of Bonn, Sigmund-Freud-Str. 25, 53105 Bonn, Germany

Ramon Bataller, MD
Liver Unit, Hospital Clinic,Villarroel 170, Barcelona 08036, Spain

Mototsugu Kato, MD
Department of Endoscopy, HokkaIDo University Hospital, Nishi-5, Kita-14, Kita-ku, Sapporo 060-8648, Japan

Lee Bouwman, Dr
Leiden University Medical Centre, department of surgery, Albinusdreef 2 PO Box 9600, 230 RC Leiden, The Netherlands

Yuji Naito, Professor
Kyoto Prefectural University of Medicine, Kamigyo-ku, Kyoto 602-8566, Japan

Takayuki Yamamoto, MD
Inflammatory Bowel Disease Center, Yokkaichi Social Insurance Hospital, 10-8 Hazuyamacho, Yokkaichi 510-0016, Japan

Alex B Lentsch, PhD, Associate Professor
Department of Surgery, Division of Trauma and Critical Care, University of Cincinnati College of Medicine, 231 Albert Sabin Way, Cincinnati OH 45267-0558, United States

Ruben Zamora, PhD
Department of Surgery,University of Pittsburgh, W1540 Biomedical Science Tower 200 Lothrop St., Pittsburgh PA 15213, United States

Ryuichi Iwakiri, Dr
Department of Medicine and Gastrointestinal Endoscopy, Saga Medical School, 5-1-1 Nabeshima, Saga 849-8501, Japan

Gianluigi Giannelli, MD
Dipartimento di Clinica Medica, Immunologia e Malattie Infettive, Sezione di Medicina Interna, Policlinico, Piazza G. Cesare 11, 70124 Bari, Italy

Francis Seow-Choen, Professor
Seow-Choen Colorectal Centre, Mt Elizabeth Medical Centre, Singapore, 3 Mt Elizabeth Medical Centre #09-10 , 228510, Singapore

Bo-Rong Pan, Professor
Outpatient Department of Oncology, The Fourth Military Medical University, 175 Changle West Road,Xi'an 710032, Shaanxi Province, China

Stephen E Roberts, Dr
Unit of Health-Care Epidemiology, Department of Public Health, University of Oxford, Old Rd, Oxford OX3 7LF, United Kingdom

Michael F Byrne , MD
Clinical Associate Professor, Division of GastroenterologyVancouver General Hospital, 100-2647 Willow Street Vancouver BC V5Z 3P1, Canada

Da-Jun Deng, Professor
Department of Cancer Etiology, Peking University School of Oncology, 1 Da-Hong-Luo-Chang Street, Western District, Beijing 100034, China

María Isabel Torres López, Professor
Experimental Biology, University of Jaen, araje de las Lagunillas s/n, Jaén 23071, Spain

Noriaki Tanaka, Professor
Department of Gastroenterological Surgery, Transplant and Surgical Oncology, Okayama University Graduate School of Medicine and Dentistry, 2-5-1, Shikata-cho, Okayama 700-8558, Japan

Minoti Vivek Apte, Associate Professor
Pancreatic Research Group, South Western Sydney Clinical School, The University of New South Wales. Liverpool, NSW 2170, Australia

Saúl Villa-Trevio, MD, PhD
Departamento de Biología Celular, Centro de Investigación y de Estudios Avanzados del IPN (Cinvestav), Ave. IPN No. 2508. Col. San Pedro, Zacatenco, C.P. 07360, México, DF, Mexico

Rudi Schmid, MD
211 Woodland Road, Kentfield, California 94904, United States

Masato Kusunoki, Professor and Chairman
Second Department of Surgery, Mie University School of Medicine, Mie, 2-174 Edobashi, Tsu MIE 514-8507, Japan

Ignacio Gil-Bazo, MD, PhD
Cancer Biology and Genetics Program,
Memorial-Sloan Kettering Cancer Center, 1275 York Avenue. Box 241, New York 10021, United States

Shannon S Glaser, Dr
Department of Internal Medicine, Scott & White Hospital, 702 SW HK Dodgen Loop, Medcial Research Building, Temple 76504, United States

Jay Pravda, MD
Inflammatory Disease Research Center, Gainesville, Florida, 32614-2181, United States

Raul J Andrade, Associate Professor
Department of Medicine, University of Malaga, Boulevar louis pasteur 32, málaga 29010, Spain

Dariusz Marek Lebensztejn, Associate Professor
IIIrd Department of Pediatrics, Medical University of Bialystok, 17 Waszyngtona Str, Bialystok 15-274, Poland

Simon D Taylor-Robinson, MD
Department of Medicine A, Imperial College London, Hammersmith Hospital, Du Cane Road, London W12 0HS, United Kingdom

Nick Paul Thompson, MD
Department of Medicine, Freeman Hospital, Newcastle Upon Tyne, NE7 7DN, Unite Kingdom

Francesco Feo, Professor
Dipartimento di Scienze Biomediche, Sezione di Patologia Sperimentale e Oncologia, Università di Sassari, Via P, Manzella 4, 07100 Sassari, Italy

PO Box 2345, Beijing 100023, China
www.wjgnet.com
wjg@wjgnet.com

World J Gastroenterol 2007 February 28; 13(4): 653
World Journal of Gastroenterology ISSN 1007-9327

Meetings

MAJOR MEETINGS COMING UP

Meeting Falk Research Workshop: Morphogenesis and Cancerogenesis of the Liver
25-26 January 2007
Goettingen
symposia@falkfoundation.de

Meeting Canadian Digestive Diseases Week (CDDW)
16-20 February 2007
Banff-AB
cagoffice@cag-acg.org
www.cag-acg.org/cddw/cddw2007.htm

Meeting Falk Symposium 158: Intestinal Inflammation and Colorectal Cancer
23-24 March 2007
Sevilla
symposia@falkfoundation.de

Meeting BSG Annual Meeting
26-29 March 2007
Glasgow
www.bsg.org.uk/

NEXT 6 MONTHS

Meeting 42nd Annual Meeting of the European Association for the Study of the Liver
11-15 April 2007
Barcelona
easl2007@easl.ch
www.easl.ch/liver-meeting/

Meeting Falk Symposium 159: IBD 2007 - Achievements in Research and Clinical Practice
4-5 May 2007
Istanbul
symposia@falkfoundation.de

Meeting European Society for Paediatric Gastroenterology, Hepatology and Nutrition Congress 2007
9-12 May 2007
Barcelona
espghan2007@colloquium.fr

Digestive Disease Week
19-24 May 2007
Washington Convention Center, Washington DC

Meeting Gastrointestinal Endoscopy Best Practices: Today and Tomorrow, ASGE Annual Postgraduate Course at DDW
23-24 May 2007
Washington-DC
tkoral@asge.org

Meeting ESGAR 2007 18th Annual Meeting and Postgraduate Course
12-15 June 2007
Lisbon
fca@netvisao.pt

Meeting Falk Symposium 160: Pathogenesis and Clinical Practice in Gastroenterology
15-16 June 2007
Portoroz
symposia@falkfoundation.de

Meeting ILTS 13th Annual International Congress
20-23 June 2007
Rio De Janeiro
www.ilts.org

Meeting 9th World Congress on Gastrointestinal Cancer
27-30 June 2007
Barcelona
meetings@imedex.com

EVENTS AND MEETINGS IN 2007

Meeting Falk Research Workshop: Morphogenesis and Cancerogenesis of the Liver
25-26 January 2007
Goettingen
symposia@falkfoundation.de

Meeting Canadian Digestive Diseases Week (CDDW)
16-20 February 2007
Banff-AB
cagoffice@cag-acg.org
www.cag-acg.org/cddw/cddw2007.htm

Meeting Falk Symposium 158: Intestinal Inflammation and Colorectal Cancer
23-24 March 2007
Sevilla
symposia@falkfoundation.de

Meeting BSG Annual Meeting
26-29 March 2007
Glasgow
www.bsg.org.uk/

Meeting 42nd Annual Meeting of the European Association for the Study of the Liver
11-15 April 2007
Barcelona
easl2007@easl.ch
www.easl.ch/liver-meeting/

Meeting Falk Symposium 159: IBD 2007 - Achievements in Research and Clinical Practice
4-5 May 2007
Istanbul
symposia@falkfoundation.de

Meeting European Society for Paediatric Gastroenterology, Hepatology and Nutrition Congress 2007
9-12 May 2007
Barcelona
espghan2007@colloquium.fr

Meeting Gastrointestinal Endoscopy Best Practices: Today and Tomorrow, ASGE Annual Postgraduate Course at DDW
23-24 May 2007
Washington-DC
tkoral@asge.org

Meeting ESGAR 2007 18th Annual Meeting and Postgraduate Course
12-15 June 2007
Lisbon
fca@netvisao.pt

Meeting Falk Symposium 160: Pathogenesis and Clinical Practice in Gastroenterology
15-16 June 2007
Portoroz
symposia@falkfoundation.de

Meeting ILTS 13th Annual International Congress
20-23 June 2007
Rio De Janeiro
www.ilts.org

Meeting 9th World Congress on Gastrointestinal Cancer
27-30 June 2007
Barcelona
meetings@imedex.com

Meeting 15th International Congress of the European Association for Endoscopic Surgery
4-7 July 2007
Athens
info@eaes-eur.org
congresses.eaes-eur.org/

Meeting 39th Meeting of the European Pancreatic Club
4-7 July 2007
Newcastle
www.e-p-c2007.com

Meeting XXth International Workshop on Heliobacter and related bacteria in cronic degistive inflammation
20-22 September 2007
Istanbul
www.heliobacter.org

Meeting Falk Workshop: Mechanisms of Intestinal Inflammation
10 October 2007
Dresden
symposia@falkfoundation.de

Meeting Falk Symposium 161: Future Perspectives in Gastroenterology
11-12 October 2007
Dresden
symposia@falkfoundation.de

Meeting Falk Symposium 162: Liver Cirrhosis - From Pathophysiology to Disease Management
13-14 October 2007
Dresden
symposia@falkfoundation.de

American College of Gastroenterology Annual Scientific Meeting
12-17 October 2007
Pennsylvania Convention Center
Philadelphia, PA

Meeting APDW 2007 - Asian Pacific Digestive Disease Week 2007
15-18 October 2007
Kobe
apdw@convention.co.jp
www.apdw2007.org

15th United European Gastroenterology Week, UEGW
27-31 October 2007
Le Palais des Congrès de Paris, Paris, France

Meeting The Liver Meeting® 2007 - 57th Annual Meeting of the American Association for the Study of Liver Diseases
2-6 November 2007
Boston-MA
www.aasld.org

Gastro 2009, World Congress of Gastroenterology and Endoscopy London, United Kingdom 2009

PO Box 2345, Beijing 100023, China
www.wjgnet.com
wjg@wjgnet.com

World J Gastroenterol 2007 January 28; 13(4): 654-656
World Journal of Gastroenterology ISSN 1007-9327

Instructions to authors

GENERAL INFORMATION

World Journal of Gastroenterology (*WJG, World J Gastroenterol* ISSN 1007-9327 CN 14-1219/R) is a weekly journal of more than 48 000 circulation, published on the 7th, 14th, 21st and 28th of every month.

Original Research, Clinical Trials, Reviews, Comments, and Case Reports in esophageal cancer, gastric cancer, colon cancer, liver cancer, viral liver diseases, *etc.*, from all over the world are welcome on the condition that they have not been published previously and have not been submitted simultaneously elsewhere.

Indexed and abstracted in

Current Contents®/Clinical Medicine, Science Citation Index Expanded (also known as SciSearch®) and Journal Citation Reports/Science Edition, *Index Medicus*, MEDLINE and PubMed, Chemical Abstracts, EMBASE/Excerpta Medica, Abstracts Journals, *Nature Clinical Practice Gastroenterology and Hepatology*, CAB Abstracts and Global Health. ISI JCR 2003-2000 IF: 3.318, 2.532, 1.445 and 0.993.

Published by

The WJG Press

SUBMISSION OF MANUSCRIPTS

Manuscripts should be typed double-spaced on A4 (297 mm × 210 mm) white paper with outer margins of 2.5 cm. Number all pages consecutively, and start each of the following sections on a new page: Title Page , Abstract, Introduction, Materials and Methods, Results, Discussion, acknowledgements, References, Tables, Figures and Figure Legends. Neither the editors nor the Publisher is responsible for the opinions expressed by contributors. Manuscripts formally accepted for publication become the permanent property of The WJG Press, and may not be reproduced by any means, in whole or in part without the written permission of both the authors and the Publisher. We reserve the right to put onto our website and copy-edit accepted manuscripts. Authors should also follow the guidelines for the care and use of laboratory animals of their institution or national animal welfare committee.

Authors should retain one copy of the text, tables, photographs and illustrations, as rejected manuscripts will not be returned to the author(s) and the editors will not be responsible for the loss or damage to photographs and illustrations in mailing process.

Online submission

Online submission is strongly advised. Manuscripts should be submitted through the Online Submission System at: http://www.wjgnet.com/index.jsp. Authors are highly recommended to consult the ONLINE INSTRUCTIONS TO AUTHORS (http://www.wjgnet.com/wjg/help/instructions.jsp) before attempting to submit online. Authors encountering problems with the Online Submission System may send an email you describing the problem to wjg@wjgnet.com for assistance. If you submit your manuscript online, do not make a postal contribution. A repeated online submission for the same manuscript is strictly prohibited.

Postal submission

Send 3 duplicate hard copies of the full-text manuscript typed double-spaced on A4 (297 mm × 210 mm) white paper together with any original photographs or illustrations and a 3.5 inch computer diskette or CD-ROM containing an electronic copy of the manuscript including all the figures, graphs and tables in native Microsoft Word format or *.rtf format to:

Editorial Office

World Journal of Gastroenterology
Editorial Department: Apartment 1066, Yishou Garden,
58 North Langxinzhuang Road,
PO Box 2345, Beijing 100023, China
E-mail: wjg@wjgnet.com
http: //www.wjgnet.com
Telephone: +86-10-85381892
Fax: +86-10-85381893

MANUSCRIPT PREPARATION

All contributions should be written in English. All articles must be submitted using a word-processing software. All submissions must be typed in 1.5 line spacing and in word size 12 with ample margins. The letter font is Tahoma. For authors from China, one copy of the Chinese translation of the manuscript is also required (excluding references). Style should conform to our house format. Required information for each of the manuscript sections is as follows:

Title page

Full manuscript title, running title, all author(s) name(s), affiliations, institution(s) and/or department(s) where the work was accomplished, disclosure of any financial support for the research, and the name, full address, telephone and fax numbers and email address of the corresponding author should be included. Titles should be concise and informative (removing all unnecessary words), emphasize what is new, and avoid abbreviations. A short running title of less than 40 letters should be provided. List the author(s)' name(s) as follows: initial and/or first name, middle name or initial(s) and full family name.

Abstract

An informative, structured abstract of no more than 250 words should accompany each manuscript. Abstracts for original contributions should be structured into the following sections: AIM: Only the purpose should be included. METHODS: The materials, techniques, instruments and equipments, and the experimental procedures should be included. RESULTS: The observatory and experimental results, including data, effects, outcome, *etc.* should be included. Authors should present *P* value where necessary, and the significant data should accompany. CONCLUSION: Accurate view and the value of the results should be included.

The format of structured abstracts is at: http://www.wjgnet.com/wjg/help/11.doc

Key words

Please list 5-10 key words that could reflect content of the study mainly from *Index Medicus*.

Text

For most article types, the main text should be structured into the following sections: INTRODUCTION, MATERIALS AND METHODS, RESULTS and DISCUSSION, and should include in appropriate Figures and Tables. Data should be presented in the body text or in Figures and Tables, but not in both.

Illustrations

Figures should be numbered as 1, 2, 3 and so on, and mentioned clearly in the main text. Provide a brief title for each figure on a separate page. No detailed legend should be involved under the figures. This part should be added into the text where the figures are applicable. Digital images: black and white photographs should be scanned and saved in TIFF format at a resolution of 300 dpi; color images should be saved as CMYK (print files) but not as RGB (screen-viewing files). Place each photograph in a separate file. Print images: supply images of size no smaller than 126 mm × 85 mm printed on smooth surface paper; label the image by writing the Figure number and orientation using an arrow. Photomicrographs: indicate the original magnification and stain in the legend. Digital Drawings: supply files in EPS if created by freehand and illustrator, or TIFF from photoshops. EPS files must be accompanied by a version in native file format for editing purposes. Existing line drawings should be scanned at a resolution of 1200 dpi and as close as possible to the size where they will appear when printed. Please use uniform legends for the same subjects. For example: Figure 1 Pathological changes of atrophic gastritis after treatment. A: ...; B: ...; C: ...; D: ...; E: ...; F: ...; G: ...

Tables

Three-line tables should be numbered as 1, 2, 3 and so on, and mentioned clearly in the main text. Provide a brief title for each table. No detailed legend should be included under the tables. This part should be added into the text where the tables are applicable. The information should complement but not duplicate that contained in the text. Use one horizontal line under the title, a second under the column heads, and a third below the Table, above any footnotes. Vertical and italic lines should be omitted.

Notes in tables and illustrations

Data that are not statistically significant should not be noted. $^{a}P<0.05$, $^{b}P<0.01$ should be noted ($P>0.05$ should not be noted). If there are other series of *P* values, $^{c}P<0.05$ and $^{d}P<0.01$ are used. Third series of *P* values can be expressed as $^{e}P<0.05$ and $^{f}P<0.01$. Other notes in tables or under

illustrations should be expressed as ^1F, ^2F, ^3F; or some other symbols with a superscript (Arabic numerals) in the upper left corner. In a multi-curve illustration, each curve should be labeled with ●, ○, ■, □, ▲, △, *etc.* in a certain sequence.

Acknowledgments

Brief acknowledgments of persons who have made genuine contributions to the manuscripts and who endorse the data and conclusions are included. Authors are responsible for obtaining written permission to use any copyrighted text and/or illustrations.

REFERENCES

Coding system

The author should code the references according the citation order in text in Arabic numerals, put references codes in square brackets, superscript it at the end of citation content or the author name of the citation. For those citation content as the narrate part, the coding number and square brackets should be typeset normally. For example, Crohn's disease (CD) is associated with increased intestinal permeability[1,2]. If references are directly cited in the text, they would be put together with the text, for example, from references [19,22-24], we know that...

When the authors code the references, please ensure that the order in text is the same as in reference part and also insure the spelling accuracy of the first author's name. Do not code the same citation twice.

PMID requirement

PMID roots in the abstract serial number indexed by PubMed (http://www.ncbi.nlm.nih.gov/entrez/query.fcgi?db=PubMed). The author should supply the PMID for journal citation. For those references that have not been indexed by PubMed, a printed copy of the first page of the full reference should be submitted.

The accuracy of the information of the journal citations is very important. Through reference testing system, the authors and editor could check the authors name, title, journal title, publication date, volume number, start page, and end page. We will interlink all references with PubMed in ASP file so that the readers can read the abstract of the citations online immediately.

Style for journal references

Authors: the first author should be typed in bold-faced letter. The surname of all authors should be typed with the initial letter capitalized and followed by their name in abbreviation (For example, Lian-Sheng Ma is abbreviated as Ma LS, Bo-Rong Pan as Pan BR). Title of the cited article and italicized journal title (Journal title should be in its abbreviation form as shown in PubMed), publication date, volume number (in black), start page, and end page [PMID: 11819634]

Note: The author should test the references through reference testing system (http://www.wjgnet.com/cgi-bin/index.pl)

Style for book references

Authors: the first author should be typed in bold-faced letter. The surname of all authors should be typed with the initial letter capitalized and followed by their name in abbreviation (For example, Lian-Sheng Ma is abbreviated as Ma LS, Bo-Rong Pan as Pan BR) Book title. Publication number. Publication place: Publication press, Year: start page and end page.

Format

Journals

English journal article (list all authors and include the PMID where applicable)

1 **Grover VP**, Dresner MA, Forton DM, Counsell S, Larkman DJ, Patel N, Thomas HC, Taylor-Robinson SD. Current and future applications of magnetic resonance imaging and spectroscopy of the brain in hepatic encephalopathy. *World J Gastroenterol* 2006; **12**: 2969-2978 [PMID: 16718775]

Chinese journal article (list all authors and include the PMID where applicable)

2 **Lin GZ**, Wang XZ, Wang P, Lin J, Yang FD. Immunologic effect of Jianpi Yishen decoction in treatment of Pixu-diarrhoea. *Shijie Huaren Xiaohua Zazhi* 1999; **7**: 285-287

In press

3 **Tian D**, Araki H, Stahl E, Bergelson J, Kreitman M. Signature of balancing selection in Arabidopsis. *Proc Natl Acad Sci U S A* 2006; In press

Organization as author

4 **Diabetes Prevention Program Research Group**. Hypertension, insulin, and proinsulin in participants with impaired glucose tolerance. *Hypertension* 2002; **40**: 679-686 [PMID: 12411462]

Both personal authors and an organization as author

5 **Vallancien G**, Emberton M, Harving N, van Moorselaar RJ; Alf-One Study Group. Sexual dysfunction in 1, 274 European men suffering from lower urinary tract symptoms. *J Urol* 2003; **169**: 2257-2261 [PMID: 12771764]

No author given

6 21st century heart solution may have a sting in the tail. *BMJ* 2002; **325**: 184 [PMID: 12142303]

Volume with supplement

7 **Geraud G**, Spierings EL, Keywood C. Tolerability and safety of frovatriptan with short- and long-term use for treatment of migraine and in comparison with sumatriptan. *Headache* 2002; **42** Suppl 2: S93-99 [PMID: 12028325]

Issue with no volume

8 **Banit DM**, Kaufer H, Hartford JM. Intraoperative frozen section analysis in revision total joint arthroplasty. *Clin Orthop Relat Res* 2002; (**401**): 230-238 [PMID: 12151900]

No volume or issue

9 Outreach: bringing HIV-positive individuals into care. *HRSA Careaction* 2002; 1-6 [PMID: 12154804]

Books

Personal author(s)

10 **Sherlock S**, Dooley J. Diseases of the liver and billiary system. 9th ed. Oxford: Blackwell Sci Pub, 1993: 258-296

Chapter in a book (list all authors)

11 **Lam SK**. Academic investigator's perspectives of medical treatment for peptic ulcer. In: Swabb EA, Azabo S. Ulcer disease: investigation and basis for therapy. New York: Marcel Dekker, 1991: 431-450

Author(s) and editor(s)

12 **Breedlove GK**, Schorfheide AM. Adolescent pregnancy. 2nd ed. Wieczorek RR, editor. White Plains (NY): March of Dimes Education Services, 2001: 20-34

Conference proceedings

13 **Harnden P**, Joffe JK, Jones WG, editors. Germ cell tumours V. Proceedings of the 5th Germ Cell Tumour Conference; 2001 Sep 13-15; Leeds, UK. New York: Springer, 2002: 30-56

Conference paper

14 **Christensen S**, Oppacher F. An analysis of Koza's computational effort statistic for genetic programming. In: Foster JA, Lutton E, Miller J, Ryan C, Tettamanzi AG, editors. Genetic programming. EuroGP 2002: Proceedings of the 5th European Conference on Genetic Programming; 2002 Apr 3-5; Kinsdale, Ireland. Berlin: Springer, 2002: 182-191

Electronic journal (list all authors)

Morse SS. Factors in the emergence of infectious diseases. Emerg Infect Dis serial online, 1995-01-03, cited 1996-06-05; 1(1): 24 screens. Available from: URL: http//www.cdc.gov/ncidod/EID/eid.htm

Patent (list all authors)

16 **Pagedas AC**, inventor; Ancel Surgical R&D Inc., assignee. Flexible endoscopic grasping and cutting device and positioning tool assembly. United States patent US 20020103498. 2002 Aug 1

Inappropriate references

Authors should always cite references that are relevant to their article, and avoid any inappropriate references. Inappropriate references include those that are linked with a hyphen and the difference between the two numbers at two sides of the hyphen is more than 5. For example, [1-6], [2-14] and [1, 3, 4-10, 22] are all considered as inappropriate references. Authors should not cite their own unrelated published articles.

Statistical data

Present as mean ± SD or mean ± SE.

Statistical expression

Express t test as t (in italics), F test as F (in italics), chi square test as χ^2 (in Greek), related coefficient as r (in italics), degree of freedom as γ (in Greek), sample number as n (in italics), and probability as P (in italics).

Units

Use SI units. For example: body mass, m (B) = 78 kg; blood pressure, p(B) = 16.2/12.3 kPa; incubation time, t (incubation) = 96 h, blood glucose concentration, c (glucose) 6.4 ± 2.1 mmol/L; blood CEA mass concentration, p (CEA) = 8.6 24.5 μg/L; CO_2 volume fraction, 50 mL/L CO_2 not 5% CO_2; likewise for 40 g/L formaldehyde, not 10% formalin; and mass fraction, 8 ng/g, *etc.* Arabic numerals such as 23, 243, 641 should be read 23 243 641.

The format about how to accurately write common units and quantum is at: http://www.wjgnet.com/wjg/help/15.doc

Abbreviations

Standard abbreviations should be defined in the abstract and on first mention in the text. In general, terms should not be abbreviated unless they are used repeatedly and the abbreviation is helpful to the reader. Permissible abbreviations are listed in Units, Symbols and Abbreviations: A Guide for Biological and Medical Editors and Authors (Ed. Baron DN, 1988) published by The Royal Society of Medicine, London. Certain commonly used abbreviations, such as DNA, RNA, HIV, LD50, PCR, HBV, ECG, WBC, RBC, CT, ESR, CSF, IgG, ELISA, PBS, ATP, EDTA, mAb, can be used directly without further mention.

Italics

Quantities: *t* time or temperature, *c* concentration, *A* area, *l* length, *m* mass, *V* volume.
Genotypes: *gyr*A, *arg* 1, *c myc*, *c fos*, *etc.*
Restriction enzymes: *Eco*RI, *Hin*dI, *Bam*HI, *Kbo* I, *Kpn* I, *etc.*
Biology: *H pylori, E coli, etc.*

SUBMISSION OF THE REVISED MANUSCRIPTS AFTER ACCEPTED

Please revise your article according to the revision policies of *WJG*. The revised version including manuscript and high-resolution image figures (if any) should be copied on a floppy or compact disk. Author should send the revised manuscript, along with printed high-resolution color or black and white photos, copyright transfer letter, the final check list for authors, and responses to reviewers by a courier (such as EMS) (submission of revised manuscript by e-mail or on the *WJG* Editorial Office Online System is NOT available at present).

Language evaluation

The language of a manuscript will be graded before sending for revision. (1) Grade A: priority publishing; (2) Grade B: minor language polishing; (3) Grade C: a great deal of language polishing; (4) Grade D: rejected. The revised articles should be in grade B or grade A.

Copyright assignment form

Please downloaded CAF from http://www.wjgnet.com/wjg/help/9.doc.

We certify that the material contained in this manuscript:

Ms:

Title:

is original, except when appropriately referenced to other sources, and that written permission has been granted by any existing copyright holders. We agree to transfer to WJG all rights of our manuscript, including: (1) all copyright ownership in all print and electronic formats; (2) the right to grant permission to republish or reprint the stated material in whole or in part, with or without a fee; (3) the right to print copies for free distribution or sale; (4) the right to republish the stated material in a collection of articles or in any other format. We also agree that our article be put on the Internet.

Criteria for authorship: The WJG requests and publishes information about contributions of each author named to the submitted study. Authorship credit should be based on (1)direct participation in the study, including substantial contributions to conception and design of study, or acquisition of data, or analysis and interpretation of data; (2) manuscript writing, including drafting the article, or revising it critically for important intellectual content; (3)supportive work, including statistical analysis of data, or acquisition of funding, or administration, technology and materials support, or supervision, or supportive contributions. Authors should meet at least one of the three conditions. The WJG does not publish co-first authors and co-corresponding authors.

We hereby assign copyright transfer to WJG if this paper is accepted.

Author Name in full (Full names should be provided, with first name first, followed by middle names and family name at the last, eg, Eamonn MM Quigley). Handwritten names are not accepted.

Author Name in abbreviation (Family name is put first in full, followed by middle names and first name in abbreviation with first letter in capital, eg, Quigley EMM). Handwritten names are not accepted.

1 Full Name: _____
Abbreviation Name: _____
Signed: _____
Date: _____

2 Full Name: _____
Abbreviation Name: _____
Signed: _____
Date: _____

3 Full Name: _____
Abbreviation Name: _____
Signed: _____
Date: _____

4 Full Name: _____
Abbreviation Name: _____
Signed: _____
Date: _____

5 Full Name: _____
Abbreviation Name: _____
Signed: _____
Date: _____

6 Full Name: _____
Abbreviation Name: _____
Signed: _____
Date: _____

7 Full Name: _____
Abbreviation Name: _____
Signed: _____
Date: _____

8 Full Name: _____
Abbreviation Name: _____
Signed: _____
Date: _____

9 Full Name: _____
Abbreviation Name: _____
Signed: _____
Date: _____

10 Full Name: _____
Abbreviation Name: _____
Signed: _____
Date: _____

Final check list for authors

The format is at: http://www.wjgnet.com/wjg/help/13.doc

Responses to reviewers

Please revise your article according to the comments/suggestions of reviewers. The format for responses to the reviewers' comments is at: http://www.wjgnet.com/wjg/help/10.doc

Proof of financial support

For paper supported by a foundation, authors should provide a copy of the document and serial number of the foundation.

Publication fee

Authors of accepted articles must pay publication fee.
EDITORIAL and LETTERS TO THE EDITOR are free of change.

World Journal of Gastroenterology®

Volume 13 Number 5
February 7, 2007

National Journal Award
2005

The WJG Press

The WJG Press, Apartment 1066 Yishou Garden, 58 North Langxinzhuang Road, PO Box 2345, Beijing 100023, China
Telephone: +86-10-85381892
Fax: +86-10-85381893
E-mail: wjg@wjgnet.com
http: //www.wjgnet.com

ISSN 1007-9327 CN 14-1219/R Local Post Offices Code No. 82-261

World Journal of Gastroenterology www.wjgnet.com Volume 13 Number 5 Feb 07 2007

ISSN 1007-9327
CN 14-1219/R

World Journal of Gastroenterology®

Indexed and Abstracted in:

Current Contents®/Clinical Medicine, Science Citation Index Expanded (also known as SciSearch®) and Journal Citation Reports/Science Edition, *Index Medicus*, MEDLINE and PubMed, Chemical Abstracts, EMBASE/Excerpta Medica, Abstracts Journals, *Nature Clinical Practice Gastroenterology and Hepatology*, CAB Abstracts and Global Health.
ISI JCR 2003-2000 IF: 3.318, 2.532, 1.445 and 0.993.

Volume 13 Number 5
February 7, 2007

World J Gastroenterol
2007 February 7; 13(5): 657-820
Online Submissions
www.wjgnet.com/wjg/index.jsp
www.wjgnet.com
Printed on Acid-free Paper

A Weekly Journal of Gastroenterology and Hepatology

National Journal Award
2005

World Journal of Gastroenterology®

Volume 13 Number 5
February 7, 2007

The WJG Press

Contents

World Journal of Gastroenterology
Volume 13 **Number** 5 **February** 7, 2007

Contents

World Journal of Gastroenterology
Volume 13 **Number** 5 **February** 7, 2007

Contents

Responsible E-Editor for this issue: Wen-Hua Ma

C-Editor for this issue: Dr. Eberhard Hildt

Responsible S-Editor for this issue: Xing-Xia Yang

World Journal of Gastroenterology (*World J Gastroenterol , WJG*), a leading international journal in gastroenterology and hepatology, has an established reputation for publishing first class research on esophageal cancer, gastric cancer, liver cancer, viral hepatitis, colorectal cancer, and *H pylori* infection, providing a forum for both clinicians and scientists, and has been indexed and abstracted in Current Contents®/Clinical Medicine, Science Citation Index Expanded (also known as SciSearch®) and Journal Citation Reports/Science Edition, *Index Medicus*, MEDLINE and PubMed, Chemical Abstracts, EMBASE/Excerpta Medica, Abstracts Journals, *Nature Clinical Practice Gastroenterology and Hepatology*, CAB Abstracts and Global Health. ISI JCR 2003-2000 IF: 3.318, 2.532, 1.445 and 0.993. *WJG* is a weekly journal published by The WJG Press. The publication date is on 7th, 14th, 21st, and 28th every month. The *WJG* is supported by The National Natural Science Foundation of China, No. 30224801 and No.30424812, which was founded with a name of *China National Journal of New Gastroenterology* on October 1,1995, and renamed as *WJG* on January 25, 1998.

PUBLISHED BY
The WJG Press

PRINTED BY
Printed in Beijing on acid-free paper by Beijing Kexin Printing House

Print ISSN 1007-9327
CN 14-1219/R

EDITORIAL OFFICE
World Journal of Gastroenterology,
The WJG Press, Apartment 1066 Yishou Garden, 58 North Langxinzhuang Road, PO Box 2345, Beijing 100023, China
Telephone: +86-10-85381892
Fax: +86-10-85381893
E-mail: wjg@wjgnet.com
http://www.wjgnet.com

SUBSCRIPTION AND AUTHOR REPRINTS
Jing Wang
The WJG Press, Apartment 1066 Yishou Garden, 58 North Langxinzhuang Road, PO Box 2345, Beijing 100023, China
Telephone: +86-10-85381892
Fax: +86-10-85381893
E-mail: j.wang@wjgnet.com
http://www.wjgnet.com

SUBSCRIPTION INFORMATION
Institutional Price 2007: USD 1500.00
Personal Price 2007: USD 700.00

INSTRUCTIONS TO AUTHORS
Full instructions are available online at http://www.wjgnet.com/wjg/help/instructions.jsp. If you do not have web access please contact the editorial office.

PO Box 2345, Beijing 100023, China
www.wjgnet.com
wjg@wjgnet.com

World J Gastroenterol 2007 February 7; 13(5): 657-670
World Journal of Gastroenterology ISSN 1007-9327

REVIEW

Role of ischaemic preconditioning in liver regeneration following major liver resection and transplantation

D Gomez, S Homer-Vanniasinkam, AM Graham, KR Prasad

D Gomez, KR Prasad, Department of Hepatobiliary Surgery and Transplantation, St. James's University Hospital, United Kingdom
S Homer-Vanniasinkam, Department of Vascular Surgery, Leeds General Infirmary, Leeds, United Kingdom
AM Graham, Department of Biomedical Sciences, University of Bradford, Bradford, United Kingdom
Correspondence to: KR Prasad, Consultant Hepatobiliary and Transplantation Surgery, Department of Hepatobiliary Surgery and Transplantation, St. James's University Hospital, Beckett Street, Leeds LS9 7TF, United Kingdom. raj.prasad@leedsth.nhs.uk
Telephone: +44-113-2065921 Fax: +44-113-2448182
Received: 2006-11-11 Accepted: 2006-12-21

Abstract

Liver ischaemic preconditioning (IPC) is known to protect the liver from the detrimental effects of ischaemic-reperfusion injury (IRI), which contributes significantly to the morbidity and mortality following major liver surgery. Recent studies have focused on the role of IPC in liver regeneration, the precise mechanism of which are not completely understood. This review discusses the current understanding of the mechanism of liver regeneration and the role of IPC in this setting. Relevant articles were reviewed from the published literature using the Medline database. The search was performed using the keywords "liver", "ischaemic reperfusion", "ischaemic preconditioning", "regeneration", "hepatectomy" and "transplantation". The underlying mechanism of liver regeneration is a complex process involving the interaction of cytokines, growth factors and the metabolic demand of the liver. IPC, through various mediators, promotes liver regeneration by up-regulating growth-promoting factors and suppresses growth-inhibiting factors as well as damaging stresses. The increased understanding of the cellular mechanisms involved in IPC will enable the development of alternative treatment modalities aimed at promoting liver regeneration following major liver resection and transplantation.

Key words: Liver regeneration; Ischaemic reperfusion; Ischaemic preconditioning; Hepatectomy; Transplantation

Gomez D, Homer-Vanniasinkam S, Graham AM, Prasad KR. Role of ischaemic preconditioning in liver regeneration following major liver resection and transplantation. *World J Gastroenterol* 2007; 13(5): 657-670

http://www.wjgnet.com/1007-9327/13/657.asp

INTRODUCTION

Ischaemic-reperfusion injury (IRI) is an inevitable phenomenon that results following major liver surgery, including partial hepatectomy and liver transplantation. As a consequence, parenchymal cell injury and liver dysfunction[1,2] of varied severity leads to significant morbidity and mortality post-surgery[3-5], in particular, in patients with liver cirrhosis and steatosis[6-9]. In addition, IRI significantly impairs liver regeneration following hepatectomy[10,11].

Due to the inevitability of ischaemia and reperfusion in liver surgery, various investigators have attempted to elucidate methods to limit the detrimental effects of IRI and improve liver function and regeneration of the remnant liver[12,13]. These include hypothermic perfusion of the liver[14], intermittent liver inflow occlusion[15,16] and ischaemic preconditioning (IPC)[17]. Liver IPC is an endogenous mechanism consisting of a short period of vascular occlusion followed by reperfusion that renders the liver more tolerant to subsequent prolonged episodes of ischaemia. Besides having protective effects on IRI following major liver resection and transplantation[17-19], it has been suggested that IPC is also beneficial in liver regeneration[20]. This article describes the current understanding of the liver regeneration cascade as published and gives a balanced review on the mechanisms by which IPC influences liver regeneration.

MECHANISMS OF LIVER REGENERATION

Liver regeneration is a complex and multi-factorial process that is mediated by interactions between regenerative cytokines, growth factors and metabolic demand of the liver following surgery and IRI.

The regenerative cytokine network and the priming pathway

During the first few hours following IRI, regenerative cytokines are produced that render the resting hepatocytes responsive to growth factors required for cellular division and proliferation[21,22]. This period is known as the "priming phase". Various mediators have been implicated as possible triggers of the regenerative cytokine network including gastrointestinal lipopolysaccharide (LPS)[23,24], Toll-like receptor-myeloid differentiation factor 88 (Myd88) signaling pathways[25-27], components from the complement cascade[28], nitric oxide (NO)[29-31] and prostaglandins[32].

Studies have identified tumour necrosis factor-alpha (TNF-α) and interleukin-6 (IL-6) as important regenerative cytokines[21,33,34]. Akerman and co-workers showed that

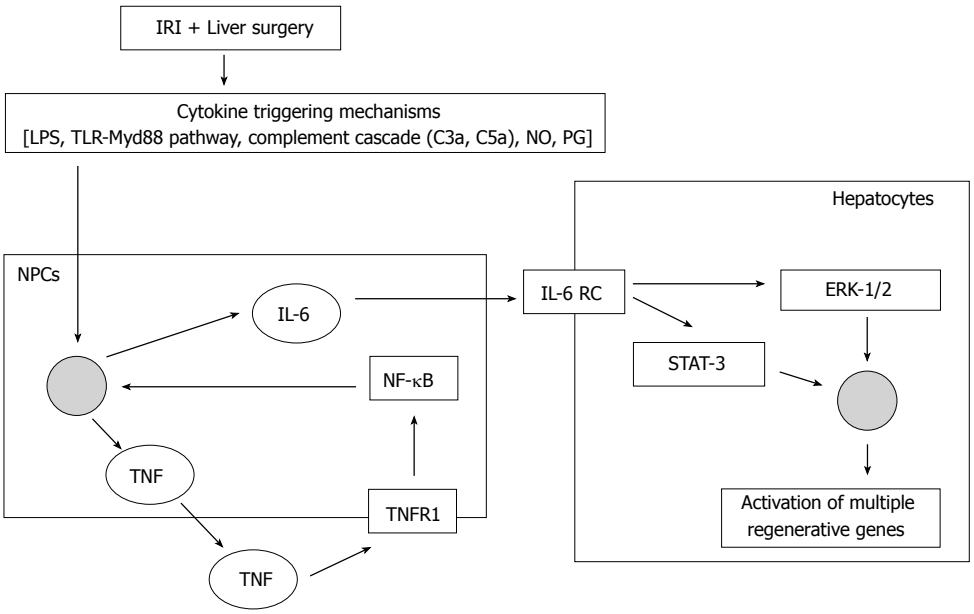

Figure 1 Current proposed mechanisms of the priming pathway of liver regeneration. IRI: Ischaemic reperfusion injury; LPS: Lipo-polysaccharide; TLR: Toll-like receptor; MyD88: Myeloid differentiation factor 88; NO: Nitric oxide; PG: Prostaglandins; NPCs: Non-parenchymal cells; TNF: Tumour necrosis factor; TNFR1: TNF receptor type I; NF-κB: Nuclear factor-kappaB; IL-6: Interleukin-6; IL-6 RC: IL-6 receptor complex; ERK-1/2: Extracellular regulated kinases 1/2; STAT-3: Signal transducer and activator of transcription-3.

anti-TNF antibodies led to delayed DNA synthesis in the regenerating rat liver and inhibited the increase in IL-6 levels following partial hepatectomy[35]. The initiation of liver growth by TNF-α was shown to be dependent on its binding to TNF-receptor type 1 (TNF-R1)[36]. Mice deficient of TNF-R1 exhibited a delay in liver regeneration and increased mortality following liver resection, which was subsequently reversed by recombinant IL-6 injection[37]. However, IL-6 lacking mice demonstrated impaired liver regeneration despite the presence of TNF-α, suggesting that TNF-R1 signaling results in the release of IL-6[38]. IL-6 deficient mice not only showed impaired ability to regenerate, but also had increased IRI following liver resection[39]. However, Wuestefeld *et al*[40] reported that mice deficient in IL-6 and its common signal transducer, glycoprotein 130 (gp130) had no defects in DNA replication following partial hepatectomy. The groups of Zimmers and Blindenbacher have suggested that the levels of serum IL-6 present following liver resection in mice are critical in modulating its regenerative effects[41,42]. This may account for the difference in results observed in studies attempting to determine the effect of IL-6 in liver regeneration. It has been suggested that other mediators such as stem cell factor and oncostatin M may play a role in enhancing the effects of IL-6 on hepatocyte regeneration[43-45].

Non-parenchymal liver cells [Kupffer cells and sinusoidal endothelial cells (SECs)] are involved in the priming phase (Figure 1)[46]. Following stimulation from cytokine triggering mechanisms, TNF-α binds to TNF-R1 on non-parenchymal liver cells and stimulates the production of IL-6[47], *via* the activation of the transcription factor nuclear factor-kappa B (NF-κB)[48-50]. Ping and colleagues demonstrated that the secretion of regenerative cytokines, such as IL-6 by rat liver SECs was mediated by the phosphatidylinositol 3-kinase (PI 3-kinase)/Akt signaling pathway[51], *via* NF-κB activation[50]. The transcription factor NF-κB is also known to be an important component of pro-survival cellular signaling responses, and hence its activation will not only stimulate IL-6 production but also activate survival genes[52,53].

IL-6 acts directly on hepatocytes by binding to the IL-6 receptor complex and induces the translocation of signal transducer and activator of transcription-3 (STAT-3) to the nucleus. This initiates a cascade of events that leads to progression of the cell cycle, culminating in the synthesis of DNA and subsequent cellular mitosis[54,55].

Growth factors and growth-factor signaling systems in liver regeneration

Following this priming phase, cell cycle progression is then dependent on growth factors, such as hepatocyte growth factor (HGF), transforming growth factor-alpha (TGF-α) and epidermal growth factor (EGF)[56,57]. The two main growth-promoting signaling systems involved in liver regeneration are the HGF and its receptor (Met) and the epidermal growth factor receptor (EGFR) and its relatively large family of ligands. The effect of growth factors and their corresponding signaling systems may be dependent on the metabolic state of the hepatocytes and the presence or absence of other effectors[58].

HGF is produced by non-parenchymal cells of the rat liver following liver injury[59-61] and partial hepatectomy[62], and acts on its receptor on hepatocytes. Several authors have demonstrated that HGF is crucial in promoting liver regeneration following partial hepatectomy and transplantation in animal models[63-67]. HGF administration to recipients of reduced-size liver grafts in rats illustrated early regeneration and provided hepatoprotection against rejection-related injuries[64,68,69]. These essential signals are regulated by HGF, *via c-met*, the gene on the HGF-receptor.

EGF is mainly produced in the salivary glands in rodents and plays an important role in hepatocyte proliferation by binding to the EGFR on hepatocytes[57]. Sialoadenectomy-induced decrease in circulating EGF in mice and rat models resulted in impaired liver regeneration following partial hepatectomy, which was reversed by the administration of EGF[70,71]. In addition, combined administration of

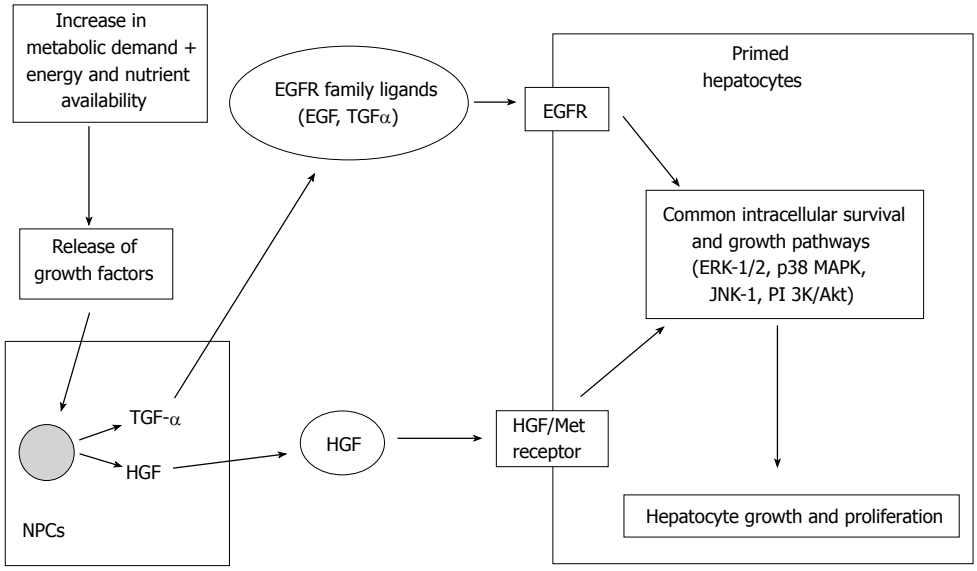

Figure 2 Potentiation of growth factor signaling pathways involved in cell cycle progression in liver regeneration. NPCs: Non-parenchymal cells; HGF: Hepatocyte growth factor; EGF: Epidermal growth factor; TGF-α: Transforming growth factor-α; EGFR: Epidermal growth factor receptor; ERK-1/2: Extracellular regulated kinases 1/2; JNK: c-jun-NH2-terminal kinase; PI 3K/Akt: Phosphatidylinositol 3-kinase/Akt-signal pathway.

EGF and insulin increases the DNA synthesis following liver resection in cirrhotic rats[72]. Results from these studies suggest that EGF has a direct effect on hepatocyte proliferation.

TGF-α is produced in non-parenchymal cells, mainly the Kupffer cells. Mead and Fausto demonstrated that TGF-α may function as a physiological inducer of hepatocyte DNA synthesis during liver regeneration by an autocrine mechanism by binding to EGFR in both rat and culture models[73]. Besides TGF-α, there are many ligands for EGFR, including EGF, amphiregulin, heparin-binding EGF-like growth factor (HB-EGF) and epiregulin[57]. Although TGF-α expression increases following partial hepatectomy in mice, TGF-α lacking mice do not display diminished liver regeneration[74,75]. This may be due to the fact that ligands such as EGF can also stimulate EGFR and activate common intracellular growth signaling pathways. Studies have shown that other growth factors, such as HB-EGF[50,76,77], amphiregulin[78], insulin and glucagon[79,80] may also play a role in liver regeneration.

Although these two growth-promoting signaling systems are largely independent, some integration may exist. Scheving *et al*[81] demonstrated that EGFR kinase inhibition by PKI166 (selective, potent inhibitor of EGFR kinase) blocked the mitogenic effects of HGF in cultured rat hepatocytes, suggesting EGFR may regulate HGF-mediated hepatocyte proliferation. Nevertheless, various regenerative pathways are initiated by HGF/*c-met* and the EGFR signaling mechanisms (Figure 2), which include the activation of mitogen-activated protein kinases (MAPKs), such as extracellular signal-regulated kinases 1 and 2 (ERK-1/2; aka p42/44 MAPKs), c-jun-NH2-terminal kinases 1 and 2 (JNK-1/2; aka p46/p54 SAPK) and p38 MAPKs. Collectively, these MAPKs have been shown to play essential roles in cell growth, transformation differentiation and apoptosis[82-84].

ERK-1/2 activation has been shown to correlate with hepatocyte proliferation in animal studies and *in vitro* models[85-87]. Besides being responsive to growth factor signals, studies have demonstrated that ERK-1/2 activity can also be induced by cytokines such as TNF-α[88]. Hence, the ERK-1/2 may be a signaling pathway that integrates both growth factor and cytokine signaling. Serandour *et al*[89] demonstrated that a combination of EGF and TNF-α induced hepatocyte proliferation by 30%, compared to EGF alone in a hepatocyte-liver epithelial cell co-culture model. This study suggested that TNF-α mediated extracellular matrix remodeling was required for continued hepatocyte replication and proliferation. Hence, this study reiterates the importance of the interaction of cytokines and growth factors in the liver regeneration cascade. Although ERK-1/2 has been identified to have a key role in hepatocyte growth, inhibition of ERK-1/2 does not significantly alter proliferation of regenerating rat hepatocytes. However, inhibition of p38 MAPKs results in decreased DNA synthesis, suggesting that p38 MAPKs activation is prerequisite for hepatocyte proliferation[90]. JNK-1 and p38 MAPKs are involved in the regulatory control of the induction of nuclear proteins, such as cyclin D1. The activation of cyclin D1 is one of the earliest steps in the pathway of resting cells to enter the pre-replicative phase of the cell cycle.

Metabolic demand of the liver

The increased metabolic demand imposed on the remnant liver following partial hepatectomy are likely to be interconnected with the activation of the mechanisms involved in DNA replication to sustain liver function. This is likely to be dependent on energy levels and nutrient availability.

Mitochondria are the predominant source of the high energy phosphates that are essential for energy-dependent processes in cells. Mitochondrial activity has been shown to be correlated with the recovery of liver function and subsequent regeneration[91,92]. Maruyama *et al*[93] showed the recovery of liver weight following hepatectomy was proportional to the energy (ATP) levels of the remnant liver in rats.

Amino acid deprivation has been shown to inhibit the regeneration process in rat livers following liver resection[94]. Nelsen *et al*[95] showed that selective amino acid deprivation in culture and protein deprivation in mice impaired hepatocyte cyclin D1 expression and that

transfection of cyclin D1 promoted cell cycle progression under these conditions. Hence, amino acids regulate hepatocyte proliferation *via* cyclin D1.

The absence of bile acids in the intestine has been shown to delay liver regeneration following partial hepatectomy in rats[96]. Following liver surgery or injury, bile flow is stimulated[97] which results in the release of bile from the gallbladder and its return through the entero-hepatic circulation exposes the remnant hepatocytes to an increase in relative bile acid flux. This early phase of bile acid overload and subsequent bile acid signaling is necessary for normal liver regeneration. However, liver-specific functions such as synthesis of clotting factors and albumin and the continuous formation of bile are impaired following partial hepatectomy and results in transient cholestasis[98]. The formation of bile is dependent on the active secretion of bile salts and other biliary constituents into the bile canaliculus by specific bile acid and organic anion transporters[99]. Gerloff *et al*[100] demonstrated that the expression of two ATP-dependent transporters [bile salt acid pump (*Bsep*) and multi-organic anion transporter (*Mrp2*)] was unchanged or slightly increased following partial hepatectomy in rats and this provided a potential mechanism by which the regenerating liver cells maintained or increased bile secretion. The authors in this study also suggested that the down-regulation of certain transporters [sodium-taurocholate cotransporter (*Ntcp*) and organic anion transporting polypeptides (*Oatp1 and Oatp2*)] could be a protective mechanism against the potentially hepatotoxic bile salts[100]. The differential regulation of hepatobiliary transporters during the regeneration process are likely to be mediated by cytokines such as TNF-α[101]. Recently, Huang *et al*[102] showed that bile acid activation of nuclear receptor-dependent signaling pathways regulated the regeneration process by sensing the liver's functional capacity following partial hepatectomy in mice. When inadequate function causes bile acids to build up, the resultant nuclear receptors activation not only induces negative feedback pathways that protect hepatocytes from bile acid toxicity but also increases the capacity of the liver to manage the overload by promoting liver growth[102].

Results from recent studies have implicated the mammalian target of rapamycin (mTOR) complex as a sensor of nutrient-energy levels and its downstream mediators, such as p70 S6 kinase, are thought to regulate protein translation and cell growth[103,104]. Inhibition of the mTOR complex leads to diminish DNA replication following partial hepatectomy in mice and rat models[105,106]. The activity of p70 S6 kinase has been shown to increase following partial hepatectomy[106] and mice lacking the S6 kinase demonstrated diminished hepatocyte proliferation[107]. Hence, energy is required for energy-dependent signaling pathways and processing the available nutrients for the regeneration process to proceed.

ISCHAEMIC PRECONDITIONING IN LIVER REGENERATION

Since IPC was first described by Murry *et al*[108], this strategy has been developed more widely and is currently practiced in major liver surgery in several centers. The mechanism of IPC is thought to be divided into two phases; early (classical/acute) pre-conditioning and delayed pre-conditioning. The hepatoprotective effects of early preconditioning occur within minutes after reperfusion and are maintained for 1 to 2 h[109]. This phase is thought to be mediated by pre-existing substances. The "second window of protection", delayed pre-conditioning, re-appears 24 to 72 h following IPC. The underlying mechanism is thought to rely on the modification of gene expression resulting in protein production as its effectors[110]. Various substances have been implicated as key effectors in liver IPC including adenosine[111-114], protein kinase C[115-117], NO[118-121], heat-shock proteins[122,123], tyrosine kinases[124], MAPKs[117], oxidative stress[125,126] and NF-κB[127,128].

The beneficial effects of IPC on the liver following IRI include decrease in severity of liver necrosis[129], anti-apoptotic effects[130], preservation of liver microcirculation[131,132] and improvement in survival rate[119], and more recently, its role in liver regeneration is currently being evaluated. For IPC to influence liver regeneration, its key effectors must be involved in either promoting or up-regulating mediators that are involved in the regeneration cascade or exert an inhibitory effect on growth-inhibitory factors of liver regeneration or *vice versa* (Figure 3).

Up-regulation of the regenerative cytokine network

Tumour necrosis factor-alpha and interleukin-6: The initiation of the regenerative response is dependent on the early activation of TNF-α and IL-6 responsive transcription factors[38,54]. Studies evaluating the effect of IPC in stimulating the release of TNF-α and IL-6 have produced conflicting findings. Tsuyama *et al*[133] reported that IPC prolonged survival, suppressed liver necrosis induced by IRI and inhibited the release of TNF-α at 1 h, and IL-6 at 2 and 5 h of the reperfusion phase in mice. IPC has also been shown to reduce TNF-α production in normothermic and cold ischaemic conditions[125,134,135].

In contrast, Bedirli and others demonstrated that IPC inhibited the production of TNF-α, but not IL-6 during the late (24 and 48 h) phases of reperfusion in rats following partial hepatectomy[136]. This study suggested that IL-6 is an important mediator in IPC-treated rats in promoting hepatocyte proliferation following liver resection[136]. Using a TNF gene-deleted mice model, Teoh *et al*[137] demonstrated that pre-treatment with low dose IL-6 prior to hepatic ischaemia conferred equivalent hepatoprotection and earlier cell cycle entry as IPC compared to non-IPC-treated mice at 2 h of reperfusion. Taken together, these studies emphasize the importance of IL-6 as a hepatoprotective and pro-proliferative mediator during the early and late phases of reperfusion following IRI. Although IPC attenuates the late onset prolonged release of TNF-α (up to 44 h) that mediates liver IRI in rats[138,139] and mice[140], IPC itself is associated with the early increase (10 min) in liver and serum TNF-α following hepatic ischaemia[140]. Injection of low dose TNF-α 30 min prior to liver ischaemia conferred similar hepatoprotection as IPC[140]. Both IPC and pre-treatment with low dose TNF-α injection were shown to stimulate earlier and more

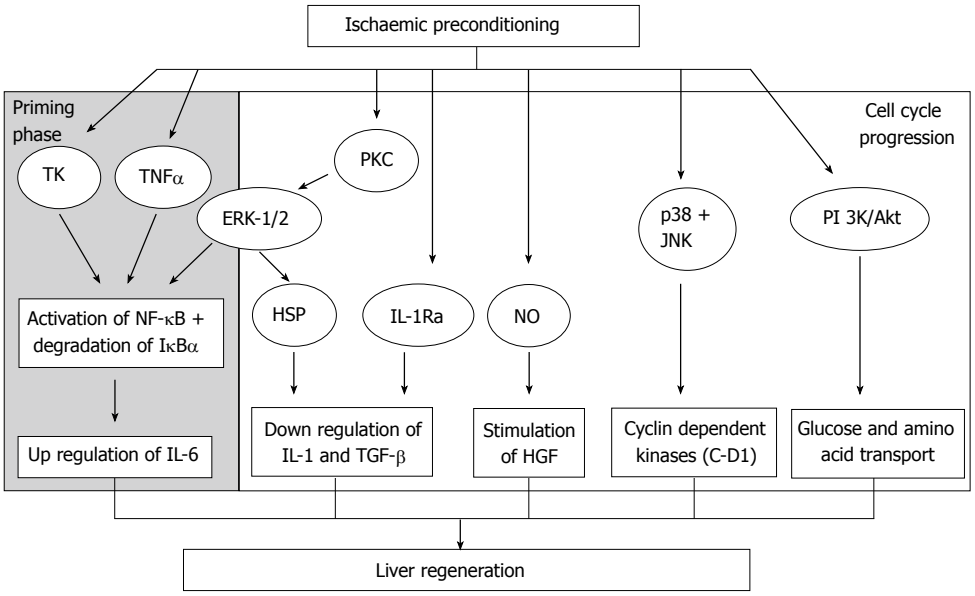

Figure 3 The effect of ischaemic preconditioning and its effectors on the signaling pathways of liver regeneration. TK: Tyrosine kinase; PKC: Protein kinase C; NF-κB: Nuclear factor-kappaB; IκBα: Inhibitory binding protein for NF-κB; ERK-1/2: Extracellular regulated kinases 1/2; HSPs: Heat shock proteins; NO: Nitric oxide; IL1-RA: Interleukin-1 receptor antagonist; HGF: Hepatocyte growth factor; ROS: Reactive oxygen species; PI 3K/Akt: Phosphatidylinositol 3-kinase/Akt-signal pathway; JNK: c-jun-NH2-terminal kinase; C-D1: Cyclin D1; IL-1: Interleukin-1; TGF-β: Transforming growth factor-β.

vigorous cell cycle entry following liver IRI compared to naïve mice during the first 24 h of the reperfusion period[140].

The differences reported among studies investigating the influence of IPC on the regenerative cytokine network may be related to the differences in experimental models and protocols employed. In addition, both TNF-α and IL-6 are known to be important components in other cellular signaling responses. For example, high levels of serum TNF-α following liver ischaemia in rats is thought to mediate liver IRI[138,139]. Investigators have suggested that the mechanism of action of IL-6 in promoting liver regeneration appear to be separate from those involved in the modulation of IRI[39,141]. The hepatoprotective mechanisms against IRI may involve the anti-inflammatory properties of IL-6 and the down regulation of TNF-α production[39,142,143]. This could potentially explain the differences in results obtained.

Nevertheless, the influence of IPC in promoting the early release of TNF-α and the up regulation of IL-6 during the reperfusion phase, and subsequent modulation of the hepatocellular proliferation process should not be discounted. In addition, these conflicting results may indicate that IPC can potentiate hepatocyte proliferation *via* at least two different pathways; liver regeneration *via* a TNF-α/IL-6-dependent pathway and a mitogen-induced proliferative pathway that does not require TNF-α or IL-6[144,145].

Down-regulation of inhibitory mediators of liver regeneration

Hepatocyte growth is controlled by a balance of both growth-promoting and growth-inhibiting factors[65,146]. While those cytokines and pathways previously described promote liver regeneration following liver resection, there are various mediators that are involved directly or indirectly in inhibiting the liver regeneration process.

Interleukin-1 and transforming growth factor-beta as inhibitors of liver regeneration: IL-1 is a mediator of acute inflammation[147] and is a significant down-regulator of hepatocyte proliferation[148]. IL-1β delays and inhibits hepatocyte proliferation in both culture models[149] and following partial hepatectomy in rats[148]. Other investigators have implicated IL-1α as a mediator of IRI and an inhibitor of liver regeneration[150]. Besides antagonizing the stimulatory effects of growth factors such as HGF[150], IL-1 strongly inhibits hepatocyte DNA synthesis leading to impaired liver regeneration in primary culture models[149]. TGF-β is another inhibitor of hepatocyte DNA synthesis[151-153] and antagonizes the stimulatory effects of HGF during liver regeneration in both *in vitro* and experimental hepatectomy models[152,154]. This anti-regenerative effect of TGF-β is thought to be modulated by the induction of oxidative stress in hepatocytes[155,156].

Results from several studies have suggested that IPC antagonizes the effects of these inhibitory cytokines. Previous studies have shown that the release of IL-1 is potentially influenced by NO during IRI in a variety of cell types[157-159]. In IPC-treated rats that underwent reduced size liver transplantation, an increase in IL-1α levels were noted following NO synthesis inhibition[150]. This practice abolished the benefits of IPC on hepatic IRI, oxidative stress and liver regeneration[3,150]. Furthermore, the detrimental effects of NO inhibition were not observed when rats subjected to this treatment were subsequently treated with an IL-1 receptor antagonist (IL-1-RA)[150]. IL-1α has also been shown to be involved in pulmonary injury following liver IRI. IPC mediated by NO, reduced IL-1α release and protected against pulmonary damage[160]. Data from these studies suggests that IPC, through increased NO availability, inhibits the release of IL-1, thereby protecting the liver graft and the lungs against liver IRI and preventing inhibition of liver regeneration. Hence, one proposed mechanism by which IPC promotes liver regeneration is by inhibiting the release of growth-inhibitory cytokines from Kupffer cells, such as IL-1, which is dependent on up-regulation of the NO pathway.

The mechanism by which IPC inhibits IL-1 production may also be related to the induction of intracellular

stress proteins[161,162], such as heat shock protein 70 (HSP 70). IPC induces over-expression of HSP 70 in isolated hepatocytes[163], and reduces liver IL-1 synthesis under normothermic conditions[164]. Besides expressing cytoprotective effects[165,166], HSP induction leads to the down-regulation of IL-1 synthesis in pancreatic[161,167] and lung[162,168] cell studies. The induction of HSP mediated by IPC may be independent of the NO pathway as the increase in HSP by IPC was not modified when NO synthesis was inhibited[150]. These results suggest that IPC potentiates the overexpression of HSP, *via* an NO independent pathway, leading to hepato-protection against IRI and ameliorates liver regeneration due to decrease inhibitor production.

Another proposed mechanism by which IPC promotes liver regeneration could be due to the stimulation of IL-1-RA. IL-1-RA is an acute phase protein that has been shown to inhibit the effects of IL-1α and IL-1β by competing for type I and type Ⅱ IL-1 receptors[169]. This leads to a decrease in the inflammatory response[169] and abrogates liver IRI *in vivo*[170]. A recent study on gene expression profiling on patients undergoing partial hepatectomy revealed that IPC stimulated the expression of the IL-1-RA gene[171]. Hence, liver over-expression of IL-1-RA following IPC directly inhibits the effect of high IL-1 concentrations induced by IRI and results in reduced liver injury and necrosis[171]. Although no study has formally assessed the effect of IL-1-RA on markers of liver regeneration, IL-1-RA could be indirectly involved in the regeneration process by antagonizing the inhibitory effects of IL-1 on hepatocyte proliferation.

Inhibitory binding protein for NF-κB (IκB-α) and NF-κB activity: The transcriptional activities of NF-κB are tightly controlled by its inhibitory proteins, especially IκB-α[172]. The phosphophorylation and subsequent degradation of IκB-α leads to the liberation of NF-κB proteins allowing binding to a variety of promoters and triggers gene expression. Data from studies examining the role of NF-κB as an effector of IPC have demonstrated conflicting results. IPC facilitated the activation of transcription factor NF-κB in an *in vivo* murine model, and this was parallel to the degradation of its inhibitory protein, IκB-α[173]. Ricciardi and co-workers found that IPC increased IκB-α phosphorylation and NF-κB concentration prior to cold ischemia in pig liver grafts. Data from this study suggested that the underlying mechanism involved was related to the activation of second messengers of tyrosine kinase[127]. Another proposed mechanism for NF-κB activation and degradation of IκB-α could be mediated by TNF-α. The release of TNF-α by IPC and pre-treatment with low-dose TNF-α was shown to increase IκB-α degradation and increase NF-κB DNA binding in a mouse model[140]. However, Li *et al*[174] observed that IPC inhibited the activity of the transcription factor NF-κB during the early reperfusion phase (1 and 2 h), and this was accompanied by diminished TNF-α expression and reduced IRI in liver transplantation rat model.

One explanation for this contradictory evidence might be the different experimental models and methodology used. Nevertheless, these results indicate that IPC does attenuate the nuclear levels of the transcription factor NF-κB. It is possible that other mediators may have an effect in determining the increase or inhibition of NF-κB activity and its corresponding cellular signaling responses.

Increased production of growth factors

Hepatocyte growth factor (HGF): Franco-Gou *et al*[175] demonstrated an increase in both liver and plasma HGF levels following IPC in reduced size liver transplantation rat model, and this was associated with an increase in hepatocyte proliferation. The modulation of HGF levels by IPC could be mediated by the generation of NO and its effect on TGF-β and HGF concentrations. IPC reduced the levels of TGF-β with an associated increase in HGF levels[150]. Similar results were seen with NO preconditioning treatment[150]. This suggests that IPC reduced TGF-β levels with a parallel increase in HGF and subsequent hepatocyte proliferation, possibly mediated by NO.

HGF may also exhibit the ability to promote hepatocyte survival. In a liver IRI rat model, pre-treatment with HGF inhibited the production of reactive oxygen species and its damaging effects[176]. Similar results were observed in a hypoxia-reoxygenation-induced oxidative stress model in hepatocytes[177]. These results suggest that the anti-apoptotic effect of HGF could pave the way for hepatocyte proliferation following IRI.

Activation of downstream mitogen-activated protein kinases (MAPKs)

Extracellular signal-regulated kinases 1 and 2 (ERK-1/2): ERK-1/2 is predominantly activated by growth-promoting factors. Studies have shown that protein kinase C plays a pivotal role in the activation of ERK-1/2 signaling pathway[163,178] that participates in the preservation of hepatocytes[163]. A number of reports have indicated that protein kinase C was critical for the development of IPC in rat, rabbit and human myocardiocytes[179,180]. Gao and associates showed that the activation of protein kinase C and its downstream ERK-1/2 mediators were increased in IPC-treated *in vivo* and *in vitro* models[163]. Data from this study also suggested that the expression of HSP70 was reduced and the protective effect of IPC was diminished when ERK-1/2 activity was reduced by a MAPK inhibitor (PD-98059). HSP70 expression and the cytoprotective effect of IPC were also reduced by a protein kinase C inhibitor (chelerythrine) in both *in vitro* and *in vivo* settings. Hence, this suggests that IPC increased the activation of ERK-1/2, *via* protein kinase C. The increased activation of protein kinase C-dependent ERK-1/2 by IPC may also increase the expression of HSP70. The up-regulation of ERK-1/2 by IPC may help in promoting liver regeneration in both the priming phase and growth factor signaling pathways.

p38 mitogen-activated protein kinases and c-jun-NH2-terminal kinase 1: Both p38 MAPKs and JNK-1 are known to modulate proliferative or apoptotic signaling pathways[181]. The activation of MAPKs and its corresponding downstream signaling pathway is regulated by specific stimuli and is also dependent on cell type. The co-activation of NF-κB protects the hepatocyte from

apoptosis and is involved in the priming of hepatocytes to enter the cell cycle[22,182].

Carini and co-investigators demonstrated that hypoxic preconditioning activated the p38 signaling pathway in rat hepatocytes subjected to hypoxia-re-oxygenation injury *in vitro*[117]. Teoh *et al*[173] demonstrated that proliferating hepatocytes were identified earlier in IPC-treated livers in a murine model of partial liver ischaemia, and this corresponded with the earlier activation and sustained maintenance of p38 and JNK-1. This suggests that IPC stimulus could prime quiescent hepatocytes to enter the cell cycle early, hence, setting up a regenerative response to compensate for hepatocyte injury by IRI.

Activation of survival and proliferative pathways

Phosphatidylinositol 3-kinase (PI 3-kinase)/Akt signaling pathway: The activation of the PI 3-kinase/Akt cascade has been shown to have a positive impact on cell survival and proliferation[183-186], inhibition of apoptosis and encourage the uptake of glucose and amino acids following stimulation by various growth-promoting factors in certain cells[187-189]. Data from the Izuishi group showed significant Akt activation following IPC in an *in vivo* model and suggested that this might contribute to the up regulation of glucose and amino acid transport after IRI required for liver regeneration[190].

Activation of nuclear proteins

Cyclin D1: Cyclin and cyclin-dependent kinases are involved in cell cycle regulation[191], in particular, the D group cyclins[192]. Cyclin D1 is a nuclear protein required for cell cycle progression in the G_1 phase[192-194], and controls hepatocyte proliferation[195]. IPC-treated livers showed earlier expression of cyclin D1 protein that corresponded with enhanced entry of hepatocytes into the cell cycle[173]. Cai and co-workers demonstrated that IPC stimulated cyclin D1 mRNA and protein expression during the early reperfusion phase in IPC-treated rat livers[196]. The early production of cyclin D1 could be mediated by the activation of the p38 MAPK pathway[182]. The cyclin D1 promoter region includes binding sites for NF-κB[197] and NF-κB activation is evident in hepatocytes during the early phase of regeneration following partial hepatectomy[48,198]. There is a close link between the activation of NF-κB by degradation of IκB-α cyclin D1 activation and cell cycle progression. IPC can modulate these transcription factors and increase cell proliferation, which is possibly one of the protective mechanisms against IRI.

Energy metabolism

Results obtained from an experimental model of 70% hepatectomy indicated that liver regeneration was closely correlated to the ATP levels of the liver remnant[93]. Studies have shown that IPC in normothermic conditions preserved the adenine nucleotide pool[199,200] and this is thought to be a consequence of the down regulation of cellular metabolism[199,201]. In a rat model of hypothermic transplant preservation injury, hepatocytes exposed to IPC had higher ATP concentrations and increased protein synthesis[202]. This improvement in energy metabolism is thought to contribute to hepatocyte viability following IRI[202]. Besides improvement in energy metabolism, Yoshizumi *et al*[203] also demonstrated an increase in bile production in IPC-treated rats. However, Franco-Gou and colleagues demonstrated similar energy metabolism (ATP, adenine nucleotides, ATP/ADP ratio and energy charge) in the IPC- and non-IPC-treated rat livers[175]. The difference in results obtained could be related to the difference in experimental models used. However, the role of IPC in modulating liver energy metabolism, which involves the preservation of ATP should not be discounted.

CLINICAL IMPLICATIONS OF ISCHAEMIC PRECONDITIONING IN LIVER SURGERY

The use of IPC as a surgical strategy to limit the detrimental effects of IRI during liver surgery has been extensively researched. Encouraging findings in animal studies in both warm ischaemia[203] and transplantation models[119], led to the first human trial which demonstrated that IPC reduced the severity of post-operative liver injury as well as alleviating endothelial cell injury[17]. Further human liver resection studies have shown that IPC reduces post-operative serum aminotransferase levels in both steatotic[204] and cirrhotic[205] livers and improves post-reperfusion haemodynamic stability[206] (Table 1). Although IPC is protective against IRI[207,208], it did not influence the morbidity and mortality rates in human studies[204,209,210]. In the transplant setting, Jassem *et al*[211] reported lower serum aminotransferase levels and shorter intensive care stay in IPC-treated cadaveric donor allografts. Other studies have not shown IPC to be beneficial in terms of graft function. Azoulay *et al*[212] found that although IPC protected cadaveric liver grafts against IRI, this beneficial effect was counter-balanced by decreased early graft function. Cescon and colleagues demonstrated similar protective effects against IRI, but IPC showed no clinical benefit (primary graft function and survival rates) in liver transplantation from deceased donors[213]. Although gaining popularity, the incongruous evidence of the clinical effects of IPC has precluded its widespread adoption in liver transplantation units.

Following major liver resection and IRI, the ability of the liver to regenerate is crucial to maintain liver function. This also has implication in live donor orthotopic liver transplantation and transplantation of segmental liver grafts. Since Yamada and co-workers first demonstrated that IPC significantly increased the regenerative capacity of the remaining hepatocytes in a rat model of IRI[20], various investigators have attempted to elucidate the role of IPC on liver regeneration using both culture and animal model studies as described above. At present, although there is no clinical trial published on the effect of IPC on liver regeneration, there are studies evaluating methods of monitoring liver regeneration. Special radiological imaging techniques currently available not only show volume of regeneration, but also determine functional ability of the remnant and regenerated liver[214,215]. This is another step towards assessing the role of IPC in liver regeneration in the clinical scenario.

Table 1 Previous published human studies on the results of ischaemic preconditioning following liver resection and transplantation

Study group	Sample[1]	Surgery	IPC[2]	Ischaemia and reperfusion time (min)[3]	Parameters assessed	Outcome of IPC
Clavien *et al*[17] (2000)	24 (12)	Liver resection	10I + 10R	IPC and control (TI: 30)	PT, Bilirubin, ALT, AST, Histology, Caspase-3 and 8 activity, SEC apoptosis, Blood loss, Transfusion, ITU stay, LOS	Protective against IRI Beneficial in patients with steatosis
Clavien *et al*[204] (2003)	100 (50)	Liver resection	10I + 10R	IPC (TI: 36 ± 5.9, Op: 225 ± 73), Control (TI: 35 ± 6.8, Op: 240 ± 92)	PT, Bilirubin, ALT, AST, Histology, Hepatic ATP, Blood loss, Transfusion, ITU stay, LOS	Protective against IRI Beneficial in younger patients, those with steatosis and longer periods of occlusion
Li *et al*[205] (2004)	29 (14)	Liver resection	5I + 5R	IPC (TI: 18 ± 3.6, Op: 191.3 ± 74.9), Control (TI: 17.4 ± 2.3, Op: 208.2 ± 45.3)	Bilirubin, ALT, AST, Histology, Caspase-3 activity, SEC apoptosis, LOS	Protective against IRI, mainly HCC patients with cirrhosis Shorter hospital stay
Nuzzo *et al*[209] (2004)	42 (21)	Liver resection	10I + 10R	IPC (TI: 54 ± 19, Op: 321 ± 92), Control (TI: 36 ± 14, Op: 339 ± 112)	PT, Bilirubin, ALT, AST, Transfusion, Morbidity, Mortality	Reduces operative bleeding Protective against IRI
Chouker *et al*[206] (2004)	68 (22)	Liver resection	10I + 10R	IPC (TI: 32 ± 6.3, Op: 251 ± 46), Control without PR (TI: NA, Op: 52 ± 30), Control with PR (TI: 35 ± 11, Op: 257 ± 83)	ALT, AST, Fluid loss, Transfusion, [4]Cardiovascular status	Protective against IRI Improves haemodynamic stability
Chouker *et al*[207] (2005)	75 (25)	Liver resection	10I + 10R	IPC (TI: 35.5 ± 2.7, LR: 32.2 ± 2.0), Control without PR (TI: NA, LR: 39 ± 4.5), Control with PR (TI: 35.6 ± 2.6, LR: 33.2 ± 2.3)	IL-6, IL-8, Cytochrome c, Adhesion molecules [B_2-integrins (CD18)], Histology (neutrophil infiltration)	Protective against IRI by attenuating neutrophil activation and IL-8 release
Chouker *et al*[208] (2005)	73 (25)	Liver resection	10I + 10R	IPC (TI: 35.12 ± 13.6, LR: 31.50 ± 9.1), Control without PR (TI: NA, LR: 34.77 ± 16.5), Control with PR (TI: 34.2 ± 10.9, LR: 32.13 ± 10)	PT, ALT, AST, α-GST	Protective against IRI Prevented early rise of α-GST
Koneru *et al*[210] (2005)	62 (34)	Transplant	5I + 5R	IPC (CI: 384 ± 92, WI: 41 ± 5.8), Control (CI: 415 ± 87, WI: 37 ± 5.6)	INR, Bilirubin, ALT, AST, Histology (apoptosis, hepatocyte swelling), LOS, Survival (6 mo)	No beneficial effect
Azoulay *et al*[212] (2005)	91 (46)	Transplant	10I + 10R	IPC (CI: 436 ± 116, Op: 441 ± 119), Control (CI: 461 ± 96, Op: 462 ± 98)	PT, Bilirubin, ALT, AST, Histology, Graft function, Morbidity, Mortality	Better ischaemic tolerance Decreased early graft function
Jassem *et al*[211] (2005)	23 (9)	Transplant	10I + 10R	IPC (CI: 620 ± 190, WI: 43.9 ± 13), Control (CI: 665 ± 280, WI: 40.4 ± 9)	AST, INR, Lactate, ITU stay, Histology (neutrophil infiltration, platelet deposition), Graft function	Protective against IRI Reduces inflammatory response Shorter ITU stay
Cescon *et al*[213] (2006)	47 (23)	Transplant	10I + 15R	[5]IPC [TI: 388 (259-830), Op: 440 (225-725)], Control [TI: 383 (279-695), Op: 465 (280-1015)]	PT, Bilirubin, ALT, AST, Histology (neutrophil, lymphocyte infiltration, iNOS, apoptosis), Graft function, Survival (1 yr)	Protective against IRI No clinical benefit

[1]Patients stated in brackets are the number of patients who had ischaemic preconditioning treatment; [2]IPC was performed by portal triad clamping in all these studies; [3]Ischaemia and operative times are presented as mean ± SD unless otherwise stated; [4]Cardiovascular status refers to mean arterial pressure, central venous pressure, heart rate, stroke volume index, systemic vascular resistance index, fluid infusion and catecholamines requirements; [5]Ischaemia and reperfusion times in this study were presented as median (range). I: Ischaemia; R: Reperfusion; IPC: Ischaemic preconditioning group; PR: Pringle maneuver; TI: Total ischaemia time; CI: Cold ischaemia time; WI: Warm ischaemia time; Op: Total operative time; LR: Liver resection time; ITU: Intensive therapy unit; LOS: Length of hospital stay; PT: Pro-thrombin time; INR: International normalized ratio of pro-thrombin time; ALT: Alanine aminotransferase; AST: Aspartate aminotransferase; α-GST: Alpha-Gluthathione S-Transferase; iNOS: Inducible form of nitric oxide synthase; ATP: Adenosine triphosphate; HCC: Hepatocellular carcinoma; IL: Interleukin; SEC: Sinusoidal endothelial cell; IRI: Ischaemia-reperfusion injury.

With the increasing laboratory evidence of protection against IRI and improved liver regeneration by IPC, several aspects of this strategy could be developed pharmacologically that may be more clinical applicable than IPC itself. This is especially in cases with a background of chemotherapy-induced steatohepatitis[216] and cirrhosis[217,218]. Pharmacologic agents targeting mediators of IPC that can be potentially developed include HGF, IL-6 and IL-1-RA. However, several issues such as the timing of administration of these agents, therapeutic doses and immunological response of the recipient need to be determined. Further understanding of the mechanistic pathways of IPC may pave the way for the development of these agents that are capable of conferring protection against IRI and promote liver regeneration.

CONCLUSION

Liver regeneration is of clinical significance in view of the increasing number of major liver resections and the increasing use of marginal donor liver and split-liver allografts for transplantation. Successful patient outcome often depends on liver regeneration, particularly in patients with cirrhotic and steatotic livers. Regeneration of the liver following IRI and major liver surgery is a complex process that involves the integration of a network of cytokines, growth factors, kinases, transcription factors and metabolic demands of the liver.

In comparison with the evidence available on the effect of IPC on IRI, its role in liver regeneration is still undetermined. However, current research has demonstrated that the beneficial effects of IPC on liver regeneration is mediated by up regulating growth-

promoting factors, suppressing growth-inhibitory factors and preserving energy levels for regeneration. Nevertheless, more studies are still required to further delineate the underlying pathophysiology of IPC and impact on mediators of liver regeneration. It is also important to determine whether the beneficial effect of IPC in the laboratory setting is reproducible in clinical practice. By understanding the underlying mechanisms by which IPC influences liver regeneration, other strategies as alternatives to IPC, could be developed to modulate the regenerative pathways in the clinical setting and improve outcomes of patients following major liver resection and transplantation. The assessment of IPC on liver regeneration in human studies is clearly the next step.

REFERENCES

1 **Bilzer M**, Gerbes AL. Preservation injury of the liver: mechanisms and novel therapeutic strategies. *J Hepatol* 2000; **32**: 508-515
2 **Serracino-Inglott F**, Habib NA, Mathie RT. Hepatic ischemia-reperfusion injury. *Am J Surg* 2001; **181**: 160-166
3 **Belghiti J**, Noun R, Malafosse R, Jagot P, Sauvanet A, Pierangeli F, Marty J, Farges O. Continuous versus intermittent portal triad clamping for liver resection: a controlled study. *Ann Surg* 1999; **229**: 369-375
4 **Huguet C**, Gavelli A, Bona S. Hepatic resection with ischemia of the liver exceeding one hour. *J Am Coll Surg* 1994; **178**: 454-458
5 **Lemasters JJ**, Thurman RG. Reperfusion injury after liver preservation for transplantation. *Annu Rev Pharmacol Toxicol* 1997; **37**: 327-338
6 **Ezaki T**, Seo Y, Tomoda H, Furusawa M, Kanematsu T, Sugimachi K. Partial hepatic resection under intermittent hepatic inflow occlusion in patients with chronic liver disease. *Br J Surg* 1992; **79**: 224-226
7 **Selzner M**, Clavien PA. Fatty liver in liver transplantation and surgery. *Semin Liver Dis* 2001; **21**: 105-113
8 **Glanemann M**, Langrehr JM, Stange BJ, Neumann U, Settmacher U, Steinmüller T, Neuhaus P. Clinical implications of hepatic preservation injury after adult liver transplantation. *Am J Transplant* 2003; **3**: 1003-1009
9 **Behrns KE**, Tsiotos GG, DeSouza NF, Krishna MK, Ludwig J, Nagorney DM. Hepatic steatosis as a potential risk factor for major hepatic resection. *J Gastrointest Surg* 1998; **2**: 292-298
10 **Foschi D**, Castoldi L, Lesma A, Musazzi M, Benevento A, Trabucchi E. Effects of ischaemia and reperfusion on liver regeneration in rats. *Eur J Surg* 1993; **159**: 393-398
11 **Watanabe M**, Chijiiwa K, Kameoka N, Yamaguchi K, Kuroki S, Tanaka M. Gadolinium pretreatment decreases survival and impairs liver regeneration after partial hepatectomy under ischemia/reperfusion in rats. *Surgery* 2000; **127**: 456-463
12 **Arii S**, Teramoto K, Kawamura T. Current progress in the understanding of and therapeutic strategies for ischemia and reperfusion injury of the liver. *J Hepatobiliary Pancreat Surg* 2003; **10**: 189-194
13 **Teoh NC**, Farrell GC. Hepatic ischemia reperfusion injury: pathogenic mechanisms and basis for hepatoprotection. *J Gastroenterol Hepatol* 2003; **18**: 891-902
14 **Azoulay D**, Eshkenazy R, Andreani P, Castaing D, Adam R, Ichai P, Naili S, Vinet E, Saliba F, Lemoine A, Gillon MC, Bismuth H. In situ hypothermic perfusion of the liver versus standard total vascular exclusion for complex liver resection. *Ann Surg* 2005; **241**: 277-285
15 **Uchinami M**, Muraoka R, Horiuchi T, Tabo T, Kimura N, Naito Y, Yoshikawa T. Effect of intermittent hepatic pedicle clamping on free radical generation in the rat liver. *Surgery* 1998; **124**: 49-56
16 **Smyrniotis V**, Kostopanagiotou G, Theodoraki K, Farantos C, Arkadopoulos N, Gamaletsos E, Condi-Paphitis A, Fotopoulos A, Dimakakos P. Ischemic preconditioning versus intermittent vascular inflow control during major liver resection in pigs. *World J Surg* 2005; **29**: 930-934
17 **Clavien PA**, Yadav S, Sindram D, Bentley RC. Protective effects of ischemic preconditioning for liver resection performed under inflow occlusion in humans. *Ann Surg* 2000; **232**: 155-162
18 **Koti RS**, Seifalian AM, Davidson BR. Protection of the liver by ischemic preconditioning: a review of mechanisms and clinical applications. *Dig Surg* 2003; **20**: 383-396
19 **Jaeschke H**. Molecular mechanisms of hepatic ischemia-reperfusion injury and preconditioning. *Am J Physiol Gastrointest Liver Physiol* 2003; **284**: G15-G26
20 **Yamada F**, Abe T, Saito T, Tsuciya T, Ishii S, Gotoh M. Ischemic preconditioning enhances regenerative capacity of hepatocytes after prolonged ischemia. *Transplant Proc* 2001; **33**: 956
21 **Webber EM**, Bruix J, Pierce RH, Fausto N. Tumor necrosis factor primes hepatocytes for DNA replication in the rat. *Hepatology* 1998; **28**: 1226-1234
22 **Fausto N**. Liver regeneration. *J Hepatol* 2000; **32**: 19-31
23 **Cornell RP**, Liljequist BL, Bartizal KF. Depressed liver regeneration after partial hepatectomy of germ-free, athymic and lipopolysaccharide-resistant mice. *Hepatology* 1990; **11**: 916-922
24 **Poltorak A**, He X, Smirnova I, Liu MY, Van Huffel C, Du X, Birdwell D, Alejos E, Silva M, Galanos C, Freudenberg M, Ricciardi-Castagnoli P, Layton B, Beutler B. Defective LPS signaling in C3H/HeJ and C57BL/10ScCr mice: mutations in Tlr4 gene. *Science* 1998; **282**: 2085-2088
25 **Akira S**, Takeda K, Kaisho T. Toll-like receptors: critical proteins linking innate and acquired immunity. *Nat Immunol* 2001; **2**: 675-680
26 **Seki E**, Tsutsui H, Iimuro Y, Naka T, Son G, Akira S, Kishimoto T, Nakanishi K, Fujimoto J. Contribution of Toll-like receptor/myeloid differentiation factor 88 signaling to murine liver regeneration. *Hepatology* 2005; **41**: 443-450
27 **Su GL**, Wang SC, Aminlari A, Tipoe GL, Steinstraesser L, Nanji A. Impaired hepatocyte regeneration in toll-like receptor 4 mutant mice. *Dig Dis Sci* 2004; **49**: 843-849
28 **Strey CW**, Markiewski M, Mastellos D, Tudoran R, Spruce LA, Greenbaum LE, Lambris JD. The proinflammatory mediators C3a and C5a are essential for liver regeneration. *J Exp Med* 2003; **198**: 913-923
29 **Jin ZG**, Wong C, Wu J, Berk BC. Flow shear stress stimulates Gab1 tyrosine phosphorylation to mediate protein kinase B and endothelial nitric-oxide synthase activation in endothelial cells. *J Biol Chem* 2005; **280**: 12305-12309
30 **Schoen JM**, Wang HH, Minuk GY, Lautt WW. Shear stress-induced nitric oxide release triggers the liver regeneration cascade. *Nitric Oxide* 2001; **5**: 453-464
31 **Wang HH**, Lautt WW. Does nitric oxide (NO) trigger liver regeneration? *Proc West Pharmacol Soc* 1997; **40**: 17-18
32 **Schoen Smith JM**, Lautt WW. The role of prostaglandins in triggering the liver regeneration cascade. *Nitric Oxide* 2005; **13**: 111-117
33 **Trautwein C**, Rakemann T, Niehof M, Rose-John S, Manns MP. Acute-phase response factor, increased binding, and target gene transcription during liver regeneration. *Gastroenterology* 1996; **110**: 1854-1862
34 **Iwai M**, Cui TX, Kitamura H, Saito M, Shimazu T. Increased secretion of tumour necrosis factor and interleukin 6 from isolated, perfused liver of rats after partial hepatectomy. *Cytokine* 2001; **13**: 60-64
35 **Akerman P**, Cote P, Yang SQ, McClain C, Nelson S, Bagby GJ, Diehl AM. Antibodies to tumor necrosis factor-alpha inhibit liver regeneration after partial hepatectomy. *Am J Physiol* 1992; **263**: G579-G585
36 **Chen G**, Goeddel DV. TNF-R1 signaling: a beautiful pathway. *Science* 2002; **296**: 1634-1635
37 **Yamada Y**, Kirillova I, Peschon JJ, Fausto N. Initiation of liver growth by tumor necrosis factor: deficient liver regeneration in mice lacking type I tumor necrosis factor receptor. *Proc Natl Acad Sci USA* 1997; **94**: 1441-1446
38 **Cressman DE**, Greenbaum LE, DeAngelis RA, Ciliberto G, Furth

EE, Poli V, Taub R. Liver failure and defective hepatocyte regeneration in interleukin-6-deficient mice. *Science* 1996; **274**: 1379-1383

39 **Camargo CA**, Madden JF, Gao W, Selvan RS, Clavien PA. Interleukin-6 protects liver against warm ischemia/reperfusion injury and promotes hepatocyte proliferation in the rodent. *Hepatology* 1997; **26**: 1513-1520

40 **Wuestefeld T**, Klein C, Streetz KL, Betz U, Lauber J, Buer J, Manns MP, Müller W, Trautwein C. Interleukin-6/glycoprotein 130-dependent pathways are protective during liver regeneration. *J Biol Chem* 2003; **278**: 11281-11288

41 **Zimmers TA**, McKillop IH, Pierce RH, Yoo JY, Koniaris LG. Massive liver growth in mice induced by systemic interleukin 6 administration. *Hepatology* 2003; **38**: 326-334

42 **Blindenbacher A**, Wang X, Langer I, Savino R, Terracciano L, Heim MH. Interleukin 6 is important for survival after partial hepatectomy in mice. *Hepatology* 2003; **38**: 674-682

43 **Ren X**, Hogaboam C, Carpenter A, Colletti L. Stem cell factor restores hepatocyte proliferation in IL-6 knockout mice following 70% hepatectomy. *J Clin Invest* 2003; **112**: 1407-1418

44 **Nakamura K**, Nonaka H, Saito H, Tanaka M, Miyajima A. Hepatocyte proliferation and tissue remodeling is impaired after liver injury in oncostatin M receptor knockout mice. *Hepatology* 2004; **39**: 635-644

45 **Kamiya A**, Kojima N, Kinoshita T, Sakai Y, Miyaijma A. Maturation of fetal hepatocytes in vitro by extracellular matrices and oncostatin M: induction of tryptophan oxygenase. *Hepatology* 2002; **35**: 1351-1359

46 **Malik R**, Selden C, Hodgson H. The role of non-parenchymal cells in liver growth. *Semin Cell Dev Biol* 2002; **13**: 425-431

47 **Selzner N**, Selzner M, Odermatt B, Tian Y, Van Rooijen N, Clavien PA. ICAM-1 triggers liver regeneration through leukocyte recruitment and Kupffer cell-dependent release of TNF-alpha/IL-6 in mice. *Gastroenterology* 2003; **124**: 692-700

48 **FitzGerald MJ**, Webber EM, Donovan JR, Fausto N. Rapid DNA binding by nuclear factor kappa B in hepatocytes at the start of liver regeneration. *Cell Growth Differ* 1995; **6**: 417-427

49 **Kirillova I**, Chaisson M, Fausto N. Tumor necrosis factor induces DNA replication in hepatic cells through nuclear factor kappaB activation. *Cell Growth Differ* 1999; **10**: 819-828

50 **Sakuda S**, Tamura S, Yamada A, Miyagawa J, Yamamoto K, Kiso S, Ito N, Higashiyama S, Taniguchi N, Kawata S, Matsuzawa Y. NF-kappaB activation in non-parenchymal liver cells after partial hepatectomy in rats: possible involvement in expression of heparin-binding epidermal growth factor-like growth factor. *J Hepatol* 2002; **36**: 527-533

51 **Ping C**, Lin Z, Jiming D, Jin Z, Ying L, Shigang D, Hongtao Y, Yongwei H, Jiahong D. The phosphoinositide 3-kinase/Akt-signal pathway mediates proliferation and secretory function of hepatic sinusoidal endothelial cells in rats after partial hepatectomy. *Biochem Biophys Res Commun* 2006; **342**: 887-893

52 **Wang CY**, Mayo MW, Korneluk RG, Goeddel DV, Baldwin AS. NF-kappaB antiapoptosis: induction of TRAF1 and TRAF2 and c-IAP1 and c-IAP2 to suppress caspase-8 activation. *Science* 1998; **281**: 1680-1683

53 **De Smaele E**, Zazzeroni F, Papa S, Nguyen DU, Jin R, Jones J, Cong R, Franzoso G. Induction of gadd45beta by NF-kappaB downregulates pro-apoptotic JNK signalling. *Nature* 2001; **414**: 308-313

54 **Debonera F**, Aldeguer X, Shen X, Gelman AE, Gao F, Que X, Greenbaum LE, Furth EE, Taub R, Olthoff KM. Activation of interleukin-6/STAT3 and liver regeneration following transplantation. *J Surg Res* 2001; **96**: 289-295

55 **Li W**, Liang X, Kellendonk C, Poli V, Taub R. STAT3 contributes to the mitogenic response of hepatocytes during liver regeneration. *J Biol Chem* 2002; **277**: 28411-28417

56 **Matsumoto K**, Nakamura T. Hepatocyte growth factor: molecular structure, roles in liver regeneration, and other biological functions. *Crit Rev Oncog* 1992; **3**: 27-54

57 **Michalopoulos GK**, Khan Z. Liver regeneration, growth factors, and amphiregulin. *Gastroenterology* 2005; **128**: 503-506

58 **Bucher NL**. Liver regeneration: an overview. *J Gastroenterol Hepatol* 1991; **6**: 615-624

59 **Kinoshita T**, Tashiro K, Nakamura T. Marked increase of HGF mRNA in non-parenchymal liver cells of rats treated with hepatotoxins. *Biochem Biophys Res Commun* 1989; **165**: 1229-1234

60 **Noji S**, Tashiro K, Koyama E, Nohno T, Ohyama K, Taniguchi S, Nakamura T. Expression of hepatocyte growth factor gene in endothelial and Kupffer cells of damaged rat livers, as revealed by in situ hybridization. *Biochem Biophys Res Commun* 1990; **173**: 42-47

61 **Hu Z**, Evarts RP, Fujio K, Marsden ER, Thorgeirsson SS. Expression of hepatocyte growth factor and c-met genes during hepatic differentiation and liver development in the rat. *Am J Pathol* 1993; **142**: 1823-1830

62 **Ping C**, Xiaoling D, Jin Z, Jiahong D, Jiming D, Lin Z. Hepatic sinusoidal endothelial cells promote hepatocyte proliferation early after partial hepatectomy in rats. *Arch Med Res* 2006; **37**: 576-583

63 **Burr AW**, Toole K, Chapman C, Hines JE, Burt AD. Anti-hepatocyte growth factor antibody inhibits hepatocyte proliferation during liver regeneration. *J Pathol* 1998; **185**: 298-302

64 **Uchiyama H**, Yanaga K, Nishizaki T, Soejima Y, Yoshizumi T, Sugimachi K. Effects of deletion variant of hepatocyte growth factor on reduced-size liver transplantation in rats. *Transplantation* 1999; **68**: 39-44

65 **Masson S**, Daveau M, Hiron M, Lyoumi S, Lebreton JP, Ténière P, Scotté M. Differential regenerative response and expression of growth factors following hepatectomy of variable extent in rats. *Liver* 1999; **19**: 312-317

66 **Tomiya T**, Ogata I, Yamaoka M, Yanase M, Inoue Y, Fujiwara K. The mitogenic activity of hepatocyte growth factor on rat hepatocytes is dependent upon endogenous transforming growth factor-alpha. *Am J Pathol* 2000; **157**: 1693-1701

67 **Okamoto K**, Suzuki S, Kurachi K, Sunayama K, Yokoi Y, Konno H, Baba S, Nakamura S. Beneficial effect of deletion variant of hepatocyte growth factor for impaired hepatic regeneration in the ischemically damaged liver. *World J Surg* 2002; **26**: 1260-1266

68 **Ikegami T**, Nishizaki T, Uchiyama H, Kakizoe S, Yanaga K, Sugimachi K. Deletion variant of hepatocyte growth factor prolongs allograft survival after liver transplantation in rats. *Surgery* 1999; **125**: 602-607

69 **Tashiro H**, Fudaba Y, Itoh H, Mizunuma K, Ohdan H, Itamoto T, Asahara T. Hepatocyte growth factor prevents chronic allograft dysfunction in liver-transplanted rats. *Transplantation* 2003; **76**: 761-765

70 **Jones DE**, Tran-Patterson R, Cui DM, Davin D, Estell KP, Miller DM. Epidermal growth factor secreted from the salivary gland is necessary for liver regeneration. *Am J Physiol* 1995; **268**: G872-G878

71 **Noguchi S**, Ohba Y, Oka T. Influence of epidermal growth factor on liver regeneration after partial hepatectomy in mice. *J Endocrinol* 1991; **128**: 425-431

72 **Hashimoto M**, Kothary PC, Eckhauser FE, Raper SE. Treatment of cirrhotic rats with epidermal growth factor and insulin accelerates liver DNA synthesis after partial hepatectomy. *J Gastroenterol Hepatol* 1998; **13**: 1259-1265

73 **Mead JE**, Fausto N. Transforming growth factor alpha may be a physiological regulator of liver regeneration by means of an autocrine mechanism. *Proc Natl Acad Sci USA* 1989; **86**: 1558-1562

74 **Webber EM**, Wu JC, Wang L, Merlino G, Fausto N. Overexpression of transforming growth factor-alpha causes liver enlargement and increased hepatocyte proliferation in transgenic mice. *Am J Pathol* 1994; **145**: 398-408

75 **Russell WE**, Kaufmann WK, Sitaric S, Luetteke NC, Lee DC. Liver regeneration and hepatocarcinogenesis in transforming growth factor-alpha-targeted mice. *Mol Carcinog* 1996; **15**: 183-189

76 **Kiso S**, Kawata S, Tamura S, Inui Y, Yoshida Y, Sawai Y, Umeki S, Ito N, Yamada A, Miyagawa J, Higashiyama S, Iwawaki T, Saito M, Taniguchi N, Matsuzawa Y, Kohno K. Liver regeneration in heparin-binding EGF-like growth factor transgenic mice after partial hepatectomy. *Gastroenterology* 2003; **124**: 701-707

77 **Mitchell C**, Nivison M, Jackson LF, Fox R, Lee DC, Campbell JS, Fausto N. Heparin-binding epidermal growth factor-like growth factor links hepatocyte priming with cell cycle progression during liver regeneration. *J Biol Chem* 2005; **280**: 2562-2568

78 **Berasain C**, García-Trevijano ER, Castillo J, Erroba E, Lee DC, Prieto J, Avila MA. Amphiregulin: an early trigger of liver regeneration in mice. *Gastroenterology* 2005; **128**: 424-432

79 **Bucher ML**, Swaffield MN. Regulation of hepatic regeneration in rats by synergistic action of insulin and glucagon. *Proc Natl Acad Sci USA* 1975; **72**: 1157-1160

80 **Hwang TL**, Chen MF, Chen TJ. Augmentation of liver regeneration with glucagon after partial hepatectomy in rats. *J Formos Med Assoc* 1993; **92**: 725-728

81 **Scheving LA**, Stevenson MC, Taylormoore JM, Traxler P, Russell WE. Integral role of the EGF receptor in HGF-mediated hepatocyte proliferation. *Biochem Biophys Res Commun* 2002; **290**: 197-203

82 **Seger R**, Krebs EG. The MAPK signaling cascade. *FASEB J* 1995; **9**: 726-735

83 **Terada Y**, Inoshita S, Nakashima O, Kuwahara M, Sasaki S, Marumo F. Regulation of cyclin D1 expression and cell cycle progression by mitogen-activated protein kinase cascade. *Kidney Int* 1999; **56**: 1258-1261

84 **Fanger GR**. Regulation of the MAPK family members: role of subcellular localization and architectural organization. *Histol Histopathol* 1999; **14**: 887-894

85 **Coutant A**, Rescan C, Gilot D, Loyer P, Guguen-Guillouzo C, Baffet G. PI3K-FRAP/mTOR pathway is critical for hepatocyte proliferation whereas MEK/ERK supports both proliferation and survival. *Hepatology* 2002; **36**: 1079-1088

86 **Thoresen GH**, Guren TK, Christoffersen T. Role of ERK, p38 and PI3-kinase in EGF receptor-mediated mitogenic signalling in cultured rat hepatocytes: requirement for sustained ERK activation. *Cell Physiol Biochem* 2003; **13**: 229-238

87 **Borowiak M**, Garratt AN, Wüstefeld T, Strehle M, Trautwein C, Birchmeier C. Met provides essential signals for liver regeneration. *Proc Natl Acad Sci USA* 2004; **101**: 10608-10613

88 **Argast GM**, Campbell JS, Brooling JT, Fausto N. Epidermal growth factor receptor transactivation mediates tumor necrosis factor-induced hepatocyte replication. *J Biol Chem* 2004; **279**: 34530-34536

89 **Sérandour AL**, Loyer P, Garnier D, Courselaud B, Théret N, Glaise D, Guguen-Guillouzo C, Corlu A. TNFalpha-mediated extracellular matrix remodeling is required for multiple division cycles in rat hepatocytes. *Hepatology* 2005; **41**: 478-486

90 **Spector MS**, Auer KL, Jarvis WD, Ishac EJ, Gao B, Kunos G, Dent P. Differential regulation of the mitogen-activated protein and stress-activated protein kinase cascades by adrenergic agonists in quiescent and regenerating adult rat hepatocytes. *Mol Cell Biol* 1997; **17**: 3556-3565

91 **Ozawa K**, Fujimoto T, Nakatani T, Asano M, Aoyama H, Tobe T. Changes in hepatic energy charge, blood ketone body ratio, and indocyanine green clearance in relation to DNA synthesis after hepatectomy. *Life Sci* 1982; **31**: 647-653

92 **Ngala Kenda JF**, de Hemptinne B, Lambotte L. Role of metabolic overload in the initiation of DNA synthesis following partial hepatectomy in the rat. *Eur Surg Res* 1984; **16**: 294-302

93 **Maruyama H**, Harada A, Kurokawa T, Kobayashi H, Nonami T, Nakao A, Takagi H. Duration of liver ischemia and hepatic regeneration after hepatectomy in rats. *J Surg Res* 1995; **58**: 290-294

94 **McGowan J**, Atryzek V, Fausto N. Effects of protein-deprivation on the regeneration of rat liver after partial hepatectomy. *Biochem J* 1979; **180**: 25-35

95 **Nelsen CJ**, Rickheim DG, Tucker MM, McKenzie TJ, Hansen LK, Pestell RG, Albrecht JH. Amino acids regulate hepatocyte proliferation through modulation of cyclin D1 expression. *J Biol Chem* 2003; **278**: 25853-25858

96 **Ueda J**, Chijiiwa K, Nakano K, Zhao G, Tanaka M. Lack of intestinal bile results in delayed liver regeneration of normal rat liver after hepatectomy accompanied by impaired cyclin E-associated kinase activity. *Surgery* 2002; **131**: 564-573

97 **Sainz GR**, Monte MJ, Barbero ER, Herrera MC, Marin JJ. Bile secretion by the rat liver during synchronized regeneration. *Int J Exp Pathol* 1997; **78**: 109-116

98 **Xu HS**, Rosenlof LK, Jones RS. Bile secretion and liver regeneration in partially hepatectomized rats. *Ann Surg* 1993; **218**: 176-182

99 **Meier PJ**. Molecular mechanisms of hepatic bile salt transport from sinusoidal blood into bile. *Am J Physiol* 1995; **269**: G801-G812

100 **Gerloff T**, Geier A, Stieger B, Hagenbuch B, Meier PJ, Matern S, Gartung C. Differential expression of basolateral and canalicular organic anion transporters during regeneration of rat liver. *Gastroenterology* 1999; **117**: 1408-1415

101 **Geier A**, Dietrich CG, Voigt S, Kim SK, Gerloff T, Kullak-Ublick GA, Lorenzen J, Matern S, Gartung C. Effects of proinflammatory cytokines on rat organic anion transporters during toxic liver injury and cholestasis. *Hepatology* 2003; **38**: 345-354

102 **Huang W**, Ma K, Zhang J, Qatanani M, Cuvillier J, Liu J, Dong B, Huang X, Moore DD. Nuclear receptor-dependent bile acid signaling is required for normal liver regeneration. *Science* 2006; **312**: 233-236

103 **Kim DH**, Sabatini DM. Raptor and mTOR: subunits of a nutrient-sensitive complex. *Curr Top Microbiol Immunol* 2004; **279**: 259-270

104 **Avruch J**, Lin Y, Long X, Murthy S, Ortiz-Vega S. Recent advances in the regulation of the TOR pathway by insulin and nutrients. *Curr Opin Clin Nutr Metab Care* 2005; **8**: 67-72

105 **Jiang YP**, Ballou LM, Lin RZ. Rapamycin-insensitive regulation of 4e-BP1 in regenerating rat liver. *J Biol Chem* 2001; **276**: 10943-10951

106 **Goggin MM**, Nelsen CJ, Kimball SR, Jefferson LS, Morley SJ, Albrecht JH. Rapamycin-sensitive induction of eukaryotic initiation factor 4F in regenerating mouse liver. *Hepatology* 2004; **40**: 537-544

107 **Volarevic S**, Stewart MJ, Ledermann B, Zilberman F, Terracciano L, Montini E, Grompe M, Kozma SC, Thomas G. Proliferation, but not growth, blocked by conditional deletion of 40S ribosomal protein S6. *Science* 2000; **288**: 2045-2047

108 **Murry CE**, Jennings RB, Reimer KA. Preconditioning with ischemia: a delay of lethal cell injury in ischemic myocardium. *Circulation* 1986; **74**: 1124-1136

109 **Jenkins DP**, Baxter GF, Yellon DM. The pathophysiology of ischaemic preconditioning. *Pharmacol Res* 1995; **31**: 219-224

110 **Ishida T**, Yarimizu K, Gute DC, Korthuis RJ. Mechanisms of ischemic preconditioning. *Shock* 1997; **8**: 86-94

111 **Peralta C**, Hotter G, Closa D, Gelpí E, Bulbena O, Roselló-Catafau J. Protective effect of preconditioning on the injury associated to hepatic ischemia-reperfusion in the rat: role of nitric oxide and adenosine. *Hepatology* 1997; **25**: 934-937

112 **Howell JG**, Zibari GB, Brown MF, Burney DL, Sawaya DE, Olinde JG, Granger DN, McDonald JC. Both ischemic and pharmacological preconditioning decrease hepatic leukocyte/endothelial cell interactions. *Transplantation* 2000; **69**: 300-303

113 **Arai M**, Thurman RG, Lemasters JJ. Involvement of Kupffer cells and sinusoidal endothelial cells in ischemic preconditioning to rat livers stored for transplantation. *Transplant Proc* 1999; **31**: 425-427

114 **Arai M**, Thurman RG, Lemasters JJ. Contribution of adenosine A(2) receptors and cyclic adenosine monophosphate to protective ischemic preconditioning of sinusoidal endothelial cells against Storage/Reperfusion injury in rat livers. *Hepatology* 2000; **32**: 297-302

115 **Carini R**, De Cesaris MG, Splendore R, Bagnati M, Albano E. Ischemic preconditioning reduces Na(+) accumulation and cell killing in isolated rat hepatocytes exposed to hypoxia. *Hepatology* 2000; **31**: 166-172

116 **Ricciardi R**, Meyers WC, Schaffer BK, Kim RD, Shah SA, Wheeler SM, Donohue SE, Sheth KR, Callery MP, Chari RS. Protein kinase C inhibition abrogates hepatic ischemic preconditioning responses. *J Surg Res* 2001; **97**: 144-149

117 **Carini R**, De Cesaris MG, Splendore R, Vay D, Domenicotti C, Nitti MP, Paola D, Pronzato MA, Albano E. Signal pathway involved in the development of hypoxic preconditioning in rat

hepatocytes. *Hepatology* 2001; **33**: 131-139
118 **Peralta C**, Closa D, Hotter G, Gelpí E, Prats N, Roselló-Catafau J. Liver ischemic preconditioning is mediated by the inhibitory action of nitric oxide on endothelin. *Biochem Biophys Res Commun* 1996; **229**: 264-270
119 **Yin DP**, Sankary HN, Chong AS, Ma LL, Shen J, Foster P, Williams JW. Protective effect of ischemic preconditioning on liver preservation-reperfusion injury in rats. *Transplantation* 1998; **66**: 152-157
120 **Koti RS**, Yang W, Dashwood MR, Davidson BR, Seifalian AM. Effect of ischemic preconditioning on hepatic microcirculation and function in a rat model of ischemia reperfusion injury. *Liver Transpl* 2002; **8**: 1182-1191
121 **Koti RS**, Seifalian AM, McBride AG, Yang W, Davidson BR. The relationship of hepatic tissue oxygenation with nitric oxide metabolism in ischemic preconditioning of the liver. *FASEB J* 2002; **16**: 1654-1656
122 **Kume M**, Yamamoto Y, Saad S, Gomi T, Kimoto S, Shimabukuro T, Yagi T, Nakagami M, Takada Y, Morimoto T, Yamaoka Y. Ischemic preconditioning of the liver in rats: implications of heat shock protein induction to increase tolerance of ischemia-reperfusion injury. *J Lab Clin Med* 1996; **128**: 251-258
123 **Ishikawa Y**, Yamamoto Y, Kume M, Yamagami K, Yamamoto H, Kimoto S, Sakai Y, Yamamoto M, Yamaoka Y. Heat shock preconditioning on mitochondria during warm ischemia in rat livers. *J Surg Res* 1999; **87**: 178-184
124 **Ricciardi R**, Schaffer BK, Kim RD, Shah SA, Donohue SE, Wheeler SM, Quarfordt SH, Callery MP, Meyers WC, Chari RS. Protective effects of ischemic preconditioning on the cold-preserved liver are tyrosine kinase dependent. *Transplantation* 2001; **72**: 406-412
125 **Peralta C**, Bulbena O, Xaus C, Prats N, Cutrin JC, Poli G, Gelpi E, Roselló-Catafau J. Ischemic preconditioning: a defense mechanism against the reactive oxygen species generated after hepatic ischemia reperfusion. *Transplantation* 2002; **73**: 1203-1211
126 **Sindram D**, Rüdiger HA, Upadhya AG, Strasberg SM, Clavien PA. Ischemic preconditioning protects against cold ischemic injury through an oxidative stress dependent mechanism. *J Hepatol* 2002; **36**: 78-84
127 **Ricciardi R**, Shah SA, Wheeler SM, Quarfordt SH, Callery MP, Meyers WC, Chari RS. Regulation of NFkappaB in hepatic ischemic preconditioning. *J Am Coll Surg* 2002; **195**: 319-326
128 **Funaki H**, Shimizu K, Harada S, Tsuyama H, Fushida S, Tani T, Miwa K. Essential role for nuclear factor kappaB in ischemic preconditioning for ischemia-reperfusion injury of the mouse liver. *Transplantation* 2002; **74**: 551-556
129 **Peralta C**, Hotter G, Closa D, Prats N, Xaus C, Gelpí E, Roselló-Catafau J. The protective role of adenosine in inducing nitric oxide synthesis in rat liver ischemia preconditioning is mediated by activation of adenosine A2 receptors. *Hepatology* 1999; **29**: 126-132
130 **Yadav SS**, Sindram D, Perry DK, Clavien PA. Ischemic preconditioning protects the mouse liver by inhibition of apoptosis through a caspase-dependent pathway. *Hepatology* 1999; **30**: 1223-1231
131 **Caban A**, Oczkowicz G, Abdel-Samad O, Cierpka L. Influence of ischemic preconditioning and nitric oxide on microcirculation and the degree of rat liver injury in the model of ischemia and reperfusion. *Transplant Proc* 2006; **38**: 196-198
132 **Szijártó A**, Hahn O, Lotz G, Schaff Z, Madarász E, Kupcsulik PK. Effect of ischemic preconditioning on rat liver microcirculation monitored with laser Doppler flowmetry. *J Surg Res* 2006; **131**: 150-157
133 **Tsuyama H**, Shimizu K, Yoshimoto K, Nezuka H, Ito H, Yamamoto S, Hasebe K, Onishi I, Muraoka K, Ninomiya I, Tani T, Hashimoto T, Yagi M, Miwa K. Protective effect of ischemic preconditioning on hepatic ischemia-reperfusion injury in mice. *Transplant Proc* 2000; **32**: 2310-2313
134 **Peralta C**, Prats N, Xaus C, Gelpí E, Roselló-Catafau J. Protective effect of liver ischemic preconditioning on liver and lung injury induced by hepatic ischemia-reperfusion in the rat. *Hepatology* 1999; **30**: 1481-1489
135 **Fernández L**, Heredia N, Peralta C, Xaus C, Roselló-Catafau J, Rimola A, Marco A, Serafín A, Deulofeu R, Gelpí E, Grande L. Role of ischemic preconditioning and the portosystemic shunt in the prevention of liver and lung damage after rat liver transplantation. *Transplantation* 2003; **76**: 282-289
136 **Bedirli A**, Kerem M, Pasaoglu H, Erdem O, Ofluoglu E, Sakrak O. Effects of ischemic preconditioning on regenerative capacity of hepatocyte in the ischemically damaged rat livers. *J Surg Res* 2005; **125**: 42-48
137 **Teoh N**, Field J, Farrell G. Interleukin-6 is a key mediator of the hepatoprotective and pro-proliferative effects of ischaemic preconditioning in mice. *J Hepatol* 2006; **45**: 20-27
138 **Colletti LM**, Remick DG, Burtch GD, Kunkel SL, Strieter RM, Campbell DA. Role of tumor necrosis factor-alpha in the pathophysiologic alterations after hepatic ischemia/reperfusion injury in the rat. *J Clin Invest* 1990; **85**: 1936-1943
139 **Rüdiger HA**, Clavien PA. Tumor necrosis factor alpha, but not Fas, mediates hepatocellular apoptosis in the murine ischemic liver. *Gastroenterology* 2002; **122**: 202-210
140 **Teoh N**, Leclercq I, Pena AD, Farrell G. Low-dose TNF-alpha protects against hepatic ischemia-reperfusion injury in mice: implications for preconditioning. *Hepatology* 2003; **37**: 118-128
141 **Selzner M**, Camargo CA, Clavien PA. Ischemia impairs liver regeneration after major tissue loss in rodents: protective effects of interleukin-6. *Hepatology* 1999; **30**: 469-475
142 **Clavien PA**, Camargo CA, Gorczynski R, Washington MK, Levy GA, Langer B, Greig PD. Acute reactant cytokines and neutrophil adhesion after warm ischemia in cirrhotic and non-cirrhotic human livers. *Hepatology* 1996; **23**: 1456-1463
143 **Mizuhara H**, O'Neill E, Seki N, Ogawa T, Kusunoki C, Otsuka K, Satoh S, Niwa M, Senoh H, Fujiwara H. T cell activation-associated hepatic injury: mediation by tumor necrosis factors and protection by interleukin 6. *J Exp Med* 1994; **179**: 1529-1537
144 **Ohmura T**, Ledda-Columbano GM, Piga R, Columbano A, Glemba J, Katyal SL, Locker J, Shinozuka H. Hepatocyte proliferation induced by a single dose of a peroxisome proliferator. *Am J Pathol* 1996; **148**: 815-824
145 **Ledda-Columbano GM**, Curto M, Piga R, Zedda AI, Menegazzi M, Sartori C, Shinozuka H, Bluethmann H, Poli V, Ciliberto G, Columbano A. In vivo hepatocyte proliferation is inducible through a TNF and IL-6-independent pathway. *Oncogene* 1998; **17**: 1039-1044
146 **Enami Y**, Kato H, Murakami M, Fujioka T, Aoki T, Niiya T, Murai N, Ohtsuka K, Kusano M. Anti-transforming growth factor-beta1 antibody transiently enhances DNA synthesis during liver regeneration after partial hepatectomy in rats. *J Hepatobiliary Pancreat Surg* 2001; **8**: 250-258
147 **Raz R**, Durbin JE, Levy DE. Acute phase response factor and additional members of the interferon-stimulated gene factor 3 family integrate diverse signals from cytokines, interferons, and growth factors. *J Biol Chem* 1994; **269**: 24391-24395
148 **Boulton R**, Woodman A, Calnan D, Selden C, Tam F, Hodgson H. Nonparenchymal cells from regenerating rat liver generate interleukin-1alpha and -1beta: a mechanism of negative regulation of hepatocyte proliferation. *Hepatology* 1997; **26**: 49-58
149 **Nakamura T**, Arakaki R, Ichihara A. Interleukin-1 beta is a potent growth inhibitor of adult rat hepatocytes in primary culture. *Exp Cell Res* 1988; **179**: 488-497
150 **Franco-Gou R**, Roselló-Catafau J, Casillas-Ramirez A, Massip-Salcedo M, Rimola A, Calvo N, Bartrons R, Peralta C. How ischaemic preconditioning protects small liver grafts. *J Pathol* 2006; **208**: 62-73
151 **Nakamura T**, Tomita Y, Hirai R, Yamaoka K, Kaji K, Ichihara A. Inhibitory effect of transforming growth factor-beta on DNA synthesis of adult rat hepatocytes in primary culture. *Biochem Biophys Res Commun* 1985; **133**: 1042-1050
152 **Scotté M**, Masson S, Lyoumi S, Hiron M, Ténière P, Lebreton JP, Daveau M. Cytokine gene expression in liver following minor or major hepatectomy in rat. *Cytokine* 1997; **9**: 859-867
153 **Russell WE**, Coffey RJ, Ouellette AJ, Moses HL. Type beta transforming growth factor reversibly inhibits the early proliferative response to partial hepatectomy in the rat. *Proc Natl Acad Sci USA* 1988; **85**: 5126-5130

154 **Bissell DM**, Wang SS, Jarnagin WR, Roll FJ. Cell-specific expression of transforming growth factor-beta in rat liver. Evidence for autocrine regulation of hepatocyte proliferation. *J Clin Invest* 1995; **96**: 447-455

155 **Herrera B**, Fernández M, Alvarez AM, Roncero C, Benito M, Gil J, Fabregat I. Activation of caspases occurs downstream from radical oxygen species production, Bcl-xL down-regulation, and early cytochrome C release in apoptosis induced by transforming growth factor beta in rat fetal hepatocytes. *Hepatology* 2001; **34**: 548-556

156 **Herrera B**, Murillo MM, Alvarez-Barrientos A, Beltrán J, Fernández M, Fabregat I. Source of early reactive oxygen species in the apoptosis induced by transforming growth factor-beta in fetal rat hepatocytes. *Free Radic Biol Med* 2004; **36**: 16-26

157 **Liu P**, Xu B, Spokas E, Lai PS, Wong PY. Role of endogenous nitric oxide in TNF-alpha and IL-1beta generation in hepatic ischemia-repefusion. *Shock* 2000; **13**: 217-223

158 **Liu P**, Xu B, Hock CE. Inhibition of nitric oxide synthesis by L-name exacerbates acute lung injury induced by hepatic ischemia-reperfusion. *Shock* 2001; **16**: 211-217

159 **Kim YM**, Talanian RV, Li J, Billiar TR. Nitric oxide prevents IL-1beta and IFN-gamma-inducing factor (IL-18) release from macrophages by inhibiting caspase-1 (IL-1beta-converting enzyme). *J Immunol* 1998; **161**: 4122-4128

160 **Franco-Gou R**, Roselló-Catafau J, Peralta C. Protection against lung damage in reduced-size liver transplantation. *Crit Care Med* 2006; **34**: 1506-1513

161 **Ye J**, Laychock SG. A protective role for heme oxygenase expression in pancreatic islets exposed to interleukin-1beta. *Endocrinology* 1998; **139**: 4155-4163

162 **LoCicero J**, Xu X, Zhang L. Heat shock protein suppresses the senescent lung cytokine response to acute endotoxemia. *Ann Thorac Surg* 1999; **68**: 1150-1153

163 **Gao Y**, Shan YQ, Pan MX, Wang Y, Tang LJ, Li H, Zhang Z. Protein kinase C-dependent activation of P44/42 mitogen-activated protein kinase and heat shock protein 70 in signal transduction during hepatocyte ischemic preconditioning. *World J Gastroenterol* 2004; **10**: 1019-1027

164 **Serafín A**, Roselló-Catafau J, Prats N, Gelpí E, Rodés J, Peralta C. Ischemic preconditioning affects interleukin release in fatty livers of rats undergoing ischemia/reperfusion. *Hepatology* 2004; **39**: 688-698

165 **Morimoto RI**, Santoro MG. Stress-inducible responses and heat shock proteins: new pharmacologic targets for cytoprotection. *Nat Biotechnol* 1998; **16**: 833-838

166 **Santoro MG**. Heat shock factors and the control of the stress response. *Biochem Pharmacol* 2000; **59**: 55-63

167 **Hsu BR**, Juang JH, Chen ST, Hsu S, Fu SH. Cobalt-Protoporphyrin treatment renders islets tolerant to interleukin-1 beta suppression. *Transplant Proc* 2004; **36**: 1181-1182

168 **Yoo CG**, Lee S, Lee CT, Kim YW, Han SK, Shim YS. Anti-inflammatory effect of heat shock protein induction is related to stabilization of I kappa B alpha through preventing I kappa B kinase activation in respiratory epithelial cells. *J Immunol* 2000; **164**: 5416-5423

169 **Gabay C**, Smith MF, Eidlen D, Arend WP. Interleukin 1 receptor antagonist (IL-1Ra) is an acute-phase protein. *J Clin Invest* 1997; **99**: 2930-2940

170 **Harada H**, Wakabayashi G, Takayanagi A, Shimazu M, Matsumoto K, Obara H, Shimizu N, Kitajima M. Transfer of the interleukin-1 receptor antagonist gene into rat liver abrogates hepatic ischemia-reperfusion injury. *Transplantation* 2002; **74**: 1434-1441

171 **Barrier A**, Olaya N, Chiappini F, Roser F, Scatton O, Artus C, Franc B, Dudoit S, Flahault A, Debuire B, Azoulay D, Lemoine A. Ischemic preconditioning modulates the expression of several genes, leading to the overproduction of IL-1Ra, iNOS, and Bcl-2 in a human model of liver ischemia-reperfusion. *FASEB J* 2005; **19**: 1617-1626

172 **Henkel T**, Machleidt T, Alkalay I, Krönke M, Ben-Neriah Y, Baeuerle PA. Rapid proteolysis of I kappa B-alpha is necessary for activation of transcription factor NF-kappa B. *Nature* 1993; **365**: 182-185

173 **Teoh N**, Dela Pena A, Farrell G. Hepatic ischemic preconditioning in mice is associated with activation of NF-kappaB, p38 kinase, and cell cycle entry. *Hepatology* 2002; **36**: 94-102

174 **Li XC**, Ma YF, Wang XH. Role of NF-kappaB as effector of IPC in donor livers before liver transplantation in rats. *Transplant Proc* 2006; **38**: 1584-1587

175 **Franco-Gou R**, Peralta C, Massip-Salcedo M, Xaus C, Serafín A, Roselló-Catafau J. Protection of reduced-size liver for transplantation. *Am J Transplant* 2004; **4**: 1408-1420

176 **Oe S**, Hiros T, Fujii H, Yasuchika K, Nishio T, Iimuro Y, Morimoto T, Nagao M, Yamaoka Y. Continuous intravenous infusion of deleted form of hepatocyte growth factor attenuates hepatic ischemia-reperfusion injury in rats. *J Hepatol* 2001; **34**: 832-839

177 **Ozaki M**, Haga S, Zhang HQ, Irani K, Suzuki S. Inhibition of hypoxia/reoxygenation-induced oxidative stress in HGF-stimulated antiapoptotic signaling: role of PI3-K and Akt kinase upon rac1. *Cell Death Differ* 2003; **10**: 508-515

178 **Boulton TG**, Nye SH, Robbins DJ, Ip NY, Radziejewska E, Morgenbesser SD, DePinho RA, Panayotatos N, Cobb MH, Yancopoulos GD. ERKs: a family of protein-serine/threonine kinases that are activated and tyrosine phosphorylated in response to insulin and NGF. *Cell* 1991; **65**: 663-675

179 **Ladilov YV**, Balser C, Piper HM. Protection of rat cardiomyocytes against simulated ischemia and reoxygenation by treatment with protein kinase C activator. *Circ Res* 1998; **82**: 451-457

180 **Rehring TF**, Shapiro JI, Cain BS, Meldrum DR, Cleveland JC, Harken AH, Banerjee A. Mechanisms of pH preservation during global ischemia in preconditioned rat heart: roles for PKC and NHE. *Am J Physiol* 1998; **275**: H805-H813

181 **Crenesse D**, Gugenheim J, Hornoy J, Tornieri K, Laurens M, Cambien B, Lenegrate G, Cursio R, De Souza G, Auberger P, Heurteaux C, Rossi B, Schmid-Alliana A. Protein kinase activation by warm and cold hypoxia- reoxygenation in primary-cultured rat hepatocytes-JNK(1)/SAPK(1) involvement in apoptosis. *Hepatology* 2000; **32**: 1029-1036

182 **Ono K**, Han J. The p38 signal transduction pathway: activation and function. *Cell Signal* 2000; **12**: 1-13

183 **Coffer PJ**, Jin J, Woodgett JR. Protein kinase B (c-Akt): a multifunctional mediator of phosphatidylinositol 3-kinase activation. *Biochem J* 1998; **335** (Pt 1): 1-13

184 **Datta SR**, Brunet A, Greenberg ME. Cellular survival: a play in three Akts. *Genes Dev* 1999; **13**: 2905-2927

185 **Kim I**, Kim HG, So JN, Kim JH, Kwak HJ, Koh GY. Angiopoietin-1 regulates endothelial cell survival through the phosphatidylinositol 3'-Kinase/Akt signal transduction pathway. *Circ Res* 2000; **86**: 24-29

186 **Fulton D**, Gratton JP, McCabe TJ, Fontana J, Fujio Y, Walsh K, Franke TF, Papapetropoulos A, Sessa WC. Regulation of endothelium-derived nitric oxide production by the protein kinase Akt. *Nature* 1999; **399**: 597-601

187 **Tsakiridis T**, McDowell HE, Walker T, Downes CP, Hundal HS, Vranic M, Klip A. Multiple roles of phosphatidylinositol 3-kinase in regulation of glucose transport, amino acid transport, and glucose transporters in L6 skeletal muscle cells. *Endocrinology* 1995; **136**: 4315-4322

188 **Kohn AD**, Summers SA, Birnbaum MJ, Roth RA. Expression of a constitutively active Akt Ser/Thr kinase in 3T3-L1 adipocytes stimulates glucose uptake and glucose transporter 4 translocation. *J Biol Chem* 1996; **271**: 31372-31378

189 **Marte BM**, Downward J. PKB/Akt: connecting phosphoinositide 3-kinase to cell survival and beyond. *Trends Biochem Sci* 1997; **22**: 355-358

190 **Izuishi K**, Fujiwara M, Hossain MA, Usuki H, Maeta H. Significance of phosphoinositide 3-kinase pathway on ischemic preconditioning followed by ischemia reperfusion in mice liver. *Transplant Proc* 2003; **35**: 132-133

191 **Hunter T**, Pines J. Cyclins and cancer. II: Cyclin D and CDK inhibitors come of age. *Cell* 1994; **79**: 573-582

192 **Pestell RG**, Albanese C, Reutens AT, Segall JE, Lee RJ, Arnold A. The cyclins and cyclin-dependent kinase inhibitors in hormonal regulation of proliferation and differentiation. *Endocr Rev* 1999; **20**: 501-534

193 **Baldin V**, Lukas J, Marcote MJ, Pagano M, Draetta G. Cyclin D1 is a nuclear protein required for cell cycle progression in G1. *Genes Dev* 1993; **7**: 812-821
194 **Pagano M**, Theodoras AM, Tam SW, Draetta GF. Cyclin D1-mediated inhibition of repair and replicative DNA synthesis in human fibroblasts. *Genes Dev* 1994; **8**: 1627-1639
195 **Albrecht JH**, Hansen LK. Cyclin D1 promotes mitogen-independent cell cycle progression in hepatocytes. *Cell Growth Differ* 1999; **10**: 397-404
196 **Cai FG**, Xiao JS, Ye QF. Effects of ischemic preconditioning on cyclinD1 expression during early ischemic reperfusion in rats. *World J Gastroenterol* 2006; **12**: 2936-2940
197 **Guttridge DC**, Albanese C, Reuther JY, Pestell RG, Baldwin AS. NF-kappaB controls cell growth and differentiation through transcriptional regulation of cyclin D1. *Mol Cell Biol* 1999; **19**: 5785-5799
198 **Cressman DE**, Greenbaum LE, Haber BA, Taub R. Rapid activation of post-hepatectomy factor/nuclear factor kappa B in hepatocytes, a primary response in the regenerating liver. *J Biol Chem* 1994; **269**: 30429-30435
199 **Peralta C**, Bartrons R, Riera L, Manzano A, Xaus C, Gelpí E, Roselló-Catafau J. Hepatic preconditioning preserves energy metabolism during sustained ischemia. *Am J Physiol Gastrointest Liver Physiol* 2000; **279**: G163-G171
200 **Peralta C**, Bartrons R, Serafin A, Blázquez C, Guzmán M, Prats N, Xaus C, Cutillas B, Gelpí E, Roselló-Catafau J. Adenosine monophosphate-activated protein kinase mediates the protective effects of ischemic preconditioning on hepatic ischemia-reperfusion injury in the rat. *Hepatology* 2001; **34**: 1164-1173
201 **Selzner N**, Selzner M, Jochum W, Clavien PA. Ischemic preconditioning protects the steatotic mouse liver against reperfusion injury: an ATP dependent mechanism. *J Hepatol* 2003; **39**: 55-61
202 **Compagnon P**, Wang HB, Southard JH, Mangino MJ. Ischemic preconditioning in a rodent hepatocyte model of liver hypothermic preservation injury. *Cryobiology* 2002; **44**: 269-278
203 **Yoshizumi T**, Yanaga K, Soejima Y, Maeda T, Uchiyama H, Sugimachi K. Amelioration of liver injury by ischaemic preconditioning. *Br J Surg* 1998; **85**: 1636-1640
204 **Clavien PA**, Selzner M, Rüdiger HA, Graf R, Kadry Z, Rousson V, Jochum W. A prospective randomized study in 100 consecutive patients undergoing major liver resection with versus without ischemic preconditioning. *Ann Surg* 2003; **238**: 843-850; discussion 851-852
205 **Li SQ**, Liang LJ, Huang JF, Li Z. Ischemic preconditioning protects liver from hepatectomy under hepatic inflow occlusion for hepatocellular carcinoma patients with cirrhosis. *World J Gastroenterol* 2004; **10**: 2580-2584
206 **Choukèr A**, Schachtner T, Schauer R, Dugas M, Löhe F, Martignoni A, Pollwein B, Niklas M, Rau HG, Jauch KW, Peter K, Thiel M. Effects of Pringle manoeuvre and ischaemic preconditioning on haemodynamic stability in patients undergoing elective hepatectomy: a randomized trial. *Br J Anaesth* 2004; **93**: 204-211
207 **Choukèr A**, Martignoni A, Schauer R, Dugas M, Rau HG, Jauch KW, Peter K, Thiel M. Beneficial effects of ischemic preconditioning in patients undergoing hepatectomy: the role of neutrophils. *Arch Surg* 2005; **140**: 129-136
208 **Choukér A**, Martignoni A, Schauer RJ, Dugas M, Schachtner T, Kaufmann I, Setzer F, Rau HG, Löhe F, Jauch KW, Peter K, Thiel M. Alpha-gluthathione S-transferase as an early marker of hepatic ischemia/reperfusion injury after liver resection. *World J Surg* 2005; **29**: 528-534
209 **Nuzzo G**, Giuliante F, Vellone M, De Cosmo G, Ardito F, Murazio M, D'Acapito F, Giovannini I. Pedicle clamping with ischemic preconditioning in liver resection. *Liver Transpl* 2004; **10**: S53-S57
210 **Koneru B**, Fisher A, He Y, Klein KM, Skurnick J, Wilson DJ, de la Torre AN, Merchant A, Arora R, Samanta AK. Ischemic preconditioning in deceased donor liver transplantation: a prospective randomized clinical trial of safety and efficacy. *Liver Transpl* 2005; **11**: 196-202
211 **Jassem W**, Fuggle SV, Cerundolo L, Heaton ND, Rela M. Ischemic preconditioning of cadaver donor livers protects allografts following transplantation. *Transplantation* 2006; **81**: 169-174
212 **Azoulay D**, Del Gaudio M, Andreani P, Ichai P, Sebag M, Adam R, Scatton O, Min BY, Delvard V, Lemoine A, Bismuth H, Castaing D. Effects of 10 minutes of ischemic preconditioning of the cadaveric liver on the graft's preservation and function: the ying and the yang. *Ann Surg* 2005; **242**: 133-139
213 **Cescon M**, Grazi GL, Grassi A, Ravaioli M, Vetrone G, Ercolani G, Varotti G, D'Errico A, Ballardini G, Pinna AD. Effect of ischemic preconditioning in whole liver transplantation from deceased donors. A pilot study. *Liver Transpl* 2006; **12**: 628-635
214 **Kwon AH**, Matsui Y, Ha-Kawa SK, Kamiyama Y. Functional hepatic volume measured by technetium-99m-galactosyl-human serum albumin liver scintigraphy: comparison between hepatocyte volume and liver volume by computed tomography. *Am J Gastroenterol* 2001; **96**: 541-546
215 **Sugai Y**, Komatani A, Hosoya T, Yamaguchi K. Response to percutaneous transhepatic portal embolization: new proposed parameters by 99mTc-GSA SPECT and their usefulness in prognostic estimation after hepatectomy. *J Nucl Med* 2000; **41**: 421-425
216 **Vauthey JN**, Pawlik TM, Ribero D, Wu TT, Zorzi D, Hoff PM, Xiong HQ, Eng C, Lauwers GY, Mino-Kenudson M, Risio M, Muratore A, Capussotti L, Curley SA, Abdalla EK. Chemotherapy regimen predicts steatohepatitis and an increase in 90-day mortality after surgery for hepatic colorectal metastases. *J Clin Oncol* 2006; **24**: 2065-2072
217 **Melendez J**, Ferri E, Zwillman M, Fischer M, DeMatteo R, Leung D, Jarnagin W, Fong Y, Blumgart LH. Extended hepatic resection: a 6-year retrospective study of risk factors for perioperative mortality. *J Am Coll Surg* 2001; **192**: 47-53
218 **Choti MA**, Sitzmann JV, Tiburi MF, Sumetchotimetha W, Rangsin R, Schulick RD, Lillemoe KD, Yeo CJ, Cameron JL. Trends in long-term survival following liver resection for hepatic colorectal metastases. *Ann Surg* 2002; **235**: 759-766

S- Editor Liu Y **L- Editor** Negro F **E- Editor** Bi L

PO Box 2345, Beijing 100023, China
www.wjgnet.com
wjg@wjgnet.com

World J Gastroenterol 2007 February 7; 13(5): 671-675
World Journal of Gastroenterology ISSN 1007-9327

REVIEW

Clinical role and importance of fluorescence *in situ* hybridization method in diagnosis of *H pylori* infection and determination of clarithromycin resistance in *H pylori* eradication therapy

Özlem Yilmaz, Ebru Demiray

Özlem Yilmaz, Ebru Demiray, Dokuz Eylül University, Faculty of Medicine, Department of Microbiology and Clinical Microbiology, 35340 Inciraltı-IZMIR, Turkey
Correspondence to: Özlem Yilmaz, Department of Microbiology and Clinical Microbiology, Faculty of Medicine, Dokuz Eylül University, Inciraltı 35340, Izmir, Turkey. ozlem.yilmaz@deu.edu.tr
Telephone: +90-232-4124506 Fax: +90-232-2590541
Received: 2006-09-20 Accepted: 2006-10-16

Yilmaz Ö, Demiray E. Clinical role and importance of fluorescence *in situ* hybridization method in diagnosis of *H pylori* infection and determination of clarithromycin resistance in *H pylori* eradication therapy. *World J Gastroenterol* 2007; 13(5): 671-675

http://www.wjgnet.com/1007-9327/13/671.asp

Abstract

H pylori is etiologically associated with gastritis, gastric and duodenal ulcers, gastric adenocarcinoma and mucosa-associated lymphoid tissue (MALT) lymphoma. Eradicating *H pylori* may convert rapidly the outcome of related diseases with the use of more accurate diagnostic molecular tests. Indeed some of the tests cannot give the evidence of current infection; *H pylori* can be detected by noninvasive and invasive methods, the latter requiring an endoscopy. Eradication failure is a big problem in *H pylori* infection. Recently, clarithromycin resistance in *H pylori* strains is increasing and eradication therapy of this bacterium is becoming more difficult. Molecular methods have frequently been applied besides phenotypic methods for susceptibility testing to detect clarithromycin resistance due to mutations in the 2143 and 2144 positions of 23S rRNA gene. Fluorescence *in situ* hybridization (FISH) method on paraffin embedded tissue is a rapid, accurate and cost-effective method for the detection of *H pylori* infection and to determine clarithromycin resistance within three hours according to the gold standards as a non-culture method. This method can also be applied to fresh biopsy samples and the isolated colonies from a culture of *H pylori*, detecting both the culturable bacillary forms and the coccoid forms of *H pylori*, besides the paraffin embedded tissue sections. This technique is helpful for determining the bacterial density and the results of treatment where clarithromycin has been widely used in populations to increase the efficacy of the treatment and to clarify the treatment failure *in vitro*.

Key words: *H pylori*; Fluorescence *in situ* hybridization method; Clarithromycin resistance

INTRODUCTION

H pylori is etiologically associated with gastritis, gastric and duodenal ulcers, gastric adenocarcinoma and mucosa-associated lymphoid tissue (MALT) lymphoma[1-3]. The prevalence of *H pylori* infection is 70%-90% in developing countries and 25%-50% in developed countries[2,4]. Person-to-person spread is the most probable mode of transmission. Fecal-oral and oral-oral transmission are also reported[5]. *H pylori* has been classified as a class I carcinogen by International Agency for Cancer Research (IACR)[6]. *H pylori* can be detected by noninvasive and invasive methods, the latter requiring an endoscopy. Noninvasive testing for *H pylori* can be done by measuring exhaled ^{13}C urea breath test (UBT), by serology, by stool antigen tests, by stool PCR and by analyzing body materials such as saliva and urine[2,7]. Invasive tests include endoscopy, with biopsy of the affected region followed by histopathologic examination of stained specimens to demonstrate the presence of the bacterium, rapid urease test, biopsy PCR and culture of the bacterium[1]. UBT, histopathology and culture of the organism, although not easily and routinely performed, are considered the gold standard for the diagnosis of *H pylori* infection[1,8].

Seven and fourteen days of triple therapy are recommended to eradicate *H pylori* according to Maastricht 2-2002 Consensus report. The triple therapy comprises a proton pump inhibitor in combination with two antibiotics, including amoxicillin, clarithromycin, or metronidazole[9-11]. Clarithromycin is a key component of most treatment recommendations to eradicate *H pylori*[12]. Resistance of *H pylori* to clarithromycin is regarded as a particular dilemma, since this drug is a part of both established therapy regimens. Thus, macrolide resistance is a frequent cause for failure of *H pylori* eradication therapy[10]. In industrialized countries approximately 10% of the

H pylori strains are clarithromycin-resistant. In developing countries, resistance rates to clarithromycin are higher, varying between 25% to 50%, while they are 5%-10% in the USA and as high as 10% in Europe[10,13,14]. Recently, the clarithromycin resistance rates are reported 16.8% and 52%-56% in Turkey[15-17]. In routine clinical laboratories the detection of clarithromycin resistance for *H pylori* is mainly based on phenotypic methods performed after culture: agar diffusion for the E-test or the agar dilution method, which is preferred as a reference method. However, there are some disadvantages of these methods such as results are not available until 48-96 h after inoculation of the agar plates[10,18]. Because *H pylori* is a fastidious organism, there are also some problems in application of culture and antibiotic susceptibility testing. Therefore easy, cheap and practicable methods are required for the detection of *H pylori* and determination of resistance, which is very important before the treatment if the resistance reaches 15%-20% in the area[7,19]. When the bacterial culture cannot be used routinely, the patient should benefit from the determination of macrolide resistance using non-invasive genotype-based methods[18].

Resistance of *H pylori* to clarithromycin is mainly due to major point mutations within an adenine-to-guanine transition at positions A2142G, A2143G and A2144G and to an adenine-to-cytosine transversion at positions A2142C and A2143C, which are included in the peptidyltransferase-encoding region of the 23S rRNA[9,11,20-23]. Mutations A2142G and A2143G are the most often observed, with the A2142C mutation being less common[24]. Other point mutations A2115G, G2141A, and T2717C have also been reported, though they appear to be very rare[18,25-27].

Detection of point mutations conferring resistance to clarithromycin for *H pylori* by molecular methods may constitute a more reliable approach and is attracting more attention[18]. Some molecular-based methods have been developed. PCR-based methods have been used to determine susceptibility to clarithromycin from biopsy specimens or cultured *H pylori* strains and stool specimens[7,28-30]. Fluorescence *in situ* hybridization (FISH) method for detection of *H pylori* and determination of its genotypic macrolide susceptibility in gastric biopsy specimens is a cultivation independent, reliable, sensitive and specific method[9,10,24]. Detection of *H pylori* and clarithromycin resistance genotype simultaneously in gastric biopsy specimens by FISH method may be a good tool for research in the future for the drug resistance mechanisms and to search for the eradication failure in developing countries, such as clarithromycin and similar antibiotics[23,31].

CLARITHROMYCIN ACTIVITY AND MECHANISM OF RESISTANCE

Clarithromycin activity

Clarithromycin is a bacteriostatic antibiotic, which belongs to a group of macrolides binding to peptidyl transferase loop of domain V of the 23S rRNA molecule. This binding interferes with protein elongation, and thus effectively blocks bacterial protein synthesis. The antibacterial activity of clarithromycin is similar to that of other macrolides, but clarithromycin is better absorbed in the gastric mucus layer, more acid-stable, and therefore more effective against *H pylori*[13,26,32]. Resistance to clarithromycin is thought to develop when substitutions in one amino acid at or near this binding site on the ribosome prevent the drug from binding, thereby making it ineffective[13].

Clarithromycin resistance

Resistance to clarithromycin in *H pylori* is caused by point mutations in three adjacent 23S rRNA nucleotides, namely 2142, 2143 and 2144. In *H pylori* these substitutions cause decreased affinity of the ribosomes for several macrolides, resulting in increased resistance. It can be induced by an adenine (A) to guanine (G) substitution at one of these positions or an adenine (A) to cytosine (C) substitution solely at position 2142. The A2142G and A2142C were significantly more frequently present in isolates with a higher minimal inhibitory concentration (MIC) for clarithromycin (> 64 mg/L), whereas the A2143G substitution was often found in isolates with a lower MIC (< 64 mg/L). Occasionally, other 23S rRNA mutations have also been reported for *H pylori*; some of them are associated with high-level resistance, while others are associated with low-level resistance[26,32]. Occasionally three described mutations, in which the adenine residues at positions 2143 and 2144 are replaced by guanine (A2143G and A2144G) or cytosine (A2143C), are localized within the peptidyl transferase region of the 23S rRNA gene[9,11,22,31].

H pylori contains two 23S rRNA genes and mutations are generally found in both copies, however, heterogeneity has been described. Heterogeneity still results in clarithromycin resistance, but it generally appears to be associated with lower resistance levels than in homogenic isolates. The higher prevalence of homogeneity over heterogeneity in *H pylori* may reflect a high efficiency of DNA recombination. The mutation in one copy of the 23S rRNA may be easily transferred to the other 23S rRNA gene by efficient homologous DNA recombination under selective pressure, conferring higher levels of clarithromycin resistance[11,22,24,26,31,32]. As expected, clarithromycin resistance coincides with resistance to other macrolides. The A2142G and A2142C mutations are linked to high-level cross-resistance to all macrolides, whereas the A2143G mutation gives rise to high-level resistance to erythromycin and intermediate-level resistance to clindamycin and streptogramin[26,32].

DETECTION OF CLARITHROMYCIN RESISTANCE

Molecular tests

The association between point mutations in the 23S rRNA gene and macrolide resistance in *H pylori* potentially provides a new approach for diagnosing macrolide resistant *H pylori* strains[33]. Numerous molecular-based methods are now available to assess clarithromycin in *H pylori*, such as PCR-RFLP, PCR-OLA, PCR-DEIA, PCR-

LipA, PCR-PHFA, 3M-PCR, real-time PCR hybridization assay, FISH, FRET, DNA sequencing by conventional and real-time (pyrosequencing) techniques. Most assays are polymerase chain reaction (PCR)-based using different methods to study the amplicons. The PCR-based molecular techniques are quicker than microbiological susceptibility testing, and more importantly, they can be performed directly on gastric biopsies and gastric juice[33].

Restriction fragment length polymorphism (RFLP) is a simple method based on the occurrence of restriction site within the amplicon. This assay allows for the detection of the previously mentioned 23S rRNA mutations using the restriction endonucleases, *Mbo*II (A2142G) *Bbs*I (A2142G), *Bsa*I (A2143G) and *Bce*AI (A2142C). As the PCR-RFLP was initially not able to detect the A2142C mutation, a 3'-mismatch reverse primer PCR method (3M-PCR) was developed[23,25,27]. However, the mutations are identified by the absence of a band, which is a less preferable endpoint than a positive endpoint[27].

Other methods, such as PCR-DNA enzyme immunoassay (DEIA), PCR oligonucleotide ligation assay (OLA), preferential homoduplex formation (PHFA) and PCR-line probe assay (LipA), include an additional hybridization step after the PCR. The PCR products were hybridized with labeled oligonucleotide probes under highly stringent conditions and hybrids were subsequently detected with specific antibodies or streptavidin-alkaline phosphatase[13,18,22,27,34,35]. The PHFA has been applied to direct detection of *H pylori* and clarithromycin resistant mutants in gastric juice samples[27]. The PHFA uses double labeled amplicons. Many of the assays are based on the principle of reverse hybridization with labeled probes for up to seven mutations and the wild type, immobilized either in microtitre wells (DEIA) or on nitrocellulose (LİPA). In these assays, PCR products are hybridized to the probes under highly stringent conditions and the resultant hybrids are detected colorimetrically. In the DEIA, the detection system is an enzyme linked immunoabsorbent assay with a labeled anti-double stranded DNA monoclonal antibody. Other more complex microtitre plate based systems such as the OLA use labeled capture and reporter probes[35].

Recently, several real-time PCR hybridization assays have been developed. The real-time PCR technique, which is powerful advancement of the basic PCR method, is developed based on amplification of a fragment of the 23S rRNA gene of *H pylori* followed by the melting curve analysis by biprobes and hyprobes[18,36]. In these assays a 23S rDNA fragment is amplified in the presence of a fluorescent-labeled mutation and anchor probe. Biprobes are sequence-specific probes labeled with the fluorophore Cy5. When the probe hybridizes to the target sequence, Cy5 is excited by the energy transfer from SybrGreen I, resulting in an increase of emitted light[29,36-38]. After completion of the PCR, the temperature is increased to determine the melting point of the mutation probe. The temperature at which the fluorescent signal drops indicates the point at which the mutation probe dissociates (melting point). When there are mismatches present in the target sequence, lower melting temperatures are obtained compared to the matched hybrid. This technique is simple and quick, and if applied directly to gastric tissue, results can be obtained within 3 h[13,27,29,34-38].

A technique named fluorescence resonance energy transfer (FRET) can be applied. In the first article in 1999, a DNA double strand specific fluorophor SYBR Green I and a second fluor dye Cy5 on a probe were used to test *H pylori* strains. This method was then applied to gastric biopsies[26].

In contrast with all the above approaches, DNA sequencing provides the gold standard reference method for mutation detection although it is not technically feasible or cost effective for routine laboratory determination of *H pylori* resistance markers. Nevertheless, knowledge of nucleotide sequences has proved invaluable for validation of the various assays mentioned above, particularly where a resistant phenotype is not associated with any of the more common mutations[35].

A recent development in rapid sequencing based on the principle of pyrosequencing, a real time DNA sequence analysis of short (25-30 bp) DNA stretches, has been applied to rapid identification of *H pylori*. Available data suggest this new technique can offer an accurate and rapid method for sequence analysis of PCR amplicons providing easily interpreted results within hours[35].

Fluorescence in situ hybridization

In situ hybridization (ISH) uses a labeled probe to detect and localize specific RNA or DNA sequences in a tissue or on a chromosome. ISH relies on DNA's ability to re-anneal, or hybridize, with a complimentary strand when at the correct temperature. "*In situ*" means "in the original place" in Latin, so ISH involves a labeled nucleic acid probe hybridizing with a DNA or RNA sequence *in situ* (in the cells) so that the location of the sequence of interest can be detected in the cells, tissue, or chromosome. Like Northern and Southern blots, ISH indicates the presence of a particular RNA or DNA sequence, but ISH differs from blots in that the labeled probe reveals the actual location of the sequence in the cells. The probe can be either radioactively labeled and detected by autoradiography or fluorescently labeled (abbreviated FISH) and detected by immunocytochemistry. The specificity of the probe depends on the permeability of the cells, the type of probes, the labeling technique, and the hybridization conditions, so specificity of ISH can be adjusted according to the desired results[39,40].

Fluorescence *in situ* hybridization (FISH) is to identify the presence of specific chromosomes or chromosomal regions through hybridization or fluorescence-labeled DNA probes to denatured chromosomal DNA[41]. FISH uses fluorescent molecules to vividly paint genes on chromosomes. This technique is particularly useful for gene mapping and for identifying chromosomal abnormalities. FISH involves the preparation of short sequences of single stranded DNA, called probes, which are complementary to the DNA sequences that researchers wish to paint and examine. These probes hybridize, or bind, to the complementary DNA and, because they are labeled with fluorescent tags, allow researchers to see the location of those sequences of DNA[41,42]. This technique allows the detection of whole bacteria in their natural habitat by fluorescence microscopy of prepared

specimens. Fluorescent signals indicate the presence of complementary chromosomal DNA; the absence of fluorescent signals indicates absence of complementary chromosomal DNA[43]. Unlike most other techniques used to study chromosomes, which require that the cells be actively dividing, FISH can also be performed on non-dividing cells, making it a highly versatile procedure[41,42,44].

Despite their small size, bacteria are accessible to the tools of cytology, such as immunofluorescence microscopy for localizing proteins in fixed cells with specific antibodies, fluorescence microscopy with the green fluorescent protein for localizing proteins in live cells, and FISH for localizing chromosomal regions and plasmids within cells[45].

The bacterial FISH technology is based on the specific DNA-DNA hybridization of defined oligonucleotides with the abundant copies of ribosomal RNA of a bacterial species (16S rRNA, 23S rRNA). The oligonucleotides, which are labeled with fluorescent dyes, penetrate the bacterial cells and bind to their target sequence. This technique allows the detection of whole bacteria in their natural habitat by fluorescence microscopy of prepared specimens, i.e. the gastric mucosa of infected humans or from animal models[43,46].

FISH is a rapid, accurate and also cost-effective method for the detection of *H pylori* and determination of macrolide resistance in cultured *H pylori* colonies. It can also be used directly on biopsy specimens for histopathological and microbiological examination[12,47]. In this assay intact *H pylori* are hybridized with fluorescent-labeled *H pylori*-specific 16S and 23S rRNA probes. The labeled bacteria were subsequently visualized by fluorescence microscopy. This assay allows detection of *H pylori* and clarithromycin resistance simultaneously. Moreover, this assay does not require DNA preparation and can directly be applied to gastric biopsy samples[9,23,26,27,32,35,48].

For *H pylori* a species-specific detection is performed by the 16S rRNA-specific oligonucleotide Hpy-1, labeled in green. Simultaneously to the species detection a genotypic antibiotic resistance determination is possible (labeled in red). The resistance against the macrolide clarithromycin, which is a major antibiotic used in the triple therapy against *H pylori* infections, is based on three defined point mutations in the 23S rRNA. These point mutations can be targeted specifically with the ClaWT, ClaR1, ClaR2, and ClaR3 probes. Different mutations correlate with different MICs of the antibiotics, ClaR1 > 64 mg/L, ClaR2, and ClaR3 between 8 and 64 mg/L[46,47].

CONCLUSION

The gold standard for accurate diagnosis of an *H pylori* infection is either culturing of the pathogen or concordant positive results obtained by histology and the rapid urease test or the ^{13}C-urea breath test (UBT)[24]. After culturing for the pathogen of gastric biopsies, probably most laboratories use disk diffusion or E-test for the determination of macrolide resistance. Both methods require further sub-culturing for several days and cannot identify the type of point mutations present in the strain[12].

The major advantage of FISH is the fact that the rRNA-targeted fluorescence-labeled oligonucleotide probes can be used for accurate determination of macrolide susceptibility, thus providing the clinician with important information with which to make a proper treatment recommendation[24,49]. Whilst the E-test is a phenotypic clarithromycin resistance measurement, FISH is an established genotypic technique for the detection of *H pylori* and discrimination between the clarithromycin-susceptible wild type and clarithromycin-resistant mutants[11,49]. FISH is a reliable fast method for the detection of clarithromycin-resistant *H pylori* mutants, and results are available within 3 h after an endoscopy. The probes are commercially available, and the method is cost-effective and can be applied in any laboratory without the need for special equipment or facilities, except for a fluorescence microscope[11,47,49].

REFERENCES

1 **Vinette KM**, Gibney KM, Proujansky R, Fawcett PT. Comparison of PCR and clinical laboratory tests for diagnosing *H. pylori* infection in pediatric patients. *BMC Microbiol* 2004; **4**: 5
2 **Kabir S**. Detection of *Helicobacter pylori* in faeces by culture, PCR and enzyme immunoassay. *J Med Microbiol* 2001; **50**: 1021-1029
3 **Ruiz-Bustos E**, Ochoa JL, Wadström T, Ascencio F. Isolation and characterisation of putative adhesins from *Helicobacter pylori* with affinity for heparan sulphate proteoglycan. *J Med Microbiol* 2001; **50**: 215-222
4 **Dunn BE**, Cohen H, Blaser MJ. *Helicobacter pylori*. *Clin Microbiol Rev* 1997; **10**: 720-741
5 **Young KA**, Akyon Y, Rampton DS, Barton SG, Allaker RP, Hardie JM, Feldman RA. Quantitative culture of *Helicobacter pylori* from gastric juice: the potential for transmission. *J Med Microbiol* 2000; **49**: 343-347
6 **Parsonnet J**, Harris RA, Hack HM, Owens DK. Should we treat *H. pylori* infection to prevent gastric cancer? *Gastroenterology* 1997; **112**: 1044-1045
7 **Sen N**, Yilmaz O, Simşek I, Küpelioğlu AA, Ellidokuz H. Detection of *Helicobacter pylori* DNA by a simple stool PCR method in adult dyspeptic patients. *Helicobacter* 2005; **10**: 353-359
8 **Park CS**, Kim J. Rapid and easy detection of *Helicobacter pylori* by in situ hybridization. *J Korean Med Sci* 1999; **14**: 15-20
9 **Rüssmann H**, Kempf VA, Koletzko S, Heesemann J, Autenrieth IB. Comparison of fluorescent in situ hybridization and conventional culturing for detection of *Helicobacter pylori* in gastric biopsy specimens. *J Clin Microbiol* 2001; **39**: 304-308
10 **Jüttner S**, Vieth M, Miehlke S, Schneider-Brachert W, Kirsch C, Pfeuffer T, Lehn N, Stolte M. Reliable detection of macrolide-resistant *Helicobacter pylori* via fluorescence in situ hybridization in formalin-fixed tissue. *Mod Pathol* 2004; **17**: 684-689
11 **Feydt-Schmidt A**, Rüssmann H, Lehn N, Fischer A, Antoni I, Störk D, Koletzko S. Fluorescence in situ hybridization vs. epsilometer test for detection of clarithromycin-susceptible and clarithromycin-resistant *Helicobacter pylori* strains in gastric biopsies from children. *Aliment Pharmacol Ther* 2002; **16**: 2073-2079
12 **Rüssmann H**, Adler K, Haas R, Gebert B, Koletzko S, Heesemann J. Rapid and accurate determination of genotypic clarithromycin resistance in cultured *Helicobacter pylori* by fluorescent in situ hybridization. *J Clin Microbiol* 2001; **39**: 4142-4144
13 **Graham DY**, Qureshi WA. Antibiotic-resistant *H. pylori* infection and its treatment. *Curr Pharm Des* 2000; **6**: 1537-1544
14 **Graham SK**, Graham DY. Contemporary diagnosis and management of *H. pylori*-associated gastrointestinal diseases. 2nd ed. USA, Pennsylvania: Handbooks in Health Care Co, 2002: 12-25

15 **Çırak MY**, Ünal S, Turet S, Dumlu GŞ, Dumlu İ, Engin D, Değertekin B, Karakan T, Cindoruk M. Klaritromisine dirençli ve duyarlı *Helicobacter pylori* suşlarının midedeki dağılımı. 21. Ulusal Gastroenteroloji Haftası 31 Ağustos-5 Eylül 2004, Antalya SB07/9. *Turk J Gastroenterol* 2004; **15** suppl 1: 41

16 **Önder GF**, Aydın A, Akarca US, Özütemiz Ö, İtler T. Ülkemizde *Helicobacter pylori*'nin klaritromisine direncinin real time PCR yöntemi ile araştırılması. 21. Ulusal Gastroenteroloji Haftası 31 Ağustos-5 Eylül 2004, Antalya SB07/5. *Turk J Gastroenterol* 2004; 15 Suppl 1: 40

17 **Özden A**, Bozdayı G, Bağlan P, Azap A, Özkan M, Koç Ö, Soykan İ, Çetinkaya H, Bahar K. *Helicobacter pylori'* nin klaritromisine karşı direncinin sıklığı. 21. Ulusal Gastroenteroloji Haftası 31 Ağustos-5 Eylül 2004, Antalya SB07/6. *Turk J Gastroenterol* 2004; **15** suppl 1: 40

18 **Oleastro M**, Ménard A, Santos A, Lamouliatte H, Monteiro L, Barthélémy P, Mégraud F. Real-time PCR assay for rapid and accurate detection of point mutations conferring resistance to clarithromycin in *Helicobacter pylori*. *J Clin Microbiol* 2003; **41**: 397-402

19 **Mégraud F**. Resistance of *Helicobacter pylori* to antibiotics. *Aliment Pharmacol Ther* 1997; **11** Suppl 1: 43-53

20 **Versalovic J**, Shortridge D, Kibler K, Griffy MV, Beyer J, Flamm RK, Tanaka SK, Graham DY, Go MF. Mutations in 23S rRNA are associated with clarithromycin resistance in *Helicobacter pylori*. *Antimicrob Agents Chemother* 1996; **40**: 477-480

21 **Taylor DE**, Ge Z, Purych D, Lo T, Hiratsuka K. Cloning and sequence analysis of two copies of a 23S rRNA gene from *Helicobacter pylori* and association of clarithromycin resistance with 23S rRNA mutations. *Antimicrob Agents Chemother* 1997; **41**: 2621-2628

22 **Debets-Ossenkopp YJ**, Sparrius M, Kusters JG, Kolkman JJ, Vandenbroucke-Grauls CM. Mechanism of clarithromycin resistance in clinical isolates of *Helicobacter pylori*. *FEMS Microbiol Lett* 1996; **142**: 37-42

23 **Trebesius K**, Panthel K, Strobel S, Vogt K, Faller G, Kirchner T, Kist M, Heesemann J, Haas R. Rapid and specific detection of *Helicobacter pylori* macrolide resistance in gastric tissue by fluorescent in situ hybridisation. *Gut* 2000; **46**: 608-614

24 **van Doorn LJ**, Glupczynski Y, Kusters JG, Mégraud F, Midolo P, Maggi-Solcà N, Queiroz DM, Nouhan N, Stet E, Quint WG. Accurate prediction of macrolide resistance in *Helicobacter pylori* by a PCR line probe assay for detection of mutations in the 23S rRNA gene: multicenter validation study. *Antimicrob Agents Chemother* 2001; **45**: 1500-1504

25 **Lascols C**, Lamarque D, Costa JM, Copie-Bergman C, Le Glaunec JM, Deforges L, Soussy CJ, Petit JC, Delchier JC, Tankovic J. Fast and accurate quantitative detection of *Helicobacter pylori* and identification of clarithromycin resistance mutations in *H. pylori* isolates from gastric biopsy specimens by real-time PCR. *J Clin Microbiol* 2003; **41**: 4573-4577

26 **Mégraud F**. *H pylori* antibiotic resistance: prevalence, importance, and advances in testing. *Gut* 2004; **53**: 1374-1384

27 **Mégraud F**. Resistance of *Helicobacter pylori* to antibiotics and its impact on treatment options. *Drug Resist Updat* 2001; **4**: 178-186

28 **Clayton CL**, Kleanthous H, Coates PJ, Morgan DD, Tabaqchali S. Sensitive detection of *Helicobacter pylori* by using polymerase chain reaction. *J Clin Microbiol* 1992; **30**: 192-200

29 **Gramley WA**, Asghar A, Frierson HF, Powell SM. Detection of *Helicobacter pylori* DNA in fecal samples from infected individuals. *J Clin Microbiol* 1999; **37**: 2236-2240

30 **Makristathis A**, Barousch W, Pasching E, Binder C, Kuderna C, Apfalter P, Rotter ML, Hirschl AM. Two enzyme immunoassays and PCR for detection of *Helicobacter pylori* in stool specimens from pediatric patients before and after eradication therapy. *J Clin Microbiol* 2000; **38**: 3710-3714

31 **Rüssmann H**, Feydt-Schmidt A, Adler K, Aust D, Fischer A, Koletzko S. Detection of *Helicobacter pylori* in paraffin-embedded and in shock-frozen gastric biopsy samples by fluorescent in situ hybridization. *J Clin Microbiol* 2003; **41**: 813-815

32 **Gerrits MM**. Molecular mechanisms of antibiotic resistance in *Helicobacter pylori*. Netherlands: Erasmus MC, 2004: 21-28

33 **Xia HX**, Fan XG, Talley NJ. Clarithromycin resistance in *Helicobacter pylori* and its clinical relevance. *World J Gastroenterol* 1999; **5**: 263-266

34 **Owen RJ**. Molecular testing for antibiotic resistance in *Helicobacter pylori*. *Gut* 2002; **50**: 285-289

35 **Simala-Grant JL**, Taylor DE. Molecular biology methods for the characterization of *Helicobacter pylori* infections and their diagnosis. *APMIS* 2004; **112**: 886-897

36 **Schabereiter-Gurtner C**, Hirschl AM, Dragosics B, Hufnagl P, Puz S, Kovách Z, Rotter M, Makristathis A. Novel real-time PCR assay for detection of *Helicobacter pylori* infection and simultaneous clarithromycin susceptibility testing of stool and biopsy specimens. *J Clin Microbiol* 2004; **42**: 4512-4518

37 **Chisholm SA**, Owen RJ, Teare EL, Saverymuttu S. PCR-based diagnosis of *Helicobacter pylori* infection and real-time determination of clarithromycin resistance directly from human gastric biopsy samples. *J Clin Microbiol* 2001; **39**: 1217-1220

38 **Gibson JR**, Saunders NA, Burke B, Owen RJ. Novel method for rapid determination of clarithromycin sensitivity in *Helicobacter pylori*. *J Clin Microbiol* 1999; **37**: 3746-3748

39 **In Situ Hybridization.** Available from: URL: http://www.bio.davidson.edu/courses/Molbio/MolStudents/spring2003/Baxter/MolecularTool.html

40 **Gene Tests.** Available from: URL: http://www.genetests.org

41 **National Human Genome Research Institute.** Available from: URL: http://www.genome.gov/10000206

42 **Aol Lifestream.** Available from: URL: http://members.aol.com/chrominfo/fishinfo.htm

43 **FISH -** (**Fluoresence In Situ Hybridization**)**.** Available from: URL: http://www.accessexcellence.org/RC/VL/GG/fish.html

44 **Watson JD**, Baker TA, Bell SP, Gann A, Levine M, Losick R. Molecular biology of the gene. 5th ed. San Francisco: Pearson Education, 2004: 692

45 **Fluorescence In Situ Hybridization**. Available from: URL: http://pollux.mpk.med.uni-muenchen.de/alpha1/forschung/FISH.html

46 **Morris JM**, Reasonover AL, Bruce MG, Bruden DL, McMahon BJ, Sacco FD, Berg DE, Parkinson AJ. Evaluation of seaFAST, a rapid fluorescent in situ hybridization test, for detection of *Helicobacter pylori* and resistance to clarithromycin in paraffin-embedded biopsy sections. *J Clin Microbiol* 2005; **43**: 3494-3496

47 **Kempf VA**, Trebesius K, Autenrieth IB. Fluorescent In situ hybridization allows rapid identification of microorganisms in blood cultures. *J Clin Microbiol* 2000; **38**: 830-838

48 **Temizkan G**, Arda N. Moleküler biyolojide kullanılan yöntemler. İst. Üniv. BİYOGEM Yayın No. 2, İstanbul: Nobel Tıp Kitabevi, 2004: 121-138

49 **Demiray E**, Tümer S, Yılmaz Ö, Altungöz O, Yorukoglu K, Soytürk M, Simsek I. Detection of *Helicobacter pylori* and clarithromycin resistance by fluorescence in situ hybridization (FISH) method in Turkish dyspeptic patients. European Helicobacter Study Group XIX. International Workshop September 7-9, 2006,Wroclaw, Poland, 13.10. *Helicobacter* 2006; **11**: 399-400

S- Editor Wang J **L- Editor** Zhu LH **E- Editor** Ma WH

PO Box 2345, Beijing 100023, China
www.wjgnet.com
wjg@wjgnet.com

World J Gastroenterol 2007 February 7; 13(5): 676-682
World Journal of Gastroenterology ISSN 1007-9327

ESOPHAGEAL CANCER

Alterations of glutathione S-transferase and matrix metalloproteinase-9 expressions are early events in esophageal carcinogenesis

Laszlo Herszenyi, Istvan Hritz, Istvan Pregun, Ferenc Sipos, Mark Juhasz, Bela Molnar, Zsolt Tulassay

Laszlo Herszenyi, Istvan Hritz, Istvan Pregun, Ferenc Sipos, Mark Juhasz, Bela Molnar, Zsolt Tulassay, 2nd Department of Medicine, Semmelweis University, Hungarian Academy of Science, Clinical Gastroenterology Research Unit, Budapest, Hungary

Correspondence to: Laszlo Herszenyi, MD, PhD, 2nd Department of Medicine, Semmelweis University, H-1088 Budapest, Szentkiralyi u. 46, Hungary. hersz@bel2.sote.hu
Telephone: +36-1-2660816 Fax: +36-1-2660816
Received: 2006-10-07 Accepted: 2006-12-15

Abstract

AIM: To investigate the role of glutathione S-transferase (GST) and matrix metalloproteinase-9 (MMP-9) expressions in the development and progression of reflux esophagitis-Barrett's metaplasia-dysplasia-adenocarcinoma sequence in the esophagus.

METHODS: GST and MMP-9 expressions were analyzed in 51 paraffin-embedded tissue samples by immunohistochemistry including patients with reflux esophagitis (n = 7), Barrett's metaplasia (n = 14), Barrett and esophagitis (n = 8), Barrett and dysplasia (n = 7), esophageal adenocarcinoma (n = 8) and a control group without any histological changes (n = 7). Immunostaining was determined semiquantitatively. Statistical analysis with one-way ANOVA, LSD test and correlation analysis were performed. P value of < 0.05 was considered significant.

RESULTS: GST expression was significantly higher while MMP-9 expression was significantly lower in control group compared to Barrett's metaplasia and the other groups. No major changes were observed between Barrett, esophagitis, and Barrett and concomitant esophagitis. Barrett and concomitant dysplasia, and adenocarcinoma revealed a significant lower expression of GST and higher levels of MMP-9 compared to all other groups. Adenocarcinoma showed almost no expression of GST and significantly higher levels of MMP-9 than Barrett and concomitant dysplasia. Alterations of GST and MMP-9 were inversely correlated (r = - 0.82).

CONCLUSION: Decreased GST and increased expression of MMP-9 in Barrett's metaplasia-dysplasia-adenocarcinoma sequence as compared to normal tissue suggest their association with esophageal tumorigenesis. Loss of GST and gain of MMP-9 in Barrett with dysplasia compared to non-dysplastic metaplasia indicate that these alterations may be early events in carcinogenesis. Quantification of these parameters in Barrett's esophagus might be useful to identify patients at higher risk for progression to cancer.

Key words: Glutathione S-transferase; Matrix metalloproteinase-9; Barrett's metaplasia; Esophagus; Adenocarcinoma; Dysplasia

Herszenyi L, Hritz I, Pregun I, Sipos F, Juhasz M, Molnar B, Tulassay Z. Alterations of glutathione S-transferase and matrix metalloproteinase-9 expressions are early events in esophageal carcinogenesis. *World J Gastroenterol* 2007; 13(5): 676-682

http://www.wjgnet.com/1007-9327/13/676.asp

INTRODUCTION

Esophageal cancer is still one of the most widespread diseases, and the early diagnosis of esophageal carcinoma correlates closely with improvement in prognosis. Barrett's esophagus (BE) is a precancerous condition of the lower esophagus in which the normal stratified squamous epithelium is replaced with specialized metaplastic columnar epithelium. Barrett's mucosa represents a type of epithelium that is completely different from the normal esophageal mucosa. BE is the main precancerous condition in the development of esophageal adenocarcinoma[1,2].

BE is diagnosed in up to 20% of patients with documented chronic gastroesophageal reflux disease (GERD). Follow-up studies have shown that BE has a 30- to 125-fold increased risk of developing into an adenocarcinoma, which emerges at a rate of approximately one cancer per 100 patient-years[3]. Barrett's adenocarcinoma displays the most rapidly increasing incidence for gastrointestinal tract cancer in the Western world. Diagnosis of Barrett's adenocarcinoma is usually made late, and consequently, is associated with poor prognosis[4-6].

Carcinogens are one of the inducing etiological factors for esophageal adenocarcinoma. Glutathione S-transferase (GST), a family of detoxification enzymes, plays an important role in the prevention of cancer by detoxifying numerous potentially carcinogenic compounds,

which can cause oxidative damage to cells[7]. Therefore, a reduction in these anti-oxidant enzymes can increase the risk of carcinogenesis[8]. Decreased GST enzyme activity has been reported in BE, and an inverse correlation was demonstrated between GST enzyme activity and tumor incidence in the gastrointestinal tract[9,10]. It has been suggested that down-regulation of GST expression could be an early event in the development of BE[11].

The degradation of the extracellular matrix (ECM), including the basement membrane, which is a specialized matrix composed of type Ⅳ collagen, laminin, entactin, proteoglycans and glycosaminoglycans, is an important feature of cancer cell invasion, and proteolytic enzymes play an important role in this event[12].

Several human solid tumors have been reported to have increased levels of proteolytic enzymes in cancer tissue, strongly suggesting that proteases may be important in tumor invasion and metastasis. With respect to the gastrointestinal tract, we have previously demonstrated that proteolytic enzymes may have a role not only in the process of gastric[13] or colorectal cancer invasion[14], but also in the progression of gastrointestinal precancerous changes into cancer[15].

Matrix metalloproteinases (MMPs) degrade components of the ECM and connective tissue surrounding the tumor cells and the basement membrane. MMPs are classified as gelatinases, collagenases, stromelysins, membrane-type matrix metalloproteinases, based mainly on the *in vivo* substrate specificity of the individual MMP. It was initially believed that MMPs, *via* breakdown of the physical barrier, were primarily involved in tumor invasion[16]. There is growing evidence, however, that the MMPs have an expanded role, as they are important for the creation and maintenance of a microenvironment that facilitates growth and angiogenesis of tumors at primary and metastatic sites[17,18].

Type Ⅳ collagen is an important protein of the basement membrane. Type Ⅳ collagenase, matrix metalloproteinase-9 (MMP-9) (gelatinase B), has been reported to be especially important in the process of tumor invasion and metastasis[19,20]. Several MMPs (gelatinase A: MMP-2; stromelysin: MMP-3; matrilysin: MMP-7; metalloelastase: MMP-12; collagenase-3: MMP-13) are expressed by tumor cells in esophageal squamous cell and adenocarcinomas, suggesting that these MMPs are responsible for tumor aggressiveness and prognosis in human esophageal carcinomas[21-24].

In the specific case of MMP-9, increased expressions have been observed in gastric cancer[25-27] and esophageal squamous cell carcinoma[28-30], but its behaviour in esophageal adenocarcinoma and in preinvasive lesions of esophageal carcinogenesis is still uncertain.

On the other hand, GST and MMP-9 as actors either in cancer prevention or in carcinogenesis have not been evaluated in the same experimental setting. Therefore, the aim of the present study was to investigate the role of GST and MMP-9 expressions using immunohistochemical analysis in the development and progression of reflux esophagitis-BE-dysplasia-adenocarcinoma sequence in the esophagus.

MATERIALS AND METHODS

Tissue specimens were obtained endoscopically from in- and outpatients with upper abdominal complaints at the 2nd Department of Medicine, Semmelweis University, Budapest.

Informed consent was obtained from all patients involved in the study, and a local ethical permission has been obtained. The patients comprised of 33 males and 18 females. The median age was 64 years with a range from 22 to 83 years. The endoscopic specimens were fixed in formalin and embedded in paraffin wax, sliced serial step sections of 4 μm thickness. GST and MMP-9 immunohistochemical expressions were analyzed in a total of 51 paraffin-embedded tissue samples by immunohistochemistry including patients with reflux esophagitis (n = 7) (4 males, 3 females, mean age 61 years, range 36-68 years); BE (n = 14) (9 males, 5 females, mean age 66 years, range 48-69 years); BE and esophagitis (n = 8) (6 males, 2 females, mean age 67 years, range 55-71 years); BE and dysplasia (n = 7) (4 males, 3 females, mean age 68 years, range 52-72 years); and esophageal adenocarcinoma (n = 8) (6 males, 2 females, mean age 71 years, range 64-83 years). Esophageal biopsies from patients with functional dyspepsia without any histological changes were used as controls (n = 7) (4 males, 3 females, mean age 49 years, range 22-56 years).

GST immunohistochemistry

The 4 micron thick tissue sections were dewaxed and rehydrated. Endogenous peroxidase activity was blocked by incubation for 30 min at room temperature in 3% hydrogen peroxide. After washing the sections 3 times in PBS for 5 min, non-specific blocking was done with 1% BSA-PBS solution for 10 min at room temperature. Next, the slides were incubated with diluted polyclonal rabbit anti-human GSTP1 antibody (1 μL GSTP1 antibody and 150 μL PBS) (Clone: A3600, DAKO) at 37℃ for 60 min in a humidified chamber. After washing the specimens 3 times in PBS, signal conversion was carried out with the LSAB2 system (DAKO) as described in the manual. Finally, haematoxylin co-staining was performed.

MMP-9 immunohistochemistry

After deparaffinization in xylene and rehydration through graded ethanol, endogenous peroxidase activity was blocked by incubation for 30 min at room temperature in 3% hydrogen peroxide. After washing the sections 3 times in PBS for 5 min, non-specific blocking was carried out with 1% BSA-PBS solution for 10 min at room temperature. Next, the slides were incubated with optimally diluted monoclonal anti-human MMP-9 antibody (Clone: 36020.111, R&D Systems) at 37℃ for 60 min in a humidified chamber. After washing the samples 3 times in PBS, signal conversion was carried out with the LSAB2 system (DAKO) as described in the manual. Finally, haematoxylin co-staining was performed.

Immunohistochemical analysis of GST and MMP-9

Known immunohistochemically-positive tissue sections

Table 1 GST immunohistochemical expression according to a semiquantitative score in various types of mucosal lesions of the esophagus

Histology	Score (mean ± SD)
Normal epithelium (Control group)[a] (n = 7)	2.85 ± 0.24
Reflux esophagitis (n = 7)	1.14 ± 0.24
Barrett's metaplasia (n = 14)	1.60 ± 0.34
Barrett's metaplasia and reflux esophagitis (n = 8)	1.12 ± 0.35
Barrett's metaplasia and dysplasia[b] (n = 7)	0.58 ± 0.37
Adenocarcinoma[b,c] (n = 8)	0.18 ± 0.25

[a]$P < 0.00001$ *vs* the other groups; [b]$P < 0.005$ *vs* the other groups (normal epithelium, reflux esophagitis, barrett's metaplasia, barrett's metaplasia and Reflux esophagitis); [c]$P < 0.05$ *vs* barrett's metaplasia and dysplasia.

Table 2 MMP-9 immunohistochemical expression according to a semiquantitative score in various types of mucosal lesions of the esophagus

Histology	Score (mean ± SD)
Normal epithelium (Control goup)[b] (n = 7)	0.28 ± 0.39
Reflux esophagitis (n = 7)	1.71 ± 0.39
Barrett's metaplasia (n = 14)	1.46 ± 0.41
Barrett's metaplasia and reflux esophagitis (n = 8)	1.75 ± 0.26
Barrett's metaplasia and dysplasia[a] (n = 7)	2.16 ± 0.25
Adenocarcinoma[a,c] (n = 8)	2.62 ± 0.35

[b]$P < 0.00001$ *vs* the other groups; [a]$P < 0.05$ *vs* the other groups (normal epithelium, reflux esophagitis, barrett's metaplasia, barrett's metaplasia and Reflux esophagitis); [c]$P < 0.05$ *vs* barrett's metaplasia and dysplasia.

were used as positive controls, and negative control sections were processed immunohistochemically after having replaced the primary antibody by PBS. None of the control sections exhibited immunoreactivity. Immunostaining was determined semiquantitatively, as previously described[31]. Essentially, the intensity of staining for GST and MMP-9 under a light microscope was graded from 0 to 3, denoting no staining or light, moderate, or intense staining. An immunohistochemical staining score was calculated for each histologic area by multiplying the staining intensity level (0 to 3) by the proportion of cells in each area staining with the given intensity. The immunohistochemical staining score for an area with 100% of cells with intense staining, for example, would be 1 × 3, equalling 3, whereas an area with 50% cells with moderate staining and 40% without any staining would have a score of 0.5 × 2 plus 0.4 × 1, equalling 1.4. Two independent investigators without knowledge of the clinical outcomes evaluated the degree of immunohistochemical staining intensity. There was less than 5% variance between the results of the two counts.

Statistical analysis

Statistical analysis with one-way ANOVA, LSD test and correlation analysis were performed by the Statistica for Windows 4.3 program package. P value of < 0.05 was considered significant.

RESULTS

The immunohistochemical expression scores of GST and MMP-9 in various types of mucosal lesions of the esophagus (n = 51) are shown in Tables 1 and 2.

Expression of GST (Table 1) in normal esophageal epithelium (control group) was significantly higher compared to BE and the other groups ($P < 0.00001$), while no major changes were observed between BE, esophagitis, and BE with concomitant esophagitis.

BE with concomitant dysplasia, and adenocarcinoma revealed a significantly lower expression of GST compared to all other groups ($P < 0.005$). Adenocarcinoma showed almost no expression of GST and a significantly lower expression than BE and concomitant dysplasia ($P < 0.05$).

The semiquantitative score of MMP-9 (Table 2) in the normal esophageal epithelium (control group) was significantly lower compared to BE and the other groups ($P < 0.00001$); while no major changes were observed between BE, esophagitis, and BE with concomitant esophagitis.

Significantly higher expression levels of MMP-9 have been observed in BE with concomitant dysplasia and adenocarcinoma compared to all other groups ($P < 0.05$). Finally, MMP-9 expression was significantly higher in adenocarcinoma compared to BE and concomitant dysplasia ($P < 0.05$).

GST and MMP-9 were expressed mainly within the cytoplasm and cytoplasmic membranes of the esophageal epithelium in dysplastic or adenocarcinoma cells (Figures 1 and 2). Immunoexpressions of GST and MMP-9 in the esophageal tissues were inversely correlated (r = - 0.82; P = 0.001) (Figure 3).

DISCUSSION

Despite advances in diagnosis and therapy, esophageal adenocarcinoma remains an aggressive and usually lethal tumor. BE is the main precancerous condition in the development of esophageal adenocarcinoma; however, its pathogenesis is poorly understood. BE typically progresses from metaplasia with atypia to dysplasia and adenocarcinoma. It is of great clinical importance to correctly identify changes with a high risk for malignant transformation, as high-grade dysplasias and early adenocarcinomas in patients with BE have a high chance for cure[32]. The identification of high-risk lesions in BE by histologic evaluation has drawbacks, especially regarding sampling errors and frequent intra- and inter-observer discrepancies in the histopathologic grading/staging of these lesions. Several new biomarkers are being tested to help in better determining the risk of cancer development.

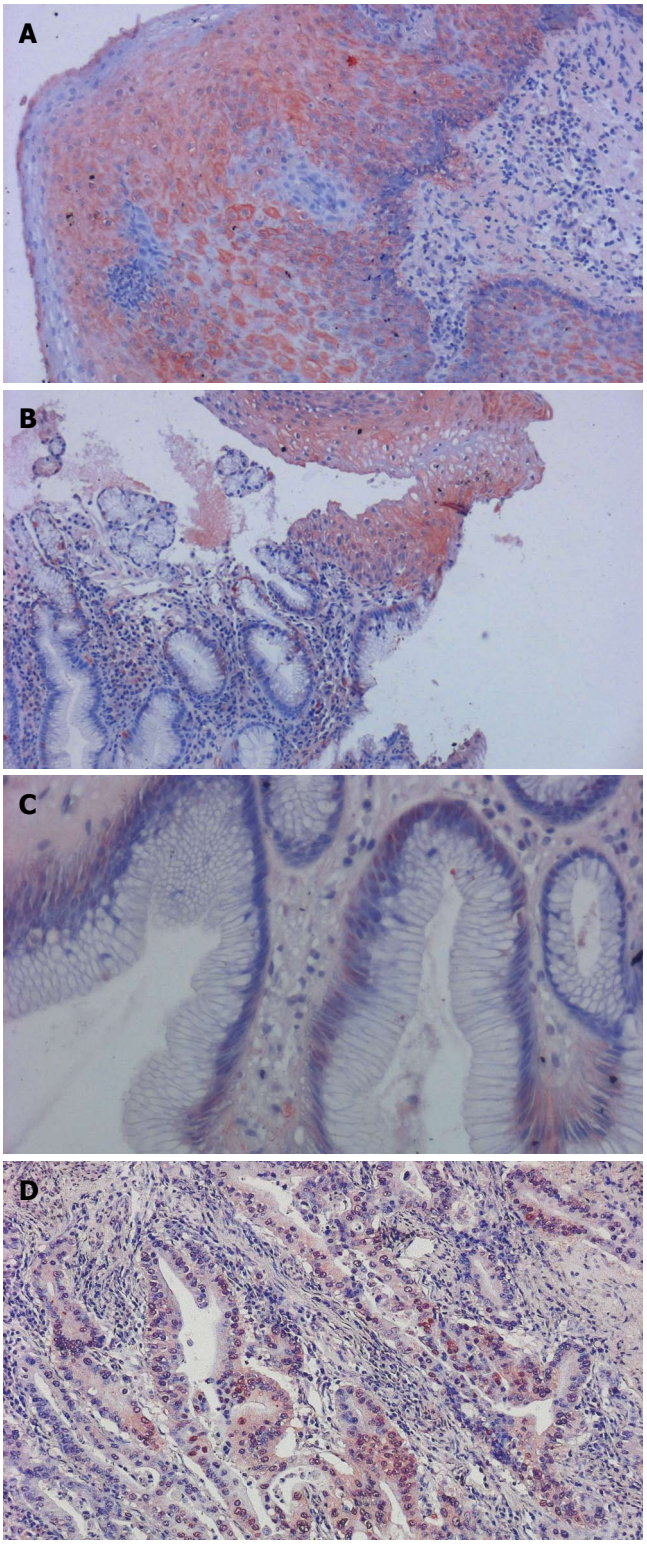

Figure 1 Expression of GST in different esophageal tissues. **A**: GST strong positive staining was observed in the normal esophagus (200 ×); **B**: Normal esophageal epithelium (top) with Barrett's metaplasia (bottom) (200 ×); **C**: Normal esophageal epithelium shows strong positive immunostaining compared to the weaker GST expression in Barrett's metaplasia (400 ×); **D**: Adenocarcinoma showing almost no expression of GST (200 ×); GST was mainly expressed within the cytoplasm.

Although most of the biological markers need to be evaluated further, at present, aneuploidy status, p16 and p53 gene abnormalities, or allelic losses are the most extensively documented alterations[33].

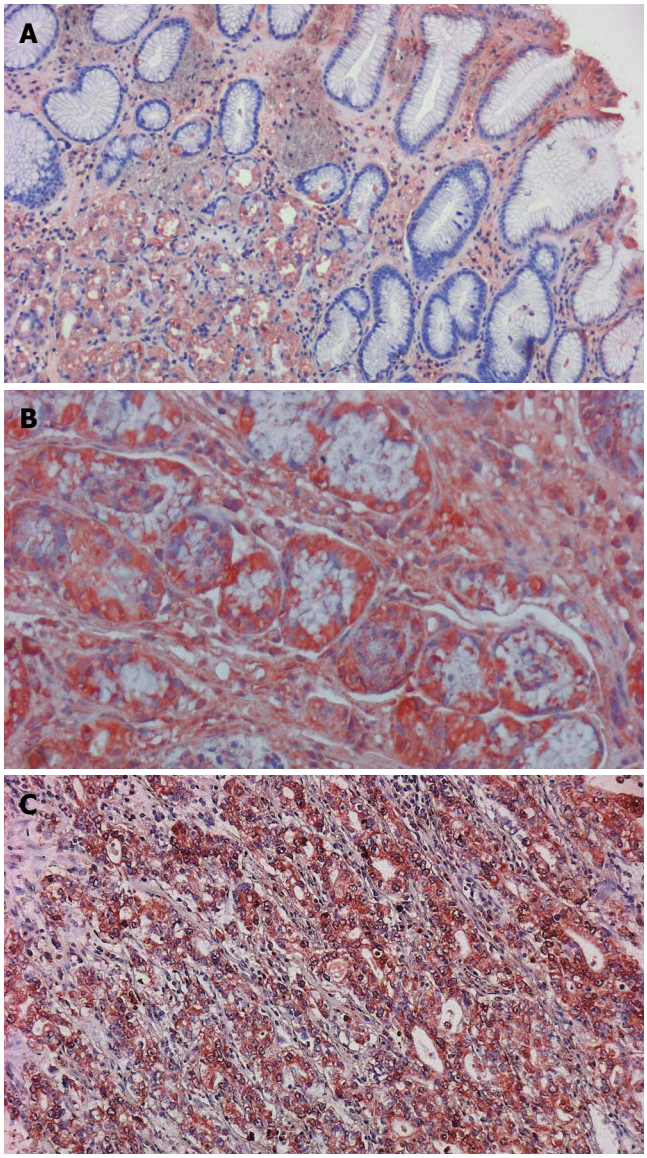

Figure 2 Expression of MMP-9 in different esophageal tissues. Strong positive immunostaining of MMP-9 in (**A**) Barrett's metaplasia (400 ×), (**B**) dysplasia (400 ×) and (**C**) adenocarcinoma (200 ×) of the esophagus. Cytoplasm of the metaplastic and dysplastic cells and cytoplasmic membranes of the esophageal adenocarcinoma cells were stained brown. Barrett's metaplasia with concomitant dysplasia and adenocarcinoma show the most intensive expression of MMP-9.

Immunostaining with a variety of antibodies provides a better understanding of the process of malignant transformation and helps to identify early markers of malignant transformation in BE[34].

Given the lack in the literature of the evaluation of GST and MMP-9 expressions in the same experimental setting, we evaluated the behaviour of detoxification enzyme GST, and one member of the matrix metalloproteinases family, MMP-9, in the development and progression of normal epithelium, reflux esophagitis, BE, dysplasia and adenocarcinoma sequence in the esophagus.

A number of findings in our study confirmed that GST is involved in esophageal carcinogenesis and progression. We have demonstrated that GST expression was significantly higher in normal esophageal epithelium compared to the other groups. On the other hand, BE with dysplasia, and adenocarcinoma revealed a significantly

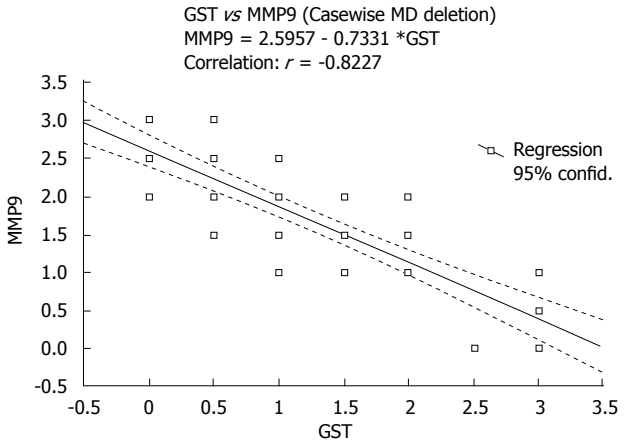

Figure 3 The correlation between immunohistochemical expressions of GST and MMP9 in different esophageal tissues. Immunohistochemical expressions of GST and MMP9 were inversely correlated (r = - 0.82; P = 0.001).

lower expression of GST, while adenocarcinoma expressed almost no GST.

Our findings are similar to the results reported by van Lieshout *et al*[9] and Cobbe *et al*[11]. They reported that the expression of GST appeared to be reduced in BE compared to normal esophageal squamous epithelium. In contrast to the van Lieshout *et al*[9] and Cobbe *et al*[11] studies, we also demonstrated that BE with concomitant dysplasia, and adenocarcinoma revealed a significantly lower expression of GST. Brabander *et al*[10] also found that GST expression was highest in the basal layer of normal esophageal squamous epithelium and lowest in adenocarcinoma cells, with BE cells showing intermediate staining intensity.

These results suggest that decreased GST expression could be an early event in the development of BE and may contribute to the risk of development and progression of adenocarcinoma in BE. The observed reduction in GST expression in BE may, therefore, contribute to the increased risk in this tissue.

Degradation of the ECM and basement membrane by tumor cells is a critical step in the process of tumor invasion and metastasis. MMP-9 is one member of the matrix metalloproteinases family, which is capable of degrading several components of the ECM. Increased expression of MMP-9 has been found in various carcinomas. With respect to the gastrointestinal tract, increased MMP-9 expressions have been observed in gastric[25-27] and colorectal cancer[35-38]. In the specific case of the esophagus, increased expression of MMP-9 has been demonstrated in esophageal squamous cell carcinoma[28-30], but its role and behaviour in esophageal adenocarcinoma and BE is not well established.

The relatively small number of patients in our study can be explained by the known data about the epidemiology of BE and esophageal adenocarcinoma in Hungary; since only 4% of patients with esophageal cancers were diagnosed to have adenocarcinoma and its proportion remained stable over the observed last decade, it seems that contrary to North American and Western European countries, the prevalence of adenocarcinoma has been, until now, very low in Hungary[39].

In the present study, immunohistochemical analysis revealed a progressive increase in the expression of MMP-9 with increasing severity of esophageal lesions. MMP-9 expression was significantly lower in normal esophageal epithelium compared to other groups. BE with concomitant dysplasia revealed a significantly higher expression of MMP-9 compared to BE, reflux esophagitis or BE with concomitant esophagitis. We observed that MMP-9 expression was significantly higher in adenocarcinoma compared to BE or BE with concomitant dysplasia. These results suggest that over-expression of MMP-9 plays an important role in the progression to esophageal adenocarcinoma, and MMP-9 protein may serve as a marker for invasiveness. Our results indicate that the activation of MMP-9 may be an early event in esophageal carcinogenesis.

Our findings are relevant from both, biological and clinical points of view. Despite the advance in preoperative and postoperative medical care of esophageal carcinoma patients, their prognosis has improved only marginally. Therefore, it would be useful to have additional biomarkers to help clinicians better determine the risk of esophageal cancer development. In esophageal cancer, novel targeted treatments are still in an early phase of development. It can be speculated that the relevance of MMP-9 in esophageal carcinogenesis may also support a possible therapeutic approach[40]. Indeed, this can be obtained directly by inhibition of MMP-9. Phase II-trials with the matrix metalloproteinase inhibitor prinomastat in patients with esophageal adenocarcinoma are under evaluation[41].

The present study showed that expressions of GST and MMP-9 were reversely or negatively correlated, thus suggesting a concomitant down-regulation and up-regulation, respectively, of these systems. GST plays an important protective role in the prevention of cancer by detoxifying potentially carcinogenic compounds, while MMP-9 should be considered an aggressive factor, playing a crucial role in the progression of esophageal carcinogenesis.

In conclusion, our results demonstrate a significantly lower expression of GST and a significantly higher expression of MMP-9, respectively, in the BE-dysplasia-adenocarcinoma sequence as compared to normal esophageal tissue. The simultaneous down-regulation of GST and up-regulation of MMP-9 strongly suggest their association with esophageal tumorigenesis and particularly, their specific role in the biology of esophageal adenocarcinoma. Loss of GST and gain of MMP-9 in BE with concomitant dysplasia compared to non-dysplastic BE indicate that these alterations may be early events in esophageal carcinogenesis. Together with other biological markers, quantification of these parameters in BE might be useful to identify patients at higher risk for progression to adenocarcinoma, to prevent tumor development and to improve prognosis.

REFERENCES

1 **Shaheen NJ**. Advances in Barrett's esophagus and esophageal adenocarcinoma. *Gastroenterology* 2005; **128**: 1554-1566

2 **Jankowski JA**, Harrison RF, Perry I, Balkwill F, Tselepis C. Barrett's metaplasia. *Lancet* 2000; **356**: 2079-2085

3 **Kim R**, Weissfeld JL, Reynolds JC, Kuller LH. Etiology of Barrett's metaplasia and esophageal adenocarcinoma. *Cancer Epidemiol Biomarkers Prev* 1997; **6**: 369-377
4 **Olliver JR**, Hardie LJ, Gong Y, Dexter S, Chalmers D, Harris KM, Wild CP. Risk factors, DNA damage, and disease progression in Barrett's esophagus. *Cancer Epidemiol Biomarkers Prev* 2005; **14**: 620-625
5 **Wong A**, Fitzgerald RC. Epidemiologic risk factors for Barrett' s esophagus and associated adenocarcinoma. *Clin Gastroenterol Hepatol* 2005; **3**: 1-10
6 **Jankowski JA**, Anderson M. Review article: management of oesophageal adenocarcinoma -- control of acid, bile and inflammation in intervention strategies for Barrett's oesophagus. *Aliment Pharmacol Ther* 2004; **20** Suppl 5: 71-80; discussion 95-96
7 **Zhu X**, Zhang SH, Zhang KH, Li BM, Chen J. Value of endoscopic methylene blue and Lugol's iodine double staining and detection of GST-Pi and telomerase in the early diagnosis of esophageal carcinoma. *World J Gastroenterol* 2005; **11**: 6090-6095
8 **Coles B**, Ketterer B. The role of glutathione and glutathione transferases in chemical carcinogenesis. *Crit Rev Biochem Mol Biol* 1990; **25**: 47-70
9 **van Lieshout EM**, Tiemessen DM, Witteman BJ, Jansen JB, Peters WH. Low glutathione and glutathione S-transferase levels in Barrett's esophagus as compared to normal esophageal epithelium. *Jpn J Cancer Res* 1999; **90**: 81-85
10 **Brabender J**, Lord RV, Wickramasinghe K, Metzger R, Schneider PM, Park JM, Hölscher AH, DeMeester TR, Danenberg KD, Danenberg PV. Glutathione S-transferase-pi expression is downregulated in patients with Barrett's esophagus and esophageal adenocarcinoma. *J Gastrointest Surg* 2002; **6**: 359-367
11 **Cobbe SC**, Scobie GC, Pohler E, Hayes JD, Kernohan NM, Dillon JF. Alteration of glutathione S-transferase levels in Barrett's metaplasia compared to normal oesophageal epithelium. *Eur J Gastroenterol Hepatol* 2003; **15**: 41-47
12 **Liotta LA**, Stetler-Stevenson WG. Tumor invasion and metastasis: an imbalance of positive and negative regulation. *Cancer Res* 1991; **51**: 5054s-5059s
13 **Plebani M**, Herszènyi L, Cardin R, Roveroni G, Carraro P, Paoli MD, Rugge M, Grigioni WF, Nitti D, Naccarato R. Cysteine and serine proteases in gastric cancer. *Cancer* 1995; **76**: 367-375
14 **Herszènyi L**, Plebani M, Carraro P, De Paoli M, Roveroni G, Cardin R, Tulassay Z, Naccarato R, Farinati F. The role of cysteine and serine proteases in colorectal carcinoma. *Cancer* 1999; **86**: 1135-1142
15 **Farinati F**, Herszényi L, Plebani M, Carraro P, De Paoli M, Cardin R, Roveroni G, Rugge M, Nitti D, Grigioni WF, D' Errico A, Naccarato R. Increased levels of cathepsin B and L, urokinase-type plasminogen activator and its inhibitor type-1 as an early event in gastric carcinogenesis. *Carcinogenesis* 1996; **17**: 2581-2587
16 **Sato H**, Seiki M. Membrane-type matrix metalloproteinases (MT-MMPs) in tumor metastasis. *J Biochem* 1996; **119**: 209-215
17 **Nelson AR**, Fingleton B, Rothenberg ML, Matrisian LM. Matrix metalloproteinases: biologic activity and clinical implications. *J Clin Oncol* 2000; **18**: 1135-1149
18 **Auvinen MI**, Sihvo EI, Ruohtula T, Salminen JT, Koivistoinen A, Siivola P, Rönnholm R, Rämö JO, Bergman M, Salo JA. Incipient angiogenesis in Barrett's epithelium and lymphangiogenesis in Barrett's adenocarcinoma. *J Clin Oncol* 2002; **20**: 2971-2979
19 **Stetler-Stevenson WG**, Aznavoorian S, Liotta LA. Tumor cell interactions with the extracellular matrix during invasion and metastasis. *Annu Rev Cell Biol* 1993; **9**: 541-573
20 **Roeb E**, Schleinkofer K, Kernebeck T, Pötsch S, Jansen B, Behrmann I, Matern S, Grötzinger J. The matrix metalloproteinase 9 (mmp-9) hemopexin domain is a novel gelatin binding domain and acts as an antagonist. *J Biol Chem* 2002; **277**: 50326-50332
21 **Shima I**, Sasaguri Y, Kusukawa J, Yamana H, Fujita H, Kakegawa T, Morimatsu M. Production of matrix metalloproteinase-2 and metalloproteinase-3 related to malignant behavior of esophageal carcinoma. A clinicopathologic study. *Cancer* 1992; **70**: 2747-2753
22 **Yamashita K**, Mori M, Shiraishi T, Shibuta K, Sugimachi K. Clinical significance of matrix metalloproteinase-7 expression in esophageal carcinoma. *Clin Cancer Res* 2000; **6**: 1169-1174
23 **Salmela MT**, Karjalainen-Lindsberg ML, Puolakkainen P, Saarialho-Kere U. Upregulation and differential expression of matrilysin (MMP-7) and metalloelastase (MMP-12) and their inhibitors TIMP-1 and TIMP-3 in Barrett's oesophageal adenocarcinoma. *Br J Cancer* 2001; **85**: 383-392
24 **Etoh T**, Inoue H, Yoshikawa Y, Barnard GF, Kitano S, Mori M. Increased expression of collagenase-3 (MMP-13) and MT1-MMP in oesophageal cancer is related to cancer aggressiveness. *Gut* 2000; **47**: 50-56
25 **Zhang S**, Li L, Lin JY, Lin H. Imbalance between expression of matrix metalloproteinase-9 and tissue inhibitor of metalloproteinase-1 in invasiveness and metastasis of human gastric carcinoma. *World J Gastroenterol* 2003; **9**: 899-904
26 **Sun WH**, Sun YL, Fang RN, Shao Y, Xu HC, Xue QP, Ding GX, Cheng YL. Expression of cyclooxygenase-2 and matrix metalloproteinase-9 in gastric carcinoma and its correlation with angiogenesis. *Jpn J Clin Oncol* 2005; **35**: 707-713
27 **Zhang JF**, Zhang YP, Hao FY, Zhang CX, Li YJ, Ji XR. DNA ploidy analysis and expression of MMP-9, TIMP-2, and E-cadherin in gastric carcinoma. *World J Gastroenterol* 2005; **11**: 5592-5600
28 **Koyama H**, Iwata H, Kuwabara Y, Iwase H, Kobayashi S, Fujii Y. Gelatinolytic activity of matrix metalloproteinase-2 and -9 in oesophageal carcinoma; a study using in situ zymography. *Eur J Cancer* 2000; **36**: 2164-2170
29 **Samantaray S**, Sharma R, Chattopadhyaya TK, Gupta SD, Ralhan R. Increased expression of MMP-2 and MMP-9 in esophageal squamous cell carcinoma. *J Cancer Res Clin Oncol* 2004; **130**: 37-44
30 **Yamamoto H**, Vinitketkumnuen A, Adachi Y, Taniguchi H, Hirata T, Miyamoto N, Nosho K, Imsumran A, Fujita M, Hosokawa M, Hinoda Y, Imai K. Association of matrilysin-2 (MMP-26) expression with tumor progression and activation of MMP-9 in esophageal squamous cell carcinoma. *Carcinogenesis* 2004; **25**: 2353-2360
31 **Hritz I**, Kuester D, Vieth M, Herszenyi L, Stolte M, Roessner A, Tulassay Z, Wex T, Malfertheiner P. Secretory leukocyte protease inhibitor expression in various types of gastritis: a specific role of Helicobacter pylori infection. *Eur J Gastroenterol Hepatol* 2006; **18**: 277-282
32 **Theisen J**, Nigro JJ, DeMeester TR, Peters JH, Gastal OL, Hagen JA, Hashemi M, Bremner CG. Chronology of the Barrett's metaplasia-dysplasia-carcinoma sequence. *Dis Esophagus* 2004; **17**: 67-70
33 **Krishnadath KK**, Reid BJ, Wang KK. Biomarkers in Barrett esophagus. *Mayo Clin Proc* 2001; **76**: 438-446
34 **Kleeff J**, Friess H, Liao Q, Büchler MW. Immunohistochemical presentation in non-malignant and malignant Barrett's epithelium. *Dis Esophagus* 2002; **15**: 10-15
35 **Curran S**, Dundas SR, Buxton J, Leeman MF, Ramsay R, Murray GI. Matrix metalloproteinase/tissue inhibitors of matrix metalloproteinase phenotype identifies poor prognosis colorectal cancers. *Clin Cancer Res* 2004; **10**: 8229-8234
36 **Takeuchi T**, Hisanaga M, Nagao M, Ikeda N, Fujii H, Koyama F, Mukogawa T, Matsumoto H, Kondo S, Takahashi C, Noda M, Nakajima Y. The membrane-anchored matrix metalloproteinase (MMP) regulator RECK in combination with MMP-9 serves as an informative prognostic indicator for colorectal cancer. *Clin Cancer Res* 2004; **10**: 5572-5579
37 **Ishida H**, Murata N, Tada M, Okada N, Hashimoto D, Kubota S, Shirakawa K, Wakasugi H. Determining the levels of matrix metalloproteinase-9 in portal and peripheral blood is useful for predicting liver metastasis of colorectal cancer. *Jpn J Clin*

Oncol 2003; **33**: 186-191

38 **Guzińska-Ustymowicz K**. MMP-9 and cathepsin B expression in tumor budding as an indicator of a more aggressive phenotype of colorectal cancer (CRC). *Anticancer Res* 2006; **26**: 1589-1594

39 **Lakatos PL**, Lakatos L, Fuszek P, Lukovich P, Kupcsulik P, Halbász J, Schaff Z, Papp J. Incidence and pathologic distribution of esophageal cancers at the gastro-esophageal junction between 1993-2003. *Orv Hetil* 2005; **146**: 411-416

40 **Tew WP**, Kelsen DP, Ilson DH. Targeted therapies for esophageal cancer. *Oncologist* 2005; **10**: 590-601

41 **Heath EI**, Burtness BA, Kleinberg L, Salem RR, Yang SC, Heitmiller RF, Canto MI, Knisely JP, Topazian M, Montgomery E, Tsottles N, Pithavala Y, Rohmiller B, Collier M, Forastiere AA. Phase II, parallel-design study of preoperative combined modality therapy and the matrix metalloprotease (mmp) inhibitor prinomastat in patients with esophageal adenocarcinoma. *Invest New Drugs* 2006; **24**: 135-140

S- Editor Liu Y **L- Editor** Lakatos PL **E- Editor** Liu WF

PO Box 2345, Beijing 100023, China
www.wjgnet.com
wjg@wjgnet.com

World J Gastroenterol 2007 February 7; 13(5): 683-691
World Journal of Gastroenterology ISSN 1007-9327

p53-expressing conditionally replicative adenovirus CNHK500-p53 against hepatocellular carcinoma *in vitro*

Hong-Chuan Zhao, Qi Zhang, Yang Yang, Min-Qiang Lu, Hua Li, Chi Xu, Gui-Hua Chen

Hong-Chuan Zhao, Qi Zhang, Yang Yang, Min-Qiang Lu, Hua Li, Chi Xu, Gui-Hua Chen, Liver Transplantation Centre, the Third Affiliated Hospital, Sun Yat-Sen University, Guangzhou 510630, Guangdong Province, China
Supported by the Major State Basic Research Development Program (973 Program) of China, No. 2003CB515507
Correspondence to: Professor Gui-Hua Chen, Liver Transplantation Centre, the Third Affiliated Hospital, Sun Yat-Sen University, Guangzhou 510630, Guangdong Province, China. zhc0117@sina.com
Telephone: +86-20-87595523 Fax: +86-20-87595523
Received: 2006-11-07 Accepted: 2006-12-05

Key words: Conditionally replicative adenovirus; Oncolytic virotherapy; Gene therapy; p53 gene; Hepatocellular carcinoma

Zhao HC, Zhang Q, Yang Y, Lu MQ, Li H, Xu C, Chen GH. p53-expressing conditionally replicative adenovirus CNHK500-p53 against hepatocellular carcinoma *in vitro*. *World J Gastroenterol* 2007; 13(5): 683-691

http://www.wjgnet.com/1007-9327/13/683.asp

Abstract

AIM: To develop a conditionally replicative gene-viral vector system called CNHK500-p53, which contains dual promoters within the E1 region, and combines the advantages of oncolytic virus and gene therapies for hepatocellular carcinoma (HCC).

METHODS: CNHK500-p53 was constructed by using human telomerase reverse transcriptase (hTERT) promoter to drive adenovirus *E1*a gene and hypoxia response element (HRE) promoter to drive adenovirus *E1*b gene. p53 gene expressing cassette was inserted into the genome of replicative virus. Viral replication experiments, cytopathic effect (CPE) and methyl thiazolyl tetrazolium (MTT) assay were performed to test the selective replication and oncolytic efficacy of CNHK500-p53.

RESULTS: Immunohistochemistry verified that infection with CNHK500-p53 was associated with selective replication of adenovirus and production of p53 protein in telomerase-positive and hypoxia-inducible factor-dependent HCC cells. p53 protein secreted from HepG2, infected with CNHK500-p53 was significantly higher than that infected with nonreplicative adenovirus Ad-p53 *in vitro* (388 ± 34.6 μg/L *vs* 76.3 ± 13.17 μg/L). Viral replication experiments showed that replication of CNHK500-p53 and CNHK500 or WtAd5, was much stronger than that of Ad-p53 in tested HCC cell lines. CPE and MTT assay indicated that CNHK500-p53 selectively replicated in and killed HCC cells while leaving normal cells unaffected.

CONCLUSION: A more efficient gene-viral system is developed by combining selective oncolysis with exogenous expression of p53 against HCC cells.

INTRODUCTION

Hepatocellular carcinoma (HCC) is the fifth most common solid tumor worldwide, accounting for 500 000 new cases annually. The majority of patients presenting with advanced disease are not candidates for liver transplantation, surgical resection, or regional therapy. In 60% to 80% of patients with HCC, underlying liver cirrhosis and hepatic dysfunction complicate its treatment. Systemic treatments have minimal effects with significant toxicity, and cannot improve patient survival[1]. The search for alternative treatment modalities has revived the concept of using oncolytic viruses to treat cancer[2,3]. In this respect, conditional replicative adenoviruses (CRAds) appear to be attractive anticancer agents that are currently evaluated in clinical trials[4,5]. CRAds exert intrinsic anticancer activity through selective replication and lysis in cancer cells. In addition, release of CRAd progeny by infected tumor cells provides a potential to amplify the oncolytic effect by lateral spread through solid tumors.

Recent studies have shown that telomerase activity may serve as a general marker of cancer cells. Its activity in normal cells is restricted to fetal tissue, whereas it is elevated in tumors[6]. Although some tumors could activate a yet unknown alternative mechanism of telomere extension, the majority (> 85%) of human HCC cells acquire immortality by expressing telomerase reverse transcriptase (hTERT)[7]. It has been shown that hTERT expression is regulated at the transcriptional level, thereby providing a promising tool for tumor-specific gene expression.

Hypoxia occurs in virtually allsolid tumors as they outgrow their blood supply. Hypoxia augments cellular levels of hypoxia-inducible factor (HIF), a transcription

factor that regulates target genes through the binding of hypoxia response elements (HRE). Activation of the HIF pathway enables cancer cells to survive and proliferate in a hypoxic environment and contributes to a more aggressive phenotype[8,9]. Therefore, the HIF/HRE system of gene regulation, which is active under hypoxia or as a result of genetic alterations during cell transformation, is particularly attractive to specific target solid tumors.

Besides viral oncolysis, CRAds can be exploited as vectors of gene therapies by advanced virology and viral vector design to enhance their oncolysis. Many malignant neoplasms have lost the function of p53. Although many oncolytic adenoviruses use p53-dependent pathways to cause cell death, several studies have shown that replicating adenoviruses kill cells more rapidly when expressing p53[10,11].

Here we have constructed a novel gene-viral vector system called CNHK500-p53, which uses hTERT promoter to drive adenovirus *E1*a gene and HRE promoter to drive adenovirus *E1*b gene. In addition, human p53 gene was cloned into the downstream of E1A of adenovirus. E1A gene is essential for adenoviral replication, and adenovirus can hardly propagate without it. Telomerase and hypoxia are two important features of human solid tumors. Making use of these two promoters, CNHK500-p53 will replicate only in telomerase positive cancer cells undergoing hypoxia in theory. We tested the replication ability and oncolytic activity of CNHK500-p53 in HCC cell lines *in vitro*.

MATERIALS AND METHODS

Vectors, cell lines and cell culture

pXC1 (wild-type adenovirus plasmid) and pBGHE3 (a plasmid-containing right arm of adenovirus type 5 with deletion of 188-1339 bp sequence.) were purchased from Microbix Biosystems Ltd (Toronto, Canada). pGEM-3ZF and pGEM-3ZF-p53 were purchased from Promega Ltd, USA. Human HCC cell lines HepG2, Hep3B, normal human liver cell line L02, normal human fibroblast cell lines MRC-5 and BJ were purchased from the American Type Culture Collection (Manassas, VA). Human HCC cell lines SMMC-7721, Bel-7402 and wild-type adenovirus 5 (WtAd5) were obtained from Second Military Medical University (Shanghai, China). Human embryonic kidney 293 cell line was obtained from Microbix Biosystems (Toronto, Canada). Hep3B, HepG2, SMMC-7721, Bel-7402 and human embryonic kidney 293 cells were cultured in DMEM (Life Technologies, Rockville, MD). L02 was cultured in RPMI 1640 medium. BJ was cultured in modified Eagle's medium (MEM). All the media were supplemented with 10% heat-inactivated fetal bovine serum (Life Technologies), 4mmol/L L-glutamine, 100 units/mL penicillin, and 100 μg/mL streptomycin and cultured under a 5% CO_2 atmosphere at 37℃.

Construction of adenovirus vectors

Complete cDNA sequence of p53 gene was amplified by PCR from plasmid pGEM-3ZF-p53 by using the upstream primer VT182 (5'CCG GAA TTC (*EcoRI*) GCC ATG GAG GAG CCG CAG TCA GA3') and downstream primer VT183(5'CGC GGA TCC (*BamHI*) TTA TCA GTC TGA GTC AGG CCC TTC TG3'). Synthetic DNA sequence was released with endonucleases *EcoRI* and *BamHI* (New England Biolabs, Beverley, MA) and ligated into plasmid pClon15 (made by ourselves, which contains the sequence of mouse cytomegalovirus promoter + multiple clone site + SV40 poly A) to generate pClon15-p53. pClon15-p53 was digested with endonucleases *AgeI* and *NotI* (New England Biolabs), a 1917-bp fragment containing mouse cytomegalovirus promoter + p53 gene + SV40 polyA was excised and inserted into *AgeI* and *NotI* sites of pSG500, which was constructed in our previous study and contained hTERT promoter core sequence with three extra E-boxes downstream and HRE promoter[12]. The plasmid resulting from the insertion of p53 gene cassette into the pSG500 in orthograde orientation was designated as pSG500-p53. pSG500-p53 and pSG500 were transfected by Lipofectamine 2000 (Life Technologies) into 293 cells together with pBHGE3. Viral plaques appeared 9-14 d after cotransfection and were sublimated three times. Recombinant adenoviruses, extracted using QIAamp DNA blood mini kit (Qiagen, Valencia, CA), were verified by PCR and named CNHK500-p53 and CNHK500. Ad-p53 was used as a control, which is a nonreplicative adenovirus vector carrying a SV40 early promoter-driven human p53 expression cassette[13]. A similar procedure was used by replacing the p53 gene with a 1538-bp fragment of the green fluorescent protein (GFP) expression cassette, obtained from plasmid pCA13-GFP (Takara Ltd, Japan), to derive conditionally replicative adenovirus CNHK500-GFP and nonreplicative adenovirus Ad-GFP. The nonreplicative adenovirus Ad-blank was used as a control.

Production and purification of adenovirus

Viruses were purified by CsCl density purification and propagated in 293 cells. After 72 h, the detached cells were harvested by centrifugation at 1000 × *g* for 5 min at 4℃, resuspended in 10 mL cold PBS (free Ca^{2+} and Mg^{2+}), and then lysed with three cycles of freeze and thaw. Lysate was collected by centrifugation at 1500 × *g* for 10 min at 4℃, and the supernatant was placed on a gradient prepared with equal parts of CsCl in PBS and then centrifuged at 15000 × *g* for 2 h at 12℃. The virus band was removed and placed in a preformed CsCl gradient by ultracentrifugation for 18 h and dialyzed into 10 mmol/L Tris-HCl (pH 7.4) containing 10 mmol/L $MgCl_2$ and 10% glycerol. Titers of the purified adenovirus were determined by plaque assays of the tissue culture infectious dose 50 methods and shown as plaque forming unit per milliliter (pfu/mL). All viral preparations were free of endotoxin.

Viral replication assay

Monolayer cells, including logarithmically growing Hep3B, HepG2, SMMC-7721 (10^5 cells/well), and contact-inhibition BJ, L02 (10^6 cells/well) were cultured in six-well dishes overnight and infected with CNHK500-p53, WtAd5, Ad-p53 at a multiplicity of infection (MOI) of 5.0 pfu/cell. Virus inocula were removed after 2 h. The cells then were washed twice with PBS and incubated at 37℃ for 0, 12, 24, 48, or 96 h. Lysates of cells were prepared with three cycles of freeze and thaw. Serial dilutions of

the lysates were titered on human embryonic kidney 293 cells with the tissue culture infectious dose 50 methods, normalized with that at the beginning of infection, and reported as multiples.

Western blot analysis of E1A and E1B protein

HepG2, Hep3B and BJ were seeded in 6-well plates at a density of 5×10^5 cells/well and infected with CNHK500-p53 or wtAd5 at a MOI of 1 after 24 h of incubation. Two days after viral infection, cells were harvested and lysed with M-PER mammalian protein extraction reagent (PI-ERCE, Rockford, IC). Concentration of the extracted protein was measured with a biophotometer (Eppendorf AG, Hamburg, Germany). Total proteins (20 μg) were separated on 10% SDS-polyacrylamide gel, electroblotted onto PROTRAN nitrocellulose transfer membrane (Schleicher & Schuell Inc, Dassel. Germany) and blocked with 5% fat-free milk in Tris-buffered saline (TBS: 10 mMTris, pH 7.5, 0.9% NaCl) containing 0.1% Tween-20 (TBST) at room temperature for 1 h. The membrane was incubated with either rabbit polyclonal antibody against Ad-E1A protein (Santa Cruz Biotechnology) or rat anti-Ad5 E1B 55k monoclonal antibody overnight at 4℃ and repeatedly washed in TBST. After incubation for 1 h with appropriate secondary horseradish peroxidase-conjugated anti-bodies and extensive washing with TBST, immunocomplexes on the membrane were detected with LumiGLOTM reagent and visualized with Kodak BiomaxMR film. To detect the expression of E1A and E1B under hypoxic condition, CNHK500-p53 infected cells were exposed to 0.1% hypoxia for 16 h before harvest.

ELISA determination of p53 gene expression

HepG2 cells were seeded in 24-well plates at a density of 5×10^4 cells/well and cultured for 24 h, followed by infection with CNHK500-p53 and Ad-p53 at a MOI of 0.1. On days 3, 5, 7, and 10 post-infection, the supernatants of cell cultures were collected and assayed for p53 gene expression levels using the ELISA kit of p53 (Chemicon International, Temecula, CA) and the manipulation was done according to the manufacturer's instructions.

Evaluation of oncolytic activity of virus vector

Cytopathic effect (CPE): Hep3B, HepG2, Bel-7402 (2×10^4 Cells/well) and BJ (6×10^4 cells/well) were dispensed in 24-well plates. The culture solution was removed on the second day, and 1 mL serum free DMEM and virus were added to each well. The multiplicity of infection (MOI) of each well was 0.01, 0.1, 1, 10 and 100, respectively. The culture plate was then incubated for 90 min in a 37℃ incubator under the condition of 5% CO_2 in DMEM containing 5% serum.

Methyl thiazolyl tetrazolium (MTT) assay: MTT assay was performed to determine cell viability at various viral MOIs. HepG2, Hep3B and BJ cells were plated at a density of 1×10^4 cells/well in 96-well plates (Falcon) and 24 h later, the cells were infected with CNHK500-p53 at serial MOIs from 0.001 to 100. After 7 d of incubation, cell viability was measured by MTT assay using a non-radioactive cell proliferation kit (Roche Molecular Biochemicals) according to its protocol, and the spectrophotometrical absorbance of samples was measured with a microplate reader model 550 (BIO-RAD Laborato-ries, Tokyo, Japan) at 570 nm with a reference of 655 nm. Percentage of cell survival was calculated using the formula: % cell survival = (OD value of infected cells/OD value of uninfected control cells) × 100%. Eight replicate samples were taken at each MOI and each experiment was repeated at least 3 times. IC_{50} of CNHK500-p53, CNHK500, and WtAd5 was calculated in HepG2 and BJ 7 d after infection. Statistical analysis was performed using Student's *t* test for differences among groups. $P < 0.05$ was considered statistically significant.

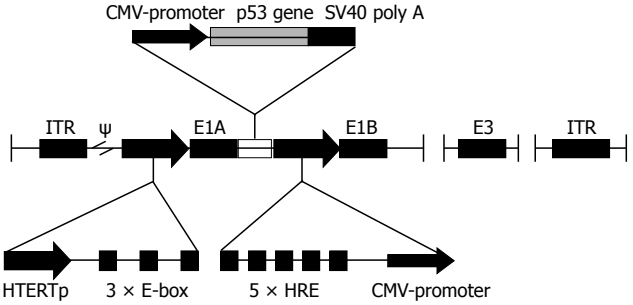

Figure 1 Schematic diagram of the CNHK500-p53 adenoviral construct. A 310-bp fragment of human telomerase reverse transcriptase (hTERT) promoter with three E-boxes (CACGTG) downstream of the core sequence replaced the endogenous E1A promoter (digested with *NotI* and *XhoI*) to control the expression of E1A. A 241-bp fragment of hypoxia response element (HRE) promoter replaced the endogenous E1B promoter to control the expression of E1B. A 1805-bp fragment of transgene expression cassette containing cytomegalovirus (CMV) promoter + p53 + SV40 poly A was inserted into the downstream of E1A (digested with *AgeI* + *NotI*) to generate CNHK500-p53. ITR, inverted terminal repeat; ψ, the adenovirus 5 packing signal.

Replication between CNHK500-GFP and Ad-GFP

HepG2, Bel-7402 (1×10^5 cells/well), and BJ (1×10^6 cells/well) were inoculated into six-well plates, respectively. When the cells were confluent, CNHK500-EGFP or Ad-EGFP was added to each well at the MOI of 1 and then washed with PBS 2 h later. Cells were then coated with 1.25% agarose. On days 3, 7 and 10, the cells were observed under a fluorescence microscope and significant changes were photographed. Fluorescence microscopy was performed with routine methods with fluorescence in isothiocyanate (FITC), with the excitement and emission wavelength being 475 nm and 490 nm, respectively.

RESULTS

To make a conditional replicative gene-viral vector, we adopted a design as shown in Figure 1, in which the adenovirus *E1*a gene was placed under the control of hTERT promoter plus three extra E-boxes, and *E1*b gene was controlled by HRE promoter, p53 gene-expressing cassette was inserted between E1A and HRE promoter. CNHK500-p53 was successfully made and verified by PCR. We were able to produce the adenovirus with high titers (2×10^{10} pfu/mL).

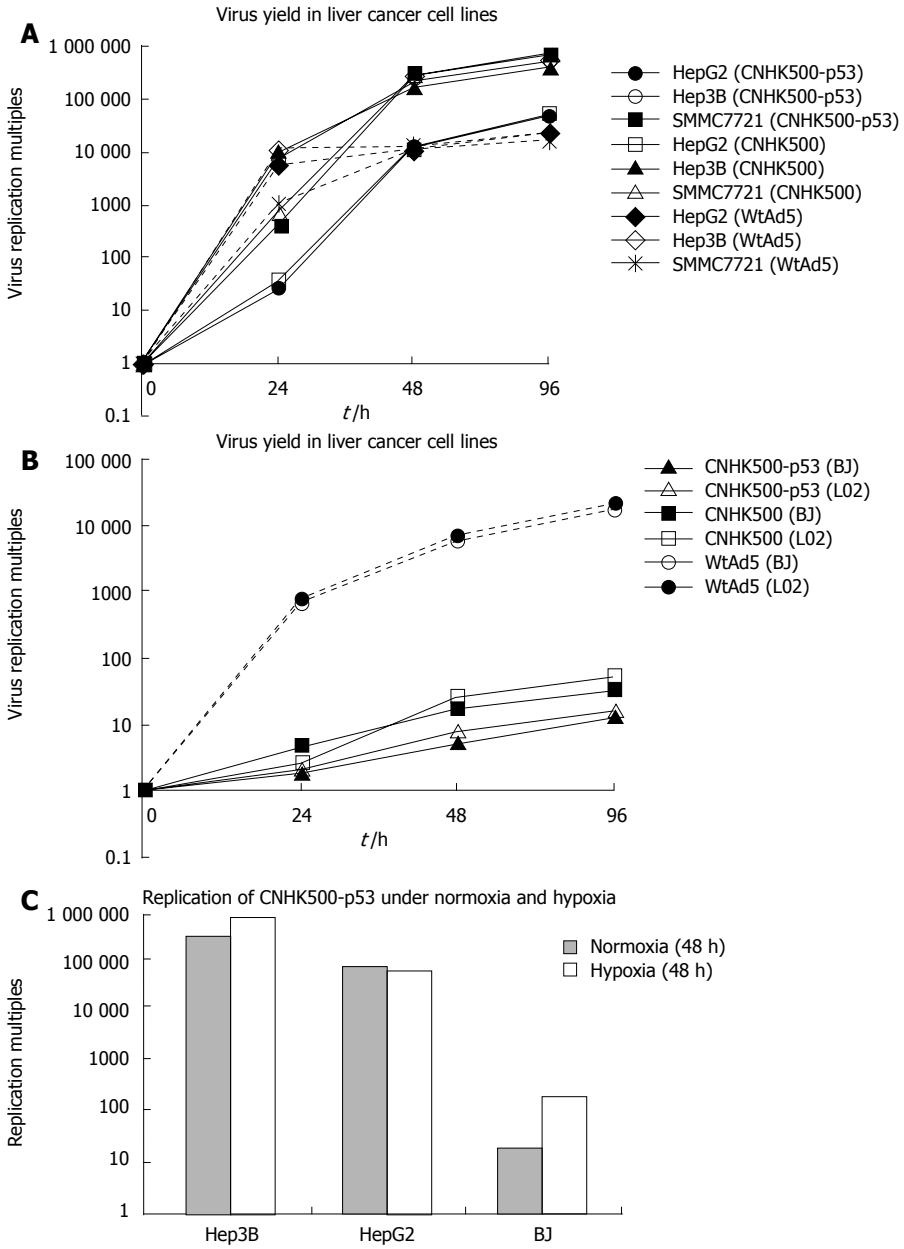

Figure 2 Selective replication of CNHK500-p53 *in vitro*. **A**: Human HCC cell lines HepG2, Hep3B, and SMMC-7721 were infected with CNHK500-p53 at a MOI of 5. Cells and media were harvested, and lysates were prepared from each group at diverse time points 0 h, 24 h, 48 h, and 96 h. Viral titers were measured with the tissue culture infectious dose 50 method, normalized with that at the beginning of infection, and shown as multiples. CNHK500-p53 replicated similarly as CNHK500 and WtAd5 in all of the tested telomerase-positive cancer cells; **B**: Comparison of replication capability of CNHK500-p53, CNHK500 and WtAd5 in telomerase-negative normal cell lines. At diverse time points 0 h, 24 h, 48 h, and 96 h after infection, cells and medium were harvested, and viral titers were measured as described previously. In all of the tested normal cell lines, the replication capability of CNHK500-p53 and CNHK500 was severely attenuated than that of WtAd5; **C**: Forty-eight hours after infection with CNHK500-p53 in HepG2, Hep3B and BJ, CNHK500-p53 showed enhanced replication ability both in HepG2, Hep3B and in BJ under hypoxia condition, but was higher in HepG2, Hep3B than in BJ.

Selective replication of CNHK500-p53

Selective replication of the new recombinant adenovirus CNHK500-p53 was evaluated using telomerase-positive HCC cell lines Hep3B, HepG2, SMMC-7721 and telomerase-negative normal cell lines BJ, L02. In HepG2, Hep3B and SMMC-7721, the replicative multiples increased to 47 230-, 459 837- and 669 251- fold respectively after 96 h of CNHK500-p53 replication, similar to those of CNHK500 and WtAd5 (Figure 2A). However, in normal cell lines BJ, L02, the replicative multiples of CNHK500-p53 and CNHK500 were only 12.8-, 16.3- and 31-, 53- fold at 96 h, and attenuated as much as 1354-, 1325- and 559-, 407.5- fold when compared with WtAd5 (Figure 2B). CNHK500-p53 showed enhanced replication ability both in HepG2, Hep3B and in BJ under hypoxia condition, but was higher in HepG2 and Hep3B cells than in normal BJ cells (Figure 2C). As hTERT promoter regulates *E1*a gene, E1A protein could be detected in telomerase positive hepatocellular cells HepG2 and Hep3B, but not in telomerase negative normal cells BJ. Under normoxic condition, E1B protein could hardly be detected due to poor activity of HRE promoter. When HCC cells were exposed to hypoxia, E1B protein was induced as a result of increased activity of HRE promoter (Figure 3A).

Expression of p53 produced by CNHK500-p53

To verify that the p53 expressed by CNHK500-p53 could secrete efficiently into the media, the conditioned media from 5×10^4 HepG2 cells infected with CNHK500-p53 or Ad-p53 at a MOI of 0.1 were collected and analyzed for the presence of p53 protein by ELISA. The quantity of p53 expressed by CNHK500-p53 and Ad-p53 on d 3, 5, 7, and 10 post-infection is shown in Figure 3B, indicating that p53 expression in CNHK500-p53 was 5.1 times more than that in Ad-p53 in HepG2 on d 7. Western blot analysis revealed a clear band of M_r 53 000 in the conditioned media after HepG2 cells were infected

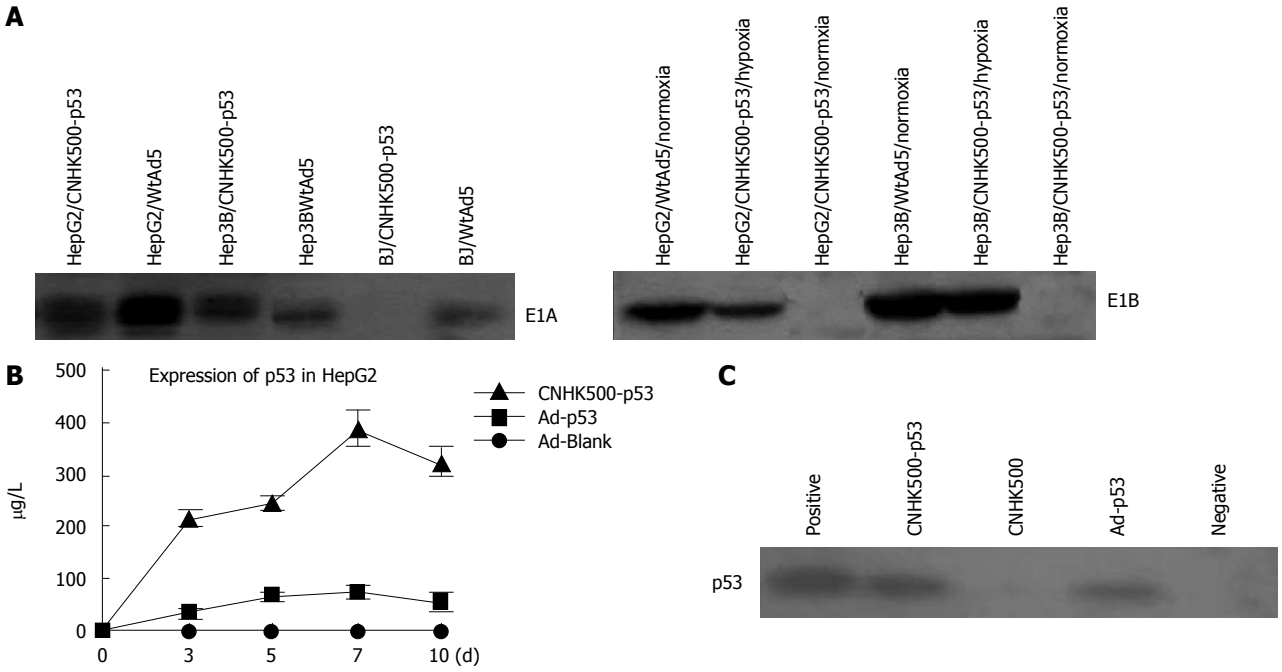

Figure 3 **A**: E1A and E1B expression identified by Western blot demonstrating that all HCC cells infected with CNHK500-p53 or WtAd5 were positive for E1A expression, however, normal BJ cells were negative for E1A expression when they were infected with CNHK500-p53, and positive only when they were infected with WtAd5, while E1B of CNHK500-p53 was only expressed under hypoxia condition in HepG2 and Hep3B, and expressed both under normal and hypoxia condition with WtAd5; **B**: ELISA assay showing that p53 protein secreted from a HepG2, infected with CNHK500-p53, was significantly higher than that infected with nonreplicative adenovirus Ad-p53 and Ad-Blank *in vitro* ($P < 0.05$); **C**: Western blot showing enhanced p53 expression in HepG2 infected with CNHK500-p53.

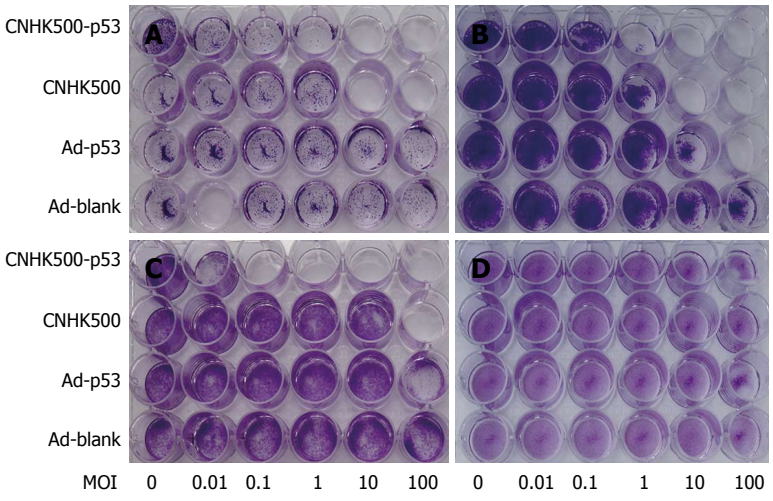

Figure 4 Cytopathic effects associated with CNHK500-p53, CNHK500, Ad-p53, and Ad-Blank infection in HCC cell lines HepG2 (**A**), Hep3B (**B**), Bel-7402 (**C**), and normal cell line BJ (**D**). Seven days after virus infection, all the cells were stained with crystal violet and photographed. Comparison with other viruses, CNHK500-p53 showed the strongest selective cytolysis against HCC cell lines. Infection with CNHK500-p53 at MOI of 0.1-1 was sufficient to induce its lytic effects in Bel-7402, HepG2, and Hep3B, although the sensitivity varied among the cell types. In contrast, no apparent cytopathic effects were observed in BJ even at MOI of 100 after CNHK500-p53 infection, which was similar to other viruses.

with CNHK500-p53 or Ad-p53 at a MOI of 1 on d 3, suggesting that the protein in the media was p53 protein (Figure 3C).

Selective cytolysis of CNHK500-p53

CPE was used to determine whether CNHK500-p53 infection induces selective cell lysis. HCC cell lines (HepG2, Hep3B, and Bel-7402) and the normal cell line (BJ) were infected with CNHK500-p53, CNHK500, Ad-p53, and Ad-Blank at various MOIs, fixed in methanol and stained with crystal violet 7 d after infection to visualize viable cells. CNHK500-p53 showed the strongest selective cytolysis effect among the viruses and killed all cancer cell lines in a dose-dependent fashion (Figure 4). Infection with CNHK500-p53 at a MOI of 0.1-1 was sufficient to induce its lytic effects, although the sensitivity varied among the cell types. In contrast, no apparent CPE was observed in BJ cells 7 d after CNHK500-p53 infection. Cytotoxicity of CNHK500-p53 was also assessed by MTT assay. HepG2, Hep3B and MRC-5, BJ cells were infected with CNHK500-p53 at various viral MOIs. As shown in Figure 5A, CNHK500-p53 induced more rapid cell death in HCC cells than in normal BJ cells 7 d after infection. Furthermore CNHK500-p53 showed a different ability to kill HepG2 and Bel-7402 with the IC_{50} being 0.012 and 0.28 of MOI. On the contrary, the IC_{50} in normal BJ cells was as high as 352.1 of MOI, suggesting that more than 29 341- or 1257-fold of CNHK500-p53 was needed to kill half BJ compared with HepG2 and Bel-7402. Comparison with CNHK500 and WAd5 infection, CNHK500-p53 not

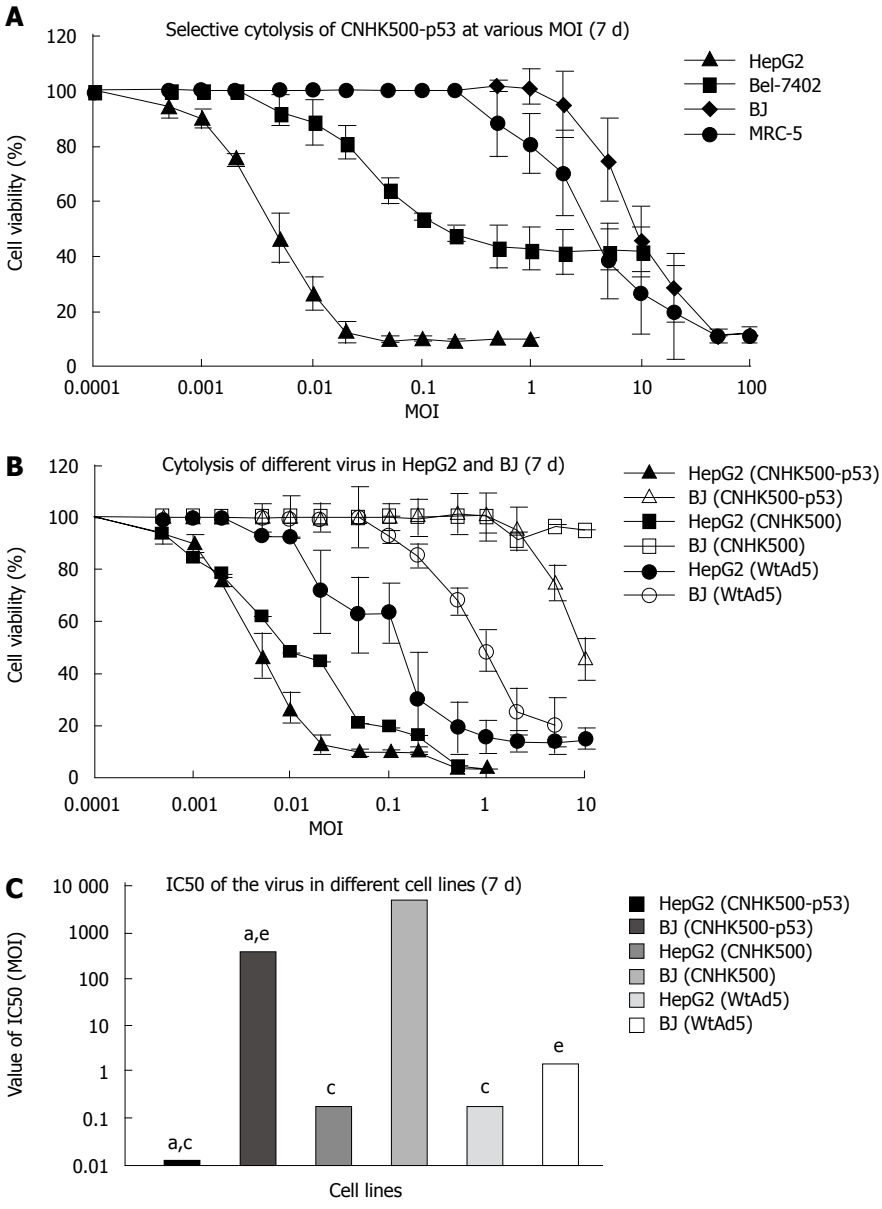

Figure 5 Oncolytic efficacy induced by CNHK500-p53 infection evaluated by MTT assay. Statistical analysis was performed using Student's *t* test for differences among groups. Statistical significance was defined as $P < 0.05$. **A**: HCC cell lines HepG2, Bel-7402 and normal cell lines BJ, MRC-5 were infected at different MOI of 0.001-100 pfu/cell of CNHK500-p53. Cell viability was measured by MTT assay 7 d after infection. CNHK500-p53 induced a more powerful oncolysis in HCC cell lines than in normal cell lines ($P < 0.05$); **B**: Seven days after infection with virus, CNHK500-p53 not only showed more powerful cytolysis than CNHK500 and WtAd5 in HepG2, but also less profound cytolysis than WtAd5 in BJ ($P < 0.05$); **C**: IC50 of CNHK500-p53, CNHk500, and WtAd5 demonstrated significant differences among groups with $^{a,c,e}P < 0.05$.

only demonstrated more apparent cytolysis against HepG2 than CNHK500 and WtAd5 but less profound cytotoxicity than WAd5 against BJ (Figure 5B and C).

Replication of gene-viral system and expression of GFP gene

To determine the selective replication of CNHK500-GFP, HCC cell lines including HepG2, Bel-7402 and normal cell line BJ were observed under fluorescent microscope at different time points after being infected with CNHK500-GFP and Ad-GFP. By conducting GFP expression, CNHK500-GFP demonstrated a greater replicative ability than Ad-GFP in HCC cell lines, with no significant difference in normal cell line. After 3, 7 and 10 d of infection with CNHK500-GFP and Ad-GFP, only a few scattered cells emitted fluorescence in normal cell line. However, in HCC cell lines, CPE such as deformation and aggregation appeared 3 d after infection, and the fluorescence emission spread from a single cell to many cells within a large area 7 d after infection. Bel-7402 cells were particularly sensitive to CNHK500-GFP, many cells died with GFP degradation and fluorescence extinction 10 d after infection (Figure 6), showing selective replication of CNHK500-derivative and correct insertion of GFP gene.

DISCUSSION

Besides conventional approaches, CRAds specifically killing tumor cells while sparing normal cells have been introduced as new agents for cancer therapy in the past decade[14,15]. The efficacy of CRAds against cancer, including HCC, is however, limited by several factors, mainly including tumor specificity and oncolysis[16].

With the advancement in molecular biology and understanding of the function of viral genes, it has become possible to genetically re-engineer viruses to make them selectively kill tumor cells over normal tissue. At present, tumor specificity has been achieved in oncolytic adenoviruses mainly (1) by altering viral genes that attenuate replication in normal tissue but not in tumor cells such as ONYX015 with E1B 55KD deleted[15],

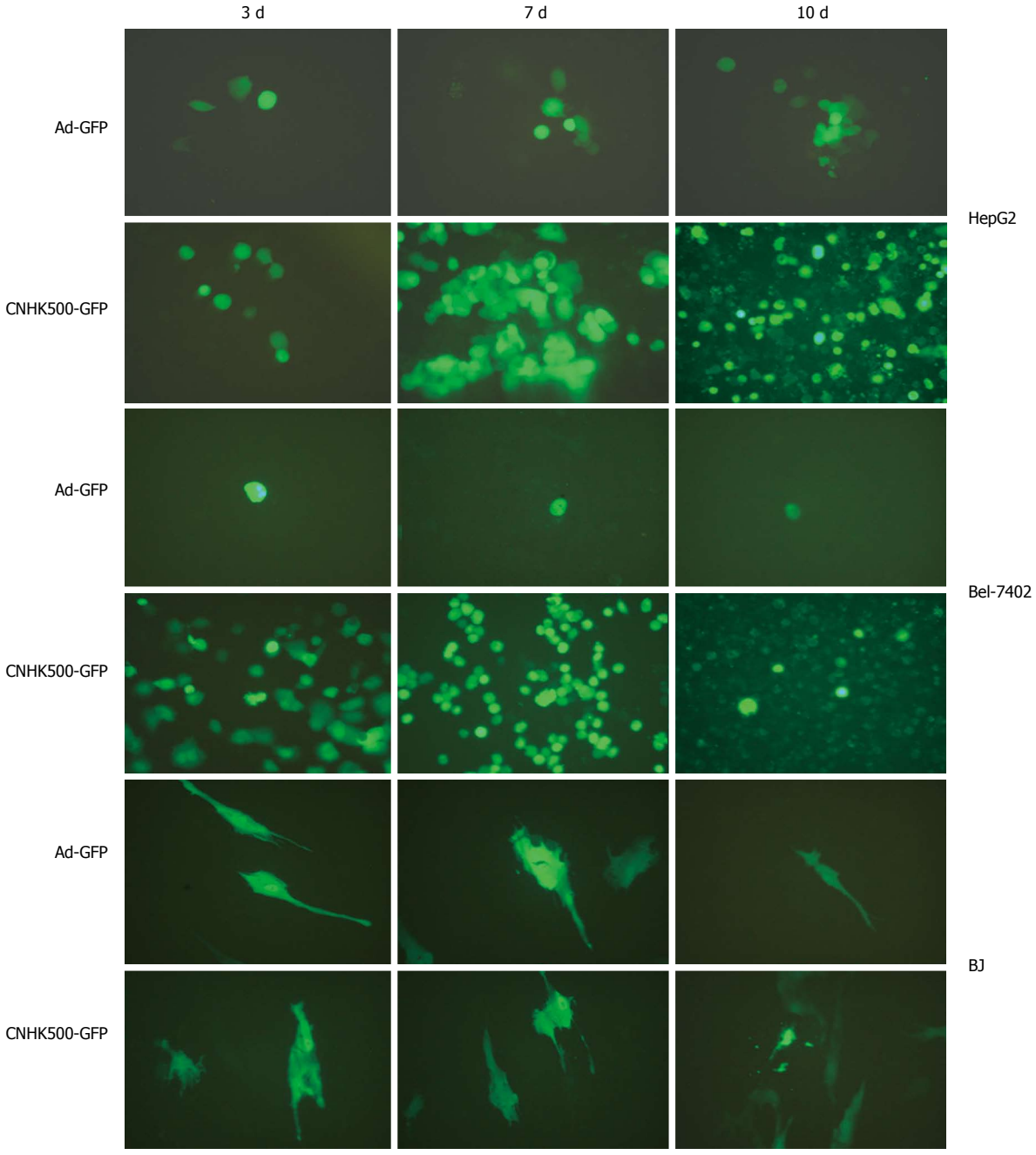

Figure 6 Fluorescent photos of HCC cell lines HepG2, Bel-7402 and normal cell line BJ infected with replicative virus CNHK500-GFP and nonreplicative virus Ad-GFP (200 magnifications).

(2) by placing viral genes that initiate viral replication under the control of promoter sequences that are active in tumor cells such as using AFP promoter to restrict viral replication in AFP-producing HCC[17,18], and (3) by modifing viral coat proteins that function in host cell infection.

Studies showed that adenovirus-induced oncolysis can benefit from combined gene therapy[11,19]. Cancer gene therapy typically involves delivery of tumor suppressor, enzyme/pro-drug gene, cytotoxic/pro-apoptotic gene, immunogene, anti-angiogenic gene directly into tumor cells[20]. After more than two decades of study, the tumor suppressor p53 gene is widely regarded as the "genome guardian." It has been estimated that at least half of all human malignancies, including HCC, are related to a mutation of the p53 gene[21].

In our previous study, we constructed a CRAd containing dual promoters within the E1 region, designated as CNHK500[12], in which the viral *E1*a gene is regulated by hTERT promoter and *E1*b gene by HRE promoter. Since telomerase is highly activated in most malignant tumors but inactive in normal somatic cells[22], CNHK500 can selectively replicate in telomerase-positive cancer cells. At the same time, its replication ability is further attenuated in normal cells as hypoxia microenvironment seldom exists among normal tissues. However, it may propagate very well in solid tumors because HRE promoter is transcriptally activated due to hypoxia, a unique feature

of human solid tumors[23]. A further study suggested that CNHK500 is tumor-selective *in vitro* and *vivo* when compared with CNHK300 and WtAd5[24]. To enhance the oncolytic potency of CNHK500, we constructed a new CRAd CNHK500-p53 by combining oncolytic virotherapy with gene therapy, which expresses functional p53 during viral replication in HCC cells as verified by PCR, Western blot, and ELISA assay. We evaluated the efficacy of CNHK500 and CNHK500-p53 against human HCC cell lines *in vitro*.

We found that exogenous expression of p53 by CNHK500-p53 could lead to enhanced oncolytic potency compared with its parent CNHK500 on most HCC cell lines, while the ability of selective replication was not significantly different between them. The superior efficacy of CNHK500-p53 was independent of the cellular p53 genetic background. It was reported that the expressed p53 gene appears to exert its anticancer activities by one or more of the following mechanisms: (1) simultaneously triggering apoptotic pathways in tumor cells by a transcription-dependent mechanism in cell nuclei[25,26] and by a transcription-independent mechanism in mitochondria[27] and Golgi apparatus[28]; (2) activating immune response factors such as natural killer cells[29] to exert "bystander effects"; (3) inhibiting DNA repair and antiapoptosis functions in tumor cells[30]; (4) down-regulating the expression of multidrug resistance genes[31] to revert the resistance of tumor cells against radio- and chemotherapies as well as the vascular endothelial growth factor gene[32] to block the blood supply to tumor tissue and matrix metalloproteinase[33] to suppress tumor cell adhesion, infiltration, and metastasis; (5) blocking the transcription of survival signals in tumor cells[34,35], thus inhibiting the growth of tumor cells in any stage of the cell cycle. Hence, dysfunctional p53 of HCC cells might delay conditionally replicative adenovirus-induced cell death, thus limiting conditionally replicative adenovirus efficacy.

In conclusion, CNHK500-p53 has the selective replicative ability in HCC cell lines and a higher oncolytic efficacy than its parent CNHK500 *in vitro*. The enhanced oncolytic efficacy may be related to the expression of p53 gene carried by CNHK500-p53. Further experiments are needed to warrant its potential therapeutic effect against HCC.

ACKNOWLEDGMENTS

We are grateful to Laboratory of Viral and Gene Therapy, Eastern Hepatobiliary Surgery Hospital, Second Military Medical University, Shanghai, China, for its help in constructing recombinant adenoviruses.

COMMENTS

Background

Hepatocellular carcinoma (HCC) is one of the most frequent and lethal malignancies worldwide especially in China. According to the reports of American cancer society (ACS) in 2005, the 5-year survival rate of HCC is only about 8.3%. Therefore, development of effective alternative approaches is needed. Replication-selective virus-mediated gene therapy holds great promise for the treatment of cancer, including HCC.

Research frontiers

So far, 656 cancer gene therapy clinical protocols are in different phase of evaluation worldwide. Unfortunately, successful delivery and targeted expression of therapeutic gene into cancer cells still are very difficult to achieve. The main problem is due to the very low *in vivo* transduction and expression efficacy of available vectors. In this respect, conditionally replicative adenoviruses appear as attractive vectors. Combination of oncolytic virotherapy and gene therapy may be an effective alternative approach against cancer.

Innovations and breakthroughs

In order to construct tumor-specific conditionally replicative adenoviruses, adenovirus E1A gene expression was driven by the hTERT promoter and E1B gene by the hypoxia response (HRE) promoter through genetic engineering, which assures adenovirus replication only in telomerase-positive cells exposed to hypoxia. Besides, human p53 gene was cloned into the downstream of E1A of adenovirus to enhance oncolysis. It was different from other study in adenovirus reconstruction methods. Meanwhile, the recombinant adenovirus was verified by PCR assay, and showed tumor-specific replication and enhanced oncolysis against HCC cell lines *in vitro*.

Applications

The results of our present study demonstrate that p53-expressing conditionally replicative adenovirus has the selectively replictive ability in HCC cell lines and a higher oncolytic efficacy than non-p53-expressing conditionally replicative adenovirus *in vitro*. The enhanced oncolytic efficacy may be related to the expression of p53 gene. Further experiments are needed to warrant its potential therapeutic effect against HCC.

Terminology

CRAds: conditional replicative adenoviruses, recombinant adenoviruses modified to selectively replicate in cancer cells; Oncolytic virotherapy: one of the cancer therapies by obtaining a virus that replicates and preferentially kills cancer cells, leaving the surrounding normal tissues relatively intact; Cancer gene therapy: Cancer gene therapy can be defined as transfer of nucleic acids into tumor or normal cells to eradicate or reduce tumor mass by direct killing of cells, immunomodulation or correction of genetic errors, and reversion of malignant status. Initially started with lots of optimism and enthusiasm, cancer gene therapy has shown limited success in treatment of patients.

Peer review

This is an interesting manuscript. In this manuscript, Hing-Chuan Zhao *et al* take advantage of the selective expression of hTERT and HIF in tumoral cells to express under their respective promoters E1A and E1B assuring adenovirus replication only in telomerase cancerous cells exposed to hypoxia. The data are clearly presented. They show the selective replication and expression of adenoviral proteins as well as the selective cytopathic effect of their adenovirus.

REFERENCES

1 **Thomas MB**, Abbruzzese JL. Opportunities for targeted therapies in hepatocellular carcinoma. *J Clin Oncol* 2005; **23**: 8093-8108
2 **Nemunaitis J**, Edelman J. Selectively replicating viral vectors. *Cancer Gene Ther* 2002; **9**: 987-1000
3 **Ring CJ**. Cytolytic viruses as potential anti-cancer agents. *J Gen Virol* 2002; **83**: 491-502
4 **Alemany R**, Balagué C, Curiel DT. Replicative adenoviruses for cancer therapy. *Nat Biotechnol* 2000; **18**: 723-727
5 **Heise C**, Kirn DH. Replication-selective adenoviruses as oncolytic agents. *J Clin Invest* 2000; **105**: 847-851
6 **Huang TG**, Savontaus MJ, Shinozaki K, Sauter BV, Woo SL. Telomerase-dependent oncolytic adenovirus for cancer treatment. *Gene Ther* 2003; **10**: 1241-1247
7 **Tahara H**, Nakanishi T, Kitamoto M, Nakashio R, Shay JW, Tahara E, Kajiyama G, Ide T. Telomerase activity in human liver tissues: comparison between chronic liver disease and hepatocellular carcinomas. *Cancer Res* 1995; **55**: 2734-2736
8 **Semenza GL**. Targeting HIF-1 for cancer therapy. *Nat Rev Cancer* 2003; **3**: 721-732

9 **Safran M**, Kaelin WG. HIF hydroxylation and the mammalian oxygen-sensing pathway. *J Clin Invest* 2003; **111**: 779-783
10 **Dix BR**, O'Carroll SJ, Myers CJ, Edwards SJ, Braithwaite AW. Efficient induction of cell death by adenoviruses requires binding of E1B55k and p53. *Cancer Res* 2000; **60**: 2666-2672
11 **van Beusechem VW**, van den Doel PB, Grill J, Pinedo HM, Gerritsen WR. Conditionally replicative adenovirus expressing p53 exhibits enhanced oncolytic potency. *Cancer Res* 2002; **62**: 6165-6171
12 **Qi Z**, Linhui P, Hongping W. Construction of CNHK500, a conditionally replicating adenovirus driven by the human telomerase reverse transcriptase promoter and hypoxia response promoter. *Zhonghua Shiyan Waike Zazhi* 2004; **21**: 1366-1368
13 **Ameyar M**, Shatrov V, Bouquet C, Capoulade C, Cai Z, Stancou R, Badie C, Haddada H, Chouaib S. Adenovirus-mediated transfer of wild-type p53 gene sensitizes TNF resistant MCF7 derivatives to the cytotoxic effect of this cytokine: relationship with c-myc and Rb. *Oncogene* 1999; **18**: 5464-5472
14 **Post DE**, Khuri FR, Simons JW, Van Meir EG. Replicative oncolytic adenoviruses in multimodal cancer regimens. *Hum Gene Ther* 2003; **14**: 933-946
15 **Bischoff JR**, Kirn DH, Williams A, Heise C, Horn S, Muna M, Ng L, Nye JA, Sampson-Johannes A, Fattaey A, McCormick F. An adenovirus mutant that replicates selectively in p53-deficient human tumor cells. *Science* 1996; **274**: 373-376
16 **Curiel DT**. The development of conditionally replicative adenoviruses for cancer therapy. *Clin Cancer Res* 2000; **6**: 3395-3399
17 **Sangro B**, Herraiz M, Prieto J. Gene therapy of neoplastic liver diseases. *Int J Biochem Cell Biol* 2003; **35**: 135-148
18 **Ohashi M**, Kanai F, Tateishi K, Taniguchi H, Marignani PA, Yoshida Y, Shiratori Y, Hamada H, Omata M. Target gene therapy for alpha-fetoprotein-producing hepatocellular carcinoma by E1B55k-attenuated adenovirus. *Biochem Biophys Res Commun* 2001; **282**: 529-535
19 **Zhang Q**, Nie M, Sham J, Su C, Xue H, Chua D, Wang W, Cui Z, Liu Y, Liu C, Jiang M, Fang G, Liu X, Wu M, Qian Q. Effective gene-viral therapy for telomerase-positive cancers by selective replicative-competent adenovirus combining with endostatin gene. *Cancer Res* 2004; **64**: 5390-5397
20 **Hernandez-Alcoceba R**, Sangro B, Prieto J. Gene therapy of liver cancer. *World J Gastroenterol* 2006; **12**: 6085-6097
21 **Shiraishi K**, Kato S, Han SY, Liu W, Otsuka K, Sakayori M, Ishida T, Takeda M, Kanamaru R, Ohuchi N, Ishioka C. Isolation of temperature-sensitive p53 mutations from a comprehensive missense mutation library. *J Biol Chem* 2004; **279**: 348-355
22 **Shay JW**, Wright WE. Telomeres and telomerase: implications for cancer and aging. *Radiat Res* 2001; **155**: 188-193
23 **Binley K**, Askham Z, Martin L, Spearman H, Day D, Kingsman S, Naylor S. Hypoxia-mediated tumour targeting. *Gene Ther* 2003; **10**: 540-549
24 **Su CQ**, Sham J, Xue HB, Wang XH, Chua D, Cui ZF, Peng LH, Li LF, Jiang LH, Wu MC, Qian QJ. Potent antitumoral efficacy of a novel replicative adenovirus CNHK300 targeting telomerase-positive cancer cells. *J Cancer Res Clin Oncol* 2004; **130**: 591-603
25 **Matsuda K**, Yoshida K, Taya Y, Nakamura K, Nakamura Y, Arakawa H. p53AIP1 regulates the mitochondrial apoptotic pathway. *Cancer Res* 2002; **62**: 2883-2889
26 **Taha TA**, Osta W, Kozhaya L, Bielawski J, Johnson KR, Gillanders WE, Dbaibo GS, Hannun YA, Obeid LM. Down-regulation of sphingosine kinase-1 by DNA damage: dependence on proteases and p53. *J Biol Chem* 2004; **279**: 20546-20554
27 **Chipuk JE**, Kuwana T, Bouchier-Hayes L, Droin NM, Newmeyer DD, Schuler M, Green DR. Direct activation of Bax by p53 mediates mitochondrial membrane permeabilization and apoptosis. *Science* 2004; **303**: 1010-1014
28 **Bennett M**, Macdonald K, Chan SW, Luzio JP, Simari R, Weissberg P. Cell surface trafficking of Fas: a rapid mechanism of p53-mediated apoptosis. *Science* 1998; **282**: 290-293
29 **Rosenblum MD**, Olasz E, Woodliff JE, Johnson BD, Konkol MC, Gerber KA, Orentas RJ, Sandford G, Truitt RL. CD200 is a novel p53-target gene involved in apoptosis-associated immune tolerance. *Blood* 2004; **103**: 2691-2698
30 **Sah NK**, Munshi A, Nishikawa T, Mukhopadhyay T, Roth JA, Meyn RE. Adenovirus-mediated wild-type p53 radiosensitizes human tumor cells by suppressing DNA repair capacity. *Mol Cancer Ther* 2003; **2**: 1223-1231
31 **Krishna R**, Mayer LD. Multidrug resistance (MDR) in cancer. Mechanisms, reversal using modulators of MDR and the role of MDR modulators in influencing the pharmacokinetics of anticancer drugs. *Eur J Pharm Sci* 2000; **11**: 265-283
32 **Pal S**, Datta K, Mukhopadhyay D. Central role of p53 on regulation of vascular permeability factor/vascular endothelial growth factor (VPF/VEGF) expression in mammary carcinoma. *Cancer Res* 2001; **61**: 6952-6957
33 **Ala-aho R**, Grénman R, Seth P, Kähäri VM. Adenoviral delivery of p53 gene suppresses expression of collagenase-3 (MMP-13) in squamous carcinoma cells. *Oncogene* 2002; **21**: 1187-1195
34 **Yin Y**, Liu YX, Jin YJ, Hall EJ, Barrett JC. PAC1 phosphatase is a transcription target of p53 in signalling apoptosis and growth suppression. *Nature* 2003; **422**: 527-531
35 **Rother K**, Johne C, Spiesbach K, Haugwitz U, Tschöp K, Wasner M, Klein-Hitpass L, Möröy T, Mössner J, Engeland K. Identification of Tcf-4 as a transcriptional target of p53 signalling. *Oncogene* 2004; **23**: 3376-3384

S- Editor Liu Y **L- Editor** Wang XL **E- Editor** Liu WF

PO Box 2345, Beijing 100023, China
www.wjgnet.com
wjg@wjgnet.com

World J Gastroenterol 2007 February 7; 13(5): 692-698
World Journal of Gastroenterology ISSN 1007-9327

COLORECTAL CANCER

Early apoptosis and cell death induced by ATX-S10Na (Ⅱ)-mediated photodynamic therapy are Bax- and p53-dependent in human colon cancer cells

Makoto Mitsunaga, Akihito Tsubota, Kohichi Nariai, Yoshihisa Namiki, Makoto Sumi, Tetsuya Yoshikawa, Kiyotaka Fujise

Makoto Mitsunaga, Akihito Tsubota, Kohichi Nariai, Yoshihisa Namiki, Makoto Sumi, Tetsuya Yoshikawa, Kiyotaka Fujise, Institute of Clinical Medicine and Research, Jikei University School of Medicine, Kashiwa, Chiba, Japan
Makoto Mitsunaga, Kiyotaka Fujise, Division of Gastroenterology and Hepatology, Department of Internal Medicine, Jikei University School of Medicine, Tokyo, Japan
Supported by a grant from the Jikei University School of Medicine
Correspondence to: Makoto Mitsunaga, MD, Institute of Clinical Medicine and Research, Jikei University School of Medicine, 163-1 Kashiwa-shita, Kashiwa, Chiba 277-8567, Japan. mit@jikei.ac.jp
Telephone: +81-4-71641111 Fax: +81-4-71668638
Received: 2006-10-20 Accepted: 2006-12-20

Abstract

AIM: To investigate the roles of Bax and p53 proteins in photosensitivity of human colon cancer cells by using lysosome-localizing photosensitizer, ATX-S10Na (Ⅱ).

METHODS: HCT116 human colon cancer cells and Bax-null or p53-null isogenic derivatives were irradiated with a diode laser. Early apoptosis and cell death in response to photodynamic therapy were determined by MTT assays, annexin V assays, transmission electron microscopy assays, caspase assays and western blotting.

RESULTS: Induction of early apoptosis and cell death was Bax- and p53-dependent. Bax and p53 were required for caspase-dependent apoptosis. The levels of anti-apoptotic Bcl-2 family proteins, Bcl-2 and Bcl-x_L, were decreased in Bax- and p53-independent manner.

CONCLUSION: Our results indicate that early apoptosis and cell death of human colon cancer cells induced by photodynamic therapy with lysosome-localizing photosensitizer ATX-S10Na (Ⅱ) are mediated by p53-Bax network and low levels of Bcl-2 and Bcl-x_L proteins. Our results might help in formulating new therapeutic approaches in photodynamic therapy.

Key words: Photodynamic therapy; ATX-S10Na (Ⅱ); Apoptosis; Bax; p53

Mitsunaga M, Tsubota A, Nariai K, Namiki Y, Sumi M, Yoshikawa T, Fujise K. Early apoptosis and cell death induced by ATX-S10Na (Ⅱ)-mediated photodynamic therapy are Bax- and p53-dependent in human colon cancer cells. *World J Gastroenterol* 2007; 13(5): 692-698

http://www.wjgnet.com/1007-9327/13/692.asp

INTRODUCTION

Photodynamic therapy (PDT) is a therapeutic procedure involving the use of tissue-penetrating laser light after the administration of tumor-localizing photosensitizers, and is used for the efficient treatment of a variety of solid and superficial cancers[1]. Tumor cell death in response to PDT is induced *via* apoptosis and/or necrosis, and depends on various conditions, such as tumor cell type, intensity of laser irradiation, and subcellular localization and concentration of the photosensitizer[2-4]. Localizing photosensitizers in cytoplasmic organelles generate reactive oxygen species by photochemical reactions, resulting in induction of cell damage[1,5,6]. Cell damage modes and the initial subcellular targets are related to the localization sites of the photosensitizers, specifically, mitochondria and lysosomes[7]. Mitochondria-localizing photosensitizers, such as silicon phthalocyanine (Pc) 4, cause rapid dissipation of the mitochondrial membrane potential and result in the release of cytochrome *c*[8]. In contrast, the hydrophilic chlorine photosensitizer ATX-S10Na (Ⅱ), localizes mainly in lysosomes[9,10] and activates apoptotic pathways *via* mitochondrial destabilization following the photodamage of lysosomes[11]. Lysosomal proteases released by lysosomal photodamage, in turn activate caspases directly and/or indirectly subsequent to mitochondrial damage[12]. Nonetheless, the mechanisms by which lysosome-localizing photosensitizers activate apoptotic pathways are not fully understood.

Members of the p53 tumor suppressor gene family play various roles in response to DNA damage, such as cell cycle regulation, DNA repair, and induction of apoptosis[13,14]. Expression of the wild-type p53 induced by chemotherapy or radiation increases the sensitivity to apoptosis, whereas a mutated or deleted p53 alters the sensitivity[15]. Furthermore, p53 regulates pro-apoptotic Bcl-2 family proteins[16,17], and these proteins localize to mitochondria and heterodimerize through a BH3 domain with anti-apoptotic Bcl-2 family members, such as

Bcl-xL[18,19]. Bax modulates the mitochondrial pathway of apoptosis by allowing the efflux of apoptogenic proteins. The shift in the balance of the pro-apoptotic and anti-apoptotic Bcl-2 family members regulates the translocation of cytochrome *c* from mitochondria to cytosol[20]. Although various studies indicate the involvement of Bax and p53 in PDT-mediated apoptosis[21-24], there are conflicting reports about whether the induction of apoptosis correlates with cell death.

The aim of the present study was to elucidate the roles of Bax and p53 in response to lysosomal photodamage induced by ATX-S10Na (Ⅱ)-PDT, which might contribute to more effective clinical use of PDT in cancer therapy. We used an established human colon cancer cell line, HCT116, which expresses wild-type Bax and p53, and derivative lines of HCT116 that differ from the parental line by virtue of a selective knockout of either Bax or p53[25,26].

MATERIALS AND METHODS

Reagents

ATX-S10Na (Ⅱ), 13, 17-bis (1-carboxypropionyl) carbamoylethyl-8-ethenyl-2-hydroxy-3-hydroxyiminoethylidene-2, 7, 12, 18-tetramethylporphyrin sodium salt was provided by Photochemical Co. (Okayama, Japan), and was dissolved in phosphate-buffered saline (PBS).

Cell cultures

Bax-null or p53-null derivatives of the wild-type HCT116 cell line, generated by targeted homologous recombination to create homozygous deletion, were a generous gift from B. Vogelstein (Johns Hopkins Oncology Center, Baltimore, MD, USA)[27,28]. Cells were maintained in McCoy's 5A medium (GIBCO-BRL, Bethesda, MD, USA) supplemented with 10% fetal calf serum (Thermo Trace, Melbourne, Australia) and 1% penicillin/streptomycin (GIBCO-BRL) in a 37℃, 5% CO_2, fully humidified incubator and passaged twice weekly.

PDT protocols

Exponentially growing cells were seeded in 96-well microplates or 35-mm dishes to approximately 30% confluence 48 h before PDT. ATX-S10Na (Ⅱ) was added to the culture medium to a final concentration of 20 μg/mL 24 h before PDT. Medium was replaced with fresh medium, and the cells were irradiated with a diode laser (Hamamatsu Photonics, Hamamatsu, Japan) at a wavelength of 670 nm. The energy fluence rate was 0.167 W/m^2 as measured using LaserMate power meter (Coherent, Auburn, CA, USA). Exposure for 5 min resulted in an incident energy fluence of 5 J/cm^2.

MTT assays

Cytotoxicity of PDT was determined by colorimetric assay with 2-(2-methoxy-4-nitrophenyl)-3-(4-nitrophenyl)-5-(2, 4-disulfophenyl)-2H-tetrazolium, monosodium salt reagent (Cell Counting Kit-8, Wako Pure Chemical Industries, Osaka, Japan). Following PDT, cells were incubated in 96-well microplates for 24 h. Ten microliters of Cell Counting Kit-8 reagent[27] were added to each well, and cells were incubated at 37℃ for 4 h. After thorough mixing, the absorbance of each well was measured at 450 nm with an Ultramark microplate reader (Bio-Rad Laboratories, Hercules, CA, USA).

Annexin V assays

Cells were collected by trypsinization and washed with ice-cold PBS, suspended in 500 μL annexin V binding buffer containing 5 μL of propidium iodide (PI) and 5 μL of annexin V-FITC (BioVision, Mountain View, CA, USA), and incubated for 15 min at room temperature in the dark. Fluorescence was measured on a BD LSR flow cytometer (Becton Dickinson, NY, USA) and processed with Cell Quest software (Becton Dickinson) for analysis.

Cell cycle analysis

Cells were collected and washed in cold PBS, fixed in 70% ethanol pre-chilled at -20℃, washed, resuspended in 25 μg/mL of PI with 100 μg/mL RNase A, and incubated for 30 min at 37℃. Fluorescence was measured on a BD LSR flow cytometer. Data were analyzed using the MODFIT 2.0 program (Verity Software).

Transmission electron microscopy assays

Ultrastructural appearances of apoptotic cells were confirmed by electron microscopy. Following PDT, cells were prefixed with 2% glutaraldehyde, post-fixed with 1% osmic acid, dehydrated in graded ethanol, embedded in resin, and cut into sections on an ultramicrotome. The cells were examined by a transmission electron microscope (TEM) (H-7500, Hitachi, Tokyo, Japan).

Quantification of caspases 3, 8 and 9 activity

Activities of caspases 3, 8 and 9 were measured by Caspase Fluorometric Assay kits (R&D Systems Inc., Minneapolis, MN, USA) according to the instructions provided by the manufacturer. Briefly, cells in 35-mm dishes were washed twice with ice-cold PBS and lysed in 100 μL of lysis buffer. Next, 50 μL of cell lysates were transferred to a 96-well plate containing reaction buffer, and were incubated for 2 h at 37℃ with 5 μL of caspase 3-, 8- or 9-specific fluorescent substrate DEVD-AFC, IETD-AFC and LEHD-AFC, respectively. Plates were read with an ARVOsx-2 fluorescence microplate reader (Wallac, Turku, Finland) using an excitation light of 400 nm and an emission light of 505 nm.

Preparation of protein extracts and immunoblotting

Cells in 35-mm dishes were washed twice with ice-cold PBS, lysed in 100 μL of lysis buffer [50 mmol/L HEPES (pH 7.4), 1% Triton X-100, 0.5% sodium deoxycholate, 150 mmol/L sodium chloride, 5 mmol/L EDTA with protease inhibitors pepstatin A (2 μg/mL), aprotinin (10 μg/mL), leupeptin (10 μg/mL) and phenylmethylsulfonyl fluoride (100 μg/mL)] and sonicated. The lysates were centrifuged at 10000 × *g* at 4℃ for 10 min. The supernatant was recovered and protein concentration was determined by the BCA protein assay (Pierce, Rockford, IL, USA). Twenty microgram of proteins were loaded on an SDS-polyacrylamide gel. After electrophoresis, proteins were electrotransferred onto a nitrocellulose membrane (Bio-Rad). Membranes were blocked with 5% nonfat milk

in Tris-buffered saline with 0.05% Tween-20 (TBS-T) for 2 h at room temperature, and then probed with primary antibodies for 1 h at room temperature or overnight at 4℃. Horseradish peroxidase (HRP)-labeled secondary antibodies were used for signal detection and blots were visualized with Enhanced Chemiluminescence (ECL) Western blotting detection reagents (Amersham Pharmacia Biotech, Piscataway, NJ, USA) and recorded on an X-ray film. For cytosolic fractionation, cells were harvested in digitonin lysis buffer (75 mmol/L NaCl, 1 mmol/L NaH_2PO_4, 8 mmol/L Na_2HPO_4, 250 mmol/L sucrose and 190 μg/mL of digitonin), supplemented with protease inhibitors, and incubated on ice for 5 min. Samples were centrifuged at 10000 × *g* at 4℃ for 30 min and the resulting supernatant was used for Western blotting. Antibodies were as follows: mouse monoclonal p53 (DO-1) (Calbiochem, San Diego, CA, USA), mouse monoclonal Bcl-2 (100) and rabbit polyclonal Bax (N-20), Bcl-x$_{S/L}$ (S-18) and β-tubulin (H-235) (Santa Cruz Biotechnology, Santa Cruz, CA, USA), mouse monoclonal cytochrome *c* (7H8.2C12) (BD Pharmingen, San Diego, CA, USA), and HRP-labeled secondary anti-mouse and anti-rabbit antibodies (Santa Cruz). The image of the specific protein band on the membrane was scanned, and the intensity of the image was analyzed by an NIH Image J program version 1.31.

Statistical analysis

Data are expressed as mean ± SD. Differences between groups were evaluated by *t*-test. *P* values < 0.05 were considered statistically significant.

RESULTS

Bax- and p53-dependent cell death and apoptosis in response to ATX-S10Na (Ⅱ)-PDT

To determine the role of Bax and p53 in ATX-S10Na (Ⅱ)-PDT, we first examined the cells' phototoxicity by MTT assays 24 h after laser irradiation. The extent of ATX-S10Na (Ⅱ) phototoxicity was dependent on the intensity of laser irradiation (Figure 1A) and the concentration of ATX-S10Na (Ⅱ) (data not shown). Wild-type HCT116 cells were significantly more sensitive to ATX-S10Na (Ⅱ)-PDT than Bax-null or p53-null cells at 5 J/cm^2 (Figure 1A). Laser irradiation greater than 10 J/cm^2 resulted in global phototoxic cell death, thereby preventing the accumulation of cells with PDT-mediated regulatory responses. Thus, laser irradiation at 5 J/cm^2 was chosen for further studies. Next, to determine the role of early apoptosis in Bax and p53 dependence of phototoxicity, we examined ATX-S10Na (Ⅱ)-PDT-mediated apoptosis by flow cytometry with annexin V and cell cycle analysis that determines a population of cells with sub-G_1 DNA content 3 or 6 h after laser irradiation. The percentage of early apoptotic, annexin V-positive and PI-negative, cells was significantly reduced in Bax-null or p53-null cells compared with wild-type HCT116 cells (Figures 1B and D). In contrast, the percentage of late apoptotic or necrotic, annexin V-positive and PI-positive, cells was not significantly different (Figure 1C). These results indicate that Bax and p53 play a central role in early apoptosis induced by ATX-S10Na (Ⅱ)-PDT. TEM studies revealed that untreated cells have thickened mitochondria and numerous cytoplasmic vesicles. In contrast, when treated with PDT, the sections contained many apoptotic cells with condensed chromatin, apoptotic bodies in the cytoplasm and cell membrane budding (Figure 1E). The percentage of apoptotic cells was higher in the wild-type than Bax-null or p53-null cells 6 h after laser irradiation.

Roles of Bax and p53 in caspase-dependent ATX-S10Na (Ⅱ)-PDT-induced apoptosis

Since caspases are early effectors for triggering PDT-mediated apoptosis[28,29], we examined the roles of Bax and p53 in caspase activation by ATX-S10Na (Ⅱ)-PDT. Caspase-3 activity increased in intensity in laser irradiation- and time-dependent manners within 24 h following PDT in wild-type HCT116 cells (data not shown). As shown in Figure 2, activities of caspase-3 and -9 apparently increased in wild-type HCT116 cells 6 h after laser irradiation. In contrast, it was significantly inhibited in Bax-null or p53-null cells. These results indicate that the caspase-dependent apoptotic process induced by ATX-S10Na (Ⅱ)-PDT was Bax- and p53-dependent. Activation of caspase-8 was slightly increased compared with caspase-9, indicating that the mitochondrial pathway of apoptosis is the major process in response to ATX-S10Na (Ⅱ)-PDT. In Bax-null HCT116 cells, caspase-9 activity was significantly but not completely inhibited, and the protein level of cytochrome *c* released from mitochondria was reduced but not absent (Figure 3), indicating that the mitochondrial pathway of apoptosis is induced by ATX-S10Na (Ⅱ)-PDT, even though Bax was absent. In p53-null cells, caspase-9 activity was slightly inhibited, and the protein level of cytochrome *c* released from mitochondria was not reduced (Figure 3), indicating that p53 is required for ATX-S10Na (Ⅱ)-PDT-mediated apoptosis.

Decreased levels of anti-apoptotic proteins Bcl-2 and Bcl-x$_L$ in response to ATX-S10Na (Ⅱ)-PDT play a role in early apoptosis, and are Bax- and p53-independent

Previous studies indicated that the levels of anti-apoptotic proteins Bcl-2 and Bcl-x$_L$ were reduced and pro-apoptotic proteins Bcl-x$_S$, Bak and Bad, but not Bid, were up-regulated in response to PDT[30-33]. Therefore, we determined the association of Bax and p53 with anti-apoptotic Bcl-2 family proteins in ATX-S10Na (Ⅱ)-PDT. Immunoblots demonstrated no significant changes in Bax and p53 expression (Figure 3). In contrast, Bcl-2 and Bcl-x$_L$ expression were decreased to similar levels in each cell type, indicating that Bax- and p53-independent downregulation of Bcl-2 and Bcl-x$_L$ plays a role in early apoptosis induced by ATX-S10Na (Ⅱ)-PDT.

DISCUSSION

Many studies have shown that PDT kills tumor cells *via* apoptosis and/or necrosis *in vivo* and *in vitro*. Although cell death in response to PDT depends on various conditions, the role of Bax or p53 in PDT remains controversial. This study was designed to determine the role of these proteins in ATX-S10Na (Ⅱ)-PDT by using an isogenic set

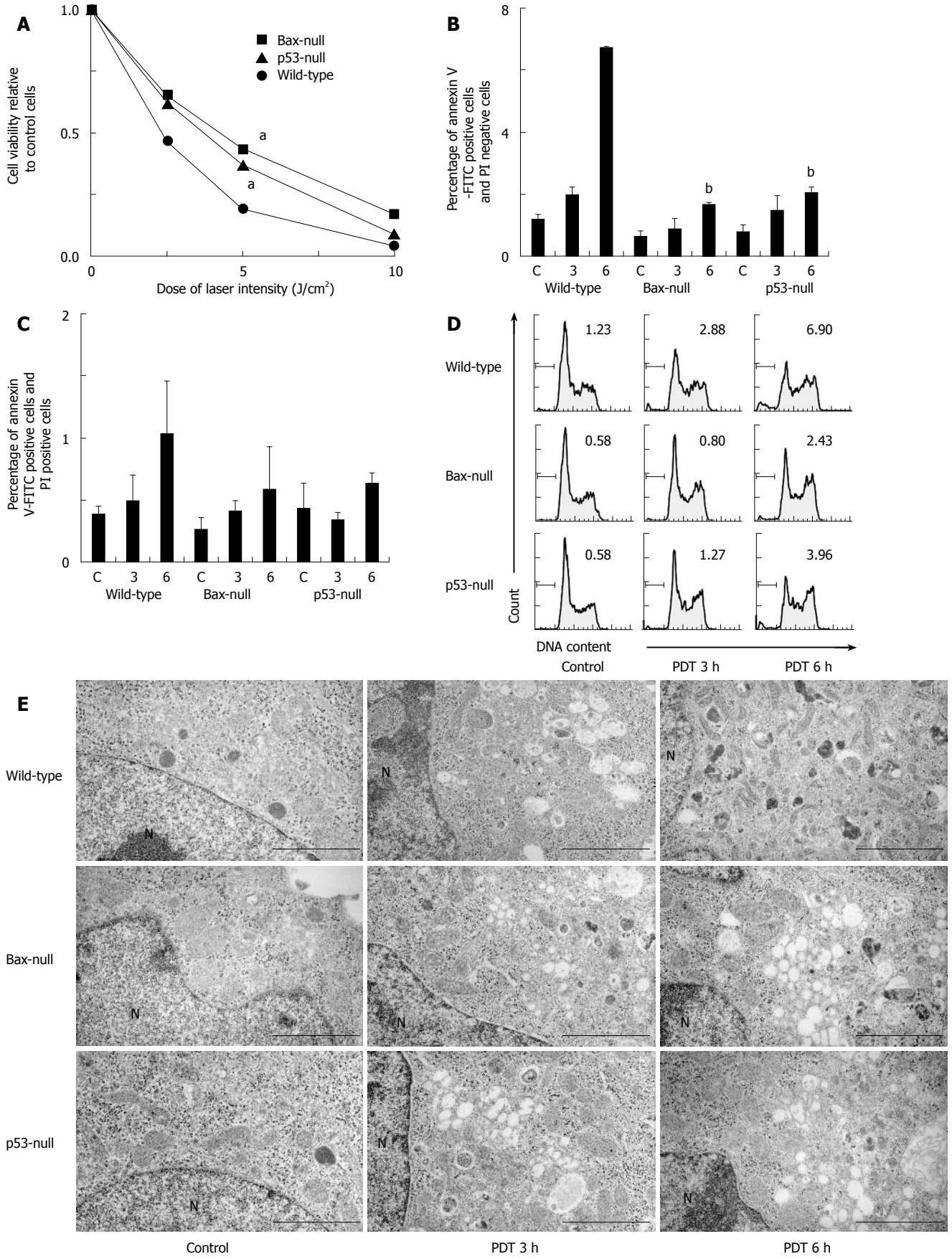

Figure 1 ATX-S10Na(Ⅱ)-PDT-mediated cell death and early apoptosis were Bax- and p53-dependent. Cells were treated with, or without, ATX-S10Na(Ⅱ)-PDT and harvested at each indicated time point following irradiation. **A**: Phototoxicity was determined by MTT assay 24 h after laser irradiation. Data are expressed as a ratio of cell viability relative to untreated control cells. Data represent the mean ± SD of three independent experiments ($^aP < 0.05$ *vs* wild-type cells). **B**, **C**: Early apoptotic changes (**B**) and late apoptotic or necrotic changes (**C**) were determined by annexin V apoptosis assays at 3 or 6 h after laser irradiation. Data are expressed as a percentage of annexin V-positive and PI-negative (**B**) or annexin V-positive and PI-positive cells (**C**). Data represent the mean ± SD of three independent experiments ($^bP < 0.05$ *vs* wild-type cells). **D**: Cell cycle distributions were determined by flow cytometry at 3 or 6 h after laser irradiation. Data are expressed as a percentage of sub-G_1 fraction. **E**: Morphological changes in response to ATX-S10Na(Ⅱ)-PDT were determined by transmission electron microscopy assays at 3 or 6 h following laser irradiation. Typical subcellular changes in response to PDT are shown (original magnification × 12 000). Scale bar: 15 μm, N: nuclei.

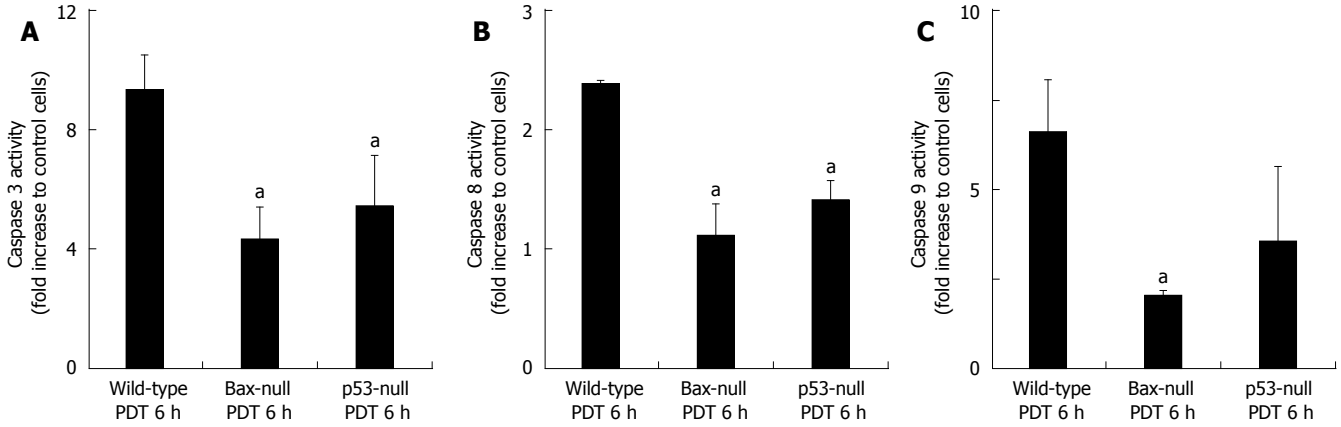

Figure 2 Induction of apoptosis by ATX-S10Na (Ⅱ)-PDT was caspase-dependent. Cells were treated with, or without, ATX-S10Na (Ⅱ)-PDT, harvested and lysed at 6 h after laser irradiation. Induction of caspase activity was assayed. **A**: caspase-3; **B**: caspase-8; **C**: caspase-9. Data represent the mean ± SD of three independent experiments ($^aP < 0.05$ *vs* wild-type cells).

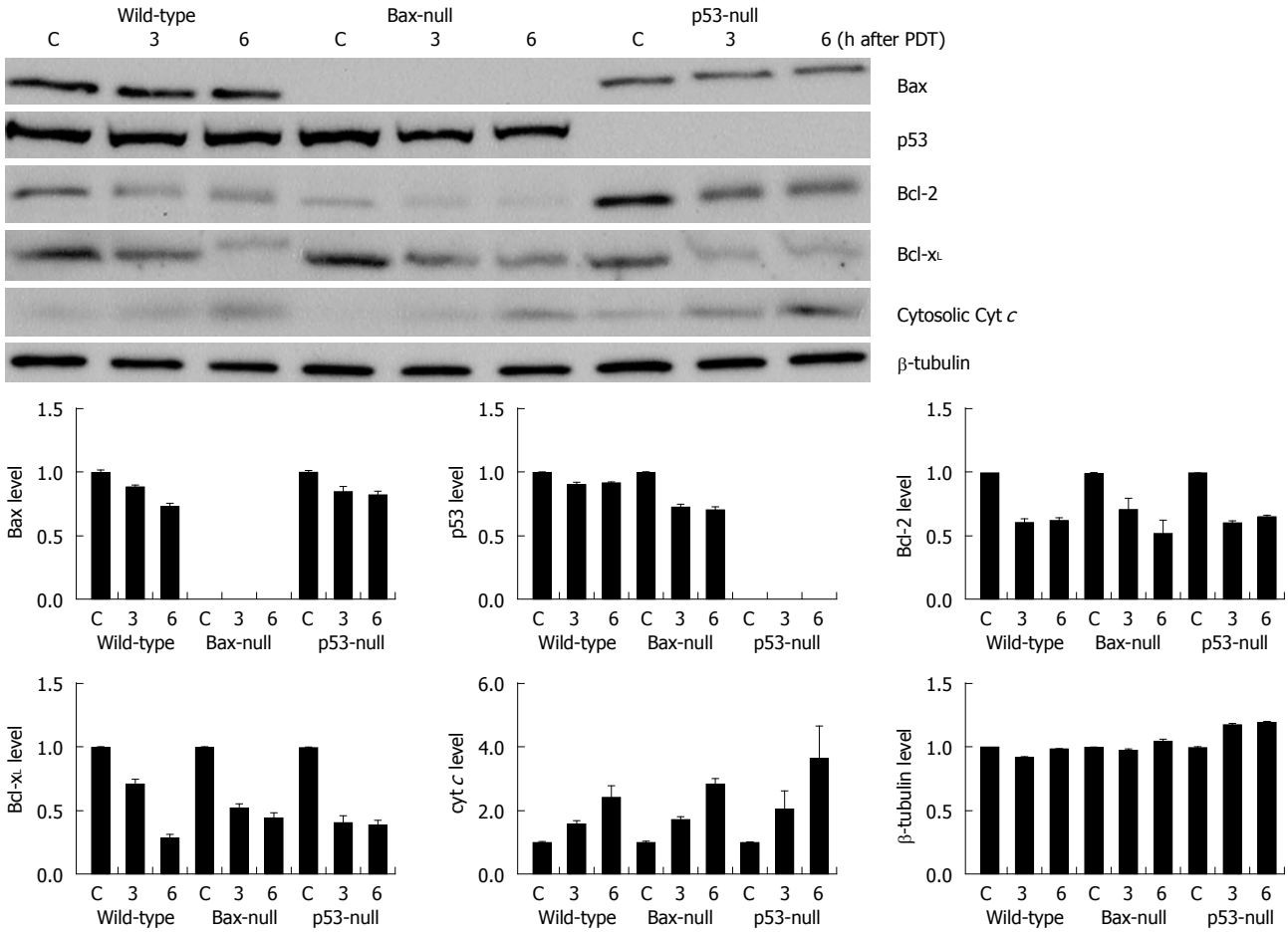

Figure 3 Low levels of Bcl-2 and Bcl-xL played a role in ATX-S10Na(Ⅱ)-PDT. Cells were treated with, or without, ATX-S10Na(Ⅱ)-PDT, harvested and lysed at 3 or 6 h after laser irradiation. Western blot analysis was performed. Each protein level was quantified by using NIH Image J program. Data represent the mean ± SD of three independent experiments.

of human colon cancer cell lines derived from HCT116. Our results indicated that ATX-S10Na (Ⅱ)-PDT induced Bax- and p53-dependent cell death and early apoptosis of human colon cancer cells. ATX-S10Na (Ⅱ)-PDT induced caspase-dependent apoptosis and reduced the levels of anti-apoptotic proteins Bcl-2 and Bcl-xL. Apoptosis was mediated mainly through a Bax-regulated mitochondrial pathway. Taken together, these results suggest that Bax and p53 play a central role in inducing early apoptosis and cell death by ATX-S10Na (Ⅱ)-PDT.

Various experiments have shown that the pro-apoptotic Bcl-2 family protein Bax plays a role in the mitochondrial pathway of apoptosis by translocating from the cytosol to the mitochondria[20]. Our present experiments revealed that

wild-type HCT116 cells were significantly more sensitive to ATX-S10Na (Ⅱ)-PDT than Bax-null cells, as determined by MTT assays (Figure 1). Induction of early apoptosis by ATX-S10Na (Ⅱ)-PDT was also Bax-dependent, as determined by the annexin V assay and cell cycle analysis (Figure 1). Bax was required for caspase activation and cytochrome *c* release, but the mitochondrial pathway of apoptosis was not completely inhibited in the absence of Bax (Figures 2 and 3). The protein level of Bax did not apparently change in the wild-type or p53-null cells (Figure 3). These findings suggest that Bax plays a central role in PDT-mediated cell death and the mitochondrial pathway of apoptosis. As Bax was a major mediator of p53-dependent apoptosis, early apoptosis was apparently processed without Bax activation. Contrary to our findings, earlier reports showed that DU-145 human prostate cancer cells that lack Bax expression do not show release of cytochrome *c* from mitochondria, loss of mitochondrial potential, caspase activation or apoptosis, but do have an altered sensitivity to overall cell death[24]. In contrast, a comparison of the PDT response of wild-type and Bax-null HCT116 human colon cancer cells showed reduced release of cytochrome *c* but it was not completely blocked in Bax-null cells. In both cell lines, caspase-dependent apoptosis was triggered and cell killing was equally sensitive; however, no significant differences in the activation of caspase-3 were found[34]. The authors concluded that the commitment to cell death after PDT occurs at a step prior to and irrespective of Bax activation. Differences between our results and the above findings may be due to cellular differences unrelated to Bax expression, intensity of laser irradiation or type of photosensitizer.

The tumor suppressor protein p53 plays an important role in response to various stress conditions[13,14]. Our present experiments revealed that wild-type HCT116 cells were significantly more sensitive to ATX-S10Na (Ⅱ)-PDT (Figure 1). In addition, induction of early apoptosis by ATX-S10Na (Ⅱ)-PDT was p53-dependent (Figure 1). p53 was required for caspase-3 activation (Figure 2). The mitochondrial pathway of apoptosis was not significantly inhibited in the absence of p53 (Figures 2 and 3). These findings suggest that p53 might play a role in PDT-mediated early apoptosis and cell death. Consistent with our findings, HL60 human promyelocytic leukemia cells that express wild-type p53 are more photosensitive than p53-deleted or mutated HL60 cells[21]. Introduction of the wild-type p53 gene into the HT29 colon cancer cells induced growth arrest but not cell death by PDT[23]. In non-isogenic colon carcinoma cell lines, increased photosensitivity of a wild-type p53 phenotype was observed compared with a mutated p53 phenotype[22]. Taken together, it is conceivable that Bax and p53 play central roles both, in cell death and in early apoptosis induced by ATX-S10Na (Ⅱ)-PDT.

The ratio of pro-apoptotic to anti-apoptotic Bcl-2 family members helps determine the threshold for inducing mitochondrial-related apoptosis[20]. Overexpression of Bcl-2 in Chinese hamster ovary (CHO) cells inhibited apoptosis and partly protected against cell death induced by PDT[35]. Reduction of Bcl-2 protein levels by Bcl-2 antisense oligonucleotides in radiation-induced fibrosarcoma (RIF-1) cells resulted in sensitization to PDT-mediated apoptotic death[31]. Our experiments revealed that decreased levels of Bcl-2 and Bcl-xL were Bax- or p53-independent in response to ATX-S10Na (Ⅱ)-PDT. Cytochrome *c* release from mitochondria was not completely inhibited in the absence of Bax or p53 (Figure 3). These findings suggest that reduced levels of anti-apoptotic Bcl-2 family proteins, that are Bax- or p53-independent, played a role in cytochrome *c* release and apoptosis induced by ATX-S10Na (Ⅱ)-PDT. Low levels of these proteins could be the result of caspase activation or photochemical targets of PDT. PDT using mitochondrial photosensitizer phthalocyanine Pc 4, directly damaged Bcl-2 and Bcl-xL, and contributed in the induction of apoptosis[33,36].

In conclusion, Bax and p53 play a central role in the apoptotic process and cell death induced by ATX-S10Na (Ⅱ)-PDT in human colon cancer cells. Low levels of anti-apoptotic Bcl-2 family proteins Bcl-2 and Bcl-xL, which are Bax- and/or p53-independent, play a role in the early apoptotic process. Bax and p53 can induce apoptosis and cell death in response to ATX-S10Na (Ⅱ)-PDT, which might help in the design of new therapeutic approaches.

ACKNOWLEDGMENTS

We thank Yoko Yumoto, Yuko Arai and Eiko Uga for technical help, Hisako Arai and Hiroyuki Sasaki for TEM analysis, Hisao Tajiri for critical reading of the manuscript, Bert Vogelstein for providing the HCT116 cell lines and Photochemical Co. for providing ATX-S10Na (Ⅱ).

REFERENCES

1 **Dougherty TJ**, Gomer CJ, Henderson BW, Jori G, Kessel D, Korbelik M, Moan J, Peng Q. Photodynamic therapy. *J Natl Cancer Inst* 1998; **90**: 889-905
2 **Agarwal ML**, Clay ME, Harvey EJ, Evans HH, Antunez AR, Oleinick NL. Photodynamic therapy induces rapid cell death by apoptosis in L5178Y mouse lymphoma cells. *Cancer Res* 1991; **51**: 5993-5996
3 **He XY**, Sikes RA, Thomsen S, Chung LW, Jacques SL. Photodynamic therapy with photofrin II induces programmed cell death in carcinoma cell lines. *Photochem Photobiol* 1994; **59**: 468-473
4 **Luo Y**, Chang CK, Kessel D. Rapid initiation of apoptosis by photodynamic therapy. *Photochem Photobiol* 1996; **63**: 528-534
5 **Oleinick NL**, Evans HH. The photobiology of photodynamic therapy: cellular targets and mechanisms. *Radiat Res* 1998; **150**: S146-S156
6 **Oleinick NL**, Morris RL, Belichenko I. The role of apoptosis in response to photodynamic therapy: what, where, why, and how. *Photochem Photobiol Sci* 2002; **1**: 1-21
7 **Peng Q**, Moan J, Nesland JM. Correlation of subcellular and intratumoral photosensitizer localization with ultrastructural features after photodynamic therapy. *Ultrastruct Pathol* 1996; **20**: 109-129
8 **Chiu SM**, Oleinick NL. Dissociation of mitochondrial depolarization from cytochrome c release during apoptosis induced by photodynamic therapy. *Br J Cancer* 2001; **84**: 1099-1106
9 **Nakajima S**, Sakata I, Takemura T, Maeda T, Hayashi H, Kubo Y. Tumor localizing and photosensitization of photochlorin ATX-S10. In: Spinelli S, Fante D, Marchesanin R. Photodynamic therapy and biomedical lasers. Amsterdam: Elsevier Science, 1992: 531-534
10 **Mori M**, Kuroda T, Obana A, Sakata I, Hirano T, Nakajima S, Hikida M, Kumagai T. In vitro plasma protein binding and cellular uptake of ATX-S10(Na), a hydrophilic chlorin photosensitizer. *Jpn J Cancer Res* 2000; **91**: 845-852
11 **Nagata S**, Obana A, Gohto Y, Nakajima S. Necrotic and

apoptotic cell death of human malignant melanoma cells following photodynamic therapy using an amphiphilic photosensitizer, ATX-S10(Na). *Lasers Surg Med* 2003; **33**: 64-70
12 **Reiners JJ**, Caruso JA, Mathieu P, Chelladurai B, Yin XM, Kessel D. Release of cytochrome c and activation of pro-caspase-9 following lysosomal photodamage involves Bid cleavage. *Cell Death Differ* 2002; **9**: 934-944
13 **el-Deiry WS**. Regulation of p53 downstream genes. *Semin Cancer Biol* 1998; **8**: 345-357
14 **Bunz F**, Hwang PM, Torrance C, Waldman T, Zhang Y, Dillehay L, Williams J, Lengauer C, Kinzler KW, Vogelstein B. Disruption of p53 in human cancer cells alters the responses to therapeutic agents. *J Clin Invest* 1999; **104**: 263-269
15 **Lowe SW**, Bodis S, McClatchey A, Remington L, Ruley HE, Fisher DE, Housman DE, Jacks T. p53 status and the efficacy of cancer therapy in vivo. *Science* 1994; **266**: 807-810
16 **Yin XM**, Oltvai ZN, Korsmeyer SJ. BH1 and BH2 domains of Bcl-2 are required for inhibition of apoptosis and heterodimerization with Bax. *Nature* 1994; **369**: 321-323
17 **Korsmeyer SJ**. BCL-2 gene family and the regulation of programmed cell death. *Cancer Res* 1999; **59**: 1693s-1700s
18 **Zha J**, Harada H, Osipov K, Jockel J, Waksman G, Korsmeyer SJ. BH3 domain of BAD is required for heterodimerization with BCL-XL and pro-apoptotic activity. *J Biol Chem* 1997; **272**: 24101-24104
19 **Lutz RJ**. Role of the BH3 (Bcl-2 homology 3) domain in the regulation of apoptosis and Bcl-2-related proteins. *Biochem Soc Trans* 2000; **28**: 51-56
20 **Tsujimoto Y**. Role of Bcl-2 family proteins in apoptosis: apoptosomes or mitochondria? *Genes Cells* 1998; **3**: 697-707
21 **Fisher AM**, Danenberg K, Banerjee D, Bertino JR, Danenberg P, Gomer CJ. Increased photosensitivity in HL60 cells expressing wild-type p53. *Photochem Photobiol* 1997; **66**: 265-270
22 **Fisher AM**, Rucker N, Wong S, Gomer CJ. Differential photosensitivity in wild-type and mutant p53 human colon carcinoma cell lines. *J Photochem Photobiol B* 1998; **42**: 104-107
23 **Zhang WG**, Li XW, Ma LP, Wang SW, Yang HY, Zhang ZY. Wild-type p53 protein potentiates phototoxicity of 2-BA-2-DMHA in HT29 cells expressing endogenous mutant p53. *Cancer Lett* 1999; **138**: 189-195
24 **Chiu SM**, Xue LY, Usuda J, Azizuddin K, Oleinick NL. Bax is essential for mitochondrion-mediated apoptosis but not for cell death caused by photodynamic therapy. *Br J Cancer* 2003; **89**: 1590-1597
25 **Bunz F**, Dutriaux A, Lengauer C, Waldman T, Zhou S, Brown JP, Sedivy JM, Kinzler KW, Vogelstein B. Requirement for p53 and p21 to sustain G2 arrest after DNA damage. *Science* 1998; **282**: 1497-1501
26 **Zhang L**, Yu J, Park BH, Kinzler KW, Vogelstein B. Role of BAX in the apoptotic response to anticancer agents. *Science* 2000; **290**: 989-992
27 **Ishiyama M**, Miyazono Y, Sasamoto K, Ohkura Y, Uedo K. A highly water-soluble disulfonated tetrazolium salt as a chromogenic indicator for NADH as well as cell viability. *Talanta* 1997; **44**: 1299-1305
28 **Kessel D**, Luo Y. Photodynamic therapy: a mitochondrial inducer of apoptosis. *Cell Death Differ* 1999; **6**: 28-35
29 **Lam M**, Oleinick NL, Nieminen AL. Photodynamic therapy-induced apoptosis in epidermoid carcinoma cells. Reactive oxygen species and mitochondrial inner membrane permeabilization. *J Biol Chem* 2001; **276**: 47379-47386
30 **Kessel D**, Castelli M. Evidence that bcl-2 is the target of three photosensitizers that induce a rapid apoptotic response. *Photochem Photobiol* 2001; **74**: 318-322
31 **Srivastava M**, Ahmad N, Gupta S, Mukhtar H. Involvement of Bcl-2 and Bax in photodynamic therapy-mediated apoptosis. Antisense Bcl-2 oligonucleotide sensitizes RIF 1 cells to photodynamic therapy apoptosis. *J Biol Chem* 2001; **276**: 15481-15488
32 **Kessel D**, Castelli M, Reiners JJ. Apoptotic response to photodynamic therapy versus the Bcl-2 antagonist HA14-1. *Photochem Photobiol* 2002; **76**: 314-319
33 **Xue LY**, Chiu SM, Fiebig A, Andrews DW, Oleinick NL. Photodamage to multiple Bcl-xL isoforms by photodynamic therapy with the phthalocyanine photosensitizer Pc 4. *Oncogene* 2003; **22**: 9197-9204
34 **Chiu SM**, Xue LY, Azizuddin K, Oleinick NL. Photodynamic therapy-induced death of HCT 116 cells: Apoptosis with or without Bax expression. *Apoptosis* 2005; **10**: 1357-1368
35 **He J**, Agarwal ML, Larkin HE, Friedman LR, Xue LY, Oleinick NL. The induction of partial resistance to photodynamic therapy by the protooncogene BCL-2. *Photochem Photobiol* 1996; **64**: 845-852
36 **Xue LY**, Chiu SM, Oleinick NL. Photochemical destruction of the Bcl-2 oncoprotein during photodynamic therapy with the phthalocyanine photosensitizer Pc 4. *Oncogene* 2001; **20**: 3420-3427

S- Editor Liu Y **L- Editor** Lakatos PL **E- Editor** Liu WF

PO Box 2345, Beijing 100023, China
www.wjgnet.com
wjg@wjgnet.com

World J Gastroenterol 2007 February 7; 13(5): 699-708
World Journal of Gastroenterology ISSN 1007-9327

Survey of molecular profiling during human colon cancer development and progression by immunohistochemical staining on tissue microarray

Wei-Chang Chen, Mao-Song Lin, Bao-Feng Zhang, Jing Fang, Qiong Zhou, Ying Hu, Heng-Jun Gao

Wei-Chang Chen, Department of Gastroenterology, the First Affiliated Hospital, Soochow University, Suzhou 215006, Jiangsu Province, China
Mao-Song Lin, Department of Gastroenterology, Taizhou People's Hospital, Taizhou 225300, Jiangsu Province, China
Bao-Feng Zhang, Jing Fang, Qiong Zhou, Ying Hu, Heng-Jun Gao, National Engineering Center for Biochip at Shanghai, Shanghai 201203, China
Supported by grant from the National 863 Project about Functional Genomic and Biochip, No. 2002AA2Z2021; and 135 Medical Important Talent Foundation of Jiangsu Province, No. 37RC2002037
Correspondence to: Dr. Wei-Chang Chen, Department of Gastroenterology, the First Affiliated Hospital of Soochow University, Suzhou 215006, Jiangsu Province, China. weichangchen@126.com
Telephone: +86-512-65223637-8374 Fax: +86-512-65228072
Received: 2006-09-28 Accepted: 2006-12-14

Abstract

AIM: To explore the molecular events taking place during human colon cancer development and progression through high-throughput tissue microarray analysis.

METHODS: We constructed two separate tissue microarrays containing 1.0 mm or 1.5 mm cylindrical samples acquired from 112 formalin-fixed and paraffin-embedded blocks, including carcinomas (n = 85), adenomatous polyps (n = 18), as well as normal para-cancerous colon tissues (n = 9). Immunohistochemical staining was applied to the analysis of the consecutive tissue microarray sections with antibodies for 11 different proteins, including p53, p21, bcl-2, bax, cyclin D1, PTEN, p-Akt1, β-catenin, c-myc, nm23-h1 and Cox-2.

RESULTS: The protein expressions of p53, bcl-2, bax, cyclin D1, β-catenin, c-myc, Cox-2 and nm23-h1 varied significantly among tissues from cancer, adenomatous polyps and normal colon mucosa (P = 0.003, P = 0.001, P = 0.000, P = 0.000, P = 0.034, P = 0.003, P = 0.002, and P = 0.007, respectively). Chi-square analysis showed that the statistically significant variables were p53, p21, bax, β-catenin, c-myc, PTEN, p-Akt1, Cox-2 and nm23-h1 for histological grade (P = 0.005, P = 0.013, P = 0.044, P = 0.000, P = 0.000, P = 0.029, P = 0.000, P = 0.008, and P = 0.000, respectively), β-catenin, c-myc and p-Akt1 for lymph node metastasis (P = 0.011, P = 0.005, and P = 0.032, respectively), β-catenin, c-myc, Cox-2 and nm23-h1 for distance metastasis (P = 0.020, P = 0.000, P = 0.026, and P = 0.008, respectively), and cyclin D1, β-catenin, c-myc, Cox-2 and nm23h1 for clinical stages (P = 0.038, P = 0.008, P = 0.000, P = 0.016, and P = 0.014, respectively).

CONCLUSION: Tissue microarray immunohistochemical staining enables high-throughput analysis of genetic alterations contributing to human colon cancer development and progression. Our results implicate the potential roles of p53, cyclin D1, bcl-2, bax, Cox-2, β-catenin and c-myc in development of human colon cancer and that of bcl-2, nm23-h1, PTEN and p-Akt1 in progression of human colon cancer.

Key words: Colon cancer; Immunohistochemistry; Tissue microarray

Chen WC, Lin MS, Zhang BF, Fang J, Zhou Q, Hu Y, Gao HJ. Survey of molecular profiling during human colon cancer development and progression by immunohistochemical staining on tissue microarray. *World J Gastroenterol* 2007; 13(5): 699-708

http://www.wjgnet.com/1007-9327/13/699.asp

INTRODUCTION

Colorectal cancer (CRC) is one of the most frequent cancers in the Western world. At present time, with the development of living conditions and changes of life behaviors, CRC has become more and more frequent in China. The prognosis in advanced cases is poor, and more than one-third of the patients will die from progressive disease because the overall survival is about 40% (15%-65%) after 5 years[1]. The development and progression of CRC, like others cancers, are results of multiple genetic alterations, so investigation of molecular changes in tumors representing the entire disease spectrum may enhance our understanding of mechanism involved in CRC tumorigenesis. Because CRC is one of the first major epithelial cancers in which molecular alterations were

described to occur in a systematic fashion during disease progression, studies of single molecular markers have not been successful in defining the biology of this disease[2]. This has prompted investigators to explore multiple molecules regulating the tumorigenesis in an effort to identify biologically aggressive tumors and appropriately select patients for adjuvant systemic or targeted therapies. However, with the progression of molecular biology and the development of oncogene research, the cancer-related genes and genetic alterations have been found rapidly. The evaluation of the clinical utility of each of these genes would require multiple consecutive experiments with hundreds of tumors. This would be both time-consuming and labor-intensive.

As a new biological technique which allows rapid visualization of molecular targets in thousands of tissues specimens at a time, either at the DNA, RNA, or protein level, tissue microarray (TMA) can facilitate rapid translation of molecular discoveries to clinical applications[3]. So it brings us a high-throughput and rapid technique which can help us complete the time- and people-consuming work. Here, we constructed two tissue microarrays containing samples from different stages of human colon cancer, adenomatous polyps and corresponding normal para-cancerous colon tissues to survey the gene alterations that may contribute to clinical behaviors of the colon cancer. We decided to investigate the role of protein expressions which had been shown correlated with the development and progression as well as metastases of colon cancer in previous studies. In this study, 11 different proteins (p53, p21, cyclin D1, bcl-2, bax, β-catenin, c-myc, PTEN p-Akt1, Cox-2 and nm23-h1) expressions were assayed by using immunohistochemical (IHC) staining to consecutive formalin-fixed tissue microarray sections. The aim was to obtain a comprehensive survey of the frequency of the target molecular alterations and the relationship between the alterations and the clinicopathological features in human colon cancer.

A number of proteins have been associated with human carcinogenesis and may be relevant to CRC. Among these molecules, we chose 11 cancer-related genes (p53, p21, cyclin D1, bcl-2, bax, β-catenin, c-myc, PTEN p-Akt1, Cox-2 and nm23-h1) which are altered during the development and progression of CRC according to the previous study reports[4-11]. Among these molecules, p53, p21, cyclin D1, bcl-2 and bax play pivotal roles in cell cycle regulation and apoptosis. Akt/protein kinase B (PKB), which is included in phosphatidyl inositol-3-OH kinase (PI3K) signaling, controls many intracellular processes, such as the suppression of apoptosis and the promotion of the cell cycle[12]. PTEN on 10q23.3 encodes a dual-specificity phosphatase that negatively regulates the phosphoinositol-3-kinase/Akt pathway and mediates cell-cycle arrest and apoptosis[13,14]. β-catenin is a member of the cadherin-catenin complex that mediates homotypic cell-cell adhesion[15]. It also plays a role in the *Wnt* signaling pathway through regulating target genes like *c-myc*. Cox-2 was elevated in human colon cancers, and the Cox-2 inhibitor, celecoxib, inhibited intestinal tumor multiplicity in a mouse model and reduced the number of adenomatous polyps in a familial adenomatous polyposis patient[16,17]. The human *nm23* gene, a candidate metastatic suppressor gene, consists of two genes, *nm23-h1* and *nm23-h2*. *Nm23-h1* aberration has been shown to be correlated with the metastatic potential of colorectal cancer in some studies[9,18]. More of these molecules were studied previously by conventional pathological or molecular biological technologies and the numbers of selected target molecules were lesser, but in this study we would assay 11 proteins at a time by IHC staining on TMA.

Many investigators and clinicians consider cancer of the colon and rectum to be two distinct diseases, thus, we chose to evaluate only the patients with colon cancer treated with surgery alone in an effort to optimize the homogeneity of the study population. In addition, all the tumor specimens selected according our data were from sporadic colon cancer patients.

MATERIALS AND METHODS

Materials

Demographic and clinical data were collected retrospectively. None of the patients received radiotherapy or chemotherapy before surgery. Formalin-fixed and paraffin-embedded tumors, adenomatous polyps and para-cancerous tissues specimens were from the archives of the Department of Gastroenterology, the First Affiliated Hospital of Soochow University and National Engineering Center for Biochip at Shanghai. All specimens were viewed by one pathologist (Jing Fang). The specimens that were interpretable for IHC included: (1) Eighty-five cancers including different grades, such as high (n = 11), moderate (n = 50), low differentiated (n = 24); (2) eighteen adenomatous polyps removed at colonoscopy; (3) nine para-cancerous colon tissues resected from colon tissues at least 5 cm apart from the corresponding cancer tissues.

Construction and sectioning of tissue microarray

The colon cancer microarray was constructed as previously described[3]. Briefly, fresh sections were cut from the donor block and stained with hematoxylin-eosin (HE), these slides were used to guide the samplings from morphologically representative regions of the tissues. A tissue array instrument (Beecher Instruments, Silver Spring, MD) was used to create holes in a recipient paraffin block and to acquire tissue cores from the donor block by a thin-walled needle with an inner diameter of 1.0 mm or 1.5 mm, held in an X-Y precision guide. The cylindrical samples were retrieved from the selected regions in the donors and extruded directly into the recipient blocks with defined array coordinates. After the construction of the array block, multiple 4-μm thick sections were cut with a microtom using an adhesive-coated tape sectioning system (Instrumedics, Hackensack, NJ) (Figure 1).

Tissue loss was a significant factor for tissue array-based analysis with previously reported rates of tissue damage ranging from 15% to 33%[19-21]. In our analysis the rates of lost cases attributable to tissue damage were less than 5% for the different markers and damaged tissues

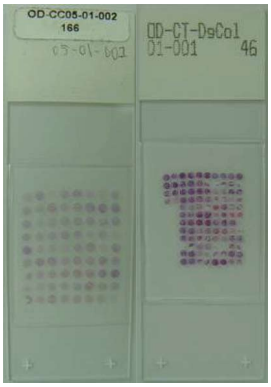

Figure 1 HE staining of 4-μm thick section of the tissue microarray.

were excluded from clinicopathological analyses of the respective markers.

IHC on formalin-fixed tissue microarray sections

IHC staining for the target genes to sections of the formalin-fixed samples on the tissue microarray was carried out by using the Envision ready-to-use methods. Slides were deparaffinized in xylene and rehydrated through graded concentrations of ethanol to distilled water, and endogenous peroxidase activity was blocked by incubation with 30 mL/L H_2O_2 in methanol for 10 min at room temperature. Then sections were submitted to antigen retrieval in a pressure cooker containing 0.01 mmol/L natrium citricium buffer for 10 min. Slides were subsequently incubated in 100 mL/L normal goat serum for 20 min at room temperature. Sections were permeabilized in PBS-Triton and incubated overnight with primary antibody at 4℃. The antibodies were used in PBS-Triton with variable dilution. Mouse anti-human monoclonal antibodies to p53 (clone Do-7; 1:50 dilution; Beijing Zhongshan Golden Bridge Biotechnology Co. Ltd.), p21 (clone DCS-60.2; 1:50 dilution; Beijing Zhongshan Golden Bridge Biotechnology Co. Ltd.), bcl-2 (clone 100/D5; 1:50 dilution; Shanghai Chang-Do Biotechnology Co. Ltd), bax (clone 2D2; 1:50; Beijing Zhongshan Golden Bridge Biotechnology Co. Ltd), β-catenin (clone CAT-5H10; 1:50 dilution; Beijing Zhongshan Golden Bridge Biotechnology Co. Ltd), c-myc (clone 9E11; 1:50 dilution; Shanghai Chang-Do Biotechnology Co. Ltd), Cox-2 (clone COX229; 1:50 dilution; Beijing Zhongshan Golden Bridge Biotechnology Co. Ltd), nm23-h1 (1:50 dilution; Shanghai Chang-Do Biotechnology Co. Ltd) and rabbit anti-human antibody to PTEN (FL-403; 1:100 dilution; Santa Cruz Biotechnology Inc, USA), p-Akt1 (1:50 dilution; Upstate, USA), cyclin D1 (clone SP4; 1:50 dilution; Shanghai Chang-Do Biotechnology Co. Ltd) were used. Each section was then incubated with Envision^{+TM}, peroxidase, mouse or rabbit (GeneTech) for 30 min. Finally, the sections were reacted with 0.02% 3, 3'-diaminoberzidine and 0.005% H_2O_2 in 0.05 mmol/L Tris-Hcl buffer and counterstained by hematoxylin.

The evaluation of the immunohistochemical staining was performed independently by two authors without knowledge of the clinicopathological information. P53, p21 and cyclin D1 immunoreactivities were observed in the nuclei of the cells, while bcl-2, bax, PTEN, p-Akt1, c-myc, Cox-2 and nm23-h1 in the cytoplasm. Only the immunoreactivity in the nucleus or cytoplasm of β-catenin was seemed as positive. The immunoreactive scores besides β-catenin and c-myc were determined by the sum of extension and intensity as reported previously[22] and were modified for some markers according to clinicopathological correlations. The intensity of the staining was scored using the following scale: 0, no staining of the tumor cells; +, mild staining; ++, moderate staining; and +++, marked staining. The area of staining was evaluated and recorded as a percentage: 0, less than 5%; +, 5%-25%; ++, 26%-50%; 3+, 51%-75%; and ++++, more than 75%. The combined score was recorded and graded as follows: -, 0-1; +, 2; ++, 3-5; +++, 6-7. More than 10% of the cancer cells showing elevated β-catenin labeling in the cytoplasm was recorded as positive expression. According to the immunostaining of c-myc in our study, we considered less than 40% cells expressed c-myc as negative.

Statistical analysis

Computerized statistical analyses were performed using the Statistical Package for the Social Sciences (SPSS), version 13.0. Clinical and histopathologic information and the results from the immunohistochemical studies of the tissue microarray were entered into a database. The variances of molecular expressions among different tissues and associations between molecular variables and clinicopathological data were analyzed with χ^2 test, but when the numbers of the cells in crosstables which had expected count less than 5 exceeded 25% or the minimum expected counts were less than 1, the Fisher's exact test was used. The relations among these molecules were analyzed by Spearman's bivariates correlation test. In all statistical analyses, a two-tailed P value $\leqslant$ 0.05 was considered statistically significant.

RESULTS

Clinicopathological data

Complete histological and clinical data of the patients were collected from patients' records. The median age for the study population was 58 years (range, 30-86 years). There were 24 patients with median age less than 58 years. There was a male predominance in the cancer patients (male: female ratio = 48:37). Thirty-two patients had positive lymph node metastasis, whereas 53 had negative. Fourteen patients had distant metastasis, and 71 had no distant metastasis. The clinical stages of these patients were strictly identified as A (n = 15), B (n = 33), C (n = 23) and D (n = 14) according to Dukes stage. After the second diagnostic assessment, there were 24 low, 50 moderately and 11 high differentiated tissues in these cancer tissue blocks according to the histological grades, while 18 tissues were diagnosed as adenomatous polyps and 9 were normal colon mucosa epithelium tissues.

Expression of p53, p21, cyclin D1, bcl-2 and bax

Owing to the short half-life of p53 protein, and its low expression levels in normal cells, wild-type p53 levels cannot be detected by IHC. In cancer cells, most p53 mutations lead to products that accumulate in the nuclei and can easily be detected by IHC. Positive immunostaining most

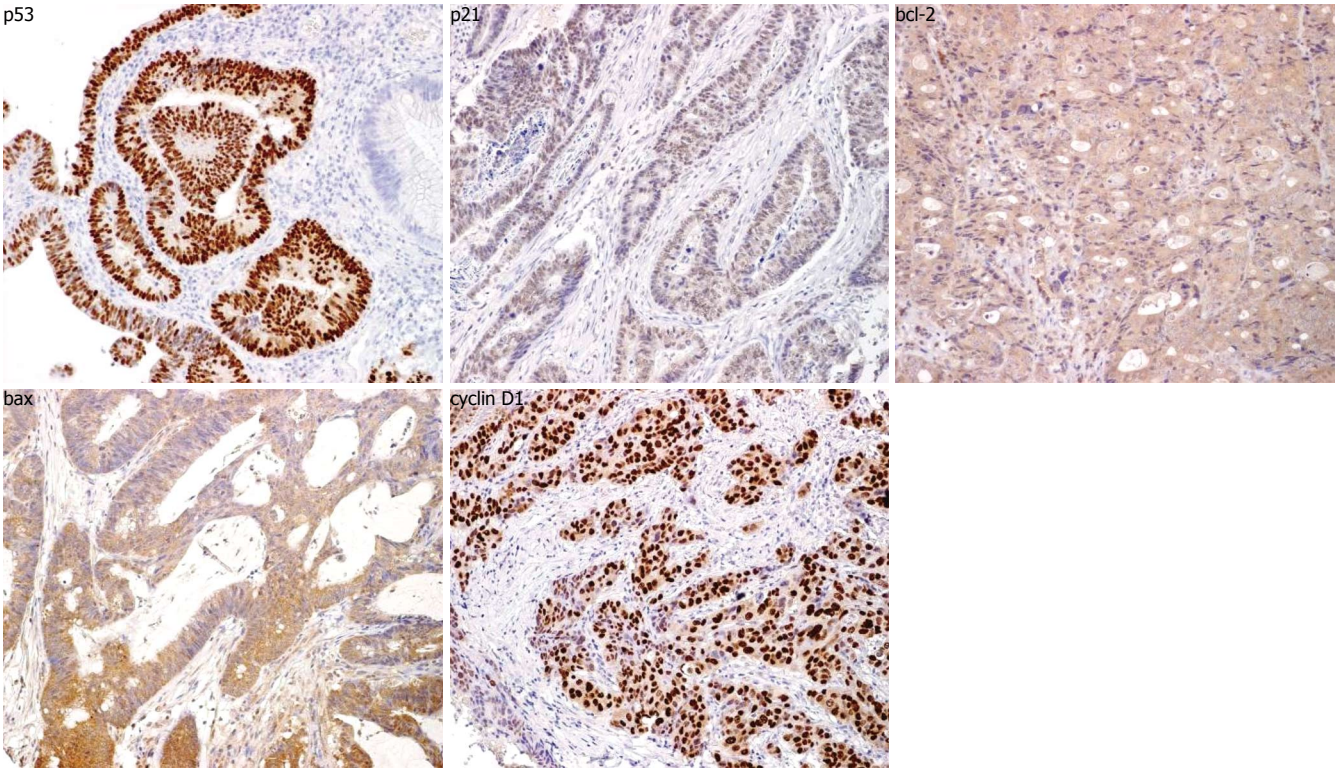

Figure 2 Immunophenotype of the investigated antigens (p53, p21, cyclin D1, bcl-2 and bax) in colon cancer (original magnification x 200). Positive stainings of p53, p21 and cyclin D1 were located in the cell nuclei, while those of bcl-2 and bax were in the cytoplasm.

Table 1 Comparison of IHC results (p53, p21, cyclin D1, bcl-2 and bax) among varying tissues

Groups	*n*	p53				*P*	p21				*P*	Cyclin D1				*P*	bcl-2				*P*	bax				*P*
		-	+	++	+++		-	+	++	+++		-	+	++	+++		-	+	++	+++		-	+	++	+++	
Cancer	85	39	6	19	21		19	9	28	26		17	16	30	22		5	1	46	32		21	9	39	16	
Adenomas	18	15	2	1	0	0.003[2]	8	5	4	1	0.000[1]	3	7	8	0	0.000[1]	1	1	7	8	0.001[2]	0	0	9	9	0.000[1]
Benign tissue	9	9	0	0	0		9	0	0	0		8	1	0	0		2	3	3	0		0	1	1	7	
Total	112	63	8	20	21		36	14	32	27		28	24	38	22		8	5	56	40		21	10	49	32	

[1]Chi-square test; [2]Fisher's exact test.

commonly represents accumulation of the stable protein product of a mutated *p53* gene that has lost its cell cycle-regulatory function. In this study, expression of p53 was identified in 46 of 85 (54%) colon cancer cell nuclei and 3 of 18 (16.66%) adenomas but absent in normal colon mucosa. Positive stainings of p21 and cyclin D1 were also located in the cell nuclei, while bcl-2 and bax were in the cytoplasm (Figure 2). The expression profiles of p21, cyclin D1, bcl-2 and bax are summarized in Table 1, which shows differences among these various tissues (cancer, adenomas, normal mucosa) regarding the IHC results of the cell cycle and apoptosis-associated protein. The relation between the immunohistochemical pattern and clinicopathological features is presented in details in Table 2. We found positive correlation between p53 and bcl-2 (r = 0.245, P = 0.010), while no significant correlation between p53 and bax (r = -0.081, P = 0.395).

Expression of Cox-2 and nm23-h1

Cox-2 and nm23-h1 were all correlated with the colon cancer progression as previously reported[8,9]. The protein expression of Cox-2 was detected in 81 of 85 (95%) colon cancer cytoplasm and 16 of 18 (88.88%) adenomas, and 6 of 9 (66.66%) normal mucosa (Figure 3). Sixty-two colon cancer patients showed a strong positive staining of nm23-h1 (score ++~+++) in the cell cytoplasm. The details of the two genes expression profiles are shown in Table 3 and the relations with clinicopathological parameters are presented in Table 4.

Expression of PTEN, p-Akt1, β-catenin, c-myc

Expressions of PTEN, p-Akt1, β-catenin, c-myc proteins were detected in the cell cytoplasm (Figure 4). Immunohistochemical results of PTEN, p-Akt1No showed no significant difference among the different tissues (data not shown). Significant difference in the expressions of β-catenin and c-myc was found among the benign mucosa, adenomas and malignant tissues (Table 5). β-catenin protein expression had a positive correlation with c-myc expression (r = 0.483, P = 0.000), thereby suggesting their

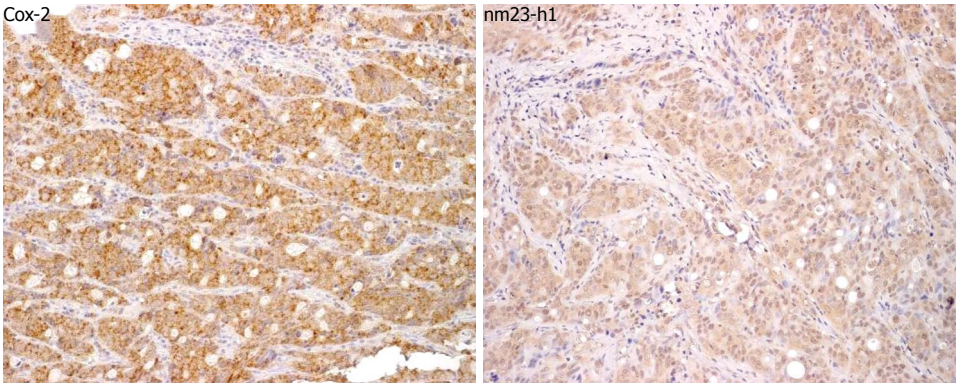

Figure 3 Immunophenotype of the investigated antigens (Cox-2 and nm23-h1) in colon cancer (original magnification x 200). The protein expressions of Cox-2 and nm23-h1 were detected in the cytoplasm.

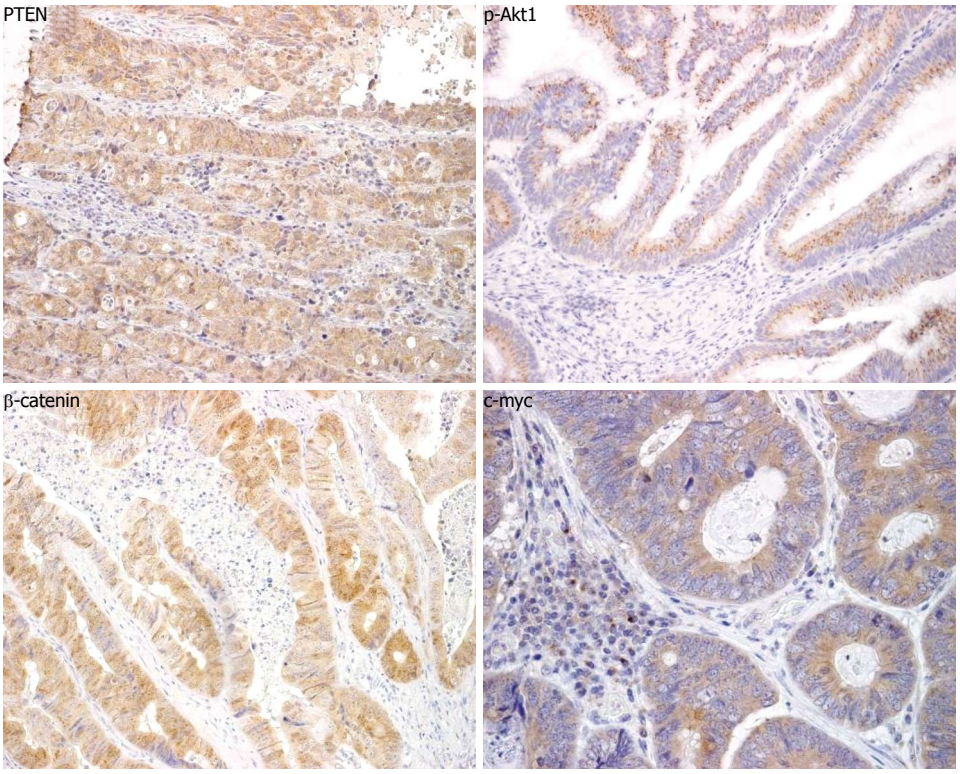

Figure 4 Immunophenotype of the investigated antigens (PTEN, p-Akt1, β-catenin and c-myc) in colon cancer (original magnification x 200). Expressions of PTEN, p-Akt1, β-catenin and c-myc were detected in the cell cytoplasm.

potent roles in *Wnt* pathway during the colon carcinogenesis. Correlations of the protein expression profiles with the clinicopathological features are shown in Tables 6 and 7.

DISCUSSION

Colon carcinogenesis is characterized by distinct morphological, genetic and cellular events. Development and progression of colon cancer to metastasis and lethal state are believed to be driven by multiple genetic alterations, the nature of which has remained poorly understood. Several pathways, such as cell cycle and apoptosis regulation, *Wnt* and PI3K/Akt pathways and so on, have been suggested to be involved in the progression[5,22,23]. However, the specific molecular alterations are largely dependent on the genetic background of the individual tumor. Therefore, investigations of molecular changes in tumors representing the entire disease spectrum may enhance our understanding of mechanisms involved in colon tumorigenesis.

To efficiently investigate the various molecules potentially relevant for colon tumor biology and to determine their potential clinical significance, large-scale analysis of multiple molecules in the same tumor tissues is required. The newly evolved and recently validated tissue microarray technique allows such molecular profiling of cancer specimens by immunohistochemistry[24,25]. In 1998, Kononen *et al*[24] introduced tissue microarrays (TMAs) as a powerful technology to rapidly visualize molecular targets such as genes and gene products in thousands of tissue specimens at a time. Furthermore, the use of TMAs for immunophenotyping of malignant tumors has recently been validated by Hoos *et al*[25] who demonstrated immunohistochemical analysis to characterize the significance of alterations in the p53 pathway and other cell cycle-related molecules in a histopathologically well-characterized cohort of patients with Hurthle cell (HC) neoplasm. In this study, two tumor tissue microarrays were constructed that allowed us to investigate the pattern of protein expressions of multiple genes and the relationships between the gene alterations and biological behaviors of colon cancer. We found that

Table 2 p53, p21, cyclin D1, bcl-2 and bax status in relation to clinicopathological parameters

Clinicopathalogical parameters		Total	p53				P	p21				P	cyclin D1				P	bcl-2				P	bax				P
			-	+	++	+++		-	1+	2+	3+		-	1+	2+	3+		-	+	++	+++		-	+	++	+++	
Age	< 58	39	17	5	8	9	0.301[1]	10	4	13	12	0.966[1]	8	6	13	12	0.752[1]	3	1	21	13	0.654[2]	11	3	17	8	0.772[1]
	⩾ 58	46	22	1	11	12		9	5	15	14		9	10	17	10		2	0	25	19		10	6	22	8	
Gender	Male	48	24	2	10	12	0.608[1]	12	1	17	16	0.040[1]	11	9	16	12	0.891[1]	5	1	26	16	0.139[2]	14	6	20	8	0.579[1]
	Female	37	15	4	9	9		7	8	11	10		6	7	14	10		0	0	20	16		7	3	19	8	
Histological grade	Low	24	18	0	3	3		10	4	3	6		9	4	8	3		3	1	16	4		11	3	9	1	
	Moderate	50	17	3	13	17	0.005[2]	6	3	21	18	0.013[2]	5	9	20	16	0.082[2]	2	0	24	23	0.075[2]	8	6	25	11	0.044[2]
	High	11	4	3	3	1		3	2	4	2		3	3	2	3		0	0	6	5		2	0	5	4	
Lymph node metastasis	Negative	53	19	4	16	14	0.067[1]	9	4	19	19	0.199[1]	11	11	20	11	0.575[1]	2	0	29	21	0.407[2]	10	6	26	11	0.457[1]
	Positive	32	20	2	3	7		10	5	9	7		6	5	10	11		3	1	17	11		11	3	13	5	
Distant metastasis	Negative	71	30	6	18	17	0.292[2]	14	8	23	23	0.644[2]	12	16	24	19	0.100[2]	3	0	39	29	0.052[2]	17	7	32	15	0.694[2]
	Positive	14	9	0	1	4		5	1	5	3		5	0	6	3		2	1	8	3		4	2	7	1	
Dukes stage	A	15	5	2	6	2		3	2	5	5		2	7	4	2		0	0	9	6		2	2	8	3	
	B	33	10	2	9	12	0.061[2]	3	2	13	13	0.286[2]	7	4	15	7	0.038[2]	1	0	18	14	0.487[2]	6	3	16	8	0.716[2]
	C	23	15	2	3	3		8	4	5	5		3	5	5	10		2	0	12	9		9	2	8	4	
	D	14	9	0	1	4		5	1	5	3		5	0	6	3		2	1	8	3		4	2	7	1	

[1] Chi-square test; [2] Fisher's exact test.

Table 3 Comparison of IHC results of Cox-2 and nm23-h1among varying tissues

Histology	n	Cox-2				P	nm23-h1				P
		-	+	++	+++		-	+	++	+++	
Cancer	85	4	4	30	47	0.002	5	7	33	29	0.007
Adenomas	18	2	0	13	3		2	1	13	2	
Benign tissue	9	3	0	1	5		4	1	2	1	
Total	112	9	4	44	55		11	9	48	32	

Fisher's exact test.

Table 4 Cox-2 and nm23-h1 status in relation to clinicopathological data

Groups		n	Cox-2				P	nm23-h1				P
			-	+	++	+++		-	+	++	+++	
Age (yr)	< 58	39	3	1	17	18	0.239	4	3	21	10	0.272
	⩾ 58	46	1	3	13	29		1	4	22	19	
Gender	Male	48	1	2	17	28	0.628	5	5	24	14	0.157
	Female	37	3	2	13	19		0	2	19	15	
Histological grade	Low	24	3	3	12	6		3	6	13	2	
	Moderate	50	1	1	14	33	0.008	2	0	23	24	0.000
	High	11	0	0	4	7		0	1	7	3	
Lymph node metastasis	Negative	53	1	2	17	33	0.223	2	3	29	18	0.434
	Positive	32	3	2	13	14		3	4	14	11	
Distant metastasis	Negative	71	1	3	27	40	0.026	3	3	39	26	0.008
	Positive	14	3	1	3	7		2	4	4	3	
Dukes stage	A	15	0	1	3	11	0.016	1	1	11	2	0.014
	B	33	0	0	12	21		0	1	16	16	
	C	23	1	2	12	8		2	1	12	8	
	D	14	3	1	3	7		2	4	4	3	

Fisher's exact test.

Table 5 Comparison of the IHC results of β-caternin and c-myc among varying tissues

Histological characteristics	Total	β-caternin		P	c-myc		P
		-	+		-	+	
Cancer	85	15	70	0.034	16	68	0.003
Adenomas	18	5	13		4	14	
Benign tissue	9	5	4		6	2	
Total	112	25	87		26	84	

Fisher's exact test.

Table 6 PTEN and p-Akt1 status in relation to clinicopathological data

Clinicopathological parameters		Total	PTEN				P	p-Akt1				P
			-	+	++	+++		-	+	++	+++	
Age	< 58	39	3	2	20	14	0.860[2]	10	0	16	13	0.408[1]
	⩾ 58	46	2	2	22	20		9	3	19	15	
Gender	Male	48	4	4	24	16	0.167[2]	14	0	19	15	0.096[1]
	Female	37	1	0	18	18		5	3	16	13	
Histological grade	Low	24	4	2	14	4		11	3	6	4	
	Moderate	50	1	2	24	23	0.029[2]	8	0	26	16	0.000[2]
	High	11	0	0	4	7		0	0	3	8	
Lymph node metastasis	Negative	53	3	2	22	26	0.132[2]	7	1	26	19	0.032[1]
	Positive	32	2	2	20	8		12	2	9	9	
Distant metastasis	Negative	71	2	3	37	29	0.060[2]	13	3	31	24	0.275[2]
	Positive	14	3	1	5	5		6	0	4	4	
Dukes stage	A	15	0	1	7	7	0.281[2]	1	0	6	8	0.106[2]
	B	33	1	1	15	16		4	1	17	11	
	C	23	1	1	15	6		8	2	8	5	
	D	14	3	1	5	5		6	0	4	4	

[1] Chi-square test; [2] Fisher's exact test.

Table 7 β-catenin and c-myc status in relation to clinicopathological data

Clinicopathological parameters		Total	β-caternin		*P*	c-myc		*P*
			-	+		-	+	
Age	< 58	39	6	33	0.983[1]	9	29	0.117[1]
	⩾ 58	46	7	39		5	41	
Gender	Male	48	8	40	0.689[1]	10	38	0.237[1]
	Female	37	5	32		4	32	
Histological grade	Low	24	10	14		11	13	
	Moderate	50	3	47	0.000[2]	3	46	0.000[2]
	High	11	0	11		0	11	
Lymph node metastasis	Negative	53	4	49	0.011[1]	4	48	0.005[1]
	Positive	32	9	23		10	22	
Distant metastasis	Negative	71	8	63	0.020[1]	6	65	0.000[1]
	Positive	14	5	9		8	5	
Dukes stage	A	15	0	15		0	15	
	B	33	2	31	0.008[2]	2	31	0.000[2]
	C	23	6	17		4	19	
	D	14	5	9		8	5	

[1]Chi-square test; [2]Fisher's exact test.

the 1.0-1.5 mm cores used to create the arrays were easy to work with, included enough tumor tissue that histological relationships were easily evaluated, and focused attention on limited regions of tumor, thus ensuring high reproducibility of scoring. Furthermore, at the same time, we could study the morphous of cells and protein expression parallely and avoid the variance in results in different experiment conditions as seen in the conventional technology.

The cell cycle-regulatory machinery is a complex system of proteins regulating each other's activity and controlling the division of cells[26]. We selected p53, p21, cyclin D1 and bcl-2/bax for analysis as target proteins participating in the regulation of proliferation and apoptosis, which are known to be deranged in cancer cell cycles, and which have been shown to affect survival of colorectal carcinomas. The p53 tumor suppressor plays a pivotal role in cell cycle regulation and apoptosis. Mutations in the *p53* gene are among the most common mutations encountered in human malignancy. Wild-type p53 along with other cellular growth factors activate *p21* gene expression and the corresponding p21 protein triggers cell-cycle arrest in the G_1 phase[27]. In colorectal cancer cells, mutated p21 neither suppressed apoptosis nor affected cell survival[28]. In addition to cell-cycle control, p53 mediates programmed cell death through the bcl-2/bax apoptotic pathway[29]. In this study, we observed that p53 was undetectable in normal colon tissue and over-expressed in only three adenomas and 54% of the adenocarcinomas. When the expression of p53 with clinicopathological parameters was compared, only the significant relation with histological grade could be seen, thereby indicating that p53 may be involved in the late stage of colon carcinogenesis and in the malignant progression of colon cancer. As to the others genes, there were significant differences among the three groups (normal mucosa, adenoma and cancer) regarding the immunohistochemical results (cyclin D1, $P = 0.000$; bcl-2, $P = 0.001$; bax, $P = 0.000$). Comparing these markers with the clinicopathological features, we observed the correlation of histological grades with bax, and Dukes stage with cyclin D1. Thus, we can speculate that cyclin D1, bcl-2 and bax aberrations may involve in the colon cancer development and the decreased expression of bax can accelerate the cancer tissue further differentiate into advanced stage, and malignant colon tissue highly expressed cyclin D1 may acquire the invasive potent. In addition, though the difference of this protein expression between distant metastasis-positive group and -negative group was not significant ($P = 0.052$) in this study, colon cancer with alteration of bcl-2 expression may facilitate to metastasize to distance sites. In our study, p21 over-expression was found in 64 of 82 (78.04%) cancers and was correlated with advanced stage colorectal cancer, which is in agreement with a previous report[30]. Furthermore, IHC revealed that some cancer cells expressed both p21 and p53, suggesting that p21 can also be activated by a p53-independent mechanism. A previous study reported that p53 can inhibit bcl-2 gene expression by transcriptional activation of the pro-apoptotic bax gene. But the relationship between p53 and bax in this cohort tissue was not established. However, our results showed that the expression of p53 had positive correlation with bcl-2. The precise mechanism of regulation of bcl-2/bax pathway through p53 needs further study.

There are two distinct Cox isoenzymes, namely constitutive Cox-1 and inducible Cox-2. It was reported that Cox-2 elevated in human esophagus, skin, and colon cancers, and the Cox-2 inhibitor, celecoxib, inhibited intestinal tumor multiplicity in a mouse model and reduced the number of adenomatous polyps in a familial adenomatous polyposis patient[16,17]. Enhanced Cox-2 expression has been related to tumor differentiation, distant metastasis and Dukes stage[31,32]. In present study, Cox-2 immunoreactivity was increased in the colon carcinoma (91%) and adenomas (88%). However, the expression of Cox-2 was correlated with less advanced grade, fewer distant metastases and lower Dukes stage in these cohort colon cancer tissues. These results indicate that Cox-2 over-expression might be an early event during the tumorigenesis in the colon and its role in progression of colon cancer deserves further investigation. Although a reduced expression of nm23-h1 has been shown to be correlated with a high metastatic potential in some human cancers, such as colorectal cancers, conflicting data have been reported[9,33]. In our study, expression of nm23-h1 was detected in 79 of 85 (92.94%) cancers, 16 of 18 (88.88%) adenomas and 4 of 8 (50%) normal tissues. The decreasing tendency of expression of nm23-h1 was found to be associated with the aggravation of differentiation, distant metastasis in the cohort patients. Therefore, the exact role of nm23-h1 in development and progression of the colon cancer needs further studies.

β-catenin is known to complex with E-cadherin to form intercellular junctions. It also participates in the *Wnt*-signaling pathway, which frequently is disrupted in colorectal carcinomas by adenomatous polyposis

coli (APC) or β-catenin mutations[15]. Translocation of β-catenin to the nucleus with transcription start of cyclin D1 and metalloproteinase 7 could lead to more aggressive colorectal carcinomas[34]. C-myc was also found to be involved in the *Wnt* pathway and seemed as a target gene of β-catenin/TCF[35]. It has been extensively documented that c-myc is over-expressed at RNA and protein levels at both early and late stages of the colorectal tumorigenesis[36]. Previous immunohistochemical studies with β-catenin showed distinct subcellular expression patterns in the colorectal carcinomas, adenomas, and benign epithelium, whereas benign tissue almost universally expressed β-catenin on the plasma membrane only, adenomas and carcinomas expressed β-catenin to varying degrees in the cytoplasm and in the nucleus as well[6,36,37]. This finding is not surprising, given the intracellular pathway described above. However, correlations between alterations of β-catenin expression in colorectal cancer and outcome variables have not been consistent[38-40]. In this study, different expressions of these two molecules were found among the varying types of tissues. β-catenin was expressed in 70 of 85 (82.83%) cancer tissues, 13 of 18 (72.22%) adenomas and only 4 of 9 (44.44%) para-cancerous normal mucosa. Similarly, positive expression of c-myc was detected in 68 of 84 (80.95%) colon cancers, 14 of 18 (77.77%) adenomas as well as 25% benign tissues. In addition to the results which showed positive correlation between the β-catenin and c-myc in our study ($r = 0.483$, $P = 0.000$), we can assume that over-expression of β-catenin in the cytoplasm and c-myc might be early events during the carcinogenesis in human colon *via* involving in the *Wnt* pathway which always distorts during colon tumorigenesis. However, the cancer tissues in the cohort with over-expression of β-catenin or c-myc exhibited less capacity to differentiate into advanced grade and invasive potential, which are contradicted to some previous reports[40,41]. The exact roles of β-catenin and c-myc aberration in progression of colon cancer requires further investigations.

The phosphatidylinositol-3 kinase (PI3K)/Akt is an important survival signal pathway that has been shown to be crucial in the regulation of balance between pro-apoptotic and survival (anti-apoptotic) signal[42]. The phosphorylated Akt level can monitor cell growth and resistance to apoptosis, indicating that activation of Akt plays an important role during the progression of colorectal carcinomas by helping promote cell growth and rescue cells from apoptosis. PTEN is a phosphatase that negatively regulates the phosphoinositol-3-kinase/Akt pathway and mediates cell-cycle arrest and apoptosis[43]. One study reported that PTEN protein expression was abnormal when compared the cancer with benign tissue[44], but same phenomenon was not found among the cohort patients including in this study. However, at the same time, PTEN expression detected by us was found to be related to tumor histological grade and p-Akt1 was related to lymph node metastasis. In this study, the expression profiles demonstrated that though did not involve in the early development of tumorigenesis, these two molecules may conduce to the lately progression of colon cancer which showed lymph node or distant metastasis. Contradiction between the results of p-Akt1 expression in our study and a previous study[11] which reported that Akt over-expression occurred frequently during human colon carcinogenesis might be because the gene background (FAP, HNPCC or sporadic CRC) of the patients studied were not strictly identified and the antibody used which was a polyclonal antibody in our study.

In summary, tissue microarrays (TMAs) combined with immunohistochemical staining for colon cancer, adenomas and normal mucosa showed that TMAs technology with 1.0 to 1.5 mm core tissue adequately represents the immunohistochemical pattern of the colon tissue. It considerably reduces the cost and labor needed to process tissue slides and enrich the technical spectrum of histopathology. The over-expressions of p53, cyclin D1, bcl-2, Cox-2, β-catenin and c-myc and the low or no expression of bax might be involved in the colon tumorigenesis and PTEN, p-Akt1 may contribute to the progression of colon cancer at late stage. No or low expression of nm23-h1 in colon cancer may contribute to the cancer cells acquired the invasion and distant metastasis potential. Further study needs to investigate the precise mechanism of colon cancer development and progression.

COMMENTS

Background

Studies of single molecular marker have not been successful in defining the biology of the colon cancer, so we explored multiple molecules regulating the colon tumorigenesis by using tissue microarray combining with immunohistochemical staining which can help us complete the time- and people-consuming work.

Research frontiers

In this study, the most worthwhile hotspot I think was investigating 11 molecules expressions by using the tissue microarray which allows rapid visualization of molecular targets at a time in protein level.

Innovations and breakthroughs

Firstly I should mention that in this study, we explored 11 molecular expressions at a time during colon carcinogenesis which was seldom found in our country. In addition, the expressions of these molecules were detected by using tissue micoarray which is a new high-throughput biological technique.

Applications

Tissue microarray can facilitate rapid translation of molecular discoveries to clinical applications used, so we can speculate that the tissue microarray technology which is fast, convenient and economic may have potential dominant position in macro-scale detection of tissue specimens in cancer studies.

Terminology

In 1998, Kononen and Kalloiniemi developed tissue microarrays (TMAs) whereby an ordered array of tissue samples are placed on a single slide. Once constructed, the TMA can be probed with a molecular target (DNA, RNA or protein) for analysis by immunohistochemistry, fluorescence *in situ* hybridization (FISH) or other molecular detection methods, enabling high-throughput *in situ* analysis of specific molecular targets in hundreds or even thousands of tissue specimens.

Peer review

In this study, the authors investigated the expressions of 11 cancer related genes involving cell proliferation, cell cycle, apoptosis, as well as signal pathway in human colon cancer, adenoma and para-cancerous mucosa by using tissue microarray, a new biological technique, combining with immunohistochemical staining at a time. The results from this study may manifest the colon cancer situation at some level and have some reference values in our country.

REFERENCES

1 **Pohl C**, Hombach A, Kruis W. Chronic inflammatory bowel disease and cancer. *Hepatogastroenterology* 2000; **47**: 57-70
2 **Fearon ER**, Hamilton SR, Vogelstein B. Clonal analysis of human colorectal tumors. *Science* 1987; **238**: 193-197
3 **Kallioniemi OP**, Wagner U, Kononen J, Sauter G. Tissue microarray technology for high-throughput molecular profiling of cancer. *Hum Mol Genet* 2001; **10**: 657-662
4 **Serrano R**, Gómez M, Farre X, Méndez M, De La Haba J, Morales R, Sanchez L, Barneto I, Aranda E. Tissue microarrays (TMAS) in colorectal cancer: Study of clinical and molecular markers. *ASCO Meeting Abstracts* 2004; **22**: 9665
5 **Chung DC**. The genetic basis of colorectal cancer: insights into critical pathways of tumorigenesis. *Gastroenterology* 2000; **119**: 854-865
6 **Hao X**, Tomlinson I, Ilyas M, Palazzo JP, Talbot IC. Reciprocity between membranous and nuclear expression of beta-catenin in colorectal tumours. *Virchows Arch* 1997; **431**: 167-172
7 **He TC**, Sparks AB, Rago C, Hermeking H, Zawel L, da Costa LT, Morin PJ, Vogelstein B, Kinzler KW. Identification of c-MYC as a target of the APC pathway. *Science* 1998; **281**: 1509-1512
8 **Kim JY**, Lim SJ, Park K. Cyclooxygenase-2 and c-erbB-2 expression in colorectal carcinoma assessed using tissue microarrays. *Appl Immunohistochem Mol Morphol* 2004; **12**: 67-70
9 **Messinetti S**, Giacomelli L, Fabrizio G, Giarnieri E, Gabatel R, Manno A, Feroci D, Guerriero G, Masci E, Vecchione A. CD44v6 and Nm23-H1 protein expression related to clinicopathological parameters in colorectal cancer. *Ann Ital Chir* 2003; **74**: 45-51
10 **Zhou XP**, Loukola A, Salovaara R, Nystrom-Lahti M, Peltomäki P, de la Chapelle A, Aaltonen LA, Eng C. PTEN mutational spectra, expression levels, and subcellular localization in microsatellite stable and unstable colorectal cancers. *Am J Pathol* 2002; **161**: 439-447
11 **Roy HK**, Olusola BF, Clemens DL, Karolski WJ, Ratashak A, Lynch HT, Smyrk TC. AKT proto-oncogene overexpression is an early event during sporadic colon carcinogenesis. *Carcinogenesis* 2002; **23**: 201-205
12 **Itoh N**, Semba S, Ito M, Takeda H, Kawata S, Yamakawa M. Phosphorylation of Akt/PKB is required for suppression of cancer cell apoptosis and tumor progression in human colorectal carcinoma. *Cancer* 2002; **94**: 3127-3134
13 **Di Cristofano A**, Pandolfi PP. The multiple roles of PTEN in tumor suppression. *Cell* 2000; **100**: 387-390
14 **Weng L**, Brown J, Eng C. PTEN induces apoptosis and cell cycle arrest through phosphoinositol-3-kinase/Akt-dependent and -independent pathways. *Hum Mol Genet* 2001; **10**: 237-242
15 **Wong NA**, Pignatelli M. Beta-catenin-a linchpin in colorectal carcinogenesis? *Am J Pathol* 2002; **160**: 389-401
16 **Soslow RA**, Dannenberg AJ, Rush D, Woerner BM, Khan KN, Masferrer J, Koki AT. COX-2 is expressed in human pulmonary, colonic, and mammary tumors. *Cancer* 2000; **89**: 2637-2645
17 **Masferrer JL**, Leahy KM, Koki AT, Zweifel BS, Settle SL, Woerner BM, Edwards DA, Flickinger AG, Moore RJ, Seibert K. Antiangiogenic and antitumor activities of cyclooxygenase-2 inhibitors. *Cancer Res* 2000; **60**: 1306-1311
18 **Martinez JA,** Prevot S, Nordlinger B, Nguyen TM, Lacarriere Y, Munier A, Lascu I, Vaillant JC, Capeau J, Lacombe ML. Overexpression of nm23-H1 and nm23-H2 genes in colorectal carcinomas and loss of nm23-H1 expression in advanced tumour stages. *Gut* 1995; **37**: 712-720
19 **Mucci NR**, Akdas G, Manely S, Rubin MA. Neuroendocrine expression in metastatic prostate cancer: evaluation of high throughput tissue microarrays to detect heterogeneous protein expression. *Hum Pathol* 2000; **31**: 406-414
20 **Schraml P**, Kononen J, Bubendorf L, Moch H, Bissig H, Nocito A, Mihatsch MJ, Kallioniemi OP, Sauter G. Tissue microarrays for gene amplification surveys in many different tumor types. *Clin Cancer Res* 1999; **5**: 1966-1975
21 **Richter J**, Wagner U, Kononen J, Fijan A, Bruderer J, Schmid U, Ackermann D, Maurer R, Alund G, Knönagel H, Rist M, Wilber K, Anabitarte M, Hering F, Hardmeier T, Schönenberger A, Flury R, Jäger P, Fehr JL, Schraml P, Moch H, Mihatsch MJ, Gasser T, Kallioniemi OP, Sauter G. High-throughput tissue microarray analysis of cyclin E gene amplification and overexpression in urinary bladder cancer. *Am J Pathol* 2000; **157**: 787-794
22 **Lynch HT**, Smyrk TC. Identifying hereditary nonpolyposis colorectal cancer. *N Engl J Med* 1998; **338**: 1537-1538
23 **Bienz M**, Clevers H. Linking colorectal cancer to Wnt signaling. *Cell* 2000; **103**: 311-320
24 **Kononen J**, Bubendorf L, Kallioniemi A, Bärlund M, Schraml P, Leighton S, Torhorst J, Mihatsch MJ, Sauter G, Kallioniemi OP. Tissue microarrays for high-throughput molecular profiling of tumor specimens. *Nat Med* 1998; **4**: 844-847
25 **Hoos A**, Urist MJ, Stojadinovic A, Mastorides S, Dudas ME, Leung DH, Kuo D, Brennan MF, Lewis JJ, Cordon-Cardo C. Validation of tissue microarrays for immunohistochemical profiling of cancer specimens using the example of human fibroblastic tumors. *Am J Pathol* 2001; **158**: 1245-1251
26 **Cordon-Cardo C**. Mutations of cell cycle regulators. Biological and clinical implications for human neoplasia. *Am J Pathol* 1995; **147**: 545-560
27 **el-Deiry WS**, Tokino T, Velculescu VE, Levy DB, Parsons R, Trent JM, Lin D, Mercer WE, Kinzler KW, Vogelstein B. WAF1, a potential mediator of p53 tumor suppression. *Cell* 1993; **75**: 817-825
28 **Lu Y**, Yamagishi N, Yagi T, Takebe H. Mutated p21(WAF1/CIP1/SDI1) lacking CDK-inhibitory activity fails to prevent apoptosis in human colorectal carcinoma cells. *Oncogene* 1998; **16:** 705-712
29 **Chao DT**, Korsmeyer SJ. BCL-2 family: regulators of cell death. *Annu Rev Immunol* 1998; **16**: 395-419
30 **Viale G**, Pellegrini C, Mazzarol G, Maisonneuve P, Silverman ML, Bosari S. p21WAF1/CIP1 expression in colorectal carcinoma correlates with advanced disease stage and p53 mutations. *J Pathol* 1999; **187**: 302-307
31 **Fujita T**, Matsui M, Takaku K, Uetake H, Ichikawa W, Taketo MM, Sugihara K. Size- and invasion-dependent increase in cyclooxygenase 2 levels in human colorectal carcinomas. *Cancer Res* 1998; **58:** 4823-4826
32 **Zhang H**, Sun XF. Overexpression of cyclooxygenase-2 correlates with advanced stages of colorectal cancer. *Am J Gastroenterol* 2002; **97**: 1037-1041
33 **Zeng ZS**, Hsu S, Zhang ZF, Cohen AM, Enker WE, Turnbull AA, Guillem JG. High level of Nm23-H1 gene expression is associated with local colorectal cancer progression not with metastases. *Br J Cancer* 1994; **70**: 1025-1030
34 **Brabletz T**, Jung A, Dag S, Hlubek F, Kirchner T. beta-catenin regulates the expression of the matrix metalloproteinase-7 in human colorectal cancer. *Am J Pathol* 1999; **155**: 1033-1038
35 **Smith DR**, Myint T, Goh HS. Over-expression of the c-myc proto-oncogene in colorectal carcinoma. *Br J Cancer* 1993; **68**: 407-413
36 **Kobayashi M**, Honma T, Matsuda Y, Suzuki Y, Narisawa R, Ajioka Y, Asakura H. Nuclear translocation of beta-catenin in colorectal cancer. *Br J Cancer* 2000; **82**: 1689-1693
37 **Iwamoto M**, Ahnen DJ, Franklin WA, Maltzman TH. Expression of beta-catenin and full-length APC protein in normal and neoplastic colonic tissues. *Carcinogenesis* 2000; **21**: 1935-1940
38 **Günther K**, Brabletz T, Kraus C, Dworak O, Reymond MA, Jung A, Hohenberger W, Köckerling T, Kockerling F, Ballhausen WG. Predictive value of nuclear beta-catenin expression for the occurrence of distant metastases in rectal cancer. *Dis Colon Rectum* 1998; **41**: 1256-1261
39 **Hugh TJ**, Dillon SA, Taylor BA, Pignatelli M, Poston GJ, Kinsella AR. Cadherin-catenin expression in primary colorectal cancer: a survival analysis. *Br J Cancer* 1999; **80**: 1046-1051
40 **Maruyama K**, Ochiai A, Akimoto S, Nakamura S, Baba S, Moriya Y, Hirohashi S. Cytoplasmic beta-catenin accumulation as a predictor of hematogenous metastasis in human

colorectal cancer. *Oncology* 2000; **59**: 302-309

41 **Masramon L**, Arribas R, Tórtola S, Perucho M, Peinado MA. Moderate amplifications of the c-myc gene correlate with molecular and clinicopathological parameters in colorectal cancer. *Br J Cancer* 1998; **77**: 2349-2356

42 **Khor TO**, Gul YA, Ithnin H, Seow HF. Positive correlation between overexpression of phospho-BAD with phosphorylated Akt at serine 473 but not threonine 308 in colorectal carcinoma. *Cancer Lett* 2004; **210**: 139-150

43 **Stambolic V**, Suzuki A, de la Pompa JL, Brothers GM, Mirtsos C, Sasaki T, Ruland J, Penninger JM, Siderovski DP, Mak TW. Negative regulation of PKB/Akt-dependent cell survival by the tumor suppressor PTEN. *Cell* 1998; **95**: 29-39

44 **Taniyama K**, Goodison S, Ito R, Bookstein R, Miyoshi N, Tahara E, Tarin D, Urquidi V. PTEN expression is maintained in sporadic colorectal tumours. *J Pathol* 2001; **194**: 341-348

S- Editor Liu Y **L- Editor** Kumar M **E- Editor** Bai SH

PO Box 2345, Beijing 100023, China
www.wjgnet.com
wjg@wjgnet.com

World J Gastroenterol 2007 February 7; 13(5): 709-716
World Journal of Gastroenterology ISSN 1007-9327

BASIC RESEARCH

Neural mechanism of acupuncture-modulated gastric motility

Yu-Qing Li, Bing Zhu, Pei-Jing Rong, Hui Ben, Yan-Hua Li

Yu-Qing Li, Bing Zhu, Pei-Jing Rong, Hui Ben, Yan-Hua Li, Institute of Acupuncture-Moxibustion, China Academy of Chinese Medical Sciences, 16 Nanxiaojie of Dongzhimennei, Beijing 100700, China
Bing Zhu, Faculty of Acupuncture, Hubei College of Traditional Chinese Medicine, Wuhan 430061, Hubei Province, China
Supported by National Natural Science Foundation of China, No. C30100245; National Basic Research 973 Program, No. 2005CB523308
Co-correspondence: Pei-Jing Rong
Correspondence to: Bing Zhu, MD, PhD, PhD, Institute of Acupuncture-Moxibustion, China Academy of Chinese Medical Sciences, 16 Nanxiaojie of Dongzhimennei, Beijing 100700, China. zhubing@mail.cintcm.ac.cn
Telephone: +86-10-64014411-2772 Fax: +86-10-64013968
Received: 2006-08-21 Accepted: 2006-11-29

Abstract

AIM: To investigate the acupuncture-modulated gastric motility and its underlying neural mechanism.

METHODS: Intragastric pressure and/or waves of gastric contraction in rats were recorded by intrapyloric balloon and changes of gastric motility induced by acupuncture stimulation were compared with the background activity before any stimulation. Gastro-vagal or splanchnic-sympathetic nerves were recorded or cut respectively for investigating the involvement of autonomic nerve pathways. Spinalization experiment was also performed.

RESULTS: Acupuncture-stimulation by exciting Aδ and/or C afferent fibers, could only modulate gastric motility. Acupuncture-stimulation on fore- and hind-limbs evoked a moderate gastric motility followed by increased vagus discharges with unchanged sympathetic activity, while the same stimulus to the acupoints in abdomen resulted in reversed effects on gastric motility and autonomic nervous activities. The inhibitory gastric response was completely abolished by splanchnic denervation, but the facilitative gastric response to stimulation of acupoints in limbs was not influenced, which was opposite to the effect when vagotomy was performed. The similar depressive effects were produced by the stimulation at the acupoints homo-segmental to the gastric innervation in the animals with or without spinalization. However, the facilitation induced by the stimulation at the acupoints hetero-segmental to the gastric innervation was not observed in the spinalized animals.

CONCLUSION: Facilitative effects of stimulating hetero-segmental acupoints are involved in the intact preparation of vagal nerves and spinal cord, while the inhibitory response induced by stimulating homo-segmental acupoints is involved in the intact preparation of sympathetic nerves. Only the acupuncture-stimulation with intensity over the threshold of Aδ and/or C afferent fibers can markedly modulate gastrointestinal motility.

Key words: Gastric motility; Acupuncture-stimulation; Intensity of acupuncture stimulation; Aδ-fiber; C-fiber; Autonomic nervous system; Supraspinal circuit

Li YQ, Zhu B, Rong PJ, Ben H, Li YH. Neural mechanism of acupuncture-modulated gastric motility. *World J Gastroenterol* 2007; 13(5): 709-716

http://www.wjgnet.com/1007-9327/13/709.asp

INTRODUCTION

Acupuncture, a commonly used neuromodulating technique, has been widely accepted in the treatment of pain syndromes[1]. It modulates the functions of visceral organs by inducing activation of the somato-visceral reflexes and change of the autonomic nervous system[2-4].

Electro-acupuncture therapy is increasingly adopted in Western countries. Acupuncture involves stimulating specific somatic points on the body by puncturing the skin with a needle. Heat, pressure or impulses of electrical energy can also stimulate the points. It was reported that the nervous system, neurotransmitters and endogenous substances respond to electro-acupuncture. Abundant information is now available concerning the neurobiological mechanisms of acupuncture related with the neural pathways and neurotransmitters/hormonal factors that mediate autonomic regulation, pain relief and other therapeutics[5]. Being a kind of traditional technique with a long history, acupuncture has been used to treat a variety of diseases including pain. Electrophysiological studies showed that acupuncture might inhibit the neuron discharge induced by pain of both somatic and visceral sources at different levels of the central nervous system, which gives a good explanation for the clinic phenomena in which acupuncture produces quick effect on somatic and visceral pain and relatively slow and long post-effect. Though there are data relating the modulation of somatic afferent inputs on visceral nociception or dysfunction, evidence for the role of acupuncture in this process is not sufficient.

The Committee of NIH published a report on the indications of acupuncture in November 1997. The summary of the consensus statement indicates that there is clear evidence that needle acupuncture treatment is effective on postoperative and chemotherapy-induced nausea and vomiting during pregnancy and post-operative dental pain[6]. Recent investigations suggest that acupuncture modulations on visceral functional activities can be mediated via the autonomic nervous system[2,4,7-9].

In the present study, therefore, we investigated the modulation of gastric motility by manual/electrical acupuncture at representative meridian-acupoints in different parts of the body and its underlying mechanism involved in different afferent fibers, autonomic nervous system and the supraspinal center.

MATERIALS AND METHODS

Animal preparation

All animal experiments were carried out in accordance with the National Institute of Health Guide for the Care and Use of Laboratory Animals and approved by the Institutional Animal Care and Use Committee of China Academy of Chinese Medical Sciences. Experiments were performed on 48 adult male Sprague-Dawley rats weighing 250-300 g. The rats were fasted overnight with free access to water and anesthetized with an intraperitoneal injection of urethane (1.0-1.2 g/kg). The trachea was cannulated and a catheter was inserted into one of the jugular veins for infusion of necessary solutions or anesthetics. The abdomen was opened by midline, and then a small longitudinal incision was made in the duodenum about 2-3 cm from the pylorus. A small balloon made of condom was inserted via the incision into the pyloric area and fixed. Another catheter (1 mm in inner diameter) was also inserted into the same incision to drain digestive juices secreted from the stomach. The balloon was filled with about 0.2-0.5 mL warm water, which gave the pressure at about 80-150 mmH_2O. Pressure in the balloon was measured by a transducer (TP-400T, Nihon Kohden) through a thin polyethylene tube (1.5 mm in outer diameter) and then input into a polygraph amplifier (RM-6000, Nihon Kohden) and led to a data acquisition system (Power-Lab/8 s, AD Instruments) for further analysis. Demi-fasting gastric motor activity was recorded as a control for at least 1 h before any stimulation was applied.

Changes of gastric motility induced by the stimulation were compared with the background activity in terms of intragastric pressure and/or waves of gastric contraction. If the changes of gastric motility during stimulation were 20% more or less than the background activity, the response was considered to have an excitatory or inhibitory regulation.

Blood pressure in a common carotid artery and heart rate were continuously monitored. The rectal temperature was kept constantly around 37℃ by a feedback-controlled heating blanket.

Recording of neural activity, severance of autonomic nerves and transection of spinal cord

To investigate whether vagal or sympathetic pathways are involved in the stimulatory or inhibitory effects of acupuncture on gastric motility, subdiaphragmatic gastro-vagal or sympathetic postganglionic nerves coming from a celiac ganglion and innervating the gut branch were dissected under microscope. Discharges of the vagal or sympathetic nerves were put into a polygraph (RM-6000, Nihon Kohden) amplifier through bipolar platinum wire electrodes and input into a data acquisition system (Power-Lab) for further analysis. In experiments, gastro-vagal nerves were cut in subdiaphragmatic bilateral truncal vagotomy (an additional cervical bilateral vagotomy was also performed in several cases) or postgangliotic nerves innervating the gut branch were cut in sympathetomy (an additional bilateral splanchnicotomy was also performed in several cases) in 24 rats.

In spinalization experiments, laminectomy was performed in C_8-T_1 of 10 animals. Frozen physiological saline was used to produce a reversible cold block (five rats), or transected with knife to determine the involvement of supraspinal circuit in acupuncture-induced effect on gastric motility.

Acupuncture stimulation

A needle (0.3 mm in diameter) was inserted into the skin and its underlying muscles at different acupoints on the body. The needle was rotated clockwise and anti-clockwise at 2 Hz for 30 s. Based on the anatomical localization in rats as compared with that in human body, the stimulated acupoints included St-13 (acupoint of Stomach-Meridian in upper-chest), Li-11 (acupoint of Large intestine-Meridian in forelimb), Cv-6 (acupoint of conception-vessel) and St-21 (acupoint of Stomach-Meridian in abdomen), Bl-21 (T_{12} segment, acupoint of Bladder-Meridian in dorsum) and St-36 (acupoint of Stomach-Meridian in hindlimb).

In electroacupuncture experiments, acupoints were stimulated by a pair of needle-electrodes inserted 0.3 cm deep into the skin and electroacupuncture intensities were chosen as the multiples of the threshold for the activation of Aδ-fiber or C-fiber, including 0.8 (0.8-$T_{A\delta}$, non-noxious stimuli, 1.42 ± 0.36 mA) and 2-times of the Aδ-fiber reflex threshold (2-$T_{A\delta}$, slight nociceptive stimuli, 3.62 ± 0.44 mA), and 1.5 times (1.5-T_C, strong nociceptive stimuli, 7.68 ± 0.53 mA) of C-fiber reflex threshold.

The thresholds of Aδ-fiber and C-fiber reflexes were decided by electrical stimulation of the sural nerve territory, which could elicite a two-component reflex response in the ipsilateral biceps femoris muscle. The first-component had a low threshold (1.64 ± 0.33 mA) response with a short latency (13.2 ± 1.4 ms) and duration (24.2 ± 1.5 ms). The second-component had a longer latency (158.8 ± 10.7 ms) and duration (243.8 ± 31.5 ms) and a higher threshold (4.84 ± 0.67 mA). These electrophysiological features clearly suggested that the two-components were produced due to the different afferent volleys activated by sural nerve stimulation. According to our previous study, it seems that the first component with a low-threshold and a short-latency could be elicited by activating the Aδ-fibers, whereas the second with a higher threshold and a longer latency might result from the activation of the unmyelinated C-fiber afferents[10].

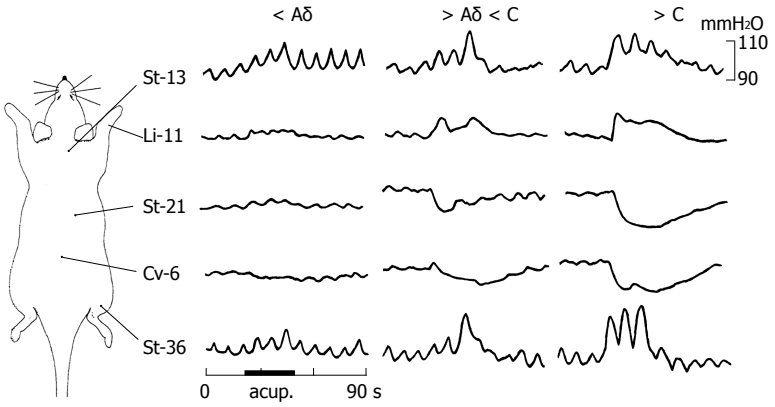

Figure 1 Gastric motility response to electro-acupuncture stimulation with different intensities. Gastric motility was recorded for 90 s, of which the first 20 s was the duration of spontaneous background of gastric activity, 21-50 s was the period of acupuncture stimulation at acupoints, poststimuli activity was recorded for 51-90 s. *Dash line* represents located abdominal acupoints.

Experimental procedures

The rats were kept in supine position and gastric motor activity was first analyzed visually to detect the waves of contractions. A standard protocol was employed for the determination of effects of acupuncture-stimulation on gastric motility response. A background gastric activity was recorded for 5-10 min followed by a test of the responses to manual or electro-acupuncture at the acupoints for 30 s. The post-stimuli response was recorded for another 5-10 min.

After a series of experiments was finished, the rats were sacrificed under deep anesthesia (urethane, 2 g/kg ip).

Statistical analysis

The data obtained before and after intervention between the two groups were compared statistically by independent *t*-test and paired *t*-test respectively. $P < 0.05$ was considered statistically significant. All data were expressed as mean ± SE.

RESULTS

Gastric motor characteristic

Gastric motor characteristics were observed in 42 rats. When the intrapyloric balloon pressure was increased to about 80-200 mmH_2O, the rhythmic waves of contractions in pyloric area were observed. When the pressure was maintained at about 100 mmH_2O by expanding the volume of the balloon with warm-water, rhythmic contractions occurred at a rate of four to six per minute and these rhythmically gastric contractions could be recorded in either the spinalized rats or the rats with intact central nervous system. The gastric contractions could also be recorded after denervation of gastric nerve branches of the vagal or splanchnic nerves.

Gastric motility response to electro-acupuncture stimulation with different intensities

The response of gastric motility to the activation of Aδ-/C-fibers was elicited by stimulating the ipsilateral sural nerve. The effects of acupuncture stimulation to Li-11 in the forelimb, St-13 in upper-breast, St-21 and Cv-6 in the abdomen and St-36 in the hindlimb on gastric motility were studied. As illustrated by an representative example in Figure 1 in combination with data in Figure 2,

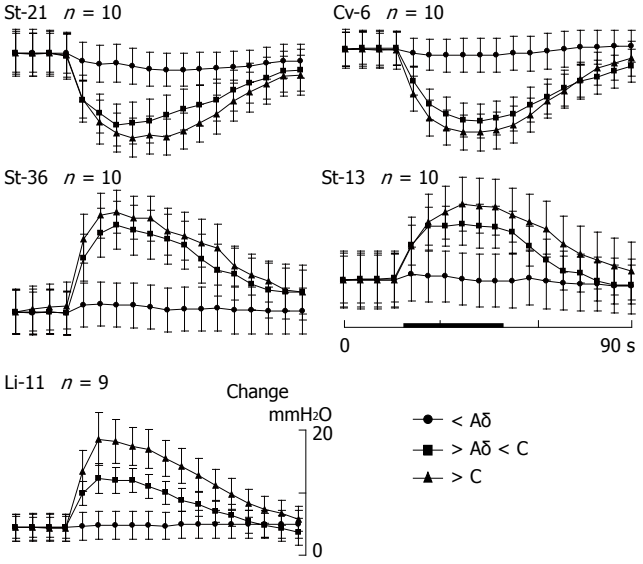

Figure 2 Quantitative analysis of gastric motility in strength-dependent response to electro-acu puncture-stimulation applied to the acupoints on different parts of body. "< Aδ": the intensity of the stimulation less than the threshold for activation of Aδ-fiber; "> Aδ < C": the intensity of the stimulation over the threshold for activation of Aδ-fiber, but less than the threshold for activation of C-fiber; "> C": the intensity of the stimulation over the threshold for activation of C-fiber.

the acupuncture stimulation with the intensity of 0.8-$T_{Aδ}$ (1.42 ± 0.36 mA) at the above five acupoints did not produce any significant influences on the gastric motility. The acupuncture stimulation with the intensity of 2-$T_{Aδ}$ (3.62 ± 0.44 mA) at the acupoints of Li-11, St-13 and St-36 elicited a mild-moderate facilitation on the gastric motility, whereas the acupuncture stimulation with the same intensity to the acupoints of St-21 and Cv-6 brought about a moderate depression of gastric motility. The acupuncture stimulation with the intensity of 1.5-T_C (7.68 ± 0.53 mA) at the acupoints of Li-11, St-13 and St-36 resulted in a strong excitatory gastric motility. In contrast, a strong inhibition on the gastric motility was induced by the same acupuncture stimulation at the acupoints of St-21 and Cv-6.

Electro-acupuncture stimulation could induce regulatory effects on gastric motility. Moreover, facilitation/depression on the gastric motility induced by acupuncture stimulation was intensity-dependent. Only the stimulation with an intensity over the threshold for activation of Aδ- and/or C-fibers could modulate gastric

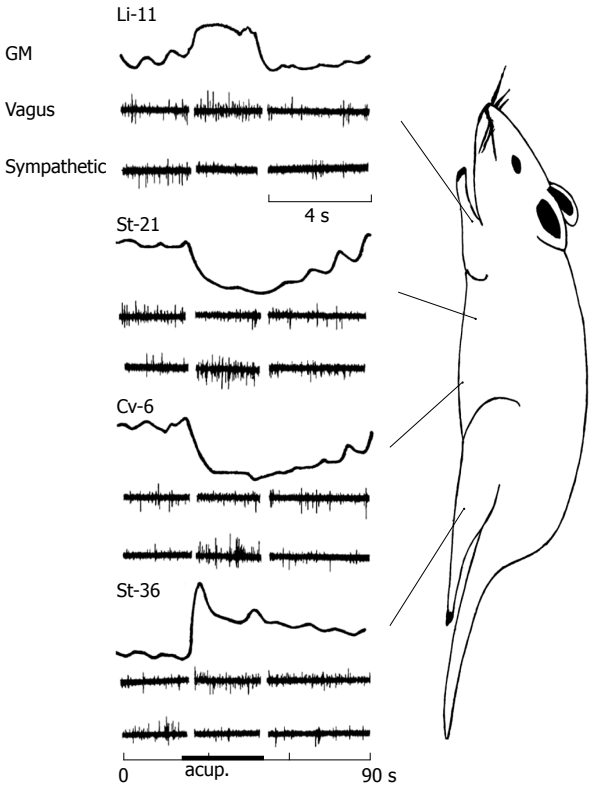

Figure 3 Gastric motility and autonomic nerve responses to acupuncture stimulation at different acupoints. In each acupoint stimulus, gastric motility (GM), activities of gastric vagal (vagus) and postganglionic sympathetic nerve branches to the stomach (symp), were simultaneously recorded.

motility ($P < 0.05$, $P < 0.001$) and the powerful effects were produced when the strongest electro-acupuncture stimulation, *i.e.* 1.5-Tc, was given ($P < 0.05$, $P < 0.001$).

Gastric motility and activity of autonomic nerves in response to acupuncture stimulation

Gastric motility in the most rats showed various responses to acupuncture stimulation at some representative acupoints on several meridians and different parts of the body. Manual acupuncture stimulation at either Li-11 in forelimb or St-36 in hindlimb led to a moderate facilitation of gastric motility with a rapid enhancement at the beginning of stimulation, followed by a tonic gastric contraction lasting throughout the period of acupuncture stimulation. The typical effects of acupuncture stimulations at Li-11 or St-36 acupoints on discharges of the branches of both gastric vagal and postganglionic sympathetic nerves to the stomach are shown in Figure 3. Acupuncture stimulation at either Li-11 ($n = 10$) or St-36 ($n = 16$) acupoints markedly increased vagal discharges (339.42 ± 133.2 spikes/min *vs* 381.6 ± 135.42 spikes/min, $P < 0.05$). The latency of increased discharges was about 2-3 s after the onset of stimulation. The facilitated response lasted for 30 s with a maximum response at about 10 s after the onset of acupuncture stimulation. In contrast to vagus response, spontaneous activity of the sympathetic nerve branch was not clearly influenced by acupuncture stimulation at either Li-11 ($n = 12$) or St-36 acupoints ($n = 12$) ($P > 0.05$). Generally, in the animals with high spontaneous activity of sympathetic nerves, the same acupuncture stimulation could mildly inhibit the discharges. However, the stimulation could produce a slight excitation in the animals with lower spontaneous sympathetic activity.

The same stimulus to the acupoints of either St-21 or Cv-6 in abdomen, resulted in high suppression with a rapid onset on gastric tonic motility, followed by an obvious inhibition on the rhythmic wave of contraction. The suppression maintained throughout the period of acupuncture stimulation. In the autonomic nerve participation, acupuncture stimulation at either St-21 ($n = 12$) or Cv-6 ($n = 10$) acupoints markedly increased sympathetic discharges (476.4 ± 150.78 spikes/min *vs* 638.82 ± 171.78 spikes/min, $P < 0.05$). In most cases, spontaneous vagal activity could also be inhibited slightly ($P > 0.05$, $n = 12$) or remained unchanged (Figure 3).

Effect of acupuncture stimulation on gastric motility involved in autonomic nerves

In order to discover their contribution to the facilitation/inhibition of acupoint-visceral reflex responses, denervation of the vagal or sympathetic nerves was performed in the present study.

The effect of acu-stimulation on gastric motility was examined in the rats after amputation of bilateral splanchnic nerves just beneath the diaphragm.

The inhibitory gastric response induced by acupuncture stimulation to acupoints of St-21 ($n = 9$), Cv-6 ($n = 9$) or Bl-21 ($n = 9$) was completely abolished after sympathectomy of the bilateral splanchnic nerves, but the facilitative gastric response induced by acupuncture stimulation to acupoint of Li-11 ($n = 9$) was not influenced significantly and St-36 ($n = 9$) was only less influenced by splanchnic denervation (Figure 4 and Figure 5A).

Bilateral subdiaphragmatic vagotomy was performed to determine the vagal involvement in the stimulatory or inhibitory effects of acupuncture on gastric motility (in some experiments, additional vagotomy of bilateral vagal nerves was also performed at the cervical level to observe the different results from those obtained in the rats after incomplete subdiaphragmatic vagotomy). As shown in Figure 4 and the cumulative results in Figure 5B, the bilateral vagotomy did not abolish the suppressive gastric response induced by acupuncture stimulation to the acupoints of either St-21 ($n = 9$), Cv-6 ($n = 9$) in abdomen, or Bl-21 in middle-dorsum ($n = 9$). However, the bilateral vagotomy completely depleted the facilitative gastric response provoked by acupuncture stimulation to the acupoints of Li-11 in forelimb ($n = 9$) or St-36 in hindlimb ($n = 9$).

Effect of acupuncture stimulation on gastric motility involved in supraspinal circuit

During acute spinalization at C_8-T_1 level, steady gastric motility could still be recorded. But for avoiding the spinal shock, 30-min period of rest was necessary.

In pre-spinalized animals, as shown in Figures 6 and 7, the gastric motility was inhibited by acupoints of St-21, Cv-6 or Bl-21, and facilitated by St-36 acupoint. Acupuncture stimulation at the acupoints of St-21 ($n =$

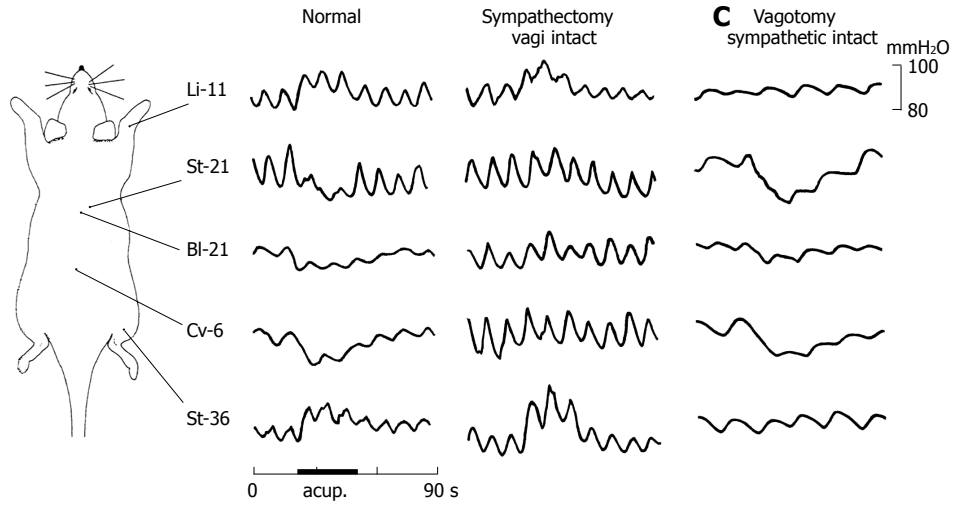

Figure 4 Effect of acupuncture stimulation on gastric motility in animals with intact autonomic nervous system, after sympathectomy of bilateral splanchnic nerves just beneath the diaphragm but intact vagi and bilateral subdiaphragmatic vagotomy but intact sympathetic nerve.

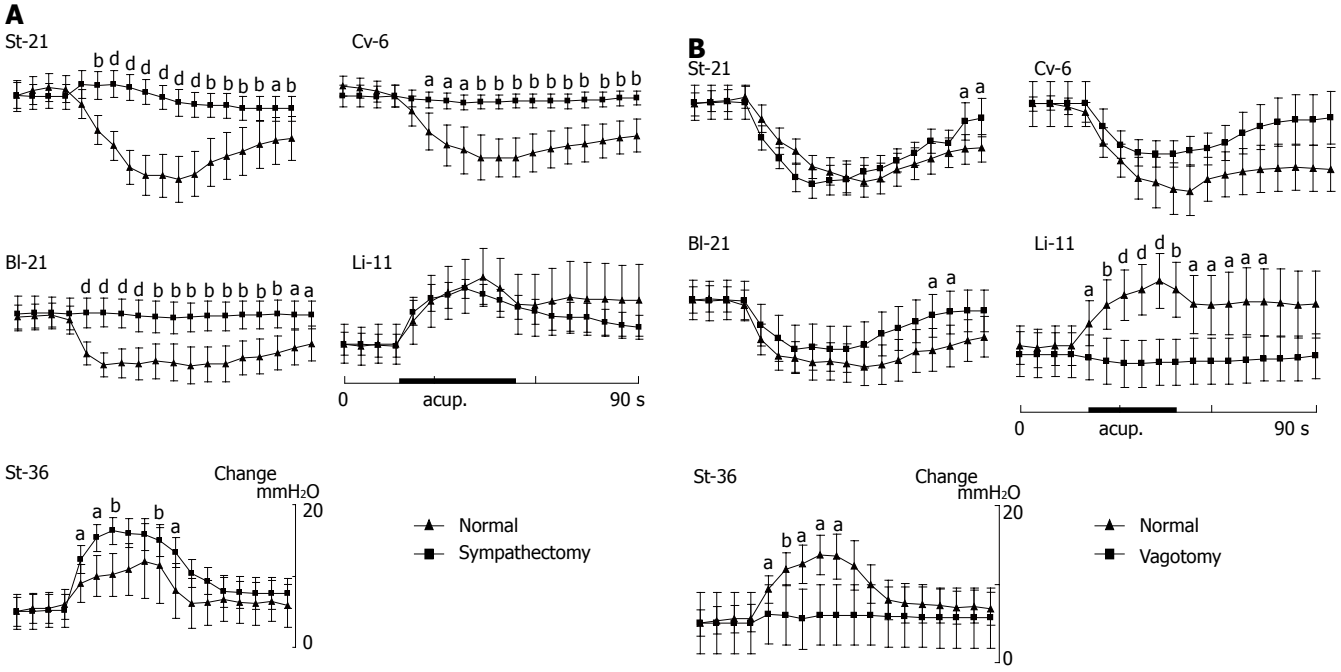

Figure 5 Analysis of the changes in gastric motility induced by acupuncture stimulation in rats after bilateral sympathectomy (**A**) of splanchnic nerves and vagotomy (**B**), respectively. $^{a}P < 0.05$, $^{b}P < 0.01$ and $^{d}P < 0.001$ *vs* animals with intact autonomic nervous system.

10), Cv-6 (n = 10) or Bl-21(n = 10) could inhibit gastric motility in the spinalized rats. On the contrary, gastric facilitative response induced by St-36 (n = 10) acupuncture stimulation disappeared completely after spinalization.

DISCUSSION

Our previous study showed that acupuncture-stimulation had facilitative or inhibitory effect on gastric motility depending on the different stimulated acupoints on different parts of the body[10]. In this study, we investigated how strong the stimulation and what autonomic nervous system can effectively modulate the gastric motility.

Modulation of gastric motility induced by acupuncture stimulation involved in activation of fine-diameter afferent fibers

The flexion reflex is usually described as an EMG discharge that mainly consists of two-components separated by periods of an EMG absence. The present results are very similar to those described by Falinower *et al*[11] and by our recent observation[12] in which sural nerve stimulation evoked a two-component reflex in the flexor muscles of the ipsilateral hindlimb. Based on accumulative electrophysiological and pharmacological evidence, the first-component is triggered by activities of small diameter Aδ-fibers, and the second-component is mediated by the unmyelinated C-fibers.

The present study demonstrated that electro-acupuncture stimulation with the strength below $T_{A\delta}$ could not effectively trigger regulatory effects on gastric motility, regardless of the locations of acupoints. Only electro-acupuncture stimulation with the strength exceeding the thresholds for activation of Aδ and/or C-fibers could profoundly modulate gastric motility. Moreover, the effects were strength-dependent and the powerful effects were

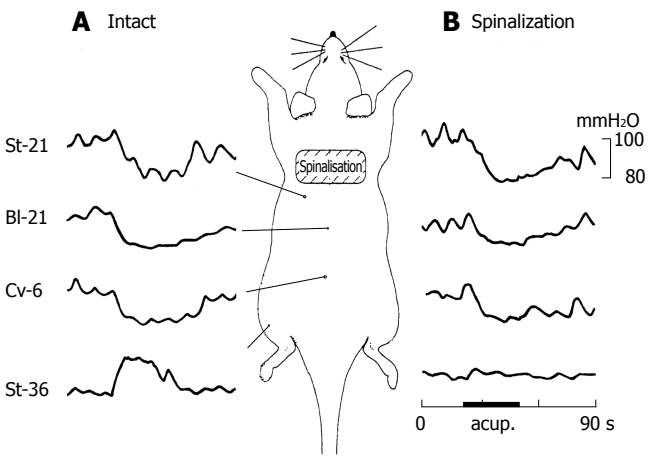

Figure 6 Effects of acupuncture stimulation involving the supraspinal circuit on gastric motility in normal (**A**) and spinalized (**B**) rats.

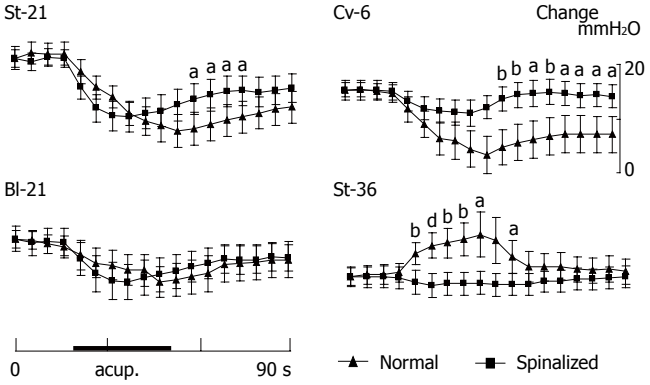

Figure 7 Effects of acupuncture stimulation at different acupoints on the regulation of gastric motility in normal and spinalized rats. Triangle-lines represent the pre-spinalized effects and square-lines indicate the post-spinalized effects. $^{a}P < 0.05$, $^{b}P < 0.01$ and $^{d}P < 0.001$ *vs* the control gastric motility of pre-spinalization.

observed when the strongest stimulation was given.

Electro-acupuncture stimulation has been known to excite various afferent fibers of rats including groups Ⅱ-Ⅲ[13], groups Ⅲ-Ⅳ[14] or groups Ⅱ-Ⅳ[15]. Koizumi *et al*[16] performed a systematical analysis of the relationship between the magnitude of cutaneo-intestinal reflex response and groups of stimulated afferent fibers. Their results indicate that stimulation of groups Ⅱ-Ⅲ cutaneous fibers in the T_{10} spinal nerve could not produce any changes in jejunal motility, while stimulation of groups Ⅱ-Ⅲ-Ⅳ fibers could always induce inhibitory responses. Stimulation of the sural afferent nerves of the hindlimb could elicit facilitative jejunal reflex, which was obtained when the stimulus intensity could activate group Ⅲ fibers and the maximal facilitation appeared when the stimulus intensity could activate group Ⅳ afferent fibers. Noguchi *et al*[17] reported that when electro-acupuncture stimulation intensity at hindlimb was less than 1.5-mA (only activation of group Ⅱ fibers), equivalently to 0.8-$T_{A\delta}$ (1.42 ± 0.36 mA) electro-acu puncyure-stimulation in our present study, there was no significant response of duodenal motility. When the intensity of electro-acupuncture stimulation exceeded 2.0-5.0-mA (activation of groups Ⅱ-Ⅲ and Ⅳ fibers), equivalently to 2-$T_{A\delta}$ (3.62 ± 0.44 mA) electro-acu-stimulation in our study, a slight increase was observed in duodenal motility. The maximal excitatory response of duodenal motility to electro-acupuncture stimulation was observed in 10-mA (activation of various afferent fibers) at hindlimb, which was equivalent to1.5-T_C (7.68 ± 0.53 mA) electro-acu puncyure-stimulation in our study. These studies demonstrated that stimulating groups Ⅲ-Ⅳ, particularly group Ⅳ or C afferent fibers of hindlimb, could produce an excitatory intestinal reflex response. On the other hand, stimulation of only group Ⅳ abdominal nerves produces an inhibitory intestinal reflex response.

These data suggest that only acupuncture stimulation with an intensity strong enough to excite Aδ (or group Ⅲ) and/or C (or group Ⅳ) afferent fibers, can lead to markedly excitatory/inhibitory modulation of gastro-intestinal motility.

Facilitation of gastric motility induced by acupuncture stimulation involved in vagal nerve and supraspinal circuit

The present study showed that acupuncture stimulation to the acupoints on face, neck, forelimbs, upper chest-dorsum and hindlinbs produced a facilitative response of gastric motility. These effects were involved in intact preparation of vagal nerves and the spinal cord, but did not require intact preparation of the splanchnic nerves.

Motor activity of the stomach, like other gastrointestinal organs, is modulated by the changes in vagal activity. It was reported that electro-acupuncture at acupoints of St-36 and Pc-6 (Neiguan, located in forelimb) enhances the gastric migrating myoelectrical complex in dogs by reducing the length of phase-I and increasing the length of phases Ⅱ and Ⅲ[18]. Ouyang *et al*[19] observed that electro-acupuncture at Pc-6 and St-36 substantially accelerates gastric emptying of liquid in dogs. The accelerating effect of electro-acupuncture on gastric emptying may be attributed to the improvement in gastric tone and antral contractile activity. Enhanced vagal activity by electro-acupuncture suggests a possible involvement of vagal pathways in its regulation of gastric motility. Xu[20] found that the regulatory effect of electro-acupuncture on gastric dysrhythmia in rabbits could be abolished after vagotomy. Sato *et al*[9] showed that acupuncture-like stimulation could elicit an excitatory gastric response when it is applied to the hindlimb. These findings suggest that acupuncture provokes a reflex that has cutaneous and muscle nerves as its afferent pathway, and the gastric vagus as its efferent pathway. In our study, acupuncture stimulation at St-36 could facilitate gastric motility by increasing the activity of gastric efferent nerves. However, this facilitation of gastric motility disappeared in spinalized rats. The facilitative duodenal response by electro-acupuncture stimulation to a hindpaw is a supraspinal reflex response involving vagal excitatory nerves, cutting the splanchnic nerve branches to the duodenal does not affect the enhanced duodenal response[17].

Facilitation in gastric motility and increase in parasympathetic activity by (electro-) acupuncture

stimulation to all acupoints except for those of abdomen and middle-dorsum (the acupoints of homo-segmental to the innervation of stomach) are accompanied with a decrease in sympathetic activity or a breakage of possible "sympathetic dominance"[21,22], suggesting that these effects require the participation of supraspinal center.

Inhibition of gastric motility induced by acupuncture stimulation involved in sympathetic nerve and propriospinal circuit

The present study showed that acupuncture stimulation to the acupoints on lower-chest, middle-dorsum and whole abdomen could induce an inhibitory response of gastric motility with an increase in the activities of sympathetic and/or a slight inhibition in the activity of vagal nerves innervating the stomach, suggesting that these effects are involved in intact preparation of sympathetic (splanchnic) nerves, but do not require intact preparation of bilateral vagal nerves and high spinal cord.

Sato *et al*[9] showed that the abdominal acupuncture-like stimulation could elicit suppressive response of gastric motility, indicating that acupuncture provokes a reflex that has cutaneous and muscle nerves as its afferent pathway, and the sympathetic gastric branches as its efferent pathway. This inhibition is accompanied with an increase in the activity of efferent nerves of sympathetic gastric branches and can be observed in spinalized rats. The inhibitory duodenal response to electro-acupuncture stimulation in abdomen is a propriospinal reflex response involving splanchnic excitatory nerves, cutting the vagal nerve branches to the duodenal does not affect the suppressed duodenal response[17]. Using duplex Doppler sonography, Choi *et al*[23] found that the frequency of intestinal motility is increased during acupuncture stimulation at St-36 acupoint. Acupuncture on the lower abdomen causes a transient relaxation of the stomach, which can be abolished by splanchnic ganglionectomy but not by truncal vagotomy[24].

In conclusion, acupuncture stimulation to the acupoints on face, neck, forelimbs, upper chest-dorsum and hindlinbs, which are distant to the region of gastric innervation, produces a facilitative response of gastric motility with increased activities of vagus and/or a slight inhibition in the activity of sympathetic nerves. These effects are involved in the intact preparation of vagal nerves and spinal cord, but do not require intact preparation of the splanchnic nerves. Acupuncture stimulation to the acupoints on lower-chest, middle-dorsum and whole abdomen, which are homo-segmental to the region of gastric innervation, induces an inhibitory response of gastric motility with increased activities of sympathetic nerves and/or a slight inhibition in the activity of vagal nerves. These effects are involved in intact preparation of sympathetic nerves, but do not require intact preparation of bilateral vagal nerves and high spinal cord. Only the acupuncture stimulation with its intensity greater than the threshold for activation of Aδ and/or C afferent fibers can induce markedly excitatory/inhibitory modulation of gastrointestinal motility.

ACKNOWLEDGMENTS

We gratefully acknowledge Professor XC Yu for the help in preparation of this manuscript.

REFERENCES

1 **Ma SX**. Neurobiology of Acupuncture: Toward CAM. *Evid Based Complement Alternat Med* 2004; **1**: 41-47
2 **Knardahl S**, Elam M, Olausson B, Wallin BG. Sympathetic nerve activity after acupuncture in humans. *Pain* 1998; **75**: 19-25
3 **Haker E**, Egekvist H, Bjerring P. Effect of sensory stimulation (acupuncture) on sympathetic and parasympathetic activities in healthy subjects. *J Auton Nerv Syst* 2000; **79**: 52-59
4 **Sato A**. Neural mechanisms of autonomic responses elicited by somatic sensory stimulation. *Neurosci Behav Physiol* 1997; **27**: 610-621
5 **Mayer DJ**. Biological mechanisms of acupuncture. *Prog Brain Res* 2000; **122**: 457-477
6 **Consensus Development Panel Program and Abstracts**. NIH Consensus Statement Online 1997: 15
7 **Chang CS**, Chou JW, Wu CY, Chang YH, Ko CW, Chen GH. Atropine-induced gastric dysrhythmia is not normalized by electroacupuncture. *Dig Dis Sci* 2002; **47**: 2466-2472
8 **Chang CS**, Ko CW, Wu CY, Chen GH. Effect of electrical stimulation on acupuncture points in diabetic patients with gastric dysrhythmia: a pilot study. *Digestion* 2001; **64**: 184-190
9 **Sato A**, Sato Y, Suzuki A, Uchida S. Neural mechanisms of the reflex inhibition and excitation of gastric motility elicited by acupuncture-like stimulation in anesthetized rats. *Neurosci Res* 1993; **18**: 53-62
10 **Li YQ**, Zhu B, Rong PJ, Ben H, Li YH. Effective regularity in modulation on gastric motility induced by different acupoint stimulation. *World J Gastroenterol* 2006; **12**: 7642-7648
11 **Falinower S**, Willer JC, Junien JL, Le Bars D. A C-fiber reflex modulated by heterotopic noxious somatic stimuli in the rat. *J Neurophysiol* 1994; **72**: 194-213
12 **Zhu B**, Xu WD, Rong PJ, Ben H, Gao XY. A C-fiber reflex inhibition induced by electroacupuncture with different intensities applied at homotopic and heterotopic acupoints in rats selectively destructive effects on myelinated and unmyelinated afferent fibers. *Brain Res* 2004; **1011**: 228-237
13 **Kawakita K**, Funakoshi M. Suppression of the jaw-opening reflex by conditioning a-delta fiber stimulation and electroacupuncture in the rat. *Exp Neurol* 1982; **78**: 461-465
14 **Noguchi E**, Ohsawa H, Kobayashi S, Shimura M, Uchida S, Sato Y. The effect of electro-acupuncture stimulation on the muscle blood flow of the hindlimb in anesthetized rats. *J Auton Nerv Syst* 1999; **75**: 78-86
15 **Ohsawa H**, Yamaguchi S, Ishimaru H, Shimura M, Sato Y. Neural mechanism of pupillary dilation elicited by electro-acupuncture stimulation in anesthetized rats. *J Auton Nerv Syst* 1997; **64**: 101-106
16 **Koizumi K**, Sato A, Terui N. Role of somatic afferents in autonomic system control of the intestinal motility. *Brain Res* 1980; **182**: 85-97
17 **Noguchi E**, Ohsawa H, Tanaka H, Ikeda H, Aikawa Y. Electro-acupuncture stimulation effects on duodenal motility in anesthetized rats. *Jpn J Physiol* 2003; **53**: 1-7
18 **Qian L**, Peters LJ, Chen JD. Effects of electroacupuncture on gastric migrating myoelectrical complex in dogs. *Dig Dis Sci* 1999; **44**: 56-62
19 **Ouyang H**, Yin J, Wang Z, Pasricha PJ, Chen JD. Electroacupuncture accelerates gastric emptying in association with changes in vagal activity. *Am J Physiol Gastrointest Liver Physiol* 2002; **282**: G390-G396
20 **Xu G**. Regulating effect of electro-acupuncture on dysrythmia of gastro-colonic electric activity induced by erythromycine in rabbits. *Zhenci Yanjiu* 1994; **19**: 71-74
21 **Daniel EE**. Electrical and contractile responses of the pyloric

region to adrenergic and cholinergic drugs. *Can J Physiol Pharmacol* 1966; **44**: 951-979
22 **Kim CH**, Zinsmeister AR, Malagelada JR. Mechanisms of canine gastric dysrhythmia. *Gastroenterology* 1987; **92**: 993-999
23 **Choi M**, Jung J, Seo M, Lee K, Nam T, Yang I, Yoon Y, Yoon J. Ultrasonographic observation of intestinal mobility of dogs after acupunctural stimulation on acupoints ST-36 and BL-27. *J Vet Sci* 2001; **2**: 221-226
24 **Tada H**, Fujita M, Harris M, Tatewaki M, Nakagawa K, Yamamura T, Pappas TN, Takahashi T. Neural mechanism of acupuncture-induced gastric relaxations in rats. *Dig Dis Sci* 2003; **48**: 59-68

S- Editor Liu Y **L- Editor** Wang XL **E- Editor** Liu WF

PO Box 2345, Beijing 100023, China
www.wjgnet.com
wjg@wjgnet.com

World J Gastroenterol 2007 February 7; 13(5): 717-724
World Journal of Gastroenterology ISSN 1007-9327

BASIC RESEARCH

Experimental study of therapeutic efficacy of Baicalin in rats with severe acute pancreatitis

Xi-Ping Zhang, Ling Zhang, Jin-Xian He, Rui-Ping Zhang, Qi-Hui Cheng, Yi-Feng Zhou, Bei Lu

Xi-Ping Zhang, Bei Lu, Department of General Surgery, Hangzhou First People's Hospital, Hangzhou 310006, Zhejiang Province, China
Ling Zhang, Class s0201 of Seven Year's Clinical Medicine, Shanxi Medical University, Taiyuan 030001, Shanxi Province, China
Jin-Xian He, Grade 03, Department of Clinical Medicine, School of Medcine, Zhejiang University, Hangzhou 310058, Zhejiang Province, China
Rui-Ping Zhang, First Affiliated Hospital, Shanxi Medical University, Taiyuan 030001, Shanxi Province, China
Qi-Hui Cheng, Department of Gynaecology and Obstetrics, Hangzhou First People's Hospital, Hangzhou 310006, Zhejiang Province, China
Yi-Feng Zhou, Department of Gastroenterology, Hangzhou First People's Hospital, Hangzhou 310006, Zhejiang Province, China
Supported by Technological Foundation Project of Traditional Chinese Medicine Science of Zhejiang Province, No. 2003C130 and No. 2004C142; Foundation Project for Medical Science and Technology of Zhejiang province, No. 2003B134; Grave Foundation Project for Technological and Development of Hangzhou, No. 2003123B19; Intensive Foundation Project for Technology of Hangzhou, No. 2004Z006; Foundation Project for Medical Science and Technology of Hangzhou, No. 2003A004; and Foundation Project for Technology of Hangzhou, No. 2005224
Correspondence to: Xi-Ping Zhang, MD, Department of General Surgery, Hangzhou First People's Hospital, 261 Huansha Road, Hangzhou 310006, Zhejiang Province, China. zxp99688@vip.163.com
Telephone: +86-571-87065701 Fax:+86-571-87914773
Received: 2006-08-19 Accepted: 2006-12-12

Abstract

AIM: To observe the therapeutic efficacy of Baicalin in rats with severe acute pancreatitis (SAP) and explore its therapeutic mechanisms.

METHODS: The SAP rat models were randomly divided into the model control group, Baicalin treatment group, octreotide treatment group and sham operation group. All groups were randomly subdivided into 3 h, 6 h and 12 h groups with 15 rats in each group. The survival, ascites volume and pathological changes of pancreas in all rats were observed at different time points after operation. The plasma amylase content and serum TNF-α, IL-6, malonaldehyde (MDA) and PLA_2 contents were also determined.

RESULTS: The survival was not obviously different between the treated groups, and was significantly higher in treated groups at 12 h compared to the model control group ($P < 0.05$, 15 *vs* 10). The ascites/body weight ratio at 3 h and 6 h was significantly lower in Baicalin treatment group compared to the model control group and octreotide treatment group ($P < 0.05$, 1.00 *vs* 2.02 and 1.43 and $P < 0.001$, 2.29 (1.21) *vs* 2.70 (0.80) and 2.08 (2.21), respectively). The contents of amylase, TNF-α, IL-6, MDA and PLA_2 were significantly lower in the treated groups than in the model control group ($P < 0.05$, 4342 *vs* 5303, 5058 *vs* 6272 in amylase, $P < 0.01$, 21.90 *vs* 36.30, 23.80 *vs* 39.70, 36 *vs* 54.35 in MDA and 56.25 *vs* 76.10 in PlA_2, or $P < 0.001$, 65.10 and 47.60 *vs* 92.15 in TNF-α, 3.03 *vs* 5.44, 2.88 *vs* 6.82, 2.83 *vs* 5.36 in IL-6, respectively). The pathological scores of pancreas in the treated groups were significantly lower than that in the model control group ($P < 0.05$, 9.00 *vs* 10.05, 6.00 *vs* 9.00, 8.00 *vs* 10.05), but no marked difference was found between the treated groups.

CONCLUSION: The Baicalin injection has significant therapeutic effects on SAP rats, its effects are similar to those of octreotide. The Baicalin injection is also cheap and has a big application range, quite hopefully to be used in clinical treatment of SAP.

Key words: Severe acute pancreatitis; Baicalin; Octreotide; Rats; Serum amylase; TNF-α; IL-6; Malonaldehyde; PLA_2

Zhang XP, Zhang L, He JX, Zhang RP, Cheng QH, Zhou YF, Lu B. Experimental study of therapeutic efficacy of Baicalin in rats with severe acute pancreatitis. *World J Gastroenterol* 2007; 13(5): 717-724

http://www.wjgnet.com/1007-9327/13/717.asp

INTRODUCTION

As one of the life-threatening severe diseases, severe acute pancreatitis (SAP) has acute onset, rapid progression, multiple complications, and its mortality has reached 20%-30%. The pathogenesis of SAP is still unknown, and no breakthrough has ever been made in its treatment. Currently, mainly somatostatin and its analog octreotide are effective drugs for SAP treatment in the clinic.

Octreotide, also named sandostatin, as an analog of

natural somatostain plays an important role in improving the survival rate of SAP animals, inhibiting secretion of pancreatin and alleviating multiple organ injury[1-3]. However, the expensive price, short half-life and inconvenient administration of these drugs have restrained their clinical popularization, especially in remote poor areas. So, it is necessary to find some cheap and highly effective drugs.

In "Qing Yi Tang" which is a representative prescription of Chinese medicine for SAP treatment, the enormous clinical practices also suggest its sound therapeutic effects on SAP[4]. Scutellaria baicalensis georgi is a main material in "Qing Yi Tang" while Baicalin (monomer) is its main active constituent. The intravenous administration with very low price can overcome the shortcomings of oral administration of "Qing Yi Tang", including poor absorption and inconvenience. The *in vitro* experiments of Baicalin have proved[5-7]: it has anti-bacterial, anti-viral and anti-inflammatory activities. It can also inhibit platelet aggregation and eliminate oxygen-free radicals. In animal experiments, Baicalin with choleretic effectcan can relieve fever, inhibit the thrombin-induced transforming process from fibringen to fibrin, lower endotoxin generation, treat and prevent endotoxemia-induced disseminated intravascular coagulation. In addition, the initial metabolite of Baicalin in body is baicalein that can more effectively inhibit pancreatin. All these pharmacologic effects can antagonize many processes during SAP onset. Its several effects are similar to those of somatostatin and its analog such as octreotide, but it has a broader application range. It is theoretically feasible to use it for SAP treatment.

Presently, to the best of our knowledge, there has not been any study report on Baicalin treatment of SAP internationally. In this experiment, we have established the SAP rat model, discussed the effects of Baicalin in treating SAP rats, compared its effects with those of octreotide and observed the therapeutic efficacy of Baicalin and explored its therapeutic mechanisms in order to provide the reliable basis for Baicalin treatment of SAP.

MATERIALS AND METHODS

Experimental animals and reagents

Clean grade healthy male Sprague-Dawley (SD) rats weighing 250-300 g were purchased from the Experimental Animal Center of Medical School, Zhejiang University, China. Sodium taurocholate and sodium pentobarbital were purchased from Sigma Company, USA. Octreotide was purchased from Swiss Pharmaceutical Company Novartis, and 5% Baicalin injection (China National Invention Patent Number ZL200310122673.6) was prepared by the first author with 305 mmol/L osmotic pressure. The TNF-α ELISA kit was purchased from Jingmei Bioengineering Corporation (China) and the calculation unit for content is pg/mL (ng/L). The IL-6 ELISA kit was purchased from Shanghai Shenxiong Biotech Company (China) and the calculation unit for content is pg/mL (ng/L). The serum malonaldehyde (MDA) kit was purchased from Nanjing Jiancheng Bioengineering Research Institute, China. The calculation units for content are respectively nmol/mL. The serum secretory phospholipase A_2 enzyme assay ELA kit (PLA_2) was purchased from R&D System Ins, USA and the calculation unit for content is U/mL.

Animal grouping

The improved Aho's method[8] was adopted to prepare SAP rat models *via* retrograde injection of 3.5% sodium taurocholate to the pancreatic duct through epidural catheter and duodenal papilla. The 135 SAP rat models were randomly divided into model control group, Baicalin treatment group and octreotide treatment group with 45 rats in each group; other 45 rats were selected as sham operation group, which only received laparotomy. All groups were then randomly subdivided into 3 h, 6 h and 12 h groups with 15 rats in each group.

Observation index

We examined the rat mortality at 3 h, 6 h and 12 h after operation and calculated the survival, observed the gross changes of pancreas and ascites volume. Ascites/body weight ratio was measured as follows: Dry gauze was used to wipe intra-abdominal hydrops; then, a scale was used to weigh the weights of gauze before and after its soaking; the difference between weights (g) was converted into ascites volume (mL); and ascites/body weight ratio was thus obtained. After mercy killing the rats anesthetized by sodium pentobarbital in batches, the samples of pancreas were collected, fixed according to the requirements, and the pathological changes of pancreas after hematoxylin-eosin (HE) staining were observed. The contents of plasma amylase and serum TNF-α, IL-6, MDA and PLA_2 were determined *via* blood sampling from heart. The full automatic biochemical analyzer was used to determine the plasma amylase level and the calculation unit for content is U/L. The serum TNF-α, IL-6 and PLA_2 levels were determined by ELISA method.

Pancreatic pathological score

A modified Schmidt's pathological score system was used (Table 1) and two pathologists in double-blind control condition performed the evaluation of severity of pancreatic tissue pathology. We modified the pathological score of pancreas, because the Schmidt's pathological score[9] was too difficult and complex to be used in our experiment.

Preparation methods of animal models

Fasting but water restraint was imposed on all rat groups 12 h prior to the operation. The rats were anesthetized by intraperitoneal injection of 2% sodium pentobarbital (0.25 mL/100 g), then laid and fixed, and the routine shaving, disinfection and draping were performed. We first established the right external jugular vein transfusion passage to use the microinfusion pump for continuous transfusion (1 mL/h per 100 g) and then used 3.5% sodium taurocholate to prepare SAP model.

Model control group: After entering the abdomen *via* median epigastric incision, we confirmed the bile-pancreatic duct, hepatic hilus and common hepatic duct, disclosed the pancreas, identified the duodenal papilla inside the duodenum duct wall, and then used a No. 5 needle to drill a hole in the mesenteric avascular

Table 1 Improved Schmidt score of pathological changes of the pancreas

Edema		Acinar necrosis (necrotic cells/HPF)		Inflammation and perivascular infiltrate (intralobular or perivascular leukocytes/HPF)		Hemorrhage and fat necross (focus)	
Absent	0	Absent	0	0-1	0	Absent
Focal expansion of interlobular septae	1	1-4	1	2-10	1	1-2
Same as 1 + diffuse expansion of interlobar; Septae/diffuse expansion of interlobar septae	2	5-10	2	11-20	2	3-4
Same as 2 + expansion of interacinar septae	3	11-16	3	21-30	3	5-6
Same as 3 + expansion of intercellular spaces	4	> 16	4	> 30/microabscesses	4	> 7

area. After inserting a segmental eqidural catheter into the duodenum cavity *via* the hole, we inserted the bile-pancreatic duct toward the direction of the papilla in a retrograde way, used the microvascular clamp to nip the duct head temporarily and meanwhile used another microvascular clamp to temporarily occlude the common hepatic duct at the confluence of the hepatic duct. After connecting the anesthetic tube end with the transfusion converter, we transfused 3.5% sodium taurocholate (0.1 mL/100 g) by retrograde transfusion *via* the microinjection pump (made by Zhejiang University) at a speed of 0.2 mL/min, then stayed for 4-5 min after injection and removed the microvascular clamp and eqidural catheter. After checking for bile leakage, we sutured the hole in the lateral duodenal wall, used the disinfected cotton ball to absorb up the anesthetic in the abdominal cavity and closed the abdomen. During the laparotomy in the sham operation group, we performed pancreas and duodenum turning over, observed pathological changes of multiple organs and finally closed the abdomen.

Dosage and methods

In Baicalin treatment group, the animal experiments of 5% Baicalin injection were completed including the acute toxicity test and SAP rat treatment by small, middle and large dose. The large dose could achieve the best therapeutic effect (dose is 10 mg/h per 100 g) and the dosage referred to the result of the previous preliminary experiment. Ten minutes after successful modeling, Baicalin treatment group was first injected 5% Baicalin injection 10 mg/100 g *via* the external jugular vein passage, followed by continuous intravenous administration (10 mg/h per 100 g) by microinfusion pump; octreotide treatment group was first injected octreotide 0.2 μg/100 *g via* the external jugular vein passage, followed by continuous intravenous transfusion (10 mg/h per 100 g) by microinfusion pump at a transfusion speed of 0.2 μg/h per 100 g. All above dosages have been proved as effective dosages in the previous preliminary experiment. Both of the sham operation group and model control group were injected saline of equivalent volume at the corresponding time points after operation.

Statistical analysis

The values were presented as mean ± SD for nomal distribution variables or median and quartile range for highly skewed variables. The significance of differences among the four groups was tested using the Kruskal-Wallis test for highly skewed data and analysis of variance (ANOVA) for normal distribution data. Multiple comparisons were subjected to Bonfferoni correction test. The Chi-square test was used to evaluate equality of frequencies for discrete variables. Correlations were tested using the Spearman rank correlation coefficients. A P value less than or equal to 0.05 was considered statistically significant. All statistical analyses were conducted using SPSS version 11.5 for windows.

Table 2 Comparison of ascites/body weight ratio [M (Q_R)]

Groups	3 h	6 h	12 h
Sham operation	0.28 (0.23)	0.44 (0.15)	0.39 (0.22)
Model control	2.02 (0.89)	2.62 (0.97)	2.70 (0.80)
Baicalin treatment	1.00 (1.30)	1.16 (0.73)	2.29 (1.21)
Octreotide treatment	1.43 (0.62)	2.15 (0.88)	2.08 (2.21)

RESULTS

Survival rate

The mortality rates of the model control group were 0% (0/15), 13.33% (2/15) and 33.33% (5/15) at 3 h, 6 h and 12 h, respectively, while those of Baicalin treatment group and octreotide treatment group were 0% at different time points. The whole sham operation group survived at different time points. The survival rate of the model control group was 66.67% (10/15) at 12 h, while the survival rate of each of Baicalin treatment group and octreotide treatment group was 100% at 12 h, indicating a marked difference ($P < 0.05$).

Comparison of ascites/body weight ratio among all groups

The ascites/body weight ratio of the model control group and treatment group significantly exceeded the sham operation group at different time points ($P < 0.001$), while there was no significant difference between the octreotide treatment group and model control group at different time points. Ascites/body weight ratio of the Baicalin treatment group was significantly less than the model control group ($P < 0.01$) and octreotide treatment group at 3 h ($P < 0.05$). Ascites/body weight ratio of the Baicalin treatment group was significantly less than the model control group and octreotide treatment group at 6 h ($P < 0.001$). However, there was no significant difference among the Baicalin treatment group, model control group and octreotide treatment group at 12 h (Table 2).

Table 3 Comparison of different indexes of blood [*M* (Q_R)]

Indexes	Sham operation			Model control			Baicalin treatment			Octreotide treatment		
	3 h	6 h	12 h	3 h	6 h	12 h	3 h	6 h	12 h	3 h	6 h	12 h
Amylase (U/L)	1582 (284)	1769 (362)	1618 (302)	5303 (1373)	6276 (1029)	7538 (2934)	4342 (1496)	5130 (1591)	5571 (2307)	5419 (1670)	5058 (1314)	6531 (2280)
TNF-α (ng/L)	3.90 (3.20)	4.00 (1.70)	5.30 (3.00)	41.44 (37.72)	92.15 (23.12)	65.02 (26.81)	44.93 (45.84)	65.10 (27.51)	47.65 (25.52)	39.30 (30.60)	47.60 (16.50)	54.50 (41.40)
IL-6 (ng/L)	1.8460 (0.35)	1.74 (0.84)	2.04 (0.82)	5.44 (1.03)	6.82 (0.81)	5.36 (0.75)	3.03 (0.87)	2.88 (1.39)	2.83 (0.60)	2.65 (1.37)	3.08 (1.210)	2.46 (1.35)
MDA (nmol/mL)	9.90 (9.90)	16.50 (13.20)	16.50 (13.20)	36.30 (13.40)	39.70 (9.90)	54.35 (19.00)	21.90 (13.45)	23.80 (14.60)	36.00 (11.60)	29.60 (18.60)	33.00 (9.90)	40.30 (16.80)

Table 4 Comparison of serum PLA2 content (mean ± SD)

Groups	3 h	6 h	12 h
Sham operation	14.62 ± 3.02	17.49 ± 3.82	19.02 ± 5.07
Model control	76.10 ± 16.70	101.46 ± 14.67	105.33 ± 18.10
Baicalin treatment	56.25 ± 22.43	67.91 ± 20.61	66.86 ± 22.10
Octreotide treatment	74.37 ± 19.94	63.13 ± 26.31	53.63 ± 12.28

Comparison of plasma amylase content among all groups

The plasma amylase content in the model control group and two treatment groups significantly exceeded that in the sham operation group at different time points ($P < 0.001$). However, there was no significant difference between the Baicalin treatment group and octreotide treatment group at different time points. Although the plasma amylase content of the Baicalin treatment group was lower than that of the model control group at different time points, the difference did not reach statistical significance at 6 h and 12 h, but reached statistical significance at 3 h ($P < 0.05$). Although plasma amylase content was significantly less in the octreotide treatment group compared to the model control group at 6 h ($P < 0.05$), no significant difference was observed at 3 h and 12 h (Table 3).

Comparison of serum TNF-α content among all groups

Serum TNF-α content significantly exceeded in the model control group and treatment groups compared to the sham operation group at different time points ($P < 0.001$). There was no significant difference in serum TNF-α content among the model control group, Baicalin treatment group and octreotide treatment group at 3 h and 12 h. However, at 6 h, both Baicalin treatment group and octreotide treatment group had significantly less serum TNF-α content compared to the model control group ($P < 0.001$); and the octreotide treatment group had significantly less serum TNF-α content than the Baicalin treatment group ($P < 0.01$) (Table 3).

Comparison of serum IL-6 content among all groups

The serum IL-6 content at 3 h and 6 h was significantly higher in the model control group and treated groups than in the sham operation group ($P < 0.001$). Baicalin treatment group and octreotide treatment group had no significant difference in serum IL-6 content at all time points. The Baicalin treatment group and octreotide treatment group had significantly lower serum IL-6 content than the model control group at all time points ($P < 0.001$). However, the model control group had significantly higher serum IL-6 content than the sham operation group at 12 h ($P < 0.001$), and so had the Baicalin treatment group ($P < 0.01$), but no significant difference was found between the octreotide treatment group and the sham operation group (Table 3).

Comparison of serum MDA content among all groups

Serum MDA content significantly exceeded in the model group, Baicalin treatment group and octreotide treatment group compared to the sham operation group at different time points ($P < 0.05$). Serum MDA content was significantly less in the Baicalin treatment group than the model group ($P < 0.01$). Similarly, serum MDA content was significantly less in the octreotide treatment group than the model group at 6 h and 12 h ($P < 0.05$). However, serum MDA content was significantly less in the Baicalin treatment group compared to the octreotide treatment group at 12 h ($P < 0.05$) (Table 3).

Comparison of serum PLA_2 content among all groups

Serum PLA_2 content significantly exceeded in the model group and treatment groups compared to the sham operation group at different time points ($P < 0.001$). At 3 h, the Baicalin treatment group had significantly less serum PLA_2 content than the model group ($P < 0.01$), while there was no marked difference between the octreotide treatment group and the model group, and the Baicalin treatment group had significantly less serum PLA_2 content than the octreotide treatment group ($P < 0.01$). At 6 h and 12 h, the Baicalin treatment group and octreotide treatment group had significantly less serum PLA_2 content than the model group ($P < 0.001$). At 6 h, there was no marked difference between the Baicalin treatment group and the octreotide treatment group, whereas at 12 h, the octreotide treatment group had significantly less serum PLA_2 content than the Baicalin treatment group ($P < 0.001$) (Table 4).

Macroscopic and microscopic pathological changes of the pancreas

Sham operation group: Macroscopically, there were only some amber ascitic fluid within the abdominal cavity, and no pathological changes visible to naked eyes in other

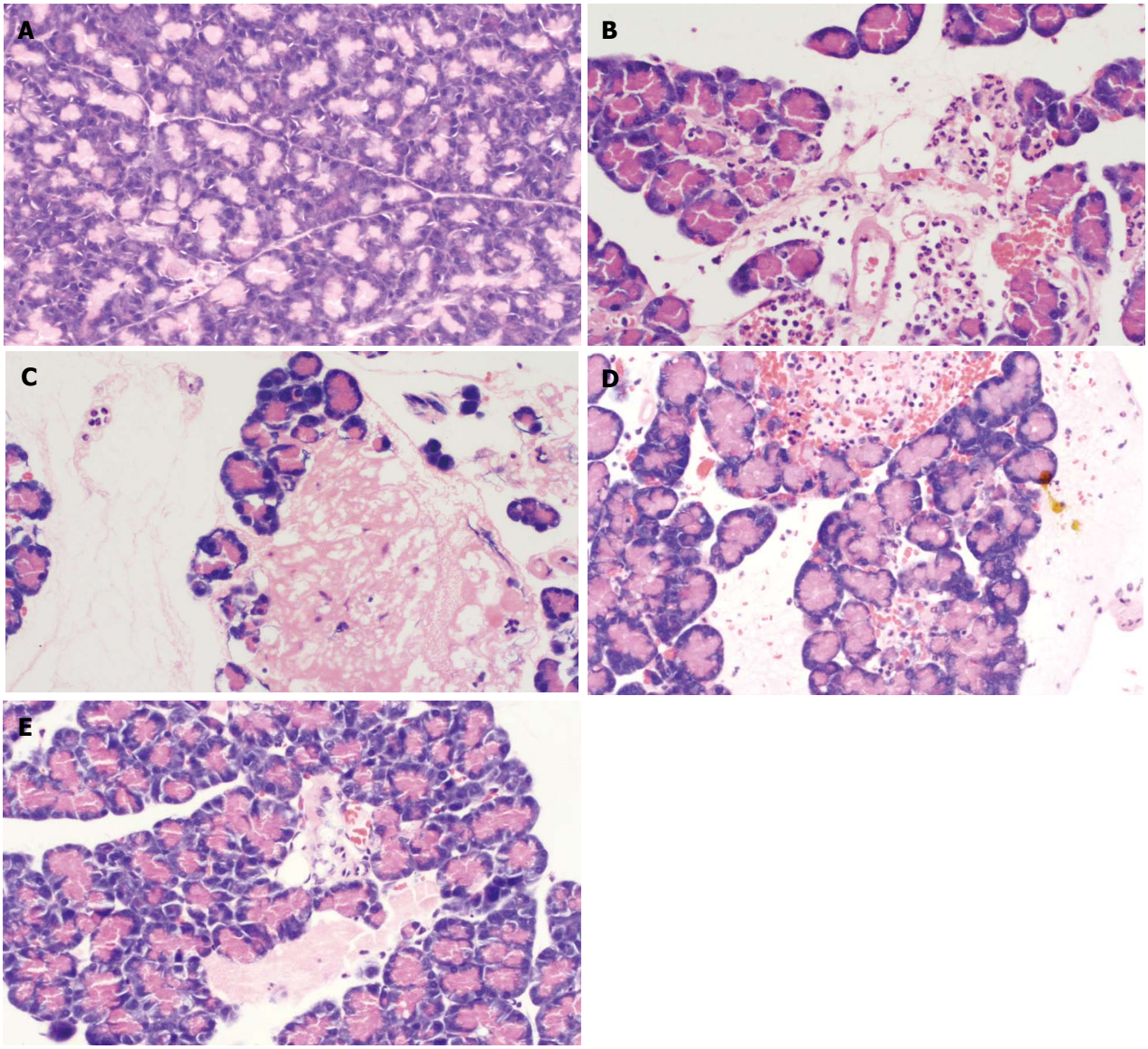

Figure 1 **A**: Sham operation group at 12 h (normal pancreas); **B**: Model control group at 12 h (Interacinar edema accompanied with piecemeal necrosis of acinus, a great deal of neutrophil infilatration among acini); **C**: Model control group at 12 h (Massive acinus necrosis); **D**: Baicalin treatment group at 12 h (interlobular and interacinar edema, focal necrosis of acinus, relatively much neutrophil infiltration among acini); **E**: Octreotide treatment group at 12 h (Interlobular edema accompanied with focal necrosis of acinus).

organs. The overall structure of the pancreas remained intact. There were no hemorrhagic changes in the pancreas, which was yellowish without volume reduction, and no significant abnormality in the pancreas, peripancreatic and epiploon at all time points. Microscopically, most remained normal with intact gland structure, mild interstitial edema occurred in very few cases, neutrophil infiltration was occasional, and no acinar cell and fat necrosis and hemorrhage were observed (Figure 1A).

Model control group: Macroscopically, pathological changes of the pancreas tail were a little more obvious than those of the pancreas head; 5 min after model induction, the pancreas manifested edema, hemorrhage and necrosis. The overall severity of the pathological changes at 3 h, 6 h and 12 h increased with time after modeling. In the 3 h group, small amount of ascitic fluid mostly slightly bloody visible to naked eyes, obvious hyperemia and edema of the pancreas, partly jellly-like edema, hemorrhage and necrosis were observed. Most ascitic fluid after 6 h and 12 h was bloody with the larger average amount than that at 3 h. The amount and characters of ascitic fluid increased and deepened with time after modeling; the degree and range of the pancreas edema, hemorrhage and necrosis became more obvious than those at 3 h; many saponified spots on peripancreatic great epiploon and peritoneum, jelly-like change, contour vanishing, quite obvious hemorrhage and necrosis changes of the pancreatic tissue were also observed. Microscopically, in the 3 h group, obvious pancreas interstitial hyperemia and edema, small amount of inflammatory cell infiltration, sporadic focal necrosis and interstitial hemorrhage occurred among which some were hemorrhagic or lytic necrosis; in the 6 h group, pancreas interstitial edema and hemorrhage, visible focal or lamellar necrosis, comparatively large area of inflammatory cell infiltration around were observed; and in the 12 h group, obvious pancreas interstitial edema, interstitial

Table 5 Comparison of pathological lesion score for pancreas (M (Q_R))

Groups	3 h	6 h	12 h
Sham operation	0.00 (1.00)	0.00 (1.00)	0.00 (1.00)
Model control	8.00 (2.00)	9.00 (3.00)	10.50 (1.50)
Baicalin treatment	7.00 (1.50)	7.00 (3.00)	9.00 (4.00)
Octreotide treatment	7.00 (2.00)	6.00 (2.00)	8.00 (2.00)

hemorrhage, large area of necrosis, lobule contour damage with a large amount of inflammatory cell infiltration were observed (Figures 1B and C).

Treatment group: Macroscopically, in the 3 h group, the pancreatic tissue with hyperemia and edema changes, milder hemorrhage and necrosis than those of model control group were observed; in the 6 h and 12 h groups, compared with the model control group, relatively limited pancreas hemorrhage and necrosis, lighter ascitic fluid color, obviously less ascitic fluid, decreased distribution and area of saponified spot, milder pancreas hemorrhage and necrosis, and relatively integrated overall pancreas structure were observed. The pathological changes of pancreatic tissue of the octreotide treatment group resembled those of the Baicalin treatment group. Microscopically, the pathological changes of most cases in the treatment group were milder than those of the model control group at the corresponding time points, such as decreased degree of interstitial edema, reduced inflammatory cell infiltration, more clear cell structure than that of the model control group, reduced pancreas interstitial erythrocyte exudation, small amount of focal hemorrhage and necrosis with little lamellar hemorrhage and necrosis, and reduced hemorrhage and necrosis range. The pathological changes of pancreatic tissue of the octreotide treatment group resembled those of the Baicalin treatment group (Figures 1D and E).

Comparison of pancreas pathological score among all groups

Pancreas pathological scores of the model control group, Baicalin treatment group and octreotide treatment group significantly exceeded those of the sham operation group at different time points ($P < 0.001$). Pancreas pathological score of the Baicalin treatment group was significantly less than that of the model control group at 12 h ($P < 0.01$). Moreover, pancreas pathological score of the octreotide treatment group was significantly less compared to the model control group at 6 h and 12 h ($P < 0.01$). However, there was no significant difference between the Baicalin treatment group and the octreotide treatment group at different time points (Table 5).

DISCUSSION

Severe acute pancreatitis (SAP) induces inflammatory reactions of pancreatic tissue itself or even systemic reactions, which is by a large portion related to excessive generation and cascade reactions of inflammatory mediators, mainly including endotoxin, oxygen-free radical, PLA_2, bradykinin, complement, acute-phase protein, vasoactive amine, arachidonic acid metabolite, cytokine (lymphokine) and PAF[10-14]. This study mainly investigates the therapeutic effects of Baicalin and octreotide by observing plasma amylase content and serum TNF-α and IL-6 content.

Table 6 Comparison of therapeutic efficacy of octreotide and Baicalin

Therapeutic efficacy	Curative	
	Baicalin	Octreotide
Improve survival rate	++	++
Decrease ascites volume	++	+
Decrease amylase	+	+
Decrease TNF-α	+	++
Decrease IL-6	++	+
Decrease MDA	+	++
Decrease PLA_2	++	+
Protect pancreatic tissue	++	++

++: Represents significant effect; +: Represents normal effect; -: No effect.

TNF-α participates in onset and progression of early-phase inflammations of acute pancreatitis (AP), and is also related to AP severity[15,16]. Excessive generation of TNF-α, or imbalance between it and other cytokines will stimulate cascade reactions, induce generation of IL-1, IL-6, IL-8, *etc*, later generate inflammatory mediators, and aggravate cell damage. Current studies found serum TNF-α had two aspects in regulating apoptosis, namely inducing apoptosis and promoting inflammation healing when its concentration was low, while leading to necrosis of pancreatic acinar cell when its concentration was high[17].

IL-6, mainly generated by monocyte after induction of IL-1, TNF, *etc*, has intensive inflammation-causing activity[18-21]. IL-6 can both directly increase the permeability of vascular endothelial cell, and has synergistic effect with TNF-α, *etc* to constitute a network of inflammatory mediators[20]. IL-6 level in serum can reflect AP severity[18,23,24]. It is generally recognized that the PLA_2 content or activity rises when SAP occurs[25]. The abnormal release and activation of PLA_2 can change lecithin into hemolytic lecithin, cause lysis and breakdown of pancreatic cell membrane, and lead to autodigestion of the pancreas[26-28]. The excessive free radicals generated in body during SAP may cause the accumulation of MDA, a lipid oxidative product. MDA content in serum can indicate the level of free radical overproduction[29,30].

In addition, a great quantity of endotoxin can induce TNF-α, stimulate or promote cytokine release including IL-1β[31], IL-6, TNF, and further mediate activation of leucocyte and platelet in multiple organs, such as pancreas, kidney and lung, and release lysosome, oxygen-free radical and lipid inflammatory substance. The excessive cytokines and inflammatory factors can cause waterfall-like cascade reactions, induce iNOS expression all over the body, generate a great deal of NO, damage blood vessel endothelium, and cause tissue necrosis[32-36].

Octreotide, a medicine currently adopted in the clinic for SAP treatment, mainly achieves its therapeutic effects

by inhibiting secretion of pancreatin and other digestive enzymes, and loosening the oddi sphincter. The most important is that octreotide can block the excessive expression of inflammatory mediators and cytokines, reduce iNOS mRNA expression and NO synthesis, and then alleviate injury of multiple organs, such as pancreas and lung[37,38]. This experiment found that compared with the model control group, both the Baicalin and octreotide treatment groups could effectively reduce the generation of ascites, plasma amylase content, and serum TNF-α, IL-6, MDA and PLA_2 content, alleviate pathological changes of pancreatic tissue, and lower mortality of SAP rats.

Compared with the octreotide group, Baicalin can more significantly inhibit the generation of ascites and excessive release of IL-6 and PLA_2 (Table 6). In addition, Baicalin also has features, such as a broad range of pharmacological actions, low side effect, and low price[37,39]. Therefore, using Baicalin to treat SAP will be an effective and cost-effective therapy for SAP.

REFERENCES

1 **Paran H**, Mayo A, Paran D, Neufeld D, Shwartz I, Zissin R, Singer P, Kaplan O, Skornik Y, Freund U. Octreotide treatment in patients with severe acute pancreatitis. *Dig Dis Sci* 2000; **45**: 2247-2251

2 **Küçüktülü U**, Alhan E, Erçin C, Cinel A, Calik A. Effects of octreotide on acute pancreatitis of varying severity in rats. *Eur J Surg* 1999; **165**: 891-896

3 **Shor NA**, Levina VP, Ioffe IV, Andreeva IV, Chumak IuF, Zhadanov VI, Zelenyĭ II. Application of octreotide in patients with acute pancreatitis. *Klin Khir* 2004; **(2)**: 15-17

4 **Li YY**, Gao ZF, Dui DH. Therapeutic effect of qingyi decoction and tetrandrine in treating severe acute pancreatitis in miniature pigs and serum drug level determination. *Zhongguo Zhongxiyi Jiehe Zazhi* 2003; **23**: 832-836

5 **Zhao YN**, Ding Y, Wang RF, Xing DM, Cheng J, Du L. A new approach to investigate the pharmacokinetics of traditional chinese medicine YL2000. *Am J Chin Med* 2004; **32**: 921-929

6 **Nakamura N**, Hayasaka S, Zhang XY, Nagaki Y, Matsumoto M, Hayasaka Y, Terasawa K. Effects of baicalin, baicalein, and wogonin on interleukin-6 and interleukin-8 expression, and nuclear factor-kappab binding activities induced by interleukin-1beta in human retinal pigment epithelial cell line. *Exp Eye Res* 2003; **77**: 195-202

7 **Shen YC**, Chiou WF, Chou YC, Chen CF. Mechanisms in mediating the anti-inflammatory effects of baicalin and baicalein in human leukocytes. *Eur J Pharmacol* 2003; **465**: 171-181

8 **Aho HJ**, Nevalainen TJ, Aho AJ. Experimental pancreatitis in the rat. Development of pancreatic necrosis, ischemia and edema after intraductal sodium taurocholate injection. *Eur Surg Res* 1983; **15**: 28-36

9 **Schmidt J**, Rattner DW, Lewandrowski K, Compton CC, Mandavilli U, Knoefel WT, Warshaw AL. A better model of acute pancreatitis for evaluating therapy. *Ann Surg* 1992; **215**: 44-56

10 **Klar E**, Werner J. New pathophysiologic knowledge about acute pancreatitis. *Chirurg* 2000; **71**: 253-264

11 **Saĭdalikhodzhaeva OZ**, Iuldashev NM, Daniiarov AN, Muratova UZ. Pancreatic enzyme activity in early phases of acute experimental pancreatitis in rats. *Ross Fiziol Zh Im I M Sechenova* 2002; **88**: 526-529

12 **Vasilescu C,** Herlea V, Buttenschoen K, Beger HG. Endotoxin translocation in two models of experimental acute pancreatitis. *J Cell Mol Med* 2003; **7**: 417-424

13 **Tomita Y**, Kuwabara K, Furue S, Tanaka K, Yamada K, Ueno M, Ono T, Maruyama T, Ajiki T, Onoyama H, Yamamoto M, Hori Y. Effect of a selective inhibitor of secretory phospholipase A2, S-5920/LY315920Na, on experimental acute pancreatitis in rats. *J Pharmacol Sci* 2004; **96**: 144-154

14 **Chvanov M**, Petersen OH, Tepikin A. Free radicals and the pancreatic acinar cells: role in physiology and pathology. *Philos Trans R Soc Lond B Biol Sci* 2005; **360**: 2273-2284

15 **Jin SL**, Niu WP, Qiu SQ. The changes of serum TNF-α and its receptor in patents with acute pancreatitis. *Zhonghua Putong Waike Zazhi* 1998; **13**: 287

16 **Li ZJ**, Xu YQ, Wang HM, Chen W. The effect of continuous high-volume hemofiltration therapy on TNF-alpha of pancreatitis patients complicated with acute renal function failure. *Xibao Yu Fenzi Mianyixue Zazhi* 2003; **19**: 373-375

17 **Zhang XP**, Lin Q. Study progress of the relationship between mediators of inflammation and apoptosis in acute panreatiti. *Shijie Huaren Xiaohua Zazhi* 2005; **13**: 2773-2777

18 **Chao KC,** Chao KF, Chuang CC, Liu SH. Blockade of interleukin 6 accelerates acinar cell apoptosis and attenuates experimental acute pancreatitis in vivo. *Br J* Surg 2006; **93**: 332-338

19 **Suzuki S**, Miyasaka K, Jimi A, Funakoshi A. Induction of acute pancreatitis by cerulein in human IL-6 gene transgenic mice. *Pancreas* 2000; **21**: 86-92

20 **Norman J**, Franz M, Messina J, Riker A, Fabri PJ, Rosemurgy AS, Gower WR. Interleukin-1 receptor antagonist decreases severity of experimental acute pancreatitis. *Surgery* 1995; **117**: 648-655

21 **Fink G**, Yang J, Carter G, Norman J. Acute pancreatitis-induced enzyme release and necrosis are attenuated by IL-1 antagonism through an indirect mechanism. *J Surg Res* 1997; **67**: 94-97

22 **Masamune A,** Shimosegawa T, Fujita M, Satoh A, Koizumi M, Toyota T. Ascites of severe acute pancreatitis in rats transcriptionally up-regulates expression of interleukin-6 and -8 in vascular endothelium and mononuclear leukocytes. *Dig Dis Sci* 2000; **45**: 429-437

23 **Brady M**, Christmas S, Sutton R, Neoptolemos J, Slavin J. Cytokines and acute pancreatitis. *Baillieres Best Pract Res Clin Gastroenterol* 1999; **13**: 265-289

24 **Inagaki T**, Hoshino M, Hayakawa T, Ohara H, Yamada T, Yamada H, Iida M, Nakazawa T, Ogasawara T, Uchida A, Hasegawa C, Miyaji M, Takeuchi T. Interleukin-6 is a useful marker for early prediction of the severity of acute pancreatitis. *Pancreas* 1997; **14**: 1-8

25 **Kiriyama S**, Kumada T, Tanikawa M. Recent advances in biochemical diagnosis and assessment of severity in acute pancreatitis. *Nihon Rinsho* 2004; **62**: 2035-2039

26 **Aufenanger J**, Samman M, Quintel M, Fassbender K, Zimmer W, Bertsch T. Pancreatic phospholipase A2 activity in acute pancreatitis: a prognostic marker for early identification of patients at risk. *Clin Chem Lab Med* 2002; **40**: 293-297

27 **Camargo EA**, Esquisatto LC, Esquisatto MA, Ribela MT, Cintra AC, Giglio JR, Antunes E, Landucci EC. Characterization of the acute pancreatitis induced by secretory phospholipases A2 in rats. *Toxicon* 2005; **46**: 921-926

28 **Mayer JM**, Raraty M, Slavin J, Kemppainen E, Fitzpatrick J, Hietaranta A, Puolakkainen P, Beger HG, Neoptolemos JP. Severe acute pancreatitis is related to increased early urinary levels of the activation Peptide of pancreatic phospholipase A(2). *Pancreatology* 2002; **2**: 535-542

29 **Kleinhans H**, Mann O, Schurr PG, Kaifi JT, Hansen B, Izbicki JR, Strate T. Oxygen radical formation does not have an impact in the treatment of severe acute experimental pancreatitis using free cellular hemoglobin. *World J Gastroenterol* 2006; **12**: 2914-2918

30 **Li ZD**, Ma QY, Wang CA. Effect of resveratrol on pancreatic oxygen free radicals in rats with severe acute pancreatitis. *World J Gastroenterol* 2006; **12**: 137-140

31 **Keck T**, Friebe V, Warshaw AL, Antoniu BA, Waneck G, Benz S, Hopt UT, Fernández-del-Castillo C. Pancreatic proteases in serum induce leukocyte-endothelial adhesion and pancreatic microcirculatory failure. *Pancreatology* 2005; **5**: 241-250

32 **Zhang JX**, Dang SC, Qu JG, Wang XQ, Chen GZ. Changes of

gastric and intestinal blood flow, serum phospholipase A2 and interleukin-1beta in rats with acute necrotizing pancreatitis. *World J Gastroenterol* 2005; **11**: 3578-3581

33 **Liu LR**, Xia SH. Role of platelet-activating factor in the pathogenesis of acute pancreatitis. *World J Gastroenterol* 2006; **12**: 539-545

34 **Cosen-Binker LI**, Binker MG, Cosen R, Negri G, Tiscornia O. Influence of hydrocortisone, prednisolone, and NO association on the evolution of acute pancreatitis. *Dig Dis Sci* 2006; **51**: 915-925

35 **Stimac D**, Fisić E, Milić S, Bilić-Zulle L, Perić R. Prognostic values of IL-6, IL-8, and IL-10 in acute pancreatitis. *J Clin Gastroenterol* 2006; **40**: 209-212

36 **Zhang XP**, Li ZF, Liu XG, Wu YT, Wang JX, Wang KM, Zhou YF. Effects of emodin and baicalein on rats with severe acute pancreatitis. *World J Gastroenterol* 2005; **11**: 2095-2100

37 **Hirota M**, Sugita H, Maeda K, Ichibara A, Ogawa M. Concept of SIRS and severe acute pancreatitis. *Nihon Rinsho* 2004; **62**: 2128-2136

38 **Zhang XP**, Xie Q. Study progress of Somatostain and its analog to treat acute pancreatitis. *Zhongguo Zhongxiyi Jiehe Waike Zazhi* 2005; **11**: 365-367

39 **Zhang XP**, Tian H, Cheng QH. The current situation in pharmacological study on Baicalin. *Zhongguo Yaolixue Tongbao* 2003; **19**: 17-20

S- Editor Liu Y **L- Editor** Kumar M **E- Editor** Bai SH

PO Box 2345, Beijing 100023, China
www.wjgnet.com
wjg@wjgnet.com

World J Gastroenterol 2007 February 7; 13(5): 725-731
World Journal of Gastroenterology ISSN 1007-9327

BASIC RESEARCH

Antidiabetic effects of chitooligosaccharides on pancreatic islet cells in streptozotocin-induced diabetic rats

Bing Liu, Wan-Shun Liu, Bao-Qin Han, Yu-Ying Sun

Bing Liu, Wan-Shun Liu, Bao-Qin Han, Yu-Ying Sun, Department of Marine Life Science, Ocean University of China, Yushan Road, No. 5, Qingdao, Shandong Province, China
Supported by the National High Technology Research and Development Program of China (863 Program, 2001AA625050) and the National Key Research and Development Program of China during the Tenth Five-Year Plan Period, No. 2001BA708B04-07
Correspondence to: Wan-Shun Liu, College of Marine Life Science, Ocean University of China, Qingdao 266003, Shandong Province, China. iceicecream1221@126.com
Telephone: +86-532-82032105 Fax: +86-532-82032105
Received: 2006-11-11 Accepted: 2006-11-29

Abstract

AIM: To investigate the effect of chitooligosaccharides on proliferation of pancreatic islet cells, release of insulin and 2 h plasma glucose in streptozotocin-induced diabetic rats.

METHODS: *In vitro*, the effect of chitooligosaccharides on proliferation of pancreatic islet cells and release of insulin was detected with optical microscopy, colorimetric assay, and radioimmunoassay respectively. *In vivo*, the general clinical symptoms, 2 h plasma glucose, urine glucose, oral glucose tolerance were examined after sixty days of feeding study to determine the effect of chitooligosaccharides in streptozotocin-induced diabetic rats.

RESULTS: Chitooligosaccharides could effectively accelerate the proliferation of pancreatic islet cells. Chitooligosaccharides (100 mg/L) had direct and prominent effect on pancreastic β cells and insulin release from islet cells. All concentrations of chitooligosaccharides could improve the general clinical symptoms of diabetic rats, decrease the 2 h plasma glucose and urine glucose, and normalize the disorders of glucose tolerance.

CONCLUSION: Chitooligosaccharides possess various biological activities and can be used in the treatment of diabetes mellitus.

Key words: Chitooligosaccharides; Diabetes mellitus; Two hours plasma glucose; Oral glucose; Tolerance test; Pancreastic islet cells; Streptozotocin

Liu B, Liu WS, Han BQ, Sun YY. Antidiabetic effects of chitooligosaccharides on pancreatic islet cells in streptozotocin-induced diabetic rats. *World J Gastroenterol* 2007; 13(5): 725-731

http://www.wjgnet.com/1007-9327/13/725.asp

INTRODUCTION

Diabetes mellitus (DM) is a highly prevalent disease all over the world. Its long-term tissue complications that affect small and large blood vessels are directly connected with the time of patients suffering from hyperglycemia. Chitosan is a polycationic copolymer consisting of β-1, 4-linked 2-acetamido- D-glucose and β-1, 4-linked 2-amino-D-glucose units. Crab and shrimp shell wastes are currently utilized as the major industrial source of biomass for large-scale production of chitosan. Chitosan which is biodegradable, non-toxic and biocompatible has been shown to be particularly useful in many fields[1], including food, cosmetics, biomedicine, agriculture and environmental protection. Furthermore, it can be used as a bioactive material due to its biodegradable, non-toxic and non-allergenic natures. However, chitosan shows its biological activity only in acidic medium because of its poor solubility at pH above 6.5 and low absorbability of non-digestible and high molecular polysaccharides. Therefore, recent studies on chitosan have attracted interest in converting it to chitooligosaccharides(COS), because COS not only are water-soluble but also possess versatile functional properties such as antitumor enhancing properties[2,3], immunostimulating effects[2,4], antimicrobial activity[5], free radical scavenging activity[6-8], protective effects against infections[9], arthritis controlling activity[10], plant disease controlling activity[11,12] and angiotensin I converting enzyme inhibitory activity[13]. However, little attention has been paid to its activity in diabetes mellitus and related mode of action.

In the present study, soluble chitooligosaccharides with low molecular weight were prepared by enzymatic hydrolysis of chitosan with chitosanase as previously described[14]. The purpose of this study was to examine the effect of chitooligosaccharides on proliferation of pancreatic islet cells and release of insulin *in vitro*.

MATERIALS AND METHODS

Materials

Chitosan (minimum 90% deacetylated, M_r: 500 000) was purchased from Jinan Haidebei Marine Bioengineering

Co., Ltd (Shangdong, China). Chitooligosaccharides were prepared by enzymatic hydrolysis of chitosan with chitosanase. NIT-1 cell line was from Institute of Medicine, Ocean University of China. Male Wistar rats (200 ± 20 g) were from Laboratory Animal Centre, Institute of Medicine, Ocean University of China. Streptozotocin (STZ) was from Sigma Chemical Co. Tissue-culture medium and reagents were from Gibco. All chemicals were purchased from Sigma Chemical unless otherwise stated.

Cell culture

Rat islets were isolated from the pancreas of male Wistar rats by collagenase digestion as previously described[15,16] and dispersed into single cells by shaking in a low calcium medium[17]. The viability of cells after isolation, determined using the fluorochrome-media-ted viability test (see below) was ⩾ 98%. The islets were placed on glass coverslips in 35-mm petri plates and cultured in RPMI-1640 medium containing 20% fetal bovine serum (FBS), L-glutamine, and penicillin/streptomycin. NIT-1 cell line, a widely used β cell line for insulin secretion studies, was established from non-obese diabetic (NOD) mice transgenic for the SV40 T antigen under control of the insulin promoter, and cultured in DMEM containing 10% FBS and antibiotics (100 IU/mL of penicillin and 100 μg/mL of streptomycin). All cultures were kept at 37℃ in 950 mL/L O_2 and 50 mL/L CO_2. The medium was changed every two days. The islet cells cultured under these conditions spread out as a monolayer within 14 d and exhibited normal responses of insulin release to glucose stimulation, as described in previous studies[18,19].

Effects of COS on proliferation of pancreastic islet cells and insulin release

COS were dissolved in Dulbecco's modified Eagle's medium (DMEM) without FBS and then diluted with medium to form the five degrades (10, 100, 500, 1000, and 2000 mg/L). The structure and function of cultured islet cells were observed under inverted phase contrast microscope. MTT assay was used to estimate the cell viability. Pancreastic islet cells were digested by 0.25% trypsin until appearance of unicellular suspension. Then 100 μL suspension with the concentration of 5.0×10^4 cells/mL was transplanted into 96-well plates. Each well had three parallels. After incubated for 24 h, the medium was changed with COS at different concentrations. Cells were incubated with 0.5 mg/mL of MTT in the last 4 h of the culture period (48 h). The medium was then decanted, 200 μL DMSO was added to the wells, and the absorbance was determined at *492 nm* using an ELISA reader. The proliferation rate was calculated (PR = A/A0 × 100%). Furthermore, the effect of COS on the viability of pancreastic islet cells was also examined at 12, 24, 36, 48, 60, 72, 96, 120, 144, 168, 192 and 216 h to study the effect of COS on the growth phase of pancreastic islet cells in 9 d. At the same time, freshly dispersed islet cells were transplanted into 24-well plates at the concentration of 5.0×10^4 cells/mL, then divided into groups and stimulated with 100 mg/L COS for 14 d. The incubation medium was collected every 2 d and then stored at -20℃ until assay. Control group was maintained in basal RPMI 1640. Each well had five parallels. At the end of the stimulation period, insulin was measured using a radio-immunoassay kit for human insulin from Linco. The experiments were performed in triplicate.

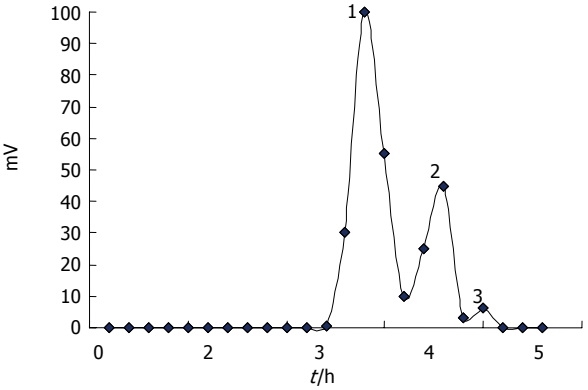

Figure 1 Chromatogram of chitooligosaccharids on Sephadex G-25 colum.

Effect of COS on streptozotocin-induced diabetic rats

Male Wistar rats were rendered diabetic by intraperitoneal injection of STZ at 65 mg/kg. The rats whose fasting blood glucose level was above 11.11 mmol/L were used for experiments after seven days. Then the rats were randomly divided into metformin treatment group, positive control group (DM) and COS treatment groups. Test samples were given intragastrically by gavage needle for 60 successive days. COS treatment groups were given chitooligosaccharides at the concentration of 250, 500, 1500 mg/kg daily. Normal control group and DM group received an equal volume of distilled water about 10 mL/kg. Metformin treatment group was given metformin at a concentration of 200 mg/kg daily. Two-hour plasma glucose (2hPG) and urine glucose were measured every 10 d. Oral glucose tolerance was examined after 60 d of feeding study. Plasma glucose was immediately measured in duplicate using a Beckman glucose analyzer Ⅱ (Beckman, Palo Alto, CA).

Statistical analysis

ANOVA was performed with Duncan's multiple range tests. SAS was used to compare the means (SAS Institute, Inc., Cary, NC, USA). $P < 0.05$ was considered statistically significant, $P < 0.01$ was considered very statistically significant.

RESULTS

Physicochemical properties and HPLC analysis of chitooligosaccharides

Chitooligosaccharides were prepared by enzymatic hydrolysis of chitosan. Components of the hydrolysis product were separated by Sephadex G-25 (Figure 1), and component 1 analyzed by TSK-GEL G3000PWXL had an average molecular weight of 1200 u, and a degree of deacetylation of 90% by the first derivative method of UV spectrometry.

Effects of COS on proliferation of pancreastic islet cells and insulin release

The influence of COS on pancreastic islet cell viability

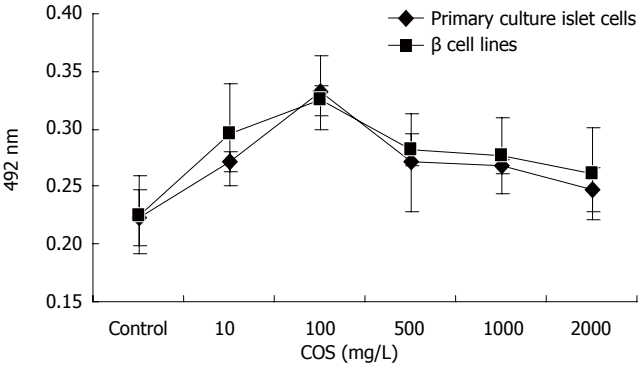

Figure 2 Effect of COS on proliferation of primary culture islet cells and β cell lines.

was assessed by MTT assay (Figure 2). Cell viability in the presence of different concentrations of COS was significantly higher than that in the absence of different concentrations of COS. The maximum stimulatory effect on cell viability was achieved at 100 mg/ L concentration among the five samples (Figures 3A and B), the proliferation rate was 148.43% and 143.71% respectively, and had a significant difference compared with the nomal control group (Figures 3C and D, $P < 0.01$), suggesting that COS could accelerate the proliferation of pancreastic islet cells in 9 d, and exert direct effects on pancreastic β cells, promote the growth of pancreastic islet cells to maximal density in 72 h, decease the time of latent phase and logarithm growth phase of pancreatic β cells (Figure 4A). The maximum stimulatory effect on cell growth phase was also achieved at 100 mg/L concentration among the five samples ($P < 0.01$)

As can be seen in Figure 4B, the results showed that exposure of primary cultured pancreatic cells to COS (100 mg/L) could continuously increase the secretion of insulin from the 6^{th} to the 14^{th} day, and had a significant difference compared with the normal control group ($P < 0.05$).

Effect of COS in streptozotocin-induced diabetic rats

All concentrations of chitooligosaccharides could decrease the 2hPG in 60 d (Figure 4C), the best effect was observed in the 500 mg/kg treatment group, with the 2hPG decreased to 16.14 mmol/L. The decrease rate was 47.48% compared with 2hPG before treatment.

The test of glucose tolerance was used to further evaluate the effects of different concentrations of chitooligosaccharides on improving the sensitivity of insulin. AS shown in Figure 4D, if the area under the DM group curve was regard as 100%, then AUC of the normal control group accounted for only 17.69% AUC of the DM group, while all concentrations of chitooligosaccharides could decrease AUC (Table 1). The best effect was observed in the medium dosage (500 mg/kg) treatment group, accounting for 68.69% of the area under the DM group curve ($P < 0.01$).

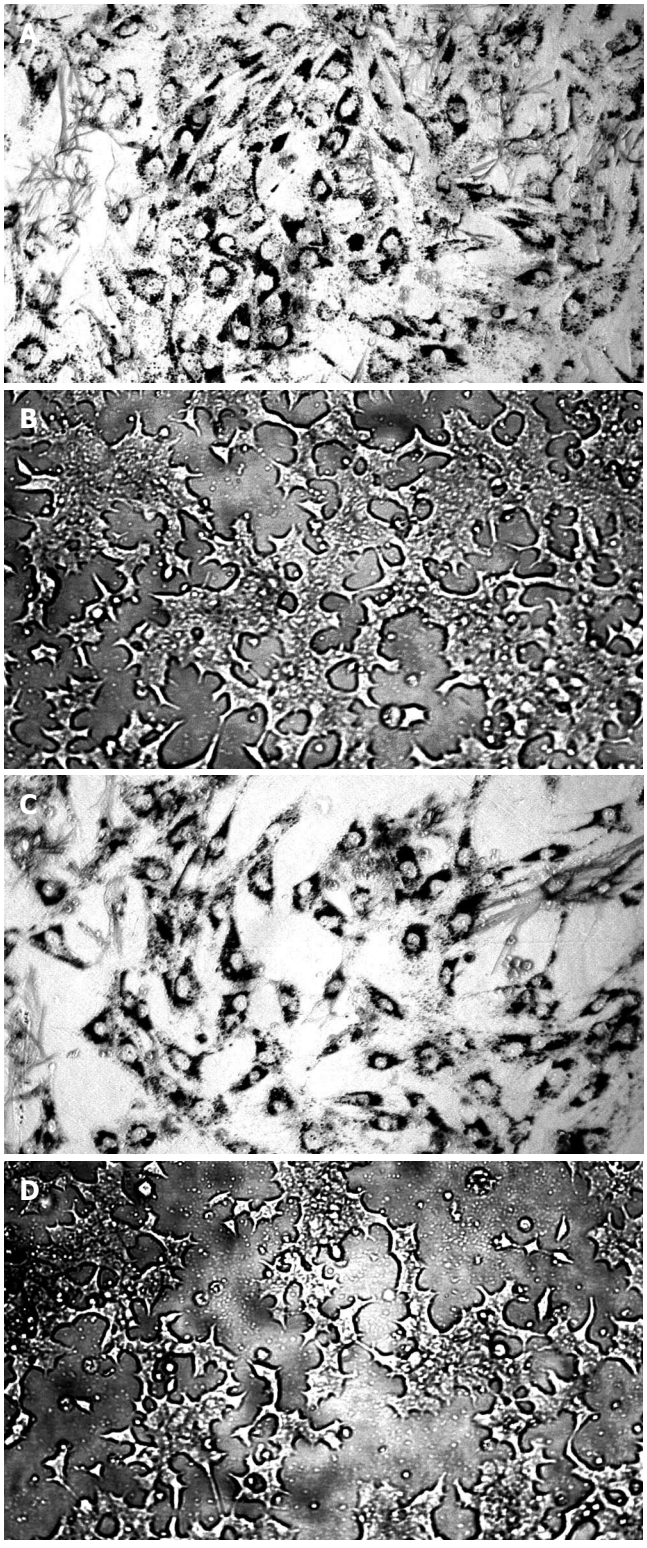

Figure 3 Photomicrograph of COS on the 48h proliferation of pancreatic islet cells and β cells (× 100) in control group (**A**) and 100 mg/L COS treatment group (**B**) of pancreatic islet cells, control group (**C**) and 100 mg/L COS treatment group (**D**) of β cell lines.

DISCUSSION

COS possess various biological activities and can be used in a number of industries. Unlike high molecular weight chitosan, COS which are readily soluble in water due to their shorter chain and free amino groups in D-glucosamine units and easily absorbed through the intestine, can quickly get into the blood flow and have systemic biological effects in the organism. In food industry, COS attract a greater interest as antimicrobial agents, antioxidants and enhancers of nutritional quality

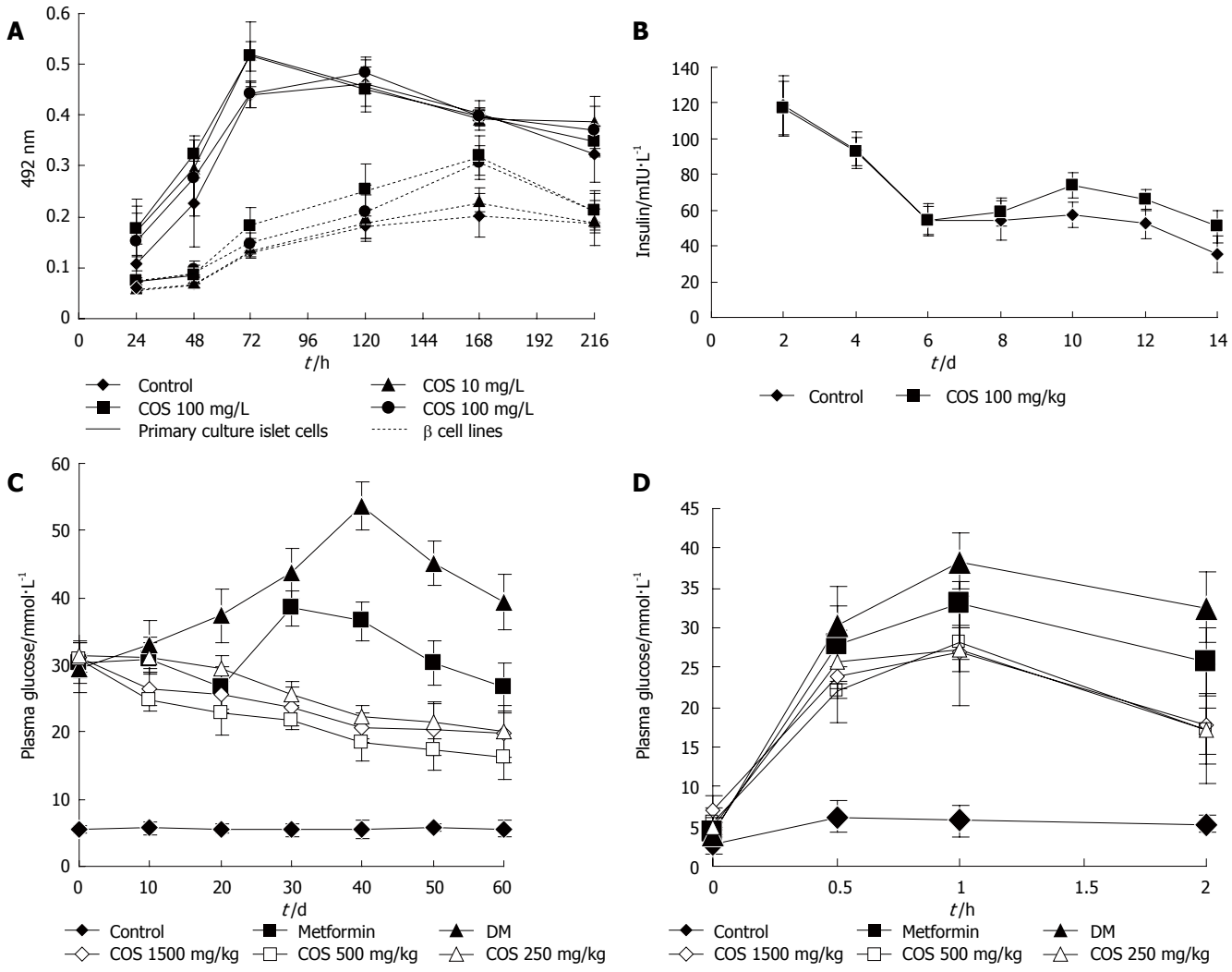

Figure 4 Effect of COS on growth phase of primary culture islet cells and β cell lines (**A**), insulin release from pancreatic islet cells (**B**), changes in 2 h plasma glucose (**C**), and in glucose tolerance test (**D**) after 60 d.

Table 1 Effect of COS on changes of plasma glucose in glucose tolerance test and AUC after 60 d (n = 9, mean ± SD)

Group	Concentration	Plasma glucose tolerance/mmol/L				AUC	AUC
	mg/kg	0 h	0.5 h	1 h	2 h	mmol/L	%
Control	-	2.75 ± 1.14[b]	6.27 ± 1.99[b]	5.78 ± 1.99[b]	5.34 ± 1.06[b]	21.66 ± 6.18[b]	17.69
Met	200	4.42 ± 1.72	28.01 ± 4.71	32.98 ± 2.98	25.64 ± 4.26	105.33 ± 3.74	86.05
DM	-	4.08 ± 1.40	30.20 ± 5.14	38.41 ± 3.41	32.54 ± 4.41	122.40 ± 12.05	100
COS-H	1500	7.01 ± 1.99	23.88 ± 5.86	27.04 ± 6.81[b]	17.88 ± 7.41[b]	85.79 ± 23.90[b]	70.09
COS-M	500	5.54 ± 1.77	22.05 ± 0.79[a]	28.17 ± 2.19[b]	17.01 ± 3.00[b]	84.08 ± 5.93[b]	68.69
COS-L	250	5.03 ± 0.51	25.62 ± 3.28	27.18 ± 2.72[b]	17.17 ± 4.42[b]	86.07 ± 8.06[b]	70.32

[a]$P < 0.05$, [b]$P < 0.01$ *vs* DM group.

of food[20,21], and also have various potential applications in agricultural industry[5]. Chemical and enzymatic methods are widely used to produce COS and chemical hydrolysis is more commonly used. However, chemical hydrolysis has some drawbacks to be commercialized, due to the production of some toxic compounds, higher risk associated with environmental pollution, and lower production yields. COS prepared by acid hydrolytic methods cannot serve as bioactive materials in general due to the possible contamination of toxic chemical compounds. Therefore, lack of proper technology for large-scale manufacture of COS with desired molecular weights has made its use difficult in human beings in the past years. Enzymatic processes which are generally carried out in batch reactors are preferred to chemical methods. This is due to minimized adverse chemical modifications of products during enzymatic hydrolysis and promotion of their biological activities. The properties of COS, such as DP, DA, charge distribution and nature of chemical modification in the molecules strongly influence its

observed biological activities. Therefore, molecular weight is considered a principal characteristic of COS that highly correlates to their biological activities. We have successfully obtained highly deacetylated (90%) chitooligosaccharides with a molecular weight of 1200 u by enzymatic hydrolysis and investigated its effect on the proliferation of pancreatic islet cells and release of insulin, lowering 2h plasma glucose and normalizing oral glucose tolerance *in vivo* and *in vitro*.

Type 2 diabetes characterized by peripheral insulin resistance followed by failure of compensation for pancreatic β cells and ultimately frank hyperglycemia[22], is traditionally considered discrete pathophysiological lesions. Proliferation of pancreatic β cells is slow and has a limited potential for regeneration (< 1% of the cells enter mitosis over 24 h in the adult state). Pancreatic β cells maintain the blood glucose concentration within a narrow range by modulating insulin secreting rate in response to the glucose levels in blood. Proper insulin secretion requires the coordinated functioning of numerous β cells that form pancreatic islets. This coordination depends on a network of communication mechanisms whereby β cells interact with extracellular signals and adjacent cells *via* connexin channels. The structure and function of primary culture islet cells and β cell lines were observed under inverted phase contrast microscope, and the viability of pancreatic islet cells and β cell lines was determined by MTT colorimetric assay indirectly in our study. In order to ensure adequate access of COS to pancreatic islet cell surfaces, we performed COS-stimulated insulin release experiments using monolayer cultures of rat islets. The results indicated that all concentrations of COS could markedly increase the viability of pancreatic islet cells. COS at the concentration of 100 mg/L effectively accelerated the proliferation of pancreatic islet cells and had direct effects on pancreastic β cells and release of insulin. Exposure of primary culture pancreatic cells to COS (100 mg/L) could continuously increase the secretion of insulin from 6 to14 d, as compared to the normal control group.

To study the specific role of COS in endocrine pancreatic function, we performed *in vivo* experiments of islet function in STZ-DM mice and measured the 2hPG and OGTT. Fasting plasma glucose and random plasma glucose used to be measured as the standard about the effect of lowering the plasma glucose. However neither fasting plasma glucose nor random plasma glucose can represent the actual glucose tolerance and insulin action[23-25]. The gold standards for assessment of insulin action and glucose homeostasis are the euglycemic, hyperinsulinemic and hyperglycemic clamp studies[26-28]. Clinically, single-value glucose determinations are probably the most commonly used marker of glucose homeostasis. Assessment of glucose tolerance in a clinical setting has traditionally been conducted using the glucose tolerance test[29,30]. Since 2 h plasma glucose is far more sensitive than fasting plasma glucose, we chose 2 h plasma glucose and oral glucose tolerance test as the standard to evaluate the effect of chitooligosaccharides in STZ -induced diabetic rats.

Our findings suggest that all concentrations of chitooligosaccharides can decrease 2hPG in 60 d. The best effect was observed in the medium dosage (500 mg/kg) treatment group, with the plasma glucose level decreased to 16.14 mmol/L compared to the DM group ($P < 0.01$). The medium dosage of chitooligosaccharides also had the best effect on glucose tolerance, accounting for 68.69% of the area under the DM group curve. The mechanism of chitooligosaccharides in decreasing the plasma glucose is perhaps due to the following reasons. Chitooligosaccharide is an alkaline, which can increase the pH values in the body fluid and the sensitivity of insulin. Chitooligosaccharides can regulate the function of the endocrine system, and reduce the secretion of insulin to normal, thus maintaining the normal metabolism of plasma glucose. Chitooligosaccharides can promote the proliferation of β cells and recovery of the function of damaged β cells.

Insulin is the primary hormone that regulates glucose uptake in mammals. In addition, a recent study demonstrated that insulin resistance itself itself at the level of β cells may contribute to the failure of pancreatic compensation, suggesting a theory for the pathogenesis of type 2 diabetes[31]. Indeed, mice with STZ -induced damage in β cells lose their ability to respond adequately to glucose stimulation and have progressive glucose intolerance. In the present study, we demonstrated that patients treated with COS had a normal β cell hyperplastic response to insulin resistance, with their 2hPG and urine glucose decreased, and the disorders of glucose tolerance normalized, indicating that COS play an important role in maintenance of glucose homeostasis *in vivo*.

In conclusion, COS possess various biological activities and can be used in the treatment of diabetes mellitus. COS can increase insulin secretion of pancreatic cells and improve the overgrowth of β cells and isolated pancreatic islet cells, decrease the 2hPG, and normalize the disorders of glucose tolerance in STZ-induced diabetic rats *in vivo*. Further study should be directed towards understanding their molecular mechanisms.

ACKNOWLEDGMENTS

We thank Mrs. Lie-Huan Chen for her help in revising this paper.

COMMENTS

Background

Chitin and chitosan can be isolated from different sources, crab and shrimp shell wastes are currently utilized as the major industrial source of biomass for the large-scale production of chitooligosaccharide (COS). Several methods have been recently used to prepare COS, and enzymatic preparation methods capture a great interest due to their safety and non-toxicity. COS possesses various biological activities and has been shown to be particularly useful in many fields. However, little attention has been paid to its activity in diabetes mellitus and related mode of action.

Research frontiers

Type 2 diabetes is characterized by peripheral insulin resistance followed by failure of compensation for pancreatic β cells and ultimately hyperglycemia. Type 2 diabetes is traditionally consodered discrete pathophysiological lesions. The proliferation of pancreatic β cells is slow with a limited potential for regeneration (< 1% of the cells enter mitosis over 24 h in the adult state). Pancreatic β cells maintain the blood glucose concentration within a narrow range by modulating insulin secreting rate in response to the glucose levels in blood. Proper insulin

secretion requires the coordinated functioning of numerous β cells that form pancreatic islets. This coordination depends on a network of communication mechanisms whereby β cells interact with extracellular signals and adjacent cells *via* connexin channels. Our study indicated that COS could increase insulin secretion of pancreatic cells and improve the overgrowth of β cells and isolated pancreatic islet cells, and decrease 2hPG, normalize the disorders of glucose tolerance of STZ-induced diabetic rats *in vivo*.

Innovations and breakthroughs

Soluble chitooligosaccharides with lower molecular weight were prepared by enzymatic hydrolysis of chitosan with t chitosanase. Enzymatic processes are generally carried out in batch reactors and are preferred to chemical methods. Our study indicated that COS could increase insulin secretion of pancreatic cells and improve the overgrowth of β cells and isolated pancreatic islet cells, decrease the 2hPG, and normalize the disorders of glucose tolerance of STZ-induced diabetic rats *in vivo*.

Applications

COS possesses various biological activities and can be utilized in a number of industries. Unlike high molecular weight chitosan, COS which is readily soluble in water due to its shorter chain and free amino groups in D-glucosamine units and easily absorbed through the intestine, can quickly get into the blood flow and has systemic biological effects in the organism. However, lack of proper technology for large-scale manufacture of COS with desired molecular weights has made its use difficult in human beings in the past years. Enzymatic processes which are generally carried out in batch reactors are preferred to chemical methods. This is due to minimized adverse chemical modifications of products during enzymatic hydrolysis and its biological activities. We have successfully obtained highly deacetylated (90%) chitooligosa-ccharide with a molecular weight of 1200 u by enzymatic hydrolysis and investigated its effect on the proliferation of pancreatic islet cells and release of insulin, lowering the 2 h plasma glucose and normalizing the oral glucose tolerance *in vivo* and *in vitro*. Our study indicate that COS could increase insulin secretion of pancreatic cells and improve the overgrowth of β cells and isolated pancreatic islet cells, and decrease the 2hPG, normalize the disorders of glucose tolerance in STZ-induced diabetic rats *in vivo*.

Terminology

Chitin, chitosan and chitooligosaccharides: Chitin is a natural polymer, the second most abundant organic resource on the earth next to cellulose. Chitosan is a polycationic copolymer consisting of β-1, 4-linked 2-acetamido-D-glucose and β-1, 4-linked 2-amino-D-glucose units. Both chitin and chitosan are copolymers of β (1-4) linked Nacetyl-β-glucosamine and glucosamine units. The proportion of N-acetyl-glucosamine units in total number of units determines the degree of deacetylation. The degree of deacetylation has an inverse relationship with the number of N-acetyl-glucosamine units, thus deacetylation of chitosan is achieved by removing Nacetyl group. In chitosan, the degree of deacetylation is higher than 50%. Chitooligosaccharide obtained by hydrolysis or degradation of chitosan, is not only water-soluble but also more effective than chitosan. NIT-1 cell line: NIT-1 cell line, a widely used β cell line in insulin secretion studies, is established from non-obese diabetic (NOD) mice transgenic for the SV40 T antigen under control of the insulin promoter; Streptozotocin (STZ): 2-deoxy-2-(3-methyl-3-nitrosourea)-1-D-glucopyranose is actively transported into pancreatic β cells *via* the Glut-2 glucose transporter. It reacts at many sites in DNA but in particular at the ring nitrogen and exocyclic oxygen atoms of the DNA bases, predominantly producing 7-methylguanine, 3-methyladenine (3-meA), and *O*6-methylguanine adducts.

Peer review

This is a good descriptive study in which authors analyzed the antidiabetic effects of chitooligosaccharide (COS) on proliferation of pancreatic islet cells in streptozotocin-induced diabetic rats. The results are interesting and suggest that COS is a potential therapeutic substance that could be used in the treatment of diabetes mellitus. The authors also studies the interesting questions about the molecular mechanism involved in COS biological activity.

REFERENCES

1 **Felt O**, Buri P, Gurny R. Chitosan: a unique polysaccharide for drug delivery. *Drug Dev Ind Pharm* 1998; **24**: 979-993
2 **Suzuki K**, Mikami T, Okawa Y, Tokoro A, Suzuki S, Suzuki M. Antitumor effect of hexa-N-acetylchitohexaose and chitohexaose. *Carbohydr Res* 1986; **151**: 403-408
3 **Nishimura K**, Nishimura S, Nishi N, Saiki I, Tokura S, Azuma I. Immunological activity of chitin and its derivatives. *Vaccine* 1984; **2**: 93-99
4 **Shibata Y**, Foster LA, Metzger WJ, Myrvik QN. Alveolar macrophage priming by intravenous administration of chitin particles, polymers of N-acetyl-D-glucosamine, in mice. *Infect Immun* 1997; **65**: 1734-1741
5 **Hadwiger LA**, Beckman JM. Chitosan as a Component of Pea-Fusarium solani Interactions. *Plant Physiol* 1980; **66**: 205-211
6 **Chiang MT**, Yao HT, Chen HC. Effect of dietary chitosans with different viscosity on plasma lipids and lipid peroxidation in rats fed on a diet enriched with cholesterol. *Biosci Biotechnol Biochem* 2000; **64**: 965-971
7 **Park PJ**, Je JY, Kim SK. Free radical scavenging activity of chitooligosaccharides by electron spin resonance spectrometry. *J Agric Food Chem* 2003; **51**: 4624-4627
8 **Je JY**, Park PJ, Kim SK. Free radical scavenging properties of hetero-chitooligosaccharides using an ESR spectroscopy. *Food Chem Toxicol* 2004; **42**: 381-387
9 **Tokoro A**, Kobayashi M, Tatewaki N, Suzuki K, Okawa Y, Mikami T, Suzuki S, Suzuki M. Protective effect of N-acetyl chitohexaose on Listeria monocytogenes infection in mice. *Microbiol Immunol* 1989; **33**: 357-367
10 **Lee SH**, Suh JS, Kim HS, Lee JD, Song J, Lee SK. MR evaluation of radiation synovectomy of the knee by means of intra-articular injection of holmium-166-chitosan complex in patients with rheumatoid arthritis: results at 4-month follow-up. *Korean J Radiol* 2003; **4**: 170-178
11 **Lin W**, Hu X, Zhang W, Rogers WJ, Cai W. Hydrogen peroxide mediates defence responses induced by chitosans of different molecular weights in rice. *J Plant Physiol* 2005; **162**: 937-944
12 **Vander P**, V rum KM, Domard A, Eddine El Gueddari N, Moerschbacher BM. Comparison of the ability of partially N-acetylated chitosans and chitooligosaccharides to elicit resistance reactions in wheat leaves *Plant Physiol* 1998; **118**: 1353-1359
13 **Park PJ**, Je JY, Kim SK. Angiotensin I converting enzyme (ACE) inhibitory activity of hetero-chitooligosaccharides prepared from partially different deacetylated chitosans. *J Agric Food Chem* 2003; **51**: 4930-4934
14 **Zhang H**, Du Y, Yu X, Mitsutomi M, Aiba S. Preparation of chitooligosaccharides from chitosan by a complex enzyme. *Carbohydr Res* 1999; **320**: 257-260
15 **Khan FA**, Goforth PB, Zhang M, Satin LS. Insulin activates ATP-sensitive K(+) channels in pancreatic beta-cells through a phosphatidylinositol 3-kinase-dependent pathway. *Diabetes* 2001; **50**: 2192-2198
16 **Hopkins WF**, Satin LS, Cook DL. Inactivation kinetics and pharmacology distinguish two calcium currents in mouse pancreatic B-cells. *J Membr Biol* 1991; **119**: 229-239
17 **Lernmark A**. The preparation of, and studies on, free cell suspensions from mouse pancreatic islets. *Diabetologia* 1974; **10**: 431-438
18 **Rocheleau JV**, Head WS, Nicholson WE, Powers AC, Piston DW. Pancreatic islet beta-cells transiently metabolize pyruvate. *J Biol Chem* 2002; **277**: 30914-30920
19 **Patterson GH**, Knobel SM, Arkhammar P, Thastrup O, Piston DW. Separation of the glucose-stimulated cytoplasmic and mitochondrial NAD(P)H responses in pancreatic islet beta cells. *Proc Natl Acad Sci USA* 2000; **97**: 5203-5207
20 **Tarsi R**, Corbin B, Pruzzo C, Muzzarelli RA. Effect of low-molecular-weight chitosans on the adhesive properties of oral streptococci. *Oral Microbiol Immunol* 1998; **13**: 217-224
21 **Tarsi R**, Muzzarelli RA, Guzmán CA, Pruzzo C. Inhibition of Streptococcus mutans adsorption to hydroxyapatite by low-molecular-weight chitosans. *J Dent Res* 1997; **76**: 665-672
22 **Warram JH**, Martin BC, Krolewski AS, Soeldner JS, Kahn CR. Slow glucose removal rate and hyperinsulinemia precede the development of type II diabetes in the offspring of diabetic

parents. *Ann Intern Med* 1990; **113**: 909-915
23 **Ramachandran A**, Snehalatha C, Vijay V, Viswanathan M. Fasting plasma glucose in the diagnosis of diabetes mellitus: a study from southern India. *Diabet Med* 1993; **10**: 811-813
24 **Lee CH**, Fook-Chong S. Evaluation of fasting plasma glucose as a screening test for diabetes mellitus in Singaporean adults. *Diabet Med* 1997; **14**: 119-122
25 **Finch CF**, Zimmet PZ, Alberti KG. Determining diabetes prevalence: a rational basis for the use of fasting plasma glucose concentrations? *Diabet Med* 1990; **7**: 603-610
26 **Hollenbeck CB**, Chen N, Chen YD, Reaven GM. Relationship between the plasma insulin response to oral glucose and insulin-stimulated glucose utilization in normal subjects. *Diabetes* 1984; **33**: 460-463
27 **Hollenbeck C**, Reaven GM. Variations in insulin-stimulated glucose uptake in healthy individuals with normal glucose tolerance. *J Clin Endocrinol Metab* 1987; **64**: 1169-1173
28 **Bogardus C**, Lillioja S, Nyomba BL, Zurlo F, Swinburn B, Esposito-Del Puente A, Knowler WC, Ravussin E, Mott DM, Bennett PH. Distribution of in vivo insulin action in Pima Indians as mixture of three normal distributions. *Diabetes* 1989; **38**: 1423-1432
29 **Engelgau MM**, Aubert RE, Thompson TJ, Herman WH. Screening for NIDDM in nonpregnant adults. A review of principles, screening tests, and recommendations. *Diabetes Care* 1995; **18**: 1606-1618
30 **Modan M**, Harris MI. Fasting plasma glucose in screening for NIDDM in the U.S. and Israel. *Diabetes Care* 1994; **17**: 436-439
31 **Kulkarni RN**, Winnay JN, Daniels M, Brüning JC, Flier SN, Hanahan D, Kahn CR. Altered function of insulin receptor substrate-1-deficient mouse islets and cultured beta-cell lines. *J Clin Invest* 1999; **104**: R69-R75

S- Editor Wang J **L- Editor** Wang XL **E- Editor** Liu WF

PO Box 2345, Beijing 100023, China
www.wjgnet.com
wjg@wjgnet.com

World J Gastroenterol 2007 February 7; 13(5): 732-739
World Journal of Gastroenterology ISSN 1007-9327

CLINICAL RESEARCH

A randomized, double-blind, placebo-controlled trial assessing the efficacy and safety of tegaserod in patients from China with chronic constipation

San-Ren Lin, Mei-Yun Ke, Jin-Yan Luo, Yao-Zong Yuan, Ji-Yao Wang, Shelley diTommaso, Verena Walter, Jiaqing Huang

San-Ren Lin, The 3rd Hospital, Beijing Medical University, Beijing, China
Mei-Yun Ke, Peking Union Medical College Hospital, Beijing, China
Jin-Yan Luo, The 2nd Hospital of Xian Jiaotong University, Shanxi, China
Yao-Zong Yuan, Shanghai Ruijin Hospital, Shanghai, China
Ji-Yao Wang, Shanghai Zhongshan Hospital, Shanghai, China
Shelley diTommaso, Verena Walter, Novartis Pharma AG, Basel, Switzerland
Jiaqing Huang, Novartis Pharmaceuticals Corp, East Hanover, New Jersey, United States
Correspondence to: Jiaqing Huang, MD, PhD, Novartis Pharmaceuticals Corporation, Gastroenterology/Urology Therapeutic Area, Clinical Development and Medical Affairs, One Health Plaza, Building 405/2019, East Hanover, NJ 07936, United States. jiaqing.huang@novartis.com
Telephone: +1-862-7787103 Fax: +1-973-7812390
Received: 2006-10-19 Accepted: 2006-12-21

Abstract

AIM: To evaluate the efficacy and safety of tegaserod, 6 mg twice daily (b.i.d.), in men and women with chronic constipation (CC) from China.

METHODS: This was a multicenter, double-blind, placebo-controlled study. Following a 2-wk treatment-free baseline period, patients were randomized to receive either tegaserod (6 mg b.i.d.) or placebo (b.i.d.) for 4 wk. An analysis of covariance with repeated measures was used to determine the overall effect of treatment for the primary efficacy variable; the change from baseline in the number of complete spontaneous bowel movements (CSBMs) during the 4-wk treatment period. Secondary efficacy endpoints included other measures of response in terms of CSBMs, and patients' daily and weekly assessment of bowel habits. Safety was also assessed, based on the incidence and severity of adverse events (AEs).

RESULTS: A total of 607 patients were randomized to receive either tegaserod (n = 304) or placebo (n = 303). Tegaserod treatment resulted in a rapid and significant increase from baseline in the adjusted mean number of CSBMs per week over wk 1-4 compared with placebo (1.39 *vs* 0.91, P = 0.0002). A statistically significant difference in favor of tegaserod was also observed for a mean increase $\geqslant$ 1 CSBM/wk over wk 1-4 (47.7% *vs* 35.0%, tegaserod *vs* placebo, respectively, P = 0.0018) and for the absolute number of $\geqslant$ 3 CSBMs/wk over wk 1-4 (25.0% *vs* 14.5%, tegaserod *vs* placebo, respectively, P = 0.0021). Improvements in other symptoms of CC were also seen in the tegaserod group, including improved stool form and reduced straining. In addition, more patients in the tegaserod group reported satisfactory relief from their constipation symptoms. The frequency and severity of AEs was comparable between tegaserod and placebo groups, with the exception of a greater incidence of diarrhea in patients receiving tegaserod (3.6%) compared with placebo (1.7%).

CONCLUSION: Tegaserod treatment improved multiple symptoms of CC and was associated with a favorable safety profile.

Key words: Chronic constipation; tegaserod; China; Complete spontaneous bowel movement; Placebo-controlled; Stool

Lin SR, Ke MY, Luo JY, Yuan YZ, Wang JY, diTommaso S, Walter V, Huang J. A randomized, double-blind, placebo-controlled trial assessing the efficacy and safety of tegaserod in patients from China with chronic constipation. *World J Gastroenterol* 2007; 13(5): 732-739

http://www.wjgnet.com/1007-9327/13/732.asp

INTRODUCTION

Chronic constipation/chronic idiopathic constipation (CC) is a gastrointestinal (GI) motility and sensory disorder that is commonly reported in many regions of the world, including Asia[1], North America[2], and Europe[3]. An epidemiological study conducted in Beijing concluded that 6.1% of the adult population were suffering from the symptoms of CC[4]. This compares with a survey of 3282 people in Hong Kong, of whom 14% were deemed to be suffering from CC[1]. The disorder is more common in women and elderly people[5]. The symptoms of CC impact on patients' quality of life (QoL) and result in frequent visits to physicians, particularly by older patients[1,6]. In

Hong Kong, approximately 25% (n = 820) of those surveyed were reported to visit a physician as a result of their symptoms[1].

The diagnosis of CC has primarily centered on the infrequency of the patients' bowel movements (BMs). However, CC is also associated with other symptoms that include straining, hard stools, feelings of incomplete evacuation, abdominal bloating, and abdominal discomfort/pain. While the pathophysiology of CC is still unclear, a proportion of patients with CC are assumed to have impaired GI motility[7]. This prolongs the length of time that stools remain in the bowel, allowing increased absorption of water from the stools which become hard and difficult to pass. Rome Ⅱ criteria refined the diagnosis of CC by providing a consensus definition that is frequently used in clinical research, and can serve as a useful guide for physicians[8]. The Rome Ⅱ criteria combine symptoms of straining, stool form and feelings of incomplete evacuation with measures of bowel frequency (less than three BMs per week).

A systematic review concluded that there were too few well-designed, randomized, placebo-controlled trials to support the efficacy of many of the available treatments for CC such as bulking laxatives (e.g., psyllium), osmotic laxatives [lactulose or polyethylene glycol (PEG)], and stimulant laxatives (senna or bisacodyl)[2]. Furthermore, other symptoms can be aggravated by laxative treatment (e.g., bloating)[9]. A further review found good evidence for the efficacy of PEG and tegaserod (Grade A recommendation) and moderate evidence to support the efficacy of lactulose and psyllium (Grade B recommendation)[10]. Other treatments for CC include the modification of patients' eating habits (increasing the consumption of dietary fiber/bulking agents), biofeedback training (where patients are taught relaxation and defecation techniques), and in severe cases, surgery. Evidence for the efficacy of these agents, however, is limited[7,11].

Targeting the pathophysiological basis of CC by stimulating intestinal motility and secretion may be a more appropriate approach for the treatment of the disorder, rather than using conventional treatments. Tegaserod is a selective agonist at the serotonin receptor, 5-HT$_4$, and has been shown to augment the release of neurotransmitters from the enteric nerves, hence stimulating intestinal peristalsis and secretion[12,13]. Two pivotal, randomized, placebo-controlled trials have demonstrated that tegaserod [2 mg or 6 mg twice daily (b.i.d.)] effectively treats the multiple symptoms of CC[14,15]. Tegaserod also effectively relieves the multiple symptoms of patients with irritable bowel syndrome (IBS) who suffer from constipation[16-18]. The majority of patients in the pivotal CC studies were Caucasian. Given that CC is a common disorder in China, the aim of the current study was to evaluate the efficacy and safety of tegaserod in men and women with CC from China.

MATERIALS AND METHODS

Study design

This was a randomized, multicenter, placebo-controlled, double-blind, parallel-group study, designed to evaluate the efficacy and safety of tegaserod in men and women with CC in China.

After completing an initial screening phase of up to 28 d, patients entered a 2-wk baseline period without study medication. At the end of the baseline period, eligible patients were randomized to receive either tegaserod 6 mg b.i.d. or placebo for 4 wk using a randomization list generated by Novartis Drug Supply Management, using Almedica Drug Label System, version 5.3 a, Almedica Technology Group Inc. All Novartis staff, other than the Drug Supply Management and the Biostatistics Quality Assurance Group, remained blind to the allocation of treatment until database lock. Randomization was performed in blocks using a 1:1 ratio. The randomization list was reviewed and locked by the Biostatistics Quality Assurance group. The identity of the treatments was concealed by using study tablets that were identical in appearance. The study was conducted in accordance with the Declaration of Helsinki and was reviewed by the Independent Ethics Committee or Institutional Review Board for each center.

Patient selection

Men and women 18 years of age or older with at least a 6-mo history of CC were eligible to participate in the study. CC was defined, according to a modification of Rome Ⅱ criteria, as less than three complete spontaneous bowel movements (CSBMs) per week accompanied by one or more of the following symptoms on more than 25% of occasions: very hard and/or hard stools (type 1 and/or 2 on the Bristol Stool Form Scale[19]), sensation of incomplete evacuation following at least 25% of BMs, and straining on at least 25% of days. All CC-related symptoms were confirmed by patient electronic diary (eDiary) data recorded during the baseline period.

Patients were excluded from entering the study if they had inflammatory bowel disease or other structural bowel disease, CC resulting from bowel surgery (with mechanical outlet obstruction, congenital anorectal malformation or clinically significant rectocele), abdominal pain/discomfort as the most bothersome symptom in the past 6 mo, past or current history or diagnosis of IBS, significant disorders or diseases that may interfere with completion of the study, or if they failed to complete the daily or weekly eDiary assessments during baseline. Patients who planned to use concomitant medications affecting bowel habits (including natural/homeopathic products) 1 wk prior to entry into baseline and during the study were also excluded, as were patients who used laxatives on more than two separate occasions during baseline. However, laxative use (bisacodyl, 15 mg/d) as a rescue medication was allowed for patients who did not experience a BM for at least 72 h.

Patients were excluded from the treatment phase if CC was not confirmed by the baseline eDiary data, if loose or watery stools were reported for 3 or more days during the baseline period, or for lack of compliance with the study protocol.

Assessments

The primary efficacy variable was the change from

baseline in the number of CSBMs per week during the 4-wk treatment period. Secondary efficacy variables included two response rates in terms of CSBMs: patients with a mean increase of one or more CSBM relative to baseline, and patients with an absolute number of three or more CSBMs per week during the 4-wk treatment period. Additional secondary efficacy variables included assessment of patients' bowel habits [i.e., stool form, frequency, and straining (which was recorded daily regardless of BM)], and patients' satisfaction with bowel habits, bothersomeness of constipation, distension/bloating, and abdominal discomfort/pain. Following each BM, patients were asked to record the time of the BM, whether the BM was accompanied by a feeling of complete evacuation (yes/no), and stool form (using the Bristol Stool Form Scale[19]). Patients evaluated their satisfaction with bowel habit on a 5-point scale ranging from 'not at all satisfied' to 'a very great deal satisfied', and bothersomeness of constipation, abdominal distension/bloating and abdominal discomfort/pain on a 5-point scale, which ranged from 'not at all bothersome' to 'a very great deal bothersome'. During the treatment phase of the study, patients also recorded whether they experienced satisfactory relief of constipation symptoms (yes/no) on a weekly basis.

The safety of tegaserod 6 mg b.i.d. *vs* placebo was evaluated by recording the frequency and severity of all adverse events (AEs) and serious adverse events (SAEs), by monitoring hematology, blood chemistry, urine and vital signs, and by performing electrocardiogram (ECG) evaluations. Other outcomes assessed but not presented in this paper included: patients' assessment of constipation on quality of life (PAC-QoL questionnaire) and patients' perception of study medication (PPSM questionnaire).

Statistical analysis

Planned enrollment was for 600 (n = 300 per arm) randomized patients with CC recruited from 15 centers across China. An assumption was made that the population distribution would be similar to that observed in the two pivotal CC trials[14,15]. Based on this assumption, the study was powered to detect a difference (tegaserod-placebo) in a change from baseline of 0.6 CSBMs/wk at a two-sided significance level of 5%. All statistical analyses were carried out with SAS® software (version 8.2).

As stated earlier, the primary efficacy variable was the change from baseline in the number of CSBMs per week during the 4-wk treatment period. Secondary efficacy variables included two response rates in terms of CSBMs: patients with a mean increase of one or more CSBMs relative to baseline, and patients with an absolute number of three or more CSBMs per week during the 4-wk treatment period. Additional secondary efficacy variables included assessment of patients' bowel habits [i.e., stool form, frequency, and straining (which was recorded daily regardless of BM)], and patients' satisfaction with bowel habits, bothersomeness of constipation, distension/bloating, abdominal discomfort/pain, and satisfaction with symptom relief (recorded weekly).

All efficacy analyses were performed on the intent-to-treat (ITT) population. Safety analyses included all patients who received at least one dose of study medication. An analysis of covariance (ANCOVA) model with repeated measures was used to analyze the overall effect of treatment for the primary efficacy variable (change from baseline in number of CSBM per week). The model included terms for treatment, week, study center, and baseline data as well as baseline data by week, and treatment by week interactions. To be defined as 'complete', BMs had to be associated with a sensation of complete evacuation. The BM was defined as spontaneous if no laxatives were taken during the 24 h prior to the BM.

Statistical analyses of the secondary efficacy variables [response rate relative to baseline (one or more CSBM per week) and response rate in terms of the absolute number of CSBMs (three or more CSBMs per week)] were carried out using a logistic regression model, with treatment and study center as factors, and the number of CSBMs per week at baseline as covariate.

Based on the daily eDiary assessments, the change from baseline was determined for the following variables: 1) the number of SBMs per week, 2) the number of days per week with no stools, hard or very hard stools, 3) the weekly mean straining score, and 4) the number of days with (too much) straining. The same ANCOVA model that was used for the primary endpoint was repeated for these variables. The number of patients with or without satisfactory relief [determined using a weekly eDiary assessment (patients were asked to consider whether they had satisfactory relief from their symptoms of CC in the past week)] were analyzed using Cochran Mantel Haenszel (CMH) tests, with center as a stratification factor.

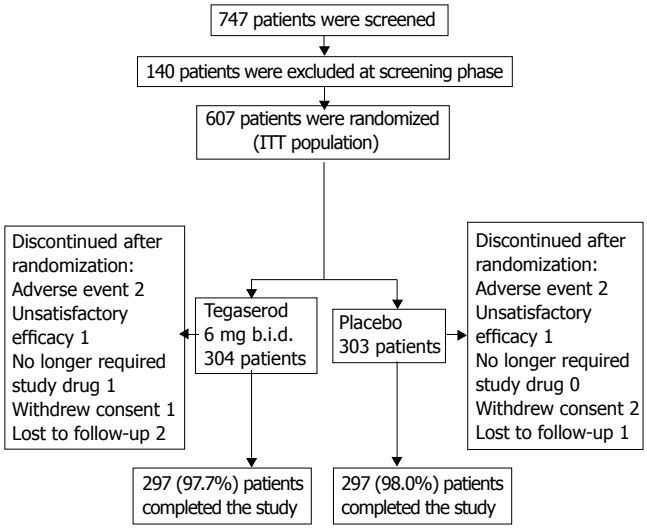

Figure 1 Participant flow.

RESULTS

Baseline

A total of 747 patients were screened for participation in this study, and 607 patients (81.3%) were randomized from a total of 15 centers to receive treatment with tegaserod 6 mg b.i.d. (n = 304) or placebo (n = 303) (Figure 1). The main reasons for screening failure were unacceptable laboratory values (5.0%), withdrawal of consent (4.3%)

Table 1 Patient demographic and baseline characteristics (ITT population)

Demographic variable	Tegaserod 6 mg b.i.d. (*n* = 304)	Placebo (*n* = 303)
Age (yr)		
Median	34.5	35
Range	18-80	18-78
Age group, years (*n*, %)		
< 35	152 (50.0)	151 (49.8)
35-64	132 (43.4)	135 (44.6)
⩾ 65	20 (6.6)	17 (5.6)
Sex (*n*, %)		
Male	70 (23.0)	61 (20.1)
Female	234 (77.0)	242 (79.9)
Race (*n*, %)		
Oriental	303 (99.7)	303 (100.0)
Other	1 (0.3)	0
Mean duration of constipation symptoms, months (SD)	100.3 (90.7)	94.9 (93.1)

and 'other' (4.3%). Most patients completed the double-blind treatment period (97.7% in the tegaserod group and 98.0% in the placebo group). One patient randomized to receive tegaserod did not receive study medication and was therefore excluded from the safety population.

Demographic and baseline variables were comparable between the tegaserod and placebo groups and most patients were Oriental [99.7% (tegaserod) *vs* 100.0% (placebo)] (Table 1).

Prior to randomization, the duration of patients' constipation symptoms was approximately 8 years in the tegaserod and placebo groups (Table 1). The mean number of CSBMs per week during the 2-wk baseline period was 0.36 in the tegaserod group and 0.31 in the placebo group. The most bothersome symptoms reported by patients subsequently randomized to tegaserod or placebo was straining (53.0% *vs* 56.1%), followed by feeling of incomplete evacuation (15.1% *vs* 15.2%), hard stools (13.5% *vs* 13.9%) and infrequent defecation (14.5% *vs* 11.9%). Laxative use in both treatment groups was comparable during the baseline period (35.5% and 36.0% of patients, randomized to tegaserod and placebo, respectively).

Primary efficacy variable

An increase from baseline in the overall number of CSBMs per week during the 4-wk treatment period was observed in patients receiving tegaserod (adjusted mean 1.39) and placebo (adjusted mean 0.91) (treatment difference; 0.48, 95% confidence interval; 0.23-0.73), yielding a statistically significant difference in favor of tegaserod ($P = 0.0002$, Figure 2 and Table 2). Tegaserod treatment significantly increased the number of CSBMs per week from baseline during each week of treatment, compared with placebo ($P < 0.05$) (Figure 3 and Table 2). Subgroup analysis revealed that men treated with tegaserod showed a greater increase from baseline in the overall number of CSBMs per week (wk 1-4) compared with women treated with tegaserod (the mean increase in the number of CSBMs per week was 1.67 in men and 1.29 in women).

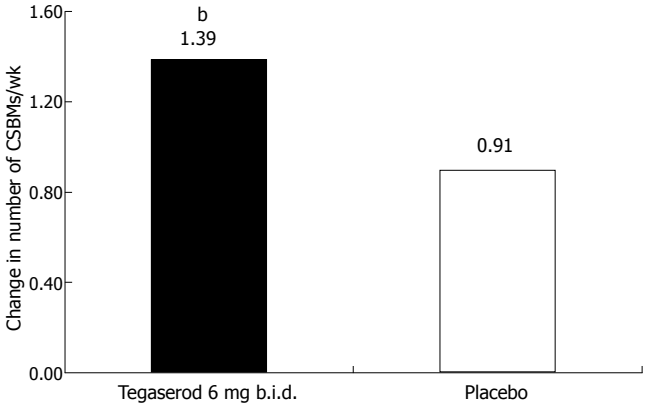

Figure 2 Change from baseline in the number of CSBMs per week (wk 1-4) by treatment (ITT population). Footnote: [b]*P* = 0.0002 *vs* placebo; Mean number of CSBMs per week at baseline: tegaserod 0.36; placebo 0.31.

Table 2 Treatment differences in change from baseline in number of CSBMs/wk for wk 1-4 (ITT population)

Time period		Tegaserod 6 mg b.i.d. *n* = 304	Placebo *n* = 303
wk 1-4	*n*	303	303
	Mean (SD)	1.38 (1.759)	0.89 (1.444)
	Adjusted mean[1]	1.39	0.91
	Median	0.75	0.25
	Min, max	-2.0, 9.0	-1.5, 7.5
	Tegaserod-placebo	0.48	
	(95% CI)[2]	(0.23, 0.73)	
	P value[3]	0.0002	
wk 1	Tegaserod–placebo	0.34	
	(95% CI)[2]	(0.05, 0.64)	
	P value[3]	0.0226	
wk 2	Tegaserod-placebo	0.54	
	(95% CI)[2]	(0.24, 0.84)	
	P value[3]	0.0004	
wk 3	Tegaserod–placebo	0.57	
	(95% CI)[2]	(0.27, 0.86)	
	P value[3]	0.0002	
wk 4	Tegaserod–placebo	0.47	
	(95% CI)[2]	(0.17, 0.77)	
	P value[3]	0.002	

CSBM: complete spontaneous bowel movement; SD: standard deviation; CI: confidence interval. Change from baseline (cfb) = post-baseline–baseline. A positive cfb indicates an increase in the number of CSBMs/wk. [1]Adjusted mean cfb. Calculated from least square mean estimate of repeated measures analysis. [2]Treatment difference (> 0 favors tegaserod). [3]Repeated measures model: cfb in number of CSBMs/wk = treatment (patient) + week + center + baseline + baseline *week + treatment *week.

Secondary efficacy variables

Analysis of response, defined as a mean increase of one or more CSBMs per week relative to baseline during the 4-wk treatment period, showed that treatment with tegaserod was significantly more effective than treatment with placebo [overall, tegaserod (47.7%) *vs* placebo (35.0%), $P = 0.0018$). While overall response was statistically significant for all 4 wk combined, statistical significance for individual weeks was reached at wk 2, 3 and 4 of treatment (Figure 4A).

Overall, treatment with tegaserod was superior to

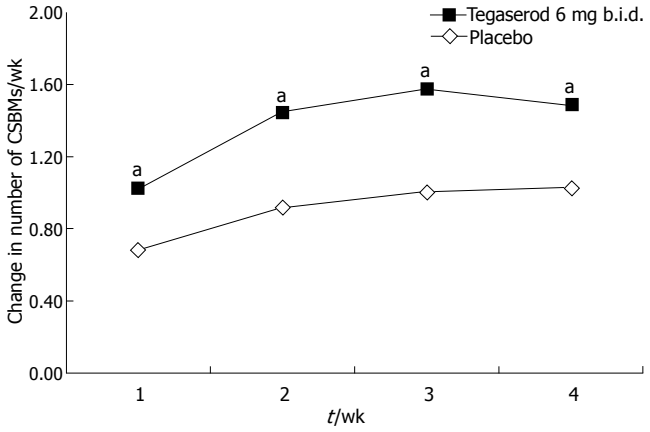

Figure 3 Change from baseline in the number of CSBMs per week by study week and treatment (ITT population). Footnote: $^{a}P < 0.05$ *vs* placebo; Mean number of CSBMs per week at baseline: tegaserod 0.36; placebo 0.31.

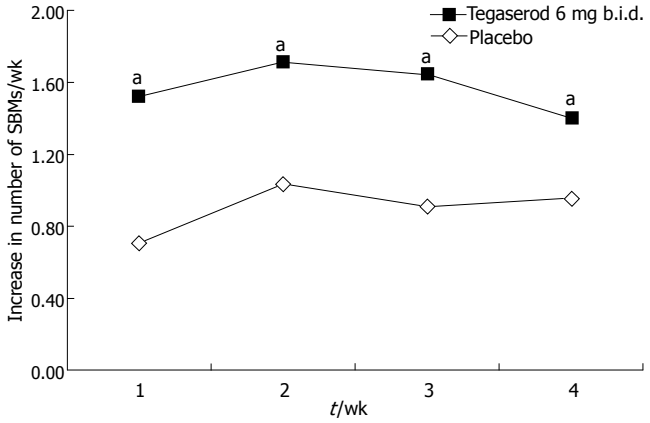

Figure 5 Change from baseline in number of SBMs per week by study week and treatment (ITT population). $^{a}P < 0.05$ *vs* placebo; Mean number of SBMs per week at baseline: tegaserod 2.33; placebo 2.26.

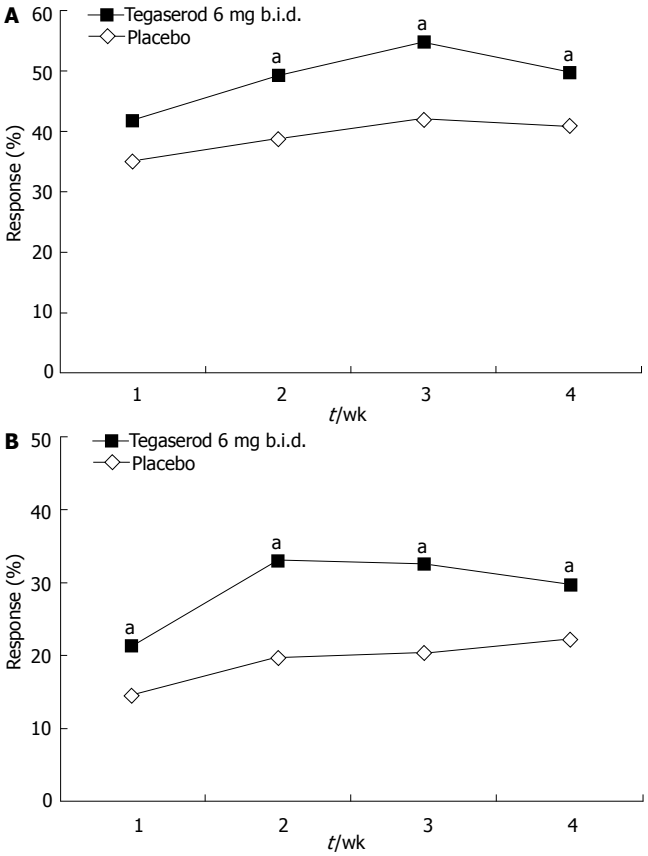

Figure 4 **A:** Response rate relative to baseline (increase of ≥ 1 CSBM per week) by week (ITT population); **B:** Absolute response rate (increase of ≥ 3 CSBM per week) (ITT population). $^{a}P < 0.05$ *vs* placebo; Mean number of CSBMs per week at baseline: tegaserod 0.36; placebo 0.31.

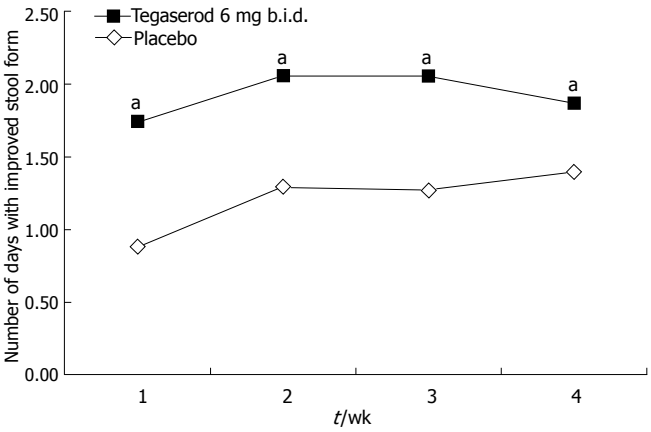

Figure 6 Change from baseline in number of days per week with no stool, hard, or very hard stools by treatment (ITT population). $^{a}P < 0.05$ *vs* placebo; An improvement was defined as a decrease in the number of days with no stool, hard, or very hard stools (Bristol stool score of 1 or 2[19]) relative to baseline.

treatment with placebo in terms of the absolute response rate (three or more CSBMs per week) [tegaserod (25.0%) *vs* placebo (14.5%), $P = 0.0021$]. This difference was statistically significant at each week of treatment (Figure 4B).

Assessment of constipation symptoms

Improvements in constipation symptoms were observed in patients receiving tegaserod over wk 1-4. Tegaserod significantly increased the number of SBMs per week compared with placebo (adjusted mean 1.57 *vs* 0.89, $P < 0.0001$), and this was statistically significant for each of the 4 wk of treatment ($P < 0.05$) (Figure 5). Compared with placebo, treatment with tegaserod also decreased the overall number of days per week (wk 1-4) with no stools, hard or very hard stools (adjusted mean -1.94 *vs* -1.19, $P < 0.0001$) and this was statistically significant for each of the 4 wk of treatment ($P < 0.05$) (Figure 6). Treatment with tegaserod also resulted in a decrease in the weekly mean straining score (adjusted mean -0.41 *vs* -0.33, $P = 0.0282$) and a decrease in the number of days per week with straining (adjusted mean -1.65 *vs* -1.24, $P = 0.0085$).

Significantly more patients receiving tegaserod than placebo responded positively to the question of whether they had 'satisfactory relief from their constipation symptoms over the past week of treatment' at all 4 wk of treatment (wk 1: 52.5% *vs* 35.0%; wk 2: 54.9% *vs* 40.5%; wk 3: 56.5% *vs* 41.3%; wk 4: 57.8% *vs* 44.2%; all $P < 0.05$) and at end of treatment (57.8% *vs* 43.9, $P < 0.05$) (Figure 7).

Trends in favor of tegaserod were observed for

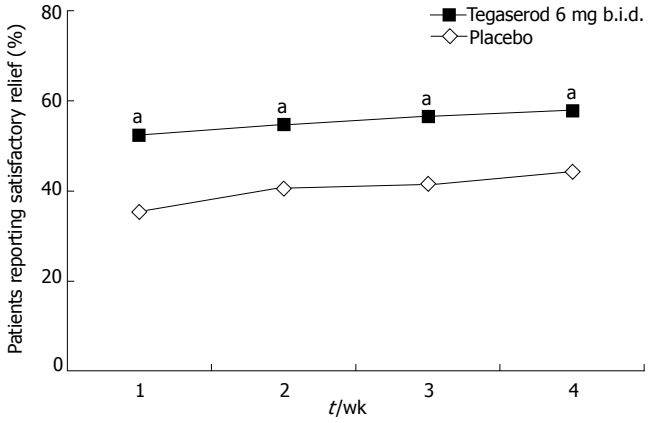

Figure 7 Satisfactory relief of constipation symptoms by week and treatment period (ITT population). $^{a}P < 0.05$ *vs* placebo.

the following secondary variables: bothersomeness of constipation, distension/bloating and abdominal discomfort/pain. Statistical significance was observed in wk 3 (bothersomeness of distension/bloating and abdominal pain/discomfort) and in wk 1-3 (bothersomeness of constipation). The number of patients using laxatives during the double-blind treatment period was higher in the placebo group (31.4%) compared with the tegaserod group (27.0%), although this difference was not statistically significant.

Safety assessments

The AEs reported in this study were mostly mild and transient. The overall frequency of AEs was similar in both the tegaserod and placebo groups (9.9% *vs* 11.2%) (Table 3). Diarrhea was the most common AE, reported by 3.6% of patients in the tegaserod group and 1.7% of patients in the placebo group. The study investigators considered the majority of cases of diarrhea to be mild (no cases were reported to be severe), and transient [median duration of first episode of diarrhea: 2 d (tegaserod group) *vs* 3 d (placebo group)]. All cases of abdominal pain were reported to be mild or moderate in severity and were reported with equal frequency in both groups (1.7% in each group).

The number of discontinuations due to AEs was the same in both treatment groups (0.7% each) (AEs resulting in discontinuation included diarrhea, dizziness, hypertension, rash, tinnitus, venous thrombosis in the limb, and vertigo). Other reasons for discontinuation included unsatisfactory therapeutic effect (0.3% in each group), patients no longer requiring study drug due to symptom improvement (0.3% in the tegaserod group and 0.0% in the placebo group), withdrawal of consent (0.3% in the tegaserod group and 0.7% in the placebo group) and patients lost to follow-up (0.7% in the tegaserod group and 0.3% in the placebo group). Five SAEs were reported, none of which were considered to be related to the study drug [one case of ureteric cancer in the tegaserod group (0.3%) and one case each of ankle fracture, pregnancy, hemorrhoid surgery, and venous thrombosis in the limb in the placebo group (1.3% in total)]. No cases of ischemic colitis were reported during this study, and no deaths occurred. Laboratory and ECG evaluations, and vital signs were comparable between treatment groups.

Table 3 Incidence of most frequent AEs, regardless of relationship to study drug (safety population)

Adverse event	Tegaserod 6 mg b.i.d. (n = 303) (%)	Placebo (n = 303) (%)
Diarrhea	11 (3.6)	5 (1.7)
Abdominal pain	5 (1.7)	5 (1.7)
Nasopharyngitis	1 (0.3)	7 (2.3)
Transaminases increased	3 (1.0)	1 (0.3)
Nausea	1 (0.3)	3 (1.0)
Abdominal distension	3 (1.0)	0
Dizziness	2 (0.7)	0
Leukopenia	1 (0.3)	1 (0.3)
Urinary tract inflammation	1 (0.3)	1 (0.3)
Abdominal pain upper	0	2 (0.7)

DISCUSSION

This is the first randomized, double-blind, placebo-controlled trial designed to evaluate the efficacy and safety of tegaserod in an adult population of men and women from China, who met the Rome Ⅱ diagnostic criteria for CC. The recent Rome Ⅲ criteria, published after this study was conducted, have further refined diagnostic criteria for CC[20].

The key efficacy analyses demonstrated that tegaserod improves multiple symptoms of CC. The results revealed that treatment with tegaserod was associated with a rapid and significant increase from baseline in the number of CSBMs at wk 1, which was sustained over each of the 4 wk of treatment. Secondary efficacy analyses also showed statistically significant improvements for tegaserod over placebo with regard to evaluation of bowel habits and satisfaction with constipation relief.

The responder rate for mean increase of one or more CSBM per week during the 4-wk treatment period [tegaserod (47.7%) *vs* placebo (35.0%)] was similar to the results obtained with Caucasian patients[14,15] suggesting that patients from China with CC respond in a similar fashion to those from Western countries.

Subgroup analysis confirmed that tegaserod relieved the multiple symptoms of CC in both men and women. This observation has clinical relevance, as fewer data are available in men, and further confirms the results from other pivotal studies[14,15].

Treatment with tegaserod was associated with a safety profile similar to that seen with placebo, although slightly more patients receiving tegaserod than placebo reported mild and transient diarrhea. Diarrhea is a predictable pharmacological event, and is likely due to tegaserod's promotile effect that stimulates peristalsis, reduces stool hardness and accelerates orocecal transit, promoting stool expulsion[12,13]. The increased incidence of diarrhea following treatment with tegaserod was similar to that reported in all other clinical studies of patients with CC from different ethnic groups[14,15,17,18].

The primary efficacy variable used in this study was the change from baseline in the number of CSBMs per week.

The assessment of SBMs discounts laxative-induced BMs, while further characterizing SBMs as 'complete' ensures that measurements are not simply based on an increase in the number of small hard pellets that are passed, which would leave symptoms unimproved for the patient. Hence, the definition of CSBM used in this study provides a subjective measure of BMs that are associated with a sense of complete evacuation, while in addition, providing an objective measure of the number of BMs. This assessment of CSBMs is considered to be able to detect changes that are meaningful to the patient.

Medications, such as laxatives, which are traditionally used to treat CC, may improve the frequency of BMs, but they do not treat the underlying causes of CC and have no proven effect on the multiple symptoms including straining, incomplete evacuation, abdominal bloating and abdominal discomfort/pain[9,21]. Therefore, in order to control their symptoms, patients often rely on multiple treatments, which are often ineffective. These include the increased intake of fiber, modifications in lifestyle and diet, and the use of prescription/non-prescription laxatives. This has led to high patient dissatisfaction and frustration with current treatments for CC[1], and hence there is a need for simple, safe, and effective first-line therapies to treat the multiple symptoms of patients with this disorder.

In conclusion, this was the first rigorously designed study to evaluate the efficacy and safety of tegaserod in an adult population of men and women from China with CC. The results of key efficacy analyses demonstrated that compared with placebo, tegaserod 6 mg b.i.d. increased the frequency of CSBMs, improved multiple symptoms of constipation, and was associated with a safety profile that is similar to that of placebo. Therefore, tegaserod offers an effective treatment option for patients from China with CC.

ACKNOWLEDGMENTS

The study design, collection, analysis and interpretation of the data was sponsored by Novartis Pharma AG. The authors would like to acknowledge the editorial support and contribution of Nicci Crofts of ACUMED® to this manuscript. ACUMED's contribution was funded by Novartis Pharma AG.

COMMENTS

Background

Chronic constipation/idiopathic constipation (CC) affects 11% to 14% of the Chinese population; however, currently prescribed first-line therapies for CC are suboptimal. Tegaserod is a selective partial agonist at the serotonin receptor, 5-HT$_4$, which is a well tolerated and effective treatment for the multiple symptoms of CC in Caucasian patients. However, its efficacy in patients from Asia-Pacific countries is unknown.

Research frontiers

There has been increasing interest in the use of serotonergic agents, such as tegaserod, for the treatment of gastrointestinal motility disorders. This study is the first randomized, double-blind, placebo-controlled trial designed to evaluate the efficacy and safety of tegaserod in men and women from China with CC.

Innovations and breakthroughs

The placebo-controlled trials demonstrating the promotile action of tegaserod on the gut (Degen *et al*, 2000 and Prather *et al*, 2000) led to the design of phase Ⅲ trials of tegaserod in patients with irritable bowel syndrome whose predominant symptom was constipation (IBS-C) and patients with CC. These studies demonstrated that treatment with tegaserod relieved multiple symptoms of these burdensome conditions (Johanson *et al*, 2004; Kamm *et al*, 2005; Müller-Lissner *et al*, 2001; Novick *et al*, 2002; Tack *et al*, 2005). As these studies were performed predominantly in patients from Western countries, this study aimed to evaluate the efficacy of tegaserod for the treatment of CC in patients from China.

Applications

The results of this study demonstrated that compared with placebo, tegaserod 6 mg b.i.d. increased the frequency of CSBMs, improved multiple symptoms of constipation, and was well tolerated in both men and women with CC from China.

Terminology

Complete spontaneous bowel movement (CSBM): The term 'CSBM' refers to the spontaneous occurrence of a bowel movement associated with a feeling of complete evacuation. Assessing bowel movements as 'spontaneous' discounts laxative-induced bowel movements, but further characterizing spontaneous bowel movements as 'complete' (CSBMs) ensures that measurements are not simply based on an increase in the number of small hard pellets that are passed, which would leave symptoms unimproved for the patient. The definition of CSBM used in this study therefore provides a subjective measure of bowel movements that are associated with a sense of complete evacuation, while in addition, providing an objective measure of the number of bowel movements. Tegaserod: A selective partial agonist of the 5-HT$_4$ receptor.

Peer review

This is an excellently designed, performed and presented study examining the efficacy of tegaserod in Chinese patients with chronic idiopathic constipation.

REFERENCES

1 **Cheng C**, Chan AO, Hui WM, Lam SK. Coping strategies, illness perception, anxiety and depression of patients with idiopathic constipation: a population-based study. *Aliment Pharmacol Ther* 2003; **18**: 319-326
2 **Brandt LJ**, Prather CM, Quigley EM, Schiller LR, Schoenfeld P, Talley NJ. Systematic review on the management of chronic constipation in North America. *Am J Gastroenterol* 2005; **100** Suppl 1: S5-S21
3 **Garrigues V**, Gálvez C, Ortiz V, Ponce M, Nos P, Ponce J. Prevalence of constipation: agreement among several criteria and evaluation of the diagnostic accuracy of qualifying symptoms and self-reported definition in a population-based survey in Spain. *Am J Epidemiol* 2004; **159**: 520-526
4 **Guo XK**, Pan MY, Han G, Fang S, Lu XC, Guo H. A cluster, stratified, randomized epidemiologic survey and analysis of related factors on adult chronic constipation in Beijing area. *Chin J Dig* 2002; **22**: 637-638
5 **Lembo A**, Camilleri M. Chronic constipation. *N Engl J Med* 2003; **349**: 1360-1368
6 **Norton C**. Constipation in older patients: effects on quality of life. *Br J Nurs* 2006; **15**: 188-192
7 **Wald A**. Pathophysiology, diagnosis and current management of chronic constipation. *Nat Clin Pract Gastroenterol Hepatol* 2006; **3**: 90-100
8 **Drossman DA**, Corazziari E, Talley NJ, Thompson WG, Whitehead W. Rome II: The Functional Gastrointestinal Disorders. 2nd ed. McLean, VA: Degnon Associates, 2000
9 **Xing JH**, Soffer EE. Adverse effects of laxatives. *Dis Colon Rectum* 2001; **44**: 1201-1209
10 **Ramkumar D**, Rao SS. Efficacy and safety of traditional medical therapies for chronic constipation: systematic review. *Am J Gastroenterol* 2005; **100**: 936-971
11 **Schiller LR**. New and emerging treatment options for chronic constipation. *Rev Gastroenterol Disord* 2004; **4** Suppl 2: S43-S51
12 **Degen L**, Matzinger D, Merz M, Appel-Dingemanse S, Maecke H, Beglinger C. Tegaserod (HTF 919), a 5-HT4 receptor partial agonist, accelerates gastrointestinal (GI) tract. *Neurogastroenterol Motil* 2000; **12**: 382

13 **Prather CM**, Camilleri M, Zinsmeister AR, McKinzie S, Thomforde G. Tegaserod accelerates orocecal transit in patients with constipation-predominant irritable bowel syndrome. *Gastroenterology* 2000; **118**: 463-468
14 **Johanson JF**, Wald A, Tougas G, Chey WD, Novick JS, Lembo AJ, Fordham F, Guella M, Nault B. Effect of tegaserod in chronic constipation: a randomized, double-blind, controlled trial. *Clin Gastroenterol Hepatol* 2004; **2**: 796-805
15 **Kamm MA**, Müller-Lissner S, Talley NJ, Tack J, Boeckxstaens G, Minushkin ON, Kalinin A, Dzieniszewski J, Haeck P, Fordham F, Hugot-Cournez S, Nault B. Tegaserod for the treatment of chronic constipation: a randomized, double-blind, placebo-controlled multinational study. *Am J Gastroenterol* 2005; **100**: 362-372
16 **Müller-Lissner SA**, Fumagalli I, Bardhan KD, Pace F, Pecher E, Nault B, Rüegg P. Tegaserod, a 5-HT(4) receptor partial agonist, relieves symptoms in irritable bowel syndrome patients with abdominal pain, bloating and constipation. *Aliment Pharmacol Ther* 2001; **15**: 1655-1666
17 **Novick J**, Miner P, Krause R, Glebas K, Bliesath H, Ligozio G, Rüegg P, Lefkowitz M. A randomized, double-blind, placebo-controlled trial of tegaserod in female patients suffering from irritable bowel syndrome with constipation. *Aliment Pharmacol Ther* 2002; **16**: 1877-1888
18 **Tack J**, Müller-Lissner S, Bytzer P, Corinaldesi R, Chang L, Viegas A, Schnekenbuehl S, Dunger-Baldauf C, Rueegg P. A randomised controlled trial assessing the efficacy and safety of repeated tegaserod therapy in women with irritable bowel syndrome with constipation. *Gut* 2005; **54**: 1707-1713
19 **O'Donnell LJ**, Virjee J, Heaton KW. Detection of pseudodiarrhoea by simple clinical assessment of intestinal transit rate. *BMJ* 1990; **300**: 439-440
20 **Longstreth GF**, Thompson WG, Chey WD, Houghton LA, Mearin F, Spiller RC. Functional bowel disorders. *Gastroenterology* 2006; **130**: 1480-1491
21 **Müller-Lissner SA**, Kamm MA, Scarpignato C, Wald A. Myths and misconceptions about chronic constipation. *Am J Gastroenterol* 2005; **100**: 232-242

S- Editor Liu Y **L- Editor** Lutze M **E- Editor** Lu W

PO Box 2345, Beijing 100023, China
www.wjgnet.com
wjg@wjgnet.com

World J Gastroenterol 2007 February 7; 13(5): 740-747
World Journal of Gastroenterology ISSN 1007-9327

CLINICAL RESEARCH

Influence of age on outcome of total laparoscopic fundoplication for gastroesophageal reflux disease

F Pizza, G Rossetti, P Limongelli, G Del Genio, V Maffettone, V Napolitano, L Brusciano, G Russo, S Tolone, M Di Martino, A Del Genio

F Pizza, G Rossetti, P Limongelli, G Del Genio, V Maffettone, V Napolitano, L Brusciano, G Russo, S Tolone, M Di Martino, A Del Genio, 1st Division of General and Gastrointestinal Surgery, Second University of Naples, Via Pansini 5, Naples 80131, Italy
Correspondence to: Francesco Pizza, MD, Via Villa Albertini, 39 bis, 80037 Nola, Naples, Italy. francesco_pizza@libero.it
Telephone: +39-333-8275449 Fax: +39-81-5666721
Received: 2006-05-01 Accepted: 2006-12-27

Abstract

AIM: To demonstrate that age does not influence the choice of treatment for gastroesophageal reflux disease (GERD). We hypothesized that the outcome of total fundoplication in patients > 65 years is similar to that of patients aged ⩽ 65 years.

METHODS: Four hundred and twenty consecutive patients underwent total laparoscopic fundoplication for GERD. Three hundred and fifty-five patients were younger than 65 years (group Y), and 65 patients were 65 years or older (group E). The following elements were considered: presence, duration, and severity of GERD symptoms; presence of a hiatal hernia; manometric evaluation, 24 h pH-monitoring data, duration of operation; incidence of complications; and length of hospital stay.

RESULTS: Elderly patients more often had atypical symptoms of GERD and at manometric evaluation had a higher rate of impaired esophageal peristalsis in comparison with younger patients. A mild intensity of heartburn often leads physicians to underestimate the severity of erosive esophagitis. The duration of the operation was similar between the two groups. The incidence of intraoperative and postoperative complications was low and the difference was not statistically significant between the two groups. An excellent outcome was observed in 92.9% young patients and 91.9% elderly patients.

CONCLUSION: Laparoscopic antireflux surgery is a safe and effective treatment for GERD even in elderly patients, warranting low morbidity and mortality rates and a significant improvement of symptoms comparable to younger patients.

Key words: Gastroesophageal reflux disease; Esophagitis; Impaired peristalsis; Hiatal hernia; Laparoscopic total fundoplication

Pizza F, Rossetti G, Limongelli P, Del Genio G, Maffettone V, Napolitano V, Brusciano L, Russo G, Tolone S, Di Martino M, Del Genio A. Influence of age on outcome of total laparoscopic fundoplication for gastroesophageal reflux disease. *World J Gastroenterol* 2007; 13(5): 740-747

http://www.wjgnet.com/1007-9327/13/740.asp

INTRODUCTION

The population of elderly is rapidly growing globally, e.g. in the USA nearly 20 million of people will be more than 85 years old in the next fifty years[1]. Digestive diseases are common causes of morbidity and mortality in the elderly[2]. Among them gastroesophageal reflux disease (GERD) is usually more severe than in younger patients, which is frequently under-diagnosed and less treated[2]. This results in an increase of esophageal mucosal injuries and subsequent complications. Therefore, a more aggressive treatment has been advocated in these patients[3]. However, a higher morbidity and mortality of open surgery in the elderly, limited the number of these patients referred for surgical treatment. Moreover, their shorter life expectancy made surgery to be deemed a cost-ineffective strategy.

The advent of laparoscopic fundoplication has greatly reduced the morbidity of antireflux surgery and by now, it should be considered the surgical treatment of choice for GERD[4]. The aim of the current study is to review the outcome of young and elderly patients undergoing laparoscopic antireflux surgery for the treatment of GERD.

MATERIALS AND METHODS

From September 1992 to December 2005, 420 consecutive patients, 171 male and 249 female, mean age 42.8 years (range 12-80) with GERD underwent laparoscopic Nissen-Rossetti fundoplication. The preoperative and postoperative data were prospectively collected. Demographic data were obtained at the time of first visit. Sixty-five patients older than 65 years of age were defined as the elderly group (EG) whereas the remaining 355 younger than 65

years of age were defined as the young group (YG). Ethics board approval for collecting and using these data was obtained.

Preoperative evaluation

Preoperatively all patients underwent Upper Gastrointestinal Endoscopy (UE), X-ray of barium swallow, esophageal manometry and 24-h pH monitoring. They were off peptic medications for thirty days. The medical evaluation included a structured questionnaire based on modified DeMeester symptom scoring system (Table 1). Measurement of hiatal hernia size was performed at the end of endoscopic examination after deflation of the stomach or by X-ray of barium swallow with video-fluoroscopy. The hernia size was measured as the distance between the centre of the diaphragmatic hiatus and the superior aspect of gastric folds. A hiatal hernia was deemed to be present if either gastric folds or a hernia pouch was present above the diaphragm between swallows. Esophagitis severity was assessed by means of Savary-Miller grading system. The location of Barrett's esophagus was noted; and the esophageal strictures, paraesophageal hernias and reinterventions were excluded from the study. Stationary esophageal manometry was carried out using 8-channel perfusion catheters, 4 disposed radially and oriented at 90° to each other and 4 positioned longitudinally at intervals of 5 cm. The catheter was perfused with distilled water using a low-compliance capillary pump at a constant infusion rate of 0.8 mL/min at 1.2 kg/cm^2. A system of pressure transducers transmitted data to an acquisition device (ACQ1^{TM}-Menfis bioMedica-Bologna, Italy) and from there to a personal computer. A specific software package (Dyno 2000^{TM}-Menfis bioMedica-Bologna, Italy) was used for data acquisition and processing. The following variables were assessed: (1) pressure of the lower esophageal sphincter; (2) relaxation of the lower esophageal sphincter (LES) in response to swallowing; (3) amplitude and propagation of peristalsis (esophageal peristalsis was considered impaired when < 30 mmHg). The LES was studied by both the stationary and the rapid pull-through methods. Esophagogastric pH monitoring was carried out using two glass probes which were connected to a portable, solid-state recorder (Digitrapper Proxima^{TM}-Synetics Medical, Sweden): the electrodes were placed, respectively, 5 cm above the proximal margin and 5 cm below the distal margin of the LES, identified by means of stationary manometry. For statistical analysis, results were expressed as a mean value ± SD; correlations among the various parameters were analysed using Fischer's exact test. The Wilcoxon signed rank test was used to compare the preoperative and postoperative modified DeMeester symptom score. American Society of Anaesthesiologists (ASA) grade was recorded at the time of surgery.

Postoperative evaluation

On an outpatient basis, the patients came to our department each six months for the first postoperative year and, after, each year and were invited to fulfil a standardized questionnaire dealing with presence of typical or atypical symptoms and based on the modified DeMeester score (Table 1). Satisfaction of the procedure and the will of undergoing the same operation after knowing its effects were defined as excellent outcome

Instrumental follow-up after surgery included: X-ray of barium swallow (performed at 1 year after surgery), esophageal manometry (performed at 6 mo, 1 year, and 2 years after surgery) and 24 h pH monitoring (performed at 1 year after surgery).

Statistical analysis was carried out using SPSS for Windows (version 12.0, SPSS Inc. Chicago, IL). Results were expressed as mean ± SD unless otherwise indicated. Student's *t* test, the Chi-square test, the Fischer's exact test and the Wilcoxon signed rank test were used as appropriate. *P* value < 0.05 was considered statistically significant.

Table 1 Modified DeMeester scoring system

Symptoms	Score	Description
Dysphagia	0	None
	1	Occasional transient episodes
	2	Require liquids to clear
	3	Impaction requiring medical attention
Heartburn	0	None
	1	Occasional brief episodes
	2	Frequent episodes requiring medical treatment
	3	Interference with daily activities
Regurgitation	0	None
	1	Occasional episodes
	2	Predictable by posture
	3	Interference with daily activities

Table 2 Preoperative evaluation: data and ASA score in EG and YG

Demographics	EG (> 65 yr)	YG (< 65 yr)	*P*
Age (mean yr ± SD)	72.6 ± 2.1	48.2 ± 3.2	< 0.05
Male:Female	1:1.5	1:1.7	NS
ASA score	2.2 ± 0.43	1.82 ± 0.51	< 0.05
Weight (mean ± SD)	64.4 ± 5.1	65.3 ± 6.4	NS

Table 3 Incidence of pre-operative symptoms in EG and YG

Symptoms	EG (%)	YG (%)	*P*
Heartburn	44/65 (67.7)	298/355 (83.9)	< 0.05
Acid regurgitation	39/65 (60.0)	277/355 (78.0)	< 0.05
Solid food dysphagia	22/65 (33.8)	27/355 (7.6)	< 0.05
Chest pain	18/65 (27.7)	51/355 (14.4)	< 0.05
Respiratory complication (chronic cough, sleep apnoea, asthma, laryngitis)	27/65 (41.5)	19/355 (5.4)	< 0.05

RESULTS

Preoperative data

Demographics data and ASA score of the two groups are listed in Table 2. In the YG, the mean duration of preoperative symptoms was 4.6 ± 2.3 years (range 1-11) whereas in the EG it was 8.3 ± 2.5 years (range 5-22). Tables 3 and 4 depict the incidence and severity of typical and atypical

Table 4 Severity of preoperative symptoms in EG and YG (mean ± SD)

Symptoms	EG	YG	*P*
Heartburn	1.7 ± 0.87	2.7 ± 0.74	< 0.05
Acid regurgitation	1.5 ± 0.96	2.3 ± 0.89	< 0.05
Solid food dysphagia	1.6 ± 0.76	0.5 ± 0.2	< 0.05
Chest pain	1.6 ± 0.82	1.5 ± 0.87	> 0.05
Respiratory complication (chronic cough, sleep apnoea, asthma, laryngitis)	1.8 ± 1.04	1.0 ± 0.45	< 0.05

Table 5 Preoperative manometric evaluation in EG and YG

Manometry	EG	YG	*P*
LES pressure (mmHg)	11.2 ± 1.5	11.0 ± 1.2	> 0.05
Impaired esophageal peristalsis (< 30 mmHg) N° of patients	43/65 (66.2%)	114/355 (32.1%)	< 0.05

Table 6 Preoperative evaluation: incidence, size of HH and pH metric data in NERD, ERD and Barrett patients in EG and YG

	EG NERD	YG NERD	*P*	EG ERD	YG ERD	*P*	EG Barrett	YG Barrett	*P*
Patients *n* (%)	15/65 (23.1)	220/355 (62)	< 0.05	45/65 (69.2)	125/355 (35.2)	< 0.05	5/65 (7.7)	10/355 (2.8)	< 0.05
Hiatal Hernia *n* (%)	13/15 (86.7)	148/220 (67.3)	< 0.05	39/45 (86.7)	97/125 (77.6)	< 0.05	4/5 (80)	8/10 (80)	-
Hiatal Hernia size (cm)	1.2 ± 0.18	0.3 ± 0.1	< 0.05	4.1 ± 1.9	2.3 ± 0.2	< 0.05			
De Meester score	13.1 ± 1.2	12.4 ± 1.2	> 0.05	17.5 ± 1.4	14.3 ± 1.2	> 0.05	18.2 ± 1.3	16.2 ± 1.4	> 0.05
(%) time pH < 4 (total)	11 ± 3	6 ± 2	< 0.05	26 ± 3	11 ± 5	< 0.05	27 ± 6	27 ± 5	> 0.05
(%) time pH < 4 (supine)	12 ± 4	7 ± 2	< 0.05	28 ± 4	13 ± 4	< 0.05	29 ± 5	30 ± 8	> 0.05
(%) time pH < 4 (upright)	9 ± 4	5 ± 2	< 0.05	15 ± 5	5 ± 3	< 0.05	25 ± 2	22 ± 7	> 0.05

symptoms in both groups. At manometric evaluation, no statistically significant differences in the mean LES pressure were found when the two groups were compared (*P* = NS) but the EG had a higher rate of impaired esophageal peristalsis (defined as peristaltic waves with a pressure value lower than 30 mmHg) in comparison with their younger counterparts (*P* < 0.05) (Table 5). Incidence of Hiatal Hernia (HH) was 89.2% (58/65) in elderly patients and 71.3% (253/355) in young patients (*P* < 0.05).

Table 6 shows the prevalence of HH and esophagitis and pH metric values either in Non-erosive reflux disease (NERD) and in Erosive reflux disease (ERD) patients. In the EG, 45/65 (69.2%) patients presented with esophagitis (ERD group): 11 of 45 (24.4%) had a grade I esophagitis while 34 out of 45 (75.6%) had a grade Ⅱ-Ⅲ esophagitis. In the YG, 125/355 (35.2%) patients presented with esophagitis (ERD group): 76 out of 125 (60.8 %) had a grade I esophagitis while 49 of 125 (39.2%) had a grade Ⅱ-Ⅲ esophagitis.

Therefore, in the EG, a significant higher grade of esophagitis has been found along with a higher incidence of Barrett esophagus (Table 6).

A pathologic DeMeester score was found at pH-monitoring in all patients of both subgroups: in the YG, it was 12.4 ± 1.2 and 14.3 ± 1.2, whereas in the EG it was 13.1 ± 11.2 and 17.5 ± 1.4 respectively for NERD and ERD subgroups. The mean percentage of total time < 4 at 24-h pH monitoring in NERD and ERD subgroups, is shown in Table 6.

Perioperative results

All the interventions were completed *via* laparoscopic approach. Mean operative time was 45 ± 14 min in YG and 61 ± 15 min in EG. No mortality was observed in both groups. A major complication occurred in 4/420 patients (1.0%), all among the YG. Mean postoperative hospital stay was 2.4 ± 0.9 d in YG (range 1-5) and 3.8 ± 1.0 d in EG (range 1-7) (*P* < 0.05). Normal activity resumed in 8.3 ± 3.4 d in YG and 12.5 ± 9.0 d in EG (*P* < 0.05) (Table 7).

Table 7 Perioperative results in EG and YG

Intraoperative results	EG	YG	*P*
Operative time (m)	61 ± 15	45 ± 15	< 0.05
Operative blood loss (mL)	50 (0-120)	30 (0-100)	< 0.05
Major complications	0	4/355 (1.1%)[1]	-
Mortality	0	0	-
Postoperative recovery			
Post operative hospital stay (d)	3.8 ± 1.0	2.4 ± 0.9	< 0.05
Resumption of normal activity (d)	12.5 ± 9.0	8.3 ± 3.4	< 0.05

[1]1/335 intraoperative mucosal tear, 3/335 postoperative bleeding (1 splenectomy).

Postoperative results

We followed up clinically 408 (97.1%) of 420 patients, 62 (95.3%) patients in the EG and 338 (95.2%) patients in YG. Two patients in the EG died four years after surgery for no surgery correlated event. In the YG, the mean follow-up was 83.2 ± 7 mo (range 6-141) whereas in EG it was 60 ± 8 mo (range 6-95).

An excellent outcome was observed in 314/338 (92.9%) younger patients and in 57/62 (91.9%) elderly patients (*P* > 0.05). Both groups showed significant improvement

Table 8 Postoperative symptoms score in EG and YG (mean symptom score ± SD)

Symptoms	EG		*P*	YG		*P*
	Preop.	Postop.		Preop.	Postop.	
Heartburn	1.7 ± 0.87	0.2 ± 0.12	< 0.05	2.7 ± 0.74	0.3 ± 0.11	< 0.05
Acid regurgitation	1.5 ± 0.96	0.3 ± 0.13	< 0.05	2.3 ± 0.89	0.2 ± 0.12	< 0.05
Solid food dysphagia	1.6 ± 0.76	0.4 ± 0.12	< 0.05	0.5 ± 0.2	0.2 ± 0.15	< 0.05
Chest pain	1.6 ± 0.82	0.3 ± 0.21	< 0.05	1.5 ± 0.87	0.2 ± 0.13	< 0.05
Respiratory complication (chronic cough, sleep apnoea, asthma, laryngitis)	1.8 ± 1.04	0.3 ± 0.11	< 0.05	1.0 ± 0.45	0.2 ± 0.12	< 0.05

Preop: preoperative; Postop: postoperative.

Table 9 Postoperative side effects in EG and YG

	EG	YG	*P*
Postoperative side effects: number patients (%)			
Dysphagia	2/62 (3.2%)[1]	11/338 (3.3%)[2]	> 0.05
Heartburn	2/62 (3.2%)[3]	12/338 (3.6%)[4]	> 0.05
Hyperflautolence	1/62 (1.6%)	6/338 (1.8%)	> 0.05
Early satiety	2/62 (3.2%)	9/338 (2.7%)	> 0.05
Bloating	1/62 (1.6%)	3/338 (0.9%)	> 0.05
Chest pain	0	2/338 (0.6%)	> 0.05

[1]2 dilation; [2]5 dilation, 6 laparoscopic re-fundoplication; [3]2 reassumed peptic medications; [4]8 reassumed peptic medications, 4 laparoscopic re-fundoplication.

Table 10 Postoperative manometric evaluation at 24 mo after surgery in EG and YG

Manometry	EG (36 Pts)		*P*	YG (230 Pts)		*P*
	Preop.	Postop.		Preop.	Postop.	
N-HPZ pressure (mmHg)	11.2 ± 1.5	28.2 ± 1.5	< 0.05	11.0 ± 1.2	28.1 ± 1.2	< 0.05
Increase of mean peristalsis waves patients *n* (%)		28/36 (77.8%)			100/230 (43.5%)	

Preop: preoperative; Postop: postoperative.

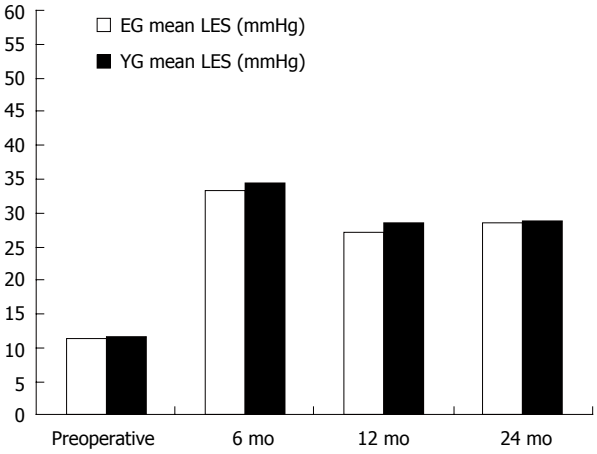

Figure 1 Modification in LES (mean in mmHg) in EG and YG.

in clinical symptom score (Table 8). At 6 mo, persisting postoperative dysphagia (DeMeester score 2-3) leading to > 15% of weight loss was observed in 11 (3.3%) of 338 patients in YG, 2 patients in the group with preoperative impaired peristalsis and 9 in the group with normal esophageal motility (Table 9). In EG, persisting postoperative dysphagia was relieved in 2 (3.2%) of 62 patients, both in group with normal preoperative esophageal peristalsis (Table 9).

No statistically significant difference was observed between patients with normal and impaired peristalsis. Five patients in YG and both 2 patients in EG were treated with endoscopic dilatation, whereas 6 patients in YG underwent a laparoscopic redo-funduplication with partial resolution of dysphagia. Recurrent heartburn was observed and confirmed with 24 h pH monitoring follow-up in 14/408 patients (3.4%), which was due to a disrupted wrap, an herniated wrap, and a slipped Nissen detected at X-ray barium in 7, 4, and 3 cases, respectively.

Ten patients reassumed their peptic medications; the remaining 4 patients, all in YG, underwent redofunduplication with partial resolution of symptoms. Respiratory symptoms showed a significant improvement in both groups (Table 9). Other data regarding hyper-flatulence, early satiety and bloating are depicted in Table 9.

Esophageal manometric follow-up (performed at 6, 12, and 24 mo after surgery) was made in 331 (81.1%) of 408 patients at 6 mo (48/62, 77.4% in EG and 283/338, 83.7% in YG), 275/408 (67.4%) at 12 mo (38/62, 61.3% in EG and 237/338, 70.1% in YG), and 266/408 (65.2%) at 24 mo (36/62, 58.1% in EG and 230/338, 68.0% in YG). Stationary esophageal manometry showed a significant improvement in the mean new high pressure zone (N-HPZ) value in comparison with preoperative values in the two groups ($P < 0.05$) (Table 10 and Figure 1); Manometric evaluation at 24 mo after surgery showed an increase of mean peristalsis waves in 28/36 (77.8%) patients of the EG and 100/230 (43.5%) patients of the YG.

Twenty-four hour pH monitoring at 1 year after surgery was performed in 205/408 (50.2%) patients. There was a significant postoperative decrease in DeMeester score and percentage of time pH < 4 during 24 h (Table 11).

DISCUSSION

Gastroesophageal reflux disease (GERD) is a common disorder in the western population; periodically symptoms

Table 11 De Meester score and percentage of reflux time during 24 h in EG and YG, preoperative and 1 yr after surgery

	Preoperative	1 yr after surgery
DeMeester score		
EG	15.1 ± 1.1	1.2 ± 0.7
YG	13.4 ± 1.5	1.1 ± 0.2
(%) time pH < 4		
EG	9.1 ± 0.6	1.4 ± 0.3
YG	8.2 ± 0.7	0.9 ± 0.8

occur in approximately 20% of adults in USA[5]. Its cost has been estimated to be $24.1 billion annually[2].

By 2020 more than 16% of population in USA are expected to be more than 65 years old while nearly 20 million ought to be more than 85 years old[6]. In the elderly, the prevalence of GERD is nearly the same among the general population, but complicated GERD appears to be more common than in young people[6].

Several authors have reported a higher incidence of esophagitis as well as Barrett esophagus in older patients[7-11]. Collen[7] found that esophagitis and Barrett esophagus were almost twice in patients aged 60 years than in young people (81% *vs* 47%, $P < 0.002$). Zhu[8] observed that the percentage of time with pH < 4 was 32.5% in older patients with GERD *vs* 12.9% in younger ones ($P < 0.05$). Furthermore, among elderly patients with esophagitis, nearly 21% had grade Ⅲ-Ⅳ disease compared with only 3.4% of younger patients ($P = 0.002$). Cameron[9] demonstrated that the prevalence of Barrett's esophagus increased with age to reach a plateau by the seventh decade. Fass[11] reported that the mean incidence rate of erosive esophagitis was 74% in the elderly and 64% in the younger patients and the frequency of symptoms was lower in the elderly group. David[12] demonstrated that the prevalence of severe esophagitis increased with age: only 12% in GERD patients < 21 years old in comparison with 37% in patients > 70 years old had severe esophagitis.

Also in our study, the elderly group (EG) had a higher rate of erosive esophagitis (69.2% *vs* 35.2.%) and a lower rate of Grade I esophagitis (22.2% *vs* 60.8%). Moreover, incidence of Barrett's esophagus as well as mean percentage of total time < 4 at pH-monitoring were significantly higher in the EG (Table 7). The frequency of reflux episodes has been reported to be similar either in the elderly or in young people whereas the duration of individual reflux episodes seems to be longer in the elderly[13]. However, it is not clear which factors lead to a more severe GERD in the elderly.

The etiopathogenesis of GERD seems to be multifactorial. The alteration may include a defective antireflux barrier, abnormal esophageal-clearance, altered esophageal mucosal resistance, and delayed gastric emptying[14].

Hiatal hernia (HH) as a structural defect of the antireflux barrier is a determining factor of GERD, by impairing both the diaphragmatic component and the clearance of acid refluxate from the distal esophagus[15]. HH has been identified in 60% of patients > 60 years old[16]. Furthermore, several studies found a higher frequency of esophagitis in patients with HH compared with patients without HH, and the severity was proportional to the size of HH. In our study, we noted a significant higher rate of HH in the EG (Table 6). Previous studies excluded any adverse effect of aging on the lower esophageal sphincter (LES) of healthy subjects[17,18]. Similarly, we did not find any significant difference in LES pressure between the EG and the YG. However, an impaired esophageal peristalsis (waves pressure < 30 mmHg) has been found in 66.7% of the EG and 33.4% of the YG (Table 5). It is not clear whether impaired peristalsis is a cause of or affects a more severe GERD, since we noted an increased amplitude of peristaltic waves both in the EG and in the YG at the postoperative manometric follow-up evaluation (Figure 1).

Changes in motility seen in older patients is related to long- term esophageal acid exposure rather than to effects of aging on esophageal smooth muscle and on collagen production that is increased in chronic inflammation[18,19]. In our study, the mean duration of preoperative symptoms was significantly longer in the EG. Probably a vicious circle begins in these subjects between cardia incontinence, increasing reflux and impaired peristalsis determining a reduction of esophageal clearing[20]. The realization of antireflux procedure seems to break this circle. Some authors described the increased amplitude of peristalsis in patients undergoing total fundoplication[21,22].

Besides, Sonnemberg showed an age dependent fall in salivary bicarbonate production while physiologic levels of gastric acid secretion remained stable in advanced age. These factors may increase esophageal acid exposure because of delayed acid clearance[23]. We found elderly patients having less frequency and severity of symptoms like heartburn and acid regurgitation than younger patients[24] (Tables 3 and 4). Raiha[24] hypothesized that typical symptoms should not be considered as expression of acid reflux in older patients. However, it is not clear which factors reduce frequency and severity of these symptoms although these patients have a higher rate of acid exposure and develop a more severe esophagitis.

Several studies have shown that altered esophageal pain perception to acid in the elderly is the result of an ageing process that may be responsible for an increased severity of GERD[11]. On the other hand, frequency and severity of atypical symptoms have been reported to be higher in elderly people with GERD[24]. Also in our study, we found a statistically significant higher rate of atypical symptoms such as dysphagia for solids, chest pain and respiratory symptoms in the EG (Tables 3 and 4).

Therefore, a mild intensity of heartburn often leads physicians to underestimate the severity of erosive esophagitis and its complications.

Surgical correction of GERD has been shown to be a cost-effective treatment by reducing long-term complications such as Barrett esophagus and stricture and by eliminating the need of a life-long medical therapy especially for young patients. However, a high morbidity and mortality rate of open surgery performed in the elderly, limited the number of these patients referred to surgical units[25]. Since a laparoscopic Nissen fundoplication

has been reported for the first time, a growing number of antireflux procedures have been performed in the USA[26]. Several studies showed laparoscopic surgery to be a safe and effective treatment for GERD being able to improve quality of life and warranting an early return to daily activities[27].

In elderly population with GERD, laparoscopic surgery has proven to be effective with low morbidity and mortality rates. Richter[2] observed that Laparoscopic Nissen Fundoplication did not increase the mortality, morbility and hospital stay in the elderly patients compared to younger surgical patients. Kalmoz[28] showed that age should not be considered a contraindication to laparoscopic surgical treatment of GERD as 97% of elderly patients would choose surgical treatment again if necessary. Bammer[29] reported that laparoscopic surgery is a good option for the treatment of severe GERD in octo- and nonagenarians, with an excellent follow-up in 93% of elderly patients. Except for preoperative disease severity, we did not find any significant difference in perioperative and postoperative results as well as in subjective and objective outcome between the two groups. The only observed differences in the operative time and blood loss seem to be related to the high ASA scores and the higher incidence and size of hiatal hernia in the EG.

Statistically significant improvement in heartburn, acid regurgitation, chest pain and respiratory complications of GERD was observed in both EG and YG (Table 9). An excellent outcome was observed in 314/338 (92.9%) younger patients and in 57/62 (91.9%) elderly patients.

A poor outcome was observed in 27 patients, 23/338 (7.1%) in YG and 4/62 (6.5%) in EG; persisting dysphagia occurred in 11/338 (3.3%) in YG and 2/62 (3.2%) in EG; and 12/338 (3.6%) in YG and 2/62 (3.2%) in EG had recurrent of heartburn. Differences between the two groups were not statistically significant also regarding the incidence of other side effects (flatulence, early satiety, etc) (Table 10). Outcome was not dependent on the presence of disordered esophageal motility.

There have been debates in literature regarding the realization of partial fundoplication in patients with defective esophageal peristalsis, and it seemed reasonable therefore, to choose this kind of wrap in elderly patients. Many authors supported the realization of a partial fundoplication in patients with impaired esophageal peristalsis to lower the incidence of persistent postoperative dysphagia[30-32]; moreover, partial wrap was considered as effective as total wrap to control gastroesophageal reflux, and short-term follow-up seemed to validate the choice of partial fundoplication[33,34]. Later on, partial antireflux procedure showed its inadequacy to assure a good protection from reflux at a long-term follow-up[35-37]. Livingston[38] reported a 1.4% recurrence rate of reflux in patients with total fundoplication versus 6.7% in those with partial fundoplication. At a long-term follow-up, Fernando[39] observed that 38% of Toupet patients used PPI versus 20% with Nissen. Jobe[40], in a ten years follow-up, noted a recurrence rate for reflux until 51% in patients treated with partial fundoplication (Toupet and Dor). Moreover, total fundoplication seems not to determinate a higher incidence of postoperative dysphagia compared with the partial wraps, even in patients with impaired peristalsis[41,42]. Patti[43] analysed the long-term results of patients treated with partial versus total antireflux procedures: efficacy was higher for total fundoplication (recurrence of reflux in 4% of patients with total fundoplication versus 19% in patients with partial fundoplication), while the incidence of postoperative dysphagia was similar in both groups, even in patients with impaired esophageal peristalsis (8% Toupet versus 9% Nissen). Pessaux[44], at a three-month follow-up, noted a dysphagia rate of 4.2% in patients treated with Nissen fundoplication versus 5.9% with Nissen-Rossetti wrap and 6.9% in those treated with Toupet. In a prospective randomized trial, Bessell[45] concluded that calibrating the antireflux wrap according to esophageal motility was not necessary, because the postoperative persistent dysphagia rate was similar between patients with total or partial wrap. Velanovich[46] did not find any statistically significant difference in postoperative dysphagia rate related to esophageal motility disorders (MD) (15.8% MD+ versus 16.4% MD-) in a group of patients undergoing total fundoplication.

Besides, total wrap seems to bring about an improvement of esophageal peristalsis. Heider[47] observed an increase of 47% of mean peristaltic waves in distal esophagus compared with preoperative time ($P < 0.01$), with the normalization of the esophageal motility in 74% of patients. Diaz de Liano[48], at 1 year follow-up, noted an augment of esophageal peristalsis in 43% of patients with impaired peristalsis undergoing total fundoplication. Scheffer[49] showed an increase of mean amplitude of peristalsis from a preoperative value of 57 mmHg to 86 mmHg at 3 mo follow-up and 92 mmHg at 2 years after surgery in a group of 34 patients. Oleynikov[50] in a trial comparing total and partial fundoplication noticed that in patients undergoing partial wrap, the mean amplitude of peristaltic waves increased from 27.8 mmHg before surgery to 35.6 mmHg postoperatively ($P > 0.05$), while in patients treated with total fundoplication, these values were respectively 28.2 mmHg versus 49.0 mmHg ($P < 0.05$). These evidences strongly support the choice of performing a total fundoplication also in elderly patients, which is often affected by severe impairment of esophageal peristalsis.

Our choice since 1972, has always been favorable to the total fundoplication, without section of short gastric vessel. We usually perform intraoperative endoscopy and manometry in order to calibrate antireflux wrap[51]. Usually, we calibrate the n-HPZ at values ranging from 20 to 45 mmHg ('hypercalibrated Nissen'), building the wrap around the gastroscope (with a diameter of 9 mm). This hypercalibration, in contrast with the 'floppy Nissen' of Donahue and DeMeester[52], resulted from the retrospective evaluation of a former series in which we used to calibrate the fundoplication to pressure values similar to those of a normal sphincter ('normocalibrated Nissen': 10-20 mmHg). This experience was followed by a high rate of gastroesophageal reflux recurrence (28.5%) in the first 12 mo after surgery[51], demonstrating that high pressure zone (HPZ) values of the Nissen-Rossetti wrap decrease after surgery with time (Figure 1). It is effective to

protect from GERD while avoiding a persistent dysphagia because a routine intraoperative manometric control of the wrap is always performed at the end of the procedure. Our preference for total calibrated wrap led us to consider it also in the treatment of patients affected with severe motility disorders such as achalasia and epiphrenic diverticula with excellent results[52,53].

In conclusion, laparoscopic antireflux surgery, is a safe and effective treatment for GERD even in elderly patients warranting low morbidity and mortality rates and a significant improvement of symptoms comparable to younger patients. Preoperative defective esophageal peristalsis is not a contraindication to total laparoscopic fundoplication.

REFERENCES

1 **Greenwald DA**. Aging, the gastrointestinal tract, and risk of acid-related disease. *Am J Med* 2004; **117** Suppl 5A: 8S-13S
2 **Richter JE**. Gastroesophageal reflux disease in the older patient: presentation, treatment, and complications. *Am J Gastroenterol* 2000; **95**: 368-373
3 **Glaser K**, Wetscher GJ, Klingler A, Klingler PJ, Eltschka B, Hollinsky C, Achem SR, Hinder RA. Selection of patients for laparoscopic antireflux surgery. *Dig Dis* 2000; **18**: 129-137
4 **Johnson LF**, Demeester TR. Twenty-four-hour pH monitoring of the distal esophagus. A quantitative measure of gastroesophageal reflux. *Am J Gastroenterol* 1974; **62**: 325-332
5 **Shaheen N**, Ransohoff DF. Gastroesophageal reflux, Barrett esophagus, and esophageal cancer: clinical applications. *JAMA* 2002; **287**: 1982-1986
6 **Hazzard WR**. Demographic peristalsis. Implications of the age wave for gastroenterologists. *Gastroenterol Clin North Am* 2001; **30**: 297-311, vii
7 **Collen MJ**, Abdulian JD, Chen YK. Gastroesophageal reflux disease in the elderly: more severe disease that requires aggressive therapy. *Am J Gastroenterol* 1995; **90**: 1053-1057
8 **Zhu H**, Pace F, Sangaletti O, Bianchi Porro G. Features of symptomatic gastroesophageal reflux in elderly patients. *Scand J Gastroenterol* 1993; **28**: 235-238
9 **Cameron AJ**, Lomboy CT. Barrett's esophagus: age, prevalence, and extent of columnar epithelium. *Gastroenterology* 1992; **103**: 1241-1245
10 **Reynolds JC**. Influence of pathophysiology, severity, and cost on the medical management of gastroesophageal reflux disease. *Am J Health Syst Pharm* 1996; **53**: S5-S12
11 **Fass R**, Pulliam G, Johnson C, Garewal HS, Sampliner RE. Symptom severity and oesophageal chemosensitivity to acid in older and young patients with gastro-oesophageal reflux. *Age Ageing* 2000; **29**: 125-130
12 **Johnson DA**, Fennerty MB. Heartburn severity underestimates erosive esophagitis severity in elderly patients with gastroesophageal reflux disease. *Gastroenterology* 2004; **126**: 660-664
13 **Whitaker M**. Proton pump inhibitors in the elderly population. *Eur J Gastroenterol Hepatol* 2002; **14** Suppl 1: S5-S9
14 **Gawrieh S**, Shaker R. Medical management of nocturnal symptoms of gastro-oesophageal reflux disease in the elderly. *Drugs Aging* 2003; **20**: 509-516
15 **Stilson WL**, Sanders I, Gardiner GA, Gorman HC, Lodge DF. Hiatal hernia and gastroesophageal reflux. A clinicoradiological analysis of more than 1,000 cases. *Radiology* 1969; **93**: 1323-1327
16 **Khajanchee YS**, Urbach DR, Butler N, Hansen PD, Swanstrom LL. Laparoscopic antireflux surgery in the elderly. *Surg Endosc* 2002; **16**: 25-30
17 **Richter JE**, Wu WC, Johns DN, Blackwell JN, Nelson JL, Castell JA, Castell DO. Esophageal manometry in 95 healthy adult volunteers. Variability of pressures with age and frequency of "abnormal" contractions. *Dig Dis Sci* 1987; **32**: 583-592
18 **Hollis JB**, Castell DO. Esophageal function in elderly man. A new look at "presbyesophagus". *Ann Intern Med* 1974; **80**: 371-374
19 **Thomson AB**. Gastro-Oesophageal reflux in the elderly: role of drug therapy in management. *Drugs Aging* 2001; **18**: 409-414
20 **Dodds WJ**, Dent J, Hogan WJ, Helm JF, Hauser R, Patel GK, Egide MS. Mechanisms of gastroesophageal reflux in patients with reflux esophagitis. *N Engl J Med* 1982; **307**: 1547-1552
21 **Lundell L**, Abrahamsson H, Ruth M, Rydberg L, Lönroth H, Olbe L. Long-term results of a prospective randomized comparison of total fundic wrap (Nissen-Rossetti) or semi-fundoplication (Toupet) for gastro-oesophageal reflux. *Br J Surg* 1996; **83**: 830-835
22 **Sonnenberg A**, Steinkamp U, Weise A, Berges W, Wienbeck M, Rohner HG, Peter P. Salivary secretion in reflux esophagitis. *Gastroenterology* 1982; **83**: 889-895
23 **Soergel KH**, Zboralske FF, Amberg JR. Presbyesophagus: esophageal motility in nonagenarians. *J Clin Invest* 1964; **43**: 1472-1479
24 **Räihä I**, Hietanen E, Sourander L. Symptoms of gastro-oesophageal reflux disease in elderly people. *Age Ageing* 1991; **20**: 365-370
25 **Leggett PL**, Bissell CD, Churchman-Winn R, Ahn C. A comparison of laparoscopic Nissen fundoplication and Rossetti's modification in 239 patients. *Surg Endosc* 2000; **14**: 473-477
26 **DeMeester TR**, Bonavina L, Albertucci M. Nissen fundoplication for gastroesophageal reflux disease. Evaluation of primary repair in 100 consecutive patients. *Ann Surg* 1986; **204**: 9-20
27 **Hinder RA**, Filipi CJ, Wetscher G, Neary P, DeMeester TR, Perdikis G. Laparoscopic Nissen fundoplication is an effective treatment for gastroesophageal reflux disease. *Ann Surg* 1994; **220**: 472-481; discussion 481-483
28 **Kamolz T**, Bammer T, Granderath FA, Pasiut M, Pointner R. Quality of life and surgical outcome after laparoscopic antireflux surgery in the elderly gastroesophageal reflux disease patient. *Scand J Gastroenterol* 2001; **36**: 116-120
29 **Bammer T**, Hinder RA, Klaus A, Libbey JS, Napoliello DA, Rodriquez JA. Safety and long-term outcome of laparoscopic antireflux surgery in patients in their eighties and older. *Surg Endosc* 2002; **16**: 40-42
30 **Bittner HB**, Meyers WC, Brazer SR, Pappas TN. Laparoscopic Nissen fundoplication: operative results and short-term follow-up. *Am J Surg* 1994; **167**: 193-198; discussion 199-200
31 **Siewert JR**, Feussner H, Walker SJ. Fundoplication: how to do it? Peri-esophageal wrapping as a therapeutic principal in gastro-esophageal reflux prevention. *World J Surg* 1992; **16**: 326-334
32 **Waring JP**, Hunter JG, Oddsdottir M, Wo J, Katz E. The preoperative evaluation of patients considered for laparoscopic antireflux surgery. *Am J Gastroenterol* 1995; **90**: 35-38
33 **Patti MG**, Arcerito M, Feo CV, De Pinto M, Tong J, Gantert W, Tyrrell D, Way LW. An analysis of operations for gastroesophageal reflux disease: identifying the important technical elements. *Arch Surg* 1998; **133**: 600-606; discussion 606-607
34 **Lund RJ**, Wetcher GJ, Raiser F, Glaser K, Perdikis G, Gadenstätter M, Katada N, Filipi CJ, Hinder RA. Laparoscopic Toupet fundoplication for gastroesophageal reflux disease with poor esophageal body motility. *J Gastrointest Surg* 1997; **1**: 301-308; discussion 308
35 **Horvath KD**, Jobe BA, Herron DM, Swanstrom LL. Laparoscopic Toupet fundoplication is an inadequate procedure for patients with severe reflux disease. *J Gastrointest Surg* 1999; **3**: 583-591
36 **Farrell TM**, Archer SB, Galloway KD, Branum GD, Smith CD, Hunter JG. Heartburn is more likely to recur after Toupet fundoplication than Nissen fundoplication. *Am Surg* 2000; **66**: 229-236; discussion 236-237
37 **Eubanks TR**, Omelanczuk P, Richards C, Pohl D, Pellegrini

CA. Outcomes of laparoscopic antireflux procedures. *Am J Surg* 2000; **179**: 391-395
38 **Livingston CD**, Jones HL, Askew RE, Victor BE, Askew RE. Laparoscopic hiatal hernia repair in patients with poor esophageal motility or paraesophageal herniation. *Am Surg* 2001; **67**: 987-991
39 **Fernando HC**, Luketich JD, Christie NA, Ikramuddin S, Schauer PR. Outcomes of laparoscopic Toupet compared to laparoscopic Nissen fundoplication. *Surg Endosc* 2002; **16**: 905-908
40 **Jobe BA**, Wallace J, Hansen PD, Swanstrom LL. Evaluation of laparoscopic Toupet fundoplication as a primary repair for all patients with medically resistant gastroesophageal reflux. *Surg Endosc* 1997; **11**: 1080-1083
41 **Baigrie RJ**, Watson DI, Myers JC, Jamieson GG. Outcome of laparoscopic Nissen fundoplication in patients with disordered preoperative peristalsis. *Gut* 1997; **40**: 381-385
42 **Beckingham IJ**, Cariem AK, Bornman PC, Callanan MD, Louw JA. Oesophageal dysmotility is not associated with poor outcome after laparoscopic Nissen fundoplication. *Br J Surg* 1998; **85**: 1290-1293
43 **Patti MG**, Robinson T, Galvani C, Gorodner MV, Fisichella PM, Way LW. Total fundoplication is superior to partial fundoplication even when esophageal peristalsis is weak. *J Am Coll Surg* 2004; **198**: 863-869; discussion 869-870
44 **Pessaux P**, Arnaud JP, Ghavami B, Flament JB, Trebuchet G, Meyer C, Huten N, Champault G. Laparoscopic antireflux surgery: comparative study of Nissen, Nissen-Rossetti, and Toupet fundoplication. Société Française de Chirurgie Laparoscopique. *Surg Endosc* 2000; **14**: 1024-1027
45 **Bessell JR**, Finch R, Gotley DC, Smithers BM, Nathanson L, Menzies B. Chronic dysphagia following laparoscopic fundoplication. *Br J Surg* 2000; **87**: 1341-1345
46 **Velanovich V**, Mahatme A. Effects of manometrically discovered nonspecific motility disorders of the esophagus on the outcomes of antireflux surgery. *J Gastrointest Surg* 2004; **8**: 335-341
47 **Heider TR**, Behrns KE, Koruda MJ, Shaheen NJ, Lucktong TA, Bradshaw B, Farrell TM. Fundoplication improves disordered esophageal motility. *J Gastrointest Surg* 2003; **7**: 159-163
48 **Díaz de Liaño A**, Oteiza F, Ciga MA, Aizcorbe M, Trujillo R, Cobo F. Nonobstructive dysphagia and recovery of motor disorder after antireflux surgery. *Am J Surg* 2003; **185**: 103-107
49 **Scheffer RC**, Samsom M, Frakking TG, Smout AJ, Gooszen HG. Long-term effect of fundoplication on motility of the oesophagus and oesophagogastric junction. *Br J Surg* 2004; **91**: 1466-1472
50 **Oleynikov D**, Eubanks TR, Oelschlager BK, Pellegrini CA. Total fundoplication is the operation of choice for patients with gastroesophageal reflux and defective peristalsis. *Surg Endosc* 2002; **16**: 909-913
51 **Del Genio A**, Izzo G, Di Martino N, Maffettone V, Landolfi V, Martella A, Barbato D. Intraoperative esophageal manometry: our experience. *Dis Esophagus* 1997; **10**: 253-261
52 **DeMeester TR**, Johnson LF. Evaluation of the Nissen antireflux procedure by esophageal manometry and twenty-four hour pH monitoring. *Am J Surg* 1975; **129**: 94-100
53 **Del Genio A**, Rossetti G, Maffetton V, Renzi A, Brusciano L, Limongelli P, Cuttitta D, Russo G, Del Genio G. Laparoscopic approach in the treatment of epiphrenic diverticula: long-term results. *Surg Endosc* 2004; **18**: 741-745
54 **Rossetti G**, Brusciano L, Amato G, Maffettone V, Napolitano V, Russo G, Izzo D, Russo F, Pizza F, Del Genio G, Del Genio A. A total fundoplication is not an obstacle to esophageal emptying after heller myotomy for achalasia: results of a long-term follow up. *Ann Surg* 2005; **241**: 614-621

S- Editor Liu Y **L- Editor** Ma JY **E- Editor** Ma WH

PO Box 2345, Beijing 100023, China
www.wjgnet.com
wjg@wjgnet.com

World J Gastroenterol 2007 February 7; 13(5): 748-753
World Journal of Gastroenterology ISSN 1007-9327

CLINICAL RESEARCH

Chios mastic treatment of patients with active Crohn's disease

Andriana C Kaliora, Maria G Stathopoulou, John K Triantafillidis, George VZ Dedoussis, Nikolaos K Andrikopoulos

Andriana C Kaliora, Maria G Stathopoulou, George VZ Dedoussis, Nikolaos K Andrikopoulos, Department of Science of Dietetics-Nutrition, Harokopio University, Athens, Greece
John K Triantafillidis, Department of Gastroenterology, Saint Panteleimon General State Hospital, Nicea, Athens, Greece
Supported by a grant from the Chios Gum Mastic Growers Association
Correspondence to: Dr. Andriana C Kaliora, Department of Science of Dietetics-Nutrition, Harokopio University of Athens, 70 El. Venizelou ave., Kallithea 17671, Athens, Greece. akaliora@hua.gr
Telephone: +30-210-9549303
Received: 2006-11-02 Accepted: 2006-12-21

Key words: Chios mastic; Crohn's disease; C-reactive protein; Cytokines; Antioxidant potential; Conservative treatment

Kaliora AC, Stathopoulou MG, Triantafillidis JK, Dedoussis GVZ, Andrikopoulos NK. Chios mastic treatment of patients with active Crohn's disease. *World J Gastroenterol* 2007; 13(5): 748-753

http://www.wjgnet.com/1007-9327/13/748.asp

Abstract

AIM: To evaluate the effectiveness of mastic administration on the clinical course and plasma inflammatory mediators of patients with active Crohn's disease (CD).

METHODS: This pilot study was conducted in patients with established mild to moderately active CD, attending the outpatient clinics of the hospital, and in healthy controls. Ten patients and 8 controls were recruited for a 4-wk treatment with mastic caps (6 caps/d, 0.37 g/cap). All patients successfully completed the protocol. CD Activity Index (CDAI), Nutritional Risk Index (NRI), C-reactive protein (CRP), interleukin-6 (IL-6), tumor necrosis factor-alpha (TNF-α), monocyte chemotactic protein-1 (MCP-1), and total antioxidant potential (TAP) were evaluated in the plasma at baseline and at the end of the treatment period. Results were expressed as mean values ± SE and $P < 0.05$ was considered to indicate statistical significance.

RESULTS: Patients exhibited significant reduction of CDAI (222.9 ± 18.7 *vs* 136.3 ± 12.3, $P = 0.05$) as compared to pretreament values. Plasma IL-6 was significantly decreased (21.2 ± 9.3 pg/mL *vs* 7.2 ± 2.8 pg/ mL, $P = 0.027$), and so did CRP (40.3 ± 13.1 mg/mL *vs* 19.7 ± 5.5, $P = 0.028$). TAP was significantly increased (0.15 ± 0.09 *vs* 0.57 ± 0.15 mmol/L uric acid, $P = 0.036$). No patient or control exhibited any kind of side effects.

CONCLUSION: The results suggest that mastic significantly decreased the activity index and the plasma levels of IL-6 and CRP in patients with mildly to moderately active CD. Further double-blind, placebo-controlled studies in a larger number of patients are required to clarify the role of this natural product in the treatment of patients with CD.

INTRODUCTION

Crohn's disease (CD) is a chronic inflammatory disease of unknown etiology that may affect any level of the gastrointestinal tract[1-3]. It is well established that immunological mechanisms are involved in the pathogenesis of the disease. Inflammatory cytokines, such as interleukin-6 (IL-6) and tumor necrosis factor-alpha (TNF-α), have a pivotal role in induction and amplification of the inflammatory cascade. Particularly, IL-6 stimulates T-cell and B-cell proliferation and differentiation[4], while it mediates the hepatic expression of acute phase proteins[5]. Increased concentration of TNF-α and monocyte chemoattractant protein-1 (MCP-1) have been reported in patients with CD[6]. Additionally, during chronic inflammation, when sustained production of reactive oxygen and nitrogen species occurs, antioxidant defenses may weaken, resulting in a situation termed oxidative stress[7]. Thus, in patients with CD, elevated oxidized low-density lipoprotein levels have been reported compared to healthy controls[6].

Despite the large number of therapeutic agents available today, none can be considered as completely satisfactory either due to resistant cases or because of significant side effects. To our knowledge, there are only scattered reports of natural compounds that potentially reverse relapse in CD. Trebble and co-workers[8] demonstrated an anti-inflammatory activity of fish oil and antioxidant supplementation evaluated in mononuclear cells of CD patients, while Lavy *et al*[9] demonstrated the effectiveness of the antioxidant β-carotene in a rat model as a prophylactic dietary measure in reducing the effects of acid induced enteritis, thus raising the possibility that patients with CD may benefit from the consumption of natural β-carotene. Also the flavonoid rutin, a well-established antioxidant compound, has been suggested as a therapeutic agent in CD. Rutin has been shown to attenuate pro-inflammatory cytokine production in both colonic

mucosa and peritoneal macrophages of experimental animals[10]. Treatment with food phytochemicals has been shown to be safe, sustainable and practical and changes of dietary habits have been advocated in the therapy of CD[11].

Pistacia lentiscus var. Chia (Anacardiaceae), well known as Chios mastic gum, is an evergreen shrub widely distributed in the Mediterranean region. Many ancient Greek authors, including Dioscurides and Theophrastus, mentioned Chios mastic for its healing properties in intestines, stomach and liver. Mastic has also been reported to possess antioxidant[12] and antibacterial[13] activity. With reference to gastrointestinal disorders, the effectiveness of the resin against peptic ulcers is evident[14] in most studies, while only in two reports there is no effect on *H pylori* eradication *in vivo*[15,16]. Furthermore, regarding gastric mucosa, the plant has been shown to be hepatoprotective in tetrachloride-intoxicated rats[17] and to suppress the extent of iron-induced lipid peroxidation in rat liver homogenates[18], without any toxic effect. A major constituent of mastic, namely oleanolic acid, is among the best-known triterpenes with biological properties against chemically induced liver injury in laboratory animals, exerting anti-inflammatory and antitumor-promotion effects[19]. This background information led us to examine the effects of supplementation with mastic in patients with active CD. This study is the first ever reported to evaluate mastic for possible clinical effectiveness in patients with CD.

MATERIALS AND METHODS

Study population

Ten consecutive patients with established CD and eight healthy controls were recruited to participate in the trial. All patients were attending the outpatient clinic of the Department of Gastroenterology, Saint Panteleimon General State Hospital in Nicea, Athens. Clinical evidence of mild to moderate Crohn's disease exacerbation was defined by a score of CD Activity Index (CDAI) higher than 150. Patients with clinical evidence of recurrence and CDAI higher than 400 were excluded from the study. Patients receiving mesalazine or antibiotics during the time of relapse were asked to continue treatment. None was receiving elemental diet or parenteral nutrition or antioxidant/mineral supplements and none was under treatment with immunosuppressives, immunomodulators and/or corticosteroids. Eight healthy volunteers with normal serum concentrations of C-reactive protein (CRP) (< 5 mg/L) and albumin (> 40 g/L) served as controls. Assessed by Medical History questionnaires, controls included in the study were healthy persons without chronic inflammatory disorder. Exclusion criteria for control recruitment were a body mass index (BMI) higher than 30 and anti-inflammatory drug treatment or antioxidant vitamin/mineral supplementation prior to trial. All volunteers gave a written consent after having received thourough information about the aims and procedure of the study. The Ethical Committees of both Harokopio University and Saint Panteleimon General State Hospital approved the protocol. Table 1 shows some demographic characteristics of patients and controls.

Table 1 Demographic characteristics and medications of patients with CD and controls

Characteristic	Patients	Controls
Age (yr)		
Mean	36.9	31.5
Range	18-73	25-45
Sex		
Female	5	4
Male	5	4
Duration of disease (yr)	6.4 (± 3.9)	-
Concomitant medication		-
None	3	
Mesalazine	3	-
Metronidazole	2	
Azathioprine	2	
Location of Crohn's disease		-
Small bowel	4	-
Small and large bowel	6	-
Fistulizing disease	3	-

Preparation of mastic caps

A UV source device (Jost/Ba-ro, Type FDLT 250/-80 × 2500) was used for sterilization of the Chios Mastic resin. Then, the sterilized mastic granules were milled to fine powder (particle size < 400 μm) by using a Hosokawa Alpine Mill (Fine Impact Mill 100 UP2). The encapsulation of powder was performed using the Profill Capsule filling System (Torpac Inc.). Capsule cells (capsugel, V caps, size 0) were made of Hpromellose (hydroxypropyl methylcellulose) and each contained 0.37 (± 0.02) g of mastic powder.

Intervention trial protocol

Dissolution time was measured according to standard methods[20] and was found to last approximately 7 min. Patients and healthy controls were subjected to a 4-wk supplementation with mastic caps (6 caps/d, 2.2 g in total) over a period from June 2005 to January 2006. Dietary assessment was accomplished applying Food Frequency Questionnaire (FFQ) and 24 h recalls. Dietary instructions were given to both healthy controls and patients as to maintain consumption of food rich in anti-inflammatory and antioxidant ingredients as poor as initially assessed by FFQ and 24 h recall interviews. Assessment of compliance during the trial was tested applying 24 h recalls twice a week. Mastic, either in the form of gum or as a sweet or bread ingredient, and fish oil, either crude or in the form of supplement, was not allowed in either group. The daily energy intake was evaluated by means of 24 h recalls. Blood samples were obtained for plasma isolation and subjected to CRP and albumin measurements prior and after the trial. At the same time points, plasma cytokine and antioxidant potential measurements were performed. Body weight was measured using electronic scales initially and at the end of the trial.

Disease activity index evaluation

The Crohn's Disease activity was evaluated by means

of the CDAI[21]. The CDAI incorporates eight related variables: the number of liquid or very soft stools per day, the severity of abdominal pain or cramping, general well being, the presence or absence of extraintestinal manifestations of CD, the presence or absence of an abdominal mass, the use of antidiarrheal drugs, hematocrit, and body weight. Scores range from 0 to 600 with higher scores indicating more severe disease activity. A score of 151 to 200 corresponds with mild disease activity; moderate disease has a score of 201 to 400, and scores of 401 or greater represent severe disease activity.

Biochemical measurements

CRP concentrations were analyzed immunoturbidimetrically on a Beckman Synchron CX5 fully automated chemistry analyzer. Albumin was measured by means of the bromocresol green method on the same analyzer.

Cytokine assays

Plasma cytokines from patients with CD and controls were assessed by quantitative enzyme-linked immunosorbent assays (ELISA) (R & D Systems Abingdon, UK) according to the manufacturer's instructions. Sensitivity limits of TNF-α, IL-6, and MCP-1 ELISAs are, respectively, 1.6 pg/mL, 0.70 pg/mL and 5.0 pg/mL. Plasma cytokines from patients with CD and controls were assessed in duplicate.

Plasma total antioxidant potential assay

Total antioxidant potential (TAP) in plasma was assessed by a colorimetric, quantitative assay for TAP in aqueous samples (OxisResearch Portland, USA) according to the manufacturer's instructions. The results of the assay were expressed as mmol/L of uric acid equivalents. The sensitivity of the assay is 30 μmol/L uric acid equivalents.

Statistical analysis

Results were expressed as mean ± SE. The Mann-Whitney Test was used for comparing differences between patients and controls prior the intervention. Differences reported primarily and at the end of the study within individual groups, were tested for significance by the Wilcoxon signed ranks test. Calculated $P < 0.05$ was considered to indicate statistical significance.

RESULTS

Alterations of CDAI and induction of remission

The CDAI score was assessed at baseline and after the 4 wk treatment with mastic. All patients receiving mastic showed a reduction of the CDAI as compared to pretreatment values. The reduction of the mean CDAI value was statistically significant (from 222.9 ± 18.7 to 136.3 ± 12.3, $P = 0.05$) (Figure 1). The two main elements of CDAI showing the most striking improvement were the number of liquid stools per day and the score of general well being.

Nutritional risk index

One of the clinically useful measures of nutritional status in CD is the Nutritional Risk Index (NRI), which is calculated based on serum albumin levels and body weight using the following equation: NRI = [1.519 × albumin (g/L)] + [0.417 × (current weight/usual weight) × 100]. A NRI > 100 denotes absence of nutritional risk. NRI values between 97.5 and 99.9 correspond to a mild nutritional risk, NRI values from 83.5 to 97.5 to moderate nutritional risk, and NRI values lower than 83.5 to severe nutritional risk.

The patients' "usual weight" was the body weight at the time of remission, as reported in medical records at the hospital and confirmed by each single patient. NRI of healthy controls was normal at the start of the study and remained unchanged after the mastic supplementation (data not shown). The mean NRI value of CD patients increased from 87.5 ± 3.7 before treatment to 91.5 ± 3.2 at the end of treatment ($P = 0.059$). This increase was evident at the end of the second week of mastic supplementation and remained constant thereafter until the end of the trial.

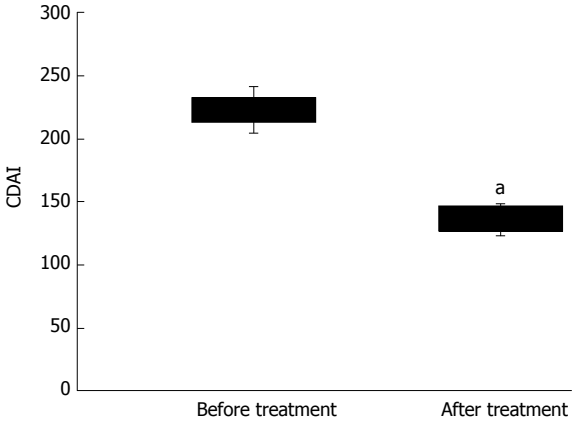

Figure 1 Crohn's disease activity index (CDAI) was decreased in patients with active Crohn's disease ($n = 10$) after 4-wk treatment with mastic caps ($^aP < 0.05$). Horizontal bars represent the mean value (± SE).

CRP

Prior to mastic treatment, CRP levels were significantly higher in CD patients (40.3 ± 13.1 mg/mL) than in healthy controls (2.4 ± 0.7 mg/L) ($P = 0.002$). Treatment with mastic caps of healthy controls resulted in no modifications in CRP values (2.3 ± 0.6 mg/L), which remained at concentrations ⩽ 5.0 mg/mL in all individuals. In CD patients, mean CRP levels were significantly decreased after treatment (from 40.3 ± 13.1 mg/mL to 19.7 ± 5.5, $P = 0.028$) (Figure 2).

IL-6 plasma concentration

IL-6 was below detection in healthy controls prior to therapy, while in patients it was significantly elevated compared to controls ($P = 0.034$). As with CRP, IL-6 in controls remained unaltered, while in patients it decreased significantly (from 21.2 ± 9.3 pg/mL to 7.2 ± 2.8 pg/mL, $P = 0.027$) (Figure 3).

TNF-α plasma concentration

Patients with active CD had TNF-α plasma concentrations 10-fold higher compared to controls before therapy (27.1 ± 9.7 pg/mL *vs* 2.6 ± 1.5 pg/mL, $P = 0.009$). After

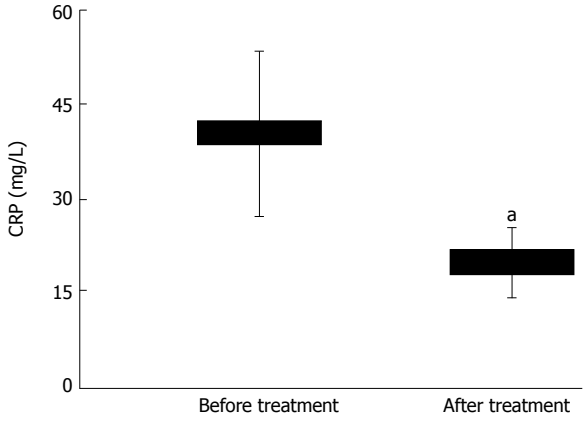

Figure 2 C-reactive protein (CRP) concentrations in patients with active Crohn's disease (n = 10) before and after 4-wk treatment with mastic caps ($^aP < 0.05$). Horizontal bars represent the mean value (± SE).

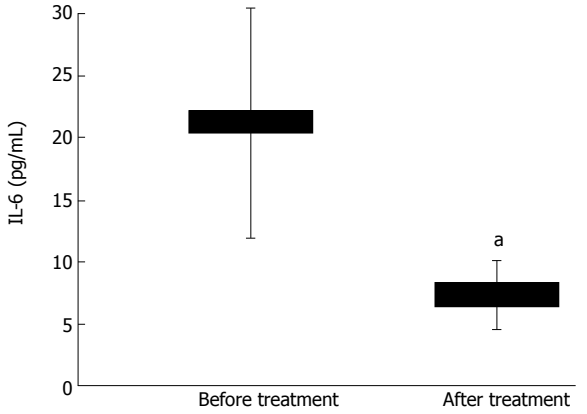

Figure 3 Plasma concentrations of interleukin-6 (IL-6) were suppressed in patients with active Crohn's disease (n = 10) after 4-wk treatment with mastic caps ($^aP < 0.05$). Horizontal bars represent the mean value (± SE).

treatment, plasma TNF-α decreased in patients, although this decrease did not reach statistical significance (27.1 ± 9.7 pg/mL to 16.4 ± 4.7 pg/mL, $P = 0.114$).

MCP-1 plasma concentration

In the case of MCP-1, patients with active CD had MCP-1 plasma concentrations 2.5-fold higher compared to controls (140.7 ± 43.9 pg/mL *vs* 57.5 ± 11.8 pg/mL, $P = 0.368$). Although not statistically significant, a decrease was observed in MCP-1 in CD patients at the end of the trial (76.6 ± 20.9 pg/ mL, $P = 0.074$).

Plasma TAP

TAP was significantly different between the two groups before mastic treatment (healthy controls, 0.4 ± 0.06 *vs* CD patients, 0.15 ± 0.09 mmol/L uric acid, $P = 0.003$). As shown in Figure 4, TAP was significantly increased in individual groups after mastic treatment (controls, 0.4 ± 0.06 *vs* 0.5 ± 0.05 mmol/L uric acid, $P = 0.025$; CD patients, 0.15 ± 0.09 *vs* 0.57 ± 0.15 mmol/L uric acid, $P = 0.036$).

Side-effects

No patient exhibited any side effects. However, during the third day of treatment, one female patient with CD of the small and large bowel reported an abrupt onset of constipation. She was advised to reduce the dose for two days. After that, she continued treatment without further complaints. No other untoward effect was reported.

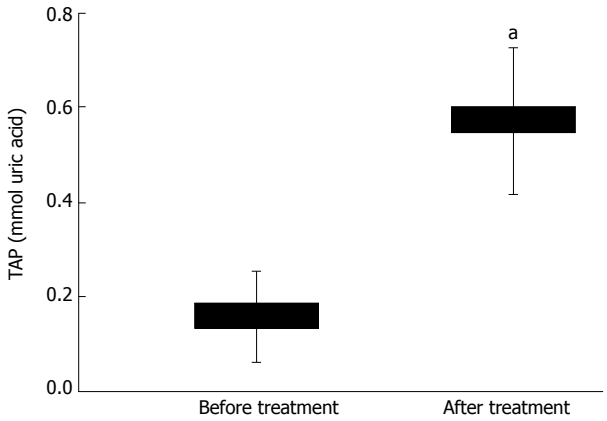

Figure 4 Plasma total antioxidant potential (TAP) was upregulated in patients with active Crohn's disease (n = 10) after 4-wk treatment with mastic caps ($^aP < 0.05$), indicating absorption of antioxidants and an improved *in vivo* antioxidant status. Horizontal bars represent the mean value (± SE).

DISCUSSION

Chios mastic has been previously shown to exert various biological properties *in vitro*[12], in experimental animal models[18] and in humans[14]. In the current study, we demonstrated that mastic was effective in the regulation of inflammation, evaluated by CRP, IL-6, TNF-α and MCP-1 in plasma, as well as in the regulation of oxidative stress, evaluated by TAP. In more details, mastic treatment significantly decreased the CDAI, which probably occurred through decrease of the pro-inflammatory IL-6, inducing remission in seven out of ten patients. Another important observation was that mastic resulted in improvement of the nutritional status, as shown by NRI.

Nutritional support in patients with CD has a primary role in inducing remission and malnutrition is very common in CD. While several factors, such as malabsorption and increased resting energy expenditure in underweight patients, may contribute to malnutrition[22], decreased oral intake is the primary cause. The methods used to support patients with CD are enteral and parenteral nutrition, in terms of protein-calorie intake. NRI is one of the most useful measures of nutritional status and points out severely malnourished patients when less than 83.5[23]. Hereby we show that NRI in patients supplemented with mastic was increased, however not significantly, perhaps due to the limited number of subjects. Particularly, NRI was increased in nine out of ten patients supplemented with mastic, two of whom experienced no nutritional risk (data not shown). The main element of NRI showing improvement was body weight gain. Based upon the fact that daily energy intake was unchanged during the trial (data not shown), increase in body weight and in NRI is due to the fact that mastic treatment resulted in decrease of liquid stools and therefore improvement in nutrient absorption.

The observed decrease in NRI in one of the patients was due to body weight loss, despite the fact that the number of liquid stools decreased. The daily energy intake of this young patient was gradually reduced and, according to her statement long after the end of the protocol, she was on a diet for weight loss.

The importance of IL-6 in patients with CD has been well documented. In patients with active CD, mRNA for IL-6 is overexpressed in the inflamed mucosa[24] and IL-6 is thought to play a crucial role in the pathogenesis of CD. Elevated IL-6 in plasma of patients with CD has been previously described[25]. Accordingly, we report that in patients with CD plasma concentration of IL-6 was significantly higher versus the control group. Significant decrease in IL-6 with mastic treatment was observed in patients following a decrease in plasma CRP (Figure 2). Because IL-6 is the main cytokine factor responsible for hepatic induction of acute phase proteins in CD, respective decrement in CRP is reasonable. In view of the fact that (1) oleoresins consist of triterpenes[26] with established anti-inflammatory and antioxidant effects[19,27] and (2) mastic contains antioxidant phenolic compounds[28], it is more likely that the plasma IL-6 decrease observed in CD patients was due to these compounds.

TNF-α showed an unsignificant (P = 0.114) 1.6-fold decrease in CD patients. On the other hand, the difference in TNF-α concentrations between patients and controls at baseline was significant. The data reported about TNF-α in CD are somewhat contradictory. Whereas some groups were able to demonstrate increased concentrations of TNF-α in CD compared to healthy controls[29], others were not[30]. Because TNF-α induces MCP-1 secretion via the activation of nuclear factor-kappa B[31], it is likely that the slight decrease in MCP-1 was due to the lower activation of the nuclear factor-kappa B pathway secondary to the decrease in TNF-α.

Oxidative stress has been proven to upregulate IL-6 gene expression[32]. We show that mastic treatment resulted in increase of plasma TAP in CD patients (Figure 4) as well as in controls. Plasma is a heterogenous solution of diverse antioxidants and an increase in the antioxidant capacity indicates absorption of antioxidants and an improved *in vivo* antioxidant status[33]. Whether the antioxidant triterpenes and phenolics contained in mastic[12] are absorbed or act on the exposed gastrointestinal mucosa, remains uncertain. Generally, our knowledge on the absorption and bioavailability of polyphenols is still limited, and the few studies in humans show that some are well absorbed and others hardly absorbed[34]. The unabsorbed may remain in the lumen and become available for fermentation in the colon. A substantial proportion of the gastrointestinal mucosa is therefore exposed to these compounds, or to their bacterial and systemic metabolites[35]. However, phenolic compounds do not seem to be absorbed as well as vitamins C and E, and hence their concentrations can be much higher in the lumen of the gastrointestinal tract than are ever achieved in plasma or other body tissues, making the action in the gastrointestinal tract more likely. Even less are the data on the absorption of triterpenes. Glycyrrhetinic acid, the triterpene derivative of glycyrrhizin, has been shown to be bioactive in experimental gastric lesion models[36] and has also been detected in the serum of experimental animals[37].

In conclusion, subjecting CD patients with mild to moderate activity to mastic treatment seems to improve the clinical features of the disease and to regulate inflammation and antioxidant status. The use of natural products as primary treatment in CD should attract wider support and research, with increasing awareness of the harm of the long-term use of corticosteroids. Whether it is time for gastroenterologists to embrace the concept that natural products, such as mastic, may be beneficial to CD needs further research in larger cohorts.

ACKNOWLEDGMENTS

We wish to thank the Chios Mastic Growers Association, especially Dr. Christos Kartalis, for the production and kind donation of Chios mastic caps, exclusively for the needs of the trial.

REFERENCES

1 **Triantafillidis JK**, Emmanouilidis A, Manousos O, Nicolakis D, Kogevinas M. Clinical patterns of Crohn's disease in Greece: a follow-up study of 155 cases. *Digestion* 2000; **61**: 121-128
2 **Triantafillidis JK**, Emmanouilidis A, Nicolakis D, Ifantis T, Cheracakis P, Merikas EG. Crohn's disease in the elderly: clinical features and long-term outcome of 19 Greek patients. *Dig Liver Dis* 2000; **32**: 498-503
3 **Triantafillidis JK**, Emmanouilidis A, Nicolakis D, Cheracakis P, Kogevinas M, Merikas E, Hereti I, Argyros N. Surgery for Crohn's disease in Greece: a follow-up study of 79 cases. *Hepatogastroenterology* 2001; **48**: 1072-1077
4 **Kishimoto T**. The biology of interleukin-6. *Blood* 1989; **74**: 1-10
5 **Ramadori G**, Armbrust T. Cytokines in the liver. *Eur J Gastroenterol Hepatol* 2001; **13**: 777-784
6 **Grip O**, Janciauskiene S, Lindgren S. Circulating monocytes and plasma inflammatory biomarkers in active Crohn's disease: elevated oxidized low-density lipoprotein and the anti-inflammatory effect of atorvastatin. *Inflamm Bowel Dis* 2004; **10**: 193-200
7 **Grisham MB**. Oxidants and free radicals in inflammatory bowel disease. *Lancet* 1994; **344**: 859-861
8 **Trebble TM**, Stroud MA, Wootton SA, Calder PC, Fine DR, Mullee MA, Moniz C, Arden NK. High-dose fish oil and antioxidants in Crohn's disease and the response of bone turnover: a randomised controlled trial. *Br J Nutr* 2005; **94**: 253-261
9 **Lavy A**, Naveh Y, Coleman R, Mokady S, Werman MJ. Dietary Dunaliella bardawil, a beta-carotene-rich alga, protects against acetic acid-induced small bowel inflammation in rats. *Inflamm Bowel Dis* 2003; **9**: 372-379
10 **Kwon KH**, Murakami A, Tanaka T, Ohigashi H. Dietary rutin, but not its aglycone quercetin, ameliorates dextran sulfate sodium-induced experimental colitis in mice: attenuation of pro-inflammatory gene expression. *Biochem Pharmacol* 2005; **69**: 395-406
11 **Levi AJ**. Diet in the management of Crohn's disease. *Gut* 1985; **26**: 985-988
12 **Dedoussis GV**, Kaliora AC, Psarras S, Chiou A, Mylona A, Papadopoulos NG, Andrikopoulos NK. Antiatherogenic effect of Pistacia lentiscus via GSH restoration and downregulation of CD36 mRNA expression. *Atherosclerosis* 2004; **174**: 293-303
13 **Huwez FU**, Thirlwell D, Cockayne A, Ala'Aldeen DA. Mastic gum kills Helicobacter pylori. *N Engl J Med* 1998; **339**: 1946
14 **Al-Said MS**, Ageel AM, Parmar NS, Tariq M. Evaluation of mastic, a crude drug obtained from Pistacia lentiscus for gastric and duodenal anti-ulcer activity. *J Ethnopharmacol* 1986; **15**: 271-278

15 **Loughlin MF**, Ala'Aldeen DA, Jenks PJ. Monotherapy with mastic does not eradicate Helicobacter pylori infection from mice. *J Antimicrob Chemother* 2003; **51**: 367-371
16 **Bebb JR**, Bailey-Flitter N, Ala'Aldeen D, Atherton JC. Mastic gum has no effect on Helicobacter pylori load *in vivo*. *J Antimicrob Chemother* 2003; **52**: 522-523
17 **Janakat S**, Al-Merie H. Evaluation of hepatoprotective effect of Pistacia lentiscus, Phillyrea latifolia and Nicotiana glauca. *J Ethnopharmacol* 2002; **83**: 135-138
18 **Ljubuncic P**, Song H, Cogan U, Azaizeh H, Bomzon A. The effects of aqueous extracts prepared from the leaves of Pistacia lentiscus in experimental liver disease. *J Ethnopharmacol* 2005; **100**: 198-204
19 **Liu J**. Oleanolic acid and ursolic acid: research perspectives. *J Ethnopharmacol* 2005; **100**: 92-94
20 **Fernández MF**, Boris S, Barbés C. Probiotic properties of human lactobacilli strains to be used in the gastrointestinal tract. *J Appl Microbiol* 2003; **94**: 449-455
21 **Summers RW**, Switz DM, Sessions JT, Becktel JM, Best WR, Kern F, Singleton JW. National Cooperative Crohn's Disease Study: results of drug treatment. *Gastroenterology* 1979; **77**: 847-869
22 **Chan AT**, Fleming CR, O'Fallon WM, Huizenga KA. Estimated versus measured basal energy requirements in patients with Crohn's disease. *Gastroenterology* 1986; **91**: 75-78
23 **Duerksen DR**, Nehra V, Bistrian BR, Blackburn GL. Appropriate nutritional support in acute and complicated Crohn's disease. *Nutrition* 1998; **14**: 462-465
24 **Arai F**, Takahashi T, Furukawa K, Matsushima K, Asakura H. Mucosal expression of interleukin-6 and interleukin-8 messenger RNA in ulcerative colitis and in Crohn's disease. *Dig Dis Sci* 1998; **43**: 2071-2079
25 **Gross V**, Andus T, Caesar I, Roth M, Schölmerich J. Evidence for continuous stimulation of interleukin-6 production in Crohn's disease. *Gastroenterology* 1992; **102**: 514-519
26 **Assimopoulou AN**, Papageorgiou VP. GC-MS analysis of penta- and tetra-cyclic triterpenes from resins of Pistacia species. Part I. Pistacia lentiscus var. Chia. *Biomed Chromatogr* 2005; **19**: 285-311
27 **Andrikopoulos NK**, Kaliora AC, Assimopoulou AN, Papapeorgiou VP. Biological activity of some naturally occurring resins, gums and pigments against in vitro LDL oxidation. *Phytother Res* 2003; **17**: 501-507
28 **Kaliora AC**, Mylona A, Chiou A, Petsios DG, Andrikopoulos NK. Detection and identification of simple phenolics in Pistacia lentiscus resin. *J Liq Chrom Rel Technol* 2004; **27**: 289-300
29 **Maeda M**, Watanabe N, Neda H, Yamauchi N, Okamoto T, Sasaki H, Tsuji Y, Akiyama S, Tsuji N, Niitsu Y. Serum tumor necrosis factor activity in inflammatory bowel disease. *Immunopharmacol Immunotoxicol* 1992; **14**: 451-461
30 **Youngman KR**, Simon PL, West GA, Cominelli F, Rachmilewitz D, Klein JS, Fiocchi C. Localization of intestinal interleukin 1 activity and protein and gene expression to lamina propria cells. *Gastroenterology* 1993; **104**: 749-758
31 **Ping D**, Boekhoudt GH, Rogers EM, Boss JM. Nuclear factor-kappa B p65 mediates the assembly and activation of the TNF-responsive element of the murine monocyte chemoattractant-1 gene. *J Immunol* 1999; **162**: 727-734
32 **Cho IJ**, Lee AK, Lee SJ, Lee MG, Kim SG. Repression by oxidative stress of iNOS and cytokine gene induction in macrophages results from AP-1 and NF-kappaB inhibition mediated by B cell translocation gene-1 activation. *Free Radic Biol Med* 2005; **39**: 1523-1536
33 **Cao G**, Booth SL, Sadowski JA, Prior RL. Increases in human plasma antioxidant capacity after consumption of controlled diets high in fruit and vegetables. *Am J Clin Nutr* 1998; **68**: 1081-1087
34 **Manach C**, Williamson G, Morand C, Scalbert A, Rémésy C. Bioavailability and bioefficacy of polyphenols in humans. I. Review of 97 bioavailability studies. *Am J Clin Nutr* 2005; **81**: 230S-242S
35 **Halliwell B**, Zhao K, Whiteman M. The gastrointestinal tract: a major site of antioxidant action? *Free Radic Res* 2000; **33**: 819-830
36 **Yano S**, Harada M, Watanabe K, Nakamaru K, Hatakeyama Y, Shibata S, Takahashi K, Mori T, Hirabayashi K, Takeda M. Antiulcer activities of glycyrrhetinic acid derivatives in experimental gastric lesion models. *Chem Pharm Bull* (Tokyo) 1989; **37**: 2500-2504
37 **Hou YC**, Ching H, Chao PD, Tsai SY, Wen KC, Hsieh PH, Hsiu SL. Effects of glucose, fructose and 5-hydroxymethyl-2-furaldehyde on the presystemic metabolism and absorption of glycyrrhizin in rabbits. *J Pharm Pharmacol* 2005; **57**: 247-251

S- Editor Liu Y **L- Editor** Negro F **E- Editor** Bi L

PO Box 2345, Beijing 100023, China
www.wjgnet.com
wjg@wjgnet.com

World J Gastroenterol 2007 February 7; 13(5): 754-760
World Journal of Gastroenterology ISSN 1007-9327

CLINICAL RESEARCH

Cytomegalovirus infection in severe ulcerative colitis patients undergoing continuous intravenous cyclosporine treatment in Japan

Masaaki Minami, Michio Ohta, Teruko Ohkura, Takafumi Ando, Naoki Ohmiya, Yasumasa Niwa, Hidemi Goto

Masaaki Minami, Takafumi Ando, Naoki Ohmiya, Yasumasa Niwa, Hidemi Goto, Department of Gastroenterology, Nagoya University Graduate School of Medicine, 65 Tsurumai-cho, Showa-ku, Nagoya 466-8550, Japan
Michio Ohta, Teruko Ohkura, Department of Bacteriology, Nagoya University Graduate School of Medicine, 65 Tsurumai-cho, Showa-ku, Nagoya 466-8550, Japan
Correspondence to: Masaaki Minami, Department of Gastroenterology, Nagoya University Graduate School of Medicine, 65 Tsurumai-cho, Showa-ku, Nagoya 466-8550, Japan. myminami@med.nagoya-u.ac.jp
Telephone: +81-52-7442144 Fax: +81-52-7442159
Received: 2006-08-07 Accepted: 2007-01-04

Abstract

AIM: To investigate active cytomegalovirus (CMV) infection following the cyclosporine A (CyA) treatment of steroid-refractory ulcerative colitis (UC).

METHODS: Twenty-three patients with severe UC not responding to steroid therapy (male 14, and female 9) enrolled at Nagoya University Hospital from 1999 to 2005. They received continuous intravenous infusion of CyA (average 4 mg/kg per day) for 1 mo. Serum and colonic biopsy samples were collected before CyA treatment and 4 d, 10 d, 20 d, and 30 d after treatment. Patients were evaluated for CMV by using serology (IgM antibody by ELISA), quantitative real-time PCR for CMV DNA, and histopathological assessment of hematoxylin and eosin (HE)-stained colonic biopsies. CMV infection was indicated by positive results in any test.

RESULTS: No patients had active CMV infection before CyA treatment. Eighteen of 23 UC patients treated with CyA were infected with active CMV (IgM antibody in 16/23 patients, 69.6%; CMV DNA in 18/23 patients, 78.2%; and inclusion bodies in 4/23 patients, 17.3%). There was no difference in the active CMV-infection rate between males and females. Active CMV infection was observed after approximately 8 d of CyA treatment, leading to an exacerbation of colitis. Fifteen of these 18 patients with active CMV infection (83.3%) required surgical treatment because of severe deteriorating colitis. Treatment with ganciclovir rendered surgery avoidable in three patients.

CONCLUSION: Our results suggest that active CMV infection in severe UC patients treated with CyA is associated with poor outcome. Further, ganciclovir is useful for treatment of CMV-associated UC after immunosuppressive therapy.

Key words: Cytomegalovirus; Cyclosporine; Ulcerative colitis; Ganciclovir

Minami M, Ohta M, Ohkura T, Ando T, Ohmiya N, Niwa Y, Goto H. Cytomegalovirus infection in severe ulcerative colitis patients undergoing continuous intravenous cyclosporine treatment in Japan. *World J Gastroenterol* 2007; 13(5): 754-760

http://www.wjgnet.com/1007-9327/13/754.asp

INTRODUCTION

Cytomegalovirus (CMV) infection is one of the most common infectious complications after immunosuppressive therapy. It occurs mainly as a secondary infection in CMV-seropositive patients. CMV infection is a common viral infection in humans, occurring in 40%-100% of adults[1]. CMV infections are generally asymptomatic or are manifested as a mild mononucleosis-like syndrome[2]. Significant CMV disease may occur in various organs such as the retina, lung, and gastrointestinal tract, and the target organ is related to the etiology of immunosuppression[1]. Gastrointestinal (GI) CMV infection is rare in immunocompetent individuals. Clinically significant GI CMV infection generally occurs in immunecompromised patients[3]. In the gastrointestinal tract, CMV disease can occur in all locations, from the mouth to the rectum, and generally involves the formation of ulcers in the mucosa, often accompanied by hemorrhage[1].

Ulcerative colitis (UC) is common all over the world and is generally more frequent than Crohn's disease (CD)[4]. UC is thought to result from the inappropriate and progressive activation of the mucosal immune system driven by the presence of normal luminal flora. The aberrant response is most likely facilitated by defects in both the barrier function of the intestinal epithelium and the mucosal immune system[4].

Cyclosporine A (CyA) selectively inhibits immune

responses mediated by T lymphocytes by modulating the interaction of calcineurin-calmodulin[5]. This recognition has led to its use in patients with severe UC, with variable results. In an uncontrolled study, approximately 60%-80% of patients suffering from severe corticosteroid-refractory ulcerative colitis responded to cyclosporine therapy[6,7]. Since an intravenous infusion of CyA has clinical benefits in patients with steroid-resistant UC, it has been generally accepted that CyA selectively blocks the activation of helper and cytotoxic T cells and acts by inhibiting the nuclear factor of activated T cells and cytokine gene expression[8].

In Japan, patients with severe, corticosteroid-refractory or corticosteroid-dependent UC are frequently treated with strong immunosuppressive agents, including CyA. Therefore, patients with inflammatory bowel disease (IBD) are expected to be at an increased risk of infection with CMV. Despite the frequent use of immunosuppressive drugs in patients with UC, data on the frequency of CMV infection and its clinical significance in patients with UC are limited. The aim of this study was to describe our experience with active CMV infection following treatment with CyA for UC.

MATERIALS AND METHODS

Patients

Twenty-three patients with severe UC enrolled at Nagoya University Hospital from 1999 to 2005. They did not respond to a minimum of 7 d of intravenous systemic steroid therapy (prednisolone, more than 30 mg/d). The diagnosis of UC was based on clinical, endoscopic, radiological, and histological parameters. The study was approved by the Ethical Committee of the Graduate School of Medicine, Nagoya University, and all samples were obtained with informed consent in accordance with the Helsinki Declaration.

CyA treatment

Twenty-three patients received a continuous intravenous infusion of CyA in the form of Sandimmun solution (Novartis Pharma KK, Tokyo, Japan) at an average daily dose of 4 mg/kg for 1 mo. The CyA dose was adjusted to maintain a whole-blood CyA concentration of less than 500 pg/L. Complete blood cell counts, C-reactive protein (CRP), liver function tests (aspartate aminotransferase and alanine aminotransferase), renal function tests (creatinine and blood urea nitrogen), and clinical evaluation were performed before CyA treatment and then 4 d, 10 d, 20 d, and 30 d after treatment.

Collection of specimens and blood serum samples

Serum samples and colonic biopsy specimens were obtained from all patients before CyA treatment and then 4 d, 10 d, 20 d, and 30 d after treatment. Multiple biopsy samples were obtained from the inflamed area during colonoscopy for histopathological examination of inflammatory activity and CMV inclusion bodies; these samples were fixed in buffered neutral formalin. EDTA-treated venous blood (5 mL) was obtained from each patient under aseptic conditions for serological studies. The plasma was separated by centrifugation.

Histopathology

The colonic biopsy samples were paraffinized, sectioned, and stained with hematoxylin and eosin (HE). These sections were microscopically evaluated for the presence of characteristic cytomegalic cells and "owl's eye" nuclear inclusion bodies. Histologically, the activity of IBD was classified according to a standard system described previously [9].

Sample preparation

For the PCR assays, DNA was extracted from 200 μL of plasma by using the QIAamp Blood Kit (QIAGEN Ltd, Tokyo, Japan), eluted in 100 μL of distilled water, and stored at -30℃ until analysis.

Serological tests

The presence of anti-CMV IgM antibodies in all sera were tested by using the CMV IgM ELISA kit (Genesis Diagnosis Ltd., UK), a commercially available kit, by using the positive and negative controls provided with the kit. Virus-specific IgM antibodies were measured in the plasma regardless of the PCR results.

Real-time semi-quantitative PCR assay

The PCR primers used were from the immediate early (IE) gene[10]. The upstream primer was 5'-GACTAGTGT GTGATGATGCTGGCCAAG-3', and the downstream primer was 5'-GCTACAATAGCCTCTTCCTCATC TG-3'. A fluorogenic probe (5'-carboxyfluorescein-AGCCTGAGGTTATCAGTGTAATGAAGCGCC-3') was located between the PCR primers[11]. PCR was carried out by using a TaqMan PCR kit (PE Applied Biosystems, Foster City, CA), as described previously[11]. Briefly, 10 μL of the DNA extraction solution from the samples was added to a PCR mixture containing 10 mmol/L of Tris (pH 8.3); 50 mmol/L of KCl; 10 mmol/L of EDTA; 5 mmol/L of $MgCl_2$; 100 mmol/L of dATP, dCTP, dGTP, and dTTP; 0.2 mmol/L of each primer; 0.1 mmol/L of fluorogenic probe; and 1.25 U of AmpliTaq Gold (PE Applied Biosystems). After activation of the AmpliTaq Gold for 10 min at 95℃, 50 cycles each of 15 s at 95℃ and 1 min at 62℃ were carried out in a Model 7700 Sequence Detector (PE Applied Biosystems). Real-time fluorescent measurements were taken and a threshold cycle (C_T) value for each sample was calculated by determining the point at which the fluorescence exceeded a threshold limit (10 × SD of the base line). For a positive control, a plasmid that contained the IE gene was constructed using the pGEM-T vector (Promega, Madison, WI) and was termed pGEM-IE. A standard graph was constructed using the C_T values obtained from the serially diluted pGME-IE. The C_T values from the clinical samples were plotted on the standard curve, and the copy number was calculated automatically by using Sequence Detector v1.6 (PE Applied Biosystems), a software package for data analysis. Samples were defined as negative when the C_T value exceeded 50 cycles[12]. The DNA copy numbers in

Table 1 Clinical and epidemiological characteristics of patients

	Male	Female	Total
Age, yr (median, range)	30 (18-56)	29 (8-56)	27 (8-56)
Gender	14	9	23
CMV infection diagnosed	11	7	18
Recent corticosteroid therapy	14	9	23
Outcome: Surgery	9	6	15
Ganciclovir therapy	2	1	3

Table 2 Utility of various tests for detection of infection with CMV in CyA treated patient with UC

Parameter	Real-time PCR (%)	Serum IgM antibodies (%)	Inclusion bodies in HE stained biopsy (%)
Number	18	16	4
Sensitivity	100	88.88	22.22
Specificity	100	100	100
PPV	100	100	100
NPV	100	71.4	26.3

the plasma were expressed per milliliters. The minimum detection level was 100 copies/mL of plasma.

Criteria for diagnosis of CMV infection

Positive results in any tests (IgM antibody, CMV DNA, or inclusion bodies in HE stained sections) were considered as evidence of CMV infection.

Statistical analysis

The results were expressed as mean ± SD. The *P* values below 0.05 were considered significant. The accuracy of each test was calculated considering a positive result in any test for CMV as evidence of infection.

RESULTS

Twenty-three patients were treated with intravenous CyA and they evidenced no severe side effects of the drug, such as renal failure or liver failure. The patient characteristics are listed in Table 1. All patients had received corticosteroids before the initiation of treatment with CyA. The degree of the severity of UC in all patients was pan colitis. Prior to treatment with CyA, active CMV infection was not observed in any of the patients. Eighteen of the 23 UC patients treated with CyA were infected with CMV (IgM antibodies in 16/23 patients, 69.6%; CMV DNA in 18/23 patients, 78.2%; and inclusion bodies in 4/23 patients, 17.3%). The rate of CMV detection by real-time PCR was significantly higher than other methods ($P < 0.05$). There was no difference in the CMV infection rate between males and females (males, 11/14; 78.57% and females, 7/9; 77.7%) (Table 2). With the exception of four of the tissue sections, all the sections from our UC patients who were treated with CyA were negative for CMV as demonstrated by histochemistry. After CyA treatment, none of the CMV-positive patients had pneumonia, hepatitis, retinitis, nephritis, or pancreatitis. Their only clinical symptoms were those of gastrointestinal disorder caused by colitis.

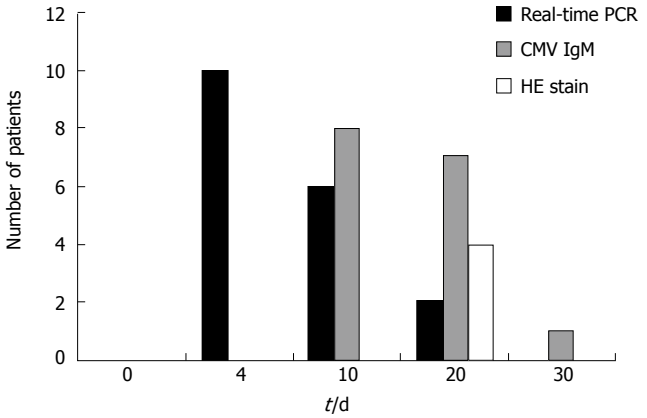

Figure 1 Comparison of initial CMV detection by day among the three methods (Real-time PCR, CMV IgM, and HE stain).

The median time of onset of the CMV infection after CyA treatment was 8.5 d (range: 4-20 d).

Real-time PCR detection is the most rapid of the three methods used (CMV IgM, HE biopsy, and real-time PCR results) (Figure 1). In particular, the HE biopsy method is slower and less sensitive than the other methods.

All patients showed an improvement in their symptoms after the initiation of the CyA treatment. Four CMV-negative patients treated with CyA showed a drastic improvement in their symptoms, and one CMV-negative patient who received CyA showed slight improvement. The degree of hematochezia progressively decreased after CyA treatment. CMV-negative patients continued to show an improvement in their symptoms during CyA treatment; further, even though CyA treatment was terminated, no deterioration in the degree of bowel symptoms was observed. On the other hand, all CMV-infected patients demonstrated an aggravation of the symptoms of colitis, i.e., an increase in the body temperature and the degree of hematochezia; after CMV infection ($P < 0.05$) (Figure 2). Further, the inflammatory values, i.e., the white blood cell (WBC) count and the CRP values worsened after CMV infection ($P < 0.05$) (Figure 3). However, an assessment of liver and renal functions after infection did not reveal any deterioration (Figure 4). After 10 d of CyA administration, CMV DNA was detected in 16 of the 18 UC patients, however, the clinical symptoms were improving. On the other hand, after 20 d, the clinical symptoms worsened in the CMV infected patients and CMV IgM and the histopathology results were positive. The values of the CMV IgM titer and the number of CMV DNA copies both increased after infection (Figure 5). The increased CMV load was followed by an increase in the severity of colitis.

Fifteen of these 18 patients with CMV infection (83.3%) required surgical treatment because of uncontrolled, severe deteriorating colitis. Perforation of the colon was observed in one of the patients after CMV infection; he underwent an emergency total colectomy. Nevertheless, in our study,

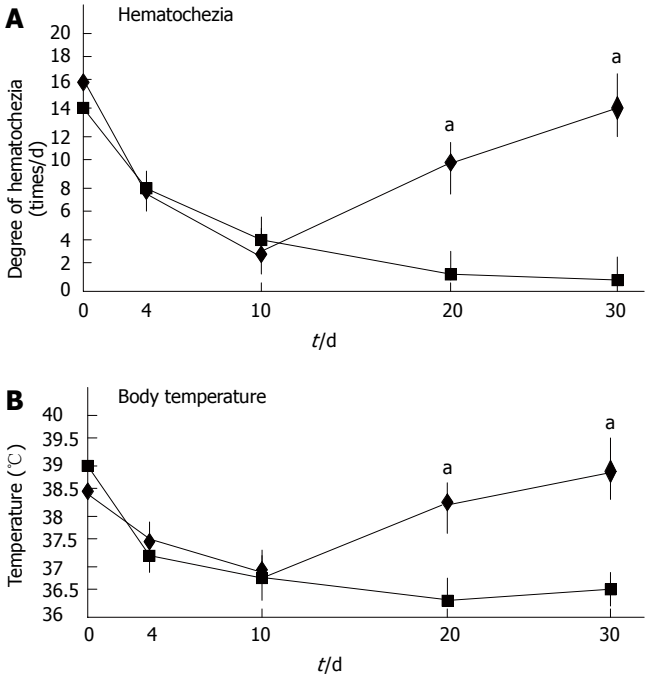

Figure 2 Change in clinical symptoms (hematochezia and body temperature) between CMV-positive and CMV-negative UC patients during intravenous CyA treatment. Panel **A** showed the change in the degree of hematochezia. Panel **B** showed the change in body temperature. The mean values of each group were plotted. Symbols: ◆, CMV positive; ■, CMV negative. $^{a}P < 0.05$.

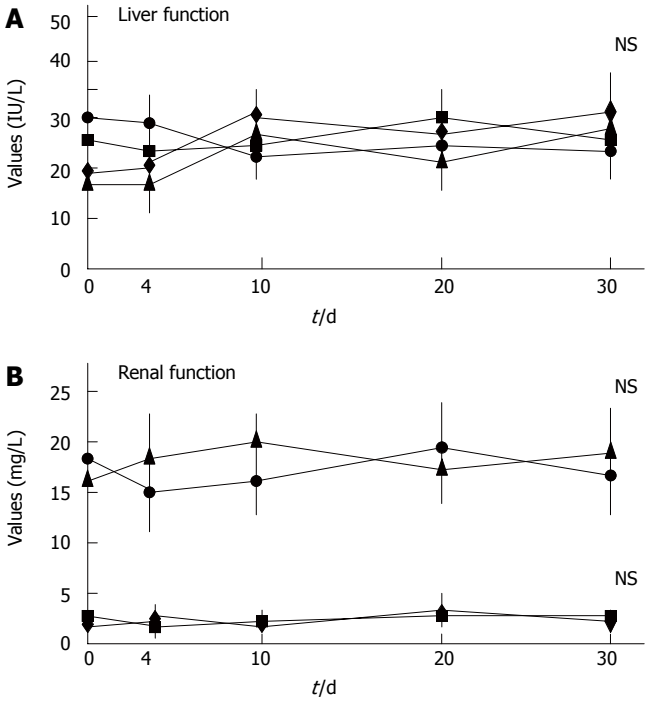

Figure 4 Change in liver function and renal function between CMV-positive and CMV-negative UC patients during intravenous CyA treatment. Panel A showed the change in liver function. The mean values of each group were plotted. Symbols: ◆, aspartate aminotransferase in CMV positive; ■, aspartate aminotransferase in CMV negative; ▲, alanine aminotransferase in CMV positive; ●, alanine aminotransferase in CMV negative. Panel B showed the change in renal function. The mean values of each group were plotted. Symbols: ◆, creatinine in CMV positive; ■, creatinine in CMV negative; ▲, blood urea nitrogen in CMV positive; ●, blood urea nitrogen in CMV negative, respectively. NS represented not significant.

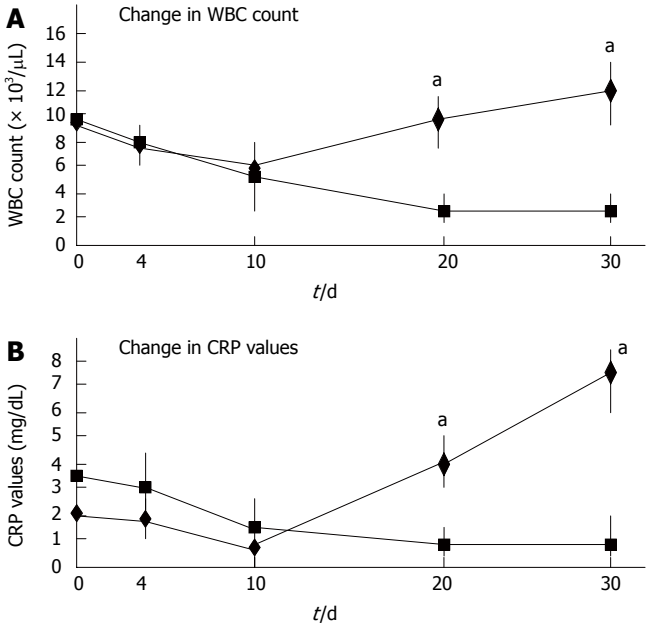

Figure 3 Change in inflammation markers between CMV-positive and CMV-negative UC patients during intravenous CyA treatment. Panel **A** showed the change in WBC count. Panel **B** showed the change in CRP value. The mean values of each group were plotted. Symbols: ◆, CMV positive; ■, CMV negative. $^{a}P < 0.05$.

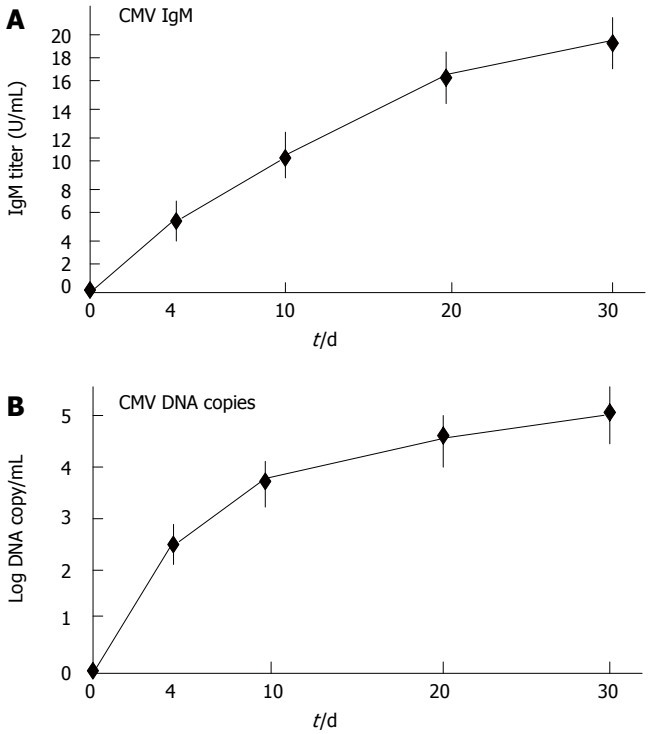

Figure 5 Change in mean CMV IgM value and CMV viral DNA load after CMV infection. Panel **A** showed the change in mean CMV IgM value after infection. Panel **B** showed the change in mean CMV viral load after infection.

there were no deaths among the UC patients after CMV infection.

Only three patients (males 2, and female 1) showed an improvement in the severity of colitis and did not require

a colorectomy since they were treated with ganciclovir following the identification of the CMV infection. The CMV IgM values did not decrease after ganciclovir treatment. However, in these three patients, the CMV DNA copy number decreased and did not show any further increase. Further, CMV infection was detected in one of the patients by an HE histopathological study. After ganciclovir administration, the owl's eye sign in the colon tissue was not observed. Thus, the three patients who were treated with ganciclovir were not reinfected with CMV although CyA treatment was continued.

DISCUSSION

We clarified a possible relationship between CMV infection and UC treated with CyA. We showed a significant deterioration in the clinical symptoms and the inflammatory response after active CMV infection. However, no impairment in hepatic or renal function was observed since we could not detect either CMV hepatitis or acute renal failure. Our results suggest that CMV infection in patients with severe UC treated with CyA is associated with a poor outcome because of severe deterioration in UC.

In general, a primary CMV infection, which is usually acquired early in life, is overcome by the humoral and cellular immunological response. Thereafter, the virus remains latent, particularly in endothelial cells and monocytes. Reactivation occurs during the use of immunosuppressive drugs. The viral load is the highest during active infection and the lowest during the latency stage in immunocompetent persons. We observed that CyA treatment may cause the reactivation of CMV and a subsequent deterioration in colitis. During a CMV infection, an increase in intestinal permeability has been shown to occur in kidney transplant recipients[14]. This defect in the barrier function may facilitate the exposure of the mucosal immune system to antigens from the luminal flora. CMV may also spread from the mucosa to the bloodstream because of such a defect in the barrier function, leading to CMV viremia in the bloodstream.

Steroid-resistant UC is defined as persistent active disease despite high-dose systemic corticosteroid therapy. A history of steroid resistance increases the possibility of complications such as CMV infection. CMV infections were detected in 4.6% to 13% of the patients diagnosed with UC[15,16]. Up to 33% of the patients with severe steroid-refractory UC were found to harbor the CMV virus. CMV was detected in 25% of the patients with steroid-refractory UC as compared to only 2.5% of patients with medically non-refractory UC. All the cases of UC with CMV infection in other investigations were clinically severe and steroid-resistant, and approximately 70% of the cases suffered from an acute exacerbation of symptoms and required immediate emergency surgeries. These results may suggest that CMV is not a coincidental occurrence but an exacerbating factor[17].

Although it is important to prevent the development of CMV disease[18], the availability of rapid, sensitive, and reliable methods for the early diagnosis of CMV infection is desirable[15]. As mentioned above, CMV disease can take many forms, depending upon the type of patient group under consideration. A consensus is available from the international CMV workshop for the definition of CMV disease[19]. The guidelines are purposefully rigorous and have aided the interpretation of clinical trial data and population based studies. However, they are likely to lead to an under appreciation of the contribution of CMV to patient morbidity. This is particularly true in the case of the histopathological diagnoses of CMV. Gastrointestinal symptoms along with histopathologically detected CMV are widely acceptable diagnostic criteria for CMV infections. In particular, the histopathological study of colon tissue is considered acceptable for CMV detection. Many CMV inclusion bodies were found in the surgical specimens of the UC cases in which CMV infection was detected, whereas CMV infection had not been detected by biopsy prior to surgery. CMV infection was observed in only 1 of the 55 cases investigated by endoscopic biopsy; however, it was detected in 8 of the 39 surgical cases[17]. Thus, it was rather difficult to detect CMV infection by biopsy, possibly because of sampling limitations. The characteristic inclusion bodies are not readily visible in routinely performed HE staining and CMV-infected cells are not always cytomegalic; therefore, the histopathological examination of the colonic biopsies had the lowest sensitivity. It has been suggested that CMV inclusion bodies are found more frequently in the right colon than in the left[16]; hence, multiple biopsies were taken from the colon, particularly from the inflamed and ulcerated areas, considering the fact that CMV exhibits tropism for the inflamed sites[20]. Therefore, it is likely that the false-negative results in the present study were related to sampling errors. Although our study did not confirm this, an immunohistochemical study of biopsy specimens may be more useful in diagnosis; however, immunohistochemistry is not a convenient tool for routine diagnosis.

The investigation of plasma CMV DNA is a simple, noninvasive, and nontraumatic method for evaluating and monitoring the CMV infection in patients. Procedures such as endoscopy and biopsies are traumatic and uncomfortable for a UC patient. The CMV-associated disease is generally the result of the reactivation of latent viruses rather than reinfection with the virus, and the measurement of CMV antibodies is often of no diagnostic use.

The real-time PCR assay was found to be as useful as the pp65 antigenemia assay because they were highly correlated[12]. Unlike the conventional qualitative PCR assay, which is not beneficial for determining the termination of antiviral therapy[21], this assay showed that the copy numbers of CMV DNA decreased and disappeared in response to anti-CMV therapy. Additionally, with this PCR method there is almost no room for bias due to subjective assessments by technicians. One investigator reported that real-time PCR is more sensitive (92%) than the pp65 test (88%) with regard to positive findings. Further, the correlations between real-time PCR and the pp65 antigenemia assay were statistically

significant[22]. The advantage of quantitative techniques is that by defining a "threshold value" of CMV load, they may allow a distinction between the commonly occurring, clinically irrelevant CMV infection and the levels of active CMV replication that are likely to lead to clinical disease[23].

However, there is still disagreement with regard to the optimal type of sample material, for example, leukocyte fractions versus plasma versus whole blood, and to the desirable sensitivity, which depends on the initial sample volume.

We used a quantitative CMV PCR assay that was able to quantify CMV DNA in plasma over the 100 copies/mL. The assay is fully controlled for maximal efficiency ~~in~~ at all steps. This is achieved by employing the widely used principle of an "internal control" and taking it one step further as a control for extraction efficacy.

Although the quantitative results obtained with different assays are difficult to compare because of the absence of an international standard, the results obtained with quantitative PCR correlate well with those of a number of other assays, and its sensitivity is generally higher[24]. The high sensitivity of the quantitative PCR assay is partly due to the use of a relatively large sample volume and the concentration of the DNA contained therein. Using plasma appears to avoid the loss of sensitivity as reported previously as compared to using whole blood or leukocytes[25]. Using plasma may also avoid the possibility of amplifying "latent" CMV from leukocytes. The exclusion of CMV DNA of intracellular origin may increase the clinical relevance of latent CMV detection; this in turn may decrease the predictive value of the test for active CMV infection[26]. Plasma is also easier to handle than cellular fractions such as leukocyte preparations and is better standardized, particularly in leukopenic patients. In HIV-positive individuals, the CMV load in whole blood and plasma has also been shown to be an important indicator of pathogenesis[27]. The presence of CMV DNA in the blood of HIV-positive patients identifies a group of patients who are almost 20 times more likely to progress to CMV disease than those who remain negative for CMV DNA in their blood[28]. In addition, an increasing CMV load in the blood was associated with an increased risk of disease progression[28]. CMV load was correlated with tissue samples obtained at the postmortem examinations of the HIV patients with histological evidence of CMV inclusions, and it was found that a viral load of > 5 000 000 genomes/μg DNA is required before CMV inclusions are observed[29]. It should be noted that some of these manifestations do not satisfy the criteria outlined for the diagnosis of CMV disease. Thus, it appears likely that cases of CMV colitis may also be dismissed because they do not meet the definition of CMV infection, despite the presence of clinical symptoms and CMV DNA in the blood. It is important to appreciate that with the advent of more sensitive molecular-based assays, a reappraisal of many of these definitions may be required.

In conclusion, a CMV infection in patients with steroid-resistant UC should be ruled out prior to initiating aggressive immunosuppressive therapy such as CyA for steroid-resistant UC. Further, ganciclovir as an anti-viral agent is useful for the treatment of CMV-associated UC after immunosuppressive therapy.

ACKNOWLEDGMENTS

We thank the members of the Departments of First Internal Medicine, Gastroenterology division, and Bacteriology, Nagoya University Graduate School of Medicine, for their technical advice.

COMMENTS

Background

Cytomegalovirus (CMV) infection is one of the most common infectious complications after immunosuppressive therapy. Ulcerative colitis (UC) is thought to result from the inappropriate and progressive activation of the mucosal immune system driven by the presence of normal luminal flora. Cyclosporine A (CyA) selectively inhibits immune responses mediated by T lymphocytes by modulating the interaction of calcineurin-calmodulin. This recognition has led to its use in patients with severe UC. In Japan, patients with severe UC are frequently treated with CyA and are expected to be at an increased risk of infection with CMV. Despite the frequent use of immunosuppressive drugs in patients with UC, data on the frequency of CMV infection and its clinical significance in patients with UC are limited.

Research frontiers

The aim of this study was to describe our experience with active CMV infection following treatment with CyA for UC in Japan.

Innovations and breakthroughs

Twenty-three patients with severe UC not responding to steroid therapy at Nagoya University Hospital received continuous intravenous infusion of CyA (average 4 mg/kg per day) for 1 mo. Serum and colonic biopsy samples were collected from all patients before CyA treatment and 4 d, 10 d, 20 d, and 30 d after treatment and were evaluated for CMV by using serology (IgM antibody by ELISA), quantitative real-time PCR for CMV DNA, and histopathological assessment of hematoxylin and eosin -stained colonic biopsies.

Applications

No patients had active CMV infection before CyA treatment. Eighteen of 23 UC patients treated with CyA were infected with active CMV (IgM antibody in 16/23 patients, 69.6%; CMV DNA in 18/23 patients, 78.2%; and inclusion bodies in 4/23 patients, 17.3%). Fifteen of these 18 patients with active CMV infection (83.3%) required surgical treatment because of severe deteriorating colitis. Treatment with ganciclovir rendered surgery avoidable in three patients. Active CMV infection in severe UC patients treated with CyA is associated with poor outcome. Further, ganciclovir is useful for treatment of CMV-associated UC after immunosuppressive therapy.

Terminology

CMV infection is one of the most common infectious complications in immune-compromised patients. UC is chronic inflammation colitis thought to result from the inappropriate and progressive activation of the mucosal immune system driven by the presence of normal luminal flora. CyA is a drug to inhibit immune responses selectively mediated by T lymphocytes by modulating the interaction of calcineurin-calmodulin.

Peer review

Severe ulcerative colitis is a potentially life-threatening condition. Traditional treatment for such patients is high-dose intravenous corticosteroids but up to 40% of patients become refractory to this treatment. In these patients CyA therapy has been shown to have an initial positive clinical response in many patients. However, i.v. cyclosporine is recommended only as short term "bridging" therapy to induce remission followed by azathioprine or 6-mercaptopurine maintenance therapy. In the present study Minami and coworkers investigated the frequency of the development of a CMV infection during a continuous intravenous cyclosporine treatment in ulcerative colitis and the clinical outcome in CMV infected vs. non infected patients. The study is of interest.

REFERENCES

1 **Goodgame RW**. Gastrointestinal cytomegalovirus disease. *Ann Intern Med* 1993; **119**: 924-935
2 **Betts RF**. Syndromes of cytomegalovirus infection. *Adv Intern Med* 1980; **26**: 447-466
3 **Surawicz CM**, Myerson D. Self-limited cytomegalovirus colitis in immunocompetent individuals. *Gastroenterology* 1988; **94**: 194-199
4 **Podolsky DK**. Inflammatory bowel disease. *N Engl J Med* 2002; **347**: 417-429
5 **Liu J**, Farmer JD, Lane WS, Friedman J, Weissman I, Schreiber SL. Calcineurin is a common target of cyclophilin-cyclosporin A and FKBP-FK506 complexes. *Cell* 1991; **66**: 807-815
6 **Sandborn WJ**, Tremaine WJ. Cyclosporine treatment of inflammatory bowel disease. *Mayo Clin Proc* 1992; **67**: 981-990
7 **Lichtiger S**, Present DH, Kornbluth A, Gelernt I, Bauer J, Galler G, Michelassi F, Hanauer S. Cyclosporine in severe ulcerative colitis refractory to steroid therapy. *N Engl J Med* 1994; **330**: 1841-1845
8 **Ina K**, Kusugami K, Shimada M, Tsuzuki T, Nishio Y, Binion DG, Imada A, Ando T. Suppressive effects of cyclosporine A on neutrophils and T cells may be related to therapeutic benefits in patients with steroid-resistant ulcerative colitis. *Inflamm Bowel Dis* 2002; **8**: 1-9
9 **Truelove SC**, Richards WC. Biopsy studies in ulcerative colitis. *Br Med J* 1956; **1**: 1315-1318
10 **Akrigg A**, Wilkinson GW, Oram JD. The structure of the major immediate early gene of human cytomegalovirus strain AD169. *Virus Res* 1985; **2**: 107-121
11 **Heid CA**, Stevens J, Livak KJ, Williams PM. Real time quantitative PCR. *Genome Res* 1996; **6**: 986-994
12 **Tanaka N**, Kimura H, Iida K, Saito Y, Tsuge I, Yoshimi A, Matsuyama T, Morishima T. Quantitative analysis of cytomegalovirus load using a real-time PCR assay. *J Med Virol* 2000; **60**: 455-462
13 **Verdonk RC**, Haagsma EB, Van Den Berg AP, Karrenbeld A, Slooff MJ, Kleibeuker JH, Dijkstra G. Inflammatory bowel disease after liver transplantation: a role for cytomegalovirus infection. *Scand J Gastroenterol* 2006; **41**: 205-211
14 **de Maar EF**, Kleibeuker JH, Boersma-van Ek W, The TH, van Son WJ. Increased intestinal permeability during cytomegalovirus infection in renal transplant recipients. *Transpl Int* 1996; **9**: 576-580
15 **Einsele H**, Ehninger G, Hebart H, Wittkowski KM, Schuler U, Jahn G, Mackes P, Herter M, Klingebiel T, Löffler J, Wagner S, Müller CA. Polymerase chain reaction monitoring reduces the incidence of cytomegalovirus disease and the duration and side effects of antiviral therapy after bone marrow transplantation. *Blood* 1995; **86**: 2815-2820
16 **Hinnant KL**, Rotterdam HZ, Bell ET, Tapper ML. Cytomegalovirus infection of the alimentary tract: a clinicopathological correlation. *Am J Gastroenterol* 1986; **81**: 944-950
17 **Takahashi Y**, Tange T. Prevalence of cytomegalovirus infection in inflammatory bowel disease patients. *Dis Colon Rectum* 2004; **47**: 722-726
18 **Goodrich JM**, Mori M, Gleaves CA, Du Mond C, Cays M, Ebeling DF, Buhles WC, DeArmond B, Meyers JD. Early treatment with ganciclovir to prevent cytomegalovirus disease after allogeneic bone marrow transplantation. *N Engl J Med* 1991; **325**: 1601-1607
19 **Ljungman P**, Plotkin SA. Workshop of CMV disease: definitions, clinical severity scores, and new syndromes. *Scand J Infect Dis Suppl* 1995; **99**: 87-89
20 **Goodman ZD**, Boitnott JK, Yardley JH. Perforation of the colon associated with cytomegalovirus infection. *Dig Dis Sci* 1979; **24**: 376-380
21 **Gerna G**, Zipeto D, Parea M, Revello MG, Silini E, Percivalle E, Zavattoni M, Grossi P, Milanesi G. Monitoring of human cytomegalovirus infections and ganciclovir treatment in heart transplant recipients by determination of viremia, antigenemia, and DNAemia. *J Infect Dis* 1991; **164**: 488-498
22 **Piiparinen H**, Höckerstedt K, Grönhagen-Riska C, Lautenschlager I. Comparison of two quantitative CMV PCR tests, Cobas Amplicor CMV Monitor and TaqMan assay, and pp65-antigenemia assay in the determination of viral loads from peripheral blood of organ transplant patients. *J Clin Virol* 2004; **30**: 258-266
23 **Emery VC**, Sabin CA, Cope AV, Gor D, Hassan-Walker AF, Griffiths PD. Application of viral-load kinetics to identify patients who develop cytomegalovirus disease after transplantation. *Lancet* 2000; **355**: 2032-2036
24 **Preiser W**, Bräuninger S, Schwerdtfeger R, Ayliffe U, Garson JA, Brink NS, Franck S, Doerr HW, Rabenau HF. Evaluation of diagnostic methods for the detection of cytomegalovirus in recipients of allogeneic stem cell transplants. *J Clin Virol* 2001; **20**: 59-70
25 **Boeckh M**, Gallez-Hawkins GM, Myerson D, Zaia JA, Bowden RA. Plasma polymerase chain reaction for cytomegalovirus DNA after allogeneic marrow transplantation: comparison with polymerase chain reaction using peripheral blood leukocytes, pp65 antigenemia, and viral culture. *Transplantation* 1997; **64**: 108-113
26 **Hamprecht K**, Steinmassl M, Einsele H, Jahn G. Discordant detection of human cytomegalovirus DNA from peripheral blood mononuclear cells, granulocytes and plasma: correlation to viremia and HCMV infection. *J Clin Virol* 1998; **11**: 125-136
27 **Bowen EF**, Sabin CA, Wilson P, Griffiths PD, Davey CC, Johnson MA, Emery VC. Cytomegalovirus (CMV) viraemia detected by polymerase chain reaction identifies a group of HIV-positive patients at high risk of CMV disease. *AIDS* 1997; **11**: 889-893
28 **Shinkai M**, Bozzette SA, Powderly W, Frame P, Spector SA. Utility of urine and leukocyte cultures and plasma DNA polymerase chain reaction for identification of AIDS patients at risk for developing human cytomegalovirus disease. *J Infect Dis* 1997; **175**: 302-308
29 **Mattes FM**, McLaughlin JE, Emery VC, Clark DA, Griffiths PD. Histopathological detection of owl's eye inclusions is still specific for cytomegalovirus in the era of human herpesviruses 6 and 7. *J Clin Pathol* 2000; **53**: 612-614

S- Editor Liu Y **L- Editor** Alpini GD **E- Editor** Ma WH

PO Box 2345, Beijing 100023, China
www.wjgnet.com
wjg@wjgnet.com

World J Gastroenterol 2007 February 7; 13(5): 761-767
World Journal of Gastroenterology ISSN 1007-9327

CLINICAL RESEARCH

Patients without hepatocellular carcinoma progression after transarterial chemoembolization benefit from liver transplantation

Aiman Obed, Alexander Beham, Kerstin Püllmann, Heinz Becker, Hans J Schlitt, Thomas Lorf

Aiman Obed, Alexander Beham, Hans J Schlitt, Department of Surgery, University of Regensburg, Regensburg 93053, Germany
Heinz Becker, Thomas Lorf, Department of Surgery, University of Goettingen, Goettingen 37073, Germany
Correspondence to: Dr. Alexander Beham, Klinik und Poliklinik für Chirurgie, der Universität Regensburg, Klinikum Regensburg,Franz-Josef-Strauss Allee 11, Regensburg 93053, Germany. alexander.beham@klinik.uni-regensburg.de
Telephone: +49-941-9446987 Fax: +49-941-9446802
Received: 2006-04-28 Accepted: 2006-08-22

Key words: Liver transplantation; Hepatocellular carcinoma

Obed A, Beham A, Püllmann K, Becker H, Schlitt HJ, Lorf T. Patients without hepatocellular carcinoma progression after transarterial chemoembolization benefit from liver transplantation. *World J Gastroenterol* 2007; 13(5): 761-767

http://www.wjgnet.com/1007-9327/13/761.asp

Abstract

AIM: To assess the outcome of patients, who underwent transarterial chemoembolization (TACE) for hepatocellular carcinoma (HCC) and subsequently liver transplantation (OLT) irrespective of tumor size when no tumor progression was observed.

METHODS: Records, imaging studies and pathology of 84 patients with HCC were reviewed. Ten patients were not treated at all, 67 patients had TACE and 35 of them were listed for OLT. Tumor progression was monitored by ultrasound and AFP level every 6 wk. Fifteen patients showed signs of tumor progression without transplantation. The remaining 20 patients underwent OLT. Further records of 7 patients with HCC seen in histological examination after OLT were included.

RESULTS: The patients after TACE without tumor progression underwent transplantation and had a median survival of 92.3 mo. Patients, who did not qualify for liver transplantation or had signs of tumor progression had a median survival of 8.4 mo. The patients without treatment had a median survival of 3.8 mo. Independent of International Union Against Cancer (UICC) stages, the patients without tumor progression and subsequent OLT had longer median survival. No significant difference was seen in the OLT treated patients if they did not fulfill the Milan criteria.

CONCLUSION: Selection of patients for OLT based on tumor progression results in good survival. The evaluation of HCC patients should not only be based on tumor size and number of foci but also on tumor progression and growth behavior under therapy.

INTRODUCTION

Hepatocellular carcinoma (HCC) is the third leading cause of cancer related mortality and the fifth most common cancer[1] worldwide. Nearly 500 000 cases are diagnosed each year in the United States and the incidence increased from 1.4 cases per 100 000 between 1976 and 1980 to 2.4 cases per 100 000 from 1990 to 1995. Furthermore, the associated mortality rate and hospitalization showed an increase of 41% and 46%, which demands a significant challenge in the management of HCC patients[2].

The stage of disease divides HCC therapy into curative versus palliative approaches. Curative treatments are reserved for patients without portal vein invasion or distant metastases and include percutaneous ablation, surgical resection and liver transplantation[3-5]. Palliative attempts include liver-directed therapies, rarely systemic chemotherapy, and are offered when local extra-hepatic spread or distant metastases are present. Palliative therapy via transarterial chemoembolization (TACE) may be offered for unresectable HCC. TACE involves the injection of chemotherapeutic agents into the hepatic artery[6,7]. Multiple large randomized and controlled trials have failed to demonstrate a beneficial effect in survival of patients treated with TACE, but meta-analysis of these trials show a slight beneficial effect in survival in comparison with conservative treatment[8].

For localized HCC in curative situations, which is defined by the absence of macro-vascular invasion and metastatic disease with well-preserved hepatic function, the initial treatment of choice is hepatic resection. In case of cirrhosis, optimal candidates for surgical resection show a single lesion less than 5 cm in size, with no complications of end-stage liver disease and no significant portal hypertension (portal pressure gradient less than 10 mmHg). Nevertheless, after 5 years there are significant

recurrence rates (70%) in HCC patients after surgical resection, and the 5-year survival rate is 30%. Taken together only about 5% of patients are ideal candidates for hepatic resection[9-11]. Therefore liver transplantation (OLT) is the only curative approach that addresses the HCC lesion as well as the underlying liver cirrhosis[12-15].

Initial reports of liver transplantation in patients with HCC showed poor outcomes with a recurrence rate up to 50% and a 5-year survival of less than 40%. In these reports many patients underwent OLT in the setting of advanced HCC. As a consequence the Milan criteria have been put forward to provide guidelines that help select HCC patients for curative OLT. The goal of this effort was to achieve comparable survival rates in liver transplanted patients with HCC and patients without concomitant neoplasias[12].

Patients fulfilling the criteria (single nodule < 5 cm or up to three nodules each < 3 cm) have a favorable prognosis with 3-year survival rates of 75% up to 85% and a recurrence rate of less than 15%. However, a retrospective cohort analysis showed comparable survival rates in patients who had solitary nodules less than 6.5 cm or 3 nodules with a combined diameter of less than 8 cm[13], demonstrating that OLT is a potentially curative approach for patients with HCC extending the Milan criteria.

However, the general scarcity of donor livers hampers timely liver transplantation. In the interim specific therapy such as TACE can be initiated to stabilize the patient's health condition. Because the Milan criteria do not take into account tumor progression following non-surgical intervention strategies, patients treated with TACE cannot be necessarily evaluated on the basis of these criteria. We therefore selected patients for liver transplantation based on the lack of tumor progression during the waiting time and determined the clinical outcome in patients who were treated with TACE and subsequently underwent liver transplantation.

MATERIALS AND METHODS

Study design and characteristics of patients

From January 1995 to March 2002, 77 patients with HCC were seen at the Department of Surgery, University of Goettingen. The diagnosis of HCC was confirmed in all patients either by biopsy of the tumor or by a serum alpha-fetoprotein (AFP) measurement. In addition, in 7 patients who underwent OLT, HCC was diagnosed in the histological examination of the explanted organ.

Patient demographics showed a male: female ratio of 70:14 and a mean age of 59 ± 11.4 years (range 31-84). The main underlying disease of HCC was liver cirrhosis (n = 63, 75%), which could be assigned to the diagnoses of alcohol (n = 23), hepatits C (n = 22) and hepatitis B (n = 18) (Table 1).

Age, gender, Child-Pugh score and tumor stage of all patients are shown in Tables 2 and 3. At the time of HCC diagnosis, 10 (12%) patients had no evidence of impaired liver function, 28 (33%) patients presented with class A, 29 (35%) with class B, and 17 (20%) with class C impaired liver function according to the Child-Pugh classification.

Table 1 Diagnostic chart of patients with HCC

Diagnoses	*n*	Age (yr, mean ± SD)
No liver disease	10	61 ± 12.2
Fibrosis	3	66.7 ± 0.6
Alcohol induced cirrhosis	23	60 ± 8.3
Hepatitis (C) cirrhosis	22	55.9 ± 9.9
Hepatitis (B) cirrhosis	18	55 ± 14.1
Others[1]	8	56 ± 16.9
Total	84	59 ± 11.4

[1] Haemochromatosis 2, Caroli-syndrome 1, primary biliary cirrhosis 1, primary sclerosing cholangitis 1, hepatitis C 1, acute liver faliure 1, cryptogene cirrhosis 1. The majority of patients had liver cirrhosis secondary to viral hepatitis and alcohol-related liver disease.

Table 2 Cirrhosis scoring of study patients according to Child-Pugh Score

Child-Pugh Score	*n*	Age	Gender	
		(yr, mean ± SD)	Male	Female
A	28	56 ± 13.2	26	2
B	29	57 ± 9.7	25	4
C	17	56 ± 9.1	15	2
Total	74	56.3 ± 11.3	66	8

HCC was classified at hospital admission.

Table 3 Staging of the patients according to UICC

UICC stage	*n*	No cirrhosis	Cirrhosis	Age (yr, mean ± SD)
Ⅰ	5	1	4	52 ± 11.7
Ⅱ	13	1	12	60 ± 13.5
Ⅲ	11	3	8	60.8 ± 8.0
Ⅳ	55	5	50	58 ± 11.6
Total	84	10	74	59 ± 11.4

Table 4 Treatment modalities of patients with HCC

Treatment	*n*	No cirrhosis	Cirrhosis
No treatment	10	3	7
TACE, not listed for OLT	32	6	41
TACE, died waiting for OLT	15		
TACE and liver transplantation	20	0	20
Liver transplantation	7	1	6
Total	84	10	74

The tumor staging according to the UICC criteria of patients used in this study is shown in Table 3.

Ten (12%) out of 84 patients were not treated because they died before the treatment was started (n = 4), they refused treatment (n = 1) or TACE could not be done due to their cardio-pulmonary risk (n = 5). The remaining 74 patients were treated as seen in Table 4. In 7 transplanted patients, the HCC was diagnosed after liver transplantation and therefore they were not treated before OLT. In the other 67 patients TACE was done and 35 of them were listed for OLT. The reasons for not listing a patient for

liver transplantation were no additional liver cirrhosis (n = 10), age older than 65 (n = 11) and persistent alcohol disease (n = 11). From the initial 35 patients who were listed for OLT, 15 showed tumor progression after TACE and were therefore subsequently removed from the transplantation list. These patients showed a median time of tumor progression of 3.1 mo. The remaining 20 patients underwent OLT with a median time on waiting list of 7.6 mo.

Chest X-ray, computed tomography (CT) and staging by the TNM scoring system of the UICC was performed in all the patients. Tumors that were first identified by histopathology of the explanted liver were classified as incidental tumors.

Selection criteria for OLT

Patients were selected for OLT based on the guidelines of Transplantions Gesellschaft (DTG). In addition, patients with extrahepatic tumor manifestation did not qualify for OLT. Tumor size or number of tumors were not taken into account for listing the patient. The patients received TACE and were restaged every 6 wk during waiting time. Evidence of tumor progression resulted in removement of the patients from the waiting list.

Transaterial chemoembolization protocol

Patients were listed for OLT and immediately obtain TACE. TACE was performed in cases of advanced HCC stage or when tumors progressed during the staging work-up every 6 wk. Patients in advanced tumor stage (downstaging group) were listed when they responded to the first TACE treatment cycle. Sixty-seven patients were subjected to selective TACE before transplantation. The chemoembolization solution contained 50 mg epirubicin, 10 mL lipiodol and 3 mL water-soluble contrast material. Embolization was performed until blood flow to the tumor stopped.

The following day CT scanning was performed to determine the lipiodol uptake by the tumor tissue. Each TACE cycle was repeated every 6 wk and ultrasound, CT scan and AFP levels were assessed. Response to TACE is defined as constant size of the tumor and/stable AFP levels. Patients showing a positive response to TACE remained on the waiting list and were monitored by a CT scan (every 3 mo) and determination of AFP level (monthly). Patients with tumor progression under TACE treatment were discharged from the waiting list (non-responder).

Post-transplantation management and follow-up

Immunosuppressive therapy following OLT consisted of a drug regimen of Prograf in combination with corticosteroids. Corticosteroids were gradually tapered and discontinued within 3 mo. Prograf was continued for one year after OLT unless side-effects were seen. The frequency of the outpatient visits thereafter varied according to the patient conditions and types of complications. No anti-cancer treatment was given after transplantation. All patients were followed up weekly in the outpatient clinic for the first month after discharged from the hospital. Screening for tumor recurrence was assessed by determination of a-fetoprotein (AFP) and ultrasonography every 3 mo. A routine CT scan of the abdomen and chest was performed every year, and additional imaging techniques (bone scan, magnetic resonance imaging) were done if HCC recurrence was suspected. The medical records and pathologic reports were analyzed retrospectively.

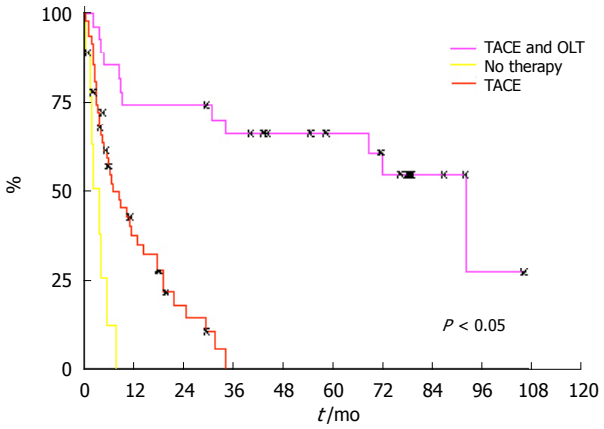

Figure 1 Survival probabilities for the first 5 yr after treatment. Overall HCC patient survival who had received TACE and OLT, only TACE and patients who received no treatment.

Statistical analysis

We analyzed the statistical significance on recurrence and survival of tumor-related risk factors, tumor size, number of nodules, and Milan criteria. We used the Kaplan-Meier method to measure survival and the log-rank test to analyze statistical differences. Results are expressed as mean ± SD. One-way ANOVA was used for comparisons between the groups when one measurement per experiment was available. Non-normally distributed data was calculated after rank transformation. Data were calculated by univariate ANOVA. Tukey's-HSD test was used for post hoc comparisons. $P < 0.05$ was considered significant in difference. Survival was estimated using Kaplan-Meier/log-rank analysis. All calculations were performed using SPSS 10.0®, standard version.

RESULTS

Tumor progression after TACE

Chemoembolization was well tolerated in the majority of patients. The most common complaints after TACE were pain, transient fever, and nausea. No patient developed major complications, which required surgical intervention. After TACE, 20 (29.2%) showed response and 47 (70.1%) showed tumor progression.

Tumor progression defines a group with good survival after OLT

As expected, the patients without treatment had the worst outcome with a median survival of 3.8 mo as seen in Figure 1. The Patients who were treated with TACE but did not qualify for liver transplantation due missing sighs of liver cirrhosis (n = 10), age older than 65 (n = 11), persistent alcohol disease (n = 11) or tumor progression (n = 15) had a median survival of 8.4 mo (Figure 1). The

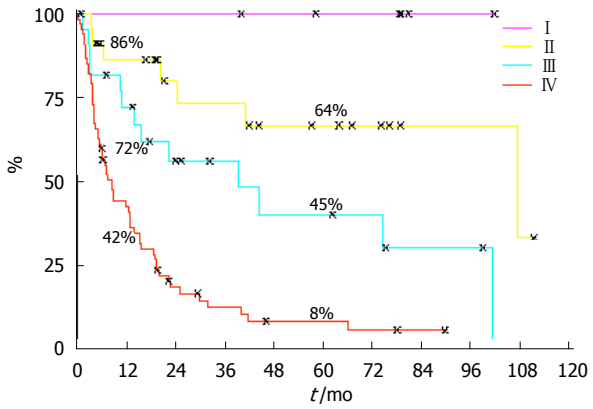

Figure 2 Kaplan-Meier patient survival curves showing survival dependent on UICC stage.

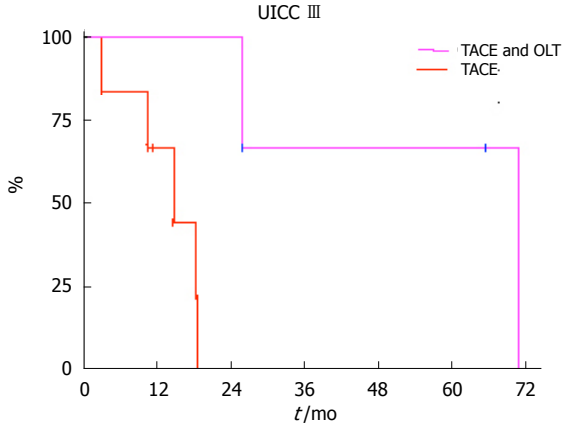

Figure 4 Kaplan-Meier patient survival curves. OLT improved survival UICC stage Ⅲ.

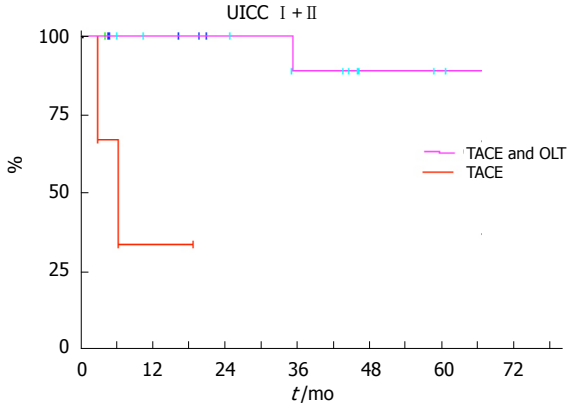

Figure 3 Kaplan-Meier patient survival curves demonstrating that OLT improved survival UICC stage Ⅰ and Ⅱ.

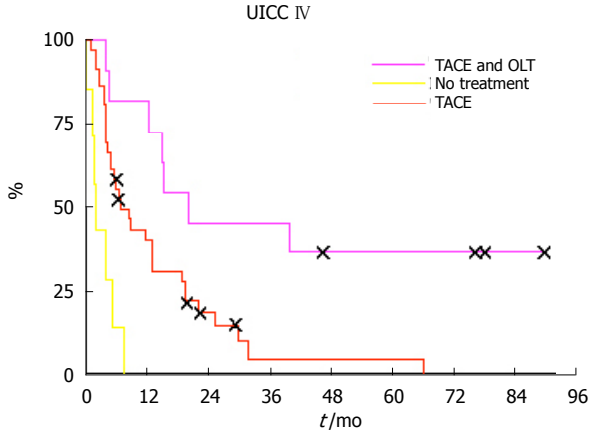

Figure 5 Kaplan-Meier patient survival curves. OLT improved survival UICC stage Ⅳ.

patients who showed no signs of tumor progression during waiting time had an average of 3 sessions of TACE (range, 1 to 10) before OLT. The TACE treated and liver transplanted patients (n = 20) had a significant better outcome compared with TACE treated patients with a median survival of 92.3 mo (Figure 1). The time of median survival in the transplanted group is comparable to OLT patients with non-malignant diseases (median survival of 101.6 mo) and confirms the selection criteria for OLT are suitable to select HCC patients for liver transplantation.

Survival dependent on UICC stage

Survival analysis revealed that the patient overall survival was dependent on the UICC stage. Patients with UICC stage Ⅰ (n = 5) had an overall survival of 100%, stage Ⅱ (n = 13) 64%, stage Ⅲ (n = 11) 45% and stage Ⅳ only 8% (n = 55) (Figure 2).

Lack of tumor progression and subsequent OLT improves survival irrespective of UICC stage

Patients, who fulfilled the selection criteria for liver transplantation and had no signs of tumor progression, underwent subsequently OLT. Independent of UICC stage, the patients with TACE and OLT had a better survival (Figures 3, 4 and 5). None of the patients with UICC stage Ⅰ on the waiting list showed signs of tumor progression. In UICC stage Ⅱ and Ⅲ, 4 patients had signs of tumor progression during waiting time. Seven of the UICC stage Ⅳ patients displayed signs of tumor progression. Independent of the UICC stage the patients without tumor progression and subsequent OLT had a significant better median survival. Patients who did not fulfill the criteria for liver transplantation or showed signs of tumor progression in UICC stage Ⅲ had a median survival of 14.2 mo compared to 39.5 mo in the liver transplanted group (Figure 4). In UICC stage Ⅳ patients the median survival was 8.6 versus 15.6 mo, respectively. The patients who were not treated at all had the worst survival with a median survival time of 3.8 mo (Figure 5). Taken together, independent of the UICC stage, the survival was significantly better in patients who qualified for liver transplantation and without any evidence of tumor progression while waiting for OLT (P > 0.05).

Patients without tumor progression have a comparable outcome irrespective of the Milan criteria

Patients, who fullfilled the Milan criteria, are considered to have an excellent outcome. Interestingly, in our study there was no significant difference (P = 0.19) in survival

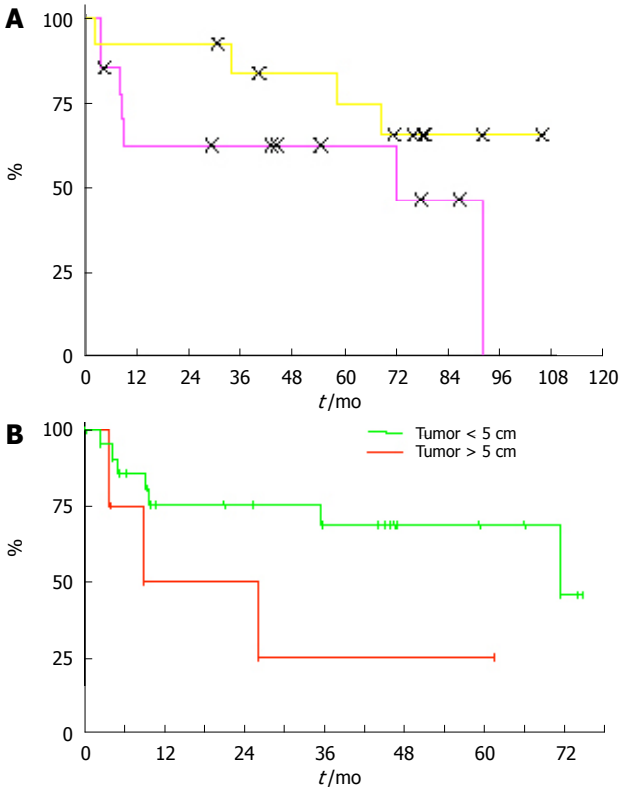

Figure 6 Survival probabilities for the first 5 years after liver transplantation according to the Milan criteria (**A**) and tumor size (**B**).

of patients, who fullfilled the Milan criteria compared to the more advanced patients (Figure 6A). However, the patients with tumors less than 5cm had a significantly better median survival ($P = 0.03$) compared to patients with tumors larger than 5 cm (Figure 6B).

DISCUSSION

Liver transplantation is the only approach that addresses the multifocal hepatocellular carcinoma and also treats the underlying cirrhosis but the limited availability of donor organs and the subsequent immunosuppression urge criteria of patient selection. Our data suggest that patients, who do not show signs of tumor progression after TACE treatment benefit from OLT irrespective of UICC stage. Without tumor progression, even patients outside of the Milan criteria do have a good outcome. Therefore we suggest that patient selection for OLT should be based on tumor size and additionally on assessment of tumor progression.

The current UNOS policy for organ allocation among patients with HCC favors those with tumors confined within the limits of diameter and number of nodules defined by the Milan criteria[12]. These were derived from a prospective study showing significantly better recurrence-free survival for 35 patients meeting the proposed criteria than for 13 patients with HCC exceeding criteria because of preoperative tumor stage underestimation based on pathologic analysis of the liver explants (92% *vs* 59% at 4 years). Other study groups proposed to "expand" the limits concerning OLT for HCC[16], because studies using the extended UCSF criteria (solitary tumor < 6.5 cm, three or fewer nodules with the largest lesion < 4.5 cm, total tumor diameter < 8 cm or without gross vascular invasion) do not worse the outcome of patients after OLT[13]. Therefore, concerns arise whether the Milan criteria may be too restrictive, thus excluding patients who would otherwise benefit from OLT. The decision for OLT is based on tumor size and number of tumor within the liver but not on growth behavior of the tumor or response of the tumor after bridging therapy. In our present study, 12 patients were found to have tumor characteristics exceeding the Milan criteria and underwent OLT. These patients were selected on the tumor progression after TACE and the difference in survival among those patients compared to patients meeting the Milan criteria did not reach statistical significance ($P = 0.19$). Thus patients without tumor progression not fulfilling the Milan criteria might benefit from OLT.

Vitale *et al*[17] described a very low occurrence of drop-outs from waiting list, though they had a quite long median waiting time of 11 mo[18]. In their study they used the following criteria to exclude patients from OLT: short-listing, general contraindication to transplant, extrahepatic spread, vascular invasion or poorly differentiated HCC (G3) at pre-OLT percutaneous biopsy. Size and number were not considered absolute selection criteria. They suggest that adoption of different selection criteria accounting more for tumor biology (grading) rather than tumor size and number and a use of a pre-OLT multimodal strategy probably may guarantee a lower number of drop-outs. Our results demonstrate that patients who show no further tumor progression under TACE treatment significantly ($P < 0.05$) benefit from OLT. It seems to be an easier biological grading method than the routine percutaneous biopsy for liver lesions because of the given potential risk of tumor seeding along the biopsy tract.

Furthermore, current imaging techniques have a high incidence of false-negative and false-positive results when evaluating HCC in cirrhosis. Only in 14.3% of OLT patients, tumor diameter was correctly identified by pretransplant radiological examinations shown by Sotiropoulos *et al*[19,20]. Sensitivity of radiological imaging was especially poor for tumors between 1 and 2 cm and less than 1 cm (21% and 0%, respectively), indicating that detection of small HCCs, especially in end-stage cirrhotic livers, remains problematic. A critical appraisal of patient characteristics together with great caution when interpreting imaging studies is recommended to determine candidacy for transplantation. Otherwise many patients are not given the opportunity to undergo OLT.

TACE involves the injection into the hepatic artery of chemotherapeutic agents such as doxorubicin, mitomycin, or cisplatin with lipiodol, to promote intra-tumor retention of the medications. TACE has the advantage of treating larger tumor-areas, being repeatable and perhaps downstaging patients. Disadvantages of TACE include significant toxicity and acute liver failure, especially when treating large areas[17]. Even if downstaging by TACE has been reported, TACE has not been shown to improve survival or recurrence of HCC after transplantion. Even in patients who were not transplanted, multiple large randomized controlled trials have failed to demonstrate

a survival benefit. Only a small survival benefit in comparison with conservative treatment was seen in meta-analysis of these trials. In addition, none of the current studies have examined the ability of TACE to sustain patients on the transplantation waiting list. Our data demonstrate that the patients, who have no tumor progression after TACE benefit substantially from OLT. Whether these patients would progress without TACE remains speculative[19,21-26].

In contrast to other malignant diseases, assessment of HCC patients on the waiting list should not only account for the current stage, it although should evaluate the tumor progression. Multiple genetic lesions within the HCC cells, which modulate growth, cell cycle, apoptosis and invasion, define tumor progression[27-31]. These genetic lesions are not defined in number and location and therefore prospective evaluation based on molecular pattern is not possible. On the other hand it is practicable to assess tumor growth by size and AFP levels.

Therefore, we conclude that the growth behavior of the tumor (defined as progression under anti-cancer therapy) could provide simple but helpful information about the recurrence rate and the outcome of HCC patients after OLT. We propose that growth behavior (P0 for no progression and P1 for progression) should be added to staging systems for classification of HCC to select patients for OLT[32-34].

REFERENCES

1 **Jemal A**, Tiwari RC, Murray T, Ghafoor A, Samuels A, Ward E, Feuer EJ, Thun MJ. Cancer statistics, 2004. *CA Cancer J Clin* 2004; **54**: 8-29

2 **El-Serag HB**, Mason AC. Rising incidence of hepatocellular carcinoma in the United States. *N Engl J Med* 1999; **340**: 745-750

3 **Llovet JM**, Fuster J, Bruix J. Intention-to-treat analysis of surgical treatment for early hepatocellular carcinoma: resection versus transplantation. *Hepatology* 1999; **30**: 1434-1440

4 **Sakon M**, Umeshita K, Nagano H, Eguchi H, Kishimoto S, Miyamoto A, Ohshima S, Dono K, Nakamori S, Gotoh M, Monden M. Clinical significance of hepatic resection in hepatocellular carcinoma: analysis by disease-free survival curves. *Arch Surg* 2000; **135**: 1456-1459

5 **Orlando A**, Cottone M, Virdone R, Parisi P, Sciarrino E, Maringhini A, Caltagirone M, Simonetti RG, Pagliaro L. Treatment of small hepatocellular carcinoma associated with cirrhosis by percutaneous ethanol injection. A trial with a comparison group. *Scand J Gastroenterol* 1997; **32**: 598-603

6 **A comparison of lipiodol chemoembolization and conservative treatment for unresectable hepatocellular carcinoma**. Groupe d'Etude et de Traitement du Carcinome Hépatocellulaire. *N Engl J Med* 1995; **332**: 1256-1261

7 **Fontana RJ**, Hamidullah H, Nghiem H, Greenson JK, Hussain H, Marrero J, Rudich S, McClure LA, Arenas J. Percutaneous radiofrequency thermal ablation of hepatocellular carcinoma: a safe and effective bridge to liver transplantation. *Liver Transpl* 2002; **8**: 1165-1174

8 **Oldhafer KJ**, Chavan A, Frühauf NR, Flemming P, Schlitt HJ, Kubicka S, Nashan B, Weimann A, Raab R, Manns MP, Galanski M. Arterial chemoembolization before liver transplantation in patients with hepatocellular carcinoma: marked tumor necrosis, but no survival benefit? *J Hepatol* 1998; **29**: 953-959

9 **Ringe B**, Pichlmayr R, Wittekind C, Tusch G. Surgical treatment of hepatocellular carcinoma: experience with liver resection and transplantation in 198 patients. *World J Surg* 1991; **15**: 270-285

10 **Iwatsuki S**, Starzl TE, Sheahan DG, Yokoyama I, Demetris AJ, Todo S, Tzakis AG, Van Thiel DH, Carr B, Selby R. Hepatic resection versus transplantation for hepatocellular carcinoma. *Ann Surg* 1991; **214**: 221-228; discussion 228-229

11 **Bismuth H**, Chiche L, Adam R, Castaing D. Surgical treatment of hepatocellular carcinoma in cirrhosis: liver resection or transplantation? *Transplant Proc* 1993; **25**: 1066-1067

12 **Mazzaferro V**, Regalia E, Doci R, Andreola S, Pulvirenti A, Bozzetti F, Montalto F, Ammatuna M, Morabito A, Gennari L. Liver transplantation for the treatment of small hepatocellular carcinomas in patients with cirrhosis. *N Engl J Med* 1996; **334**: 693-699

13 **Yao FY**, Ferrell L, Bass NM, Watson JJ, Bacchetti P, Venook A, Ascher NL, Roberts JP. Liver transplantation for hepatocellular carcinoma: expansion of the tumor size limits does not adversely impact survival. *Hepatology* 2001; **33**: 1394-1403

14 **Herrero JI**, Sangro B, Quiroga J, Pardo F, Herraiz M, Cienfuegos JA, Prieto J. Influence of tumor characteristics on the outcome of liver transplantation among patients with liver cirrhosis and hepatocellular carcinoma. *Liver Transpl* 2001; **7**: 631-636

15 **McPeake JR**, O'Grady JG, Zaman S, Portmann B, Wight DG, Tan KC, Calne RY, Williams R. Liver transplantation for primary hepatocellular carcinoma: tumor size and number determine outcome. *J Hepatol* 1993; **18**: 226-234

16 **Broelsch CE**, Frilling A, Malago M. Should we expand the criteria for liver transplantation for hepatocellular carcinoma--yes, of course! *J Hepatol* 2005; **43**: 569-573

17 **Vitale A**, Brolese A, Zanus G, Bassanello M, Montin U, Gringeri E, D'Amico F, Ciarleglio FA, Carraro A, Cappuzzo G, Bridda A, D'Amico DF, Cillo U. Multimodal therapy before liver transplantation for hepatocellular carcinoma. *Hepatol Res* 2005

18 **Fisher RA**, Maluf D, Cotterell AH, Stravitz T, Wolfe L, Luketic V, Sterling R, Shiffman M, Posner M. Non-resective ablation therapy for hepatocellular carcinoma: effectiveness measured by intention-to-treat and dropout from liver transplant waiting list. *Clin Transplant* 2004; **18**: 502-512

19 **Sotiropoulos GC**, Malagó M, Molmenti E, Paul A, Nadalin S, Brokalaki EI, Verhagen R, Dirsch O, Gerken G, Lang H, Broelsch CE. Efficacy of transarterial chemoembolization prior to liver transplantation for hepatocellular carcinoma as found in pathology. *Hepatogastroenterology* 2005; **52**: 329-332

20 **Sotiropoulos GC**, Malagó M, Molmenti E, Paul A, Nadalin S, Brokalaki E, Kühl H, Dirsch O, Lang H, Broelsch CE. Liver transplantation for hepatocellular carcinoma in cirrhosis: is clinical tumor classification before transplantation realistic? *Transplantation* 2005; **79**: 483-487

21 **Biselli M**, Andreone P, Gramenzi A, Trevisani F, Cursaro C, Rossi C, Ricca Rosellini S, Cammà C, Lorenzini S, Stefanini GF, Gasbarrini G, Bernardi M. Transcatheter arterial chemoembolization therapy for patients with hepatocellular carcinoma: a case-controlled study. *Clin Gastroenterol Hepatol* 2005; **3**: 918-925

22 **Arimura E**, Kotoh K, Nakamuta M, Morizono S, Enjoji M, Nawata H. Local recurrence is an important prognostic factor of hepatocellular carcinoma. *World J Gastroenterol* 2005; **11**: 5601-5606

23 **Veltri A**, Moretto P, Doriguzzi A, Pagano E, Carrara G, Gandini G. Radiofrequency thermal ablation (RFA) after transarterial chemoembolization (TACE) as a combined therapy for unresectable non-early hepatocellular carcinoma (HCC). *Eur Radiol* 2006; **16**: 661-669

24 **Liem MS**, Poon RT, Lo CM, Tso WK, Fan ST. Outcome of transarterial chemoembolization in patients with inoperable hepatocellular carcinoma eligible for radiofrequency ablation. *World J Gastroenterol* 2005; **11**: 4465-4471

25 **Decaens T**, Roudot-Thoraval F, Bresson-Hadni S, Meyer C, Gugenheim J, Durand F, Bernard PH, Boillot O, Boudjema K, Calmus Y, Hardwigsen J, Ducerf C, Pageaux GP, Dharancy S, Chazouilleres O, Dhumeaux D, Cherqui D, Duvoux C. Impact of pretransplantation transarterial chemoembolization on survival and recurrence after liver transplantation for hepatocellular carcinoma. *Liver Transpl* 2005; **11**: 767-775

26 **Guan YS**, Sun L, Zhou XP, Li X, Zheng XH. Hepatocellular carcinoma treated with interventional procedures: CT and MRI follow-up. *World J Gastroenterol* 2004; **10**: 3543-3548
27 **Pérez Saborido B**, Meneu JC, Moreno E, García I, Moreno A, Fundora Y. Is transarterial chemoembolization necessary before liver transplantation for hepatocellular carcinoma? *Am J Surg* 2005; **190**: 383-387
28 **Marui Y**, McCall J, Gane E, Holden A, Duncan D, Yeong ML, Chow K, Munn S. Liver transplantation for hepatocellular carcinoma in New Zealand: a prospective intent-to-treat analysis. *N Z Med J* 2005; **118**: U1532
29 **Lambert B**, Praet M, Vanlangenhove P, Troisi R, de Hemptinne B, Gemmel F, Van Vlierberghe H, Van de Wiele C. Radiolabeled lipiodol therapy for hepatocellular carcinoma in patients awaiting liver transplantation: pathology of the explant livers and clinical outcome. *Cancer Biother Radiopharm* 2005; **20**: 209-214
30 **Yamashiki N**, Tateishi R, Yoshida H, Shiina S, Teratani T, Sato S, Mine N, Kondo Y, Kawabe T, Omata M. Ablation therapy in containing extension of hepatocellular carcinoma: a simulative analysis of dropout from the waiting list for liver transplantation. *Liver Transpl* 2005; **11**: 508-514
31 **Johnson EW**, Holck PS, Levy AE, Yeh MM, Yeung RS. The role of tumor ablation in bridging patients to liver transplantation. *Arch Surg* 2004; **139**: 825-829; discussion 829-830
32 **Huynh H**. Overexpression of tumour suppressor retinoblastoma 2 protein (pRb2/p130) in hepatocellular carcinoma. *Carcinogenesis* 2004; **25**: 1485-1494
33 **Liu LX**, Jiang HC, Liu ZH, Zhu AL, Zhou J, Zhang WH, Wang XQ, Wu M. Gene expression profiles of hepatoma cell line BEL-7402. *Hepatogastroenterology* 2003; **50**: 1496-1501
34 **Figueras J**, Ibañez L, Ramos E, Jaurrieta E, Ortiz-de-Urbina J, Pardo F, Mir J, Loinaz C, Herrera L, López-Cillero P, Santoyo J. Selection criteria for liver transplantation in early-stage hepatocellular carcinoma with cirrhosis: results of a multicenter study. *Liver Transpl* 2001; **7**: 877-883

S- Editor Wang J **L- Editor** Ma JY **E- Editor** Liu WF

PO Box 2345, Beijing 100023, China
www.wjgnet.com
wjg@wjgnet.com

World J Gastroenterol 2007 February 7; 13(5): 768-773
World Journal of Gastroenterology ISSN 1007-9327

CLINICAL RESEARCH

Esophageal mesenchymal tumors: Endoscopy, pathology and immunohistochemistry

Xuan Zhu, Xiao-Qian Zhang, Bi-Min Li, Ping Xu, Kun-He Zhang, Jiang Chen

Xuan Zhu, Xiao-Qian Zhang, Bi-Min Li, Ping Xu, Department of Gastroenterology, First Affiliated Hospital, Nanchang University, Nanchang 330006, Jiangxi Province, China
Kun-He Zhang, Jiang Chen, Department of Digestive Diseases, First Affiliated Hospital, Nanchang University, Nanchang 330006, Jiangxi Province, China
Supported by the Scientific and Technological Foundation of the Jiangxi Provincial Department of Science and Technology
Correspondence to: Dr. Xuan Zhu, Department of Gastroenterology, the First Affiliated Hospital, Nanchang University, Nanchang 330006, Jiangxi Province, China. jyyfyzx@163.com
Telephone: +86-791-8692505 Fax: +86-791-8623153
Received: 2006-10-09 Accepted: 2006-12-26

Abstract

AIM: To study the endoscopic, pathological and immunohistochemical features of esophageal mesenchymal tumors.

METHODS: Twenty-nine patients diagnosed as esophageal mysenchymal tumors by electronic endoscopy and endoscopic ultrasound (EUS) were observed under light microscopes, and all tissues were stained by the immunohistochemical method. The expression of CD117, CD34, SMA and desmin were measured by staining intensity of cells and positive cell ratios.

RESULTS: Endoscopically, esophageal gastrointestinal stromal tumors (GISTs) and leiomyomas (LMs) had similar appearances, showing submucosal protuberant lesions. They all showed low echo images originated from the muscularis propria or muscularis mucosa on EUS. Endoscopy and EUS could not exactly differentiate esophageal GISTs from LMs. Microscopically, there were two kinds of cells: spindle cell type and epitheloid cell type in esophageal GISTs. Leiomyomas and leiomyosarcomas were only of spindle cell type. One malignancy was found in five cases of esophageal GISTs, and one malignancy in 24 cases of leiomyomas and leiomyosarcomas. Using Fisher's exact method, the differences of malignant lesion proportion were not significant between esophageal LMs and GISTs, 1/5 *vs* 1/24 ($P > 0.05$). All cases of esophageal GISTs were positive for CD117, and 3 cases were also positive for CD34. The 24 cases of leiomyomas and leiomyosarcomas were all negative for CD117 and CD34. The differences of positive rates of CD117 and CD34 were significant between esophageal GISTs and LMs, 5/5 *vs* 0/24, 3/5 *vs* 0/24 ($P < 0.005$). All leiomyomas and leiomyosarcomas were positive for SMA, and desmin. Among 5 cases of esophageal GISTs, 2 cases were SMA positive, and 1 case was desmin positive. The differences in positive rates and expression intensity of SMA and desmin were significant between esophageal LMs and GISTs, 24/24 *vs* 2/5, 24/24 *vs* 1/5 ($P < 0.005$).

CONCLUSION: The most common esophageal mesenchymal tumors are leiomyomas, and esophageal GISTs are less common. Most of esophageal LMs and GISTs are benign. Endoscopy and EUS are the effective methods to diagnose esophageal mesenchymal tumors and they can provide useful information for the treatment of these tumors. However, they cannot exactly differentiate esophageal GISTs from LMs. Pathological, especially immunohistochemical features are useful to differentiate GISTs from leiomyomas.

Key words: Esophageal mesenchymal tumors; Gastrointestinal stromal tumors; Leiomyomas; Endoscopy; Pathology; Immunohistochemistry

Zhu X, Zhang XQ, Li BM, Xu P, Zhang KH, Chen J. Esophageal mesenchymal tumors: Endoscopy, pathology and immunohistochemistry. *World J Gastroenterol* 2007; 13(5): 768-773

http://www.wjgnet.com/1007-9327/13/768.asp

INTRODUCTION

Traditionally, the gastrointestinal mesenchymal tumors (GIMTs) have been almost uniformly classified as gastrointestinal leiomyomas (LMs). However, recent evidence indicates that most mesenchymal tumors of the gastrointestinal tract are gastrointestinal stromal tumors (GISTs)[1]. It is difficult to differentiate esophageal GISTs from LMs because of their similar appearance. GISTs frequently have malignant potential, therefore, it is important to differentiate GISTs from LMs. GISTs arising in the gastrointestinal tract have been known quite well. Whether there are the same stromal tumors in the esophagus, and whether stromal tumors are the most

frequent mesenchymal tumors of the esophagus, are big concern of clinical doctors[2,3].

MATERIALS AND METHODS

Specimen collection

All the patients were in- and outpatients from the First Affiliated Hospital of Nanchang University during June 2004 to November 2005 and they all met with the following two criteria: (1) Endoscopically, the tumors showed submucosal protuberant lesions, and they showed low echo images originated from the muscularis propria or muscularis mucosa on EUS. (2) Microscopically, they were diagnosed as esophageal mesenchymal tumors. All tissue specimens were obtained by the following 3 methods: biopsy, endoscopic mucosal resection (EMR) or surgical operation.

Methods

All tissue specimens were fixed in 10% formalin and processed routinely for paraffin embedding. Sections of 4-mm thick were stained with hematoxylin and eosin, and observed by light microscopy. Then all cases were stained for CD117, CD34, SMA, and desmin. All antibodies were purchased from Beijing Zhongshan Corporation. The detailed procedures were carried out according to instructions of the kits.

Criteria for histopathology

First, esophageal mesenchymal tumors: According to the criteria of 2005 WHO Oncopathology and Genetics[4], if spindle cells and epitheloid cells were shown microscopically, esophageal mesenchymal tumors can be diagnosed. Sencond, criteria for assessing malignancy of gastrointestinal stromal tumors: according to the criteria of 2005 WHO Oncopathology and Genetics and the advice of Singer and Miettinen[4-6], GISTs were diagnosed as malignant when the following criteria were met: tumor size $\geqslant$ 5 cm, nuclear mitotic figure > 5/50 HPF. GISTs were diagnosed as benign: tumor size < 5 cm, nuclear mitotic figure < 5/50 HPF. GISTs were diagnosed as potentially malignant: tumor size $\geqslant$ 5 cm, nuclear mitotic figure < 5/50 HPF or tumor size < 5 cm, nuclear mitotic figure > 5/50 HPF. At the same time, tumor hemorrhage/necrosis, peripheral invasive growth, lymph node metastasis and metastasis to another organ are all considered also. Third, criteria for leiomyosarcomas: according to the criteria of 2005 WHO Oncopathology and Genetics and internal reports[4,7,8], tumor size $\geqslant$ 5 cm, nuclear mitotic figure > 5/50 HPF, tumor hemorrhage/necrosis, peripheral invasive growth and metastasis.

Assessment for immunohistochemical results

Positive results were indicated if the cytoplasm was stained brown, and cell membrane was stained positive for CD34 and CD117. The categories were (+): more than 10% of cells stained; (-): less than 10% of cells stained. Positive control: CD117, an indicator of the known GISTs; CD34, an indicator of vascular endothelial cells in tumors; SMA, an indicator of normal smooth muscles in vascular walls or esophageal walls; Desmin, an indicator of normal smooth muscles in esophageal walls. Negative control: the primary antibody was replaced by PBS for negative control.

Table 1 Clinical findings of 29 cases of esophageal mesenchymal tumors

Tumor type	*n*	Dysphagia	Heart burn/ retrosternal pain	Hemorrhage	Stomachache	Asymptomatic
LMs	24	4	7	1	2	10
GISTs	5	1	1	1	0	2
Total	29	5	8	2	2	12

Tested by Fisher's exact method, the differences of symptoms are not significant between esophageal LMs and GISTs ($P > 0.05$).

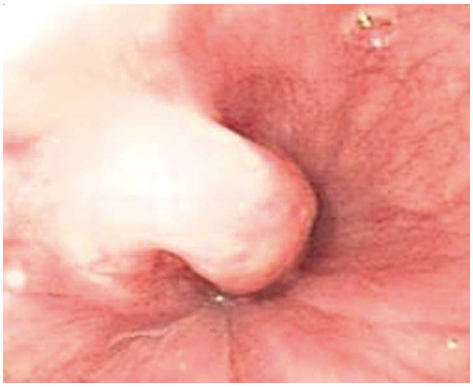

Figure 1 Endoscopic image of esophageal stromal tumors.

Statistical analysis

Data was tested using Fisher's exact method. A P value less than 0.05 was considered statistically significant.

RESULTS

Clinical data

Among 29 cases of esophageal mesenchymal tumors diagnosed by endoscopy, pathology and immunohistochemistry, 5 cases were esophageal GISTs, 23 cases were leiomyomas and 1 case was leiomyosarcoma. In the group of esophageal GISTs, 3 cases were male, and 2 cases were female. Their age ranged from 44-63 years (mean 52 ± 7.8 years). In the group of leiomyomas and leiomyosarcomas, 13 cases were male, and 11 cases were female. Their age was between 24-68 years (mean 55 ± 10.2 years). The symptoms of esophageal mesenchymal tumors are summarized in Table 1.

Endoscopic and EUS characteristics

Endoscopically, GISTs showed submucosal protuberant lesions such as hemisphere, nodosity, strip or irregular shape, and had smooth surface, wide bases and the same color as its adjacent mucosa (Figures 1 and 2). The malignant lesions showed ulceration or hemorrhage, and had no clear boundaries with the normal tissue. Benign tumors varied from 0.5-3 cm in size. One malignant tumor

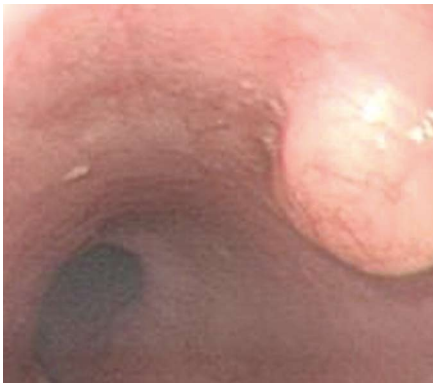

Figure 2 Endoscopic image of leiomyomas.

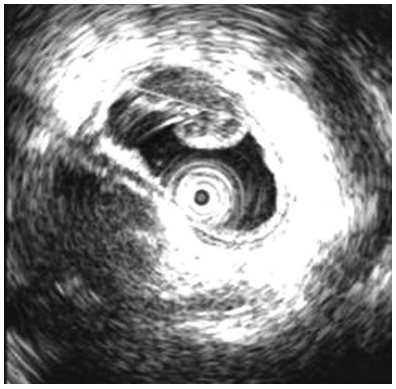

Figure 3 EUS image of esophageal stromal tumors: originated from muscularis propria.

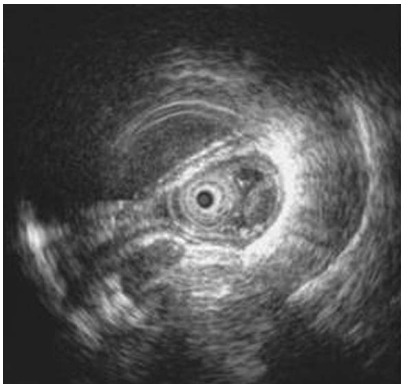

Figure 4 EUS image of leiomyomas: originated from muscularis mucosa.

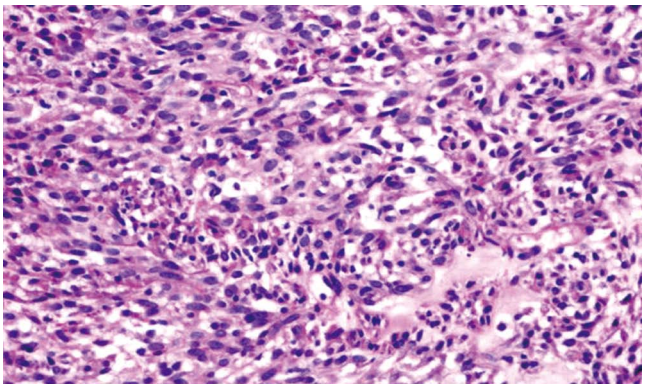

Figure 5 Malignant esophageal stromal tumor: tumor cells were intensely stained, but there was no visible mitoschisis. (HE × 200).

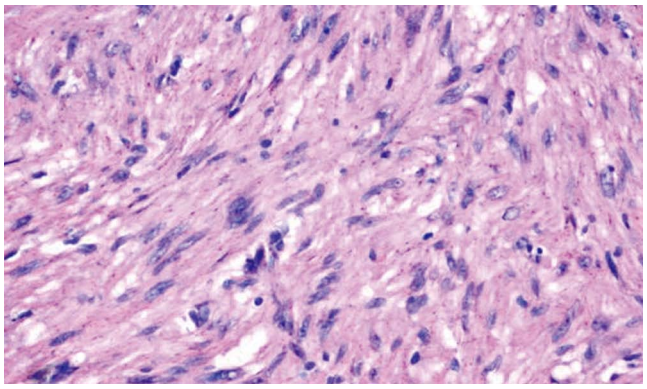

Figure 6 Esophageal leiomyoma: cells were all spindle, with abundant eosinophilic cytoplasm (HE × 200).

was especially large, extending to the cardia and body of the stomach. LMs showed submucosal protuberant lesions such as polyps, hemisphere, pillar, dumb bell, with smooth surfaces. Tumors varied between 0.5-3 cm in size, and had clear borders. One leiomyosarcoma showed irregular nodosity. Its size was 3 cm × 4 cm with anabrotic surfaces.

On EUS, GISTs showed round, spindle-shaped or irregular low echo images originated from the muscularis propria or muscularis mucosa, from which internal echoes were homogeneous or heterogeneous. Two cases were originated from the muscularis mucosa and 3 cases from the muscularis propria (Figures 3 and 4). LMs also showed low echo images originated from the muscularis propria or muscularis mucosa and their internal echoes were homogeneous or heterogeneous. Eleven cases were originated from the muscularis mucosa and 12 cases were originated from the muscularis propria. Endoscopy and EUS could not differentiate esophageal GISTs from LMs because of their similar appearances.

Pathological characteristics

Among 5 cases of GISTs, 4 cases were of spindle cell type, and one case was of epitheloid cell type. There was no mixture of cell types. The cells of GISTs were more intense than leiomyomas, and had a less eosinophilic cytoplasm. The spindle cells were arranged in braid, sarciniform, or cord-like and their nuclei were rod -like. The epitheloid cells were round, orbicular-ovate or polygon and their nuclei were conspicuous. According to the above mentioned criteria, there was 1 case of malignancy at the inferior segment of the esophagus, which size was uncertain, with hemorrhage and necrosis on its surface. Microscopically, the tumor cells were intense, but there was no visible mitoschisis (Figure 5).

Twenty three cases of LMs were composed of well-differentiated smooth muscle cells of spindle cell type and the cells were arranged as braid, sarciniform. The tumors were moderately cellular with abundant eosinophilic cytoplasm (Figure 6). According to the criteria, there was one leiomyosarcoma, which size was 3 cm × 4 cm, with ulceration and bleeding on its surface and without clear borders. Microscopically, there were abundant spindle cells with a few mitoschisis.

Among 29 cases of esophageal mesenchymal tumors, one case with malignancy (20%) was found in 5 cases of esophageal GISTs, and one case with malignancy (4.2%) was found in 24 cases of leiomyomas and leiomyosarcomas. Using Fisher's exact method, the differences of malignant lesions proportion were not significant between esophageal LMs and GISTs, 1/5 *vs* 1/24 ($P > 0.05$).

Immunohistochemical results

Twenty nine cases of esophageal mesenchymal tumors

Table 2 Expression of CD117 in 29 cases of esophageal mesenchymal tumors

Tumor type	*n*	Positive rate (%)
GISTs	5	5
LMs	24	0
	$P < 0.003$	

Table 3 Expression of CD34 in 29 cases of esophageal mesenchymal tumors

Tumor type	*n*	Positive rate (%)
GISTs	5	3 (60)
LMs	24	0
	$P < 0.003$	

Table 4 Expression of SMA in 29 cases of esophageal mesenchymal tumors

Tumor type	*n*	Positive rate (%)
LMs	24	24 (100)
GISTs	5	2 (40)
	$P < 0.003$	

Table 5 Expression of desmin in 29 cases of esophageal mesenchymal tumors

Tumor type	*n*	Positive rate (%)
LMs	24	24 (100)
GISTs	5	1 (20)
	$P < 0.003$	

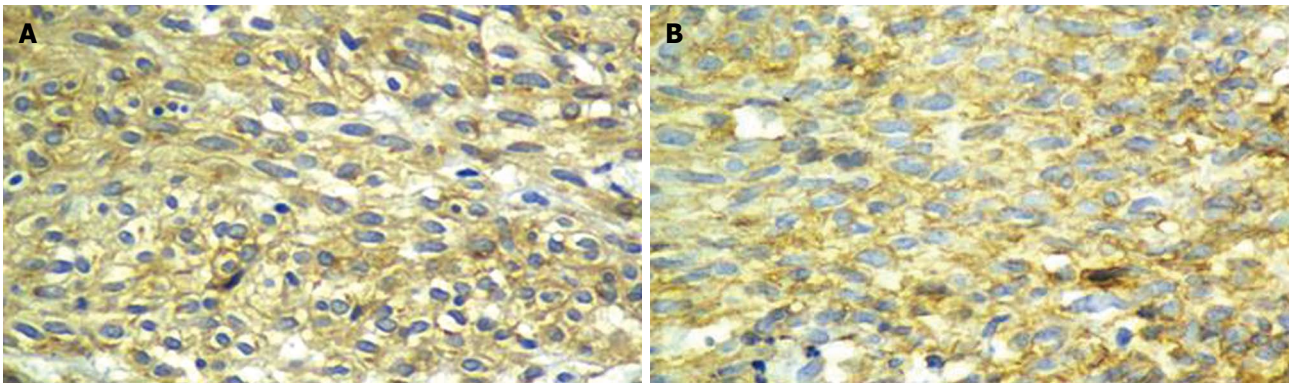

Figure 7 Expression of CD117(× 200) and CD 34 (× 400) in malignant esophageal stromal tumor: showing yellow or brown granules in cell cytoplasm and (or) membrane. **A**: CD117; **B**: CD34.

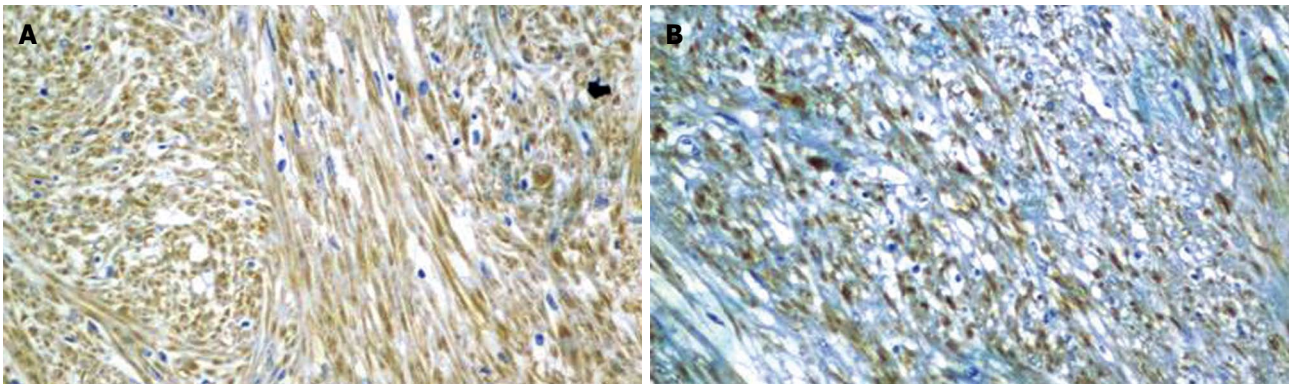

Figure 8 Expression of SMA (**A**) and Desmin (**B**) in esophageal leiomyomas (× 200): showing yellow or brown granules in cell cytoplasm.

were all stained positive for CD117, CD34, SMA and desmin. The results are summarized in Table 2, Table 3, Table 4 and Table 5, Figures 7 and 8.

DISCUSSION

Gastrointestinal mesenchymal tumors have long been classified as LMs, including leiomyoma and leiomyosarcoma. In 1983 Mazur and Clark introduced the term of gastrointestinal stromal tumors (GISTs). GISTs are a kind of potentially malignant tumor. Most scholars believe that the stomach is the predilective site of GISTs, next are the intestines, the colon and the rectum. And GISTs seldom occur in the esophagus[9,10].

Gouveia[11] reported that esophageal GISTs, though less in number, were also made up of fusiform cells, and their mitotic index was low. CD117 and CD34 were expressed, and the malignant degree was low. Among 57 cases of esophageal mesenchymal tumors, studied by Madalie[12], 14 cases of esophageal GISTs were found, and only 2 cases were malignant. Wang[13] reported that 9 cases of GISTs were found among 44 cases of esophageal mesenchymal tumors, and 3 cases were malignant. In our study, among 29 cases of esophageal mesenchymal tumors, 5 cases were demonstrated to be GISTs by endoscopy, pathology, and immunochemistry, and the other 24 cases were LMs. This result further proved that esophageal GISTs exist in the gastrointestinal tract, though they are fewer in number than esophageal LMs, accounting for only 20%[12-14].

Esophageal mesenchymal tumors mostly occur in people of middle and old age, especially over 50 years old, occasionally in children. In the current study, all the 5 cases were over 40 years old, and 3 of them were over 50 years old (the youngest one was 40 years old). The mean age was 52 years. Esophageal leiomyomas may occur at any age. In our group, age of patients with LMs was from 20 to 70 years, and males were slightly more than females. The clinical manifestations of esophageal mesenchymal tumors are closely correlated with the size, nature, and growth pattern of the tumor. In the earlier period, clinical symptoms are nonspecific. When the tumor volume becomes bigger grossly and grows intracavitarily, symptoms such as dysphagia, heart burn, and retrosternal pain may become obvious. Some patients may have upper gastrointestinal hemorrhage.

The appearance of esophageal GISTs and leiomyomas are similar under the endoscope. They are generally globular, hemispheroid, polypoid, with tubercular eminences. The surface of benign GIMTs is smooth, while there is ulceration or hemorrhage on the surface of malignant GIMTs. EUS can not only examine the wall of the esophagus, but can also estimate the topography of the extent, location of lesions, and their relation to the surrounding organs[15,16]. EUS can discriminate GIMTs from other protrusion lesions of the esophagus. Usually esophageal mesenchymal tumors show a low echo image. Though EUS can help doctors to make therapeutic decisions by surgery or by endoscopy, it cannot help doctors to judge the type of the GIMTs.

Esophageal GISTs originate from between the walls of the esophagus. They are a kind of proliferation of spindle cells or epithelioid cells. No matter where the tumor is originated, the cells of GISTs are more abundant than that of leiomyomas and have less eosinophilic cytoplasm. The tumor cells are interlaced，dispersed, or paliformly arranged. In our study, cell nests made up of spindle cells were found in three cases of esophageal GISTs. These cell nests can only be found in GISTs, but not in LMs. This result is coincident with that of Franquemont[17].

There is no definite criterium for differentiation between benign and malignant esophageal mesenchymal tumors. We determined the nature of tumors according to their infiltration, metastasis, volume, and nuclear mitotic figure. In the present study, one case of interstitialoma occurred at the inferior segment of the esophagus. Its diameter was more than 5 cm. There was ulceration and hemorrhage on the surface, but no obvious mitoschisis. This tumor can still be judged as malignant. Kimiyoshi[18] suggested a criterium for differentiation between benign and malignant GISTs: hemorrhage or necrosis, the diameter of the tumor > 5 cm, Ki-67 labeling index (LI) > 3%. If the tumor has any one of the items above, it is malignant. If none of the items above can be found, then it is benign. Kimiyoshi also found that cellulosity, nuclear atypia, and mitoschisis were not related to the nature of the tumor. This is different from the traditional diagnostic criteria. And further studies are needed. Leiomyosarcomas are not common, and its diagnostic criteria are not well studied. According to the criteria of WHO, there was only 1 case of leiomyosarcoma in the present study. The tumor occurred at the inferior segment of the esophagus. Intensive fusiform cells could be seen under the microscope. Mitoschisis could be seen accidently. The diagnosis was low potential malignant leiomyosarcoma. The incidence of esophageal leiomyosarcoma is low.

In our study, the difference between the ratio of malignant GISTs (1/5) and that of leiomyosarcoma (1/24) was insignificant. It showed that the biological behaviour of GISTs was related to the site of the tumor. Esophageal GISTs are not as malignant as those in the gastrointestine. It was also noted that 1 case of esophageal leiomyosarcoma and 1 case of esophageal interstitialoma both occurred in the inferior segment of the esophagus adjacent to the cardia. Whether the predilection site for malignant lobus intermedius tumor is the inferior segment of the esophagus is still to be studied.

In 1998, Kindblom *et al*[19] found that GISTs expressed CD117, which provided an effective means to study GISTs. CD117 is sensitive and specific. Studies reported that the sensitivity was 90%-100%[20,21]. In this study, all 5 cases of esophageal interstitialoma expressed CD117, while no case of leiomyoma expressed CD117. Both the sensitivity and specificity were 100%. This result is coincident with most overseas studies. However, not all GISTs expressed CD117. Debiec-Rychter found that in some of the malignant or recurrent cases of GISTs, CD117 was not expressed[22]. CD34 is a sensitive immunochemistry marker of GISTs. CD34 was expressed in 60%-70% cases of GISTs[23,24], but barely expressed in leiomyomas and myoschwannomas[25,26]. In our group the sensitivity of CD34 was 60%, and the specificity was 100%. Smooth muscle actin(SMA) is widespread and strong positive in smooth muscles, and also positive in GISTs. This shows that some GIST cells could differentiate into smooth muscles. Desmin is a key index for diagnosis and differential diagnosis of GIMTs, which is strongly expressed in smooth muscles, while barely expressed in GISTs. In this group, desmin was positive in all 24 cases of leiomyoma (leiomyosarcoma); only positive in 1 GIST. This is consistent with previous reports[27,28].

Our study provided evidence that all esophageal mesenchymal tumors had the same immunohistochemical features, and combined detection of CD117, CD34, SMA and desmin can help differentiate esophageal GISTs from LMs.

In summary, the present study demonstrates that

the traditional classification is not precise by combined analysis of the clinical, endoscopic, pathological and immunohistochemical features of esophageal mesenchymal tumors. Clinical findings, endoscopy and EUS can be helpful for diagnosis of esophageal mesenchymal tumors, but cannot determine the nature of tumors. Pathology and immunohistochemistry play an important role in their diagnosis and differential diagnosis.

REFERENCES

1 **O'leary T**, Berman JJ. Gastrointestinal stromal tumors: answers and questions. *Hum Pathol* 2002; **33**: 456-458
2 **Lewin KJ**, Appleman HD. Tumors of the esophagus and stomach. Atlas of tumor. Pathology. Washington DC: AFIP, 1996: 151
3 **Miettinen M**, Sarlomo-Rikala M, Sobin LH, Lasota J. Esophageal stromal tumors: a clinicopathologic, immunohistochemical, and molecular genetic study of 17 cases and comparison with esophageal leiomyomas and leiomyosarcomas. *Am J Surg Pathol* 2000; **24**: 211-222
4 **Hamilton SR**. Hamilton, Aaltonen LA. The classification of WHO oncopathology and genetics in 2005 (Section of digestive system). *J Diagno Pathol corporation* 2005; 14-16
5 **Singer S**, Rubin BP, Lux ML, Chen CJ, Demetri GD, Fletcher CD, Fletcher JA. Prognostic value of KIT mutation type, mitotic activity, and histologic subtype in gastrointestinal stromal tumors. *J Clin Oncol* 2002; **20**: 3898-3905
6 **Miettinen M**, El-Rifai W, H L Sobin L, Lasota J. Evaluation of malignancy and prognosis of gastrointestinal stromal tumors: a review. *Hum Pathol* 2002; **33**: 478-483
7 **Zeng ZY**, Huang KH, Zan J, Li CQ, Wang LY, Chen WX. Clinic and pathological features of leiomyomas on up-gastrointestinal tract. *Guangdong Yixue* 2003; **24**: 56-58
8 **Yang YH**, Chen ZS, Xie G, Xie CY, Yu J, Wu XG. Analysis on clinic, pathological and immunohistochemical features of Gastrointestinal mesenchymal tumors. *Shiyong Yiyuan Linchuang Zazhi* 2005; **2**: 77-78
9 **Miettinen M**, Lasota J. Gastrointestinal stromal tumors--definition, clinical, histological, immunohistochemical, and molecular genetic features and differential diagnosis. *Virchows Arch* 2001; **438**: 1-12
10 **Luo RZ**, Liang XM, He JH. Gastrointestinal stromal tumors: a clinicopathologic and immunohistochemical study of 154 cases. *Guangdong Yixue* 2004; **25**: 244-246
11 **Gouveia AM**, Pimenta AP, Lopes JM, Capelinha AF, Ferreira SS, Valbuena C, Oliveira MC. Esophageal GIST: therapeutic implications of an uncommon presentation of a rare tumor. *Dis Esophagus* 2005; **18**: 70-73
12 **Ma DL**, Liu XH, Bai CG, Wu LL, Xie Q. Studies on clinical, histological, immunohistochemical features of esophageal mesenchymal tumors. *Zhonghua Waike Zazhi* 2002; **40**: 237
13 **Wang ZD**, Wang XL, Wang YJ, Yang HC, Wang Y, Wu GX. Esophageal gastrointestinal stromal tumors: an immunohistochemical and clinicopathologic study. *Zhenduan Binglixue Zazhi* 2005; **12**: 31-33
14 **Hou YY**, Wang J, Zhu XZ, Tao K. A comparative study of esophageal stromal tumors and smooth muscle tumors. *Zhonghua Binglixue Zazhi* 2002; **31**: 116-119
15 **Oğuz D**, Filik L, Parlak E, Dişibeyaz S, Ciçek B, Kaçar S, Aydoğ G, Sahin B. Accuracy of endoscopic ultrasonography in upper gastrointestinal submucosal lesions. *Turk J Gastroenterol* 2004; **15**: 82-85
16 **Lowe AS**, Kay CL. Noninvasive competition for endoscopic ultrasound. *Gastrointest Endosc Clin N Am* 2005; **15**: 209-224, xi
17 **Franquemont DW**. Differentiation and risk assessment of gastrointestinal stromal tumors. *Am J Clin Pathol* 1995; **103**: 41-47
18 **Yokoi K**, Tanaka N, Shoji K, Ishikawa N, Seya T, Horiba K, Kanazawa Y, Yamashita K, Ohaki Y, Tajiri T. A study of histopathological assessment criteria for assessing malignancy of gastrointestinal stromal tumor, from a clinical standpoint. *J Gastroenterol* 2005; **40**: 467-473
19 **Kindblom LG**, Remotti HE, Aldenborg F, Meis-Kindblom JM. Gastrointestinal pacemaker cell tumor (GIPACT): gastrointestinal stromal tumors show phenotypic characteristics of the interstitial cells of Cajal. *Am J Pathol* 1998; **152**: 1259-1269
20 **Ignjatović M**. Gastrointestinal stromal tumors. *Vojnosanit Pregl* 2002; **59**: 183-202
21 **Miettinen M**, Lasota J. Gastrointestinal stromal tumors (GISTs): definition, occurrence, pathology, differential diagnosis and molecular genetics. *Pol J Pathol* 2003; **54**: 3-24
22 **Debiec-Rychter M**, Wasag B, Stul M, De Wever I, Van Oosterom A, Hagemeijer A, Sciot R. Gastrointestinal stromal tumours (GISTs) negative for KIT (CD117 antigen) immunoreactivity. *J Pathol* 2004; **202**: 430-438
23 **Fletcher CD**, Berman JJ, Corless C, Gorstein F, Lasota J, Longley BJ, Miettinen M, O'Leary TJ, Remotti H, Rubin BP, Shmookler B, Sobin LH, Weiss SW. Diagnosis of gastrointestinal stromal tumors: A consensus approach. *Hum Pathol* 2002; **33**: 459-465
24 **Joensuu H**, Fletcher C, Dimitrijevic S, Silberman S, Roberts P, Demetri G. Management of malignant gastrointestinal stromal tumours. *Lancet Oncol* 2002; **3**: 655-664
25 **Erlandson RA**, Klimstra DS, Woodruff JM. Subclassification of gastrointestinal stromal tumors based on evaluation by electron microscopy and immunohistochemistry. *Ultrastruct Pathol* 1996; **20**: 373-393
26 **Rosai J**, Ackerman LV. Ackman's Surgical Pathology, St.Louis: Mosby, 1996: 645-647
27 **Yamaguchi J**, Sawada N, Tobioka H, Takakuwa R, Goto T, Sakuma Y, Ikeda T, Satoh M, Mori M. Electron microscopic and immunohistochemical studies of gastrointestinal stromal tumors. *Med Electron Microsc* 1999; **32**: 213-220
28 **Yamaguchi U**, Hasegawa T, Masuda T, Sekine S, Kawai A, Chuman H, Shimoda T. Differential diagnosis of gastrointestinal stromal tumor and other spindle cell tumors in the gastrointestinal tract based on immunohistochemical analysis. *Virchows Arch* 2004; **445**: 142-150

S- Editor Liu Y **L- Editor** Zhu LH **E- Editor** Ma WH

PO Box 2345, Beijing 100023, China
www.wjgnet.com
wjg@wjgnet.com

World J Gastroenterol 2007 February 7; 13(5): 774-780
World Journal of Gastroenterology ISSN 1007-9327

CLINICAL RESEARCH

High-altitude gastrointestinal bleeding: An observation in Qinghai-Tibetan railroad construction workers on Mountain Tanggula

Tian-Yi Wu, Shou-Quan Ding, Jin-Liang Liu, Jian-Hou Jia, Rui-Chen Dai, Dong-Chun Zhu, Bao-Zhu Liang, De-Tang Qi, Yong-Fu Sun

Tian-Yi Wu, Physiological Research Group of Ministry of Railway, PRC, High Altitude Medical Research Institute, Xining 810012, Qinghai Province, China
Shou-Quan Ding, 12th Hospital of Qinghai-Tibetan Railroad Construction Company, Golmud 816000, Qinghai Province, China
Jin-Liang Liu, Jian-Hou Jia, 20th Hospital of Qinghi-Tibetan Railroad Construction Company, Golmud 816000, Qinghai Province, China
Rui-Chen Dai, Dong-Chun Zhu, Public Health Bureau of Qinghai-Tibetan Railroad Construction Company, Golmud 816000, Qinghai Province, China
Bao-Zhu Liang, De-Tang Qi, China Railroad Construction Company, Beijing 100844, China
Yong-Fu Sun, Ministry of Railway, Beijing 100844, China
Supported by the grant LS-CNNSF-30393130, and 973 Program 2006 CB 504100, CB708514, China
Correspondence to: Tian-Yi Wu, MD, Professor of Physiology and Medicine, National Key Laboratory of High Altitude Medicine, High Altitude Medical Research Institute, Nanchua West Road No. 344, Xining 810012, Qinghai Province, China. wutianyiqh@hotmail.com
Telephone: +86-971-6250870 Fax: +86-971-6142232
Received: 2006-03-03 Accepted: 2006-10-17

Abstract

AIM: To investigate the gastrointestinal bleeding (GIB) in people from lowland to high altitude and in workers on Mountain Tanggula and its causes as well as treatment and prophylaxis.

METHODS: From 2001 to October 2003, we studied GIB in 13502 workers constructing the railroad on Mountain Tanggula which is 4905 m above the sea level. The incidence of GIB in workers at different altitudes was recorded. Endoscopy was performed when the workers evacuated to Golmud (2808 m) and Xining (2261 m). The available data on altitude GIB were analyzed.

RESULTS: The overall incidence of GIB was 0.49% in 13502 workers. The incidence increased with increasing altitude. The onset of symptoms in most patients was within three weeks after arrival at high altitude. Bleeding manifested as hematemesis, melaena or hematochezia, and might be occult. Endoscopic examination showed that the causes of altitude GIB included hemorrhage gastritis, gastric ulcer, duodenal ulcer, and gastric erosion. Experimental studies suggested that acute gastric mucosal lesion (AGML) could be induced by hypoxic and cold stress, which might be the pathogenesis of altitude GIB. Those who consumed large amount of alcohol, aspirin or dexamethasone were at a higher risk of developing GIB. Persons who previously suffered from peptic ulcer or high-altitude polycythemia were also at risk of developing GIB. Early diagnosis, evacuation, and treatment led to early recovery.

CONCLUSION: GIB is a potentially life threatening disease, if it is not treated promptly and effectively. Early diagnosis, treatment and evacuation lead to an early recovery. Death due to altitude GIB can be avoided if early symptoms and signs are recognized.

Key words: High altitude; Gastrointestinal bleeding; Hypoxic stress; Acute gastric mucosal lesion; Risk factors

Wu TY, Ding SQ, Liu JL, Jia JH, Dai RC, Zhu DC, Liang BZ, Qi DT, Sun YF. High-altitude gastrointestinal bleeding: An observation in Qinghai-Tibetan railroad construction workers on Mountain Tanggula. *World J Gastroenterol* 2007; 13(5): 774-780

http://www.wjgnet.com/1007-9327/13/774.asp

INTRODUCTION

Although cardiac, respiratory and neurological symptoms are more common among mountaineers and persons from lowland going to the high altitude, little work has been done on the effect of hypoxia on digestive system in either patients with altitude illness or in healthy individuals at high altitude. In fact, symptoms of the digestive system such as anorexia, epigastric discomfort, epigastralgia, heart burn, dyspepsia, nausea, vomiting, diarrhea, haematemesis, piles and peptic ulcers are frequently found in mountaineers and altitude sojourners[1,2]. Moreover, epidemiological and clinical studies suggest that gastrointestinal bleeding (GIB) is not uncommon at high altitude, and is often life-threatening[3,4]. There are two diagnostic criteria for acute mountain sickness (AMS), one is the ESQ Ⅲ[5] and the other is the Lake Louise consensus scoring system[6]. Gastrointestinal symptoms include nausea/vomiting, loss of appetite, stomach/abdominal pain, constipation,

however, the GIB is not included in the diagnostic criteria. Furthermore, data on GIB are available from Japanese, Chinese, and Peruvians, but rarely reported in western people[7].

Altitude problems are of great importance for the railroad construction workers at high altitude. The construction of railroad on Mountain Tanggula offered a unique opportunity for investigation and study of AMS, high altitude pulmonary edema (HAPE), and high altitude cerebral edema (HACE), as well as high altitude GIB. This paper describes the incidence, clinical features, and risk factors for GIB in the railroad construction workers on Mountain Tanggula.

MATERIALS AND METHODS

Areas and subjects

Between June 29, 2001 and October 31, 2003, altitude gastrointestinal problems including altitude GIB were studied at two hospitals near the construction site. One hospital is located on the Fenghoushan at an altitude of 4779 m and the other hospital is situated in the Kekexili area at an altitude of 4505 m. These two hospitals received patients from the construction sites, working at altitudes between 3486 m and 4905 m. A total of 8014 workers worked at Fenghoushan and 5488 in Kekexili over the past three years. The weather conditions in the two surveying regions and the evacuated areas in Golmud and Xining are summarized in Table 1.

The weather and climatologic data were provided by the Tanggula Meteorological Observatory Station and the Qinghai Weather Bureau. Workers were not only exposed to a hypoxic environment, but also to severe cold. The temperature in winter ranged between -27℃ and -36℃, with an annual average temperature of -3℃ to -7℃.

A questionnaire was delivered to the persons to be investigated, including age, gender, ethnicity, occupation, place of birth, length of time at low altitude, length of time after ascending to high altitude, history of smoking and consumption of alcoholic beverages, current and past medical history, and family history.

All subjects underwent a careful medical evaluation before and after ascending to high altitude. Physical examination, routine blood tests, chest roentgenograms, electrocardiograms, *etc* were performed. The protocol was approved by the Qinghai High Altitude Medical Research Institute Committee on Human Research. Informed consent was obtained verbally for each subject.

Diagnosis

The diagnosis of AMS was made using the Lake Louise scoring system (LLSS) in which two or more of symptoms monitored were defined as AMS[6]. The clinical diagnosis of GIB was based on the following criteria: (1) occurrence in unacclimatized individuals who were rapidly exposed to altitudes exceeding 3000 m; (2) onset of typical symptoms including epigastric discomfort, epigastric pain, haematemesis, melaena, or hematochezia; (3) significant decrease in hemoglobin concentration (Hb) or hematocrit value (Hct); (4) endoscopic diagnosis of GIB after descending to the Golmud (2808 m) or Xining (2261 m); (5) disappearance of symptoms and signs after treatment with blood transfusion and oxygen. Outcome was assessed according to the clinical and laboratory results.

Table 1 Weather conditions in the two surveying regions and the two evacuated areas-Golmud and Xining

Area	Fenghoushan	Kekexili	Golmud	Xining
Altitude (m)	4905	4505	2808	2261
PB (mmHg)	417	440	538	585
Average annual temperature (℃)	-7.0	-2.6	3.6	6.7
Annual precipitation (mm)	317	291	42	371
Annual sunshine time (h)	2712	2764	3101	2793
Relative humility (%)	57	58	34	57

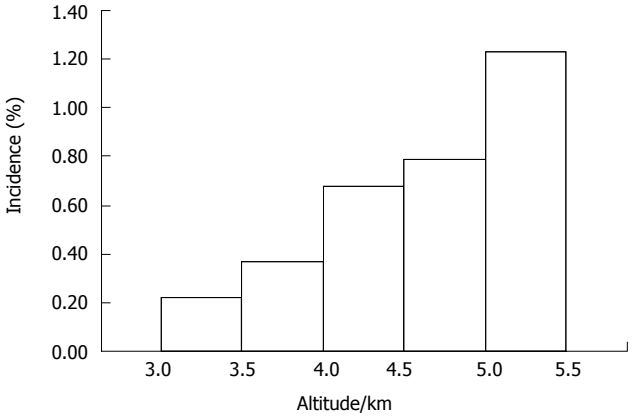

Figure 1 Frequency distribution of altitudes in patients with gastrointestinal bleeding diagnosed at two hospitals on Mountain Tanggula. The incidence of GIB increases with increasing altitude.

Statistical analysis

Statistical analysis was made by the IBM 3990 system. The incidence (cumulative case rate over a defined period in a defined population) of GIB in these populations was calculated. The frequency of risk factors for GIB was examined, using two by two tables, odds ratios, and chi square test. Comparison of mean numerical values was made by t test. $P < 0.05$ was considered statistically significant.

RESULTS

Overall incidence

We selected two typical areas where the local hospitals are located to investigate the altitude illness. From 2001 to 2003, GIB was found in 66 cases of 13502 workers on Mountain Tanggula during the period with an incidence of 0.49%.

Predisposing factors

The incidence of GIB was also found to be dependent upon many variables, including altitude, length of stay at high altitude, age, sex, labouring conditions, and ethnicity.

Altitude: The incidence of GIB at various altitudes is shown in Figure 1. Occurrence of GIB was rarely found below 3500 m. The highest frequency of GIB

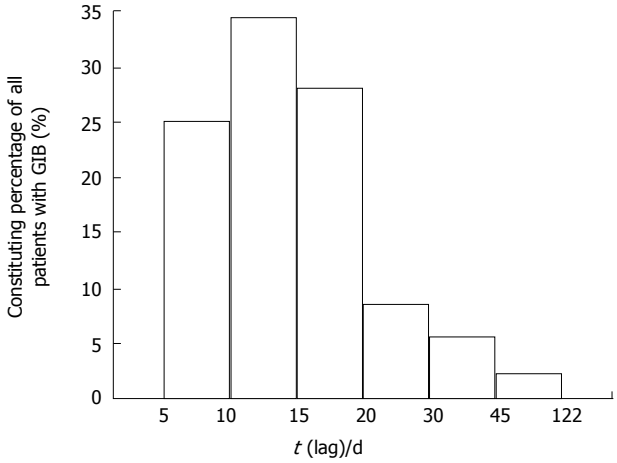

Figure 2 Time lag between ascent and onset of illness.

was observed between 4500 m and 5000 m, its incidence increased gradually with altitudes being 0.2% at 3500 m and 1.1% at 4905 m ($P < 0.01$).

Onset time of symptoms: Symptoms suggestive of GIB occurred in 17 out of 66 cases (25.8%) within 5-10 d after arrival at high altitude, in 24 cases (36.3%) within 11-15 d, 14 cases (21.2%) within 16-20 d, the remaining 11 cases(16.7%) within 21-122 d (16.7%) (Figure 2). The onset time of most symptoms was within three weeks after arrival at high altitude.

Age and gender: Many of the patients were young or middle-age adults, and the oldest was 46 years of age. The mean age of all cases was 34 ± 7.8 years.

GIB occurred frequently in men. Since the total number of females was small (21 persons), and could be neglected.

Occupation: The incidence of GIB in workers and carders was 0.51% and 0.46%, respectively. There was no significant difference between the two groups ($P > 0.05$).

Ethnicity: Interestingly, all the GIB patients were Han Chinese lowlanders. Over one-third of the workers were native highlanders (most of them were Tibetans who permanently lived at altitudes from 2500 m to 3200 m) and no GIB was found in them.

Endoscopic findings

All patients with altitude GIB were evacuated to the hospitals in Golmud or Xining. Among them, 28 had an endoscopic examination either at admission or within 24 h after admission and others were not able or refused to undergo an endoscopic examination. Endoscopic examination showed gastric ulcer in 11 cases, duodenal ulcer in 4, combined ulcers in 4, hemorrhage erosion in 5, bleeding gastritis in 4 and chronic atrophic gastritis in 1, respectively.

Risk factors

GIB was obviously related to drinking alcohol and use of aspirin and/or dexamethasone in 3 patients. Case one was a 37-year old railroad worker from lowland to a construction site at 4505 m. During the ascent, he was given 8 mg dexamethasone followed by 4 mg every eight hours for AMS prophylaxis. In the morning after arrival at 4505 m, he complained of severe headache. He was given 0.5 g of aspirin and dexamethasone, which did not relieve his headache. He drank approximately 300 mL of liquor (50% alcohol). After eight hours he suddenly became incapacitated with symptoms of upset stomach, abdominal pain, and severe fatigue. At about 6.0 AM on the third day, he had melaena and tarry black stool, thus aspirin and dexamethasone were immediately stopped. Within a few hours his condition became progressively worsened, and he was promptly evacuated to the Golmud Hospital (2808 m). At admission, his BP was 90/50 mmHg and Hb level was below 65 g/L. Gastro-fiberscopic examination was performed within six hours after admission and revealed diffuse gastric bleeding and erosion, and linear gastric ulcer combined with duodenal ulcer. Supplementary oxygen was given and an intravenous drip was put up. After 600 mL whole blood transfusion over about five hours, and administration of H_2 blocker (ranitidine), his BP gradually increased (110/80 mmHg), and malaena was stopped. He slowly improved over two weeks, his Hb increased to 105 g/L. He was discharged 21 d after admission and returned to his lowland home.

In addition to this case, we encountered 2 similar cases at the Kekexili construction site. Case two was a healthy young man who took aspirin and dexamethasone to prevent AMS and drank alcohol in the evening, he had brisk melaena in the next morning. Case three was a middle age worker, with a previous history of gastric peptic ulcer. He took aspirin for headache, after drinking 100 mL of hard liquor, he developed acute melaena.

Polycythemia (Hb > 210 g/L) was found in 5 patients with GIB having lived at altitude above 4000 m for more than 45 d.

Moreover six patients with GIB had a previous history of potential peptic ulcer and 5 had chronic gastritis.

Outcomes

Once the diagnosis was confirmed, the patients were either evacuated to the Golmud Hospital (2808 m), or treated as outpatients or sent to Xining (2261 m). Their conditions gradually improved after effective treatments.

DISCUSSION

Nomenclature and relation between AMS and altitude GIB

High-altitude GIB is a distinct clinical entity. However, the different terms of this syndrome have been used by different authors. The term "hypoxic gastric bleeding" is used loosely in some Peruvian scientists[8], "altitude digestive hemorrhage" is also used for this illness[9]. Since hemorrhage could occur in buccal mucosa, digestive mucosa, finger nails, as well as in gastrointestinal tract, urinary tract, retina and gums[10,11], it is named as "high altitude hemorrhage syndrome". GIB is one of the clinical manifestations of this syndrome[11]. However, GIB is almost an independent digestive mucosal lesion, causing gastrointestinal bleeding at high altitude. We hold that the term "high altitude gastrointestinal bleeding" (altitude GIB) is more suitable for this condition.

We also noted that approximately 58% of GIB patients are accompanied with AMS, and about 42% have altitude GIB alone. However, GIB has not been found to be associated with HAPE or HACE. Thus whether altitude GIB is a gastrointestinal type of AMS should be further studied.

Incidence of altitude GIB

The incidence of altitude GIB among workers constructing Qinghai-Tibetan highway on Mountain Tanggula from 1978 to 1984 was 1.1%[4]. The incidence of altitude GIB in workers constructing the Qinghai-Tibetan railroad at the same mountainous areas was 0.49% in 2001-2003, which is much lower than the reported incidence in mountaineers on Everest. During 1988 the China-Japan-Nepal Friendship Expedition to Mountain Qomolungma (Everest), a total of 52 Japanese mountaineers climbed from Tibetan (north) side (5154 m) to the summit (7790 m), five on the north side suffered from upper alimentary bleeding with an incidence of 9.6%[12], suggesting that the incidence of GIB increases with the increase of altitude.

Liu[13] reported that the occurrence of GIB in soldiers stationed between 3700 m and 5380 m for one year is 0.8% of the total patients and 1.5% of AMS cases at a Chinese Army Hospital located at the foot of Mountain Karakoram (3550 m) during the same period. However, endoscopy examination showed that the incidence of acute gastric mucosal lesion (AGML) in mountaineers is as high as 16%-49%[14-16], suggesting that some subclinical GIB exists.

Clinical features of altitude GIB

Of the 66 cases, 17 had altitude GIB within 10 d after arrival at above 3500 m. Most patients (55) had altitude GIB within 20 d, and 11 had altitude GIB after 21 d. These observations were incomparable with the onset of HAPE or HACE. In general, the mean time of HAPE or HACE occurrence after arrival at above 3500 m was three days with a range of 1-5 d.

The victims of GIB include both mountaineers and native highlanders[8,17]. Macedo[8] reported that two adult male native Quechua Indians presented a sudden and severe gastric bleeding of unknown etiology in the Andes. However, in our GIB patients, there were no Tibetan natives. It is possible that these individuals have greater genetic resistance to hypoxia at high altitude.

At high altitude, GIB may be manifested as haematemesis (vomiting of blood, either bright red or brown in color), melaena (tarry black, sticky stool) or hematochezia (fresh red blood per rectum, ruling out the diagnosis of piles). However, hemorrhage was manifested as melaena in almost all 64 patients except for two with haematemesis. Bleeding, however, might be occult, with normal appearance of stools. Occult blood in stools was detected in 10 mountaineers by Naito *et al*[18] using "OC-Hemodia Kit" which can detect only human hemoglobin without cross-reaction in any other animals during their Iwate Karakoram expedition in 1989, a total of 8 persons presented a positive reaction, suggesting that silent bleeding from gastrointestinal mucosa commonly exists in mountaineers.

GIB gives rise to symptoms and signs depending upon the rate and extent of bleeding. In our experiences, acute moderate bleeding (blood loss greater than 500 to 1000 mL) results in drowsiness, dizziness, oliguria, sweating and pallor. BP changes occur first in the form of orthostatic hypotension. Pulse rate seems to be a far less accurate parameter, particularly at high altitude, as tachycardia is common amongst such mountaineers. Acute massive bleeding is characterized by loss of greater than 1500 mL or 25% of the circulating blood volume within a period of minutes to hours, decreased systolic and diastolic BP, increased pulse rate, decreased hemoglobin concentration or Hct values. It is a critical indicator for the desperate situation. Therefore any patient experiencing malaena with or without hematemesis or associated symptoms or hypotension, should be evacuated promptly and hospitalized immediately for further evaluation and treatment[4].

Endoscopic findings and causes of altitude GIB

Endoscopy is highly advisable. Sugie *et al*[19] found gastro-duodenal mucosa lesions in 13 out of 22 mountaineers at Mountain Xixapangma (5020 m). The results of arterial blood gas analysis reported by Sugie *et al*[20] are as follows: PaO2 = 43 mmHg, PaCO2 = 23.5 mmHg, pH = 7.51, BE = 1.0. Zhao and Li[15,16] reported that the incidence of gastro-duodenal mucosal lesions is 49% in 51 young healthy male subjects at the altitude between 3658 m and 4200 m. Occasionally, upper digestive hemorrhage may occur in gastric cancer patients at altitude[21,22].

Saito[12] reported a male mountaineer on Mt. Everest expedition who developed massive GIB and serious anemia at the altitude of 7028 m. Endoscopy after his arrival at sea level, showed no abnormality[23]. Zhou[24] reported a case of a healthy lowland Han subject who developed GIB during a sojourn at Lhasa (3658 m) and died of recurrent massive GIB. Postmortem revealed diffuse superficial erosion in the stomach but no peptic ulcers.

Mechanism of altitude GIB

The mechanism of altitude GIB remains unclear. Pathological studies in patients died of altitude GIB revealed significant dilatation of arterioles and venules, formation of extensive blood capillaries in gastric mucosa[25] and hemorrhage into the gastric mucosa[26]. Different kinds of stress can cause AGML. It was reported that cold or hypoxic stress can induce AGML in rats[27,28]. However, on high mountains, cold stress usually accompanies the effects of hypoxic stress in mountaineers, suggesting that hypoxemia is probably the main factor for AGML in mountaineers who are healthy at sea level[19]. Kamiyama *et al*[29] have attributed the potential difference (PD) to the indicator of gastric integrity or gastric mucosa defensive mechanism that may play an important role in the pathogenesis of hypoxia-induced AGML. The PD is closely related to the transport of electrolytes by gastric mucosa cells depending on aerobic metabolism. Hypoxemia may cause changes

in tissue levels of oxygen resulting in decrease of PD. Strenuous exertion and hard work increase hypoxia stress and induce injury of gastric mucosa capillaries[14,17]. Naito *et al*[30] noted that peroxidation of phosohatidylcholine in gastric mucosa is another possible mechanism underlying AGML at high altitude. It was reported that ulcer index (UI) and phosphatidylcholine hydroperoxide (PCOOH) are higher in hypoxia group than in control group, though thiobarbituric acid (TBA) substance does not differ between the two groups, suggesting that lipid peroxidation in gastric mucosa may play a role in the pathogenesis of hypoxia-induced AGML. Acute diffuse lesions induced by stresses are pathologically and clinically distinct from gastro-duodenal mucosa lesions and present as an upper alimentary bleeding.

Fisk factors for altitude GIB

Alcohol: It is historically believed that alcohol could relieve and protect against AMS[4]. More recently, Houston[31] has recommended less alcohol use on mountains. It appears that alcohol may also be a risk factor for GIB at altitude. Ravenhill[32] has observed that alcohol increases the severity of symptoms of AMS. Those who drink a little alcohol under a simulated hypoxic condition (7620 m), may impair their mental and physical function[33]. Steele[34] has described three Sherpas who had severe epigastric pain, nausea and vomiting after heavy drinking on Mountain Everest. Zhou[24] reported three young men in Lhasa who developed massive gastric hemorrhage due to acute hemorrhagic gastritis after a hard drinking. High altitude native populations, such as Quechua Indians, like to drink inferior rough alcohol, which may be the aetiology of the increased prevalence of gastric ulceration[26]. From 1978 to 1984 when the Qinghai-Tibetan Highway was under construction, the incidence of GIB was higher (1.93%) in workers who drank more of it than in those (0.95%) who drank it less[4], suggesting that drinking alcohol increases the risk of developing GIB at altitude and alcohol should be avoided.

Aspirin or other NSAID agents: Aspirin has been shown to be effective in treating headache due to AMS[35]. Aspirin alone is not very effective in preventing headache due to AMS, whereas aspirin in combination with dexamethasone can achieve rather good results[36]. There is strong but not conclusive evidence that major bleeding episodes could result from acute, diffuse hemorrhagic lesions in the upper GI tract after ingestion of aspirin. Thus, relief of headache due to AMS is a difficult matter because aspirin and other non-steroidal anti-inflammatory drugs (NSAID) lead to GIB[7,37]. It was reported that drugs such as paracetamol (acetaminophen) or ibuprofen, have a strong anti-inflammatory action on headache or other pains and do not cause gastrointestinal bleeding[38].

Dexamethasone: Dexamethasone has been used in the prevention and treatment of AMS[39,40] because administration of it for a short time does not result in any problems at high altitude[31]. However, dexamethasone is one of the drugs that are strongly suspected of being ulcerogenic, especially in patients with a prior history of peptic ulcer disease, and may increase the risk of GIB at altitude. Concomitant use of dexamethasone, aspirin and alcohol has an additive or synergistic effect on the upper GI tract mucosa, and could lead to rapid and serious GIB as in our cases.

High altitude polycythemia: Polycythemia is a common feature seen in altitude residents and patients with hypoxemia[15,16,24]. Digestive symptoms such as epigastric pain, dyspepsia, anorexia, vomiting, and diarrhea can be frequently eliminated in 89%-100% of patients with high altitude polycythemia (HAPC)[24]. GIB is a common complication of HAPC. In our series five patients with GIB had HAPC. Zhou[24] reported polycythemia in 21 young male Chinese soldiers (mean age 26.6 years) stationed in Lhasa (3658 m) who had no previous history of peptic ulcer. GIB occurred following development of HAPC. They found that exposure to cold, strenuous exertion, and drinking alcohol are the main predisposing causes.

Zhao and Li[15,16] have reported their endoscopic examinations in 98 patients with HAPC (Hb > 210 g/L) in Lhasa, showing superficial gastritis in 29, gastric ulcer in 26, duodenal ulcer in 12, complex ulcers in 5, and atrophic gastritis in 3. Chu and Sun[41] examined 5 patients with HAPC (mean Hb = 225 g/L) in Madou (4300 m), diffuse bleeding and erosion as well as ulcerous necrosis were observed in their stomach, and electromicroscopic examination showed the ultrastructural characteristics of their gastric mucosal biopsies, such as irregularly arranged thick microvilli, microfilament enlargement of secretory canaliculus, and high density of enlarged mitochondria in parietal cells, increased zymogen granules and rough endoplasmic reticulum in principal cells, proliferation of vascular endothelial cells, microvilli-like appearance of their surface and basement membrance thickening. Such gastric mucosal lesions may be associated with gastric mucosal ischemia caused by microvascular thrombosis due to excessive polycythemia.

Peptic ulcerations at high altitude: Clinical observations on the Himalayas and Andes suggest that peptic ulcer occurs more frequently at high altitude than at sea level[21,24,42]. At high altitude, the ulceration rate is higher in gastric ulcer than in duodenal ulcer[43,44]. Berrio *et al*[42] reported that 100 cases of GIB have been diagnosed by endoscopic examinations in General Hospital at La Oroya (3800 m), gastric ulcer accounting for 33%, duodenal ulcer accounting for 23%, gastric erosion accounting for 23%, neoplasias accounting for 2%, respectively. The prevalence of gastric ulcer increases with increasing altitude, while the prevalence of duodenal ulcer does not[42]. Upper digestive hemorrhage is a common complication of peptic ulceration at high altitude[42,45], the hemorrhagic rate is 20%-66%[9,45].

It is well known that the incidence of gastric ulcers and bleeding is increasing in high altitude residents chronically exposed to a hypoxic environment[42,45-47]. In addition, hypoxic and cold stress-induced gastric mucosal lesion may explain in part, the high incidence of gastric ulcers in altitude populations.

In the present 66 cases of GIB, 4 had a previous history of peptic ulcer. Among them, GIB occurred

rapidly in 1 patient after using aspirin, suggesting that persons with known peptic ulceration should not go to high altitude mountains unless their symptoms have been well controlled before they go to high altitude mountains as complications in the field can be fatal[37].

Course and prognosis of altitude GIB

Altitude GIB can be life threatening and acute massive bleeding due to secondary effects of shock-increasing anoxia, cellular dysfunction and acidosis at high mountains may lead to death[4]. We have reported that the mortality of altitude GIB is as high as 6.8% in Qinghai-Tibetan Highway construction workers on Mountain Tanggula[4].

The emergency measures taken for acute altitude GID include early evacuation or just descent with oxygen inhalation and saline-infusion or blood transfusion. Drugs, such as H_2 blockers or proton pump inhibitors have been shown to be more effective in ameliorating GIB[4]. Mountaineers and highlanders should know well about the symptomatic self care (SSC) for altitude GIB[48], that is when symptoms such as epigastric pain or dyspepsia are present, a H2-receptor antagonist is effective for ulcers and GIB and the current therapy for altitude GIB.

In conclusion, early diagnosis, treatment and evacuation lead to an early recovery. Death due to altitude GIB can be avoided if early symptoms and signs are recognized.

REFERENCES

1 **Bhattacharjya B,** editor. Mountain Sickness. Toronto: Bristol John Wright & Sons LTD, 1964
2 **Hu HC**, Wu TY, Li TL, editors. High Altitude Disease. (In Chinese). Xining: Qinghai Publishing House, 1997: 65-68
3 **Berrios J.** Consideraciones sobre la pathologia digestive en los habitentes de las grandes alturas del Peru. (In Spanish). *Rev Gastroenterol Peru* 1982; **2**: 21-28
4 **Wu TY.** Take note of altitude gastrointestinal bleeding. *Newsletter Int Soc Mountain Med* 2001; **10**: 9-11
5 **Sampson JB**, Cymerman A, Burse RL, Maher JT, Rock PB. Procedures for the measurement of acute mountain sickness. *Aviat Space Environ Med* 1983; **54**: 1063-1073
6 **Roach RC,** Bärtsch P, Hackett PH, Oelz O. The Lake Louse acute mountain sicknedd scoring system. In: Sutton JR, Houston CS, Coates G, editors. Hypoxia and Molecular Biology. Burlington, VT: Queen City Press, 1995: 272-274
7 **Editorial.** October case discussion. *ISMM Newsletter* 1999; **9**: 13-15
8 **Macedo Dianderas J**. Hemorragias gastricas por hipoxia de altura. (In Spanish). *Arch Inst Biol Andina Lima* 1968; **2**: 183-187
9 **Monge ES**, Diaz JF. Aparato gastrointestinal. En: C.C. Monge and F. Leon-Velarde, editors. El RETO Fisiologico de vivir en los ANDES. (In Spanish). Lima: Universidad Peruana Cayatano Heredia, 2003: 227-229
10 **Heath D**. The morbid anatomy of high altitude. *Postgrad Med J* 1979; **55**: 502-511
11 **Li SP**. High-altitude hemorrhage syndrome. *J Wilderness Med* 1993; **4**: 115-117
12 **Saito A.** The medical reports of the China-Japan-Nepal Friendship Expedition to Mt. Qomolungma/Sagamatha (Everest). *Jap J Mount Med* 1989; **9**: 83-87
13 **Liu MF**. Upper alimentary bleeding at high altitude. In: Lu YD, Li KX, Yin ZY, editors. High Altitude Medicine and Physiology. (In Chinese). Tianjing: Tianjing Science & Technology Press, 1995: 586
14 **Nakashima M,** Saito A, Endo K, Matsubayashi. K, Jin-Nouchi Y, Seto T, Demizu A, Hirata K. Sugie T, Kan N, Tobe T, Nayashi K, Adachi M, Kubo S. The report of Kyoto University Medical Research Expedition to Xixabangma (8027 m) 1999 (KUMREX' 90). *Jap J Mount Med* 1990; **10:** 135-144
15 **Zhao GB**, Li R. The gastrointestinal mucosal lesions in patients with high altitude polycythemia. *Zhonghua Yixue Zazhi* 1991; **71**: 611-612
16 **Zhao GB**, Li L. Impairment of the digestive system in high altitude erythrocythemia. *Zhonghua Neike Zazhi* 1991; **30**: 492-494
17 **Macedo Dianderas J**, Hemorragia gastricas en la altura (4540 m. Sebre el nivel del mar). (In Spanish). *Arch Inst Biol Andina Lima* 1965; **1**: 53-56
18 **Naito H**, Matuno A, Sakai I, Kamiyama Y, Doi T, Kobari M, Rahman M. Takita A, and Matsuda T. Gastrointestinal symptoms in high mountain climbing-Medical report in Iwate Karakoram Friendship Expedition on 1989. In: G. Ueda, JT Reeves, M Sekigushi, editors. High Altitude Medicine. Matsumoto: Shinshu University Press, 1992: 286-299
19 **Sugie T,** Adachi M, Jin-Nouchi Y, Matsubayashi K, Nakashima M, Saito A. Gastroduodenal mucosa lesion at high altitude. *Jap J Mount Med* 1991; **11**: 55-58
20 **Sugie T**, Kan N, Saito A, Tobe T, Adachi M, Jin-Nouchi Y, Matsubayashi K, Nakashima M. Acute gastric mucosal lesion at the high altitude. In: Sutton JR, Coates G, Houston C, editors. Hypoxia and Mountain Medicine. Burlington: Queen City Printers Inc., 1992: 320
21 **Berrios J**, Zapata C, Nago A, Bussaleu A, Farfan G. Estudio comparativo de la patologia digestiva de las grandes Alturas y del nivel del mar en el Peru. (In Spanish). En: III Jornades Cientificas. En bomenaje al centenario del nacimiento del professor doctor Carlos Monge Medrano. Enero 21-26 de 1985. Lima: Universidad Peruana Cayatano Heredia, 1985: 197
22 **Villanueva Palacios J**, López de Guimaraes D, Avila Polo F. Upper digestive tract hemorrhage in the Peruvian Andes: report of 115 cases observed in Huaraz. *Rev Gastroenterol Peru* 1976; **16**: 99-104
23 **Masuyama M**. A discussion on the October case discussion. *ISMM Newsletter* 1999; **9**: 13-15
24 **Cao ZW**. editor. High Altitude Polycythemia. Beijing: Military Medical Science Press, 1996: 96-97
25 **Zevallos G,** Meiller M. Algunos aspectos histopathologicos de la ulcers gastroduodenal en la altura. (In Spanish). *Rev Asoc Med Prov Yauli* (Peru) 1959; **4**: 66-73
26 **Heath D**, Williams DR, editors. High Altitude Medicine and Pathology. Oxford: Oxford University Press, 1995: 258-259
27 **Kamiyama Y**, Sakai I, Naito H, Kobari M, Matsuno S, Tsuchiya T, Oketani K. Pathogenesis and prevention of experimental acute gastric ulcers by cold restraint stress. In: Ueda G, Kusama GS, Voelkel NF, editors. High Altitude Medical Science. Matsumoto: Shinshu University Press, 1988: 454-457
28 **Aichi M**. Experimental studies on development of gastric mucosal damage following acute hypoxemia in Rats (author's transl). *Nihon Shokakibyo Gakkai Zasshi* 1980; **77**: 1223-1233
29 **Kamiyama Y**, Matsuno S, Sakai I, and Naito H. Pathogenesis of experimental acute mucosal lesion induced by hypoxia in rats. In: Ueda G, Reeves JT, Sekiguch IM. editors. High Altitude Medicine. Matsumoto: Shinshu University Press, 1992: 280-285
30 **Naito H**, Masuko T, Kamiyama Y, Sakai I, Matsuno S. A possible role of lipid peroxidation in the pathogenesis of acute gastric mucosal lesion induced by hypoxia. Abstracts of the Third World Congress on Mountain Medicine. Matsumoto: Shinshu University Press, 1998: 111
31 **Houston CS**. editor. Go Higher, Oxygen, Man, and Mountain. 4th edition. Shrewsbury: Swan Hill Press, 1998: 157, 164
32 **Ravenhill TH**. Some experience of mountain sickness in the Andes. *J Tropical Med & Hygiene* 1913; **16**: 313-320
33 **Nettles JL**, Olson RN. Effects of alcohol on hypoxia. *JAMA* 1965; **194**: 1193-1194
34 **Steele P**. Medicine on Mount Everest 1971. *Lancet* 1971; **2**: 32-39
35 **Burtscher M**, Likar R, Nachbauer W, Philadelphy M. Aspirin for prophylaxis against headache at high altitudes: randomised, double blind, placebo controlled trial. *BMJ* 1998;

316: 1057-1058
36 **Burtscher MB**, Philadelphy M, Likar R, and Nachbauer W. Aspirin versus diamox plus aspirin for headache during physical activity at high altitude (Abst.) In: Roach RC, Wagner PD, Hackett PH, editors. Hypoxia: Into the Next Millennium. New York: Plenum/Kluwer, 1999: 133
37 **Ward MP**, Milledge JS, West JB, editors. High Altitude Medicine and Physiology. New York: Oxford University Press Inc, 2000: 326-327
38 **Broome JR**, Stoneham MD, Beeley JM, Milledge JS, Hughes AS. High altitude headache: treatment with ibuprofen. *Aviat Space Environ Med* 1994; **65**: 19-20
39 **Hackett PH**, Roach RC, Wood RA, Foutch RG, Meehan RT, Rennie D, Mills WJ. Dexamethasone for prevention and treatment of acute mountain sickness. *Aviat Space Environ Med* 1988; **59**: 950-954
40 **Rabold M.** Dexamethasone for prophylaxis and treatment of acute mountain sickness. *J Wilderness Med* 1992; **2**: 54-60
41 **Chu XQ**, Sun HF. Ultrastructural characteristics of gastric mucosa inpatients with high altitude polycythemia. Abstracts of the Third World Congress on Mountain Medicine and High Altitude Physiology. Matsumoto: Shinshu Universith Press, 1998: 164
42 **Berríos J**, Sedano O, Calle E, Montero F, Manrique J, Hinostroza E. Upper digestive hemorrhage in the inhabitants of high altitudes in Peru. *Rev Gastroenterol Peru* 1996; **16**: 13-18
43 **Garrido-Klinge G**, Pena L. Ulcera peptica en la altura. (In Spanish). *Diagnostico* (Peru) 1982; **10**: 70-72
44 **Garrido-Klinge G**, Pena L. The gastro-duodenal ulcer in high altitudes. *Gastroenterology* 1959; **37**: 390-400
45 **Garrido-Klinge G**, Pena L. La ulcera gastroduodenal en las grandes Alturas (Andes Peruanos). (In Spanish). *An Fac Med* (Lima) 1960; **43**: 419-436
46 **Maccagno FV**. Ulcera gastro-duodenal en la altura. (In Spanish). *Rev Asoc Med Prov Yauli* (Peru) 1960; **5**: 74-100
47 **Garrido-Klinge G**, Pena L. Ulcera peptica en la altura. (In Spanish). *Diagnostico* (Peru) 1982; **10**: 70-72
48 **Editorial**. The Symptomatic Self Care for prevention and treatment of patients with peptic ulcerations. Chinese Health News, 1999-11-11

S- Editor Wang GP **L- Editor** Wang XL **E- Editor** Ma WH

PO Box 2345, Beijing 100023, China
www.wjgnet.com
wjg@wjgnet.com

World J Gastroenterol 2007 February 7; 13(5): 781-784
World Journal of Gastroenterology ISSN 1007-9327

RAPID COMMUNICATION

Differences in characteristics of patients with and without known risk factors for hepatocellular carcinoma in the United States

Jon D Dorfman, Richard Schulick, Michael A Choti, Jean-Francois H Geschwind, Ihab Kamel, Michael Torbenson, Paul J Thuluvath

Jon D Dorfman, Richard Schulick, Michael A Choti, Department of Surgery, The Johns Hopkins University School of Medicine, Baltimore, MD 21205, United States
Jean-Francois H Geschwind, Ihab Kamel, Department of Radiology, The Johns Hopkins University School of Medicine, Baltimore, MD 21205, United States
Michael Torbenson, Department of Pathology, The Johns Hopkins University School of Medicine, Baltimore, MD 21205, United States
Paul J Thuluvath, Department of Medicine, The Johns Hopkins University School of Medicine, Baltimore, MD 21205, United States
Correspondence to: Paul J Thuluvath, MD, FRCP, The Johns Hopkins Hospital, Rm 429, 1830 E. Monument Street, Baltimore, MD 2105, United States. pjthuluv@jhmi.edu
Telephone: +1-410-6145389 Fax: +1-410-6149612
Received: 2006-09-21 Accepted: 2006-12-13

Abstract

AIM: To examine the clinical characteristics of a subgroup of patients with hepatocellular carcinoma (HCC) and compare them to those with known risk factors.

METHODS: We used the HCC database of 306 patients seen at our institution from January 1, 1995 to December 31, 2001. Of the 306 patients, 63 (20%, group 1) had no known risk factors (hepatitis C virus, hepatitis B virus, alcohol, hemochromatosis or cirrhosis from any cause) and 243 (group 2) had one or more risk factors.

RESULTS: The median age was similar in both groups, but there were disproportionate numbers of younger (< 30 years old), older (> 80 years) patients, women (33% *vs* 18%), and Caucasians (81% *vs* 52%) in group 1 as compared to group 2. There were fewer Asians (2% *vs* 11%) and African Americans (13% *vs* 27%) in group 1. Abdominal pain (70% *vs* 37%) was more common while gastrointestinal bleeding (0% *vs* 11%) and ascites (4% *vs* 17%) were less common in group 1 compared to group 2. Group 1 had larger tumor burden (median size 9.4 cm *vs* 5.7 cm) at the time of presentation, but there were no differences in the site (right, left or bilateral lesions), or number of tumors between the two groups.

CONCLUSION: HCC patients without identifiable risk factors have different characteristics and clinical presentation compared to those with known risk factors. Absence of cirrhosis and larger tumor burden may explain the differences in the presenting symptoms.

Key words: Hepatocellular carcinoma; Patient characteristics; Risk factors

Dorfman JD, Schulick R, Choti MA, Geschwind JFH, Kamel I, Torbenson M, Thuluvath PJ. Differences in characteristics of patients with and without known risk factors for hepatocellular carcinoma in the United States. *World J Gastroenterol* 2007; 13(5): 781-784

http://www.wjgnet.com/1007-9327/13/781.asp

INTRODUCTION

Hepatocellular carcinoma (HCC) is a common cancer in the world with more than 500 000 new cases reported per year[1,2]. The disease is unevenly distributed worldwide with a higher incidence in South-East Asia and Sub-Saharan Africa than in other regions of the world[1,2]. Although it is less common in the United States and Western Europe, there are data to suggest that the incidence may be increasing secondary to hepatitis C virus (HCV)[1-5]. The common risk factors that predispose to HCC include hepatitis B virus (HBV), hepatitis C virus (HCV), aflatoxin, and cirrhosis in general[6-9]. In addition, hemochromatosis, alcoholism, and non-alcoholic fatty liver disease (NAFLD cirrhosis) increase the risk of developing HCC[10]. In the United States, alcoholism and hepatitis C are the leading predisposing causes of HCC[11]. However, a significant proportion of patients develop HCC despite the absence of any known risk factors including cirrhosis. There is only limited information on the differences in the characteristics and outcomes of patients with or without risk factors who develop liver cancer in the USA.

The purpose of this study was to define the clinical characteristics and presentation of patients without identifiable risk factors and compare them to those with known risk factors.

MATERIALS AND METHODS

For the purpose of this study, we studied patients who

Table 1 Patient characteristics *n* (%)

Category	Group 1 (*n* = 63)	Group 2 (*n* = 243)	*P*
Sex			
Male	42 (67)	198 (82)	< 0.05
Female	21 (33)	45 (18)	
Age (yr)			
Median (range)	66 (18–87)	61 (23–87)	
< 30	5 (8)	3 (1)	< 0.01
30-39.9	3 (5)	10 (4)	
40-49.9	6 (10)	35 (14)	
50-59.9	9 (14)	65 (27)	
60-69.9	10 (16)	76 (31)	
70-79.9	17 (27)	44 (18)	
> 80	8 (13)	7 (3)	
Unknown	5 (8)	3 (1)	
Race			
Asian	1 (2)	27 (11)	< 0.05
African American	8 (31)	66 (27)	
Caucasian	51 (81)	125 (51)	
Hispanic	1 (2)	8 (3)	
Other	1 (1)	12 (5)	
Unknown	1 (1)	5 (2)	
Country			
US born	58 (92)	201 (83)	
Immigrant	2 (3)	28 (11)	
Foreign visitor	3 (5)	14 (6)	

Table 2 Symptoms and signs at presentation *n* (%)

	Group 1 (*n* = 46)	Group 2 (*n* = 217)	*P*
Symptoms			
Abdominal pain	32 (70)	81 (37)	< 0.001
Fatigue	7 (15)	39 (18)	
Anorexia	7 (15)	22 (10)	
Nausea and vomiting	7 (15)	23 (11)	
Change in bowel habits	3 (7)	15 (7)	
Gastrointestinal bleed	0 (0)	24 (11)	< 0.05
None	8 (17)	85 (39)	< 0.01
Signs			
Weight loss	12 (26)	38 (18)	
Abdominal mass	4 (9)	14 (7)	
Jaundice	3 (7)	26 (12)	
Fever	3 (7)	14 (7)	
Ascites	2 (4)	37 (17)	< 0.05
Encephalopathy	1 (2)	19 (9)	
None	25 (54)	113 (52)	

presented to the Johns Hopkins Hospital with HCC from January 1, 1995 to December 31, 2001. A retrospective database was created with the approval of the Institutional Review Board. Patients with HCC were identified for inclusion in the database by searching the medical records using an ICD-9 code for liver cancer (155.0) and the Database of Pathology Departments using the term "hepatocellular carcinoma". The information was collected on all patients using the hospital's electronic patient record.

To be included in the study, a patient was 18 years or older, visited Johns Hopkins Hospital during the designated period, and had a confirmatory diagnosis of HCC. HCC was diagnosed based on histological confirmation or an elevated alpha fetoprotein (AFP) > 400 IU/mL with a liver image showing characteristic features of HCC. In the absence of elevated AFP or histological confirmation, characteristic liver image along with a clinical history compatible with HCC was necessary[12]. A compatible clinical history included known cirrhosis, HBV or HCV infection, hemochromatosis or history of alcoholism.

The risk factors for HCC were defined as HBV, HCV, cirrhosis from any cause (based on imaging and/or liver histology), aflatoxin, alcoholism, hemochromatosis, pre-malignant liver tumors and rare metabolic syndromes that are known to predispose to HCC. Patients without any known identifiable risk factors were included in group 1 and compared to those patients with one or more risk factors (group 2).

Statistical analysis was performed with SPSS version 10.0. Statistical tests included chi-square and Student-*t* tests. $P < 0.05$ was considered statistically significant.

RESULTS

Three hundred and six patients were seen with HCC at our institution from January 1, 1995 to December 31, 2001. Of the 306 patients, 63 (20%, group 1) had no known risk factors (HCV, HBV, alcohol, hemochromatosis or cirrhosis from any cause) and 243 (group 2) had one or more risk factors.

Of the 243 patients (group 2) with a known risk factor for HCC, hepatitis B was documented in 49 (20%), hepatitis C was present in 110 (45%) and 115 (47%) acknowledged moderate or abusive alcohol use. Rare disorders such as Wilson's disease, porphyria cutaneous tarda, autoimmune hepatitis, schistosomiasis, and sclerosing cholangitis were noted in one patient each. Cirrhosis was documented by histology in 164 (67%).

Demographic data of both groups are shown in Table 1. There was a male predominance in both groups but there was a higher proportion of females in group 1 (2:1 *vs* 9:2) compared to group 2. The median age was greater in group 1 with a disproportionate distribution of patients at the extremes of age.

Presenting signs and symptoms are shown in Table 2, with complete data available in 263 of the 306 patients. The most common presenting symptom in each group was abdominal pain, but it was more common in group 1. Other statistically significant differences noted were the frequency of gastrointestinal bleeding and the presence of ascites. Weight loss was comparable in both groups. As expected , HCC was not diagnosed during routine screening or surveillance in any patient of group 1 but in 46 (21%) of group 2 ($P < 0.001$).

Diagnostic imaging data revealed differences between groups 1 and 2 (Table 3). We excluded studies that were not done at our institution since films were not available for confirmation. Imaging studies showed a larger tumor diameter (median 9.3 cm, range 4-25 cm *vs* 5.7 cm, range 0.7-20 cm) in group 1 than 2. Approximately half of the patients (52% and 48%) in both groups had a solitary tumor, and the majority of tumors were located in the right liver (67% and 60%). A higher proportion of patients in group 2 had bilateral tumors (7% *vs* 24%, P = NS). Portal vein involvement was similar in both groups.

Histological examination demonstrated fibrolamellar

Table 3 Tumor imaging characteristics

	Group 1	Group 2
Size	*n* = 24	*n* = 159
Median (cm)	9.3	5.7
Minimum (cm)	4	0.7
Maximum (cm)	25	20
	n (%)	*n* (%)
< 2 (cm)	0 (0)	15 (9)
2.01-5.0	2 (8)	59 (37)
5.01-10.0	13(54)	68 (43)
> 10.0	9 (38)	7 (11)
Focality	*n* = 25	*n* = 149
Unifocal	13 (52)	72 (48)
Multifocal	12 (48)	77 (52)
Hemiliver	*n* = 30	*n* = 162
Right	20 (67)	97 (60)
Left	5 (17)	27 (17)
Bilateral	5 (7)	38 (24)

Please note that size could not be determined in 6 patients in group 1 and 3 in group 2. Similarly 'focality' could not be determined in 5 patients in group 1 and 13 in group 2.

variant HCC in 6/63 patients of group 1 and 0/243 patients of group 2.

DISCUSSION

In this study, we described the characteristics of patients who presented to a tertiary care center in the United States without known risk factors for HCC and compared them to those with one or more identifiable risk factors. The patients in group 1 without identifiable risk factors had a relatively higher proportion of women and Caucasians. The age distribution of this group was asymmetrical, with a disproportionate number of patients less than 30 years old and older than 80 years. The increased frequency of younger HCC patients in this group could be explained by the fibrolamellar variant of HCC that is known to affect younger patients without risk factors. This tumor was exclusively seen in group 1, 4 out of the 6 patients less than 30 years old had fibrolamellar variant. While fibrolamellar variant could explain the disproportionate number of younger patients in group 1, another explanation must be found for the increased number of patients over the age of 80 years in this group. It is certainly possible that these patients may have had occult viral hepatitis or alcohol use, and examination of liver tissue or peripheral blood monocytes may have detected occult HBV and HCV infections in some of them. The retrospective nature of this study also did not permit us to determine whether these patients had adequate tests to rule out viral hepatitis. Another demographic difference between the two groups of patients was the ratio of males to females. Group 1 had a relatively higher proportion of female patients, and it is possible that some of these patients may have progressed from adenoma.

The clinical presentation was also different in both groups. Group 2 was more likely to present without any symptoms (40% *vs* 17%) and this could be partly explained by the fact that many of these patients (19%) were diagnosed with HCC during surveillance or screening. Abdominal pain was the most common symptom in both groups, but it was more common in group 1 and this could be explained by the larger tumor burden. Despite the smaller (40% smaller) tumor size in group 2, portal vein involvement and metastases were similar in both groups, suggesting that there may be differences in tumor biology.

Our study suggested that there were differences in patient characteristics, symptoms, and tumor size in patients who presented with and without known risk factors for HCC. Absence of cirrhosis and tumor size may explain the differences in symptoms, and there is a suggestion that tumor biology may be different in these groups. The higher proportions of women and older patients without risk factors remain poorly explained. It is important to note that our study had all the inherent weaknesses of a retrospective study. It is more than likely that a more detailed diagnostic work-up may have revealed more risk factors in both groups. In addition, we could not independently confirm the laboratory test results in many patients. The prospective and complete collection of data on risk factors and tumor characteristics of patients diagnosed with HCC will further distinguish the differences between patients who present with and without risk factors.

Most patients with HCC have known risk factors such as HCV, HBV, or cirrhosis. Genetic changes that lead to HCC are complex and poorly understood, and most studies have focused on the genetic changes in the 'high risk' population[13,14]. Genetic changes that lead to HCC take place over 30-50 years, and this may partly explain the difficulty to define the sequential molecular changes that lead to HCC. There is increasing circumstantial evidence that the development of HCC, like most other cancers, is a multi-step process including inactivation or loss of tumor suppressor genes, activation or over expression of multiple oncogenes and heterozygosity of multiple chromosomes[13-18]. There is experimental evidence that p53, Rb1 and Wnt pathways are important molecular pathways involved in the development of HCC. The early genetic changes may vary depending on the etiology of liver disease and geographic location. Even in the same patient, there may be considerable genetic heterogeneity among different tumor nodules, suggesting that we may not find a common unifying pathway in the pathogenesis of HCC. However, accumulating evidence indicates that hepatocytes with multiple genetic changes may expand in a clonal fashion leading to dysplastic nodules and liver cancer. The molecular mechanisms of liver cancer in patients without known risk factors are difficult to explain. It is possible that many of these patients have been exposed to known or unknown carcinogens. Prospective studies should be designed to identify hitherto unidentified factors including the role of obesity or non-alcoholic fatty liver disease, occult HBV or HCV infections and genetic predisposition.

REFERENCES

1 **Parkin DM**, Bray FI, Devesa SS. Cancer burden in the year 2000. The global picture. *Eur J Cancer* 2001; **37** Suppl 8: S4-S66

2 **el-Serag HB**. Epidemiology of hepatocellular carcinoma. *Clin Liver Dis* 2001; **5**: 87-107, vi
3 **El-Serag HB**, Mason AC. Rising incidence of hepatocellular carcinoma in the United States. *N Engl J Med* 1999; **340**: 745-750
4 **Nair S**, Shiv Kumar K, Thuluvath PJ. Mortality from hepatocellular and biliary cancers: changing epidemiological trends. *Am J Gastroenterol* 2002; **97**: 167-171
5 **Davila JA**, Morgan RO, Shaib Y, McGlynn KA, El-Serag HB. Hepatitis C infection and the increasing incidence of hepatocellular carcinoma: a population-based study. *Gastroenterology* 2004; **127**: 1372-1380
6 **Beasley RP**, Hwang LY, Lin CC, Chien CS. Hepatocellular carcinoma and hepatitis B virus. A prospective study of 22 707 men in Taiwan. *Lancet* 1981; **2**: 1129-1133
7 **Kiyosawa K**, Akahane Y, Nagata A, Furuta S. Hepatocellular carcinoma after non-A, non-B posttransfusion hepatitis. *Am J Gastroenterol* 1984; **79**: 777-781
8 **Chen CJ**, Wang LY, Lu SN, Wu MH, You SL, Zhang YJ, Wang LW, Santella RM. Elevated aflatoxin exposure and increased risk of hepatocellular carcinoma. *Hepatology* 1996; **24**: 38-42
9 **Fattovich G**, Stroffolini T, Zagni I, Donato F. Hepatocellular carcinoma in cirrhosis: incidence and risk factors. *Gastroenterology* 2004; **127**: S35-S50
10 **Marrero JA**, Fontana RJ, Su GL, Conjeevaram HS, Emick DM, Lok AS. NAFLD may be a common underlying liver disease in patients with hepatocellular carcinoma in the United States. *Hepatology* 2002; **36**: 1349-1354
11 **El-Serag HB**. Hepatocellular carcinoma: recent trends in the United States. *Gastroenterology* 2004; **127**: S27-S34
12 **Saini S**, Ralls PW, Balfe DM, Bree RL, DiSantis DJ, Glick SN, Kidd R, Levine MS, Megibow AJ, Mezwa DG, Shuman WP, Greene FL, Laine LA, Lillemoe K. Liver lesion characterization. American College of Radiology. ACR Appropriateness Criteria. *Radiology* 2000; **215** Suppl: 193-199
13 **Okuda K**. Hepatocellular carcinoma. *J Hepatol* 2000; **32**: 225-237
14 **Moradpour D**, Blum HE. Pathogenesis of hepatocellular carcinoma. *Eur J Gastroenterol Hepatol* 2005; **17**: 477-483
15 **Feitelson MA**, Pan J, Lian Z. Early molecular and genetic determinants of primary liver malignancy. *Surg Clin North Am* 2004; **84**: 339-354
16 **Kew MC**. Synergistic interaction between aflatoxin B1 and hepatitis B virus in hepatocarcinogenesis. *Liver Int* 2003; **23**: 405-409
17 **Szabó E**, Páska C, Kaposi Novák P, Schaff Z, Kiss A. Similarities and differences in hepatitis B and C virus induced hepatocarcinogenesis. *Pathol Oncol Res* 2004; **10**: 5-11
18 **Koike K**. Molecular basis of hepatitis C virus-associated hepatocarcinogenesis: lessons from animal model studies. *Clin Gastroenterol Hepatol* 2005; **3**: S132-S135

S- Editor Liu Y **L- Editor** Wang XL **E- Editor** Lu W

PO Box 2345, Beijing 100023, China
www.wjgnet.com
wjg@wjgnet.com

World J Gastroenterol 2007 February 7; 13(5): 785-790
World Journal of Gastroenterology ISSN 1007-9327

RAPID COMMUNICATION

Clinical benefits of biochemical markers of bone turnover in Egyptian children with chronic liver diseases

Karam A Mahdy, Hanaa H Ahmed, Fathia Mannaa, Azza Abdel-Shaheed

Karam A Mahdy, Medical Biochemistry Department, National Research Centre, Egypt
Hanaa H Ahmed, Hormones Department, National Research Centre, Egypt
Fathia Mannaa, Medical Physiology Department, National Research Centre, Egypt
Azza Abdel-Shaheed, Child Health Department, National Research Centre, Egypt
Supported by the National Research Centre during the research plan from 2001-2004 by projects 5/4/5 and 5/5/5 in collaboration with National Liver Institute of Menoufyia University
Correspondence to: Karam A Mahdy, Medical Biochemistry Department, National Research Centre, El Bohouth Street, Dokki 12311, Cairo, Egypt. karammahdy@yahoo.com
Telephone: +2-2-3371499 Fax: +2-2-3370931
Received: 2006-08-23 Accepted: 2006-12-20

Abstract

AIM: To investigate the association between serum insulin-like growth factor 1 (IGF-1), osteocalcin, and parathyroid hormone (PTH) levels with the etiology and clinical condition of patients with chronic liver disease.

METHODS: Eighty children with hepatocellular damage were divided into 3 groups according to the etiology of disease infection: bilharziasis (9 patients), hepatitis B virus (HBV, 12 patients) and hepatitis C virus (HCV, 29 patients). The Child score index was found as A in 24 patients, B in 22 patients, C in 4 patients. Thirty healthy children served as control group. HBsAg, HBcAbIgM, HBcAbIgG, and anti-HCV were detected using ELISA technique. HCV-RNA was measured by reverse transcription polymerase chain reaction (RT-PCR). Anti-bilharzial antibodies were detected by indirect haem-agglutination test. Liver function tests were performed using autoanalyser. Serum IGF-1, osteocalcin and PTH levels were measured by ELISA technique. Abdominal ultrasonography was also conducted.

RESULTS: Serum IGF-1 level was significantly lower in all patient groups with liver diseases, while serum osteocalcin and PTH levels were significantly elevated in patients with HBV and HCV infections compared with the control group. Serum osteocalcin and PTH concentrations were measured with the severity of liver disease from Child A to C. Child A patients unexpectedly showed significantly reduced IGF-1 levels in comparison to patients staged as Child B or C. Serum osteocalcin level was negatively correlated with albumin (14.7 ± 0.54 *vs* 3.6 ± 0.10, $P < 0.05$), while that for PTH was positively correlated with total protein (70.1 ± 2.17 *vs* 6.7 ± 0.10, $P < 0.05$) in patients with HCV infection.

CONCLUSION: Low serum IGF-1 level seems to play a critical role in the bone loss in patients with chronic liver disease. Elevated biochemical markers of bone remodeling suggest high-turnover in patients with viral infection and reflect severity of the clinical stage.

Key words: Liver disease; Bone turnover; Insulin-like growth factor-1; Osteocalcin; Parathyroid hormone

Mahdy KA, Ahmed HH, Mannaa F, Abdel-Shaheed A. Clinical benefits of biochemical markers of bone turnover in Egyptian children with chronic liver diseases. *World J Gastroenterol* 2007; 13(5): 785-790

http://www.wjgnet.com/1007-9327/13/785.asp

INTRODUCTION

Bone tissues are metabolically active and undergo continuous remodeling throughout their life. Skeletal remodeling is achieved by two counteracting processes: bone formation which is accomplished through osteoblasts and bone resorption that is attributed to osteoclast activity[1]. Bone manifestations are well-known as extrahepatic complications of chronic liver disease[2]. Patients with chronic liver disease are at increased risk of developing hepatic osteodystrophy manifested as osteomalacia or osteoporosis[3]. Osteoporosis can be described as a disturbance in the bone remodeling process. Bone loss is a result of an imbalance of the bone remodeling process, where bone resorption exceeds bone formation[4].

The prevalence of osteoporosis in patients with chronic liver diseases ranges from 10% to 60%[5,6]. In general, secondary factors such as malabsorption and nutritional deficiencies may cause bone changes in chronic liver disease[7]. Insulin like growth factor (IGF) family is considered as important anabolic hormones, which play a role in anabolic metabolism and stimulating DNA synthesis, cell proliferation and meiotic division throughout life[8]. Since most circulating IGFs are synthesized by hepatocytes, lower levels of these parameters could be found in patients with liver diseases[8].

Regulation of bone metabolism is achieved by various factors such as mechanical motion, minerals, and hormones, all influencing bone turnover[4]. Osteocalcin is a protein produced by osteoblasts. Its level is reduced in the presence of osteodystrophia and can be recommended as a very sensitive and specific marker for bone formation/turnover[9].

Parathyroid hormone has a dual effect on bone cells. It can stimulate osteoblast activity and lead to substantial increase in bone density. In contrast, when secreted continuously at relatively high rates, as in hyperparathyroidism patients it can stimulate oseoclast-mediated bone resorption and suppress osteoblast activity[1]. The anabolic effect of parathyroid hormone (PTH) on osteoblasts is probably both direct and indirect via growth factors such as insulin like growth factor-1 (IGF-1) and transforming growth factor-β (TGF-β)[1].

However, the role of hepatocellular dysfunction in hepatic osteodystrophy is not clear. Therefore, this study aimed to clarify the influence of hepatocellular dysfunction on bone loss, and to outline the clinical benefits of controlling serum IGF-1, osteocalcin and parathyroid hormone levels in children with chronic liver diseases.

MATERIALS AND METHODS

Eighty children were enrolled in this study, from Liver Institute, Menoufyia University Inpatient and Outpatient Clinic and divided into: (1) Bilharziasis group: 9 patients (males whose age ranged from 6 to 15 years). (2) HBV group: 12 patients (10 males and 2 females whose age ranged from 3 to 15 years). (3) HCV group: 29 patients (22 males and 7 females whose age ranged from 2 to 16 years). (4) Control group: 30 apparently healthy children (22 males and 8 females whose age ranged from 3 to 15 years) with no history or clinical evidence of liver disease or any other diseases. (5) History was obtained from all individuals and clinical examination was carried out.

Specimen collection

Under complete aseptic condition, 5 mL of blood was taken from all the patients and controls. Each blood sample was divided into two portions: a small portion (1.8 mL) was taken on 3.8% Na-citrate as anticoagulant (0.02 mL) to obtain plasma and a larger portion of blood sample was allowed to clot. Sera were separated and stored at -80℃ till being tested, while the plasma sample was used immediately to measure prothrombin time and concentration.

Serological test

Hepatitis surface antigen (HBsAg), hepatitis B core antibody IgM (HBcAb IgM) and hepatitis B core antibody IgG (HBcAb IgG) were measured by ELISA technique using kits from Dia-Sorin Biomedica Co., according to the methods of Boniolo *et al*[10], Tedder and Wilson[11] and Hoofangle *et al*[12] respectively.

Anti-HCV was detected by third generation of ELISA using kit from the Biochem ImmunoSystem Inc[13], HCV-RNA extraction was carried out by reverse transcription polymerase chain reaction (RT-PCR) according to the method described by Ravaggi *et al*[14]. Anti-bilharzial antibodies were detected by indirect haem-agglutination test (IHA) according to the method of Hoshino *et al*[15], using kits of Fumoze-France.

Table 1 Serum IGF-1, osteocalcin and PTH levels in patient groups and control group (mean ± SE)

	Control (n = 30)	Bilharziasis (n = 9)	HBV (n = 12)	HCV (n = 29)
IGF-1 (ng/mL)	277.1 ± 12.2	94.0 ± 4.30[b]	105.1± 10.3[b]	230.0 ± 10.5[b]
Osteocalcin (ng/mL)	5.7 ± 0.3	6.8 ± 0.66	16.5 ± 0.76[b]	14.7 ± 0.54[b]
PTH (ng/mL)	61.6 ± 2.7	63.3 ± 3.03	83.4 ± 4.30[b]	70.1 ± 2.17[a]

[a]$P < 0.05$, [b]$P < 0.01$ *vs* control group.

Liver function tests

Serum AST, ALT, alkaline phosphatase (ALP), GGT , total and direct bilirubin, total protein, and albumin levels were measurd using EKTOCHEM 750XRC analyzer. Prothrombin time and concentration were also estimated in plasma according to the method of Poller[16].

Biochemical markers of bone turnover

Serum insulin like growth factor-1 (IGF-1), osteocalcin and PTH levels were measured by ELISA technique using kits of BioSource-Belgium[17-19].

Abdominal ultrasonography

To assess the size and echopattern of the liver, the size of the spleen and the presence of ascitis or any other abnormalities in the abdomen were detected using RT-X200 Prob 3.5 MHZ convex of General Electric Company -USA.

Statistical analysis

The obtained data are presented as mean ± SE. The difference between two groups was calculated using unpaired *t*-test, while the difference between more than two groups was calculated using one way analysis of variance ANOVA according to Snedecor and Cochran[20]. Least significant difference (LSD) test was used to compare the means of Child classification according to Walter and Duncan[21] at probability 0.05.

RESULTS

Patients with chronic liver diseases were divided into three groups according to the etiology: group 1 (9 patients with bilharziasis whose mean age was 10.8 ± 1 years), group 2 (12 patients with HBV whose mean age was 11.5 ± 0.6 years, and group 3 (29 patients with HCV infection whose mean age was 11.8 ± 1.5 years). Thirty children whose mean age was 10.5 ± 0.5 years and were sex matched with normal liver served as control group.

Table 1 depicts the results of serum IGF-1, osteocalcin and PTH levels in patients with either bilharziasis or HBV and HCV infections as well as in controls. The results revealed that patients with bilharziasis and those with either HBV or HCV infections showed a significant

Table 2 Liver function tests in different patient groups and control group (mean ± SE)

	Control (n = 30)	Bilharziasis (n = 9)	HBV (n = 12)	HCV (n = 29)
ALT (U/L)	20.5 ± 0.9	38.0 ± 6.8[a]	72.6 ± 12.4[a]	107.0 ± 28.1[a]
AST (U/L)	18.4 ± 0.8	46.0 ± 7.5[a]	71.2 ± 10.8[a]	120.0 ± 21.8[a]
ALP (U/L)	74.0 ± 9.3	82.0 ± 11.8	214.0 ± 41.2[a]	165.0 ± 28.9[a]
GGT (U/L)	26.0 ± 2.1	37.6 ± 9.9	54.0 ± 1.5[a]	59.9 ± 11.1[a]
T. bilirubin (mg/dL)	0.84 ± 0.03	0.9 ± 0.16	1.8 ± 0.20[a]	1.3 ± 0.13[a]
T. protein (mg/dL)	6.9 ± 0.10	7.1 ± 0.30	6.8 ± 0.20	6.7 ± 0.10[a]
Albumin (mg/dL)	4.0 ± 0.06	3.9 ± 0.10	3.5 ± 0.19[a]	3.6 ± 0.10[a]
Prothrombin (%)	93.0 ± 1.3	77.0 ± 4.0[a]	69.0 ± 6.0[a]	65.6 ± 2.50[a]

[a]$P < 0.05$ *vs* control group.

Table 3 Alterations in serum IGF-1, osteocalcin and PTH levels according to the severity of the disease from class A to C (mean ± SE)

Severity	A (n = 24)	B (n = 22)	C (n = 4)	LSD at 0.05
IGF-1 (ng/mL)	152.6[b] ± 7	186.8[a] ± 20.3	196.0[a] ± 36.4	32.67
Osteocalcin (ng/mL)	12.6[b] ± 0.9	14.6[a] ± 0.9	15.8[a] ± 1.2	1.73
PTH (ng/mL)	71.3[b] ± 3.0	70.3[b] ± 2.7	86.5[a] ± 4.3	5.36

Within each row the means followed by different letters are significantly different. LSD: Least significance difference. [a]$P < 0.05$, [b]$P < 0.01$ *vs* control group.

Table 4 Effect of age and sex on serum IGF-1, osteocalcin and PTH (mean ± SE)

	Age (yr)			Sex		
	3-9	10-16	P	Male	Female	P
IGF-1 (ng/mL)	153.2 ± 59.3	182.6 ± 84.5	0.268	175.2 ± 84.2	177.1 ± 58.4	0.948
Osteocalcin (ng/mL)	13.8 ± 4.7	13.7 ± 4.2	0.941	13.1 ± 4.1	16.4[a] ± 4.1	0.037
PTH (ng/mL)	71.1 ± 14.0	72.3 ± 13.8	0.786	73.1 ± 13.8	67.2 ± 13.1	0.249

[a]$P < 0.05$ *vs* males.

decrease ($P < 0.01$) in serum IGF-1 level compared to the controls. The most significant decrease in serum IGF-1 was recorded in patients with bilharziasis followed by HBV-infected and HCV-infected patients. Serum osteocalcin level showed a significant increase ($P < 0.01$) in patients with HBV and HCV infection compared to the controls. The most significant increase in serum osteocalcin level was observed in HBV-infected patients. Patients suffering from bilharziasis had no significant ($P > 0.05$) change in serum osteocalcin level compared to the controls. Serum PTH level was significantly increased in HBV-infected patients ($P < 0.01$) and in those with HCV infection ($P < 0.05$) compared to the controls. No significant change in serum PTH level was detected in patients with bilharziasis compared to the controls (Table 1).

Liver function tests in patients with bilharziasis or HBV and HCV infection as well as in the control are presented in Table 2. Serum ALT and AST activities showed a significant ($P < 0.05$) increase in all patient groups compared to the control group. The most significant increase in serum ALT and AST activities was recorded in the patients suffering from HCVinfection. The activities of ALP, GGT and total bilirubin in serum revealed a significant increase ($P < 0.05$) in patients with HBV and HCV infection compared to the control, while no significant change ($P > 0.05$) was recorded in patients with bilharziasis as compared to the control group. Serum total protein level showed significant decrease ($P < 0.05$) in patients with HCV infection, whereas patients with either bilharziasis or HBV had no significant ($P > 0.05$) change as compared to the control (Table 2). Serum albumin level revealed a significant ($P < 0.05$) decrease in patients suffering from either HBV or HCV infection compared to the control. No significant change in serum albumin level was observed in patients with bilharziasis compared to the control. Patients suffering from either bilharziasis or HBV and HCV infection had a significant ($P < 0.05$) decrease in prothrombin concentration compared to the control. The most significant decrease in prothrombin concentration was detected in HCV-infected patients (Table 2).

Alterations in serum IGF-1, osteocalcin and PTH level according to the severity of the disease from Child class A to C are depicted in Table 3. Significant ($P < 0.05$) change was detected in the three serum markers (IGF-1, osteocalcin and PTH) in each grade of the disease. The mean values of the three serum markers were markedly increased with the severity of the disease and the highest value was recorded in Child class C of the disease using LSD at probability 0.05.

Noteworthy, our results revealed that serum IGF-1, osteocalcin and PTH levels were not age or sex dependent except for osteocalcin level which was higher in females (Table 4).

On correlating the three bone markers with each other and liver function indices using Pearson correlation, there was only significant negative correlation between serum osteocalcin and albumin ($r = -0.409$, $P = 0.027$) and significant positive correlation between PTH and total protein ($r = 0.451$, $P = 0.014$) in patients with HCV infection (Figure 1A and B), while no significant correlation was recorded between IGF-1, PTH or osteocalcin in our patients.

DISCUSSION

Patients with chronic liver disease are prone to develop hepatic osteodystrophy. In the majority of cases it is

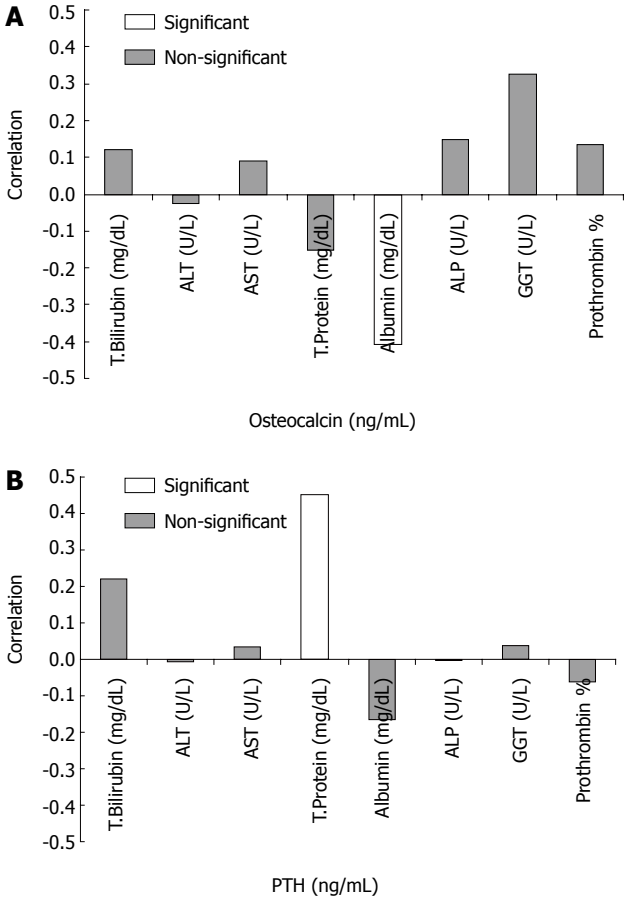

Figure 1 Correlation coefficient between serum osteocalcin and albumin levels (**A**) & between serum PTH and total protein levels (**B**) in patients with HCV infection.

characterized by development of osteoporosis and/or osteomalacia with possible persistence of minor or major disability[3]. Osteoporosis reflects loss of bone (both matrix and its mineral) and osteomalacia is due to defective mineralization of osteoid[22]. Osteoporosis is a frequent complication of end-stage liver disease irrespective of its etiology. The prevalence varies between 9% and 60%, the highest being observed in cholestatic disorders and alcoholic liver disease[23].

The present study aimed at elucidating the influence of bilharziasis, hepatitis B or C infections on the development of osteoporosis in children. Serum levels of IGF-1, osteocalcin and PTH were measured and correlated with the routine liver functions as well as the child-pough score. The results of the present work showed that serum IGF-1 level was significantly decreased in all children infected with bilharziasis, HBV and HCV, while unexpectedly it showed significant increase with the severity of liver diseases from A to B or C classification but its level was still lower than that in the control.

These results are greatly supported by the finding of Hassan *et al*[24] who showed a significant reduction in the level of IGF-1 in children with schistosomiasis with or without hepatic fibrosis. Also, our results are in agreement with the findings of Orsini *et al*[25] who found similar results in hepatosplenic schistosomiasis patients and the results of Mazziotti *et al*[26] in patients with hepatocellular carcinoma (HCC) and hepatitis C virus-related cirrhosis. The reduction in IGF-1 level also can precede the diagnosis of HCC[26]. Similarly, decreased serum IGF-1 level has been recorded both in patients with viral cirrhosis[9,27] and in patients with hepatitis B infection without cirrhosis[28].

In schistosomiasis patients with hepatic fibrosis, the depressed circulation of IGF-1, free T4 and growth hormone may be responsible for stunted stature[24]. Moreover, low serum IGF-1 level in hepatosplenic schistosomiasis patients has been found to be related to the clinical form of hepatosplenic schistosomiasis[25]. The level of IGF-1 is elevated in patients with schistosomiasis with or without liver fibrosis and relates to its clinical form[25], suggesting that the severity of liver dysfunction can affect the level of IGF-1. As liver function of patients with bilharziasis is usually better than those with cirrhosis due to HBV and HCV infection and usually scored as child A, this may partly explain the relatively unexpected low level of IGF-1 in our patients with less sever liver affection (child A group).

The present study recorded a significant increase in serum osteocalcin level in patients with viral hepatitis infection only. Also a negative correlation was obtained with the level of serum albumin in patients with HCV infection. Moreover, serum osteocalcin level was significantly increased in child B and C patients than in child A patients.

It has been reported that serum osteocalcin level is higher in cirrhotic patients than in control, suggesting that cirrhotic patients have high bone turnover. In addition, osteodystrophy associated with hepatic cirrhosis is due to a defect in alpha-hydroxylation (1, $25(OH)_2D$) by the kidney due to the decrease in its primary substrate, the liver $25(OH)_2D$. This could be attributed to the reduced availability of vitamin D, inadequate conversion of vitamin D to $25(OH)_2D$, accelerated metabolism of $25(OH)_2D$, and urinary loss of $25(OH)_2D$ with its transport protein[29]. However, some studies reported that serum osteocalcin level is low in cirrhotic patients and osteopenia in these patients is not due to a decrease in bone formation[30,31], but may be a consequence of hepatic osteodystrophy due to low plasma vitamin D and calcium levels[31].

Concerning the changes in serum PTH level, the present study recorded significant increase in patients with Hepatitis B and C infections. As regard a positive correlation was obtained with serum total protein level among the group of HCV infection. Moreover, serum PTH was significantly increased in class B and C patients than patients of class A.

In hepatocellular dysfunction some previous studies reported that serum PTH level is high in patients with primary biliary cirrhosis[32], liver cirrhosis[33], HBV infection[34], as well as in dogs with schistosomiasis[35] and in children with cholestatic and non-cholestatic liver disease[36]. On the other hand, other studies reported that PTH is unchanged in patients with chronic viral liver disease[37] and post hepatic cirrhosis[38]. Kirch and co-workers[33] have found a significant correlation between PTH and the parameters of liver functions such as prothrombin, albumin and bilirubin, suggesting that the increasing PTH level is related to liver dysfunction. This may explain why the elevation of PTH level is due

to the impaired liver function rather than secondary hyperparathyroidism[33]. Moreover, elevated PTH-related protein was observed with hyperglobulinemia and hypoalbuminemia in dogs with schistosomiasis[35], and this may explain the obtained positive correlation between PTH and serum total protein levels in patients with HCV infection due to hyperglobulinemia observed in our study.

Hepatic osteodystrophy (HOD) begins at the stage of chronic non-cirrhotic liver injury and bone loss is connected with liver damage, suggesting that the principal pathogenesis of HOD is attributed to intestinal Ca-malabsorption as a result of low serum albumin and villous atrophy[39]. Lower ionized calcium resulting from deficient intestinal absorption due to low $25(OH)_2D$, leads to increase in PTH level[36].

The significant rise in serum osteocalcin level in our female patients indicated that their bone turnover was accelerated. This result is in agreement with Steinberg *et al*[40] who found that female sex is a risk factor for bone turnover and low bone density.

In conclusion, serum IGF-1, osteocalcin and PTH appear to be markers of bone metabolism in children with hepatocellular damage. Low level of IGF-1 seems to play a role in the bone mass loss in patients with chronic liver disease. Elevated biochemical markers of bone remodeling suggest high bone turnover in children with viral infections. Fortification of diet by ergocalciferol is essential in patients with chronic liver disease and regular bone density measurements are necessary in these patients.

REFERENCES

1 **Seibel MJ**. Bone metabolism, mineral homeostasis and its pharmacological modulation. *Clin Lab* 2004; **50**: 255-264
2 **Iber F**. Bone disease in chronic liver disease. *Am J Gastroenterol* 1989; **84**: 1229-1230
3 **Rabinovitz M**, Shapiro J, Lian J, Block GD, Merkel IS, Van Thiel DH. Vitamin D and osteocalcin levels in liver transplant recipients. Is osteocalcin a reliable marker of bone turnover in such cases? *J Hepatol* 1992; **16**: 50-55
4 **Ravn P**, Fledelius C, Rosenquist C, Overgaard K, Christiansen C. High bone turnover is associated with low bone mass in both pre- and postmenopausal women. *Bone* 1996; **19**: 291-298
5 **Guañabens N**, Parés A, Mariñoso L, Brancós MA, Piera C, Serrano S, Rivera F, Rodés J. Factors influencing the development of metabolic bone disease in primary biliary cirrhosis. *Am J Gastroenterol* 1990; **85**: 1356-1362
6 **Bonkovsky HL**, Hawkins M, Steinberg K, Hersh T, Galambos JT, Henderson JM, Millikan WJ, Galloway JR. Prevalence and prediction of osteopenia in chronic liver disease. *Hepatology* 1990; **12**: 273-280
7 **Compston JE**. Hepatic osteodystrophy: vitamin D metabolism in patients with liver disease. *Gut* 1986; **27**: 1073-1090
8 **Wu YL**, Ye J, Zhang S, Zhong J, Xi RP. Clinical significance of serum IGF-I, IGF-II and IGFBP-3 in liver cirrhosis. *World J Gastroenterol* 2004; **10**: 2740-2743
9 **Delmas PD**, Wahner HW, Mann KG, Riggs BL. Assessment of bone turnover in postmenopausal osteoporosis by measurement of serum bone Gla-protein. *J Lab Clin Med* 1983; **102**: 470-476
10 **Boniolo A**, Dovis M, Matteja R. Use of an enzyme-linked immunosorbent assay for screening hybridoma antibodies against hepatitis B surface antigen. *J Immunol Methods* 1982; **49**: 1-15
11 **Tedder RS**, Wilson-Croome R. IgM-antibody response to the hepatitis B core antigen in acute and chronic hepatitis B. *J Hyg* (Lond) 1981; **86**: 163-172
12 **Hoofnagle JH**, Gerety RJ, Barker LF. Antibody to hepatitis-B-virus core in man. *Lancet* 1973; **2**: 869-873
13 **Alter HJ**, Prince AM. Transfusion-associated non-A, non-B hepatitis: an assessment of the causative agent and its clinical impact. *Transfus Med Rev* 1988; **2**: 288-293
14 **Ravaggi A**, Primi D, Cariani E. Direct PCR amplification of HCV RNA from human serum. *PCR Methods Appl* 1992; **1**: 291-292
15 **Hoshino S**, Camargo ME, da Silva LC. Standardization of a hemagglutination test for schistosomiasis with formalin-treated human erythrocytes. *Am J Trop Med Hyg* 1970; **19**: 463-470
16 **Poller L**. Laboratory control of anticoagulant therapy. *Semin Thromb Hemost* 1986; **12**: 13-19
17 **Blum WF**, Albertsson-Wikland K, Rosberg S, Ranke MB. Serum levels of insulin-like growth factor I (IGF-I) and IGF binding protein 3 reflect spontaneous growth hormone secretion. *J Clin Endocrinol Metab* 1993; **76**: 1610-1616
18 **Coleman RE**, Mashiter G, Fogelman I, Whitaker KD, Caleffi M, Moss DW, Rubens RD. Osteocalcin: a potential marker of metastatic bone disease and response to treatment. *Eur J Cancer Clin Oncol* 1988; **24**: 1211-1217
19 **Goltzman D**, Henderson B, Loveridge N. Cytochemical bioassay of parathyroid hormone: characteristics of the assay and analysis of circulating hormonal forms. *J Clin Invest* 1980; **65**: 1309-1317
20 **Snedecor GW**, Cochran WG. Statistical Methods, 7th ed. Ames, Iowa: The Iowa State University Press, 1980
21 **Walter A,** Duncan DB. Multiple range and multiple test. *Biometrics* 1969; **11**: 1-24
22 **Sherlock S**, Dooley J. Cholestatis. In: Diseases of the liver and biliary system.10th ed., Sherlock S, Dooley J (editors), Oxford: Blackwell Scientific Publications, 1997: 217-273
23 **Schiefke I**, Fach A, Wiedmann M, Aretin AV, Schenker E, Borte G, Wiese M, Moessner J. Reduced bone mineral density and altered bone turnover markers in patients with non-cirrhotic chronic hepatitis B or C infection. *World J Gastroenterol* 2005; **11**: 1843-1847
24 **Hassan AH**, Abd el Moneim MA, Abd el Aal AA, Abou Aly SA, Ahmed SH, Soliman AT, el Kersh MM. Circulating growth hormone, insulin-like growth factor I, cortisol and free thyroxine in children with schistosomiasis with and without hepatic fibrosis. *J Trop Pediatr* 1991; **37**: 25-30
25 **Orsini M**, Rocha RS, Disch J, Katz N, Rabello A. The role of nutritional status and insulin-like growth factor in reduced physical growth in hepatosplenic Schistosoma mansoni infection. *Trans R Soc Trop Med Hyg* 2001; **95**: 453-456
26 **Mazziotti G**, Sorvillo F, Morisco F, Carbone A, Rotondi M, Stornaiuolo G, Precone DF, Cioffi M, Gaeta GB, Caporaso N, Carella C. Serum insulin-like growth factor I evaluation as a useful tool for predicting the risk of developing hepatocellular carcinoma in patients with hepatitis C virus-related cirrhosis: a prospective study. *Cancer* 2002; **95**: 2539-2545
27 **Gallego-Rojo FJ**, Gonzalez-Calvin JL, Muñoz-Torres M, Mundi JL, Fernandez-Perez R, Rodrigo-Moreno D. Bone mineral density, serum insulin-like growth factor I, and bone turnover markers in viral cirrhosis. *Hepatology* 1998; **28**: 695-699
28 **Chui SH**, Chan K, Chui AK, Shek LS, Wong RN. The effects of a Chinese medicinal suppository (Vitalliver) on insulin-like growth factor 1 and homocysteine in patients with hepatitis B infection. *Phytother Res* 2005; **19**: 674-678
29 **Suzuki K**, Arakawa Y, Chino S, Yagi K. Hepatic osteodystrophy. *Nihon Rinsho* 1998; **56**: 1604-1608
30 **Resch H**, Pietschmann P, Krexner E, Woloszczuk W, Willvonseder R. Peripheral bone mineral content in patients with fatty liver and hepatic cirrhosis. *Scand J Gastroenterol* 1990; **25**: 412-416
31 **Crosbie OM**, Freaney R, McKenna MJ, Hegarty JE. Bone density, vitamin D status, and disordered bone remodeling in end-stage chronic liver disease. *Calcif Tissue Int* 1999; **64**: 295-300

32 **Fonseca V**, Epstein O, Gill DS, Menon RK, Thomas M, McIntyre N, Dandona P. Hyperparathyroidism and low serum osteocalcin despite vitamin D replacement in primary biliary cirrhosis. *J Clin Endocrinol Metab* 1987; **64**: 873-877
33 **Kirch W**, Höfig M, Ledendecker T, Schmidt-Gayk H. Parathyroid hormone and cirrhosis of the liver. *J Clin Endocrinol Metab* 1990; **71**: 1561-1566
34 **Wiczkowski A**. The influence of hypervolemia on the secretion of atrial natriuretic peptide, the renin-angiotensin-aldosterone system's activity and concentration of vasopressin, parathormone and calcitonin in hepatitis B virus infected patients with chronic liver diseases. *Przegl Epidemiol* 1994; **48**: 433-440
35 **Fradkin JM**, Braniecki AM, Craig TM, Ramiro-Ibanez F, Rogers KS, Zoran DL. Elevated parathyroid hormone-related protein and hypercalcemia in two dogs with schistosomiasis. *J Am Anim Hosp Assoc* 2001; **37**: 349-355
36 **Mehany NL,** Mostafa AA, El-karaksy H, El-Asrag HA and El-Bayoumy AS. Vitamin D metabolism and related biochemical parameters in children with chronic liver diseases. *Arab J Lab Med* 2000; **26**: 331-348
37 **Duarte MP**, Farias ML, Coelho HS, Mendonça LM, Stabnov LM, do Carmo d Oliveira M, Lamy RA, Oliveira DS. Calcium-parathyroid hormone-vitamin D axis and metabolic bone disease in chronic viral liver disease. *J Gastroenterol Hepatol* 2001; **16**: 1022-1027
38 **Karan MA**, Erten N, Tascioglu C, Karan A, Sindel D, Dilsen G. Osteodystrophy in posthepatitic cirrhosis. *Yonsei Med J* 2001; **42**: 547-552
39 **Nakano A**, Kanda T, Abe H. Bone changes and mineral metabolism disorders in rats with experimental liver cirrhosis. *J Gastroenterol Hepatol* 1996; **11**: 1143-1154
40 **Steinberg KK**, Bonkovsky HL, Caudill SP, Bernhardt RK, Hawkins M. Osteocalcin and bone alkaline phosphatase in the serum of women with liver disease. *Ann Clin Lab Sci* 1991; **21**: 305-314

S- Editor Liu Y **L- Editor** Wang XL **E- Editor** Ma WH

PO Box 2345, Beijing 100023, China
www.wjgnet.com
wjg@wjgnet.com

World J Gastroenterol 2007 February 7; 13(5): 791-795
World Journal of Gastroenterology ISSN 1007-9327

RAPID COMMUNICATION

Per rectal portal scintigraphy as a useful tool for predicting esophageal variceal bleeding in cirrhotic patients

Taned Chitapanarux, Ong-ard Praisontarangkul, Satawat Thongsawat, Pises Pisespongsa, Apinya Leerapun

Taned Chitapanarux, Ong-ard Praisontarangkul, Satawat Thongsawat, Pises Pisespongsa, Apinya Leerapun, Division of Gastroenterology, Department of Internal Medicine, Faculty of Medicine, Chiang Mai University, Chiang Mai 50200, Thailand
Supported by the Gastroenterological Association of Thailand
Correspondence to: Dr. Taned Chitapanarux, Department of Internal Medicine, Faculty of Medicine, Chiang Mai University, Chiang Mai 50200, Thailand. thaitaned@yahoo.com
Telephone: +66-53-945482 Fax: +66-53-945481
Received: 2006-10-24 Accepted: 2007-01-08

Abstract

AIM: To investigate potential roles of per rectal portal scintigraphy in diagnosis of esophageal varices and predicting the risk of bleeding.

METHODS: Fifteen normal subjects and fifty cirrhotic patients with endoscopically confirmed esophageal varices were included. Patients were categorized into bleeder and non-bleeder groups according to history of variceal bleeding. All had completed per rectal portal scintigraphy using ^{99m}Technetium pertechnetate. The shunt index was calculated from the ratio of ^{99m}Technetium pertechnetate in the heart and the liver. Data were analyzed using Student's *t*-test and receiver operating characteristics.

RESULTS: Cirrhotic patients showed a higher shunt index than normal subjects (63.80 ± 25.21 *vs* 13.54 ± 6.46, $P < 0.01$). Patients with variceal bleeding showed a higher shunt index than those without bleeding (78.45 ± 9.40 *vs* 49.35 ± 27.72, $P < 0.01$). A shunt index of over 20% indicated the presence of varices and that of over 60% indicated the risk of variceal bleeding.

CONCLUSION: In cirrhotic patients, per rectal portal scintigraphy is a clinically useful test for identifying esophageal varices and risk of variceal bleeding.

Key words: Portal scintigraphy; Portal hypertension; Cirrhosis; Esophageal varices; Bleeding

Chitapanarux T, Praisontarangkul O, Thongsawat S, Pisespongsa P, Leerapun A. Per rectal portal scintigraphy as a useful tool for predicting esophageal variceal bleeding in cirrhotic patients. *World J Gastroenterol* 2007; 13(5): 791-795

http://www.wjgnet.com/1007-9327/13/791.asp

INTRODUCTION

Esophageal variceal bleeding is a serious and potentially life-threatening complication of liver cirrhosis[1-4]. No simple noninvasive method which accurately predicts esophageal variceal bleeding is available so far and endoscopists have had to perform endoscopy every 3 to 6 mo to evaluate patients with previously bleeding esophageal varices[5,6]. However, this approach is costly and not all patients with liver cirrhosis and esophageal varices are good candidates for such procedures[7].

Per rectal portal scintigraphy is a noninvasive method for evaluation of portosystemic shunting using portal shunt index (SI) calculated from radioactivity curves of the liver and the heart. In humans, such an SI shows a good correlation with portal pressure measured by percutaneous transhepatic portography or intraoperative method[8]. Portal scintigraphy is also clinically useful, especially in establishing prognosis of cirrhotic patients with varying shunt indices[9]. Evaluating portal pressure using per rectal portal scintigraphy may be easily performed and might provide information on risk of variceal bleeding.

The aim of this study was to determine the benefit of per rectal portal scintigraphy for evaluation of non-bleeding esophageal varices, bleeding esophageal varices and normal control subjects. We also compared different portal shunt indices, Child-Pugh grades and endoscopic appearances in various groups and examined the correlation between the portal SI and risk of variceal bleeding.

MATERIALS AND METHODS

Normal subjects and patients

Normal subjects: Normal adult volunteers of both sexes, with a minimum age of 18 years, were recruited. An attempt was made to obtain subjects in well distributed age groups, and equal in number for both sexes. All of the subjects were in good health, with no history of the liver and vascular diseases, or use of medication, alcohol or any substances that might affect the liver. The liver function test was normal, and tests for viral hepatitis (B, C) were negative or revealed immunized status. Hepatic ultrasonography was also performed to rule out structural liver disease or hepatocellular carcinoma.

Patients: Cirrhotic patients of either alcoholic or viral in etiology who had signs of portal hypertension, and a history or physical signs suggesting esophageal varices, or even esophageal variceal bleeding, were asked to participate in this study. Only patients with endoscopically confirmed esophageal varices were included. The esophageal varices were graded according to criteria developed by the Japanese Research Society for Portal Hypertension[10]. Thorough medical examination and interview for the history of gastrointestinal bleeding were performed. Only cirrhotic patients with esophageal varices were included in this study. The initial laboratory tests performed in this study included complete blood count, liver function test, viral hepatitis (B, C) profile, and renal function test. All patients were graded according to Child-Pugh classification. The etiology of bleeding was considered to be variceal if either actively bleeding varices were observed by endoscopy or if varices were endoscopically found without other sources of bleeding.

Informed consent were obtained from all patients and the protocol was in conformity with the ethical guidelines of the Declaration of Helsinki and the Clinical Research Committee at Chiang Mai University Hospital.

Measurement of the portal shunt index

The procedure used for per rectal portal scintigraphy was the same for both normal subjects and cirrhotic patients[9]. After fasting overnight for at least 6 h, the rectum was emptied by administration of laxatives (unison enema 100 mL). A polyethylene device (Terumo® feeding tube Fr.8) was inserted deep into the rectum with the tip of the tube being placed in the upper rectum, 20 cm above the anal verge, to avoid absorption into the systemic circulation via the inferior rectal vein in the lower rectum. To generate time-activity curves, a gammascinti camera with a large field of view (Apex SP4, El-Scint Co., Israel), equipped with a low-energy, multipurpose, parallel-hold collimator was used. The collimator was positioned over the patient's abdomen so that the field of view would always include the heart, the liver, and the spleen. Ten millicuries (2 mL) of ^{99m}Technetium pertechnetate, followed by 15 mL of air, was infused into the rectum through the tube. The sequential images were generated from counts in their areas of interest (AOI). For color display, the summed images were reconstructed by grouping of 20 s per image from the original 60 images. ^{99m}Technetium pertechnetate is commonly used in diagnostic scanning and imaging both in clinics and research. The procedure is safe and readily applicable because of the amount and short half life of radioactive substance used. Portal pressure increases shortly after an episode of variceal bleeding[11] and is stable over 72 h after bleeding[12]. Therefore, per rectal portal scintigraphy in patients of the bleeding group was performed 72 h after bleeding when the portal pressure returned to baseline level in order to determine the risk of that episode of bleeding.

Calculation of the portal shunt index

To calculate the amount of blood that entered the portal system and went to the liver and the heart, we used the portal SI[8]. This index was derived from the ratio of ^{99m}Technetium pertechnetate in the heart and the liver at the exact time as shown in the following equation.

$$SI = \frac{\sum_{0}^{(n+25)/5} x_i(H)}{\sum_{0}^{(n+25)/5} x_i(L) + \sum_{0}^{(n+25)/5} x_i(H)} \times 100\%$$

n = time at which radionuclides appeared in the area of the liver (s).

n' = time at which radionuclides appeared in the area of the heart (s).

$Xi\ (L)$ = the count per 5 s over the AOI of the liver.

$Xi\ (H)$ = the count per 5 s over the AOI of the heart.

In normal portal circulation, the transit time of blood circulation from the liver to the heart via hepatic veins and inferior vena cava was 18-26 s, and the scinti images were acquired in 5 s per image. The SI was calculated at the time of n + 25 s. The results were shown as the pattern of time-activity curves and summed-images.

Statistical analysis

Results were expressed as mean ± SD. The significance of difference between mean values was evaluated by Student's *t*-test. Differences with probability values of less than 0.05 were considered to be significant. The selection of an appropriate cutoff point of portosystemic shunt for the presence of esophageal varices and the risk of variceal bleeding was analyzed by the receiver operating characteristic (ROC)[13].

RESULTS

The normal control group consisted of eight male and seven female subjects (aged 28-59 years, mean 44.3 years). Fifty cirrhotic patients (45 males and 5 females), of various etiologies, aged between 30 and 70 years (mean 46.9 years) were recruited in this study. The baseline characteristics of all study patients are shown in Table 1. The patients were categorized into two groups according to their history of variceal bleeding, namely a non-bleeding group including 25 patients and a bleeding group with 25 patients. Bleeding was the first episode in all 25 patients in the bleeding group. All patients had received neither endoscopic variceal surveillance nor prophylactic treatment to prevent variceal bleeding. The two groups of patients showed similar baseline characteristics with the exception of alanine aminotransferase, total bilirubin, and prothrombin time. The severity of liver disease in the bleeding group was higher than that of the non-bleeding group. In the non-bleeding group, etiologies of liver disease were alcoholic in 9, hepatitis viral B in 6, hepatitis viral C in 5, and alcoholic and virus in 5 cases. In the bleeding group, etiologies of liver disease were alcoholic in 20, hepatitis virus B in 3, and alcoholic and virus in 2 cases. The mean SI in normal subjects was 13.54% ± 6.46%. For the cirrhotic patients, the mean SI was 63.80% ± 25.21%. Normal subjects were found to have significantly lower average SI than cirrhotic patients with esophageal varices ($P < 0.01$). If cirrhotic

Table 1 Baseline characteristics of the study patients

	Control (n = 15)	Non bleeder (n = 25)	Bleeder (n = 25)
Age (yr)	44.27 ± 8.48	49.32 ± 10.25	44.25 ± 8.86
Sex (M/F)	8/7	20/5	25/0
Presence of ascites (%)	0	10 (40)	7 (28)
Hepatic encephalopathy (%)	0	0	3 (12)
Serum albumin (g/dL)	4.55 ± 0.26	3.16 ± 0.54	2.76 ± 0.83
Alanine aminotransferase (U/L)	18.93 ± 4.03	51.88 ± 45.9	77.12 ± 61.41[b]
Serum bilirubin (mg/dL)	0.65 ± 0.19	2.49 ± 1.16	5.27 ± 6.55[b]
Prothrombin time (s)	-	2.67 ± 1.02	3.27 ± 2.43[b]
Etiology of cirrhosis			
Alcohol	-	9	20
Hepatitis B virus	-	6	3
Hepatitis C virus	-	5	0
Alcohol and virus	-	5	2
Child-Pugh A	-	13	8
B	-	9	9
C	-	3	8

[b]$P < 0.01$ *vs* bleeder and non bleeder group.

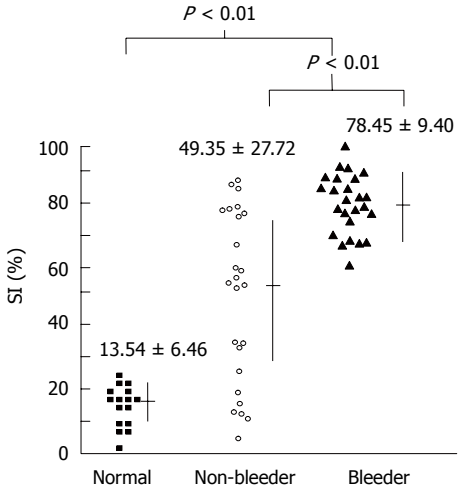

Figure 1 Comparison of portal shunt index in normal subjects and cirrhotic patients, with and without variceal bleeding. Data shown as mean (horizontal bar) ± SD (vertical bar).

patients were grouped as non-bleeding and bleeding, the mean SIs were 49.35% ± 27.72% and 78.45% ± 9.40%, respectively. The average SI in bleeding group was significantly higher than in non-bleeding group ($P < 0.01$), as shown in Figure 1.

Analysis was done to discover any difference in SIs when the patients were sub-grouped according to etiologies (i.e. alcoholic, viral, or both), presence of ascites, endoscopic appearances and Child-Pugh grade. Details are shown in Table 2. The mean SI was 78.87% ± 22.05% in cirrhosis from alcohol, 56.67% ± 24.08% in cirrhosis from virus, and 41.23% ± 23.47% in cirrhosis from alcohol plus viruses. The average SI in the etiology group of alcohol significantly differed from that of virus, and also that of alcohol plus virus ($P < 0.05$). The mean SI was 62.87% ± 28.62% in cirrhotic patients without ascites and 65.92% ± 23.64% in cirrhotic patients with ascites. The difference between both groups was not significant ($P = 0.35$). We used Child-Pugh classification to estimate the severity of liver disease in both bleeding and non-bleeding groups as a whole. The mean SI was 52.60% ± 25.31% in Child-Pugh grade A, 69.29% ± 22.34% in Child-Pugh grade B, and 76.64% ± 22.01% in Child-Pugh grade C. The SI in Child-Pugh grade A differed significantly ($P < 0.05$) from those in Child-Pugh grades B and C. Although the SI in Child-Pugh grade B seemed to be lower than that in Child-Pugh grade C, the difference was not statistically significant ($P = 0.20$).

Portal shunt index and endoscopic appearances of esophageal varices

The esophageal varices were endoscopically graded according to the Japanese Research Society for Portal Hypertension by color, forms, location, diameters, and the red color sign (RCS). Variceal forms were classified into three types: straight (F_1), enlarged tortuous (F_2), and largest sized (F_3). The mean SI was 57.03% ± 27.63% in F_1 group, 67.47% ± 24.99% in F_2 group, and 72.65% ± 8.77% in F_3 group (Table 2). Mean SI in F_3 group was higher than in F_2 and F_1 groups. The difference between the groups was statistically significant ($P < 0.05$). Mean SI in RCS-negative group was 52.94% ± 26.31% and in RCS-positive group was 68.16% ± 23.78%. The difference between both groups was not significant ($P = 0.054$).

Portal shunt index and risk of esophageal variceal bleeding

The receiver operating characteristic (ROC) showed the cutoff point of portal SI between normal subjects and cirrhotic patients at 20% with a 90.0% sensitivity and 53.3% specificity. The cutoff point of portal SI between the cirrhotic patients with and without variceal bleeding was 60% with a 96.0% sensitivity and 72.0% specificity (Figure 2). Basically, the cirrhotic patients with esophageal varices who had a portal SI of more than 60% might have high risk of variceal bleeding, and the patients who had a portal SI more than 20% were likely to develop esophageal varices.

Table 2 Portal shunt index in cirrhotic patients according to the etiologies of cirrhosis, presence of ascites, Child-Pugh grade and endoscopic appearances

			n	Portal shunt index (%)
Etiology of cirrhosis				
	Alcohol		29	78.87 ± 22.05
	Virus[1]		14	56.67 ± 24.08
	Alcohol with virus[1]		7	41.23 ± 23.47
Ascites	Absence		33	62.87 ± 28.62
	Presence		17	65.92 ± 23.64
Severity of liver diseases		Child A	21	52.60 ± 25.31
		Child B	18	69.29 ± 22.34
		Child C	11	76.64 ± 22.01
Endoscopic appearances		F_1	14	50.03 ± 27.63
		F_2	20	67.47 ± 24.99
		F_3	16	72.65 ± 8.77
		RCS-positive	27	68.16 ± 23.78
		RCS-negative	23	52.04 ± 26.31

[1] Including hepatitis B virus and hepatitis C virus.

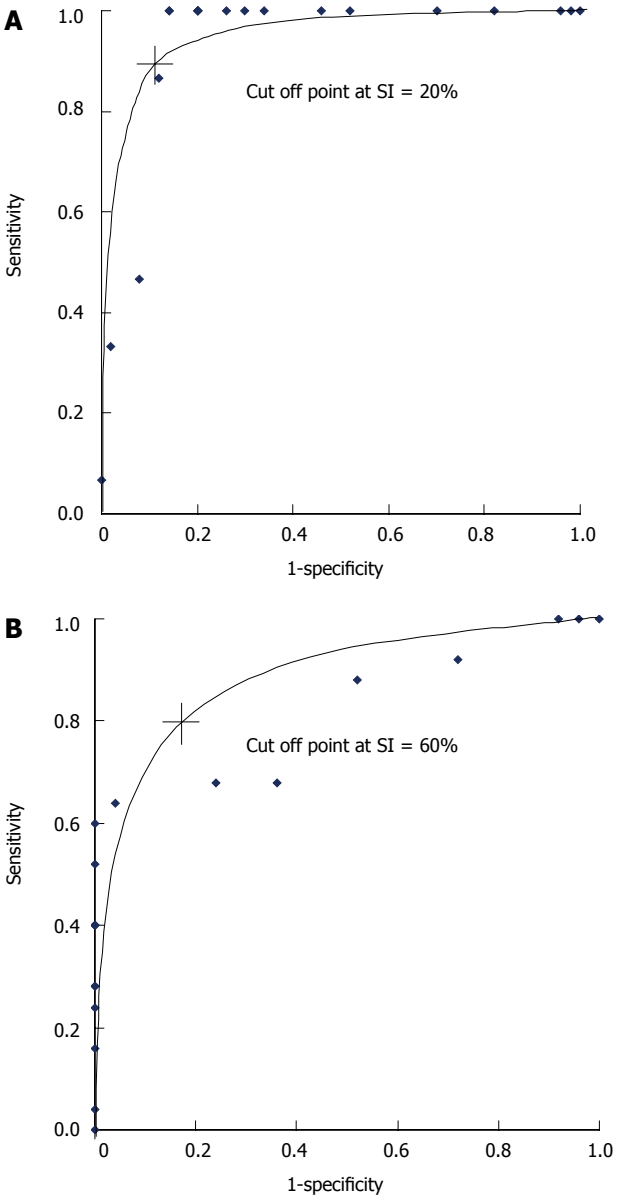

Figure 2 ROC curves of the portal shunt indices. **A**: Between normal subjects and cirrhotic patients with esophageal varices; **B**: Between cirrhotic patients with and without variceal bleeding (bleeder *vs* non-bleeder). + Indicates a cutoff point with maximum discrimination.

DISCUSSION

In this study, we used per rectal portal scintigraphy to detect and investigate portosystemic shunting in order to determine the difference among the bleeding, the non-bleeding cirrhotic and the normal control groups. We found that the SI was higher in the bleeders compared with other groups. The SI correlated with the severity of liver disease and the size of esophageal varices. Bleeding from the varices was a major complication of portal hypertension that may vary according to the severity of portal hypertension. The cumulative survival rate of patients with esophageal varices was significantly lower than that of patients without varices[14]. The cumulative survival rate of patients with portosystemic shunting seen by scintillation splenoportography was also significantly lower than that of patients without such a shunt [15]. Many factors could potentially be used to predict variceal bleeding in cirrhotic patients with esophageal varices. These predictors include the following: (1) local factors such as variceal size, vessel radius, or red color sign; (2) hemodynamic factors: portal pressure > 12 mmHg, blood volume, and collateral blood flow; and (3) severity of liver disease[10]. In general, the direct measurement of portal pressure is performed invasively and not readily available in many clinical settings. In those circumstances, indirect measurement of portal pressure, such as portosystemic shunt evaluation may be used instead. Recently, various methods of measuring portosystemic shunt have been developed, and the relationships between the risk of variceal bleeding and the extent of portosystemic shunt have been studied.

Per rectal portal approach in the measurement of portal circulation using various radionuclides has been described as a relatively non-invasive method by many researchers[9,16-19]. In our present study, we chose to perform non-invasive per rectal portal scintigraphy using ^{99m}Technetium pertechnetate because this radionuclide is well absorbed by the rectum, has a short half life and large doses could be used[20]; it also generates images useful for diagnosis and is economical. The SI from per rectal scintigraphy also correlated well with the degree of portal pressure[9]. In this study, the mean SI in cirrhotic patients with esophageal varices was significantly higher than that in normal subjects. The cutoff level of SI indicating development of esophageal varices derived from the ROC was 20%. All six cirrhotic patients with esophageal varices whose SIs were less than 20% belonged to Child-Pugh grade A and had less severe variceal forms without red color signs than patients with esophageal varices and an SI more than 20%. None of these six patients with small varices bled.

We also studied the association between Child-Pugh class, etiology of cirrhosis and portal scintigraphy in cirrhotic patients with esophageal varices. The mean SI

in Child-Pugh grade C was higher than that of Child-Pugh grade B and grade A, with a significant difference between grade C and A. The SI tended to be higher in patients with more severe liver disease. Because the Child-Pugh classification correlated well with the severity of liver disease, serial measurement of portal circulation by SI might be helpful in investigating the progress of cirrhosis. The SI in alcoholic cirrhosis was significantly higher than other etiologies because of more severe liver disease in alcoholic group. The SI in patients with alcohol and virus cirrhosis was lower compared with cirrhosis induced by alcohol or virus alone. This might possibly result from the small number of patients in alcohol with virus group. The SIs in cirrhotic patients with and without ascites were not significantly different. In comparison of the SI in different variceal forms, there were significant differences among the size of varices. Higher SIs were found in patients with higher variceal forms. There was a good relationship between SI and the size of esophageal varices.

The SI values in the present study were significantly different in cirrhotic patients with and without variceal bleeding. It was presumed that an increasing flow of blood through the collateral of inferior mesenteric veins measured by portal scintigraphy reflected the increasing pressure in the portal system, the development and the size of esophageal varices. This increasing pressure was at a certain level, adequately high for the varices to rupture. So the higher the SI, the higher was the risk of bleeding. In this study, the SI was clearly demonstrated to be a useful predictor of the risk of bleeding. By ROC, an SI of more than 60% correlated with esophageal variceal bleeding. We presumed that if cirrhotic patients had an SI of more than 20%, they would have adequate portal pressure to develop the esophageal varices, and if the SI was more than 60% they carried the risk of variceal bleeding. However, further prospective, longitudinal studies are needed to confirm these results.

In conclusion, this study suggests that portosystemic shunt, represented by the SI and evaluated by per rectal portal scintigraphy, is higher in cirrhotic patients with esophageal varices. The magnitude of blood shunting through these tributaries correlates well with the etiology and severity of cirrhosis and the risk of variceal bleeding. An SI of more than 60% in cirrhotic patients with esophageal varices reflects a high risk of variceal bleeding.

REFERENCES

1 **Van Ruiswyk J**, Byrd JC. Efficacy of prophylactic sclerotherapy for prevention of a first variceal hemorrhage. *Gastroenterology* 1992; **102**: 587-597

2 **Thomopoulos KC**, Labropoulou-Karatza C, Mimidis KP, Katsakoulis EC, Iconomou G, Nikolopoulou VN. Non-invasive predictors of the presence of large oesophageal varices in patients with cirrhosis. *Dig Liver Dis* 2003; **35**: 473-478

3 **de Franchis R**. Evaluation and follow-up of patients with cirrhosis and oesophageal varices. *J Hepatol* 2003; **38**: 361-363

4 **Mendez C**, Marsano L, Wright R. Complications of cirrhosis. *J Ky Med Assoc* 2003; **101**: 403-414

5 **von Herbay A**, Frieling T, Häussinger D. Color Doppler sonographic evaluation of spontaneous portosystemic shunts and inversion of portal venous flow in patients with cirrhosis. *J Clin Ultrasound* 2000; **28**: 332-339

6 **Yin XY**, Lu MD, Huang JF, Xie XY, Liang LJ. Color Doppler velocity profile assessment of portal hemodynamics in cirrhotic patients with portal hypertension: correlation with esophageal variceal bleeding. *J Clin Ultrasound* 2001; **29**: 7-13

7 **Burkart DJ**, Johnson CD, Ehman RL, Weaver AL, Ilstrup DM. Evaluation of portal venous hypertension with cine phase-contrast MR flow measurements: high association of hyperdynamic portal flow with variceal hemorrhage. *Radiology* 1993; **188**: 643-648

8 **Shiomi S**, Kuroki T, Kurai O, Kobayashi K, Ikeoka N, Monna T, Ochi H. Portal circulation by technetium-99m pertechnetate per-rectal portal scintigraphy. *J Nucl Med* 1988; **29**: 460-465

9 **Shiomi S**, Kuroki T, Ueda T, Takeda T, Ikeoka N, Nishiguchi S, Nakajima S, Kobayashi K, Ochi H. Clinical usefulness of evaluation of portal circulation by per rectal portal scintigraphy with technetium-99m pertechnetate. *Am J Gastroenterol* 1995; **90**: 460-465

10 **The general rules for recording endoscopic findings on esophageal varices.** *Jpn J Surg* 1980; **10**: 84-87

11 **Pomier-Layrargues G**, Villeneuve JP, Willems B, Huet PM, Marleau D. Systemic and hepatic hemodynamics after variceal hemorrhage: effects of propranolol and placebo. *Gastroenterology* 1987; **93**: 1218-1224

12 **Ready JB**, Robertson AD, Goff JS, Rector WG. Assessment of the risk of bleeding from esophageal varices by continuous monitoring of portal pressure. *Gastroenterology* 1991; **100**: 1403-1410

13 **Dawson-Saunders B**. Evaluating Diagnostic Procedures. In: Dawson-Saunders B, Trapp RG, editors. Basic&Clinical Biostatistics. 2 nd ed. Connecticut: Appleton&Lange, 1994: 243-246

14 **Baker LA**, Smith C, Lieberman G. The natural history of esophageal varices; a study of 115 cirrhotic patients in whom varices were diagnosed prior to bleeding. *Am J Med* 1959; **26**: 228-237

15 **Syrota A**, Paraf A, Gaudebout C, Desgrez A. Significance of intra- and extrahepatic portasystemic shunting in survival of cirrhotic patients. *Dig Dis Sci* 1981; **26**: 878-885

16 **Castell DO**, Grace ND, Wennar MH, Chalmers TC, Moore EW. Evaluation of portal circulation in hepatic cirrhosis. A new method using xenon. *Gastroenterology* 1969; **57**: 533-541

17 **Tonami N**, Nakajima K, Hisada K, Tanaka N, Kobayashi K. A noninvasive method for evaluating portal circulation by administration of Ti-201 per rectum. *J Nucl Med* 1982; **23**: 965-972

18 **Yen CK**, Pollycove M, Crass R, Lin TH, Baldwin R, Lamb J. Portasystemic shunt fraction quantification with colonic iodine-123 iodoamphetamine. *J Nucl Med* 1986; **27**: 1321-1326

19 **Wang JY**, Chen SL, Chen FZ, Xu WG, Hu DC, Chen XF, Jin G, Liu HY. A non-invasive method for evaluating cirrhotic portal hypertension by administration of ^{99m}Tc-MIBI per rectum. *J Gastroenterol Hepatol* 1995; **10**: 169-173

20 **Urbain D**, Jeghers O, Ham HR. Per-rectal portal scintigraphy: comparison between technetium-99m, thallium-201, and iodine-123-HIPDM. *J Nucl Med* 1988; **29**: 2020-2021

S- Editor Liu Y **L- Editor** Zhu LH **E- Editor** Ma WH

PO Box 2345, Beijing 100023, China
www.wjgnet.com
wjg@wjgnet.com

World J Gastroenterol 2007 February 7; 13(5): 796-800
World Journal of Gastroenterology ISSN 1007-9327

RAPID COMMUNICATION

Increased plasma malondialdehyde and fructosamine in anemic *H pylori* infected patients: Effect of treatment

G Vijayan, RC Sundaram, Zachariah Bobby, Abdoul Hamide, N Selvaraj, N Rattina Dasse

G Vijayan, RC Sundaram, Zachariah Bobby, N Selvaraj, N Rattina Dasse, Department of Biochemistry, Jawaharlal Institute of Postgraduate Medical Education and Research, Pondicherry 605006, India
Abdoul Hamide, Department of Medicine, Jawaharlal Institute of Postgraduate Medical Education and Research, Pondicherry 605006, India
Correspondence to: Dr. Zachariah Bobby, Assistant Professor, Department of Biochemistry, Jawaharlal Institute of Postgraduate Medical Education and Research, Pondicherry 605006, India. zacbobby@yahoo.com
Telephone: +91-413-2273078 Fax: +91-413-2372067
Received: 2006-07-01 Accepted: 2006-12-30

Abstract

AIM: To unravel the possible association of malondialdehyde (MDA) and fructosamine in anemic *H pylori* infected patients and to observe the alteration in MDA and fructosamine levels in these patients after treatment for one month.

METHODS: Fructosamine, MDA and glucose were estimated in 22 anemic *H pylori* infected patients and 16 healthy controls. Hematological parameters were also evaluated in both the groups using Sysmex-K-100 automated cell counter. The *H pylori* infected patients were randomly divided into two groups. *H pylori* infected patients in Group Ⅰ received both iron supplementation and anti-*H pylori* therapy, while patients in Group Ⅱ received only iron supplementation. All the biochemical and hematological parameters were estimated after one month of treatment.

RESULTS: In anemic *H pylori* infected patients, while MDA (5.41 ± 2.16 *vs* 2.26 ± 0.50; $P < 0.05$) and fructosamine (2.64 ± 0.93 *vs* 1.60 ± 0.35; $P < 0.05$) were significantly increased, iron (32.72 ± 14.93 *vs* 110.25 ± 26.58; $P < 0.05$), hemoglobin (6.9 ± 2.6 *vs* 12.66 ± 0.74; $P < 0.05$) and ferritin (28.82 ± 16.27 *vs* 140.43 ± 30.72; $P < 0.05$) levels were significantly decreased compared with the controls. With partial correlation analysis, fructosamine was found to have a significant positive correlation with MDA. In Group Ⅰ, while MDA level decreased significantly (3.11 ± 1.73 *vs* 5.50 ± 2.46; $P < 0.05$), there was a significant increase in iron (84.09 ± 29.51 *vs* 36.09 ± 17.81; $P < 0.05$), hemoglobin (10.40 ± 1.11 *vs* 7.42 ± 1.90; $P < 0.05$) and ferritin (116.91 ± 63.34 *vs* 30.46 ± 17.81; $P < 0.05$) levels after one month. There was no significant change in the levels of fructosamine in group Ⅰ after treatment. Similarly, no significant alterations were noted in the levels of MDA, fructosamine, hemoglobin or ferritin in Group Ⅱ patients after one month of treatment.

CONCLUSION: An increased level of fructosamine and MDA was found in anemic *H pylori* infected patients. Present data supports the premise that lipid peroxides *per se* do play a role in the glycation of plasma proteins. Furthermore, the findings from this study indicate that treatment for both anemia and *H pylori* infections is required for lowering the levels of lipid peroxides in these patients.

Key words: *H pylori*; Anemia; Fructosamine; Malondialdehyde; Iron; Glycation

Vijayan G, Sundaram RC, Bobby Z, Hamide A, Selvaraj N, Rattina Dasse N. Increased plasma malondialdehyde and fructosamine in anemic *H pylori* infected patients: Effect of treatment. *World J Gastroenterol* 2007; 13(5): 796-800

http://www.wjgnet.com/1007-9327/13/796.asp

INTRODUCTION

H pylori, a gram negative bacillus is the most common pathogenic bacteria in the world[1]. Even though approximately half of the population in the world has *H pylori* infection, the prevalence and severity vary greatly among countries and population groups within the same countries. The overall prevalence of *H pylori* is strongly correlated with socio-economic conditions[1]. The prevalence among middle aged adults is over 80% in many developing countries as compared with 20%-50% in industrialized countries[2].

Accumulating evidences suggest an association between gastric *H pylori* infection and low iron stores and anemia[3-6]. Epidemiological studies have demonstrated a close relationship between serum ferritin and presence of anti-*H pylori* IgG[3,4]. A fall in serum ferritin reflects declining body iron stores and is an accepted marker of iron deficiency. It has also been found that eradication of *H pylori* infection in iron-deficient anemic patients was found to reverse the iron deficiency status in both children and adults[5,6].

Spontaneous nonenzymatic modifications of protein are commonly reported in tissues with slow turnover and they are considered by several authors as a possible common mechanism involved in the progression of many pathological conditions[6]. Among the nonenzymatic processes, oxidative stress and glycation have aroused a particular interest in recent years[7,8].

Glycation is a non-enzymatic condensation reaction between reducing sugars and free amino groups at NH_2-terminus or susceptible ε-amino groups of lysine residues of proteins. The reaction is initiated by the reversible formation of a schiff base, which undergoes a rearrangement to form a relatively stable Amadori product[9]. The pathological consequences of these alterations very much depend on the nature of proteins involved as well as on their function and concentration in a particular organ[9]. The rate of formation of glycated protein is considered to depend on the ambient concentration of glucose and half life of the protein[9]. However, there is convincing evidence that concentrations of nonenzymatically glycated protein are increased in many non-diabetic pathological states[10-13]. Elevated concentrations of glycated hemoglobin have been found in myocardial infarction, chronic renal failure, and nephrotic syndrome patients with normal blood glucose concentrations[10-12]. Similarly high concentrations of fructosamine are reported in non-diabetic chronic renal failure and rheumatic arthritis patients[12,13]. Increased levels of glycated hemoglobin (HbA_{1C}) have also been documented in iron deficiency anemic patients without any history of diabetes[14-16].

We have recently demonstrated that lipid peroxides *per se* can enhance the process of protein glycation[17]. This result was in agreement with the findings of Jain *et al*[18]. We have also demonstrated that the process of lipid peroxidation and glycation are closely associated in patients with chronic renal failure, hyperthyroid, asthma, nephrotic syndrome and patients with rheumatoid arthritis[19-24].

Even though there are substantial reports demonstrating the presence of excess lipid peroxides in patients with *H pylori* infection, there is a dearth of information regarding the levels of glycated proteins in these patients with anemia. Given the importance of glycated protein in causing pathological complication in various diseases, it was deemed pertinent to investigate the levels of glycated plasma protein and the possible association with the levels of lipid peroxides in *H pylori* infected patients who were anemic. Furthermore, we explored the effect of treatment on the levels of these parameters. This study is the first to describe an association between lipid peroxides and glycated protein in anemic *H pylori* infected patients.

MATERIALS AND METHODS

Blood sample (3 mL) was obtained from 22 anemic patients with *H pylori* infection and 16 age matched healthy subjects. Anemic patients were recruited from the outpatient department of our institute, JIPMER, Pondicherry, India. Only patients of 13 years of age or older were enrolled for this study. Anemic patients were selected based on the hemoglobin levels (Hb < 11 g/dL) and peripheral blood smear suggesting iron deficiency anemia. Selected patients underwent detailed physical examination and laboratory evaluation.

One milliliter of the whole blood in EDTA was used for the analysis of hemoglobin and red cell indices using Sysmex-K-100 automated cell counter (Sysmex Singapore Pvt. Ltd, Singapore). The rest of the sample was centrifuged at 3000 r/min for 10 min. The plasma was separated and analyzed for lipid peroxides, fructosamine, iron, ferritin and glucose. Plasma ferritin level was determined by ELISA using human ferritin enzyme immunoassay test kit (IBL Immunobiological Laboratories, Hamburg, Germany). Fructosamine was measured by p-indonitrotetrazolium violet kinetic method using the Raichem Kits (Haemagen Diagnostics, San Diego, CA) adapted to 550 Express Plus Analyzer (Ciba Corning Diag., Oberlin, OH). The concentration of lipid peroxides in plasma was measured by thiobarbituric acid method[25]. Plasma iron and glucose were measured by fully automated ferrozine and glucose oxidase methods respectively in Ciba Corning 550 Express Plus. All patients who were found to have iron deficiency by the above parameters underwent stool examination on three consecutive days for the presence of hookworm ova on microscopy and for occult blood by benzidine test.

After informed consent, upper gastrointestinal endoscopy was done and multiple biopsy specimens were obtained from the antral mucosa for rapid urease test and histology. Tissue sections were stained for *H pylori* with Geimsa. *H pylori* infection was defined as a visible organism seen under microscopy and a positive rapid urease test. Patients with histories of consumption of nonsteroidal anti-inflammatory drugs (NSAIDs), anticoagulants or corticosteroids, those with hematological disorders or stool samples positive for occult blood or hookworm ova, and those with duodenal or gastric ulcers or carcinoma stomach at endoscopy were excluded from the study.

Patients positive for *H pylori* infection by rapid urease test and on histology were randomly assigned to two groups (Group I and Ⅱ) by creating block sizes of six or eight and linking to five-digit random numbers (Rand Corporation; New York: The Free Press, 1955). Patients in Group I received oral ferrous sulfate tablets 200 mg thrice a day for 1 mo, and a 14-d course of anti-*H pylori* therapy consisting of clarithromycin 250 mg bid, lansoprazole 30 mg bid and tinidazole 500 mg bid. Those in Group Ⅱ received only oral ferrous sulfate tablets as above. All the above-mentioned biochemical and hematological parameters were assayed after 1 mo therapy. This study was approved by the ethics committee of JIPMER. Informed consent was obtained from all subjects.

Statistical analysis

Student's *t* test was used to estimate the differences between the groups. Correlation was assessed by the partial correlation analysis. All results are presented as mean ± SD. $P < 0.05$ was considered statistically significant.

RESULTS

All the parameters tested in both the *H pylori* infected

Table 1 Comparison of biochemical and hematological parameters in *H pylori* infected anemic patients and controls

Parameters	Control group (n = 16)	Test group (n = 22)
Hemoglobin (g/dL)	12.66 ± 0.74	6.9 ± 2.6[a]
Iron (μg/dL)	110.25 ± 26.58	32.72 ± 14.93[a]
Ferritin (ng/mL)	140.43 ± 30.72	28.82 ± 16.27[a]
Fructosamine (nmol/L)	1.60 ± 0.35	2.64 ± 0.93[a]
MDA (mmol/L)	2.26 ± 0.50	5.41 ± 2.16[a]
Glucose (mg/dL)	81.19 ± 9.74	83.50 ± 8.27

[a]$P < 0.05$ *vs* control group.

group and healthy controls are given in Tables 1 and 2. Fructosamine levels were significantly higher in *H pylori* infected patients compared to controls. Levels of lipid peroxides were significantly increased in the test group than the healthy age-matched controls. In the test group, a significant correlation ($r = 0.50$, $P = 0.02$) was observed between fructosamine and MDA using partial correlation analysis controlling for blood glucose level. As previously reported, hemoglobin, serum iron and ferritin levels were significantly reduced in *H pylori* infected patients when compared with controls.

Response to therapy

Patients in group I had a greater increase in mean hemoglobin level (2.98 g/dL) after one mo than those in Group Ⅱ (1.07 g/dL). The increases in mean serum iron (48 μg /dL *vs* 15.91 μg/dL) and ferritin levels (86.45 ng/mL *vs* 25.28 ng/mL) after one mo of treatment were also more marked in Group I than in Group Ⅱ. There was also a significantly decreased MDA levels in Group I when compared with Group Ⅱ after one mo of treatment. However, there was no significant alteration in fructosamine levels in both the groups after one mo of treatment.

DISCUSSION

Free radicals and other reactive oxygen species (ROS) are generated by all aerobic cells and are known to participate in a great variety of deleterious reactions[26]. The oxidative damage caused by free radicals is believed to play a pivotal role in the pathogenesis of *H pylori* infection[27-29]. Lipid peroxidation is one of the reactions set into motion as a consequence of the formation of these radicals in cells and tissues[26]. The initiation of lipid peroxidation has been considered the proximal cause of cell membrane destruction and cell damage[26]. Increased amounts of malondialdehyde (MDA) have been found in patients infected with *H pylori*[30-32]. Our results also indicate an increased lipid peroxidation in *H pylori* infected patients.

Lipid peroxidation can damage proteins, lipids, carbohydrates and nucleic acids. Plasma membranes are the critical targets of lipid peroxides[26]. Apart from participating in these deleterious reactions, lipid peroxides *in vitro* have been found to enhance the glycation of proteins[18]. We have also recently reported that MDA can enhance the glycation of hemoglobin *per se*[17].

Table 2 Changes in hematological and biochemical parameters of groups after treatment

Parameters	Group Ⅰ (*H pylori* treatment + oral iron therapy) (n = 11)	Group Ⅱ (Oral iron therapy) (n = 11)
Hemoglobin (g/dL)		
Baseline	7.42 ± 1.90	6.38 ± 2.37
1 mo after therapy	10.40 ± 1.11[a]	7.45 ± 1.94
Iron (μg/dL)		
Baseline	36.09 ± 18.97	29.36 ± 9.10
1 mo after therapy	84.09 ± 29.51[a]	45.27 ± 21.36[a]
Ferritin (ng/mL)		
Baseline	30.46 ± 17.81	27.18 ± 15.26
1 mo after therapy	116.91 ± 63.34[a]	52.46 ± 39.21
Fructosamine (nmol/L)		
Baseline	2.28 ± 0.62	2.99 ± 1.06
1 mo after therapy	2.13 ± 0.63	2.27 ± 0.97
MDA (mmol/L)		
Baseline	5.50 ± 2.46	5.32 ± 1.94
1 mo after therapy	3.11 ± 1.73[a]	3.81 ± 1.61

[a]$P < 0.05$ *vs* the baseline value before treatment.

We have found that lipid peroxides are closely associated with glycated hemoglobin in hyperthyroid, chronic renal failure and asthma patients[20-22]. We observed a significant association between MDA and fructosamine in non-diabetic asthma, nephrotic syndrome, rheumatoid arthritis and chronic renal failure patients[19,22-24].

In the present study, the levels of fructosamine were increased significantly in anemic patients infected with *H pylori* when compared with healthy controls. Among the various methods proposed for the measurement of glycated serum proteins, fructosamine is the method of choice for the clinicians[9]. As albumin is the most abundant protein in serum and contains multiple lysine residues, measurement of fructosamine is mainly the determination of glycated albumin[9].

In anemic patients, the concentrations of HbA_{1C} have been reported to be increased[14-16]. Several hypotheses have been formulated to explain the increase in glycated hemoglobin concentrations in these patients. It has been proposed that in iron deficiency the quarternary structure of the hemoglobin molecule may be altered, thus glycation of the β-globin chains occur more readily[14]. According to some investigators, the increase in glycated hemoglobin in non-diabetic anemic patients is mainly attributed to the decrease in hemoglobin levels in these patients[16].

To our knowledge, no study to date has attempted to clarify whether there is any increase in glycated protein levels in anemic, *H pylori* infected patients and whether this increase is the consequence of an increased lipid peroxidation among these patients.

To verify this hypothesis, we tested a well-defined group of anemic, *H pylori* infected patients before and after one month of treatment. In our study, the increased MDA was found to be significantly associated with increased fructosamine concentrations ($r = 0.50$, $P = 0.02$) before treatment, even when the proposed effect of

glucose on the concentrations of fructosamine was refuted by partial correlation analysis. The mechanism by which MDA enhances the glycation process has not been clearly elucidated. MDA is thought to enhance the process of protein glycation by acting as an anchor between sugar and hemoglobin moieties[18]. It has also been suggested that oxidative stress can facilitate the autoxidation of glucose to dicarbonyl intermediates, an early step in the Maillard reaction[33].

There was a significant decrease in MDA levels in *H pylori* infected patients after one month of treatment with both ferrous sulfate and anti-*H pylori* therapy. Previous reports have indicated that the levels of lipid peroxides decrease significantly after treatment for *H pylori* infection[30,32]. Similarly, in iron deficiency anemia it has been found that supplementation with iron reduces the levels of glycated hemoglobin[14]. There was no significant decrease in MDA levels in the test group treated with only oral iron. In both the test groups, there was no significant reduction in fructosamine levels after one month of treatment. There also existed no significant association in the anemic *H pylori* infected group between fructosamine and MDA after one month of treatment. One reason for these observed results can be attributed to the half-life of glycated proteins.

Recent studies have uncovered a myriad of pathological events induced by glycated albumin. These include increasing the expression of extracellular matrix protein, activation of protein kinase C, and stimulating the expression of transforming growth factor β_1 and its primary signaling receptor, the TGF-β type Ⅱ receptor. Apart from these alterations, glycated albumin has been found to alter the levels of NF-κB. These data support the hypothesis that glycated albumin is a sufficient stimulus to set into motion pathogenic signaling pathways. Several investigators have also reported that *H pylori* can activate NF-κB in human gastric mucosa *in vivo* and cultured gastric epithelial cells *in vitro*, thus the pathogenesis may be mediated through NF-κB[34-36]. Studies have shown that these alterations in molecular pathways play an essential role in the *H pylori* induced inflammation and associated complications.

In conclusion, this study gives a snapshot of an increased glycated serum protein and lipid peroxide levels in *H pylori* infected patients who were anemic as well. These data from the present study also supports the notion that alteration in the levels of MDA in anemic *H pylori* infected patients may be the basis for enhanced levels of fructosamine. Furthermore, the findings from our study indicate that treatment for both anemia and *H pylori* are required for reducing the levels of lipid peroxides in these patients.

It would be interesting to investigate the levels of fructosamine in non-anemic *H pylori* infected patients and it is worthwhile to investigate if additional supplementation of antioxidants would potentiate any further attenuation of protein glycation in *H pylori* infected patients when compared with the regular therapy. A longer follow-up investigation after treatment would shed more light into the above-mentioned alterations in anemic *H pylori* infected subjects.

REFERENCES

1 **Malaty HM**, Graham DY. Importance of childhood socioeconomic status on the current prevalence of Helicobacter pylori infection. *Gut* 1994; **35**: 742-745
2 **Valle JD**. Peptic ulcer disease and related disorders. In: Harrison's Priniciples of Internal Medicine. 15th ed. New York, USA: McGraw Hill, 2001: 1649-1664
3 **Berg G**, Bode G, Blettner M, Boeing H, Brenner H. Helicobacter pylori infection and serum ferritin: A population-based study among 1806 adults in Germany. *Am J Gastroenterol* 2001; **96**: 1014-1018
4 **Milman N**, Rosenstock S, Andersen L, Jørgensen T, Bonnevie O. Serum ferritin, hemoglobin, and Helicobacter pylori infection: a seroepidemiologic survey comprising 2794 Danish adults. *Gastroenterology* 1998; **115**: 268-274
5 **Marignani M**, Angeletti S, Bordi C, Malagnino F, Mancino C, Delle Fave G, Annibale B. Reversal of long-standing iron deficiency anaemia after eradication of Helicobacter pylori infection. *Scand J Gastroenterol* 1997; **32**: 617-622
6 **Choe YH**, Kim SK, Son BK, Lee DH, Hong YC, Pai SH. Randomized placebo-controlled trial of Helicobacter pylori eradication for iron-deficiency anemia in preadolescent children and adolescents. *Helicobacter* 1999; **4**: 135-139
7 **Kennedy AL**, Lyons TJ. Glycation, oxidation, and lipoxidation in the development of diabetic complications. *Metabolism* 1997; **46**: 14-21
8 **Hunt JV**, Dean RT, Wolff SP. Hydroxyl radical production and autoxidative glycosylation. Glucose autoxidation as the cause of protein damage in the experimental glycation model of diabetes mellitus and ageing. *Biochem J* 1988; **256**: 205-212
9 **Lapolla A**, Traldi P, Fedele D. Importance of measuring products of non-enzymatic glycation of proteins. *Clin Biochem* 2005; **38**: 103-115
10 **Chowdhury TA**, Lasker SS. Elevated glycated haemoglobin in non-diabetic patients is associated with an increased mortality in myocardial infarction. *Postgrad Med J* 1998; **74**: 480-481
11 **Cecchin E**, De Marchi S, Panarello G, De Angelis V. Rheological abnormalities of erythrocyte deformability and increased glycosylation of hemoglobin in the nephrotic syndrome. *Am J Nephrol* 1987; **7**: 18-21
12 **Sabater J**, Quereda C, Herrera I, Pascual J, Villafruela JJ, Ortuño J. Nonenzymatic glycosylation of hemoglobin and total plasmatic proteins in end-stage renal disease. *Am J Nephrol* 1991; **11**: 37-43
13 **Rodríguez-García J**, Requena JR, Rodríguez-Segade S. Increased concentrations of serum pentosidine in rheumatoid arthritis. *Clin Chem* 1998; **44**: 250-255
14 **Coban E**, Ozdogan M, Timuragaoglu A. Effect of iron deficiency anemia on the levels of hemoglobin A1c in nondiabetic patients. *Acta Haematol* 2004; **112**: 126-128
15 **Brooks AP**, Metcalfe J, Day JL, Edwards MS. Iron deficiency and glycosylated haemoglobin A. *Lancet* 1980; **2**: 141
16 **El-Agouza I**, Abu Shahla A, Sirdah M. The effect of iron deficiency anaemia on the levels of haemoglobin subtypes: possible consequences for clinical diagnosis. *Clin Lab Haematol* 2002; **24**: 285-289
17 **Selvaraj N**, Bobby Z, Sathiyapriya V. Effect of lipid peroxides and antioxidants on glycation of hemoglobin: an in vitro study on human erythrocytes. *Clin Chim Acta* 2006; **366**: 190-195
18 **Jain SK**, Palmer M. The effect of oxygen radicals metabolites and vitamin E on glycosylation of proteins. *Free Radic Biol Med* 1997; **22**: 593-596
19 **Selvaraj N**, Bobby Z, Das AK, Ramesh R, Koner BC. An evaluation of level of oxidative stress and protein glycation in nondiabetic undialyzed chronic renal failure patients. *Clin Chim Acta* 2002; **324**: 45-50
20 **Selvaraj N**, Bobby Z, Koner BC, Das AK. Reassessing the increased glycation of hemoglobin in nondiabetic chronic renal failure patients: a hypothesis on the role of lipid peroxides. *Clin Chim Acta* 2005; **360**: 108-113
21 **Mohan Kumar KM**, Bobby Z, Selvaraj N, Kumar Das A,

Chandra Koner B, Sen SK, Ramesh R, Ranganathan P. Possible link between glycated hemoglobin and lipid peroxidation in hyperthyroidism. *Clin Chim Acta* 2004; **342**: 187-192

22 **Sathiyapriya V**, Bobby Z, Vinod Kumar S, Selvaraj N, Parthibane V, Gupta S. Evidence for the role of lipid peroxides on glycation of hemoglobin and plasma proteins in non-diabetic asthma patients. *Clin Chim Acta* 2006; **366**: 299-303

23 **Balamurugan R**, Bobby Z, Selvaraj N, Nalini P, Koner BC, Sen SK. Increased protein glycation in non-diabetic pediatric nephrotic syndrome: possible role of lipid peroxidation. *Clin Chim Acta* 2003; **337**: 127-132

24 **Babu NP**, Bobby Z, Selvaraj N, Harish BN. Increased fructosamine in non-diabetic rheumatoid arthritis patients: role of lipid peroxides and glutathione. *Clin Chem Lab Med* 2006; **44**: 848-852

25 **Satoh K**. Serum lipid peroxide in cerebrovascular disorders determined by a new colorimetric method. *Clin Chim Acta* 1978; **90**: 37-43

26 **Freeman BA**, Crapo JD. Biology of disease: free radicals and tissue injury. *Lab Invest* 1982; **47**: 412-426

27 **Naito Y**, Yoshikawa T. Molecular and cellular mechanisms involved in Helicobacter pylori-induced inflammation and oxidative stress. *Free Radic Biol Med* 2002; **33**: 323-336

28 **Giamarellos-Bourboulis EJ**, Tzivras M, Kourtesas D, Arnaoutis TP, Delladatsima I, Dionyssiou-Asteriou A, Davaris P, Vafiadis-Zouboulis I, Archimandritis A. Lipid peroxidation in chronic gastritis; any influence of Helicobacter pylori? *Prostaglandins Leukot Essent Fatty Acids* 2003; **68**: 257-261

29 **Davies GR**, Simmonds NJ, Stevens TR, Sheaff MT, Banatvala N, Laurenson IF, Blake DR, Rampton DS. Helicobacter pylori stimulates antral mucosal reactive oxygen metabolite production *in vivo*. *Gut* 1994; **35**: 179-185

30 **Drake IM**, Mapstone NP, Schorah CJ, White KL, Chalmers DM, Dixon MF, Axon AT. Reactive oxygen species activity and lipid peroxidation in Helicobacter pylori associated gastritis: relation to gastric mucosal ascorbic acid concentrations and effect of *H pylori* eradication. *Gut* 1998; **42**: 768-771

31 **Farinati F**, Della Libera G, Cardin R, Molari A, Plebani M, Rugge M, Di Mario F, Naccarato R. Gastric antioxidant, nitrites, and mucosal lipoperoxidation in chronic gastritis and Helicobacter pylori infection. *J Clin Gastroenterol* 1996; **22**: 275-281

32 **Santra A**, Chowdhury A, Chaudhuri S, Das Gupta J, Banerjee PK, Mazumder DN. Oxidative stress in gastric mucosa in Helicobacter pylori infection. *Indian J Gastroenterol* 2000; **19**: 21-23

33 **Slatter DA**, Murray M, Bailey AJ. Formation of a dihydropyridine derivative as a potential cross-link derived from malondialdehyde in physiological systems. *FEBS Lett* 1998; **421**: 180-184

34 **Hattori Y**, Kakishita H, Akimoto K, Matsumura M, Kasai K. Glycated serum albumin-induced vascular smooth muscle cell proliferation through activation of the mitogen-activated protein kinase/extracellular signal-regulated kinase pathway by protein kinase C. *Biochem Biophys Res Commun* 2001; **281**: 891-896

35 **Cohen MP**, Shea E, Chen S, Shearman CW. Glycated albumin increases oxidative stress, activates NF-kappa B and extracellular signal-regulated kinase (ERK), and stimulates ERK-dependent transforming growth factor-beta 1 production in macrophage RAW cells. *J Lab Clin Med* 2003; **141**: 242-249

36 **Campbell J**, Ciesielski CJ, Hunt AE, Horwood NJ, Beech JT, Hayes LA, Denys A, Feldmann M, Brennan FM, Foxwell BM. A novel mechanism for TNF-alpha regulation by p38 MAPK: involvement of NF-kappa B with implications for therapy in rheumatoid arthritis. *J Immunol* 2004; **173**: 6928-6937

S- Editor Liu Y **L- Editor** Ma JY **E- Editor** Ma WH

PO Box 2345, Beijing 100023, China
www.wjgnet.com
wjg@wjgnet.com

World J Gastroenterol 2007 February 7; 13(5): 801-803
World Journal of Gastroenterology ISSN 1007-9327

CASE REPORT

Esophagotracheal fistula caused by gastroesophageal reflux 9 years after esophagectomy

Kiyotomi Maruyama, Satoru Motoyama, Manabu Okuyama, Yusuke Sato, Kaori Hayashi, Yoshihiro Minamiya, Jun-ichi Ogawa

Kiyotomi Maruyama, Satoru Motoyama, Manabu Okuyama, Yusuke Sato, Kaori Hayashi, Yoshihiro Minamiya, Jun-ichi Ogawa, Department of Surgery, Akita University School of Medicine, 1-1-1 Hondo, Akita, Japan
Correspondence to: Kiyotomi Maruyama, Department of Surgery, Akita University School of Medicine, 1-1-1 Hondo, Akita 010-8543, Japan. kiyomaru@doc.med.akita-u.ac.jp
Telephone: +81-18-8846132
Received: 2006-11-03 Accepted: 2006-12-21

Abstract

Fistula between digestive tract and airway is one of the complications after esophagectomy with lymph node dissection. A case of esophagotracheal fistula secondary to esophagitis 9 years after esophagectomy and gastric pull-up for treatment of esophageal carcinoma is described. It was successfully treated with transposition of a pedicled pectoralis major muscle flap.

Key words: Esophagus; Fistula; Surgery; Complications; Esophagitis; Reflux

Maruyama K, Motoyama S, Okuyama M, Sato Y, Hayashi K, Minamiya Y, Ogawa J. Esophagotracheal fistula caused by gastroesophageal reflux 9 years after esophagectomy. *World J Gastroenterol* 2007; 13(5): 801-803

http://www.wjgnet.com/1007-9327/13/801.asp

INTRODUCTION

The denervated stomach as an esophageal substitute recovers intraluminal acidity with time. Increased risk for acid reflux after incurs prolonged esophageal exposure to gastric acid which may lead to esophageal mucosal injury. A patient with esophagotracheal fistula caused by reflux esophagitis 9 years after esophagectomy with postoperative radiation therapy was treated with transposition of a pedicled pectoralis major muscle flap. This complication caused by esophagitis has been described.

CASE REPORT

A 59-year old man presented with a sudden onset of dyspnea and increasing cough productive of gastric contents and saliva. Significant past medical history included an esophagectomy with a reconstruction of gastric tube pulled up through the posterior mediastinum 9 years earlier for esophageal squamous cell carcinoma (pT1, pN0, pM0, pStage I), followed by irradiation (58 Gy) due to positive for malignancy of proximal surgical margin of the esophagus with histological examination. After the operation he had relapses of gastric ulcer and reflux esophagitis. There was no evidence of cancer recurrence over the follow-up period.

He was symptom-free except for cough after swallowing and regurgitation. None of abnormal shadows was detected in chest radiographs. Upper gastrointestinal endoscopy showed a fistula with a diameter of 5 mm on the anterior wall of the esophagus, 20 mm proximal to the esophagogastric anastomosis (Figure 1A), and a gastric ulcer just below the anastomosis (Figure 1B). No malignant feature was detected around the fistula and pathological examination of biopsy specimens from the gastric ulcer showed chronic inflammation. Bronchoscopic examination demonstrated the fistula in the membranous portion of the trachea, 90 mm distal to the vocal cord and 50 mm proximal to the bifurcation (Figure 2). Computed tomography confirmed the fistula located on a level with the upper wedge of sternum and no image of cancer recurrence (Figure 3). Twenty-four pH monitoring in the cervical esophagus was failed because of his rejection.

The patient received proton pomp inhibitors before operation with a slight improvement in his clinical symptoms, but no apparent improvement in the bronchoscopic examination. Surgery was performed 20 d after administration. A cuff of spiral endotracheal tube (8 mm in diameter) was situated below the fistula in the trachea. With the patient in the supine position, a U-shaped skin incision in the anterior cervix and median sternotomy to the 3rd rib were made. Previous radiation therapy made the procedure difficult. After lysis of adhesions, cervical esophagus and the upper portion of gastric tube were freed. Then, the common wall between esophagus and trachea was carefully dissected free in a cranial to caudal direction until the fistula was identified. No malignant changes were found macroscopically. The wall of the fistula was cut sharply, taking care to avoid tearing of the membranous portion of trachea widely. The fistula orifice in the esophageal wall was closed primarily in layers and the orifice in the trachea was also sutured primarily. The

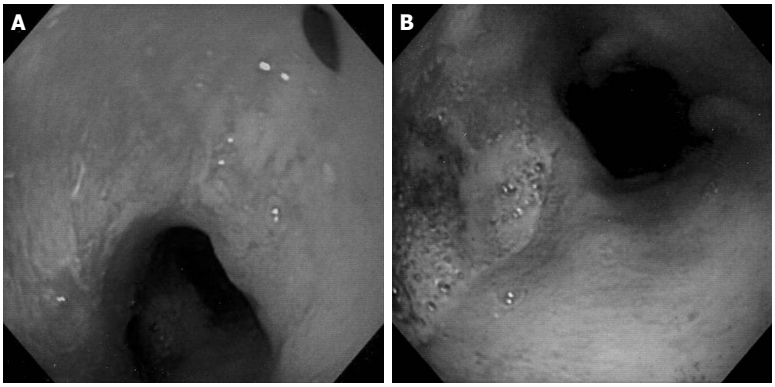

Figure 1 Upper gastrointestinal endoscopy showing a fistula in the esophagus, 20 mm proximal to the anastomosis (**A**), and a gastric ulcer just below the anastomosis (**B**).

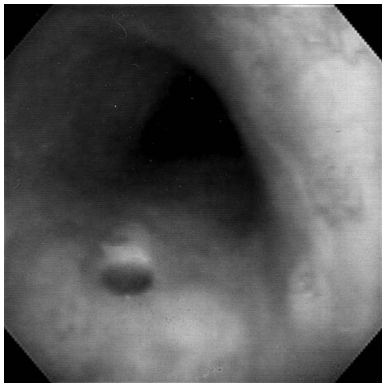

Figure 2 Bronchoscopic examination showing a fistula in the membranous portion of the trachea, 90 mm distal to the vocal cord.

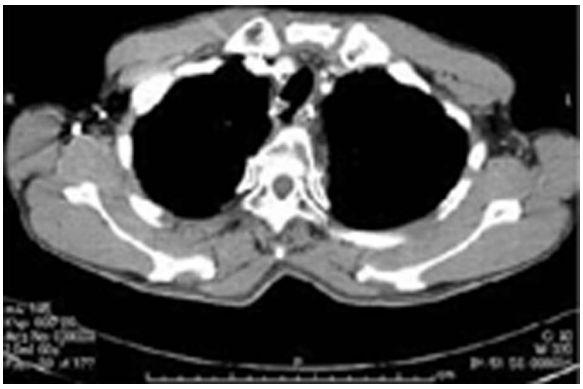

Figure 3 Computed tomography showing an esophagotracheal fistula located on a level with the upper wedge of sternum.

medial wedge of the left clavicle, 1st and 2nd ribs, and the left half of the sternum to the 2nd rib were excised. The left pectoralis major muscle flap was inserted and fixed between the trachea and the gastric tube. His endotracheal tube was extubated immediately after the operation. The patient's postoperative course was uneventful. On the 16th postoperative day, feeding was started when no leak was found after a gastrograffin swallow revealed no leak. The patient was discharged on the 28th postoperative day. He had no evidence of esophagitis, gastric ulcer and fistula 9 mo after the operation.

DISCUSSION

Fistulae between digestive tract and airway are recognized as complications after esophagectomy. The digestive tracts include residual esophagus, esophagogastric anastomosis and gastric tube. Leakage from esophagogastric anastomosis can lead to localized mediastinitis and represents a possible cause of tracheoesophagogastric fistula. Gastric tube-to-airway fistula develops due to peptic ulcer, ischemia of gastric tube or airway, radiation or abscess in the mediastinum. Fistula between cervical esophagus and trachea is the rarest case in these three types of fistulae. This fistula caused by gastroesophageal reflux after esophagectomy has not been reported previously.

Peptic ulcers of pulled-up gastric tubes often cause hemorrhage, perforation and penetration[1]. Gutschow e*t al*[2] reported that the denervated stomach as an esophageal substitute recovers a normal intraluminal acidity with time, so that more than 3 years after surgery the 24-hour pH profile in the gastric cavity of almost all patients is similar to that in healthy subjects. Shibuya[3] showed that sever esophagitis is found in 75.6% of remnant esophagus after esophagectomy for esophageal cancer. Gutschow *et al*[2] showed that 38.5% of patients have reflux esophagitis in the remnant esophagus for 3 years or more after esophagectomy. In our patient, endoscopic examination more than 4 years after esophagectomy revealed often severe esophagitis and gastric ulcer. Although he was treated with a proton pomp inhibitor every time, he discontinued himself taking drugs because of symptom-free. Therefore, it is strongly suggested that repetition of severe esophagitis and postoperative radiation therapy influenced formation of his fistula. In this patient, *H pylori*-IgG was positive. Although evaluation of his gastric emptying was not made, he often had reflux-symptom after esophagectomy.

Myocutaneous or muscle flap, because of their rich blood supply, can be used to fill the dead space after fistulectomy and add vital tissue to prevent recurrent fistulization[1,4-6]. In the part of cervical area, sternocleidomastoid muscle and pectoralis major have been used. If the esophagus and/or gastric tube cannot be preserved, continuity of the gastrointestinal tract may be reconstructed with, for example, colonic or small bowel interposition[7].

No significant relationship has been found between reflux symptoms, such as heart burn and regurgitation, and endoscopic findings after esophagectomy in the previous reports[3,8]. Patients with denervated stomach may be free from symptoms of gastric ulcer. Therefore, endoscopic examination is necessary at least once a year for early detection of ulceration and esophagitis. Fistulae between digestive tract and airway are grave complications of esophagectomy because they frequently result in respiratory failure and life-threatening conditions. If gastric ulcer or esophagitis is detected in endoscopic examination after esophagectomy, this therapy should be

started immediately regardless of the interval between the examination and esophagectomy.

REFERENCES

1 **Hayashi K**, Ando N, Ozawa S, Tsujizuka K, Kitajima M, Kaneko T. Gastric tube-to-tracheal fistula closed with a latissimus dorsi myocutaneous flap. *Ann Thorac Surg* 1999; **68**: 561-562

2 **Gutschow C**, Collard JM, Romagnoli R, Salizzoni M, Hölscher A. Denervated stomach as an esophageal substitute recovers intraluminal acidity with time. *Ann Surg* 2001; **233**: 509-514

3 **Shibuya S**, Fukudo S, Shineha R, Miyazaki S, Miyata G, Sugawara K, Mori T, Tanabe S, Tonotsuka N, Satomi S. High incidence of reflux esophagitis observed by routine endoscopic examination after gastric pull-up esophagectomy. *World J Surg* 2003; **27**: 580-583

4 **Marty-Ané CH**, Prudhome M, Fabre JM, Domergue J, Balmes M, Mary H. Tracheoesophagogastric anastomosis fistula: a rare complication of esophagectomy. *Ann Thorac Surg* 1995; **60**: 690-693

5 **Stal JM**, Hanly PJ, Darling GE. Gastrobronchial fistula: an unusual complication of esophagectomy. *Ann Thorac Surg* 1994; **58**: 886-887

6 **Sakamoto K**, Ogawa M, Yamamoto S, Mugita N, Saishoji T, Azuma KS, Hayashida K. Closure of a gastric tube-tracheal fistula by transposition of a pedicled sternocleidomastoid muscle flap. *Surg Today* 1997; **27**: 181-185

7 **Buskens CJ**, Hulscher JB, Fockens P, Obertop H, van Lanschot JJ. Benign tracheo-neo-esophageal fistulas after subtotal esophagectomy. *Ann Thorac Surg* 2001; **72**: 221-224

8 **Yuasa N**, Sasaki E, Ikeyama T, Miyake H, Nimura Y. Acid and duodenogastroesophageal reflux after esophagectomy with gastric tube reconstruction. *Am J Gastroenterol* 2005; **100**: 1021-1027

S- Editor Liu Y **L- Editor** Wang XL **E- Editor** Lu W

PO Box 2345, Beijing 100023, China
www.wjgnet.com
wjg@wjgnet.com

World J Gastroenterol 2007 February 7; 13(5): 804-805
World Journal of Gastroenterology ISSN 1007-9327

CASE REPORT

A case of biliary gastric fistula following percutaneous radiofrequency thermal ablation of hepatocellular carcinoma

Angela Falco, Dante Orlando, Roberto Sciarra, Luciano Sergiacomo

Angela Falco, Dante Orlando, Luciano Sergiacomo, Department of Internal Medicine, "S. Massimo" Civil Hospital, Penne, Italy
Roberto Sciarra, Department of Radiology, "S. Massimo" Civil Hospital, Penne, Italy
Correspondence to: Angela Falco, MD, PhD, Department of Internal Medicine, "S. Massimo" Civil Hospital, Via Btg Alpini L' Aquila, Penne (Pe) 65017, Italy. angela.falco@email.it
Telephone: +39-85-8276220 Fax: +39-85-8276308
Received: 2006-09-29 Accepted: 2006-10-23

Abstract

Percutaneous radiofrequency thermal ablation (RFA) is an effective and safe therapeutic modality in the management of liver malignancies, performed with ultrasound guidance. Potential complications of RFA include liver abscess, ascites, pleural effusion, skin burn, hypoxemia, pneumothorax, subcapsular hematoma, hemoperitoneum, liver failure, tumour seeding, biliary lesions. Here we describe for the first time a case of biliary gastric fistula occurred in a 66-year old man with a Child's class A alcoholic liver cirrhosis as a complication of RFA of a large hepatocellular carcinoma lesion in the Ⅲ segment. In the light of this case, RFA with injection of saline between the liver and adjacent gastrointestinal tract, as well as laparoscopic RFA, ethanol injection (PEI), or other techniques such as chemoembolization, appear to be more indicated than percutaneous RFA for large lesions close to the gastrointestinal tract.

Key words: Radiofrequency thermal ablation; Hepatocellular carcinoma; Biliary gastric fistula; Complications

Falco A, Orlando D, Sciarra R, Sergiacomo L. A case of biliary gastric fistula following percutaneous radiofrequency thermal ablation of hepatocellular carcinoma. *World J Gastroenterol* 2007; 13(5): 804-805

http://www.wjgnet.com/1007-9327/13/804.asp

INTRODUCTION

Percutaneous radiofrequency thermal ablation (RFA) is an emerging therapeutic modality in the management of liver malignancies[1], particularly in patients who cannot undergo surgery[2]. The increasing attractiveness of this technique is due to its effectiveness, safety and low morbidity rate[1,2]. Compared with ethanol injection (PEI), the first percutaneous therapy to be introduced, RFA is characterized by the need of a reduced number of treatment sessions. Both therapies are generally performed with ultrasound (US) guidance which allows considerable ease of application, due to their low costs and no X-ray exposure. Nevertheless, a number of potential complications of RFA have been described, occurring with a rate of almost 9%[3], including liver abscess, ascites, pleural effusion, skin burn, hypoxemia, pneumothorax, subcapsular hematoma, hemoperitoneum, liver failure, and tumour seeding. In addition, biliary lesions have been described in 1% of a large number of patients included in a review of the literature in this field[3], and two case reports describing enterobiliary[4] and biliary pleural[5] fistulae have been published so far.

CASE REPORT

Here we describe a case of biliary gastric fistula occurred in a 66-year old man with a Child's class A alcoholic liver cirrhosis as a complication of RFA of a large (4.0 cm × 4.5 cm) hepatocellular carcinoma (HCC) lesion in the III segment. Written informed consent was obtained from the patient before treatment. The ablation was performed under US-guidance [Eidos (EUB-525), Esaote, Genova, Italy] using a 3.5 MHz sector probe, with a lateral guide for electrode placement. The treatment was made under general anesthesia using a 20-cm long, 18-gauge electrode to apply the RF current (MIRAS RC, Invatec Italia, Brescia, Italy). The procedure lasted 30 min without apparent complications. In the night following the intervention, the patient experienced transient retching, responsive to metoclopramide administration, and moderate abdominal pain. An enhanced computed axial tomography (CT) scan of the abdomen, performed 22 d after the procedure, showed the presence of aerobilia within the left portion of the liver attributed to a biliary gastric fistula (Figure 1A). A subsequent conventional contrast-enhanced study of the first gastrointestinal tract, showed a fistulous tract starting from the lesser curvature of the stomach with concomitant spasm of the greater curvature, causing a communication with the left portion of the liver (Figure 1B).

DISCUSSION

Biliary gastric fistulae can be diagnosed on the basis of both direct and indirect radiological signs. The diagnosis

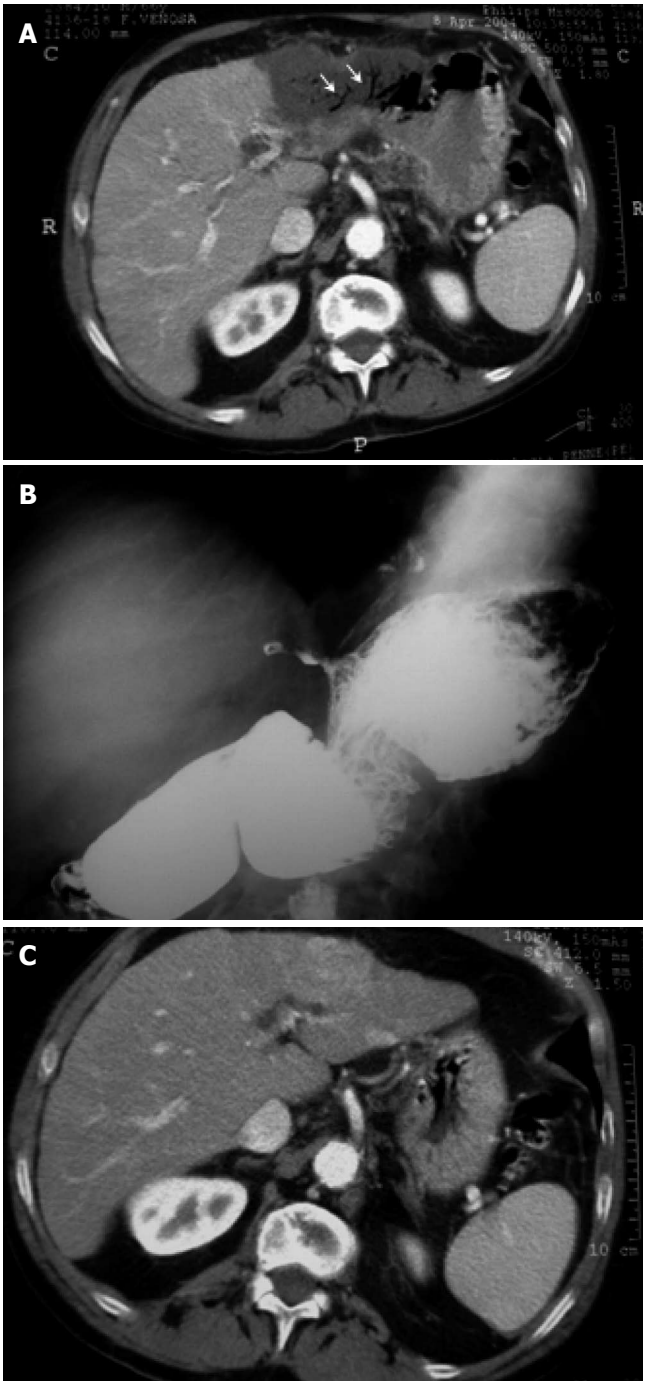

Figure 1 Enhanced CT abdominal scan performed after the percutaneous procedure showing air inclusions in the bile ducts within the left portion of the liver (**A**), radiograph of the first gastrointestinal tract showing a biliary gastric fistula starting from the lesser curvature of the stomach with concomitant spasm of the greater curvature (**B**), and enhanced CT scan of the abdomen performed before percutaneous thermal ablation of the HCC lesion in the III liver segment showing a left portion of the liver without aerobilia (**C**).

with indirect radiological criteria was made by enhanced CT. The presence of aerobilia confined to the left portion of the liver (Figure 1A), in the absence of surgery for biliary-digestive by-pass procedures and the fact that the thermoablative treatment was performed after a previous CT in which the fistula was not present (Figure 1C), led to the hypothesis of a iatrogenic alteration. This was confirmed by a conventional contrast-enhanced study of the first gastrointestinal tract, showing a fistulous tract starting from the lesser curvature of the stomach with concomitant spasm of the greater curvature, causing a communication with the left portion of the liver (Figure 1B).

Perforation of the gastrointestinal tract, a possible major complication of RFA of hepatic nodules, can be difficult to recognize as its clinical manifestations can be attributed to the normal course of the so called "post-ablation syndrome". Indeed, mild to moderate abdominal pain is not uncommon after RFA of large lesions, particularly when they abut the Glisson's capsule containing nerve endings.

We describe here for the first time in the literature a case of biliary gastric fistula as a possible complication of thermal ablation of HCC lesions. A recent study has shown the efficacy and safety of percutaneous RFA of HCC abutting the gastrointestinal tract[6]. Nevertheless, in the light of this case and previous descriptions of enterobiliary fistulae occurred following the same therapeutic modality, RFA with injection of saline between the liver and adjacent gastrointestinal tract, as well as laparoscopic RFA, PEI, or other techniques such as chemoembolization, appear to be more indicated than percutaneous RFA for large lesions close to the gastrointestinal tract.

REFERENCES

1 **Rossi S**, Buscarini E, Garbagnati F, Di Stasi M, Quaretti P, Rago M, Zangrandi A, Andreola S, Silverman D, Buscarini L. Percutaneous treatment of small hepatic tumors by an expandable RF needle electrode. *AJR Am J Roentgenol* 1998; **170**: 1015-1022

2 **Livraghi T**, Goldberg SN, Lazzaroni S, Meloni F, Ierace T, Solbiati L, Gazelle GS. Hepatocellular carcinoma: radiofrequency ablation of medium and large lesions. *Radiology* 2000; **214**: 761-768

3 **Mulier S**, Mulier P, Ni Y, Miao Y, Dupas B, Marchal G, De Wever I, Michel L. Complications of radiofrequency coagulation of liver tumours. *Br J Surg* 2002; **89**: 1206-1222

4 **Bessoud B**, Doenz F, Qanadli SD, Nordback P, Schnyder P, Denys A. Enterobiliary fistula after radiofrequency ablation of liver metastases. *J Vasc Interv Radiol* 2003; **14**: 1581-1584

5 **Liberale G**, Delhaye M, Ansay J, Houben JJ, Coppens E, Gelin M, Donckier V. Biliary pleural fistula as a complication of radiofrequency ablation for liver metastasis. *Acta Chir Belg* 2004; **104**: 448-450

6 **Choi D**, Lim HK, Kim MJ, Kim SH, Lee WJ, Kim SH, Lim JH, Paik SW, Koh KC, Yoo BC. Therapeutic efficacy and safety of percutaneous radiofrequency ablation of hepatocellular carcinoma abutting the gastrointestinal tract. *AJR Am J Roentgenol* 2004; **183**: 1417-1424

S- Editor Wang J **L- Editor** Wang XL **E- Editor** Liu WF

PO Box 2345, Beijing 100023, China
www.wjgnet.com
wjg@wjgnet.com

World J Gastroenterol 2007 February 7; 13(5): 806-808
World Journal of Gastroenterology ISSN 1007-9327

CASE REPORT

Spontaneous rupture of a hepatic hydatıd cyst into the peritoneum causing only mild abdominal pain: A case report

Kemal Karakaya

Kemal Karakaya, Department of General Surgery, Zonguldak Karaelmas University, Faculty of Medicine, Kozlu, Zonguldak 67600, Turkey
Correspondence to: Kemal Karakaya, Department of General Surgery, Zonguldak Karaelmas University, Faculty of Medicine, Kozlu, Zonguldak 67600, Turkey. knkarakaya@gmail.com
Telephone: +90-372-2660509 Fax: +90-372-2660509
Received: 2006-11-21 Accepted: 2006-12-25

Abstract

Hydatid disease is an endemic disease in certain areas of the world. It is located mostly in the liver. Spontaneous rupture of the hydatid cyst into the peritoneum is a rare condition, which is accompanied by serious morbidity and mortality generally. We present herein a case with a spontaneous rupture of a hepatic hidatid disease into the peritoneum without any serious symptoms. A 15-year-old boy was admitted to the emergency room with a mild abdominal pain lasting for a day. Physical examination revealed only mild abdominal tenderness. There was no history of trauma or complaints related to hydatid diseases. Ultrasonography showed a large amount of free fluid and a cystic lesion with irregular borders in the liver. He was operated on. Postoperative albendazol therapy was given for 2 mo. No recurrence or secondary hydatidosis was seen on CT investigation in the 3rd, 6th and 12th mo following surgery.

Key words: Hydatid disease; Spontaneous rupture; Liver

Karakaya K. Spontaneous rupture of a hepatic hydatıd cyst into the peritoneum causing only mild abdominal pain: A case report. *World J Gastroenterol* 2007; 13(5): 806-808

http://www.wjgnet.com/1007-9327/13/806.asp

INTRODUCTION

Hydatid disease is a parasitic infestation caused by Echinococcus granulosus[1-3]. Hydatid disease is an endemic problem in Turkey as well as in sheep-bearing regions of the world[1,2,4].

Although hepatic hydatid disease may be asymptomatic for many years, it can become symptomatic due to expansion, rupture or pyogenic infection[2,3,5]. Hydatid cyst rupture may cause mild to fatal complications[2,5]. Rupture of the hepatic hydatid disease generally occurs into the biliary tree. Rupture of the cyst in the peritoneal cavity is rare and generally followed by anaphylactic reactions.

In this study, we present a case of a spontaneous rupture of a hepatic hydatid cyst into the peritoneum, in which the patient was admitted to the emergency room for mild abdominal pain without any other symptom. Spontaneous rupture of the hepatic hydatid cyst into peritoneum without any serious symptom is unusual.

CASE REPORT

A 15-year-old boy perceived sudden abdominal pain in the epigastrium and right upper quadrant a day ago. After a short duration his pain was ameliorated spontaneously. The following day he perceived mild pain in the right lower quadrant. He had no pruritis, erythema or any other symptom except the abdominal pain. No history of blunt trauma was found.

Physical examination revealed a blood pressure of 100/70 mmHg, and a pulse rate of 78 beats/min. The patient was afebrile. Abdominal palpation revealed mild tenderness. He was comfortable on his movements. There was no history of nausea, vomiting or loss of appetite. Laboratory investigations were normal except mild leukocytosis (WBC: 11 000/mm^3).

Abdominal ultrasonography showed a large amount of free fluid and a cystic lesion measuring 10 cm × 12 cm with irregular borders in the right lobe of the liver. The anterior border of the cyst was incomplete. Floating membrane image was seen. The biliary ducts were normal in calibration.

The abdomen was exposed through a right paramedian incision. Approximately 3500 mL clear fluid was aspirated from the intraperitoneal space. There was a hydatid cyst in the right lobe of the liver. The cyst was 13 cm in size and had a ruptured area of 5 cm × 7 cm anteriorly (Figure 1). There were firm adhesions between the liver and right diaphragm. There was no daughter vesicle in the abdominal cavity. The germinative membrane was taken out completely (Figure 2). No biliary leakage was seen. We could not find any other pathological evidence on exploration. The cyst pouch was irrigated with hypertonic saline (20%) and then followed by isotonic saline. The peritoneal cavity was irrigated with isotonic saline. Introflexion procedure was performed. Latex drains were

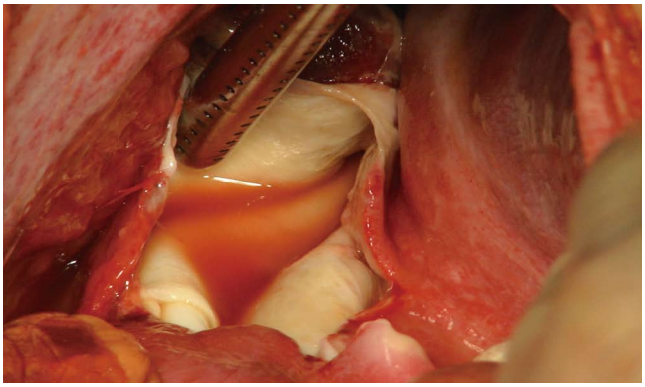

Figure 1 Ruptured hydatid cyst in the liver.

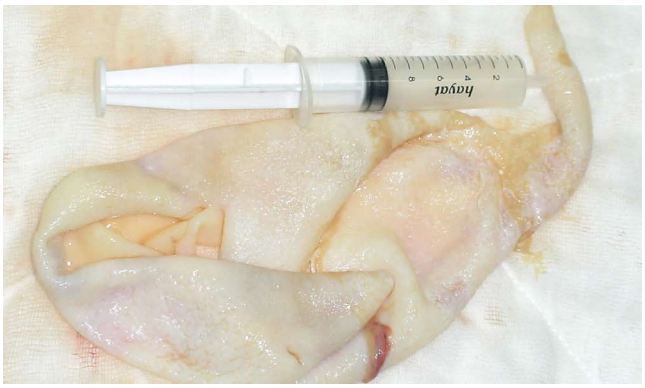

Figure 2 Germinative membrane extracted totally.

placed into the sub-hepatic and recto-vesicle areas.

The patient was discharged from the hospital on the 9th postoperative day without any complication. Postoperative albendazole therapy (10 mg/kg) was prescribed for 2 mo under the liver enzyme and blood count monitoring. The patient was controlled as an outpatient. Postoperative follow up was uneventful for 13 mo. No recurrence or secondary hydatidosis was seen on CT investigation in the 3rd, 6 th and 12th mo following surgery.

DISCUSSION

The hydatid cyst is typically filled with clear fluid (hydatid fluid). The cyst consists of an internal cellular layer (germinal layer) and an outer, acellular layer (laminated layer). As the cyst expands gradually, a granulomatous host reaction followed by a fibrous reaction forms a connective tissue layer, which is called a pericyst[1].

Hydatid disease is a serious health problem in endemic areas as well as in Turkey [6,7]. The diagnosis and appropriate surgical therapy is usually delayed because most of the hydatid cysts remain asymptomatic until it is getting complicated [1-3,7,8].

Precautions for the hydatid disease are mostly insufficient. Treatment of dogs with antihelmintic is the main procedure to control the parasite (Echinococcus spp.)[9]. In rural areas of Turkey this treatment is not applied routinely. In the rural area, sheep are home-slaughtered routinely. Dogs can access to the infected viscera. This is true in almost all of the developing or underdeveloped countries in the world[9].

Initially almost all of the hydatid cysts are asymptomatic. Later in time some symptoms depending on the involved organ, localisation of the cyst and pressure effect of the cyst on the surrounding tissues and structures develop[1,7,10]. Abdominal pain is the most commonly encountered symptom. The second one is the symptoms arising from the pressure effect of the cyst[7,8,11]. It is known that rupture of the cyst ameliorates the abdominal pain and the patient feels comfortable to some degree[2]. Later in time rupture of the hydatid cyst produces symptoms and signs of allergy or peritoneal irritation almost all the time[10]. No history of previous abdominal pain or any other symptom relating to the hydatid cyst was present in the case presented here.

Diagnosis of the hydatid cyst is mainly based on ultrasonography and computed tomography (CT)[1-3,7,8,10,11]. CT is especially valuable for the 3-dimensional localisation of the cyst preoperatively[8,11]. MRI, magnetic resonance cholangio pancreatography (MRCP), scintigraphy scans and laparoscopy may be useful for diagnosis of the rare, undiagnosed cases and for its complications. As we made the diagnosis of a ruptured hepatic hydatid cyst by US examination, the other investigational techniques were not used for preoperative evaluation.

Surgery is the preferred treatment for the cure of the hydatid disease[3,6,8]. Surgical procedures may differ from percutaneous aspiration instillation and reaspiration to complete excision of the cyst[1,6,7]. We performed introfleksion procedure on the patient. Rupture of the cyst is usually related to increased intracystic pressure. This may be related to trauma, or over enlargement of the cyst[2,10]. Perforation of the hydatid cyst may cause dissemination of the parasite and increased morbidity and mortality rate[1,2,9]. As cyst size increases, risk of rupture increases[5]. Cyst size measured 13 cm preoperatively in our case. Intraperitoneal rupture of the hydatid cyst can cause abdominal pain, allergy and anaphylaxis[1,2,5]. Mild abdominal tenderness was present in our patient on admission. The patient had no history of trauma or any event that increases intra-abdominal pressure such as coughing or constipation.

Medical treatment with albendazole is described elsewhere[1,6,7,10,11]. The patient was treated with albendazole 10 mg/kg for 2 mo under liver enzyme and blood count monitoring. Postoperative follow up was uneventful.

Intra-peritoneal hydatidosis is a major problem for the patients who have hydatid cyst rupture. The patient presented here had no recurrence or secondary hydatidosis.

In endemic regions, it is useful to consider hydatid cyst disease for patients with abdominal pain admitted to the emergency room. Rupture of the hydatid cyst may be fatal.

REFERENCES

1 **Eckert J**, Deplazes P. Biological, epidemiological, and clinical aspects of echinococcosis, a zoonosis of increasing concern. *Clin Microbiol Rev* 2004; **17**: 107-135

2 **Erdogmus B**, Yazici B, Akcan Y, Ozdere BA, Korkmaz U, Alcelik A. Latent fatality due to hydatid cyst rupture after a severe

cough episode. *Tohoku J Exp Med* 2005; **205**: 293-296
3 **Sayek I**, Yalin R, Sanaç Y. Surgical treatment of hydatid disease of the liver. *Arch Surg* 1980; **115**: 847-850
4 **Altintaş N**. Cystic and alveolar echinococcosis in Turkey. *Ann Trop Med Parasitol* 1998; **92**: 637-642
5 **Kantarci M**, Onbas O, Alper F, Celebi Y, Yigiter M, Okur A. Anaphylaxis due to a rupture of hydatid cyst: imaging findings of a 10-year-old boy. *Emerg Radiol* 2003; **10**: 49-50
6 **Yagci G**, Ustunsoz B, Kaymakcioglu N, Bozlar U, Gorgulu S, Simsek A, Akdeniz A, Cetiner S, Tufan T. Results of surgical, laparoscopic, and percutaneous treatment for hydatid disease of the liver: 10 years experience with 355 patients. *World J Surg* 2005; **29**: 1670-1679
7 **Hatipoglu AR**, Coskun I, Karakaya K, Ibis C. Retroperitoneal localization of hydatid cyst disease. *Hepatogastroenterology* 2001; **48**: 1037-1039
8 **Schwartz SI**. Liver. 7th ed. Schwartz SI, Shires GT, Spencer FC, Daly JM, Fischer JE, Galloway AC, editors. Principles of Surgery. International Edition: McGraw-Hill Book Company, 1999: 1403-1405
9 **Oku Y**, Malgor R, Benavidez U, Carmona C, Kamiya H. Control program against hydatidosis and the decreased prevalence in Uruguay. International Congress Series 1267; 2004: 98-104
10 **Derici H**, Tansug T, Reyhan E, Bozdag AD, Nazli O. Acute intraperitoneal rupture of hydatid cysts. *World J Surg* 2006; **30**: 1879-1883; discussion 1884-1885
11 **Langer B**, Gallinger S. Cystic disease of the liver. In: Zuidema GD,Turcotte JG, editors. Shackelford's Surgery of the Alimentary Tract. Philadelphia, London, Toronto, Montreal, Sydney, Tokyo: WB Saunders Company, 1996: 531-540

S- Editor Liu Y **L- Editor** Zhu LH **E- Editor** Ma WH

PO Box 2345, Beijing 100023, China
www.wjgnet.com
wjg@wjgnet.com

World J Gastroenterol 2007 February 7; 13(5): 809-812
World Journal of Gastroenterology ISSN 1007-9327

CASE REPORT

Carcinosarcoma of the liver with mesenchymal differentiation

Shinichi Sumiyoshi, Masataka Kikuyama, Yuji Matsubayashi, Fujito Kageyama, Yoshihiro Ide, Yoshimasa Kobayashi, Hirotoshi Nakamura

Shinichi Sumiyoshi, Masataka Kikuyama, Yuji Matsubayashi, Fujito Kageyama, Department of Gastroenterology, Hamamatsu Rosai Hospital, Hamamatsu, Japan
Yoshihiro Ide, Department of Pathology, Hamamatsu Rosai Hospital, Hamamatsu, Japan
Yoshimasa Kobayashi, Hirotoshi Nakamura, Second Division, Department of Internal Medicine, Hamamatsu University School of Medicine, Hamamatsu, Japan
Correspondence to: Shinichi Sumiyoshi, MD, Second Division, Department of Internal Medicine, Hamamatsu University School of Medicine, Hamamatsu, Japan, 1-20-1 Handayama, Hamamatsu 431-3192, Japan. sumishin@hama-med.ac.jp
Telephone: +81-53-4352263 Fax: +81-53-4352354
Received: 2006-10-22 Accepted: 2007-01-08

Abstract

We report an extremely rare case where a mesenchymal differentiation, especially embryonal sarcoma, was demonstrated in cholangiocarcinoma. At autopsy, a yellowish-white tumor (15 cm x 12 cm) was found in the right hepatic lobe, and there were several daughter nodules in both hepatic lobes. Histologically, most of the main tumor and all of the daughter nodules examined showed sarcomatous changes (spindle cells, pleomorphic cells and hyalization). Histologic examination of a part of the main tumor disclosed a focus of adenocarcinoma within the tumor. The frequent transitions between the adenocarcinomatous areas and the sarcomatous areas suggested that sarcomatous transformation occurred in the cholangiocarcinoma and then spread rapidly. Immunohistochemically, the adenocarcinomatous elements were positive for cytokeratin, carcinoembryonic antigen (CEA) and epithelial membrane antigen, and negative in the sarcomatous cells. Vimentin was positive only in the sarcomatous elements. The findings of the present case support the view that carcinosarcomas represent carcinomas that develop sarcomatous elements via metaplasia of the epithelial element.

Key words: Cholangiocarcinoma; Carcinosarcoma; Mesenchymal differentiation

Sumiyoshi S, Kikuyama M, Matsubayashi Y, Kageyama F, Ide Y, Kobayashi Y, Nakamura H. Carcinosarcoma of the liver with mesenchymal differentiation. *World J Gastroenterol* 2007; 13(5): 809-812

http://www.wjgnet.com/1007-9327/13/809.asp

INTRODUCTION

Cholangiocarcinoma is usually a moderately to well differentiated adenocarcinoma with considerable demoplastic reactions. Nakajima *et al*[1] reported that 92 of 102 cases of cholangiocarcinoma were mucin-producing adenocarcinomas, and the remaining were adenosquamous (3 cases), squamous (3 cases), mucinous (1 case), or anaplastic carcinoma (3 cases). Only brief descriptions of sarcomatous changes and sarcomatous variants of cholangiocarcinoma can be found in a few studies or reviews dealing with a large series of cholangiocarcinoma cases[1,2] . However, detailed clinicopathological studies of sarcomatous changes in cholangiocarcinoma have not been reported in English and Japanese literature to the best of our knowledge.

Because we recently encountered an autopsy case of cholangiocarcinoma showing sarcomatous changes, we report this case to emphasize the autopsy findings, as well as the histogenesis of sarcomatous changes in cholangiocarcinoma.

CASE REPORT

A 74-year old Japanese woman was admitted to our hospital complaining of pain in the right hypochondrium and underwent a cholecystectomy. The main laboratory data were as follows: red blood cells 378 × 10^4/mm^3, white blood cells 5200/mm^3, serum total protein 8.0 g/dL, total bilirubin 0.8 mg/dL, serum glutamic-oxaloacetic transaminase 46 IU/L, serum glutamic-pyruvic transaminase 58 IU/L, lactic acid dehydrogenase 416 IU/L, alkaline phosphatase 476 IU/L, γ-glutamyl transpeptidase 119 IU/L, and C- reactive protein 2.9 mg/dL. Carcinoembryonic antigen (CEA) was 51.5 ng/mL, but serum α-fetoprotein (AFP), a protein induced by vitamin K absence or antagonists (PIVKA-Ⅱ) and carbohydrase antigen 19-9 (CA19-9) were within the normal range. Hepatitis B core (HBc) antibody, hepatitis C antibody (HCV-Ab), and human immunodeficiency virus (HIV) were all negative. A computed tomography scan of the abdomen revealed a low-density mass with renal invasion in all segments of the right hepatic lobe, without lymph node swelling or dilatation of the intrahepatic bile ducts. Magnetic resonance imaging revealed hypointensity on the T1-weighted images and heterogeneous hyperintensity on the T2-weighted images (Figures 1A and B). Angiography showed a malignant blush in the right lobe (not shown). A sonographically guided hepatic tumor biopsy showed the

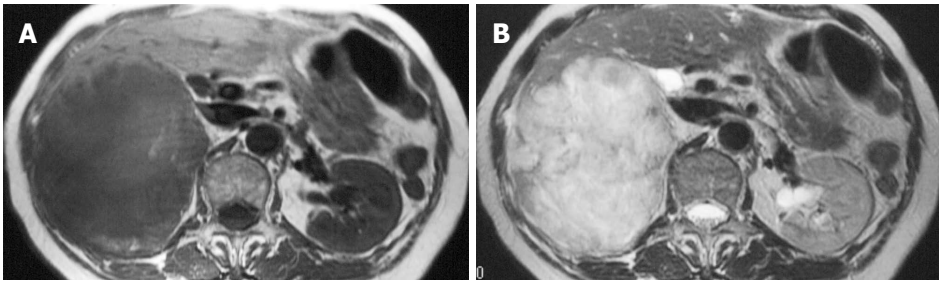

Figure 1 Magnetic resonance imaging showing hypointense areas in the right lobe of the liver on a T1-weighted image (**A**) and an inhomogeneously hyperintense mass on a T2-weighted image (**B**).

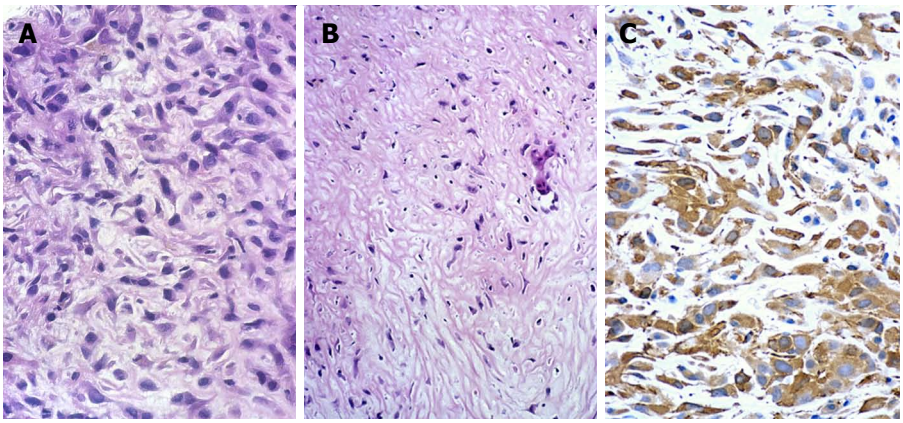

Figure 2 Needle biopsy showing a sarcomatous area consisting of interlacing bundles of atypical spindle cells [hematoxylin-eosin stain; magnification x 200 (**A**), x 100 (**B**)] and immunohistochemical staining showing positive α-SMA (**C**).

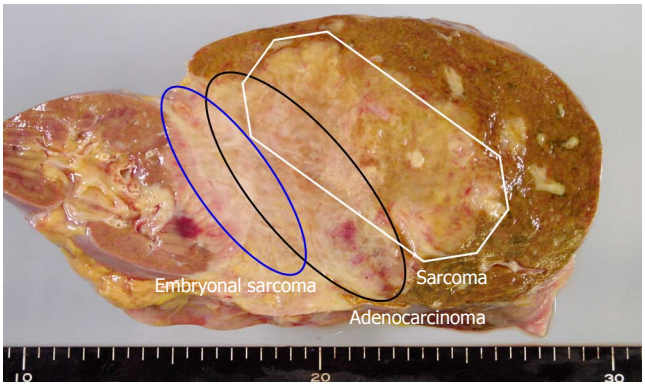

Figure 3 Gross appearance of hepatic tumor.

proliferation of spindle cells. An immunohistochemical study showed that α-smooth muscle actin (SMA) was positive, and keratin, vimentin, desmin, CEA, and S-100 protein were negative, thus leiomyosarcoma was suspected (Figure 2). Her general condition gradually worsened and she died of hepatic failure and disseminated intravascular coagulation (DIC) after two months.

Autopsy findings

The gross findings were a yellowish-white tumor (15 cm × 12 cm) with blurred borders in the right hepatic lobe (Figure 3) where the right branch of the portal vein and right kidney were occluded.

Microscopically, the majority of the main tumor and all daughter nodules examined showed a sarcomatous appearance. Elongated cells were arranged in bundles, occasionally interlacing. These histologic features were similar to those of fibrosarcoma or leiomyosarcoma. That is, these areas were composed of nonadhesive spindle-shaped or fusiform cells, and to a lesser degree, pleomorphic giant or multinuclear cells, the majority of the latter showing bizarre nuclei and prominent nucleoli (Figure 4). These sarcomatous areas looked like malignant leiomyosarcoma. There were many foci of coagulative necrosis within these sarcomatous areas. In addition, there was a well-differentiated tubular adenocarcinoma within the tumor (Figure 5). There were direct transitions between adenocarcinomatous elements and sarcomatous elements. However, the transitions were unclear. A hydropsy-like part was recognized at the side edge of the tumor, and tumor cells floating in mucinous cytoplasm were evidence of undifferentiated (embryonal) sarcoma (Figure 6).

These two elements on the representative section of tumor were mapped (Figure 3), showing adenocarcinomatous elements within the tumor and a considerable amount of sarcomatous elements surrounding this carcinoma. There were no histologic elements suggestive of hepatocellular carcinoma.

The nontumorous hepatic tissue showed nonspecific reactive changes with mild fibrous enlargement of the portal tracts, but not liver cirrhosis. There were no regenerative nodules throughout the liver, and HBsAg was not detected in the liver by orcein stain.

Primary antisera to keratin, vimentin, desmin, AFP, CEA, and S-100 protein were obtained from DAKO Corporation. Keratin was weakly positive in the adenocarcinoma cells. There was positive staining for CEA at the part of tubular adenocarcinoma. Vimentin was expressed only in the sarcomatous cells. There were no positive reactions for AFP, desmin, S-100 protein, or CA19-9 in the tumor cells.

It was diagnosed as cholangiocarcinoma and carcino-

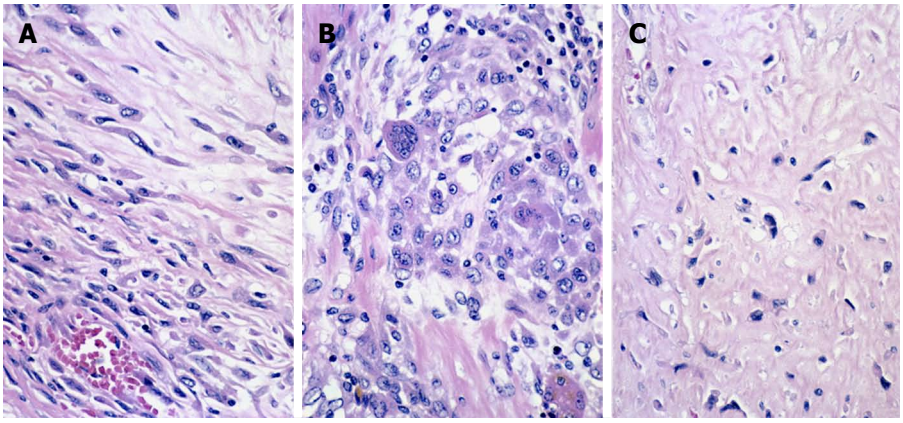

Figure 4 Spindle cells (**A**), pleomorphic areas (**B**), or hyalization (**C**) in leiomyosarcoma (hematoxylin-eosin stain; magnification x 160).

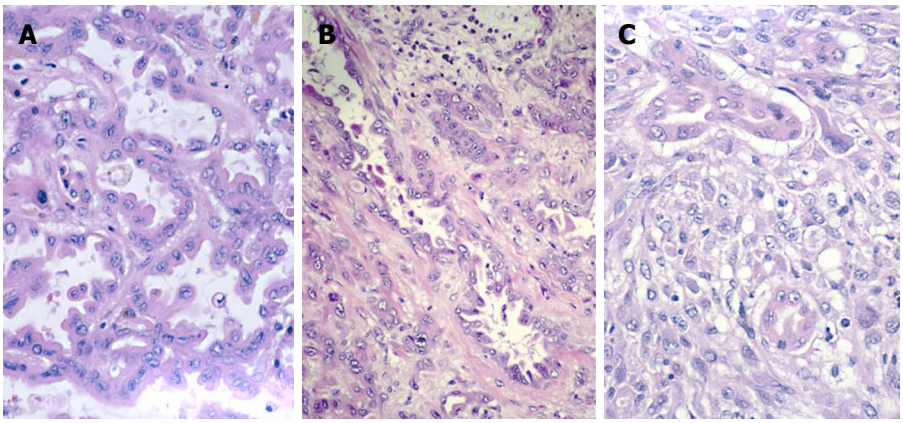

Figure 5 Cholangiocarcinoma focus (**A**) (hematoxylin-eosin stain; magnification x160), component surrounded by fibrosis (**B**) (hematoxylin-eosin stain; magnification x100), intimately mixed carcinomatous and sarcomatous components (**C**) (hematoxylin-eosin stain; magnification x 160).

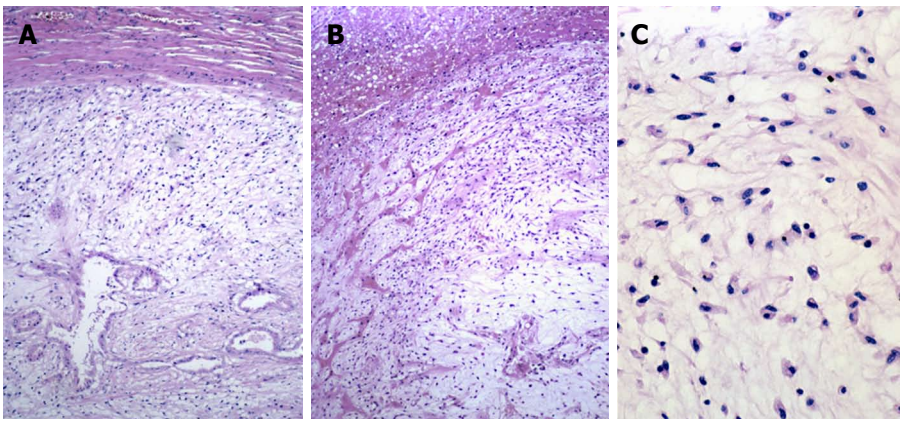

Figure 6 Sarcomatous portion of the tumor consisting of undifferentiated (embryonal) sarcoma [hematoxylin-eosin stain; magnification x 25 (**A**, **B**), x 160 (**C**)].

sarcoma with mesenchymal differentiation that specialized and coexisted in a lobe corollary tumor.

DISCUSSION

Sarcomatous transformation of primary cancer of the liver in adults is most common in hepatocellular carcinoma (HCC), especially after anticancer chemotherapy or transarterial embolization therapy[3]. In our patient, there were no lesions resembling HCC, and AFP was negative in the tumor, so that the derivation of sarcomatous cells from HCC was excluded.

Histologic mapping of a whole section of the main tumor showed adenocarcinomatous and sarcomatous elements within the main tumor. Considering the mapping, the sarcomatous elements would be interpreted as the result of the metaplastic transformation of pre-existing adenocarcinoma cells[4].

In our case, direct transitions between sarcoma and adenocarcinoma in the main tumor suggested that the sarcomatous changes might have developed secondarily from pre-existing cholangiocarcinoma. Most of the daughter nodules showed such sarcomatous changes, suggesting that sarcomatous elements grow and spread more rapidly than the adenocarcinomatous elements.

Thompson *et al*[5] stated that the carcinomatous and sarcomatous components may be monoclonal in origin and derived from single stem cells. Genetic analysis is one possible solution to this problem, as reported in esophageal carcinosarcoma[6].

What is more, various other hypotheses have been proposed to explain the biphasic appearance of sarcomatoid carcinomas[7,8]. Briefly, the explanations include the collision theory of independent neoplastic growth from multipotent stem cell origins, epithelial to mesenchymal conversion by epithelial-stromal interaction, and a combination of the two. The salient features in our case were the presence of dysplasia and adenocarcinoma *in situ*, morphological "transition" between carcinomatous and sarcomatous tissues in relation to expansion of invasion, and the detection of sarcomatous characteristics by immunohistochemistry in the epithelial component, which strongly support the histogenesis of epithelial to mesenchymal conversion. Gentile *et al*[9] reported that the presence of productive retroviral infection in the sarcomatous cells is related with tumor progression from the carcinomatous to the sarcomatous phase. The examination I performed confirmed that it was negative for viruses, but it was related with an unknown virus. However, why sarcomatous changes develop is a mystery.

In summary, sarcomatoid carcinoma derived from cholangiocarcinoma is an extremely rare tumor composed of mixed malignant epithelial and mesenchymal cells, with only 12 cases[10-12] reported to date who died of liver failure due to extensive metastatic growth of sarcomatoid carcinoma despite postoperative chemotherapy. The histologic features, stage, and outcome of the reported cases indicate that this neoplasm generally pursues a highly aggressive and malignant biological course with rapid growth and wide local infiltration, leading to a poor prognosis. Radical surgery with adjuvant chemotherapy, and close follow-up are necessary for the management of this disease.

REFERENCES

1 **Nakajima T**, Kondo Y, Miyazaki M, Okui K. A histopathologic study of 102 cases of intrahepatic cholangiocarcinoma: histologic classification and modes of spreading. *Hum Pathol* 1988; **19**: 1228-1234

2 **Okuda K**, Nakashima T. Primary carcinoma of the liver. 4th ed. In: Berk JE, editor. Bockus gastroenterology. Philadelphia: WB Saunders, 1985: 3361-3364

3 **Kakizoe S**, Kojiro M, Nakashima T. Hepatocellular carcinoma with sarcomatous change. Clinicopathologic and immunohistochemical studies of 14 autopsy cases. *Cancer* 1987; **59**: 310-316

4 **Nakajima T**, Kondo Y. A clinicopathologic study of intrahepatic cholangiocarcinoma containing a component of squamous cell carcinoma. *Cancer* 1990; **65**: 1401-1404

5 **Thompson L**, Chang B, Barsky SH. Monoclonal origins of malignant mixed tumors (carcinosarcomas). Evidence for a divergent histogenesis. *Am J Surg Pathol* 1996; **20**: 277-285

6 **Iwaya T**, Maesawa C, Tamura G, Sato N, Ikeda K, Sasaki A, Othuka K, Ishida K, Saito K, Satodate R. Esophageal carcinosarcoma: a genetic analysis. *Gastroenterology* 1997; **113**: 973-977

7 **Lopez-Beltran A**, Pacelli A, Rothenberg HJ, Wollan PC, Zincke H, Blute ML, Bostwick DG. Carcinosarcoma and sarcomatoid carcinoma of the bladder: clinicopathological study of 41 cases. *J Urol* 1998; **159**: 1497-1503

8 **Guarino M**, Tricomi P, Giordano F, Cristofori E. Sarcomatoid carcinomas: pathological and histopathogenetic considerations. *Pathology* 1996; **28**: 298-305

9 **Gentile R**, Castellaneta A. Carcinosarcoma of the colon, one or two tumors? *Pathologica* 1997; **89**: 62-68

10 **Nomura K**, Aizawa S, Ushigome S. Carcinosarcoma of the liver. *Arch Pathol Lab Med* 2000; **124**: 888-890

11 **Eriguchi N**, Aoyagi S, Hara M, Okuda K, Fukuda S, Tamae T, Kanazawa N. Malignant sarcomatoid tumor of the liver: report of a case. *Surg Today* 2001; **31**: 170-173

12 **Wang XW**, Liang P, Li HY. Primary hepatic carcinosarcoma: a case report. *Chin Med J* (Engl) 2004; **117**: 1586-1587

S- Editor Liu Y **L- Editor** Wang XL **E- Editor** Ma WH

PO Box 2345, Beijing 100023, China
www.wjgnet.com
wjg@wjgnet.com

World J Gastroenterol 2007 February 7; 13(5): 813-815
World Journal of Gastroenterology ISSN 1007-9327

CASE REPORT

Metastatic melanoma to the common bile duct causing obstructive jaundice: A case report

Radoje B Colovic, Nikica M Grubor, Miodrag D Jovanovic, Marjan T Micev, Natasa R Colovic

Radoje B Colovic, Nikica M Grubor, Miodrag D Jovanovic, Marjan T Micev, Natasa R Colovic, Institute for Digestive Diseases, First Surgical Clinic, Clinical Center of Serbia, Koste Todorovica 6, Belgrade 11000, Serbia
Correspondence to: Radoje B Colovic, Institute for Digestive Diseases, First Surgical Clinic, Clinical Center of Serbia, Koste Todorovica 6, Belgrade 11000, Serbia. marcolov@eunet.yu
Telephone: +381-11-3610715 Fax: +381-11-3615569
Received: 2006-10-10 Accepted: 2006-12-29

Abstract

Metastatic melanoma to the common bile duct is very rare with only 18 cases reported so far. We report a 46 year old women who, 18 mo after excision of a skin melanoma, developped a painless progressive obstructive jaundice. At operation a melanoma within the distal third of the common bile duct was found. There were no other secondaries within the abdomen. The common bile duct, including the tumor, was resected and anastomosed with Roux-en-Y jejunal limb. The patient survived 31 mo without any sign of local recurrence and was submitted to three other operations for axillar and brain secondaries, from which she finally died. Radical resection of metastatic melanoma to the common bile duct may result in lifelong relief of obstructive jaundice. It is safe and relatively easy to perform. In other cases, a less aggressive approach, stenting or bypass procedures, should be adopted.

Key words: Metastatic melanoma; Common bile duct; Jaundice

Colovic RB, Grubor NM, Jovanovic MD, Micev MT, Colovic NR. Metastatic melanoma to the common bile duct causing obstructive jaundice: A case report. *World J Gastroenterol* 2007; 13(5): 813-815

http://www.wjgnet.com/1007-9327/13/813.asp

INTRODUCTION

The great majority of malignant melanomas arise from the skin, squamous mucose membranes, retina, and leptomeninges. They can metastasize to almost every organ of the body. The intraabdominal viscera are involved in diffuse metastatic disease in approximately 60% of patients[1-3]. DasGupta and Brasfield in 1964 reported a 15% involvement of the gallbladder and 6% involvement of the remainder of the biliary tree[2].

CASE REPORT

A 46-year-old woman was admitted to our hospital with painless progressive obstructive jaundice. Previously she had been submitted to excision of a skin melanoma on the back in a local hospital. Our laboratory data showed an elevated bilirubin (235.9 μmol/L, direct bilirubin 138.4 μmol/L), alkaline phosphatase (1540 U/L), gama GT (638 U/L), SGOT (525 U/L), SGPT (870/U/L), and ESR (76/1 h). Ultrasonography showed a dilated gallbladder and common bile duct and suspected stone within the distal third of the common bile duct. In December 1996, a cholecystectomy was performed. An operative cholangiography through the cystic duct showed a tumorous mass within the distal common bile duct causing almost complete obstruction (Figure 1). The duodenum was mobilized, the common bile duct was opened and a piece of dark soft tumour tissue was removed. Frozen section biopsy showed a malignant melanoma. The common bile duct was then carefully dissected and transected 1 cm away from the lower edge of the tumor. The duct was proximally resected close to the convergence of the hepatic ducts. The distal end of the common bile duct was oversewn and the proximal end was anastomosed with Roux-en-Y jejunal limb. A careful search showed no other secondaries within the abdomen.

The recovery was uneventful. Histopathology revealed ill-defined epithelioid tumor cell aggregates infiltrating bile ducts and the surrounding fibro-adipose structures. There was strong brown granular intracytoplasmic pigmentation in some parts of the infiltrate (Figures 2 and 3). Fontana-Masson histochemical staining confirmed melanin pigment and positive strong anti-S100 protein and anti-HMB45 immunoreactivity with weak positivity to anti-melan A antibodies proved the diagnosis of a metastatic melanoma. The patient survived 31 mo without any signs of local recurrence. She had to be submitted to another three surgeries for the axillar and brain secondaries, which were a final cause of her death.

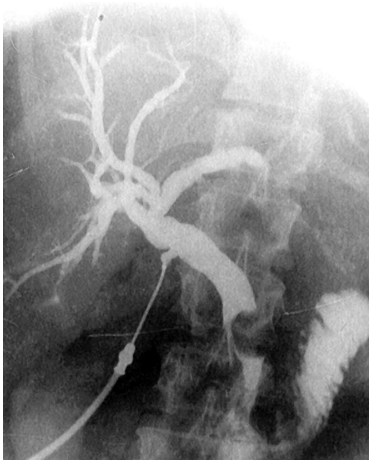

Figure 1 Showing filling defect within the distal common bile duct causing almost complete obstruction.

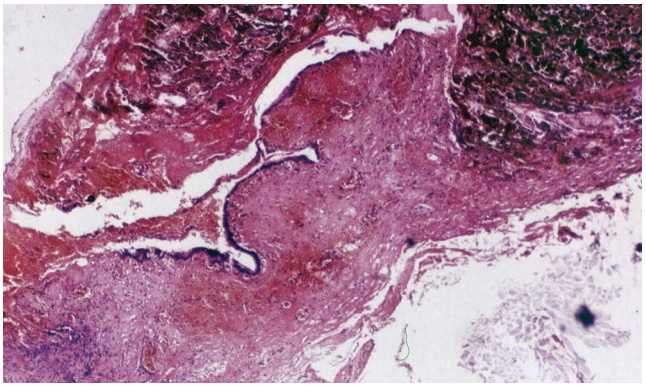

Figure 2 A pigmented malignant tumour evidently infiltrates extrahepatic bile duct. Later histochemical and immunohistochemical analyses showed melanoma cells (HE, × 13).

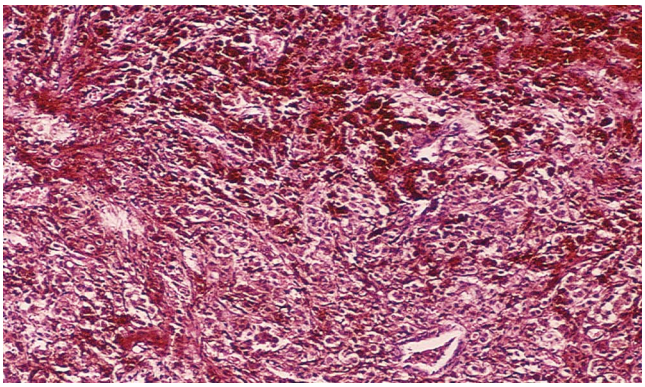

Figure 3 Higher magnification of the same tumour field showed insular and trabecular-to-solid histological organization of melanoma cells. Most of the cells were hyperpigmented with massive intracytoplasmic melanosome granules (HE, × 64).

DISCUSSION

The first case of a metastatic melanoma to the bile duct was described by Spigelberg in 1895, and the second by Duval in 1908[4]. A search throughout Medline showed 18 metastatic melanomas to the common bile duct reported so far[4-19]. Within this period, about 20 cases of primary malignant melanomas of the common bile duct have been described. However, in spite of confirmatory immunohistochemical stains, electron microscopic studies, the presence of junctional activity adjacent to the tumour, and tests to rule out other possible remote or concurrent primary sites, absolute exclusion of a metastatic melanoma from an unknown occult site or regressed site is not entirely possible[20]. The melanoma secondaries usually arise from the primary skin lesion but occasionally they may arise from primary or metastatic melanoma of the gallbladder[7,12,16].

Patients with metastatic melanoma to the common bile duct usually present with progressive painless obstructive jaundice[4,19]. Rarely the patients have hematobilia[10], pain[5,8], or cholangitis[19]. Laboratory data show a cholestatic jaundice. On ultrasonography this tumour is echogenic with little or no acoustic shadowing[9]. The exact preoperative diagnosis of the tumour is established, almost exclusively when localised at the Vater's papilla so that a biopsy can be taken[18], or on the basis of histologic examination of a small fragment of the tissue retrieved from the bile duct with a Dormia basket after papilotomy[19].

The current literature has few recommendations with regard to appropriate treatment of the melanoma metastases to the bile ducts[14,19]. It seems reasonable to perform radical surgical resection in patients with potentially curable disease and isolated deposits in the bile duct[14,19]. We believe it is paticularly indicated if resection is not too dangerous and if it is relatively easy to perform, as in the present case. A resection may be necessary in cases of serious hematobilia[10]. If there is a concurrent metastatic disease elsewhere, it is prudent to adopt a less aggressive approach in order to relieve obstructive jaundice, such as the bypass procedures[14], or stenting[18,19].

REFERENCES

1 **Pomerantz H**, Margolin HN. Metastases to the gastrointestinal tract from malignant melanoma. *Am J Roentgenol Radium Ther Nucl Med* 1962; **88**: 712-717
2 **Dasgupta TK**, Brasfield RD. Metastatic melanoma of the gastrointestinal tract. *Arch Surg* 1964; **88**: 969-973
3 **Patel JK**, Didolkar MS, Pickren JW, Moore RH. Metastatic pattern of malignant melanoma. A study of 216 autopsy cases. *Am J Surg* 1978; **135**: 807-810
4 **Cohen AJ**, Thompson LD, Jaques DP, d'Avis JC. Biliary tract melanoma. *Mil Med* 1990; **155**: 5-8
5 **Zaide EC**. Malignant melanoma of the choledochus. *Arq Oncol* 1963; **26**: 254-255
6 **Cole HS**, Freston JW. Recurrent melanoma presenting with obstructive jaundice. Report of two cases. *Rocky Mt Med J* 1973; **70**: 42-46
7 **Armbruster C**. Pancreatocephaloduodenectomy for melanoma metastasis in the terminal ductus choledochus. *Zentralbl Chir* 1973; **98**: 681-682
8 **Bowdler DA**, Leach RD. Metastatic intrabiliary melanoma. *Clin Oncol* 1982; **8**: 251-255
9 **Daunt N**, King DM. Metastatic melanoma in the biliary tree. *Br J Radiol* 1982; **55**: 873-874
10 **McArthur MS**, Teergarden DK. Metastatic melanoma presenting as obstructive jaundice with hemobilia. *Am J Surg* 1983; **145**: 830-832

11 **O'Connell JB**, Whittemore DM, Russell JC, Ellis WA, Becker DR. Malignant melanoma metastatic to the cystic and common bile ducts. *Cancer* 1984; **53**: 184-186
12 **Verbanck JJ**, Rutgeerts LJ, van Aelst FJ, Tytgat JH, Decoster JM, Noyez DN, Theunynck PJ, Geboes KJ. Primary malignant melanoma of the gallbladder, metastatic to the common bile duct. *Gastroenterology* 1986; **91**: 214-218
13 **Kohler B**, Riemann JF. Obstructive jaundice due to an intraductal melanoma metastasis. *Endoscopy* 1987; **19**: 79-80
14 **England MD**, Sarr MG. Metastatic melanoma: an unusual cause of obstructive jaundice. *Surgery* 1990; **107**: 595-596
15 **Parquier JN**, Peetrons P, Liénard D, Maisonnier H, Jeanmart L. Jaundice secondary to a metastasis of a malignant melanoma at the level of the common bile duct. *J Belge Radiol* 1991; **74**: 201-204
16 **Zhang ZD**, Myles J, Pai RP, Howard JM. Malignant melanoma of the biliary tract: a case report. *Surgery* 1991; **109**: 323-328
17 **Thompson JF**, Mathur MN, Coates AS. Common bile duct obstruction due to intraluminal metastatic melanoma. *Aust N Z J Surg* 1993; **63**: 502-504
18 **Sans M**, Llach J, Bordas JM, Andreu V, Campo A, Castells A, Mondelo E, Terés J, Rodés J. Metastatic malignant melanoma of the papilla of Vater: an unusual case of obstructive cholestasis treated with biliary prostheses. *Endoscopy* 1996; **28**: 791-792
19 **Garas G**, Bramston B, Edmunds SE. Malignant melanoma metastatic to the common bile duct. *J Gastroenterol Hepatol* 2000; **15**: 1348-1351
20 **Wagner MS**, Shoup M, Pickleman J, Yong S. Primary malignant melanoma of the common bile duct: a case report and review of the literature. *Arch Pathol Lab Med* 2000; **124**: 419-422

S- Editor Liu Y **L- Editor** Zhu LH **E- Editor** Ma WH

PO Box 2345, Beijing 100023, China
www.wjgnet.com
wjg@wjgnet.com

World J Gastroenterol 2007 February 7; 13(5): 816
World Journal of Gastroenterology ISSN 1007-9327

ACKNOWLEDGMENTS

Acknowledgments to Reviewers of *World Journal of Gastroenterology*

Many reviewers have contributed their expertise and time to the peer review, a critical process to ensure the quality of *World Journal of Gastroenterology*. The editors and authors of the articles submitted to the journal are grateful to the following reviewers for evaluating the articles (including those were published and those were rejected in this issue) during the last editing period of time.

Takeshi Azuma, Associate Professor
Second Department of Internal Medicine, University of Fukui, Faculty of Medical Sciences, Matsuoka-cho, YoshIDa-gun, Fukui 910-1193, Japan

Patrick Bertolino
AW Morrow Gastroenterology and Liver Centre, Centenary Institute of Cancer Medicine and Cell Biology, Locked Bag No 6, Newtown, NSW 2042, Australia

Josep M Bordas, MD
Department of Gastroenterology IMD, Hospital Clinic", Llusanes 11-13 at, Barcelona 08022, Spain

Ravi S Chari, MD, Associate Professor
Division of Hepatobiliary Surgery and Liver Transplantation, Departments of Surgery and Cancer Biology,1313 21st Avenue South Suite 801 Oxford House, Vanderbilt University Medical Center,Nashville, TN 37232-4753, United States

John Y Chiang, MD, PhD, Professor
Department of Biochemistry and Molecular Pathology, Northeastern Ohio Univ. College of Medicine, 4209 State Route 44, P.O. Box 95, Rootstown, OH 44272, United States

Parimal Chowdhury, Professor
Department of Physiology and Biophysics, College of Medicine University of Arkansas for Medical Sciences, 4301 W Markham Street Little Rock, Arkansas 72205, United States

Zong-Jie Cui, PhD, Professor
Institute of Cell Biology, Beijing Normal University, 19 XinJieKouWaiDaJie, Beijing 100875, China

Jean-Francois Dufour, Professor
Department of Clinical Pharmacology Inselspital, University of Berne35 Murtenstrasse 3010 Berne, Switzerland

Bijan Eghtesad, Dr, Associate Professor
Department of General Surgery, Cleveland Clinic Foundation, 9500 Euclid Avenue, Cleveland OH 44195, United States

Ronnie Fass, MD
Department of Internal Medicine, University of Arizona, Southern Arizona Via Health Care System G1 Section (1-111G-1)3401 S.4th Avenue, Tucson AZ 85723-0001, United States

Kazuma Fujimoto, Professor
Department of Internal Medicine, Saga Medical School, Nabeshima, Saga, Saga 849-8501, Japan

Andreas Geier, Associate Professor
Department of Internal Medicine III, University Hospital Aachen (UKA), Aachen University (RWTH), Pauwelsstrasse 30, D-52074 Aache, Germany

Rick Greupink, Dr
University of Groningen, A. Deusinglaan 1, Groningen 9713AV, The Netherlands

David J Hackam, MD, PhD
Division of Pediatric Surgery, Children's Hospital of Pittsburgh, Room 4A-486 DeSoto Wing, 3705 Fifth Avenue, Pittsburgh, Pennsylvania 15213. United States

Martin Hennenberg
Dipl-Biol, Medizinische Klinik & Poliklinik I, Uni-Klinik Bonn, Sigmund-Freud Str. 25, 53105 Bonn, Martin

Dusan M Jovanovic, Professor
Institute of Oncology, Institutski Put 4, Sremska Kamenica 21204, Serbia

Serdar Karakose, Professor
Department of Radiology, Meram Medical Faculty, Selcuk University, Konya 42080, Turkey

Peter Laszlo Lakatos, MD, PhD, Assistant Professor
1st Department of Medicine, Semmelweis University, Koranyi S 2A, Budapest H1083, Hungary

Philippe Mathurin, MD
Service d'Hépato-gastroentérologie, Hôpital Claude Huriez 2ème étage Est, Avenue Michel Polonovski, 59037 Lille, France

Bo-Rong Pan, Professor
Outpatient Department of Oncology, The Fourth Military Medical University, 175 Changle West Road,Xi'an 710032, Shaanxi Province, China

Raffaele Pezzilli, MD,
Department of Internal Medicine and Gastroenterology, Sant'Orsola-Malpighi Hospital, Via Massarenti, 9, Bologna 40138, Italy

Jay Pravda, MD
Inflammatory Disease Research Center, Gainesville, Florida, 32614-2181, United States

Lun-Xiu Qin, Professor
Liver Cancer Institute and Zhongshan Hospital, Fudan University, 180 Feng Lin Road, Shanghai 200032, China

Vasiliy I Reshetnyak, MD, PhD, Professor
Scientist Secretary of the Scientific Research Institute of General Reanimatology, 25-2, Petrovka str., 107031, Moscow, Russia

Hiroki Sasaki, PhD
Genetics Division, National Cancer Center Research Institute, 1-1, Tsukiji 5-chome, Chuo-ku, Tokyo 104-0045, Japan

Roland M Schmid, Professor
Chairman of the 2nd Department of Internal Medicine, Technical University of Munich, Ismaninger Straße 22, D- 81675 München, Germany

Tomohiko Shimatani, Assistant Professor
Department of General Medicine, Hiroshima University Hospital, 1-2-3 Kasumi, Minami-ku, Hiroshima 7348551, Japan

Pentti Sipponen, Professor, Head of the Division
Huslab, Helsinki University Cental Hospital, Division of Pathology Pathology, Jorvi Hospita, Huslab, Helsinki University Central Hospital, Espoo 02740, Finland

Gisela Sparmann, MD
Division of Gastroenterology, Department of Internal Medicine, University of Rostock, Ernst-Heydemann-Str. 6, Rostock D-18057, Germany

Qin Su, Professor
Department of Pathology, Cancer Hospital and Cancer Institute, Chinese Academy of Medical Sciences and Peking Medical College, PO Box 2258, Beijing 100021, China

Claudia Veltkamp, MD
Department of Gastroenterology, University of Heidelberg, INF 410, 69120 Heidelberg, Germany

Silvana Zanlungo, Professor
Departamento de Gastroenterología, Pontificia Universidad Católica de Chile, Marcoleta 367, Casilla 114-D, Santiago, Chile

Shu Zheng, Professor
Scientific Director of Cancer Institute, Zhejiang University, Secondary Affiliated Hospital, Zhejiang University, 88# Jiefang Road, Hangzhou 310009, Zhejiang Province, China

PO Box 2345, Beijing 100023, China
www.wjgnet.com
wjg@wjgnet.com

World J Gastroenterol 2007 February 7; 13(5): 817
World Journal of Gastroenterology ISSN 1007-9327

Meetings

MAJOR MEETINGS COMING UP

Meeting Falk Research Workshop: Morphogenesis and Cancerogenesis of the Liver
25-26 January 2007
Goettingen
symposia@falkfoundation.de

Meeting Canadian Digestive Diseases Week (CDDW)
16-20 February 2007
Banff-AB
cagoffice@cag-acg.org
www.cag-acg.org/cddw/cddw2007.htm

Meeting Falk Symposium 158: Intestinal Inflammation and Colorectal Cancer
23-24 March 2007
Sevilla
symposia@falkfoundation.de

Meeting BSG Annual Meeting
26-29 March 2007
Glasgow
www.bsg.org.uk/

NEXT 6 MONTHS

Meeting 42nd Annual Meeting of the European Association for the Study of the Liver
11-15 April 2007
Barcelona
easl2007@easl.ch
www.easl.ch/liver-meeting/

Meeting Falk Symposium 159: IBD 2007 - Achievements in Research and Clinical Practice
4-5 May 2007
Istanbul
symposia@falkfoundation.de

Meeting European Society for Paediatric Gastroenterology, Hepatology and Nutrition Congress 2007
9-12 May 2007
Barcelona
espghan2007@colloquium.fr

Digestive Disease Week
19-24 May 2007
Washington Convention Center, Washington DC

Meeting Gastrointestinal Endoscopy Best Practices: Today and Tomorrow, ASGE Annual Postgraduate Course at DDW
23-24 May 2007
Washington-DC
tkoral@asge.org

Meeting ESGAR 2007 18th Annual Meeting and Postgraduate Course
12-15 June 2007
Lisbon
fca@netvisao.pt

Meeting Falk Symposium 160: Pathogenesis and Clinical Practice in Gastroenterology
15-16 June 2007
Portoroz
symposia@falkfoundation.de

Meeting ILTS 13th Annual International Congress
20-23 June 2007
Rio De Janeiro
www.ilts.org

Meeting 9th World Congress on Gastrointestinal Cancer
27-30 June 2007
Barcelona
meetings@imedex.com

EVENTS AND MEETINGS IN 2007

Meeting Falk Research Workshop: Morphogenesis and Cancerogenesis of the Liver
25-26 January 2007
Goettingen
symposia@falkfoundation.de

Meeting Canadian Digestive Diseases Week (CDDW)
16-20 February 2007
Banff-AB
cagoffice@cag-acg.org
www.cag-acg.org/cddw/cddw2007.htm

Meeting Falk Symposium 158: Intestinal Inflammation and Colorectal Cancer
23-24 March 2007
Sevilla
symposia@falkfoundation.de

Meeting BSG Annual Meeting
26-29 March 2007
Glasgow
www.bsg.org.uk/

Meeting 42nd Annual Meeting of the European Association for the Study of the Liver
11-15 April 2007
Barcelona
easl2007@easl.ch
www.easl.ch/liver-meeting/

Meeting Falk Symposium 159: IBD 2007 - Achievements in Research and Clinical Practice
4-5 May 2007
Istanbul
symposia@falkfoundation.de

Meeting European Society for Paediatric Gastroenterology, Hepatology and Nutrition Congress 2007
9-12 May 2007
Barcelona
espghan2007@colloquium.fr

Meeting Gastrointestinal Endoscopy Best Practices: Today and Tomorrow, ASGE Annual Postgraduate Course at DDW
23-24 May 2007
Washington-DC
tkoral@asge.org

Meeting ESGAR 2007 18th Annual Meeting and Postgraduate Course
12-15 June 2007
Lisbon
fca@netvisao.pt

Meeting Falk Symposium 160: Pathogenesis and Clinical Practice in Gastroenterology
15-16 June 2007
Portoroz
symposia@falkfoundation.de

Meeting ILTS 13th Annual International Congress
20-23 June 2007
Rio De Janeiro
www.ilts.org

Meeting 9th World Congress on Gastrointestinal Cancer
27-30 June 2007
Barcelona
meetings@imedex.com

Meeting 15th International Congress of the European Association for Endoscopic Surgery
4-7 July 2007
Athens
info@eaes-eur.org
congresses.eaes-eur.org/

Meeting 39th Meeting of the European Pancreatic Club
4-7 July 2007
Newcastle
www.e-p-c2007.com

Meeting XXth International Workshop on Heliobacter and related bacteria in cronic degistive inflammation
20-22 September 2007
Istanbul
www.heliobacter.org

Meeting Falk Workshop: Mechanisms of Intestinal Inflammation
10 October 2007
Dresden
symposia@falkfoundation.de

Meeting Falk Symposium 161: Future Perspectives in Gastroenterology
11-12 October 2007
Dresden
symposia@falkfoundation.de

Meeting Falk Symposium 162: Liver Cirrhosis - From Pathophysiology to Disease Management
13-14 October 2007
Dresden
symposia@falkfoundation.de

American College of Gastroenterology Annual Scientific Meeting
12-17 October 2007
Pennsylvania Convention Center
Philadelphia, PA

Meeting APDW 2007 - Asian Pacific Digestive Disease Week 2007
15-18 October 2007
Kobe
apdw@convention.co.jp
www.apdw2007.org

15th United European Gastroenterology Week, UEGW
27-31 October 2007
Le Palais des Congrès de Paris, Paris, France

Meeting The Liver Meeting® 2007 - 57th Annual Meeting of the American Association for the Study of Liver Diseases
2-6 November 2007
Boston-MA
www.aasld.org

Gastro 2009, World Congress of Gastroenterology and Endoscopy London, United Kingdom 2009

PO Box 2345, Beijing 100023, China
www.wjgnet.com
wjg@wjgnet.com

World J Gastroenterol 2007 February 7; 13(5): 818-820
World Journal of Gastroenterology ISSN 1007-9327

Instructions to authors

GENERAL INFORMATION

World Journal of Gastroenterology (*WJG, World J Gastroenterol* ISSN 1007-9327 CN 14-1219/R) is a weekly journal of more than 48 000 circulation, published on the 7th, 14th, 21st and 28th of every month.

Original Research, Clinical Trials, Reviews, Comments, and Case Reports in esophageal cancer, gastric cancer, colon cancer, liver cancer, viral liver diseases, *etc.*, from all over the world are welcome on the condition that they have not been published previously and have not been submitted simultaneously elsewhere.

Indexed and abstracted in

Current Contents®/Clinical Medicine, Science Citation Index Expanded (also known as SciSearch®) and Journal Citation Reports/Science Edition, *Index Medicus*, MEDLINE and PubMed, Chemical Abstracts, EMBASE/Excerpta Medica, Abstracts Journals, *Nature Clinical Practice Gastroenterology and Hepatology*, CAB Abstracts and Global Health. ISI JCR 2003-2000 IF: 3.318, 2.532, 1.445 and 0.993.

Published by

The WJG Press

SUBMISSION OF MANUSCRIPTS

Manuscripts should be typed double-spaced on A4 (297 mm × 210 mm) white paper with outer margins of 2.5 cm. Number all pages consecutively, and start each of the following sections on a new page: Title Page , Abstract, Introduction, Materials and Methods, Results, Discussion, acknowledgements, References, Tables, Figures and Figure Legends. Neither the editors nor the Publisher is responsible for the opinions expressed by contributors. Manuscripts formally accepted for publication become the permanent property of The WJG Press, and may not be reproduced by any means, in whole or in part without the written permission of both the authors and the Publisher. We reserve the right to put onto our website and copy-edit accepted manuscripts. Authors should also follow the guidelines for the care and use of laboratory animals of their institution or national animal welfare committee.

Authors should retain one copy of the text, tables, photographs and illustrations, as rejected manuscripts will not be returned to the author(s) and the editors will not be responsible for the loss or damage to photographs and illustrations in mailing process.

Online submission

Online submission is strongly advised. Manuscripts should be submitted through the Online Submission System at: http://www.wjgnet.com/index.jsp. Authors are highly recommended to consult the ONLINE INSTRUCTIONS TO AUTHORS (http://www.wjgnet.com/wjg/help/instructions.jsp) before attempting to submit online. Authors encountering problems with the Online Submission System may send an email you describing the problem to wjg@wjgnet.com for assistance. If you submit your manuscript online, do not make a postal contribution. A repeated online submission for the same manuscript is strictly prohibited.

Postal submission

Send 3 duplicate hard copies of the full-text manuscript typed double-spaced on A4 (297 mm × 210 mm) white paper together with any original photographs or illustrations and a 3.5 inch computer diskette or CD-ROM containing an electronic copy of the manuscript including all the figures, graphs and tables in native Microsoft Word format or *.rtf format to:

Editorial Office

World Journal of Gastroenterology
Editorial Department: Apartment 1066, Yishou Garden,
58 North Langxinzhuang Road,
PO Box 2345, Beijing 100023, China
E-mail: wjg@wjgnet.com
http: //www.wjgnet.com
Telephone: +86-10-85381892
Fax: +86-10-85381893

MANUSCRIPT PREPARATION

All contributions should be written in English. All articles must be submitted using a word-processing software. All submissions must be typed in 1.5 line spacing and in word size 12 with ample margins. The letter font is Tahoma. For authors from China, one copy of the Chinese translation of the manuscript is also required (excluding references). Style should conform to our house format. Required information for each of the manuscript sections is as follows:

Title page

Full manuscript title, running title, all author(s) name(s), affiliations, institution(s) and/or department(s) where the work was accomplished, disclosure of any financial support for the research, and the name, full address, telephone and fax numbers and email address of the corresponding author should be included. Titles should be concise and informative (removing all unnecessary words), emphasize what is new, and avoid abbreviations. A short running title of less than 40 letters should be provided. List the author(s)' name(s) as follows: initial and/or first name, middle name or initial(s) and full family name.

Abstract

An informative, structured abstract of no more than 250 words should accompany each manuscript. Abstracts for original contributions should be structured into the following sections: AIM: Only the purpose should be included. METHODS: The materials, techniques, instruments and equipments, and the experimental procedures should be included. RESULTS: The observatory and experimental results, including data, effects, outcome, *etc.* should be included. Authors should present *P* value where necessary, and the significant data should accompany. CONCLUSION: Accurate view and the value of the results should be included.

The format of structured abstracts is at: http://www.wjgnet.com/wjg/help/11.doc

Key words

Please list 5-10 key words that could reflect content of the study mainly from *Index Medicus*.

Text

For most article types, the main text should be structured into the following sections: INTRODUCTION, MATERIALS AND METHODS, RESULTS and DISCUSSION, and should include in appropriate Figures and Tables. Data should be presented in the body text or in Figures and Tables, but not in both.

Illustrations

Figures should be numbered as 1, 2, 3 and so on, and mentioned clearly in the main text. Provide a brief title for each figure on a separate page. No detailed legend should be involved under the figures. This part should be added into the text where the figures are applicable. Digital images: black and white photographs should be scanned and saved in TIFF format at a resolution of 300 dpi; color images should be saved as CMYK (print files) but not as RGB (screen-viewing files). Place each photograph in a separate file. Print images: supply images of size no smaller than 126 mm × 85 mm printed on smooth surface paper; label the image by writing the Figure number and orientation using an arrow. Photomicrographs: indicate the original magnification and stain in the legend. Digital Drawings: supply files in EPS if created by freehand and illustrator, or TIFF from photoshops. EPS files must be accompanied by a version in native file format for editing purposes. Existing line drawings should be scanned at a resolution of 1200 dpi and as close as possible to the size where they will appear when printed. Please use uniform legends for the same subjects. For example: Figure 1 Pathological changes of atrophic gastritis after treatment. A: ...; B: ...; C: ...; D: ...; E: ...; F: ...; G: ...

Tables

Three-line tables should be numbered as 1, 2, 3 and so on, and mentioned clearly in the main text. Provide a brief title for each table. No detailed legend should be included under the tables. This part should be added into the text where the tables are applicable. The information should complement but not duplicate that contained in the text. Use one horizontal line under the title, a second under the column heads, and a third below the Table, above any footnotes. Vertical and italic lines should be omitted.

Notes in tables and illustrations

Data that are not statistically significant should not be noted. $^{a}P<0.05$, $^{b}P<0.01$ should be noted ($P>0.05$ should not be noted). If there are other series of *P* values, $^{c}P<0.05$ and $^{d}P<0.01$ are used. Third series of *P* values can be expressed as $^{e}P<0.05$ and $^{f}P<0.01$. Other notes in tables or under

illustrations should be expressed as ^1F, ^2F, ^3F; or some other symbols with a superscript (Arabic numerals) in the upper left corner. In a multi-curve illustration, each curve should be labeled with ●, ○, ■, □, ▲, △, *etc.* in a certain sequence.

Acknowledgments

Brief acknowledgments of persons who have made genuine contributions to the manuscripts and who endorse the data and conclusions are included. Authors are responsible for obtaining written permission to use any copyrighted text and/or illustrations.

REFERENCES

Coding system

The author should code the references according the citation order in text in Arabic numerals, put references codes in square brackets, superscript it at the end of citation content or the author name of the citation. For those citation content as the narrate part, the coding number and square brackets should be typeset normally. For example, Crohn's disease (CD) is associated with increased intestinal permeability[1,2]. If references are directly cited in the text, they would be put together with the text, for example, from references [19,22-24], we know that...

When the authors code the references, please ensure that the order in text is the same as in reference part and also insure the spelling accuracy of the first author's name. Do not code the same citation twice.

PMID requirement

PMID roots in the abstract serial number indexed by PubMed (http://www.ncbi.nlm.nih.gov/entrez/query.fcgi?db=PubMed). The author should supply the PMID for journal citation. For those references that have not been indexed by PubMed, a printed copy of the first page of the full reference should be submitted.

The accuracy of the information of the journal citations is very important. Through reference testing system, the authors and editor could check the authors name, title, journal title, publication date, volume number, start page, and end page. We will interlink all references with PubMed in ASP file so that the readers can read the abstract of the citations online immediately.

Style for journal references

Authors: the first author should be typed in bold-faced letter. The surname of all authors should be typed with the initial letter capitalized and followed by their name in abbreviation (For example, Lian-Sheng Ma is abbreviated as Ma LS, Bo-Rong Pan as Pan BR). Title of the cited article and italicized journal title (Journal title should be in its abbreviation form as shown in PubMed), publication date, volume number (in black), start page, and end page [PMID: 11819634]

Note: The author should test the references through reference testing system (http://www.wjgnet.com/cgi-bin/index.pl)

Style for book references

Authors: the first author should be typed in bold-faced letter. The surname of all authors should be typed with the initial letter capitalized and followed by their name in abbreviation (For example, Lian-Sheng Ma is abbreviated as Ma LS, Bo-Rong Pan as Pan BR) Book title. Publication number. Publication place: Publication press, Year: start page and end page.

Format

Journals

English journal article (list all authors and include the PMID where applicable)

1 **Grover VP**, Dresner MA, Forton DM, Counsell S, Larkman DJ, Patel N, Thomas HC, Taylor-Robinson SD. Current and future applications of magnetic resonance imaging and spectroscopy of the brain in hepatic encephalopathy. *World J Gastroenterol* 2006; **12**: 2969-2978 [PMID: 16718775]

Chinese journal article (list all authors and include the PMID where applicable)

2 **Lin GZ**, Wang XZ, Wang P, Lin J, Yang FD. Immunologic effect of Jianpi Yishen decoction in treatment of Pixu-diarrhoea. *Shijie Huaren Xiaohua Zazhi* 1999; **7**: 285-287

In press

3 **Tian D**, Araki H, Stahl E, Bergelson J, Kreitman M. Signature of balancing selection in Arabidopsis. *Proc Natl Acad Sci U S A* 2006; In press

Organization as author

4 **Diabetes Prevention Program Research Group**. Hypertension, insulin, and proinsulin in participants with impaired glucose tolerance. *Hypertension* 2002; **40**: 679-686 [PMID: 12411462]

Both personal authors and an organization as author

5 **Vallancien G**, Emberton M, Harving N, van Moorselaar RJ; Alf-One Study Group. Sexual dysfunction in 1, 274 European men suffering from lower urinary tract symptoms. *J Urol* 2003; **169**: 2257-2261 [PMID: 12771764]

No author given

6 21st century heart solution may have a sting in the tail. *BMJ* 2002; **325**: 184 [PMID: 12142303]

Volume with supplement

7 **Geraud G**, Spierings EL, Keywood C. Tolerability and safety of frovatriptan with short- and long-term use for treatment of migraine and in comparison with sumatriptan. *Headache* 2002; **42** Suppl 2: S93-99 [PMID: 12028325]

Issue with no volume

8 **Banit DM**, Kaufer H, Hartford JM. Intraoperative frozen section analysis in revision total joint arthroplasty. *Clin Orthop Relat Res* 2002; (**401**): 230-238 [PMID: 12151900]

No volume or issue

9 Outreach: bringing HIV-positive individuals into care. *HRSA Careaction* 2002; 1-6 [PMID: 12154804]

Books

Personal author(s)

10 **Sherlock S**, Dooley J. Diseases of the liver and billiary system. 9th ed. Oxford: Blackwell Sci Pub, 1993: 258-296

Chapter in a book (list all authors)

11 **Lam SK**. Academic investigator's perspectives of medical treatment for peptic ulcer. In: Swabb EA, Azabo S. Ulcer disease: investigation and basis for therapy. New York: Marcel Dekker, 1991: 431-450

Author(s) and editor(s)

12 **Breedlove GK**, Schorfheide AM. Adolescent pregnancy. 2nd ed. Wieczorek RR, editor. White Plains (NY): March of Dimes Education Services, 2001: 20-34

Conference proceedings

13 **Harnden P**, Joffe JK, Jones WG, editors. Germ cell tumours V. Proceedings of the 5th Germ Cell Tumour Conference; 2001 Sep 13-15; Leeds, UK. New York: Springer, 2002: 30-56

Conference paper

14 **Christensen S**, Oppacher F. An analysis of Koza's computational effort statistic for genetic programming. In: Foster JA, Lutton E, Miller J, Ryan C, Tettamanzi AG, editors. Genetic programming. EuroGP 2002: Proceedings of the 5th European Conference on Genetic Programming; 2002 Apr 3-5; Kinsdale, Ireland. Berlin: Springer, 2002: 182-191

Electronic journal (list all authors)

Morse SS. Factors in the emergence of infectious diseases. Emerg Infect Dis serial online, 1995-01-03, cited 1996-06-05; 1(1): 24 screens. Available from: URL: http//www.cdc.gov/ncidod/EID/eid.htm

Patent (list all authors)

16 **Pagedas AC**, inventor; Ancel Surgical R&D Inc., assignee. Flexible endoscopic grasping and cutting device and positioning tool assembly. United States patent US 20020103498. 2002 Aug 1

Inappropriate references

Authors should always cite references that are relevant to their article, and avoid any inappropriate references. Inappropriate references include those that are linked with a hyphen and the difference between the two numbers at two sides of the hyphen is more than 5. For example, [1-6], [2-14] and [1, 3, 4-10, 22] are all considered as inappropriate references. Authors should not cite their own unrelated published articles.

Statistical data

Present as mean ± SD or mean ± SE.

Statistical expression

Express t test as t (in italics), F test as F (in italics), chi square test as χ^2 (in Greek), related coefficient as r (in italics), degree of freedom as γ (in Greek), sample number as n (in italics), and probability as P (in italics).

Units

Use SI units. For example: body mass, m (B) = 78 kg; blood pressure, p(B) = 16.2/12.3 kPa; incubation time, t (incubation) = 96 h, blood glucose concentration, c (glucose) 6.4 ± 2.1 mmol/L; blood CEA mass concentration, p (CEA) = 8.6 24.5 μg/L; CO_2 volume fraction, 50 mL/L CO_2 not 5% CO_2; likewise for 40 g/L formaldehyde, not 10% formalin; and mass fraction, 8 ng/g, *etc.* Arabic numerals such as 23, 243, 641 should be read 23 243 641.

The format about how to accurately write common units and quantum is at: http://www.wjgnet.com/wjg/help/15.doc

Abbreviations

Standard abbreviations should be defined in the abstract and on first mention in the text. In general, terms should not be abbreviated unless they are used repeatedly and the abbreviation is helpful to the reader. Permissible abbreviations are listed in Units, Symbols and Abbreviations: A Guide for Biological and Medical Editors and Authors (Ed. Baron DN, 1988) published by The Royal Society of Medicine, London. Certain commonly used abbreviations, such as DNA, RNA, HIV, LD50, PCR, HBV, ECG, WBC, RBC, CT, ESR, CSF, IgG, ELISA, PBS, ATP, EDTA, mAb, can be used directly without further mention.

Italics

Quantities: *t* time or temperature, *c* concentration, *A* area, *l* length, *m* mass, *V* volume.
Genotypes: *gyr*A, *arg* 1, *c myc*, *c fos*, *etc.*
Restriction enzymes: *Eco*RI, *Hin*dI, *Bam*HI, *Kbo* I, *Kpn* I, *etc.*
Biology: *H pylori, E coli, etc.*

SUBMISSION OF THE REVISED MANUSCRIPTS AFTER ACCEPTED

Please revise your article according to the revision policies of *WJG*. The revised version including manuscript and high-resolution image figures (if any) should be copied on a floppy or compact disk. Author should send the revised manuscript, along with printed high-resolution color or black and white photos, copyright transfer letter, the final check list for authors, and responses to reviewers by a courier (such as EMS) (submission of revised manuscript by e-mail or on the *WJG* Editorial Office Online System is NOT available at present).

Language evaluation

The language of a manuscript will be graded before sending for revision. (1) Grade A: priority publishing; (2) Grade B: minor language polishing; (3) Grade C: a great deal of language polishing; (4) Grade D: rejected. The revised articles should be in grade B or grade A.

Copyright assignment form

Please downloaded CAF from http://www.wjgnet.com/wjg/help/9.doc.

We certify that the material contained in this manuscript:

Ms:

Title:

is original, except when appropriately referenced to other sources, and that written permission has been granted by any existing copyright holders. We agree to transfer to WJG all rights of our manuscript, including: (1) all copyright ownership in all print and electronic formats; (2) the right to grant permission to republish or reprint the stated material in whole or in part, with or without a fee; (3) the right to print copies for free distribution or sale; (4) the right to republish the stated material in a collection of articles or in any other format. We also agree that our article be put on the Internet.

Criteria for authorship: The WJG requests and publishes information about contributions of each author named to the submitted study. Authorship credit should be based on (1)direct participation in the study, including substantial contributions to conception and design of study, or acquisition of data, or analysis and interpretation of data; (2) manuscript writing, including drafting the article, or revising it critically for important intellectual content; (3)supportive work, including statistical analysis of data, or acquisition of funding, or administration, technology and materials support, or supervision, or supportive contributions. Authors should meet at least one of the three conditions. The WJG does not publish co-first authors and co-corresponding authors.

We hereby assign copyright transfer to WJG if this paper is accepted.

Author Name in full (Full names should be provided, with first name first, followed by middle names and family name at the last, eg, Eamonn MM Quigley). Handwritten names are not accepted.

Author Name in abbreviation (Family name is put first in full, followed by middle names and first name in abbreviation with first letter in capital, eg, Quigley EMM). Handwritten names are not accepted.

1 Full Name: _____
Abbreviation Name: _____
Signed: _____
Date: _____

2 Full Name: _____
Abbreviation Name: _____
Signed: _____
Date: _____

3 Full Name: _____
Abbreviation Name: _____
Signed: _____
Date: _____

4 Full Name: _____
Abbreviation Name: _____
Signed: _____
Date: _____

5 Full Name: _____
Abbreviation Name: _____
Signed: _____
Date: _____

6 Full Name: _____
Abbreviation Name: _____
Signed: _____
Date: _____

7 Full Name: _____
Abbreviation Name: _____
Signed: _____
Date: _____

8 Full Name: _____
Abbreviation Name: _____
Signed: _____
Date: _____

9 Full Name: _____
Abbreviation Name: _____
Signed: _____
Date: _____

10 Full Name: _____
Abbreviation Name: _____
Signed: _____
Date: _____

Final check list for authors

The format is at: http://www.wjgnet.com/wjg/help/13.doc

Responses to reviewers

Please revise your article according to the comments/suggestions of reviewers. The format for responses to the reviewers' comments is at: http://www.wjgnet.com/wjg/help/10.doc

Proof of financial support

For paper supported by a foundation, authors should provide a copy of the document and serial number of the foundation.

Publication fee

Authors of accepted articles must pay publication fee.
EDITORIAL and LETTERS TO THE EDITOR are free of change.

World Journal of
Gastroenterology ®
Volume 13 Number 6
February 14, 2007

National Journal Award
2005

The WJG Press

The WJG Press, Apartment 1066 Yishou Garden, 58 North
Langxinzhuang Road, PO Box 2345, Beijing 100023, China
Telephone: +86-10-85381901
Fax: +86-10-85381893
E-mail: wjg@wjgnet.com
http: //www.wjgnet.com

ISSN 1007-9327 CN 14-1219/R Local Post Offices Code No. 82-261

World Journal of Gastroenterology
www.wjgnet.com
Volume 13
Number 6
Feb 14
2007

ISSN 1007-9327
CN 14-1219/R

World Journal of
Gastroenterology®

Indexed and Abstracted in:

Current Contents®/Clinical Medicine, Science Citation Index Expanded (also known as SciSearch®) and Journal Citation Reports/Science Edition, *Index Medicus*, MEDLINE and PubMed, Chemical Abstracts, EMBASE/Excerpta Medica, Abstracts Journals, *Nature Clinical Practice Gastroenterology and Hepatology*, CAB Abstracts and Global Health.
ISI JCR 2003-2000 IF: 3.318, 2.532, 1.445 and 0.993.

Volume 13 Number 6
February 14, 2007

World J Gastroenterol
2007 February 14; 13(6): 821-984
Online Submissions
www.wjgnet.com/wjg/index.jsp
www.wjgnet.com
Printed on Acid-free Paper

A Weekly Journal of Gastroenterology and Hepatology

National Journal Award
2005

World Journal of Gastroenterology®

Volume 13 Number 6
February 14, 2007

The WJG Press

Contents

World Journal of Gastroenterology
Volume 13 **Number** 6 **February** 14, 2007

Contents

World Journal of Gastroenterology
Volume 13 **Number** 6 **February** 14, 2007

Contents

Responsible E-Editor for this issue: Wei Lu

C-Editor for this issue: Ming Li, Associate Professor

Responsible S-Editor for this issue: Ye Liu

World Journal of Gastroenterology (*World J Gastroenterol , WJG*), a leading international journal in gastroenterology and hepatology, has an established reputation for publishing first class research on esophageal cancer, gastric cancer, liver cancer, viral hepatitis, colorectal cancer, and *H pylori* infection, providing a forum for both clinicians and scientists, and has been indexed and abstracted in Current Contents®/Clinical Medicine, Science Citation Index Expanded (also known as SciSearch®) and Journal Citation Reports/Science Edition, *Index Medicus*, MEDLINE and PubMed, Chemical Abstracts, EMBASE/Excerpta Medica, Abstracts Journals, *Nature Clinical Practice Gastroenterology and Hepatology*, CAB Abstracts and Global Health. ISI JCR 2003-2000 IF: 3.318, 2.532, 1.445 and 0.993. *WJG* is a weekly journal published by The WJG Press. The publication date is on 7th, 14th, 21st, and 28th every month. The *WJG* is supported by The National Natural Science Foundation of China, No. 30224801 and No.30424812, which was founded with a name of *China National Journal of New Gastroenterology* on October 1,1995, and renamed as *WJG* on January 25, 1998.

PUBLISHED BY
The WJG Press

PRINTED BY
Printed in Beijing on acid-free paper by Beijing Kexin Printing House

 Print ISSN 1007-9327
CN 14-1219/R.

EDITORIAL OFFICE
World Journal of Gastroenterology,
The WJG Press, Apartment 1066 Yishou Garden, 58 North Langxinzhuang Road, PO Box 2345, Beijing 100023, China
Telephone: +86-10-85381892
Fax: +86-10-85381893
E-mail: wjg@wjgnet.com
http://www.wjgnet.com

SUBSCRIPTION AND AUTHOR REPRINTS
Jing Wang
The WJG Press, Apartment 1066 Yishou Garden, 58 North Langxinzhuang Road, PO Box 2345, Beijing 100023, China
Telephone: +86-10-85381892
Fax: +86-10-85381893
E-mail: j.wang@wjgnet.com
http://www.wjgnet.com

SUBSCRIPTION INFORMATION
Institutional Price 2007: USD 1500.00
Personal Price 2007: USD 700.00

INSTRUCTIONS TO AUTHORS
Full instructions are available online at http://www.wjgnet.com/wjg/help/instructions.jsp. If you do not have web access please contact the editorial office.

PO Box 2345, Beijing 100023, China
www.wjgnet.com
wjg@wjgnet.com

World J Gastroenterol 2007 February 14; 13(6): 821-825
World Journal of Gastroenterology ISSN 1007-9327

EDITORIAL

The hepatic sinusoidal endothelial lining and colorectal liver metastases

Filip Braet, Keissuke Nagatsuma, Masaya Saito, Lilian Soon, Eddie Wisse, Tomokazu Matsuura

Filip Braet, Lilian Soon, Eddie Wisse, Australian Key Centre for Microscopy and Microanalysis, Electron Microscopy Unit, The University of Sydney, NSW 2006, Australia
Keissuke Nagatsuma, Department of Pathology, The Jikei University School of Medicine, Tokyo, Japan
Masaya Saito, Division of Gastroenterology and Hepatology, Department of Internal Medicine, The Jikei University School of Medicine, Tokyo, Japan
Tomokazu Matsuura, Department of Laboratory Medicine, The Jikei University School of Medicine, Tokyo, Japan
Correspondence to: Professor Filip Braet, Australian Key Centre for Microscopy and Microanalysis, Electron Microscope Unit, Madsen Building F09, University of Sydney, Sydney, NSW 2006, Australia. filip.braet@emu.usyd.edu.au
Telephone: +61-2-93517619 Fax: +61-2-93517682
Received: 2006-11-08 Accepted: 2006-12-21

Abstract

Colorectal cancer (CRC) is a common malignant disease and the severe nature of cases in men and women who develop colorectal cancer makes this an important socio-economic health issue. Major challenges such as understanding and modeling colorectal cancer pathways rely on our understanding of simple models such as outlined in this paper. We discuss that the development of novel standardized approaches of multidimensional (correlative) biomolecular microscopy methods facilitates the collection of (sub) cellular tissue information in the early onset of colorectal liver metastasis and that this approach will be crucial in designing new effective strategies for CRC treatment. The application of X-ray micro-computed tomography and its potential in correlative imaging of the liver vasculature will be discussed.

Key words: Apoptosis; Australia; Correlative microscopy; Endothelial cells; Hepatic metastasis; Colorectal cancer; CC531; Gaps; Interferon gamma; Kupffer cells; Natural killer cells; Nitric oxide; Macrophages; Modeling; Phagocytosis; Plugging; Pit cells; Stellate cells; X-ray micro-computed tomography

Braet F, Nagatsuma K, Saito M, Soon L, Wisse E, Matsuura T. The hepatic sinusoidal endothelial lining and colorectal liver metastases. *World J Gastroenterol* 2007; 13(6): 821-825

http://www.wjgnet.com/1007-9327/13/821.asp

INTRODUCTION

Colorectal cancer (CRC) is a common malignant disease, with the majority of deaths attributable to hepatic metastasis. In the Western world, it is the second cause of cancer death in women after breast cancer, and the third cause of cancer death in men after lung and prostate cancer, being responsible for about 492 000 deaths p.a. worldwide and 4500 deaths p.a. in Australia[1]. In addition, the statistical data reveal that the risk of developing CRC disproportionately strikes individuals in the age group 65 years and older, illustrating its health longevity impact on the ageing population. At the first diagnosis of CRC, 20% of the patients already have liver metastasis and 30% of the patients will develop metastasis afterwards. 80% of the patients who die of CRC have metastases in the liver and prognosis is generally poor[2].

It is obvious that once the tumour cells have immigrated to the liver, they cross the hepatic sinusoidal endothelial barrier and by the time liver metastases form, most steps in the metastatic cascade have been completed. Consequently, exploring the preceding stages of CRC metastasis, proliferation and new blood vessel formation as well as mechanisms to disturb cell survival are to date of main interest as they are largely unexplored. As discussed in the following sections, the availability of new reconstructing and modeling techniques provide liver cancer biologists with an invaluable tool to bridge the gap between bench science and the development of potential novel liver CRC (immuno) therapeutic strategies.

COLORECTAL CANCER AND THE HEPATIC SINUSOIDAL IMMUNE SYSTEM

When the tumour cells invade the vascular bed and metastasise to the liver, they encounter the liver specific immune defence mechanisms. This hepatic sinusoidal immune system involves the hepatic-specific natural killer cells (NK) (pit cells)[3], Kupffer cells (KC) (liver-associated macrophages)[4] and hepatic endothelial cells (HEC)[5], and is proven to play an important role in protecting the liver from invading colon carcinoma cells[6]. The conventional paradigm of CRC liver metastasis is based on a multi-step process characterized by a series of structural, cellular and molecular events, which give the tumour cells the ability to proceed through the many phases of liver metastasis. Based on literature survey the following common sequence of key-events within the liver sinusoids are involved in the

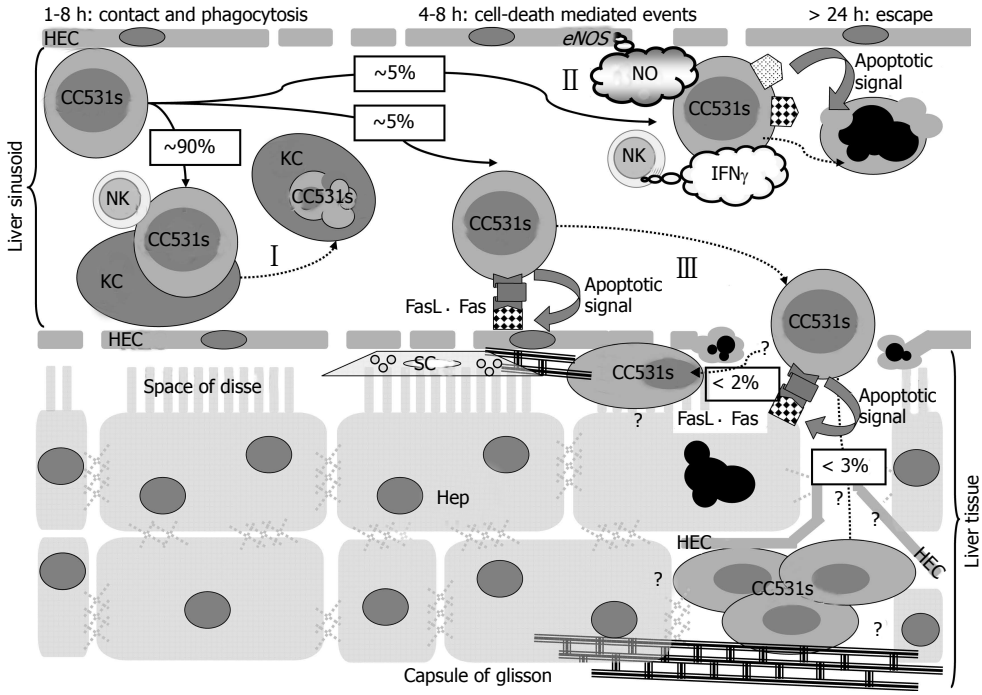

Figure 1 Schematic representation of the local hepatic sinusoidal immune defence system in the different steps of CRC liver metastasis (Steps Ⅰ to Ⅲ) as outlined in detail in the "*Phagocytosis, Apoptosis, Endothelial Retraction and Tumour Survival*"-section. The subsequent steps in the metastatic cascade as denoted by question marks illustrate that considerable work remains, especially once CRC cells traverse the sinusoidal endothelial lining and invade the liver tissue.

process of CRC liver metastasis: Tumour cells approach the liver tissue through finer branches of the portal vein, where they will be trapped in either the finest branch of the portal veins, or the portal hepatic sinusoids. These sinusoids are narrow and tortuous. The diameter of sinusoids is much smaller than the diameter of CRC cells. NK and KC are mobile cells and can be seen moving along the hepatic sinusoid in *in vivo* microscopy experiments (our unpublished data). At this stage, the NK and KC are seen to be associated with the majority of the tumour cells, resulting in cytolysis and subsequent phagocytosis of the majority of the cancer cells[7-9]. Subsequently, specific adhesion of tumour cells within the hepatic microcirculation and active extravasation of the surviving cancer cells through the damaged hepatic endothelium takes place[10]. Both are believed to be essential events for cancer metastasis in the liver[11]; although others postulate that tumour cells develop exclusively intravascularly during the early stages[12]. However, it has been demonstrated that endothelial damage and gap formation occurs in both scenarios, enabling large cellular surface interactions between the tumour cells and the hepatocytes[9-11].

In a later stage, matrix proteins derived from the stellate cells (SC) (liver-associated fibroblasts) are believed to provide a substrate for migration of tumour cells and infiltrating immuno-competent cells, whereas later on tight structures of matrix proteins surrounding tumour nodules provide a barrier for establishment of direct KC- and NK-cell-to-tumour-cell-contact and/or targeted therapies[9,13]. This is supported by the observation that large numbers of KC and NK cells were not activated at later phases in the metastasis process[14]. Finally, CRC cells spread throughout the liver, followed by the abdominal and peritoneal cavity[9,15].

PHAGOCYTOSIS, APOPTOSIS, ENDOTHELIAL RETRACTION AND TUMOUR SURVIVAL

Our previous microscopy and fine structural immunochemistry studies significantly contributed to the above model and as depicted in figure 1 we were able to demonstrate that KC, NK and HECs all work together in concert as one immune-surveillance guardian in the defence against CRC liver metastasis (Figure 1)[6]. Furthermore, it was shown that phagocytosis and apoptosis are key processes in three central steps in the complex CRC liver metastatic cascade, briefly: (Step Ⅰ) When CC531s colon carcinoma cells encounter the liver sinusoid about 90% of the tumour cells are eliminated by a synergistic action between KC and NK cells[9]; (Step Ⅱ) We have proven that HECs express FasL and that about 5% of the colorectal CC531s cell population express functional Fas under influence of IFNγ and NO released in the sinusoid by NK and HECs, respectively. In this situation, the IFNγ-activated pathway supports the immune system by inducing apoptosis in CC531s cells[16]; (Step Ⅲ) Conversely, Fas expressing HEC undergo apoptosis by FasL expressing CC531s cells. As a result, about 5% of the CC531s cells are able to escape the local immune system and provide themselves a gateway towards the liver tissue as the HECs retracts. Next the CC531s cells have free access to the Fas expressing hepatocytes (Hep) which undergo in turn apoptosis by the FasL bearing CC531s cells and as a result invade the liver tissue[17]. Reconstruction data obtained *via* the aid of confocal laser scanning microscopy indicated that surviving cancer cells are primarily confined to the Space of Disse and to the Glisson capsule, suggesting that metastasis would initiate from this extracellular matrix-rich region.

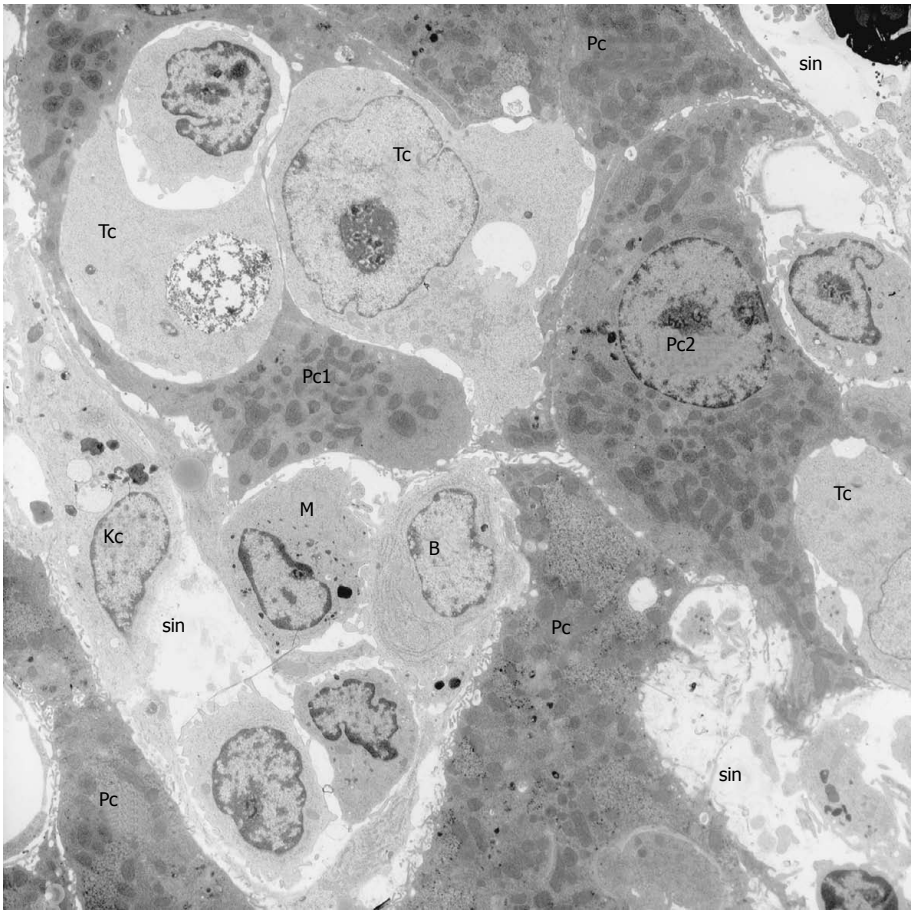

Figure 2 Transmission electron microscopy photomicrograph at low magnification (6700 x) of rat liver one week after i.v. injection of one million CC531s colon cancer cells. Tumour cells (Tc) can be recognized by a ribosome-rich, bulky cytoplasm containing few organelles. Tumour cell nuclei are large and contain mostly euchromatin. In this picture, tumour cells have already taken position in the liver parenchyma and compress or deform the parenchymal cells (Pc1 and Pc2). In this stage, tumour cells are so numerous that defending cells, such as Kupffer cells (Kc) and monocytes (M) in the hepatic sinusoids (sin) and B lymphocytes (B) seem to be no longer involved as in earlier stages. At this stage of tumour cell settlement, rebuilding of the hepatic tissue sets in and soon small visible white spots of metastasis will be seen on the surface of the liver.

Overall, based on our combined light-, laser- and electron microscopic *in vivo* and *in situ* studies, we believe that the majority of tumour cells entering the liver will be destroyed in this first confrontation with hepatic sinusoidal cells. The trouble is supposed to be the fact that only a very few tumour cells need to escape from the hepatic sinusoids and after settling in the liver parenchymal tissue, as depicted in the photograph (Figure 2), they form metastases and start spreading new tumour cells in the hepatic tissue (i.e., secondary metastasis). It is also supposed that after leaving the hepatic sinusoids, the tumour cells are not chased by the local hepatic sinusoidal immune cells, and that the liver tissue has to rely from that moment onwards on other cellular- and immune defence systems, such as those offered by cytotoxic T cells, monocyte-derived macrophages and others.

RECONSTRUCTING AND MODELING COLORECTAL HEPATIC METASTASIS WITH CORRELATIVE THREE-DIMENSIONAL IMAGING TECHNIQUES

In the past, mainly two-dimensional structural tissue information has been generated about the metastasis pathways of CRC tumour formation in the liver. Attempts to target specific CRC pathways for therapeutic intervention, such as apoptosis by cell-death mediated drug delivery and/or new blood vessel outgrowth by specific anti-angiogenic drug release, partly failed because of our limited structural and molecular understanding about the tumour's complex cell- and tissue microenvironment using two-dimensional imaging. New concepts and progress in cell biology have been discovered thanks to improved correlative microscopy techniques that continue to rely predominantly on advances in new, three-dimensional (3D) reconstructing and modeling techniques[18,19]. Ideally, 3D correlative microscopy can be defined as an imaging platform aiming to cross-correlate information with multiple microscopy techniques on the same tissue(s) and/or cell(s). There is growing evidence from the literature that this approach facilitates the understanding of cellular and/or rare events by providing the possibility to collect new qualitative and quantitative information in a large sample volume[20,21]. In the past our group successfully applied different biomolecular microscopy methods on our CC531s CRC model. The data conferred under the above section were obtained by combining confocal laser scanning-[9,22], live cell-[23], atomic force-[24], scanning electron-[10,17] and transmission electron[16,25] microscopy data. In line, we started up correlative confocal laser scanning microscopy-[9,18] and X-ray micro-computed tomography (CT)[26] studies as defined above to quantitatively collect the spatial and temporal cell- and tissue architecture at different resolution levels of CRC hepatic metastasis (*vide infra*).

In a recent study[27], we applied the impregnation method in which en bloc staining of perfused-fixed hepatic tissue with osmium tetroxide and uranyl acetate was shown

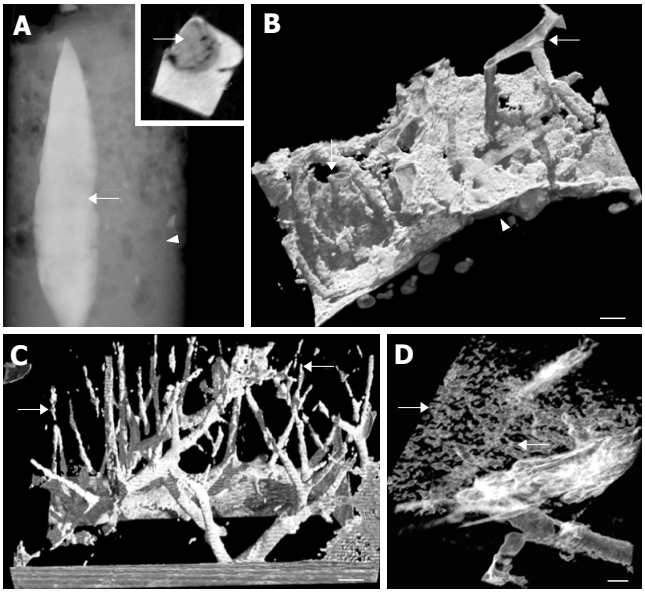

Figure 3 X-ray micro-computed tomography (CT) image set of hepatic tissue. For detailed recording and subsequent image processing settings we refer to Ananda *et al* (27). **A**: Low -magnification data showing an overview of a glutaraldehyde perfused-fixed and subsequently osmium tetroxide/uranyl acetate *en bloc* stained liver lobule (arrow) versus the unstained sample mounting support (arrowhead). Note, inset shows the corresponding Z-info at an ad random height of the main image; **B**: X-ray micro CT 3D reconstruction image showing the portal venous blood vessels (arrow) and hepatic tissue (arrowhead); **C**: X-ray micro CT reconstruction after density histogram image filtering, showing the intricate pattern of hepatic sinusoids (arrow) in 3D context. Note the absence of liver tissue information under this image processing condition (compare with B for the difference); **D**: Conversely, using different opacity thresholds resulted in the visualization of the hepatic cords, i.e. parenchymal tissue, (arrow). (Courtesy to Ms. S. Ananda and Ms. V. Marsden). Scale Bars (B-D), 500 μm.

to be successful to reconstruct and model a large sample volume of the macro- and microvasculature of hepatic tissue with X-ray micro-computed tomography (Figure 3). Furthermore, we demonstrated that correlative laser light optical imaging provided a limit of confidence for X-ray micro CT imaging of the hepatic vasculature as the large blood vessels such as the hepatic portal veins, and the smaller blood vessels i.e., the hepatic sinusoidal vascular bed could be visualized[27]. When applying the established contrasting method to the CC531s CRC metastasis model[9] it was observed that the dense array of blood vessels was interrupted in the liver tissue samples bearing the CRC cells when compared to the controls[27]. This is in line with the earlier observations made by Maehara[28] who showed tumour-induced reorganization of the auricular vascular bed after barium sulphate contrasting. Based on these data we forth casting the ability to correlate information in large tissue volumes from the X-ray micro CT models with reconstruction data obtained from confocal laser scanning microscopy on the same sample and region of interest by using fluorescent- and X-ray dense fiducial markers. This will definitely bridge the resolution gap from the micrometre to nanometre scale in studying cancer-mediated events, respectively.

In conclusion. Advanced multidimensional correlative microscopy methods and modeling techniques will feature heavily in the future quest to understand and to quantitatively define the spatial and temporal mechanisms regulating the pathways of CRC liver metastasis. There will be no doubt that elucidating the subcellular and molecular events of tumour-mediated cell-death processes (apoptosis) and collecting simultaneously additional structural and functional data in tumour-induced new blood vessel formation (angiogenesis) will be of main interest in future combined imaging studies as this approach will most probably result in an accurate correlative representation of the liver architecture and the tumour's microvasculature. One may hope that the combination of correlative insights gathered will be a breakthrough in the study of liver tumours and this will facilitate novel targeted cancer therapies in the long-term.

ACKNOWLEDGMENTS

The authors acknowledge the facilities as well as technical and administrative assistance from staff in the NANO Major National Research Facility at the "Australian Key Centre for Microscopy and Microanalysis" of The University of Sydney. T.M. and F.B. also acknowledge the support of the "Japan Association for the Advancement of Medical Equipment" (H17-nano-013 No. 141/Japanese Government-Ministry of Welfare and Labour). The authors are grateful to Ms. A Simpson, Ms. E Kable, Ms. E Korkmaz & Dr. L Cole, for excellent technical assistance, to Dr K Vekemans for providing hepatic tissue (Figure 3A), and to Mr. G Cohn, Mr. A Restov & Dr. A Jones for supporting Ms. S Ananda and Ms. V Marsden in soft X-ray imaging.

COMMENTS

Background

Major challenges such as understanding and modeling colorectal liver metastases pathways rely on the understanding of simple models derived from large biomolecular image data sets.

Research frontiers

This paper elegantly demonstrated that the development of novel standardized approaches of multidimensional (correlative) biomolecular microscopy methods facilitated the collection of (sub) cellular tissue information in the early onset of colorectal liver metastasis and that this approach is crucial in designing new effective strategies for colorectal cancer treatment.

Innovations and breakthroughs

Advanced multidimensional correlative microscopy methods and modeling techniques will feature heavily in the future quest to understand and to quantitatively define the spatial and temporal mechanisms regulating the pathways of colorectal cancer liver metastasis.

Applications

There is no doubt that the "correlative insights"-approach, as discussed in depth in this "invitation expert review"-paper, will be a breakthrough in the study of liver tumours and will facilitate the design of novel targeted cancer therapies.

Terminology

Colorectal cancer is a common malignancy that frequently metastasizes to the liver. Identifying the mechanisms regulating the nanobiology of colorectal liver metastasis, as well as gaining a better understanding of the interaction between the metastatic tumour cell and the different types of liver cells, including the liver

vasculature, is a first when new therapeutic approaches wanted to be designed.

Peer review

How and why colorectal cancer cells metastasize to the liver has always been a subject of continuing interest. The authors describe this concept nicely, supported by excellent pictures.

REFERENCES

1 **Australian Institute of Health and Welfare**. Cancer in Australia 2000. Cancer series no. 23. Canberra, 2003
2 **Hamady ZZ**, Kotru A, Nishio H, Lodge JP. Current techniques and results of liver resection for colorectal liver metastases. *Br Med Bull* 2004; **70**: 87-104
3 **Nakatani K**, Kaneda K, Seki S, Nakajima Y. Pit cells as liver-associated natural killer cells: morphology and function. *Med Electron Microsc* 2004; **37**: 29-36
4 **Naito M**, Hasegawa G, Ebe Y, Yamamoto T. Differentiation and function of Kupffer cells. *Med Electron Microsc* 2004; **37**: 16-28
5 **Enomoto K**, Nishikawa Y, Omori Y, Tokairin T, Yoshida M, Ohi N, Nishimura T, Yamamoto Y, Li Q. Cell biology and pathology of liver sinusoidal endothelial cells. *Med Electron Microsc* 2004; **37**: 208-215
6 **Vekemans K**, Braet F. Structural and functional aspects of the liver and liver sinusoidal cells in relation to colon carcinoma metastasis. *World J Gastroenterol* 2005; **11**: 5095-5102
7 **Kan Z**, Ivancev K, Lunderquist A, McCuskey PA, McCuskey RS, Wallace S. In vivo microscopy of hepatic metastases: dynamic observation of tumor cell invasion and interaction with Kupffer cells. *Hepatology* 1995; **21**: 487-494
8 **Rushfeldt C**, Sveinbjørnsson B, Seljelid R, Smedsrød B. Early events of hepatic metastasis formation in mice: role of Kupffer and NK-cells in natural and interferon-gamma-stimulated defense. *J Surg Res* 1999; **82**: 209-215
9 **Timmers M**, Vekemans K, Vermijlen D, Asosingh K, Kuppen P, Bouwens L, Wisse E, Braet F. Interactions between rat colon carcinoma cells and Kupffer cells during the onset of hepatic metastasis. *Int J Cancer* 2004; **112**: 793-802
10 **Vekemans K**, Timmers M, Vermijlen D, De Zanger R, Wisse E, Braet F. CC531s colon carcinoma cells induce apoptosis in rat hepatic endothelial cells by the Fas/FasL-mediated pathway. *Liver Int* 2003; **23**: 283-293
11 **Vidal-Vanaclocha F**. Role of sinusoidal endothelium in the pathogenesis of liver disease. In: Vidal-Vanaclocha F, editor. Functional Heterogeneity of Liver Tissue. Austin: R.G. Landes Company, 1997: 110-132
12 **Mook OR**, Van Marle J, Vreeling-Sindelárová H, Jonges R, Frederiks WM, Van Noorden CJ. Visualization of early events in tumor formation of eGFP-transfected rat colon cancer cells in liver. *Hepatology* 2003; **38**: 295-304
13 **Shimizu S**, Yamada N, Sawada T, Ikeda K, Kawada N, Seki S, Kaneda K, Hirakawa K. In vivo and in vitro interactions between human colon carcinoma cells and hepatic stellate cells. *Jpn J Cancer Res* 2000; **91**: 1285-1295
14 **Griffini P**, Smorenburg SM, Vogels IM, Tigchelaar W, Van Noorden CJ. Kupffer cells and pit cells are not effective in the defense against experimentally induced colon carcinoma metastasis in rat liver. *Clin Exp Metastasis* 1996; **14**: 367-380
15 **Lopes Cardozo AM**, Gupta A, Koppe MJ, Meijer S, van Leeuwen PA, Beelen RJ, Bleichrodt RP. Metastatic pattern of CC531 colon carcinoma cells in the abdominal cavity: an experimental model of peritoneal carcinomatosis in rats. *Eur J Surg Oncol* 2001; **27**: 359-363
16 **Vekemans K**, Braet F, Muyllaert D, Wisse E. Nitric oxide from rat liver sinusoidal endothelial cells induces apoptosis in IFN gamma-sensitized CC531s colon carcinoma cells. *J Hepatol* 2004; **41**: 11-18
17 **Vekemans K**, Braet F, Wisse E. DiO-labeled CC531s colon carcinoma cells traverse the hepatic sinusoidal endothelium via the Fas/FasL pathway. *J Gastrointest Surg* 2004; **8**: 371-372; author reply 372
18 **Robinson JM**, Takizawa T, Pombo A, Cook PR. Correlative fluorescence and electron microscopy on ultrathin cryosections: bridging the resolution gap. *J Histochem Cytochem* 2001; **49**: 803-808
19 **Grabenbauer M**, Geerts WJ, Fernadez-Rodriguez J, Hoenger A, Koster AJ, Nilsson T. Correlative microscopy and electron tomography of GFP through photooxidation. *Nat Methods* 2005; **2**: 857-862
20 **Koster AJ**, Klumperman J. Electron microscopy in cell biology: integrating structure and function. *Nat Rev Mol Cell Biol* 2003; **Suppl**: SS6-SS10
21 **Takizawa T**, Robinson JM. Correlative microscopy of ultrathin cryosections in placental research. *Methods Mol Med* 2006; **121**: 351-369
22 **Timmers M**, Vermijlen D, Vekemans K, De Zanger R, Wisse E, Braet F. Tracing DiO-labelled tumour cells in liver sections by confocal laser scanning microscopy. *J Microsc* 2002; **208**: 65-74
23 **Vekemans K**, Timmers M, Vermijlen D, Zanger RD, Wisse E, Braet F. Cytotoxic reactions of CC531s towards liver sinusoidal endothelial cells: a microscopical study. *Comp Hepatol* 2004; **3** Suppl 1: S49
24 **Braet F**, Vermijlen D, Bossuyt V, De Zanger R, Wisse E. Early detection of cytotoxic events between hepatic natural killer cells and colon carcinoma cells as probed with the atomic force microscope. *Ultramicroscopy* 2001; **89**: 265-273
25 **Vermijlen D**, Luo D, Froelich CJ, Medema JP, Kummer JA, Willems E, Braet F, Wisse E. Hepatic natural killer cells exclusively kill splenic/blood natural killer-resistant tumor cells by the perforin/granzyme pathway. *J Leukoc Biol* 2002; **72**: 668-676
26 **Ritman EL**. Micro-computed tomography-current status and developments. *Annu Rev Biomed Eng* 2004; **6**: 185-208
27 **Ananda S**, Marsden V, Vekemans K, Korkmaz E, Tsafnat N, Soon L, Jones A, Braet F. The visualization of hepatic vasculature by X-ray micro-computed tomography. *J Electron Microsc* (Tokyo) 2006; **55**: 151-155
28 **Maehara N**. Experimental microcomputed tomography study of the 3D microangioarchitecture of tumors. *Eur Radiol* 2003; **13**: 1559-1565

S- Editor Liu Y **L- Editor** Worthley DL **E- Editor** Lu W

PO Box 2345, Beijing 100023, China
www.wjgnet.com
wjg@wjgnet.com

World J Gastroenterol 2007 February 14; 13(6): 826-829
World Journal of Gastroenterology ISSN 1007-9327

REVIEW

Current role of bloodless liver resection

Spiros G Delis, Juan Madariaga, A Bakoyiannis, Ch Dervenis

Spiros G Delis, A Bakoyiannis, Ch Dervenis, Liver Surgical Unit, A Surgical Clinic, Agia Olga Hospital, Athens, Greece
Juan Madariaga, Department of Surgery, Division of Transplantation & Liver Surgery, University Of Miami School of Medicine, Miami, Florida, United States
Correspondence to: Spiros G Delis MD, PhD, Liver Unit, A Surgical Clinic, Agia Olga Hospital, 3-5 Agias Olgas str., Athens, Greece. sdelis55@hotmail.com
Telephone: +3-210-5012849 Fax: +3-210-5012849
Received: 2006-06-29 Accepted: 2006-07-18

Abstract

Liver resections are demanding operations which can have life threatening complications although they are performed by experienced liver surgeons. Recently new technologies are applied in the field of liver surgery, having one goal: safer and easier liver operations. The aim of this article is to address the issue of bloodless liver resection using radiofrequency energy. Radionics, Cool-tip™ System and Tissue Link are some of the devices which are using radiofrequency energy. All information included in this article, refers to these devices in which we have personal experience in our unit of liver surgery. These devices take advantage of its unique combination of radiofrequency current and internal electrode cooling to perform sealing of the small vessels and biliary radicals. Dissection is also feasible with the cool-tip probe. For the purposes of this study patient sex, age, type of disease and type of surgical procedure in association with the duration of parenchymal transection, blood loss, length of hospital stay, morbidity and mortality were analyzed. Cool-tip RF device may provide a unique, simple and rather safe method of bloodless liver resections if used properly. It is indicated mostly in cirrhotic patients with challenging hepatectomies (segment Ⅷ, central resections). The total operative time is eliminated and the average blood loss is significantly decreased. It is important to note that this technique should not be applied near the hilum or the vena cava to avoid damage of these structures.

Key words: Bloodless liver resection; Radiofrequency; Cool-tip; Tissue link; Hepatectomy

Delis SG, Madariaga J, Dervenis C, Bakoyiannis A. Current role of bloodless liver resection. *World J Gastroenterol* 2007; 13(6): 826-829

http://www.wjgnet.com/1007-9327/13/826.asp

INTRODUCTION

Bleeding after liver resection remains a significant factor affecting prognosis. The concept of introducing new bloodless techniques to facilitate surgical resection of liver tumors have stimulated hepatobiliary surgeons. This has taken the form of vascular occlusion of the inflow (Pringle), the outflow or both (total vascular exclusion). Ischemic preconditioning or hemi-hepatic inflow vascular occlusion are alternative methods better tolerated in patients with cirrhosis. Although vascular occlusion techniques have been proven effective to control intraoperative bleeding, the pathophysiologic effects are still poorly analyzed and difficult to predict for patients with decreased hepatic reserve[1-5].

PATHOPHYSIOLOGIC EFFECTS OF VASCULAR OCCLUSION

The Pringle maneuver places the surgical candidate at a high risk for liver damage due to ischemia and subsequent postoperative liver failure[4,5]. The spectrum of mechanism leading to ischemia-reperfusion (I-R) injury is large and involves metabolic and mitochondrial changes as adenosine triphosphate depletion, Kupffer cell activation, release of reactive oxygen species, cytokine secretion and microcirculatory disturbances. Granulocytes have been strongly suggested to play a key role in the amplification of I-R injury ending in apoptosis, necrosis and organ failure[6,7]. A recent paper by Kukita showed that the Pringle maneuver in hepatectomy caused remnant liver injury in a pig model by expression of iNOS, a marker related to I-R injury[8].

THE USE OF RADIOFREQUENCY DEVICES IN LIVER RESECTION

Recent efforts have aimed to perform bloodless liver resections in the setting of parenchymal transection with new sophisticated devices[9-14] avoiding inflow occlusion. The Cool–tip radiofrequency device (Radionics, Tyco Healthcare) and the Tissue Link equivalent both use radiofrequency energy transmitted through the electrode to the adjacent liver parenchyma causing ion vibration with heat production. In fact the devices are able to achieve both necrosis of the liver tissue and sealing of blood vessels up to 3 mm in diameter by collagen fusion[9]. The saline circuit at the tip of the RF needle offers better ion agitation thus preventing charring with eschar formation.

DISCUSSION

The unique function to enhance heat conduction with a better tumoricidal effect makes these devices an advantageous tool for liver transactions. These findings lend important functional support to the concept of bloodless liver resection in cirrhotic patients and demanding segmentectomies (segment Ⅷ, central hepatectomy etc). There is also a theoretical advantage of further liver necrosis beyond the demarcation line with increase of the surgical margin as proved by enzymatic analysis in frozen liver specimens[13]. However, the effect of this amount of necrotic tissue on cirrhotic patients with limited liver remnant reserve is not clear.

From our own experience, in more than 30 liver resections in fibrotic or even cirrhotic livers with both devices, the negative effect is minimal. We noted one case of hyperbilirubinemia postoperatively in a thrombocytopenic patient with hepatitis C related cirrhosis after a segment Ⅴ-Ⅵ resection for a 5 cm single hepatocellular carcinoma (HCC). However the enzymes declined sharply the following days. In challenging segmentectomies the adjacent liver damage is not avoided but overall it is not harmful. The high postoperative aspartate aminotransferase (AST) levels reflect the coagulation-necrosis pattern at the raw surface of the remnant liver parenchyma and the maximum AST value is well correlated with the transection area[13]. It is worth noting that parenchymal degeneration is limited to the transection surface, which differs from the whole-liver ischemic damage caused by the Pringle maneuver. In addition coagulation induced by RF might be less prone to infection as we noted in our series, in opposition to ischemic necrosis due to inflow occlusion.

There is growing evidence that radio frequency (RF) is implicate in the enzymatic mechanism of cell division causing cell apoptosis[13]. In this regard, as already reported, an exciting possibility of tissue ablation beyond the histologic margins exists but needs further studies to establish its clinical effectiveness.

Complications relating to biliary tree following RF ablation are described in the literature[12]. Such complications remain to be the main problem with major resections using RF and regardless of the ultimate advantageous function of a bloodless RF device the liver surgical principles of hilar dissection should not be overlooked. There is a sense that, although the technique simplifies parenchymal transection, it cannot alter the conventional thought that such devices must only be used by experienced hepatobiliary surgeons. At the beginning of the learning curve with these new techniques we experienced two bile leaks suggesting that the dissecting sealer provides secure sealing of small bile ducts.

Even major anatomic liver resections can usually be performed without inflow occlusion and with infrequent need for blood transfusion. The results compare favorably with reports in which inflow occlusion was used routinely[2]. Most of the blood loss during major resections occurred from small branches or side holes of the middle hepatic vein. Unfortunately this anatomic structure appeared to be more difficult to visualize with the RF devises compared with CUSA or the traditional Kelly crashing technique and is correlated with similar findings pointed out by Poon[11]. However the likelihood of vessel identification is strongly affected by operator experience. Although Poon *et al*[11] suggest selective use of Tissue Link for wedge resections and segmentectomies our experience with application of both Radionics and Tissue Link in major liver resections is promising regarding blood loss and transection time. Even though the transection time appears to be longer with our approach due to the lower transection speed of the device we demonstrate better control of capillary bleeding with subsequent less total operative time. An additional advantage of the RF devices is their potential effectiveness in the laparoscopic era of liver resection although it is still premature.

OUR EXPERIENCE

In our series a total of 36 patients underwent liver resections using the Radiofrequency Cool-Tip device (Radionics, Tyco Healthcare) in the Liver Unit of Agia Olga Hospital.

Patients and methods

Twelve patients had HCC, 20 had liver metastasis from colon cancer (CRM), 1 cystic ovarian metastasis (OM) of segment Ⅲ, 1 focal nodular hyperplasia (FNH), 1 liver metastasis from renal tumor (RM) and 1 intrahepatic cholangiocarcinoma (ICC). Sixteen major and twenty minor hepatectomies have been performed using this new device. A redo hepatectomy of segment Ⅵ combined with wedge lung resection for an upper lobe metastatic lesion and a laparoscopic segment Ⅲ resection were included, both for CRM. Eight of our CRM patients had significant steatosis (> 30%) due to preoperative chemotherapy. All cases of HCC had underlying Child A cirrhosis with normal platelet counts except for a hepatitis B, C and Delta carrier with a low platelet count (PLT 84000/mL) due to mild portal hypertension and pegylated interferon treatment.

Technique

The RF device was set at 95 watts on the 480 kHz electrosurgical generator. RF should last 30-60 s to obtain a zone of tissue necrosis with a radius of 1 cm and 3 cm in depth. Once RF ablation has been completed (proven by increase tissue impedance) a common scalpel was used to divide the tissue. The probes were moved along the transection line to accomplish both dissection and liver coagulation. Small vessels < 5 mm and biliary radicles are sealed by collagen fusion although major intrasegmentary vessels (middle hepatic vein branch to segment Ⅷ) require clips or sutures.

Results

The median transection time was 44 min (range 26 to 81 min).The operative time for parenchymal transection was primarily affected due to two independent factors: (a) the raw liver surface (major hepatectomies defined as more than 3 segments resected were prolonged with median transection time 62 min and range 47 to 81 min compared to minor liver resections; median 30 min) and (b) the underlying liver disease. Radionics required more time to

perform resections in cirrhotic livers (median 45 min; range 30 to 70 min) compared to the non-cirrhotic control[5] (median 30 min; range 25 to 50 min). Intraoperative blood loss was 100 mL (range 30 to 300 mL). Stitches were not placed except in the group of patients who underwent major hepatectomies or challenging segmental resections.

All patients had a postoperative increase of liver enzymes which normalized within 7 d. Serial monitoring of liver function in the first 7 postoperative days revealed peak serum aspartate aminotransferase (median 504.5 U/L, range 101 to 856 U/L) on d 1 or 3 with a rapid decline thereafter by d 7. Median peak postoperative serum bilirubin level was 1, 17 mg/dL (range 0.45 to 3.48 mg/dL).

Resected specimens were carefully examined for depth of tissue coagulation along the transection margin. Depth of tissue coagulation was 3 to 5 mm while providing an additional tumor negative margin at the resection border.

The in hospital mortality rate was zero. Procedure related complications included two bile leaks managed conservatively after major hepatectomies at the beginning of our learning curve. It is obvious that sealing of biliary radicles requires more time than vessels and therefore meticulous ablation is mandatory. No liver failure was reported in our series even in the cirrhotic group of patients. No reoperation was documented for rebleeding. The length of hospital stay ranged from 3 to 12 d with a mean value of 7 d.

We concluded that RF assisted liver resections can achieve low morbidity with minimal blood loss particularly in cirrhotic livers or challenging segmentectomies avoiding the sequela associated with the inflow occlusion techniques.

OTHER DEVICES USED IN LIVER RESECTION

A different approach for liver transection was introduced by Habbib and associates[10] with sequential RF needle insertion around the tumor until a necrotic rim is achieved. The transection of the parenchyma follows in a bloodless field. However the technique is applied much easier in the periphery of the liver compare to the hilum. Furthermore multiple insertions of the needle close to the tumor margin require superior Ultrasound (US) skills especially in demanding segmentectomies or central resections. Practically, once the ablation process starts, the sensitivity of the US to credibly detect tumor stereo tactic structure and ablation interface in real time decreases significantly.

Another interesting device introduced recently is the high frequency supported jet cutting device (HF jet) which allows rapid resections with minimal blood loss and no electrolyte disturbances. However, it is still undergoing experimental studies and it is difficult to translate experimental success to the clinical arena yet.

CONCLUSION

Although Bloodless cutting devices are promising there are several issues worth noting: (1) The techniques are still in progress and no randomization exists to compare the bloodless liver resection with the traditional approaches. (2) The bile leak rate is not reported thoroughly due to the fact that some groups use the bloodless devices combined with clips or staples and rely on intraoperative cholangiograms to early diagnose and treat. (3) Although the device provides excellent coagulation and is strongly recommended for cirrhotic patients, limited experience exists in patients with advanced cirrhosis, portal hypertension and low platelet count. (4) Sufficient data is not available with regard to liver resection in jaundiced patients with hilar cholangiocarcinoma wherein CUSA or water-jet seems to be more efficient. However, the RF devices are effective tools in a selective group of liver surgical patients. A randomized prospective trial comparing hepatectomies under intermittent Pringle maneuver or without clamping using modern equipment would be appropriate.

Although limited data regarding efficacy of the most popular transaction devices (CUSA, Hydro-Jet) including dissecting RF sealer is available the cost-effectiveness of expensive devices is not thoroughly analyzed. Two randomized controlled trials comparing clamp crushing technique versus CUSA and CUSA versus Hydrojet using inflow occlusion are published 15, 16. Both had critical limitations which included normal and cirrhotic livers. In the most recent prospective randomized study by Clavien and associates, 17 conclude that clamp crushing technique is the most efficient device in terms of resections time, blood loss and blood transfusion frequency compared with CUSA, Hydrojet and dissecting RF sealer. Pringle was applied routinely in the group of clamp crushing transection but not in the equivalent groups of bloodless liver resection. Even though Kelly crashing was proved the most cost-efficient, no marginal livers (cirrhotic, cholestatic) were included in the study.

REFERENCES

1 **Torzilli G**, Makuuchi M, Inoue K. The vascular control in liver resection: revisitation of a controversial issue. *Hepatogastroenterology* 2002; **49**: 28-31
2 **Cunningham JD**, Fong Y, Shriver C, Melendez J, Marx WL, Blumgart LH. One hundred consecutive hepatic resections. Blood loss, transfusion, and operative technique. *Arch Surg* 1994; **129**: 1050-1056
3 **Clavien PA**, Yadav S, Sindram D, Bentley RC. Protective effects of ischemic preconditioning for liver resection performed under inflow occlusion in humans. *Ann Surg* 2000; **232**: 155-162
4 **Wu CC**, Hwang CR, Liu TJ, P'eng FK. Effects and limitations of prolonged intermittent ischaemia for hepatic resection of the cirrhotic liver. *Br J Surg* 1996; **83**: 121-124
5 **Farges O**, Malassagne B, Flejou JF, Balzan S, Sauvanet A, Belghiti J. Risk of major liver resection in patients with underlying chronic liver disease: a reappraisal. *Ann Surg* 1999; **229**: 210-215
6 **Choukèr A**, Martignoni A, Schauer R, Dugas M, Rau HG, Jauch KW, Peter K, Thiel M. Beneficial effects of ischemic preconditioning in patients undergoing hepatectomy: the role of neutrophils. *Arch Surg* 2005; **140**: 129-136
7 **Serracino-Inglott F**, Habib NA, Mathie RT. Hepatic ischemia-reperfusion injury. *Am J Surg* 2001; **181**: 160-166
8 **Kukita K**, Katsuramaki T, Kikuchi H, Meguro M, Nagayama M, Kimura H, Isobe M, Hirata K. Remnant liver injury after hepatectomy with the pringle maneuver and its inhibition by an iNOS inhibitor (ONO-1714) in a pig model. *J Surg Res* 2005; **125**: 78-87
9 **Strasberg SM**, Drebin JA, Linehan D. Use of a bipolar vessel-sealing device for parenchymal transection during liver surgery. *J Gastrointest Surg* 2002; **6**: 569-574

10 **Weber JC**, Navarra G, Jiao LR, Nicholls JP, Jensen SL, Habib NA. New technique for liver resection using heat coagulative necrosis. *Ann Surg* 2002; **236**: 560-563
11 **Poon RT**, Fan ST, Wong J. Liver resection using a saline-linked radiofrequency dissecting sealer for transection of the liver. *J Am Coll Surg* 2005; **200**: 308-313
12 **DeMatteo RP**, Fong Y, Jarnagin WR, Blumgart LH. Recent advances in hepatic resection. *Semin Surg Oncol* 2000; **19**: 200-207
13 **Di Carlo I**, Barbagallo F, Toro A, Sofia M, Guastella T, Latteri F. Hepatic resections using a water-cooled, high-density, monopolar device: a new technology for safer surgery. *J Gastrointest Surg* 2004; **8**: 596-600
14 **Sakamoto Y**, Yamamoto J, Kokudo N, Seki M, Kosuge T, Yamaguchi T, Muto T, Makuuchi M. Bloodless liver resection using the monopolar floating ball plus ligasure diathermy: preliminary results of 16 liver resections. *World J Surg* 2004; **28**: 166-172
15 **Takayama T**, Makuuchi M, Kubota K, Harihara Y, Hui AM, Sano K, Ijichi M, Hasegawa K. Randomized comparison of ultrasonic vs clamp transection of the liver. *Arch Surg* 2001; **136**: 922-928
16 **Rau HG**, Wichmann MW, Schinkel S, Buttler E, Pickelmann S, Schauer R, Schildberg FW. Surgical techniques in hepatic resections: Ultrasonic aspirator versus Jet-Cutter. A prospective randomized clinical trial. *Zentralbl Chir* 2001; **126**: 586-590
17 Lesurtel M, Selzner M, Petrowsky H, McCormack L, Clavien PA. How should transection of the liver be performed?: a prospective randomized study in 100 consecutive patients: comparing four different transection strategies. *Ann Surg* 2005; **242**: 814-822, discussion 822-823

S- Editor Wang J **L- Editor** Alpini GD **E- Editor** Lu W

PO Box 2345, Beijing 100023, China
www.wjgnet.com
wjg@wjgnet.com

World J Gastroenterol 2007 February 14; 13(6): 830-836
World Journal of Gastroenterology ISSN 1007-9327

REVIEW

Novel approaches towards conquering hepatitis B virus infection

Guo-Yi Wu, Hong-Song Chen

Guo-Yi Wu, Hong-Song Chen, Hepatology Institute, People's Hospital, Peking University, Beijing 100044, China
Supported by the National Basic Research Program, No. 2005CB522902; the Municipal Science and Technique Program, H030230150130
Correspondence to: Dr. Hong-Song Chen, Hepatology Institute, People's Hospital, Peking University, Beijing 100044, China. chen2999@sohu.com
Telephone: +86-13501196710 Fax: +86-10-68318386
Received: 2006-12-11 Accepted: 2007-01-09

Abstract

Currently approved treatments for hepatitis B virus (HBV) infection include the immunomodulatory agent, IFN-α, and nucleos(t)ide analogues. Their efficacy is limited by their side effects, as well as the induction of viral mutations that render them less potent. It is thus necessary to develop drugs that target additional viral antigens. Chemicals and biomaterials by unique methods of preventing HBV replication are currently being developed, including novel nucleosides and newly synthesized compounds such as capsid assembling and mRNA transcription inhibitors. Molecular therapies that target different stages of the HBV life cycle will aid current methods to manage chronic hepatitis B (CHB) infection. The use of immunomodulators and gene therapy are also under consideration. This report summarizes the most recent treatment possibilities for CHB infection. Emerging therapies and their potential mechanisms, efficacy, and pitfalls are discussed.

Key words: Hepatitis B virus; Antiviral drugs; Drug evaluation; Immunomodulatory agents; Gene therapy

Wu GY, Chen HS. Novel approaches towards conquering hepatitis B virus infection. *World J Gastroenterol* 2007; 13(6): 830-836

http://www.wjgnet.com/1007-9327/13/830.asp

INTRODUCTION

The hepatitis B virus (HBV) is a major world health problem, Leading to 1.2 million deaths per year according to the World Health Organization (WHO)[1]. HBV infection can result in acute, fulminant, or chronic disease, liver cirrhosis, and the development of hepatocellular carcinomas (HCC). There is a vaccine, but no 100% effective antiviral treatment available for patients with chronic hepatitis B (CHB). The response rate to IFN therapy, as measured by the loss of hepatitis B e antigen (HBeAg), is less than 40%[2]. This treatment is even less effective in Asian patients (primarily Chinese), particularly for those with below normal alanine transaminase (ALT) levels[3]. IFN therapy is also associated with many disabling side effects and is therefore only suitable for some patients.

Since HBV DNA replication occurs via reverse transcription[4], the use of reverse transcriptase inhibitors is an attractive target for anti-HBV therapy. Nucleoside analogues are chemically synthesized drugs that mimic natural nucleosides. In China, three nucleoside/nucleotide drugs are used to manage chronic HBV infection: lamivudine (3TC), adefovir dipivoxil (ADV), and entecavir (ETV). Although all three are potent viral suppressors, none is able to permanently eradicate HBV[5]. As a result, the durability of the antiviral response is suboptimal once treatment is halted. In some patients, HBV DNA levels and ALT concentrations increase and result in a potentially life-threatening recurrence of disease[6,7]. Patients can only be safely withdrawn from nucleos(t)ide therapy if HBeAg seroconverts to anti-HBe or HBV DNA diminishes to undetectable levels[8,9]. To prevent disease recurrence, long-term polymerase inhibitor maintenance therapy is often required[10]. In addition, prolonged use of nucleoside/nucleotide is associated with the emergence of drug-resistant mutants[11,12], and clinically characterized by increasing serum HBV DNA and ALT levels[10,13]. Each drug has a different profile of resistant mutations[14], so it is essential that each is appropriately managed. These findings underscore a requirement for new and better-tolerated therapies for hepatitis B virus infection.

In this report, we review different strategies for drug design, and evaluate their effectiveness *in vitro*, in models of HBV replication *in vivo*, and in clinical trials.

NUCLEOSIDE ANALOGUES

Orally applied nucleoside and nucleotide analogs have been important therapies against HBV infection throughout the last decade. The nucleoside analogs, lamivudine and entecavir, and the nucleotide analog, adefovir dipivoxil, are approved for use in humans. Many similar compounds are being tested in preclinical or clinical settings (Table 1).

Table 1 Anti-HBV nucleoside/nucleotide analogues under development

Phase	Drugs	Company
Phase Ⅲ	Emtricitabine (FTC)	Gilead (California, USA)
	Tenofovir DF	Gilead (California, USA)
	Telbivudine (L-dT)	Idenix (Massachusetts, USA)
	Clevudine (L-FMAU)	Gilead/Triangle (California, USA)
Phase Ⅱ	Elvucitabine (β-L-Fd4C)	Achillion (Connecticut, USA)
	Valtorcitabine (val-L-dC)	Idenix (Massachusetts, USA)
	Amdoxovir (DAPD)	Triangle (California, USA)
	Racivir [(+/-)-FTC]	Pharmasset (New Jersey, USA)
	LB80380	LG Life Sciences (Seoul, Korea)
Phase Ⅰ	Alamifovir (purine nucleoside analogue)	Lilly/Mitsubishi (Indiana, USA/Osaka, Japan)
	MIV 210 (FLG prodrug)	Medivir/GSK (Huddinge, Sweden/Brentford, UK)
	Hepavir B (PMEA prodrug)	Ribapharm (California, USA)
Pre-clinical	β-L-FddC	Biochem/GSK (Sante-Foy, Canada/Brentford, UK)
	6- [2- (phosphonomethoxy) alkoxy]-2, 4-diaminopyrimidines	Rega Institute for Medical Research, K.U.Leuven (Leuven, Belgium)
	2-benzenesulfonylalkyl-5-substituted-sulfanyl-[1, 3, 4]-oxadiazoles	National University of Singapore (Singapore)

EMTRICITABINE (FTC)

Emtricitabine is a nucleoside analogue used for treatment against human immunodeficiency virus (HIV) and also has clinical activity against HBV. It has a similar structure to lamivudine, differing only in a fluorine at its 5 prime end. In a randomized double-blind study, patients received 200 mg of emtricitabine (n = 167) or a placebo (n = 81) once daily for 48 wk and underwent a pretreatment and end-of-treatment liver biopsy. Following treatment, 62% of patients who had received emtricitabine had improved liver histology, while only 25% of the placebo patients showed improvement ($P < 0.001$). Significant improvement was also demonstrated between subgroups that were positive ($P < 0.001$) and negative ($P = 0.002$) for hepatitis B e (HBe) antigen. Serum HBV DNA levels were below 400 copies/mL in 54% (n = 167) of the emtricitabine group and only 2% (n = 81) of the placebo group ($P < 0.001$), while alanine aminotransferase levels were normal in 65% (109/167) of the emtricitabine group and 25% (20/81) of the control group ($P < 0.001$). At wk 48, 20 of 159 patients (13%) from the emtricitabine group in whom HBV DNA was detected at the end of treatment, had virus with resistance mutations (95% confidence interval, 8%-18%). The rate of seroconversion to anti-HBe (12%) and loss of HBe antigen were not different between arms, and the safety profiles of emtricitabine and placebo were similar during treatment. Forty-eight weeks of emtricitabine treatment resulted in significant histologic, virologic, and biochemical improvement in chronic HBV infected patients, regardless of whether HBe antigen was detectable[15].

Phase Ⅲ clinical trials are underway to determine the long-term safety and efficacy of emtricitabine, however its role as a monotherapy may be limited by its structural similarity to lamivudine and the corresponding risk of drug resistance.

TENOFOVIR (VIREAD, PMPA)

Tenofovir was FDA approved in 2001 for use in HIV infected adults in combination with other antiretroviral agents. Lamivudine-associated and ADEFOVIR-resistant mutations were not detected when tenofovir was used in a clinical trial. Thus, tenofovir may be a highly effective rescue drug in HBV-infected patients who show altered responsiveness to lamivudine and ADEFOVIR[16]. An additional double-blind, placebo-controlled trial showed that tenofovir may be a useful component of antiretroviral therapy for HIV/HBV co-infected patients. Importantly, tenofovir is equivalent to adefovir in its ability to reduce HBV DNA levels, and may, in fact, be superior[17]. If HBV treatment can be deferred until combination antiretroviral therapy for HIV infection is needed, the combination of tenofovir plus lamivudine or emtricitabine will be the potent HBV therapy and a solid backbone for HIV combination antiretroviral therapy, and a potent treatment for HBV and it likely decreases the emergence of HBV resistance. It will decrease the chance that HBV resistance will emerge as well[18].

CLEVUDINE (L-FMAU)

Clevudine is a nucleoside analog with an unnatural beta-L configuration, and *in vitro* studies suggest that it is effective against lamivudine-resistant HBV mutants. In the Woodchuck model, a daily clevudine dose of 10 mg/kg resulted in a 100 million copies' decrease in viral load. Interestingly, a delayed rebound in viral load was observed after drug cessation in a dose-dependent manner. No evidence of clevudine toxicity was observed in treated animals, however, further studies are being conducted to assess its long-term efficacy and safety[19]. Clinical trials show that clevudine is one of the most potent analogs available for treating HBV, and that its antiviral effects can last up to 6 mo after treatment, as illustrated by sustained normalization of ALT levels[18]. The mechanism by which clevudine elicits its anti-hepadna virus activity is distinct from other nucleoside analogs. It acts as a competitive inhibitor by binding to the catalytic site of HBV polymerase and inhibiting the priming of HBV DNA chain elongation. Nucleoside inhibitors, in general, interfere with viral polymerase activity through competitive inhibition and incorporation into the viral DNA strands[20].

TELBIVUDINE (LdT)

Telbivudine is a novel nucleoside analog that is being developed for the oral treatment of chronic HBV. It is a highly specific and selective inhibitor of replication *in vitro*, and specifically targets the HBV DNA polymerase. Unlike other nucleoside antivirals, telbivudine does not act against other viruses or induce mitochondrial toxicity by targeting mammalian DNA polymerases. Telbivudine preferentially inhibits HBV second-strand (DNA-dependent) DNA synthesis, in contrast to LdC and lamivudine, which are first-strand (RNA-dependent) DNA synthesis inhibitors[21].

Telbivudine has a significantly higher rate of response than the standard HBV treatment, lamivudine, as well as superior viral suppression capability. It is generally well tolerated, with a low adverse effect profile, and no toxicity at its effective treatment dose.

Preclinical and clinical studies show that telbivudine has good pharmacokinetic properties that support once-daily dosing, and are not affected by gender, food intake, or liver health. Patients with moderate to severe renal impairment do require dose adjustment, however, which is also necessary for other drugs of this class.

Phase Ⅱb clinical trial results illustrate that patients with chronic HBV who are treated with telbivudine have significantly greater virologic and biochemical responses than those treated with lamivudine. Combination therapies revealed similar results to those obtained using telbivudine alone. These data support the ongoing phase Ⅲ evaluation of telbivudine as a treatment for patients with chronic HBV[22].

OTHER NUCLEOSIDE ANALOGS

Additional nucleoside analogs that have favorable toxicity profiles and a promise of increased effectiveness against HBV are in various stages of clinical development. The phase Ⅲ trials of emtricitabine, clevudine, tenofovir, and telbivudine will help define the efficacy and safety profiles of these drugs, while the profiles of newer and more potent drugs like LB80380 remain to be confirmed. It is important to recognize, however, that many of these compounds share cross-resistance profiles with existing nucleoside analogues such as lamivudine, adefovir, and entecavir[23,24]. As a result, these drugs may not offer much advantage over current treatment regimens. Current research efforts are focusing on the development of drugs that offer low rates of resistance or little cross-resistance with other nucleoside analogues.

NOVEL MOLECULAR TARGETS OF HBV THERAPY

Because HBV pol carries out the enzymatic functions of reverse transcription and DNA synthesis, it is the primary target of HBV antiviral development[25]. Nucleoside and nucleotide analogues are the primary class of antiviral agents used for this purpose. In recent years, several compounds that specifically attack molecular targets other than HBV pol have been identified, including inhibitors of HBV encapsidation and HBcAg translation. Encapsidation occurs when the viral RNA, pol, and core are assembled into the nucleocapsid prior to viral replication[26].

HETEROARYLDIHYDROPYRIMIDINE (HAP)

The heteroaryldihydropyrimidines (HAPs), including BAY41-4109, BAY38-7690, and BAY39-5493, are a new class of antivirals that inhibit production of HBV virions. HAPs show more favorable (50% and 90%) inhibitory concentrations (IC50 and IC90) than lamivudine in a cell-based HBV replication assay. They act as allosteric effectors, binding the HBV core protein and resulting in its degradation, which subsequently inhibits nucleocapsid formation[27]. HAPs inhibit HBV replication in a transgenic mouse model with an efficacy similar to that of lamivudine[28]. Since these drugs destabilize preformed capsids, they may be used to treat blood products in order to lower the HBV transmission rates. Thus, HAPs may become a valuable addition to anti-HBV therapy. None of them has yet been tested in humans, but the clinical trial results of Bay 41-4109 are expected.

PHENYLPROPENAMIDES

The phenylpropenamides represent another group of compounds that inhibit encapsidation[29]. The phenylpropenamide derivatives, AT-61 and AT-130, are synthesized and shown to inhibit HBV replication. These agents inhibit encapsidation by directly preventing nucleocapsid formation, a mechanism distinct from that used by HAPs. In a cell-based replication system, the phenylpropenamides are not as potent as lamivudine in inhibiting HBV replication (the IC50 is approximately 10 times higher), but are active against the lamivudine-resistant YMDD mutant[29,30]. These drugs are specific for HBV and have no activity against related viruses such as woodchuck hepatitis virus (WHV) and DHB. Although this class of compounds has a favorable toxicity profile, clinical trials are still required.

HELIOXANTHIN ANALOGUES

Helioxanthin was originally isolated from the shrub, Taiwania ctyptomerioides, and its derivative, 5-4-2, was synthesized in the laboratory. Helioxanthin and 5-4-2 belong to a class of small molecules that inhibit the HBV DNA as well as the HBV RNA and viral protein expression. Their structures are different from other anti-HBV compounds, suggesting that they may have a unique mode of action. Cheng YC *et al*[31] found that helioxanthin and 5-4-2 inhibited HBV mRNA levels in HepG2 2.2.15, as well as the HBV transcripts, 3.5 kb and 2.4/2.1 kb. The HBV core protein also decreased after treatment. Anti-HBV activity was evaluated *in vitro* using the HBV stably transfected hepatoma cell lines, Wl0 (adr, wt) and DM2 (adr, rtL180M/rtM204V, lamivudine-resistant), and helioxanthin and 5-4-2 inhibited both wild type and mutated HBV. Since the core protein activates the pregenomic/pre C promoters, it is possible that the decrease in 3.5 kb transcript results from a lack of transactivation by the core protein. Helioxanthin and 5-4-2 profoundly inhibited

pregenomic/preC and preS/S promoter activity using a gene reporter system, suggesting that they target multiple steps of the viral life cycle. The detailed mechanism of action by this class of compounds is being explored, and clinical trials are still required.

GLUCOSIDASE AND PEPTIDE INHIBITORS OF CAPSID ASSEMBLY

The heavy glycosylation of HBV envelope proteins is important for viral assembly. As a result, specific glucosidase inhibitors have been developed to inhibit the assembly process. N-nonyl-deoxynojirimycin (N-nonyl-DNJ) is an inhibitor of N-linked glycan processing and the endoplasmic reticulum (ER) glucosidase. Researchers show the N-nonyl-DNJ has antiviral activity in the woodchuck model of HBV infection[32]. Another glucosidase inhibitor, N-nonyl-deoxygalactojirimycin (N-nonyl-DGJ), exerts its antiviral activity prior to viral envelopment, thus may prevent proper encapsidation of the HBV pregenomic RNA. These agents show promise in inhibiting viral replication using the WHV model, but toxicity may limit their clinical efficacy. Using a molecular approach to screen a phage display library, Dyson *et al*[34] identified peptide aptamers that specifically interfere with the interaction between core particles and envelop proteins during assembly[33]. These peptides bind specifically to the tip of the core protein shell that comprises conserved amino acid residues within the nucleocapsid. This is important because of the risk of drug resistance. One candidate peptide inhibited HBV replication in a cell-based assay and exhibited no toxicity.

These promising approaches underscore the importance of identifying other molecular targets that may be used in combination therapies.

IMMUNOMODULATORY AGENTS

A variety of immunomodulatory therapies have been developed over the last few decades to manage CHB. These therapies are designed to eliminate the virus by activating either nonspecific host immune responses or HBV-specific CD4+ T helper and CD8+ cytotoxic lymphocytes[35]. The nonspecific modalities include the use of TLRs, thymosin, IFN-α, and IFN-γ, and the specific modalities include dendritic cell and cytotoxic T-lymphocyte (CTL)-based therapies. In recent years, the APOBEC family has shown promise as an anti-HBV drug.

APOBEC3G

To replicate efficiently, viruses must overcome innate defense mechanisms. Human APOBEC3G is a cytidine deaminase that represents one such barrier by conferring broad intracellular antiretroviral protection. This enzyme is packaged in virions and acts during reverse transcription to deaminate deoxycytidine residues to deoxyuridine (dU) within the growing minus-strand of viral DNA. These dU-rich reverse transcripts are either degraded or result in proviruses that are largely nonfunctional due to a G-to-A hypermutation. Most lentiviruses escape APOBEC3G inhibition by expressing a protein, Vif, which prevents deaminase incorporation into the virion and triggers its proteasomal degradation. However, APOBEC3G is capable of blocking a wide spectrum of distantly related retroviruses. Turelli *et al*[36] show APOBEC3G-mediated inhibition of HBV and DHBV DNA production in human HuH-7 hepatoma cells and avian hepatoma cells. Thus, the viral and cellular interaction partners required for anti-hepadnaviral APOBEC3G action are conserved among these species. Rosler C *et al*[37] found that core-associated HBV RNA is not reduced in the presence of A3G, and that wild-type levels of pgRNA associate with HBV core protein in the presence or absence of A3G. Yang DL *et al*[38] showed a dose dependent decrease in the levels of intracellular core-associated HBV DNA, however, as well as a decrease in the extracellular production of HBsAg and HBeAg following APOBEC3G treatment. The levels of intracellular core-associated viral RNA also decreased, but the expression of HBcAg in transfected cells remained the same. Consistent with these *in vitro* results, levels of HBsAg in the sera of mice decreased dramatically. A larger 1.5-log10 decrease in serum HBV DNA and liver HBV RNA levels were observed in APOBEC3G-treated versus control groups. These findings suggest that APOBEC3G suppresses HBV replication and antigen expression both *in vivo* and *in vitro*, and is a promising advance in HBV therapy.

THERAPEUTIC VACCINATION

HBV persistence is thought to result from poor HBV-specific T cell responses[39]. This has resulted in efforts to stimulate HBV-specific T cells using therapeutic vaccines[40]. Mancini-Bourgine *et al*[41] conducted a phase Ⅰ study to evaluate the effectiveness of an HBV DNA vaccine that encodes HBV envelope proteins in ten chronic HBV carriers who did not respond to current antiviral therapies. Patients received four 1 mg intramuscular injections of the vaccine and an increased frequency of HBV specific T cell responses was observed. HBV DNA levels declined in five patients, and one patient successfully cleared the infection.

Yuan *et al*[42] constructed a hepatitis B immunogenic complex therapeutic vaccine from a combination of yeast-derived recombinant HBsAg and human anti-HBs immunoglobulin (YIC). Its safety profile and the immune responses it elicited were examined in a phase Ⅰ clinical trial. IFN-γ levels were higher in all eight subjects studied ($P = 0.015$) and IL-2 levels increased in seven of the eight subjects ($P = 0.002$). These results show that the hepatitis B immunogenic complex therapeutic vaccine (YIC) can induce a potent anti-HBs response.

Wu *et al*[43] also developed an innovative minovirus vaccine to induce hepatitis B virus specific cytotoxic T-lymphocyte responses. They proved that their mimovirus could induce an HBsAg28-39-specific CTL response *in vivo*. This type of vaccine is now under the phase Ⅱ clinical trial in China.

The promise of these approaches requires further examinations in a large randomized study.

DENDRITIC CELL VACCINATION

Dendritic cells (DCs) function as antigen-presenting cells. Peripheral DCs phagocytose microbes and viruses, and migrate to the regional lymph nodes where they mature and present foreign protein peptides to naive T cells[44]. These T cells then become activated, and acquire direct antiviral function as well as the ability to produce a variety of cytokines, including IFN, IL-2, IL-12, and IL-18. Many viruses, including HBV, are able to escape immune surveillance and persist in the host without evoking an immune response. Zheng *et al*[45] studied the functional defects of DCs in patients with CHB and showed that human leukocyte antigen (HLA) class Ⅱ and B7 expression are not upregulated on these cells, leading to inadequate IL-12 levels to fight against infection. Although DC vaccination shows promise, it is still in the preclinical phase. With advances in technology, DC-based therapy may be an important method of managing CHB[46].

TLR LIGANDS

TLRs play an important role in innate immune recognition and regulation[47]. They belong to a family of evolutionarily conserved receptors that recognize structural patterns on different pathogens[48]. After finding a particular virus or microbe, TLRs activate phagocytes and DCs to mount an immune response[49]. In an HBV transgenic mouse model, Isogawa *et al*[50] showed that a single injection of a TLR ligand can inhibit HBV replication in hepatocytes by inducing the production of antiviral cytokines. These data support the further development of this approach.

CTL-BASED THERAPY

CTL-based immunotherapy is based on the concept that HBV-specific CTLs control infection by suppressing HBV replication in infected humans[51]. Vitiello *et al*[52] developed a lipopeptide-based vaccine containing one CTL epitope from the HBV core region. This vaccine induced an HBV-specific CTL response in healthy volunteers in a phase Ⅰ clinical trial that was comparable to CTL responses observed during acute HBV infection. In a phase Ⅱ trial in patients with chronic HBV, however, CTL-based therapy was much less effective for suppressing HBV DNA[53]. This therapeutic approach may still be clinically useful if it is designed to recognize multiple CTL epitopes.

CYTOKINES

Cytokines play a major role in controlling viral infections[54]. In a transgenic mouse model, type 1 IFNs (α and β) were shown to inhibit HBV viral replication[55,56]. IFN-γ also prevents HBV replication by activating natural killer T (NKT) cells and T cells[57], however, clinical trials with IFN-γ did not show much benefit in patients with CHB[58]. Robek *et al*[59] reported that IFN-λ inhibits HBV replication and induces IFN-stimulated gene expression using a mechanism distinct from that used by IFN-α, -β, or -γ. Thus, IFN-λ may be useful as a therapeutic agent in the management of CHB.

Because of its ability to induce T cell proliferation, IL-2 is hypothesized to be an important immunostimulatory molecule, especially during chronic viral diseases[54]. IL-2 downregulates HBV gene expression in a transgenic mouse model and in patients with HIV, intermittent rIL-2 therapy prolongs CD4 T cell survival[60]. As a result, rIL-2 may be used as an adjunct therapy to prime other forms of immunomodulation such as therapeutic vaccination[61].

Cavanaugh *et al*[62] demonstrated the antiviral efficacy of IL-12 in an HBV transgenic mouse model, however the overall reduction in viral titers was modest compared to other anti-HBV treatments[63]. Kimura *et al*[64] showed that IL-18 also inhibits HBV replication in a transgenic mouse mode, but its efficacy in humans remains to be tested.

While many of these cytokines may not be potent as single agents they may help understand the mechanisms used by various immunomodulatory strategies to control HBV infection[61].

ADOPTED CELL THERAPY

Sun *et al* isolated peripheral blood mononuclear cells from patients and activated them by anti-CD3 monoclonal antibody, interleukin-2 and interferon-γ *in vitro* for 10 d to produce multifactors activated immune cells (MAICs). When the cells have expanded and activated effectively 10 d later, these patients were transfused with these cells. Significant HBV inhibition was observed in 8 out of 14 until 1 year after transfusion. These findings strongly suggest that MAICs transfusion can effectively inhibit the replication of hepatitis B virus.

GENE THERAPY

Researchers are developing novel nucleic acid-based interventions against HBV. These tools for manipulating gene expression are an attractive means of targeting HBV at different stages of its life cycle, with the ultimate goal of completely eradicating the virus[66]. Although this approach is not realistic for clinical use at this time, tremendous advances in this field have been made over the past few years. There are three gene therapy approaches: the use of antisense oligodeoxyribonucleic acids (ODNs), ribozymes, and short interfering RNAs (siRNAs). Some researches have shown significant results using these treatments, but the mode of delivering nucleic acid-based therapies remains a problem. Since HBV primarily replicates in hepatocytes, it is important that these compounds target the liver in order to reduce the required dose and minimize nonspecific effects[67]. Safety is also a potential concern with this therapeutic approach[68], as is the issue of host enzymes biodegrading these compounds and rendering them ineffective. Nonspecific activation of the immune system is further noted as a risk of administering nucleic acid-based compounds[69]. Advances in delivery strategies and an improved understanding of the mechanisms of these technologies should lead to safer and more efficacious nucleic acid-based therapeutic approaches.

CONCLUSIONS

Treatment of chronic HBV requires inhibiting hepatitis B virus replication or eliminating the virus from cells. The major problem with current treatments is the emergence of drug resistant variants over time. Novel therapies that target unique molecules or require shorter treatment time are still in demand. Several new anti-HBV nucleoside analogues are in different stages of clinical trials, and in the next decade we should see an increase in the use of agents designed to target specific molecules. The greatest challenge in the future of HBV treatment is the achievement of a safe, cost-effective, and durable regimen that takes advantage of novel therapeutic modalities.

REFERENCES

1 **World Health Organization warns of growing "crisis of suffering"**. 1997. Available from: URL: http://www.who.ch/whr/1997/presse.htm
2 **Wong DK**, Cheung AM, O'Rourke K, Naylor CD, Detsky AS, Heathcote J. Effect of alpha-interferon treatment in patients with hepatitis B e antigen-positive chronic hepatitis B. A meta-analysis. *Ann Intern Med* 1993; **119**: 312-323
3 **Lok AS**, Lai CL, Wu PC, Leung EK. Long-term follow-up in a randomised controlled trial of recombinant alpha 2-interferon in Chinese patients with chronic hepatitis B infection. *Lancet* 1988; **2**: 298-302
4 **Summers J**, Mason WS. Replication of the genome of a hepatitis B--like virus by reverse transcription of an RNA intermediate. *Cell* 1982; **29**: 403-415
5 **Hoofnagle JH**, Lau D. New therapies for chronic hepatitis B. *J Viral Hepat* 1997; **4** Suppl 1: 41-50
6 **Lau GK**, Piratvisuth T, Luo KX, Marcellin P, Thongsawat S, Cooksley G, Gane E, Fried MW, Chow WC, Paik SW, Chang WY, Berg T, Flisiak R, McCloud P, Pluck N. Peginterferon Alfa-2a, lamivudine, and the combination for HBeAg-positive chronic hepatitis B. *N Engl J Med* 2005; **352**: 2682-2695
7 **Akuta N**, Suzuki F, Kobayashi M, Matsuda M, Sato J, Suzuki Y, Sezaki H, Hosaka T, Someya T, Kobayashi M, Saitoh S, Arase Y, Ikeda K, Kumada H. Virological and biochemical relapse after discontinuation of lamivudine monotherapy for chronic hepatitis B in Japan: comparison with breakthrough hepatitis during long-term treatment. *Intervirology* 2005; **48**: 174-182
8 **Lok AS**, Heathcote EJ, Hoofnagle JH. Management of hepatitis B: 2000--summary of a workshop. *Gastroenterology* 2001; **120**: 1828-1853
9 **Liaw YF**, Leung N, Guan R, Lau GK, Merican I, McCaughan G, Gane E, Kao JH, Omata M. Asian-Pacific consensus statement on the management of chronic hepatitis B: a 2005 update. *Liver Int* 2005; **25**: 472-489
10 **Lok AS**. The maze of treatments for hepatitis B. *N Engl J Med* 2005; **352**: 2743-2746
11 **Lai CJ**, Terrault NA. Antiviral therapy in patients with chronic hepatitis B and cirrhosis. *Gastroenterol Clin North Am* 2004; **33**: 629-654, x-xi
12 **Lau DT**, Khokhar MF, Doo E, Ghany MG, Herion D, Park Y, Kleiner DE, Schmid P, Condreay LD, Gauthier J, Kuhns MC, Liang TJ, Hoofnagle JH. Long-term therapy of chronic hepatitis B with lamivudine. *Hepatology* 2000; **32**: 828-834
13 **Locarnini S**, Hatzakis A, Heathcote J, Keeffe EB, Liang TJ, Mutimer D, Pawlotsky JM, Zoulim F. Management of antiviral resistance in patients with chronic hepatitis B. *Antivir Ther* 2004; **9**: 679-693
14 **Doo E**, Liang TJ. Molecular anatomy and pathophysiologic implications of drug resistance in hepatitis B virus infection. *Gastroenterology* 2001; **120**: 1000-1008
15 **Lim SG**, Ng TM, Kung N, Krastev Z, Volfova M, Husa P, Lee SS, Chan S, Shiffman ML, Washington MK, Rigney A, Anderson J, Mondou E, Snow A, Sorbel J, Guan R, Rousseau F. A double-blind placebo-controlled study of emtricitabine in chronic hepatitis B. *Arch Intern Med* 2006; **166**: 49-56
16 **van Bömmel F**, Zöllner B, Sarrazin C, Spengler U, Hüppe D, Möller B, Feucht HH, Wiedenmann B, Berg T. Tenofovir for patients with lamivudine-resistant hepatitis B virus (HBV) infection and high HBV DNA level during adefovir therapy. *Hepatology* 2006; **44**: 318-325
17 **Levy V**, Grant RM. Antiretroviral therapy for hepatitis B virus-HIV-coinfected patients: promises and pitfalls. *Clin Infect Dis* 2006; **43**: 904-910
18 **Lee HS**, Chung YH, Lee K, Byun KS, Paik SW, Han JY, Yoo K, Yoo HW, Lee JH, Yoo BC. A 12-week clevudine therapy showed potent and durable antiviral activity in HBeAg-positive chronic hepatitis B. *Hepatology* 2006; **43**: 982-988
19 **Peek SF**, Cote PJ, Jacob JR, Toshkov IA, Hornbuckle WE, Baldwin BH, Wells FV, Chu CK, Gerin JL, Tennant BC, Korba BE. Antiviral activity of clevudine [L-FMAU, (1-(2-fluoro-5-methyl-beta, L-arabinofuranosyl) uracil)] against woodchuck hepatitis virus replication and gene expression in chronically infected woodchucks (Marmota monax). *Hepatology* 2001; **33**: 254-266
20 **Chong Y**, Chu CK. Understanding the unique mechanism of L-FMAU (clevudine) against hepatitis B virus: molecular dynamics studies. *Bioorg Med Chem Lett* 2002; **12**: 3459-3462
21 **Kim JW**, Park SH, Louie SG. Telbivudine: a novel nucleoside analog for chronic hepatitis B. *Ann Pharmacother* 2006; **40**: 472-478
22 **Lai CL**, Leung N, Teo EK, Tong M, Wong F, Hann HW, Han S, Poynard T, Myers M, Chao G, Lloyd D, Brown NA. A 1-year trial of telbivudine, lamivudine, and the combination in patients with hepatitis B e antigen-positive chronic hepatitis B. *Gastroenterology* 2005; **129**: 528-536
23 **Tenney DJ**, Levine SM, Rose RE, Walsh AW, Weinheimer SP, Discotto L, Plym M, Pokornowski K, Yu CF, Angus P, Ayres A, Bartholomeusz A, Sievert W, Thompson G, Warner N, Locarnini S, Colonno RJ. Clinical emergence of entecavir-resistant hepatitis B virus requires additional substitutions in virus already resistant to Lamivudine. *Antimicrob Agents Chemother* 2004; **48**: 3498-3507
24 **Fung SK**, Lok AS. Management of hepatitis B patients with antiviral resistance. *Antivir Ther* 2004; **9**: 1013-1026
25 **Köck J**, Schlicht HJ. Analysis of the earliest steps of hepadnavirus replication: genome repair after infectious entry into hepatocytes does not depend on viral polymerase activity. *J Virol* 1993; **67**: 4867-4874
26 **Deres K**, Schröder CH, Paessens A, Goldmann S, Hacker HJ, Weber O, Krämer T, Niewöhner U, Pleiss U, Stoltefuss J, Graef E, Koletzki D, Masantschek RN, Reimann A, Jaeger R, Gross R, Beckermann B, Schlemmer KH, Haebich D, Rübsamen-Waigmann H. Inhibition of hepatitis B virus replication by drug-induced depletion of nucleocapsids. *Science* 2003; **299**: 893-896
27 **Stray SJ**, Bourne CR, Punna S, Lewis WG, Finn MG, Zlotnick A. A heteroaryldihydropyrimidine activates and can misdirect hepatitis B virus capsid assembly. *Proc Natl Acad Sci USA* 2005; **102**: 8138-8143
28 **Weber O**, Schlemmer KH, Hartmann E, Hagelschuer I, Paessens A, Graef E, Deres K, Goldmann S, Niewoehner U, Stoltefuss J, Haebich D, Ruebsamen-Waigmann H, Wohlfeil S. Inhibition of human hepatitis B virus (HBV) by a novel non-nucleosidic compound in a transgenic mouse model. *Antiviral Res* 2002; **54**: 69-78
29 **King RW**, Ladner SK, Miller TJ, Zaifert K, Perni RB, Conway SC, Otto MJ. Inhibition of human hepatitis B virus replication by AT-61, a phenylpropenamide derivative, alone and in combination with (-)beta-L-2',3'-dideoxy-3'-thiacytidine. *Antimicrob Agents Chemother* 1998; **42**: 3179-3186
30 **Delaney WE**, Edwards R, Colledge D, Shaw T, Furman P, Painter G, Locarnini S. Phenylpropenamide derivatives AT-61 and AT-130 inhibit replication of wild-type and lamivudine-resistant strains of hepatitis B virus in vitro. *Antimicrob Agents Chemother* 2002; **46**: 3057-3060
31 **Cheng YC**, Ying CX, Leung CH, Li Y. New targets and inhibitors of HBV replication to combat drug resistance. *J Clin Virol* 2005; **34** Suppl 1: S147-S150

32 **Block TM**, Lu X, Mehta AS, Blumberg BS, Tennant B, Ebling M, Korba B, Lansky DM, Jacob GS, Dwek RA. Treatment of chronic hepadnavirus infection in a woodchuck animal model with an inhibitor of protein folding and trafficking. *Nat Med* 1998; **4**: 610-614

33 **Dyson MR**, Murray K. Selection of peptide inhibitors of interactions involved in complex protein assemblies: association of the core and surface antigens of hepatitis B virus. *Proc Natl Acad Sci USA* 1995; **92**: 2194-2198

34 **Böttcher B**, Tsuji N, Takahashi H, Dyson MR, Zhao S, Crowther RA, Murray K. Peptides that block hepatitis B virus assembly: analysis by cryomicroscopy, mutagenesis and transfection. *EMBO J* 1998; **17**: 6839-6845

35 **Sprengers D**, Janssen HL. Immunomodulatory therapy for chronic hepatitis B virus infection. *Fundam Clin Pharmacol* 2005; **19**: 17-26

36 **Turelli P**, Mangeat B, Jost S, Vianin S, Trono D. Inhibition of hepatitis B virus replication by APOBEC3G. *Science* 2004; **303**: 1829

37 **Rösler C**, Köck J, Kann M, Malim MH, Blum HE, Baumert TF, von Weizsäcker F. APOBEC-mediated interference with hepadnavirus production. *Hepatology* 2005; **42**: 301-309

38 **Lei YC**, Hao YH, Zhang ZM, Tian YJ, Wang BJ, Yang Y, Zhao XP, Lu MJ, Gong FL, Yang DL. Inhibition of hepatitis B virus replication by APOBEC3G in vitro and in vivo. *World J Gastroenterol* 2006; **12**: 4492-4497

39 **Koziel MJ**. The immunopathogenesis of HBV infection. *Antivir Ther* 1998; **3**: 13-24

40 **Beckebaum S**, Cicinnati VR, Gerken G. DNA-based immunotherapy: potential for treatment of chronic viral hepatitis? *Rev Med Virol* 2002; **12**: 297-319

41 **Mancini-Bourgine M**, Fontaine H, Scott-Algara D, Pol S, Bréchot C, Michel ML. Induction or expansion of T-cell responses by a hepatitis B DNA vaccine administered to chronic HBV carriers. *Hepatology* 2004; **40**: 874-882

42 **Liu SA**, Xu DZ, Zhang JP, Huang KL, Yao J, Xu LF, Yuan ZH, Wen YM. Immune response for phase I clinical trial of a hepatitis B immunogenic complex therapeutic vaccine, YIC. *Zhonghua Ganzangbing Zazhi* 2006; **14**: 89-92

43 **Wu YZ**, Zhao JP, Wan Y, Jia ZC, Zhou W, Bian J, Ni B, Zou LY, Tang Y. Mimovirus: a novel form of vaccine that induces hepatitis B virus-specific cytotoxic T-lymphocyte responses in vivo. *J Virol* 2002; **76**: 10264-10269

44 **Akbar SM**, Horiike N, Onji M, Hino O. Dendritic cells and chronic hepatitis virus carriers. *Intervirology* 2001; **44**: 199-208

45 **Zheng BJ**, Zhou J, Qu D, Siu KL, Lam TW, Lo HY, Lee SS, Wen YM. Selective functional deficit in dendritic cell--T cell interaction is a crucial mechanism in chronic hepatitis B virus infection. *J Viral Hepat* 2004; **11**: 217-224

46 **Akbar SM**, Furukawa S, Hasebe A, Horiike N, Michitaka K, Onji M. Production and efficacy of a dendritic cell-based therapeutic vaccine for murine chronic hepatitis B virus carrierer. *Int J Mol Med* 2004; **14**: 295-299

47 **Moynagh PN**. TLR signalling and activation of IRFs: revisiting old friends from the NF-kappaB pathway. *Trends Immunol* 2005; **26**: 469-476

48 **Akira S**, Takeda K. Toll-like receptor signalling. *Nat Rev Immunol* 2004; **4**: 499-511

49 **Tosi MF**. Innate immune responses to infection. J Allergy Clin Immunol 2005; **116**: 241-249; quiz 250

50 **Isogawa M**, Robek MD, Furuichi Y, Chisari FV. Toll-like receptor signaling inhibits hepatitis B virus replication in vivo. *J Virol* 2005; **79**: 7269-7272

51 **BenMohamed L**, Wechsler SL, Nesburn AB. Lipopeptide vaccines--yesterday, today, and tomorrow. *Lancet Infect Dis* 2002; **2**: 425-431

52 **Livingston BD**, Crimi C, Grey H, Ishioka G, Chisari FV, Fikes J, Grey H, Chesnut RW, Sette A. The hepatitis B virus-specific CTL responses induced in humans by lipopeptide vaccination are comparable to those elicited by acute viral infection. *J Immunol* 1997; **159**: 1383-1392

53 **Heathcote J**, McHutchison J, Lee S, Tong M, Benner K, Minuk G, Wright T, Fikes J, Livingston B, Sette A, Chestnut R. A pilot study of the CY-1899 T-cell vaccine in subjects chronically infected with hepatitis B virus. The CY1899 T Cell Vaccine Study Group. *Hepatology* 1999; **30**: 531-536

54 **Stevceva L**. Cytokines and their antagonists as therapeutic agents. *Curr Med Chem* 2002; **9**: 2201-2207

55 **Robek MD**, Wieland SF, Chisari FV. Inhibition of hepatitis B virus replication by interferon requires proteasome activity. *J Virol* 2002; **76**: 3570-3574

56 **Wieland SF**, Guidotti LG, Chisari FV. Intrahepatic induction of alpha/beta interferon eliminates viral RNA-containing capsids in hepatitis B virus transgenic mice. *J Virol* 2000; **74**: 4165-4173

57 **Kakimi K**, Lane TE, Chisari FV, Guidotti LG. Cutting edge: Inhibition of hepatitis B virus replication by activated NK T cells does not require inflammatory cell recruitment to the liver. *J Immunol* 2001; **167**: 6701-6705

58 **Carreño V**, Moreno A, Galiana F, Bartolomé FJ. Alpha- and gamma-interferon versus alpha-interferon alone in chronic hepatitis B. A randomized controlled study. *J Hepatol* 1993; **17**: 321-325

59 **Robek MD**, Boyd BS, Chisari FV. Lambda interferon inhibits hepatitis B and C virus replication. *J Virol* 2005; **79**: 3851-3854

60 **Kovacs JA**, Lempicki RA, Sidorov IA, Adelsberger JW, Sereti I, Sachau W, Kelly G, Metcalf JA, Davey RT, Falloon J, Polis MA, Tavel J, Stevens R, Lambert L, Hosack DA, Bosche M, Issaq HJ, Fox SD, Leitman S, Baseler MW, Masur H, Di Mascio M, Dimitrov DS, Lane HC. Induction of prolonged survival of CD4+ T lymphocytes by intermittent IL-2 therapy in HIV-infected patients. *J Clin Invest* 2005; **115**: 2139-2148

61 **Liu M**, Acres B, Balloul JM, Bizouarne N, Paul S, Slos P, Squiban P. Gene-based vaccines and immunotherapeutics. *Proc Natl Acad Sci USA* 2004; **101** Suppl 2: 14567-14571

62 **Cavanaugh VJ**, Guidotti LG, Chisari FV. Interleukin-12 inhibits hepatitis B virus replication in transgenic mice. *J Virol* 1997; **71**: 3236-3243

63 **Carreño V**, Zeuzem S, Hopf U, Marcellin P, Cooksley WG, Fevery J, Diago M, Reddy R, Peters M, Rittweger K, Rakhit A, Pardo M. A phase I/II study of recombinant human interleukin-12 in patients with chronic hepatitis B. *J Hepatol* 2000; **32**: 317-324

64 **Kimura K**, Kakimi K, Wieland S, Guidotti LG, Chisari FV. Interleukin-18 inhibits hepatitis B virus replication in the livers of transgenic mice. *J Virol* 2002; **76**: 10702-10707

65 **Sun J**, Gao Y, Chen HS, Wang SX, Li RB, Jiang D, Wei L, Wang Y. Transfusion of multi-factors activated immune cells as a novel treatment for patients with chronic hepatitis B. *J Clin Virol* 2006; **35**: 26-32

66 **Wu J**, Nandamuri KM. Inhibition of hepatitis viral replication by siRNA. *Expert Opin Biol Ther* 2004; **4**: 1649-1659

67 **Konishi M**, Wu CH, Wu GY. Delivery of hepatitis B virus therapeutic agents using asialoglycoprotein receptor-based liver-specific targeting. *Methods Mol Med* 2004; **96**: 163-173

68 **Ryther RC**, Flynt AS, Phillips JA, Patton JG. siRNA therapeutics: big potential from small RNAs. *Gene Ther* 2005; **12**: 5-11

69 **Sullenger BA**, Gilboa E. Emerging clinical applications of RNA. *Nature* 2002; **418**: 252-258

S- Editor Liu Y **L- Editor** Ma JY **E- Editor** Lu W

PO Box 2345, Beijing 100023, China
www.wjgnet.com
wjg@wjgnet.com

World J Gastroenterol 2007 February 14; 13(6): 837-844
World Journal of Gastroenterology ISSN 1007-9327

Soluble forms of extracellular cytokeratin 18 may differentiate simple steatosis from nonalcoholic steatohepatitis

Yusuf Yilmaz, Enver Dolar, Engin Ulukaya, Semra Akgoz, Murat Keskin, Murat Kiyici, Sibel Aker, Arzu Yilmaztepe, Selim Gurel, Macit Gulten, Selim Giray Nak

Yusuf Yilmaz, Uludag University Medical School, Department of Internal Medicine, Bursa, Turkey
Enver Dolar, Murat Keskin, Murat Kiyici, Selim Gurel, Macit Gulten, Selim Giray Nak, Uludag University Medical School, Department of Gastroenterology, Bursa, Turkey
Engin Ulukaya, Arzu Yilmaztepe, Uludag University Medical School, Department of Biochemistry, Bursa, Turkey
Semra Akgoz, Uludag University Medical School, Department of Statistics, Bursa, Turkey
Sibel Aker, Uludag University Medical School, Department of Pathology, Bursa, Turkey
Correspondence to: Yusuf Yilmaz, MD, Uludag Universitesi Tip Fakultesi Ic Hastaliklari Gorukle, Bursa 16059, Turkey. yusufyilmaz@uludag.edu.tr
Telephone: +90-533-4403995 Fax: +90-224-4434119
Received: 2006-11-17 Accepted: 2006-12-19

Abstract

AIM: To investigate whether serum levels of two soluble forms of extracellular cytokeratin 18 (M30-antigen and M65-antigen) may differentiate nonalcoholic steatohepatitis (NASH) from simple steatosis in patients with nonalcoholic fatty liver disease (NAFLD).

METHODS: A total of 83 patients with suspected NAFLD and 49 healthy volunteers were investigated. Patients with suspected NAFLD were classified according to their liver histology into four groups: definitive NASH (n = 45), borderline NASH (n = 24), simple fatty liver (n = 9), and normal tissue (n = 5). Serum levels of caspase-3 generated cytokeratin-18 fragments (M30-antigen) and total cytokeratin-18 (M65-antigen) were determined by ELISA.

RESULTS: Levels of M30-antigen and M65-antigen were significantly higher in patients with definitive NASH compared to the other groups. An abnormal value (> 121.60 IU/L) of M30-antigen yielded a 60.0% sensitivity and a 97.4% specificity for the diagnosis of NASH. Sensitivity and specificity of an abnormal M65-antigen level (> 243.82 IU/L) for the diagnosis of NASH were 68.9% and 81.6%, respectively. Among patients with NAFLD, M30-antigen and M65-antigen levels distinguished between advanced fibrosis and early-stage fibrosis with a sensitivity of 64.7% and 70.6%, and a specificity of 77.3% and 71.2%, respectively.

CONCLUSION: Serum levels of M30-antigen and M65-antigen may be of clinical usefulness to identify patients with NASH. Further studies are mandatory to better assess the role of these apoptonecrotic biomarkers in NAFLD pathophysiology.

Key words: Steatosis; Steatohepatitis; Cytokeratin 18; M30-antigen; M65-antigen

Yilmaz Y, Dolar E, Ulukaya E, Akgoz S, Keskin M, Kiyici M, Aker S, Yilmaztepe A, Gurel S, Gulten M, Nak SG. Soluble forms of extracellular cytokeratin 18 may differentiate simple steatosis from non-alcoholic steatohepatitis. *World J Gastroenterol* 2007; 13(6): 837-844

http://www.wjgnet.com/1007-9327/13/837.asp

INTRODUCTION

Nonalcoholic fatty liver disease (NAFLD) is a common condition comprising a wide spectrum of liver damage associated with metabolic disorders, including central obesity, dyslipidemia, hypertension, and hyperglycemia. The spectrum of disease is variable, ranging from simple steatosis with benign prognosis, to nonalcoholic steatohepatitis (NASH), advanced fibrosis and cirrhosis, conferring increase in morbidity and mortality[1,2].

NASH could be present in one third of NAFLD cases and appears to have a higher likelihood of progression to cirrhosis. Furthermore, an increased risk of hepatocellular carcinoma and end-stage liver disease has been reported among patients with NASH[3,4]. It follows that early recognition of subjects with NASH is crucial to prevent the development of severer forms of liver disease and improve the clinical outcome. Differentiation of simple steatosis from NASH requires histopathologic evaluation[5]. In this regard, liver biopsy remains the most sensitive and specific means of providing important diagnostic and prognostic information[6,7]. Nonetheless, given that liver biopsy is an expensive procedure, with occasional complications and poor patient acceptance[8-11], the search for surrogate markers to replace liver biopsy is highly recommended.

A growing body of evidence has recently suggested that dysregulation of hepatocyte apoptosis could play an important role in the progression of NAFLD to

NASH[12-14]. During apoptosis, a number of intracellular proteins are cleaved by caspases. A neoepitope in cytokeratin 18 (CK18), termed M30-antigen, becomes available at an early caspase cleavage event during apoptosis and is not detectable in vital or necrotic cells[15-18]. A monoclonal antibody, M30, specifically recognizes a fragment of CK18 cleaved at Asp396 (M30-antigen)[19]. By contrast, the cytosolic pool of uncleaved CK18 (also termed M65-antigen) is released from cells during necrosis[19]. These findings implicate that assessments of different forms of CK18 in patient sera (M30-antigen for apoptosis and M65-antigen for necrosis) could be used to examine different cell death modes *in vivo*. Two robust immunoassays are currently available to measure the levels of M30-antigen and M65-antigen[20-22].

In this study, we have measured different forms of CK18 (M30-antigen and M65-antigen) in serum from NAFLD patients as an approach for differentiating simple steatosis from NASH. Specifically, we wanted to establish a reliable diagnostic model by using these non-invasive biomarkers.

MATERIALS AND METHODS

Study participants

Between November 2005 and October 2006, we enrolled a total of 83 patients (38 females and 45 males, age range: 25-76 years) with suspected NAFLD. By the ATP Ⅲ Expert Panel of the U.S. National Cholesterol Education Program criteria[23], approximately one third of participants had the metabolic syndrome. Patients with viral hepatitis, hemochromatosis, Wilson's disease, autoimmune hepatitis, primary biliary cirrhosis, sclerosing cholangitis, biliary obstruction, alpha-1 antitrypsin deficiency, or malignancies were excluded from the present study. None of the subjects was using any medications, including estrogens, amiodarone, steroids, tamoxifen, or herbal supplements. Furthermore we excluded patients with daily alcohol intake exceeding 20 g/d or previous abdominal surgery. For control purposes, 49 healthy age- and gender-matched volunteers were recruited. All controls were judged to be in good health, with normal results on liver function tests and confirmed as having normal liver by ultrasound. Subjects with a consumption of alcohol > 20 g/d or who were taking any medication were not included in the control group.

A written informed consent was obtained from all participants. The study protocol was reviewed and approved by the Ethics Committee of the Uludag University Medical School.

Clinical assessment

All subjects underwent physical examination, anthropometric measurements and biochemical screening. Liver ultrasound (US) scanning was performed to assess the degree of steatosis. All US procedures were performed by the same operator. Liver steatosis was assessed semiquantitatively on a scale of 0 to 3: 0, absent; 1, mild; 2, moderate; and 3, severe. Computed tomography (CT) evaluation of liver parenchyma was performed in all NAFLD patients. An experienced pathologist examined liver histology according to the NIDDK NASH Clinical Research Network scoring system[24]. Patients with suspected NAFLD were classified according to their liver histology into four groups: definitive NASH (n = 45), borderline NASH (n = 24), simple fatty liver (n = 9), and normal tissue (n = 5). In a secondary analysis, patients with borderline NASH, simple fatty liver, and normal tissue were grouped together and analyzed as a single group which is named as no-NASH.

Histological analysis

Ultrasonography-guided liver biopsies were performed under conscious sedation using a 16-gauge Klatskin needle. The length of histological specimens was not smaller than 2.5 cm. All biopsy specimens were placed in formalin solution for fixation and embedded in paraffin blocks. Serial sections (sectioned at 4 μm intervals) were stained with hematoxylin-eosin, Masson's trichrome. An experienced pathologist blinded to clinical data scored the liver biopsies according to the NIDDK NASH Clinical Research Network scoring system[24]. Steatosis was scored from 0 to 3 with a four grades scoring system from S0 to S3: S0: no steatosis or less than 5%, S1: 5%-33%, S2: 33%-66%, S3: > 66%. Lobular inflammation was graded as follows: stage 0, no foci; stage 1: < 2 foci per 200 × field; stage 2: 2-4 foci per 200 × field; stage 3: > 4 foci per 200 × field. Fibrosis was staged as follows: stage 0: no fibrosis; stage 1: perisinusoidal or periportal fibrosis with 3 different patterns: 1A: mild, zone 3, perisinusoidal; 1B: moderate, zone 3, perisinusoidal fibrosis, and 1C portal/periportal fibrosis; stage 2: perisinusoidal and portal/periportal fibrosis; stage 3: bridging fibrosis; stage 4: cirrhosis. The histological NASH score was defined as the unweighted sum of the scores for steatosis (0-3), lobular inflammation (0-3), and ballooning (0-2); thus ranging from 0 to 8. Cases with scores of 0 to 2 were considered as having simple steatosis; on the other hand, cases with scores of 5 or greater were diagnosed as definitive NASH[24]. Cases with activity scores of 3 and 4 were considered as borderline (probable) NASH.

ELISA assays

Blood samples were centrifuged at 2500 g for 10 min, and serum aliquots were stored at -80℃ until immediately before analysis. All samples were analyzed in duplicate and in a blinded fashion. Serum levels of M30-antigen and M65-antigen were determined by commercially available immunoassays (M30-Apoptosense ELISA kit and M65 ELISA kit, Peviva AB, Bromma, Sweden) according to the manufacturer's instructions. The M65-ELISA assay measures native soluble CK18 (M65-antigen), whereas the M30-Apoptosense ELISA kit measures the levels of the CK18-Asp396 neo-epitope (M30-antigen). Briefly, samples were placed into wells coated with a mouse monoclonal antibody as a catcher. After washing, a horseradish peroxidase conjugated antibody (M30 or M65) was used for detection. Reference concentrations of M30-antigen or M65-antigen were used to prepare assay calibration. The absorbance was determined with an ELISA reader at 450 nm.

Table 1 General and biochemical characteristics of patients with suspected NAFLD

Characteristic	Entire cohort (n = 83)	Definitive NASH (n = 45)	Borderline NASH (n = 24)	Simple steatosis (n = 9)	Normal tissue (n = 5)
Male gender	54.2%	62.2%	50.0%	44.4%	20.0%
Age (yr)	48.9 ± 9.1	47.8 ± 8.8	48.7 ± 6.2	53.1 ± 10.1	52.4 ± 19.2
Body mass index (kg/m^2)	30.3 ± 4.8	30.2 ± 4.1	31.1 ± 6.5	29.5 ± 3.7	28.0 ± 3.0
Waist circumference (cm)	99 ± 9	101 ± 8	100 ± 9	94 ± 10	93 ± 11
Waist/hip ratio	0.93 (0.01-1.08)	0.95 (0.09-1.08)	0.93 (0.09-1.02)	0.8 (0.74-1.05)	0.86 (0.01-0.87)
Hypertension	33.7%	28.9%	50%	22.2%	20%
Systolic blood pressure (mmHg)	122 ± 13	124 ± 13	121 ± 13	121 ± 16	115 ± 11
Diastolic blood pressure (mmHg)	77 ± 10	80 ± 9	76 ± 11	71 ± 10	72 ± 9
Diabetes mellitus	14.5%	13.3%	16.7%	22.2%	0%
Fasting glucose (mg/dL)	103 ± 22	102 ± 21	105 ± 25	109 ± 25	93 ± 7
Fasting insulin (μU/mL)[1]	24 (1-298)	34 (3-298)	21 (1-281)	20 (1-110)	11 (1-16)
HOMA index	3.0 (0.2-16.5)	3.1 (0.3-16.5)	2.9 (0.3-8.1)	2.6 (0.2-4.9)	2.3 (1.6-3.8)
Hyperlipidemia history	83.1%	80.0%	91.7%	77.8%	80%
Total cholesterol (mg/dL)	213 ± 40	213 ± 44	224 ± 31	190 ± 27	199 ± 49
Triglycerides (mg/dL)[1]	149 (38-424)	151 (38-424)	164 (90-398)	102 (49-286)	149 (44-182)
Metabolic syndrome	34.9%	37.8%	33.3%	33.3%	20.0%
Lp(a) (mg/dL)[1]	10 (2-157)	9 (2-98)	20 (2-157)	6 (2-68)	19 (5-32)
Microalbuminuria (μg/mL)[1]	1.0 (0.2-48.4)	4.2 (0.2-48.4)	0.7 (0.2-3.8)	0.65 (0.3-8.9)	0.4 (0.2-1.0)
AST (IU/L)[1]	42 (16-102)	44 (18-95)	33 (16-102)	32 (17-65)	28 (19-91)
ALT (IU/L)[1]	60 (10-184)	68 (23-184)	47 (12-146)	47 (19-84)	35 (10-149)
AST/ALT ratio	0.68 (0.34-1.90)	0.65 (0.34-0.95)	0.71 (0.45-1.42)	0.77 (0.59-1.21)	0.8 (0.6-1.9)
ALP (UI/L)[1]	82 (19-154)	84 (44-152)	85 (43-132)	94 (19-154)	76 (61-131)
GGT (UI/L)[1]	47 (15-526)	52 (16-526)	29 (15-199)	65 (22-164)	73 (17-124)
LDH (UI/L)[1]	196 (132-379)	198 (143-375)	193 (132-295)	184 (163-379)	171 (152-340)
Total Bilirubin (mg/dL)[1]	0.7 (0.1-2.5)	0.7 (0.1-2.5)	0.6 (0.1-1.7)	0.5 (0.1-0.8)	0.8 (0.4-2.1)
HbA1c	5.6 (4.6-9.9)%	5.7 (4.7-9.9)%	5.5 (4.6-7.7)%	5.6 (5.1-7.4)%	5.5 (5.4-6.2)%
Transferrin saturation	19 (2-48)%	20 (2-48)%	17 (5-29)%	23.5 (11-44)%	18 (8-28)%
Ferritin (ng/mL)[1]	77 (6-406)	93 (6-399)	69 (12-297)	96 (10-406)	23 (9-61)
Positive ANA	21.6%	23.9%	20.8%	0%	40.0%
Positive AMA	1.2%	2.1%	0%	0%	0%
Positive ASMA	7.2%	4.3%	4.4%	0%	20.0%
Positive LKM-1	0%	0%	0%	0%	0%

[1]Data expressed as median (minimum-maximum); HOMA: homeostasis model assessment; HDL: high-density lipoprotein; Lp(a): lipoprotein(a); AST: aspartate aminotransferase; ALT: alanine aminotransferase; ALP: alkaline phosphatase; GGT: gamma glutamyl transpeptidase; LDH: lactate dehydrogenase; HbA1c: glycated hemoglobin; ANA: antinuclear antibodies; AMA: antimitochondrial antibodies; ASMA: anti-smooth muscle antibody; LKM-1, liver-kidney microsomal antigen.

Statistical analysis

Variables are presented as counts and percentages or means ± SD, unless otherwise indicated. Pearson's χ^2 test was used for comparison of categorical variables. Between group mean differences were tested by the Mann-Whitney U test or the Kruskal-Wallis test, as appropriate. The sensitivity, specificity, positive predictive value, and negative predictive value of the serum biomarkers in predicting definitive NASH were calculated using receiver operating characteristic (ROC) analyses. Diagnostic properties were expressed as percentages, with 95% confidence intervals (95% CIs). Cut-off values for serum biomarkers were determined using the MedCalc demo statistical software (Mariakerke, Belgium). Univariate (simple) and multivariate (forward stepwise) regression models were used to assess the independent predictors of definitive NASH in patients with suspected NAFLD. A $P < 0.05$ was retained for statistical significance. All computations were made using SPSS 10.0 (SPSS Inc., Chicago, IL, USA).

RESULTS

Patients Characteristics

The control (n = 49) and NAFLD (n = 83) groups were well balanced for age and gender (data not shown). Table 1 shows the clinical and biochemical characteristics of the NAFLD patients stratified by their liver histology into four groups: definitive NASH (n = 45), borderline NASH (n = 24), simple fatty liver (n = 9), and normal tissue (n = 5).

There was a statistically significant difference in microalbuminuria ($P < 0.05$), ALT levels ($P < 0.05$) and AST/ALT ratio ($P < 0.05$) between the four groups. By contrast, there were no statistically significant differences between the groups in age, gender, BMI, waist circumference, history of hypertension, hyperlipidemia, diabetes, or prevalence of the metabolic syndrome. Values of alkaline phosphatase, gamma-glutamyl transferase, lactic acid dehydrogenase, ferritin, and homeostasis model assessment-estimated insulin resistance (HOMA) were not significantly different across the four patient groups. 27% of patients with suspected NAFLD had positive serological testing for autoantibodies.

Histopathology

The histological features of patients with suspected NAFLD are presented in Table 2. Of 83 subjects, 5 had normal biopsies with < 5% steatosis. Nine subjects had steatosis alone. In the present study, 24 patients with suspected NAFLD had histological borderline NASH.

Table 2 Histological findings in 83 patients with suspected NAFLD

Variable	Definition	Score	Entire cohort (n = 83) (%)	Definitive NASH (n = 45) (%)	Borderline NASH (n = 24) (%)	Simple steatosis (n = 9) (%)	Normal tissue (n = 5) (%)
Steatosis	< 5%	0	8.40	0	8.30	0	100
	5%-33%	1	39.80	13.30	75.00	100	0
	> 33%-66%	2	30.10	46.70	16.70	0	0
	> 66%	3	21.70	40.00	0	0	0
Lobular inflammation (foci per 200 × field)	No foci	0	15.70	0	0	88.90	100
	< 2 foci	1	26.50	8.90	70.80	11.10	0
	2-4 foci	2	43.40	64.40	29.20	0	0
	> 4 foci	3	14.50	26.70	0	0	0
Ballooning	None	0	12	0	0	55.60	100
	Few balloon cells	1	24.10	6.70	70.90	44.40	0
	Many cells/prominent ballooning	2	63.90	93.30	29.10	0	0
Fibrosis stage	None	0	54.20	33.30	66.70	100	100
	Mild, zone 3, perisinusoidal	1A	8.40	11.10	8.30	0	0
	Moderate, zone 3, perisinusoidal	1B	3.60	6.70	0	0	0
	Portal/periportal	1C	13.30	15.60	16.60	0	0
	Perisinusoidal and portal/periportal	2	13.30	22.20	4.20	0	0
	Bridging fibrosis	3	7.20	11.10	4.20	0	0
	Cirrhosis	4	0	0	0	0	0

Table 3 Imaging findings in 83 patients with suspected NAFLD

Steatosis		Entire cohort (n = 83)	Definitive NASH (n = 45)	Borderline NASH (n = 24)	Simple steatosis (n = 9)	Normal tissue (n = 5)
Sonographic grade of hepatosteatosis	Mild	44.00%	27.50%	50.00%	77.80%	100.00%
	Moderate	40.00%	55%	31.80%	11.10%	0%
	Severe	16.00%	17.50%	18.20%	11.10%	0%
Liver attenuation on CT (HU)		43.8 ± 14.6	36.9 ± 11.9	49.5 ± 15.1	55.2 ± 6.2	64.1 ± 3.3

Criteria for definitive NASH, as proposed by the NASH Clinical Research Network[24], were fulfilled by 45 patients. Among patients with definitive NASH, liver biopsy showed that steatosis was mild in 13.3%, moderate in 46.7%, and severe in 40.0%. Lobular inflammation and ballooning were present in all biopsy specimens from definitive NASH patients in varying amounts. 77% of definitive NASH patients exhibited fibrosis. No liver biopsy demonstrated cirrhosis.

Imaging

Ultrasound and CT findings are summarized in Table 3. Among the 83 subjects with suspected NAFLD, ultrasonographic examination revealed mild steatosis in 44%, moderate steatosis in 40% and severe steatosis in 16% of cases. By CT scans, the mean (SD) absolute liver density value of the entire study cohort was 43.8 ± 14.6 Hounsfield units (HU).

Serum biomarkers

As shown in Table 4, the serum levels of M-30 antigen were markedly higher in the definitive NASH group than in the control ($P < 0.001$), simple fatty liver ($P < 0.01$) and borderline NASH ($P < 0.001$) groups. Serum levels of M-30 antigen did not differ between patients with definitive NASH and subjects with normal biopsy.

Serum concentrations of M-65 antigen were higher in the patients with definitive NASH than in those with borderline NASH ($P < 0.001$), simple fatty liver ($P < 0.01$), normal tissue ($P < 0.05$), or in healthy individuals ($P < 0.001$). Serum levels of both biomarkers did not differ between the possible NASH, simple steatosis, and normal biopsy groups compared with the control group.

Subjects with possible NASH, simple fatty liver, or normal tissue were then grouped together (no-NASH group, n = 38) for a secondary analysis. The results of this analysis showed that the serum levels of both biomarkers were markedly higher in the definitive NASH group than in the no-NASH group ($P < 0.001$ for both biomarkers).

Diagnostic value of serum biomarkers for the prediction of definitive NASH

Table 5 lists the sensitivity, specificity, positive predictive value, and negative predictive value of the M30-antigen and the M65-antigen in predicting definitive NASH. In addition, the area under the ROC curve (ROC AUC) for both biomarkers was determined. The ROC AUC provides a measure of the overall discriminative ability of a test. In general, ROC AUC $\geqslant$ 7 indicates acceptable discrimination, ROC AUC $\geqslant$ 8 excellent discrimination

Table 4 Concentrations of serum M30-antigen and M65-antigen in the study groups

Biomarker	Definitive NASH (n = 45)	Borderline NASH (n = 24)	Simple steatosis (n = 9)	Normal tissue (n = 5)	Healthy volunteers (n = 49)	No-NASH (n = 38)	[1]P
M30-antigen (IU/L)	200.4 ± 183.1	69.8 ± 37.1	60.1 ± 36.8	81.0 ± 17.5	43.3 ± 45.9	69.0 ± 34.9	< 0.001
[2]P	Reference category	< 0.001	< 0.01	NS	< 0.001	< 0.001	
M65-antigen (IU/L)	362.8 ± 178.7	210.6 ± 59.6	215.3 ± 78.2	207.0 ± 47.4	150.9 ± 44.1	211.2 ± 61.5	< 0.001
[2]P	Reference category	< 0.001	< 0.01	< 0.05	< 0.001	< 0.001	

[1]P value calculated using Kruskal-Wallis test. [2]Comparisons between definitive NASH patients and other patient groups were performed by Mann-Whitney U Test.

Table 5 Diagnostic performance of serum M30-antigen and M65-antigen levels for the diagnosis of definitive NASH

Patient category	Serum biomarker	Cut-off value[1] (IU/L)	Sensitivity (95% CI)	Specificity (95% CI)	Positive predictive value (%)	Negative predictive value (%)	Negative likelihood ratio	Area under the ROC curve (95% CI)
Borderline NASH	M30-antigen	121.6	60 (44.3-74.3)	95.8 (78.8-99.3)	96.40	56.10	0.42	0.783 (0.668-0.783)
	M65-antigen	241.34	68.9 (53.3-81.8)	83.3 (62.6-95.2)	88.60	58.80	0.37	0.809 (0.697-0.894)
Simple steatosis	M30-antigen	109.64	62.2 (46.5-76.2)	100 (66.2-100.0)	100.00	34.60	0.38	0.83 (0.703-0.918)
	M65-antigen	186.77	93.3 (81.7-98.5)	66.7 (30.1-92.1)	93.30	66.70	0.10	0.807 (0.677-0.902)
Normal tissue	M30-antigen	96.5	64.4 (48.8-78.1)	100 (48.0-100.0)	100.00	23.80	0.36	0.724 (0.508-0.841)
	M65-antigen	227.18	73.3 (58.1-85.4)	80 (28.8-96.7)	97.10	25.00	0.33	0.809 (0.673-0.906)
Healthy controls	M30-antigen	82.52	75.6 (60.5-87.1)	85.7 (72.7-94.0)	82.90	79.20	0.29	0.881 (0.798-0.938)
	M65-antigen	189.64	91.4 (77.6-98.6)	68.1 (36.1-94.2)	92.00	68.20	0.18	0.94 (0.839-0.980)
No-NASH	M30-antigen	121.6	60 (44.3-74.3)	97.4 (86.1-99.6)	96.40	67.30	0.41	0.787 (0.683-0.869)
	M65-antigen	243.82	68.9 (53.3-81.8)	81.6 (65.7-92.2)	81.60	68.90	0.38	0.809 (0.708-0.887)

[1]Cut-off value corresponding to the highest accuracy value (minimal false negative and false positive results).

and ROC AUC $\geqslant$ 9 outstanding discrimination (very unusual). As shown in Table 5, both biomarkers revealed good discriminative ability for predicting definitive NASH. Notably, M30-antigen and M65-antigen gave similar diagnostic abilities.

Relationship between liver fibrosis and serum biomarkers

Table 6 shows the sensitivity, specificity, positive predictive value, and negative predictive value of M30-antigen and M65-antigen in differentiating early liver fibrosis from advanced fibrosis. Serum levels of both M30-antigen ($P < 0.01$) and M65-antigen ($P < 0.01$) were higher in patients with advanced fibrosis compared to those with early fibrosis. Both biomarkers appeared to have similar diagnostic ability.

Relationship between transaminases and serum biomarkers

We found a weak, albeit significant, positive correlation between M30-antigen levels with both AST ($r = 0.441$, $P < 0.001$) and ALT values ($r = 0.425$, $P < 0.001$). Similarly, concentrations of M65-antigen were positively related to both AST ($r = 0.490$, $P < 0.001$) and ALT ($r = 0.473$, $P < 0.001$).

Multivariate analysis

To assess the independent contribution of M30-antigen, M60-antigen as well as CT findings in identifying subjects with definitive NASH, simple and multiple linear regression analyses were performed (Table 7). Simple regression analysis showed that AST/ALT ratio, microalbuminuria, waist/hip ratio, CT density as well as levels of M30-antigen and M-65 antigen were all significantly associated with the presence of definitive NASH (data not shown). Variables associated with definitive NASH on univariate analysis were then entered into a multivariate model. The model showed that the addition of M-30 antigen to computed tomography yielded a 86.1% sensitivity and a 83.3% specificity for NASH. Similarly, the addition of M-60 antigen to computed tomography yielded a 83.3% sensitivity and a 83.3% specificity for NASH.

DISCUSSION

The results of our study show that different forms of CK18 in patient sera (M30-antigen and M65-antigen) may be of clinical usefulness in discriminating NASH from simple fatty liver or NAFLD patients with severe fibrosis from subjects with early fibrosis.

NAFLD is increasingly recognized as one of the most common causes of liver disease worldwide[25,26]. In this regard, in view of the epidemic of the metabolic syndrome, the prevalence of NAFLD is expected to continue to increase in future years[25]. A liver biopsy remains the gold standard for the evaluation of liver histology and is therefore a key test used to establish the diagnosis of NAFLD[1]. Unfortunately, it is an invasive procedure associated with discomfort and some risk[8,9]. It is therefore not suitable for the evaluation of all individuals with suspected NAFLD. The limitations of a liver biopsy have led to considerable interest and attempts to diagnose this condition with laboratory tests and imaging modalities.

Although simple fatty liver has been considered a benign disease, NASH appears to be a common cause of cryptogenic cirrhosis and may even result in hepatocellular carcinoma[26-28]. To date, the pathophysiological pathways

Table 6 Diagnostic performance of serum M30-antigen and M65-antigen levels in discriminating NAFLD patients with severe fibrosis from subjects with early fibrosis

	Cut-off value[1] (IU/L)	Sensitivity (95% CI) (%)	Specificity (95% CI) (%)	Positive predictive value (%)	Negative predictive value (%)	Negative likelihood ratio	Area under the curve (95% CI)
M30-antigen	121.6	64.7 (38.4-85.7)	77.3 (65.3-86.7)	42.30	89.50	0.46	0.733 (0.624-0.824)
M65-antigen	243.82	70.6 (44.1-89.6)	71.2 (58.7-81.7)	38.70	90.40	0.41	0.742 (0.635-0.832)

[1]Cut-off value corresponding to the highest accuracy value (minimal false negative and false positive results).

Table 7 Diagnostic value of serum biomarkers in combination with CT scans for the diagnosis of definitive NASH according to multivariate regression analysis

		P	Odds ratio	95% CI	Sensitivity (%)	Specificity (%)	Positive predictive value (%)	Negative predictive value (%)	Accuracy (%)
Combination	CT	0.001	0.891	0.831-0.955	86.10	83.30	86.10	83.30	84.80
	M30-antigen	0.002	1.029	1.011-1.048					
Combination	CT	0.003	0.916	0.865-0.971	83.30	83.30	85.70	86.60	83.30
	M65-antigen	0.003	1.015	1.005-1.025					

involved in liver damage and in the progression of pure fatty liver to NASH remain largely unknown. Currently, the most accepted theory to explain the pathogenesis of NAFLD is the so-called "two-hit" hypothesis[29]. According to this model, the development of hepatic steatosis constitutes the first hit, and cellular events leading to hepatic inflammation constitute the second hit.

Experimental and clinical data have suggested a role for hepatocyte apoptosis in liver inflammation and tissue damage, regeneration of parenchyma, and fibrosis[30-33]. In this regard, a reduction in hepatocyte apoptosis has been shown to result in decreased liver fibrosis in animal models of cholestasis[32]. Of interest is also the observation that fibrosis has been suggested to rely on induction of hepatic stellate cells apoptosis[32]. In the clinical setting, Bantel *et al*[34] have previously shown that sera from patients with HCV infection had a markedly higher caspase activation than controls. In addition, measurements of caspase activity in serum were found to be related to the extent of steatosis or presence of fibrosis.

Recently, there has been a growing interest in measuring different CK18 forms in peripheral blood as a means to examine different cell death modes. Intriguingly, a recent report by Wieckowska *et al*[35] has shown that measurement of serum M30-antigen levels may allow discrimination of definitive NASH patients from simple fatty liver with high sensitivity and specificity. However, the sample size in this study was small, and no attempt was made to study the concentrations of M-30 antigen in patients with possible NASH.

Our present results confirm and expand previous findings[35] on the potential clinical usefulness of different forms of CK18 (M30-antigen and M65-antigen) as biochemical assays to accurately distinguish definitive NASH from simple fatty liver. Notably, we are also able to investigate a group of patients with possible NASH and to establish reliable cutoffs for the differential diagnosis of possible NASH from definitive NASH. Appropriate cut-off values for serum M-30 antigen and M-65 antigen were 121.60 IU/L (sensitivity, 60.0%; specificity, 95.8%; positive predictive value, 96.4%; negative predictive value, 56.1%) and 241.34 IU/L (sensitivity, 68.9%; specificity, 83.3%; positive predictive value, 88.6%; negative predictive value, 58.8%), respectively. Altogether, these biochemical findings seem to indicate that possible NASH more closely resembles the clinical and pathophysiological features of simple fatty liver than those of definitive NASH.

Importantly, it remains a clinically crucial issue to distinguish definitive NASH from more benign forms of NAFLD[1]. The appropriate cut-off values for serum M-30 antigen and M-65 antigen that distinguish between NASH and no-NASH (borderline NASH, simple fatty liver, normal tissue) were 121.60 IU/L (sensitivity, 60.0%; specificity, 97.4%; positive predictive value, 96.4%; negative predictive value, 67.3%) and 243.82 IU/L (sensitivity, 68.9%; specificity, 81.6%; positive predictive value, 81.6%; negative predictive value, 68.9%), respectively. Of great interest, multivariate regression analysis showed that the combination of M-30 antigen and CT increased the sensitivity and specificity for definitive NASH to 86.1% and 83.3%, respectively. Similarly, the combination of M-65 antigen and CT increased the sensitivity and specificity for NASH to 83.3% and 83.3%, respectively. Altogether, our data suggest that measurement of different forms of CK18 in combination with CT has greater diagnostic utility for the identification of patients with definitive NASH than the use of either test alone.

A weak, albeit significant, correlation between serum forms of CK18 (both M30-antigen and M65-antigen) and levels of hepatic transaminases was found. Although it has been suggested that aminotransferases are released during necrosis at a higher rate than in apoptosis[36], we found that hepatic transaminases were significantly correlated with levels of both M-30 antigen (a marker of apoptosis) and M-65 antigen (a marker of necrosis). To quantify the rates of apoptosis and necrosis in patients with definitive NASH, we also determined the M30:M65 ratio[22] as a means to investigate mode of cell death of hepatocytes

(data not shown). Of note, differently from other forms of NAFLD, the mode of such cellular death was apoptosis dominant in definitive NASH individuals compared to other NAFLD patient groups.

In summary, the results of the present study suggest that noninvasive monitoring of different forms of CK18 (M30-antigen and M65-antigen) in sera of patients with suspected NAFLD may represent a reliable tool to differentiate definitive NASH from simple fatty liver. Additionally, these biomarkers may be useful for identifying NAFLD patients with more severe liver fibrosis. Further validation studies in larger groups of patients are needed to confirm our findings.

ACKNOWLEDGMENTS

The authors thank the assistance of the Research Fellows and the Scientific Staff at the Uludag University Medical School. Also, we are indebted to Dr. Enzo Emanuele for revising our manuscript.

COMMENTS

Background

Liver biopsy remains the gold standard for assessing histologic lesions of non-alcoholic fatty liver disease (NAFLD). Unfortunately, it is an invasive procedure associated with discomfort and some risk. The limitations of a liver biopsy have led to considerable interest and attempts to diagnose this condition with laboratory tests and imaging modalities.

Research frontiers

As liver biopsy is impossible to perform as a diagnostic mass-screening tool, great effort is currently being spent in the validation of simple non-invasive markers of liver injury in patients with NAFLD. Specifically, the early identification of patients with nonalcoholic steatohepatitis (NASH) is of clinical importance because of the prognostic implications.

Innovations and breakthroughs

We demonstrated that noninvasive monitoring of different forms of cytokeratin-18 (M30-antigen and M65-antigen) in sera of patients with suspected NAFLD may represent a reliable tool to differentiate definitive NASH from simple fatty liver. Additionally, these biomarkers may be useful for identifying NAFLD patients with severer liver fibrosis.

Applications

In patients with non-alcoholic fatty liver disease, measurement of different forms of cytokeratin-18 in patient sera, a simple and non-invasive biomarker reliably predicts the presence or absence of NASH.

Terminology

Cytokeratin-18: a cytoskeletal protein found primarily in epithelial cells; M30-antigen: a fragment of cytokeratin-18 cleaved at Asp396 by caspases (a marker of apoptosis); M65-antigen: full-length soluble cytokeratin-18 (a marker of necrosis).

Peer review

This manuscript is pertinent, timely, with a fairly rigorous statistical approach to an important clinical question: what would be the best biological markers in human NAFLD.

REFERENCES

1 **Brunt EM**. Nonalcoholic steatohepatitis. *Semin Liver Dis* 2004; **24**: 3-20
2 **Sheth SG**, Gordon FD, Chopra S. Nonalcoholic steatohepatitis. *Ann Intern Med* 1997; **126**: 137-145
3 **Bugianesi E**, Leone N, Vanni E, Marchesini G, Brunello F, Carucci P, Musso A, De Paolis P, Capussotti L, Salizzoni M, Rizzetto M. Expanding the natural history of nonalcoholic steatohepatitis: from cryptogenic cirrhosis to hepatocellular carcinoma. *Gastroenterology* 2002; **123**: 134-140
4 **Marrero JA**, Fontana RJ, Su GL, Conjeevaram HS, Emick DM, Lok AS. NAFLD may be a common underlying liver disease in patients with hepatocellular carcinoma in the United States. *Hepatology* 2002; **36**: 1349-1354
5 **Angulo P**. Nonalcoholic fatty liver disease. *N Engl J Med* 2002; **346**: 1221-1231
6 **Van Ness MM**, Diehl AM. Is liver biopsy useful in the evaluation of patients with chronically elevated liver enzymes? *Ann Intern Med* 1989; **111**: 473-478
7 **Sorbi D**, Boynton J, Lindor KD. The ratio of aspartate aminotransferase to alanine aminotransferase: potential value in differentiating nonalcoholic steatohepatitis from alcoholic liver disease. *Am J Gastroenterol* 1999; **94**: 1018-1022
8 **McGill DB**, Rakela J, Zinsmeister AR, Ott BJ. A 21-year experience with major hemorrhage after percutaneous liver biopsy. *Gastroenterology* 1990; **99**: 1396-1400
9 **Poynard T**, Ratziu V, Bedossa P. Appropriateness of liver biopsy. *Can J Gastroenterol* 2000; **14**: 543-548
10 **Ratziu V**, Charlotte F, Heurtier A, Gombert S, Giral P, Bruckert E, Grimaldi A, Capron F, Poynard T. Sampling variability of liver biopsy in nonalcoholic fatty liver disease. *Gastroenterology* 2005; **128**: 1898-1906
11 **Younossi ZM**, Gramlich T, Liu YC, Matteoni C, Petrelli M, Goldblum J, Rybicki L, McCullough AJ. Nonalcoholic fatty liver disease: assessment of variability in pathologic interpretations. *Mod Pathol* 1998; **11**: 560-565
12 **Canbay A**, Higuchi H, Bronk SF, Taniai M, Sebo TJ, Gores GJ. Fas enhances fibrogenesis in the bile duct ligated mouse: a link between apoptosis and fibrosis. *Gastroenterology* 2002; **123**: 1323-1330
13 **Takehara T**, Tatsumi T, Suzuki T, Rucker EB, Hennighausen L, Jinushi M, Miyagi T, Kanazawa Y, Hayashi N. Hepatocyte-specific disruption of Bcl-xL leads to continuous hepatocyte apoptosis and liver fibrotic responses. *Gastroenterology* 2004; **127**: 1189-1197
14 **Feldstein AE**, Canbay A, Angulo P, Taniai M, Burgart LJ, Lindor KD, Gores GJ. Hepatocyte apoptosis and fas expression are prominent features of human nonalcoholic steatohepatitis. *Gastroenterology* 2003; **125**: 437-443
15 **Ueno T**, Toi M, Linder S. Detection of epithelial cell death in the body by cytokeratin 18 measurement. *Biomed Pharmacother* 2005; **59** Suppl 2: S359-S362
16 **Caulín C**, Salvesen GS, Oshima RG. Caspase cleavage of keratin 18 and reorganization of intermediate filaments during epithelial cell apoptosis. *J Cell Biol* 1997; **138**: 1379-1394
17 **Ku NO**, Liao J, Omary MB. Apoptosis generates stable fragments of human type I keratins. *J Biol Chem* 1997; **272**: 33197-33203
18 **MacFarlane M**, Merrison W, Dinsdale D, Cohen GM. Active caspases and cleaved cytokeratins are sequestered into cytoplasmic inclusions in TRAIL-induced apoptosis. *J Cell Biol* 2000; **148**: 1239-1254
19 **Leers MP**, Kölgen W, Björklund V, Bergman T, Tribbick G, Persson B, Björklund P, Ramaekers FC, Björklund B, Nap M, Jörnvall H, Schutte B. Immunocytochemical detection and mapping of a cytokeratin 18 neo-epitope exposed during early apoptosis. *J Pathol* 1999; **187**: 567-572
20 **Ueno T**, Toi M, Bivén K, Bando H, Ogawa T, Linder S. Measurement of an apoptotic product in the sera of breast cancer patients. *Eur J Cancer* 2003; **39**: 769-774
21 **Canbay A**, Kip SN, Kahraman A, Gieseler RK, Nayci A, Gerken G. Apoptosis and fibrosis in non-alcoholic fatty liver disease. *Turk J Gastroenterol* 2005; **16**: 1-6
22 **Kramer G**, Erdal H, Mertens HJ, Nap M, Mauermann J, Steiner G, Marberger M, Bivén K, Shoshan MC, Linder S. Differentiation between cell death modes using measurements of different soluble forms of extracellular cytokeratin 18. *Cancer Res* 2004; **64**: 1751-1756

23 **Executive Summary of The Third Report of The National Cholesterol Education Program (NCEP) Expert Panel on Detection, Evaluation, And Treatment of High Blood Cholesterol In Adults (Adult Treatment Panel III)**. *JAMA* 2001; **285**: 2486-2497
24 **Kleiner DE**, Brunt EM, Van Natta M, Behling C, Contos MJ, Cummings OW, Ferrell LD, Liu YC, Torbenson MS, Unalp-Arida A, Yeh M, McCullough AJ, Sanyal AJ. Design and validation of a histological scoring system for nonalcoholic fatty liver disease. *Hepatology* 2005; **41**: 1313-1321
25 **Falck-Ytter Y**, Younossi ZM, Marchesini G, McCullough AJ. Clinical features and natural history of nonalcoholic steatosis syndromes. *Semin Liver Dis* 2001; **21**: 17-26
26 **Neuschwander-Tetri BA**, Caldwell SH. Nonalcoholic steatohepatitis: summary of an AASLD Single Topic Conference. *Hepatology* 2003; **37**: 1202-1219
27 **Matteoni CA**, Younossi ZM, Gramlich T, Boparai N, Liu YC, McCullough AJ. Nonalcoholic fatty liver disease: a spectrum of clinical and pathological severity. *Gastroenterology* 1999; **116**: 1413-1419
28 **Teli MR**, James OF, Burt AD, Bennett MK, Day CP. The natural history of nonalcoholic fatty liver: a follow-up study. *Hepatology* 1995; **22**: 1714-1719
29 **Day CP**, James OF. Steatohepatitis: a tale of two "hits"? *Gastroenterology* 1998; **114**: 842-845
30 **Jaeschke H**, Gores GJ, Cederbaum AI, Hinson JA, Pessayre D, Lemasters JJ. Mechanisms of hepatotoxicity. *Toxicol Sci* 2002; **65**: 166-176
31 **Rust C**, Gores GJ. Locoregional management of hepatocellular carcinoma. Surgical and ablation therapies. *Clin Liver Dis* 2001; **5**: 161-173
32 **Canbay A**, Friedman S, Gores GJ. Apoptosis: the nexus of liver injury and fibrosis. *Hepatology* 2004; **39**: 273-278
33 **Jaeschke H**, Lemasters JJ. Apoptosis versus oncotic necrosis in hepatic ischemia/reperfusion injury. *Gastroenterology* 2003; **125**: 1246-1257
34 **Bantel H**, Lügering A, Heidemann J, Volkmann X, Poremba C, Strassburg CP, Manns MP, Schulze-Osthoff K. Detection of apoptotic caspase activation in sera from patients with chronic HCV infection is associated with fibrotic liver injury. *Hepatology* 2004; **40**: 1078-1087
35 **Wieckowska A**, Zein NN, Yerian LM, Lopez AR, McCullough AJ, Feldstein AE. In vivo assessment of liver cell apoptosis as a novel biomarker of disease severity in nonalcoholic fatty liver disease. *Hepatology* 2006; **44**: 27-33
36 **Que FG**, Gores GJ. Cell death by apoptosis: basic concepts and disease relevance for the gastroenterologist. *Gastroenterology* 1996; **110**: 1238-1243

S- Editor Liu Y **L- Editor** Mihm S **E- Editor** Lu W

PO Box 2345, Beijing 100023, China
www.wjgnet.com
wjg@wjgnet.com

World J Gastroenterol 2007 February 14; 13(6): 845-850
World Journal of Gastroenterology ISSN 1007-9327

Adherence and invasion of mouse-adapted *H pylori* in different epithelial cell lines

Mao-Jun Zhang, Fan-Liang Meng, Xiao-Yun Ji, Li-Hua He, Jian-Zhong Zhang

Mao-Jun Zhang, Fan-Liang Meng, Xiao-Yun Ji, Li-Hua He, Jian-Zhong Zhang, Department of Diagnostics, National Institute for Communicable Disease Control and Prevention, Chinese Center for Disease Control and Prevention, Beijing 102206, China
Supported by the National Natural Science Foundation of China, No. 30370078
Correspondence to: Dr. Jian-Zhong Zhang, Department of Diagnostics, National Institute for Communicable Disease Control and Prevention, Chinese Center for Disease Control and Prevention, PO Box 5, Changping, Beijing 102206, China. helico99@sina.com
Telephone: +86-10-61739456 Fax: +86-10-61730233
Received: 2007-01-14 Accepted: 2007-02-09

Abstract

AIM: To assess the adhesion and invasion abilities of different mouse adapted *H pylori* strains in different cell lines *in vitro* and investigate their effects on the virulence factors cagA and vacA.

METHODS: The adherence and invasion abilities of different *H pylori* strains in different epithelial cell lines were examined by the gentamycin protection assay. The null mutants of cagA and vacA were processed by direct PCR mutation method. The morphologic changes of different cell lines after *H pylori* attachment were examined by microscopy.

RESULTS: The densities of adherence to and invasion into cells *in vitro* were different from those in the mouse infection experiments. 88-3887 strain could invade and adhere to cells stronger than SS1 and X47. All tested strains had better adhering and invasive abilities in SCG-7901 cell. CagA and vacA minus mutants had the same invasion and adherent abilities as their wild types. In all strains and cell lines tested, only AGS cell had the significant hummingbird phenotype after inoculation with the 88-3887 wild-type.

CONCLUSION: Both the host cells and the bacteria play important parts in the invasion and adhesion abilities of *H pylori*. CagA and VacA are not related to the ability of invasion and adhesion of *H pylori* in different cell lines *in vitro*.

Key words: *H pylori*; Adherence; Invasion; Cell line

Zhang MJ, Meng FL, Ji XY, He LH, Zhang JZ. Adherence and invasion of mouse-adapted *H pylori* in different epithelial cell lines. *World J Gastroenterol* 2007; 13(6): 845-850

http://www.wjgnet.com/1007-9327/13/845.asp

INTRODUCTION

Infection with the human gastric pathogen *H pylori* can develop into chronic gastritis, peptic ulcer and gastric cancer[1-4]. Adhesion to the gastric epithelium and the host responses take the crucial role in the pathogenesis of *H pylori* infections.

Adherence is considered to be associated with both colonization and virulence properties of *H pylori*. A mouse infection model has been used to investigate the pathogenesis of *H pylori*[5-8]. Results from Dr. Berg. DE and colleagues suggested that different *H pylori* strains had gradient colonization abilities in various mouse cell lines *in vivo* (unpublished data). Studies at cellular levels showed *H pylori* induced the secretion of pro-inflammatory cytokines, cell proliferation, and apoptosis of epithelial cells and the cell lines were used as models for the investigation of the interaction between the bacteria and hosts *in vitro*[9-12]. There were proofs that *H pylori* were not present in the gastric epithelial cells but in the mucus layer overlying the gastric tissue[1,13]. However, there were also a number of biopsy studies[14-16] and cell culture infection models[17-21] that provided increasing evidence for the intracellular survival of *H pylori*. Internalization into the host cell should be considered a major strategy to evade the host immune response of the bacteria. Amieva *et al*[22] proved that the intercellular *H pylori* may be released to repopulate the extracellular environment again. It is well accepted that *H pylori* infection is hard to be eradicated in some cases, and triple drug therapy often fails to eliminate *H pylori* in infected patients[23-25].

In this study, the adherence and invasion abilities of 3 mouse-adapted *H pylori* strains, which colonized the mice at different densities in different epithelial cells lines, were assessed by gentamycin adherence and invasiveness assay. Moreover, to investigate whether the virulence factors cagA and vacA could affect these abilities, mutants in these genes were established to examine their capacities to adhere to epithelial cells and compared to their wild-type counterparts.

MATERIALS AND METHODS

Bacteria and culture condition

The backgrounds of 3 mouse passed *H pylori* strains are shown in Table 1. All these mouse passed strains were

kindly offered by Dr. Berg DE, (Washington University, School of Medicine, St. Louis, MO 63110). The mouse inoculation experiments were done with C57BL/6J IL-12 KO mouse by Dr Berg DE's lab and the results from all these 4 strains were obtained. 88-3887 is a mouse adapted strain parentally from *H pylori* 26695. So far, there has been no reported data on the mouse colonization capacity of 88-3887 cagA::cam and SS1 vacA::cam.

Wild type *H pylori* strains of SS1, X47 and 88-3887 were grown in an *H pylori* selective medium (Columbia Agar Base supplemented with 5% sheep blood and 0.25 mg/mL vancomycin, 0.2 mg/mL amphotericin B, 0.2 mg/mL polymyxin B and 0.3 mg/mL trimethoprim) and incubated at 37℃ in a microaerobic atmosphere containing 5% O_2, 10% CO_2 and 85% N_2. CagA and vacA null mutants (88-3887 cagA::cam, SS1 vacA::cam) were grown in an *H pylori* selective medium with 20 μg/mL chloramphenicol and cultured under the same condition as wild type strains.

Generation of H pylori allelic replacement mutants

The null mutants for cagA::cam and vacA::cam were generated by direct PCR method as described previously[26,27]. Chloramphenicol resistance cassette (cat) was amplified using primers C1 and C2 designated from the pBlueScript Ⅱ SK plasmid. The alleles in which cagA and vacA were replaced by cat were generated by the PCR method. The PCR products containing those ΔcagA (cagA::cam) and ΔvacA (vacA::cam) alleles were used to transform the wild-type *H pylori* strains 88-3887 and SS1 with selection for Camr (20 μg/mL). The primers for 88-3887 ΔcagA (88-3887 ΔcagA::cam) were cagA-P1, cagA-P2, cagA-P3 and cagA-P4. Primers for SS1 ΔvacA (SS1 ΔvacA::cam) mutant were vacA-P1, vacA-P2, vacA-P3 and vacA-P4. The sequences of the primers are listed in Table 2. All mutations were confirmed by specific PCR using cat, vacA and cagA genes.

Preparation of cell line cultures

AGS cells (ATCC CRL 1739, human gastric adenocarcinoma epithelial cell line), SGC-7901 cells (human gastric cancer cell line from laboratory collection), MDCK cells (ATCC CCL-34, Marbin-Darby canine kidney epithelial cell line) were seeded to generate 2×10^5 cells in RPMI 1640 medium supplemented with 10% FCS (Gibco BRL, Eggenstein, Germany) per well in 24-well tissue culture plates. The plates were incubated at 37℃ in 5% CO_2 for 24 h. The culture medium was replaced with fresh RPMI1640 medium without FCS for 2 h before the inoculation of bacteria.

Adherence and invasiveness assay

The 24 h cultured bacteria were harvested from plates with phosphate-buffered saline (PBS) and washed by centrifugation at 5000 r/min for 5 min at 4℃ 3 times. The pellets were suspended in PBS to 1 OD600 (approximately 108 CFU/mL), and 0.1 mL of this suspension was inoculated into each duplicate host cell wells to achieve a multiplicity of infection (MOI) of 100. As a control, 0.1 mL of PBS was added to each host cell lines. Infection was carried out at 37℃ in 5% CO_2 for 5 h. After 5 h infection, the monolayer was then washed 3 times with 1 mL RPMI1640 with 10% FCS medium and reincubated under the same conditions for another 2 h. Cell culture medium containing 25 mg/mL of gentamicin was added to each of the wells for the enumeration of intracellular bacteria (In preliminary experiments, 25 mg/mL of gentamicin could kill all *H pylori* isolates after a 2 h exposure and 0.1% saponin had no influence on *H pylori* culture compared with PBS). Following incubation, all monolayers (with or without gentamicin) were washed 5 times with RPMI 1640 and lysed with 0.1% saponin (Sigma cat#S-7900) in PBS. The suspensions were serial diluted. Both the intracellular bacteria and the total cell-associated bacteria were estimated by counting the number of CFU on *H pylori* selective plates. Results are expressed as the average from 3 independent experiments. Wild type *H pylori* strains and their mutants were inoculated into different cell lines respectively and mixed simultaneously. For the mix infection, the bacteria were counted on the normal selective medium and the selective medium with 20 μg/mL chloramphenicol separately.

Table 1 Background of mouse passed *H pylori* strains

H pylori strains	CagA	Tissue tropism	CFU/g of mouse stomach tissue
SS1	+	Antrum	10^6
X47	-	Corpus	10^6
88-3887	+	[1]None	10^4

[1]Same distribution densities in antrum and corpus.

Table 2 Primers for null mutant of cagA and vacA of *H pylori*

Primer	Sequence (5'-3')
C1	GATATAGATTGAAAAGTGGAT
C2	TTATCAGTGCGACAAACTGGG
CagA-P1	CCCAAGCTGATCAGAGTGAG
CagA-P2	ATCCACTTTTCAATCTATATCGGCTTCGTTAGTCATTG TTTCTCC
CagA-P3	CCCAGTTTGTCGCACTGATAAGGTGGTTTCCAAAAAT CTTAAAGGATT
CagA-P4	GGTTGCACGCATTTTCCCTTAATC
VacA-P1	CTACGGTGTATGATGACGCTCA
VacA-P2	ATCCACTTTTCAATCTATATCCACAAAGGGTGCGAC TTTAGAC
VacA-P3	CCCAGTTTGTCGCACTGATAAGATCAATCAAGCTTG AATTTCA
VacA-P4	TTAGAAACTATACCTCATTCCTAAA

Image capture

After the co-culture of bacteria and different cells for 5 h, the monolayer cells were washed by PBS and the images were obtained under the microscope (Olympus BX 51).

RESULTS

Invasion and adherence abilities of H pylori strains in different cell lines

SS1, X47 strains had higher capacities to colonize the mice than 88-3887 but the intensities of their invasion and adherence in the cell lines were quite different. 88-3887

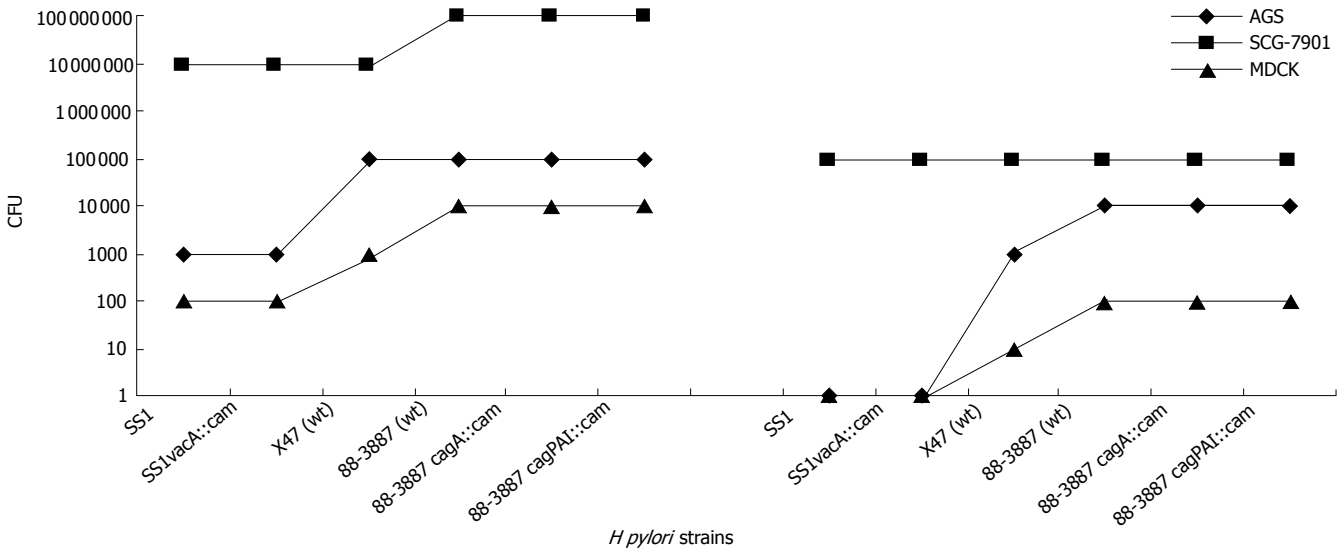

Figure 1 Levels of adherence and invasion of *H pylori* in different cell lines. Bacteria were added to AGS cell monolayer at an MOI of 100 for 5 h at 37℃ in a humidified atmosphere with 5% CO_2. Data were obtained by adherence and invasiveness assays in three independent experiments and are expressed as CFU per well of AGS cells. The left side 3 refrangible lines indicate the ability of the adherence in 3 different cell lines. The right sides indicate the invasiveness ability in the 3 cell lines. Values represent the mean CFU of viable bacteria recovered per well of a 24-well tissue culture tray.

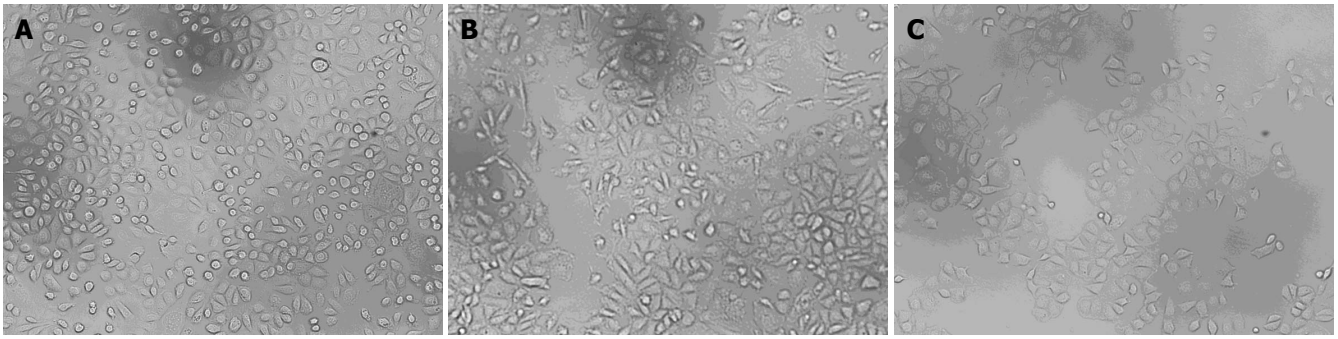

Figure 2 Images showing morphologic changes induced by *H pylori* attachment. After co-culture of the bacteria with different cells for 5 h, the monolayer AGS cells were washed with PBS and the images were captured by microscopic Olympus BX51. **A**: AGS cell; **B**: The hummingbird/scattering appearance of AGS after being attached with 88-3887 wild-type, 5 h; **C**: AGS with *H pylori* 88-3887 cagA minus mutant (88-3887 cagA::cam), 5 h.

could invade and adhere to the cells better than SS1 and X47. The intensity of SS1 was lowest among the three tested strains. Each of the three *H pylori* strains had the highest adherent and invasive ability in the SCG-7901 cell. 88-3887 ΔcagA::cam and SS1 ΔvacA::cam had the same invasiveness and adherence ability as their wild type counterparts, respectively. The effects of different bacteria in different cell lines are shown in Figure 1.

Morphologic changes of different cell lines after inoculation with H pylori

Cell morphology was examined under the microscope after 5 h co-culture. Fifty percent AGS cells became elongated like the hummingbird phenotype after attachment with 88-3887 wild type strain, while there were no such hummingbird like changes in AGS cell after inoculation with 88-3887 ΔcagA::cam. There were no significant hummingbird like phenotype in AGS after attachment with X47, SS1 and SS1vacA::cam strains. MDCK cells were scattered and slightly elongated after inoculation with 88-3887, 88-3887 ΔcagA::cam, SS1 and SS1 ΔvacA::cam strains. After inoculation with X47 wild type strains, MDCK cells changed to round shape. The attachment of the 5 tested *H pylori* strains caused the SCG-7901 cells to become scattered, and there was no significant difference in phenotypic changes between different strains. The morphologic images are shown in Figure 2.

DISCUSSION

H pylori is one of the most prevalent and persistent infectious agents in humans[28-30]. Adhesion is considered to be a major process for *H pylori* to colonize the host tissue and cause diseases. Intimate attachment to the host cells could facilitate the bacterium's colonization, efficient delivery of effecter proteins such as cagA and vacA from the bacteria to the host cell and gain of nutrients from the environment. Bacteria with better adherence properties would colonize the host at higher densities and cause severe damage of the host[31,32]. Although *H pylori* have generally been considered as an extracellular pathogen, a number of *in vitro* infection experiments and biopsy

examinations have shown that it is capable of occasionally entering mammalian cells[33]. This penetration action may be one of the mechanisms for survival of the bacteria. In the present study, all tested *H pylori* strains adhered to SCG-7901, AGS and MDCK cells in a gradient way and the densities were 10^{7-8}, 10^{3-5} and 10^{2-4} CFU/mL, respectively. The intensities of the adhering ability in different cells in vitro were quite different from those in the mouse infection models *in vivo* and the *H pylori* adherence capacities in human cells were stronger than that in the canine kidney epithelial cells. According to this study, the invasive capacity was always consistent with the adhesion ability in all the tested cell lines, the higher the adhesion capacity, the better the invasion ability. Our results are consistent with previous evidence of the invasion ability in mammalian cells of *H pylori*[22,34] and it may imply the varied attachment mechanisms among different host species during *H pylori* infection. It also supports the view that both the host and bacterial factors mediate the adhesion and invasion of *H pylori*.

In the present study, the gentamicin protection assay was relatively simple, reproducible and measureable. Bacteria were determined after recovery from an additional 2 h incubation with gentamicin in the medium. The internalized bacteria were protected since the gentamicin could not penetrate the mammalian cell membranes. All the calculated data were repeated 3 times and each host cell had duplicate wells for each *H pylori* strain for validation.

CagA is present in some *H pylori* strains with enhanced virulence, and has been identified as an important risk factor for development of severe gastric diseases. *H pylori* strains are divided into two groups named type Ⅰ and type Ⅱ strains, based on whether they express cagA or not[35,36]. It was previously described that cagA was an effector protein of *H pylori* that was translocated *via* a type Ⅳ secretion system into gastric epithelial cells, interacted with different components in the host cell signal transduction pathways and the actin binding proteins, which ultimately affect the cytoskeletal organization[37-40]. This study showes no correlation between the presence of cagA with the ability of adhesion and invasion of *H pylori*. The only hummingbird response of AGS cell was induced by 88-3887 wild type strain but not the cagA minus mutant. This result is consistent with the previous conclusion that cagA plays a crucial role in the host cytoskeleton change. However, neither SS1 (cagA+) nor X47 (cagA-) could induce the same morphologic changes in the tested cells. Apart from AGS with the 88-3887 wild type, the other tested host cells attached with *H pylori* presented the under stress phenotypic changes such as cell scattering, elongation, and roundness in shape. These induced changes were not necessarily associated with cagA or vacA. It has been discovered that translocated cagA forms a physical complex with tyrosine phosphatase SHP-2, which plays an important role in the signal transduction pathway of the cell skeleton. According to the sequences constituting the SHP-2 binding site, cagA proteins can be sub-classified into East Asian and Western types, which have different binding and transforming activities[41,42]; while SS1 and 88-3887 all belong to the Western type. However, this could not explain why SS1 did not induce the same phenotypic change in AGS as 88-3887. SS1 also harbors cagA and could achieve high level mouse colonization. But this is controversial to the fact that the cag PAI in this strain is incomplete, as it lacks one open reading frame in the so-called 'left half' of the island[43,44]. On the other hand, we had no evidence to support that the gene defect SS1 strain caused different effects on AGS phenotypic changes from that of 88-3887 strain. Dana *et al*[45] reported that mouse adapted strains had a reduced capacity to induce inflammatory responses in AGS cells and suggests that such bacteria are more easily to colonize mice. The present results may indicate that the effector function of cagA in the host cell cytoskeletal rearrangement is pivotal and bacterium and host dependent. In different hosts, different *H pylori* strains invade *via* alternate receptor mechanisms, and various signal transduction pathways. The high degree genetic diversities of *H pylori* may be generated depending on the geographic origin or the ethnic origin of the host.

VacA cytotoxin is also considered to be an important virulence factor in *H pylori*, since it induces large cytoplasmic vacuoles in cultured mammalian cells. VacA is present in all *H pylori* strains and has been shown to be related to the colonization and intracellular survival of the bacteria[46,47]. This study shows that vacA has no effect on the adhesion and invasion abilities of *H pylori*. Our results are conflict with Terebiznik's data but consistent with Amieva *et al*[22]'s observation that the internalization of *H pylori* did not require vacA or cagA[48]. The phenotypic changes of the host cells attached with SS1 vacA minus mutant were the same as the wild type *H pylori* strains.

In summary, this study assesses the adherence and invasiveness abilities of different mouse adapted *H pylori* strains in different mammalian cell lines. The results imply that both the host-genetic and the microbial factors are involved in the development of the pathogenic infection outcome. VacA and cagA constitute important virulence factors of *H pylori* and both are delivered into the host cells depending on the intimate contact between bacteria and the gastric epithelial cells. This study suggests that neither vacA nor cagA is associated with the adhesion and invasion abilities of *H pylori* in different mammalian cell models. The phenotypic changes induced by *H pylori* are also host and bacterium dependent.

ACKNOWLEDGMENTS

We are grateful to Dr. Douglas E Berg for his kind donation of the pBlueScript Ⅱ SK plasmid and the entire mouse adapted *H pylori* strains.

REFERENCES

1 **Marshall BJ**, Warren JR. Unidentified curved bacilli in the stomach of patients with gastritis and peptic ulceration. *Lancet* 1984; **1**: 1311-1315

2 **Graham DY**, Lew GM, Evans DG, Evans DJ, Klein PD. Effect of triple therapy (antibiotics plus bismuth) on duodenal ulcer healing. A randomized controlled trial. *Ann Intern Med* 1991; **115**: 266-269

3 **Parsonnet J**, Hansen S, Rodriguez L, Gelb AB, Warnke RA, Jellum E, Orentreich N, Vogelman JH, Friedman GD.

Helicobacter pylori infection and gastric lymphoma. *N Engl J Med* 1994; **330**: 1267-1271
4 **Williams MP**, Pounder RE. Helicobacter pylori: from the benign to the malignant. *Am J Gastroenterol* 1999; **94**: S11-S16
5 **Taylor JM**, Ziman ME, Huff JL, Moroski NM, Vajdy M, Solnick JV. Helicobacter pylori lipopolysaccharide promotes a Th1 type immune response in immunized mice. *Vaccine* 2006; **24**: 4987-4994
6 **Tan S**, Fraley CD, Zhang M, Dailidiene D, Kornberg A, Berg DE. Diverse phenotypes resulting from polyphosphate kinase gene (ppk1) inactivation in different strains of Helicobacter pylori. *J Bacteriol* 2005; **187**: 7687-7695
7 **Suto H**, Zhang M, Berg DE. Age-dependent changes in susceptibility of suckling mice to individual strains of Helicobacter pylori. *Infect Immun* 2005; **73**: 1232-1234
8 **Akada JK**, Ogura K, Dailidiene D, Dailide G, Cheverud JM, Berg DE. Helicobacter pylori tissue tropism: mouse-colonizing strains can target different gastric niches. *Microbiology* 2003; **149**: 1901-1909
9 **Crabtree JE**, Farmery SM, Lindley IJ, Figura N, Peichl P, Tompkins DS. CagA/cytotoxic strains of Helicobacter pylori and interleukin-8 in gastric epithelial cell lines. *J Clin Pathol* 1994; **47**: 945-950
10 **Day AS**, Su B, Ceponis PJ, Jones NL, Yau E, Sieveking D, Sherman PM. Helicobacter pylori infection induces interleukin-18 production in gastric epithelial (AGS) cells. *Dig Dis Sci* 2004; **49**: 1830-1835
11 **Ledig S**, Wagner S, Manns MP, Beil W, Athmann C. Role of the receptor-mediated apoptosis in Helicobacter pylori in gastric epithelial cells. *Digestion* 2004; **70**: 178-186
12 **Karabay G**, Nacar A, Can F, Demirbilek M, Bacanli D, Take G, Yazici AC. Apoptosis and proliferation in gastric epithelium due to Helicobacter pylori: an immunohistochemical and ultrastructural study. *Acta Gastroenterol Belg* 2006; **69**: 191-196
13 **Molyneux AJ**, Harris MD. Helicobacter pylori in gastric biopsies--should you trust the pathology report? *J R Coll Physicians Lond* 1993; **27**: 119-120
14 **el-Shoura SM**. Helicobacter pylori: I. Ultrastructural sequences of adherence, attachment, and penetration into the gastric mucosa. *Ultrastruct Pathol* 1995; **19**: 323-333
15 **Engstrand L**, Graham D, Scheynius A, Genta RM, El-Zaatari F. Is the sanctuary where Helicobacter pylori avoids antibacterial treatment intracellular? *Am J Clin Pathol* 1997; **108**: 504-509
16 **Noach LA**, Rolf TM, Tytgat GN. Electron microscopic study of association between Helicobacter pylori and gastric and duodenal mucosa. *J Clin Pathol* 1994; **47**: 699-704
17 **Bukholm G**, Tannaes T, Nedenskov P, Esbensen Y, Grav HJ, Hovig T, Ariansen S, Guldvog I. Colony variation of Helicobacter pylori: pathogenic potential is correlated to cell wall lipid composition. *Scand J Gastroenterol* 1997; **32**: 445-454
18 **Evans DG**, Evans DJ, Graham DY. Adherence and internalization of Helicobacter pylori by HEp-2 cells. *Gastroenterology* 1992; **102**: 1557-1567
19 **Petersen AM**, Blom J, Andersen LP, Krogfelt KA. Role of strain type, AGS cells and fetal calf serum in Helicobacter pylori adhesion and invasion assays. *FEMS Immunol Med Microbiol* 2000; **29**: 59-67
20 **Segal ED**, Falkow S, Tompkins LS. Helicobacter pylori attachment to gastric cells induces cytoskeletal rearrangements and tyrosine phosphorylation of host cell proteins. *Proc Natl Acad Sci USA* 1996; **93**: 1259-1264
21 **Wilkinson SM**, Uhl JR, Kline BC, Cockerill FR. Assessment of invasion frequencies of cultured HEp-2 cells by clinical isolates of Helicobacter pylori using an acridine orange assay. *J Clin Pathol* 1998; **51**: 127-133
22 **Amieva MR**, Salama NR, Tompkins LS, Falkow S. Helicobacter pylori enter and survive within multivesicular vacuoles of epithelial cells. *Cell Microbiol* 2002; **4**: 677-690
23 **Axon AT**. Eradication of Helicobacter pylori. *Scand J Gastroenterol Suppl* 1996; **214**: 47-53; discussion 57-60
24 **Belhoussine-Idrissi L**, Boedeker EC. Helicobacter pylori infection: treatment. *Curr Opin Gastroenterol* 2002; **18**: 26-33
25 **Vakil N**, Go MF. Treatment of Helicobacter pylori infection. *Curr Opin Gastroenterol* 2000; **16**: 32-39
26 **Zeng X**, He LH, Yin Y, Zhang MJ, Zhang JZ. Deletion of cagA gene of Helicobacter pylori by PCR products. *World J Gastroenterol* 2005; **11**: 3255-3259
27 **Jeong JY**, Mukhopadhyay AK, Dailidiene D, Wang Y, Velapatiño B, Gilman RH, Parkinson AJ, Nair GB, Wong BC, Lam SK, Mistry R, Segal I, Yuan Y, Gao H, Alarcon T, Brea ML, Ito Y, Kersulyte D, Lee HK, Gong Y, Goodwin A, Hoffman PS, Berg DE. Sequential inactivation of rdxA (HP0954) and frxA (HP0642) nitroreductase genes causes moderate and high-level metronidazole resistance in Helicobacter pylori. *J Bacteriol* 2000; **182**: 5082-5090
28 **Montecucco C**, Rappuoli R. Living dangerously: how Helicobacter pylori survives in the human stomach. *Nat Rev Mol Cell Biol* 2001; **2**: 457-466
29 **Bourke B**, Jones NL. Pathogenesis of Helicobacter pylori infection. *Curr Opin Gastroenterol* 2001; **17**: 24-29
30 **Magalhães Queiroz DM**, Luzza F. Epidemiology of Helicobacter pylori infection. *Helicobacter* 2006; **11** Suppl 1: 1-5
31 **Sokurenko EV**, Courtney HS, Maslow J, Siitonen A, Hasty DL. Quantitative differences in adhesiveness of type 1 fimbriated Escherichia coli due to structural differences in fimH genes. *J Bacteriol* 1995; **177**: 3680-3686
32 **Sokurenko EV**, Chesnokova V, Dykhuizen DE, Ofek I, Wu XR, Krogfelt KA, Struve C, Schembri MA, Hasty DL. Pathogenic adaptation of Escherichia coli by natural variation of the FimH adhesin. *Proc Natl Acad Sci USA* 1998; **95**: 8922-8926
33 **Petersen AM**, Krogfelt KA. Helicobacter pylori: an invading microorganism? A review. *FEMS Immunol Med Microbiol* 2003; **36**: 117-126
34 **Kwok T**, Backert S, Schwarz H, Berger J, Meyer TF. Specific entry of Helicobacter pylori into cultured gastric epithelial cells via a zipper-like mechanism. *Infect Immun* 2002; **70**: 2108-2120
35 **Cabral MM**, Mendes CM, Castro LP, Cartelle CT, Guerra J, Queiroz DM, Nogueira AM. Apoptosis in Helicobacter pylori gastritis is related to cagA status. *Helicobacter* 2006; **11**: 469-476
36 **Xiang Z**, Censini S, Bayeli PF, Telford JL, Figura N, Rappuoli R, Covacci A. Analysis of expression of CagA and VacA virulence factors in 43 strains of Helicobacter pylori reveals that clinical isolates can be divided into two major types and that CagA is not necessary for expression of the vacuolating cytotoxin. *Infect Immun* 1995; **63**: 94-98
37 **Bagnoli F**, Buti L, Tompkins L, Covacci A, Amieva MR. Helicobacter pylori CagA induces a transition from polarized to invasive phenotypes in MDCK cells. *Proc Natl Acad Sci USA* 2005; **102**: 16339-16344
38 **Higashi H**, Yokoyama K, Fujii Y, Ren S, Yuasa H, Saadat I, Murata-Kamiya N, Azuma T, Hatakeyama M. EPIYA motif is a membrane-targeting signal of Helicobacter pylori virulence factor CagA in mammalian cells. *J Biol Chem* 2005; **280**: 23130-23137
39 **Selbach M**, Moese S, Backert S, Jungblut PR, Meyer TF. The Helicobacter pylori CagA protein induces tyrosine dephosphorylation of ezrin. *Proteomics* 2004; **4**: 2961-2968
40 **Higashi H**, Nakaya A, Tsutsumi R, Yokoyama K, Fujii Y, Ishikawa S, Higuchi M, Takahashi A, Kurashima Y, Teishikata Y, Tanaka S, Azuma T, Hatakeyama M. Helicobacter pylori CagA induces Ras-independent morphogenetic response through SHP-2 recruitment and activation. *J Biol Chem* 2004; **279**: 17205-17216
41 **Higashi H**, Tsutsumi R, Muto S, Sugiyama T, Azuma T, Asaka M, Hatakeyama M. SHP-2 tyrosine phosphatase as an intracellular target of Helicobacter pylori CagA protein. *Science* 2002; **295**: 683-686
42 **Higashi H**, Tsutsumi R, Fujita A, Yamazaki S, Asaka M, Azuma T, Hatakeyama M. Biological activity of the Helicobacter pylori virulence factor CagA is determined by variation in the tyrosine phosphorylation sites. *Proc Natl Acad Sci USA* 2002; **99**: 14428-14433
43 **Tomb JF**, White O, Kerlavage AR, Clayton RA, Sutton GG, Fleischmann RD, Ketchum KA, Klenk HP, Gill S, Dougherty

BA, Nelson K, Quackenbush J, Zhou L, Kirkness EF, Peterson S, Loftus B, Richardson D, Dodson R, Khalak HG, Glodek A, McKenney K, Fitzegerald LM, Lee N, Adams MD, Hickey EK, Berg DE, Gocayne JD, Utterback TR, Peterson JD, Kelley JM, Cotton MD, Weidman JM, Fujii C, Bowman C, Watthey L, Wallin E, Hayes WS, Borodovsky M, Karp PD, Smith HO, Fraser CM, Venter JC. The complete genome sequence of the gastric pathogen Helicobacter pylori. *Nature* 1997; **388**: 539-547

44 **Salama N**, Guillemin K, McDaniel TK, Sherlock G, Tompkins L, Falkow S. A whole-genome microarray reveals genetic diversity among Helicobacter pylori strains. *Proc Natl Acad Sci USA* 2000; **97**: 14668-14673

45 **Philpott DJ**, Belaid D, Troubadour P, Thiberge JM, Tankovic J, Labigne A, Ferrero RL. Reduced activation of inflammatory responses in host cells by mouse-adapted Helicobacter pylory isolates. *Cell Microbiol* 2002; **4**: 285-296

46 **Cover TL**. The vacuolating cytotoxin of Helicobacter pylori. *Mol Microbiol* 1996; **20**: 241-246

47 **Figueiredo C**, Machado JC, Yamaoka Y. Pathogenesis of Helicobacter pylori Infection. *Helicobacter* 2005; **10** Suppl 1: 14-20

48 **Terebiznik MR**, Vazquez CL, Torbicki K, Banks D, Wang T, Hong W, Blanke SR, Colombo MI, Jones NL. Helicobacter pylori VacA toxin promotes bacterial intracellular survival in gastric epithelial cells. *Infect Immun* 2006; **74**: 6599-6614

S- Editor Wang J **L- Editor** Zhu LH **E- Editor** Lu W

PO Box 2345, Beijing 100023, China
www.wjgnet.com
wjg@wjgnet.com

World J Gastroenterol 2007 February 14; 13(6): 851-857
World Journal of Gastroenterology ISSN 1007-9327

BASIC RESEARCH

Proteasome inhibition-induces endoplasmic reticulum dysfunction and cell death of human cholangiocarcinoma cells

Yucel Ustundag, Steven F Bronk, Gregory J Gores

Yucel Ustundag, Steven F Bronk, Gregory J Gores, Mayo Clinic College of Medicine, Rochester, MN 55905, United States
Supported by NIH grants DK63947 (to GJG) and the Mayo and Palumbo Foundations
Correspondence to: Gregory J Gores, MD, Professor of Medicine, Mayo Clinic College of Medicine, 200 First Street SW, Rochester, Minnesota 55905, United States. gores.gregory@mayo.edu
Telephone: +1-507-2840686 Fax: +1-507-2840762
Received: 2006-10-12 Accepted: 2006-12-09

Abstract

AIM: To determine if proteasome inhibition induces apoptosis in human cholangiocarcinoma cells, and if so, to elucidate the cellular mechanisms.

METHODS: Studies were performed in the human KMCH, KMBC, and Mz-ChA-1 cholangiocarcinoma, and normal rat cell lines. MG132, a peptide aldehyde, which inhibits the chymotrypsin-like activity of the proteaosome was employed for this study. Apoptosis was assessed morphologically by 4′-6-Diamidino-2-phenylindole (DAPI) nuclear staining and fluorescence microscopy. Mitochondrial membrane potential was examined using a fluorescent unquenching assay. Ultrastructural changes during cell death were examined using transmission electron microscopy (TEM). Caspase 3/7 activity was assessed using an enzymatic-based fluorescent assay. Cytosolic-free calcium concentrations were measured using Fura-2 and digitized fluorescent microscopy.

RESULTS: MG132, a proteasome inhibitor, induced apoptosis in all the cholangiocarcinoma cell lines examined. In contrast, minimal cytotoxicity was observed in normal rat cholangiocytes. Apoptosis was time- and -concentration-dependent. There was no change in the mitochondrial membrane potential between treated and untreated cells. Ultrastructural examination by transmission electron microscopy displayed the classic features of apoptosis, but in addition, there was also dramatic vacuolization of the endoplasmic reticulum (ER). Unexpectedly, no increase in caspase 3/7 activity was observed in MG132 treated cells, nor did the pancaspase inhibitor, Q-VD-OPh prevent cell death. The protein synthesis inhibitor, cycloheximide, blocked apoptosis induced by proteosome inhibitor indicating that ER dysfunction was dependent upon the formation of new proteins.

CONCLUSION: Proteosome inhibition induces ER dysfunction and caspase-independent cell death selectively in human cholangiocarcinoma cells. Proteasome inhibitors warrant evaluation as anticancer agents for the treatment of human cholangiocarcinoma.

Key words: MG132; Cholangiocarcinoma; Proteosome; Apoptosis; Calcium

Ustundag Y, Bronk SF, Gores GJ. Proteasome inhibition-induces endoplasmic reticulum dysfunction and cell death of human cholangiocarcinoma cells. *World J Gastroenterol* 2007; 13(6): 851-857

http://www.wjgnet.com/1007-9327/13/851.asp

INTRODUCTION

Cholangiocarcinoma is a malignant disease arising from the epithelial cells, termed cholangiocytes, lining the intra and extrahepatic bile duct. Unfortunately, the incidence of disease is increasing in many Western countries[1,2]. Surgery and liver transplantation are the only curative treatment options; however, disease recurrence is common even after ostensibly curative surgical procedures[3,4]. Non-surgical therapy is palliative and there is no proven medical therapy for this neoplasm. Thus, cholangiocarcinoma is a devastating disease which frequently causes death. Additional therapies are needed for the treatment of this cancer. Cholangiocarcinoma has many phenotypic similarities with the hematologic malignancy multiple myeloma. For example, both neoplasms are IL-6 dependent, evade apoptosis by overexpression of the Bcl-2 family protein Mcl-1, and are associated with genetic silencing of the tumor suppressor gene *p16*[5,6]. Recently, targeted inhibition of the proteasome has been shown to be effective anticancer therapy for multiple myeloma[7]. In contrast, the effect of proteasome inhibition as therapy for cholangiocarcinoma is unknown.

Proteasomes are complex macromolecular structures which enzymatically degrade ubiquinated proteins[8]. The barrel shaped 20S proteasome is a very large ATP dependent proteolytic complex which has 4 rings that enclose a central hollow where proteolysis takes place[9]. Its 2 central β-rings contain multiple chymotrypsin-like, two trypsin-like and two caspase-like activities. The outer 2 alpha rings encircle a small opening through

which polypeptide substrates enter. These alpha rings are essential for assembly of the whole particle. The ubiquitin-proteasome pathway plays an important role in signal transduction, transcriptional regulation and response to stress[10,11]. Inhibition of this pathway can trigger cell cycle arrest at G1-S and G2-M phases of the cell cycle and apoptotic pathways[12]. Although proteasome inhibition may be predicted to have nonspecific cytotoxicity, malignant cells are much more sensitive to the proapoptotic effects of proteasome inhibition than normal cells[13]. The potential explanation for this selectivity appears to be due to the fact that cancer cells have more defective proteins accumulating at much higher rates than normal cells. This increases their dependency on optimal proteasome function to dispose of these proteins. Proteosome failure leads to the accumulation of these proteins which are toxic to the cell.

In cancer cells, the accumulation of proteins, due to proteasome inhibition induces cell death by multiple mechanisms. Loss of proteasome function can lead to accumulation of pro-apoptotic mediators which trigger the cellular apoptotic machinery[14,15]. For example proteasome inhibition leads to cellular accumulation of the proapoptotic BH3 domain only protein of the Bcl-2 family, Bim[15]. Bim dependent cell death is associated with mitochondrial dysfunction and activation of intracellular caspases, cysteine proteases which trigger canonical apoptotic programs[15]. By preventing activation of the pro-survival transcription factor, NF-κB, proteasome inhibition can also trigger apoptosis[16]. More recently, proteasome inhibitors have also been associated with cell death by inducing endoplasmic reticulum (ER) dysfunction[17]. Thus, the mechanisms of cell death by proteasome inhibition are complex and likely cell type specific.

The overall objective of this study was to determine if proteasome inhibition induces apoptosis in cholangiocarcinoma cell lines. The results demonstrate that proteasome inhibition induces caspase-independent cell death of human cholangiocarcinoma cell lines. This cell death pathway is associated with structural abnormalities of the ER. Proteasome inhibition appears to induce ER dysfunction and cell death in human cholangiocarcinoma cells.

MATERIALS AND METHODS

Reagents

MG132 was from Calbiochem (San Diego CA). Bortezomib was obtained from the Mayo Clinic Formulary (Rochester, MN). DMEM (Life Technologies, Gaithersburg, MD), fetal bovine serum (Summit Biotechnology, Fort Collins, CO), Penicillin-streptomycin (Bio-Whittaker, Walkersville, MD), gentamycin (GIBCO BRL, Life Technologies, Grand Island, NY), and O-VD-OPh (Enzyme Systems, Livermore, CA), ECL (Amersham, Arlington Heights, IL), BAPTA, AM (Invitrogen, Eugene, OR) staurosporine (Sigma Chemicals Co, St Louis, MO) and cycloheximide (Sigma Chemicals Co, St Louis, MO) were purchased as indicated.

Cell lines

The human cholangiocarcinoma cell lines KMCH-1, KMBC, Mz-ChA-1, and normal rat cholangiocyte cell line were cultured in Dulbecco's modified Eagle medium supplemented with 10% fetal bovine serum, penicillin G (100 000 U/L), streptomycin (100 mg/L) and gentamycin (100 mg/dL) as described previousl[18-20]. The normal rat cholangiocyte cell line was a generous gift from Nicholas F. LaRusso, Mayo Clinic, Rochester, MN[21]. Cells were maintained in a humidified incubator under an atmosphere containing 10% CO_2 at 37℃.

Quantitation of apoptosis

Morphologic features of apoptosis were quantified by assessing the characteristic nuclear changes of apoptosis (i.e., chromatin condensation and nuclear fragmentation) using the nuclear binding dye 4',6-diamino-2-phenylindole dihydrochloride (Sigma chemicals, St. Louis, MO) and fluorescent microscopy[22].

Caspase 3/7 assay

Cells were cultured in 96 well plates (Corning, NY, NY). Cellular caspase activation was assessed using the Apo-One™ homogeneous caspase-3/7 Assay according to the supplier's instructions (the Apo-ONE™ Homogenous Caspase 3/7 activity kit-Promega Corporation, Madison WI, USA). The Apo-One™ Reagent was added directly to the cells in a 1:1 (Apo-One™ Reagent: cell culture medium) ratio of reagent to sample. After gently mixing by shaking at 300-500 r/min on a plate shaker for 30 s, the fluorescence of each well was measured at an excitation wave length of 485 and an emission wavelength of 530 nm using a fluorescent plate reader[23].

Transmission electron microscopy

Cultured KMCH cells were fixed using Triump's fixative as previously described[24]. Briefly, the media was aspirated and replaced with equal volume of Trump's fixative (1% glutaraldehyde and 4% formaldehyde in 0.1 mol/L phosphate buffer, pH 7.2). Specimens were post-fixed with 1% osmium tetroxide in 0.1 M cacodylate buffer and embedded in Spurr's resin. Thin sections (70 nm) were cut and placed on copper grids and double stained with uranyl acetate and lead citrate. The tissue was examined and photographed with a transmission electron microscope (1200 EXII; JEOL, Peabody, MA) operating at 60 kV. Electron micrographs of cholangiocarcinoma cells each were examined by two masked observers.

Measurement of cytosolic free calcium (Ca_i^{++})

Ca_i^{++} was measured in cultured KMCH cells loaded with fura-2 using multiparameter digitized videomicroscopy as previously described by us[25]. The microscope was a Zeiss IM-35 inverted florescence microscope (Thormwood, NY) equipped with phase contrast optics. A low light intensified video camera (Model 66, MTI-Dage, Michigan City, IN) collected florescent images which were digitized with a QVG/AFA-123 video acquisition and display board set (Imaging technologies, Woburn, MA) operating in a MicroPDP 11/23 computer (Digital Equipment Corporation, Maynard, MA). Ca_i^{++} was quantified by ratio imaging of fura-2

fluorescence excited at 340 and 380 nm. Fluorescence was taken through a 395 nm dichroic reflector and a 470-550 emission filter. By using a Kd of 224 nmol/L for the fura-2-Ca_i^{++} complex, the mean values of pixel ratios for each cell were converted to Ca_i^{++} as described previously by Gyrinkiewicz *et al*[26]. Rmin, Rmax and sfb2/sb2 values were calculated from measurements with fura-2 free acid solutions in capillary tubes (Vitro Dynamics, Inc., Rockaway, NJ) set on the microscope stage[27]. To test whether the involvement of Ca^{2+} homeostasis could be the key to the specific vulnerability of cholangiocarcinoma cells to proteasome inhibition, we co-treated KMCH cell cultures with an intracellular Ca^{2+} chelator, BAPTA-AM (5 μmol/L) with MG132 for 24 h.

Quantification of mitochondrial membrane potential

The mitochondrial membrane potential in KMCH cells was measured by using a fluorescence unquenching assay as previously described in detail by us[28]. This assay is based on the concept of resonance energy transfer between the mitochondrial membrane potential-sensitive dyes tetramethylrhodamine ethyl ester and mitotracker green. Cellular fluorescence was depicted using the multiparameter digitized fluorescence microscopy system described above and quantified by a software program (Universal Imaging Co) as previously described elsewhere in detail[29].

Immunocytochemistry for cellular NFκB localization

Cells, cultured on collagen-coated glass cover slips, were fixed with 4% paraformaldehyde. Cells were then permeabilized with 0.5% Triton-X in PBS and blocked with PBS containing 1% bovine serum albumin. To ascertain the cellular localization, cytoplasmic *vs* nuclear, for the p65 subunit of NFκB, cells were next incubated with a polyclonal rabbit anti-p65 immunoglobulin G (sc-372, Santa Cruz Biotechnology, Santa Cruz, CA) in blocking buffer (1:1500) at 4℃ overnight. After washing, Cy3-conjugated goat anti-rabbit Ig (Jackson Immuno Research Labs, West Grove, PA) in blocking buffer (1:1000) was added for one hour at room temperature. Cells were then imaged by confocal microscopy (Zeiss LSM 510, Carl Zeiss, Inc.,Thornwood, NJ), as described previously in detail[30].

Statistical analysis

All data represent at least three independent experiments and are expressed as the mean ± SE unless otherwise indicated. All of the data were expressed as means from three individual experiments. Differences between groups were determined by using the Student's *t*-test for unpaired observations.

RESULTS

Proteasome inhibition induces apoptosis selectively in human cholangiocarcinoma cells

MG132 was employed to inhibit proteasome proteolytic activity**.** Proteasome inhibition by MG132 induced apoptosis in all three human cholangiocarcinoma cells. Apoptosis was time-dependent and was maximal (65% ± 2%) at a MG132 concentration of 1 μmol/L at 24 h. Apoptosis was also concentration-dependent as maximal apoptosis (90%) was observed at 24 h in KMCH cells treated with 10 μmol/L MG132 (Figure 1A, B, and C). In contrast, minimal cytotoxicity was observed in normal rat cholangiocytes treated with 10 μmol/L MG132 (Figure 1B and C). As assessed by nuclear morphology, dead cells had the classic features of apoptosis (Figure 1C). We selected the KMCH cells for further mechanistic studies as this cell has been frequently employed for studies of human cholangiocarcinoma[31].

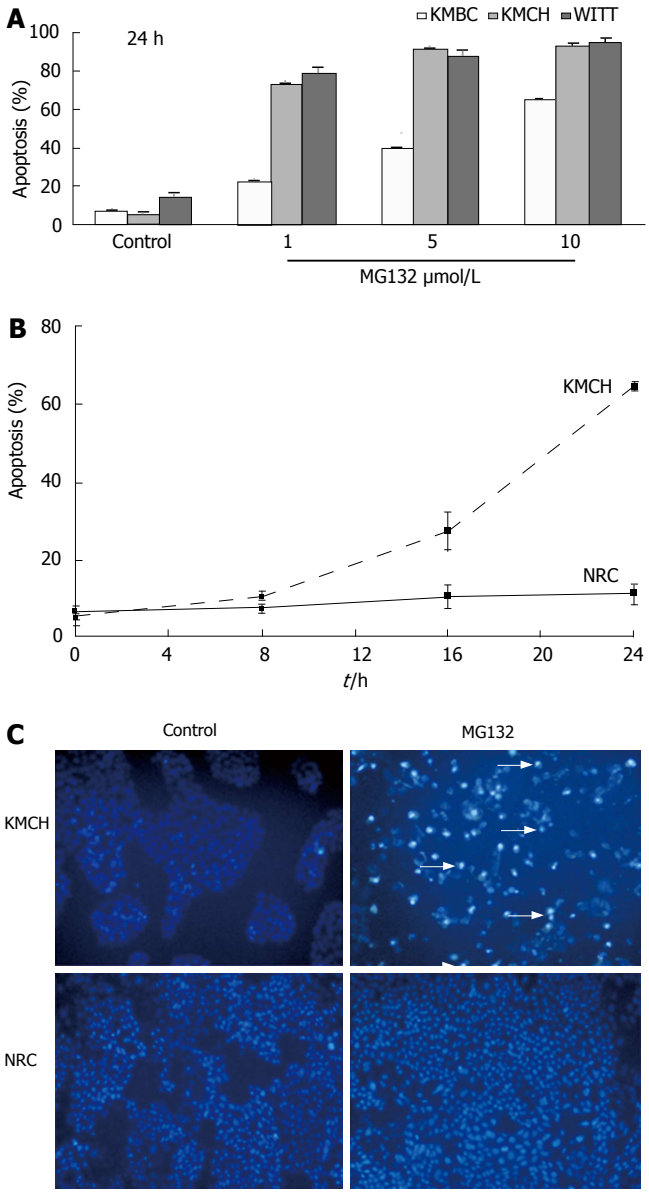

Figure 1 Morphologic assessment of MG132 induced death in KMCH, KMBC and Mz-ChA-1 cholangiocarcinoma and normal rat cholangiocytes (NRC) cell lines. **A**: MG132 induces apoptosis in all cholangiocarcionoma cell lines was maximal (> 90%) with a MG132 concentration of 10 (μmol/L); **B**: MG132 (1 μmol/L) induced apoptosis in the human KMCH cholangiocarcinoma cell line, but not in the nontransformed NRC cells; **C**: Apoptosis had the classic nuclear appearance as assessed by DAPI staining and fluorescence microscopy.

Proteasome inhibition induces caspase-independent cell death

In many models, but not all, apoptosis is caspase-dependent. To determine if MG132 mediated apoptosis is caspase-

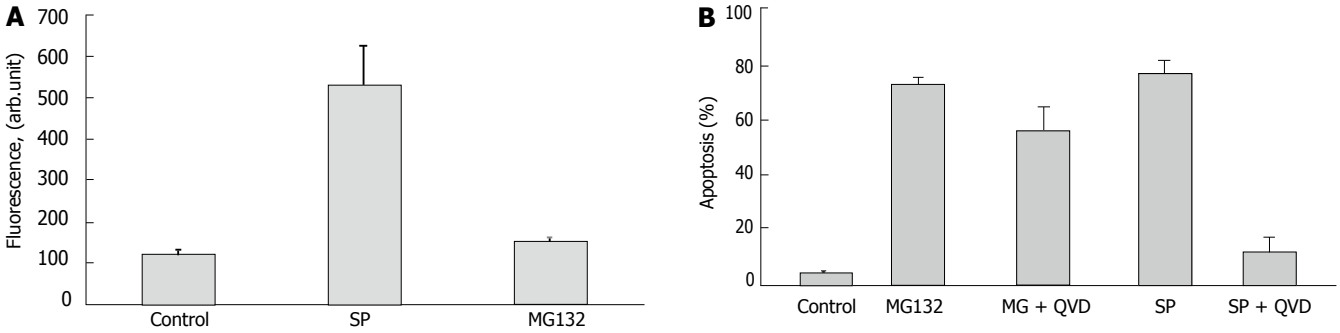

Figure 2 Caspase 3/7 activity and apoptosis in MG132 and staurosporine (SP) treated KMCH cells **A**: Cells were treated with MG132 1 μmol/L and SP 5 μmol/L for 16 h. Caspase 3/7 activity was increased SP cells ($P < 0.05$). In contrast, caspase activity was not different for MG132 treated cells *vs* controls. **B**: Cell death was assessed by morphologic criteria using DAPI and fluorescence microscopy. Cells were treated with SP or MG1321 for 24 h in the absence or presence of the pancaspase inhibitor, QVD at 5 μmol/L. Note QVD blocked staurosporine, but not MG132, induced apoptosis. Data represent the mean ± SE of three separate studies.

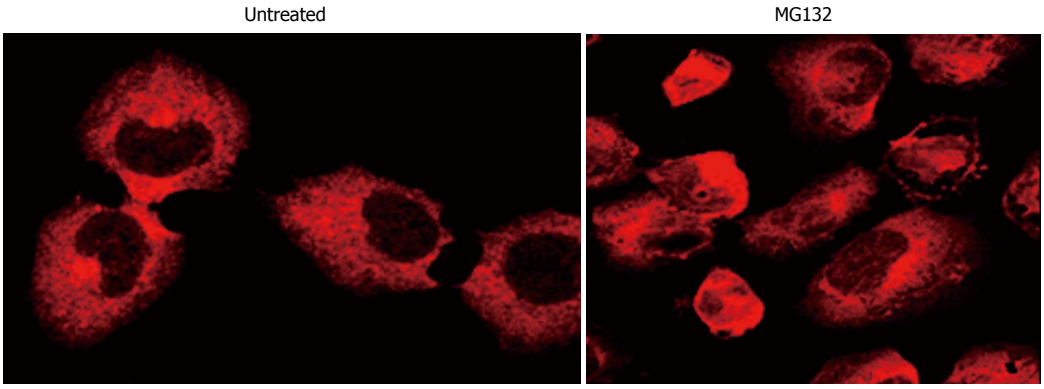

Figure 3 Immunofluorescence for cell localization of the p65 NF-κB subunit. Cellular compartmentation of the p65 NF-κB subunit was examined in KMCH cells by confocal laser scanning microscopy. The p65 NFκB subunit was completely cytoplasmic in untreated KMCH cholangiocarcinoma cells; its localization also remained cytoplasmic following exposure to MG132 (1 μmol/L) for 24 h.

dependent in KMCH cells, we initially measured caspase activity (Figure 2A). Unexpectedly, an increase in caspase 3/7 activity was not observed in MG132 treated cells, although a 5-fold increase was readily observed in staurosporine treated cells, an agent which induces caspase-dependent cell death[32]. Consistent with this observation, MG132 mediated apoptosis was also not inhibited by the pancaspase inhibitor QVD-OPh[33]. In contrast, QVD-(0Ph) readily inhibited staurosporine mediated apoptosis (Figure 2B). Thus, in human cholangiocarcinoma cells, proteasome inhibition is associated with caspase- independent cell death.

NFκB is not constitutively activated in cholangiocarcinoma cells

Several effects of proteasome inhibitors including apoptosis seem to be mediated through inhibition of NF-κB by blocking the degradation of I-κB[34]. Since this transcription factor is constitutively activated in many malignant cells, we examined NF-κB activation in cholangiocarcinoma by im munocytochemistry[35,36]. NF-κB nuclear immunoreactivity was not identified in cholangiocarcinoma cells (Figure 3). Thus, NF-κB is not constitutively activated in this cell type. Therefore, proteasome inhibition cannot induce apoptosis by blocking this pathway in this cell type.

Proteasome inhibition induces an ER stress pathway of apoptosis

To further examine the mechanisms of cell by MG132 in these cells, ultrastructural studies of the MG132 treated cells were performed. Both in MG132 and bortezomib treated cells, prominent ER vacuolization was observed. This observation was extremely pronounced and readily apparent in all apoptotic cells (Figure 4A). Thus, proteasome inhibition is associated with morphologic evidence for ER dysfunction. The specificity of proteasome inhibition in this cell type was verified by examining mitochondrial function. The mitochondrial membrane potential is a sensitive indicator of mitochondrial function. In contrast to the ER structure and function alterations, proteasome inhibition by MG132 did not perturb the mitochondrial membrane potential. Indeed, integrated mitochondrial membrane fluorescence (average fluorescent intensity x pixels above background) was observed to be 168736 ± 17699 and 143269 ± 8859 in untreated and treated cells following 24 h of incubation, respectively (P = NS). Thus, proteasome inhibition by MG132 induces significant ER structural alterations in the absence of mitochondrial dysfunction.

Because the ER stress pathway of cell death can be associated with sustained increases in cytosolic-free Ca^{++}, we next measured cytosolic-free Ca_i^{++} in MG132 treated KMCH cells. Sustained, but very modest, increases in cytosolic-free Cai^{++} were observed after treatment with MG132 and bortezomib. Cytosolic-free Cai^{++} concentrations increased only 2 fold (129 ± 3 nmol/L to 244 ± 33 nmol/L with 1 μmol/L MG132 and 292 ± 54 nmol/L with 1 μmol/L bortezomib, $P < 0.05$). (Figure

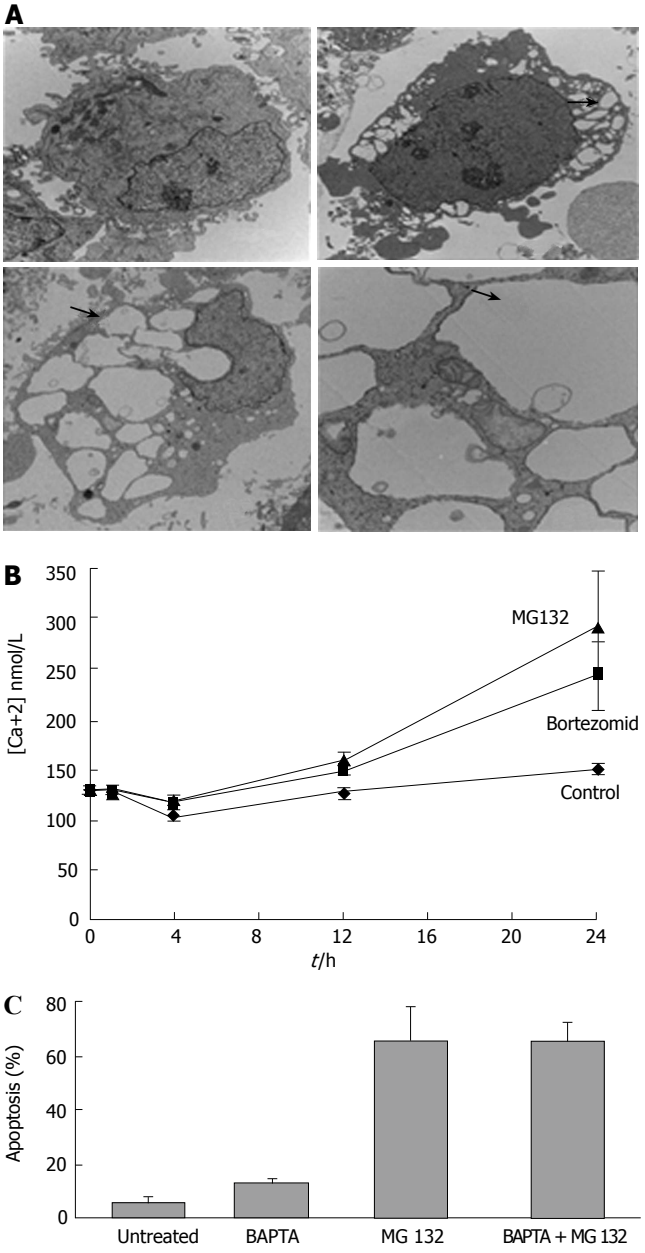

Figure 4 **A**: Morphologic features of apoptosis induced by proteasome inhibitors, MG132 and bortezomib in KMCH cells. On the left up panel, transmission electron microscopic appearance of untreated cholangiocarcinoma cell is depicted (bar = 0.5 μm). In the right up panel, exposure to MG132 (1 μmol/L) for 24 h results in a distinctly dilated ER (arrowhead) (bar = 2 μm) . On the bottom-left panel, similar results are observed with MG 132 (0.5 μmol/L) for 24 h (arrowhead) (bar = 2 μm). Note apoptotic morphology also characterized by condensation of heterochromatin; On the bottom-right panel, high magnification image of cytoplasm shows dilated ER (arrowhead) (bar = 2 μm); **B**: Ca_i^{++} increases following treatment with proteasome inhibitors in KMCH cells. The time course of Ca_i^{++} changes is demonstrated. At 24 h, Ca_i^{++} levels were significantly increased in MG132 1 mol/L and Bortezomib 1 μmol/L treated cells than untreated KMCH cells ($P < 0.05$); **C**: Intracellular Ca_i^{++} chelation with BAPTA does not prevent apoptosis by MG132.

4B). Co-treatment of BAPTA-AM, a potent calcium-chelator, with MG132 did not reduce MG132 induced apoptosis (Figure 4C). Taken together, proteasome inhibition induces ER dysfunction and apoptosis in human cholangiocarcinoma cells. This ER dysfunction is characterized by morphologic changes in the ER and modest elevations in cytosolic-free calcium. However, the latter is unlikely to be the mediator of cell death.

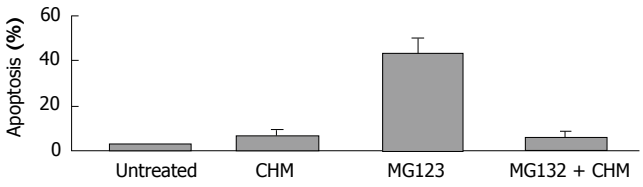

Figure 5 The translational inhibitor cycloheximide inhibits MG132 induced cell death in KMCH cells. The translational inhibitor, cycloheximide (CHM) 50 μmol/L, completely inhibited MG132 1 μmol/L induced apoptosis in KMCH cells co-treated with both agents for 24 h. Cell death was assessed by morphologic criteria using DAPI and fluorescence microscopy. Data represent the mean ± SE of three separate studies.

Cycloheximide inhibits MG132 induced apoptosis

Proteasome inhibitors allow cellular protein synthesis to continue while they block degradation of damaged or unfolded proteins. Accumulation of unfolded proteins in the ER can trigger ER dysfunction and cell death. To ascertain if this is the mechanism of proteasome inhibitor mediated cell death in cholangiocarcinoma cells, the cells were co-incubated with MG132 plus cycloheximide, a protein synthesis inhibitor[37]. Cycloheximide remarkably blocked MG132 induced apoptosis (7.5 *vs* 64.5%, $P < 0.05$) (Figure 5). This observation suggests active protein synthesis is necessary for the cytotoxicity of proteasome inhibition in human cholangiocarcinomas.

DISCUSSION

The principal findings of this study relate to the mechanism of cell death in human cholangiocarcinoma cells by proteasome inhibition. The results demonstrated that (1) proteasome inhibition induces apoptosis in cholangiocarcinoma cells; (2) the cell death is caspase-independent; and (3) is associated with morphologic changes of the ER; and (4) the cell death is dependent upon protein synthesis. The results support the further exploration of proteasome inhibition as a therapeutic strategy for human cholangiocarcinoma. The proteasome inhibitor MG132 induced time- and concentration-dependent cell death in all cholangiocarcinoma cell lines examined. These data suggest proteasome inhibitors are potential anti-cancer drugs for this neoplasm. This class of agents is currently employed for the treatment of multiple myeloma. Although, the efficacy of proteasome inhibitors for the treatment of solid tumors has been disappointing, this may not be necessarily true for cholangiocarcinoma. Despite the fact that cholangiocarcinoma is an epithelial cell tumor, it has many phenotypic features similar to multiple myeloma including interleukin 6 dependent survival signaling pathways[38]. From this prospective, proteasome inhibitors may be anti-cancer drugs for cholangiocarcinoma as well.

Proteasome inhibitors have been reported to trigger caspase-dependent apoptosis by caspase-3 and 8 activation in multiple myeloma and chronic lymphocytic leukemia cells[16,39]. The caspase dependent apoptosis can be induced by preventing proteasome degradation of Bim, a potent proapoptotic member of the Bcl-2 family of proteins. Bim accumulation then triggers the mitochondrial pathway of

apoptosis. Nevertheless, MG132 induced apoptosis was found to be caspase independent in cholangiocarcinoma cell lines as an increase of caspase-3/7 activity was not observed in our studies. Likewise, there was no inhibition of apoptosis by a pancaspase inhibitor. Consistent with the lack of caspase activity, the mitochondrial membrane potential was also unperturbed in treated cells. This observation suggests proteasome inhibition triggers an alternative cell death pathway in these cells. Proteasome inhibitors have several anti-tumoral mechanisms. One of them is by inactivation of the transcription factor, NF-κB. Indeed, inhibition of NF-κB is a prominent mechanism by which proteasome inhibition induces apoptosis. In response to cellular stress; I-κB is degraded by proteasomes and NF-κB released activating transcription of genes for several factors including apoptosis inhibitors[16]. However, our current study demonstrated that NF-κB is not constitutively active in KMCH, KMBC and Mz-ChA-1 cholangiocarcinoma cell lines and, therefore, proteosome inhibitors can not induce cell death in these cells by blocking NF-κB activation.

The ER can be involved as a primary target organelle in apoptosis. Secretory proteins or proteins for plasma membrane are modified and acquire their correct folding conformation in the ER. Proteins that are unable to fold properly in the ER are degraded by the proteasome. It is proposed that proteasome inhibition can cause the accumulation of misfolded proteins, resulting in excessive ER stress[17]. Transformed cells are particularly sensitive to the ER cell death pathway[40]. Indeed, our ultrastructural studies demonstrated marked alterations of ER morphology by proteasome inhibition. Similar morphologic findings have also been reported in glioma cells undergoing apoptosis after treatment with proteasome inhibitor, bortezomib[41]. The protein synthesis inhibitor cycloheximide did reduce cell death by the proteasome inhibitor MG132. This observation suggests that accumulation of misfolded or unfolded proteins following protein inhibition likely contributes to the ER morphologic changes and cell death observed in the current study. The ability of MG132 to induce cell death in the cells by a selective mechanism is of therapeutic interest. Drugs such as bortezomib warrant further attention as therapeutic agents in the treatment of cholangiocarcinoma.

ACKNOWLEDGMENTS

The superb secretarial service of Erin Bungum is gratefully acknowledged.

REFERENCES

1 **Patel T**. Increasing incidence and mortality of primary intrahepatic cholangiocarcinoma in the United States. *Hepatology* 2001; **33**: 1353-1357
2 **Gores GJ**. Cholangiocarcinoma: current concepts and insights. *Hepatology* 2003; **37**: 961-969
3 **Jarnagin WR**, Fong Y, DeMatteo RP, Gonen M, Burke EC, Bodniewicz BS J, Youssef BA M, Klimstra D, Blumgart LH. Staging, resectability, and outcome in 225 patients with hilar cholangiocarcinoma. *Ann Surg* 2001; **234**: 507-517; discussion 517-519
4 **Meyer CG**, Penn I, James L. Liver transplantation for cholangiocarcinoma: results in 207 patients. *Transplantation* 2000; **69**: 1633-1637
5 **San-Miguel J**, García-Sanz R, López-Pérez R. Analysis of methylation pattern in multiple myeloma. *Acta Haematol* 2005; **114** Suppl 1: 23-26
6 **Yang B**, House MG, Guo M, Herman JG, Clark DP. Promoter methylation profiles of tumor suppressor genes in intrahepatic and extrahepatic cholangiocarcinoma. *Mod Pathol* 2005; **18**: 412-420
7 **Johnson JR**, Temple R. Food and Drug Administration requirements for approval of new anticancer drugs. *Cancer Treat Rep* 1985; **69**: 1155-1159
8 **Lee DH**, Goldberg AL. Proteasome inhibitors: valuable new tools for cell biologists. *Trends Cell Biol* 1998; **8**: 397-403
9 **Tanaka K**, Yoshimura T, Kumatori A, Ichihara A, Ikai A, Nishigai M, Kameyama K, Takagi T. Proteasomes (multi-protease complexes) as 20 S ring-shaped particles in a variety of eukaryotic cells. *J Biol Chem* 1988; **263**: 16209-16217
10 **Adams J**, Palombella VJ, Elliott PJ. Proteasome inhibition: a new strategy in cancer treatment. *Invest New Drugs* 2000; **18**: 109-121
11 **Adams J**. Preclinical and clinical evaluation of proteasome inhibitor PS-341 for the treatment of cancer. *Curr Opin Chem Biol* 2002; **6**: 493-500
12 **Hershko A**, Ciechanover A. The ubiquitin system. *Annu Rev Biochem* 1998; **67**: 425-479
13 **Richardson PG**, Barlogie B, Berenson J, Singhal S, Jagannath S, Irwin D, Rajkumar SV, Srkalovic G, Alsina M, Alexanian R, Siegel D, Orlowski RZ, Kuter D, Limentani SA, Lee S, Hideshima T, Esseltine DL, Kauffman M, Adams J, Schenkein DP, Anderson KC. A phase 2 study of bortezomib in relapsed, refractory myeloma. *N Engl J Med* 2003; **348**: 2609-2617
14 **Luciano F**, Jacquel A, Colosetti P, Herrant M, Cagnol S, Pages G, Auberger P. Phosphorylation of Bim-EL by Erk1/2 on serine 69 promotes its degradation via the proteasome pathway and regulates its proapoptotic function. *Oncogene* 2003; **22**: 6785-6793
15 **Nikrad M**, Johnson T, Puthalalath H, Coultas L, Adams J, Kraft AS. The proteasome inhibitor bortezomib sensitizes cells to killing by death receptor ligand TRAIL via BH3-only proteins Bik and Bim. *Mol Cancer Ther* 2005; **4**: 443-449
16 **Mitsiades N**, Mitsiades CS, Poulaki V, Chauhan D, Fanourakis G, Gu X, Bailey C, Joseph M, Libermann TA, Treon SP, Munshi NC, Richardson PG, Hideshima T, Anderson KC. Molecular sequelae of proteasome inhibition in human multiple myeloma cells. *Proc Natl Acad Sci USA* 2002; **99**: 14374-14379
17 **Fribley A**, Zeng Q, Wang CY. Proteasome inhibitor PS-341 induces apoptosis through induction of endoplasmic reticulum stress-reactive oxygen species in head and neck squamous cell carcinoma cells. *Mol Cell Biol* 2004; **24**: 9695-9704
18 **Murakami T**, Yano H, Maruiwa M, Sugihara S, Kojiro M. Establishment and characterization of a human combined hepatocholangiocarcinoma cell line and its heterologous transplantation in nude mice. *Hepatology* 1987; **7**: 551-556
19 **Yano H**, Maruiwa M, Iemura A, Mizoguchi A, Kojiro M. Establishment and characterization of a new human extrahepatic bile duct carcinoma cell line (KMBC). *Cancer* 1992; **69**: 1664-1673
20 **Knuth A**, Gabbert H, Dippold W, Klein O, Sachsse W, Bitter-Suermann D, Prellwitz W, Meyer zum Büschenfelde KH. Biliary adenocarcinoma. Characterisation of three new human tumor cell lines. *J Hepatol* 1985; **1**: 579-596
21 **Vroman B**, LaRusso NF. Development and characterization of polarized primary cultures of rat intrahepatic bile duct epithelial cells. *Lab Invest* 1996; **74**: 303-313
22 **Kwo P**, Patel T, Bronk SF, Gores GJ. Nuclear serine protease activity contributes to bile acid-induced apoptosis in hepatocytes. *Am J Physiol* 1995; **268**: G613-G621
23 **Niles A**, Humpal-Winter J. The Apo-One Homogeneous Caspase-3/7 Assay: A simplified "solution" for apoptosis detection. *Cell Notes* 2001; **2**: 2-3
24 **Komuro A**, Hodge DO, Gores GJ, Bourne WM. Cell death during corneal storage at 4 degrees C. *Invest Ophthalmol Vis Sci* 1999; **40**: 2827-2832

25 **Groskreutz JL**, Bronk SF, Gores GJ. Ruthenium red delays the onset of cell death during oxidative stress of rat hepatocytes. *Gastroenterology* 1992; **102**: 1030-1038
26 **Grynkiewicz G**, Poenie M, Tsien RY. A new generation of Ca2+ indicators with greatly improved fluorescence properties. *J Biol Chem* 1985; **260**: 3440-3450
27 **Spivey JR**, Bronk SF, Gores GJ. Glycochenodeoxycholate-induced lethal hepatocellular injury in rat hepatocytes. Role of ATP depletion and cytosolic free calcium. *J Clin Invest* 1993; **92**: 17-24
28 **Fujii Y**, Johnson ME, Gores GJ. Mitochondrial dysfunction during anoxia/reoxygenation injury of liver sinusoidal endothelial cells. *Hepatology* 1994; **20**: 177-185
29 **Gee KR**, Brown KA, Chen WN, Bishop-Stewart J, Gray D, Johnson I. Chemical and physiological characterization of fluo-4 Ca(2+)-indicator dyes. *Cell Calcium* 2000; **27**: 97-106
30 **Ribeiro A**, Bronk SF, Roberts PJ, Urrutia R, Gores GJ. The transforming growth factor beta(1)-inducible transcription factor TIEG1, mediates apoptosis through oxidative stress. *Hepatology* 1999; **30**: 1490-1497
31 **Chiorean MV**, Guicciardi ME, Yoon JH, Bronk SF, Kaufmanns SH, Gores GJ. Imatinib mesylate induces apoptosis in human cholangiocarcinoma cells. *Liver Int* 2004; **24**: 687-695
32 **Caserta TM**, Smith AN, Gultice AD, Reedy MA, Brown TL. Q-VD-OPh, a broad spectrum caspase inhibitor with potent antiapoptotic properties. *Apoptosis* 2003; **8**: 345-352
33 **Tamaoki T**, Nomoto H, Takahashi I, Kato Y, Morimoto M, Tomita F. Staurosporine, a potent inhibitor of phospholipid/Ca++dependent protein kinase. *Biochem Biophys Res Commun* 1986; **135**: 397-402
34 **Hideshima T**, Chauhan D, Richardson P, Mitsiades C, Mitsiades N, Hayashi T, Munshi N, Dang L, Castro A, Palombella V, Adams J, Anderson KC. NF-kappa B as a therapeutic target in multiple myeloma. *J Biol Chem* 2002; **277**: 16639-16647
35 **Ni H**, Ergin M, Huang Q, Qin JZ, Amin HM, Martinez RL, Saeed S, Barton K, Alkan S. Analysis of expression of nuclear factor kappa B (NF-kappa B) in multiple myeloma: downregulation of NF-kappa B induces apoptosis. *Br J Haematol* 2001; **115**: 279-286
36 **Bargou RC**, Emmerich F, Krappmann D, Bommert K, Mapara MY, Arnold W, Royer HD, Grinstein E, Greiner A, Scheidereit C, Dörken B. Constitutive nuclear factor-kappaB-RelA activation is required for proliferation and survival of Hodgkin's disease tumor cells. *J Clin Invest* 1997; **100**: 2961-2969
37 **Park J**, Tadlock L, Gores GJ, Patel T. Inhibition of interleukin 6-mediated mitogen-activated protein kinase activation attenuates growth of a cholangiocarcinoma cell line. *Hepatology* 1999; **30**: 1128-1133
38 **Wettstein FO**, Noll H, Penman S. Effect of Cycloheximide on Ribosomal Aggregates Engaged in Protein Synthesis In Vitro. *Biochim Biophys Acta* 1964; **87**: 525-528
39 **Duechler M**, Linke A, Cebula B, Shehata M, Schwarzmeier JD, Robak T, Smolewski P. In vitro cytotoxic effect of proteasome inhibitor bortezomib in combination with purine nucleoside analogues on chronic lymphocytic leukaemia cells. *Eur J Haematol* 2005; **74**: 407-417
40 **Linder S**, Shoshan MC. Lysosomes and endoplasmic reticulum: targets for improved, selective anticancer therapy. *Drug Resist Updat* 2005; **8**: 199-204
41 **Wagenknecht B**, Hermisson M, Groscurth P, Liston P, Krammer PH, Weller M. Proteasome inhibitor-induced apoptosis of glioma cells involves the processing of multiple caspases and cytochrome c release. *J Neurochem* 2000; **75**: 2288-2297

S- Editor Wang J **L- Editor** Glaser SS **E- Editor** Lu W

PO Box 2345, Beijing 100023, China
www.wjgnet.com
wjg@wjgnet.com

World J Gastroenterol 2007 February 14; 13(6): 858-865
World Journal of Gastroenterology ISSN 1007-9327

BASIC RESEARCH

Pancreatic carcinoma coexisting with chronic pancreatitis versus tumor-forming pancreatitis: Diagnostic utility of the time-signal intensity curve from dynamic contrast-enhanced MR imaging

Yoshitsugu Tajima, Tamotsu Kuroki, Ryuji Tsutsumi, Ichiro Isomoto, Masataka Uetani, Takashi Kanematsu

Yoshitsugu Tajima, Tamotsu Kuroki, Ryuji Tsutsumi, Takashi Kanematsu, Department of Surgery, Nagasaki University Graduate School of Biomedical Sciences, Japan
Ichiro Isomoto, Masataka Uetani, Department of Radiology and Radiation Biology, Nagasaki University Graduate School of Biomedical Sciences, Japan
Correspondence to: Yoshitsugu Tajima, MD, Department of Surgery, Nagasaki University Graduate School of Biomedical Sciences, 1-7-1 Sakamoto, Nagasaki 852-8501, Japan. ytajima@net.nagasaki-u.ac.jp
Telephone: +81-9-58497316 Fax: +81-9-58497319
Received: 2006-10-25 Accepted: 2006-12-23

Abstract

AIM: To evaluate the ability of the time-signal intensity curve (TIC) of the pancreas obtained from dynamic contrast-enhanced magnetic resonance imaging (MRI) for differentiation of focal pancreatic masses, especially pancreatic carcinoma coexisting with chronic pancreatitis and tumor-forming pancreatitis.

METHODS: Forty-eight consecutive patients who underwent surgery for a focal pancreatic mass, including pancreatic ductal carcinoma (n = 33), tumor-forming pancreatitis (n = 8), and islet cell tumor (n = 7), were reviewed. Five pancreatic carcinomas coexisted with longstanding chronic pancreatitis. The pancreatic TICs were obtained from the pancreatic mass and the pancreatic parenchyma both proximal and distal to the mass lesion in each patient, prior to surgery, and were classified into 4 types according to the time to a peak: 25 s and 1, 2, and 3 min after the bolus injection of contrast material, namely, type-Ⅰ, Ⅱ, Ⅲ, and Ⅳ, respectively, and were then compared to the corresponding histological pancreatic conditions.

RESULTS: Pancreatic carcinomas demonstrated type-Ⅲ (n = 13) or Ⅳ (n = 20) TIC. Tumor-forming pancreatitis showed type-Ⅱ (n = 5) or Ⅲ (n = 3) TIC. All islet cell tumors revealed type-Ⅰ. The type-Ⅳ TIC was only recognized in pancreatic carcinoma, and the TIC of carcinoma always depicted the slowest rise to a peak among the 3 pancreatic TICs measured in each patient, even in patients with chronic pancreatitis.

CONCLUSION: Pancreatic TIC from dynamic MRI provides reliable information for distinguishing pancreatic carcinoma from other pancreatic masses, and may enable us to avoid unnecessary pancreatic surgery and delays in making a correct diagnosis of pancreatic carcinoma, especially, in patients with longstanding chronic pancreatitis.

Key words: Pancreatic carcinoma; Chronic pancreatitis; Focal pancreatic mass; Tumor-forming pancreatitis; Differential diagnosis; Dynamic magnetic resonance imaging; Time-signal intensity curve

Tajima Y, Kuroki T, Tsutsumi R, Isomoto I, Uetani M, Kanematsu T. Pancreatic carcinoma coexisting with chronic pancreatitis versus tumor-forming pancreatitis: The diagnostic utility of the time-signal intensity curve from dynamic contrast-enhanced MR imaging. *World J Gastroenterol* 2007; 13(6): 858-865

http://www.wjgnet.com/1007-9327/13/858.asp

INTRODUCTION

The differential diagnosis between carcinoma and benign lesion in the pancreas is extremely important because surgical resection offers the only chance of a cure in patients with pancreatic carcinoma or, conversely, may result in unnecessary risk of morbidity and mortality for benign lesions. Recent advances in imaging techniques have enabled us to precisely detect pancreatic carcinoma, however, it still remains difficult to distinguish chronic pancreatitis from this dismal pancreatic malignancy because chronic pancreatitis occasionally presents as a focal pancreatic swelling or mass with similar clinical and radiologic features to pancreatic carcinoma[1-3]. To complicate this issue even further, chronic pancreatitis may develop into pancreatic carcinoma[4-7], and also pancreatic carcinoma may develop obstructive chronic pancreatitis secondary to pancreatic ductal obstruction[2,8,9].

Both pancreatic carcinoma and chronic pancreatitis

possess a large degree of fibrosis[10-13], which is associated with a gradual progressive enhancement on contrast-enhanced computed tomography (CT) and dynamic magnetic resonance imaging (MRI)[2,3,14,15], making the distinction of these entities difficult. We recently demonstrated a time-signal intensity curve (TIC) of the pancreas obtained from dynamic contrast-enhanced MRI to be a reliable and non-invasive monitoring technique for a precise evaluation of pancreatic fibrosis[16]. In this study, we investigated the ability of the pancreatic TIC from dynamic MRI to differentiate pancreatic carcinoma from other focal pancreatic masses, especially in patients with chronic pancreatitis.

MATERIALS AND METHODS

We evaluated 48 consecutive patients who underwent surgery for focal pancreatic masses due to focal solid tumors or focal enlargement of the pancreas, between March 1999 and May 2006. The pancreatic masses with cystic components, such as cystadenocarcinoma, intraductal papillary-mucinous neoplasm, solid-pseudopapillary tumor, or pseudocyst, were excluded. The patients ranged in age from 45 to 82 years, with a mean of 65 years. There were 30 men and 18 women. From the clinical and radiologic findings, 34 patients were suspected of having pancreatic carcinoma, 7 of having focal chronic pancreatitis (so-called tumor-forming pancreatitis), and 7 of having islet cell tumor. The surgical interventions consisted of a pancreaticoduodenectomy (PD, n = 13), a pylorus-preserving pancreaticoduodenectomy (PPPD, n = 18), a duodenum-preserving pancreatic head resection (DPPHR, n = 1), a middle pancreatectomy (MP, n = 2), a distal pancreatectomy (DP, n = 13), and a hepaticojejunostomy together with biopsies of the pancreas (n = 1). The postoperative histological evaluations of the surgical specimens revealed the pancreatic masses to be pancreatic ductal carcinoma in 33, tumor-forming pancreatitis in 8, and an islet cell tumor in 7.

All 48 patients received dynamic contrast-enhanced MRI of the pancreas prior to surgery. The pancreatic MRI was conducted by using the 1.5-T superconducting system (SIGNA Horizon LXTM; GE Medical Systems, Milwaukee, WI). We used a fat-suppressed three-dimensional fast spoiled gradient re-called echo sequence with the following imaging parameters: TR/TE, 6.0-6.1/1.3-1.4 msec; flip angle, 20°; section thickness, 6-8 mm; no intersection gap; matrix, 256 × 160; 1 excitation; field of view, 32-36 cm. The dynamic series comprised 5 individual dynamic images, obtained before and 25 s and 1, 2 and 3 min after the rapid bolus injection of 0.1 mmol of meglumine gadopentetate (Magnevist®; Schering, Berlin, Germany)/kg of body weight. The contrast medium was administered intravenously at approximately 3 mL/s followed by flushing with 20 mL saline solution. The original MRI data were then loaded onto a workstation, and the regions of interest (ROI) were placed at 3 different parts of the pancreas in each patient, i.e., the pancreatic mass and the non-tumorous pancreatic parenchyma both proximal (head-sided) and distal (tail-sided) to the mass lesion. The ROI ranged in size from 0.2 to 1 cm^2. The pancreatic TIC was then generated as a percentage increase in the signal intensity (SI), according to the following enhancement formula: (SIpost-SIpre)/SIpre × 100, where SIpre and SIpost represent the pre- and post-contrast SIs, respectively. [16]The patterns of pancreatic TIC were classified into 4 types (Figure 1): type-Ⅰ, characterized by a rapid rise to a peak (25 s after injection of contrast material) followed by a rapid decline; type-Ⅱ, with a slow rise to a peak (1 min after administration of contrast material) followed by a slow decline; and type-Ⅲ or Ⅳ, with an even slower rise to a peak (2 or 3 min after the administration of contrast material) followed by a slow decline or plateau.

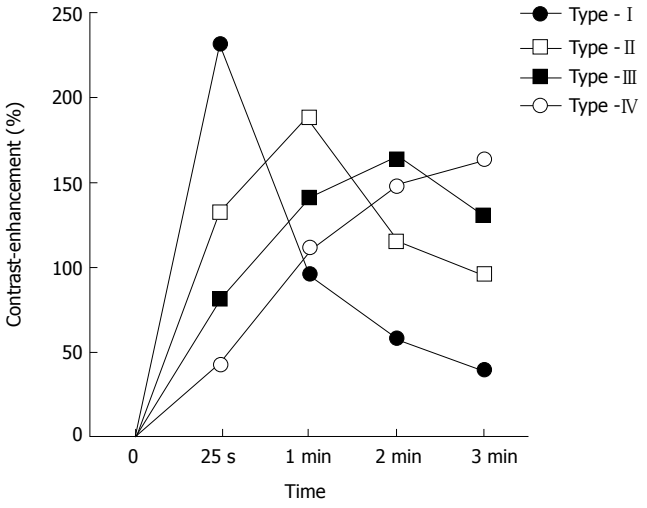

Figure 1 Patterns of the time-signal intensity curve (TIC) from dynamic contrast-enhanced magnetic resonance imaging of the pancreas.

A retrospective review of the preoperative pancreatic MRI study and pancreatic histology was performed, and the patterns of TIC from dynamic MRI measured at the 3 parts of the pancreas were then compared with the corresponding histological pancreatic sections in each patient.

RESULTS

The clinicopathological characteristics and the results of a pancreatic MRI study of 33 patients with pancreatic ductal carcinoma are described in Table 1.

Pancreatic carcinomas developed in a normal pancreas in 28 patients, whose preoperative diagnosis based on the clinical and radiologic findings was identical to the histological diagnosis. Pancreatic carcinomas demonstrated type-Ⅲ (n = 12) or type-Ⅳ (n = 16) TIC. In contrast, the pancreatic parenchyma proximal to the tumor showed type-Ⅰ TIC, while the distal pancreas revealed type-Ⅰ (n = 5) or type-Ⅱ (n = 23) TIC (Figure 2). A histological study of the distal pancreas showing type-Ⅱ TIC revealed obstructive chronic pancreatitis with mild to severe fibrosis.

Five patients had pancreatic carcinoma in the background of longstanding chronic pancreatits. Two

Table 1 Clinicopathological characteristics and pancreatic TIC profiles in patients with focal pancreatic mass due to pancreatic carcinoma

Case No.	Age	Sex	Location of focal mass	Preoperative diagnosis	Underlying chronic pancreatitis	operative procedure	Type of pancreatic TIC of			Histopathology of		
							proximal pancreas	focal mass	distal pancreas	proximal pancreas	focal mass	distal pancreas
1	53	M	Ph	Carcinoma	No	PD	I	Ⅲ	I	Normal	IDC	Normal
2	64	M	Ph	Carcinoma	No	PD	I	Ⅲ	I	Normal	IDC	Normal
3	73	F	Ph	Carcinoma	No	PD	I	Ⅲ	Ⅱ	Normal	IDC	TACP
4	52	F	Ph	Carcinoma	No	PD	I	Ⅲ	Ⅱ	Normal	IDC	TACP
5	69	M	Ph	Carcinoma	No	PPPD	I	Ⅲ	Ⅱ	Normal	IDC	TACP
6	70	F	Ph	Carcinoma	No	PPPD	I	Ⅲ	Ⅱ	Normal	IDC	TACP
7	53	M	Ph	Carcinoma	No	PPPD	I	Ⅲ	Ⅱ	Normal	IDC	TACP
8	78	F	Ph	Carcinoma	No	PPPD	I	Ⅲ	Ⅱ	Normal	IDC	TACP
9	57	M	Ph	Carcinoma	No	PPPD	I	Ⅲ	Ⅱ	Normal	IDC	TACP
10	59	F	Pb	Carcinoma	No	DP	I	Ⅲ	Ⅱ	Normal	IDC	TACP
11	75	F	Pb	Carcinoma	No	DP	I	Ⅲ	Ⅱ	Normal	IDC	TACP
12	75	F	Pb	Carcinoma	No	DP	I	Ⅲ	Ⅱ	Normal	IDC	TACP
13	54	F	Ph	Carcinoma	No	PD	I	Ⅳ	I	Normal	IDC	Normal
14	63	M	Ph	Carcinoma	No	PPPD	I	Ⅳ	I	Normal	IDC	Normal
15	57	F	Ph	Carcinoma	No	PPPD	I	Ⅳ	I	Normal	IDC	Normal
16	67	M	Ph	Carcinoma	No	PD	I	Ⅳ	Ⅱ	Normal	IDC	TACP
17	67	M	Ph	Carcinoma	No	PD	I	Ⅳ	Ⅱ	Normal	IDC	TACP
18	59	M	Ph	Carcinoma	No	PD	I	Ⅳ	Ⅱ	Normal	IDC	TACP
19	74	M	Ph	Carcinoma	No	PD	I	Ⅳ	Ⅱ	Normal	IDC	TACP
20	69	M	Ph	Carcinoma	No	PD	I	Ⅳ	Ⅱ	Normal	IDC	TACP
21	73	M	Ph	Carcinoma	No	PD	I	Ⅳ	Ⅱ	Normal	IDC	TACP
22	74	M	Ph	Carcinoma	No	PPPD	I	Ⅳ	Ⅱ	Normal	IDC	TACP
23	61	M	Ph	Carcinoma	No	PPPD	I	Ⅳ	Ⅱ	Normal	IDC	TACP
24	64	F	Ph	Carcinoma	No	PPPD	I	Ⅳ	Ⅱ	Normal	IDC	TACP
25	63	M	Ph	Carcinoma	No	PPPD	I	Ⅳ	Ⅱ	Normal	IDC	TACP
26	68	M	Ph	Carcinoma	No	PPPD	I	Ⅳ	Ⅱ	Normal	IDC	TACP
27	65	M	Pb	Carcinoma	No	DP	I	Ⅳ	Ⅱ	Normal	IDC	TACP
28	76	M	Pb	Carcinoma	No	DP	I	Ⅳ	Ⅱ	Normal	IDC	TACP
29	59	M	Ph	Carcinoma	Yes	PD	Ⅱ	Ⅲ	Ⅱ	CP	IDC	CP
30	75	F	Ph	Carcinoma	Yes	PPPD	Ⅱ	Ⅳ	Ⅱ	CP	IDC	CP
31	57	F	Ph	TF- pancreatitis	Yes	palliative	Ⅱ	Ⅳ	Ⅱ	CP	IDC	CP
32	67	M	Ph	TF-pancreatitis	Yes	PD	Ⅱ	Ⅳ	Ⅲ	CP	IDC	CP
33	79	F	Ph	Carcinoma	Yes	PPPD	Ⅲ	Ⅳ	Ⅲ	CP	IDC	CP

TIC: time-signal intensity curve; Ph: pancreatic head; Pb: pancreatic body; TF: tumor-forming; PD: pancreaticoduodenectomy; PPPD: pylorus-preserving pancreaticoduodenectomy; DP: distal pancreatectomy; N: normal; IDC: invasive ductal carcinoma; CP: chronic pancreatitis; TACP: tumor-associated chronic pancreatitis.

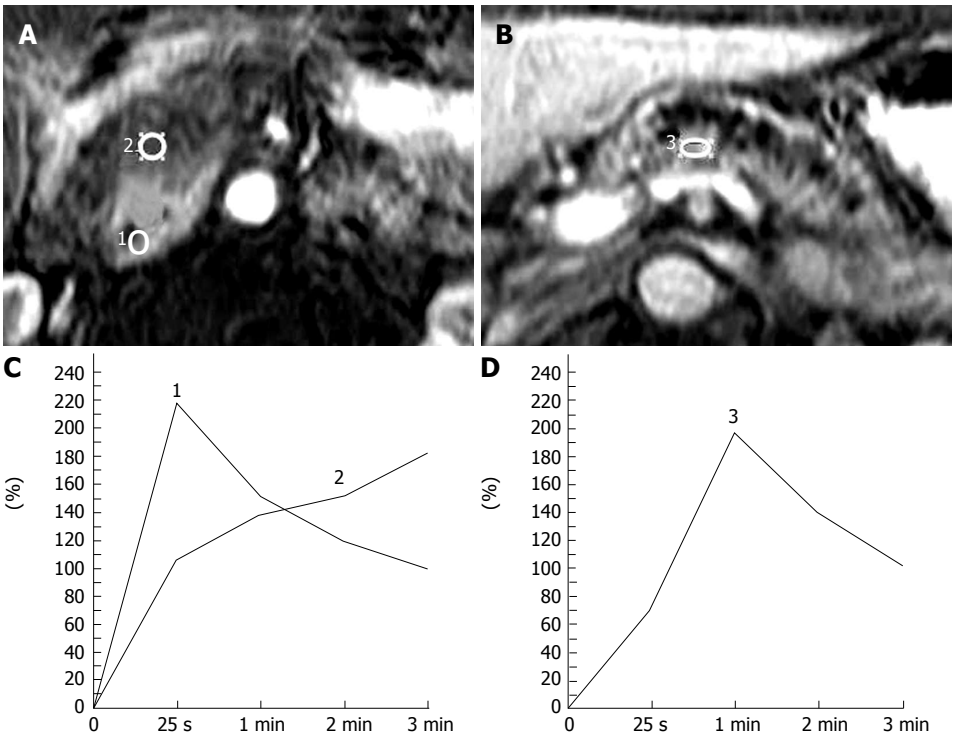

Figure 2 Representative pancreatic TIC profiles in patients with pancreatic ductal carcinoma developed in a normal pancreas. **A**, **B**: Dynamic contrast-enhanced MRI images of the pancreas in a 59-year-old man with carcinoma of the head of the pancreas. The ROIs are placed at the pancreatic mass (No.2 ROI) and the non-tumorous pancreatic parenchyma both proximal (No.1 ROI) and distal (No.3 ROI) to the mass lesion; **C**: Pancreatic TICs obtained from the no.1 and no. 2 ROIs as in (**A**) demonstrate type-Ⅰ and type-Ⅳ, respectively; **D**: Pancreatic TIC obtained from the No.3 ROI as in Figure 2**B** shows type-Ⅱ.

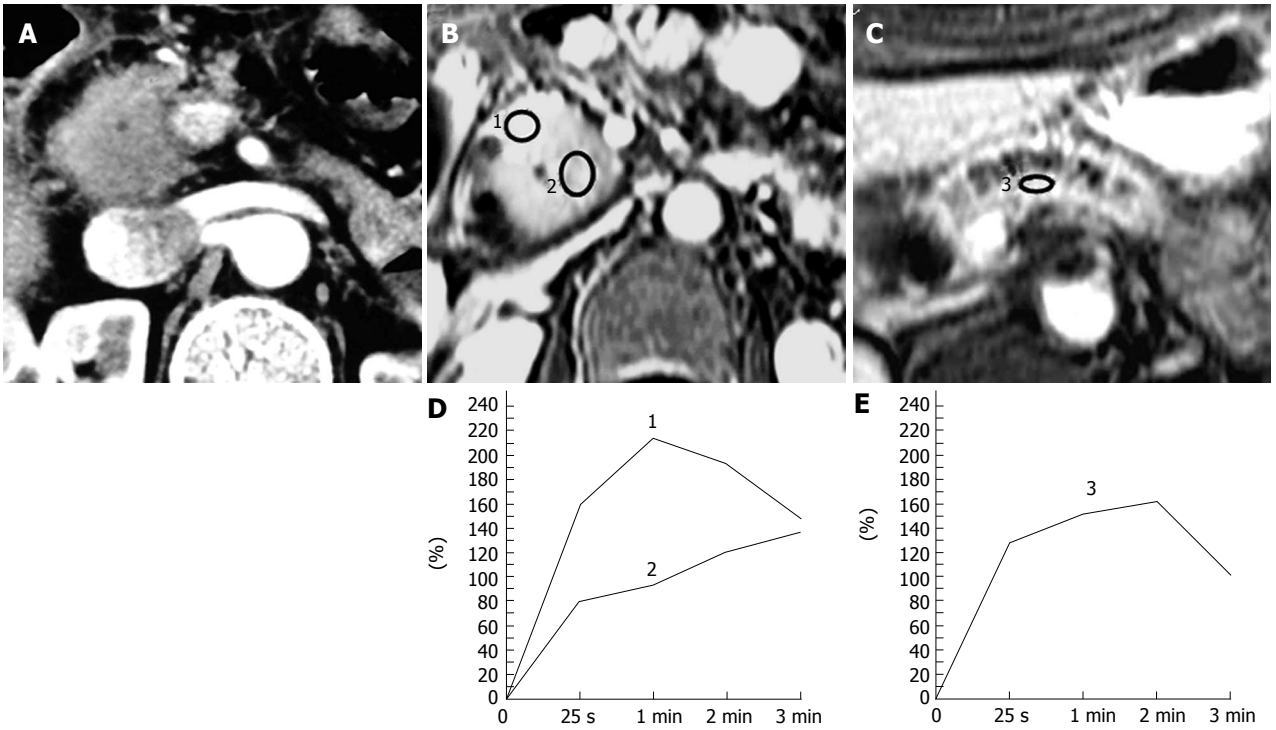

Figure 3 Pancreatic carcinoma occurring in a 67-year-old man with a longstanding chronic pancreatitis. **A**: An abdominal contrast-enhanced CT image shows a focal enlargement of the head of the pancreas. The tumor-to-parenchymal attenuation difference is obscure. The patient underwent a laparotomy under a diagnosis of tumor-forming pancreatitis presenting with obstructive jaundice and was found to have pancreas head carcinoma during the operation; **B**, **C**: Dynamic contrast-enhanced MRI images of the pancreas. The ROIs are placed at the focally enlarged pancreas head (No.2 ROI), the proximal side of the head of the pancreas (No.1 ROI) , and the body of the pancreas (No.3 ROI); **D**: Pancreatic TICs obtained from the No.1 and No.2 ROIs as in (**B**) demonstrate type-Ⅱ and type-Ⅳ, respectively; **E**: Pancreatic TIC obtained from the No.3 ROI as in (**C**) shows type-Ⅲ.

Table 2 Clinicopathological characteristics and pancreatic TIC profiles in patients with focal pancreatic mass due to chronic pancreatitis

Case No.	Age	Sex	Location of focal mass	Preoperative diagnosis	Underlying chronic pancreatitis	Operative procedure	Type of pancreatic TIC of			Histopathology of		
							proximal pancreas	focal mass	distal pancreas	proximal pancreas	focal mass	distal pancreas
1	70	M	Ph	TF-pancreatitis[1]	Yes	PPPD	Ⅱ	Ⅱ	Ⅱ	CP	CP	CP
2	55	M	Pb	TF-pancreatitis	Yes	MP	Ⅱ	Ⅱ	Ⅱ	CP	CP	CP
3	62	M	Ph	TF-pancreatitis	Yes	PPPD	Ⅱ	Ⅱ	Ⅲ	CP	CP	CP
4	47	M	Pb	TF-pancreatitis	Yes	DP	Ⅱ	Ⅱ	Ⅲ	CP	CP	CP
5	63	M	Ph	TF-pancreatitis[1]	Yes	PPPD	Ⅲ	Ⅲ	Ⅱ	CP	CP	CP
6	45	F	Pb	TF-pancreatitis	Yes	DP	Ⅲ	Ⅲ	Ⅲ	CP	CP	CP
7	60	M	Pt	TF-pancreatitis	No	DP	Ⅰ	Ⅱ	Ⅱ	Normal	CP	CP
8	51	F	Pt	TF-pancreatitis	No	DP	Ⅰ	Ⅲ	Ⅲ	Normal	CP	CP

TIC: time-signal intensity curve; Ph: pancreatic head, Pb: pancreatic body, Pt: pancreatic tail; TF: tumor-forming; PPPD: pylorus-preserving pancreaticoduodenectomy; MP: middle pancreatectomy; DP: distal pancreatectomy; CP: chronic pancreatitis; [1]Suspicious of carcinoma.

of them underwent surgery under a diagnosis of tumor-forming pancreatitis and were confirmed to be pancreatic carcinoma during the operation: one patient underwent a pancreaticoduodenectomy, while the other received a palliative operation because of the far advanced stage of the disease. The TIC profiles of 5 carcinomas coexisting with chronic pancreatitis showed type-Ⅲ (n = 1) or type-Ⅳ (n = 4) TIC. Although the proximal and distal pancreas demonstrated type-Ⅱ or type-Ⅲ pancreatic TIC, pancreatic carcinoma displayed a distinctive TIC profile in every patient, depicting the slowest rise to a peak among the 3 pancreatic TICs measured in each individual pancreas (Figure 3).

In 8 patients with tumor-forming pancreatitis, 6 lesions were associated with longstanding chronic pancreatitis and 2 lesions were recognized in a normal pancreas (Table 2). Preoperative diagnosis of these patients was tumor-forming pancreatitis, but in 2 patients, who underwent a pylorus-preserving pancreaticoduodenectomy together with lymphadenectomy, the possibility of carcinoma of the head of the pancreas could not be ruled out and the definitive diagnosis of chronic pancreatitis was confirmed after surgery. The focal pancreatic masses due to tumor-forming pancreatitis demonstrated the TIC of type-Ⅱ (n =

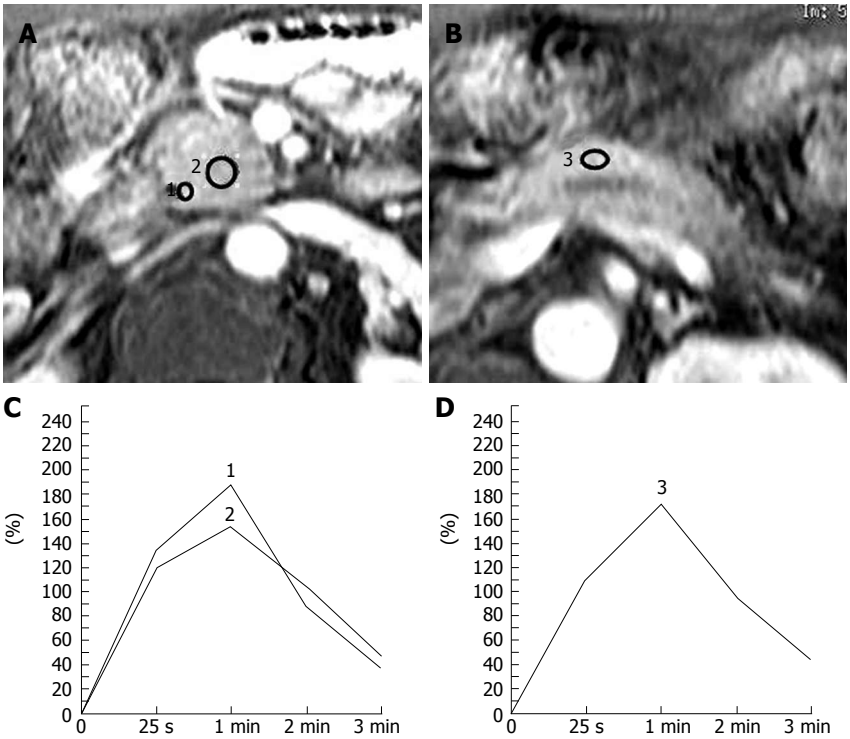

Figure 4 Tumor-forming pancreatitis in a 70-year-old man with a long history of alcohol abuse. The patient underwent a pylorus-preserving pancreaticoduodenectomy together with lymphadenectomy for a suspected pancreas head carcinoma associated with obstructive jaundice and was confirmed to be chronic pancreatitis after surgery. **A**, **B**: Dynamic contrast-enhanced MRI images of the pancreas. The ROIs are placed at the pancreatic mass (No.2 ROI) and the pancreatic parenchyma both proximal (nNo.1 ROI) and distal (No.3 ROI) to the mass lesion; **C**: Both of the pancreatic TICs obtained from the No.1 and no.2 ROIs as in Figure 4A demonstrate type-Ⅱ; **D**: Pancreatic TIC obtained from the No.3 ROI as in Figure 4B also shows type-Ⅱ.

Table 3 Clinicopathological characteristics and pancreatic TIC profiles in patients with focal pancreatic mass due to islet cell tumor

Case No.	Age	Sex	Location of focal mass	Preoperative diagnosis	Underlying chronic pancreatitis	Operative procedure	Type of pancreatic TIC of			Histopathology of		
							proximal pancreas	focal mass	distal pancreas	proximal pancreas	focal mass	distal pancreas
1	63	M	Ph	Insulinoma	No	PPPD	I	I	I	Normal	Insulinoma	Normal
2	68	M	Pb	Insulinoma	No	MP	I	I	I	Normal	Insulinoma	Normal
3	82	M	Pb	Islet cell tumor	No	DP	I	I	I	Normal	Glucagonoma	Normal
4	47	F	Pb	Islet cell tumor	No	DP	I	I	I	Normal	Glucagonoma	Normal
5	70	M	Ph	Islet cell tumor	No	DPPHR	I	I	I	Normal	NFICT	Normal
6	46	F	Pb	Islet cell tumor	No	DP	I	I	I	Normal	NFICT	Normal
7	69	F	Pb	Islet cell tumor	No	DP	I	I	I	Normal	NFICT	Normal

TIC: time-signal intensity curve; Ph: pancreatic head, Pb: pancreatic body; PPPD: pylorus-preserving pancreaticoduodenectomy; DPPHR: duodenum-preserving pancreatic head resection; MP: middle pancreatectomy; DP: distal pancreatectomy; NFICT: non-functioning islet cell tumor.

5) or type-Ⅲ (n = 3). Meanwhile, the TICs of the proximal and distal pancreas varied in type from type- I to type-Ⅲ. In comparing 3 pancreatic TICs measured for each patient, the TIC profile of the focal mass was identical to TICs of both the proximal and distal pancreas in 3 patients (Figure 4), or equal to at least one of these TICs in 5 patients.

In 7 patients with islet cell tumors, a correct diagnosis was made preoperatively on the basis of their characteristic clinical and radiologic features. The tumors demonstrated type- I TIC, and the TICs of the proximal and distal pancreas also showed type- I (Table 3). The histological study revealed the non-tumorous pancreatic parenchyma to be normal in these cases.

Overall, pancreatic ductal carcinomas demonstrated type-Ⅲ (n = 13) or Ⅳ (n = 20) TIC, and the type-Ⅳ TIC was only recognized in pancreatic carcinoma among the 48 series of focal pancreatic mass. Moreover, the TIC profile of carcinoma always depicted the slowest rise to a peak among the 3 pancreatic TICs measured in each patient. Tumor-forming pancreatitis showed type-Ⅱ (n = 5) or Ⅲ (n = 3) TIC, and the TICs of the focal mass due to chronic pancreatitis were identical to at least one of the TICs in the proximal and distal pancreas in each patient. All islet cell tumors revealed type- I TIC.

DISCUSSION

The differentiation between pancreatic carcinoma coexisting with chronic pancreatitis and focal mass due to chronic pancreatitis continues to be a challenge. Although various diagnostic modalities have been proposed to help differentiate these 2 pancreatic entities[17-22], the accuracy of each method varies and no single non-invasive method for making a correct diagnosis has yet been suggested. The presence of a focal pancreatic mass is generally indicative of a neoplasm, and thus the patients are often subjected to

major pancreatic surgery such as pancreaticoduodenectomy for presumed pancreatic malignancy that proves later to be benign in 5% to 11% of all cases[23-26]. In our series, 2 of 8 patients with tumor-forming pancreatitis underwent a pancreas head resection along with lymphadenectomy, because pancreatic carcinoma could not be ruled out. Conversely, 2 patients with preoperative diangnosis of tumor-forming pancreatitis were revealed to have pancreatic malignancy during operation. An accurate preoperative differential diagnosis is needed to avoid such unnecessary surgery and delays in making a correct diagnosis of pancreatic carcinoma.

The present study on the differentiation of focal pancreatic masses with dynamic contrast-enhanced MRI demonstrated that pancreatic ductal carcinomas exhibit a characteristic TIC profile which is different from other focal masses of the pancreas. The type-Ⅳ TIC was a unique profile indicative of pancreatic carcinoma since no other focal pancreatic masses displayed type-Ⅳ TIC. A representative TIC profile pattern of the pancreas with carcinoma was comprised of type- Ⅰ TIC in the proximal pancreas, type-Ⅳ TIC in the mass lesion, and type-Ⅱ TIC in the distal pancreas. Our previous study demonstrated the fibrosis ratios of pancreas with type-Ⅰ, Ⅱ, or Ⅲ TICs as to be 3.5% (range, 1.5-10.1), 15.9% (range, 7.5-25.2), and 22.6% (range, 17.8-27.3), respectively[16]. In the present study, the type-Ⅱ TIC of the distal pancreas in patients with pancreatic carcinoma also reflected the increase in fibrosis in the distal pancreas due to obstructive chronic pancreatitis. Similar findings of delayed enhancement of the pancreas distal to pancreatic carcinoma have been noted on both dual-phase CT examinations[2] and a dynamic MRI study[8].

On the other hand, there was an overlap in the TIC profile between pancreatic carcinoma and tumor-forming pancreatitis in this study, i.e., type-Ⅲ TIC. The type-Ⅲ TIC accounted for 39% (13/33) of pancreatic carcinoma and 38% (3/8) of tumor-forming pancreatitis. However, the series of pancreatic TICs measured in 3 parts of the individual pancreas provided helpful information for distinguishing these 2 pancreatic pathologies. The TIC profile of a mass due to carcinoma always depicted the slowest rise to a peak among the 3 pancreatic TICs, even in carcinomas occurring in patients known to have longstanding chronic pancreatitis, while the TIC profile of the focal mass due to chronic pancreatitis was identical to at least one of the proximal and distal pancreatic TICs in individual patients. Chronic pancreatitis has a risk for pancreatic carcinoma with an incidence of 2% after 10 years and 5.9% after 20 years of documented chronic pancreatitis[4], and the diagnosis of pancreatic carcinoma in this setting may therefore be difficult or even impossible[1,24,25,27,28]. Thus far, at the time of detection, the majority of patients with pancreatic carcinoma associated with chronic pancreatitis tend to be surgically unresectable. However, our findings suggest that the pancreatic TIC from dynamic MIR is a potential diagnostic tool for detecting pancreatic carcinoma in patients with longstanding chronic pancreatitis, which enable us to distinguish pancreatic carcinoma from tumor-forming pancreatitis.

The major morphologic change of chronic pancreatitis is the progressive destruction of the exocrine parenchyma with replacement by dense fibrous tissue[1-3]. However, pancreatic carcinomas also possess an abundant degree of fibrosis[10,12] since pancreatic carcinoma cells induce fibrosis by the stimulation of pancreatic stellate cells[29,30]. Fibrosis diminishes the amount of aqueous protein in the pancreatic acini and the capillary network of the pancreas that may underlie both the loss of signal intensity in the pancreas on fat-suppressed T1-weighted images and the diminished enhancement on dynamic contrast-enhanced images[31,32]. Experimental and clinical studies have demonstrated alcoholic or occlusive chronic pancreatitis and pancreatic carcinoma to be associated with tissue fibrosis, a reduced blood vessel density[33,34], and a decreased pancreatic blood flow[35-38]. In contrast, pancreatic islet cell tumors are hypervascular neoplasms[39] and it is therefore reasonable that all pancreatic islet cell tumors showed type- Ⅰ TIC in this study. The number of blood vessels, the amount of aqueous protein, and the degree of fibrosis in the pancreas, along with the difference in the mass-to-pancreatic parenchymal contrast, may together play a role in the MRI contrast-enhancement of pancreatic masses. However, there is a considerable discrepancy in the reported results of the blood vessel count and the degree of fibrosis in pancreatic carcinoma, tumor-forming pancreatitis, tumor-associated chronic pancreatitis, and the normal pancreas[10,33,34,40-44]. To clarify the precise pancreatic pathology based on the pancreatic TIC from dynamic MRI, a qualitative assessment of the changes in pancreatic microcirculation during neovascularization and the obliteration of the small vessels by fibrosis or cancer cells is thus called for.

In conclusion, pancreatic TIC from dynamic MRI was found to provide reliable information for differentiating pancreatic carcinoma from a focal mass due to chronic pancreatitis and for also detecting pancreatic carcinoma associated with longstanding chronic pancreatitis. This imaging technique may therefore make it possible to eliminate the number of exploratory laparotomies as well as unnecessary major pancreatic surgery and delays in making a correct diagnosis of pancreatic carcinoma, especially in patients associated with chronic pancreatitis.

REFERENCES

1 **Steer ML**, Waxman I, Freedman S. Chronic pancreatitis. *N Engl J Med* 1995; **332**: 1482-1490

2 **Johnson PT**, Outwater EK. Pancreatic carcinoma versus chronic pancreatitis: dynamic MR imaging. *Radiology* 1999; **212**: 213-218

3 **Kim T**, Murakami T, Takamura M, Hori M, Takahashi S, Nakamori S, Sakon M, Tanji Y, Wakasa K, Nakamura H. Pancreatic mass due to chronic pancreatitis: correlation of CT and MR imaging features with pathologic findings. *AJR Am J Roentgenol* 2001; **177**: 367-371

4 **Lowenfels AB**, Maisonneuve P, Cavallini G, Ammann RW, Lankisch PG, Andersen JR, Dimagno EP, Andrén-Sandberg A, Domellöf L. Pancreatitis and the risk of pancreatic cancer. International Pancreatitis Study Group. *N Engl J Med* 1993; **328**: 1433-1437

5 **Malka D**, Hammel P, Maire F, Rufat P, Madeira I, Pessione F, Lévy P, Ruszniewski P. Risk of pancreatic adenocarcinoma in chronic pancreatitis. *Gut* 2002; **51**: 849-852
6 **Bansal P**, Sonnenberg A. Pancreatitis is a risk factor for pancreatic cancer. *Gastroenterology* 1995; **109**: 247-251
7 **Talamini G**, Falconi M, Bassi C, Sartori N, Salvia R, Caldiron E, Frulloni L, Di Francesco V, Vaona B, Bovo P, Vantini I, Pederzoli P, Cavallini G. Incidence of cancer in the course of chronic pancreatitis. *Am J Gastroenterol* 1999; **94**: 1253-1260
8 **Tsuda T**, Mochizuki T, Kikuchi K, Tanaka H, Sugata S, Ikezoe J. Late-phase enhancement of the upstream portion of pancreatic adenocarcinoma on dual-phase helical CT. *Abdom Imaging* 2001; **26**: 635-639
9 **Müller MF**, Meyenberger C, Bertschinger P, Schaer R, Marincek B. Pancreatic tumors: evaluation with endoscopic US, CT, and MR imaging. *Radiology* 1994; **190**: 745-751
10 **Imamura T**, Iguchi H, Manabe T, Ohshio G, Yoshimura T, Wang ZH, Suwa H, Ishigami S, Imamura M. Quantitative analysis of collagen and collagen subtypes I, III, and V in human pancreatic cancer, tumor-associated chronic pancreatitis, and alcoholic chronic pancreatitis. *Pancreas* 1995; **11**: 357-364
11 **Cubilla AL**, Fitzgerald PJ. Tumors of the exocrine pancreas. In: Atlas of tumor pathology. 2nd ed. Volume Fascicle 19. Washington DC: Armed Forces Institute of Pathology, 1984: 1-40
12 **Longnecker DS.** Pancreas. In: Damjanov I, Linder J, editors. Anderson's Pathology. 10th ed. St. Louis: Mosby-Year Book, 1996: 1891-1916
13 **Ritchie AC**. Pancreas. In: Ritchie AC, editor. Boyd's textbook of pathology, 9th ed. Philadelphia: Lea & Febiger, 1990: 1202-1234
14 **McNulty NJ**, Francis IR, Platt JF, Cohan RH, Korobkin M, Gebremariam A. Multi--detector row helical CT of the pancreas: effect of contrast-enhanced multiphasic imaging on enhancement of the pancreas, peripancreatic vasculature, and pancreatic adenocarcinoma. *Radiology* 2001; **220**: 97-102
15 **Gabata T**, Matsui O, Kadoya M, Yoshikawa J, Miyayama S, Takashima T, Nagakawa T, Kayahara M, Nonomura A. Small pancreatic adenocarcinomas: efficacy of MR imaging with fat suppression and gadolinium enhancement. *Radiology* 1994; **193**: 683-688
16 **Tajima Y**, Matsuzaki S, Furui J, Isomoto I, Hayashi K, Kanematsu T. Use of the time-signal intensity curve from dynamic magnetic resonance imaging to evaluate remnant pancreatic fibrosis after pancreaticojejunostomy in patients undergoing pancreaticoduodenectomy. *Br J Surg* 2004; **91**: 595-600
17 **Boadas J**, Mora J, Urgell E, Puig P, Roca M, Cussó X, Capellà G, Lluís F, Farré A. Clinical usefulness of K-ras gene mutation detection and cytology in pancreatic juice in the diagnosis and screening of pancreatic cancer. *Eur J Gastroenterol Hepatol* 2001; **13**: 1153-1159
18 **Gansauge S**, Gansauge F, Negri G, Galle P, Müller J, Nüssler AK, Poch B, Beger HG. The role of anti-p53-autoantibodies in pancreatic disorders. *Int J Pancreatol* 1996; **19**: 171-178
19 **Maire F**, Micard S, Hammel P, Voitot H, Lévy P, Cugnenc PH, Ruszniewski P, Puig PL. Differential diagnosis between chronic pancreatitis and pancreatic cancer: value of the detection of KRAS2 mutations in circulating DNA. *Br J Cancer* 2002; **87**: 551-554
20 **Kitano M**, Kudo M, Maekawa K, Suetomi Y, Sakamoto H, Fukuta N, Nakaoka R, Kawasaki T. Dynamic imaging of pancreatic diseases by contrast enhanced coded phase inversion harmonic ultrasonography. *Gut* 2004; **53**: 854-859
21 **Ichikawa T**, Sou H, Araki T, Arbab AS, Yoshikawa T, Ishigame K, Haradome H, Hachiya J. Duct-penetrating sign at MRCP: usefulness for differentiating inflammatory pancreatic mass from pancreatic carcinomas. *Radiology* 2001; **221**: 107-116
22 **van Kouwen MC**, Jansen JB, van Goor H, de Castro S, Oyen WJ, Drenth JP. FDG-PET is able to detect pancreatic carcinoma in chronic pancreatitis. *Eur J Nucl Med Mol Imaging* 2005; **32**: 399-404
23 **Proca DM**, Ellison EC, Hibbert D, Frankel WL. Major pancreatic resections for chronic pancreatitis. *Arch Pathol Lab Med* 2001; **125**: 1051-1054
24 **Smith CD**, Behrns KE, van Heerden JA, Sarr MG. Radical pancreatoduodenectomy for misdiagnosed pancreatic mass. *Br J Surg* 1994; **81**: 585-589
25 **van Gulik TM**, Reeders JW, Bosma A, Moojen TM, Smits NJ, Allema JH, Rauws EA, Offerhaus GJ, Obertop H, Gouma DJ. Incidence and clinical findings of benign, inflammatory disease in patients resected for presumed pancreatic head cancer. *Gastrointest Endosc* 1997; **46**: 417-423
26 **Abraham SC**, Wilentz RE, Yeo CJ, Sohn TA, Cameron JL, Boitnott JK, Hruban RH. Pancreaticoduodenectomy (Whipple resections) in patients without malignancy: are they all 'chronic pancreatitis'? *Am J Surg Pathol* 2003; **27**: 110-120
27 **Shemesh E**, Czerniak A, Nass S, Klein E. Role of endoscopic retrograde cholangiopancreatography in differentiating pancreatic cancer coexisting with chronic pancreatitis. *Cancer* 1990; **65**: 893-896
28 **Leung TK**, Lee CM, Wang FC, Chen HC, Wang HJ. Difficulty with diagnosis of malignant pancreatic neoplasms coexisting with chronic pancreatitis. *World J Gastroenterol* 2005; **11**: 5075-5078
29 **Apte MV**, Haber PS, Darby SJ, Rodgers SC, McCaughan GW, Korsten MA, Pirola RC, Wilson JS. Pancreatic stellate cells are activated by proinflammatory cytokines: implications for pancreatic fibrogenesis. *Gut* 1999; **44**: 534-541
30 **Bachem MG**, Schünemann M, Ramadani M, Siech M, Beger H, Buck A, Zhou S, Schmid-Kotsas A, Adler G. Pancreatic carcinoma cells induce fibrosis by stimulating proliferation and matrix synthesis of stellate cells. *Gastroenterology* 2005; **128**: 907-921
31 **Semelka RC**, Shoenut JP, Kroeker MA, Micflikier AB. The pancreas. In MRI of the Abdomen with CT Correlation, Semelka RC , Shoenut JP, editors. New York: Raven Press, 1993: 84-98
32 **Semelka RC**, Shoenut JP, Kroeker MA, Micflikier AB. Chronic pancreatitis: MR imaging features before and after administration of gadopentetate dimeglumine. *J Magn Reson Imaging* 1993; **3**: 79-82
33 **Zhao P**, Tu J, van den Oord JJ, Fevery J. Damage to duct epithelium is necessary to develop progressing lesions of chronic pancreatitis in the cat. *Hepatogastroenterology* 1996; **43**: 1620-1626
34 **De Angelis C**, Valente G, Spaccapietra M, Angonese C, Del Favero G, Naccarato R, Andriulli A. Histological study of alcoholic, nonalcoholic, and obstructive chronic pancreatitis. *Pancreas* 1992; **7**: 193-196
35 **Schilling MK**, Redaelli C, Reber PU, Friess H, Signer C, Stoupis C, Büchler MW. Microcirculation in chronic alcoholic pancreatitis: a laser Doppler flow study. *Pancreas* 1999; **19**: 21-25
36 **Kakugawa Y**, Giaid A, Yanagisawa M, Baynash AG, Melnyk P, Rosenberg L, Duguid WP. Expression of endothelin-1 in pancreatic tissue of patients with chronic pancreatitis. *J Pathol* 1996; **178**: 78-83
37 **Lewis MP**, Lo SK, Reber PU, Patel A, Gloor B, Todd KE, Toyama MT, Sherman S, Ashley SW, Reber HA. Endoscopic measurement of pancreatic tissue perfusion in patients with chronic pancreatitis and control patients. *Gastrointest Endosc* 2000; **51**: 195-199
38 **Sofuni A**, Iijima H, Moriyasu F, Nakayama D, Shimizu M, Nakamura K, Itokawa F, Itoi T. Differential diagnosis of pancreatic tumors using ultrasound contrast imaging. *J Gastroenterol* 2005; **40**: 518-525
39 **Van Hoe L**, Gryspeerdt S, Marchal G, Baert AL, Mertens L. Helical CT for the preoperative localization of islet cell tumors of the pancreas: value of arterial and parenchymal phase images. *AJR Am J Roentgenol* 1995; **165**: 1437-1439
40 **Zhongqiu W**, Guangming L, Jieshou L, Xinhua Z, Ziqian C, Kui M. The comparative study of tumor angiogenesis and CT enhancement in pancreatic carcinoma. *Eur J Radiol* 2004; **49**:

274-280
41 **Rzepko R**, Jaśkiewicz K, Klimkowska M, Nałecz A, Izycka-Swieszewska E. Microvascular density in chronic pancreatitis and pancreatic ductal adenocarcinoma. *Folia Histochem Cytobiol* 2003; **41**: 237-239
42 **Ueda T**, Oda T, Kinoshita T, Konishi M, Nakahashi C, Takahashi S, Hasebe T, Fukao K, Ochiai A. Neovascularization in pancreatic ductal adenocarcinoma: Microvessel count analysis, comparison with non-cancerous regions and other types of carcinomas. *Oncol Rep* 2002; **9**: 239-245
43 **Cho SG**, Lee DH, Lee KY, Ji H, Lee KH, Ros PR, Suh CH. Differentiation of chronic focal pancreatitis from pancreatic carcinoma by in vivo proton magnetic resonance spectroscopy. *J Comput Assist Tomogr* 2005; **29**: 163-169
44 **Banerjee SK**, Zoubine MN, Mullick M, Weston AP, Cherian R, Campbell DR. Tumor angiogenesis in chronic pancreatitis and pancreatic adenocarcinoma: impact of K-ras mutations. *Pancreas* 2000; **20**: 248-255

S- Editor Liu Y **L- Editor** Smith RC **E- Editor** Ma WH

PO Box 2345, Beijing 100023, China
www.wjgnet.com
wjg@wjgnet.com

World J Gastroenterol 2007 February 14; 13(6): 866-873
World Journal of Gastroenterology ISSN 1007-9327

BASIC RESEARCH

Embryonic stem cells develop into hepatocytes after intrasplenic transplantation in CCl_4-treated mice

Kei Moriya, Masahide Yoshikawa, Ko Saito, Yukiteru Ouji, Mariko Nishiofuku, Noriko Hayashi, Shigeaki Ishizaka, Hiroshi Fukui

Kei Moriya, Ko Saito, Mariko Nishiofuku, Hiroshi Fukui, Division of Hepatology, Third Department of Internal Medicine, Nara Medical University, 840 Shijo-cho, Kashihara, Nara 634-8521, Japan
Masahide Yoshikawa, Yukiteru Ouji, Noriko Hayashi, Shigeaki Ishizaka, Division of Developmental Biology, Department of Parasitology, Nara Medical University, 840 Shijo-cho, Kashihara, Nara 634-8521, Japan
Correspondence to: Masahide Yoshikawa, Division of Developmental Biology, Department of Parasitology, Nara Medical University, 840 Shijo-cho, Kashihara, Nara 634-8521, Japan. myoshika@naramed-u.ac.jp
Telephone: +81-744-298857 Fax: +81-744-24712
Received: 2006-10-04 Accepted: 2006-12-15

Abstract

AIM: To transplant undifferentiated embryonic stem (ES) cells into the spleens of carbon tetrachloride (CCl_4)-treated mice to determine their ability to differentiate into hepatocytes in the liver.

METHODS: CCl_4, 0.5 mL/kg body weight, was injected into the peritoneum of C57BL/6 mice twice a week for 5 wk. In group 1 (n = 12), 1 x 10^5 undifferentiated ES cells (0.1 mL of 1 x 10^6/mL solution), genetically labeled with GFP, were transplanted into the spleens 1 d after the second injection. Group 2 mice (n = 12) were injected with 0.2 mL of saline twice a week, instead of CCl_4, and the same amount of ES cells was transplanted into the spleens. Group 3 mice (n = 6) were treated with CCl_4 and injected with 0.1 mL of saline into the spleen, instead of ES cells. Histochemical analyses of the livers were performed on post-transplantation d (PD) 10, 20, and 30.

RESULTS: Considerable numbers of GFP-immunopositive cells were found in the periportal regions in group 1 mice (CCl_4-treated) on PD 10, however, not in those untreated with CCl_4 (group 2). The GFP-positive cells were also immunopositive for albumin (ALB), alpha-1 antitrypsin, cytokeratin 18, and hepatocyte nuclear factor 4 alpha on PD 20. Interestingly, most of the GFP-positive cells were immunopositive for DLK, a hepatoblast marker, on PD 10. Although very few ES-derived cells were demonstrated immunohistologically in the livers of group 1 mice on PD 30, improvements in liver fibrosis were observed. Unexpectedly, liver tumor formation was not observed in any of the mice that received ES cell transplantation during the experimental period.

CONCLUSION: Undifferentiated ES cells developed into hepatocyte-like cells with appropriate integration into tissue, without uncontrolled cell growth.

Key words: Embryonic stem cells; Hepatic differentiation; Intrasplenic transplantation; Carbon tetrachloride

Moriya K, Yoshikawa M, Saito K, Ouji Y, Nishiofuku M, Hayashi N, Ishizaka S, Fukui H. Embryonic stem cells develop into hepatocytes after intrasplenic transplantation in CCl_4-treated mice. *World J Gastroenterol* 2007; 13(6): 866-873

http://www.wjgnet.com/1007-9327/13/866.asp

INTRODUCTION

Embryonic stem (ES) cells are self-renewing and multipotent cells derived from the inner cell masses of preimplantation blastocysts[1,2], and have many characteristics of an optimal cell source for cell-replacement therapy. Theoretically, ES cells are able to be produced limitlessly, and various kinds of cell-types have been generated *in vitro* and *in vivo*. Thus, ES cells are considered to have potential to become an optimal cell source for cell-replacement therapy.

We previously showed that mouse ES cells have an ability to differentiate into hepatocyte-like cells *in vitro* using an attached culture of embryoid bodies (EBs)[3] and demonstrated that introduction of transcription factor gene hepatocyte nuclear factor 3 beta, which plays an important role in liver development, led to an efficient induction of ES cells into hepatocyte-like cells[4,5]. The *in vitro* capability of ES cells to differentiate into hepatocyte-like cells has also been proven by other investigators[6-21]. In general, the methods used in those studies can be divided into spontaneous and directed differentiation. For spontaneous differentiation, the formation of embryoid bodies (EBs) has been mostly utilized[6-11]. With directed differentiation, different processes of enrichment of a specific differentiated cell type that use elements to promote the differentiation of ES cells into an endodermal lineage, such as the addition of growth factors (GFs) and

hormones[12-20], and the constitutive expression of hepatic transcription factors[21], have been utilized.

In contrast to a number of reports of hepatic differentiation of ES cells *in vitro*, the behavior of transplanted ES cells in the liver has not been reported, except for the formation of teratomas[9,22]. According to the results of a study that utilized intravenous transplantation of a relatively large number of undifferentiated ES cells (2×10^6/mouse)[9], tumor formation was observed in the livers of all carbon tetrachloride (CCl_4)-treated mice, but not in mice with normal livers. Although the tumors formed in the livers contained ES-derived mature hepatocytes, few cells seemed to have been integrated into the ordinary structure of the residual normal livers. Recently, bone marrow stem cells (BMSCs) were demonstrated to differentiate into hepatocytes and integrate into the liver after intravenous transplantation in CCl_4-treated mice, even without *in vitro* induction directed toward an endoderm or hepatocyte lineage[23]. Those results suggested that the livers in CCl_4-mice provide a microenvironment necessary for the lodging of BMSCs or ES cells, and their subsequent differentiation into hepatocytes.

In the present study, we investigated whether ES cells are able to differentiate into hepatocytes *in vivo*. For this purpose, we transplanted a reduced number of undifferentiated ES cells (1×10^5/mouse) into the spleens of CCl_4-treated experimental and CCl_4-untreated control mice, expecting that tumors would develop in the livers. We found that the native ES cells migrated to the liver and developed into hepatocyte-like cells in CCl_4-treated mice, but not in the CCl_4-untreated control mice. Further, localization of migrated ES cells in the CCl_4-mice livers was found in the periportal regions on post-transplantation day (PD) 10 and the cells were immuno-positive for albumin (ALB), alpha-1 antitrypsin (α1AT), and cytokeratin 18 (CK18) on PD 20. Hepatocyte nuclear factor 4 alpha (HNF4α), an important transcription factor for mature hepatocytes, was also detected immunohistochemically. Interestingly, most of the GFP-positive cells showed immuno-positivity to DLK, a hepatoblast marker, on PD 10. Although there were very few ES-derived cells demonstrated immunohistologically in the livers on PD 30, improvements in liver fibrosis were observed. Unexpectedly, formation of liver tumors was not observed in any of the mice that received transplanted cells during the experimental period.

Our results suggest that undifferentiated ES cells can develop into hepatocyte-like cells with appropriate integration into tissue without invariably leading to uncontrolled cell growth. In the future era of cell growth control, undifferentiated ES cells may be directly used for therapeutic transplantation as well as terminally differentiated derivatives.

MATERIALS AND METHODS

Murine ES cell line

We utilized G4-2 cells from a mouse ES cell line (129/SvJ mouse ES cells, a kind gift from Dr. Hitoshi Niwa, RIKEN Center for Developmental Biology, Kobe, Japan). The G4-2 cells were derived from EB3 ES cells[24,25] and carried an enhanced green fluorescent protein (EGFP) gene under the control of the CAG expression unit. EB3 ES cells are a subline derived from E14tg2a ES cells[26] and carry the blasticidin S-resistant selection marker gene driven by the Oct-3/4 promoter (active under undifferentiated status). For the present study, undifferentiated G4-2 cells were maintained on gelatin-coated dishes without feeder cells in Dulbecco's modified Eagle's medium (DMEM; Sigma; St. Louis, MO) supplemented with 10% fetal bovine serum (FBS; GIBCO/BRL; Grand Island, NY;), 0.1 mmol/L 2-mercaptoethanol (Sigma), 10 mmol/L nonessential amino acids (GIBCO/BRL), 1 mmol/L sodium pyruvate (Sigma), and 1400 U/mL of leukemia inhibitory factor (LIF; GIBCO/BRL). For some of the experiments, G4-2 cells were cultured in medium containing 10 μg/mL of blasticidin S to eliminate differentiated cells.

Preparation of graft cells

Culture dishes (9 cm in diameter), used to maintain the undifferentiated ES colonies, were washed with 8 mL of ice-cold phosphate-buffered saline (PBS, pH 7.4) 3 times and then treated with 1.0 mL of 0.025% trypsin/PBS for 2 min at 37℃. Five milliliters of ES maintenance medium containing 10% FBS was added to the culture dish to stop trypsin activity. Single cell solutions were easily obtained by repeated pipetting. Cells were washed with ice-cold PBS 3 times and finally prepared for transplantation in a PBS solution at a cell concentration of 1×10^6/mL.

CCl_4 treatment

To induce liver damage, CCl_4 at 0.5 mL/kg of body weight was injected into the peritoneum twice a week for 5 wk.

Grouping of experimental animals

Female C57BL/6 mice were purchased from Japan SLC (Shizuoka, Japan) at 6 wk of age and used as experimental animals. All procedures including the surgical steps were performed in accordance with the Guidelines of Nara Medical University for experiments involving animals and recombinant DNA. The mice were divided into 3 groups. Group 1 (n = 12) received CCl_4 treatment and transplantation of graft cells. One day after the second injection of CCl_4, 1×10^5 GFP-positive undifferentiated ES cells (0.1 mL of 1×10^6/mL solution) were transplanted into the spleen. Briefly, a 1-cm incision was made on the left flank and the spleen was extracted through the incision. Then, 0.1 mL of the graft cell solution (1×10^6 cells/mL) was slowly infused into the inferior pole of the spleen using a 31-gauge needle and a Hamilton syringe. Once the infusion was complete, the syringe was left in place for 1 min. Group 2 mice (n = 12) were injected in the same manner with 0.2 mL of saline twice a week, instead of CCl_4, and transplanted with the same amount of ES cells into the spleen as Group 1. Group 3 mice (n = 6) were treated with CCl_4 and injected with 0.1 ml of saline into the spleen in the same manner, instead of ES cells. Grouping and an outline of the experiments are shown in Figure 1.

Tissue preparation

The livers were thoroughly perfused *via* the heart with 4% paraformaldehyde to wash out contaminating blood cells. For fixation, the perfused livers were incubated with 4% paraformaldehyde overnight, then soaked in 30% sucrose for 3 d. Tissues were frozen on dry ice and then sectioned into 5-μm slices using a cryostat in preparation for dyeing.

Immunohistochemistry and double immunofluorescence for GFP

Immunohistochemical analysis was performed in accordance with previously reported methods[27]. Frozen tissue sections were desiccated completely at room temperature using a dryer, washed with phosphate-buffered saline (PBS) 3 times for 5 min each, and soaked in PBS containing 5% bovine serum albumin (BSA) once for 5 min. Sections were incubated overnight with anti-GFP (1:1000, Molecular Prove Inc, OR, USA and Nacalai Tesque Inc, Kyoto, Japan), anti-ALB (1:100, Biogenesis Ltd, England, UK), anti-α1AT (1:100, Zymed Laboratories Inc, CA, USA), anti-CK18 (1:100, Chemicon International Inc, CA, USA), anti-CK19 (1:100, Abcam Ltd, Cambridge, UK), anti-HNF4α (1:50, Santa Cruz Biotechnology Inc, CA, USA), and anti-DLK[28] (1:100) antibodies. Tissue sections were then washed with PBS 3 times for 5 min each and incubated with biotin-conjugated anti-rat (anti-rabbit or anti-mouse) IgG (1:200, Vector Laboratories Inc, CA, USA) secondary antibodies for 1 h at 37℃, then washed 3 times for 5 min each with diluted water. Next, for the purpose of intrinsic peroxidase elimination, the tissue sections were immersed in 3% hydrogen peroxide (H_2O_2) for 30 min, then washed 3 times for 5 min each with PBS. The sections were incubated with Vectastain ABC^R reagent (Vector Laboratories Inc, CA, USA) for 2 h at 37℃, then washed 3 times for 5 min with diluted water and treated with 0.02 mol/L Tris-HCl buffer (pH 7.5) containing 4% diaminobenzidine tetrahydrochloride (Vector Laboratories Inc, CA, USA) in the presence of 0.0004% H_2O_2 for 2 min at room temperature. Stained sections were rinsed with diluted water, and immersed in ethanol and xylene for complete dehydration. Finally, the sections were enclosed with Entellan-new^R.

For fluorescent immunohistochemistry, tissue sections were incubated with Alexa Fluor^R 488 and 546 goat anti-rat (anti-rabbit or anti-mouse) IgG (H + L) conjugate (Molecular Prove Inc, OR, USA) secondary antibodies for 1 h, then washed 3 times for 5 min each with PBS. Sections were mounted on glass slides from an Anti-fade Kit (Molecular Prove Inc, OR, USA). Positive cells in the liver were observed using a Provis microscope (Olympus, Tokyo) equipped with a charge coupled device (CCD) camera. A total of 10 different areas in each liver section were analyzed independently for each mouse.

RESULTS

Migration of ES cells into CCl_4-treated mouse livers

GFP-immuno-positivity was examined in the liver specimens 10 d after intrasplenic transplantation (PD 10 of 1 × 10^5 GFP-positive ES cells (groups 1 and 2) or intrasplenic injection of saline (group 3) (Figure 2). A distinct distribution of immunoreactivity against GFP was observed in the liver sections of group 1 mice, which were treated with CCl_4 and grafted with ES cells (Figure 2A). Further, GFP-positive cells were present in the periportal regions of the hepatic lobules. However, no GFP-positive cells were detected in liver sections from group 2 mice (not treated with CCl_4, grafted with ES cells) (Figure 2B), or in those from group 3 mice (treated with CCl_4, not grafted with ES cells) (Figure 2C).

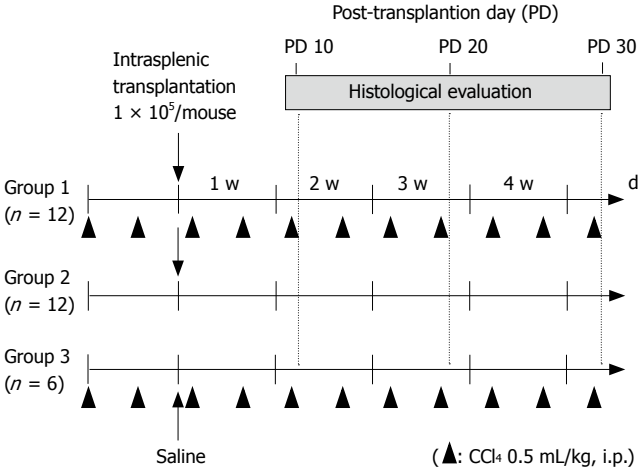

Figure 1 Grouping of experimental animals. Female C57BL/6 mice were divided into 3 groups. Intraperitoneal injection of CCl_4 at 0.5 mL/kg body weight was performed twice a week in group 1 mice (n = 12) and group 3 mice (n = 6), while 0.2 mL of saline was injected instead of CCl_4 in group 2 mice (n = 12). One day after the second intraperitoneal injection of CCl_4 or saline, 1 x 10^5 GFP-positive undifferentiated ES cells (0.1 mL of 1 x 10^6/mL solution) were transplanted into the spleens in groups 1 and 2, whereas no cell transplantation was performed with group 3.

GFP-immuno-positivity was also examined in the liver specimens on PD 20 and 30 (Figure 3). Immunoreactivity to GFP was detected in the liver sections from group 1 mice on PD 20 (Figure 3B), though the intensity was weaker than that on PD 10. On PD 30, scant or no GFP-immuno-positivity was detected in group 1 mice (Figure 3C). We also counted the number of GFP-positive cells in 10 microscopic fields, focusing on the periportal area. The average numbers of GFP-positive cells around the portal vein on PD 10, 20, and 30 were 65 ± 18, 26 ± 15, and 4.0 ± 2.0 respectively, in each microscopic field at 400 × magnification (Figure 3D).

Expression of hepatocyte-related markers in GFP-positive cells

Nearly all of the GFP-positive cells had disappeared from the livers of the transplanted mice by PD 30, however, considerable numbers of GFP-positive cells were present in the hepatic lobules for a limited period in those in group 1. Next, we utilized immunohistochemistry to examine the expressions of ALB, α1AT, and CK18 on PD 20 (Figure 4A). ALB immuno-positivity was observed homogeneously throughout the hepatic lobules without discrimination between the periportal regions and the other parts. Immuno-positivity for α1AT and CK18 was also observed throughout the lobules, though some cells located in the

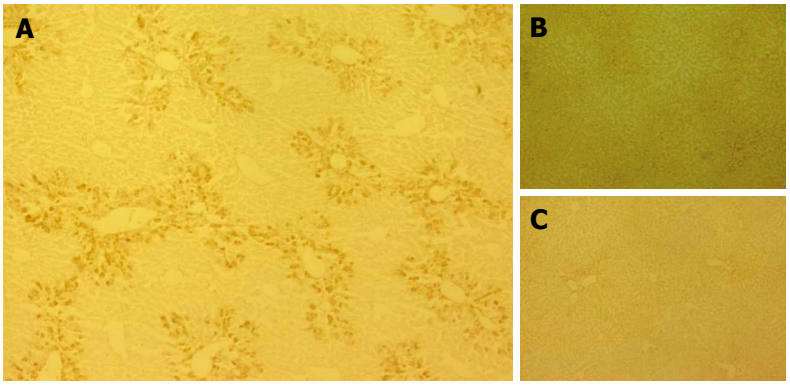

Figure 2 Migration of ES cells into CCl_4-treated mouse livers. GFP-immuno-positivity was examined in the liver specimens on PD 10. **A**: Immunoreactivity against GFP was clearly observed in the liver sections of Group 1 mice and GFP was predominantly distributed in the portal regions; **B**, **C**: No GFP-positive cells were detected in liver sections of group 2 (**B**) and group 3 mice (**C**).

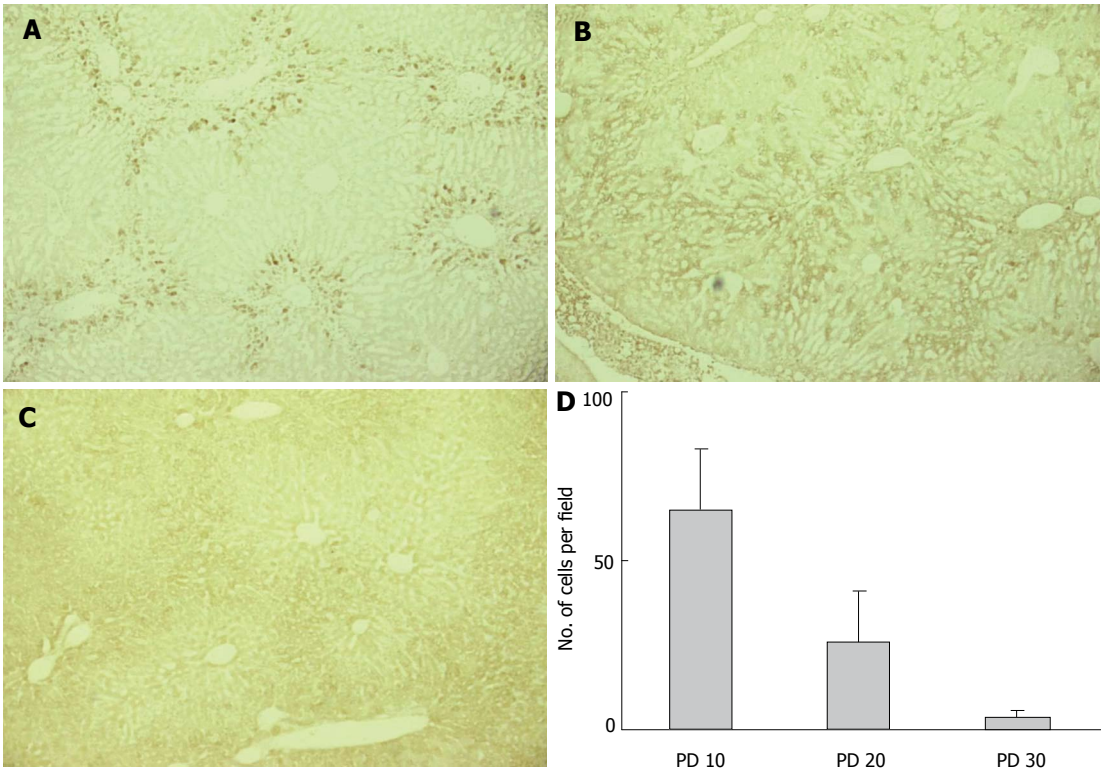

Figure 3 Disappearing GFP-immuno-positivity. GFP-immuno-positivity on PD 10, 20, and 30 was examined using liver specimens from group 1 mice. **A**: GFP-immunoreactivity was clearly observed in the periportal regions on PD 10; **B**: GFP-immunoreactivity was still detected on PD 20, though the intensity was weaker than on PD 10. Cells presenting GFP-immunoreactivity were more inwardly distributed in the hepatic lobules, as compared to PD 10; **C**: Scant or no GFP-immuno-positivity was detected on PD 30; **D**: The average numbers of GFP-positive cells around the portal vein were determined after examining 10 microscopic fields in the periportal area at 400 x magnification.

periportal area showed a higher level of intensity. Double immunofluorescent studies on PD 20 demonstrated that most of the GFP-immuno-positive cells expressed ALB, α1AT, and CK18 (Figure 4B). Further, the expression of HNF4α, a transcription factor necessary for complete differentiation of hepatocytes *in vivo*[29], was confirmed in GFP-immuno-positive cells (Figure 4C). In contrast to the expression of hepatocyte-related markers on GFP-positive cells, there were no CK19-positive ES-derived cells (Figure 4D).

Expression of hepatoblast marker on GFP-positive cells

Next, we used an antibody against DLK for an immunohistochemical examination of the involvement of recapitulating developmental processes. DLK is a molecule identified as a possible hepatoblast marker and known to be strongly expressed on hepatoblasts in mouse embryonic livers until embryonic d 16.5, after which it becomes downregulated and disappears by birth[28]. Immunoreactivity against DLK was clearly observed in the periportal regions on PD 10 (Figure 5A, left), though few DLK-immuno-positive cells were present in the hepatic lobules on PD 20 (Figure 5A, right). A double immunofluorescent study on PD 10 showed that the DLK-immuno-positive cells were also GFP-immuno-positive (Figure 5C).

Decreased fibrosis after ES transplantation

Liver fibrosis was histologically evaluated using picro-Sirius red staining. Representative liver sections stained with Sirius red are shown in Figure 6. The five-week treatment with CCl_4 induced liver fibrosis in group C mice, whereas decreased fibrosis was observed in group 1, which received ES cells (Figure 6B).

Tumor formation

All of the livers in the experimental animals were removed and the lobes sliced into 2-mm widths, with specimens from the middle lobes used for microscopic analysis. No tumor formation was observed macroscopically or

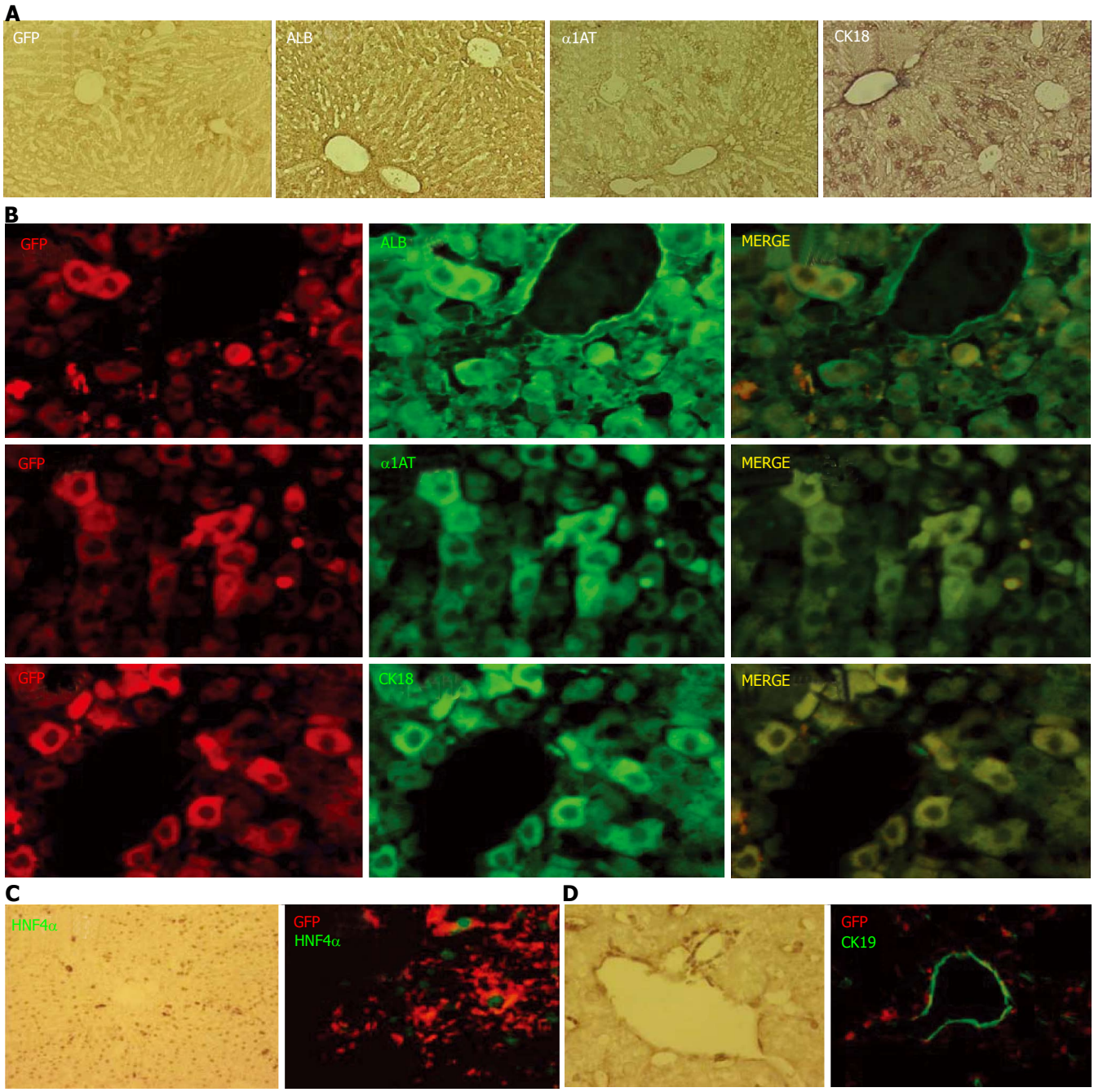

Figure 4 Expression of hepatocyte-related markers on GFP-positive cells. **A**: Prior to conducting immunofluorescent studies, the expression of GFP, ALB, α1AT, and CK18 on PD 20 was examined using a conventional method; **B**, **C**: Double immunofluorescent studies on PD 20 demonstrated that most of the GFP-immuno-positive cells expressed ALB, α1AT, and CK18; **C**: Expression of HNF4α was confirmed in the GFP-immuno-positive cells; **D**: There were no CK19-positive ES-derived cells.

microscopically in any of the livers. All of the spleens were also examined macroscopically and microscopically, and no tumors were found. Further, no tumor development in any organs other than the liver and spleen was observed for up to 30 d after transplantation.

DISCUSSION

In the present study, we demonstrated that ES cells migrated to the liver and differentiated into hepatocyte-like cells after intrasplenic transplantation. It is reasonable to speculate that generation of a favorable microenvironment is required in the recipient liver for undifferentiated ES cells to differentiate into hepatocytes. We adopted a method of repeated CCl_4 administration to induce undifferentiated ES cells into hepatocyte-like cells. It has been reported that BMSCs intravenously transplanted into mice that received repeated CCl_4 treatments migrated to the liver and differentiated into hepatocytes[23], suggesting that a favorable condition was generated in the CCl_4-treated livers to trap exogenously administered BMSCs and allow them differentiate into hepatocyte-like cells. Although the mechanisms by which a CCl_4-treated liver favors hepatic differentiation of BMSCs remain to be elucidated, we considered that CCl_4 treatment provides a suitable condition for ES cells to differentiate into

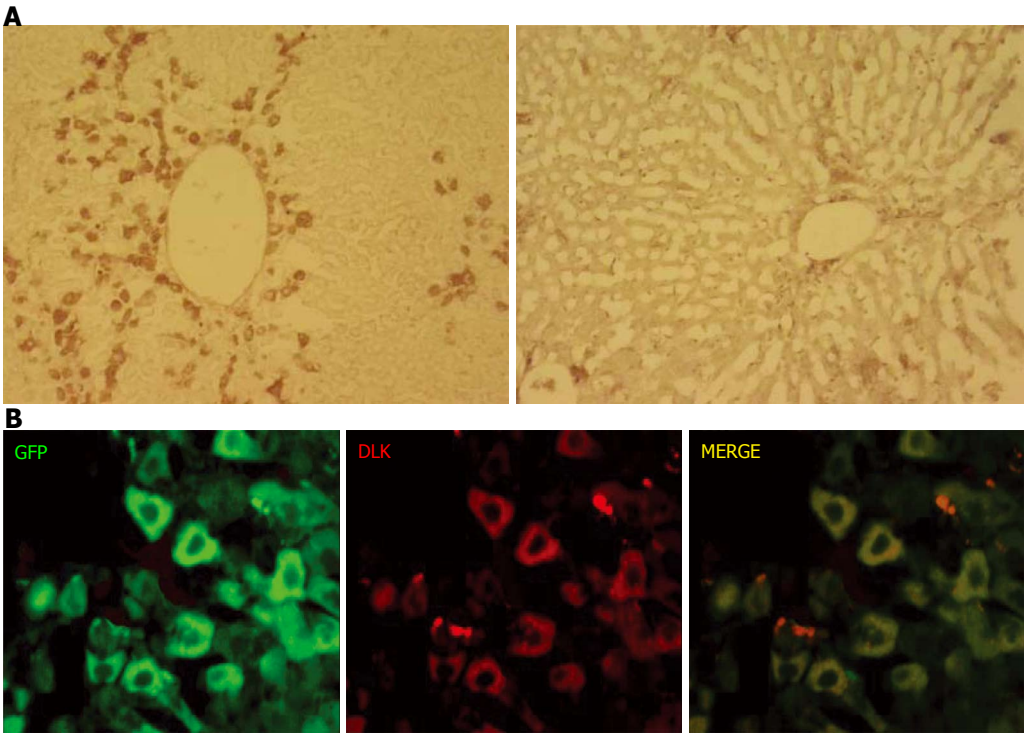

Figure 5 Expression of hepatoblast marker DLK on GFP-positive cells. **A**: DLK-immuno-positivity was examined on PD 10 (left) and PD 20 (right). A number of cells showed immunoreactivity against DLK on PD 10, whereas there were few on PD 20; **B**: Most of GFP-immunopositive cells on PD 10 were positive for DLK.S.

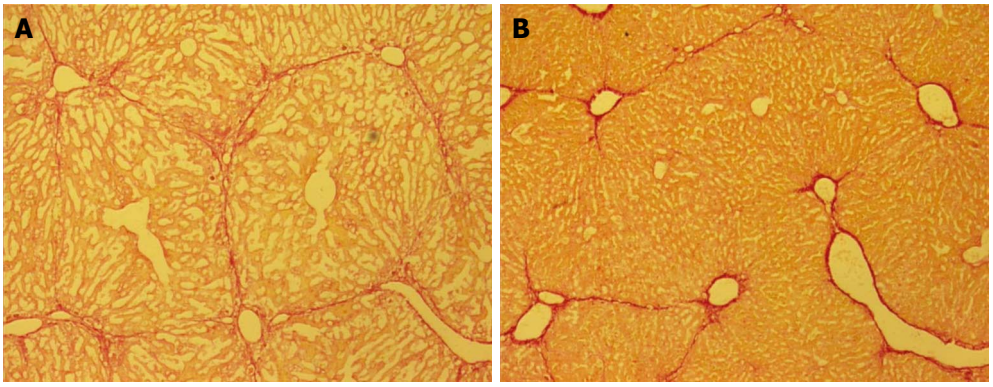

Figure 6 Decreased fibrosis after ES transplantation. Liver fibrosis was histologically evaluated on PD 30 using picro-Sirius red staining. Representative liver histology results for group 3 (**A**) and group 1 (**B**) mice. Decreased fibrosis was observed in group 1 mice, as compared to those in group 3.

hepatocyte-like cells in a manner similar to that for BMSCs. In addition to the differentiation of BMSCs into hepatocyte-like cells *in vivo*, that of hematopoietic stem cells (HSCs) into hepatocyte-like cells has been reported using a coculture with hepatocytes from CCl_4-treated livers[30]. Based on those reports, we transplanted ES cells into CCl_4-treated livers of mice with the expectation that they would differentiate into hepatocyte-like cells.

We found that ES cells migrated into the livers of the CCl_4-treated mice, whereas no such migration was observed in CCl_4-untreated mice. The migrated ES cells, shown by GFP-immuno-positivity, were distributed in the periportal regions on PD 10 and 20, and disappeared by PD 30. GFP-immuno-positive ES-derived cells in the livers on PD 20 were also immuno-positive for the hepatocyte-related markers ALB, α1AT, and CK18, suggesting their successful differentiation into hepatocyte-like cells. Further, the expression of HNF4α, an important transcription factor for hepatocyte maturation, was also observed in the ES-derived cells in our immunohistochemical examination. These results suggest that a CCl_4-treated liver has the ability to support homing and hepatic differentiation of undifferentiated ES cells.

It is difficult to fully elucidate the mechanisms involved with generation of ES-derived hepatocyte-like cells in the liver. However, we considered that recapitulation of the developmental process in the liver may have a role. In the present study, we tested for immunopositive reactions to DLK, which is a molecule that has been identified as a possible hepatoblast marker and shown to be strongly expressed on hepatoblasts in mouse embryonic livers until embryonic d 16.5, after which it was downregulated and disappeared by birth[28]. DLK-positive cells were detected and found to have a similar distribution as GFP-positive cells in the CCl_4-treated livers, as they were markedly present in the periportal regions on PD 10 and few in number on PD 20. Most of the GFP-positive cells were also immuno-positive for DLK on PD 10. These results strongly suggest that mechanisms similar to those related to hepatocyte development are involved in generating ES-derived hepatocyte-like cells. Apart from the involvement of recapitulated liver development, it is known that oval

cells are activated to proliferate following extensive and chronic liver damage with inhibited proliferation of hepatocytes[31,32]. Those cells are considered to represent a type of hepatic stem cells derived from the canal of Hering[33-35]. Although we did not examine for the presence of oval cells in the present study, some GFP-positive grafted cells may also express markers for those cells, as shown in the case of BMC transplantation to CCl_4-treated mice.

Because of the risk of tumor formation, we transplanted small numbers of undifferentiated ES cells in the present study. Using a rat model of Parkinson's disease, it was initially reported that transplantation of small numbers of mouse ES cells increases the influence of the host tissue and allows for default differentiation[36]. Therefore, we used 10^5 cells for intrasplenic transplantation, which was 20-fold fewer than the number of transplanted ES cells in a previous report[9], in which teratoma formation in the liver was documented. Nevertheless, we expected teratoma development, because ES cells in an undifferentiated state were utilized as graft cells. However, no tumors developed in the livers or spleens in the mice that received transplants up to the end of the 30-d experimental period. This observation might be explained by the disappearance of GFP-immuno-positive cells from the liver by PD 30. PCR analysis of liver tissue specimens collected on PD 30 using a GFP-specific primer set failed to reveal PCR products (data not shown), suggesting the absence of transplanted ES cells or ES-derived cells in the liver. A previous study[23] reported that transplanted BMSC cells were retained in the liver under conditions of persistent CCl_4 treatment. We consider that one of the reasons for the elimination of grafted ES cells seen in our study was because of the allogeneic transplantation method utilized, as the grafted ES cells were derived from 129SVJ mice and the donor mice were C57BL6, even though 129SVJ and C57BL6 are classified as the same haplotype, $H\text{-}2^b$. It is conceivable that an immunological barrier may eliminate non-self-grafted cells, leading to the absence of ES-derived cells and no occurrence of tumor formation.

Interestingly, a reduction of liver fibrosis was observed on PD 30 in CCl_4-treated mice that underwent ES-cell transplantation, despite the absence of grafted cells in the liver. It has been reported that transplantation of BMSCs[37] and BM-derived mesenchymal stem cells[38] had a protective effect against fibrosis in livers chronically damaged by administration of CCl_4. However, no results of the effects of ES cells on hepatic fibrosis are known to have been reported. Thus, there may be some common mechanisms underlying the improvement of hepatic fibrosis following the transplantation of cells with stem cell characteristics, as has been reported in the case of BMSCs.

Recently, it was reported that mouse undifferentiated ES cells fused with mouse bone marrow cells and neural stem cells *in vitro*[39,40]. Further, hybrid hepatocytes were produced by cell fusion between embryoid body-derived cynomolgus monkey ES cells and hepatocytes from uPA/SCID mice[41]. In the present study, we did not investigate whether generation of GFP-immuno-positive hepatocyte-like cells in the liver was due simply to the differentiation of the transplanted ES cells, or to cell fusion between ES cells and hepatocytes. In the near future, we intend to perform FISH analyses using a set of mouse chromosome X- and Y-specific probes.

In conclusion, we found that undifferentiated ES cells grafted into the spleen migrated to the liver and developed into hepatocyte-like cells without apparent tumor formation in CCl_4-treated mice. Although a prolonged presence of grafted cells in the liver was not observed, a beneficial effect of inhibiting fibrosis was obtained by the present single transplantation method. In the coming era of control of cell growth, undifferentiated ES cells may be directly used for therapeutic transplantation as well as terminally differentiated derivatives.

REFERENCES

1 **Evans MJ**, Kaufman MH. Establishment in culture of pluripotential cells from mouse embryos. *Nature* 1981; **292**: 154-156
2 **Martin GR**. Isolation of a pluripotent cell line from early mouse embryos cultured in medium conditioned by teratocarcinoma stem cells. *Proc Natl Acad Sci USA* 1981; **78**: 7634-7638
3 **Yamada T**, Yoshikawa M, Kanda S, Kato Y, Nakajima Y, Ishizaka S, Tsunoda Y. In vitro differentiation of embryonic stem cells into hepatocyte-like cells identified by cellular uptake of indocyanine green. *Stem Cells* 2002; **20**: 146-154
4 **Kanda S**, Shiroi A, Ouji Y, Birumachi J, Ueda S, Fukui H, Tatsumi K, Ishizaka S, Takahashi Y, Yoshikawa M. In vitro differentiation of hepatocyte-like cells from embryonic stem cells promoted by gene transfer of hepatocyte nuclear factor 3 beta. *Hepatol Res* 2003; **26**: 225-231
5 **Ishizaka S**, Shiroi A, Kanda S, Yoshikawa M, Tsujinoue H, Kuriyama S, Hasuma T, Nakatani K, Takahashi K. Development of hepatocytes from ES cells after transfection with the HNF-3beta gene. *FASEB J* 2002; **16**: 1444-1446
6 **Abe K**, Niwa H, Iwase K, Takiguchi M, Mori M, Abé SI, Abe K, Yamamura KI. Endoderm-specific gene expression in embryonic stem cells differentiated to embryoid bodies. *Exp Cell Res* 1996; **229**: 27-34
7 **Jones EA**, Tosh D, Wilson DI, Lindsay S, Forrester LM. Hepatic differentiation of murine embryonic stem cells. *Exp Cell Res* 2002; **272**: 15-22
8 **Miyashita H**, Suzuki A, Fukao K, Nakauchi H, Taniguchi H. Evidence for hepatocyte differentiation from embryonic stem cells in vitro. *Cell Transplant* 2002; **11**: 429-434
9 **Chinzei R**, Tanaka Y, Shimizu-Saito K, Hara Y, Kakinuma S, Watanabe M, Teramoto K, Arii S, Takase K, Sato C, Terada N, Teraoka H. Embryoid-body cells derived from a mouse embryonic stem cell line show differentiation into functional hepatocytes. *Hepatology* 2002; **36**: 22-29
10 **Kumashiro Y**, Asahina K, Ozeki R, Shimizu-Saito K, Tanaka Y, Kida Y, Inoue K, Kaneko M, Sato T, Teramoto K, Arii S, Teraoka H. Enrichment of hepatocytes differentiated from mouse embryonic stem cells as a transplantable source. *Transplantation* 2005; **79**: 550-557
11 **Asahina K**, Fujimori H, Shimizu-Saito K, Kumashiro Y, Okamura K, Tanaka Y, Teramoto K, Arii S, Teraoka H. Expression of the liver-specific gene Cyp7a1 reveals hepatic differentiation in embryoid bodies derived from mouse embryonic stem cells. *Genes Cells* 2004; **9**: 1297-1308
12 **Hamazaki T**, Iiboshi Y, Oka M, Papst PJ, Meacham AM, Zon LI, Terada N. Hepatic maturation in differentiating embryonic stem cells in vitro. *FEBS Lett* 2001; **497**: 15-19
13 **Kuai XL**, Cong XQ, Li XL, Xiao SD. Generation of hepatocytes from cultured mouse embryonic stem cells. *Liver Transpl* 2003;

9: 1094-1099
14 **Hu AB**, Cai JY, Zheng QC, He XQ, Shan Y, Pan YL, Zeng GC, Hong A, Dai Y, Li LS. High-ratio differentiation of embryonic stem cells into hepatocytes in vitro. *Liver Int* 2004; **24**: 237-245
15 **Kania G**, Blyszczuk P, Jochheim A, Ott M, Wobus AM. Generation of glycogen- and albumin-producing hepatocyte-like cells from embryonic stem cells. *Biol Chem* 2004; **385**: 943-953
16 **Jochheim A**, Hillemann T, Kania G, Scharf J, Attaran M, Manns MP, Wobus AM, Ott M. Quantitative gene expression profiling reveals a fetal hepatic phenotype of murine ES-derived hepatocytes. *Int J Dev Biol* 2004; **48**: 23-29
17 **Shirahashi H**, Wu J, Yamamoto N, Catana A, Wege H, Wager B, Okita K, Zern MA. Differentiation of human and mouse embryonic stem cells along a hepatocyte lineage. *Cell Transplant* 2004; **13**: 197-211
18 **Imamura T**, Cui L, Teng R, Johkura K, Okouchi Y, Asanuma K, Ogiwara N, Sasaki K. Embryonic stem cell-derived embryoid bodies in three-dimensional culture system form hepatocyte-like cells in vitro and in vivo. *Tissue Eng* 2004; **10**: 1716-1724
19 **Kubo A**, Shinozaki K, Shannon JM, Kouskoff V, Kennedy M, Woo S, Fehling HJ, Keller G. Development of definitive endoderm from embryonic stem cells in culture. *Development* 2004; **131**: 1651-1662
20 **Teratani T**, Yamamoto H, Aoyagi K, Sasaki H, Asari A, Quinn G, Sasaki H, Terada M, Ochiya T. Direct hepatic fate specification from mouse embryonic stem cells. *Hepatology* 2005; **41**: 836-846
21 **Levinson-Dushnik M**, Benvenisty N. Involvement of hepatocyte nuclear factor 3 in endoderm differentiation of embryonic stem cells. *Mol Cell Biol* 1997; **17**: 3817-3822
22 **Choi D**, Oh HJ, Chang UJ, Koo SK, Jiang JX, Hwang SY, Lee JD, Yeoh GC, Shin HS, Lee JS, Oh B. In vivo differentiation of mouse embryonic stem cells into hepatocytes. *Cell Transplant* 2002; **11**: 359-368
23 **Terai S**, Sakaida I, Yamamoto N, Omori K, Watanabe T, Ohata S, Katada T, Miyamoto K, Shinoda K, Nishina H, Okita K. An in vivo model for monitoring trans-differentiation of bone marrow cells into functional hepatocytes. *J Biochem* 2003; **134**: 551-558
24 **Niwa H**, Miyazaki J, Smith AG. Quantitative expression of Oct-3/4 defines differentiation, dedifferentiation or self-renewal of ES cells. *Nat Genet* 2000; **24**: 372-376
25 **Nishimura F**, Yoshikawa M, Kanda S, Nonaka M, Yokota H, Shiroi A, Nakase H, Hirabayashi H, Ouji Y, Birumachi J, Ishizaka S, Sakaki T. Potential use of embryonic stem cells for the treatment of mouse parkinsonian models: improved behavior by transplantation of in vitro differentiated dopaminergic neurons from embryonic stem cells. *Stem Cells* 2003; **21**: 171-180
26 **Hooper M**, Hardy K, Handyside A, Hunter S, Monk M. HPRT-deficient (Lesch-Nyhan) mouse embryos derived from germline colonization by cultured cells. *Nature* 1987; **326**: 292-295
27 **Hsu SM**, Raine L, Fanger H. Use of avidin-biotin-peroxidase complex (ABC) in immunoperoxidase techniques: a comparison between ABC and unlabeled antibody (PAP) procedures. *J Histochem Cytochem* 1981; **29**: 577-580
28 **Tanimizu N**, Nishikawa M, Saito H, Tsujimura T, Miyajima A. Isolation of hepatoblasts based on the expression of Dlk/Pref-1. *J Cell Sci* 2003; **116**: 1775-1786
29 **Li J**, Ning G, Duncan SA. Mammalian hepatocyte differentiation requires the transcription factor HNF-4alpha. *Genes Dev* 2000; **14**: 464-474
30 **Jang YY**, Collector MI, Baylin SB, Diehl AM, Sharkis SJ. Hematopoietic stem cells convert into liver cells within days without fusion. *Nat Cell Biol* 2004; **6**: 532-539
31 **Petersen BE**, Zajac VF, Michalopoulos GK. Hepatic oval cell activation in response to injury following chemically induced periportal or pericentral damage in rats. *Hepatology* 1998; **27**: 1030-1038
32 **Paku S**, Schnur J, Nagy P, Thorgeirsson SS. Origin and structural evolution of the early proliferating oval cells in rat liver. *Am J Pathol* 2001; **158**: 1313-1323
33 **Theise ND**, Saxena R, Portmann BC, Thung SN, Yee H, Chiriboga L, Kumar A, Crawford JM. The canals of Hering and hepatic stem cells in humans. *Hepatology* 1999; **30**: 1425-1433
34 **Saxena R**, Theise N. Canals of Hering: recent insights and current knowledge. *Semin Liver Dis* 2004; **24**: 43-48
35 **Zhang Y**, Bai XF, Huang CX. Hepatic stem cells: existence and origin. *World J Gastroenterol* 2003; **9**: 201-204
36 **Bjorklund LM**, Sánchez-Pernaute R, Chung S, Andersson T, Chen IY, McNaught KS, Brownell AL, Jenkins BG, Wahlestedt C, Kim KS, Isacson O. Embryonic stem cells develop into functional dopaminergic neurons after transplantation in a Parkinson rat model. Proc *Natl Acad Sci USA* 2002; 99: 2344-2349
37 **Sakaida I**, Terai S, Yamamoto N, Aoyama K, Ishikawa T, Nishina H, Okita K. Transplantation of bone marrow cells reduces CCl4-induced liver fibrosis in mice. *Hepatology* 2004; **40**: 1304-1311
38 **Zhao DC**, Lei JX, Chen R, Yu WH, Zhang XM, Li SN, Xiang P. Bone marrow-derived mesenchymal stem cells protect against experimental liver fibrosis in rats. *World J Gastroenterol* 2005; **11**: 3431-3440
39 **Terada N**, Hamazaki T, Oka M, Hoki M, Mastalerz DM, Nakano Y, Meyer EM, Morel L, Petersen BE, Scott EW. Bone marrow cells adopt the phenotype of other cells by spontaneous cell fusion. *Nature* 2002; **416**: 542-545
40 **Ying QL**, Nichols J, Evans EP, Smith AG. Changing potency by spontaneous fusion. *Nature* 2002; **416**: 545-548
41 **Okamura K**, Asahina K, Fujimori H, Ozeki R, Shimizu-Saito K, Tanaka Y, Teramoto K, Arii S, Takase K, Kataoka M, Soeno Y, Tateno C, Yoshizato K, Teraoka H. Generation of hybrid hepatocytes by cell fusion from monkey embryoid body cells in the injured mouse liver. *Histochem Cell Biol* 2006; **125**: 247-257

S- Editor Wang J **L- Editor** Alpini GD **E- Editor** Lu W

PO Box 2345, Beijing 100023, China
www.wjgnet.com
wjg@wjgnet.com

World J Gastroenterol 2007 February 14; 13(6): 874-881
World Journal of Gastroenterology ISSN 1007-9327

BASIC RESEARCH

Effects of hypothalamic paraventricular nuclei on apoptosis and proliferation of gastric mucosal cells induced by ischemia/reperfusion in rats

Li Li, Yong-Mei Zhang, Wei-Li Qiao, Lin Wang, Jian-Fu Zhang

Li Li, Department of Pathophysiology, Xuzhou Medical College, 84 West Huaihai Road, Xuzhou 221002, Jiangsu Province, China
Yong-Mei Zhang, Wei-Li Qiao, Jian-Fu Zhang, Department of Physiology, Xuzhou Medical College, 84 West Huaihai Road, Xuzhou 221002, Jiangsu Province, China
Yong-Mei Zhang, Jian-Fu Zhang, Department of Neurobiology; Xuzhou Medical College, 84 West Huaihai Road, Xuzhou 221002, Jiangsu Province, China
Lin Wang, Department of Histology and Embryology, Xuzhou Medical College, 84 West Huaihai Road, Xuzhou 221002, Jiangsu Province, China
Supported by grants from the National Natural Science Foundation of China, No. 30370533, 30570671 and the Educational Department Science Research Foundation of Jiangsu Province, No. 99KJB310005, 05KJB310134
Correspondence to: Professor Jian-Fu Zhang, Department of Physiology, Xuzhou Medical College, Xuzhou 221002, Jiangsu Province, China. jfzhang@xzmc.edu.cn
Telephone: +86-516-85748461 Fax: +86-516-83262004
Received: 2006-10-23 Accepted: 2006-12-29

Abstract

AIM: To investigate the effects of electrical stimulation of hypothalamic paraventricular nuclei (PVN) on gastric mucosal cellular apoptosis and proliferation induced by gastric ischemia/reperfusion (I/R) injury.

METHODS: For different experimental purposes, stimulating electrode plantation or electrolytic destruction of the PVN was applied, then the animals' GI/R injury model was established by clamping the celiac artery for 30 min and allowing reperfusing the artery for 30 min, 1 h, 3 h or 6 h respectively. Then histological, immunohistochemistry methods were used to assess the gastric mucosal damage index, the gastric mucosal cellular apoptosis and proliferation at different times.

RESULTS: The electrical stimulation of PVN significantly attenuated the GI/R injury at 30 min, 1 h and 3 h after reperfusion. The electrical stimulation of PVN decreased gastric mucosal apoptosis and increased gastric mucosal proliferation. The electrolytic destruction of the PVN could eliminate the protective effects of electrical stimulation of PVN on GI/R injury. These results indicated that the PVN participated in the regulation of GI/R injury as a specific area in the brain, exerting protective effects against the GI/R injury, and the protection was associated with the inhibition of cellular apoptosis and the promotion of gastric mucosal proliferation.

CONCLUSION: Stimulating PVN significantly inhibits the gastric mucosal cellular apoptosis and promots gastric mucosal cellular proliferation. This may explain the protective mechanisms of electrical stimulation of PVN against GI/R injury.

Key words: Hypothalamic paraventricular nuclei; Gastric ischemia/reperfusion; Proliferation; Apoptosis

Li L, Zhang YM, Qiao WL, Wang L, Zhang JF. Effects of hypothalamic paraventricular nuclei on apoptosis and proliferation of gastric mucosal cells induced by ischemia/reperfusion in rats. *World J Gastroenterol* 2007; 13(6): 874-881

http://www.wjgnet.com/1007-9327/13/874.asp

INTRODUCTION

Since the 1980s, ischemia-reperfusion (I/R) injury of organs has been frequently encountered as a complex phenomenon in medicine and biology. Researches have been focused on I/R injury of organs such as the heart, brain, lungs, and the kidneys. In recent years, there has been an increase in the available information concerning the acute gastric mucosal injury induced by I/R, or gastric I/R injury[1-4]. The investigative key points have focused on the effects of individual factors on gastric mucosal injury induced by gastric I/R, including increase of oxygen free radicals and endothelin level, microvascular dysfunction, polymorphonuclear leukocyte infiltration, nitric oxide release, gastric acid secretion, prostaglandin decrease and so on[5-15]. Some researchers have quested the best methods to protect the gastric mucosa against gastric I/R injury, such as the endothelin converting enzyme inhibitor phosphoramidon[16], the anti-reactive oxygen species drug, tetrahydrabioptin[9] and the adhesion molecules of anti-leukocytes[17]. However, little is known about the systemic regulation of gastric I/R injury, particularly the role of related central nuclei.

It has been known that the gastric mucosal tissue integrity depends upon the interplay between cell renewal

and death of damaged or aged cells. The gastric mucosa has a high renewal rate, and all gastric mucosal surface epithelial cells are replaced within 3-5 d as the exfoliated surface mucosal cells are replaced by cells migrating from the glandular foveolar and neck area[18]. The mucosa is maintained by the balance between proliferation and apoptosis of gastric mucosal cells. To study the imbalance between proliferation and apoptosis is of great significance in understanding the causes of gastric lesions.

Recently, literature reviews revealed that I/R could induce tissue injury and cellular apoptosis in many important organs[19-25]. Apoptosis of gastric mucosal cells has also been studied under varied conditions in rats, including ethanol, non-steroidal anti-inflammatory drugs, retinoic acids, *H pylori* infection[26-30]. Some reports of gastric mucosal cellular apoptosis induced by gastric I/R are contradictory. Fukuyama *et al*[31], for example, reported that apoptosis is not induced in the gastric mucosa after gastric I/R. Wada *et al*[32] demonstrated that gastric I/R induces significant apoptosis in the gastric mucosa. However, the central regulation of gastric mucosal cellular apoptosis and proliferation induced by gastric I/R in rats has not yet been fully elucidated.

In his early study[33], Salim pointed out that hypothalamus, especially the paraventricular nuclei (PVN), is extraordinarily complex in its structure and function. It participates in the regulation of various activities of the stomach, including secretion, electrical activation and gastric motor. Our previous study[34] showed that PVN and its associated nuclei could regulate the development of restraint and cold-water immersion stress-induced ulcer in stomach and that PVN is involved in the regulation of gastric I/R injury as one of the specific CNS areas attenuating gastric I/R injury[35]. The cellular mechanisms responsible for the attenuation of GI/R injury by electrical stimulation of PVN are still unknown.

The aim of our study is to investigate the molecular mechanisms of stimulating PVN in protecting against gastric I/R injury, to observe the characteristics of gastric mucosal cellular apoptosis and proliferation induced by gastric I/R at various times. It is believed that any progress in this field will help better understand the pathology of gastric I/R injury at cellular level.

MATERIALS AND METHODS

Reagents

M30 CytoDEATH monoclonal antibody was obtained from Roche (Basel, Switzerland). Mouse anti-rat proliferative nucleolus monoclonal antibody (proliferative cell nuclear antigen, PCNA), PowerVision^{TM} two-step immunohistochemistry detection kit, and 3.3' -diaminobenzidine (DAB; Maixin-Bio Co., China) substrate solution were obtained from Zhongshan Biotech Co. (Beijing, China).

Animals

Groups of six adult male Sprague-Dawley rats, weighing 180-220g,were supplied by the Experimental Animal Center of Xuzhou Medical College (usage certificate of experimental animals, No: SYXK (su) 2002-0038). All experiments were carried out in accordance with the National Institute of Health Guide for the Care and Use of Laboratory Animals. The animals were housed under controlled temperature (22-24℃) and photoperiod (12 h light: 12 h dark) in wire-mesh-floor cages to prevent ingestion of hair and feces. The animals were fasted for 24 h before the experiment with free access to tap water. The animals were allocated to different groups to serve as gastric I/R injury models for different purposes in the experiments.

Electrical stimulation of PVN

Three days before the experiment, the rats were anesthetized with sodium pentobarbital (40 mg/kg i.p.) and mounted onto a stereotaxic apparatus. The scalp was incised, and a 0.5 mm hole was drilled in the cranium dorsal to the target site. The coordinates of PVN for the placement of electrodes were taken from the atlas of Paxinos and Watson[36] as follows: AP 1.5 mm, LR 0.4 mm, H 7.7-7.8 mm, and the incisor bar was positioned 3.3 mm below the center of the aural bars.

The concentric bipolar stimulating electrode is consisted of an insulated outer barrel formed from the needle of a medical syringe (0.4 mm in diameter) and an inner Ni-Cr wire, insulated except for the tip, which protrudes about 0.2 mm from the barrel. The stimulating electrode was inserted into PVN and fixed to the cranium with dental cement.

During the experiment, the rat was also anesthetized with sodium pentobarbital (40 mg/kg i.p.). PVN was stimulated before the induction of gastric I/R injury. The electrical stimulating parameters have been described previously[35]. Stimulation was performed 5 times with uniphasic, constant current square wave pulses (pulse width 0.2 ms, intensity 0.4 mA, frequency 50 Hz, duration 1 min), at 5 min intervals. In the sham PVN stimulation group, only the electrode was inserted, and no current was passed.

Electrical destruction of PVN

Three days before the experiment, the rat was anesthetized with sodium pentobarbital (40 mg/kg i.p.) and mounted onto a stereotaxic apparatus. The coordinates of PVN for the placement of destructing electrodes was similar to that of the stimulating electrodes. The destructing electrodes was in bilateral PVN. The destructing electrode were placed a single stainless steel wire, 0.3 mm in diameter, with a naked tip about 0.3 mm, and void of insulation. Bilateral lesions were then made by passing a positive DC of 1 mA for 10 s. The lesion electrode was immediately removed after destruction. Sham operations were performed with the same surgical procedures, and no current was passed.

Preparation of gastric I/R model

The animal, were kept fasting for 24 h with free access to water before experiment. All experiments were carried out under anesthesia with sodium pentobarbital (40 mg/kg i.p.), the supplemental dose of the anesthetic was given i.p. to maintain animal anesthesia throughout the experiment. GastricI/R injury was induced according to the method of

Wada *et al*[37]. Briefly, the abdominal cavity was cut open, and the celiac artery and its adjacent tissues were carefully isolated. The celiac artery was first clamped with a small vascular clamp for 30 min to induce ischemia, and was then released to allow reperfusion for 30 min, 1 h, 3 h or 6 h respectively. Sham-operated animals underwent all of the surgical procedures except for the arterial clamping. At the end of each experiment, the rats with gastric I/R injury or sham-operated groups were killed by exsanguination via the abdominal aorta under anesthesia[38], while the rats with embedded electrode in PVN were killed by decapitation under deep anesthesia. The stomach was removed rapidly, opened along the great curvature, rinsed with ice-cold phosphate buffered saline (PBS, 0.1 mol/L), and spread onto a cold plate. The gastric mucosa was carefully examined grossly and microscopically.

Assessment of gastric mucosal injury index

Quantitative histological assessment of mucosal injury was performed with the method described by Guth *et al*[39] with slight modifications. The index is based on a cumulative-length scale. In which an individual lesion limited within the mucosal epithelium (including the pinpoint erosions, ulcers and hemorrhagic spots) is scored by giving points for its length. The score is 1 for a lesion $\leqslant$ 1 mm, 2 for a lesion > 1 mm and $\leqslant$ 2 mm, for a lesion > 2 mm $\leqslant$ 3 mm, and so on. For a lesion with a width > 1 mm, the lesion score is doubled. The sum of the scores represents the GMDI. To avoid the researcher's bias, the GMDI was determined by a researcher who was unfamiliar with the details of the experiment.

Immunohistochemical staining

Immunohistochemistry was performed with the streptavidin-peroxidase (SP) method[40]. The primary antibodies used were polyclonal antibody against proliferating cell nuclear antigen (PCNA), monoclonal antibody against M30 CytoDEATH. The gastric tissue samples were fixed in Bouin's fixative for paraffin tissue slices. Five-μm thick sections were, deparaffinized, rehydrated, and boiled. The dewaxed sections were heated in a microwave oven (700 W) for 12 min to retrieve the antigens, and cooled to room temperature. The endogenous peroxide was blocked with 3% hydrogen peroxide (H_2O_2) for 15 min in methanol. The sections were washed with PBS (0.01 mol/L), blocked with 10% goat serum for 15 min to reduce the non-specific antibody binding, and then incubated with the primary antibody (M30CytoDEATh 1:10, PCNA 1:50) at 4℃ overnight. The sections were washed twice for 5 min with PBS, incubated with the secondary anti-mouse immunoglobulin (Santa Cruz Inc., USA) conjugated with biotin at room temperature for 30 min, washed again with PBS (0.01 mol/L), and incubated with SP complex for 15 min. The reaction products of peroxidase were visualized by incubation with 0.05 mol/L Tris-HCl buffer (pH 7.6) containing 20 mg 3.3'-diaminobenzidine (DAB, Maixin-Bio Co. China) and 100 μL 5% H_2O_2 per 100 mL. The brown color signifying the presence of the antigen bound to the antibodies was detected by light microscopy. Finally, the sections were counterstained for nuclei with hematoxylin. The sections obtained from the control group were stained according to the same method except that PBS was substituted for the specific primary antibody. M30 CytoDEATH staining was quantified by calculating the average ratio of positive cells in 10 vision fields under a 400 × microscope. PCNA staining was quantified by calculating the average ratio of positive cells in 10 vision fields under a 100 × microscope.

Histological verification of stimulated or destructed PVN sites

At the end of each experiment, the PVN site was marked by passing a positive direct current of 1 mA for 10 s. The experimental rats were killed by decapitation under deep anesthesia, and the brains were removed and fixed in 10% formalin for 7 d. Frozen coronal serial sections (45 μm) were cut through the hypothalamus and mounted and stained with 1% neutral red to verify the sites of electrical stimulation under a light microscope. The data from rats whose target sites failed to meet the histological criteria were deleted from the statistical analysis.

Statistical analysis

All results are expressed as mean ± SE. Data were compared by an analysis of variance (ANOVA) followed by Student-Newman-keuls (SNK) test. All calculations were performed with SPSS 10.0 for Windows, $P < 0.05$ was considered statistically significant.

RESULTS

Histological verification of stimulated PVN sites

By referring to Paxinos and Watson's Stereotaxic Atlas[36], histological verification was performed at all sites of electrical stimulation (Figure 1)

Effects of electrical stimulation and electrolytic destruction of PVN on gastric I/R injury in rats

Our previous experiments confirmed that the GMDI of the gastric I/R injury only group is similar to that of sham electrically stimulated PVN plus gastric I/R injury group (sham PVN + gastric I/R injury) at the different time points during reperfusion. Thus, we compared the differences between GI/R only and PVN + gastric I/R injury groups in subsequent experiments.

As shown in Figure 2, gastric mucosal injury was not found (the GMDI being zero) in the sham-operated group. The stimulated PVN + normal stomach group or the destructed PVN + normal stomach group was similar to that of normal rat group. In the gastric I/R injury group, the GMDI was 94.67 ± 25.57 at 1 h after reperfusion. The GMDI was significantly lower in the electrical stimulation of PVN + gastric I/R injury group than in the gastric I/R injury only group at 1 h after reperfusion (94.67 ± 25.57 *vs* 54.83 ± 12.64, $P < 0.05$). The GMDI was not significantly different in the bilateral PVN destruction + gastric I/R injury group compared with that in the gastric I/R injury injury only group or sham stimulating PVN plus gastric I/R injury group (106.94 ± 20.91 *vs* 94.67 ± 25.57, $P > 0.05$), but was markedly higher than that gastric I/R injury the electrical stimulation of PVN + GI/R group (106.94

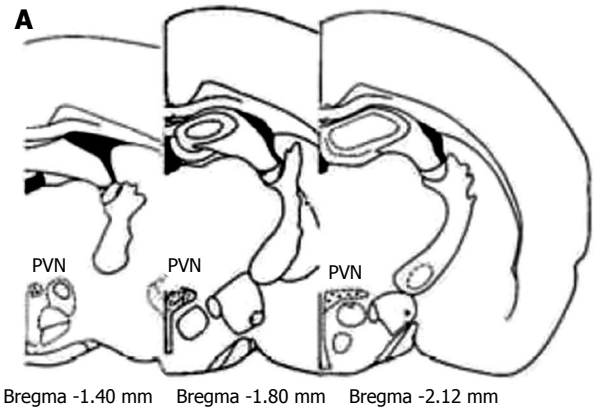

Figure 1 Sites of the stimulating electrode tip in PVN. **A**: Standard atlas sections of the rat brain showing the distributions of stimulating sites of the experimental animals; **B**: Photomicrographs of stimulating sites in the rat brain. The section stained with neutral red, showing the position of stimulating electrode tip by passing a positive DC of 1 mA for 10 s, which indicates a placement within the PVN.

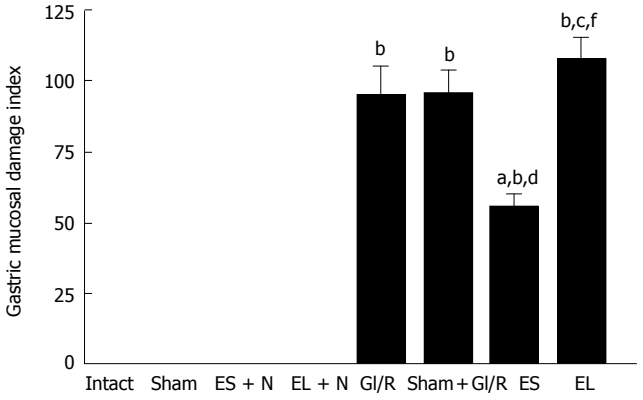

Figure 2 Effect of electrical stimulation and bilateral electrolytic destruction of PVN on gastric mucosal damage induced by I/R at 1 h after reperfusion in rats. Intact: normal rat; sham: sham-operation (electrode was inserted, with no current passing and no artery clamped); ES + N: intact stomach after electrical stimulation of the PVN. EL + N: intact stomach after bilateral electrolytic destruction of the PVN; GI/R injury: gastric ischemia-reperfusion injury; Sham+GI/R injury: sham electrical stimulation of the PVN plus GI/R injury; ES: electrical stimulation of the PVN plus GI/R injury; EL: bilateral electrolytic destruction of the PVN plus GI/R injury. Values of GMDI are mean ± SE (n = 6). $^{b}P < 0.01$ *vs* intact, $^{d}P < 0.01$ ES *vs* ES + N, $^{f}P < 0.01$ EL *vs* EL + N, $^{a}P < 0.05$, ES *vs* GI-R, $^{c}P < 0.05$, EL *vs* ES.

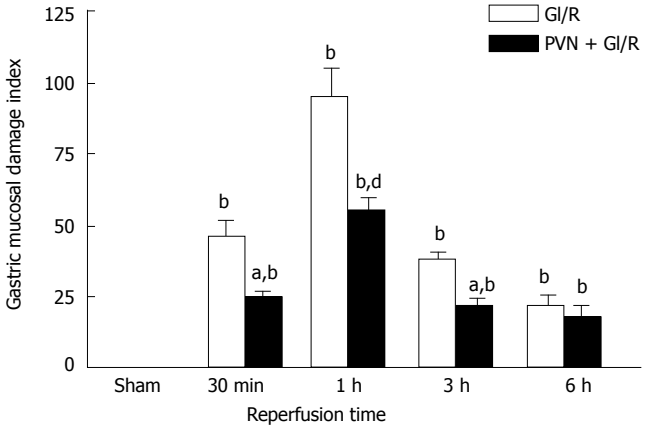

Figure 3 Effect of electrical stimulation of PVN on gastric mucosal damage induced by I/R at different times in rats. Sham: sham-operation(electrode was inserted, with no current passing and no artery clamped); GI/R: gastric ischemia/reperfusion was maintained for 30 min, 1 h, 3 h and 6 h after 30 min of ischemia, respectively; PVN + GI/R: electrical stimulation of the PVN plus GI/R. Values: Each column represents mean ± SE (n = 6). $^{b}P < 0.01$ *vs* sham; $^{a}P < 0.05$, $^{d}P < 0.01$, PVN + GI/R *vs* GI/R at different times.

± 20.91 *vs* 54.83 ± 12.64, $P < 0.05$).

As shown in Figure 3, in the gastric I/R injury group, the gastric mucosal lesions appeared 30 min after reperfusion, the GMDI reached maximum at 1h after reperfusion (94.67 ± 25.57), but then declined. In the group of PVN + gastric I/R, the GMDI was significantly lower than that the gastric I/R group at 30 min, 1 h and 3 h after reperfusion ($P < 0.01$). At 6 h after reperfusion, there was no significant difference ($P > 0.05$) between the GI/R group and the stimulating PVN + gastric I/R group.

Effect of electrical simulation of PVN on apoptosis of gastric mucosal cells induced by GI/R in rats

As shown in Figure 4, the M30 CytoDEATH positive apoptotic cells (i.e. apoptotic cells) were distributed predominantly in the upper part of the gastric glands and epithelial cells, where the cytoplasm was stained brown. In the normal gastric mucosa (Figure 4A and B), the few apoptotic cells were apparent. In the GI/R injury group, the percentage of apoptotic cells increased rapidly at the onset of reperfusion, and peaked at 1 h after reperfusion (6.32 times higher than that in the normal gastric mucosa, $P < 0.01$) (Figure 4C). Electrical stimulation of PVN markedly decreased the percentage of M30 CytoDEATH positive cells at 1 h after reperfusion (Figure 4 D), which declined to the basal level at 6 h after reperfusion (Figure 4E and F). Figure 4G indicates the negative control group.

As shown in Figure 5, the electrical stimulation of PVN significantly decreased the percentage of M30 CytoDEATH positive cells throughout the 6 h reperfusion ($P < 0.05$ or $P < 0.01$).

Effect of electrical stimulation of PVN on proliferation of gastric mucosal cells induced by GI/R in rats

As shown in Figure 6, the proliferating-positive cells were found in the normal gastric mucosa, which were distributed predominantly in the glandular neck area of the gastric mucosa (Figure 6 A and B). The percentage of proliferating cells decreased rapidly at 1 h after reperfusion

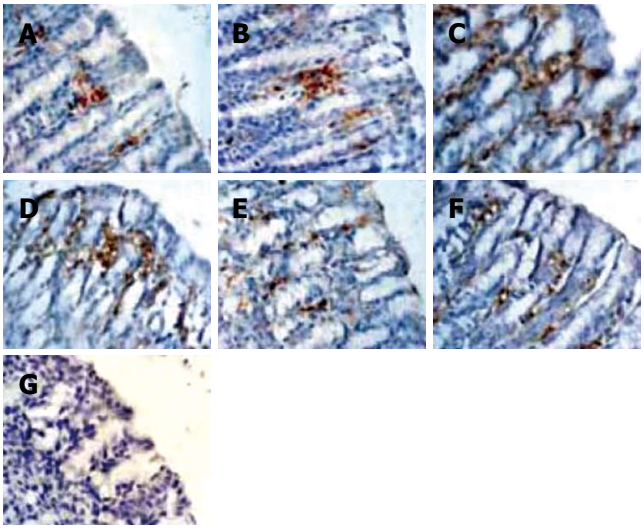

Figure 4 Histological exhibition of electrical stimulation of PVN on gastric mucosal apoptosis induced by I/R at different times in rats. The apoptotic-positive cells were probed with anti-M30 CytoDEATH antibody and counter-stained with hematoxylin in rat gastric mucosa (× 400). **A**: normal gastric mucosa; **B**: sham operation; **C**: GI/R at 1 h after reperfusion; **D**: PVN + GI/R at 1 h after reperfusion; **E**: GI/R at 6 h after reperfusion; **F**: PVN+GI/R at 6 h after reperfusion; **G**: negative control group.

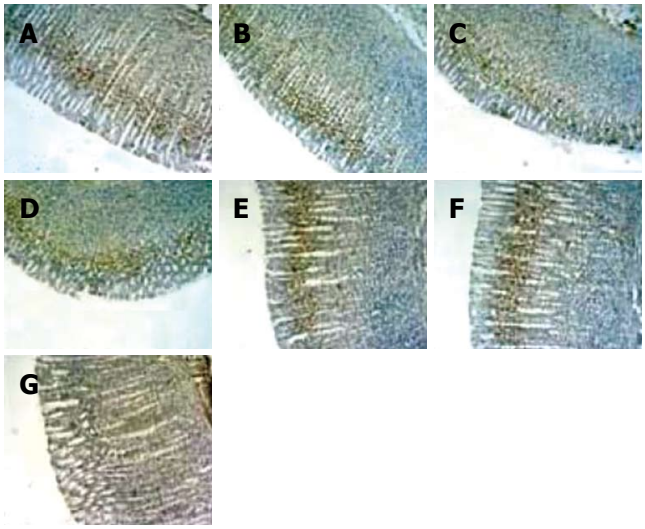

Figure 6 Histological exhibition of electrical stimulation of PVN on gastric mucosal cellular proliferation induced by I/R at different times in rats. Proliferating-positive cells were probed with anti-mouse anti-proliferating cell nuclear antigen (PCNA) antibody and counter stained with hematoxylin in gastric mucosa (× 100). **A**: normal control gastric mucosa; **B**: gastric mucosa after sham operation; **C**: GI/R, 1 h after reperfusion; **D**: PVN + GI/R, 1 h after reperfusion; **E**: GI/R, 6 h after reperfusion; **F**: PVN + GI-R, 6 h after reperfusion; **G**: negative control group.

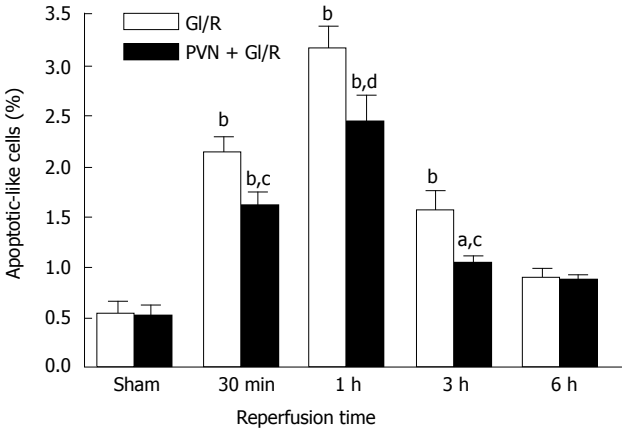

Figure 5 Effect of electrical stimulation of PVN on gastric mucosal cellular apoptosis induced by I/R at different time points in rats. Sham: sham-operation; GI/R: reperfusion was maintained for 30 min, 1 h, 3 h and 6 h after 30 min of ischemia, respectively; PVN + GI/R: electrical stimulation of PVN plus GI/R. The percentage of apoptotic cells was taken by counting the cells in 10 microscopic fields (× 400). Each column represents mean ± SE (n = 6). $^{a}P < 0.05$, $^{b}P < 0.01$, GI/R *vs* sham-operation; $^{c}P < 0.05$, $^{d}P < 0.01$, PVN + GI/R *vs* GI/R at each time point.

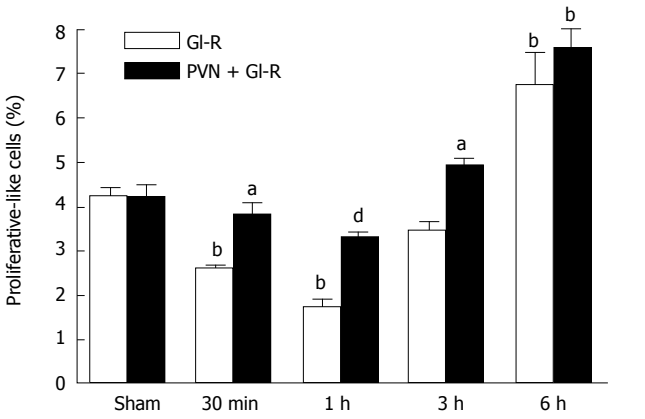

Figure 7 Effect of electrical stimulation of PVN on gastric mucosal proliferation induced by I/R at different times in rats. Sham: sham-operation; GI/R: reperfusion was maintained for 30 min, 1 h, 3 h and 6 h after 30 min of ischemia, respectively; PVN+GI/R: electrical stimulation of PVN plus GI/R. The percentage of proliferating cells was taken by using cell count in 10 microscopic fields (× 100). Each column represents an average value expressed in mean ± SE (n = 6). $^{b}P < 0.01$, GI/R *vs* sham operation; $^{a}P < 0.05$ and $^{d}P < 0.01$, PVN + GI/R *vs* GI/R.

(Figure 6C). The percentage of proliferating positive cells were significantly higher in the stimulating PVN + gastric I/R injury group than in the gastric I/R injury group (Figure 6D). The proliferating-positive cells accumulated in both the gastric I/R injury only group and the stimulating PVN + gastric I/R injury group at 6 h after reperfusion, and the crowding was not significantly different at this time (Figure 6E and F). Figure 6G negative control group.

Figure 7 also showes that the electrical stimulation of PVN significantly increased the percentage of proliferating-positive cells at 30 min (1.47 times), 1 h (1.89 times) and 3 h (1.43 times) after reperfusion compared with the respective values in the gastric I/R injury group.

DISCUSSION

In our present study, the gross gastric mucosa damage index was determined to evaluate the extent of gastric I/R injury. Immunohistochemistry was also used to assess the processes of gastric mucosal cellular apoptosis and proliferation in gastric I/R injury by detecting the apoptotic cells with the M30 CytoDEATH monoclonal antibody (which binds to a caspase-cleaved formalin-

resistant epitope of the cytokeratin 18 cytoskeletal protein in the cytoplasm of apoptotic cells) and by labelling the proliferating cells with multi-clonal antibodies to PCNA (an assistant factor of DNA polymerase)[41,42]. We assessed these variables at different times from 30 min to 6 h after reperfusion. We reasoned that our histological analysis the process would help us better understand the cellular mechanisms responsible for the reperfusion injury.

In our analysis of the GMDI data, which was obtained with gastric I/R injury model of anesthetized (sodium pentobarbital, 40 mg·kg^{-1}i.p.) rats, it was noticed that the gastric mucosal damage was localized within the mucosal epithelium, the lesions started to occur at 30 min after reperfusion, reached their peak at 1 h and then subsided. We dynamically observed the changes of apoptosis and proliferation of gastric mucosal cells at different times from 30 min to 6 h after gastric I/R injury, Histological study of the normal gastric mucosa revealed a few apoptotic cells in the superficial layer of gastric mucosa and proliferating cells only in the gastric glandular neck area. These patterns contrast with previous reports [43,44], supporting the notion that cell renewal and apoptosis are two essential processes maintaining the homeostasis of normal gastric mucosa. The pattern of simultaneous change in gastric mucosal cellular apoptosis during reperfusion is similar to that of gastric I/R injury; i.e., the level of apoptosis also reached its peak at 1 h after reperfusion when the gastric mucosal injury was most serious, and then declined. In contrast, the level of gastric mucosal cellular proliferation induced by ischemia/reperfusion also reached its minimum at 1 h after reperfusion, but the level of proliferation reached its maximum at 6 h after reperfusion, indicating that the proliferating process of gastric mucosal cells is slower than the apoptosis process. It is widely accepted that the gastric mucosal integrity depends on the balance between apoptosis and proliferation, which explains the equilibrium between cell renewal and death of damaged or aged cells, and that ischemia/reperfusion may induce mucosal injury by altering this balance.

In our present study, techniques of electrical stimulation and electrolytic destruction were adopted and the role of electrical stimulation of PVN in gastric mucosal injury, cellular apoptosis, and proliferation induced by gastric I/R injury were observed. It was found that PVN stimulation protected against gastric I/R injury. In the electrical stimulation of PVN plus gastric I/R group, the GMDI was significantly lower than that in the gastric I/R injury only group at 30 min, 1 h and 3 h after reperfusion. After bilateral PVN destruction, the GMDI was not significantly different from that in the gastric I/R only group, but it was significantly higher than that in electrical stimulation of PVN plus gastric I/R group ($P < 0.05$). Furthermore, our results also revealed that the electrical stimulation of PVN markedly decreased the expression of apoptotic-positive cells, and increased the expression of proliferating positive cells at 0.5, 1, 3 h after reperfusion, respectively. These results indicate that PVN participates in the regulation of gastric mucosal cellular apoptosis and proliferation after gastric I/R in rats. Inhibiting gastric mucosal cellular apoptosis and promoting gastric mucosal cellular proliferation might mediate the dramatic protective effect of PVN on gastric mucosal injury. Our data also support the notion that PVN is a specific center in the brain that maintains the integrity of gastric mucosa and modifies the equilibrium between gastric mucosal apoptosis and proliferation.

Our previous experimental results have testified that the protective effect against gastric I/R injury is related to the excitation of PVN neurons. We focused on the microinjection of L-glutamic acid (a neuronal stimulant) into PVN, and found that the chemical stimulation produces a similar effect to that of 0.4 mA electrical stimulation of PVN[35], and the histological evidence from present study illustrates that the destroyed locus is only restricted within PVN. These results imply that the protection against gastric I/R injury resulted from the excitation of PVN neurons rather than from the excitation of nerve fibers passing PVN or spreading the stimulating current. Therefore, PVN is closely related to the gastric mucosal cellular apoptosis and proliferation induced by gastric I/R, suggesting that PVN is one of the specific brain areas in regulating the gastric I/R injury.

The research on the neuro-endocrine mechanism of the protection of stimulating PVN on gastric I/R injury has been limited except for our previous reports. Our previous study indicates that PVN stimulation, electrical or chemical, activates its neurons to affect the activity of nucleus tractus solitarius (NTS)-dorsal vagal complex (DVC) through its descending fibers and then accomplish the protection against gastric I/R injury by the mediating vagus and sympathetic nerves[45]. Our another study also discovered that electrical stimulation of PVN significantly increases the stress gastric ulceration, while electrolytic lesion of PVN decreases it. PVN is an important brain site in regulating the development of stress-induced gastric ulcers, and is involved in classical neurotransmitters of ACh, NE and 5-HT, with the parasympathetic, sympathetic nervous systems and the three endocrine glands (thyroid, adrenal and gonad) taking part in the effect[34]. Nevertheless, when compared with our previous study on stress-induced gastric ulcer, in our present study the stimulating PVN attenuated gastric mucosal damage induced by gastric I/R, instead of aggravating it, as mentioned above, the contradictory results cannot be satisfactorily explained. It might be wise to regard the PVN as an extremely complicated regulatory mechanism integrating various stress information. Hence the mechanism of the protective effect of PVN against gastric I/R injury may not be a simple one. Recently, Tarnawski reviewed cellular and molecular mechanisms of gastrointestinal ulcer healing, and pointed out that the healing processes are controlled by many cytokines, growth factors (EGF, PDGF, KGF, HGF, TGFβ, VEGF, angiopoietins) and transcription factors activated by tissue injury in spatially and temporally coordinated manners[46]. It will be of interest to further examine this hypothesis in our experimental system.

In future, our further investigation will involve gathering more information and understand the mechanisms of PVN protecting against gastric reperfusion injury. At present, some efforts are being made in our laboratory to assess the effect of molecular mechanisms

and signaling pathways of the protective effect of PVN.

COMMENTS

Background

Little is known about the systemic regulation of gastric I/R injury, particularly the role of related central nuclei. The present study found that the paraventricular nuclei (PVN) exerts protective effects against gastric I/R injury as a specific area in the brain, and the protection is associated with the inhibition of cellular apoptosis and promotion of gastric mucosal proliferation.

Research frontiers

The present study discussed the cellular mechanisms responsible for the gastric I/R injury and the possible cellular mechanisms of the attenuation of gastric I/R injury by electrical stimulation of PVN.

Innovations and breakthroughs

Our previous study showed that PVN is involved in the regulation of gastric I/R injury as one of the specific CNS areas attenuating gastric I/R injury. The cellular mechanisms responsible for the attenuation of gastric I/R injury by electrical stimulation of PVN are still unknown. It was the first time in this study to investigate the molecular mechanisms of stimulating PVN in protecting against gastric I/R injury, to observe the characteristics of gastric mucosal cellular apoptosis and proliferation induced by gastric I/R at various times.

Applications

The present study would help better understand the pathology of gastric I/R injury at cellular level and the regulation role of PVN in gastric function.

Terminology

M30 CytoDEATH is a caspase-cleaved formalin-resistant epitope of cytokeratin 18 cytoskeletal protein in the cytoplasm of apoptotic cells. PCNA is a proliferating cell nuclear antigen as an assistant factor of DNA polymerase.

Peer review

This is an interesting manuscript that links central neural mechanisms with protection of gastric mucosa following gastric I/R injury and found that stimulating PVN significantly inhibits gastric mucosal cellular apoptosis and promots gastric mucosal cellular proliferation, which is probably one of the protective mechanisms of electrical stimulation of PVN against gastric I/R injury. It was suggested that more methods should be performed to clarify the change patterns of gastric mucosal cellular apoptosis and proliferation.

REFERENCES

1 **De La Lastra CA**, Cabeza J, Motilva V, Martin MJ. Melatonin protects against gastric ischemia-reperfusion injury in rats. *J Pineal Res* 1997; **23**: 47-52

2 **Kishimoto Y**, Wada K, Nakamoto K, Ashida K, Kamisaki Y, Kawasaki H, Itoh T. Quantitative analysis of cyclooxygenase-2 gene expression on acute gastric injury induced by ischemia-reperfusion in rats. *Life Sci* 1997; **60**: PL127-PL133

3 **Kitano M**, Wada K, Kamisaki Y, Nakamoto K, Kishimoto Y, Kawasaki H, Itoh T. Effects of cimetidine on acute gastric mucosal injury induced by ischemia-reperfusion in rats. *Pharmacology* 1997; **55**: 154-164

4 **Wada K**, Kamisaki Y, Kitano M, Nakamoto K, Itoh T. Protective effect of cystathionine on acute gastric mucosal injury induced by ischemia-reperfusion in rats. *Eur J Pharmacol* 1995; **294**: 377-382

5 **Andrews FJ**, Malcontenti-Wilson C, O'Brien PE. Polymorphonuclear leukocyte infiltration into gastric mucosa after ischemia-reperfusion. *Am J Physiol* 1994; **266**: G48-G54

6 **Blebea J**, Bacik B, Strothman G, Myatt L. Decreased nitric oxide production following extremity ischemia and reperfusion. *Am J Surg* 1996; **172**: 158-161; discussion 161-162

7 **Brzozowski T**, Konturek PC, Konturek SJ, Drozdowicz D, Kwiecieñ S, Pajdo R, Bielanski W, Hahn EG. Role of gastric acid secretion in progression of acute gastric erosions induced by ischemia-reperfusion into gastric ulcers. *Eur J Pharmacol* 2000; **398**: 147-158

8 **Brzozowski T**, Konturek PC, Konturek SJ, Sliwowski Z, Drozdowicz D, Stachura J, Pajdo R, Hahn EG. Role of prostaglandins generated by cyclooxygenase-1 and cyclooxygenase-2 in healing of ischemia-reperfusion-induced gastric lesions. *Eur J Pharmacol* 1999; **385**: 47-61

9 **Ishii M**, Shimizu S, Nawata S, Kiuchi Y, Yamamoto T. Involvement of reactive oxygen species and nitric oxide in gastric ischemia-reperfusion injury in rats: protective effect of tetrahydrobiopterin. *Dig Dis Sci* 2000; **45**: 93-98

10 **Michida T**, Kawano S, Masuda E, Kobayashi I, Nishimura Y, Tsujii M, Hayashi N, Takei Y, Tsuji S, Nagano K. Role of endothelin 1 in hemorrhagic shock-induced gastric mucosal injury in rats. *Gastroenterology* 1994; **106**: 988-993

11 **Morishita T**, Guth PH. Effect of exogenous acid on the rat gastric mucosal microcirculation in hemorrhagic shock. *Gastroenterology* 1987; **92**: 1958-1964

12 **Nakamoto K**, Wada K, Kitano M, Kishimoto Y, Ashida K, Kamisaki Y, Kawasaki H, Itoh T. The role of endogenous acid in the development of acute gastric ulcer induced by ischemia-reperfusion in the rat. *Life Sci* 1998; **62**: PL63-PL69

13 **Smith GS**, Mercer DW, Cross JM, Barreto JC, Miller TA. Gastric injury induced by ethanol and ischemia-reperfusion in the rat. Differing roles for lipid peroxidation and oxygen radicals. *Dig Dis Sci* 1996; **41**: 1157-1164

14 **Sonoda M**, Asakuno G, Matsuki M, Satomi A, Ishida K, Sakagishi Y. Radical trapping by PBN during reperfusion in rabbit gastric mucosa. *Free Radic Res Commun* 1993; **19** Suppl 1: S185-S191

15 **Wada K**, Kamisaki Y, Ohkura T, Kanda G, Nakamoto K, Kishimoto Y, Ashida K, Itoh T. Direct measurement of nitric oxide release in gastric mucosa during ischemia-reperfusion in rats. *Am J Physiol* 1998; **274**: G465-G471

16 **Hassan M**, Kashimura H, Matsumaru K, Nakahara A, Fukutomi H, Muto H, Goto K, Tanaka N. Phosphoramidon, an endothelin converting enzyme inhibitor attenuates local gastric ischemia-reperfusion injury in rats. *Life Sci* 1997; **61**: PL141-PL147

17 **Andrews FJ**, Malcontenti-Wilson C, O'Brien PE. Expression of adhesion molecules and leukocyte recruitment into gastric mucosa following ischemia-reperfusion. *Dig Dis Sci* 1997; **42**: 326-332

18 **Stachura J**, Tarnawski A, Dabroś W. Apoptosis: genetically programmed physiologic cell loss in normal gastric oxyntic mucosa and in mucosa of grossly healed gastric ulcer. *J Clin Gastroenterol* 1993; **17** Suppl 1: S70-S77

19 **Granger DN**, Korthuis RJ. Physiologic mechanisms of postischemic tissue injury. *Annu Rev Physiol* 1995; **57**: 311-332

20 **Han H**, Iwanaga T, Fujita T. Species-differences in the process of apoptosis in epithelial cells of the small intestine: an ultrastructural and cytochemical study of luminal cell elements. *Arch Histol Cytol* 1993; **56**: 83-90

21 **MacLellan WR**, Schneider MD. Death by design. Programmed cell death in cardiovascular biology and disease. *Circ Res* 1997; **81**: 137-144

22 **Potten CS**. The significance of spontaneous and induced apoptosis in the gastrointestinal tract of mice. *Cancer Metastasis Rev* 1992; **11**: 179-195

23 **Schlossberg H**, Zhang Y, Dudus L, Engelhardt JF. Expression of c-fos and c-jun during hepatocellular remodeling following ischemia/reperfusion in mouse liver. *Hepatology* 1996; **23**: 1546-1555

24 **Tagami M**, Ikeda K, Nara Y, Fujino H, Kubota A, Numano F, Yamori Y. Insulin-like growth factor-1 attenuates apoptosis in hippocampal neurons caused by cerebral ischemia and reperfusion in stroke-prone spontaneously hypertensive rats. *Lab Invest* 1997; **76**: 613-617

25 **Yin T**, Sandhu G, Wolfgang CD, Burrier A, Webb RL, Rigel DF, Hai T, Whelan J. Tissue-specific pattern of stress kinase activation in ischemic/reperfused heart and kidney. *J Biol Chem* 1997; **272**: 19943-19950

26 **Kusuhara H**, Matsuyuki H, Matsuura M, Imayoshi T, Okumo-

to T, Matsui H. Induction of apoptotic DNA fragmentation by nonsteroidal anti-inflammatory drugs in cultured rat gastric mucosal cells. *Eur J Pharmacol* 1998; **360**: 273-280
27 **Li H**, Andersson EM, Helander HF. Reactions from rat gastric mucosa during one year of Helicobacter pylori infection. *Dig Dis Sci* 1999; **44**: 116-124
28 **Piotrowski J**, Piotrowski E, Skrodzka D, Slomiany A, Slomiany BL. Induction of acute gastritis and epithelial apoptosis by Helicobacter pylori lipopolysaccharide. *Scand J Gastroenterol* 1997; **32**: 203-211
29 **Piotrowski J**, Slomiany A, Slomiany BL. Activation of apoptotic caspase-3 and nitric oxide synthase-2 in gastric mucosal injury induced by indomethacin. *Scand J Gastroenterol* 1999; **34**: 129-134
30 **Slomiany BL**, Piotrowski J, Slomiany A. Role of basic fibroblast growth factor in the suppression of apoptotic caspase-3 during chronic gastric ulcer healing. *J Physiol Pharmacol* 1998; **49**: 489-500
31 **Fukuyama K**, Iwakiri R, Noda T, Kojima M, Utsumi H, Tsunada S, Sakata H, Ootani A, Fujimoto K. Apoptosis induced by ischemia-reperfusion and fasting in gastric mucosa compared to small intestinal mucosa in rats. *Dig Dis Sci* 2001; **46**: 545-549
32 **Wada K**, Nakajima A, Takahashi H, Yoneda M, Fujisawa N, Ohsawa E, Kadowaki T, Kubota N, Terauchi Y, Matsuhashi N, Saubermann LJ, Nakajima N, Blumberg RS. Protective effect of endogenous PPARgamma against acute gastric mucosal lesions associated with ischemia-reperfusion. *Am J Physiol Gastrointest Liver Physiol* 2004; **287**: G452-G458
33 **Salim AS**. The hypothalamus and gastric mucosal injuries: origin of stress-induced injury? *J Psychiatr Res* 1988; **22**: 35-42
34 **Zhang JF**, Zheng F. The role of paraventricular nucleus of hypothalamus in stress-ulcer formation in rats. *Brain Res* 1997; **761**: 203-209
35 **Zhang JF**, Zhang YM, Yan CD, Zhou XP. Neuroregulative mechanism of hypothalamic paraventricular nucleus on gastric ischemia-reperfusion injury in rats. *Life Sci* 2002; **71**: 1501-1510
36 **Paxinos G**, Watson C. The rat brain in stereotaxic coordinates. 2nd ed. Sydney: Academic press, 1986: 23-26
37 **Wada K**, Kamisaki Y, Kitano M, Kishimoto Y, Nakamoto K, Itoh T. A new gastric ulcer model induced by ischemia-reperfusion in the rat: role of leukocytes on ulceration in rat stomach. *Life Sci* 1996; **59**: PL295-PL301
38 **Ichikawa H**, Naito Y, Takagi T, Tomatsuri N, Yoshida N, Yoshikawa T. A specific peroxisome proliferator-activated receptor-gamma (PPAR-gamma) ligand, pioglitazone, ameliorates gastric mucosal damage induced by ischemia and reperfusion in rats. *Redox Rep* 2002; **7**: 343-346
39 **Guth PH**, Aures D, Paulsen G. Topical aspirin plus HCl gastric lesions in the rat. Cytoprotective effect of prostaglandin, cimetidine, and probanthine. *Gastroenterology* 1979; **76**: 88-93
40 **Nardone G**, Staibano S, Rocco A, Mezza E, D'armiento FP, Insabato L, Coppola A, Salvatore G, Lucariello A, Figura N, De Rosa G, Budillon G. Effect of Helicobacter pylori infection and its eradication on cell proliferation, DNA status, and oncogene expression in patients with chronic gastritis. *Gut* 1999; **44**: 789-799
41 **Maga G**, Hubscher U. Proliferating cell nuclear antigen (PCNA): a dancer with many partners. *J Cell Sci* 2003; **116**: 3051-3060
42 **Majka J**, Burgers PM. The PCNA-RFC families of DNA clamps and clamp loaders. *Prog Nucleic Acid Res Mol Biol* 2004; **78**: 227-260
43 **Olivares D**, Gisbert JP, Pajares JM. Helicobacter pylori infection and gastric mucosal epithelial cell apoptosis. *Rev Esp Enferm Dig* 2005; **97**: 505-520
44 **Luo JC**, Shin VY, Yang YH, Wu WK, Ye YN, So WH, Chang FY, Cho CH. Tumor necrosis factor-alpha stimulates gastric epithelial cell proliferation. *Am J Physiol Gastrointest Liver Physiol* 2005; **288**: G32-G38
45 **Zhang JF**, Zhang YM, Yan CD, Zhou XP, Qi YJ. Protective effects of paraventricular nucleus stimulation and vasopressin on gastric ischemia-reperfusion injury in rats. *Shengli Xuebao* 2002; **54**: 133-138
46 **Tarnawski AS**. Cellular and molecular mechanisms of gastrointestinal ulcer healing. *Dig Dis Sci* 2005; **50** Suppl 1: S24-S33

S- Editor Wang J **L- Editor** Wang XL **E- Editor** Ma WH

PO Box 2345, Beijing 100023, China
www.wjgnet.com
wjg@wjgnet.com

World J Gastroenterol 2007 February 14; 13(6): 882-888
World Journal of Gastroenterology ISSN 1007-9327

BASIC RESEARCH

Effect of BN52021 on NFκ-Bp65 expression in pancreatic tissues of rats with severe acute pancreatitis

Shi-Hai Xia, Dian-Chun Fang, Chun-Xiu Hu, Hui-Ying Bi, Yin-Zhi Yang, Yao Di

Shi-Hai Xia, Dian-Chun Fang, Chun-Xiu Hu, Hui-Ying Bi, Yin-Zhi Yang, Yao Di, Department of Gastroenterology, Southwest Hospital, Third Military Medical University, Chongqing 400038, China
Supported by the National Natural Science Foundation of China, No. 30300465
Correspondence to: Dr. Dian-Chun Fang, Department of Gastroenterology, Southwest Hospital, Third Military Medical University, Chongqing 400038, China. xshhcx@sina.com
Telephone: +86-23-68754124 Fax: +86-23-68754124
Received: 2006-10-22 Accepted: 2007-01-09

Abstract

AIM: To investigate dynamic changes and significance of expression of NF-κBp65 in pancreatic tissues of rats with severe acute pancreatitis (SAP), as well as BN52021 effects.

METHODS: Wistar male rats were randomly divided into negative control group (NC group, n = 60), SAP-model group (SAP group, n = 60), and BN52021-treated group (BN group, n = 60), and each of the above groups was respectively divided into 6 subgroups at different time points after operation (1 h, 2 h, 3 h, 6 h, 12 h, and 24 h) (n = 10). By RT-PCR and Western blot, NF-κBp65 mRNA and its protein expression in pancreatic tissues of rats were detected respectively.

RESULTS: The expression of NF-κBp65 mRNA dynamically changed in both SAP groups and BN groups. The mRNA level was higher in SAP groups than NC groups at 2 h, 3 h, 12 h, and 24 h after operation (P < 0.05), higher in BN groups than NC groups at all time points (P < 0.05), and higher in BN groups than SAP group at 1 h (P < 0.05). The NF-κBp65 protein level was higher in SAP groups than NC groups at 1 h, 3 h, and 6 h (P < 0.01), and 2 h, 12 h, and 24 h (P < 0.05), higher in BN groups than NC groups at all time points (P < 0.05), and lower in BN groups than SAP groups at 1 h, 3 h, and 6 h (P < 0.05).

CONCLUSION: The expression of NF-κBp65 in pancreatic tissues is dynamically changed and the changes play an important role in pathogenesis of SAP. BN52021 exerts therapeutic effects through reducing the expression level of NF-κBp65 protein in the early stage of SAP.

Key words: BN52021; Pancreatitis; NF-κB; Signal transduction

Xia SH, Fang DC, Hu CX, Bi HY, Yang YZ, Di Y. Effect of BN52021 on NF-κBp65 expression in pancreatic tissues of rats with severe acute pancreatitis. *World J Gastroenterol* 2007; 13(6): 882-888

http://www.wjgnet.com/1007-9327/13/882.asp

INTRODUCTION

Up to now, the precise pathogenesis of Severe acute pancreatitis (SAP) with a high mortality has not been completely elucidated although the theories of self-digestion, leukocyte over-activation, microcirculatory disorder, bacterial shifting and secondary infection, i.e. the second attack, immune functional change, cell apoptosis and oxygen free radicals etc. have explained the pathogenesis of SAP from different angles[1,2].

NF-κBp65 is a type of protein that can bind many kinds of cytokines and adhesion molecules at the κB site of their gene promoters to enhance transcription of the genes. It plays an important role in cellular signal transduction in different theories of SAP pathogenesis[3]. For example, the activation of NF-κBp65 is the decisive factor in many pathological states and it especially has a close relationship with the occurrence and pathophysiological process of severe infections[4]. In SAP pathogenesis, the clinical course of SAP is dependent on the over-activated inflammatory cells and inflammatory factors expressed, in which platelet activating factor (PAF) is a crucial transmitter for systematic inflammatory reaction of SAP. PAF was found to have the ability to activate NF-κB in 1994[5], and the studies since then have shown that PAF receptor (PAF-R) is a target gene of NF-κB[6]. All these findings have attracted researchers to further study the relationship between PAF and NF-κB.

BN52021 (ginkgolide B) is a specific antagonist to PAF-R. In recent years, studies at home and abroad have showed that it has significant physiological activities, such as platelet aggregration inhibition, anti-inflammation, and anti-shock, etc. BN52021 has significant effects in treatment of animals with SAP[7,8]. But the exact pathogenesis of BN52021 on SAP is unknown. This study was aimed at dynamically investigating the changes and significance of the expression of NF-κBp65 mRNA and its protein in pancreatic tissues and effects of BN52021 in rats with SAP.

MATERIALS AND METHODS

Main reagents and apparatus

BN52021 and sodium taurocholate were purchased from Sigma (USA), amylase kit was from Beijing Kemei Reagent Co. (Beijing, China), trizol and diethyl pyrocarbonate (DEPC) were from Invitrogen Company (USA), RT kit was from IBM Fermentas Company (Lithuania), dNTPs and the RNA enzyme inhibitor were from TaKaRa Company (Japan), DNA Tag enzyme was from Promega (USA), Primary antibody of NF-κBp65 rabbit-anti-rat serum and the enhanced chemiluminescence (ECL) system were from Santa Cruz Biotechnology (USA), secondary antibody of sheep-antirabbit was from Beijing Dingguo Biotechnology Co., Ltd. (Beijing, China), polyvinylidene fluoride (PVDF film) was from Millipore Corp. (USA), prestained marker was from Beijing Tianwei Time Biotechnology Co., Ltd. (Beijing, China), β-actin was from Beijing Zhongshan Biotechnology Co., Ltd. (Beijing, China), DYY-12 electrophoresis system and electric trans-blot SD were from Beijing Liuyi Instrument Factory (Beijing, China), type-2720 PCR apparatus was from ABI Company (USA), and gel scanning & imaging system and vertical electrophoresis system were from Bio-Rad (USA).

Animal grouping and model preparation

One hundred and eighty Wistar male rats (weighing 0.20-0.23 kg, 6-8 wk old, Grade Ⅱ, Certificate SCXK 2002-001) were provided by Laboratory Animal Center of PLA Academy of Military Medical Sciences, China. All rats were maintained in an environment of controlled temperature (22℃-25℃), humidity (55%-58%), and lighting (12 h light/12 h dark), with free access to tap water and regular chow diet. They were randomly divided into the negative controlled group (NC group, n = 60), SAP-modeled group (SAP group, n = 60), and BN52021-treated group (BN group, n = 60), and each of the above groups was respectively divided into 6 subgroups at different time points after operation (1 h, 2 h, 3 h, 6 h, 12 h, and 24 h) (n = 10). SAP models were prepared according to the method by Aho *et al*[9]. Wistar male rats were weighed, marked and fasted for 24 h before the operation, with free access to water. Anaesthesia was conducted by abdominal cavity injection of 0.4% sodium pentobarbital (40 mg/kg). Rats were fixed in dorsal decubitus. The skin was prepared and sterilized. And a 2-cm incision was made along the middle line of the upper belly and the abdominal cavity was entered. The duodenum and pancreaticobiliary duct were searched, the hepatic end of the pancreaticobiliary duct was clipped with a non-invasive vascular clip, pancreaticobiliary duct retrograde centesis was conducted with an obtuse (pointless) needle through duodenum seromuscular layer, and then 5% sodium taurocholate (0.1 mL/100 g) was injected in the retrograde direction of pancreaticobiliary duct with a micro-syringe, at an injection rate of 0.20 mL/min. After the injection of the drug, the part of pancreaticobiliary duct entering the duodenum was clipped with a non-invasive vascular clip for 10 min, and then the vascular clip was removed. After making sure that there was no active bleeding in the abdominal cavity, the abdomen was closed in two layers, and the wound was covered with sterile gauze. For the rats in NC group, the duodenum was merely stirred and pancreas was touched several times after opening the abdomen, and then the abdomen was closed. For the BN group, BN52021 (5 mg/kg: dissolved with Me_2SO) was injected intravenously within 15 min after the operation; and for the groups of NC and SAP, the same volume of physiological saline (0.9% NaCl) was injected through femoral vein.

Table 1 Scoring standard of pathological change for pancreatic tissue of rats with SAP

Pathological grading	Pathological change	Scores
Edema	Inter-lobule local edema, widened pleura	1
	Inter-lobule diffuse edema, widened intra-lobule clearance	2
	Increased intra-lobule clearance, alveolus swollen, and separated	3
Inflammatory	White cells < 20/visual field under high-power microscope	1
Cell infiltration	White cells 20-50/visual field under high-power microscope	2
	White cells > 30/visual field under high-power microscope, or micro-abscess occurs	3
Hemorrhage	Parenchymal hemorrhage < 20%	1
	Parenchymal hemorrhage 20%-50%	2
	Parenchymal hemorrhage > 50%	3
Necrosis	Necrosis area < 20%	1
	Necrosis area 20%-50%	2
	Necrosis area > 50%	3

Sample collection and storage

The rats in each group received anaesthesia at respective time points after the operation (1 h, 2 h, 3 h, 6 h, 12 h, and 24 h), and venous blood was collected from the right atrium. After a 10 min water bath at 37℃, and then a centrifugation for 10 min at 3000 g/min, the supernatant of the blood was respectively placed into sterilized EP tubes, and stored in a refrigerator at -20℃ for determination of serum amylase. Meanwhile, two portions of pancreatic tissues of each group were treated differently; one portion was placed in liquid nitrogen overnight, and then frozen in a refrigerator at -80℃ for further use, and another portion was fixed with 40 g/L neutral buffer formaldehyde, embedded with paraffin wax, cut into slices, and then HE stained for pathological observation and scoring.

Determination of serum amylase

Determination of serum amylase was conducted using a fully automatic biochemical apparatus and an amylase kit.

Pathological observation and scoring of pancreas

Pathological observation and scoring for pancreatic tissue samples (Table 1)[10]: 10 visual fields under a high-power microscope (HE stain, × 400) were randomly selected, and pathological changes of each item in the table were graded and scored, with a score of 0 for pathological changes of items not included in Table 1.

Primers

NF-κBp65 primer was prepared according to the previous

method as reported[11]. The NF-κBp65 and β-actin primers were synthesized by Shanghai Yingjun Biotechnology Co. Ltd. (Table 2).

Determination of NF-κBp65 mRNA expression by RT-PCR

First, the total RNA of pancreatic tissues was extracted with Trizol Reagent for each group. Then, the integraty of the total RNA was examined by agarose electrophoresis, its concentration and purity were determined by a UV spectrophotometer, and the total RNA concentration of the sample was calculated. According to instructions of the RT reagent kit, 1 μg of the total RNA was used, and OligdT18 was used as a primer to produce 20 μL of the reaction system. PCR reaction was conducted by using 4 μL cDNA-RT product, 3 μL 10 × PCR buffer, 3 μL dNTPs of 200 μmol/L, 3 μL upstream primer of 10 pmol/μL, 3 μL downstream primer of 10 pmol/μL, 1μL Taq enzyme, and 13 μL deionized double-distilled water. Thermal cycle conditions were as follows: Predegeneration for 4 min at 94℃, 45 s at 94℃, 1 min at 72℃; after 35 cycles, an extension was conducted for another 5 min at 72℃. For each PCR reaction, a negative control with the same volume of deionized double-distilled water instead of cDNA was used, and meanwhile, amplification was conducted to control DNA contamination. The housekeeping gene was amplified, i.e. β-actin, as internal reference for gene quantitative expression. The sequence of PCR product was determined by Shanghai Yingjun Biotechnology Co., Ltd., and the results were in accordance with the corresponding mRNA. To 5 μL of RT-PCR product, 1 μL of supernatant buffer (containing 0.2 mg/mL ethidium bromde) was added, electrophoresis was conducted on gels containing 1.5% agarose at 80 V for 45 min, and photographed with Quantity One Gel Imaging System. A semiquantitative analysis of the experimental results was conducted.

Determination of NF-κBp65 protein expression by Western blot

The prepared total protein was added to gel-added buffer at a ratio of 1:2 and then heated in water at 100℃ for 5 min. For its vertical plating electrophoresis, the added volume was 15 μL. Each sample was palced on 2 parallel glue plates, one of which was used for staining and the other for membrane transferring. The voltage and time of electrophoresis were 80 v, 10 min and 120 v, 60 min for concentrating glue and isolating glue, respectively. The gels and membranes were placed among 6 sheets of filter paper and then between 2 foamy pads and put into electrical transfer tank containing buffer. After precooling for 10 min in icy water, the gel and membrane were galvanized for trans-printing for 4 h at a current of 1 mA/cm^2. The trans-printed gel was stained to determine whether the trans-printing was complete. The trans-printed product was put into a solution containing 0.5% bovine serum albumin, slightly shaken and enclosed for 1 h. NF-κBp65 antibody (diluted in 1:400) was added and placed at 4℃ overnight. After the labeled PVDF membrane was washed with 0.05% Tween-20 buffer (TBST) for 5 min three times, it was incubated with IgG labeled with HRP (diluted in 1:200) at 4℃ overnight. The membrane was washed with 0.05% TBST again for 5 min three times. The liquid of ECL A and that of ECL B were mixed at an equal volume (0.125 mL liquid/cm^2 membrane). The PVDF membrane was immerged in the mixed liquid for 1 min. Then the membrane was put on the freshness-retaining membrane. The trans-printing membrane was fixed in the developing tray and pictured using medical film for 30 s to 1 min, developed for 1-3 min and fixed for 1 min. Finally, the membrane was cleaned with water and dried up. The PVDF membrane was put into the desorption liquid, shaken at 50℃ for 30 min, enclosed, added with β-actin antibody (diluted in 1:200) and placed at 4℃ overnight. Then the above-mentioned process was repeated again for imaging. The results were photographed, saved in a computer, analysis was conducted by using Image-Pro Plus 4.5 image-analyzing software, and the integrated optical density (IOD) was calculated. The optical density ratio of target protein and β -actin in the same membrane was taken as the value of the fi nal experimental results.

Table 2 PCR primer series, position and segment length of NF-κBp65 and β-actin.

Gene	Primer series (5'-3')	Gene No.	Position	Length
NF-κBp65	GAAGAAGCGAGACCTGGAG	NM_199267	424-442	398 bp
	TCCGGAACACAATGGCCAC		821-803	
β-actin	TCCTAGCACCATGAA GATC	NM_031144	1044-1062	190 bp
	AAACGCAGCTCAGTAACAG		1233-1215	

Statistical analysis

The above experiments were repeated 3 times, the average values were calculated as the final data, and expressed as mean ± SEM. Data were processed with SPSS11.5 statistical software, normal test was conducted using *t* test and single-factor analysis of variance. Results were considered statistically significant when $P < 0.05$ or $P < 0.01$.

RESULTS

Serum amylase

It showed that the serum amylase in the SAP groups and the BN groups significantly increased at each time point than those in the NC groups ($P < 0.05$); however, the values in the BN groups significantly decreased at 3 h, 6 h, and 24 h than those in the SAP groups ($P < 0.05$) (Table 3).

Pathological observation and scoring

The pathological results showed that there was no obvious abnormality in abdominal cavity at all time points, and the pancreatic structure was almost normal in NC groups; in the SAP groups, hemorrhagic ascites occurred, necrosis foci were present in the pancreas, a number of saponifying spots occurred in the mesentery and greater omentum, and inflammatory cells infiltrated in pancreatic stroma and glandular lobule, and diffuse bleeding and piecemeal necrosis occurred and over time, the pathological changes were exacerbated; in the BN groups, the pathological changes were less serious than those in the SAP groups. It

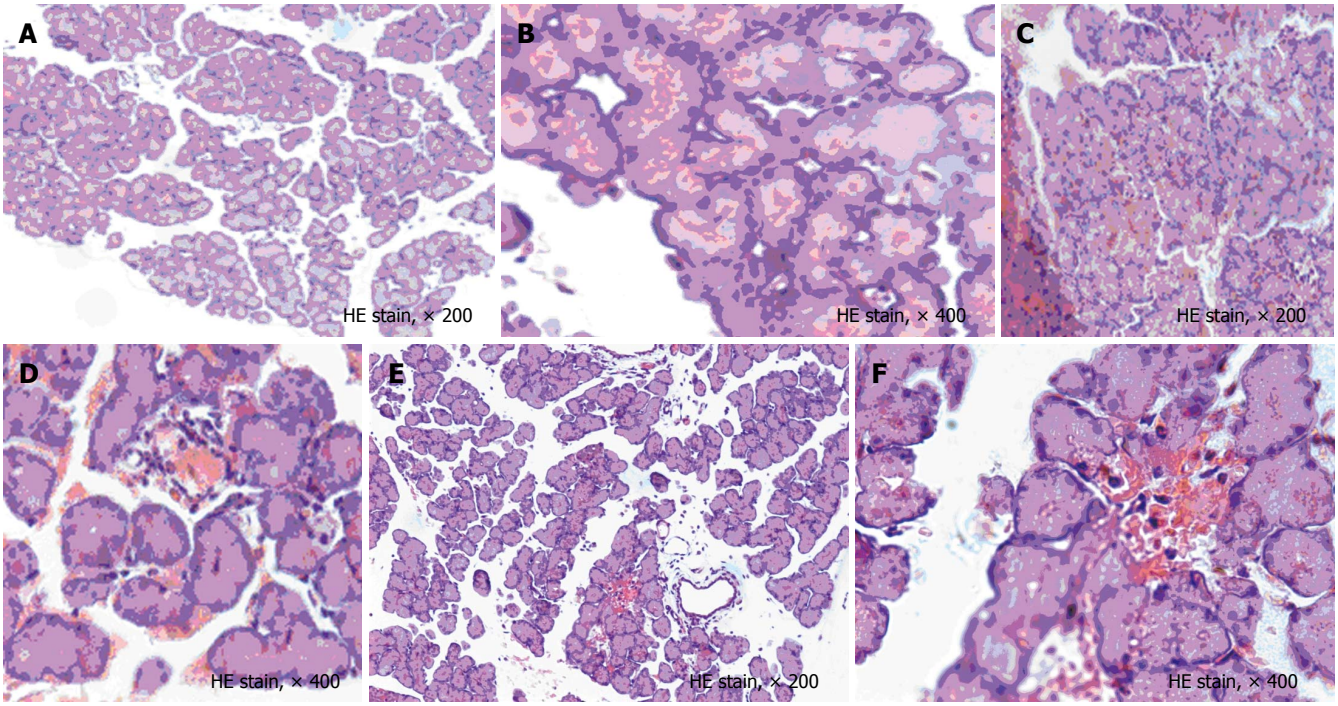

Figure 1 Pathological change of pancreatic tissues at 6 h after operation in each group. **A** and **B**: In NC group, the pancreatic structure was almost normal; **C** and **D**: In SAP group, inflammatory cells infiltrated, diffuse bleeding and piecemeal necrosis were occurred; **E** and **F**: In BN group, the pathological changes were less serious than those in SAP group.

Table 3 Level of serum amylase at each time point in each group after operation (U/L) *n* = 10, mean ± SD

Groups	Time points					
	1 h	2 h	3 h	6 h	12 h	24 h
NC	1835.6 ± 613.2	1491.5 ± 507.0	1530.4 ± 247.0	1400.2 ± 447.5	2153.2 ± 236.3	337 ± 43.7
SAP	2560.5 ± 121.5[a]	2810.5 ± 147.2[a]	4799.3 ± 107.0[a]	4919.7 ± 139.6[a]	3486.3 ± 181.8[a]	2283 ± 127.0[a]
BN	2214.5 ± 109.1[b]	3331.7 ± 196.4[b]	4185 ± 147.8[b,c]	3784.7 ± 124.1[b,c]	3454 ± 264.1[b]	1360.4 ± 161.4[b,c]

[a]$P < 0.05$, [b]$P < 0.05$ *vs* NC group; [c]$P < 0.05$ *vs* SAP group.

Table 4 Scores of pancreatic tissues at each time point in each group after operation *n* = 10, mean ± SD

Groups	Time points					
	1 h	2 h	3 h	6 h	12 h	24 h
NC	0.12 ± 0.05	0.11 ± 0.06	0.12 ± 0.05	0.13 ± 0.04	0.12 ± 0.06	0.13 ± 0.05
SAP	4.82 ± 0.35[a]	7.65 ± 0.40[a]	8.85 ± 0.39[a]	9.15 ± 0.55[a]	10.10 ± 0.65[a]	11.75 ± 0.25[a]
BN	5.55 ± 0.30[b]	6.65 ± 0.42[b]	5.95 ± 0.19[b,c]	5.55 ± 0.36[b,c]	6.72 ± 0.30[b,c]	9.95 ± 0.58[b]

[a]$P < 0.05$, [b]$P < 0.05$ *vs* NC group; [c]$P < 0.05$ *vs* SAP group.

was shown that the scores in the SAP groups and the BN groups significantly increased at all time points than those in the NC groups ($P < 0.05$); however, the scores in the BN groups markedly decreased at 3 h, 6 h, and 24 h than those in the SAP groups ($P < 0.05$) (Figure 1, Table 4).

NF-κBp65 mRNA expression in the pancreatic tissues and effects of BN52021 on it

The expression of NF-κBp65 mRNA was dynamically changed in both SAP groups and BN groups in a dual-peak manner. The two peaks of the expression appeared at 1 h and 24 h in the SAP groups and at 1 h and 12 h in the BN groups and then the expression reached its lowest level at 6 h. The mRNA level was higher in SAP groups than NC groups at 2 h, 3 h, 12 h, and 24 h after operation ($P < 0.05$), higher in BN groups than NC groups at all time points ($P < 0.05$), and higher in BN group than SAP group at 1 h ($P < 0.05$) (Figure 2, Table 5).

NF-κBp65 protein expression in the pancreatic tissue and effects of BN52021 on it

The NF-κBp65 protein level was markedly higher in SAP groups than NC groups at 1 h, 3 h, and 6 h ($P < 0.01$), and 2 h, 12 h, and 24 h ($P < 0.05$), also higher in BN groups than NC groups at all time points ($P < 0.05$), but lower in BN group than SAP groups at 1 h, 3 h, and 6 h ($P < 0.05$) (Figure 3, Table 6).

DISCUSSION

Studies in recent years confirmed that cytokines and adhesion molecules play an important role in pathogenesis of SAP. NF-κBp65, which is a type of protein that can bind many kinds of cytokines and adhesion molecules at the κB site of their gene promoters to enhance transcription of the genes, plays an important role in the occurrence and development of SAP[4,11]. Meanwhile, it is one member of the family of transcription-regulating protein and a homologous or heterogenous dimmer that contains 5 subunits of p50, p52, p65, cRel and RelB.

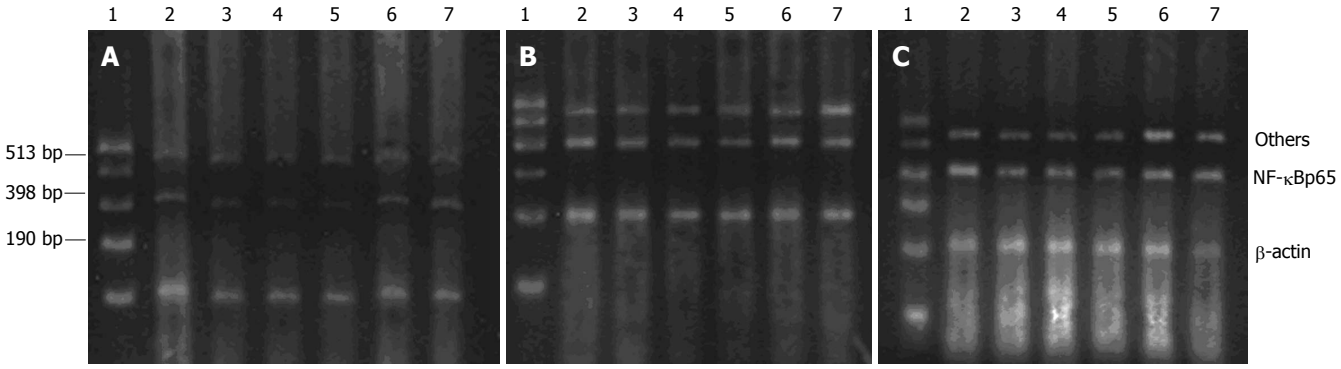

Figure 2 Expression of NF-κBp65 mRNA at all time points in each group after operation. **A**: NC group; **B**: SAP group; **C**: BN group. 1: Marker, 2: 1 h, 3: 2 h, 4: 3 h, 5: 6 h, 6: 12 h, 7: 24 h.

Table 5 Absorbance values of NF-κBp65 mRNA in pancreatic tissue at each time in each group after operation n = 10, mean ± SD

Groups	Time points					
	1 h	2 h	3 h	6 h	12 h	24 h
NC	220.01 ± 94.51	186.30 ± 51.52	167.19 ± 51.55	114.91 ± 55.96	123.91 ± 54.78	131.08 ± 66.84
SAP	340.47 ± 119.14	269.03 ± 66.03[a]	229.45 ± 50.34[a]	197.07 ± 96.02	307.42 ± 100.62[a]	376.97 ± 0.22[a]
BN	470.80 ± 122.78[b,c]	268.70 ± 87.64[b]	267.95 ± 49.66[b]	277.64 ± 83.37[b]	337.21 ± 103.02[b]	340.24 ± 0.44[b]

[a]P < 0.05, [b]P < 0.05 *vs* NC group; [c]P < 0.05 *vs* SAP group.

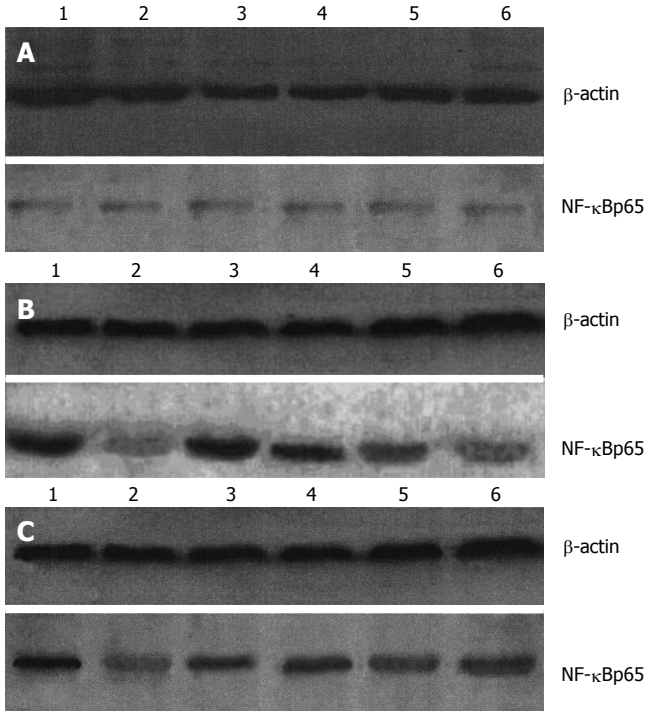

Figure 3 Expression of NF-κBp65 protein at all time points in each group after operation. **A**: NC group; **B**: SAP group; **C**: BN group. 1: 1 h, 2: 2 h, 3: 3 h, 4: 6 h, 5: 12 h, 6: 24 h.

Table 6 Absorbance values of NF-κBp65 protein in pancreatic tissue at each time point in each group after operation. n = 10, mean ± SD

Groups	Time points					
	1 h	2 h	3 h	6 h	12 h	24 h
NC	0.05 ± 0.00	0.09 ± 0.01	0.07 ± 0.01	0.05 ± 0.01	0.06 ± 0.01	0.10 ± 0.02
SAP	1.43 ± 0.06[a]	0.80 ± 0.05[d]	1.58 ± 0.02[a]	1.38 ± 0.03[a]	0.87 ± 0.09[d]	0.90 ± 0.05[d]
BN	1.04 ± 0.02[b,c]	0.72 ± 0.02[b]	1.01 ± 0.04[b,c]	0.95 ± 0.03[b,c]	0.75 ± 0.02[b]	0.76 ± 0.01[b]

[a]P < 0.05, [b]P < 0.05, [d]P < 0.05 *vs* NC group; [c]P < 0.05 *vs* SAP group.

Under normal condition, it binds to its inhibiting protein single IκB (including IκBα, IVBβ and IκBε) and has no activity. Upon stimulation of cells by such activating signals as endotoxin or TNF-α, it separates from IκB and enters the cellular nucleus and binds with specific κB sequence of DNA to enhance transcription of genes of infl ammatory media and cytokines. In 1997, Dunn *et al*, for the first time, found that activation of NF-κBp65 is an important early event in the occurrence of acute pancreatitis (AP) through establishing bile-originated AP by ligation of pancreatic duct. Blinman *et al* showed that the activity of NF-κBp65 is significantly enhanced and the expression of IL-6 and KC increases in the pancreatic tissues in the early stage of edematous pancreatitis in rats induced by litorin. Therefore, they believe that the activation of NF-κBp65 plays an important role in pathogenesis of AP; IL-1, IL-6, IL-8, IL-10 and TNF are associated with AP. Since the production of these inflammatory cytokines is regulated by NF-κBp65 and activator protein 1, it is believed that NF-κBp65 plays the major role in the infl ammatory media regulating network[12,13].

In this study, we found that the expression of NF-κBp65 mRNA and protein were significantly higher in SAP groups than in NC groups at all time points. Moreover, the expression markedly increased in the early stage, dynamically changed in dual-peak and time-dependent

manners. These findings confirm that NF-κBp65 plays an important role in the occurrence and development of SAP. The mechanisms include: SAP causes severe endotoxemia, and LPS and endotoxin component bind with their respective binding protein and CD14 molecule on cell membrane to form an LPS-LBP-CD14 complex to activate the signal transduction of Toll-like receptor 4, and the signal transduction further activates gene transcription of cytokines (such as IL-1, IL-6 and IL-8)[14]. In SAP, the pancreatic elastase is activated to activate NF-κBp65 to exert its inflammation-inducing effects through the TLR4/NF-κB pathway. Consequently, damage of pancreatic self-digestion function and injuries of other organs outside of pancreas occur[15]. In SAP, PLA2 is activated to activate expression of NF-κBp65 of target cells in tissues[16]. NF-κBp65 is firstly activated in the pancreatic tissue to release cytokines. The cytokines start the "waterfall reaction" of inflammatory media through the "triggering role". The inflammatory media such as PAF are released into the blood. Though the activation of NF-κB in the pancreatic tissues can be partly inhibited by intra- and extracellular pathways of negative feedback of NF-κBp65, the inflammatory media can again activate NF-κBp65 in other organs outside of pancreas (neutrophils, Kuffer cells, liver, lung and intestines, etc.) to produce more inflammatory media. As a result, they participate in the development of SAP and aggravate the injuries of pancreas and other organs or even cause SIRS, ARDS and MOF[4].

BN52021, one of the effective components of Chinese medicine ginkgo biloba leaf and a strong antagonist against the inflammatory medium of PAF, can not only block the signal transduction of PAF but also decrease blood concentration of PAF to exert its biological effect[17]. This study showed that BN52021 could decrease serum amylase level and alleviate pathological changes in SAP, which is consistent with that reported by other researchers[18,19]. The expression of NF-κBp65 mRNA was significantly higher in SAP and BN groups than in NC group at all time points after operation. However, it was markedly higher in BN groups than in SAP group at 1 h after the operation. The reason for the latter might be that the Me_2SO used for dissolution of BN52021 can aggravate inflammatory reaction in the early stage of SAP, resulting in enhancement of NF-κBp65 mRNA expression, however, the mechanism needs to be further elucidated. Our results suggest that BN52021 does not significantly affect the expression of NF-κBp65 mRNA. The expression of NF-κBp65 protein was significantly lower in BN groups than in SAP groups at 1, 3 and 6 h after operation. However, it was still markedly higher in BN groups than in NC groups at all time points after operation. These findings suggest that BN52021 can inhibit the expression of NF-κBp65 protein in the early stage, to some extent, which might be one mechanism of its therapeutic effects on SAP. However, there was difference in the effect of BN52021 on NF-κBp65 mRNA expression and its protein expression. We believe that BN52021 causes downstream changes in signal transduction, leading to the difference, the mechanism of which also needs to be further studied.

In summary, the increase of NF-κBp65 expression plays an important role in pathogenesis of SAP. BN52021 can decrease serum level of amylase and alleviate pathological changes in SAP. Meanwhile, it can decrease expression of NF-κBp65 protein in pancreatic tissues in the early stage of SAP to exert its therapeutic effects.

COMMENTS

Background

BN52021 (ginkgolide B) is a specific antagonist to platelet activating factor receptor (PAF-R). In recent years, studies at home and abroad have shown that it has significant physiological activities, such as platelet aggregration inhibition, anti-inflammation, and anti-shock. BN52021 has significant effects in treatment of animals with severe acute pancreatitis (SAP). But the exact pathogenesis of BN52021 on SAP is unknown. This study was aimed to dynamically investigate the changes and significance of the expression of NF-κBp65 mRNA and its protein in pancreatic tissues and effects of BN52021 in rats with SAP.

Research frontiers

To explore molecule mechanism of BN52021 on severe acute pancreatitis.

Innovations and breakthroughs

BN52021 has remarkable curative effects in acute pancreatitis. But the mechanism of BN52021 hasn't been researched extensively. The study explored the significance of NF-κBp65 in platelet activating factor receptor signal transduction.

Applications

The results may provide theortic and experimental evidence for study, and application of BN52021, and new approaches for therapy of severe acute pancreatitis.

Terminology

NF-κBp65 is a type of protein that can bind many kinds of cytokines and adhesion molecules at the κB site of their gene promoters to enhance transcription of the genes. It plays an important role in cellular signal transduction in different theories of pathogenesis of severe acute pancreatitis. BN52021, namely code of ginkgolide B, one of the effective components of Chinese medicine ginkgo biloba leaf and a strong antagonist against the inflammatory medium of platelet activating factor (PAF), can not only block the signal transduction of PAF but also decrease blood content of PAF to exert its biological effect. It has significant physiological activities, such as platelet aggregration inhibition, anti-inflammation, and anti-shock.

Peer review

The results show that the expression of NF-κBp65 in pancreatic tissues dynamically changed and the changes played an important role in pathogenesis of severe acute pancreatitis (SAP). BN52021 exerted some kind of therapeutic effect through reducing the expression level of NF-κBp65 proteins in the early stage of SAP.

REFERENCES

1 **Tenner S**, Banks PA. Acute pancreatitis: nonsurgical management. *World J Surg* 1997; **21**: 143-148
2 **Klar E**, Messmer K, Warshaw AL, Herfarth C. Pancreatic ischaemia in experimental acute pancreatitis: mechanism, significance and therapy. *Br J Surg* 1990; **77**: 1205-1210
3 **Tak PP**, Firestein GS. NF-kappaB: a key role in inflammatory diseases. *J Clin Invest* 2001; **107**: 7-11
4 **Gray KD**, Simovic MO, Chapman WC, Blackwell TS, Christman JW, Washington MK, Yull FE, Jaffal N, Jansen ED, Gautman S, Stain SC. Systemic nf-kappaB activation in a transgenic mouse model of acute pancreatitis. *J Surg Res* 2003; **110**: 310-314
5 **Siebenlist U**, Franzoso G, Brown K. Structure, regulation and function of NF-kappa B. *Annu Rev Cell Biol* 1994; **10**: 405-455
6 **Chaqour B**, Howard PS, Richards CF, Macarak EJ. Mechanical stretch induces platelet-activating factor receptor gene expression through the NF-kappaB transcription factor. *J Mol*

Cell Cardiol 1999; **31**: 1345-1355
7 **McKenna DJ**, Jones K, Hughes K. Efficacy, safety, and use of ginkgo biloba in clinical and preclinical applications. *Altern Ther Health Med* 2001; **7**: 70-86, 88-90
8 **Liu LR**, Xia SH. Role of platelet-activating factor in the pathogenesis of acute pancreatitis. *World J Gastroenterol* 2006; **12**: 539-545
9 **Aho HJ**, Koskensalo SM, Nevalainen TJ. Experimental pancreatitis in the rat. Sodium taurocholate-induced acute haemorrhagic pancreatitis. *Scand J Gastroenterol* 1980; **15**: 411-416
10 **Wu JX**, Yuan YZ, Xu JY, Qin LF, Li DG, Lu HM. Pathological Characteristics of Acute Necrotizing Pancreatitis in Rats and the Methods of Evaluation. *Zhongguo Shiyan Dongwu Xuebao* 2002; **10**: 210-213
11 **Butcher HL**, Kennette WA, Collins O, Zalups RK, Koropatnick J. Metallothionein mediates the level and activity of nuclear factor kappa B in murine fibroblasts. *J Pharmacol Exp Ther* 2004; **310**: 589-598
12 **Bi HY**, Xia SH. Role of NF-κB in systemic inflammatory response syndrome. *Shijie Huaren Xiahua Zazhi* 2004; **12**: 2873-2841
13 **Shi C**, Zhao X, Lagergren A, Sigvardsson M, Wang X, Andersson R. Immune status and inflammatory response differ locally and systemically in severe acute pancreatitis. *Scand J Gastroenterol* 2006; **41**: 472-480
14 **Nishimune H**, Vasseur S, Wiese S, Birling MC, Holtmann B, Sendtner M, Iovanna JL, Henderson CE. Reg-2 is a motoneuron neurotrophic factor and a signalling intermediate in the CNTF survival pathway. *Nat Cell Biol* 2000; **2**: 906-914
15 **Hietaranta A**, Mustonen H, Puolakkainen P, Haapiainen R, Kemppainen E. Proinflammatory effects of pancreatic elastase are mediated through TLR4 and NF-kappaB. *Biochem Biophys Res Commun* 2004; **323**: 192-196
16 **Luo SF**, Lin WN, Yang CM, Lee CW, Liao CH, Leu YL, Hsiao LD. Induction of cytosolic phospholipase A2 by lipopolysaccharide in canine tracheal smooth muscle cells: involvement of MAPKs and NF-kappaB pathways. *Cell Signal* 2006; **18**: 1201-1211
17 **Vogensen SB**, Strømgaard K, Shindou H, Jaracz S, Suehiro M, Ishii S, Shimizu T, Nakanishi K. Preparation of 7-substituted ginkgolide derivatives: potent platelet activating factor (PAF) receptor antagonists. *J Med Chem* 2003; **46**: 601-608
18 **Wang XP**, Yu YZ, Xu JY. The therapeutic effect of Ginkgolides on acute pancreatitis in rats and its mechanisms. *Zhongguo Yaolixue Tongbao* 1995; **11**: 199-201
19 **Ji Z**, Wang B, Li S, Tang Y, Ding TK, Ma YG. The role of platelet activating factor in pathogenesis of acute pancreatitis in dogs. *Zhonghua Waike Zazhi* 1997; **35**: 108-110

S- Editor Liu Y **L- Editor** Zhu LH **E- Editor** Lu W

PO Box 2345, Beijing 100023, China
www.wjgnet.com
wjg@wjgnet.com

World J Gastroenterol 2007 February 14; 13(6): 889-894
World Journal of Gastroenterology ISSN 1007-9327

CLINICAL RESEARCH

Serum γ-glutamyltransferase, alanine aminotransferase, and aspartate aminotransferase activity in Iranian healthy blood donor men

Hossein Khedmat, Farahnaz Fallahian, Hassan Abolghasemi, Bashir Hajibeigi, Zohre Attarchi, Farshid Alaeddini, Mohammad Taghi Holisaz, Masoumeh Pourali, Shahin Sharifi, Nasrin Zarei

Hossein Khedmat, Farahnaz Fallahian, Mohammad Taghi Holisaz, Farshid Alaeddini, Baqiyatallah University of Medical Sciences, Iran
Hassan Abolghasemi, Bashir Hajibeigi, Zohre Attarchi, Masoumeh Pourali, Shahin Sharifi, Nasrin Zarei, Iranian Blood Transfusion Organization Research Center, Tehran, Iran
Correspondence to: Hossein Khedmat, associate professor, Department of Internal Medicine, Baqiyatallah Hospital, Baqiyatallah University of Medical Sciences, Mollasadra Ave. Tehran, IR, Iran. dr.khedmat@gmail.com
Telephone: +98-21-88037560 Fax: +98-21-88037560
Received: 2006-08-19 Accepted: 2006-12-18

Abstract

AIM: To determine serum γ-glutamyltransferase (GGT), alanine aminotransferase (ALT), and aspartate aminotransferase (AST) activity, and to assess their correlation with demographic and clinical findings in healthy blood donors.

METHODS: This cross-sectional study was performed in 934 male blood donors, aged 18 to 68 years, who consecutively attended Tehran blood transfusion service in 2006. All participants were seronegative for HBV or HCV infections, non alcohol users, and all underwent a standard interview and anthropometric tests. Clinical and biochemical parameters including AST, ALT, and GGT activities were determined. Patients taking drugs known to cause hepatic fat deposition were excluded. For AST, ALT, and GGT variables, we used 33.33 and 66.66 percentiles, so that each of them was divided into three tertiles.

RESULTS: Mean AST, ALT, and GGT activities were 25.26 ± 12.58 U/L (normal range 5-35 U/L), 33.13 ± 22.98 (normal range 5-35 U/L), and 25.11 ± 18.32 (normal range 6-37 U/L), respectively. By univariate analyses, there were significant associations between increasing AST, ALT, or GGT tertiles and age, body weight, body mass index, and waist and hip circumferences ($P < 0.05$). By multiple linear regression analyses, ALT was found to be positively correlated with dyslipidemia (B = 6.988, $P = 0.038$), whereas ALT and AST were negatively correlated with age. AST, ALT, and GGT levels had positive correlation with family history of liver disease (B = 15.763, $P < 0.001$), (B = 32.345, $P < 0.001$), (B = 24.415, $P < 0.001$), respectively.

CONCLUSION: Although we did not determine the cutoffs of the upper normal limits for AST, ALT, and GGT levels, we would suggest screening asymptomatic patients with dyslipidemia and also subjects with a family history of liver disease.

Key words: γ-glutamyltransferase; Alanine aminotransferase; Aspartate aminotransferase; Blood donor

Khedmat H, Fallahian F, Abolghasemi H, Hajibeigi B, Attarchi Z, Alaeddini F, Holisaz MT, Pourali M, Sharifi S, Zarei N. Serum γ-glutamyltransferase, alanine aminotransferase, and aspartate aminotransferase activity in Iranian healthy blood donor men. *World J Gastroenterol* 2007; 13(6): 889-894

http://www.wjgnet.com/1007-9327/13/889.asp

INTRODUCTION

The level of aspartate aminotransferase (AST), alanine aminotransferase (ALT), γ-glutamyltransferase (GGT) elevation that is considered abnormal varies widely and has recently been brought into question[1]. There is also debate as to whether or not different cutoffs are indicated for normal ranges of liver enzymes. Several studies have shown that variation in serum AST ALT or GGT in the population is associated with risk of development of cardiovascular disease, type 2 diabetes, stroke, or hypertension[2,3]. Nonalcoholic fatty liver disease (NAFLD) is a common explanation for abnormal liver-test results in blood donors, and it is the cause of asymptomatic elevation of aminotransferase levels in up to 90 percent of cases once other causes of liver disease are excluded[4]. Associations between abnormal values and also the prevalence and the risk factors for fatty liver have not undergone a formal evaluation in a representative sample of the general population. NAFLD is emerging as a component of the metabolic syndrome, although it is not known whether markers of NAFLD, including elevated concentrations of AST, and ALT, predict the development

of metabolic syndrome. The third report of the National Cholesterol Education Program expert panel on Detection, Evaluation, and Treatment of High Blood Cholesterol in Adults (ATP Ⅲ) defines metabolic syndrome as involving three or more of the following criteria[5]:

- Central/abdominal obesity as measured by waist circumference: for men > 40 inches (102 cm) and for women > 35 inches (88 cm).
- Fasting plasma triglycerides ⩾ 150 mg/dL (1.69 mmol/L)
- HDL cholesterol for men < 40 mg/dL (1.04 mmol/L), and for women < 50 mg/dL (1.29 mmol/L)
- Blood pressure ⩾ 130/85 mmHg
- Fasting plasma glucose ⩾ 110 mg/dL (6.1 mmol/L)

Also frequently seen with metabolic syndrome but not included in the ATP Ⅲ criteria are prothrombotic and proinflammatory tendencies. All of the factors associated with metabolic syndrome are interrelated. Obesity and lack of exercise tend to lead to insulin resistance. Insulin resistance has a negative effect on lipid production, increasing VLDL (very low-density lipoprotein), LDL and triglyceride levels in the bloodstream and decreasing HDL (high-density lipoprotein). This can lead to fatty plaque deposits in the arteries enhancing the risks for cardiovascular disease, blood clots, and strokes. Excess insulin increases renal sodium retention, which increases blood pressure and can lead to hypertension.

Our aim was to determine serum γ-glutamyltransferase, alanine aminotransferase, and aspartate aminotransferase activity and to investigate their relationship with several components of the metabolic syndrome in 934 healthy male blood donors in Tehran blood transfusion center from 15 February to 22 March 2006.

MATERIALS AND METHODS

Clinical and laboratory assessment

Nine hundred thirty four apparently healthy Iranian men, who attended to Tehran blood transfusion center for blood donation during a 37-d period from 15 February to 22 March 2006, were consecutively enrolled in the cross-sectional study. A standard interview, anthropometrics, and biochemical analyses were conducted for each participant. Samples from all donations were tested according to the recognized screening test algorithms for hepatitis B surface antigen, anti-HCV, anti-HIV1/2, syphilis, and for AST, ALT and GGT levels. Samples repeatedly reactive or indeterminate for HBsAg were further analyzed with a second independent HBsAg enzyme immunoassay (EIA), and if further reactive, were tested by a neutralization assay. Samples repeatedly reactive or indeterminate for anti-HCV were confirmed with an additional independent anti-HCV EIA and with a HCV-RIBA assay. Samples repeatedly reactive or indeterminate for HIV were confirmed with a second independent anti-HIV1/2 test, a p24 Ag assay and a HIV western blot. Samples reactive to venereal disease research laboratory (VDRL) were tested by fluorescent Treponemal antibody absorbed (FTA-ABS) as confirmatory test for syphilis infection.

The following conditions were excluded: seropositivity for hepatitis B surface antigen, and or antibody to hepatitis C virus, approved by confirmatory tests of hepatitis B and C viruses, alcohol consumption, use of drugs which may produce fatty liver as asparaginase, tetracycline, warfarin, amiodarone, tamoxifen, estrogens, bleomycin, diltiazem, nifedipine, methotrexate, corticosteroids, and salicylates. Cigarette smoking was not considered a criterion for exclusion. As number of female blood donors were limited (56 subjects), their data were not included. Personal and family history of hypertension, ischemic heart disease, stroke, dyslipidemia, diabetes mellitus, chronic liver disease according to diagnosis of physician, cigarette smoking, medication history, demographic findings such as body weight, height, body mass index, waist and hip circumferences, waist to hip ratio, and blood pressure were recorded. All anthropometric measurements were made by the same physician. Former and present smokers were defined as ever smokers. Established diagnosis of diabetes was considered if random blood sugar > 200 mg/dL (⩾ 11.1 mmol/L) plus symptoms of diabetes or the patient was a known case of diabetes by a physician. Dyslipidemia was diagnosed in the case of documented use of anti-lipemic medication, or the fasting levels of total cholesterol above 200 mg/dL or triglycerides above 170 mg/dL. The diagnosis of hypertension was based on the following criteria: systolic blood pressure ⩾ 140 mmHg and or diastolic blood pressure ⩾ 90 mmHg measured within 30 min in the sitting position using a brachial sphygmomanometer or ongoing use of antihypertensive treatment. Personal history of ischemic heart disease, stroke, family history of diabetes, family history of chronic liver disease in first relatives were recorded if the diagnoses were approved by a physician.

Venous blood was drawn from antecubital vein. AST, ALT and GGT levels were detected by auto-analyzer. AST, ALT and GGT in serum were determined by ELISA method. Furthermore, to eliminate effect of freeze-thawing of samples that may lower enzyme activity values, ALT, AST, and GGT testing was conducted on samples which were immediately carried to the laboratory. We did not exclude people with known diabetes that is likely to be affected more commonly with fatty liver disease, to avoid bias in conclusions. The study proposal and the protocol were approved by the ethics committee of Baqiyatallah University of Medical Sciences, and a written informed consent was obtained from each participant.

Statistical analysis

Analysis was performed using SPSS software version 13.0. For numerical variables we used mean value, standard deviation, median, 5^{th} and 95^{th} percentiles, maximum and minimum. For categorical variables we used number and percent. Since AST, ALT, and GGT values were not gaussian distributed, the levels of these variables were logarithm neperian (Ln) transformed. For measurement of their mean, we changed the amounts to normal Log and then we used exponential of mean and used that as mean of variables.

We used 33.33 and 66.66 percentiles and each variable was divided into three groups. For associations of them with numerical variables variance analyses, and for analyzing statistical difference among categorical variables in relation to AST, ALT, and GGT levels, chi-square tests

Table 1 AST tertiles according to characteristics of the study population

Variable	AST			*P*
	< 21	21-25	> 25	
Age (mean ± SD), yr	42.1 ± 11.4	40.9 ± 11.2	39.5 ± 10.2	0.020 (group 1 *vs* group 3)
Body weight (mean ± SD), km	80.6 ± 11.9	82.1 ± 12.8	85.7 ± 13.4	0.000 (group 1, 2 *vs* group 3)
Height (mean ± SD), cm	174.4 ± 6.9	174.9 ± 6.4	175.3 ± 6.8	0.232
Body mass index (BMI) (mean ± SD)	26.6 ± 3.7	26.9 ± 3.9	27.9 ± 4.3	0.000 (group 1, 2 *vs* group 3)
Waist circumference (mean ± SD), cm	94.3 ± 8.6	95.5 ± 9.7	97.3 ± 9.7	0.000 (group 1, 2 *vs* group 3)
Hip circumference (mean ± SD), cm	100.7 ± 8.2	101.5 ± 9.4	103 ± 9.1	0.001 (group 1, 2 *vs* group 3)
Waist to hip ratio (WHR) (mean ± SD)	0.94 ± 0.04	0.94 ± 0.05	0.94 ± 0.05	0.449
Diabetes mellitus (% positive)	2.7	1.3	1.0	0.226
Family history of diabetes (% positive)	23.3	18.8	18.6	0.271
Family history of liver disease (% positive)	0.3	1.6	1.3	0.276
Hypertension (% positive)	3.7	2.6	2.3	0.574
Dyslipidemia (% positive)	6.3	4.9	8.1	0.262
Smoking habit (% positive)	24.0	21.7	19.7	0.435

Table 2 ALT tertiles according to characteristics of the study population

Variable	ALT			*P*
	< 22	22-34	> 34	
Age (mean ± SD), yr	42.1 ± 11.9	41.5 ± 10.9	38.9 ± 9.9	0.001 (group 1, 2 *vs* group 3)
Body weight (mean ± SD), kg	79.0 ± 11.5	83.0 ± 11.4	86.5 ± 14.4	0.000 (all of groups)
Height (mean ± SD), cm	174.45 ± 6.76	174.67 ± 6.69	175.4 ± 6.6	0.173
Body mass index (BMI) (mean ± SD)	25.94 ± 3.4	27.29 ± 3.6	28.1 ± 4.6	0.000 (all of groups)
Waist circumference (mean ± SD), cm	93.2 ± 9.5	95.7 ± 8.6	98.1 ± 9.5	0.000 (all of groups)
Hip circumference (mean ± SD), cm	99.5 ± 9.0	102.0 ± 8.2	104.1 ± 9.2	0.001 (all of groups)
Waist to hip ratio (WHR) (mean ± SD)	0.94 ± 0.04	0.94 ± 0.05	0.94 ± 0.05	0.152
Diabetes mellitus (% positive)	2.0	1.0	1.9	0.571
Family history of diabetes (% positive)	20.6	21.8	18.2	0.538
Family history of liver disease (% positive)	0.3	1.3	1.6	0.268
Hypertension (% positive)	3.6	2.4	2.6	0.621
Dyslipidemia (% positive)	4.9	7.4	7.1	0.402
Smoking habit (% positive)	21.64	23.57	20.2	0.602

were performed. If it was a difference between groups, in analysis variance, we used LSD test for showing the group that had significant difference. All reported *P* values are two tailed, and those < 0.05 were considered statistically significant. Multiple linear regression analyses were conducted to assess variables that are associated with increased AST, ALT, or GGT levels, and all the variables entered the model and then those that had a *P* value less than 0.1 were maintained in the equation.

RESULTS

The mean age of 934 participants was 40.83 ± 10.96 (range of 18.00 to 68.00) years. The mean body mass index, waist circumference, and waist to hip ratio (WHR) were 27.09 ± 3.98, 95.62 ± 9.41 centimeter, and 0.93 ± 0.04, respectively. Mean AST, ALT, and GGT activities were 25.26 ± 12.58 U/L (normal range 5-35 U/L), 33.13 ± 22.98 U/L (normal range 5-35 U/L), and 25.11 ± 18.32 U/L (normal range 6-37 U/L), respectively. Mean (Transformation Ln) of AST, ALT, and GGT were 23.76, 28.45, and 20.52, respectively. Considering 5th and 95th percentiles of AST (16, 42), ALT (13, 70), or GGT (8, 58) U/L, the 95th percentiles values were high in the population studied. Subjects were divided into three groups according to liver enzyme tertiles. In AST tertiles, AST level was < 21, 21-25 U/L, and AST > 25 U/L in groups 1, 2, and 3, respectively. In ALT tertiles, ALT level was < 22, 22-34, and > 34 U/L in groups 1, 2, and 3, respectively. In GGT tertiles, GGT level was < 15 U/L, 15-25 U/L, and > 25 U/L in groups 1, 2, and 3, respectively.

Comparative demographic, clinical and biochemical characteristics of our study population in AST, ALT, and GGT tertile groups by univariate analyses are shown in Tables 1, 2, and 3. Univariate analyses show significant associations between increasing AST, ALT, or GGT tertiles and age, body weight, body mass index, central adiposity, waist and hip circumferences ($P < 0.05$). Moreover, evidence that increasing ALT, AST, and GGT tertiles are associated with demographic parameters of the metabolic syndrome (body weight, body mass index, waist circumference and hip circumference), support the conclusion that most of the abnormalities are probably due to NAFLD. The mean body mass index in our study population of 27.09 ± 3.98 could implicate a potentially important public health attention.

Table 4 shows correlation of our study characteristics with AST, ALT, or GGT levels in multiple linear regression.

In multiple linear regression analysis, AST was found

Table 3 GGT tertiles according to characteristics of the study population

Variable	GGT			*P*
	< 15	15-25	> 25	
Age (mean ± SD), yr	38.8 ± 11.4	42.4 ± 11.2	41.3 ± 10.1	0.000 (group 1 *vs* group 2, 3)
Body weight (mean ± SD), kg	79.1 ± 11.2	83.8 ± 12.6	85.7 ± 13.9	0.000 (group 1 *vs* group 2, 3)
Height (mean ±SD), cm	174.6 ± 6.5	174.9 ± 7.0	175.1 ± 6.6	0.675
Body mass index (BMI) (mean ± SD)	25.9 ± 3.3	27.6 ± 4.3	27.9 ± 4.0	0.000 (group 1 *vs* group 2, 3)
Waist circumference (mean ± SD), cm	92.9 ± 9.1	96.5 ± 9.5	97.8 ± 8.9	0.000 (group 1 *vs* group 2, 3)
Hip circumference (mean ± SD), cm	99.2 ± 8.9	102.8 ± 9.0	103.7 ± 8.5	0.001 (group 1 *vs* group 2, 3)
Waist to hip ratio (WHR) (mean ± SD)	0.94 ± 0.04	0.94 ± 0.04	0.94 ± 0.05	0.103
Diabetes mellitus (% positive)	0.6	2.0	2.3	0.217
Family history of diabetes (% positive)	19.1	22.1	19.5	0.608
Family history of liver disease (% positive)	0.0	1.0	2.3	0.023
Hypertension (% positive)	2.2	2.7	3.6	0.582
Dyslipidemia (% positive)	5.1	7.1	7.2	0.486
Smoking habit (% positive)	19.49	23.29	22.7	0.471

to be inversely related with age and smoking habit (B = -0.125, $P = 0.002$; B = -1.874, $P = 0.076$, respectively).

ALT was negatively correlated with age (B = -0.317, $P = 0.000$), and positively with a personal history of dyslipidemia (B = 6.988, $P = 0.038$). For AST, ALT, and GGT levels positive associations were found with a family history of liver disease (B = 15.763, $P < 0.001$; B = 32.345, $P < 0.001$; and B = 24.415, $P < 0.001$, respectively).

Table 4 Correlation of the study population characteristics with AST, ALT, and GGT levels

Dependent variable	Independent variable	Coefficients		*P*
		B	Std. Error	
AST	Age	-0.125	0.039	0.002
	Family history of liver disease	15.763	4.029	0.000
	Smoking habit	-1.874	1.056	0.076
ALT	Age	-0.317	0.071	0.000
	Family history of liver disease	32.345	7.258	0.000
	Dyslipidemia	6.988	3.363	0.038
GGT	Family history of liver disease	24.415	5.791	0.000

DISCUSSION

In the general population, the estimated NAFLD prevalence ranges from 3% to 24%, with most estimates in the 6% to 14% range. NAFLD appears to be most strongly associated with obesity. It appears to be more common in men, and it increases with increasing age and after menopause. More advanced stages of NAFLD are associated with older age and higher body mass index[6]. In Ruhl *et al*[7] study, elevated ALT was associated with younger age corresponding to our study in which increasing ALT and AST tertiles were inversely related to age.

NAFLD is the major cause of elevation of ALT and it is in fact considered the hepatic manifestation of metabolic syndrome[8]. In a study of 10368 adults aged 20 years and over, participating in the Tehran Lipid and Glucose Study[9], the age-standardized prevalence of the metabolic syndrome was 33.7%.

Several studies have shown that variation in serum GGT in the population is associated with risk of death or development of cardiovascular disease, type 2 diabetes, stroke, or hypertension. Whitfield JB *et al*[2] estimated the relative importance of genetic and environmental sources of variation in GGT. There were highly significant correlations between GGT and body mass index, serum lipids, lipoproteins, glucose, insulin, and blood pressure. These correlations were more attributable to genes that affect both GGT and known cardiovascular risk factors than to environmental factors.

Nakanishi N *et al*[3] investigated the association between serum GGT and risk of metabolic syndrome and type 2 diabetes mellitus. The results of the article indicate that serum GGT may be an important predictor for developing metabolic syndrome and type 2 diabetes mellitus. Kim HC, *et al*[10] showed that the serum ALT and GGT levels were significantly associated with metabolic syndrome in men but not in women.

In the present study, correlation between family history of liver disease and increased liver enzymes may be attributable to genes that affect AST, ALT, and GGT and also known metabolic syndrome risk factors and environmental factors. Although we did not exclude other etiologies of hepatitis in families of blood donors, the association of family history of hepatitis with increasing AST, ALT, or GGT levels may show a genetic predisposition. As fatty liver is the most common cause of liver function test abnormality, further investigation is needed for genetic and dietary habits as predisposing factors for liver abnormality. Interaction of genetic and environmental factors might be the trigger of inflammatory cascades leading to metabolic syndrome. Rising liver enzymes activity may be the hepatic manifestation of ongoing inflammation and metabolic syndrome. The liver plays an important role in maintaining normal glucose concentration. It is also a major site of insulin clearance[11]. Type 2 diabetes mellitus is a public health problem of epidemic dimension and its prevalence is on the rise. Many risk factors, including the metabolic syndrome, have been implicated in its development[12].

There are controversies about normal ranges of liver enzymes in the general population. Furthermore, the level of elevation that is considered abnormal varies widely and has recently been brought into question. There is also a

debate as to whether or not different cutoffs are indicated for normal ranges of liver enzymes in men and women. Given all the controversy, it is clear that more acceptable and accurate means of noninvasive diagnostic approach to NAFLD as the most common cause of liver function test abnormality is needed. In addition, the use of higher cutoff values for normal ALT, AST, or GGT would lower the estimated prevalence of occult liver disease in the population.

Mohammadnejad M *et al*[13] showed that serum ALT activity was independently associated with body mass index and male gender, but not with age. The upper normal limit for non-overweight women (BMI of less than 25) was 34 U/L, and for non-overweight men 40 U/L. This article suggested that the normal range of ALT should be defined for male and female separately. Using this level of upper limit value for ALT activity, the authors of this paper may lose some men with NAFLD who need screenings. Our study corresponds with their data with respect to the association of liver enzymes and body mass index but we also noted liver enzyme correlation with age, body weight, and waist and hip circumferences.

Ruhl and Everhart[7] reviewed data from the third US National Health and Nutrition Examination Survey (1988-1994) in which adult participants underwent anthropometric measurements. Abnormal ALT was defined as ALT > 43 U/L for men or women. Serum ALT levels as a surrogate marker for NAFLD were elevated in 2.8% of the study population. Moreover, using recently suggested lower normal values for ALT (> 30 U/L for men and > 19 U/L for women), they found elevated levels in 12.4% of men and 13.9% of women. Clark JM and Diehl AM[1] in their editorial comment on Ruhl C *et al*[7] acknowledged that occult liver disease may be more common than previously suspected. They agreed that the association of ALT abnormalities with the metabolic syndrome supports the conclusion that the ALT elevations are due to NAFLD. The conditions associated with fatty liver disease presenting with normal liver enzymes and the mechanism involved in its development remain to be fully elucidated.

The hypothesis that fatty liver with normal liver enzymes occurs more frequently in arterial hypertensive patients was tested by Donati G *et al*[14] and they found that the condition is associated with insulin resistance. Essential hypertension is considered an insulin resistant state[15], and approximately 50% of patients with arterial hypertension are reported to be insulin resistant with hyperinsulinemia[16], a value much higher than that is found in the general population.

Our study population was consisted of healthy blood donors who are a better sample to indicate the burden of occult liver disease and NAFLD in the general population compared to the sampling from gastroenterology clinics or referred patients with metabolic syndrome. History of personal hypertension had no statistically significant association with increasing liver enzyme levels. It is noteworthy that hypertensive patients are not good candidates for blood donation and, because most of them have already been excluded from our study, interpretation of our findings in this regard is limited.

Our study has some limitations. The vast majority of our participants were male; and the volunteer blood donors are healthier than general population. In this study, all the biochemical and clinical variables predicting the presence of metabolic syndrome were not examined. We did not consider the racial, ethnicity, genetic and environmental sources of variation in AST, ALT, and GGT; amount of regular physical activity, eating habits, and biochemical characteristics of metabolic syndrome. We did not determine cutoffs of liver enzymes for estimation of non-alcoholic fatty liver disease, although NAFLD is reported even in normal range of liver enzymes. A better understanding of the factors that modulate liver disease progression is critical, so that we can target selected patients for more aggressive monitoring, lifestyle interventions, and pharmacotherapy.

In conclusion, variation within the normal ranges of AST, ALT, and GGT in healthy subjects is associated with some components of metabolic syndrome. In adult healthy men, those in the highest AST, ALT, and GGT levels, present with family history of liver disease; and those in the highest ALT levels, present with dyslipidemia. It is reasonable to recommend screening those with dyslipidemia that is also a risk factor for atherosclerosis and premature cardiovascular disease. Moreover, screening subjects with evidence of abdominal obesity and family history of liver disease is necessary.

The follow-up of these individuals would determine if certain amounts of AST, ALT, and GGT values might be considered as early predictors of subsequent fatty liver and the metabolic syndrome. In this way, the health-related outcomes of AST, ALT, and GGT values and the needed optimal frequency of their visiting would be determined. The health benefits of screening for fatty liver and other components of metabolic syndrome seems as necessary as performing tests for evidence of viral hepatitis B and C infections.

ACKNOWLEDGMENTS

The authors would like to thank managers of Blood Transfusion Organization Research Center for the accompanying illustrations, the financial support, and technical assistance. Also, we thank Dr. Mohammad Miri, Masoud Taremi, Tajbakhsh Rajabi and Mitra Khari for their assistance.

REFERENCES

1 **Clark JM**, Diehl AM. Defining nonalcoholic fatty liver disease: implications for epidemiologic studies. *Gastroenterology* 2003; **124**: 248-250

2 **Whitfield JB**, Zhu G, Nestler JE, Heath AC, Martin NG. Genetic covariation between serum gamma-glutamyltransferase activity and cardiovascular risk factors. *Clin Chem* 2002; **48**: 1426-1431

3 **Nakanishi N**, Suzuki K, Tatara K. Serum gamma-glutamyltransferase and risk of metabolic syndrome and type 2 diabetes in middle-aged Japanese men. *Diabetes Care* 2004; **27**: 1427-1432

4 **Angulo P**. Nonalcoholic fatty liver disease. *N Engl J Med* 2002; **346**: 1221-1231

5 Executive Summary of The Third Report of The National

Cholesterol Education Program (NCEP) Expert Panel on Detection, Evaluation, And Treatment of High Blood Cholesterol In Adults (Adult Treatment Panel III). *JAMA* 2001; **285**: 2486-2497

6 **Clark JM**. The epidemiology of nonalcoholic fatty liver disease in adults. *J Clin Gastroenterol* 2006; **40** Suppl 1: S5-S10

7 **Ruhl CE**, Everhart JE. Determinants of the association of overweight with elevated serum alanine aminotransferase activity in the United States. *Gastroenterology* 2003; **124**: 71-79

8 **Gasbarrini G**, Vero V, Miele L, Forgione A, Hernandez AP, Greco AV, Gasbarrini A, Grieco A. Nonalcoholic fatty liver disease: defining a common problem. *Eur Rev Med Pharmacol Sci* 2005; **9**: 253-259

9 **Azizi F**, Salehi P, Etemadi A, Zahedi-Asl S. Prevalence of metabolic syndrome in an urban population: Tehran Lipid and Glucose Study. *Diabetes Res Clin Pract* 2003; **61**: 29-37

10 **Kim HC**, Choi SH, Shin HW, Cheong JY, Lee KW, Lee HC, Huh KB, Kim DJ. Severity of ultrasonographic liver steatosis and metabolic syndrome in Korean men and women. *World J Gastroenterol* 2005; **11**: 5314-5321

11 **Michael MD**, Kulkarni RN, Postic C, Previs SF, Shulman GI, Magnuson MA, Kahn CR. Loss of insulin signaling in hepatocytes leads to severe insulin resistance and progressive hepatic dysfunction. *Mol Cell* 2000; **6**: 87-97

12 **Abuissa H**, Bel DS, O'keefe JH. Strategies to prevent type 2 diabetes. *Curr Med Res Opin* 2005; **21**: 1107-1114

13 **Mohamadnejad M**, Pourshams A, Malekzadeh R, Mohamadkhani A, Rajabiani A, Asgari AA, Alimohamadi SM, Razjooyan H, Mamar-Abadi M. Healthy ranges of serum alanine aminotransferase levels in Iranian blood donors. *World J Gastroenterol* 2003; **9**: 2322-2324

14 **Donati G**, Stagni B, Piscaglia F, Venturoli N, Morselli-Labate AM, Rasciti L, Bolondi L. Increased prevalence of fatty liver in arterial hypertensive patients with normal liver enzymes: role of insulin resistance. *Gut* 2004; **53**: 1020-1023

15 **Ferrannini E**, Buzzigoli G, Bonadonna R, Giorico MA, Oleggini M, Graziadei L, Pedrinelli R, Brandi L, Bevilacqua S. Insulin resistance in essential hypertension. *N Engl J Med* 1987; **317**: 350-357

16 **Pollare T**, Lithell H, Berne C. Insulin resistance is a characteristic feature of primary hypertension independent of obesity. *Metabolism* 1990; **39**: 167-174

S- Editor Liu Y **L- Editor** Mihm S **E- Editor** Lu W

PO Box 2345, Beijing 100023, China
www.wjgnet.com
wjg@wjgnet.com

World J Gastroenterol 2007 February 14; 13(6): 895-900
World Journal of Gastroenterology ISSN 1007-9327

RAPID COMMUNICATION

Higher radiation dose with a shorter treatment duration improves outcome for locally advanced carcinoma of anal canal

Kim Huang, Daphne Haas-Kogan, Vivian Weinberg, Richard Krieg

Kim Huang, Daphne Haas-Kogan, Richard Krieg, Department of Radiation Oncology, University of California, San Francisco, CA, United States
Vivian Weinberg, Comprehensive Cancer Center Biostatistics Core, University of California, San Francisco, CA, United States
Correspondence to: Richard Krieg, MD, Department of Radiation Oncology, Suite H1031, PO Box 1708, University of California, San Francisco, 1600 Divisidero St, San Francisco, CA 941151708, United States. krieg@radonc17.ucsf.edu
Telephone: +1-415-3537175 Fax: +1-415-3539883
Received: 2006-09-13 Accepted: 2007-01-10

Key words: Anal carcinoma; Locally advanced; Chemoradiation

Huang K, Haas-Kogan D, Weinberg V, Krieg R. Higher radiation dose with a shorter treatment duration improves outcome for locally advanced carcinoma of anal canal. *World J Gastroenterol* 2007; 13(6): 895-900

http://www.wjgnet.com/1007-9327/13/895.asp

Abstract

AIM: To assess whether radiation dose and duration of treatment influence local control and survival of patients with locally advanced anal cancer treated with definitive chemoradiation.

METHODS: Twenty-eight consecutive patients who were treated with definitive radiation therapy for bulky anal cancers (> 5 cm in size) were reviewed. Nineteen patients had T3 lesions, 8 patients had T4 lesions, and 15 patients had lymph node involvement. The median tumor size was 7.5 cm. All but one patient received concurrent chemoradiation. The median radiation dose was 54 Gy. The median duration of treatment was 58 d.

RESULTS: With a median follow-up of 2.5 years in all patients and 7.8 years in living patients, the 2-year local recurrence-free probability was 57% and overall survival rate was 67%. Neither radiation dose nor duration of treatment alone was predictive of either time to local failure or overall survival. However, longer treatment breaks can potentially mask an advantage over higher radiation doses. Therefore, we examined those patients who received $\geqslant$ 54 Gy within 60 d, comparing them to the rest of the patients. Of patients who received $\geqslant$ 54 Gy within 60 d, local progression-free probability was 89% versus 42% for the rest of the group (P = 0.01).

CONCLUSION: Local failure is a significant problem in locally advanced carcinomas of the anal canal. Higher radiation doses with limited treatment breaks may offer an increase in local control and survival.

INTRODUCTION

Combined chemoradiation has been established as the standard treatment for epidermoid anal cancer by randomized trials that have demonstrated improvements in local control and disease free survival compared to radiation alone[1,2]. Administered with radiation, the combination of 5-flurouracil (5-FU) and mitomycin C is the regimen of choice, providing superior disease-free survival compared to 5-FU alone[3]. However, for locally advanced anal cancer, especially lesions greater than 5 cm, local control rates of only 50% have been achieved[4,5]. Higher radiation dose has been shown to improve outcome in some studies[6-9]. A phase Ⅱ radiation dose escalation trial for anal cancer performed by the Radiation Therapy Oncology Group (RTOG) showed increased colostomy rates with increased doses compared to patients treated with a lower dose in a previous RTOG trial[10]. The worse outcome may in part be attributed to a mandatory 2 wk break in this trial. It is unclear if increasing the radiation dose in patients with locally advanced anal cancer receiving combined modality therapy will improve the results compared with doses of 45-50 Gy[10].

In order to assess whether higher radiation doses improve clinical outcome for patients with locally advanced anal cancer, we retrospectively reviewed treatment outcomes of patients with bulky (> 5 cm) epidermoid anal cancer. Radiation dose, treatment time, as well as patient, tumor and treatment related factors were evaluated for prognosis.

MATERIALS AND METHODS

Subjects

This work has been approved by the Institutional Review

Board of the University of California, San Francisco. Between 1982 and 2000, 28 consecutively treated patients underwent definitive radiation therapy for documented bulky anal cancers (disease greater than 5 cm in primary tumor or lymph nodes). Patients who had local excision prior to radiotherapy were excluded. Of 28 patients, 27 had bulky disease at primary sites and one had bulky lymph node disease. One patient was treated for bulky recurrent disease after abdominoperineal resection.

Treatment

One patient declined treatment with chemotherapy and was treated with radiation alone, while the other 27 patients received concurrent chemoradiation. Chemotherapy consisted of 5-FU and mitomycin C in 23 patients, 5-FU and cisplatin in one patient and 5-FU alone in three patients. 5-FU was given at 1000 mg/m^2 over 4 d. Generally mitomycin C was given at 10 mg/m^2. Cisplatin was given at 75 mg/m^2 every 4 wk. One patient was treated with induction 5-FU and cisplatin with progressive disease, followed by 5-FU and mitomycin C concurrently with radiation. All patients received 2 cycles of chemotherapy generally at an interval of 4 wk concurrently with radiation, except for one patient who died of fulminant hepatitis after receiving only one cycle of chemotherapy. Two patients received 5-FU alone during the second cycle after severe hematologic toxicity associated with the first cycle of chemotherapy with 5-FU and mitomycin.

Radiation was administered utilizing 6 or 18 MV photons. Treatment fields were AP/PA to the whole pelvis and bilateral inguinal regions, followed by a lateral field boost plus/minus electron field boost to cover the inguinal regions. The first field reduction was at 30.6 Gy to the true pelvis, followed by subsequent field reductions at 36 Gy and 45 Gy. For patients who had a CD4 count < 200, the initial field was the true pelvis to minimize toxicity. Before 1985, radiation doses of 40-50 Gy were planned, while after 1985, target radiation doses were increased to 54-60 Gy. Five patients did not receive the planned doses of radiation, secondary to toxicity in 3 patients, receiving 36 Gy, 50.4 Gy and 51.4 Gy, respectively, and noncompliant in 2 patients, receiving 50.4 Gy and 45 Gy, respectively. The radiation doses ranged from 31 to 65 Gy, with a median of 54 Gy. The dose per fraction ranged from 1.6 to 2.0 Gy once daily. The lower dose per fraction of 1.6 to 2.0 Gy was used in the early 80's when radiation was first used concurrently with chemotherapy.

Follow-up

All the patients were evaluated at least once a week during radiotherapy. The patients were then evaluated every 1-2 mo for the first 6 mo, followed by every 3 mo for the next 6-12 mo, every 4-6 mo from 18 mo through 3 years, and annually thereafter. At each follow-up visit, a physical examination, including digital rectal examination, and palpation of the inguinal regions was performed. Acute and late effects on normal tissues were graded according to the CTCAE v3 scoring criteria.

Table 1 Distribution of patients by the 2002 American Joint Committee on Cancer Staging Classification[1]

Stage	N0	N1	N2	N3	Total
T3	6	3	6	4	19
T4	6	0	1	1	8
Total	12	3	7	5	27

[1]One patient who had recurrent disease with an initial stage of T2N0 was not included in this table.

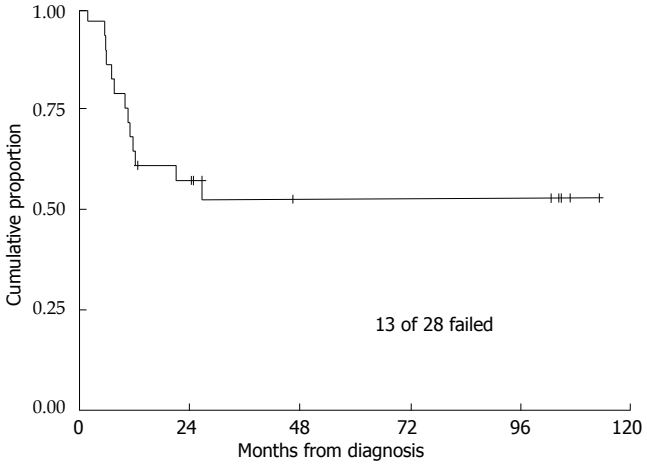

Figure 1 Kaplan-Meier estimate of the probability of local freedom from progression.

Statistical analysis

This is a retrospective analysis of treatment outcomes for bulky anal carcinoma treated at UCSF. Descriptive statistics (mean, median, and proportions) were calculated to characterize the patient, disease, and treatment features. Estimates of survival rates and recurrence-free probabilities were calculated using the Kaplan-Meier product limit method. Durations were calculated from the date of diagnosis. Univariate analyses were performed to evaluate factors that may be predictors of outcome. The log rank test was used to compare distributions of subsets.

RESULTS

Patient characteristics

The cohort included 10 women and 18 men with a median age of 63 years (range 30-79 years). Eight patients had cloacgenic carcinoma and 20 patients had squamous cell carcinoma. Table 1 shows the T- and N-stage distributions of the patients according to the 2002 AJCC staging classification. Nineteen patients had T3 lesions, 8 patients had T4 lesions, 1 had recurrent disease and 15 patients had pathologically involved lymph nodes. The median tumor size was 7.5 (range 5.5-12) cm. Four patients were human immunodeficiency virus (HIV) positive with CD4 counts of 63 180 238 and 347, respectively.

Treatment outcome

With a median follow-up of 2.5 (range 0.2-17.3) years for

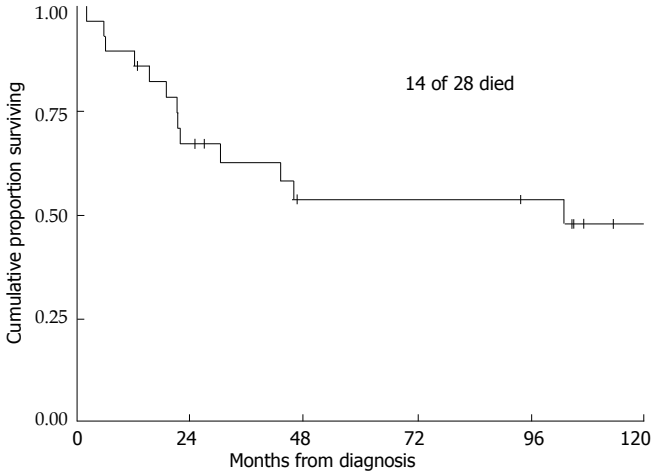

Figure 2 Kaplan-Meier estimate of the probability of overall survival.

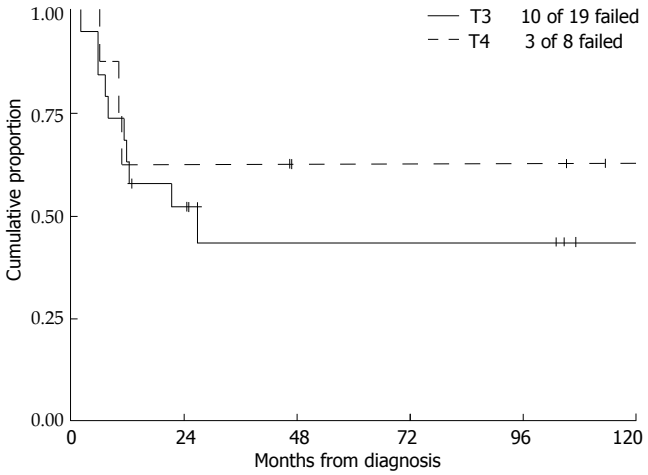

Figure 3 Kaplan-Meier estimate of the probability of local freedom from progression in comparison of patients with T3 versus T4 disease.

all patients and 7.8 (range 1.1-17.3) years for living patients, the 2-year and 5-year local recurrence-free probabilities and 95% confidence intervals (CI) were 57% (95% CI: 37%-73%) and 52% (95% CI: 32%-69%), respectively (Figure 1). The 2- and 5-year overall survival estimates were 67% (95% CI: 46%-81%) and 54% (33%-71%), respectively (Figure 2). The 2- and 5-year colostomy-free survival estimates were 42% (95% CI: 24%-60%) and 33% (95% CI: 16%-51%), respectively. Sixteen patients had persistent abnormalities at the completion of radiotherapy. In 12 of the 16 patients, biopsies of the persistent abnormalities revealed pathological documentation of residue disease in 5 patients. The single patient with a bulky lymph node experienced a lymph node failure, with a concurrent distant failure 25 mo after diagnosis. In the 4 patients who were HIV positive, 2 experienced local failures, 1 experienced a regional failure, and one died of fulminant hepatitis during treatment after receiving only 36 Gy, presumably secondary to chemotherapy. In patients treated with 5-FU alone with concurrent radiation, 2 out of 3 experienced local failures. The patient who did not receive any chemotherapy also had a local recurrence.

Toxicity

Acute side effects of radiation therapy and chemotherapy were moderate to severe. Twenty patients had acute grade 3 or 4 toxicities including 15 patients with grade 3 dermatological toxicities, 1 patient with grade 3 gastrointestinal toxicity, and 5 patients with grade 3 and 4 with grade 4 hematologic toxicities. The worst acute toxicity was dermatological in 10 patients, hematologic in 5 patients, both dermatological and hematologic in 4 patients, and gastrointestinal in 1 patient. In patients who received $\geqslant$ 54 Gy, 15 out of 17 patients experienced grade 3 or 4 toxicity, compared to 5 out of 11 patients who received less than 54 Gy. In the 4 patients who were HIV positive, one did not have any grade 3 or 4 acute toxicity, one had grade 3 dermatological toxicity, 1 had grade 3 dermatological and hematologic toxicities, 1 had grade 3 dermatological toxicity and grade 4 hematologic toxicity and died of fulminant hepatitis after receiving 30 Gy of radiation.

The median duration of treatment was 58 (range 31-112) d. In patients who received $\geqslant$ 54 Gy, the median duration of treatment was 60 d compared to 44 d in those who received < 54 Gy. Twenty-two patients had treatment breaks longer than 3 d. Ten patients had only one treatment break and 12 had more than 1 treatment break. The median length of total treatment breaks was 11 (range 0-53) d. Twelve patients had treatment breaks totaling longer than 14 d. The median dose at the first treatment break was 30.6 (range 3.6-52.2) Gy. Three patients had treatment breaks due to non-compliance, and the rest of patients due to toxicity. For patients who received $\geqslant$ 54 Gy, 16 out of 17 patients had a break longer than 3 d, compared to 6 out of 11 patients who received < 54 Gy.

Disease control

Univariate analyses revealed that male gender and HIV infection were each associated with worse overall survival (P = 0.02 and P = 0.01, respectively). Excluding HIV positive patients, male gender demonstrated a trend towards worse survival (P = 0.08). There was no significant difference in local control (Figure 3) or survival when comparing patients with T3 and T4 disease. Nodal stage, tumor size and type of chemotherapy were not predictive of either time to failure or overall survival. Neither radiation dose nor duration of treatment alone was statistically associated with either time to failure or overall survival.

Time and dose consideration

Even though radiation dose or duration of treatment alone was not statistically correlated with either time to failure or overall survival, these two factors were interrelated. Patients who received $\geqslant$ 54 Gy were more likely to experience treatment breaks resulting in longer treatment duration, potentially masking an advantage over higher radiation doses. Therefore, we examined those patients who received $\geqslant$ 54 Gy within 60 d, and compared them to the rest of the group (Figure 4). Patients who received $\geqslant$ 54 Gy within 60 d had significantly improved local progression-free and overall survival rates compared to

Table 2 Subgroup analysis of local control based on total radiation dose and overall treatment time

Fraction of patients controlled locally	High dose (> 54 Gy)	Low dose (< 54 Gy)
Short duration (≤ 60 d)	8/9[b]	4/9
Long duration (> 60 d)	2/8	1/2

[b]$P = 0.01$ *vs* the rest of the subgroups.

those whose treatments spanned longer than 60 d or who received less than 54 Gy (2-year local progression-free and overall survival probabilities of 89% (95% CI: 43%-98%) and 100% for treatments within 60 d compared to 42% (95% CI: 20%-62%) and 53% (95% CI: 29%-72%) for the rest of the group ($P = 0.01$ and $P = 0.02$, respectively). Of patients who received ≥ 54 Gy, 8 out of 9 patients were locally controlled if the treatment was completed within 60 d. However, for those patients who received ≥ 54 Gy with treatment durations longer than 60 d, only 2 out of 8 were locally controlled. For those patients who received less than 54 Gy, only 5 out of 11 were locally controlled (Table 2). The mean total dose in patients who received less than 54 Gy was 46 Gy.

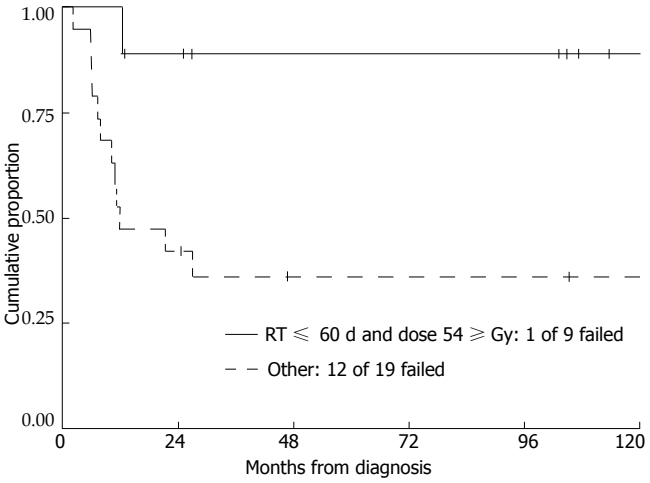

Figure 4 Kaplan-Meier estimate of the probability of local freedom from progression comparing patients who received > 54 Gy within 60 d *vs* the rest of the patients.

DISCUSSION

In the current study, neither total radiation dose nor treatment time alone was prognostic for local control or survival. The two factors were interrelated in that it took a longer treatment time to deliver an overall higher radiation dose: 35 d for 45 Gy and 45 d for 60 Gy. In addition, higher radiation doses resulted in higher toxicity rates and therefore a higher likelihood of treatment breaks. In this study, patients who received ≥ 54 Gy within 60 d had significantly improved local progression-free (Figure 4) and overall survival compared to those whose treatment spanned longer than 60 d or who received less than 54 Gy. This confirms a dose response in the treatment of locally advanced anal cancer with chemoradiation, although prolonged treatment breaks negate the advantage of higher dose.

Total radiation dose has been shown to impact outcome in anal carcinoma treated with combined chemoradiation[6-9]. Constantinou *et al*[6] found that radiation doses of ≥ 54 Gy were associated with significantly improved survival (84% *vs* 47%) and local control (77% *vs* 61%) in anal cancer patients treated with chemoradiation. About 30% of patients in their study had T3 or T4 lesions. In a group of patients treated with chemoradiation using continuous infusion of 5-FU, local control increased from 50% in those receiving < 45 Gy, to 73% in those receiving 50-54 Gy and 83% in those receiving > 60 Gy[9]. Nigh *et al*[8] reported a dose response with improved local control at higher doses: 64% at < 45 Gy, 77% at 45-55 Gy and 92% at > 55 Gy. At MD Anderson, local control was 50% for all stages receiving 45-49 Gy and 90% for those patients receiving greater than or equal to 55 Gy[7].

Overall treatment time has similarly been shown to impact outcome in treatment of anal cancer[10-15]. In the second phase of the dose escalation study RTOG 9208 without the mandatory break, the 1-year colostomy rate decreased from 23% to 11%[10,14]. In an European Organization for Research and Treatment of Cancer (EORTC) trial with a similar design to RTOG 9208 including a 2 wk break at 36 Gy (but slightly different chemotherapy with 5-FU given continuously during radiation), the 3-year local control and colostomy-free interval were 88% and 81% respectively, which compared favorably to the earlier EORTC randomized trial with a 6 wk break and mitomycin C given only on the first day of radiation[12]. Built in breaks > 37.5 d correlate with poorer loco-regional control in patients treated with a median of 40 Gy to the pelvis and a 20 Gy boost with either external beam radiation or brachytherapy[15]. Ceresoli *et al*[13] found that overall treatment times longer than 70 d were related to a worse disease-free survival in a group of patients treated with a median radiation dose of 56 Gy. Overall treatment times > 75 d were associated with poorer local control (69% *vs* 85%) in a study by Allal[11].

Increased toxicities have been observed in patients treated with higher radiation doses. In the second phase of the dose escalation study RTOG 9208 without the mandatory break, 50% of patients required treatment interruptions lasting at least 7 d. In our study, 71% of patients had treatment breaks longer than 3 d. Fourteen patients had grade 3 or greater dermatological toxicities requiring treatment breaks. One way to decrease toxicities is to use conformal radiation therapy. Indeed, one study showed that conformal radiotherapy enhanced tolerance to treatment, shortened treatment time to 6 wk and significantly decreased acute toxicities[16]. In another study, intensity-modulated radiotherapy (IMRT) improved conformality and reduced normal structure dose without compromising local control in the treatment of anal cancer[17]. We have investigated the potential to improve coverage of tumor volumes while maximizing sparing of normal tissues such as the skin and bowel using IMRT and have adopted IMRT as the preferred treatment technique for locally advanced anal cancer. Grade 3 or greater

hematologic toxicity was observed in 9 patients. Cisplatin-based combined modality therapy may generate less acute toxicity and a wider therapeutic index. In a retrospective analysis of patients treated with 55 Gy of radiation and continuous infusion of cisplatin and 5-FU, local control and survival were comparable to the best results reported with mitomycin C and 5-FU, with greater than 90% of patients completing treatment without significant treatment interruptions[18].

Hoffman *et al*[19] previously reported our institutional experience of treating HIV positive anal cancer patients with chemoradiation. Excellent disease control with acceptable morbidity was achieved in patients with a CD4 count of greater than or equal to 200[19]. There were 4 HIV positive patients with locally advanced disease in the group reported herein. Their disease control and survival were poor and toxicities were significant, although the small number of patients precluded firm conclusions regarding the role played by their HIV status.

The ideal chemotherapy regimen has yet to be established. An Eastern Oncology Group trial tested concurrent cisplatin, 5-FU, and 59.4 Gy of radiation with a 2-wk break after 36 Gy, which resulted in a complete response rate of 68%[20]. Adjuvant chemotherapy after combined chemoradiation is being tested in the ACT Ⅱ randomized trial from the United Kingdom[21]. The recently closed randomized trial RTOG 9811 compares concurrent chemoradiation with 5-FU and mitomycin C versus induction chemotherapy and concurrent chemoradiation with 5-FU and cisplatin. In addition, for T3, T4, node positive and any lesions with residual disease after 45 Gy, a boost of 10-14 Gy is included to achieve total doses of 55-59 Gy. The result from this trial may answer some of the questions pertaining to the best treatment regimen for anal cancer.

In conclusion, local failure is a significant problem in locally advanced carcinomas of the anal canal. Although the number of patients in this study was relatively small, we believe that higher radiation doses with limited treatment breaks may offer an increase in local control and survival.

COMMENTS

Background

There is controversy in the field regarding whether higher radiation doses improve outcome in anal cancer. Local control rate for locally advanced anal cancer is around 50%, which clearly needs to be improved. This paper tries to address the interrelation of time and dose and generates the hypothesis of higher radiation doses with shorter treatment duration improve outcome in locally advance anal cancer.

Research frontiers

The current focus of research is in the delivery of intensity modulated radiation therapy to treat anal cancer. The highly conformal dose distribution allows more sparing of normal tissues and high dose to the tumor, therefore, fewer toxicities and treatment breaks and hopefully improved tumor control.

Innovations and breakthroughs

Constantinou *et al* found that radiation doses of ⩾ 54 Gy were associated with significantly improved survival (84% *vs* 47%) and local control (77% *vs* 61%) in anal cancer patients treated with chemoradiation. Other studies addressed treatment time to some extent. This is the only study looking at radiation doses and treatment time in locally advanced anal cancer.

Applications

To achieve improved local control in locally advanced anal cancer patients, radiation doses of at least 54 Gy should be given concurrently with chemotherapy. Treatment breaks should be minimized to realize the effect of the higher doses of radiation. Modern techniques such as intensity-modulated radiotherapy may be a means to deliver higher doses of radiation while minimizing toxicities and treatment breaks.

Terminology

Total radiation dose is the final dose that is delivered to the gross tumor. Overall treatment time is the entire duration of radiation from beginning to end including any mandatory or elective treatment breaks. Intensity-modulated radiotherapy is a technique which delivers radiation in multiple fields of varying radiation intensity so that the dose distribution can be highly conformal around the target and minimizing doses to nearby critical tissues.

Peer review

The paper addresses one of the controversies in the field, that is, whether higher radiation dose improves outcome in locally advanced anal cancer. The data suggests higher radiation dose with shorter treatment duration improves outcome in this group of patients.

REFERENCES

1 **Bartelink H**, Roelofsen F, Eschwege F, Rougier P, Bosset JF, Gonzalez DG, Peiffert D, van Glabbeke M, Pierart M. Concomitant radiotherapy and chemotherapy is superior to radiotherapy alone in the treatment of locally advanced anal cancer: results of a phase III randomized trial of the European Organization for Research and Treatment of Cancer Radiotherapy and Gastrointestinal Cooperative Groups. *J Clin Oncol* 1997; **15**: 2040-2049

2 **Epidermoid anal cancer: results from the UKCCCR randomised trial of radiotherapy alone versus radiotherapy, 5-fluorouracil, and mitomycin. UKCCCR Anal Cancer Trial Working Party**. UK Co-ordinating Committee on Cancer Research. *Lancet* 1996; **348**: 1049-1054

3 **Flam M**, John M, Pajak TF, Petrelli N, Myerson R, Doggett S, Quivey J, Rotman M, Kerman H, Coia L, Murray K. Role of mitomycin in combination with fluorouracil and radiotherapy, and of salvage chemoradiation in the definitive nonsurgical treatment of epidermoid carcinoma of the anal canal: results of a phase III randomized intergroup study. *J Clin Oncol* 1996; **14**: 2527-2539

4 **Gerard JP**, Ayzac L, Hun D, Romestaing P, Coquard R, Ardiet JM, Mornex F. Treatment of anal canal carcinoma with high dose radiation therapy and concomitant fluorouracil-cisplatinum. Long-term results in 95 patients. *Radiother Oncol* 1998; **46**: 249-256

5 **Peiffert D**, Bey P, Pernot M, Guillemin F, Luporsi E, Hoffstetter S, Aletti P, Boissel P, Bigard MA, Dartois D, Baylac F. Conservative treatment by irradiation of epidermoid cancers of the anal canal: prognostic factors of tumoral control and complications. *Int J Radiat Oncol Biol Phys* 1997; **37**: 313-324

6 **Constantinou EC**, Daly W, Fung CY, Willett CG, Kaufman DS, DeLaney TF. Time-dose considerations in the treatment of anal cancer. *Int J Radiat Oncol Biol Phys* 1997; **39**: 651-657

7 **Hughes LL**, Rich TA, Delclos L, Ajani JA, Martin RG. Radiotherapy for anal cancer: experience from 1979-1987. *Int J Radiat Oncol Biol Phys* 1989; **17**: 1153-1160

8 **Nigh SS**, Smalley SR, Elman AJ, Paradelo JC, Kooser JA, Reddi R, Evans RG.Conservative Therapy for Anal Carcinoma: an Analysis of Prognostic Factors. *Int J Radiat Oncol Biol Phys* 1991; **21**: 224

9 **Rich TA**, Ajani JA, Morrison WH, Ota D, Levin B. Chemoradiation therapy for anal cancer: radiation plus continuous infusion of 5-fluorouracil with or without cisplatin. *Radiother Oncol* 1993; **27**: 209-215

10 **John M**, Pajak T, Flam M, Hoffman J, Markoe A, Wolkov H,

Paris K. Dose escalation in chemoradiation for anal cancer: preliminary results of RTOG 92-08. *Cancer J Sci Am* 1996; **2**: 205-211

11 **Allal AS**, Mermillod B, Roth AD, Marti MC, Kurtz JM. The impact of treatment factors on local control in T2-T3 anal carcinomas treated by radiotherapy with or without chemotherapy. *Cancer* 1997; **79**: 2329-2335

12 **Bosset JF**, Roelofsen F, Morgan DA, Budach V, Coucke P, Jager JJ, Van der Steen-Banasik E, Trivière N, Stüben G, Puyraveau M, Mercier M. Shortened irradiation scheme, continuous infusion of 5-fluorouracil and fractionation of mitomycin C in locally advanced anal carcinomas. Results of a phase II study of the European Organization for Research and Treatment of Cancer. Radiotherapy and Gastrointestinal Cooperative Groups. *Eur J Cancer* 2003; **39**: 45-51

13 **Ceresoli GL**, Ferreri AJ, Cordio S, Villa E. Role of dose intensity in conservative treatment of anal canal carcinoma. Report of 35 cases. *Oncology* 1998; **55**: 525-532

14 **John M**, Pajak T, Krieg R, Pinover WH, Myerson R. Dose Escalation without Split-course in Chemoradiation for Anal Cancer: Results of a Phase II RTOG Study. *Int J Radiat Oncol Biol Phys*. 1997; **39**: 203

15 **Weber DC**, Kurtz JM, Allal AS. The impact of gap duration on local control in anal canal carcinoma treated by split-course radiotherapy and concomitant chemotherapy. *Int J Radiat Oncol Biol Phys* 2001; **50**: 675-680

16 **Vuong T**, Devic S, Belliveau P, Muanza T, Hegyi G. Contribution of conformal therapy in the treatment of anal canal carcinoma with combined chemotherapy and radiotherapy: results of a phase II study. *Int J Radiat Oncol Biol Phys* 2003; **56**: 823-831

17 **Milano MT**, Jani AB, Farrey KJ, Rash C, Heimann R, Chmura SJ. Intensity-modulated radiation therapy (IMRT) in the treatment of anal cancer: toxicity and clinical outcome. *Int J Radiat Oncol Biol Phys* 2005; **63**: 354-361

18 **Hung A**, Crane C, Delclos M, Ballo M, Ajani J, Lin E, Feig B, Skibber J, Janjan N. Cisplatin-based combined modality therapy for anal carcinoma: a wider therapeutic index. *Cancer* 2003; **97**: 1195-1202

19 **Hoffman R**, Welton ML, Klencke B, Weinberg V, Krieg R. The significance of pretreatment CD4 count on the outcome and treatment tolerance of HIV-positive patients with anal cancer. Int J Radiat *Oncol Biol Phys* 1999; **44**: 127-131

20 **Martenson JA**, Lipsitz SR, Wagner H, Kaplan EH, Otteman LA, Schuchter LM, Mansour EG, Talamonti MS, Benson AB. Initial results of a phase II trial of high dose radiation therapy, 5-fluorouracil, and cisplatin for patients with anal cancer (E4292): an Eastern Cooperative Oncology Group study. *Int J Radiat Oncol Biol Phys* 1996; **35**: 745-749

21 **James R**, Meadows HM. The second UK phase III anal cancer trial of chemoradiation and maintenance therapy (ACT II): preliminary results on toxicity and outcome. *Proc ASCO* 2003, **22**: 287

S- Editor Liu Y **L- Editor** Zhu LH **E- Editor** Lu W

PO Box 2345, Beijing 100023, China
www.wjgnet.com
wjg@wjgnet.com

World J Gastroenterol 2007 February 14; 13(6): 901-905
World Journal of Gastroenterology ISSN 1007-9327

RAPID COMMUNICATION

Endoscopic sphincterotomy in patients with stenosis of ampulla of Vater: Three-year follow-up of exocrine pancreatic function and clinical symptoms

Nils Ewald, Axel Michael Marzeion, Reinhard Georg Bretzel, Hans Ulrich Kloer, Philip Daniel Hardt

Nils Ewald, Axel Michael Marzeion, Reinhard Georg Bretzel, Hans Ulrich Kloer, Philip Daniel Hardt, Third Medical Department and Policlinic, University Hospital Giessen and Marburg, Giessen Site, D-35392 Giessen, Germany
Correspondence to: Dr. Nils Ewald, Third Medical Department and Policlinic, University Hospital Giessen and Marburg, Giessen Site, D-35392 Giessen,
Germany. nils.ewald@innere.med.uni-giessen.de
Telephone: +49-641-9942751 Fax: +49-641-9942757
Received: 2006-11-13 Accepted: 2007-01-21

Key words: Endoscopic sphincterotomy; Fecal elastase; Chronic pancreatitis; Papillary stenosis; Oddi dysfunction

Ewald N, Marzeion AM, Bretzel RG, Kloer HU, Hardt PD. Endoscopic sphincterotomy in patients with stenosis of ampulla of Vater: Three-year follow-up of exocrine pancreatic function and clinical symptoms. *World J Gastroenterol* 2007; 13(6): 901-905

http://www.wjgnet.com/1007-9327/13/901.asp

Abstract

AIM: To investigate retrospectively the long-term effect of endoscopic sphincterotomy (ES) including exocrine pancreatic function in patients with stenosis of ampulla of Vater.

METHODS: After diagnostic endoscopic retrograde cholangiopancreatography (ERCP) and ES because of stenosis of the ampulla of Vater (SOD Type Ⅰ), follow-up examinations were performed in 60 patients (mean follow-up time 37.7 mo). Patients were asked about clinical signs and symptoms at present and before intervention using a standard questionnaire. Before and after ES exocrine pancreatic function was assessed by determination of immunoreactive fecal elastase 1. Serum enzymes indicating cholestasis as well as serum lipase and amylase were measured.

RESULTS: Eighty percent of patients reported an improvement in their general condition after ES. The fecal elastase 1 concentrations (FEC) in all patients increased significantly after ES. This effect was even more marked in patients with pathologically low concentrations (< 200 μg/g) of fecal elastase prior to ES. The levels of serum lipase and amylase as well as serum alcaline phosphatase (AP) and gamma-glutamyltranspeptidase (GGT) decreased significantly after ES.

CONCLUSION: The results of this study demonstrate that patients with stenosis of the ampulla of Vater can be successfully treated with endoscopic sphincterotomy. The positive effect is not only indicated by sustained improvement of clinical symptoms and cholestasis but also by improvement of exocrine pancreatic function.

INTRODUCTION

Endoscopic sphincterotomy (ES) has been introduced as a treatment for sphincter of Oddi dysfunction (SOD)[1,2]. At least in SOD type I, which is caused by structural changes of the papilla in the majority of patients, ES is the treatment of choice[3,4]. In most of the recent papers the focus of clinical interest has been put on aspects of cholestasis.

Gallstones, bile duct microlithiasis and sludge may repeatedly induce ductal lesions leading to obstruction and stenosis of the papilla of Vater[5-7]. In addition to the resulting problems concerning the bile duct system, chronic obstruction of the papilla of Vater may also contribute to lesions of the pancreas. This might also play a role in the pathogenesis of chronic pancreatitis. Segmental or diffuse dilation of the main pancreatic duct as part of the spectrum of chronic pancreatitis has given rise to the concept of obstruction and pancreatic ductal hypertension as an important pathogenetic mechanism of chronic pancreatitis[8,9]. Data from an autopsy study also showed that the incidence of chronic pancreatitis is higher in patients with gallstones which emphasises the role of gallstones, sludge and papillary stenosis in the pathogenesis of chronic pancreatitis[10].

The former gold standard imaging technique, endoscopic retrograde cholangiopancreaticographie (ERCP), is based on ductal abnormalities. Pancreatographic changes correlate with exocrine dysfunction[11]. As an indirect pancreatic function test measurement of fecal elastase-1 concentrations (FEC) shows a 93%-100% sensitivity for moderate and 96%-100% sensitivity for severe exocrine pancreatic insufficiency as well as a specificity of 93%-98%[12,13].

The aim of this study was to investigate the long-term effects of ES not only regarding clinical symptoms

and parameters of cholestasis, but also with a focus on exocrine pancreatic function.

MATERIALS AND METHODS

Patients

Nineteen male and 41 female patients aged between 21 and 80 years (mean age 57.4 ± 15.2 years) were investigated retrospectively. The follow-up period averaged 37.7 ± 7.0 mo (ranging from 28-51 mo). The mean body mass index was 24.4 ± 4.0 kg/m² (ranging from 18.4-35.5 kg/m²).

All patients, who initially presented with signs of either cholestasis or pancreatic inflammation and abdominal complaints, underwent ERCP and endoscopic sphincterotomy (ES) in our department after giving their informed consent. The period between the first ES and follow-up averaged 37.7 mo. Follow-up consisted of assessing clinical and laboratory data of the patients before and after ES by using the patients' records and personal interviewing based on a standardized questionnaire. Patients with malignancy of the pancreas and/or the bile duct system were not included.

ERCP and ES

All patients underwent ERCP and ES in our department. All procedures were performed by one experienced investigator using standard techniques. Radiological changes of the pancreatic duct system were evaluated according to the Cambridge classification[14]. In all patients ES was performed because of SOD type 1 [clinical symptoms, laboratory findings and findings in imaging techniques (ultrasound or ERCP)]. For ES a single use precurved sphincterotome (Wilson-Cook Medical Inc., NC, USA) and a single use guidewire 0.18 inch (Medwork, Neuss, Germany) were used. ES was performed as sphincterotomy of the pancreatic and/or biliary segment of the sphincter of Oddi. Some patients underwent ES more than once because of recurrent symptoms and/or signs of cholestasis and/or pancreatic inflammation. In some cases a precut of the papilla was necessary.

Questionnaire

The questionnaire included the following items: age, sex, and body mass index (BMI). The intensity of clinical symptoms such as nausea, emesis, and quantity of abdominal pain were assessed using the visual analogue scale (0 = not present, 10 = maximum complaint).

Laboratory methods

Blood samples were taken routinely prior to and after ES and checked for the following parameters: serum lipase (normal range 20-160 U/L), serum alpha-amylase (< 53 U/L), serum aspartate aminotransferase (AST/SGOT; male 5-20, female 5-17 U/L), serum alanine aminotransferase (ALT/SGPT; male 5-23, female 5-17 U/L), alcaline phosphatase (AP; male adult 60-170 U/L, female adult 40-160 U/L), gamma-glutamyltranspeptidase (GGT; male 6-28 U/L, female 4-18 U/L), and bilirubin (< 1.0 mg/dL). Fecal elastase-1 was determined by ELISA using two monoclonal antibodies specific for human elastase-1, which bind to different epitopes of the enzyme (elastase-1 stool kit; Schebo-Biotech, Giessen, Germany). Results were expressed in μg/g stool. Values < 200 μg/g were considered to represent exocrine insufficiency, values > 200 μg/g were regarded as normal.

Table 1 ERCP findings in 60 patients

	Patients *n* (%)
Papilla	
Papillitis (chronic/acute)	20 (33)
Periampullary diverticulum	7 (12)
Pancreas	
Pancreas divisum	0
Pancreatitis Cambridge 0	2 (3)
Pancreatitis Cambridge Ⅰ	11 (18)
Pancreatitis Cambridge Ⅱ	25 (42)
Pancreatitis Cambridge Ⅲ	10 (17)
No pancreatogram	12 (20)
Bile duct system	
Cholangitis	10 (17)
Biliary sludge and stones	15 (25)
Bile duct dilation (any)	31 (52)
Common bile duct stenosis	4 (6)
Negative cholecystography	7 (12)

Table 2 Amount and kind of sphincterotomies in 60 patients

	Patients *n* (%)
Biliary sphincterotomy	35 (58)
Pancreatic spincterotomy	3 (5)
Both	22 (37)
Amount of necessary sphincterotomies	
One	34 (57)
Two	10 (17)
Three	9 (15)
Four and more	7 (12)

Statistical analysis

Results are expressed as mean ± SD and range of values if not otherwise indicated. Statistics were carried out by the Statistical Package for Social Sciences (SPSS) for Windows, version 11.01. Wilcoxon-test was performed to test for significant differences between pre-treatment and post-treatment values. $P < 0.05$ was considered statistically significant.

RESULTS

Table 1 shows findings in ERCP, Table 2 indicates the amount as well as the kind of ES (biliary/pancreatic sphincterotomy). Fifty patients (83%) showed either impaired exocrine pancreatic function (fecal elastase-1 < 200 μg/g) or were classified as Cambridge Ⅰ-Ⅲ based on radiological changes of the pancreas irrespective of the initial indication for ERCP.

Clinical symptoms

After ES, 80% of the patients reported a general relief of

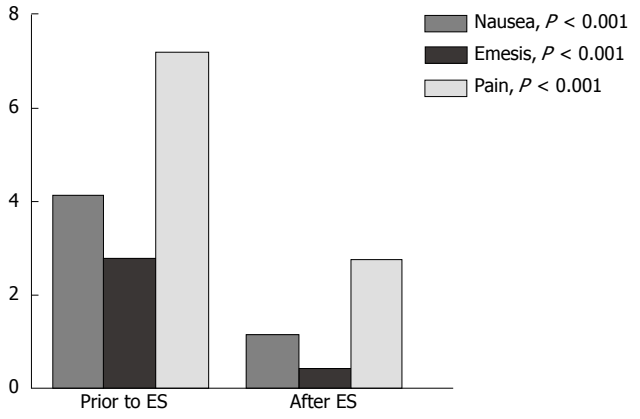

Figure 1 Clinical symptoms prior to and after endoscopic sphincterotomy due to the visual analogue scale (0 = not present, 10 = maximum complaint), *n* = 55.

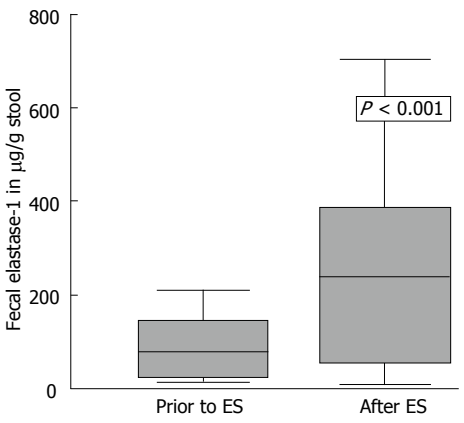

Figure 2 Levels of fecal elastase-1 of patients with initially impaired exocrine pancreatic function (< 200 μg/g; *n* = 26) prior to and after endoscopic sphincterotomy. Medians and interquartiles given.

symptoms, 6.7% reported the same general condition by their own assessment, whereas only 5.0% reported a worse condition. No data were given in 8.3% of all patients. There was a significant reduction of clinical symptoms such as nausea, emesis and abdominal pain after ES (Figure 1).

Laboratory findings

Serum enzymes indicating cholestasis such as Gamma-glutamyltranspeptidase, alcaline phosphatase and bilirubin showed a significant reduction after ES. Serum alpha-amylase and serum lipase also significantly decreased to normal levels after ES (data given in Table 3).

Exocrine pancreatic function

In all the 60 patients, fecal elastase-1 increased significantly from a mean of 264.38 ± 184.01 μg/g (range 10-741 μg/g) prior to ES to 337.05 ± 185.35 μg/g (range 10-816 μg/g) after ES ($P < 0.05$) (Figure 2). In patients with very low levels of fecal elastase-1 (< 200 μg/g) prior to ES, fecal elastase-1 rose significantly from a mean of 82.46 ± 60.22 μg/g (range 15-187 μg/g) to 253.42 ± 200.18 μg/g (range 10-705 μg/g) after ES ($P = 0.001$). In seven patients with fecal elastase-1 levels between 200 and 300 μg/g prior to ES, fecal elastase-1 increased significantly from a mean of 262 ± 36.47 μg/g (range 212-297 μg/g) prior to ES to 442.29 μg/g (range 360-610 μg/g) after ES ($P = 0.018$).

Table 3 Levels of GGT, AP, bilirubin, serum lipase and serum alpha-amylase in all patients (*n* = 60) prior to and after endoscopic sphincterotomy (mean ± SD)

	Prior to ES	After ES	*P*
GGT (U/L)	102.13 ± 146.21 (range 4-711)	41.02 ± 69.24 (range 7-337)	= 0.001
AP (U/L)	205.23 ± 214.88 (35-1645)	146.62 ± 135.2 (36-1047)	= 0.001
Bilirubin (mg/dL)	1.4 ± 2.44 (0.3-15.0)	0.65 ± 0.75 (0.1-6.0)	< 0.001
Serum lipase (U/L)	817.37 ± 1391.45 (11-7200)	29.60 ± 13.18 (6-71)	< 0.001
Serum amylase (U/L)	192.92 ± 336.44 (15-1714)	61.63 ± 19.98 (21-102)	< 0.05

ES: Endoscopic sphincerotomy.

DISCUSSION

In sphincter of Oddy dysfunction (SOD), especially in type 1 displaying structural changes of the papilla in most cases, endoscopic sphincterotomy (ES) has been introduced as a definitive treatment[3]. Most of the available research efforts focus on the beneficial effects of ES concerning clinical symptoms and parameters of cholestasis. In the present study all patients with cholestatic problems prior to ES showed an improvement after treatment. In 94% of our patients biliary sphincterotomy could effectively improve cholestasis as indicated by the normalized GGT and AP. Obviously these positive effects, lasting a mean of three years so far, are results from optimized biliary drainage without stenting. This is remarkable because pancreatobiliary drainage by endoscopic placement of an endoprothesis (needing exchange of stents at intervals of 2 to 4 mo) is accompanied with complications and shows poor long-term results[15,16].

Since papillary stenosis has been suggested to play a possible role as a pathogenetic factor in pancreatitis[6,17,18], the present study included patients with pancreatitis type symptoms and focused on changes in exocrine pancreatic function. Therapeutical approaches in patients with chronic pancreatitis aim to alleviate pain, prevent attacks of pancreatitis, reduce the effects of pancreatic insufficiency and manage complications no matter what the etiology of chronic pancreatitis might be. Medical management may include oral analgesics, enzymatic replacement, diet, and abstinence from alcohol. If obstruction of the pancreatic duct is present, invasive options must be considered. Endoscopic therapeutic techniques such as insertion of endoprothesis, balloon or catheter dilation or sphincterotomy are applied increasingly[19]. The facilitation of pancreatic ductal drainage should lead to a reduction of ductal pressure which is the rationale for the endoscopic intervention. The exact role of increased pressure in the pancreatic ductal system in the pathogenesis of chronic pancreatitis is not known, although elevated pressures have been documented in different animal models and human beings[20-22]. It was reported that patients with chronic pancreatitis and pain have higher main pancreatic duct pressures than controls and experience pain relief after surgical decompression[23]. Cholelithiasis, bile duct microlithiasis and biliary sludge might induce

papillitis or papillary stenosis followed by recurrent or permanent elevation of pancreatic ductal pressure with the consequence of chronic pancreatitis. This role of cholelithiasis and sludge in the pathogenesis of chronic pancreatitis still remains a controversy. However, several reports indicate that in patients who are thought to have 'idiopathic' pancreatitis, bile duct microlithiasis, sludge and bile crystals may account for the pancreatitis[24-28]. There are individual reports on patients with sphincter of Oddi dysfunction or stenosis and recurrent episodes of pancreatitis which have been treated successfully with sphincterotomy.

In this study the long term effect of ES on pancreatic function and clinical symptoms of 60 patients with stenosis of ampulla of Vater was investigated. Regarding the clinical symptoms such as abdominal pain, nausea and emesis, most of our patients (80%) experienced a long-term improvement after ES. In the majority of patients we could also observe an improvement of exocrine pancreatic function as measured by FEC. It must be stressed that the follow-up study was performed at least 28 mo (maximum 51 mo) after endoscopic treatment. Other studies have reported similar immediate symptomatic improvements in patients who underwent dilation of the pancreatic duct followed by placement of an endoprothesis, but the long-term results are not very promising as symptomatic stent occlusion often occurs[15,29]. As reported elsewhere[30], in some of our patients several sphincterotomies (up to six) had to be performed, if symptoms and pathological laboratory findings persisted. It appears possible, that recurrent cholestasis or clinical symptoms can be caused by papillary restenosis which is a known complication of sphincterotomy, usually occurring years after intervention[31]. We think that the patients' long-term clinical improvement concerning pancreatic pathology is due to a decrease of pancreatic ductal pressure after overcoming the underlying pathogenetic factor of papillary stenosis. Few of our patients (11.7%) reported no improvement or even aggravation in their clinical condition after ES. Most of these cases were classified as chronic pancreatitis Ⅲ according to the Cambridge-Classification. They showed persisting impaired exocrine pancreatic function after ES indicated by persisting reduced FEC. This sub-group of patients had proven advanced structural and functional abnormalities, which were probably progressive and irreversible. Since pain is often a cardinal symptom of chronic pancreatitis, many studies focus on it beside other clinical symptoms when judging the effect of treatment. This is the first time that the effect of endoscopic spincterotomy on exocrine pancreatic function based on fecal elastase-1 was investigated. In summary, all patients showed a significant increase in fecal elastase-1 levels after ES, which was even more marked in patients with pathologically low concentrations of fecal elastase-1 prior to ES, indicating that endoscopic sphincterotomy has positive effects on exocrine pancreatic function. A similar effect was found in patients with low, but still normal fecal elastase-1 levels (200-300 μg/g) prior to ES. The results are due to effective treatment of the underlying ethiological factor which leads to normalized ductal pressure of the pancreas and regeneration of pancreatic parenchyma. In contrast to the common belief of irreversibel structural and functional impairment of the pancreas in chronic pancreatitis, the findings of the present study confirm that there is at least a subset of patients with chronic pancreatitis in which a recovery of functional capacity is possible[32].

In conclusion, patients with stenosis of the ampulla of Vater can be successfully treated with endoscopic sphincterotomy. The positive effect is indicated not only by sustained improvement of biliary type clinical symptoms and laboratory markers of cholestasis, but also by improvement of exocrine pancreatic function and pancreatitis type clinical symptoms. Without question there is a need for prospective, randomized, controlled trials which investigate endoscopic sphincterotomy versus pancreatobiliary stenting and conservative medical therapy in chronic pancreatitis.

COMMENTS

Background

Endoscopic sphincterotomy has been introduced as a treatment for sphincter of Oddi dysfunction. In most recent papers the focus of clinical interest has been put on aspects of cholestasis. In addition to the resulting problems concerning the bile duct system, chronic obstruction of the papilla of Vater may also contribute to lesions of the pancreas, and may also play a role in the pathogenesis of chronic pancreatitis. The aim of this study was to investigate the long-term effects of ES not only on clinical symptoms and parameters of cholestasis, but also on exocrine pancreatic function.

Innovations and breakthroughs

The study showed that patients with stenosis of the ampulla of Vater could be successfully treated with endoscopic sphincterotomy. The positive effect was indicated not only by sustained improvement of biliary type clinical symptoms and laboratory markers of cholestasis, but also by improvement of exocrine pancreatic function and pancreatitis type clinical symptoms. The improvement in exocrine pancreatic function and pancreatic regeneration after endoscopic sphincterotomy is remarkable.

Applications

There is a definite need for prospective, randomized, controlled trials which investigate endoscopic sphincterotomy versus pancreatobiliary stenting and conservative medical therapy in chronic pancreatitis.

Terminology

Sphincter of Oddi dysfunction (SOD): Sphincter of Oddi dysfunction refers to structural or functional disorders involving the sphincter of Oddi that may result in impedance of bile and pancreatic juice flow. Geenen *et al* have divided SOD patients into three types. Type Ⅰ patients exhibit all three criteria (biliary pain, abnormal liver serology and bile duct dilation). Type Ⅱ patients have typical biliary pain and either abnormal liver serology or dilation of the bile duct, but not both. In type Ⅲ patients, the extrahepatic bile duct is not dilated, and abnormal liver serology is not found, whereas pain is present.

Peer review

The authors retrospectively audited a series of 60 patients with stenosis of the ampulla Vater (SOD) who had undergone endoscopic sphincterotomy (ES) and their 3-year follow-up concerning symptom improvement & pancreatic exocrine function. I agree with the acceptance of this manuscript for publication in the WJG.

REFERENCES

1 **Hogan WJ**, Geenen JE. Biliary dyskinesia. *Endoscopy* 1988; **20** Suppl 1: 179-183

2 **Sugawa C**, Park DH, Lucas CE, Higuchi D, Ukawa K. Endoscopic sphincterotomy for stenosis of the sphincter of Oddi. *Surg Endosc* 2001; **15**: 1004-1007

3 **NIH state-of-the-science statement on endoscopic retrograde cholangiopancreatography (ERCP) for diagnosis and therapy**. *NIH Consens State Sci Statements* 2002; **19**: 1-26
4 **Bistritz L**, Bain VG. Sphincter of Oddi dysfunction: managing the patient with chronic biliary pain. *World J Gastroenterol* 2006; **12**: 3793-3802
5 **Bernhard JP**, Laugier R. The pathogenesis of chronic pancreatitis. In: Johnson CD, Imrie CW, editors. Pancreatic disease: progress and prospects. Berlin: Springer Verlag, 1991: 185-193
6 **Tarnasky PR**, Hoffman B, Aabakken L, Knapple WL, Coyle W, Pineau B, Cunningham JT, Cotton PB, Hawes RH. Sphincter of Oddi dysfunction is associated with chronic pancreatitis. *Am J Gastroenterol* 1997; **92**: 1125-1129
7 **Ros E**, Navarro S, Bru C, Garcia-Pugés A, Valderrama R. Occult microlithiasis in 'idiopathic' acute pancreatitis: prevention of relapses by cholecystectomy or ursodeoxycholic acid therapy. *Gastroenterology* 1991; **101**: 1701-1709
8 **Karanjia ND**, Singh SM, Widdison AL, Lutrin FJ, Reber HA. Pancreatic ductal and interstitial pressures in cats with chronic pancreatitis. *Dig Dis Sci* 1992; **37**: 268-273
9 **Okazaki K**, Yamamoto Y, Nishimori I, Nishioka T, Kagiyama S, Tamura S, Sakamoto Y, Nakazawa Y, Morita M, Yamamoto Y. Motility of the sphincter of Oddi and pancreatic main ductal pressure in patients with alcoholic, gallstone-associated, and idiopathic chronic pancreatitis. *Am J Gastroenterol* 1988; **83**: 820-826
10 **Olsen TS**. The incidence and clinical relevance of chronic inflammation in the pancreas in autopsy material. *Acta Pathol Microbiol Scand A* 1978; **86**A: 361-365
11 **Bozkurt T**, Braun U, Leferink S, Gilly G, Lux G. Comparison of pancreatic morphology and exocrine functional impairment in patients with chronic pancreatitis. *Gut* 1994; **35**: 1132-1136
12 **Löser C**, Möllgaard A, Fölsch UR. Faecal elastase 1: a novel, highly sensitive, and specific tubeless pancreatic function test. *Gut* 1996; **39**: 580-586
13 **Stein J**, Jung M, Sziegoleit A, Zeuzem S, Caspary WF, Lembcke B. Immunoreactive elastase I: clinical evaluation of a new noninvasive test of pancreatic function. *Clin Chem* 1996; **42**: 222-226
14 **Sarner M**, Cotton PB. Classification of pancreatitis. *Gut* 1984; **25**: 756-759
15 **Smits ME**, Badiga SM, Rauws EA, Tytgat GN, Huibregtse K. Long-term results of pancreatic stents in chronic pancreatitis. *Gastrointest Endosc* 1995; **42**: 461-467
16 **Devière J**, Devaere S, Baize M, Cremer M. Endoscopic bili**ary** drainage in chronic pancreatitis. *Gastrointest Endosc* 1990; **36**: 96-100
17 **Cattell RB**, Colcock BP, Pollack JL. Stenosis of the sphincter of Oddi. *N Engl J Med* 1957; **256**: 429-435
18 **Doubilet H**, mulholland JH. Eight-year study of pancreatitis and sphincterotomy. *J Am Med Assoc* 1956; **160**: 521-528
19 **Geenen JE,** Rolny P. Endoscopic therapy of acute and chronic pancreatitis. *Gastrointest Endosc* 1991; **37**: 377-382
20 **Bradley EL.** Pancreatic duct pressure in chronic pancreatitis. *Am J Surg* 1982; **144**: 313-316
21 **Binmoeller KF**, Rathod VD, Soehendra N. Endoscopic therapy of pancreatic strictures. *Gastrointest Endosc Clin N Am* 1998; **8**: 125-142
22 **Frey CF**, Smith GJ. Description and rationale of a new operation for chronic pancreatitis. *Pancreas* 1987; **2**: 701-707
23 **Nealon WH**, Townsend CM, Thompson JC. Operative drainage of the pancreatic duct delays functional impairment in patients with chronic pancreatitis. A prospective analysis. *Ann Surg* 1988; **208**: 321-329
24 **Feller ER**. Endoscopic retrograde cholangiopancreatography in the diagnosis of unexplained pancreatitis. *Arch Intern Med* 1984; **144**: 1797-1799
25 **Lee SP**, Nicholls JF, Park HZ. Biliary sludge as a cause of acute pancreatitis. *N Engl J Med* 1992; **326**: 589-593
26 **Marotta PJ**, Gregor JC, Taves DH. Biliary sludge: a risk factor for 'idiopathic' pancreatitis? *Can J Gastroenterol* 1996; **10**: 385-388
27 **Testoni PA**, Caporuscio S, Bagnolo F, Lella F. Idiopathic recurrent pancreatitis: long-term results after ERCP, endoscopic sphincterotomy, or ursodeoxycholic acid treatment. *Am J Gastroenterol* 2000; **95**: 1702-1707
28 **Ponchon T**, Bory RM, Hedelius F, Roubein LD, Paliard P, Napoleon B, Chavaillon A. Endoscopic stenting for pain relief in chronic pancreatitis: results of a standardized protocol. *Gastrointest Endosc* 1995; **42**: 452-456
29 **Binmoeller KF**, Jue P, Seifert H, Nam WC, Izbicki J, Soehendra N. Endoscopic pancreatic stent drainage in chronic pancreatitis and a dominant stricture: long-term results. *Endoscopy* 1995; **27**: 638-644
30 **Elton E**, Howell DA, Parsons WG, Qaseem T, Hanson BL. Endoscopic pancreatic sphincterotomy: indications, outcome, and a safe stentless technique. *Gastrointest Endosc* 1998; **47**: 240-249
31 **Freeman ML**, Nelson DB, Sherman S, Haber GB, Herman ME, Dorsher PJ, Moore JP, Fennerty MB, Ryan ME, Shaw MJ, Lande JD, Pheley AM. Complications of endoscopic biliary sphincterotomy. *N Engl J Med* 1996; **335**: 909-918
32 **Mergener K**, Baillie J. Chronic pancreatitis. *Lancet* 1997; **350**: 1379-138**5**

S- Editor Liu Y **L- Editor** Wang XL **E- Editor** Lu W

PO Box 2345, Beijing 100023, China
www.wjgnet.com
wjg@wjgnet.com

World J Gastroenterol 2007 February 14; 13(6): 906-911
World Journal of Gastroenterology ISSN 1007-9327

RAPID COMMUNICATION

Unsedated ultrathin upper endoscopy is better than conventional endoscopy in routine outpatient gastroenterology practice: A randomized trial

Lucio Trevisani, Viviana Cifalà, Sergio Sartori, Giuseppe Gilli, Giancarlo Matarese, Vincenzo Abbasciano

Lucio Trevisani, Viviana Cifalà, Sergio Sartori, Giancarlo Matarese, Vincenzo Abbasciano, Digestive Endoscopy Centre, Department of Internal Medicine, S. Anna Hospital, Ferrara, Italy
Giuseppe Gilli, Health Physics Department, S. Anna Hospital, Ferrara, Italy
Correspondence to: Dr. Lucio Trevisani, Centro di Endoscopia Digestiva, Azienda Ospedaliera-Universitaria "Arcispedale S. Anna", C.so Giovecca 203, Ferrara 44100, Italy. tvl@unife.it
Telephone: +39-532-237558 Fax: +39-532-236932
Received: 2006-10-16 Accepted: 2006-11-23

Abstract

AIM: to compare the feasibility and patients' tolerance of esophagogastroduodenoscopy (EGD) using a thin endoscope with those of conventional oral EGD and to determine the optimal route of introduction of small-caliber endoscopes.

METHODS: One hundred and sixty outpatients referred for diagnostic EGD were randomly allocated to 3 groups: conventional (C)-EGD (9.8 mm in diameter), transnasal (TN)-EGD and transoral (TO)-EGD (5.9 mm in diameter). Pre-EGD anxiety was measured using a 100-mm visual analogue scale (VAS). After EGD, patients and endoscopists completed a questionnaire on the pain, nausea, choking, overall discomfort, and quality of the examination either using VAS or answering some questions. The duration of EGD was timed. Blood oxygen saturation (SaO_2) and heart rate (HR) were monitored during EGD.

RESULTS: Twenty-one patients refused to participate in the study. The 3 groups were well-matched for age, gender, experience with EGD, and anxiety. EGD was completed in 91.1% (41/45), 97.5% (40/41), and 96.2% (51/53) of cases in TN-EGD, TO-EGD, and C-EGD groups, respectively. TN-EGD lasted longer (3.11 ± 1.60 min) than TO-EGD (2.25 ± 1.45 min) and C-EGD (2.49 ± 1.64 min) ($P < 0.05$). The overall tolerance was higher ($P < 0.05$) and the overall discomfort was lower ($P < 0.05$) in TN-EGD group than in C-EGD group. EGD was tolerated "better than expected" in 73.2% of patients in TN-EGD group and 55% and 39.2% of patients in TO-EGD and C-EGD groups, respectively ($P < 0.05$). Endoscopy was tolerated "worst than expected" in 4.9% of patients in TN-EGD group and 17.5% and 23.5% of patients in TO-EGD and C-EGD groups, respectively ($P < 0.05$). TN-EGD caused mild epistaxis in one case. The ability to insufflate air, wash the lens, and suction of the thin endoscope were lower than those of conventional instrument ($P < 0.001$). All biopsies performed were adequate for histological assessment.

CONCLUSION: Diagnostic TN-EGD is better tolerated than C-EGD. Narrow-diameter endoscope has a level of diagnostic accuracy comparable to that of conventional gastroscope, even though some technical characteristics of these instruments should be improved. Transnasal EGD with narrow-diameter endoscope should be proposed to all patients undergoing diagnostic EGD.

Key words: Diagnotic esophagogastroduodenoscopy; Endoscopy; Gastroscopy

Trevisani L, Cifalà V, Sartori S, Gilli G, Matarese G, Abbasciano V. Unsedated ultrathin upper endoscopy is better than conventional endoscopy in routine outpatient gastroenterology practice: A randomized trial. *World J Gastroenterol* 2007; 13(6): 906-911

http://www.wjgnet.com/1007-9327/13/906.asp

INTRODUCTION

Esophagogastroduodenoscopy (EGD) is a safe and quick procedure, and can be carried out without sedation[1]. However, it can evoke anxiety, feelings of vulnerability, embarrassment, and discomfort[2]. The fears and concerns associated with the endoscopic procedure decrease patient's compliance, making EGD execution more difficult[2-4], and in many countries EGD is performed using conscious sedation[5]. Although usually safe, sedation is not free from adverse effects[6-8], and produces a 30%-50% increase of the EGD costs, either direct (medications, additional time required to sedate and recover the patients, additional personnel needed to monitor the patients) or indirect (time lost from work by both the patient and patient's escort)[9,10].

Narrow-diameter endoscopes (< 6 mm) were developed in the early 1990s with the aim of reducing patient discomfort and avoiding the cost and risks of conscious sedation. These endoscopes can also be

introduced through the nose, as reported by Shaker in 1994[11]. Either this study or a cancer screening program in Japan[12] showed that the transnasal unsedated procedure is safe and well tolerated, and allows adequate visualization of the upper gastrointestinal tract. However, the use of these endoscopes is still limited to a small subset of patients[10], even though they have been reported to be suitable not only for diagnostic purposes, but also for interventional procedures, such as PEG and placement of nasoenteric feeding tubes[13-16].

In this randomized trial, we compared the unsedated small-caliber endoscopy using the transnasal and transoral routes with unsedated conventional endoscopy. Our primary aims were to compare the patients' tolerance to small-caliber and conventional endoscopes, to determine the optimal route of introduction of small-caliber endoscopes, and to evaluate the differences in the general handling of small-caliber and conventional instruments. Secondary objectives were to evaluate duration and safety of the procedure.

MATERIALS AND METHODS

Study population

One hundred and sixty consecutive outpatients, undergoing elective diagnostic EGD and fulfilling the eligibility criteria, were randomly assigned to three groups by a computer-generated randomization list and asked to participate in the study. Inclusion criteria were age between 18 and 70 years, and capability (evaluated by the endoscopist) of fully understanding and filling up the questionnaire of the study. Exclusion criteria were history of gastrectomy, esophagectomy, or other upper-gastrointestinal (GI) tract surgery, history of sinus or nasal septum surgery, planned endoscopic therapy, coagulopathy or anticoagulant therapy, psychiatric diseases or long-term psychiatric drug addiction, presence of neoplastic or other serious concomitant diseases, pregnancy.

In the control group (C-EGD), unsedated EGD was performed with pharyngeal topical anesthesia, using a Fujinon EG-250WR5 videoendoscope (outer diameter of the insertion tube is 9.8 mm). In the transnasal-EGD (TN-EGD) and transoral-EGD (TO-EGD) groups, unsedated EGD was performed with pharyngeal or nasal topical anesthesia alone, using a Fujinon EG-270N5 videoendoscope (outer diameter of the insertion tube is 5.9 mm), which was introduced through the nose or the mouth. The patients underwent EGD in the left lateral position, and all procedures were carried out by three endoscopists well trained in unsedated narrow-diameter transnasal and transoral endoscopy.

The study protocol was approved by the Ethical Committee of our hospital, and all patients enrolled gave their written informed consent to participate in the study.

Outcome measurements

Pre-EGD assessment: Age, gender, prior experience of endoscopic examination, blood oxygen saturation (SaO_2), and heart rate (HR) were recorded. Since anxiety was hypothesized to be a potential factor of discomfort, all patients were asked to rate their pre-EGD anxiety level using a 100-mm visual analogue scale (VAS), with 100 being the highest level. The patients were asked also to specify what they dreaded more about endoscopic examination among the following six items: fear of pain, fear of vomiting, fear of stifling, fear of complications, fear of endoscopic findings, and others.

Monitored parameters: SaO_2 and HR were continuously monitored during EGD. An abnormal vital sign was defined as HR > 130 bpm or decrease in SaO_2 below 90% for over one minute. The duration of EGD was timed in all patients. A procedure was considered complete if gastric retroflexion was accomplished, the second portion of the duodenum was reached, and all indicated biopsies were obtained. If the transnasal route failed, a switch was made to the oral route using the same instrument, and EGD was considered unsuccessful according to the study design. The occurrence of complications was recorded after each procedure.

Post-EGD assessment: Data were collected from both the patient and the endoscopist. The sensation of pain and overall discomfort were quantified on a 100-mm VAS (0 = non existent, 100 = unbearable), and the overall tolerance to EGD was assessed as very poor, poor, fair, good, excellent. Patients scored their sensation of nausea and choking on a 100-mm VAS, and indicated also their tolerance by answering the questions of "how did you tolerate EGD, and what you were expecting?" and choosing one of the following 3 items: worse than expected, as expected, better than expected.

Endoscopists scored the level of difficulty in introduction of the gastroscope on a 100-mm VAS. Endoscopists' satisfaction was assessed with 100-mm VAS for the performances of the endoscopes, with regard to the adequacy of the view, the air insufflation/washing of the lens, and suction.

Statistical analysis

Statistical analysis was performed by using Statgraphics V4 (STSC Inc.; Rockville, MD, USA) and SPSS V8 (SPSS Inc.; Chicago, IL, USA) statistical software packages. Gender and previous experience of endoscopic examination were analyzed by the chi square test. Age and pre-endoscopic anxiety levels were analyzed using the Kruskal-Wallis non parametric test. Kruskal-Wallis test was also used to analyze the duration of EGD, difficulty in introduction of the gastroscope, nausea, choking, and performances of the endoscope. ANOVA-RM was used to compare physicians' and patients' opinions about intubation pain, overall discomfort, and overall tolerance.

The statistical power of the sample size was also evaluated, and levels over 90% were found in the most part of the tests applied. $P < 0.05$ was considered statistically significant.

RESULTS

Twenty-one out of 160 patients who were considered eligible and randomized into TN-EGD group ($n = 9$), TO-EGD group ($n = 11$), and C-EGD group ($n = 1$), refused

Table 1 Demographic and clinical data of the patients

	TN-EGD	TO-EGD	C-EGD	*P*
Patients (*n*)	45	41	53	
Gender (m/f)	22/23	15/26	24/29	NS
Age (yr; mean ± SD)	45.73 ± 12.59	43.92 ± 14.97	43.83 ± 13.68	NS
Patients with previous EGD, *n* (%)	17 (37.7)	17 (41.4)	19 (35.8)	NS
Baseline anxiety score in VAS (mean ± SD)	45.36 ± 27.71	44.34 ± 32.25	45.84 ± 30.35	NS
Baseline oxygen saturation (%; mean ± SD)	98.58 ± 1.41	98.48 ± 1.38	98.47 ± 1.54	NS
Baseline hart rate (bpm; mean ± SD)	84.92 ± 16.12	86.07 ± 15.80	86.32 ± 15.01	NS
Successful completion EGD, *n* (%)	41 (91.1)	40 (97.5)	51 (96.2)	NS
Duration of EGD (min; mean ± SD)	3.11 ± 1.60	2.25 ± 1.45	2.49 ± 1.64	< 0.05
Tachycardia, *n* (%)	1 (2.4)	1 (2.5)	3 (5.9)	NS
Blood oxygen desaturation, *n* (%)	0 (0)	0 (0)	2 (3.9)	NS
Biopsy during EGD, *n* (%)	19 (46.3)	16 (40.0)	24 (47.0)	NS
Complications, *n* (%)	1 (2.4)	0 (0)	0 (0)	NS

Table 2 Patients' and endoscopists' evaluations (mean ± SD)

	TN-EGD (*n* = 41)	TO-EGD (*n* = 40)	C-EGD (*n* = 51)	*P*	Statistical procedure
Patients' assessment					
Intubation (pain)	24.49 ± 21.70	20.08 ± 23.46	26.53 ± 31.18	NS	ANOVA-RM
Overall discomfort	22.49 ± 23.59	32.35 ± 28.65	34.02 ± 31.21	NS	ANOVA-RM
Choking	9.66 ± 13.44	19.72 ± 25.80	25.37 ± 33.77	NS	Kruskal-Wallis
Nausea/Vomiting	21.80 ± 26.89	39.57 ± 34.40	35.39 ± 34.27	NS	Kruskal-Wallis
Overall tolerance	3.95 ± 0.71	3.70 ± 0.72	3.29 ± 0.90	< 0.001	ANOVA-RM
Endoscopists' assessment					
Difficulty in intubation	10.97 ± 16.71	6.57 ± 10.37	9.61 ± 14.78	NS	Kruskal-Wallis
Intubation (pain)	16.34 ± 18.37	15.00 ± 17.48	20.10 ± 25.56	NS	ANOVA-RM
Overall discomfort	8.22 ± 9.76	14.85 ± 16.84	23.04 ± 27.31	NS	ANOVA-RM
Overall tolerance	4.56 ± 0.59	4.18 ± 0.93	3.63 ± 1.08	< 0.01	ANOVA-RM

to participate in the study. One hundred and thirty-nine patients (61 males and 78 females) entered the study. The three groups were well-matched for age, gender, previous experience of endoscopic examination, blood oxygen saturation, heart rate, and baseline anxiety score (Table 1). In all groups the most common cause of fear before EGD was fear of stifling (44 cases on the whole). Seven out of 139 patients (5.0%) did not complete EGD and were excluded from any subsequent analysis. EGD was successfully completed in 91.1% (41/45) of patients in TN-EGD group, 97.5% (40/41) in TO-EGD group, and 96.2% (51/53) in C-EGD group, respectively. TN-EGD failed in 4 cases (8.9%) due to difficult insertion of the endoscope through the nose or intolerance. These patients were excluded from any subsequent analysis.

The duration of the procedure was significantly longer in TN-EGD group than in TO-EGD and C-EGD groups (3.11 ± 1.6 min *vs* 2.25 ± 1.45 min and 2.49 ± 1.64 min, respectively; $P < 0.05$). Such a difference was not due to a higher frequency of biopsy sampling that was similar in the three groups (Table 1).

No complication occurred in C-EGD and TO-EGD groups. One patient (2.4%) in TN-EGD group had mild and self-limiting epistaxis. Occurrence of abnormal vital signs (blood oxygen desaturation and tachycardia) was less frequent in TN-EGD group than in the other two groups, but the difference was not statistically significant (Table 1).

Endoscopists' assessment showed no difference in the intubation difficulty among the three groups (Table 2). Likewise, on the basis of patients' evaluation, no difference was found in choking or nausea/vomiting among the three groups.

ANOVA-RM analysis of the factor "method" (TN-EGD *vs* TO-EGD *vs* C-EGD) independently of the observer (patient or endoscopist), showed that the overall tolerance was significantly higher in TN-EGD and TO-EGD groups than in C-EGD group ($P < 0.001$ and $P < 0.01$, respectively). TN-EGD and TO-EGD groups did not differ from each other. Conversely, no difference was observed in intubation pain and overall discomfort (Table 2). ANOVA-RM analysis of the factor "observer" (patient *vs* endoscopist) independently of the method, showed that endoscopist underestimated the levels of intubation pain ($P < 0.01$) and overall discomfort ($P < 0.001$), and overrated the overall tolerance ($P < 0.001$) in comparison with the patient. Contemporaneous analysis of both factors "observer" and "method", a significant difference was observed in overall discomfort and overall tolerance between TN-EGD and C-EGD ($P < 0.05$) (Figures 1A and B). All these results had a power greater than 90%, even though some differences were observed according to the factor considered (method, observer, and their combination).

Seventy-three point two percent of patients in TN-EGD group, 55% in TO-EGD group, and 39.2% in C-EGD group tolerated EGD better than expected (Table 3). EGD was tolerated worst than expected by 4.9%, 17.5%, and 23.5% of patients, respectively. Frequency

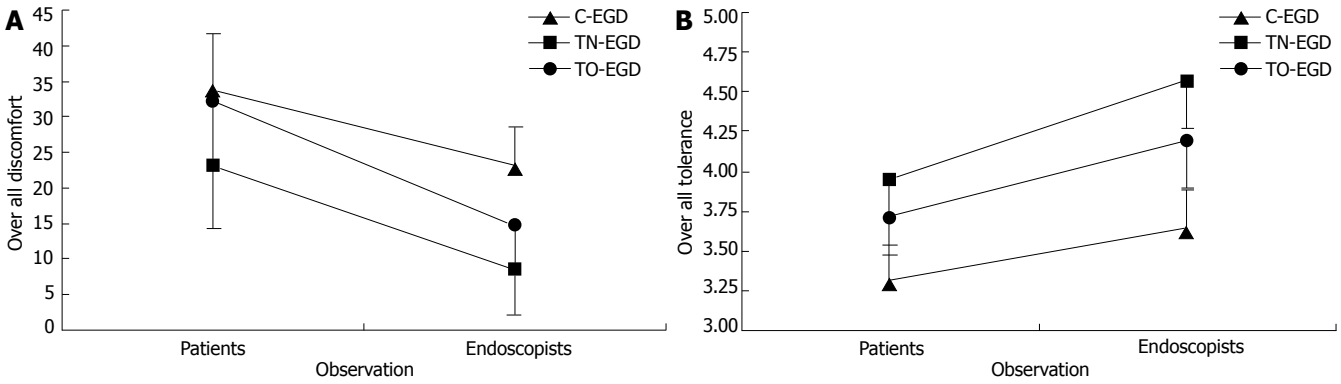

Figure 1 Overall discomfort (**A**) and overall tolerance (**B**) at EGD for patients and endoscopists in the three groups of patients. Statistical difference can be observed comparing TN-EGD *vs* C-EGD.

Table 3 Answers to the questions of "how did you tolerate EGD and what you were expecting of?"

	TN-EGD (n = 41)	TO-EGD (n = 40)	C-EGD (n = 51)
Worse than expected, n (%)	2 (4.9)	7 (17.5)	12 (23.5)
As expected, n (%)	9 (21.9)	11 (27.5)	19 (37.3)
Better than expected, n (%)	30 (73.2)	22 (55.0)	20 (39.2)

Table 4 Results of the endoscopists' evaluation of the performances of endoscopes

	TN-EGD (n = 41)	TO-EGD (n = 40)	C-EGD (n = 51)	P
Endoscopists' score (mean ± SD)				
Image quality	87.85 ± 14.34	89.57 ± 11.00	91.98 ± 11.85	NS
Suction	81.90 ± 9.98	84.82 ± 11.82	94.37 ± 7.49	< 0.001
Air insufflation/washing of the lens	83.90 ± 13.70	85.80 ± 13.34	94.76 ± 6.49	< 0.001
Reaching of the second portionof the duodenum, n (%)	41 (100)	40 (100)	51 (100)	NS
Adequate biopsy sampling, n (%)	19/19 (100)	16/16 (100)	24/24 (100)	NS

analysis showed a statistically significant trend ($P < 0.05$) due to the difference between TN-EGD and C-EGD ($P < 0.01$).

On the basis of the endoscopists' rating scores, the ability to insufflate air/wash the lens, and suction of ultrathin endoscope were lower than those of conventional endoscope ($P < 0.001$) (Table 4). No difference was observed in image quality, and the second portion of the duodenum was reached in all cases with both instruments. In no case the examination was not completed because of the higher flexibility of ultrathin endoscope.

Biopsies were taken at the operator's discretion in 59 cases (19 in TN-EGD group, 16 in TO-EGD group, and 24 in C-EGD group). All biopsies were adequate (Table 3), EGD needed to be repeated in no case because of inadequate histopathologic results.

DISCUSSION

Narrow-diameter endoscopes have been put on the market about ten years before, but their use in clinical practice is still limited to a small subset of patients, either in the United States[10] or in countries such as Italy, where EGD is performed without routine conscious sedation. It is still debated whether the best way of introduction of these instruments is the transnasal or the peroral route, as until now few comparisons have been published in literature. Some randomized trials suggested that the peroral route may be easier to perform and slightly preferred by both patients and endoscopists[17-20]. Conversely, in our series TN-EGD caused less discomfort and was better tolerated. Indeed, univariate analysis seemed to suggest that both TN-EGD and TO-EGD were better tolerated than C-EGD, but multivariate analysis revealed that only TN-EGD showed significantly lower discomfort and higher tolerance than C-EGD. Moreover, TN-EGD patients answered the questions of "how did you tolerate EGD and what you were expecting of?" more positively than the other patients. Our results partially agree with those of Preiss *et al*[21] who observed that patients' acceptance of the EGD is significantly better with the ultrathin endoscope introduced through the nose (but not through the mouth) than with the standard endoscope, as choking was lower. More recently, Thota *et al*[22] reported that the transnasal route is better tolerated than the transoral route, but a 4-mm videoendoscope was used in their study. Conversely, in a randomized trial comparing ultrathin endoscopy through both the transnasal and oral routes with standard EGD, Birkner *et al*[23] observed that patients' opinion about the overall assessment is significantly better in the standard oral EGD. However, this result may be biased by the presence of higher anxiety levels in ultrathin endoscope groups than in control group. Indeed, anxiety is well known to decrease patient compliance, making EGD execution more difficult[3,24]. Such a bias could also explain the surprising observation that patients who underwent peroral EGD with a 6-mm endoscope complained of greater gagging than those who underwent peroral EGD with a 9.8-mm endoscope. Indeed, a lot of trials reported that patient discomfort is lower when small-caliber endoscopes are used[17,25] or no difference is found in tolerance related to endoscope

size[26]. To our knowledge no other study has reported that increasing diameters of the instrument can improve the feasibility and tolerance of unsedated upper endoscopy. Unlike the trial of Birkner[23], our three groups were well-matched for parameters such as gender, age, previous experience of EGD, and anxiety, which can influence the tolerance to endoscopy[24,27]. In our study, transnasal EGD failed in only 4 out of 45 patients (8.9%) because of inability to insert the endoscope through the nose. Once the nasal tract was passed, it was possible to complete all the EGD procedures, including exploration of the second part of the duodenum. Our failure rate is similar to that reported by other authors who used endoscopes with outer diameter of 5.9 mm[21]. Today, endoscopes with a smaller diameter have become available, so it is likely that failure rate will decrease and patients' acceptance will improve in the near future, as the larger-endoscope diameter is considered a predictive factor for procedure failure[19,22].

All biopsy samples taken in our patients were of good quality, and EGD never needed to be repeated because of inadequate histopathologic results. This confirms that biopsy sampling can successfully be done using small diameter endoscopes[17,26,28].

According to other trials[21,29], in our study the percentage of abnormal vital signs was similar in the three groups of patients. However, it has recently been reported that TN-EGD is associated with fewer adverse effects on cardiopulmonary function than TO-EGD[30].

Our study confirmed that the performances of the narrow endoscope were acceptable. Unlike some prior reports[23,26], our experience indicates that image quality and handling of ultrathin and standard endoscopes are similar. Compared to the older color wheel technology, the new ultrathin technology using a color chip similar to that used in standard endoscopes is therefore not susceptible to image distortion. Conversely, the ability to insufflate air, wash the lens, and suction of ultrathin endoscope were lower than those of conventional endoscope. These limits do not compromise diagnostic EGD, but might hamper operative endoscopy, even though some studies suggested that ultrathin endoscopes can work well also in some interventional procedures[13-16].

The average duration of TN-EGD is significantly longer than that of TO-EGD, either in our study or in many other prior reports[17,23,31,32], probably because gastroenterologists are commonly not familiar with the introduction of endoscopes through the nose. Conversely, some authors have not found any difference in duration of EGD between oral and nasal route[21] and a prospective study reported that the duration of transnasal technique is even shorter than peroral technique[33]. However, in this latter study, the time spent to perform transoral EGD was unusually long (11 min).

In conclusion, small-caliber peroral or transnasal EGD has good technical performances, and is safe, generally well accepted and preferred by the patients to conventional EGD. In our opinion, unsedated EGD with narrow-diameter endoscopes should be proposed to all patients undergoing diagnostic EGD. As transnasal EGD seems better tolerated than peroral endoscopy, endoscopists should acquire more familiarity with this route of introduction. The growing skill of endoscopists, as well as further technical improvements in the ultrathin endoscopes, will probably lead to the increasing use of transnasal gastroscopy in the near future.

REFERENCES

1 **al-Atrakchi HA**. Upper gastrointestinal endoscopy without sedation: a prospective study of 2000 examinations. *Gastrointest Endosc* 1989; **35**: 79-81
2 **Brandt LJ**. Patients' attitudes and apprehensions about endoscopy: how to calm troubled waters. *Am J Gastroenterol* 2001; **96**: 280-284
3 **Campo R**, Brullet E, Montserrat A, Calvet X, Moix J, Rué M, Roqué M, Donoso L, Bordas JM. Identification of factors that influence tolerance of upper gastrointestinal endoscopy. *Eur J Gastroenterol Hepatol* 1999; **11**: 201-204
4 **Dominitz JA**, Provenzale D. Patient preferences and quality of life associated with colorectal cancer screening. *Am J Gastroenterol* 1997; **92**: 2171-2178
5 **Bell GD**. Premedication, preparation, and surveillance. *Endoscopy* 2002; **34**: 2-12
6 **Gattuso SM**, Litt MD, Fitzgerald TE. Coping with gastrointestinal endoscopy: self-efficacy enhancement and coping style. *J Consult Clin Psychol* 1992; **60**: 133-139
7 **Woloshynowych M**, Oakley DA, Saunders BP, Williams CB. Psychological aspects of gastrointestinal endoscopy: a review. *Endoscopy* 1996; **28**: 763-767
8 **Conlong P**, Rees W. The use of hypnosis in gastroscopy: a comparison with intravenous sedation. *Postgrad Med J* 1999; **75**: 223-225
9 **Mokhashi MS**, Hawes RH. Struggling toward easier endoscopy. *Gastrointest Endosc* 1998; **48**: 432-440
10 **Sorbi D**, Chak A. Unsedated EGD. *Gastrointest Endosc* 2003; **58**: 102-110
11 **Shaker R**. Unsedated trans-nasal pharyngoesophagogastrodu odenoscopy (T-EGD): technique. *Gastrointest Endosc* 1994; **40**: 346-348
12 **Nozaki R**, Fujiyoshi T, Tamura M, Tsuchiya A, Takagi K, Takano M. Evaluation of small calibre transnasal panendoscopes for upper GI screening examination. *Dig Endosc* 1995; **7**: 155-159
13 **Bajaj JS**, Shaker R. Another indication for transnasal, unsedated upper-GI endoscopy. *Gastrointest Endosc* 2005; **62**: 667-668
14 **Dumortier J**, Lapalus MG, Pereira A, Lagarrigue JP, Chavaillon A, Ponchon T. Unsedated transnasal PEG placement. *Gastrointest Endosc* 2004; **59**: 54-57
15 **Fang JC**, Hilden K, Holubkov R, DiSario JA. Transnasal endoscopy vs. fluoroscopy for the placement of nasoenteric feeding tubes in critically ill patients. *Gastrointest Endosc* 2005; **62**: 661-666
16 **Vitale MA**, Villotti G, D'Alba L, De Cesare MA, Frontespezi S, Iacopini G. Unsedated transnasal percutaneous endoscopic gastrostomy placement in selected patients. *Endoscopy* 2005; **37**: 48-51
17 **Craig A**, Hanlon J, Dent J, Schoeman M. A comparison of transnasal and transoral endoscopy with small-diameter endoscopes in unsedated patients. *Gastrointest Endosc* 1999; **49**: 292-296
18 **Dean R**, Dua K, Massey B, Berger W, Hogan WJ, Shaker R. A comparative study of unsedated transnasal esophagogastrod uodenoscopy and conventional EGD. *Gastrointest Endosc* 1996; **44**: 422-424
19 **Dumortier J**, Napoleon B, Hedelius F, Pellissier PE, Leprince E, Pujol B, Ponchon T. Unsedated transnasal EGD in daily practice: results with 1100 consecutive patients. *Gastrointest Endosc* 2003; **57**: 198-204
20 **Zaman A**, Hahn M, Hapke R, Knigge K, Fennerty MB, Katon RM. A randomized trial of peroral versus transnasal unsedated endoscopy using an ultrathin videoendoscope.

Gastrointest Endosc 1999; **49**: 279-284
21 **Preiss C**, Charton JP, Schumacher B, Neuhaus H. A randomized trial of unsedated transnasal small-caliber esoph agogastroduodenoscopy (EGD) versus peroral small-caliber EGD versus conventional EGD. *Endoscopy* 2003; **35**: 641-646
22 **Thota PN**, Zuccaro G, Vargo JJ, Conwell DL, Dumot JA, Xu M. A randomized prospective trial comparing unsedated esophagoscopy via transnasal and transoral routes using a 4-mm video endoscope with conventional endoscopy with sedation. *Endoscopy* 2005; **37**: 559-565
23 **Birkner B**, Fritz N, Schatke W, Hasford J. A prospective randomized comparison of unsedated ultrathin versus standard esophagogastroduodenoscopy in routine outpatient gastroenterology practice: does it work better through the nose? *Endoscopy* 2003; **35**: 647-651
24 **Trevisani L**, Sartori S, Gaudenzi P, Gilli G, Matarese G, Gullini S, Abbasciano V. Upper gastrointestinal endoscopy: are preparatory interventions or conscious sedation effective? A randomized trial. *World J Gastroenterol* 2004; **10**: 3313-3317
25 **Mulcahy HE**, Riches A, Kiely M, Farthing MJ, Fairclough PD. A prospective controlled trial of an ultrathin versus a conventional endoscope in unsedated upper gastrointestinal endoscopy. *Endoscopy* 2001; **33**: 311-316
26 **Dumortier J**, Ponchon T, Scoazec JY, Moulinier B, Zarka F, Paliard P, Lambert R. Prospective evaluation of transnasal esophagogastroduodenoscopy: feasibility and study on performance and tolerance. *Gastrointest Endosc* 1999; **49**: 285-291
27 **Abuksis G**, Mor M, Segal N, Shemesh I, Morad I, Plaut S, Weiss E, Sulkes J, Fraser G, Niv Y. A patient education program is cost-effective for preventing failure of endoscopic procedures in a gastroenterology department. *Am J Gastroenterol* 2001; **96**: 1786-1790
28 **Saeian K**, Townsend WF, Rochling FA, Bardan E, Dua K, Phadnis S, Dunn BE, Darnell K, Shaker R. Unsedated transnasal EGD: an alternative approach to conventional esophagogastroduodenoscopy for documenting Helicobacter pylori eradication. *Gastrointest Endosc* 1999; **49**: 297-301
29 **Garcia RT**, Cello JP, Nguyen MH, Rogers SJ, Rodas A, Trinh HN, Stollman NH, Schlueck G, McQuaid KR. Unsedated ultrathin EGD is well accepted when compared with conventional sedated EGD: a multicenter randomized trial. *Gastroenterology* 2003; **125**: 1606-1612
30 **Yagi J**, Adachi K, Arima N, Tanaka S, Ose T, Azumi T, Sasaki H, Sato M, Kinoshita Y. A prospective randomized comparative study on the safety and tolerability of transnasal esophagogast roduodenoscopy. *Endoscopy* 2005; **37**: 1226-1231
31 **Campo R**, Montserrat A, Brullet E. Transnasal gastroscopy compared to conventional gastroscopy: a randomized study of feasibility, safety, and tolerance. *Endoscopy* 1998; **30**: 448-452
32 **Shaker R**, Saeian K. Unsedated transnasal laryngo-esophagogastroduodenoscopy: an alternative to conventional endoscopy. *Am J Med* 2001; **111** Suppl 8A: 153S-156S
33 **Krakamp B**, Parusel M, Saers T. Prospective study comparing conventional and transnasal esophagogastroduodenoscopy for routine diagnosis. *Dtsch Med Wochenschr* 2004; **129**: 82-86

S- Editor Wang J **L- Editor** Wang XL **E- Editor** Lu W

PO Box 2345, Beijing 100023, China
www.wjgnet.com
wjg@wjgnet.com

World J Gastroenterol 2007 February 14; 13(6): 912-915
World Journal of Gastroenterology ISSN 1007-9327

RAPID COMMUNICATION

Use of probiotics for prevention of radiation-induced diarrhea

P Delia, G Sansotta, V Donato, P Frosina, G Messina, C De Renzis, G Famularo

P Delia, G Sansotta, V Donato, P Frosina, G Messina, C De Renzis, G Famularo, Institute of Radiology, Oncologic Radiotherapy Unit, Azienda Ospedaliera Universitaria, Messina and Department of Internal Medicine, San Camillo Hospital, Rome, Italy
Correspondence to: Dr. Giuseppe Famularo, Department of Internal Medicine, San Camillo Hospital, Circonvallazione Gianicolense, 00152 Rome,
Italy. gfamularo@scamilloforlanini.rm.it
Telephone: +39-6-58704325 Fax: +39-6-58704557
Received: 2006-10-29 Accepted: 2007-01-18

Abstract

AIM: To investigate the efficacy of a high-potency probiotic preparation on prevention of radiation-induced diarrhea in cancer patients.

METHODS: This was a double-blind, placebo-controlled trial. Four hundred and ninety patients who underwent adjuvant postoperative radiation therapy after surgery for sigmoid, rectal, or cervical cancer were assigned to either the high-potency probiotic preparation VSL#3 (one sachet *t.i.d.*,) or placebo starting from the first day of radiation therapy. Efficacy endpoints were incidence and severity of radiation-induced diarrhea, daily number of bowel movements, and the time from the start of the study to the use of loperamide as rescue medication.

RESULTS: More placebo patients had radiation-induced diarrhea than VSL#3 patients (124 of 239 patients, 51.8%, and 77 of 243 patients, 31.6%; $P < 0.001$) and more patients given placebo suffered grade 3 or 4 diarrhea compared with VSL#3 recipients (55.4% and 1.4%, $P < 0.001$). Daily bowel movements were 14.7 ± 6 and 5.1 ± 3 among placebo and VSL#3 recipients ($P < 0.05$), and the mean time to the use of loperamide was 86 ± 6 h for placebo patients and 122 ± 8 h for VSL#3 patients ($P < 0.001$).

CONCLUSION: Probiotic lactic acid-producing bacteria are an easy, safe, and feasible approach to protect cancer patients against the risk of radiation-induced diarrhea.

Key words: Probiotics; Radiation therapy; Diarrhea

Delia P, Sansotta G, Donato V, Frosina P, Messina G, De Renzis C, Famularo G. Use of probiotics for prevention of radiation-induced diarrhea. *World J Gastroenterol* 2007; 13(6): 912-915

http://www.wjgnet.com/1007-9327/13/912.asp

INTRODUCTION

Almost all regimens of radiation therapy may disturb the colonization resistance of the indigenous gut flora. This is the main mechanism underlying the pathophysiology of acute radiation-induced enteritis and colitis, which are a common and potentially severe complication among cancer patients treated with radiation therapy. Attempts to treat this complication with antibiotics, sucralfate, anti-inflammatory drugs such as mesalazine and balsalazide, glutamine, octreotide, proteolytic enzymes, and hyperbaric oxygen have so far provided inconclusive clinical results with failure of treatment occurring in a substantial proportion of patients[1-9]. Furthermore, prophylactic use of sucralfate does not reduce the burden of radiation-induced bowel toxicity but rather, is associated with more severe gastrointestinal symptoms including bleeding and fecal incontinence[10,11]. In the light of these contradictory findings, we urgently need innovative approaches that target other steps in the pathophysiology of radiation-induced diarrhea.

The term probiotic refers to a product or preparation containing viable and defined microorganisms in a number thought to be sufficient to alter by implantation or colonization the host's microflora and thereby exert beneficial effects[12,13]. Experimental studies in animal models and clinical trials of patients with inflammatory bowel disease (IBD) have consistently shown that use of probiotic organisms may effectively down-modulate the severity of intestinal inflammation through altering the composition and the metabolic and functional properties of gut indigenous flora[12,13]. Experience with probiotic organisms for the prevention of enteritis and colitis in cancer patients receiving radiation therapy is limited, however we have recently shown in a small pilot trial of feasibility and safety that both the incidence and severity of radiation-induced diarrhea were appreciably reduced with pre-emptive treatment with VSL#3, a new high potency preparation of probiotic lactobacilli, during adjuvant radiotherapy after surgery for abdominal and pelvic cancer[14]. The present study was undertaken to assess and compare the benefits of probiotic therapy with VSL#3 on clinically relevant endpoints in a greater sample of 490 patients, including 190 subjects we enrolled in our earlier trial.

MATERIALS AND METHODS

Four hundred ninety consecutive patients attending the outpatient clinics of the Cancer X-Ray Unit of the University of Messina, Italy, from May 1999 to December 2005, who had received adjuvant postoperative radiation therapy after surgery for sigmoid, rectal, or cervical cancers were randomly assigned to either treatment with VSL#3 (VSL Pharmaceuticals, Fort Lauderdale, MD), one sachet *t.i.d.*, or a VSL#3-identical appearing placebo starting from the first day of radiation therapy until the end of the scheduled cycles of radiation therapy. The design of the study was approved by the Ethics Committee of our hospital, and all patients gave written informed consent to participate. The study was double-blind, parallel-group, and placebo-controlled and was performed in accordance with the Declaration of Helsinki and standards of good clinical practice.

Each sachet of VSL#3 contained 450 billions/g of viable lyophilized bacteria, including four strains of lactobacilli (*L. casei, L. plantarum, L. acidophilus, and L. delbruekii subsp. bulgaricus*), three strains of bifidobacteria (*B. longum, B. breve, and B. infantis*), and one strain of *Streptococcus salivarius subsp. thermophilus*. Patients were eligible for inclusion if they had no contraindication for probiotic or antibiotic therapy or radiation therapy. We excluded by randomization patients with a Karnofsky performance score $\leqslant$ 70, a life expectancy $\leqslant$ 1 year, persistent vomiting or diarrhea, fistulizing disease, known Crohn's disease or ulcerative colitis, intra-abdominal abscesses or fever (more than 37.5℃) at the time of enrolment, or clinical, microbiological, or imaging evidence of sepsis syndrome, and requirement for continuous antibiotic treatment or use of antibiotics in the last 2 wk before initiation of VSL#3 therapy.

At base-line, patients provided a medical history and had a physical examination (consisting of vital signs, 12-lead electrocardiogram, neurological examination, and laboratory testing). The study subjects were followed up weekly during the scheduled cycle of radiation therapy and then 1 mo after completion of radiation therapy. At each visit, clinical symptoms, concomitant medications, and any adverse events were reviewed, and a physical examination and laboratory studies were performed. Efficacy endpoints were incidence and severity of radiation-induced diarrhea, number of patients who discontinued radiotherapy because of diarrhea, daily number of bowel movements, and the time from the start of the study to the use of loperamide as rescue medication for diarrhea. The randomization was balanced between treatment groups in terms of sex, age, nodal involvement, tumor grade and size, local invasion at operation, invasion of contiguous structures at histology, and postoperative complications. The total X-ray dose the patients were given was between 60 and 70 Gy. We measured the severity of gastrointestinal toxicity according to World Health Organization grading, with grade 0 indicating no toxicity, grade 1 indicating self-limited toxicity lasting less than 2 d, grade 2 indicating self-limited symptoms lasting more than 2 d, grade 3 referring to symptoms requiring treatment, and grade 4 indicating severe toxicity with dehydration and/or hemorrhage.

Statistical analysis

Statistical analysis of results was performed using Kaplan-Meier estimates. $P < 0.05$ was taken as significant.

RESULTS

Two hundred thirty nine out of 245 patients in the placebo group (97.5%) completed the study as 6 patients were withdrawn after a few sessions of radiation therapy due to the occurrence of severe diarrhea resistant to loperamide and the usual standard of care; these patients were excluded from the analysis of results. Two hundred forty three among the 245 patients in the VSL#3 group (99.1%) completed the study, one patient withdrew his consent after the first session of radiation therapy, and one patient died of myocardial infarction after three sessions of radiation therapy; both patients were excluded from analysis of the results.

More patients in the placebo group had radiation-induced enteritis and colitis compared with the VSL#3 group (124 of 239, 51.8%, versus 77 of 243 patients, 31.6%; $P < 0.001$). Furthermore, patients given the placebo suffered more severe toxicity compared with VSL#3 recipients as grade 3 or 4 diarrhea was documented in 69 of 124 (55.4%) placebo-treated patients and 8 of 77 (1.4%) VSL#3-treated patients ($P < 0.001$), whereas 50 of 124 placebo-treated patients had grade 1 or 2 diarrhea compared with 34 of 77 VSL#3 recipients (NS). Even though the difference did not reach statistical significance, there was clearly a trend in favor of the treatment with VSL#3 compared with the placebo.

The mean daily number of bowel movements for patients with radiation-induced diarrhea was 14.7 $\pm$ 6 and 5.1 $\pm$ 3 among placebo and VSL#3 recipients, respectively ($P < 0.05$), and the mean time to the use of loperamide as rescue medication for diarrhea was 86 $\pm$ 6 h for patients receiving placebo versus 122 $\pm$ 8 h for patients receiving VSL#3 ($P < 0.001$).

No tumor- or treatment-related deaths or deaths from other causes were recorded in either group during the period of radiation therapy, and no case of bacteremia, sepsis, or septic shock due to the probiotic lactobacilli was reported among the VSL#3 recipients during the treatment period with the probiotic preparation or during the six months beyond active treatment. Likewise, no case of bacteremia, sepsis, or septic shock due to organisms other than the probiotic lactobacilli was recognized during the period of active treatment. We did not recognize any other toxicity reasonably attributable to VSL#3.

DISCUSSION

We have clearly demonstrated in a large sample of patients the benefits of probiotic therapy with VSL#3 for the prevention and/or reduction of both the incidence and severity of enteritis and colitis associated with adjuvant radiation treatment after surgery for abdominal and pelvic cancer. Significantly fewer patients treated with VSL#3 had grade 3 or 4 diarrhea during the period of radiation treatment compared with patients given placebo, in

addition to the usual standard of care. We also observed a trend in favor of VSL#3 in terms of reduced incidence in grade 1 or 2 intestinal toxicity, even though the difference between the two groups did not reach statistical significance.

The findings of this study have reiterated those of our early pilot trial[14] and strongly support our working hypothesis that using probiotic lactobacilli may be an easy, cheap, safe, and feasible approach to effectively protect patients against the risk of radiation-induced diarrhea, which is a severe and potentially lethal complication of radiation therapy for abdominal and pelvic cancer. However, apart from our two studies with VSL#3, experience with probiotic organisms in this setting is limited. Our Medline search yielded indeed only one other study with probiotics, i.e. the double-blind and randomized trial by Urbancsek and colleagues who reported favorable results with *Lactobacillus GG* treatment[15]. In contrast, we used VSL#3, which is a high-potency preparation with unique characteristics compared with traditional probiotics, in particular, because of the enormously high bacterial concentration and the presence of a consortium of different bacterial species with potential synergistic relations between different strains that may greatly enhance the suppression of potential pathogens[12]. Whether treatment with VSL#3 could be more effective than using *Lactobacillus GG* or other probiotic organisms is unknown for several reasons, including the lack of a well-designed head-to-head comparison between the different probiotic preparations. However, the composite mixture of VSL#3 with a large number of probiotic strains possessing very different and specialized metabolic and immunoregulatory activities is a unique feature of this preparation, and may explain its wide spectrum of biological activities. One additional important point is that results of experimental studies and double-blind placebo-controlled clinical trials have consistently validated VSL#3 as a therapeutic tool to down-modulate intestinal inflammation in several animal and human models of IBD[13]. In contrast, clinical trials of *Lactobacillus GG* treatment for IBD patients have provided conflicting results and the true clinical efficacy of this probiotic strain is still substantially unclear[16-18].

Clinical and experimental studies of VSL#3 in patients with ulcerative colitis and animal models of IBD have provided insights into the mechanisms underlying the efficacy of probiotic lactobacilli of VSL#3 to protect patients against radiation-induced diarrhea. VSL#3 lactobacilli lower the production of proinflammatory cytokines and several other effectors of inflammation and tissue injury, such as nitric oxide and metalloproteinases, interfere with the pro-inflammatory signal transduced by toll-like receptors, exert a significant protection upon the integrity of the intestinal epithelial barrier, and down-modulate the process of apoptosis. This latter mechanism is of utmost importance because the triggering of an unregulated process of apoptosis is regarded as the main factor ultimately responsible for the radiation-induced injury of the intestinal epithelium[19]. Furthermore, probiotic bacteria up-regulate the innate immune response in the gut and are thus part of a protective mechanism against invasive organisms, which is important when ileal and colonic protection against invading organisms is severely impaired as a result of exposure to radiation. All these mechanisms are likely to synergistically contribute to the down-modulation of gut inflammation and host protection against intestinal colonization by invasive pathogens and their subsequent translocation into portal circulation also in patients irradiated for therapeutic purposes.

Treatment with VSL#3 proved in our study to be remarkably safe and we did not recognize any toxicity reasonably attributable to VSL#3 over the time-span of probiotic treatment. Furthermore, we observed no case of bacteremia, sepsis, or septic shock due to the probiotic lactobacilli of VSL#3, which is in agreement with results of other clinical trials of VSL#3 in IBD patients. Previous clinical experience with this probiotic preparation has indeed demonstrated the remarkable safety of VSL#3 bacteriotherapy even with dosages significantly greater than those used in this trial. This does strongly reinforce the view that probiotic treatment with VSL#3 should be regarded as remarkably safe even in the setting of intestinal inflammation associated with severely altered barrier function as it may occur in patients with radiation-induced enteritis and colitis.

REFERENCES

1 **Donner CS**. Pathophysiology and therapy of chronic radiation-induced injury to the colon. *Dig Dis* 1998; **16**: 253-261
2 **Valls A**, Pestchen I, Prats C, Pera J, Aragón G, Vidarte M, Algara M. Multicenter double-blind clinical trial comparing sucralfate vs placebo in the prevention of diarrhea secondary to pelvic irradiation. *Med Clin* (Barc) 1999; **113**: 681-684
3 **Kneebone A**, Mameghan H, Bolin T, Berry M, Turner S, Kearsley J, Graham P, Fisher R, Delaney G. Effect of oral sucralfate on late rectal injury associated with radiotherapy for prostate cancer: A double-blind, randomized trial. *Int J Radiat Oncol Biol Phys* 2004; **60**: 1088-1097
4 **Dodd MJ**, Miaskowski C, Greenspan D, MacPhail L, Shih AS, Shiba G, Facione N, Paul SM. Radiation-induced mucositis: a randomized clinical trial of micronized sucralfate versus salt & soda mouthwashes. *Cancer Invest* 2003; **21**: 21-33
5 **Resbeut M**, Marteau P, Cowen D, Richaud P, Bourdin S, Dubois JB, Mere P, N'Guyen TD. A randomized double blind placebo controlled multicenter study of mesalazine for the prevention of acute radiation enteritis. *Radiother Oncol* 1997; **44**: 59-63
6 **Jahraus CD**, Bettenhausen D, Malik U, Sellitti M, St Clair WH. Prevention of acute radiation-induced proctosigmoiditis by balsalazide: a randomized, double-blind, placebo controlled trial in prostate cancer patients. *Int J Radiat Oncol Biol Phys* 2005; **63**: 1483-1487
7 **Kozelsky TF**, Meyers GE, Sloan JA, Shanahan TG, Dick SJ, Moore RL, Engeler GP, Frank AR, McKone TK, Urias RE, Pilepich MV, Novotny PJ, Martenson JA. Phase III double-blind study of glutamine versus placebo for the prevention of acute diarrhea in patients receiving pelvic radiation therapy. *J Clin Oncol* 2003; **21**: 1669-1674
8 **Yavuz MN**, Yavuz AA, Aydin F, Can G, Kavgaci H. The efficacy of octreotide in the therapy of acute radiation-induced diarrhea: a randomized controlled study. *Int J Radiat Oncol Biol Phys* 2002; **54**: 195-202
9 **Martin T**, Uhder K, Kurek R, Roeddiger S, Schneider L, Vogt HG, Heyd R, Zamboglou N. Does prophylactic treatment with proteolytic enzymes reduce acute toxicity of adjuvant pelvic irradiation? Results of a double-blind randomized trial. *Radiother Oncol* 2002; **65**: 17-22
10 **Kneebone A**, Mameghan H, Bolin T, Berry M, Turner S,

Kearsley J, Graham P, Fisher R, Delaney G. The effect of oral sucralfate on the acute proctitis associated with prostate radiotherapy: a double-blind, randomized trial. *Int J Radiat Oncol Biol Phys* 2001; **51**: 628-635

11 **Martenson JA**, Bollinger JW, Sloan JA, Novotny PJ, Urias RE, Michalak JC, Shanahan TG, Mailliard JA, Levitt R. Sucralfate in the prevention of treatment-induced diarrhea in patients receiving pelvic radiation therapy: A North Central Cancer Treatment Group phase III double-blind placebo-controlled trial. *J Clin Oncol* 2000; **18**: 1239-1245

12 **Famularo G**, De Simone C, Matteuzzi D, Pirovano F. Traditional and high-potency probiotic preparations for oral bacteriotherapy. *BioDrugs* 1999; **12**: 455-470

13 **Famularo G**, Mosca L, Minisola G, Trinchieri V, De Simone C. Probiotic lactobacilli: a new perspective for the treatment of inflammatory bowel disease. *Curr Pharm Des* 2003; **9**: 1973-1980

14 **Delia P**, Sansotta G, Donato V, Messina G, Frosina P, Pergolizzi S, De Renzis C, Famularo G. Prevention of radiation-induced diarrhea with the use of VSL#3, a new high-potency probiotic preparation. *Am J Gastroenterol* 2002; **97**: 2150-2152

15 **Urbancsek H**, Kazar T, Mezes I, Neumann K. Results of a double-blind, randomized study to evaluate the efficacy and safety of Antibiophilus in patients with radiation-induced diarrhoea. *Eur J Gastroenterol Hepatol* 2001; **13**: 391-396

16 **Zocco MA**, dal Verme LZ, Cremonini F, Piscaglia AC, Nista EC, Candelli M, Novi M, Rigante D, Cazzato IA, Ojetti V, Armuzzi A, Gasbarrini G, Gasbarrini A. Efficacy of Lactobacillus GG in maintaining remission of ulcerative colitis. *Aliment Pharmacol Ther* 2006; **23**: 1567-1574

17 **Bousvaros A**, Guandalini S, Baldassano RN, Botelho C, Evans J, Ferry GD, Goldin B, Hartigan L, Kugathasan S, Levy J, Murray KF, Oliva-Hemker M, Rosh JR, Tolia V, Zholudev A, Vanderhoof JA, Hibberd PL. A randomized, double-blind trial of Lactobacillus GG versus placebo in addition to standard maintenance therapy for children with Crohn's disease. *Inflamm Bowel Dis* 2005; **11**: 833-839

18 **Prantera C**, Scribano ML, Falasco G, Andreoli A, Luzi C. Ineffectiveness of probiotics in preventing recurrence after curative resection for Crohn's disease: a randomised controlled trial with Lactobacillus GG. *Gut* 2002; **51**: 405-409

19 **Paris F**, Fuks Z, Kang A, Capodieci P, Juan G, Ehleiter D, Haimovitz-Friedman A, Cordon-Cardo C, Kolesnick R. Endothelial apoptosis as the primary lesion initiating intestinal radiation damage in mice. *Science* 2001; **293**: 293-297

S- Editor Liu Y **L- Editor** Zhu LH **E- Editor** Lu W

PO Box 2345, Beijing 100023, China
www.wjgnet.com
wjg@wjgnet.com

World J Gastroenterol 2007 February 14; 13(6): 916-920
World Journal of Gastroenterology ISSN 1007-9327

RAPID COMMUNICATION

Self-expandable metallic stents for palliation of patients with malignant gastric outlet obstruction caused by stomach cancer

Tae Oh Kim, Dae Hwan Kang, Gwang Ha Kim, Jeong Heo, Geun Am Song, Mong Cho, Dong Heon Kim, Mun Sup Sim

Tae Oh Kim, Dae Hwan Kang, Gwang Ha Kim, Jeong Heo, Geun Am Song, Mong Cho, Department of Internal Medicine, Pusan National University College of Medicine, Busan, Korea
Dong Heon Kim, Mun Sup Sim, Department of General Surgery, Pusan National University College of Medicine, Busan, Korea
Correspondence to: Dae Hwan Kang, MD, Department of Internal Medicine, Pusan National University College of Medicine, 1-10 Ami-dong, Soe-gu, Busan 602-739, Korea. sulsulpul@yahoo.co.kr
Telephone: +82-51-2407869 Fax: +82-51-2448180
Received: 2006-09-25 Accepted: 2007-01-05

Abstract

AIM: To ascertain clinical outcome and complications of self-expandable metal stents for endoscopic palliation of patients with malignant obstruction of the gastrointestinal (GI) tract.

METHODS: A retrospective review was performed throughout August 2000 to June 2005 of 53 patients with gastric outlet obstruction caused by stomach cancer. All patients had symptomatic obstruction including nausea, vomiting, and decreased oral intake. All received self-expandable metallic stents.

RESULTS: Stent implantation was successful in all 53 (100%) patients. Relief of obstructive symptoms was achieved in 43 (81.1%) patients. No immediate stent-related complications were noted. Seventeen patients had recurrent obstruction (tumor ingrowth in 14 patients, tumor overgrowth in 1 patient, and partial distal stent migration in 2 patients). The mean survival was 145 d. Median stent patency time was 187 d.

CONCLUSION: Endoscopic placement of self-expandable metallic stents is a safe and effective treatment for the palliation of patients with inoperable malignant gastric outlet obstruction caused by stomach cancer.

Key words: Self-expandable metallic stents; Malignant gastric outlet obstruction; Stomach cancer

Kim TO, Kang DH, Kim GH, Heo J, Song GA, Cho M, Kim DH, Sim MS. Self-expandable metallic stents for palliation of patients with malignant gastric outlet obstruction caused by stomach cancer. *World J Gastroenterol* 2007; 13(6): 916-920

http://www.wjgnet.com/1007-9327/13/916.asp

INTRODUCTION

Malignant obstruction of the stomach is a preterminal event that causes nausea, vomiting, dysphagia, and nutritional deficiencies leading to progressive deterioration in a patient's quality of life. It is generally managed by surgical intervention. Because a subgroup of these patients consists of people who are elderly or have advanced, metastatic disease or other medical illness, surgery may be impossible in such patients.

Endoscopic placement of self-expandable metallic stents (SEMS) has been used for palliative treatment of patients with malignant obstruction of the gastrointestinal (GI) tract for over a decade[1,2]. Endoscopic stent placement is a safe and feasible treatment option for patients with malignant gastric outlet obstruction. In retrospective comparative studies, patients who underwent an open gastrojejunostomy had delayed oral intake after surgery[3], higher procedure-related morbidity, higher 30-d mortality[4], and a longer length of hospital stay[4-6], and incurred greater hospital charges[5] than patients who underwent an endoscopic stent insertion. To date, there has been no study that assesses clinical outcome after SEMS insertion for malignant gastric outlet obstruction caused by stomach cancer only, rather than by pancreatic, biliary, or duodenal cancer. Here we report results from a 5-year, single-center experience with the use of SEMS to palliate patients hospitalized with gastric outlet obstruction because of inoperable gastric cancer.

MATERIALS AND METHODS

Patients

Between August 2000 and June 2005, 103 patients with malignant gastroduodenal and jejunal stenosis underwent endoscopic procedures with uncovered SEMS. Obstruction was caused by stomach cancer in 53 (51.3%) patients, by recurrent malignant obstruction after gastric surgery in 20 (19.4%), by pancreatic cancer in 14 (13.6%), by bile

duct cancer in 7 (6.8%), by duodenal cancer in 3 (2.9%), by ampullary cancer in 2 (2.0%), by gallbladder cancer in 2 (2.0%) and unclassified in 2 (2.0%) patients. Only patients with malignant obstruction due to stomach cancer were included in this study. The diagnosis of malignant tumor and gastric outlet obstruction was established by means of endoscopy, duodenography and computed tomography. Fifty three patients (35 men, 18 women; mean age 64.0 years, range 34-85 years) with malignant gastric outlet obstruction who were treated with SEMS were followed at our outer-patient department, inpatient department or by phone calls. None of the patients were operative candidates based on the presence of advanced, metastatic disease or medical comorbidity. All patients had symptomatic obstructions such as nausea, vomiting, bloating, and abdominal pain. The degree and site of the stenosis were usually evaluated before endoscopy, using radiographs taken after oral contrast opacification; the gastric outlet area was divided into the antropyloric portion (40 patients), pyloric and duodenal bulb portion (8 patients), body and antropyloric portion (5 patients). Patient demographics are summarized in Table 1.

Table 1 Patient demographics

Total number of patients	53
Mean age, yr (range)	64.0 (34-85)
Male/Female	35/18
Present illness	
Stomach cancer	53 (100%)
Location of obstruction	
Antropyloric	40 (75.5%)
Pylorus and duodenal bulb	8 (15.1%)
Body and antropyloric	5 (9.4%)

Equipments

The stents used in this study were the SEMS (NiTi-S®, Pyloric(TTS), Taewoong, South Korea), 18 mm in diameter and 60, 80, 100, or 120 mm in length. These stents are constructed from a nickel-titanium alloy with or without an outer membrane. The covered stent is coated with polyurethane in the body and the proximal flare portion. The diameters are 18 mm and 26 mm in the body and flare portions, respectively. The stent is tightly mounted on a delivery system with an outer diameter of 10-11 Fr and an overall length of 180 cm. This long and slim delivery system allowed us to insert and deploy the stent through the working channel of the therapeutic endoscope. A 300-cm long, 0.035- or 0.025-inch diameter biliary guidewire (Zebra, Microvasive, USA, or Metro, Wilson Cook, USA) or a 260-cm long, 0.035-inch diameter exchange guidewire (Radiofocus M, Terumo, Tokyo, Japan) was used. The endoscopes used were a 2-channel endoscope with a working channel of 3.7 mm (GIF-2T200, Olympus Co., Japan) or a therapeutic duodenoscope with a working channel of 4.2 mm (TJF 200, Olympus Co., Japan).

Endoscopic techniques

We placed all stents under endoscopic and fluoroscopic guidance. Stent insertion was performed under conscious sedation using titrated doses of midazolam administrated by an experienced endoscopist or a nurse with appropriate monitoring. After identification of the stenosis, a guidewire was passed through it using a standard endoscopic retrograde cholangiopancreatography (ERCP) catheter. The length of the stenosis was determined by the stricture identified with a water-soluble, iodinated contrast medium. The stent chosen extended at least an additional 1-2 cm in length on each side of the stenosis to allow an adequate margin of stent. An undeployed SEMS delivery system was passed through the working channel of the endoscope over the guidewire so that the ends of the undeployed stent were equidistant from the ends of the stenosis. The stent was deployed from the distal end with frequent repositioning of the proximal position in the desired location because of a tendency for it to move away from the scope. The adequacy of stent placement was assessed at the conclusion of each procedure using a combination of endoscopy and fluoroscopy. An oral contrast opacification was obtained immediately after the procedure. Technical endoscopic success was defined as correct placement of the stent across the stricture with an established patency confirmed fluoroscopically. Uncovered stents were used primarily in all cases. The patients provided informed consent before endoscopic stent insertion.

Oral intake was allowed immediately after the procedure, beginning with liquid followed by a semisolid or soft diet, if possible. When uncovered stents were occluded by tumor ingrowth, a covered stent was reimplanted through the first stent to palliate tumor ingrowth through openings between the mesh. A good clinical outcome was defined as an immediate improvement in the patient's oral intake, thereby obviating the need for other palliative options. Follow-up investigations were performed only if symptoms recurred.

Statistical analysis

Survival was calculated using the Kaplan-Meier estimator. The date of censoring was the date of death. Cumulative stent patency was also tabulated using Kaplan-Meier plots. Censored data were determined by patients without stent occlusion and still alive, while events were determined by patients with stent occlusion, dislocation, or death.

RESULTS

Stent implantation

Stent implantation was successful in all 53 patients, and we used uncovered stents initially to prevent migration. A complementary hydrostatic dilation of the stent was not needed.

Clinical outcomes and complications

Relief of major clinical symptoms (nausea, abdominal distension, reflux symptoms, vomiting) was achieved in 43

Table 2 Clinical outcomes after stent insertion in 53 patients with stomach cancer

Technical success, *n* (%)	53 (100)
Clinical success, *n* (%)	43 (81.1)
Tolerated diet, %	43 (81.1)
Regular diet, %	9.3 (4/43)
Soft diet	58.1 (25/43)
Liquid diet	32.6 (14/43)
30-d mortality, *n* (%)	10 (18.9)
Reintervention, *n* (%)	17 (32.1)
Tumor ingrowth	14 (26.4)
Tumor overgrowth	1 (1.9)
Stent migration	2 (3.8)
Mean follow up period, d	145 (4-718)
Mean survival, d (SD)	145 (± 150.4)
Mean stent patency, d (range)	187 (33-335)

of 53 (81.1%) patients. A total of 4 of 43 (9.3%) patients could eat solid food, 25 patients (58.1%) tolerated a soft diet, and 14 patients (32.6%) continued to take liquids alone. Of the 53, 10 (18.9%) patients had intermittent episodes of vomiting, and their diets were modified as necessary (Table 2).

During the stent-insertion procedure, no major complications such as serious bleeding, bowel perforation, infection, or procedure-related mortality were noted. After the insertion of the stent, only minor complications such as mild abdominal pain occurred. During follow-up, stent-related problems required treatment in 17 patients (32.1%). Distal stent migration occurred partially in 2 patients (3.8%), 36 and 149 d after stent insertion, respectively, with resultant recurrence of obstructive symptoms. A second stent was inserted to overlap the first, which resulted in immediate relief of symptoms. Stent obstruction caused by proximal and distal tumor overgrowth occurred in 1 patient (1.9%) at 331 d after deployment. Tumor ingrowth through the stent mesh was observed in 14 patients (26.4%) at a mean of 78.4 d after the initial procedure. We defined early restenosis as a stent obstruction from tumor ingrowth within 4 wk after first stent implantation, and identified its development in 5 of 43 (11.6%) patients. Occlusion was identified clinically, radiologically, and endoscopically. We reimplanted covered stents in those who had tumor ingrowth or overgrowth.

Survival and stent patency

The mean follow-up period for the patients was 145 d (range, 4-718 d). The mean survival was 145 d (SD; ± 150.4 d) (Figure 1), and median stent patency time was 187 d (95% CI, 39-335) (Figure 2). The overall 30-d mortality was 10 of 53 patients (18.9%).

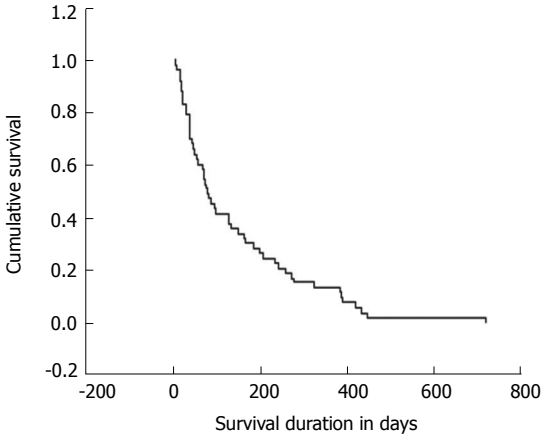

Figure 1 Survival curve of 53 patients with malignant gastric outlet obstruction caused by stomach cancer treated with SEMS.

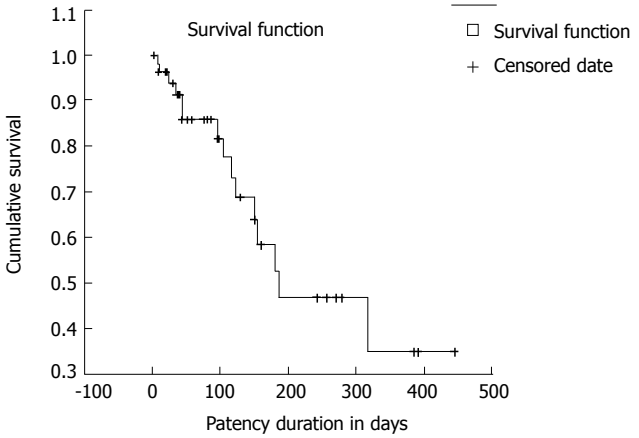

Figure 2 Survival curve showing the probability of stent patency among 53 patients with malignant gastric outlet obstruction caused by stomach cancer treated with SEMS.

DISCUSSION

Malignant gastric outlet obstruction is a distressing complication of gastric cancer that results in inexorable deterioration of patient quality of life. Although surgical palliation is an available option in such patients, the results of palliative gastric bypass surgery are poor with high rates of morbidity and mortality[6-8]. Because of the limitations of surgery and because many patients are elderly, frail, and in an advanced stage of disease, various techniques for restoration of bowel function by non-surgical means (eg, balloon dilation and laser photoablation) have been proposed; all have met with limited success[9,10].

Since the endoscopic application of SEMS to malignant gastric outlet obstruction in the early 1990s, the use of SEMS to pass through an obstructing neoplasm with minimal morbidity has become increasingly widespread. SEMS insertion becomes popular for treatment of malignant gastric outlet obstruction because it provides prolonged patency and simple, safe, and effective palliation in these patients.

However, the results of previous studies suggested limitations in stent patency and overall survival; these studies included heterogeneous patient groups with different causes of gastric outlet obstruction or using different types of stents. To explore the effect and complications of pyloric stents in patients with stomach cancer, we excluded patients with gastric outlet obstruction resulting from other types of cancer. To date, this is the first and largest study of endoscopic stenting for malignant gastric outlet obstruction

resulting from stomach cancer only.

The results of the present study are similar or superior to those of prior published studies of enteral stent insertion for malignant gastric outlet obstruction with respect to technical success[11-15]. When we had difficulties performing the procedure, we modified the stenting technique, including using a more hydrophilic Terumo guidewire, stiffer guidewire, or a therapeutic duodenoscope; these modifications helped us overcome difficulties and achieve successful stenting. In our study, enteral stent placement allowed 81.1% of patients to resume an oral diet, an outcome similar to that reported in other studies[11,12,14-16]. The complications related to stent insertion in the present study are less than those noted in previous studies[12-14].

Restenosis by tumor ingrowth is the most common problem of uncovered stents, and some studies describe the use of covered stents to prevent this complication. Despite their ability to prevent tumor ingrowth, covered stents have been reported to migrate more often (more than 20%) than uncovered stents[17,18]. Stent migration could cause bleeding, perforation, or obstruction and require operation. Recently, a new double-layered combination stent (outer uncovered and inner covered dual stent, a Combi pyloric stent) was developed to prevent tumor ingrowth and migration and prolong stent patency in patients with gastric outlet obstruction. More data are needed to confirm the above results. Based on these results, we used uncovered stents initially. Recurrent stenosis of the stent because of progressive tumor ingrowth was a problem because most of the stents used were uncovered. Tumor ingrowth occurred in 14 (26.4%) patients at a mean of 78.4 d in our study. Overall recurrent stenosis rates of 8%-46% at an interval of 2-21 wk (mean, 7.5 wk) have been reported in other studies[14,15,19-24]. It is difficult to compare our results with results of other studies because other reports included patients with a variety of cancers. Early restenosis within 4 wk after stenting occurred in 5 (11.6%) patients in the current study. This result is similar to our previous result (14.3% for total gastric outlet obstruction patients and 10% for stomach cancer patients) and lower than our results for patients with recurrent malignant obstruction after gastric surgery (60%, unpublished data). Obstruction by tumor ingrowth usually is managed with placement of additional covered stents through the original stent.

Stent patency is influenced partly by tumor ingrowth and survival, which are also influenced by disease type. Survival is influenced by underlying diseases also. Our results of mean patient survival time and median stent patency time are somewhat longer than previously reported results[2,5,13-15], however, as stated, comparisons are difficult because ours is the sole report addressing gastric outlet obstruction resulting from stomach cancer only. Thus, the reason for these differences is not clear, but the primary illnesses that caused the gastric outlet obstruction can be the most important factor. In most western reports, the most common primary illness related to gastric outlet obstruction is pancreatic cancer, and most gastric outlet obstruction develops in the terminal stage in patients with pancreatic or biliary cancer. While in our report, stomach cancer was the sole primary disease. When compared with surgical palliation, endoscopic stenting decreases the length of hospital stay and improves survival and oral intake.

All published series on SEMS in the upper gastrointestinal tract are retrospective. The studies all differ in stent types used, and the populations differ with regard to the demographic characteristics and etiologic causes of the upper GI obstruction. There are no exact criteria regarding the selection of an uncovered stent versus a covered stent; studies are retrospective with varying definitions of complications; and a variety of stent types and insertion methods are used. Although our study is also retrospective with several similar limitations, it includes a more homogeneous patient group compared to previous studies.

In conclusion, SEMS placement is a safe and effective treatment for the palliation of patients with inoperable malignant gastric outlet obstruction caused by stomach cancer. Therefore, it should be considered as the primary choice over palliative resection for the palliation of obstruction in such patients.

REFERENCES

1 **Baron TH**. Expandable metal stents for the treatment of cancerous obstruction of the gastrointestinal tract. *N Engl J Med* 2001; **344**: 1681-1687

2 **Baron TH**, Harewood GC. Enteral self-expandable stents. *Gastrointest Endosc* 2003; **58**: 421-433

3 **Maetani I**, Tada T, Ukita T, Inoue H, Sakai Y, Nagao J. Comparison of duodenal stent placement with surgical gastrojejunostomy for palliation in patients with duodenal obstructions caused by pancreaticobiliary malignancies. *Endoscopy* 2004; **36**: 73-78

4 **Wong YT**, Brams DM, Munson L, Sanders L, Heiss F, Chase M, Birkett DH. Gastric outlet obstruction secondary to pancreatic cancer: surgical vs endoscopic palliation. *Surg Endosc* 2002; **16**: 310-312

5 **Yim HB**, Jacobson BC, Saltzman JR, Johannes RS, Bounds BC, Lee JH, Shields SJ, Ruymann FW, Van Dam J, Carr-Locke DL. Clinical outcome of the use of enteral stents for palliation of patients with malignant upper GI obstruction. *Gastrointest Endosc* 2001; **53**: 329-332

6 **Monson JR**, Donohue JH, McIlrath DC, Farnell MB, Ilstrup DM. Total gastrectomy for advanced cancer. A worthwhile palliative procedure. *Cancer* 1991; **68**: 1863-1868

7 **Smith JW**, Brennan MF. Surgical treatment of gastric cancer. Proximal, mid, and distal stomach. *Surg Clin North Am* 1992; **72**: 381-399

8 **Lillemoe KD**, Barnes SA. Surgical palliation of unresectable pancreatic carcinoma. *Surg Clin North Am* 1995; **75**: 953-968

9 **Moses FM**, Peura DA, Wong RK, Johnson LF. Palliative dilation of esophageal carcinoma. *Gastrointest Endosc* 1985; **31**: 61-63

10 **Suzuki H**, Miho O, Watanabe Y, Kohyama M, Nagao F. Endoscopic laser therapy in the curative and palliative treatment of upper gastrointestinal cancer. *World J Surg* 1989; **13**: 158-164

11 **Kim JH**, Yoo BM, Lee KJ, Hahm KB, Cho SW, Park JJ, Kim SS, Park HC, Kim JH. Self-expanding coil stent with a long delivery system for palliation of unresectable malignant gastric outlet obstruction: a prospective study. *Endoscopy* 2001; **33**: 838-842

12 **Maetani I**, Tada T, Shimura J, Ukita T, Inoue H, Igarashi Y, Hoshi H, Sakai Y. Technical modifications and strategies for stenting gastric outlet strictures using esophageal endoprostheses. *Endoscopy* 2002; **34**: 402-406

13 **Nassif T**, Prat F, Meduri B, Fritsch J, Choury AD, Dumont JL, Auroux J, Desaint B, Boboc B, Ponsot P, Cervoni JP. Endoscopic palliation of malignant gastric outlet obstruction

using self-expandable metallic stents: results of a multicenter study. *Endoscopy* 2003; **35**: 483-489

14 **Telford JJ**, Carr-Locke DL, Baron TH, Tringali A, Parsons WG, Gabbrielli A, Costamagna G. Palliation of patients with malignant gastric outlet obstruction with the enteral Wallstent: outcomes from a multicenter study. *Gastrointest Endosc* 2004; **60**: 916-920

15 **Kim GH**, Kang DH, Lee DH, Heo J, Song GA, Cho M, Yang US. Which types of stent, uncovered or covered, should be used in gastric outlet obstructions? *Scand J Gastroenterol* 2004; **39**: 1010-1014

16 **Jung GS**, Song HY, Seo TS, Park SJ, Koo JY, Huh JD, Cho YD. Malignant gastric outlet obstructions: treatment by means of coaxial placement of uncovered and covered expandable nitinol stents. *J Vasc Interv Radiol* 2002; **13**: 275-283

17 **Jung GS**, Song HY, Kang SG, Huh JD, Park SJ, Koo JY, Cho YD. Malignant gastroduodenal obstructions: treatment by means of a covered expandable metallic stent-initial experience. *Radiology* 2000; **216**: 758-763

18 **Park KB**, Do YS, Kang WK, Choo SW, Han YH, Suh SW, Lee SJ, Park KS, Choo IW. Malignant obstruction of gastric outlet and duodenum: palliation with flexible covered metallic stents. *Radiology* 2001; **219**: 679-683

19 **Feretis C**, Benakis P, Dimopoulos C, Georgopoulos K, Milas F, Manouras A, Apostolidis N. Palliation of malignant gastric outlet obstruction with self-expanding metal stents. *Endoscopy* 1996; **28**: 225-228

20 **Pinto IT**. Malignant gastric and duodenal stenosis: palliation by peroral implantation of a self-expanding metallic stent. *Cardiovasc Intervent Radiol* 1997; **20**: 431-434

21 **Bethge N**, Breitkreutz C, Vakil N. Metal stents for the palliation of inoperable upper gastrointestinal stenoses. *Am J Gastroenterol* 1998; **93**: 643-645

22 **Nevitt AW**, Vida F, Kozarek RA, Traverso LW, Raltz SL. Expandable metallic prostheses for malignant obstructions of gastric outlet and proximal small bowel. *Gastrointest Endosc* 1998; **47**: 271-276

23 **Yates MR**, Morgan DE, Baron TH. Palliation of malignant gastric and small intestinal strictures with self-expandable metal stents. *Endoscopy* 1998; **30**: 266-272

24 **Soetikno RM**, Lichtenstein DR, Vandervoort J, Wong RC, Roston AD, Slivka A, Montes H, Carr-Locke DL. Palliation of malignant gastric outlet obstruction using an endoscopically placed Wallstent. *Gastrointest Endosc* 1998; **47**: 267-270

S- Editor Liu Y **L- Editor** Zhu LH **E- Editor** Ma WH

PO Box 2345, Beijing 100023, China
www.wjgnet.com
wjg@wjgnet.com

World J Gastroenterol 2007 February 14; 13(6): 921-924
World Journal of Gastroenterology ISSN 1007-9327

RAPID COMMUNICATION

Clinical considerations and therapeutic strategy for sigmoid volvulus in the elderly: A study of 33 cases

Michael Safioleas, Constantinos Chatziconstantinou, Evangelos Felekouras, Michael Stamatakos, Ioannis Papaconstantinou, Anastasios Smirnis, Panagiotis Safioleas, Alkiviades Kostakis

Michael Safioleas, Michael Stamatakos, Anastasios Smirnis, Panagiotis Safioleas, Alkiviades Kostakis, 2nd Department of Propedeutic Surgery, School of Medicine, Athens University, Laiko Hospital, Greece
Constantinos Chatziconstantinou, Department of Radiology, Laiko Hospital, Athens, Greece
Evangelos Felekouras, Ioannis Papaconstantinou, 1st Department of Surgery, School of Medicine, Athens University, Laiko Hospital, Greece
Correspondence to: Professor Michael Safioleas, MD, PhD, 2nd Department of Propedeutic Surgery, School of Medicine, Athens University, Laiko Hospital, 7 Kyprou Ave, Filothei, Athens 15237, Greece. stamatakosmih@yahoo.gr
Telephone: +30-210-6812188
Received: 2006-10-18 Accepted: 2006-12-25

Abstract

AIM: To evaluate different types of treatment for sigmoid volvulus and clarify the role of endoscopic intervention versus surgery.

METHODS: A retrospective review of the clinical presentation and imaging characteristics of 33 sigmoid volvulus patients was presented, as well as their diagnosis and treatment, in combination with a literature review.

RESULTS: In 26 patients endoscopic detorsion was achieved after the first attempt and one patient died because of uncontrollable sepsis despite prompt operative treatment. Seven patients had unsuccessful endoscopic derotation and were operated on. On two patients with gangrenous sigmoid, Hartmann's procedure was performed. In five patients with viable colon, a sigmoid resection and primary anastomosis was carried out. Three patients had a lavage "on table" prior to anastomosis, while in the remaining 2 patients a diverting stoma was performed according to the procedure of the first author. Ten patients were operated on during their first hospital stay (3 to 8 d after the deflation). All patients had viable colon; 7 patients had a sigmoid resection and primary anastomosis, 2 patients had sigmoidopexy and one patient underwent a near-total colectomy. Two patients (sigmoidectomy-sigmoidopexy) had recurrences of volvulus 43 and 28 mo after the initial surgery. Among 15 patients who were discharged from the hospital after non-operative deflation, 3 patients were lost to follow-up. Of the remaining 12 patients, 5 had a recurrence of volvulus at a time in between 23 d and 14 mo. All the five patients had been operated on and in four a gangrenous sigmoid was found. Three patients died during the 30 d postoperative course. The remaining seven patients were admitted to our department for elective surgery. In these patients, 2 subtotal colectomies, 3 sigmoid resections and 2 sigmoidopexies were carried out. One patient with subtotal colectomy died. Taken together of the results, it is evident that after 17 elective operations we had only one death (5.9%), whereas after 15 emergency operations 6 patients died, which means a mortality rate of 40%.

CONCLUSION: Although sigmoid volvulus causing intestinal obstruction is frequently successfully encountered by endoscopic decompression, however, the principal therapy of this condition is surgery. Only occasionally in patients with advanced age, lack of bowel symptoms and multiple co-morbidities might surgical repair not be considered.

Key words: Volvulus; Celiotomy; Large bowel obstruction; Decompression; Sigmoidectomy

Safioleas M, Chatziconstantinou C, Felekouras E, Stamatakos M, Papaconstantinou I, Smirnis A, Safioleas P, Kostakis A. Clinical considerations and therapeutic strategy for sigmoid volvulus in the elderly: A study of 33 cases. *World J Gastroenterol* 2007; 13(6): 921-924

http://www.wjgnet.com/1007-9327/13/921.asp

INTRODUCTION

Although sigmoid volvulus is uncommon in Western Europe, it nevertheless constitutes the third leading cause of large bowel obstruction in adults[1]. The main predisposing factor to sigmoid volvulus is a long, redundant sigmoid colon with an elongated mesentery, which is prone to twisting on itself. Sigmoid volvulus is an abdominal emergency occurring more commonly in the elderly, particularly in individuals with dementia or a psychiatric illness[1,2] and has a high mortality rate up to 50% in each episode[3]. In elderly patients who have no

signs of peritonitis or bowel gangrene an initial attempt with non-operative reduction is justified. After a successful non-operative reduction, an elective resection of the sigmoid colon is recommended as the risks of elective surgery are less compared with those associated with recurrent volvulus. We report the results of a series of 33 adult patients with a mean follow-up of 4.5 year (range 2-18 year) supporting this assumption.

MATERIALS AND METHODS

In the period of 1984-2003, 33 patients (18 males and 15 females) ranging in age between 58 and 89 year, were treated for sigmoid volvulus at the 2nd Department of Propaedeutic Surgery, Medical School, Athens University, Laiko General Hospital in Greece. The hospital records of these thirty three patients were retrospectively reviewed. All patients were admitted to our department on an emergency basis due to abdominal pain, vomiting and abdominal distention. Among these patients, 7 were institutionalized. Abdominal radiographs and CT scans were indicative of sigmoid volvulus (Figures 1 and 2), showing marked bowel dilatation and fluid levels, while the outline of twisted loop was evident.

RESULTS

All patients were actively resuscitated by means of nasogastric suction and correction of fluid-electrolyte imbalance, while broad-spectrum antibiotics were started immediately after admission. Subsequently, all patients, without signs of peritonitis, underwent sigmoidoscopy post bowel preparation with edema. In 26 patients detorsion was achieved after the first attempt. However, one patient developed septic peritonitis four days after detorsion and even though he was immediately operated on, he passed away.

Seven patients had unsuccessful endoscopic derotation and were operated on within 48 h after their admission. In two patients with gangrenous sigmoid, Hartmann's procedure was performed, however, one patient died. In five patients with viable colon, sigmoid resection and primary anastomosis were carried out (Figure 3). Three patients had a lavage "on table" prior to anastomosis, while in the remaining 2 patients a diverting stoma according to the technique of the first author (MS) was used (Figure 4).

Ten patients were operated on during their first hospital stay (3 to 8 d after the deflation). All patients had viable colon; 7 patients had a sigmoid resection and primary anastomosis, 2 patients had sigmoidopexy and one patient underwent a near-total colectomy. Two patients (sigmoidectomy-sigmoidopexy) had recurrences of volvulus 43 and 28 mo after the initial surgery. Among 15 patients who were discharged from the hospital after the non-operative deflation, 3 patients were lost to follow-up. Of the remaining 12 patients, 5 had a recurrence of volvulus at a time in between 23 d and 14 mo. All the five patients had been operated on and in four a gangrenous sigmoid was found. Three patients died during the 30 d postoperative course. The remaining seven patients were admitted to our department for elective surgery. In these

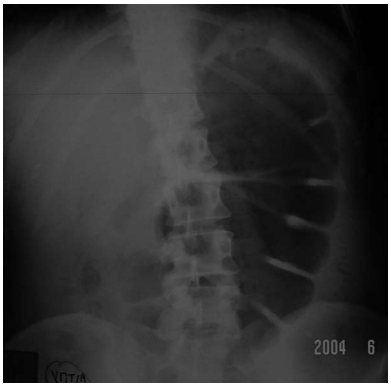

Figure 1 Plain abdominal film showing sigmoid volvulus.

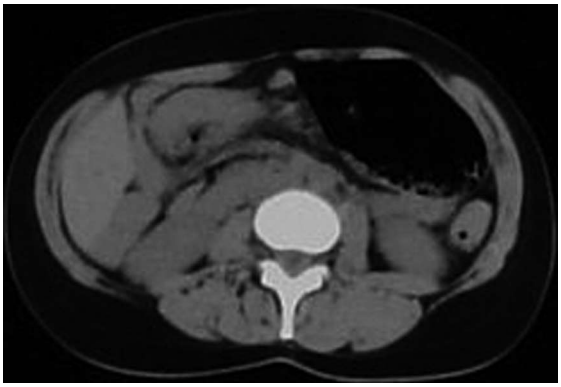

Figure 2 CT scan showing dilated colon due to its torsion.

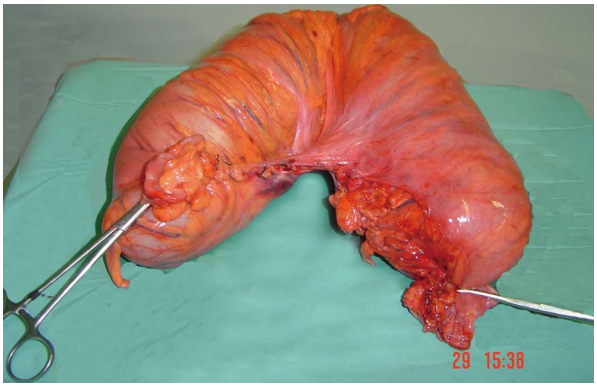

Figure 3 Surgical specimen of sigmoid volvulus showing the distention of the bowel.

patients, 2 subtotal colectomies, 3 sigmoid resections and 2 sigmoidopexies were carried out. One patient with subtotal colectomy died. Taken together of the results, it is evident that after 17 elective operations we had only one death (mortality rate: 5.9%), whereas after 15 emergency operations 6 patients died (mortality rate: 40%). In Figure 5 the course of 33 patients is schematically depicted.

DISCUSSION

Sigmoid volvulus is the most common cause of strangulation of the colon and is also the cause for 1% to 7% of all intestinal obstructions in Western countries[4]. Many patients with sigmoid volvulus have clinical findings

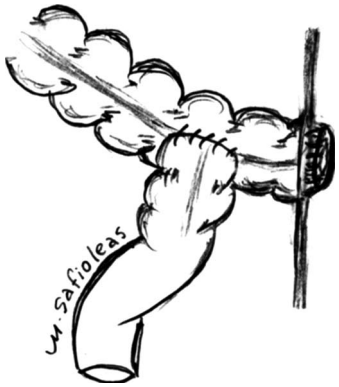

Figure 4 Schematic representation of the procedure described by Michael Safioleas, i.e. Sigmoidectomy, primary anastomosis and diverting stoma. The technique is introduced in International Journal of Colorectal Disease 2006 vol: 21.

indicating a disorder of bowel movement[5,6], such as constipation and abdominal distention long before the development of a sigmoid volvulus. Some researchers have claimed that sigmoid volvulus might be one of the disorders allied with Hirschsprung's disease[7]. It is also a fact that patients undergoing sigmoidectomy for sigmoid volvulus frequently suffer from elongation and dilatation of the remaining colon and some even require surgery for revolvulus[8]. The disease is rare in children[9]; however, if it occurs, it may result in acute intestinal obstruction, unlike in adults where the obstruction may be subacute and progressive[10]. In our series 19 patients had a history of undetermined abdominal pain during the period of 3 to 9 mo. Moreover, besides chronic constipation and despite the use of laxatives[2,11], other risk factors that predispose to sigmoid volvulus are considered as follows: (1) a course with high fiber diet, (2) pregnancy, (3) pelvic tumors or cysts, (4) previous abdominal surgery. Concerning the last factor, the presence of a band attaching the sigmoid colon to the abdominal wall can act as an axis for volvulus. Furthermore, it is supposed that the loss of ganglion cells is only a consequence, not a cause, since the exact cause leading to sigmoid volvulus is not clear[12].

All these conditions may produce a large, redundant sigmoid colon, in association with mesocolon, long and narrow at its parietal attachment, resulting in the two ends of the loop being close together, under which condition, the bowel is capable of becoming torted around its central mesenteric axis.

Although sigmoid volvulus has been well studied for many decades, its treatment appears to be still evolving[3]; however, over the past two decades, resection and primary anastomosis has emerged as the preferable treatment for this disease[13]. Whether endoscopic deflation is feasible to perform prior to surgery is an optimal choice. Unfortunately endoscopic detorsion is not always successful. In Western countries a 30% failure has been reported[14-16].

In our department, since 1995, we have always followed such a strategy. Initially, we attempt an endoscopic deflation and if it is unsuccessful we proceed to an emergency operation; while if detorsion has been achieved the operation is performed after 3 to 8 d by a semi-elective or elective way. In the majority of cases resection of the involved sigmoid colon is carried out, in which case primary anastomosis is the goal, either after "on table" lavage, or applying a diverting stroma[17].

In the presence of megacolon, a near-total colectomy

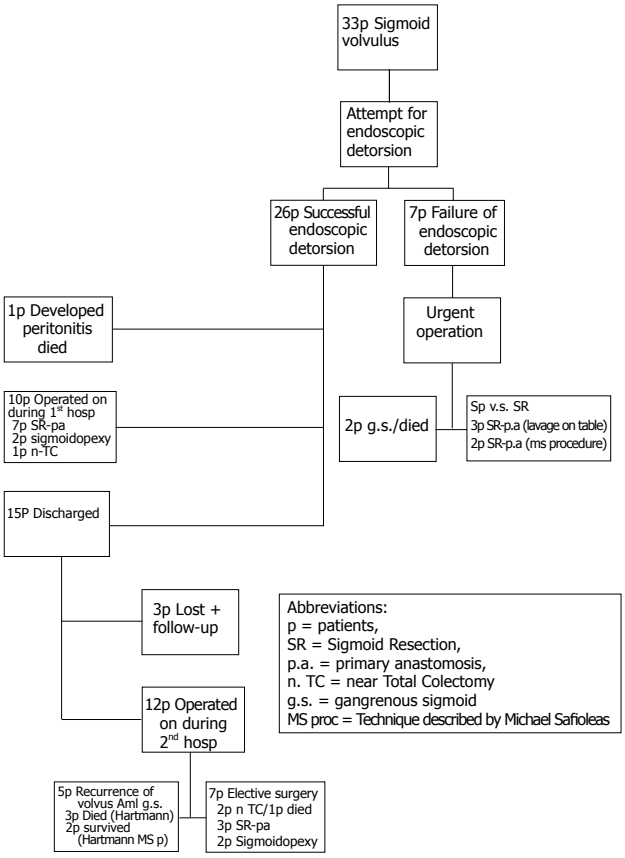

Figure 5 Schematic depiction of the course of 33 patients suffering from volvulus of the sigmoid colon and treated in our department.

is required. Furthermore, various procedures have been adopted for sigmoid volvulus in adult patients, such as mesosigmoidoplasty, sigmoidopexy, tube sigmoid colostomy or mesocoloplasty. In patients with sigmoid resection a recurrence is possible in approximately 25% to 35% cases[5,13,18]. The mortality rate ranges from 1% to 9% for viable colon[15,19], and 25% for gangrenous volvulus[15]. Colonic resection for non-gangrenous sigmoid volvulus has an acceptably low rate of complications, particularly when it is done as a semi-elective procedure, i.e., subsequent to endoscopic detorsion and deflation[20]. Finally, recurrent volvulus after resection has been reported at an incidence rate ranging from 24% to 33% of cases[5,18].

In conclusion, even though sigmoid volvulus causing intestinal obstruction is frequently encountered in endoscopic decompression, this condition should be definitely treated by surgery; and only occasionally in patients with advanced age, lack of bowel symptoms, having multiple co-morbidities might surgical repair not be considered.

REFERENCES

1 **Grossmann EM**, Longo WE, Stratton MD, Virgo KS, Johnson FE. Sigmoid volvulus in Department of Veterans Affairs Medical Centers. *Dis Colon Rectum* 2000; **43**: 414-418
2 **Dülger M**, Cantürk NZ, Utkan NZ, Gonullu NN. Management of sigmoid colon volvulus. *Hepatogastroenterology* 2000; **47**: 1280-1283
3 **Madiba TE**, Thomson SR. The management of sigmoid volvulus. *J R Coll Surg Edinb* 2000; **45**: 74-80

4 **Frizelle FA**, Wolff BG. Colonic volvulus. *Adv Surg* 1996; **29**: 131-139
5 **Morrissey TB**, Deitch EA. Recurrence of sigmoid volvulus after surgical intervention. *Am Surg* 1994; **60**: 329-331
6 **Strom PR**, Stone HH, Fabian TC. Colonic atony in association with sigmoid volvulus: its role in recurrence of obstructive symptoms. *South Med J* 1982; **75**: 933-936
7 **Tomita R**, Ikeda T, Fujisaki S, Tanjoh K, Munakata K. Hirschsprung's disease and its allied disorders in adults' histological and clinical studies. *Hepatogastroenterology* 2003; **50**: 1050-1053
8 **Furuya Y**, Yasuhara H, Yanagie H, Naka S, Takenoue T, Shinkawa H, Niwa H, Kikuchi T, Nagao T. Role of ganglion cells in sigmoid volvulus. *World J Surg* 2005; **29**: 88-91
9 **Campbell JR**, Blank E. Sigmoid volvulus in children. *Pediatrics* 1974; **53**: 702-705
10 **Hinshaw DB**, CARTER R. Surgical management of acute volvulus of the sigmoid colon; a study of 55 cases. *Ann Surg* 1957; **146**: 52-60
11 **Khanna AK**, Kumar P, Khanna R. Sigmoid volvulus: study from a north Indian hospital. *Dis Colon Rectum* 1999; **42**: 1081-1084
12 **Collure DW**, Hameer HR. Loss of ganglion cells and marked attenuation of bowel wall in cecal dilatation. *J Surg Res* 1996; **60**: 385-388
13 **Ballantyne GH**. Review of sigmoid volvulus: history and results of treatment. *Dis Colon Rectum* 1982; **25**: 494-501
14 **Sinha RS**. A clinical appraisal of volvulus of the pelvic colon with special reference to aetiology and treatment. *Br J Surg* 1969; **56**: 838-840
15 **Mishra SB**, Sahoo KP. Primary resection and anastomosis for volvulus of sigmoid colon. *J Indian Med Assoc* 1986; **84**: 265-268
16 **Faranisi CT**. An approach to the management of volvulus of the sigmoid colon. *Cent Afr J Med* 1990; **36**: 31-33
17 **Safioleas MC**, Moulakakis KG, Stamatakos MK. A new therapeutic surgical method in patients with left-sided colonic emergencies. *Int J Colorectal Dis* 2006; **21**: 186-187
18 **Chung YF**, Eu KW, Nyam DC, Leong AF, Ho YH, Seow-Choen F. Minimizing recurrence after sigmoid volvulus. *Br J Surg* 1999; **86**: 231-233
19 **De U**. Sigmoid volvulus in rural Bengal. *Trop Doct* 2002; **32**: 80-82
20 **Degiannis E**, Levy RD, Sliwa K, Hale MJ, Saadia R. Volvulus of the sigmoid colon at Baragwanath Hospital. *S Afr J Surg* 1996; **34**: 25-28

S- Editor Liu Y **L- Editor** Zhu LH **E- Editor** Lu W

PO Box 2345, Beijing 100023, China
www.wjgnet.com
wjg@wjgnet.com

World J Gastroenterol 2007 February 14; 13(6): 925-929
World Journal of Gastroenterology ISSN 1007-9327

RAPID COMMUNICATION

Validity and cost comparison of ^{14}carbon urea breath test for diagnosis of *H Pylori* in dyspeptic patients

Shahid Rasool, Shahab Abid, Wasim Jafri

Shahid Rasool, Shahab Abid, Wasim Jafri, Section of Gastroenterology, Department of Medicine, The Aga Khan University Hospital, Karachi, Pakistan.
Supported by University Research Council Grant, No. 041F431YC
Correspondence to: Dr. Shahab Abid, MBBS, FCPS, Associate Professor, Department of Medicine, Aga Khan University Hospital, Stadium Road, Karachi, Pakistan. shahab.abid@aku.edu
Telephone: +92-21-4864656 Fax: +92-21-4934294
Received: 2006-10-17 Accepted: 2006-12-22

Abstract

AIM: To validate and compare the cost of microdose ^{14}C urea breath test (UBT) with histology and rapid urease test for the diagnosis of *H Pylori*.

METHODS: Ninety-four consecutive patients with dyspeptic symptoms undergoing gastroscopy were enrolled. Gastric biopsies were taken for histology and rapid urease test. UBT was performed after gastroscopy by microdose ^{14}C urea capsules. Sensitivity, specificity and accuracy of UBT were calculated and compared with histology and rapid urease test. Cost comparison of these tests was also performed.

RESULTS: *H pylori* was diagnosed by histology and rapid urease test in 66 (70%) and 61 (65%) patients, while ^{14}C UBT detected infection in 63 (67%). Accuracy of UBT was 93% in comparison with histology while its positive and negative predictive values were 97% and 84%, respectively. Comparison of ^{14}C UBT with rapid urease test gives an accuracy of 96%, with positive and negative predictive values of 95% and 97%, respectively. These results were highly reproducible with a Kappa test (P value < 0.001). Cost of histology or rapid urease test with gastroscopy was 110 USD or 95 USD respectively while the cost of UBT was 15 USD.

CONCLUSION: Microdose ^{14}C UBT was comparable to histology and rapid urease test. ^{14}C UBT is an economical, self sufficient and suitable test to diagnose active *H pylori* infection in less developed countries.

Key words: *H pylori*; Microdose; ^{14}C urea breath test; Diagnosis; Reliable; Economical

Rasool S, Abid S, Jafri W. Validity and cost comparison of ^{14}carbon urea breath test for diagnosis of *H Pylori* in dyspeptic patients. *World J Gastroenterol* 2007; 13(6): 925-929

http://www.wjgnet.com/1007-9327/13/925.asp

INTRODUCTION

H Pylori is a gram negative, microaerophilic human pathogen which is prevalent worldwide. *H Pylori* infection causes gastritis and is associated with development of peptic ulcer disease, gastric carcinoma, lymphoma, micronutrient deficiencies and ischemic heart disease[1,2]. The International Agency for Research on Cancer classified *H Pylori* as group 1 carcinogen (a definite cause of cancer in humans)[3].

H Pylori can be diagnosed by invasive techniques requiring endoscopy and biopsy such as histology, tissue culture and detection of *H Pylori* by polymerase chain reaction. The non-invasive techniques for the diagnosis of *H Pylori* include serum *H Pylori* antibody titer, urea breath test (UBT) and *H Pylori* stool antigen test. A reliable, non-invasive and economical diagnosis is a best choice for the management of *H Pylori* in both test and treatment.

Among the non-invasive tests, UBT is supposed to be a gold standard test for the diagnosis of *H Pylori* infection. UBT is based on enzymatic hydrolysis of labeled urea in the stomach by urease, an enzyme produced in abundance by *H Pylori*. In the presence of *H Pylori* infection, urea is hydrolyzed to ammonia and carbon dioxide (CO_2). This labeled CO_2 is exhaled and measured for radioactivity. Bacteria other than *H Pylori* that produce urease in a small amount cannot survive in the gastric mucosa.

There are two types of UBT, ^{13}C UBT and ^{14}C UBT. The former is difficult to analyze because it requires sophisticated infrastructure such as a mass spectrometer, technical expertise and therefore costly while ^{14}C UBT is an easily available technique that uses ^{14}C urea capsules with a 5, 3 or 1 uCi dose. The microdose 1 uCi (Helicap) utilizes a very low dose of radiation[4,5]. Considering these facts, in 1997 the Nuclear Regulatory Commission permitted *in vivo* diagnostic use of capsules containing 1 uCi of ^{14}C urea without a license[6]. The equipment is small, portable and can be placed on a desktop. Microdose ^{14}C UBT is claimed to be a reliable and economical diagnostic test for *H Pylori* infection, which may be used even in remote areas with limited resources.

This prospective study was done to determine the validity and cost of microdose ^{14}C UBT in comparison with histology and rapid urease test for the diagnosis of *H Pylori*.

MATERIALS AND METHODS

All consecutive men and non-pregnant women with dyspeptic symptoms undergoing gastroscopy were considered for enrollment.

Dyspepsia was defined as the presence of one or more of the postprandial fullness, early satiation, or epigastric pain or burning for the last three months with symptom onset at least six months before diagnosis according to the latest Rome Ⅲ criteria[7].

Inclusion criteria

Patients of both genders with dyspepsia were 18-70 years in age. Patients with a history of recent intake of proton pump inhibitor and antibiotics were enrolled only if four weeks have passed since last systemic antibacterial or bismuth medication therapy and 1 wk since last use of proton pump inhibitor or H2-receptor antagonist.

Exclusion criteria

Pregnant women, patients who had gastric surgery, patients with a history of *H Pylori* eradication therapy in the past six months and patients with active gastrointestinal bleeding were excluded from the study.

Ethical clearance

Study protocol was approved by the institutional ethical review committee. Written informed consent was obtained from all patients before enrollment.

Endoscopy and biopsy sampling

After overnight fast, esophago-gastro-duodenoscopy was performed with Olympus or Pentax videoscope. Six biopsies were taken, three from antrum and other three from the body of stomach from each patient. Two biopsies, one from the antrum and the other from the body were used for rapid urease test and the other four (two from antrum and two from body) for histology.

Rapid urease test

Rapid urease test kit (Pronto Dry, Medical Instrument Corp., France) was used to detect the presence of *H Pylori* urease[8]. Result was read in 30 min and 1 h after sampling. The color change from yellow to pink was considered positive and no color change as a negative result. Results were interpreted by either endoscopist or his assistant who were blinded about the results of UBT and histology.

Histology

Four biopsy specimens (two from corpus and two from antrum) were processed separately for histological examination according to standard procedure. Hematoxylin and eosin (HE) and Giemsa staining was performed on these samples. Results were interpreted by a pathologist who was blinded about the results of UBT and rapid urease test. Pathologist commented on the active and chronic *H Pylori* infection based on the presence of *H Pylori* along with neutrophils, eosinophils, lymphocytes, lymphoid follicles, and intestinal metaplasia according to the classification by Genta RM *et al*[9].

^{14}C UBT

Patients swallowed 37 kBq (1 uCi) of an encapsulated form of ^{14}C-urea/citric acid composition (Helicap, Noster System AB Stockholm, Sweden) with water after endoscopy. Breath samples were collected with a special dry cartridge system (Heliprobe Breath Card, Noster System AB Stockholm, Sweden) after 10 min. Patients exhaled gently into the cartridge mouthpiece until the indicator membrane changed in color from orange to yellow. Breath card was inserted into a β-scintillation counter (Heliprobe-analyser, Noster System AB Stockholm, Sweden) and activity was counted for 250 s. This is a portable machine that can be placed on a desktop. Results were expressed both as counts per minute (HCPM) and as grade (0: not infected, CPM < 25; 1: equivocal, CPM 25-50; 2: infected, CPM > 50), which was suggested by the producer according to the counts obtained from the cartridges[10]. Grades 0 and 1 were considered negative for the detection of *H Pylori*.

Statistical analysis

The statistical package for social science SPSS (release 11.5, standard version, copyright © SPSS) was used for data analysis. The descriptive analysis was done for demographic features. Results were presented as mean ± SD in number (percentage).

Sensitivity, specificity, positive and negative predictive values of UBT with 95% confidence intervals were calculated against histology and rapid urease test. Kappa test was applied to check the reproducibility of the results. Cost comparison of these diagnostic methods was also performed.

RESULTS

Ninety-four consecutive patients with dyspeptic symptoms undergoing gastroscopy were enrolled for the validity of microdose ^{14}C UBT. There were 60 (64%) men and the mean age of study group was 40.8 ± 12.8 years. *H Pylori* infection was diagnosed by histology in 66 (70%) patients and by rapid urease test in 61 (65%) patients. UBT detected active *H Pylori* infection in 63 (67%) patients. Demographic characteristics of the patients and results of these diagnostic tests are summarized in Table 1.

^{14}C UBT vs histology

In comparison with histology, UBT has a sensitivity and specificity of 92% (95% CI: 87%-95%) and 93% (95% CI: 79%-99%), respectively. The positive predictive value (PPV) of ^{14}C UBT was found to be 97% (95% CI: 91%-99%) and negative predictive value (NPV) was 84% (95% CI: 72%-89%) compared with histology. These results show that UBT has an accuracy of 93% as compared with

Table 1 Patient demographics and results of *H Pylori* detection by various tests (n = 94), mean ± SD

Parameters	n (%)
Gender	
Male	60 (64)
Female	34 (36)
Age (yr)	40.8 + 12.8
Histopathology	
Positive	66 (70)
Negative	28 (30)
UBT	
Positive	63 (67)
Negative	31 (33)
Rapid urease test	
Positive	61 (65)
Negative	33 (35)

histology. Kappa test result was 0.805 with P value < 0.001, indicating that these results were reproducible (Table 2).

^{14}C UBT vs rapid urease test

In comparison of UBT and rapid urease test, the sensitivity and specificity of UBT were 98% (95% CI: 93%-99%) and 91% (95% CI: 80%-94%). The PPV and NPV were 95% (95% CI: 89%-97%) and 97% (95% CI: 86%-99%), respectively. UBT has an accuracy of 96% in comparison with rapid urease test. Result of Kappa test was 0.881 ($P \leqslant 0.001$) which showed a good response (Table 2).

Four patients with histological evidence of *H Pylori* infection had negative results with UBT and rapid urease test. The discordant results between histology, UBT and rapid urease test are shown in Table 3.

Cost analysis

At the time of this study, the cost of gastroscopy was 90 USD while the cost of histology and rapid urease test was 20 USD and 5 USD in our institute. Therefore, the overall cost of *H Pylori* diagnosis by histology was 110 USD and 95 USD by rapid urease test. The cost of UBT was only 15 USD in our institute.

DISCUSSION

Current guidelines for the management of *H Pylori* infection recommend eradication treatment without performing endoscopy in patients under 45 years of age who have no remarkable symptoms[11-13]. The use of non-invasive tests has been advocated in different strategies for management of dyspeptic patients in the primary care based on clinical and economical analyses[14,15].

Invasive diagnostic tests for *H Pylori* diagnosis need gastroscopy that requires sedation and monitoring during the procedure by trained staff and expertise. These diagnostic tests are costly and require an established healthcare infrastructure.

In practical terms, invasive tests for the diagnosis of *H Pylori* are not feasible, especially in less developed countries. An economical, reliable and office based diagnostic test is therefore, more appropriate in settings of

Table 2 Sensitivity and specificity of ^{14}C UBT against histopathology and rapid urease test for *H Pylori* diagnosis (n = 94)

UBT compared to:	Sensitivity (95% CI)	Specificity (95% CI)	PPV (95% CI)	NPV (95% CI)	Accuracy
Histopathology	92% (87-95)	93% (79-99)	97% (91-99)	84% (72-89)	93%
Rapid urease test	98% (93-99)	91% (80-94)	95% (89-97)	97% (86-99)	96%

UBT: urea breath test; PPV: positive predictive value; NPV: negative predictive value; CI: confidence interval.

Table 3 Discordant results between histopathology, ^{14}C UBT and rapid urease test for *H Pylori* diagnosis (n = 94)

Groups	Patients (n)	Histopathology	UBT	RUT
Group 1	59	+	+	+
	2	+	+	-
	1	+	-	+
	4	+	-	-
Group 2	1	-	+	+
	1	-	+	-
	26	-	-	-

UBT: urea breath test; RUT: rapid urease test; +: positive; -: negative.

under privileged and cost constraint societies.

Other factors that determine choice of diagnostic tests apart from accuracy, in primary care setting include the availability of test, ease to perform, cost, self-sufficiency and acceptance by the patients. Present study has shown that microdose ^{14}C UBT has all these features.

Our study has demonstrated a high accuracy of microdose ^{14}C UBT for the detection of *H Pylori* infection comparable to histological diagnosis of *H Pylori*. The results of present study are comparable to other studies, with a sensitivity and specificity of more than 90% for the diagnosis of *H pylori* infection[16-18].

The sensitivity and specificity of ^{14}C UBT were 98% and 91% while PPV and NVP were 95% and 97% respectively, compared with rapid urease test. The overall accuracy was 96%. These results are similar to another study that found a 93% sensitivity, 96% specificity and 95% accuracy in comparison with rapid urease test[19]. Moreover, studies using a combination of histopathology and rapid urease test as a gold standard has also reported a comparable sensitivity and specificity of ^{14}C UBT above 90%[20,21].

H Pylori Stool Antigen (HpSA) test is a promising non-invasive test. This test seems to be equivalent to the UBT in terms of its yield of diagnosing *H Pylori*[22]. However, collection of stools may be a disagreeable task for many patients and it is difficult to manage in office based settings. *H Pylori* serum antibody test is another non-invasive test. It has a low sensitivity and specificity and it does not indicate active *H Pylori* infection because antibody titers can remain high for a long period despite adequate treatment[23]. It is one of the best tests for estimation of sero-prevalence of *H Pylori*, unfortunately it is not an ideal

test for the diagnosis of active *H Pylori* infection.

It has been shown that UBT becomes false negative during treatment with proton pump inhibitors and H-2 blockers[24,25]. However, it has been observed recently that addition of citric acid in the urea capsule may diminish the negative effect of acid inhibitory drugs on the accuracy of ^{14}C UBT[26]. Although we used an acidified ^{14}C urea capsule (Helicap), we preferred to discontinue anti-acid medications for at least seven days before the test. Controversies exist regarding the best diagnostic test for *H Pylori* among patients with active upper GI bleeding. ^{13}C UBT was found better than histology and rapid urease test by a few studies in patients with active upper GI bleeding[27,28]. However, validity of ^{14}C UBT in patients with active upper GI bleeding has never been assessed.

Concerns about the radiation hazard can be raised against ^{14}C UBT. However, it has been found in practice that by using microdose ^{14}C UBT, only a small amount of isotope was used and the test actually entailed low radiation exposure (3 mSv)[29,30].

Nearly the entire ingested isotope is rapidly excreted in urine or breath within 72 h. Recently safety of microdose ^{14}C UBT has been established even in young children[31].

In conclusion, microdose ^{14}C UBT is a highly sensitive and specific non-invasive test comparable to the invasive methods such as histology and rapid urease test used for *H Pylori* diagnosis. This test requires no sophisticated infrastructure. ^{14}C UBT is self-sufficient and easy to perform with readily available results. In our opinion, this is one of the best options for detection of *H Pylori* infection in office based settings, especially in less developed countries.

ACKNOWLEDGMENTS

The authors want to thank Mr. Mohammad Islam for his statistical advice and Ms. Rozina Wasaya for her support in endoscopy.

COMMENTS

Background

H pylori is one of the most prevalent infection organisms, especially in low socio-economic societies. It is associated with intestinal and extra-intestinal manifestations including malignancy. There is a need to establish cost-effective eradication strategies especially in less developed countries.

Research frontiers

Microdose ^{14}C Urea Breath Test (UBT) is carried out without the use of sophisticated equipment and specialized trained personnel. There is a need to compare the diagnostic usefulness of ^{14}C UBT with other diagnostic modalities such as histopathology and rapid urease test for *H pylori* detection. This comparison will help establish the value of ^{14}C UBT in resource constraint settings.

Innovations and breakthrough

^{14}C UBT is not a commonly used diagnostic method and there are only few studies about the accuracy of ^{14}C UBT for *H pylori* diagnosis. This study concluded that the sensitivity and specificity of microdose ^{14}C UBT is comparable to mostly used invasive diagnostic tests, such as histopathology and rapid urease test.

Application

Microdose ^{14}C UBT may be utilized for the non-invasive diagnosis of *H pylori* especially in the areas lacking an established health care structure. It can be used in accordance with the "test and treatment" policy in patients with dyspepsia without remarkable features.

Terminology

Dyspepsia is defined as the presence of one or more symptoms of the postprandial fullness, early satiation, epigastric pain or burning for the past three months with symptom onset at least six months before the diagnosis according to the latest Rome Ⅲ criteria. ^{14}C UBT is available in 5, 3 and 1 uCi dose. The microdose 1 uCi (Helicap) utilizes a very low dose of radiation.

Peer review

This is an interesting paper which addresses an important issue in the diagnosis of *H pylori* infection. Authors reported that the microdose ^{14}C UBT is a simple, less expensive and accurate test to diagnose *H pylori* infection. The paper is well written and conclusions are supported by results.

REFERENCES

1 **Fennerty MB**. Helicobacter pylori: why it still matters in 2005. *Cleve Clin J Med* 2005; **72** Suppl 2: S1-S7; discussion S14-S21
2 **Zhang C**, Yamada N, Wu YL, Wen M, Matsuhisa T, Matsukura N. Helicobacter pylori infection, glandular atrophy and intestinal metaplasia in superficial gastritis, gastric erosion, erosive gastritis, gastric ulcer and early gastric cancer. *World J Gastroenterol* 2005; **11**: 791-796
3 **Schistosomes, liver flukes and Helicobacter pylori**. IARC Working Group on the Evaluation of Carcinogenic Risks to Humans. Lyon, 7-14 June 1994. *IARC Monogr Eval Carcinog Risks Hum* 1994; **61**: 1-241
4 **Hamlet AK**, Erlandsson KI, Olbe L, Svennerholm AM, Backman VE, Pettersson AB. A simple, rapid, and highly reliable capsule-based 14C urea breath test for diagnosis of Helicobacter pylori infection. *Scand J Gastroenterol* 1995; **30**: 1058-1063
5 **Bielański W**, Konturek SJ, Dobrzańska MJ, Pytko-Polończyk J, Sito E, Marshall BJ. Microdose 14C-urea breath test in detection of Helicobacter pylori. *J Physiol Pharmacol* 1996; **47**: 91-100
6 **Radioactive drug: capsules containing carbon-14 urea for "in vivo" diagnostic use for humans**. USA: Nuclear Radioactive Committee, 1998: 10 CFR §30.21
7 **Tack J**, Talley NJ, Camilleri M, Holtmann G, Hu P, Malagelada JR, Stanghellini V. Functional gastroduodenal disorders. *Gastroenterology* 2006; **130**: 1466-1479
8 **Marshall BJ**, Warren JR, Francis GJ, Langton SR, Goodwin CS, Blincow ED. Rapid urease test in the management of Campylobacter pyloridis-associated gastritis. *Am J Gastroenterol* 1987; **82**: 200-210
9 **Genta RM**, Lew GM, Graham DY. Changes in the gastric mucosa following eradication of Helicobacter pylori. *Mod Pathol* 1993; **6**: 281-289
10 **Hegedus O**, Rydén J, Rehnberg AS, Nilsson S, Hellström PM. Validated accuracy of a novel urea breath test for rapid Helicobacter pylori detection and in-office analysis. *Eur J Gastroenterol Hepatol* 2002; **14**: 513-520
11 **Current European concepts in the management of Helicobacter pylori infection**. The Maastricht Consensus Report. European Helicobacter Pylori Study Group. *Gut* 1997; **41**: 8-13
12 **The report of the Digestive Health InitiativeSM International Update Conference on Helicobacter pylori**. *Gastroenterology* 1997; **113**: S4-S8
13 **Lam SK**, Talley NJ. Report of the 1997 Asia Pacific Consensus Conference on the management of Helicobacter pylori infection. *J Gastroenterol Hepatol* 1998; **13**: 1-12
14 **Pathak CM**, Bhasin DK, Khanduja KL. Urea breath test for Helicobacter pylori detection: present status. *Trop Gastroenterol* 2004; **25**: 156-161
15 **McColl KE**, Murray LS, Gillen D, Walker A, Wirz A, Fletcher J, Mowat C, Henry E, Kelman A, Dickson A. Randomised trial of endoscopy with testing for Helicobacter pylori compared with non-invasive H pylori testing alone in the management of dyspepsia. *BMJ* 2002; **324**: 999-1002

16 **Oztürk E**, Yeşilova Z, Ilgan S, Arslan N, Erdil A, Celasun B, Ozgüven M, Dağalp K, Ovali O, Bayhan H. A new, practical, low-dose 14C-urea breath test for the diagnosis of Helicobacter pylori infection: clinical validation and comparison with the standard method. *Eur J Nucl Med Mol Imaging* 2003; **30**: 1457-1462
17 **Peura DA**, Pambianco DJ, Dye KR, Lind C, Frierson HF, Hoffman SR, Combs MJ, Guilfoyle E, Marshall BJ. Microdose 14C-urea breath test offers diagnosis of Helicobacter pylori in 10 minutes. *Am J Gastroenterol* 1996; **91**: 233-238
18 **Faigel DO**, Childs M, Furth EE, Alavi A, Metz DC. New noninvasive tests for Helicobacter pylori gastritis. Comparison with tissue-based gold standard. *Dig Dis Sci* 1996; **41**: 740-748
19 **Tewari V**, Nath G, Gupta H, Dixit VK, Jain AK. 14C-urea breath test for assessment of gastric Helicobacter pylori colonization and eradication. *Indian J Gastroenterol* 2001; **20**: 140-143
20 **Gomes AT**, Coelho LK, Secaf M, Módena JL, Troncon LE, Oliveira RB. Accuracy of the 14C-urea breath test for the diagnosis of Helicobacter pylori. *Sao Paulo Med J* 2002; **120**: 68-71
21 **Artiko VM**, Obradović VB, Petrović NS, Davidović BM, Grujić-Adanja GS, Nastić-Mirić DR, Milosavlijević TN. 14C-urea breath test in the detection of Helicobacter pylori infection. *Nucl Med Rev Cent East Eur* 2001; **4**: 101-103
22 **Roth DE**, Taylor DN, Gilman RH, Meza R, Katz U, Bautista C, Cabrera L, Velapatiño B, Lebron C, Razúri M, Watanabe J, Monath T. Posttreatment follow-up of Helicobacter pylori infection using a stool antigen immunoassay. *Clin Diagn Lab Immunol* 2001; **8**: 718-723
23 **Fauchãre JL**. Evaluation of the anti- Helicobacter pylori serum antibody response. In: Lee A, Mégraud F, editors. Helicobacter pylori: techniques for clinical diagnosis and basic research. 2 ed. London Saunders, 1996: 33-45
24 **Graham DY**, Opekun AR, Hammoud F, Yamaoka Y, Reddy R, Osato MS, El-Zimaity HM. Studies regarding the mechanism of false negative urea breath tests with proton pump inhibitors. *Am J Gastroenterol* 2003; **98**: 1005-1009
25 **Graham DY**, Opekun AR, Jogi M, Yamaoka Y, Lu H, Reddy R, El-Zimaity HM. False negative urea breath tests with H2-receptor antagonists: interactions between Helicobacter pylori density and pH. *Helicobacter* 2004; **9**: 17-27
26 **Chey WD**, Chathadi KV, Montague J, Ahmed F, Murthy U. Intragastric acidification reduces the occurrence of false-negative urea breath test results in patients taking a proton pump inhibitor. *Am J Gastroenterol* 2001; **96**: 1028-1032
27 **Gisbert JP**, Abraira V. Accuracy of Helicobacter pylori diagnostic tests in patients with bleeding peptic ulcer: a systematic review and meta-analysis. *Am J Gastroenterol* 2006; **101**: 848-863
28 **Winiarski M**, Bielanski W, Plonka M, Dobrzanska M, Kaminska A, Bobrzynski A, Ronturek PC, Konturek SJ. The usefulness of capsulated 13C-urea breath test in diagnosis of Helicobacter pylori infection in patients with upper gastrointestinal bleeding. *J Clin Gastroenterol* 2003; **37**: 34-38
29 **Stubbs JB**, Marshall BJ. Radiation dose estimates for the carbon-14-labeled urea breath test. *J Nucl Med* 1993; **34**: 821-825
30 **Leide-Svegborn S**, Stenström K, Olofsson M, Mattsson S, Nilsson LE, Nosslin B, Pau K, Johansson L, Erlandsson B, Hellborg R, Skog G. Biokinetics and radiation doses for carbon-14 urea in adults and children undergoing the Helicobacter pylori breath test. *Eur J Nucl Med* 1999; **26**: 573-580
31 **Gunnarsson M**, Leide-Svegborn S, Stenström K, Skog G, Nilsson LE, Hellborg R, Mattsson S. No radiation protection reasons for restrictions on ^{14}C urea breath tests in children. *Br J Radiol* 2002; **75**: 982-986

S- Editor Liu Y **L- Editor** Ma JY **E- Editor** Lu W

PO Box 2345, Beijing 100023, China
www.wjgnet.com
wjg@wjgnet.com

World J Gastroenterol 2007 February 14; 13(6): 930-933
World Journal of Gastroenterology ISSN 1007-9327

RAPID COMMUNICATION

Omeprazole-based triple therapy with low-versus high-dose of clarithromycin plus amoxicillin for *H pylori* eradication in Iranian population

Ali Asghar Keshavarz, Homayoon Bashiri, Mahtab Rahbar

Ali Asghar Keshavarz, Department of Gastroenterology and Hepatology, Emam Reza Hospital, Kermanshah University of Medical Sciences, Kermanshah, Iran
Homayoon Bashiri, Department of Internal Medicine Emam Reza Hospital, Kermanshah, Iran
Mahtab Rahbar, Department of Pathology, Emam Reza Hospital, Kermanshah, Iran
Correspondence to: Dr. Ali Asghar Keshavarz, Emam Reza Hospital, Kermanshah University of Medical Sciences, Kermanshah, Iran. dr_keshavarz@yahoo.com
Telephone: +98-831-7244800 Fax: +98-831-7244700
Received: 2006-10-26 Accepted: 2007-01-05

Key words: Triple therapy; *H pylori*; Amoxicillin; Clarithromycin; Low-dose regimen

Keshavarz AA, Bashiri H, Rahbar M. Omeprazole-based triple therapy with low-versus high-dose of clarithromycin plus amoxicillin for *H pylori* eradication in Iranian population. *World J Gastroenterol* 2007; 13(6): 930-933

http://www.wjgnet.com/1007-9327/13/930.asp

Abstract

AIM: To investigate the efficacy and tolerability of *H pylori* eradication in an omeprazole-based triple therapy with high- and low-dose of clarithromycin and amoxicillin.

METHODS: One hundred and sixty *H pylori* positive patients were randomly assigned to two groups based on the following 2 wk investigation; (1) group A or low-dose regimen received omeprazole 20 mg b.i.d, clarithromycin 250 mg b.i.d and amoxicillin 500 mg b.i.d; and (2) group B or high-dose regimen received omeprazole 20 mg b.i.d, clarithromycin 500 mg b.i.d and amoxicillin 1000 mg b.i.d. During the study *H pylori* status was assessed by histology and rapid urease test prior and by ^{13}C-urea breath test 6 wk after the therapy. Standard questionnaires were administered to determine the compliance to treatment and possible adverse events of therapy. Data were subject to χ^2 to compare the eradication rates in the two groups. The significant level of 95% ($P \leqslant 0.05$) was considered statistically different.

RESULTS: We found that the per-protocol eradication rate was 88% (68/77) in group A, and 89% (67/75) in group B. The intension-to-treat eradication rate was 85% (68/80) in group A and 83.75% (67/80) in group B. Overall adverse events were 26% in group A and 31% in group B. The adverse events were generally mild in nature and tolerated well in both groups with a compliance of 98% in group A *vs* 96% in group B.

CONCLUSION: The omeprazole-based low dose regimen of clarithromycin and amoxicillin for two weeks in *H pylori* eradication is as effective as high dose regimen in Iranian population.

INTRODUCTION

H pylori is associated with chronic active gastritis, peptic ulcer diseases, gastric adenocarcinoma and mucosa-associated lymphoid tissue lymphoma[1-3]. Numerous treatment regimens for *H pylori* eradication with particular attention to duration and dosage have been adopted in various geographic regions of world with contradictory results[4-6]. The goal of all these attempts is to obtain a cheap, safe, tolerable and acceptable *H pylori* eradication rate regimen. An *H pylori* regimen should achieve at least an 80% eradication rate[7,8]. Classical triple therapy based on H2-receptor antagonist or a proton pump inhibitor (PPI) due to high prevalence (75.2%) of *H pylori* resistance to metronidazole in Iran, is not accompanied by acceptable eradication rates[9,10]. In a randomized study of two weeks treatment in Iranian duodenal ulcer patients with bismuth triple therapy (bismuth, metronidazole and amoxicillin), the cure rate for *H pylori* was 46.0% by per-protocol (PP) analyses[11]. Furazolidone, a cheap antibiotic, has been focus of attention as a substitute for clarithromycin or metronidazole in few clinical trials of bismuth triple and quadruple therapy in Iran[12,13]. In a bismuth quadruple therapy with two different doses of furazolidone, intention-to-treat (ITT) and PP eradication rates were 72% with low and 92% with high dose of furazolidone respectively[13]. Regardless of this study, in practice its higher doses are accompanied by poor compliance and severe side-effects, and so far no Hp consensus group has recommended its routine use. To keep in mind these facts and overcome the above shortcomings, the first line of therapy as suggested by European, American, and Asian-Pacific guidelines for *H pylori* eradication that combines a PPI with clarithromycin and either amoxicillin

or metronidazole should be considered as first line of *H pylori* treatment in Iranian patients. Based on high resistance of *H pylori* strains to metronidazole in Iran, non-metronidazole containing regimens are recommended for *H pylori* eradication in our country. Since short-term regimens are not effective in *H pylori* eradication in Iranian patients, a 10-14 d therapy is needed[14]. As this regimen is costly for routine use in developing countries, dose reduction is an option to decrease its cost. There are limited studies that have evaluated the efficacy of both clarithromycin and amoxicillin in low-dose regimens in *H pylori* eradication with a PPI-based triple therapy[15-19]. Therefore, we tried to investigate the efficacy and tolerability of omeprazole-based triple therapy with high and low doses of clarithromycin and amoxicillin in *H pylori* eradication in Iranian population.

MATERIALS AND METHODS

Between October 2004 and September 2005, 160 consecutive *H pylori*-infected patients, 18-80 years of age, were recruited for this study. The patients were excluded from enrolment if they had taken proton pump inhibitors, bismuth preparations or antibiotics within 4 wk prior to the study; had histories of gastric or duodenal surgery, allergy to medications or endoscopic evidence of gastric malignancy, gastric outlet obstruction, bleeding or if they had clinically significant cardiovascular, hepatic, pulmonary metabolic or psychiatric diseases. The *H pylori* infection was defined as positive when both rapid urease test and histology were positive for *H pylori* documentation. In the biopsy rapid test, two biopsy specimens (one from antrum and one from corpus on the greater curvature) were examined. Four biopsy specimens (two from antrum and two from the mid-corpus on the greater and lesser curvature) underwent histopathological assessment. Eligible patients were randomized to receive the two following regimens: group A or low-dose regimen (n = 80) received omeprazole 20 mg b.i.d, clarithromycin 250 mg b.i.d and amoxicillin 500 mg b.i.d, and group B or high-dose regimen (n = 80) received omeprazole 20 mg b.i.d, clarithromycin 500 mg b.i.d and amoxicillin 1000 mg b.i.d for two weeks. Eradication was confirmed by ^{13}C-urea breath test 6 wk after completion of treatment. Results under 5 cut-off were considered negative. Adverse events were prospectively evaluated. They were assessed as mild (discomfort not interfering with daily activity); moderate (discomfort interfering with daily activity); and severe (discomfort resulting in discontinuation of therapy). Compliance was checked by pill count at the end of treatment. Poor compliance was defined as taking less than 70% of pills. Eradication rates were evaluated by ITT and PP analyses. The eradication and adverse event rates in the two treatment groups were compared using χ^2 test. A P value less than 0.05 was considered statistically significant. Data were analyzed using the SPSS for Windows (version 11.5; SPSS, Inc, Chicago, Illinois, USA).

RESULTS

Demographic and outcome data of two eradication regimen groups are summarized in Table 1. No significant difference was found between the two groups of patients with regard to clinical variables. Five patients (2 in group A and 3 in group B) with poor compliance and 3 (1 in group A and 2 in group B) with incomplete follow-up therapy were excluded from PP analysis for *H pylori* eradication. The per-protocol eradication rate was 88% in group A, and 89% in group B. The ITT eradication rate was 85% in group A and 83.75% in group B. The differences were not statistically significant between the two groups by ITT and PP. All the patients receiving at least one dose of medications were included in adverse event analysis, and 26% of the group A and 31% of group B reported at least one adverse event during the therapy. Diarrhea was the most common adverse event in both groups (5% in group A *vs* 9% in group B). All but 5 (2 in group A and 3 in group B) complied with the eradication therapies and took more than 70% of assigned tablets. Both groups displayed similar compliance rates (98% in group A *vs* 96% in group B).

Table 1 Demographic data and outcomes of two enrolled groups

Data	Group A (n = 80)	Group B (n = 80)
Mean age (yr) (mean ± SD)	52.4 ± 13	53.1 ± 12.3
Gender (male/female)	55/25	57/23
Eradication rate		
Intension-to-treat	85% (68/80)	83.75% (67/80)
Per-protocol	88% (68/77)	89% (67/75)
Adverse events		
Mild	20% (15)	22% (17)
Moderate	5% (5)	8% (6)
Severe	1.25% (1)	2.5% (2)
Compliance	98% (78/80)	96% (77/80)

DISCUSSION

The results of this study confirm that efficacy of low and high dose regimens of clarithromycin and amoxicillin and comparable omeprazole dose (20 mg b.i.d) are equal in *H pylori* eradication in Iranian population. The treatments were well tolerated and associated with a high compliance rate. Many studies have compared different doses of clarithromycin in *H pylori* eradication, with contradictory results, but those that have evaluated clarithromycin-amoxicillin combination in low-dose regimens for *H pylori* eradication are scarce[15]. Hp consensus groups have generally recommended a 500 mg b.i.d dosage of clarithromycin for *H pylori* eradication[7,8]. However, some issues with regard to the clarithromycin dosage need to be addressed. MACHI study produced disappointing results for low-dose clarithromycin regimens, with an eradication rate of 79.5% by intension-to-treat analysis compared with 90.6% for the clarithromycin 500 mg b.i.d regimen[16]. A meta-analysis also showed that pooled eradication rate of the clarithromycin 500 mg b.i.d regimen was 86.6% by ITT analysis and 89.5% by PP analysis, which were significantly higher than those achieved with the clarithromycin 250 mg b.i.d regimen, 78.2% by ITT and 83.3% by PP analyses[19]. However, even in that meta-analysis, subgroup analysis

showed that proton pump inhibitor dosing frequency affected the efficacy of *H pylori* eradication. On the basis of proton pump inhibitor b.i.d regimens, the *H pylori* eradication rates by pooled PP analysis were 86.1% and 89.6% in the clarithromycin 250mg b.i.d and 500 mg b.i.d regimens, respectively. In contrast, a recent Japanese study showed that clarithromycin 200 mg b.i.d regimen was as effective as 400 mg b.i.d[18]. In addition, a multi-center study performed in France demonstrated a somewhat higher, although not significant, eradication rate with low-dose clarithromycin triple therapy compared with the conventional regimen[17]. In a study by Miwa H *et al*[15]using different doses of omeprazole-clarithromycin-amoxicillin, in their low-dose group of omeprazole 20 mg, amoxicillin 750 mg and clarithromycin 200 mg all b.i.d, the eradication rates by ITT and PP were 82.5% and 90% respectively. In our study, the eradication rate of low-dose regimen was 85% and 88% by ITT and PP analysis, respectively. Because of the high metronidazole resistance in our country (75.2%)[10] and low eradication rate of *H pylori* with metronidazole containing regimens and shortcomings with other applied *H pylori* eradication regimens in Iran, the first line of *H pylori* treatment as suggested by most *H pylori* consensus groups, the PPI-based therapy with low-dose regimen of clarithromycin-amoxicillin seems to be a good option to overcome its high cost in developing countries. In a study by Malekzadeh *et al*[14] using a 7-d conventional therapy with clarithromycin, regardless of low prevalence of *H pylori* resistance to clarithromycin in their report (1.2%), the eradication rate was unacceptably low (35.5% in ITT). This low eradication rate has been attributed to the high prevalence of cancer in the areas of the study, their conclusion was that patients in this high-prevalence cancer area may have a higher bacterial load in gastric mucosa with different biological behaviors, Cag A strains or host-immune response. It has been estimated that the rate of eradication increased by 9% by extending duration of therapy from 7 to 10 d[20]. Based on these reports and our results, efficacy of proton pump triple therapy with conventional and low-dose regimens of clarithromycin and amoxicillin with 7, 10 and 14 d requires more evaluation in different geographic regions of Iran by further multi-center head-to-head comparison studies in our country. In conclusion, two weeks triple therapy with a proton pump inhibitor and low-dose regimen of clarithromycin and amoxicillin is as effective as high-dose regimen, and has acceptable eradication rate and the best cost-benefit ratio in Iranian population.

REFERENCES

1 **Go MF**. Review article: natural history and epidemiology of Helicobacter pylori infection. *Aliment Pharmacol Ther* 2002; **16** Suppl 1: 3-15

2 **Uemura N**, Okamoto S, Yamamoto S, Matsumura N, Yamaguchi S, Yamakido M, Taniyama K, Sasaki N, Schlemper RJ. Helicobacter pylori infection and the development of gastric cancer. *N Engl J Med* 2001; **345**: 784-789

3 **Hsu PI**, Lai KH, Lo GH, Tseng HH, Lo CC, Chen HC, Tsai WL, Jou HS, Peng NJ, Chien CH, Chen JL, Hsu PN. Risk factors for ulcer development in patients with non-ulcer dyspepsia: a prospective two year follow up study of 209 patients. *Gut* 2002; **51**: 15-20

4 **Zanten SJ**, Bradette M, Farley A, Leddin D, Lind T, Unge P, Bayerdörffer E, Spiller RC, O'Morain C, Sipponen P, Wrangstadh M, Zeijlon L, Sinclair P. The DU-MACH study: eradication of Helicobacter pylori and ulcer healing in patients with acute duodenal ulcer using omeprazole based triple therapy. *Aliment Pharmacol Ther* 1999; **13**: 289-295

5 **Lamouliatte H**, Samoyeau R, De Mascarel A, Megraud F. Double vs. single dose of pantoprazole in combination with clarithromycin and amoxycillin for 7 days, in eradication of Helicobacter pylori in patients with non-ulcer dyspepsia. *Aliment Pharmacol Ther* 1999; **13**: 1523-1530

6 **Vallve M**, Vergara M, Gisbert JP, Calvet X. Single vs. double dose of a proton pump inhibitor in triple therapy for Helicobacter pylori eradication: a meta-analysis. *Aliment Pharmacol Ther* 2002; **16**: 1149-1156

7 **Malfertheiner P**, Mégraud F, O'Morain C, Hungin AP, Jones R, Axon A, Graham DY, Tytgat G. Current concepts in the management of Helicobacter pylori infection--the Maastricht 2-2000 Consensus Report. *Aliment Pharmacol Ther* 2002; **16**: 167-180

8 **Lam SK**, Talley NJ. Report of the 1997 Asia Pacific Consensus Conference on the management of Helicobacter pylori infection. *J Gastroenterol Hepatol* 1998; **13**: 1-12

9 **Siavoshi F**, Safari F, Malekzadeh R. Antimicrobial susceptibility of *H pylori* isolated from adults and children. Abstract book of 4th Iranian. *H pylori* infection congress; 2004: 27-28

10 **Mohammadi M**, Doroud D, Massarrat S, Farahvash MJ. Clarithromycin resistance in Iranian H. pylori strains before introduction of clarithromycin. *Helicobacter* 2003; **8**: 80

11 **Kaviani MJ**, Malekzadeh R, Vahedi H, Sotoudeh M, Kamalian N, Amini M, Massarrat S. Various durations of a standard regimen (amoxycillin, metronidazole, colloidal bismuth sub-citrate for 2 weeks or with additional ranitidine for 1 or 2 weeks) on eradication of Helicobacter pylori in Iranian peptic ulcer patients. A randomized controlled trial. *Eur J Gastroenterol Hepatol* 2001; **13**: 915-919

12 **Roghani HS**, Massarrat S, Pahlewanzadeh MR, Dashti M. Effect of two different doses of metronidazole and tetracycline in bismuth triple therapy on eradication of Helicobacter pylori and its resistant strains. *Eur J Gastroenterol Hepatol* 1999; **11**: 709-712

13 **Fakheri H**, Merat S, Hosseini V, Malekzadeh R. Low-dose furazolidone in triple and quadruple regimens for Helicobacter pylori eradication. *Aliment Pharmacol Ther* 2004; **19**: 89-93

14 **Malekzadeh R**, Merat S, Derakhshan MH, Siavoshi F, Yazdanbod A, Mikaeli J, Sotoudemanesh R, Sotoudeh M, Farahvash MJ, Nasseri-Moghaddam S, Pourshams A, Dolatshahi S, Abedi B, Babaei M, Arshi S, Majidpour A. Low Helicobacter pylori eradication rates with 4- and 7-day regimens in an Iranian population. *J Gastroenterol Hepatol* 2003; **18**: 13-17

15 **Miwa H**, Ohkura R, Murai T, Nagahara A, Yamada T, Ogihara T, Watanabe S, Sato N. Effectiveness of omeprazole-amoxicillin-clarithromycin (OAC) therapy for Helicobacter pylori infection in a Japanese population. *Helicobacter* 1998; **3**: 132-138

16 **Lind T**, Veldhuyzen van Zanten S, Unge P, Spiller R, Bayerdörffer E, O'Morain C, Bardhan KD, Bradette M, Chiba N, Wrangstadh M, Cederberg C, Idström JP. Eradication of Helicobacter pylori using one-week triple therapies combining omeprazole with two antimicrobials: the MACH I Study. *Helicobacter* 1996; **1**: 138-144

17 **Bigard MA**, Delchier JC, Riachi G, Thibault P, Barthelemy P. One-week triple therapy using omeprazole, amoxycillin and clarithromycin for the eradication of Helicobacter pylori in patients with non-ulcer dyspepsia: influence of dosage of omeprazole and clarithromycin. *Aliment Pharmacol Ther* 1998; **12**: 383-388

18 **Kihira K**, Satoh K, Saifuku K, Kawakami S, Fukazawa K, Ishino Y, Kimura K, Sugano K. Rabeprazole, amoxycillin and low- or high-dose clarithromycin for cure of Helicobacter pylori infection. *Aliment Pharmacol Ther* 2000; **14**: 1083-1087

19 **Huang J**, Hunt RH. The importance of clarithromycin dose in the management of Helicobacter pylori infection: a meta-analysis of triple therapies with a proton pump inhibitor, clarithromycin and amoxycillin or metronidazole. *Aliment Pharmacol Ther* 1999; **13**: 719-729

20 **Calvet X**, García N, López T, Gisbert JP, Gené E, Roque M. A meta-analysis of short versus long therapy with a proton pump inhibitor, clarithromycin and either metronidazole or amoxycillin for treating Helicobacter pylori infection. *Aliment Pharmacol Ther* 2000; **14**: 603-609

S- Editor Liu Y **L- Editor** Ma JY **E- Editor** Lu W

PO Box 2345, Beijing 100023, China
www.wjgnet.com
wjg@wjgnet.com

World J Gastroenterol 2007 February 14; 13(6): 934-938
World Journal of Gastroenterology ISSN 1007-9327

RAPID COMMUNICATION

Growth inhibitory effect of wild-type *Kras*2 gene on a colonic adenocarcinoma cell line

Hong Li, Hou-Fa Cao, Jun Wan, Yuan Li, Mei-Ling Zhu, Po Zhao

Hong Li, Hou-Fa Cao, Inpatient Department of Medical Health Center, Chinese PLA General Hospital, Beijing 100853, China
Jun Wan, Yuan Li, Mei-Ling Zhu, Department of Nanlou Digestion, Chinese PLA General Hospital , Beijing 100853, China
Po Zhao, Department of Pathology, Chinese PLA General Hospital, Beijing 100853, China
Supported by a grant from National Natural Science Foundation of China for Young Scholars, No. 30200326
Correspondence to: Dr. Po Zhao, Department of Pathology, Chinese PLA General Hospital, Beijing 100853, China. zhaopo@301hospital.com.cn
Telephone: +86-10-66937736
Received: 2006-12-01 Accepted: 2007-01-13

Abstract

AIM: To observe the growth inhibitory effect of wild-type *Kras*2 gene on a colonic adenocarcinoma cell line Caco-2.

METHODS: Recombinant plasmid pCI-neo-*Kras*2 with wild type *Kras*2 open reading frame was constructed. The Caco-2 cells were transfected with either pCI-neo or pCI-neo-*Kras2* using Lipofectamine 2000. The expression of wild type *Kras*2 was examined by Northern blot analysis. And the expression of wild type *Kras*2 protein was examined by Western blot analysis. The effects of wild-type *Kras*2 on cell proliferation were analyzed by monotetrazolium (MTT) assay, meanwhile analyses of cell cycle and spontaneous apoptosis rate were carried out by flow cytometry (FCM).

RESULTS: The plasmid of pCI-neo-*Kras*2 was successfully established. The growth rate of cells transfected with pCI-neo-*Kras*2 was significantly lower than the control cells transfected with the empty pCI-neo vector ($P < 0.05$). Cell cycle analysis revealed arrest of the pCI-neo-*Kras*2 transfected cells in G_0/G1 phases, decreased DNA synthesis and decreased fractions of cells in S phase. The proliferative index of cells transfected with pCI-neo-*Kras*2 was decreased compared with the control cells (49.78% *vs* 64.21%), while the apoptotic rate of Caco-2 cells with stable *Kras*2 expression increased (0.30% *vs* 0.02%).

CONCLUSION: The wild-type *Kras*2 gene effectively inhibits the growth of the colonic adenocarcinoma cell line Caco-2.

Key words: Colonic adenocarcinoma; Wild-type *Kras*2; Cell cycle; Apoptosis

Li H, Cao HF, Wan J, Li Y, Zhu ML, Zhao P. Growth inhibitory effect of wild-type *Kras*2 gene on a colonic adenocarcinoma cell line. *World J Gastroenterol* 2007; 13(6): 934-938

http://www.wjgnet.com/1007-9327/13/934.asp

INTRODUCTION

A number of molecular studies have shown that colon carcinogenesis results from an accumulation of epigenetic and genetic alterations, including activation of the proto-oncogenes, and inactivation of the mutations of tumor suppressor genes or of DNA repair genes[1]. Previously extensive studies have been done on the activation of the *K-ras*2 proto-oncogene[2-4] and have revealed the association between colon carcinogenesis and the frequency of RAS mutations. Approximately 50% of colorectal tumors contain K-*ras*2 gene mutations, leading to activation of the *K-ras*2 oncogene, which is an early event in carcinogenesis. A recent study on *Kras*2, however, demonstrated that the wild-type *Kras*2 inhibited the growth, colony formation and *in vivo* tumor formation of lung cancer cells[5]. In addition, wild-type *Kras*2 has also been shown to inhibit colony formation and tumor development by transformed NIH/3T3 cells. These results indicated wild-type *kras*2 might exert its tumor suppressor effect in carcinogenesis. In the current study, we attempted to investigate the tumor suppressive effect of wild-type *Kras*2 on the proliferation of a colon cancer cell line. We transfected the wild-type *Kras*2 gene into Caco-2 cell, a human colon adenocarcinoma cell line, and established a stably transfected cell line by G418 selection. The effects of wild-type *Kras*2 on cell growth, cell cycle distribution and apoptosis were analyzed in Caco-2 cells.

MATERIALS AND METHODS

Cell culture

Human colon tumor cell line Caco-2 was purchased from American Type Culture Center (ATCC) (Rockville, MD, USA) and was maintained in MEM-NEAA medium supplemented with 10% FCS and 100 U/mL penicillin-

streptomycin in a humidified atmosphere with 5% CO_2 at 37℃.

Cloning of wild-type Kras2 gene and plasmid construction

Appropriate institutional approval for human tissue studies and the informed consent from all subjects were both obtained. The wild-type *Kras*2 cDNA fragment was amplified by PCR. Briefly, total RNA from human peripheral blood was extracted by Trizol reagent (Invitrogen) and the Reverse Transcription System kit (Promega) was used to synthesize the cDNA. The primer sets Y1: 5'-ACCCACGCGTATGACTGAATATAAAC-3' and Y2: 5'-AACGTCGACTTACATAATTACACACT-3' (Shanghai Oke Corp.) with *Mlu* I and *Sal* I enzyme sites respectively were used to amplify the wild-type *Kras*2 cDNA. The PCR product was harvested from 1% agarose gel, digested by *Mul* I and *Sal* I enzymes and inserted into the pCI-neo vector at *Mul I* and *Sal I* cloning sites to construct the pCI-neo-*Kras*2 expression vector. All ligation products were transformed into DH5 competent cells. The constructs were confirmed by restriction enzyme mapping and DNA sequencing.

Cell transfection and stable screening

For transfection experiment, Caco-2 cells were seeded into 100-mm culture dishes and grown until 80% confluence. The empty plasmid pCI-neo and the pCI-neo-*Kras*2 were stably transfected using Lipofectamine 2000 reagent (Invitrogen), according to the manufacturer's instruction. Caco-2 cells were selected with 1.2 mg/mL G418 for 2 wk and maintained in normal MEM medium containing 0.6 mg/mL G418 (Amresco USA).

RNA isolation and Northern blot analysis

A total of 1.5×10^5 viable Caco-2 cells transfected with the pCI-neo empty vector or *Kras*2 stably expressing cells were plated into one well of six-well plates with 5 mL of culture medium and cultured until 90% cell confluence. Total RNA was isolated in 2 mL of TRIZOL reagent according to the manufacturer's instruction. Twenty micrograms of total RNA were electrophoresed through a 1% agarose gel containing formaldehyde and were transferred to a Hybond N^+ membrane (Amersham). The membrane was hybridized with a [^{32}P]-labeled *Kras*2 cDNA probe in 5 mL hybridization buffer containing 50% deionized formamide, 0.5 × Denhardt's solution, 0.5% sodium dodecyl sulfate (SDS), and 1 mg of salmon sperm DNA (Sigma). After hybridization overnight at 50℃, the membrane was washed according to the manufacturer's instruction and exposed to BioMax-MS film (Eastman Kodak) for 2 d at -80℃. The autoradiographic bands were performed in quantitative analysis using Image software.

Monotetrazolium (MTT) assays

The cancer cells with stable expression of wild-type *Kras*2 and the control cells were separately seeded at the same time into 96-well culture plates and then routinely cultured for 6 d. MTT was added to the culture wells and the 570 nm wave-length absorption value (*A* value) was assayed at 5 h, 1, 2, 3, 4, 5 and 6 d after seeding of cells. The cell growth curves were protracted using the following formula, GI = Nc-Nt/Nc × 100%. Nc and Nt represent the *A* value of the control and the experimental group cells. All experiments were performed in triplicate and repeated 3 times.

Cell cycle analysis

Cell cycle analysis was performed by propidium iodide (PI) staining. Briefly, Caco-2 cells were firstly seeded into 10-cm dishes at 5×10^5. After further cultured for 2 d, the cells were trypsinized and harvested in PBS followed by two washes with PBS. After that the cells were resuspended in PBS at 1-2 × 10^6/mL and fixed with 70% cool ethanol for at least 1 h. Next, the cells were washed twice and centrifuged at 1000 × *g* for 3 min. The pelleted cells were resuspended in 1 mL PBS and added with 50 μL of RNase A stock solution (10 g/mL) and mixed well, and then incubated for 3 h at 4℃. Finally, the cells were pelleted and added with 1 mL of PI staining solution (3.8 mmol/L sodium citrate, 50 μg/mL PI in PBS) and incubated for 1 h at room temperature. After that the cells were analyzed by flow cytometry on an FACSCalibur (Becton Dickinson Immunocytometry Systems, San Jose, CA) exciting at 488-nm, and the DNA-linked red fluorescence (PI) was measured through a 600-nm wavelength filter. This experiment was performed three times.

Western blot analysis

A total of 50 μg of proteins in whole cell lysates was separated by SDS-polyacrylamide gel electrophoresis and transferred to PVDF membranes (Millipore, Bedford, MA). After blocking with 5% (w/v) nonfat milk, the blots were incubated with the first anti-*Kras*2 antibody (F234, sc-30; SantaCruz Biotechnology, Santa Cruz, CA; 1:100 dilution in a blocking solution, 2 h at room temperature) or with the anti-GAPDH antibody (Sigma Chemical, St. Louis, MO; 1:2000 dilution in a blocking solution, 1 h at room temperature). The blots were then washed with PBST and incubated with a secondary antibody (Amersham Biosciences, Buckinghamshire, UK). Positive signal bands were detected using ECL plus (Amersham Biosciences).

Statistical analysis

The results for MTT assay and cell cycle analysis were presented as the mean ± SD of three replicate culture wells. Analysis was performed using Statview software. All data were evaluated for paired variables to compare between two groups. $P < 0.05$ was considered to be statistically significant.

RESULTS

Identification of the expression vector of Kras2 gene

The plasmids including pCI-neo and pCI-neo-*Kras*2 were digested with *Mul* I and *Sal* I enzymes and the 576 bp and 5472 bp products were observed. The 576 bp *Kras*2 cDNA was inserted into the pCI-neo vector. And the inserted fragment was verified by sequencing.

Transcription of the Kras2 gene in Caco-2 cells

To measure the expression level of *Kras*2 gene in Caco-2 cells, northern blot analysis was used to detect the *Kras*2

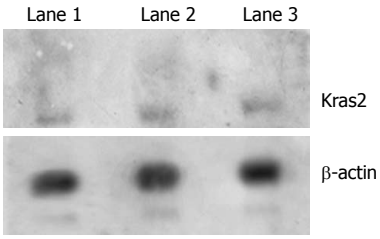

Figure 1 mRNA expression of wild-type *Kras*2 in Caco-2 cell.

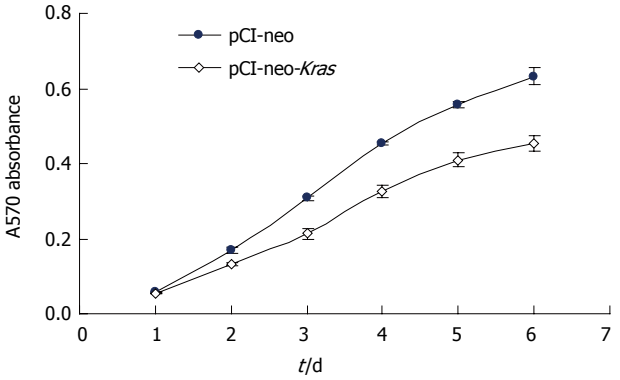

Figure 2 Growth inhibitory effect of wild-type *Kras*2 on Caco-2 cell.

mRNA. β-actin mRNA was also detected as an inner control. Consistent with the information provided by ATCC, the *Kras*2 transcript was not detected in Caco-2 cells (Figure 1).

Suppression of Caco-2 cell growth by wild-type Kras2

To determine the effect of wild-type *Kras*2 on the proliferative capacity of Caco-2 cells, a cell growth curve was generated by MTT assay. As shown in Figure 2, the growth rate of cells transfected with pCI-neo-*Kras*2 was significantly lower than the control cells transfected with the empty pCI-neo vector beginning from the third day after cell seeding.

Effect of wild-type Kras2 on cell cycle and apoptosis of Caco-2 cells

To detect the effect of wild-type *Kras*2 on cell differentiation and apoptosis of Caco-2 cells, cell cycle distribution and the apoptosis rate were analyzed by flow cytometry. The proliferative index of cells transfected with pCI-neo-*Kras*2 was decreased, compared with the control cells (49.78% *vs* 64.21%) (Table 1). As shown in Figure 3, the pCI-neo-*Kras*2 transfected cells were arrested in G_0/G1 phases, compared with control cells, and the apoptotic rate of Caco-2 cells with stable *Kras*2 expression was increased (0.30% *vs* 0.02%).

Expression of wild-type Kras2 gene

To determine whether the expression level of the *Kras*2 protein was different between the cells transfected with pCI-neo-*Kras*2 and the control cells transfected with the empty pCI-neo vector, we performed Western blot analysis on both cell lines using a monoclonal *Kras*2 antibody. The results showed that the Caco2 cell line without pCI-neo-*Kras*2 transfection expressed a faint protein product (Figure 4, lane A), and pCI-neo-*Kras*2 stably transfected cell line (lane B) expressed a 21 kDa product of *Kras*2. GAPDH was used as an internal control for loading volume.

Table 1 Influence of wild-type *Kras*2 gene on cell cycle of Caco-2 cells (%)

Cell lines	G0/G1 phase	S phase	G2/M phase	Proliferative index
pCI-neo	35.79	40.04	24.17	64.21
PCI-neo-*Kras*2	50.22	32.88	16.9	49.78

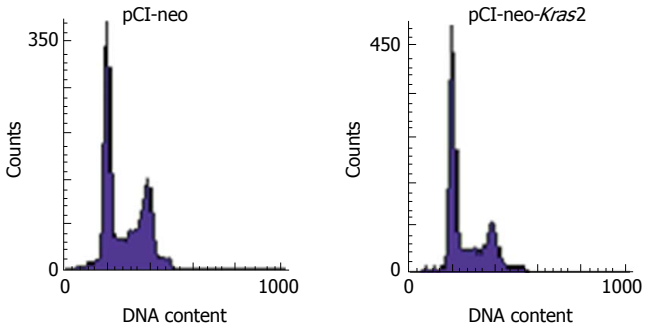

Figure 3 Effect of the wild-type *Kras*2 on cell cycle of Caco-2 cells.

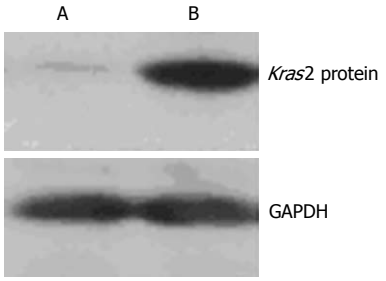

Figure 4 Expression of the wild-type *Kras*2 protein in cell lines.

DISCUSSION

Human colon carcinogenesis and tumor progression are considered to be the result of multigene alterations. Activating point mutations in *ras* gene are widely correlated with human colon carcinogenesis and progression, and have been detected in more human tumor types and at a higher frequency (25%-30% of all human tumors) than other oncogenes[6-9]. For example, *ras* mutations are detected in 40%-50% of colon carcinomas[10,11], 80% of pancreatic carcinomas[12-15], and 30%-50% of lung adenocarcinomas[16-20]. *Kras*2 mutations account for > 90% of the activating *ras* mutations observed in these tumor types. The oncogenic alleles of *ras* genes are generally perceived to be dominant because their transforming ability exists when normal alleles are also expressed[21]. However, recent evidence from both *in vivo* and *in vitro* studies suggested that the dominance of the *ras* oncogene might result from overexpression of the mutant *ras* allele or from deletion of the wild-type allele. Previous studies also suggested that the wild-type *Kras*2 allele could suppress the oncogenic potential of the mutant

*Kras*2 allele[5]. Heterozygous *Kras*2 deficient mice were highly susceptible to chemically induced lung tumors compared to wild-type littermates. All tumors displayed an activated *Kras*2 because of a chemically induced mutation. Experimental evidence demonstrated that wild-type *Kras*2 inhibited cell growth, colony formation and tumor development in a murine lung tumor cell line containing an activated *Kras*2 allele. In addition, the loss of wild-type *Kras*2 was found in 67%-100% of chemically induced mouse lung adenocarcinomas harboring a mutant *Kras*2 allele[5]. Moreover, results from epidemiological investigations showed that loss of heterozygosity (LOH) of chromosome 12p was detected in nearly 50% of human lung adenocarcinomas and large cell carcinomas, and *Kras*2 mutations were detected at codon 12 in about 40% of human lung cancers[22]. We also observed that high frequent loss of heterozygosity in this domain occurred in carcinogenesis and progression of colon carcinoma[23]. These findings suggest that wild-type *Kras*2 is a tumor suppressor and is frequently lost during tumor progression.

Several mutational events common to tumor cells in colorectal cancer have been identified. It is not known whether the accumulation of these mutations occurs in a specific sequence. However, certain stages in the disease development do correlate with the presence of particular mutations[24]. In the genetic model of human colon tumorigenesis, activation of *Kras*2 mutation has been identified to promote colon carcinogenesis and progression, meanwhile, masking the potential tumor suppressor effect of the wild-type *Kras*2. To elucidate whether the wild-type *Kras*2 is a tumor suppressor in more tumor types, we hypothesized that the *K-ras2* plays double roles of both "oncogenic" and "anti-oncogenic" effects. In physiological state, *K-ras2* is a proto-oncogene, which is transformed to an oncogene by activating point mutation, whereas the wild-type *K-ras* can still maintain its tumor-suppressor function. To explore the biological role of the wild-type *K-ras* gene, it is necessary to exclude the interference of activated mutations of *K-ras*. Therefore, it is reasonable to select Caco-2 cells as the cell model in this study[25]. To our knowledge, this is the first report on the relationship between the presence of wild-type *Kras*2 and the growth and apoptotic properties of human colon cancer cells. Our results demonstrated that the wild-type *Kras*2 effectively inhibited the proliferation, and meanwhile promoted apoptosis of colon cancer cells. Ras is a GTP/GDP binding protein, affecting cell growth and proliferation *via* several signaling pathways[25]. In this study, wild-type *Kras*2 inhibited the growth of Caco-2 human colon cancer cells mainly through cell cycle arrest in G_0/G1 phase, decreased DNA synthesis, and decreased fractions of cells in S phase.

Aberrant apoptosis mechanism also exists in colon cancer. Previous studies have demonstrated that the activating mutation of Ras inhibited apoptosis in colon cancer cells[26]. Here, we showed that the exogenous expression of wild-type *Kras*2 increased the apoptotic rate of Caco-2 cells (0.30% *vs* 0.02%), possibly via a mechanism involving Ras G-proteins and Raf-1 kinase, which needs to be further investigated[27].

Taken together, through exogenous expression of the wild-type *Kras*2 gene in Caco-2 colon cancer cells, we firstly demonstrate that the wild-type *Kras*2 gene is a potential tumor suppressor in human colon cancer. Our study also implies that increase of the expression level of wild-type *Kras*2 gene might be a gene therapeutic strategy for human colon cancer.

COMMENTS

Background

Conventional viewpoints suggest *ras* gene is closely related to carcinogenesis and progression of colon carcinoma. About 30 percent of tumors display mutation of *ras* gene, in which the most frequent one is *Kras*2, and a relatively high frequency of *Kras*2 mutation is seen in colon carcinoma, pancreas carcinoma and lung carcinoma. Recent studies raised doubt about the dominant oncogene roles of *Kras*2 gene, and showed the frequent loss of wild type *Kras*2 in human and mouse lung adenocarcinomas, and that loss of heterozygosity on chromosome 12p12-13 in *Kras*2 gene existed in non-small-cell lung cancer. In addition, wild-type *Kras*2 has also been shown to inhibit colony formation and tumor development by transformed NIH/3T3 cells. These results indicate that wild-type *kras*2 probably has a tumor suppressor effect in carcinogenesis.

Research frontiers

We investigated the tumor suppressive effect of wild-type *Kras*2 on cell proliferation of a colon cancer cell line.

Innovations and breakthroughs

To our knowledge, this is the first report on the relationship between the presence of wild-type *Kras*2 and the growth and apoptosis properties of human colon cancer cells.

Applications

This study demonstrates that the wild-type *Kras*2 gene is a potential tumor suppressor in human colon cancer. Strikingly and of great potential clinical relevance, our results indicate that increase in the expression level of wild-type *Kras*2 gene might be a beneficial gene therapeutic strategy for human colon cancer.

Terminology

*Kras*2, namely v-Ki-ras2 Kirsten rat sarcoma viral oncogene homolog, is on chromosome 12p12-13, and is one of the three members of the *ras* gene: *Hras*1, *Nras* and *K-ras*2. Apoptosis, also called programmed cell death, or "cell suicide": A form of cell death in which a programmed sequence of events leads to the elimination of cells without releasing harmful substances into the surrounding area. Apoptosis plays a crucial role in biological development and maintaining health by eliminating old cells, and unhealthy cells. Cell cycle, the sequence of stages that a cell passes through between one cell division and the next. A cell cycle can be divided into four main stages: the M phase, when nuclear and cytoplasmic division occurs; the G1 phase; the S phase, in which DNA replication occurs; and the G2 phase, a relatively quiescent period.

Peer review

This is an interesting paper that challenges dogma of role of *Kras*2 in CRC. The study with appropriate methods investigating the effect of re-introduction of wild-type *Kras*2 in colorectal cancer cell lines on cell growth, proliferation and apoptosis. A major finding of the study was that re-expression of wild-type *Kras*2 inhibited cell growth and proliferation along with induction of the apoptosis in the studied cell line. It is worthy of publication in *WJG*.

REFERENCES

1 **Halatsch ME**, Hirsch-Ernst KI, Weinel RJ, Kahl GF. Differential activation of the c-Ki-ras-2 proto-oncogene in human colorectal carcinoma. *Anticancer Res* 1998; **18**: 2323-2325
2 **Rodenhuis S**, Slebos RJ. Clinical significance of ras oncogene activation in human lung cancer. *Cancer Res* 1992; **52**: 2665s-2669s
3 **Perentesis JP**, Bhatia S, Boyle E, Shao Y, Shu XO, Steinbuch

M, Sather HN, Gaynon P, Kiffmeyer W, Envall-Fox J, Robison LL. RAS oncogene mutations and outcome of therapy for childhood acute lymphoblastic leukemia. *Leukemia* 2004; **18**: 685-692

4 **Wang Y**, Wang Y, Stoner G, You M. ras mutations in 2-acetylaminofluorene-induced lung and liver tumors from C3H/HeJ and (C3H x A/J)F1 mice. *Cancer Res* 1993; **53**: 1620-1624

5 **Zhang Z**, Wang Y, Vikis HG, Johnson L, Liu G, Li J, Anderson MW, Sills RC, Hong HL, Devereux TR, Jacks T, Guan KL, You M. Wildtype Kras2 can inhibit lung carcinogenesis in mice. *Nat Genet* 2001; **29**: 25-33

6 **Spandidos DA**, Sourvinos G, Tsatsanis C, Zafiropoulos A. Normal ras genes: their onco-suppressor and pro-apoptotic functions (review). *Int J Oncol* 2002; **21**: 237-241

7 **Adjei AA**. Blocking oncogenic Ras signaling for cancer therapy. *J Natl Cancer Inst* 2001; **93**: 1062-1074

8 **Bos JL**. ras oncogenes in human cancer: a review. *Cancer Res* 1989; **49**: 4682-4689

9 **Anderson MW**, Reynolds SH, You M, Maronpot RM. Role of proto-oncogene activation in carcinogenesis. *Environ Health Perspect* 1992; **98**: 13-24

10 **Perucho M**, Goldfarb M, Shimizu K, Lama C, Fogh J, Wigler M. Human-tumor-derived cell lines contain common and different transforming genes. *Cell* 1981; **27**: 467-476

11 **Vogelstein B**, Fearon ER, Hamilton SR, Kern SE, Preisinger AC, Leppert M, Nakamura Y, White R, Smits AM, Bos JL. Genetic alterations during colorectal-tumor development. *N Engl J Med* 1988; **319**: 525-532

12 **Mariyama M**, Kishi K, Nakamura K, Obata H, Nishimura S. Frequency and types of point mutation at the 12th codon of the c-Ki-ras gene found in pancreatic cancers from Japanese patients. *Jpn J Cancer Res* 1989; **80**: 622-626

13 **Shibata D**, Almoguera C, Forrester K, Dunitz J, Martin SE, Cosgrove MM, Perucho M, Arnheim N. Detection of c-K-ras mutations in fine needle aspirates from human pancreatic adenocarcinomas. *Cancer Res* 1990; **50**: 1279-1283

14 **Bremner R**, Balmain A. Genetic changes in skin tumor progression: correlation between presence of a mutant ras gene and loss of heterozygosity on mouse chromosome 7. *Cell* 1990; **61**: 407-417

15 **Pinto MM**, Emanuel JR, Chaturvedi V, Costa J. Ki-ras mutations and the carcinoembryonic antigen level in fine needle aspirates of the pancreas. Acta Cytol 1997; 41: 427-434

16 **Mills NE**, Fishman CL, Rom WN, Dubin N, Jacobson DR. Increased prevalence of K-ras oncogene mutations in lung adenocarcinoma. *Cancer Res* 1995; **55**: 1444-1447

17 **Rodenhuis S**, Slebos RJ, Boot AJ, Evers SG, Mooi WJ, Wagenaar SS, van Bodegom PC, Bos JL. Incidence and possible clinical significance of K-ras oncogene activation in adenocarcinoma of the human lung. *Cancer Res* 1988; **48**: 5738-5741

18 **Suzuki Y**, Orita M, Shiraishi M, Hayashi K, Sekiya T. Detection of ras gene mutations in human lung cancers by single-strand conformation polymorphism analysis of polymerase chain reaction products. *Oncogene* 1990; **5**: 1037-1043

19 **Reynolds SH**, Anna CK, Brown KC, Wiest JS, Beattie EJ, Pero RW, Iglehart JD, Anderson MW. Activated protooncogenes in human lung tumors from smokers. *Proc Natl Acad Sci USA* 1991; **88**: 1085-1089

20 **Li S**, Rosell R, Urban A, Font A, Ariza A, Armengol P, Abad A, Navas JJ, Monzo M. K-ras gene point mutation: a stable tumor marker in non-small cell lung carcinoma. *Lung Cancer* 1994; **11**: 19-27

21 **Li J**, Zhang Z, Dai Z, Plass C, Morrison C, Wang Y, Wiest JS, Anderson MW, You M. LOH of chromosome 12p correlates with Kras2 mutation in non-small cell lung cancer. *Oncogene* 2003; **22**: 1243-1246

22 **Diaz R**, Ahn D, Lopez-Barcons L, Malumbres M, Perez de Castro I, Lue J, Ferrer-Miralles N, Mangues R, Tsong J, Garcia R, Perez-Soler R, Pellicer A. The N-ras proto-oncogene can suppress the malignant phenotype in the presence or absence of its oncogene. *Cancer Res* 2002; **62**: 4514-4518

23 **Li H**, Wan J, Li Y, Zhu ML, Zhao P. Loss of heterozygosity on chromosome 12p12-13 region in Chinese patients with colon carcinoma. *Zhonghua Yixue Yichuanxue Zazhi* 2005; **22**: 694-697

24 **Fearon ER**, Vogelstein B. A genetic model for colorectal tumorigenesis. *Cell* 1990; **61**: 759-767

25 **Shields JM**, Pruitt K, McFall A, Shaub A, Der CJ. Understanding Ras: 'it ain't over 'til it's over'. *Trends Cell Biol* 2000; **10**: 147-154

26 **Davies H**, Bignell GR, Cox C, Stephens P, Edkins S, Clegg S, Teague J, Woffendin H, Garnett MJ, Bottomley W, Davis N, Dicks E, Ewing R, Floyd Y, Gray K, Hall S, Hawes R, Hughes J, Kosmidou V, Menzies A, Mould C, Parker A, Stevens C, Watt S, Hooper S, Wilson R, Jayatilake H, Gusterson BA, Cooper C, Shipley J, Hargrave D, Pritchard-Jones K, Maitland N, Chenevix-Trench G, Riggins GJ, Bigner DD, Palmieri G, Cossu A, Flanagan A, Nicholson A, Ho JW, Leung SY, Yuen ST, Weber BL, Seigler HF, Darrow TL, Paterson H, Marais R, Marshall CJ, Wooster R, Stratton MR, Futreal PA. Mutations of the BRAF gene in human cancer. *Nature* 2002; **417**: 949-954

27 **Raines KW**, Cao GL, Lee EK, Rosen GM, Shapiro P. Neuronal nitric oxide synthase-induced S-nitrosylation of H-Ras inhibits calcium ionophore-mediated extracellular-signal-regulated kinase activity. *Biochem J* 2006; **397**: 329-336

S- Editor Liu Y **L- Editor** Zhu LH **E- Editor** Ma WH

PO Box 2345, Beijing 100023, China
www.wjgnet.com
wjg@wjgnet.com

World J Gastroenterol 2007 February 14; 13(6): 939-944
World Journal of Gastroenterology ISSN 1007-9327

RAPID COMMUNICATION

Construction of recombinant attenuated Salmonella typhimurium DNA vaccine expressing *H pylori* ureB and IL-2

Can Xu, Zhao-Shen Li, Yi-Qi Du, Yan-Fang Gong, Hua Yang, Bo Sun, Jing Jin

Can Xu, Zhao-Shen Li, Yi-Qi Du, Yan-Fang Gong, Hua Yang, Bo Sun, Jing Jin, Department of Gastroenterology, Changhai Hospital, Second Military Medical University, Shanghai 200433, China
Supported by the National Natural Science Foundation of China, No. 30170427
Correspondence to: Dr. Can Xu, Department of Gastroenterology, Changhai Hospital, Second Military Medical University, Shanghai 200433, China. xxccan@sohu.com
Telephone: +86-21-25070539 Fax: +86-21-25074635
Received: 2006-08-08 Accepted: 2006-12-21

Abstract

AIM: To construct a recombinant live attenuated Salmonella typhimurium DNA vaccine encoding *H pylori* ureB gene and mouse IL-2 gene and to detect its immunogenicity *in vitro* and *in vivo.*

METHODS: *H pylori* ureB and mouse IL-2 gene fragments were amplified by polymerase chain reaction (PCR) and cloned into pUCmT vector. DNA sequence of the amplified ureB and IL-2 genes was assayed, then cloned into the eukaryotic expression vector pIRES through enzyme digestion and ligation reactions resulting in pIRES-ureB and pIRES-ureB-IL-2. The recombinant plasmids were used to transform competent *E. coli* DH5α, and the positive clones were screened by PCR and restriction enzyme digestion. Then, the recombinant pIRES-ureB and pIRES-ureB-IL-2 were used to transform LB5000 and the recombinant plasmids extracted from LB5000 were finally introduced into the final host SL7207. After that, recombinant strains were grown *in vitro* repeatedly. In order to detect the immunogenicity of the vaccine *in vitro*, pIRES-ureB and pIRES-ureB-IL-2 were transfected to COS-7 cells using Lipofectamine^{TM}2000, the immunogenicity of expressed UreB and IL-2 proteins was assayed with SDS-PAGE and Western blot. C57BL/6 mice were orally immunized with 1×10^8 recombinant attenuated Salmonella typhimurium DNA vaccine. Four weeks after vaccination, mice were challenged with 1×10^7 CFU of live *H pylori* SS1. Mice were sacrificed and the stomach was isolated for examination of *H pylori* 4 wk post-challenge.

RESULTS: The 1700 base pair ureB gene fragment amplified from the genomic DNA was consistent with the sequence of *H pylori* ureB by sequence analysis. The amplified 510 base pair fragment was consistent with the sequence of mouse IL-2 in gene bank. It was confirmed by PCR and restriction enzyme digestion that *H pylori* ureB and mouse IL-2 genes were inserted into the eukaryotic expression vector pIRES. The experiments *in vitro* showed that stable recombinant live attenuated Salmonella typhimurium DNA vaccine carrying ureB and IL-2 genes was successfully constructed and the specific strips of UreB and IL-2 expressed by recombinant plasmids were detected through Western blot. Study *in vivo* showed that the positive rate of rapid urease test of the immunized group including ureB and ureB-IL-2 was 37.5% and 12.5% respectively, and was significantly lower than that (100%) in the control group ($P < 0.01$).

CONCLUSION: Recombinant attenuated Salmonella typhimurium DNA vaccine expressing UreB protein and IL-2 protein with immunogenicity can be constructed. It can protect mice against *H pylori* infection, which may help the development of a human-use *H pylori* DNA vaccine.

Key words: *H pylori*; DNA vaccine; ureB gene; Salmonella typhimurium

Xu C, Li ZS, Du YQ, Gong YF, Yang H, Sun B, Jin J. Construction of recombinant attenuated Salmonella typhimurium DNA vaccine expressing *H pylori* ureB and IL-2. *World J Gastroenterol* 2007; 13(6): 939-944

http://www.wjgnet.com/1007-9327/13/939.asp

INTRODUCTION

H pylori infection can lead to chronic gastritis, peptic ulcer disease, and is also a risk factor for gastric adenocarcinoma and mucosa-associated lymphoid tissue (MALT) lymphoma[1-4]. More than 50% of the human population worldwide are infected with *H pylori*. About 10%-20% of all the patients have severe diseases such as gastric or duodenal ulcer and gastric cancer. The current therapy, based on the use of proton-pump inhibitor and antibiotics[5-7], is efficacious but faces potential problems like patient compliance, increasingly reported antibiotic resistance, and side effects such as abdominal pain, nausea, diarrhea[8]. Vaccination of humans against *H pylori*

infection may be an effective and economic approach to its control.

Studies of *H pylori* vaccine have focused on the individual *H pylori* proteins or the whole bacterial cell sonicates as antigens which need mucosal adjuvants like cholera toxin or *E. coli* labile toxin to elicit effective protection[9-11]. However, their use in humans is hampered by extremely high toxicity of mucosal adjuvants[12,13]. Recently, DNA vaccine without such mucosal adjuvants has been demonstrated to induce both humoral and cellular immunity and is becoming a promising treatment for viral, bacterial and parasitic pathogens[14,15]. Protective immunity against HIV, influenza virus, rabies virus, malaria and tuberculosis has been shown in animal models[16-19]. DNA vaccine of *H pylori* is seldom reported.

It was reported that coexpression of cytokine genes together with antigen-encoding genes in DNA vaccination vectors can increase both humoral and cellular immune response[20,21]. No information is available about the effects of cytokine-derived adjuvant in combination with *H pylori* vaccine.

In the present study we constructed a recombinant live attenuated Salmonella typhimurium DNA vaccine carrying *H pylori* ureB gene and mouse IL-2 gene, and identified its immunogenicity in transfected COS-7 cells *in vitro* and its prophylactic immunization *in vivo*.

MATERIALS AND METHODS

Bacteria and mammalian cell line and culture conditions

Attenuated Salmonella typhimura LB5000 and SL7207 kindly provided by Professor Bruce Stocker of Stanford University, USA, were cultured in Amp (-) LB medium. *E. coli* DH5α was grown in LB medium containing 50mg ampicillin per liter. *H pylori* strain CCUG17874 (NCTC11638) kindly provided by the Italian IRIS Research Center was cultured on *H pylori* selective agar plates with 10% defibrillated sheep blood and antibiotics (Merck Company, Germany) at 37℃ under microaerophilic conditions with 5% O_2, 10% CO_2 and 85% N_2. COS-7 cell line and recombinant plasmid pCIneo-IL-2 were provided by the Department of Immunology, Secondary Military Medical University of China. The mammalian expression vector pIRES was purchased from Clontech, USA.

PCR amplication of ureB and IL-2 gene fragments

Genomic DNA of *H pylori* was extracted as previously described using CTAB[22]. According to the complete DNA sequence of *H pylori* published and multiple clone sites of pIRES, the primers to amplify ureB containing *Nhe I* site in P1 and *Xho I* site in P2 respectively were designed (P1: 5' GCTAGCCACCATGAAAAAGATTAGCAGAAAAG 3', P2: 5' CTCGAGCTAGAAAATGCTAAAGAGTTG CGCC 3'). The primers to amplify IL-2 containing *Sal I* site in P3 and *Not I* site in P4 were designed (P3: 5' GTC-GACCACCATGTACAGCATGCAGCTCG3', P4: 5' GCGGCCGCTTATTGAGGGCTTGTTGAGATG 3'). Amplication conditions for ureB were as follows: at 95℃ for 5 min, then 35 cycles at 95℃ for 30 s, at 55℃ for 50 s and at 72℃ for 90 s, followed by 10 min at 72℃. Amplication conditions for IL-2 were at 95℃ for 5 min, then 30 cycles at 95℃ for 30 s, at 55℃ for 40 s and at 72℃ for 1 min, followed by 5 min at 72℃. The amplified products were analyzed on 1.2% agarose gels stained with ethidium bromide.

Sequencing analysis of ureB and IL-2

The PCR products were separated using a QIAquick gel extraction kit (QIAGEN, CA, USA). Purified ureB and IL-2 fragments were each subcloned into TA cloning vector pUCmT (Takara, Dalian, China) resulting in pUCmT-ureB and pUCmT-IL-2, then the nucleotide sequences of ureB and IL-2 were analyzed using an automatic sequencer.

Construction of recombinant pIRES-ureB and pIRES-ureB-IL-2

Fragments of *Nhe I* and *Xho I*-digested pUCmT-ureB were inserted into the *Nhe I*/*Xho I* site of eukaryotic expression vector pIRES, through a serial of enzyme digestion and ligation reactions resulting in pIRES-ureB. Fragments of *Sal I* and *Not I*-digested pUCmT-IL-2 were inserted into the *Sal I*/*Not I* site of pIRES-ureB. The recombinant pIRES-ureB and pIRES-ureB-IL-2 were all confirmed by PCR and restriction enzyme digestion.

In vitro transfection and expression of UreB and IL-2

Recombinant plasmids of pIRES-ureB and pIRES-ureB-IL-2 were transfected into COS-7 cells respectively in order to detect the proteins expressed by pIRES-ureB and pIRES-ureB-IL-2. COS-7 cell line was cultured at 37℃, in Dulbecco's modified Eagle's medium supplemented with 10% FBS (Gibco-BRL, UK), 100 U/mL penicillin and 100 μg/mL streptomycin, 15 mmol/L HEPES, 2 mmol/L *L*-glutamine. The mixture of pIRES-ureB and Lipofectamine ™2000 (Invitrogen, USA) or pIRES-ureB-IL-2 and Lipofectamine™2000 were added to the COS-7 cells. Forty-eight hours after transfection, the cells were washed with PBS and protein extraction reagent was added. The lysate was collected and centrifuged at 12000 × *g* for 5 min at 4℃.

Supernatant containing proteins was electrophoretically analyzed in a 10% polyacrylamide gel, subsequently electrotransferred onto nitrocellulose membranes. Nonspecific binding sites were blocked with 2% bovine serum albumin (BSA), then rabbit anti-*H pylori* or rabbit anti-IL-2 antibodies and peroxidase-labeled anti-rabbit immunoglobulin G (IgG) were added. The antigens were visualized by chemiluminescence (Bio-Rad, Germany) according to the manufacturer's instructions.

Construction of recombinant attenuated Salmonella typhimurium carrying H pylori ureB and mouse IL-2 genes

Recombinant pIRES-ureB and pIRES-ureB-IL-2 were used to transform attenuated Salmonella typhimurium LB5000 for methylation decoration using calcium chloride, then the recombinant plasmids extracted were transformed into the final host strain SL7207 by electroporation. The attenuated Salmonella typhimurium SL7207 carrying ureB gene and SL7207 carrying both ureB and IL-2 genes were

cultured in LB medium to 80 generations. The recombinant plasmids in transformed SL7207 were isolated from every 10 generations and identified by restriction enzymes and PCR.

Immunization

Prior to immunization, mice were left overnight without solid food and 4 h without water. One hundred μL of 3% sodium bicarbonate was given orally using a stainless steel catheter tube to neutralize the stomach pH. Immediately after that, mice in the vaccination group were orally given 5×10^8 live attenuated salmonella typhimurium DNA vaccine ureB or ureB-IL-2 in a total volume of 200 μL, mice in the control group were given 200 μL PBS. Mice had free access to water and food after immunization.

Challenge of mice

Four weeks after immunization, all mice were challenged with 200 μL *H pylori* SS1 (1×10^7 CFU). Before challenge, all mice were prepared as described above.

Assessment of H pylori in gastric tissue

Four weeks after challenge, all mice were sacrificed and the stomach was carefully removed from each mouse under aseptic conditions. The stomach was washed 3 times in sterile PBS to remove food residues. A part of the antral region was used for rapid urease test to measure the urease activity.

Statistical analysis

Differences in *H pylori* strain-induced urease activity in stomach of immunized and non- immunized mice were evaluated using a two-tailed Fisher's exact test.

RESULTS

Sequence analysis of ureB and IL-2

Sequence analysis of ureB and IL-2 showed that the sequences of amplified fragments were consistent with those of *H pylori* ureB and mouse IL-2 published in the gene bank respectively.

Recombinant plasmids confirmed by PCR and restriction enzyme digestion

After pUCmT-ureB and pIRES were digested by both *Nhe* I and *Xho* I, a 1700 bp fragment of ureB was directly cloned into *Nhe* I/*Xho* I site of pIRES, resulting in a recombinant plasmid pIRES-ureB. IL-2 was inserted into the *Sal* I/*Not* I site of pIRES-ureB to get pIRES-ureB-IL-2. Both PCR and restriction enzyme digestion demonstrated that recombinant plasmids contained the ureB and IL-2 genes. PCR and restriction enzyme digestion products were analyzed on agarose gel (Figure 1).

Immunoreactivity of expressed recombinant proteins

Identification of pIRES-ureB and pIRES-ureB-IL-2 *in vitro* expression was carried out. The lysate of COS-7 cells transfected by pIRES-ureB and pIRES-ureB-IL-2 was analyzed by Western blot (Figure 2A and B). It revealed the band about 66 000 in relative molecular weight

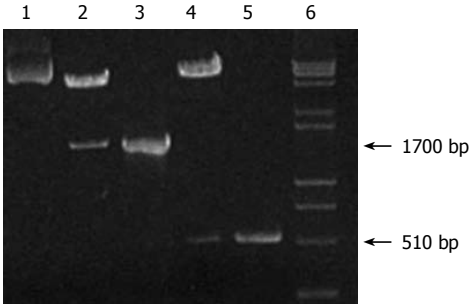

Figure 1 Agarose gel electrophoresis analysis of recombinant pIRES-ureB-IL-2. Lane 1: pIRES after digestion with Nhe I and Xho I as a negative control, lane 2: pIRES-ureB-IL-2 after digestion with Nhe I and Xho I, lane 3: PCR product of ureB, lane 4: pIRES-ureB-IL-2 after digestion with SalI and Not I, lane 5: PCR product of IL-2, lane 6: DNA Marker (DL2000 + 15000).

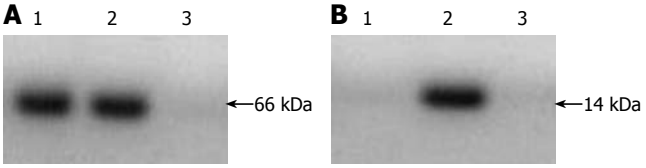

Figure 2 Western blot analysis of expressed UreB protein products (**A**) and IL-2 protein products (**B**). Lane 1: COS-7 cells transfected by pIRES-ureB, lane 2: COS-7 cells transfected by pIRES-ureB-IL-2, lane 3: COS-7 cells transfected by pIRES as a control.

corresponded to UreB protein and 14 000 to IL-2 protein, but the control transfected with pIRES had no specific band.

Recombinant attenuated Salmonella typhimurium DNA vaccine and its stability in vitro

After transformed by pIRES-ureB-IIL-2, recombinant plasmid extracted from LB5000 was used to transform SL7207. Plasmid stability is essential to assure the stable expression of antigens encoded by genes which were cloned into the plasmids. Therefore, SL7207 carrying pIRES-ureB-IIL-2 was grown *in vitro* up to 80 generations to examine the plasmid stability. The objective fragments (1.7 kb and 510 bp) could be seen on the map of agarose gel of PCR products and those of restriction enzyme digested recombinant plasmid isolated from transformed SL7207 (Figure 3A and B).

Rapid urease test results of gastric mucosa

All mice in the control PBS group were infected with *H pylori*. In contrast, 62.5% and 87.5% of mice immunized with ureB and ureB-IL-2 were resistant to *H pylori* ($P < 0.01$). The negative rate of rapid urease test in ureB-IL-2 group was significantly higher than that in ureB group ($P < 0.05$, Table 1).

DISCUSSION

DNA vaccine or genetic vaccine can induce immune response to DNA-encoded proteins after naked DNA is

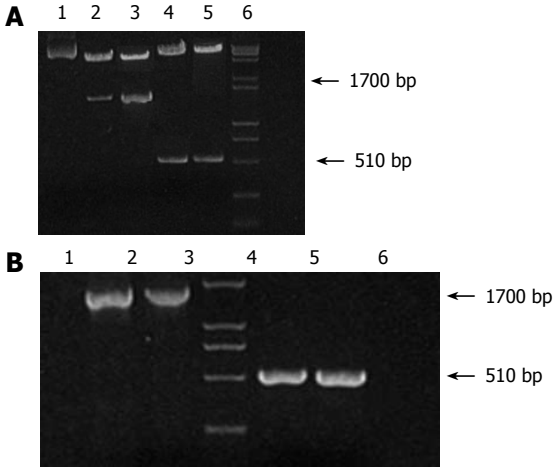

Figure 3 Agarose gel electrophoresis analysis of recombinant attenuated Salmonella typhimurium DNA vaccine strain with restriction enzyme digestion (**A**) (lane1: pIRES after digestion with Nhe I and Xho I, lanes 2-3: recombinant plasmid pIRES-ureB-IL-2 from strains of different generations after digestion with Nhe I and Xho I, lanes 4-5: pIRES-ureB-IL-2 from strains of different generations after digestion with Sal I and Not I, lane 6: DNA marker: (DL2000 + 15000) and identification of recombinant attenuated Salmonella typhimurium DNA vaccine strain carrying ureB by PCR (**B**) (lane1: product amplified from pIRES as a negative control, Lane4: Marker (DL2000); Lanes 2-3: ureB amplified from strains of different generations, lane 4: marker-DL2000, lanes 5-6: IL-2 amplified from strains of different generations.

Table 1 Rapid urease test results of gastric mucosa in different groups

Group	Positive (*n*)	Negative (*n*)	Total (*n*)	Negative rate (%)
PBS	10	0	10	0
ureB	9	15	24	62.5[b]
ureB-IL-2	3	21	24	87.5[a,b]

[a]$P < 0.05$ *vs* ureB group; [b]$P < 0.01$ *vs* PBS group.

injected into a host. DNA vaccines have been widely used in laboratory animals to elicit comprehensive humoral and cellular immune responses. Clinical trials have shown that DNA vaccines are safe and well tolerated[15,23]. Moreover, some reports have demonstrated that DNA vaccine could produce long-lasting immunity[24-25]. The vaccine itself is a recombinant plasmid with heat stability and does not need to be purified. It can be used to protect against and treat tumors[26-29].

However, this approach has not been fully explored in *H pylori* vaccine. The available *H pylori* vaccine is a protein vaccine, including *H pylori* whole cells or one of the recombinant proteins of *H pylori* as an antigen of the vaccine in combination with mucosal adjuvants such as cholera toxin or heat-labile toxin of enterotoxigenic *E. coli* [11,30,31]. The manufacture of such vaccines is complicated, and some mucosal adjuvants have gastrointestinal toxicity. It was reported that mucosal immunization with *Helicobacter heilmannii* urease B or *H pylori* urease, given nasally with cholera toxin, could protect BALB/c mice against *H heilmannii* infection and significantly reduce the preexisting infection[32]. However, immunization aggravates gastric corpus atrophy.

Urease is an enzyme consisting of six UreA subunits and six UreB subunits. Urease negative *H pylori* strains are unable to colonize the stomach of gnotobiotic piglets, demonstrating its role in the colonization. Urease may intervene directly or indirectly in induction of tissue damage in the stomach. Moreover, it may play an additional role in adhesion and stimulation of inflammatory cells. Urease is a highly conserved protein among gastric *H pylori* species and a potential antigen for prophylactic and therapeutic vaccines against *H pylori* infection among different animals[33-35], suggesting that it is an ideal antigen candidate for *H pylori* vaccine.

It has been shown that live attenuated bacteria carrier including attenuated strains of Salmonella *in vitro* could deliver DNA vaccines to human cells, thus allowing vaccination via mucosal surfaces and specific targeting of professional antigen presenting cells in mucosa-associated lymphoid tissue tumors[36,37].

Several studies have shown that co-administration of cytokine proteins or of cytokine-expressing plasmids can modulate the immune response to DNA vaccination[40,41]. Enhancement of antigen-specific antibody response and T cell response has been demonstrated by vaccine co-expressing DNA and immune adjuvants like IL-2 or granulocyte macrophage colony stimulating factor (GM-CSF) gene[40,41].

In this study, we constructed a live recombinant attenuated Salmonella typhimurium DNA vaccine strain expressing UreB protein and mouse IL-2 protein. The complete ureB gene fragment and mouse IL-2 gene were amplified and then sequence analysis was performed after they were cloned respectively into the TA cloning vector pUCmT. Purified ureB and IL-2 were cloned into eukaryotic expression vector pIRES. Both the enzyme digestion and PCR confirmed the successful construction of recombinant plasmid pIRES-ureB and pIRES-ureB-IL-2. Recombinant attenuated Salmonella typhimurium carrying *H pylori* ureB gene and mouse IL-2 was successfully constructed after recombinant plasmid was used to transform LB5000 and SL7207. Since the stability of the protective antigen is very important for a vaccine, we assayed the stability of the recombinant plasmid *in vitro*. PCR and restriction enzyme digestion confirmed the presence of pIRES-ureB-IL-2 in all transformed strains of SL7207 up to the 80th generation, demonstrating the stability of the recombinant plasmid in SL7207.

It was also shown *in vitro* in our present study that COS-7 cellls transfected by pIRES-ureB-IL-2 could express 66000 UreB and 14000 IL-2, but COS-7 cells transfected by pIRES could not express them. The pIRES-ureB-IL-2 DNA vaccine we constructed could express UreB protein which can react with anti-*H pylori* protein and IL-2 which can react with anti-mouse IL-2 protein.

We also demonstrated that a single dose of ureB or both ureB and adjuvant IL-2 delivered by the live attenuated Salmonella typhimurium SL7207 strain could protect C57BL/6 mice against *H pylori* colonization in the stomach. No protection was observed in the control group. Compared with ureB group, ureB-IL-2 group

appeared to induce a better protection against *H pylori* infection with a significantly higher negative rate of rapid urease test, suggesting that adjuvant IL-2 may improve the protective immunization level.

In summary, recombinant attenuated Salmonella typhimurium DNA vaccine encoding *H pylori* ureB gene and mouse IL-2 gene can express UreB and IL-2 with immunogenicity. DNA vaccine can protect against *H pylori* challenge in animal models. The therapeutic effect of DNA vaccine on *H pylori* infection and its mechanism should be further studied.

COMMENTS

Background

Studies of *H pylori* vaccine have focused on the individual *H pylori* proteins or the whole bacterial cell sonicates as antigens which need mucosal adjuvants like cholera toxin or *Escherichia coli* labile toxin to elicit effective protection. However, clinical trials have shown the intestinal toxicity of mucosal adjuvants. Recently, DNA vaccine without such mucosal adjuvants has been demonstrated to induce humoral and cellular immunity and is becoming a promising treatment for viral, bacterial and parasitic pathogens. Protective immunity against HIV, influenza virus, rabies virus, malaria and tuberculosis has been shown in animal models. DNA vaccine against *H pylori* is seldom reported.

Research frontiers

It was reported that co-expression of cytokine genes and antigen-encoding genes in DNA vaccination vectors can increase humoral and cellular immune response. No information is available about the effects of cytokine-derived adjuvant in combination with H pylori vaccine.

Innovations and breakthroughs

Recombinant attenuated Salmonella typhimurium DNA vaccine encoding *H pylori* ureB gene and mouse IL-2 gene can express UreB and IL-2 with immunogenicity. DNA vaccine against *H pylori* and adjuvant IL-2 may improve the protective immunization level.

Applications

H pylori vaccine can prevent *H pylori* infection in human beings.

Peer review

The manuscript by Dr. Xu *et al* described an interesting study on the construction of a recombinant attenuated S. typhimurium DNA vaccine for *Helicobacter pylori* infection. The authors have coexpressed *H pylori* ureB and cytokine IL-2 which can improve the potential immunogenicity and protective efficacies of the vaccine.

REFERENCES

1 **Isakov V**, Malfertheiner P. *Helicobacter pylori* and nonmalignant diseases. *Helicobacter* 2003; **8** Suppl 1: 36-43
2 **Miwa H**, Sakaki N, Sugano K, Sekine H, Higuchi K, Uemura N, Kato M, Murakami K, Kato C, Shiotani A, Ohkusa T, Takagi A, Aoyama N, Haruma K, Okazaki K, Kusugami K, Suzuki M, Joh T, Azuma T, Yanaka A, Suzuki H, Hashimoto H, Kawai T, Sugiyama T. Recurrent peptic ulcers in patients following successful Helicobacter pylori eradication: a multicenter study of 4940 patients. *Helicobacter* 2004; **9**: 9-16
3 **Takahashi S**. Long-term Helicobacter pylori infection and the development of atrophic gastritis and gastric cancer in Japan. *J Gastroenterol* 2002; **37** Suppl 13: 24-27
4 **Al-Akwaa AM**, Siddiqui N, Al-Mofleh IA. Primary gastric lymphoma. *World J Gastroenterol* 2004; **10**: 5-11
5 **Suzuki H**, Masaoka T, Nomura S, Hoshino Y, Kurabayashi K, Minegishi Y, Suzuki M, Ishii H. Current consensus on the diagnosis and treatment of H. pylori-associated gastroduodenal disease. *Keio J Med* 2003; **52**: 163-173
6 **Perri F**, Qasim A, Marras L, O'Morain C. Treatment of Helicobacter pylori infection. *Helicobacter* 2003; **8** Suppl 1: 53-60
7 **Anagnostopoulos GK**, Kostopoulos P, Margantinis G, Tsiakos S, Arvanitidis D. Omeprazole plus azithromycin and either amoxicillin or tinidazole for eradication of Helicobacter pylori infection. *J Clin Gastroenterol* 2003; **36**: 325-328
8 **Cameron EA**, Powell KU, Baldwin L, Jones P, Bell GD, Williams SG. Helicobacter pylori: antibiotic resistance and eradication rates in Suffolk, UK, 1991-2001. *J Med Microbiol* 2004; **53**: 535-538
9 **Kotloff KL**, Sztein MB, Wasserman SS, Losonsky GA, DiLorenzo SC, Walker RI. Safety and immunogenicity of oral inactivated whole-cell Helicobacter pylori vaccine with adjuvant among volunteers with or without subclinical infection. *Infect Immun* 2001; **69**: 3581-3590
10 **Jeremy AH**, Du Y, Dixon MF, Robinson PA, Crabtree JE. Protection against Helicobacter pylori infection in the Mongolian gerbil after prophylactic vaccination. *Microbes Infect* 2006; **8**: 340-346
11 **Durrani Z**, Rijpkema S. Orogastric vaccination of guinea pigs with Helicobacter pylori sonicate and a high dose of cholera toxin lowers the burden of infection. *FEMS Immunol Med Microbiol* 2003; **36**: 169-173
12 **Holmgren J**, Adamsson J, Anjuère F, Clemens J, Czerkinsky C, Eriksson K, Flach CF, George-Chandy A, Harandi AM, Lebens M, Lehner T, Lindblad M, Nygren E, Raghavan S, Sanchez J, Stanford M, Sun JB, Svennerholm AM, Tengvall S. Mucosal adjuvants and anti-infection and anti-immunopathology vaccines based on cholera toxin, cholera toxin B subunit and CpG DNA. *Immunol Lett* 2005; **97**: 181-188
13 **Pizza M**, Giuliani MM, Fontana MR, Monaci E, Douce G, Dougan G, Mills KH, Rappuoli R, Del Giudice G. Mucosal vaccines: non toxic derivatives of LT and CT as mucosal adjuvants. *Vaccine* 2001; **19**: 2534-2541
14 **Martin JE**, Sullivan NJ, Enama ME, Gordon IJ, Roederer M, Koup RA, Bailer RT, Chakrabarti BK, Bailey MA, Gomez PL, Andrews CA, Moodie Z, Gu L, Stein JA, Nabel GJ, Graham BS. A DNA vaccine for Ebola virus is safe and immunogenic in a phase I clinical trial. *Clin Vaccine Immunol* 2006; **13**: 1267-1277
15 **Schalk JA**, Mooi FR, Berbers GA, van Aerts LA, Ovelgönne H, Kimman TG. Preclinical and clinical safety studies on DNA vaccines. *Hum Vaccin* 2006; **2**: 45-53
16 **Muthumani K**, Zhang D, Dayes NS, Hwang DS, Calarota SA, Choo AY, Boyer JD, Weiner DB. Novel engineered HIV-1 East African Clade-A gp160 plasmid construct induces strong humoral and cell-mediated immune responses in vivo. *Virology* 2003; **314**: 134-146
17 **Soboll G**, Horohov DW, Aldridge BM, Olsen CW, McGregor MW, Drape RJ, Macklin MD, Swain WF, Lunn DP. Regional antibody and cellular immune responses to equine influenza virus infection, and particle mediated DNA vaccination. *Vet Immunol Immunopathol* 2003; **94**: 47-62
18 **Carvalho LJ**, Daniel-Ribeiro CT, Goto H. Malaria vaccine: candidate antigens, mechanisms, constraints and prospects. *Scand J Immunol* 2002; **56**: 327-343
19 **Ha SJ**, Jeon BY, Kim SC, Kim DJ, Song MK, Sung YC, Cho SN. Therapeutic effect of DNA vaccines combined with chemotherapy in a latent infection model after aerosol infection of mice with Mycobacterium tuberculosis. *Gene Ther* 2003; **10**: 1592-1599
20 **Chang SY,** Lee KC, Ko SY, Ko HJ, Kang CY. Enhanced efficacy of DNA vaccination against Her-2/neu tumor antigen by genetic adjuvants. *Int J Cancer* 2004; **111**: 86-95
21 **Buonocore F**, Mazzini M, Forlenza M, Randelli E, Secombes CJ, Zou J, Scapigliati G. Expression in Escherchia coli and purification of sea bass (Dicentrarchus labrax) interleukin 1beta, a possible immunoadjuvant in aquaculture. *Mar Biotechnol* (NY) 2004; **6**: 53-59
22 **Xu C**, Li ZS, Tu ZX, Xu GM, Gong YF, Man XH. Distribution of cagG gene in Helicobacter pylori isolates from Chinese patients with different gastroduodenal diseases and its clinical

and pathological significance. *World J Gastroenterol* 2003; **9**: 2258-2260

23 **Liu MA**, Wahren B, Karlsson Hedestam GB. DNA vaccines: recent developments and future possibilities. *Hum Gene Ther* 2006; **17**: 1051-1061

24 **Medjitna TD**, Stadler C, Bruckner L, Griot C, Ottiger HP. DNA vaccines: safety aspect assessment and regulation. *Dev Biol* (Basel) 2006; **126**: 261-270; discussion 327

25 **Fuller DH**, Loudon P, Schmaljohn C. Preclinical and clinical progress of particle-mediated DNA vaccines for infectious diseases. *Methods* 2006; **40**: 86-97

26 **Henke A**. DNA immunization--a new chance in vaccine research? *Med Microbiol Immunol* 2002; **191**: 187-190

27 **Abdelnoor AM**. Plasmid DNA vaccines. *Curr Drug Targets Immune Endocr Metabol Disord* 2001; **1**: 79-92

28 **Donnelly J**, Berry K, Ulmer JB. Technical and regulatory hurdles for DNA vaccines. *Int J Parasitol* 2003; **33**: 457-467

29 **Reisfeld RA**, Niethammer AG, Luo Y, Xiang R. DNA vaccines designed to inhibit tumor growth by suppression of angiogenesis. *Int Arch Allergy Immunol* 2004; **133**: 295-304

30 **Guy B**, Hessler C, Fourage S, Haensler J, Vialon-Lafay E, Rokbi B, Millet MJ. Systemic immunization with urease protects mice against *Helicobacter pylori* infection. *Vaccine* 1998; **16**: 850-856

31 **Keenan JI**, Rijpkema SG, Durrani Z, Roake JA. Differences in immunogenicity and protection in mice and guinea pigs following intranasal immunization with *Helicobacter pylori* outer membrane antigens. *FEMS Immunol Med Microbiol* 2003; **36**: 199-205

32 **Dieterich C**, Bouzourène H, Blum AL, Corthésy-Theulaz IE. Urease-based mucosal immunization against Helicobacter heilmannii infection induces corpus atrophy in mice. *Infect Immun* 1999; **67**: 6206-6209

33 **Dunn BE,** Phadnis SH. Structure, function and localization of Helicobacter pylori urease. *Yale J Biol Med* 1998; **71**: 63-73

34 **Sougioultzis S**, Lee CK, Alsahli M, Banerjee S, Cadoz M, Schrader R, Guy B, Bedford P, Monath TP, Kelly CP, Michetti P. Safety and efficacy of E coli enterotoxin adjuvant for urease-based rectal immunization against *Helicobacter pylori*. *Vaccine* 2002; **21**: 194-201

35 **Hocking D**, Webb E, Radcliff F, Rothel L, Taylor S, Pinczower G, Kapouleas C, Braley H, Lee A, Doidge C. Isolation of recombinant protective Helicobacter pylori antigens. *Infect Immun* 1999; **67**: 4713-4719

36 **Thole JE**, van Dalen PJ, Havenith CE, Pouwels PH, Seegers JF, Tielen FD, van der Zee MD, Zegers ND, Shaw M**.** Live bacterial delivery systems for development of mucosal vaccines. *Curr Opin Mol Ther* 2000; **2**: 94-99

37 **Dietrich G**, Spreng S, Favre D, Viret JF, Guzman CA. Live attenuated bacteria as vectors to deliver plasmid DNA vaccines. *Curr Opin Mol Ther* 2003; **5**: 10-19

38 **Sirard JC**, Niedergang F, Kraehenbuhl JP. Live attenuated Salmonella: a paradigm of mucosal vaccines. *Immunol Rev* 1999; **171**: 5-26

39 **Nobiron I**, Thompson I, Brownlie J, Collins ME. Cytokine adjuvancy of BVDV DNA vaccine enhances both humoral and cellular immune responses in mice. *Vaccine* 2001; **19**: 4226-4235

40 **McGettigan JP**, Koser ML, McKenna PM, Smith ME, Marvin JM, Eisenlohr LC, Dietzschold B, Schnell MJ. Enhanced humoral HIV-1-specific immune responses generated from recombinant rhabdoviral-based vaccine vectors co-expressing HIV-1 proteins and IL-2. *Virology* 2006; 344: 363-377

41 **Niethammer AG**, Xiang R, Ruehlmann JM, Lode HN, Dolman CS, Gillies SD, Reisfeld RA. Targeted interleukin 2 therapy enhances protective immunity induced by an autologous oral DNA vaccine against murine melanoma. *Cancer Res* 2001; **61**: 6178-6184

S- Editor Liu Y **L- Editor** Wang XL **E- Editor** Ma WH

PO Box 2345, Beijing 100023, China
www.wjgnet.com
wjg@wjgnet.com

World J Gastroenterol 2007 February 14; 13(6): 945-949
World Journal of Gastroenterology ISSN 1007-9327

RAPID COMMUNICATION

Oral absorption of hyaluronic acid and phospholipids complexes in rats

Si-Ling Huang, Pei-Xue Ling, Tian-Min Zhang

Si-Ling Huang, Pei-Xue Ling, Tian-Min Zhang, Working Station for Postdoctoral Scientific Research, Institute of Biopharmaceuticals of Shandong Province, Jinan 250108, Shandong Province, China
Supported by the Natural Science Foundation of Shandong Province, China. No. Y2005C31
Correspondence to: Professor Dr. Pei-Xue Ling, Working Station for Postdoctoral Scientific Research, Institute of Biopharmaceuticals of Shandong Province, Jinan 250108, Shandong Province, China. peixue.ling@bausch.com
Telephone: +86-531-88937780-1301 Fax: +86-531-88937780-1822
Received: 2006-09-05 Accepted: 2006-12-30

Abstract

AIM: To prepare a complex of hyaluronic acid (HA) and phospholipids (PL), and study the improvement effect of PL on the oral absorption of HA.

METHODS: The complex of HA-PL (named Haplex) was prepared by film dispersion and sonication method, its physico-chemical properties were identified by infrared spectra and differential scanning calorimetry (DSC). The oral absorption of Haplex was studied. Thirty-two healthy rats were divided into 4 groups randomly: (1) a normal saline (NS) control group; (2) an HA group; (3) a mixture group and (4) a Haplex group. After intragastric administration, the concentration of HA in serum was determined.

RESULTS: The physico-chemical properties of Haplex were different from HA or PL or their mixture. After Haplex was administered to rats orally, the serum concentration of HA was increased when compared with the mixture or HA control groups from 4 h to 10 h ($P < 0.05$). The $\Delta AUC_{0\text{-}12\ h}$ of Haplex was also greater than that of the other three groups ($P < 0.05$).

CONCLUSION: The method of film dispersion and sonication can prepare HA and PL complex, and PL can enhance the oral absorption of exogenous HA.

Key words: Hyaluronic acid; Phospholipids; Complex; Oral absorption; Infrared spectrum; Thermochemistry

Huang SL, Ling PX, Zhang TM. Oral absorption of hyaluronic acid and phospholipids complexes in rat. *World J Gastroenterol* 2007; 13(6): 945-949

http://www.wjgnet.com/1007-9327/13/945.asp

INTRODUCTION

Hyaluronic acid (HA) is an acidic linear mucopolysaccharide, having regularly alternating units of *N*-acetylglucosamine and *D*-glucuronic acid linked by 1, 4- or 1, 3-β-glycosidic bonds. HA distributes widely in connective tissues, vitreous body, and joint fluid of vertebrates. Its relative molecular mass (M_r) is 2×10^5-7×10^6, it possesses an important function of water keeping[1]. As is well known, the unique viscoelastic and lubricating properties of HA along with its biocompatibility and nonimmunogenicity have led to its wide uses in cosmetic, health care, medical, pharmaceutical applications, and so on.

It has been shown that HA can be absorbed by rats after oral administration in our previous experiments. As skin care and healthy food, HA can increase the precurosor which synthesizes HA *in vivo*. It can play a systemic role by increasing the concentration of endogenous HA from dermis to epidermis, therefore delaying aging is possible[2,3]. However, several limitations exist and influence the gastrointestinal absorption of exogenous HA when it is administered orally, such as high M_r and poor liposolubility of HA.

Phospholipids (PL) contains glycerol with a phosphate ester and two fatty acid ester side chains. They are the major building blocks of biological membranes and are tissue compatible[4]. PL is a series of amphiprotic materials, which can improve the gastrointestinal absorption of drugs. Since the 1980s, drugs especially plants extracts, complex with PL began to be a common trial to increase their oral bioavailability. The results indicate that PL complex play an important role in increasing the drug therapeutic effects, and the technique is easy to practise[5,6]. Consequently, in our experiment, PL was used as an absorption enhancer and the complex of HA and PL was prepared, which was named Haplex. The physico-chemical properties of Haplex were identified by infrared spectrum and differential scanning calorimetry. Haplex was administered to rats orally to prove if PL can enhance the oral absorption of HA.

MATERIALS AND METHODS

Reagents

HA was obtained from Shandong Freda Biochemical Limited Company, China. Egg lecithin was obtained from Lipoid Company, Germany. HA radioimmunoassay kit (HA RIA Kit) was obtained from Shanghai Naval Medical

Research Institute, China. The other agents were all analytically pure.

Animals

Wistar rats (female, 260-300 g in weight) were obtained from the Animal Resource Center of Shandong University. Animals were housed at a constant temperature of 22 ± 2℃, and fed on standard pellet chow and water *ad libitum*. All experiments were carried out in accordance with the China Animal Welfare Legislation and were approved by Shandong University Ethics Committee of the Care and Use of Laboratory Animals.

Haplex preparation

The Haplex was prepared by film dispersion and sonication method[7,8]. The mixture of HA and PL was obtained by grinding in mortar.

Infrared spectra

We detected the position changes of main functional groups of Haplex by attenuated total reflectance infrared spectrum. Samples were spread on the KBr crystal glass plate and impacted. The spectral resolution was 8.0 cm, scanning range was 4000-500 cm^{-1} and the result was the average value of 200 times.

Differential scanning calorimetry

The thermochemical property changes of Haplex were detected by DSC. Its operational conditions were as follows: flow rate of N_2 50 mL/min, scanning range of temperature 0-400℃ and raising rate 5℃/min.

Animal screening

Some diseases could increase the concentration of HA in blood; therefore, the healthy animals should be screened before the experiment. The serum concentration range of HA was lower than plasma in rodent animals. The concentration range of HA in the plasma of healthy rats was 46-260 mg/L[9]. In this experiment, we found that the serum concentration of HA in most rats was lower than 180 mg/L, so these rats were selected for the following experiments.

Group and administration

Thirty-two healthy rats were divided into 4 groups with 8 rats in each group. The 4 groups were: a normal saline (NS) control group; an HA group; a mixture group and a Haplex group. All selected rats were fasted (but free drinking) for 12 h before experiment, and were anesthetized by intraperitoneal injection of Pentobarbital before drawing blood. The rats were intragastrically administrated with HA dosage of 60 mg/kg body weight using an intragastric injector. The injector was inserted into the stomach of rats at a depth of 4-6 cm, and the solution was pushed out.

Blood drawing and detection

The blood was drawn from subclavian vein at 0, 1, 2, 4, 7, 10 and 12 h after administration, and then was centrifuged after the serum separation. The serum was collected and stored in refrigerator at -80℃. After that, the concentration of HA in serum was detected using HA RIA Kit.

Statistical analysis

The data were presented as mean ± SD, and t test was performed between groups. $P < 0.05$ was considered statistically significant.

Because HA was inherent ingredient of serum, the concentration of HA in blank blood should be precluded when we analyze the data. The absorption effect was evaluated by the net increasing value of area under HA concentration-time curve ($\Delta AUC_{0\text{-}t}$). In our experiment, the time of drawing blood was 0-12 h after administration. The value of $\Delta AUC_{0\text{-}12\,h}$ was calculated by trapezoidal rule, and the formula was expressed as follows:

$$\Delta AUC_{0\text{-}12\,h} = \mathrm{SUM}\{(t_{i+1}-t_i)[(C_i - C_0) + (C_{i+1} - C_0)]/2\}$$

In this formula, t_i and C_i represent the time of drawing blood and the serum concentration of HA at t_i. C_0 indicates the serum concentration of HA at 0 h after administration.

RESULTS

Infrared absorption

The results of IR are shown in Figure 1. As shown in Figure 1, the absorption peak of C=O and C-N of HA in Haplex shifted to superior position, the dissociated carboxy group of HA was also changed. The stretching vibration peak of P=O and P-O-C of PL in Haplex was budged too ($\upsilon_{P=O}$ moved to superior position, $\upsilon_{P\text{-}O\text{-}C}$ moved to the opposition). These changes indicated that the interactions of HA and PL in Haplex happened between the carboxyl group and amide group of HA and the polar head of PL, which belonged to ionic bond interaction and hydrophobic interaction[10-12].

Thermochemical properties

The DSC curves (Figure 2) showed that the endothermic phase transition peak and the exothermic oxygenolysis peak of PL in Haplex both disappeared. But the thermochemical property of HA had no obvious difference. The results revealed that as a mucopolysaccharide, HA could protect PL and weaken the sensibility of PL to temperature[13].

In a word, IR and DSC indicated that the physico-chemical properties of Haplex were different from HA, PL and their mixture. The results proved that the complex formed between HA and PL.

Oral absorption of Haplex in rats

The basic principle of HA RIA Kit was the competitive binding reaction between ^{125}I-HA in kit, non-marked HA in serum and HA binding protein (HABP). The amount of ^{125}I-HA-HABP complex was determined[14]. The rat serum samples were collected. After setting the standard curve, the concentrations of HA in serum samples were determined.

The drug concentration-time curves are shown in Figure 3. Compared with NS group, an evident absorption peak appeared in 4-12 h after administration in the

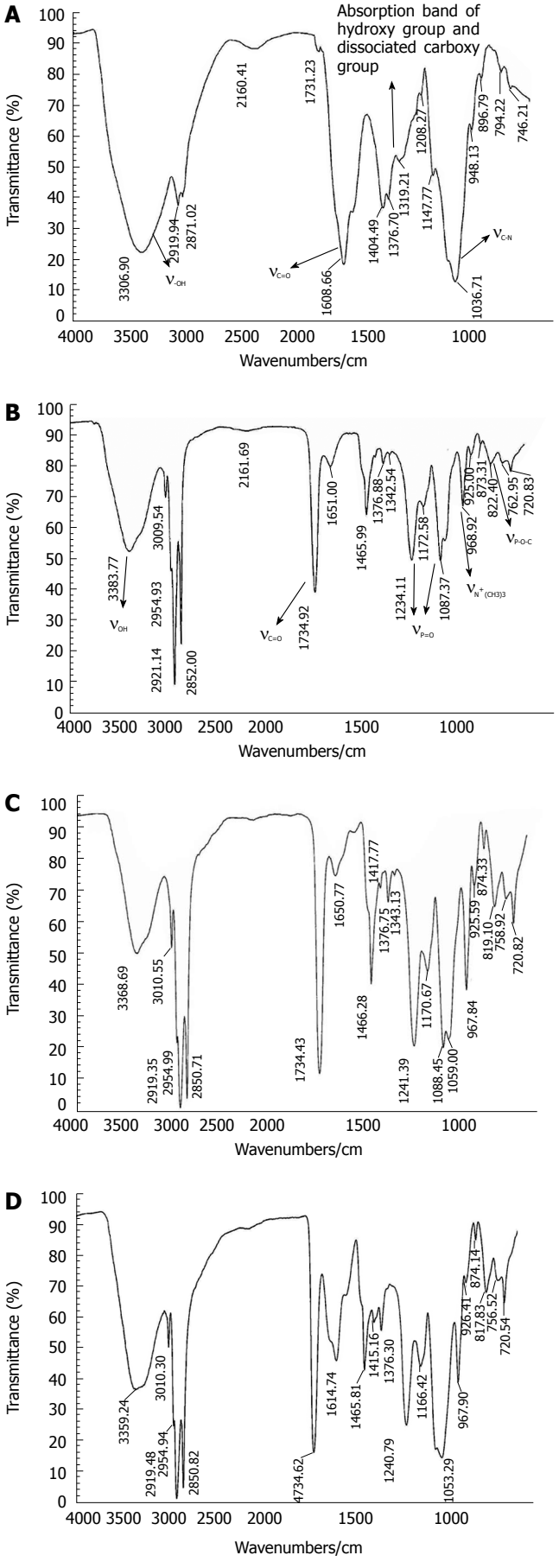

Figure 1 The IR spectra of HA, PL, Haplex, physical mixture of HA and PL. **A**: HA; **B**: PL; **C**: Mixture of HA and PL; **D**: Haplex.

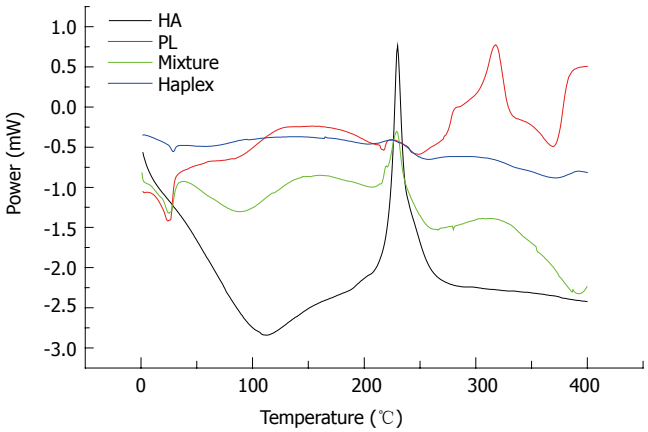

Figure 2 DSC curves of HA, PL, Haplex, physical mixture of HA and PL.

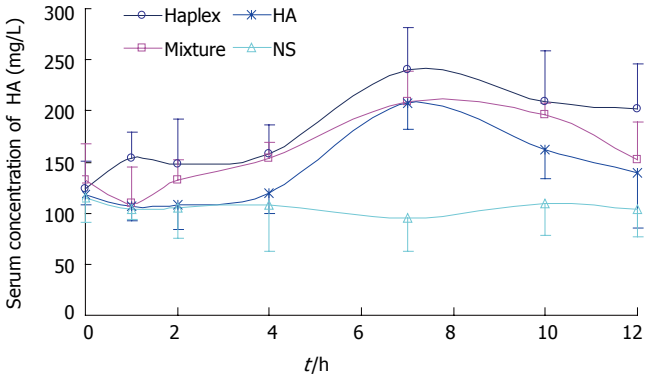

Figure 3 Serum concentration-time curves of HA after single oral dose of Haplex (n = 8).

Table 1 Comparison of ΔAUC$_{0\text{-}12\ h}$ after oral administration

Groups	ΔAUC$_{0\text{-}12\ h}$ (ng·h/mL)
Haplex	777.9 ± 318.3[a]
Mixture	451.6 ± 401.3
HA	381.8 ± 340.8

[a]$P < 0.05$ *vs* HA group.

other three groups ($P < 0.01$). From 0 h to 12 h after administration, the serum concentration of HA in Haplex group was higher than in HA group ($P < 0.05$ in 4-10 h after administration) and the mixture group. However, the serum concentration of HA in mixture group was higher than that in HA group at some certain time points only. The calculation results of ΔAUC$_{0\text{-}12\ h}$ (Table 1) were coincident with Figure 3.

Therefore, the oral absorption experiment demonstrated that: (1) exogenous HA was absorbed into blood after oral administration; (2) after the formation of the complex, PL in Haplex could promote the oral absorption of exogenous HA, increase the HA concentration in serum and prolong the time of HA absorption. However, during the experiment, no

absorption peak appeared in the NS control group. It indicated that oral administration of NS could not increase the HA concentration in serum, and not influence the absorption of HA. And it is thus rational to use NS to dissolve HA and Haplex.

DISCUSSION

The results of animal experiments indicated that PL could enhance the oral absorption of HA after the formation of Haplex. The mechanism of the enhancement effect might be related to the following elements.

PL is an important component of cell membrane and the exogenous PL has strong affinity to cell surfaces. In the Haplex, HA and PL combined together, PL could facilitate HA binding to the cells. On the other hand, in the presence of excess water, PL could form lipid spheres. The polar head groups are oriented to the water; the fatty acyl chains could form a palisade structure, with their ends abutting in the center of the membrane. Similarly, Haplex might form the structure of liposome when it entered into the gastrointestinal fluid. Therefore, when Haplex got close to the gastrointestinal mucous membrane cells, fusion, pinocytosis and phagocytosis might occur due to liposome's double molecular constitution. These contributions could improve the absorption of HA into gastrointestinal mucous membrane. Moreover, due to the smaller particle diameter of PL in Haplex, it could increase the contact area and the contact time between Haplex and intestine wall. All these effects benefit the absorption of HA[5,15-17].

The synovial fluid of normal joints contains several molecular species, the most important constitute of which is HA. HA plays critical role in the physiology of joint function, including lubrication of the synovial surfaces. In addition, synovial fluids contains phospholipids. The presence of HA and PL complexes could provide excellent protection of the cartilage surface from enzymes and free radicals in the synovial fluid, so it could be used as an oral protectant of joint function[18].

HA is a slow-release carrier due to its bioadhesion and biocompatibility properties[19]. After the formation of complex, HA could improve the absorption of PL because of the three dimensions network of HA, and enhance the health care effect of PL.

Haplex could be made in different types of oral praeparatum, including liquid and solid preparation. The nutrition additives and other active components could be added into Haplex if required. The increased effectiveness of active components might attribute to both the bioadhension property of HA and the absorption facilitation property of PL. Haplex thus may be used in skin care and joint disease prevention.

COMMENTS

Background

Hyaluronic acid(HA) is an endogenous glycosaminoglycan, it possesses unique viscoelastic and lubricating properties, and is widely used in cosmetic, health care, medical, pharmaceutical applications, and so on. When exogenous HA is administrated orally, it can increase the concentration of endogenous HA from dermis to epidermis, thereby, it can play systemic roles to delay aging and prevent joints diseases. Phospholipids(PL) are a series of amphiprotic materials, they can improve the gastrointestinal absorption and reduce side effects of drugs.

Research frontiers

In this study, the authors prepared the complexes and mixture of HA and PL. The oral absorption of HA both contained in complex and mixture were studied in rats after intragastric administration.

Innovations and breakthroughs

Because of the high relative molecular mass and poor liposolubility of HA, its gastrointestinal absorption was limited when it is administered orally. In this study, the authors proved that the serum concentration of HA increased when Haplex was administrated orally. So PL could improve the oral absorption of HA after they formed complexes.

Applications

This study provided an evidence for the development of oral praeparatum containing HA. The complex could be used in the fields of healthy food development and joint function protection.

Peer review

This is a descriptive study that shows the improvement effect of phospholipids (PL) on the oral absorption of hyaluronic acid (HA) using a complex between both named Haplex. The manuscript is easy to understand and in general terms well written.

REFERENCES

1 **Kaufmann J**, Mohle K, Hofmann HJ, Arnold K. Molecular dynamics study of hyaluronic acid in water. *J Mol Struct* (Theochem) 1998; **422**: 109-121

2 **Ling PX**. Hyaluronan. Beijing: Zhongguo Qinggongye Chubanshe, 2000: 122-134

3 **Yamamoto H**. Antiaging and cosmetic effects of dietary hyaluronic acid (cxtracellular matrix extract). *New Food Ind* 1998; **40**: 33-41

4 **Cao D**, Qiu AY, Wang XG. The structure, nature, function and researching situation of phospholipids. *Liangshi yu Youzhi* 2004; **5**: 3-7

5 **Zhai GX**, Lou HX, Zou LJ, Bi DZ. Advancement of drugs and phospholipids complex. *Zhongguo Yaoxue Zazhi* 2001; **36**: 801-803

6 **Wu JM**, Chen DW, Sun B, Li SM, Zhang RH. Review of natrual principles complex with phospholipid in pharmacy. *Zhongguo Yaoxue Zazhi* 1998; **33**: 9-11

7 **Pasquali-Ronchetti I**, Quaglino D, Mori G, Bacchelli B, Ghosh P. Hyaluronan-phospholipid interactions. *J Struct Biol* 1997; **120**: 1-10

8 **Ghosh P**, Hutadilok N, Adam N, Lentini A. Interactions of hyaluronan (hyaluronic acid) with phospholipids as determined by gel permeation chromatography, multi-angle laser-light-scattering photometry and 1H-NMR spectroscopy. *Int J Biol Macromol* 1994; **16**: 237-244

9 **Reed RK**, Lilja K, Laurent TC. Hyaluronan in the rat with special reference to the skin. *Acta Physiol Scand* 1988; **134**: 405-411

10 **Tian F**, Zeng GM, Wang DM, Xi SQ. FTIR study on molecular mechanism of the interactions between rare earth ions and dipalmitoylphosphatidylcholine cast-dry film. *Wuli Huaxue Xuebao* 1995; **8**: 134-138

11 **Wang QH**, Feng YY, Yang SL, Chen LF. Study on the phosphatidycholine by means of infrared and ultraviolet spectroscopy. *Nanjing Shida Xuebao* (Natural Sci) 1994; **17**: 51-53

12 **Zhang XL**, Liu LY, Wu GZ. Preparation and quality analysis of the hyaluronic acid from human umbilical cord. *Zhongguo Yaofang* 1999; **1**0: 10-11

13 **Ohtake S**, Schebor C, de Pablo JJ. Effects of trehalose on the phase behavior of DPPC-cholesterol unilamellar vesicles. *Biochim Biophys Acta* 2006; **1758**: 65-73

14 **Li SL**. Nuclear Medicine. 6th ed. Beijing: Renmin Weisheng Chubanshe, 2004: 33-35
15 **Li L**. Medicinal value of phospholipids. *Liangshi yu Youzhi* 2001; **8**: 34-36
16 **Desai MP**, Labhasetwar V, Amidon GL, Levy RJ. Gastrointestinal uptake of biodegradable microparticles: effect of particle size. *Pharm Res* 1996; **13**: 1838-1845
17 **Ling PX**, Tang X, Wang FS, Zhu MH, Zhang TM. Current status in research on complex of drug with phospholipid. *Zhongguo Yaoxue Zazhi* 2005; **40**: 401-402
18 **Kawano T**, Miura H, Mawatari T, Moro-Oka T, Nakanishi Y, Higaki H, Iwamoto Y. Mechanical effects of the intraarticular administration of high molecular weight hyaluronic acid plus phospholipid on synovial joint lubrication and prevention of articular cartilage degeneration in experimental osteoarthritis. *Arthritis Rheum* 2003; **48**: 1923-1929
19 **Yerushalmi N**, Arad A, Margalit R. Molecular and cellular studies of hyaluronic acid-modified liposomes as bioadhesive carriers for topical drug delivery in wound healing. *Arch Biochem Biophys* 1994; **313**: 267-273

S- Editor Liu Y **L- Editor** Ma JY **E- Editor** Ma WH

PO Box 2345, Beijing 100023, China
www.wjgnet.com
wjg@wjgnet.com

World J Gastroenterol 2007 February 14; 13(6): 950-954
World Journal of Gastroenterology ISSN 1007-9327

RAPID COMMUNICATION

Detection of aberrant methylation in fecal DNA as a molecular screening tool for colorectal cancer and precancerous lesions

Zhao-Hui Huang, Li-Hua Li, Fan Yang, Jin-Fu Wang

Zhao-Hui Huang, Li-Hua Li, Fan Yang, Oncology Institute of Wuxi, the Fourth Affiliated Hospital of Soochow University, Wuxi 214062, Jiangsu Province, China
Jin-Fu Wang, College of life sciences, Zhejiang University, Hangzhou 310012, Zhejiang Province, China
Supported by grant from Scientific and Technologic Bureau of Wuxi, No. CS055010
Correspondence to: Zhao-Hui Huang, Oncology Institute of Wuxi, The Fourth Affiliated Hospital of Soochow University, 200 Huihe Road, Wuxi 214062, Jiangsu Province, China. hzhwxsy@yahoo.com.cn
Telephone: +86-510-88683506 Fax: +86-510-88683507
Received: 2006-12-14 Accepted: 2007-01-06

Abstract

AIM: To investigate the feasibility of detecting methylated fecal DNA as a screening tool for colorectal carcinoma (CRC) and precancerous lesions.

METHODS: Methylated secreted frizzled-related protein gene 2 (*SFRP2*), hyperplastic polyposis protein gene (*HPP1*) and O^6-methylguanine-DNA methyltransferase gene (*MGMT*) in stools from 52 patients with CRC, 35 patients with benign colorectal diseases and 24 normal individuals were analyzed using methylation-specific PCR.

RESULTS: Methylated *SFRP2*, *HPP1* and *MGMT* were detected in 94.2%, 71.2%, 48.1% of CRC patients and 52.4%, 57.1%, 28.6% of adenoma patients, respectively. The overall prevalence of fecal DNA with at least one methylated gene was 96.2% and 81.8% in patients with CRC and precancerous lesions, respectively. In contrast, only one of the 24 normal individuals revealed methylated DNA. These results indicated a 93.7% sensitivity and a 77.1% specificity of the assay for detecting CRC and precancerous lesions.

CONCLUSION: Methylation testing of fecal DNA using a panel of epigenetic markers may be a simple and promising non-invasive screening method for CRC and precancerous lesions.

Key words: Colorectal cancer; Methylation; Feces; Secreted frizzled-related protein gene 2; Hyperplastic polyposis protein gene; Methylguanine-DNA methyltransferase gene

Huang ZH, Li LH, Yang F, Wang JF. Detection of aberrant methylation in fecal DNA as a molecular screening tool for colorectal cancer and precancerous lesions. *World J Gastroenterol* 2007; 13(6): 950-954

http://www.wjgnet.com/1007-9327/13/950.asp

INTRODUCTION

Colorectal carcinoma (CRC) is one of the leading causes of cancer-related death in the world. Detection of early-stage cancer and precancerous lesions seems to be a key measure to reduce its death rate[1]. Most deaths due to CRC are preventable through screening, which involves the search for neoplasms (cancer and precancerous lesions) in asymptomatic individuals. Several CRC screening tests, including fecal occult-blood testing (FOBT), barium enema, colonoscopy and sigmoidoscopy, have been available for years. However, none of these methods has been established as a well-accepted screening tool, because of their low compliance rates or low sensitivity and/or specificity. More optimized screening methods should be established with a high sensitivity and specificity for early-stage cancers and precancerous lesions.

Epigenetic gene silencing is increasingly recognized to play a crucial role in human tumors[2]. One of the principal epigenetic mechanisms known to be involved in carcinogenesis is the methylation of cytosine residues in CpG-rich sequences (CpG islands) located within the promoter regions of genes regulating cell proliferation, apoptosis, and DNA repair. DNA methylation within gene promoters results in aberrant gene silencing, which can make an important contribution to the emergence of neoplasias. A number of genes can now be hypermethylated in colorectal tumors[3]. Aberrant promoter methylation often occurs very early during CRC carcinogenesis[4]. Moreover, it has been shown recently that DNA hypermethylation can be detected in DNA from stools of patients with colorectal tumor, suggesting that fecal DNA methylation analysis might provide a valuable approach to non-invasive screening for early colorectal lesions[5-8]. Lenhard *et al*[9] reported that a single methylation marker hypermethylated in cancer 1 (*HIC1*) can be used to detect CRC. Methylated *HIC1* has been found in 42% and 31% of fecal samples from patients with CRC and adenoma, respectively. Aberrant methylation of vimentin gene was also reported in fecal DNA from 43 out of 94

CRC patients, with a sensitivity of 46% and a specificity of 90%, respectively[10]. These studies suggested that a panel of methylated genes might be required to improve the detection sensitivity for CRC. However, to date, methylation markers have not been assessed thoroughly in stools. Few studies have been performed on methylated fecal DNA in CRC patients in parallel with healthy individuals and patients with benign colorectal diseases, and most of these investigations only analyzed a small number of samples.

In the present study, we analyzed methylation of three genes: secreted frizzled-related protein gene 2 (*SFRP2*), hyperplastic polyposis protein gene (*HPP1*) and O^6-methylguanine-DNA methyltrans- ferase gene (*MGMT*) in stools from patients with CRC and benign colorectal diseases as well as from normal controls, and evaluated the feasibility of detecting hypermethylation in stools as a non-invasive screening tool for CRC and precancerous lesions.

MATERIALS AND METHODS

Materials

Fifty-two CRC patients, 35 patients with benign colorectal diseases (including 21 with adenomas, 8 with hyperplastic polyps and 6 with ulcerative colitis) and 24 patients with endoscopically normal colons, undergoing colonoscopy for routine clinical indications in the 4th Affiliated Hospital of Soochow University, were enrolled in this study (Table 1). In addition, fifteen CRC tissue samples and 8 normal colon samples that were resected at the time of surgery or colonoscopy were obtained from Wuxi Tumor Resource Bank. The study was approved by the ethical committee of our institution.

Stool specimens were collected by patients and sent to laboratory within 2 h after defecation, aliquoted and stored at -80℃ until analysis.

Methods

DNA isolation: DNA was isolated from stool samples (200 mg) using the QIAamp DNA Stool Mini Kit (Qiagen). Genomic DNA was purified from colon tissue samples using the QIAamp DNA Mini Kit. The extracted DNA was quantitated by UV spectrum and stored at -20℃.

Methylation-specific PCR (MSP): Stool DNA was modified with sodium bisulfite as previously described[11]. Blood DNA treated *in vitro* with SssI methyltransferase was used as a positive control for methylated alleles, and placental DNA was used as a negative control for MSP assay.

The bisulfite-modified DNA was subjected to PCR in a blinded manner using primer pairs designed to amplify specifically the methylated or unmethylated alleles of respective genes (Table 2). PCR products were analyzed by 2.5% agarose gel electrophoresis. To verify the reliability of MSP, ten PCR products from methylated amplicon of *SFRP2* were randomly selected and bidirectionally sequenced.

Table 1 Characteristics of patients

Characteristics	Colorectal cancer *n* = 52	Benign control *n* = 35	Normal control *n* = 24
Sex			
Male	31	20	13
Female	21	15	11
Age			
Mean ± SD	63.5 ± 11.8	60.0 ± 10.3	59.6 ± 8.2
Range	25-81	31-79	35-68
Dukes stage			
A + B	27	Na	Na
C + D	25	Na	Na
Nodal status			
Positive	23	Na	Na
Negative	29	Na	Na
Tumor size			
> 5 cm	19	Na	Na
≤ 5 cm	33	Na	Na
Tumor locus			
Rectum	24	Na	Na
Distal colon	16	Na	Na
Proximal colon	12	Na	Na

Na: not applicable.

Table 2 Primers for MSP

Primer	Sequences (5′-3′)	Annealing temperature	Product size (bp)
SRFP2-MF	GGGTCGGAGTTTTTCGGAGTTGCGC	62℃	138
SRFP2-MR	CCGCTCTCTTCGCTAAATACGACTCG		
SRFP2-UF	TTTTGGGTTGGAGTTTTTTGGAGTTGTGT	58℃	145
SRFP2-UR	AACCCACTCTCTTCACTAAATACAACTCA		
HPP1-MF	TTTAGCGGACGATTTTTTCGTTTCG	57℃	122
HPP1-MR	AACGACGACGATAACAATAA		
HPP1-UF	TTTAGTGGATGATTTTTTTGTTTTG	57℃	122
HPP1-UR	AACAACAACAATAACAATAA		
MGMT-MF	TTTCGACGTTCGTAGGTTTTCGC	56℃	81
MGMT-MR	GCACTCTTCCGAAAACGAAACG		
MGMT-UF	TTTGTGTTTTGATGTTTGTAGGTTTTTGT	59℃	93
MGMT-UR	AACTCCACACTCTTCCAAAAACAAAACA		

U: unmethylated; M: methylated; F: forward; R: reverse.

Statistical analysis

Statistical probabilities were analyzed by 2 × 2 contingency tables using binomial distribution of differences, Fisher's exact test or Pearson's chi-square test. Calculations were performed using SPSS10.0 software. $P < 0.05$ was considered statistically significant.

RESULTS

Methylated *SFRP2*, *HPP1* and *MGMT* were found in 14, 11 and 8 of 15 CRC tissue samples, respectively. In contrast, none of the 8 samples from normal colonic epithelia revealed any detectable methylated DNA.

MSP was performed on all the 111 stool samples, including 15 fecal samples from CRC patients with matched CRC tissue samples, to analyze *SFRP2*, *HPP1* and *MGMT* (Figure 1). The conversion rate of unmethylated cytosines by bisulfite was measured by sequencing random PCR products from methylated MSP for *SFRP2* (Figure 2).

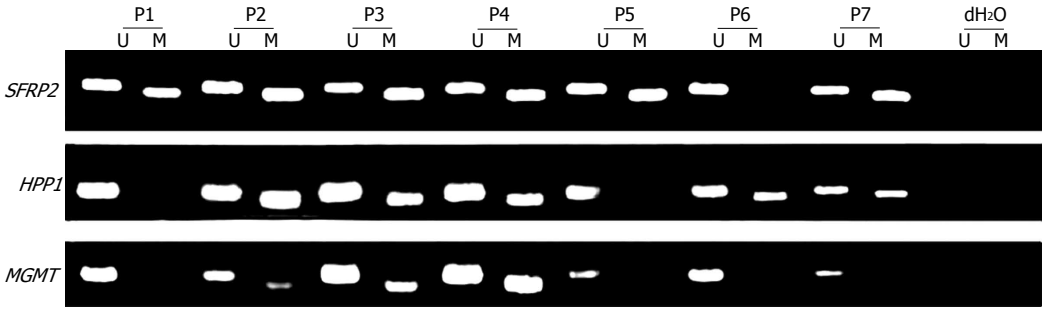

Figure 1 Representative results from methylation-specific PCR analysis performed in stool samples from patients with colorectal cancer.

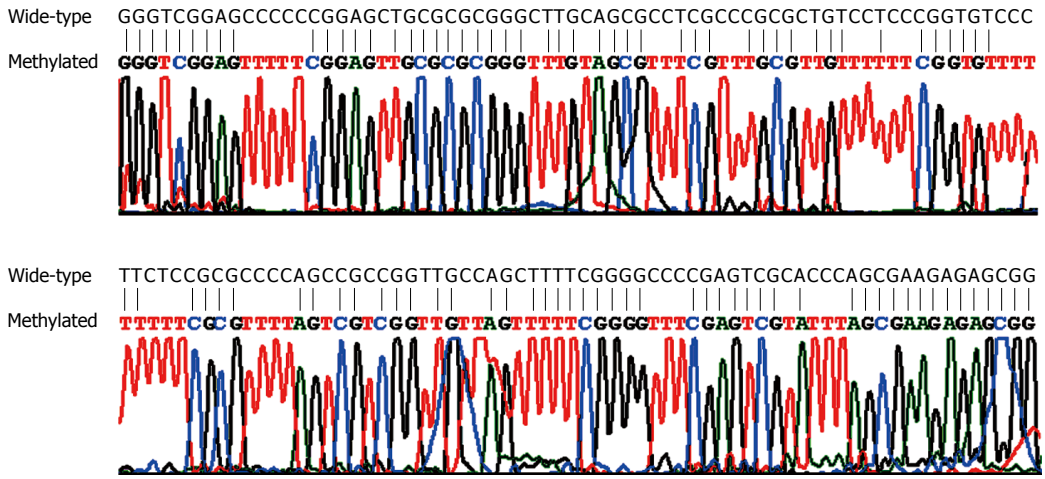

Figure 2 Sequence comparison between amplicons of methylated *SFRP2* and wild-type *SFRP2*.

A total of 10 PCR products were sequenced bidirectionally, revealing only 1 unconverted non-CpG cytosine. A total of 39 non-CpG cytosines were present in the genomic sequence matching with the amplicon of *SFRP2*. By, assuming error-free PCR, > 99.7% of unmethylated cytosines were converted, which assured the reliability of the positive results of MSP. In addition, the sequencing results revealed that CpGs in the amplicon were uniformly methylated (Figure 2), indicating that complete methylation or hypermethylation occurred at *SFRP2*.

The MSP results of fecal DNA are listed in Table 3. Of the 10 patients with advanced adenomas (characterized by size > 1 cm, villous histology, and high-grade dysplasia), 8 had detectable promoter hypermethylation in at least one gene. The sensitivity and specificity of MSP for detecting advanced adenoma were 80% and 83.7%, respectively. Of the 6 patients with ulcerative colitis (UC), one was positive for *SFRP2* and *HPP1*. Colonoscopy with biopsy for this patient revealed high-grade dysplasia. One colonoscopically negative control revealed methylation of *SFRP2*. The sensitivity of *SFRP2*, *HPP1* and *MGMT* assay for detecting CRC and precancerous lesions (including 10 advanced adenomas and 1 UC with dysplasia) was 90.5%, 71.4% and 46.0%, respectively. The specificity of *SFRP2*, *HPP1* and *MGMT* for detecting CRC and precancerous lesions was 83.3%, 85.4% and 93.8%, respectively. These results indicated a 93.7% sensitivity and a 77.1% specificity of the combined test of the three genes for detecting CRC and precancerous lesions.

To examine the coincidence of methylation status between fecal DNA and DNA in its original colon caner, 15 pairs of samples with matched tissue and fecal samples were tested for their methylation status. Methylated *SFRP2*, *HPP1* and *MGMT* were found in 14, 11 and 8 of 15 CRC tissue samples, respectively. In contrast, none of the 8 samples from normal colonic epithelia revealed any detectable methylated DNA. The MSP results were highly consistent between paired fecal and tissue samples, except that two patients had detectable methylated *HPP1* or *MGMT* only in tissue samples.

No correlation was observed between stool DNA hypermethylation and nodal status, Dukes stage, tumor size or tumor locus (data not shown).

DISCUSSION

In this study, we explored the feasibility of detecting methylated fecal DNA as a screening tool for CRC and precancerous lesions. The results showed that DNA methylation could be detected in feces of patients with CRC and precancerous lesions with a high sensitivity (93.7%) and specificity (77.1%).

We detected DNA methylation of *SFRP2*, *HPP1* and *MGMT* in fecal samples from patients with colorectal tumor and non-tumor diseases. It has been shown that these three genes can be methylated in patients with CRC and precancerous lesions[6-8,12-16]. Of the genes chosen for this study, *SFRP2* gene belongs to a new class of tumor suppressor genes (*SFRPs*), which are secreted glycoproteins working as inhibitory modulators of a putative tumorigenic pathway (the Wnt signaling pathway). Aberrant promoter methylation of *SFRP* genes has been described in CRC

by several studies[7,15]. Müller *et al*[7] reported that *SFRP2* is methylated differentially in stools of patients with or without CRC, and *SFRP2* hypermethylation is proposed as a sensitive marker, detecting 77%-90% of CRCs. However, the sample size used in their study was small and the prevalence of methylated *SFRP2* in patients with benign colorectal diseases and in other races or ethnic group was not addressed. In this study, we detected methylated *SFRP2* in fecal samples from Chinese patients with CRC, benign colorectal diseases and in healthy individuals, simultaneously. Our results show that hypermethylated *SFRP2* is detectable in stools of Chinese patients with CRC and precancerous lesions, suggesting that it is a sensitive marker for detecting CRC in healthy controls with 94.2% of sensitivity and 95.2% of specificity, higher than those in a previous report[8]. The different results may be due to the assay-related differences or a different patient population. In addition, methylation of this gene was found in one colonoscopically negative case, which may be most likely owing to the *SFRP2* methylation occurring frequently in premaligant aberrant crypt foci (ACF) that is overlooked at colonoscopy[15].

HPP1 encodes a transmembrane protein containing follistatin and epidermal growth factor–like domains and contains a CpG island in its promoter region that can be aberrantly hypermethylated in CRC and its precursor lesions[13,14,16-18], indicating that *HPP1* gene methylation is an early epigenetic alteration in colorectal carcinogenesis and may be a valuable molecular marker for early diagnosis of CRC. The results of our study indicate that *HPP1* methylation could be frequently detected in most stool samples from patients with CRC (71.2%) and advanced adenoma (57.1%).

MGMT is an important DNA repair enzyme that protects cells from the carcinogenic effects of alkylating agents by removing adducts from the O^6 position of guanine, thus preventing G:C to A:T transition. It was reported that *MGMT* gene inactivation caused by promoter methylation plays a key role in a great variety of human tumors[12]. Leung *et al*[6] showed that 45% hypermethylated *MGMT* are detected in stools of CRC patients in a small-scale feasibility study without healthy subjects as controls. The positive rate of *MGMT* hypermethylation in our study was comparable with their results.

Of the three genes, *SFRP2* is the most informative marker, reaching a sensitivity of 90.5% for CRC and precancerous lesions. In our study, all the 32 samples with methylated *MGMT* revealed methylated *SFRP2*, suggesting that combined detecting of *MGMT* could not increase the detection rate of *SFRP2* for CRC, while a combined test of *SFRP2* and *HPP1* increased the detection rate (93.7%) for CRC and precancerous lesions.

No significant correlation was found between the presence of methylation in fecal DNA and any clinicopathologic characteristics of cancer in our study, indicating that these methylation markers in later stage CRC are as sensitive as in early stage CRC, and may be equivalently sensitive to proximal or distal cancers. However, Ebert *et al*[16] reported that *HPP1* methylation is linked to the location of the primary tumor in the colon and is more frequently methylated in colon cancer compared to rectal cancer. The reasons for the divergent results may include assay-related differences, different patient population and samples.

Table 3 Methylation of *SFRP2*, *HPP1* and *MGMT* in stool samples *n* (%)

Diagnosis	No	Gene locus			Total
		SFRP2	*HPP1*	*MGMT*	
Cancer	52	49 (94.2)	37 (71.2)	25 (48.1)	50 (96.2)
Adenomas	21	11 (52.4)	12 (57.1)	6 (28.6)	15 (71.4)
Advanced adenomas	10	7 (70.0)	7 (70.0)	4 (40.0)	8 (80.0)
Hyperplastic polyp	8	3 (37.5)	2 (25.0)	1 (12.5)	3 (37.5)
Ulcerative colitis	6	1 (16.7)	1 (16.7)	0 (0)	1 (16.7)
Normal	24	1 (4.2)	0 (0)	0 (0)	1 (4.2)

Adenomas are the precursor of most sporadic CRCs. Hyperplastic polyp-serrated adenoma to carcinoma sequence is characterized by recognizable histological changes. Colorectal lesions, starting with dysplastic ACF, hyperplastic polyp (HP) and benign tubular adenoma have the potential to progress to advanced adenomas, which have a significant potential to transform into CRC[17]. Although both ACF and HP are common lesions and the great majority would not transform into clinically significant polyps. HP occurring in the right colon and in the setting of hyperplastic polyposis has the greatest potential to transform into CRC[17,18]. It is unclear if these lesions with methylated DNA would develop into cancer. However, DNA methylation is more common in advanced adenomas. All these findings suggest that methylation may reflect the malignant potential of these lesions. UC-associated CRC is different from sporadic carcinoma. The molecular mechanisms underlying the progression of UC to dysplasia and carcinoma have not been fully understood. One of the UC patients with methylated *SFRP2* and *HPP1* in feces was also diagnosed with high-grade dysplasia, indicating that DNA methylation is not only a frequent event in colorectal tumor, but also detectable in fecal samples from patients with HP and UC. Although detection of early stage CRC represents an important screening goal, efforts should be directed toward detection of dysplastic cells present in patients with benign diseases, such as adenoma, HP and UC. Whether hypermethylation of these three genes can identify these non-malignant diseases, including self-limiting HPs, non-dysplastic ACF and UC, is still unclear. Recent studies indicate that methylation patterns can define a subset of HPs with a significant malignant potential[17,19]. Thus, patients with methylated fecal DNA may belong to high-risk individuals and need more accurate/specific clinical examinations and follow-up.

Although FOBT is a valuable noninvasive screening method that reduces the risk of CRC-related death, it has a limited sensitivity. Colonoscopy, with a high sensitivity and specificity for detection of CRC and large adenomas, requires a thorough bowel preparation, which causes discomfort and small but non-negligible risk of major complications in patients. In contrast, using aberrant gene methylation as a molecular marker seems to offer a potentially powerful approach to population-based

screening for CRC and precancerous lesions. However, further prospective study is needed to validate the epigenetic markers. In addition, simplified, non-expensive and automatized assays may be important for population-based screening.

REFERENCES

1 **Jemal A**, Siegel R, Ward E, Murray T, Xu J, Smigal C, Thun MJ. Cancer statistics, 2006. *CA Cancer J Clin* 2006; **56**: 106-130
2 **Baylin SB**, Ohm JE. Epigenetic gene silencing in cancer - a mechanism for early oncogenic pathway addiction? *Nat Rev Cancer* 2006; **6**: 107-116
3 **Kondo Y**, Issa JP. Epigenetic changes in colorectal cancer. *Cancer Metastasis Rev* 2004; **23**: 29-39
4 **Chan AO**, Broaddus RR, Houlihan PS, Issa JP, Hamilton SR, Rashid A. CpG island methylation in aberrant crypt foci of the colorectum. *Am J Pathol* 2002; **160**: 1823-1830
5 **Belshaw NJ**, Elliott GO, Williams EA, Bradburn DM, Mills SJ, Mathers JC, Johnson IT. Use of DNA from human stools to detect aberrant CpG island methylation of genes implicated in colorectal cancer. *Cancer Epidemiol Biomarkers Prev* 2004; **13**: 1495-1501
6 **Leung WK**, To KF, Man EP, Chan MW, Bai AH, Hui AJ, Chan FK, Lee JF, Sung JJ. Detection of epigenetic changes in fecal DNA as a molecular screening test for colorectal cancer: a feasibility study. *Clin Chem* 2004; **50**: 2179-2182
7 **Müller HM**, Oberwalder M, Fiegl H, Morandell M, Goebel G, Zitt M, Mühlthaler M, Ofner D, Margreiter R, Widschwendter M. Methylation changes in faecal DNA: a marker for colorectal cancer screening? *Lancet* 2004; **363**: 1283-1285
8 **Petko Z**, Ghiassi M, Shuber A, Gorham J, Smalley W, Washington MK, Schultenover S, Gautam S, Markowitz SD, Grady WM. Aberrantly methylated CDKN2A, MGMT, and MLH1 in colon polyps and in fecal DNA from patients with colorectal polyps. *Clin Cancer Res* 2005; **11**: 1203-1209
9 **Lenhard K**, Bommer GT, Asutay S, Schauer R, Brabletz T, Göke B, Lamerz R, Kolligs FT. Analysis of promoter methylation in stool: a novel method for the detection of colorectal cancer. *Clin Gastroenterol Hepatol* 2005; **3**: 142-149
10 **Chen WD**, Han ZJ, Skoletsky J, Olson J, Sah J, Myeroff L, Platzer P, Lu S, Dawson D, Willis J, Pretlow TP, Lutterbaugh J, Kasturi L, Willson JK, Rao JS, Shuber A, Markowitz SD. Detection in fecal DNA of colon cancer-specific methylation of the nonexpressed vimentin gene. *J Natl Cancer Inst* 2005; **97**: 1124-1132
11 **Herman JG**, Graff JR, Myöhänen S, Nelkin BD, Baylin SB. Methylation-specific PCR: a novel PCR assay for methylation status of CpG islands. *Proc Natl Acad Sci USA* 1996; **93**: 9821-9826
12 **Esteller M**, Hamilton SR, Burger PC, Baylin SB, Herman JG. Inactivation of the DNA repair gene O6-methylguanine-DNA methyltransferase by promoter hypermethylation is a common event in primary human neoplasia. *Cancer Res* 1999; **59**: 793-797
13 **Young J**, Biden KG, Simms LA, Huggard P, Karamatic R, Eyre HJ, Sutherland GR, Herath N, Barker M, Anderson GJ, Fitzpatrick DR, Ramm GA, Jass JR, Leggett BA. HPP1: a transmembrane protein-encoding gene commonly methylated in colorectal polyps and cancers. *Proc Natl Acad Sci USA* 2001; **98**: 265-270
14 **Sato F**, Shibata D, Harpaz N, Xu Y, Yin J, Mori Y, Wang S, Olaru A, Deacu E, Selaru FM, Kimos MC, Hytiroglou P, Young J, Leggett B, Gazdar AF, Toyooka S, Abraham JM, Meltzer SJ. Aberrant methylation of the HPP1 gene in ulcerative colitis-associated colorectal carcinoma. *Cancer Res* 2002; **62**: 6820-6822
15 **Suzuki H**, Watkins DN, Jair KW, Schuebel KE, Markowitz SD, Chen WD, Pretlow TP, Yang B, Akiyama Y, Van Engeland M, Toyota M, Tokino T, Hinoda Y, Imai K, Herman JG, Baylin SB. Epigenetic inactivation of SFRP genes allows constitutive WNT signaling in colorectal cancer. *Nat Genet* 2004; **36**: 417-422
16 **Ebert MP**, Mooney SH, Tonnes-Priddy L, Lograsso J, Hoffmann J, Chen J, Röcken C, Schulz HU, Malfertheiner P, Lofton-Day C. Hypermethylation of the TPEF/HPP1 gene in primary and metastatic colorectal cancers. *Neoplasia* 2005; **7**: 771-778
17 **Wynter CV**, Walsh MD, Higuchi T, Leggett BA, Young J, Jass JR. Methylation patterns define two types of hyperplastic polyp associated with colorectal cancer. *Gut* 2004; **53**: 573-580
18 **Goldstein NS**, Bhanot P, Odish E, Hunter S. Hyperplastic-like colon polyps that preceded microsatellite-unstable adenocarcinomas. *Am J Clin Pathol* 2003; **119**: 778-796
19 **Wynter CV**, Kambara T, Walsh MD, Leggett BA, Young J, Jass JR. DNA methylation patterns in adenomas from FAP, multiple adenoma and sporadic colorectal carcinoma patients. *Int J Cancer* 2006; **118**: 907-915

S- Editor Liu Y **L- Editor** Wang XL **E- Editor** Lu W

PO Box 2345, Beijing 100023, China
www.wjgnet.com
wjg@wjgnet.com

World J Gastroenterol 2007 February 14; 13(6): 955-959
World Journal of Gastroenterology ISSN 1007-9327

RAPID COMMUNICATION

Clinical study on safety of adult-to-adult living donor liver transplantation in both donors and recipients

Bin Liu, Lu-Nan Yan, Wen-Tao Wang, Bo Li, Yong Zeng, Tian-Fu Wen, Ming-Qing Xu, Jia-Yin Yang, Zhe-Yu Chen, Ji-Chun Zhao, Yu-Kui Ma, Jiang-Wen Liu, Hong Wu

Bin Liu, Lu-Nan Yan, Wen-Tao Wang, Bo Li, Yong Zeng, Tian-Fu Wen, Ming-Qing Xu, Jia-Yin Yang, Zhe-Yu Chen, Ji-Chun Zhao, Yu-Kui Ma, Jiang-Wen Liu, Hong Wu, The Liver Transplantation Division, Department of Surgery, West China Hospital, Sichuan University, Chengdu 610041, Sichuan Province, China

Correspondence to: Lu-Nan Yan, MD, Liver Transplantation Division, Department of Surgery, West China Hospital, Sichuan University. Chengdu 610041, Sichuan Province, China. surgeryliubin@163.com

Telephone: +86-28-85422476 Fax: +86-28-85423724
Received: 2006-11-14 Accepted: 2006-12-30

Abstract

AIM: To investigate the safety of adult-to-adult living donor liver transplantation (A-A LDLT) in both donors and recipients.

METHODS: From January 2002 to July 2006, 50 cases of A-A LDLT were performed at West China Hospital, Sichuan University, consisting of 47 cases using right lobe graft without middle hepatic vein (MHV), and 3 cases using dual grafts (one case using two left lobe, 2 using one right lobe and one left lobe). The most common diagnoses were hepatitis B liver cirrosis, 30 (60%) cases; and hepatocellular carcinoma, 15 (30%) cases in adult recipients. Among them, 10 cases had the model of end-stage liver disease (MELD) with a score of more than 25. Donor screening consisted of reconstruction of the hepatic blood vessels and biliary system with 3-dimension computed tomography and volumetry of whole liver and right liver volume. Various improved surgical techniques were adopted in the procedures for both donors and recipients .

RESULTS: Forty-nine right lobes and 3 left lobes (2 left lobe grafts for 1 recipient, 1 left lobe graft for 1 recipient who had received right lobe graft donated by relative living donor) were obtained from 52 living donors. The 49 right lobe grafts, without MHV, weighed 400 g-850 g (media 550 g), and the ratio of graft volume to recipient standard liver volume (GV/SLV) ranged from 31.74% to 71.68% (mean 45.35%). All donors' remnant liver volume was over 35% of the whole liver volume. There was no donor mortality. With a follow-up of 2-52 mo (media 9 mo), among 50 adult recipients, complications occurred in 13 (26%) cases and 4 (8%) died postoperatively within 3 mo. Their 1-year actual survival rate was 92%.

CONCLUSION: When preoperative CT volumetry shows volume of remnant liver is more than 35%, the ratio of right lobe graft to recipients standard liver volume exceeding 40%, A-A LDLT using right lobe graft without MHV should be a very safe procedure for both donors and recipients, otherwise dual grafts liver transplantation should be considered.

Key words: Adult-to-adult living donor liver transplantation; Middle hepatic vein; Dual grafts; Right lobe graft; Standard liver volume; Grafts; Weight; Complication

Liu B, Yan LN, Wang WT, Li B, Zeng Y, Wen TF, Xu MQ, Yang JY, Chen ZY, Zhao JC, Ma YK, Liu JW, Wu H. Clinical study on safety of adult-to-adult living donor liver transplantation both in donors and recipients. *World J Gastroenterol* 2007; 13(6): 955-959

http://www.wjgnet.com/1007-9327/13/955.asp

INTRODUCTION

With the shortage of donation of livers worldwide, the first pediatric living donor liver transplantation (LDLT) was performed by Raia in Brazil in 1989[1]. Yamaoka reported the first case of adult to adult LDLT (A-A LDLT) in 1993[2]. Fan reported for the first time a case of A-A LDLT using extended right lobe graft in 1997[3]. Since then, its application has successfully expanded from pediatric to adult patients. But A-A LDLT has not become effective for patients with end-stage liver disease until 2000. The risk of donors has obviously increased with A-A LDLT. Although liver transplantation was performed for donors because of remnant liver failure[4,5], the mortality of donors was about 0.2%-0.3%[6]. If recipient's body weight is much higher than donor's, the graft can not meet the needs of metabolism, thus resulting in small-for-size syndrome[7], or even the death of recipient. So it is a serious problem at present to make both donors and recipients safe, and for recipients to receive an adequate volume of graft for metabolism.

Since July 2001 we have performed the first case of pediatric LDLT in our hospital. A-A LDLT was performed

in January 2002[8,9]. Till July 2006, 62 cases of LDLT have been performed, including 50 cases of A-A LDLT. This article aims to discuss about our experience how to make both donors and recipients safe in A-A LDLT and the indications for dual grafts liver transplantation.

MATERIALS AND METHODS

Materials of recipients

From January 2002 to July 2006, 50 cases of right lobe graft A-A LDLT were performed in our hospital, including 47 right lobe graft without middle hepatic vein (MHV) liver transplantation and 3 dual graft liver transplantation (dual relative donated left lobe grafts 1, relative right lobe graft and relative left lobe graft 1, relative right lobe graft and cadaveric left lobe graft 1[10]). Among the 50 recipients there were 43 men, and 7 women, aged 18-63 years (mean age of 39 years). Primary diseases of recipients included liver cirrhosis after hepatitis B, 30 cases (12 of them had acute liver failure); diffuse ischemic intrahepatic biliary stenosis (DI IBS), 2; Budd-Chiari syndrome with liver cirrhosis[11], 1; postoperative liver failure after three right lobe hepatectomy caused by hepatic trauma, 1; hepatocellular carcinoma, 15; and cholangiocarcinoma, 1. There were 15 (30%) cases at risk among the 50 cases, including 7 cases of acute severe hepatitis, 5 fulminant liver failure, 2 DI IBS with liver failure, and 1 liver failure after hepatectomy. All these patients underwent A-A LDLT at emergency. According to Child-Pugh classification, there were 18 cases of grade A, 7 of grade B, and 25 of grade C. By United Network for Organ Sharing classification, there were 10 cases of stage Ⅰ, 10 of stage Ⅱa, 12 of stage Ⅱb, and 18 of stage Ⅲ. The model of end-stage liver disease scores were: ≤ 18, 35 cases; 19-24, 5 cases; 25-30, 1 case; and > 30, 9 cases. Among 16 malignant cases, no one exceeded 18 scores.

Materials of donors

There were 52 cases, including 16 men and 36 women, with an age range of 9-65 years (mean age 38 years).The relationship between recipients and donors included father 3, mother 8, brother 14, sister 3, spouse 7 (grafts were all donated by wives in this group), children 3, and others 5.

The donors and recipients were blood group identical in 39 cases and compatible in 13 cases. All donors in this group voluntarily donated part of their liver. The ethical aspect of this study was approved by the Ethical Committee of our hospital.

Preoperative evaluation for donors

Physical examination and retrospective analysis of donors' medical records were performed before their operations. The donors and recipients must be blood group identical or compatible. Hepatitis, syphilis, HIV, or Epstein-Barr virus, cytomegalovirus, tuberculosis infection constituted an ineligibility for potential donor. Hepatic blood vessels and biliary system were reconstructed before operation, and the volume of the total liver and right hemiliver were evaluated and calculated with 3-dimension computed tomography (3-D CT). As a potential donor, the right lobe graft volume should not exceed 65% of the total liver, while if the ratio of right lobe graft volume to recipients' standard liver volume is less than 40%, the recipients should undergo dual graft liver transplantation.

To minimize the risk and complications of donors, we have adopted the following managements: (1) to abandon preoperative endoscopic retrograde cholangiopancreatography (ERCP), instead of cholangiography intraoperatively; (2) to study the tracks and variations of hepatic artery with 3-D CT before operation; (3) to abandon routine hepatic puncture for biopsy before operation unless patients were supposed to have fatty liver[12].

Operative approaches in donors

Using right Mercedes (Chevron with vertical extension) incision from xiphoid process to midaxillary line, we unfolded abdominal cavity with suspended abdominal puller. All donated livers were right lobe grafts without MHV. We identified hepatic incision line (the line from the gallbladder fossa below the inferior vena cava) with intraoperative ultrasonography to confirm the tracks of MHV, aided by observing the color change of right and left lobes when right hepatic artery and right tributaries of portal vein (PV) were clamped. Without clamping hepatic blood vessel, we resected liver with cavitron ultrasonic surgical dissector, using temporarily bipolar electric coagulation hemostasis to deal with the section plane. According to the caliber of conduits, we selected different methods of hemostasis such as titanium clamp or ligation. The crassitude tributaries of MHV could be transitorily clamped for anastomosis via interpositioning a vein graft when grafts were planted. Operation should be performed meticulously when dissociating around hepatic hilar. One should carefully analyze the cholangiographic film intraoperatively in order to know whether there are branches or variations in the right hepatic duct, snip connective tissue and bile duct of hilar plate, meanwhile carefully distinguish minute orifica of hepatic ducts, making markers with thin sutures for anastomosis when planting grafts.

We dissected liver tissue till making total right lobe graft dissociated with heparinizing the whole donor body, in turn clamped and cut off the right hepatic artery, right tributary of PV and right hepatic vein, placed the graft into the container filled with 4℃ University of Wisconsin (UW) solution, then removed it to back table for perfusion.

We continuously stitched the orifica of the right tributary of PV with 5-0 sutures, while the orifica of right hepatic duct were stitched at intervals with 6-0 sutures, without interfering with the blood flow in the trunk and left tributary of PV, and the bile flow direction in common hepatic duct.

Bench

We perfused the grafts from PV with 2 liters of 4℃ UW solution, rinsed biliary tracts, repaired orificia of hepatic vein, and kept it as large as possible so as to provide sufficient venous outflow. On back table, we anastomosed recipients' great saphenous vein or cadaveric iliac blood vessels to crassitude tributaries of MHV. We measured and

recorded the hepatic vasculatures and the orificia caliber of bile duct and weight of grafts, then calculated the ratio of grafts to recipients' weight (GRWR)[13] and the ratio of grafts volume to recipients' standard liver volume (GV/SLV)[14].

Operative techniques in recipients

Operation was performed following the routine procedures of our hospital[9,15]. When resecting recipients' liver, we attentively reserved posterohepatic inferior vana cava' s (IVC) integrality, dissociated right hepatic vein cling to IVC, reserved the orifica of right hepatic vein (RHV), along with the end axis enlarged IVC downward, making it suitable for donor's RHV and anastomosis[12]. It was necessary to make ellipsed incision on suitable parts of IVC when the orificia of crassitude tributaries of right hepatic inferior vein or MHV were jointed with IVC by interpositioning the great saphenous vein or cryopreserved cadaveric blood vessels. We adopted end-to-end anastomosis of grafts' right tributaries of PV to recipient's PV trunk, maintained a suitable length for PV trunk after anastomosis, then opened blood flow in hepatic vein and PV, recovered blood perfusion of grafts and ended nonhepatic phase period. With loupe, we finished hepatic artery anastomosis and adopted end-to-end anastomosis of right hepatic duct to common hepatic duct, or Roux-en-Y choledochojejunostomy. If right hepatic duct had many tributaries and their caliber $\leqslant$ 2 mm, biliary tracts should be reconstructed under microscope[16].

Splenectomy should be performed at the same time if donors suffered from splenomegaly and hypersplenism (blood platelet $\leqslant$ 30×10^9/L). If PV pressure was > 25 cmH_2O, splenic artery ligation should be performed for recipients in order to alleviate PV pressure[17].

RESULTS

Preoperative CT evaluation of hepatic volume

We have evaluated the volume of remnant liver with CT. According to the volume of the total liver and right lobe grafts with MHV and right lobe grafts without MHV, we calculated the volume of remnant liver with and without MHV after resection. The evaluation results of 50 donors showed that the volume of remnant liver with MHV < 30% in 10 cases, 30%-35% in 24 cases, > 35% in 16 cases, while the volume of remnant liver without MHV < 30% in 0 case, 30%-35% in 5 cases, and > 35% in 45 cases. According to the Fan criteria[13], the volume of remnant liver should exceed 30%. In this study, there were 10 cases with a volume of remnant liver with MHV of less than 30%, which would be ineligible for potential donor, thus reducing the donor pool. According to Lee criteria[14], the volume of remnant liver should exceed 35%, resulting in just 16 cases of donors. The volume of remnant liver without MHV ranged from 30% to 35% in 5 cases. Considering the safety of 3 among 5 cases whose volume of remnant liver was less than 35%; we adopted dual grafts liver transplantation.

Cinical results in donors

Among 52 donors, we resected right lobe grafts in 49 cases and left lobe grafts in 3 cases (2 left lobe grafts for 1 recipient, 1 left lobe graft for 1 recipient who had received right lobe graft donated by a relative living donor). Grafts of 49 cases were all without MHV, and the weight ranged from 400 g to 850 g (mean weight 550 g). The ratio of right lobe graft to recipient's standard liver volume was 31.74%-71.68% (mean 45.35%). The ratio of graft to recipient's body weight was 0.72%-1.31% (mean 0.91%). Intraoperative total blood loss volume of donors ranged from 250 mL to 735 mL (mean 345 mL), and these blood was all retransfused with autologous blood recovery system. Only 4 cases in this group received allogeneic RBC transfusion of 200 mL to make up the intraoperative blood loss. Operation time varied from 380 min to 620 min (mean 425 min).

Donors had the following complications: transient chyle leakage, recovered after symptomatic treatment; portal venous thromobosis, received second thrombectomy, mending leakage with a patch of great saphenous vein; subphrenic effusion, cured by surgical drainage; and pleural effusion, recovered after repeated thoracic cavity puncture. There was no donor death, and the hospitalized time ranged from 7 to 30 d (mean 11 d). All donors are well and have returned to their daily life and work.

Clinical results in recipients

GRWR was 0.72%-1.17%. There were 12 cases > 1.0%, 31 cases 0.8%-1.0%, and 7 cases < 0.8%. Mean intraoperative blood loss volume was 980 mL. We used autologous blood recovery system for patients with benign diseases. No allogeneic blood transfusion (44%) was made in 22 cases, and the mean operation time was 542 min (range 365-1400 min). Five cases with fulminant liver failure received venous bypass during operation, while the other 45 cases did not.

Among the 50 cases, except for right hepatic vein, we additionally anastomosed right inferior hepatic vein to IVC in 19 cases, and interposed vein grafts on Ⅴ segmental tributaries (V5) of MHV in 20 cases, and on Ⅷ segmental tributaries (V8) in 13 cases (single tributary in 9 cases and double tributary in 12 cases).

We found PV variations in 9 cases, and right anterior and posterior sectoral PV and left PV all directly arise from the PV trunk. So there were two PV orificas on the section plane of right hemiliver, we connected orifica of right anterior and posterior sectoral PV to form a big one, then anastomosed it to recipients' PV trunk in 7 cases, and anastomosed two orificas to both right and left PV in 2 cases.

We adopted end-to-end anastomosis of right hepatic duct to recipients' common bile duct in 34 cases of bile duct anastomosis. Three cases received T tube drainage, while 31 cases did not. Among 16 cases who underwent choledochojejunostomy, 3 cases had 3 hepatic duct orificas, 11 cases had 2, and 2 cases had 1. Thirty-three orificas were routinely anastomosed with magnifying glasses. There were 11 orificas in 5 cases with calibers less than 2 mm, for which operative microscope was used for the anastomosis.

All cases in this study were followed up for 2-52 mo (mean 9 mo). Four (8%) patients died at 21 d, 27 d, 31 d, and 42 d after operation respectively. The causes

included: small-for-size syndrome 1, multiple organs failure caused by pulmonary infection 2, and renal failure 1. Complications occurred in 13 (26%) cases which included hepatic artery embolization (2), biliary leakage (2), subphrenic abscess (1), anastomotic bleeding in Roux-Y jejunojejunostomy (1), hepatic venous stenosis (1), small-for-size syndrome (1), pulmonary infection (3), and renal failure (2). The one-year survival rate was 92%.

DISCUSSION

Making donors safe

Based on familial relationship or friendship, a healthy adult voluntarily donates part of liver, who hopes this will be safe for both donors and recipients. For a surgeon, there is great pressure to ensure operations successful for both donors and recipients. The rationality of LDLT has not been acknowledged worldwide until the first pediatric case was performed in 1989[1].

Pediatric LDLT is that an adult donates small part of liver for a child patient. Donor's safety can be ensured and risk is low. In 1993 Yamaoka *et al*[2] and in 1997 Fan *et al*[3] respectively successfully performed A-A LDLT using right hemiliver. Compared with pediatric LDLT, the risk of A-A LDLT obviously increased when resecting the right hemiliver. So this operation has not been extensively performed in Europe and America, especially as one donor died of gas gangrene of the stomach in America in 2002[18], enthusiasm for A-A LDLT was lessened with one disaster after another. Data in 2006 indicated that there were more than 2000 LDLT cases in America, 1000 in Europe, 2000 in Asia, respectively. The number of donor deaths have reached 14 all over the world with a mortality of about 0.2%-0.3%. So donor's safety has been widely and closely noticed[19].

If we resect too much of a donor's liver, the volume of remnant liver will become too small to meet the needs of the donor's metabolism, leading to dysfunction of liver after operation, liver failure, or even death. On the other hand, if we resect too small part of donor liver, the graft also cannot meet the needs of a donor's metabolism. It is still a challenging subject attempting to tackle this contradication. At present, it is well acknowledged that the volume of total liver and right hemiliver can be calculated with 3-D CT. Fan thought that it was effective to ensure the safety of donors provided the volume of evaluated remnant liver exceeded 30% of the total liver[13]. So he advocated that we should resect the right lobe graft with MHV, while Huang recently thought the volume of evaluated remnant liver exceeded 35% of total liver[4], and suggested that we should resect right lobe graft without MHV.

In this paper we consecutively calculated the volume of donor's liver in 50 A-A LDLT cases. The results show that if we resect the right lobe graft with MHV, the volume of remnant liver was < 30% in 10 cases, 30%-35% in 24 cases, and > 35% in 16 cases. According to the Fan's criteria, 10 cases could not be the candidates for donor, thus dramatically lowering the score of donor liver. Otherwise if we resect right hemiliver without MHV, none case had remnant liver volume < 30%, 5 cases 30%-35% , and the others > 35%. According to Fan's criteria, all donors in this study can be candidates for donors, donor pool can be enlarged, while donor safety should be addressed with the increased risk. Alternatively, according to Huang's criteria, 5 cases in this group would be ineligible for donors, donor safety could be enhanced while the donor pool was being reduced.

Both to maximize to make donors safe and to prevent reduction of donor pool, we resected 47 right lobe grafts without MHV among 52 cases, the other 3 cases received dual grafts liver transplantation. In this way, we have not only ensured donor safety, but achieved satisfactory results.

Making recipients safe

Being different from total liver transplantation, the recipients only received parts of donor's liver in A-A LDLT. It is still controversial discerning the optimal volume of graft for metabolism. At present, there are two standards worldwide: one is GRWR and the other is GV/SLV. It is generally thought that the former should be more than 0.8%[13], and the latter should be more than 40%[14]. In 49 cases of this group, GV/SLV ranged from 31.74% to 71.66% (mean 45.35%), and GRWR from 0.72% to 1.31% (mean 0.91%). Among these cases, GRWR was < 0.8% in 7 cases, and GV/SLV was < 40% in 6 cases, but GV/SLV all exceeded 40% in 3 cases according preoperative CT evaluation, and the other 3 cases whose GV/SLV < 40% underwent dual grafts LDLT. After resection during operation, GV/SLV < 40% was found in 6 cases. This result showed that there are differences between CT evaluation and grafts real weight. Yet clinical study in this group proved that a little error did not influence clinical prognosis. So preoperative CT evaluation has instructive significance for clinical practice.

One case in this group did not receive reconstruction for crassitude tributaries of MHV at its inception in our hospital, causing right anterior lobe of right hemiliver congestion and swelling, and liver dysfunction, small-for-size syndrome and death finally[12]. GV/SLV in this case was 52.98%, which was not definitely related to graft size.

Occurrence of small-for-size syndrome was related to not only small size of grafts, circumfluence of hepatic vein or other factors, but also high pressure in PV, or hyperperfusion of PV which lead to injury of epithelioid cell in hepatic sinus of grafts[20]. Ito *et al*[17] proved that portal hypertension, ligating splenic artery could make PV pressure decrease by 5-10 cmH_2O, obtaining more satisfying clinical results. Therefore, 5 cases in this group with splenoparectasis and blood platelet < 30×10^9/L were routinely underwent splnectomy, other 6 cases with PV pressure > 25 cmH_2O underwent ligation of splenic artery, the results were satisfactory.

About dual grafts

It was effective to use dual grafts to solve the problem of too small size of graft and make donors safe. This approach was first reported by Lee *et al*[21]. It requires 3 operation groups performing 3 operations simultaneously, and the cost is high; while if we adopt double left lobe grafts for liver transplantation, we have to turn over 180° and place ectopically at the location of right one. Therefore, surgical techniques became demanding,

increasing the risk of complications. Therefore it is not a popular procedure worldwide[19]. We adopted one smaller right lobe graft and one left lobe graft, and placed them at primary locations, which have overcome the shortcomings of difficulties for operation[10]. Additionally, it was quite strict controlling the indications of right lobe graft LDLT in South Korea that almost 31% A-A LDLT cases underwent dual graft liver transplantation[4]. Only 3 of 50 cases received dual grafts liver transplantation in this study, while other 47cases underwent right lobe graft LDLT. These protocols can not only make both donors and recipients safe, but also obviously reduce medical cost and consumption of medical materials. The clinical results were satisfactory.

In our experience, right lobe grafts without MHV is adopted, volume of remnant liver is more than 35%, preoperative evaluation with CT and the ratio of right lobe graft to recipients standard liver volume exceeding 40%, are all effective indices to make both donors and recipients safe in right hemiliver LDLT, otherwise we should expect to adopt dual grafts liver transplantation.

REFERENCES

1 **Raia S**, Nery JR, Mies S. Liver transplantation from live donors. *Lancet* 1989; **2**: 497

2 **Fujita S**, Tanaka K, Tokunaga Y, Uemoto S, Sano K, Manaka D, Shirahase I, Shinohara H, Yamaoka Y, Ozawa K. Living-related liver transplantation for biliary atresia. *Clin Transplant* 1993; **7**: 571-577

3 **Lo CM**, Fan ST, Liu CL, Wei WI, Lo RJ, Lai CL, Chan JK, Ng IO, Fung A, Wong J. Adult-to-adult living donor liver transplantation using extended right lobe grafts. *Ann Surg* 1997; **226**: 261-269; discussion 269-270

4 **Brown RS**, Russo MW, Lai M, Shiffman ML, Richardson MC, Everhart JE, Hoofnagle JH. A survey of liver transplantation from living adult donors in the United States. *N Engl J Med* 2003; **348**: 818-825

5 **Akabayashi A**, Slingsby BT, Fujita M. The first donor death after living-related liver transplantation in Japan. *Transplantation* 2004; **77**: 634

6 **Hwang S**, Lee SG, Lee YJ, Sung KB, Park KM, Kim KH, Ahn CS, Moon DB, Hwang GS, Kim KM, Ha TY, Kim DS, Jung JP, Song GW. Lessons learned from 1,000 living donor liver transplantations in a single center: how to make living donations safe. *Liver Transpl* 2006; **12**: 920-927

7 **Tanaka K**, Ogura Y. "Small-for-size graft" and "small-for-size syndrome" in living donor liver transplantation. *Yonsei Med J* 2004; **45**: 1089-1094

8 **Yan LN**, Wen TF, Li B. A case report of adult-to-adult living donor liver transplantation. *Zhonghua Gandan Waike Zazhi*, 2002, **8**: 634-635

9 **Yan LN**. Contemporary liver transplantation. Beijing: People's Military Medical Press, 2004: 599-652

10 **Chen Z**, Yan L, Li B, Zeng Y, Wen T, Zhao J, Wang W, Yang J, Ma Y, Liu J. Successful adult-to-adult living donor liver transplantation combined with a cadaveric split left lateral segment. *Liver Transpl* 2006; **12**: 1557-1559

11 **Yan L**, Li B, Zeng Y, Wen T, Zhao J, Wang W, Xu M, Yang J, Ma Y, Chen Z, Wu H. Living donor liver transplantation for Budd-Chiari syndrome using cryopreserved vena cava graft in retrohepatic vena cava reconstruction. *Liver Transpl* 2006; **12**: 1017-1019

12 **Yan LN**, Li B, Zeng Y, Wen TT, Zhao JC, Wang WT, Yang JY, Xu MQ, Ma YK, Chen ZY, Wu H. Adult-to-adult living donor liver transplantation. *Sichuan Daxue Xuebao Yixueban* 2006; **37**: 88-92

13 **Fan ST**, Lo CM, Liu CL, Yong BH, Chan JK, Ng IO. Safety of donors in live donor liver transplantation using right lobe grafts. *Arch Surg* 2000; **135**: 336-340

14 **Kawasaki S**, Makuuchi M, Matsunami H, Hashikura Y, Ikegami T, Nakazawa Y, Chisuwa H, Terada M, Miyagawa S. Living related liver transplantation in adults. *Ann Surg* 1998; **227**: 269-274

15 **Yan LN**. Liver Surgery. Beijing: People's Medical Publishing House, 2002: 201-262

16 **Yan LN**, Li B, Zeng Y, Wen TF, Zhao JC, Wang WT, Yang JY, Xu MQ, Ma YK, Chen ZY, Liu JW, Wu H. Adult-to-adult living donor liver transplantation using right lobe graft: report of 24 cases. *Zhonghua Yixue Zazhi* 2006; **86**: 411-415

17 **Ito T**, Kiuchi T, Yamamoto H, Oike F, Ogura Y, Fujimoto Y, Hirohashi K, Tanaka AK. Changes in portal venous pressure in the early phase after living donor liver transplantation: pathogenesis and clinical implications. *Transplantation* 2003; **75**: 1313-1317

18 **Miller C**, Florman S, Kim-Schluger L, Lento P, De La Garza J, Wu J, Xie B, Zhang W, Bottone E, Zhang D, Schwartz M. Fulminant and fatal gas gangrene of the stomach in a healthy live liver donor. *Liver Transpl* 2004; **10**: 1315-1319

19 **Sugawara Y**, Makuuchi M. Safe liver harvesting from living donors. *Liver Transpl* 2006; **12**: 902-903

20 **Lo CM**, Liu CL, Fan ST. Portal hyperperfusion injury as the cause of primary nonfunction in a small-for-size liver graft-successful treatment with splenic artery ligation. *Liver Transpl* 2003; **9**: 626-628

21 **Lee SG**, Hwang S, Park KM, Kim KH, Ahn CS, Lee YJ, Cheon JY, Joo SH, Moon DB, Joo CW, Min PC, Koh KS, Han SH, Choi KT, Hwang KS. Seventeen adult-to-adult living donor liver transplantations using dual grafts. *Transplant Proc* 2001; **33**: 3461-3463

S- Editor Liu Y **L- Editor** Ma JY **E- Editor** Lu W

PO Box 2345, Beijing 100023, China
www.wjgnet.com
wjg@wjgnet.com

World J Gastroenterol 2007 February 14; 13(6): 960-963
World Journal of Gastroenterology ISSN 1007-9327

CASE REPORT

Gastric adenocarcinoma inducing portal hypertension: A rare presentation

Pradipta Ghosh, Katsumi Miyai, Mario Chojkier

Pradipta Ghosh, Mario Chojkier, Department of Medicine, Division of Gastroenterology and Hepatology, University of California, San Diego; San Diego, California, United States
Katsumi Miyai, Department of Pathology, University of California, San Diego; San Diego, California, United States
Mario Chojkier, Veterans Affairs Medical Center, Cancer Center, University of California, San Diego, California, United States
Correspondence to: Dr. Pradipta Ghosh, Department of Medicine, University of California, San Diego, San Diego, CA 92161, USA 3350 La Jolla Village Dr. (9111-D), San Diego, CA 92161-0002, United States. prghosh@ucsd.edu
Telephone: +1-858-5342766
Received: 2006-09-23 Accepted: 2006-12-22

Abstract

Advanced gastric cancer usually presents with symptoms due to direct extension into adjacent viscera, distant metastases from lymphatic or hematogenic dissemination and peritoneal seeding. However, portal hypertension as a presentation of metastatic gastric cancer is rare and usually seen in association with other malignancies, e.g. hepatocellular and pancreatic carcinoma. We report a case of signet ring adenocarcinoma of the stomach that presented with esophageal and duodenal varices and bleeding due to portal hypertensive gastropathy. Pagetoid spread of cancer cells likely caused early metastasis and the unusual presentation. We also discussed the pathophysiology of development of portal hypertension in association with malignancies.

Key words: Advanced Gastric adenocarcinoma; Signet ring; Portal hypertension

Ghosh P, Miyai K, Chojkier M. Gastric adenocarcinoma inducing portal hypertension: A rare presentation. *World J Gastroenterol* 2007; 13(6): 960-963

http://www.wjgnet.com/1007-9327/13/960.asp

INTRODUCTION

Portal hypertension in the setting of malignancy could arise from different mechanisms: intraluminal obstruction of portal vein (either due to tumor thrombus[1-3] or as a result of deep vein thrombosis due to a paraneoplastic hypercoagulable state, extraluminal compression due to metastatic lymph nodes or tumor tissue, and acquired portal vein aneurysm[4]. Hepatocellular carcinoma and pancreatic adenocarcinoma are the commonest tumors reported in literature to present as variceal bleeding[5-10]. A case of ovarian cancer presenting similarly has been reported[11]. Gastric adenocarcinoma associated with portal venous thrombosis has been retrospectively recognized using imaging studies and post-mortem analysis[3] or encountered during the course of treatment of the primary tumor[12]. However, initial presentation as portal hypertension is rare and to our knowledge, has not been reported. We report a case of signet ring adenocarcinoma of the gastric cardia that presented as portal hypertension associated with upper gastrointestinal bleeding. The mechanism of portal hypertension was radiographically confirmed as due to a metastatic lymph node compressing the main and left portal veins.

CASE REPORT

An 80-year old man presented with 14-kg weight loss and melena for three weeks prior to hospital admission. He was pale, had bilateral pleural effusions, moderate ascites and guiac-positive melenic stool. Past medical history was significant for gastroesophageal reflux disease, systemic arterial hypertension and depression. There was no history of known liver disease or of alcohol consumption.

Laboratory studies confirmed the presence of normocytic anemia (hemoglobin 8.0 gm/dL), normal coagulation parameters, liver and chemistry panels. An eso phagogastroduodenoscopy revealed two columns of grade 1 esophageal varices (Figure 1A and B), moderately severe portal hypertensive gastropathy (Figure 1C) and duodenal varices (Figure 1D). On retroflexed view we identified a nodular growth in the cardia of the stomach (Figure 1E, star) infiltrating into the distal esophagus (Figure 1B). Portal hypertensive gastropathy was felt to be the cause of gastrointestinal bleeding.

Histopathological examination of the biopsies obtained from the nodularity in the cardia revealed a poorly-differentiated infiltrative malignancy characterized by moderately-sized cells with abundant vacuolated cytoplasm, occasional signet ring cells (Figure 2A and B), nuclear pleomorphism and the presence of mitotic figures. Immunohistochemical staining for CK7 was positive in the malignant cells (not shown), while CK20 was negative. Mucicarmine stain showed cytoplasmic positivity (Figure

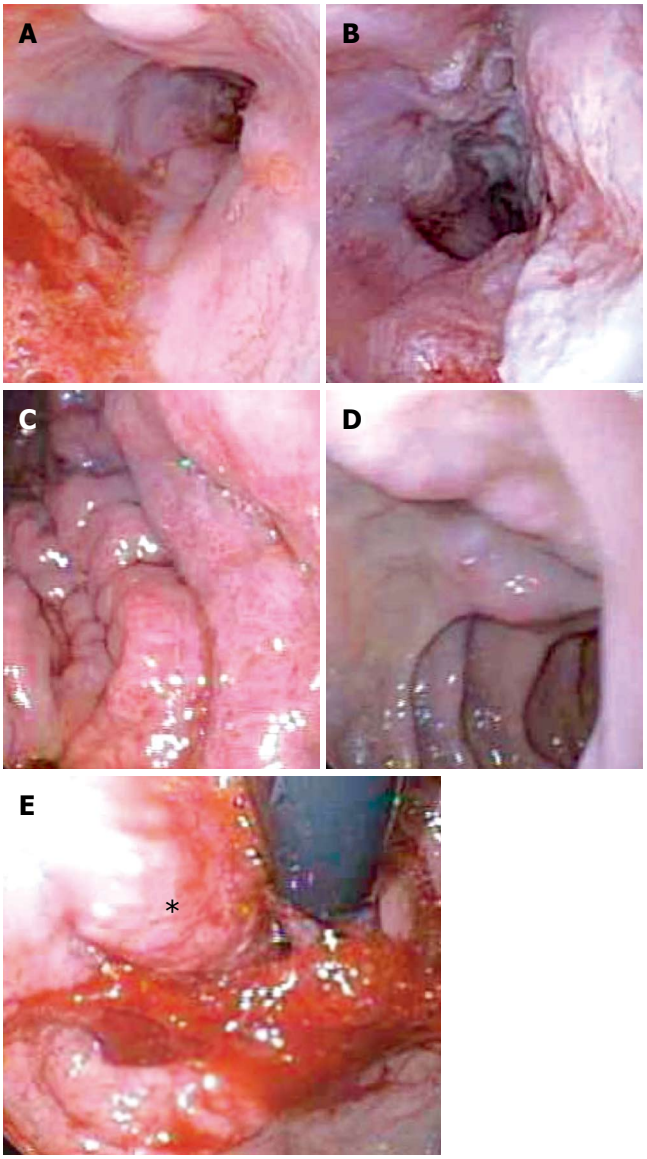

Figure 1 Esophagogastroduodenoscopy demonstratring grade 1 esophageal varices (**A**), tumor invasion of distal third of the esophagus (**B**), moderate portal hypertensive gastropathy (**C**), duodenal varices (**D**), retroflexed view of the nodular tumor in the gastric fundus (**E**).

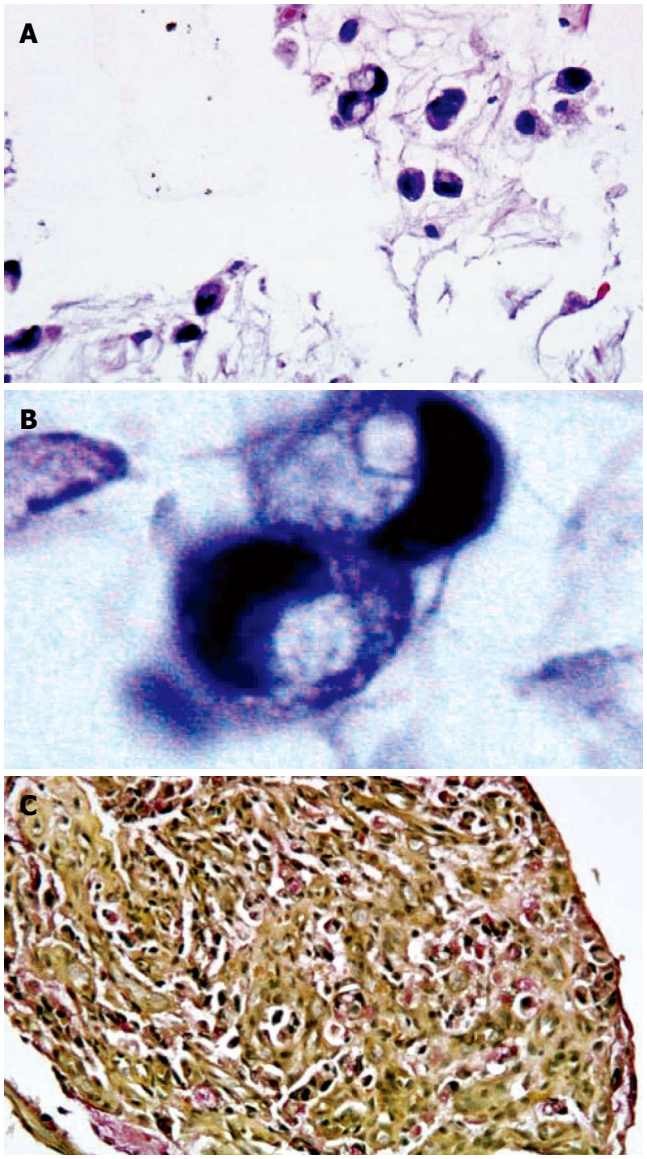

Figure 2 Histology and immunohistochemistry of biopsies from gastric: Light microscopy with hematoxylin and eosin staining of tumor tissue at 40X and 100X with oil magnifications demonstrating moderately-sized cells with abundant vacuolated cytoplasm (**A**) and occasional signet ring cells (**B**), and mucicarmine stain demonstrating intracytoplasmic positive staining (**C**).

2C), differentiating these tumor cells from muciphages in the lamina propria.

In the absence of other causes of portal hypertension, we postulated that the endoscopic appearance was best explained by portal venous obstruction. A color Doppler ultrasonography of the hepatic venous system demonstrated reversal of flow in the left portal vein with appropriate direction of flow in the right and main portal veins. The liver and hepatic arteries appeared normal. A computerized tomography of the abdomen after administration of intravenous contrast revealed a soft tissue mass (Figure 3A and B, star) measuring 5 cm in diameter displacing the pancreatic head and neck inferiorly. The superior mesenteric, splenic (Figure 3B, arrow) and main portal veins were all seen passing through this mass with severe attenuation of all three vessels. The presence of ascites and bilateral pleural effusions was confirmed by both studies.

Due to the advanced stage of the tumor carrying a poor prognosis in this elderly and frail patient, palliative surgery or systemic chemotherapy was considered counterproductive. He was discharged to hospice and subsequently passed away within three months from the time of diagnosis. At autopsy, metastatic disease to the segment VI of the liver was confirmed. A soft tissue mass was found encasing the spleno-portal venous system without vascular invasion or luminal thrombosis, correlating to that seen on CT image ante-mortem. Histopathologic characterization of this mass confirmed it as a lymph node metastasis from primary gastric adenocarcinoma almost replacing the entire normal architecture.

DISCUSSION

Advanced gastric cancer presenting as portal hypertension is unusual. Hepatocellular carcinoma is associated with

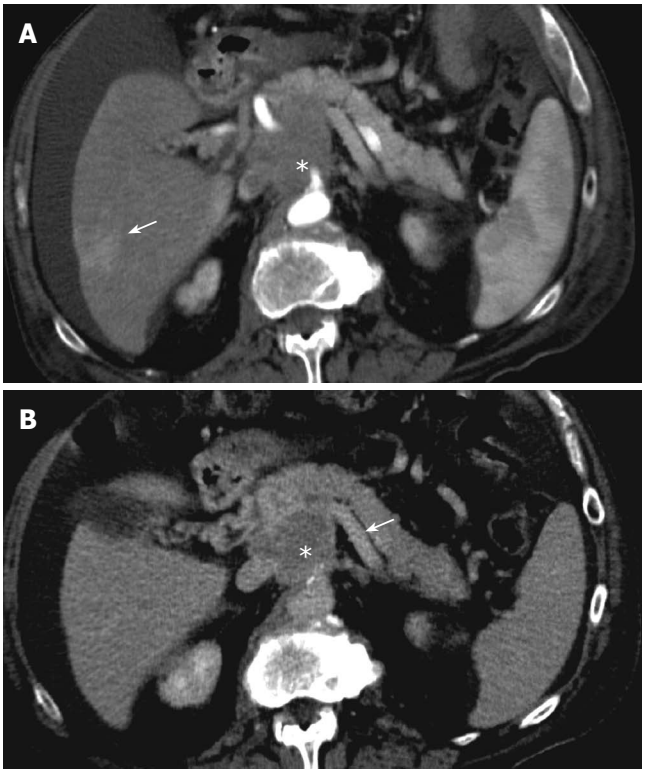

Figure 3 Contiguous helical CT scan of the abdomen at 5 mm collimation with intravenous contrast captured in arterial phase (**A**) and portal venous phase (**B**) at the level of the pancreas. A 5 cm soft tissue mass (star) was seen with severe attenuation of the splenic (**B**, arrow), main portal and superior mesenteric veins. An area of increased attenuation within the segment VI of the liver was visualized in arterial phase (**A**, arrow) concerning for metastasis.

tumor invasion of the portal and hepatic veins whereas pancreatic cancer affects the splenic vein with isolated left-sided portal hypertension. Alpha-feto protein producing hepatoid adenocarcinoma of the stomach also tends to invade the veins and metastasize to the liver[3]. In our patient serum level of alpha-feto protein was normal and not expressed within tumor cells. Gastric signet ring adenocarcinoma with metastasis to ovaries (Krukenberg tumors)[13,14], bones, meninges[15], colon, gingiva, tonsils, breasts, para-aortic lymph nodes and cervix has been reported in the literature.

Our case report not only adds to the variety of presentations of this type of cancer, but also provides an example of unusual clinical and endoscopic mimicry. The presence of esophageal and duodenal varices and absence of gastric varices suggested main portal trunk and left portal venous obstruction with effective decompression of the splenic venous system. The absence of splenomegaly, presence of an unusually enlarged inferior mesenteric vein (not shown), multiple perigastric collaterals indicated that indeed the left sided portal circulation was decompressed even though there was no obvious spleno-renal shunt. Esophageal varices usually arise due to increased pressure in the left gastric (coronary) vein that drains into the left portal vein, and less often into the main portal vein. Duodenal varices are a rare occurrence and the incidence is estimated to be 0.4% in the setting of portal hypertension[16]. The afferent vessel is usually the superior or inferior pancreaticoduodenal vein originating in the portal vein trunk or superior mesenteric vein. In our case, superior mesenteric as well as main portal veins were attenuated by encompassing metastatic mass, explaining the occurrence of esophageal and duodenal varices.

Signet ring adenocarcinoma is a rare, distinct type of gastric cancer. A retrospective analysis of this type of tumor has revealed an equal incidence in both genders: a younger age and larger tumor at presentation[17]. The histological type is commonly scirrhous and infiltrative. As in other gastric cancers, patients with early signet ring cell carcinoma have a good prognosis. However, these patients at the advanced stage have a poorer prognosis depending on the extent of vascular microinvasion and tumor location[17]. Pagetoid spread of the signet ring cells beneath the epithelial lining of gastric foveolae/glands is likely the cause of early lymphatic/vascular metastasis as in our case.

REFERENCES

1 **Tanaka A**, Takeda R, Mukaihara S, Hayakawa K, Takasu K, Terajima H, Yamaoka Y, Chiba T. Tumor thrombi in the portal vein system originating from gastrointestinal tract cancer. *J Gastroenterol* 2002; **37**: 220-228
2 **Ishikawa M**, Koyama S, Ikegami T, Fukutomi H, Gohongi T, Yuzawa K, Fukao K, Fujiwara M, Fujii K. Venous tumor thrombosis and cavernous transformation of the portal vein in a patient with gastric carcinoma. *J Gastroenterol* 1995; **30**: 529-533
3 **Araki T**, Suda K, Sekikawa T, Ishii Y, Hihara T, Kachi K. Portal venous tumor thrombosis associated with gastric adenocarcinoma. *Radiology* 1990; **174**: 811-814
4 **Yang DM**, Yoon MH, Kim HS, Jin W, Hwang HY, Kim HS. CT findings of portal vein aneurysm caused by gastric adenocarcinoma invading the portal vein. *Br J Radiol* 2001; **74**: 654-656
5 **Jain A**, Jain S, Chowdhury V, Mukhopadhyay S, Aggarwal A, Kar P. Profuse variceal hemorrhage as a presenting feature of pancreatic adenocarcinoma in a young non-icteric patient. *J Assoc Physicians India* 1999; **47**: 730-732
6 **Nakaba H**, Miyata M, Hamaji M, Izukura M, Okumura K, Kawashima Y. Gastric varices formation due to pancreatic tumor: a case of successful resection of cystadenocarcinoma. *Jpn J Surg* 1991; **21**: 583-586
7 **Mullan FJ**, McKelvey ST. Pancreatic carcinoma presenting as bleeding from segmental gastric varices: pitfalls in diagnosis. *Postgrad Med J* 1990; **66**: 401-403
8 **Joya Seijo MD**, del Valle Loarte P, Marco Martínez J, Herrera Merino N, Agud Aparicio JL. Sinistral portal hypertension with bleeding gastric varices as initial manifestation of renal-cell carcinoma. *An Med Interna* 2004; **21**: 283-284
9 **Smith TA**, Brand EJ. Pancreatic cancer presenting as bleeding gastric varices. *J Clin Gastroenterol* 2001; **32**: 444-447
10 **Chang CY**. Pancreatic adenocarcinoma presenting as sinistral portal hypertension: an unusual presentation of pancreatic cancer. *Yale J Biol Med* 1999; **72**: 295-300
11 **Wallace W**, Mulholland K, Epanomeritakis E. Bleeding gastric varices--a rare complication of ovarian cancer. *Int J Clin Pract* 2005; **59**: 119-120
12 **Heyne JP**, Pfleiderer SO, Trebing G, Scheele J, Kaiser WA. Palliative portal vein stent placement for lymphatic recurrence of gastric cancer. *Int J Colorectal Dis* 2005; **20**: 67-71
13 **Kakushima N**, Kamoshida T, Hirai S, Hotta S, Hirayama T, Yamada J, Ueda K, Sato M, Okumura M, Shimokama T, Oka Y. Early gastric cancer with Krukenberg tumor and review of cases of intramucosal gastric cancers with Krukenberg tumor. *J Gastroenterol* 2003; **38**: 1176-1180
14 **Yada-Hashimoto N**, Yamamoto T, Kamiura S, Seino H, Ohira

H, Sawai K, Kimura T, Saji F. Metastatic ovarian tumors: a review of 64 cases. *Gynecol Oncol* 2003; **89**: 314-317

15 **Lisenko Y**, Kumar AJ, Yao J, Ajani J, Ho L. Leptomeningeal carcinomatosis originating from gastric cancer: report of eight cases and review of the literature. *Am J Clin Oncol* 2003; **26**: 165-170

16 **Hashizume M**, Tanoue K, Ohta M, Ueno K, Sugimachi K, Kashiwagi M, Sueishi K. Vascular anatomy of duodenal varices: angiographic and histopathological assessments. *Am J Gastroenterol* 1993; **88**: 1942-1945

17 **Yokota T**, Kunii Y, Teshima S, Yamada Y, Saito T, Kikuchi S, Yamauchi H. Signet ring cell carcinoma of the stomach: a clinicopathological comparison with the other histological types. *Tohoku J Exp Med* 1998; **186**: 121-130

S- Editor Liu Y **L- Editor** Wang XL **E- Editor** Ma WH

PO Box 2345, Beijing 100023, China
www.wjgnet.com
wjg@wjgnet.com

World J Gastroenterol 2007 February 14; 13(6): 964-969
World Journal of Gastroenterology ISSN 1007-9327

CASE REPORT

Fatal liver failure caused by reactivation of lamivudine-resistant hepatitis B virus: A case report

Yuka Suzuki, Hiroshi Yotsuyanagi, Chiaki Okuse, Yoshihiko Nagase, Hideaki Takahashi, Kyoji Moriya, Michihiro Suzuki, Kazuhiko Koike, Shiro Iino, Fumio Itoh

Yuka Suzuki, Chiaki Okuse, Yoshihiko Nagase, Hideaki Takahashi, Michihiro Suzuki, Fumio Itoh, Division of Gastroenterology and Hepatology, Department of Internal Medicine, St. Marianna University School of Medicine, 2-16-1 Sugao, Miyamae-ku, Kawasaki 216-8511, Japan
Hiroshi Yotsuyanagi, Kyoji Moriya, Kazuhiko Koike, Division of Infectious Diseases, Department of Internal Medicine, University of Tokyo, 7-3-1 Hongo, Bunkyo-ku, Tokyo 113-0033, Japan
Shiro Iino, Center for Liver Diseases, Seizankai Kiyokawa Hospital, 2-31-12 Asagayaminami, Suginami, Tokyo 166-0004, Japan
Correspondence to: Hiroshi Yotsuyanagi, MD, PhD, Division of Infectious Diseases, Department of Internal Medicine, University of Tokyo, 7-3-1 Hongo, Bunkyo-ku, Tokyo 113-0033, Japan. hyotsu-tky@umin.ac.jp
Telephone: +81-3-58008720 Fax: +81-3-58008796
Received: 2006-07-05 Accepted: 2006-12-29

Abstract

We present a case of fetal liver failure caused by the activation of lamivudine-resistant hepatitis B virus (HBV) nine months after lamivudine treatment. A 57-year old man visited our hospital for the treatment of decompensated chronic hepatitis B. Lamivudine was started in December 2001. Subsequently, serum HBV was negative for HBV DNA with seroconversion from HBeAg to anti-HBe and improvement of liver function. However, HBV DNA and HBeAg were again detected in September 2002. He was complicated by breakthrough hepatitis and admitted to our hospital in November for severely impaired liver function. Vidarabine treatment was started and serum HBV DNA and alanine aminotransferase (ALT) decreased transiently. However, after the start of α-interferon treatment, HBV DNA level increased and liver function deteriorated. He died 1 mo after admission. An analysis of amino acid sequences in the polymerase region revealed that rtM204I/V with rtL80I/V occurred at the time of viral breakthrough. After the start of antiviral treatment, rtL180M was detected in addition to rtM204I/V and rtL80I/V, and became predominant in the terminal stage of the disease. HBV clone with a high replication capacity may be produced by antiviral treatment leading to the worsening of liver function. Antiviral therapy for patients with breakthrough hepatitis in advanced liver disease should be carefully performed.

Key words: Hepatitis B virus; Lamivudine; Polymerase; Interferon; Tyrosine-methionine-aspartate-aspartate

Suzuki Y, Yotsuyanagi H, Okuse C, Nagase Y, Takahashi H, Moriya K, Suzuki M, Koike K, Iino S, Itoh F. Fatal liver failure caused by reactivation of lamivudine-resistant hepatitis B virus: A case report. *World J Gastroenterol* 2007; 13(6): 964-969

http://www.wjgnet.com/1007-9327/13/964.asp

INTRODUCTION

Lamivudine is a nucleoside analogue that interrupts the reverse transcription of hepatitis B viral (HBV) pregenomic RNA. Lamivudine is effective for controlling chronic hepatitis B and currently recommended as the first line of treatment for chronic active hepatitis B[1,2]. Even for patients with decompensated liver cirrhosis, lamivudine improves liver function and extends transplantation free intervals[3-10]. Since more than 10% of patients with chronic HBV infection are estimated to develop liver cirrhosis and may eventually suffer from decompensated liver cirrhosis or hepatocellular carcinoma, the role of lamivudine in the treatment of advanced liver disease caused by chronic HBV infection is large[11-14].

The major problems concerning lamivudine treatment are the viral and biochemical breakthroughs caused by drug resistance. Amino acid mutation in the highly conserved tyrosine-methionine-aspartate-aspartate (YMDD) motif can occur six months after treatment and often increases alanine aminotransferase (ALT) level. Although the increase is usually mild, a marked increase in ALT level leading to fatal hepatic failure has been reported[15-17]. Factors other than the YMDD motif mutation that are associated with the worsening of liver function remain to be clarified.

Here, we report a case of fatal hepatic failure caused by lamivudine-resistant HBV. A serial analysis of viral amino acid sequences indicated that the acquisition of mutations outside the YMDD motif might be related to the deteriolation of the patient's condition.

CASE REPORT

A 57-year old man visited our hospital in September 2001

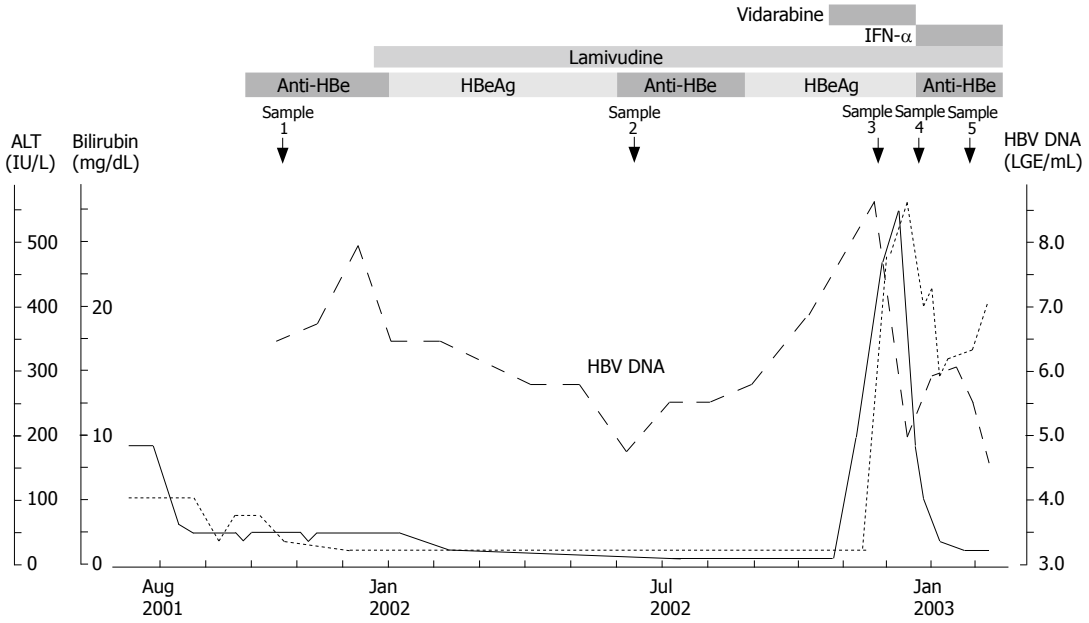

Figure 1 Clinical course of our patient. HBV DNA level was quantified by transcription-mediated amplification assay. The levels of HBV DNA started to increase 8 mo after treatment with reappearance of HBeAg. Breakthrough hepatitis developed 12 mo after treatment. The timing of serum sample analysis for mutations is shown by the arrowhead.

for the treatment of decompensated chronic hepatitis B. In 1978, He was found to be positive for serum HBs antigen (HBsAg). In July 2001, he was admitted to a nearby hospital for ascites where he was diagnosed as having decompensated cirrhosis with exacerbated chronic hepatitis B. The symptomatic control of his ascites improved his general condition. For further treatment, he was referred to our hospital.

On his first visit, he showed no symptoms or signs of worsening hepatic failure or encephalopathy. No ascites or leg edema was observed. His bulbar conjunctiva was slightly jaundiced. Dilated vasculature was observed in his neck and chest. His ALT, total bilirubin and albumin were 50 IU/L, 3.1 mg/dL and 3.7 g/dL, and his prothrombin time was 76%. He was diagnosed as having liver cirrhosis with a Child-Pugh score of 8. He was negative for HBe antigen (HBeAg) and his HBV DNA level measured by transcription-mediated amplification and hybridization protection assay[18] was $10^{6.5}$ genome copies/mL.

In November 2001, he was found to be positive for HBeAg and showed an increase in HBV DNA level. Because he had a history of decompensated chronic hepatitis B, lamivudine treatment (100 mg/d) was started in December. Figure 1 shows the clinical course. The high serum levels of bilirubin and ALT decreased and normalized within 6 mo after lamivudine treatment was started. The patient became negative for HBV DNA and HBeAg.

However, in September 2002, he was found to be positive for HBeAg again and showed an increase in HBV DNA level. In November 2002, he observed jaundice of his bulbar conjunctiva and was admitted to our hospital. Although he was alert, his bulbar conjunctiva and skin were jaundiced. His ALT, total bilirubin, were 474 IU/L, 11.4 mg/dL and 4.3 g/dL. His HBV DNA level was $10^{8.6}$ genome copies/mL. He was diagnosed as having breakthrough hepatitis caused by lamivudine-resistant mutants of HBV. HBV with an amino acid substitution in the YMDD motif in the domain C of polymerase region was detected.

Because interferon is not indicated in patients with decompensated cirrhosis, vidarabine, which is effective for the control of active HBV infection[19-21], was administered together with lamivudine under informed consent. Liver function improved transiently with a decrease in HBV DNA within 2 wk. As prolonged vidarabine administration may induce several complications[22], vidarabine was switched to interferon-α. After the start of interferon-α treatment, HBV DNA level increased and liver function worsened. He died of hepatic failure and rupture of esophageal varices 1 mo after his admission.

The histolopathology of the patient's liver after necropsy showed cirrhosis with zonal necrosis. Hepatocyte regeneration was scarce (Figure 2).

To elucidate the viral factors affecting early viral breakthrough and fatal outcome, amino acid sequences of the upstream polymerase region (aa 1-250) of HBV DNA in serum were examined at 5 points as shown in Figure 1. The methods were as follows.

First, DNA was extracted from 100 μL of a serum sample using the QIAamp DNA blood mini kit (Qiagen Inc., Valencia, CA). Three fragments spanning the upper polymerase region of HBV DNA were amplified by nested PCR with the primers shown in Table 1. The first stage of amplification was carried out using a thermal cycler for 40 cycles (94℃ for 1 min, 55℃ for 1 min, 72℃ for 1 min) in 100 μL of reaction mixture containing 200 mmol/L dNTPs, 1.0 mmol/L each of the primers and 1 × PCR buffer [50 mmol/L KCl, 10 mmol/L Tris-HCl (pH 8.3), 1.5 mmol/L $MgCl_2$ and 0.001% (w/v) gelatin] and 2 units of Ampli-Taq polymerase gold (Perkin Elmer Cetus Corp., CT). Two microliters of the PCR products was subjected to the second stage of amplification under the same conditions as the first stage.

Second, PCR products were purified using Wizard PCR preps DNA purification resin (Promega, WI) and cloned into a plasmid vector using the TA cloning kit (PCR cloning kit Qiagen, CA). Four clones were selected from

Table 1 Primers used for amplification and sequencing of polymerase region of HBV

Region 1		
Outer sense	nt 2222-2241	CTTACTTTTGGAAGAGAAAC
Outer antisense	nt 2490-2509	GGACAGTAGAAGAATAAAG
Inner sense	nt 2222-2241	CTTACTTTTGGAAGAGAAAC
Inner antisense	nt 2478-2497	GAATAAAGCCCAGTAAAGTT
Region 2		
Outer sense	nt 2413-2434	GCGTCGCAGAAGATCTCAATC
Outer antisense	nt 2816-2835	GTTCCCAAGAATATGGTGAC
Inner sense	nt 2434-2452	CTCGGGAATCTCAATGTTAG
Inner antisense	nt 2816-2835	GTTCCCAAGAATATGGTGAC
Region 3		
Outer sense	nt 2490-2509	CTTTATTCTTCTACTGTACC
Outer antisense	nt 3121-3143	CGATTGGTGGAGGCAGGAGGAGG
Inner sense	nt 2637-2656	ATGCCTGCTAGGTTTTATCC
Inner antisense	nt 3121-3143	CGATTGGTGGAGGCAGGAGGAGG

each plate, from which recombinant plasmid DNA was purified using a commercially available kit (Plasmid midi kit, Qiagen, Valencia, CA). Nucleotide sequences were determined bidirectionally using the dye terminator cycle sequencing ready reaction kit (PE Applied Biosystems, CA) and the PCR primers. Sequencing was performed using an automated DNA sequencer (ABI 377: PE Applied Biosystems).

The determined amino acid sequences in the polymerase region are shown in Figure 3. No amino acid sequence changes were found at the start of lamivudine treatment. At the time of viral breakthrough, rtM204I with rtL80I became dominant. After the start of interferon treatment, rtM204I was replaced by rtM204V and rtL80I by rtL80V. At the final stage of the disease, mutation rtL180M appeared besides rtM204V and rtL80V.

DISCUSSION

Lamivudine monotherapy is effective in suppressing HBV replication and ameliorating liver disease in chronic hepatitis B patients regardless of HBeAg positivity. A one-year study of HBeAg-positive chronic hepatitis B patients showed that 16% of these patients become seroconverted to anti-HBe and 72% of these patients showed normalization of their ALT levels[23]. Furthermore, treatment with lamivudine is associated with histologic improvement not only in terms of necroinflammatory score but also in terms of fibrosis score after long-term treatment[24].

One advantage of lamivudine is that it can be used safely in patients with decompensated cirrhosis[3-10]. In contrast to IFN-α, lamivudine is well tolerated without any significant side effects even in patients with decompensated cirrhosis. Furthermore, lamivudine can improve liver function and survival prognosis.

However, the emergence of a drug-resistant mutant is a big problem in lamivudine treatment. A large-scale Asian study showed that lamivudine resistant HBV infection occurred in 23% of patients in year one and 65% of patients in year five. Hepatitis flares, which occurred more commonly in patients with lamivudine resistant mutations, occurred in 10% of patients in year one, and in 18% to

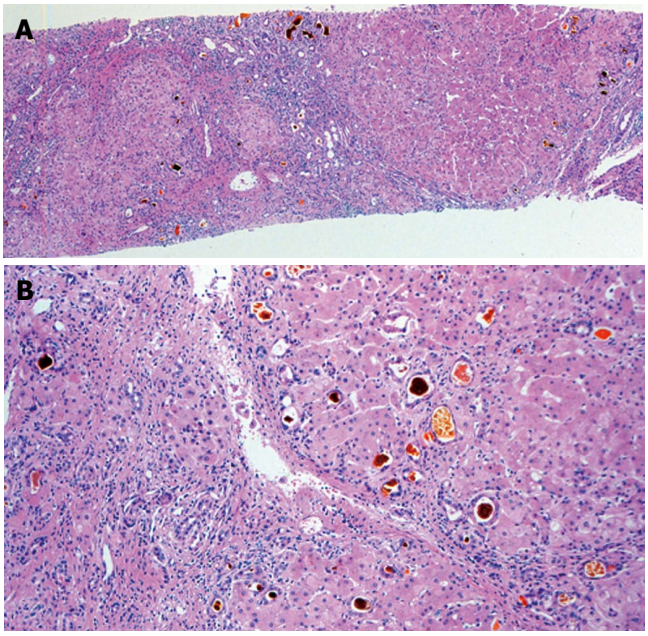

Figure 2 Histopathological findings of liver specimens showing irregularly-shaped parenchymal cells with massive necrosis (**A**) and scarce hepatocyte regeneration (**B**) surrounded by extensive fibrosis (**A**: HE × 20; **B**: HE × 80).

21% of patients in years two to five. Among patients with lamivudine resistant HBV infection, occurrence of hepatic decompensation increased significantly in patients with lamivudine resistant HBV infection for more than 4 years (from 0% to 6%)[25]. In this large-scale Asian study, liver-disease-related death occurred in two patients.

The prognosis of patients with lamivudine-resistant HBV infection, particularly those with advanced liver disease, may be determined by the timing and severity of breakthrough hepatitis. However, the viral factors that may influence the severity of this hepatitis remain to be clarified. A recent study indicated that patients with a normal ALT level even after the emergence of a YMDD motif mutant are characterized by HBeAg negativity during pretreatment, HBeAg loss during therapy, a longer duration from the commencement of therapy until the emergence of YMDD mutant, and lack of mixed-type YMDD mutants[26]. In contrast, patients with severely exacerbated hepatitis after the emergence of a YMDD mutant tend to have more substitutions in the reverse transcriptase (rt) region within the polymerase gene at the time of hepatitis exacerbation than those without hepatitis exacerbation[26].

Our patient acquired amino acid mutations in the polymerase region one after the other. Amino acid changes in rtM204/I appeared at the time of viral breakthrough. After the initial treatment with vidarabine, rtM204/V substituted for rtM204/I in one of the four clones. During the interferon treatment, rtM204/V became predominant.

Another mutation observed in our patient was rtL80I/V. Ogata *et al*[27] showed that rtL180M is accompanied with rtM204I in some patients with resistance to lamivudine. Because the mutation at aa position 80 was found at the same time as that at aa position 204 in our patient, it is not clear whether the mutation at aa position 80 affects the clinical course.

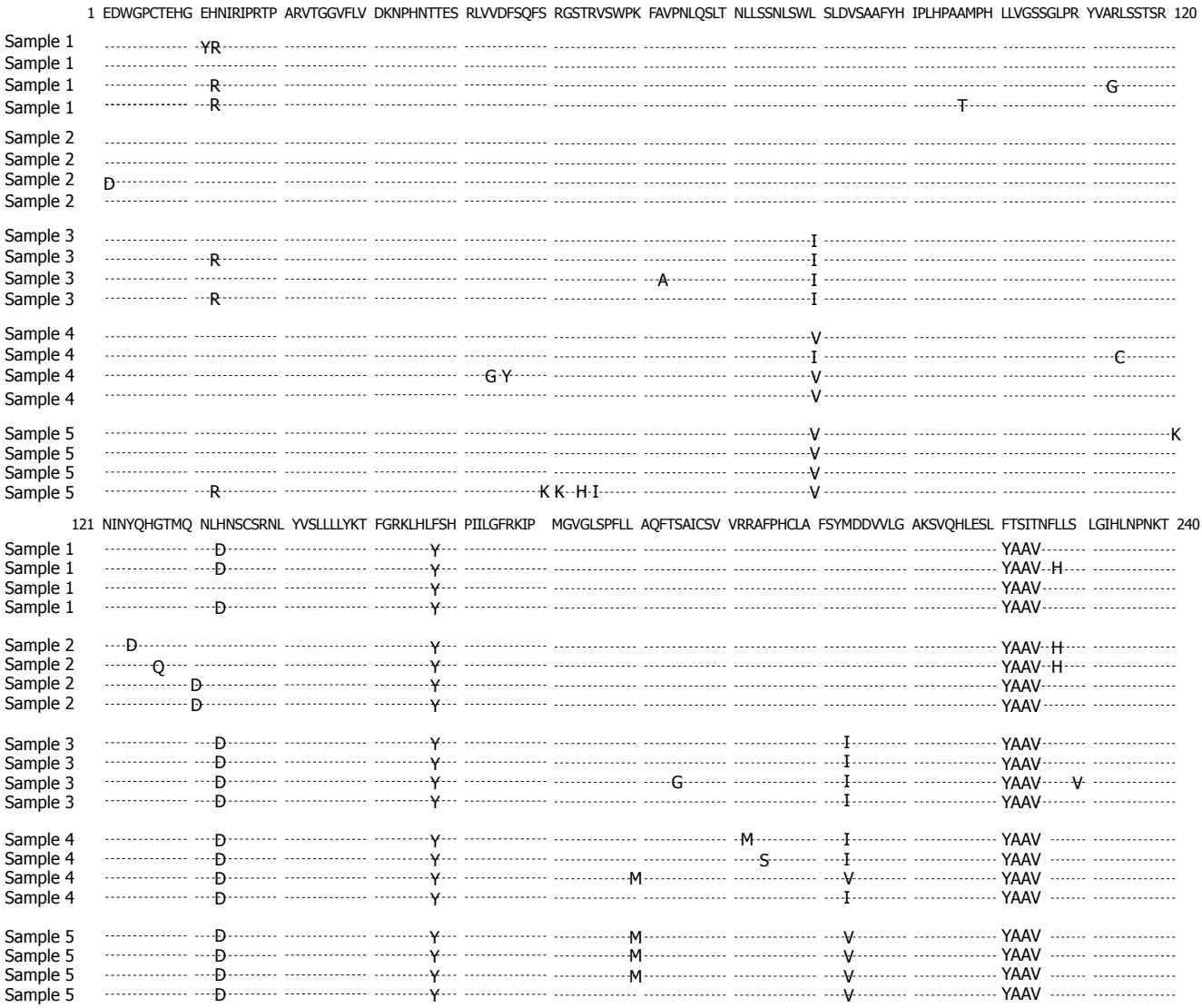

Figure 3 Comparison of amino acid sequences of HBV polymerase gene of isolates before lamivudine treatment (sample 1) and four sequential isolates (samples 2-5) during treatment. A HBV mutant with substitutions of isoleucine for leucine at residue 80 (rtL80I) in combination with isoleucine for methionine at residue 204 (rtM204I) was observed 12 mo after treatment (sample 3). After vidarabine treatment, another HBV mutant with substitutions of valine for leucine at residue 80 (rtL80V) and valine for methionine at residue 204 (rtM204V) was observed (sample 4). These mutations predominated in combination with methionine for leucine at residue 180 (rtL180M) after interferon treatment (sample 5). The published HBV DNA sequence of hepatitis B virus variant (genotype C, AB033550, Okamoto *et al*) was used for comparison.

At the final stage of the disease with deterioration of the condition of the patient, rtL180M, rtM204I/V and rtL80I/V became predominant. Natsuizaka *et al*[28] showed that rtL180M and rtM204V are related to the exacerbation of hepatitis. Interestingly, a patient with a marked elevation in HBV DNA level in Ogata's report had rtL180M in addition to rtL80I and rtM204I. Therefore, the acquisitions of rtL80I/V and rt180M in addition to rtM204I/V may be associated with a severe exacerbation of hepatitis. Large-scale studies are necessary to elucidate this hypothesis.

In our patient, vidarabine decreased HBV DNA levels and improved liver function. Although the long-term use of vidarabine is contraindicated because of its possible side effects including irreversible neurotoxicity[22], its short-term use is effective for controlling active HBV infection and herpes simplex viral infection.

Vidarabine was replaced by interferon-α because adefovir dipivoxil was not available in 2002. Serum HBV DNA and bilirubin levels increased again, which led to a fatal outcome, and HBV clones that have rtL180M became predominant, indicating that withdrawal of vidarabine and administration of interferon may be dangerous for the treatment of severe breakthrough hepatitis. Since interferon may potentially precipitate immunological flares and liver failure[29], nucleotide analogues that are effective for lamivudine-resistant HBV such as adefovir dipivoxil[30-32], entecavir[33-35] and tenofovir[36,37], should be used for the treatment of severe breakthrough hepatitis instead of vidarabine or interferon.

In conclusion, antiviral therapy should be considered in the treatment of patients with hepatic failure after breakthrough hepatitis caused by HBV mutants to lamivudine. The serial acquisition of amino acid mutations outside the YMDD motif in the polymerase region may be associated with severe hepatitis.

REFERENCES

1 **Lok AS**, McMahon BJ. Chronic hepatitis B: update of

recommendations. *Hepatology* 2004; **39**: 857-861
2 **Liaw YF**, Leung N, Guan R, Lau GK, Merican I, McCaughan G, Gane E, Kao JH, Omata M. Asian-Pacific consensus statement on the management of chronic hepatitis B: a 2005 update. *Liver Int* 2005; **25**: 472-489
3 **Villeneuve JP**, Condreay LD, Willems B, Pomier-Layrargues G, Fenyves D, Bilodeau M, Leduc R, Peltekian K, Wong F, Margulies M, Heathcote EJ. Lamivudine treatment for decompensated cirrhosis resulting from chronic hepatitis B. *Hepatology* 2000; **31**: 207-210
4 **Yao FY**, Bass NM. Lamivudine treatment in patients with severely decompensated cirrhosis due to replicating hepatitis B infection. *J Hepatol* 2000; **33**: 301-307
5 **Kapoor D**, Guptan RC, Wakil SM, Kazim SN, Kaul R, Agarwal SR, Raisuddin S, Hasnain SE, Sarin SK. Beneficial effects of lamivudine in hepatitis B virus-related decompensated cirrhosis. *J Hepatol* 2000; **33**: 308-312
6 **Sponseller CA**, Bacon BR, Di Bisceglie AM. Clinical improvement in patients with decompensated liver disease caused by hepatitis B after treatment with lamivudine. *Liver Transpl* 2000; **6**: 715-720
7 **Fontana RJ**, Keeffe EB, Carey W, Fried M, Reddy R, Kowdley KV, Soldevila-Pico C, McClure LA, Lok AS. Effect of lamivudine treatment on survival of 309 North American patients awaiting liver transplantation for chronic hepatitis B. *Liver Transpl* 2002; **8**: 433-439
8 **Yao FY**, Terrault NA, Freise C, Maslow L, Bass NM. Lamivudine treatment is beneficial in patients with severely decompensated cirrhosis and actively replicating hepatitis B infection awaiting liver transplantation: a comparative study using a matched, untreated cohort. *Hepatology* 2001; **34**: 411-416
9 **Hann HW**, Fontana RJ, Wright T, Everson G, Baker A, Schiff ER, Riely C, Anschuetz G, Gardner SD, Brown N, Griffiths D. A United States compassionate use study of lamivudine treatment in nontransplantation candidates with decompensated hepatitis B virus-related cirrhosis. *Liver Transpl* 2003; **9**: 49-56
10 **Manolakopoulos S**, Karatapanis S, Elefsiniotis J, Mathou N, Vlachogiannakos J, Iliadou E, Kougioumtzan A, Economou M, Triantos C, Tzourmakliotis D, Avgerinos A. Clinical course of lamivudine monotherapy in patients with decompensated cirrhosis due to HBeAg negative chronic HBV infection. *Am J Gastroenterol* 2004; **99**: 57-63
11 **Fattovich G**, Brollo L, Giustina G, Noventa F, Pontisso P, Alberti A, Realdi G, Ruol A. Natural history and prognostic factors for chronic hepatitis type B. *Gut* 1991; **32**: 294-298
12 **Liaw YF**, Tai DI, Chu CM, Chen TJ. The development of cirrhosis in patients with chronic type B hepatitis: a prospective study. *Hepatology* 1988; **8**: 493-496
13 **Liaw YF**, Lin DY, Chen TJ, Chu CM. Natural course after the development of cirrhosis in patients with chronic type B hepatitis: a prospective study. *Liver* 1989; **9**: 235-241
14 **Fattovich G**, Giustina G, Schalm SW, Hadziyannis S, Sanchez-Tapias J, Almasio P, Christensen E, Krogsgaard K, Degos F, Carneiro de Moura M. Occurrence of hepatocellular carcinoma and decompensation in western European patients with cirrhosis type B. The EUROHEP Study Group on Hepatitis B Virus and Cirrhosis. *Hepatology* 1995; **21**: 77-82
15 **Kim JW**, Lee HS, Woo GH, Yoon JH, Jang JJ, Chi JG, Kim CY. Fatal submassive hepatic necrosis associated with tyrosine-methionine-aspartate-aspartate-motif mutation of hepatitis B virus after long-term lamivudine therapy. *Clin Infect Dis* 2001; **33**: 403-405
16 **Wang JH**, Lu SN, Lee CM, Lee JF, Chou YP. Fatal hepatic failure after emergence of the hepatitis B virus mutant during lamivudine therapy in a patient with liver cirrhosis. *Scand J Gastroenterol* 2002; **37**: 366-369
17 **Kagawa T**, Watanabe N, Kanouda H, Takayama I, Shiba T, Kanai T, Kawazoe K, Takashimizu S, Kumaki N, Shimamura K, Matsuzaki S, Mine T. Fatal liver failure due to reactivation of lamivudine-resistant HBV mutant. *World J Gastroenterol* 2004; **10**: 1686-1687
18 **Kamisango K**, Kamogawa C, Sumi M, Goto S, Hirao A, Gonzales F, Yasuda K, Iino S. Quantitative detection of hepatitis B virus by transcription-mediated amplification and hybridization protection assay. *J Clin Microbiol* 1999; **37**: 310-314
19 **Hoofnagle JH**, Minuk GY, Dusheiko GM, Schafer DF, Johnson R, Straus S, Jones EA, Gerin JL, Ishak K. Adenine arabinoside 5'-monophosphate treatment of chronic type B hepatitis. *Hepatology* 1982; **2**: 784-788
20 **Weller IV**, Lok AS, Mindel A, Karayiannis P, Galpin S, Monjardino J, Sherlock S, Thomas HC. Randomised controlled trial of adenine arabinoside 5'-monophosphate (ARA-AMP) in chronic hepatitis B virus infection. *Gut* 1985; **26**: 745-751
21 **Marcellin P**, Ouzan D, Degos F, Brechot C, Metman EH, Degott C, Chevalier M, Berthelot P, Trepo C, Benhamou JP. Randomized controlled trial of adenine arabinoside 5'-monophosphate in chronic active hepatitis B: comparison of the efficacy in heterosexual and homosexual patients. *Hepatology* 1989; **10**: 328-331
22 **Hoofnagle JH**, Hanson RG, Minuk GY, Pappas SC, Schafer DF, Dusheiko GM, Straus SE, Popper H, Jones EA. Randomized controlled trial of adenine arabinoside monophosphate for chronic type B hepatitis. *Gastroenterology* 1984; **86**: 150-157
23 **Lai CL**, Chien RN, Leung NW, Chang TT, Guan R, Tai DI, Ng KY, Wu PC, Dent JC, Barber J, Stephenson SL, Gray DF. A one-year trial of lamivudine for chronic hepatitis B. Asia Hepatitis Lamivudine Study Group. *N Engl J Med* 1998; **339**: 61-68
24 **Dienstag JL**, Goldin RD, Heathcote EJ, Hann HW, Woessner M, Stephenson SL, Gardner S, Gray DF, Schiff ER. Histological outcome during long-term lamivudine therapy. *Gastroenterology* 2003; **124**: 105-117
25 **Lok AS**, Lai CL, Leung N, Yao GB, Cui ZY, Schiff ER, Dienstag JL, Heathcote EJ, Little NR, Griffiths DA, Gardner SD, Castiglia M. Long-term safety of lamivudine treatment in patients with chronic hepatitis B. *Gastroenterology* 2003; **125**: 1714-1722
26 **Suzuki F**, Akuta N, Suzuki Y, Sezaki H, Arase Y, Hosaka T, Someya T, Kobayashi M, Saitoh S, Ikeda K, Kobayashi M, Matsuda M, Satoh J, Watahiki S, Kumada H. Clinical and virological features of non-breakthrough and severe exacerbation due to lamivudine-resistant hepatitis B virus mutants. *J Med Virol* 2006; **78**: 341-352
27 **Ogata N**, Fujii K, Takigawa S, Nomoto M, Ichida T, Asakura H. Novel patterns of amino acid mutations in the hepatitis B virus polymerase in association with resistance to lamivudine therapy in japanese patients with chronic hepatitis B. *J Med Virol* 1999; **59**: 270-276
28 **Natsuizaka M**, Hige S, Ono Y, Ogawa K, Nakanishi M, Chuma M, Yoshida S, Asaka M. Long-term follow-up of chronic hepatitis B after the emergence of mutations in the hepatitis B virus polymerase region. *J Viral Hepat* 2005; **12**: 154-159
29 **Janssen HL**, Brouwer JT, Nevens F, Sanchez-Tapias JM, Craxi A, Hadziyannis S. Fatal hepatic decompensation associated with interferon alfa. European concerted action on viral hepatitis (Eurohep). *BMJ* 1993; **306**: 107-108
30 **Perrillo R**, Schiff E, Yoshida E, Statler A, Hirsch K, Wright T, Gutfreund K, Lamy P, Murray A. Adefovir dipivoxil for the treatment of lamivudine-resistant hepatitis B mutants. *Hepatology* 2000; **32**: 129-134
31 **Hadziyannis SJ**, Tassopoulos NC, Heathcote EJ, Chang TT, Kitis G, Rizzetto M, Marcellin P, Lim SG, Goodman Z, Wulfsohn MS, Xiong S, Fry J, Brosgart CL. Adefovir dipivoxil for the treatment of hepatitis B e antigen-negative chronic hepatitis B. *N Engl J Med* 2003; **348**: 800-807
32 **Marcellin P**, Chang TT, Lim SG, Tong MJ, Sievert W, Shiffman ML, Jeffers L, Goodman Z, Wulfsohn MS, Xiong S, Fry J, Brosgart CL. Adefovir dipivoxil for the treatment of hepatitis B e antigen-positive chronic hepatitis B. *N Engl J Med* 2003; **348**: 808-816
33 **Chang TT**, Gish RG, Hadziyannis SJ, Cianciara J, Rizzetto M, Schiff ER, Pastore G, Bacon BR, Poynard T, Joshi S, Klesczewski KS, Thiry A, Rose RE, Colonno RJ, Hindes RG. A dose-ranging study of the efficacy and tolerability of entecavir

in Lamivudine-refractory chronic hepatitis B patients. *Gastroenterology* 2005; **129**: 1198-1209

34 **Chang TT**, Gish RG, de Man R, Gadano A, Sollano J, Chao YC, Lok AS, Han KH, Goodman Z, Zhu J, Cross A, DeHertogh D, Wilber R, Colonno R, Apelian D. A comparison of entecavir and lamivudine for HBeAg-positive chronic hepatitis B. *N Engl J Med* 2006; **354**: 1001-1010

35 **Lai CL**, Shouval D, Lok AS, Chang TT, Cheinquer H, Goodman Z, DeHertogh D, Wilber R, Zink RC, Cross A, Colonno R, Fernandes L. Entecavir versus lamivudine for patients with HBeAg-negative chronic hepatitis B. *N Engl J Med* 2006; **354**: 1011-1020

36 **van Bömmel F**, Wünsche T, Mauss S, Reinke P, Bergk A, Schürmann D, Wiedenmann B, Berg T. Comparison of adefovir and tenofovir in the treatment of lamivudine-resistant hepatitis B virus infection. *Hepatology* 2004; **40**: 1421-1425

37 **van der Eijk AA**, Hansen BE, Niesters HG, Janssen HL, van de Ende M, Schalm SW, de Man RA. Viral dynamics during tenofovir therapy in patients infected with lamivudine-resistant hepatitis B virus mutants. *J Viral Hepat* 2005; **12**: 364-372

S- Editor Wang GP **L- Editor** Wang XL **E- Editor** Lu W

PO Box 2345, Beijing 100023, China
www.wjgnet.com
wjg@wjgnet.com

World J Gastroenterol 2007 February 14; 13(6): 970-972
World Journal of Gastroenterology ISSN 1007-9327

CASE REPORT

Stent placement is effective on both postoperative hepatic arterial pseudoaneurysm and subsequent portal vein stricture: A case report

Toshiaki Ichihara, Tsutomu Sato, Hideaki Miyazawa, Satoshi Shibata, Manabu Hashimoto, Koichi Ishiyama, Yuzo Yamamoto

Toshiaki Ichihara, Tsutomu Sato, Hideaki Miyazawa, Satoshi Shibata, Manabu Hashimoto, Koichi Ishiyama, Yuzo Yamamoto, Departments of Gastroenterological Surgery and Radiology, Akita University School of Medicine, Hondo, Akita 010-8543, Japan
Correspondence to: Toshiaki Ichihara, Departments of Gastroenterological Surgery, Akita University School of Medicine, 1-1-1 Hondo, Akita 010-8543, Japan. ichihara@gipc.akita-u.ac.jp
Telephone: +81-18-8362614 Fax: +81-18-8846126
Received: 2006-11-17 Accepted: 2007-01-17

Abstract

To treat postoperative bleeding after hepato-pancreato-biliary surgery, interventional radiology has become essential. We report a case of coincidental pseudoaneurysm and jejunal varices that were both successfully treated by stent-grafts. After a pancreaticoduodenectomy, the patient developed a pseudoaneurysm in the hepatic artery and a stenosis in its periphery. After establishing hepatic arterial flow by placing stent-grafts over both the pseudoaneurysm and the stenosis, the pseudoaneurysm was embolized with microcoils. Nine months later, the patient developed jejunal varices caused by a severe stricture in the main trunk of the portal vein. Percutaneous transhepatic portography was performed and stent-grafts were placed over the stenotic segment. A venoplasty using stent-grafts normalized the portal blood flow and the jejunal varices vanished. Although stenosis occurred due to scarred tissues from leakage after pancreaticoduodenectomy, stent-grafts were useful for managing jejunal bleeding post-operatively.

Key words: Extrahepatic portal vein stenosis; Jejunal varices; Interventional radiology; Stent-graft

Ichihara T, Sato T, Miyazawa H, Shibata S, Hashimoto M, Ishiyama K, Yamamoto Y. Stent placement is effective on both postoperative hepatic arterial pseudoaneurysm and subsequent portal vein stricture: A case report. *World J Gastroenterol* 2007; 13(6): 970-972

http://www.wjgnet.com/1007-9327/13/970.asp

INTRODUCTION

Postoperative bleeding is one of the leading causes of death after pancreaticoduodenectomy[1]. In particular, delayed hemorrhage occurring five or more days post-operatively[2] is difficult to manage because the hepatic artery and/or the portal vein are frequently affected. That is, not only hemostasis, but also the maintenance of hepatic blood flow has to be considered in treating these patients. Above all other methods, embolization using an interventional radiology (IVR) technique has been used for surgical treatment because of its efficacy and minimal invasiveness[3]. In this paper we report jejunal varices due to a portal venous stricture and a coincidental pseudoaneurysm in the hepatic artery after a pancreaticoduodenectomy. These complications occurred metachronously and each was successfully treated with an IVR technique using stent-grafts. Although treatment for this condition has not yet been standardized, we give a detailed account of our approach.

CASE REPORT

Treatment of pseudoaneurysm in the hepatic artery

In July 2004, a 64-year-old woman underwent a pancreaticoduodenectomy with a Child's reconstruction for carcinoma of the distal bile duct[4]. During the postoperative course, a minor leak from the hepaticojejunostomy occurred, which was resolved within ten days. However, on the 26th postoperative day, 250 mL of blood through an intraabdominal drain was collected.

Angiography was carried out immediately. As shown in Figure 1A, there was no extravasation, but a severe stricture in the proper hepatic artery and pseudoaneurysm at the cutting stump of the gastroduodenal artery were noted. To secure the hepatopetal arterial flow, an angioplasty was performed. Two pieces of stent-grafts, each 2.5 mm in diameter and 13 mm or 23 mm in length (MULTI LINK Penta®, GUIDANT Indianapolis, IN, USA) were introduced sequentially through the stenotic segment and the pseudoaneurysm in the hepatic artery (Figure 1B). After stenting, embolization of the pseudoaneurysm was attempted using microcoils (GDC Detachable coil®: Boston scientific; Natick, MA, USA) to stop the inflow into the pseudoaneurysmal lumen (Figure 1C). The patency of the hepatic artery and the disappearance of the pseudoaneurysm were confirmed by arteriography 8 d after treatment

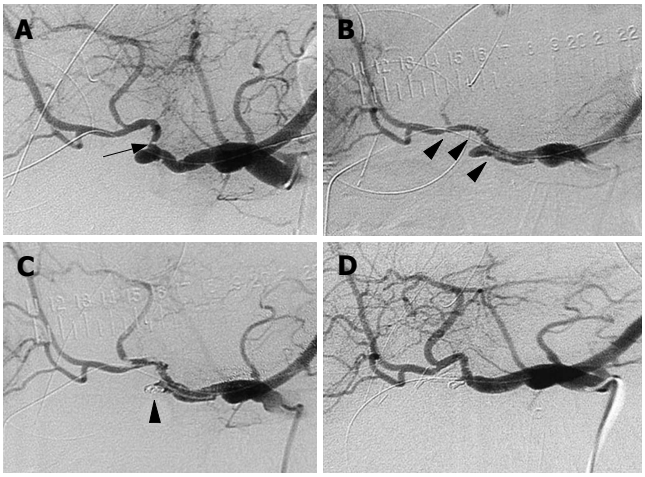

Figure 1 **A**: A severe stricture of a narrow segment in the proper hepatic artery and a bulging at the stump of the gastroduodenal artery were seen. An arrow indicates a stricture; **B**: The stent-graft for an angioplasty was introduced through the stenotic segment to secure the hepatopetal arterial flow. Arrow heads indicate the stent-graft placed in the hepatic artery; **C**: After the stenting, embolization of the pseudoaneurysm was attempted to stop the inflow into the pseudoaneurysmal lumen using microcoils. An arrow head indicates microcoils placed in the pseudoaneurysmal lumen; **D**: The patency of the hepatic artery and disappearance of the pseudoaneurysm were confirmed by arteriography 8 d after the treatment.

(Figure 1D). The patient was discharged from the hospital 4 wk after treatment.

Treatment of jejunal varices caused by extrahepatic obliteration of the portal vein

This patient did well for 9 mo after hospital discharge. In April 2005, however, she was readmitted with gastrointestinal bleeding. Laboratory data upon admission showed severe anemia and hyperammoninemia. Gastrointestinal fiberscopy showed bleeding from a varix in the lifted limb of the jejunum near the hepaticojejunostomy.

Angiography was performed. Hepatic arterial flow was normal as seen in Figure 1D. However, celiac and superior mesenteric arteriography during the portal phase (Figure 2A and B) revealed a severe stricture at the main trunk of the portal vein, adjacent to the microcoils that had been inserted 10 mo earlier. Hepatofugal collaterals had also developed *via* the left gastric vein and the inferior mesenteric vein. Moreover, collateral vessels were observed around the hepaticojejunostomy creating jejunal varices in the lifted limb toward the hepatic hilum. These jejunal varices were identified as the source of the intestinal bleeding. Since an abdominal computed tomography showed no recurrent tumor, the portal vein stenosis was most likely caused by inflammatory changes that occurred after a leak at the hepaticojejunostomy.

Because the main flow of the portal vein was not completely interrupted, percutaneous transhepatic portography (PTP) into the mesenteric side of the portal vein beyond the stenosis was performed. As seen in Figure 2A and B, PTP findings were consistent with those obtained by conventional angiography. To maintain the main stream of the portal vein, two pieces of uncovered-type, self-expandable metallic stent-grafts, 8 mm in diameter and 20 or 30 mm in length (LUMINEXX®, BARD, Covington, GA, USA) were placed in succession over the stenotic segment. The stent-grafts were then mechanically dilated using a balloon dilator (Power Flex®; Cordis, Miami, FL, USA), resulting in full expansion of the grafts. However, portal blood flow was not corrected immediately. We speculated that possible causes for this were vasospasm of the portal system and/or thrombi generated during stenting and dilation. Therefore, a heparin-coated catheter was left in the mesenteric side of the portal trunk, and urokinase (Nihon Pharmaceutical Co., Tokyo, Japan) 240 000 U a day (Nihon Pharmaceutical Co., Tokyo, Japan) was infused for 7 d. As shown in Figure 3A and B, portography after the urokinase infusion revealed good portal blood flow through the stent-grafts and the jejunal varices had disappeared. Before placement of the stent-grafts, portal venous pressure was 32 cmH_2O, which dropped to 25 cmH_2O after correcting portal blood flow. Gastrointestinal fiberscopy confirmed the absence of jejunal varices around the hepaticojejunostomy. Currently, the patient is doing well without repetitive episodes of gastrointestinal bleeding for 9 mo after the procedure.

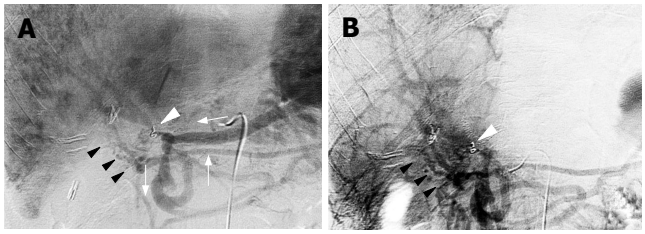

Figure 2 **A**: Portal phase of the celiac arteriography showed a severe stricture at the main trunk of the portal vein. Hepatopetal collaterals through mesenteric veins were observed forming jejunal varices (black arrow heads) in the lifted jejunal limb. A white arrow head indicates the stricture and white arrows indicate the direction of blood flow; **B**: Portal venous phase of the superior mesenteric arteriogram also depicts hepatopetal collaterals and jejunal varices (black arrows) around the hepaticojejunostomy. White arrow heads indicate the stricture of the portal vein adjacent to the microcoils placed in the pseudoaneurysm.

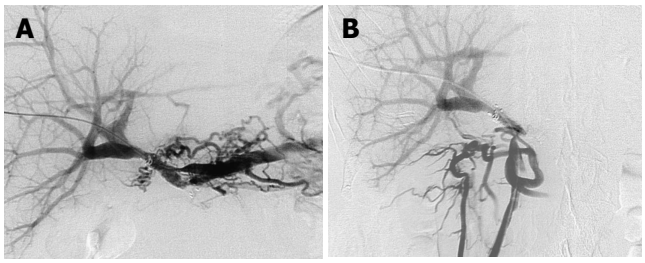

Figure 3 Portography after urokinase infusion showed a good portal blood flow and collaterals forming jejunal varices had disappeared. **A**: Catheter tip was placed in the splenic vein; **B**: Catheter tip was placed in the superior mesenteric vein.

DISCUSSION

Treatment of pseudoaneurysms in the hepatic artery

Rupture of a pseudoaneurysm of the hepatic artery is the main cause of postoperative death after pancreaticoduodenectomy[5]. In the majority of cases, there is concurrent leakage at the site of the pancreatico-intestinal or

choledocho-jejunal anastomosis. Therefore, reentering the previously scarred operative field for repair is not easy and hemostasis by suturing the bleeding point often fails because of a re-encroachment on the affected vessels[6]. On the other hand, using a remote approach like IVR *via* blood vessels is minimally invasive, thus preferable in these situations. However, when hepatic arterial flow is interrupted by IVR to stop hemorrhage, consecutive events such as liver cell necrosis, a breakdown of the choledochojejunostomy, and multiple liver abscesses could occur. Therefore, when using IVR after embolizing pseudoaneurysms, patient outcomes depend a great deal on the maintenance of hepatic arterial flow. In this case, stent-grafts in the hepatic artery prior to the embolization of a pseudoaneurysm were used. However, using stent-grafts in these cases is controversial. For example, several radiologists have suggested that placing a stent-graft in blood vessels with inflammatory changes is inappropriate[7]. Conversely, Paci *et al*[8] reported the efficacy of stent-grafts in the treatment of pseudoaneurysms in hepatic arteries. We used stent-grafts to secure hepatic arterial flow by dilating the stenotic part of the artery and guiding the blood flow into the proper direction out of the pseudoaneurysmal lumen, avoiding the possibility of migrating microcoils interfering with arterial flow to the liver.

Treatment of jejunal varices caused by extrahepatic obliteration of the portal vein

In cases of varices generated in the intestines, extrahepatic portal obstruction often plays a causative role[9]. Jejunal varices caused by portal venous obliteration could be treated with either a shunt for portal decompression[10,11], an angioplasty by an IVR technique such as balloon dilation, stenting to correct the portal blood flow[12] or embolizing varices by an IVR technique to stop inflow[13,14]. Making a treatment choice is complex, involving various factors such as portal hemodynamics, the extent of liver fibrosis, and the cause of portal venous obliteration. However, a priority is establishing a permanent correction of portal blood flow assuring long-lasting effectiveness of hemostasis. That is, re-bleeding from jejunal varices or newly-developed gastroesophageal varices could occur if hepatopetal flow through the main portal trunk is impaired.

Since in this case, there was a possibility for normal portal venous flow, an angioplasty using either stent-grafts or balloons was used. If the portal vein had been completely obstructed by inflammatory changes and the obstructed segments were wider than an inch in length as occurred in our previous cases[15,16], treatments other than angioplasty would have been chosen.

In addition, it was possible to dilate the stricture and secure a lumen of 8 mm in diameter using a balloon dilator. This mechanically-forced dilation could inadvertently interfere with an immediate correction of portal blood flow, however, a urokinase infusion through the portal vein to resolve thrombi attached was valuable[15,16].

Another unsolved issue using this intervention is the duration of patency of the stent-grafts. Funaki *et al* [17]reported that patency was maintained with their stents in portal veins for lengths of time ranging from 4 to 29 mo ,and in most cases stents were obstructed by malignancies. Since we have only followed our patient for 14 mo, continued surveillance to determine patency of the stent is essential.

REFERENCES

1 **Trede M**, Schwall G. The complications of pancreatectomy. *Ann Surg* 1988; **207**: 39-47
2 **Kim J**, Kim JK, Yoon W, Heo SH, Lee EJ, Park JG, Kang HK, Cho CK, Chung SY. Transarterial embolization for postoperative hemorrhage after abdominal surgery. *J Gastrointest Surg* 2005; **9**: 393-399
3 **Sato N**, Yamaguchi K, Shimizu S, Morisaki T, Yokohata K, Chijiiwa K, Tanaka M. Coil embolization of bleeding visceral pseudoaneurysms following pancreatectomy: the importance of early angiography. *Arch Surg* 1998; **133**: 1099-1102
4 **Child CG**. Carcinoma of the duodenum. Ann Surg 1943; **118**: 838-842
5 **Brodsky JT**, Turnbull AD. Arterial hemorrhage after pancreatoduodenectomy. The 'sentinel bleed'. *Arch Surg* 1991; **126**: 1037-1040
6 **Otah E**, Cushin BJ, Rozenblit GN, Neff R, Otah KE, Cooperman AM. Visceral artery pseudoaneurysms following pancreatoduodenectomy. *Arch Surg* 2002; **137**: 55-59
7 **Bürger T**, Halloul Z, Meyer F, Grote R, Lippert H. Emergency stent-graft repair of a ruptured hepatic artery secondary to local postoperative peritonitis. *J Endovasc Ther* 2000; **7**: 324-327
8 **Paci E**, Antico E, Candelari R, Alborino S, Marmorale C, Landi E. Pseudoaneurysm of the common hepatic artery: treatment with a stent-graft. *Cardiovasc Intervent Radiol* 2000; **23**: 472-474
9 **Moncure AC**, Waltman AC, Vandersalm TJ, Linton RR, Levine FH, Abbott WM. Gastrointestinal hemorrhage from adhesion-related mesenteric varices. *Ann Surg* 1976; **183**: 24-29
10 **Chen VT**, Wei J, Liu YC. A new procedure for management of extrahepatic portal obstruction. Proximal splenic-left intrahepatic portal shunt. *Arch Surg* 1992; **127**: 1358-1360
11 **Katoh H**, Shimozawa E, Kojima T, Tanabe T. Modified splenorenal shunt with splenopancreatic disconnection. *Surgery* 1989; **106**: 920-924
12 **Hiraoka K**, Kondo S, Ambo Y, Hirano S, Omi M, Okushiba S, Katoh H. Portal venous dilatation and stenting for bleeding jejunal varices: report of two cases. *Surg Today* 2001; **31**: 1008-1011
13 **Sato T**, Asanuma Y, Ishida H, Hashimoto M, Tanaka J, Andoh H, Yasui O, Kurokawa T, Komatsuda T, Konno K, Heianna J, Koyama K: A case of extrahepatic portosystemic shunt without portal hypertension treated by laparoscopically assisted embolization. *Surgery* 1999; **126**: 984-986
14 **Sato T**, Yasui O, Kurokawa T, Hashimoto M, Asanuma Y, Koyama K. Jejunal varix with extrahepatic portal obstruction treated by embolization using interventional radiology: report of a case. *Surg Today* 2003; **33**: 131-134
15 **Smith SC**, Winters KJ, Lasala JM. Stent thrombosis in a patient receiving chemotherapy. *Cathet Cardiovasc Diagn* 1997; **40**: 383-386
16 **Bilodeau L**, Hearn JA, Dean LS, Roubin GS. Prolonged intracoronary urokinase infusion for acute stent thrombosis. *Cathet Cardiovasc Diagn* 1993; **30:** 141-146
17 **Funaki B**, Rosenblum JD, Leef JA, Hackworth CA, Szymski GX, Alonso EM. Angioplasty treatment of portal vein stenosis in children with segmental liver transplants: mid-term results. *AJR Am J Roentgenol* 1997; **169**: 551-554

S- Editor Liu Y **L- Editor** Zhu LH **E- Editor** Lu W

PO Box 2345, Beijing 100023, China
www.wjgnet.com
wjg@wjgnet.com

World J Gastroenterol 2007 February 14; 13(6): 973-974
World Journal of Gastroenterology ISSN 1007-9327

CASE REPORT

Knot formation in the feeding jejunostomy tube: A case report and review of the literature

Guo-Shiou Liao, Huan-Fa Hsieh, Meng-Hang Wu, Teng-Wei Chen, Jyh-Cherng Yu, Yao-Chi Liu

Guo-Shiou Liao, Department of Surgery, Tri-Service General Hospital Penghu Branch, National Defense Medical Center, Taiwan, China
Teng-Wei Chen, Jyh-Cherng Yu, Yao-Chi Liu, Division of General Surgery, Department of Surgery, Tri-Service General Hospital, National Defense Medical Center, Taipei, Taiwan, China
Huan-Fa Hsieh, Department of Surgery, Yee-Zen General Hospital, Taiwan, China
Meng-Hang Wu, Department of Surgery, Show Chwan Memorial Hospital, Changhua, Taiwan, China
Correspondence to: Dr. Jyh-Cherng Yu, Division of General Surgery, Department of Surgery, Tri-Service General Hospital, National Defense Medical Center, 325, Cheng-Kung Road 2nd section, Taipei 114, Taiwan, China. bmws22008@yahoo.com.tw
Telephone: +886-2-87927191 Fax: +886-2-87927372
Received: 2006-07-17 Accepted: 2007-01-17

Abstract

Jejunostomy feeding tubes provide surgeons with an excellent method for providing nutritional support, but there are several complications associated with a tube jejunostomy, including complications resulting from placement of the tube, mechanical problems related to the location or function and development of focally thickened small-bowel folds. A 76-year old man who presented with multiple medical diseases was admitted to our hospital due to aspiration pneumonia with acute respiratory failure and septic shock. He underwent exploratory laparotomy with feeding jejunostomy using a 14-French nasogastric tube for nutritional support. However, occlusion of the feeding tube was found 30 d after operation, and a rare complication of knot formation in the tube occurred after a new tube was replaced. On the following day, the tube was removed and replaced with a similar tube, which was placed into the jejunum for only 15 cm. The patient's feedings were maintained smoothly for two months. Knot formation in the feeding tube seems to be very rare. To our knowledge, this is the third case in the literature review. Its incidence is probably related to the length of the tube inserted into the lumen.

Key words: Feeding jejunostomy tube; Complications; Knot formation

Liao GS, Hsieh HF, Wu MH, Chen TW, Yu JC, Liu YC. Knot formation of the feeding jejunostomy tube: A case report and review of the literature. *World J Gastroenterol* 2007; 13(6): 973-974

http://www.wjgnet.com/1007-9327/13/973.asp

INTRODUCTION

During the past 3 decades, enteral nutrition has become increasingly popular because of improved nutritional formulas, advances in catheter technology, and development of less invasive techniques (including endoscopic, fluoroscopic, and laparoscopic techniques) for placement of feeding tubes for this purpose[1]. As a result, jejunostomy tubes are used more frequently than before. Despite the benefit of the enteral route for maintaining nutrition, complications have been reported in 2%-12% of patients in whom jejunostomy tubes were placed[2].

CASE REPORT

Here we present a case of 76-year old man who had a history of bilateral middle cerebral artery stenosis with multiple cerebral infarctions and was bedridden for five years. He was living in a nursing home when he was admitted to our hospital due to the impression of aspiration pneumonia with acute respiratory failure and septic shock. He underwent exploratory laparotomy with feeding jejunostomy using a 14-French nasogastric tube for enteral feedings. However, occlusion of the feeding tube was found 30 d after operation. We tried flushing the tube with warm water through a large piston syringe by gentle push-and-pull motions, but in vain. So we replaced it with a new tube. When we inserted the 14-French nasogastric tube into the upper jejunum, we advanced it at least one third of a meter distally beyond its entrance site. When the patency of the tube was checked, we were unable to put any feedings through the tube. An abdominal roentgenographic study demonstrated that a knot was formed in the tube (Figure 1, arrow).

On the following day, with the patient under intravascular general anesthesia and local anesthesia, the tube was removed (Figure 2), and replaced with a similar tube which was inserted into the jejunum only for 15 cm. The patient's feedings were maintained smoothly for two months.

DISCUSSION

An enterostomal device, which is inserted percutaneously

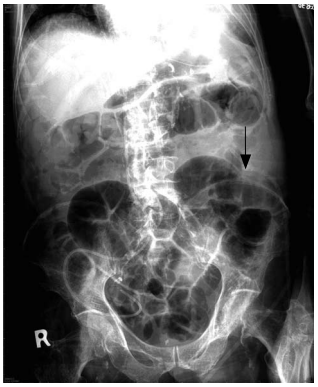

Figure 1 Abdominal roentgenographic study showing knot formation in the tube (arrow).

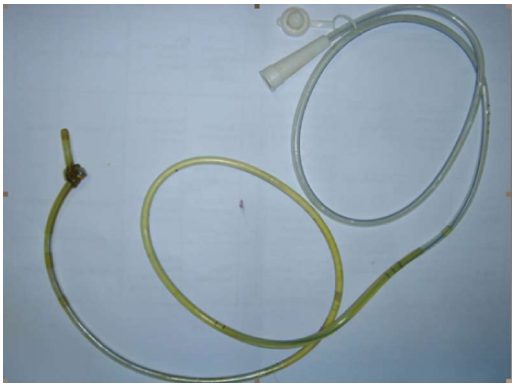

Figure 2 Knot formation in the feeding tube.

through a stoma created on the abdomen (gastrostomy or jejunostomy), can be placed by surgical, endoscopic, laparoscopic, or radiologic techniques[3]. It is indicated when the nasal route is contraindicated or when the patient is expected to need long-term enteral feedings. Jejunostomy tube may be placed for long-term postpyloric enteral feedings when bypassing the stomach is desirable. Patients who will benefit from jejunostomy feedings include those with gastric disease, abnormal gastric and duodenal emptying, upper gastrointestinal obstruction or fistula, absent gag reflex, or significant risk of esophageal reflux and aspiration[4,5].

Abnormalities related to the placement of the tube include complications resulting from placement of the tube (i.e., small-bowel obstruction, nonobstructive small bowel narrowing, sealed-off extraluminal tracks or collections, extravasation of contrast material to the skin, jejunal hematomas, small bowel intussusception, and pneumatosis cystoides intestinalis), mechanical problems related to the location or function (i.e., coiling, kinking, occlusion, malpositioning, disruption, or knotting of the jejunostomy tube and retrograde flow of contrast material) and development of focally thickened small bowel folds as an isolated finding at or just distal to the intraluminal end of the tube[1,6-8].

To avoid a clogged feeding tube, enteral feeding devices should be thoroughly flushed every 4 to 6 h during continuous feedings and whenever feedings are on hold, before and after administration of feedings and medications or after the residuals are checked. A large syringe (30 to 60 mL) should always be used for flushing to prevent rupture of the tube. The tube should be irrigated with 20 to 30 mL of tepid water. No fluid has been found to be superior to water for maintaining patency. A stylet should never be used to unclog a tube because it can puncture the tube or part of the gastrointestinal tract. We may try one of the newer plastic declogging devices to mechanically unclog a feeding tube[9-11].

Coiling, kinking, malpositioning, occlusion, or disruption of the jejunostomy tube have been frequently found in patients, but knot formation in the feeding tube seems to be rare[12,13]. To our knowledge, this seems to be the third case in the literature review. Its occurrence is probably greater when the tube is inserted farther into the lumen, suggesting that the mechanism of knot formation is similar to that of supercoiling and concatenate formation. To avoid knot formation the feeding tube should not be inserted too long into the lumen. No more than 15 cm seems appropriate in our experience.

REFERENCES

1 **Carucci LR**, Levine MS, Rubesin SE, Laufer I, Assad S, Herlinger H. Evaluation of patients with jejunostomy tubes: imaging findings. *Radiology* 2002; **223**: 241-247
2 **Pagana KD**. Preventing complications in jejunostomy tube feedings. *Dimens Crit Care Nurs* 1987; **6**: 28-38
3 **Keymling M**. Technical aspects of enteral nutrition. *Gut* 1994; **35**: S77-S80
4 **Abdel-Lah Mohamed A**, Abdel-Lah Fernández O, Sánchez Fernández J, Pina Arroyo J, Gómez Alonso A. Surgical access routes in enteral nutrition. *Cir Esp* 2006; **79**: 331-341
5 **Kaur N**, Gupta MK, Minocha VR. Early enteral feeding by nasoenteric tubes in patients with perforation peritonitis. *World J Surg* 2005; **29**: 1023-1027; discussion 1027-1028
6 **Tapia J**, Murguia R, Garcia G, de los Monteros PE, Oñate E. Jejunostomy: techniques, indications, and complications. *World J Surg* 1999; **23**: 596-602
7 **Prahlow JA**, Barnard JJ. Jejunostomy tube failure: malnutrition caused by intraluminal antegrade jejunostomy tube migration. *Arch Phys Med Rehabil* 1998; **79**: 453-455
8 **Cataldi-Betcher EL**, Seltzer MH, Slocum BA, Jones KW. Complications occurring during enteral nutrition support: a prospective study. *JPEN J Parenter Enteral Nutr* 1983; **7**: 546-552
9 **Nicholas JM**, Cornelius MW, Tchorz KM, Tremblay LN, Spiegelman ER, Easley KA, Small W, Feliciano DV, Powell MA, Poklepovic J. A two institution experience with 226 endoscopically placed jejunal feeding tubes in critically ill surgical patients. *Am J Surg* 2003; **186**: 583-590
10 **Myers JG**, Page CP, Stewart RM, Schwesinger WH, Sirinek KR, Aust JB. Complications of needle catheter jejunostomy in 2,022 consecutive applications. *Am J Surg* 1995; **170**: 547-550; discussion 550-551
11 **Holmes JH**, Brundage SI, Yuen P, Hall RA, Maier RV, Jurkovich GJ. Complications of surgical feeding jejunostomy in trauma patients. *J Trauma* 1999; **47**: 1009-1012
12 **Myers A**, Thurston W, Ho CS. Spontaneous knotting of a transgastric jejunostomy tube: case report. *Can Assoc Radiol J* 1997; **48**: 22-24
13 **Cappell MS**, Scarpa PJ, Nadler S, Miller SH. Complications of nasoenteral tubes. Intragastric tube knotting and intragastric tube breakage. *J Clin Gastroenterol* 1992; **14**: 144-147

S- Editor Liu Y **L- Editor** Wang XL **E- Editor** Lu W

PO Box 2345, Beijing 100023, China
www.wjgnet.com
wjg@wjgnet.com

World J Gastroenterol 2007 February 14; 13(6): 975-977
World Journal of Gastroenterology ISSN 1007-9327

CASE REPORT

Acute pancreatitis and amiodarone: A case report

Yen-Yuan Chen, Ching-Yu Chen, Kai-Kuen Leung

Yen-Yuan Chen, Ching-Yu Chen, Kai-Kuen Leung, Department of Family Medicine, National Taiwan University Hospital, Taipei, Taiwan, China
Correspondence to: Dr. Kai-Kuen Leung, Department of Family Medicine, National Taiwan University Hospital, No. 7, Chung-Shan South Road, Taipei 10016, Taiwan, China. kkleung@ha.mc.ntu.edu.tw
Telephone: +886-2-23123456-2147 Fax: +886-2-23118674
Received: 2006-12-06 Accepted: 2007-01-23

Abstract

Amiodarone, a class Ⅲ antiarrhythmic drug, is one of the most effective drugs used in the treatment of ventricular and paroxysmal supraventricular tachyarrhythmia. Adverse effects of amiodarone including pulmonary toxicity, hepatotoxicity, aggravation of arrhythmia, and thyroid diseases are well understood. A 66-year old woman with acute pancreatitis was admitted to our hospital with the complaint of epigastralgia radiating to both flanks for two months. Her symptoms and elevation of pancreatic enzymes did not respond to conventional medical treatment of pancreatitis for 18 d. No known causal factors for pancreatitis such as biliary tract stone, hypertriglyceridemia and alcohol consumption could be identified. Under the suspicion of amiodarone-induced acute pancreatitis, amiodarone was substituted by propafenone. Her symptoms soon alleviated and serum lipase level declined. Three months after hospital discharge, the abdominal pain did not recur. Amiodarone was approved to treat recurrent ventricular fibrillation or sustained ventricular tachyarrhythmia that has been resistant to other medications since 1986. Pancreatitis is a very rare adverse effect associated with the use of amiodarone, and only four cases of amiodarone-induced pancreatitis have been reported in literature. We report a patient who developed acute pancreatitis during amiodarone therapy.

Key words: Acute pancreatitis; Amiodarone; Amylase; Lipase

Chen YY, Chen CY, Leung KK. Acute pancreatitis and amiodarone: A case report. *World J Gastroenterol* 2007; 13(6): 975-977

http://www.wjgnet.com/1007-9327/13/975.asp

INTRODUCTION

Amiodarone has been approved to treat recurrent ventricular fibrillation or sustained ventricular tachyarrhythmia which has been resistant to other medications since 1986. A recent study showed that amiodarone is more effective than propafenone and sotalol against paroxysmal atrial fibrillation, suggesting that amiodarone is the first choice of treatment for maintaining sinus rhythm in patients with paroxysmal atrial fibrillation[1]. Although amiodarone is effective in treating atrial and ventricular arrhythmias, adverse effects are common and increase markedly after a year of treatment. Adverse effects may occur in many organ systems, such as pulmonary, cardiac, central nervous systems, as well as in thyroid, liver and gastrointestinal tract, and some of them can be very serious and even fatal[2]. Pancreatitis is a very rare adverse effect associated with the use of amiodarone, and only four cases of acute pancreatitis induced by amiodarone have been reported in the literature[3-6]. We report a patient who developed acute pancreatitis during amiodarone therapy.

CASE REPORT

A 66-year old woman was admitted to our hospital because of epigastrialgia and flank pain for two months. The patient had a long history of rheumatic heart disease involving mitral and aortic valves. She received aortic valve replacement in 1973 and mitral valve replacement in 1999. She had paroxysmal atrial fibrillation with rapid ventricular response controlled by quinidine and digoxin for many years. However, tachyarrhythmia attacked her very frequently in recent years, so she received a radiofrequency catheter ablation in 2000. At that time, electrophysiological study revealed sick sinus syndrome and a cardiac pacemaker (DDDR) was implanted. After ablation therapy, she experienced exertional dyspnea and orthopnea with the severity of New York Heart Association function class Ⅱ. Coronary angiography revealed no sign of coronary artery stenosis. She visited the heart clinic regularly and was treated with warfarin, spirololactone, furosemide and digitalis.

She did not smoke cigarettes or drink alcoholic beverages. According to her medical records, she had no chronic diseases such as diabetes mellitus, hypertension, hyperlipidemia and chronic hepatitis. She did not have any exposure to toxic chemicals or travel overseas. Cholecystectomy was performed in 1981 due to gall bladder stones and acute cholecystitis. She did not

Table 1 Clinical characteristics of reported cases of amiodarone-induced pancreatitis and the present case

Authors and year	Age/Sex	Serum amylase level (normal value)	Serum lipase level (normal value)	Pancreatitis developed during the use of amiodarone	Resolved following the removal of amiodarone	Re-challenge of amiodarone	Association between amiodarone and pancreatitis
Sastri SV, *et a*l 1990	67/M	64 (0-45)	38 (6-20)	Yes	No	No	Questionable
Munoz RAI, *et al* 1996	67/M	387 (70-220)	546 (not applicable)	Yes	Yes	No	Possible
Bosch X, *et al* 1997	46/F	1480 (17-115)	946 (0-190)	Yes	Yes	Yes	Definite
Famularo G, *et al* 2004	80/M	732 (0-95)	548 (10-140)	Yes	Yes	No	Possible
Present case 2006	66/F	109 (0-220)	395 (0-30)	Yes	Yes	No	Possible

experience any right upper abdominal discomfort after the operation. Total hysterectomy and bilateral salpingo-oophorectomy were done in 1984 due to uterine myoma and right ovarian cyst. The post-operation course was uneventful.

Approximately three months before this admission, amiodarone (200 mg per day) was given due to recurrent paroxysmal atrial fibrillation. The dosage was reduced to 100 mg daily one month before admission. About two months before this admission, she began to suffer from a constant pain at her epigastrium. It was a dull pain with radiation to her flanks. The pain did not change with body positions, but it slightly got worse after meals. She had no nausea, vomiting or diarrhea. She lost her appetite and 2 kilograms of her body weight within one month.

On admission, physical examination was unremarkable except for mild knocking pain on both flanks. The patient had no fever and jaundice. Laboratory examinations including urine analysis, complete blood count, liver and renal functions were within normal range. Serum amylase was 109 U/L (normal value < 220 U/L) and serum lipase was 395 U/L (normal value < 30 U/L). Ultrasound and triphase dynamic computer tomography of the abdomen demonstrated no dilatation of intrahepatic ducts or common bile duct, no stones, no pancreatic enlargement or necrosis, and no fluid accumulation. Because of the persisted elevation of serum lipase, endoscopic ultrasonography was done for a better visualization of the pancreas. The result revealed a reticular pattern over the whole pancreas that suggested the diagnosis of pancreatitis. Under the impression of pancreatitis, her oral intake was prohibited except for medications including amiodarone. Her abdominal symptoms persisted and serum lipase level was still high after three weeks of conventional medical treatments.

Because no causal factor for pancreatitis was found after the initial work-up, acute pancreatitis induced by amiodarone was suspected. So amiodarone was substituted by propafenone (400 mg) after a three-day overlapping of both drugs. After amiodarone was discontinued, her abdominal pain soon subsided and serum lipase gradually returned to nearly normal level at discharge. Three months after discharge, she was totally free of abdominal symptoms and her follow-up check of serum amylase and lipase level was normal.

DISCUSSION

Pancreatitis is usually presented with moderate to severe abdominal pain sometimes radiated to the flanks, accompanied with increased serum amylase and lipase and a variable degree of morphological changes in the pancreas. Gallstones and alcohol are the most common causes of acute pancreatitis. Other etiologies include hypertriglyceridemia, trauma, infection and drugs. Many medications have been reported in the literature to be related to the development of pancreatitis[7,8]. However, there is no clinical feature that can differentiate drug-induced pancreatitis from other factor caused-pancreatitis. Drug-induced pancreatitis is diagnosed by the following criteria: pancreatitis developed during treatments, resolved following the removal of the drug, and re-development following re-challenge of the offending drug[9]. A "definite" association can be made if the suspected drug meets all three criteria. If a relationship is supported by not all three criteria, the drug is classified as having a "possible" association. A drug is classified as "questionable" if it is supported by inadequate or contradictory evidence[9]. The summaries of four reported cases and our present case and the association between pancreatitis and amiodarone are shown in Table 1.

How do we explain the discrepancy between serum amylase and lipase in our patient? Although the elevation of amylase and lipase is an important indicator for acute pancreatitis, normoamylasemia has been reported in 19% of patients with acute pancreatitis[10]. Elevated lipase and normal amylase may occur in acute pancreatitis due to a longer time interval since onset of attack, pancreatitis caused by alcohol abuse or by hypertriglyceridemia[11]. Lipase level usually peaks at 24 h after the onset of acute pancreatitis and normalizes within 8 to 14 d from the onset of acute pancreatitis. Compared with serum amylase, serum lipase rises slightly later and remains elevated longer. Since our patient sought medical help two months after the onset of acute abdominal pain, her serum amylase might would have returned to a normal limit. Therefore, the possibility of acute pancreatitis could not be excluded due the normoamylasemia from the very beginning. Postmortem samples from patients who have received a long-term treatment with amiodarone reveal high concentrations of amiodarone and its metabolites in adipose tissue, liver, lung and pancreas[12]. Chronic deposition of amiodarone in pancreatic tissues may explain the prolonged elevation of lipase in our patient. The findings in ultrasound and computer tomography of the abdomen are required for the diagnosis of pancreatitis. However, in our patient, no obvious abnormality was found in abdominal ultrasonography and computer tomography. The only abnormal finding was a reticular

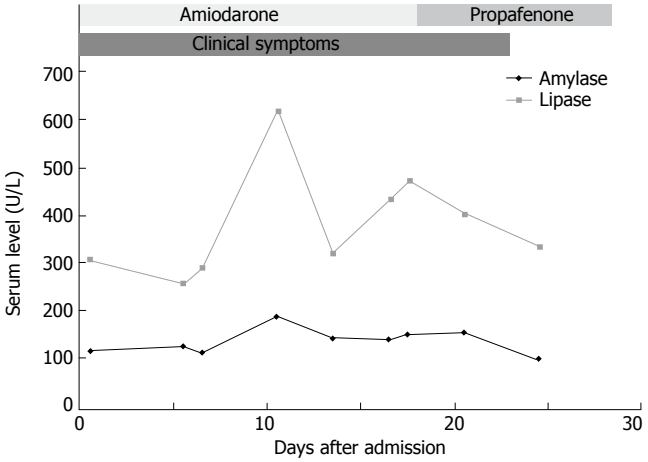

Figure 1 Temporal relationship between amiodarone therapy and the change of clinical symptoms and major laboratory data.

pattern in endoscopic ultrasonography that highly suggested pancreatitis. Our finding is similar to Bosch's patient whose abdominal ultrasonography and computer tomography were normal[5]. The temporal relationship between amiodarone therapy and the change of clinical symptoms and major laboratory data of this patient are shown in Figure 1.

Before reaching the conclusion that pancreatitis is induced by amiodarone, other etiological factors of pancreatitis should be ruled out. In our patient, no other etiological cause was found from her medical history, physical examination, laboratory results and image studies. Since we did not re-challenge with amiodarone due to ethical concerns, our patient fulfilled the "possible" diagnosis of amiodarone-induced pancreatitis. The possible mechanisms of drug-induced acute pancreatitis include pancreatic duct constriction, immunosuppression, direct cellular toxicity, osmotic or metabolic changes, and arteriolar thrombosis[13], but the exact mechanism of pancreatitis induced by amiodarone is still unknown.

Only four cases of acute pancreatitis induced by amiodarone have been reported in the literature[3-6]. Our case is the first Asian patient with acute pancreatitis induced by amiodarone. Although acute pancreatitis induced by amiodarone seems to be less severe than pancreatitis caused by gallstones or alcohol abuse, physicians and patients should completely understand the adverse effects of amiodarone including acute pancreatitis when they decide to use amiodarone.

REFERENCES

1 **Roy D**, Talajic M, Dorian P, Connolly S, Eisenberg MJ, Green M, Kus T, Lambert J, Dubuc M, Gagné P, Nattel S, Thibault B. Amiodarone to prevent recurrence of atrial fibrillation. Canadian Trial of Atrial Fibrillation Investigators. *N Engl J Med* 2000; **342**: 913-920
2 **Connolly SJ**. Evidence-based analysis of amiodarone efficacy and safety. *Circulation* 1999; **100**: 2025-2034
3 **Sastri SV**, Diaz-Arias AA, Marshall JB. Can pancreatitis be associated with amiodarone hepatotoxicity? *J Clin Gastroenterol* 1990; **12**: 70-73
4 **Muñoz Ruiz AI**, Calvo Elipe A, Guerrero Vega E, Gorgojo Martínez JJ, Vera López E, Gilsanz Fernández C. Pancreatitis and inappropriate ADH secretion syndrome associated with amiodarone. *An Med Interna* 1996; **13**: 125-126
5 **Bosch X**, Bernadich O. Acute pancreatitis during treatment with amiodarone. *Lancet* 1997; **350**: 1300
6 **Famularo G**, Minisola G, Nicotra GC, De Simone C. Acute pancreatitis caused by amiodarone. *Eur J Emerg Med* 2004; **11**: 305-306
7 **Wilmink T**, Frick TW. Drug-induced pancreatitis. *Drug Saf* 1996; **14**: 406-423
8 **Napier S**, Thomas M. 36 year old man presenting with pancreatitis and a history of recent commencement of Orlistat case report. *Nutr J* 2006; **5**: 19
9 **Sura ME**, Heinrich KA, Suseno M. Metronidazole-associated pancreatitis. *Ann Pharmacother* 2000; **34**: 1152-1155
10 **Clavien PA**, Robert J, Meyer P, Borst F, Hauser H, Herrmann F, Dunand V, Rohner A. Acute pancreatitis and normoamylasemia. Not an uncommon combination. *Ann Surg* 1989; **210**: 614-620
11 **Yadav D**, Agarwal N, Pitchumoni CS. A critical evaluation of laboratory tests in acute pancreatitis. *Am J Gastroenterol* 2002; **97**: 1309-1318
12 **Maggioni AP**, Maggi A, Volpi A, D'Aranno V, Tognoni G, Giani P. Amiodarone distribution in human tissues after sudden death during Holter recording. *Am J Cardiol* 1983; **52**: 217-218
13 **Underwood TW**, Frye CB. Drug-induced pancreatitis. *Clin Pharm* 1993; **12**: 440-448

S- Editor Liu Y **L- Editor** Wang XL **E- Editor** Lu W

PO Box 2345, Beijing 100023, China
www.wjgnet.com
wjg@wjgnet.com

World J Gastroenterol 2007 February 14; 13(6): 978-979
World Journal of Gastroenterology ISSN 1007-9327

CASE REPORT

Virtual colonoscopy-induced perforation in a patient with Crohn's disease

Sunny H Wong, Vincent WS Wong, Joseph JY Sung

Sunny H Wong, Vincent WS Wong, Joseph JY Sung, Institute of Digestive Disease and Department of Medicine and Therapeutics, The Chinese University of Hong Kong, Hong Kong, China
Correspondence to: Professor Joseph Sung, Department of Medicine and Therapeutics, 9/F Prince of Wales Hospital, 30-32 Ngan Shing Street, Shatin, Hong Kong, China. joesung@cuhk.edu.hk
Telephone: +852-26323132 Fax: +852-26373852
Received: 2006-11-28 Accepted: 2007-01-22

Abstract

We report a case of sigmoid colon perforation in a patient with Crohn's disease undergoing computed-tomographic (CT) colonography. A 70-year-old patient with Crohn's disease with terminal ileitis and sigmoid stricture underwent CT colonography after incomplete conventional colonoscopy. During the procedure, the colon was inflated by air insufflation and the patient developed abdominal pain with radiological evidence of retroperitoneal and intraperitoneal free gas. Hartmann's operation was performed. This case highlights that CT colonography is not risk-free. The risk of perforation may be higher in patients with inflammatory bowel disease.

Key words: Perforation; Colonography; Crohn's disease; Stricture; Hartmann's; Inflammatory bowel disease

Wong SH, Wong VWS, Sung JJY. Virtual colonoscopy-induced perforation in a patient with Crohn's disease. *World J Gastroenterol* 2007; 13(6): 978-979

http://www.wjgnet.com/1007-9327/13/978.asp

INTRODUCTION

Computed-tomographic (CT) colonography is a relatively non-invasive tool to examine the colon. It was once thought to be almost risk-free when compared to conventional colonoscopy. However, cases of colonic perforation during CT colonography were reported in normal subjects undergoing primary screening of colonic carcinoma. It is obvious that CT colonography carries a low but definite risk of colonic perforation. A few cases of perforation were also reported in diseased colons, as in patients suffering from ulcerative colitis and colonic carcinoma. In this article, we report a case of colonic perforation in a patient with Crohn's disease undergoing CT colonography.

CASE REPORT

A 70-year-old gentleman suffered from Crohn's disease for more than 10 years. He presented with chronic loose stool diarrhea. He did not have per-rectal bleeding, abdominal pain or other extra-intestinal symptoms. His body weight remained static at around 42 kg. Colonoscopy in 2005 showed a stricture at the sigmoid colon with aphthous ulcers, and a barium enema follow-through study showed terminal ileal narrowing. Tissue biopsy of the colon showed active chronic colitis with hyperplastic crypts consistent with Crohn's disease.

Since 2004, the patient had worsened diarrhea and progressive weight loss to 40 kg. His hemoglobin dropped from 13.1 to 12.0 g/dL. Plasma C-reactive protein increased to 33.5 mg/L. He was treated with sulphasalazine and iron supplements. A regular colonoscopy was arranged to assess disease extent and to rule out colorectal cancer, but the endoscope failed to advance beyond the tight sigmoid stricture even using a pediatric colonoscope.

The patient was admitted to our hospital for computed tomographic (CT) colonography on 7 July 2006 for further evaluation. A 20-French Foley catheter without balloon inflation was inserted with the tip in the rectum, and air was introduced into the large bowel through manual insufflation. Immediately after air insufflation, the patient complained of lower abdominal pain. Plain CT film demonstrated large amounts of free retroperitoneal air and a small amount of intraperitoneal free gas (Figure 1).

The patient was diagnosed to have iatrogenic colonic perforation. During emergency surgery, a 3 mm perforation at the anti-mesenteric side of proximal sigmoid was noticed, and there was a tight stricture at descending colon just 1 cm proximal to the perforation. A left hemicolectomy was performed to resect the stricture and perforated segment. The distal transverse colon was brought out as end colostomy. He subsequently had uneventful recovery apart from transient perioperative atrial fibrillation.

DISCUSSION

CT colonography is a relatively non-invasive imaging technique to examine the colon. Adequate bowel preparation is essential. During the procedure, air or

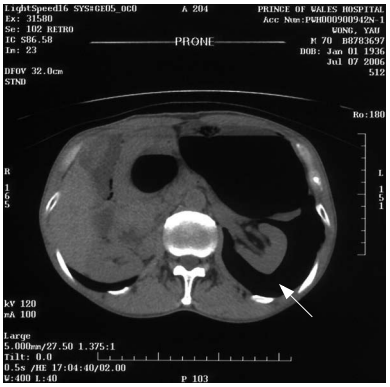

Figure 1 Plain CT scan of the abdomen after air insufflation during CT colonoscopy. Extensive retroperitoneal gas was detected (arrow).

carbon dioxide is insufflated through a rectal catheter. Helical CT scans of the abdomen and pelvis during a breath-hold are then performed to give a 3-dimensional 'fly-through' reconstruction, allowing examination of the colonic surface with a simulated endoscopic view.

CT colonography has been most extensively evaluated for the detection of colonic polyps and cancer. In 1233 asymptomatic patients in the United States, the sensitivity and specificity of CT colonography in detecting adenomatous polyps of at least 10 mm in size were 92 percent and 96 percent, respectively[1]. Less commonly, CT colonography has also been utilized in patients with Crohn's disease. The greatest advantage of CT colonography lies in patients with strictures, adhesions or obstructing tumors which prevent complete colonoscopic examination. Studies have shown that CT colonography can detect thickened bowel wall and deep ulcers in patients with Crohn's disease[2].

Since CT colonography does not involve the insertion of an endoscope, it is generally perceived as a safe procedure. The International Working Group on Virtual Colonography reviewed a total of 21 923 CT colonography procedures and reported only 2 cases of colonic perforations with a rate of 0.009%[3]. Nevertheless, it is noteworthy that most of the reported series involve people with normal colon, some undergoing primary screening only. In patients with colonic diseases, the diseased colonic wall may not accommodate a high intraluminal pressure as well as a normal colon. In addition, strictures may prevent the even distribution of the air insufflated, resulting in an increased intraluminal pressure locally. This may have accounted for the close proximity between the perforation site and stricture in our patient. There are case reports of colonic perforations in patients with ulcerative colitis[4] or carcinoma of the colon[5].

In conclusion, our case highlights that CT colonography is not risk-free. The risk of perforation may be higher in patients with inflammatory bowel disease. Prospective studies should be conducted to further evaluate the risk of CT colonography in these patients.

REFERENCES

1 **Pickhardt PJ**, Choi JR, Hwang I, Butler JA, Puckett ML, Hildebrandt HA, Wong RK, Nugent PA, Mysliwiec PA, Schindler WR. Computed tomographic virtual colonoscopy to screen for colorectal neoplasia in asymptomatic adults. *N Engl J Med* 2003; **349**: 2191-2200

2 **Tarján Z**, Zágoni T, Györke T, Mester A, Karlinger K, Makó EK. Spiral CT colonography in inflammatory bowel disease. *Eur J Radiol* 2000; **35**: 193-198

3 **Pickhardt PJ**. Incidence of colonic perforation at CT colonography: review of existing data and implications for screening of asymptomatic adults. *Radiology* 2006; **239**: 313-316

4 **Coady-Fariborzian L**, Angel LP, Procaccino JA. Perforated colon secondary to virtual colonoscopy: report of a case. *Dis Colon Rectum* 2004; **47**: 1247-1249

5 **Kamar M**, Portnoy O, Bar-Dayan A, Amitai M, Munz Y, Ayalon A, Zmora O. Actual colonic perforation in virtual colonoscopy: report of a case. *Dis Colon Rectum* 2004; **47**: 1242-1244; discussion 1244-1246

S- Editor Liu Y **L- Editor** Zhu LH **E- Editor** Lu W

PO Box 2345, Beijing 100023, China
www.wjgnet.com
wjg@wjgnet.com

World J Gastroenterol 2007 February 14; 13(6): 980
World Journal of Gastroenterology ISSN 1007-9327

ACKNOWLEDGMENTS

Acknowledgments to Reviewers of *World Journal of Gastroenterology*

Many reviewers have contributed their expertise and time to the peer review, a critical process to ensure the quality of *World Journal of Gastroenterology*. The editors and authors of the articles submitted to the journal are grateful to the following reviewers for evaluating the articles (including those published in this issue and those rejected for this issue) during the last editing time period.

Yik-Hong Ho, Professor
Department of Surgery, School of Medicine, James Cook University, Townsville 4811, Australia

Olivier Detry, Dr
Department of Abdominal Surgery and Transplantation, University of Liège, CHU Sart Tilman B35, B-4000 Liège, Belgium

Kazuhiro Hanazaki, MD
Kohasu, Okocho, Nankoku, Kochi, 783-8505, Japan

Osman Cavit Ozdogan, Associate Professor
Department of Gastroenterology, Liver Unit, Marmara University School of Medicine, Istanbul 34662, Turkey

Frank A Anania, Professor
Division of Division Digestive Diseases, 615 Michael Street, Room 255 Whitehead Biomedical Research Building, Atlanta, GA 30322, United States

Sri Prakash Misra, Professor
Moti Lal Nehru Medical College, Allahabad 211001, India

Filip Braet, Associate Professor
Australian Key Centre for Microscopy and Microanalysis, Madsen Building (F09), The University of Sydney, Sydney NSW 2006, Australia

Wei Tang, MD, EngD, Assistant Professor
Department of surgery, Graduate School of Medicine, The University of Tokyo, Tokyo 113-8655, Japan

Corlu Anne, PhD
Inserm U522, Hôpital Pontchaillou, rue Henri Le guilloux, Rennes 35033, France

Leonard R Johnson, Professor
Department of Physiology, University Tennessee College of Medicine, 894 Union Ave, Memphis, TN 38163, United States

Markus W Büchler, MD
Department of General Surgery, University of Heidelberg, Im Neuenheimer Feld 110, Heidelberg D-69120, Germany

Silvana Zanlungo, Prof
Departamento de Gastroenterología, Pontificia Universidad Católica de Chile, Marcoleta 367, Casilla 114-D, Santiago, Chile

Marie-Catherine Vozenin-brotons, PhD
UPRES EA 27-10, IRSN/IGR, 39 rue C. Desmoulins, Villejuif Cedex 94305, France

Ta-Sen Yeh, MD, PhD
Department of Surgery, Chang Gung Memorial Hospital, 5 Fu-Hsing Street, Taoyuan, Taiwan, China

Sri Prakash Misra, Professor
Moti Lal Nehru Medical College, Allahabad 211001, India

Paolo Gionchetti, MD
Internal Medicine and gastroenterology, University of Bologna-Italy, Policlinico S.Orsola,Pad.25,via Massarenti 9, Bologna 40138, Italy

Yvan Vandenplas, Professor
Department of Pediatrics, AZ-VUB, Laarbeeklaan 101, Brussels 1090, Belgium

Yik-Hong Ho, Professor
Department of Surgery, School of Medicine, James Cook University, Townsville 4811, Australia

Ian C Roberts-Thomson, Professor
Department of Gastroenterology and Hepatology, The Queen Elizabeth Hospital, 28 Woodville Road, Woodville South 5011, Australia

Ala Sharara, MD
Division of Gastroenterology, Director, Endoscopy Unit, American University of Beirut Medical Center, Associate Consulting Professor, Duke University Medical Center, PO Box 11-0236, Riad El Solh 110 72020, Beirut, Lebanon

Reza Malekzadeh, Professor
Digestive Disease Research Center, Tehran University of Medical Sciences, Shariati Hospital, Kargar Shomali Avenue, 19119 Tehran, Iran

Daniel Lindsay Worthley, Dr
Department of Gastroenterology and Hepatology, Flinders Medical Centre, Room 3D230, Bedford Park, SA 5042, Australia

Sri Prakash Misra, Professor
Moti Lal Nehru Medical College, Allahabad 211001, India

Wang-Xue Chen, Dr
Institute for Biological Sciences, National Research Concil Canada, 100 Sussex Drive, Room 3100, Ottawa, Ontario K1A 0R6, Canada

Silvana Zanlungo, Professor
Departamento de Gastroenterología, Pontificia Universidad Católica de Chile, Marcoleta 367, Casilla 114-D, Santiago, Chile

Shu Zheng, Professor
Scientific Director of Cancer Institute, Zhejiang University, Secondary Affiliated Hospital, Zhejiang University, 88# Jiefang Road, Hangzhou 310009, Zhejiang Province, China

Yaron Niv, Professor
Department of Gastroenterology, Rabin Medical Center, Beilinson Campus, Tel Aviv University, 2 Hadekel St., Pardesia 42815, Israel

Fernando Alvarez, Professor
Service de gastroentérologie, hépatologie et nutrition, Hôpital Sainte-Justine, 3175 Côte Ste-Catherine, Montréal, Québec, Canada H3T 1C5, Canada

Mauro Bernardi, Professor
University of Bologna, Semeiotica Medica-Policlinico S. Orsola-Malpighi-Via Massarenti, 9, Bologna 40138, Italy

Pierre Brissot, Professor
Liver Disease Unit And Inserm U-522, University Hospital Pontchaillou, 2, Rue Henri Le Guilloux, Rennes 35033, France

Katsuhisa Omagari, MD
Second Department of Internal Medicine, Nagasaki University School of Medicine, 1-7-1 Sakamoto, Nagasaki-city 852-8501, Japan

Akihito Tsubota, Assistant Professor
Institute of Clinical Medicine and Research, Jikei University School of Medicine, 163-1 Kashiwa-shita, Kashiwa, Chiba 277-8567, Japan

Silvio Nadalin, Dr
Department of General Surgery and Transplantation, University of Essen, Hufelandstrasse 55, D- 45122 Essen, Germany

Luigi Bonavina, Professor
Department of Surgery, Policlinico San Donato, University of Milano, via Morandi 30, Milano 20097, Italy

Takayuki Yamamoto, MD
Inflammatory Bowel Disease Center, Yokkaichi Social Insurance Hospital, 10-8 Hazuyamacho, Yokkaichi 510-0016, Japan

Masahiro Arai, MD, PhD
Department of Gastroenterology, Toshiba General Hospital, 6-3-22 Higashi-ooi, Shinagawa-ku, Tokyo 140-8522, Japan

PO Box 2345, Beijing 100023, China
www.wjgnet.com
wjg@wjgnet.com

World J Gastroenterol 2007 February 14; 13(6): 981
World Journal of Gastroenterology ISSN 1007-9327

Meetings

MAJOR MEETINGS COMING UP

Meeting Falk Research Workshop: Morphogenesis and Cancerogenesis of the Liver
25-26 January 2007
Goettingen
symposia@falkfoundation.de

Meeting Canadian Digestive Diseases Week (CDDW)
16-20 February 2007
Banff-AB
cagoffice@cag-acg.org
www.cag-acg.org/cddw/cddw2007.htm

Meeting Falk Symposium 158: Intestinal Inflammation and Colorectal Cancer
23-24 March 2007
Sevilla
symposia@falkfoundation.de

Meeting BSG Annual Meeting
26-29 March 2007
Glasgow
www.bsg.org.uk/

NEXT 6 MONTHS

Meeting 42nd Annual Meeting of the European Association for the Study of the Liver
11-15 April 2007
Barcelona
easl2007@easl.ch
www.easl.ch/liver-meeting/

Meeting Falk Symposium 159: IBD 2007 - Achievements in Research and Clinical Practice
4-5 May 2007
Istanbul
symposia@falkfoundation.de

Meeting European Society for Paediatric Gastroenterology, Hepatology and Nutrition Congress 2007
9-12 May 2007
Barcelona
espghan2007@colloquium.fr

Digestive Disease Week
19-24 May 2007
Washington Convention Center, Washington DC

Meeting Gastrointestinal Endoscopy Best Practices: Today and Tomorrow, ASGE Annual Postgraduate Course at DDW
23-24 May 2007
Washington-DC
tkoral@asge.org

Meeting ESGAR 2007 18th Annual Meeting and Postgraduate Course
12-15 June 2007
Lisbon
fca@netvisao.pt

Meeting Falk Symposium 160: Pathogenesis and Clinical Practice in Gastroenterology
15-16 June 2007
Portoroz
symposia@falkfoundation.de

Meeting ILTS 13th Annual International Congress
20-23 June 2007
Rio De Janeiro
www.ilts.org

Meeting 9th World Congress on Gastrointestinal Cancer
27-30 June 2007
Barcelona
meetings@imedex.com

EVENTS AND MEETINGS IN 2007

Meeting Falk Research Workshop: Morphogenesis and Cancerogenesis of the Liver
25-26 January 2007
Goettingen
symposia@falkfoundation.de

Meeting Canadian Digestive Diseases Week (CDDW)
16-20 February 2007
Banff-AB
cagoffice@cag-acg.org
www.cag-acg.org/cddw/cddw2007.htm

Meeting Falk Symposium 158: Intestinal Inflammation and Colorectal Cancer
23-24 March 2007
Sevilla
symposia@falkfoundation.de

Meeting BSG Annual Meeting
26-29 March 2007
Glasgow
www.bsg.org.uk/

Meeting 42nd Annual Meeting of the European Association for the Study of the Liver
11-15 April 2007
Barcelona
easl2007@easl.ch
www.easl.ch/liver-meeting/

Meeting Falk Symposium 159: IBD 2007 - Achievements in Research and Clinical Practice
4-5 May 2007
Istanbul
symposia@falkfoundation.de

Meeting European Society for Paediatric Gastroenterology, Hepatology and Nutrition Congress 2007
9-12 May 2007
Barcelona
espghan2007@colloquium.fr

Meeting Gastrointestinal Endoscopy Best Practices: Today and Tomorrow, ASGE Annual Postgraduate Course at DDW
23-24 May 2007
Washington-DC
tkoral@asge.org

Meeting ESGAR 2007 18th Annual Meeting and Postgraduate Course
12-15 June 2007
Lisbon
fca@netvisao.pt

Meeting Falk Symposium 160: Pathogenesis and Clinical Practice in Gastroenterology
15-16 June 2007
Portoroz
symposia@falkfoundation.de

Meeting ILTS 13th Annual International Congress
20-23 June 2007
Rio De Janeiro
www.ilts.org

Meeting 9th World Congress on Gastrointestinal Cancer
27-30 June 2007
Barcelona
meetings@imedex.com

Meeting 15th International Congress of the European Association for Endoscopic Surgery
4-7 July 2007
Athens
info@eaes-eur.org
congresses.eaes-eur.org/

Meeting 39th Meeting of the European Pancreatic Club
4-7 July 2007
Newcastle
www.e-p-c2007.com

Meeting XXth International Workshop on Heliobacter and related bacteria in cronic degistive inflammation
20-22 September 2007
Istanbul
www.heliobacter.org

Meeting Falk Workshop: Mechanisms of Intestinal Inflammation
10 October 2007
Dresden
symposia@falkfoundation.de

Meeting Falk Symposium 161: Future Perspectives in Gastroenterology
11-12 October 2007
Dresden
symposia@falkfoundation.de

Meeting Falk Symposium 162: Liver Cirrhosis - From Pathophysiology to Disease Management
13-14 October 2007
Dresden
symposia@falkfoundation.de

American College of Gastroenterology Annual Scientific Meeting
12-17 October 2007
Pennsylvania Convention Center
Philadelphia, PA

Meeting APDW 2007 - Asian Pacific Digestive Disease Week 2007
15-18 October 2007
Kobe
apdw@convention.co.jp
www.apdw2007.org

15th United European Gastroenterology Week, UEGW
27-31 October 2007
Le Palais des Congrès de Paris, Paris, France

Meeting The Liver Meeting® 2007 - 57th Annual Meeting of the American Association for the Study of Liver Diseases
2-6 November 2007
Boston-MA
www.aasld.org

Gastro 2009, World Congress of Gastroenterology and Endoscopy London, United Kingdom 2009

PO Box 2345, Beijing 100023, China
www.wjgnet.com
wjg@wjgnet.com

World J Gastroenterol 2007 February 14; 13(6): 982-984
World Journal of Gastroenterology ISSN 1007-9327

Instructions to authors

GENERAL INFORMATION

World Journal of Gastroenterology (*WJG, World J Gastroenterol* ISSN 1007-9327 CN 14-1219/R) is a weekly journal of more than 48 000 circulation, published on the 7th, 14th, 21st and 28th of every month.

Original Research, Clinical Trials, Reviews, Comments, and Case Reports in esophageal cancer, gastric cancer, colon cancer, liver cancer, viral liver diseases, *etc.*, from all over the world are welcome on the condition that they have not been published previously and have not been submitted simultaneously elsewhere.

Indexed and abstracted in

Current Contents®/Clinical Medicine, Science Citation Index Expanded (also known as SciSearch®) and Journal Citation Reports/Science Edition, *Index Medicus*, MEDLINE and PubMed, Chemical Abstracts, EMBASE/Excerpta Medica, Abstracts Journals, *Nature Clinical Practice Gastroenterology and Hepatology*, CAB Abstracts and Global Health. ISI JCR 2003-2000 IF: 3.318, 2.532, 1.445 and 0.993.

Published by

The WJG Press

SUBMISSION OF MANUSCRIPTS

Manuscripts should be typed double-spaced on A4 (297 mm × 210 mm) white paper with outer margins of 2.5 cm. Number all pages consecutively, and start each of the following sections on a new page: Title Page , Abstract, Introduction, Materials and Methods, Results, Discussion, acknowledgements, References, Tables, Figures and Figure Legends. Neither the editors nor the Publisher is responsible for the opinions expressed by contributors. Manuscripts formally accepted for publication become the permanent property of The WJG Press, and may not be reproduced by any means, in whole or in part without the written permission of both the authors and the Publisher. We reserve the right to put onto our website and copy-edit accepted manuscripts. Authors should also follow the guidelines for the care and use of laboratory animals of their institution or national animal welfare committee.

Authors should retain one copy of the text, tables, photographs and illustrations, as rejected manuscripts will not be returned to the author(s) and the editors will not be responsible for the loss or damage to photographs and illustrations in mailing process.

Online submission

Online submission is strongly advised. Manuscripts should be submitted through the Online Submission System at: http://www.wjgnet.com/index.jsp. Authors are highly recommended to consult the ONLINE INSTRUCTIONS TO AUTHORS (http://www.wjgnet.com/wjg/help/instructions.jsp) before attempting to submit online. Authors encountering problems with the Online Submission System may send an email you describing the problem to wjg@wjgnet.com for assistance. If you submit your manuscript online, do not make a postal contribution. A repeated online submission for the same manuscript is strictly prohibited.

Postal submission

Send 3 duplicate hard copies of the full-text manuscript typed double-spaced on A4 (297 mm × 210 mm) white paper together with any original photographs or illustrations and a 3.5 inch computer diskette or CD-ROM containing an electronic copy of the manuscript including all the figures, graphs and tables in native Microsoft Word format or *.rtf format to:

Editorial Office

World Journal of Gastroenterology
Editorial Department: Apartment 1066, Yishou Garden,
58 North Langxinzhuang Road,
PO Box 2345, Beijing 100023, China
E-mail: wjg@wjgnet.com
http: //www.wjgnet.com
Telephone: +86-10-85381892
Fax: +86-10-85381893

MANUSCRIPT PREPARATION

All contributions should be written in English. All articles must be submitted using a word-processing software. All submissions must be typed in 1.5 line spacing and in word size 12 with ample margins. The letter font is Tahoma. For authors from China, one copy of the Chinese translation of the manuscript is also required (excluding references). Style should conform to our house format. Required information for each of the manuscript sections is as follows:

Title page

Full manuscript title, running title, all author(s) name(s), affiliations, institution(s) and/or department(s) where the work was accomplished, disclosure of any financial support for the research, and the name, full address, telephone and fax numbers and email address of the corresponding author should be included. Titles should be concise and informative (removing all unnecessary words), emphasize what is new, and avoid abbreviations. A short running title of less than 40 letters should be provided. List the author(s)' name(s) as follows: initial and/or first name, middle name or initial(s) and full family name.

Abstract

An informative, structured abstract of no more than 250 words should accompany each manuscript. Abstracts for original contributions should be structured into the following sections: AIM: Only the purpose should be included. METHODS: The materials, techniques, instruments and equipments, and the experimental procedures should be included. RESULTS: The observatory and experimental results, including data, effects, outcome, *etc.* should be included. Authors should present *P* value where necessary, and the significant data should accompany. CONCLUSION: Accurate view and the value of the results should be included.

The format of structured abstracts is at: http://www.wjgnet.com/wjg/help/11.doc

Key words

Please list 5-10 key words that could reflect content of the study mainly from *Index Medicus*.

Text

For most article types, the main text should be structured into the following sections: INTRODUCTION, MATERIALS AND METHODS, RESULTS and DISCUSSION, and should include in appropriate Figures and Tables. Data should be presented in the body text or in Figures and Tables, but not in both.

Illustrations

Figures should be numbered as 1, 2, 3 and so on, and mentioned clearly in the main text. Provide a brief title for each figure on a separate page. No detailed legend should be involved under the figures. This part should be added into the text where the figures are applicable. Digital images: black and white photographs should be scanned and saved in TIFF format at a resolution of 300 dpi; color images should be saved as CMYK (print files) but not as RGB (screen-viewing files). Place each photograph in a separate file. Print images: supply images of size no smaller than 126 mm × 85 mm printed on smooth surface paper; label the image by writing the Figure number and orientation using an arrow. Photomicrographs: indicate the original magnification and stain in the legend. Digital Drawings: supply files in EPS if created by freehand and illustrator, or TIFF from photoshops. EPS files must be accompanied by a version in native file format for editing purposes. Existing line drawings should be scanned at a resolution of 1200 dpi and as close as possible to the size where they will appear when printed. Please use uniform legends for the same subjects. For example: Figure 1 Pathological changes of atrophic gastritis after treatment. A: ...; B: ...; C: ...; D: ...; E: ...; F: ...; G: ...

Tables

Three-line tables should be numbered as 1, 2, 3 and so on, and mentioned clearly in the main text. Provide a brief title for each table. No detailed legend should be included under the tables. This part should be added into the text where the tables are applicable. The information should complement but not duplicate that contained in the text. Use one horizontal line under the title, a second under the column heads, and a third below the Table, above any footnotes. Vertical and italic lines should be omitted.

Notes in tables and illustrations

Data that are not statistically significant should not be noted. $^{a}P<0.05$, $^{b}P<0.01$ should be noted ($P>0.05$ should not be noted). If there are other series of *P* values, $^{c}P<0.05$ and $^{d}P<0.01$ are used. Third series of *P* values can be expressed as $^{e}P<0.05$ and $^{f}P<0.01$. Other notes in tables or under

illustrations should be expressed as ^1F, ^2F, ^3F; or some other symbols with a superscript (Arabic numerals) in the upper left corner. In a multi-curve illustration, each curve should be labeled with ●, ○, ■, □, ▲, △, *etc.* in a certain sequence.

Acknowledgments

Brief acknowledgments of persons who have made genuine contributions to the manuscripts and who endorse the data and conclusions are included. Authors are responsible for obtaining written permission to use any copyrighted text and/or illustrations.

REFERENCES

Coding system

The author should code the references according the citation order in text in Arabic numerals, put references codes in square brackets, superscript it at the end of citation content or the author name of the citation. For those citation content as the narrate part, the coding number and square brackets should be typeset normally. For example, Crohn's disease (CD) is associated with increased intestinal permeability[1,2]. If references are directly cited in the text, they would be put together with the text, for example, from references [19,22-24], we know that...

When the authors code the references, please ensure that the order in text is the same as in reference part and also insure the spelling accuracy of the first author's name. Do not code the same citation twice.

PMID requirement

PMID roots in the abstract serial number indexed by PubMed (http://www.ncbi.nlm.nih.gov/entrez/query.fcgi?db=PubMed). The author should supply the PMID for journal citation. For those references that have not been indexed by PubMed, a printed copy of the first page of the full reference should be submitted.

The accuracy of the information of the journal citations is very important. Through reference testing system, the authors and editor could check the authors name, title, journal title, publication date, volume number, start page, and end page. We will interlink all references with PubMed in ASP file so that the readers can read the abstract of the citations online immediately.

Style for journal references

Authors: the first author should be typed in bold-faced letter. The surname of all authors should be typed with the initial letter capitalized and followed by their name in abbreviation (For example, Lian-Sheng Ma is abbreviated as Ma LS, Bo-Rong Pan as Pan BR). Title of the cited article and italicized journal title (Journal title should be in its abbreviation form as shown in PubMed), publication date, volume number (in black), start page, and end page [PMID: 11819634]

Note: The author should test the references through reference testing system (http://www.wjgnet.com/cgi-bin/index.pl)

Style for book references

Authors: the first author should be typed in bold-faced letter. The surname of all authors should be typed with the initial letter capitalized and followed by their name in abbreviation (For example, Lian-Sheng Ma is abbreviated as Ma LS, Bo-Rong Pan as Pan BR) Book title. Publication number. Publication place: Publication press, Year: start page and end page.

Format

Journals

English journal article (list all authors and include the PMID where applicable)

1 **Grover VP**, Dresner MA, Forton DM, Counsell S, Larkman DJ, Patel N, Thomas HC, Taylor-Robinson SD. Current and future applications of magnetic resonance imaging and spectroscopy of the brain in hepatic encephalopathy. *World J Gastroenterol* 2006; **12**: 2969-2978 [PMID: 16718775]

Chinese journal article (list all authors and include the PMID where applicable)

2 **Lin GZ**, Wang XZ, Wang P, Lin J, Yang FD. Immunologic effect of Jianpi Yishen decoction in treatment of Pixu-diarrhoea. *Shijie Huaren Xiaohua Zazhi* 1999; **7**: 285-287

In press

3 **Tian D**, Araki H, Stahl E, Bergelson J, Kreitman M. Signature of balancing selection in Arabidopsis. *Proc Natl Acad Sci U S A* 2006; In press

Organization as author

4 **Diabetes Prevention Program Research Group**. Hypertension, insulin, and proinsulin in participants with impaired glucose tolerance. *Hypertension* 2002; **40**: 679-686 [PMID: 12411462]

Both personal authors and an organization as author

5 **Vallancien G**, Emberton M, Harving N, van Moorselaar RJ; Alf-One Study Group. Sexual dysfunction in 1, 274 European men suffering from lower urinary tract symptoms. *J Urol* 2003; **169**: 2257-2261 [PMID: 12771764]

No author given

6 21st century heart solution may have a sting in the tail. *BMJ* 2002; **325**: 184 [PMID: 12142303]

Volume with supplement

7 **Geraud G**, Spierings EL, Keywood C. Tolerability and safety of frovatriptan with short- and long-term use for treatment of migraine and in comparison with sumatriptan. *Headache* 2002; **42** Suppl 2: S93-99 [PMID: 12028325]

Issue with no volume

8 **Banit DM**, Kaufer H, Hartford JM. Intraoperative frozen section analysis in revision total joint arthroplasty. *Clin Orthop Relat Res* 2002; (**401**): 230-238 [PMID: 12151900]

No volume or issue

9 Outreach: bringing HIV-positive individuals into care. *HRSA Careaction* 2002; 1-6 [PMID: 12154804]

Books

Personal author(s)

10 **Sherlock S**, Dooley J. Diseases of the liver and billiary system. 9th ed. Oxford: Blackwell Sci Pub, 1993: 258-296

Chapter in a book (list all authors)

11 **Lam SK**. Academic investigator's perspectives of medical treatment for peptic ulcer. In: Swabb EA, Azabo S. Ulcer disease: investigation and basis for therapy. New York: Marcel Dekker, 1991: 431-450

Author(s) and editor(s)

12 **Breedlove GK**, Schorfheide AM. Adolescent pregnancy. 2nd ed. Wieczorek RR, editor. White Plains (NY): March of Dimes Education Services, 2001: 20-34

Conference proceedings

13 **Harnden P**, Joffe JK, Jones WG, editors. Germ cell tumours V. Proceedings of the 5th Germ Cell Tumour Conference; 2001 Sep 13-15; Leeds, UK. New York: Springer, 2002: 30-56

Conference paper

14 **Christensen S**, Oppacher F. An analysis of Koza's computational effort statistic for genetic programming. In: Foster JA, Lutton E, Miller J, Ryan C, Tettamanzi AG, editors. Genetic programming. EuroGP 2002: Proceedings of the 5th European Conference on Genetic Programming; 2002 Apr 3-5; Kinsdale, Ireland. Berlin: Springer, 2002: 182-191

Electronic journal (list all authors)

Morse SS. Factors in the emergence of infectious diseases. Emerg Infect Dis serial online, 1995-01-03, cited 1996-06-05; 1(1): 24 screens. Available from: URL: http//www.cdc.gov/ncidod/EID/eid.htm

Patent (list all authors)

16 **Pagedas AC**, inventor; Ancel Surgical R&D Inc., assignee. Flexible endoscopic grasping and cutting device and positioning tool assembly. United States patent US 20020103498. 2002 Aug 1

Inappropriate references

Authors should always cite references that are relevant to their article, and avoid any inappropriate references. Inappropriate references include those that are linked with a hyphen and the difference between the two numbers at two sides of the hyphen is more than 5. For example, [1-6], [2-14] and [1, 3, 4-10, 22] are all considered as inappropriate references. Authors should not cite their own unrelated published articles.

Statistical data

Present as mean ± SD or mean ± SE.

Statistical expression

Express t test as t (in italics), F test as F (in italics), chi square test as χ^2 (in Greek), related coefficient as r (in italics), degree of freedom as γ (in Greek), sample number as n (in italics), and probability as P (in italics).

Units

Use SI units. For example: body mass, m (B) = 78 kg; blood pressure, p(B) = 16.2/12.3 kPa; incubation time, t (incubation) = 96 h, blood glucose concentration, c (glucose) 6.4 ± 2.1 mmol/L; blood CEA mass concentration, p (CEA) = 8.6 24.5 μg/L; CO_2 volume fraction, 50 mL/L CO_2 not 5% CO_2; likewise for 40 g/L formaldehyde, not 10% formalin; and mass fraction, 8 ng/g, *etc.* Arabic numerals such as 23, 243, 641 should be read 23 243 641.

The format about how to accurately write common units and quantum is at: http://www.wjgnet.com/wjg/help/15.doc

Abbreviations

Standard abbreviations should be defined in the abstract and on first mention in the text. In general, terms should not be abbreviated unless they are used repeatedly and the abbreviation is helpful to the reader. Permissible abbreviations are listed in Units, Symbols and Abbreviations: A Guide for Biological and Medical Editors and Authors (Ed. Baron DN, 1988) published by The Royal Society of Medicine, London. Certain commonly used abbreviations, such as DNA, RNA, HIV, LD50, PCR, HBV, ECG, WBC, RBC, CT, ESR, CSF, IgG, ELISA, PBS, ATP, EDTA, mAb, can be used directly without further mention.

Italics

Quantities: *t* time or temperature, *c* concentration, *A* area, *l* length, *m* mass, *V* volume.
Genotypes: *gyr*A, *arg* 1, *c myc*, *c fos*, *etc.*
Restriction enzymes: *Eco*RI, *Hin*dI, *Bam*HI, *Kbo* I, *Kpn* I, *etc.*
Biology: *H pylori, E coli, etc.*

SUBMISSION OF THE REVISED MANUSCRIPTS AFTER ACCEPTED

Please revise your article according to the revision policies of *WJG*. The revised version including manuscript and high-resolution image figures (if any) should be copied on a floppy or compact disk. Author should send the revised manuscript, along with printed high-resolution color or black and white photos, copyright transfer letter, the final check list for authors, and responses to reviewers by a courier (such as EMS) (submission of revised manuscript by e-mail or on the *WJG* Editorial Office Online System is NOT available at present).

Language evaluation

The language of a manuscript will be graded before sending for revision. (1) Grade A: priority publishing; (2) Grade B: minor language polishing; (3) Grade C: a great deal of language polishing; (4) Grade D: rejected. The revised articles should be in grade B or grade A.

Copyright assignment form

Please downloaded CAF from http://www.wjgnet.com/wjg/help/9.doc.

We certify that the material contained in this manuscript:

Ms:

Title:

is original, except when appropriately referenced to other sources, and that written permission has been granted by any existing copyright holders. We agree to transfer to WJG all rights of our manuscript, including: (1) all copyright ownership in all print and electronic formats; (2) the right to grant permission to republish or reprint the stated material in whole or in part, with or without a fee; (3) the right to print copies for free distribution or sale; (4) the right to republish the stated material in a collection of articles or in any other format. We also agree that our article be put on the Internet.

Criteria for authorship: The WJG requests and publishes information about contributions of each author named to the submitted study. Authorship credit should be based on (1)direct participation in the study, including substantial contributions to conception and design of study, or acquisition of data, or analysis and interpretation of data; (2) manuscript writing, including drafting the article, or revising it critically for important intellectual content; (3)supportive work, including statistical analysis of data, or acquisition of funding, or administration, technology and materials support, or supervision, or supportive contributions. Authors should meet at least one of the three conditions. The WJG does not publish co-first authors and co-corresponding authors.

We hereby assign copyright transfer to WJG if this paper is accepted.

Author Name in full (Full names should be provided, with first name first, followed by middle names and family name at the last, eg, Eamonn MM Quigley). Handwritten names are not accepted.

Author Name in abbreviation (Family name is put first in full, followed by middle names and first name in abbreviation with first letter in capital, eg, Quigley EMM). Handwritten names are not accepted.

1 Full Name: _____

Abbreviation Name: _____

Signed: _____

Date: _____

2 Full Name: _____

Abbreviation Name: _____

Signed: _____

Date: _____

3 Full Name: _____

Abbreviation Name: _____

Signed: _____

Date: _____

4 Full Name: _____

Abbreviation Name: _____

Signed: _____

Date: _____

5 Full Name: _____

Abbreviation Name: _____

Signed: _____

Date: _____

6 Full Name: _____

Abbreviation Name: _____

Signed: _____

Date: _____

7 Full Name: _____

Abbreviation Name: _____

Signed: _____

Date: _____

8 Full Name: _____

Abbreviation Name: _____

Signed: _____

Date: _____

9 Full Name: _____

Abbreviation Name: _____

Signed: _____

Date: _____

10 Full Name: _____

Abbreviation Name: _____

Signed: _____

Date: _____

Final check list for authors

The format is at: http://www.wjgnet.com/wjg/help/13.doc

Responses to reviewers

Please revise your article according to the comments/suggestions of reviewers. The format for responses to the reviewers' comments is at: http://www.wjgnet.com/wjg/help/10.doc

Proof of financial support

For paper supported by a foundation, authors should provide a copy of the document and serial number of the foundation.

Publication fee

Authors of accepted articles must pay publication fee.
EDITORIAL and LETTERS TO THE EDITOR are free of change.

World Journal of Gastroenterology®

Volume 13 Number 7
February 21, 2007

National Journal Award
2005

The WJG Press

The WJG Press, Apartment 1066 Yishou Garden, 58 North Langxinzhuang Road, PO Box 2345, Beijing 100023, China
Telephone: +86-10-85381892
Fax: +86-10-85381893
E-mail: wjg@wjgnet.com
http: //www.wjgnet.com

ISSN 1007-9327 CN 14-1219/R Local Post Offices Code No. 82-261

World Journal of Gastroenterology www.wjgnet.com Volume 13 Number 7 Feb 21 2007

ISSN 1007-9327
CN 14-1219/R

WJG

World Journal of Gastroenterology®

Indexed and Abstracted in:

Current Contents®/Clinical Medicine, Science Citation Index Expanded (also known as SciSearch®) and Journal Citation Reports/Science Edition, *Index Medicus*, MEDLINE and PubMed, Chemical Abstracts, EMBASE/Excerpta Medica, Abstracts Journals, *Nature Clinical Practice Gastroenterology and Hepatology*, CAB Abstracts and Global Health.
ISI JCR 2003-2000 IF: 3.318, 2.532, 1.445 and 0.993.

Volume 13 Number 7
February 21, 2007

World J Gastroenterol
2007 February 21; 13(7): 985-1148
Online Submissions
www.wjgnet.com/wjg/index.jsp
www.wjgnet.com
Printed on Acid-free Paper

A Weekly Journal of Gastroenterology and Hepatology

National Journal Award
2005

World Journal of Gastroenterology®

Volume 13 Number 7
February 21, 2007

The WJG Press

Contents

World Journal of Gastroenterology
Volume 13 **Number** 7 **February** 21, 2007

Contents

World Journal of Gastroenterology
Volume 13 **Number** 7 **February** 21, 2007

Contents

Responsible E-Editor for this issue: Wen-Hua Ma

C-Editor for this issue: Dr. Osman Cavit Ozdogan

Responsible S-Editor for this issue: Jing Wang

World Journal of Gastroenterology (*World J Gastroenterol , WJG*), a leading international journal in gastroenterology and hepatology, has an established reputation for publishing first class research on esophageal cancer, gastric cancer, liver cancer, viral hepatitis, colorectal cancer, and *H pylori* infection, providing a forum for both clinicians and scientists, and has been indexed and abstracted in Current Contents®/Clinical Medicine, Science Citation Index Expanded (also known as SciSearch®) and Journal Citation Reports/Science Edition, *Index Medicus*, MEDLINE and PubMed, Chemical Abstracts, EMBASE/Excerpta Medica, Abstracts Journals, *Nature Clinical Practice Gastroenterology and Hepatology*, CAB Abstracts and Global Health. ISI JCR 2003-2000 IF: 3.318, 2.532, 1.445 and 0.993. *WJG* is a weekly journal published by The WJG Press. The publication date is on 7th, 14th, 21st, and 28th every month. The *WJG* is supported by The National Natural Science Foundation of China, No. 30224801 and No.30424812, which was founded with a name of *China National Journal of New Gastroenterology* on October 1,1995, and renamed as *WJG* on January 25, 1998.

PUBLISHED BY
The WJG Press

PRINTED BY
Printed in Beijing on acid-free paper by Beijing Kexin Printing House

Print ISSN 1007-9327
CN 14-1219/R

EDITORIAL OFFICE
World Journal of Gastroenterology,
The WJG Press, Apartment 1066 Yishou Garden, 58 North Langxinzhuang Road, PO Box 2345, Beijing 100023, China
Telephone: +86-10-85381892
Fax: +86-10-85381893
E-mail: wjg@wjgnet.com
http://www.wjgnet.com

SUBSCRIPTION AND AUTHOR REPRINTS
Jing Wang
The WJG Press, Apartment 1066 Yishou Garden, 58 North Langxinzhuang Road, PO Box 2345, Beijing 100023, China
Telephone: +86-10-85381892
Fax: +86-10-85381893
E-mail: j.wang@wjgnet.com
http://www.wjgnet.com

SUBSCRIPTION INFORMATION
Institutional Price 2007: USD 1500.00
Personal Price 2007: USD 700.00

INSTRUCTIONS TO AUTHORS
Full instructions are available online at http://www.wjgnet.com/wjg/help/instructions.jsp. If you do not have web access please contact the editorial office.

World Journal of Gastroenterology®

Editorial Board

2007-2009

Published by The WJG Press, PO Box 2345, Beijing 100023, China
Fax: +86-10-85381893 E-mail: wjg@wjgnet.com http://www.wjgnet.com

The *World Journal of Gastroenterology* Editorial Board consists of 916 members, representing a team of worldwide experts in gastroenterology and hepatology. They are from 55 countries, including Albania (1), Argentina (2), Australia (26), Austria (9), Belarus (1), Belgium (13), Brazil (1), Bulgaria (1), Canada (23), Chile (1), China (49), Croatia (2), Cuba (1), Czech (1), Denmark (5), Egypt (3), Finland (4), France (36), Germany (96), Greece (3), Hungary (2), Iceland (1), India (6), Iran (2), Ireland (4), Israel (6), Italy (71), Japan (163), Lebanon (3), Lithuania (1), Macedonia (1), Malaysia (3), Mexico (3), Monaco (1), Netherlands (21), New Zealand (1), Nigeria (1), Norway (3), Pakistan (1), Poland (6), Portugal (2), Russia (3), Serbia (1), Singapore (3), Slovakia (1), Slovenia (1), South Africa (1), South Korea (13), Spain (29), Sweden (9), Switzerland (12), Turkey (8), United Arab Emirates (1), United Kingdom (61), and United States (192).

Louis Libbrecht, *Leuven*
Etienne M Sokal, *Brussels*
Gert A Van Assche, *Leuven*
Yvan Vandenplas, *Brussels*
Eddie Wisse, *Keerbergen*

Brazil
Heitor Rosa, *Goiania*

Bulgaria
Zahariy Krastev, *Sofia*

Canada
Fernando Alvarez, *Québec*
David Armstrong, *Ontario*
Olivier Barbier, *Québec*
Nancy Baxter, *Toronto*
Matthew Bjerknes, *Toronto*
Frank J Burczynski, *Winnipeg*
Michael F Byrne, *Vancouver*
Wang-Xue Chen, *Ottawa*
Hugh J Freeman, *Vancouver*
Chantal Guillemette, *Québec*
Samuel S Lee, *Calgary*
Gary A Levy, *Toronto*
John K Marshall, *Ontario*
Donna-Marie McCafferty, *Calgary*
Thomas I Michalak, *St. John's*
Gerald Y Minuk, *Manitoba*
Paul Moayyedi, *Hamilton*
Eldon Shaffer, *Calgary*
Morris Sherman, *Toronto*
Alan BR Thomson, *Edmonton*
EF Verdu, *Ontario*
John L Wallace, *Calgary*
Eric M Yoshida, *Vancouver*

Chile
Silvana Zanlungo, *Santiago*

China
Henry LY Chan, *Hongkong*
Xiao-Ping Chen, *Wuhan*
Zong-Jie Cui, *Beijing*
Da-Jun Deng, *Beijing*
Sheung-Tat Fan, *Hong Kong*
Jin Gu, *Beijing*
De-Wu Han, *Taiyuan*
Ming-Liang He, *Hong Kong*
Wayne HC Hu, *Hong Kong*
Chee-Kin Hui, *Hong Kong*
Ching Lung Lai, *Hong Kong*
Kam Chuen Lai, *Hong Kong*
James YW Lau, *Hong Kong*
Yuk Tong Lee, *Hong Kong*
Suet Yi Leung, *Hong Kong*
Wai-Keung Leung, *Hong Kong*
Jing-Yun Ma, *Beijing*
Lun-Xiu Qin, *Shanghai*
Qin Su, *Beijing*
Wai-Man Wong, *Hong Kong*
Hong Xiao, *Beijing*
Dong-Liang Yang, *Wuhan*
Winnie Yeo, *Hong Kong*
Yuan Yuan, *Shenyang*
Man-Fung Yuen, *Hong Kong*
Jian-Zhong Zhang, *Beijing*
Xin-Xin Zhang, *Shanghai*
Shu Zheng, *Hangzhou*

Croatia
Tamara Cacev, *Zagreb*
Marko Duvnjak, *Zagreb*

Cuba
Damian Casadesus Rodriguez, *Havana*

Czech
Milan Jirsa, *Praha*

Denmark
Peter Bytzer, *Copenhagen*
Hans Gregersen, *Aalborg*
Jens H Henriksen, *Hvidovre*
Fin Stolze Larsen, *Copenhagen*
SØren MØller, *Hvidovre*

Egypt
Abdel-Rahman El-Zayadi, *Giza*
Sanaa Moharram Kamal, *Cairo*
Ayman Yosry, *Cairo*

Finland
Irma Elisabet Jarvela, *Helsinki*
Katri Maria Kaukinen, *Tampere*
Minna Nyström, *Helsinki*
Pentti Sipponen, *Espoo*

France
Bettaieb Ali, *Dijon*
Corlu Anne, *Rennes*
Denis Ardid, *Clermont-Ferrand*
Charles Paul Balabaud, *Bordeaux*
Soumeya Bekri, *Rouen*
Jacques Belghiti, *Clichy*
Pierre Brissot, *Rennes*
Patrice Philippe Cacoub, *Paris*
Franck Carbonnel, *Besancon*
Laurent Castera, *Pessac*
Bruno Clément, *Rennes*
Jacques Cosnes, *Paris*
Thomas Decaens, *Cedex*
Francoise Lunel Fabiani, *Angers*
Gérard Feldmann, *Paris*
Jean Fioramonti, *Toulouse*
Catherine Guettier, *Villejuif*
Chantal Housset, *Paris*
Juan Lucio Iovanna, *Marseille*
Rene Lambert, *Lyon*
Philippe Mathurin, *Lille*
Tamara Matysiak–Budnik, *Paris*
Francis Mégraud, *Bordeaux*
Richard Moreau, *Clichy*
Thierry Piche, *Nice*
Raoul Poupon, *Paris*
Jean Rosenbaum, *Bordeaux*
Jose Sahel, *Marseille*
Jean-Philippe Salier, *Rouen*
Jean-Yves Scoazec, *Lyon*
Khalid Ahnini Tazi, *Clichy*
Baumert F Thomas, *Strasbourg*
Emmanuel Tiret, *Paris*
MC Vozenin-brotons, *Villejuif*
Jean-Pierre Henri Zarski, *Grenoble*
Jessica Zucman-Rossi, *Paris*

Germany
HD Allescher, *Garmisch-Partenkirchen*
Martin Anlauf, *Kiel*
Rudolf Arnold, *Marburg*
Max G Bachem, *Ulm*
Thomas F Baumert, *Freiburg*
Daniel C Baumgart, *Berlin*
Hubert Blum, *Freiburg*
Thomas Bock, *Tuebingen*
Katja Breitkopf, *Mannheim*
Dunja Bruder, *Braunschweig*
Markus W Büchler, *Heidelberg*
Christa Buechler, *Regensburg*
Reinhard Buettner, *Bonn*
Elke Cario, *Essen*
Uta Dahmen, *Essen*
CF Dietrich, *Bad Mergentheim*
Rainer Josef Duchmann, *Berlin*
Paul Enck, *Tuebingen*
Fred Fändrich, *Kiel*
Ulrich Robert Fölsch, *Kiel*
Helmut Friess, *Heidelberg*
Peter R Galle, *Mainz*
Nikolaus Gassler, *Aachen*
Andreas Geier, *Aachen*
Dieter Glebe, *Giessen*
Burkhard Göke, *Munich*
Florian Graepler, *Tuebingen*
Axel M Gressner, *Aachen*
Veit Gülberg, *Munich*
Rainer Haas, *Munich*
Eckhart Georg Hahn, *Erlangen*
Stephan Hellmig, *Kiel*
Martin Hennenberg, *Bonn*
Johannes Herkel, *Hamburg*
Klaus Herrlinger, *Stuttgart*
Eberhard Hildt, *Berlin*
Joerg C Hoffmann, *Berlin*
Ferdinand Hofstaedter, *Regensburg*
Werner Hohenberger, *Erlangen*
RG Jakobs, *Ludwigshafen*
Jutta Keller, *Hamburg*
Andrej Khandoga, *Munich*
Sibylle Koletzko, *München*
Stefan Kubicka, *Hannover*
Joachim Labenz, *Siegen*
Frank Lammert, *Bonn*
Thomas Langmann, *Regensburg*
Christian Liedtke, *Aachen*
Matthias Löhr, *Mannheim*
Christian Maaser, *Muenster*
Ahmed Madisch, *Dresden*
Michael Peter Manns, *Hannover*
Stephan Miehlke, *Dresden*
Sabine Mihm, *Göttingen*
Silvio Nadalin, *Essen*
Markus F Neurath, *Mainz*
Johann Ockenga, *Berlin*
Florian Obermeier, *Regensburg*
Gustav Paumgartner, *Munich*
Ulrich Ks Peitz, *Magdeburg*
Markus Reiser, *Bochum*
Steffen Rickes, *Magdeburg*
Gerhard Rogler, *Regensburg*
Tilman Sauerbruch, *Bonn*
Dieter Saur, *Munich*
Andreas Schäffler, *Regensburg*
Hans Scherubl, *Berlin*
Joerg Schirra, *Munich*
Volker Schmitz, *Bonn*
Roland M Schmid, *München*
AG Schreyer, *Regensburg*
Tobias Schroeder, *Essen*
Hans Seifert, *Oldenburg*
Manfred V Singer, *Mannheim*
Gisela Sparmann, *Rostock*
Jurgen M Stein, *Frankfurt*
Ulrike Susanne Stein, *Berlin*
Manfred Stolte, *Bayreuth*
Christian P Strassburg, *Hannover*
WR Stremmel, *Heidelberg*
Harald F Teutsch, *Ulm*
Robert Thimme, *Freiburg*
HL Tillmann, *Leipzig*
Tung-Yu Tsui, *Regensburg*
Axel Ulsenheimer, *Munich*
Patrick Veit, *Essen*
Claudia Veltkamp, *Heidelberg*
Siegfried Wagner, *Deggendorf*
Henning Walczak, *Heidelberg*
Fritz von Weizsacker, *Berlin*
Jens Werner, *Heidelberg*
Bertram Wiedenmann, *Berlin*
Reiner Wiest, *Regensburg*
Stefan Wirth, *Wuppertal*
Stefan JP Zeuzem, *Homburg*

Greece

Elias A Kouroumalis, *Heraklion*
Ioannis E Koutroubakis, *Heraklion*
Spiros Sgouros, *Athens*

Hungary

Peter Laszlo Lakatos, *Budapest*
Zsuzsa Szondy, *Debrecen*

Iceland

H Gudjonsson, *Reykjavik*

India

KA Balasubramanian, *Vellore*
Sujit K Bhattacharya, *Kolkata*
Yogesh K Chawla, *Chandigarh*
Radha K Dhiman, *Chandigarh*
Sri Prakash Misra, *Allahabad*
ND Reddy, *Hyderabad*

Iran

Reza Malekzadeh, *Tehran*
Seyed Alireza Taghavi, *Shiraz*

Ireland

Billy Bourke, *Dublin*
Ronan A Cahill, *Cork*
Anthony P Moran, *Galway*

Israel

Simon Bar-Meir, *Hashomer*
Abraham Rami Eliakim, *Haifa*
Yaron Ilan, *Jerusalem*
Avidan U Neumann, *Ramat-Gan*
Yaron Niv, *Pardesia*
Ran Oren, *Tel Aviv*

Italy

Giovanni Addolorato, *Roma*
Luigi E Adinolfi, *Naples*
Domenico Alvaro, *Rome*
V Annese, *San Giovanni Rotond*
Adolfo Francesco Attili, *Roma*
Giovanni Barbara, *Bologna*
Gabrio Bassotti, *Perugia*
Pier Maria Battezzati, *Milan*
Stefano Bellentani, *Carpi*
Luca Saverioq Belli, *Milan*
Antomio Benedetti, *Ancona*
Mauro Bernardi, *Bologna*
Livia Biancone, *Rome*
Luigi Bonavina, *Milano*
Flavia Bortolotti, *Padova*
Giuseppe Brisinda, *Rome*
Giovanni Cammarota, *Roma*
Antonino Cavallari, *Bologna*
Giuseppe Chiarioni, *Valeggio*
Michele Cicala, *Rome*
Amedeo Columbano, *Cagliari*
Massimo Conio, *Sanremo*
Dario Conte, *Milano*
Gino Roberto Corazza, *Pavia*
Francesco Costa, *Pisa*
Antonio Craxi, *Palermo*
Roberto De Giorgio, *Bologna*
Giovanni D De Palma, *Naples*
Fabio Farinati, *Padua*
Francesco Feo, *Sassari*
Stefano Fiorucci, *Perugia*
Andrea Galli, *Firenze*
Valeria Ghisett, *Turin*
Gianluigi Giannelli, *Bari*
Edoardo G Giannini, *Genoa*
Paolo Gionchetti, *Bologna*
Mario Guslandi, *Milano*
Pietro Invernizzi, *Milan*
Giacomo Laffi, *Firenze*
Giovanni Maconi, *Milan*
Lucia Malaguarnera, *Catania*
ED Mangoni, *Napoli*
Giulio Marchesini, *Bologna*
Fabio Marra, *Florence*
Marco Marzioni, *Ancona*
Giuseppe Montalto, *Palermo*
Giovanni Monteleone, *Rome*
Giovanni Musso, *Torino*
Gerardo Nardone, *Napoli*
Valerio Nobili, *Rome*
Luisi Pagliaro, *Palermo*
Fabrizio R Parente, *Milan*
F Perri, *San Giovanni Rotondo*
Raffaele Pezzilli, *Bologna*
A Pilotto, *San Giovanni Rotondo*
Mario Pirisi, *Novara*
Paolo Del Poggio, *Treviglio*
Gabriele Bianchi Porro, *Milano*
Piero Portincasa, *Bari*
Bernardino Rampone, *Siena*
Claudio Romano, *Messina*
Marco Romano, *Napoli*
Gerardo Rosati, *Potenza*
Mario Del Tacca, *Pisa*
Pier Alberto Testoni, *Milan*
Enrico Roda, *Bologna*
Domenico Sansonno, *Bari*
Vincenzo Savarino, *Genova*
Roberto Testa, *Genoa*
Dino Vaira, *Bologna*

Japan

Kyoichi Adachi, *Izumo*
Yasushi Adachi, *Sapporo*
Taiji Akamatsu, *Matsumoto*
Sk Md Fazle Akbar, *Ehime*
Takafumi Ando, *Nagoya*
Akira Andoh, *Otsu*
Taku Aoki, *Tokyo*
Masahiro Arai, *Tokyo*
Tetsuo Arakawa, *Osaka*
Yasuji Arase, *Tokyo*
Masahiro Asaka, *Sapporo*
Hitoshi Asakura, *Tokyo*
Takeshi Azuma, *Fukui*
Yoichi Chida, *Fukuoka*
Takahiro Fujimori, *Tochigi*
Jiro Fujimoto, *Hyogo*
Kazuma Fujimoto, *Saga*
Mitsuhiro Fujishiro, *Tokyo*
Yoshihide Fujiyama, *Otsu*
Hirokazu Fukui, *Tochigi*
Hiroyuki Hanai, *Hamamatsu*
Kazuhiro Hanazaki, *Kochi*
Naohiko Harada, *Fukuoka*
Makoto Hashizume, *Fukuoka*
Tetsuo Hayakawa, *Nagoya*
Kazuhide Higuchi, *Osaka*
Keisuke Hino, *Ube*
Keiji Hirata, *Kitakyushu*
Yuji Iimuro, *Nishinomiya*
Kenji Ikeda, *Tokyo*
Fumio Imazeki, *Chiba*
Yutaka Inagaki, *Kanagawa*
Yasuhiro Inokuchi, *Yokohama*
Haruhiro Inoue, *Yokohama*
Masayasu Inoue, *Osaka*
Akio Inui, *Kagoshima*
Hiromi Ishibashi, *Nagasaki*
Shunji Ishihara, *Izumo*
Toru Ishikawa, *Niigata*
Kei Ito, *Sendai*
Masayoshi Ito, *Tokyo*
Hiroaki Itoh, *Akita*
Ryuichi Iwakiri, *Saga*
Yoshiaki Iwasaki, *Okayama*
Terumi Kamisawa, *Tokyo*
Hiroshi Kaneko, *Aichi-Gun*
Shuichi Kaneko, *Kanazawa*
Takashi Kanematsu, *Nagasaki*
Mitsuo Katano, *Fukuoka*
Junji Kato, *Sapporo*
Mototsugu Kato, *Sapporo*
Shinzo Kato, *Tokyo*
Norifumi Kawada, *Osaka*
Sunao Kawano, *Osaka*
Mitsuhiro Kida, *Kanagawa*
Yoshikazu Kinoshita, *Izumo*
Tsuneo Kitamura, *Chiba*
Seigo Kitano, *Oita*
Kazuhiko Koike, *Tokyo*
Norihiro Kokudo, *Tokyo*
Satoshi Kondo, *Sapporo*
Shoji Kubo, *Osaka*
Shigeki Kuriyama, *Kagawa*
Masato Kusunoki, *Tsu Mie*
Katsunori Iijima, *Sendai*
Shin Maeda, *Tokyo*
Masatoshi Makuuchi, *Tokyo*
Osamu Matsui, *Kanazawa*
Yasuhiro Matsumura, *Chiba*
Yasushi Matsuzaki, *Tsukuba*
Kiyoshi Migita, *Omura*
Tetsuya Mine, *Kanagawa*
Hiroto Miwa, *Hyogo*
Masashi Mizokami, *Nagoya*
Yoshiaki Mizuguchi, *Tokyo*
Motowo Mizuno, *Hiroshima*
Morito Monden, *Suita*
Hisataka S Moriwaki, *Gifu*
Yasuaki Motomura, *Iizuka*
Yoshiharu Motoo, *Kanazawa*
Kazunari Murakami, *Oita*
Kunihiko Murase, *Tusima*
Masahito Nagaki, *Gifu*
Masaki Nagaya, *Kawasaki*
Yuji Naito, *Kyoto*
Hisato Nakajima, *Tokyo*
Hiroki Nakamura, *Yamaguchi*
Shotaro Nakamura, *Fukuoka*
Mikio Nishioka, *Niihama*
Shuji Nomoto, *Nagoya*
Susumu Ohmada, *Maebashi*
Masayuki Ohta, *Oita*
Tetsuo Ohta, *Kanazawa*
Kazuichi Okazaki, *Osaka*
Katsuhisa Omagari, *Nagasaki*
Saburo Onishi, *Nankoku*
Morikazu Onji, *Ehime*
Satoshi Osawa, *Hamamatsu*
Masanobu Oshima, *Kanazawa*
Hiromitsu Saisho, *Chiba*
Hidetsugu Saito, *Tokyo*
Yutaka Saito, *Tokyo*
Isao Sakaida, *Yamaguchi*
Michiie Sakamoto, *Tokyo*
Yasushi Sano, *Chiba*
Hiroki Sasaki, *Tokyo*
Iwao Sasaki, *Sendai*
Motoko Sasaki, *Kanazawa*
Chifumi Sato, *Tokyo*
Shuichi Seki, *Osaka*
Hiroshi Shimada, *Yokohama*
Mitsuo Shimada, *Tokushima*
Tomohiko Shimatan, *Hiroshima*
Hiroaki Shimizu, *Chiba*
Ichiro Shimizu, *Tokushima*
Yukihiro Shimizu, *Kyoto*
Shinji Shimoda, *Fukuoka*
Tooru Shimosegawa, *Sendai*
Tadashi Shimoyama, *Hirosaki*
Ken Shirabe, *Iizuka*
Yoshio Shirai, *Niigata*
Katsuya Shiraki, *Mie*
Yasushi Shiratori, *Okayama*

Masayuki Sho, *Nara*
Yasuhiko Sugawara, *Tokyo*
Hidekazu Suzuki, *Tokyo*
Minoru Tada, *Tokyo*
Tadatoshi Takayama, *Tokyo*
Tadashi Takeda, *Osaka*
Koji Takeuchi, *Kyoto*
Kiichi Tamada, *Tochigi*
Akira Tanaka, *Kyoto*
Eiji Tanaka, *Matsumoto*
Noriaki Tanaka, *Okayama*
Shinji Tanaka, *Hiroshima*
Wei Tang, *Tokyo*
Hideki Taniguchi, *Yokohama*
Kyuichi Tanikawa, *Kurume*
Akira Terano, *Shimotsugagun*
Hitoshi Togash, *Yamagata*
Kazunari Tominaga, *Osaka*
Takuji Torimura, *Fukuoka*
Minoru Toyota, *Sapporo*
Akihito Tsubota, *Chiba*
Shingo Tsuji, *Osaka*
Takato Ueno, *Kurume*
Shinichi Wada, *Tochigi*
Hiroyuki Watanabe, *Kanazawa*
Toshio Watanabe, *Osaka*
Yuji Watanabe, *Ehime*
Chun-Yang Wen, *Nagasaki*
Koji Yamaguchi, *Fukuoka*
Takayuki Yamamoto, *Yokkaichi*
Takashi Yao, *Fukuoka*
Masashi Yoneda, *Tochigi*
Hiroshi Yoshida, *Tokyo*
Masashi Yoshida, *Tokyo*
Norimasa Yoshida, *Kyoto*
Kentaro Yoshika, *Toyoake*
Masahide Yoshikawa, *Kashihara*

Lebanon
Bassam N Abboud, *Beirut*
Ala I Sharara, *Beirut*
Joseph Daoud Boujaoude, *Beirut*

Lithuania
Limas Kupcinskas, *Kaunas*

Macedonia
Vladimir Cirko Serafimoski, *Skopje*

Malaysia
Andrew Seng Boon Chua, *Ipoh*
Khean-Lee Goh, *Kuala Lumpur*
Jayaram Menon, *Sabah*

Mexico
Garcia-Compean Diego, *Monterrey*
Saúl Villa-Treviño, *México*
JK Yamamoto-Furusho, *México*

Monaco
Patrick Rampal, *Monaco*

Netherlands
Ulrich Beuers, *Amsterdam*
Gerd Bouma, *Amsterdam*
Lee Bouwman, *Leiden*
J Bart A Crusius, *Amsterdam*
Rick Greupink, *Groningen*
Janine K Kruit, *Groningen*
Ernst Johan Kuipers, *Rotterdam*
Ton Lisman, *Utrecht*
Yi Liu, *Amsterdam*
Servaas Morré, *Amsterdam*
Chris JJ Mulder, *Amsterdam*
Michael Müller, *Wageningen*
Amado Salvador Peña, *Amsterdam*
Robert J Porte, *Groningen*
Ingrid B Renes, *Rotterdam*
Andreas Smout, *Utrecht*
RW Stockbrugger, *Maastricht*
Luc JW van der Laan, *Rotterdam*
Karel van Erpecum, *Utrecht*
GP VanBerge-Henegouwen, *Utrecht*

New Zealand
Ian David Wallace, *Auckland*

Nigeria
Samuel Babafemi Olaleye, *Ibadan*

Norway
Trond Berg, *Oslo*
Tom Hemming Karlsen, *Oslo*
Helge Lyder Waldum, *Trondheim*

Pakistan
Muhammad S Khokhar, *Lahore*

Poland
Tomasz Brzozowski, *Cracow*
Robert Flisiak, *Bialystok*
Hanna Gregorek, *Warsaw*
DM Lebensztejn, *Bialystok*
Wojciech G Polak, *Wroclaw*
Marek Hartleb, *Katowice*

Portugal
MP Cecília, *Lisbon*
Miguel Carneiro De Moura, *Lisbon*

Russia
Vladimir T Ivashkin, *Moscow*
Leonid Lazebnik, *Moscow*
Vasiliy I Reshetnyak, *Moscow*

Serbia
DM Jovanovic, *Sremska Kamenica*

Singapore
Bow Ho, *Kent Ridge*
Khek-Yu Ho, *Singapore*
Francis Seow-Choen, *Singapore*

Slovakia
Anton Vavrecka, *Bratislava*

Slovenia
Sasa Markovic, *Ljubljana*

South Africa
Michael C Kew, *Parktown*

South Korea
Byung Ihn Choi, *Seoul*
Ho Soon Choi, *Seoul*
M Yeo, *Suwon*
Sun Pyo Hong, *Gyeonggi-do*
Jae J Kim, *Seoul*
Jin-Hong Kim, *Suwon*
Myung-Hwan Kim, *Seoul*
Chang Hong Lee, *Seoul*
Jong Kyun Lee, *Seoul*
Eun-Yi Moon, *Seoul*
Jae-Gahb Park, *Seoul*
Dong Wan Seo, *Seoul*
Dong jin Suh, *Seoul*

Spain
Juan G Abraldes, *Barcelona*
Agustin Albillos, *Madrid*
Raul J Andrade, *Málaga*
Luis Aparisi, *Valencia*
Fernando Azpiroz, *Barcelona*
Ramon Bataller, *Barcelona*
Josep M Bordas, *Barcelona*
Xavier Calvet, *Sabadell*
Andres Cardenas, *Barcelona*
Vicente Carreño, *Madrid*
Jose Castellote, *Barcelona*
Antoni Castells, *Barcelona*
Vicente Felipo, *Valencia*
Juan C Garcia-Pagán, *Barcelona*
Jaime Bosch Genover, *Barcelona*
Jaime Guardia, *Barcelona*
Angel Lanas, *Zaragoza*
María Isabel Torres López, *Jaén*
José M Mato, *Derio*
Juan F Medina, *Pamplona*
MA Muñoz-Navas, *Pamplona*
Julian Panes, *Barcelona*
Miguel Minguez Perez, *Valencia*
Miguel Perez-Mateo, *Alicante*
Josep M Pique, *Barcelona*
Jesus M Prieto, *Pamplona*
Sabino Riestra, *Pola De Siero*
Luis Rodrigo, *Oviedo*
Manuel Romero-Gómez, *Sevilla*

Sweden
Curt Einarsson, *Huddinge*
Ulf Hindorf, *Lund*
Hanns-Ulrich Marschall, *Stockholm*
Lars Christer Olbe, *Molndal*
Matti Sallberg, *Stockholm*
Magnus Simrén, *Göteborg*
Xiao-Feng Sun, *Linköping*
Ervin Tóth, *Malmö*
Weimin Ye, *Stockholm*

Switzerland
Chrish Beglinger, *Basel*
Pierre A Clavien, Zurich
Jean-Francois Dufour, *Bern*
Franco Fortunato, *Zürich*
Jean Louis Frossard, *Geneva*
Gerd A Kullak-Ublick, *Zurich*
Pierre Michetti, *Lausanne*
Francesco Negro, *Genève*
Bruno Stieger, *Zurich*
Arthur Zimmermann, *Berne*
Radu Tutuian, *Zurich*
Stephan Robert Vavricka, *Zurich*

Turkey
Yusuf Bayraktar, *Ankara*
Figen Gurakan, *Ankara*
Aydin Karabacakoglu, *Konya*
Serdar Karakose, *Konya*
Hizir Kurtel, *Istanbu*
Osman Cavit Ozdogan, *Istanbul*
Özlem Yilmaz, *Izmir*
Cihan Yurdaydin, *Ankara*

United Arab Emirates
Sherif M Karam, *Al-Ain*

United Kingdom
David Adams, *Birmingham*
NK Ahluwalia, *Stockport*
CG Antoniades, *London*
Anthony TR Axon, *Leeds*
Qasim Aziz, *Manchester*
Nicholas M Barnes, *Birmingham*
Jim D Bell, *London*
Mairi Brittan, *London*
Simon Scott Campbell, *Manchester*
Simon R Carding, *Leeds*
Paul Jonathan Ciclitira, *London*

Tatjana Crnogorac-Jurcevic, *London*
Amar Paul Dhillon, *London*
Emad M El-Omar, *Aberdeen*
Annette Fristscher-Ravens, *London*
Elizabeth Furrie, *Dundee*
Daniel Richard Gaya, *Edinburgh*
Subrata Ghosh, *London*
William Greenhalf, *Liverpool*
Indra Neil Guha, *Southampton*
Peter Clive Hayes, *Edinburgh*
Gwo-Tzer Ho, *Edinburgh*
Anthony R Hobson, *Salford*
Stefan G Hübscher, *Birmingham*
Robin Hughes, *London*
Pali Hungin, *Stockton*
David Paul Hurlstone, *Sheffield*
Janusz AZ Jankowski, *Oxford*
Brian T Johnston, *Belfast*
David EJ Jones, *Newcastle*
Michael A Kamm, *Harrow*
Peter Karayiannis, *London*
Laurens Kruidenier, *Harlow*
Patricia F Lalor, *Birmingham*
Hong-Xiang Liu, *Cambridge*
K E L McColl, *Glasgow*
Stuart AC McDonald, *London*
Dermot Patrick Mcgovern, *Oxford*
Giorgina Mieli-Vergani, *London*
Nikolai V Naoumov, *London*
John P Neoptolemos, *Liverpool*
James Neuberger, *Birmingham*
Mark S Pearce, *Newcastle Upon Tyne*
D Mark Pritchard, *Liverpool*
Stephen E Roberts, *Swansea*
Marco Senzolo, *Padova*
Soraya Shirazi-Beechey, *Liverpool*
Robert Sutton, *Liverpool*
Simon D Taylor-Robinson, *London*
Ulrich Thalheimer, *London*
Nick Paul Thompson, *Newcastle*
David Tosh, *Bath*
Frank Ivor Tovey, *London*
Chris Tselepis, *Birmingham*
Diego Vergani, *London*
Geoffrey Warhurst, *Salford*
Peter James Whorwell, *Manchester*
Karen Leslie Wright, *Bath*
Min Zhao, *Foresterhill*

United States

Gary A Abrams, *Birmingham*
Golo Ahlenstiel, *Bethesda*
BS Anand, *Houston*
Frank A Anania, *Atlanta*
Gavin Edward Arteel, *Louisville*
Jasmohan Singh Bajaj, *Milwaukee*
Jamie S Barkin, *Miami Beach*
Kim Elaine Barrett, *San Diego*
Marc Basson, *Detroit*
Timothy R Billiar, *Pittsburgh*
Edmund J Bini, *New York*
Jennifer D Black, *Buffalo*
Herbert L Bonkovsky, *Farmington*
Andrea D Branch, *New York*
Robert S Bresalier, *Houston*
Alan L Buchman, *Chicago*
Alan Cahill, *Philadelphia*
John M Carethers, *San Diego*
David L Carr-Locke, *Boston*
Ravi S Chari, *Nashville*
Jiande Chen, *Galveston*
Xian-Ming Chen, *Rochester*
Ramsey Chi-man Cheung, *Palo Alto*
William D Chey, *Ann Arbor*
John Y Chiang, *Rootstown*
Parimal Chowdhury, *Arkansas*
Raymond T Chung, *Boston*
James M Church, *Cleveland*
Mark G Clemens, *Charlotte*
Vincent Coghlan, *Beaverton*
David Cronin II, *New Haven*
John Cuppoletti, *Cincinnati*
Peter V Danenberg, *Los Angeles*
Kiron Moy Das, *New Brunswick*
Sharon DeMorrow, *Temple*
Deborah L Diamond, *Seattle*
Peter Draganov, *Florida*
Bijan Eghtesad, *Cleveland*
Hala El-Zimaity, *Houston*
Michelle Embree-Ku, *Providence*
Ronnie Fass, *Tucson*
Mark A Feitelson, *Philadelphia*
Ariel E Feldstein, *Cleveland*
Alessandro Fichera, *Chicago*
Chris E Forsmark, *Gainesville*
Chandrashekhar R Gandhi, *Pittsburgh*
Susan L Gearhart, *Baltimore*
Xupeng Ge, *Boston*
John P Geibel, *New Haven*
Xin Geng, *New Brunswick*
Jean-Francois Geschwind, *Baltimore*
Ignacio Gil-Bazo, *New York*
Shannon S Glaser, *Temple*
Ajay Goel, *Dallas*
Julia Butler Greer, *Pittsburgh*
David R Graham, *Houston*
Anna S Gukovskaya, *Los Angeles*
Sanjeev Gupta, *Bronx*
David J Hackam, *Pittsburgh*
Stephen B Hanauer, *Chicago*
Gavin Harewood, *Rochester*
Alan W Hemming, *Gainesville*
Samuel B Ho, *San Diego*
Hongjin Huang, *Alameda*
Jamal A Ibdah, *Columbia*
Atif Iqbal, *Omaha*
Hajime Isomoto, *Rochester*
Hartmut Jaeschke, *Tucson*
Dennis M Jensen, *Los Angeles*
Leonard R Johnson, *Memphis*
Peter James Kahrilas, *Chicago*
AN Kalloo, *Baltimore*
Neil Kaplowitz, *Los Angeles*
Rashmi Kaul, *Tulsa*
Jonathan D Kaunitz, *Los Angeles*
Ali Keshavarzian, *Chicago*
Miran Kim, *Providence*
Joseph B Kirsner, *Chicago*
Leonidas G Koniaris, *Miami*
Burton I Korelitz, *New York*
Robert J Korst, *New York*
Richard A Kozarek, *Seattle*
Michael Kremer, *Chapel Hill*
Shiu-Ming Kuo, *Buffalo*
Daryl Tan Yeung Lau, *Galvesto*
Joel E Lavine, *San Diego*
Dirk J van Leeuwen, *Lebanon*
Glen A Lehman, *Indianapolis*
Alex B Lentsch, *Cincinnati*
Andreas Leodolter, *La Jolla*
Gene LeSage, *Houston*
Ming Li, *New Orleans*
Zhiping Li, *Baltimore*
LM Lichtenberger, *Houston*
GR Lichtenstein, *Philadelphia*
Otto Schiueh-Tzang Lin, *Seattle*
Martin Lipkin, *New York*
Edward V Loftus, *Rocheste*
Robin G Lorenz, *Birmingham*
JD Luketich, *Pittsburgh*
Henry Thomson Lynch, *Omaha*
Patrick M Lynch, *Houston*
Peter J Mannon, *Bethesda*
John Frank Di Mari, *Texas*
John M Mariadason, *Bronx*
WM Mars, *Pittsburgh*
Laura E Matarese, *Pittsburgh*
Lynne V McFarland, *Washington*
Kevin McGrath, *Pittsburgh*
Harihara Mehendale, *Monroe*
Howard Mertz, *Nashville*
George W Meyer, *Sacramento*
G Michalopoulos, *Pittsburgh*
James Michael Millis, *Chicago*
Smruti Ranjan Mohanty, *Chicago*
Satdarshan Singh Monga, *Pittsburgh*
Timothy H Moran, *Baltimore*
Steven F Moss, *Providence*
Masaki Nagaya, *Boston*
Laura Eleanor Nagy, *Cleveland*
Hiroshi Nakagawa, *Philadelphia*
Douglas B Nelson, *Minneaplis*
Brant K Oelschlager, *Washington*
Curtis T Okamoto, *Los Angeles*
Stephen JD O'Keefe, *Pittsburgh*
Dimitry Oleynikov, *Omaha*
Natalia A Osna, *Omaha*
Stephen J Pandol, *Los Angeles*
Pankaj Jay Pasricha, *Gaveston*
Zhiheng Pei, *New York*
Michael A Pezzone, *Pittsburgh*
CS Pitchumoni, *New Brunswiuc*
Jay Pravda, *Gainesville*
M Raimondo, *Jacksonville*
GS Raju, *Galveston*
Murray B Resnick, *Providence*
Adrian Reuben, *Charleston*
Douglas K Rex, *Indianapolis*
Victor E Reyes, *Galveston*
Richard A Rippe, *Chapel Hill*
Marcos Rojkind, *Washington*
Hemant Kumar Roy, *Evanston*
Shawn David Safford, *Norfolk*
NJ Shaheen, *Chapel Hill*
Stuart Sherman, *Indianapolis*
Shivendra Shukla, *Columbia*
Alphonse E Sirica, *Virginia*
Shanthi V Sitaraman, *Atlanta*
Shanthi Srinivasan, *Atlanta*
Michael Steer, *Boston*
Gary D Stoner, *Columbus*
Liping Su, *Chicago*
Christina Surawicz, *Seattle*
Gyongyi Szabo, *Worcester*
Yvette Taché, *Los Angeles*
Seng-Lai Tan, *Seattle*
Andrzej Tarnawski, *Long Beach*
Andrzej S Tarnawski, *Orange*
K-M Tchou-Wong, *New York*
Neil D Theise, *New York*
PJ Thuluvath, *Baltimore*
Swan Nio Thung, *New York*
Natalie J Torok, *Sacramento*
RA Travagli, *Baton Rouge*
G Triadafilopoulos, *Stanford*
James F Trotter, *Denver*
Chung-Jyi Tsai, *Lexington*
Hugo E Vargas, *Scottsdale*
Scott A Waldman, *Philadelphia*
Jian-Ying Wang, *Baltimore*
Steven David Wexner, *Weston*
Keith Tucker Wilson, *Baltimore*
Jacqueline L Wolf, *Boston*
Jackie Wood, *Ohio*
George Y Wu, *Farmington*
Jian Wu, *Sacramento*
Samuel Wyllie, *Houston*
Wen Xie, *Pittsburgh*
Yoshio Yamaoka, *Houston*
Francis Y Yao, *San Francisco*
Min You, *Tampa*
Zobair M Younossi, *Virginia*
Liqing Yu, *Winston-Salem*
David Yule, *Rochester*
Ruben Zamora, *Pittsburgh*
Michael E Zenilman, *New York*
Zhi Zhong, *Chapel Hill*

PO Box 2345, Beijing 100023, China
www.wjgnet.com
wjg@wjgnet.com

World J Gastroenterol 2007 February 21; 13(7): 985-992
World Journal of Gastroenterology ISSN 1007-9327

REVIEW

p53 gene in treatment of hepatic carcinoma: *Status quo*

Yong-Song Guan, Zi La, Lin Yang, Qing He, Ping Li

Yong-Song Guan, Zi La, Lin Yang, Qing He, Ping Li, Department of Radiology and Oncology, West China Hospital of Sichuan University, Chengdu 610041, Sichuan Province, China
Correspondence to: Dr. Yong-Song Guan, State Key Laboratory of Biotherapy, West China Hospital, West China Medical School, Sichuan University-Gaopeng Street, Keyuan Road 4, Chengdu 610041, Sichuan Province, China. yongsongguan@yahoo.com
Telephone: +86-28-85422601 Fax: +86-28-85538359
Received: 2006-11-30 Accepted: 2007-01-16

Abstract

Hepatocellular carcinoma (HCC) is one of the 10 most common cancers worldwide. There is no ideal treatment for HCC yet and many researchers are trying to improve the effects of treatment by changing therapeutic strategies. As the majority of human cancers seem to exhibit either abnormal p53 gene or disrupted p53 gene activation pathways, intervention to restore wild-type p53 (wt-p53) activities is an attractive anti-cancer therapy including HCC. Abnormalities of p53 are also considered a predisposition factor for hepatocarcinogenesis. p53 is frequently mutated in HCC. Most HCCs have defects in the p53-mediated apoptotic pathway although they carry wt-p53. High expression of p53 *in vivo* may exert therapeutic effects on HCC in two aspects: (1) High expression of exogenous p53 protein induces apoptosis of tumor cells by inhibiting proliferation of cells through several biologic pathways and (2) Exogenous p53 renders HCC more sensitive to some chemotherapeutic agents. Several approaches have been designed for the treatment of HCC *via* the p53 pathway by restoring the tumor suppression function from inactivation, rescuing the mutated p53 gene from instability, or delivering therapeutic exogenous p53. Products with p53 status as the target have been studied extensively *in vitro* and *in vivo*. This review elaborates some therapeutic mechanisms and advances in using recombinant human adenovirus p53 and oncolytic virus products for the treatment of HCC.

Key words: p53 gene; Hepatocellular carcinoma; Therapeutic strategies; Advances; Prospects

Guan YS, La Z, Yang L, He Q, Li P. p53 gene in treatment of hepatic carcinoma: *Status quo*. *World J Gastroenterol* 2007; 13(7): 985-992

http://www.wjgnet.com/1007-9327/13/985.asp

INTRODUCTION

The concept of human gene therapy[1,2] derives from fundamental discoveries[3,4] on the nature and working[5] of the gene. Since the essential principles of molecular genetics and gene transfer in bacteria were established in the 1960s, gene transfer into animals and humans using either viral vector and/or genetically modified cultured cells has become inevitable[6]. Since then, this concept has promoted thousands of researchers to attempt to realize their long-cherished dreams of eradicating some of the obstinate human diseases. Broadly defined, the concept of gene therapy involves transfer of genetic materials[6] into cells, tissues, or whole organs, with the goal of eliminating diseases or at least improving the clinical condition of patients[7]. As a milestone of gene therapy, the first approved clinical protocol started trials in September, 1990[8]. Gene therapy provides great opportunities for treating diseases due to genetic disorders, infections and cancer[9]. Hepatocellular carcinoma (HCC) is one of the 10 most common cancers worldwide with its highest prevalence in Southeast Asia and sub-Saharan Africa[10]. Although great efforts have been made to overcome this cancer, no ideal treatment is available at present[11]. In recent years, many researchers are trying to improve the effects of treatment by changing therapeutic strategies[12]. As the majority of human cancers seem to exhibit either abnormal p53 gene[13] or disrupted p53 gene activation pathways[14], intervention to restore wild-type p53 (wt-p53) activities is an attractive anti-cancer therapy[14,15]. This review elaborates some therapeutic mechanisms and advances in using recombinant human adenovirus p53[16] and oncolytic virus[17] products for the treatment of HCC.

CARCINOGENESIS OF LIVER CELLS AND p53 GENE

Cancer predisposition, onset and therapeutic response can be critically determined by the integrity of tumor suppressor p53[15]. Tumor suppressor protein p53 can protect cells from growth and division[18], thus mediating cell-cycle arrest[19], DNA repair[20] and apoptosis[13,14,19,21] after its activation by multiple forms of cellular stresses[19]. p53 mutations[22] in plasma DNA are associated with several cancers, and abnormalities of p53 are also considered a predisposition factor for HCC (Table 1). Mutant p53 (mt-p53) may be a marker of HCC carcinogen exposure[22]. For example, in aflatoxin B1-exposed patients[23], R249S tumor protein p53[24], one of the cancer-associated mutants, encodes p53, and is considered a

Table 1 Abnormal p53 status detected in HCC with probable mechanisms

Endogenous status of p53 or its pathways	Probable mechanisms
Mutation of p53 gene	Point mutation, allele deletion, insertion, *etc.*
Loss of or decrease in wt-p53 expression	Enhanced p53 degradation, complex formation
Hyperactivities of negative regulators of p53	No p53 mutation, over-expressed negative regulators of p53 attenuate its function
Increased diversity of p53 aberration	Progression of HCC
Presence of serum anti-p53 antibodies	Over-expression of wt-p53, presence of mt-p53, or both

Table 2 Approaches for restoring tumor suppression function of p53 in the treatment of HCC

Strategies	Therapeutic effects
Chemotherapy or radiotherapy	Inducing p53-dependent apoptosis in tumor cells with wt-p53
Supplying exogenous wt-p53 by gene delivery	Suppressing growth of both mutant and wild-type p53-containing tumor cells
Overexpression of ARF	Blocking p53 degradation pathways to induce p53 triggered tumor cell death
Interruption of MDM2-p53 interaction	Preventing MDM2-mediated p53 ubiquitinationand degradation to restore transactivation
Molecules stabilizing the active conformation of the protein	Rescuing mt-p53 to restore p53 function

genetic alteration during hepatocarcinogenesis[23]. Here R249S as a mutant of p53 core domain, is a structural mutation[25], and constitutes one of the "hot spots" associated with cancer.

There is evidence that the level of p53 alterations is high in HCC, since it was reported that p53 increases the frequency of HCC prediction from 79.5% to 86.3%[26], showing that serum concentration of p53 protein may be a convenient and useful non-invasive screening test for prediction of HCC. A study[27] showed that attenuated p53 function and telomere-induced chromosomal instability play a critical and cooperative role in the progression of chronic liver damage to hepatocellular carcinoma. Loss of p53 expression or presence of abnormal forms of the protein is frequently associated with HCC cell lines. Bressac *et al*[28] studied the p53 gene at the DNA, RNA, and protein level in seven human HCC-derived cell lines, and found that six of them show p53 abnormalities, suggesting that alterations in p53 may be important events in the transformation of hepatocytes[29] into the malignant phenotype. p53 gene is frequently mutated in high-grade[30] HCC. Inactivation of this multiple tumor suppressor gene plays an important role in the progression of chronic liver damage to hepatocellular carcinoma by directly or indirectly inducing chromosome instability, cell proliferation and neovascularization[31]. Kondo *et al*[32] performed dual-color fluorescence *in situ* hybridization to evaluate loss of the p53 gene, and revealed that loss of the p53 gene occurs in HCC, and diversity of the p53 gene aberration increases with the progression of chronic liver damage to HCC.

Other factors for hepatocarcinogenesis are correlated with abnormal functioning of p53, such as hepatitis B virus (HBV)[23,33] and hepatitis C virus (HCV)[34]. HBV gene encodes HBV protein x (HBx)[33], a protein as a transcriptional activator[35] and plays an important role in viral replication in HBV-infected cells. HBx as an oncoprotein[36], can bind to the C terminus of p53 and inhibit several critical p53-mediated cellular processes, including DNA sequence-specific binding, transcriptional transactivation, and apoptosis[37]. HBx integration and inactivation of p53 by mutations and regional allelic deletions are frequently found in tumors associated with HBV infection[38]. HBx up-regulates survivin[39] expression in hepatoma tissues. Survivin is an inhibitor of apoptosis and found in many common human cancers but not in normal tissues. Survivin is suppressed by wt-p53 and over-expressed in 41%-70% of HCCs from Asia, its over-expression is associated with aberrant p53 nuclear positivity[40].

In addition to its aberration, as p53 responds to a variety of genotoxic[34] and cytotoxic[41] agents in the presence of a potent inhibitor[42] of p53, the liver's ability to handle such toxic agents is influenced, thus inducing hepatocarcinogenesis.

Anti-p53 antibodies (p53-Abs) are products triggered by accumulation of a mutated form of p53 protein and probably a large quantity of wt-p53 protein[43]. As a specific serological marker for p53 gene expression changes in HCC, the presence of p53-Abs is independent of serum alpha fetoprotein and other conventional tumor markers[44]. It was reported that serum p53-Abs have a specificity of 100% for detecting malignancy[44], suggesting that its use in combination with markers may increase the diagnostic sensitivity of cancer.

MECHANISMS OF p53 THERAPY FOR HCC

Restoration of tumor suppression function of p53 has been speculated in several clinical lines for the treatment of HCC (Table 2).

p53 is frequently mutated in HCC[31]. Most HCCs have defects in the p53-mediated[37] apoptotic pathway although they carry wt-p53. Sometimes, p53 in HCC is wild-type but has inactive function[45]. Signal to and activation of p53 can lead to wt-p53 expression, thus suppressing the transformed phenotype of hepatocytes and increasing the effects of both chemotherapeutic agents and radiation therapy[46]. Repression of p53 can be partial or complete[45] in HCC, and activation of p53 can be achieved by single small molecules, such as the well known antimalaria drug quinacrine[45]. Supplying exogenous wt-p53 in cancer cells by gene delivery is effective in suppressing tumor growth of both mutant and wild-type p53-containing tumors[14]. The murine double minute 2 gene (MDM2) is an oncogene and contains a p53-DNA binding site and produces a phosphoprotein that forms a tight complex with both mutant and wild-type p53 protein, thus inhibiting p53-mediated transactivation and inducing p53 degradation[47]. There is a MDM2-p53 auto-regulatory feedback loop[48] that regulates the function of p53 protein and expression

of the MDM2 gene. Expression of the MDM2 gene can be regulated by the level of wild-type p53 protein, while the MDM2 protein, in turn, can form a complex with p53 and decrease its ability to act as a positive transcription factor at the MDM2 gene-responsive element. Several approaches have now been used to interrupt MDM2-p53 interaction to increase functional p53 levels and p53-mediated therapeutic effectiveness[49]. ADP-ribosylation factor (ARF) proteins are critical regulators of the protein secreting pathway[50]. In a human HCC cell line[51], adenosine diphosphate (ADP) and adenosine triphosphate (ATP) are degraded to adenosine and treatment of HCC cells with adenosine can inhibit growth of HCC cells and activate caspase-3, indicating that adenosine is an apoptotic agent with cytotoxicity. ARF is considered a tumor suppressor[52], and can initiate cellular response to aberrant oncogene activation by binding to and inhibiting the activity of MDM2. The human counterpart[53] of MDM2 (HDM2), like the murine protein, can inactivate the transactivation ability of human p53. ARF and p53 bind to MDM2 on different sites. ARF-p53 complex is formed depending on the mediation by MDM2 and can enhance p53 stability[54]. Blockage of p53 degradation pathways either by over-expression of ARF or interruption of MDM2-p53 interaction can effectively induce p53-triggered tumor cell death[14].

High expression of p53[55] *in vivo* may exert therapeutic effects on HCC in two aspects: (1) High expression of exogenous p53 protein induces apoptosis of tumor cells by inhibiting proliferation of cells through several biologic pathways and (2) exogenous p53 renders HCC more sensitive to some chemotherapeutic agents.

In addition, p53 down-regulates the expression of genes involved in angiogenesis[56], by the angiogenesis-inhibiting properties of wt-p53 protein[13].

It is very difficult to treat HCC due to drug resistance. It is necessary to reverse multiple drug resistance to human HCC cells and to find out the related mechanisms. The expression and activity of P-glycoprotein as well as the multiple drug resistance gene (MDR) products, are elevated in HCC cells with mt-p53[57]. Expression of mt-p53 enhances drug resistance to HCC cells and reduces their uptake of chemotherapeutic agents. In contrast to the increased expression of MDR by mt-p53, wt-p53 inhibits transcription of MDR[58]. Therefore, restoration of wt-p53 activity in HCC cells leads to the sensitivity of HCC cells to chemotherapeutic agents because of the decreased expression of P-glycoprotein encoded by MDR.

APPROACHES OF p53 THERAPY FOR HCC

Studies indicate that it is necessary to deliver therapeutic genes into cells with high specificity and efficiency in order to increase the effect of gene therapy against cancer[5,7,9,11]. A key factor for the success of gene therapy is the development of delivery systems[5,7,9] that are capable of efficiently transferring genes into a variety of tissues, without any associated pathogenic effects[7]. These techniques permit the isolation and insertion of genes into the recombinant delivery systems[5]. Two kinds of gene transfer vectors, namely viral and non-viral, are available at present.

Viruses are recognized natural gene carriers[5] and provide inspiration of gene therapy. Viruses have been engineered as gene delivery vectors[59]. However, their limits such as selective disadvantage[60], immunogenicity and toxicity[61], inefficient gene transfer and short-lived[62] or inadequate expression in transfected liver cells[63], require us to search other delivery systems.

Non-viral vectors have several advantages over viral vectors[61]. The transferred gene is in the form of a plasmid[64] that is on the surface or in the interior of the vector. Such vectors include liposome[61], molecular conjugates[65], nanoparticles[66] with strong anti-tumor effect on human HCC, naked DNA[67] and complexed DNA[68]. Better transfection efficiency can be achieved with delivery systems such as cationic lipids and cationic polymers[63].

To date, tissue-specific expression[69], self-replicating[70] and integrating plasmid[71] systems have been reported for gene therapy of HCC. Iodized oil emulsion[72] has a particular affinity to hypervascular hepatic tumors and is now commonly used in HCC chemoembolization, suggesting that it can be applied to the liver as a non-viral gene transfer system for intra-arterial gene delivery with selective gene expression in tumor cells.

THERAPEUTIC PRODUCTS WITH p53 STATUS AS TARGET

Recombinant adenovirus p53 (rAd-p53) and oncolytic virus are the promising therapeutic products for the treatment of HCC mostly applied *in vitro* and *in vivo* at present. With the introduction of exogenous wt-p53 expressed by the recombinant adenoviral vector, the expression of both p53 and p21 proteins is found to be up-regulated in cells[55]. Inhibition of cell growth and apoptosis can be achieved[55]. Oncolytic viruses[73,74] are a number of defective viruses, which cannot replicate in normal cells but are able to grow in tumor cells, finally leading to their lysis.

The two kinds of viruses and their characteristics were compared (Table 3).

Recombinant adenovirus p53 (rAd-p53)

Since human adenovirus vector systems have a lager host range and lower pathogenicity to humans[75], and the binding affinity for epithelium[76] is important because most of human tumors are of the epithelial origin, and serotype 4 of species E[77,78] shows a specific binding affinity for HCC cells[76], they are generally used for the expression of proteins in human beings or other species with some advantages. The E1 region of adenovirus has been identified as a subregion of the viral genome present in transformed cells and is responsible for transformation[79]. Recombinant human adenoviruses constructed with the E1 region replaced by exogenous DNA become replication-defective and yield a relatively low degree of acute toxicity[80]. Since recombinant adenoviral vector expresses wt-p53 (Ad-p53), p53 gene can be transfected into HCC cell lines[55]. Experiments showed that tumor cells transduced with the wt-p53 gene can inhibit *in vivo*

Table 3 Comparison of several characteristics of rAd-p53 with oncolytic virus products

Products	Characteristics
rAd-p53	p53 gene is transfected into HCC cells with recombinant adenoviral vector expressing wt-p53
Advexin	Larger host range, low pathogenicity to human, replication-impaired adenoviral vector carrying the p53 gene
Gendicine	The first commercial gene therapy product in the world approved by SFDA
SCH58500	Replication-deficient type 5 adenovirus vector expressing human wt-p53 under control of cytomegalovirus promoter
Oncolytic viruses	Incapable of replicating in normal cells but selectively replicating in p53-defective tumor cells to lyse them
ONYX-015	Tumor-selective replicating virus, the prototype for oncolytic adenoviral therapy
CNHK300-mE	Replication-competent with advantages of both gene and virus therapies

tumor growth of adjacent nontransduced cells, suggesting that Ad-p53 is also anti-angiogenic[81], partially by the bystander effect induced by the wt-p53 gene transfer on adjacent tumor cells.

Oncolytic viruses

As HCC cells with p53 defects have lost their cellular surveillance mechanisms, oncolytic viruses interfering with the main surveillance pathways such as those controlled by p53[73], could replicate selectively in them and cause lysis. E1A gene of adenovirus is an apoptosis-inducing gene and E1B gene of adenovirus is an apoptosis-inhibiting gene. The 55-kilodalton (55kDa) protein from the E1B-region of adenovirus binds to and inactivates the p53 gene[82]. Because of a deletion in E1B, the 55-kDa E1B protein is not expressed and the mutant adenovirus, termed ONYX-015[83], is able to replicate only in wt-p53 deficient cells. The E1B55K-defective adenovirus ONYX-015 is a prototype[73,82,83] of oncolytic viruses and can selectively replicate in and kill p53-deficient HCC cells, the success of cancer gene therapy is not promising unless it is carefully designed based on the biology of a specific[84] tumor type. To enhance the efficiency of such oncolytic viruses, another E1B 55kDa-deficient adenovirus armed with a mouse endostatin gene has been constructed for anti-tumor activities against HCC, and termed as CNHK200-mE[85]. With the synergistic effect of carrier virus and therapeutic gene, a novel approach has been established with the vector system termed as gene-viral vector[86] or gene-viral therapeutic system wherein an anti-tumor gene is inserted into the genome of a replicative virus specific for tumor cells to combine the advantages of gene and virus therapies. Using the human telomerase reverse transcriptase (hTERT) promoter to drive the expression of adenovirus E1A gene and clone the therapeutic gene mouse endostatin into the adenovirus genome, CNHK300-murine endostatin (CNHK300-mE)[87] is constructed, showing potential effects in the treatment of HCC.

EMPIRICAL STUDIES OF p53 THERAPY FOR HCC

Activation of p53 by either chemotherapy or radiotherapy induces p53-dependent apoptosis in tumor cells with wt-p53[14].

In the treatment of HCC, p53 products are injected into liver tissue by a variety of routes[55,72,82,88-92]. When p53 products are injected intratumorally[55,88,89], introduction of exogenous wt-p53 can inhibit cell growth, the expression of both p53 and p21 proteins is up-regulated in tumor cells. Intraarterial gene delivery into animal hepatic tumors can lead to selective gene expression in tumor cells[72]. Antegrade intraportal and retrograde intrabiliary routes are compared, induce transgene expression in periportal areas of liver with no significant difference in transduction efficacy, and no apparent complications are observed apart from very mild elevation of serum biochemical parameters[90]. The effect of bile and pancreatic juice on gene delivery has been studied under the guide of endoscopic retrograde cholangiopancreatography (ERCP)[92], showing that neither bile nor pancreatic juice affects transgene expression. Intrasplenic injection of p53 products can transfer gene into the portal venous circulation. When p53 products are injected intravenously, barriers such as the endothelial lining of tumor vasculature impair the efficiency of adenoviral vectors for gene delivery into HCCs[65,82], which can be overcome by direct injection of p53 products into tumor tissues[89]. Other gene delivery routes have also been reported[91].

High-volume hydrodynamic injection of a gene *via* the hepatic artery with inferior vena cava/portal vein occlusion can achieve a high level of gene expression in HCC rat model[67]. This gene transfer technique may have potential in clinical gene therapy for HCC. Oncolytic adenovirus-mediated gene therapy induces tumor-cell apoptosis and reduces tumor angiogenesis, leading to inhibition of HCC growth in animal model[88]. Because CNHK200-mE is capable of selectively replicating in HCC cells, thus suppressing tumor growth and antiangiogenic activity in nude mice[85], it can be used as a potential agent in the treatment of HCC.

CLINICAL RESEARCHES OF p53 THERAPY FOR HCC

After *in vitro* and *in vivo* experiments, different adenovirus-mediated p53 gene therapies for various tumors have been evaluated[46]. It was reported that when recombinant adenovirus p53 (SCH 58500) is administered by hepatic arterial infusion, and it distributes more predominantly in liver tissues than in tumors[93].

Intratumoural injection of Ad-p53 can lead to over-expression of p53 in cancer cells by inducing cell growth arrest and apoptosis, and overcome resistance or increase the effectiveness of radiation therapy and chemotherapy[94].

Hepatic artery embolization for the treatment of HCC was first reported in 1979[95]. Since the 1980s, transcatheter arterial chemo-embolization (TACE) has been applied

to various HCCs apart from those with humoral hypercalcemia[96]. TACE as a local ablative treatment is able to control local disease and prolong a similar survival to that of surgical resection[11]. However, the recurrence of HCC after successful control of local tumor spread is high due to the non-curative procedure. In contrast to necrosis resulting from TACE, apoptosis is not commonly accompanied with inflammation that causes collateral cell damage, suggesting that the effects of intra-tumoral or intraarterial injection of p53 products in combination with TACE, on tumor tissue ischemia and necrosis, may be synergic and can improve survival.

In addition, inhibitors of p53-mediated apoptosis might be used to transiently decrease apoptosis in normal tissues when patients receive high doses of radiation or chemotherapy[97]. Emulsion of iodized oil and contrast medium can be used as a nonviral gene transfer system for intraarterial gene delivery[72].

CHALLENGES AND PROSPECTS

p53 is an ideal target for anti-cancer drug design[14]. Blockage of p53 degradation pathways can effectively induce p53 triggered tumor cell death[14]. Since unlike most other tumor suppressor genes, mt-p53 is over-expressed in tumor cells, a promising approach involving reactivation of tumor-suppressing function to mt-p53[21,25]. Further understanding of the mechanisms of how to restore p53 activity, may lead to discovery of more potent analogs and new strategies[11,73,91] for p53-targeting in tumor therapy.

More genes previously unknown have been identified that are involved in the regulation of p53 transcriptional activity and their over-expression inhibits p53 target promoters and p53-mediated apoptosis, suggesting that these genes play a role as p53 inhibitors and may have oncogenic activity[98].

As hepatocarcinogenesis is a multistage process involving a number of genes[99,100], attention should be paid to the target genes whose altered expression actually mediates neoplastic phenotype. There is an urgent need to establish simple and low-cost tests for detecting expression of p53-related genes in HCC[99,100] that are hallmarks of HCC development. Continuous monitoring of serum p53 protein is important in early detection of recurrence of HCC, and immunodetection of serum p53 is valuable[101] for post-operative monitoring during follow-up in preoperatively positive patients.

Nevertheless, about 40% of cancers retain wt-p53, and there may be mutations of other genes in cells with p53 mutations. Therefore, the mechanisms of p53 in HCC therapies should be further studied.

It was reported that hepatic arterial administration of p53 products cannot substantially increase transduction of tumor cells, and ligation of the hepatic artery following infusion of adenovirus or addition of lipiodol infusion has no effect on the transduction of tumor cells[102], suggesting that better administration approaches must be developed for more efficient transduction of tumor cells.

Safety and research ethics must be emphasized. Human gene therapy can lead to serious adverse effects and even death[103]. In a gene therapy experiment in 1999[104], death of Jesse Gelsinger was found to be directly linked to the viral vector used for the treatment. This tragic event has raised new questions about the prospects for human gene therapy, which not only achieves a therapeutic effect but also has potential adverse effects.

Another task at present is to find out the key points of tumor resistance to rAd-p53[105-108]. Since exogenous wt-p53 was introduced, inhibition of tumor growth has become unnecessary for human cancer cells carrying mt-p53[105]. In some cancer cells, wt-p53 is inactivated by different mechanisms. Since the presence of mt-p53 may induce genome instability of human cancer cells and mutator ability, they can escape the effects of exogenous wt-p53 and contribute to the failure of wt-p53 gene therapy. On the contrary, exogenous wt-p53 in other cancers can have effects only on those expressing wt-p53. For example, alterations of p53 gene are uncommon in differentiated thyroid neoplasm but can be frequently detected in anaplastic thyroid carcinoma[107], suggesting that impaired p53 function may contribute to the undifferentiated and highly aggressive phenotype of these tumors. It was reported that exogenous expression of wt-p53 has influence on thyroid tumorigenic properties only in cells bearing altered p53, whereas it has no effect on cells expressing wt-p53 activity[106], indicating that the endogenous p53 status seems to be essential for the effectiveness of p53-based gene therapy for some cancers. Another study[108] evaluated the therapeutic effects of truncated Bid gene (tBid) on p53-resistent HCC and demonstrated that this gene only targets AFP-producing cells but not non-AFP producing ones[109]. The introduction of tBid can not only significantly but also specifically kill HCC cells that produce AFP, indicating that death of HCC cells is induced by an apoptotic pathway independent of p53 status[108].

CONCLUSION

p53 is an ideal target for the design of anti-cancer therapeutic strategies. p53 is frequently mutated in a significant portion of HCCs, and can mediate defective apoptotic pathways in HCC carrying wild type of p53. Several approaches have been designed for the treatment of HCC *via* the p53 pathway by restoring tumor suppression function from inactivation, rescuing mutated p53 gene from instability, or delivering therapeutic exogenous p53. Products with p53 status as the target have been studied extensively *in vitro* and *in vivo*. Although their therapeutic effects are limited, further study is needed to elucidate the mechanisms of p53 in HCC therapies, the role of endogenous p53 status, novel genes involved in the regulation of p53 transcriptional activity, the establishment of simple and low-cost tests for detecting expression of p53-related genes in HCC, better administration approaches of exogenous p53, safety and research ethics, and the key points of resistance to rAd-p53 in HCC.

COMMENTS

Background

Hepatocellular carcinoma (HCC) is one of the 10 most common cancers

worldwide. There are no ideal therapies for advanced HCC so far, and many researchers are trying to improve the effects of treatment by changing therapeutic strategies including application of gene therapy.

Research frontiers

About 50% of human cancers are associated with mutations in the core domain of tumor suppressor p53, thus p53 is regarded as the most frequently mutated gene. It is an attractive approach to the treatment of HCC by restoring wild type p53 activity.

Innovations and breakthroughs

Several approaches have been designed for the treatment of HCC *via* the p53 pathway by restoring tumor suppression function from inactivation, rescuing the mutated p53 gene from instability, or delivering therapeutic exogenous p53. Products with p53 status as the target have been studied extensively *in vitro* and *in vivo*.

Applications

p53 pathway can be used as a target in the treatment of HCC.

Terminology

Gene Therapy: The treatment of certain disorders, especially those caused by genetic anomalies or deficiencies, by introducing specifically engineered genes into patient cells. **p53 gene**: It is a tumor suppressor gene providing instructions for making a protein called tumor protein 53 (TP53). Through the effect of the protein it produces, *TP53* is a tumor suppressor gene regulating the cycle of cell division by protecting cells from growing and dividing too fast or in an uncontrolled way. The p53 protein is located in the nuclei of cells throughout the body and can bind directly to DNA. When the DNA in cells becomes damaged, this protein plays a critical role in determining whether the DNA is repaired or the cells undergo programmed cell death (apoptosis). If the DNA can be repaired, p53 activates other genes to repair the damage. If the DNA cannot be repaired, the p53 tumor protein protects cells from dividing and signals it to undergo apoptosis. This process protects cells with mutated or damaged DNA from dividing, which helps prevent the development of tumors. Because the p53 tumor protein is essential for regulating cell division, it has been nicknamed the "guardian of the genome. **Vector**: Any device of transportation or movement. In this article, it denotes "a virus used to deliver genetic material into cells" or "a piece of DNA carrying DNA fragments into host cells".

Peer review

This review elaborates some therapeutic mechanisms and advances in using recombinant human adenovirus p53 and oncolytic virus products in the treatment of HCC. This review is helpful for many readers. The prospects should be expanded.

REFERENCES

1 **Editorial: Playing with genes**. *Br Med J* 1976; **1**: 302
2 **Stetten D**. What men fear. *Perspect Biol Med* 1978; **21**: 515-523
3 **Friedmann T**. Progress toward human gene therapy. *Science* 1989; **244**: 1275-1281
4 **Friedmann T**. The evolving concept of gene therapy. *Hum Gene Ther* 1990; **1**: 175-181
5 **Gonçalves MA**. A concise peer into the background, initial thoughts and practices of human gene therapy. *Bioessays* 2005; **27**: 506-517
6 **Wolff JA**, Lederberg J. An early history of gene transfer and therapy. *Hum Gene Ther* 1994; **5**: 469-480
7 **Verma IM**, Weitzman MD. Gene therapy: twenty-first century medicine. *Annu Rev Biochem* 2005; **74**: 711-738
8 **Blaese RM**, Culver KW, Miller AD, Carter CS, Fleisher T, Clerici M, Shearer G, Chang L, Chiang Y, Tolstoshev P, Greenblatt JJ, Rosenberg SA, Klein H, Berger M, Mullen CA, Ramsey WJ, Muul L, Morgan RA, Anderson WF. T lymphocyte-directed gene therapy for ADA- SCID: initial trial results after 4 years. *Science* 1995; **270**: 475-480
9 **Park TG**, Jeong JH, Kim SW. Current status of polymeric gene delivery systems. *Adv Drug Deliv Rev* 2006; **58**: 467-486
10 **Seeff LB**, Hoofnagle JH. Epidemiology of hepatocellular carcinoma in areas of low hepatitis B and hepatitis C endemicity. *Oncogene* 2006; **25**: 3771-3777
11 **Müller C**. Hepatocellular carcinoma--rising incidence, changing therapeutic strategies. *Wien Med Wochenschr* 2006; **156**: 404-409
12 **Llovet JM**. Updated treatment approach to hepatocellular carcinoma. *J Gastroenterol* 2005; **40**: 225-235
13 **Cheah PL**, Looi LM. p53: an overview of over two decades of study. *Malays J Pathol* 2001; **23**: 9-16
14 **Wang W**, Rastinejad F, El-Deiry WS. Restoring p53-dependent tumor suppression. *Cancer Biol Ther* 2003; **2**: S55-S63
15 **Haupt S**, Haupt Y. Importance of p53 for cancer onset and therapy. *Anticancer Drugs* 2006; **17**: 725-732
16 **Peng Z**. Current status of gendicine in China: recombinant human Ad-p53 agent for treatment of cancers. *Hum Gene Ther* 2005; **16**: 1016-1027
17 **Ries SJ**. Elucidation of the molecular mechanism underlying tumor-selective replication of the oncolytic adenovirus mutant ONYX-015. *Future Oncol* 2005; **1**: 763-766
18 **Levine AJ**. p53, the cellular gatekeeper for growth and division. *Cell* 1997; **88**: 323-331
19 **Bálint E E**, Vousden KH. Activation and activities of the p53 tumour suppressor protein. *Br J Cancer* 2001; **85**: 1813-1823
20 **Selivanova G**, Wiman KG. p53: a cell cycle regulator activated by DNA damage. *Adv Cancer Res* 1995; **66**: 143-180
21 **Bykov VJ**, Wiman KG. Novel cancer therapy by reactivation of the p53 apoptosis pathway. *Ann Med* 2003; **35**: 458-465
22 **Hagiwara N**, Mechanic LE, Trivers GE, Cawley HL, Taga M, Bowman ED, Kumamoto K, He P, Bernard M, Doja S, Miyashita M, Tajiri T, Sasajima K, Nomura T, Makino H, Takahashi K, Hussain SP, Harris CC. Quantitative detection of p53 mutations in plasma DNA from tobacco smokers. *Cancer Res* 2006; **66**: 8309-8317
23 **Laurent-Puig P**, Zucman-Rossi J. Genetics of hepatocellular tumors. *Oncogene* 2006; **25**: 3778-3786
24 **Friedler A**, DeDecker BS, Freund SM, Blair C, Rüdiger S, Fersht AR. Structural distortion of p53 by the mutation R249S and its rescue by a designed peptide: implications for "mutant conformation". *J Mol Biol* 2004; **336**: 187-196
25 **Bullock AN**, Henckel J, DeDecker BS, Johnson CM, Nikolova PV, Proctor MR, Lane DP, Fersht AR. Thermodynamic stability of wild-type and mutant p53 core domain. *Proc Natl Acad Sci USA* 1997; **94**: 14338-14342
26 **El Far MA**, Atwa MA, Yahya RS, El Basuni MA. Evaluation of serum levels of p53 in hepatocellular carcinoma in Egypt. *Clin Chem Lab Med* 2006; **44**: 653-656
27 **Farazi PA**, Glickman J, Horner J, Depinho RA. Cooperative interactions of p53 mutation, telomere dysfunction, and chronic liver damage in hepatocellular carcinoma progression. *Cancer Res* 2006; **66**: 4766-4773
28 **Bressac B**, Galvin KM, Liang TJ, Isselbacher KJ, Wands JR, Ozturk M. Abnormal structure and expression of p53 gene in human hepatocellular carcinoma. *Proc Natl Acad Sci USA* 1990; **87**: 1973-1977
29 **Nagao M**, Nakajima Y, Hisanaga M, Kayagaki N, Kanehiro H, Aomatsu Y, Ko S, Yagita H, Yamada T, Okumura K, Nakano H. The alteration of Fas receptor and ligand system in hepatocellular carcinomas: how do hepatoma cells escape from the host immune surveillance in vivo? *Hepatology* 1999; **30**: 413-421
30 **Jeng YM**, Peng SY, Lin CY, Hsu HC. Overexpression and amplification of Aurora-A in hepatocellular carcinoma. *Clin Cancer Res* 2004; **10**: 2065-2071
31 **Hirohashi S**. Pathology and molecular mechanisms of multistage human hepatocarcinogenesis. *Princess Takamatsu Symp* 1991; **22**: 87-93
32 **Kondo M**, Marusawa H, Ueda Y, Katsurada A, Kawasome C, Takami S, Kinoshita M, Ikai I, Yamaoka Y, Chiba T. Diverse p53 gene aberration in hepatocellular carcinoma detected by dual-color fluorescence in situ hybridization. *J Gastroenterol Hepatol* 2004; **19**: 1066-1073
33 **Dewantoro O**, Gani RA, Akbar N. Hepatocarcinogenesis in viral Hepatitis B infection: the role of HBx and p53. *Acta Med*

Indones 2006; **38**: 154-159
34 **Cho JW**, Park K, Kweon GR, Park JC, Lee JC, Baek WK, Jang BC, Suh SI, Suh MH. Modulation of cell death sensitivity by mutant p53 in HCV core-expressing cells. *Int J Mol Med* 2005; **15**: 475-480
35 **Wu CG**, Salvay DM, Forgues M, Valerie K, Farnsworth J, Markin RS, Wang XW. Distinctive gene expression profiles associated with Hepatitis B virus x protein. *Oncogene* 2001; **20**: 3674-3682
36 **Mathonnet G**, Lachance S, Alaoui-Jamali M, Drobetsky EA. Expression of hepatitis B virus X oncoprotein inhibits transcription-coupled nucleotide excision repair in human cells. *Mutat Res* 2004; **554**: 305-318
37 **Elmore LW**, Hancock AR, Chang SF, Wang XW, Chang S, Callahan CP, Geller DA, Will H, Harris CC. Hepatitis B virus X protein and p53 tumor suppressor interactions in the modulation of apoptosis. *Proc Natl Acad Sci USA* 1997; **94**: 14707-14712
38 **Cougot D**, Neuveut C, Buendia MA. HBV induced carcinogenesis. *J Clin Virol* 2005; **34** Suppl 1: S75-S78
39 **Zhang X**, Dong N, Yin L, Cai N, Ma H, You J, Zhang H, Wang H, He R, Ye L. Hepatitis B virus X protein upregulates survivin expression in hepatoma tissues. *J Med Virol* 2005; **77**: 374-381
40 **Kannangai R**, Wang J, Liu QZ, Sahin F, Torbenson M. Survivin overexpression in hepatocellular carcinoma is associated with p53 dysregulation. *Int J Gastrointest Cancer* 2005; **35**: 53-60
41 **Lacabanne V**, Viguier M, Guillet JG, Choppin J. A wild-type p53 cytotoxic T cell epitope is presented by mouse hepatocarcinoma cells. *Eur J Immunol* 1996; **26**: 2635-2639
42 **Eipel C**, Schuett H, Glawe C, Bordel R, Menger MD, Vollmar B. Pifithrin-alpha induced p53 inhibition does not affect liver regeneration after partial hepatectomy in mice. *J Hepatol* 2005; **43**: 829-835
43 **Lutz W**, Nowakowska-Swirta E. Gene p53 mutations, protein p53, and anti-p53 antibodies as biomarkers of cancer process. *Int J Occup Med Environ Health* 2002; **15**: 209-218
44 **Müller M**, Meyer M, Schilling T, Ulsperger E, Lehnert T, Zentgraf H, Stremmel W, Volkmann M, Galle PR. Testing for anti-p53 antibodies increases the diagnostic sensitivity of conventional tumor markers. *Int J Oncol* 2006; **29**: 973-980
45 **Gurova KV**, Hill JE, Guo C, Prokvolit A, Burdelya LG, Samoylova E, Khodyakova AV, Ganapathi R, Ganapathi M, Tararova ND, Bosykh D, Lvovskiy D, Webb TR, Stark GR, Gudkov AV. Small molecules that reactivate p53 in renal cell carcinoma reveal a NF-kappaB-dependent mechanism of p53 suppression in tumors. *Proc Natl Acad Sci USA* 2005; **102**: 17448-17453
46 **Horowitz J**. Adenovirus-mediated p53 gene therapy: overview of preclinical studies and potential clinical applications. *Curr Opin Mol Ther* 1999; **1**: 500-509
47 **Momand J**, Zambetti GP, Olson DC, George D, Levine AJ. The mdm-2 oncogene product forms a complex with the p53 protein and inhibits p53-mediated transactivation. *Cell* 1992; **69**: 1237-1245
48 **Wu X**, Bayle JH, Olson D, Levine AJ. The p53-mdm-2 autoregulatory feedback loop. *Genes Dev* 1993; **7**: 1126-1132
49 **Zhang** H. MDM2 oncogene as a novel target for human cancer therapy. *Curr Pharm Des* 2000; **6**: 393-416
50 **Stearns T**, Willingham MC, Botstein D, Kahn RA. ADP-ribosylation factor is functionally and physically associated with the Golgi complex. *Proc Natl Acad Sci USA* 1990; **87**: 1238-1242
51 **Wen LT**, Knowles AF. Extracellular ATP and adenosine induce cell apoptosis of human hepatoma Li-7A cells via the A3 adenosine receptor. *Br J Pharmacol* 2003; **140**: 1009-1018
52 **Rocha S**, Perkins ND. ARF the integrator: linking NF-kappaB, p53 and checkpoint kinases. *Cell Cycle* 2005; **4**: 756-759
53 **Brown DR**, Deb S, Muñoz RM, Subler MA, Deb SP. The tumor suppressor p53 and the oncoprotein simian virus 40 T antigen bind to overlapping domains on the MDM2 protein. *Mol Cell Biol* 1993; **13**: 6849-6857
54 **Lin J**, Zhu MH. Interactive pathway of ARF-mdm2-p53. *Ai Zheng* 2003; **22**: 328-330
55 **Guo Y**, Zeng Y, Wang K, Zhu X, Luo H, Zheng M, Li M, Chen J. Therapeutic potential of recombinant adenovirus expressing p53 in hepatocellular carcinoma cell lines. *Zhonghua Ganzangbing Zazhi* 2001; **9** Suppl: 43-45
56 **Oliveira AM**, Ross JS, Fletcher JA. Tumor suppressor genes in breast cancer: the gatekeepers and the caretakers. *Am J Clin Pathol* 2005; **124** Suppl: S16-S28
57 **Chan KT**, Lung ML. Mutant p53 expression enhances drug resistance in a hepatocellular carcinoma cell line. *Cancer Chemother Pharmacol* 2004; **53**: 519-526
58 **Li YX**, Lin ZB, Tan HR. Wild type p53 increased chemo-sensitivity of drug-resistant human hepatocellular carcinoma Bel7402/5-FU cells. *Acta Pharmacol Sin* 2004; **25**: 76-82
59 **Zhang X**, Godbey WT. Viral vectors for gene delivery in tissue engineering. *Adv Drug Deliv Rev* 2006; **58**: 515-534
60 **Büning H**, Ried MU, Perabo L, Gerner FM, Huttner NA, Enssle J, Hallek M. Receptor targeting of adeno-associated virus vectors. *Gene Ther* 2003; **10**: 1142-1151
61 **Miyazaki M**, Obata Y, Abe K, Furusu A, Koji T, Tabata Y, Kohno S. Gene transfer using nonviral delivery systems. *Perit Dial Int* 2006; **26**: 633-640
62 **Palmer DH**, Mautner V, Mirza D, Oliff S, Gerritsen W, van der Sijp JR, Hubscher S, Reynolds G, Bonney S, Rajaratnam R, Hull D, Horne M, Ellis J, Mountain A, Hill S, Harris PA, Searle PF, Young LS, James ND, Kerr DJ. Virus-directed enzyme prodrug therapy: intratumoral administration of a replication-deficient adenovirus encoding nitroreductase to patients with resectable liver cancer. *J Clin Oncol* 2004; **22**: 1546-1552
63 **Kodama K**, Katayama Y, Shoji Y, Nakashima H. The features and shortcomings for gene delivery of current non-viral carriers. *Curr Med Chem* 2006; **13**: 2155-2161
64 **Noireaux V**, Libchaber A. A vesicle bioreactor as a step toward an artificial cell assembly. *Proc Natl Acad Sci USA* 2004; **101**: 17669-17674
65 **Kim JW**, Lee HS. Tumor targeting by doxorubicin-RGD-4C peptide conjugate in an orthotopic mouse hepatoma model. *Int J Mol Med* 2004; **14**: 529-535
66 **Barraud L**, Merle P, Soma E, Lefrançois L, Guerret S, Chevallier M, Dubernet C, Couvreur P, Trépo C, Vitvitski L. Increase of doxorubicin sensitivity by doxorubicin-loading into nanoparticles for hepatocellular carcinoma cells in vitro and in vivo. *J Hepatol* 2005; **42**: 736-743
67 **Tada M**, Hatano E, Taura K, Nitta T, Koizumi N, Ikai I, Shimahara Y. High volume hydrodynamic injection of plasmid DNA via the hepatic artery results in a high level of gene expression in rat hepatocellular carcinoma induced by diethylnitrosamine. *J Gene Med* 2006; **8**: 1018-1026
68 **Meyer F**, Ball V, Schaaf P, Voegel JC, Ogier J. Polyplex-embedding in polyelectrolyte multilayers for gene delivery. *Biochim Biophys Acta* 2006; **1758**: 419-422
69 **Uto H**, Ido A, Hori T, Hirono S, Hayashi K, Tamaoki T, Tsubouchi H. Hepatoma-specific gene therapy through retrovirus-mediated and targeted gene transfer using an adenovirus carrying the ecotropic receptor gene. *Biochem Biophys Res Commun* 1999; **265**: 550-555
70 **Min KA**, Lee SK, Kim CK. Improved gene expression pattern using Epstein-Barr virus (EBV)-based plasmid and cationic emulsion. *Biomaterials* 2005; **26**: 1063-1070
71 **Wilson GM**, Deeley RG. An episomal expression vector system for monitoring sequence-specific effects on mRNA stability in human cell lines. *Plasmid* 1995; **33**: 198-207
72 **Kim YI**, Chung JW, Park JH, Han JK, Hong JW, Chung H. Intraarterial gene delivery in rabbit hepatic tumors: transfection with nonviral vector by using iodized oil emulsion. *Radiology* 2006; **240**: 771-777
73 **Cherubini G**, Petouchoff T, Grossi M, Piersanti S, Cundari E, Saggio I. E1B55K-deleted adenovirus (ONYX-015) overrides G1/S and G2/M checkpoints and causes mitotic catastrophe and endoreduplication in p53-proficient normal cells. *Cell Cycle* 2006; **5**: 2244-2252
74 **O'Shea CC**, Johnson L, Bagus B, Choi S, Nicholas C, Shen

A, Boyle L, Pandey K, Soria C, Kunich J, Shen Y, Habets G, Ginzinger D, McCormick F. Late viral RNA export, rather than p53 inactivation, determines ONYX-015 tumor selectivity. *Cancer Cell* 2004; **6**: 611-623

75 **Gonçalves MA**, de Vries AA. Adenovirus: from foe to friend. *Rev Med Virol* 2006; **16**: 167-186

76 **Zhang LQ**, Mei YF, Wadell G. Human adenovirus serotypes 4 and 11 show higher binding affinity and infectivity for endothelial and carcinoma cell lines than serotype 5. *J Gen Virol* 2003; **84**: 687-695

77 **Ebner K**, Rauch M, Preuner S, Lion T. Typing of human adenoviruses in specimens from immunosuppressed patients by PCR-fragment length analysis and real-time quantitative PCR. *J Clin Microbiol* 2006; **44**: 2808-2815

78 **Jacobs SC**, Davison AJ, Carr S, Bennett AM, Phillpotts R, Wilkinson GW. Characterization and manipulation of the human adenovirus 4 genome. *J Gen Virol* 2004; **85**: 3361-3366

79 **Bos JL**, Jochemsen AG, Bernards R, Schrier PI, van Ormondt H, van der Eb AJ. Deletion mutants of region E1a of AD12 E1 plasmids: effect on oncogenic transformation. *Virology* 1983; **129**: 393-400

80 **Wills KN**, Maneval DC, Menzel P, Harris MP, Sutjipto S, Vaillancourt MT, Huang WM, Johnson DE, Anderson SC, Wen SF. Development and characterization of recombinant adenoviruses encoding human p53 for gene therapy of cancer. *Hum Gene Ther* 1994; **5**: 1079-1088

81 **Nishizaki M**, Fujiwara T, Tanida T, Hizuta A, Nishimori H, Tokino T, Nakamura Y, Bouvet M, Roth JA, Tanaka N. Recombinant adenovirus expressing wild-type p53 is antiangiogenic: a proposed mechanism for bystander effect. *Clin Cancer Res* 1999; **5**: 1015-1023

82 **Heise C**, Sampson-Johannes A, Williams A, McCormick F, Von Hoff DD, Kirn DH. ONYX-015, an E1B gene-attenuated adenovirus, causes tumor-specific cytolysis and antitumoral efficacy that can be augmented by standard chemotherapeutic agents. *Nat Med* 1997; **3**: 639-645

83 **Rothmann T**, Hengstermann A, Whitaker NJ, Scheffner M, zur Hausen H. Replication of ONYX-015, a potential anticancer adenovirus, is independent of p53 status in tumor cells. *J Virol* 1998; **72**: 9470-9478

84 **Stoff-Khalili MA**, Dall P, Curiel DT. Gene therapy for carcinoma of the breast. *Cancer Gene Ther* 2006; **13**: 633-647

85 **Li G**, Sham J, Yang J, Su C, Xue H, Chua D, Sun L, Zhang Q, Cui Z, Wu M, Qian Q. Potent antitumor efficacy of an E1B 55kDa-deficient adenovirus carrying murine endostatin in hepatocellular carcinoma. *Int J Cancer* 2005; **113**: 640-648

86 **Qian Q**, Sham J, Che X, Xu J, Xue H, Cui Z, Zhu B, Wu M. Gene-viral vectors: a promising way to target tumor cells and express anticancer genes simultaneously. *Chin Med J (Engl)* 2002; **115**: 1213-1217

87 **Li GC**, Yang JM, Nie MM, Su CG, Sun LC, Qian YZ, Fang GE, Sham J, Wu MC, Qian QJ. Potent antitumoral effects of a novel gene-viral therapeutic system CNHK300-mEndostatin in hepatocellular carcinoma. *Chin Med J (Engl)* 2005; **118**: 179-185

88 **Ye Z**, Wang X, Hao S, Zhong J, Xiang J, Yang J. Oncolytic adenovirus-mediated E1A gene therapy induces tumor-cell apoptosis and reduces tumor angiogenesis leading to inhibition of hepatocellular carcinoma growth in animal model. *Cancer Biother Radiopharm* 2006; **21**: 225-234

89 **Yoon SK**, Armentano D, Wands JR, Mohr L. Adenovirus-mediated gene transfer to orthotopic hepatocellular carcinomas in athymic nude mice. *Cancer Gene Ther* 2001; **8**: 573-579

90 **Kuriyama S**, Yoshiji H, Nakai S, Deguchi A, Uchida N, Kimura Y, Inoue H, Kinekawa F, Ogawa M, Nonomura T, Masaki T, Kurokohchi K, Watanabe S. Adenovirus-mediated gene transfer into rat livers: comparative study of retrograde intrabiliary and antegrade intraportal administration. *Oncol Rep* 2005; **13**: 69-74

91 **White SA**, LoBuglio AF, Arani RB, Pike MJ, Moore SE, Barlow DL, Conry RM. Induction of anti-tumor immunity by intrasplenic administration of a carcinoembryonic antigen DNA vaccine. *J Gene Med* 2000; **2**: 135-140

92 **Xie X**, Forsmark CE, Lau JY. Effect of bile and pancreatic juice on adenoviral-mediated gene delivery: implications on the feasibility of gene delivery through ERCP. *Dig Dis Sci* 2000; **45**: 230-236

93 **Atencio IA**, Grace M, Bordens R, Fritz M, Horowitz JA, Hutchins B, Indelicato S, Jacobs S, Kolz K, Maneval D, Musco ML, Shinoda J, Venook A, Wen S, Warren R. Biological activities of a recombinant adenovirus p53 (SCH 58500) administered by hepatic arterial infusion in a Phase 1 colorectal cancer trial. *Cancer Gene Ther* 2006; **13**: 169-181

94 **Roth JA**. Adenovirus p53 gene therapy. *Expert Opin Biol Ther* 2006; **6**: 55-61

95 **Roche A**, Franco D, Dhumeaux D, Bismuth H, Doyon D. Emergency hepatic arterial embolization for secondary hypercalcemia in hepatocellular carcinoma. *Radiology* 1979; **133**: 315-316

96 **Suzuki K**, Kono N, Ono A, Osuga Y, Kiyokawa H, Mineo I, Matsuda Y, Miyoshi S, Kawata S, Minami Y. Transcatheter arterial chemo-embolization for humoral hypercalcemia of hepatocellular carcinoma. *Gastroenterol Jpn* 1988; **23**: 29-36

97 **Strom E**, Sathe S, Komarov PG, Chernova OB, Pavlovska I, Shyshynova I, Bosykh DA, Burdelya LG, Macklis RM, Skaliter R, Komarova EA, Gudkov AV. Small-molecule inhibitor of p53 binding to mitochondria protects mice from gamma radiation. *Nat Chem Biol* 2006; **2**: 474-479

98 **Llanos S**, Efeyan A, Monsech J, Dominguez O, Serrano M. A high-throughput loss-of-function screening identifies novel p53 regulators. *Cell Cycle* 2006; **5**: 1880-1885

99 **Feitelson MA**, Pan J, Lian Z. Early molecular and genetic determinants of primary liver malignancy. *Surg Clin North Am* 2004; **84**: 339-354

100 **Zhu MH**, Ni CR, Zhu Z, Li FM, Zhang SM. Determination of expression of eight p53-related genes in hepatocellular carcinoma with tissue microarrays. *Ai Zheng* 2003; **22**: 680-685

101 **Attallah AM**, Abdel-Aziz MM, El-Sayed AM, Tabll AA. Detection of serum p53 protein in patients with different gastrointestinal cancers. *Cancer Detect Prev* 2003; **27**: 127-131

102 **Maron DJ**, Tada H, Moscioni AD, Tazelaar J, Fraker DL, Wilson JM, Spitz FR. Intra-arterial delivery of a recombinant adenovirus does not increase gene transfer to tumor cells in a rat model of metastatic colorectal carcinoma. *Mol Ther* 2001; **4**: 29-35

103 **Smith L**, Byers JF. Gene therapy in the post-Gelsinger era. *JONAS Healthc Law Ethics Regul* 2002; **4**: 104-110

104 **Walters J**. Why did Jesse die? *Update* 2001; **17**: E1

105 **Vinyals A**, Peinado MA, Gonzalez-Garrigues M, Monzó M, Bonfil RD, Fabra A. Failure of wild-type p53 gene therapy in human cancer cells expressing a mutant p53 protein. *Gene Ther* 1999; **6**: 22-33

106 **Moretti F**, Nanni S, Farsetti A, Narducci M, Crescenzi M, Giuliacci S, Sacchi A, Pontecorvi A. Effects of exogenous p53 transduction in thyroid tumor cells with different p53 status. *J Clin Endocrinol Metab* 2000; **85**: 302-308

107 **Moretti F**, Farsetti A, Soddu S, Misiti S, Crescenzi M, Filetti S, Andreoli M, Sacchi A, Pontecorvi A. p53 re-expression inhibits proliferation and restores differentiation of human thyroid anaplastic carcinoma cells. *Oncogene* 1997; **14**: 729-740

108 **Miao J**, Chen GG, Chun SY, Yun JP, Chak EC, Ho RL, Lai PB. Adenovirus-mediated tBid overexpression results in therapeutic effects on p53-resistant hepatocellular carcinoma. *Int J Cancer* 2006; **119**: 1985-1993

109 **Luo X**, Budihardjo I, Zou H, Slaughter C, Wang X. Bid, a Bcl2 interacting protein, mediates cytochrome c release from mitochondria in response to activation of cell surface death receptors. *Cell* 1998; **94**: 481-490

S- Editor Liu Y **L- Editor** Wang XL **E- Editor** Lu W

PO Box 2345, Beijing 100023, China
www.wjgnet.com
wjg@wjgnet.com

World J Gastroenterol 2007 February 21; 13(7): 993-996
World Journal of Gastroenterology ISSN 1007-9327

REVIEW

Metallothionein: An overview

N Thirumoorthy, KT Manisenthil Kumar, A Shyam Sundar, L Panayappan, Malay Chatterjee

N Thirumoorthy, College of Pharmacy, Kovai Estate, Kalapatti Road, Tamilnadu, India
KT Manisenthil Kumar, A Shyam Sundar, L Panayappan, Malay Chatterjee, Department of Pharmaceutical Technology, Jadavpur University, Kolkata, India
Correspondence to: N Thirumoorthy, KMCH, College of Pharmacy, Kovai Estate, Kalapatti Road, Coimbatore 641 035, Tamilnadu, India. tmoorthyn@yahoo.com
Telephone: +91-98-43255552 Fax: +91-422-2628645
Received: 2006-07-27 Accepted: 2007-01-10

Abstract

Metallothioneins (MTs) were discovered in 1957 by Margoshes and Vallee and identified as low-molecular weight and sulphydryl rich proteins. It is not surprising that most mammalian tissues contain age related basal levels of MTs since they are involved in metalloregulatory processes that include cell growth and multiplication. In an effort to understand the biology of this intriguing tumor, various biomarkers such as oncogenes, p53 tumor suppressor gene, waf 1 protein, proliferating cell nuclear antigen, telomerase, microsatellite markers and cytogenetic changes have been examined. One biomarker which has recently shown to be expressed in various human tumors but still less reported in carcinoma is MT. Immunohistochemical detection of MT proteins in cold acetone-fixed paraffin embedded liver sections was performed by the streptavidin-avidin-biotin immuno-peroxidase complex method.

Key words: Metallothioneins; Protective function; Immuno-histochemical detection; Anti-oxidant character; Metal regulatory gene; Oncogene; Apoptosis; Genotoxic; Non-genotoxic environment; Detoxification

Thirumoorthy N, Manisenthil Kumar KT, Shyam Sundar A, Panayappan L, Chatterjee M. Metallothionein: An overview. *World J Gastroenterol* 2007; 13(7): 993-996

http://www.wjgnet.com/1007-9327/13/993.asp

INTRODUCTION

Metallothioneins (MTs) were discovered in 1957 by Margoshes and Vallee and identified as low-molecular weight sulphydryl rich proteins. Due to their high metal content and unusual bioinorganic structure, they are distinguished as metalloproteins. It is not surprising that most mammalian tissues contain age related basal levels of MTs since they are involved in metalloregulatory processes that include cell growth and multiplication. The presence of high levels of MTs in developing mammalian cells is well documented and it has been suggested that the MT-expressed protein is similar to onco-developmental gene products such as alpha-fetoprotein[1].

Classification of MTs

MT is a small protein with a high affinity for divalent heavy metal ions. MTs are a family of Mr 6000 proteins comprised of MT-Ⅰ, MT-Ⅱ, MT-Ⅲ and MT-Ⅳ classes with multiple isoforms within each class. MT-Ⅰ and MT-Ⅱ are ubiquitously expressed and are stress inducible. MT-Ⅰ isoform inducibility is reported to depend on the embryonic germ layer from which a tumor is derived[2].

MTs are a group of ubiquitous low molecular mass cysteine-rich intracellular metal binding proteins. In human, MTs are encoded by a family of genes consisting of 10 functional MT isoforms and the encoded proteins are conventionally subdivided into four groups: MT-1, MT-2, MT-3 and MT-4 proteins. While a single MT-2A gene encodes MT-2 protein, MT-1 protein comprises many subtypes encoded by a set of MT-1 genes (MT-1A, MT-1B, MT-1E, MT-1F, MT-1G, MT-1H and MT-1X), accounting for the micro-heterogeneity of the MT-1 protein. Different MT genes in humans possibly play different functional roles during development or under various physiological conditions[3,4].

The known functions of MTs include metalloregulatory roles in cell growth and differentiation, and enhanced synthesis of MTs in rapidly proliferating tissues suggests its crucial role in normal and neoplastic cell growth[5].

Characteristics of MTs

These intracellular proteins are characterized by their unusual high cysteine content (30%) and lack of aromatic amino acids. Because of their rich thiol content, MTs bind a number of trace metals including cadmium, mercury, platinum and silver, and also protect cells and tissues against heavy metal toxicity. Additionally MTs are among the most abundant intracellular aspects for biologically essential metals, zinc and copper. MT metal-thiolate fractions being dynamic and of high affinity also facilitate metal exchange in tissues[6].

They are present in a great variety of eukaryotes[3], functioning as anti-oxidants; they also play a protective role against hydroxyl free radicals. This is relevant in tumors (nasopharyngeal carcinoma) which are known to be

markedly radio-sensitive, where radiotherapy (which kills cells *via* free-radical-induced apoptosis) is the treatment of choice[7].

MT AS TUMOR MARKER

Alteration in MT function due to carcinogenesis

Development of carcinogenesis is a dynamic process in which irregulation of gene function occurs. Time is crucial in this process. During a latency period of several years or even decades, the genetic material of cells is subject to multiple 'hits' by damaged substances, carcinogens, etc. Accumulation of damage leads to altered gene function and colonal expansion of mutated cells. However, most of these early lesions never develop into more aggressive and invasive states, but disappear spontaneously. This feature of carcinogenesis does not solely influence the initial phase of this process but actively intervenes and changes the course of the disease[5].

Protective functions of MT

MTs have a high binding affinity to bivalent metal ions. A number of studies have demonstrated the presence or enhanced synthesis of MT in rapidly proliferating normal cells, regenerating cells and cancer cells. The studies have suggested a relationship between high expression of MT protein and aggressive neoplastic cell growth. Due to their nucleophilicity, MTs have been shown to protect cells against the cytotoxic effects of electrophilic anticancer drugs. However, protection of cells by MT from the cytotoxic effect of agents such as 1-β-D-arabinofuranosyl cytosine and nuclear factor DF-α must involve mechanisms other than simple covalent binding[8].

Relation between MT and apoptosis

Recent reports of various studies have shown that the enhanced expression of MT in cells induces the anti-apoptotic effects and a lack of MT in MT null cells increases the susceptibility to apoptic cell death after exposure to certain anticancer drugs. The down-regulation of MT in MCF-7 cells within 18-mer antisense has not only shown inhibition in growth but also initiated apoptosis[8].

MTs INVOLVED IN PATHOPHYSIOLOGICAL PROCESSES IN HUMAN

Role of MT in detoxification

MTs play a homeostatic role in the control and detoxification of the heavy metals; several evidences indicate that MT has the capacity to scavenge reactive oxygen metabolite (ROM), particularly the hydroxyl radical. These substances which are produced continuously during normal aerobic metabolism may become noxious in situations of imbalance with endogenous antioxidants and then can induce DNA damage, lipid peroxidation, enzyme oxidation, *etc.*, leading to cellular destruction, chromosomal aberrations and finally to cancer. Paradoxically, by anticancer treatment such as radiotherapy, chemotherapy and photodynamic therapy, tumor cells are killed by generating toxic amounts of ROM[2].

MT was considered as a potential prognostic marker in invasive ductal carcinoma of the breast[9], skin[10], cervix[11] and pancreas[12]. Irregular cell growth, due to increased cell proliferation or failure of cells to undergo apoptosis is recognized as a major contributory factor to the malignant process.

Dual functions of MT

MTs appear to perform dual functions of influencing the growth and survival of tumor cells as they are known to have metallo-regulatory functions in cellular repair processes, growth and differentiation and to play a protective role in oxidative stress by scavenging free radicals, thus protecting the cell against apoptosis induced by oxidative stress. MT can be induced by a number of endogenous and exogenous stimuli including glucocorticoids, interferon, interleukin-1, progesterone, vitamin D_3 endotoxins, serum factors, and heavy metals, storage of metal ions and regulation of cellular zinc[1].

MT and its response to anti-cancer drugs

The association of MT expression with spontaneous mutagenesis response to anti-cancer drugs and tumor progression has emerged in recent years. This has been more significant in the later stage, with reliable methods for detecting the two isoforms of MT-Ⅰ and MT-Ⅱ by immunohistochemistry in archival tissues. MT over expression has been associated with more malignant and higher grade tumors in some cancers and with more differentiated lower grade tumors in others[6].

Over expression of MT

The *in vitro* studies suggest that MT over expression in ovarian cancer may induce chemo-resistance. It has been proposed that the sequestration of drugs or their metabolites may prevent the reaction of these compounds with the respective intracellular target, thus decreasing the efficacy of certain anti-cancer drugs.

Recurrence of drug resistant ovarian tumors that initially appear to respond well to chemotherapy may be explained by over expression of drug resistance proteins such as MT.

Another opinion of the same investigators is that growth factor signals might activate transcription factors that control the expression of drug-resistant enzymes and proteins. However, two independent groups of investigators were unable to find a direct causal relationship between MT expression and chemo-resistance[1].

Genotoxic and non-genotoxic effects

Humans are exposed to mixtures of genotoxic and non-genotoxic environmental chemicals that may be linked to cancer. Robust biomarkers of somatic stem cell mutation and mutant clonal expansion may provide cancer surrogates that are useful for risk assessment. Acquired mutation of a selectable endogenous reporter gene like glucose-6-phosphate dehydrogenase (G6PD) within a colonic crypt stem cell induces a crypt-restricted phenotype change.

Stem cell mutation

Stable crypt-restricted immunopositivity for MT is a recently described stem cell mutation marker for mouse colon that can be assayed in paraffin-fixed tissue sections and has been validated against the G6PD assay. MT-immunopositive crypt frequency has shown a dose response to three different chemical mutagens that further confirmed the evidence that it is a somatic mutation marker[13].

Low levels of MTs and their susceptibility

Accumulating evidence indicates that cells with low levels of intracellular MT are more susceptible to DNA damage and apoptotic death after exposure to stress stimuli including oxidative stress, whereas prior induction of MT appears to confer protection. The findings of changes in unicellular localization of MT from cytoplasm to the nucleus during early differention of myoblasts coincide with increased apoptosis of newly formed myotubes[14].

Markers of carcinogenesis

The basal expression of MT in normal cells has generally been associated with heavy metal detoxification, intracellular trace elements storage and scavenging of free radicals. Authors Tridip and Thirumoorthy studied the roles of alterations of hepatic levels of trace elements and significance of the expression of MT and Ki-67 proteins as important markers of carcinogenesis in the development of pre-malignant phenotype and the reported dose (0.5 ppm) of vanadium in suppressing 2-AAF-induced carcinogenicity. Several reports are available to show that, over expression and up-regulation of MT and Ki-67 proteins are associated with the carcinogenic processes. But the reports documenting the anti-neoplastic potential of chemo-preventive agents in modulating these indicts are meager.

It was reported that the chemo-preventive potential of vanadium is suppressing in MT and Ki-67 expression in preneoplastic rat liver. The role of vanadium on p53 expression and induction of apoptosis in a defined rat model of experimental hepato-carcinogenesis has also been brought into focus[15].

MT as anti-oxidants

MTs can function as antioxidants. It has been suggested that intracellular oxidants may play a role in anticancer drug mediated programmed cell death and it was observed that MT expression can be regulated by ambient oxygen levels. This has led to speculation that MT may be an inducible anti-apoptotic gene product[6].

Proteins like MT may play an important role in carcinogenesis, including tumor cell pathology and drug resistance. It was shown that colorectal and gastric carcinogenesis was associated with a significant increase in the level of manganese (Mn-SOD) containing superoxide dismutase, an antioxidant enzyme that detoxifies superoxide to hydrogen peroxide[2].

Factors influencing synthesis of MT

The synthesis of MT is regulated by polymorphic genes and induced by many factors such as metals, hormones, cytokinen, drugs and physical and oxidative stresses. Tumor MT levels have also been reported to correlate with resistance to anticancer reagent[16].

MT regulates intracellular concentration of zinc and other metal ions. MT over expression can influence transcription, replication and protein synthesis, and might explain why MT over expression is associated with high-grade tumors, including carcinomas of the head and neck[17].

IMMUNOSTAINING OF MT

Positive control

Immunohistochemical detection of MT protein in cold acetone-fixed paraffin embedded liver sections was performed by the streptavidin-avidin-biotin-immuno peroxidase complex method (Jin *et al*, 2002). Briefly, 5 μm thin sections on poly-L-lysine coated slides were deparaffinized and rehydrated. Endogenous peroxidase activity was blocked with 1% H_2O_2 in 0.1 mol/L Tris-NaCl (pH 7.6) for 30 min. After incubation with 5% normal goat serum for 1 h at 37℃, sections were incubated overnight at 40C with the primary antibody rabbit anti-rat MT-1 in 1% BSA using 1:50 dilution. Sections were then incubated with a bio-tinylated secondary antibody goat anti-rabbit IgG (Sigma) for 30 min at 37℃ with 1:200 dilutions.

This was followed by incubation with streptavidin peroxidase (1:100) for 1 h and subsequent chromogen development with 0.5% of 3, 3'-diamino benzedrine tetra hydrochloride (DAB) and 0.33% H_2O_2 in 0.5 mol/L Tris-NaCl as substrate. The sections were then counterstained with Harris haematoxylin (H&E), then dehydrated, mounted and served as positive control.

Negative control

Negative control was prepared following the above steps but by omitting the primary antibody. MT immuno-staining was considered positive when the nuclei and cytoplasm of the hepatocytes were stained prominently (purplish brown/reddish brown). MT immunoreactivity was expressed as percentage of immuno-positive cells. A total of 10 high power fields were randomly chosen. The numbers of positive cells were determined in relation to the total number of cells in the field[15].

REFERENCES

1 **Tan Y**, Sinniah R, Bay BH, Singh G. Metallothionein expression and nuclear size in benign, borderline, and malignant serous ovarian tumours. *J Pathol* 1999; **189**: 60-65

2 **Janssen AM**, van Duijn W, Kubben FJ, Griffioen G, Lamers CB, van Krieken JH, van de Velde CJ, Verspaget HW. Prognostic significance of metallothionein in human gastrointestinal cancer. *Clin Cancer Res* 2002; **8**: 1889-1896

3 **Kägi JH**, Schäffer A. Biochemistry of metallothionein. *Biochemistry* 1988; **27**: 8509-8515

4 **Jin R**, Bay BH, Chow VT, Tan PH, Lin VC. Metallothionein 1E mRNA is highly expressed in oestrogen receptor-negative human invasive ductal breast cancer. *Br J Cancer* 2000; **83**: 319-323

5 **Jin R**, Chow VT, Tan PH, Dheen ST, Duan W, Bay BH. Metallothionein 2A expression is associated with cell proliferation in breast cancer. *Carcinogenesis* 2002; **23**: 81-86

6 **Kondo Y**, Woo ES, Michalska AE, Choo KH, Lazo JS. Metallothionein null cells have increased sensitivity to anticancer drugs. *Cancer Res* 1995; **55**: 2021-2023
7 **Jayasurya A**, Bay BH, Yap WM, Tan NG. Correlation of metallothionein expression with apoptosis in nasopharyngeal carcinoma. *Br J Cancer* 2000; **82**: 1198-1203
8 **Abdel-Mageed AB**, Agrawal KC. Activation of nuclear factor kappaB: potential role in metallothionein-mediated mitogenic response. *Cancer Res* 1998; **58**: 2335-2338
9 **Schmid KW**, Ellis IO, Gee JM, Darke BM, Lees WE, Kay J, Cryer A, Stark JM, Hittmair A, Ofner D. Presence and possible significance of immunocytochemically demonstrable metallothionein over-expression in primary invasive ductal carcinoma of the breast. *Virchows Arch A Pathol Anat Histopathol* 1993; **422**: 153-159
10 **Zelger B**, Hittmair A, Schir M, Ofner C, Ofner D, Fritsch PO, Böcker W, Jasani B, Schmid KW. Immunohistochemically demonstrated metallothionein expression in malignant melanoma. *Histopathology* 1993; **23**: 257-263
11 **Lim K**, Evans A, Adams M, Fish R, Dhundee J, Dallimone N, Jasani B. Association of immunohistochemically detachable metallothionein (IDMT) expression with malignant transformation in cervical neoplasia. *J pathol* 1996; **178**: 48A
12 **Ohshio G**, Imamura T, Okada N, Wang ZH, Yamaki K, Kyogoku T, Suwa H, Yamabe H, Imamura M. Immunohistochemical study of metallothionein in pancreatic carcinomas. *J Cancer Res Clin Oncol* 1996; **122**: 351-355
13 **Donnelly ET**, Bardwell H, Thomas GA, Williams ED, Hoper M, Crowe P, McCluggage WG, Stevenson M, Phillips DH, Hewer A, Osborne MR, Campbell FC. Metallothionein crypt-restricted immunopositivity indices (MTCRII) correlate with aberrant crypt foci (ACF) in mouse colon. *Br J Cancer* 2005; **92**: 2160-2165
14 **Lewin B**, Genes VI. Oxford-NewYork-Tokyo: Oxford University Press, 1997: 849-850
15 **Chakraborty T**, Samanta S, Ghosh B, Thirumoorthy N, Chatterjee M. Vanadium induces apoptosis and modulates the expressions of metallothionein, Ki-67 nuclear antigen, and p53 during 2-acetylaminofluorene-induced rat liver preneoplasia. *J Cell Biochem* 2005; **94**: 744-762
16 **Hishikawa Y**, Koji T, Dhar DK, Kinugasa S, Yamaguchi M, Nagasue N. Metallothionein expression correlates with metastatic and proliferative potential in squamous cell carcinoma of the oesophagus. *Br J Cancer* 1999; **81**: 712-720
17 **Raleigh JA**, Chou SC, Calkins-Adams DP, Ballenger CA, Novotny DB, Varia MA. A clinical study of hypoxia and metallothionein protein expression in squamous cell carcinomas. *Clin Cancer Res* 2000; **6**: 855-862

S- Editor Liu Y **L- Editor** Ma JY **E- Editor** Lu W

PO Box 2345, Beijing 100023, China
www.wjgnet.com
wjg@wjgnet.com

World J Gastroenterol 2007 February 21; 13(7): 997-1002
World Journal of Gastroenterology ISSN 1007-9327

Cytochrome P450 levels are altered in patients with esophageal squamous-cell carcinoma

I Bergheim, E Wolfgarten, E Bollschweiler, AH Hölscher, C Bode, A Parlesak

I Bergheim, C Bode, A Parlesak, Department of Physiology of Nutrition, Hohenheim University (140e), Stuttgart 70599, Germany
E Wolfgarten, E Bollschweiler, AH Hölscher, Department of Visceral and Vascular Surgery, University of Cologne, Cologne, Germany
Correspondence to: Ina Bergheim, PhD, Hohenheim University (140b), Fruwirthstrasse 12, Stuttgart 70599, Germany. bergheim@uni-hohenheim.de
Telephone: +49-711-45924102 Fax: +49-711-45924343
Received: 2006-08-10 Accepted: 2007-01-23

Abstract

AIM: To investigate the role of cytochrome P450 (CYP) in the carcinogenesis of squamous-cell carcinoma (SCC) in human esophagus by determining expression patterns and protein levels of representative CYPs in esophageal tissue of patients with SCC and controls.

METHODS: mRNA expression of CYP2E1, CYP2C, CYP3A4, and CYP3A5 was determined using RT-PCR in both normal and malignant esophageal tissues of patients with untreated esophageal SCC (n = 21) and in controls (n = 10). Protein levels of CYP2E1, CYP2C8, CYP3A4, and CYP3A5 were measured by Western blot.

RESULTS: Within the group of SCC patients, mRNA expression of CYP 3A4 and CYP2C was significantly lower in malignant tissue (-39% and -74%, respectively, $P < 0.05$) than in normal tissue. Similar results were found in CYP3A4 protein levels. Between groups, CYP3A4, CYP3A5, and CYP2C8 protein concentration was significantly higher in non-malignant tissue of SCC patients (4.8-, 2.9-, and 1.9-fold elevation, $P < 0.05$) than in controls. In contrast, CYP2E1 protein levels were significantly higher in controls than in SCC patients (+46%, $P < 0.05$).

CONCLUSION: Significant differences exist in protein levels of certain CYPs in non-malignant esophageal tissue (e.g. CYP2C8, CYP3A4, CYP3A5, and CYP2E1) between SCC patients and healthy subjects and may contribute to the development of SCC in the esophagus.

Key words: Squamous-cell carcinoma; Cytochrome P450; Western blot; RT-PCR; Human

Bergheim I, Wolfgarten E, Bollschweiler E, Hölscher AH, Bode C, Parlesak A. Cytochrome P450 levels are altered in patients with esophageal squamous-cell carcinoma. *World J Gastroenterol* 2007; 13(7): 997-1002

http://www.wjgnet.com/1007-9327/13/997.asp

INTRODUCTION

Worldwide, esophageal cancer is one of the ten most common cancers[1] with an overall 5-year survival rate of 3%-10%[2]. Although the entity of adenocarcinoma is rising[3], the majority of carcinomas of the esophagus are squamous-cell carcinoma (SCC)[1]. Results of several epidemiological studies indicate that hot beverage, alcohol and tobacco are key risk factors for the development of carcinoma in the esophagus[1,4]. However, despite intense research[5], the role of xenobiotica-metabolizing enzymes in the development of esophageal SCC is not fully understood due to the lack of successful pharmacological therapies.

Cytochrome P450 (CYP) is a multi-gene superfamily of heme-containing enzymes catalyzing the oxidative metabolism of many compounds[6]. CYP families 1, 2, and 3, which are the main CYP families participating in the metabolism of xenobiotics, are highly expressed within the liver. However, several CYPs have been shown to be also expressed in extrahepatic tissues such as the esophagus[7]. CYPs not only function in the detoxification but may also be involved in the activation of potential (pro-) carcinogens. The alimentary tract is exposed to a large variety of compounds, including potential (pro-) carcinogens. Indeed, it has been proposed that extrahepatic tissue might play an important role in the CYP-mediated metabolism of xenobiotic compounds and therefore might affect the susceptibility of certain organs to the development of malignancies. However, knowledge on regulation and localization of CYPs outside the liver (i.e., the esophagus) is limited and should be clarified.

CYPs may play a critical role not only in the development of SCC in the esophagus but also in the treatment of SCC. Therefore, the aim of the present study was to determine mRNA expression and protein concentrations of representative CYPs (e.g., CYP2C, CYP2E1, CYP3A4, and CYP3A5) in macroscopically normal esophageal tissue of patients with untreated SCC and in disease-free controls. Furthermore, as the expression of CYPs may be altered throughout the development of carcinoma, levels of CYPs were also

measured in SCC and compared to those determined in macroscopically normal neighboring esophageal tissue of the same patients.

MATERIALS AND METHODS

Subjects and tissue specimens

The study was approved by the Ethics Committee of the Medical Clinic of the University of Cologne, Germany. Informed consent was obtained from all subjects included in the study. All subjects underwent endoscopy for medical screening. Of the 31 subjects enrolled, 21 had an untreated SCC of the esophagus. Ten subjects with a negative diagnosis of SCC in the esophagus or malignancies in the gastrointestinal tract and no history of esophageal SCC or other malignancies served as controls. Only subjects without medication known to affect expression of the investigated CYPs were included in the current study. All study participants completed a questionnaire concerning smoking and anthropometrical parameters (Table 1). Using a standard pinch forceps, two biopsies were obtained from macroscopically normal esophageal tissue of controls and patients with SCC. Furthermore, in SCC subjects two biopsies were taken from carcinoma. Biopsies were placed immediately in liquid nitrogen, and stored at -80℃ until analysis. Histopathological analysis of SCC was performed by an experienced pathologist. Tumor staging was based on differentiation and varied from poorly differentiated (G1: n = 2, G1-2: n = 2), moderately differentiated (G2: n = 8, G2-3: n = 4) to well differentiated (G3: n = 5). In controls, the absence of SCC, inflammation, and any other pathological changes of the esophagus were confirmed endoscopically by an experienced physician.

Table 1 Characteristics of untreated esophageal SCC patients and controls (mean ± SE)

Parameter	Patients	Controls	*P*
n	21	10	
Age	56.7 ± 1.9	51.1 ± 3.5	0.118
Sex (Female/Male)	7/14	5/5	0.425
BMI	23.8 ± 1.4	25.1 ± 0.6	0.370
Cigarette usage (Yes/No)	10/11	3/7	0.242

BMI: body mass index.

Isolation of total RNA-protein

Both total RNA and protein were isolated using Trizol reagent following the instructions of the manufacturer (Invitrogene, Gaithersburg, MD, USA). Briefly, tissue was homogenized in Trizol reagent, chloroform was added and phases were separated into RNA and protein phases. RNA was precipitated using isopropanol, washed with ethanol and resuspended in RNAase-free water. Protein was precipitated using isopropanol and washed three times in 0.3 mol/L guanidin hydrochlorid in 95% ethanol solution. The protein pellet was dried, resuspended and the concentration of protein in each sample was determined using a commercially available Bradford assay (BioRad, Munich, Germany).

Reverse transcription and PCR

Using a first-strand cDNA synthesis kit (Invitrogen, Gaithersburg, MD, USA) cDNA was synthesized from 200 ng of total RNA. For the amplification of CYPs the following primer sequences were used: CYP2C8-19, detecting CYP2C isoformes 8 to 19: sense GCTAAAGTCCAGGAAGAGATTGA and antisense TCCTGCTGAGAAAGGCATGAAGT[8]; CYP2E1: sense AGCACAACTCTGAGATATGG and antisense ATAGTCACTGTACTTGAACT[8]; CYP3A4: sense CCAAGCTATGCTCTTCACCG and antisense TCAGGCTCCACTTACGGTGC[9]; CYP3A5: sense TGTCCAGCAGAAACTGCAAA and antisense TTGAAGAAGTCCTTGCGTGTC [9] . The PCR reaction mixture consisted of 0.6 μL of cDNA, 10 × PCR buffer, 200 μmol/L dNTPs (Boehringer, Mannheim, Germany), BSA (0.25 mg/mL), DMSO (2% v/v), 0.5 μmol/LM of specific primer and 0.5 U Taq-polymerase (Promega, Madison, WI, USA), and water to a final volume of 10 μL. For amplification of the four cytochrome P450 cDNAs, PCR-conditions were as follows: at 94℃ for 3 s, at 45°C for 3 s, at 72℃ for 30 s, for 32 cycles. Amplification of histone 3.3 (primer sequences: sense CGTGCTAGCTGGATGTCTT and antisense CCACTGAACTTCTGATTCGC[10]) was performed applying the following conditions: at 94℃ for 3 s, at 45℃ for 3 s, and at 72℃ for 30 s, for 30 cycles. All measurements were carried out at least in duplicate in a rapid cycler (Idaho Tec., USA) within the linear range of the reaction. PCR products were separated in a 1.5% agarose gel, stained with ethidium bromide and photographed using a digital camera from Biometra (Goettingen, Germany). To ensure the success of PCR, human liver cDNA was used as a positive control. RT-PCR analysis was performed in triplicate, whenever possible. However, in case of a reduced mRNA availability, measurements were conducted in duplicate.

Immunoblot analysis

Antibodies used for the detection of CYP2E1 and CYP3A4 were a generous gift of Dr. M. Ingelman-Sundberg, Karolinska Institute, Stockholm, Sweden. Primary antibodies for the measurements of CYP2C8 and CYP3A5 were purchased from Chemicon, Inc. (Frankfurt, Germany).

On each blot, protein extracted from human liver was used as standard. Twenty to 30 μg of total protein and serial dilutions of standard protein (12.5, 25, and 50 μg) were separated by sodium dodecylsulphate-polyacryamide gel electrophoresis (SDS-PAGE) and transferred to nitrocellulose membranes. After blocked in 5% non-fat milk in Tris-buffered saline-Tween 20 (TBST, 0.01% v/v Tween 20), membranes were probed with dilutions of primary antibodies in TBS, followed by an incubation with the secondary antibody. The protein/antibody complex was visualized by enhanced chemiluminescence (SuperSignal® West Dura, Pierce, KTM, Bad Godesberg,

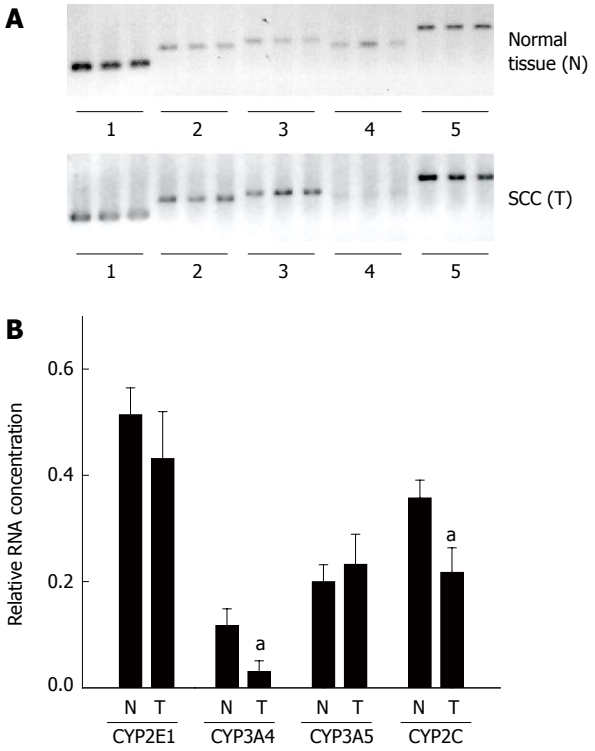

Figure 1 CYP3A5, CYP2E1, CYP3A4, and CYP2C mRNA expression in esophagus of untreated SCC patients. **A**: Representative photomicrograph of RT-PCR products of untreated esophageal SCC patients (N = normal esophageal tissue, T = tumor tissue obtained from SCC patients). Measurements were carried out either in triplicate or in case of reduced mRNA availability in duplicate. Lanes 1, 6: histone 3.3, lanes 2, 7: CYP2C, lanes 3, 8: CYP2E1, lanes 4, 9: CYP3A4, lanes 5, 10: CYP3A5; **B**: Densitometric analysis of CYP2C, CYP2E1, CYP3A4, and CYP3A5 mRNA expression in normal esophageal tissue and SCC. Results are normalized to histone 3.3 expression. Data are means ± SE. $^{a}P < 0.05$ *vs* normal tissue.

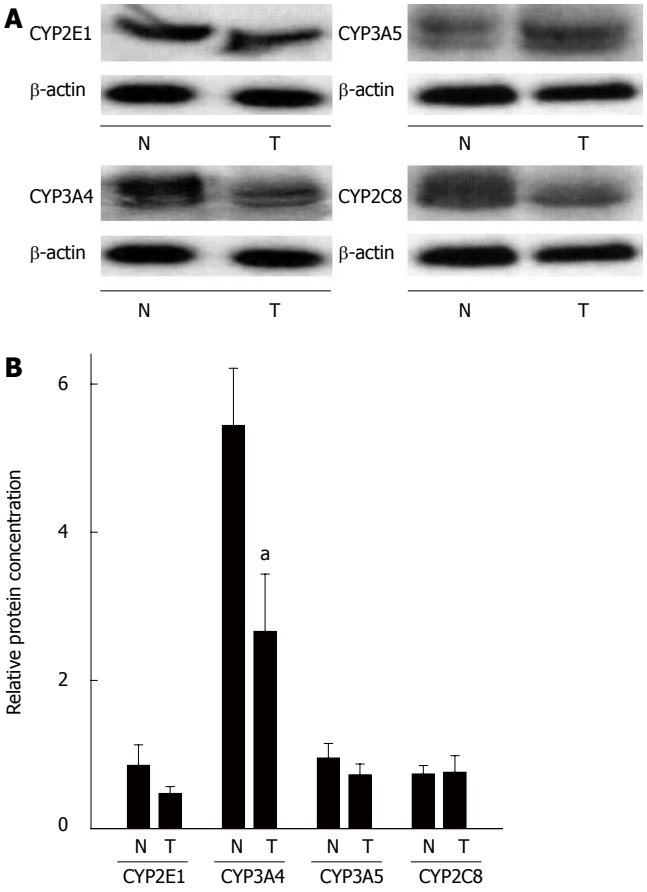

Figure 2 Protein levels of CYP2C8, CYP2E1, CYP3A4, and CYP3A5 in macroscopically normal tissue and SCC patients **A**: Representative Western blots of CYP2C8, CYP2E1, CYP3A4, and CYP3A5 in macroscopically normal esophageal tissue (N) and SCC (T) esophageal SCC patients; **B**: Quantitative analysis of blots. Results are normalized to β-actin. Data are means ± SE. $^{a}P < 0.05$ *vs* normal tissue.

Germany). Densitometric analysis was performed using the software AIDA (Raytest, Isotopenmessgeraete, Straubenhardt, Germany). Signal intensities of the samples were adjusted to the intensities of the serially diluted standards. To ensure equal loading, all blots were stained with Ponceau red. Haptene signals were normalized to β-actin using a commercially available antibody (Sigma Chemical Co., Munich, Germany).

Statistical analysis

Results are presented as means ± SE unless otherwise indicated. Fisher´s exact test was used to compare lifestyle data. The Mann-Whitney *U*-test was used for the comparison of relative mRNA concentration and protein levels measured in normal esophageal tissue obtained from patients with SCC and disease-free controls. Wilcoxon's *t*-test was used for the comparison of relative mRNA expression and protein concentration measured in normal esophageal tissue and SCC of the same patient. $P < 0.05$ was considered statistically significant.

RESULTS

The majority of the 31 patients were of normal weight and their age ranged from 38-71 years. No differences were found in smoking habits between patients and controls (Table 1).

CYP expression and protein levels in normal esophageal tissue and untreated esophageal SCC patients

High quality of undegraded mRNA from normal esophageal tissue and SCC was obtained from 12 out of 21 patients with esophageal SCC. Expression of histone 3.3 mRNA, used as housekeeping gene, was detected in all samples. The results of RT-PCR measurements are summarized in Figure 1. In addition to RNA measurements, protein levels of CYPs were determined in normal esophageal tissue and in patients with SCC (n = 21) (Figure 2).

CYP2E1: In SCC patients, expression of CYP2E1 did not differ between normal esophageal tissue and SCC. Similarly, no differences were found in CYP2E1 protein levels between normal tissue and SCC.

CYP 3A5: CYP3A5 mRNA expression and CYP3A5 protein levels were comparable in normal esophageal tissue and SCC.

CYP2 (8-19): Expression of CYP2C (8-19) was significantly lower in tissue obtained from SCC patients that in normal neighboring esophageal tissue. Specifically, mRNA expression of CYP2C (8-19) was about 39%

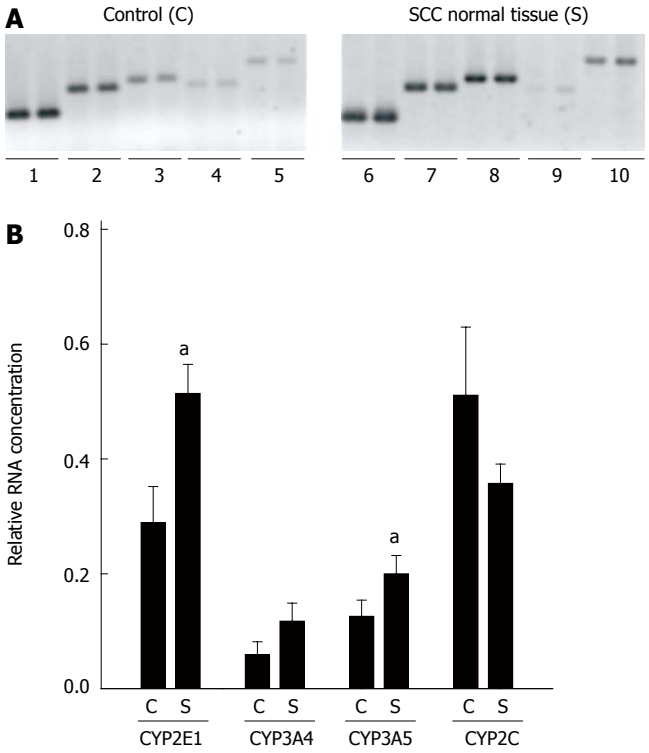

Figure 3 Expression of CYP2C8, CYP2E1, CYP3A4, and CYP3A5 in macroscopically normal tissue of SCC patients and controls. **A**: Representative photomicrograph of RT-PCR products determined in normal tissue of patients with untreated esophageal SCC (S) and controls (C). All measurements were carried out in dupilcate. Lanes 1, 6: histone 3.3, lanes 2, 7: CYP2C, lanes 3, 8: CYP2E1, lanes 4, 9: CYP3A4, lanes 5, 10: CYP3A5; **B**: Quantitative analysis of CYP2C, CYP2E1, CYP3A4, and CYP3A5 mRNA expression in normal esophageal tissue of SCC patients and controls. Results are normalized to histone 3.3 expression. Data are means ± SE. $^aP < 0.05$ *vs* normal tissue.

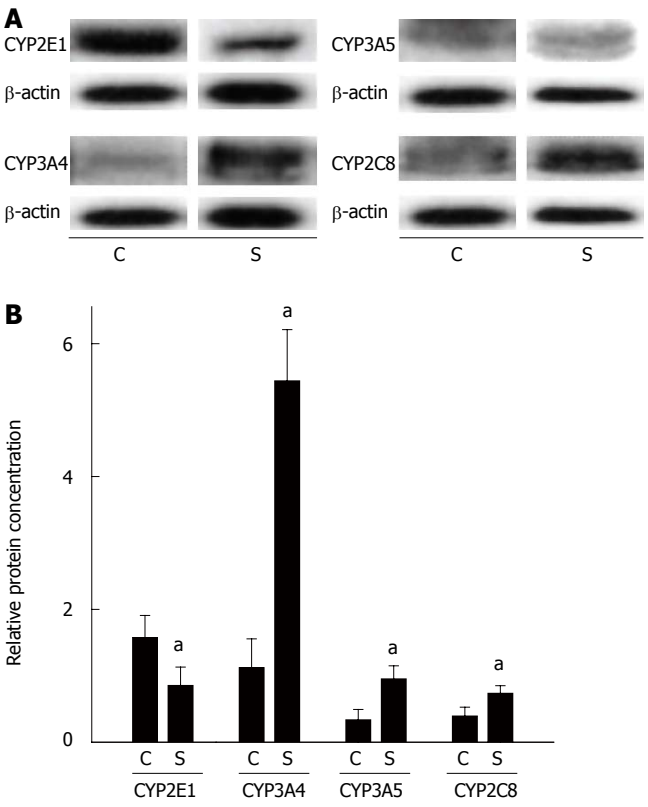

Figure 4 CYP3A5, CYP2E1, CYP3A4, and CYP2C protein levels in esophagus of SCC patients and disease-free controls. **A**: Representative Western blot of CYPs determined in normal tissue of untreated esophageal SCC patients (S) and disease-free controls (C); **B**: Quantitative analysis of CYP2C, CYP2E1, CYP3A4, and CYP3A5 protein levels in normal esophageal tissue of SCC patients and disease-free controls. Results are normalized to β-actin. Data are means ± SE. $^aP < 0.05$ *vs* disease-free controls.

lower ($P < 0.05$) in tissue of SCC patients than in normal tissue. In addition, protein concentration of CYP2C8 was determined, however no differences were found between SCC and normal tissue.

CYP3A4: CYP3A4 mRNA expression was significantly lower in SCC than in normal neighboring esophageal tissue. Specifically, mRNA expression of CYP3A4 was about 74 % lower in SCC than in normal tissue ($P < 0.05$). Furthermore, protein levels of CYP3A4 were significantly lower (by about 51%) in SCC than in normal esophageal tissue ($P < 0.05$).

Expression and protein levels of CYPs in normal esophageal tissue of SCC patients and controls

Furthermore, expression of CYP2C, CYP2E1, CYP3A4, and CYP3A5 mRNA and CYP2C8, CYP2E1, CYP3A4, as well as CYP3A5 protein concentrations were determined in normal esophageal tissue of untreated SCC patients ($n = 21$) and compared with those in 10 disease-free controls. Representative agarose gels depicting RT-PCR measurements and semiquantitative analysis of RT-PCR are shown in Figure 3. Expression of the housekeeping gene histone 3.3 was detected in all samples. Results of the comparisons of protein levels are summarized in Figure 4.

CYP2E1: Expression of CYP2E1 was found to be significantly higher by about 43 % in normal tissue obtained from patients with esophageal SCC than in disease-free controls ($P < 0.05$). Interestingly, CYP2E1 protein levels were significantly lower in normal tissue of SCC patients than in esophageal tissue obtained from disease-free controls (about -46%, $P < 0.05$).

CYP3A5: Expression of CYP3A5 mRNA in normal esophageal tissue was about 37 % higher in tissue obtained from SCC patients than in controls. Similar differences were found in protein levels, with protein levels of CYP3A5 being significantly higher by about 2.9-fold in normal esophageal tissue obtained from patients with esophageal SCC than in controls ($P < 0.05$).

CYP2C (8-19): No differences were found in CYP2C (8-19) mRNA expression between normal tissue of patients with esophageal SCC and controls. CYP2C8 protein levels were about 1.9-fold higher in normal tissue of SCC patients than in controls ($P < 0.05$).

CYP3A4: Similar to CYP2C (8-19), mRNA expression did not differ between normal tissue of patients with SCC and controls. However, when protein levels of CYP3A4 were compared between normal tissue of patients with SCC and controls, CYP3A4 protein concentration was found to be about 4.8-fold higher in normal tissue of SCC patients than in controls ($P < 0.05$).

Table 2 Correlation between mRNA expression and protein levels of CYP2E1, CYP3A4, CYP3A5, and CYP2C8 in normal esophageal tissue and SCC

Normal esophageal tissue	Spearmen R	*P*
CYP2E1	-0.09	0.72
CYP3A4	0.07	0.76
CYP3A5	0.19	0.41
CYP2C8	0.07	0.76
Esophageal SCC		
CYP2E1	0.02	0.96
CYP3A4	0.16	0.65
CYP3A5	0.49	0.15
CYP2C8	-0.22	0.53

Relation of protein levels and mRNA expression of CYPs in normal esophageal mucosa of SCC patients and disease-free controls

Since it has been shown before by others and our group[11-13] that mRNA expression and protein concentration of CYP450 are not related in tissues of some digestive organs (e.g. colon), non-parametric correlation analysis of mRNA expression and protein levels for each CYP investigated was performed. Indeed, no significant correlations were found between mRNA expression and protein levels in any of the CYPs investigated (Table 2).

DISCUSSION

Different protein levels of CYPs in normal tissue of untreated esophageal SCC patients and controls

Esophageal cancer is the third most common gastrointestinal cancer[1] with the majority of tumors being SCC[4]. It was reported that interindividual differences in CYP gene expression may contribute to the interindividual susceptibility to environmental (pro-) carcinogens and subsequently the development of malignancies[14]. Despite this hypothesis, only a few extensive studies have determined mRNA and/or protein expression of CYPs in esophageal tissue and esophageal carcinoma of humans, respectively[14-17] and most of these studies did not distinguish between adenocarcinoma and SCC. The presence of CYP2C-, CYP2E- and CYP3A- in normal esophageal tissue and SCC has been shown by others before[14-17]. However, some of the available data are contradictory and most studies determined either the expression or the protein levels in normal esophageal tissue and SCC. For example, using immunohistochemistry Murray *et al*[16] detected CYP3A, CYP1A, and CYP2C9 in most of the malignant tissue from patients with esophageal malignancies, but only CYP1A was detected in unaffected normal tissue of patients. Lechevrel *et al*[14] detected CYP3A4/5 and CYP2E1 protein and mRNA in some patients with adenocarcinoma or SCC in the esophagus. However, CYPs levels varied considerably between individuals and only CYP3A5 and CYP2E1 mRNA could be identified by RT-PCR. In the current study, CYP3A4 protein levels and CYP3A4 and CYP2C mRNA expression were found to be significantly lower in SCC than in its neighboring normal tissue. However, even more important, protein concentrations of CYP3A4, CYP3A5, and CYP2C8 were significantly higher in non-malignant esophageal tissue of patients with SCC than in tissues of healthy controls, while those of CYP2E1 were moderately reduced. At the level of mRNA expression, only CYP2E1 and CYP3A5 expression differed between groups. This finding can be considered to be of higher importance in carcinogenesis of the esophagus, as perpetually modified metabolism patterns of xenobiotics might result either in reduced detoxification of carcinogens or in elevated production of carcinogens from pro-carcinogens. The latter case might be of special importance due to strikingly increased amounts of CYP3A4 and CYP3A5 protein in non-malignant specimens from patients with SCC. These data suggest that the amount of CYPs might not only vary extensively between SCC and normal surrounding tissue but also between patients with SCC and healthy subjects. However, as in the present study CYP levels were only determined in SCC, it remains to be determined if expression and protein levels of CPYs are also altered in earlier stages of the disease (e.g., intraepithelial neoplasia of low and high grade). Furthermore, protein concentration of some CYPs (e.g., CYP2E1, CP2C8, CYP3A4, and CYP3A5) is considerably altered in normal tissue of patients with SCC compared to control subjects without malignancies. Hence, significant differences in protein concentration of these CYPs appear to be present before the development of malignancies in patients with SCC, suggesting that these enzymes are likely associated with the development of malignancies in the esophagus.

CYP mRNA is not related to protein levels either in normal esophageal tissue or in esophageal SCC

It has been suggested that expression of CYPs is not solely regulated at the level of gene transcription[18]. For instance, several studies performed in rodents and humans have reported a dissociation of mRNA expression and protein levels of CYP2C8 and CYP2E1, CYP3A4 and CYP3A5 in colon, duodenum and kidney, respectively[12,13,18]. Furthermore, *in vitro* studies performed in rat hepatocytes indicate that CYP2E1 is regulated by posttranscriptional ligand-dependent stabilization of the enzyme[19]. Similar mechanisms have been described for CYP3A in rats and humans[20,21]. Using cultured hepatocytes it also has been shown that only 60%-70% of mRNAs encoding for CYP2E1 are translated[22]. Indeed, in the present study, no correlation was found between protein and mRNA levels, suggesting that expression of certain CYPs (e.g., CYP2C8, CYP2E1, CYP3A4, and CYP3A5) in esophageal musoca might not solely be regulated at the level of transcription.

In conclusion, similar to the findings of others[14-17] interindividual variability along with a substantial dissociation of mRNA expression pattern and protein levels seems to be a characteristic of CYP expression. Although it is difficult to interpret the higher and lower levels of CYPs found in the present study, continued work focussing on the CYPs identified to have differential expression in pa-

tients with SCC is needed to determine their metabolic implications.

ACKNOWLEDGMENTS

The antibodies against human CYP2E1 and CYP3A4 were kindly provided by Dr. M Ingelman-Sundberg.

REFERENCES

1 **Glade MJ**. Food, nutrition, and the prevention of cancer: a global perspective. American Institute for Cancer Research/ World Cancer Research Fund, American Institute for Cancer Research, 1997. *Nutrition* 1999; **15**: 523-526
2 **Eloubeidi MA**, Desmond R, Arguedas MR, Reed CE, Wilcox CM. Prognostic factors for the survival of patients with esophageal carcinoma in the U.S.: the importance of tumor length and lymph node status. *Cancer* 2002; **95**: 1434-1443
3 **Bollschweiler E**, Wolfgarten E, Gutschow C, Hölscher AH. Demographic variations in the rising incidence of esophageal adenocarcinoma in white males. *Cancer* 2001; **92**: 549-555
4 **Bollschweiler E**, Wolfgarten E, Nowroth T, Rosendahl U, Mönig SP, Hölscher AH. Vitamin intake and risk of subtypes of esophageal cancer in Germany. *J Cancer Res Clin Oncol* 2002; **128**: 575-580
5 **Metzger R**, Schneider PM, Warnecke-Eberz U, Brabender J, Hölscher AH. Molecular biology of esophageal cancer. *Onkologie* 2004; **27**: 200-206
6 **Sheweita SA**. Drug-metabolizing enzymes: mechanisms and functions. *Curr Drug Metab* 2000; **1**: 107-132
7 **Ding X**, Kaminsky LS. Human extrahepatic cytochromes P450: function in xenobiotic metabolism and tissue-selective chemical toxicity in the respiratory and gastrointestinal tracts. *Annu Rev Pharmacol Toxicol* 2003; **43**: 149-173
8 **Hakkola J**, Pasanen M, Purkunen R, Saarikoski S, Pelkonen O, Mäenpää J, Rane A, Raunio H. Expression of xenobiotic-metabolizing cytochrome P450 forms in human adult and fetal liver. *Biochem Pharmacol* 1994; **48**: 59-64
9 **Kivistö KT**, Griese EU, Fritz P, Linder A, Hakkola J, Raunio H, Beaune P, Kroemer HK. Expression of cytochrome P 450 3A enzymes in human lung: a combined RT-PCR and immunohistochemical analysis of normal tissue and lung tumours. *Naunyn Schmiedebergs Arch Pharmacol* 1996; **353**: 207-212
10 **Futscher BW**, Blake LL, Gerlach JH, Grogan TM, Dalton WS. Quantitative polymerase chain reaction analysis of mdr1 mRNA in multiple myeloma cell lines and clinical specimens. *Anal Biochem* 1993; **213**: 414-421
11 **Eliasson E**, Johansson I, Ingelman-Sundberg M. Substrate-, hormone-, and cAMP-regulated cytochrome P450 degradation. *Proc Natl Acad Sci USA* 1990; **87**: 3225-3229
12 **Bergheim I**, Bode C, Parlesak A. Decreased expression of cytochrome P450 protein in non-malignant colonic tissue of patients with colonic adenoma. *BMC Gastroenterol* 2005; **5**: 34
13 **Bergheim I**, Bode C, Parlesak A. Distribution of cytochrome P450 2C, 2E1, 3A4, and 3A5 in human colon mucosa. *BMC Clin Pharmacol* 2005; **5**: 4
14 **Lechevrel M**, Casson AG, Wolf CR, Hardie LJ, Flinterman MB, Montesano R, Wild CP. Characterization of cytochrome P450 expression in human oesophageal mucosa. *Carcinogenesis* 1999; **20**: 243-248
15 **Ribeiro Pinto LF**, Teixeira Rossini AM, Albano RM, Felzenszwalb I, de Moura Gallo CV, Nunes RA, Andreollo NA. Mechanisms of esophageal cancer development in Brazilians. *Mutat Res* 2003; **544**: 365-373
16 **Murray GI**, Shaw D, Weaver RJ, McKay JA, Ewen SW, Melvin WT, Burke MD. Cytochrome P450 expression in oesophageal cancer. *Gut* 1994; **35**: 599-603
17 **Nakajima T**, Wang RS, Nimura Y, Pin YM, He M, Vainio H, Murayama N, Aoyama T, Iida F. Expression of cytochrome P450s and glutathione S-transferases in human esophagus with squamous-cell carcinomas. *Carcinogenesis* 1996; **17**: 1477-1481
18 **Hakkak R**, Korourian S, Ronis MJ, Ingelman-Sundberg M, Badger TM. Effects of diet and ethanol on the expression and localization of cytochromes P450 2E1 and P450 2C7 in the colon of male rats. *Biochem Pharmacol* 1996; **51**: 61-69
19 **Eliasson E**, Mkrtchian S, Ingelman-Sundberg M. Hormone- and substrate-regulated intracellular degradation of cytochrome P450 (2E1) involving MgATP-activated rapid proteolysis in the endoplasmic reticulum membranes. *J Biol Chem* 1992; **267**: 15765-15769
20 **Feierman DE**, Melnikov Z, Zhang J. The paradoxical effect of acetaminophen on CYP3A4 activity and content in transfected HepG2 cells. *Arch Biochem Biophys* 2002; **398**: 109-117
21 **Zangar RC**, Hernandez M, Novak RF. Posttranscriptional elevation of cytochrome P450 3A expression. *Biochem Biophys Res Commun* 1997; **231**: 203-205
22 **Kocarek TA**, Zangar RC, Novak RF. Post-transcriptional regulation of rat CYP2E1 expression: role of CYP2E1 mRNA untranslated regions in control of translational efficiency and message stability. *Arch Biochem Biophys* 2000; **376**: 180-190

S- Editor Liu Y **L- Editor** Wang XL **E- Editor** Ma WH

PO Box 2345, Beijing 100023, China
www.wjgnet.com
wjg@wjgnet.com

World J Gastroenterol 2007 February 21; 13(7): 1003-1009
World Journal of Gastroenterology ISSN 1007-9327

Successful initial ablation therapy contributes to survival in patients with hepatocellular carcinoma

Manabu Morimoto, Kazushi Numata, Kazuya Sugimori, Kazuhito Shirato, Atsushi Kokawa, Hiroyuki Oka, Kingo Hirasawa, Ryonho Koh, Hiromi Nihommatsu, Katsuaki Tanaka

Manabu Morimoto, Kazushi Numata, Kazuya Sugimori, Kazuhito Shirato, Atsushi Kokawa, Hiroyuki Oka, Kingo Hirasawa, Ryonho Koh, Hiromi Nihommatsu, Katsuaki Tanaka, Gastroenterological Center, Yokohama City University Medical Center, 4-57 Urafune-cho, Minami-ku, Yokohama 232-0024, Japan
Correspondence to: Manabu Morimoto, MD, Gastroenterological Center, Yokohama City University Medical Center, 4-57, Urafunecho, Minami-ku, Yokohama City, 232-0024, Japan. morimoto@urahp.yokohama-cu.ac.jp
Telephone: +81-45-2615656 Fax: +81-45-2619492
Received: 2006-11-27 Accepted: 2007-01-15

Key words: Percutaneous ethanol injection; Radiofrequency ablation; Successful initial treatment; Overall survival; Prognostic factor

Morimoto M, Numata K, Sugimori K, Shirato K, Kokawa A, Oka H, Hirasawa K, Koh R, Nihommatsu H, Tanaka K. Successful initial ablation therapy contributes to survival in patients with hepatocellular carcinoma. *World J Gastroenterol* 2007; 13(7): 1003-1009

http://www.wjgnet.com/1007-9327/13/1003.asp

Abstract

AIM: To evaluate the outcome predictors of percutaneous ablation therapy in patients with unresectable hepatocellular carcinoma (HCC), especially to identify whether the initial treatment response contributes to the survival of the patients.

METHODS: The study cohort included 153 patients with single (102) and two or three (51) HCC nodules 5 cm or less in maximum diameter. As an initial treatment, 110 patients received radiofrequency ablation and 43 patients received percutaneous ethanol injection.

RESULTS: The Kaplan-Meier estimates of overall 3- and 5-year survival rates were 75% and 59%, respectively. The log-rank test revealed statistically significant differences in the overall survivals according to Child-Pugh class (P = 0.0275), tumor size (P = 0.0130), serum albumin level (P = 0.0060), serum protein induced by vitamin K absence or antagonist Ⅱ level (P = 0.0486), and initial treatment response (P = 0.0130). The independent predictors of survival were serum albumin level (risk ratio, 3.216; 95% CI, 1.407-7.353; P = 0.0056) and initial treatment response (risk ratio, 2.474; 95% CI, 1.076-5.692; P = 0.0330) based on the Cox proportional hazards regression models. The patients had a serum albumin level 3.5 g/dL and the 3- and 5-year survival rates of 86% and 82%.

CONCLUSION: In HCC patients treated with percutaneous ablation therapy, serum albumin level and initial treatment response are the independent outcome predictors.

INTRODUCTION

Hepatocellular carcinoma (HCC) is one of the most prevalent human cancers with an increasing incidence worldwide[1], and about 70% of HCC is found in Asia[2]. Surveillance with ultrasonography (US) and alpha-fetoprotein in cirrhosis can detect small HCC at an early stage. For early stage patients (single HCC ⩽ 5 cm or ⩽ 3 nodules ⩽ 3 cm), surgery is considered the first treatment option, however, because of accompanying chronic liver disease, many HCC patients can not undergo surgical resection[3-5]. As non-surgical treatment, various local ablation therapies such as percutaneous ethanol injection (PEI)[6,7] or percutaneous radiofrequency (RF) ablation have been proposed, and encouraging results of survival rates have been reported[8-10].

Although many reports of the prognostic predictors after surgical resection of early stage HCC have been reported[11-13], there have been few reports of the prognostic predictors after percutaneous ablation therapy. Sala *et al* in recent years reported that "Child-Pugh class" and "initial treatment response" as prognostic factors of the survival in those who received percutaneous ablation therapy[14]; however, most of the cases (83%) were treated with PEI. The current state of the main percutaneous ablation therapy changes from PEI to RF ablation; therefore, to establish an optimal therapeutic strategy based on the current state, we started this cohort study after 2000 when RF ablation was introduced in our institution.

In this study, we examined a group of HCC patients whose tumors were percutaneously treated using RF ablation or PEI and analyzed the factors pertinent to the prognosis. This approach permits (1) establishment of an

optimal protocol in the percutaneous ablation therapy; and (2) assessment of the prognostic factors in RF ablation and PEI.

MATERIALS AND METHODS

Patients

Between May 2000 and March 2005, 226 patients were diagnosed for the first time as having HCC lesions using US and contrast-enhanced CT and were hospitalized at Yokohama City University Medical Center. The criteria for entry in this study were (1) the presence of either a solitary lesion or up to three lesions, (2) a maximum tumor diameter of 5 cm or less, (3) patients who did not meet with the surgical criteria (resection or transplantation), (4) the lesion was detectable using US, and (5) no evidence existing of portal thrombosis, extrahepatic metastasis, or uncontrollable ascites. Seventy-three patients were excluded from the study and 153 patients were enrolled. The patients' characteristics are depicted in Table 1. Ninety-three of the enrolled patients were men and 60 were women, ranging in age from 51 to 87 years (mean, 69 years). One hundred and thirty-three patients were Child-Pugh class A, and 20 patients were Child-Pugh class B. All had underlying cirrhosis due to hepatitis C virus (n = 134), hepatitis B virus (n = 8), alcohol use (n = 7), or other factors (n = 4). One hundred and two patients presented with solitary tumors and 51 patients had 2-3 lesions. The greatest tumor diameters $\leqslant$ 3 cm were seen in 120 patients, and > 3 cm in 33 patients. A confirmed diagnosis of HCC was made by the pathological examination of biopsied specimens obtained using a 21-gauge fine needle (Sonopsy, Hakko, Tokyo, Japan) and/or the radiological criteria[15] in all patients. Patients with a tumor more than 3 cm in maximum diameter were treated with transcatheter arterial chemoembolization (TACE) followed by RF ablation or PEI.

The entire protocol was approved by the hospital ethics committee and was performed in compliance with the Helsinki Declaration. Written informed consent was obtained from all patients and relatives.

Table 1 Characteristics of patients

Variables	All patients (n = 153)	PEI (n = 43)	RF ablation (n = 110)	P
Age (yr)				
mean ± SD	69 ± 7	69 ± 7	68 ± 7	NS
Sex				
Male/Female	93/60	22/21	71/39	NS
Etiology				
HCV	134	38	96	
HBV	8	1	7	NS
Alcohol	7	2	5	
Others	4	2	2	
Child-Pugh class				
A/B	133/20	37/6	96/14	NS
Tumor size (cm)				
$\leqslant$ 3/> 3	120/33	33/10	87/23	NS
Tumor number				
Single/Multiple	102/51	19/24	83/27	< 0.05
Serum alpha-fetoprotein level (ng/mL)				
mean ± SD	781 ± 8180	2501 ± 15289	109 ± 282	NS
Serum PIVKA-II level (ng/mL)				
mean ± SD	347 ± 1258	565 ± 1467	262 ± 1169	NS
Serum albumin level (g/dL)				
mean ± SD	3.8 ± 0.5	3.7 ± 0.5	3.8 ± 0.5	NS
Initial treatment response				
Successful/Unsuccessful	125/28	35/8	90/20	NS

RF: radiofrequency; PEI: percutaneous ethanol injection; NS: not significant; HCV: hepatitis C virus; HBV: hepatitis B virus; PIVKA-Ⅱ: protein induced vitamin K absence or antagonist Ⅱ.

Treatment procedures

Percutaneous ethanol injection: Based on the reports of Llovet *et al*[16] and Livraghi *et al*[17], we selected PEI without selecting RF ablation when a tumor satisfied the following criteria: (1) existing in a subcapsular location, (2) existing in a location adjacent to a major vessel and another organ (heart, gallbladder, stomach and bowel), and (3) demonstrating poor differentiation. Patients with impaired clotting tests, or with a lower platelet count less than 5×10^{10}/L were considered as being contraindicated for RF ablation and were treated by PEI. Ten patients (23% of patients treated by PEI) with tumors more than 3 cm in diameter were treated with TACE followed by PEI[18].

We used a real-time convex scanner or linear-array scanner with 3.5-MHz probes and a lateral attachable apparatus for needle guidance (Core-Vision 6000™, Toshiba Medical Co., Tokyo, Japan). First, it was confirmed under US guidance that a 15- or 20-cm, 21-gauge puncture needle with a closed conical tip and three terminal side holes (PEIT needle; Hakko, Tokyo, Japan) was correctly positioned within the lesion, and 99.5% absolute ethyl alcohol was then slowly injected. Caution was taken to inject the deepest portions of the lesion first and then the more central and superficial portions, to prevent superficial spreading of the ethanol from masking the view for subsequent injections. We usually used one or more PEIT needles for each treatment session, and ethanol was injected into the tumor at one or more locations until the lesion was completely filled. Treatment was given twice a week. A treatment series usually consisted of six or more sessions, and the total dose of ethanol varied with the volume of the lesion, the texture, patient compliance, and distribution of the ethanol.

Radiofrequency ablation: We selected the RF ablation for the cases with low risks of tumor seeding and the hemorrhage based on the previous reports[16,17,19]. Twenty-three patients (21% of patients treated by RF ablation) with tumors more than 3 cm in diameter were treated with TACE followed by RF ablation[20].

At the beginning, grounding was achieved by attaching 2 or 4 pads to the patient's thighs. A conscious sedation, consisting of a combination of intramuscular

administration of pentazocine (Pentazin™ 15 mg, Sankyo Pharmaceuticals, Tokyo, Japan) and hydroxyzine chloride (Atarax-P™ 25 mg, Pfizer Japan, Tokyo, Japan), was administered before treatment. Local anesthesia was achieved by injecting 1% lidocaine hydrochloride (Xylocaine™, Astra Japan, Tokyo, Japan). Sixty-five of 112 patients were treated with hooked, 15-gauge, 25-cm-long electrodes, which are expandable by 10 hooks to a maximum dimension of 3 or 3.5 cm (Le Veen Needle Electrode; Radiotherapeutics, Mountain View, CA), and RF ablation was applied using a generator (RTC 2000; Boston Scientific Japan, Tokyo, Japan). For the remaining 47 tumors, 17-gauge, cooled electrodes with a dimention of 2 or 3 cm (Cool-tip needle; Radionics, Burlington, MA) were used, attached to a 500-kHz RF generator (Radionics, Burlington, MA) capable of producing power of 200 W. A peristaltic pump (Watson-Marlow, Wilmington, MA) was used to infuse 0℃ normal saline solution into the lumen of the electrodes to maintain the temperature below 25℃. For tumors more than 2 cm in diameter, several insertions were performed to obtain complete ablation of the entire tumors.

Transcatheter arterial chemoembolization: Thirty-three patients with tumors more than 3 cm in diameter were treated with TACE followed by RF ablation or PEI. We performed TACE by selectively introducing a microcatheter into the right or left hepatic artery or a segmental branch of the hepatic artery and injecting a mixture of iodized oil (Lipiodol; Andre Guerbet, Aulnay-sous-Bois, France) and epirubicin hydrochloride (30-50 mg per body surface) (Farmorubicin; Pharmacia and Upjohn, Tokyo, Japan) or styrene maleic acid neocarzinostatin (1.0-3.0 mg per body surface) (SMANCS; Yamanouchi Pharmaceutical, Tokyo, Japan). This was followed by introduction of a gelatin sponge (1 mm × 1 mm × 1 mm) (Spongel; Yamanouchi Pharmaceutical, Tokyo, Japan).

Evaluation of initial treatment response and follow-up

Initial treatment response was assessed by contrast-enhanced CT 1, 3, and 6 mo after initial treatment session. Successful initial treatment was defined as the absence of an enhanced area within the tumor assessed by contrast enhanced CT 6 mo after initial treatment session. If the presence of residual viable tumor within the treated area was defined by CT within 6 mo after initial treatment, the case was judged to be unsuccessful in the initial treatment. After the evaluation of initial treatment response, patients were followed up every 3 mo by contrast enhanced CT and/or US.

When the residual viable tumor and/or distant recurrence were detected by the follow-up CT, percutaneous ablation therapy was added if they were within 3 lesions, and TACE was selected for patients who were ineligible for percutaneous ablation therapy, with large and/or multifocal HCC who did not have vascular invasion or extrahepatic spread[15]. The above-mentioned treatment was repeated at once whenever the tumor recurrence was detected, until uncontrolled ascites or intravascular tumor thrombus appeared and serum bilirubin level reached 3 mg/dL or higher.

Statistical analysis

The end point of the study was the survival. The baseline characteristics of patients were expressed as mean ± standard deviation. Differences in proportions among the groups were analyzed by the Chi-square test. Mean quantitative values were compared by the Student's *t* test. Follow-up data was dealt with from the beginning of the treatment and was maintained until the death or the last visit of the patients before April 30, 2006. The Kaplan-Meier method was used to calculate the survival rate and the log-rank test was used to analyze differences.

As pretreatment factors, fifteen variables were assessed in the univariate analysis: age (< 70 *vs* ≥ 70 years); sex (male *vs* female); cause of underlying cirrhosis (HCV *vs* HBV *vs* alcohol *vs* others); Child-Pugh class (A *vs* B); tumor size (≤ 3 cm *vs* > 3 cm); tumor number (single *vs* multiple); serum alpha-fetoprotein levels (<400 *vs* ≥ 400 ng/mL); serum protein induced by vitamin K absence or antagonist Ⅱ (PIVKA-Ⅱ) level (< 300 *vs* ≥ 300 ng/mL); and serum albumin level (≤ 3.5 *vs* > 3.5g/dL); serum alanine aminotransferase (ALT) level (<80 *vs* ≥ 80 U/L); serum bilirubin level (<2 *vs* ≥ 2 mg/dL); serum platelet count (<9 *vs* ≥ 9 × 10^9/L); prothrombin activity (≤ 70 *vs* > 70%); encephalopathy (none *vs* yes); and ascites (none *vs* yes). As treatment factors, two variables were assessed in the univariate analysis: type of treatment (PEI *vs* RF ablation); and initial treatment response (successful *vs* unsuccessful). Significant variables ($P < 0.05$) were included in a stepwise Cox regression analysis. Data analyses were performed with SPSS software (version 10.0J; SPSS, Tokyo, Japan). All *P* values were derived from two-tailed tests and $P < 0.05$ was accepted as statistically significant.

RESULTS

Treatment response and survival

In general, the percutaneous ablation procedures were well tolerated in all the patients. Both cardiac and respiratory parameters remained stable throughout the treatment. The regimen of conscious sedation and local anesthesia used in this study was adequate for these ablation methods. None of the patients experienced bleeding as a result of these percutaneous ablation techniques.

No local tumor residue was found in 125 of 153 (82%) patients as assessed by contrast enhanced CT 6 mo after the initial treatment (defined as successful initial treatment) (Figure 1). The remaining 28 (18%) patients judged as having residual viable tumor by contrast enhanced CT within 6 mo after the initial treatment (defined as unsuccessful initial treatment), were re-treated by RF ablation or PEI until no vascularities could be recognized within the tumor by contrast enhanced CT. With regard to the type of treatment, successful initial treatment was obtained in 90 (82%) of 110 patients treated with RF ablation, and in 35 (81%) of 43 patients treated with PEI, and no significant difference was observed between the two types of treatment. After a median follow-up of 34 mo (range, 1-66), the 1-, 3-, and 5-year survival rates were 95%, 75%, and 59%, respectively (Figure 2). At the time of the analysis, 83 (54%) patients had tumor recurrence

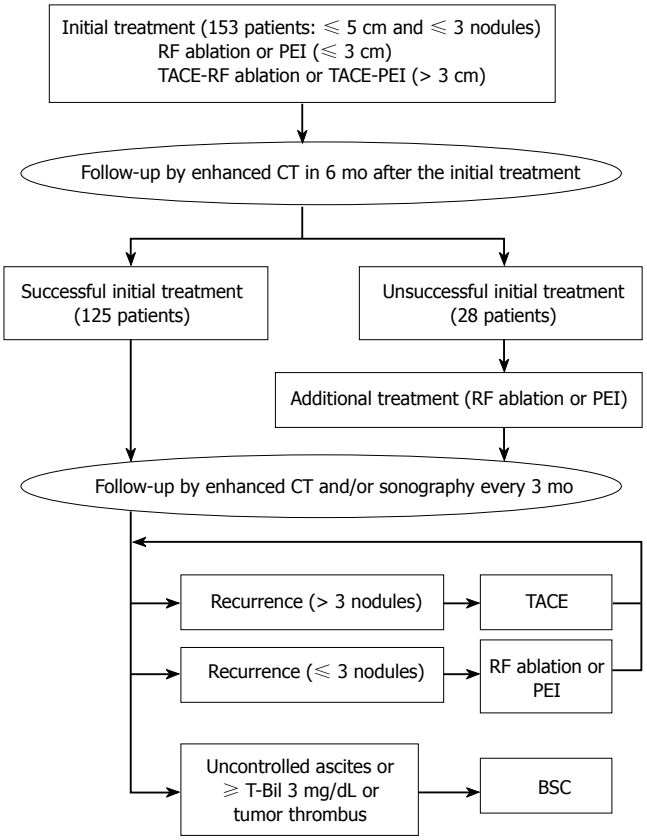

Figure 1 Follow-up chart of overall treatment design.

Table 2 Univariate analysis for factors associated with survival

Variables	Patients	*P*
Pre-treatment factors		
Age (yr)		
< 70/≥ 70	74/79	0.0923
Sex		
Male/Female	93/60	0.7284
Child-Pugh class		
A/B	133/20	0.0275
Tumor size (cm)		
≤ 3/> 3	120/33	0.0130
Tumor number		
Single/Multiple	102/51	0.6298
Serum alpha-fetoprotein level (ng/mL)		
< 400/≥ 400	142/11	0.0722
Serum PIVKA-Ⅱ level (ng/mL)		
< 300/≥ 300	133/20	0.0486
Serum albumin level (g/dL)		
≤ 3.5/> 3.5	50/103	0.0060
Treatment factors		
Type of ablation therapy		
RF ablation/PEI	110/43	0.9829
Initial treatment response		
Successful/Unsuccessful	125/28	0.0130

RF: radiofrequency; PEI: percutaneous ethanol injection; NS: not significant; PIVKA-Ⅱ: protein induced vitamin K absence or antagonist Ⅱ.

(incomplete local treatment and/or distant recurrence), 24 patients died and 3 were l lost to follow-up. With regard to the type of treatment, tumor recurrences were observed in 58 (53%) of 110 patients treated with RF ablation, and in 25 (58%) of 43 patients treated with PEI. Death was due to tumor progression in 18 patients and due to liver failure in 6 patients.

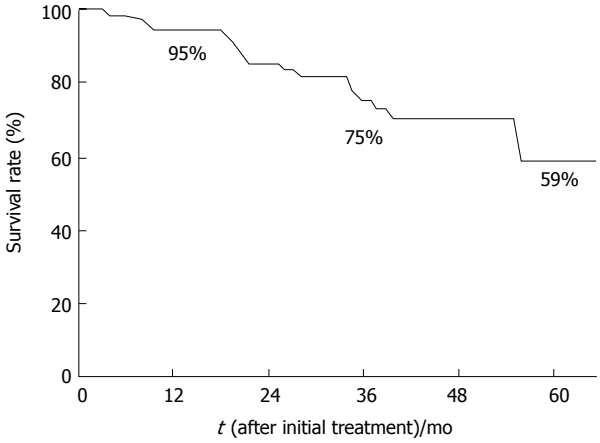

Figure 2 Overall probability of survival.

Table 3 Multivariate analysis for factors associated with survival

Variables	Risk ratio (95% CI)	*P*
Tumor size (cm)		
> 3	1.0	
≤ 3	0.459 (0.179-1.174)	0.104
Serum PIVKA-Ⅱ level (ng/mL)		
≥ 300	1.0	
< 300	0.542 (0.191-1.535)	0.249
Serum albumin level (g/dL)		
> 3.5	1.0	
≤ 3.5	3.216 (1.407-7.353)	0.006
Initial treatment response		
Successful	1.0	
Unsuccessful	2.474 (1.076-5.692)	0.033

Abbreviations: PIVKA-Ⅱ, protein induced vitamin K absence or antagonist Ⅱ.

Factors for survival

In the univariate analysis, 5 variables were associated with survival (Table 2). Of the pre-treatment factors, Child-Pugh classification, tumor size, serum albumin level, and serum PIVKA-Ⅱ level were found to be significant predictors of survival. And of the treatment factors, initial treatment response was found to be a significant predictor of survival while the type of ablation therapy (RF ablation *vs* PEI) was not ($P = 0.9829$). Multivariate analysis disclosed two independent predictors: serum albumin level ≤ 3.5g/dL *vs* >3.5g/dL (risk ratio 3.216, 95%CI: 1.407-7.353, $P = 0.0056$) and successful initial treatment *vs* unsuccessful initial treatment (risk ratio 2.474, 95%CI: 1.076-5.692, $P = 0.0330$) (Table 3). When only pre-treatment factors were included in the multivariate analysis, serum albumin level (risk ratio 3.199, 95%CI: 1.405-7.281, $P = 0.0056$) was proved to be an independent predictor.

The sole predictive factor for survival in patients with a serum albumin level > 3.5g/dL proved to be the initial treatment response; therefore the survival was examined

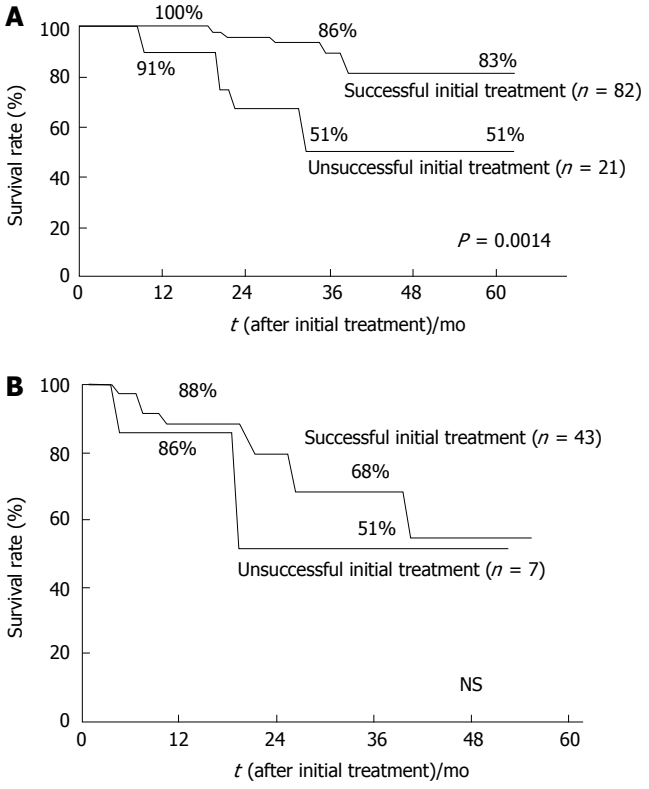

Figure 3 Overall probability of survival according to initial treatment response. **A**: In patients with a serum albumin level > 3.5 g/dL; **B**: In patients with a serum albumin level ≤ 3.5 g/dL.

in case groups with serum albumin levels > 3.5g/dL (n = 103) and ≤ 3.5g/dL (n = 50) according to the initial treatment response. In patients with a serum albumin level > 3.5g/dL, the 1-, 3-, and 5-year survival rates in patients who were judged as having had a successful initial treatment were 100%, 86%, and 83%, respectively (n = 82), and the survival rates in patients who were judged as having had an unsuccessful initial treatment were 91%, 51%, and 51% at 1-, 3-, and 5-year, respectively (n = 21) (P = 0.0014) (Figure 3A). On the other hand, in patients with a serum albumin level ≤ 3.5g/dL, the multivariate analysis proved no independent predictors for survival. The survival rates in 43 patients with a successful initial treatment were 88% and 68% at 1 and 3 years, and in 7 patients with an unsuccessful initial treatment, the survival rates were 86% and 51% at 1 and 3 years, respectively (P = 0.3813) (Figure 3B).

Initial treatment response was significantly associated with the tumor number (P = 0.0031), tumor size (P = 0.0441), serum alpha-fetoprotein level (P = 0.0156), and serum PIVKA-Ⅱ level (P = 0.0071), however it was not associated with the etiology of underlying cirrhosis, Child-Pugh class, and type of ablation therapy (Table 4).

Table 4 Comparison of clinical background between successful initial treatment group and unsuccessful initial treatment group

	Initial treatment	
	Successful (n = 125)	Unsuccessful (n = 28)
Sex		
Male/Female	75/50	18/10
Age (yr)		
< 70/≥ 70	67/58	12/16
Etiology		
HCV/HBV/Alcohol/Others	108/6/7/4	26/2/0/0
Child-Pugh class		
A/B	110/15	23/5
Serum albumin level (g/dL)		
≤ 3.5/> 3.5	43/82	7/21
Tumor size (cm)		
≤ 3/> 3	102/23	18/10[a]
Tumor number		
Single/Multiple	90/35	12/16[a]
Type of ablation therapy		
RF ablation/PEI	90/35	20/8
Serum alpha-fetoprotein level (ng/mL)		
< 400/≥ 400	119/6	23/5[a]
Serum PIVKA-Ⅱ level (ng/mL)		
< 300/≥ 300	113/12	20/8[a]

RF: radiofrequency; PEI: percutaneous ethanol injection; HCV: hepatitis C virus; HBV: hepatitis B virus; PIVKA-Ⅱ: protein induced vitamin K absence or antagonist Ⅱ. [a]P < 0.05 *vs* the successful initial treatment group.

DISCUSSION

In the current study, we examined a group of HCC patients whose tumors were percutaneously treated using RF ablation or PEI and analyzed the predictors that contributed to the prognosis. Multivariate analysis disclosed two independent predictors: serum albumin level and initial treatment response. In the cases with a serum albumin level > 3.5 g/dL, our data consistently showed that a successful initial treatment was the most predictive factor for long-term survival.

Examinations of the factor that could contribute to the long-term survival of patients undergoing percutaneous ablation therapy, have been reported previously; however, most of them were evaluations using PEI. Pompili *et al* evaluated the therapeutic efficacy of PEI for patients with Child-Pugh class A and tumors > 5 cm in diameter, and reported that alpha-fetoprotein level and liver function were factors which contributed to survival[21]. Ebara *et al* evaluated the therapeutic efficacy of PEI for patients with ≤ 3 lesions of small HCC, and found that alpha-fetoprotein level and liver function were factors contributed to the suvival[22]. Recently, Sala *et al*[14] and Xu *et al*[23] reported the prognostic predictors after percutaneous ablation therapies. However, most of the cases were treated with PEI in the former study[14], and in the latter study[23], 63% of treated cases were recurrent HCC and the selection for ablation procedures (microwave *vs* RF ablation) was not fully clarified. To establish an optimal therapeutic protocol after the introduction of RF ablation, we started this cohort study after 2000 when RF ablation was introduced in our institution. In this study, 72% of the patients were treated with RF ablation, and this may reflect the current state of the available percutaneous ablation procedures.

In our study, the serum albumin level was shown as the most important pre-treatment predictor for survival. Hepatic functional reserve as indicated by the serum albumin level has generally been identified to be a good

prognostic factor for survival. The serum albumin level has been shown to be one of the prognostic factors in HCC patients treated with hepatic resection[24] and PEI[25]. Ikeda *et al* reported that the serum albumin level was one of the independent factors associated with the carcinogens in HCV positive viral hepatitis[26]. In this study, 88% of patients had hepatitis C virus infection; therefore, the serum albumin level is selected as a significant factor that may provide for the recurrence of HCC after successful percutaneous local ablation therapy.

Furthermore, initial treatment response was shown as a second significant predictor for survival. Sala *et al* recently reported that initial treatment response was an outcome predictor of the survival after ablation therapy and initial complete tumor necrosis should be considered a relevant therapeutic target irrespective of tumor size and liver function[14]. In the present study, the impact of extensive tumor necrosis on survival has been observed in patients with good liver functional reserve (serum albumin level > 3.5 g/dL); however, it was not found in patients with poor liver functional reserve (serum albumin level ⩽ 3.5 g/dL). Therefore, in patients with poor liver function reserve, optimal selection of patients as candidates for ablation therapies and of the appropriate therapeutic schedule for each single patient to control the tumor growth, avoiding a clinically significant worsening of liver function, is essential to obtain an improvement in survival.

Treatment response was generally judged by CT at one month after the treatment based on the WHO criteria[15], however in this study, the initial treatment response was judged by CT at 6 mo after the initial treatment. This difference of the surveillance after the initial treatment may be explained as follows. First, 22% of our patients underwent TACE prior to ablation therapy, so it was difficult to achieve a detailed evaluation of treatment response with CT because of dense lipiodol accumulation in the treated area[27]. Second, 72% of the patients received RF ablation therapy, resulting in an inflammatory increased vascular flow rim of the outline of the ablated zone for about one month following treatment, which can disturb the evaluation of the local treatment by contrast-enhanced CT[28].

In this study, alpha-fetoprotein level, PIVKA-Ⅱ level, tumor size, and tumor number were significant factors for the initial treatment response by univariate analysis. Although there are few reports which have examined the factors for initial treatment response following percutaneous ablation therapy, there are several reports as to what contributes to local recurrence when RF ablation is selected. Lencioni *et al* showed that tumor size and type of ablation therapy were the factors for local recurrence-free survival in those cases treated with RF ablation and PEI[29]. Lin *et al* reported that tumor number, tumor size, histopathological (Edmondson's) grade, and type of ablation therapy were significant factors of local recurrence[30].

In summary, we demonstrated that the best candidates for percutaneous ablation therapy are those patients who have good hepatic functional reserve and can be expected to achieve successful initial treatment. Attempts to fully ablate large tumors (3-5 cm in diameter) are achieved successfully by the combined use of TACE, however, further studies are needed to clarify whether or not the combined use of TACE in RF ablation will be a therapeutic option to achieve complete tumor necrosis for the treatment of large HCC tumors.

REFERENCES

1 **Parkin DM**, Bray F, Ferlay J, Pisani P. Estimating the world cancer burden: Globocan 2000. *Int J Cancer* 2001; **94**: 153-156
2 **Bosch FX**, Ribes J, Borràs J. Epidemiology of primary liver cancer. *Semin Liver Dis* 1999; **19**: 271-285
3 **Primary liver cancer in Japan.** Clinicopathologic features and results of surgical treatment. *Ann Surg* 1990; **211**: 277-287
4 **Arii S**, Yamaoka Y, Futagawa S, Inoue K, Kobayashi K, Kojiro M, Makuuchi M, Nakamura Y, Okita K, Yamada R. Results of surgical and nonsurgical treatment for small-sized hepatocellular carcinomas: a retrospective and nationwide survey in Japan. The Liver Cancer Study Group of Japan. *Hepatology* 2000; **32**: 1224-1229
5 **Fong Y**, Sun RL, Jarnagin W, Blumgart LH. An analysis of 412 cases of hepatocellular carcinoma at a Western center. *Ann Surg* 1999; **229**: 790-799; discussion 799-800
6 **Ebara M**, Ohto M, Sugiura N, Kita K, Yoshikawa M, Okuda K, Kondo F, Kondo Y. Percutaneous ethanol injection for the treatment of small hepatocellular carcinoma. Study of 95 patients. *J Gastroenterol Hepatol* 1990; **5**: 616-626
7 **Castells A**, Bruix J, Bru C, Fuster J, Vilana R, Navasa M, Ayuso C, Boix L, Visa J, Rodés J. Treatment of small hepatocellular carcinoma in cirrhotic patients: a cohort study comparing surgical resection and percutaneous ethanol injection. *Hepatology* 1993; **18**: 1121-1126
8 **Rossi S**, Di Stasi M, Buscarini E, Quaretti P, Garbagnati F, Squassante L, Paties CT, Silverman DE, Buscarini L. Percutaneous RF interstitial thermal ablation in the treatment of hepatic cancer. *AJR Am J Roentgenol* 1996; **167**: 759-768
9 **Livraghi T**, Goldberg SN, Lazzaroni S, Meloni F, Solbiati L, Gazelle GS. Small hepatocellular carcinoma: treatment with radio-frequency ablation versus ethanol injection. *Radiology* 1999; **210**: 655-661
10 **Curley SA,** Izzo F, Delrio P, Ellis LM, Granchi J, Vallone P, Fiore F, Pignata S, Daniele B, Cremona F. Radiofrequency ablation of unresectable primary and metastatic hepatic malignancies: results in 123 patients. *Ann Surg* 1999; **230**: 1-8
11 **Suehiro T**, Sugimachi K, Matsumata T, Itasaka H, Taketomi A, Maeda T. Protein induced by vitamin K absence or antagonist II as a prognostic marker in hepatocellular carcinoma. Comparison with alpha-fetoprotein. *Cancer* 1994; **73**: 2464-2471
12 **Arii S**, Tanaka J, Yamazoe Y, Minematsu S, Morino T, Fujita K, Maetani S, Tobe T. Predictive factors for intrahepatic recurrence of hepatocellular carcinoma after partial hepatectomy. *Cancer* 1992; **69**: 913-919
13 **Nagao T,** Inoue S, Goto S, Mizuta T, Omori Y, Kawano N, Morioka Y. Hepatic resection for hepatocellular carcinoma. Clinical features and long-term prognosis. *Ann Surg* 1987; **205**: 33-40
14 **Sala M**, Llovet JM, Vilana R, Bianchi L, Solé M, Ayuso C, Brú C, Bruix J. Initial response to percutaneous ablation predicts survival in patients with hepatocellular carcinoma. *Hepatology* 2004; **40**: 1352-1360
15 **Bruix J**, Sherman M, Llovet JM, Beaugrand M, Lencioni R, Burroughs AK, Christensen E, Pagliaro L, Colombo M, Rodés J. Clinical management of hepatocellular carcinoma. Conclusions of the Barcelona-2000 EASL conference. European Association for the Study of the Liver. *J Hepatol* 2001; **35**: 421-430
16 **Llovet JM**, Vilana R, Brú C, Bianchi L, Salmeron JM, Boix L, Ganau S, Sala M, Pagès M, Ayuso C, Solé M, Rodés J, Bruix J. Increased risk of tumor seeding after percutaneous radiofrequency ablation for single hepatocellular carcinoma. *Hepatology* 2001; **33**: 1124-1129
17 **Livraghi T,** Solbiati L, Meloni MF, Gazelle GS, Halpern

EF, Goldberg SN. Treatment of focal liver tumors with percutaneous radio-frequency ablation: complications encountered in a multicenter study. *Radiology* 2003; **226**: 441-451

18 **Tanaka K,** Okazaki H, Nakamura S, Endo O, Inoue S, Takamura Y, Sugiyama M, Ohaki Y. Hepatocellular carcinoma: treatment with a combination therapy of transcatheter arterial embolization and percutaneous ethanol injection. *Radiology* 1991; **179**: 713-717

19 **Morimoto M,** Sugimori K, Shirato K, Kokawa A, Tomita N, Saito T, Tanaka N, Nozawa A, Hara M, Sekihara H, Shimada H, Imada T, Tanaka K. Treatment of hepatocellular carcinoma with radiofrequency ablation: radiologic-histologic correlation during follow-up periods. *Hepatology* 2002; **35**: 1467-1475

20 **Yamakado K,** Nakatsuka A, Ohmori S, Shiraki K, Nakano T, Ikoma J, Adachi Y, Takeda K. Radiofrequency ablation combined with chemoembolization in hepatocellular carcinoma: treatment response based on tumor size and morphology. *J Vasc Interv Radiol* 2002; **13**: 1225-1232

21 **Pompili M,** Rapaccini GL, Covino M, Pignataro G, Caturelli E, Siena DA, Villani MR, Cedrone A, Gasbarrini G. Prognostic factors for survival in patients with compensated cirrhosis and small hepatocellular carcinoma after percutaneous ethanol injection therapy. *Cancer* 2001; **92**: 126-135

22 **Ebara M,** Okabe S, Kita K, Sugiura N, Fukuda H, Yoshikawa M, Kondo F, Saisho H. Percutaneous ethanol injection for small hepatocellular carcinoma: therapeutic efficacy based on 20-year observation. *J Hepatol* 2005; **43**: 458-464

23 **Xu HX**, Lu MD, Xie XY, Yin XY, Kuang M, Chen JW, Xu ZF, Liu GJ. Prognostic factors for long-term outcome after percutaneous thermal ablation for hepatocellular carcinoma: a survival analysis of 137 consecutive patients. *Clin Radiol* 2005; **60**: 1018-1025

24 **Chen MF,** Tsai HP, Jeng LB, Lee WC, Yeh CN, Yu MC, Hung CM. Prognostic factors after resection for hepatocellular carcinoma in noncirrhotic livers: univariate and multivariate analysis. *World J Surg* 2003; **27**: 443-447

25 **Kuriyama H,** Okada S, Okusaka T, Ueno H, Ikeda M. Prognostic factors in patients with small hepatocellular carcinoma treated by percutaneous ethanol injection. *J Gastroenterol Hepatol* 2002; **17**: 1205-1210

26 **Ikeda K,** Saitoh S, Suzuki Y, Kobayashi M, Tsubota A, Koida I, Arase Y, Fukuda M, Chayama K, Murashima N, Kumada H. Disease progression and hepatocellular carcinogenesis in patients with chronic viral hepatitis: a prospective observation of 2215 patients. *J Hepatol* 1998; **28**: 930-938

27 **Nakamura H,** Hashimoto T, Oi H, Sawada S. Transcatheter oily chemoembolization of hepatocellular carcinoma. *Radiology* 1989; **170**: 783-786

28 **Goldberg SN,** Gazelle GS, Mueller PR. Thermal ablation therapy for focal malignancy: a unified approach to underlying principles, techniques, and diagnostic imaging guidance. *AJR Am J Roentgenol* 2000; **174**: 323-331

29 **Lencioni RA,** Allgaier HP, Cioni D, Olschewski M, Deibert P, Crocetti L, Frings H, Laubenberger J, Zuber I, Blum HE, Bartolozzi C. Small hepatocellular carcinoma in cirrhosis: randomized comparison of radio-frequency thermal ablation versus percutaneous ethanol injection. *Radiology* 2003; **228**: 235-240

30 **Lin SM**, Lin CJ, Lin CC, Hsu CW, Chen YC. Radiofrequency ablation improves prognosis compared with ethanol injection for hepatocellular carcinoma < or = 4 cm. *Gastroenterology* 2004; **127**: 1714-1723

S- Editor Liu Y **L- Editor** Ma JY **E- Editor** Ma WH

PO Box 2345, Beijing 100023, China
www.wjgnet.com
wjg@wjgnet.com

World J Gastroenterol 2007 February 21; 13(7): 1010-1017
World Journal of Gastroenterology ISSN 1007-9327

LIVER CANCER

Rab23 is a potential biological target for treating hepatocellular carcinoma

Yun-Jian Liu, Qian Wang, Wen Li, Xiao-Hui Huang, Mao-Chuan Zhen, Shu-Hong Huang, Lian-Zhou Chen, Ling Xue, Hong-Wei Zhang

Yun-Jian Liu, Qian Wang, Wen Li, Xiao-Hui Huang, Maochuan Zhen, Lian-Zhou Chen, Department of Hepatobiliary Surgery, First Affiliated Hospital of Sun Yat-Sen University, Guangzhou 510080, Guangdong Province, China
Ling Xue, Depatment of Pathology, First Affiliated Hospital of Sun Yat-Sen University, Guangzhou 510080, Guangdong Province, China
Shu-Hong Huang, Hong-Wei Zhang, Institute of Developmental Biology, School of Life Sciences, Shandong University, Jinan 250100, Shandong Province, China
Correspondence to: Qian Wang, PhD, Department of Hepatobiliary Surgery, First Affiliated Hospital of Sun Yat-Sen University, Guangzhou 510080, Guangdong Province, China. wangqian00@hotmail.com
Telephone: +86-13929572752
Received: 2006-12-11 Accepted: 2007-01-23

Abstract

AIM: To elucidate the role of Rab23 in hepatocellular carcinoma (HCC) by assessing the expression of Rab23 in HCC tissue and in HCC cell lines.

METHODS: Primary tumors (n = 100) were stained with Rab23 antibodies using immunohistochemistry and *in situ* hybridization in tissue microarrays. Relationships between gene expression and pathology parameters were analysed. The biological significance of Rab23 in Hep-3B cells was examined by knocking down Rab23 gene expression. We designed a pair of double-stranded RNAs against human rab23 and transfected siRNA into Hep-3B cells. Rab23 expression in these cells was examined using RT-PCR and Western blots. We investigated cell growth by MTT assays and fluorescence-activated cell sorting.

RESULTS: High cytoplasmic and nuclear expression of Rab23 was found in 38 of 71 (53.5%) and in 49 of 68 HCC patients (72%) respectively, which correlated with tumor size. HCC cell lines expressed Rab23. In Hep3B cells, siRNA for Rab23 decreased Rab23 mRNA by 4.5-fold and protein expression by 2-fold. Survival rates at 24 and 48 h for Hep-3B cells transfected with siRNA were lower and about 30% Hep-3B cells were apoptotic. Knocking down rab23 suppressed Hep3B cell growth, suggesting that rab23 could play an important role in Hep3B cell growth.

CONCLUSION: Rab23 is overexpressed and/or activated in HCC. Rab23 may be both a HCC predictor and a target for treating HCC.

Key words: Rab23; Sonic hedgehog; Hepatocellular carcinoma; Tissue microarray; siRNA

Liu YJ, Wang Q, Li W, Huang XH, Zhen MC, Huang SH, Chen LZ, Xue L, Zhang HW. Rab23 is a potential biological target for treating hepatocellular carcinoma. *World J Gastroenterol* 2007; 13(7): 1010-1017

http://www.wjgnet.com/1007-9327/13/1010.asp

INTRODUCTION

Hepatocellular carcinoma (HCC) is the most frequent primary malignant tumor of the liver. HCC is the third leading global cause of cancer-related death. Over 54% of HCC cases occur in China. Hepatitis B virus is a common causal agent of liver cancer, and other factors have also been found. However, the molecular mechanisms contributing to tumor progression to HCC remain unknown[1].

In recent years, targeted therapies for a variety of HCCs have achieved clinically significant response rates and have given oncologists the chance to develop individual-based strategies for patient therapy. One rationale for such therapeutic approaches is to detect target molecules in the tumor. There is a growing list of such target molecules, the levels of which are now routinely estimated by IHC staining in biopsy specimens or surgically removing tumor material. Such assays not only generate important data for therapeutic decisions, but also provide information relevant to the prognosis of patients[2].

An example is targeting of the hedgehog (Hh) pathway. Dysregulation of this pathway has been implicated in the genesis of cancers from multiple tissue types[3]. Moreover, from embryogenesis to adulthood, skin and gastrointestinal progenitors are regulated by Hh signaling[4-6]. This pathway is activated when sonic hedgehog (SHH) or Indian hedgehog (IHH) ligands bind to their receptor, patched (PTC). When unoccupied by ligand, PTC is a tumor suppressor that binds to and represses smoothened (SMO)[7], preventing the SMO proto-oncoprotein from

activating downstream transcription factors, such as GLi1. Conversely, when ligand binds to PTC, SMO is released and GLi1 is activated, resulting in the transcription of target genes including PTC and Gli1[7]. Hh signaling is now known to play a critical role in the gastrointestinal tract in both health and disease. Most recently, two research groups have simultaneously reported abnormal activation of the SHH pathway in HCC[8,9]. Although the investigators paid much attention to the relationships between hedgehog signaling and HCC, little is known about this pathway in carcinogenesis.

One regulator of SHH signaling is Rab23. In 1994, the full-length cDNA encoding Rab23, a novel Ras-related small GTPase, was isolated using the sequence of a previously described GTPases[10]. Northern analysis revealed that Rab23 mRNA is predominantly expressed in the brain, which places the protein together with Rab3a and Rab15, in the group of small GTPases characteristic of the nervous system[11]. Rab23, a new member of the RAB family expressed in retina, is composed of 7 exons spanning a 34 kb domain of genomic DNA. It is located in the pericentromeric region of chromosome 6 between microsatellite markers D6S257 and D6S1659, within the critical region of RP25[12] and localized at the plasma membrane and the endocytic pathway[12,13]. Rab23 is a negative regulator of SHH[13,14]. It acts on upstream of Gli transcription factors in patterning neural cell types in the spinal cord. The primary target of Rab23 is the Gli2 activator. Rab23 and Gli3 repressors have additive effects on patterning. Analysis of Gli3 protein suggests that Rab23 also has a role in promoting the production of Gli3 repressor. Although the patched and smoothened membrane proteins can change subcellular location in response to SHH, analysis demonstrates that Rab23 does not work through either patched or smoothened membrane protein. Instead, Rab23 appears to regulate subcellular localization of essential components of the hedgehog pathway that act both on downstream of smoothened and on upstream of Gli proteins[15].

Until now there have no reports about Rab23 expression in HCC or even in other human tumors. Since Rab23 is a negative regulator of SHH signaling which can induce malignant carcinoma, dysregulation of Rab23 also may result in HCC. If it is true, we may be able to find a new target for diagnosis and treatment of HCC. In the present study, we evaluated the hypothesis that increases in Rab23 signaling induce hepatocarcinogenesis by regulating Hh signaling in HCC tissues.

MATERIALS AND METHODS

Overall experimental design

We compared Rab23 expression in non-neoplastic and malignant human livers by IHC and *in situ* hybridization using tissue microarrays. Furthermore, since it has been confirmed that there is hedgehog signaling in Hep-3B cells[8,9], we examined the biological significance of the Rab23 gene in Hep-3B cells by knocking down Rab23 gene expression. To identify a possible role of Rab23 in HCC, we designed a pair of double-stranded RNAs (dsRNAs) against human Rab23, and transfected siRNAs into Hep-3B cells. We examined Rab23 expression in these cells using RT-PCR and Western blots. We investigated cell growth by MTT assays and fluorescence-activated cell sorting.

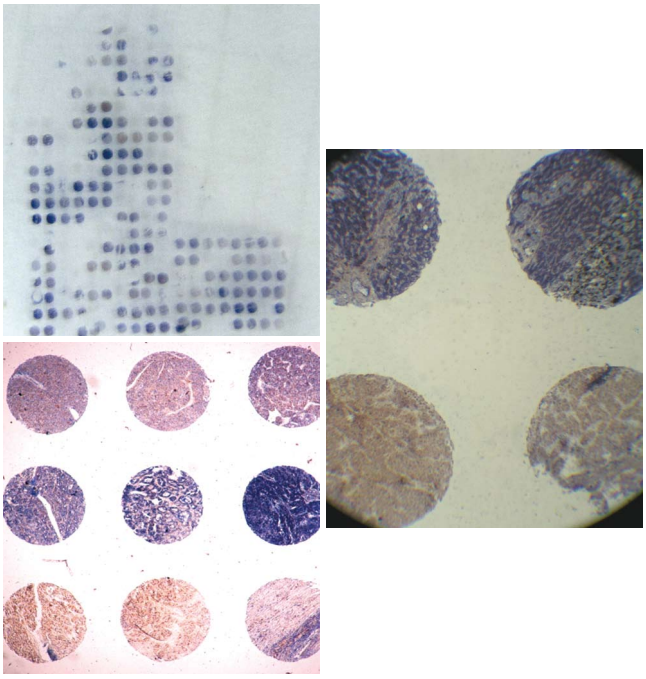

Figure 1 *In situ* hybridization using tissue microarrays.

Patient material

HCC samples from 100 patients were used in this study. All of them were from Sun Yat-Sen University (Guangzhou, China) and selected over a 4-year period (1993-1997). Twenty-five tumor adjacent liver tissue samples were also used. None of the patients received chemotherapy or radiation therapy. Each specimen was fixed in alcoholic formalin for 8-12 h and embedded in paraffin.

Construction of tissue microarray

A hundred archived formalin-fixed and paraffin-embedded anonymous, representative specimens of HCC were also assessed. Non-necrotic areas in tumor for coring into a tissue microarray (TMA) were marked using an indelible pen on a hematoxylin and eosin (HE) stained whole section from donor blocks. TMAs were assembled from formalin-fixed and paraffin-embedded tumor tissue samples as previously described[16] by using a precision instrument (Beecher Instruments, Silver Spring, MD). Cores (600 μm in diameter) were randomly arrayed in triplicate across the recipient block with asymmetrical placement for orientation. TMA coordinates and clinicopathological data were stored for reference. TMA slides were sectioned and mounted on Superfrost®/Plus microscope slides as 6-μm sections (Figure 1). Hematoxylin and eosin (H&E) stained TMA sections were used as morphological references.

Immunohistochemistry

Paraffin-embedded tissue sections were deparaffinized. Slides from each case were exposed to affinity purified rabbit anti-Rab23 primary antibody (BD Biosciences, San Jose, CA, USA) and diluted in PBS for 2 h at room temperature. Detection was carried out using Elivision TM Plus Polymer HRP (Mouse/Rabbit) immunohistochemistry kits (Maixin.Bio, Fuzhou,China). Location of peroxidase was visualized with diaminobenzidione(DAB). Hematoxylin was used for counterstaining. Sections were thoroughly washed with PBS between steps. Negative controls (absence of primary antibody) were run for each experiment. We defined a positive sample as one in which more than one third of one tissue chip was stained brown.

In situ hybridization

In situ hybridization was performed according to the manufacturer's instructions (Roche Molecular Biochemicals, Mannheim, Germany) and the published *in situ* hybridization protocol[17,18]. Sense and antisense probes were obtained by T3 or T7 *in vitro* transcription using a DIG RNA labeling kit from Roche (Mannheim, Germany). Rab23 (AY585189) was cloned into BamH1 of pBluescriptSK+. Tissue sections (8-μm thick) were mounted onto poly-L-lysine slides. Following deparaffinization, tissue sections were rehydrated in a series of ethanol dilutions. To enhance the signal and facilitate probe penetration, sections were immersed in 0.3% Triton X-100 solution for 15 min at room temperature and in proteinase K solution (20 μg/mL) for 20 min at 37℃, respectively. Sections were incubated with 4% (w/v) paraformaldehyde/phosphate-buffered saline (PBS) for 5 min at 4℃. After washed with PBS, slides were incubated with prehybridization solution (50% formamide, 50% 4 × SSC) for 2 h at 37℃. Probe was added to each tissue section at a concentration of 1 μg/mL and hybridized overnight at 42℃. After high stringency washing, the sections were incubated with an alkaline phosphatase-conjugated sheep anti-digoxigenin antibody, which catalyzes a color reaction with nitro-blue-tetrazolium (NBT)/5-bromo-4-chloro-3-indolyl phosphate (BCIP) substrate (Roche, Mannheim, Germany). A blue color indicated strong hybridization.

Culture of Hep-3B cell line

Hep-3B cells kindly donated by Professor Shi-Gang Xiong (Department of Pathology, Keck School of Medicine, University of Southern California, USA.), were cultured in Dulbecco's minimal essential medium (DMEM; Gibco BRL, Gaithersburg, MD, USA) supplemented with 10% fetal bovine serum (FBS; Bio-Whittaker, Walkersville, MD, USA), 100 IU/mL penicillin, and 100 μg/mL streptomycin. Cultures were incubated at 37℃ in a humidified atmosphere containing 50 mL/L CO_2, and the medium was changed twice a week. Cell viability was tested by trypan blue exclusion. All experiments were performed with Hep-3B cells from passages 6-15, which were exposed to serum-free culture medium containing 0.1% bovine serum albumin for 24 h.

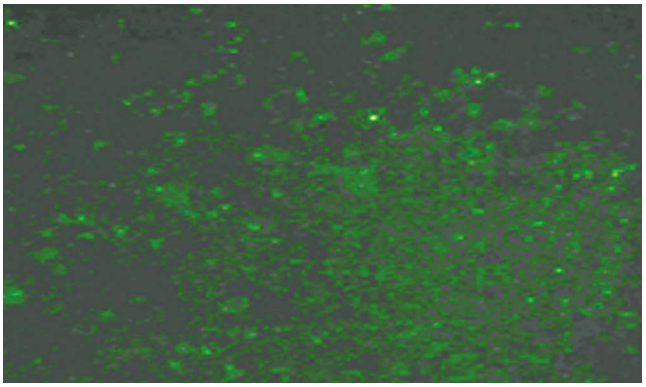

Figure 2 Rab23 gene silencing in Hep-3B cells. Green fluorescence could be detected in siRNA-transfected Hep-3B cells (negative control group).

Rab23 gene silencing in Hep-3B cells

Hep-3B cells were harvested by trypsinization and seeded 24 h prior to transfection, on 6-well plates at a density of 300 000 cells/well in 2 mL DMEM with 10% FBS. When the Hep-3B cells were at 90%-95% confluence, the culture medium was replaced with 1 mL of DMEM with or without 10% FBS. Following an overnight incubation, cells received 1 mL of complete medium and were incubated until 72 h post transfection.

According to the design principle of siRNA[19-21], short interfering RNA for Rab23 and negative control siRNA were designed. The target gene sequence of Rab23 is 5`-3` CCA GAA CTA ACG CAT TCA TCA A. The siRNA sequence (siRNA Duplex) is CCA GAA CUA ACG CAU UCA A dT dA dAdT GGU CUU GAU UGC GUA AGU U. The sequence of negative control siRNA is: sense 5`-UUC UCC GAA CGU GUC ACG UTT-3`, Anti-sense 5`-ACG UGA CAC GUU CGG AGA ATT-3`. Short interfering RNAs (siRNAs) for Rab23 were purchased from Guangzhou Ribobio CO., Ltd (Guangzhou, China) and negative control siRNAs were purchased from Shanghai GenePharma Co., Ltd (Shanghai, China). Double-strand RNA (final concentration of 50 and 100 nmol/L) in OPTI-MEM (80 μL) and oligofectamine (4 μL) in OPTI-MEM (15 μL) were mixed and allowed to stand at room temperature for 20 min according to the manufacturer's directions (Invitrogen, Carlsbad, USA). The mixture was added directly into a culture of Hep-3B cells (1×10^5/mL) in OPTI-MEM (0.4 mL). After 24 h, the consequences of transfection were watched through fluorescence of the cells (Figure 2). Transfection efficiency was normalized by monitoring luciferase activity from total cell lysates using the firefly luciferase (FLuc) assay kit (Promega, madison, USA). Cells were analyzed after 12 h by MTT assay. After 48 h they were analyzed by fluorescence-activated cell sorting, Western blots and RT-PCR . All experiments were performed in triplicate.

RNA isolation and two-step real-time RT-PCR

Two-step real-time RT-PCR was performed to compare the expression of Rab23 in normal liver tissue samples and Hep-3B cell lines. Total RNA was extracted using

TRIzol reagent (Sigma) according to the manufacturer's instructions. Reverse transcription with oligo (dT) priming was used to generate cDNAs from total RNA (2 μg) extracts. The synthesized cDNAs for Rab23 and β-actin were amplified using specific sets of primers. Optimal oligonucleotide primers were designed using Beacon Designer 2.0 software (MWG Biotech, High Point, NC). The primers used to amplify human Rab23 were synthesized according to the following sequences: forward primer: 5' GTA GTA GCC GAA GTG GGA 3', reverse primer: 5' CCT TTG TTT GTT GGGTCT C 3' according to ABO34244 in the gene bank. β-actin primer was designed based on published cDNA sequences: forward primer 5'TCA TCA CCA TTG GCA ATG AG3', reverse primer 5' CAC TGT GTT GGC GTA CAG GT 3'. Each PCR mixture contained the appropriate set of forward and reverse primers (0.2 μmol/L), each dNTP at 0.25 mmol/L, 1.25 U Taq polymerase, and 2.5 mmol/L $MgCl_2$ in a PCR buffer. The PCR procedure consisted of 28 cycles of denaturation at 95℃ for 1 min, annealing at 58℃ for 1 min, and extension at 72℃ for 1 min, with initial denaturation of sample cDNA at 95℃ for 3 min and an additional extension period of 10 min after the last cycle. The PCR products were subjected to 1.5% agarose gel electrophoresis stained with ethidium bromide and quantitated by densitometry using an Image Master VDS system and associated software (Pharmacia, USA).

Protein extraction and Western blotting

Cells were washed with cold PBS and lysed by the addition of a lysis buffer containing 1% Nonidet P-40, 50 mmol/L Tris (pH 7.5), 150 mmol/L NaCl, 0.1% SDS, and protease inhibitor cocktail (Boehringer Mannhein, Lewes, U.K.) for 20 min at 4℃. Insoluble materials were removed by centrifugation at 15000 r/min for 15 min at 4℃. The supernatant was saved and the protein concentration was determined using a Bio-Rad protein assay kit (Bio-Rad, Hercules, CA). Cell extracts (50 μg/lane) were separated *via* 10% gel electrophoresis and electroblotted onto PVDF membranes. Nonspecific binding sites were blocked by incubating nitrocellulose sheets for 1 h in phosphate-buffered saline containing 5% low-fat dry milk. Membranes were probed with primary antibodies overnight at 4℃, followed by a secondary horseradish peroxidase-conjugated second antibody. Blots were developed using an enhanced chemiluminescence detection system (ECL, Amersham Pharmacia Biotech) according to the manufacturer's instructions.

MTT assay

The cell proliferation and viability were determined by MTT assay as previously described[18]. Briefly, cells (5×10^3 cells per well) were seeded in 96-well microtiter plates (Nunc, Denmark). After different treatments for 12 , 24 , 48 h or 72 h, an aliquot (50 μL) of MTT (Sigma) solution (2 mg/mL in PBS) was added to each well and the plates were incubated for an additional 4 h at 37℃. MTT solution in medium was aspirated off. To achieve solubilization of the formazan crystal formed in viable cells, 150 μL DMSO was added to each well. The absorbance was read at 490 nm on a Dias automatic microwell plate reader with DMSO as the blank.

Fluorescence-activated cell sorting

After treatment for 48 h, cells were washed with cold sterile phosphate-buffered saline (PBS), and harvested in 70% cold alcohol solution for immediate analysis in a Becton Dickinson FACScan flow cytometer (Becton Dickinson, San Jose, CA). Data were acquired and analyzed using CellQuest software (BD Biosciences). The flow cytometer was calibrated daily with CaliBRITE 3 (BD biosciences) for fluorescence sensitivity and spectral overlap.

Statistical analysis

For immunohistochemistry and *in situ* hybridization results, Fisher's exact test or a binomial proportion analysis was used. $P < 0.05$ was considered statistically significant. Results of RT-PCR, Western blotting and MTT assays were expressed as mean ± SE of at least three separate experiments. Results were analyzed by one-way analysis of variance (ANOVA) followed by the Student-Neumann-Keuls test. Again, differences with P values of < 0.05 were considered statistically significant.

RESULTS

Expression of Rab23 in normal liver tissues and HCCs by immunohistochemistry

The expression of Rab23 in normal liver tissues has not been reported. Slight or no membranous staining of Rab23 in normal liver tissue was detected in our study. There was also no cytoplasmic or nuclear staining of Rab23 in normal liver tissues (Figure 3A). Conversely, expression of Rab23 was found in HCCs, and the expression rate was 53.5% (38 of 71 samples were positive, Table 1). Most samples expressed Rab23 in nuclei of HCC cells (Figure 3B and C). The results of expression of Rab23 correlated with tumor size ($P < 0.01$, Table 1), suggesting that Rab23 might be a useful prognostic indicator in HCC .

Expression of Rab23 in normal liver tissue and HCCs by in situ hybridization

No expression of Rab23 could be detected by *in situ* hybridization in five normal liver tissue samples (Figure 3D). To confirm this result, we also checked the transcripts by RT-PCR, and got the same result (data not shown).

To assess the frequency of Rab23 activation in HCC, we examined its expression in tissue samples derived from 100 different HCC cases (Table 1). We found positive staining for Rab23 in 38 of 71 (72%) HCC cases (Figure 3E and F). Further analyses again showed that activation of Rab23 correlated with tumor size ($P < 0.01$, Table 1).

Low expression of Rab23 in Hep-3B cell line when it was silenced by siRNA

Hep-3B cells were divided into three groups: a transfected group, a blank control group, and a negative control group. After 24 h of treatment with siRNA, Hep-3B cells were

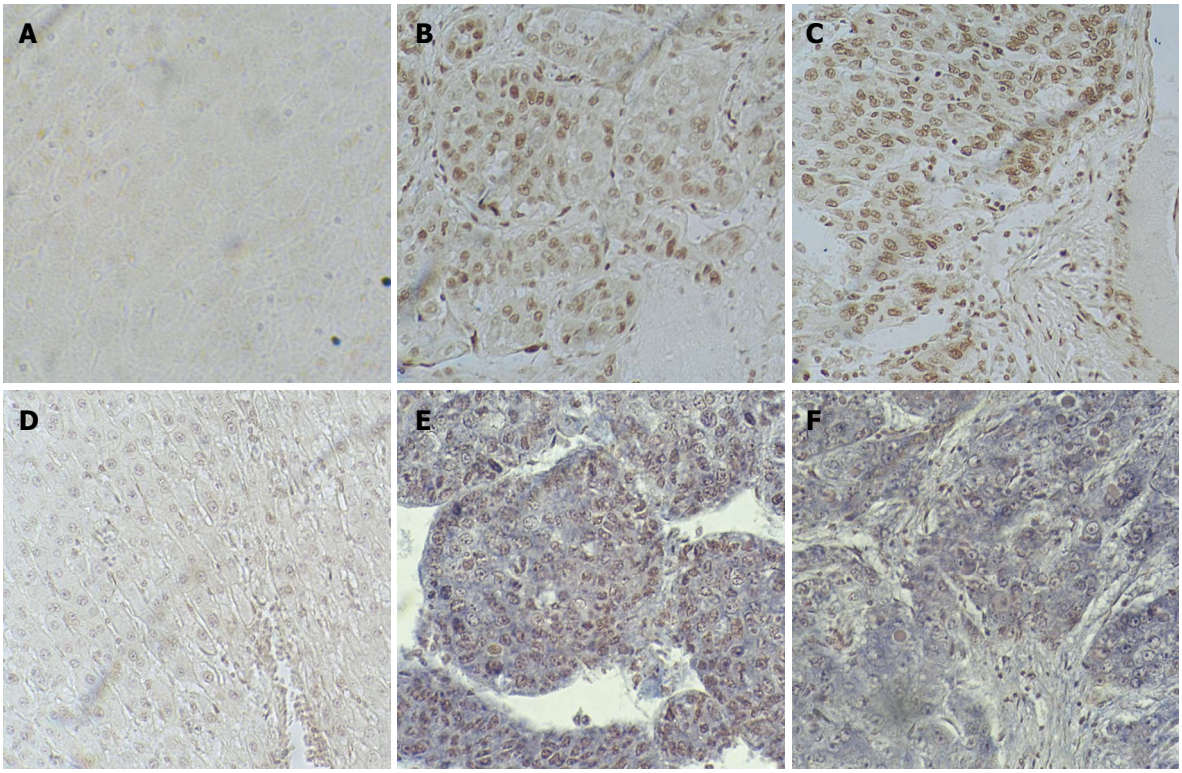

Figure 3 Expression of Rab23 in normal liver tissues and HCCs as seen by immunohistochemistry (**A-C**) and *in situ* hybridization (**D-F**).

Table 1 Expression of Rab23 in HCC (*in-situ* hybridization and immunohistochemistry)

	In-situ hybridization			limmunohistochemistry		
	Pos	Neg	*P*	Pos	Neg	*P*
Normal	0	5		0	5	
Paracarcinoma	0	18		0	18	
HCC	38	33		48	19	
Tumor Differentiation						
Well	4	3		6	1	
Mod and poor	34	30	0.3028	42	18	0.2681
Metastasis						
Yes	9	5		10	4	
No	29	28	0.2663	38	15	0.2591
Tumor size						
Small	3	11		4	13	
Large	35	22	0.0072	35	15	0.001
Age						
⩾ 50 yr	14	10		15	9	
< 50 yr	24	23	0.5613	33	10	0.2149
Sex						
Male	29	26		44	15	
Female	9	7	0.8036	4	4	0.1156
HBsAg						
Pos	34	31		46	17	
Neg	4	2	0.2721	2	2	0.2517
AFP						
⩾ 20 μg/L	26	24		35	12	
< 20 μg/L	12	9	0.6917	13	7	0.4314

Statistical analysis was performed by Fisher's exact test or Binomial proportions analysis. A *P* value < 0.05 was considered statistically significant. Pos: positive signal; Neg: Negative signal; Well: Well-differentiated tumors; Mod-poor: Moderately to poorly differentiated tumors.

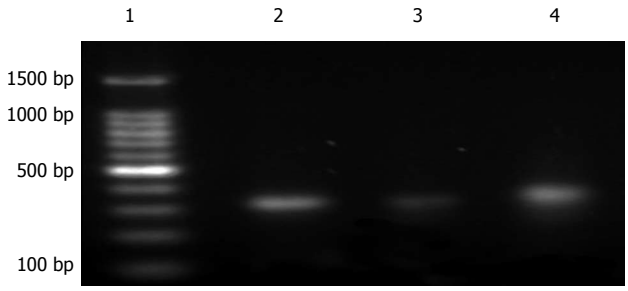

Figure 4 Electrophoresis of the RT-PCR products of Rab23 mRNA in Hep-3B cells after being silenced by siRNA. Lane 1: marker 1500; Lane 2: blank control group; Lane 3: transfection group; Lane 4: negative control group.

harvested and total RNA was extracted. RT-PCR was done as described previously[18]. The expression levels in the transfected group decreased almost 4.5 fold compared with the blank control group. There was no statistical significance between the blank control group and the negative control group (Figure 4,Figure 5, Figure 6).

Expression of Rab23 protein in Hep-3B cells decreased when it was silenced by siRNA

We used the same method for preparing Hep-3B cells for Western blots as for preparing cells for RT-PCR. After 24 h of treatment, Hep-3B cells were harvested and protein was extracted. Western blots were run according to a protocol described previously[22]. The expression levels in the transfected group decreased to almost half the level of the blank control group. There was no statistical

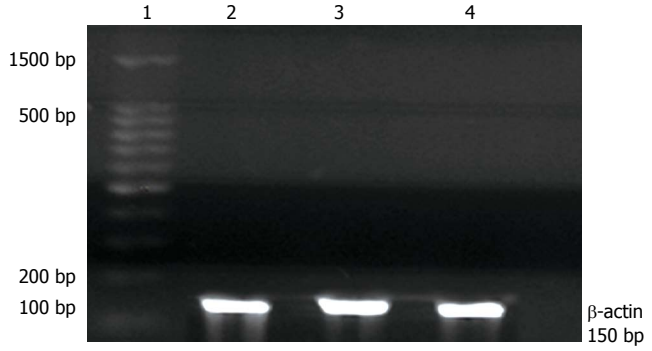

Figure 5 Electrophoresis of the RT-PCR products of β-actin mRNA in Hep-3B cells. Lane 1: marker 1500; Lane 2: blank control group; Lane 3: transfection group; Lane4: negative control group.

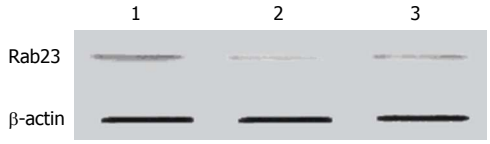

Figure 7 Western blot results for Rab23 in Hep-3B cells after being silenced by siRNA. Lane 1: blank control group; Lane 2: transfection group; Lane 3: negative control group.

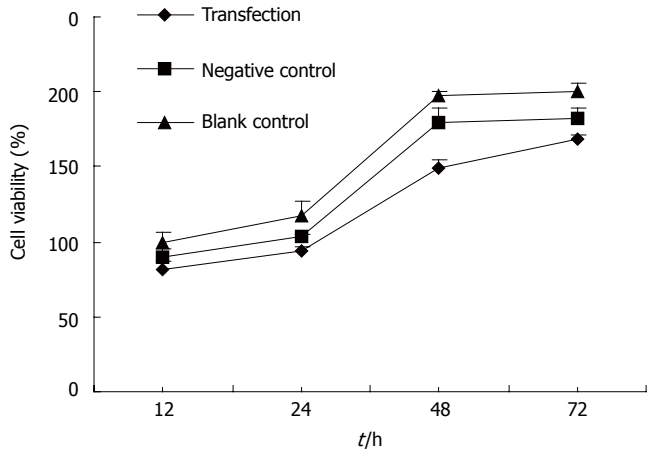

Figure 9 The results of MTT assays. At 48 h and 72 h, growth of Hep-3B cells was inhibited after being interferenced by siRNA against Rab23 gene. the survival rate of the transfection group decreased compared with controls. $P < 0.01$ *vs* control group. Again, there was no significant difference between blank and negative control groups, $P > 0.05$.

significance between the blank control group and the negative control group (Figure 7, Figure 8).

Viability of Hep-3B cells decreased after being transfected

Here we determined whether inhibition of the expression of Rab23 in Hep-3B cells also inhibits the proliferation of these cells by MTT assay. Forty-eight hours and 72 h after adding siRNA, the survival rate of the transfected group decreased compared with controls ($P < 0.05$, Figure 9). Again, there was no significant difference between the blank and negative control groups.

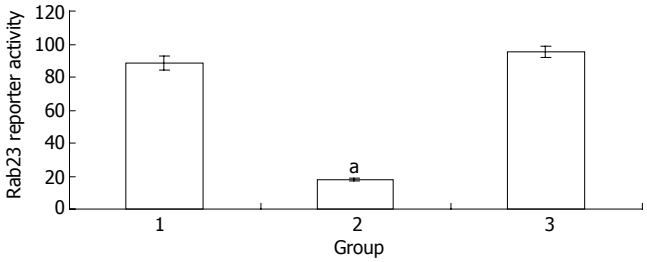

Figure 6 Electrophoresis of the RT-PCR products of Rab23 mRNA in Hep-3B cells after being silenced by siRNA. Lane 1: blank control group; Lane 2: transfection group; Lane 3: negative control group. [a]$P < 0.05$ *vs* control.

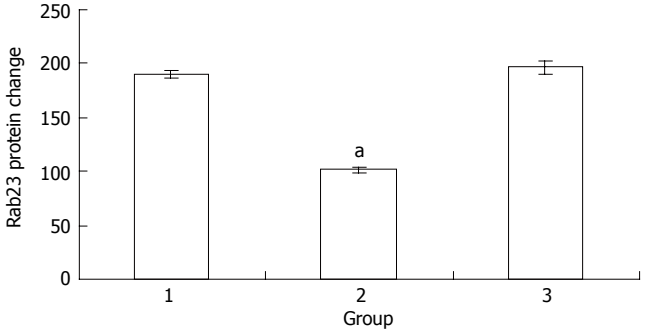

Figure 8 Western blot result for Rab23 in Hep-3B cells after being silenced by siRNA. Lane 1: blank control group; Lane 2: transfection group; Lane 3: negative control group. [a]$P < 0.05$ *vs* control.

Apoptosis rate of Hep-3B cells increased after the Rab23 gene was silenced by siRNA

Forty-eight hours after siRNA treatment, Hep-3B cells were tested by fluorescence- activated cell sorting. Apoptosis skewness was seen in the transfected group. The apoptotic rate of Hep-3B was 30% in the blank control group but 0% in the negative control groups (Figure 10).

DISCUSSION

The worldwide incidence of liver cancer is expected to rise over the next decade. This is serious because the prevalence and mortality rate of HCC are rather high at present[23]. Furthermore, the mechanisms underlying the initiation and progression of HCC remain elusive. One candidate mechanism involves the hedgehog (Hh) pathway. Dysregulation of this pathway has been implicated in the genesis of several kinds of cancer derived from multiple tissue types[3], including HCC[8,9]. One aspect of Hh signaling is negative regulation of this pathway by Rab23[13,15]. Rab23 acts on upstream of Gli transcription factors in patterning neural cell types in the spinal cord. The primary target of Rab23 is the Gli2 activator. Rab23 and Gli3 repressor have additive effects on pattering. Analysis of the Gli3 protein suggests that Rab23 also has a role in promoting the expression of Gli3 repressor. Although the membrane proteins patched and smoothened can change subcellular location in response to SHH, analysis demonstrates that Rab23 does not work through either patched or smoothened. Instead, Rab23 appears to

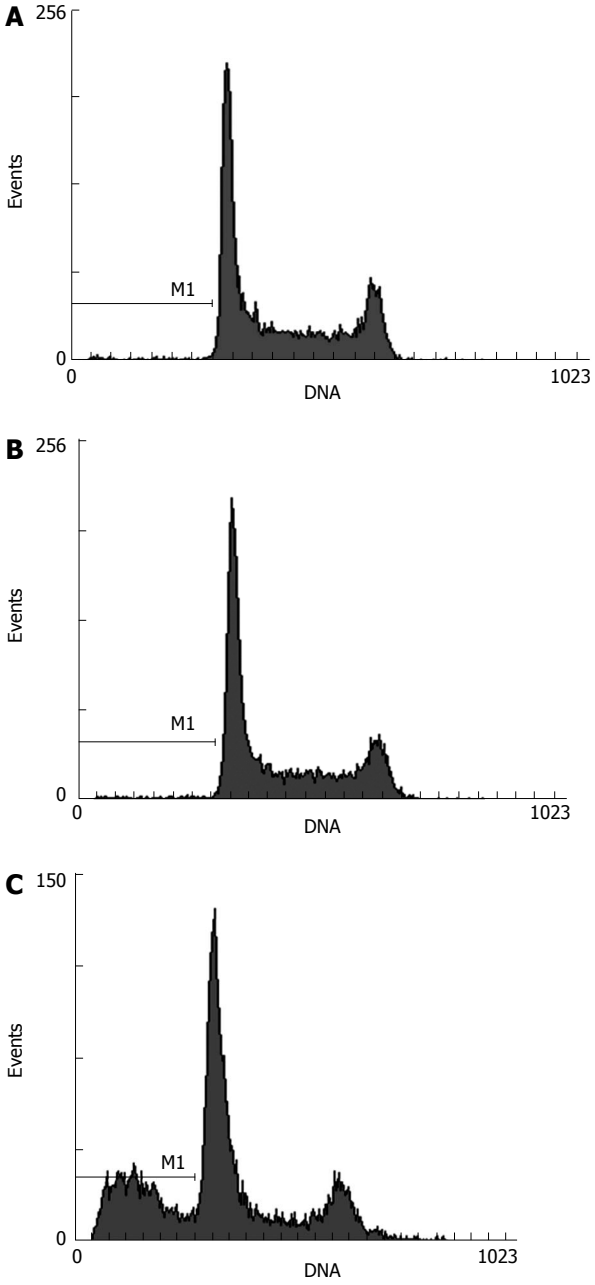

Figure 10 Apoptotic rate of Hep-3B cells measured by flow cytometry. in negative control (**A**), blank control (**B**) and transfected (**C**) groups.

regulate subcellular localization of essential components of the hedgehog pathway that act both on downstream of smoothened and on upstream of Gli proteins[14].

There are no reports about studies of Rab23 in HCC or even in any other human tumors. Since Rab23 is a negative regulator of SHH which can induce malignant carcinoma, Rab23 may also contribute to tumorigenesis in HCC.

Our results identify one potential mechanism underlying hepatocarcinogenesis, namely dysregulation of Rab23 and SHH signaling. In this study, we found that the aberrant expression of Rab23 was a general event during the development of HCC, and that the expression of the Rab23 gene correlated with tumor size. These findings are strongly supported by our studies of Hep3B cells in which Rab23 was silenced by siRNA, which inhibited cell proliferation and increased apoptosis. Further studies are now needed to identify the mechanisms by which Rab23 expression might contribute to dysregulation of SHH signaling and HCC tumorigenesis. Rab23 plays an important role in tumorigenesis of HCC and other human tumors. Also, Rab23 may be a new biological target for prognosis and treatment of HCC.

ACKNOWLEDGMENTS

The authors thank Dr. Ningning Wang, Department of Medical Statistics and Epidemics, School of Public Health, Sun Yat-Sen University, for her valuable advice on statistics.

REFERENCES

1 **Tien LT**, Ito M, Nakao M, Niino D, Serik M, Nakashima M, Wen CY, Yatsuhashi H, Ishibashi H. Expression of beta-catenin in hepatocellular carcinoma. *World J Gastroenterol* 2005; **11**: 2398-2401
2 **Iimuro Y**, Fujimoto J. Strategy of gene therapy for liver cirrohosis and hepatocellular carcinoma. *J Hepatobiliary Pancreat Surg* 2003; **10**: 45-47
3 **Beachy PA**, Karhadkar SS, Berman DM. Tissue repair and stem cell renewal in carcinogenesis. *Nature* 2004; **432**: 324-331
4 **Clatworthy JP**, Subramanian V. Stem cells and the regulation of proliferation, differentiation and patterning in the intestinal epithelium: emerging insights from gene expression patterns, transgenic and gene ablation studies. *Mech Dev* 2001; **101**: 3-9
5 **Ruiz i Altaba A**, Sánchez P, Dahmane N. Gli and hedgehog in cancer: tumours, embryos and stem cells. *Nat Rev Cancer* 2002; **2**: 361-372
6 **van den Brink GR**, Bleuming SA, Hardwick JC, Schepman BL, Offerhaus GJ, Keller JJ, Nielsen C, Gaffield W, van Deventer SJ, Roberts DJ, Peppelenbosch MP. Indian Hedgehog is an antagonist of Wnt signaling in colonic epithelial cell differentiation. *Nat Genet* 2004; **36**: 277-282
7 **Taipale J**, Beachy PA. The Hedgehog and Wnt signalling pathways in cancer. *Nature* 2001; **411**: 349-354
8 **Sicklick JK**, Li YX, Jayaraman A, Kannangai R, Qi Y, Vivekanandan P, Ludlow JW, Owzar K, Chen W, Torbenson MS, Diehl AM. Dysregulation of the Hedgehog pathway in human hepatocarcinogenesis. *Carcinogenesis* 2006; **27**: 748-757
9 **Huang S**, He J, Zhang X, Bian Y, Yang L, Xie G, Zhang K, Tang W, Stelter AA, Wang Q, Zhang H, Xie J. Activation of the hedgehog pathway in human hepatocellular carcinomas. *Carcinogenesis* 2006; **27**: 1334-1340
10 **Chavrier P**, Simons K, Zerial M. The complexity of the Rab and Rho GTP-binding protein subfamilies revealed by a PCR cloning approach. *Gene* 1992; **112**: 261-264
11 **Olkkonen VM**, Peterson JR, Dupree P, Lütcke A, Zerial M, Simons K. Isolation of a mouse cDNA encoding Rab23, a small novel GTPase expressed predominantly in the brain. *Gene* 1994; **138**: 207-211
12 **Marcos I**, Borrego S, Antiñolo G. Molecular cloning and characterization of human RAB23, a member of the group of Rab GTPases. *Int J Mol Med* 2003; **12**: 983-987
13 **Evans TM**, Ferguson C, Wainwright BJ, Parton RG, Wicking C. Rab23, a negative regulator of hedgehog signaling, localizes to the plasma membrane and the endocytic pathway. *Traffic* 2003; **4**: 869-884
14 **Eggenschwiler JT**, Espinoza E, Anderson KV. Rab23 is an essential negative regulator of the mouse Sonic hedgehog signalling pathway. *Nature* 2001; **412**: 194-198
15 **Eggenschwiler JT**, Bulgakov OV, Qin J, Li T, Anderson KV. Mouse Rab23 regulates hedgehog signaling from smoothened

to Gli proteins. *Dev Biol* 2006; **290**: 1-12
16 **Packeisen J**, Korsching E, Herbst H, Boecker W, Buerger H. Demystified...tissue microarray technology. *Mol Pathol* 2003; **56**: 198-204
17 **Ma X**, Sheng T, Zhang Y, Zhang X, He J, Huang S, Chen K, Sultz J, Adegboyega PA, Zhang H, Xie J. Hedgehog signaling is activated in subsets of esophageal cancers. *Int J Cancer* 2006; **118**: 139-148
18 **Ma X**, Chen K, Huang S, Zhang X, Adegboyega PA, Evers BM, Zhang H, Xie J. Frequent activation of the hedgehog pathway in advanced gastric adenocarcinomas. *Carcinogenesis* 2005; **26**: 1698-1705
19 **Amarzguioui M**, Prydz H. An algorithm for selection of functional siRNA sequences. *Biochem Biophys Res Commun* 2004; **316**: 1050-1058
20 **Reynolds A**, Leake D, Boese Q, Scaringe S, Marshall WS, Khvorova A. Rational siRNA design for RNA interference. *Nat Biotechnol* 2004; **22**: 326-330
21 **Ui-Tei K**, Naito Y, Takahashi F, Haraguchi T, Ohki-Hamazaki H, Juni A, Ueda R, Saigo K. Guidelines for the selection of highly effective siRNA sequences for mammalian and chick RNA interference. *Nucleic Acids Res* 2004; **32**: 936-948
22 **Li W**, Zhang J, Huang Q, Zhu H, Zhang X. Long-term administering low anticoagulant activity heparin can lessen rat hepatic fibrosis induced by either CCl(4) or porcine serum injection. *Hepatol Res* 2006; **36**: 115-123
23 **Marrero JA**. Hepatocellular carcinoma. *Curr Opin Gastroenterol* 2005; **21**: 308-312

S- Editor Liu Y **L- Editor** Wang XL **E- Editor** Ma WH

PO Box 2345, Beijing 100023, China
www.wjgnet.com
wjg@wjgnet.com

World J Gastroenterol 2007 February 21; 13(7): 1018-1026
World Journal of Gastroenterology ISSN 1007-9327

COLORECTAL CANCER

Decreased fragile histidine triad expression in colorectal cancer and its association with apoptosis inhibition

Jie Cao, Xiao-Ping Chen, Wang-Lin Li, Jie Xia, Hong Du, Wei-Biao Tang, Hui Wang, Xi-Wen Chen, Huan-Qing Xiao, Yu-Yuan Li

Jie Cao, Wang-Lin Li, Jie Xia, Wei-Biao Tang, Hui Wang, Xi-Wen Chen, Huan-Qing Xiao, Department of Gastrointestinal Surgery, Affiliated Guangzhou First People's Hospital, Guangzhou Medical College, Guangzhou 510180, Guangdong Province, China
Xiao-Ping Chen, Center of Hepatic Surgery, Tongji Hospital, Tongji Medical College, Huazhong University of Science and Technology, Wuhan 430030, Hubei Province, China
Hong Du, Department of Pathology, Affiliated Guangzhou First People's Hospital, Guangzhou Medical College, Guangzhou 510180, Guangdong Province, China
Yu-Yuan Li, Department of Gastroenterology, Affiliated Guangzhou First People's Hospital, Guangzhou Medical College, Guangzhou 510180, Guangdong Province, China
Supported by the Natural Science Foundation of Guangdong Province, No. 06020005
Correspondence to: Jie Cao, MD, Department of Gastrointestinal Surgery, Affiliated Guangzhou First People's Hospital, Guangzhou Medical College, 1# Pang Fu Road, Guangzhou 510180, Guangdong Province, China. czhongt@126.com
Telephone: +86-20-81048185 Fax: +86-20-81045937
Received: 2006-11-14 Accepted: 2007-01-18

Abstract

AIM: To detect the expression of fragile histidine triad (FHIT) in normal colorectal tissue, colorectal adenoma and colorectal cancer (CRC) tissue, and to analyze its relationship with the clinicopathological features of CRC, and apoptosis-associated proteins (Bcl-2, Bax, survivin) and apoptosis in colorectal cancer.

METHODS: FHIT mRNA analysis was performed by nested reverse transcription-polymerase chain reaction (RT-PCR) assay. Tissue microarray (TMA) was established to detect the expression of FHIT, Bcl-2, Bax and survivin genes in 80 CRC tissue specimens, 16 colorectal adenoma tissue specimens and 16 hemorrhoid (PPH) tissue specimens during the same period of time as the control. Citrate-microwave-SP was used as immunohistochemical method. The relationship between clinicopathological factors, such as differentiation grades and 5-year survival rate was observed. TUNEL assay was used to detect the apoptosis index in 80 CRC tissue specimens.

RESULTS: Ten out of 26 (38.5%) CRC tissue specimens expressed aberrant FHIT transcripts, none of the aberrant FHIT transcripts was observed in the matched normal tissue and colorectal adenoma tissue by nested RT-PCR assay. The positive rate of FHIT gene expression in normal colorectal tissue, colorectal adenoma and carcinoma tissue was 93.75%, 68.75% and 46.25%, respectively. Clinicopathological analysis of patients showed that the decreased FHIT gene expression was not associated with age, sex, serum CEA levels, tumor site and size, histological classification. However, the expression of FHIT was correlated with differentiation grades, pathological stages, lymph node metastases and 5-year survival rate after operation. The positive rate of apoptosis-associated proteins (Bax, Bcl-2 and survivin) in CRC tissue was 72.50%, 51.25% and 77.50%, respectively. The expression of these apoptosis-associated proteins in CRC tissue was correlated with the expression of FHIT. The mean apoptosis index in FHIT negative tumors was significantly lower than that in FHIT positive tumors (5.41 ± 0.23 *vs* 0.56 ± 0.10, $P < 0.01$).

CONCLUSION: The FHIT gene plays an important role in the regulation of apoptosis and decreased FHIT expression plays a key role in the initiation and progression of colorectal carcinoma.

Key words: Colorectal cancer; Fragile histidine triad; Expression; Apoptosis

Cao J, Chen XP, Li WL, Xia J, Du H, Tang WB, Wang H, Chen XW, Xiao HQ, Li YY. Decreased fragile histidine triad expression in colorectal cancer and its association with apoptosis inhibition. *World J Gastroenterol* 2007; 13(7): 1018-1026

http://www.wjgnet.com/1007-9327/13/1018.asp

INTRODUCTION

Colorectal cancer is the second leading cause of death in the United States, where the cumulative lifetime risk of developing colorectal cancer in both men and women is 6%[1]. In China, colorectal cancer is the fourth leading cause of death[2].

The fragile histidine triad (FHIT) gene, is a tumor suppressor gene located at the fragile site FRA3B on chromosome 3p14.2 that can be identified by positional

cloning, a region of the genome showing loss of heterozygosity (LOH) in a variety of cancers[3,4]. FHIT is involved in carcinogenesis of many human tissues, including digestive tract tissue. The FHIT gene contains an open reading frame (ORF) of 444 base pairs (bps) encoding a protein of 147 amino acids, which appears to be ubiquitously expressed in human tissues. Large deletions within FHIT transcripts occur frequently in multiple malignancies[5,6]. Most of the deletions described to date in the FHIT gene involve loss of one or more coding exons and lead to a truncated protein[6]. Loss of FHIT protein expression and abnormal FHIT transcripts, including deletions and insertions of exons, have been found in lung and breast cancers, as well as in head and neck cancers[7-11]. Ohta *et al*[3] reported that aberrant transcripts of the FHIT gene have been observed in 38% of CRC cases. It was also reported that the FHIT gene plays an important role in both oncogenesis and progression of CRC[12-14]. However, Thiagalingam *et al*[15] showed that there is no evidence that the FHIT gene is involved in CRC carcinogenesis. The clinicopathological significance of FHIT alterations in CRC still remains unclear.

The role of FHIT expression in the development of colorectal cancer (CRC) is poorly understood. Recently, tissue microarray (TMA) technique has been developed, which can significantly increase the throughput of immunohistochemistry (IHC) tumor analysis. TMA is composed of a large number of small tissue cores punched out from different tumors. These tissue core specimens obtained from tissue blocks, are then arranged into a single recipient paraffin block[16]. This approach allows analysis of a large number of different tumor samples in one IHC experiment. Arrays as large as 1000 samples have been reported[17]. TMA can be used to test the prognostic significance of antibodies against proteins encoded by differentially expressed genes using a large number of archival patient samples. Decreased p53 expression is correlated with lymph node metastasis in CRC[18]. In our present study, an expanded repertoire of TMA technique was used to demonstrate the novel relationship between FHIT expression and clinicopathological factors, such as differentiation, pathological stages, lymph node metastasis and 5-year survival rate.

The presence of FHIT gene mutations correlates significantly with decreased FHIT expression in human CRC. Several well integrated biochemical subroutines promote CRC cell growth and inhibit apoptosis, tipping the balance of colon epithelial cells towards an unrestricted proliferation and outliving the sequence of mutations required for carcinogenesis. Apoptosis is essential for successful embryonic development and maintenance of normal tissue homeostasis[19]. The present study was to test the hypothesis that decreased FHIT expression inhibits apoptosis and decreases apoptosis-associated protein expression, to characterize FHIT mRNA and protein expression in normal colorectal tissue, and adenoma and adenocarcinoma tissue, and to investigate the mechanism of FHIT gene inactivation and its association with apoptosis inhibition in the development and progression of human CRC.

MATERIALS AND METHODS

Colorectal carcinoma tissue samples

Human colorectal tissue specimens were obtained from patients at the Department of Gastrointestinal Surgery, Affiliated Guangzhou First People's Hospital, Guangzhou Medical College, China, from January 1997 to June 2000. All tissue specimens were snap- frozen and stored at -80℃. There were 48 male and 32 female patients with an average age of 62 years (range 32-81 years). Of the 80 specimens of human colorectal carcinoma we examined, 20, 22, 23 and 15 were classified as Dukes' stage A, B, C and D, respectively. Histologically, well-differentiated CRC was found in 16, moderately-differentiated CRC in 44, and poorly-differentiated in 22 specimens, respectively (Table 1). As a control, 16 normal colorectal tissue specimens and 16 colorectal adenoma specimens were also obtained. These tissue specimens were snap-frozen in liquid nitrogen, embedded in paraffin and stored at -80℃. Sections of each paraffin block were stained with hematoxylin and eosin.

RT-PCR assay

Total RNA was isolated from 26 colorectal cancer and 26 normal adjacent colonic tissue specimens, and 14 adenoma and 14 normal adjacent colonic tissue specimens with TRIzol™ reagent (Life Technologies). Nested RT-PCR was carried out as described previously[20]. A 24 μL mixture of total RNA (10 μg), 0.4 mmol/L oligo (dT) (New England Biolabs), and QH_2O was prepared. After incubation for 10 min at 70℃, the mixture was quickly cooled on ice, and 16 μL of RT-PCR mixture containing 8 μL of 5 × first strand buffer (Invitrogen) (250 mmol/L Tris–HCl pH 8.3, 375 mmol/L KCl, 15 mmol/L $MgCl_2$), 4 μL of 0.1 M DTT (Invitrogen), 2 μL 10 mmol/L deoxynucleotide mixture (dATP, dTTP, dCTP and dGTP, 10 mmol/L each) (Roche), 2 μL of RNase inhibitor (40 U/μL) (Roche) was added. The reaction proceeded in GeneAmp 2400 (Applied Biosystems) at 45℃ for 2 min. After 400 U of SuperScript™ RnaseH-reverse transcriptase (200 U/μL) (Invitrogen) was added and incubated for 45 min at 60℃, the reaction was inactivated at 70℃ for 15 min and at 94℃ for 3 min. cDNA was used as a template in the following RT-PCR.

Mutation analysis of FHIT mRNA transcripts and aberrant splicing in human CRC by sequencing

Mutation screening in aberrant RT-PCR products was performed using an ABI 377 automated sequencer with a pEGM-T vector as described previously[21]. Aberrant migrating bands were directly sequenced after isolation of bands from low melting agarose and purification on columns.

Analysis of FHIT, Bax, Bcl-2 and survivin protein expression by TMA-IHC

Construction of tissue microarray (TMA): Archival paraffin-embedded, formalin-fixed tissues from 80 Chinese CRC, 16 colonic adenoma and 16 noncancerous normal mucosa patients were collected. Two independent experienced pathologists selected representative areas from

Table 1 Expression of FHIT and clinical or pathological factors

	n	FHIT expression		χ^2	*P*
		Positive	Negative		
Age					
< 60	34	16	18	0.16	0.901
⩾ 60	46	21	25		
Sex					
M	42	19	23	0.04	0.849
F	38	18	20		
Differentiated					
Well	16	12	4	4.84	0.028
Moderately	44	20	24		
Poorly	20	5	15		
Dukes					
A, B	45	27	18	7.82	0.005
C, D	35	10	25		
Lymph node metastasis					
Positive	16	11	5	4.07	0.006
Negative	64	26	38		
Survival					
⩾ 5 yr	35	23	12	5.77	0.016
< 5 yr	18	5	13		

each donor tumor block, and then one 1-mm core was taken from a representative area of the tumor and inserted into a recipient paraffin block to create the TMA[6]. One TMA slide contained 112 samples. We employed the TMA technique to explore the expression of FHIT, Bax, Bcl-2 and survivin in colorectal tumor specimens and its correlation with apoptosis status by TMA-IHC and TMA-TUNEL. We investigated consecutively-cut serial sections and examined the same tumor region in three dimensions.

Immunohistochemical analysis of FHIT, Bax, Bcl-2 and survivin expression in human CRC by TMA-IHC: Immunohistochemical studies were performed using a citrate-microwave-streptavidin peroxydase technique. Immunohistochemical detection was done using anti-FHIT, anti-Bax, anti-Bcl-2 and anti-survivin antibodies, respectively. Endogenous peroxidase activity was quenched by methanol containing 3% hydrogen peroxide (Sigma, Taufkirchen, Germany). Nonspecific binding was blocked by applying normal rabbit serum in a humidity chamber at a dilution of 1:10 for 30 min. Primary antibodies were applied overnight at 4℃. The secondary antibody (goat to mouse immunoglobulins, DAKO, Denmark) was applied for 1 h at room temperature. Peroxidase–antiperoxidase (PAP rabbit, DAKO) conjugate diluted at 1:100 in phosphate-buffered saline (PBS) was applied for 45 min at room temperature. The sections were stained with diaminobenzidine tetrahydrochloride (DAB, Sigma) and then counterstained with hematoxylin. Negative control staining was performed by omitting the primary antibody. As a positive control for FHIT protein in immunohistochemical studies, we used paraffin sections of lung cancer positive for FHIT protein.

Quantitative measurements: Quantitative analysis of immune reactions related to the total tissue area was performed. We measured the percentage of positive immune reactivity with these antibodies in the tissue epithelium (normal and tumor). Histological images were captured with an OLYMPUS BX50 system microscope with an objective at magnification X 40, through a video camera, and digitized by appropriate software. In each section, 500 cells per core were calculated. The relative level of specific immunostaining and its localization were also judged. The relative intensity of cell immunostaining was evaluated semi-quantitatively. The data of tissue array were confirmed by a pathologist at the Department of Pathology of Affiliated Guangzhou First People's Hospital.

Hierarchical clustering and tree-view analysis: Hierarchical clustering was performed by the Cluster program (available at http://rana.lbl.gov/) as described previously in two dimensions: tumors were grouped together based on the relation of their immunostaining profiles, and antibodies were grouped based on tumors they stained. The clustered data were visualized with the Tree-view software tool programs originally developed for analyzing cDNA microarray data (Available at http://rana.lbl.gov/), which graphically displayed the results of the analysis as dendrograms and arrays, wherein the rows and columns corresponded to the raw staining data, presented in the order determined.

Detection of cell apoptosis state in human CRC by TUNEL assay

Cell apoptosis was detected in 80 CRC specimens by TMA-TUNEL assay (Apotag Peroxidase Kit, Oncor, Gaithersburg, MD) with the Apop-Tag™ peroxidase kit (Zhongshan Biotech, Beijing). For the evaluation of TUNEL index, the number of TUNEL-positive colonic epithelial cells was recorded using the × 40 objective lens. The case was considered positive for TUNEL if any colonic epithelial cells showed TUNEL staining. The TUNEL index was determined as the number of TUNEL-positive colonic epithelial cells expressed as a percentage of the total number of counted colonic epithelial cells. Necrotic areas were excluded.

Statistical analysis

Results were presented as mean ± SD. All statistical analyses were carried out using SPSS 11.0 for Windows statistical software (SPSS Inc, USA). The relationship between the clinicopathological variables and FHIT loci and protein alterations was examined by Fisher's exact test. The relationship between the expression of FHIT and prognosis of CRC was analyzed by Cox-Mantel test. $P < 0.05$ was considered statistically significant. All experiments were performed three times.

RESULTS

Analysis of aberrant splice of FHIT gene in human CRC

Expression of FHIT mRNA was detected by nested RT-PCR. According to the results, 34.6% samples with abnormal FHIT expression displayed two transcript categories: normal FHIT transcript (PCR products = 707 bp) and aberrant FHIT transcript (PCR products = 336 bp and 239 bp), respectively (Figure 1). However, the samples with normal FHIT expression only showed a normal FHIT transcript size.

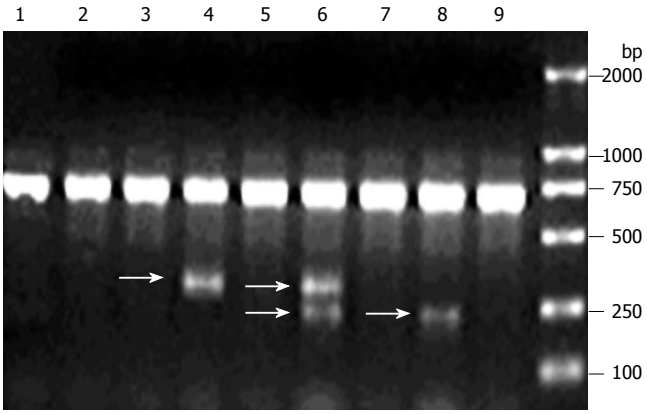

Figure 1 Frequency of intragenic deletions in FHIT transcripts in human CRC. Gel photo of FHIT RT-PCR products showing that the full length FHIT was the predominant transcript in samples 1-3, 5, 7 and 9. Both full length FHIT and shorter fragments representing transcripts containing deletions in FHIT could be seen in samples 4, 6 and 7. The arrow shows the gel position of splice variants.

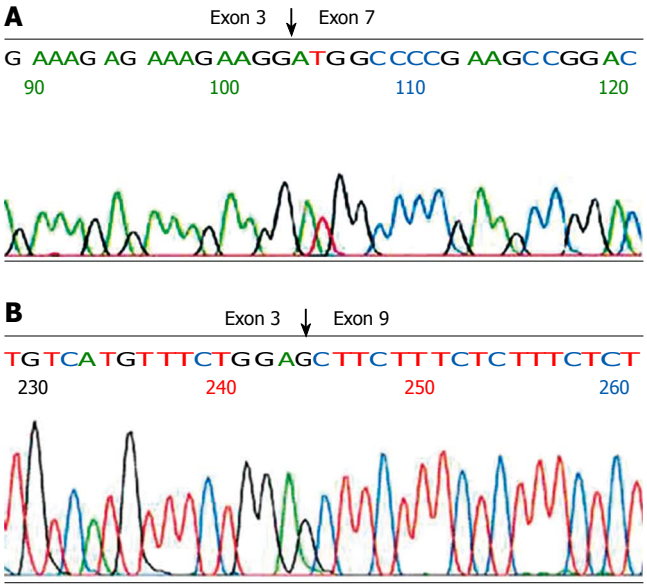

Figure 2 Sequencing analysis of aberrant FHIT transcripts. **A**: Deletion of exons 4-6 in the FHIT gene; **B**: Deletion of exons 4-8 in the FHIT gene.

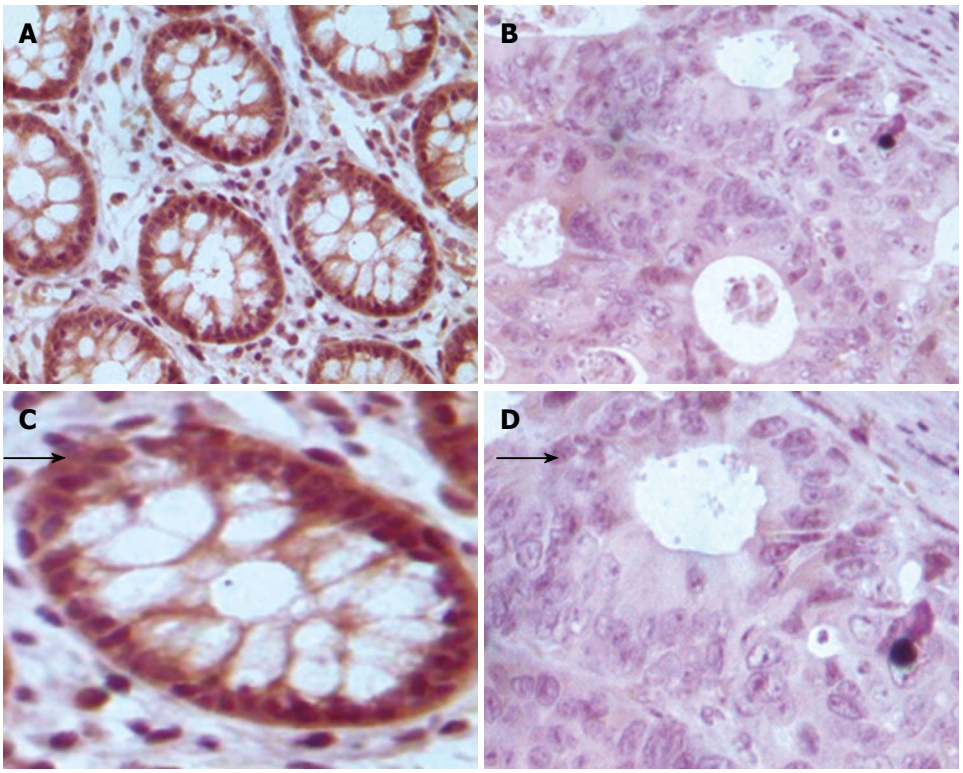

Figure 3 TMA-IHC assay showing significantly decreased FHIT expression in normal colonic mucosal samples (**A**), CRC tissue samples (**B**), and magnified views of the respective samples **A** and **B** (**C** and **D**).

Mutation analysis of FHIT gene in human CRC by sequencing

Aberrant RT-PCR products were sequenced after isolation of bands from low melting agarose and purification on columns. In the 336 bp fragment, Exon 3 was spliced to exon 7 (E3/E7), and thus the transcript lacked exons 4-6 (Figure 2A). In the 239 bp fragment, Exon 3 was spliced to exon 9 containing an E3/E9 aberrant transcript (Figure 2B).

Clinicopathological features and their relation to expression of FHIT in human CRC

The correlation between FHIT protein expression and clinicopathological data in the 80 carcinoma specimens is shown in Table 1, and a photograph of a representative specimen is provided in Figure 3. FHIT negative CRC was found in 43 and FHIT FHIT positive CRC was found in 37 specimens. Fifty-three percent (32 of 60) of specimens with well-differentiated CRC had positive

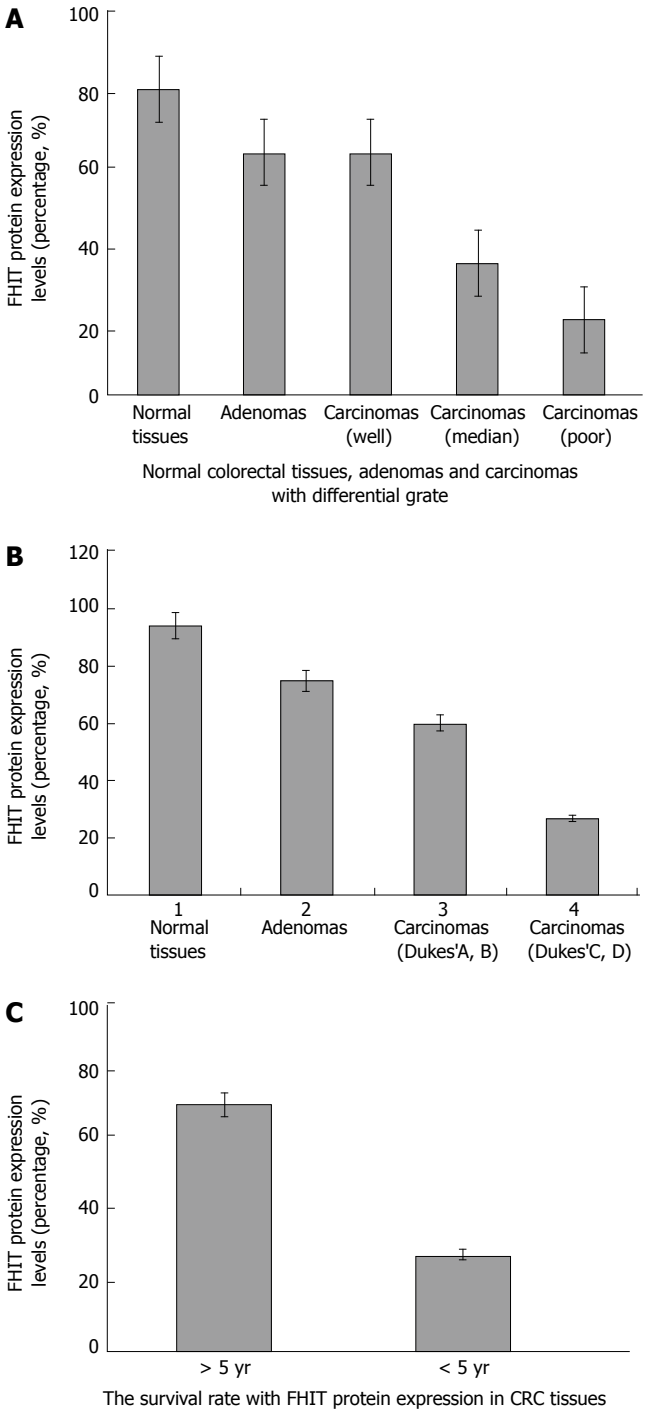

Figure 4 Relationships between FHIT expression and CRC differentiation grade (**A**) and stage (**B**), and survival rate (**C**) CRC patients.

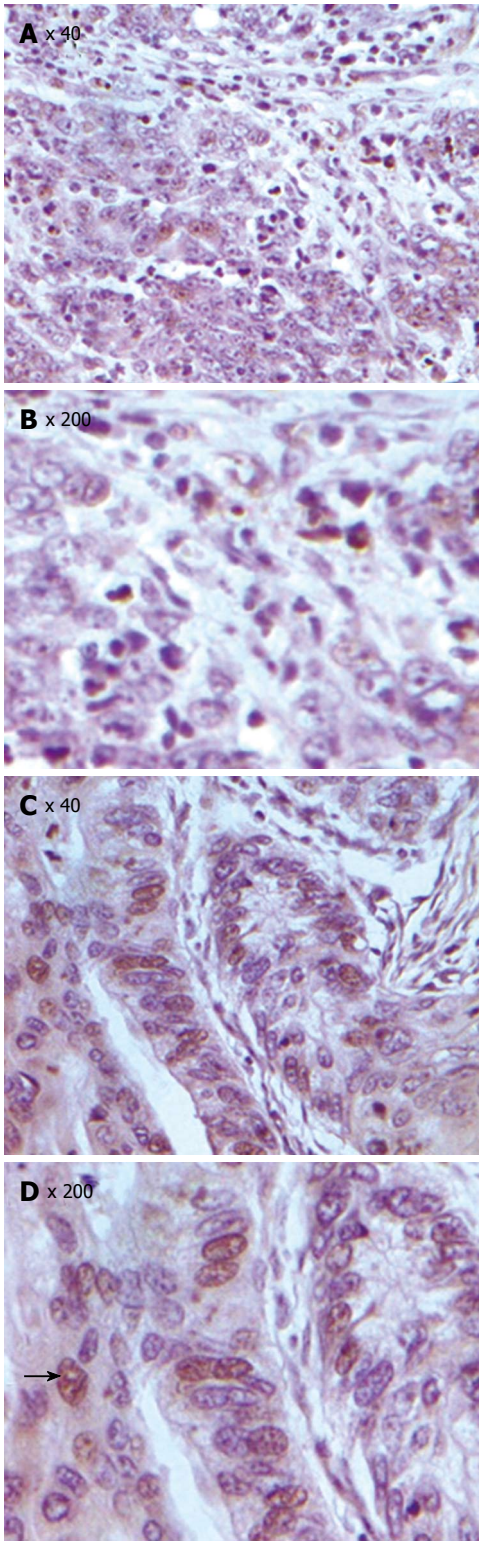

Figure 5 TUNEL assay showing significantly decreased apoptosis in FHIT-negative CRC cells (**A**), FHIT-positive CRC cells (**C**), and magnified views of the respective samples **A** and **C** (**B** and **D**).

FHIT expression, whereas 25% (5 of 20) of specimens with poorly-differentiated CRC had positive FHIT expression ($P < 0.05$), while 93.75% (15 of 16) and 75% (12 of 16) had positive FHIT expression in the normal colorectal tissue specimens and colorectal adenoma specimens, respectively (Figure 4A and Table 1). Sixty percent (27 of 45) of specimens with Dukes' A and B had positive FHITexpression, whereas only 28% (10 of 35) of specimens with Dukes' C and D had positive FHIT expression ($P < 0.005$) (Figure 4B and Table 1). Moreover, prognosis of the FHIT-negative cases was much poorer than the FHIT-positive cases (Figure 4C and Table 1). There was no significant correlation between other clinicopathological factors and FHIT expression.

Apoptosis status in human CRC as assessed by TUNEL

The role of FHIT protein in apoptosis as a proapoptic factor was detected by TUNEL assay. Aberrant expression of the FHIT gene was related to colonic epithelial cell apoptosis (Figures 5 and 6, Table 2). The apoptosis index was 5.41 ± 0.23 in colorectal cancer with normal FHIT

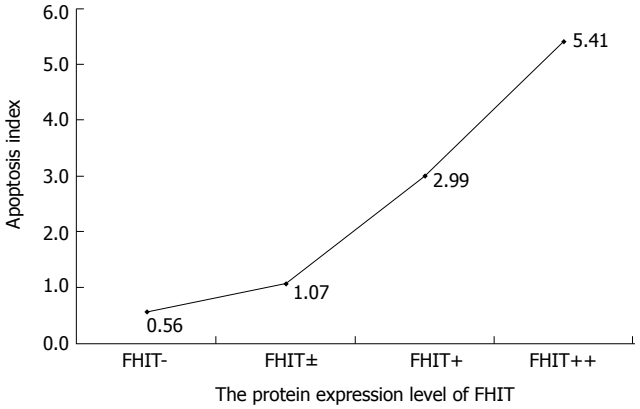

Figure 6 Decreased FHIT expression and apoptosis inhibition in human CRC. Reduced apoptosis index was detected in the same number of cells per field in CRC with FHIT-negative expression.

Table 2 Relationship between FHIT expression and apoptosis index (AI) in human CRC

FHIT	*n*	AI
-	11	0.56 ± 0.10
+/-	15	1.07 ± 0.16
+	17	2.99 ± 0.32
++	37	5.41 ± 0.23

expression and 0.56 ± 0.10 in tumors with absent FHIT expression. The rate of apoptosis was significantly lower in tumors with aberrant FHIT expression than in tumors with normal FHIT expression ($P < 0.05$).

Expression of Bax, Bcl-2 and survivin and its correlation with FHIT alteration

Since growth inhibitory effect of FHIT- expressing cells is related to apoptosis, we determined whether FHIT protein is related with other members in the apoptotic pathway. Of the CRC tissue specimens, 54% (43 of 80) had positive FHIT expression, whereas the remaining 46% (37 of 80) had no detectable FHIT expression by TMA-IHC assay (Figure 7, Figure 8, Figure 9 and Figure 10). Seventy-seven percent of FHIT protein-negative CRC specimens showed decreased Bax expression, whereas 75% and 60% FHIT protein-negative specimens displayed increased Bcl-2 and survivin expression (Figure 7, Figure 8, Figure 9 and Figure 10). The difference was statistically significant (Table 3).

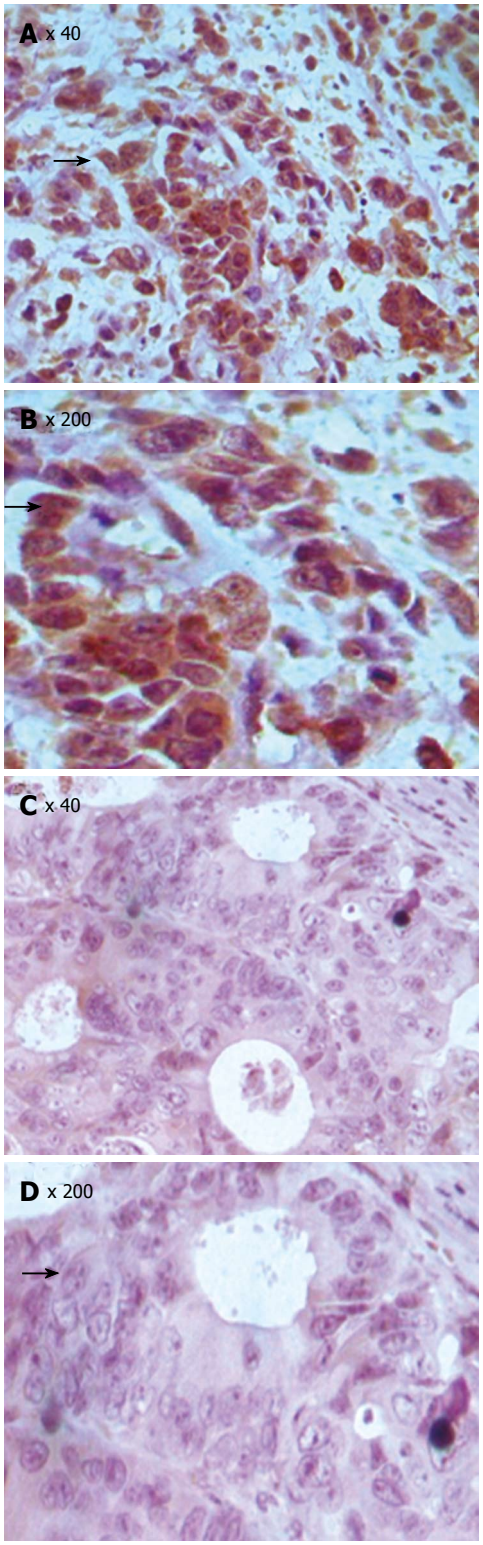

Figure 7 TMA-IHC showing significantly decreased Bax expression in FHIT positive CRC tissue samples (**A**), FHIT-negative CRC tissue samples (**C**), and magnified views of the respective samples **A** and **C** (**B** and **D**).

DISCUSSION

In the present study, frequent allelic loss was observed on chromosome 3p in lung cancer and preneoplastic bronchial lesions, indicating that inactivation of putative tumor suppressor genes on chromosome 3p may be involved in early steps of lung carcinogenesis. Ohta *et al*[3] have identified the FHIT gene on chromosome 3p14.2, spanning the FRA3B common fragile site and the t (3:8) break point associated with hereditary renal cell carcinomas. The FHIT gene is more than 1 Mb in size, encoding a 1.1-kb cDNA with 10 small exons and a cytoplasmic Mr 16 800 protein with diadenosine triphosphate (Ap3A) hydrolase activity [4]. In this study, truncated FHIT transcripts were observed frequently alongside full-length transcripts and sequence analysis of the truncated gene transcripts revealed mainly

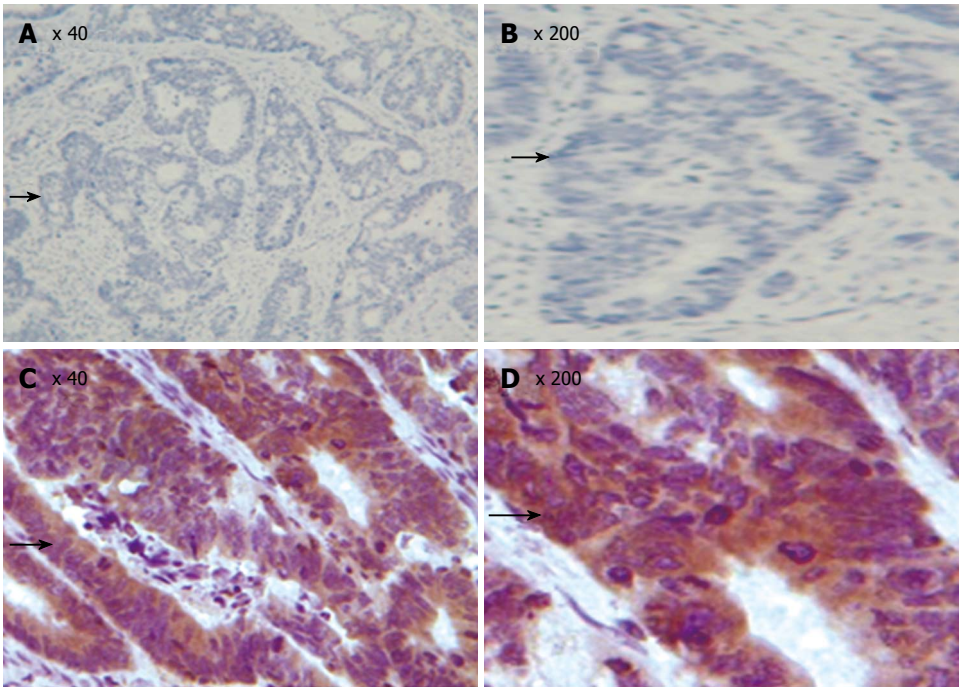

Figure 8 TMA-IHC showing significantly increased Bcl-2 expression FHIT positive CRC tissue samples (**A**), FHIT-negative CRC tissue samples (**C**), and magnified views of the respective samples **A** and **C** (**B** and **D**).

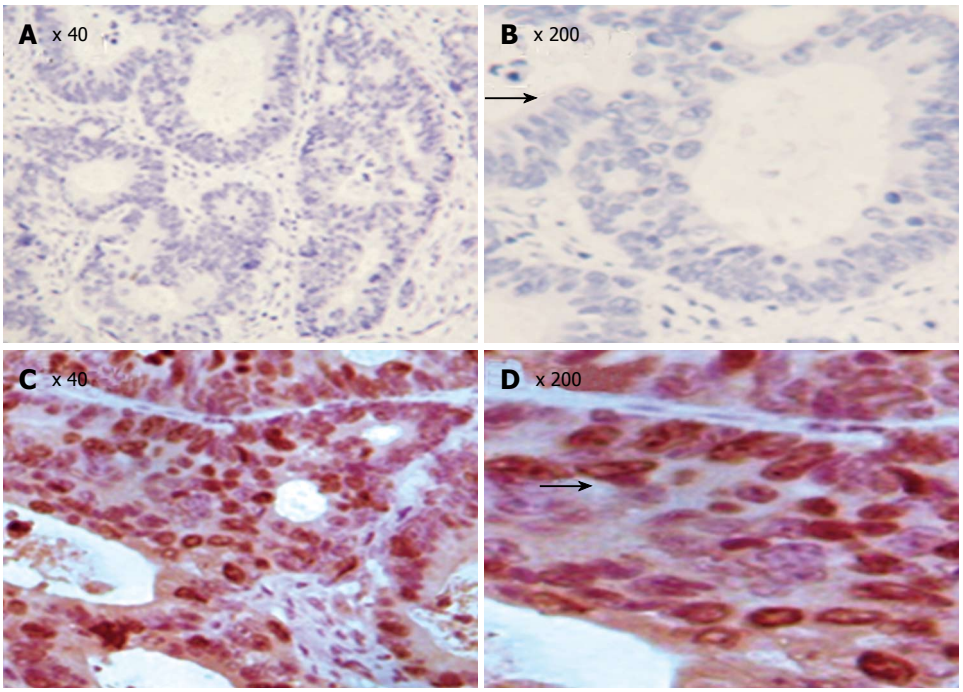

Figure 9 TMA-IHC showing significantly increased survivin expression in FHIT-positive CRC tissue samples (**A**), FHIT-negative CRC tissue samples (**C**), and magnified views of the respective samples **A** and **C** (**B** and **D**).

exon skipping and alternate RNA processing events. To elucidate the possible molecular mechanisms responsible for this loss of protein expression, we used RT-PCR for FHIT transcript analysis and cDNA sequencing for mutation detection. We found that 34.6% of the samples with decreased FHIT expression had an additional aberrant FHIT transcript product. However, aberrant FHIT was not identified in the samples with normal FHIT expression. These data suggest that loss and rearrangement of the FHIT gene derived from FRA3B breaks or gaps in the large FHIT intronic region may give rise to aberrant cDNA splicing and result in loss of FHIT protein, suggesting that the majority of aberrant FHIT transcripts lack exons 4-6 and 4-8. Our results indicate that higher incidence of aberrant processing of FHIT mRNA and mutation result in FHIT down-regulation in human CRC.

Loss of FHIT protein expression has been found in lung and breast cancers, as well as in head and neck cancers[7-10]. Ohta and colleagues[2] have reported significant loss or reduction of FHIT expression in 39% CRC patients. However, Thiagalingam *et al*[15] showed that the FHIT gene is not involved in CRC carcinogenesis. In this study, we demonstrated that loss of FHIT expression was associated with poorly- and well-differentiated CRC and frequent lymph node metastasis by TMA-IHC assay, indicating that FHIT plays a role in the progression of

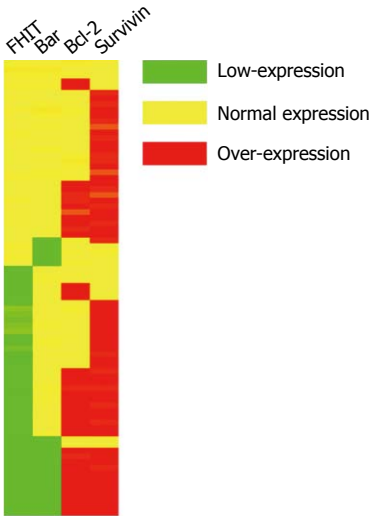

Figure 10 Tree-view of differential protein expression data from 80 CRC tissue samples. Tree-view demonstrated the FHIT protein expression related to Bax, Bcl-2 and survivin protein expression. Red indicates up-regulation, green indicates down-regulation, and yellow indicates no significant change.

Table 3 Expression of Bax, Bcl-2, survivin and correlation with FHIT alteration

		n	FHIT expression		χ^2	*P*
			Positive	Negative		
Bax	+	62	25	37	3.89	0.048
	-	18	12	6		
Bcl-2	+	58	32	26	6.75	0.009
	-	22	5	17		
Survivin	+	41	11	30	12.76	0
	-	39	26	13		

CRC because loss of FHIT protein is intimately associated with the development of CRC. Lack of FHIT gene expression and consequent protein expression can be due to deletions, mutations, or epigenetic modifications.

These results strongly indicate that aberrant expression of the FHIT gene is related to the development and progression of CRC. However, the relationship between FHIT expression and apoptosis has not been studied in human CRC, and the decreased apoptosis in FHIT deficient CRC has not been explained. We therefore designed this study to investigate the differential patterns of apoptosis-related protein expression associated with difference in FHIT expression, in order to identify specific changes that might reflect the pathway by which FHIT affects apoptosis. We performed TUNEL analysis in this study to assess apoptosis status and observed decreased apoptosis in FHIT negative CRC tissue samples compared to FHIT-positive CRC tissue samples. The apoptosis index was 5.41 ± 0.23 in tumors with normal FHIT expression and 0.56 ± 0.10 in tumors with aberrant expression. The rate of apoptosis in tumors with aberrant FHIT expression was significantly lower than that in tumors with normal FHIT expression ($P < 0.01$). Furthermore, we conducted tissue microarray analysis to identify differentially expressed proteins in relevant apoptosis pathways. For this initial pathway, we chose three key proteins belonging to the Bcl/Bax pathway (Bcl2 and Bax) and survivin-caspase pathway (survivin). In this study, the FHIT-negative CRC tissue samples were associated with down-regulation of Bax and up-regulation of Bcl-2. It is known that the Bax gene is an apoptosis-promoting member of the BCL-2 gene family, and apoptosis is known to be accelerated when the Bax function is predominant[22]. On the other hand, over-expression of Bcl-2 seems to be associated with the blocking of apoptosis. The ability of Bcl-2 to inhibit apoptosis is dependent on the expression of Bcl-2 and formation of hetero- and homo-dimers between members of the Bcl-2 family[23]. We observed a significant correlation between FHIT protein expression and members of the Bcl/Bax pathway in human CRC ($P < 0.05$). Survivin is minimally expressed in normal adult tissues but over-expressed in a wide range of human cancers, including cancer of the breast, lung, esophagus and urinary bladder. Survivin is one member of inhibitors of apoptosis and appears to block apoptosis by interfering with the caspase activation pathway[24]. In the present study, we demonstrated that survivin, an inhibitor of apoptosis protein family, was significantly increased in FHIT-negative CRC, indicating that FHIT plays a critical role in FHIT-induced apoptosis, occurring through inactivation of the survivin-caspase signal pathway. Accordingly, future investigations must address protein-protein interactions that lead to these changes in expression and apoptosis, thus allowing us to place FHIT at its correct position within the pathways, ultimately helping to elucidate the precise mechanism by which its expression modulates apoptosis in human CRC.

In conclusion, decreased FHIT expression is caused by mutations of the FHIT gene in human CRC. Down-regulation of FHIT is associated with down-regulation of Bax and up-regulation of Bcl-2 and survivin, which results in alterations in apoptosis status. Differential FHIT expression in human CRC plays a role in control of cell growth and apoptosis. FHIT is a potentially important growth suppressor gene that plays a role in the development and progression of human CRC. FHIT may be a candidate for therapeutic modulation of apoptosis in human CRC.

ACKNOWLEDGMENTS

We thank Dr. Ziqiang Yuan at Department of Molecular Genetics, Albert Einstein College of Medicine, NY, USA for revising the manuscript.

REFERENCES

1 **Hawk ET**, Levin B. Colorectal cancer prevention. *J Clin Oncol* 2005; **23**: 378-391
2 **Li M**, Gu J. Changing patterns of colorectal cancer in China over a period of 20 years. *World J Gastroenterol* 2005; **11**: 4685-4688
3 **Ohta M**, Inoue H, Cotticelli MG, Kastury K, Baffa R, Palazzo J, Siprashvili Z, Mori M, McCue P, Druck T, Croce CM, Huebner K. The FHIT gene, spanning the chromosome 3p14.2 fragile site and renal carcinoma-associated t(3;8) breakpoint, is abnormal in digestive tract cancers. *Cell* 1996; **84**: 587-597
4 **Boldog F**, Gemmill RM, West J, Robinson M, Robinson L, Li E, Roche J, Todd S, Waggoner B, Lundstrom R, Jacobson J, Mullokandov MR, Klinger H, Drabkin HA. Chromosome 3p14 homozygous deletions and sequence analysis of FRA3B. *Hum Mol Genet* 1997; **6**: 193-203

5 **Hayashi S**, Tanimoto K, Hajiro-Nakanishi K, Tsuchiya E, Kurosumi M, Higashi Y, Imai K, Suga K, Nakachi K. Abnormal FHIT transcripts in human breast carcinomas: a clinicopathological and epidemiological analysis of 61 Japanese cases. *Cancer Res* 1997; **57**: 1981-1985

6 **Huebner K**, Hadaczek P, Siprashvili Z, Druck T, Croce CM. The FHIT gene, a multiple tumor suppressor gene encompassing the carcinogen sensitive chromosome fragile site, FRA3B. *Biochim Biophys Acta* 1997; **1332**: M65-M70

7 **Siprashvili Z**, Sozzi G, Barnes LD, McCue P, Robinson AK, Eryomin V, Sard L, Tagliabue E, Greco A, Fusetti L, Schwartz G, Pierotti MA, Croce CM, Huebner K. Replacement of Fhit in cancer cells suppresses tumorigenicity. *Proc Natl Acad Sci USA* 1997; **94**: 13771-13776

8 **Wistuba II**, Behrens C, Virmani AK, Mele G, Milchgrub S, Girard L, Fondon JW, Garner HR, McKay B, Latif F, Lerman MI, Lam S, Gazdar AF, Minna JD. High resolution chromosome 3p allelotyping of human lung cancer and preneoplastic/preinvasive bronchial epithelium reveals multiple, discontinuous sites of 3p allele loss and three regions of frequent breakpoints. *Cancer Res* 2000; **60**: 1949-1960

9 **Sozzi G**, Sard L, De Gregorio L, Marchetti A, Musso K, Buttitta F, Tornielli S, Pellegrini S, Veronese ML, Manenti G, Incarbone M, Chella A, Angeletti CA, Pastorino U, Huebner K, Bevilaqua G, Pilotti S, Croce CM, Pierotti MA. Association between cigarette smoking and FHIT gene alterations in lung cancer. *Cancer Res* 1997; **57**: 2121-2123

10 **Campiglio M**, Pekarsky Y, Menard S, Tagliabue E, Pilotti S, Croce CM. FHIT loss of function in human primary breast cancer correlates with advanced stage of the disease. *Cancer Res* 1999; **59**: 3866-3869

11 **Pavelić K**, Krizanac S, Cacev T, Hadzija MP, Radosević S, Crnić I, Levanat S, Kapitanović S. Aberration of FHIT gene is associated with increased tumor proliferation and decreased apoptosis-clinical evidence in lung and head and neck carcinomas. *Mol Med* 2001; **7**: 442-453

12 **Hibi K**, Taguchi M, Nakamura H, Hirai A, Fujikake Y, Matsui T, Kasai Y, Akiyama S, Ito K, Takagi H. Alternative splicing of the FHIT gene in colorectal cancers. *Jpn J Cancer Res* 1997; **88**: 385-388

13 **Luceri C**, Guglielmi F, De Filippo C, Caderni G, Mini E, Biggeri A, Napoli C, Tonelli F, Cianchi F, Dolara P. Clinicopathologic features and FHIT gene expression in sporadic colorectal adenocarcinomas. *Scand J Gastroenterol* 2000; **35**: 637-641

14 **Hao XP**, Willis JE, Pretlow TG, Rao JS, MacLennan GT, Talbot IC, Pretlow TP. Loss of fragile histidine triad expression in colorectal carcinomas and premalignant lesions. *Cancer Res* 2000; **60**: 18-21

15 **Thiagalingam S**, Lisitsyn NA, Hamaguchi M, Wigler MH, Willson JK, Markowitz SD, Leach FS, Kinzler KW, Vogelstein B. Evaluation of the FHIT gene in colorectal cancers. *Cancer Res* 1996; **56**: 2936-2939

16 **Kononen J**, Bubendorf L, Kallioniemi A, Bärlund M, Schraml P, Leighton S, Torhorst J, Mihatsch MJ, Sauter G, Kallioniemi OP. Tissue microarrays for high-throughput molecular profiling of tumor specimens. *Nat Med* 1998; **4**: 844-847

17 **Knösel T**, Emde A, Schlüns K, Chen Y, Jürchott K, Krause M, Dietel M, Petersen I. Immunoprofiles of 11 biomarkers using tissue microarrays identify prognostic subgroups in colorectal cancer. *Neoplasia* 2005; **7**: 741-747

18 **Cao J**, Li WL, Du H, Tang WB, Wang H.FHIT and p53 expression in human colonic carcinoma. *Chin J Exp Surg* 2006; **23**: 787-789

19 **Vaux DL**, Korsmeyer SJ. Cell death in development. *Cell* 1999; **96**: 245-254

20 **Druck T**, Hadaczek P, Fu TB, Ohta M, Siprashvili Z, Baffa R, Negrini M, Kastury K, Veronese ML, Rosen D, Rothstein J, McCue P, Cotticelli MG, Inoue H, Croce CM, Huebner K. Structure and expression of the human FHIT gene in normal and tumor cells. *Cancer Res* 1997; **57**: 504-512

21 **Virgilio L**, Shuster M, Gollin SM, Veronese ML, Ohta M, Huebner K, Croce CM. FHIT gene alterations in head and neck squamous cell carcinomas. *Proc Natl Acad Sci USA* 1996; **93**: 9770-9775

22 **Yang E**, Zha J, Jockel J, Boise LH, Thompson CB, Korsmeyer SJ. Bad, a heterodimeric partner for Bcl-XL and Bcl-2, displaces Bax and promotes cell death. *Cell* 1995; **80**: 285-291

23 **Reed JC**. Bcl-2 and the regulation of programmed cell death. *J Cell Biol* 1994; **124**: 1-6

24 **Altieri DC**. Survivin, versatile modulation of cell division and apoptosis in cancer. *Oncogene* 2003; **22**: 8581-8589

S- Editor Liu Y **L- Editor** Wang XL **E- Editor** Ma WH

PO Box 2345, Beijing 100023, China
www.wjgnet.com
wjg@wjgnet.com

World J Gastroenterol 2007 February 21; 13(7): 1027-1031
World Journal of Gastroenterology ISSN 1007-9327

Hepatitis B virus infection and replication in primarily cultured human fetal hepatocytes

Min Lin, Qun Chen, Li-Ye Yang, Wen-Yu Li, Xi-Biao Cao, Jiao-Ren Wu, You-Peng Peng, Mo-Rui Chen

Min Lin, Li-Ye Yang, Wen-Yu Li, Xi-Biao Cao, Jiao-Ren Wu, You-Peng Peng, Mo-Rui Chen, Chaozhou Central Hospital, Chaozhou 521000, Guangdong Province, China
Qun Chen, Guangdong Medical College, Zhanjiang 524023, Guangdong Province, China
Supported by the Social Development Plan, Guangdong Province, No. 20051010057
Correspondence to: Dr. Li-Ye Yang, Chaozhou Central Hospital, Chaozhou 521021, Guangdong Province, China. yangleeyee@sina.com
Telephone: +86-768-2224092-2210 Fax: +86-768-2229563
Received: 2006-12-18 Accepted: 2007-01-26

Abstract

AIM: To investigate the infection and replication of hepatitis B virus (HBV) in primarily cultured human fetal hepatocytes (HFHs).

METHODS: The human fetal hepatocytes were cultured in serum-free medium, HBV-positive serum was added into the medium to study the susceptibility of hepatocytes to HBV infection. The supernatant was collected for ELISA assay of HBsAg and HBeAg, and quantitative fluorescence PCR for HBV-DNA assay daily. Albumin and HBcAg, CK8 and CK18 expressions were detected by immunohistochemistry in cultured hepatocytes. Content of lactate dehydrogenate (LDH) was measured to find out the integrity of the cell membrane.

RESULTS: A stable hepatocyte culture system was established. HBV could infect the hepatocytes and replicate, and HBcAg expression could be detected by immunohistochemistry in hepatocyte-like cells. HBV-DNA in the supernatant could be detected from d 2 to d 18 and HBsAg and HBeAg were positive on d 3-d 18 after HBV infection. HBV in medium increased from d 0 to d 6 and subsequently decreased as the cells were progressively loosing their hepatocyte phenotypes.

CONCLUSION: HBV could infect human fetal hepatocytes and replicate. This *in vitro* model allowed a detailed study on early events associated with human HBV entry into cells and subsequent replication.

Key words: Hepatitis B virus; Infection; Human fetal hepatocytes; Culture

Lin M, Chen Q, Yang LY, Li WY, Cao XB, Wu JR, Peng YP, Chen MR. Hepatitis B virus infection and replication in primarily cultured human fetal hepatocytes. *World J Gastroenterol* 2007; 13(7): 1027-1031

http://www.wjgnet.com/1007-9327/13/1027.asp

INTRODUCTION

Hepatitis B virus (HBV) infection is one of the commonest infections in the world. According to some reports, about 400 million people have been infected with HBV, and about 5% are chronically infected[1]. Chronic hepatitis B can cause cirrhosis and liver cancer[2-4]. It is estimated that there are more than one million deaths of this infection and 320 thousand deaths from liver cancer associated with HBV each year in the world[5]. There are about 400 million people with chronic hepatitis B worldwide[6]. HBV exhibits a very narrow host range and shows a strong tropism for liver parenchyma cells. It has therefore, been assumed that the susceptibility to HBV infection is restricted to differentiated cells. It was found by some authors that human primarily cultured hepatocytes were more susceptible than other kinds of cells to HBV infection[7,8]. Here we describe a system of experimental infection by HBV virus using primary human fetal hepatocytes. Infection was obtained by co-cultivation of human fetal hepatocytes with HBV-positive serum. The infected fetal hepatocytes *in vitro* were found to initiate viral DNA replication, and they produced infectious viral particles into medium.

MATERIALS AND METHODS

Primary culture of human fetal hepatocytes

Hepatocytes were prepared from 6 wk old human fetal liver. Embryos procurement was approved by the Ethics Committee of Chaozhou Central Hospital. The sera from the mothers were negative for hepatitis C virus (HCV), HBV and human immunodeficiency virus (HIV) by ELISA (Shanghai SIIC Ke-Hua Biotechnology). Firstly, we used Hank's liquid to wash the aborted fetus 3 times, and liver tissues were taken out. Secondly, the liver tissues were cut with scissors into 0.1-0.5 mm^3 pieces. At last, the little pieces were shattered with 5 mL syringe to single cells or cell aggregates. Viability, assessed by the trypan blue exclusion test, was between 70% and 90%. The cells

were seeded into 12-well culture dishes (Orange Scientific) at about 2×10^5 cells per well and incubated with 1 mL of 10% FBS (Gibco) in DMEM (Dulbecco's Modified Eagle's Medium)/F12 (Nutrient Mixture F-12 HAM) (1:1) (Sigma-Aldrich) supplemented with 0.1 U/L penicillin, 0.1 ng/L streptomycin, and 0.1 ng/L fluconazole at 37℃ under 5% CO_2 in air. The medium was changed after the first 48 h with serum-free medium. The serum-free medium was composed of DMEM/F12 (1:1) and 0.01 nmol/L nicotinamide, 0.02 ng/L epidermal growth factor (EGF), 0.02 ng/L basic fibroblast growth factor (bFGF), 0.365 ng/L glutamate, B27 (1:50) (Sigma), 0.1 U/L penicillin, 0.1 ng/L streptomycin, and 0.1 ng/L fluconazole.

Viral sources

A serum sample for infection test from HBV carriers was analyzed. The patient was anti-HbsAb positive as detected by the ELISA (Shanghai SIIC Ke-Hua Biotechnology), and HBV-DNA in the serum sample was quantified with fluorescence quantitative polymerase chain reaction (FQ-PCR) assay (Da-An Gene Corp). The patient had received no antiviral therapy prior to the study, and not infected with HCV or HIV. The sera were stored at -80℃ until use. The number of serum HBV was 7.6×10^7 copy/mL as quantified by FQ-PCR.

In vitro infection

After 24 h culture in serum-free medium as mentioned above, infection was obtained by incubation 1 mL serum-free culture medium with 5% dimethyl sulphoxide (DMSO) and 100 μL HBV serum. Following 24 h exposure, cells were washed 6 times with 3 mL Hank's liquid and incubated in 1 mL fresh serum-free medium as described above. The medium was changed every day, and the supernatant was collected at various times during the culture period and stored at -80℃. We used one-well cells without HBV serum sample as negative control.

Detection of HBV-DNA by FQ-PCR

To qualify these DNA molecules, virus DNA was extracted from the culture medium using an alkaline lysis method for FQ-PCR analyses[9]. For detection of HBV-DNA in cultured cells, all of the cells were digested by trypsin-EDTA (0.25%-0.01 mmol/L) solution and centrifugated, then were washed six times with PBS. Cells were lysed with 0.05 mol/L Tris-HCl (pH 7.4)-1% sodium dodecyl sulfate (SDS)-0.02 mol/L NaCl-0.02 mol/L EDTA and incubated with 0.5 g/L of proteinase K at 37℃ overnight[9]. Total DNA was extracted by an alkaline lysis method.

HBV-DNA was measured by FQ-PCR diagnostic kit from Da-An Gene Corp. with Lightcycler™ Roche. In this reaction, the nucleotide sequences of the primers were as follows: P1: 5'ATCCTGCTGCTATGCCTCATC TT3' (23 bp), P2: 5'ACAGTGGGGGAAAGCCCTACG AA3' (23 bp), FISH: 5'TGGCTAGTTTACTAGTGCCA TTTG3' (25 bp)[10].

QT-PCR amplification was performed using Roche QT-PCR system with 2 min initial denaturation at 93℃ for 40 cycles of 5 s at 93℃ and 45 s at 57℃, followed by 1 s of extension at 37℃.

Detection of HBsAg and HbeAg by ELISA

HBsAg and HBeAg levels in the supernatant were detected using the monoclonal Ⅱ enzyme-linked immunosorbent assay. ELISA kits were obtained from Shanghai SIIC Ke-Hua Biotechnology. Titers were expressed as the ratios against cut-off values (A450 of negative control + 0.05 for HBsAg and + 0.05 for HBeAg).

Periodic acid- Schiff's staining

To discriminate liver cells from stromal cells for general observation of morphology, cells were stained with periodic acid-Schiff's reagent (PAS) by standard methods[12]. The reagents were from Shanghai Zhu-Chun Biotechnology.

Detection of albumin and HBcAg by immunohistochemical staining

The cells were fixed in 0.4% formaldehyde in PBS at room temperature for 15 min, and washed 3 times by PBS. After that, they were incubated for 15 min with 0.25% Triton-X100 and washed 3 times by PBS. Cells were then incubated with the following dilutions of primary antibodies for 1 h at room temperature: antibody to cytokeratin-8 (CK-8) and cytokeratin-18 (CK-18) (Beijing Zhong-Shan Biotechnology), which were diluted at 1:100 in PBS; antibody to HBcAg (1:1) (Fuzhou Maxim Biotechnology); and antibody to human albumin diluted at 1:1000 in PBS (Sigma). Other steps were performed according to manufacturer's instruction of SP-9000 kits, and AEC served as chromagens.

Determination of integrity of cell membranes

Content of LDH was measured using automatic blood biochemistry analysis (HITACHI 7060) with Roche reagents. LDH was expressed as U/L released into the medium to find out the integrity of the cell membrane every 24 h.

Statistical analysis

The statistical analysis was performed with SPSS 13.0 statistic software.

RESULTS

Properties and phenotypes of cultured hepatocytes

Single cells or cell aggregates were isolated from fetal human livers. The initial cell population was an obvious mixture of hematopoietic and epithelial cells. For instance, red blood cells were copious, although these were rapidly removed at the first medium change. They were plated onto plastic dishes with serum containing medium. After 12 h, the hepatocytes started to attach to the dishes but did not proliferate. After 48 h, the media became serum free, and the HFHs began to show two kinds of state, including cell aggregates or spheroid and scattered cells. The spheroid was made up of many epithelial cells, and fibroblast-like cells migrated from them (Figure 1A). With the elongation of culture time, the percentage of fibroblast-like cells gradually increased and the percentage of flat epithelial cells gradually decreased. After 3-5 wk, fibroblast-like cells proliferated to form a monolayer (Figure 1C).

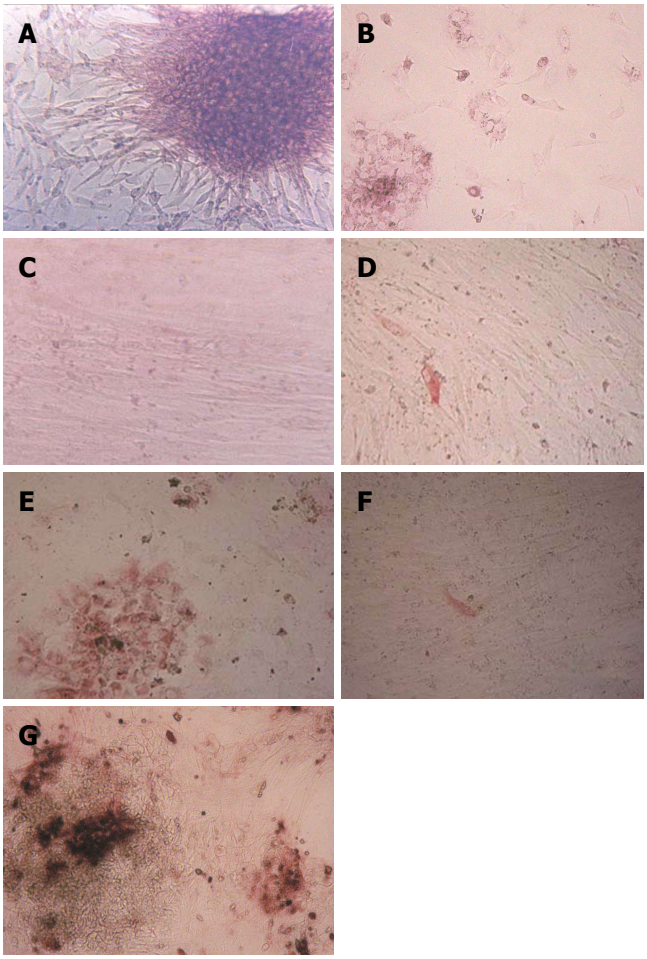

Figure 1 Morphology, PAS and S-P staining of the HFHs under light microscope. **A:** Isolated HFHs formed epithelial-like spheroid and they were surrounded by fibroblast-like cells in culture after 48 h; **B:** HFHs were stained by PAS, the majorities of cultured cells were positive; **C:** HFHs state *in vitro* for 50 d; **D:** HFHs were positive for CK8 in hepatocytes *in vitro* for 50 d (S-P); **E:** HFHs expressed liver marker CK18 *in vitro* for 14 d (S-P); **F:** Only a few of hepatocytes were positive for CK18 *in vitro* for 50 d (S-P); **G:** HFHs expressed ALB *in vitro* for 14 d (S-P). (Original magnification, × 40).

To confirm the phenotypes of HFHs after 2 wk, cells were analyzed by PAS staining. The majority of cells were stained, and these cells were multiangular and flat, their morphology were similar to that of hepatocytes (Figure 1B), Furthermore, we performed S-P staining using primary antibodies against ALB, CK8 and CK18, the results showed clearly that these proteins were expressed in about 90% cells, confirming that the cells expressed hepatocyte phenotypes (Figure 1E and 1G). After 50 d, only less than 1% cells expressed CK8 and CK18 (Figure 1F). The above-mentioned results were also reported by HU *et al*[11]. CK8 and CK18 are cytoskeletal proteins characteristic of hepatocytes, they play a very important role in maintaining the structure of hepatocytes, and are expressed in the hepatocyte cytoplasm of the fetal hepatocytes *in vivo*. Thus, they are good markers for hepatocytes. As culture time extending, the cells that expressed hepatocyte phenotypes gradually decreased, while those cells that expressed fibroblast phenotypes gradually increased. In our opinion, there were two factors to explain this situation: (1) the fibroblast-like cells

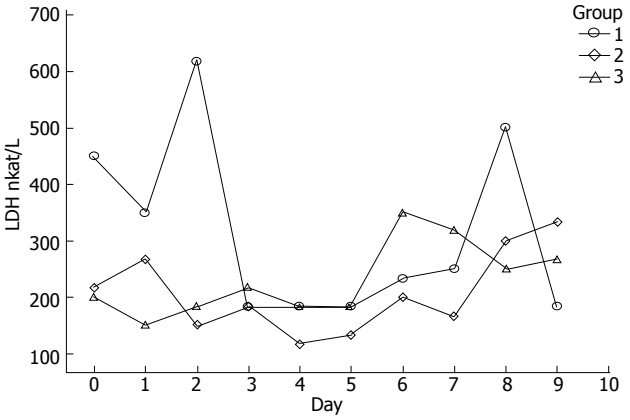

Figure 2 Lactate dehydrogenase (LDH) released in primary human hepatocytes.

proliferated faster than hepatocyte-like cells. Therefore, after several weeks culture, fibroblast-like cells proliferated to form a monolayer and few hepatocyte-like cells could be observed; (2) HFHs could change their phenotypes from hepatocytes to mesenchymal cells, this phenomenon has also been reported by other studies[9].

In the course of this study, it was visually apparent that the tendency of LDH increased with culture time in serum-free medium (Figure 2). The amount of LDH in the supernatant ranged from 620 nkat/L to 130 nkat/L.

Production of viral antigens in fetal liver cells

The serum-free culture medium was collected periodically and the levels of HBsAg and HBeAg were analyzed. As shown in Figures 3A and 3B, the HBsAg and HBeAg were first detected at d 3 after the infection and continued to appear positive during the following 16 d. They must have been synthesized in liver cells because the wash liquid (time zero) and medium from d 1 to d 2 were negative for HBsAg and HBeAg. Thus, the human fetal hepatocytes should be infected by wild virus and replicated HBV.

Human fetal hepatocytes were cultured for 24 h with HBV serum, washed, and incubated with serum-free medium. The supernatant was taken every day and assayed for HBsAg and HBeAg.

Detection of HBV-DNA in media and cultured cells

The culture media were collected from d 0 to d 18 (the day of human HBV serum deprivation was indicated as d 0), and were measured by FQ-PCR. HBV-DNA appeared at d 2, and reached a secretion peak from d 3 to d 6. The tendency began to decrease on d 6. Because there was no HBV-DNA in the medium at d 0-2 after infection, HBV-DNA was detected in the serum-free medium from d 3 to d 18 (Figure 4). Therefore, they must have been released from the infected hepatocytes, and the hepatocytes must release and replicate virus DNA. The results of HBV-DNA in liver cells are shown in Table 1.

Detection of HBcAg by immunohistochemical staining

To estimate the population of infected cells, immunohistochemical staining was used to assay HBcAg. HBcAg was detected in about 10% of hepatocyte-like cells 3 d after infection (Figure 5A), whereas no HBcAg was found

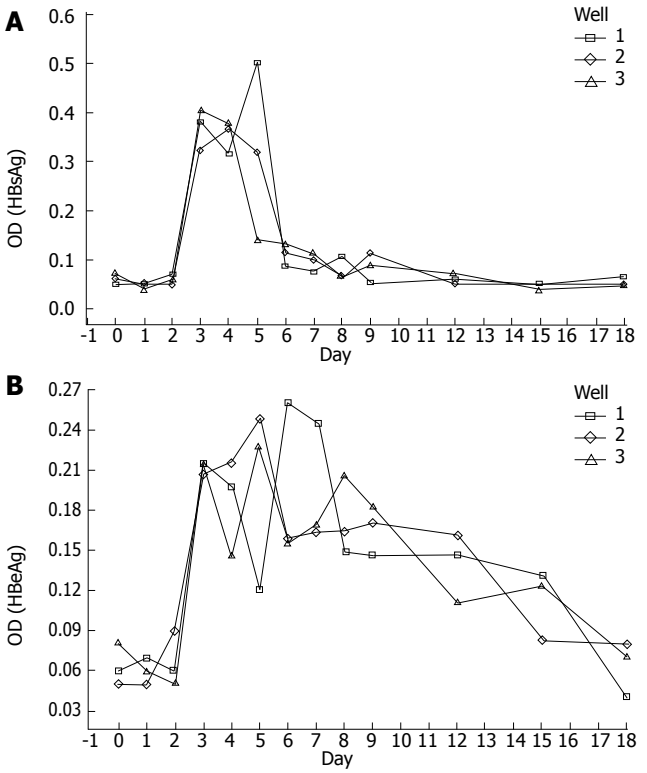

Figure 3 HBsAg (**A**) and HBeAg (**B**) in supernatant detected by ELISA (OD: optical denisity).

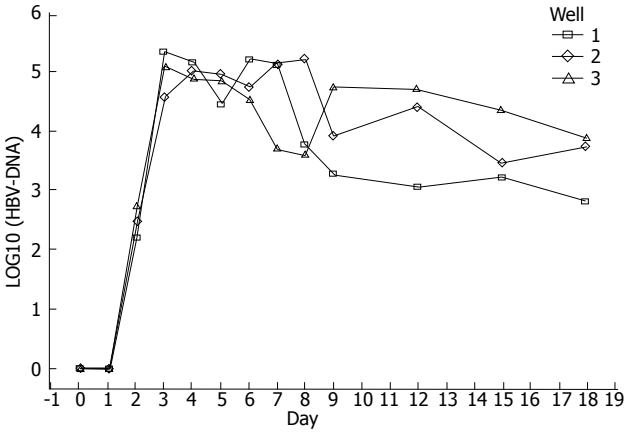

Figure 4 HBV-DNA in media detected by FQ-PCR.

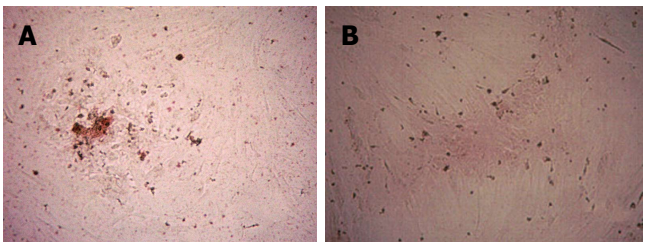

Figure 5 Detection of HBcAg by immunohistochemistry staining (S-P). **A:** The HBcAg positive in hepatocytes; **B:** Negative control for HBcAg. Original magnification, × 40.

Table 1 Cells quantified by FQ-PCR on d 18

Well	Cell number	HBV-DNA (copy/L)
1	1.0×10^4	2.092×10^9
2	1.5×10^4	8.506×10^9
3	1.1×10^5	1.371×10^{10}

in the negative control (Figure 5 B).

DISCUSSION

Replication of HBV has been achieved in human hepatoma cell lines using integrated or transfected HBV genomes as templates[13-16]. Duck cells and adult human liver cells were also successfully infected by HBV[17,18]. However, no signs of viral penetration, replication, or particle production have been observed except for a transient expression of some viral markers in hepatoma cell lines[14-15]. Duck cells and adult human liver cells could not perfectly analogue the process of the HBV infection in human fetal hepatocytes[17,18], and human fetal hepatocytes were used in a few experiments for HBV infection[19,20]. We demonstrated in this study that primary cultures of fetal human hepatocytes could maintain HBV infection *in vitro* and support the replication of HBV DNA.

In this study, an evidence of virus DNA replication in primary human fetal hepatocytes was testified from d 2 to d 18 after infection by FQ-PCR, another evidence was that HBsAg and HBeAg appeared positive from d 3 to d 18 by ELISA. The process of HBV replication and release continued for 16 d. The results were similar to other experiments with DMSO supplement[18]. But the HBV secretion time in our experiment was longer than the experiments without DMSO[19-21]. The data demonstrated that viral replication *in vitro* might be strongly enhanced by DMSO.

Previous studies of primary hepatocytes provided very little information about the quantity of HBV-DNA in the culture medium[21-23]. In their reports, DNA or RNA used to be detected by Southern blot or Northern blot[14,18,23]. The procedures of these methods were complicated, and the results were not stable. In our experiment, we used FQ-PCR to measure the HBV-DNA in the supernatant and cultured cells. FQ-PCR combines gene amplification and molecule hybridization with fluorescence physics, conducts the whole process of DNA amplification and PCR products analysis in an enclosed tube, and real-time detection as well as auto-analysis under computer control[10]. As a result, the cross-contamination of conventional PCR products and incapacity of quantification can be eliminated fundamentally[10]. Furthermore, the specificity and sensitivity increased remarkably. This method could provide reliable and precise data for HBV quantification.

The quantity of HBV in medium increased from d 0 to d 6 and decreased from d 7 to d 18 in the infection process. From d 0 to d 6, HBV replicated in infected cells and released to the medium, and then the free HBV infected other hepatocytes. With the increasing number of hepatocytes, it formed one infected cycle in cells and

the quantity of HBV increased in the medium. From d 7 to d 18, a part of cells gradually lost their hepatocyte phenotypes and HBV infection susceptibility, and the cycle was broken. Meanwhile, a part of floating cells and cell spheroid died gradually, subsequently, the quantity of HBV decreased.

In this study, we found that the presence of HbeAg was more correlated with HBV-DNA in the medium than that of HBsAg. According to our knowledge, HBeAg was a marker of extensive viral replication in HBsAg-positive sera of patients with hepatitis B virus infection[24]. The presence of HBeAg in the serum correlated well with hepatitis B-DNA[24]. Therefore, our results were similar to the status in human body.

By immunohistochemical analysis, we were able to observe a part of infection of the hepatocytes in the cultures. Similar results have previously been reported[23]. Recently, Tuttleman *et al*[17] used primary duck hepatocytes to infect HBV and only 10% of the primary duck hepatocytes displayed HBcAg[25]. The events could be observed in duck hepatocytes and human fetal liver cells. According to some reports, the procedure of liver cell isolation could destroy the capacity for infection of all but some cells. As it is well known, human hepatocytes were hard to maintain in cultures, such as albumin expression. Such phenotypes are easily lost within one week culture when the cells are inoculated in serum-containing medium. In our observation, the shape of the hepatocytes was polygonal at 48 h. With elongation of culture time, some hepatocytes gradually changed and extended in shape and became fibroblast-like, meanwhile they lost hepatocyte phenotypes such as ALB, CK18 and CK8 expressions. So it is likely that some flat cells may lessen the susceptibility to HBV infection.

HBV infection in primary fetal hepatocyte cultures is suitable for cloning virus because of the limited infectivity of the cells. However, our system *in vitro* has been found very useful for studying the early events in viral entry into cells as well as viral replication.

REFERENCES

1 **Lee WM**. Hepatitis B virus infection. *N Engl J Med* 1997; **337**: 1733-1745
2 **Liu CJ**, Chen BF, Chen PJ, Lai MY, Huang WL, Kao JH, Chen DS. Role of hepatitis B virus precore/core promoter mutations and serum viral load on noncirrhotic hepatocellular carcinoma: a case-control study. *J Infect Dis* 2006; **194**: 594-599
3 **Whitworth A**. Ten years later: liver cancer treatment reevaluated. *J Natl Cancer Inst* 2006; **98**: 958-959
4 **Kremsdorf D**, Soussan P, Paterlini-Brechot P, Brechot C. Hepatitis B virus-related hepatocellular carcinoma: paradigms for viral-related human carcinogenesis. *Oncogene* 2006; **25**: 3823-3833
5 **Di Bisceglie AM**, Rustgi VK, Hoofnagle JH, Dusheiko GM, Lotze MT. NIH conference. Hepatocellular carcinoma. *Ann Intern Med* 1988; **108**: 390-401
6 **Yan JC**, Ma JY, Pan BR, Ma LS. The study of chronic hepatitis B in China. *Shijie Huaren Xiaohua Zazhi* 2001; **9**: 611-616
7 **Guha C**, Mohan S, Roy-Chowdhury N, Roy-Chowdhury J. Cell culture and animal models of viral hepatitis. Part I: hepatitis B. *Lab Anim (NY)* 2004; **33**: 37-46
8 **Walter E**, Keist R, Niederöst B, Pult I, Blum HE. Hepatitis B virus infection of tupaia hepatocytes in vitro and in vivo. *Hepatology* 1996; **24**: 1-5
9 **Klintschar M**, Neuhuber F. Evaluation of an alkaline lysis method for the extraction of DNA from whole blood and forensic stains for STR analysis. *J Forensic Sci* 2000; **45**: 669-673
10 **Cheng G**, He YS, Zhou XY. Fluorescence quantitative PCR and its application in detection of hepatitis B virus. *Zhonghua Jianyan Yixue Zazhi* 1999; **22**: 135-136
11 **Roberts GP**. Histochemical detection of sialic acid residues using periodate oxidation. *Histochem J* 1977; **9**: 97-102
12 **Hu A**, Cai J, Zheng Q, He X, Pan Y, Li L. Hepatic differentiation from embryonic stem cells in vitro. *Chin Med J (Engl)* 2003; **116**: 1893-1897
13 **Lu X**, Block TM, Gerlich WH. Protease-induced infectivity of hepatitis B virus for a human hepatoblastoma cell line. *J Virol* 1996; **70**: 2277-2285
14 **Tsurimoto T**, Fujiyama A, Matsubara K. Stable expression and replication of hepatitis B virus genome in an integrated state in a human hepatoma cell line transfected with the cloned viral DNA. *Proc Natl Acad Sci USA* 1987; **84**: 444-448
15 **Sells MA**, Chen ML, Acs G. Production of hepatitis B virus particles in Hep G2 cells transfected with cloned hepatitis B virus DNA. *Proc Natl Acad Sci USA* 1987; **84**: 1005-1009
16 **Sureau C**, Romet-Lemonne JL, Mullins JI, Essex M. Production of hepatitis B virus by a differentiated human hepatoma cell line after transfection with cloned circular HBV DNA. *Cell* 1986; **47**: 37-47
17 **Tuttleman JS**, Pugh JC, Summers JW. In vitro experimental infection of primary duck hepatocyte cultures with duck hepatitis B virus. *J Virol* 1986; **58**: 17-25
18 **Gripon P**, Diot C, Thézé N, Fourel I, Loreal O, Brechot C, Guguen-Guillouzo C. Hepatitis B virus infection of adult human hepatocytes cultured in the presence of dimethyl sulfoxide. *J Virol* 1988; **62**: 4136-4143
19 **Jiang YG**, Li QF, Qing M, Wang YM, Primary human fetal hepatocytes with HBV infection in vitro. *Shijie Huaren Xiaohua Zazhi* 2000; **8**: 403-405
20 **Wang F**, Wang YM, Tang B, Liu J, Liu GD, Wang XH. Assays for HBV infection in primary human fetal hepatocytes cultured in vitro, *Disan Junyidaxue Xuebao* 2004; **26**: 74-77
21 **Tang B**, Wang YM, Wang F, Liu J, Zhang R. Susceptibility change to HBV in primary culture of first trimester human fetal hepatocytes. *Zhonghua Ganzangbing Zazhi* 2004; **12**: 21-24
22 **Galle PR**, Hagelstein J, Kommerell B, Volkmann M, Schranz P, Zentgraf H. In vitro experimental infection of primary human hepatocytes with hepatitis B virus. *Gastroenterology* 1994; **106**: 664-673
23 **Ochiya T**, Tsurimoto T, Ueda K, Okubo K, Shiozawa M, Matsubara K. An in vitro system for infection with hepatitis B virus that uses primary human fetal hepatocytes. *Proc Natl Acad Sci USA* 1989; **86**: 1875-1879
24 **Lu ZR**, Lei H. Textbook of Diagnostics (Engl). 1st ed. Oxford: Chin Sci Pub, 2006: 301
25 **Zhou GY**, Jiang XC, Textbook of Pathology (Engl). 1st ed. Oxford: Chin Sci Pub, 2006: 243

S- Editor Liu Y **L- Editor** Ma JY **E- Editor** Lu W

PO Box 2345, Beijing 100023, China
www.wjgnet.com
wjg@wjgnet.com

World J Gastroenterol 2007 February 21; 13(7): 1032-1041
World Journal of Gastroenterology ISSN 1007-9327

BASIC RESEARCH

Role of soluble factors and three-dimensional culture in *in vitro* differentiation of intestinal macrophages

Tanja Spoettl, Martin Hausmann, Katrin Menzel, Heidi Piberger, Hans Herfarth, Juergen Schoelmerich, Frauke Bataille, Gerhard Rogler

Tanja Spoettl, Martin Hausmann, Katrin Menzel, Heidi Piberger, Hans Herfarth, Juergen Schoelmerich, Frauke Bataille, Gerhard Rogler, Department of Internal Medicine I, and Institute of Pathology, University of Regensburg, Regensburg 93042, Germany
Supported by the Deutsche Forschungsgemeinschaft (SFB585, Ro 1236/3-2) and the BMBF Kompetenznetz-CED
Correspondence to: Gerhard Rogler, MD, PhD, Department of Internal Medicine I, University Hospital of Zuerich, Raemistrasse 100, 8091 Zuerich, Switzerland. gerhard.rogler@usz.ch
Telephone: +49-941-9447180 Fax: +49-941-9447179
Received: 2006-05-16 Accepted: 2006-09-20

Abstract

AIM: To examine the factor(s) involved in differentiation of intestinal macrophages (IMACs) using a recently established *in vitro* model.

METHODS: To test whether soluble or membrane bound factors induce IMAC-differentiation, freshly elutriated monocytes (MO) were incubated with conditioned media or cell membranes of intestinal epithelial cells (IEC) or cultured with IEC in transwell systems. To determine the importance of an active migration of MO, three-dimensional aggregates from a 1:1-mixture of MO and IEC were examined by immunohistochemistry and flow cytometry. Apoptosis was examined by caspase-3 Western blots. Extracellular matrix production in differentiation models was compared by immunohistochemistry.

RESULTS: IMAC differentiation was observed in a complex three-dimensional co-culture model (multicellular spheroid, MCS) with IEC after migration of MO into the spheroids. By co-culture of MO with conditioned media or membrane preparations of IEC no IMAC differentiation was induced. Co-culture of MO with IEC in transwell-cultures, with the two cell populations separated by a membrane also did not result in intestinal-like differentiation of MO. In contrast to IEC-spheroids with immigrating MO in mixed MCS of IEC and MO only a small subpopulation of MO was able to survive the seven day culture period.

CONCLUSION: Intestinal-like differentiation of MO *in vitro* is only induced in the complex three-dimensional MCS model after immigration of MO indicating a role of cell-matrix and/or cell-cell interactions during the differentiation of IMACs.

Key words: Intestinal macrophages; Intestinal epithelial cells; Multicellular spheroids; Inflammatory bowel disease; Tolerance differentiation

Spoettl T, Hausmann M, Menzel K, Piberger H, Herfarth H, Schoelmerich J, Bataille F, Rogler G. Role of soluble factors and three-dimensional culture in *in vitro* differentiation of intestinal macrophages. *World J Gastroenterol* 2007; 13(7): 1032-1041

http://www.wjgnet.com/1007-9327/13/1032.asp

INTRODUCTION

Macrophages represent a component of the innate immune system which is of central importance. One of the largest populations of macrophages in the body is intestinal macrophages (IMACs)[1]. They are localized directly underneath the epithelial barrier at the sites of antigen entry, in particular in the sub-epithelial region of the small and large intestine and in the subepithelial domes of Peyer's patches[2-4]. IMACs constitute 10%-20% of mononuclear cells in the human lamina propria[2,5-8]. They undergo a specific process of differentiation. This specific differentiation is believed to be essential for the specific functions of IMACs in the mucosal innate but also adaptive immune system. As IMACs are central players of both systems, a better understanding of the factors determining their differentiation may allow the definition of new targets for therapeutic interventions during acute and chronic mucosal inflammation. The importance of IMACs is supported by the finding that NOD2/CARD15, the first gene identified to increase susceptibility to Crohn's disease, is mainly expressed in macrophages in the colonic mucosa[9,10].

The phenotype of IMACs is remarkable: Less than 10% of the macrophages (MACs) isolated from normal colonic mucosa express the typical MO/MAC-specific surface markers CD14, CD16, CD11b, CD11c[11-13]. Furthermore, the expression of co-stimulatory molecules B7-1 (CD80) and B7-2 (CD86) on IMACs is low[14,15]. In

addition, the expression of pattern recognition receptor (PRR) toll like receptor (TLR) 2 and TLR 4 is also down-regulated in IMACs on transcriptional and translational levels[16]. The prototypic MO/MAC functions such as generation of superoxide radicals (oxidative burst reaction) are absent in normal mucosal IMACs due to a lack of NADPH-oxidase subunit expression[17], indicating that normal IMACs constitute a non-reactive cell population, which might be important for the induction of tolerance in the intestinal mucosa. A disturbance of the differentiation process followed by a reactive cell type retaining PRRs and activation functions could be followed by chronic inflammation.

Recently we used a three-dimensional co-culture model (multicellular spheroid model, MCS-model) of intestinal epithelial cells (IEC) and monocytes (MO) to induce the *in vitro* differentiation of intestinal-like macrophages[18]. We demonstrated that IEC clearly play an important role in the differentiation of IMACs. Freshly elutriated MO, which adhered and infiltrated IEC-MCS, changed their phenotype during a seven-day co-culture period[18]. Typical MO/MAC specific surface antigens such as CD14, CD16, CD11b and CD11c, which were detectable on invading cells after 24 h, were down-regulated after seven days. This differentiation was of functional relevance as seen by the loss of LPS-induced IL-1β transcription in IEC-MCS/MO co-cultures compared to control experiments[18]. As the gut specific differentiation of IMACs is of great functional importance and the MCS-model resembled the differentiation process *in vitro*, we addressed the question of which factor(s) induce the specific IMAC-differentiation.

Little is known about the direct interaction between IEC and MO/MAC. In normal intestinal mucosa tissue IMAC are separated from IEC by the basement membrane[2,4]. Doe and co-workers[19] have localized IMACs beneath the luminal epithelium[19]. It has been shown that IMACs or dendritic cells can transmigrate and return again across the basement membrane[20] and that the basement membrane is as easily permeable for large molecules as complement factors[21]. Martin and co-workers[22] found that murine MO/MAC and IEC are coupled by gap junctions and that gap junctional communication may provide a tool by which inflammatory cells regulate IEC function and vice versa.

In the present study, we aimed to study whether the induction of intestinal like differentiation of MAC is induced by soluble or secreted proteins, whether direct cell-cell interactions are necessary, whether cell-matrix interactions play a major role and whether all MO or just a subpopulation of MO is capable of differentiating into IMACs.

MATERIALS AND METHODS

Monocyte isolation and cell culture

Primary blood MO were obtained by leukapheresis of healthy donors, followed by density gradient centrifugation over Ficoll/Hypaque as described previously[18]. Two intestinal epithelial cell lines (HT-29 and WiDr) and a control cell line of non-intestinal origin (urothelial carcinoma, J82) were used. All cell lines were cultured under standard tissue-culture conditions[23,24]. The isolation of monocytes was approved by the local institutional review board.

Conditioned medium

Confluent monolayers of IEC lines or the control cell line were incubated with cell culture medium with or without fetal calf serum (FCS). After 48 h the medium was removed, centrifuged and stored at -20℃. Freshly elutriated MO were incubated in conditioned medium for up to seven days.

Immunohistochemistry

Immunohistochemical staining was carried out according to the standard alkaline phosphatase anti-alkaline phosphatase (APAAP) or diaminobenzidine (DAB) technique[25]. The following monoclonal antibodies against MO/MAC-antigens were used: anti-CD68 (clone: KP1, Dako, Hamburg, Germany), anti-CD11b (clone: BEAR1, Immunotech, Hamburg, Germany), anti-CD11c (clone: BU15, Immunotech, Hamburg, Germany), anti-CD14 (clone: RMO52, Immunotech, Hamburg, Germany) and anti-CD16 (clone: 3G8, Immunotech, Hamburg, Germany). For detection of extracellular matrix antibodies against fibronectin (clone: 568, Progen, Heidelberg, Germany), laminin (clone: 4C7, Dako, Hamburg, Germany) and collagen Ⅳ (clone: CIV 22.(1), Dako, Hamburg, Germany) were used.

Cell ELISA

Fixed MO were washed with NKH buffer (0.14 mol/L NaCl, 5 mmol/L KCl and 2 mmol/L HEPES, all Merck, Darmstadt, Germany) and unspecific binding was blocked with 10% FCS in NAG buffer (0.1% NaN_3, 2 mmol/L HEPES, 0.2% gelatine, all Merck, Darmstadt, Germany and 0.2% BSA, Sigma-Aldrich, Deisenhofen, Germany). Antibodies against CD68, CD14, CD16 and β_2-microglobuline (anti-β_2M, Dianova, Hamburg, Germany) as a positive control were applied. After rinsing, rabbit anti-mouse IgG (Dako, Hamburg, Germany) was added and incubated with peroxidase-conjugated goat-anti-rabbit antibody (Immunotech, Hamburg, Germany). Subsequent incubation with 1.2-phenylendiamine-dihydrochloride substrate (OPD, Fluka, Deisenhofen, Germany) for exact 12 min resulted in a yellow color. The reaction was stopped with 1 mol/L H_2SO_4 (Merck, Darmstadt, Germany) and the extinction was determined photometrically. As a reference value the extinction of ß$_2$M was set 1. All measured values were standardized on the β_2M-extinction.

Proliferation and cell viability assay (MTS-test)

A total of 100 000 MO per well were grown either in conditioned media of IEC or in control media in 96-well plates for seven days. A colorimetric assay (MTS, Endogen, Woburn, Germany) for quantification of cell proliferation and cell viability was performed according to the manufacturer's protocol. The absorption was measured 8 h after addition of the MTS-labeling mixture.

Cell membranes

IEC or control cells were washed with PBS, resuspended in homogenization buffer (Tris 50 mmol/L, EDTA 1 mmol/L, PMSF 1 mmol/L, benzamidine 1 mmol/L, saccharose 0.25 mmol/L) and lyzed by sonification. Cell membranes were isolated in three subsequent centrifugation steps (400 × *g* for 10 min, 8500 × *g* for 10 min, 25000 × *g* for 30 min). During the third centrifugation step, the cell membranes were sedimented, re-suspended in PBS and incubated in 96-well plates to allow adherence to the plastic surface. After 30 min the supernatants were removed and replaced by a suspension of freshly elutriated MO.

Transwell co-cultures

IEC were seeded onto filter inserts with a pore size of 12 μm or 3 μm (preventing IEC from transmigration through the membranes). After formation of an IEC-monolayer the supernatant was removed and freshly elutriated MO in medium supplemented with 2% of human AB-serum were added to each filter insert. After seven days of incubation migrated cells were fixed for immunohistochemistry. Cells in suspension were collected separately and subjected to flow cytometrical analysis.

Generation of MCS

MCS from only IEC or from a 1:1 mixture of IEC and MO were generated according to the liquid overlay culture technique[18]. Mixed spheroids were also generated with addition of a blocking anti-Fas antibody (Upstate Biotechnology, Lake Placid, USA) to the cell suspension 30 min before seeding.

Flow cytometry

Flow cytometry was performed using a Coulter EPICS® XL-MCL (Coulter, Krefeld, Germany). Cells were double stained with a FITC-conjugated anti-CD14 antibody (clone Tük4, Coulter, Krefeld, Germany) and a PE-conjugated anti-CD33 antibody (clone MY9, Coulter, Krefeld, Germany) as described previously.

Data acquisition and analysis were performed using WIN-MDI software (http://facs.scripps.edu/help/html/).

Immunoblotting

Cells were resuspended in RIPA buffer (1% Nonidet P-40, 0.5% sodium deoxycholate, 0.1% SDS, 1 mmol/L Na_3VO_4, 50 mmol/L NaF and 1 tablet of complete proteinase inhibitor cocktail [Boehringer, Mannheim, Germany] per 50 mL PBS) for 10 min on ice and centrifuged (12000 ×*g* for 15 min at 4℃). The protein concentration of the supernatant (protein fraction) was determined by BCA protein assay (Sigma-Aldrich Chemie, Deisenhofen, Germany). Thirty μg of protein was mixed with an equivalent volume of 2 × protein loading buffer containing 2-β-mercaptoethanol and boiled for 5 min before it was loaded onto SDS polyacrylamide gels. After electrophoresis, proteins were transferred onto nitro-cellulose membranes using the Xcell blot module (Invitrogen BV/NOVEX; Gronigen, Netherlands) and blocked in TBST (50 mmol/L Tris-HCl, pH 7.5, 150 mmol/L NaCl, 0.05% Tween 20) containing 5% non-fat dry milk powder. Protein immunoblots were performed using specific antibodies to caspase-3 (clone 19, Transduction Laboratories, Lexington, USA) and β-actin (clone JLA20, Calbiochem, Cambridge, USA). The membranes were further incubated with peroxidase-conjugated secondary antibodies and protein bands were visualized using a chemoluminescence kit (ECL Plus ™, Amersham, Buckinghamshire, UK) according to the manufacturer's protocol.

RESULTS

Recently we demonstrated *in vitro* differentiation of MO into IMACs in complex three- dimensional co-culture models (MCS model) with IEC after migration of MO into the IEC complexes. Here we further studied whether soluble factors or cell-cell interactions might be more relevant to this differentiation.

IEC-conditioned media did not induce differentiation of IMACs

To test whether soluble factors secreted by IEC induce the intestinal-like differentiation of MO, freshly elutriated MO were incubated with IEC-conditioned medium for seven days. Immunohistochemical analysis of MO showed no intestinal-like differentiation. CD14, CD16, CD11b and CD11c, which are down-regulated during differentiation of IMACs and therefore absent on MAC from normal non-inflamed mucosa, were all detectable. CD14 was expressed by 70%-80%, CD16 by 50%-60%, CD11b by 80%-90% and CD11c by 90%-100% of the MO/MAC incubated in HT-29-conditioned medium for seven days. Same results obtained with conditioned medium of the second tested IEC line WiDr were not significantly different from the values obtained with the MO/MAC incubated in control media (Figure 1). When cells were analysed by flow cytometry these findings were confirmed as no down-regulation of CD14, CD16, CD11b and CD80 expression could be observed in MO after seven-day co-culture with IEC-conditioned media (CD14 expression shown in Figure 2).

The results were further confirmed and quantified using the cell-ELISA technique able to detect minor changes in antigen expression. As a positive control and for reference values we determined the expression of the MAC housekeeping gene β_2M (Figure 3A). All other values were standardized in relation to $ß_2$M-expression. The antigen expression of MO/MAC, incubated in IEC-conditioned medium did not differ significantly from that of cells, incubated in control medium. The expression of CD16 was always slightly decreased, but could also be observed in control experiments and was not specific for IEC-conditioned media (Figure 3B).

IMAC differentiation was not induced by IEC-membrane bound factors

To determine whether membrane-bound factors of IEC induce the intestinal-like differentiation of MO, freshly elutriated blood MO were co-cultured with membrane preparations of IEC as described in Materials and

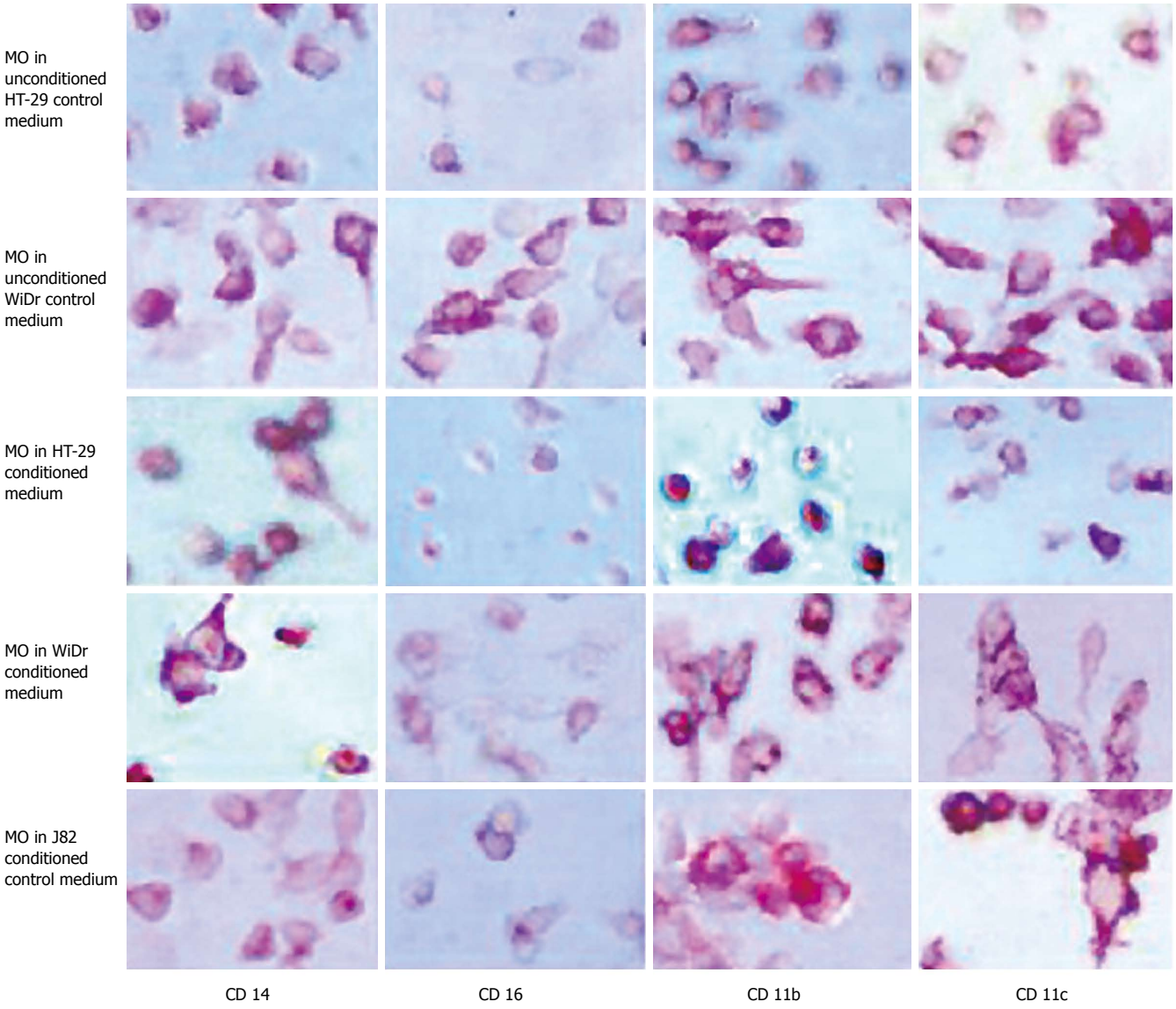

Figure 1 Immunohistochemical detection of MO/MAC antigen expression after 7 d of culture in IEC conditioned medium. Freshly elutriated MO were incubated in unconditioned control media, conditioned media of the IEC lines HT-29 and WiDr and conditioned medium of the control cell line J82 of non-intestinal origin for seven days. Antigen expression was determined by immunohistochemistry (APAAP-method). Expression of the MO/MAC specific antigens CD14, CD16, CD11b and CD11c was determined. All tested antigens were detectable on the cells after the seven-day culture period. Incubation in IEC-conditioned medium had no influence on antigen expression.

Methods. After an incubation period of seven days MO co-cultured with IEC-membranes showed no differentiation into intestinal-like MAC. The tested antigens CD14, CD16, CD11b and CD11c were still detectable after seven days of culture of MO/MAC together with membrane preparations of the IEC line HT-29. MO/MAC incubated for seven days without membrane preparations showed the same pattern of antigen expression (Figure 4).

Same results were obtained with membranes of a second intestinal epithelial cell line (WiDr) and the control cell line J82 (data not shown).

IMAC differentiation was not observed in transwell culture

To test whether a short direct contact between MO and IEC is able to induce intestinal-like differentiation of MO, we incubated MO and IEC in so called "transwell-cultures". MO were added to IEC grown in filter inserts. When filters with a pore size of three μm were used, only MO were able to migrate through the membrane as confirmed by negative staining for the epithelial cell marker EP-4 and positive staining for the MO/MAC-marker CD33 (Figure 5A). Twelve-μm long filters allowed also IEC to migrate through the membranes. IEC could be easily distinguished from MO/MAC by morphology and showed no expression of the tested MO/MAC-specific antigens. MO either migrated through the IEC layer or stayed in the upper compartment of transwell-culture. Antigen expression of cells adherent to the plastic dishes after transmigration was examined by immunohistochemistry. MO/MAC were all positive for the intracellular MO/MAC marker CD68 and showed a high expression of CD14, CD16, CD11b and CD11c after the seven day culture period (Figure 5B). Non adherent cells from the upper or lower compartment of the filter insert were analysed by

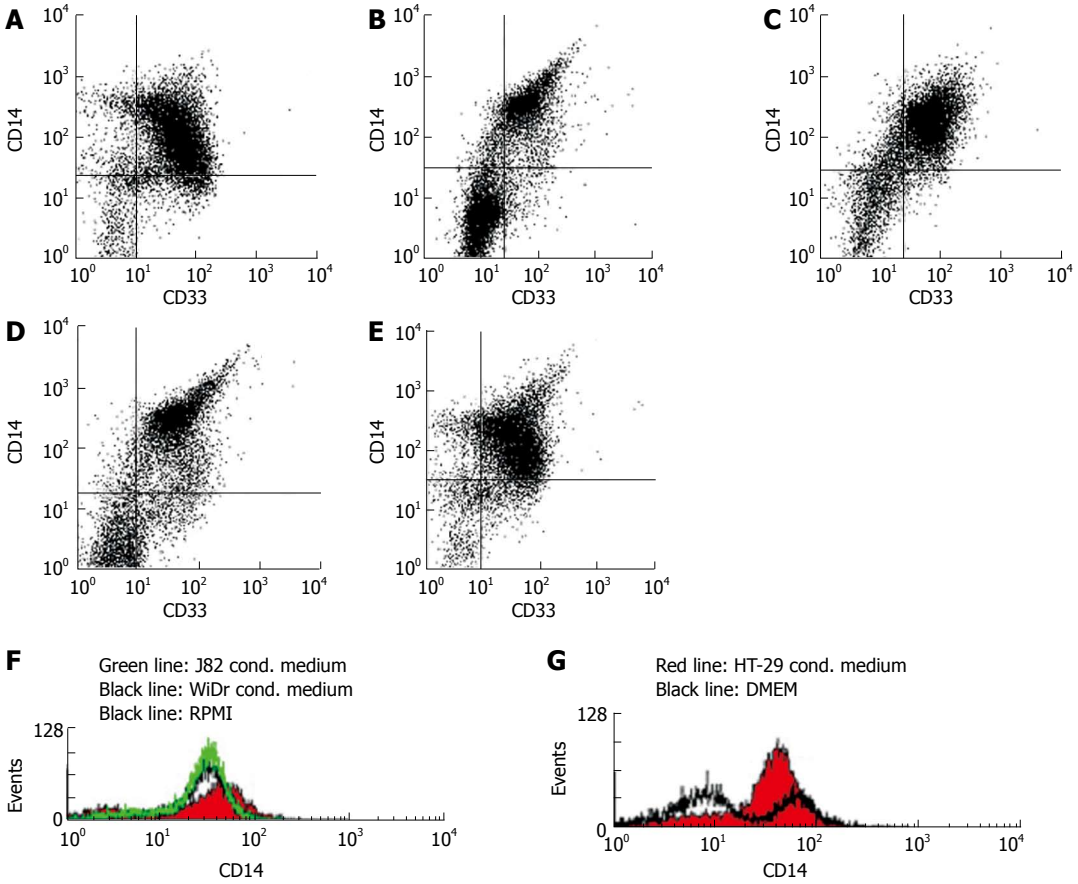

Figure 2 Flow cytometrical quantification of MO/MAC antigen expression after seven days of culture in IEC conditioned medium. **A**: Ninety-two percent of CD33+ cells (MO/MAC) showed expression of CD14 in MO cultured in unconditioned control medium (RPMI) without FCS supplemented with 2% human AB serum for seven days; **B**: Ninety-five percent of CD33+ cells (MO/MAC) were CD14-positiv in MO cultured in WiDr conditioned medium without FCS supplemented with 2% human AB serum for seven days; **C**: Ninety-two percent of CD33+ cells (MO/MAC) were CD14-positive in MO cultured in J82 conditioned medium (control cell line of non-intestinal origin) without FCS supplemented with 2% human AB serum for seven days; **D**: Ninety-four percent of CD33+ cells (MO/MAC) showed expression of CD14 in MO cultured in unconditioned control medium (DMEM) without FCS supplemented with 2% human AB serum for seven days; **E**: Ninety-eight percent of CD33+ cells (MO/MAC) were CD14-positive in MO cultured in HT-29 conditioned medium without FCS supplemented with 2% human AB serum for seven days; **F**: No down-regulation of CD14 expression was observed on histogram of CD14 expressing mononuclear cells after seven days of culture in RPMI (control medium), J82 (control cell line) or WiDR conditioned medium; **G**: Histogram of CD14 expressing mononuclear cells after seven days of culture in DMEM (control medium) and HT-29 conditioned medium.

flow cytometry and showed a similar antigen pattern with high CD14, CD16 and CD11b expressions (Figure 5C and D).

Immigration of MO into MCS was relevant to IMAC differentiation

To test whether the process of invading the three-dimensional IEC-spheroids is necessary for the differentiation of MO into IMACs, we generated "mixed spheroids" from a 1:1-mixture of IEC and MO. In these experiments MO were added during the generation of MCS and did not invade the three-dimensional aggregates.

Flow cytometrical analysis showed 15.2% MO/MAC inside spheroids of the control cell line J82 after 24 h of co-culture. This percentage was nearly constant during a seven-day culture period (13.2%, d 7, n = 5). In spheroids with the IEC line HT-29 a different effect could be observed. After 24 h 21.7% MO/MAC inside the spheroids could be detected. On day seven of co-culture the percentage of MO/MAC inside the spheroids decreased to 1.4% (n = 4). Similar results could be obtained with spheroids of the IEC line WiDr. The percentage of MO/MAC inside the spheroids decreased from 14.6% (24 h) to 2.4% (d 7, n = 4) (Figure 6A). Remaining MO/MAC inside the aggregates showed no differentiation into IMACs. The results showed that active invasion of the aggregates by MO was an essential step in the process of IMAC differentiation.

To test whether the observed decrease in the relative amount of MO in "mixed spheroids" is due to Fas-induced apoptosis, we added a blocking anti-Fas antibody to the cell suspensions before generating "mixed spheroids". Addition of the anti-Fas antibody did not change the results significantly. The number of MO/MAC decreased from 14.2% (24 h) to 0.8% (7d) in HT-29 MCS and from 20% (24 h) to 2.3% (7d) in WiDr spheroids. In control experiments with J82 spheroids the number of MO/MAC was almost constant with 13.9% at 24 h and 12% on day seven (n = 3) (Figure 6B).

In addition, Western-blots for caspase-3 were

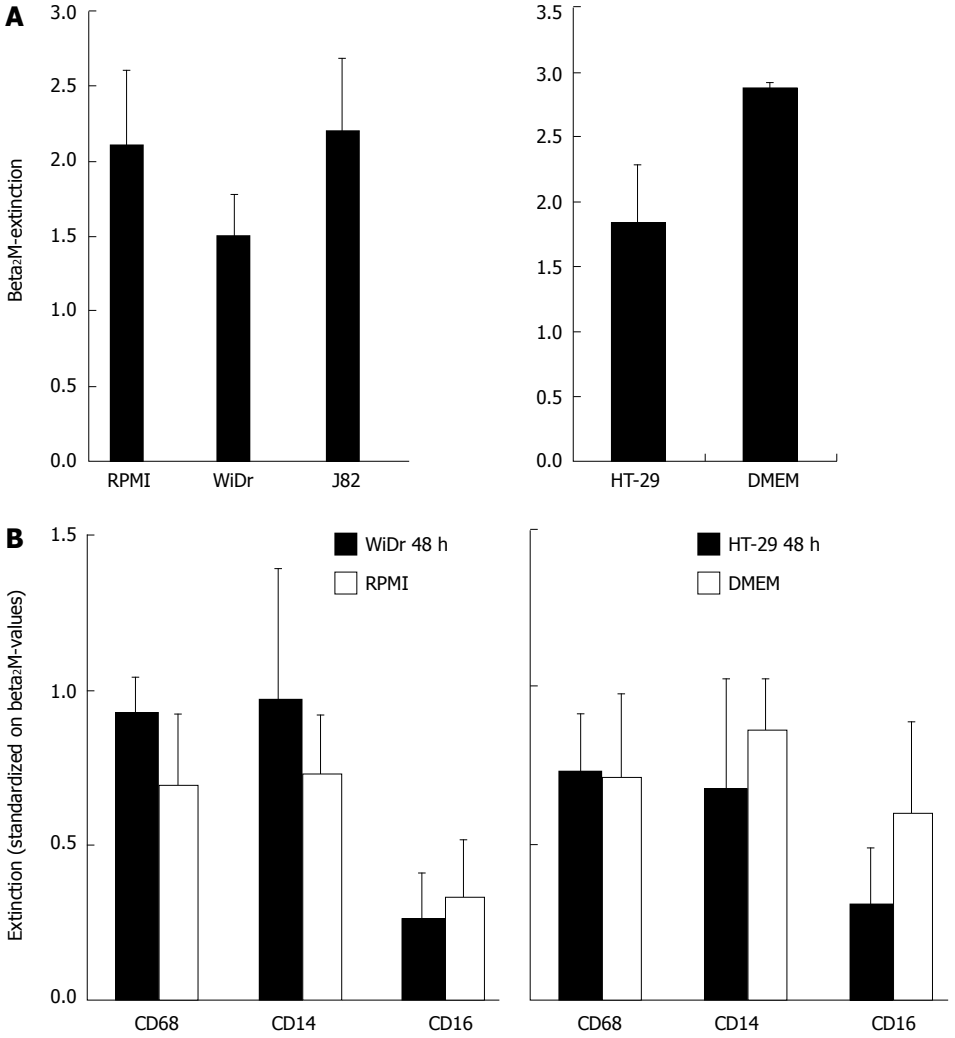

Figure 3 Cell ELISA of MO/MAC antigen expression after seven days of co-culture with IEC conditioned media. **A**: Freshly elutriated MO were incubated in conditioned medium of the IEC line WiDr or control media (left graph) of HT-29 and control media (right graph) for seven days. Expression of the housekeeping antigen β2M was determined an extinction is given as absolute value; **B**: CD68, CD14 and CD16 antigen expression of MO incubated in conditioned medium of the IEC line WiDr or non-conditioned control medium (left graph) or HT-29 and control medium (right graph) after seven days was also determined by cell ELISA. Values are standardized on β_2M-extinction.

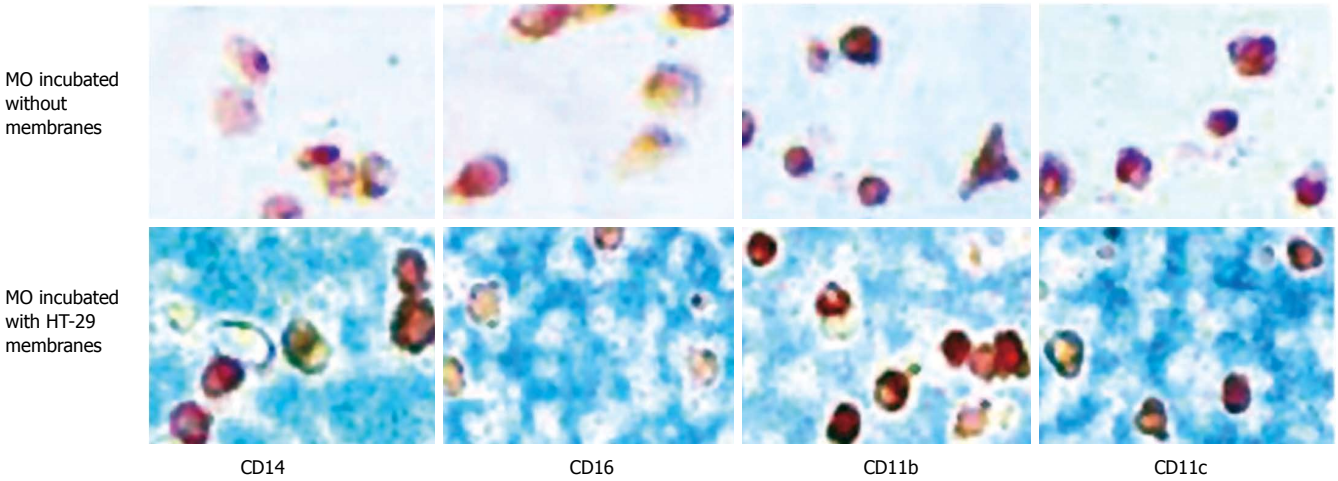

Figure 4 MO/MAC antigen expression after seven days of culture with IEC membranes. Freshly elutriated MO were incubated for seven days with membrane preparations of the IEC line HT-29 or without membranes. Antigen expression was determined by immunohistochemistry (APAAP-method). There was no difference in expression of CD14, CD16, CD11b and CD11c in cells incubated with or without IEC membranes.

performed. After 24 h and three days no activated caspase-3 was detected in "mixed MCS" of IEC and MO or in control cells and MO (Figure 7).

Potential role of extracellular matrix in IMAC differentation

The expression of extracellular matrix (ECM) proteins (fibronectin, laminin and collagen IV) in the "normal" and mixed spheroids was determined by immunohistochemistry. Laminin and collagen IV were not detectable in both mixed spheroids and spheroids invaded by MO. In contrast, a strong expression of fibronectin could be detected in spheroids invaded by MO, which was

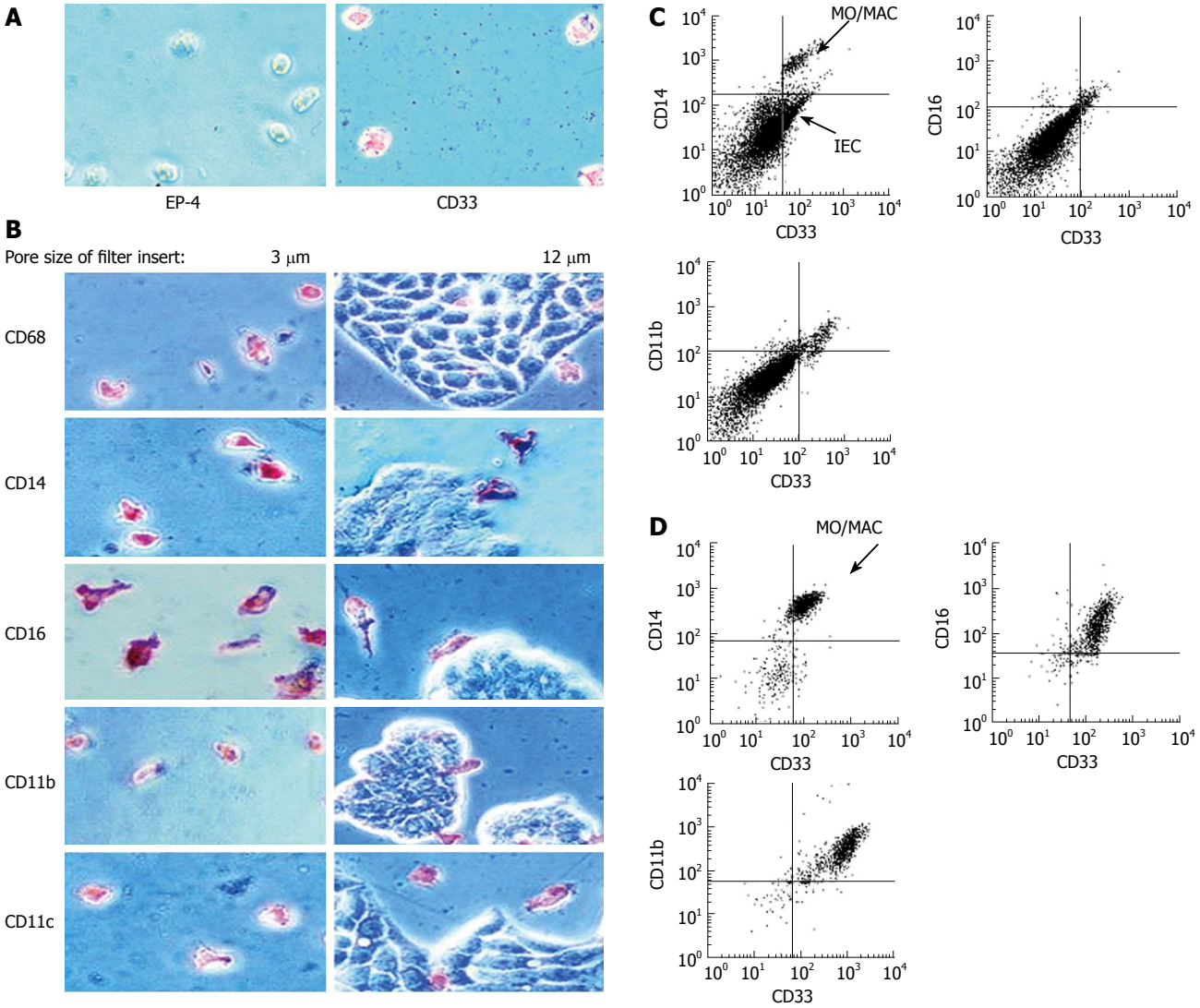

Figure 5 Antigen expression of MO/MAC incubated with IEC in trans-well cultures. Freshly elutriated MO were incubated with the IEC line HT-29 seeded on filter inlays for seven days. Depending on pore size of the inlays only MO or MO and IEC could migrate through the filter. Antigen expression of migrating and non-migrating cells was examined by immunohistochemistry (APAAP-method) and flow cytometry. **A**: Migrating cells adhered to the plastic surface of the cell culture plate. When filters with a pore size of 3 μm were used, only MO were able to migrate through the membrane. Migrating cells were all negative for the epithelial cell specific marker EP-4 and positive for the MO/MAC-marker CD33; **B**: Migrating cells showed expression of CD68, CD14, CD16, CD11b and CD11c (left column). Twelve μm pores allowed migration of MO and IEC. None of the tested antigens was expressed by IEC (right column); **C**: Non migrating cells which remained in the upper compartment of the filter insert were examined by flow cytometry. The CD33-positive cell population (MO/MAC) showed also expression of CD14, CD16 and CD11b; **D**: Migrating cells which did not adhere to the plastic dish were examined by flow cytometry. Cells showed CD33-expression and were positive for CD14, CD16 and CD11b.

up-regulated from three to seven days of culture and was absent in mixed spheroids incubated for the same time. The expression of fibronectin was localized in the inner region of aggregates (Figure 8).

DISCUSSION

As IMACs are essential players in local immune responses and the innate immune system of intestinal barrier, their specific phenotype must be of importance. Compared to IMACs from inflammatory bowel disease (IBD) patients, IMACs from normal intestinal mucosa show a down-regulation of several surface markers, co-stimulatory molecules and proteins necessary for LPS-induced signal transduction[11-13,16], which may be responsible for the induction of tolerance.

Recently we have shown that MO differentiate into IMACs after immigration into the MCS co-culture with IEC *in vitro*[18]. In this study, factor(s) inducing IMAC differentiation *in vitro* were analysed. We showed that the specific IMAC differentiation was not mediated by soluble or membrane bound factors of IEC alone, as no intestinal-like differentiation was observed in freshly elutriated MO cultured together with IEC-conditioned medium or IEC-membranes. Also "weak interactions" between MO and IEC in trans-well cultures, in which MO and IEC (monolayers) were only separated by filter membranes, were not sufficient for differentiation. IMAC differentiation could only be induced in the complex three-dimensional MCS model with close contact between MO, IEC and ECM[18]. Loss of MO observed in 1:1 "mixed spheroids" of the IEC lines HT-29 and WiDr was obviously not due to apoptosis, as we could neither block this effect by adding an anti-Fas antibody nor detect

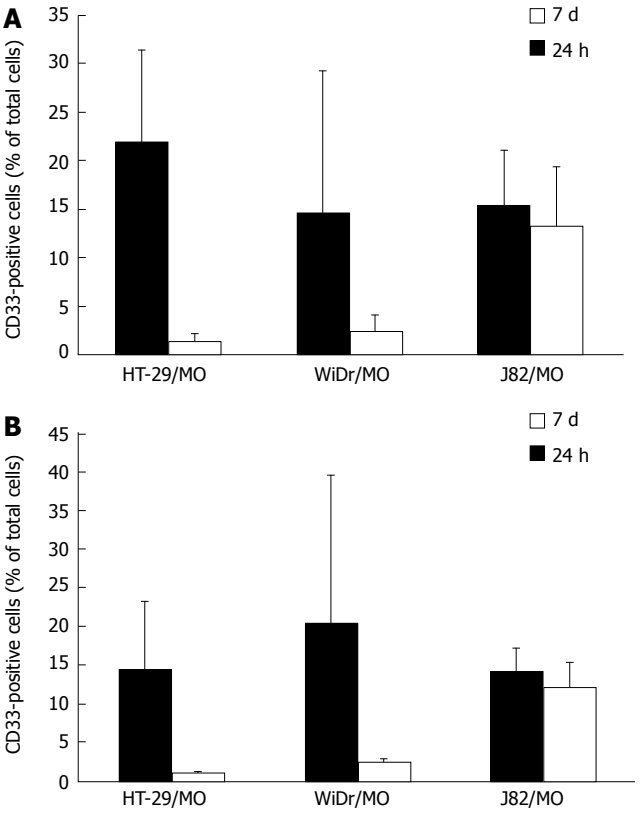

Figure 6 Mixed spheroids of MO and IEC or the control cell line. Mixed spheroids of the IEC lines HT-29 and WiDr or the control cell line J82 and MO were generated and cultured for seven days, disaggregated and examined by flow cytometry. **A**: There was a strong decrease of surviving MO/MAC (CD33+ cells) inside IEC spheroids compared to control spheroids over the seven-day culture period. In HT-29 spheroids the percentage decreased from 21.7% (24 h) to 1.4% (7 d). In WiDr spheroids a slighter decrease was observed with 14.6% MO/MAC after 24 h and 2.4% after seven days. In spheroids of the control cell line J82 no selection of a MO/MAC subpopulation could be observed. The number of MO/MAC inside the aggregates was nearly constant with 15.2% (24 h) and 13.2 (7 d); **B**: Addition of a blocking anti-Fas antibody 30 min before generation of the mixed spheroids did not change the results. In IEC-MCS a strong decrease of MO/MAC was observed (HT-29: 14.2% 24 h, 0.8% 7 d, WiDr: 20.1% 24 h, 2.3% 7 d). The MO/MAC number in control cell MCS was nearly constant with 13.9% (24 h) and 12.0% (7 d).

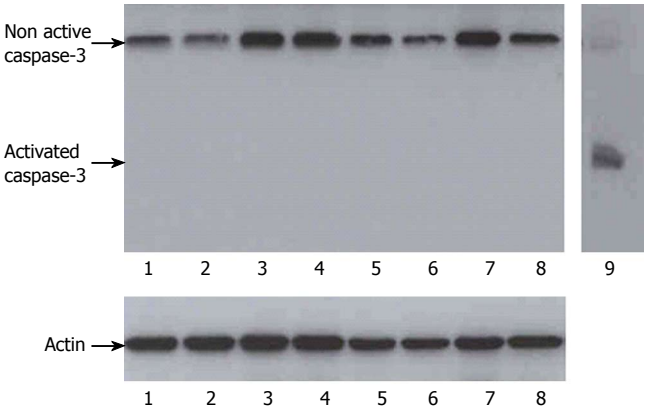

Figure 7 Western-blot for caspase-3 of mixed spheroids after 24 h and three days. Mixed spheroids of IEC and MO, control cells and MO or control spheroids generated only from IEC or control cells were disaggregated after 24 h and three days of culture. Western-blots for activated caspase-3 were performed. Lane 1: HT-29 without MO 24 h; lane 2: HT-29/MO (1:1) 24 h; lane 3: J82 without MO 24 h; lane 4: J82/MO (1:1) 24 h; lane 5: HT-29 without MO 3 d; lane 6: HT-29/MO (1:1) 3 d; lane 7: J82 without MO 3 d; lane 8: J82/MO (1:1) 3 d; lane 9: positive control for activated caspase-3. No activated caspase-3 could be detected in co-cultures of MO and IEC or in spheroids generated only from IEC.

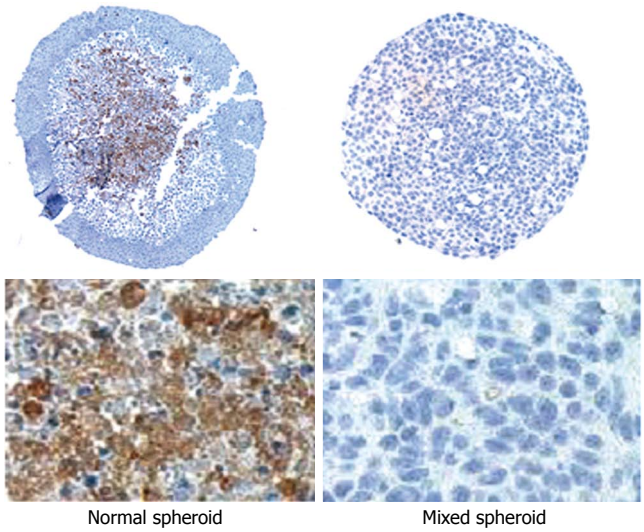

Figure 8 Immunohistochemical staining for the ECM-protein fibronectin in "normal" and mixed spheroids of the IEC line HT-29 after seven days. Fibronectin could be detected in spheroids invaded by MO and cultured for seven days. Expression was preferentially localized in the center of aggregates. In mixed spheroids cultured for seven days no fibronectin expression was observed.

activated caspase-3 during the incubation period.

Although MCS do not resemble the *in vivo* situation where IMACs are separated from the IEC by the basement membrane, many conditions such as O_2-gradient, pH or ECM production are similar to those in the body[26-28]. In MCS, cells are also able to form cell-cell and cell-matrix contacts which are found *in vivo*[29-31] and may therefore be regarded as a useful model to study the important aspects of IMAC differentiation.

In general, interactions between different cell types, special cytokine milieus and contact with components of the ECM can trigger cells to develop a special phenotype. Hohn and co-workers[32] showed that components of the basement membrane and ECM are involved in choriocarcinoma cell differentiation. Hanspal *et al*[33] have demonstrated the importance of cell-cell interactions during the regulation of erythropoiesis. The ECM protein, vitronectin, controls the differentiation of cerebellar granular cells[34]. It was reported that ECM also plays a role in the differentiation of embryonic stem cells[35] and skeletal muscle cells[36]. Armstrong *et al*[37] have shown that ECM proteins have effects on MAC differentiation, growth and function.

Jacob *et al*[38] induced differentiation of MO to MAC *in vitro* by culturing MO on different ECM protein substrates, and found that specific markers associated with differentiation are changes in the expression of cell surface antigens. FACS analysis showed a down-regulation of CD14 occurring in a substrate dependent manner, which was the highest in MO maintained on fibronectin in their study[38].

In our experiments, MCS invaded by MO and cultured

for seven days contained a large amount of ECM protein fibronectin. In addition, the expression of fibronectin was up-regulated during the culture period, which is correlated with the previously described down-regulation of CD14 and other MO-specific surface markers[18]. In mixed spheroids no fibronectin expression could be detected, which could be due to a stronger degradation of ECM proteins by the larger amount of MO added or a lack of synthesis induction. Fibronectin present in the described co-culture model seems to be an important factor contributing to the *in vitro* differentiation of IMACs as well as the active invasion of MO into the three-dimensional aggregates, indicating that only a subpopulation of blood MO is able to differentiate into IMACs.

The loss of MO in the "mixed spheroids" could have several reasons. First, differentiation into the intestinal phenotype is necessary for survival in the epithelial cell environment. Second, the higher number of mononuclear cells in the mixed spheroids compared to the model with MO invasion induces factors that lead to cell death or prevent the synthesis of survival factors. Third, we cannot exclude that this is a self protection effect of the tumor cell lines used and that MO only enter the MCS in the MCS model.

We cannot exclude that there is a pre-primed subpopulation of MO in the peripheral blood that is especially suited to get in contact with IEC. According to such a hypothesis only this pre-primed subpopulation would enter the MCS model or the mucosa and further differentiate into IMACs. This natural selection would not be observed in co-cultures of all elutriated peripheral MO with conditioned media, membrane preparations or in mixed spheroids. The number of differentiating cells would be too low to reach a significant difference. In the present study, we investigated this possibility of a pre-primed subpopulation of MO suited for IMAC differentiation.

To understand the differentiation process of IMACs in healthy individuals may further help to find an approach for the therapy of IBD. Local induction of a tolerogenic and anergic IMAC cell type could down-regulate or stop mucosal inflammation. A therapeutic approach inducing differentiation of this cell type would be one step up the inflammatory cascade not aimed at T-cells but at the site of the first contact with antigen entry in the mucosa.

REFERENCES

1 **Lee SH**, Starkey PM, Gordon S. Quantitative analysis of total macrophage content in adult mouse tissues. Immunochemical studies with monoclonal antibody F4/80. *J Exp Med* 1985; **161**: 475-489

2 **Pavli P**, Doe WF. Intestinal macrophages. In: Mac Dermott RP, Stenson WF, editors. Inflammatory bowel disease. New York: Elsevier, 1992: 177-188

3 **LeFevre ME**, Hammer R, Joel DD. Macrophages of the mammalian small intestine: a review. *J Reticuloendothel Soc* 1979; **26**: 553-573

4 **Bockman DE**, Boydston WR, Beezhold DH. The role of epithelial cells in gut-associated immune reactivity. *Ann N Y Acad Sci* 1983; **409**: 129-144

5 **Bull DM**, Bookman MA. Isolation and functional characterization of human intestinal mucosal lymphoid cells. *J Clin Invest* 1977; **59**: 966-974

6 **Donnellan WL**. The structure of the colonic mucosa. The epithelium and subepithelial reticulohistiocytic complex. *Gastroenterology* 1965; **49**: 496-514

7 **Golder JP**, Doe WF. Isolation and preliminary characterization of human intestinal macrophages. *Gastroenterology* 1983; **84**: 795-802

8 **Pavli P**, Woodhams CE, Doe WF, Hume DA. Isolation and characterization of antigen-presenting dendritic cells from the mouse intestinal lamina propria. *Immunology* 1990; **70**: 40-47

9 **Hugot JP**, Chamaillard M, Zouali H, Lesage S, Cézard JP, Belaiche J, Almer S, Tysk C, O'Morain CA, Gassull M, Binder V, Finkel Y, Cortot A, Modigliani R, Laurent-Puig P, Gower-Rousseau C, Macry J, Colombel JF, Sahbatou M, Thomas G. Association of NOD2 leucine-rich repeat variants with susceptibility to Crohn's disease. *Nature* 2001; **411**: 599-603

10 **Ogura Y**, Bonen DK, Inohara N, Nicolae DL, Chen FF, Ramos R, Britton H, Moran T, Karaliuskas R, Duerr RH, Achkar JP, Brant SR, Bayless TM, Kirschner BS, Hanauer SB, Nuñez G, Cho JH. A frameshift mutation in NOD2 associated with susceptibility to Crohn's disease. *Nature* 2001; **411**: 603-606

11 **Andus T**, Rogler G, Daig R, Falk W, Schölmerich J, Gross V. The role of macrophages. In: Tygat GNJ, Bartelsman JFWM, van Deventer SJH, editors. Inflammatory bowel disease. The Netherlands: Kluwer Dordrecht, 1995: 281-297

12 **Rogler G**, Hausmann M, Vogl D, Aschenbrenner E, Andus T, Falk W, Andreesen R, Schölmerich J, Gross V. Isolation and phenotypic characterization of colonic macrophages. *Clin Exp Immunol* 1998; **112**: 205-215

13 **Rogler G**, Andus T, Aschenbrenner E, Vogl D, Falk W, Schölmerich J, Gross V. Alterations of the phenotype of colonic macrophages in inflammatory bowel disease. *Eur J Gastroenterol Hepatol* 1997; **9**: 893-899

14 **Rugtveit J**, Bakka A, Brandtzaeg P. Differential distribution of B7.1 (CD80) and B7.2 (CD86) costimulatory molecules on mucosal macrophage subsets in human inflammatory bowel disease (IBD). *Clin Exp Immunol* 1997; **110**: 104-113

15 **Barbosa IL**, Gant VA, Hamblin AS. Alveolar macrophages from patients with bronchogenic carcinoma and sarcoidosis similarly express monocyte antigens. *Clin Exp Immunol* 1991; **86**: 173-178

16 **Hausmann M**, Kiessling S, Mestermann S, Webb G, Spöttl T, Andus T, Schölmerich J, Herfarth H, Ray K, Falk W, Rogler G. Toll-like receptors 2 and 4 are up-regulated during intestinal inflammation. *Gastroenterology* 2002; **122**: 1987-2000

17 **Hausmann M**, Spöttl T, Andus T, Rothe G, Falk W, Schölmerich J, Herfarth H, Rogler G. Subtractive screening reveals up-regulation of NADPH oxidase expression in Crohn's disease intestinal macrophages. *Clin Exp Immunol* 2001; **125**: 48-55

18 **Spöttl T**, Hausmann M, Kreutz M, Peuker A, Vogl D, Schölmerich J, Falk W, Andreesen R, Andus T, Herfarth H, Rogler G. Monocyte differentiation in intestine-like macrophage phenotype induced by epithelial cells. *J Leukoc Biol* 2001; **70**: 241-251

19 **Pavli P**, Maxwell L, Van de Pol E, Doe F. Distribution of human colonic dendritic cells and macrophages. *Clin Exp Immunol* 1996; **104**: 124-132

20 **D'Amico G**, Bianchi G, Bernasconi S, Bersani L, Piemonti L, Sozzani S, Mantovani A, Allavena P. Adhesion, transendothelial migration, and reverse transmigration of in vitro cultured dendritic cells. *Blood* 1998; **92**: 207-214

21 **Fujigaki Y**, Nagase M, Kojima K, Yamamoto T, Hishida A. Glomerular handling of immune complex in the acute phase of active in situ immune complex glomerulonephritis employing cationized ferritin in rats. Ultrastructural localization of immune complex, complements and inflammatory cells. *Virchows Arch* 1997; **431**: 53-61

22 **Martin CA**, Homaidan FR, Palaia T, Burakoff R, el-Sabban ME. Gap junctional communication between murine macrophages and intestinal epithelial cell lines. *Cell Adhes Commun* 1998; **5**: 437-449

23 **Marshall CJ**, Franks LM, Carbonell AW. Markers of neoplastic

transformation in epithelial cell lines derived from human carcinomas. *J Natl Cancer Inst* 1977; **58**: 1743-1751
24 **Noguchi P**, Wallace R, Johnson J, Earley EM, O'Brien S, Ferrone S, Pellegrino MA, Milstien J, Needy C, Browne W, Petricciani J. Characterization of the WIDR: a human colon carcinoma cell line. *In Vitro* 1979; **15**: 401-408
25 **Aigner A**, Neumann S. Immunchemie: Grundlagen, Anwendungen, Perspektiven. Jena: Gustav Fischer**,** 1997
26 **Inch WR**, McCredie JA, Sutherland RM. Growth of nodular carcinomas in rodents compared with multi-cell spheroids in tissue culture. *Growth* 1970; **34**: 271-282
27 **Mueller-Klieser W**. Multicellular spheroids. A review on cellular aggregates in cancer research. *J Cancer Res Clin Oncol* 1987; **113**: 101-122
28 **Konur A**, Kreutz M, Knüchel R, Krause SW, Andreesen R. Cytokine repertoire during maturation of monocytes to macrophages within spheroids of malignant and non-malignant urothelial cell lines. *Int J Cancer* 1998; **78**: 648-653
29 **Sutherland RM**. Cell and environment interactions in tumor microregions: the multicell spheroid model. *Science* 1988; **240**: 177-184
30 **Olive PL**, Durand RE. Drug and radiation resistance in spheroids: cell contact and kinetics. *Cancer Metastasis Rev* 1994; **13**: 121-138
31 **Davies CD**, Müller H, Hagen I, Gårseth M, Hjelstuen MH. Comparison of extracellular matrix in human osteosarcomas and melanomas growing as xenografts, multicellular spheroids, and monolayer cultures. *Anticancer Res* 1997; **17**: 4317-4326
32 **Hohn HP**, Grümmer R, Bosserhoff S, Graf-Lingnau S, Reuss B, Bäcker C, Denker HW. The role of matrix contact and of cell-cell interactions in choriocarcinoma cell differentiation. *Eur J Cell Biol* 1996; **69**: 76-85
33 **Hanspal M**. Importance of cell-cell interactions in regulation of erythropoiesis. *Curr Opin Hematol* 1997; **4**: 142-147
34 **Wechsler-Reya RJ**. Caught in the matrix: how vitronectin controls neuronal differentiation. *Trends Neurosci* 2001; **24**: 680-682
35 **Czyz J**, Wobus A. Embryonic stem cell differentiation: the role of extracellular factors. *Differentiation* 2001; **68**: 167-174
36 **Osses N**, Brandan E. ECM is required for skeletal muscle differentiation independently of muscle regulatory factor expression. *Am J Physiol Cell Physiol* 2002; **282**: C383-C394
37 **Armstrong JW**, Chapes SK. Effects of extracellular matrix proteins on macrophage differentiation, growth, and function: comparison of liquid and agar culture systems. *J Exp Zool* 1994; **269**: 178-187
38 **Jacob SS**, Shastry P, Sudhakaran PR. Monocyte-macrophage differentiation in vitro: modulation by extracellular matrix protein substratum. *Mol Cell Biochem* 2002**; 233:** 9-17

S- Editor Liu Y **L- Editor** Wang XL **E- Editor** Ma WH

PO Box 2345, Beijing 100023, China
www.wjgnet.com
wjg@wjgnet.com

World J Gastroenterol 2007 February 21; 13(7): 1042-1052
World Journal of Gastroenterology ISSN 1007-9327

BASIC RESEARCH

Evidence for a sequential transfer of iron amongst ferritin, transferrin and transferrin receptor during duodenal absorption of iron in rat and human

Vasantha L Kolachala, B Sesikeran, K Madhavan Nair

Vasantha L Kolachala, Division of Digestive Diseases, Department of Medicine, Emory University, Atlanta, GA, United States
B Sesikeran, K Madhavan Nair, National Institute of Nutrition, Indian Council of Medical Research, Jamai-Osmania PO, Hyderabad 500007, India
Supported by Council of Scientific and Industrial research, India: schemes no (812) 93-EMR-11 to KMN
Correspondence to: K Madhavan Nair, National Institute of Nutrition, Indian Council of Medical Research, Jamai-Osmania PO, Hyderabad 500007, India. nairthayil@gmail.com
Telephone: +91-40-27008921 Fax: +91-40-27019074
Received: 2006-10-31 Accepted: 2007-01-04

Abstract

AIM: To elucidate the sequential transfer of iron amongst ferritin, transferrin and transferrin receptor under various iron status conditions.

METHODS: Incorporation of ^{59}Fe into mucosal and luminal proteins was carried out in control WKY rats. The sequential transfer of iron amongst ferritin, transferrin and transferrin receptor was carried out in iron deficient, control and iron overloaded rats. The duodenal proteins were subjected to immunoprecipitation and quantitation by specific ELISA and *in situ* localization by microautoradiography and immunohistochemistry in tandem duodenal sections. Human duodenal biopsy (n = 36) collected from subjects with differing iron status were also stained for these proteins.

RESULTS: Ferritin was identified as the major protein that incorporated iron in a time-dependent manner in the duodenal mucosa. The concentration of mucosal ferritin was significantly higher in the iron excess group compared to control, iron deficient groups (731.5 ± 191.96 *vs* 308.3 ± 123.36, 731.5 ± 191.96 *vs* 256.0 ± 1.19, $P < 0.005$), while that of luminal transferrin which was significantly higher than the mucosal did not differ among the groups (10.9 ± 7.6 *vs* 0.87 ± 0.79, 11.1 ± 10.3 *vs* 0.80 ± 1.20, 6.8 ± 4.7 *vs* 0.61 ± 0.63, $P < 0.001$). *In situ* grading of proteins and iron, and their superimposition, suggested the occurrence of a sequential transfer of iron. This was demonstrated to occur through the initial binding of iron to luminal transferrin then to absorptive cell surface transferrin receptors. The staining intensity of these proteins varied according to the iron nutrition in humans, with intense staining of transferrin receptor observed in iron deficient subjects.

CONCLUSION: It is concluded that the intestine takes up iron through a sequential transfer involving interaction of luminal transferrin, transferrin-transferrin receptor and ferritin.

Key words: Mucosa; Lumen; Iron-binding proteins

Kolachala VL, Sesikeran B, Nair KM. Evidence for a sequential transfer of iron amongst ferritin, transferrin and transferrin receptor during duodenal absorption of iron in rat and human. *World J Gastroenterol* 2007; 13(7): 1042-1052

http://www.wjgnet.com/1007-9327/13/1042.asp

INTRODUCTION

Iron homeostasis is accomplished by regulating absorption in the proximal small intestine and is regulated according to the body's needs. Failure to maintain this equilibrium leads to pathological conditions resulting in either iron deficiency or iron overload. Iron deficiency anemia remains the most important micronutrient deficiency world wide. Iron is essential because of its unique ability to serve as both an electron donor and acceptor. Because of iron's virtual insolubility and potential toxicity under physiological conditions, special molecules have evolved for its acquisition, transport and storage in soluble, nontoxic form. In humans, heme iron is absorbed more efficiently than non-heme iron[1]. Recent studies demonstrate that non-heme iron is transported into the cell in the ferrous [Fe (Ⅱ)] form, mainly by carrier divalent metal transporter 1 (DMT1)-also known as natural resistance associated macrophage protein 2 (Nramp2) or divalent cation transporter 1 (DCT1)[2] . However, iron absorption is not impaired by mutation of DMT-1, suggesting that DMT-1 is not the only transporter operating within the endosomes of crypt cells. Studies of Conrad *et al*[3], showed that ferric iron is absorbed by β3 integrin and mobilferrin pathway which is shared with other nutritional metals .

In last few decades, several candidate proteins involved

in the transmembrane transport of iron have been identified[4] . Several years ago, Granick *et al* demonstrated that ferritin sequesters iron and provides the block to iron uptake. Although this model remains unproven, the hypothesis that the amount of mucosal ferritin dictates the extent of iron absorbed by the enterocytes is still intriguing. It has been postulated that iron absorption was the primary method of maintaining body iron homeostasis and was regulated by a mucosal receptor that blocked iron absorption when it became satiated with iron. For two decades, it was believed that ferritin was the receptor that regulates iron absorption, and that apoferritin enhances iron absorption while holoferritin blocks iron uptake. This hypothesis was disproved by immunological studies showing that there was little or no apoferritin in the absorptive cells of iron deficient animals[5]. Despite the close relationship between ferritin levels and intestinal iron absorption[6] it is not clear whether this protein plays a passive or active role in transport regulation.

There are studies to argue for[7-11] and against[12-14] the view that transferrin (Tf) is an important mediator of iron absorption. The proposal that mucosal Tf acts as a shuttle protein for iron absorption was suggested by Huebers *et al*[15]. Selective localization of transferrin in the duodenal epithelium in rat[16,17] and in human[17] , and the co-localization of transferrin receptor (TfR) and transferrin in coated pits on the basal and lateral membranes of crypt cells in mouse have been demonstrated[18]. However, an ultrastructural study of Parmley *et al*[19] failed to identify TfR on the surface of enterocyte microvilli. Thus, the role of transferrin and transferrin receptor in the duodenal uptake was not identified with certainty. In 1983, it was postulated that transferrin was secreted into the intestinal lumen to bind iron and enter the absorptive cell as a transferrin iron complex in a manner similar to non-intestinal cells[15]. Recent studies of transferrin receptor knockout mice ($TfR^{-/-}$) provide new insights regarding the physiologic role of the transferrin/transferrin receptor cycle. Homozygous $TfR^{-/-}$ animals die *in utero* with impaired erythropoiesis and defective neurological development. Thus, the $TfR^{-/-}$ mice provide a convincing demonstration that the transferrin/transferrin receptor cycle plays a central role in the maintenance of normal iron metabolism. Whether transferrin is associated with receptor and whether it plays any role in iron absorption at this site is yet to be determined. A protein called hereditary hemochromatosis (HFE) has been shown to interact with transferrin receptor 1 (TfR1)[20] to influence the rate of receptor mediated uptake of transferrin-bound iron[21-24] . Thus, these investigations of exact localization of mucosal transferrin and transferrin receptor, inside or outside the enterocytes, are conflicting. Therefore, an attempt was made to describe the sequential movement of iron across intestine. The events were sequenced by *in situ* localization of iron by microautoradiography and immunohistochemistry of ferritin, transferrin and transferrin receptor in serial sections of intestine.

MATERIALS AND METHODS

Radioactive $^{59}FeCl_3$ (sp.act 4.0 Ci/g iron in 0.01 mol/L HCl) was obtained from BRIT (Mumbai, India). Photographic emulsion LM-1 was obtained from Amersham (Amersham International plc, UK). SIH universal anti-rabbit kit, human and rat serotransferrin was obtained from Sigma Aldrich Co (St. Louis, USA). Ferritin, transferrin antisera against purified proteins were produced in New Zealand white rabbits. Polyclonal antiserum against rat placental transferrin receptor was a gift from James D. Cook, M.D (University of Kansas Medical Center, Kansas City, USA). All other chemicals used were of analytic grade and procured locally.

Studies in rats

Rats from National Centre for Laboratory Animal Sciences (National Institute of Nutrition, Hyderabad) were used for the study. All animal experiments were approved by the institutional animal ethics committee.

Incorporation of radioactive iron into various iron binding protein was carried out in *Wistar/Kyoto* (*WKY*) adult male normal rats (body weight 200 g). Food was withheld for 16-18 h before administering 1 mL of 7-10 μci of $^{59}FeCl_3$ in 0.01N HCl by gavage. Rats were sacrificed at various time intervals starting at 15, 30 min, 1, 2, 4 and 12 h to study the time-dependent incorporation of iron into luminal and mucosal proteins of various segments. All the subsequent operations were carried out on ice. The luminal content was collected by flushing with 5-10 mL of saline containing protease inhibitors. The mucosal scrapings were obtained by scrapping off the everted segments with a glass slide. The intestinal contents obtained from three rats from each group were pooled together for each time point. The contents were homogenized in 1:4 v/v of saline containing a cocktail of protease inhibitors (PMSF 75 μg/mL, leupeptin 1 μg/mL and iodoacetate186 μg/mL), and subjected to 60% ammonium sulphate fractionation. A clear supernatant was prepared for subsequent analysis.

Further to explore the specific role of duodenal transferrin and ferritin during iron absorption, time-dependent (5 min-4 h) incorporation of radioactive iron into these proteins, along with quantitation by specific ELISA and immunoprecipitation techniques for ferritin and transferrin, was carried out in control, iron-deficient, and excess iron fed rats. For this, 74 *WKY* male weanling rats (body weight 37.5 ± 7.63) were randomly selected and housed individually into iron deficient (n = 30), control (n = 24) and iron excess (n = 24) groups. They were allowed to have free access to food and water for 7 weeks. The rats were placed on one of the three diets each containing identical protein, fat, carbohydrate, and complete vitamin and fiber supplements. The diets were produced in accordance with the recommendations of American Institute of Nutrition (AIN93)[25]. The diet also contained a balanced mineral mix, differing only in the iron content. The deficient group received iron deficient semi-synthetic diet containing < 10 mg iron/kg diet, while the iron adequate and excess groups received diet containing 35 and 250 mg/kg diet, respectively. At the end of this period rats were administered 7-10 μCi of radioactive iron and sacrificed at different time points. Duodenal segments

of intestine were collected at 5, 15, 30 min, 1, 2, 4 h and processed. Homogenates of luminal and mucosal contents were analyzed for ferritin and transferrin by specific sandwich ELISA. Incorporation of radiolabelled iron into these proteins was studied by imunoprecipitation with specific antibodies.

Finally, studies were carried out to understand the sequential movement of iron across intestine under various iron status conditions. *WKY* male weanling rats (body weight 36.8 ± 6.56) were equally (n = 8) distributed into iron deficient, control and iron overload groups. For iron overloading, in addition to iron excess diet as mentioned above, we gave 4 intra-peritonial injections of 1 mL of imferon, an iron sorbitol citric acid complex in water (50 mg of iron/mL, Rallies India Ltd, Mumbai, India) at weekly intervals. After 7 wk, rats were fasted overnight and given 100 μCi of $^{59}FeCl_3$ with 0.25 mg of carrier iron as ferrous sulphate by gavage. Duodenal segment of intestine were collected at 5, 15, 30 min, 1, 2, 4, 16 h. The segments were flushed with formalin, cut opened longitudinally and fixed in 10% neutral formalin for 12 h. These intestinal segments were rolled longitudinally (Swiss-roll), and further processed for microautoradiography and immunohistochemistry.

Western blotting and autoradiography

The protein content was estimated by the method of Bradford[26]. Both luminal and mucosal proteins (100 μg) were subjected to 4%-20% PAGE along with rat liver ferritin as a marker. The separated protein bands were visualized by autoradiography and probed with ferritin antibody.

ELISA of ferritin and transferrin

Ferritin and transferrin proteins in the luminal and mucosal contents were quantified using a specific sandwich ELISA system developed by us.

Immunoprecipitation

In order to understand the role of different iron binding proteins during absorption, luminal contents and mucosal proteins were lyophilized. Duodenal mucosal and luminal proteins obtained at initial time points (5, 15, 30 min) were reconstituted and subjected to immunoprecipitation with ferritin and transferrin antisera. Equal volumes (1 mL) of duodenal mucosal and luminal proteins (2-4 mg) and 1:32 diluted ferritin and transferrin antisera were incubated at 37℃ for 1 h and at 4℃ overnight. The specificity of ferritin and transferrin antisera was demonstrated by replacing immune serum with non-immune serum in the immunoprecipitation protocol. The immunoprecipitate was collected and washed three times with PBS. ^{59}Fe radioactivity in the fraction was counted in a gamma counter (Packard Autogamma, Cobra Ⅱ). A known activity of $^{59}FeCl_3$ was run with samples to correct for decay and counting efficiency of the gamma counter.

Preparation of intestinal sections for microautoradiography and immunohistochemistry

An automatic tissue processor (Shandon, Processor 2LE) using ascending grades of isopropyl alcohol and chloroform was used. The processed tissue samples were embedded in paraffin (58-60℃) using a Leica tissue-embedding unit. A set of 10 serial sections of 4 μ thickness were taken from each block using Reichert-Jung 2030 rotary manual microtome. The sections were mounted on chromalum-gelatin coated glass slides and further processed for immunohistochemistry and microautoradiography according to standard procedures.

Microautoradiography

In situ localization of radiolabelled iron was carried out in dehydrated sections. The sections were processed with photographic emulsion according to the manufacturer's guidelines (Amersham LM-1, Amersham UK). These sections were stained with hematoxylin, dehydrated and mounted with DPX mounting medium. For signals, the sections were viewed under light microscope (Leitz Ortholux) and photographed.

Immunohistochemistry

Serial sections were used for immunohistochemical localization of transferrin, transferrin receptor and ferritin, using respective antisera. The binding of each antiserum to their respective proteins was done using Sigma SIH kit. Counter-staining was done with Mayer's hematoxylin. Control slides were layered with non-immune serum instead of primary antiserum. The localization of the antigen was done using goat anti-rabbit HRPO conjugate. The comparison of staining intensity and the quantification of positively stained cells was carried out under light microscope with the magnification set at 10 ×, 25 × or 40 ×. In addition, the distribution of intestinal mucosal ferritin, transferrin and transferrin receptor in relation to iron status was evaluated in human biopsy specimens.

Human duodenal mucosal biopsy

Endoscopic intestinal (duodenal) biopsy specimens were collected by a gastroenterologist from 30 males and 6 females attending the Gastroenterology Department of Gandhi Hospital (Secunderabad, India) for various upper GI tract related ailments. Informed oral consent was obtained from all the subjects. All the subjects were classified based on their hematological and iron status parameters. Accordingly, a cut off value of hemoglobin < 13 g/dL for male and < 12 g/dL for female was classified as anemia, while anemia with serum ferritin < 12 μg/L as iron deficiency anemia. Biopsy specimens of 3-4 mm were collected and immediately spread on a wire mesh. These specimens were then immersed in 10% neutral buffered formalin solution and processed for immunohistochemistry of ferritin, transferrin and transferrin receptor, as described earlier.

Haematological and iron status indicators

Fasting blood samples were collected from rats and human subjects to estimate haemoglobin and iron status parameters. Hemoglobin was estimated by an automated hematology counter (Serono system 9000 Rx). Quantitation

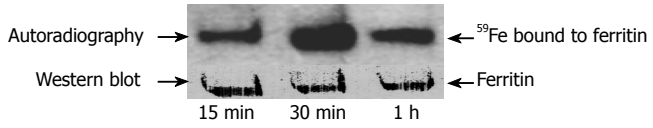

Figure 1 Ferritin takes up radiolabelled iron in a time dependent manner and has a direct role in iron absorption: Upper panel: Autoradiogram of duodenal proteins. Duodenal mucosal proteins (100 μg) obtained after 15 min, 30 min, 1 h after an oral dose of 7-10 μCi of $^{59}FeCl_3$ were subjected to 4%-20% PAGE and dehydrated. The radioactive bands were developed on X-ray film. As shown in the figure, one radioactive band corresponding to ferritin whose intensity was maximal at 30 min and then decreased with time. Lower panel: These proteins were subjected to western blot with ferritin antibody.

of human and rat serum ferritin, rat mucosal, and luminal ferritin and transferrin was estimated by homologous sandwich ELISA systems developed by us. Liver iron was estimated by dry ashing followed by an estimation of iron in the mineral solution by bathophenathroline method[1].

RESULTS

Initially, a kinetic study was carried out to understand the *in vivo* time course of iron absorption of ^{59}Fe given by oral gavage to rats with normal iron status condition. Specific activity of duodenal mucosa was found to be highest, followed by jejunum, ileum and stomach at all time points studied. The specific activity of ^{59}Fe was found to increase with time and attained a peak at 30 min in duodenal mucosa (data not shown).

Ferritin takes up radio-labelled iron in a time dependent manner and has a direct role in iron absorption

In order to understand the role of ferritin in iron absorption, an autoradiogram was performed with proteins obtained from 60% ammonium sulphate precipitation of luminal and mucosal fractions after oral administration of ^{59}Fe. As shown in Figure 1, upper panel, rats with normal iron status showed a single radioactive protein band identical to purified rat liver ferritin. The intensity of the radioactive band associated with ferritin increased with time and showed maximal band intensity at 30 min and decreased subsequently with no change in the ferritin protein band intensity (Figure 1, lower panel). These results suggested that intestinal ferritin is an important component of the intestinal iron transport system and seems to take up iron and facilitate its transfer across the mucosal cells. Thus these results demonstrate that ferritin is not just a sink but takes up iron and releases it in a time-dependent manner during the absorptive process.

To determine the specific role of iron binding proteins like ferritin, transferrin and transferrin receptor, rats were given different amounts of iron. Haematological and iron status parameters indicated the induction of iron deficiency and iron overloading in respective groups (data not shown). Table 1 shows the ferritin and transferrin concentrations in the intestinal luminal and mucosal contents of rats with various iron status parameters. The concentration of ferritin was higher in mucosa than in the lumen of duodenum in all the groups. In iron excess group, there was a significantly higher concentration of ferritin, both in lumen and mucosa, compared to deficient and control groups. In contrast, the transferrin concentration was significantly higher in lumen than in mucosa within the group and was similar between the groups.

Table 1 Ferritin and transferrin concentrations in rat duodenum under various iron status conditions

Parameter	Control	Iron deficient	Iron excess
Ferritin (ng/mg protein)			
Lumen	126.0^{a} ± 61.42	105.8^{a} ± 35.81	228.8^{c} ± 73.54
Mucosa	308.3^{c} ± 123.36	256.0^{c} ± 1.19	731.5^{e} ± 191.96
Transferrin (μg/mg protein)			
Lumen	10.9^{b} ± 7.6	11.1^{b} ± 10.3	6.8^{b} ± 4.7
Mucosa	0.87^{d} ± 0.79	0.80^{d} ± 1.20	0.61^{d} ± 0.63

Values with different superscript letters within each column and row are significantly different at $^{a,c,e}P < 0.005$ for ferritin and $^{b,d}P < 0.001$ for transferrin by one way ANOVA ($n = 5$).

Reciprocal relationship between luminal transferrin and mucosal ferritin iron

To understand the interaction between luminal transferrin and mucosal ferritin after oral administration of ^{59}Fe, rats were sacrificed at 5, 15 and 30 min. As shown in Figure 2A the percentage of radioactive iron in duodenal lumen was found to decrease with time. The highest luminal specific activity was seen in iron-deficient rats followed by control and iron excess fed rats. In deficient and control rats, there was a progressive increase in specific activity while in the excess iron fed group, the radioactivity was retained at the site of absorption (Figure 2B). This was supported by the findings on luminal and mucosal radioactivity, which showed a faster transit of iron from lumen to mucosa in iron-deficient and control rats. On the other hand, in the iron excess fed rats luminal radioactivity showed slower transit as indicated by increase in the radioactivity from 30 min onwards. The plasma radioactivity during the same time periods reflected the slower transit of duodenal iron in iron excess fed rats (plasma specific activity of 150 ± 20 dpm/mL during 15-60 min) which showed no peak in plasma iron as compared to the iron-deficient and control groups (plasma specific activity of 700 ± 50 and 400 ± 50 dpm/mL, respectively). The luminal transferrin iron declined with time in all the groups while that of mucosal ferritin increased only in deficient and sufficient groups during the 5-30 min of iron uptake (Figure 2). As shown in Figure 2B percentage of ferritin bound iron reached a peak and showed a decline confirming the release of iron from ferritin in deficient and control groups. In the iron excess group the percentage ferritin-bound iron did not change with time, confirming the blockage of iron in this group.

Microautradiography demonstrate the sequential transfer of radiolabelled iron

In order to study the *in vivo* translocation of iron after oral administration of radiolabelled iron, duodenal

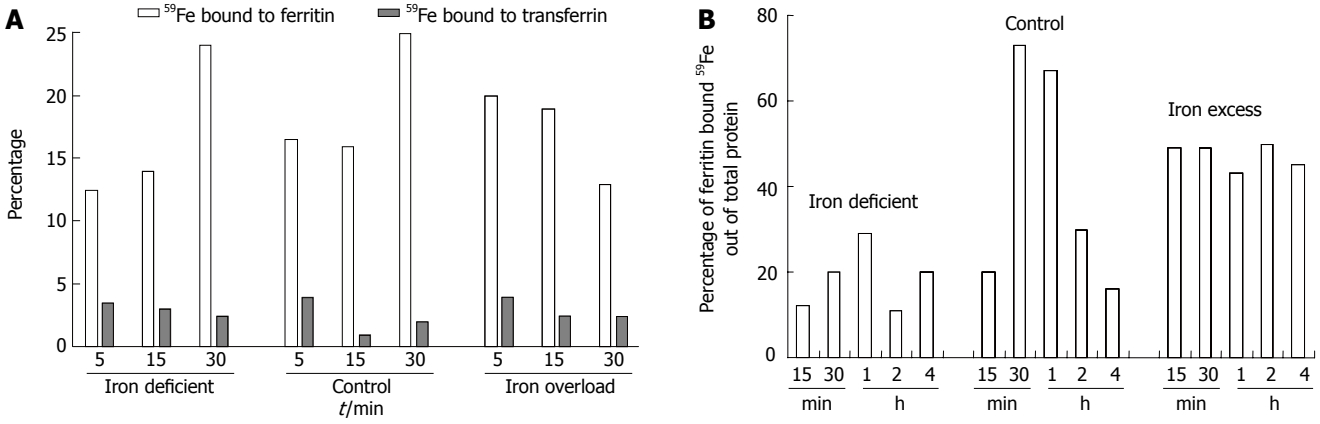

Figure 2 Reciprocal relationship between luminal transferrin and mucosal ferritin. **A**: Luminal and mucosal proteins collected after oral administration of ^{59}Fe after various time intervals were subjected to immunoprecipitation with ferritin and transferrin antibodies. The bar graph represents percentage incorporation of ^{59}Fe in luminal transferrin (crossed bars) and mucosal ferritin (open bars) of duodenum; **B**: Percentage of ferritin bound iron out of total protein bound iron with time, in various iron status conditions.

Table 2 Summary of *in situ* grading of sequential autoradiographic and immunohistochemical staining signals

Radioactive iron/protein	Iron status	Basal	5 min	15 min	30 min	2h
^{59}Fe	ID	-	SUR+	IE+++	IE+++	-
	OL	-	SUR+++	IE±	IE±	-
Tf	ID	IV±	IV++	IE+++ IV++		IE+ IV++
	OL	IV±	IE± IV±	IE± IV±		
TfR	ID	SUR±	SUR++	IE++	IE+	SUR±
	OL	SUR±	SUR++	SUR+	-	-
Fe	ID	IE± IV±	-	-		IE±
	OL	IE±	-		IE±	IE± IV+++

Tf: transfferin; TfR: Transferrin receptor; Fe: Ferritin; ID: Iron deficient; OL: Iron overload; IE: Intra epithelial; IV: Intra vascular; SUR: Surface; Grading +: minimal staining; ++: good; +++: intense; –: nil.

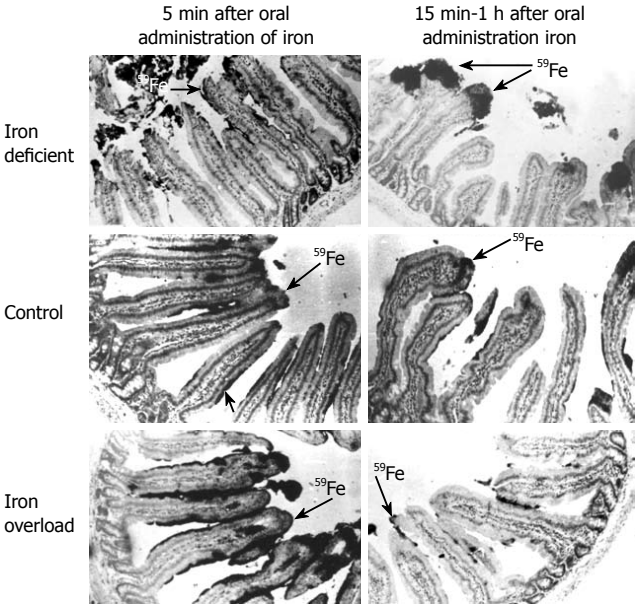

Figure 3 Microautoradiography demonstrated the sequential transfer of iron: Microautoradiography of duodenal sections of intestine obtained after oral administration of 100 μCi of $^{59}FeCl_3$ and 250 g of carrier iron in iron deficient top panel (ID), control middle panel (C) and iron overload bottom panel (OL) rats. These photographs illustrate the progressive transfer of iron into the villi (25 x).

segments were processed for microautoradiography under various iron status conditions. Table 2 shows the grading of staining intensities of radiolabelled iron, ferritin, transferrin/transferrin receptor in the iron deficient and iron excess groups. The radioactivity at 5 min was localized on the surface of the villi in the iron deficient group (top left panel ID, 5 min) (Figure 3). Subsequently, the radioactivity was present in the columnar epithelial cells (absorptive cells) at the tip of the villi between 15 min to 1 h in iron deficient (top right, panel ID, 15, 30 min, 1 h, and Table 2). At 2 and 4 h most of the radioactive iron was seen inside the villi in the lamina propria. A similar trend was observed in the control group (middle, panel C, 5 min and 15, 30 min, 1 h). However, in iron-overloaded intestine, high intensity radioactivity was noticed at 5 min on the surface (bottom left, panel OL, 5 min) but was minimal signals at 15 and 30 min (bottom right panel OL, 15 min and Table 2). The radioactive signals at 15 and 30 min associated with iron were maximal intraepithelially in iron-deficient rats and plasma radioactivity indicated maximum absorption. In iron-overloaded rats the signal was maximal at 5 min and seen only at the absorptive surface and retained at the site of absorption (Table 2).

Ferritin appears in the epithelial cells after oral administration of iron

Immunohistochemistry with ferritin antibody demonstrated that at 5 min, ferritin staining was maximal intraepithelially in iron-deficient intestine (Figure 4), while intense staining was seen both intraepithelially and intravascularly, in iron-overloaded intestine (Figure 4 top right, panel OL, 5 min Fe). The intensity of staining within the villi at 1 h (bottom left panel ID-1 h, Fe) was minimal and similar to that seen at basal status in iron deficient intestine. On the other hand, the staining intensity was

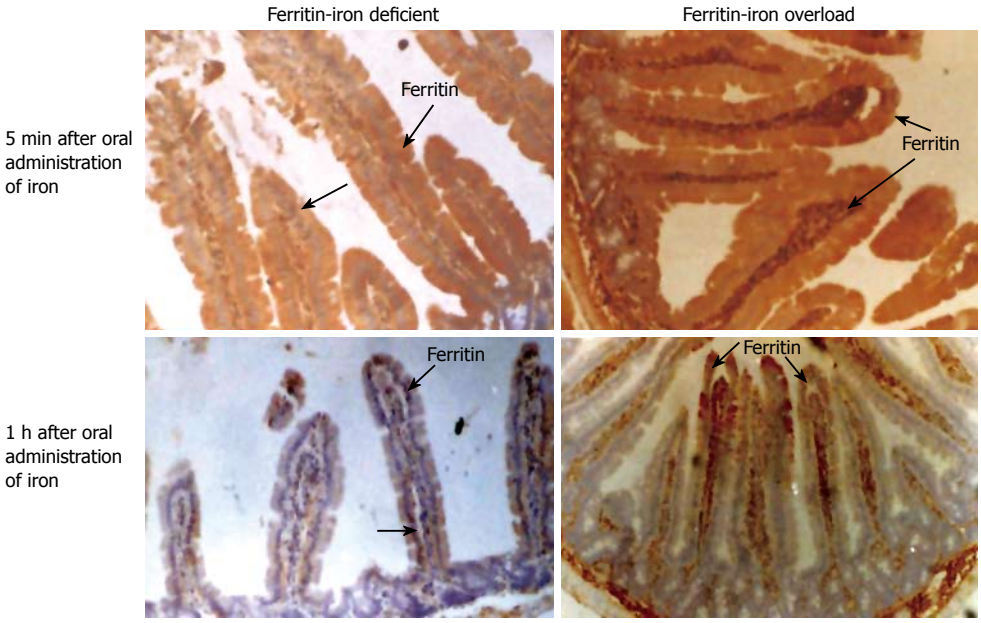

Figure 4 Ferritin appears in the epithelial cells after oral administration of ^{59}Fe: Immunohistochemical localization of ferritin (Fe) in the duodenal sections of intestine of iron deficient left panel (ID) and iron overload right panel (OL) rats at various time points after oral administration of radioactive iron (25 X).

lower in iron-loaded intestine after 15 min indicating the presence of holoferritin and blocking of iron absorption (Table 2).

Microautoradiography and immunohistocheminstry with transferrin and transferrin receptor demonstrates the in vivo uptake of iron through transferrin receptor

The *in situ* localization of radioactive iron in the iron deficient group indicated its presence on the cell surface (5 min) and then intraepithelially (15, 30 min) in the villi (Table 2). The intensity of transferrin staining was found to be maximal at the tip of the epithelial cells at 15 min (Figure 5, left panel ID 15 min Tf) and subsequently decreased to basal status. Staining of the blood vessels for transferrin started to appear from 2 h onwards in ID (bottom left panel ID, 2 h Tf). The staining for transferrin at 15 min within the epithelial cells was not observed in iron-overload group (Table 2). In the iron-overload group, staining due to transferrin was minimal at 5-30 min (Figure 5B, top left panel Tf, OL 30 min). In both groups, the transferrin receptor was localized mainly on the surface of the duodenal villi, thus demonstrating margination of transferrin receptor after oral administration of iron (right top panel Figure 5A, TfR, Basal). This, however, at 15 min was internalized at the tip of the epithelial cells along with iron and transferrin (Figure 5A). After 2hr TfR reappeared on the surface of the villi in the iron deficient (Figure 5A, middle right panel, TfR, ID, 15 min, 2 h) demonstrating the *in vivo* receptor recycling. In contrast, in the iron-overload group TfR was seen only at the surface even at 30 min and 1 h (Figure 5B, bottom panel, TfR, OL, 15 min, 1h) showing no internalization of receptor.

The radioactive signals at 15 min were maximal intraepithelially in the iron deficient group. During this time period, transferrin and its receptor were also co-localized maximally within the epithelial cells (Figure 5C). The intensities of both these proteins subsequently diminished and minimal staining was seen at the margin of the absorptive surface. The intensity of transferrin receptor staining was maximal along the entire margin during different time points in the iron-overloaded intestine. This was a striking difference between the two extreme conditions. Microautoradiography along with the immunohistochemistry of ferritin and the transferrin/transferrin receptor demonstrated the *in vivo* internalization of transferrin and its receptor along with radiolabelled iron and recycling of the receptor to the surface. This clearly shows a transferrin-mediated iron uptake at the absorptive surface of the rat intestine.

Staining intensity of ferritin, transferrin/ transferrin receptor in human duodenal biopsy under different iron nutritional status

In addition, we have performed immonohistochemistry of ferritin, transferrin/transferrin receptor in human duodenal biopsy specimens collected from various iron status conditions. All the subjects were classified according to their indicators of iron status such as haemoglobin, serum ferritin (Table 3). According to these parameters, 13 of them belonged to normal group, 6 had iron-deficient anemia, 14 anemia, one each had blood transfused, iron injected and iron given orally as supplement. Representative immunohistochemical images for ferritin, transferrin and transferrin receptor of duodenal biopsy from normal, iron deficient anemia and blood transfused are given in Figure 6. The staining intensity for ferritin varied according to iron status and thus staining was +++ normal (top left), ± iron deficient (middle left panel Fe ID) and ++ in blood transfused (Figure 6 bottom left panel Fe BT) subjects. The intensity of transferrin staining was also similar to that of ferritin staining in normal, iron-deficient and in blood transfused subjects (center top, middle and bottom panels respectively). The transferrin receptor on the other hand, stained more intensely with a grading score of (+++) in

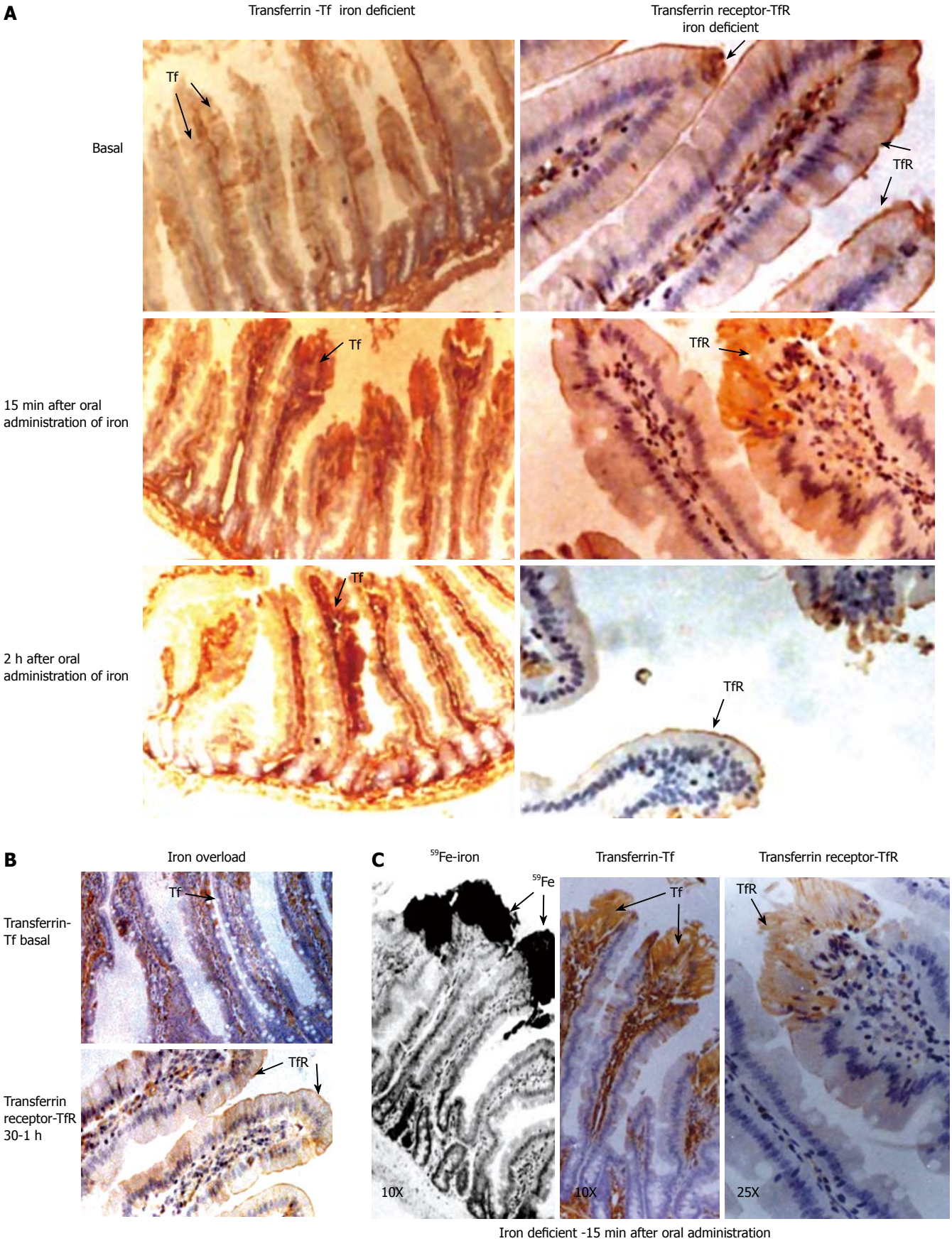

Figure 5 Microautoradiography and immunohistocheminstry with transferrin and transferrin receptor demonstrates the in vivo uptake of iron through transferrin receptor. **A**: Immunohistochemical localization of transferrin left panel (Tf) and transferrin receptor right panel (TfR) in the duodenal sections of intestine of iron deficient rat (ID); **B**: transferrin stain in iron over loaded rat (top panel) (OL)at basal status and tranferrin receptor on the surface of the epithelial cells showing no internalization(bottom panel) in iron overloaded condition after oral administration of radioactive iron (10X); **C**: Co-localization of iron, transferrin and transferrin receptors in the duodenal sections of intestines of iron deficient rats obtained 15 min after oral administration of radioactive iron. Microautoradiographic localization of iron immunohistochemical localization of transferrin transferring receptor.

Table 3 Classification of human subjects according to iron status indicators

	Sex	No	Age (yr)	Hb (g/dL)	PCV	RBC M/cu mm	Serum ferritin (μg/L)
Normal	M	12	36.5 ± 10.6	14.8 ± 0.9	44.5 ± 3.3	5.8 ± 0.7	43 ± 22.1
	F	1	7.2	12.4	36	4.5	71.7
Iron deficient anemia	M	4	24.5 ± 20.9	7.4 ± 2.6	23.3 ± 9.0	4.1 ± 1.7	7.2 ± 4.0
	F	2	20.5	7.3	26.5	3.5	6.5
	M	10	44.3 ± 16.5	11.1 ± 1.64	33.6 ± 5.2	4.5 ± 1.4	75.3 ± 32.2
Anemia	F	4	21 ± 6.6	6.8 ± 3.0	20.8 ± 9.0	2.1 ± 1.2	57.4 ± 13.4
Iron supplements	F						
Blood transfusion	M	1	32	9.5	29	4.7	28.6
Iron injection	F	1	32	8.4	27	4.3	101
Oral iron	F	1	20	9.7	30	3	38

Values are mean ± SD. Cut off values for defining deficiency, Hb: Male < 13 g/dL, Female < 12 g/dL, serum ferritin < 12 μg/L.

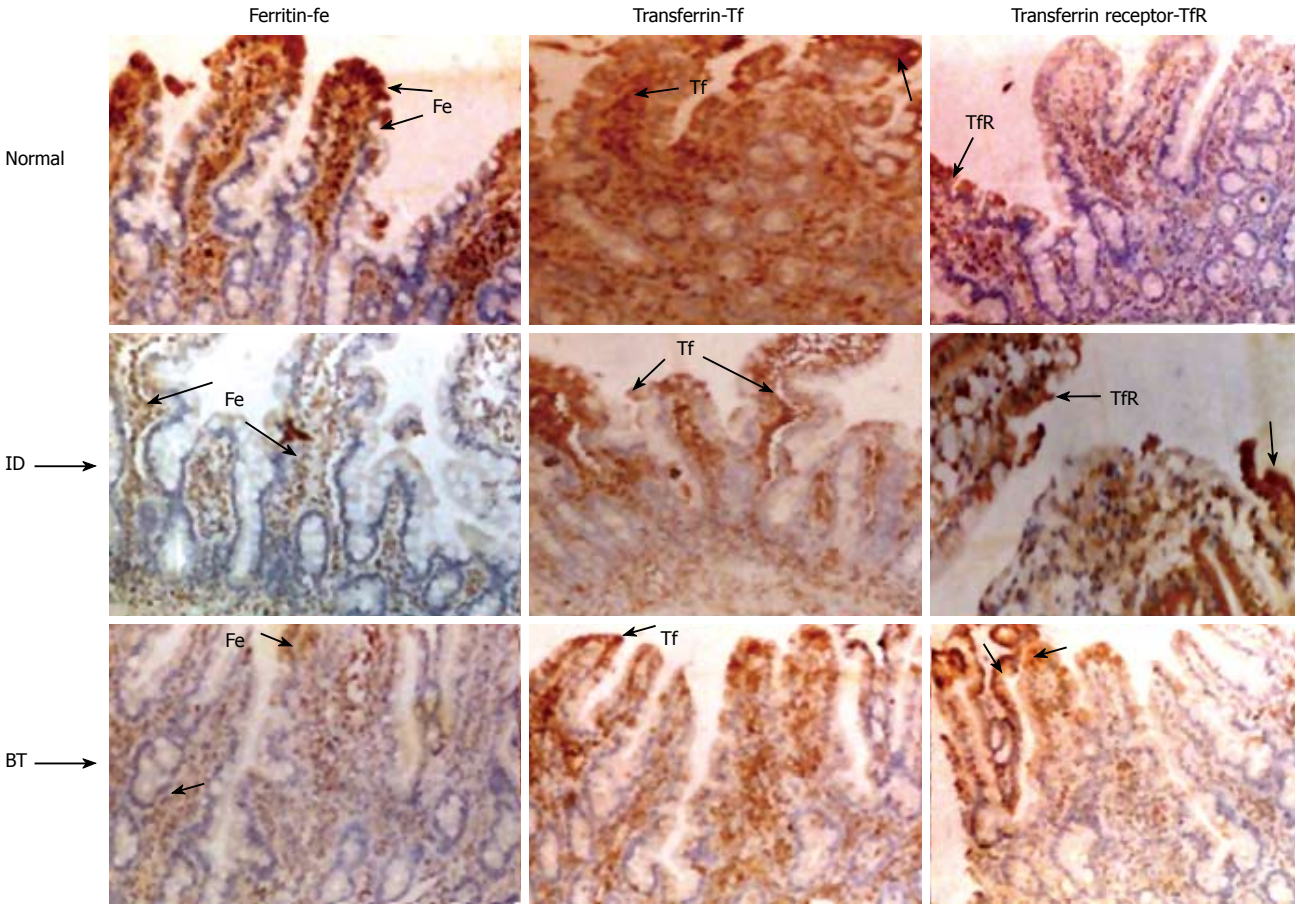

Figure 6 Staining intensity of ferritin, transferrin and transferrin receptor in human duodenal biopsy under different iron nutritional status: Immunohistochemical localization of ferritin (Fe), transferrin (Tf) and transferrin receptor (TfR) in the duodenal biopsy sections of normal (top panel, N), iron deficient (middle panel, ID) and blood transfused (bottom panel, BT) human subjects. Staining intensity; ± represents Light, + normal, ++ good, +++ intense.

the iron-deficient subjects (Figure 6 middle right panel ID TfR) compared to + in normal (top right panel, TfR) and blood transfused subjects (bottom right panel BT TfR).

DISCUSSION

Ferritin, transferrin and transferrin receptor are the important proteins that regulate iron homeostasis in almost all the cells. However, the actions of these proteins in the absorptive cells remain unclear. Data on the role of these proteins were obtained mainly by studying one protein at a time. By attempting to sequence serially the role of these proteins together, during intestinal uptake, we were able to provide evidence for *in vivo* receptor mediated uptake of iron.

The radioactive signals at 15 to 30 min associated with iron were maximal intraepithelially in iron deficient rats. Along with iron, both transferrin and transferrin receptor

were co-localized at this time. The intensities of both these proteins were subsequently decreased and minimal amounts were seen at the margin of absorptive surface in iron deficient intestine. In addition, ferritin appeared intraepithelial in iron deficient and control groups, suggesting its modulation during the absorptive phase. Presence of most of the radiolabelled signal only on absorptive surface at 5 min and beyond in iron-overloaded rats suggest its restricted entry into the duodenum due to the presence of mucosal holo ferritin. This is supported by the intense ferritin staining seen both intraepithelial and intravascular in iron overloaded intestine, especially during absorptive phase and beyond. Further, the presence of transferrin receptor along the entire margin during different phases of iron uptake suggests no internalization of transferrin receptor in iron excess condition.

It is interesting to note that the concentration of mucosal ferritin and the iron associated with it was similar in control and iron deficient groups, and was significantly lower than that seen in the excess iron fed group. This could be due to the regulatory role of mucosal ferritin at the site of adsorption in the case of iron excess, while in the case of normal and iron deficient duodenum it could release the incorporated iron.

A positive relationship between *in situ* localization of ferritin and better iron status was demonstrated in rats and humans. The results on autoradiography of rat duodenal mucosal and luminal preparations suggests that intestinal ferritin takes up iron and releases it in a time dependent manner during the absorptive process. This is supported by the findings on localization of iron in the duodenal mucosa during absorption which showed a positive relationship, with better iron status at 5 min and a negative relationship at 15 min-1h. Similarly in human subjects, the intensity of ferritin staining was lowest in iron deficient subjects, highest in normal subjects and in between in the case of the blood transfused subjects. These observations suggest that mucosal ferritin is an important component of the intestinal iron transport system which takes up iron and facilitates its transfer across the mucosal cells

The studies of Miyoshi *et al*[27] support the presence of ferritin in duodenum. Their studies showed accumulation of iron in the apical area of duodenal villous cells with in ferritin. The presence of maximal ^{55}Fe radioactivity at 5 min over the brush border and terminal web was demonstrated by Bedard *et al*[28]. They observed that during the next 3 h, radioactivity was present almost exclusively in absorptive cells and in lamina propria. In contrast, Conrad and Crosby[29] observed very little radioactivity in the small intestinal mucosa of iron-depleted and iron overload rats from 2-48 h after gastric administration of ^{59}Fe. This discrepancy may be due to the fact that they did not included time points earlier than 2 h. Because it is an inducible protein, it is possible that ferritin expression at the sites of absorption may be related to the iron status. This suggests that iron absorption is probably dependent on the relative concentrations of mucosal apo and holo ferritins, and is inhibited in conditions of iron overload and enhanced in iron deficiency.

Quantitatively, the amount of transferrin in the lumen is 10 times higher than that of mucosa and is not dependent on iron nutritional status (Table 1). The observation on identical amounts of luminal transferrin, irrespective of iron nutritional status, implies that this protein may be presenting equal amount of iron for absorption. The net amount of iron, which is taken up by the mucosa, thus depends on mucosal transferrin receptors. Duodenal mucosal transferrin receptor showed reciprocal relationship with iron status. The significance of this may be to present equal amounts of iron for absorption through binding to luminal transferrin. Consequently, the amount of iron absorbed by the mucosa may depend only on the mucosal transferrin receptor which has inverse relationship with better iron status.

Huebers *et al*[8,15] suggest that luminal transferrin acts as a shuttle protein for iron uptake. Autoradiographic studies by Conrad and Crosby[30] and Bedard *et al*[28] also suggest that intestinal crypt cells are able to take up transferrin-bound iron from circulation. According to some other investigators, however, transferrin is unlikely to be a major transporter of iron from lumen to the baso-lateral membrane[31-33]. According to Idzerda[34], the transferrin gene is not expressed in the intestine and, therefore, cannot be synthesized. Thus, it is possible that the luminal transferrin may be imported from plasma, as hypothesized by Parmley *et al*[19].

Although the receptor mediated cellular uptake of iron is well known and takes place in all dividing cells, such a mechanism operating in the intestine has not been documented earlier. The results of this study, in conjunction with earlier observations[5,35-37], allow us to propose a model for intestinal iron absorption whereby., the recycling of transferrin and transferrin receptors enables luminal transferrin bound iron to enter the enterocytes. The receptor density at the absorptive surface, which is inversely proportional to better iron nutritional status, might regulate this iron uptake process.

The presence of transferrin and its receptor on the margin during basal condition, and the appearance of both the receptor and the ligand at 15 min intraepithelially along with the radiolabelled iron in iron depleted rat intestine, support the above model. The appearance of TfR after 2 h on the margin of villi suggests that the receptor protein returned to the surface after releasing iron. In contrast, there was no evidence of intraepithelial transferrin and transferrin receptor in iron overloaded intestine, as evidenced by the presence of receptor on the margin even at 30 min.

Though the staining intensity of transferrin in duodenal section was high in control subjects, there was no obvious difference between iron deficient subject and blood transfused subjects. Staining for transferrin was intense in the apical portion and blood vessels, while that of transferrin receptor was more concentrated at the epithelial lining of duodenum (Figure 6). The higher intensity of transferrin receptor in iron deficient subjects and minimal in control and blood transfused subjects suggests a role for it in iron absorption. This is supported

by the reciprocal relationship observed between transferrin receptor and ferritin staining. Similar finding on TfR staining at the margin of the villi was observed by Banerjee *et al*[36] . The ultrastructural studies of Levine *et al*[31] have shown that transferrin receptor and transferrin are co-localized in coated pits on the basal and lateral membranes of crypt cells. Further, Anderson *et al*[35] confirmed that the TfR is a prominent protein on the basal and lateral membranes of intestinal epithelial cells.

The above findings, along with earlier observation, suggest that luminal transferrin must be presenting equal amount of iron for absorption since this protein does not respond to iron status. The net amount of iron taken up by mucosa depends on mucosal transferrin receptors, which respond reciprocally with better iron status. These results suggest that mucosal ferritin, luminal transferrin and mucosal cell surface transferrin receptors are closely related to iron status and interact with each other in carrying iron across the intestinal mucosa.

ACKNOWLEDGMENTS

Vasantha L Kolachala was the recipient of an Indian Council of Medical Research Fellowship. Grateful acknowledgement also to Dr. Rupender Prasad (Mahavir Hospital, Hyderbad, India), and Dr. A Vidyasagar and Dr. B Prahlad (Gandhi Hospital, Hyderabad, India) for their help in providing human biopsy specimens.

REFERENCES

1 **Bothwell TH**, Charlton RW. Current problems of iron overload. *Recent Results Cancer Res* 1979; **69**: 87-95
2 **Touret N**, Furuya W, Forbes J, Gros P, Grinstein S. Dynamic traffic through the recycling compartment couples the metal transporter Nramp2 (DMT1) with the transferrin receptor. *J Biol Chem* 2003; **278**: 25548-25557
3 **Conrad ME**, Umbreit JN, Moore EG, Hainsworth LN, Porubcin M, Simovich MJ, Nakada MT, Dolan K, Garrick MD. Separate pathways for cellular uptake of ferric and ferrous iron. *Am J Physiol Gastrointest Liver Physiol* 2000; **279**: G767-G774
4 **Conrad ME**, Umbreit JN. Pathways of iron absorption. *Blood Cells Mol Dis* 2002; **29**: 336-355
5 **Brittin GM**, Raval D. Duodenal ferritin synthesis during iron absorption in the iron-deficient rat. *J Lab Clin Med* 1970; **75**: 811-817
6 **Whittaker P**, Skikne BS, Covell AM, Flowers C, Cooke A, Lynch SR, Cook JD. Duodenal iron proteins in idiopathic hemochromatosis. *J Clin Invest* 1989; **83**: 261-267
7 **Pollack S**, Lasky FD. A new iron-binding protein isolated from intestinal mucosa. *J Lab Clin Med* 1976; **87**: 670-679
8 **Huebers H**, Huebers E, Rummel W, Crichton RR. Isolation and characterization of iron-binding proteins from rat intestinal mucosa. *Eur J Biochem* 1976; **66**: 447-455
9 **Savin MA**, Cook JD. Mucosal iron transport by rat intestine. *Blood* 1980; **56**: 1029-1035
10 **Osterloh K**, Forth W. Determination of transferrin-like immunoreactivity in the mucosal homogenate of the duodenum, jejunum, and ileum of normal and iron deficient rats. *Blut* 1981; **43**: 227-235
11 **Johnson G**, Jacobs P, Purves LR. Iron binding proteins of iron-absorbing rat intestinal mucosa. *J Clin Invest* 1983; **71**: 1467-1476
12 **Cox TM**, Mazurier J, Spik G, Montreuil J, Peters TJ. Iron binding proteins and influx of iron across the duodenal brush border. Evidence for specific lactotransferrin receptors in the human intestine. *Biochim Biophys Acta* 1979; **588**: 120-128
13 **Simpson RJ**, Osterloh KR, Raja KB, Snape SD, Peters TJ. Studies on the role of transferrin and endocytosis in the uptake of Fe3+ from Fe-nitrilotriacetate by mouse duodenum. *Biochim Biophys Acta* 1986; **884**: 166-171
14 **Worwood M**, Edwards A, Jacobs A. Non-ferritin iron compound in rat small intestinal mucosa during iron absorption. *Nature* 1971; **229**: 409-410
15 **Huebers HA**, Huebers E, Csiba E, Rummel W, Finch CA. The significance of transferrin for intestinal iron absorption. *Blood* 1983; **61**: 283-290
16 **Isobe K**, Isobe Y. Localization of transferrin in rat duodenal mucosa by immunoperoxidase technique. *Nihon Ketsueki Gakkai Zasshi* 1983; **46**: 797-807
17 **Mason DY**, Taylor CR. Distribution of transferrin, ferritin, and lactoferrin in human tissues. *J Clin Pathol* 1978; **31**: 316-327
18 **Levine DS**, Woods JW. Immunolocalization of transferrin and transferrin receptor in mouse small intestinal absorptive cells. *J Histochem Cytochem* 1990; **38**: 851-858
19 **Parmley RT**, Barton JC, Conrad ME. Ultrastructural localization of transferrin, transferrin receptor, and iron-binding sites on human placental and duodenal microvilli. *Br J Haematol* 1985; **60**: 81-89
20 **Parkkila S**, Waheed A, Britton RS, Bacon BR, Zhou XY, Tomatsu S, Fleming RE, Sly WS. Association of the transferrin receptor in human placenta with HFE, the protein defective in hereditary hemochromatosis. *Proc Natl Acad Sci USA* 1997; **94**: 13198-13202
21 **Gross CN**, Irrinki A, Feder JN, Enns CA. Co-trafficking of HFE, a nonclassical major histocompatibility complex class I protein, with the transferrin receptor implies a role in intracellular iron regulation. *J Biol Chem* 1998; **273**: 22068-22074
22 **Roy CN**, Blemings KP, Deck KM, Davies PS, Anderson EL, Eisenstein RS, Enns CA. Increased IRP1 and IRP2 RNA binding activity accompanies a reduction of the labile iron pool in HFE-expressing cells. *J Cell Physiol* 2002; **190**: 218-226
23 **Salter-Cid L**, Brunmark A, Li Y, Leturcq D, Peterson PA, Jackson MR, Yang Y. Transferrin receptor is negatively modulated by the hemochromatosis protein HFE: implications for cellular iron homeostasis. *Proc Natl Acad Sci USA* 1999; **96**: 5434-5439
24 **Waheed A**, Grubb JH, Zhou XY, Tomatsu S, Fleming RE, Costaldi ME, Britton RS, Bacon BR, Sly WS. Regulation of transferrin-mediated iron uptake by HFE, the protein defective in hereditary hemochromatosis. *Proc Natl Acad Sci USA* 2002; **99**: 3117-3122
25 **Reeves PG**, Nielsen FH, Fahey GC. AIN-93 purified diets for laboratory rodents: final report of the American Institute of Nutrition ad hoc writing committee on the reformulation of the AIN-76A rodent diet. *J Nutr* 1993; **123**: 1939-1951
26 **Bradford MM**. A rapid and sensitive method for the quantitation of microgram quantities of protein utilizing the principle of protein-dye binding. *Anal Biochem* 1976; **72**: 248-254
27 **Miyoshi H**, Ashida K, Hirata I, Ohshiba S, Naitoh T. Transferrin is not involved in initial uptake process of iron in rat duodenal mucosa. Ultrastructural study by x-ray energy spectrometry. *Dig Dis Sci* 1995; **40**: 1484-1490
28 **Bédard YC**, Pinkerton PH, Simon GT. [Iron absorption by the duodenal mucosa (author's transl)]. *Nouv Rev Fr Hematol* 1973; **13**: 727-743
29 **Crosby WH**, Conrad ME, Wheby MS. The rate of iron accumulation in iron storage disease. *Blood* 1963; **22**: 429-440
30 **Bédard YC**, Pinkerton PH, Simon GT. Uptake of circulating iron by the duodenum of normal mice and mice with altered iron stores, including sex-linked anemia: high resolution radioautographic study. *Lab Invest* 1976; **34**: 611-615
31 **Levine PH**, Levine AJ, Weintraub LR. The role of transferrin

in the control of iron absorption: studies on a cellular level. *J Lab Clin Med* 1972; **80**: 333-341
32 **Schümann K**, Osterloh K, Forth W. Independence of in vitro iron absorption from mucosal transferrin content in rat jejunal and ileal segments. *Blut* 1986; **53**: 391-400
33 **Mazurier J**, Montreuil J, Spik G. Visualization of lactotransferrin brush-border receptors by ligand-blotting. *Biochim Biophys Acta* 1985; **821**: 453-460
34 **Idzerda RL**, Huebers H, Finch CA, McKnight GS. Rat transferrin gene expression: tissue-specific regulation by iron deficiency. *Proc Natl Acad Sci USA* 1986; **83**: 3723-3727
35 **Anderson GJ**, Powell LW, Halliday JW. The endocytosis of transferrin by rat intestinal epithelial cells. *Gastroenterology* 1994; **106**: 414-422
36 **Banerjee D**, Flanagan PR, Cluett J, Valberg LS. Transferrin receptors in the human gastrointestinal tract. Relationship to body iron stores. *Gastroenterology* 1986; **91**: 861-869
37 **El-Shobaki FA**, Rummel W. Mucosal transferrin and ferritin factors in the regulation of iron absorption. *Res Exp Med* (Berl) 1977; **171**: 243-253

S- Editor Liu Y **L- Editor** Banati RB **E- Editor** Ma WH

PO Box 2345, Beijing 100023, China
www.wjgnet.com
wjg@wjgnet.com

World J Gastroenterol 2007 February 21; 13(7): 1053-1059
World Journal of Gastroenterology ISSN 1007-9327

BASIC RESEARCH

Influence of heme oxygenase-1 gene transfer on the viability and function of rat islets in *in vitro* culture

Xiao-Bo Chen, Yong-Xiang Li, Yang Jiao, Wei-Ping Dong, Ge Li, Jing Chen, Jian-Ming Tan

Xiao-Bo Chen, Yong-Xiang Li, Yang Jiao, Wei-Ping Dong, Jian-Ming Tan, Department of Renal Transplantation and Urology, the First People's Hospital, Shanghai Jiao Tong University; Shanghai Clinical Medical Center of Organ Transplantation , Shanghai 200080, China
Ge Li, Jing Chen, State Key Laboratory of Genetic Engineering, Institute of Genetics, School of Life Sciences, Fudan University, Shanghai 200433, China
Supported by the National Natural Science Foundation of China, No. 30571759 and Social Development Foundation of Shanghai, No. 2002-53
Correspondence to: Dr Jian-Ming Tan, Department of Renal Transplantation and Urology, the First People's Hospital, Shanghai Jiao Tong University; Shanghai Clinical Medical Center of Organ Transplantation, Shanghai 200080, China. jmtan156@yahoo.com.cn
Telephone: +86-21-63069482 Fax: +86-21-63069482
Received: 2006-10-14 Accepted: 2006-11-14

Abstract

AIM: To investigate the influence of heme oxygenase-1 (HO-1) gene transfer on the viability and function of cultured rat islets *in vitro.*

METHODS: Islets were isolated from the pancreata of Sprague-Dawley rats by intraductal collagenase digestion, and purified by discontinuous Ficoll density gradient centrifugation. Purified rat islets were transfected with adenoviral vectors containing human HO-1 gene (Ad-HO-1) or enhanced green fluorescent protein gene (Ad-EGFP), and then cultured for seven days. Transfection was confirmed by fluorescence microscopy and Western blot. Islet viability was evaluated by acridine orange/propidium iodide fluorescent staining. Glucose-stimulated insulin release was detected using insulin radioimmunoassay kits and was used to assess the function of islets. Stimulation index (SI) was calculated by dividing the insulin release upon high glucose stimulation by the insulin release upon low glucose stimulation.

RESULTS: After seven days culture, the viability of cultured rat islets decreased significantly (92% ± 6% *vs* 52% ± 13%, $P < 0.05$), and glucose-stimulated insulin release also decreased significantly (6.47 ± 0.55 mIU/L/30IEQ *vs* 4.57 ± 0.40 mIU/L/30IEQ, 14.93 ± 1.17 mIU/L/30IEQ *vs* 9.63 ± 0.71 mIU/L/30IEQ, $P < 0.05$). Transfection of rat islets with adenoviral vectors at an MOI of 20 was efficient, and did not impair islet function. At 7 d post-transfection, the viability of Ad-HO-1 transfected islets was higher than that of control islets (71% ± 15% *vs* 52% ± 13%, $P < 0.05$). There was no significant difference in insulin release upon low glucose stimulation (2.8 mmol/L) among Ad-HO-1 transfected group, Ad-EGFP transfected group, and control group ($P > 0.05$), while when stimulated by high glucose (16.7 mmol/L) solution, insulin release in Ad-HO-1 transfected group was significantly higher than that in Ad-EGFP transfected group and control group, respectively (12.50 ± 2.17 mIU/L/30IEQ *vs* 8.87 ± 0.65 mIU/L/30IEQ; 12.50 ± 2.17 mIU/L/30IEQ *vs* 9.63 ± 0.71 mIU/L/30IEQ, $P < 0.05$). The SI of Ad-HO-1 transfected group was also significantly higher than that of Ad-EGFP transfected group and control group, respectively (2.21 ± 0.02 *vs* 2.08 ± 0.05; 2.21 ± 0.02 *vs* 2.11 ± 0.03, $P < 0.05$).

CONCLUSION: The viability and function of rat islets decrease over time in *in vitro* culture, and heme oxygenase-1 gene transfer could improve the viability and function of cultured rat islets.

Key words: Islet viability; Islet function; Heme oxygenase-1; Gene transfer; Adenoviral vectors

Chen XB, Li YX, Jiao Y, Dong WP, Li G, Chen J, Tan JM. Influence of heme oxygenase-1 gene transfer on the viability and function of rat islets in *in vitro* culture. *World J Gastroenterol* 2007; 13(7): 1053-1059

http://www.wjgnet.com/1007-9327/13/1053.asp

INTRODUCTION

Diabetes affects more than 200 million people worldwide[1]. The mainstay treatment for type Ⅰ diabetic patients is chronic insulin injection. While exogenous insulin therapy has dramatically reduced mortality in diabetes, patients often succumb to the long-term sequelae of diabetic angiopathy, either in the form of nephropathy, neuropathy or retinopathy. Vascularized pancreas transplantation reliably restores normoglycemia and maintains long-term glucose homeostasis, but it has significant surgical morbidity and mortality[2]. In 2000, with the success of the 'Edmonton protocol', which had produced insulin independence in 85% of type Ⅰ diabetic patients one year after allogeneic islets transplantation combined with a non-steroid immunosuppressive regimen, islet transplantation has progressed from research to clinical reality[3].

The technique to maintain isolated islet preparations in tissue culture has been adopted by most islet transplant centers. Islet culture for a brief period (24 to 72 h) has emerged as the current standard procedure prior to clinical transplantation[4,5]. It offers advantages over immediate infusion post-isolation, enabling assessment of islet quality and safety, and reducing islet immunogenicity as well as recipient travel to the transplantation site and immunosuppression before transplantation[6]. But *in vitro* culture of islets has been shown to result in loss of viable tissue over time, and a decrease in glucose responsiveness has been observed in those islets which survive[7,8].

Several phenomena, including activation of free radicals, apoptosis and necrosis, may be responsible for these effects. Therefore, approaches towards enhancing islets resistance to these insults would facilitate both clinical and investigative trials. As a cellular graft, islets are especially suited for gene therapy. An attractive strategy for protecting islets in *in vitro* culture is to use gene therapy to transduce islets with cytoprotective genes that can make islets more resistant to injury.

Heme oxygenase-1 (HO-1) is the rate-limiting enzyme in the heme degradative pathway that catalyzes the oxidation of heme into biliverdin, carbon monoxide (CO), and free iron[9,10], and it has been described as a ubiquitous inducible stress protein capable of cytoprotection *via* radical scavenging and apoptosis prevention. Overexpression of HO-1 by chemical induction or gene therapy has been used to reduce the deleterious effects of oxidative stress and apoptosis in various cell types and animal models[11-14].

Compared with chemical induction, gene transfer can provide effective, targeted, and relatively persistent expression of HO-1. The aim of the present study was to investigate the influence of HO-1 gene transfer on the viability and function of cultured rat islets, and to explore the potential value of HO-1 gene transfer in islet transplantation.

MATERIALS AND METHODS

Animals

Twenty male Sprague-Dawley rats weighing 250 to 300 g were purchased from Shanghai Experimental Animal Center of Chinese Academy of Sciences.

Rat islet isolation and culture

Rat islets were isolated from the pancreata of the outbred male Sprague-Dawley rats by a collagenase digestion technique and discontinuous Ficoll density gradient centrifugation[15]. The main bile duct was located and clamped at both ends. Ten milliliters of collagenase *P* (Roche Applied Science, Indianapolis, Ind, USA) solution (1 g/L, pH 7.8) was injected into the duct and then the distended pancreas was surgically resected, and incubated at 38℃ for 15 min. The digested gland was vigorously shaken for 10 s and the digestion was stopped by Hank's solution (4℃) with 100 mL/L fetal calf serum (Gibco, BRL, USA). The tissue was filtered through a 600 μm screen, and then washed by Hank's solution twice. Islets were purified by centrifugation at 3000 r/min for 20 min on discontinuous Ficoll (Pharmacia Fine Chemicals, Uppsala, Sweden) gradients. After several washes with Hank's solution, islets were suspended in RPMI-1640 medium (Gibco, BRL, USA) containing 100 mL/L fetal calf serum (Gibco, BRL, USA), 20 mmol/L HEPES (Sigma-Aldrich Chemicals, Louis Mo, USA), 100 kU/L of penicillin and 100 g/L of streptomycin at 37℃ in a humidified atmosphere of 50 mL/L CO_2. Islets purity was assessed by dithizone (Sigma-Aldrich Chemicals, Louis Mo, USA) staining, and islets were counted and scored in size. An algorithm was used for the calculation of 150 μm-diameter islet equivalent number (IEQ).

Adenoviral vectors

Adenoviral vectors were prepared by use of the AdEasy system (Stratagene, Baltimore, USA). Human HO-1 cDNA was cloned into pAdTrack-CMV. Once constructed, the shuttle vector was linearized with *Pme* I and co-transformed into *E. coli* BJ5183 together with pAdEasy-1, the supercoiled viral DNA plasmid. Transformants were selected on kanamycin and the recombinants were subsequently identified by restriction digestion. Once a recombinant was identified, it was produced in bulk using the recombination-deficient XL10-Gold® strain. Purified recombinant adenoviral plasmid DNA was then linearized by *Pac* I to expose its inverted terminal repeats (ITR) and transfected into HEK293 cells where deleted viral genes necessary for virus assembly were complemented *in vivo*. The pAdEasy-1 vector will not replicate in cells other than complementing cells (293 cells). This vector has been developed to infect but not replicate in non-permissive target cells. Ad-EGFP was generated using the same system and supplied by the Institute of Genetics of Fudan University. Viral titers were determined by plaque assay and expressed as plaque forming units per mL (pfu/mL). Viral titers of Ad-HO-1 and Ad-EGFP were 1.96×10^9 and 1.99×10^9 pfu/mL, respectively.

Adenovirus infection

Aliquots of 30 IEQ were resuspended in 0.5 mL serum-free culture medium and placed in a 24-well culture plate and incubated with Ad-HO-1 and Ad-EGFP vectors at a multiplicity of infection (MOI) of 20 at 37℃ for 4 h with agitation every 1 h. MOI was calculated using the assumption that islets contain on average 1000 cells. After infection, islets were washed twice with culture medium and incubated for at least 48 h before further analysis to allow for transgene expression. Control islets were mock infected. Mock infected islets underwent a similar procedure, but were not exposed to viruses during the incubation period and were not incubated with any vectors.

Western blot analysis

Islet cells (48 h post-transfection) were washed with cold phosphate buffered saline (PBS) and lysed in 2% SDS, Tris-HCl 60 mmol/L (pH 6.8) buffer, incubated at 95℃, sonicated in a water bath at 37℃ and centrifuged at 12 000 r/min for 15 min. Assessment of the total protein content was carried out with the BCA detection kit (Pierce Biotechnology, Rockford, IL, USA). Aliquots corresponding to 100 μg of protein were subjected to electrophoresis on a 15% SDS-PAGE pre-cast gel

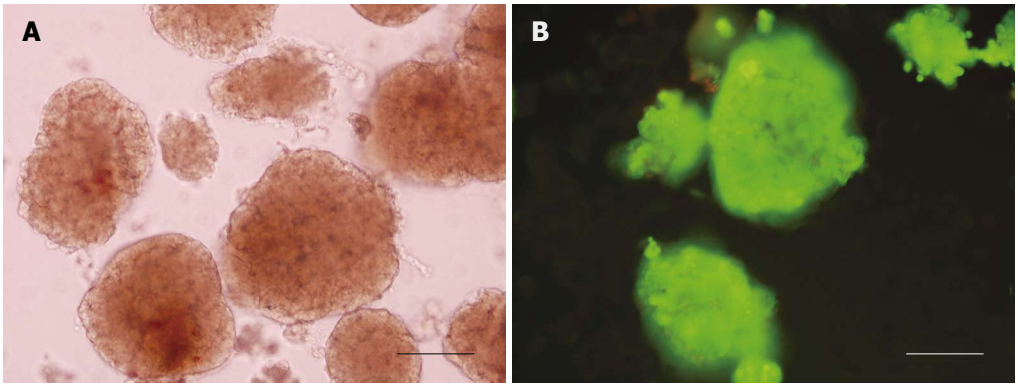

Figure 1 Purity and viability of freshly isolated rat islets. **A**: Islets stained with DTZ (red staining indicates islets; islet purity was above 90%); **B**: Islets stained with AO/PI (green staining indicated live cells, red staining indicated dead cells; islet via bility was above 90%). Bar = 150 μm, × 200 magnification.

and transferred electrophoretically to a nitrocellulose membrane. The membranes were incubated with 50 g/L non-fat dry milk in TBS (20 mmol/L Tris, 500 mmol/L NaCl, pH 7.5) overnight at 4℃ to block non-specific binding. The blots are then incubated with the murine antihuman HO-1 monoclonal antibodies (StressGen, Victoria, BC, Canada) at a dilution of 1:200 for 2 h at room temperature; this was followed by a 1 h incubation with the AP-conjugated rabbit antimouse polyclonal antibody (Promega, USA) at a dilution of 1:1000. The protein bands were visualized by the NBT + BCIP staining system (Haoyang Biological Manufacture Co, Ltd, Tianjin, China).

Islet viability

Islet viability was evaluated by acridine orange (AO)/propidium iodide (PI) (Sigma-Aldrich Chemicals, Louis Mo, USA) fluorescent staining. The fluorescent dye, containing 10 μL AO (670 μmol/L) and 1mL PI (750 μmol/L), was used at a 1:10 dilution. After the islets were washed twice with Hank's solution, the fluorescent dye was added to each well. Ten minutes later, islets were analyzed under a fluorescence microscope. Living cells were identified by green staining (AO), whereas dead cells showed a brown-red staining (PI).

Islet function

In vitro function of freshly isolated islets and cultured islets was assessed by glucose-stimulated insulin release. Islets of different groups were washed with PBS twice, and incubated first in low (2.8 mmol/L) and then in high (16.7 mmol/L) concentrations of glucose in culture medium. The static incubation assay was performed in a 24-well flat-bottomed culture plate with 30 IEQ/well and 3 duplicate wells for each islet group. Supernatant from each well was collected after each 1 h incubation, and the concentration was measured using an insulin radioimmunoassay kit (Jiuding Biotech Co, Ltd, Tianjin, China). Stimulation index (SI) was calculated by dividing the insulin release upon high glucose by the insulin release upon low glucose stimulation.

Statistical analysis

Data are expressed as mean ± SD. Statistical and graphical analysis was performed with software of SPSS10.0. Analyses were performed using the two-tailed Student's t-test where appropriate.

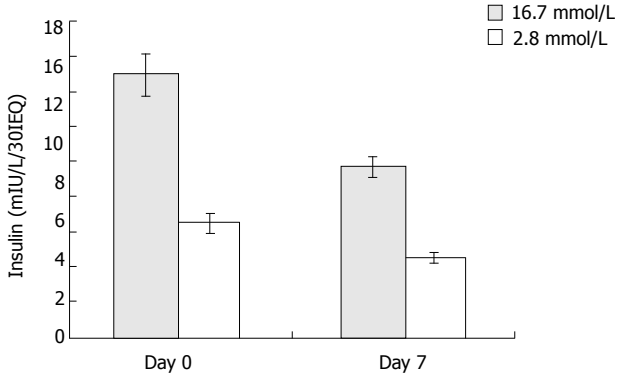

Figure 2 Effect of culture on glucose-stimulated insulin release. The insulin release upon either high or low glucose stimulation decreased conspicuously after seven days culture, $P < 0.05$

RESULTS

Purity and viability of freshly isolated rat islets

The purity of freshly isolated islets was above 90% calculated from the ratio of dithizone stained cells to dithizone nonstained cells as a percentage of the total cell number (Figure 1A). The viability of freshly isolated islets was above 90% calculated from the ratio of AO staining cells (living cells) to PI staining cells (dead cells) as a percentage of the total cell number (Figure 1B).

Effect of in vitro culture on insulin release

The glucose-stimulated insulin release was used to assess the function of cultured rat islets. As shown in Figure 2, after 7 d culture, the insulin release upon low and high glucose stimulation decreased from 6.47 ± 0.55 to 4.57 ± 0.40 mIU/L/30IEQ, and from 14.93 ± 1.17 to 9.63 ± 0.71 mIU/L/30IEQ, respectively. In other words, islet function decreased conspicuously over time in *in vitro* culture.

Exogenous gene expression in adenovirus-transduced rat islets

Typical fluorescence micro-photographs of rat islets transfected with Ad-EGFP at an MOI of 20 were taken at 48 h post-transfection. As shown in Figure 3A and B, the fluorescence in Ad-EGFP transfected islets was intense. Western blot was used to detect the expression of human HO-1 protein in three groups of islets. Figure 4 shows that human HO-1 protein was detected in Ad-HO-1 transfected islets but not in uninfected or Ad-

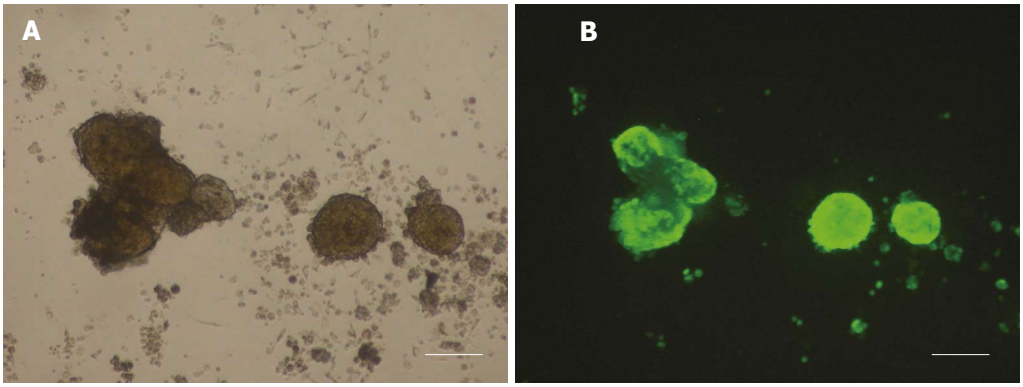

Figure 3 Ad-EGFP transduced islets. Microphotographs were taken at 48 h post-transfection (**A**, **B**). Fluorescence was intense at an MOI of 20 (**B**). Bar = 200 μm, × 100 magnification.

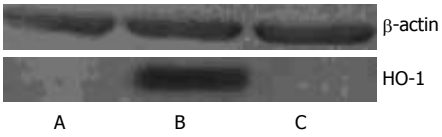

Figure 4 Western blot for hHO-1. Islets infected with Ad-HO-1, Ad-EGFP, or mock infected for 48 h were examined by Western blot. HO-1 expression was only detected in Ad-HO-1 group. A: control group; B: Ad-HO-1 group; C: Ad-EGFP group.

EGFP transfected islets. Therefore, adenovirus mediated exogenous gene transfer into rat islets was successful.

Effect of HO-1 gene transfer on the viability of cultured rat islets

The viability of islets was assessed by AO/PI fluorescent staining.

Representative pictures are shown in Figure 5. The viability of control islets was greatly reduced as shown by the large number of dead cells within the islets (Figure 5A). Nevertheless, the number of dead cells was reduced when islets were transfected with HO-1 gene (Figure 5B). Quantitative analysis of islet viability was performed by using fluorescence microscopy to determine the proportion of living cells within islets. As shown in Figure 5C, islet viability decreased greatly after 7 d culture (92% ± 6% *vs* 52% ± 13%, $P < 0.05$), but HO-1 gene transfer could reverse the viability reduction (71% ± 15% *vs* 52% ± 13%, $P < 0.05$).

Influence of adenoviral transfection on insulin release

Since adenoviral transfection at a high transfecting dose may damage islets and interfere with their biologic function[16], glucose-stimulated insulin release was employed to evaluate the influence of adenoviral transfection at an MOI of 20 on insulin release. As shown in Figure 6, there was no significant difference in glucose-stimulated insulin release between Ad-EGFP transfected islets and control islets at 7 d post-transfection (4.30 ± 0.40 *vs* 4.57 ± 0.40 mIU/L/30IEQ, 8.87 ± 0.65 *vs* 9.63 ± 0.71 mIU/L/30IEQ, respectively). It demonstrated that adenoviral transfection at an MOI of 20 was safe for islets.

Effect of HO-1 gene transfer on the function of cultured rat islets

After 7 d culture post transfection, the insulin release upon low and high glucose of uninfected (control islets), Ad-EGFP transfected, and Ad-HO-1 transfected islets were 4.57 ± 0.40 *vs* 9.63 ± 0.71 mIU/L/30IEQ, 4.30 ± 0.40 *vs* 8.87 ± 0.65 mIU/L/30IEQ, 5.67 ± 0.99 *vs* 12.50 ± 2.17 mIU/L/30IEQ, respectively. SI of control group, Ad-EGFP group, and Ad-HO-1 group were 2.11 ± 0.03, 2.08 ± 0.05, 2.21 ± 0.02, respectively. As shown in Figures 6 and 7, the insulin release upon high level glucose stimulation and SI of Ad-HO-1 transfected islets were significantly higher than those of Ad-EGFP transfected islets and control islets ($P < 0.05$). Therefore, HO-1 gene transfer can improve the function of cultured islets.

DISCUSSION

With recent advances in techniques of islet isolation and the introduction of more potent and less diabetogenic immunosuppressive therapies, islet transplantation has progressed from research to clinical reality, and it has been regarded as a safe and viable route to achieve insulin independence in a population of patients with type Ⅰ diabetes[3]. Many transplant protocols incorporate a period of short-term (24 to 72 h) islet culture before transplantation for the recipient to be treated with immunodepleting agents[4,5,17,18], and to provide time for *in vitro* assessment of islet quality. Short-term islet culture indeed has some benefits, such as purification of the islet preparation, immunomodulation[6], and possibly improved allograft survival. However, cultured islets are known to degrade rapidly[19,20], and lose viability and functional responsiveness to glucose stimulation with the extension of culturing time[7,8]. Islet loss as high as 30% to 50% has been reported after 48 hours of culture[21].

The islet, once removed from its natural surroundings within the pancreas and placed within the alien environment of the culture plate, becomes deprived of normal physiological organization and exposed to a number of hostile factors, such as hypoxia, activation of free radicals, apoptosis and necrosis that cause its premature demise. The quality of the transplanted islets is of the utmost importance to successfully achieve normal levels of glucose in transplant recipients, therefore, preservation of viability and function of islets post-isolation is a pre-requisite in islet transplantation. Pancreatic islets, as a cellular graft, are especially suited for gene therapy, as they can be infected efficiently *ex vivo* and then transplanted with minimal systemic exposure of the recipient to the vector.

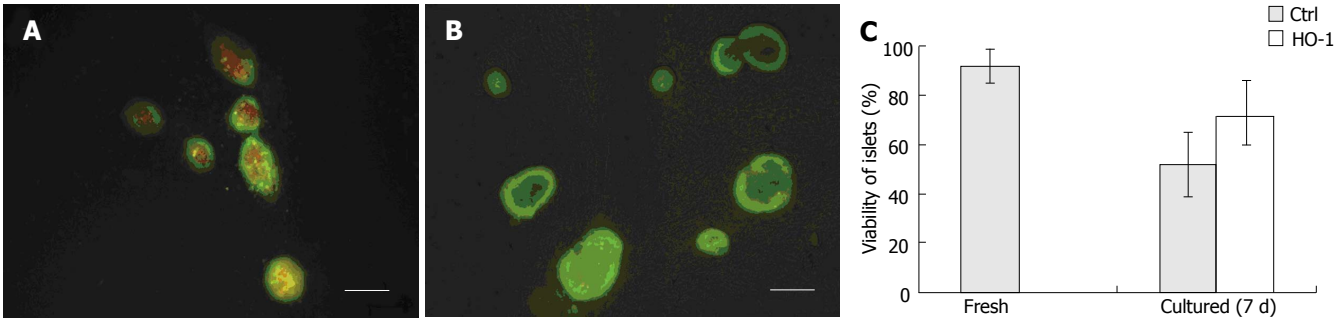

Figure 5 Effect of HO-1 gene transfer on the viability of cultured rat islets. At 7 d post-transfection, the control group showed the presence of numerous dead cells (red) at the center of the islets (**A**), while the Ad-HO-1 group showed more living cells (**B**). Bar = 200 Um, × 100 magnification. The islet viability was decreased greatly after 7 d culture ($P < 0.05$), whereas HO-1 gene transfer could reduce the loss of islet viability ($P < 0.05$).

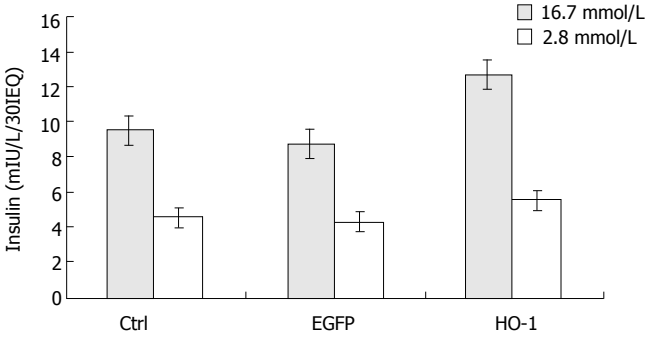

Figure 6 Effect of HO-1 gene transfer on insulin release of cultured rat islets. At 7 d post-transfection, no significant difference in glucose-stimulated insulin release was detected between Ad-EGFP transfected islets and control islets, however, the insulin release upon high glucose stimulation of Ad-HO-1 transfected islets was significantly higher than that of Ad-EGFP transfected islets and control islets, $P < 0.05$.

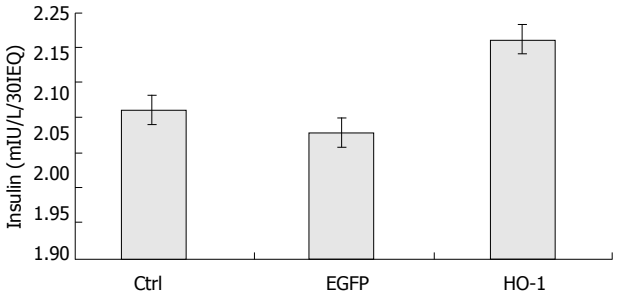

Figure 7 Effect of HO-1 gene transfer on stimulation index of cultured rat islets. The SI of Ad-HO-1 transfected islets was significantly higher than that of Ad-EGFP transfected islets and control islets, $P < 0.05$.

HO-1 has been identified as a ubiquitous stress protein induced in many cell types by various stimulants, such as hemolysis, inflammatory cytokines, oxidative stress, heat shock, heavy metals, and endotoxin[22]. HO-1 is the rate-limiting enzyme of heme degradation into its byproducts biliverdin, CO, and iron[9,10]. Biliverdin is subsequently reduced into bilirubin, a powerful anti-oxidant, and it may inhibit the generation of reactive oxygen species[23].

CO has a cytoprotective role in different systems[24-26], including pancreatic β-cells[27]. Heme catabolism by HO-1 also releases free iron, which has the potential to exacerbate the cytotoxic effects of reactive oxygen species[28,29].

However, generation of intracellular free iron upregulates the expression of ferritin[28,29], which has a high capacity to store free iron[29]. Ferritin has been shown to protect endothelial cells against activated neutrophils as well as H_2O_2-mediated cytotoxicity[29], suggesting that some of the effects of HO-1 may be mediated by ferritin[28,29]. As HO-1 is not expressed constitutively, it has been demonstrated that overexpression of HO-1 by chemical induction can protect islet cells from apoptosis and improve *in vivo* function after transplantation[22]. Compared with chemical induction, gene transfer can provide effective, targeted, and relatively persistent expression of HO-1.

Adenoviral vectors are useful for efficient gene delivery to differentiated and non-proliferating cells, such as isolated pancreatic islets[30]. In addition, adenoviral vectors can be produced in high titers and there is no risk of insertional mutagenesis as their genomes are not integrated into chromosomes. In the present study, recombinant adenoviral vectors were generated by use of the AdEasy system, and employed to transfect rat islets at an MOI of 20. According to fluorescence photographs taken at 48 h post-transfection, the expression of EGFP was intense. Furthermore, human HO-1 protein was detected by Western blot in Ad-HO-1 transfected islets at the same time. This demonstrated that recombinant adenoviral vectors were efficient to deliver exogenous genes into rat islets *in vitro*. Insulin release upon glucose stimulation was a measure of islet function, which was a prerequisite to any gene therapy program for diabetes treatment by islet transplantation[31]. In our experiments, no significant difference in glucose-stimulated insulin release was detected between Ad-EGFP transfected islets and control islets at 7 d post-transfection. This is consistent with the results reported by others showing that adenoviral vectors at a low transfecting dose (MOI 20) provided effective transfer of a marker gene into islet cells without impairing cell function[16].

Even though many clinical islet transplant protocols culture islets for only 24 to 72 h, islets were cultured for seven days in our study. This culture period was selected to minimize the effects of isolation factors on islet function, while maximizing the effect of culture. After

seven days culturing, the insulin release upon either low or high concentration glucose stimulation was significantly lower than that of freshly isolated islets ($P < 0.05$). This is consistent with previous reports showing that islet function degrades in *in vitro* culture over time. Nevertheless, the insulin release upon high concentration glucose stimulation and stimulation index (SI) of Ad-HO-1 transfected islets were significantly higher than those of Ad-EGFP transfected islets and control islets ($P < 0.05$). As glucose-stimulated insulin release was a favourable marker of the function of islets, our study demonstrated that HO-1 gene transfer conferred cytoprotection and improved islet function in *in vitro* culture. This was probably related to the effect of CO, which was not only a stimulator of insulin release but also a trigger of the transients of $[Ca^{2+}]$ i assumed to coordinate the secretory activity of the β-cells[32]. Furthermore, results of fluorescence microscopy studies with AO/PI staining indicated that HO-1 gene transfection significantly improved islet viability and survival during *in vitro* culture.

Despite the efficient transfection capacity of adenoviral vectors, the transgene cannot integrate into the host cell genome, leading to transient transgenic expression. In our study, we found that the EGFP expression time in cultured islets was more than 3 wk (data not shown). However, for some therapeutic strategies, such as islet cytoprotection in *in vitro* culture or early after transplantation, temporal expression of the cytoprotective transgene mediated by adenoviral vectors is still recommended because the factors related to early islet injury usually play a major role in the outcome of islet transplantation.

In summary, we demonstrated that adenoviral vectors could successfully transfer exogenous HO-1 gene into rat islet cells, and HO-1 gene transfer could improve rat islet viability and function in *in vitro* culture. Strategies using HO-1 gene transfer to islets might lead to better outcome in islet transplantation.

ACKNOWLEDGMENTS

We thank the staff of the Diabetes Research Laboratory, the First Affiliated Hospital of Shanghai Jiao Tong University, for helping us to isolate rat islets.

COMMENTS

Background

With recent advances in methods of islet isolation and the introduction of more potent and less diabetogenic immunosuppressive therapies, islet transplantation has progressed from research to clinical reality. Islet culture for a brief period (24 to 72 h) has emerged as the current standard procedure prior to clinical transplantation. Short-term islet culture indeed have some benefits, such as purification of the islet preparation, immunomodulation, assessment of islet quality, and possibly improved allograft survival. But *in vitro* culture of islets has been shown to result in a loss of viability over time, and a decrease in glucose responsiveness has been observed for those islets which survive.

As a cellular graft, islets are especially suited for gene therapy applications. HO-1 has been described as a ubiquitous inducible stress protein capable of cytoprotection via radical scavenging and apoptosis prevention. Overexpression of HO-1 can be chemically induced, but compared with chemical induction, gene transfer can provide effective, targeted, and relatively persistent expression of HO-1. It's an attractive strategy to protect islets *in vitro* culture by using gene therapy to transduce islets with cytoprotective gene that can make islets more resistant to injury.

Research frontiers

Although advances in islet isolation and less diabetogenic immunosuppression have moved islet transplantation forward from research to clinical reality, many challenges have to be faced with, such as keeping islet viable, single donor grafts, limited donor supply, tolerance induction.

Innovations and breakthroughs

Overexpression of HO-1 by chemical induction can protect islet cells from apoptosis and improve islet function. We used gene technique to modify rat islets *in vitro*, and found that HO-1 gene transfer could protect islet viability and function after seven days culture. Compared with chemical induction, gene transfer can provide effective, targeted, and relatively persistent expression of HO-1.

Applications

HO-1 gene transfer can improve islet viability and function. It suggests a potential therapeutic application for HO-1 gene in improving islet survival/function in islet transplantation.

Terminology

Islet equivalent (IEQ): islets with an average diameter of 150 μm.

Peer review

In this manuscript, Chen *et al.* have analyzed whether adenovirus-mediated gene transfer of heme oxygenase-1 into rat isolated pancreatic islets, affect the long term viability of the cells. This manuscript is well written, experiments and analyses of data are adequately performed.

REFERENCES

1 **Boyle JP**, Honeycutt AA, Narayan KM, Hoerger TJ, Geiss LS, Chen H, Thompson TJ. Projection of diabetes burden through 2050: impact of changing demography and disease prevalence in the U.S. *Diabetes Care* 2001; **24**: 1936-1940
2 **Stratta RJ**. Mortality after vascularized pancreas transplantation. *Surgery* 1998; **124**: 823-830
3 **Shapiro AM**, Lakey JR, Ryan EA, Korbutt GS, Toth E, Warnock GL, Kneteman NM, Rajotte RV. Islet transplantation in seven patients with type 1 diabetes mellitus using a glucocorticoid-free immunosuppressive regimen. *N Engl J Med* 2000; **343**: 230-238
4 **Hering BJ**, Kandaswamy R, Harmon JV, Ansite JD, Clemmings SM, Sakai T, Paraskevas S, Eckman PM, Sageshima J, Nakano M, Sawada T, Matsumoto I, Zhang HJ, Sutherland DE, Bluestone JA. Transplantation of cultured islets from two-layer preserved pancreases in type 1 diabetes with anti-CD3 antibody. *Am J Transplant* 2004; **4**: 390-401
5 **Hering BJ**, Kandaswamy R, Ansite JD, Eckman PM, Nakano M, Sawada T, Matsumoto I, Ihm SH, Zhang HJ, Parkey J, Hunter DW, Sutherland DE. Single-donor, marginal-dose islet transplantation in patients with type 1 diabetes. *JAMA* 2005; **293**: 830-835
6 **Kim SC**, Han DJ, Kim IH, Woo KO, We YM, Kang SY, Back JH, Kim YH, Kim JH, Lim DG. Comparative study on biologic and immunologic characteristics of the pancreas islet cell between 24 degrees C and 37 degrees C culture in the rat. *Transplant Proc* 2005; **37**: 3472-3475
7 **Schmied BM**, Ulrich A, Matsuzaki H, Ding X, Ricordi C, Moyer MP, Batra SK, Adrian TE, Pour PM. Maintenance of human islets in long-term culture. *Differentiation* 2000; **66**: 173-180
8 **Cui YF**, Ma M, Wang GY, Han DE, Vollmar B, Menger MD. Prevention of core cell damage in isolated islets of Langerhans by low temperature preconditioning. *World J Gastroenterol* 2005; **11**: 545-550
9 **Maines MD**. The heme oxygenase system: a regulator of second messenger gases. *Annu Rev Pharmacol Toxicol* 1997; **37**: 517-554
10 **Katori M**, Busuttil RW, Kupiec-Weglinski JW. Heme oxygenase-1 system in organ transplantation. *Transplantation* 2002; **74**: 905-912

11 **Tobiasch E**, Günther L, Bach FH. Heme oxygenase-1 protects pancreatic beta cells from apoptosis caused by various stimuli. *J Investig Med* 2001; **49**: 566-571

12 **Tsuburai T**, Suzuki M, Nagashima Y, Suzuki S, Inoue S, Hasiba T, Ueda A, Ikehara K, Matsuse T, Ishigatsubo Y. Adenovirus-mediated transfer and overexpression of heme oxygenase 1 cDNA in lung prevents bleomycin-induced pulmonary fibrosis via a Fas-Fas ligand-independent pathway. *Hum Gene Ther* 2002; **13**: 1945-1960

13 **McCarter SD**, Akyea TG, Lu X, Bihari A, Scott JR, Badhwar A, Dungey AA, Harris KA, Feng Q, Potter RF. Endogenous heme oxygenase induction is a critical mechanism attenuating apoptosis and restoring microvascular perfusion following limb ischemia/reperfusion. *Surgery* 2004; **136**: 67-75

14 **Wang XH**, Wang K, Zhang F, Li XC, Li J, De W, Guo J, Qian XF, Fan Y. Heme oxygenase-1 alleviates ischemia/reperfusion injury in aged liver. *World J Gastroenterol* 2005; **11**: 690-694

15 **Sutton R**, Peters M, McShane P, Gray DW, Morris PJ. Isolation of rat pancreatic islets by ductal injection of collagenase. *Transplantation* 1986; **42**: 689-691

16 **Weber M**, Deng S, Kucher T, Shaked A, Ketchum RJ, Brayman KL. Adenoviral transfection of isolated pancreatic islets: a study of programmed cell death (apoptosis) and islet function. *J Surg Res* 1997; **69**: 23-32

17 **Stock PG**, Bluestone JA. Beta-cell replacement for type I diabetes. *Annu Rev Med* 2004; **55**: 133-156

18 **Markmann JF**, Deng S, Huang X, Desai NM, Velidedeoglu EH, Lui C, Frank A, Markmann E, Palanjian M, Brayman K, Wolf B, Bell E, Vitamaniuk M, Doliba N, Matschinsky F, Barker CF, Naji A. Insulin independence following isolated islet transplantation and single islet infusions. *Ann Surg* 2003; **237**: 741-749; discussion 749-750

19 **Brendel MD**, Kong SS, Alejandro R, Mintz DH. Improved functional survival of human islets of Langerhans in three-dimensional matrix culture. *Cell Transplant* 1994; **3**: 427-435

20 **Korbutt GS**, Pipeleers DG. Cold-preservation of pancreatic beta cells. *Cell Transplant* 1994; **3**: 291-297

21 **London NJ**, Swift SM, Clayton HA. Isolation, culture and functional evaluation of islets of Langerhans. *Diabetes Metab* 1998; **24**: 200-207

22 **Pileggi A**, Molano RD, Berney T, Cattan P, Vizzardelli C, Oliver R, Fraker C, Ricordi C, Pastori RL, Bach FH, Inverardi L. Heme oxygenase-1 induction in islet cells results in protection from apoptosis and improved in vivo function after transplantation. *Diabetes* 2001; **50**: 1983-1991

23 **Stocker R**, Yamamoto Y, McDonagh AF, Glazer AN, Ames BN. Bilirubin is an antioxidant of possible physiological importance. *Science* 1987; **235**: 1043-1046

24 **Brouard S**, Otterbein LE, Anrather J, Tobiasch E, Bach FH, Choi AM, Soares MP. Carbon monoxide generated by heme oxygenase 1 suppresses endothelial cell apoptosis. *J Exp Med* 2000; **192**: 1015-1026

25 **Peyton KJ**, Reyna SV, Chapman GB, Ensenat D, Liu XM, Wang H, Schafer AI, Durante W. Heme oxygenase-1-derived carbon monoxide is an autocrine inhibitor of vascular smooth muscle cell growth. *Blood* 2002; **99**: 4443-4448

26 **Maines MD**. Heme oxygenase 1 transgenic mice as a model to study neuroprotection. *Methods Enzymol* 2002; **353**: 374-388

27 **Günther L**, Berberat PO, Haga M, Brouard S, Smith RN, Soares MP, Bach FH, Tobiasch E. Carbon monoxide protects pancreatic beta-cells from apoptosis and improves islet function/survival after transplantation. *Diabetes* 2002; **51**: 994-999

28 **Ferris CD**, Jaffrey SR, Sawa A, Takahashi M, Brady SD, Barrow RK, Tysoe SA, Wolosker H, Barañano DE, Doré S, Poss KD, Snyder SH. Haem oxygenase-1 prevents cell death by regulating cellular iron. *Nat Cell Biol* 1999; **1**: 152-157

29 **Balla G**, Jacob HS, Balla J, Rosenberg M, Nath K, Apple F, Eaton JW, Vercellotti GM. Ferritin: a cytoprotective antioxidant strategem of endothelium. *J Biol Chem* 1992; **267**: 18148-18153

30 **Wilson JM**. Adenoviruses as gene-delivery vehicles. *N Engl J Med* 1996; **334**: 1185-1187

31 **Fernandes JR**, Duvivier-Kali VF, Keegan M, Hollister-Lock J, Omer A, Su S, Bonner-Weir S, Feng S, Lee JS, Mulligan RC, Weir GC. Transplantation of islets transduced with CTLA4-Ig and TGFbeta using adenovirus and lentivirus vectors. *Transpl Immunol* 2004; **13**: 191-200

32 **Lundquist I**, Alm P, Salehi A, Henningsson R, Grapengiesser E, Hellman B. Carbon monoxide stimulates insulin release and propagates Ca^{2+} signals between pancreatic beta-cells. *Am J Physiol Endocrinol* Metab 2003; **285**: E1055-E1063

S- Editor Wang J **L- Editor** Zhu LH **E- Editor** Lu W

PO Box 2345, Beijing 100023, China
www.wjgnet.com
wjg@wjgnet.com

World J Gastroenterol 2007 February 21; 13(7): 1060-1066
World Journal of Gastroenterology ISSN 1007-9327

BASIC RESEARCH

Uric acid enhances T cell immune responses to hepatitis B surface antigen-pulsed-dendritic cells in mice

Xiao-Jun Ma, De-Ying Tian, Dong Xu, Dao-Feng Yang, Hui-Fen Zhu, Zhi-Hui Liang, Zheng-Gang Zhang

Xiao-Jun Ma, De-Ying Tian, Dong Xu, Dao-Feng Yang, Zheng-Gang Zhang, Department of Infectious Diseases, Tongji Hospital, Tongji Medical College, Huazhong University of Science and Technology, Wuhan 430030, Hubei Province, China
Hui-Fen Zhu, Zhi-Hui Liang, Department of Immunology, Tongji Medical College, Huazhong University of Science and Technology, Wuhan 430030, Hubei Province, China
Supported by the National Natural Science Foundation of China, No. 30471533
Correspondence to: Dr. De-Ying Tian, Department of Infectious Diseases, Tongji Hospital, Tongji Medical College, Huazhong University of Science and Technology, Jiefang Avenue 1095,Wuhan 430030, Hubei Province, China. langz2004@126.com
Telephone: +86-27-69807982 Fax: +86-27-83613408
Received: 2006-11-12 Accepted: 2006-12-25

Abstract

AIM: To study the induction of T cellular immune responses in BALB/c mice immunized with uric acid and dendritic cells (DCs) pulsed with hepatitis B virus surface antigen (HBsAg).

METHODS: DCs were generated from bone-marrow cells of BABL/c mice, and then pulsed or unpulsed with HBsAg protein (HBsAg-pulsed-DCs or unpulsed-DCs) in vitro. BABL/c mice were immunized with HBsAg-pulsed-DCs (1×10^6) and uric acid, injected through the tail vein of each mouse. The mice in control groups were immunized with HBsAg-pulsed-DCs alone, unpulsed-DCs alone or 200 μg uric acid alone or PBS alone. The immunization was repeated 7 d later. Cytotoxic T lymphocytes (CTLs) *in vivo* were determined by the CFSE labeled spleen lysis assay. Spleen cells or spleen T cells were isolated, and re-stimulated *in vitro* with HBsAg for 120 h or 72 h. Production of IFN-γ and IL-4 secreted by spleen cells were determined by ELISA method; proliferation of spleen T cells were detected by flow cytometry.

RESULTS: The cytotoxicities of HBsAg-specific-CTLs, generated after immunization of HBsAg-pulsed-DCs and uric acid, were 68.63% ± 11.32% and significantly stronger than that in the control groups ($P < 0.01$). Compared with control groups, in mice treated with uric acid and HBsAg-pulsed-DCs, the spleen T cell proliferation to HBsAg re-stimulation was stronger (1.34 ± 0.093 *vs* 1.081 ± 0.028, $P < 0.01$), the level of IFN-γ secreted by splenocytes was higher (266.575 ± 51.323 *vs* 135.223 ± 32.563, $P < 0.01$) , and IL-4 level was lower (22.385 ± 2.252 *vs* 40.598 ± 4.218, $P < 0.01$).

CONCLUSION: Uric acid can strongly enhance T cell immune responses induced by HBsAg-pulsed-DCs vaccine. Uric acid may serve as an effective adjuvant of DC vaccine against HBV infection.

Key words: Uric acid; Dendritic cells; Hepatitis B virus surface antigen; Cytotoxic T lymphocytes; Mouse

Ma XJ, Tian DY, Xu D, Yang DF, Zhu HF, Liang ZH, Zhang ZG. Uric acid enhances T cell immune responses to hepatitis B surface antigen-pulsed-dendritic cells in mice. *World J Gastroenterol* 2007; 13(7): 1060-1066

http://www.wjgnet.com/1007-9327/13/1060.asp

INTRODUCTION

It is generally accepted that dendritic cells (DCs) are the most efficient and powerful antigen presenting cells and play a center role in exciting T cell immune reactions. T-cell mediated immune responses, especially Hepatitis B virus (HBV) specific- cytotoxic T lymphocyte (CTL) response, may play an important role in resolving HBV infection[1,2]. hepatitis B surface antigen (HBsAg) pulsed DCs can activate lymphocytes to become HBsAg-specific CTLs or specific $CD4^+$ T cells *in vivo*[3]. Shimizu *et al*[4] immunized HBV transgenic mice with DCs loading HBsAg, and found that DC vaccine could break tolerance to HBV and induce an effective anti-viral immune response. Chen *et al*[5] reported that HBsAg-pulsed DCs from the peripheral blood could effectively suppress HBV replication in chronic hepatitis B patients. However, anti-HBV immune effects of DC vaccine are varied and instable. This may be due to the diversity of DC vaccine preparations; however, the main cause may be the insufficiency of DC vaccines. For example, some researchers carried out similar immune therapy in volunteers, but no evident immune response was shown[3,6-8]. Therefore, the basic research of DC vaccine as well as how to improve the immune response to DC vaccine is still a significant challenge.

Recently, it was reported that uric acid (UA) could stimulate DCs to mature, promote DCs to present foreign antigens and stimulate T lymphocytes[9,10]. These findings demonstrate the adjuvant effects of uric acid and encourage the potential application of uric acid in

vaccination.

This study aimed to observe the T cell immune response after immunization with HBsAg pulsed DCs (HBsAg-pulsed-DCs) and uric acid in mice. The results demonstrated that administration of uric acid could enhance the T cell immune response to HBsAg-pulsed-DCs.

MATERIALS AND METHODS

Mice

Male or female BALB/c (H-2^d) mice aged 8 to 10 wk were obtained from the Department of Experimental Animals, Tongji Medical College, Huazhong University of Science and Technology, Wuhan, China. All animal experiments followed the guidelines for the care and use of animals established by Tongji Medical College, Huazhong University of Science and Technology, and were approved by the Ethics Committee of Tongji Medical College.

Agents

Uric acid (UA, Sigma-aldrich) was dissolved at a concentration of 5 mg/mL in 0.1 mol/L sodium borate buffer (pH 8.5) for more than 72 h[9,11]. The HBsAg protein was synthesized by Shanghai SanGon Company, China. The purity (> 99%) of the protein was confirmed by high performance liquid chromatography (HPLC) and mass spectrometry. Carboxy-fluorescein diacetate, succinimidyl ester (CFSE, Molecular Probes, USA) was dissolved in dimethyl sulfoxide (DMSO) at a concentration of 10 mmol/L.

Preparation and culture of bone marrow DCs

DCs were prepared as described previously[12]. Briefly, bone marrow cells were collected from the femur and tibiae of BALB/c mice, and DCs were grown from precursors at a starting concentration of 2×10^6 cells per ml in complete RPMI 1640 (RPMI 1640 supplemented with 10% inactivated fetal calf serum, 2 mmol/L L-glutamine, 100 U/mL penicillin G and 100 μg/mL streptomycin), and cultured in six-well flat bottom plates (Falcon) at 37℃, 5% CO_2 for 3 h and then non-adherent cells were washed out. rmGM-CSF at 10 ng/mL (PeproTech, Rocky Hill, NJ) and rmIL-4 at 10 ng/mL (PeproTech, Rocky Hill, NJ) were added to the culture. On days 3, 5 and 7, half of the medium was replaced with a fresh medium. On day 7, cells were incubated with uric acid (100, 200 and 400 μg/mL) or 1 μg/mL lipopolysaccharide (LPS, Sigma), respectively. Serum-free RPMI 1640 was used as control. On day 9, cells and culture supernatants were collected for further experiments and analysis.

Analysis of cell surface markers on DCs by flow cytometry

Expression of DC cell surface molecules (CD11c, CD83, IA/IE, CD86) were determined by flow cytometric analysis. Cells were washed twice with an ice cold FACScan buffer (PBS containing 2% FCS and 0.1% sodium azide). The same buffer was used for the incubation with antibodies as well as for all washes. Twenty percent of mixed sera of mice and rats were used to prevent nonspecific antibody binding. FITC-conjugated anti-mouse CD1lc (Clone: N418, eBioscience) and IA/IE(Clone: M5/114.15.2, eBioscience) or PE-conjugated anti-mouse CD83 (Clone:Michel-17, eBioscience) and CD86 (Clone: RMMP-2, Caltag Laboratories) were added, respectively, to the cells and the samples were left on ice for 45 min in the dark. Fluorescence profiles were generated on an FACScan flow cytometer (Becton Dickinson). Histogram was produced with the CellQuest software package.

Measurement of IL-12P70 concentrations

The concentration of IL-12P70 in DC culture supernatants was determined by using an enzyme-linked immunosorbent assay (ELISA) kit (R&D Systems) according to the manufacturer's instructions.

Preparation of HBsAg-pulsed-DCs

Mature DCs stimulated by 1 μg/mL LPS were collected and used to pulse with HBsAg. The procedure for pulsing DCs was the same as previously described[13]. Briefly, 1×10^6 mature DCs were incubated with 10 μg/mL HBsAg for 6 h. DCs were washed three times and resuspended in PBS.

Immunization of mice

Totally 1×10^6 HBsAg-pulsed-DCs (total volume 200 μL) were injected through the tail vein of each mouse, together with 200 μg uric acid. The mice immunized with HBsAg-pulsed-DCs (1×10^6) or unpulsed-DCs (1×10^6) alone were used as controls. The mice treated with 200 μg uric acid or 200 μL PBS alone were used as controls as well. Ten mice were in each group. The immunization was repeated 7 d later.

Assay of CTL cytotoxic activity in vivo

Seven days after immunization with DCs for the second and last time, each mouse received spleen cells labeled with CFSE. To prepare target cells to detect in vivo cytotoxic activity[14,15], erythrocytes were removed from naive BALB/c spleen cell suspensions by lysis in ammonium chloride solution. The cells were then washed and split into two populations. One population was pulsed with 10 μg/mL HBsAg, incubated at 37℃ for 4 h, and labeled with a high concentration of CFSE (5.0 μmol/L) (CFSE^{high} cells). Another population as control target cells was left without HBsAg and was labeled with a low concentration of CFSE (0.5 μmol/L) (CFSE^{low} cells)[16]. An equal number of cells from each population were mixed together, and each mouse received a total of 2×10^7 mixed cells in 400 μL of PBS. Cells were intravenously injected into all mice as above. And 10 h later, the mice were sacrificed and their spleen cells were obtained. Cell suspensions were analyzed by flow cytometry, and each population was detected for their differential CFSE fluorescence intensities. Up to 1×10^4 CFSE-positive cells were collected for analysis. To calculate specific lysis, the following formula was used: Ratio = (percentage CFSE^{low}/percentage CFSE^{high}). Percentage specific lysis = [1- (ratio unprimed/ratio primed) × 100][14,15].

Cytokine production by spleen cells

Spleen cells from the immunized mice were depleted

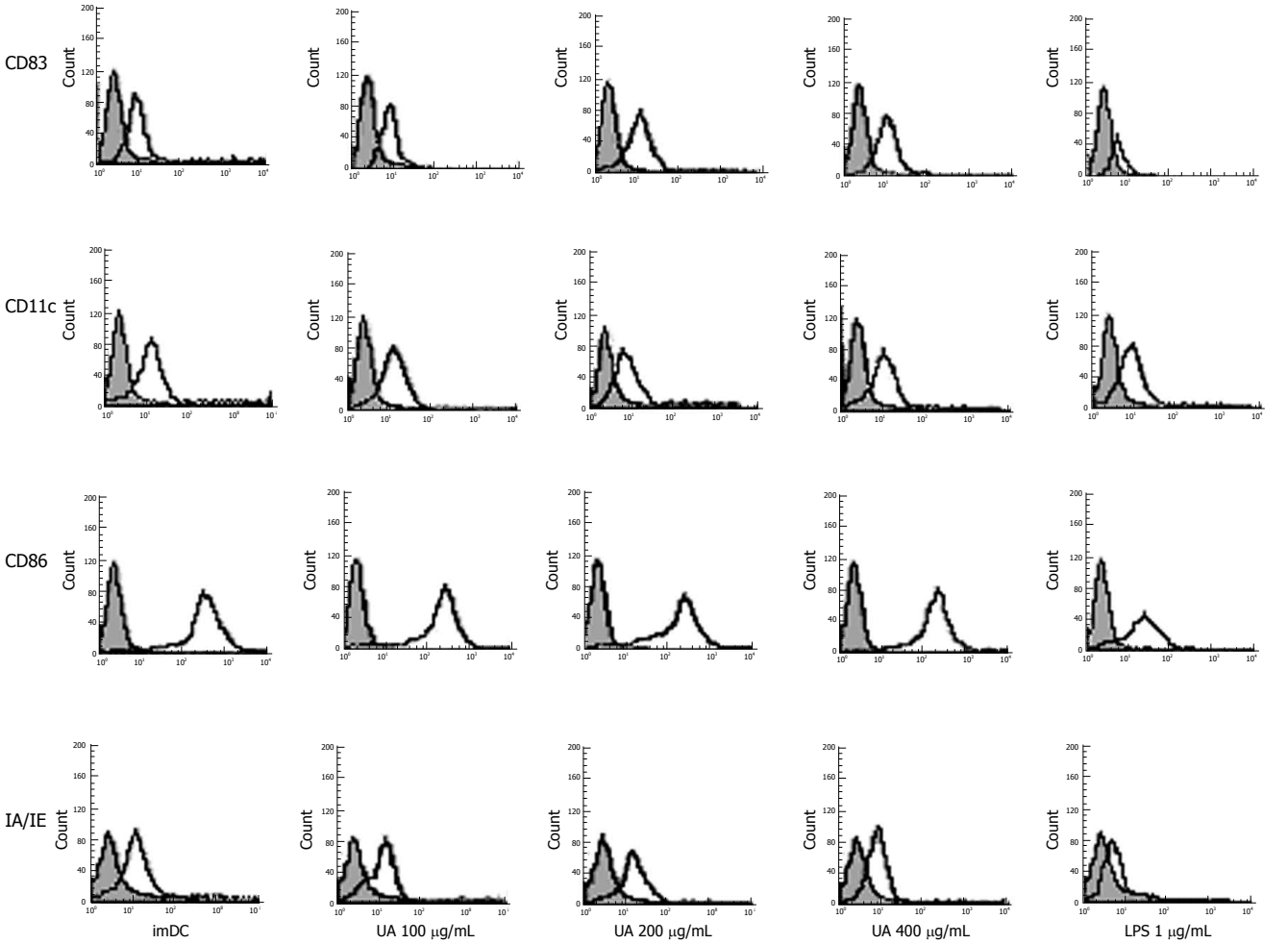

Figure 1 The cell surface markers analysis on dendritic cells by flow cytometry after exposure to uric acid or LPS. Bone marrow-derived DCs were stimulated with 100, 200 and 400 μg/mL uric acid or 1 μg/mL LPS or Serum-free RPMI media 1640 for 48 h and immunostained with mAbs against CD11c, CD83, CD86 and IA/IE molecules (open histograms). Shade histograms represent the isotype control mAb staining of the cells. The histograms (Figure 1) and data (Table 1) are representative of five independent experiments.

of erythrocytes and washed twice with PBS. The cells obtained were resuspended with complete RPMI 1640, and seeded in duplicate into flat-bottomed 24-well microtitration plates(Costar, Brumath, France) at 2×10^6 cells per well in 1 mL of culture medium containing 10 μg/mL HBsAg. The cell-free culture supernatants were harvested after 72 h and assayed for IFN-γ and IL-4 activity. The cytokine concentrations were determined by using a commercial ELISA kit (eBioscience Inc.) according to the manufacturer's instructions, and the standard curves corresponding to known amounts of mouse recombinant IFN-γ, IL-4. The sensitivity limits for the assays are 15 pg/mL for IFN-γ, and 4 pg/mL for IL-4.

Cell proliferative response of spleen T cells

Erythrocytes were removed from the spleen cells of mice 14 d after immunization as above. The cells were resuspended with complete RPMI 1640, and then T cells were separated by a nylon wool column method[17]. In brief, 1×10^8 cells were drained through a nylon wool column (Polysciences. Inc., Warrington, PA) for 45 min at 37℃, and then nonadherent T cells were collected after two washes. T cells were labeled with 2.5 μmol/L CFSE and washed three times in the medium as described above, counted, and resuspended at a concentration of 1×10^6 cells/mL. The samples were seeded in triplicate into 24-well microtitration plates (Costar, Brumath, France) at 2×10^6 cells per well in 2 mL of culture medium containing 10 μg/mL HBsAg or PBS. T cells from the untreated mice were used as the negative control; and T cells from the untreated mice stimulated with 10 μg/mL concanavalin A (ConA) and 10 μg/mL HBsAg or PBS was served as the positive controls. The plates were incubated for 72 h in 5% CO_2 at 37℃. Cell proliferation was estimated by flow cytometry[16]. Histogram was produced with the Motif 3.0 software package.

Statistical analysis

All data were presented as mean ± SD and analyzed using the Student-Newman-Keuls test and LSD multiple comparisons with SPSS11.5 software in the experiments. $P < 0.05$ was regarded as statistically significant.

RESULTS

Cell surface markers on DCs

We demonstrated an increase in CD83, IA/IE, and CD86 expression by DCs, stimulated with uric acid previously (Figure 1, Table 1). The effect of uric acid was dose-dependent and was still observed when the uric acid was

Table 1 Surface molecular expression of DCs (%, mean ± SD)

Group	*n*	CD11C	CD83	CD86	MHC
RMPI-1640	5	72.85 ± 1.64	21.66 ± 5.34[f]	37.77 ± 1.62[f]	27.34 ± 1.81[f]
UA100	5	73.16 ± 1.05	47.71 ± 4.75[b,d]	78.48 ± 2.98[b,f]	75.83 ± 2.49[b,f]
UA200	5	73.18 ± 0.95	52.23 ± 0.83[b]	80.14 ± 1.01[b]	79.47 ± 0.92[b]
UA400	5	73.36 ± 1.46	52.33 ± 0.94[b]	81.08 ± 1.25[b]	80.36 ± 1.22[b]
LPS	5	73.44 ± 1.33	53.28 ± 1.12[b]	82.50 ± 2.29[bb]	81.42 ± 2.21[b]

[b]$P < 0.001$ *vs* RMPI-1640; [d]$P < 0.01$ *vs* LPS; [f]$P < 0.001$ *vs* LPS.

Table 2 IL-12 p70 production in DC supernatants (mean ± SD, *n* = 5, ng/mL)

Group	imDC	UA100	UA200	UA400	LPS
IL-12P70	2.53 ± 0.27	3.52 ± 0.22[b]	3.99 ± 0.28[b]	4.37 ± 0.19[b]	4.38 ± 0.17[b]

[b]$P < 0.001$ *vs* imDC.

Table 3 IFN-γ production of spleen cells (mean ± SD, *n* = 10, pg/mL)

Group	IL-4	γ-IFN
PBS	40.598 ± 4.218	135.223 ± 32.563
UA	39.387 ± 3.657	141.500 ± 32.654
Unpulsed-DC	37.352 ± 3.238	149.32 ± 37.354
HBsAg-pulsed-DC	22.385 ± 2.252[b]	266.575 ± 51.323[b]
UA-DC	15.123 ± 1.353[d]	429.216 ± 59.232[d]

[b]$P < 0.01$, [d]$P < 0.001$ *vs* PBS group.

administered at 100 μg/mL. After stimulation with uric acid (100-400 μg/mL), the percentage of various markers increased from 2.0- fold to 3.0-fold. The stimulatory effect elicited by uric acid at a concentration of 200-400 μg/mL was similar to that induced by LPS (1 μg/mL). After stimulation with uric acid or LPS, the CD11c expression in each group was high and similar, including the imDC group.

IL-12 p70 production in DC supernatants

Using the ELISA technique, the IL-12 p70 secretion by DCs was detected 48h after stimulation with uric acid or LPS. IL-12p70 production was markedly increased in response to uric acid stimulation in a dose-dependent manner. The IL-12p70 production stimulated by 200-400 μg/mL uric acid was similar to LPS treatment (Table 2).

Cytokine production by spleen cells

The supernatants of cultured immune spleen cells were evaluated for the production of IL-4 (Th2 cytokine) or IFN-γ (Th1 cytokine) in response to HBsAg re-stimulation on day 14 (Figure 2, Table 3).

The production of IL-4 in mice immunized with HBsAg-pulsed-DCs and uric acid was lower than that of mice immunized with HBsAg-pulsed-DCs alone or unpulsed-DCs alone or PBS alone($P < 0.001$ for all) (Figure 2A).

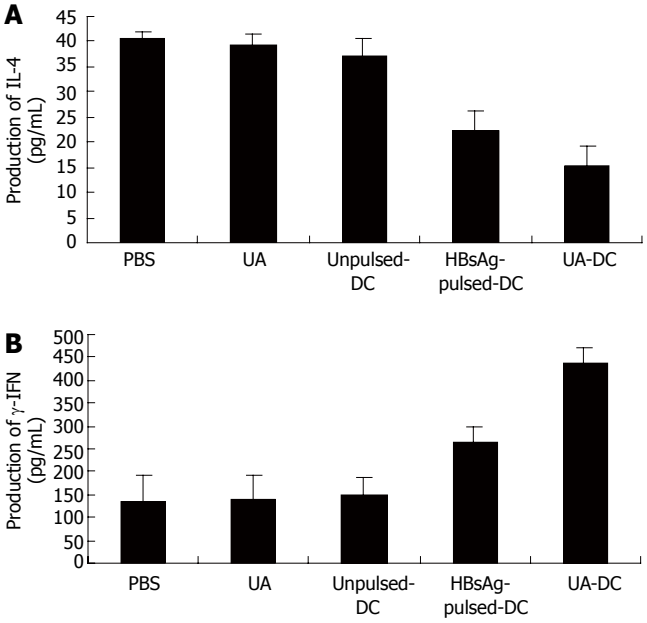

Figure 2 Cytokine production by splenocytes. Fourteen days after immunization, spleen cells were isolated, then stimulated with HBsAg (10 μg/mL) *in vitro*. Values were measured at 72 h for IL-4 (**A**), IFN-γ (**B**) by ELISA. The results are representative of ten samples from each group. The data show the mean ± SD.

The production of IFN-γ (Figure 2B) in mice immunized with HBsAg-pulsed-DCs and uric acid was significantly greater ($P < 0.001$ for all) than that in mice immunized with HBsAg-pulsed-DCs alone. Spleen cells from mice immunized with unpulsed-DCs alone or PBS alone produced a few IFN-γ.

Spleen cells from mice immunized with uric acid alone failed to enhance the secretion of IFN-γ or inhibit the secretion of the IL-4 (Figure 2).

Cell proliferative response in spleen T cells

Fourteen days after immunization, CFSE-labeled-T cells from each mouse were re-stimulated with 10 μg/mL HBsAg or PBS for 72 h *in vitro*, and cellular proliferations were assayed by flow cytometry (Figure 3, Table 4).

A strong proliferative response to HBsAg re-stimulation was observed in T cells of mice immunized with HBsAg-pulsed-DCs and uric acid (Figure 3).

Proliferative response to HBsAg re-stimulation was also observed in T cells of mice treated with HBsAg-pulsed-DCs. Insignificant proliferation was observed in T cells of mice treated with unpulsed-DCs. No proliferation to HBsAg re-stimulation was observed in T cells of mice treated with uric acid alone or PBS (Figure 3).

PBS re-stimulation *in vitro* failed to stimulate T cell proliferation in each mouse (Table 4).

Determination of HBsAg-specific-CTL cytotoxicity

We directly determined the activity of HBsAg-specific-CTLs with an in vivo cytotoxicity assay. The extent of lysis of HBsAg-pulsed spleen cells was expressed as R-values (Figure 4) and the cytotoxicity activity of HBsAg-specific-CTLs were calculated (Table 5).

A significant strong cytotoxicity of HBsAg-specific CTLs was observed in the mice immunized with HBsAg-pulsed-DCs and uric acid; whereas immunization with

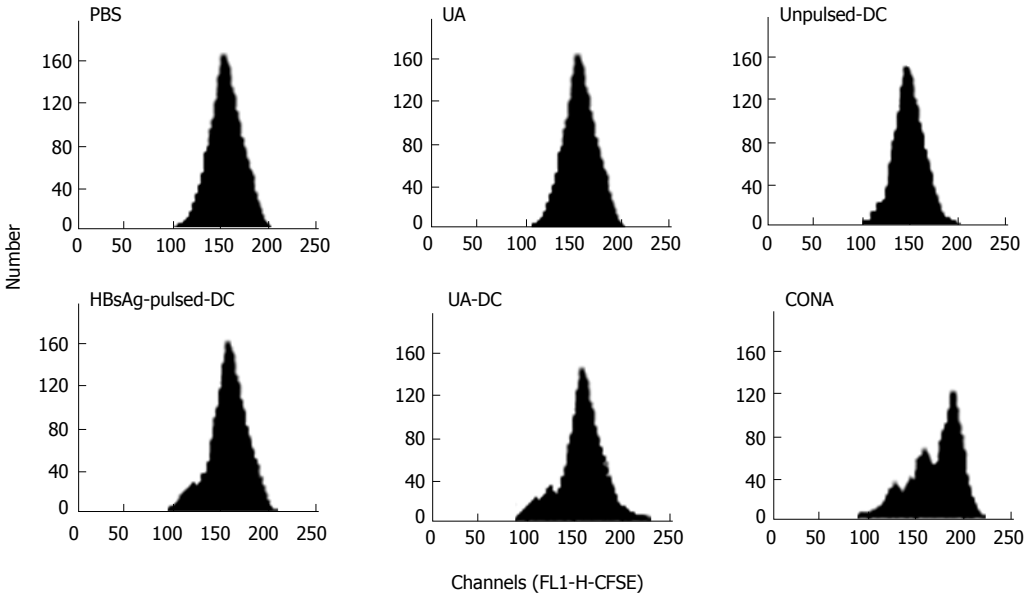

Figure 3 Celluar proliferative response in spleen T cells after stimulation with HBsAg or PBS for 72 h *in vitro*. Celluar proliferative response was estimated by flow cytometry. Spleen T cells of PBS group mice were cultured with HBsAg or PBS and ConA, used as ConA group. Histogram was produced by the modfit 3.0 software packages. These results showed were from individual mice that were representative of per experiment group.

Table 4 T cell proliferative response

Group	*n*	SI (HBsAg)	SI (PBS)
PBS	10	1.09 ± 0.028	1.062 ± 0.027
UA	10	1.17 ± 0.035	1.067 ± 0.031
Unpulsed-DC	10	1.19 ± 0.055	1.076 ± 0.035
HBsAg-pulsed-DC	10	1.34 ± 0.093[b]	1.081 ± 0.028
UA-DC	10	1.59 ± 0.156[d]	1.081 ± 0.029
ConA	10	2.53 ± 0.179[d]	2.487 ± 0.146

[b]$P \leqslant 0.01$, [d]$P \leqslant 0.001$, *vs* PBS group.

Table 5 HBsAg-specific CTL cytotoxicity (%, mean ± SD, *n* = 10)

Group	PBS	UA	Unpulsed-DC	HBsAg-pulsed-DC	UA-DC
Cytotoxicity	3.51 ± 1.14	3.52 ± 1.15	6.32 ± 2.18	27.32 ± 7.32[b]	68.63 ± 11.32[d]

[b]$P \leqslant 0.01$, [d]$P \leqslant 0.001$, *vs* PBS group.

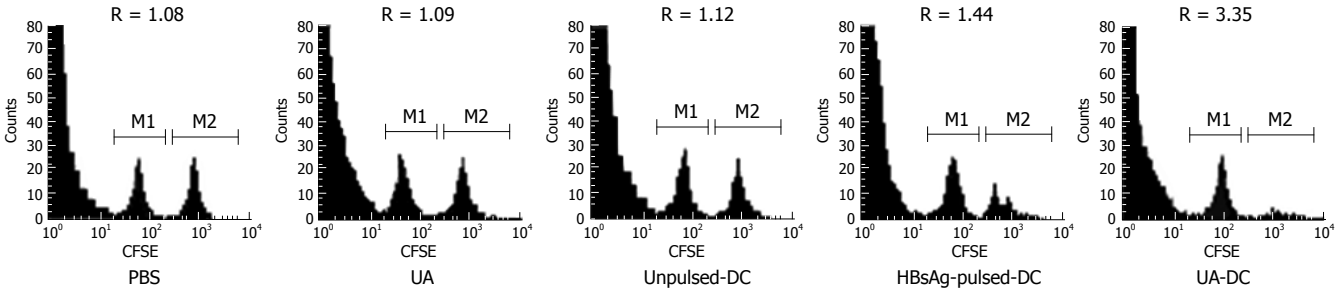

Figure 4 Analyze CTL activity against HBsAg of immunization mice by flow cytometry in vivo at 2 wk. Flow cytometric analysis of each mouse was adoptively transferred with a 1:1 mixture of Protein-pulsed ($CFSE^{high}$) and unpulsed ($CFSE^{low}$) naive mouse splenocytes 10 h previously. Then ratio between percentage of $CFSE^{low}$ cells and $CFSE^{high}$ cells were calculated. HBsAg-specific CTL cytotocity was determined (Table 5). These histogram results were from individual mice that were representative of ten experiments.

HBsAg-pulsed-DCs alone or unpulsed-DCs induced low cytotoxicities of HBsAg-specific CTLs (Table 5).

In mice immunized with uric acid 200 μg alone or PBS, R values or CTL cytotoxicity were similar ($P > 0.05$) (Figure 4). It demonstrated that no significant specific lysis was observed and immunization with uric acid 200 μg alone failed to induce HBsAg-specific CTLs.

DISCUSSION

It has been shown that T-cell mediated immune responses are very important in overcoming HBV infection[1,2] and DCs can efficiently prime T-cell response, so the development of a vaccine of DCs has attracted considerable interest[18,19].

Several studies indicated that uric acid had excellent immune adjuvant activity, which could promote the specific immune response to vaccines efficiently[9,11]. Shi and colleagues have shown that the generation of responses from specific CTL activity was significantly enhanced, when uric acid was injected into mice along with the gp120 protein of the human immunodeficiency virus (HIV)[9]. Hu and colleagues showed that eliminating uric acid, by administration of allopurinol or uricase, delayed tumor

immune rejection, whereas subcutaneous administration of uric acid enhanced the rejection process[11].

Uric acid crystals might be the biologically active form. It was shown that preformed crystals were highly stimulatory, whereas soluble uric acid was not[9-11]. The concentrations of uric acid that stimulated DCs corresponded to one at which uric acid crystals were precipitated. Injection of purified uric acid (> 70 μg /mL) was shown to boost CTL responses in spleen cells isolated from mice, which had been primed with particulate antigens, by triggering increased DC expression of the costimulatory molecules CD86 and CD80[9,11]. Allopurinol and uricase treatment, which substantially reduced plasma uric acid concentrations, was shown to markedly inhibit this T-cell priming. Uric acid crystals are known to stimulate monocytes to produce inflammatory mediators[20], and it seems likely that DCs are stimulated in a similar way.

As highly specialized antigen presenting cells (APC), DCs play a central role in antigen presentation to $CD4^+$ or $CD8^+$ T cells and allogeneic T cell proliferation[8]. It has been known that phenotypic and functional maturation was critical for DCs to activate immune responses effectively[21]. In a previous study, it was reported that uric acid could promote expression of co-stimulatory molecules (CD86, CD80) on DC surfaces[9]. Our data showed that uric acid promoted maturation of DCs ($CD83^{high}$) and up-regulated the expression of co-stimulatory molecules CD86, and IA/IE (MHC-I molecule).

DCs have a crucial role in determining the type of T cell mediated response[22,23]. IL-12 is an important immune modulatory molecule, which specifically promotes Th1 cell differentiation and suppresses Th2 cell function, and induces a Th1 cell immune response[24]. In this study, uric acid could promote DCs to secrete IL-12p70 in vitro; after combination of immunization with uric acid, in spleen cells of mice, production of IFN-γ was significantly up-regulated, and IL-4 production was down-regulated. This indicated that uric acid might enhance Th1 cell immune responses by promoting DC to secrete IL-12. And then Th1 cells can induce the proliferation of CTLs and amplification of $CD8^+$ T cell responses[25].

In addition, we showed that combination immunization of uric acid and HBsAg-pulsed-DCs could elicit a strong T cell-mediated immune response. Compared with HBsAg-pulsed-DCs vaccine alone, combination immunization elicited significantly greater T cell immune responses as evidenced by T cell proliferation to HBsAg re-stimulation, Th1 cytokine secretion and HBsAg-specific CTL responses. Uric acid may enhance the T cell immune responses by stimulating DC maturation and enhance its functions.

In hyperuricemia, it is well-known that uric acid can precipitate in the joints, where they cause gout, and/or in other tissues causing inflammation[26]. Therefore, the dose of uric acid administration is of crucial importance. In our study, the dose of uric acid was 200 μg. According to Shi and Hu *et al*[9,11], this dose of uric acid was safe and had an adjuvant effect.

We immunized both treated and control mice with 200 μg uric acid alone for two weeks. As expected, the T cell mediated immune responses were not enhanced. It demonstrated that uric acid has no adjuvant activity in the absence of exogenous antigens. It is important that no autoimmunity is induced, using uric acid as an adjuvant of vaccine.

In the murine model, combination of uric acid and HBsAg-pulsed-DCs seemed to be very effective. However, the anti-HBV effect of this vaccine strategy must be tested further in the HBV animal model.

In summary, we have demonstrated that uric acid can strongly enhance T cell immune responses to HBsAg-pulsed-DCs. We conclude that uric acid might serve as an effective adjuvant for DC vaccine against HBV infection. This strategy provides a model to develop therapeutic vaccines against HBV infection.

ACKNOWLEDGMENTS

We are grateful to Professor Zuo-Ya Li, and Guan-Xin Shen for valuable advice on ELISA.

REFERENCES

1 **Meyer zum Büschenfelde KH.** Immunopathology of chronic liver diseases. *Verh Dtsch Ges Pathol* 1995; **79**: 186-197
2 **Bertoletti A**, Gehring AJ. The immune response during hepatitis B virus infection. *J Gen Virol* 2006; **87**: 1439-1449
3 **Akbar SM**, Horiike N, Onji M. Immune therapy including dendritic cell based therapy in chronic hepatitis B virus infection. *World J Gastroenterol* 2006; **12**: 2876-2883
4 **Shimizu Y**, Guidotti LG, Fowler P, Chisari FV. Dendritic cell immunization breaks cytotoxic T lymphocyte tolerance in hepatitis B virus transgenic mice. *J Immunol* 1998; **161**: 4520-4529
5 **Chen M**, Li YG, Zhang DZ, Wang ZY, Zeng WQ, Shi XF, Guo Y, Guo SH, Ren H. Therapeutic effect of autologous dendritic cell vaccine on patients with chronic hepatitis B: a clinical study. *World J Gastroenterol* 2005; **11**: 1806-1808
6 **Santini SM**, Belardelli F. Advances in the use of dendritic cells and new adjuvants for the development of therapeutic vaccines. *Stem Cells* 2003; **21**: 495-505
7 **Sallusto F**, Lanzavecchia A. Efficient presentation of soluble antigen by cultured human dendritic cells is maintained by granulocyte/macrophage colony-stimulating factor plus interleukin 4 and downregulated by tumor necrosis factor alpha. *J Exp Med* 1994; **179**: 1109-1118
8 **Banchereau J**, Steinman RM. Dendritic cells and the control of immunity. *Nature* 1998; **392**: 245-252
9 **Shi Y**, Evans JE, Rock KL. Molecular identification of a danger signal that alerts the immune system to dying cells. *Nature* 2003; **425**: 516-521
10 **Jerome KR**, Corey L. The danger within. *N Engl J Med* 2004; **350**: 411-412
11 **Hu DE**, Moore AM, Thomsen LL, Brindle KM. Uric acid promotes tumor immune rejection. *Cancer Res* 2004; **64**: 5059-5062
12 **Inaba K**, Inaba M, Romani N, Aya H, Deguchi M, Ikehara S, Muramatsu S, Steinman RM. Generation of large numbers of dendritic cells from mouse bone marrow cultures supplemented with granulocyte/macrophage colony-stimulating factor. *J Exp Med* 1992; **176**: 1693-1702
13 **Overwijk WW**, Surman DR, Tsung K, Restifo NP. Identification of a Kb-restricted CTL epitope of beta-galactosidase: potential use in development of immunization protocols for "self" antigens. *Methods* 1997; **12**: 117-123
14 **Coles RM**, Mueller SN, Heath WR, Carbone FR, Brooks AG. Progression of armed CTL from draining lymph node to

spleen shortly after localized infection with herpes simplex virus 1. *J Immunol* 2002; **168**: 834-838
15 **Salio M**, Palmowski MJ, Atzberger A, Hermans IF, Cerundolo V. CpG-matured murine plasmacytoid dendritic cells are capable of in vivo priming of functional CD8 T cell responses to endogenous but not exogenous antigens. *J Exp Med* 2004; **199**: 567-579
16 **Lyons AB**. Analysing cell division in vivo and in vitro using flow cytometric measurement of CFSE dye dilution. *J Immunol Methods* 2000; **243**: 147-154
17 **Dixon DM**, Misfeldt ML. Proliferation of immature T cells within the splenocytes of athymic mice by Pseudomonas exotoxin A. *Cell Immunol* 1994; **158**: 71-82
18 **Böcher WO**, Dekel B, Schwerin W, Geissler M, Hoffmann S, Rohwer A, Arditti F, Cooper A, Bernhard H, Berrebi A, Rose-John S, Shaul Y, Galle PR, Löhr HF, Reisner Y. Induction of strong hepatitis B virus (HBV) specific T helper cell and cytotoxic T lymphocyte responses by therapeutic vaccination in the trimera mouse model of chronic HBV infection. *Eur J Immunol* 2001; **31**: 2071-2079
19 **Akbar SM**, Furukawa S, Hasebe A, Horiike N, Michitaka K, Onji M. Production and efficacy of a dendritic cell-based therapeutic vaccine for murine chronic hepatitis B virus carrierer. *Int J Mol Med* 2004; **14**: 295-299
20 **Landis RC**, Yagnik DR, Florey O, Philippidis P, Emons V, Mason JC, Haskard DO. Safe disposal of inflammatory monosodium urate monohydrate crystals by differentiated macrophages. *Arthritis Rheum* 2002; **46**: 3026-3033
21 **Cella M**, Sallusto F, Lanzavecchia A. Origin, maturation and antigen presenting function of dendritic cells. *Curr Opin Immunol* 1997; **9**: 10-16
22 **Santana MA**, Esquivel-Guadarrama F. Cell biology of T cell activation and differentiation. *Int Rev Cytol* 2006; **250**: 217-274
23 **Tan P**, Anasetti C, Hansen JA, Melrose J, Brunvand M, Bradshaw J, Ledbetter JA, Linsley PS. Induction of alloantigen-specific hyporesponsiveness in human T lymphocytes by blocking interaction of CD28 with its natural ligand B7/BB1. *J Exp Med* 1993; **177**: 165-173
24 **Kourilsky P**, Truffa-Bachi P. Cytokine fields and the polarization of the immune response. *Trends Immunol* 2001; **22**: 502-509
25 **Gately MK**, Wolitzky AG, Quinn PM, Chizzonite R. Regulation of human cytolytic lymphocyte responses by interleukin-12. *Cell Immunol* 1992; **143**: 127-142
26 **Gentili A**. The advanced imaging of gouty tophi. *Curr Rheumatol Rep* 2006; **8**: 231-235

S- Editor Liu Y **L- Editor** Zhu LH **E- Editor** Ma WH

PO Box 2345, Beijing 100023, China
www.wjgnet.com
wjg@wjgnet.com

World J Gastroenterol 2007 February 21; 13(7): 1067-1073
World Journal of Gastroenterology ISSN 1007-9327

CLINICAL RESEARCH

Feasibility and safety of autologous bone marrow mononuclear cell transplantation in patients with advanced chronic liver disease

Andre Castro Lyra, Milena Botelho Pereira Soares, Luiz Flavio Maia da Silva, Marcos Fraga Fortes, André Goyanna Pinheiro Silva, Augusto César de Andrade Mota, Sheilla A Oliveira, Eduardo Lorens Braga, Wilson Andrade de Carvalho, Bernd Genser, Ricardo Ribeiro dos Santos, Luiz Guilherme Costa Lyra

Andre Castro Lyra, Milena Botelho Pereira Soares, Luiz Flavio Maia da Silva, Marcos Fraga Fortes, André Goyanna Pinheiro Silva, Eduardo Lorens Braga, Wilson Andrade de Carvalho, Ricardo Ribeiro dos Santos, Luiz Guilherme Costa Lyra, Hospital Sao Rafael, Salvador, Bahia, Brazil
Andre Castro Lyra, Eduardo Lorens Braga, Luiz Guilherme Costa Lyra, Gastro-Hepatology Unit, Federal University of Bahia, Salvador, Bahia, Brazil
Milena Botelho Pereira Soares, Augusto César de Andrade Mota, Sheilla A Oliveira, Ricardo Ribeiro dos Santos, Centro de Pesquisas Goncalo Moniz, Fundacao Oswaldo Cruz, Salvador, Bahia, Brazil
Sheilla A Oliveira, Centro de Pesquisas Aggeu Magalhaes, Fundaçao Oswaldo Cruz, Recife, Pernambuco, Brazil
Bernd Genser, BGStats Consulting, Graz, Austria
Supported by IMBT-MCT/CNPq and Monte Tabor/Hospital Sao Rafael
Correspondence to: André Castro Lyra, Gastro-Hepatology Unit, Federal University of Bahia, R Socrates Guanaes Gomes 84/401, Salvador, Bahia 40296720, Brazil. aclyra@atarde.com.br
Telephone: +55-71-32357048 Fax: +55-71-32357048
Received: 2006-10-14 Accepted: 2006-11-14

Abstract

AIM: To evaluate the safety and feasibility of bone marrow cell (BMC) transplantation in patients with chronic liver disease on the waiting list for liver transplantation.

METHODS: Ten patients (eight males) with chronic liver disease were enrolled to receive infusion of autologous bone marrow-derived cells. Seven patients were classified as Child-Pugh B and three as Child-Pugh C. Baseline assessment included complete clinical and laboratory evaluation and abdominal MRI. Approximately 50 mL of bone marrow aspirate was prepared by centrifugation in a ficoll-hypaque gradient. At least of 100 millions of mononuclear-enriched BMCs were infused into the hepatic artery using the routine technique for arterial chemoembolization for liver tumors. Patients were followed up for adverse events up to 4 mo.

RESULTS: The median age of the patients was 52 years (range 24-70 years). All patients were discharged 48 h after BMC infusion. Two patients complained of mild pain at the bone marrow needle puncture site. No other complications or specific side effects related to the procedure were observed. Bilirubin levels were lower at 1 (2.19 ± 0.9) and 4 mo (2.10 ± 1.0) after cell transplantation that baseline levels (2.78 ± 1.2). Albumin levels 4 mo after BMC infusion (3.73 ± 0.5) were higher than baseline levels (3.47 ± 0.5). International normalized ratio (INR) decreased from 1.48 (SD = 0.23) to 1.43 (SD = 0.23) one month after cell transplantation.

CONCLUSION: BMC infusion into hepatic artery of patients with advanced chronic liver disease is safe and feasible. In addition, a decrease in mean serum bilirubin and INR levels and an increase in albumin levels are observed. Our data warrant further studies in order to evaluate the effect of BMC transplantation in patients with advanced chronic liver disease.

Key words: Bone marrow; Cell transplantation; Liver failure; Stem cell; Cirrhosis

Lyra AC, Soares MBP, da Silva LFM, Fortes MF, Silva AGP, Mota ACA, Oliveira SA, Braga EL, de Carvalho WA, Genser B, dos Santos RR, Lyra LGC. Feasibility and safety of autologous bone marrow mononuclear cell transplantation in patients with advanced chronic liver disease. *World J Gastroenterol* 2007; 13(7): 1067-1073

http://www.wjgnet.com/1007-9327/13/1067.asp

INTRODUCTION

Chronic liver disease may progress to end-stage liver disease (ESLD), liver failure and death. Patients with ESLD may experience serious complications such as encephalopathy, ascites and esophagogastric variceal hemorrhage. Liver transplantation is the only available therapy for patients with chronic liver failure. Because of the shortage of donated organs, up to 10%-15% of these patients die without receiving an organ in developed countries[1]. In some undeveloped countries the number of deaths on the waiting list might be greater. In some regions

of Brazil it takes an average of more than two years until liver transplantation. Therefore, alternative methods such as cell therapy are necessary to increase patient survival on the liver transplant waiting list. Several sources of stem cells have been proposed for cell therapy. Embryonic stem cells are the most potent in terms of their differentiation potential but may be oncogenic when transplanted *in vivo* and their use has been a matter of controversy because of ethical issues[2]. A number of studies during the last decade have identified cells both within and outside the liver that have properties of hepatic stem cells and might differentiate into hepatocytes or bile duct epithelial cells[3-5]. Hematopoietic tissue is most accessible and of special interest , and it has been demonstrated that bone marrow contains multipotent adult progenitor cells that can generate a variety of cell types found in other tissues[6-8].

Studies in animal models of liver diseases have demonstrated that bone marrow cell (BMC) transplantation may accelerate the liver regeneration process, reduce hepatic fibrosis and improve liver function and survival rate[9-11]. However, its mechanism is still controversial. Several studies have suggested that hematopoietic cells may generate hepatocyte-like cells, while others hypothesized that they should act mainly by fusion with hepatocytes or by paracrine effect[12-15]. Fusion between hepatocytes and hematopoietic cells produces heterokaryotic hybrid cells that initially contain the genetic elements and organelles of both cell types and may then express the hepatocyte phenotype. Several studies suggest that cytokines and growth factors produced by infused hematopoietic cells may support liver function and repair in adult animals without forming new hepatocytes from the infused cells[15]. Based on the findings from other studies that suggest improvement of liver fibrosis in experimental models of liver disease and because bone marrow cell transplantation itself is already an established treatment for hematological and oncological diseases, we conducted a clinical trial to evaluate the safety and feasibility of autologous BMC therapy in patients with chronic liver disease on the waiting list for liver transplantation.

MATERIALS AND METHODS

Subjects

The study group comprised 10 patients with chronic liver disease (8 males, 2 females, age: 24 to 70 years) on the waiting list for liver transplantation. They were enrolled to receive infusion of autologous BMC from September 2005 to January 2006. Informed written consent was obtained from all subjects. The study protocol conformed to the ethical guidelines of the 1975 Declaration of Helsinki and was approved by the Ethics Committee of Hospital São Rafael, Salvador, Brazil and by the Brazilian National Ethics Committee (CONEP). Eligible patients had all the following inclusion criteria: age range between 18-75 years, advanced chronic liver disease of different etiologies classified as Child Pugh B or C, absence of liver tumors and appropriate use of contraception method for women of child-bearing potential. Patients were excluded from the study if they had one or more of the following exclusion criteria: risk for bone marrow aspiration, sepsis, human immunodeficiency virus infection, active hepatic encephalopathy, liver tumor, history of malignant neoplasm except for non-melanoma skin cancer, decompensated heart failure, platelet count < 30000/mm^3, international normalized ratio (INR) > 2.2, renal failure (creatinine > 2.5 mg/dL), participation in other clinical trials, pregnancy or lactation.

Baseline assessment included complete clinical and laboratorial evaluation as well as abdominal magnetic resonance imaging to exclude liver tumor. Laboratory tests consisted of complete blood count, serum bilirubin levels, prothrombin time, serum blood glucose, urea, creatinine, alpha-fetoprotein, total proteins and albumin levels, serum aminotransferase concentrations, alkaline phosphatase and gamma-glutamyl transferase levels, thyroid stimulating hormone (TSH) concentrations. Patients were followed up for adverse events with clinical and laboratory evaluations on d 1, 2, 3, 7, 15, 30, 45, 60, 90, 120 after BMC transplantation.

Bone marrow cell therapy

Approximately 50 mL of bone marrow was aspirated from the iliac crest. An enriched fraction of bone marrow mononuclear cells was prepared by centrifugation of total bone marrow in a ficoll-hypaque gradient. At least 100 millions of mononuclear-enriched BMC suspended in 20 mL of saline was infused into the hepatic artery of included patients by a catheter, using the routine technique for arterial chemoembolization of liver tumors[16].

Statistical analysis

Exploratory data analysis was conducted to calculate means, standard deviations and 95% confidence intervals of measurements (laboratory tests, Child Pugh score at baseline at 1 and 4 mo). Relative mean changes at 1 and 4 mo with respect to the baseline level were calculated. To examine the development of laboratory parameters after BMC infusion individual response profiles were plotted as a function of weeks after intervention. In addition, estimates of the mean response profiles and 95% confidence intervals were obtained by calculating moving averages of patients' measurements over a period of 4 weeks and by applying linear interpolation. All statistical analyses were conducted by the statistical software package STATA (StataCorp. 2005. Stata Statistical Software: Release 8. College Station, TX: StataCorp LP).

RESULTS

The median age of the study population was 52 years (range 24-70 years). Four patients had alcoholic liver disease, 4 had chronic hepatitis C, one had chronic cholestatic liver disease and one cryptogenic cirrhosis (Table 1). Seven patients were classified as Child-Pugh B and 3 patients as Child-Pugh C. None had a liver tumor.

The number of BMCs infused in each patient is shown in Table 1. All patients were discharged 48 h after BMC infusion. Two patients complained of mild pain at the bone marrow needle puncture site. No other complications

Table 1 Clinical characteristics of studied patients and the number of transplanted autologous BMCs

Patient ID	Age (yr)	Sex	Etiology of cirrhosis	BMCs transplanted (*n*)
JWOR	49	Male	Alcohol + HCV	2.8×10^8
FMB	60	Male	Alcohol	5.2×10^8
EAS	63	Female	HCV	3.2×10^8
RNR	24	Male	Cholestatic	13.1×10^8
IAN	49	Male	Alcohol + HCV	2.6×10^8
NPA	55	Female	Cryptogenic	3.5×10^8
RBC	49	Male	Alcohol	4.8×10^8
RMV	66	Male	HCV	3.4×10^8
GAFL	70	Male	Alcohol	1.6×10^8
ABSF	40	Male	HCV	2.4×10^8

Table 2 Characteristics of the distribution of serum bilirubin, albumin and INR levels in 10 patients with chronic liver failure at baseline, 1 and 4 mo after transplantation of autologous BMCs

Bilirubin (mg/dL)	Minimum	Maximum	Mean	Median	Standard deviation	Relative mean change from baseline (%)
Baseline	1.2	4.83	2.78	2.45	1.16	
1 mo	0.5	3.56	2.19	2.28	0.91	-21
4 mo	0.72	4.16	2.1	1.87	1.04	-24
Albumin (unit)						
Baseline	2.5	4.4	3.47	3.5	0.51	
1 mo	2.9	4.5	3.44	3.25	0.52	-1
4 mo	3.1	4.8	3.73	3.6	0.51	7
INR (unit)						
Baseline	1.08	1.89	1.46	1.48	0.23	
1 mo	1.1	1.94	1.44	1.43	0.23	-1
4 mo	1.16	1.75	1.42	1.43	0.18	-3

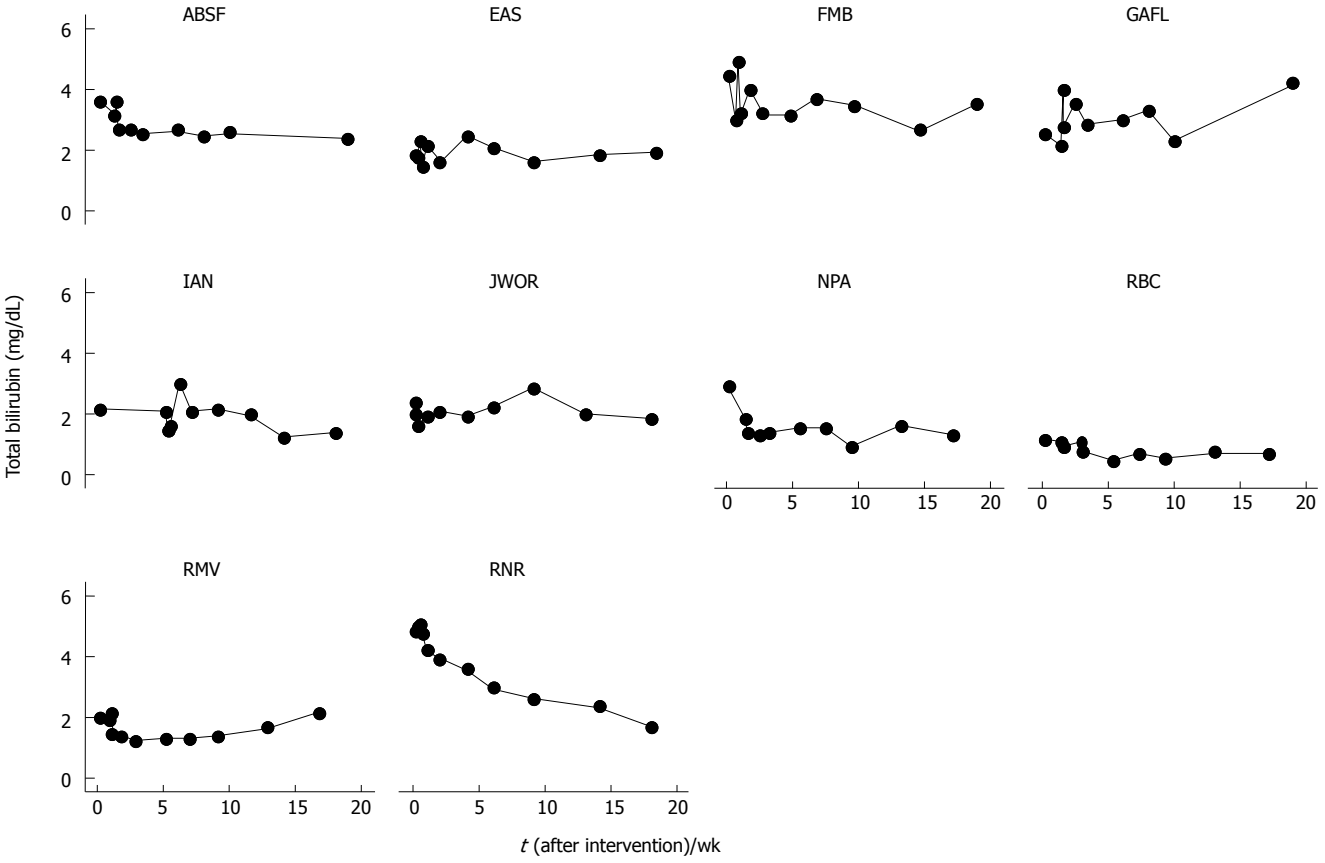

Figure 1 Serum bilirubin levels in 10 patients with chronic liver disease as a function of weeks after transplantation of autologous BMCs.

or specific side effects related to the infusion procedure were reported. A 70-year old patient with a history of previous episodes of hepatic encephalopathy developed reversible grade I encephalopathy 33 d after BMC infusion. The episode was controlled without requirement of hospitalization and was not considered an adverse event since 3 identical episodes were documented for this patient in the last year before his inclusion in the study.

Total bilirubin levels were 21% lower at 1 mo (2.19 ± 0.91) and 24% lower at 4 mo (2.10 ± 1.04) after BMC transplantation that baseline levels (2.78 ± 1.16) (Table 2). When individual response profiles were evaluated, a decrease in total bilirubin levels was observed in 7 of 10 patients after BMC transplantation (Figure 1). The mean profile of bilirubin levels after BMC infusion is shown in Figure 2.

Albumin levels were 1% lower at 1 mo (3.44 ± 0.52) and 7% higher at 4 mo after BMC infusion (3.73 ± 0.51) that baseline levels (3.47 ± 0.51) (Table 2). The analysis of individual levels showed an increase in albumin levels

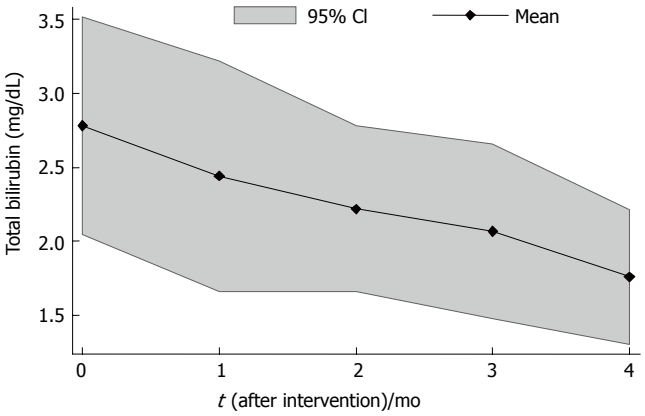

Figure 2 Mean profile of serum total bilirubin levels including a 95% confidence band in 10 patients with chronic liver disease as a function of weeks after transplantation of autologous BMCs.

in 6 patients and a reduction in 1 patient 4 mo after BMC transplantation (Figure 3). The mean profile of serum albumin levels is shown in Figure 4.

INR levels were 1% lower at 1 mo (1.44 ± 0.23) and 4% lower at 4 mo (1.42 ± 0.18) after BMC transplantation that baseline levels (1.46 ± 0.23) (Table 2). INR levels reduced in 7 patients and increased in 1 patient after BMC transplantation (Figure 5). The mean profiles of INR levels are shown in Figure 6.

The data about other relevant laboratory parameters (WBC, hemoglobin, ALT, AST, GGT, creatinine) before and after the intervention are shown in Table 3.

Table 3 Characteristics of the distribution of laboratory parameters in 10 patients with chronic liver failure at baseline, 1 and 4 mo after BMC transplantation

	Minimum	Maximum	Mean	Median	Standard deviation	Relative mean change from baseline (%)
Hemoglobin (g/dL)						
Baseline	11.30	16.90	13.16	12.2	1.90	
1 mo	9.50	16.00	12.26	11.95	1.81	-8
4 m	10.30	15.10	12.80	12.7	1.47	-3
WBC (x 10^3/mm^3)						
Baseline	2.60	5.40	3.94	4	0.97	
1 mo	2.30	5.10	3.35	2.85	1.04	-15
4 mo	2.30	6.00	3.60	3.25	1.14	-9
GGT (U/L)						
Baseline	50.00	543.00	172.20	139	147.50	
1 mo	48.00	474.20	157.20	134.5	129.00	-9
4 mo	47.00	489.67	163.50	132.5	133.25	-5
AST (U/L)						
Baseline	29.00	192.00	100.60	92.5	56.24	
1 mo	26.00	173.00	86.90	79	47.58	-14
4 mo	29.00	180.00	85.80	64	46.87	-15
ALT(U/L)						
Baseline	11.00	120.00	56.00	43	35.54	
1 mo	22.00	115.00	54.80	42.5	32.71	-2
4 mo	17.00	131.00	53.50	41	34.97	-4
Creatinine (mg/dL)						
Baseline	0.60	1.50	0.86	0.8	0.26	
1 mo	0.70	1.30	0.90	0.85	0.20	5
4 mo	0.60	1.20	0.87	0.85	0.19	1

DISCUSSION

There is an urgent need to search for alternatives to whole organ transplantation. Based on the ability of stem cells to differentiate into specific cell types according to their environment, cell transplantation has become an attractive therapeutic method for the treatment of patients with liver disease aiming, at least, at a temporary support of hepatic function until a liver becomes available for organ transplantation.

This phase I study aimed to evaluate the feasibility and safety of autologous bone marrow cell transplantation into the hepatic artery of patients with advanced chronic liver disease. In the present study, we infused BMCs into the hepatic artery using the same routine technique for arterial chemoembolization of liver tumors which is feasible and not associated with serious local side effects[16], and used the hepatic artery for cell infusion since the blood inflow to the liver could be mostly secured. Our results confirmed the feasibility and safety of BMC infusion into hepatic artery in such patients. BMC transplantation was well tolerated to all patients and only two patients complained of mild pain at the bone marrow needle puncture site. We did not detect any other side effects. The episode of reversible hepatic encephalopathy 33 d after BMC infusion in a 70-year old man with alcoholic cirrhosis was not interpreted as an adverse event related to the procedure because identical episodes were observed in the previous year.

In addition to the evaluation of safety and feasibility, our results indicated that there were alterations of liver function parameters after transplantation of autologous BMCs in patients with advanced chronic liver disease. Four months after BMC transplantation the mean serum bilirubin and INR levels decreased while the mean albumin levels increased. Of note, 7 patients had their bilirubin levels reduced while 6 patients had their albumin levels increased. The greatest reduction in the bilirubin levels was observed in a 24-year old patient (R.N.R.) with chronic cholestatic liver disease who had the highest amount of transplanted BMCs (13.1×10^8) compared to the others (Table 1). The number of transplanted BMCs was lower in patients with cirrhosis caused by HCV and in the 70-year old patient.

Recently, two phase I studies using granulocyte-colony stimulating factor (G-CSF) to mobilize BMCs in patients with chronic liver disease were conducted[17,18]. Gaia *et al*[17] evaluated the feasibility and safety of BMC mobilization in 8 patients with end stage liver cirrhosis following G-CSF administration. Mobilization (monitored by the number of CD34 + ve cells) was observed in all patients after G-CSF administration, which was well tolerated and free of adverse events. Child-Pugh score decreased by 2 or more points in four patients, increased in one patient, while it was unchanged (or decreased by less than 2 points) in three patients. Overall, the MELD score decreased from a median pre-treatment value of 17.5 (range 11-20) to 14.5

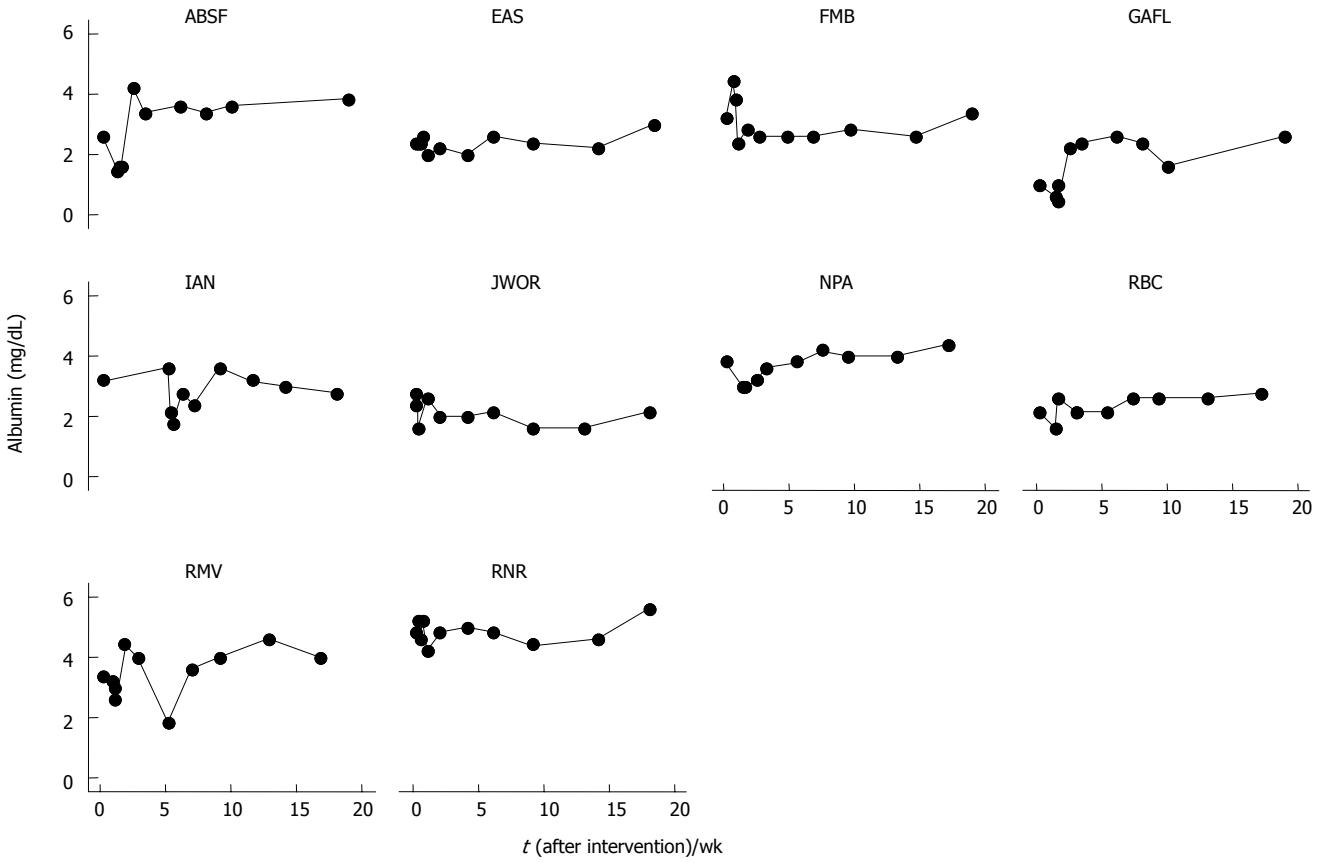

Figure 3 Serum albumin levels in 10 patients with chronic liver disease as a function of weeks after transplantation of autologous BMCs.

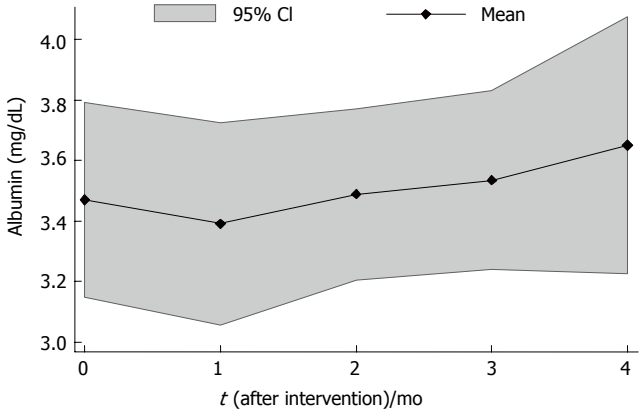

Figure 4 Mean profile of serum albumin levels including a 95% confidence band in 10 patients with chronic liver failure as a function of weeks after transplantation of autologous BMCs.

(range 9-20) at end of follow-up. In another study Gordon *et al*[18] evaluated the safety and tolerability of autologous CD34+ cell injection into five patients with liver insufficiency. Included patients were given subcutaneously 520 μg G-CSF and CD34+ cells were collected and then returned to the patients via the hepatic artery or the portal vein. No major complications or specific side effects related to the procedure were observed. Three of the five patients showed a reduction in serum bilirubin and four of five showed an increase in serum albumin. The results of these two studies appear to be in agreement with ours. The choice of utilizing purified stem cells instead of mononuclear cell fraction depends on a future comparison of the efficacy in the two cell populations. In addition, purification procedures to obtain a specific cell population increase the costs of the therapy.

Studies in animal models of liver diseases have demonstrated that bone marrow cell transplantation decreases hepatic fibrosis and improves survival rate. Sakaida *et al*[11] investigated the effect of BMC transplantation on mice with established liver fibrosis induced by carbon tetrachloride (CCl_4) administration. Four weeks after BMC transplantation, the mice had significantly reduced liver fibrosis, as assessed by hydroxyproline content in the livers, compared to mice treated with CCl_4 alone. Similar results have been observed in other studies[9,19,20]. In addition, improvement in several parameters of liver function, such as albumin and bilirubin levels and prothrombin time has been reported[8,12,21]. These experimental studies suggest that BMC infusion may be responsible for the potential beneficial effects on liver function as observed in our clinical study.

Our study was not able to evaluate the efficacy of BMC infusion in patients with liver disease due to its design. Controlled studies would be required to address this issue. Further studies are also necessary to determine the number of BMCs required for achievement of therapeutic effect, which may vary with the patient's age and the etiology of liver disease.

In summary, BMC infusion into the hepatic artery of patients with advanced chronic liver disease is safe and

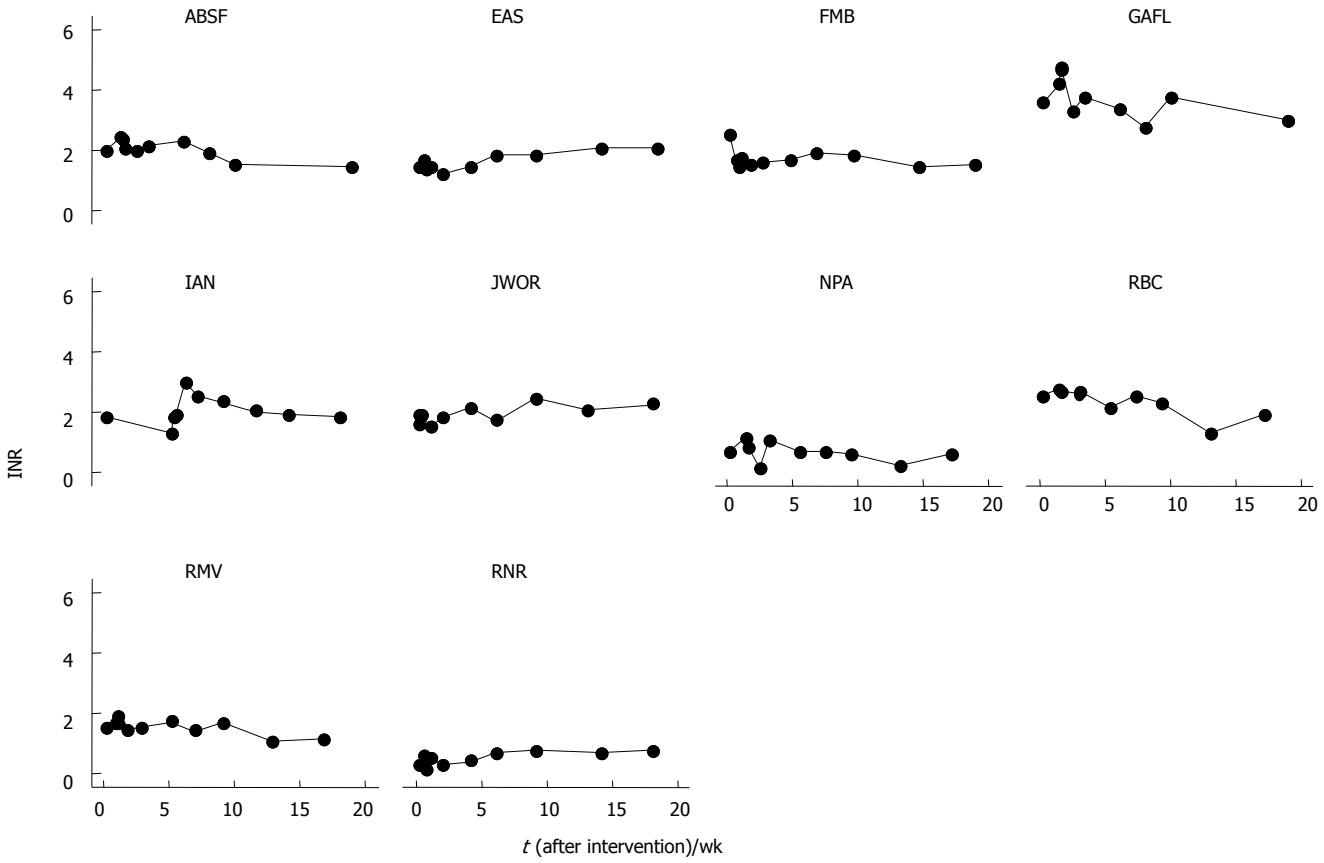

Figure 5 INR levels in 10 patients with chronic liver failure as a function of weeks after transplantation of autologous BMCs.

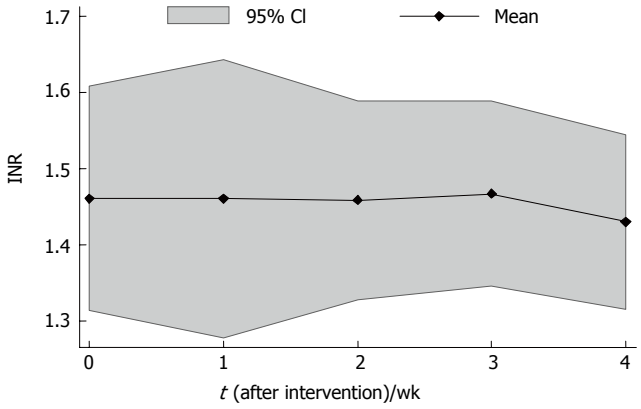

Figure 6 Mean profile of INR levels including a 95% confidence band in 10 patients with chronic liver failure as a function of weeks after transplantation of autologous bone marrow cells.

feasible. In addition, in most patients there is a decrease in mean serum bilirubin and INR levels, and an elevation of serum albumin. Our results warrant further studies in order to evaluate the effects of BMC transplantation in patients with advanced chronic liver disease.

ACKNOWLEDGMENTS

We thank Dr Patricia Seixas A Brandrao, Heleni F de Carvalho, Andrea da S Sant'Ana, Dr. Paulo Engracio M de Souza, Dr Sonia M Duarte Cathala and Dr. Gabriela Fortes for their invaluable assistance in the care of the patients and Carol O Ramos, Luciano Coelho, Amanda A. Mascarenhas and Carlos Daniel VB de Carvalho for their support in the organization of the clinical data.

REFERENCES

1 **Allen KJ**, Buck NE, Williamson R. Stem cells for the treatment of liver disease. *Transpl Immunol* 2005; **15**: 99-112
2 **Teramoto K**, Hara Y, Kumashiro Y, Chinzei R, Tanaka Y, Shimizu-Saito K, Asahina K, Teraoka H, Arii S. Teratoma formation and hepatocyte differentiation in mouse liver transplanted with mouse embryonic stem cell-derived embryoid bodies. *Transplant Proc* 2005; **37**: 285-286
3 **Haque S**, Haruna Y, Saito K, Nalesnik MA, Atillasoy E, Thung SN, Gerber MA. Identification of bipotential progenitor cells in human liver regeneration. *Lab Invest* 1996; **75**: 699-705
4 **Theise ND**, Saxena R, Portmann BC, Thung SN, Yee H, Chiriboga L, Kumar A, Crawford JM. The canals of Hering and hepatic stem cells in humans. *Hepatology* 1999; **30**: 1425-1433
5 **Yasui O**, Miura N, Terada K, Kawarada Y, Koyama K, Sugiyama T. Isolation of oval cells from Long-Evans Cinnamon rats and their transformation into hepatocytes in vivo in the rat liver. *Hepatology* 1997; **25**: 329-334
6 **Alison MR**, Poulsom R, Jeffery R, Dhillon AP, Quaglia A, Jacob J, Novelli M, Prentice G, Williamson J, Wright NA. Hepatocytes from non-hepatic adult stem cells. *Nature* 2000; **406**: 257
7 **Braun KM**, Sandgren EP. Cellular origin of regenerating parenchyma in a mouse model of severe hepatic injury. *Am J Pathol* 2000; **157**: 561-569
8 **Lagasse E**, Connors H, Al-Dhalimy M, Reitsma M, Dohse M, Osborne L, Wang X, Finegold M, Weissman IL, Grompe M. Purified hematopoietic stem cells can differentiate into hepa-

tocytes *in vivo*. *Nat Med* 2000; **6**: 1229-1234
9 **Fang B**, Shi M, Liao L, Yang S, Liu Y, Zhao RC. Systemic infusion of FLK1(+) mesenchymal stem cells ameliorate carbon tetrachloride-induced liver fibrosis in mice. *Transplantation* 2004; **78**: 83-88
10 **Sakaida I**, Terai S, Nishina H, Okita K. Development of cell therapy using autologous bone marrow cells for liver cirrhosis. *Med Mol Morphol* 2005; **38**: 197-202
11 **Sakaida I**, Terai S, Yamamoto N, Aoyama K, Ishikawa T, Nishina H, Okita K. Transplantation of bone marrow cells reduces CCl4-induced liver fibrosis in mice. *Hepatology* 2004; **40**: 1304-1311
12 **Vassilopoulos G**, Wang PR, Russell DW. Transplanted bone marrow regenerates liver by cell fusion. *Nature* 2003; **422**: 901-904
13 **Wang X**, Willenbring H, Akkari Y, Torimaru Y, Foster M, Al-Dhalimy M, Lagasse E, Finegold M, Olson S, Grompe M. Cell fusion is the principal source of bone-marrow-derived hepatocytes. *Nature* 2003; **422**: 897-901
14 **Quintana-Bustamante O**, Alvarez-Barrientos A, Kofman AV, Fabregat I, Bueren JA, Theise ND, Segovia JC. Hematopoietic mobilization in mice increases the presence of bone marrow-derived hepatocytes *via in vivo* cell fusion. *Hepatology* 2006; **43**: 108-116
15 **Thorgeirsson SS**, Grisham JW. Hematopoietic cells as hepatocyte stem cells: a critical review of the evidence. *Hepatology* 2006; **43**: 2-8
16 **Ahrar K**, Gupta S. Hepatic artery embolization for hepatocellular carcinoma: technique, patient selection, and outcomes. *Surg Oncol Clin N Am* 2003; **12**: 105-126
17 **Gaia S**, Smedile A, Omedè P, Olivero A, Sanavio F, Balzola F, Ottobrelli A, Abate ML, Marzano A, Rizzetto M, Tarella C. Feasibility and safety of G-CSF administration to induce bone marrow-derived cells mobilization in patients with end stage liver disease. *J Hepatol* 2006; **45**: 13-19
18 **Gordon MY**, Levicar N, Pai M, Bachellier P, Dimarakis I, Al-Allaf F, M'Hamdi H, Thalji T, Welsh JP, Marley SB, Davies J, Dazzi F, Marelli-Berg F, Tait P, Playford R, Jiao L, Jensen S, Nicholls JP, Ayav A, Nohandani M, Farzaneh F, Gaken J, Dodge R, Alison M, Apperley JF, Lechler R, Habib NA. Characterization and clinical application of human CD34+ stem/progenitor cell populations mobilized into the blood by granulocyte colony-stimulating factor. *Stem Cells* 2006; **24**: 1822-1830
19 **Zhao DC**, Lei JX, Chen R, Yu WH, Zhang XM, Li SN, Xiang P. Bone marrow-derived mesenchymal stem cells protect against experimental liver fibrosis in rats. *World J Gastroenterol* 2005; **11**: 3431-3440
20 **Oyagi S**, Hirose M, Kojima M, Okuyama M, Kawase M, Nakamura T, Ohgushi H, Yagi K. Therapeutic effect of transplanting HGF-treated bone marrow mesenchymal cells into CCl4-injured rats. *J Hepatol* 2006; **44**: 742-748
21 **Jang YY**, Collector MI, Baylin SB, Diehl AM, Sharkis SJ. Hematopoietic stem cells convert into liver cells within days without fusion. *Nat Cell Biol* 2004; **6**: 532-539

S- Editor Wang J **L- Editor** Wang XL **E- Editor** Ma WH

PO Box 2345, Beijing 100023, China
www.wjgnet.com
wjg@wjgnet.com

World J Gastroenterol 2007 February 21; 13(7): 1074-1078
World Journal of Gastroenterology ISSN 1007-9327

RAPID COMMUNICATION

Hepatitis C risk assessment, testing and referral for treatment in urban primary care: Role of race and ethnicity

Stacey B Trooskin, Victor J Navarro, Robert J Winn, David J Axelrod, A Scott McNeal, Maricruz Velez, Steven K Herrine, Simona Rossi

Stacey B Trooskin, Victor J Navarro, Maricruz Velez, Steven K Herrine, Simona Rossi, Division of Gastroenterology and Hepatology, Thomas Jefferson University, Philadelphia, PA 19107, United States
Robert J Winn, Department of Family Medicine, Thomas Jefferson University, Philadelphia, PA 19107, United States
David J Axelrod, Division of Internal Medicine, Thomas Jefferson University, Philadelphia, PA 19107, United States
A Scott McNeal, Delaware Valley Community Health Inc., Philadelphia, PA 19107, United States
Supported by an educational grant from Roche
Correspondence to: Dr. Victor Navarro, Thomas Jefferson University, Division of Gastroenterology and Hepatology, 132 South 10th Street, Suite 480 Main Building, Philadelphia, PA 19107, United States. victor.navarro@jefferson.edu
Telephone: +1-215-9555271
Received: 2006-11-15 Accepted: 2007-01-26

Abstract

AIM: To determine rates of hepatitis C (HCV) risk factor ascertainment, testing, and referral in urban primary care practices, with particular attention to the effect of race and ethnicity.

METHODS: Retrospective chart review from four primary care sites in Philadelphia; two academic primary care practices and two community clinics was performed. Demographics, HCV risk factors, and other risk exposure information were collected.

RESULTS: Four thousand four hundred and seven charts were reviewed. Providers documented histories of injection drug use (IDU) and transfusion for less than 20% and 5% of patients, respectively. Only 55% of patients who admitted IDU were tested for HCV. Overall, minorities were more likely to have information regarding a risk factor documented than their white counterparts (79% *vs* 68%, $P < 0.0001$). Hispanics were less likely to have a risk factor history documented, compared to blacks and whites ($P < 0.0001$). Overall, minorities were less likely to be tested for HCV than whites in the presence of a known risk factor (23% *vs* 35%, $P = 0.004$). Among patients without documentation of risk factors, blacks and Hispanics were more likely to be tested than whites (20% and 24%, *vs* 13%, $P < 0.005$, respectively).

CONCLUSION: (1) Documentation of an HCV risk factor history in urban primary care is uncommon, (2) Racial differences exist with respect to HCV risk factor ascertainment and testing, (3) Minority patients, positive for HCV, are less likely to be referred for subspecialty care and treatment. Overall, minorities are less likely to be tested for HCV than whites in the presence of a known risk factor.

Key words: Hepatitis C; Minority groups; Urban health; Primary health care; Risk assessment

Trooskin SB, Navarro VJ, Winn RJ, Axelrod DJ, McNeal AS, Velez M, Herrine SK, Rossi S. Hepatitis C risk assessment, testing and referral for treatment in urban primary care: Role of race and ethnicity. *World J Gastroenterol* 2007; 13(7): 1074-1078

http://www.wjgnet.com/1007-9327/13/1074.asp

INTRODUCTION

Several studies have suggested that hepatitis C (HBV) manage-ment is suboptimal in primary care settings[1-5]. In fact, only 59% of primary care physicians (PCPs) reported asking patients about HCV risk factors[3]. A similar conclusion was made by another study which found that 46% and 62% of physicians reported that they routinely asked patients about a history of blood transfusion and injection drug use, respectively[4]. Shehab reported that HCV testing is rarely initiated in primary care clinics based on physician identified risk factors such as transfusion prior to 1992 or a history of injection drug use[1]. Similar studies among urban primary care practices, comprising patients at highest risk for exposure to HCV risk factors, have not been reported. Such a study would be important to better assess the feasibility of implementing wide scale risk assessment, testing, and treatment strategies.

The purpose of this retrospective cohort study is to assess the rates of HCV risk factor ascertainment, testing and referral for treatment in urban primary care practices, with particular attention to the effect of race and ethnicity as determined by systematic review of the medical records.

MATERIALS AND METHODS

A retrospective chart review was conducted in four

Table 1 Population demographics

Primary care practice	Total	Mean age	Gender (% male)	Insured (%)	Race				
					White (%)	Black (%)	Hisp (%)	OTH (%)	Unknown (%)
Clinic #1	1182	40	34	62	1	4	84	< 0.5	11
Clinic #2	948	41	62	57	4	65	7	1	24
Clinic #3	1089	42	34	95	26	37	2	5	31
Clinic #4	1188	48	43	98	45	22	2	6	26

urban primary care clinic sites in Philadelphia. These sites included two federally qualified health clinics serving predominantly minority populations and two university-based primary care practices; a family medicine practice and an internal medicine practice. Each of the four study sites is unique in the population that it serves. Clinic #1 is a community clinic which serves a predominantly Hispanic population (84%), comprised of mostly female patients (66%); in 2005 this clinic served approximately 15 000 patients. Clinic #2 is a community clinic which serves a predominantly black population (65%-70%); this clinic served approximately 7000 patients in 2005. The majority of the patients attending the two community clinics are either uninsured, or covered by a Medicaid HMO. The two university-based practices serve racially diverse populations. Approximately 60% of the patients attending the Family Medicine university-based practice (clinic #3, patient population served in 2005, 23 000) are black. The majority of the patients attending the practice have traditional insurance. Those with Medicare coverage and the uninsured make up a small percentage of the patient population, 6% and 5% respectively. Approximately 45% of the patients attending the Internal Medicine university-based practice (patients served in 2005, 21 000) are black (clinic #4), and the majority of the patients attending the practice have traditional insurance.

Random charts were selected at systematic intervals, based upon practice size, so that a total of approximately 1000 charts were reviewed from each practice. The number of charts required was calculated by taking into account the prevalence of risk factors among minority and non-minority subjects, the rate of risk factors recognized, the proportion of persons at risk screened for HCV and of those who tested positive. All these assumptions were derived from previous studies and from the authors' experience.

All patient visits in each selected chart were reviewed by a team of trained chart reviewers. No identifying information was collected. Data were available dating back to the patients' first visit, with a mean of 3.6 years (standard deviation 4.9 years) prior to the patients' most recent documented visit. Specific data collected included sex, age, race/ethnicity, as well as documentation of HCV risk factors. An HCV risk factor was broadly defined as any potential exposure to HCV; these included injection drug use, blood transfusion prior to 1992, percutaneous exposure as in the case of an exposed health care worker), non-injection drug use, tattoos, body piercing, history of sexually transmitted diseases, incarceration, and unprotected sex[9]. When documentation of an HCV risk factor was identified, it was determined if HCV testing was ordered and if the patient was referred for subspecialty care.

Statistical analysis

Data were collected using a standardized data collection instrument. All chart reviewers were trained and accompanied by an investigator. An investigator (SBT, VJN) re-reviewed at least 10% of all charts at random to check for accuracy. Trained data entry personnel entered the data into data management software (Microsoft Access). All data were analyzed using SAS v 9.14. Descriptive statistics and frequency tables were generated. Chi-square tests and logistic regression were used to assess statistical differences.

RESULTS

Study cohort

The total number of charts reviewed was 4407. One thousand one hundred eighty two charts were sampled from clinic #1; 948 charts from clinic #2; and 1089 from clinic #3 and 1 188 charts were reviewed from clinic #4 (Table 1). In order to facilitate a comparison of HCV management practices between races, we included only those charts in which race information was recorded. Approximately 23% of the charts reviewed did not include the race or ethnicity of the patient with clinic #1 having the lowest percentage of undocumented race/ethnicity (11%). Clinic #2 was missing approximately 24% of race/ethnicity documentation as compared to 26% for the Internal Medicine university-based practice and 31% for the Family Medicine university-based practice. Of the 3 413 charts with documented race/ethnicity which were included in the analysis, 1333, 1103, and 846 were reported as black, Hispanic, and white patients, respectively. Racial/ethnic groups were similar with respect to the average age of patients at the time of review (mean age 43). Forty-four percent of blacks were male, as compared to 34% of Hispanics and 45% of whites.

Documentation rate of HCV risk factors and the effect of race/ethnicity

Primary care providers documented a history (positive or negative) of IDU and/ or transfusion, arguably the most important risk factors for HCV acquisition, for 12% and 2% of patients, respectively. Only 0.48% (n = 21) of the total study population (n = 4407) were documented as having a positive history of transfusion prior to 1992. A history of percutaneous exposure as a health care

Table 2 Prevalence of HCV risk factors documented in patient charts by race/ethnicity

HCV risk factor	Black *n* = 1333		Hispanic *n* = 1103		White *n* = 846	
	Info available *n* (%)	With risk factor *n* (%)	Info available *n* (%)	With risk factor *n* (%)	Info available *n* (%)	With risk factor *n* (%)
IDU	241 (18)	54 (22)	48 (4.4)[e]	19 (40)	134 (16)	11 (8.2)
Transfusion	22 (1.7)	7 (32)	11 (1.0)	2 (18)	29 (3.4)	9 (31)
HCV needle stick	1 (0.1)	1 (100)	2 (0.2)	2 (100)	1 (0.1)	1 (100)
History of drug use	957 (72)[a]	359 (38)[b,c]	820 (74)[a]	94 (11)	535 (63)	53 (10)
History of STD	517 (39)[b]	350 (68)[b,c]	550 (50)[b]	185 (34)	164 (19)	53 (32)
History of HIV testing	452 (34)[b]	390 (86)	396 (36)[b]	305 (77)[a]	119 (14)	108 (91)
Tattoos	15 (1.1)	11 (73)	2 (0.2)	1 (50)	21 (2.5)	17 (80)
Piercing	2 (0.2)	0 (0)	1 (0.1)	0 (0)	1 (0.1)	1 (100)
Prostitution	9 (0.7)	6 (67)	3 (0.3)	2 (67)	1 (0.12)	1 (100)
Incarceration	38 (2.8)	36 (95)	12 (1.1)	12 (100)	4 (0.5)	3 (75)

[a]$P < 0.05$ *vs* whites; [c]$P < 0.05$ *vs* Hispanics; [b]$P < 0.001$ *vs* whites; [e]$P < 0.05$ *vs* blacks and whites.

worker was rarely specified ($n = 4$). Patients' histories of prostitution, incarceration, tattoos or body piercing were recorded for less than 2% of patients. Ascertainment of a history of non-injection drug use and sexually transmitted diseases occurred for 67% and 34% of patients, respectively (Table 2).

When documentation of HCV risk factor ascertainment was compared between different races/ethnicities, overall, minorities were more likely to have information regarding a risk factor documented than their white counterparts (79% *vs* 68%, $P < 0.0001$). Hispanics were much less likely to have had a history of IDU (positive or negative) documented than other groups; (4.4% ascertainment rate compared with 18% and 16% for blacks and whites, respectively) ($P < 0.0001$). Blacks and Hispanics were more likely to have had a documented history of non-IDU (72% and 74%, respectively) as compared to whites (63%, $P < 0.05$). Hispanics were more likely to have a chart entry regarding sexually transmitted diseases than were blacks (50% *vs* 39%) and blacks were more likely to have this history documented than whites (39% *vs* 19%, $P < 0.001$). Statistical comparisons were not used to assess differences between racial/ethnic groups for prostitution, incarceration, tattoos or body piercing due to the low rate of ascertainment.

Among patients who denied IDU, higher rates of other risk factors were reported among minorities. For example, 64% (29/45) of the minorities who denied IDU admitted non-injection drug use as compared to 31% (5/16) of the whites ($P < 0.05$). In addition, 25% of minorities (55/216) who denied IDU had a history of an STD documented as compared to 5% (7/123) of whites ($P < 0.05$).

Overall, females (74%, $n = 2\ 469$) were more likely than males (71%, $n = 1\ 818$) to have information regarding a risk factor history (positive or negative history) documented in the chart ($P = 0.0091$). However, among those individuals who had risk factor information documented, males (54%) were more likely to have a positive risk factor history than females (30%) ($P < 0.0001$). Among individuals with a documented positive HCV risk factor, there was no difference in the percentage of males and females tested for HCV ($P = 0.176$).

The odds of having documented information regarding HCV risk factors decreased by 1.4% with each additional year of age ($P < 0.0001$). Among those individuals who had risk factor information documented ($n = 3113$), the odds of having a positive risk factor history decreased by 1.7% with each additional year of age ($P < 0.0001$). Among individuals with a documented positive HCV risk factor ($n = 1158$), the odds of being tested increased by 1.3% with each additional year of age ($P = 0.025$).

HCV testing

Overall, minorities were less likely to be tested for HCV than whites in the presence of a known risk factor (23% *vs* 35%, $P = 0.004$). Of the 12% of patients for whom information regarding IDU was recorded ($n = 531$), 19% admitted this behavior. Of this group (blacks $n = 54$, Hispanics $n = 19$, whites $n = 11$), 55%-58% were tested for HCV, with no differences among the race or ethnic groups. Of the 21 patients documented as having a history of blood transfusion prior to 1992, approximately 67% were tested for HCV. Because the rate of documentation was so low for a history of transfusion, comparisons between racial/ethnic groups could not be made with respect to the rate of testing in the presence of this risk factor. Thirty-six percent of patients with tattoos and 50% of individuals with body piercing and with no identified other risk factor were tested for HCV (Table 3). Of those patients with a history of incarceration, 30% were tested. In the absence of IDU or prior blood transfusion, a history of sexually transmitted disease, non-injection drug use, engaging in sexual activity with or as a commercial sex worker, or a history of HIV testing were associated with testing rates of 19%, 22%, 33% and 24%, respectively. Due to the low rate of documentation of risk factors by the physicians, it was not possible to compare rates of testing between racial groups for piercing, incarceration, prostitution, and tattoos.

Among patients who denied risk factors when asked,

Table 3 Rates of testing among individuals with a documented non conventional HCV risk factor but no conventional risk factors

	Number with only non-conventional risk factors[1]	Tested (%)
Tattoos	33	36.4
Piercing	4	50.0
History of drug use	513	21.6
Prostitution	6	33.3
Incarceration	60	30.0
History of STD	706	19.4
History of HIV testing	903	24.1

[1]Patient may be included in more than one category.

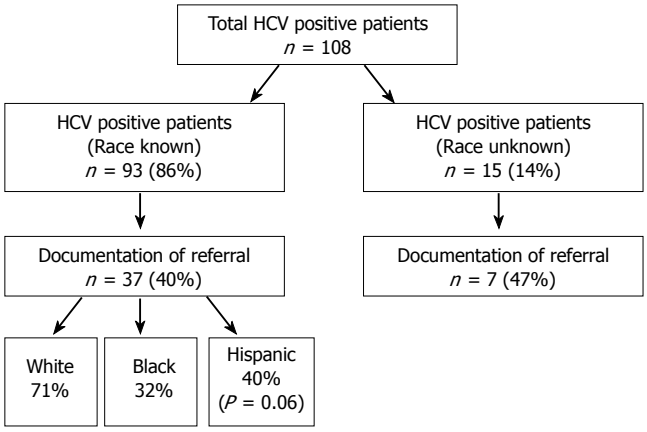

Figure 1 HCV referral practices.

the proportion tested for HCV was higher for blacks (20%, $n = 187$) and Hispanics (24%, $n = 29$) than for whites (13%, $n = 123$) ($P < 0.05$).

Overall, seven percent of patients in whom no risk factors were documented ($n = 3212$) were still tested for HCV. Hispanics (9.9%, $n = 848$) were more likely to be tested than both blacks (5.4%, $n = 737$) and whites (6.4%, $n = 733$) in the absence of any documented risk factor.

HCV referral practices

Of the 93 patients who were identified as being HCV positive (and for whom race/ethnicity was known), 37 (40%) had chart documentation of referral to a specialist. Of this group, 71% of white patients were referred, as compared to 40% of Hispanics ($P = 0.06$), and 32% of blacks (Figure 1). Among HCV positive patients whose race was not known ($n = 15$), 47% were referred to a specialist. Of these, 10 patients were from clinic #2, which serves a predominantly black population.

DISCUSSION

Overall, minorities were more likely to have information regarding HCV risk factors documented than their white counterparts. However, the ascertainment of IDU and blood transfusion prior to 1992, arguably the most important risk factors for HCV acquisition, was low, 12% and 1.8% respectively. Perhaps the greatest significance of these findings is that even in populations with expected high rates of risk factors, recommended management practices for risk factor ascertainment are infrequently followed[9].

Overall, minorities were less likely to be tested for HCV than whites in the presence of a known risk factor. The underlying reason for this is unknown but deserves further study. Rates of testing among patients who had a documented history of IDU or blood transfusion prior to 1992 were low, regardless of race. This finding demonstrates that recommendations regarding HCV testing practices are infrequently followed[9-12]. The reason for low rates of testing among minorities in the presence of a risk factor is likely to be multifactorial. Practitioners may be more likely to ask minority patients about risk behaviors, given an implicit understanding of the surrounding urban community and the epidemiology of HCV, but less likely to test if the provider feels that the patient would not be a candidate for treatment or if the patient would not opt for treatment.

Minorities were more likely than non-minorities to be tested for HCV in the absence of a recorded risk factor, or if such a history was denied. This finding could be explained by undocumented factors which might have led to testing, or the more frequent documentation of non-intravenous drug use in this population, which might be, in turn, interpreted as a risk for the acquisition of HCV. Unfortunately, medical record information did not allow us to more carefully assess these factors.

The rate of referral among patients who tested positive for HCV differed among the race groups. Specifically, minorities were less likely than whites to be referred for subspecialty evaluation. Although of potential significance, this finding may have been affected by missing referral information, local resources, as well as patient and provider perception of the need for and benefit of treatment.

Our study is limited in scope due to several factors. We performed the study in a relatively small number of practices which may reflect idiosyncrasies of a few treating physicians or have been affected by patient demographics which were unique to the local area. Moreover, we could not assess whether cultural, educational, or economic factors affected risk assessment and testing practices. Despite these limitations, the low rate of testing in a potentially high-risk population has serious implications; any strategy to test patients at risk for acquisition of HCV must be preceded by a plan that increases the rate of risk factor ascertainment in primary care.

Therefore, recommendations must be developed for physicians to increase the rate of identification of individuals who may have been exposed to HCV in the past as well as appropriate testing. Although primary care physicians are responsible for screening for multiple health problems during a routine health care visit, the benefits of identifying HCV risk factors and infection must not be overlooked. Risk factor screening and identification allows for patients to be educated regarding the risks of injection drug use and needle sharing. Appropriate testing and diagnosis of HCV allows for the patient to be evaluated

for treatment and receive counseling regarding alcohol cessation. In addition to physician education, patient education campaigns must also be developed to increase patient compliance with testing recommendations made by their physicians.

ACKNOWLEDGMENTS

The authors thank Sidney Cohen, MD for his assistance in preparation of the manuscript.

COMMENTS

Background

The increasing prevalence of hepatitis C virus (HCV) infection in the United States makes it an important challenge for primary care physicians (PCPs) and subspecialists. There are several potential benefits to diagnosing hepatitis C in a primary care setting.Diagnosis provides the patient with the opportunity to be counseled regarding behaviors that may transmit the infection to others such as sharing needles in the context of IDU. Diagnosis also allows the health care provider to educate the patient regarding behaviors that may hasten the progression of liver disease such as alcohol intake. Furthermore, early diagnosis allows the patient to be provided with appropriate preventive services such as hepatitis A and B vaccines. Lastly, early diagnosis allows the patient to be evaluated for hepatitis C therapy at a time when treatment may be more effective; prior to progression to fibrotic liver disease.

Research frontiers

Several studies have suggested that hepatitis C management is suboptimal in primary care settings. The purpose of this retrospective cohort study is to assess the rates of HCV risk factor ascertainment, testing and referral for treatment in urban primary care practices, with particular attention to the effect of race and ethnicity as determined by systematic review of the medical records.

Related publications

This publication is the first to result from our studies related to HCV management in primary care settings. Three additional manuscripts are in preparation. However, there are several articles, cited throughout this manuscript, from other investigators, that can provide additional information related to HCV management in primary care.

Innovations and breakthroughs

Very few studies have examined hepatitis C risk assessment, testing and referral for treatment in urban primary care settings. Moreover, no studies have examined racial differences within these practices. The findings indicate that (1) Documentation of an HCV risk factor history in urban primary care is uncommon, (2) Racial differences exist with respect to HCV risk factor ascertainment and testing, and (3) Minority patients, positive for HCV, were less likely to be referred for subspecialty care and treatment. Overall, minorities were less likely to be tested for HCV than whites in the presence of a known risk factor.

Applications

The findings presented may be applied in a number of settings where advances in the identification, testing and referral of primary care patients, specifically racial and ethnic minorities are sought. The results of this study may be of interest to epidemiologists and other public health professionals. The findings of this study address a deficit in the literature related to HCV in minorities and provide the background for future studies and intervention endeavors aimed at improving HCV identification and management in primary care settings.

Peer review

The results show that risk factors are often missed and minority patients are less likely to be tested for HCV and to be referred for treatment. The authors conclude that, although their investigation has some selection biases, the results indicate the existence of a consistent reservoir of infection in subgroups of patients, [specifically] black and Hispanic. Although "expected" given the characteristics of the population selected, the results are interesting.

REFERENCES

1 **Shehab TM**, Orrego M, Chunduri R, Lok AS. Identification and management of hepatitis C patients in primary care clinics. *Am J Gastroenterol* 2003; **98**: 639-644
2 **Shehab TM**, Sonnad SS, Jeffries M, Gunaratnum N, Lok AS. Current practice patterns of primary care physicians in the management of patients with hepatitis C. *Hepatology* 1999; **30**: 794-800
3 **Shehab TM**, Sonnad SS, Lok AS. Management of hepatitis C patients by primary care physicians in the USA: results of a national survey. *J Viral Hepat* 2001; **8**: 377-383
4 **Navarro VJ**, St Louis TE, Bell BP. Identification of patients with hepatitis C virus infection in New Haven County primary care practices. *J Clin Gastroenterol* 2003; **36**: 431-435
5 **Nicklin DE**, Schultz C, Brensinger CM, Wilson JP. Current care of hepatitis C-positive patients by primary care physicians in an integrated delivery system. *J Am Board Fam Pract* 1999; **12**: 427-435
6 **Frischer M**, Leyland A, Cormack R, Goldberg DJ, Bloor M, Green ST, Taylor A, Covell R, McKeganey N, Platt S. Estimating the population prevalence of injection drug use and infection with human immunodeficiency virus among injection drug users in Glasgow, Scotland. *Am J Epidemiol* 1993; **138**: 170-181
7 **Wolf RC**, Case P, Pagano M. Estimation of the prevalence of injection drug use in greater Boston in 1993. *J Psychoactive Drugs* 1998; **30**: 21-24
8 **Shehab TM**, Sonnad S, Gebremariam A, Schoenfeld P. Knowledge of hepatitis C screening and management by internal medicine residents: trends over 2 years. *Am J Gastroenterol* 2002; **97**: 1216-1222
9 **Recommendations for prevention and control of hepatitis C virus (HCV) infection and HCV-related chronic disease.** Centers for Disease Control and Prevention. *MMWR Recomm Rep* 1998; **47**: 1-39
10 **Management of hepatitis C.** *NIH Consens Statement* 1997; **15**: 1-41
11 **Screening for hepatitis C virus infection in adults: recommendation statement.** *Ann Intern Med* 2004; **140**: 462-464
12 **Strader DB**, Wright T, Thomas DL, Seeff LB. Diagnosis, management, and treatment of hepatitis C. *Hepatology* 2004; **39**: 1147-1171

S- Editor Liu Y **L- Editor** Zhu LH **E- Editor** Ma WH

PO Box 2345, Beijing 100023, China
www.wjgnet.com
wjg@wjgnet.com

World J Gastroenterol 2007 February 21; 13(7): 1079-1084
World Journal of Gastroenterology ISSN 1007-9327

RAPID COMMUNICATION

A new oral formulation for the release of sodium butyrate in the ileo-cecal region and colon

Aldo Roda, Patrizia Simoni, Maria Magliulo, Paolo Nanni, Mario Baraldini, Giulia Roda, Enrico Roda

Aldo Roda, Maria Magliulo, Paolo Nanni, Department of Pharmaceutical Sciences, University of Bologna, Via Belmeloro 6, Bologna 40126, Italy
Patrizia Simoni, Mario Baraldini, Giulia Roda, Enrico Roda, Department of Internal Medicine and Gastroenterology, University of Bologna, via Massarenti 9, Bologna 40126, Italy
Correspondence to: Professor Aldo Roda, Department of Pharmaceutical Sciences, University of Bologna, Via Belmeloro 6, Bologna 40126, Italy. aldo.roda@unibo.it
Telephone: +39-51-343398 Fax: +39-51-343398
Received: 2006-11-10 Accepted: 2007-01-22

Abstract

AIM: To develop a new formulation with hydroxy propyl methyl cellulose and Shellac coating for extended and selective delivery of butyrate in the ileo-caecal region and colon.

METHODS: One-gram sodium butyrate coated tablets containing ^{13}C-butyrate were orally administered to 12 healthy subjects and 12 Crohn's disease patients and the rate of ^{13}C-butyrate absorption was evaluated by $^{13}CO_2$ breath test analysis for eight hours. Tauroursodeoxycholic acid (500 mg) was co-administered as a biomarker of oro-ileal transit time to determine also the site of release and absorption of butyrate by the time of its serum maximum concentration.

RESULTS: The coated formulation delayed the ^{13}C-butyrate release by 2-3 h with respect to the uncoated tablets. Sodium butyrate was delivered in the intestine of all subjects and a more variable transit time was found in Crohn's disease patients than in healthy subjects. The variability of the peak $^{13}CO_2$ in the kinetic release of butyrate was explained by the inter-subject variability in transit time. However, the coating chosen ensured an efficient release of the active compound even in patients with a short transit time.

CONCLUSION: Simultaneous evaluation of breath $^{13}CO_2$ and tauroursodeoxycholic acid concentration-time curves has shown that the new oral formulation consistently releases sodium butyrate in the ileo-cecal region and colon both in healthy subjects and Crohn's disease patients with variable intestinal transit time. This formulation may be of therapeutic value in inflammatory bowel disease patients due to the appropriate release of the active compound.

Key words: Sodium butyrate; Inflammatory bowel diseases; Ulcerative colitis; Crohn's disease; Controlled release formulation; Pharmacokinetics; Stable isotope; Breath test

Roda A, Simoni P, Magliulo M, Nanni P, Baraldini M, Roda G, Roda E. A new oral formulation for the release of sodium butyrate in the ileo-cecal region and colon. *World J Gastroenterol* 2007; 13(7): 1079-1084

http://www.wjgnet.com/1007-9327/13/1079.asp

INTRODUCTION

Butyric acid, a short chain fatty acid, is the main colonic bacterial product of non-starch polysaccharides[1]. Impaired butyric acid metabolism (usually as butyrate species) has been implicated in the development of ulcerative colitis (UC)[2] but there are conflicting data regarding its role in the pathogenesis of UC[3-11]. Large bowel mucosa biopsy specimens from quiescent UC patients have also shown reduced oxidation of butyrate but not of glucose and glutamine, the two other major fuel sources for colonic epithelium[3]. *In vitro* studies conducted in terminal ileal mucosa biopsy specimens from UC patients support this concept[4]. A study on colonic sodium butyrate (NaB) metabolism using ^{14}C-butyrate rectal instillation and $^{14}CO_2$-breath test in patients affected by extensive UC showed a reduction in NaB oxidation, which returned to normal on remission[10]. The authors concluded that while impaired NaB metabolism is unlikely to be a primary cause of UC, impairment of short chain fatty acid metabolism by coloncytes may be a pathogenic factor. Another study indicated that in quiescent UC patients, the rate of NaB metabolism is not impaired[11].

It has recently been demonstrated that NaB exhibits anti-inflammatory properties as documented by a strong inhibition of interleukin (IL)-12 production by suppressing both IL-12p35 and IL-12p40 mRNA accumulation, and enhances IL-10 secretion in Staphylococcus aureus cell-stimulated human monocytes[12]. Investigation of the effects of NaB on some G1 phase-related proteins in a colon carcinoma cell line (HT29) has revealed another potential pharmacological property, since NaB is able to reduce cyclin D1 and p53 level in a dose-dependent

fashion and to suppress cell growth[13]. Thus, the lack of NaB in diets poor in carbohydrates could lead to clinically relevant functional alterations. In vivo, the growth inhibitory effects of NaB on colon cancer cells appear to be somewhat less marked[14,15].

Some clinical applications of NaB treatment have already been successfully evaluated. NaB enemas seem to provide an effective treatment for acute radiation proctitis, accelerating the healing process[16,17]. Oral co-administration of NaB and mesalazine in patients with active UC seems to improve the efficacy of mesalazine monotherapy[18,19].

These considerations prompted us to develop a new oral formulation in which NaB is released in the terminal ileum and colon, the target of its potential pharmacological activity[19].

The main problem in the development of controlled release formulation is to extrapolate *in vitro* release data to those achieved during *in vivo* studies. This is particularly crucial for drugs used in patients with gastrointestinal diseases in which the intestinal transit time shows a high variability.

The colonic target release of enteric coated butyrate requires an optimized coating able to prevent an early release (duodenum-jejunum-ileum) resulting in an absorption and metabolism of butyrate before reaching the colon. The coating is expected to release NaB from the ileo-caecal region as a result of a variation of intestinal pH but a delayed release delivery kinetic would result in a loss of a relatively high amount of butyrate in the stools.

Tuleu *et al*[20] have developed pellets for colonic delivery of NaB *via* oral route. When they are administered to rats a large amount is lost in the caecum for coating dissolution problems.

Optimization of the tablets is therefore crucial to determine in the healthy subjects and patients with Inflammatory bowel disease (IBD) the exact delivery site of butyrate in the intestine thus reducing false negative data in term of efficacy due to a poor delivery of the active compound in the target area.

Sodium butyrate tablets (1 g) coated with hydroxyl propyl methylcellulose (HPMC) and natural polymer Shellac have been developed and optimized by conventional *in vitro* studies. In the present study the optimal coating thickness was optimized *in vivo* by evaluating the release of the active ingredient by the kinetics of $^{13}CO_2$ excretion in the breath of healthy subjects and Crohn's disease patients after oral administration of ^{13}C-labeled NaB included in the 1 g tablets. The rate of $^{13}CO_2$ production is the result of ^{13}C-NaB intestinal absorption and metabolism that was evaluated by the rate of production of $^{13}CO_2$ in exhaled breath over 8 h. The $^{13}C/^{12}C$ isotope ratio was measured by isotope ratio mass spectrometry (IRMS). The intestinal transit time was evaluated by simultaneous co-administration of tauroursodeoxycholic acid (TUDCA).

TUDCA was selected as a biomarker of oro-ileal transit time since it is absorbed actively only in the ileum, the time of its peak serum level reflects the oro-ileal transit time. A sensitive and specific enzyme immunoassay was performed to evaluate serum TUDCA concentration at various time intervals after administration as previously described[21].

To evaluate the kinetics of the release of NaB from the tablets, we compared the time of maximum $^{13}CO_2$ excretion with that of peak serum TUDCA concentration within individual subjects in order to overcome the high variability in intestinal transit time.

MATERIALS AND METHODS

Oral NaB formulation

Plain and coated tablets containing hydroxyl propyl methylcellulose and shellac with a pH dependent extended release coating were used in the study. Both formulations contained 1 g of NaB and three batches of tablets containg 5%, 10% and 20% w/w of ^{13}C-NaB (CIL, Andover MA, USA) were prepared.

The difference between the two tablets was the internal pre-coating of HPMC and external coating of shellac, which is resistant to desgregation up to pH 7. All other excipients of the formulations were identical. The pre-coating of HPMC was made to avoid that basic characteristics of the active ingredient in the tablet nucleus would induce an early dissolution of shellac which is resistant to acid pH and soluble to basic pH. In order to optimize the release of NaB in the colon, different thickness films of shellac (50, 80 and 120 μm) were studied. Coated tablets (Sobutir) were supplied by Promefarm srl, Milan, Italy. The different formulations were then administered to the same subjects in order to verify simultaneously the kinetic of NaB release in relation to the oro-ileal transit time evaluated by the time of the serum TUDCA peak and select the formulation that would be admitted to the complete study.

Subjects studied

The study was carried out in 12 healthy subjects (6 males and 6 females, median age 42 years, range 18-60 years) and 12 Crohn's disease patients (9 females and 4 males, median age 40 years, range 18-65 years) with a relatively mild activity index ranging from $320 \geqslant$ C.D.A.I. $\geqslant 220$[22]. To avoid any difference in the transit time, we studied only patients with the same level of activity index. In addition, the patients studied had no pure ileal or ileo-colonic involvement and they did not receive steroid or immunosuppressive treatment. All patients during the study presented diarrhoea. Before this final controlled study volunteers received the different formulations under development and between the different studies a washout period of one week was used. Thirty minutes before the study, 2 mL of blood was collected for the baseline values, as were two separate samples of breath in a 10 mL capped glass tube. After administration of the 1 g ^{13}C-NaB tablet and of 500 mg TUDCA as gelatine capsules (Tudcabil®, Pharmacia Upjohn, Milan, Italy), the subjects received a standard liquid test meal of 375 Kcal, containing 17 g of fat, 10.4 g of protein and 10 g of carbohydrates. Breath and blood samples were collected at 30 min intervals over an 8-h period (unless otherwise specified). The oro-ileal transit time was defined as the time interval between administration of TUDCA and the peak serum TUDCA (C_{max}) time[21]. The time of the maximum $^{13}CO_2$ breath excretion was used to represent the time of release and absorption of sodium butyrate. The study approved by

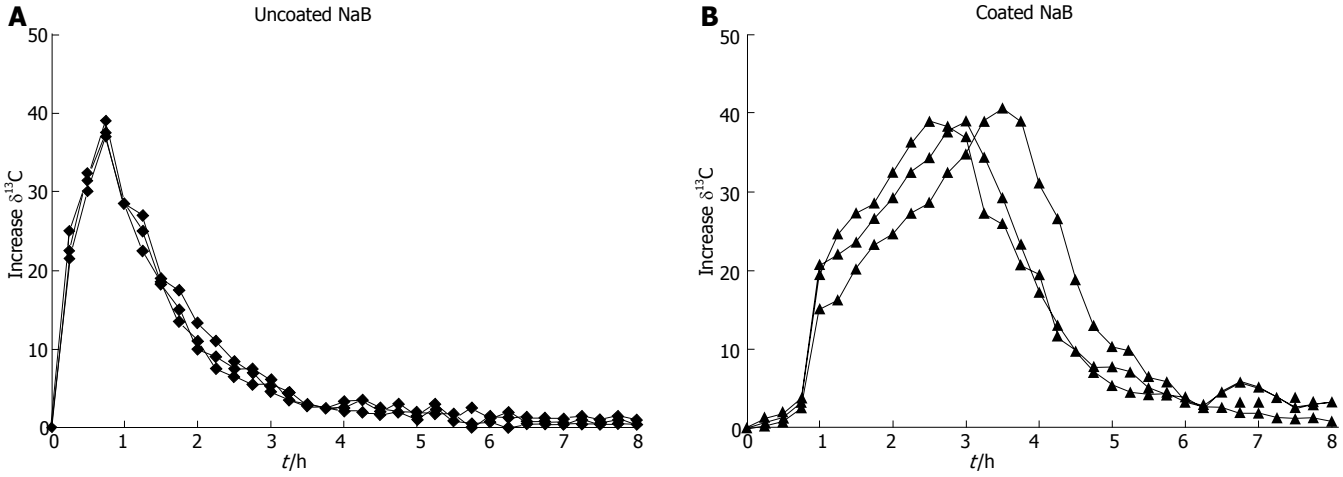

Figure 1 Excretion of breath $^{13}CO_2$ after oral administration of uncoated (**A**) and shellac-coated (**B**) 1 g NaB tablets containing 10% w/w of ^{13}C-NaB in 12 healthy subjects. The experiment of each formulation was repeated three times in the same subject for different weeks.

the Ethical Committee of University of Bologna was conducted according to the institutional guidelines.

Analytical methods

$^{13}CO_2$ breath test: $^{13}CO_2$ in each of the duplicate breath samples was analyzed by continuous flow isotope ratio mass spectrometry (IRMS; ANCA, PDZ Europa Ltd, Cheshire U.K.). The results were expressed as δ^{13}C that was calculated from:

$$\delta^{13}C = \left(\frac{^{13}C/^{12}C\ (sample)}{^{13}C/^{12}C\ (std)} - 1 \right) \times 1000$$

where $^{13}C/^{12}C$ (std) is the Pee Dee Belemnite (PDB) reference standard $^{13}C/^{12}C$ ratio, the final value was expressed as a milli percentage (δ^{13}C‰).

Serum TUDCA enzyme immunoassay

Serum TUDCA levels were determined by a specific chemiluminescent enzyme immunoassay previously developed and optimized in our laboratory[21]. The method is a solid-phase competitive format with a TUDCA-specific polyclonal antibody immobilized on 96 wells black polystyrene microtiter plates. A horseradish peroxidase (HRP)-UDCA conjugate was synthesized, purified, properly characterized, and used as enzymatic tracer.

For the TUDCA assay 100 μL of the sample (serum diluted 1/50, v/v with assay buffer: 0.05 mol/L phosphate/EDTA buffer, pH 7.4, containing 1 g/L bovine serum albumin) or of six standard TUDCA solutions with a concentration ranging from 0.01 to 1000 nmol/L was incubated in the 96-well microtiter plates coated with the antibody for 1 h at 37℃ with 100 μL of the properly diluted HRP-UDCA tracer. After washed with assay buffer, 100 μL of the chemiluminescent substrate (H_2O_2/luminol/enhancer SuperSignal ELISA Pico, Pierce, Ⅱ, USA) was added and the light signal was measured using a PMT based luminometer microtiter reader (Luminoskan Ascent, Thermo Electron Corporation MA, USA) .

TUDCA concentrations were determined by a plot of chemiluminescent (CL) signal *vs* the log of concentration and the best data fit was obtained by linear regression of the six point standards. Serum TUDCA was expressed as nmol/L of serum.

RESULTS

Optimization of NaB oral formulation

The ^{13}C-NaB dose to include in the 1 g NaB tablet was standardized by quantifying the amount of label to produce a breath CO_2 enrichment of the ^{13}C-isotope that could be accurately evaluated with respect to the baseline value representing its natural abundance.

During the course of three separate weeks, three 1-g NaB tablets containing 5%, 10% and 20% w/w of ^{13}C-NaB respectively, were administered to six healthy subjects. The excretion rate of $^{13}CO_2$ in breath was measured and the maximum value was calculated. The dose of 100 mg of the label was chosen giving a δ^{13}C‰ of 15.3 that was much higher than the baseline value of -28%. This wide cut off could allow the accurate evaluation of not only the maximum excretion of $^{13}CO_2$ but also small variations during the 8-h study period and eventually low $^{13}CO_2$ excretion resulting in patients with impaired metabolism of NaB. The coating thickness was optimized according to the kinetics of the $^{13}CO_2$ excretion accounting for the release and absorption of butyrate from the tablet. The results obtained with 50, 80 and 120 μm thickness coating suggested that the coating size of 80 μm was the most adequate to prevent a too early release and absorption of NaB as occurred with the 50 μm thickness and to ensure complete release of the active ingredient in a time comparable with the oro-ileal transit time.

The NaB tablet containing 10% w/w of ^{13}C-NaB and 80 μm-thick coating was used to evaluate the final performance of the formulation. The intra-subject variability was evaluated by administering either coated or uncoated NaB formulations three times to the same subject in separate experiments and monitoring the excretion of $^{13}CO_2$ at 15 min time intervals (Figure 1). In the uncoated tablet, the intra-subject variability was very low and the curves were almost super impossible.

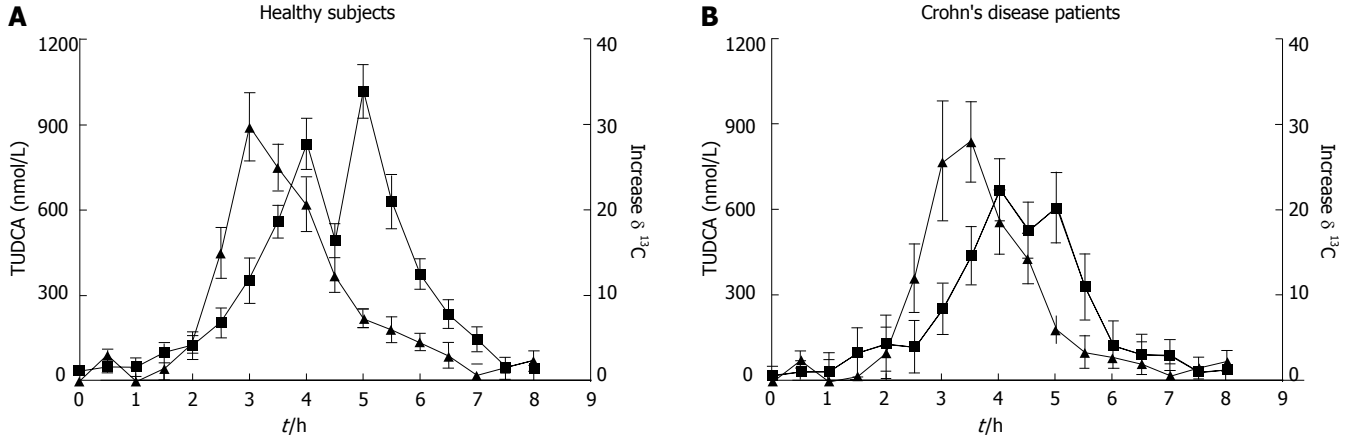

Figure 2 Profiles of the mean $^{13}CO_2$ breath excretion (▲) and serum TUDCA concentrations (■) plotted against time. Data were collected after administration of the Shellac-coated tablet containing 10% w/w of ^{13}C-butyrate and two gelatine capsules containing 250 mg each of TUDCA. Data are expressed as mean ± SD in 12 healthy subjects (**A**) and 12 Crohn's disease patients (**B**).

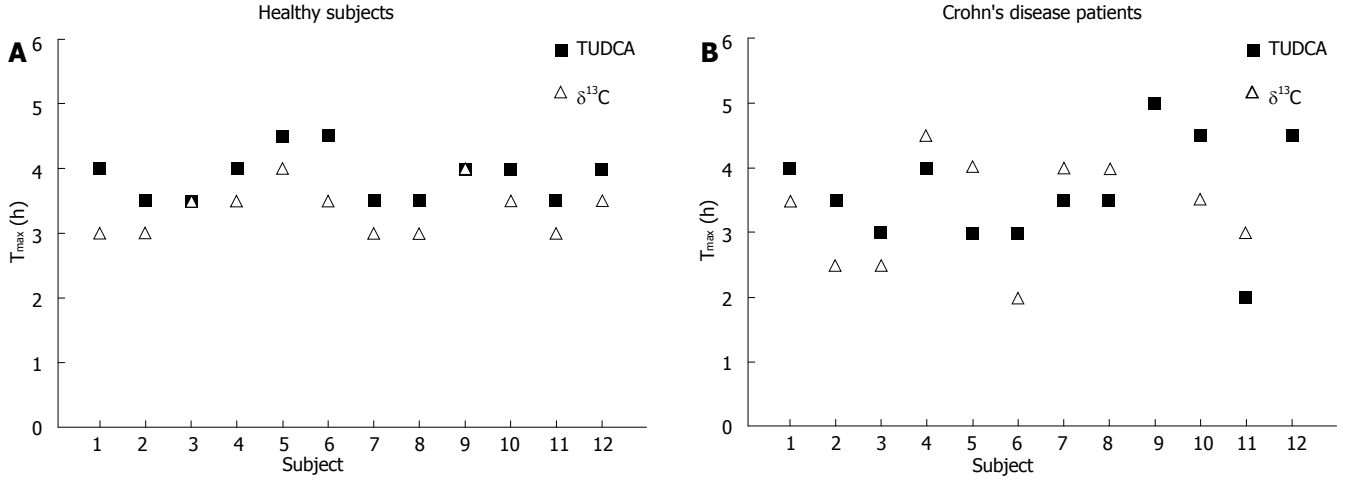

Figure 3 Tmax obtained in control subjects (**A**) and Crohn's disease patients (**B**) using serum TUDCA and $^{13}CO_2$ breath tests.

The maximum excretion was achieved 45 min after administration of the dose and the absorption started just in the first 15 min. A slightly higher variability was observed when the coated formulation was administered as a result of an intra-subject variability in gastric emptying and overall gastrointestinal transit. The mean peak $^{13}CO_2$ excretion time of the coated tablets was 180 min (range 150-225 min), showing the extended release of NaB caused by the shellac coating.

Serum TUDCA chemiluminescent enzyme immunoassay

Chemiluminescent enzyme immunoassay fulfilling all the standard requirements of accuracy and precision was used. The intra and inter studies showed that the coefficient of variation was always below 9%. The limit of quantification of 10 nmol/L allowed direct analysis of TUDCA in a 20-fold diluted serum sample.

The mean serum TUDCA profiles together with the kinetics of $^{13}CO_2$ excretion obtained in the healthy subjects and Crohn's disease patients are shown in Figure 2. The serum TUDCA profile was characterized by two peaks. The first peak was reached 180-200 min after TUDCA administration and represented the oro-ileal transit time, the second peak was observed after 300-400 min as a result of the enterohepatic circulation of the absorbed TUDCA.

In the healthy subjects peak of serum TUDCA concentration was achieved at a median of 4 h (range 3-5 h) after NaB administration. The mean peak $^{13}CO_2$ excretion time occurred slightly earlier at 3.5 h and the range of variability was similar to that of TUDCA. A similar behavior was observed in Crohn's disease patients with a higher variability due to variation in the intestinal transit time.

Top panel and bottom panel are shown in Figure 3. The Tmax was obtained in control subjects and Crohn's disease patients using the serum TUDCA and $^{13}CO_2$ breath tests. No subject and Crohn's disease patient had an earlier release of $^{13}CO_2$ after administration of the coated tablets with respect to the Tmax of TUDCA. Similarly no subject and patient missed to give a peak of $^{13}CO_2$ excretion or reported the loss of intact tablets in stools.

The ileal release was defined (a priori) as the $^{13}CO_2$ peak occurring within 30 min from the time of TUDCA peak whereas colonic release was considered as the $^{13}CO_2$

peak occurring after this interval.

The temporal correspondence between the maximum $^{13}CO_2$ excretion times, with the TUDCA time at the Cmax representing the biomarker oro-ileal transit time even if occurring at different times, usually slightly earlier suggested that the active ingredient was still delivered in the colon in high concentration and therefore we expected that it would exert its activity in IBD patients.

In all the studied subjects, NaB was efficiently released by the coated tablet, suggesting that the formulation developed could be used in these subjects to prevent an early absorption and deliver a large amount of NaB in the colon just starting from the terminal ileum as shown by the kinetic profile of $^{13}CO_2$ and serum TUDCA.

DISCUSSION

The present study was designed to evaluate a new NaB formulation able to deliver the active ingredients of 1 g tablets coated with shellac into the colon by oral administration. The coating delayed the release of the active ingredients by two-three hours with respect to the uncoated formulation, thus a large amount of NaB could reach the colon, as demonstrated by the temporal similarity between the profiles of $^{13}CO_2$ breath test and serum TUDCA concentration. In fact, TUDCA is absorbed by an active carrier-mediated mechanism only in the ileum[23, 24], and previous studies comparing the TUDCA serum levels after its oral administration with other markers of intestinal transit-time such as sulfasalazine showed that this method provides a valid and practical means of assessment of the oro-ileal transit-time[21]. Comparison of the peak times of $^{13}CO_2$ excretion and serum TUDCA concentration could confirm the efficacy of shellac coating in delivering NaB to the colon independently of intestinal transit-time variability. The dissolution of Shellac coating at pH 7 and its thickness driving the kinetics of the dissolution process has been well optimized and a large amount of NaB which starts to be delivered after two hours reaches the intact ileo-cecal region as shown by the kinetics of TUDCA intestinal absorption.

It was recently reported that topical butyrate improves the efficacy of 5-ASA in refractory distal ulcerative colitis[17], due to the presence of NaB in the colon administered topically *in situ*. Vernia *et al*[16] demonstrated in a pilot study that oral butyrate may improve the efficacy of oral mesalazine in active ulcerative colitis but a large scale investigation to confirm the present findings is still required. In this case the NaB was administered as tablets coated with a pH-dependent soluble polymer. More recently it has been reported that chronic feeding (tablets, 4 g a day for 8 wk) of this enteric coated NaB formulation (tablets, 4 g a day for 8 wk) (tablets, 4 g a day for 8 wk) can effectively induce clinical improvement/remission in mild Crohn's disease[25].

An adequate enteric coating is needed for therapy of ileo-colonic disorders since when uncoated uncoated oral formulation of NaB is administered in an uncoated oral formulation, the compound is promptly dissolved and rapidly metabolized before reaching the colon as shown by the time of the maximum $^{13}CO_2$ excretion occurring within 30-45 min after the ^{13}C butyrate oral administration. A specific enteric coated formulation has been therefore designed to deliver the drug in that portion of the intestine keeping into account the high variability of the intestinal transit time observed in IBD patients.

The amount of $^{13}CO_2$ excreted in breath was similar among the Crohn's disease patients, showing that the rate and efficiency of NaB metabolism are similar in the healthy subjects. The patients were characterized by a mild active disease accounting for the efficient metabolism of butyrate and the oral formulation was expected to deliver NaB into the colon in a similar extent as to enema administration.

Furthermore the new coated ^{13}C-NaB oral formulation containing ^{13}C-labeled butyrate can also be used to evaluate the rate of colocyte-metabolized NaB by performing $^{13}CO_2$ breath test before and after chronic administration of NaB. The impairment of NaB utilization by colonocytes that has been observed in previous studies[2-4] can then readily be evaluated by measuring the reduction in cumulative $^{13}CO_2$ excretion in the 8-h period following oral administration of colon-targeted NaB tablets. A similar approach could also be used to evaluate the effectiveness of therapies for IBD patients with mesalazine (either alone or in combination with NaB) and new formulations designed to improve NaB absorption and metabolism. The reported NaB formulation can effectively improve oral administration of NaB ensuring the release of the active compound in the lower intestine portion which is the target for its pharmacological activity.

REFERENCES

1 **Cummings JH**. Short chain fatty acids in the human colon. *Gut* 1981; **22**: 763-779
2 **Roediger WE**, Nance S. Metabolic induction of experimental ulcerative colitis by inhibition of fatty acid oxidation. *Br J Exp Pathol* 1986; **67**: 773-782
3 **Chapman MA**, Grahn MF, Boyle MA, Hutton M, Rogers J, Williams NS. Butyrate oxidation is impaired in the colonic mucosa of sufferers of quiescent ulcerative colitis. *Gut* 1994; **35**: 73-76
4 **Chapman MA**, Grahn MF, Hutton M, Williams NS. Butyrate metabolism in the terminal ileal mucosa of patients with ulcerative colitis. *Br J Surg* 1995; **82**: 36-38
5 **Finnie IA**, Taylor BA, Rhodes JM. Ileal and colonic epithelial metabolism in quiescent ulcerative colitis: increased glutamine metabolism in distal colon but no defect in butyrate metabolism. *Gut* 1993; **34**: 1552-1558
6 **Scheppach W**, Sommer H, Kirchner T, Paganelli GM, Bartram P, Christl S, Richter F, Dusel G, Kasper H. Effect of butyrate enemas on the colonic mucosa in distal ulcerative colitis. *Gastroenterology* 1992; **103**: 51-56
7 **Steinhart AH**, Hiruki T, Brzezinski A, Baker JP. Treatment of left-sided ulcerative colitis with butyrate enemas: a controlled trial. *Aliment Pharmacol Ther* 1996; **10**: 729-736
8 **Patz J**, Jacobsohn WZ, Gottschalk-Sabag S, Zeides S, Braverman DZ. Treatment of refractory distal ulcerative colitis with short chain fatty acid enemas. *Am J Gastroenterol* 1996; **91**: 731-734
9 **Scheppach W**. Treatment of distal ulcerative colitis with short-chain fatty acid enemas. A placebo-controlled trial. German-Austrian SCFA Study Group. *Dig Dis Sci* 1996; **41**: 2254-2259
10 **Den Hond E**, Hiele M, Evenepoel P, Peeters M, Ghoos Y, Rutgeerts P. In vivo butyrate metabolism and colonic permeability in extensive ulcerative colitis. *Gastroenterology*

1998; **115**: 584-590
11 **Simpson EJ**, Chapman MA, Dawson J, Berry D, Macdonald IA, Cole A. In vivo measurement of colonic butyrate metabolism in patients with quiescent ulcerative colitis. *Gut* 2000; **46**: 73-77
12 **Säemann MD**, Böhmig GA, Osterreicher CH, Burtscher H, Parolini O, Diakos C, Stöckl J, Hörl WH, Zlabinger GJ. Anti-inflammatory effects of sodium butyrate on human monocytes: potent inhibition of IL-12 and up-regulation of IL-10 production. *FASEB J* 2000; **14**: 2380-2382
13 **Coradini D**, Pellizzaro C, Marimpietri D, Abolafio G, Daidone MG. Sodium butyrate modulates cell cycle-related proteins in HT29 human colonic adenocarcinoma cells. *Cell Prolif* 2000; **33**: 139-146
14 **Otaka M**, Singhal A, Hakomori S. Antibody-mediated targeting of differentiation inducers to tumor cells: inhibition of colonic cancer cell growth in vitro and in vivo. A preliminary note. *Biochem Biophys Res Commun* 1989; **158**: 202-208
15 **Avivi-Green C**, Polak-Charcon S, Madar Z, Schwartz B. Apoptosis cascade proteins are regulated in vivo by high intracolonic butyrate concentration: correlation with colon cancer inhibition. *Oncol Res* 2000; **12**: 83-95
16 **Vernia P**, Monteleone G, Grandinetti G, Villotti G, Di Giulio E, Frieri G, Marcheggiano A, Pallone F, Caprilli R, Torsoli A. Combined oral sodium butyrate and mesalazine treatment compared to oral mesalazine alone in ulcerative colitis: randomized, double-blind, placebo-controlled pilot study. *Dig Dis Sci* 2000; **45**: 976-981
17 **Vernia P**, Annese V, Bresci G, d'Albasio G, D'Incà R, Giaccari S, Ingrosso M, Mansi C, Riegler G, Valpiani D, Caprilli R. Topical butyrate improves efficacy of 5-ASA in refractory distal ulcerative colitis: results of a multicentre trial. *Eur J Clin Invest* 2003; **33**: 244-248
18 **Pinto A**, Fidalgo P, Cravo M, Midões J, Chaves P, Rosa J, dos Anjos Brito M, Leitão CN. Short chain fatty acids are effective in short-term treatment of chronic radiation proctitis: randomized, double-blind, controlled trial. *Dis Colon Rectum* 1999; **42**: 788-795; discussion 795-796
19 **Høverstad T**, Bøhmer T, Fausa O. Absorption of short-chain fatty acids from the human colon measured by the $14CO_2$ breath test. *Scand J Gastroenterol* 1982; **17**: 373-378
20 **Tuleu C**, Andrieux C, Cherbuy C, Darcy-Vrillon B, Duée PH, Chaumeil JC. Colonic delivery of sodium butyrate via oral route: acrylic coating design of pellets and in vivo evaluation in rats. *Methods Find Exp Clin Pharmacol* 2001; **23**: 245-253
21 **Azzaroli F**, Mazzella G, Mazzeo C, Simoni P, Festi D, Colecchia A, Montagnani M, Martino C, Villanova N, Roda A, Roda E. Sluggish small bowel motility is involved in determining increased biliary deoxycholic acid in cholesterol gallstone patients. *Am J Gastroenterol* 1999; **94**: 2453-2459
22 **Best WR**, Becktel JM, Singleton JW, Kern F. Development of a Crohn's disease activity index. National Cooperative Crohn's Disease Study. *Gastroenterology* 1976; **70**: 439-444
23 **Wilson FA**. Intestinal transport of bile acids. In: Schultz SG, Field M, Frizzell RA, editors. Handbook of physiology. The gastrointestinal system. Intestinal absorption and secretion. Bethesda: Am Physiol Soc, 1991: 389-404
24 **Aldini R**, Montagnani M, Roda A, Hrelia S, Biagi PL, Roda E. Intestinal absorption of bile acids in the rabbit: different transport rates in jejunum and ileum. *Gastroenterology* 1996; **110**: 459-468
25 **Di Sabatino A**, Morera R, Ciccocioppo R, Cazzola P, Gotti S, Tinozzi FP, Tinozzi S, Corazza GR. Oral butyrate for mildly to moderately active Crohn's disease. *Aliment Pharmacol Ther* 2005; **22**: 789-794

S- Editor Liu Y L- Editor Wang XL E- Editor Lu W

PO Box 2345, Beijing 100023, China
www.wjgnet.com
wjg@wjgnet.com

World J Gastroenterol 2007 February 21; 13(7): 1085-1089
World Journal of Gastroenterology ISSN 1007-9327

RAPID COMMUNICATION

Possible role of human cytomegalovirus in pouchitis after proctocolectomy with ileal pouch-anal anastomosis in patients with ulcerative colitis

Damian Casadesus, Tatsuo Tani, Toshifumi Wakai, Satoshi Maruyama, Tsuneo Iiai, Haruhiko Okamoto, Katsuyoshi Hatakeyama

Damian Casadesus, Tatsuo Tani, Toshifumi Wakai, Satoshi Maruyama, Tsuneo Iiai, Haruhiko Okamoto, Katsuyoshi Hatakeyama, Division of Digestive and General Surgery, Niigata University Graduate School of Medical and Dental Sciences, Niigata, Japan
Correspondence to: Tatsuo Tani, MD, PhD, Division of Digestive and General Surgery, Niigata University Graduate School of Medical and Dental Sciences, 1-757 Asahimachi-dori, Niigata City 951-8510, Japan. ttani@med.niigata-u.ac.jp
Telephone: +81-25-2272228 Fax: +81-25-2270779
Received: 2006-10-24 Accepted: 2006-11-11

Abstract

AIM: To detect the presence of human cytomegalovirus (HCMV) proteins and genes on the ileal pouch of patients with ulcerative colitis who have undergone proctocolectomy with ileal pouch-anal anastomosis (IPAA).

METHODS: Immunohistochemistry, polymerase chain reaction (PCR) and PCR sequencing methods were utilized to test the presence of HCMV in pouch specimens taken from 34 patients in 86 endoscopies.

RESULTS: HCMV genes and proteins were detected in samples from 12 (35.2%) patients. The rate of detection was significant in the endoscopies from patients diagnosed with pouchitis (5 of 12, 41.6%), according to the Japanese classification of pouchitis, in comparison to patients with normal pouch (7 of 62, 11.2%; P = 0.021). In all patients with pouchitis in which the HCMV was detected, it was the first episode of pouchitis. The virus was not detected in previous biopsies taken in normal endoscopies of these patients. During the follow-up, HCMV was detected in one patient with recurrent pouchitis and in 3 patients whose pouchitis episodes improved but whose positive endoscopic findings persisted.

CONCLUSION: HCMV can take part in the inflammatory process of the pouch in some patients with ulcerative colitis who have undergone proctocolectomy with IPAA.

Key words: Human cytomegalovirus; Pouchitis; Inflammatory bowel disease; Ileal pouch-anal anastomosis

Casadesus D, Tani T, Wakai T, Maruyama S, Iiai T, Okamoto H, Hatakeyama K. Possible role of human cytomegalovirus in pouchitis after proctocolectomy with ileal pouch-anal anastomosis in patients with ulcerative colitis. *World J Gastroenterol* 2007; 13(7): 1085-1089

http://www.wjgnet.com/1007-9327/13/1085.asp

INTRODUCTION

Human cytomegalovirus (HCMV) is a ubiquitous, species-specific beta-herpes virus that can establish lifelong latency in the host after the primary infection. HCMV infection is endemic within the human population, and its role as a pathogen in the colon and ileum is still unclear. Early studies suggested that HCMV infection initiates some cases of ulcerative colitis (UC)[1,2], plays a role in UC exacerbation[3], causes self-limited colitis[4], and increases the incidence of complications, emergency surgery or death in patients with UC[3,5,6].

Pouchitis is a frequent complication in patients with UC who have undergone colectomy with ileal pouch-anal anastomosis (IPAA). The etiology of pouchitis is still unknown, but several theories have been proposed, such as genetic susceptibility, a possible novel third form of inflammatory bowel disease (IBD) in the pouch, recurrence of UC in the pouch, misdiagnosis of Crohn's disease, ischemic complication of surgery, fecal stasis, and bacterial overgrowth. Recent studies have reported HCMV infection as a cause of pouchitis in 3 immunocompetent patients[7,8]. The diagnosis of this specific infectious agent as a possible cause of pouchitis is crucial before initiating immune modifier therapy, fecal diversion, or pouch excision. We explored the presence of viral gene products and proteins in the pouches of a series of patients who have undergone proctocolectomy with IPAA.

MATERIALS AND METHODS

Patients

Enrolled in this study were 34 Japanese patients (17 females, 17 males) who underwent proctocolectomy

with IPAA at the Department of General and Digestive Surgery, Niigata University Hospital between 1990 and 2003. The patients' age ranged from 24 to 68 years (mean 34.8 ± 15.4 years). Oral and written informed consent was obtained from each patient. The study protocol adhered to the ethical guidelines of the 1975 Declaration of Helsinki and was approved by the institution's ethical committee. We reviewed the clinical and endoscopic records of all the enrolled patients. The patients had a history of UC between 1 to 5 years and underwent the operation in two or three steps. The diagnosis of pouchitis was based on clinical and endoscopic criteria according to the modified pouchitis disease activity index (mPDAI)[9] and the Japanese classification of pouchitis (JCP)[10]. JCP defines pouchitis as a condition with severe endoscopic findings, or with two or more clinical symptoms and moderate endoscopic findings. Eighty-six endoscopies were performed in 34 patients. Twenty-eight endoscopies were performed in patients complaining of symptoms, 46 endoscopies were carried out in routine controls after surgery, and 12 were performed during pouchitis follow-up. Biopsies were performed both in areas with pathological findings (edema, granularity, friability, erythema, loss of vascular pattern, mucous exudates, erosion or ulceration) and in areas with mucosa of normal appearance.

Immunohistochemistry (IHC)

Immunostaining for HCMV was performed on paraffin-embedded sections with a cocktail of two monoclonal mouse antibodies against human cytomegalovirus (clone CCH2 & DDG9, Dako Cytomation, CA, USA) at a dilution of 1:100. All paraffin-embedded samples from each patient were used for IHC. According to the company specifications, antibody CCH2 reacts with an early nuclear protein identical with non-structural DNA-binding protein p52 (UL44), whereas antibody DDG9 reacts with an immediate-early nuclear protein with a molecular weight of about 76 kDa. For both antibodies, the reactivity persists also at later stages during HCMV infection where the localization is less distinctly nuclear and appears to be in the cytoplasm. Five-μm thick sections were deparaffinized and rehydrated using graded alcohol concentrations, then the sections were digested with trypsin (Sigma Chemicals, Germany) at 37℃ for 20 min. After endogenous peroxidase was blocked by incubation with 30 mL/L hydrogen peroxide for 20 min, the sections were incubated overnight at 4℃ with the cocktail of anti-human cytomegalovirus antibodies. Control slides from the same biopsy block were incubated with PBS without the primary antibody. They were then incubated at room temperature for 30 min with goat anti-mouse immunoglobulin conjugated to a peroxidase-labeled amino-acid polymer, Simple Stain Max PO (Nichirei Histofine, Tokyo, Japan). The sections were reacted with diaminobenzidine in 50 mol/L Tris-HCL (pH 7.5) with 0.3% (vol/vol) hydrogen peroxide for 5 min and counterstained with hematoxylin.

Polymerase chain reaction (PCR) and PCR sequencing

To confirm that our probe was specific for HCMV nucleic acids, DNA samples were extracted from two paraffin sections 20 μm in size, and cut from the same biopsy specimens described above with a QIAamp DNA minikit (Qiagen, Tokyo, Japan). From each sample, 200 ng of DNA was amplified by PCR with the primer 5'-TGCAGTTTGGTCCCTTAAAG-3' and 5'-AAGAATCCTCACCTGGCTTA-3' from the HCMV large structural phosphoprotein (UL32) and the primer 5'-TCCAACACCCACAGTACCCGT-3' and 5'-CGGAAACGATGGTGTAGTTCG-3' from the HCMV glycoprotein B (UL55), using a method specific for UL32 gene[11] and UL55 gene[12]. The amplified DNA products were visualized on 2% agarose gel (NuSieve GTG agarose, FMC Bio Products, Rockland, USA) stained with 0.01% (vol/vol) ethidium bromide and visualized under ultraviolet light. The bands of UL32 gene were cut out and the DNA was analyzed by automated sequencing (ABI Prism 310 Diagnostics Systems, Applied Biosystems, Tokyo, Japan). The HCMV sequence was confirmed by NCBI Blast, and found to be identical to that of UL32. To avoid potential PCR contamination, all preparations were processed masked, no positive controls were used in any PCR reactions and a separated room was used for the preparation of the reaction mixture. The distilled water control gave negative results in each assay run, and confirmed the efficiency of these preventive measures. When IHC and/or PCR were positive, the sample was considered to be HCMV-positive, and when both of them were negative, the sample was considered to be HCMV-negative.

Statistical analysis

The results of HCMV detection are expressed in numbers of patients and percentages. The results of the cumulative-life steroid dose are given as means ± SD. Statistical significance was calculated with SPSS 13 (SPSS Inc., Chicago, IL, USA) using Fisher's exact test and Student's *t*-test when appropriate, and the results were considered significant at $P \leqslant 0.05$.

RESULTS

Twenty-eight endoscopies were performed in patients complaining of symptoms and 46 endoscopies were performed in routine controls at different time points after surgery. Four hundred and seventy-three specimens were evaluated, 103 from patients with pouchitis and 370 from patients with a normal pouch. We detected HCMV in samples from 12 endoscopies using IHC and PCR. These endoscopies were performed because the patients were complaining of symptoms (8 endoscopies) or during routine controls after surgery (4 endoscopies). Immunoreactivity was observed in the submucosal layer with predominant nuclear staining of cells (Figure 1). There were not any differences in the staining pattern between the HCMV-positive patients with and without pouchitis either using mPDAI or JCP. We performed PCR for all samples, and amplified products from both genes were detected in the same sample with positive IHC (Figure 2). No HCMV was detected in the distilled water control that was run through the same PCR reaction.

HCMV was significantly detected in endoscopies of patients diagnosed with pouchitis (5 of 12, 41.6%)

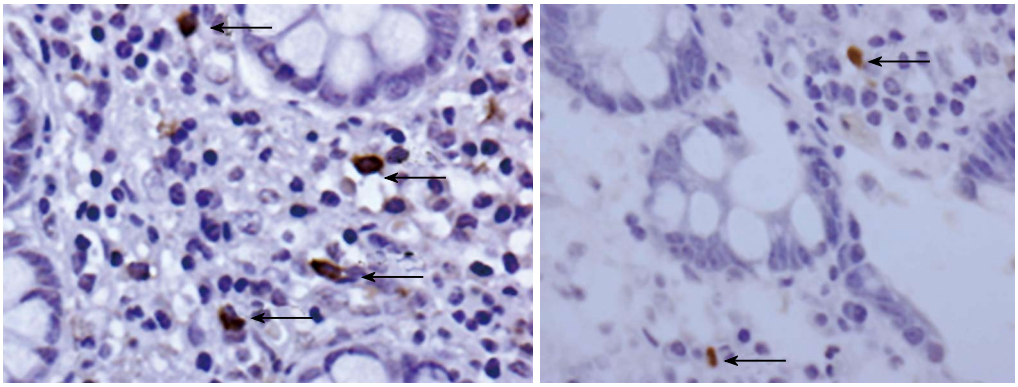

Figure 1 Immunohistochemical staining for HCMV of biopsy samples from ileoanal pouch. Cells in the submucosa (arrows) show strong nuclear staining. Original magnification x 600.

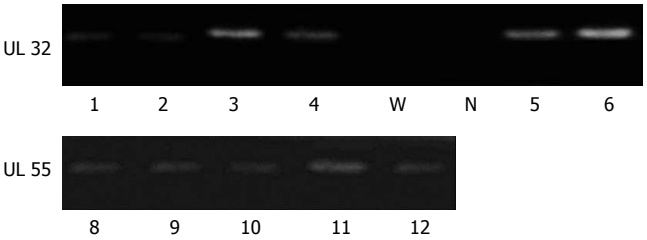

Figure 2 Agarose gel showing UL32 gene products (lanes 1-4, 5 and 6) and UL 55 gene products (lanes 8-12). W: Water; N: HCMV-negative patient.

Table 1 HCMV detection during endoscopic examinations of UC patients with proctocolectomy and ileal pouch-anal anastomosis *n* (%)

	HCMV positive	HCMV negative	*P*
mPDAI[10]			
Pouchitis	3 (27.2)	8 (72.7)	NS
No pouchitis	9 (14.2)	54 (85.7)	
JCP[11]			
Pouchitis	5 (41.6)	7 (58.3)	0.021
No pouchitis	7 (11.2)	55 (88.7)	

mPDAI: modified pouchitis disease activity index; JCP: Japanese classification of pouchitis, NS: not significant.

compared to those with normal pouch (7 of 62, 11.2%; $P = 0.021$, Table 1). According to mPDAI, HCMV was more frequently detected in patients with pouchitis (3 of 11, 27.2%) than in those with normal pouch (9 of 63, 14.2%), but this result was not statistically significant. In all patients with pouchitis in which the HCMV was detected in endoscopy, it was the first episode of pouchitis. In these patients HCMV was not detected in biopsies taken in previous normal endoscopies. The odds ratio suggested that the presence of HCMV was 5 times more frequent in patients with episodes of pouchitis than in patients without.

There was not correlation between the presence of HCMV and the duration of UC, the period of pouchitis, the number of operations, the age, and the gender of the patients. There was no significant difference between the cumulative-life steroid dose and HCMV presence. The mean of the cumulative-life steroid dose was 17152.5 mg ± 16999.0 mg in HCMV-negative patients, and 13347.8 mg ± 12966.7 mg in HCMV-positive patients ($P = 0.52$). After the diagnosis of pouchitis, all patients began treatment with oral metronidazole (500 mg/d). During the follow-up, 2 patients diagnosed with pouchitis were lost and one of them was HCMV-positive. In the samples from 12 endoscopies performed during follow-up, HCMV was detected using IHC and PCR in 4 (4 of 10, 40%) patients. One of these patients had recurrent pouchitis and 3 showed improvement of pouchitis episodes but persistent positive endoscopic findings.

DISCUSSION

It has been suggested that HCMV plays a role in the onset, exacerbation and complication of inflammatory bowel disease (IBD)[2-6,13-18]. However, the etiology of pouchitis is still unknown and the role of HCMV as a possible etiologic factor has not been studied yet. This is the first report exploring the correlation between HCMV and pouchitis in a group of patients with UC who underwent proctocolectomy with IPAA. There are three possible causes for this association: (1) the virus is a simple bystander in the inflammatory process of the pouch, (2) the virus takes part in the inflammatory process after reactivation and productive infection due to another pathogen infection, (3) the virus induces the inflammatory process after infection.

The differentiation of latently infected monocytes[19-23] into tissue macrophages, as occurs with intercurrent infections, could lead to the productive infection and dissemination of HCMV in the digestive tract mucosa of infected patients. No single identifiable causative organism has been detected as the cause of pouchitis, but the infiltration of neutrophils and the proven response to antibacterial therapy suggest that pouchitis could have a bacterial cause[24-27]. However, different facts suggest that HCMV is a real gastrointestinal pathogen and that it can be partly related to the development of pouchitis in some patients. HCMV is often detected in the absence of other pathogens, and some UC complications have been associated with the presence of HCMV[3,5,6]. Moreover, colitis and pouchitis caused by HCMV infection are known to respond to antiviral therapy[8,9,15], and immediate-early HCMV gene products enhance cytokine production and cytokine gene expression[28,29] which *in vivo* would lead to the pronounced inflammation in UC

and pouchitis. Although the pathway of HCMV infection and inflammation is still unclear, the increased production of different cytokines and arachidonic acid, as well as the increased activity of cyclooxygenase 2 after HCMV infection[30-34], could explain the inflammatory response in IBD and pouchitis. In our study on a small series of patients with pouchitis, we hypothesized that HCMV may have played an important role in the etiology of pouchitis in those cases. We detected by IHC an early protein and an immediate-early protein present during an early stage of viral infection. This result corresponds to the detection by PCR of genes that appear early after infection and then frequently decline to undetectable levels with the passage of time[35]. The presence of HCMV turned positive in the episode of pouchitis. However, other factors such as bacterial overgrowth and fecal hydrogen sulfide production[36] could also be implicated in the etiology of pouchitis episode in patients with no detectable HCMV.

The true incidence of HCMV infection in pouchitis as well as in IBD may be underestimated, as diagnostic evaluation for HCMV is not pursued in many of these patients. In our series, the patients did not receive antiviral therapy and HCMV antigenemia was not measured because a diagnosis of HCMV pouchitis was not sought on the occasion of endoscopy. However, after the antibacterial treatment, HCMV persisted in 4 patients with positive endoscopic findings, confirming the possibility of a possible role of HCMV in the etiology of pouchitis in those patients. Since multiple factors play a role in pouchitis, the clinician must exclude HCMV infection as the cause of pouchitis, especially in patients resistant to treatment, before performing fecal diversion, or pouch excision. Concomitant evaluation of the presence of HCMV may be a clinically significant component of the successful treatment of pouchitis.

In conclusion, the presence of HCMV in pouchitis could partly explain the inflammatory response in some patients with UC who have undergone proctocolectomy with IPAA. Therefore, prospective studies with a large number of patients and an analysis of the correlation between antigenemia of HCMV and immunohistological data are definitely needed to identify the specific role of this virus.

ACKNOWLEDGMENTS

The authors thank Mr. Takashi Hatano for his technical assistance. DC is in receipt of a grant from the Ministry of Education, Culture, Sports, Science and Technology of Japan.

REFERENCES

1 **Diepersloot RJ**, Kroes AC, Visser W, Jiwa NM, Rothbarth PH. Acute ulcerative proctocolitis associated with primary cytomegalovirus infection. *Arch Intern Med* 1990; **150**: 1749-1751
2 **Lortholary O**, Perronne C, Leport J, Leport C, Vildé JL. Primary cytomegalovirus infection associated with the onset of ulcerative colitis. *Eur J Clin Microbiol Infect Dis* 1993; **12:** 570-572
3 **Berk T**, Gordon SJ, Choi HY, Cooper HS. Cytomegalovirus infection of the colon: a possible role in exacerbations of inflammatory bowel disease. *Am J Gastroenterol* 1985; **80**: 355-360
4 **Surawicz CM**, Myerson D. Self-limited cytomegalovirus colitis in immunocompetent individuals. *Gastroenterology* 1988; **94**: 194-199
5 **Cooper HS**, Raffensperger EC, Jonas L, Fitts WT. Cytomegalovirus inclusions in patients with ulcerative colitis and toxic dilation requiring colonic resection. *Gastroenterology* 1977; **72**: 1253-1256
6 **Eyre-Brook IA**, Dundas S. Incidence and clinical significance of colonic cytomegalovirus infection in idiopathic inflammatory bowel disease requiring colectomy. *Gut* 1986; **27:** 1419-1425
7 **Moonka D**, Furth EE, MacDermott RP, Lichtenstein GR. Pouchitis associated with primary cytomegalovirus infection. *Am J Gastroenterol* 1998; **93**: 264-266
8 **Muñoz-Juarez M**, Pemberton JH, Sandborn WJ, Tremaine WJ, Dozois RR. Misdiagnosis of specific cytomegalovirus infection of the ileoanal pouch as refractory idiopathic chronic pouchitis: report of two cases. *Dis Colon Rectum* 1999; **42**: 117-120
9 **Shen B**, Achkar JP, Connor JT, Ormsby AH, Remzi FH, Bevins CL, Brzezinski A, Bambrick ML, Fazio VW, Lashner BA. Modified pouchitis disease activity index: a simplified approach to the diagnosis of pouchitis. *Dis Colon Rectum* 2003; **46:** 748-753
10 **Inflammatory bowel disease study group**. Atlas of endoscopic diagnosis of pouchitis. Tokyo: Kyoubundou, 2003
11 **Ashshi AM**, Klapper PE, Cooper RJ. Detection of human cytomegalovirus, human herpesvirus type 6 and human herpesvirus type 7 in urine specimens by multiplex PCR. *J Infect* 2003; **47:** 59-64
12 **Kühn JE**, Wendland T, Eggers HJ, Lorentzen E, Wieland U, Eing B, Kiessling M, Gass P. Quantitation of human cytomegalovirus genomes in the brain of AIDS patients. *J Med Virol* 1995; **47**: 70-82
13 **Cottone M**, Pietrosi G, Martorana G, Casà A, Pecoraro G, Oliva L, Orlando A, Rosselli M, Rizzo A, Pagliaro L. Prevalence of cytomegalovirus infection in severe refractory ulcerative and Crohn's colitis. *Am J Gastroenterol* 2001; **96**: 773-775
14 **Loftus EV**, Alexander GL, Carpenter HA. Cytomegalovirus as an exacerbating factor in ulcerative colitis. *J Clin Gastroenterol* 1994; **19:** 306-309
15 **Papadakis KA**, Tung JK, Binder SW, Kam LY, Abreu MT, Targan SR, Vasiliauskas EA. Outcome of cytomegalovirus infections in patients with inflammatory bowel disease. *Am J Gastroenterol* 2001; **96**: 2137-2142
16 **Pfau P**, Kochman ML, Furth EE, Lichtenstein GR. Cytomegalovirus colitis complicating ulcerative colitis in the steroid-naive patient. *Am J Gastroenterol* 2001; **96:** 895-899
17 **Vega R**, Bertrán X, Menacho M, Domènech E, Moreno de Vega V, Hombrados M, Cabré E, Ojanguren I, Gassull MA. Cytomegalovirus infection in patients with inflammatory bowel disease. *Am J Gastroenterol* 1999; **94:** 1053-1056
18 **Maté del Tío M**, Peña Sánchez de Rivera JM, Larrauri Martínez J, Garcés Jiménez MC, Barbado Hernández FJ. Association of cytomegalovirus colitis and the 1st episode of ulcerative colitis in an immunocompetent patient. *Gastroenterol Hepatol* 1996; **19**: 206-207
19 **Dankner WM**, McCutchan JA, Richman DD, Hirata K, Spector SA. Localization of human cytomegalovirus in peripheral blood leukocytes by in situ hybridization. *J Infect Dis* 1990; **161:** 31-36
20 **Ibanez CE**, Schrier R, Ghazal P, Wiley C, Nelson JA. Human cytomegalovirus productively infects primary differentiated macrophages. *J Virol* 1991; **65:** 6581-6588
21 **Sinzger C**, Plachter B, Grefte A, The TH, Jahn G. Tissue macrophages are infected by human cytomegalovirus in vivo. *J Infect Dis* 1996; **173:** 240-245
22 **Taylor-Wiedeman J**, Sissons JG, Borysiewicz LK, Sinclair JH. Monocytes are a major site of persistence of human cytomegalovirus in peripheral blood mononuclear cells. *J Gen*

Virol 1991; **72** (Pt 9): 2059-2064
23 **Yurochko AD**, Huang ES. Human cytomegalovirus binding to human monocytes induces immunoregulatory gene expression. *J Immunol* 1999; **162:** 4806-4816
24 **Iwaya A**, Iiai T, Okamoto H, Ajioka Y, Yamamoto T, Asahara T, Nomoto K, Hatakeyama K. Change in the bacterial flora of pouchitis. *Hepatogastroenterology* 2006; **53**: 55-59
25 **Lim M**, Sagar P, Finan P, Burke D, Schuster H. Dysbiosis and pouchitis. *Br J Surg* 2006; **93**: 1325-1334
26 **Abdelrazeq AS**, Kelly SM, Lund JN, Leveson SH. Rifaximin-ciprofloxacin combination therapy is effective in chronic active refractory pouchitis. *Colorectal Dis* 2005; **7**: 182-186
27 **Gosselink MP**, Schouten WR, van Lieshout LM, Hop WC, Laman JD, Ruseler-van Embden JG. Eradication of pathogenic bacteria and restoration of normal pouch flora: comparison of metronidazole and ciprofloxacin in the treatment of pouchitis. *Dis Colon Rectum* 2004; **47**: 1519-1525
28 **Geist LJ**, Monick MM, Stinski MF, Hunninghake GW. The immediate early genes of human cytomegalovirus upregulate tumor necrosis factor-alpha gene expression. *J Clin Invest* 1994; **93**: 474-478
29 **Iwamoto GK**, Monick MM, Clark BD, Auron PE, Stinski MF, Hunninghake GW. Modulation of interleukin 1 beta gene expression by the immediate early genes of human cytomegalovirus. *J Clin Invest* 1990; **85:** 1853-1857
30 **Rahbar A**, Boström L, Lagerstedt U, Magnusson I, Söderberg-Naucler C, Sundqvist VA. Evidence of active cytomegalovirus infection and increased production of IL-6 in tissue specimens obtained from patients with inflammatory bowel diseases. *Inflamm Bowel Dis* 2003; **9**: 154-161
31 **Compton T**, Kurt-Jones EA, Boehme KW, Belko J, Latz E, Golenbock DT, Finberg RW. Human cytomegalovirus activates inflammatory cytokine responses via CD14 and Toll-like receptor 2. *J Virol* 2003; **77**: 4588-4596
32 **Redman TK**, Britt WJ, Wilcox CM, Graham MF, Smith PD. Human cytomegalovirus enhances chemokine production by lipopolysaccharide-stimulated lamina propria macrophages. *J Infect Dis* 2002; **185**: 584-590
33 **Zhu H**, Cong JP, Yu D, Bresnahan WA, Shenk TE. Inhibition of cyclooxygenase 2 blocks human cytomegalovirus replication. *Proc Natl Acad Sci USA* 2002; **99**: 3932-3937
34 **Nokta MA**, Hassan MI, Loesch K, Pollard RB. Human cytomegalovirus-induced immunosuppression. Relationship to tumor necrosis factor-dependent release of arachidonic acid and prostaglandin E2 in human monocytes. *J Clin Invest* 1996; **97:** 2635-2641
35 **Greijer AE**, van de Crommert JM, Stevens SJ, Middeldorp JM. Molecular fine-specificity analysis of antibody responses to human cytomegalovirus and design of novel synthetic-peptide-based serodiagnostic assays. *J Clin Microbiol* 1999; **37**: 179-188
36 **Ohge H**, Furne JK, Springfield J, Rothenberger DA, Madoff RD, Levitt MD. Association between fecal hydrogen sulfide production and pouchitis. *Dis Colon Rectum* 2005; **48**: 469-475

S- Editor Wang J **L- Editor** Wang XL **E- Editor** Ma WH

PO Box 2345, Beijing 100023, China
www.wjgnet.com
wjg@wjgnet.com

World J Gastroenterol 2007 February 21; 13(7): 1090-1097
World Journal of Gastroenterology ISSN 1007-9327

RAPID COMMUNICATION

Frequent loss of heterozygosity in two distinct regions, 8p23.1 and 8p22, in hepatocellular carcinoma

Tomoe Lu, Hiroshi Hano, Chenxi Meng, Keisuke Nagatsuma, Satoru Chiba, Masahiro Ikegami

Tomoe Lu, Hiroshi Hano, Chenxi Meng, Keisuke Nagatsuma, Satoru Chiba, Masahiro Ikegami, Department of Pathology, Jikei University School of Medicine, Tokyo, Japan
Supported by The Jikei University Research Fund
Correspondence to: Tomoe Lu, MD, PhD, Department of Pathology, The Jikei University School of Medicine, 3-25-8 Nishishinbashi, Minato-ku, Tokyo 105-8461, Japan. luwei@jikei.ac.jp
Telephone: +81-3-34331111-231 Fax: +81-3-54720700
Received: 2006-11-25 Accepted: 2007-01-18

Abstract

AIM: To identify the precise location of putative tumor suppressor genes (TSGs) on the short arm of chromosome 8 in patients with hepatocellular carcinoma (HCC).

METHODS: We used 16 microsatellite markers informative in Japanese patients, which were selected from 61 published markers, on 8p, to analyze the frequency of loss of heterozygosity (LOH) in each region in 33 cases (56 lesions) of HCC.

RESULTS: The frequency of LOH at 8p23.2-21 with at least one marker was 63% (20/32) in the informative cases. More specifically, the frequency of LOH at 8p23.2, 8p23.1, 8p22, and 8p21 was 6%, 52%, 47%, and 13% in HCC cases. The LOH was significantly more frequent at 8p23.1 and 8p22 than the average (52% *vs* 22%, $P = 0.0008$; and 47% *vs* 22%, $P = 0.004$, respectively) or others sites, such as 8p23.2 (52% *vs* 6%, $P = 0.003$; 47% *vs* 22%, $P = 0.004$) and 8p21 (52% *vs* 13%, $P = 0.001$; 47% *vs* 13%, $P = 0.005$) in liver cancer on the basis of cases. Notably, LOH frequency was significantly higher at *D8S277*, *D8S503*, *D8S1130*, *D8S552*, *D8S254* and *D8S258* than at the other sites. However, no allelic loss was detected at any marker on 8p in the lesions of nontumor liver tissues.

CONCLUSION: Deletion of 8p, especially the loss of 8p23.1-22, is an important event in the initiation or promotion of HCC. Our results should be useful in identifying critical genes that might lie at 8p23.1-22.

Key words: Loss of heterozygosity; Chromosome; Hepatocarcinogenesis; Hepatocellular carcinoma; 8p

Lu T, Hano H, Meng C, Nagatsuma K, Chiba S, Ikegami M. Frequent loss of heterozygosity in two distinct regions, 8p23.1 and 8p22, in hepatocellular carcinoma. *World J Gastroenterol* 2007; 13(7): 1090-1097

http://www.wjgnet.com/1007-9327/13/1090.asp

INTRODUCTION

Primary liver cancer is one of the most frequent neoplasms worldwide, with both an incidence and a mortality rate that are increasing markedly. According to a recent report, the global number of new cases annually rose from 437 400 to 564 000 between 1990 and 2000, and is expected to continue to rise in the future[1-4].

Hepatocellular carcinoma (HCC), the predominant histological subtype of primary liver cancer, mostly arises against a background of chronic liver disease, usually in association with cirrhosis. Several risk factors for HCC have been reported, such as chronic infection with hepatitis B virus (HBV), and C virus (HCV) or both, alcohol-induced liver injury, and dietary exposure to aflatoxin B1 and others. Prolonged exposure to these risk factors is thought to cause an accumulation of chromosomal aberrations and altered gene expression, and eventually results in hepatocarcinogenesis[4-6]. In Japan, more than 70% of HCCs develop in patients with chronic infections with HCV[7]. Carcinogenesis is mainly researched based on virology and the viral gene itself. However, the mechanisms by which inflammation and cirrhosis contribute to tumor development and/or progression remain unclear. After the human genome was sequenced, the mechanism of generation and subsequent progression was researched at a molecular level for HCC. Histological findings suggest that the initiation and subsequent development of HCC are multistep processes involving qualitative and quantitative changes in sequentially expressed genes, especially the inactivation of tumor suppressor genes (TSGs) related to the deletion of chromosomal regions critical for hepatocarcinogenesis[8,9]. A typical alteration in many TSGs, the mutation of one allele, can be detected as a loss of heterozygosity (LOH) with informative markers in TSG regions. Therefore, LOH assays have been widely used as an indirect approach in the search for a new TSG[10]. In the last few years, genetic approaches to the detection of genome-wide LOH using microsatellite markers and chromosomal aberrations detected by comparative genomic hybridization (CGH) have indicated that frequent allelic loss in many different chromosomal regions, including 1p[11,12], 3p[13],

4q[14], 6q[15], 8p[16-19], 9p[20], 10p[21], 13q[22], 22q[23], 16q, 17p and Xq[24,25] , is closely associated with the tumorigenesis of HCC.

We have performed a genome-wide search for LOH with human genetic markers in several types of human cancer and confirmed that loss of 8p is the most frequent chromosomal alteration in prostate cancer, especially allelic loss at 8p22, which not only is an important event in the initiation of tumor, but also is closely associated with the progression of primary cancer to metastatic cancer[26].

In our comprehensive allelotyping, less than 30% of microsatellite markers located at 8p21-23, were recognized as informative for Japanese patients. We therefore undertook an allelotype based study of 33 HCCs using the selected informative markers to obtain a comprehensive view of the LOH on the most frequent altered chromosome, and to identify the location of the putative TSGs in HCC.

MATERIALS AND METHODS

Tissue collection, histopathology, and DNA extraction

Thirty-three patients with hepatocellular carcinoma who underwent liver resection were included in this study. Of these, fifty six tumor lesions and 33 adjacent morphological non-tumor lesions were obtained from surgically resected specimens. All specimens were formalin-fixed, and paraffin wax-embedded tissues were processed with routine histological methods. Use of the tissues was approved by the Ethics Committee of the Jikei University School of Medicine before the study. The study group included 26 men and 7 women, ranging in age from 31 to 76 years. Of the 33 patients, 24 (73%) had a chronic infection with HCV, HBV or both and 15 (45%) had cirrhosis in the background liver tissues. Histological diagnoses were made according to the WHO Histological Classification of Tumors of the Liver and Intrahepatic Bile Ducts (2000). According to histological grade, HCC was classified into well differentiated (WD), moderately differentiated (MD), and poorly differentiated (PD) types. In this study, clinicopathological characteristics were also classified, such as solitary or multiple tumor, growth pattern of tumor (expansive or infiltrative), infiltration of capsule or not, histological grading of tumor (well, moderately or poor differentiation), and with or without vascular and bile duct infiltration. Simultaneously, we also compared LOH frequency and etiological factors, such as chronic hepatitis with HCV or HBV infection, and cirrhosis in the background liver tissues. Fibrosis degree was classified as F1, F2, F3, and F4 according to the histological grading and staging of chronic hepatitis. In this system, liver cirrhosis was classed as F4, which is the end-stage form of liver fibrosis. Of the 33 patients who underwent liver resection, 18 had a solitary tumor nodule and 15 had multiple tumor nodules. All lesions from each case were selected and reviewed by two pathologists in order to confirm the original diagnosis. The tumor (T) and corresponding non-tumor hepatocytes (H), and remaining nonhepatocytes that were portal vein lesions (*P*) were micro-dissected from 15-μm tissue specimens after deparaffinization and nuclear staining. Normal tissues were obtained from the gallbladder or lymph nodes collected from the same patients (Figure 1). DNA was extracted using the standard phenol/chloroform method as described previously[26].

LOH analysis

Matched tumors, corresponding non-tumor liver tissues, and normal tissue DNAs were analyzed for LOH by amplification of polymorphic microsatellite markers using the polymerase chain reaction (PCR). Sixty-one published microsatellite markers, located at 8p23.3, 8p23.2, 8p23.1, 8p22, and 8p21, were selected from the Genome Database (available at http: //www. gdb. org). A total of 16 microsatellite markers were identified as informative in Japanese patients and used (Table 1).

DNA amplification was performed in 10-μL volumes containing 100 ng of genomic DNA as a template. Each PCR mixture contained 1.5 mmol/L $MgCl_2$, 100 μmol/L forward and reverse primers, 200 μmol/L each of dATP, dGTP, dTTP and dCTP, 10 μCi of [α-^{32}P] dCTP (6000 Ci/mmol, Amersham, Biosciences Corp., Piscataway, NJ), 1 U of Taq DNA polymerase (Wako Pure Chemical Industries, Ltd., Osaka, Japan), and 1 × PCR buffer. After the initial denaturation at 94℃, 35 PCR cycles, each consisting of denaturation at 94℃ for 30 s, annealing at 65℃ -50℃ for 30 s, elongation at 72℃ for 1 min, and a final extension at 72℃ for 5 min, were performed in a 96-well Hybaid thermocycler (Gene Amp PCR System 9600, Takara, Tokyo, Japan). Ten microliters of PCR products were denatured with 30-60 μL of dye solution (95% formamide, 10 mmol/LEDTA (pH 8.0), 0.2% xylene cyanol FF, and 0.02% bromophenol blue) at 95℃ for 3 min and then cooled on ice immediately. Three microliters of denatured products were separated on a 6% urea-formamide-polyacrylamide gel and electrophoresed at 40 W for 2-3 h at room temperature. The dried gel was exposed to Hyperfilm MP (Amersham Biosciences Corp.) for 3-7 d and reexposed to another film for 2-3 wk.

Criteria for LOH

A pair of regular and longer-exposed autoradiographs was reviewed independently by two of the authors (T. L. and CX. M.). Informative pairs were judged by visual inspection to show LOH, no loss or to be noninformative.

LOH was defined as a loss of intensity of 60% or greater in 1 or more alleles in the tumor (T) or corresponding hepatocytes (H) compared with the identical allele in the normal tissue (N) (Figure 1).

Statistical analysis

The differences in LOH frequency between tumor, nontumor and normal tissues for individual markers and background values were determined with Fisher's exact test.

RESULTS

The distribution of the frequency of LOH at 8p23.2, 8p23.1, 8p22 and 8p21 for hepatocellular carcinoma is shown in Table 2. Allelic loss at 8p23.2-21 was detected with at least 1 marker in 18 of 32 (56%) cases of liver cancer. More specifically, the frequency of LOH at 8p23.2, 8p23.1, 8p22, and 8p21 with at least 1 marker was 6% (1

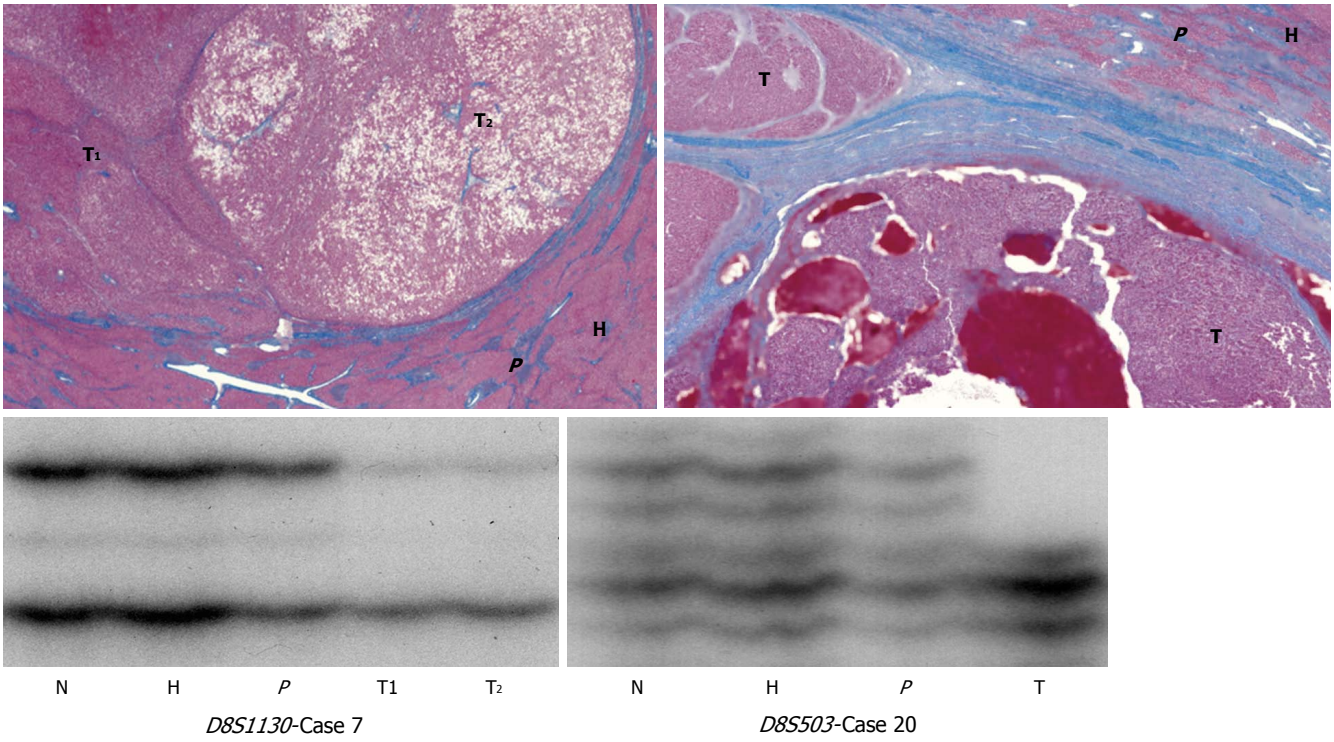

Figure 1 Representative examples of LOH in two cases of hepatocellular carcinoma (N: normal; H: hepatocytes; P: portal vein; T: tumor; number beside T indicates different lesion): case 7 showing partial loss of upper alleles in lesions of tumor 1 and tumor 2 but not in lesions of hepatocytes and portal vein at *D8S1130*; case 20 showing complete loss of upper alleles in lesion of tumor but not in surrounding non-tumor tissues at *D8S503*.

of 16), 52% (16 of 31), 47% (15 of 32), and 13% (4 of 32) for liver cancer cases respectively (Table 2). A similar result was obtained in the lesion-to-lesion comparison (data not shown). In contrast, no allelic loss at any markers on 8p was detected in the background liver tissue. The average frequency of LOH at 8p23.2-21 was 22% (58 of 264) in informative cases. We found that LOH at the 8p23.1 and 8p22 loci was significantly higher than the average in HCC cases ($P = 0.0008$, and $P = 0.004$, respectively). But allelic loss at 8p23.2 and 8p21, the loci on either side of the 8p23.1-22 region, tended to be lower than the average. On the other hand, no allelic loss (0 of 52 lesions) was detected at any informative markers on 8p23.2-21 in the surrounding liver tissues. Moreover, allelic loss at *D8S277, D8S503, D8S1130, D8S552, D8S1109, D8S254*, and *D8S258* was 25%, 42%, 39%, 43%, 24%, 43% and 50%, respectively, significantly higher than that elsewhere and the average frequency at 8p.

Correlations between LOH frequency and clinicopathological variables are summarized in Table 3. To determine whether allelic loss at 8p was associated with clinicopathological characteristics and reveal its biological role in the initiation and/or progression of tumors, we compared the frequency of LOH based on almost all of the clinicopathological findings. Corresponding to the result described above, the LOH frequency tended to be higher at 8p23.1 and 8p22 loci than at 8p23.2 and 8p21 loci for all clinicopathological findings, but no significant difference in LOH frequency was found between the liver cancer positive or negative for malignant factors. In other words, no association was detected between the deletion of 8p23.1-22 and subsequent progression of the tumors.

The distribution of LOH frequency based on the fibrosis (F) of background liver tissues, which is usually thought to be associated with hepatocarcinogenesis, was also analyzed. The frequency of LOH at 8p23.1 or 8p22 in F1, F2, F3, and F4 was 75% (3 of 4), 78% (7 of 9), 20% (1 of 5), and 38% (5 of 13), or 100% (2 of 2), 56% (5 of 9), 40% (2 of 5), and 46% (6 of 13), respectively. No statistically significant difference in LOH frequency was found on the basis of the fibrosis staging at 8p. Allelic loss at 8p even tended to be slightly more frequent in cases of tumor with earlier-stage fibrosis than in cases with advanced stage fibrosis of the background liver tissues.

DISCUSSION

Previous studies of LOH have reported that allelic loss of 8p is the most frequent chromosomal alteration in a variety of human cancers and have suggested that one or several tumor suppressor genes (TSGs) may lie within the short arm of chromosome 8[16-19]. To further identify the precise location of the putative TSGs that might potentially be involved in the tumorigenesis of HCC, we performed a high-density LOH study of HCC at 8p using recently developed microsatellite markers. Only 16 of 61 (less than 30%) were identified as informative for Japanese patients. Furthermore, among the informative markers, the informative cases for all specimens were usually lower (from 20% to 70%) for Japanese than for Westerners. The same-general tendency has been found in various other types of cancer, possibly because Japan is not multiracial like Western countries. This has led us to suggest that using this characteristic might be more efficient for identifying

Table 1 Informative microsatellite markers were selected and used in this study

No.	Locus	Markers	Genetic map (cM)	Forward	Reverse	PCR product size (bp)	result[1]
1	8p23.3	D8S7	Not listed	ACCCTGACAGCAGAGGTTTC	ACCCTGACGTTCTCCCAGTA	250-252	ni
2	8p23.2	D8S1164	Not listed	CACAAATCAGATTTTTGAAGTTGC	GGGTTAGACGGACAACCTCA	225	ni
3	8p23.2	D8S264	0.7	ACATCTGCGTCGTCTTCATA	CCAACACCTGAGTCAGCATA	121-145	in
4	8p23.2	D8S262	4.3	AGCTCAAAAGCGAAGGTGAT	GGCAACAAAGTGAGATCCTG	114-128	in
5	8p23.1	sts-X53793	Not listed	TCGACTACCCAGTGGTCTTG	GTTCAAAATGCTTGCTCGC	127	ni
6	8p23.1	D8S1742	Not listed	CCCCCACCAAGACACA	CTCAAGGGATATGAAGGGCA	130	in
7	8p23.1	D8S277	8.2	GATTTGTCCTCATGCAGTGT	ACATGTTATGTTTGAGAGGTCTG	121	in
8	8p23.1	D8S1918	Not listed	GAATGTCATGCTGGGAACG	GTAGCTCTCAAAGCAAATTATGAGC	108	ni
9	8p23.1	D8S1819	10	TCACTGAGGGACTTGGC	CGTGCTGAGAATGAGACC	207	in
10	8p23.1	D8S1140	Not listed	GACAACATCCGATAATGCTG	GAGGACATCTAGATAATTGGAAGA	378	ni
11	8p23.1	D8S503	16.2	GGTTACGAGTTTTGTCCTTTG	GAAACAAACCAATGTAGGAGTG	136	in
12	8p23.1	D8S1672	Not listed	AACTGAGATCACGCCACTCC	CCCATTGGTTTTAGAGTGGC	149	ni
13	8p23.1	AFM234ve1	Not listed	TACCGCAAAACACACCA	GCAGCCTTAGTTGACAACA	245	ni
14	8p23.1	D8S2045	Not listed	CCGATTGCTTCATCGGGAC	CGCCTCCTCCTCTGAAATCCT	120	ni
15	8p23.1	D8S1130	22.4	GAAGATTTGGCTCTGTTGGA	TGTCTTACTGCTATAGCTTTCATAA	145	in
16	8p23.1	D8S1946	Not listed	GCACAAGATCAGAGAGGTTGTG	GAGGAGAGATGGTGTTGGGA	102	ni
17	8p23.1	D8S1640	Not listed	TGCAGTCTGCGGGAGTTC	AGCAGGGTGACTGTAAAGAAGG	175	ni
18	8p23.1	D8S2060	Not listed	CTCTCCGGGAATGTAATACTGC	GAGCTGGGAGTTACTGCCTG	256	ni
19	8p23.1	D8S552	26.4	CCTGTACCATACCCCTGTATC	AAGGTTTGAATCTCTCAGTGG	132	in
20	8p23.1	D8S1109	26.4	TTCTCAGAATTGCTCATAGTGC	TCAGCTCCTCTTCTGCTGAT	241	in
21	8p23.1	D8S2066	Not listed	TTTTCTCCATCCGGTGACTC	CCAACTACGGCATGGTTTCT	175	ni
22	8p23.1-22	D8S1106	26.5	TTGTTTACCCCTGCATCACT	TTCTCAGAATTGCTCATAGTGC	149	ni
23	8p22	D8S1451	Not listed	AACCTAAGGTTCTGTGCTACATCA	AACTTACCAAGGCCGTTTAGG	149	ni
24	8p22	EST465487	Not listed	TTTGTTTGGGTGGAGGACTC	TGGACATCTGCCTAGGTCCT	250	ni
25	8p22	D8S1647	Not listed	CCAGAATTTTGAAATAGATTCATCC	AAATTTTGTAAATATCAGTGTTCCG	174	ni
26	8p22	stSG29388	32	GCAGTGAGATTTTGCTTCTGG	ATGAACATTCAATGAATCAGCA	125	ni
27	8p22	D8S1713	Not listed	CAGGGGCTGATTGTCAGAAC	GTGGCTGTCACCAAGGTCTC	113	ni
28	8p22	SGC33312	Not listed	AGGGCCTTGGGAACACTC	TCAGTTTAAATGGATGGTTTTTACT	137	ni
29	8p22	D8S2080	Not listed	GACTCAAAGAGAACCTGCCG	TAGGTTGGTGAGCACACGTC	132	ni
30	8p22	D8S2081	Not listed	ACCCAGTTACAGCACTGTAATATCA	CTCTACCCCGAAATGATGGA	147	ni
31	8p22	SHGC-24261	Not listed	AAGCAGAGATAAGCCCGACA	TTTCTTTAGATGGAGTCCATTGC	123	ni
32	8p22	SHGC-52401	Not listed	ACAGGATAGTGTTAGGCTCACATG	CATTCTCTGTATCTTTTGGGGG	120	ni
33	8p22	D8S254	Not listed	TGCCGGACATACATTAGTGA	TTGTAAACACCACAAGCAGG	65-75	in
34	8p22	D8S2001	Not listed	GACATTGAATTCCAGTATTTGTGC	GGACAAATGCCACTGCAAC	138	ni
35	8p22	SHGC-5873	Not listed	GACACACACATACAGAAAACCA	CTTACCATGAATGGAGCTTG	225	ni
36	8p22	D8S261	35.8	TGCCACTGTCTTGAAAATCC	TATGGCCCAGCAATGTGTAT	128	in
37	8p22	AFM234vf4	Not listed	GGGCACAGGCATGTGT	GGCTGCATTCTGAAAGGTTA	260-272	ni
38	8p22	D8S1948	Not listed	TTACAAAACATACCCAGTGTTTGG	CTTTTTAGTGCTTGAGACTGTCTCC	110	ni
39	8p22	D8S2028	Not listed	TCAAAAGTTTTGTTTCTATTCAGGG	TTTTTTCTGTTCCCCTCCG	178	ni
40	8p22	D8S258	40.3	CTGCCAGGAATCAACTGAG	TTGACAGGGACCCACG	144-154	in
41	8p22	D8S1949	Not listed	TGTCTTACAGCTCTCCCTCTCC	CAGTAAGGATCACCAAGACAAGG	106	ni
42	8p22	D8S1983	Not listed	ATTGGAAGAGGCAAATGGTG	TATGTACTGGATGAAGCAGGACA	175	ni
43	8p22	D8S1786	Not listed	CGAAAGATTGAGACCCCAT	GTTTCCACACCGAAGCC	209	ni
44	8p22	D8S298	42.7	AGGCTTACACCCATGGACC	ACGCAGCACACAACATCAT	155-167	in
45	8p21.3	D8S2050	Not listed	TGCCAATATCAGTGGAAGAGG	TCCTTTTTCCCTTGTTGCC	162	ni
46	8p21.3	D8S1752	Not listed	TCCTGGATCAGGCAGAAA	TCAGAGTTGGGTGAGCGA	140	in
47	8p21.3	D8S1734	44.9	GCTATCCACTTGTCCCAGA	AGCCCAGAAATAAACCCTC	114	in
48	8p21.2	D8S2256	Not listed	GTGTCTTGAGATACTGGTGA	GAGAAATGTCTTTGTTGAGG	101	ni
49	8p21.2	D8S2259	Not listed	TGAAAGCCTGTTTAGAGAGA	CTATTGCCCTGTGTTTTGCC	105	ni
50	8p21.2	D8S1220	Not listed	TTCCGTATACACATGCACCC	TAGCAGCCAGACACAGGAGC	90	ni
51	8p21.1	D8S1445	Not listed	GCAACAGAGCGAGACTCCGTC	AAGCTTACATTCTGGGTGAC	117-139	in
52	8p21.1	D8S2261	Not listed	GTATTTATTCCACAAGCATCTTA	CAACCCCATCAGTCTCTCTAAT	204	ni
53	8p21.1	D8S1444	Not listed	TTCTTCTAGATTTCCTACTA	CATTTGTTAAAAGTACAACC	91	x
54	8p21	D8S2249	Not listed	TCCACCCATTTCAGCCTTTC	CTAAAACATTTAACTTTCATT	101	ni
55	8p21	D8S2248	Not listed	ATACAGGTAGGTGAGGGCAA	TTCTGATGCTCTTCTGGAGT	136	ni
56	8p21	D8S2247	Not listed	CATTGTGGTGGAGGTCGGAG	TTCCCCCATCCCATCTGAG	122	ni
57	8p21	D8S2262	Not listed	ATGTTTTGTTCATGGGTCTTT	AAGAAAAAGGGAAGGGGCAGT	98	ni
58	8p21	D8S339	Not listed	TAGATGTTACCATTTCAC	GATTAGATCTTGGATCAG	162	ni
59	8p21	D8S2245	Not listed	CCTCTTTATCCCACTTTTCAG	CATTTTACGAATATAAGCATCC	138	ni
60	8p21	D8S2244	Not listed	ACAACTAAAGGACTTAAAGG	GACAAGAAAAGAACAAATGG	145	ni
61	8p21	D8S2246	Not listed	TAACCTGTGAATGAGAATAC	TGACAGTTTTGAGAGAATCC	169	ni

[1]ni: noninformative; in: informative.

candidate regions of deletion at 8p.

In this study, LOH at 8p was detected in 56% of informative cases of HCC. However, no allelic loss was found in corresponding hepatocytes including 18 lesions of morphogenetic non-tumor tissues and 14 lesions of cirrhotic liver tissues at any markers, the latter usually considered a

Table 2 LOH status for the 8p23.2, 8p23.1, and 8p22 in hepatocellular carcinoma

Case	Age	Sex	St/Mt	Grading	Etiology	D8S264	D8S262	8p23.2	D8S1742	D8S277	D8S1819	D8S503	D8S1130	D8S552	D8S1109	8p23.1	D8S254	D8S261	D8S258	D8S298	8p22	D8S1752	D8S1734	D8S1445	8p21	8p23.2-21
12	60	M	Mt	MD	Alcoholic	ni	ni	ni	ni	ni	ni	ni	○	ni	ni	○	○	○	●	○	●	○	○	○	○	●
11	64	M	St	MD	CH(C)+, LC	ni	ni	ni	○	○	ni	○	○	ni	○	○	○	ni	●	ni	●	○	○	○	○	●
1	42	M	St	PD	CH(B)+	ni	ni	ni	ni	○	○	ni	○	ni	●	●	●	○	ni	ni	●	○	○	○	○	●
2	59	M	St	MD	CH(-)	○	○	○	ni	ni	ni	○	○	ni	●	●	●	○	ni	○	●	ni	○	○	○	●
27	69	M	Mt	PD	CH(C)+	ni	ni	ni	○	○	ni	ni	ni	ni	●	●	○	○	○	ni	○	○	○	○	○	●
26	58	M	St	MD	CH(C)+, LC	○	ni	○	○	○	○	●	○	ni	○	●	○	○	ni	○	○	○	ni	○	○	●
15	31	F	Mt	MD	CH(C)+	ni	ni	ni	ni	ni	ni	●	ni	ni	ni	●	ni	ni	●	ni	●	○	ni	○	○	●
29	73	M	St	WD	CH(C)+	ni	ni	ni	ni	ni	ni	ni	●	ni	○	●	●	ni	●	●	●	○	○	○	○	●
6	72	M	St	MD	CH(C)+	ni	ni	ni	ni	ni	○	ni	●	ni	ni	●	○	ni	●	○	●	○	○	○	○	●
20	65	M	St	WD	Alcoholic, LC	ni	○	○	●	●	●	●	●	●	●	●	●	●	●	ni	●	●	○	○	●	●
8	74	M	Mt	MD	CH(-)	ni	○	○	●	●	ni	ni	●	ni	○	●	●	ni	ni	●	●	●	ni	ni	●	●
7	59	M	Mt	WD	CH(B)+, (C)+	○	○	○	○	●	●	ni	●	ni	ni	●	○	ni	ni	○	○	○	●	●	●	●
19	50	M	Mt	MD	CH(B)+, LC	○	●	●	●	○	ni	●	●	●	○	●	ni	ni	●	○	●	●	●	○	●	●
28	58	M	Mt	MD	CH(B)+	ni	○	○	ni	○	ni	○	●	●	○	●	●	ni	ni	ni	●	ni	○	○	○	●
5	51	M	Mt	MD	CH(B)+	ni	ni	ni	ni	ni	○	ni	●	ni	ni	●	●	ni	ni	ni	●	ni	○	○	○	●
10	71	F	Mt	MD	CH(C)+, LC	ni	ni	ni	○	○	○	●	ni	ni	ni	●	●	○	●	ni	●	○	○	○	○	●
4	57	M	Mt	MD	CH(C)+, LC	○	○	○	ni	●	○	○	○	○	○	●	○	ni	○	○	○	○	○	○	○	●
13	74	M	Mt	MD	CH(-)	ni	ni	ni	○	ni	ni	ni	●	ni	ni	●	ni	ni	ni	ni	ni	○	ni	○	○	●
18	51	M	St	WD	CH(B)+, LC	ni	ni	ni	ni	ni	○	ni	ni	○	ni	○	●	○	ni	ni	●	○	○	○	○	●
16	54	M	Mt	MD	Alcoholic, LC	ni	ni	ni	○	ni	ni	○	○	ni	ni	○	●	ni	○	ni	●	○	ni	○	○	●
25	71	M	St	MD	CH(B)+, (C)+	ni	○	○	○	ni	ni	ni	○	ni	ni	○	ni	ni	ni	ni	ni	○	ni	○	○	○
30	56	M	St	MD	CH(C)+	ni	○	○	○	○	ni	○	ni	ni	○	○	ni	ni	ni	○	○	ni	ni	○	○	○
9	57	M	St	WD	CH(C)+	ni	ni	ni	○	ni	ni	ni	○	ni	ni	○	○	ni	ni	ni	ni	○	○	○	○	○
3	51	M	St	MD	CH(B)+	ni	ni	ni	○	○	○	ni	○	ni	○	○	○	ni	○	ni	○	ni	○	○	○	○
32	54	F	St	MD	CH(B)+, LC	○	ni	○	○	○	ni	○	○	○	○	○	○	○	○	ni	○	○	○	○	○	○
21	67	M	St	WD	CH(C)+, LC	ni	ni	ni	ni	○	ni	ni	ni	ni	ni	○	ni	ni	○	○	○	ni	ni	○	○	○
33	76	F	St	WD	CH(C)+, LC	○	○	○	○	ni	ni	ni	○	ni	○	○	○	ni	ni	○	○	○	○	○	○	○
23	71	M	Mt	MD	CH(-)	ni	ni	ni	ni	ni	ni	ni	○	ni	ni	○	ni	ni	○	ni	○	ni	○	○	○	○
22	65	M	Mt	MD	CH(C)+	ni	ni	ni	ni	ni	○	ni	ni	ni	ni	○	○	ni	ni	○	○	○	○	○	○	○
31	65	F	Mt	MD	CH(C)+, LC	ni	ni	ni	○	ni	○	ni	○	○	○	○	ni	ni	ni	ni	ni	ni	○	○	○	○
17	37	F	Mt	MD	CH(B)+, LC	ni	ni	ni	ni	ni	ni	ni	ni	ni	ni	ni	ni	○	ni	ni	○	ni	ni	○	○	○
24	60	M	Mt	MD	CH(-), LC	ni	○	○	ni	○	ni	ni	ni	ni	○	○	○	ni	○	ni	○	○	○	○	○	○
LOH ●						0	1	1	3	4	2	5	9	3	4	16	10	1	8	2	15	3	2	1	4	20
Informative (32/33)						8	13	16	17	16	12	12	23	7	17	31	23	10	16	13	32	23	23	31	32	32
LOH/Informative (58/264 = 22%)						0%	8%	6%[a]	18%	25%	17%	42%	39%	43%	24%	52%[b]	43%	10%	50%	15%	47%[c]	13%	9%	3%	13%[d]	63%[e]

A total of 32 informative liver cancer cases were analyzed for LOH at the sixteen microsatellite markers. The number of informative cases and frequency of LOH was shown at the bottom. St: solitary tumor; Mt: multiple tumor; WD: well differetiation; MD: moderately differretiation; PD: poorly differentiation; CH: chronic hepatitis; LC: liver cirrhosis. ● LOH; ○ retention of heterozygosity; ni: noninformative. Significant different from the average, 52% *vs* 22%, [b]$P = 0.0008$; 47% *vs* 22%, [c]$P = 0.004$; 63% *vs* 22%, [e]$P = 0.007$; No statistically significant different from the average, 6% *vs* 22%, [a]$P = 0.207$; 13% *vs* 22%, [d]$P = 0.257$.

premalignant liver lesion. Our result suggests that allelic loss at 8p is an important event in the initiation or promotion of HCC.

Furthermore, among the informative regions 8p23.2, 8p23.1, 8p22, and 8p21, allelic loss was significantly more frequent at 8p23.1 and 8p22 than at 8p23.2 and 8p21 on both sides of the loci. Several minimal regions adjacent to frequently deleted markers were also identified, such as *D8S277, D8S503, D8S1130,* and *D8S552* at 8p23.1, and *D8S254* and *D8S258* at 8p22. On the basis of the minimal regions of overlapping deletions at 8p, we identified two sites, 8p23.1 and 8p22, possibly containing TSGs involved in human liver carcinogenesis. That is to say, the commonly deleted regions were restricted to 8p23.1-22 suggesting that the key genes exist in two distinct regions that might be closely related to the carcinogenesis of

Table 3 Distribution of LOH frequency at 8p in hepatocellular carcinoma cases by clinicopathological variables

Clinicopathological Variables	D8S 264	D8S 262	8p23.2	D8S 1742	D8S 277	D8S 1819	D8S 503	D8S 1130	D8S 552	D8S 1109	8p23.1	D8S 254	D8S 261	D8S 258	D8S 298	8p22	D8S 1752	D8S 1734	D8S 1445	8p21	8p23.2-21
Tumor size (mm)																					
> 50	0/4	0/4	0/5 (0%)	0/6	1/5	0/6	2/4	4/12	0/1	3/8	10/14 (71%)	4/10	0/5	3/7	1/6	6/13 (46%)	0/10	0/10	0/15	0/15 (0%)	10/15 (67%)
< 50	0/3	1/7	1/8 (13%)	3/11	3/11	2/6	3/7	5/11	3/6	1/9	6/17 (35%)	6/13	1/7	5/9	1/7	9/16 (56%)	3/11	2/14	1/15	4/15 (27%)	10/17 (59%)
Tumor number																					
St	0/2	0/3	0/5 (0%)	1/9	1/8	1/5	2/6	3/12	1/3	3/10	6/15 (41%)	9/18	1/6	4/7	1/7	4/13 (31%)	3/20	2/18	1/24	4/24 (17%)	17/24 (71%)
Mt	0/5	1/10	1/10 (10%)	2/7	3/8	1/6	3/6	6/11	2/4	1/7	10/16 (63%)	1/4	0/4	4/9	1/6	5/13 (38%)	0/2	0/5	0/7	0/7 (0%)	2/7 (29%)
Growth Pattern																					
Eg	0/8	1/13	1/15 (7%)	3/16	4/13	2/11	4/11	9/22	3/7	3/15	14/28 (50%)	8/20	1/8	7/14	2/13	13/26 (50%)	3/20	2/21	1/29	4/29 (14%)	18/29 (62%)
Ig	0/1	0/1	0/1 (0%)	0/1	0/3	0/2	1/1	0/1	0/0	1/2	2/5 (40%)	2/2	0/2	1/2	0/0	2/2 (100%)	0/2	0/2	0/2	0/2 (0%)	2/2 (100%)
Formation of capsule																					
Fc-	0/6	1/8	1/10 (10%)	2/3	1/4	1/4	2/3	4/7	3/4	2/5	5/6 (83%)	3/4	1/3	3/3	0/3	5/5 (100%)	2/5	1/5	0/5	2/5 (40%)	5/5 (100%)
Fc+	0/2	0/6	0/6 (0%)	1/14	3/12	1/8	3/9	5/17	0/3	2/12	11/25 (44%)	7/18	0/7	5/13	2/10	10/23 (43%)	1/18	1/18	1/26	2/26 (8%)	15/26 (58%)
Infiltration to capsule																					
Fc-Inf-	0/6	1/8	1/10 (10%)	1/5	1/7	0/7	3/5	3/8	0/4	2/8	7/11 (64%)	3/10	0/5	4/9	0/3	7/15 (47%)	1/10	1/12	0/15	1/15 (7%)	10/15 (67%)
Fc-Inf+	0/1	0/3	0/3 (0%)	1/8	1/3	0/2	1/4	3/10	0/0	1/5	5/13 (38%)	5/9	0/3	3/5	2/7	6/11 (55%)	1/10	0/8	0/13	1/13 (8%)	7/13 (54%)
Septal formation																					
Sf-	0/0	0/3	0/3 (0%)	1/7	2/6	1/7	3/5	3/8	1/4	2/5	7/13 (54%)	5/9	0/5	5/9	1/4	7/15 (47%)	1/12	0/12	0/16	1/16 (6%)	9/16 (56%)
Sf+	0/6	1/9	1/10 (10%)	2/8	1/5	0/3	1/4	3/10	1/1	2/7	5/12 (42%)	4/10	0/3	3/6	1/6	7/11 (64%)	2/9	1/9	0/12	2/12 (17%)	8/12 (67%)
Grading																					
WD	0/3	0/3	0/4 (0%)	1/4	2/4	2/4	1/2	4/6	1/4	1/2	4/8 (50%)	3/6	1/2	3/5	1/5	3/7 (43%)	1/7	1/7	1/7	2/7 (29%)	4/7 (57%)
MD	1/7	0/9	1/13 (8%)	2/13	2/12	1/9	4/12	5/17	1/12	3/6	11/21 (52%)	6/13	1/8	5/11	1/13	10/18 (56%)	2/12	1/13	0/21	2/21 (10%)	13/21 (62%)
PD	0/0	0/1	0/1 (0%)	0/1	0/3	0/1	0/1	1/3	2/3	0/1	2/3 (67%)	1/2	1/3	0/1	0/0	1/2 (50%)	0/2	0/2	0/2	0/2 (0%)	2/2 (100%)
pT																					
pT1	0/1	0/2	0/2 (0%)	0/2	0/1	0/1	0/1	1/2	0/3	0/2	0/5 (0%)	2/6	0/1	2/3	1/2	3/6 (50%)	0/6	0/6	0/6	0/6 (0%)	3/6 (50%)
pT2	1/7	0/7	1/10 (10%)	2/6	1/7	1/3	4/6	4/5	2/5	3/3	7/11 (64%)	5/8	1/4	5/7	0/4	7/11 (64%)	2/8	1/9	0/11	2/11 (18%)	8/11 (73%)
pT3	0/2	0/2	0/3 (0%)	1/4	2/2	1/3	0/2	3/8	1/5	0/1	5/8 (63%)	2/4	0/1	0/2	1/4	2/5 (40%)	1/5	1/5	1/8	2/8 (25%)	5/8 (63%)
pT4	0/0	0/0	0/0 (0%)	0/0	0/1	0/1	0/0	0/1	1/1	0/0	1/1 (100%)	1/1	0/2	0/0	0/0	1/2 (50%)	0/1	0/1	0/2	0/2 (0%)	1/2 (50%)
pN																					
pN-	1/8	0/10	1/12 (8%)	3/7	3/7	2/4	3/5	6/9	1/8	0/1	5/12 (42%)	4/9	0/0	6/7	2/7	8/13 (62%)	3/11	2/10	1/13	4/13 (31%)	9/13 (69%)
pNx	0/0	0/3	0/3 (0%)	0/6	1/5	0/4	1/4	2/9	2/6	1/5	6/12 (50%)	2/4	0/6	1/5	0/1	2/4 (50%)	0/5	0/5	0/7	0/7 (0%)	4/7 (57%)
pM																					
pM-	1/6	0/11	1/13 (8%)	2/7	1/5	1/2	3/5	3/10	3/8	2/4	6/14 (43%)	3/7	1/5	5/9	1/6	6/11 (55%)	2/10	1/11	0/13	2/13 (15%)	7/13 (54%)
pMx	0/0	0/0	0/0 (0%)	0/0	2/3	0/2	0/1	2/2	0/2	1/1	3/4 (75%)	5/6	0/1	0/1	0/0	5/7 (71%)	1/5	0/5	0/8	1/8 (13%)	7/8 (88%)
Vascular infiltration																					
V-	0/7	1/10	1/13 (8%)	2/10	3/10	1/8	4/9	6/13	2/6	2/9	9/20 (45%)	6/15	0/5	7/13	0/7	11/20 (55%)	2/16	2/18	1/21	3/21 (14%)	14/21 (67%)
V+	1/7	0/2	1/9 (11%)	1/7	1/6	1/4	1/3	3/10	1/1	2/8	7/11 (64%)	4/6	1/5	1/3	2/6	4/7 (57%)	1/6	0/5	0/9	1/9 (11%)	5/9 (56%)
Bile duct infiltration																					
B-	0/10	1/13	1/17 (6%)	3/18	4/15	2/11	4/13	10/24	3/9	3/17	15/28 (54%)	7/18	2/9	8/15	2/12	11/24 (46%)	2/19	2/20	1/27	3/27 (11%)	16/27 (59%)
B+	0/1	0/1	0/2 (0%)	0/3	0/3	1/4	1/3	0/4	1/3	1/4	3/4 (75%)	3/5	1/5	0/1	0/4	4/5 (80%)	1/4	0/4	0/5	1/5 (20%)	4/5 (80%)
Liver cirrhosis																					
LC-	0/2	0/6	0/6 (0%)	1/8	2/7	1/6	1/4	7/14	1/1	3/8	11/18 (61%)	6/11	0/4	4/7	2/8	9/16 (56%)	1/10	1/13	1/18	2/18 (11%)	12/18 (67%)

LC+	0/5	1/5	1/7 (14%)	2/9	2/9	1/6	4/8	2/9	2/6	1/9	5/13 (38%)	4/10	1/6	4/9	0/5	6/13 (46%)	2/11	1/11	0/14	2/14 (14%)	8/14 (57%)
Chronic hepatitis																					
CH-	0/1	0/3	0/4 (0%)	2/3	2/3	1/1	1/2	3/7	1/1	2/4	4/8 (50%)	4/6	1/3	2/5	1/3	5/7 (71%)	2/6	0/5	0/8	2/8 (25%)	6/8 (75%)
CH+	0/6	1/7	1/9 (11%)	1/13	2/13	1/11	4/9	6/16	2/6	2/13	12/23 (52%)	6/17	0/7	6/11	1/10	10/22 (45%)	1/17	2/19	1/24	2/24 (8%)	14/24 (58%)

Eg: expansive growth; Ig: infiltrative growth; St: solitary tumor; Mt: multiple tumor; LC: liver cirrhosis; CH: chronic hepatitis.

HCC. Our results are consistent with previously reported patterns of molecular change in HCC and other epithelial tumors. No statistically significant differences were detected in the candidate regions 8p23.1 and 8p22 between the frequency of LOH and any clinicopathologic characteristics, including etiological factors considered to contribute to tumorigenesis, and malignant factors usually important to the subsequent progression of tumors. These results led us to the hypothesis that loss of 8p is not essential for the subsequent development or progression of HCC.

Moreover, with respect to the results of allelotyping, several genes, such as angiopintin 2 (ANGPT2), AGPAT5, LOC648814, DEFB 137 and DEFB 136, LONRF1, and FLJ36980, which were adjacent to the candidate markers D8S277, D8S503, D8S1130, D8S552, and D8S1109 at 8p23.1, respectively, were analyzed for somatic mutations or expression by single nucleotide polymorphisms (SSCPs) and the reverse transcription polymerase chain reaction (RT-PCR) methods. However, no significant mutation or absence of expression of these adjacent genes was found (data not shown), indicating that alterations of those genes may not be closely related to the carcinogenesis[16-19,26]. Several new candidate cancer-susceptibility genes at 8p22, such as deleted in breast cancer 2 (DBC2), leucine zipper tumor suppressor 1 (LZTS1), and deleted in liver cancer 1 (DLC1), and mitochondrial tumor suppressor 1 (MTUS1) have been cloned[27-30]. We have analyzed these genes in the same HCC samples, but a somatic mutation or absence of expression of these candidate genes is rare in Japanese patients (data not shown), indicating that these well-known candidate genes are not the main targets of the observed LOH at 8p22. Although no significant genetic alterations were detected in HCC in the present study, it could not be denied that they had already had some epigenetic change during the pre-cancer stage or earlier in the carcinogenesis. Although detailed data have not been published, the present results strongly suggest that other unknown genes in the region 8p22-23.1 play an important role in HCC. Further studies are needed to identify critical oncogenes or TSGs, including those in 8p22-23.1. Our results should be useful for identifying the targets of deletion at 8p.

ACKNOWLEDGMENTS

We thank Miss Kana Tamura and Ms. Michiko Kasai for their help in collecting samples, Mrs. Misako Shirai and Mrs. Mamiko Owada for technique help, and Miss Michiko Takagi for photographic help.

REFERENCES

1 **Parkin DM**, Pisani P, Ferlay J. Estimates of the worldwide incidence of 25 major cancers in 1990. *Int J Cancer* 1999; **80**: 827-841
2 **Pisani P**, Bray F, Parkin DM. Estimates of the world-wide prevalence of cancer for 25 sites in the adult population. *Int J Cancer* 2002; **97**: 72-81
3 **Bosch FX**, Ribes J, Díaz M, Cléries R. Primary liver cancer: worldwide incidence and trends. *Gastroenterology* 2004; **127**: S5-S16
4 **Bruix J**, Boix L, Sala M, Llovet JM. Focus on hepatocellular carcinoma. *Cancer Cell* 2004; **5**: 215-219
5 **Feitelson MA**, Sun B, Satiroglu Tufan NL, Liu J, Pan J, Lian Z. Genetic mechanisms of hepatocarcinogenesis. *Oncogene* 2002; **21**: 2593-2604
6 **Thorgeirsson SS**, Grisham JW. Molecular pathogenesis of human hepatocellular carcinoma. *Nat Genet* 2002; **31**: 339-346
7 **Minister's Secretariat**, Ministry of Health, Labor and Welfare, Statistics and Information Dept, Vital Statistics of Japan. Age-adjusted death rates of malignant neoplasms by site, sex and calendar year (1970-2001). 2001
8 **Ng IO**, Guan XY, Poon RT, Fan ST, Lee JM. Determination of the molecular relationship between multiple tumour nodules in hepatocellular carcinoma differentiates multicentric origin from intrahepatic metastasis. *J Pathol* 2003; **199**: 345-353
9 **Maggioni M**, Coggi G, Cassani B, Bianchi P, Romagnoli S, Mandelli A, Borzio M, Colombo P, Roncalli M. Molecular changes in hepatocellular dysplastic nodules on microdissected liver biopsies. *Hepatology* 2000; **32**: 942-946
10 **Vogelstein B**, Fearon ER, Hamilton SR, Kern SE, Preisinger AC, Leppert M, Nakamura Y, White R, Smits AM, Bos JL. Genetic alterations during colorectal-tumor development. *N Engl J Med* 1988; **319**: 525-532
11 **Gisin J**, Perren A, Bawohl M, Jochum W. Rare allelic imbalances, but no mutations of the PRDX1 gene in human hepatocellular carcinomas. *J Clin Pathol* 2005; **58**: 1229-1231
12 **Mori T**, Nomoto S, Koshikawa K, Fujii T, Sakai M, Nishikawa Y, Inoue S, Takeda S, Kaneko T, Nakao A. Decreased expression and frequent allelic inactivation of the RUNX3 gene at 1p36 in human hepatocellular carcinoma. *Liver Int* 2005; **25**: 380-388
13 **Tischoff I**, Markwarth A, Witzigmann H, Uhlmann D, Hauss J, Mirmohammadsadegh A, Wittekind C, Hengge UR, Tannapfel A. Allele loss and epigenetic inactivation of 3p21.3 in malignant liver tumors. *Int J Cancer* 2005; **115**: 684-689
14 **Bando K**, Nagai H, Matsumoto S, Koyama M, Kawamura N, Onda M, Emi M. Identification of a 1-cM region of common deletion on 4q35 associated with progression of hepatocellular carcinoma. *Genes Chromosomes Cancer* 1999; **25**: 284-289
15 **Okabe H**, Ikai I, Matsuo K, Satoh S, Momoi H, Kamikawa T, Katsura N, Nishitai R, Takeyama O, Fukumoto M, Yamaoka Y. Comprehensive allelotype study of hepatocellular carcinoma: potential differences in pathways to hepatocellular carcinoma between hepatitis B virus-positive and -negative tumors. *Hepatology* 2000; **31**: 1073-1079
16 **Kahng YS**, Lee YS, Kim BK, Park WS, Lee JY, Kang CS. Loss of heterozygosity of chromosome 8p and 11p in the dysplastic nodule and hepatocellular carcinoma. *J Gastroenterol Hepatol* 2003; **18**: 430-436
17 **Chan KL**, Lee JM, Guan XY, Fan ST, Ng IO. High-density allelotyping of chromosome 8p in hepatocellular carcinoma and clinicopathologic correlation. *Cancer* 2002; **94**: 3179-3185
18 **Pineau P**, Nagai H, Prigent S, Wei Y, Gyapay G, Weissenbach J, Tiollais P, Buendia MA, Dejean A. Identification of three

distinct regions of allelic deletions on the short arm of chromosome 8 in hepatocellular carcinoma. *Oncogene* 1999; **18**: 3127-3134

19 **Piao Z**, Park C, Park JH, Kim H. Allelotype analysis of hepatocellular carcinoma. *Int J Cancer* 1998; **75**: 29-33

20 **Anzola M**, Cuevas N, Lopez-Martinez M, Martinez de Pancorbo M, Burgos JJ. p16INK4A gene alterations are not a prognostic indicator for survival in patients with hepatocellular carcinoma undergoing curative hepatectomy. *J Gastroenterol Hepatol* 2004; **19**: 397-405

21 **Kremer-Tal S**, Reeves HL, Narla G, Thung SN, Schwartz M, Difeo A, Katz A, Bruix J, Bioulac-Sage P, Martignetti JA, Friedman SL. Frequent inactivation of the tumor suppressor Kruppel-like factor 6 (KLF6) in hepatocellular carcinoma. *Hepatology* 2004; **40**: 1047-1052

22 **Chen CF**, Yeh SH, Chen DS, Chen PJ, Jou YS. Molecular genetic evidence supporting a novel human hepatocellular carcinoma tumor suppressor locus at 13q12.11. *Genes Chromosomes Cancer* 2005; **44**: 320-328

23 **Zhu GN**, Zuo L, Zhou Q, Zhang SM, Zhu HQ, Gui SY, Wang Y. Loss of heterozygosity on chromosome 10q22-10q23 and 22q11.2-22q12.1 and p53 gene in primary hepatocellular carcinoma. *World J Gastroenterol* 2004; **10**: 1975-1978

24 **Nishida N**, Fukuda Y, Komeda T, Ito T, Nishimura T, Minata M, Kuno M, Katsuma H, Ikai I, Yamaoka Y, Nakao K. Prognostic impact of multiple allelic losses on metastatic recurrence in hepatocellular carcinoma after curative resection. *Oncology* 2002; **62**: 141-148

25 **Yeh SH**, Chen PJ, Shau WY, Chen YW, Lee PH, Chen JT, Chen DS. Chromosomal allelic imbalance evolving from liver cirrhosis to hepatocellular carcinoma. *Gastroenterology* 2001; **121**: 699-709

26 **Lu W**, Takahashi H, Furusato B, Maekawa S, Ikegami M, Sudo A, Egawa S, Hano H. Allelotyping analysis at chromosome arm 8p of high-grade prostatic intraepithelial neoplasia and incidental, latent, and clinical prostate cancers. *Genes Chromosomes Cancer* 2006; **45**: 509-515

27 **Knowles MA**, Aveyard JS, Taylor CF, Harnden P, Bass S. Mutation analysis of the 8p candidate tumour suppressor genes DBC2 (RHOBTB2) and LZTS1 in bladder cancer. *Cancer Lett* 2005; **225**: 121-130

28 **Seng TJ**, Low JS, Li H, Cui Y, Goh HK, Wong ML, Srivastava G, Sidransky D, Califano J, Steenbergen RD, Rha SY, Tan J, Hsieh WS, Ambinder RF, Lin X, Chan AT, Tao Q. The major 8p22 tumor suppressor DLC1 is frequently silenced by methylation in both endemic and sporadic nasopharyngeal, esophageal, and cervical carcinomas, and inhibits tumor cell colony formation. *Oncogene* 2007; **26**: 934-944

29 **Di Benedetto M**, Pineau P, Nouet S, Berhouet S, Seitz I, Louis S, Dejean A, Couraud PO, Strosberg AD, Stoppa-Lyonnet D, Nahmias C. Mutation analysis of the 8p22 candidate tumor suppressor gene ATIP/MTUS1 in hepatocellular carcinoma. *Mol Cell Endocrinol* 2006; **252**: 207-215

30 **Di Benedetto M**, Bièche I, Deshayes F, Vacher S, Nouet S, Collura V, Seitz I, Louis S, Pineau P, Amsellem-Ouazana D, Couraud PO, Strosberg AD, Stoppa-Lyonnet D, Lidereau R, Nahmias C. Structural organization and expression of human MTUS1, a candidate 8p22 tumor suppressor gene encoding a family of angiotensin II AT2 receptor-interacting proteins, *ATIP*. *Gene* 2006; **380**: 127-136

S- Editor Liu Y **L- Editor** Zhu LH **E- Editor** Lu W

PO Box 2345, Beijing 100023, China
www.wjgnet.com
wjg@wjgnet.com

World J Gastroenterol 2007 February 21; 13(7): 1098-1102
World Journal of Gastroenterology ISSN 1007-9327

RAPID COMMUNICATION

KIT-negative gastrointestinal stromal tumors with a long term follow-up: A new subgroup does exist

Katerina Kontogianni-Katsarou, Constantina Lariou, Eugenia Tsompanaki, Christina Vourlakou, Evi Kairi-Vassilatou, Costas Mastoris, Georgia Pantazi, Agatha Kondi-Pafiti

Katerina Kontogianni-Katsarou, Evi Kairi-Vassilatou, Agatha Kondi-Pafiti, Department of Pathology, Athens Medical School, Areteion University Hospital, 76, Vas. Sophias Ave., Athens 11528, Greece
Constantina Lariou, Christina Vourlakou, Costas Mastoris, Georgia Pantazi, Department of Pathology, Evaggelismos General Hospital, Ipsiladou 45-47, Athens 10676, Greece
Eugenia Tsompanaki, Department of Statistics, School of Economics and Business, Athens University, Patision 76, Athens 10434, Greece
Supported by Hellenic State Scholarship Foundation, Department of Science Promotion, No. 19366/2005
Correspondence to: Katerina Kontogianni-Katsarou, MD, PhD, Department of Pathology, Athens Medical School, Areteion University Hospital, 1b, Agias Annis Str. 145 63, Kifisia, Greece. k.kontogianni@m2k.gr
Telephone: +30-210-8018624 Fax: +30-210-8018624
Received: 2006-10-27 Accepted: 2007-01-12

Abstract

AIM: To investigate the incidence of KIT immunohostochemical staining in (GI) stromal tumors (GISTs), and to analyze the clinical manifestations of the tumors and prognostic indicators.

METHODS: We retrospectively analyzed 50 cases of previously diagnosed GISTs. Tissue samples were assessed with KIT (CD117 antigen), CD34, SMA, desmin, S-100, NSE, PCNA, Ki-67, and BCL-2 for immunohistochemical study and pathological characteristics were analyzed for prognostic factors.

RESULTS: Fifteen tumors (30%) were negative in KIT staining. A significant association was observed between gender (male patients: 14/15) and KIT-negative staining (P = 0.003).The patients's mean age was 56.6 years. Tumors developed in stomach (n = 8), small intestine (n = 5), large intestine (n = 1) and oesophagus (n = 1). The mean tumor size was 5.72 cm. The mitotic count ranged from 0-29/50 HPF (mean: 3.4) and 73% of tumors showed no necrosis. The majority of the tumors (67%) had dual or epithelioid differentiation. Tumors were classified as very low or low risk (n = 7), intermediate risk (n = 5), and high risk (n = 3) groups. Twelve (80%) patients were alive without evidence of residual tumor for an average period of 40.25 mo (12-82 mo); three patients developed metastatic disease to the liver and eventually died within 2-12 mo (median survival: 8.6 mo).

CONCLUSION: A small subgroup of GISTs fulfils the clinical and morphological criteria of these tumors, and lacks KIT expression. These tumors predominantly developed in the stomach, being dual or epithelioid in morphology, which are classified as low risk tumors and presented a better survival status than KIT-positive tumors. The ability to diagnose GISTs still depends on immunohistochemical staining but the research should extend in gene mutations.

Key words: Gastrointestinal stromal tumors; CD 117 antigen; Immunohistochemistry; Survival

Kontogianni-Katsarou K, Lariou C, Tsompanaki E, Vourlakou C, Kairi-Vassilatou E, Mastoris C, Pantazi G, Kondi-Pafiti A. KIT-negative gastrointestinal stromal tumors with a long term follow up: A new subgroup does exist. *World J Gastroenterol* 2007; 13(7): 1098-1102

http://www.wjgnet.com/1007-9327/13/1098.asp

INTRODUCTION

Most gastrointestinal mesenchymal neoplasms are gastrointestinal stromal tumors (GISTs). Their definitions follow the WHO histological classification where the term GIST is now used for a specific group of tumors comprising the majority of all gastrointestinal stromal tumors[1]. Typically, GISTs are immunohistochemically positive for KIT tyrosine kinase receptor which is perhaps their single best defining feature[2]. Most GISTs are positive for KIT (CD117 antigen), which may show membrane, diffuse cytoplasmic or a perinuclear accentuation pattern.

Histological assessment of malignancy is essentially based on mitotic counts, the size of the lesion and presence or absence of metastasis[3-5]. A proportion of GISTs, especially the malignant tissues show mutations in the regulatory juxtamembrane domain (exon 11) of the KIT gene[6]. Until now, the treatment with selective tyrosine kinase inhibitors, such as imatinib mesylate, for patients with GISTs has hinged on the KIT positive immunostaining tumors. Although the KIT positivity by immunohistochemistry becomes invaluable in the diagnosis of GISTs, some authors believe that a small subgroup of these tumors fulfils the clinical and morphological criteria

of GISTs, and lacks KIT expression. The biological features of these tumors have rarely been addressed.

Our aim was to investigate the incidence of KIT immunohostochemical staining in 50 cases of previously diagnosed GI stromal tumors, to carried out a comprehensive examination of GISTs that are negative in CD117 expression, and to analyze the clinical manifestations and prognostic indicators of the tumors.

MATERIALS AND METHODS

Using the database of Surgery and Pathology Departments of "Evaggelismos" General Hospital and Areteion University Hospital, we collected records with a pathologic diagnosis of stromal tumor of GI tract. Fifty patients with the diagnosis of GIST between 1994-2004 were retrieved from the archives. Patient age, gender, clinical manifestations, tumor size, pathological characteristics, the presence of distant metastasis and the outcome were recorded.

Tumor specimens were fixed in 10% buffered formalin after gross examination and embedded in paraffin. Histologic sections stained with hematoxylin and eosin were evaluated for all cases. Tumors were classified as very low risk, low risk, intermediate or high risk groups based on histological parameters according to NIH Consencus Guidelines for Grading[4].

Immunohistochemistry

The tumor samples from all 50 cases were examined for various markers using commercially available immunohistochemical antibodies against KIT (CD117 antigen), (A4502, polyclonal, Dako, USA; 1:50 dilution), CD34 (clone QBEnd/10) (Novocastra Labs; 1:50), S-100 (clone S1/61/69) (Novocastra Labs; 1:40), smooth-muscle actin (SMA) (clone asm-1) (Dako; 1:200), desmin (clone DE-R-11) (Novocastra Labs; 1:100), neuron-specific enolase (NSE) (clone 5E2) (Novocastra Labs; 1:100), neurofilament protein (NFL) (clone NR4) (Novocastra Labs; 1:50), bcl-2 (clone 124) (Dako; 1:40), proliferating cell nuclear antigen (PNA) (clone PC10) (Novocastra Labs; 1:200), Ki-67 (clone MM1) (Novocastra Labs; 1:200) by a standard three-step immunoperoxidase procedure (APAAP, DAKO, Glostroup, Danmark). Appropriate positive controls were run concurrently for all antibodies tested. According to the percentage of tumor cells showing an immunopositive reaction among the total tumor cells, tumors were reported as negative ($\leqslant$ 10%) or positive (> 10%).

Statistical methods

Data was analyzed using statistical software SPSS version 12.0. Chi-square test or Fisher's exact test was done for categorical variables to assess differences among baseline patient features. Overall survival was computed by the Kaplan-Meier method. Comparison of survival between subgroups was performed by the log-rank test. The relative importance of prognostic factors for the survival was analyzed with Cox's proportional hazard model. Statistical significance would be inferred at a two-tailed P value < 0.05.

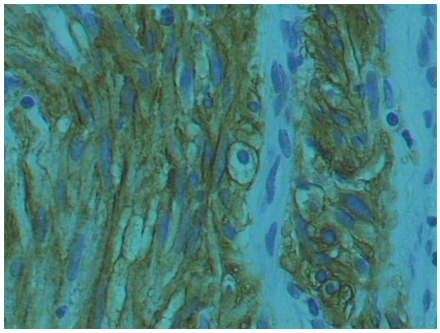

Figure 1 Histological section of GIST showing positive immunostaining for KIT (CD117 antigen) × 400.

RESULTS

Clinical and pathological data of patients with GISTs

Thirty-one (62%) patients were male and 19 (38%) female. Their age at diagnosis ranged from 26 to 89 years (mean: 62 ± 14.5). The most common symptoms were abdominal pain (72%). The most common anatomic sites of tumor origin were the small intestine (n = 23) and the stomach (n = 19). Three tumors were located in oesophagus and 5 tumors in large intestine.

The size of the tumor ranged from 0.2 cm to 30 cm (mean: 4.58 ± 5.2). The mitotic count was 0-29 per 50 HPF (× 400) (mean: 4.25 ± 2). Necrosis was present in 13 (26%) tumors. Twenty-four (48%) tumors showed evidence of dual differentiation toward smooth muscle and neural elements. Reactivity for either SMA or desmin (epithelioid features) was observed in 8 (16%) cases. There was neural differentiation (spindled features) in 7 (14%) cases. No evidence of differentiation toward either cell type, was formed even after exhaustive immunohistochemistry in 11 (22%) cases. Of the 50 tissues tested, 35 (70%) were positive for KIT staining (Figure 1), while 15 (30%) tumors lacked KIT expression. The high incidence of KIT-positive staining (57%) was in tissues diagnosed as "high risk" tumors. Twenty-four (48%) tumors were CD34 positive. The proliferative activity (PCNA labeling index) was high (> 10% labeled nuclei) in 62% of our specimens. Only 6 (12%) cases were characterized by high (> 20% labeled nyclei) Ki-67 immunoreactivity percentages. Bcl-2 protein was positively expressed in the cytoplasm of tumor cells in 26 (52%) specimens.

Complete information on patients' clinical course could be obtained in 50 (100%) cases. According to the available follow-up, patients with KIT-positive staining tumors were alive without evidence of residual tumor for an average period of 32.3 mo (12-82 mo). Tumor location, mitotic counts, risk group and metastasis seem to be related to survival, since partial likelihood ratio test of Cox regression for each of these patient's feature was less than 0.05 (Figure 2, Figure 3, Figure 4). There was an indication of association between tumor size and mitoses (P = 0.055, Fisher's Exact test).

Clinicopathological features of KIT (CD117) negative GISTs

Of the 50 tissues tested, a small subgroup of tumors (n = 15) fulfiled the clinical and morphological criteria of GISTs and lacked KIT antigen immunoexpression. The clinicopathological features of KIT-negative cases

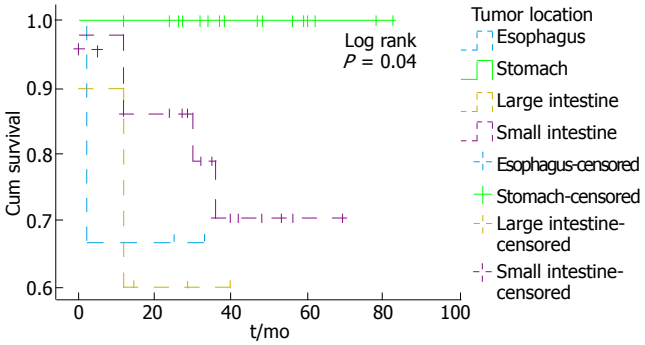

Figure 2 Cumulative survival for patients with GISTs based on tumor location.

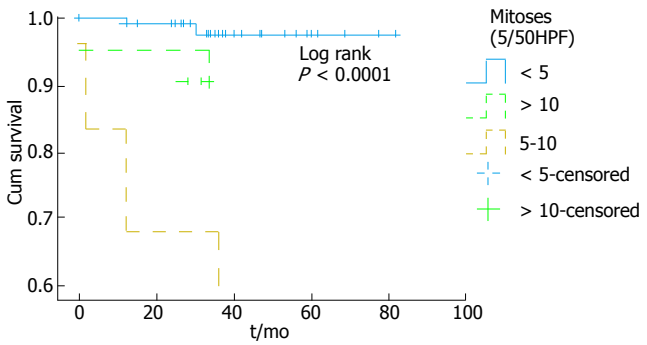

Figure 3 Cumulative survival for patients with GISTs based on mitotic counts.

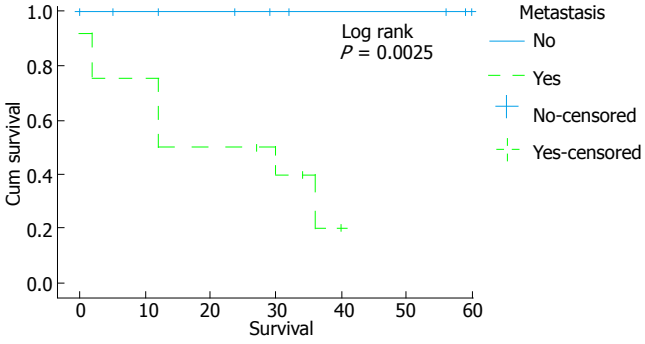

Figure 4 Cumulative survival for patients with GISTs based on metastasis status.

are shown in Table 1. A highly significant association was observed between gender and CD117 staining ($P = 0.003$). All, except one, KIT-negative tumors were observed in male patients, while the majority of female patients (18/19) expressed CD117 immunostaining (Table 2).

Patients' age at diagnosis ranged from 26 to 82 years (mean: 56.6). The majority of them (11/15) presented at the hospital with symptoms, as abdominal pain. KIT-negative GISTs developed in stomach ($n = 8$), small intestine ($n = 5$), large intestine ($n = 1$) and oesophagus ($n = 1$) (Table 3).

Tumors size ranged from 0.5 cm to 30 cm (mean: 5.72). The majority of tumors were smaller than 5 cm (9/15), and only one was > 10 cm. The mitotic count ranged from 0-29 per 50 HPF (× 400) (mean: 3.4). Twelve (80%) tumors contained less than 5/50 HPF mitoses, 2 (13%) tumors contained mitoses between 5 and 10/50 HPF and 1 (7%) tumor contained mitoses > 10/50 HPF. Absence of necrosis was present in 73% (11/15) of tumors.

Of the 15 KIT-negative samples, 6 (40%) cases had dual differentiation showing histologically mixed spindled and epithelioid type features, four (27%) cases showed histologically predominantly epithelioid type features, two (13%) cases spindled type features, and 3(20%) cases were classified as anaplastic (Table 4).

KIT-negative tumors were diagnosed as "very low" and "low risk" (benign) ($n = 7$), "intermediate risk" (uncertain malignant potential) ($n = 5$), and "high risk" tumors (malignant potential) ($n = 3$).

The clinical status was primary presentation in 12 patients. According to the available follow-up, twelve patients (80%) were alive without evidence of residual tumor for an average period of 40.25 mo (12-82 mo); three patients developed metastatic disease to the liver and eventually died within 2-12 mo (median survival: 8.6 mo).

DISCUSSION

The classification of GISTs has been a continually evolving process reflecting our increasing understanding of the biological nature of these tumors. One of the most important concepts of the recent years is that GISTs show the differentiation of the interstitial cells of Cajal (ICC)[2]. Mesenchymal tumors of GI can be identified based on the features of ICCs and can therefore designated as GISTs[4].

Histological and immunohistochemical advances, and molecular genetics provide a new era for GISTs. KIT, a type Ⅲ tyrosine kinase growth factor receptor, is the common denominator in most GISTs[7-9]. CD117, the epitope for KIT, is introduced as a new phenotypic marker for distinguishing between GISTs and non-GIST spindle cell tumors of the GI. A small subgroup of GISTs that fulfill the clinical and morphological criteria of these tumors is essentially KIT-negative by immunohistohemistry. The biological features of these tumors have rarely been addressed. In the absence of CD117 immunopositivity, the diagnosis of GISTs is challenging.

Based on this and using the latest clinical and histological criteria, we screened 50 cases of gastrointestinal stromal tumors with a long term follow-up. Generally, as it was expected, tumor location, mitotic counts, risk group and metastasis were significantly associated with survival. Of the 50 tissues tested, 35 (70%) were positive for CD117 staining and 15 (30%) were negative. A significant association was observed between gender and KIT (CD117) immunostaining. KIT-negative tumors were observed in male patients, while the majority of female patients expressed CD117 immunostaining.

The majority of KIT-negative tumors developed in stomach while KIT-positive tumors developed in small intestine. This finding is in accordance with recent studies[10]. The majority of KIT-negative tumors were smaller than 5 cm (9/15), and 80% contained mitoses less than 5/50 HPF.

Of the 15 CD117-negative samples, 6 cases had evidence of dual differentiation, 4 cases showed histologically epithelioid type features, two had spindle type features, and 3 cases were negative for all markers,

Table 1 Clinicopathological features of KIT-negative cases

Case No.	Sex	Age (yr)	Symptoms	Site	Size (cm)	Mitoses (/50 HPF)	Presence of necrosis	Morphology	Risk category	Clinical status	Survival data/mo
1	M	60	Yes	Small Intestine	4.30	1	No	Epithelioid	Low risk	Primary	Alive/12
2	M	46	No	Stomach	0.50	0	No	Mixed	Very low risk	Primary	Alive/24
3	M	50	No	Small Intestine	0.50	0	No	Anaplastic	Very low risk	Primary	Alive/24
4	M	64	Yes	Large Intestine	4.50	10	Yes	Epithelioid	High risk	Liver metastasis	Dead/12
5	M	78	Yes	Small Intestine	7.00	1	Yes	Mixed	Intermediate risk	Liver metastasis	Dead/12
6	F	53	Yes	Stomach	5.00	0	No	Spindled	Low risk	Primary	Alive/47
7	M	43	Yes	Esophagus	7.00	0	No	Mixed	Intermediate risk	Primary	Alive/25
8	M	51	Yes	Small Intestine	6.00	2	Yes	Epithelioid	Intermediate risk	Primary	Alive/12
9	M	69	No	Stomach	2.00	0	No	Mixed	Very low risk	Primary	Alive/37
10	M	54	Yes	Stomach	3.50	0	No	Spindled	Low risk	Primary	Alive/62
11	M	70	Yes	Stomach	6.00	0	No	Anaplastic	Intermediate risk	Primary	Alive/82
12	M	42	Yes	Stomach	6.00	2	No	Anaplastic	Intermediate risk	Primary	Alive/56
13	M	26	No	Stomach	0.50	0	No	Epithelioid	Very low risk	Primary	Alive/78
14	M	82	Yes	Stomach	30.00	6	Yes	Mixed	High risk	Primary	Alive/82
15	M	61	Yes	Small Intestine	3.00	29	No	Mixed	High risk	Liver metastasis	Dead/2

M = male; F = female.

Table 2 Correlation between gender and CD117 expression in patients with GISTs

		CD117 expression		
		Negative	Positive	Total
Gender	Male	14	17	31
		45.20%	54.80%	100%
	Female	1	18	19
		5.30%	94.70%	100%
Total		15	35	50

Table 3 Correlation between tumor location and CD117 expression in patients with GISTs

Tumor location	CD117 expression		
	Negative	Positive	Total
Esophagus	1	2	3
	33.30%	66.70%	100%
Stomach	8	11	19
	42.10%	57.90%	100%
Small intestine	5	18	23
	21.70%	78.30%	100%
Large intestine	1	4	5
	20%	80%	100%
Total	15	35	50
	30%	70%	100%

Table 4 Immunohistohemical findings of patients with KIT-negative GISTs

Case No.	CD117	Immunohistochemistry				CD34
		α-SMA	Desmin	S-100	NSE	
1	Negative	Positive	Positive	-	-	Positive
2	Negative	-	Positive	Positive	-	-
3	Negative	-	-	-	-	Positive
4	Negative	Positive	-	-	-	Positive
5	Negative	Positive	-	-	Positive	-
6	Negative	-	-	Positive	Positive	-
7	Negative	Positive	Positive	Positive	-	-
8	Negative	Positive	-	-	-	Positive
9	Negative	Positive	Positive	-	Positive	-
10	Negative	-	-	Positive	Positive	Positive
11	Negative	-	-	-	-	Positive
12	Negative	-	-	-	-	Positive
13	Negative	Positive	Positive	-	-	-
14	Negative	Positive	-	-	Positive	Positive
15	Negative	Positive	-	Positive	-	-

but positive for CD34 staining. Our findings support previously published data[10,11], suggesting that there is a subgroup of KIT–negative GISTs that exhibit the same clinical and morphological features as the KIT-positive tumors.

The majority of KIT-negative tumors were diagnosed as "very low" or "low risk" tumors, while the highest incidence of KIT-positive staining was found in "high risk" tumors. The majority of patients with KIT-negative tumors (80%) were alive without evidence of residual tumor for an average period of 40.25 mo and presented a better survival status than the patients with KIT-positive tumors.

Benign and malignant GISTs carry mutations in KIT gene. It is still not clear whether mutations are independent prognostic factors[12,13]. We believe that a search for gene mutation, as the c-kit gene, in KIT-negative staining tumors might clarify the diagnosis status (unpublished observations), as other authors believe that KIT mutations[11] or intragenic platelet-derived growth factor-alpha (PDGFR-a) activating mutations are present in some of these tumors[10]. The pharmaceutical development and therapeutic implications of protein tyrosine kinase inhibitors has refocused the attention on GIST. Until recently, no patient with complete response to therapy was reported[14]. Is there any value in separating these tumors with epithelioid or dual differentiation because they are often KIT-antigen negative[15]? Is this going to be the result of a better differentiation status, detection of certain molecular alterations or it may be related to more traditional criteria as size and mitosis rate? There is still challenge to identify those patients who would benefit

from receiving the new therapy.

In conclusion, our study confirms that traditional histologic criteria alone are not enough to confirm GISTs diagnosis, but are still the only criteria to estimate biological behavior in these tumors. A small subgroup of GISTs fulfils the clinical and morphological criteria of these tumors, and lacks KIT expression. These tumors predominantly develop in stomach, showing dual or epithelioid morphology; they are classified as "low risk" tumors, and present with a better survival status than KIT-positive staining tumors. The ability to diagnose GISTs still depends on the immunohistochemical staining but the research should expand in gene mutations.

REFERENCES

1 **Miettinen M**, Lasota J. Gastrointestinal stromal tumors: review on morphology, molecular pathology, prognosis, and differential diagnosis. *Arch Pathol Lab Med* 2006; **130**: 1466-1478
2 **Kindblom LG**, Remotti HE, Aldenborg F, Meis-Kindblom JM. Gastrointestinal pacemaker cell tumor (GIPACT): gastrointestinal stromal tumors show phenotypic characteristics of the interstitial cells of Cajal. *Am J Pathol* 1998; **152**: 1259-1269
3 **Miettinen M**, El-Rifai W, H L Sobin L, Lasota J. Evaluation of malignancy and prognosis of gastrointestinal stromal tumors: a review. *Hum Pathol* 2002; **33**: 478-483
4 **Fletcher CD**, Berman JJ, Corless C, Gorstein F, Lasota J, Longley BJ, Miettinen M, O'Leary TJ, Remotti H, Rubin BP, Shmookler B, Sobin LH, Weiss SW. Diagnosis of gastrointestinal stromal tumors: A consensus approach. *Hum Pathol* 2002; **33**: 459-465
5 **Berman J**, O'Leary TJ. Gastrointestinal stromal tumor workshop. *Hum Pathol* 2001; **32**: 578-582
6 **Kitamura Y**, Hirota S, Nishida T. Molecular pathology of c-kit proto-oncogene and development of gastrointestinal stromal tumors. *Ann Chir Gynaecol* 1998; **87**: 282-286
7 **Koay MH**, Goh YW, Iacopetta B, Grieu F, Segal A, Sterrett GF, Platten M, Spagnolo DV. Gastrointestinal stromal tumours (GISTs): a clinicopathological and molecular study of 66 cases. *Pathology* 2005; **37**: 22-31
8 **Hirota S**, Isozaki K, Moriyama Y, Hashimoto K, Nishida T, Ishiguro S, Kawano K, Hanada M, Kurata A, Takeda M, Muhammad Tunio G, Matsuzawa Y, Kanakura Y, Shinomura Y, Kitamura Y. Gain-of-function mutations of c-kit in human gastrointestinal stromal tumors. *Science* 1998; **279**: 577-580
9 **Miettinen M**, Lasota J. KIT (CD117): a review on expression in normal and neoplastic tissues, and mutations and their clinicopathologic correlation. *Appl Immunohistochem Mol Morphol* 2005; **13**: 205-220
10 **Debiec-Rychter M**, Wasag B, Stul M, De Wever I, Van Oosterom A, Hagemeijer A, Sciot R. Gastrointestinal stromal tumours (GISTs) negative for KIT (CD117 antigen) immunoreactivity. *J Pathol* 2004; **202**: 430-438
11 **Tzen CY**, Mau BL. Analysis of CD117-negative gastrointestinal stromal tumors. *World J Gastroenterol* 2005; **11**: 1052-1055
12 **Rubin BP**. Gastrointestinal stromal tumours: an update. *Histopathology* 2006; **48**: 83-96
13 **Miettinen M**. Gastrointestinal stromal tumors: parameters that determine biological potential and guide therapy from a surgical pathologist point of view. Society for Ultrastructural Pathology. *USCAP Meeting;* 2003: 16-20
14 **Demetri GD**. Identification and treatment of chemoresistant inoperable or metastatic GIST: experience with the selective tyrosine kinase inhibitor imatinib mesylate (STI571). *Eur J Cancer* 2002; **38** Suppl 5: S52-S59
15 **Herrera GA**. Histological perspective: a journey through evolution of classification schemes. Society for Ultrastructural Pathology. *USCAP Meeting;* 2003: 1-6

S- Editor Liu Y **L- Editor** Ma JY **E-Editor** Lu W

PO Box 2345, Beijing 100023, China
www.wjgnet.com
wjg@wjgnet.com

World J Gastroenterol 2007 February 21; 13(7): 1103-1107
World Journal of Gastroenterology ISSN 1007-9327

RAPID COMMUNICATION

NCB-02 (standardized Curcumin preparation) protects dinitrochlorobenzene-induced colitis through down-regulation of NFκ-B and iNOS

MV Venkataranganna, Md Rafiq, S Gopumadhavan, Ghouse Peer, UV Babu, SK Mitra

MV Venkataranganna, Md Rafiq, S Gopumadhavan, Ghouse Peer, UV Babu, SK Mitra, R&D Center, The Himalaya Drug Company, Bangalore-562 123, India
Correspondence to: MV Venkataranganna, PhD, Senior Research Scientist, R&D Center, The Himalaya Drug Company, Makali, Bangalore-562 123, India. venkataranganna@himalayahealthcare.com
Telephone: +91-80-23714444 Fax: +91-80-23714471
Received: 2006-10-07 Accepted: 2007-01-12

Abstract

AIM: To evaluate the efficacy and mechanism of action of NCB-02, a standardized Curcumin preparation, against 2, 4-dinitrochlorobenzene (DNCB)-induced ulcerative colitis in rats.

METHODS: Ulcerative colitis was induced in male rats by sensitizing with topical application of DNCB in acetone for 14 d and intra-colonol challenge with DNCB on day 15. A separate group of animals with vehicle treatment in similar fashion served as control group. Colitis rats were divided into different groups and treated with NCB-02 at doses of 25, 50 and 100 mg/kg b.wt p.o. for 10 d. Sulfasalazine at a dose of 100 mg/kg b.wt for 10 d served as a reference group. On day 10 after respective assigned treatment, all the animals were euthanized and the length of the colon, weight of entire colon and distal 8 cm of the colon were recorded. The distal part of the colon was immediately observed under a stereomicroscope and the degree of damage was scored. Further distal 8 cm of the colon was subject to the determination of colonic myeloperoxidase (MPO), lipid peroxidation (LPO) and alkaline phosphatase (ALP) activities. A small piece of the sample from distal colon of each animal was fixed in 10% neutral buffered formalin and embedded in paraffin wax and sectioned for immunohistochemical examination of NFκ-B and iNOS expression.

RESULTS: NCB-02 showed a dose dependent protection against DNCB-induced alteration in colon length and weight. NCB-02 treatment also showed a dose dependent protection against the elevated levels of MPO, LPO and ALP, induced by DNCB. NCB-02 demonstrated a significant effect at a dose of 100 mg/kg b.wt., which was almost equipotent to 100 mg/kg b.wt. of sulfasalazine. Treatment with sulfasalazine and curcumin at a dose of 100 mg/kg b.wt. inhibited the DNCB-induced overexpression of NFκ-B and iNOS in the colon.

CONCLUSION: Curcumin treatment ameliorates colonic damage in DNCB-induced colitic rats, an effect associated with an improvement in intestinal oxidative stress and downregulation of colonic NFκ-B and iNOS expression.

Key words: Curcumin; Colitis; Dinitrochlorobenzene; NFκ-B; iNOS

Venkataranganna MV, Rafiq Md, Gopumadhavan S, Peer G, Babu UV, Mitra SK. NCB-02 (standardized Curcumin preparation) protects dinitrochlorobenzene-induced colitis through down-regulation of NFκ-B and iNos. *World J Gastroenterol* 2007; 13(7): 1103-1107

http://www.wjgnet.com/1007-9327/13/1103.asp

INTRODUCTION

Inflammatory bowel disease (IBD), including Crohn's disease and ulcerative colitis (UC), is a chronic and relapsing inflammatory disease caused by the inflammation and sores in the lining of large intestine and characterized clinically by recurrent episodes of bloody diarrhea, cramping, abdominal pain and histologically by mucosal inflammation and injury[1]. Conventional therapy for UC includes sulfasalazine and other 5-aminosalicylic acid (5-ASA) type of compounds, and in more persistent and/or severe cases, oral, rectal and parenteral corticosteroids and immunosuppressants are administered[2]. All of these have significant toxicities and are partly or completely ineffective in significant numbers of patients[3].

Several agents used in the management of IBD, such as corticosteroids, sulfasalazine and 5-ASA, have documented regulation of Nuclear Factor Kappa-B (NFκ-B) function[2]. Given the importance of inflammatory cell activation involved in the development of IBD, there is a need for a treatment modality against IBD that can block the inflammatory processes. There is substantial evidence for the involvement of oxidative stress and profound alterations in the biosynthesis of the labile free

radical nitric oxide from L-arginine in the pathogenesis of colitis[4]. The use of medicinal plants or their active components has become an increasingly attractive approach for the treatment of UC. Curcumin, the active principle in turmeric, is a polyphenolic antioxidant and a natural yellow orange dye. Turmeric contains three curcumin analogues based on the number of hydroxyl groups present in the parent molecule. They are Curcumin (Curcumin I), demethoxy curcumin (Curcumin Ⅱ) and bis-demethoxy curcumin (Curcumin Ⅲ). Curcumin is a active constituent of *Curcuma longa*, whose anti-inflammatory properties are related in part to inhibition of the activities of the cyclooxygenase, lipoxygenase and NFκ-B in several cell systems[5-9]. Many experimental studies have demonstrated the important role of Curcumin in the attenuation of IBD and colonic cancer and it is also known to exhibit a variety of beneficial effects including antitumor, anti-HIV, antioxidant, anticataract development, septic shock, promotion of wound healing in normal and diabetic conditions, anti-asthmatic, anti-colitis, anti-fibrosis, reduction of mucosal damage, prevention of UV damage to skin, inhibition of development of cancers of the skin, stomach, colon, prostate, oral cavity and liver. Furthermore, Curcumin could also inhibit tumor metastases, pancreatitis, drug or alcohol-induced liver fibrosis, cystic fibrosis and Alzheimer's disease[10,11].

NCB-02 is a standardized extract of *Curcuma longa* containing 78% curcuminoids, 72% of which is Curcumin, 18.08% demethoxy curcumin and 9.42% bis-demethoxy Curcumin. This study was designed to evaluate its efficacy and mechanism of action against 2, 4-dinitrochloro-benzene (DNCB)-induced ulcerative colitis in rats.

MATERIALS AND METHODS

Animals

Laboratory bred Wistar male rats weighing between 220-250 g were used for the experiments. The animals were housed and acclimatized to a constant temperature of 22 ± 3℃ and were exposed to 12 h day and night cycle. The animals were fed with synthetic diet and water *ad libitum*.

Effect of NCB-02 on UC in rats induced by DNCB[12]

Forty-eight rats were divided into six groups of eight animals each and, the nape hair was depleted. About 300 μL DNCB in acetone (20 g/L) was dropped to the nape of the rats once a day for 14 d. On the 15th day, animals of Groups Ⅱ-Ⅵ were subject to intracolonol challenge of DNCB. Intra-colon challenge was done by infusing 0.25 mL of 0.1% DNCB in 50% alcohol into colon by a nylon catheter (3 mm in diameter), which was inserted into the colon at the site of 8 cm from the anus. Group I served as normal control and received 50% alcohol instead of DNCB. The animals were kept in Trendelenburg position for 1 min after DNCB administration and maintained in cages with free access to water and food.

Rats of Groups I and Ⅱ served as normal and positive controls respectively and were administered with water (vehicle) at a dose of 10 mL/kg b.wt. p.o. and Group Ⅲ rats with 100 mg/kg b.wt. p.o. of reference drug, sulfasalazine. Rats of groups Ⅳ-Ⅵ received 25, 50 and 100 mg/kg b.wt. p.o. of NCB-02, respectively. The treatment was carried out for 10 d, after challenge with DNCB. On d 10, after assigned treatment, all the animals were euthanized by exsanguinations. The entire length of the colon starting from the ceacal end was excised, opened and gently rinsed with ice-cold saline. The colon was kept flat with the mucosal surface upward on a plate prechilled to 4℃. The length of the colon, weight of entire colon and distal 8 cm of the colon were recorded. The distal part of the colon was immediately observed under stereomicroscope to note any visible damage. The degree of damage was scored macroscopically on a 0-5 scale by independent observers[13]. Further distal 8 cm of the colon was subject to the determination of colonic myeloperoxidase[14], lipid peroxides[15] and ALP activity. A small piece of the sample from distal colon of each animal was fixed in 10% neutral buffered formalin and embedded in paraffin wax and sectioned for immunohistochemical examination[16].

Myeloperoxidase (MPO) activity

MPO is an enzyme found in cells of myeloid origin, and has been used extensively as a biochemical marker of granulocyte (mainly neutrophil) infiltration into gastrointestinal tissues[14]. Samples of distal colon were homogenized in 10 mmol/L potassium phosphate buffer, pH 7.0 containing 0.5% hexadecyltrimethylammonium bromide and centrifuged for 30 min at 20000 × *g* at 4℃. An aliquot of the supernatant was then allowed to react with a solution of 1.6 mmol/L O-dianisidine and 0.1 mmol/L H_2O_2. The rate of change in absorbance was measured spectrophotometrically at 650 nm. One unit of myeloperoxidase activity was defined as degrading 1 mmol of H_2O_2 per min at 37℃ and was expressed as units per milligram of tissue sampled (U/mg tissue).

Estimation lipid peroxidation and ALP

The tissue was homogenized at a concentration of 10% w/v in 0.15 mol/L potassium chloride using a glass homogenizer. The homogenate was centrifuged at 800 × *g* and the supernatants were used for the estimation of lipid peroxides[15] and alkaline phosphatase (ALP) using Boheringer Mannheim kit.

Immunohistochemistry for NFκ-B and inducible nitric oxide synthase (iNOS)[16]

Colon sections were deparaffinized in xylene, for 2-5 min and dehydrated with 100% ethanol for 2-3 min followed with 95% ethanol for 1 min, then rinsed in distilled water. Tissue sections were incubated with primary antibody at appropriate dilution in phosphate buffered saline (PBS) for 1 h at room temperature, then incubated in biotinylated secondary antibody in PBS for 1 h at room temperature. After rinsing in PBS for 3 changes of 2 min each, sections were incubated in freshly prepared peroxidase substrate solution for 10 min at room temperature and counterstained with weak haematoxylin for 10 min after rinsing with PBS.

Table 1 Various biomarkers of colitis

	Ulcer index	Colon length	Colon Wt. (Total) (gm)	Distal Colon wt. (last 8 cm) (gm)	MPO Units/gm of tissue	LPO nmol/L per 100 mg	ALP IU/100 mg
Control	0.00 ± 0.00	19.88 ± 0.41	1.46 ± 0.05	0.52 ± 0.02	2.98 ± 0.42	145.75 ± 13.78	26.63 ± 3.45
Positive control	4.50 ± 0.25[b]	15.75 ± 0.39[b]	2.18 ± 0.13[b]	1.33 ± 0.10[b]	5.63 ± 0.46[b]	296.23 ± 23.98[b]	252.13 ± 33.69[d]
Sulfasalazine (100 mg/kg)	2.75 ± 0.39[f]	18.13 ± 0.37[h]	1.76 ± 0.05[j]	0.84 ± 0.05[h]	3.60 ± 0.29[j]	211.54 ± 32.23[j]	136.38 ± 17.69[j]
NCB-02 (25mg/kg)	3.75 ± 0.23	15.13 ± 0.37	1.98 ± 0.14	1.22 ± 0.13	4.27 ± 0.45	259.38 ± 28.71	232.38 ± 33.79
NCB-02 (50mg/kg)	3.00 ± 0.18[j]	16.50 ± 0.31	1.88 ± 0.15	1.09 ± 0.09	3.90 ± 0.32	205.69 ± 22.09[j]	186.88 ± 24.86
NCB-02 (100mg/kg)	2.63 ± 0.25[f]	18.13 ± 0.45[h]	1.69 ± 0.07[j]	0.90 ± 0.06[j]	3.73 ± 0.30[j]	174.84 ± 13.06[h]	153.13 ± 20.23[j]

[b]$P < 0.001$, [d]$P < 0.01$ *vs* control; [f]$P < 0.001$, [h]$P < 0.01$, [j]$P < 0.05$ *vs* positive control.

Statistical analysis

The values were expressed as mean ± SE. The results were analyzed statistically using one-way ANOVA followed by Dunnet's multiple comparison test using GraphPad Prism software package (Version 4.0) to find the level of significance. The minimum level of significance is fixed at $P < 0.05$.

RESULTS

Rats sensitized and challenged with DNCB showed ulcers with severe macroscopic inflammation in the colon as assessed by the colonic damage score. Colon length was significantly reduced with a significant increase in total and distal colon weight in colitic rats as compared with non-colitic control rats. There was also a significant increase in colonic MPO, LPO and ALP activity as compared with non-colitic rats (Table 1). Treatment with NCB-02 showed a dose dependent protection against DNCB-induced colonic damage as indicated by normalization of colon length, reduction in colon weight (total and distal) and decrease in the levels biochemical markers such as MPO, LPO and ALP. NCB-02 at a dose of 100 mg/kg b.wt. p.o. showed a significant effect on various parameters (Table 1). Reference drug sulfasalazine presented with a significant reversal of DNCB-induced alterations at a dose of 100 mg/kg b.wt. p.o. (Table 1).

Sulfasalazine treatment resulted in significant protection with the mean ulcer score of 2.75 ± 0.39 and NCB-02 had a dose dependent protection at 25, 50 and 100 mg/kg b.wt. with ulcer scores of 3.75 ± 0.23, 3.00 ± 0.18 and 2.63 ± 0.25 ($P < 0.001$), respectively (Table 1).

Myeloperoxidase activity is an established marker for inflammatory cell (mainly neutrophils) infiltration in rodent models of colitis, and was thus examined. MPO activity was significantly increased in colitis rats as compared with the control. NCB-02 treatment inhibited DNCB-induced MPO activity in a dose dependent manner. Both sulfasalazine and NCB-02 at a dose of 100 mg/kg b.wt. significantly protected DNCB-induced elevation of MPO activity (Table 1).

High level expression of iNOS and NFκ-B were observed in colitis rats, which is revealed by immunohistochemistry (Figures 1 and 2). This immunohistochemistry for NFκ-B and iNos expression revealed that NCB-02 at a dose 100 mg/kg b.wt. inhibited the DNCB-induced expression of these pro-inflammatory mediators of ulcerative colitis.

From the various parameters evaluated it was observed that 100 mg/kg b.wt. of NCB-02 was almost equipotent to sulfasalazine at 100 mg/kg b.wt.

DISCUSSION

In the present investigation, the beneficial effects observed with NCB-02 (Standardized Curcumin preparation) treatment were assessed based on the improvement of colon weight and length, and histologically by preservation of the colon architecture in comparison with the rats from the non-treated colitic group. The biochemical assays, such as MPO and ALP, performed in the colonic specimens confirmed the anti-inflammatory effect exerted by Curcumin at a dose of 100 mg/kg, since it was associated with significant reduction in MPO and ALP activities. MPO activity has been widely used to detect and follow intestinal inflammation, and a reduction in the activity of this enzyme can be interpreted as a manifestation of the anti-inflammatory activity of a given compound. Alkaline phosphatase activity is considered as one of the sensitive markers of inflammation in the intestine, as this enzyme activity is invariably augmented in these experimental conditions of colitis. The results obtained in this study confirm the intestinal anti-inflammatory effect previously demonstrated for Curcumin[9,17].

Earlier studies provided evidence of significantly elevated activation of NFκ-B in ulcerative colitis and Crohn's disease[18,19]. Several therapeutic agents with NFκ-B inhibitory activity, such as sulfasalazine, mesalamine, and corticosteroids have been used for the treatment of IBD. They have sundry defects such as steroid dependence and steroid resistance, decreasing glucose tolerance, hepatotoxicity and pancreatitis[2]. Now, more potent and selective treatment strategies for IBD aim at preventing NFκ-B activation in mucosal macrophages and T lymphocytes.

According to the well-described role of NFκ-B in inflammatory regulation and iNOS expression, the degree of NFκ-B expression was determined in the colonic tissue samples from animals subjected to DNCB sensitization and challenge. The inflammatory status induced by DNCB was associated with increased colonic NFκ-B expression when compared to normal tissues. Curcumin treatment resulted in inhibition of NFκ-B expression and similar

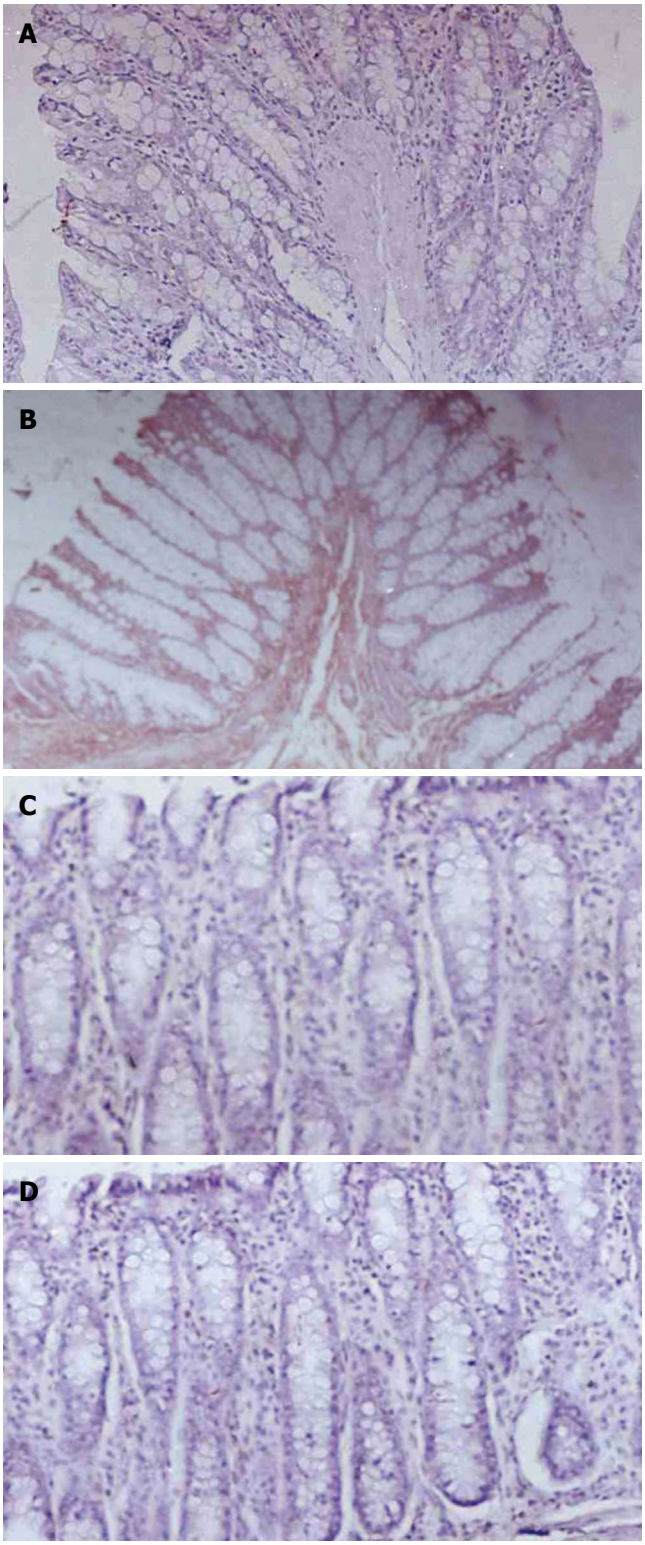

Figure 1 **A**: Section of colon in normal control showing normal structure and architecture (immunohistochemistry, 40 x); **B**: Section of colon in DNCB control showing extensive NFκ-B (brown) expression in tissue (immunohistochemistry, 40 x); **C**: Section of colon in sulfasalazine treated group showing limited NFκ-B (brown) expression (immunohistochemistry, 40 x); **D**: Section of colon in NCB-02 treated group showing minimal NFκ-B (brown) expression (immunohistochemistry, 40 x).

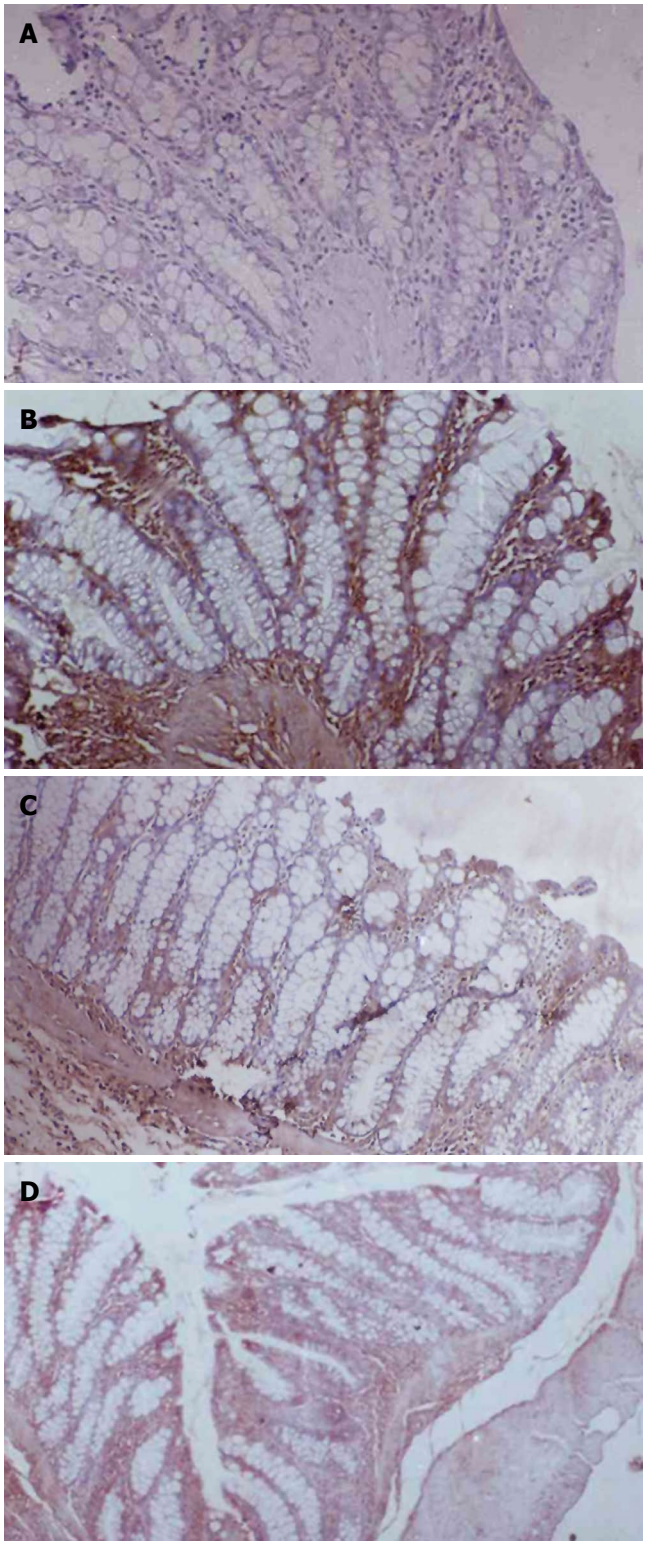

Figure 2 **A**: Section of colon in normal control showing normal structure and architecture (immunohistochemistry, 40 x); **B**: Section of colon in DNCB control showing extensive iNos (brown) expression in tissue (immunohistochemistry, 40 x), **C**: Section of colon in sulfasalazine treated group showing limited iNos (brown) expression (immunohistochemistry, 40 x); **D**: Section of colon in NCB-02 treated group showing minimal iNos (brown) expression (immunohistochemistry, 40 x).

response was observed with sulfasalazine treatment.

Nitric oxide is one of the important pro-inflammatory mediators, which plays a key role in the pathogenesis of IBD. In our study, we evaluated the effect of Curcumin on colonic iNOS activity in the DNCB-induced model of experimental colitis. DNCB administration increased colonic iNOS activity expression in rats, as detected by immunohistochemistry (Figure 2B). The intestinal anti-

inflammatory effect exerted by NCB-02, was associated with a reduction of iNOS expression (Figure 2D) when compared with DNCB control animals.

Myeloperoxidase is an enzyme found in cells of myeloid origin, and has been used extensively as a biochemical marker of granulocyte (mainly neutrophil) infiltration into gastrointestinal tissues. Our study showed that DNCB raised the levels of colonic MPO, which was ameliorated in NCB-02 and sulfasalazine treated groups.

In addition, our study gives some evidence about the mechanisms involved in the intestinal anti-inflammatory effect of Curcumin. One of the mechanisms could be its inhibition of free radical generation and antioxidant properties, which is evident from several earlier observations[9,10]. This activity may play a crucial role in the intestinal anti-inflammatory effect of the Curcumin, because intense oxidative insult is a common feature in human IBD and in the different experimental models of rat colitis, such as the trinitrobenzene sulfonic acid (TNBS) and the DNCB models in rats, and is an important mechanism for tissue damage during chronic intestinal inflammation[18].

In the last decade, it became increasingly clear that NO overproduction by iNOS is deleterious to intestinal function, which contributes significantly to gastrointestinal immunopathology in the chronic inflammatory events in IBD[16,18]. The important role attributed to NO in these intestinal conditions prompted us to study whether the beneficial effects of Curcumin on DNCB-induced colitis could be related to an effect on colonic NO production. The results in this study reveal that colonic inflammation is associated with a higher colonic iNOS expression, as evidenced by immunohistochemistry. Treatment of colitic rats with NCB-02 effectively inhibited the upregulated colonic iNOS expression.

The present study revealed that oral treatment of NCB-02 in colitic rats significantly inhibited the NFκ-B pathway, which is reported to be activated as a consequence of the intestinal inflammatory process induced by DNCB. The molecular mechanism involved in the suppressive effects of Curcumin on NFκ-B could be due to the inhibition of NFκ-B by acting as antioxidants, since NFκ-B is a redox-sensitive transcription factor and activated by oxidative stress in the inflamed intestinal mucosa via blocking the phosphorylation and degradation of IkB protein, as previously reported *in vitro* and *in vivo*[7,19].

In conclusion, Curcumin treatment ameliorates colonic damage in DNCB-induced colitic rats, an effect associated with an improvement in intestinal oxidative stress and a downregulation in colonic iNOS and NFκ-B expression. Therefore, Curcumin (NCB-02) may hold promise for the treatment of inflammatory bowel disease.

REFERENCES

1 **Furrie E**, Macfarlane S, Cummings JH, Macfarlane GT. Systemic antibodies towards mucosal bacteria in ulcerative colitis and Crohn's disease differentially activate the innate immune response. *Gut* 2004; **53**: 91-98

2 **Nikolaus S**, Fölscn U, Schreiber S. Immunopharmacology of 5-aminosalicylic acid and of glucocorticoids in the therapy of inflammatory bowel disease. *Hepatogastroenterology* 2000; **47**: 71-82

3 **Farrell RJ**, Kelleher D. Glucocorticoid resistance in inflammatory bowel disease. *J Endocrinol* 2003; **178**: 339-346

4 **Barbosa DS**, Cecchini R, El Kadri MZ, Rodríguez MA, Burini RC, Dichi I. Decreased oxidative stress in patients with ulcerative colitis supplemented with fish oil omega-3 fatty acids. *Nutrition* 2003; **19**: 837-842

5 **Han SS**, Keum YS, Seo HJ, Surh YJ. Curcumin suppresses activation of NF-kappaB and AP-1 induced by phorbol ester in cultured human promyelocytic leukemia cells. *J Biochem Mol Biol* 2002; **35**: 337-342

6 **Pan MH**, Lin-Shiau SY, Lin JK. Comparative studies on the suppression of nitric oxide synthase by curcumin and its hydrogenated metabolites through down-regulation of IkappaB kinase and NFkappaB activation in macrophages. *Biochem Pharmacol* 2000; **60**: 1665-1676

7 **Zhang F**, Altorki NK, Mestre JR, Subbaramaiah K, Dannenberg AJ. Curcumin inhibits cyclooxygenase-2 transcription in bile acid- and phorbol ester-treated human gastrointestinal epithelial cells. *Carcinogenesis* 1999; **20**: 445-451

8 **Jobin C**, Bradham CA, Russo MP, Juma B, Narula AS, Brenner DA, Sartor RB. Curcumin blocks cytokine-mediated NF-kappa B activation and proinflammatory gene expression by inhibiting inhibitory factor I-kappa B kinase activity. *J Immunol* 1999; **163**: 3474-3483

9 **Singh S**, Aggarwal BB. Activation of transcription factor NF-kappa B is suppressed by curcumin (diferuloylmethane) [corrected] *J Biol Chem* 1995; **270**: 24995-25000

10 **Ruby AJ**, Kuttan G, Babu KD, Rajasekharan KN, Kuttan R. Anti-tumour and antioxidant activity of natural curcuminoids. *Cancer Lett* 1995; **94**: 79-83

11 **Aggarwal BB**, Kumar A, Bharti AC. Anticancer potential of curcumin: preclinical and clinical studies. *Anticancer Res* 2003; **23**: 363-398

12 **Jiang XL**, Cui HF. A new chronic ulcerative colitis model produced by combined methods in rats. *World J Gastroenterol* 2000; **6**: 742-746

13 **Fan H**, Qiu MY, Mei JJ, Shen GX, Liu SL, Chen R. Effects of four regulating-intestine prescriptions on pathology and ultrastructure of colon tissue in rats with ulcerative colitis. *World J Gastroenterol* 2005; **11**: 4800-4806

14 **Perner A**, Andresen L, Normark M, Fischer-Hansen B, Sørensen S, Eugen-Olsen J, Rask-Madsen J. Expression of nitric oxide synthases and effects of L-arginine and L-NMMA on nitric oxide production and fluid transport in collagenous colitis. *Gut* 2001; **49**: 387-394

15 **Mitra SK**, Venkataranganna MV, Sundaram R, Gopumadhavan S. Antioxidant activity of AO-8, a herbal formulation *in vitro* and *in vivo* experimental models. *Phytother Res* 1999; **13**: 300-303

16 **Dong WG**, Liu SP, Yu BP, Wu DF, Luo HS, Yu JP. Ameliorative effects of sodium ferulate on experimental colitis and their mechanisms in rats. *World J Gastroenterol* 2003; **9**: 2533-2538

17 **Ukil A**, Maity S, Karmakar S, Datta N, Vedasiromoni JR, Das PK. Curcumin, the major component of food flavour turmeric, reduces mucosal injury in trinitrobenzene sulphonic acid-induced colitis. *Br J Pharmacol* 2003; **139**: 209-218

18 **Monteleone G**, Mann J, Monteleone I, Vavassori P, Bremner R, Fantini M, Del Vecchio Blanco G, Tersigni R, Alessandroni L, Mann D, Pallone F, MacDonald TT. A failure of transforming growth factor-beta1 negative regulation maintains sustained NF-kappaB activation in gut inflammation. *J Biol Chem* 2004; **279**: 3925-3932

19 **Jian YT**, Mai GF, Wang JD, Zhang YL, Luo RC, Fang YX. Preventive and therapeutic effects of NF-kappaB inhibitor curcumin in rats colitis induced by trinitrobenzene sulfonic acid. *World J Gastroenterol* 2005; **11**: 1747-1752

S- Editor Liu Y **L- Editor** Ma JY **E- Editor** Ma WH

PO Box 2345, Beijing 100023, China
www.wjgnet.com
wjg@wjgnet.com

World J Gastroenterol 2007 February 21; 13(7): 1108-1111
World Journal of Gastroenterology ISSN 1007-9327

RAPID COMMUNICATION

Primary duodenal neoplasms: A retrospective clinico-pathological analysis

Amanjit Bal, Kusum Joshi, Kim Vaiphei, JD Wig

Amanjit Bal, Kusum Joshi, Kim Vaiphei, JD Wig, Departments of Histopathology and General Surgery, Post Graduate Institute of Medical Sciences and Research, Sector-12, Chandigarh 160012, India
Correspondence to: Dr. Amanjit Bal, MD, Assistant Professor, Department of Histopathology, Post Graduate Institute of Medical Sciences and Research, Chandigarh 160012, India. docaman5@hotmail.com
Telephone: +91-172-2755136
Received:2006-12-10 Accepted: 2007-01-29

Abstract

AIM: To analyze the clinico-pathological spectrum of primary duodenal neoplasms.

METHODS: A total of 55 primary duodenal neoplasms reported in the last 10 years after excluding ampullary and periampullary tumors were included in the study. Clinical details were noted and routine hematoxylin and eosin stained paraffin sections were studied for histological subtyping of the tumors.

RESULTS: On histopathological examination primary duodenal neoplasms were categorized as: epithelial tumor in 27 cases (49.0%) including 10 cases of adenoma, 15 cases of adenocarcinoma, and 2 cases of Brunner gland adenoma; mesenchymal tumor in 9 cases (16.3%) consisting of 4 cases of gastrointestinal stromal tumor, 4 cases of smooth muscle tumor and I case of neurofibroma; lymphoproliferative tumor in 12 cases (21.8%), and neuroendocrine tumor in 7 cases (12.7%).

CONCLUSION: Although non-ampullary/periampullary duodenal adenocarcinomas are rare, they constitute the largest group. Histopathological examination of primary duodenal tumors is important for correct histological subtyping.

Key words: Duodenum; Adenocarcinoma; Stromal tumor; Neuroendocrine tumor; Lymphoma

Bal A, Joshi K, Vaiphei K, Wig JD. Primary duodenal neoplasms: A retrospective clinico-pathological analysis. *World J Gastroenterol* 2007; 13(7): 1108-1111

http://www.wjgnet.com/1007-9327/13/1108.asp

INTRODUCTION

Although the small intestine constitutes 75% of the gastrointestinal tract, tumors arising from it are rare. Small intestine tumors account for about 5% of all alimentary tract tumors and the duodenum has a higher proportion of these tumors than the jejunum and ileum[1]. Duodenal carcinomas account for 20%-25% of all small bowel malignancies, whereas sarcomas, carcinoid and lymphomas are less common[2]. Duodenal tumors pose diagnostic difficulties because of their rarity, non-specific signs and symptoms and the fact that duodenum is usually overlooked during upper gastrointestinal endoscopy. The present study was undertaken to analyze the clinico-pathological spectrum of primary duodenal neoplasms reported in the last 10 years.

MATERIALS AND METHODS

A retrospective analysis of duodenal tumors retrieved from the Department of Histopathology, PGIMER, over a period of 10 years (1997-2006) was done. A total of 60 duodenal neoplasms after excluding 163 ampullary/periampullary carcinomas were retrieved from the records. All the clinical details like age, sex, presenting symptoms were noted from the patient record files. Relative laboratory and radiological findings were obtained. The specimens were fixed in buffered formalin and processed for paraffin sections. Routine hematoxylin and eosin-stained paraffin sections were studied for histological subtyping of the tumors. Histochemical stains like periodic acid Schiff (PAS), mucicarmine and immunohistochemical stains like c-kit, smooth muscle antigen (SMA), leukocyte common antigen (LCA), CD3, CD20, cytokeratin (CK) and chromogranin, were performed wherever required for exact categorization of the tumors.

RESULTS

Of the 60 duodenal neoplasms retrieved from records, 2 metastatic tumors and 3 with direct infiltration into duodenum from the subjacent site were excluded from the study. The study comprised of 55 cases of primary duodenal neoplasm. The age of the patients ranged from 7 to 70 years and the male to female ratio was 1.9:1. On histopathological examination primary duodenal neoplasms were categorized as: epithelial tumor, mesenchymal tumor, lymphoproliferative tumor, and neuroendocrine tumor (Table 1).

Table 1 Histopathological sub-classification of primary duodenal tumors (excluding ampullary and peri-ampullary tumors)

Pathological diagnosis	Cases *n* (%) *n* = 55
Epithelial tumors	27 (49.0)
Adenoma	10
Adenocarcinoma	15
Brunneroma	2
Mesenchymal tumors	9 (16.3)
GIST	4
Benign	1
Borderline	1
Malignant	2
Smooth muscle tumors	4
Leiomyoma	2
Leiomyosarcoma	2
Neurofibroma	1
Lymphoproliferative tumors	12 (21.8)
Non-Hodgkin's lymphoma	12
B-Cell lymphoma	10
T Cell lymphoma	2
Neuroendocrine tumors	7 (12.7)
Carcinoid	5
Gastrinoma	1
Neuroendocrine carcinoma	1

Epithelial tumor

There were 27 cases (49.0%) of epithelial tumor including 10 cases of adenoma, 15 cases of adenocarcinoma, and 2 cases of Brunner gland adenoma.

Adenoma: The age range of patients with adenoma was 10-60 years and the male to female ratio was 1:2.3. All adenomas were seen in D1-D2 portion of the duodenum and classified as flat adenoma in 1 case, tubular adenoma in 4 cases, tubulovillous adenoma in 3 cases (Figure 1A), and villous adenoma in 2 cases. Two cases were associated with multiple polyposis coli.

Adenocarcinoma: The age range of patients with adenocarcinoma was 38-70 years and the male to female ratio was 2:1. Of the 15 cases, 10 were found to have adenocarcinoma in D1-D2 portion of the duodenum and 5 were found to have adenocarcinoma in D3-D4 portion of the duodenum. Adenocarcinomas were sub-categorized as well-differentiated adenocarcinoma in 8 cases, moderately-differentiated adenocarcinoma in 2 cases, poorly-differentiated adenocarcinoma in 2 cases, and signet ring cell type adenocarcinoma in 3 cases. One adenocarcinoma was documented to be arising from pre-existing adenoma (Figure 1B).

Brunner gland adenoma: They were both seen in males and in D1 portion of the duodenum. The size of tumor ranged from 3 to 4 cm and microscopic examination showed lobules of Brunner glands separated by fibrovascular septa (Figure 1C).

Mesenchymal/stromal tumor

Nine cases (16.3%) were included in this group including 4 cases of gastrointestinal stromal tumor, 4 cases of smooth muscle tumor and 1 cases of neurofibroma. The age of the patients ranged from 32 to 70 years and the male to female ratio was 1.2:1.

Gastrointestinal stromal tumor (GIST): On pathological examination of 4 cases of GIST, 2 cases were diagnosed as malignant GIST based on the mitotic count of > 10/50HPF and tumor deposits in the omentum. One case was categorized as borderline GIST (5 cm in diameter) with its mitotic count of < 5/50HPF and one case was labeled as benign GIST (Figure 1D). All the cases were positive for c-kit immunostain and negative for SMA and S-100.

Smooth muscle tumor: Leiomyoma was found in 2 cases and leiomyosarcoma in 2 cases, respectively. Leiomyosarcoma showed high mitotic count of > 5/10HPF and areas of necrosis. All the tumors were positive for SMA and negative for c-kit.

Neural tumor: There was a single case of plexiform neurofibroma positive for S-100 immunostain.

Lymphoproliferative tumor

Twelve cases (21.8%) of non-Hodgkin's lymphoma (NHL) were included in this group (Figure 1E). Their age ranged from 7 to 85 years and the male to female ratio was 5:1. All the cases were found to have primary duodenal lymphoma because of the absence of disease in other organs. On immunohistological examination of 12 cases, B-cell phenotype was documented in 10 cases (83.3%) and T-cell phenotype in 2 cases (16.6%). B-cell lymphomas were further categorized as diffuse large cell lymphoma in 8 cases and MALT lymphoma in 2 cases. T-cell duodenal lymphomas were not associated with enteropathy as there was no histologic evidence of villous atrophy.

Neuroendocrine tumor

Seven tumors (12.7%) were located in this histologic category. Of the 7 tumors, 5 were benign and labeled as carcinoid based on their characteristic organoid pattern, granular cytoplasm, salt and pepper nuclear chromatin as well as chromogranin positivity (Figure 1F). One case was suggestive of gastrinoma based upon serum gastrin levels and was associated with parathyroid and adrenal hyperplasia. However, confirmation was not possible on histopathological sections because of non-availability of gastrin immunostain. One case was labeled as malignant as it had metastatic tumor deposits in lymph nodes.

DISCUSSION

Primary neoplasms of the small intestine constituting 90% of mucosal surface area of the gastrointestinal tract are extremely rare. Duodenum constituting only 4% of the small intestine has a relatively high proportion of all the tumors as compared to the jejunum and ileum. Primary malignant duodenal tumors are uncommon accounting for only 0.3% of all gastrointestinal tumors but about 50% of all small intestinal malignancies[3]. Many hypotheses have been proposed for the low incidence of small intestinal tumors as compared to large intestine including greater fluidity of contents in the small intestine which are less irritating as compared to solid contents, rapid transit

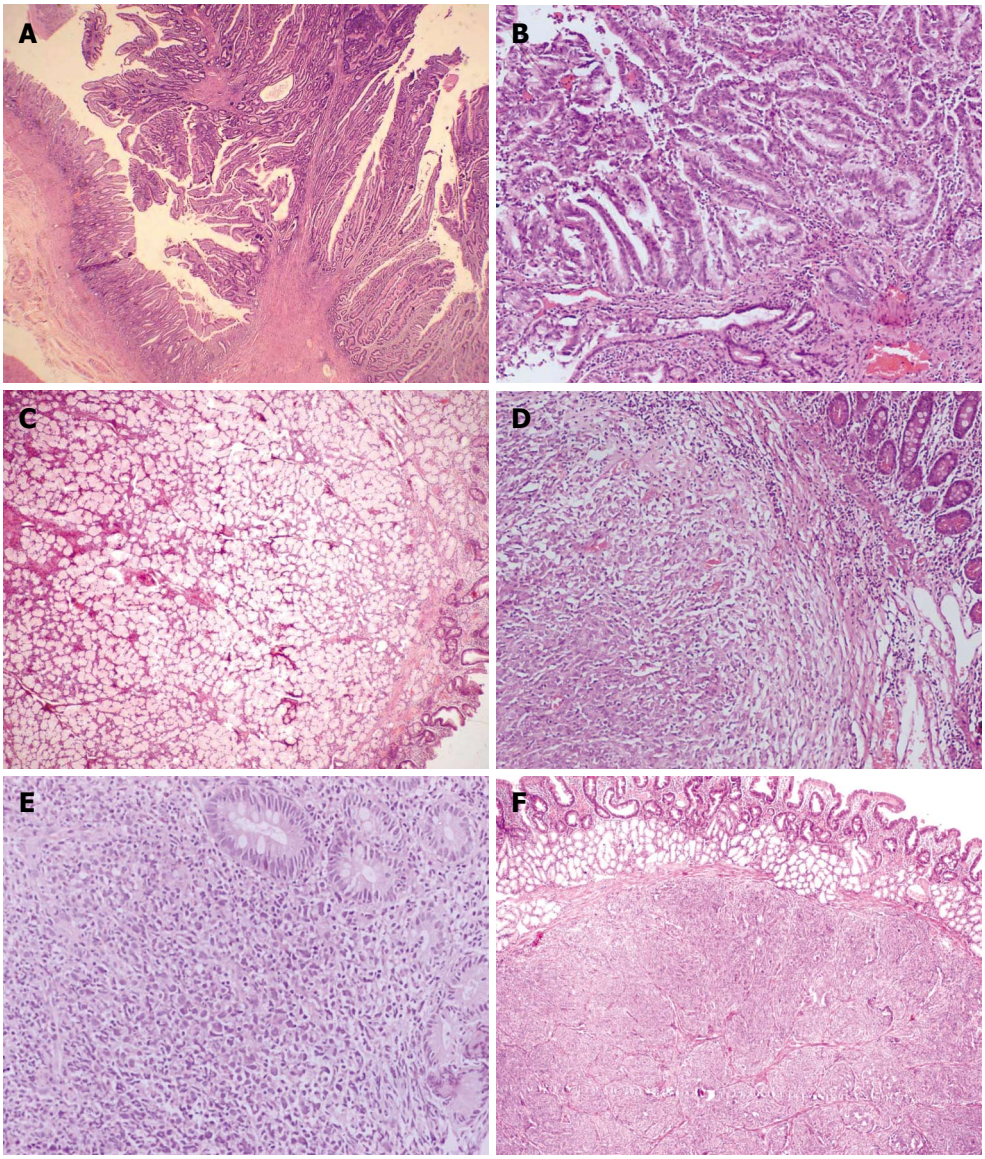

Figure1 Photomicrograph showing tubulovillous adenoma of the duodenum (**A**) (HE × 100), adenocarcinoma arising in tubulovillous adenoma of the duodenum (**B**) (HE × 200), Brunner glands separated by fibrovascular septa in Brunner gland adenoma of the duodenum (**C**) (HE × 40), spindle cell gastrointestinal stromal tumour in submucosa of the duodenum (**D**) (HE × 100), non-Hodgkin's lymphoma showing diffuse monotonus population of large cells infiltrating duodenal glands (**E**) (HE × 100), and circumscribed tumour nodule with tumour cells arranged in organoid pattern in carcinoid of the duodenum (**F**) (HE × 40).

time through small intestine thus reducing exposure to potential carcinogens, low bacterial population producing carcinogens and high concentration of lymphoid tissue producing IgA immunoglobulins[4]. It is often difficult to diagnose early duodenal tumors because of their non-specific and insidious presentation.

Adenomas are the most common duodenal tumors including adenomatous polyps and Brunner adenoma. Adenomatous polyps are more common at gastroduodenal junction and have 3%-5% risk of developing adenocarcinoma in life time[5]. Brunner gland adenomas are very rare tumors and less than 150 cases have been reported in the English literature[6]. Size of the tumor is important in differentiating adenoma from Brunner gland hyperplasia. The size less than 1 cm is referred to as Brunner gland hyperplasia. Adenocarcinoma of the duodenum not originating from the region of ampulla is an uncommon neoplasm. Since it was first described in 1746 by Hamburgur, approximately 800 cases have been described in the literature. However in these cases there is a mix of ampullary and peri-ampullary carcinomas[7]. Because of rarity of these tumors, the exact etiological factors have not been defined. Patients with familial adenomatous polyposis and Crohn's disease or celiac disease have a higher risk of developing duodenal carcinoma[8]. In the present study, there were no such associations. Only one case was arising in the background of adenoma and two cases of tubulovillous adenoma were associated with polyposis coli. Heniford *et al*[8] reported that D3-D4 is the most common site of primary duodenal adenocarcinoma. However, in the present study 10/15 adenocarcinomas were seen in D1-D2 region. D3-D4 carcinomas have better prognosis as compared to D1-D2 carcinomas because the former behave like hind gut tumors and the latter as foregut tumors[9].

The relative frequency of duodenal stromal tumors is not known. Only one study has presented a series of 190 duodenal stromal tumors[10]. According to their findings, gastrointestinal stromal tumors (GIST), the c-kit positive primary mesenchymal tumor, constitute the largest group of mesenchymal tumors in contrast to smooth muscle tumors i.e. leiomyoma and leiomyosarcoma which are now thought to be rare in the duodenum. In the present series, there were an equal number of GISTs and smooth muscle

tumors. However, the number of cases was too small to comment on the relative frequency of these tumors in duodenum. Neural tumors are extremely rare in duodenum and we encountered only one case of neurofibroma. Subclassification into benign, borderline and malignant stromal tumors based upon size, mitosis, necrosis and metastasis must be made for prognosis[11,12].

Gastrointestinal tract is the most common extranodal site of involvement by non-Hodgkin's lymphoma (NHL). Primary lymphomas of the small intestine are relatively rare and account for 4%-12% of all NHLs and 19%-38% of small bowel malignancies[13]. In the present study, duodenal lymphomas accounted for 21.8% all duodenal tumors. Recently reports have emerged about the increasing frequency of primary MALT lymphomas in the small intestine and it is proposed that small intestinal MALTs are of gastric origin due to the probable role of *H pylori*. In this review of duodenal tumors, only two cases were of MALT lymphomas, the remaining were of diffuse large B cell type and T cell lymphomas. It was reported that intestinal T cell lymphomas are more common in small intestine and a term "enteropathy associated T-cell lymphoma" (EATL) has been introduced based upon their existence in coelic disease[14]. However, no such association was seen in our cases. Histopathological examination and exact immunophenotyping of NHLs based on WHO classification are important from the prognosis point of view as T cell lymphomas have poor prognosis as compared to B cell lymphomas. MALT lymphomas in B cell group have a better prognosis.

Duodenal neuroendocrine tumors (NETs) comprise 2%-3% of all gastrointestinal endocrine tumors including gastrinoma, somatostatinoma, nonfunctional NET, and poorly-differentiated NE carcinoma and their frequency is increasing[15]. Although the majority of these tumors are nonfunctional, they can cause Zollinger-Ellison syndrome and other clinical hormonal syndromes. Gastrinomas defined as gastrin secreting tumors are associated with Zollinger-Ellison syndrome (ZES) and hereditary gastrinomas, which are associated with endocrine neoplasia type 1 (MEN1) syndrome. In the present study, there was only one case of gastrinoma associated with parathyroid and adrenal hyperplasia.

In conclusion, although non-ampullary/periampullary duodenal adenocarcinomas are rare, they constitute the largest group. Histopathological examination of primary duodenal tumors is important for the correct histological subtyping of these tumors and collecting prognostic information which influences the management.

REFERENCES

1 **Zollinger RM. Primary neoplasms of the small intestine.** *Am J Surg* 1986; **151**: 654-658
2 **Kaminski N**, Shaham D, Eliakim R. Primary tumours of the duodenum. *Postgrad Med J* 1993; **69**: 136-138
3 **Kerremans RP**, Lerut J, Penninckx FM. Primary malignant duodenal tumors. *Ann Surg* 1979; **190**: 179-182
4 **Negri E**, Bosetti C, La Vecchia C, Fioretti F, Conti E, Franceschi S. Risk factors for adenocarcinoma of the small intestine. *Int J Cancer* 1999; **82**: 171-174
5 **Ryder NM**, Ko CY, Hines OJ, Gloor B, Reber HA. Primary duodenal adenocarcinoma: a 40-year experience. *Arch Surg* 2000; **135**: 1070-1074; discussion 1074-1075
6 **Rocco A**, Borriello P, Compare D, De Colibus P, Pica L, Iacono A, Nardone G. Large Brunner's gland adenoma: case report and literature review. *World J Gastroenterol* 2006; **12**: 1966-1968
7 **Rose DM**, Hochwald SN, Klimstra DS, Brennan MF. Primary duodenal adenocarcinoma: a ten-year experience with 79 patients. *J Am Coll Surg* 1996; **183**: 89-96
8 **Heniford BT**, Iannitti DA, Evans P, Gagner M, Henderson JM. Primary nonampullary/periampullary adenocarcinoma of the duodenum. *Am Surg* 1998; **64**: 1165-1169
9 **Tocchi A**, Mazzoni G, Puma F, Miccini M, Cassini D, Bettelli E, Tagliacozzo S. Adenocarcinoma of the third and fourth portions of the duodenum: results of surgical treatment. *Arch Surg* 2003; **138**: 80-85
10 **Miettinen M**, Kopczynski J, Makhlouf HR, Sarlomo-Rikala M, Gyorffy H, Burke A, Sobin LH, Lasota J. Gastrointestinal stromal tumors, intramural leiomyomas, and leiomyosarcomas in the duodenum: a clinicopathologic, immunohistochemical, and molecular genetic study of 167 cases. *Am J Surg Pathol* 2003; **27**: 625-641
11 **Goldblum JR**, Appelman HD. Stromal tumors of the duodenum. A histologic and immunohistochemical study of 20 cases. *Am J Surg Pathol* 1995; **19**: 71-80
12 **Winfield RD**, Hochwald SN, Vogel SB, Hemming AW, Liu C, Cance WG, Grobmyer SR. Presentation and management of gastrointestinal stromal tumors of the duodenum. *Am Surg* 2006; **72**: 719-722; discussion 722-723
13 **Kohno S**, Ohshima K, Yoneda S, Kodama T, Shirakusa T, Kikuchi M. Clinicopathological analysis of 143 primary malignant lymphomas in the small and large intestines based on the new WHO classification. *Histopathology* 2003; **43**: 135-143
14 **Harris NL**, Jaffe ES, Stein H, Banks PM, Chan JK, Cleary ML, Delsol G, De Wolf-Peeters C, Falini B, Gatter KC. A revised European-American classification of lymphoid neoplasms: a proposal from the International Lymphoma Study Group. *Blood* 1994; **84**: 1361-1392
15 **Mullen JT**, Wang H, Yao JC, Lee JH, Perrier ND, Pisters PW, Lee JE, Evans DB. *Carcinoid tumors of the duodenum. Surgery* 2005; **138**: 971-977; discussion 977-978

S- Editor Liu Y **L- Editor** Wang XL **E- Editor** Ma WH

PO Box 2345, Beijing 100023, China
www.wjgnet.com
wjg@wjgnet.com

World J Gastroenterol 2007 February 21; 13(7): 1112-1118
World Journal of Gastroenterology ISSN 1007-9327

RAPID COMMUNICATION

Aqueous suspension of anise "*Pimpinella anisum*" protects rats against chemically induced gastric ulcers

Ibrahim A Al Mofleh, Abdulqader A Alhaider, Jaber S Mossa, Mohammed O Al-Soohaibani, Syed Rafatullah

Ibrahim A Al Mofleh, Department of Medicine, College of Medicine, King Saud University, Riyadh, Saudi Arabia
Abdulqader A Alhaider, Department of Pharmacology, College of Medicine, King Saud University, Riyadh, Saudi Arabia
Mohammed O Al-Sohaibani, Department of Pathology, College of Medicine, King Saud University, Riyadh, Saudi Arabia
Jaber S Mossa, Syed Rafatullah, Department of Pharmacognosy and Medicinal, Aromatic and Poisonous Plants Research Center, College of Pharmacy, King Saud University, Riyadh, Saudi Arabia
Supported by King AbdulAziz City for Science and Technology, Riyadh, Saudi Arabia, Spices Project No. AR-16-37
Correspondence to: Professor Ibrahim Abdulkarim Al Mofleh, College of Medicine, King Saud University, PO Box 2925 (59), Riyadh 11461, Saudi Arabia. iamofleh@yahoo.com
Telephone: +966-1-4671215 Fax: +966-1-4671217
Received: 2006-12-02 Accepted: 2007-01-23

Abstract

AIM: To substantiate the claims of Unani and Arabian traditional medicine practitioners on the gastroprotective potential effect of a popular spice anise, "*Pimpinella anisum* L." on experimentally-induced gastric ulceration and secretion in rats.

METHODS: Acute gastric ulceration in rats was produced by various noxious chemicals including 80% ethanol, 0.2 mol/L NaOH, 25% NaCl and indomethacin. Anti-secretory studies were undertaken using pylorus-ligated Shay rat technique. Levels of gastric non-protein sulfhydryls (NP-SH) and wall mucus were estimated and gastric tissue was also examined histologically. Anise aqueous suspension was used in two doses (250 and 500 mg/kg body weight) in all experiments.

RESULTS: Anise significantly inhibited gastric mucosal damage induced by necrotizing agents and indomethacin. The anti-ulcer effect was further confirmed histologically. In pylorus-ligated Shay rats, anise suspension significantly reduced the basal gastric acid secretion, acidity and completely inhibited the rumenal ulceration. On the other hand, the suspension significantly replenished ethanol-induced depleted levels of gastric mucosal NP-SH and gastric wall mucus concentration.

CONCLUSION: Anise aqueous suspension possesses significant cytoprotective and anti-ulcer activities against experimentally-induced gastric lesions. The anti-ulcer effect of anise is possibly prostaglandin-mediated and/or through its anti-secretory and antioxidative properties.

Key words: Spice; Anise; *Pimpinella anisum*; Cytoprotection; Gastric ulcer; Gastric secretion; Sulfhydryls; Gastric wall mucus

Al Mofleh IA, Alhaider AA, Mossa JS, Al-Sohaibani MO, Rafatullah S. Aqueous suspension of anise "*Pimpinella anisum*" protects rats against chemically induced gastric ulcers. *World J Gastroenterol* 2007; 13(7): 1112-1118

http://www.wjgnet.com/1007-9327/13/1112.asp

INTRODUCTION

Peptic ulcer is one of the most common gastrointestinal diseases. Nowadays proton pump inhibitors and H_2-recptor antagonists are the most widely used drugs to treat peptic ulcer disease. However, the use of these anti-secretory drugs may be associated with adverse events and ulcer relapse[1]. Thus, there is a need for more effective, less toxic and cost-effective anti-ulcer agents. In recent years, a widespread search has been launched to identify new anti-ulcer drugs from natural sources. Spices comprising the most important products used for flavouring foods and medicinal herbs are considered nowadays as potential bioactive agents that can interfere positively or negatively with different cellular processes. They are extensively used in medicine, pharmaceuticals, perfumery and cosmetics. Additionally they possess antioxidant, antispasmodic, carminative, anti-inflammatory and other properties[2]. A number of spices, namely large cardamom[3], black pepper[4], caraway[5], cardamom[6], clove[7], coriander[8], ginger[9], peppermint[10], saffron[11], turmeric[12] among others have been shown to possess significant gastroprotective activities. The fruits of anise plant, *pimpinella anisum* L. are locally known as aniseed and yansoon. The powder and concoction of anise in hot water are used as carminatives, antiseptics, diuretics, digestives, aphrodisiacs, and as a remedy for insomnia and constipation[13]. Furthermore, anise is used to promote digestion, improve appetite, alleviate cramps and nausea, and relieve flatulence and colic. In Unani and Arabian traditional medicine, anise fruit and its oil have been used for the treatment of various conditions including dyspepsia, nausea, abdominal colic,

seizures and epilepsy[14]. The phytotherapeutic applications of anise are based on its digestive, carminative, diuretic and expectorating action[15]. It has been recently reported that the essential oil of anise is highly effective as both larvicidal and ovicidal agents[16]. The principal constituents of anise are volatile oil, coumarins, fatty acids, flavonoid glycosides, proteins and carbohydrates. Among others, anise oil contains anethole and caryophyllene[17]. Since we have not come across a scientific report on potential gastroprotective claims of anise aqueous suspension, the present study was carried out to assess its effect on chemically induced gastric ulcers in rats.

MATERIALS AND METHODS

Plant material and preparation of aqueous suspension

Seeds of anise "*Pimpinella anisum* L" (family, Apiaceae) were purchased from local herb shops in Riyadh and identified by an expert taxonomist. The sample was preserved (voucher # Sp.Pr.17-16-37) at the herbarium of Department of Pharmacognosy, College of Pharmacy, King Saud University, Riyadh, for future reference. The seeds were ground to very fine powders (75 micron), and used as an aqueous suspension for treatment in different experiments.

Animals

Wistar albino rats of either sex, approximately at the same age, weighing 150-200 g were obtained from Animal Care Center, College of Pharmacy, King Saud University, and maintained under standard conditions of temperature, humidity and light (12 h dark, 12 h light) with free access to Purina chow and water. Before testing, the animals were fasted for 36 h with access to water *ad libitum*. The conduct of experiments and the procedure of sacrifice (using ether) were approved by the Ethics Committee of the Experimental Animal Care Society, College of Pharmacy, King Saud University, Riyadh, Saudi Arabia.

Dose selection and route of administration

The doses (250 and 500 mg/kg, body weight) selected for the experiments were based on the maximum tolerable dose value (MTD) (30 g/kg, body weight) and the preliminary experiments conducted on the pharmacological activity of anise. The aqueous suspension was administred intragastrically (i.g.) through gastric intubation in all experiments, unless stated otherwise intraperitoneally (i.p.) in anti-secretory studies.

Gastric lesions induced by necrotizing agents

The rats were administered ig 1 mL of different necrotizing agents (80% ethanol, 0.2 mol/L NaOH and 25% NaCl)[18]. Anise suspension was given 30 min before the administration of necrotizing agents. One hour after the administration of ethanol and alkalis, the rats were sacrificed and examined for lesions in the stomach. The scoring of lesions, assays of gastric wall mucus and sulfhydryls as well as histological changes in the stomach were observed as follows. The patchy lesions of stomach induced by ethanol were scored according to the method described by Schiantarelli *et al*[19] using the following scale: 0 = normal mucosa, 1 = hyperemic mucosa or up to 3 small patches, 2 = 4 to 10 small patches, 3 = more than 10 small or up to 3 medium-sized patches, 4 = 4 to 6 medium-seized patches, 5 = more than 6 medium-sized or up to 3 large patches, 6 = 4 to 6 large patches, 7 = 7 to 10 large patches, 8 = more than 10 large patches or extensive necrotic zones. "Small" was defined as up to 2 mm across (max. diameter), "medium-sized" between 2 and 4 mm across and "large" more than 4 mm across.

Histopathological evaluation

Gastric tissue samples were fixed in neutral buffered formalin for 24 h. Sections of gastric tissue were histopathologically examined to study the ulcerogenic and/or anti-ulcerogenic activity of anise. The tissues were fixed in 10% buffered formalin and processed using a VIP tissue processor. The processed tissues were embedded in paraffin blocks and sections of about 5 μm thickness were cut by employing an American optical rotary microtome. These sections were stained with haematoxylin and eosin using routine procedures[20]. The slides were examined microscopically for pathomorphological changes such as congestion, hemorrhage, edema and erosions using an arbitrary scale for severity assessment of these changes.

Gastric lesions induced by indomethacin

Indomethacin was suspended in 1.0% carboxy-methylcellulose (CMC) in water (6 mg/mL) and administered orally to the rats fasted for 36 h at a dose of 30 mg/kg, body weight. Control rats were treated similarly with an equivalent amount of the vehicle[21]. The animals were sacrificed 6 h after the treatment. Stomachs of the animals were excised off the body, rinsed with normal saline and studied accordingly [22].

Estimation of non-protein sulfhydryls

Gastric mucosal non-protein sulfhydryls (NP-SH) were measured according to the method of Sedlak and Lindsay[23]. The glandular part of the stomach was homogenized in ice-cold 0.02 mmol/L ethylenediam inetetraacetic acid (EDTA). Aliquots of 5 mL of the homogenates were mixed in 15 mL test tubes with 4 mL of distilled water and 1 mL of 50% trichloroacetic acid (TCA). The tubes were shaken intermittently for 10 min and centrifuged at 3000 *g*. Two milliliters of supernatant was mixed with 4 mL of 0.4 mol/L Tris buffer at pH 8.9, 0.1 mL of 5, 5'-dithio-bis- (2-nitrobenzoic acid) (DTNB) was added and the sample was shaken. The absorbance was measured within 5 min after addition of DTNB at 412 nm against a reagent blank.

Pylorus-ligated rats (anti-secretory studies)

The rats were fasted for 36 h with access to water *ad libitum* before the pylorus was ligated under ether anesthesia and care was taken to avoid bleeding and occlusion of blood vessels [24]. Anise suspension was administered immediately after pylorus ligation (Shay) by ip route. The rats were sacrificed at 6 h after the pylorus ligation. The stomachs were removed, with the contents collected, volumes measured, centrifuged and analyzed for titratable acidity

Table 1 Effect of aqueous anise suspension on gastric lesions induced by various necrotizing agents (mean ± SD)

Group serial	Treatment	Dose (mg/kg, i.g.)	Ulcer index		
			80% EtOH	0.2 mol/L NaOH	25% NaCl
1	Control (distilled water)	-	7.16 ± 0.40	8.00 ± 0.0	7.66 ± 0.33
2	*Pimpinella anisum*	250	6.00 ± 0.51[b]	4.66 ± 0.80[d]	6.00 ± 0.44[d]
3	*Pimpinella anisum*	500	4.00 ± 0.44[d]	3.66 ± 0.66[d]	4.00 ± 0.51[d]

Six rats were used in each group. [b]$P < 0.01$, [d]$P < 0.001$ *vs* control (distilled water) group, Student' *t*-test.

Table 2 Effect of aqueous anise suspension on ethanol-induced histopathological changes in rat stomach

Group serial	Treatment and dose (mg/kg, body weight/day)	Histopathological changes							
		Congestion	Haemorrhage	Edema	Necrosis	Inflammatory changes	Dysplastic changes	Erosions	Ulceration
1	Control (distilled water) (1 mL/rat)	-	-	-	-	-	-	-	-
2	Ethanol, 80% (1 mL/rat)	++	+++	++	++	+	+	+++	+
3	Pimpinella anisum (250) + ethanol, 80% (1 mL/rat)	+	+	+	-	-	-	+	-
4	Pimpinella anisum (500) + ethanol, 80% (1 mL/rat)	+	+	+	-	-	-	+	-

-: normal, +: moderate, ++: severe, +++: intensely severe.

against 0.01 mol/L NaOH (pH 7) and the titratable acidity was calculated.

Determination of gastric wall mucus

Gastric wall mucus was determined according to the modified procedure of Corne *et al*[25]. The glandular segment of the stomach was separated from the rumen of the stomach, weighed, and transferred immediately to 10 mL of 0.1% w/v Alcian blue solution (in 0.16 mmol/L sucrose solution buffered with 0.05 mL sodium acetate at pH 5). Tissue was stained for 2 h in Alcian blue, and excess dye was removed by two successive rinses with 10 mL of 0.25 mmol/L sucrose, first for 15 min and then for 45 min. Dye complexed with the gastric wall mucus was extracted with 10 mL of 0.5 mmol/L magnesium chloride which was intermittently shaken for 1 min at 30 min intervals for 2 h. Four milliliters of blue extract was then vigorously shaken with an equal volume of diethyl ether. The resulting emulsion was centrifuged at 4000 r/min for 10 min and the absorbance of aqueous layer was recorded at 580 nm. The quantity of Alcian blue extracted from per gram of wet glandular tissue was then calculated.

Statistical analysis

The readings shown are means ± SD. The mean determination of treatment groups was compared statistically with that of control group using *t*.

RESULTS

Effect of anise suspension on gastric lesions induced by necrotizing agents

The treatments of rats with 80% ethanol, 0.2mol/L NaOH and 25% NaCl produced extensive gastric lesions mainly confined to glandular part of the stomach in all the control (only necrotizing agents treated) animals. The ulcer index in ethanol, sodium hydroxide and sodium chloride treatment groups was 7.16 ± 0.40, 8.00 ± 0.0 and 7.66 ± 0.33, respectively. Pretreatment of rats with anise suspension at the dose of 250 mg/kg significantly prevented gastric mucosal lesions induced by all necrotizing agents used. The ulcer index was 6.00 ± 0.51 ($P < 0.01$), 4.66 ± 0.80 ($P < 0.001$), 6.00 ± 0.44 ($P < 0.001$), respectively. In stomach of rats treated with 500 mg/kg of anise suspension, the ulcer index was 4.00 ± 0.44 ($P < 0.001$), 3.66 ± 0.66 ($P < 0.001$) and 4.00 ± 0.51 ($P < 0.001$) in ethanol, sodium hydroxide and sodium chloride groups respectively (Table 1).

Effect of anise suspension on histopathological changes

Histological examination of gastric mucosa showed various histopathological changes including congestion, haemorrhage, edema, necrosis, inflammatory and dysplastic changes, erosions and ulcers in ethanol-treated rats. The histological indices such as necrosis, inflammatory and dysplastic changes and ulceration were completely inhibited in rats pretreated with both doses of anise suspension (Table 2).

Effect of anise suspension on gastric lesions induced by indomethacin

To study the anti-ulcerogenic effects of anise suspension on indomethacin-induced gastric lesions in rats, two does of anise were used (250 and 500 mg/kg). Data on ulcer index in rats pretreated with both doses are reported in Table 3. The increased ulcer index in the gastric mucosa of

Table 3 Effect of aqueous anise suspension on indomethacin-induced gastric mucosal lesions (mean ± SD)

Group serial	Treatment	Animals (*n*)	Dose (mg/kg, i.g.)	Ulcer index
1	Control (indo only)	6	-	32.16 ± 5.22
2	*Pimpinella anisum* + indo	6	250	9.66 ± 1.96[d]
3	*Pimpinella anisum* + indo	6	500	6.00 ± 2.68[d]

[d]$P < 0.001$ *vs* control (indo only) group. Indo: indomethacin.

Table 4 Effect of aqueous anise suspension on the levels of non-protein sulfhydryles (NP-SH) in glandular stomach of rats treated with 80% ethanol (mean ± SD)

Group serial	Treatment and dose (mg/kg, body weight)	NP-SH concentration (μmol/100 mg wet tissue)
1	Control (distilled water, 1 mL/rat)	11.70 ± 0.86
2	Control (80% ethanol, 1 mL/rat)	6.31 ± 0.23[b]
3	*Pimpinella anisum* (250) + 80% ethanol (1 mL/rat)	6.71 ± 0.33
4	*Pimpinella anisum* (500) + 80% ethanol (1 mL/rat)	7.68 ± 0.37[a]

Six rats were used in each group. [a]$P < 0.05$ *vs* control (80% ethanol) group, [b]$P < 0.01$ *vs* control (distilled water) group.

Table 5 Effect of anise suspension on gastric secretion, acidity and gastric lesion index in pylorus-ligated Shay rats (mean ± SD)

Group serial	Treatment	Dose (mg/kg, i.g)	Volume of gastric content (mL)	Titratable acid (mEq/L)	Ulcer index
1	Control (distilled water)	-	7.83 ± 0.38	127.21 ± 2.64	0.66 ± 0.21
2	*Pimpinella anisum*	250	3.00 ± 0.51[b]	109.33 ± 4.64[d]	0.00[d]
3	*Pimpinella anisum*	500	0.33 ± 0.33[d]	108.33 ± 5.00[d]	0.00[d]

Six rats were used in each group. [b]$P < 0.01$, [d]$P < 0.001$ *vs* control (distilled water) group.

Table 6 Effect of aqueous anise suspension on ethanol-induced gastric wall mucus concentration changes (mean ± SD)

Group serial	Treatment	Dosage (mg/kg,i.g.)	Gastric wall mucus (μg Alcian blue of wet glandular tissue)
1	Control (distilled water)	-	474.98 ± 13.86
2	80% ethanol only	-	307.92 ± 10.69[d]
3	*Pimpinella anisum* 80% ethanol	250	372.75 ± 20.87[a]
4	*Pimpinella anisum* 80% ethanol	500	391.60 ± 20.19[b]

[a]$P < 0.05$, [b]$P < 0.01$ *vs* 80% ethanol group only; [d]$P < 0.001$ *vs* control (distilled water) group.

indomethacin-treated rats (control) decreased significantly in animals treated with lower and higher anise doses (32.16 ± 5.22 *vs* 9.66 ± 1.96 and 6.00 ± 2.68, $P < 0.001$), respectively.

Effect of anise suspension on ethanol-induced mucosal NP-SH *depletion*

The level of NP-SH in the gastric mucosa of control rats was 11.70 ± 0.86 mmol/g of tissue, significantly decreased to 6.31 ± 0.23 mmol/g following the administration of ethanol. Pretreatment of rats with anise suspension at a higher dose (500 mg/kg) significantly replenished the ethanol-induced depletion of NP-SH ($P < 0.05$, Table 4).

Effect of anise suspension on gastric secretion in pylorus-ligated rats

In control rats, pylorus ligation for 6 h resulted in an accumulation of 7.83 ± 0.38 mL of gastric secretions, titratable acidity 127.21 ± 2.64 in mEq/L and an ulcer index 0.66 ± 0.33 (Table 5). The volume of gastric secretion in the rats treated with 250 and 500 mg/kg of anise suspension significantly reduced to 3.00 ± 0.51 and 0.33 ± 0.33 mL, respectively ($P < 0.001$). A significant decrease in titratable acid was also observed in the rats treated with 250 mg/kg (109.33 ± 4.64 mEq/L) and 500 mg/kg (108.33 ± 5.00 mEq/L) ($P < 0.001$). A complete inhibition of rumenal ulcers was noted in both groups of rats treated with anise suspension as compared to control group (Table 5).

Effect of anise suspension on ethanol-induced changes in gastric wall mucus

The treatment of rats with ethanol significantly decreased the Alcian blue binding capacity of gastric wall mucus (307.92 ± 10.69 μg Alcian blue/g of tissue) as compared to control rats (474.98 ± 13.86 μg/g). Pretreatment of rats with anise suspension at 250 mg/kg (372.75 ± 20.87 μg/g) and 500 mg/kg (391.60 ± 20.19 μg/g) significantly enhanced Alcian blue binding capacity of gastric mucosa ($P < 0.05$, $P < 0.01$), respectively (Table 6).

DISCUSSION

Anise spice is added to foods in several forms as whole spice, as ground spice or as isolates from its extracts and volatile oils[26]. We adopted the suspension dosage form in our experiments. In necrotizing agents-induced gastric ulcers, the lesions were characterized by multiple haemorrhage red bands of different sizes along the longitudinal axis of the glandular stomach. This model is extensively used to screen drugs for cytoprotection[27]. This study provided a substantial evidence for anti-ulcer and

anti-secretory effects of an aqueous suspension of anise. Anise suspension significantly inhibited the ulcerative lesions in all animals treated with necrotizing agents, which was further confirmed by histological findings in which necrosis, inflammatory, dysplastic changes and ulcers were abolished in rats pretreated with anise suspension. The ability of gastric mucosa to resist injury by endogenous secretions (acid, pepsin and bile) and ingested irritants (e.g., alcohol), can be attributed to a number of factors that have been referred to collectively as mucosal defense[28]. Gastric mucosal lesions induced by necrotizing agents such as ethanol and strong alkalis are due to depression of the gastric defensive mechanisms[29]. Although ethanol-induced ulcers are not inhibited by anti-secretory agents such as cimetidine, they are inhibited by agents that enhance mucosal defensive factors such as prostoglandins[30]. The current results suggest that the anti-ulcerogenic effect of anise suspension may be related to its cytoprotective activity.

Gastroduodenal ulceration is a major limitation to the use of non-steroidal anti-inflammatory drugs (NSAIDs)[31]. NSAIDs can cause damage to the gastroduodenal mucosa via several mechanisms, including their topical irritant effect on the epithelium, impairment of the mucosal barrier function, suppression of gastric prostaglandin synthesis, reduction of gastric mucosal blood flow and interference with the repair of superficial injury. The presence of acid in the lumen of stomach also contributes to the pathogenesis of NSAIDs-induced ulcers and bleeding by impairing the restitution process, interfering with haemostasis and inactivating several growth factors that are important in mucosal defence and repair[32,33]. In the present study, indomethacin-induced gastric lesions were extensively prevented by anise suspension.

Sulfhydryl compounds have been significantly implicated in the maintenance of gastric integrity, particularly when reactive oxygen species are involved in the pathophysiology of tissue damage[34]. Since anise suspension significantly enhances gastric tissue NP-SH concentration, it is conceivable that it is endowed with antioxidant properties accounting for its gastroprotective action. Hence, it may be presumed that the replenishing potential of sulfhydryl levels might play an important role in the gastroprotective activity of anise suspension-treated rats. Furthermore, the ability of anise suspension to protect against ulcers in NSAID-induced gastric damage may be due to the enhanced synthesis of mucus, bicarbonates and prostaglandins, as well as reduced acid output. Consequently these activities can promote the inhibition of basal gastric acid secretion as observed in our pylorus-ligated shay rat model[35,36]. On the other hand, it is also important to note that NSAIDs can increase gastric acid secretion, through prostaglandin inhibitory effects on parietal cells[37,38]. In the present study, anise aqueous suspension treatment significantly reduced basal gastric acid volume, titratable acidity and completely inhibited ulcer formation in rats. However, to date it is still controversial about relationship between the acid output and the genesis of acute gastric mucosal lesions (AGML). Our results support this correlation as anise suspension significantly reduced basal gastric secretion and prevented the occurrence of AGML in pylorus-ligated rats and thus, supporting the hypothesis of "no acid no ulcer" [39]. It has been postulated that histamine may be involved in the formation of pylorus-ligated ulcers and play a mediating role in the gastric secretion stimulated by gastrin, vagal stimulation, and cholinergic agents[40]. The correlation between gastric mucus and acid secretions in our experiments, clearly demonstrated that the gastric protective activity observed may be associated with correction or normalization of the altered balance between erosive action of acid and gastric mucosal defence. Gastric wall mucus is thought to play an important role as a defensive factor against gastric mucosal damage[41]. The determined gastric wall mucus is used as an indicator for gastric wall mucus secretion[42]. In the present investigation, anise suspension caused a significant enhancement of ethanol-induced gastric wall mucus depletion in rats, which further confirms the ability of anise to prevent and/or ameliorate the effects of damaging agents. These findings indicate that anise suspension preserves gastric mucus secretion and strengthens gastric mucosa defense factors in experimental rats[43,44].

The chemical constituents of anise responsible for its anti-ulcer activity are not known. However, chemical studies demonstrated that anise contains estrarole[45], anethol[46], eugenol[47], anisaldehyde, methylchanicol[48], coumarins[49] and terpenes[50] among others as the major compounds. Anise and its compounds have been identified as free radicals or active oxygen scavengers[51]. In addition, the ability of anise suspension to protect gastric mucosa against lesions induced by chemical irritants is likely by maintaining the structural integrity of gastric epithelium and balance of aggressive factors and inherent protective mechanisms[52]. Furthermore, the mucus gel and its bicarbonate gradient seem to be an important first-line defense against harmful stimuli [53].

In conclusion, anise suspension exhibits an anti-ulcer potential activity through at least one or more possible mechanisms including inhibition of basal gastric secretion, stimulation of mucus secretion, endogenous gastric mucosal prostaglandin synthesis and possible antioxidative activity.

REFERENCES

1 **Wolfe MM**, Sachs G. Acid suppression: optimizing therapy for gastroduodenal ulcer healing, gastroesophageal reflux disease, and stress-related erosive syndrome. *Gastroenterology* 2000; **118**: S9-S31

2 **Nalini N**, Sabitha K, Viswanathan P, Menon VP. Influence of spices on the bacterial (enzyme) activity in experimental colon cancer. *J Ethnopharmacol* 1998; **62**: 15-24

3 **Rafatullah S**, Galal AM, Al-Yahya MA, Al-Said MS. Gastric and duodenal antiulcer and cytoprotective effects of *Afromomum melegueta* in rats. *Int J Pharmacogn* 1995; **33**: 311-316

4 **Al-Mofleh IA**, Alhaider AA, Mossa JS, Al-Sohaibani MO, Rafatullah S, Qureshi S. Inhibition of gastric mucosal damage by *piper nigrum* (Black pepper). *Phcog Mag* 2005; **1**: 64-68

5 **Alhaider AA**, Al-Mofleh IA, Al-Sohaibani MO, Rafatullah S and Qureshi S. Effect of *Carum carvi* on experimentally induced gastric mucosal damage in wistar albino rats. *Intl J Pharmacol* 2006; **2**: 309-315

6 **Alhaider AA**, Al-Mofleh IA, Mossa JS, Al-Sohaibani MO, Qureshi S, Rafatullah S. Pharmacological and safety evaluation studies on "Cardamom" *Elettaria cardamomum*: An important ingredient of Gahwa (Arabian coffee). *Arab J Pharm Sci* 2005; **3**: 47-58

7 **Al-Mofleh IA**, Alhaider AA, Mossa JS, Al-Sohaibani MO, Qureshi S, Rafatullah S. Pharmacological studies on 'Clove' *Eugenia caryophyllata*. *Phcog Mag* 2005; **1**: 105-109

8 **Al-Mofleh IA**, Alhaider AA, Mossa JS, Al-Sohaibani MO, Rafatullah S, Qureshi S. Protection of gastric mucosal damage by *Coriandrum sativum* L. pretreatment in Wistar albino rats. *Environ Toxicol Pharmacol* 2006; **22**: 64-69

9 **al-Yahya MA**, Rafatullah S, Mossa JS, Ageel AM, Parmar NS, Tariq M. Gastroprotective activity of ginger zingiber officinale rosc., in albino rats. *Am J Chin Med* 1989; **17**: 51-56

10 **Al-Mofleh IA**, Alhaider AA, Mossa JS, Al-Sohaibani MO, Qureshi S, Rafatullah S. Antisecretagogue, antiulcer and cytoprotective effects of 'Peppermint' *Mentha piperita* L. in laboratory animals. *J Med Sci* 2006; **6**: 930-936

11 **Al-Mofleh IA**, Alhaider AA, Mossa JS, Al-Sohaibani MO, Qureshi S, Rafatullah S. Antigastric ulcer studies on "Saffron" *Crocus sativus* L. in rats. *Pakistan J Biol Sci* 2006; **9**: 1009-1013

12 **Rafatullah S**, Tariq M, Al-Yahya MA, Mossa JS, Ageel AM. Evaluation of turmeric (*Curcuma longa*) for gastric and duodenal antiulcer activity in rats. *J Ethnopharmacol* 1990; **29**: 25-34

13 **Kreydiyyeh SI**, Usta J, Knio K, Markossian S, Dagher S. Aniseed oil increases glucose absorption and reduces urine output in the rat. *Life Sci* 2003; **74**: 663-673

14 **Said HM**, Saeed A, D'Silva LA, Zubairy HN, Bano Z. Medicinal herbal: A textbook for medical students and doctors. Pakistan: Hamdard Foundation Pakistan, 1996: 1-82

15 **Besharati-Seidani A**, Jabbari A, Yamini Y. Headspace solvent microextraction: a very rapid method for identification of volatile components of Iranian *Pimpinella anisum* seed. *Anal Chim Acta* 2005; **530**: 155-161

16 **Prajapati V**, Tripathi AK, Aggarwal KK, Khanuja SP. Insecticidal, repellent and oviposition-deterrent activity of selected essential oils against Anopheles stephensi, Aedes aegypti and Culex quinquefasciatus. *Bioresour Technol* 2005; **96**: 1749-1757

17 **Leung AY**. Encyclopedia of common natural ingredients used in food, drugs and cosmetics. New York: John Wiley and Sons Inc, 1980: 409

18 **Robert A**, Nezamis JE, Lancaster C, Davis JP, Field SO, Hanchar AJ. Mild irritants prevent gastric necrosis through "adaptive cytoprotection" mediated by prostaglandins. *Am J Physiol* 1983; **245**: G113-G121

19 **Schiantarelli P**, Cadel S, Folco GC. Gastroprotective effects of morniflumate, an esterified anti-inflammatory drug. *Arzneimittelforschung* 1984; **34**: 885-890

20 **Culling CFA**. Handbook of Histopathological and Histochemical Techniques. 3rd ed. London: Butterworth and Company, 1974: 126-159

21 **Bhargava KP**, Gupta MB, Tangri KK. Mechanism of ulcerogenic activity of indomethacin and oxyphenbutazone. *Eur J Pharmacol* 1973; **22**: 191-195

22 **Szabo S**, Trier JS, Brown A, Schnoor J, Homan HD, Bradford JC. A quantitative method for assessing the extent of experimental gastric erosions and ulcers. *J Pharmacol Methods* 1985; **13**: 59-66

23 **Sedlak J**, Lindsay RH. Estimation of total, protein-bound, and nonprotein sulfhydryl groups in tissue with Ellman's reagent. *Anal Biochem* 1968; **25**: 192-205

24 **Shay H**, Komarov SA, Fels SS, Meranza D, Grunstein M, Siplet H. A simple method for uniform production of gastric ulceration in rat. *Gastroenterology* 1945; **5**: 43-61

25 **Corne SJ**, Morrissey SM, Woods RJ. Proceedings: A method for the quantitative estimation of gastric barrier mucus. *J Physiol* 1974; **242**: 116P-117P

26 **Suhaj M**. Spice antioxidants isolation and their antiradical activity: a review. *J Food Compos Anal* 2006; **19**: 531-537

27 **Robert A**, Nezamis JE, Lancaster C, Hanchar AJ. Cytoprotection by prostaglandins in rats. Prevention of gastric necrosis produced by alcohol, HCl, NaOH, hypertonic NaCl, and thermal injury. *Gastroenterology* 1979; **77**: 433-443

28 **Wallace JL**. Pathogenesis of NSAID-induced gastroduodenal mucosal injury. *Best Pract Res Clin Gastroenterol* 2001; **15**: 691-703

29 **Kinoshita M**, Noto T, Tamaki H. Effect of a combination of ecabet sodium and cimetidine on experimentally induced gastric lesions and gastric mucosal resistance to ulcerogenic agents in rats. *Biol Pharm Bull* 1995; **18**: 223-226

30 **Morimoto Y**, Shimohara K, Oshima S, Sukamoto T. Effects of the new anti-ulcer agent KB-5492 on experimental gastric mucosal lesions and gastric mucosal defensive factors, as compared to those of teprenone and cimetidine. *Jpn J Pharmacol* 1991; **57**: 495-505

31 **Wallace JL**. How do NSAIDs cause ulcer disease? *Baillieres Best Pract Res Clin Gastroenterol* 2000; **14**: 147-159

32 **Toma W**, Hiruma-Lima CA, Guerrero RO, Brito AR. Preliminary studies of Mammea americana L. (Guttiferae) bark/latex extract point to an effective antiulcer effect on gastric ulcer models in mice. *Phytomedicine* 2005; **12**: 345-350

33 **Whittle BJ**. Gastrointestinal effects of nonsteroidal anti-inflammatory drugs. *Fundam Clin Pharmacol* 2003; **17**: 301-313

34 **Blandizzi C**, Fornai M, Colucci R, Natale G, Lubrano V, Vassalle C, Antonioli L, Lazzeri G, Del Tacca M. Lansoprazole prevents experimental gastric injury induced by non-steroidal anti-inflammatory drugs through a reduction of mucosal oxidative damage. *World J Gastroenterol* 2005; **11**: 4052-4060

35 **Kimura M**, Goto S, Ihara Y, Wada A, Yahiro K, Niidome T, Aoyagi H, Hirayama T, Kondo T. Impairment of glutathione metabolism in human gastric epithelial cells treated with vacuolating cytotoxin from *Helicobacter pylori*. *Microb Pathog* 2001; **31**: 29-36

36 **Loguercio C**, Romano M, Di Sapio M, Nardi G, Taranto D, Grella A, Del Vecchio Blanco C. Regional variations in total and nonprotein sulfhydryl compounds in the human gastric mucosa and effects of ethanol. *Scand J Gastroenterol* 1991; **26**: 1042-1048

37 **Ligumsky M**, Goto Y, Debas H, Yamada T. Prostaglandins mediate inhibition of gastric acid secretion by somatostatin in the rat. *Science* 1983; **219**: 301-303

38 **Soll AH**. Mechanisms of action of antisecretory drugs. Studies on isolated canine fundic mucosal cells. *Scand J Gastroenterol Suppl* 1986; **125**: 1-8

39 **Melo JR**, de Araújo GK, da Luz MM, da Conceição SA, Lisboa FA, Moraes-Santos T, Cunha-Melo JR. Effect of acid secretion blockade on acute gastric mucosal lesions induced by Tityus serrulatus scorpion toxin in anaesthetized rats. *Toxicon* 2006; **48**: 543-549

40 **Blandizzi C**, Mengozzi G, Intorre L, Natale G, Soldani G, Del Tacca M. Inhibitory cholinergic effects of esaprazole on gastric secretion and plasma gastrin levels in the dog. *Pharmacology* 1993; **46**: 231-240

41 **Marhuenda E**, Martin MJ, De La Alarcon Lastra C. Antiulcerogenic acitivity of aescine in different experimental models. *Phytother Res* 1993; **7**: 13-16

42 **Mersereau WA**, Hinchey EJ. Role of gastric mucosal folds in formation of focal ulcers in the rat. *Surgery* 1982; **91**: 150-155

43 **Lukie BE**, Forstner GG. Synthesis of intestinal clycoproteins. Inhibition of (I- 14 C)glucosamine incorporation by sodium salicylate *in vitro*. *Biochim Biophys Acta* 1972; **273**: 380-388

44 **Davenport HW**. Destruction of the gastric mucosal barrier by detergents and urea. *Gastroenterology* 1968; **54**: 175-181

45 **Zargari A**. Medicinal plants. Tehran, Iran: Tehran University Press, 1989: 519-521

46 **Andarwulan N**, Shetty K. Phenolic content in differentiated tissue cultures of untransformed and Agrobacterium-transformed roots of anise (Pimpinella anisum L.). *J Agric Food Chem* 1999; **47**: 1776-1780

47 **Monod C**, Dortan D. Eugenol in anise oil. *Chem abstr* 1950; **45**: 3124A

48 **Reichling J**, Kemmerer B, Sauer-Gürth H. Biosynthesis of pseudoisoeugenols in tissue cultures of Pimpinella anisum. Phenylalanine ammonia lyase and cinnamic acid 4-hydroxylase activities. *Pharm World Sci* 1995; **17**: 113-119
49 **Kartnig V**, Moeckel H, Maunz B. The occurrence of cumarins and sterols in tissue-cultures of roots of Anethum graveolens and Pimpinella anisum (author's transl). *Planta Med* 1975; **27**: 1-13
50 **Burkhardt G**, Reichling J, Martin R, Becker H. Terpene hydrocarbons in Pimpinella anisum L. *Pharm Weekbl Sci* 1986; **8**: 190-193
51 **Gülçin İ**, Oktay M, Kireçci E, Küfrevioğlü Öİ. Screening of antioxidant and antimicrobial activities of anise (*Pimpinella anisum* L.) seed extracts. *Food Chem* 2003; **83**: 371-382
52 **Hills BA**, Butler BD, Lichtenberger LM. Gastric mucosal barrier: hydrophobic lining to the lumen of the stomach. *Am J Physiol* 1983; **244**: G561-G568
53 **Allen A**, Garner A. Mucus and bicarbonate secretion in the stomach and their possible role in mucosal protection. *Gut* 1980; **21**: 249-262

S- Editor Liu Y **L- Editor** Wang XL **E- Editor** Ma WH

PO Box 2345, Beijing 100023, China
www.wjgnet.com
wjg@wjgnet.com

World J Gastroenterol 2007 February 21; 13(7): 1119-1122
World Journal of Gastroenterology ISSN 1007-9327

RAPID COMMUNICATION

H pylori are associated with chronic cholecystitis

Dong-Feng Chen, Lu Hu, Ping Yi, Wei-Wen Liu, Dian-Chun Fang, Hong Cao

Dong-Feng Chen, Lu Hu, Ping Yi, Wei-Wen Liu, Dian-Chun Fang, Hong Cao, Department of Gastroenterology, Daping Hospital,Third Military Medical University, Chongqing 400042, China
Supported by the National Natural Science Foundation of China, No. 39970039
Correspondence to: Dr. Dong-Feng Chen, Department of Gastroenterology, Research Institute of Surgery, Daping Hospital, Third Military Medical University, Chongqing 400042, China. dfchen9@hotmail.com
Telephone: +86-23-68757362 Fax: +86-23-68813806
Received: 2005-08-05 Accepted: 2007-01-23

Abstract

AIM: To study whether *H pylori* are associated with chronic cholecystitis.

METHODS: The subjects were divided into three groups: *H pylori*-infected cholecystitis group, *H pylori*-negative cholecystitis group and control group. Pathologic changes of the gallbladder were observed by optic and electronic microscopes and the levels of interleukin-1, 6 and 8 (IL-1, 6 and 8) were detected by radioimmunoassay.

RESULTS: Histological evidence of chronic cholecystitis including degeneration, necrosis, inflammatory cell infiltration, were found in the region where *H pylori* colonized. Levels of IL-1, 6 and 8 in gallbladder mucosa homogenates were significantly higher in *H pylori*-infected cholecystitis group than those in *H pylori*-negative cholecystitis group and control group.

CONCLUSION: *H pylori* infection may be related to cholecystitis.

Key words: *H pylori*; Chronic cholecystitis; Interleukin; Colonization; Gallbladder mucosa

Chen DF, Hu L, Yi P, Liu WW, Fang DC, Cao H. *H pylori* are associated with chronic cholecystitis. *World J Gastroenterol* 2007; 13(7): 1119-1122

http://www.wjgnet.com/1007-9327/13/1119.asp

INTRODUCTION

H pylori have definite pathogenic action and related to gastritis, peptic ulcer and gastric carcinoma[1-3]. Previous studies have demonstrated that *H pylori* correlate with diseases of the extra-gastrointestine, the liver and the cholecyst[4-8]. We have isolated *H pylori* from the gallbladder and cultured *H pylori*, and preliminarily proved that there exist live *H pylori* in the gallbladder. In the present study, we carried out electron microscopic observation and immunohistochemistry to the relationship between *H pylori* and chronic cholecystitis.

MATERIALS AND METHODS

Subjects

A total of 81 cases with chronic cholecystitis were divided into *H pylori*-negative group (n = 59) and *H pylori*-infected group (n = 22), based on previous studies, PCR amplification and culture results for *H pylori*. Besides, a control group was used including another 20 cases who were proved to have no obvious inflammation in the gallbladder mucosa except polyps or *H pylori* infection after a cholecystectomy due to a gallbladder polyp.

Investigation of gastric mucosa metaplasia of epithelial cells of gallbladder mucosa

By histochemical staining of AB/PAS mucus, and based on histology of mucosal epithelial cells and characteristics of cells secreting mucus, an observation was made on gastric mucosa metaplasia of epithelial cells of gallbladder mucosa and colonization of *H pylori* in the epithelial cells of gallbladder mucosa. The relationship between *H pylori* and the epithelial cells of the gallbladder was observed by optic microscopy, W-S silver stain and immunohistochemical stain using anti-*H pylori* antibodies. The resected gallbladder specimens from cases with chronic cholecystitis were immobilized with 3% glutaral, embedded and sliced for transmission electron microscopic investigation.

Relationship between H pylori and cholecystitis

Inflammatory changes of epithelial cells of the gallbladder mucosa in regions where *H pylori* colonized were observed by optic microscopy and ultrastructural changes of epithelial cells of the gallbladder were observed by electron microscopy.

Assay of interleukins in homogenates of gallbladder mucosa

The radio-immune analytical reagent kits including IL-1, IL-6 and IL-8 were purchased from Dongya Research Institute of Biotechnology, Beijing. About 1 g of resected

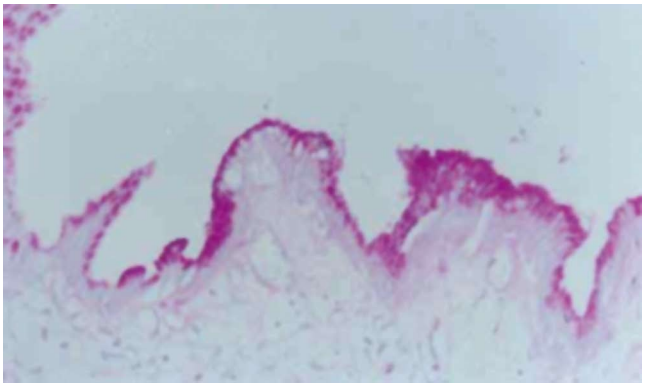

Figure 1 Specimens of chronic cholecystitis. Many positive PAS materials appear in epithelial cells of gallbladder mucosa (PAS × 200).

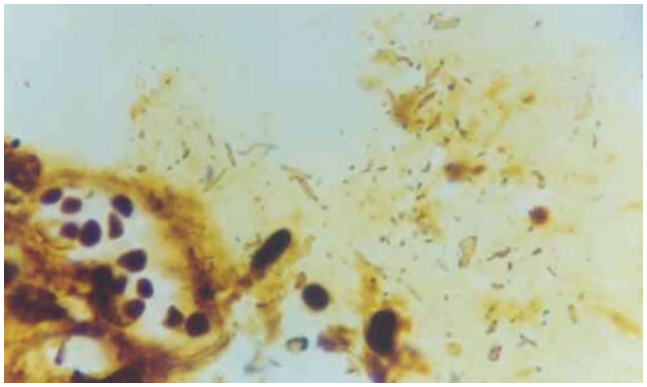

Figure 2 Helicobacter-like bacteria and inflammatory cells in mucus on gallbladder mucosa (WS × 200).

Table 1 Gastric metaplasia of gallbladder mucosa in cases with chronic cholecystitis

Group	*n*	Gastric metaplasia positive (*n*)	Gastric metaplasia negative (*n*)
Control	20	0	20
Chronic cholecystitis			
Positive *H pylori*	22	18	4
Negative *H pylori*	59	7	52

gallbladder mucosa was added into ultrapure water (Center of Molecular Biology, Research Institute of Surgery, Daping Hospital, Third Military Medical University, Chongqing) and homogenized in an IS-l homogenizer (Medical Machine Factory, Zhejiang) and the homogenates were centrifuged at 4000 r/min for l5 min, after which the supernatants were collected and frozen at -70℃. The EC-l200 radio-immune auto-γ counting device (Zhongjia Corporation of ChinaAcademy of Sciences) was employed for radio-immune assay and a fully automatic biochemical assay device of Beckman Synchron CX (USA) was used for quantification of proteins of gallbladder mucosa homogenates.

Statistical analysis

Data were expressed as mean ± SD and processed with Chi-square test and Student's t-test. $P < 0.05$ was considered significant.

RESULTS

Metaplasia of gastric mucosa in gallbladder

In cases with a gallbladder polyp, no mucus stained positive for PAS was found in gallbladder mucosa in the region beyond the polyp, nor was positive substance of PAS, i.e., metaplasia of gastric mucosa, found in epithelial cells of mucosa. In cases with chronic lithic cholecystitis, the epithelium of gallbladder mucosa was column-like. AB/PAS stain showed that neutral mucus was positive, with metaplasia of epithelial cells of gastric mucosa (Figure 1).

Gastric metaplasia of gallbladder mucosa appeared in 25 cases, accounting for 30.86% (25/81) of all cases with chronic cholecystitis, however, it was not found in the control group (Table 1). This suggested that gallbladder mucosa was apt to gastric metaplasia in cases with chronic lithiasis cholecystitis, especially in those with *H pylori* infection in the gallbladder, of gastric metaplasia of gallbladder mucosa (18/22, 81.82%) was significantly higher than that in cases with negative *H pylori* (7/59, 11.86%, $P < 0.01$). It indicated that gastric metaplasia of gallbladder mucosa might relate to *H pylori* infection in the gallbladder.

Colonization of H pylori in gallbladder and its relation to cholecystitis

The optic microscopy showed that *H pylori* were scattered or aggregated on, or located within certain distance from the epithelial cells of gallbladder mucosa and that individual *H pylori* distributed inside epithelial cells or existed in intercellular space. At the regions with *H pylori,* column-like cells secreted neutral mucus by AB/PAS stain, indicating that the gallbladder mucosa had gastric metaplasia and that gastric mucosa were absent in some regions where *H pylori* located. Electron microscopy showed that *H pylori* were located on, stuck to, or entered the epithelial cells of gallbladder mucosa, where, however, no tight junction or adhesiveness could be seen. Moreover, optic microscopy revealed degeneration of the epithelial cells of gallbladder mucosa, infiltration and exudation of inflammatory cells, exfoliation of the epithelial cells, or chronic inflammation such as mucous layer shrinkage, decrease or even disappearance of epithelial cells and glands at sites where *H pylori* were present. Sometimes, there could be seen that inflammatory cells aggregated around *H pylori* and the latter were swallowed (Figure 2). On the other hand, only a few inflammatory cells infiltrated the mucosa, with intact epithelial cells, in most cases with chronic cholecystitis without *H pylori* infection. Exceptionally, even in these cases, there emerged acute inflammatory manifestations including infiltration of large numbers of inflammatory cells, degeneration, apoptosis and exudation of epithelial cells or chronic inflammatory manifestations including atrophy of glands. In the gallbladder epithelial cells that were proved to have

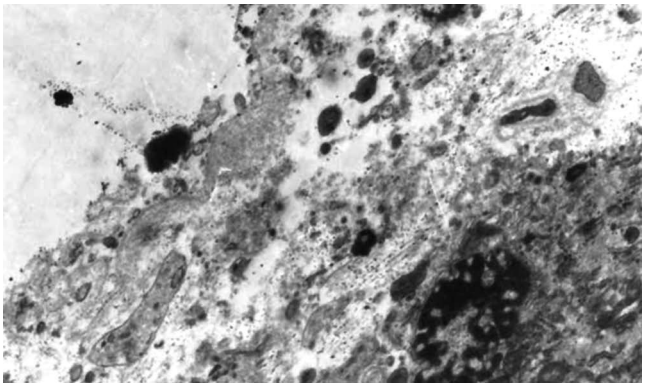

Figure 3 Electron microscopic images of *H pylori* on the epithelial cells of gallbladder (× 6000).

H pylori infection by electron microscopy, changes such as destructed epithelial cell membranes, loose cellular connection, dilatation of mitochondria, decrease or disappearance of crest, and dilatation of endoplasmic reticulum could be seen, which were severer compared with those without *H pylori* infection (Figure 3). The levels of IL-l, IL-6 and IL-8 of gallbladder mucosa homogenates were expressed as ng/g protein, and are shown in Table 2.

In cases with chronic cholecystitis, the levels of IL-l, IL-6 and IL-8 in gallbladders in both negative *H pylori* group and positive *H pylori* group were significantly higher than those in control group ($P < 0.01$). Moreover, there was a significant difference between positive *H pylori* group and negative *H pylori* group in levels of IL-1, IL-6 and IL-8 in the gallbladder ($P < 0.01$).

Table 2 Levels of IL-l, IL-6 and IL-8 of gallbladder mucosa homogenates (ng/g protein)

Groups	*n*	IL-1	IL-6	IL-8
Control	20	21.65 ± 4.28	77.10 ± 10.56	101.35 ± 19.39
Chronic cholecystitis				
Negative *H pylori*	59	68.76 ± 15.08[b]	159.54 ± 37.65[b]	152.10 ± 46.57
Positive *H pylori*	22	142.68 ± 25.41[b,d]	241.50 ± 80.60[b,d]	593.18 ± 93.59[b,d]

[b]$P < 0.01$ *vs* control group; [d]$P < 0.01$ *vs* negative *H pylori* group.

DISCUSSION

The gallbladder and stomach are originated from endoblasts and have similar tissue structures, with the mucosa covered with a slime layer [9-11]. AB/PAS stain showed that the epithelial cells of gallbladder mucosa secreted neutral mucus, with gastric metaplasia, in about 31% (25/81) of cases with cholecystolithiasis. Caselli *et al*[12-14] also demonstrated that the epithelial cells of gallbladder mucosa had gastric metaplasia in cases with cholecystolithiasis. Roa *et al*[15,16] found that pepsinogen I , Ⅱ were expressed in the epithelial cells of the gallbladder. The significance of gastric metaplasia of gallbladder mucosa lies in that the gastric metaplasia provides conditions for *H pylori* colonization in the gallbladder. The results of our study showed that compared with cases without *H pylori* infection in the gallbladder, there was a significantly higher incidence rate of gastric metaplasia in epithelial cells of gallbladder mucosa in cases with *H pylori* infection. It also proved that the gastric metaplasia of gallbladder mucosa closely correlated with *H pylori* infection in the gallbladder. Nevertheless, there were cases with *H pylori* infection but without gastric metaplasia in the gallbladder; meanwhile, there were cases with gastric metaplasia but without *H pylori* infection. These findings indicate that there is no absolute causality between gastric metaplasia and *H pylori* infection in the gallbladder. We hypothesize that many epithelial cells of the gastrointestinal tract have receptors for *H pylori* colonization factors. Therefore, *H pylori* can colonize on the epithelial cells of the gallbladder mucosa with no gastric metaplasia[17].

We also found that *H pylori* were separated from or adhered to the epithelial cells of gallbladder mucosa and that some *H pylori* penetrated through epithelial cells of the gallbladder. It that *H pylori* had a weak ability to pass through cells. At sites where *H pylori* aggregated, the epithelial cells of gallbladder mucosa were degenerated, erosive and even apoptotic. In some parts, inflammatory cells infiltrated, which became more obvious with increases in the number of *H pylori*. Electron microscopy revealed that at sites infected with *H pylori*, the integrity of the cell membrane of epithelial cells was destructed, with swelling of mitochondria and dilatation of endoplasmic reticulum. It showed that colonization of *H pylori* in the gallbladder cause inflammation of the gallbladder, mainly chronic nonsuppurative inflammation, which in turn provides an important condition for *H pylori* as one of the etiological factors leading to cholecystitis. Damage of the epithelial cells of gallbladder mucosa caused by *H pylori* may relate to specific virulence factors of *H pylori* such as cytotoxin-associated protein (CagA) and vacuoles toxin (VacA) , as well as urease, lipopolysaccharides and mucus enzyme of *H pylori*[18].

H pylori can also damage the epithelial cells of gallbladder mucosa through mediating inflammation and immunoreaction. The levels of IL-l, IL-6 and IL-8 in gallbladder mucosa homogenates in both *H pylori* negative and positive groups were significantly higher than those in control group ($P < 0.01$). It indicates that chronic lithic cholecystitis is associated with these three cytokines. We also found that in cholecystitis specimens with or without *H pylori* infection, levels of IL-1, IL-6 and IL-8 were significantly higher than those in control group, indicating that these interleukins may participate in pathogenesis of chronic cholecystitis. This may accord with the function of IL in *H pylori*-related gastritis and gastric ulcer[19,20]. After infection with *H pylori*, the urease, lipase and heat shock proteins secreted by *H pylori* can activate regional epithelial cells of mucosa and vascular endothelial cells expressing IL-1, IL-6 and other cytokines such as ICAM-I, hence stimulating and chemotaxy intravascular lymphocytes and monocytes to shift to *H pylori*-infected sites. IL-6 can activate and induce differentiation of T cells through other cytokines and enhance the function of

monocytes and NK cells, resulting in inflammation and injury at sites infected with *H pylori*. Our study verified that CagA of *H pylori* exerted strong action in stimulating epithelial cells and other cells expressing IL-8, which can activate and chemotactic neutrophils and lymphocytes[21]. In cases with chronic cholecystitis infected with *H pylori*, levels of IL-1, IL-6 and IL-8 of gallbladder mucosa were significantly higher than those in cases without *H pylori* infection. It suggests that *H pylori* participate in and aggravate cholecystitis, destruction of epithelial cells of the gallbladder and atrophy of the gallbladder[22]. Taken together, our study indicates that *H pylori* infection in the gallbladder may be one of the etiological factors leading to cholecystitis. The precise mechanism requires further verifications.

REFERENCES

1 **Tsuji S**, Kawano S. Peptic ulcer recurrence and Helicobacter pylori: evidence from Japan. *J Gastroenterol* 2003; **38**: 410-411

2 **Apostolov E**, Al-Soud WA, Nilsson I, Kornilovska I, Usenko V, Lyzogubov V, Gaydar Y, Wadström T, Ljungh A. Helicobacter pylori and other Helicobacter species in gallbladder and liver of patients with chronic cholecystitis detected by immunological and molecular methods. *Scand J Gastroenterol* 2005; **40**: 96-102

3 **Guo XL**, Wang LE, Du SY, Fan CL, Li L, Wang P, Yuan Y. Association of cyclooxygenase-2 expression with Hp-cagA infection in gastric cancer. *World J Gastroenterol* 2003; **9**: 246-249

4 **Ohara T**, Kanoh Y, Higuchi K, Arakawa T, Morisita T. Eradication therapy of Helicobacter pylori directly induces apoptosis in inflammation-related immunocytes in the gastric mucosa--possible mechanism for cure of peptic ulcer disease and MALT lymphoma with a low-grade malignancy. *Hepatogastroenterology* 2003; **50**: 607-609

5 **Gibbons AH**. Helicobacter pylori: a clinician's view. *Hosp Med* 2003; **64**: 535-538

6 **D'Elios MM**, Amedei A, Del Prete G. Helicobacter pylori antigen-specific T-cell responses at gastric level in chronic gastritis, peptic ulcer, gastric cancer and low-grade mucosa-associated lymphoid tissue (MALT) lymphoma. *Microbes Infect* 2003; **5**: 723-730

7 **Konturek PC**, Brzozowski T, Konturek SJ, Kwiecień S, Pajdo R, Drozdowicz D, Stachura J, Karczewska E, Hahn EG. Functional and morphological aspects of Helicobacter pylori-induced gastric cancer in Mongolian gerbils. *Eur J Gastroenterol Hepatol* 2003; **15**: 745-754

8 **Randi G**, Franceschi S, La Vecchia C. Gallbladder cancer worldwide: geographical distribution and risk factors. *Int J Cancer* 2006; **118**: 1591-1602

9 **Tsukanov VV**, Grishchenko NN. Association of Helicobacter pylori with chronic cholecystitis. *Eksp Klin Gastroenterol* 2003; (6):80-82

10 **Osadchuk MA**, Geras'kina TB. Chronic cholecystitis--some lithogenic aspects. *Ter Arkh* 1997; **69**: 27-30

11 **Pradhan SB**, Dali S. Relation between gallbladder neoplasm and Helicobacter hepaticus infection. *Kathmandu Univ Med J* (KUMJ) 2004; **2**: 331-335

12 **Peng XN**, Fan XG, Huang Y, Wang ZM, Cheng YP. The study on relationship between helicobacter infection and primary liver carcinoma. *Shijie Huaren Xiaohua Zazhi* 2002; **10**: 902-906

13 **Jiao JZ**, Nie QH, Zhao CL, Wu YS, Wen SX, Wu Q. Clinical relationship between Helicobacter pylori infection and chronic hepatopathy. *Shijie Huaren Xiaohua Zazhi* 2003; **11**: 851-853

14 **Huang C**, Wu ZM, Zheng ZX. Clinical significance of 13C breath test in preoperative examination for patients with cholecystolithiasis cholecystitis. *Shijie Huaren Xiaohua Zazhi* 2002; **10**: 1336-1338

15 **Chen W**, Li D, Cannan RJ, Stubbs RS. Common presence of Helicobacter DNA in the gallbladder of patients with gallstone diseases and controls. *Dig Liver Dis* 2003; **35**: 237-243

16 **Leong RW**, Sung JJ. Review article: Helicobacter species and hepatobiliary diseases. *Aliment Pharmacol Ther* 2002; **16**: 1037-1045

17 **Monstein HJ**, Jonsson Y, Zdolsek J, Svanvik J. Identification of Helicobacter pylori DNA in human cholesterol gallstones. *Scand J Gastroenterol* 2002; **37**: 112-119

18 **Roa I,** Araya JC, Shiraishi T, Yatani R, Wistuba I, Villaseca M, de Aretxabala X. Immunohistochemical demonstration of pepsinogens I and II in the gallbladder. *Rev Med Chil* 1992; **120**: 1351-1358

19 **Straubinger RK**, Greiter A, McDonough SP, Gerold A, Scanziani E, Soldati S, Dailidiene D, Dailide G, Berg DE, Simpson KW. Quantitative evaluation of inflammatory and immune responses in the early stages of chronic Helicobacter pylori infection. *Infect Immun* 2003; **71**: 2693-2703

20 **Kamangar F**, Limburg P, Taylor P, Dawsey S. Re: Helicobacter pylori and interleukin 1 genotyping: an opportunity to identify high-risk individuals for gastric carcinoma. *J Natl Cancer Inst* 2003; **95**: 760; author reply 760-761

21 **Morland CM**, Fear J, Joplin R, Adams DH. Inflammatory cytokines stimulate human biliary epithelial cells to express interleukin-8 and monocyte chemotactic protein-1. *Biochem Soc Trans* 1997; **25**: 232S

22 **Amieva MR**, Vogelmann R, Covacci A, Tompkins LS, Nelson WJ, Falkow S. Disruption of the epithelial apical-junctional complex by Helicobacter pylori CagA. *Science* 2003; **300**: 1430-1434

S- Editor Liu Y **L- Editor** Zhu LH **E- Editor** Ma WH

PO Box 2345, Beijing 100023, China
www.wjgnet.com
wjg@wjgnet.com

World J Gastroenterol 2007 February 21; 13(7): 1123-1128
World Journal of Gastroenterology ISSN 1007-9327

RAPID COMMUNICATION

Effect of parenteral and early intrajejunal nutrition on pancreatic digestive enzyme synthesis, storage and discharge in dog models of acute pancreatitis

Huan-Long Qin, Zhen-Dong Su, Lei-Guang Hu, Zai-Xian Ding, Qing-Tian Lin

Huan-Long Qin, Zhen-Dong Su, Lei-Guang Hu, Zai-Xian Ding, Qing-Tian Lin, Institute of Parenteral Nutrition and Enteral Nutrition, Department of Surgery, Shanghai Jiaotong University Affiliated Sixth People's Hospital, Yishan Rd. 600, Shanghai 200233, China
Supported by grant from the Morning Star Fund of Shanghai, China, No. 99QB14010
Correspondence to: Dr. Huan-Long Qin, Institute of Parenteral Nutrition and Enteral Nutrition, Department of Surgery, Shanghai Jiaotong University Affiliated Sixth People's Hospital, Yishan Rd. 600, Shanghai 200233, China. hlqin@sjtu.edu.cn
Telephone: +86-21-64942226 Fax: +86-21-64368920
Received: 2006-10-17 Accepted: 2007-01-04

Abstract

AIM: To study the effect of early intrajejunal nutrition on enzyme-protein synthesis and secretion during acute pancreatitis.

METHODS: Fifteen dogs were randomly divided into parenteral nutrition (n = 7) and early intrajejunal nutrition groups (n = 8). An acute pancreatitis model was induced by injecting 5% sodium taurocholate and trypsin into the pancreas via the pancreatic duct. Intrajejunal nutrition was delivered with a catheter via a jejunostomy tube after the model was established for 24 h. On d 1 and 7 and at the beginning of nutritional support, radioactive tracing and electron microscopes were used to evaluate the enzyme-protein synthesis in acinar cells, the subcellular fractionation and the change in zymogen granules after 1.85 × 10^6 Bq L-^{3}H phenylalanine was infused at 30, 60, 120, and 180 min.

RESULTS: The ^{3}H radioactivity in pancreatic acinar cells reached its peak level at 60 min, and the contents in the early intrajejunal nutrition group were higher than those in the parenteral nutrition group, which were then decreased. The mean number and area of zymogen granules did not show any significant statistical difference in both groups on d 1 or on d 7 (P > 0.05).

CONCLUSION: Early intrajejunal nutrition might be effective in dogs with acute pancreatitis.

Key words: Parenteral nutrition; Enteral nutrition; Digestive enzyme; Acute pancreatitis

Qin HL, Su ZD, Hu LG, Ding ZX, Lin QT. Effect of parenteral and early intrajejunal nutrition on pancreatic digestive enzyme synthesis, storage and discharge in dog models of acute pancreatitis. *World J Gastroenterol* 2007; 13(7): 1123-1128

http://www.wjgnet.com/1007-9327/13/1123.asp

INTRODUCTION

Beneficial effects of total enteral nutrition (TEN) have been noted in a number of diseases, such as burn, trauma, and sepsis. In comparison with parenteral nutrition (PN), TEN can reduce nosocomial infection, multiple organ failure (MOF), and the length of hospitalization[1-4]. Early enteral nutritional (EEN) support in patients with acute pancreatitis (AP) has been evaluated by some authors who reported that it can moderate the acute phase response and improve disease severity and clinical outcome[5-10]. However, the commonly encountered problems of gastric atony and outlet obstruction have limited the successful delivery of enteral nutrition to patients with severe acute pancreatitis. In addition, many surgeons believe that EEN may lead to recurrence of symptoms and delayed complications, because EEN may increase the release of digestive enzymes and lysosomal hydrolases. This action of digestive enzymes and lysosomal hydrolases may be important in the development of acute pancreatitis, as lysosomal enzymes such as cathepsin B, are known to be capable of activating trypsinogen and intracellular digestive enzymes that may trigger the autodigestive phenomenon of the pancreas[11]. However, these problems may be overcome if enteral nutrition is delivered to the jejunum as distal as possible from Treitz's ligament, thereby avoiding stimulation of the cephalic and gastric phase. Therefore, it is necessary to investigate the effect of early intrajejunal nutrition (EIN) on pancreatic acinar cell uptake of ^{3}H phenylalanine, digestive enzyme synthesis, storage and discharge in dogs with AP.

MATERIALS AND METHODS

Materials

^{3}H phenylalanine (5mCi/mL) was obtained from Amersham. CBZ-arginine-napthalamide , thymus DNA

and RNA-napthalamide, cytochrome c, 3- (N-morphplino) propanesulfonic acid (MOPS), phenylmethyl- sulfonyl fluoride (PMSF), and Triton X-100 were from Sigma Chemical. All other commercially available reagents were of the highest purity.

Animal model

Twenty-two dogs weighing 18-22 kg had free access to water. After fasting for 12-14 h, all dogs were anesthetized by intramuscular injection of ketamine (10 mL/kg) and intravenous injection of sodium pentobarbital (30 mg/kg). Under sterile conditions, middle laparotomy and duodenotomy were performed. An AP model was induced by injecting 1mg/kg of a combined solution of 5% sodium taurocholate and trypsin 8000-10000 BAEF units/mL into the pancreatic duct at a pressure of 30 cm H_2O. The common biliary duct was clamped. A catheter was placed at 30 cm distal to Treitz's ligament *via* jejunostomy. After the AP model was established, the duodenum and abdomen were closed. The neck regions of dogs were shaved and prepared in a sterile manner for catheterization. A silastic catheter (1.0 mm in inner diameter, 1.5 mm in outer diameter) was inserted through the external jugular vein to reach the superior vena cava and connected to the infusion solution. Fifteen dogs with AP survived after 7 d, and the death rate was 32% (7/22). The study was approved by our Institutional Animal Committee.

Experimental groups and nutritional solution preparation

Fifteen dogs with AP were randomly divided into PN group (n = 7) and EIN group (n = 8). The two groups were isocaloric and isonitrogenous. PN solutions consisted of 7% Vamin (SSPC, 9.4 g/1000 mL), 20% intralipid (SSPC), and 50% glucose (GS). Non-protein calorie was 50 kC (209.2 kJ/kg) and nitrogen was 0.3 g/kg.d. The total volume of solution infused was 70 mL/kg.d. The energy index supported with glucose and fat emulsion was 1:1. Multivitamins and electrolytes were also included in TPN solutions. The 0.9% saline solution was infused at 250 mL/kg during operation and postoperatively for 8 h, thereafter at 125 mL/kg. The nutrient solution was infused at a constant infusion rate by a pump (100-120 mL/h).

The EIN solution was Nutrison (Nutricia). The jejunum was infused through a jejunostomy catheter with 250 mL Nutrison and 500 mL 0.9% saline at 24 h after AP was induced, 500 mL Nutrison and 250mL 0.9% saline were infused after 48 h and continued for 7 d. The infusion rate was controlled by microcomputer-pump (Nutricia). During the EIN support period, the insufficient amount of calorie and nitrogen was supplemented by partial parenteral nutrition[4] (Table 1).

Table 1 Calories, nitrogen and liquid supplemented between two groups

Group	20% Intralipid (mL/kcal)	50% glucose (mL/kcal)	Vamin (9.4g/L) (mL/g)	0.9% saline (mL)	Nutrison (1 kal/mL)
PN group (1-7 d)	227/500	500/500	640/6.0	2500	0
EIN group (1 d)	170/375	187.5/375	468/4.4	1750	250 mL (1.6 g) + NS500 mL
EIN group (2-7 d)	113.6/250	125/250	298/2.8	1750	500 mL (3.2 g) + NS 250 mL

NS: natural saline.

Amino acid uptake

Dogs with AP were infused with radioactive ^3H phenylalanine (1.85×10^6 Bq) at beginning of PN or EIN on d 1 and 7, respectively. The abdomen was opened twice and partial pancreas was rapidly removed at 30, 60, 120 and 180 min after ^3H phenylalanine pulse infusion. After rinsed with a cold homogenization buffer containing 5 mmol/L MOPS (pH 7.0), 250 mmol/L sucrose, 1 mmol/L $MgSO_4$, and 0.1 mmol/L PMSF and trimmed of fat, the pancreas was homogenized in this cold buffer using a Brinkman polytron. The homogenate was centrifuged at 150 × g for 15 min at 4℃ to pellet unbroken cells and the resulting supernatant was used to measure ^3H phenylalanine uptake. For this purpose, an aliquot of the supernatant was mixed with an equal volume of cold 20% trichloroacetic acid (TCA) and centrifuged at 4000 × g for 15 min. The remaining radioactive ^3H phenylalanine in the resulting supernatant was quantified using a Packard liquid scintillation counter.

Protein synthesis

The pancreas was sampled at the above fixed time points. The pancreas was rinsed in cold homogenization buffer, trimmed of fat, and divided into small fragments, which were homogenized in 8 mL of homogenization buffer using 5 full up- and down strokes of a motorized glass-Teflon homogenizer. The homogenate was centrifuged at 150 × g for 15 min at 4℃ to remove unbroken cells and debris. An aliquot was mixed with an equal volume of cold 20% TCA. After incubation on ice for 1 h to precipitate proteins, the sample was centrifuged at 4000 × g for 15 min at 4℃. The pellet was washed twice in 2 mL of 10% TCA. The final pellet was dissolved using a Packard liquid scintillation counter after addition of 10 mL of Beckman Ready-Solv.

Subcellular fractionation

The pancreas was removed, homogenized and subcellularly fractionated using the method of Tartakoff and Jamieson[12] with some modifications by DeLisle *et al*[13]. Briefly, the pancreas was divided into fragments, homogenized in 8 mL homogenization buffer by 5 full up- and -down strokes of a motorized glass-Teflon homogenizer, unbroken cells and debris were removed by centrifugation at 150 × g for 15 min at 4℃. The resulting supernatant was considered to be the entire sample for later calculation and to contain 100% of all measured components, and centrifuged at 1300 × g for 15 min at 4℃, yielding the "zymogen granule" pellet and a supernatant. The latter was harvested and centrifuged at 12000 × g for 12 min at 4℃ to obtain the "lysosome-mitochondria" pellet and a 12000 × g supernatant. This supernatant was centrifuged at 105000 × r/min for 60 min at 4℃

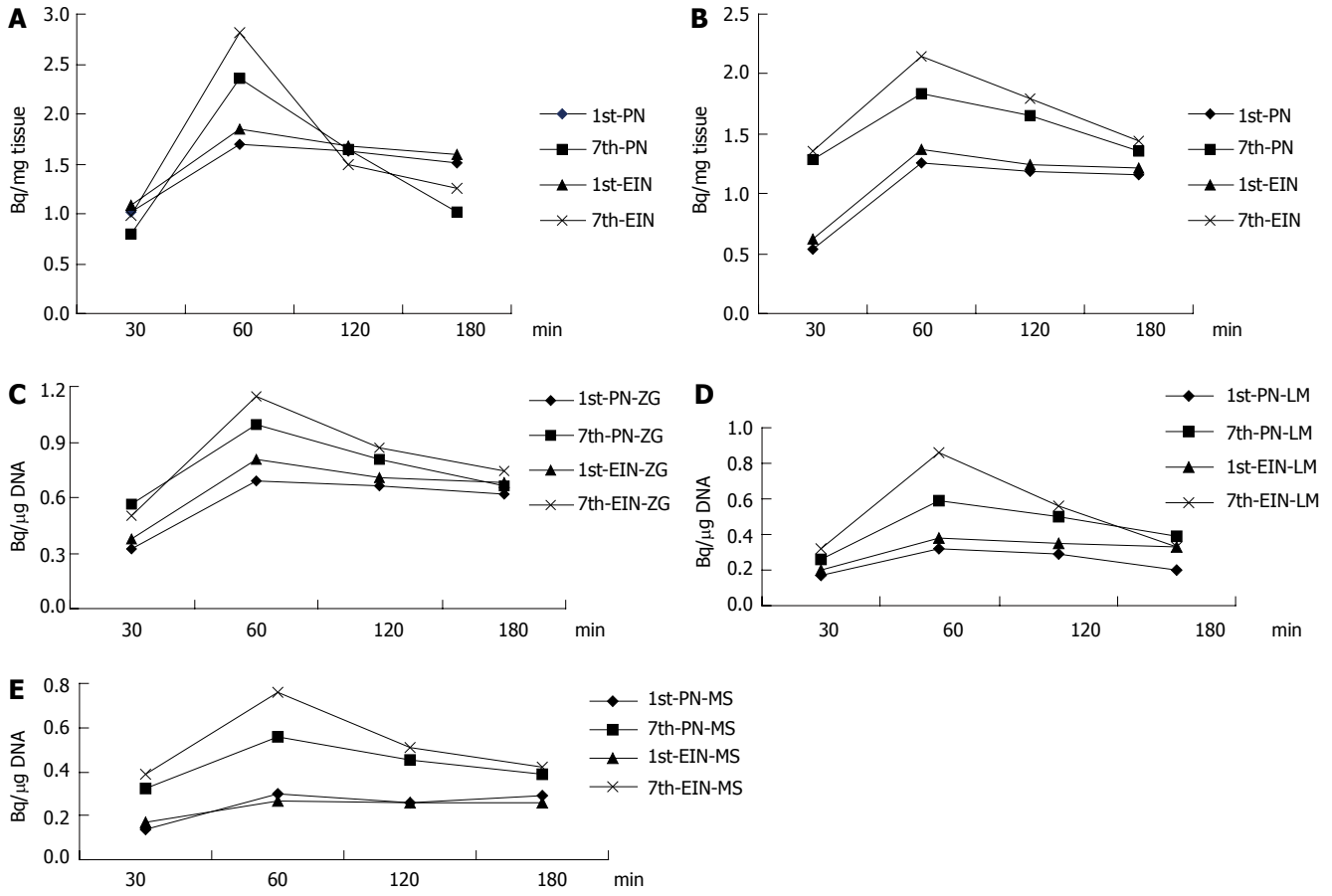

Figure 1 Change of ^{3}H radioactivity in acinar cell uptake (**A**), enzyme-protein synthesis (**B**), zymogen granules (**C**), lysosomal mitochondria (**D**), and microsomal (**E**) at different time points in two groups.

to produce a "microsomal" pellet and postmicrosomal or soluble fraction. The pellets described above were individually resuspended in 2 mL of homogenization buffer prior to measurement of marker enzymes and DNA. To measure the content of newly synthesized protein in each fraction, an aliquot of the sample or the resuspended pellet was mixed with an equal volume of 20% TCA, incubated for 1 h at 4℃ and centrifuged at 4000 × *g*. The pellet was washed as described above prior to measurement of TCA-precipitable radioactivity.

Electron microscopy

The fixation procedure used for conventional thin-section electron microscopy involved incubation with OsO4 alone (1% or 2% in phosphate buffer) at 0℃ for 30 min. After fixation, the sample was washed extensively in Veronal acetate buffer (90 mmol/L, ph 6.0), stained by incubation at 0℃ for 60 min in uranyl-magnesium acetate (0.5%) in the same buffer, washed again, dehydrated and embedded. Thin sections were doubly stained with uranyl acetate and lead nitrate, and examined under Philip EM 400 electron microscope.

A systematic randomized protocol was used to select tissue areas for morphometric analysis[14]. In each grid, 10 pictures were taken by one operator at a magnification of 150 for a total of ten negatives per sample. Two hundred and thirty pictures (PN group, n = 110; EIN group, n = 120) were printed and observed by one operator with a semi automated method using a digitizing tablet and pen, and a PC with dedicated software (Image Measure, Microscince, USA). The interstitial and vascular space, nonexocrine cells, exocrine cell nuclei, and acinar lumen space were not considered. The cross-sectional cytoplasmic area (mm^2) of exocrine cells and mature exocrine enzyme granules was directly measured on prints. In each group of samples, the mean zymogen granular number and area were obtained.

Statistical analysis

The data were collected by two blinded observers and presented as mean ± SE for multiple determinations. The statistical significance of observed changes was evaluated by t test using SPSS 10.0 statistical-software. $P < 0.05$ was considered statistically significant.

RESULTS

Pancreatic exocrine secretion stimulation test (PESST) on the first day

Acinar cell uptake of ^{3}H phenylalanine: The pancreatic acinar cell uptake of ^{3}H phenylalanine was evaluated at 60 min after the start of pulse infusion, and ^{3}H radioactivity in the EIN group was higher than that in PN group ($P < 0.05$), and then gradually decreased. There was no statistical difference between the two groups (Figure 1A).

Enzyme-protein synthesis: The maximal values for

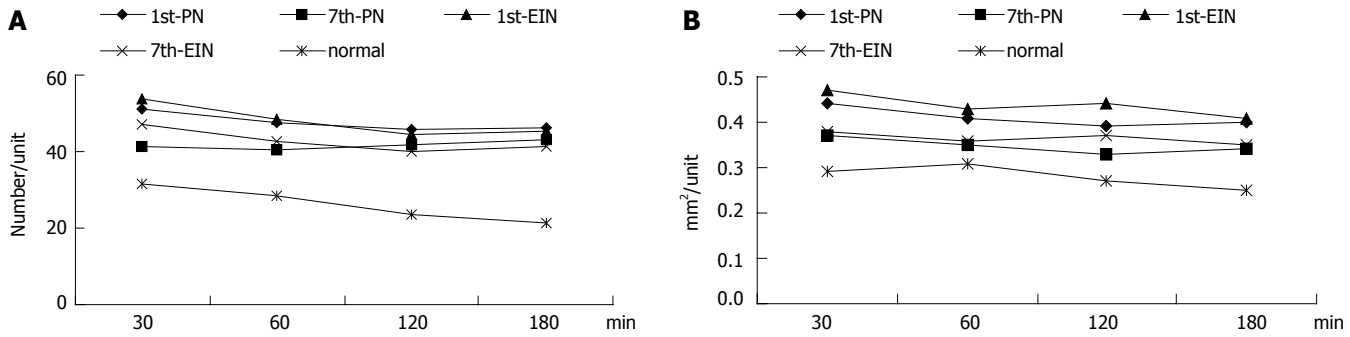

Figure 2 Change of MZGA in EIN group (**A**) and PN group (**B**) at different time points.

both groups were similar in acinar cell uptake of ^{3}H phenylalanine. The incorporation of ^{3}H-phenylalanine into enzyme protein was maximal at 60 min in both groups, and then gradually decreased. There was no difference between the two groups at 180 min (Figure 1B).

Intracellular transport of newly synthesized protein: The peak level of ^{3}H radioactivity was reached in the three subcellular fractionations at 60 min, and ^{3}H radioactivity in zymogen granules in the EIN group was higher than that in the PN group at 60min ($P < 0.05$). ^{3}H radioactivity in lysosomal-mitochondria and the microsomal subcellular fractionation did not reach statistical difference at the fixed time between the two groups, and then gradually decreased, the changes did not reach statistical difference (Figure 1C-E).

Electron microscopy

There was no difference in the submicroscopic cytology of acinar cells between the two groups. In particular, the fine structure of mature secretory granules was consistently similar. The electron density of membrane-bound mature exocrine granules had no change in this study in both PESST determinations. However, the mean zymogen granule number (MZGN) and mean zymogen granule area (MZGA) were not apparently changed on d 1 and 7 in either group, and the change in their number and unit area at different time points did not reach statistical difference (Figure 2A and B).

DISCUSSION

Traditionally, enteral nutrition is implemented after a 2-3 wk period of parenteral nutritional support[15]. This clinical strategy has been developed to provide a sufficient time period for the pancreas to rest and rehabilitate. The concept of pancreatic rest stems from the belief that stimulation of pancreatic exocrine function in patients with acute pancreatitis releases large quantities of proteolytic enzymes which result in autodigestion of the pancreas and peripancreatic tissues, causing deterioration in the patient's condition. The presence of food in the stomach and duodenum elicits gastropancreatic and duodenopancreatic reflexes that result in the stimulation of pancreatic exocrine secretion. However, these effects are insignificant when nutrients are delivered directly into the jejunum[16-25]. Kaushik *et al*[26] reported that enteral feeding can be given without stimulating pancreatic trypsin secretion provided it is delivered into the mid-distal jejunum, because the avoidance of trypsin stimulation may optimize enteral feeding in patients with acute pancreatitis.

It is known that digestive proteins and lysosomal enzymes are synthesized by polyribosomes binding to the cytoplasmic surface of endoplasmic reticulum (ER) membrane, and then transferred to the lumen of ER cisternae[27]. They are transported together to the Golgi, and normally separated from each other in the Golgi complex and condensing vacuole (CV) stage of intracellular transport. Normally, digestive enzymes and lysosomal hydrolases, which are synthesized in ribosomes attaching to the rough-surfaced endoplasmic reticulum and migrating to the Golgi complex and CV, are separated from each other by a complex sorting mechanism. Eventually, they are targeted for inclusion in distinct organelles: zymogen granules and lysosomes. In order to evaluate the effect of EIN on pancreatic acinar cell uptake of ^{3}H-phenylalanine and incorporation into zymogen protein in acute pancreatitic dogs, morphological changes were observed by determining the process of amino acid uptake, enzyme-protein synthesis, intracellular transport, and discharge of newly synthesized proteins from the pancreas within 3 h after beginning of PN and EIN on the first day. The results showed that ^{3}H phenylalanine radioactivity due to amino acid uptake and the extent of incorporation into newly synthesized proteins reached its peak level at 60 min in both groups. The parameters in the EIN group were higher than those in the PN group ($P < 0.05$), and then gradually decreased. To further analyze the effect of EIN on uptake of amino acids and enzyme-protein synthesis in subcellular fractions on the first day, we used differential and density-gradient centrifugation to determine the ^{3}H radioactivity in zymogen granules, lysosome-mitochondria and microsomal subcellular fractionation. In this study, the maximal values were obtained at 60 min in each of these fractions in lysosomes (cathepsin B), mitochondria (cytochrome oxidase) and zymogen granules (amylase), and then gradually decreased. These results suggest that the EIN alters neither amino acid uptake nor the extent of incorporation of ^{3}H radioactivity into newly synthesized proteins.

To study the possibility of recurrent pancreatitis,

PESST was performed to determine whether EIN increases ^{3}H radioactivity in lysosomes, mitochondria, and zymogen granules during AP. The results showed that the ^{3}H radioactivity in amino acid uptake, enzyme-protein synthesis, and subcellular fractionation reached its peak level at 60 min in both groups, which was higher in the EIN group than in the PN group ($P < 0.05$), and then gradually decreased. The content of ^{3}H in zymogen granules, lysosome-mitochondria and microsomal subcellular fractionation were consistent with the changes of amino acid uptake. The peak level of radioactivity on d 7 was higher than that on d 1. The tissue level of pulse-labeled proteins declined as expected due to secretion of labeled digestive zymogens into the duodenum via the pancreatic duct system. These results suggest that 7 d continuous intrajejunal nutrition can neither over-stimulate acinar cell uptake of ^{3}H nor enhance enzyme-protein synthesis and release. Cell fractionation studies indicated that intracellular transport of granules was not affected by EIN stimulation. Indeed, disappearance of pulse-labeled proteins from 10 500 × *g* pellet (total microsomal fraction enriched in rough endoplasmic reticulum elements and expected to contain Golgi elements as well) and their appearance in the 1300 × *g* pellet (enriched in zymogen granules and presumably condensing vacuoles) were not significantly different in EIN stimulation.

It is known that stored zymogens granules and lysosomal enzymes could play a key role in the development of pancreatitis and may, in fact, explain the intrapancreatic activation of digestive enzymes occurring in the course of many forms of pancreatitis[28]. Secretory proteins, on the other hand, progressively increase their concentration within the dilated Golgi cisternal rims and/or CV. The CV ultimately matures to ZG which is transported to the luminal plasmalemma and releases its contents by exocytosis. The large vacuoles containing both secretory and lysosomal enzymes in acute pancreatitis suggest that AP stimulates the process of CV maturation. Therefore, theoretically, EIN might increase intracellular transport and expand the CV compartment (formation of large vacuoles). To quantitatively assess the effect of EIN on the secretory granule cell compartment, ultrastructural morphometrical study of the pancreas under electron microscope was designed. The results showed that more ZG was accumulated in the interstitial space. The number and area of ZG were higher than those in normal. However, no gross difference in acinar cell ultrastructure was observed. These findings did not reach statistical difference between the two groups on d 1 and 7 during the nutritional support period, suggesting that EIN does not promote pancreatic acinar cell enzyme protein synthesis and release. The precise mechanism of EIN-stimulating acinar cells is unclear. However, some results indicate that receptor-triggered events of transmembrane signaling (rise of cytoplasmic Ca^{2+}) and the responsiveness and sensitivity to gastrointestinal hormones in pancreatic acinar cells are significantly inhibited[29].

In conclusion, early intrajejunal nutrition might be effective in dogs with acute pancreatitis. However, further study is needed to evaluate the effects of EIN and PN in patients with AP.

REFERENCES

1 **MacFie J**. Enteral versus parenteral nutrition. *Br J Surg* 2000; **87**: 1121-1122
2 **Neoptolemos JP**, Raraty M, Finch M, Sutton R. Acute pancreatitis: the substantial human and financial costs. *Gut* 1998; **42**: 886-891
3 **Al-Omran M**, Groof A, Wilke D. Enteral versus parenteral nutrition for acute pancreatitis. *Cochrane Database Syst Rev* 2003; (1): CD002837
4 **Qin HL**, Su ZD, Hu LG, Ding ZX, Lin QT. Effect of early intrajejunal nutrition on pancreatic pathological features and gut barrier function in dogs with acute pancreatitis. *Clin Nutr* 2002; **21**: 469-473
5 **Saluja A**, Saito I, Saluja M, Houlihan MJ, Powers RE, Meldolesi J, Steer M. In vivo rat pancreatic acinar cell function during supramaximal stimulation with caerulein. *Am J Physiol* 1985; **249**: G702-G710
6 **Abou-Assi S**, Craig K, O'Keefe SJ. Hypocaloric jejunal feeding is better than total parenteral nutrition in acute pancreatitis: results of a randomized comparative study. *Am J Gastroenterol* 2002; **97**: 2255-2262
7 **Oláh A**, Pardavi G, Belágyi T, Nagy A, Issekutz A, Mohamed GE. Early nasojejunal feeding in acute pancreatitis is associated with a lower complication rate. *Nutrition* 2002; **18**: 259-262
8 **Chen QP**. Enteral nutrition and acute pancreatitis. *World J Gastroenterol* 2001; **7**: 185-192
9 **Hallay J**, Kovács G, Szatmári K, Bakó A, Szentkereszty Z, Lakos G, Sipka S, Sápy P. Early jejunal nutrition and changes in the immunological parameters of patients with acute pancreatitis. *Hepatogastroenterology* 2001; **48**: 1488-1492
10 **McGregor CS**, Marshall JC. Enteral feeding in acute pancreatitis: just do it. *Curr Opin Crit Care* 2001; **7**: 89-91
11 **Sanabria A**. Randomized controlled trial of the effect of early enteral nutrition on markers of the inflammatory response in predicted severe acute pancreatitis. *Br J Surg* 2001; **88**: 728
12 **Tartakoff AM**, Jamieson JD. Subcellular fractionation of the pancreas. *Methods Enzymol* 1974; **31**: 41-59
13 **De Lisle RC**, Schulz I, Tyrakowski T, Haase W, Hopfer U. Isolation of stable pancreatic zymogen granules. *Am J Physiol* 1984; **246**: G411-G418
14 **Falconi M**, Caldiron E, Zancanaro C, Benati D, Talamini G, Bassi C, Pederzoli P. In vivo octreotide administration acutely reduces exocrine granule size in the human pancreas. *Pancreatology* 2001; **1**: 30-35
15 **Oláh A**, Belágyi T, Issekutz A, Gamal ME, Bengmark S. Randomized clinical trial of specific lactobacillus and fibre supplement to early enteral nutrition in patients with acute pancreatitis. *Br J Surg* 2002; **89**: 1103-1107
16 **Takács T**, Hajnal F, Németh J, Lonovics J, Pap A. Stimulated gastrointestinal hormone release and gallbladder contraction during continuous jejunal feeding in patients with pancreatic pseudocyst is inhibited by octreotide. *Int J Pancreatol* 2000; **28**: 215-220
17 **Eckerwall G**, Andersson R. Early enteral nutrition in severe acute pancreatitis: a way of providing nutrients, gut barrier protection, immunomodulation, or all of them? *Scand J Gastroenterol* 2001; **36**: 449-458
18 **Eatock FC**, Brombacher GD, Steven A, Imrie CW, McKay CJ, Carter R. Nasogastric feeding in severe acute pancreatitis may be practical and safe. *Int J Pancreatol* 2000; **28**: 23-29
19 **Lehocky P**, Sarr MG. Early enteral feeding in severe acute pancreatitis: can it prevent secondary pancreatic (super) infection? *Dig Surg* 2000; **17**: 571-577
20 **Erstad BL**. Enteral nutrition support in acute pancreatitis. *Ann Pharmacother* 2000; **34**: 514-521
21 **Duerksen DR**, Bector S, Yaffe C, Parry DM. Does jejunal

feeding with a polymeric immune-enhancing formula increase pancreatic exocrine output as compared with TPN? A case report. *Nutrition* 2000; **16**: 47-49

22 **Sahin M**, Ozer S, Vatansev C, Aköz M, Vatansev H, Aksoy F, Dilsiz A, Yilmaz O, Karademir M, Aktan M. The impact of oral feeding on the severity of acute pancreatitis. *Am J Surg* 1999; **178**: 394-398

23 **Windsor AC**, Kanwar S, Li AG, Barnes E, Guthrie JA, Spark JI, Welsh F, Guillou PJ, Reynolds JV. Compared with parenteral nutrition, enteral feeding attenuates the acute phase response and improves disease severity in acute pancreatitis. *Gut* 1998; **42**: 431-435

24 **Lobo DN**, Memon MA, Allison SP, Rowlands BJ. Evolution of nutritional support in acute pancreatitis. *Br J Surg* 2000; **87**: 695-707

25 **Kalfarentzos F**, Kehagias J, Mead N, Kokkinis K, Gogos CA. Enteral nutrition is superior to parenteral nutrition in severe acute pancreatitis: results of a randomized prospective trial. *Br J Surg* 1997; **84**: 1665-1669

26 **Kaushik N**, Pietraszewski M, Holst JJ, O'Keefe SJ. Enteral feeding without pancreatic stimulation. *Pancreas* 2005; **31**: 353-359

27 **Rosenfeld MG**, Kreibich G, Popov D, Kato K, Sabatini DD. Biosynthesis of lysosomal hydrolases: their synthesis in bound polysomes and the role of co- and post-translational processing in determining their subcellular distribution. *J Cell Biol* 1982; **93**: 135-143

28 **Watanabe O**, Baccino FM, Steer ML, Meldolesi J. Supramaximal caerulein stimulation and ultrastructure of rat pancreatic acinar cell: early morphological changes during development of experimental pancreatitis. *Am J Physiol* 1984; **246**: G457-G467

29 **Powers RE**, Saluja AK, Houlihan MJ, Steer ML. Aberration in stimulus-secretion coupling caused by a choline deficient 0.5% ethionine containing (CDE diet) (Abstract). *Federation Proc* 1985; **44**: 535

S- Editor Wang J **L- Editor** Wang XL **E- Editor** Ma WH

PO Box 2345, Beijing 100023, China
www.wjgnet.com
wjg@wjgnet.com

World J Gastroenterol 2007 February 21; 13(7): 1129-1134
World Journal of Gastroenterology ISSN 1007-9327

RAPID COMMUNICATION

Mechanisms involved in ceramide-induced cell cycle arrest in human hepatocarcinoma cells

Jing Wang, Xiao-Wen Lv, Jie-Ping Shi, Xiao-Song Hu

Jing Wang, Research Center for Eco-Environmental Sciences, The Chinese Academy of Sciences, Beijing 100085, China
Xiao-Wen Lv, Feed Research Institute, Chinese Academy of Agricultural Sciences, Beijing 100081, China
Jie-Ping Shi, Xiao-Song Hu, College of Food Science and Nutritional Engineering, China Agricultural University, Beijing, China
Correspondence to: Xiao-Song Hu, Research Center for Eco-Environmental Sciences, The Chinese Academy of Sciences, Haidian District, Beijing 100085, China. wangjing@rcees.ac.cn
Telephone: +86-10-62849321
Received: 2006-10-12 Accepted: 2007-01-18

Abstract

AIM: To investigate the effect of ceramide on the cell cycle in human hepatocarcinoma Bel7402 cells. Possible molecular mechanisms were explored.

METHODS: [3- (4, 5)-dimethylthiazol-2-yl]-2, 5-diphenyltetrazolium bromide (MTT) assay, plasmid transfection, reporter assay, FACS and Western blotting analyses were employed to investigate the effect and the related molecular mechanisms of C2-ceramide on the cell cycle of Bel7402 cells.

RESULTS: C2-ceramide was found to inhibit the growth of Bel7402 cells by inducing cell cycle arrest. During the process, the expression of p21 protein increased, while that of cyclinD1, phospho-ERK1/2 and c-myc decreased. Furthermore, the level of CDK7 was downregulated, while the transcriptional activity of PPARγ was upregulated. Addition of GW9662, which is a PPARγ specific antagonist, could reserve the modulation action on CDK7.

CONCLUSION: Our results support the hypothesis that cell cycle arrest induced by C2-ceramide may be mediated *via* accumulation of p21 and reduction of cyclinD1 and CDK7, at least partly, through PPARγ activation. The ERK signaling pathway was involved in this process.

Key words: Ceramide; Cell cycle arrest; Human hepatocarcinoma cells; P21; CyclinD1; CDK7; PPARγ; ERK

Wang J, Lv XW, Shi JP, Hu XS. Mechanisms involved in ceramide-induced cell cycle arrest in human hepatocarcinoma cells. *World J Gastroenterol* 2007; 13(7): 1129-1134

http://www.wjgnet.com/1007-9327/13/1129.asp

INTRODUCTION

Ceramide has emerged as a novel lipid second messenger with specific roles in mediating cell growth, differentiation, stress responses and apoptosis[1-3]. Ceramide is generated through the hydrolysis of sphingomyelin by the activation of sphingomyelinase (SMase). A number of stimuli have been reported to activate SMase[4-6]. Exogenously administered synthetic ceramide mimicked the action of these inducers in the regulation of various cell functions. Ceramide mediates numerous cellular functions such as differentiation, growth arrest, apoptosis and proliferation[7,8]. Ceramide is thought to be involved in modulating ceramide-activated protein kinase (CAPK), mitogen-activated protein kinase (MAPK), ceramide-activated protein phosphatase (CAPP) and phospholipaseA2 (PLA2), *etc*[9]. Apoptosis induction by ceramide is associated with Bcl-2 phosphorylation, SAPK/JNK and caspase pathway activation[10]. On the other hand, activation of PKC and Bcl-2 expression can inhibit the ceramide signal pathway[11,12]. However, the link between ceramide signaling and the cell cycle is poorly understood.

To exploit the effect of ceramide on the cell cycle, human hepatocarcinoma Bel7402 cells were employed and treated with C2-ceramide. Hepatocarcinoma occurs with high incidence in southern China and southeast Asia. Radiation is one of the agents that activates ceramide signaling[13], and therefore, it is of interest in investigating the effect of ceramide on Bel7402 cells. In this study, we observed inhibition of cell proliferation and cell cycle arrest in the G1 phase following C2-ceramide treatment in Bel7402 cells. Subsequent studies suggested that modulation might be mediated *via* accumulation of p21 and reduction of cyclinD1 and CDK7, at least partly, through PPARγ activation. The ERK signaling pathway was also involved in this process.

MATERIALS AND METHODS

Materials

C2-ceramide was purchased from Sigma. Co (St Louis Mo, USA); mouse monoclonal anti-p21, anti-cyclinD1,

anti-CDK7, anti-p-ERK and anti-c-myc were purchased from Santa Cruz Biotechnology, Inc (CA, USA); antibody of PE-E-cadherin was purchased from DAKO Co. Horseradish peroxidase-conjugated secondary antibodies were purchased from Jackson Immuno-Research Laboratories, Inc (West Grove, PA, USA). Lipofectamine and lipofectin reagents were from Gibco, Inc. RNaseA, MTT, propiudium iodide and other chemicals were all from Sigma.

Cell culture

Bel7402 cells were provided by the Institute of Zoology, Chinese Academy of Sciences, China. Cells were maintained in Dulbecco's minimal essential medium (DMEM) supplemented with 10% fetal bovine serum (FBS) in a humidified atmosphere of 95% air/5% CO_2 at 37℃. A subculture of cells was processed by enzymatic digestion (trypsin/EDTA solution: 0.25/0.02%). C2-ceramide dissolved in ethanol was used without filtration. The final concentration of ethanol in culture medium was < 0.3%.

MTT assay

Bel7402 cells were seeded onto 96-well plates at a concentration of 2.5×10^3 cells/well in DMEM plus 5% FBS. The stock of C2-ceramide was diluted with medium, and then added to wells for desired final concentrations. After exposure to C2-ceramide for the desired time, 10 μL of 5 mg/mL MTT was added to each well and incubated for 4 h, and the liquid in wells was evaporated. To dissolve the formazam, 100 μL of DMSO was added. The absorbance was determined with a microplate reader model 550 at the wavelength of 570 nm.

Cell cycle analysis

The proportions of cells in G0-G1, S, and G2-M were determined by flow cytometric analysis of DNA content. Briefly, cells were obtained by trypsinization following treatment with C2-ceramide, and then washed twice with PBS. Cells were then incubated with RNase at a concentration of 0.25 mg/mL at 37℃ for 1 h following incubation with PI (50 μg/mL in PBS) for 30 min at 4℃ in the dark. Before flow cytometry, samples were syringed through a 25-gauge needle to prevent nuclear clumping. PI was excited at 488 nm, and fluorescence was analyzed at 620 nm. All measurements were carried out under the same instrumental settings.

PE-E-cadherin labeling

Cells were washed once with cold PBS, and centrifuged to collect the cell pellet (350 g × 5 min) following treatment with C2-ceramide.The cell pellet was resuspended in cold PBS (4℃) and PE-E-cadherin and the corresponding isotype antibodies were added to the cell suspension and mixed gently. The tube was then incubated for 30-60 min in the dark at room temperature prior to flow cytometry. PE-E-cadherin binding was analyzed by flow cytometry collecting the fluorescence of 10 000 cells using a FACScan (Becton Dickinson) according to the manufacturer's instructions. All experiments were replicated three times.

Western blot analysis

To determine the expression levels of E-cadherin, p21, cyclinD1, CDK7 and c-myc, cells were lysed in buffer (150 mmol/L NaCl, 1% NP-40, 0.5% sodium deoxycholate, 0.1% SDS, 50 mmoL/L Tris, pH 8.0, 1 mmoL/L phenylmethylsulfonyl fluoride (PMSF), and 10 μg/mL aprotinin). To determine the level and phosphorylation state of ERK, cells were harvested in lysis buffer containing 50 mmol/LTES (N-tris [hydroxymethyl] methyl-2-aminoethane sulfonic acid) (pH 7.4), 2 mmol/L EGTA, 1 mmol/L EDTA, 250 mmol/L sucrose, 40 mmol/L phenylphosphate, 1 mmol/L $MgCl_2$, 2 mmoL/L Na_3VO_4, 10 mmol/L $Na_4P_2O_7$, 100 mmol/L NaF, 5 μg/mL aprotinin, 1 mmol/L PMSF, 1 μg/mL leupeptin, 5 mmol/L benzamidine, and 10 mmol/L dithiothreitol. Protein (40-80 μg) was separated by 12%-15% SDS-polyacrylamide gel in the separation buffer (25 mmol/L Tris, 250 mmol/L Glycine, 0.1% SDS). Total proteins were transferred onto a PVDF membrane after electrophoresis. Western blot analyses using anti-p21, anti-cyclinD1, anti-CDK7, anti-c-myc, anti-phospho-p42/p44ERK and anti-totalERK antibodies were performed. As an internal control, mouse monoclonal anti-β-actin antibody was used.

Transient transfection and luciferase assay for PPARγ activity

Bel7402 cells were seeded at a concentration of 1×10^5 cells/35 mm dish. After 12 h, the medium was changed from complete medium to DMEM without antibiotic. Transfection was done using LipofectAMINE reagent mixed with 2 μg of acyl-CoA oxidase promoter-luciferase plasmid pAOXPPREluc and the control pAOXBluc basic vector (kindly donated by Dr. Osumi) for 8 h. After the transfection mixture was replaced by a medium containing 10% FBS, cells were then incubated with or without different concentrations of ceramide for a desired time. Luciferase activity was measured according to the manufacturer's protocol (Promega).

Statistical analysis

All statistical analyses were performed with SPSS 10.0 statistical package for Microsoft Windows. Data were expressed as mean ± SE for all measurements. $P < 0.05$ was considered statistically significant.

RESULTS

Ceramide inhibited proliferation by halting the cell cycle in Bel7402 cells

Treatment with different concentrations of C2-ceramide for 24 h exhibited significant inhibition of cell proliferation of human hepatocarcinoma Bel7402 cells as suggested by MTT assay. Under concentrations of 0, 5, 10, 15, 30 and 60 μmmo/L, inhibitory rates were 0, 21.5% ± 1.3%, 52.7% ± 0.9%, 69.3% ± 1.2%, 77.2% ± 0.8% and 83.8% ± 1.2%, respectively (Figure 1A). Cytotoxicity was further indicated by determination of E-cadherin, which is a marker for many tumor cells with high expression. PE-E-cadherin antibodies were stained with cells to determine

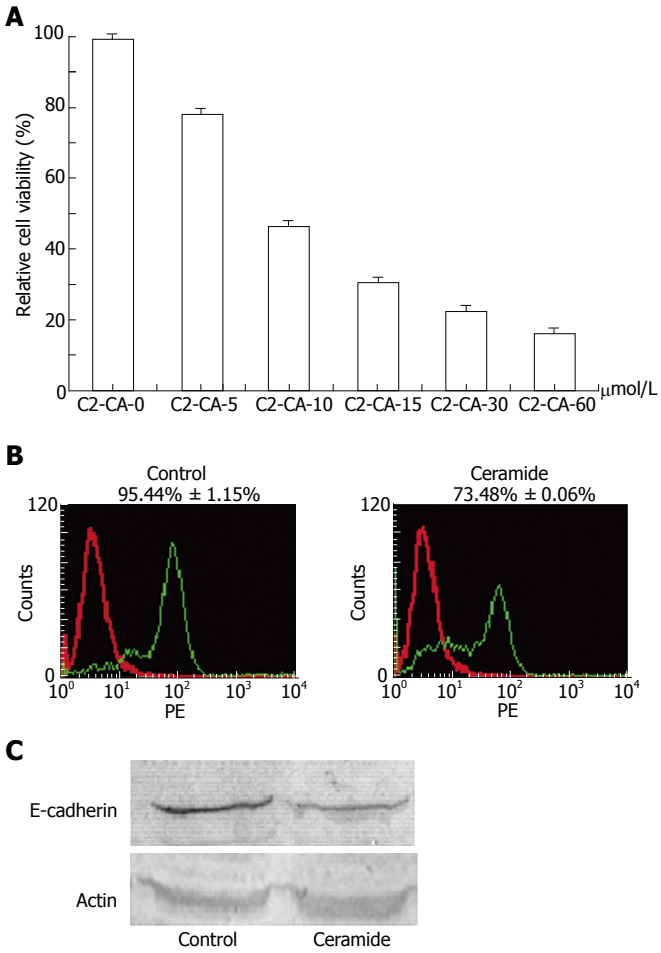

Figure 1 Ceramide inhibited proliferation by halt of cell cycle in Bel7402 cells. **A**: ceramide inhibited cell proliferation in Bel7402 cells. Cells were cultured in the medium with different concentrations of C2-ceramide for 24 h. Cell viability was analyzed by MTT assay and presented as cell proliferative rates. The results show the mean ± SE (n = 3-4); **B** and **C**: ceramide down-regulated the expression of E-cadherin. Bel7402 cells were incubated with or without 30 μmmo/L of ceramide for 24 h. Cells were then harvested and stained with anti-E-cadherin directly labeled by PE. The protein levels of E-cadherin were determined by flow cytometry. Data was represented by the mean ± SE of 3 or 4 separate experiments (**B**). Bel7402 cells were incubated with or without 30 μmmo/L of ceramide for 24 h. Cells were then harvested, lysed and resolved in 12% SDS-PAGE. The expression of E-cadherin was determined by Western blot. Actin was used as a control. Data represent the results of three separate experiments (**C**).

the expression of E-cadherin on the cell surface. Flow cytometry analysis results indicated that E-cadherin was significantly down-regulated by C2-ceramide (Figure 1B), which was also suggested by blot assay (Figure 1C). To test whether the cytotoxicity was derived from the effect on the cell cycle, flow cytometry analysis was applied following treatment with different concentrations of C2-ceramide at 0, 5, 15, 30 and 60 μmol/L. As shown in Table 1, the cell cycle was halted in the G1 phase, and the percentage of cells in the G1 phase was 35.3% ± 0.7%, 36.8% ± 1.2%, 43.9% ± 1.2%, 57.2% ± 0.6% and 76.2% ± 1.3%, respectively.

Ceramide up-regulated the expression of p21$^{WAF1/BIP1}$ and down-regulated that of cyclinD1

In order to elucidate whether molecules were involved in the G1/S transition following C2-ceramide treatment,

Table 1 Ceramide halted cell cycle in Bel7402 cells (mean ± SE, n = 3)

Ceramide (μmol/L)	G_0/G_1 (%)	S (%)	G_2/M
0	35.3 ± 0.7	44.3 ± 0.3	20.4 ± 0.1
5	36.8 ± 1.2	43.9 ± 0.4	19.3 ± 1.8[a]
15	43.9 ± 1.2[a]	41.9 ± 0.7[a]	14.2 ± 0.8[a]
30	57.2 ± 0.6[a]	28.8 ± 0.5[a]	14.0 ± 0.5[a]
60	76.2 ± 1.3[a]	8.2 ± 0.2[a]	15.6 ± 1.3[a]

[a]$P < 0.05$ *vs* control.

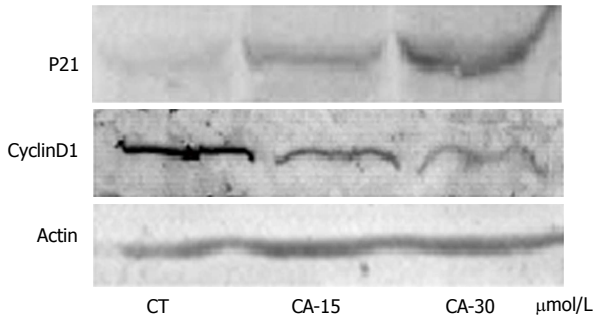

Figure 2 Ceramide up-regulated the expression of p21$^{WAF1/BIP1}$ and down-regulated that of cyclinD1. Bel7402 cells were incubated with different concentrations of ceramide as indicated for 24 h. Cells were harvested, lysed and resolved in 15% SDS-PAGE. The expression of p21 and cyclinD1 were determined by Western blot. Actin was used as a control. Data represent the results of three separate experiments.

cell extracts were prepared from Bel7402 cells treated with different concentrations of C2-ceramide. Protein expression was indicated by blot using anti-p21 and anti-cyclinD1 antibodies, respectively. As shown in Figure 2, C2-ceramide increased the expression of p21 protein, but decreased that of cyclinD1 protein.

CDK7 and PPARγ pathways involved in cell cycle arrest induced by C2-ceramide

In our previous study, we reported that C2-ceramide could activate PPARγ transcription activity in human colon cancer HT29 cells[14]. In this study, as shown in Figure 3A, C2-ceramide could also markedly activate the transcriptional activity of PPARγ in hepatocarcinoma Bel7402 cells.

Cyclin-dependent kinase 7 (CDK7) is critical for cell cycle and transcriptional programs[15]. Therefore, we investigated the expression of CDK7 by blotting. It was observed that CDK7 expression decreased following treatment with 30 μmmo/L C2-ceramide for 24 h. However, addition of the PPARγ specific antagonist GW9662 markedly reversed the inhibition (Figure 3B).

Ceramide inhibited the activation of ERK1/2 in Bel7402 cells

ERK plays a key role in cell survival in many cells. To examine whether ceramide inhibited the activation of ERK, Bel7402 cells were treated with different concentrations of C2-ceramide and phospho-ERK1/2 was determined. As shown in Figure 4, the expression of p-ERK decreased significantly with the treatment of

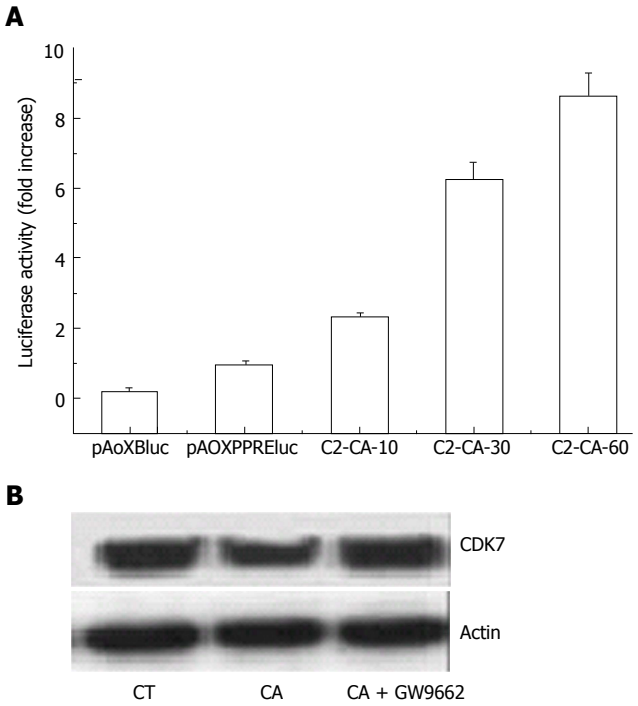

Figure 3 CDK7 and PPARγ pathways involved in cell cycle arrest induced by C2-ceramide. **A**: activation of PPARγ transcriptional activity induced by C2-ceramide. Bel7402 cells were transiently transfected with the PPAR responsive element (PPRE) reporter construct (pAOXPPREluc) or the promoter-less control vector pAOXBluc following the treatment of different concentrations of C2-ceramide as indicated, PPARγ transcriptional activity was measured as described. The bar represents the relative fold increase of luciferase activity. The results show means ± SE (n = 3); **B**: C2-ceramide down-regulated the expression of CDK7, which was blocked by GW9662. Bel7402 cells were cultured with 30 μmol/L C2-ceramide in the presence or absence of GW9662, which was claimed as a specific PPARγ antagonist for 24 h. Total proteins were extracted and resolved on SDS-PAGE followed by Western blot assay using anti-CDK7 antibody. Data represents the results of three separate experiments.

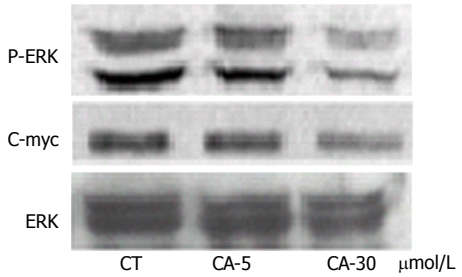

Figure 4 Ceramide inhibited activation of ERK pathway in Bel7402. Bel7402 cells were incubated with different concentrations of ceramide as indicated. Total proteins were extracted and resolved on SDS-PAGE. Phospho-ERK1/2 and c-myc were normalized to total Erk1/2 and internal standard actin was determined by Western blot. Data represents the results of three separate experiments.

C2-ceramide, while total ERK protein expression was unaffected.

To complete the study of the MAPK pathway, c-myc content was also indicated by blot using anti-c-myc antibodies. As shown in Figure 4, the modulation pattern on the expression of c-myc induced by C2-ceramide was similar to that of p-ERK.

DISCUSSION

Since ceramide was affirmed as an important lipid second messenger in 1994, the importance of ceramide in cell metabolism has been broadly investigated. Ceramide has shown inhibition of cell growth *via* apoptosis in a variety of cancers. However, the link between ceramide signaling and the cell cycle is poorly understood. The present work demonstrates that C2-ceramide halted the distribution of cell cycles in G1 phase, and the mechanisms involved were explored.

As displayed in Table 1, C2-ceramide induced cell cycle arrest in the G1 phase. Accordingly, down-regulation of E-cadherin, a marker for many tumor cells with high expression, suggested that C2-ceramide inhibited cancer cell growth (Figure 1B).

In order to elucidate the mechanisms involved in cell cycle arrest following treatment with C2-ceramide in Bel7402 cells, we firstly investigated whether the cell cycle control genes; i.e., cyclin D1 and the cyclin-dependent kinase inhibitor p21, are involved in ceramide-mediated cell cycle regulation in Bel7402 cells.

Cell cycle progression is regulated by interactions between cyclins and cyclin-dependent kinases, which are modulated by a family of negative cell cycle regulators; i.e., cyclin-dependent kinase inhibitors, which are especially involved in controlling the transition from G1 to S-phase[16,17]. The latter includes two families, the CIP/KIP family and the INK4 family. p21 is a member of the CIP/KIP family and plays a crucial role in growth arrest by a variety of mechanisms[18]. Consistent with this idea, we showed that C2-ceramide up-regulated the expression of p21 protein concomitant with inhibition of cyclin D1 protein (Figure 2).

PPARγ is clearly involved in lipid metabolism and is essential for cell differentiation[19,20]. Activation of PPARγ by its ligands can induce growth inhibition and cytotoxicity in human prostate cancer cells, colon cancer cells and liposarcoma cells, and their biological activities are attributed to inhibition of proliferation and induction of apoptosis by PPARγ[21,22]. We have previously shown C2-ceramide could induce apoptosis *via* a PPARγ dependent pathway in human colon cancer HT29 cells[14]. To examine whether the PPARγ pathway was involved in the modulation of cell cycle arrest induced by ceramide in human hepatocarcinoma Bel7402 cells, the luciferase reporter of PPRE3x-tk-luc was transfected and luciferase activity was assayed. The result shown in Figure 3A suggested that ceramide activated the transcriptional activity of PPARγ in a dose-dependent manner.

CDK7 distributes normally throughout the nucleus and cytoplasm, and in the nucleus, it attaches to a DNA template with other TFⅡH subunits initiating gene transcription[23], which is very important in modulating cell proliferation. Participating in basal transcription by phosphorylating the carboxy-terminal domain of the largest subunit of RNA polymerase Ⅱ, CDK7 is critical for the cell cycle and transcriptional programmes, which also phosphorylate other CDKs as an essential step for their activation[24,25]. Often, phosphorylation of NRs by kinases that are associated with general transcription factors (e.g. CDK7 within TFⅡH), or activated in response to a variety of signals (MAPKs, Akt, PKA, PKC),

facilitates the recruitment of coactivators or components of the transcription machinery and, therefore, cooperates with the ligand to enhance transcription activation.

Though there is much to be explored, data have shown that C2-ceramide inhibited cell proliferation through attenuation of CDK7 (Figure 3B). However, GW9662, which is a PPARγ specific antagonist, could markedly block this action. These data suggested that CDK7 was related to PPARγ, which was consistent with the opinion described above.

ERK signaling plays a key role in cell survival, and Erk1/2 are proteins belonging to the MAPK pathway, whose members are active when phosphorylated. Consequently, dephosphorylation of these proteins inhibits their activity and the transcription factor c-myc. The increase of PP2A, which is a serine/threonine phosphatase causing dephosphorylation of MAPKs[26], is one of the causes of Erk1/2 dephosphorylation. Indeed, the ERK1/2 pathway, that regulates cellular growth and proliferation, has been shown to be pro[27-30] or anti-apoptotic[31-33], depending on experimental conditions and/or cell types. To examine whether C2-ceramide can inhibit activation of ERK, phospho-ERK was determined. It was found that phospho-ERK decreased with the treatment of C2-ceramide in Bel7402 cells, however, the expression level of total ERK protein was unaffected. Accordingly, the protein expression of c-myc also decreased (Figure 4).

In summary, with consideration that there is much to be explored, it was concluded that C2-ceramide plays an important role in the inhibition of cell growth in Bel7402 cells. Our results showed that there is p21 accumulation in accordance with decreased cyclinD1, inactivation of the ERK pathway, downregulation of CDK7 and stimulation of PPARγ transcriptional activity. As such, our results support the hypothesis that suppression of hepatocarcinoma cell growth through cell cycle arrest induced by C2-ceramide may be mediated *via* accumulation of p21 and reduction of cyclinD1 and CDK7, at least partly, through PPARγ activation. The ERK signaling pathway was involved in this process.

REFERENCES

1 **Obeid LM**, Linardic CM, Karolak LA, Hannun YA. Programmed cell death induced by ceramide. *Science* 1993; **259**: 1769-1771
2 **Hannun YA**, Obeid LM. The Ceramide-centric universe of lipid-mediated cell regulation: stress encounters of the lipid kind. *J Biol Chem* 2002; **277**: 25847-25850
3 **Mathias S**, Peña LA, Kolesnick RN. Signal transduction of stress via ceramide. *Biochem J* 1998; **335** (Pt 3): 465-480
4 **Tavarini S**, Colombaioni L, Garcia-Gil M. Sphingomyelinase metabolites control survival and apoptotic death in SH-SY5Y neuroblastoma cells. *Neurosci Lett* 2000; **285**: 185-188
5 **Tomassini B**, Testi R. Mitochondria as sensors of sphingolipids. *Biochimie* 2002; **84**: 123-129
6 **Jaffrézou JP**, Levade T, Bettaïeb A, Andrieu N, Bezombes C, Maestre N, Vermeersch S, Rousse A, Laurent G. Daunorubicin-induced apoptosis: triggering of ceramide generation through sphingomyelin hydrolysis. *EMBO J* 1996; **15**: 2417-2424
7 **Levade T**, Malagarie-Cazenave S, Gouazé V, Ségui B, Tardy C, Betito S, Andrieu-Abadie N, Cuvillier O. Ceramide in apoptosis: a revisited role. *Neurochem Res* 2002; **27**: 601-607
8 **Haimovitz-Friedman A**, Kolesnick RN, Fuks Z. Ceramide signaling in apoptosis. *Br Med Bull* 1997; **53**: 539-553
9 **Hannun YA**. Functions of ceramide in coordinating cellular responses to stress. *Science* 1996; **274**: 1855-1859
10 **Raisova M**, Goltz G, Bektas M, Bielawska A, Riebeling C, Hossini AM, Eberle J, Hannun YA, Orfanos CE, Geilen CC. Bcl-2 overexpression prevents apoptosis induced by ceramidase inhibitors in malignant melanoma and HaCaT keratinocytes. *FEBS Lett* 2002; **516**: 47-52
11 **Zhang J**, Alter N, Reed JC, Borner C, Obeid LM, Hannun YA. Bcl-2 interrupts the ceramide-mediated pathway of cell death. *Proc Natl Acad Sci USA* 1996; **93**: 5325-5328
12 **Sawai H**, Okazaki T, Takeda Y, Tashima M, Sawada H, Okuma M, Kishi S, Umehara H, Domae N. Ceramide-induced translocation of protein kinase C-delta and -epsilon to the cytosol. Implications in apoptosis. *J Biol Chem* 1997; **272**: 2452-2458
13 **Haimovitz-Friedman A**, Kan CC, Ehleiter D, Persaud RS, McLoughlin M, Fuks Z, Kolesnick RN. Ionizing radiation acts on cellular membranes to generate ceramide and initiate apoptosis. *J Exp Med* 1994; **180**: 525-535
14 **Wang J**, Lv X, Shi J, Hu X. Ceramide induces apoptosis via a peroxisome proliferator-activated receptor gamma-dependent pathway. *Apoptosis* 2006; **11**: 2043-2052
15 **Xiao D**, Singh SV. Phenethyl isothiocyanate-induced apoptosis in p53-deficient PC-3 human prostate cancer cell line is mediated by extracellular signal-regulated kinases. *Cancer Res* 2002; **62**: 3615-3619
16 **Fang JY**, Lu YY. Effects of histone acetylation and DNA methylation on p21 (WAF1) regulation. *World J Gastroenterol* 2002; **8**: 400-405
17 **Chellappan SP**, Giordano A, Fisher PB. Role of cyclin-dependent kinases and their inhibitors in cellular differentiation and development. *Curr Top Microbiol Immunol* 1998; **227**: 57-103
18 **Kim JS**, Lee S, Lee T, Lee YW, Trepel JB. Transcriptional activation of p21 (WAF1/CIP1) by apicidin, a novel histone deacetylase inhibitor. *Biochem Biophys Res Commun* 2001; **281**: 866-871
19 **Rosen ED**, Sarraf P, Troy AE, Bradwin G, Moore K, Milstone DS, Spiegelman BM, Mortensen RM. PPAR gamma is required for the differentiation of adipose tissue in vivo and in vitro. *Mol Cell* 1999; **4**: 611-617
20 **Barak Y**, Nelson MC, Ong ES, Jones YZ, Ruiz-Lozano P, Chien KR, Koder A, Evans RM. PPAR gamma is required for placental, cardiac, and adipose tissue development. *Mol Cell* 1999; **4**: 585-595
21 **Chinetti G**, Griglio S, Antonucci M, Torra IP, Delerive P, Majd Z, Fruchart JC, Chapman J, Najib J, Staels B. Activation of proliferator-activated receptors alpha and gamma induces apoptosis of human monocyte-derived macrophages. *J Biol Chem* 1998; **273**: 25573-25580
22 **Takahashi N**, Okumura T, Motomura W, Fujimoto Y, Kawabata I, Kohgo Y. Activation of PPARgamma inhibits cell growth and induces apoptosis in human gastric cancer cells. *FEBS Lett* 1999; **455**: 135-139
23 **Chen J**, Larochelle S, Li X, Suter B. Xpd/Ercc2 regulates CAK activity and mitotic progression. *Nature* 2003; **424**: 228-232
24 **Bushnell DA**, Westover KD, Davis RE, Kornberg RD. Structural basis of transcription: an RNA polymerase II-TFIIB cocrystal at 4.5 Angstroms. *Science* 2004; **303**: 983-988
25 **Oelgeschläger T**. Regulation of RNA polymerase II activity by CTD phosphorylation and cell cycle control. *J Cell Physiol* 2002; **190**: 160-169
26 **Westermarck J**, Li SP, Kallunki T, Han J, Kähäri VM. p38 mitogen-activated protein kinase-dependent activation of protein phosphatases 1 and 2A inhibits MEK1 and MEK2 activity and collagenase 1 (MMP-1) gene expression. *Mol Cell Biol* 2001; **21**: 2373-2383
27 **Garg TK**, Chang JY. Oxidative stress causes ERK phosphorylation and cell death in cultured retinal pigment epithelium: prevention of cell death by AG126 and 15-deoxy-delta 12, 14-PGJ2. *BMC Ophthalmol* 2003; **3**: 5
28 **Choi YJ**, Lim SY, Woo JH, Kim YH, Kwon YK, Suh SI, Lee

SH, Choi WY, Kim JG, Lee IS, Park JW, Kwon TK. Sodium orthovanadate potentiates EGCG-induced apoptosis that is dependent on the ERK pathway. *Biochem Biophys Res Commun* 2003; **305**: 176-185

29 **Wang X**, Martindale JL, Holbrook NJ. Requirement for ERK activation in cisplatin-induced apoptosis. *J Biol Chem* 2000; **275**: 39435-39443

30 **Calabrese C**, Frank A, Maclean K, Gilbertson R. Medulloblastoma sensitivity to 17-allylamino-17-demethoxygeldanamycin requires MEK/ERKM. *J Biol Chem* 2003; **278**: 24951-24959

31 **Johnson GL**, Lapadat R. Mitogen-activated protein kinase pathways mediated by ERK, JNK, and p38 protein kinases. *Science* 2002; **298**: 1911-1912

32 **Smalley KS**. A pivotal role for ERK in the oncogenic behaviour of malignant melanoma? *Int J Cancer* 2003; **104**: 527-532

33 **Zheng B**, Fiumara P, Li YV, Georgakis G, Snell V, Younes M, Vauthey JN, Carbone A, Younes A. MEK/ERK pathway is aberrantly active in Hodgkin disease: a signaling pathway shared by CD30, CD40, and RANK that regulates cell proliferation and survival. *Blood* 2003; **102**: 1019-1027

S- Editor Liu Y **L- Editor** Lutze M **E- Editor** Lu W

PO Box 2345, Beijing 100023, China
www.wjgnet.com
wjg@wjgnet.com

World J Gastroenterol 2007 February 21; 13(7): 1135-1137
World Journal of Gastroenterology ISSN 1007-9327

CASE REPORT

Pancreatic metastasis of leiomyosarcoma in the right thigh: A case report

Yang Seok Koh, Jung Chul, Chol Kyoon Cho, Hyun Jong Kim

Yang Seok Koh, Jung Chul, Chol Kyoon Cho, Hyun Jong Kim, Division of Hepatobiliary & Pantreatic Surgery, Department of Surgery, Chonnam National University Medical School, Gwangju 501757, Korea
Correspondence to: Jung Chul Kim, Division of Hepatobiliary & pantreatic Surgery, Department of Surgery, Chonnam University Medical School, Hakdong 8, Donggu, Gwangju 501757, Korea. 3rdvivace@hanmail.net
Telephone: +82-62-2206456 Fax: +82-62-2271635
Received: 2006-12-07 Accepted: 2007-01-29

Abstract

Pancreatic tumors are primary in most of the cases. Pancreatic metastases associated with other primary malignancies, especially pancreatic metastasis of leiomyosarcoma, are uncommon. A 66-year-old woman underwent surgical resection of malignant mesenchymoma (70% osteosarcoma and 30% leiomyosarcoma) in the right thigh. In the postoperative period, a pancreatic mass was identified radiologically by abdominal computed tomography. Pylorus-preserving pancreaticoduodenectomy was performed. The surgical specimen revealed leiomyosarcoma metastasized to the pancreas. A metastatic nodule on the remnant pancreatic tail was discovered 9 mo after the first pancreatic resection, and distal pancreatectomy was performed. Cases of pancreatic metastasis from leiomyosarcoma are extremely rare, especially when the tumor was resectable. We report here a unique case of pancreatic metastasis from a leiomyosarcoma in the right thigh that had been treated surgically.

Key words: Pancreatic tumor; Leiomyosarcoma; Metastasis

Koh YS, Chul J, Cho CK, Kim HJ. Pancreatic metastasis of leiomyosarcoma in the right thigh: A case report. *World J Gastroenterol* 2007; 13(7): 1135-1137

http://www.wjgnet.com/1007-9327/13/1135.asp

INTRODUCTION

The occurrence of metastatic lesions in the pancreas is very uncommon. The incidence of metastatic pancreatic tumors is 1.6%-11% at autopsy[1,2]. The majority of patients with pancreatic metastasis have widespread diseases. Isolated, potentially resectable pancreatic metastasis is detected infrequently. Therefore, resection of metastatic tumors of the pancreas has been occasionally reported, and its role in improving the survival or quality of life is not clearly defined[3,4]. However, some recent studies have reported that surgical resection can be performed in selected patients with isolated pancreatic metastases, achieving long-term survival and good palliation[1,5]. We report here a case of pancreatic metastatic from leiomyosarcoma of the right anterior thigh, which was treated by surgical resection, and review the literature about pancreatic metastasis.

CASE REPORT

A 66-year-old woman was referred to our hospital with a mass in the right thigh (Figure 1). In September 2005, she had undergone surgical resection for this mass. Malignant mesenchymoma (70% osteosarcoma and 30% leiomyosarcoma) was diagnosed histologically. In the postoperative period, abdominal computed tomography (CT) identified a pancreatic mass. The patient complained of non-specific abdominal discomfort. Laboratory findings were all within normal limits. The levels of the tumor markers including carcinoembryonic agent and carbohydrate antigen 19-9, were within the normal ranges. Abdominal CT revealed a mass at the head of the pancreas. Magnetic resonance imaging of the abdomen showed a low-intensity mass on T1-weighted images and a non-homogeneous high-intensity mass on T2-weighted images. No evidence of other distant metastases was seen (Figure 1). At laparotomy, a fixed mass of 4 cm or so in length was palpated at the head of the pancreas, displacing the surrounding duodenum. Therefore, pylorus-preserving pancreaticoduodenectomy was performed. Macroscopic examination of the operative specimen showed a 4 cm × 3 cm lobulated solid mass with a thin wall. Microscopic examination revealed a malignant neoplasm with predominance of spindle cells. The tumor cells were immunoreactive for desmin. Metastatic leiomyosarcoma was diagnosed histologically (Figure 2). The postoperative course was uneventful. We recommended systemic chemotherapy to the patient, but she declined. Nine months after the first pancreatic resection, a follow-up abdominal CT showed development of a new 1-cm mass in the remnant tail of the pancreas (Figure 1). Distal

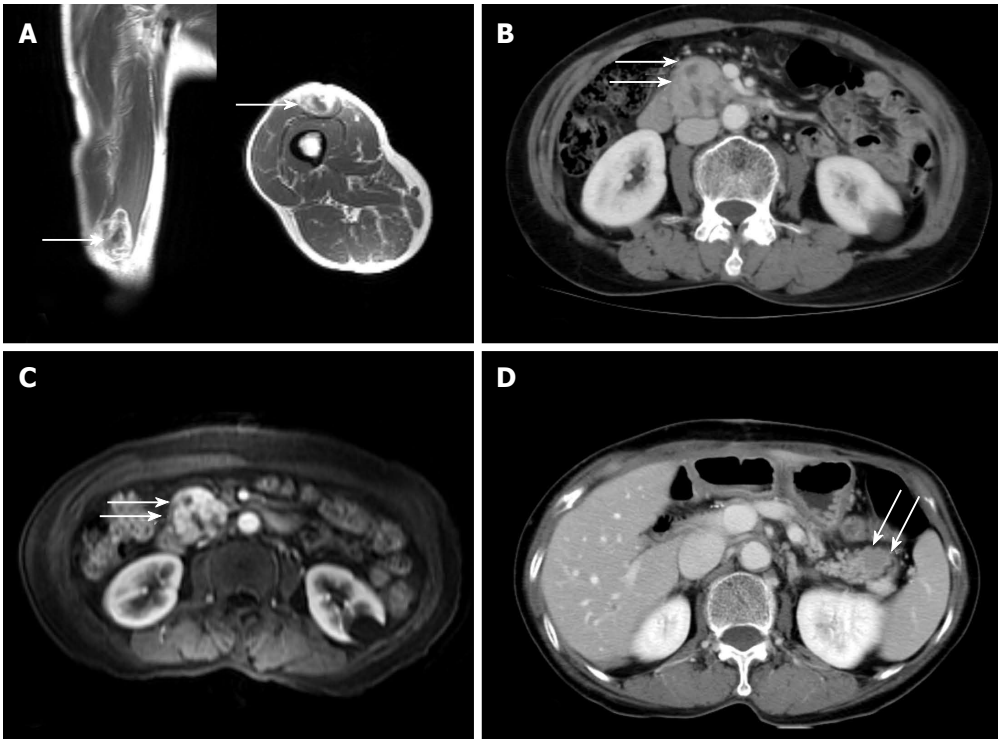

Figure 1 Radiological findings. **A**: Gadolinium-enhanced T1 weighted image showing a soft tissue tumor in the muscle of the anterior thigh; **B**: Contrast-enhanced abdominal CT scan showing a heterogeneously enhanced mass at the head of the pancreas; **C**: Gadolinium-enhanced T1 weighted image showing a well-enhanced mass with necrotic foci at the head of the pancreas; **D**: Follow-up CT obtained after 10 mo showing a low attenuated mass in the tail of the pancreas.

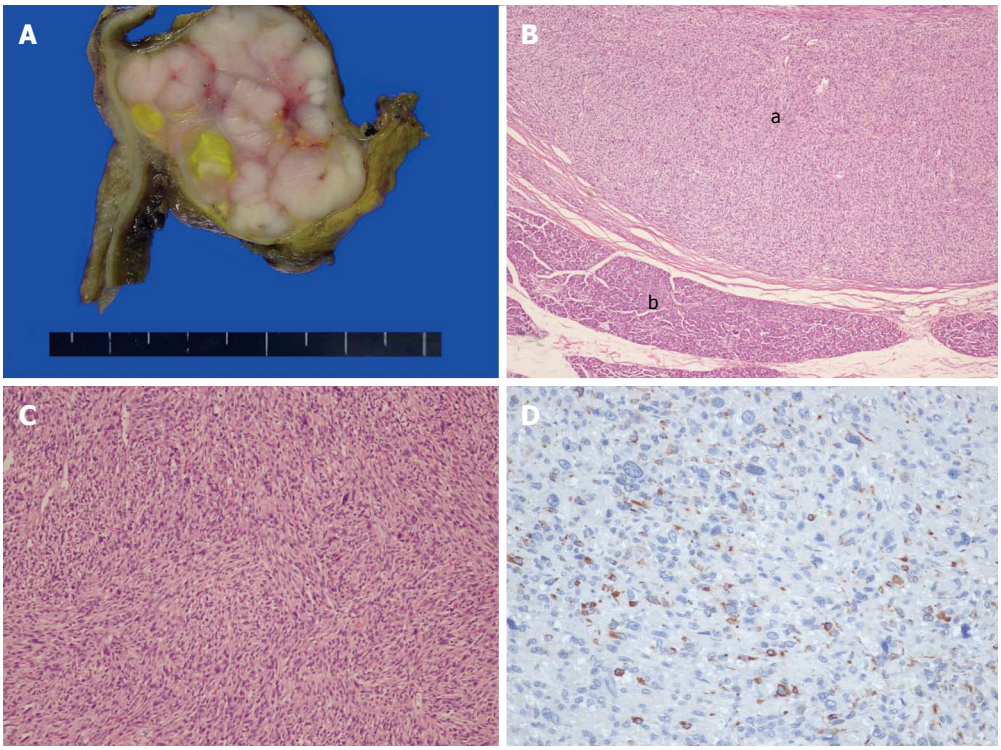

Figure 2 Gross and microscopic findings for metastatic leiomyosarcoma. **A**: The section reveals a whitish solid tumor with a lobulated pattern and a yellowish necrotic portion, abutting duodenal wall on the left side, and compressed pancreatic head tissue on the right side; **B**: Low-power view displaying eosinophilic intersecting fascicles circumscribed by a fibrous capsule (a) and adjacent normal pancreatic tissue (b) (hematoxylin and eosin stain × 40); **C**: Cellular proliferation of atypical spindle tumor cells is accompanied by nuclear atypia and hyperchromasia (hematoxylin and eosin stain × 200); **D**: Tumor cells show immunoreactivity for desmin.

pancreatectomy was performed. The tumor showed the same microscopic findings, and leiomyosarcoma was also diagnosed histologically.

DISCUSSION

Metastatic lesions in the pancreas are uncommon. Adsay *et al*[1] reviewed pathological specimens from 4955 adult autopsy cases in an attempt to identify tumors that had metastasized to the pancreas. There were only 81 (1.6%) cases of metastatic tumors, the majority of which were of epithelial origin, and the most common sites of the primary lesions were the lung, kidney, and gastrointestinal tract. However, a few cases of leiomyosarcoma with metastases to the pancreas have been reported. Primary sites of leiomyosarcomas included the uterus[6,7], ovary[8], veins[9], spermatic cord[10], intestine[3,10], retroperitoneum[2,11], and soft tissue[11,12]. To the best of our knowledge, including the present case, only 16 cases of pancreatic metastasis from leiomyosarcoma have been reported to

date in the English language literature[7,8,12].

The differential diagnosis between a solitary metastatic tumor and primary pancreatic carcinoma may be very difficult as signs and symptoms are similar for both primary and secondary tumors, and radiological imaging is unable to differentiate primary from secondary pancreatic lesions[13]. In our case, non-specific abdominal pain appeared to be the most common symptom. The symptoms of pancreatic metastases often include pain, weight loss, obstructive jaundice, and duodenal obstruction, which are very similar to the symptoms of primary pancreatic cancer[1,3,9]. Therefore, pre-operative diagnosis is challenging, and considerable caution is needed for patients with a previous history of non-pancreatic neoplastic disease. The pre-operative diagnosis of our case was primarily a non-functioning islet cell tumor of pancreas, although the patient had previously undergone surgical treatment for mesenchymoma of the left leg. Various diagnostic tools have been used to assess tumors. In recent years, 18-FDG-PET has proven to be useful for the accurate staging of tumors[3]. Percutaneous fine-needle aspiration (FNA) is found helpful in establishing the correct preoperative diagnosis, especially in patients who are not amenable to surgery, and in assisting in decisions related to the possibility and type of chemotherapy[3]. However, with the exception of postoperative histology, there is no definitive method for unambiguous diagnosis.

Metastatic tumors of the pancreas are usually diagnosed at an advanced stage, and solitary resectable metastasis occurs less frequently. Therefore, metastatic tumors of the pancreas are rarely treated surgically. Sperti *et al*[3] reported that 8/259 (3%) pancreatic resections were performed for pancreatic metastases. Therefore, our patient represents a very unusual case.

Only a few cases of pancreatic metastasis from sarcomas have been reported. Experience is limited, and the effectiveness of surgery for these types of lesions has not been clearly established. However, long-term survival may be conferred by "curative" resection for pancreatic metastasis from visceral or soft tissue sarcoma[3,7,9,14]. It is clear that surgical excision has the potential to improve prognosis if the primary site and other metastases are well-controlled. In the present unique case, pancreatic metastasis from leiomyosarcoma was diagnosed, and the patient underwent pancreatectomy twice in 10 mo. An attempt at complete tumor resection can offer patients the best hope of prolonged survival.

REFERENCES

1 **Crippa S**, Angelini C, Mussi C, Bonardi C, Romano F, Sartori P, Uggeri F, Bovo G. Surgical treatment of metastatic tumors to the pancreas: a single center experience and review of the literature. *World J Surg* 2006; **30**: 1536-1542

2 **Adsay NV**, Andea A, Basturk O, Kilinc N, Nassar H, Cheng JD. Secondary tumors of the pancreas: an analysis of a surgical and autopsy database and review of the literature. *Virchows Arch* 2004; **444**: 527-535

3 **Sperti C**, Pasquali C, Liessi G, Pinciroli L, Decet G, Pedrazzoli S. Pancreatic resection for metastatic tumors to the pancreas. *J Surg Oncol* 2003; **83**: 161-166; discussion 166

4 **Roland CF**, van Heerden JA. Nonpancreatic primary tumors with metastasis to the pancreas. *Surg Gynecol Obstet* 1989; **168**: 345-347

5 **Hiotis SP**, Klimstra DS, Conlon KC, Brennan MF. Results after pancreatic resection for metastatic lesions. *Ann Surg Oncol* 2002; **9**: 675-679

6 **Iwamoto I**, Fujino T, Higashi Y, Tsuji T, Nakamura N, Komokata T, Douchi T. Metastasis of uterine leiomyosarcoma to the pancreas. *J Obstet Gynaecol Res* 2005; **31**: 531-534

7 **Falconi M**, Crippa S, Sargenti M, Capelli P, Pederzoli P. Pancreatic metastasis from leiomyosarcoma of the broad ligament of the uterus. *Lancet Oncol* 2006; **7**: 94-95

8 **Nasu M**, Inoue J, Matsui M, Minoura S, Matsubara O. Ovarian leiomyosarcoma: an autopsy case report. *Pathol Int* 2000; **50**: 162-165

9 **Le Borgne J**, Partensky C, Glemain P, Dupas B, de Kerviller B. Pancreaticoduodenectomy for metastatic ampullary and pancreatic tumors. *Hepatogastroenterology* 2000; **47**: 540-544

10 **Wernecke K**, Peters PE, Galanski M. Pancreatic metastases: US evaluation. *Radiology* 1986; **160**: 399-402

11 **Nakamura E**, Shimizu M, Itoh T, Manabe T. Secondary tumors of the pancreas: clinicopathological study of 103 autopsy cases of Japanese patients. *Pathol Int* 2001; **51**: 686-690

12 **Boudghène FP**, Deslandes PM, LeBlanche AF, Bigot JM. US and CT imaging features of intrapancreatic metastases. *J Comput Assist Tomogr* 1994; **18**: 905-910

13 **Ishigure K**, Kaneko T, Takeda S, Inoue S, Kawase Y, Nakao A. Pancreatic metastasis from leiomyosarcoma in the back. *Hepatogastroenterology* 2003; **50**: 1675-1677

14 **Nakajima Y**, Kakizaki S, Kanda D, Shimada Y, Sohara N, Sato K, Takagi H, Mori M, Watanabe H. Pancreatic and gastric metastases of leiomyosarcoma arising in the left leg. *Int J Clin Oncol* 2005; **10**: 342-347

S- Editor Liu Y **L- Editor** Ma JY **E- Editor** Ma WH

PO Box 2345, Beijing 100023, China
www.wjgnet.com
wjg@wjgnet.com

World J Gastroenterol 2007 February 21; 13(7): 1138-1140
World Journal of Gastroenterology ISSN 1007-9327

CASE REPORT

A prophylactic approach for bone marrow transplantation from a hepatitis B surface antigen-positive donor

Abhasnee Sobhonslidsuk, Artit Ungkanont

Abhasnee Sobhonslidsuk, Artit Ungkanont, Department of Medicine, Faculty of Medicine, Ramathibodi Hospital, Mahidol University, Bangkok, Thailand
Correspondence to: Abhasnee Sobhonslidsuk, MD, Department of Medicine, Ramathibodi hospital, 270 Praram 6 Road, Rajathevee, Bangkok 10400, Thailand. teasb@mahidol.ac.th
Telephone: +66-2-2011304 Fax: +66-2-2011387
Received: 2006-12-14 Accepted: 2007-01-08

Abstract

It has been accepted that bone marrow transplantation (BMT) is the only curative therapeutic option for certain hematologic malignancies. The southeast Asia region is an endemic area of hepatitis B virus (HBV) infection; thus, BMT using a hepatitis B surface antigen (HBsAg)-positive donor is occasionally unavoidable. Organ transplantation using a HBsAg-positive donor can lead to post-transplantation de novo HBV infection and severe HBV-related hepatitis if no effective prophylactic measures are taken prior to and after transplantation. In this report, a four-level approach was designed for a patient with chronic myeloid leukemia, beginning with a booster HBV vaccination before performing BMT with a HBsAg-positive donor. Prior to BMT, the HBV viral load of the donor was reduced to an undetectable level by antiviral therapy. After BMT, hepatitis B immunoglobulin was administered intramuscularly for 1 wk together with a long-term antiviral drug, lamivudine. One year after discontinuation of lamivudine, the patient is still free of HBV infection.

Key words: Bone marrow transplantation; Hepatitis B virus; Vaccination; Hepatitis B immunoglobulin; Lamivudine.

Sobhonslidsuk A, Ungkanont A. A prophylactic approach for bone marrow transplantation from a hepatitis B surface antigen-positive donor. *World J Gastroenterol* 2007; 13(7): 1138-1140

http://www.wjgnet.com/1007-9327/13/1138.asp

INTRODUCTION

Certain hematologic malignancies can only be cured by bone marrow transplantation (BMT). In the southeast Asian region, hepatitis B virus (HBV) infection is highly prevalent. BMT from donors exhibiting the hepatitis B surface antigen (HBsAg) is therefore occasionally unavoidable. Intensive chemotherapeutic drugs used in a conditioning regimen and post-transplantion immunosuppressive drugs are required to suppress host immunity and to prevent graft versus host disease (GVHD). Using grafts with HBsAg-positive hematopoietic stem cells is associated with severe liver injury and a high mortality rate[1-3]. In this report, we present a long-term follow-up study of a seronegative patient who underwent BMT with a HBsAg-positive donor in which a four-level approach for the prevention of HBV infection was utilized.

CASE REPORT

A thirty-seven year old man, a known case of chronic myeloid leukemia with positive Philadelphia chromosome in chronic phase, was previously treated with hydroxyurea. The patient planned to receive BMT from his sole HLA-identical sibling, his sister, who had been a known hepatitis B carrier. She was anti-HBe positive and had an HBV viral load of 5260 copies/mL, as indicated by the Amplicor HBV Monitor Test (Roche Diagnostics, NJ, USA). Lamivudine (100 mg/d) was initiated to suppress HBV DNA; and 3 mo later, her HBV viral load became undetectable. His antibody to HBsAg (anti-HBs) was firstly positive at a level of 10.3 mIU/mL. A booster dose of hepatitis B vaccine was given to him, and the subsequent anti-HBs level rose to 83 mIU/mL. A conditioning regimen for BMT containing busulfan (16 mg/kg) and cyclophosphamide (120 mg/kg) was started before the initiation of BMT. GVHD was prevented using methotrexate and tacrolimus. Lamivudine (100 mg/d) was initiated 7 d prior to BMT and was continued thereafter. From the day of BMT to the 7th d post-BMT, hepatitis B immunoglobulin (HBIg) 800 IU was injected intramuscularly daily in order to maintain the anti-HBs level > 1000 IU/L. From the 7th d post-BMT, the anti-HBs level was persistently over 1000 IU/L without HBIG administration. One month after BMT, while on tacrolimus for GVHD suppression and lamivudine for HBV prophylaxis, the patient's blood test results were as follows: HBsAg negative, anti-HBs positive (at 400 mIU/mL), anti-HBc positive, HBV viral load < 200 copies per ml and HBV PCR positive. HBV PCR became negative by 6 mo after BMT. The patient had only grade I acute GVHD and limited chronic GVHD. Tacrolimus was gradually tapered

off and then discontinued at the 15th mo post-BMT, and lamivudine was stopped 3 mo later. Two and a half years after BMT or 1 year after discontinuation of lamivudine, the patient felt well, and his blood tests indicated that he was HBsAg negative, anti-HBc positive, anti-HBs positive (at 14 mIU/mL) and HBV PCR negative.

DISCUSSION

The Asia-Pacific region is an endemic area of HBV infection, with a prevalence of more than 8%[4]. Most transplantation centers have regarded HBV infection as a relative contraindication for organ transplantation[5,6]. BMT with HBsAg-positive donors has been reported to be associated with an increased incidence of HBV-related hepatitis, severe liver-related complications, fatal liver failure and death[1,2,6-11]. However, a few reports show that HBsAg might be present transiently in some patients after receiving bone marrow graft from HBsAg-positive donors[1,2]. High HBV viral load in BMT donors and the absence of anti-HBs in BMT patients are two important risk factors predisposing a patient to the development of HBV-related hepatitis post-BMT[1,2]. Oral antiviral drugs are suitable to decrease the HBV viral load of the HBsAg-positive BMT donor. Lamivudine seems to be an appropriate antiviral drug in this situation because it causes rapid viral load reduction and because HBV resistance rarely occurs in a short period of lamivudine treatment[12]. Before BMT, the anti-HBs level in the present case report was increased to 83 mIU/mL by a booster dose of HBV vaccination. In general, the persistence of anti-HBV activity after BMT may be caused by residual recipient lymphocytes that have survived intensive conditioning regimens[3]. We decided to administer HBIg intramuscular injection from d 0 to d 8 post-BMT because the residual number of patient lymphocytes was uncertain. Anti-HBs level monitoring during the early post-BMT period showed that anti-HBs levels were over 1000 mIU/mL, resulting in the decision to discontinue HBIg 7 d post-BMT. HBIg was injected intramuscularly according to the protocol employed in HBV-related liver transplantation[13]. The mechanisms by which HBIg prevents graft re-infection are not completely understood. They may decrease the spread of HBV infection by neutralizing circulating viral particles and by inducing lyses of infected cells through pathways such as antibody-dependent cellular cytotoxicity[13]. Combination therapy of HBIg and lamivudine offers synergistic protection against HBV infection and appears to be more effective than a single agent for prophylaxis after HBV-related liver transplantation[13]. A recent study proposed a three-level approach when hematopoietic stem cell transplantation (HSCT) was performed with a HBV-positive donor[6]. The three-level approach consisted of a pre-HSCT reduction of HBV viral replication in donors by lamivudine, a pre-HSCT enhancement of the recipient's anti-HBV immunity by HBV vaccination, and finally, a post-HSCT suppression of HBV viral replication in recipients with lamivudine[6]. In that paper, patients received lamivudine for 52 wk after HSCT; however, our patient received lamivudine for 72 wk, and treatment with this drug was stopped 12 wk after the discontinuation of tacrolimus. A flare of HBV infection and severe hepatitis was reported if antiviral drug was withdrawn in patients with immunosuppressive status or upon completion of chemotherapy[14]. Continuing lamivudine for at least 3 mo after completion of chemotherapy or immunosuppressive drugs has been recommended by a recent practice guideline[15]. The HBV viral load, as determined by the Amplicor HBV monitor test used in this report, is far more sensitive than the Digene Hybrid Capture assay used in a previous report[6,16]. De novo HBV infection might appear in the long-term follow-up of antiviral-prophylactic BMT patients with HBV-positive donors whose viral load was determined to be negative using a low sensitivity assay. An additional benefit of post-transplantion HBIg may be anticipated in hematopoietic stem cell transplantation. Recently, HBIg and lamivudine treatment during BMT in a child who received BMT from her HBsAg-positive mother has been reported[17]. The child received lamivudine only 1 d before BMT and continued the drug for 102 d. The details of HBV viral load and HBV PCR, however, were not mentioned in that paper[17]. The authors suggested that HBIg and lamivudine combination may be useful during the early period of BMT[17]. Intramuscular injection of HBIg sometimes requires the correction of thrombocytopenia or changing the route of administration from intramuscular to intravenous injection. Due to the large dosage of intravenous HBIg and its high cost, it may not be affordable for all patients. Our strategies for using BMT from HBsAg-positive donors will require multicenter studies with a large number of patients and a longer follow-up before this costly, four-level prophylactic approach can be put into practice.

REFERENCES

1 **Locasciulli A**, Alberti A, Bandini G, Polchi P, Arcese W, Alessandrino P, Bosi A, Testa M, Bacigalupo A. Allogeneic bone marrow transplantation from HBsAg+ donors: a multicenter study from the Gruppo Italiano Trapianto di Midollo Osseo (GITMO). *Blood* 1995; **86**: 3236-3240

2 **Lau GK**, Lie AK, Kwong YL, Lee CK, Hou J, Lau YL, Lim WL, Liang R. A case-controlled study on the use of HBsAg-positive donors for allogeneic hematopoietic cell transplantation. *Blood* 2000; **96**: 452-458

3 **Hui CK**, Cheung WW, Chan SC, Lo CM, Lau GK. Hepatitis B vaccination and preemptive treatment of hepatitis B virus in liver transplantation. *Curr Opin Organ Transplant* 2006; **11**: 594-598

4 **Lesmana LA**, Leung NW, Mahachai V, Phiet PH, Suh DJ, Yao G, Zhuang H. Hepatitis B: overview of the burden of disease in the Asia-Pacific region. *Liver Int* 2006; **26** Suppl 2: 3-10

5 **Guideline on the microbiological safety of human organs, tissues and cells used in transplantation: Advisory committee on the microbiological safety of board and tissues for transplantation**. United Kingdom Department of Health. August 2000

6 **Hui CK**, Lie A, Au WY, Ma SY, Leung YH, Zhang HY, Sun J, Cheung WW, Chim CS, Kwong YL, Liang R, Lau GK. Effectiveness of prophylactic Anti-HBV therapy in allogeneic hematopoietic stem cell transplantation with HBsAg positive donors. *Am J Transplant* 2005; **5**: 1437-1445

7 **McIvor C**, Morton J, Bryant A, Cooksley WG, Durrant S, Walker N. Fatal reactivation of precore mutant hepatitis B

virus associated with fibrosing cholestatic hepatitis after bone marrow transplantation. *Ann Intern Med* 1994; **121**: 274-275

8 **Caselitz M**, Link H, Hein R, Maschek H, Böker K, Poliwoda H, Manns MP. Hepatitis B associated liver failure following bone marrow transplantation. *J Hepatol* 1997; **27**: 572-577

9 **Cooksley WG**, McIvor CA. Fibrosing cholestatic hepatitis and HBV after bone marrow transplantation. *Biomed Pharmacother* 1995; **49**: 117-124

10 **Lau GK**, Liang R, Chiu EK, Lee CK, Lam SK. Hepatic events after bone marrow transplantation in patients with hepatitis B infection: a case controlled study. *Bone Marrow Transplant* 1997; **19**: 795-799

11 **Martin BA**, Rowe JM, Kouides PA, DiPersio JF. Hepatitis B reactivation following allogeneic bone marrow transplantation: case report and review of the literature. *Bone Marrow Transplant* 1995; **15**: 145-148

12 **Liaw YF**, Leung N, Guan R, Lau GK, Merican I, McCaughan G, Gane E, Kao JH, Omata M. Asian-Pacific consensus statement on the management of chronic hepatitis B: a 2005 update. *Liver Int* 2005; **25**: 472-489

13 **Villamil FG**. Prophylaxis with anti-HBs immune globulins and nucleoside analogues after liver transplantation for HBV infection. *J Hepatol* 2003; **39**: 466-474

14 **Hui CK**, Cheung WW, Au WY, Lie AK, Zhang HY, Yueng YH, Wong BC, Leung N, Kwong YL, Liang R, Lau GK. Hepatitis B reactivation after withdrawal of pre-emptive lamivudine in patients with haematological malignancy on completion of cytotoxic chemotherapy. *Gut* 2005; **54**: 1597-1603

15 **Keeffe EB**, Dieterich DT, Han SH, Jacobson IM, Martin P, Schiff ER, Tobias H, Wright TL. A treatment algorithm for the management of chronic hepatitis B virus infection in the United States: an update. *Clin Gastroenterol Hepatol* 2006; **4**: 936-962

16 **Lok AS**, McMahon BJ. Chronic hepatitis B: update of recommendations. *Hepatology* 2004; **39**: 857-861

17 **Tavil B**, Kuşkonmaz B, Kasem M, Demir H, Cetin M, Uçkan D. Hepatitis B immunoglobulin in combination with lamivudine for prevention of hepatitis B virus reactivation in children undergoing bone marrow transplantation. *Pediatr Transplant* 2006; **10**: 966-969

S- Editor Wang J **L- Editor** Ma JY **E- Editor** Ma WH

PO Box 2345, Beijing 100023, China
www.wjgnet.com
wjg@wjgnet.com

World J Gastroenterol 2007 February 21; 13(7): 1141-1143
World Journal of Gastroenterology ISSN 1007-9327

CASE REPORT

Lipoma within inverted Meckel's diverticulum as a cause of recurrent partial intestinal obstruction and hemorrhage: A case report and review of literature

Güldeniz Karadeniz Cakmak, Ali Ugur Emre, Oge Tascilar, Sibel Bektaş, Bulent Hamdi Uçan, Oktay Irkorucu, Kemal Karakaya, Yucel Ustundag, Mustafa Comert

Güldeniz Karadeniz Cakmak, Ali Ugur Emre, Oge Tascilar, Bulent Hamdi Uçan, Oktay Irkorucu, Kemal Karakaya, Mustafa Comert, Department of Surgery, Zonguldak Karaelmas University, School of Medicine, Kozlu-Zonguldak, Turkey
Sibel Bektaş, Department of Pathology, Zonguldak Karaelmas University, School of Medicine, Kozlu-Zonguldak, Turkey
Yucel Ustundag, Department of Gastroenterology, Zonguldak Karaelmas University, School of Medicine, Kozlu-Zonguldak, Turkey
Correspondence to: Dr. Güldeniz Karadeniz Cakmak, Zonguldak Karaelmas Universitesi, Arastirma ve Uygulama Hastanesi Bashekimligi, Kozlu-Zonguldak 67600, Turkey. gkkaradeniz@yahoo.com
Telephone: +90-372-2610159
Received: 2006-11-24 Accepted: 2007-01-15

Abstract

Lipoma within an inverted Meckel's diverticulum presenting with hemorrhage and partial intestinal obstruction is an exceptional clinical entity. We report a case of 47-year-old male with a history of recurrent episodes of partial intestinal obstruction and melena due to a subserosal lipoma located in the base of an inverted Meckel's diverticulum. According to our knowledge, this is the first case of a lipoma within a Meckel's diverticulum giving rise to this clinical scenario without the existence of heterotrophic gastric or pancreatic tissues.

Key words: Meckel's diverticulum; Lipoma; Inversion; Intestinal obstruction; Hemorrhage

Karadeniz Cakmak G, Emre AU, Tascilar O, Bektaş S, Ucan BH, Irkorucu O, Karakaya K, Ustundag Y, Comert M. Lipoma within inverted Meckel's diverticulum as a cause of recurrent partial intestinal obstruction and hemorrhage: A case report and review of literature. *World J Gastroenterol* 2007; 13(7): 1141-1143

http://www.wjgnet.com/1007-9327/13/1141.asp

INTRODUCTION

Tumor of Meckel's diverticulum occurs infrequently. Moreover, the association of a lipoma within the inverted Meckel's diverticulum as a leading point of bleeding and recurrent episodes of partial intestinal obstruction is such an unusual circumstance that might be considered quite impossible.

Meckel's diverticulum is the most prevalent congenital anomaly of the gastrointestinal tract, which is reported to occur in 1%-3% of the general population and autopsy series[1,2]. However, the lifetime risk of complication development in patients with Meckel's diverticulum was proposed to be less than 5% in recent investigations[3]. These complications included intestinal obstruction, intussusceptions, inflammation and bleeding.

Lipomas are the rare benign tumors of the small intestine with no malignant potential and mostly encountered incidentally during investigation of the gastrointestinal tract for another reason, since they are usually asymptomatic[4]. As small intestinal lipoma is relatively infrequent, it is even a rarer source of gastrointestinal bleeding.

We present a case of a 47-year-old man with fatigue, chronic abdominal pain and tarry stool due to an inverted Meckel's diverticulum with a subserosal lipoma. This is a special case that has not appeared in literature over the past 4 decades. Although the incidence of Meckel's diverticulum is high, inversion is a scarsely diagnosed entity and the association of a lipoma within the inverted Meckel's diverticulum as a leading point of lower gastrointestinal hemorrhage without the existence of heterotopic gastric and pancreatic tissues and recurrent partial intestinal obstruction is an exceptional case.

CASE REPORT

A 47-year-old man was admitted to our clinic with fatigue, recurrent episodes of constipation and abdominal pain. Melena was mentioned on admission. He denied vomiting, fever, or chills. He had had symptoms intermittently for about 4 mo, leading to several hospital visits. Over the previous 2 mo, the episodes of pain became more pronounced with radiation to his back. The patient was not using any specific medication and his medical history did not suggest a major disease. Physical examination revealed a temperature of 37℃, a pulse rate of 90 beats per minute (bpm), a blood pressure of 110/70 mmHg, and a respiration rate of 18 breaths per minute. The

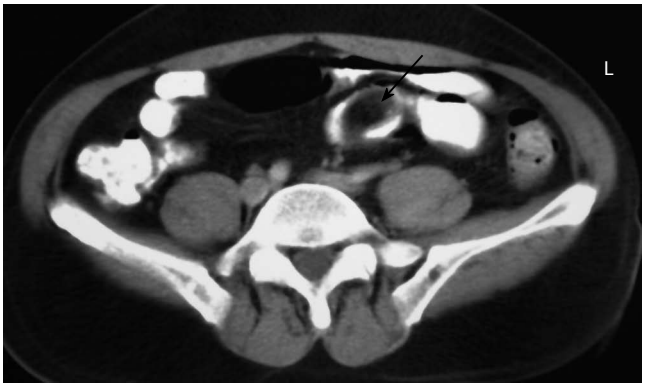

Figure 1 Contrast enhanced CT shows a hypodens, regular contoured, polypoid, 4 cm × 2 cm mass lesion with fatty density.

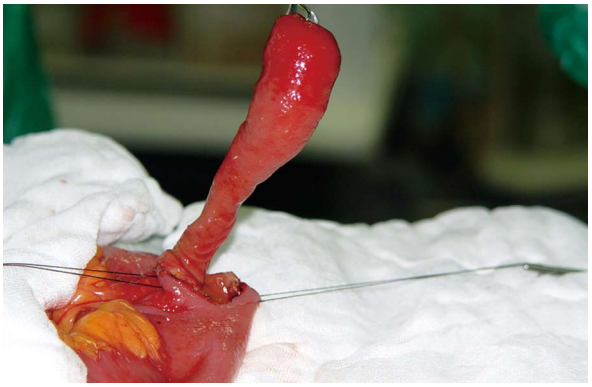

Figure 2 A pedinculated mass lesion within the inverted Meckel's diverticulum.

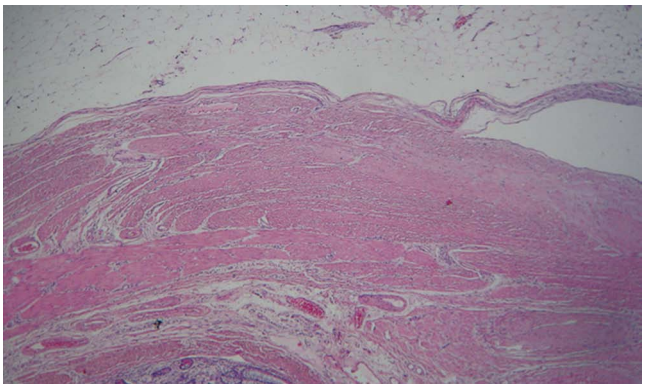

Figure 3 Microscopic appearance of a subserosal lipoma within the inverted Meckel's diverticulum (HE).

patient was pale-looking without abdominal tenderness, guarding or rebound and norm active bowel sounds were auscultated. Examination of heart and lungs revealed no abnormal findings. Rectal examination revealed tarry fecal content. Clear gastric content was obtained on nasogastric aspiration. The initial laboratory workup was as follows: hematocrit, 33%; hemoglobin, 11.2 g/dL; white blood cells, 10 500/mm^3 with a normal differential count; platelets, 195 000/mm^3; blood glucose, 87 mg/dL; blood urea, 25 mg/dL; creatinine, 0.8 mg/dL; SGOT, 32 IU/L; SGPT,25 IU/L; LDH, 54 IU/L; total bilirubin, 0.4 mg/dL; direct bilirubin, 0.2 mg/dL; and Na+, 138 meq/L; andK+, 3.7meq/L. Fecal occult blood test was positive. A gastrointestinal cause was sought in order to explain the patient's hemorrhage. He had received upper and lower gastrointestinal tract endoscopic examinations without identification of a specific bleeding etiology except a little amount of blood residue in terminal ileum. A computed tomography (CT) scan of the abdomen and pelvis revealed mildly dilated loops of proximal small bowel and a polypoid, 4 cm × 2 cm mass lesion with fatty density localized in the left lower quadrant and a suspicious filling defect in cecum (Figure 1). A pedinculated lipoma was assumed to be the underlying cause of recurrent partial intestinal obstruction and bleeding. He was taken to the operating room with the diagnosis of symptomatic small bowel lipoma. At surgery, an inverted Meckel's diverticulum induced by a pedinculated subserosal lipomatous solid mass nearly obstructing the lumen with ulcer and hemorrhage was found 40 cm from the ileocecal valve (Figure 2). Segmental resection of the ileal loop harboring the lesion was carried out and an end-to-end ileo-ileal anastomosis was performed. The lipoma within the inverted Meckel's diverticulum as a leading point of obstruction and bleeding was 5 cm long and 3 cm in diameter. Pathologic evaluation of the specimen confirmed the diagnosis of a subserosal lipoma within the inverted Meckel's diverticulum and revealed neither heterotrophic gastric and pancreatic tissue nor signs of malignancy (Figure 3). Five days after intervention, the patient was discharged from the hospital without any complication.

DISCUSSION

The omphalomesenteric duct connects the mid gut and yolk sac in seven weeks of gestation and during the eighth week, it normally undergoes obliteration[5]. Under circumstances of failure or incomplete vitelline duct obliteration, a spectrum of abnormalities appears, the most common of which is Meckel's diverticulum. Omphalomesenteric fistula, enterocysts or a fibrous band connecting the small intestine to the umbilicus are the other pathologies that can be encountered. As the location of the Meckel's diverticulum varies among individuals, they are usually detected in the antimesenteric side of the ileum within 100 cm of ileocecal valve. Meckel's diverticulum possesses various complication risks including intestinal obstruction, intussusception, inflammation and bleeding. Inversion of a Meckel's diverticula is a scarse entity with a potential of intestinal obstruction due to direct luminal obliteration or causing a lead point for intussusception[6-8]. The pathophysiology of the disease process leads to a complicated and confusing clinical picture of recurrent obstructive symptoms, chronic abdominal pain and lower gastrointestinal bleeding that may cause a delay in diagnosis and waste time. In our case, we have detected a lipoma as a leading point of inversion which causes partial obstruction and bleeding. Recurrent partial obstructive periods and abdominal pain of our patient might be attributed to luminal obstruction due to inversion

of Meckel's diverticulum which might be induced by lipomatous development. An other possible mechanism for this symptomatology might be the probable intussusseptions according to the inverted diverticulum, which has been reported as a lead point previously[6,7]. Intestinal obstruction due to intussusception as a result of a lipoma within Meckel's diverticulum has only been reported twice in literature[9,10]. Primary pathophysiologic process responsible for bleeding in Meckel's diverticulum is the ileal mucosal ulceration due to the existence of heterotrophic gastric or pancreatic tissues which has not been verified in our patient; instead a subserosal lipoma has been demonstrated with ulceration and hemorrhage.

Lipomas of the small intestine are the second most common benign tumors next to leiomyomas[11]. Their location and the peak age vary, however approximately 50% were found in the ileum, and the sixth to seventh decades of life were considered to be the most risky period[4,11]. In general, lipomas are defined to originate in the submucosal layer and are usually solitary, with variable sizes ranging from 1 cm to 30 cm[12]. They usually appear as a sessile protrusion into the lumen of the intestine. Due to motor activity of underlying muscularis propria, they tend to extrude into the bowel wall or through the luminal area progressively, which might be the responsible reason for the inversion of the Meckel's diverticulum in our case. In this manner, a pseudopedicle is formed, providing a polypoid appearance to the lesion. Although the majority of these lesions are asymptomatic and detected incidentally during the routine examinations or in surgical specimen removed for various other reasons, on rare occasions they might present with symptoms depending on their size and location. Lipomas smaller than 1 cm are generally incapable of producing symptoms, however 75% of lipomas with a size > 4 cm might give rise to gastrointestinal symptoms. Intestinal obstruction is one of the major result due to the occlusion of lumen by a large protruding lesion. Hemorrhage which is an other possible consequence might be based on an ulceration of the overlying mucosa caused by direct pressure from the lipoma or due to intussusception per se[4,12]. Preoperative diagnosis of small intestinal lipomas can be established by means of endoscopic and radiologic evaluation. Radiolucency and the so-called "squeeze sign" implying an altered configuration during peristalsis are suggestive findings observed in small intestinal series. Detection of fatty tissue density within the mass on CT scans supports the diagnosis. The "naked fat sign" which can be defined as the protrusion of fat through mucosal disruption following multiple biopsy sampling of the submucosal mass during endoscopic examination is believed to be pathognomonic[4,11].

Although more common in children, the complications of Meckel's diverticulum have also been described in adults. Gastrointestinal bleeding and intestinal obstruction are the two most common clinical problems associated with Meckel's diverticulum. Tumor within a Meckel's diverticulum is a scarce clinical entity with a reported incidence of only 2%[13]. Intestinal obstruction caused by a lipoma within the Meckel's diverticulum is so uncommon that we could only find three cases in the literature, two of which were due to intussusception[9,10], and one case of direct lumen occlusion by a large protruding lesion[14]. Moreover, the association of gastrointestinal hemorrhage and recurrent episodes of partial intestinal obstruction caused by a subserosal lipoma within an inverted Meckel's diverticulum without the existence of heterotrophic gastric or pancreatic tissue is an exceptional case, which has not been reported over the last 40 years in literature.

REFERENCES

1 **Soderlund S**. Meckel's diverticulum. A clinical and histologic study. *Acta Chir Scand Suppl* 1959; Suppl **248**: 1-233
2 **Yahchouchy EK**, Marano AF, Etienne JC, Fingerhut AL. Meckel's diverticulum. *J Am Coll Surg* 2001; **192**: 658-662
3 **Leijonmarck CE**, Bonman-Sandelin K, Frisell J, Räf L. Meckel' s diverticulum in the adult. *Br J Surg* 1986; **73**: 146-149
4 **Fernandez MJ**, Davis RP, Nora PF. Gastrointestinal lipomas. *Arch Surg* 1983; **118**: 1081-1083
5 **DeBartolo HM**, van Heerden JA. Meckel's diverticulum. *Ann Surg* 1976; **183**: 30-33
6 **Dujardin M**, de Beeck BO, Osteaux M. Inverted Meckel's diverticulum as a leading point for ileoileal intussusception in an adult: case report. *Abdom Imaging* 2002; **27**: 563-565
7 **Steinwald PM**, Trachiotis GD, Tannebaum IR. Intussusception in an adult secondary to an inverted Meckel's diverticulum. *Am Surg* 1996; **62**: 889-894
8 **Konstantakos AK**. Meckel's diverticulum-induced ileocolonic intussusception. *Am J Surg* 2004; **187**: 557-558
9 **Ahmed HU**, Wajed S, Krijgsman B, Elliot V, Winslet M. Acute abdomen secondary to a Meckel's lipoma. *Ann R Coll Surg Engl* 2004; **86:** W4-W5
10 **Formejster I**, Mattern R. Ileus due to ileo-cecal intussusception caused by lipoma coexistent with Meckel's diverticulum. *Wiad Lek* 1971; **24**: 1101
11 **Olmsted WW**, Ros PR, Hjermstad BM, McCarthy MJ, Dachman AH. Tumors of the small intestine with little or no malignant predisposition: a review of the literature and report of 56 cases. *Gastrointest Radiol* 1987; **12**: 231-239
12 **Zografos G**, Tsekouras DK, Lagoudianakis EE, Karantzikos G. Small intestinal lipoma as a cause of massive gastrointestinal bleeding identified by intraoperative enteroscopy. A case report and review of the literature. *Dig Dis Sci* 2005; **50**: 2251-2254
13 **Williams RS**. Management of Meckel's diverticulum. *Br J Surg* 1981; **68**: 477-480
14 **Krespis EN**, Sakorafas GH. Partial intestinal obstruction caused by a lipoma within a Meckel's diverticulum. *Dig Liver Dis* 2006; **38**: 358-359

S- Editor Liu Y **L- Editor** Ma JY **E- Editor** Ma WH

PO Box 2345, Beijing 100023, China
www.wjgnet.com
wjg@wjgnet.com

World J Gastroenterol 2007 February 21; 13(7): 1144
World Journal of Gastroenterology ISSN 1007-9327

ACKNOWLEDGMENTS

Acknowledgments to Reviewers of *World Journal of Gastroenterology*

Many reviewers have contributed their expertise and time to the peer review, a critical process to ensure the quality of *World Journal of Gastroenterology*. The editors and authors of the articles submitted to the journal are grateful to the following reviewers for evaluating the articles (including those were published and those were rejected in this issue) during the last editing period of time.

Akira Andoh, MD
Department of Internal Medicine, Shiga University of Medical Science, Seta Tukinowa, Otsu 520-2192, Japan

Taku Aoki, MD
Division of Hepato-Biliary-Pancreatic and Transplantation Surgery, Department of Surgery, Graduate School of Medicine, University of Tokyo,7-3-1 Hongo, Bunkyo-ku, Tokyo, 113-8655, Japan

Hitoshi Asakura, Director, Emeritus Professor
International Medical Information Center, Shinanomachi Renga Bldg.35, Shinanomachi, Shinjukuku, Tokyo 160-0016, Japan

Olivier Barbier
CHUQ-CHUL Research Center, 2705 Laurier Boulevard, Québec G1V 4G2, Canada

Yusuf Bayraktar, Professor
Department of Gastroenterology, School of Medicine, Hacettepe University, Ankara 06100, Turkey

Flavia Bortolotti, Dr
Clinica Medica 5, Via Giustiniani 2, 35100 Padova, Italy

Katja Breitkopf, Dr
Department of Medicine II, University Hospital Mannheim, University of Heidelberg, Theodor-Kutzer-Ufer 1-3, 68167 Mannheim, Germany

Paolo Del Poggio, Dr
Hepatology Unit, Department of Internal Medicine, Treviglio Hospital, Piazza Ospedale 1, Treviglio Bg 24047, Italy

Olivier Detry, Dr
Department of Abdominal Surgery and Transplantation, University of Liège, CHU Sart Tilman B35, B-4000 Liège, Belgium

Curt Einarsson, Professor
Department of Medicine, Karolinska institute, Karolinska University Hospital Huddinge, Dept of Gastroenterology and Hepatology, K 63, Huddinge SE-141 86, Sweden

Nikolaus Gassler, Professor
Institute of Pathology, University Hospital RWTH Aachen, Pauwelsstrasse 30, 52074 Aachen, Germany

Pietro Invernizzi, Dr
Division of Internal Medicine, Department of Medicine, Surgery, Dentistry, San Paolo School of Medicine, University of Milan, Via Di Rudinfi 8, 20142 Milan, Italy

Jonathan D Kaunitz, MD
Building 114, Suite 217, West Los Angeles VA Medical Center, 11301 Wilshire Boulevard, Los Angeles, California 90073, United States

Zahariy Krastev, Professor
Department of Gastroneterology, Universiti Hospital "St. Ivan Rilski",#15, blvd "Acad. Ivan Geshov", Sofia 1431, Bulgaria

Michael Kremer, MD
Skipper Bowles Center for Alcohol Studies, CB# 7178, 3011 Thurston-Bowles Building, University of North Carolina, Chapel Hill, NC 27599, United States

John K Marshall, MD, Associate Professor of Medicine
Division of Gastroenterology (4W8), McMaster University Medical Centre, 1200 Main Street West, Hamilton, Ontario L8N 3Z5, Canada

Samuel Babafemi Olaleye, Dr
Department of Physiology, University of Ibadan, Ibadan, Nigeria, Ibadan 022, Nigeria

Satoshi Osawa, MD
First Department of Medicine, Hamamatsu University School of Medicine, 1-20-1 Handayama, Hamamatsu, 431-3192, Japan

Bo-Rong Pan, Professor
Outpatient Department of Oncology, The Fourth Military Medical University, 175 Changle West Road,Xi'an 710032, Shaanxi Province, China

Richard A Rippe, Dr
Department of Medicine, The University of North Carolina at Chapel Hill, Chapel Hill, NC 27599-7038, United States

Luis Rodrigo, Professor
Gastroenterology Service, Hospital Central de Asturias, c/ Celestino Villamil, s.n., Oviedo 33.006, Spain

Manuel Romero-Gómez, MD, Professor
Hepatology Unit, Hospital Universitario de Valme, Ctra de Cádiz s/n, Sevilla 41014, Spain

Heitor Rosa, Professor
Department of Gastroenterology and Hepatology, Federal University School of Medicine, Rua 126 n.21, Goiania - GO 74093-080, Brazil

Shawn David Safford, Dr
Department of Surgery, Duke University Medical Center, 994 West Ocean View Avenue, Norfolk VA23503, United States

Manfred V Singer, Professor
Department of Medicine II, University Hospital at Mannheim, Theodor-Kutzer-Ufer 1-3, Mannheim 68167, Germany

Zsuzsa Szondy, Professor
Department of Biochemistry and Molecular Biol, University of Debrecen, Debrecen H-4012, Hungary

Wei Tang, MD, EngD, Assistant Professor
H-B-P Surgery Division, Artificial Organ and Transplantation Division, Department of surgery, Graduate School of Medicine, The University of Tokyo, Tokyo 113-8655, Japan

Andrzej Tarnawski, Professor
VA Medical Center/University of California-Irvine, 5901 East 7th St, Long Beach, CA 90822-5201, United States

Harald Vogelsang, Professor
Gastroenterology, AKH- KIM IV, Wahringer G. 18-20, Vienna A-1090, Austria

Stefan Wirth, Professor Dr
Children's Hospital, Heusnerstt. 40, Wuppertal 42349, Germany

Daniel Lindsay Worthley, Dr
Department of Gastroenterology and Hepatology, Flinders Medical Centre, Room 3D230, Bedford Park, SA 5042, Australia

PO Box 2345, Beijing 100023, China
www.wjgnet.com
wjg@wjgnet.com

World J Gastroenterol 2007 February 21; 13(7): 1145
World Journal of Gastroenterology ISSN 1007-9327

Meetings

MAJOR MEETINGS COMING UP

Meeting Falk Research Workshop: Morphogenesis and Cancerogenesis of the Liver
25-26 January 2007
Goettingen
symposia@falkfoundation.de

Meeting Canadian Digestive Diseases Week (CDDW)
16-20 February 2007
Banff-AB
cagoffice@cag-acg.org
www.cag-acg.org/cddw/cddw2007.htm

Meeting Falk Symposium 158: Intestinal Inflammation and Colorectal Cancer
23-24 March 2007
Sevilla
symposia@falkfoundation.de

Meeting BSG Annual Meeting
26-29 March 2007
Glasgow
www.bsg.org.uk/

NEXT 6 MONTHS

Meeting 42nd Annual Meeting of the European Association for the Study of the Liver
11-15 April 2007
Barcelona
easl2007@easl.ch
www.easl.ch/liver-meeting/

Meeting Falk Symposium 159: IBD 2007 - Achievements in Research and Clinical Practice
4-5 May 2007
Istanbul
symposia@falkfoundation.de

Meeting European Society for Paediatric Gastroenterology, Hepatology and Nutrition Congress 2007
9-12 May 2007
Barcelona
espghan2007@colloquium.fr

Digestive Disease Week
19-24 May 2007
Washington Convention Center, Washington DC

Meeting Gastrointestinal Endoscopy Best Practices: Today and Tomorrow, ASGE Annual Postgraduate Course at DDW
23-24 May 2007
Washington-DC
tkoral@asge.org

Meeting ESGAR 2007 18th Annual Meeting and Postgraduate Course
12-15 June 2007
Lisbon
fca@netvisao.pt

Meeting Falk Symposium 160: Pathogenesis and Clinical Practice in Gastroenterology
15-16 June 2007
Portoroz
symposia@falkfoundation.de

Meeting ILTS 13th Annual International Congress
20-23 June 2007
Rio De Janeiro
www.ilts.org

Meeting 9th World Congress on Gastrointestinal Cancer
27-30 June 2007
Barcelona
meetings@imedex.com

EVENTS AND MEETINGS IN 2007

Meeting Falk Research Workshop: Morphogenesis and Cancerogenesis of the Liver
25-26 January 2007
Goettingen
symposia@falkfoundation.de

Meeting Canadian Digestive Diseases Week (CDDW)
16-20 February 2007
Banff-AB
cagoffice@cag-acg.org
www.cag-acg.org/cddw/cddw2007.htm

Meeting Falk Symposium 158: Intestinal Inflammation and Colorectal Cancer
23-24 March 2007
Sevilla
symposia@falkfoundation.de

Meeting BSG Annual Meeting
26-29 March 2007
Glasgow
www.bsg.org.uk/

Meeting 42nd Annual Meeting of the European Association for the Study of the Liver
11-15 April 2007
Barcelona
easl2007@easl.ch
www.easl.ch/liver-meeting/

Meeting Falk Symposium 159: IBD 2007 - Achievements in Research and Clinical Practice
4-5 May 2007
Istanbul
symposia@falkfoundation.de

Meeting European Society for Paediatric Gastroenterology, Hepatology and Nutrition Congress 2007
9-12 May 2007
Barcelona
espghan2007@colloquium.fr

Meeting Gastrointestinal Endoscopy Best Practices: Today and Tomorrow, ASGE Annual Postgraduate Course at DDW
23-24 May 2007
Washington-DC
tkoral@asge.org

Meeting ESGAR 2007 18th Annual Meeting and Postgraduate Course
12-15 June 2007
Lisbon
fca@netvisao.pt

Meeting Falk Symposium 160: Pathogenesis and Clinical Practice in Gastroenterology
15-16 June 2007
Portoroz
symposia@falkfoundation.de

Meeting ILTS 13th Annual International Congress
20-23 June 2007
Rio De Janeiro
www.ilts.org

Meeting 9th World Congress on Gastrointestinal Cancer
27-30 June 2007
Barcelona
meetings@imedex.com

Meeting 15th International Congress of the European Association for Endoscopic Surgery
4-7 July 2007
Athens
info@eaes-eur.org
congresses.eaes-eur.org/

Meeting 39th Meeting of the European Pancreatic Club
4-7 July 2007
Newcastle
www.e-p-c2007.com

Meeting XXth International Workshop on Heliobacter and related bacteria in cronic degistive inflammation
20-22 September 2007
Istanbul
www.heliobacter.org

Meeting Falk Workshop: Mechanisms of Intestinal Inflammation
10 October 2007
Dresden
symposia@falkfoundation.de

Meeting Falk Symposium 161: Future Perspectives in Gastroenterology
11-12 October 2007
Dresden
symposia@falkfoundation.de

Meeting Falk Symposium 162: Liver Cirrhosis - From Pathophysiology to Disease Management
13-14 October 2007
Dresden
symposia@falkfoundation.de

American College of Gastroenterology Annual Scientific Meeting
12-17 October 2007
Pennsylvania Convention Center
Philadelphia, PA

Meeting APDW 2007 - Asian Pacific Digestive Disease Week 2007
15-18 October 2007
Kobe
apdw@convention.co.jp
www.apdw2007.org

15th United European Gastroenterology Week, UEGW
27-31 October 2007
Le Palais des Congrès de Paris, Paris, France

Meeting The Liver Meeting® 2007 - 57th Annual Meeting of the American Association for the Study of Liver Diseases
2-6 November 2007
Boston-MA
www.aasld.org

Gastro 2009, World Congress of Gastroenterology and Endoscopy London, United Kingdom 2009

PO Box 2345, Beijing 100023, China
www.wjgnet.com
wjg@wjgnet.com

World J Gastroenterol 2007 February 21; 13(7): 1146-1148
World Journal of Gastroenterology ISSN 1007-9327

Instructions to authors

GENERAL INFORMATION

World Journal of Gastroenterology (*WJG, World J Gastroenterol* ISSN 1007-9327 CN 14-1219/R) is a weekly journal of more than 48 000 circulation, published on the 7th, 14th, 21st and 28th of every month.

Original Research, Clinical Trials, Reviews, Comments, and Case Reports in esophageal cancer, gastric cancer, colon cancer, liver cancer, viral liver diseases, *etc.*, from all over the world are welcome on the condition that they have not been published previously and have not been submitted simultaneously elsewhere.

Indexed and abstracted in

Current Contents®/Clinical Medicine, Science Citation Index Expanded (also known as SciSearch®) and Journal Citation Reports/Science Edition, *Index Medicus*, MEDLINE and PubMed, Chemical Abstracts, EMBASE/Excerpta Medica, Abstracts Journals, *Nature Clinical Practice Gastroenterology and Hepatology*, CAB Abstracts and Global Health. ISI JCR 2003-2000 IF: 3.318, 2.532, 1.445 and 0.993.

Published by

The WJG Press

SUBMISSION OF MANUSCRIPTS

Manuscripts should be typed double-spaced on A4 (297 mm × 210 mm) white paper with outer margins of 2.5 cm. Number all pages consecutively, and start each of the following sections on a new page: Title Page , Abstract, Introduction, Materials and Methods, Results, Discussion, acknowledgements, References, Tables, Figures and Figure Legends. Neither the editors nor the Publisher is responsible for the opinions expressed by contributors. Manuscripts formally accepted for publication become the permanent property of The WJG Press, and may not be reproduced by any means, in whole or in part without the written permission of both the authors and the Publisher. We reserve the right to put onto our website and copy-edit accepted manuscripts. Authors should also follow the guidelines for the care and use of laboratory animals of their institution or national animal welfare committee.

Authors should retain one copy of the text, tables, photographs and illustrations, as rejected manuscripts will not be returned to the author(s) and the editors will not be responsible for the loss or damage to photographs and illustrations in mailing process.

Online submission

Online submission is strongly advised. Manuscripts should be submitted through the Online Submission System at: http://www.wjgnet.com/index.jsp. Authors are highly recommended to consult the ONLINE INSTRUCTIONS TO AUTHORS (http://www.wjgnet.com/wjg/help/instructions.jsp) before attempting to submit online. Authors encountering problems with the Online Submission System may send an email you describing the problem to wjg@wjgnet.com for assistance. If you submit your manuscript online, do not make a postal contribution. A repeated online submission for the same manuscript is strictly prohibited.

Postal submission

Send 3 duplicate hard copies of the full-text manuscript typed double-spaced on A4 (297 mm × 210 mm) white paper together with any original photographs or illustrations and a 3.5 inch computer diskette or CD-ROM containing an electronic copy of the manuscript including all the figures, graphs and tables in native Microsoft Word format or *.rtf format to:

Editorial Office

World Journal of Gastroenterology
Editorial Department: Apartment 1066, Yishou Garden,
58 North Langxinzhuang Road,
PO Box 2345, Beijing 100023, China
E-mail: wjg@wjgnet.com
http: //www.wjgnet.com
Telephone: +86-10-85381892
Fax: +86-10-85381893

MANUSCRIPT PREPARATION

All contributions should be written in English. All articles must be submitted using a word-processing software. All submissions must be typed in 1.5 line spacing and in word size 12 with ample margins. The letter font is Tahoma. For authors from China, one copy of the Chinese translation of the manuscript is also required (excluding references). Style should conform to our house format. Required information for each of the manuscript sections is as follows:

Title page

Full manuscript title, running title, all author(s) name(s), affiliations, institution(s) and/or department(s) where the work was accomplished, disclosure of any financial support for the research, and the name, full address, telephone and fax numbers and email address of the corresponding author should be included. Titles should be concise and informative (removing all unnecessary words), emphasize what is new, and avoid abbreviations. A short running title of less than 40 letters should be provided. List the author(s)' name(s) as follows: initial and/or first name, middle name or initial(s) and full family name.

Abstract

An informative, structured abstract of no more than 250 words should accompany each manuscript. Abstracts for original contributions should be structured into the following sections: AIM: Only the purpose should be included. METHODS: The materials, techniques, instruments and equipments, and the experimental procedures should be included. RESULTS: The observatory and experimental results, including data, effects, outcome, *etc.* should be included. Authors should present *P* value where necessary, and the significant data should accompany. CONCLUSION: Accurate view and the value of the results should be included.

The format of structured abstracts is at: http://www.wjgnet.com/wjg/help/11.doc

Key words

Please list 5-10 key words that could reflect content of the study mainly from *Index Medicus*.

Text

For most article types, the main text should be structured into the following sections: INTRODUCTION, MATERIALS AND METHODS, RESULTS and DISCUSSION, and should include in appropriate Figures and Tables. Data should be presented in the body text or in Figures and Tables, but not in both.

Illustrations

Figures should be numbered as 1, 2, 3 and so on, and mentioned clearly in the main text. Provide a brief title for each figure on a separate page. No detailed legend should be involved under the figures. This part should be added into the text where the figures are applicable. Digital images: black and white photographs should be scanned and saved in TIFF format at a resolution of 300 dpi; color images should be saved as CMYK (print files) but not as RGB (screen-viewing files). Place each photograph in a separate file. Print images: supply images of size no smaller than 126 mm × 85 mm printed on smooth surface paper; label the image by writing the Figure number and orientation using an arrow. Photomicrographs: indicate the original magnification and stain in the legend. Digital Drawings: supply files in EPS if created by freehand and illustrator, or TIFF from photoshops. EPS files must be accompanied by a version in native file format for editing purposes. Existing line drawings should be scanned at a resolution of 1200 dpi and as close as possible to the size where they will appear when printed. Please use uniform legends for the same subjects. For example: Figure 1 Pathological changes of atrophic gastritis after treatment. A: ...; B: ...; C: ...; D: ...; E: ...; F: ...; G: ...

Tables

Three-line tables should be numbered as 1, 2, 3 and so on, and mentioned clearly in the main text. Provide a brief title for each table. No detailed legend should be included under the tables. This part should be added into the text where the tables are applicable. The information should complement but not duplicate that contained in the text. Use one horizontal line under the title, a second under the column heads, and a third below the Table, above any footnotes. Vertical and italic lines should be omitted.

Notes in tables and illustrations

Data that are not statistically significant should not be noted. $^{a}P<0.05$, $^{b}P<0.01$ should be noted ($P>0.05$ should not be noted). If there are other series of *P* values, $^{c}P<0.05$ and $^{d}P<0.01$ are used. Third series of *P* values can be expressed as $^{e}P<0.05$ and $^{f}P<0.01$. Other notes in tables or under

illustrations should be expressed as ^1F, ^2F, ^3F; or some other symbols with a superscript (Arabic numerals) in the upper left corner. In a multi-curve illustration, each curve should be labeled with ●, ○, ■, □, ▲, △, *etc.* in a certain sequence.

Acknowledgments

Brief acknowledgments of persons who have made genuine contributions to the manuscripts and who endorse the data and conclusions are included. Authors are responsible for obtaining written permission to use any copyrighted text and/or illustrations.

REFERENCES

Coding system

The author should code the references according the citation order in text in Arabic numerals, put references codes in square brackets, superscript it at the end of citation content or the author name of the citation. For those citation content as the narrate part, the coding number and square brackets should be typeset normally. For example, Crohn's disease (CD) is associated with increased intestinal permeability[1,2]. If references are directly cited in the text, they would be put together with the text, for example, from references [19,22-24], we know that...

When the authors code the references, please ensure that the order in text is the same as in reference part and also insure the spelling accuracy of the first author's name. Do not code the same citation twice.

PMID requirement

PMID roots in the abstract serial number indexed by PubMed (http://www.ncbi.nlm.nih.gov/entrez/query.fcgi?db=PubMed). The author should supply the PMID for journal citation. For those references that have not been indexed by PubMed, a printed copy of the first page of the full reference should be submitted.

The accuracy of the information of the journal citations is very important. Through reference testing system, the authors and editor could check the authors name, title, journal title, publication date, volume number, start page, and end page. We will interlink all references with PubMed in ASP file so that the readers can read the abstract of the citations online immediately.

Style for journal references

Authors: the first author should be typed in bold-faced letter. The surname of all authors should be typed with the initial letter capitalized and followed by their name in abbreviation (For example, Lian-Sheng Ma is abbreviated as Ma LS, Bo-Rong Pan as Pan BR). Title of the cited article and italicized journal title (Journal title should be in its abbreviation form as shown in PubMed), publication date, volume number (in black), start page, and end page [PMID: 11819634]

Note: The author should test the references through reference testing system (http://www.wjgnet.com/cgi-bin/index.pl)

Style for book references

Authors: the first author should be typed in bold-faced letter. The surname of all authors should be typed with the initial letter capitalized and followed by their name in abbreviation (For example, Lian-Sheng Ma is abbreviated as Ma LS, Bo-Rong Pan as Pan BR) Book title. Publication number. Publication place: Publication press, Year: start page and end page.

Format

Journals

English journal article (list all authors and include the PMID where applicable)

1 **Grover VP**, Dresner MA, Forton DM, Counsell S, Larkman DJ, Patel N, Thomas HC, Taylor-Robinson SD. Current and future applications of magnetic resonance imaging and spectroscopy of the brain in hepatic encephalopathy. *World J Gastroenterol* 2006; **12**: 2969-2978 [PMID: 16718775]

Chinese journal article (list all authors and include the PMID where applicable)

2 **Lin GZ**, Wang XZ, Wang P, Lin J, Yang FD. Immunologic effect of Jianpi Yishen decoction in treatment of Pixu-diarrhoea. *Shijie Huaren Xiaohua Zazhi* 1999; **7**: 285-287

In press

3 **Tian D**, Araki H, Stahl E, Bergelson J, Kreitman M. Signature of balancing selection in Arabidopsis. *Proc Natl Acad Sci U S A* 2006; In press

Organization as author

4 **Diabetes Prevention Program Research Group**. Hypertension, insulin, and proinsulin in participants with impaired glucose tolerance. *Hypertension* 2002; **40**: 679-686 [PMID: 12411462]

Both personal authors and an organization as author

5 **Vallancien G**, Emberton M, Harving N, van Moorselaar RJ; Alf-One Study Group. Sexual dysfunction in 1, 274 European men suffering from lower urinary tract symptoms. *J Urol* 2003; **169**: 2257-2261 [PMID: 12771764]

No author given

6 21st century heart solution may have a sting in the tail. *BMJ* 2002; **325**: 184 [PMID: 12142303]

Volume with supplement

7 **Geraud G**, Spierings EL, Keywood C. Tolerability and safety of frovatriptan with short- and long-term use for treatment of migraine and in comparison with sumatriptan. *Headache* 2002; **42** Suppl 2: S93-99 [PMID: 12028325]

Issue with no volume

8 **Banit DM**, Kaufer H, Hartford JM. Intraoperative frozen section analysis in revision total joint arthroplasty. *Clin Orthop Relat Res* 2002; (**401**): 230-238 [PMID: 12151900]

No volume or issue

9 Outreach: bringing HIV-positive individuals into care. *HRSA Careaction* 2002; 1-6 [PMID: 12154804]

Books

Personal author(s)

10 **Sherlock S**, Dooley J. Diseases of the liver and billiary system. 9th ed. Oxford: Blackwell Sci Pub, 1993: 258-296

Chapter in a book (list all authors)

11 **Lam SK**. Academic investigator's perspectives of medical treatment for peptic ulcer. In: Swabb EA, Azabo S. Ulcer disease: investigation and basis for therapy. New York: Marcel Dekker, 1991: 431-450

Author(s) and editor(s)

12 **Breedlove GK**, Schorfheide AM. Adolescent pregnancy. 2nd ed. Wieczorek RR, editor. White Plains (NY): March of Dimes Education Services, 2001: 20-34

Conference proceedings

13 **Harnden P**, Joffe JK, Jones WG, editors. Germ cell tumours V. Proceedings of the 5th Germ Cell Tumour Conference; 2001 Sep 13-15; Leeds, UK. New York: Springer, 2002: 30-56

Conference paper

14 **Christensen S**, Oppacher F. An analysis of Koza's computational effort statistic for genetic programming. In: Foster JA, Lutton E, Miller J, Ryan C, Tettamanzi AG, editors. Genetic programming. EuroGP 2002: Proceedings of the 5th European Conference on Genetic Programming; 2002 Apr 3-5; Kinsdale, Ireland. Berlin: Springer, 2002: 182-191

Electronic journal (list all authors)

Morse SS. Factors in the emergence of infectious diseases. Emerg Infect Dis serial online, 1995-01-03, cited 1996-06-05; 1(1): 24 screens. Available from: URL: http//www.cdc.gov/ncidod/EID/eid.htm

Patent (list all authors)

16 **Pagedas AC**, inventor; Ancel Surgical R&D Inc., assignee. Flexible endoscopic grasping and cutting device and positioning tool assembly. United States patent US 20020103498. 2002 Aug 1

Inappropriate references

Authors should always cite references that are relevant to their article, and avoid any inappropriate references. Inappropriate references include those that are linked with a hyphen and the difference between the two numbers at two sides of the hyphen is more than 5. For example, [1-6], [2-14] and [1, 3, 4-10, 22] are all considered as inappropriate references. Authors should not cite their own unrelated published articles.

Statistical data

Present as mean ± SD or mean ± SE.

Statistical expression

Express *t* test as *t* (in italics), *F* test as *F* (in italics), chi square test as χ^2 (in Greek), related coefficient as *r* (in italics), degree of freedom as γ (in Greek), sample number as *n* (in italics), and probability as *P* (in italics).

Units

Use SI units. For example: body mass, m (B) = 78 kg; blood pressure, *p*(B) = 16.2/12.3 kPa; incubation time, t (incubation) = 96 h, blood glucose concentration, c (glucose) 6.4 ± 2.1 mmol/L; blood CEA mass concentration, p (CEA) = 8.6 24.5 μg/L; CO_2 volume fraction, 50 mL/L CO_2 not 5% CO_2; likewise for 40 g/L formaldehyde, not 10% formalin; and mass fraction, 8 ng/g, *etc.* Arabic numerals such as 23, 243, 641 should be read 23 243 641.

The format about how to accurately write common units and quantum is at: http://www.wjgnet.com/wjg/help/15.doc

Abbreviations
Standard abbreviations should be defined in the abstract and on first mention in the text. In general, terms should not be abbreviated unless they are used repeatedly and the abbreviation is helpful to the reader. Permissible abbreviations are listed in Units, Symbols and Abbreviations: A Guide for Biological and Medical Editors and Authors (Ed. Baron DN, 1988) published by The Royal Society of Medicine, London. Certain commonly used abbreviations, such as DNA, RNA, HIV, LD50, PCR, HBV, ECG, WBC, RBC, CT, ESR, CSF, IgG, ELISA, PBS, ATP, EDTA, mAb, can be used directly without further mention.

Italics
Quantities: *t* time or temperature, *c* concentration, *A* area, *l* length, *m* mass, *V* volume.
Genotypes: *gyr*A, *arg* 1, *c myc*, *c fos*, *etc.*
Restriction enzymes: *Eco*RI, *Hin*dI, *Bam*HI, *Kbo* I, *Kpn* I, *etc.*
Biology: *H pylori, E coli, etc.*

SUBMISSION OF THE REVISED MANUSCRIPTS AFTER ACCEPTED

Please revise your article according to the revision policies of *WJG*. The revised version including manuscript and high-resolution image figures (if any) should be copied on a floppy or compact disk. Author should send the revised manuscript, along with printed high-resolution color or black and white photos, copyright transfer letter, the final check list for authors, and responses to reviewers by a courier (such as EMS) (submission of revised manuscript by e-mail or on the *WJG* Editorial Office Online System is NOT available at present).

Language evaluation
The language of a manuscript will be graded before sending for revision. (1) Grade A: priority publishing; (2) Grade B: minor language polishing; (3) Grade C: a great deal of language polishing; (4) Grade D: rejected. The revised articles should be in grade B or grade A.

Copyright assignment form
Please downloaded CAF from http://www.wjgnet.com/wjg/help/9.doc.

We certify that the material contained in this manuscript:

Ms:

Title:

is original, except when appropriately referenced to other sources, and that written permission has been granted by any existing copyright holders. We agree to transfer to WJG all rights of our manuscript, including: (1) all copyright ownership in all print and electronic formats; (2) the right to grant permission to republish or reprint the stated material in whole or in part, with or without a fee; (3) the right to print copies for free distribution or sale; (4) the right to republish the stated material in a collection of articles or in any other format. We also agree that our article be put on the Internet.

Criteria for authorship: The WJG requests and publishes information about contributions of each author named to the submitted study. Authorship credit should be based on (1)direct participation in the study, including substantial contributions to conception and design of study, or acquisition of data, or analysis and interpretation of data; (2) manuscript writing, including drafting the article, or revising it critically for important intellectual content; (3)supportive work, including statistical analysis of data, or acquisition of funding, or administration, technology and materials support, or supervision, or supportive contributions. Authors should meet at least one of the three conditions. The WJG does not publish co-first authors and co-corresponding authors.

We hereby assign copyright transfer to WJG if this paper is accepted.

Author Name in full (Full names should be provided, with first name first, followed by middle names and family name at the last, eg, Eamonn MM Quigley). Handwritten names are not accepted.

Author Name in abbreviation (Family name is put first in full, followed by middle names and first name in abbreviation with first letter in capital, eg, Quigley EMM). Handwritten names are not accepted.

1 Full Name: _____
Abbreviation Name: _____
Signed: _____
Date: _____

2 Full Name: _____
Abbreviation Name: _____
Signed: _____
Date: _____

3 Full Name: _____
Abbreviation Name: _____
Signed: _____
Date: _____

4 Full Name: _____
Abbreviation Name: _____
Signed: _____
Date: _____

5 Full Name: _____
Abbreviation Name: _____
Signed: _____
Date: _____

6 Full Name: _____
Abbreviation Name: _____
Signed: _____
Date: _____

7 Full Name: _____
Abbreviation Name: _____
Signed: _____
Date: _____

8 Full Name: _____
Abbreviation Name: _____
Signed: _____
Date: _____

9 Full Name: _____
Abbreviation Name: _____
Signed: _____
Date: _____

10 Full Name: _____
Abbreviation Name: _____
Signed: _____
Date: _____

Final check list for authors
The format is at: http://www.wjgnet.com/wjg/help/13.doc

Responses to reviewers
Please revise your article according to the comments/suggestions of reviewers. The format for responses to the reviewers' comments is at: http://www.wjgnet.com/wjg/help/10.doc

Proof of financial support
For paper supported by a foundation, authors should provide a copy of the document and serial number of the foundation.

Publication fee
Authors of accepted articles must pay publication fee.
EDITORIAL and LETTERS TO THE EDITOR are free of change.

World Journal of Gastroenterology®

Volume 13 Number 8
February 28, 2007

National Journal Award
2005

The WJG Press

The WJG Press, Apartment 1066 Yishou Garden, 58 North Langxinzhuang Road, PO Box 2345, Beijing 100023, China
Telephone: +86-10-85381901
Fax: +86-10-85381893
E-mail: wjg@wjgnet.com
http: //www.wjgnet.com

ISSN 1007-9327 CN 14-1219/R Local Post Offices Code No. 82-261

World Journal of Gastroenterology www.wjgnet.com Volume 13 Number 8 Feb 28 2007

ISSN 1007-9327
CN 14-1219/R

World Journal of Gastroenterology®

Indexed and Abstracted in:
Current Contents®/Clinical Medicine, Science Citation Index Expanded (also known as SciSearch®) and Journal Citation Reports/Science Edition, *Index Medicus*, MEDLINE and PubMed, Chemical Abstracts, EMBASE/Excerpta Medica, Abstracts Journals, *Nature Clinical Practice Gastroenterology and Hepatology*, CAB Abstracts and Global Health.
ISI JCR 2003-2000 IF: 3.318, 2.532, 1.445 and 0.993.

Volume 13 Number 8
February 28, 2007

World J Gastroenterol
2007 February 28; 13(8): 1149-1312
Online Submissions
www.wjgnet.com/wjg/index.jsp
www.wjgnet.com
Printed on Acid-free Paper

A Weekly Journal of Gastroenterology and Hepatology

National Journal Award
2005

World Journal of Gastroenterology®

Volume 13 Number 8
February 28, 2007

The WJG Press

Contents

Contents

World Journal of Gastroenterology
Volume 13 **Number** 8 **February** 28, 2007

World Journal of Gastroenterology
Volume 13 **Number** 8 **February** 28, 2007

Contents

Responsible E-Editor for this issue: Wei Lu

C-Editor for this issue: George Y Wu, Professor

Responsible S-Editor for this issue: Ye Liu

World Journal of Gastroenterology (*World J Gastroenterol , WJG*), a leading international journal in gastroenterology and hepatology, has an established reputation for publishing first class research on esophageal cancer, gastric cancer, liver cancer, viral hepatitis, colorectal cancer, and *H pylori* infection, providing a forum for both clinicians and scientists, and has been indexed and abstracted in Current Contents®/Clinical Medicine, Science Citation Index Expanded (also known as SciSearch®) and Journal Citation Reports/Science Edition, *Index Medicus*, MEDLINE and PubMed, Chemical Abstracts, EMBASE/Excerpta Medica, Abstracts Journals, *Nature Clinical Practice Gastroenterology and Hepatology*, CAB Abstracts and Global Health. ISI JCR 2003-2000 IF: 3.318, 2.532, 1.445 and 0.993. *WJG* is a weekly journal published by The WJG Press. The publication date is on 7th, 14th, 21st, and 28th every month. The *WJG* is supported by The National Natural Science Foundation of China, No. 30224801 and No.30424812, which was founded with a name of *China National Journal of New Gastroenterology* on October 1,1995, and renamed as *WJG* on January 25, 1998.

PUBLISHED BY
The WJG Press

PRINTED BY
Printed in Beijing on acid-free paper by Beijing Kexin Printing House

 Print ISSN 1007-9327
CN 14-1219/R.

EDITORIAL OFFICE
World Journal of Gastroenterology,
The WJG Press, Apartment 1066 Yishou Garden, 58 North Langxinzhuang Road, PO Box 2345, Beijing 100023, China
Telephone: +86-10-85381892
Fax: +86-10-85381893
E-mail: wjg@wjgnet.com
http://www.wjgnet.com

SUBSCRIPTION AND AUTHOR REPRINTS
Jing Wang
The WJG Press, Apartment 1066 Yishou Garden, 58 North Langxinzhuang Road, PO Box 2345, Beijing 100023, China
Telephone: +86-10-85381892
Fax: +86-10-85381893
E-mail: j.wang@wjgnet.com
http://www.wjgnet.com

SUBSCRIPTION INFORMATION
Institutional Price 2007: USD 1500.00
Personal Price 2007: USD 700.00

INSTRUCTIONS TO AUTHORS
Full instructions are available online at http://www.wjgnet.com/wjg/help/instructions.jsp. If you do not have web access please contact the editorial office.

PO Box 2345, Beijing 100023, China
www.wjgnet.com
wjg@wjgnet.com

World J Gastroenterol 2007 February 28; 13(8): 1149-1155
World Journal of Gastroenterology ISSN 1007-9327

EDITORIAL

Practical guidelines for the treatment of inflammatory bowel disease

T Kuhbacher, UR Fölsch

T Kuhbacher, UR Fölsch, Department of Internal Medicine, University Hospital Schleswig-Holstein, Campus Kiel, Schittenhelmstr.12, Kiel 24105, Germany
Correspondence to: UR Fölsch, Department of Internal Medicine, University Hospital Schleswig-Holstein, Campus Kiel, Schittenhelmstr.12, 24105 Kiel,
Germany. urföelsch@1med.uni-kiel.de
Telephone: +49-431-5971271 Fax: +49-431-5971271
Received: 2006-07-11 Accepted: 2006-12-28

Abstract

In recent years, great progress has been made regarding the treatment of inflammatory bowel disease (IBD), particularly in the field of biological therapies. Nevertheless, the ultimate treatment is not in sight. With the development of new medication, it has become clear that we need a new understanding of IBD. Therapy needs to fit the different subtypes of IBD; e.g. mild disease in comparison to severe chronic active disease or Crohn's disease with or without fistulation or stenosis. The following article gives a practical overview of actual treatments for IBD. The intention of this article is not to provide a complete review of all new scientific developments, but to give a practical guideline for therapy of IBD.

Key words: Inflammatory bowel disease; Ulcerative colitis; Crohn's disease; Immunomodulators; Anti-tumor necrosis factor

Kuhbacher T, Fölsch UR. Practical guidelines for the treatment of inflammatory bowel disease. *World J Gastroenterol* 2007; 13(8): 1149-1155

http://www.wjgnet.com/1007-9327/13/1149.asp

INTRODUCTION

Crohn's disease and ulcerative colitis are both defined as inflammatory bowel diseases (IBD), characterized by a chronic inflammation of the gut mucosa. The clinical course of both diseases can differ from a mild form, in which the patient reaches long-term remission without taking permanent medication, to a chronic active form, in which remission is only reached by permanently taking immunosuppressives and/or biologics or by taking them for a long period of time. Patients are not only burdened by the most common symptoms of IBDs; e.g. diarrhea, bowel pain, fever and complications such as fistulation, stenosis and abscesses in Crohn's disease and megacolon in ulcerative colitis, but are also burdened by the side-effects of the therapeutics, which the patients take to achieve a normal quality of life. Therefore, it is a great responsibility for a physician to consider treatment for an individual patient.

Recent discussions in the field of IBD are concerned with recommendations for a step-down or step-up therapy. A step-down therapy means using the most effective biologic or immunosuppressive treatment on the market, even without prior use of therapeutics such as steroids, in order to reach an effective remission as soon as possible. A step-up therapy means using a "classical" treatment by, for example, starting with aminosalicylates and ending up with an immunosuppressive and/or biological. Even if using a common step-up therapy treatment, the decision about which drug to use should be based on the individual patient, considering the clinical course and diagnosed complications according to current treatment guidelines.

This article provides a short overview of IBD and practical guidelines for the actual treatment of IBD (Figures 1 and 2). It is recognized that there is still an urgent medical need for improvement in the treatment in IBD and that treatments may not be sufficient for all patients, although great progress has been made in therapeutic approaches in the last decades (especially regarding biological therapeutics). The current guidelines for IBD therapy are distinguished by the course, place and severity of the clinical disease[1-7]. In Crohn's disease, a mild active form, a moderate or severe active form or a severe chronically active form can be differentiated. Patients can also be defined as steroid-dependent or steroid-refractory. The endoscopic and clinical pattern, the segments of the body that are involved (e.g. only small colon or small and large colon and/or stomach), the complications (such as fistulation and/or stenosis) as well as the duration of the inflammation and the response (or loss of response) to steroids are taken into account in the evaluation. In ulcerative colitis, differentiation is easier because inflammation only involves the large colon, starting from the rectum to the coecum. Therefore, treatment is determined by the clinical disease course and the involved segments of the colon, such as left-sided disease or pancolitis, as well as the response to steroids

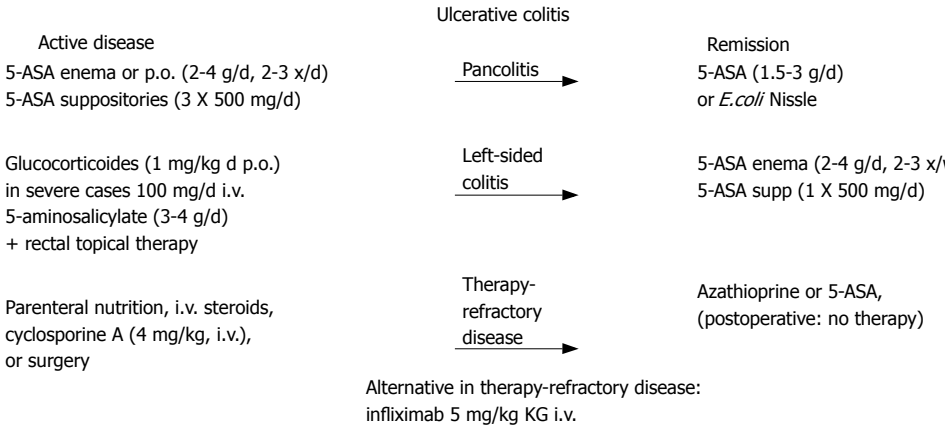

Figure 1 Short overview of the treatment regime of ulcerative colitis.

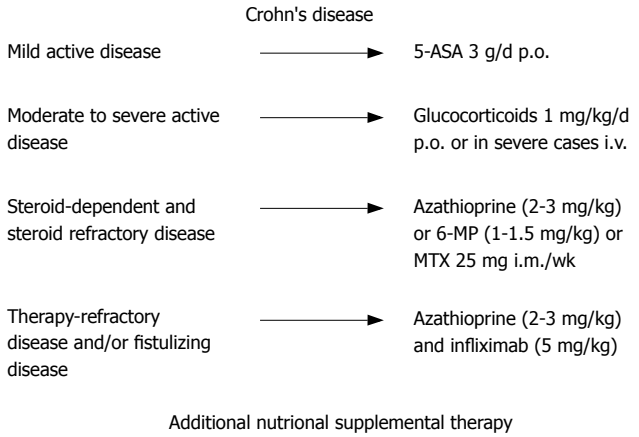

Figure 2 Short overview of treatment regimen in Crohn´s disease.

(steroid-dependent or steroid-refractory). In the following paragraphs the treatment of IBD will be discussed according to use of different therapeutic drugs.

5-Aminosalicylates (5-ASA)

5-ASA are bowel-specific drugs that are metabolized in the gut where the predominant actions occur. As a derivative of salicylic acid, 5-ASA is also an antioxidant that traps free radicals, which are potentially damaging by-products of metabolism. In the radical induction theory of ulcerative colitis, 5-ASA functions as a free radical trap as well as an anti-inflammatory drug. 5-ASA is considered to be the active moiety of sulphasalazine, which metabolizes to it. Oral and/or topical 5-ASA is recommended for mild to moderate ulcerative colitis to induce and maintain remission. The dosage of 5-ASA should be no less than 3 g/d. In practice, most patients do not like a topical treatment, but in left-sided disease, an enema with 4 g of 5-ASA 2 times per day or suppositories with 500 mg 5-ASA 3 times per day are most effective. Sometimes it is helpful for the patient to use the enema only in the evening and the suppositories in the morning. In Crohn's disease, aminosalicylates should also be used in initial therapy for mild disease, although discussion about efficacy has increased recently. In contrast to ulcerative colitis, the use of aminosalicylates for the maintenance of remission is not recommended for Crohn's disease because clinical studies have not shown success in remission maintenance[8,9]. 5-ASA is a standard treatment for ulcerative colitis, but not for Crohn's disease. In the last few years, new formulations have been on the market with varying clinical value. In some special cases; e.g. patients with an ileostoma, a formulation that sets metabolites free prior to the large bowel may be helpful. In patients with IBD and arthritis, sulphasalazine rather than 5-ASA formulations seems to be more effective regarding arthritis. In most patients, the side-effects are not very severe with headache as one of the most common side-effects. However, in some cases nephritis, pancreatitis and hair loss have been reported, which suggests regular monitoring of renal and liver enzymes at least once in three months.

Antibiotics

Antibiotics (e.g. metronidazole) play only a minor role in the additional treatment of fistulizing disease[10]. Although metronidazole (for up to 3 mo in a dosage of 400 mg 2 times per day) is often used in post-operative management after an ileocecal resection or fistula/abscess operation for Crohn's disease, this therapy is not based on study evidence. A side-effect of long-term treatment with metronidazole is polyneuropathy and monitoring is, therefore, required. Antibiotics are also used in the conservative treatment of small abscesses. Understanding the role of microbiota and antibiotics in IBD may become important in the future, but currently clinical studies have not provided support for this concern.

Corticosteroids

In patients with moderate to severe Crohn's disease or ulcerative colitis, corticosteroids are effective for the induction of clinical response and remission[11-16]. Dosages from 40-60 mg/d or 1 mg/kg per day orally are effective for the induction of remission. After the induction of remission, the steroid dose should be tapered (10 mg/wk until 40 mg; 5 mg/wk until 20 mg, followed by a tapering of 2.5 mg/wk). In severe disease, the application of parenteral glucocorticoids as soon as possible is useful for an anti-inflammatory response. Before the initiation of steroid treatment, the presence of an abscess should be excluded. In patients who have been on glucocorticoids

for more than one month, an ACTH (Adrenocorticotropic hormone)-Test should be performed before beginning tapering of the steroid. The ACTH-test can detect deficient cortisol production in the body. If there is a deficiency, hydrocortisone should be used as a substitute.

Budesonide

The benefits of glucocorticoid therapy should be carefully balanced against possible side-effects. Budesonide can reduce typical steroid side effects by a 90% first-pass metabolism in the liver and erythrocytes. Due to a special structural formulation, budesonide achieves the best anti-inflammatory effect in ileocecal inflammation[17-20]. Therefore, it is useful in therapy for Crohn's disease with ileocecal inflammation only. However, neither budesonide nor any other glucocorticosteroid should be used for a maintenance therapy due to the side-effects (e.g. Cushing-syndrome, osteoporosis or cardiomyopathy[21,22]). All patients treated with corticosteroids should additionally receive vitamin D and calcium substitution to avoid bone loss.

Immunosuppressives

The clinical course of 36% of IBD patients is defined as steroid-refractory and in 20% as steroid-dependent[23]. Immunomodulators are, therefore, recommended for the treatment of chronic active IBD. Studies have shown an efficacy for immunosuppressives that is similar to azathioprine and its metabolite, 6-mercaptopurine (6-MP; 2-3 mg/kg per day, resp. 1-1.5 mg/kg per day), in the long-term use of chronic active disease. Immunomodulators have been shown to be efficient for the control of inflammation and remission maintenance. Only limited data exists on the efficacy of immunosuppressants in fistulizing Crohn's disease and the prevention of post-operative recurrence[24-30]. Evidence-based data is missing on the post-operative use of azathioprine and many IBD referral centers are using azathioprine for the prevention of post-operative recurrence. Prior to an initiation of treatment with azathioprine or 6-MP, patients should be thiopurine methyltransferase (TPMT) genotype assessed in order to detect for a homozygous deficiency in TPMT in an effort to avert AZA or 6-MP-induced potential adverse events. All patients on azathioprine or 6-MP should be monitored weekly in the first month and after that once a month regarding their white blood count and liver enzymes because a myelosuppression or an elevation of liver enzymes subsequent to the use of azathioprine or 6-MP can occur. In such cases, the dosage of azathioprine or 6-MP should be reduced or paused until lab values are normal. In patients with gastrointestinal side-effects after the intake of azathioprine, a change to 6-MP should be considered.

Methotrexate and cyclosporine

Methotrexate is another immunomodulatory agent that is used in long-term treatment of IBD. The dosage for induction of remission in chronic active disease is 25 mg i.m. per week for 16 wk, followed by a maintenance treatment of 15 mg i.m. per week. In contrast to azathioprine and 6-MP, the data on use of methotrexate is rather scarce[31-33]. Cyclosporine is reserved for the treatment of severe steroid-refractory ulcerative colitis only. Intravenous cyclosporine (2-4 mg/kg) was able to prevent a decidered colectomy in two of three patients with severe ulcerative colitis. Due to its toxicity, use should be considered carefully; i.e. it should be used only in very severe active disease cases to avoid a colectomy. In Crohn' s disease, cyclosporine has been shown to be effective only in fistulizing, but not luminal disease[34-37].

Tacrolimus

Only very inadequate data is available for tacrolimus. Improvement of fistula drainage, but not closure was demonstrated in a randomized, placebo-controlled trial with tacrolimus[38,39].

Infliximab

Biological therapies, especially anti-TNF agents, play a pivotal role in the treatment of chronic active IBD and fistulizing disease[40-43]. The first anti-TNF agent on the market, infliximab, is a chimeric IgG1 mouse/human monoclonal antibody. Randomised, placebo-controlled trials (ACCENT I and Ⅱ) demonstrated the efficacy of infliximab (5 mg/kg, i.v.) in the induction of clinical response and remission in patients with active Crohn´ s disease. In fistulizing disease, complete fistula closure of at least 50% of the fistulas could be seen in 55% of the patients after three infusions of infliximab at wk 0, 2 and 6 (ACCENT Ⅱ). Given on a regular basis in intervals of 8-12 wk (5 mg/kg i.v.), infliximab is able to maintain remission[44-50].

In ulcerative colitis, the recently completed ACT I and ACT Ⅱ randomised, placebo-controlled trials demonstrated the efficacy of infliximab treatment in induction of remission and mucosal healing in 61.2% of the infliximab treated patients *versus* 32.4% of placebo treated patients[51,52].

Contraindications and side-effects should be taken into consideration carefully prior to infliximab therapy[53]. Due to immunogenicity, infliximab can lead to the formation of human anti-chimeric antibodies (HACA) in 30% to 75% of the patients. Additional administration of immunosuppressants; e.g. azathioprine and/or pretreatment with intravenous prednisolone, can reduce the risks of HACA formation. The main reported side-effect is an infusion reaction, which can occur as an acute allergic/anaphylactic reaction or a delayed hypersensitivity reaction. In clinical trials, observations have included infections, drug-induced lupus, cardiac failure, non-Hodgkin's lymphoma and, in post-marketing surveillance, tuberculosis, pneumonia, histoplasmosis, listeriosis and aspergillosis. To avoid a potential tuberculosis reactivation, a purified protein derivative (PPD) skin test and a chest-X-ray should be performed prior to infliximab treatment[54-67]. Patients with perianal or enterocutaneous fistulizing Crohn's disease should be treated first with infliximab. The effect of infliximab is not as effective on entero-enteral or recto-vaginal fistulas. Patients with steroid-refractory or chronic active Crohn's disease or ulcerative colitis who do not respond to immunosuppressive therapy alone should also be treated with infliximab. The recommended

treatment regimen is an induction scheme with three infusions (5 mg/kg i.v.) at 0, 2 and 6 wk, followed by a maintenance treatment of infliximab every 8 wk (5 mg/kg i.v.). Additionally, immunosuppressive therapy with azathioprine, for example, is recommended. HACA testing is not recommended routinely for every patient on infliximab, but it is recommended if there is a delayed hypersensitivity reaction or if the last infliximab infusion was more than 12 wk previous.

Adalimumab

Other TNF agents also showed efficacy in Crohn's disease. The human IgG1 antibody adalimumab, which is a therapeutic agent used for rheumatoid arthritis, was effective in open-label experience. A placebo-controlled, randomised trial was also conducted. One advantage, in comparison to infliximab, might be the completely human structure of the antibody, which leads to better tolerance and a subcutaneous route of administration. Data on adverse reactions in Crohn's disease patients are still not available, but adalimumab is well-tolerated in patients with rheumatoid arthritis[68-71].

CDP-870

Certolizumab pegol (CDP-870), which is a polyethylene-glycolated Fab-fragment of the anti-tumour necrosis factor, has been shown to be effective in the treatment of Crohn's disease in a recent published, randomised, placebo-controlled trial. At week ten, 52.8% of the certolizumab (400 mg) treated patients showed a clinical response versus 30.1% in the placebo treated group (the high placebo response was seen in a large patient subgroup with low C-reactive protein levels; this might have been due to statistical separation between treatment and placebo group[72]). The antibody was well tolerated. Ongoing trials, however, are necessary to establish efficacy in Crohn's disease.

CDP-571

CDP-571, which is a humanized IgG4 monoclonal antibody against tumour necrosis factor alpha, initially showed an induction of clinical response in controlled trials, but failed in a phase Ⅲ trial which was discontinued[73].

Onercept and eternacept

Onercept, which is a recombinant human p55 soluble receptor to TNF, and also eternacept, which is a recombinant human p75 soluble receptor to TNF, failed in a phase Ⅱ trial with Crohn's disease and both trials were discontinued[74-76].

Natalizumab

Adhesion molecule inhibiting agents, such as natalizumab, which is a humanized IgG4 antibody, demonstrated a clinical response in a clinical trial in Crohn's disease, but all trials had to be stopped immediately after cases of progressive multifocal leucencephalopathy in patients receiving natalizumab for multiple sclerosis were reported[77-79].

The antisense oligonucleotide of the adhesion molecule ICAM-1 (anti-ICAM-1) was ineffective in Crohn's disease[80].

A hopeful, novel approach for the treatment of Crohn's disease is an anti-IL-12/IL-23p40 antibody that proved effective for induction of response and remission in a phase Ⅱ study[81].

β-Interferon

The use of β-Interferon, which has been investigated in a small pilot study in ulcerative colitis with a subcutaneous administration, seems to be effective, but larger, randomised, placebo-controlled studies need to be performed to clarify the clinical efficacy[82].

In conclusion, the only biological therapeutic today, which has been proven effective in IBD and is available on the market is infliximab. The market release of new TNF agents might happen in the near future.

Probiotics

A different group of therapeutic agents for therapy of IBD are probiotics. The use of probiotics has been advocated in colonic inflammatory disease for a long time. Only recently, two controlled trials demonstrated that E. coli nissle is as effective as 5-ASA for remission maintenance in ulcerative colitis[83,84]. For remission maintenance and pouchitis, studies demonstrated the benefit of probiotics[85,86]. Due to a better understanding of the molecular events and the pathophysiological processes of this disease, it is hoped that more probiotic agents will be developed in the near future.

5-ASA

A short, practical guideline would be incomplete without discussing IBD and pregnancy. 5-ASA is not harmful during pregnancy and there is very little placental transport. 5-ASA should be avoided during breast feeding because there are no studies on 5-ASA use during breast feeding[87]. Acute disease or a flare up of IBD can be treated throughout an entire pregnancy with steroids. Glucocorticoids pass the placental barrier, but there has been no significant evidence of teratogenesis. There have been some observations of cleft lip and palate associated with the intake of steroids. In general, no increase in fetal complications have been found with use of 5-ASA compared to the general population[88].

Azathioprine or 6-mercaptupurine

The use of azathioprine or 6-mercaptupurine should not be completed during pregnancy. Extensive experience with use of these substances during pregnancy exists with other autoimmune diseases and patients who received renal transplants. No teratogenic effects in humans have been reported so far. However, it is very important to discuss all the data and possible complications with the patient and it is essential that the decision to take the drug should be made by the patient[89].

Methotrexate is contraindicated during pregnancy as it is mutagenic and teratogenic[90]. Cyclosporine is not teratogenic, but due to its side-effects, it needs to be considered very carefully and should only be used to avoid a colectomy[91]. Infliximab should not be given as

maintenance therapy during pregnancy. In very severe disease, it can be considered as an emergency therapy[92]. Nutrition has not been discussed in this article so far. However, the balance of trace elements and vitamins is essential for successful therapy. Vitamin B12 and folinic acid, for example, should be monitored in Crohn's disease patients with ileal inflammation to avoid a deficiency syndrome, which can lead to severe anemia. Also ferritin should be monitored and, if necessary, substituted orally or intravenously to avoid severe iron deficiency anemia. In severe cases of iron deficiency anemia, erythropoietin (10 000IE s.c. 3 times per week) plus iron i.v. (62.5 mg in 250 mL NaCl) is effective[93]. In severe ulcerative colitis or Crohn's disease, patients profit from short term parenteral or additional high calorie nutrition[94].

All above treatment regimens attempt to avoid complications and inflammation in IBD. However, all conservative therapy sometimes fails or is not effective enough. Examples might be therapy for refractory ulcerative colitis, which can only be successfully treated by an operation (e.g. a colectomy with an ileoanal pouch anastomosis), non-inflammatory stricture in Crohn's disease or severe fistulizing disease, in which a protective ileostoma can be very useful for supporting conservative treatment. In such cases, close collaboration with an experienced IBD surgeon is essential.

It can be summarized that although a number of new biological agents have been developed in the last decades for the treatment of IBD, there is still a great need for new pharmcotherapeutics, particularly for chronic refractory disease patients with multiple complications.

REFERENCES

1 **Hanauer SB**, Meyers S. Management of Crohn's disease in adults. *Am J Gastroenterol* 1997; **92**: 559-566

2 **Stange EF**, Schreiber S, Fölsch UR, von Herbay A, Schölmerich J, Hoffmann J, Zeitz M, Fleig WE, Buhr HJ, Kroesen AJ, Moser G, Matthes H, Adler G, Reinshagen M, Stein J.Diagnostics and treatment of Crohn's disease -- results of an evidence-based consensus conference of the German Society for Digestive and Metabolic Diseases. *Z Gastroenterol* 2003; **41**: 19-20

3 **Hoffmann JC**, Zeitz M, Bischoff SC, Brambs HJ, Bruch HP, Buhr HJ, Dignass A, Fischer I, Fleig W, Fölsch UR, Herrlinger K, Höhne W, Jantschek G, Kaltz B, Keller KM, Knebel U, Kroesen AJ, Kruis W, Matthes H, Moser G, Mundt S, Pox C, Reinshagen M, Reissmann A, Riemann J, Rogler G, Schmiegel W, Schölmerich J, Schreiber S, Schwandner O, Selbmann HK, Stange EF, Utzig M, Wittekind C.Diagnosis and therapy of ulcerative colitis: results of an evidence based consensus conference by the German society of Digestive and Metabolic Diseases and the competence network on inflammatory bowel disease. *Z Gastroenterol* 2004; **42**: 979-983

4 **Rutgeerts PJ**. Conventional treatment of Crohn's disease: objectives and outcomes. *Inflamm Bowel Dis* 2001; **7** Suppl 1: S2-S8

5 **Kühbacher T**, Schreiber S, Fölsch UR. Ulcerative colitis: conservative management and long-term effects. *Langenbecks Arch Surg* 2004; **389**: 350-353

6 **Feagan BG**. Maintenance therapy for inflammatory bowel disease. *Am J Gastroenterol* 2003; **98**: S6-S17

7 **Hanauer SB**, Present DH. The state of the art in the management of inflammatory bowel disease. *Rev Gastroenterol Disord* 2003; **3**: 81-92

8 **Cammà C**, Giunta M, Rosselli M, Cottone M. Mesalamine in the maintenance treatment of Crohn's disease: a meta-analysis adjusted for confounding variables. *Gastroenterology* 1997; **113**: 1465-1473

9 **Sutherland L**, Roth D, Beck P, May G, Makiyama K. Oral 5-aminosalicylic acid for inducing remission in ulcerative colitis. *Cochrane Database Syst Rev* 2000; (**2**): CD000543

10 **Thukral C**, Travassos WJ, Peppercorn MA. The Role of Antibiotics in Inflammatory Bowel Disease. *Curr Treat Options Gastroenterol* 2005; **8**: 223-228

11 **Summers RW**, Switz DM, Sessions JT, Becktel JM, Best WR, Kern F, Singleton JW. National Cooperative Crohn's Disease Study: results of drug treatment. *Gastroenterology* 1979; **77**: 847-869

12 **Malchow H**, Ewe K, Brandes JW, Goebell H, Ehms H, Sommer H, Jesdinsky H. European Cooperative Crohn's Disease Study (ECCDS): results of drug treatment. *Gastroenterology* 1984; **86**: 249-266

13 **Truelove SC**, Witts LJ. Cortisone in ulcerative colitis; final report on a therapeutic trial. *Br Med J* 1955; **2**: 1041-1048

14 **Modigliani R**, Mary JY, Simon JF, Cortot A, Soule JC, Gendre JP, Rene E. Clinical, biological, and endoscopic picture of attacks of Crohn's disease. Evolution on prednisolone. Groupe d'Etude Thérapeutique des Affections Inflammatoires Digestives. *Gastroenterology* 1990; **98**: 811-818

15 **Shepherd HA**, Barr GD, Jewell DP. Use of an intravenous steroid regimen in the treatment of acute Crohn's disease. *J Clin Gastroenterol* 1986; **8**: 154-159

16 **Smith RC**, Rhodes J, Heatley RV, Hughes LE, Crosby DL, Rees BI, Jones H, Evans KT, Lawrie BW. Low dose steroids and clinical relapse in Crohn's disease: a controlled trial. *Gut* 1978; **19**: 606-610

17 **Ferguson A**, Campieri M, Doe W, Persson T, Nygård G. Oral budesonide as maintenance therapy in Crohn's disease--results of a 12-month study. Global Budesonide Study Group. *Aliment Pharmacol Ther* 1998; **12**: 175-183

18 **Thomsen OO**, Cortot A, Jewell D, Wright JP, Winter T, Veloso FT, Vatn M, Persson T, Pettersson E. A comparison of budesonide and mesalamine for active Crohn's disease. International Budesonide-Mesalamine Study Group. *N Engl J Med* 1998; **339**: 370-374

19 **Hellers G**, Cortot A, Jewell D, Leijonmarck CE, Löfberg R, Malchow H, Nilsson LG, Pallone F, Pena S, Persson T, Prantera C, Rutgeerts P. Oral budesonide for prevention of postsurgical recurrence in Crohn's disease. The IOIBD Budesonide Study Group. *Gastroenterology* 1999; **116**: 294-300

20 **Löfberg R**, Rutgeerts P, Malchow H, Lamers C, Danielsson A, Olaison G, Jewell D, Ostergaard Thomsen O, Lorenz-Meyer H, Goebell H, Hodgson H, Persson T, Seidegård C. Budesonide prolongs time to relapse in ileal and ileocaecal Crohn's disease. A placebo controlled one year study. *Gut* 1996; **39**: 82-86

21 **Lukert BP**, Raisz LG. Glucocorticoid-induced osteoporosis: pathogenesis and management. *Ann Intern Med* 1990; **112**: 352-364

22 **Chun A**, Chadi RM, Korelitz BI, Colonna T, Felder JB, Jackson MH, Morgenstern EH, Rubin SD, Sacknoff AG, Gleim GM. Intravenous corticotrophin vs. hydrocortisone in the treatment of hospitalized patients with Crohn's disease: a randomized double-blind study and follow-up. *Inflamm Bowel Dis* 1998; **4**: 177-181

23 **Munkholm P**, Langholz E, Davidsen M, Binder V. Frequency of glucocorticoid resistance and dependency in Crohn's disease. *Gut* 1994; **35**: 360-362

24 **Candy S**, Wright J, Gerber M, Adams G, Gerig M, Goodman R. A controlled double blind study of azathioprine in the management of Crohn's disease. *Gut* 1995; **37**: 674-678

25 **Hawthorne AB**, Logan RF, Hawkey CJ, Foster PN, Axon AT, Swarbrick ET, Scott BB, Lennard-Jones JE. Randomised controlled trial of azathioprine withdrawal in ulcerative colitis. *BMJ* 1992; **305**: 20-22

26 **Pearson DC**, May GR, Fick GH, Sutherland LR. Azathioprine and 6-mercaptopurine in Crohn disease. A meta-analysis. *Ann Intern Med* 1995; **123**: 132-142

27 **Pearson DC**, May GR, Fick G, Sutherland LR. Azathioprine for maintaining remission of Crohn's disease. *Cochrane Database Syst Rev* 2000; (**2**): CD000067

28 **Sandborn W**, Sutherland L, Pearson D, May G, Modigliani R, Prantera C. Azathioprine or 6-mercaptopurine for inducing remission of Crohn's disease. *Cochrane Database Syst Rev* 2000; (**2**): CD000545

29 **Hanauer SB**, Korelitz BI, Rutgeerts P, Peppercorn MA, Thisted RA, Cohen RD, Present DH. Postoperative maintenance of Crohn's disease remission with 6-mercaptopurine, mesalamine, or placebo: a 2-year trial. *Gastroenterology* 2004; **127**: 723-729

30 **Korelitz BI**, Adler DJ, Mendelsohn RA, Sacknoff AL. Long-term experience with 6-mercaptopurine in the treatment of Crohn's disease. *Am J Gastroenterol* 1993; **88**: 1198-1205

31 **Sandborn WJ**. A review of immune modifier therapy for inflammatory bowel disease: azathioprine, 6-mercaptopurine, cyclosporine, and methotrexate. *Am J Gastroenterol* 1996; **91**: 423-433

32 **Kozarek RA**, Patterson DJ, Gelfand MD, Botoman VA, Ball TJ, Wilske KR. Methotrexate induces clinical and histologic remission in patients with refractory inflammatory bowel disease. *Ann Intern Med* 1989; **110**: 353-356

33 **Feagan BG**, Fedorak RN, Irvine EJ, Wild G, Sutherland L, Steinhart AH, Greenberg GR, Koval J, Wong CJ, Hopkins M, Hanauer SB, McDonald JW. A comparison of methotrexate with placebo for the maintenance of remission in Crohn's disease. North American Crohn's Study Group Investigators. *N Engl J Med* 2000; **342**: 1627-1632

34 **Lichtiger S**, Present DH, Kornbluth A, Gelernt I, Bauer J, Galler G, Michelassi F, Hanauer S. Cyclosporine in severe ulcerative colitis refractory to steroid therapy. *N Engl J Med* 1994; **330**: 1841-1845

35 **Van Assche G**, D'Haens G, Noman M, Vermeire S, Hiele M, Asnong K, Arts J, D'Hoore A, Penninckx F, Rutgeerts P. Randomized, double-blind comparison of 4 mg/kg versus 2 mg/kg intravenous cyclosporine in severe ulcerative colitis. *Gastroenterology* 2003; **125**: 1025-1031

36 **Egan LJ**, Sandborn WJ, Tremaine WJ. Clinical outcome following treatment of refractory inflammatory and fistulizing Crohn's disease with intravenous cyclosporine. *Am J Gastroenterol* 1998; **93**: 442-448

37 **Lichtenstein GR**, Abreu MT, Cohen R, Tremaine W. American Gastroenterological Association Institute technical review on corticosteroids, immunomodulators, and infliximab in inflammatory bowel disease. *Gastroenterology* 2006; **130**: 940-987

38 **Fellermann K**, Ludwig D, Stahl M, David-Walek T, Stange EF. Steroid-unresponsive acute attacks of inflammatory bowel disease: immunomodulation by tacrolimus (FK506). *Am J Gastroenterol* 1998; **93**: 1860-1866

39 **Sandborn WJ**, Present DH, Isaacs KL, Wolf DC, Greenberg E, Hanauer SB, Feagan BG, Mayer L, Johnson T, Galanko J, Martin C, Sandler RS. Tacrolimus for the treatment of fistulas in patients with Crohn's disease: a randomized, placebo-controlled trial. *Gastroenterology* 2003; **125**: 380-388

40 **van Deventer SJ**. Review article: targeting TNF alpha as a key cytokine in the inflammatory processes of Crohn's disease--the mechanisms of action of infliximab. *Aliment Pharmacol Ther* 1999; **13** Suppl 4: 3-8; discussion 38

41 **Van Assche G**, Vermeire S, Rutgeerts P. Medical treatment of inflammatory bowel diseases. *Curr Opin Gastroenterol* 2005; **21**: 443-447

42 **Rutgeerts PJ**. An historical overview of the treatment of Crohn's disease: why do we need biological therapies? *Rev Gastroenterol Disord* 2004; **4** Suppl 3: S3-S9

43 **Targan SR**, Hanauer SB, van Deventer SJ, Mayer L, Present DH, Braakman T, DeWoody KL, Schaible TF, Rutgeerts PJ. A short-term study of chimeric monoclonal antibody cA2 to tumor necrosis factor alpha for Crohn's disease. Crohn's Disease cA2 Study Group. *N Engl J Med* 1997; **337**: 1029-1035

44 **Hanauer SB**, Feagan BG, Lichtenstein GR, Mayer LF, Schreiber S, Colombel JF, Rachmilewitz D, Wolf DC, Olson A, Bao W, Rutgeerts P. Maintenance infliximab for Crohn's disease: the ACCENT I randomised trial. *Lancet* 2002; **359**: 1541-1549

45 **Present DH**, Rutgeerts P, Targan S, Hanauer SB, Mayer L, van Hogezand RA, Podolsky DK, Sands BE, Braakman T, DeWoody KL, Schaible TF, van Deventer SJ. Infliximab for the treatment of fistulas in patients with Crohn's disease. *N Engl J Med* 1999; **340**: 1398-1405

46 **Hanauer SB**. Efficacy and safety of tumor necrosis factor antagonists in Crohn's disease: overview of randomized clinical studies. *Rev Gastroenterol Disord* 2004; **4** Suppl 3: S18-S24

47 **Sandborn WJ**. New concepts in anti-tumor necrosis factor therapy for inflammatory bowel disease. *Rev Gastroenterol Disord* 2005; **5**: 10-18

48 **Travassos WJ**, Cheifetz AS. Infliximab: Use in Inflammatory Bowel Disease. *Curr Treat Options Gastroenterol* 2005; **8**: 187-196

49 **Rutgeerts P**, Feagan BG, Lichtenstein GR, Mayer LF, Schreiber S, Colombel JF, Rachmilewitz D, Wolf DC, Olson A, Bao W, Hanauer SB. Comparison of scheduled and episodic treatment strategies of infliximab in Crohn's disease. *Gastroenterology* 2004; **126**: 402-413

50 **Rutgeerts P**, D'Haens G, Targan S, Vasiliauskas E, Hanauer SB, Present DH, Mayer L, Van Hogezand RA, Braakman T, DeWoody KL, Schaible TF, Van Deventer SJ. Efficacy and safety of retreatment with anti-tumor necrosis factor antibody (infliximab) to maintain remission in Crohn's disease. *Gastroenterology* 1999; **117**: 761-769

51 **Rutgeerts P**, Feagan BG, Olson A, Johanns J, Travers S, Present D, Sands BE, Sandborn W, Olson A. A Randomized Placebo-Controlled Trial Of Infliximab Therapy for Active Ulcerative Colitis: the Act 1 Trial

52 **Sandborn WJ**, Rachmilewitz D, Hanauer SB, Lichtenstein GR, de Villiers WJ, Olson A,Joharms J, Traverse S, Colombel JF. Infliximab Induction and Maintenance Therapy for Ulcerative Colitis: the Act 2 Trial

53 **Schreiber S**, Campieri M, Colombel JF, van Deventer SJ, Feagan B, Fedorak R, Forbes A, Gassull M, Gendre JP, van Hogezand RA, Lofberg R, Modigliani R, Pallone F, Petritsch W, Prantera C, Rampton D, Seibold F, Vatn M, Zeitz M, Rutgeerts P. Use of anti-tumour necrosis factor agents in inflammatory bowel disease. European guidelines for 2001-2003. *Int J Colorectal Dis* 2001; **16**: 1-11; discussion 12-13

54 **Hanauer SB**, Wagner CL, Bala M, Mayer L, Travers S, Diamond RH, Olson A, Bao W, Rutgeerts P. Incidence and importance of antibody responses to infliximab after maintenance or episodic treatment in Crohn's disease. *Clin Gastroenterol Hepatol* 2004; **2**: 542-553

55 **Baert F**, Noman M, Vermeire S, Van Assche G, D' Haens G, Carbonez A, Rutgeerts P. Influence of immunogenicity on the long-term efficacy of infliximab in Crohn's disease. *N Engl J Med* 2003; **348**: 601-608

56 **Farrell RJ**, Alsahli M, Jeen YT, Falchuk KR, Peppercorn MA, Michetti P. Intravenous hydrocortisone premedication reduces antibodies to infliximab in Crohn's disease: a randomized controlled trial. *Gastroenterology* 2003; **124**: 917-924

57 **Cheifetz A**, Smedley M, Martin S, Reiter M, Leone G, Mayer L, Plevy S. The incidence and management of infusion reactions to infliximab: a large center experience. *Am J Gastroenterol* 2003; **98**: 1315-1324

58 **Hanauer S**, Rutgeerts P, Targan S, D'Haens G, Targan S, Kam L, Present D, Mayer L, Wagner C, LaSorda J, Sands B, Livingston R. Delayed hypersensitivity to infliximab (Remicade) reinfusion after a 2-4 year interval without treatment. *Gastroenterology*. 1999; **116**: A731

59 **Remicade** [package insert]. Malvern. PA: Centocor, 2004

60 **Vermeire S**, Noman M, Van Assche G, Baert F, Van Steen K, Esters N, Joossens S, Bossuyt X, Rutgeerts P. Autoimmunity associated with anti-tumor necrosis factor alpha treatment in Crohn's disease: a prospective cohort study. *Gastroenterology* 2003; **125**: 32-39

61 **Mohan N**, Edwards ET, Cupps TR, Oliverio PJ, Sandberg G, Crayton H, Richert JR, Siegel JN. Demyelination occurring during anti-tumor necrosis factor alpha therapy for inflammatory arthritides. *Arthritis Rheum* 2001; **44**: 2862-2869

62 **Thomas CW**, Weinshenker BG, Sandborn WJ. Demyelination during anti-tumor necrosis factor alpha therapy with

infliximab for Crohn's disease. *Inflamm Bowel Dis* 2004; **10**: 28-31
63 **Brown SL**, Greene MH, Gershon SK, Edwards ET, Braun MM. Tumor necrosis factor antagonist therapy and lymphoma development: twenty-six cases reported to the Food and Drug Administration. *Arthritis Rheum* 2002; **46**: 3151-3158
64 **Kwon HJ**, Coté TR, Cuffe MS, Kramer JM, Braun MM. Case reports of heart failure after therapy with a tumor necrosis factor antagonist. *Ann Intern Med* 2003; **138**: 807-811
65 **Keane J**, Gershon S, Wise RP, Mirabile-Levens E, Kasznica J, Schwieterman WD, Siegel JN, Braun MM. Tuberculosis associated with infliximab, a tumor necrosis factor alpha-neutralizing agent. *N Engl J Med* 2001; **345**: 1098-1104
66 **Lee JH**, Slifman NR, Gershon SK, Edwards ET, Schwieterman WD, Siegel JN, Wise RP, Brown SL, Udall JN, Braun MM. Life-threatening histoplasmosis complicating immunotherapy with tumor necrosis factor alpha antagonists infliximab and etanercept. *Arthritis Rheum* 2002; **46**: 2565-2570
67 **Velayos FS**, Sandborn WJ. Pneumocystis carinii pneumonia during maintenance anti-tumor necrosis factor-alpha therapy with infliximab for Crohn's disease. *Inflamm Bowel Dis* 2004; **10**: 657-660
68 **Papadakis KA**, Shaye OA, Vasiliauskas EA, Ippoliti A, Dubinsky MC, Birt J, Paavola J, Lee SK, Price J, Targan SR, Abreu MT. Safety and efficacy of adalimumab (D2E7) in Crohn's disease patients with an attenuated response to infliximab. *Am J Gastroenterol* 2005; **100**: 75-79
69 **Sandborn WJ**, Hanauer S, Loftus EV, Tremaine WJ, Kane S, Cohen R, Hanson K, Johnson T, Schmitt D, Jeche R. An open-label study of the human anti-TNF monoclonal antibody adalimumab in subjects with prior loss of response or intolerance to infliximab for Crohn's disease. *Am J Gastroenterol* 2004; **99**: 1984-1989
70 **Youdim A**, Vasiliauskas EA, Targan SR, Papadakis KA, Ippoliti A, Dubinsky MC, Lechago J, Paavola J, Loane J, Lee SK, Gaiennie J, Smith K, Do J, Abreu MT. A pilot study of adalimumab in infliximab-allergic patients. *Inflamm Bowel Dis* 2004; **10**: 333-338
71 **Baker DE**. Adalimumab: human recombinant immunoglobulin g1 anti-tumor necrosis factor monoclonal antibody. *Rev Gastroenterol Disord* 2004; **4**: 196-210
72 **Schreiber S**, Rutgeerts P, Fedorak RN, Khaliq-Kareemi M, Kamm MA, Boivin M, Bernstein CN, Staun M, Thomsen OØ, Innes A. A randomized, placebo-controlled trial of certolizumab pegol (CDP870) for treatment of Crohn's disease. *Gastroenterology* 2005; **129**: 807-818
73 **Sandborn WJ**, Feagan BG, Radford-Smith G, Kovacs A, Enns R, Innes A, Patel J. CDP571, a humanised monoclonal antibody to tumour necrosis factor alpha, for moderate to severe Crohn's disease: a randomised, double blind, placebo controlled trial. *Gut* 2004; **53**: 1485-1493
74 **Sandborn WJ**, Hanauer SB, Katz S, Safdi M, Wolf DG, Baerg RD, Tremaine WJ, Johnson T, Diehl NN, Zinsmeister AR. Etanercept for active Crohn's disease: a randomized, double-blind, placebo-controlled trial. *Gastroenterology* 2001; **121**: 1088-1094
75 **D'Haens G**, Swijsen C, Noman M, Lemmens L, Ceuppens J, Agbahiwe H, Geboes K, Rutgeerts P. Etanercept in the treatment of active refractory Crohn's disease: a single-center pilot trial. *Am J Gastroenterol* 2001; **96**: 2564-2568
76 **Rutgeerts P**, Lemmens L, Van Assche G, Noman M, Borghini-Fuhrer I, Goedkoop R. Treatment of active Crohn's disease with onercept (recombinant human soluble p55 tumour necrosis factor receptor): results of a randomized, open-label, pilot study. *Aliment Pharmacol Ther* 2003; **17**: 185-192
77 **Sandborn WJ**, Colombel JF, Enns R, Feagan BG, Hanauer SB, Lawrance IC, Panaccione R, Sanders M, Schreiber S, Targan S, van Deventer S, Goldblum R, Despain D, Hogge GS, Rutgeerts P. Natalizumab induction and maintenance therapy for Crohn's disease. *N Engl J Med* 2005; **353**: 1912-1925
78 **Van Assche G**, Van Ranst M, Sciot R, Dubois B, Vermeire S, Noman M, Verbeeck J, Geboes K, Robberecht W, Rutgeerts P. Progressive multifocal leukoencephalopathy after natalizumab therapy for Crohn's disease. *N Engl J Med* 2005; **353**: 362-368
79 **Kleinschmidt-DeMasters BK**, Tyler KL. Progressive multifocal leukoencephalopathy complicating treatment with natalizumab and interferon beta-1a for multiple sclerosis. *N Engl J Med* 2005; **353**: 369-374
80 **Schreiber S**, Nikolaus S, Malchow H, Kruis W, Lochs H, Raedler A, Hahn EG, Krummenerl T, Steinmann G. Absence of efficacy of subcutaneous antisense ICAM-1 treatment of chronic active Crohn's disease. *Gastroenterology* 2001; **120**: 1339-1346
81 **Mannon PJ**, Fuss IJ, Mayer L, Elson CO, Sandborn WJ, Present D, Dolin B, Goodman N, Groden C, Hornung RL, Quezado M, Yang Z, Neurath MF, Salfeld J, Veldman GM, Schwertschlag U, Strober W. Anti-interleukin-12 antibody for active Crohn's disease. *N Engl J Med* 2004; **351**: 2069-2079
82 **Nikolaus S**, Rutgeerts P, Fedorak R, Steinhart AH, Wild GE, Theuer D, Möhrle J, Schreiber S. Interferon beta-1a in ulcerative colitis: a placebo controlled, randomised, dose escalating study. *Gut* 2003; **52**: 1286-1290
83 **Rembacken BJ**, Snelling AM, Hawkey PM, Chalmers DM, Axon AT. Non-pathogenic Escherichia coli versus mesalazine for the treatment of ulcerative colitis: a randomised trial. *Lancet* 1999; **354**: 635-639
84 **Kruis W**, Schütz E, Fric P, Fixa B, Judmaier G, Stolte M. Double-blind comparison of an oral Escherichia coli preparation and mesalazine in maintaining remission of ulcerative colitis. *Aliment Pharmacol Ther* 1997; **11**: 853-858
85 **Gionchetti P**, Rizzello F, Helwig U, Venturi A, Lammers KM, Brigidi P, Vitali B, Poggioli G, Miglioli M, Campieri M. Prophylaxis of pouchitis onset with probiotic therapy: a double-blind, placebo-controlled trial. *Gastroenterology* 2003; **124**: 1202-1209
86 **Mimura T**, Rizzello F, Helwig U, Poggioli G, Schreiber S, Talbot IC, Nicholls RJ, Gionchetti P, Campieri M, Kamm MA. Once daily high dose probiotic therapy (VSL#3) for maintaining remission in recurrent or refractory pouchitis. *Gut* 2004; **53**: 108-114
87 **Diav-Citrin O**, Park YH, Veerasuntharam G, Polachek H, Bologa M, Pastuszak A, Koren G. The safety of mesalamine in human pregnancy: a prospective controlled cohort study. *Gastroenterology* 1998; **114**: 23-28
88 **Mogadam M**, Dobbins WO, Korelitz BI, Ahmed SW. Pregnancy in inflammatory bowel disease: effect of sulfasalazine and corticosteroids on fetal outcome. *Gastroenterology* 1981; **80**: 72-76
89 **Alstead EM**, Ritchie JK, Lennard-Jones JE, Farthing MJ, Clark ML. Safety of azathioprine in pregnancy in inflammatory bowel disease. *Gastroenterology* 1990; **99**: 443-446
90 **Donnenfeld AE**, Pastuszak A, Noah JS, Schick B, Rose NC, Koren G. Methotrexate exposure prior to and during pregnancy. *Teratology* 1994; **49**: 79-81
91 **Radomski JS**, Ahlswede BA, Jarrell BE, Mannion J, Cater J, Moritz MJ, Armenti VT. Outcomes of 500 pregnancies in 335 female kidney, liver, and heart transplant recipients. *Transplant Proc* 1995; **27**: 1089-1090
92 **Aberra FN**. To be or not to be: infliximab during pregnancy? *Inflamm Bowel Dis* 2006; **12**: 76-78
93 **Schreiber S**, Howaldt S, Schnoor M, Nikolaus S, Bauditz J, Gasché C, Lochs H, Raedler A. Recombinant erythropoietin for the treatment of anemia in inflammatory bowel disease. *N Engl J Med* 1996; **334**: 619-623
94 **O'Sullivan M**, O'Morain C. Nutritional Treatments in Inflammatory Bowel Disease. *Curr Treat Options Gastroenterol* 2001; **4**: 207-213

S- Editor Liu Y **L- Editor** Zhu LH **E- Editor** Che YB

PO Box 2345, Beijing 100023, China
www.wjgnet.com
wjg@wjgnet.com

World J Gastroenterol 2007 February 28; 13(8): 1156-1161
World Journal of Gastroenterology ISSN 1007-9327

EDITORIAL

New aspects in celiac disease

MI Torres, MA López Casado, A Ríos

MI Torres, Department of Experimental Biology, University of Jaén, Jaén 23071, Spain
MA López Casado, Department of Gastroenterology Pediatrics. Hospital Virgen de las Nieves, Granada
A Ríos, Department Cell Biology. University of Granada, Granada
Correspondence to: Dr. Torres MI, Department of Experimental Biology, University of Jaén, Paraje de las Lagunillas s/n, Jaén 23071, Spain. mitorres@ujaen.es
Telephone: +34-953-212762 Fax: +34-953-211875
Received: 2006-09-01 Accepted: 2006-12-21

Abstract

Celiac disease (CD) is a common autoimmune disorder characterized by an immune response to ingested gluten and has a strong HLA association with HLA-DQ2 and HLA-DQ8 molecules, but human HLA-DQ risk factors do not explain the entire genetic susceptibility to gluten intolerance. CD is caused by the lack of immune tolerance (oral tolerance) to wheat gluten. In this sense, the expression of soluble HLA-G in CD is of special interest because the molecule plays an important role in the induction of immune tolerance. The enhanced expression of soluble HLA-G found in CD may be part of a mechanism to restore the gluten intolerance. In this editorial, we review recent progress in understanding CD in relation to its prevalence, diagnosis and possible mechanisms of pathogenesis.

Key words: Celiac disease; Oral tolerance; IL-10; TGF-beta; Gluten intolerance

Torres MI, López Casado MA, Ríos A. New aspects in celiac disease. *World J Gastroenterol* 2007; 13(8): 1156-1161

http://www.wjgnet.com/1007-9327/13/1156.asp

INTRODUCTION

Celiac disease (CD) is a chronic inflammatory disease which develops in genetically predisposed individuals. CD is a T cell-mediated inflammatory disorder with autoimmune features and it has environmental and immunologic components[1,2]. It is characterised by an immune response to ingested wheat gluten and related proteins of rye and barley that leads to inflammation, villous atrophy and crypt hyperplasia in the proximal part of the small intestine[2,3]. The common presentation symptoms and signs of CD include diarrhea, abdominal distention, abdominal pain, weight loss, fatigue, and malnutrition.

The clinical classification of CD is based on the presence or lack of gastrointestinal symptoms: "classical" or "symptomatic" CD refers to presentations with diarrhea and with malabsorption syndrome, whereas "atypical" or "asymptomatic" form has no gastrointestinal manifestations[4]. CD is defined as silent when the typical enteropathy is found in patients who apparently are healthy. Potential CD refers to a risk for developing a typical CD later in life; the patients have Endomysial antibody (EMA) and tissue transglutaminase (tTG) antibodies with HLA DQ2 or DQ8 predisposing genotype[6,7], and normal or minimal abnormal mucosa. Finally, a specific manifestation of CD is refractory sprue defined as symptomatic, severe villous atrophy with increased intraepithelial lymphocytes (IELs) despite maintenance of a strict gluten-free diet[5].

Although there have been major advances in our knowledge of the disease, there are few advances in the therapy. The only accepted treatment for CD is a nutritional therapy with a gluten-free diet for lifelong[8]. Here, we review recent advances in our understanding of CD with respect to its prevalence and diagnosis, and possible mechanisms underlying the gluten intolerance.

PREVALENCE

CD is the most common food-sensitive enteropathy in humans. The prevalence is estimated in the range of 1:100 to 1:300 in North America and Europe[9,10]. Recently, it has become clear that CD is much more prevalent than previously thought. We observed in our pediatric population (south-east of Spain) a 1:75 prevalence, which is in good agreement with the studies by Fasano et al [9] and Ciclitira *et al*[10] showing a prevalence of 1:133 in the United States and 1:100 in Europe, respectively.

At the present time, the form of clinical presentation of CD is changing. In our experience, CD is a very common disorder, and most affected individuals have the atypical and silent forms of the disease, which are also the prevalent forms of disease presentation in our population. Indeed, we observed a more elevated percentage of patients associated with HLA-DQ8 molecule in CD (around 20%-25%) than have been described previously by other studies, which estimated the percentage of HLA-DQ8 patients to be about 10%[11]. Furthermore, the HLA-DQ8 CD patients are commonly associated with extraintestinal symptoms presentations, and are frequently

Table 1 Clinical manifestations of untreated celiac disease

Manifestations	Associated diseases	Genetic associated diseases
Classic symptoms:	Autoimmune diseases:	Down syndrome
		Turner syndrome
Abdominal pain	Type 1 diabetes	William syndrome
Anorexia	Thyroiditis	IgA deficiency
Diarrhea	Sjogren's syndrome	
Weight loss	IgA nephropathy	
Short stature		
Irritability	Neurologic disturbances:	
Nonclassic symptoms:	Autism	
	Depression	
Dermatitis hepertiformis	Epilepsy	
Hepatitis	Cerebellar ataxia	
Anemia		
Arthritis	Other diseases:	
Constipation		
Alopecia	Osteopenia/osteoporosis	
Pubertal delay	Infertility	
Vomiting	Intestinal adenocarcinoma	
Inflammatory bowel disease	Non-Hodgkin lymphoma	
Migraine headaches		

associated with others autoimmune diseases (unpublished results).

DIAGNOSIS

We believe that the current diagnostic criteria for CD need a revision. CD is often missed during diagnosis because many individuals do not present the disease with the classical gastrointestinal symptoms. In fact, the percentage of undiagnosed population has markedly increased, and significant risks and complications are associated with untreated CD (Table 1).

As a multi-factorial disorder, CD may present highly diverse clinical manifestations[12]. CD patients typically display extraintestinal (non-classical) symptoms or lack classical gastrointestinal symptoms such as diarrhea, abdominal pain, distention, or weight loss. In our pediatric population, the non-classical symptoms are often the most common presentation in newly diagnosed CD cases. These include autoimmune alopecia, iron deficiency, or elevated levels of liver transaminases, and they often may be the only manifestation of CD in an affected individual (Table 1).

In our experience, small bowel biopsy is critical for diagnosing symptomatic patients with negative serology for CD and with HLA compatible with the disease. Although we consider intestinal biopsy as the gold standard for CD diagnosis, in many occasions the permission for intestinal biopsy is refused. Both serologic tests and genetic study are necessary to select subjects who need intestinal biopsy (Table 2).

CD is more common in certain risk groups. Family members of known celiac patients represent the most important group of study patients. The determination of HLA typing as a first step is useful as it would exclude approximately one third of first degree relatives in a CD family. We found a high prevalence of CD between relatives, and the highest percentage was observed among daughters. The CD relatives are a population at high risk of developing gluten intolerance and we propose that an extensive study of such group should be undertaken. It is noteworthy that after the first diagnosis of CD, the family will become more self-aware in recognizing early symptoms related to the disease.

PATHOGENESIS

A defect in antigen processing by epithelial cells, together with the intrinsic properties of the gliadins, as well as the HLA-DQ haplotype of the individual are considered the principal factors involved in the pathogenesis of CD[3]. CD is strongly associated with HLA class II genes that map to the DQ locus. It has been shown that CD is associated with the expression of HLA-DQ2 and HLA-DQ8[6,7]. Several studies found that the majority of celiac patients carry DQ2 (DQA1*05/DQB1*02), with the remaining patients displaying an association with DQ8 (DQA1*0301/DQB1*0302). Collectively, these HLA genes confer up to 40% of the genetic risk for CD development.

Gliadin peptide presentation and T-cell activation are critical events in the pathogenesis of CD. Gluten peptides are not fully digested by the action of gastric, intestinal and pancreatic enzymes in CD patients. A 33-mer peptide was isolated and identified as the primary initiator of the inflammatory response to gluten in celiac patients[16]. This peptide reacted with tissue transglutaminase (tTG), the major autoantigen in CD that deamidates certain glutamine residues of gluten to glutamic acid. This in turn produces a negative charge that favours binding and presentation by HLA-DQ2 and DQ8 molecules, which are responsible for T-cell activation and subsequent production of cytokines, leading to tissue damage[17,18]. The inappropriate CD4+ T-cell activation in the lamina propia commonly observed in CD is triggered by specific gluten peptides bound to DQ2 and DQ8 heterodimers on the surface of antigen presentation cells[2,6]. The mucosal intestinal lesion is believed to be mainly induced by the production of IFN-gamma from these gluten specific T cells[1, 2]. Moreover, changes in intestinal permeability, secondary to alterations in intercellular tight junctions or in the processing of the food antigen, have also been recently implicated in the loss of tolerance to gluten[19].

Immune (oral) tolerance

The gut immune system is exposed to a wide variety of antigens derived from foods, resident bacteria and invading microorganisms. Oral tolerance is a physiological condition characterized by induction of immune unresponsiveness toward intestinal alimentary and bacterial antigens of the intestinal flora. Multiple cellular and molecular mechanisms are involved in the regulation of this fundamental property of the gut immune system[20].

CD is the most common food-sensitive enteropathy in humans and is caused by the lack of immune tolerance (oral tolerance) to wheat gluten and the prolamin fractions of rye and barley. Many different gluten peptides recognized by intestinal T cells have been identified[21]. The activation

Table 2 Diagnosis in celiac disease

Diagnostic criteria used in celiac disease	Diagnostic propose for celiac disease	Comments
Serological test: Tissue transglutaminase antibody (tTGA) Endomysial antibody (EMA) Gliadin antibodies (AGA) Total IgA	With classical symptoms: Serological test: Tissue transglutaminase antibody (tTGA) Endomysial antibody (EMA) Gliadin antibodies (AGA)	Positive serology supports a diagnosis of CD, but they are not essential. Compatible with HLA-DQ2/D8 testing and identify individuals for further biopsy evaluation. Small bowel biopsy is critical in symptomatic patients with negative serology for CD and with HLA compatible with the disease
Endoscopy	HLA-DQ2/DQ8 testing	Determination of HLA typing as a first step in diagnosis in CD family
	Capsule endoscopy (with adequate pathological interpretation)	Adequate number of biopsies and well oriented. Estimate lymphocyte infiltration and partial or total villus atrophy
	Without classical symptoms HLA-DQ2/DQ8 testing	Primordial role of HLA-typing if serology is negative and with biopsy refused or equivocal to identify individuals
	Serologic test: Tissue transglutaminase antibody (tTGA) Endomysial antibody (EMA) Gliadin antibodies (AGA)	Adequate number of biopsies and well oriented. Estimate lymphocyte infiltration and partial or total villous atrophy
	Capsule endoscopy (with adequate pathological interpretation)	

of these gluten-reactive T cells represents a key event in the pathogenesis of CD[1,2]. The mucosa of CD patients is characterized by a high proportion of intraepithelial T cells bearing gamma-delta chain of the antigenic T cell receptors (γδ IEL)[22].

Ingested gliadin, the triggering agent of the disease, can cross the epithelial barrier and elicit a harmful T cell-mediated immune response. Dendritic cells are supposed to play a pivotal role in shaping the immune response[23]. Immature dendritic cells are characterised by low levels of MHC class II expression and co-stimulatory molecules and can mediate tolerance presumably by induction of T regulatory cells (Treg cells)[24]. Moreover, IL-10 released by Treg cells can modulate the function of immature dendritic cells and inhibit their differentiation, amplifying the local presence of "tolerizing dendritic cells"[25]. IL-10-modulated dendritic cells induce anergy of effector T cells through still undefined mechanisms requiring cell-cell contact.

Therefore, the direction of the immune response toward immunity or tolerance depends on the stage of maturation and the functional properties of the dendritic cells. Gliadin peptides can contribute to overcoming the stage of unresponsiveness of immature dendritic cells by inducing phenotypic and functional dendritic cell maturation, resulting in more efficient processing and presentation of gliadin peptides to specific T lymphocytes[26].

HLA-G: molecule of immune tolerance

HLA-G is a non-classical major histocompatibility complex class I molecule selectively expressed at the maternal-foetal interface on cytotrophoblast cells, protecting the fetus from the maternal immune rejection, and creating a general state of tolerance[27]. HLA-G exhibit tolerogenic properties via interaction with inhibitory receptors presented in natural killer (NK) cells, T cells and antigen-presenting cells (APC)[28].

The presence of soluble HLA-G (sHLA-G) in the cerebrospinal fluid of multiple sclerosis[29] and allograft acceptance after transplantation[30] suggests a tolerogenic function for this molecule against innate and adaptive cellular immune responses. Interestingly, work from our lab and others have suggested that HLA-G antigens may play a protective role in inflammation[31,32]. Further analysis revealed that, sHLA-G molecules inhibit lytic activity of NK cells, induce apoptosis of CD8+ CTLs and affect CD4+ alloproliferation[33]. Thus, the immune modulatory properties of sHLA-G may suggest a potentia role in CD.

We have demonstrated an association of CD with sHLA-G expression (Figure 1A) and we found a correlation between increased levels of sHLA-G expression and CD associated with other autoimmune diseases, being dependent on a genetic link of these diseases through HLA genes[34].

The expression of soluble HLA-G in CD is of special interest because its molecule plays an important role in the induction of immune tolerance[35]. We propose that the enhanced expression of sHLA-G found in CD could be part of a mechanism to restore the gluten intolerance. HLA-G may act through inhibitory receptor (ILT) interactions that lead to development of tolerogenic dendritic cells with the induction of anergic and immunosuppressive T cells, and an arrest of maturation/activation of dendritic cells. The expression of these ILT receptors on dendritic cells is tightly controlled by inflammatory stimuli, and by cytokines[36].

Thus, a powerful anti-inflammatory response to gliadin might occur during the development of the disease with uncontrolled production of HLA-G and anti-inflammatory cytokines, such as IL-10 and TGF-beta, which counteract the inflammation and/or may cause recruitment of intra-epithelial lymphocytes, maintaining the intestinal lesions presented in CD[34].

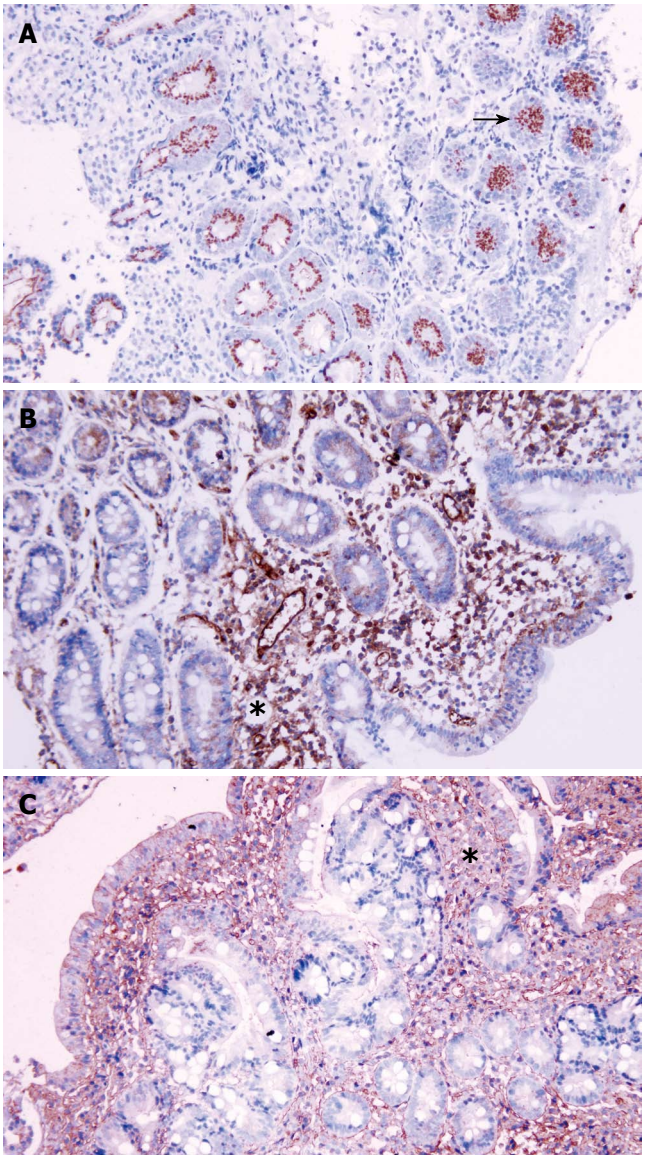

Figure 1 Immunohistochemistry analysis in celiac patients. **A**: Immunohistochemical staining for HLA-G in the Lieberkühn crypts; **B**: Immunohistochemical staining for IL-10 at the lamina propria level; **C**: Immunoreaction for TGF-beta in areas of infiltrated inflammatory cells. Arrows and asterisks: cells showing immunoreactivity (x 200).

Cytokines

The characteristics of an intestinal inflammatory response depend on the cytokines produced during this response. The production of cytokines from T cells and macrophages is of potential importance for the histological lesions that appear in CD. The CD lesions are associated with a marked infiltration of Th1 cells dominated by the synthesis of the pro-inflammatory cytokines, IFN-gamma and TNF-alpha[37]. IL-15 also has an important role in CD, because it orchestrates intraepithelial lymphocytes changes in the disease. Certain parts of gluten may stimulate the innate part of the immune system, and IL-15 is a central player in this immune response-induced by gluten, inducing the activation of IEL in CD[38]. Engineered IL-15 over-expression by epithelial cells in the intestine leads to a massive expansion of CD8+ intestinal T cells accompanied by a CD-like enteropathy[39]. Furthermore, IL-15 induces the expression of MICA, the epithelial ligand of NKG2D[40].

We found in the celiac patients increased levels of anti-inflammatory cytokines IL-10 and TGF-beta at the lamina propria level in biopsy samples of patients with villous atrophy and elevated lymphocyte infiltration (Figure 1B and C). IL-10 predominantly acts as a potent anti-inflammatory factor and a suppressive agent for Th1 responses[41]. TGF-beta is a major factor for the production of immunoglobulin A (IgA) and acts as a potent mediator of the tissue repair[42]. Interestingly, tTG, described as the major endomysial autoantigen in CD, is necessary for the activation of TGF-beta[43]. The elevated levels of IL-10 and TGF-beta are insufficient for the inhibition of the autoimmune reaction, and would modulate the immune response and induce the activation of B lymphocytes. These cytokines may play important roles in inducing HLA-G. In this regard, the possible role of IL-10 in inducing HLA-G protein expression has been already previously described in CD[34].

Table 3 Future directions in celiac disease

Unanswered questions	Future directions
Immunopathogenesis	
How is oral tolerance broken?	Restoring immunological tolerance to gluten would represent the ideal cure for CD
Gluten-specific T cells	Gluten-specific T cells could be inactivated or deleted, tolerance to gluten should be restored
Diagnosis	
What is the significance of the vast number of currently undiagnosed people with the disease?	The rate of the diagnosis will continue to increase with better diagnosis.
What is the significance of the increase number of people with extraintestinal symptoms or without classical symptoms in CD?	"the suspicion of the disease"
Genetics	
Identify the genetic risk factors that predispose to CD	Polymorphic genes located in the MHC region and CD Genetic polymorphism of cytokine genes may influence the risk of CD Associated polymorphism with serological markers HLA-G polymorphism?

FUTURE DIRECTIONS

There are many unanswered questions about CD. What is responsible for the collapse of CD oral tolerance? Restoring immunological tolerance to gluten would represent the ideal way to treat or cure this disease. However, if gluten-specific T cells could be inactivated or deleted, tolerance to gluten should be restored. What is the significance of the vast number of currently undiagnosed people with the disease? What is the significance of the increased number of people with extraintestinal symptoms

or without classical symptoms in CD? As we anticipate that the rate of the diagnosis will continue to increase, it will be important to further our understanding of the pathogenesis of CD and improve its diagnosis (Table 3). The diversity of the clinical presentation in CD can complicate the diagnosis and delay the treatment initiation. In our experience, the most important diagnostic test in CD is "the suspicion of the disease". The screening of CD should start with a serologic test (for IgA and IgG anti-endomysial and anti-tTG antibodies), and HLA typing. If the patient is genetically compatible with the disease (even with negative serology), a confirmatory small biopsy by capsule endoscopy should be followed.

Recently, many efforts have been made to identify the genetic risk factors that predispose to CD. The lack of immune tolerance in CD could occur due to genetic polymorphisms in any of the non-MHC molecules involved in the induction, regulation or expression of mucosal immune responses, such as IL-10, TGF-beta, IFN-gamma. Most of these polymorphisms affect gene transcription influencing the individual susceptibility to CD[44]. In addition, several associations between different polymorphic genes located in the MHC region and CD have been reported[45]. Furthermore, we found evidence that HLA-G is an interesting candidate as susceptibility gene in CD. These findings should open new perspectives for the identification of genetic susceptibility to CD.

REFERENCES

1 **Sollid LM**. Coeliac disease: dissecting a complex inflammatory disorder. *Nat Rev Immunol* 2002; **2**: 647-655
2 **Alaedini A**, Green PH. Narrative review: celiac disease: understanding a complex autoimmune disorder. *Ann Intern Med* 2005; **142**: 289-298
3 **Robins G**, Howdle PD. Advances in celiac disease. *Curr Opin Gastroenterol* 2005; **21**: 152-161
4 **Fasano A**. Clinical presentation of celiac disease in the pediatric population. *Gastroenterology* 2005; **128**: S68-S73
5 **Schuppan D**, Dennis MD, Kelly CP. Celiac disease: epidemiology, pathogenesis, diagnosis, and nutritional management. *Nutr Clin Care* 2005; **8**: 54-69
6 **Kim CY**, Quarsten H, Bergseng E, Khosla C, Sollid LM. Structural basis for HLA-DQ2-mediated presentation of gluten epitopes in celiac disease. *Proc Natl Acad Sci USA* 2004; **101**: 4175-4179
7 **Louka AS**, Sollid LM. HLA in coeliac disease: unravelling the complex genetics of a complex disorder. *Tissue Antigens* 2003; **61**: 105-117
8 **Fasano A**, Catassi C. Current approaches to diagnosis and treatment of celiac disease: an evolving spectrum. *Gastroenterology* 2001; **120**: 636-651
9 **Fasano A**, Berti I, Gerarduzzi T, Not T, Colletti RB, Drago S, Elitsur Y, Green PH, Guandalini S, Hill ID, Pietzak M, Ventura A, Thorpe M, Kryszak D, Fornaroli F, Wasserman SS, Murray JA, Horvath K. Prevalence of celiac disease in at-risk and not-at-risk groups in the United States: a large multicenter study. *Arch Intern Med* 2003; **163**: 286-292
10 **Ciclitira PJ**, Johnson MW, Dewar DH, Ellis HJ. The pathogenesis of coeliac disease. *Mol Aspects Med* 2005; **26**: 421-458
11 **Tighe MR**, Hall MA, Barbado M, Cardi E, Welsh KI, Ciclitira PJ. HLA class II alleles associated with celiac disease susceptibility in a southern European population. *Tissue Antigens* 1992; **40**: 90-97
12 **Meize-Grochowski R**. Celiac disease: a multisystem autoimmune disorder. *Gastroenterol Nurs* 2005; **28**: 394-402; quiz 403-404
13 **Dewar D**, Pereira SP, Ciclitira PJ. The pathogenesis of coeliac disease. *Int J Biochem Cell Biol* 2004; **36**: 17-24
14 **Kagnoff MF**. Overview and pathogenesis of celiac disease. *Gastroenterology* 2005; **128**: S10-S18
15 **Lundin KE**, Scott H, Fausa O, Thorsby E, Sollid LM. T cells from the small intestinal mucosa of a DR4, DQ7/DR4, DQ8 celiac disease patient preferentially recognize gliadin when presented by DQ8. *Hum Immunol* 1994; **41**: 285-291
16 **Shan L**, Molberg Ø, Parrot I, Hausch F, Filiz F, Gray GM, Sollid LM, Khosla C. Structural basis for gluten intolerance in celiac sprue. *Science* 2002; **297**: 2275-2279
17 **Molberg O**, Mcadam SN, Körner R, Quarsten H, Kristiansen C, Madsen L, Fugger L, Scott H, Norén O, Roepstorff P, Lundin KE, Sjöström H, Sollid LM. Tissue transglutaminase selectively modifies gliadin peptides that are recognized by gut-derived T cells in celiac disease. *Nat Med* 1998; **4**: 713-717
18 **Reif S**, Lerner A. Tissue transglutaminase--the key player in celiac disease: a review. *Autoimmun Rev* 2004; **3**: 40-45
19 **Fasano A**. Intestinal zonulin: open sesame! *Gut* 2001; **49**: 159-162
20 **Dubois B**, Goubier A, Joubert G, Kaiserlian D. Oral tolerance and regulation of mucosal immunity. *Cell Mol Life Sci* 2005; **62**: 1322-1332
21 **Arentz-Hansen H**, McAdam SN, Molberg Ø, Fleckenstein B, Lundin KE, Jørgensen TJ, Jung G, Roepstorff P, Sollid LM. Celiac lesion T cells recognize epitopes that cluster in regions of gliadins rich in proline residues. *Gastroenterology* 2002; **123**: 803-809
22 **Ebert EC**. Intra-epithelial lymphocytes: interferon-gamma production and suppressor/cytotoxic activities. *Clin Exp Immunol* 1990; **82**: 81-85
23 **Alpan O**, Rudomen G, Matzinger P. The role of dendritic cells, B cells, and M cells in gut-oriented immune responses. *J Immunol* 2001; **166**: 4843-4852
24 **Steinman RM**, Turley S, Mellman I, Inaba K. The induction of tolerance by dendritic cells that have captured apoptotic cells. *J Exp Med* 2000; **191**: 411-416
25 **Jonuleit H**, Schmitt E, Schuler G, Knop J, Enk AH. Induction of interleukin 10-producing, nonproliferating CD4(+) T cells with regulatory properties by repetitive stimulation with allogeneic immature human dendritic cells. *J Exp Med* 2000; **192**: 1213-1222
26 **Palová-Jelínková L,** Rozková D, Pecharová B, Bártová J, Sedivá A, Tlaskalová-Hogenová H, Spísek R, Tucková L. Gliadin fragments induce phenotypic and functional maturation of human dendritic cells. *J Immunol* 2005; **175**: 7038-7045
27 **McMaster MT**, Librach CL, Zhou Y, Lim KH, Janatpour MJ, DeMars R, Kovats S, Damsky C, Fisher SJ. Human placental HLA-G expression is restricted to differentiated cytotrophoblasts. *J Immunol* 1995; **154**: 3771-3778
28 **Le Rond S**, Gonzalez A, Gonzalez AS, Carosella ED, Rouas-Freiss N. Indoleamine 2,3 dioxygenase and human leucocyte antigen-G inhibit the T-cell alloproliferative response through two independent pathways. *Immunology* 2005; **116**: 297-307
29 **Fainardi E**, Rizzo R, Melchiorri L, Vaghi L, Castellazzi M, Marzola A, Govoni V, Paolino E, Tola MR, Granieri E, Baricordi OR. Presence of detectable levels of soluble HLA-G molecules in CSF of relapsing-remitting multiple sclerosis: relationship with CSF soluble HLA-I and IL-10 concentrations and MRI findings. *J Neuroimmunol* 2003; **142**: 149-158
30 **Lila N**, Rouas-Freiss N, Dausset J, Carpentier A, Carosella ED. Soluble HLA-G protein secreted by allo-specific CD4+ T cells suppresses the allo-proliferative response: a CD4+ T cell regulatory mechanism. *Proc Natl Acad Sci USA* 2001; **98**: 12150-12155
31 **Carosella ED**, Moreau P, Aractingi S, Rouas-Freiss N. HLA-G: a shield against inflammatory aggression. *Trends Immunol* 2001; **22**: 553-555
32 **Torres MI**, Le Discorde M, Lorite P, Ríos A, Gassull MA, Gil A, Maldonado J, Dausset J, Carosella ED. Expression of HLA-G in inflammatory bowel disease provides a potential way to distinguish between ulcerative colitis and Crohn's disease. *Int*

Immunol 2004; **16**: 579-583
33 **Bainbridge DR**, Ellis SA, Sargent IL. HLA-G suppresses proliferation of CD4(+) T-lymphocytes. *J Reprod Immunol* 2000; **48**: 17-26
34 **Torres MI**, López-Casado MA, Luque J, Peña J, Ríos A. New advances in coeliac disease: serum and intestinal expression of HLA-G. *Int Immunol* 2006; **18**: 713-718
35 **Rouas-Freiss N**, Paul P, Dausset J, Carosella ED. HLA-G promotes immune tolerance. *J Biol Regul Homeost Agents* 2000; **14**: 93-98
36 **Ristich V**, Liang S, Zhang W, Wu J, Horuzsko A. Tolerization of dendritic cells by HLA-G. *Eur J Immunol* 2005; **35**: 1133-1142
37 **Nilsen EM**, Lundin KE, Krajci P, Scott H, Sollid LM, Brandtzaeg P. Gluten specific, HLA-DQ restricted T cells from coeliac mucosa produce cytokines with Th1 or Th0 profile dominated by interferon gamma. *Gut* 1995; **37**: 766-776
38 **Maiuri L**, Ciacci C, Auricchio S, Brown V, Quaratino S, Londei M. Interleukin 15 mediates epithelial changes in celiac disease. *Gastroenterology* 2000; **119**: 996-1006
39 **Meresse B**, Chen Z, Ciszewski C, Tretiakova M, Bhagat G, Krausz TN, Raulet DH, Lanier LL, Groh V, Spies T, Ebert EC, Green PH, Jabri B. Coordinated induction by IL15 of a TCR-independent NKG2D signaling pathway converts CTL into lymphokine-activated killer cells in celiac disease. *Immunity* 2004; **21**: 357-366
40 **Hüe S**, Mention JJ, Monteiro RC, Zhang S, Cellier C, Schmitz J, Verkarre V, Fodil N, Bahram S, Cerf-Bensussan N, Caillat-Zucman S. A direct role for NKG2D/MICA interaction in villous atrophy during celiac disease. *Immunity* 2004; **21**: 367-377
41 **Li L**, Elliott JF, Mosmann TR. IL-10 inhibits cytokine production, vascular leakage, and swelling during T helper 1 cell-induced delayed-type hypersensitivity. *J Immunol* 1994; **153**: 3967-3978
42 **Cataldo F**, Lio D, Marino V, Scola L, Crivello A, Corazza GR. Plasma cytokine profiles in patients with celiac disease and selective IgA deficiency. *Pediatr Allergy Immunol* 2003; **14**: 320-324
43 **Hansson T**, Ulfgren AK, Lindroos E, DannAEus A, Dahlbom I, Klareskog L. Transforming growth factor-beta (TGF-beta) and tissue transglutaminase expression in the small intestine in children with coeliac disease. *Scand J Immunol* 2002; **56**: 530-537
44 **Lio D**, Scola L, Forte GI, Accomando S, Giacalone A, Crivello A, Cataldo F. TNFalpha, IFNgamma and IL-10 gene polymorphisms in a sample of Sicilian patients with coeliac disease. *Dig Liver Dis* 2005; **37**: 756-760
45 **Lie BA**, Sollid LM, Ascher H, Ek J, Akselsen HE, Rønningen KS, Thorsby E, Undlien DE. A gene telomeric of the HLA class I region is involved in predisposition to both type 1 diabetes and coeliac disease. *Tissue Antigens* 1999; **54**: 162-168

S- Editor Liu Y **L- Editor** Tan SL **E- Editor** Ma WH

PO Box 2345, Beijing 100023, China
www.wjgnet.com
wjg@wjgnet.com

World J Gastroenterol 2007 February 28; 13(8): 1162-1169
World Journal of Gastroenterology ISSN 1007-9327

GASTRIC CANCER

(-)-Epigallocatechin-3-gallate inhibits growth of gastric cancer by reducing VEGF production and angiogenesis

Bao-He Zhu, Wen-Hua Zhan, Zheng-Rong Li, Zhao Wang, Yu-Long He, Jun-Sheng Peng, Shi-Rong Cai, Jin-Ping Ma, Chang-Hua Zhang

Bao-He Zhu, Wen-Hua Zhan, Zheng-Rong Li, Zhao Wang, Yu-Long He, Jun-Sheng Peng, Shi-Rong Cai, Jin-Ping Ma, Chang-Hua Zhang, Department of Gastrointestinal & Pancreatic Surgery, First Affiliated Hospital, Sun Yat-Sen University; Gastric Center of Sun Yat-Sen University, Guangzhou 510080, Guangdong Province, China
Supported by the grants from the National Natural Science Foundation of China, No. 30571833, and the Natural Science Foundation of Guangdong Province, China, No. 05001785
Correspondence to: Wen-Hua Zhan, MD, Department of Gastrointestinal & Pancreatic Surgery, First Affiliated Hospital, Sun Yat-Sen University; Gastric Center of Sun Yat-Sen University, Guangzhou 510080, Guangdong Province, China. wenhuazhanwcwk@yahoo.com.cn
Telephone: +86-20-87331438 Fax: +86-20-87331438
Received: 2006-12-01 Accepted: 2007-01-29

Abstract

AIM: To investigate the effect of (-)-epigallocatechin-3-gallate (EGCG) on growth of gastric cancer and its possible mechanism.

METHODS: Heterotopic tumors were induced by subcutaneously injection of SGC-7901 cells in nude mice. Tumor growth was measured by calipers in two dimensions. Tumor angiogenesis was determined with tumor microvessel density (MVD) by immunohistology. Vascular endothelial growth factor (VEGF) protein level and activation of signal transducer and activator of transcription 3 (Stat3) were examined by Western blotting. VEGF mRNA expression was determined by RT-PCR and VEGF release in tumor culture medium by ELISA. VEGF-induced cell proliferation was studied by MTT assay, cell migration by gelatin modified Boyden chamber (Transwell) and *in vitro* angiogenesis by endothelial tube formation in Matrigel.

RESULTS: Intraperitoneal injection of EGCG inhibited the growth of gastric cancer by 60.4%. MVD in tumor tissues treated with EGCG was markedly reduced. EGCG treatment reduced VEGF protein level *in vitro* and *in vivo*. Secretion and mRNA expression of VEGF in tumor cells were also suppressed by EGCG in a dose-dependent manner. This inhibitory effect was associated with reduced activation of Stat3, but EGCG treatment did not change the total Stat3 expression. EGCG also inhibited VEGF-induced endothelial cell proliferation, migration and tube formation.

CONCLUSION: EGCG inhibits the growth of gastric cancer by reducing VEGF production and angiogenesis, and is a promising candidate for anti-angiogenic treatment of gastric cancer.

Key words: Epigallocatechin-3-gallate; Angiogenesis; Migration; Tube formation; Vascular endothelial growth factor; Signal transducer and activator of transcription 3; Gastric cancer

Zhu BH, Zhan WH, Li ZR, Wang Z, He YL, Peng JS, Cai SR, Ma JP, Zhang CH. (-)-Epigallocatechin-3-gallate inhibits growth of gastric cancer by reducing VEGF production and angiogenesis. *World J Gastroenterol* 2007; 13(8): 1162-1169

http://www.wjgnet.com/1007-9327/13/1162.asp

INTRODUCTION

Gastric cancer is the leading cause of cancer-related death in most countries, but the incidence has steadily decreased throughout the world in recent decades[1]. Although the exact reason for the decline is uncertain, it was reported that dietary factors play a role[2]. Epidemiological studies showed that regular drinking of green tea significantly reduces the occurrence and mortality of many types of cancer[3]. Case-control studies have provided evidence for protective effect of green tea against gastric cancer[4]. Experiment and animal model studies also demonstrated that green tea and its components have anti-cancer effect against gastric cancer[5,6], but conclusive results are not available at present[7].

(-)-Epigallocatechin-3-gallate (EGCG) is the most abundant and active component of green tea, and the beneficial properties of green tea appear to be ascribed to EGCG. The effect of EGCG on cell proliferation and apoptosis has been well established. EGCG suppresses tumor growth by inhibiting proliferation and inducing apoptosis through a variety of mechanisms[8]. Recent studies showed that EGCG has anti-angiogenic property and reduces tumor growth in mouse model by inhibiting angiogenesis[9,10]. Angiogenesis, the growth of new blood vessels from preexisting capillaries, is necessary for solid tumor growth and metastasis. Angiogenesis is initiated by the release of certain angiogenic factors from tumor cells. Vascular endothelial growth factor (VEGF), which has

been shown to be the most potent angiogenic factor, is associated with tumor-induced angiogenesis. Angiogenesis is closely associated with progression and prognosis of gastric cancer, and VEGF expression is a predictive and prognostic factor of gastric cancer[11]. Anti-angiogenic therapy targeting VEGF can inhibit growth and metastasis of gastric cancer[12]. However, whether EGCG suppresses growth of gastric cancer by anti-angiogenesis remains to be elucidated.

In this study, we investigated the effect of EGCG on angiogenesis and growth of gastric cancer with an *in vitro* and *in vivo* model. Data reported here show that EGCG suppresses growth of gastric cancer by reducing VEGF production and VEGF-induced angiogenesis.

MATERIALS AND METHODS

Cell culture

Human gastric cancer cells (SGC-7901 cells, Cell Bank of Sun Yat-Sen University, Guangzhou, China) were maintained in Dulbecco's modified Eagle's medium (DMEM) supplemented with 10% (v/v) fetal bovine serum (FBS, Gibco BRL, Gaithersburg, MD) and incubated at 37℃ in a humidified incubator containing 50 mL/L CO_2. Human umbilical vein endothelial cells (HUVECs) were prepared from fresh human umbilical cord and grown in human endothelial-serum free medium (endothelial-SFM, Gibco BRL, Gaithersburg, MD) supplemented with 10% FBS, 100 U penicillin, streptomycin and fungizone, and incubated at 37℃ in a humidified incubator containing 50 mL/L CO_2. To maintain uniform conditions, all experiments were carried out between cell passages 4-6.

Tumor growth assay

SGC-7901 cells (5×10^6 cells/0.2 mL) in SFM were inoculated subcutaneously into the dorsal area of 6-8-wk female BALB/c nude mice, weighing 18-22 g (Experimental Animal Center of Sun Yet-Sen University, Guangzhou, China). When tumors reached a volume of 50 mm^3, intraperitoneal injection of EGCG was carried out at the dosage of 1.5 mg/d per mouse ($n = 6$). The control group ($n = 6$) was treated with the same volume of PBS. Tumor growth was monitored by external measurement in two dimensions every other day with calipers. Tumor volume was determined according to the equation: $V = (L \times W^2)/2$, where V is volume, L is length and W is width. Twenty-eight days after EGCG injection, all animals were sacrificed, tumors were excised and weighed. The tumor inhibition ratio was calculated as follows: inhibition ratio (%) = $[(C-T)/C] \times 100\%$, where C is the average tumor weight of the control group and T is the average tumor weight of the EGCG-treated group. Some tumor tissues were frozen at -80℃ for Western blot analysis and others fixed in 4% formaldehyde for immunohistochemistry analysis.

All animal studies were performed according to the guides for the Care and Use of Laboratory Animals approved by Sun Yat-Sen University.

Determination of tumor microvessel density

Histologic 4-μm thick sections prepared from formaldehyde fixed and paraffin embedded tumor tissues were used for immunohistochemical analysis. After deparaffinization, rehydration, antigen retrieval and blocking of endogenous peroxidase, the specimens were incubated overnight at 4℃ with goat polyclonal anti-CD34 antibodies diluted at 1:100 (Santa Cruz Biotechnology, Santa Cruz, CA, USA). The sections were rinsed and incubated with peroxidase-conjugated second antibody followed by enzyme conjugate (HRP-streptavidin). Microvessels were revealed with diaminobenzidine (DAB) and the sections were counterstained with Mayer's hematoxylin. In negative-control staining, the primary antibodies were omitted. Tumor vasculature was quantified by the Weidner's method[13]. The area of tumor containing the maximum number of microvessels to be counted was identified by scanning the entire tumor at low power (100 ×). The number of highlighted vessels from 3 fields was then counted in this area at high power (200 ×).

Western blot analysis

SGC-7901 cells were seeded in 90 mm plates and cultured in growth medium until 70%-80% confluence. The culture medium was replaced with SFM supplemented with different concentrations of EGCG (0, 5, 10, 20, and 40 μmol/L). The cells were incubated for another 24 h. Total protein from cell lysates and tumor tissue homogenizations was extracted with mammalian cell lysis kit (Bio Basic Inc., Ontario, Canada). Protein levels were quantified with Bio-Rad protein assay kit (Bio-Rad Laboratories, Richmond, CA). Total protein (100 μg) was separated in 12% SDS–PAGE, and transferred onto PVDF membrane (Invitrogen, Carlsbad, CA, USA). The membrane was blocked with 5% skim milk and incubated at 4℃ overnight with rabbit polyclonal anti-VEGF antibody (Santa Cruz Biotechnology, Santa Cruz, CA, USA), rabbit polyclonal anti-Stat3 antibody (Santa Cruz Biotechnology, Santa Cruz, CA, USA), or goat polyclonal anti-p-Stat3 antibody (Phospho-Stat3 [tyr-705], Santa Cruz Biotechnology, Santa Cruz, CA, USA). After washing three times with 0.1% Tween 20 in Tris-saline, the membranes were incubated with biotin-labeled anti-rabbit or anti-goat IgG for 1 h at room temperature with agitation. The probe proteins were detected using enhanced chemiluminescence system (Amersham International, Piscataway, N.J., USA).

Measurement of VEGF in supernatant by ELISA

The effect of EGCG on VEGF release in tumor cells was measured by ELISA. SGC-7901 cells seeding in 90 mm plates were cultured until 70%-80% confluence. The cells were washed three times with PBS and the culture medium was replaced with SFM. EGCG was added to the medium to various concentrations (0, 5, 10, 20 and 40 μmol/L) and incubated with the cells for 24 h. The conditioned medium was harvested and centrifuged. VEGF concentration in the supernatant was measured using a VEGF ELISA kit (R & D systems, Minneapolis, Minn., USA).

RT-PCR analysis

SGC-7901 cells were seeded in 90 mm plates and cultured in growth medium until 90% confluence. The culture medium was replaced with SFM supplemented

with EGCG at different concentrations (0, 5, 10, 20 and 40 μmol/L). The cells were incubated for another 24 h. Total RNA was extracted from the cell lysates. The levels of human VEGF cDNAs were evaluated by RT-PCR and normalized by the levels of human cytoplasmic β-actin. Reverse transcription was performed with 1 μg total RNA and 100 pmol random hexamers in a total volume of 20 μL to produce first-strand cDNA. PCR experiments were performed with 1 μL of the first-strand cDNA in a 50 μL reaction mixture. Human VEGF cDNA was amplified with specific primers (sense primer: 5'TGC ATT CAC ATT TGT TGT GC 3'; antisense primer: 5'AGA CCC TGG TGG ACA TCT TC-3', a 200 bp product) and β-actin specific primers (sense primer: 5'-TCA TCA CCA TTG GCA ATG AG-3'; antisense primer: 5'-CAC TGT GTT GGC GTA CAG GT-3'; a 150 bp product). Amplification conditions were as follows: denaturation at 94℃ for 1 min, annealing at 60℃ (for β-actin at 55℃) for 1 min, and extension at 72℃ for 1 min. All PCRs were linear up to 30 cycles.

Cell proliferation assay by MTT assay

The effect of EGCG (Sigma, St. Louis, MO., USA) on endothelial cell proliferation induced by VEGF was determined by MTT assay (Sigma, St. Louis, MO., USA). Briefly, 2.5 × 10^4 HUVECs were plated in 24-well plates pre-coated with 2.0% gelatin in triplicate and cultured overnight in growth medium. Then the culture medium was changed with endothelial-SFM supplemented with 2% FBS and 20 ng/mL recombinant human vascular endothelial growth factor (hrVEGF; R & D Systems, Minneapolis, Minn., USA) in the presence of EGCG at various concentrations (0, 5, 10, 20 and 40 μmol/L). The viable cells were quantified by MTT assay at indicated time point following the manufacturer's instructions.

Cell migration assay

Endothelial cell migration induced by VEGF was assessed using a modified Boyden chamber (8 μmol/L pores, Transwell®; Corning Costar Corp., Cambridge, MA). The transwell inserts were coated with 2.0% gelatin. HUVECs were treated with EGCG at various concentrations (0, 5, 10, 20 and 40 μmol/L) for 24 h. Cells were harvested by trypsinization, washed twice with PBS, and resuspended in endothelial-SFM containing 2% FBS and EGCG at the indicated concentrations. Then the treated cells were added to the upper chamber at 2 × 10^5 cells per well and 0.6 mL endothelial-SFM containing 2% FBS and 20 ng/mL VEGF was added to the bottom chamber. After 4-h incubation at 37℃, cells on the upper surface of the membrane were mechanically removed, and the migrated cells on the lower surface of the membrane were fixed and stained with hematoxylin. The average number of migrated cells from 5 randomly chosen fields (× 200) on the lower surface of the membrane was counted. Each experiment was performed in triplicate.

Tube formation assay

Matrigel was thawed at 4℃ in an ice-water bath, and 300 μL/well was carefully added to a pre-chilled 24-well plate using a cold pipette. Matrigel was allowed to polymerize for 1 h at 37℃. After polymerization, 5 × 10^4 cells/well in endothelial-SFM with 2% serum, 20 ng/mL VEGF and EGCG at different concentrations (0, 5, 10, 20 and 40 μmol/L) was layered on top of polymerized gel. Cells were incubated for 48 h and photographed. For quantification of tube formation, the total length of tubes formed in a unit area was measured using an NIH Image program.

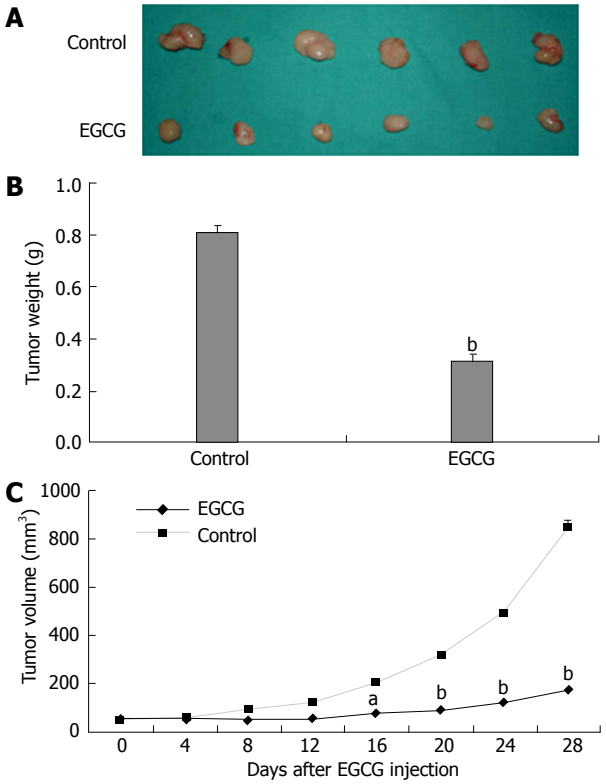

Figure 1 Inhibition of growth of human gastric cancer xenografts in an athymic mouce model. **A**: tumor tissues treated with EGCG or PBS on d 28 after treatment; **B**: an average of 60.4% suppression of primary tumor growth in the EGCG treatment group compared with control group; **C**: tumor growth suppression curve: volumes of EGCG treatment group versus PBS treatment group on indicated days. Data are presented as mean ± SE (n = 6, $^aP < 0.05$, $^bP < 0.01$).

Statistical analysis

Student's t test was used in all statistical analyses. $P < 0.05$ was considered statistically significant.

RESULTS

EGCG suppressed growth of human gastric carcer xenografts in athymic mice

To evaluate the effect of EGCG on tumor growth, tumor xenografts were created by implanting SGC-7901 cells into the dorsal area of athymic mice. Nine days after implantation, tumors reached a size of 50 mm^3. The mice were randomized into two groups and received intraperitoneal injection of EGCG or PBS, respectively. EGCG treatment markedly inhibited tumor growth when compared to control group (Figure 1A). The mean weight of tumors of EGCG treatment was significantly lower than that of control group, and an average of 60.4% suppression of primary tumor growth was observed ($P < 0.01$, Figure 1B). From d 16 after EGCG

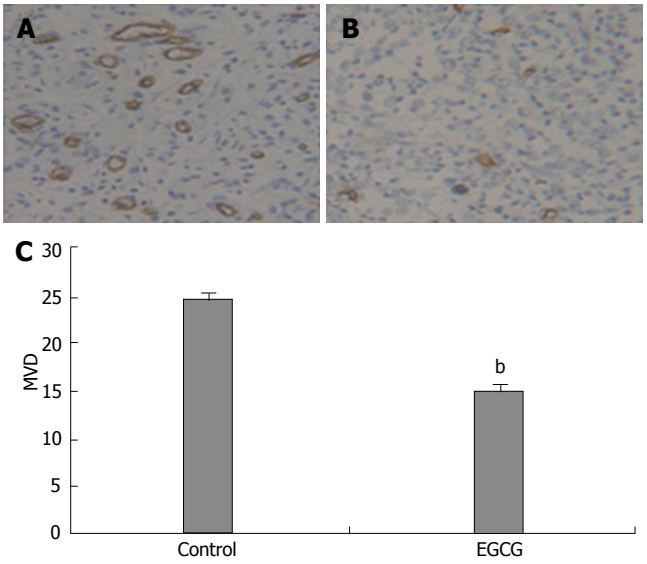

Figure 2 MVD in tumor tissues determined by a specific antibody against mouse endothelial CD34 in PBS group (**A**) and EGCG group (**B**) (200 ×) while quantitative analysis showing significant reduction of tumor MVD after EGCG treatment (**C**). Data are presented as mean ± SE (n = 6, $^bP < 0.01$).

injection, the average volume of tumors was significantly lower in EGCG treatment group than in control group (Figure 1C).

EGCG inhibited tumor neovascularization

To elucidate the anti-angiogenic activity of EGCG *in vivo*, the effect of EGCG on tumor angiogenesis was evaluated by CD34 immunostaining for capillaries in tumor tissues. The density of CD34-stained capillaries was significantly lower in EGCG treatment group (Figure 2A) than in control group (Figure 2B). Microvessel density in tumors receiving EGCG treatment was markedly reduced ($P < 0.01$, Figure 2C), and an average of 38.2% suppression was observed.

EGCG inhibited VEGF expression and Stat3 activation in vitro and in vivo

Gastric cancer had a high expression level of VEGF and Stat3, and activation of Stat3. To determine the effect of EGCG on Stat3 activation and expression of VEGF and total Stat3, the protein level of VEGF, total Stat3 and phosphorylated Stat3 in tumor cells and tissues was examined by Western blot. As shown in Figure 3, EGCG treatment down-regulated VEGF expression in cultured tumor cells in a dose-dependent manner. VEGF expression in tumor tissues treated with EGCG was also markedly reduced. Consistent with the results of VEGF expression, activation of Stat3 in cultured tumor cells was decreased in a concentration-dependent manner, and also apparently reduced in EGCG treated tumor tissues. However, EGCG treatment did not change the expression of total Stat3 either in cultured cells or in tumor tissues.

EGCG decreased VEGF secretion from tumor cells

Angiogenesis is initiated by the release of angiogenic factors from tumor cells. VEGF is the most potent angiogenic factor and associated with tumor-induced

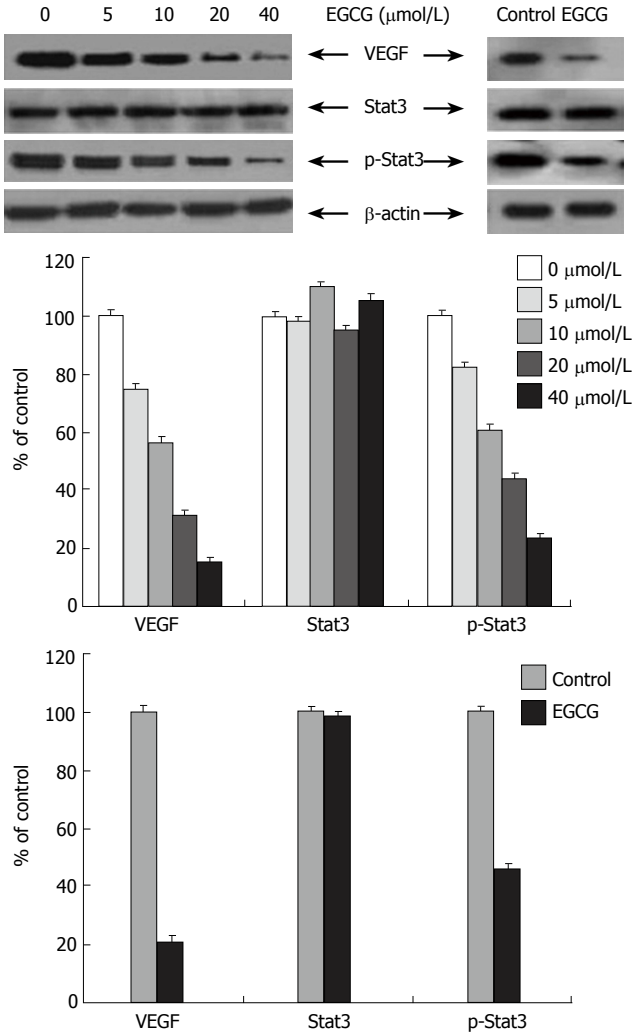

Figure 3 Suppression of VEGF expression and Stat3 activation in tumor cells and tissues by EGCG. Protein level of VEGF and phosphorylated Stat3 was dose-dependently reduced in tumor cells treated with EGCG and also markedly in EGCG treated tumor tissues. EGCG did not change expression of Stat3 in tumor cells or tumor tissues.

angiogenesis. To examine the effect of EGCG on VEGF secretion, VEGF protein level in the conditioned medium was measured by ELISA. EGCG treatment reduced VEGF secretion in the culture medium in a dose-dependent manner (Figure 4A). EGCG at the concentration of 5 μmol/L significantly reduced VEGF secretion by 16.0% ($P < 0.05$).

EGCG inhibited VEGF expression at transcription level

To determine whether the inhibitory effect of EGCG on VEGF expression is at the transcriptional level, we examined VEGF mRNA expression in tumor cells by RT-PCR, showing that VEGF mRNA expression in EGCG treated cells was reduced in a dose-dependent manner (Figure 4B). These results suggested that EGCG reduced VEGF expression by inhibiting VEGF gene transcription and decreasing VEGF mRNA expression.

EGCG inhibited endothelial cell proliferation induced by VEGF

Tumor angiogenesis is induced by VEGF mainly produced by tumor cells. VEGF-induced angiogenesis is very important

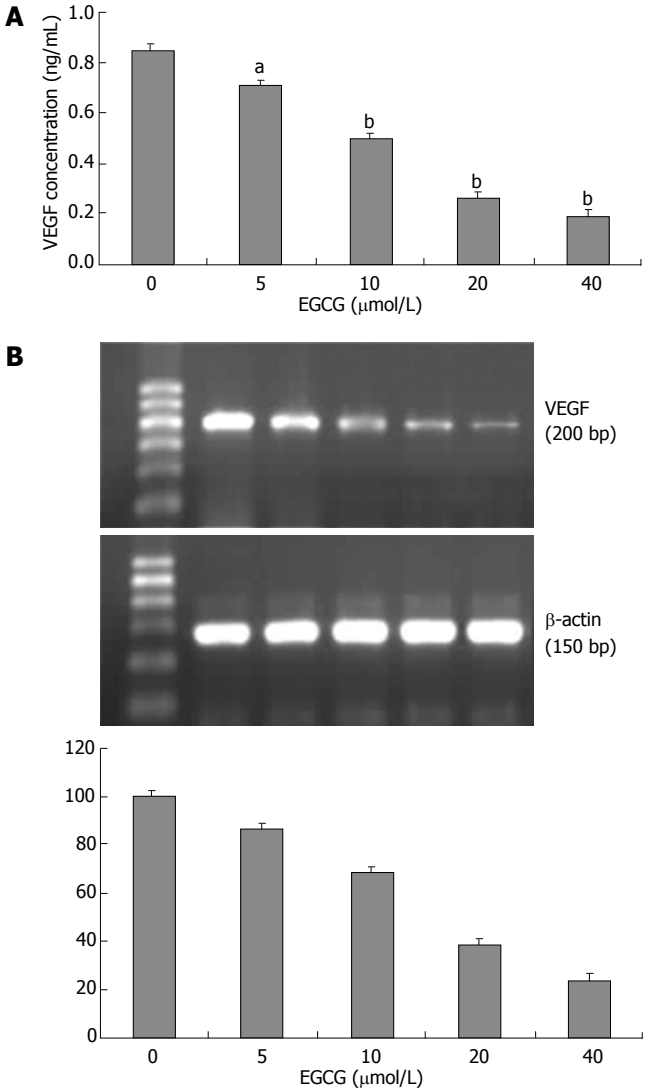

Figure 4 Decreased VEGF secretion (**A**) and inhibition of of VEGF mRNA expression (**B**) in tumor cells. SGC-7901 cells were treated with various concentrations of EGCG for 24 h and VEGF protein level in the supernatant was measured by ELISA and mRNA expression in tumor cells was examined by RT-PCR. Data are presented as mean ± SE (n = 3, $^aP < 0.05$, $^bP < 0.01$).

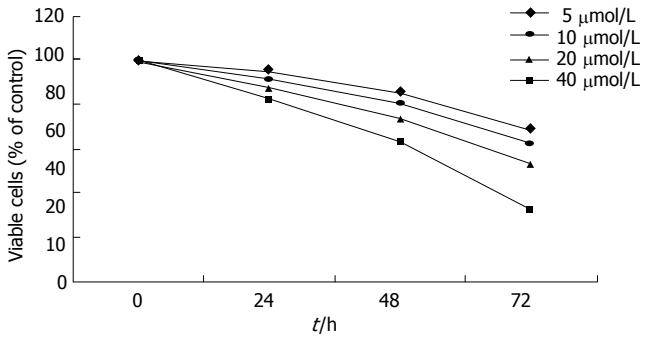

Figure 5 Inhibitory effects of EGCG on VEGF-induced proliferation of endothelial cells. HUVECs were treated with 20 ng/mL VEGF and EGCG at the indicated concentration and time. EGCG time- and dose-dependently inhibited HUVEC proliferation induced by VEGF. Values are expressed as percent of control (means ± SE, n = 3).

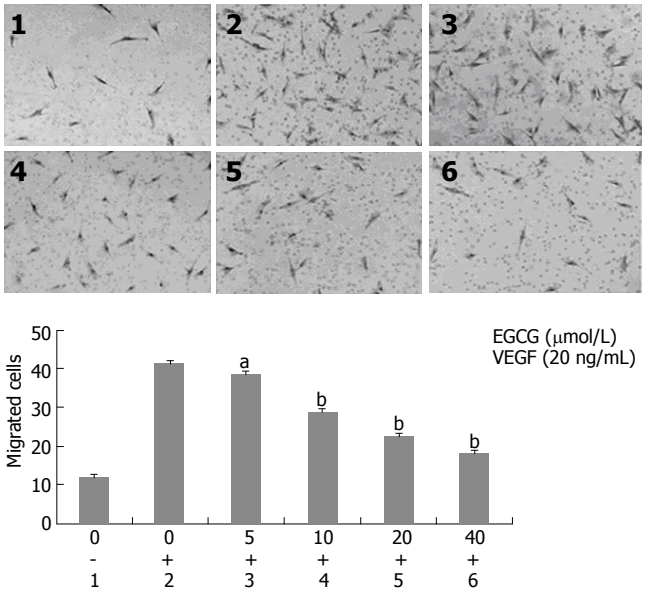

Figure 6 EGCG inhibits endothelial cell migration induced by VEGF. EGCG inhibited migration of HUVECs induced by VEGF in a dose-dependent manner. Data are presented as mean ± SE (n = 3). VEGF-induced migration without EGCG treatment was used as a control. Values significantly lower than control are indicated ($^aP < 0.05$, $^bP < 0.01$).

for tumor growth and metastasis. To further investigate whether EGCG inhibits VEGF-induced angiogenesis, we examined the effect of EGCG on VEGF-induced endothelial proliferation, migration and tuber formation. The effect of EGCG on VEGF-induced proliferation of HUVECs was determined by MTT assay. HUVECs were treated with 20 ng/mL VEGF and EGCG at the indicated concentrations for 24, 48 and 72 h. As shown in Figure 5, EGCG treatment abrogated VEGF-induced proliferation of HUVECs in a time- and dose-dependent manner.

Inhibitory effect of EGCG on endothelial cell migration induced by VEGF

Endothelial cell migration is one of the key steps in angiogenesis. We examined the inhibitory effect of EGCG on endothelial cell migration induced by VEGF. As shown in Figure 6, EGCG treatment significantly and dose-dependently inhibited migration of HUVECs induced by VEGF. EGCG at the concentration of 5 μmol/L could effectively reduce VEGF-induced endothelial cell migration ($P < 0.05$).

Inhibition of VEGF-induced tube formation by EGCG

We determined the effect of EGCG on tube formation induced by VEGF. When treated with EGCG, tube formation induced by VEGF was inhibited in a concentration-dependent manner. EGCG reduced the length of endothelial tubes even at the concentration of 5 μmol/L, and an average of 24.2% inhibition was observed ($P < 0.01$). At the concentration of 40 μmol/L, EGCG abrogated almost all tube formations induced by VEGF (Figure 7).

DISCUSSION

Despite significant advance in treatment, gastric cancer remains one of the leading causes of cancer-related death in many countries such as China[14]. Tremendous efforts

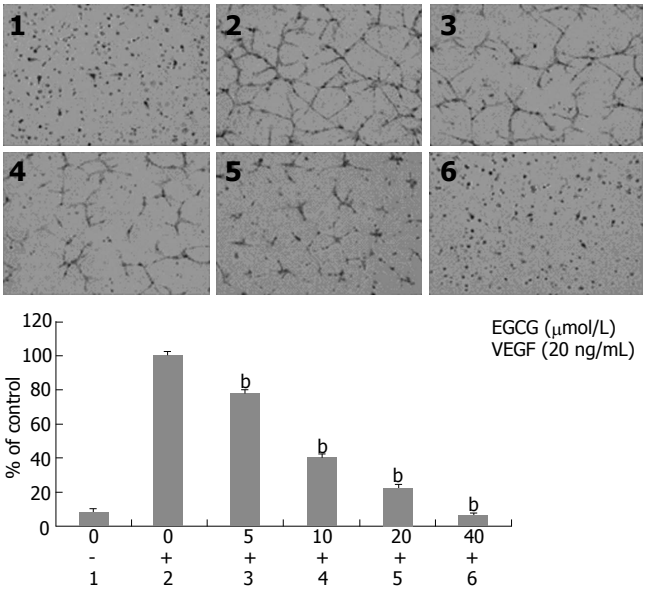

Figure 7 Inhibition of EGCG on VEGF-induced tube formation of endothelial cells. EGCG dose-dependently inhibited tube formation induced by VEGF on Matrigel. Data are expressed as percent of control. VEGF-induced tube formation without EGCG treatment was used as a control. Values significantly lower than control are indicated ($^bP < 0.01$).

have been made to identify new chemopreventive and chemotherapeutic agents and strategies. Anti-angiogenic therapy is one of the most promising novel strategies and many attempts have been made to prevent or delay tumor growth by anti-angiogenesis. As the most potent angiogenic factor, VEGF has become one of the most common targets in anti-angiogenic therapy. In this study, we demonstrated that EGCG suppressed growth of gastric cancer by reducing VEGF production and VEGF-induced angiogenesis.

Green tea has been shown to have anti-angiogenic activity and drinking tea can significantly prevent VEGF-induced corneal neovascularization[15]. As the most abundant and active component of green tea, EGCG has also been shown to have anti-angiogenic property[9]. Treatment with EGCG can inhibit tumor growth[10]. In this study, intraperitoneal injection of EGCG markedly suppressed growth of gastric cancer, and an average of 60.4% inhibition was observed. MVD in tumor tissues treated with EGCG were significantly decreased. These results suggest that EGCG inhibits growth of gastric cancer.

Previous studies indicated that EGCG inhibits VEGF expression in tumor cells[10,16]. Treatment with EGCG also dose-dependently suppresses the secretion of VEGF both in endothelial cells and in tumor cells[17]. To evaluate the effect of EGCG on expression of VEGF in gastric cancer, we determined the expression of VEGF in cultured cells and tumor tissues. As shown in Figure 3, EGCG treatment dose-dependently decreased the expression of VEGF in cultured tumor cells. In tumor tissues treated with EGCG, the expression of VEGF was markedly reduced. Treatment with EGCG also reduced VEGF secretion in tumor cells in a dose-dependent manner. EGCG dose-dependently suppressed VEGF mRNA expression (Figure 4B). These findings suggest that EGCG inhibits angiogenesis in gastric cancer by reducing production of VEGF at transcriptional level.

VEGF expression is associated with a variety of transcription factors, genes and modulators[18]. Several mechanisms have been proposed for the inhibitory effect of EGCG on VEGF expression. EGCG strongly inhibits the transcriptional activity of transcription factors, such as NF-kappa B[16,19] and activator protein-1[20]. Treatment with EGCG also decreases the constitutive activation of EGFR[16] and the expression of protein kinase C[19], transcription modulators of VEGF, suggesting that these changes are associated with inhibition of VEGF promoter activity and cellular production of VEGF. Recent studies showed that EGCG strongly inhibits the constitutive activation of Stat3 in tumor cells[16]. Stat3 is one of the key transcription factors in regulation of VEGF expression[18]. Stat3 activation directly promotes VEGF expression and stimulates tumor angiogenesis[21]. In this study, high activation level of Stat3 was observed in gastric cancer, showing that abnormally activated Stat3 expression significantly correlates with VEGF expression and microvessel density (MVD), and is an independently prognostic factor of poor survival[22]. EGCG can reduce VEGF expression by inhibiting activation of Stat3 in human head, neck and breast cancer[16]. In this study, EGCG dose-dependently inhibited activation of Stat3. In tumor cells and tissues treated with EGCG, the protein level of phosphorylated Stat3 was markedly reduced, but the total Stat3 level remained unchanged, suggesting that EGCG down-regulates VEGF expression at least in part by inhibiting Stat3 activation in gastric cancer.

It was reported that EGCG is most effective in inhibiting angiogenesis among the four main catechins of green tea[23]. Angiogenesis is initiated by the release of angiogenic factors from tumor cells, and VEGF is the most potent angiogenic factor. In this study, EGCG directly inhibited VEGF-induced angiogenesis. As shown in Figure 5, treatment with EGCG inhibited VEGF-induced HUVEC proliferation in a time- and dose-dependent manner and endothelial cell migration and tuber formation were also abrogated by EGCG, suggesting that EGCG inhibits angiogenesis in gastric cancer by inhibiting VEGF-induced angiogenesis and reducing production of VEGF.

VEGF induces angiogenesis by binding to its receptors on endothelial cell surface. It was reported that EGCG dose-dependently inhibits VEGF binding to its receptors on endothelial cell surface, and EGCG is the only catechin of green tea that could disrupt VEGF receptor binding[23]. Importantly, EGCG at low doses (0.5-10 μmol/L) markedly inhibits formation of VEGFR-2 complex[19]. The exact mechanism underlying the inhibition of VEGF receptor binding is unclear. A recent report suggested that green tea extract dose-dependently inhibits expression of VEGFR-1 and -2 on HUVECs[24]. But in our study, EGCG could not modulate VEGFR-1 and VEGFR-2 expression (data not shown). Disruption of VEGF receptor binding would block receptor tyrosine phosphorylation and VEGF-induced growth and survival signaling. Treatment with EGCG inhibits VEGF-induced VEGFR-1 and VEGFR-2

phosphorylation on endothelial cells in a time- and dose-dependent manner[25]. This disruption decreases PI3-kinase activity in a dose-dependent manner[19], suppresses VE-cadherin tyrosine phosphorylation and Akt activation[26], and also decreases the PI3 kinase-dependent activation and DNA-binding ability of NF-kappaB[19], suggesting that EGCG inhibits VEGF-induced angiogenesis by disrupting VEGF signaling pathway.

In the present study, EGCG suppressed growth of gastric cancer by targeting multiple steps of angiogenesis. EGCG at the concentration 5 μmol/L effectively inhibited VEGF production and VEGF-induced angiogenesis. EGCG at 40 μmol/L almost totally abolished tube formation induced by VEGF. Previous studies also showed that concentrations of EGCG used in anti-angiogenesis experiments are usually lower than those in anti-cancer experiments, thus strongly supporting the concept that EGCG represents a potent angiogenic inhibitor and EGCG has dual anti-angiogenesis and anti-cancer activities. EGCG might mainly act as an angiogenic inhibitor *in vivo*, and this might in part explain the discrepancy between cell line and animal model studies. The concentration of EGCG tested in cell line system usually is 10-100 μmol/L, or higher. It is much higher than that observed in plasma or tissues of animals or human beings after ingestion of tea or related tea preparations for the poor bioavailability of EGCG[27].

As an angiogenic inhibitor targeting tumor-induced angiogenesis, EGCG might have some advantages over conventional cytotoxic chemotherapy for genetic stability of endothelial cells and abnormality of tumor vasculature. EGCG is less likely to induce drug resistance and has little or no toxicity. During the treatment, EGCG treated mice did not show weight loss or unusual behavior, histopathological examination also did not reveal any detectable toxicity to liver or kidney (data not shown), suggesting that EGCG at the concentrations used does not cause any detectable toxicity. Previous studies also showed that EGCG induces apoptosis and cell cycle arrest in many cancer cells without affecting normal cells[28]. It was reported that EGCG has anti-cancer effect without any severe side effects[29]. Taken together, as a natural and non-toxic product, EGCG might be a promising candidate for anti-angiogenic treatment of gastric cancer.

REFERENCES

1 **Parkin DM**, Pisani P, Ferlay J. Estimates of the worldwide incidence of eighteen major cancers in 1985. *Int J Cancer* 1993; **54**: 594-606
2 **Kelley JR**, Duggan JM. Gastric cancer epidemiology and risk factors. *J Clin Epidemiol* 2003; **56**: 1-9
3 **Chen D**, Daniel KG, Kuhn DJ, Kazi A, Bhuiyan M, Li L, Wang Z, Wan SB, Lam WH, Chan TH, Dou QP. Green tea and tea polyphenols in cancer prevention. *Front Biosci* 2004; **9**: 2618-2631
4 **Kono S**, Ikeda M, Tokudome S, Kuratsune M. A case-control study of gastric cancer and diet in northern Kyushu, Japan. *Jpn J Cancer Res* 1988; **79**: 1067-1074
5 **Yamane T**, Takahashi T, Kuwata K, Oya K, Inagake M, Kitao Y, Suganuma M, Fujiki H. Inhibition of N-methyl-N'-nitro-N-nitrosoguanidine-induced carcinogenesis by (-)-epigallocatechin gallate in the rat glandular stomach. *Cancer Res* 1995; **55**: 2081-2084
6 **Horie N**, Hirabayashi N, Takahashi Y, Miyauchi Y, Taguchi H, Takeishi K. Synergistic effect of green tea catechins on cell growth and apoptosis induction in gastric carcinoma cells. *Biol Pharm Bull* 2005; **28**: 574-579
7 **Hoshiyama Y**, Kawaguchi T, Miura Y, Mizoue T, Tokui N, Yatsuya H, Sakata K, Kondo T, Kikuchi S, Toyoshima H, Hayakawa N, Tamakoshi A, Yoshimura T. Green tea and stomach cancer--a short review of prospective studies. *J Epidemiol* 2005; **15** Suppl 2: S109-S112
8 **Yang CS**, Lambert JD, Hou Z, Ju J, Lu G, Hao X. Molecular targets for the cancer preventive activity of tea polyphenols. *Mol Carcinog* 2006; **45**: 431-435
9 **Jung YD**, Ellis LM. Inhibition of tumour invasion and angiogenesis by epigallocatechin gallate (EGCG), a major component of green tea. *Int J Exp Pathol* 2001; **82**: 309-316
10 **Jung YD**, Kim MS, Shin BA, Chay KO, Ahn BW, Liu W, Bucana CD, Gallick GE, Ellis LM. EGCG, a major component of green tea, inhibits tumour growth by inhibiting VEGF induction in human colon carcinoma cells. *Br J Cancer* 2001; **84**: 844-850
11 **Kakeji Y**, Koga T, Sumiyoshi Y, Shibahara K, Oda S, Maehara Y, Sugimachi K. Clinical significance of vascular endothelial growth factor expression in gastric cancer. *J Exp Clin Cancer Res* 2002; **21**: 125-129
12 **Shishido T**, Yasoshima T, Denno R, Sato N, Hirata K. Inhibition of liver metastasis of human gastric carcinoma by angiogenesis inhibitor TNP-470. *Jpn J Cancer Res* 1996; **87**: 958-962
13 **Weidner N**, Semple JP, Welch WR, Folkman J. Tumor angiogenesis and metastasis--correlation in invasive breast carcinoma. *N Engl J Med* 1991; **324**: 1-8
14 **Yang L**. Incidence and mortality of gastric cancer in China. *World J Gastroenterol* 2006; **12**: 17-20
15 **Cao Y**, Cao R. Angiogenesis inhibited by drinking tea. *Nature* 1999; **398**: 381
16 **Masuda M**, Suzui M, Lim JT, Deguchi A, Soh JW, Weinstein IB. Epigallocatechin-3-gallate decreases VEGF production in head and neck and breast carcinoma cells by inhibiting EGFR-related pathways of signal transduction. *J Exp Ther Oncol* 2002; **2**: 350-359
17 **Sartippour MR**, Shao ZM, Heber D, Beatty P, Zhang L, Liu C, Ellis L, Liu W, Go VL, Brooks MN. Green tea inhibits vascular endothelial growth factor (VEGF) induction in human breast cancer cells. *J Nutr* 2002; **132**: 2307-2311
18 **Xie K**, Wei D, Shi Q, Huang S. Constitutive and inducible expression and regulation of vascular endothelial growth factor. *Cytokine Growth Factor Rev* 2004; **15**: 297-324
19 **Rodriguez SK**, Guo W, Liu L, Band MA, Paulson EK, Meydani M. Green tea catechin, epigallocatechin-3-gallate, inhibits vascular endothelial growth factor angiogenic signaling by disrupting the formation of a receptor complex. *Int J Cancer* 2006; **118**: 1635-1644
20 **Dong Z**, Ma W, Huang C, Yang CS. Inhibition of tumor promoter-induced activator protein 1 activation and cell transformation by tea polyphenols, (-)-epigallocatechin gallate, and theaflavins. *Cancer Res* 1997; **57**: 4414-4419
21 **Niu G**, Wright KL, Huang M, Song L, Haura E, Turkson J, Zhang S, Wang T, Sinibaldi D, Coppola D, Heller R, Ellis LM, Karras J, Bromberg J, Pardoll D, Jove R, Yu H. Constitutive Stat3 activity up-regulates VEGF expression and tumor angiogenesis. *Oncogene* 2002; **21**: 2000-2008
22 **Gong W**, Wang L, Yao JC, Ajani JA, Wei D, Aldape KD, Xie K, Sawaya R, Huang S. Expression of activated signal transducer and activator of transcription 3 predicts expression of vascular endothelial growth factor in and angiogenic phenotype of human gastric cancer. *Clin Cancer Res* 2005; **11**: 1386-1393
23 **Kondo T**, Ohta T, Igura K, Hara Y, Kaji K. Tea catechins inhibit angiogenesis in vitro, measured by human endothelial cell growth, migration and tube formation, through inhibition of VEGF receptor binding. *Cancer Lett* 2002; **180**: 139-144
24 **Kojima-Yuasa A**, Hua JJ, Kennedy DO, Matsui-Yuasa I. Green tea extract inhibits angiogenesis of human umbilical vein endothelial cells through reduction of expression of VEGF

receptors. *Life Sci* 2003; **73**: 1299-1313
25 **Lamy S**, Gingras D, Béliveau R. Green tea catechins inhibit vascular endothelial growth factor receptor phosphorylation. *Cancer Res* 2002; **62**: 381-385
26 **Tang FY**, Nguyen N, Meydani M. Green tea catechins inhibit VEGF-induced angiogenesis in vitro through suppression of VE-cadherin phosphorylation and inactivation of Akt molecule. *Int J Cancer* 2003; **106**: 871-878
27 **Lambert JD**, Yang CS. Cancer chemopreventive activity and bioavailability of tea and tea polyphenols. *Mutat Res* 2003; **523-524**: 201-208
28 **Chen ZP**, Schell JB, Ho CT, Chen KY. Green tea epigallocatechin gallate shows a pronounced growth inhibitory effect on cancerous cells but not on their normal counterparts. *Cancer Lett* 1998; **129**: 173-179
29 **Jatoi A**, Ellison N, Burch PA, Sloan JA, Dakhil SR, Novotny P, Tan W, Fitch TR, Rowland KM, Young CY, Flynn PJ. A phase II trial of green tea in the treatment of patients with androgen independent metastatic prostate carcinoma. *Cancer* 2003; **97**: 1442-1446

S- Editor Liu Y **L- Editor** Wang XL **E- Editor** Lu W

PO Box 2345, Beijing 100023, China
www.wjgnet.com
wjg@wjgnet.com

World J Gastroenterol 2007 February 28; 13(8): 1170-1174
World Journal of Gastroenterology ISSN 1007-9327

GASTRIC CANCER

Downregulation of survivin by RNAi inhibits growth of human gastric carcinoma cells

Guo-Ying Miao, Qi-Ming Lu, Xiu-Lan Zhang

Guo-Ying Miao, Qi-Ming Lu, Xiu-Lan Zhang, Department of Digestion, The People's Hospital of Gansu Province, Lanzhou 730000, Gansu Province, China
Correspondence to: Qi-Ming Lu, Department of Digestion, The People's Hospital of Gansu Province, Lanzhou 730000, Gansu Province, China. mguoying@tom.com
Telephone: +86-931-8281758
Received: 2006-12-09 Accepted: 2007-02-09

Key words: Gastric carcinoma; Survivin; RNA interference; Apoptosis; Gene expression

Miao GY, Lu QM, Zhang XL. Downregulation of survivin by RNAi inhibits growth of human gastric carcinoma cells. *World J Gastroenterol* 2007; 13(8): 1170-1174

http://www.wjgnet.com/1007-9327/13/1170.asp

Abstract

AIM: To investigate the inhibitory effect of a specific small survivin interfering RNA (siRNA) on cell proliferation and the expression of survivin in human gastric carcinoma cell line SGC-7901.

METHODS: To knockdown survivin expression, a small interfering RNA targeting against survivin was synthesized and transfected into SGC-7901 cells with lipofectamine™2000. The downregulation of survivin expression at both mRNA and protein levels were detected by reverse transcription-polymerase chain reaction (RT-PCR) and Western blot analysis. Cell proliferation inhibition rates were determined by methyl thiazolyl tetrazolium (MTT) assay. The effect of survivin siRNA on cell cycle distribution and cell apoptosis was determined by flow cytometry (FCM).

RESULTS: RNA interference could efficiently suppress the survivin expression in SGC-7901 cells. At 48 h after transfection, the expression inhibition rate was 44.52% at mRNA level detected by RT-PCR and 40.17% at protein level by Western blot analysis. Downregulation of survivin resulted in significant inhibition of tumor cell growth *in vitro*. The cell proliferation inhibition rates at 24, 48 and 72 h after survivin siRNA and non-siliencing siRNA transfection, were 34.06%, 47.61% and 40.36%, respectively. The apoptosis rate was 3.56% and the number of cells was increased in G_0/G_1 phase from 38.2% to 88.6%, and decreased in S and G_2/M phase at 48 h after transfection.

CONCLUSION: Downregulation of survivin results in significant inhibition of tumor growth *in vitro*. The inhibition of survivin expression can induce apoptosis of SGC-7901 cells. The use of survivin siRNA deserves further investigation as a novel approach to cancer therapy.

INTRODUCTION

Survivin was initially identified as a member of the inhibitor of apoptosis protein (IAP) family. Up to the present, overexpression of survivin has not been reported in differentiated normal tissues with exception of thymus, basal colonic epithelium endothelial cells and neural stem cells during angiogenesis[1]. However, the highly specific expression of survivin was found in many human cancers, including gastric cancer. By inhibiting apoptosis and promoting mitosis, survivin facilitates cancer cell survival and growth[2-6]. Several studies have revealed that survivin as an indispensable factor can regulate and assist completion of cytokinesis[7-10]. Recently, it has been also proven that overexpression of survivin can protect cells from apoptosis by inhibiting pro-apoptotic caspases-3 and caspases-7; when acting as a microtubule stabilizer during mitosis, it promotes cell cycle progression as well[11-14]. In addition, Asanuma K *et al*[15] reported that survivin enhanced the expression of the Fas ligand in cancer cells through up-regulation of specific protein-1-mediated gene transcription, and enabled cancer cells to counter-attack immune cells by inducing FasL-triggered apoptosis of cells in the immune surveillance system.

RNAi is a genetic interference phenomenon that is effective for suppressing gene expression. It involves post-transcriptional gene silencing *via* a process in which double-stranded RNA (dsRNA) inhibits gene expression in a sequence-dependent manner through degradation of the corresponding mRNA. Its blocking action on gene expression has been successfully observed in rat and human cells cultured *in vitro*, and the knockdown of genes in cells has been achieved[16,17].

In the present study, siRNA targeting to the survivin gene was introduced into gastric carcinoma cell line SGC-7901, which overexpresses survivin. Its effect on cancer cell growth was investigated.

MATERIALS AND METHODS

Cell lines and culture

Human gastric carcinoma cell line SGC-7901 was a present from Dr. Wei Liu. The cells were cultured in RPMI 1640 medium supplemented with 100 mL/L fetal bovine serum (FBS), 8×10^5 U/L penicillin and 0.1 g/L streptomycin in humidified incubator containing 50 mL/L CO_2 at 37℃.

siRNA preparation and transfection of short interfering RNA

siRNA oligonucleotides with two thymidine residues (tt) at the 3' end of the sequence were designed for survivin (sense, 5'-GCAUUCGUCCGGUUGCGCUtt-3'antisense, 5'-AGCGCAACCGGACGAAUGCtt-3'). Cells were treated in parallel with a non-silencing-siRNA (sense, 5'-UUCUCCGAACGUGUCACGUtt-3'; antisense, 5'-ACGUGACACGUUCGGAGAAtt-3') as control oligonucleotides were synthesized by Shanghai Genechem Co. These cells were cultured in medium without antibiotics, and 24 h before transfection resulting in a confluence of the cell monolayer by 50%-70%. Specific survivin siRNA or non-silencing siRNA (70 nmol) were mixed with lipofectamine ^{TM}2000 (Invitrogen) according to manufacturer's recommendation and added to the cells. After 6 h at 37℃, the medium was changed, and the cells were cultivated in RPMI 1640 supplemented with 10% heat-inactivated FBS.

3-(4, 5-methylthiazol-2-yl)-2, 5-diphenyl-tetrazolium bromide (MTT) assay

SGC-7901 cells (5×10^5) were placed onto 96-well plates in RPMI-1640 containing 10% FBS in a final volume of 0.1 mL. The next day, the cells were treated with siRNA. MTT was added (20 μL/well of 5 g/L solution in PBS) after culture for 24 h, 48 h and 72 h. When incubated at 37℃ for 4 h, the reaction was stopped by addition of 100 μL DMSO. The reaction product was quantified by measuring the absorbance at 490 nm using an ELISA reader (WALLAC 1420 VICTOR 2, Victor Co, Finland) and Software HT-Soft (Perkin-Elmer). All samples were assayed repeatedly in six wells.

Reverse transcription polymerase chain reaction

SGC-7901 cells (5×10^5) were seeded onto 6-well plates. Total RNA was extracted 48 h after transfection using trizol reagent. Reverse transcription was performed using one step RT-PCR kit. The primers of human survivin were 5'-GGACCGCCTAAGAGGGCGTGC-3' (forward primer) and 5'-AATGTAGAGATGCGGTGGTCCTT-3' (reverse primer). The primers of human β-actin were 5'-GTGGGCATGGGTCAGAAG-3' (forward primer) 5'-GAGGCGTACAGGGATAGCAC-3' (reverse primer). Thermal cycle conditions were as follows: 42℃ for 30 min, 94℃ for 2 min, followed by 28 cycles of 94℃ 15 s, 55℃ 30 s, 72℃ 1 min, with a final extension at 72℃ for 10 min. RT-PCR products were visualized by ethidium bromide-stained agarose gels.

Western immunoblot analysis

SGC-7901 cells (5×10^5) were seeded onto 6-well plates. Forty-eight hours after transfection, cells were collected and washed twice by cold PBS, and each well was treated with 50 μL lysis buffer (2 mmol/L Tris-HCl pH 7.4, 50 mmol/L NaCl, 25 mmol/L EDTA, 50 mmol/L NaF, 1.5 mmol/L Na_3VO_4, 1% Triton X-100, 0.1% SDS, supplemented with protease inhibitors 1 mmol/L phenylmethylsulfonylfluoride, 10 mg/L pepstatin, 10 mg/L aprotinin, and 5 mg/L leupeptin) (all from Sigma). Protein concentrations were determined using the bicinchoninic acid protein assay. Equal amounts of protein (40 μg) were separated on a 15% SDS polyacrylamide gel and transferred to a nitrocellulose membrane (Hybond C, Amersham, Freiburg, Germany). Membranes were blocked in 5% nonfat dry milk in TBS for 1 h at room temperature and probed with rabbit antisurvivin antibodies (dilution, 1:500 Santa Cruz Biotechnology, USA) overnight at 4℃. After 3 times washing with TBS containing 0.1% Tween 20, membranes were incubated with anti-rabbit IgG-horseradish-peroxidase (1:5000, Santa Cruz Biotechnology, USA), and developed by luminol mediated chemiluminescence (Appylgen Technologies Inc, China). To confirm equal protein loading, membranes were reprobed with a 1:1000 dilution of an anti-actin antibody (Santa Cruz Biotechnology, USA). Densitometric analyses were performed using Scion Image software.

Flow cytometry

SGC-7901 (5×10^5) cell lines were seeded in triplicate onto 6 well-plates, and cultured in RPMI-1640 supplemented with 100 mL/L FBS. When transfected for 48 h, the cells were collected and washed with ice-cold PBS, and fixed in 70% ethanol overnight at 4℃. The fixed cells were pelleted, washed in PBS, resuspended in PBS containing 0.1 mg/mL of propidium iodide, and analysed by flow cytometry.

Statistical analysis

Data were expressed as mean ± SD. All statistical analyses were performed using the SPSS 10.0 software package for Windows (SPSS Inc., Chicago, IL). One-way ANOVA followed by Bonferroni correction was used to compare the data among three or more groups. A value of $P < 0.01$ was considered statistically significant.

RESULTS

Expression of survivin gene in SGC-7901 cells

To examine the specific effect of survivin siRNA treatment on survivin expression in SGC-7901 line, the survivin mRNA and protein expression levels were determined quantitatively with RT-PCR and Western blot analyses, respectively. Results are displayed in Figure 1 and Figure 2. Survivin mRNA and protein were strongly expressed in gastric cancer SGC-7901 cells as reflected by RT-PCR and Western blot. The inhibition rate of survivin mRNA after transfection with specific survivin siRNA was 44.52%. The inhibition rate of survivin protein after transfection with specific survivin siRNA was 40.17%. Survivin expression was decreased significantly at 48 h after transfection with specific survivin siRNA.

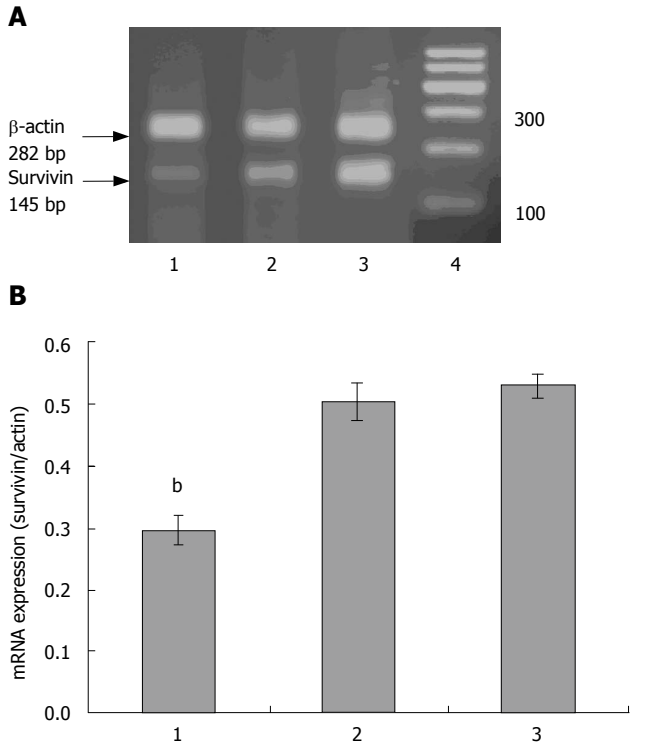

Figure 1 Expression of survivin mRNA in different groups of SGC-7901 cells. **A**: Survivin mRNA expression in RT-PCR assay; **B**: Survivin mRNA expression in SGC-7901. 1: treated with survivin siRNA; 2: treated with non-silencing siRNA; 3: untreated. Data are expressed as mean ± SD of three experiments, survivin siRNA group *vs* non-silencing siRNA group, $^bP < 0.01$; survivin siRNA group *vs* untreated group, $^bP < 0.01$.

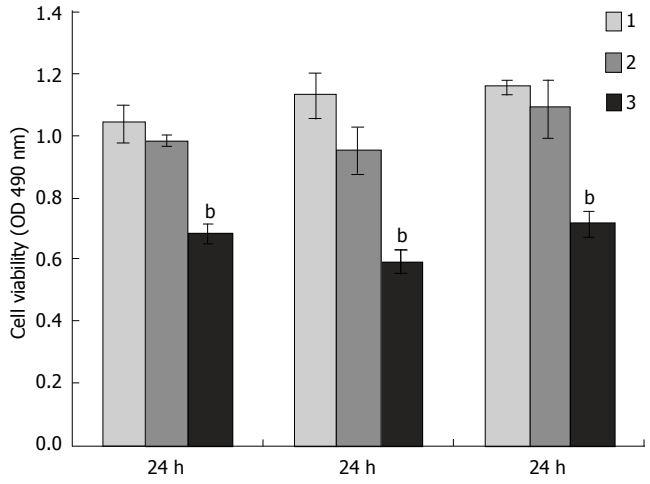

Figure 3 Effects on cell viability after non-silencing siRNA and survivin siRNA treatment. 1: untreated; 2: non-silencing siRNA; 3: survivin siRNA. Data are expressed as mean ± SD, survivin siRNA group *vs* non-silencing siRNA group, $^bP < 0.01$; survivin siRNA group *vs* untreated group, $^bP < 0.01$.

Effect of survivin siRNA on cell proliferation of gastric cancer cells

To determine whether inhibition of survivin affects cell proliferation in SGC-7901, metabolic activity at 24, 48, and 72 h was determined by the MTT assay. The cell viability was reduced significantly after treatment with specific survivin siRNA ($P < 0.01$) at 24, 48, and 72 h as compared with non-silencing siRNA treatment or untreated controls (Figure 3). The cell proliferation inhibition rates were

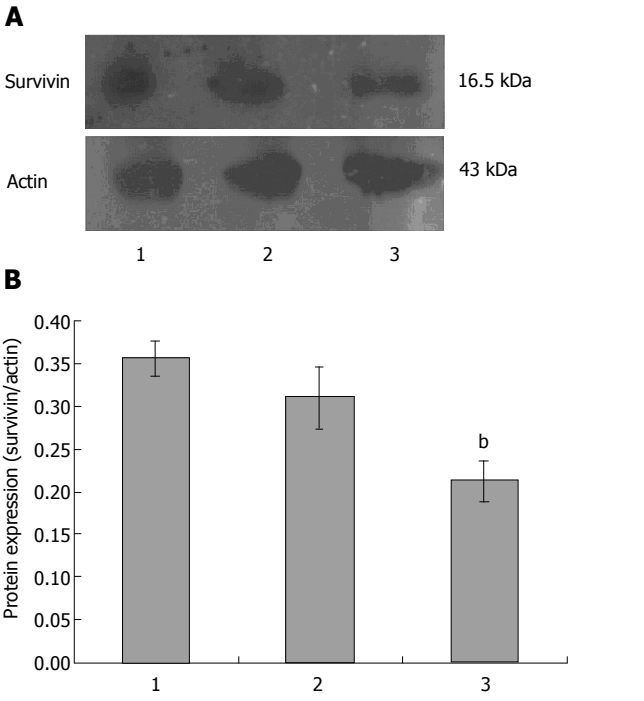

Figure 2 Western blot assay of survivin protein expression in SGC-7901 cells. **A**: Survivin protein expression in Western blot assay; **B**: Survivin protein expression in SGC-7901.1: untreated; 2: non-silencing siRNA; 3: survivin siRNA. Data are expressed as mean ± SD of three experiments, survivin siRNA group *vs* non-silencing siRNA group, $^bP < 0.01$; survivin siRNA group *vs* untreated group, $^bP < 0.01$.

Table 1 Effects of treatment with survivin-siRNA on cell cycle distribution and apoptosis 48 h after transfection

Groups	Cell cycle			Apoptosis rate
	G_0/G_1	S	G_2/M	
Untreated	38.21 ± 3.39	47.71 ± 2.73	14.00 ± 0.92	0.83 ± 0.34
Non-silencing	42.53 ± 2.78	43.28 ± 4.12	14.20 ± 2.90	1.08 ± 0.33
Sur-siRNA	88.60 ± 4.04^b	12.00 ± 3.42^b	0.10 ± 0.07^b	3.56 ± 0.91^b

Data are expressed as mean ± SD of the three experiments, sur-siRNA group *vs* non-silencing group, $^bP < 0.01$; sur-siRNA group *vs* untreated group, $^bP < 0.01$.

34.06%, 47.61% and 40.36%, respectively.

Effect of survivin siRNA on cell cycle distribution and apoptosis

Survivin has been reported to express in the G2/M phase of the cell cycle and to contribute to the aberrant progression of cancer cells through mitosis. In our study, in comparison of non-silencing siRNA group and untreated controls, specific survivin siRNA caused accumulation in the G_0/G_1 phase, and decreased the number of cells of G_2/M phase and increased hypodiploid DNA content ($P < 0.01$) at 48 h after transfection. Apoptosis rate was 3.56% in the group of specific survivin siRNA transfection (Table 1).

DISCUSSION

The balance between apoptosis and anti-apoptosis signal pathways plays a role in the pathogenesis of a variety of

cancers. It has been demonstrated that the inhibition of apoptosis promotes the mitotic progression in cancer cells[18]. Based on its specific overexpression in a vast majority of solid cancers and its anti-apoptotic function, survivin represents a suitable target for antitumor approaches. The inhibition of survivin would block the anti-apoptosis and mitotic progression in tumor cells[19], as a result, tumor development is suppressed. So, survivin has attracted considerable attention as a novel member of IAP family.

RNAi is an evolutionarily conserved phenomenon in which gene expression is suppressed by the introduction of homologous double-stranded RNAs (dsRNAs). Synthetic siRNA can trigger an RNA interference response in mammalian cells and induce strong inhibition of specific gene expression[20]. Therefore, it can be used as a powerful approach to silence mammalian gene expression for gene function studies[21-24].

Since survivin is important for the survival of various human tumors, survivin siRNA could become an effective therapeutic agent for tumors with overexpression of survivin. Survivin has been successfully down-regulated by RNAi in some previous studies[25-29]. However, the down-regulation of survivin expression by RNAi in gastric cancer SGC-7901 cells has not been performed until now.

In addition, it is reported that the effect of RNAi may be greatly different, targeting to different sequence of the gene[30-32]. It is therefore, very important to find the proper sequence. The sequence designed by Williams *et al*[26] has been confirmed effective in their research. So in our study, we synthesized this siRNA duplex with a thymidine overhang on 3' terminus *in vitro* to diminish the survivin expression of gastric carcinoma SGC-7901 cell line and to impair its growth potential. We observed that SGC-7901 cells transfected with survivin siRNA grew slowly as compared with the control groups. Survivin siRNA showed anti-proliferation function. RT-PCR and Western blot findings demonstrated that survivin mRNA and protein expression were reduced by over 40%, and survivin gene was blocked in SGC-7901 cells transfected with surviving siRNA at the level of transcription and protein expression. Flow cytometry revealed that the cell growth inhibition by survivin siRNA was a result of cell cycle arrest at G_0/G_1-phase and induction of apoptosis indicated by increased hypodiploid DNA content. The possible mechanism is that survivin is characterized by cell cycle dependent expression, i.e., it is expressed in G_2/M. Ito and co-workers transfected survivin into four human hepatocellular carcinoma cell lines and found that the number of cells in G_0/G_1 was remarkably reduced, and the number of cells in S or G2/M increased. In our study, after SGC-7901 cells were transfected with survivin siRNA, the number of cells in G_0/G_1 was remarkably increased, and the number of cells in S or G_2/M decreased. The effect showed the same mechanism. However, in the study by Kappler and co-workers, five human sarcoma cell lines transfected with specific survivin siRNA showed G_2/M arrest[26]. Ning *et al*[33] also observed a specific G_2/M arrest when using survivin-directed siRNA as a gene therapeutic approach to human bladder cancer cells. The reason remains unclear, and it may be due to different cell lines.

The above-mentioned findings confirm that chemically synthesized siRNAs can specifically block survivin gene expression, inducing cell apoptosis and inhibiting the growth of carcinoma cells.

In conclusion, our data suggest that survivin gene can be regarded as a very good target gene in genetic therapy for gastric carcinomas and the use of survivin siRNA deserves further investigations as a novel approach to cancer therapy.

ACKNOWLEDGMENTS

We would thank Dr. Juan Li (Central Laboratory of First Affiliated Hospital of Lanzhou University) for her excellent technical assistance. We would also thank Dr. Liu Wei (Institute of Pathology, Lanzhou University) for providing us the cell lines.

REFERENCES

1 **Altieri DC**. Survivin, versatile modulation of cell division and apoptosis in cancer. *Oncogene* 2003; **22**: 8581-8589
2 **Tarnawski A**, Pai R, Chiou SK, Chai J, Chu EC. Rebamipide inhibits gastric cancer growth by targeting survivin and Aurora-B. *Biochem Biophys Res Commun* 2005; **334**: 207-212
3 **Wakana Y**, Kasuya K, Katayanagi S, Tsuchida A, Aoki T, Koyanagi Y, Ishii H, Ebihara Y. Effect of survivin on cell proliferation and apoptosis in gastric cancer. *Oncol Rep* 2002; **9**: 1213-1218
4 **Kania J**, Konturek SJ, Marlicz K, Hahn EG, Konturek PC. Expression of survivin and caspase-3 in gastric cancer. *Dig Dis Sci* 2003; **48**: 266-271
5 **Zhu XD**, Lin GJ, Qian LP, Chen ZQ. Expression of survivin in human gastric carcinoma and gastric carcinoma model of rats. *World J Gastroenterol* 2003; **9**: 1435-1438
6 **Ikeguchi M**, Liu J, Kaibara N. Expression of survivin mRNA and protein in gastric cancer cell line (MKN-45) during cisplatin treatment. *Apoptosis* 2002; **7**: 23-29
7 **Lens SM**, Wolthuis RM, Klompmaker R, Kauw J, Agami R, Brummelkamp T, Kops G, Medema RH. Survivin is required for a sustained spindle checkpoint arrest in response to lack of tension. *EMBO J* 2003; **22**: 2934-2947
8 **Carvalho A**, Carmena M, Sambade C, Earnshaw WC, Wheatley SP. Survivin is required for stable checkpoint activation in taxol-treated HeLa cells. *J Cell Sci* 2003; **116**: 2987-2998
9 **Honda R**, Körner R, Nigg EA. Exploring the functional interactions between Aurora B, INCENP, and survivin in mitosis. *Mol Biol Cell* 2003; **14**: 3325-3341
10 **Beltrami E**, Plescia J, Wilkinson JC, Duckett CS, Altieri DC. Acute ablation of survivin uncovers p53-dependent mitotic checkpoint functions and control of mitochondrial apoptosis. *J Biol Chem* 2004; **279**: 2077-2084
11 **Zaffaroni N**, Pennati M, Daidone MG. Survivin as a target for new anticancer interventions. *J Cell Mol Med* 2005; **9**: 360-372
12 **Altieri DC**. Validating survivin as a cancer therapeutic target. *Nat Rev Cancer* 2003; **3**: 46-54
13 **Giodini A**, Kallio MJ, Wall NR, Gorbsky GJ, Tognin S, Marchisio PC, Symons M, Altieri DC. Regulation of microtubule stability and mitotic progression by survivin. *Cancer Res* 2002; **62**: 2462-2467
14 **Altieri DC**. Molecular circuits of apoptosis regulation and cell division control: the survivin paradigm. *J Cell Biochem* 2004; **92**: 656-663
15 **Asanuma K**, Tsuji N, Endoh T, Yagihashi A, Watanabe N. Survivin enhances Fas ligand expression via up-regulation of specificity protein 1-mediated gene transcription in colon cancer cells. *J Immunol* 2004; **172**: 3922-3929
16 **Konnikova L**, Kotecki M, Kruger MM, Cochran BH.

Knockdown of STAT3 expression by RNAi induces apoptosis in astrocytoma cells. *BMC Cancer* 2003; **3**: 23
17 **Tuschl T**, Borkhardt A. Small interfering RNAs: a revolutionary tool for the analysis of gene function and gene therapy. *Mol Interv* 2002; **2**: 158-167
18 **Kawamura K**, Sato N, Fukuda J, Kodama H, Kumagai J, Tanikawa H, Shimizu Y, Tanaka T. Survivin acts as an antiapoptotic factor during the development of mouse preimplantation embryos. *Dev Biol* 2003; **256**: 331-341
19 **Wall NR**, O'Connor DS, Plescia J, Pommier Y, Altieri DC. Suppression of survivin phosphorylation on Thr34 by flavopiridol enhances tumor cell apoptosis. *Cancer Res* 2003; **63**: 230-235
20 **Izquierdo M**. Short interfering RNAs as a tool for cancer gene therapy. *Cancer Gene Ther* 2005; **12**: 217-227
21 **Downward J**. RNA interference. *BMJ* 2004; **328**: 1245-1248
22 **Mittal V**. Improving the efficiency of RNA interference in mammals. *Nat Rev Genet* 2004; **5**: 355-365
23 **Hannon GJ**, Rossi JJ. Unlocking the potential of the human genome with RNA interference. *Nature* 2004; **431**: 371-378
24 **Stevenson M**. Therapeutic potential of RNA interference. *N Engl J Med* 2004; **351**: 1772-1777
25 **Williams NS**, Gaynor RB, Scoggin S, Verma U, Gokaslan T, Simmang C, Fleming J, Tavana D, Frenkel E, Becerra C. Identification and validation of genes involved in the pathogenesis of colorectal cancer using cDNA microarrays and RNA interference. *Clin Cancer Res* 2003; **9**: 931-946
26 **Kappler M**, Bache M, Bartel F, Kotzsch M, Panian M, Würl P, Blümke K, Schmidt H, Meye A, Taubert H. Knockdown of survivin expression by small interfering RNA reduces the clonogenic survival of human sarcoma cell lines independently of p53. *Cancer Gene Ther* 2004; **11**: 186-193
27 **Uchida H**, Tanaka T, Sasaki K, Kato K, Dehari H, Ito Y, Kobune M, Miyagishi M, Taira K, Tahara H, Hamada H. Adenovirus-mediated transfer of siRNA against survivin induced apoptosis and attenuated tumor cell growth in vitro and in vivo. *Mol Ther* 2004; **10**: 162-171
28 **Yang D**, Welm A, Bishop JM. Cell division and cell survival in the absence of survivin. *Proc Natl Acad Sci USA* 2004; **101**: 15100-15105
29 **Guan HT**, Xue XH, Wang XJ, Li A, Qin ZY. Knockdown of survivin expression by small interfering RNA suppresses proliferation of two human cancer cell lines. *Chin Med Sci J* 2006; **21**: 115-119
30 **Luo KQ**, Chang DC. The gene-silencing efficiency of siRNA is strongly dependent on the local structure of mRNA at the targeted region. *Biochem Biophys Res Commun* 2004; **318**: 303-310
31 **Overhoff M**, Alken M, Far RK, Lemaitre M, Lebleu B, Sczakiel G, Robbins I. Local RNA target structure influences siRNA efficacy: a systematic global analysis. *J Mol Biol* 2005; **348**: 871-881
32 **Guan HT**, Xue XH, Dai ZJ, Wang XJ, Li A, Qin ZY. Down-regulation of survivin expression by small interfering RNA induces pancreatic cancer cell apoptosis and enhances its radiosensitivity. *World J Gastroenterol* 2006; **12**: 2901-2907
33 **Ning S**, Fuessel S, Kotzsch M, Kraemer K, Kappler M, Schmidt U, Taubert H, Wirth MP, Meye A. siRNA-mediated down-regulation of survivin inhibits bladder cancer cell growth. *Int J Oncol* 2004; **25**: 1065-1071

S- Editor Liu Y **L- Editor** Ma JY **E- Editor** Zhou T

PO Box 2345, Beijing 100023, China
www.wjgnet.com
wjg@wjgnet.com

World J Gastroenterol 2007 February 28; 13(8): 1175-1181
World Journal of Gastroenterology ISSN 1007-9327

Selective COX-2 inhibitor, NS-398, suppresses cellular proliferation in human hepatocellular carcinoma cell lines *via* cell cycle arrest

Ji Yeon Baek, Wonhee Hur, Jin Sang Wang, Si Hyun Bae, Seung Kew Yoon

Ji Yeon Baek, Si Hyun Bae, Seung Kew Yoon, Department of Internal Medicine, College of Medicine, The Catholic University of Korea, 505 Banpo-dong, Seocho-gu 137-701, Seoul, Korea
Wonhee Hur, Jin Sang Wang, WHO Collaborating Center for Reference and Research on Viral Hepatitis, The Catholic University of Korea, 505 Banpo-dong, Seocho-gu 137-701, Seoul, Korea
Supported by the Songeui Foundation of the Catholic University of Korea for Medical Research
Correspondence to: Dr. Si Hyun Bae, Department of Internal Medicine, Kangnam St. Mary's Hospital, #505 Banpo-dong, Seocho-gu, Seoul 137-701, Korea. baesh@catholic.ac.kr
Telephone: +82-2-5901425 Fax: +82-2-34814025
Received: 2006-09-14 Accepted: 2006-12-28

Abstract

AIM: To investigate the growth inhibitory mechanism of NS-398, a selective cyclooxygenase-2 (COX-2) inhibitor, in two hepatocellular carcinoma (HCC) cell lines (HepG2 and Huh7).

METHODS: HepG2 and Huh7 cells were treated with NS-398. Its effects on cell viability, cell proliferation, cell cycles, and gene expression were respectively evaluated by water-soluble tetrazolium salt (WST-1) assay, 4'-6-diamidino-2-phenylindole (DAPI) staining, flow cytometer analysis, and Western blotting, with dimethyl sulfoxide (DMSO) as positive control.

RESULTS: NS-398 showed dose- and time-dependent growth-inhibitory effects on the two cell lines. Proliferating cell nuclear antigen (PCNA) expressions in HepG2 and Huh7 cells, particularly in Huh7 cells were inhibited in a time- and dose-independent manner. NS-398 caused cell cycle arrest in the G1 phase with cell accumulation in the sub-G1 phase in HepG2 and Huh7 cell lines. No evidence of apoptosis was observed in two cell lines.

CONCLUSION: NS-398 reduces cell proliferation by inducing cell cycle arrest in HepG2 and Huh7 cell lines, and COX-2 inhibitors may have potent chemoprevention effects on human hepatocellular carcinoma.

Key words: Selective cyclooxygenase 2 inhibitor; Cell growth; Cell cycle; Hepatocellular carcinoma cells

Baek JY, Hur W, Wang JS, Bae SH, Yoon SK. Selective COX-2 inhibitor, NS-398, suppresses cellular proliferation in human hepatocellular carcinoma cell lines *via* cell cycle arrest. *World J Gastroenterol* 2007; 13(8): 1175-1181

http://www.wjgnet.com/1007-9327/13/1175.asp

INTRODUCTION

Hepatocellular carcinoma (HCC) is one of the most common malignancies worldwide[1]. Although HCC is significantly more prevalent in Asia and Africa, a rising incidence has been reported in Western countries. Most patients present at an advanced stage when successful surgical treatment is no longer feasible and current therapeutic options achieve clinical responses in only a small percentage of cases. As a consequence, effective approaches for prevention and treatment need to be established.

Epidemiological and experimental studies have demonstrated the effect of non-steroidal anti-inflammatory drugs (NSAIDs) in the prevention of human cancers, especially those in the gastroenterological tract[2-4]. Epidemiological studies have shown that the rate of mortality of colorectal cancer in individuals taking NSAIDs is 40%-50% lower than that in non-users[4]. NSAIDs inhibit endogenous prostaglandin synthesis. The key step in the enzymatic conversion of arachidonic acid to prostaglandins is catalyzed by cyclooxygenases (COX), and represents the specific target of NSAIDs.

Two forms of cyclooxygenase, COX-1 and COX-2 have been identified. COX-1 is expressed constitutively in most tissues and appears to be responsible for prostaglandin production in various physiological functions such as platelet aggregation and maintenance of gastric mucosa. In contrast, COX-2 is induced by several inflammatory cytokines and growth factors[5] and frequently over-expressed in various tumor cells. Selective COX-2 inhibitors do not affect platelet aggregation or bleeding time and cause far fewer acute gastric erosions than several nonselective inhibitors. Therefore, selective COX-2 inhibitors such as celecoxib and NS-398 are preferable to nonselective COX-2 inhibitors.

The role of COX-2 in hepatocellular carcinogenesis

is still unclear. Previous studies have shown increased expression of COX-2 in patients with various liver diseases, suggesting its possible role in chronic liver disease and during HCC progression[6-8]. In addition, some studies have described the possible benefits of treatment with COX-2 inhibitors as indicated by their effects on human HCC cell lines[8-10]. However, contrasting results have also been reported about the expression of COX-2 or the effects of COX-2 inhibitors on HCC cell lines[11]. COX-2 may be a logical therapeutic target in various human cancers including HCC. However, information regarding the mechanisms involved in these effects is scant and sometimes contradictory[12-15].

In this study, we examined the effects and possible mechanism of NS-398, a selective COX-2 inhibitor in two human hepatoma cell lines, HepG2, and Huh7.

MATERIALS AND METHODS

Materials

Human hepatoma cell lines HepG2 (showing wild-type p53) and Huh7 (showing mutant-type p53) were obtained from the American Type Culture Collection (Rockville, MD, USA). Each cell line was cultured in Dulbecco's modified Eagle's medium (DMEM; Invitrogen, Carlsbad, CA) supplemented with 10% fetal bovine serum (FBS), essential amino acids, 100 units/mL penicillin (Invitrogen), and 100 μg/mL streptomycin (Invitrogen, Carlsbad, CA). All cells were maintained in a humidified atmosphere containing 950 mL/L air and 50 mL/L CO_2 at 37℃. NS-398 was purchased from Cayman Chemical (Ann Arbor, MI, USA) and dissolved in dimethyl sulfoxide (DMSO).

Cell viability assay

To evaluate the inhibitory growth effect of NS-398, we confirmed its cytotoxicity and proliferating activity by water-soluble tetrazolium salt (WST-1) assay (Roche Diagnostics, Mannheim, Germany). The WST-1 assay is a colorimetric method in which the dye intensity is proportional to the number of viable cells. Cells were seeded into 96-well microtiter plates at a concentration of 5×10^3 cells/well. After 12-h incubation, cells were treated with serum-free media containing various concentrations of NS-398 (0, 50, 100, and 200 μmol/L) for 24, 48, and 72 h. Because we used DMSO-dissolved NS-398, cells cultured in the serum-free media containing an equivalent volume of DMSO without NS-398 respectively were used as controls to ensure DMSO not to promote unwanted cellular effects. The final concentration of DMSO was < 0.3%. After incubation, the cells were washed with PBS and the cell proliferation reagent WST-1 was added with cell culture medium, and incubated for 4 h. Sample absorbence was analyzed using a bichromatic ELISA reader at 450 nm. All experiments were performed in triplicate.

Nuclei staining and FACS analysis

Characterization of apoptosis and/or necrosis was carried out after propidium iodide (PI) and Annexin V-FITC staining with apoptosis detection kit I (Pharmingen, San Diego, CA, USA) followed by flow cytometric analysis after 24, 48 and 72 h of 100 μmol/L NS-398 treatment in HepG2 and Huh7 according to the manufacturer's instructions. For histogram analysis after PI staining, the cells were fixed with 70% ethanol in PBS for 15 min at -20℃. The fixed cells were incubated with RNase A (100 μg/mL) for 30 min at 37℃ and then stained with PI (50 mg/mL in PBS). Fluorescence of individual nuclei and intact cells was determined using a FACScalibur flow cytometer (Beacton Dickinson, San Jose, CA).

For detection of apoptosis, cells were washed twice with ice cold PBS and stained simultaneously with FITC-conjugated Annexin V and PI for 20 min on ice in the dark with a binding buffer. Within the next hour, cells were analyzed for apoptosis. The total number of apoptotic cells was determined by calculation of Annexin V+ and PI-cells (reflecting early apoptosis) together with annexin V+ and PI+ cells (reflecting late apoptosis/secondary necrosis).

DAPI staining

4'-6-diamidino-2-phenylindole (DAPI), a DNA-binding fluorescent dye, was used to determine whether the mechanism of growth inhibition upon NS-398 treatment is apoptosis. After treatment with 100 μmol/L NS-398 for 0, 24, 48, and 72 h, the cells were washed three times with PBS, fixed in a 3.7% formaldehyde solution for 10 min, fixed once in 1 mL of methanol, and then stained with 4 μg/mL DAPI (Oncor, Gaithersburg, MD) for 10 min. Results were determined by visual observation of nuclear morphology *via* fluorescence microscopy.

Immunoblot analysis

HepG2 and Huh7 cells were seeded on 100-mm dishes at a density of 1.5×10^6 cells/dish. After seeding and overnight incubation, cells were serum-starved for 24 h and incubated in serum-free media with 100 μmol/L NS-398 for 0, 24, 48 and 72 h. Attached and floating cells were harvested together. Cells cultured in the same condition without NS-398 were used as controls. Proteins extracted from either treated or control cells were measured by Bradford assay, and subjected to SDS-PAGE. The proteins were then transferred electrophoretically to nitrocellulose membrane (Schleicher & Schuell, Dassel, Germany) at 100 V for 1 h at 4℃. To stain the proteins and to validate that equal amounts of protein were loaded in each lane and transferred efficiently, the membrane was immersed in 0.5% Ponceau S (Sigma Chemical Co., St. Louis, MD) in 1% acetic acid. The membrane was washed three times with TBS containing 0.1% Tween 20 (TBS-T). After blocking with 5% skim milk in TBST buffer for 1 h, the membrane was incubated with primary antibodies (anti-mouse COX-2 antibody, 1:500; anti-rabbit caspase-9, caspase-3 and caspase-8, 1:1000; anti-mouse poly [ADP-ribose] -polymerase (PARP) antibody, 1:1000; anti-mouse proliferating cell nuclear antigen (PCNA) antibody, 1:1000 and anti-mouse β-actin antibody, 1:2500) overnight at 4℃. The membrane was incubated with secondary antibodies for 1 h and detected with ECL reagent (Amersham-Pharmacia, UK).

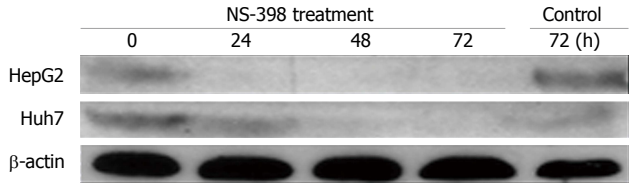

Figure 1 Immunoblot analysis for COX-2 protein levels in HepG2 and Huh7 cells. Cells were treated with 100 μmol/L NS-398 for 0, 24, 48 and 72 h. Control cells were treated with DMSO without NS-398. The upper bands represent 72 kDa COX-2-specific staining while the lower bands are β-actin controls. COX-2 expression was detectable but low in both cell lines. Decreased changes were observed in COX-2 expression with increasing time.

Statistical analysis

One-way analysis of variance (ANOVA) was performed to test the differences in cellular proliferation and apoptosis of the two cell lines treated with different NS-398 concentrations for varying times. $P < 0.05$ was considered statistically significant. Data were analyzed using the Statistical Package for Social Sciences (SPSS) (version 11.0).

RESULTS

Inhibition of COX-2 expression by NS-398

We first characterized the hepatoma cell lines by their expression of COX-2. Samples containing 50 μg of extracted protein were loaded onto the gel. Immunoblot analysis revealed that both cell lines expressed COX-2 protein. The expression of COX-2 was inhibited by NS-398. Immunoblot analysis also demonstrated different COX-2 expressions after treatment with 100 μmol/L NS-398 for different periods of time (Figure 1).

Inhibition of HepG2 and Huh7 cell viability by NS-398

To determine the effect of the selective COX-2 inhibitor NS-398 on HepG2 and Huh7 cells, cell viability was determined by WST-1 assay. Growth-inhibitory experiments were performed by treating cells with various doses of NS-398 for different periods of time. As shown in Figure 2, NS-398 reduced cell viability in a time- and dose-dependent manner on both cell lines. However, treatment with only DMSO as a control did not alter HepG2 and Huh7 cell proliferation ($P > 0.05$).

No evidence of apoptosis was observed in two cell lines

To confirm that NS-398 induces apoptosis of COX-2-expressing HepG2 and Huh7 cells, a double-staining method using FITC-conjugated Annexin V and PI, DAPI staining and Western blotting were done. In the Annexin and PI staining, the percentages of apoptotic and necrotic cells at 0, 24, 48 and 72 h after 100 μmol/L of NS-398 treatment were not significantly different in HepG2 and Huh7 cells (Figure 3). Moreover, no condensed and fragmented nuclei were found in DAPI staining (data not shown). Immunoblot analysis showed that there was no activation of caspase-3, caspase-8, caspase-9 and PARPs in HepG2 and Huh7 cells treated with 100 μmol/L of NS-398 (Figure 4). Taken together, NS-398 did not induce apoptosis in HepG2 and Huh7 cells.

NS-398 suppressed cell proliferation by inducing cell cycle arrest, especially in Huh7 cell lines

To test the effects of NS-398 on cellular proliferation, the two HCC cell lines were treated with 100 μmol/L of NS-398. We detected PCNA protein by IB analysis. As shown in Figure 5, both cell lines showed a down-regulation of PCNA expression after treatment with 100 μmol/L of NS-398 in a time dependent manner. In particular, NS-398 treatments significantly suppressed the cellular proliferation in Huh7 cells.

To determine whether suppressions of proliferation in Huh7 cells induced by NS-398 are associated with cell-cycle arrest, we measured DNA content by flow cytometry. We observed that the population of cells in sub-G1 phase increased after 100 μmol/L NS-398 treatment in both cell lines for different periods of time. A significant correlation was observed between the growth inhibition and accumulation of cells in sub-G1 phase for Huh7 at 48 h (Figure 6).

DISCUSSION

COX-2 is involved in several pathological processes such as inflammation and cancer, and inhibition of apoptosis is regarded as one mechanism by which COX-2 contributes to tumorigenesis. Recent studies demonstrated that selective COX-2 inhibitors (including NS-398) which can inhibit cell proliferation or induce apoptosis are found not only in HCC cell lines but also in colorectal[2,3], esophageal[14], bladder[15], prostatic[16], lung[17], cervix[18] carcinoma cells.

Over-expression of COX-2 has been demonstrated in patients with HCC and high COX-2 expression in non-tumor liver tissue is significantly associated with inflammatory activity[6,8,19]. These findings indicate that COX-2 expression plays an important role in hepatic inflammation and malignant transformation of hepatocytes[20]. However, the key mechanism by which COX-2 affects HCC cell growth remains unclear.

In this study, we detected the expression of COX-2 protein in HepG2 and Huh7 cells by Western blotting. Decreased changes in COX-2 protein expression were observed during the course of growth inhibition by NS-398 treatment (Figure 1). Our findings suggest that the growth-inhibitory effect on hepatocellular carcinoma cell lines is dependent on COX-2 expression[10]. However, several other studies have shown that there is no correlation between COX-2 expression and growth-inhibitory effects induced by NSAIDs[9,11,21].

NS-398-induced inhibition of cell growth is both dose- and time-dependent (Figure 2). The association of COX-2 inhibition with suppression of tumor cell proliferation remains unclear in HCC. Our findings demonstrate that NS-398 may inhibit cell growth in a dose- and time-dependent manner, due to the result of evident cell cycle arrest at G1 (Figures 2 and 6)[11]. Decreased PCNA expression supports the finding of a reduced number of cells in S phase by cell cycle analysis, which is an important event in cell cycle arrest of HepG2 (wild-type p53) and Huh-7 (p53-220Cys) induced by NS-398.

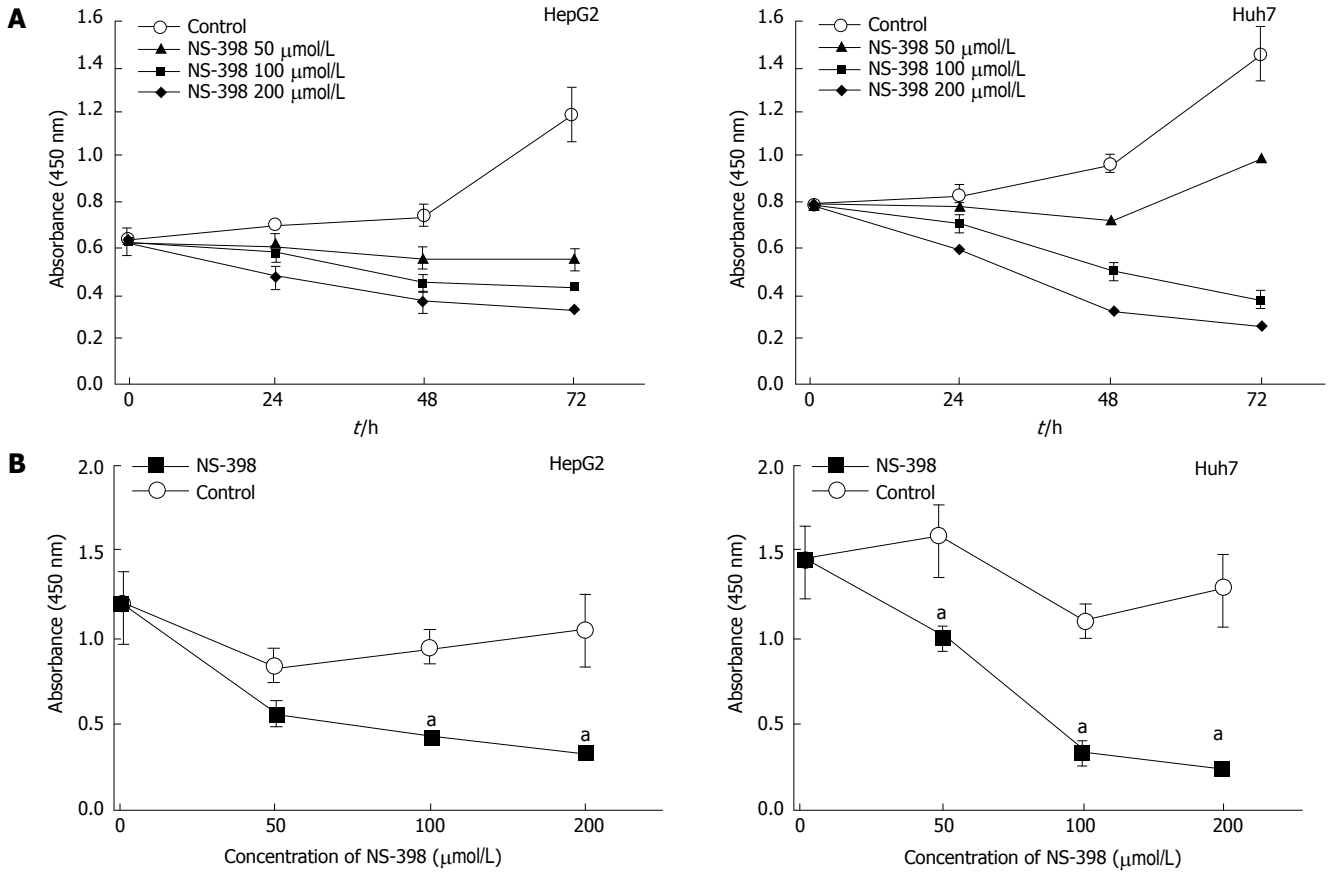

Figure 2 Proliferation of HepG2 and Huh7 cells inhibited by NS-398. **A**: Time-dependent growth-inhibitory effect of NS-398. One hundred μmol/L NS-398 was added to HepG2 and Huh7 cells, which were cultured for 24, 48 or 72 h, and subjected to WST-1 assay. Absorbance was detected at 450 nm with an ELISA plate reader, and the growth rates of both cell lines treated with NS-398 were reduced compared to controls. Control cells were treated with an equivalent volume of DMSO without NS-398, respectively; **B**: Dose-dependent growth-inhibitory effect of NS-398. Cells treated with various concentrations of NS-398 were cultured for 72 h, and quantified by WST-1 assay. Data from 3 independent experiments are shown as e mean ± SD ($^aP < 0.05$).

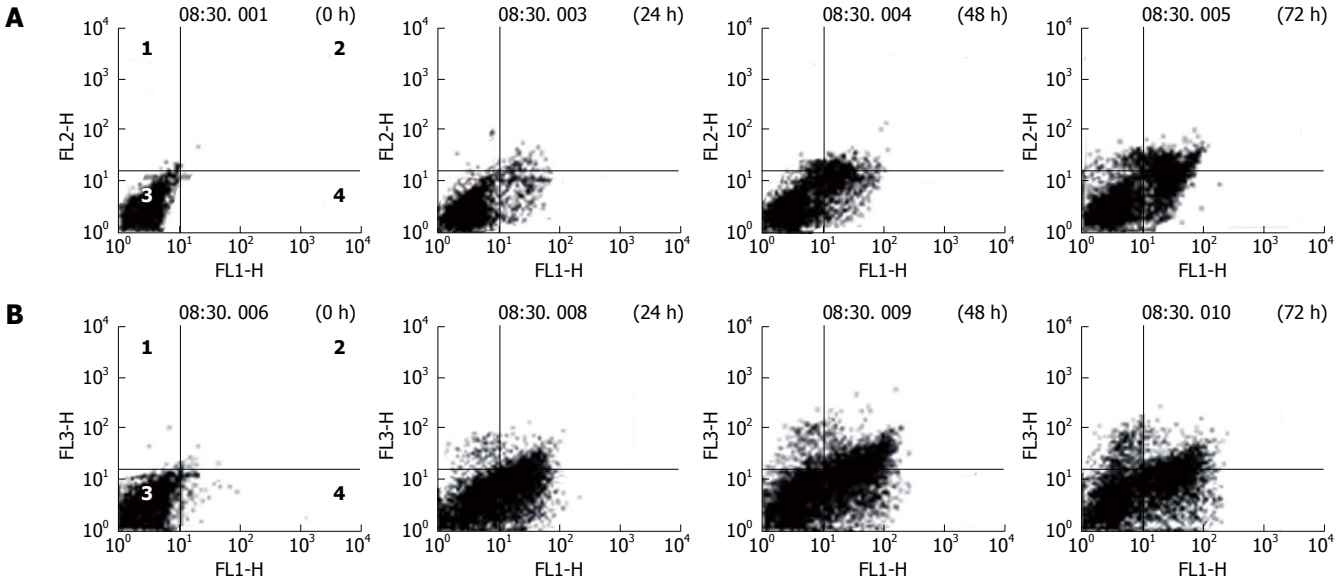

Figure 3 Flow cytometric analysis after exposure of HepG2 (**A**) and Huh7 (**B**) cells to NS-398. Cells were treated with 100 μmol/L NS-398 for 24, 48, and 72 h, stained with annexin V-FITC and propidium iodide and analyzed on a FACScalibur flow cytometer. Quadrants 2-4 represent secondary necrotic cells, viable cells, and apoptotic cells, respectively.

In particular, NS-398 treatment significantly suppressed Huh7 proliferation. Recent reports indicate a complex relationship between the tumor suppressor p53 and COX-2[22,23]. While wild-type p53 over-expression leads to increased COX-2 levels[24], opposite effects where p53 inhibits COX-2 transcription have been reported[25]. Thus,

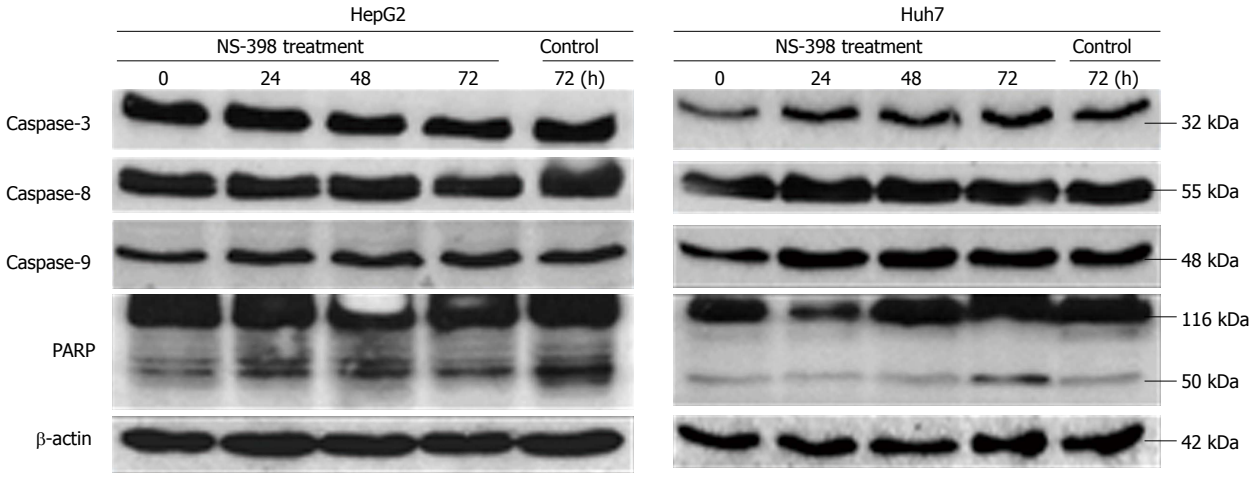

Figure 4 No evidence of activation of the caspase pathway and PARP by NS-398. No evidence of apoptosis in HepG2 and Huh7 cells was observed after NS-398 treatment. No caspase pathway activation or PARP cleavage was detected in both cell lines.

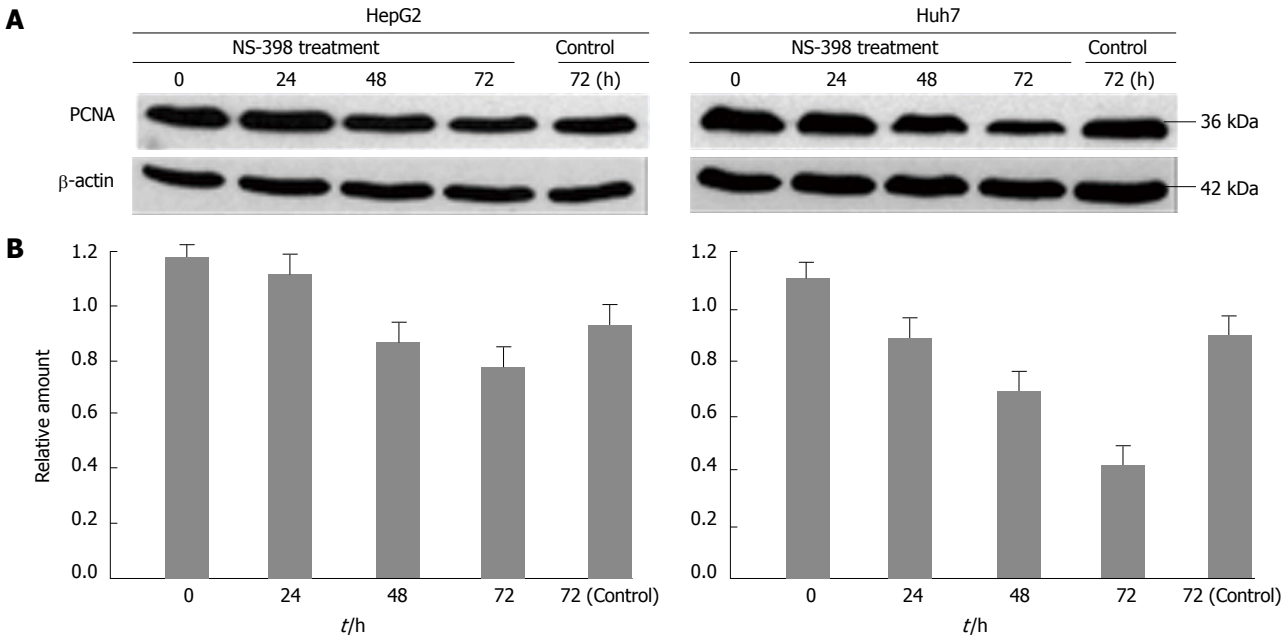

Figure 5 Inhibition of PCNA expression by NS-398. **A**: Down-regulation of PCNA expression in both cell lines after NS-398 treatment. Cells were treated for 24, 48, and 72 h with 100 μmol/L NS-398. Controls were treated with an equivalent volume of DMSO without NS-398. PCNA expressions in HepG2 and Huh7 cells were inhibited in a time-dependent (as shown above) and dose-independent (data not shown) manner; **B**: Quantification of the relative amount of each band by image analysis.

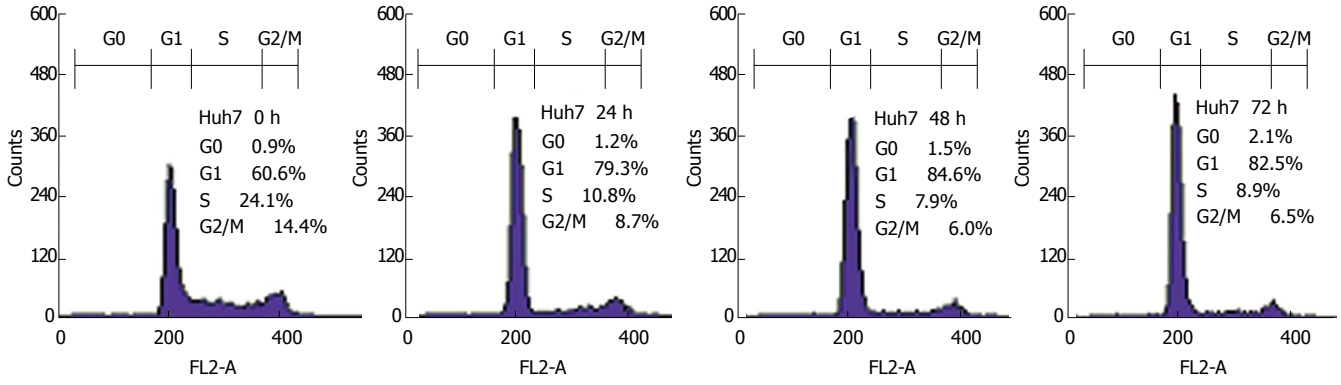

Figure 6 Inhibition of cell cycle arrest in Huh7 by NS-398. The cell cycle distribution was determined using a FACScan flow cytometer. Cells were harvested at 24, 48 and 72 h after treatment with 100 μmol/L NS-398 and collected. RNA was digested and DNA content was stained with propidium iodide (PI). Representative DNA histograms for Huh7 cells were shown.

different chemosensitivity to the selective COX-2 inhibitor NS-398 might be associated with different p53 status, including Huh-7 (mutated p53) and HepG2 (wild-type p53).

Several other studies, however, have shown that NS-398 inhibits cell proliferation and induces apoptosis *via* caspase-dependent or caspase-independent pathway in hepatoma cell lines[7,26,27]. But in our experiments, we obtained all negative data in Western blots and DAPI staining. This discrepancy may be due, at least in part, to sub-clone variation and different culture conditions[9,28].

Alteration of apoptosis is considered an important mechanism of carcinogenesis[21,26]. Caspases can be divided, based on their activity, into initiator caspases (caspase-8 and -9) and effector caspases (caspases-3, -6 and -7). In our study, no definite evidence of apoptosis was found after NS-398 treatment of both cell lines, suggesting that the major mechanism of growth inhibition by NS-398 may be anti-proliferation by cell cycle arrest rather than apoptosis.

In conclusion, selective COX-2 inhibitor, NS-398, inhibits the growth of HepG2 and Huh7 cells by inducing cell cycle arrest and is a potential candidate as an effective chemopreventive tool against human HCC.

REFERENCES

1 **Chen CJ**, Yu MW, Liaw YF. Epidemiological characteristics and risk factors of hepatocellular carcinoma. *J Gastroenterol Hepatol* 1997; **12**: S294-S308

2 **Hanif R**, Pittas A, Feng Y, Koutsos MI, Qiao L, Staiano-Coico L, Shiff SI, Rigas B. Effects of nonsteroidal anti-inflammatory drugs on proliferation and on induction of apoptosis in colon cancer cells by a prostaglandin-independent pathway. *Biochem Pharmacol* 1996; **52**: 237-245

3 **Elder DJ**, Halton DE, Hague A, Paraskeva C. Induction of apoptotic cell death in human colorectal carcinoma cell lines by a cyclooxygenase-2 (COX-2)-selective nonsteroidal anti-inflammatory drug: independence from COX-2 protein expression. *Clin Cancer Res* 1997; **3**: 1679-1683

4 **Farrow DC**, Vaughan TL, Hansten PD, Stanford JL, Risch HA, Gammon MD, Chow WH, Dubrow R, Ahsan H, Mayne ST, Schoenberg JB, West AB, Rotterdam H, Fraumeni JF, Blot WJ. Use of aspirin and other nonsteroidal anti-inflammatory drugs and risk of esophageal and gastric cancer. *Cancer Epidemiol Biomarkers Prev* 1998; **7**: 97-102

5 **Fosslien E**. Molecular pathology of cyclooxygenase-2 in neoplasia. *Ann Clin Lab Sci* 2000; **30**: 3-21

6 **Koga H**, Sakisaka S, Ohishi M, Kawaguchi T, Taniguchi E, Sasatomi K, Harada M, Kusaba T, Tanaka M, Kimura R, Nakashima Y, Nakashima O, Kojiro M, Kurohiji T, Sata M. Expression of cyclooxygenase-2 in human hepatocellular carcinoma: relevance to tumor dedifferentiation. *Hepatology* 1999; **29**: 688-696

7 **Rahman MA**, Dhar DK, Masunaga R, Yamanoi A, Kohno H, Nagasue N. Sulindac and exisulind exhibit a significant antiproliferative effect and induce apoptosis in human hepatocellular carcinoma cell lines. *Cancer Res* 2000; **60**: 2085-2089

8 **Bae SH**, Jung ES, Park YM, Kim BS, Kim BK, Kim DG, Ryu WS. Expression of cyclooxygenase-2 (COX-2) in hepatocellular carcinoma and growth inhibition of hepatoma cell lines by a COX-2 inhibitor, NS-398. *Clin Cancer Res* 2001; **7**: 1410-1418

9 **Cheng AS**, Chan HL, Leung WK, Wong N, Johnson PJ, Sung JJ. Specific COX-2 inhibitor, NS-398, suppresses cellular proliferation and induces apoptosis in human hepatocellular carcinoma cells. *Int J Oncol* 2003; **23**: 113-119

10 **Hu KQ**, Yu CH, Mineyama Y, McCracken JD, Hillebrand DJ, Hasan M. Inhibited proliferation of cyclooxygenase-2 expressing human hepatoma cells by NS-398, a selective COX-2 inhibitor. *Int J Oncol* 2003; **22**: 757-763

11 **Cheng J**, Imanishi H, Amuro Y, Hada T. NS-398, a selective cyclooxygenase 2 inhibitor, inhibited cell growth and induced cell cycle arrest in human hepatocellular carcinoma cell lines. *Int J Cancer* 2002; **99**: 755-761

12 **Cheng J**, Imanishi H, Liu W, Nakamura H, Morisaki T, Higashino K, Hada T. Involvement of cell cycle regulatory proteins and MAP kinase signaling pathway in growth inhibition and cell cycle arrest by a selective cyclooxygenase 2 inhibitor, etodolac, in human hepatocellular carcinoma cell lines. *Cancer Sci* 2004; **95**: 666-673

13 **Kern MA**, Schöneweiss MM, Sahi D, Bahlo M, Haugg AM, Kasper HU, Dienes HP, Käferstein H, Breuhahn K, Schirmacher P. Cyclooxygenase-2 inhibitors suppress the growth of human hepatocellular carcinoma implants in nude mice. *Carcinogenesis* 2004; **25**: 1193-1199

14 **Yu HP**, Shi LY, Lu WH, Su YH, Li YY, Xu SQ. Expression of cyclooxygenase-2 (COX-2) in human esophageal cancer and in vitro inhibition by a specific COX-2 inhibitor, NS-398. *J Gastroenterol Hepatol* 2004; **19**: 638-642

15 **Choi EM**, Kwak SJ, Kim YM, Ha KS, Kim JI, Lee SW, Han JA. COX-2 inhibits anoikis by activation of the PI-3K/Akt pathway in human bladder cancer cells. *Exp Mol Med* 2005; **37**: 199-203

16 **Liu XH**, Yao S, Kirschenbaum A, Levine AC. NS398, a selective cyclooxygenase-2 inhibitor, induces apoptosis and down-regulates bcl-2 expression in LNCaP cells. *Cancer Res* 1998; **58**: 4245-4249

17 **Hida T**, Leyton J, Makheja AN, Ben-Av P, Hla T, Martinez A, Mulshine J, Malkani S, Chung P, Moody TW. Non-small cell lung cancer cycloxygenase activity and proliferation are inhibited by non-steroidal antiinflammatory drugs. *Anticancer Res* 1998; **18**: 775-782

18 **Kim SH**, Song SH, Kim SG, Chun KS, Lim SY, Na HK, Kim JW, Surh YJ, Bang YJ, Song YS. Celecoxib induces apoptosis in cervical cancer cells independent of cyclooxygenase using NF-kappaB as a possible target. *J Cancer Res Clin Oncol* 2004; **130**: 551-560

19 **Kondo M**, Yamamoto H, Nagano H, Okami J, Ito Y, Shimizu J, Eguchi H, Miyamoto A, Dono K, Umeshita K, Matsuura N, Wakasa K, Nakamori S, Sakon M, Monden M. Increased expression of COX-2 in nontumor liver tissue is associated with shorter disease-free survival in patients with hepatocellular carcinoma. *Clin Cancer Res* 1999; **5**: 4005-4012

20 **Williams CS**, Mann M, DuBois RN. The role of cyclooxygenases in inflammation, cancer, and development. *Oncogene* 1999; **18**: 7908-7916

21 **Huang DS**, Shen KZ, Wei JF, Liang TB, Zheng SS, Xie HY. Specific COX-2 inhibitor NS398 induces apoptosis in human liver cancer cell line HepG2 through BCL-2. *World J Gastroenterol* 2005; **11**: 204-207

22 **Lee DW**, Park SW, Park SY, Heo DS, Kim KH, Sung MW. Effects of p53 or p27 overexpression on cyclooxygenase-2 gene expression in head and neck squamous cell carcinoma cell lines. *Head Neck* 2004; **26**: 706-715

23 **Choi EM**, Heo JI, Oh JY, Kim YM, Ha KS, Kim JI, Han JA. COX-2 regulates p53 activity and inhibits DNA damage-induced apoptosis. *Biochem Biophys Res Commun* 2005; **328**: 1107-1112

24 **Corcoran CA**, He Q, Huang Y, Sheikh MS. Cyclooxygenase-2 interacts with p53 and interferes with p53-dependent transcription and apoptosis. *Oncogene* 2005; **24**: 1634-1640

25 **Liu XH**, Kirschenbaum A, Yu K, Yao S, Levine AC. Cyclooxygenase-2 suppresses hypoxia-induced apoptosis via a combination of direct and indirect inhibition of p53 activity in a human prostate cancer cell line. *J Biol Chem* 2005; **280**: 3817-3823

26 **Kern MA**, Schubert D, Sahi D, Schöneweiss MM, Moll I, Haugg AM, Dienes HP, Breuhahn K, Schirmacher P. Proapoptotic and antiproliferative potential of selective cyclooxygenase-2 inhibitors in human liver tumor cells.

Hepatology 2002; **36**: 885-894

27 **Foderà D**, D'Alessandro N, Cusimano A, Poma P, Notarbartolo M, Lampiasi N, Montalto G, Cervello M. Induction of apoptosis and inhibition of cell growth in human hepatocellular carcinoma cells by COX-2 inhibitors. *Ann N Y Acad Sci* 2004; **1028**: 440-449

28 **Park MK**, Hwang SY, Kim JO, Kwack MH, Kim JC, Kim MK, Sung YK. NS398 inhibits the growth of Hep3B human hepatocellular carcinoma cells via caspase-independent apoptosis. *Mol Cells* 2004; **17**: 45-50

S- Editor Wang J **L-Editor** Wang XL **E- Editor** Chin GJ

PO Box 2345, Beijing 100023, China
www.wjgnet.com
wjg@wjgnet.com

World J Gastroenterol 2007 February 28; 13(8): 1182-1186
World Journal of Gastroenterology ISSN 1007-9327

LIVER CANCER

Assessment of hemodynamics in precancerous lesion of hepatocellular carcinoma: Evaluation with MR perfusion

Sheng Guan, Wei-Dong Zhao, Kang-Rong Zhou, Wei-Jun Peng, Feng Tang, Jian Mao

Sheng Guan, Department of Radiology, 1st Affiliated Hospital, Zhengzhou University, Zhengzhou 450052, Henan Province, China
Wei-Dong Zhao, Department of Radiology, 2nd Affiliated Hospital, Shanxi Medical University, Taiyuan 030001, Shanxi Province, China
Kang-Rong Zhou, Department of Radiology, Zhongshan Hospital, Fudan university, Shanghai 200032, China
Wei-Jun Peng, Feng Tang, Jian Mao, Department of Radiology, Tumor Hospital, Fudan University, Shanghai 200032, China
Supported by the grants from Foundation of Ministry of Public Health of China, No. 20011420 and National Natural Science Foundation of China, No. 30470503
Correspondence to: Dr. Kang-Rong Zhou, Department of Radiology, Zhongshan Hospital, Fudan University, Shanghai 200032, China. gs858@yahoo.com.cn
Telephone: +86-371-65167390 Fax: +86-371-66910839
Received: 2006-10-31 Accepted: 2006-12-30

Abstract

AIM: To investigate the hemodynamic changes in a precancerous lesion model of hepatocellular carcinoma (HCC).

METHODS: Hemodynamic changes in 18 Wistar rats were studied with non-invasive magnetic resonance (MR) perfusion. The changes induced by diethylnitrosamine (DEN) developed into liver nodular lesions due to hepatic cirrhosis during the progression of carcinogenesis. The MR perfusion data [positive enhancement integral (PEI)] were compared between the nodular lesions corresponding well with MR images and pathology and their surrounding hepatic parenchyma.

RESULTS: A total of 46 nodules were located by MR imaging and autopsy, including 22 dysplastic nodules (DN), 9 regenerative nodules (RN), 10 early HCCs and 5 overt HCCs. Among the 22 DNs, 6 were low-grade DN (LGDN) and 16 were high-grade DN (HGDN). The average PEI of RN, DN, early and overt HCC was 205.67 ± 31.17, 161.94 ± 20.74, 226.09 ± 34.83, 491.86 ± 44.61 respectively, and their liver parenchyma nearby was 204.84 ± 70.19. Comparison of the blood perfusion index between each RN and its surrounding hepatic parenchyma showed no statistically significant difference (P = 0.06). There were significant differences in DN (P = 0.02). During the late hepatic arterial phase, the perfusion curve in DN declined. DN had an iso-signal intensity at the early hepatic arterial phase and a low signal intensity at the portal venous phase. Of the 10 early HCCs, 4 demonstrated less blood perfusion and 6 displayed minimally increased blood flow compared to the surrounding parenchyma. Five HCCs showed significantly increased blood supply compared to the surrounding parenchyma (P = 0.02).

CONCLUSION: Non-invasive MR perfusion can detect changes in blood supply of precancerous lesions.

Key words: Liver; Perfusion; Magnetic resonance imaging; Rat

Guan S, Zhao WD, Zhou KR, Peng WJ, Tang F, Mao J. Assessment of hemodynamics in precancerous lesion of hepatocellular carcinoma: Evaluation with MR perfusion. *World J Gastroenterol* 2007; 13(8): 1182-1186

http://www.wjgnet.com/1007-9327/13/1182.asp

INTRODUCTION

The changes of blood flow in dysplastic and regenerative nodules in patients with hepatic cirrhosis have been evaluated in previous studies with computed tomography (CT) arterial portography (CTAP) and CT hepatic arteriography (CTHA) techniques[1-3]. It has been demonstrated that during the late stage of hepatic cirrhosis, sequential hemodynamic changes in blood supply of dysplastic nodules lead to the development of early hepatocellular carcinoma (HCC). The main portal venous blood supply of these nodules gradually changes into the hepatic arterial supply. However, invasive methods require simultaneous catheterization of hepatic artery and superior mesentery artery to inject contrast enhancement substances. Because of their invasiveness, these methods have limited clinical application. With the development of techniques, especially the reduction of scanning time, magnetic resonance imaging (MRI) following intravenous injection of extracellular contrast agents has recently been described and validated to assess perfusion parameters in liver[4-7]. With this method, the contrast agent in blood flow of arterial and portal vein can be measured non-invasively. The purpose of this study was to assess experimentally whether MR perfusion can demonstrate the hemodynamic changes of liver nodular lesions.

MATERIALS AND METHODS

Animal model

The study protocol was reviewed and approved by the Institutional Committee for Animal Care of Fudan University. Experiments were performed on 18 6-wk old male Wistar rats weighing 150 ± 10 g (Experimental Animal Center of Fudan University, Shanghai, China). All animals were housed in independent ventilating cabinets (IVC) at 18-22℃ with 55% humidity in a 12 h light/dark cycle with free access to clean diet. Lesions in rats were induced by diethylnitrosamine (DEN, 0.99 mg/mL, Sigma, USA) in order to develop hepatocellular carcinoma during carcinogenesis. The animals received DEN (10 mg/kg per day) in drinking water at 0.01% g/L from a fresh DEN solution prepared every two days for 100 d.

Magnetic resonance imaging

A 1.5 Tesla magnetic resonance (MR) system with a 40 mT/m maximum gradient capability (TwinSpeed, Excite II, double gradient field, General Electric, USA) and 3-inch surface coil was employed and two rats were scanned every week from the 12th wk to the 20th wk after they were exposed to carcinogen. The rats were deeply anesthetized with a mixture of urethane (25%) and diazepam (2 mg) before MR scanning. Plain scanning was performed first in order to show the position of nodules, including sequences of 3-planar-localization scanning, axial and coronal T2 weighted scanning (T2WI), and axial T1 weighted (T1WI) scanning (in-phase and out-phase).

MR perfusion scanning was only performed on the nodules of interest demonstrated by T2WI. Fast spoiled gradient-echo sequence (FSPGR) was selected and the time resolution was 4 sections/2 s. Major protocol parameters included TR/TE: 5.8-8 ms/4-2.7 ms; band width: 31.3-19.2 kHz; section thickness: 2 mm; intersection gap: 0.5 mm; matrix: 128 × 128; excitation time: 1; FOV: 8. The time of acquisition of perfusion-weighted images was at the 8th phase after the starting point of tail vein bolus injection of diluted gadolinium (0.1 mmol/mL, Magnevist; Schering, Guangzhou, China) (0.2 mmol/kg). The total scaning time was 2 min.

Pathological analysis

Within 24 h after MR imaging, the rats were killed and their liver was removed at autopsy. The whole liver was serially sectioned into 1 mm-thick sections corresponding to the coronal plane MR image. The sections were fixed in a 10% formalin solution for 48 h and paraffin-embedded. Standard hematoxylin-eosin staining was used to assess the nature of nodules and immunohistochemical staining was performed for reticulin protein, CD31, CD34 antibodies. Transmission electron microscopy was also performed to study the ultrastructure of hepatic cancer cells. Pathologic diagnosis was made by two specialists independently and all nodules were defined grossly and microscopically following the criteria and nomenclature of the International Working Party on the Terminology of Nodular Hepatocellular Lesions[8].

Image evaluation

Data processing was performed at a workstation with AW 4.2 software package (General Electric, USA). Signal intensity and time curves were derived from manually drawing regions of interest (ROIs) on nodules and surrounding hepatic parenchyma. Positive enhancement integral (PEI) representing the blood perfusion could be obtained by setting the start (8th) and end (12th) phases. Values were expressed as mean ± SD. Statistical analysis was performed with SPSS 11.0. Perfusion data between nodules and parenchyma nearby were compared with *t* test. $P < 0.05$ was considered statistically significant.

Table 1 Average of PEI in nodules and adjacent parenchyma

	PEI	SD	*t*	*P*
RN	205.67	31.17	5.30	0.06
DN	161.94	20.74	3.64	0.02[a]
eHCC	226.09	34.83		
HCC	491.86	44.61	3.74	0.02[a]
Parenchyma	204.84	70.19		

[a]$P < 0.05$.

RESULTS

A total of 46 nodules were located by MR imaging and autopsy, including 22 dysplastic nodules (DN), 9 regenerative nodules (RN), 10 early HCCs and 5 overt HCCs. Among the DN (2-7 mm, average 4.6 mm), 6 were low grade DN (LGDN) and 16 were high grade DN (HGDN). The average positive enhancement integral (PEI) of DN, early and overt HCCs was 205.67 ± 31.17,161.94 ± 20.74,226.09 ± 34.83, 491.86 ± 44.61 respectively, and their adjacent liver parenchyma was 204.84 ± 70.19 (Table 1).

By comparing the blood perfusion index between nodules and their surrounding hepatic parenchyma, we found no difference in RN ($t = -5.303$, $P = 0.06$) showing the same signal intensity as its adjacent parenchyma at both hepatic artery phase and portal vein phase of MR perfusion. There were significant differences in dysplastic nodules ($t = -3.63$, $P = 0.02$) which manifested decreased blood perfusion. At the later phase of hepatic artery, the perfusion curve in DN declined when compared with surrounding parenchyma. DN showed an iso-signal intensity at hepatic artery phase and a low signal intensity at portal vein phase (Figure 1).

Of the 10 early HCCs, 4 manifested low perfusion and the average PEI value was smaller than that of adjacent parenchyma, showing an iso-signal intensity at the phase of artery and a low signal intensity at portal vein phase. The PEI values were higher in 6 early HCCs than in parenchyma nearby, which had a relatively higher signal intensity at hepatic artery phase and a low signal intensity at portal vein phase (Figure 2). Five overt HCCs had a remarkably higher signal intensity at hepatic artery phase and their perfusion curves ran up when compared with the surrounding parenchyma at early artery phase. The PEI value of HCC was much higher than that of adjacent parenchyma and the difference was significant ($t = 3.74$, $P = 0.02$) (Figure 3).

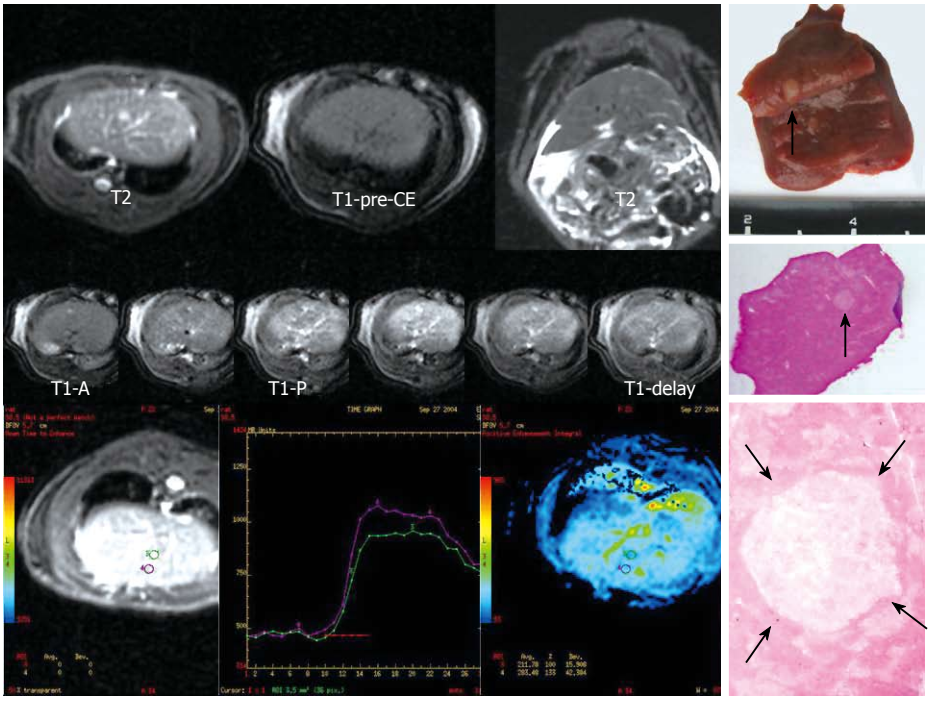

Figure 1 DN showing a high signal intensity on T2, but not on T1 and PWI.

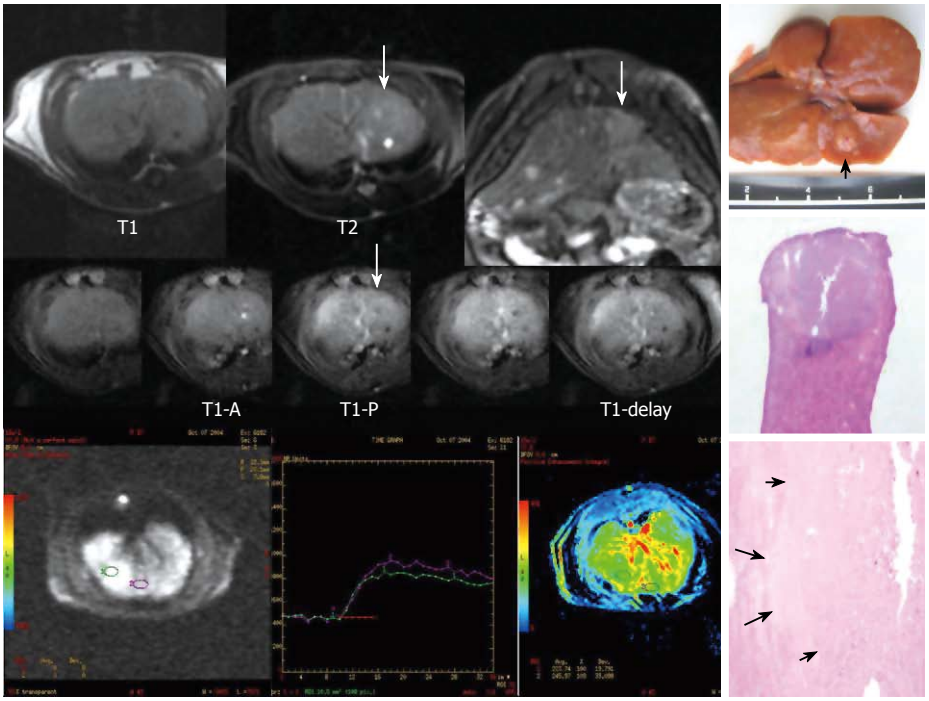

Figure 2 Early HCC showing an iso-signal intensity on T1, a high signal intensity on T2 or on T2 coronal.

DISCUSSION

There is cumulative evidence that RN at the late stage of hepatic cirrhosis can develop into HCC through an intermediate step of DN which has been considered as a precancerous lesion by the International Working Party since 1995[8,9], even though the hepatocarcinogenesis has not been clarified thoroughly. Early detection of HCC is critical to patient treatment and survival because of improved surgical techniques for resection and transplantation and new alternative therapeutic options, such as transcatheter chemoembolization or radiofrequency ablation. For surveillance of patients at risk, accurate methods capable of revealing not only HCC but also the premalignant precursor, namely DN, are required.

The imaging characteristics of DN have been previously reported[10-12]. However, the diagnosis of precancerous lesions is still difficult because of the overlapping between DN and RN, DN and early HCC on ultrasound, CT and MRI. Meanwhile, some researchers demonstrated that RN has almost the same blood flow as liver, which is mainly supplied by portal vein, and hepatic artery accounting for only a small part of total blood flow[13]. When RN progresses into DN, the blood flow in most parts of DN decreases (mainly portal vein

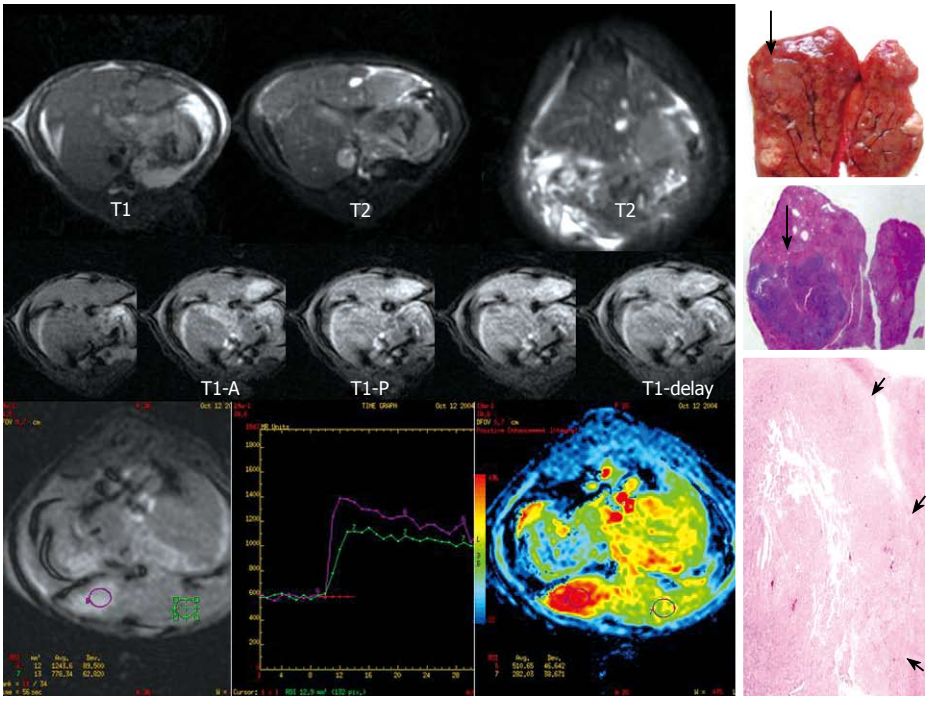

Figure 3 HCC showing an iso/low-signal intensity on T1WI, a hyper-intensity on T2.

blood supply) compared with surrounding parenchyma, and HCC always has increased blood flow (mainly hepatic artery blood supply) than its adjacent parenchyma. Until now this change has been regarded as the key-point to differentiate the nodules in liver. CTAP and CTHA are considered the best ways to make their differential diagnosis. But the application is limited in clinical practice due to their invasiveness. Non-invasive methods at present mainly focus on multi-detector spiral CT, MRI, PET and harmonic ultrasound[14-17]. To our knowledge, hemodynamic changes in hepatic nodules studied with MR perfusion have not been previously reported.

In the present study, MR perfusion demonstrated hemodynamic changes during the transition of RN to DN, early and overt HCC. The results obtained by ultra-fast MR perfusion scanning are consistent with those by invasive methods of CTAP or CTHA[18]. Moreover, hepatic artery segment of the perfusion curve in nodules declined slightly compared with surrounding parenchyma at the stage of HGDN and early HCC, suggesting that the preexisting hepatic artery is destructed in nodules. Otherwise, the positive enhancement integral representing the total blood flow would show polarization during this period. Part of them presented as increased blood flow (6/10 in early HCC; 5/16 in HGDN), but decreased blood flow was also observed at the same time in others (4/10 in early HCC; 11/16 in HGDN). The results of our pathology showed that the blood vessels in DN (including HGDN and LGDN) decreased compared with its surrounding hepatic parenchyma, and an increased number of tumor vessels were seen in HCC and even in early HCC. However, sinusoidal capillarization inside the nodules became gradually prominent during the process from RN, LGDN to HGDN and finally to HCC. This discrepancy cannot be clearly explained at present. The explanation of this phenomenon and the answer to its relationship with the alteration of nodular characteristics, and whether it corresponds with the different changes in tumor cells or in microvessles, depend on further pathologic studies.

The main advantage of MR perfusion is that this procedure provides ample information not only on the hemodynamic changes of nodular lesions in liver, but also on the parenchyma of the tumor. Therefore, this technique may be more valuable for the differential diagnosis of nodules in liver. The sequence we used in this study was fast spin gradient echo (FSPGR) which is as fast as echo-planar imaging (EPI). The ratio of time resolution was 0.5 s/section, but its signal-noise ratio (SNR) and spatial resolution were much higher than those of EPI, suggesting that this sequence is suitable for liver MR perfusion.

Nowadays, although CT perfusion (CTP) and PET are also used to study the hemodynamics, MR perfusion shows more advantages when small nodular lesions in liver and precancerous lesion of HCC are analyzed. It has been reported that MRI is more sensitive than CT and PET in revealing the small nodules in liver, especially in the hepatic parenchyma with the background of serious cirrhosis[19,20]. Moreover, MR perfusion has no side effects of radiation and has a better prospect than CT in study of hemodynamics. However, both MR imaging and CT have their technical defects at present. The scan of perfusion could only focus on ROI of one or several sections and could not cover the whole liver, while nodular lesions liver are usually multiple and located in different lobes., thus limiting its application in clinical practice. Newly developed harmonic ultrasound showing the vascular structure inside nodules more clearly, may have a broader prospect. Reports on the application of this technique in liver are few and further investigation is needed[21].

REFERENCES

1 **Takayasu K**, Muramatsu Y, Furukawa H, Wakao F, Moriyama N, Takayama T, Yamasaki S, Sakamoto M, Hirohashi S.

Early hepatocellular carcinoma: appearance at CT during arterial portography and CT arteriography with pathologic correlation. *Radiology* 1995; **194**: 101-105
2 **Kanematsu M**, Hoshi H, Imaeda T, Murakami T, Inaba Y, Yokoyama R, Nakamura H. Detection and characterization of hepatic tumors: value of combined helical CT hepatic arteriography and CT during arterial portography. *AJR Am J Roentgenol* 1997; **168**: 1193-1198
3 **Mikami S**, Kubo S, Hirohashi K, Shuto T, Kinoshita H, Nakamura K, Yamada R. Computed tomography during arteriography and arterial portography in small hepatocellular carcinoma and dysplastic nodule: a prospective study. *Jpn J Cancer Res* 2000; **91**: 859-863
4 **Materne R**, Smith AM, Peeters F, Dehoux JP, Keyeux A, Horsmans Y, Van Beers BE. Assessment of hepatic perfusion parameters with dynamic MRI. *Magn Reson Med* 2002; **47**: 135-142
5 **Cha S**. Perfusion MR imaging: basic principles and clinical applications. *Magn Reson Imaging Clin N Am* 2003; **11**: 403-413
6 **Zhao JG**, Feng GS, Kong XQ, Li X, Li MH, Cheng YS. Changes of tumor microcirculation after transcatheter arterial chemoembolization: first pass perfusion MR imaging and Chinese ink casting in a rabbit model. *World J Gastroenterol* 2004; **10**: 1415-1420
7 **Zhao JG**, Feng GS, Kong XQ, Li X, Li MH, Cheng YS. Assessment of hepatocellular carcinoma vascularity before and after transcatheter arterial chemoembolization by using first pass perfusion weighted MR imaging. *World J Gastroenterol* 2004; **10**: 1152-1156
8 **Terminology of nodular hepatocellular lesions**. International Working Party. *Hepatology* 1995; **22**: 983-993
9 **Su Q**, Bannasch P. Relevance of hepatic preneoplasia for human hepatocarcinogenesis. *Toxicol Pathol* 2003; **31**: 126-133
10 **Efremidis SC**, Hytiroglou P. The multistep process of hepatocarcinogenesis in cirrhosis with imaging correlation. *Eur Radiol* 2002; **12**: 753-764
11 **Kim MJ**, Lim JH, Lee SJ, Kim SH, Lee WJ, Lim HK, Park JM, Park CK. Correlation between the echogenicity of dysplastic nodules and their histopathologically determined fat content. *J Ultrasound Med* 2003; **22**: 327-334
12 **Lim JH**, Choi BI. Dysplastic nodules in liver cirrhosis: imaging. *Abdom Imaging* 2002; **27**: 117-128
13 **Matsui O**, Kadoya M, Kameyama T, Yoshikawa J, Takashima T, Nakanuma Y, Unoura M, Kobayashi K, Izumi R, Ida M. Benign and malignant nodules in cirrhotic livers: distinction based on blood supply. *Radiology* 1991; **178**: 493-497
14 **Lim JH**, Kim MJ, Park CK, Kang SS, Lee WJ, Lim HK. Dysplastic nodules in liver cirrhosis: detection with triple phase helical dynamic CT. *Br J Radiol* 2004; **77**: 911-916
15 **Kapanen MK**, Halavaara JT, Häkkinen AM. Assessment of vascular physiology of tumorous livers: comparison of two different methods. *Acad Radiol* 2003; **10**: 1021-1029
16 **Ward J**, Robinson PJ. How to detect hepatocellular carcinoma in cirrhosis. *Eur Radiol* 2002; **12**: 2258-2272
17 **Theise ND**, Park YN, Kojiro M. Dysplastic nodules and hepatocarcinogenesis. *Clin Liver Dis* 2002; **6**: 497-512
18 **Tajima T**, Honda H, Taguchi K, Asayama Y, Kuroiwa T, Yoshimitsu K, Irie H, Aibe H, Shimada M, Masuda K. Sequential hemodynamic change in hepatocellular carcinoma and dysplastic nodules: CT angiography and pathologic correlation. *AJR Am J Roentgenol* 2002; **178**: 885-897
19 **Rode A**, Bancel B, Douek P, Chevallier M, Vilgrain V, Picaud G, Henry L, Berger F, Bizollon T, Gaudin JL, Ducerf C. Small nodule detection in cirrhotic livers: evaluation with US, spiral CT, and MRI and correlation with pathologic examination of explanted liver. *J Comput Assist Tomogr* 2001; **25**: 327-336
20 **Krinsky GA**, Lee VS, Theise ND. Focal lesions in the cirrhotic liver: high resolution ex vivo MRI with pathologic correlation. *J Comput Assist Tomogr* 2000; **24**: 189-196
21 **Honda T**, Kumada T, Kiriyama S, Sone Y, Tanikawa M, Hisanaga Y, Toyoda H, Ishiguro H, Ogawa S, Takeshima K, Kawachi T, Hibi T, Hayashi K, Katano Y, Fukuda Y, Goto H. Comparison of contrast-enhanced harmonic ultrasonography and power Doppler ultrasonography for depicting vascularity of hepatocellular carcinoma identified by angiography-assisted CT. *Hepatol Res* 2003; **27**: 315-322

S- Editor Wang J **L- Editor** Wang XL **E- Editor** Ma WH

PO Box 2345, Beijing 100023, China
www.wjgnet.com
wjg@wjgnet.com

World J Gastroenterol 2007 February 28; 13(8): 1187-1194
World Journal of Gastroenterology ISSN 1007-9327

Comethylation of *p*16 and *MGMT* genes in colorectal carcinoma: Correlation with clinicopathological features and prognostic value

Koviljka Krtolica, Milena Krajnovic, Slavica Usaj-Knezevic, Dragan Babic, Dusan Jovanovic, Bogomir Dimitrijevic

Koviljka Krtolica, Milena Krajnovic, Bogomir Dimitrijevic, Laboratory for Radiobiology and Molecular Genetics, Institute of Nuclear Sciences "Vinca", P. O. BOX 522, Belgrade, Serbia
Slavica Usaj-Knezevic, Dusan Jovanovic, Institute of Oncology, Sremska Kamenica, Serbia
Dragan Babic, Institute for Medical Statistics of Medical University, Belgrade, Serbia
Supported by the grant 143010 from the Ministry of Science and Environment Protection of the Republic of Serbia
Correspondence to: Dr. Koviljka Krtolica, Laboratory for Radiobiology and Molecular Genetics, Institute of Nuclear Sciences "Vinca", P. O. BOX 522, Belgrade, Serbia. krtolica@vin.bg.ac.yu
Telephone: +381-11-2447485 Fax: +381-11-2447485
Received: 2006-11-29 Accepted: 2007-01-12

Abstract

AIM: To investigate the significance of *p*16 and O^6-methylguanine-DNA methyltransferase (*MGMT*) genes promoter hypermethylation and K-*ras* mutations on colorectal tumorigenesis and progression.

METHODS: *p*16 and *MGMT* methylation status was examined on 47 tumor samples, and K-*ras* mutational status was examined on 85 tumor samples. For methylation analysis, a methylation specific PCR (MS-PCR) method was used.

RESULTS: *p*16 and *MGMT* promoter methylation was found in 51% (24/47) and 43% (20/47) of CRCs, respectively, and the K-*ras* mutation was found in 44% (37/85) of CRCs. Comethylation of *p*16 and *MGMT* genes was significantly associated with lower aggressiveness of the disease within a two-year period of observation. Only 27% of patients with simultaneous *p*16 and *MGMT* methylation showed the detectible occurrence of metastasis and/or death, compared to 67% of patients without double methylation or with no methylation (3/11 *vs* 22/33, $P < 0.05$, χ^2-test). In addition, *p*16 and *MGMT* comethylation showed a trend toward an association with longer survival in patients with CRCs (35.5 ± 6.0 mo *vs* 23.1 ± 3.2 mo, $P = 0.072$, Log-rank test). Progression of the disease within a two-year period was observed in 66% of patients carrying the K-*ras* mutation, compared to only 19% of patients with wild type K-*ras* (29/44 *vs* 7/37, $P < 0.001$, χ^2-test). The presence of the K-*ras* mutation significantly correlated to shortened overall survival (20.0 ± 1.9 mo *vs* 37.0 ± 1.8 mo, $P < 0.001$, Log-rank test). The comethylation of *p*16 and *MGMT* genes was significantly associated with lower aggressiveness of the disease even when K-*ras* mutations were included in the analysis as an independent variable.

CONCLUSION: Our data suggest that comethylation of promoters of *p*16 and *MGMT* genes could have a prognostic value in patients with CRC. Specifically, concurrent methylation of both genes correlates with better prognosis.

Key words: Colorectal carcinoma; DNA methylation; *p*16; *MGMT*; K-*ras* mutation

Krtolica K, Krajnovic M, Usaj-Knezevic S, Babic D, Jovanovic D, Dimitrijevic B. Comethylation of *p*16 and *MGMT* genes in colorectal carcinoma: Correlation with clinicopathological features and prognostic value. *World J Gastroenterol* 2007; 13(8): 1187-1194

http://www.wjgnet.com/1007-9327/13/1187.asp

INTRODUCTION

Point mutations in the K-*ras* gene are among the most common genetic features of colorectal cancers (CRCs)[1]. In addition to mutational changes, epigenetic mechanisms also play an important role in the pathogenesis of this tumor type. The main epigenetic modification observed in the human genome is methylation of cytosine residues within CpG dinucleotides. Aberrant *de novo* methylation of CpG islands within the promoter region may lead to silencing of gene transcription through a complex process involving chromatin condensation and histone deacetylation[2,3]. Epigenetic silencing through DNA methylation can begin very early in tumor progression and may affect multiple genes involved in different cellular pathways, including cell cycle control, DNA repair and many others[4,5].

Inactivation of cell cycle regulatory genes, such as *p*16, confers a selective growth advantage to affected cells. This tumor suppressor gene encodes a cyclin-dependent kinase inhibitor, which is critical for maintaining the retinoblastoma (Rb) protein in its active,

non-phosphorylated state in the cyclin D-Rb pathway[6]. Promoter hypermethylation may lead to transcriptional inactivation of *p*16 resulting in abnormal cell cycling and uncontrolled cell growth, which are the hallmarks of cancer cells[7].

In addition, epigenetic modification can cause inactivation of DNA repair genes, such as O^6-methylguanine-DNA methyltransferase (*MGMT*)[8]. *MGMT* is a DNA repair protein that removes mutagenic and cytotoxic alkyl adducts from the O^6 position of guanine[9]. In the absence of *MGMT* activity, the adducts are not removed allowing the O^6-alkyl guanine to mispair with thymine during DNA replication, resulting in a G-to-A transition[10]. This kind of mutation may accumulate in the genes specifically associated with particular tumor types, such as K-*ras* in CRCs[9].

The literature suggests that hypermethylation of *p*16 and *MGMT* genes occurs as frequently in CRCs as previously reported for the K-*ras* gene[7,11,12]. Epigenetic changes usually begin very early in carcinogenesis, are potentially reversible, and can advance to gene alterations. For this reason, detection of aberrant methylation can be important for early diagnosis, prognosis and treatment of patients affected by this disease[5,13].

In the present study, we analyzed the methylation status of *p*16 and *MGMT* gene promoters in patients with primary CRC and compared the frequency of these changes with the occurrence of the K-*ras* gene mutations. In addition, we evaluated the correlation of these gene alterations with standard clinicopathological parameters, such as Dukes' stage, differentiation, location, histological and macroscopical type of tumor, patient gender and age. We also examined the possible correlation between these gene alterations and some immunohistochemical parameters that are known to be indicators of cell transformation, migration and metastasis of tumor cells. These parameters include altered expression of adhesive molecules E-cadherin and CD44, decrease or loss of laminin, which is a major component of epithelial basal membrane, and increased proliferate activity of the neoplastic cell. The ultimate aim of this study was to evaluate the influence of these genetic and epigenetic changes on disease progression and patient survival.

MATERIAL AND METHODS

Patients and tumor specimens

Tumor material in the form of formalin-fixed and paraffin-embedded tissue was obtained from 85 patients who underwent radical surgical resection (R0) at the Institute for Pathology and Forensic Medicine, Military Medical Academy, Belgrade. All patients gave informed consent prior to specimen collection according to institutional guidelines. None of the patients had preoperative or postoperative chemotherapy. The progression of the disease (occurrence of metastasis or/and death) was monitored during the two-year period following surgery, and survival over a five-year period was estimated. Mean follow-up was 31, 4 mo (range, 2 to 66 mo).

Tumor tissue chosen for analysis was routinely processed and microscopically examined for the regions enriched in neoplastic cells. Several 10 μm sections with neoplastic cell content greater than 85% were taken from each specimen and used for direct *in vitro* amplification of the K-*ras* gene by polymerase chain reaction (PCR). For K-*ras* mutational analysis, the sample of 47 was augmented with 38 samples from our previous study[14]. For analysis of *p*16 and *MGMT* methylation status, DNA was isolated from 47 samples.

Analysis of mutation status of the K-ras gene

Sections (10 μm thick) of the formalin-fixed and paraffin-embedded tumor specimens were de-paraffined and kept under 70% ethanol at 4℃ until PCR. *In vitro* amplification of 111-bp DNA fragments encompassing codons 12 and 13 of the K-*ras* gene was performed on tissue from sections as described by Almoguera *et al*[15]. Detection of K-*ras* mutations was performed on 85 patients with primary CRC by a highly selective oligonucleotide hybridization technique, as described earlier[14]. Two specimens were analyzed by single strand conformation polymorphism (SSCP) electrophoresis.

Analysis of methylation status of the p16 and MGMT genes

DNA methylation patterns in the promoter CpG islands of the *p*16 and *MGMT* genes were determined in 47 samples by methylation-specific PCR (MSP) following the bisulfite modification of isolated genomic DNA, as described by Herman *et al*[16], with some modifications[17]. Briefly, DNA was isolated from deparaffined tumor specimens using standard Proteinase K, phenol/chloroform/isoamyl alcohol extraction, and ethanol precipitation. Two μg of isolated DNA were denatured by NaOH (final 0.3 mmol/L) at 42℃ for 30 min and modified by sodium bisulfite (5.20-5.69 mol/L, pH 5.0, Sigma, USA) for 4 hr at 55℃. After incubation, DNA was purified using the DNA extraction KIT (MBI Fermentas, Lithuania), again treated by NaOH (final 0.3 mol/L), at 37℃ for 20 min, precipitated with ethanol/ammonium acetate and resuspended in 40 μL of 1 mmol/L Tris-HCl, pH 8.0. Aliquots of 4 μL of bisulfite modified DNA were used for MSP reactions. The PCR mixture contained 1 x PCR buffer (16 mmol/L ammonium sulfate, 67 mmol/L Tris-HCL, pH 8.8, 10 mmol/L 2-mercaptoethanol), 6.7 mmol/L $MgCl_2$, dNTP (each at 1.25 mmol/L) and primers (300 ng each per reaction) in a final volume of 50 μL. Reactions were hot-started at 95℃ for 5 min before the addition of 1.25 units of Taq polymerase (MBI Fermentas, Lithuania). Amplification was carried out in a Hybaid OmniGene temperature cycler for 35 cycles (30 s at 95℃, 30 s at the adequate annealing temperature, and 30 s at 72℃), followed by a final extension for 4 min at 72℃. Primers for a methylated and unmethylated promoter of the *p*16 gene were used from Herman *et al*[16] and for the *MGMT* gene from Esteller *et al*[8]. The annealing temperatures for unmethylated and methylated *p*16 amplification were 60℃ and 65℃, respectively, whereas the annealing temperature for both unmethylated and methylated *MGMT* amplification was 57℃. Controls without DNA were performed for each set of PCRs. Modified DNA from the human lymphoma cell line Raji (ECACC No:

85011429) served as positive control for methylated alleles, and modified DNA from normal lymphocytes as negative control for methylated alleles of *p*16 and *MGMT* genes. 10 μL of each PCR reaction were directly loaded on to nondenaturing 8% polyacrylamide gels, stained with $AgNO_3$ and visualized by Na_2CO_3, or 2% agarose gels, stained with SYBR Green I and visualized under UV illumination.

Immunohistochemistry

Immunohistochemistry was performed using the labeled streptavidin-biotin method (LSAB Kit+, Dako, Denmark) with microwave pretreatment for antigen retrieval. Endogenous peroxidase activity was blocked by incubating with 3% H_2O_2. Sections were then incubated with primary monoclonal antibodies against E-cadherin (HECD-1, Zymed Laboratories, San Francisco, USA), CD44 (Clone DF 1485, Dakocytomation, Denmark) and Laminin (4C7, Dakocytomation, Denmark) and Proliferation Cell Nuclear Antigen-PCNA (PC-10, Dakocytomation, Denmark) in optimal concentrations. Amino-ethyl carbazole was used as chromogen and finally Mayer's hematoxylin was used for counterstaining. The presence of a positive reaction in some normal tissue structures served as a positive control. Negative controls were prepared by replacing the primary antibody with Tris-buffered saline.

Immunostaining (membrane cytoplasmic immunoreactivity) for CD44 was calculated as the percentage of positive tumor cells in relation to the total number of tumor cells in representative fields. The presence of less then 10%, from 10% to 50%, and for more than 50% of positive tumor cells of CD44 were considered as low, moderate and extensive expression, respectively. Present, heterogenous and absent expression in the case of E-cadherin were distinguished. The loss of laminin immunoreactivity at the tumor-stroma borders was considered according to a three-point semiquantitive scale as follows: in more than 75%, between 25%-75% and in less than 25% of glandular structures. The PCNA index was considered to be low if less than 10% of tumor cell nuclei were positive, moderate for 10%-50%, and high for more than 50% of PCNA positive tumor cell nuclei.

Statistical analysis

Contingency tables were analyzed using Pearson's χ^2-test or Fisher's exact two-tailed test (*F*-test), when expected frequencies were lower than five. Continuous variables were compared with the use of Student's *t*-test. Overall survival distributions were estimated by the Kaplan-Meier method and differences were evaluated by the Log-rank test. The data was fitted to Cox's proportional risks regression model. In all tests, a *P* value less than 0.05 were considered as statistically significant.

RESULTS

K-ras mutations, p16 and MGMT promoter methylation in primary colorectal carcinomas

We detected K-*ras* mutations in 44% (37/85) of patients with CRC. The distribution of mutations was 57% (21/37) of G-to-T transversions, 32% (12/37) of G-to-A transitions and 11% (4/37) of G-to-C transversions. In codons 12 and 13, we detected mutations in 73% (27/37) and 27% (10/37), respectively.

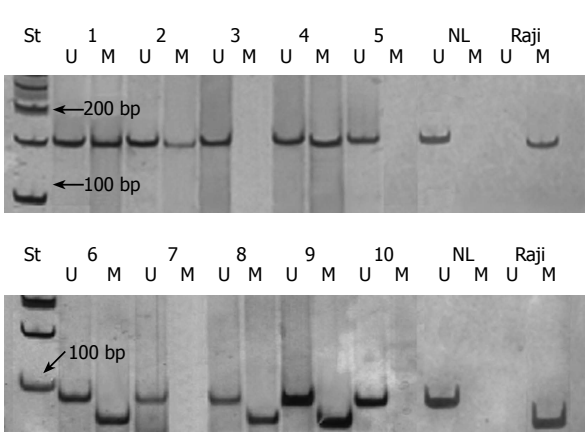

Figure 1 Analysis of *p*16 (**A**) and *MGMT* (**B**) gene methylation by MSP. The presence of a visible PCR product in lanes U indicates the presence of unmethylated genes of *p*16 (151 bp) and *MGMT* (93 bp); the presence of product in lanes M indicates the presence of methylated genes of *p*16 (150 bp) and *MGMT* (81 bp). The samples of colorectal carcinoma 1, 2 and 4 show *p*16 promoter hypermethylation, while 6, 8 and 9 show *MGMT* promoter hypermethylation. NL-normal lymphocytes as a positive control for unmethylated alleles; Raji-commercial cell line as a positive control for methylated alleles; St-molecular weight marker (50 bp).

Aberrant methylation of *p*16 and *MGMT* genes was detected in 51% (24/47) and 43% (20/47) of patients, respectively. Representative examples of the methylation analysis are shown in Figure 1A and B.

Of the total number of cases analyzed for methylation, 45% (21/47) had a mutant K-*ras* gene. Simultaneous alterations of K-*ras* and *p*16 genes were detected in 26% (12/47) of tumors. These events seemed to occur independently, as estimated by a χ^2-test (results not shown). The type of mutation at K-*ras* did not show a significant association with the *p*16 methylation by an *F*-test, although 55% (6/11) of samples with the hypermethylated *p*16 promoter carried G-to-T transversions in K-*ras*.

Simultaneous occurrence of K-*ras* mutation and *MGMT* methylation was detected in 21% (10/47) of the patients. Our results showed that *MGMT* methylation is significantly associated with a G-to-A transition in the K-*ras* gene ($P = 0.01$, *F*-test). This type of oncogene transition mutation occurs in 67% (6/9) of tumors carrying *MGMT* methylation, in contrast to only 10% (1/10) of tumors without *MGMT* methylation, but with the same type of K-*ras* mutation.

Concurrent methylation of *p*16 and *MGMT* genes was detected in 11 out of 47 (23%) cases, while simultaneous K-*ras*, *p*16 and *MGMT* alterations were present in 6 out of 47 cases (13%). Methylation of *p*16 and *MGMT* as well as K-*ras* mutation vs comethylation of *p*16 and *MGMT* genes seemed to occur independently as assessed by a χ^2-test (results not shown).

Correlation of K-ras mutations and hypermethylation of p16 and MGMT genes with clinicopathological and immunohistochemical parameters

We further examined correlation between genetic and epigenetic alterations and some clinicopathological and

Table 1 Association between *p*16 and *MGMT* methylation, K-*ras* mutations and clinicopathological features of colorectal cancer

	Methylation (%)		Mutations (%)
Variable	*p*16 (n = 46)	*MGMT* (n = 46)	K-*ras* (n = 84)
Gender			
Female	9/15 (60.0)	7/15 (46.7)	15/23 (65.2)[a]
Male	15/31 (48.4)	13/31 (41.9)	22/61 (36.1)
Dukes' stage			
A	5/9 (55.5)	5/9 (55.5)	8/21 (38.1)
B	7/10 (70.0)	4/10 (40.0)	12/24 (50.0)
C	8/15 (53.3)	8/15 (53.3)	17/39 (43.6)[4]
D	4/12 (33.3)	3/12 (25.0)	
Differentiation			
Poor	15/25 (60.0)	10/25 (40.0)	18/44 (40.9)
Moderate	8/18 (44.4)	10/18 (55.5)	16/26 (61.5)
Well	1/3 (33.3)	0/3 (0)	3/14 (21.4)
Macrosopic type[2]			
Polypoid	11/23 (47.8)	14/23 (60.7)[a]	25/48 (52.1)
Flat	13/23 (56.5)	6/23 (26.1)	12/35 (34.3)
Histological type[2]			
Mucinous	8/19 (42.1)	6/19 (31.6)	16/34 (47.1)
Tubular	16/27 (59.3)	14/27 (51.8)	21/49 (42.8)
Location[2]			
Proximal	3/3 (100)	1/3 (33.3)	5/9 (55.5)
Distal	21/43 (48.8)	19/43 (44.2)	32/74 (43.2)
Progression (2 yr)[1,3]			
Metastasis or/and death	11/25 (44.0)	9/25 (36.0)	29/44 (65.9)[b]
Without progression	12/19 (63.1)	11/19 (57.9)	7/37 (18.9)

Complete clinicopathological data were missing on one sample of colorectal cancer, and it was only included in analysis of genetic alterations; [a]$P < 0.05$; [b]$P < 0.001$ (all P values were revealed by χ^2-test); Data are missing on two[1] subjects for *p*16 and *MGMT* methylation status analysis, and on one[2] and three[3] subjects for K-*ras* mutation analysis, respectively. [4]Data for C and D Dukes' stages are considered together for K-*ras* mutation analysis.

Table 2 Association between *p*16 and *MGMT* methylation, K-*ras* mutations and immunohistochemical features of colorectal cancer

	Methylation (%)		Mutations (%)
Variable	*p*16 (n = 46)	*MGMT* (n = 46)	K-*ras* (n = 84)
E-cadherin[1,3]			
Absent	13/19 (68.4)	9/19 (47.4)	28/37 (75.7)[b]
Heterogeneous	4/14 (28.6)	7/14 (50.0)	4/23 (17.4)
Present	6/11 (54.5)	4/11 (36.4)	4/21 (19.0)
CD44 expression[1,3]			
Absent	7/11 (63.6)	6/11 (54.5)	4/22 (18.2)
Low	6/9 (66.7)	4/9 (44.4)	5/17 (29.4)
Moderate	2/7 (28.6)	4/7 (57.1)	4/10 (40.0)
Extensive	8/17 (47.0)	6/17 (35.3)	23/32 (71.9)[b]
CD44 type[2,4]			
Membranous	9/17 (52.9)	7/17 (41.2)	9/36 (25.0)
Cytoplasmic	13/26 (50.0)	12/26 (46.1)	27/44 (71.9)[b]
Laminin[1,3]			
0-25%	5/8 (62.5)	5/8 (62.5)	2/15 (13.3)
25%-75%	5/12 (41.7)	5/12 (41.7)	5/22 (22.7)
> 75%	13/24 (54.2)	10/24 (41.7)	29/44 (65.9)[b]
PCNAi[1,3]			
0	1/2 (50.0)	2/2 (100)	0/2 (0)
0-10%	5/9 (55.5)	4/9 (44.4)	3/17 (17.6)
10%-50%	6/9 (66.7)	5/9 (55.5)	3/20 (15.0)
> 50%	11/24 (45.8)	9/24 (37.5)	30/42 (71.4)[b]

Complete immunohistochemical data were missing on one sample of colorectal cancer, and it was only included in analysis of genetic alterations; [b]$P < 0.001$ (all P values were revealed by χ^2-test); Data are missing on two[1] and three[2] subjects for *p*16 and *MGMT* methylation status analysis, respectively, and on three[3] and four[4] subjects for K-*ras* mutation analysis, respectively.

immunohistochemical parameters that might be important for disease prognosis in CRC patients. The results of these analyses are summarized in Tables 1 and 2.

The presence of K-*ras* mutations was significantly more frequent in female than in male patients ($P < 0.05$, χ^2-test, Table 1). In addition, the average age of female patients carrying K-*ras* mutations was 53.3 ± 11.8 years, which was significantly lower ($P < 0.01$, t -test) than the average age for males with K-*ras* mutations (64.1 ± 8.7 years). As presented in Table 1, there was no significant association between the presence of the K-*ras* mutations and other clinicopathological features. However, the presence of K-*ras* mutations correlated significantly with the lack of E-cadherin expression, extensive expression and cytoplasmic type of CD44 antigen, decreased expression of laminin and the high PCNA index ($P < 0.001$ by χ^2-test in all cases; Table 2). These correlations were independent of the type of K-*ras* mutation, except in the case of E-cadherin, where the lack of expression of this adhesive molecule showed a significant correlation with the G-to-T transversions ($P < 0.05$, χ^2-test, results not shown).

*p*16 methylation was not associated with any of the variables considered, as presented in Table 1 and 2, though *p*16 methylation tended to be more prevalent in tumors not expressing E-cadherin ($P < 0.1$, χ^2-test). Methylation of *MGMT* gene was significantly more prevalent in polyploid than in flat colorectal carcinomas ($P < 0.05$, χ^2-test, Table 1). There was no significant association between *MGMT* methylation and any other clinicopathological features studied. In addition, comethylation of *p*16 and *MGMT* genes did not correlate with any clinicopathological or immunohistochemical parameters considered.

Survival analysis

In this study, we also monitored the progression of the disease in the two-year period following surgery. Methylation of *p*16 and *MGMT* genes, when they were considered separately, showed slight but insignificant correlation with slower progression of disease (Table 1). However, during that period, only 27% (3/11) of patients with simultaneous *p*16 and *MGMT* methylation showed the occurrence of metastasis and/or death, compared to 67% (22/33) of patients without this double or any gene methylation ($P < 0.05$, χ^2-test, Figure 2A).

This association was preserved and was even higher ($P < 0.01$, F-test, Figure 2B) when K-*ras* mutations were included as an independent variable. Namely, the progression of the disease occurred in only 2 of 6 (33%) patients with *p*16 and *MGMT* comethylation and K-*ras* mutations, while disease recurred in 13 of 14 (93%) patients with the K-*ras* mutation, but with only one methylated or both unmethylated genes. However, when both genes were unmethylated in the presence of the mutant K-*ras* gene, it was observed that all 4 patients from this group exhibited the progression of the disease within two years, compared to only 2 of 6 patients with *p*16 and *MGMT* comethylation and K-*ras* gene mutations ($P = 0.076$,

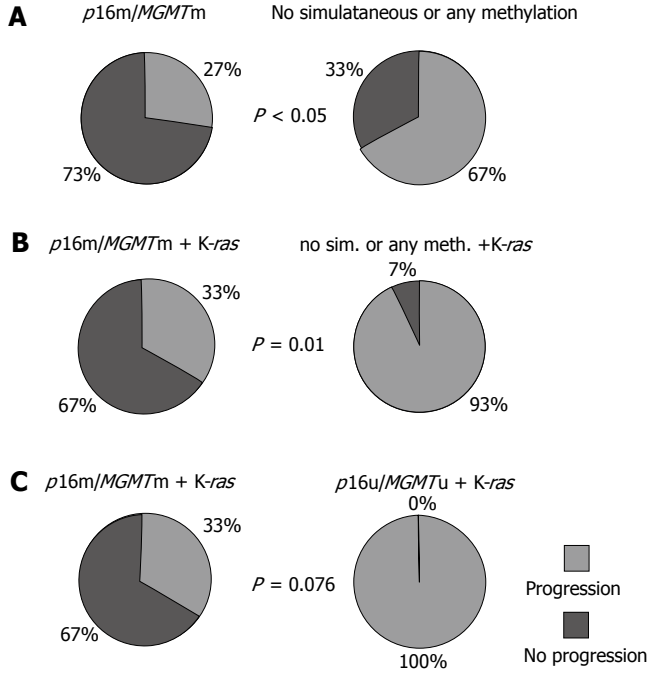

Figure 2 Graphical distribution of progression of the disease in the two-year period, as a function of simultaneous *p*16 and *MGMT* methylation status (**A**); simultaneous *p*16, *MGMT* methylation and mutated *K-ras* gene compared either to no simultaneous or any methylation of two genes (**B**) or to unmethylated both (**C**), respectively.

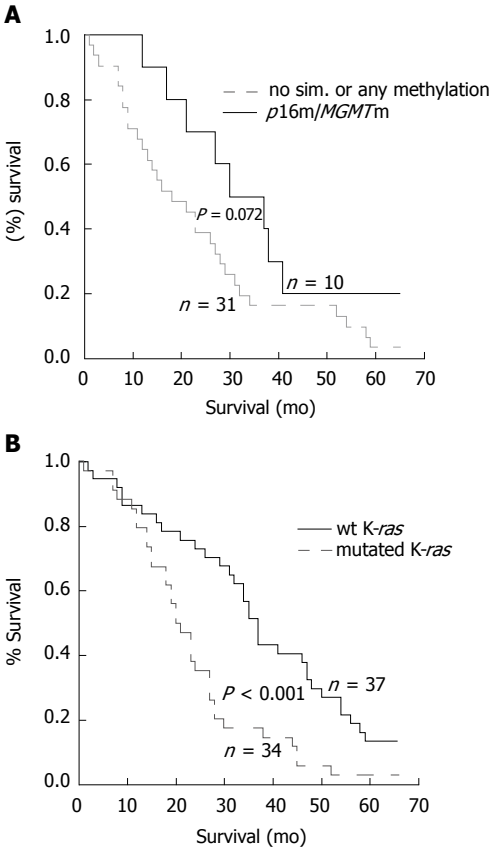

Figure 3 Overall survival among the patients with CRC according to the methylation status of *p*16 and *MGMT* genes (**A**), and mutational status of K-*ras* gene (**B**). Overall survival is longer in the group of the patients with simultaneous methylation of *p*16 and *MGMT* gene than in group with no simultaneous or any methylation ($P = 0.072$, Log-rank test). Overall survival is significantly lower in the group of patients with mutated K-*ras* than in group with unchanged, wild type K-*ras* gene ($P < 0.001$, Log-rank test). Survival curves were constructed by Kaplan-Meier method.

F-test, Figure 2C).

When the analyzed group was augmented with 38 patients from our previous study on CRC[14], we observed the progression of disease within a two-year period in 66% (29/44) of patients carrying the K-*ras* mutation, compared to only 19% (7/37) of patients with the wild type K-*ras* gene($P < 0.001$, χ^2 test, Table 1).

The Kaplan-Meier analysis of the few-year survival rate revealed a slight but insignificant influence of *p*16 and *MGMT* gene methylation on longer overall survival when the alterations of these genes were considered separately (results not shown). However, simultaneous *p*16 and *MGMT* methylation showed a trend toward association with longer survival in patients with CRCs who underwent curative surgery ($P = 0.072$, Log-rank-test, Figure 3A), as the median survival for these patients was 35.5 ± 6.0 mo in contrast to 23.1 ± 3.2 mo for patients without simultaneous or any methylation of examined genes. Multivariate analysis revealed that *p*16 and *MGMT* comethylation had no prognostic value without additional variables. By the same analysis, the presence of K-*ras* mutations significantly correlated to shortened overall survival (20.0 ± 1.9 mo *vs* 37.0 ± 1.8 mo) for 85 patients included in the analysis ($P < 0.001$, Log-rank test, Figure 3B). However, a Kaplan-Meier analysis considering simultaneous presence of K-*ras* mutations according to the methylated status of *p*16 and *MGMT* was not possible because there was a small number of samples.

DISCUSSION

The significance of *p*16 and *MGMT* methylation for tumor formation and progression, as well as correlation with the occurrence of classical genetic changes in K-*ras* genes, was the major subject of this study. While the frequency of the genetic and epigenetic alterations in these genes was similar to those previously reported[7,8,11,18,19], this is the first study to assess their cumulative and individual effects on disease progression.

While there was no clear association between methylation and standard prognostic parameters in CRC, the data obtained from survival analysis suggest that the simultaneous methylation of *p*16 and *MGMT* genes could be a better predictive factor for the course of disease. The most important finding of the current study was that comethylation of *p*16 and *MGMT* genes was significantly associated with lower aggressiveness of the disease and tended to associate with longer overall survival in patients with CRC who underwent curative surgery. More importantly, the influence of the double gene alteration was significant in spite of the simultaneous presence of K-*ras* mutations, which is another well established molecular marker of unfavorable prognosis in CRCs. Consistent with our previous findings[14] and those of the multicentric RASCAL study[20], our present results confirm that the mutated K-*ras* gene is a molecular marker for the more aggressive course of disease and was connected to reduced overall survival. In addition, we demonstrated

that K-*ras* mutation is strongly associated with parameters that are indicators of poor prognosis. These include the absence of E-cadherin expression[21], extensive expression of the cytoplasmic type of CD44 antigen[22], low expression of laminin[23] and high PCNA index[24].

The functional association between the effect of *p*16 and *MGMT* gene inactivation and K-*ras* mutation on the progression of disease is not clear. Yet, in the absence of methylation of both *p*16 and *MGMT* genes together with the mutated K-*ras*, a severe form of the disease is likely to commence. There is evidence that CRC does not evolve through a single sequence of molecular alterations, but evolves through different pathways. Each of them has distinct clinical, pathological and molecular characteristics[25]. One possible explanation for our findings could be that the colorectal tumors without comethylation of the two genes could arise through different mechanisms. These include large genetic rearrangements and chromosomal instability, with a significant degree of gene amplification and deletion[26,27] and such changes could be associated with a more aggressive course of the disease as proposed by Verma and Srivastava[13]. The other proposed pathway of colorectal carcinogenesis involves the occurrence of microsatellite instability (MSI), which is a phenotype resulting from alteration in the mismatch repair genes; e.g. *hMLH1* and *hMLH2*[28,26]. Some authors reported a relationship between MSI and CpG island methylator phenotype (CIMP+), as *hMLH1* is frequently inactivated by aberrant promoter methylation in sporadic MSI-H CRCs[29]. On the other hand, the CIMP+ phenotype is described as the occurrence of simultaneous methylation of a large number of genes, including *p*16 and *hMLH1*[29,30]. Though the biological and clinical properties of CIMP+ CRCs remain largely unknown, there is no longer doubt that those epigenetic changes mark a distinct group of tumors that have unique molecular profiles and etiology. More over, Wynter *et al*[31] demonstrated that there are at least two pathways for colorectal carcinogenesis, both implicating CIMP-high status. One group of tumors arises through *BRAF* mutations and *hMLH1* methylation, and another with K-*ras* instead of *BRAF* mutations and with *MGMT* instead of *hMLH1* promoter hypermethylation. Whitehall *et al*[32] demonstrated that methylation of *MGMT* has been linked to low levels of MSI (MSI-L) and Samowitz *et al*[33] demonstrated that the appearance of K-*ras* mutations is rare in high level MSI-H CRC. It is also known that MSI-H CRC associated with a CIMP+ phenotype is mostly located within the proximal colon[27,29]. In our study, all but three tumors have been located within the distal colon, so we can only speculate that they may not belong to the MSI-H group. We propose that in our group of analyzed patients who mostly have distal CRC, comethylation of *p*16 and *MGMT* genes together with other molecular changes suggest a pathway in signal transduction that could increase survival. Importantly this is in spite of the opposing effect of K-*ras* mutations. It would, therefore, be interesting to determine the MSI phenotype in this patient population in order to establish a possible association with observed genetic and epigenetic alteration.

Though all these questions cannot be fully resolved in the present study, our results confirm the multifactorial nature of cancer development, highlighting the molecular differences across the various classes of lesions, and exclude a single linear model of accumulating genetic alterations. In this report, we describe the association of concurrent methylation of *p*16 and *MGMT* genes with the course of disease in unselected group of CRCs. At this point, it must be noted that we did not analyze a large group of patients. However, the size of our study is still large enough to interpret the results correctly.

While some studies reported a correlation between promoter hypermethylation of the *p*16 gene and prognosis in patients with colorectal cancers[34-38], others observed no significant role of *p*16 methylation as a prognostic factor[30]. In addition, Nagasaka *et al*[39] found that methylated *MGMT* was significantly related to lower risk of recurrence in CRC. They proposed that colorectal tumors with methylated *MGMT* are less aggressive than tumors without such epigenetic change. Liang *et al*[34] proposed that geographical differences or other unknown factors supplementary to *p*16 methylation might increase tumor aggressiveness. Considering these and our previous results[14], we speculate that different geographic, environmental, and lifestyle factors could affect the genesis and clinical behavior of CRCs with different molecular profiles. Nevertheless, prospective studies that incorporate a larger number of genes and environmental factors are required to determine the relative contribution of each factor to the risk of developing CRCs with specific epigenetic and genetic profiles. We further support the notion that precise determination of molecular changes in CRCs is needed in order to overcome the risk of oversimplifying the role of a single or few genetic or epigenetic changes in tumorigenesis. Such analysis, supplemented by the conventional study of prognostic factors, introduces quality to prognostication of patients with CRC and aids the design of more efficient treatment modalities.

ACKNOWLEDGMENTS

We thank Dr. Nadezda Urosevic for reviewing the manuscript.

COMMENTS

Background

Colorectal carcinogenesis is a multistep process in which the progressive accumulation of genetic and epigenetic changes leads to a malignant transformation of normal epithelial cells of colon and rectum. Point mutations in K-*ras* gene are among the most common genetic features of colorectal cancers. In the past decade it has been shown that methylation of the promoter region of many tumor suppressor and DNA repair genes, such as *p*16 and *MGMT* has the important role in pathogenesis of this tumor type too, but its influence on disease progression remain inconclusive.

Research frontiers

Epigenetic changes usually begin very early in carcinogenesis, they are potentially reversible, and they can advance to gene alterations. For this reason, detection of aberrant methylation can be important for early diagnosis, prognosis and treatment

of patients affected by this disease.

Innovations and breakthroughs

Comethylation of *p*16 and *MGMT* genes was significantly associated with lower aggressiveness of disease within two-year period of observation ($P < 0.05$), and showed the trend toward the association with longer survival in patients with CRCs ($P = 0.072$). On the other hand, the presence of K-*ras* mutations was associated with higher aggressiveness and shortened overall survival ($P < 0.001$). The comethylation of *p*16 and *MGMT* genes was significantly associated with lower aggressiveness of disease even when K-*ras* mutations were included in analysis as an independent variable ($P < 0.01$). This is the first attempt to assess the cumulative and individual effect of these genes on the disease progression.

Applications

The results presented in this article have demonstrated that the precise determination of molecular changes in CRCs is needed in order to overcome the risk of oversimplifying the role of single or a few genetic or epigenetic changes in tumorigenesis. In addition, this study underlines the need for considering the different geographic, environmental, and lifestyle factors that could affect the genesis and clinical behavior of CRCs with different molecular profiles. Prospective studies supplemented by the conventional study of prognostic factors, could improve the quality and accuracy of patients prognosis and aid design of the more efficient treatment modalities.

Terminology

Epigenetic changes: heritable changes in gene function that do not include the changes in DNA sequence. DNA methylation: the addition of a methyl group to a cytosine residue that lies next to guanine within CpG dinucleotides. Aberrant *de novo* methylation of CpG islands within the promoter region may lead to silencing of gene transcription through a complex process involving chromatin condensation and histone deacetylation. CpG islands: CpG rich areas located in the promoter regions of many genes. Methylation-specific PCR (MSP): amplification of modified DNA by sodium bisulfite that converts unmethylated cytosines to uracils, while methylated cytosines remains unmodified.

Peer review

The authors found some interesting findings where they showed that patients with tumors where both promoters were methylated showed less death and had longer survival rates than patients with unmethylated promoters. The data is straightforward and convincing. The authors address a clinically relevant issue on CRC prognosis. They have also demonstrated initial and unique findings examining K-*ras*, *p*16 and *MGMT* modifications and patient outcome.

REFERENCES

1 **Vogelstein B**, Fearon ER, Hamilton SR, Kern SE, Preisinger AC, Leppert M, Nakamura Y, White R, Smits AM, Bos JL. Genetic alterations during colorectal-tumor development. *N Engl J Med* 1988; **319**: 525-532

2 **Jones PL**, Veenstra GJ, Wade PA, Vermaak D, Kass SU, Landsberger N, Strouboulis J, Wolffe AP. Methylated DNA and MeCP2 recruit histone deacetylase to repress transcription. *Nat Genet* 1998; **19**: 187-191

3 **Wade PA, Gegonne A**, Jones PL, Ballestar E, Aubry F, Wolffe AP. Mi-2 complex couples DNA methylation to chromatin remodelling and histone deacetylation. *Nat Genet* 1999; **23**: 62-66

4 **Baylin SB**, Herman JG, Graff JR, Vertino PM, Issa JP. Alterations in DNA methylation: a fundamental aspect of neoplasia. *Adv Cancer Res* 1998; **72**: 141-196

5 **Baylin SB**, Esteller M, Rountree MR, Bachman KE, Schuebel K, Herman JG. Aberrant patterns of DNA methylation, chromatin formation and gene expression in cancer. *Hum Mol Genet* 2001; **10**: 687-692

6 **Serrano M**, Hannon GJ, Beach D. A new regulatory motif in cell-cycle control causing specific inhibition of cyclin D/CDK4. *Nature* 1993; **366**: 704-707

7 **Herman JG**, Merlo A, Mao L, Lapidus RG, Issa JP, Davidson NE, Sidransky D, Baylin SB. Inactivation of the CDKN2/p16/MTS1 gene is frequently associated with aberrant DNA methylation in all common human cancers. *Cancer Res* 1995; **55**: 4525-4530

8 **Esteller M**, Hamilton SR, Burger PC, Baylin SB, Herman JG. Inactivation of the DNA repair gene O6-methylguanine-DNA methyltransferase by promoter hypermethylation is a common event in primary human neoplasia. *Cancer Res* 1999; **59**: 793-797

9 **Pegg AE**. Mammalian O6-alkylguanine-DNA alkyltransferase: regulation and importance in response to alkylating carcinogenic and therapeutic agents. *Cancer Res* 1990; **50**: 6119-6129

10 **Coulondre C**, Miller JH. Genetic studies of the lac repressor. IV. Mutagenic specificity in the lacI gene of Escherichia coli. *J Mol Biol* 1977; **117**: 577-606

11 **Wiencke JK**, Zheng S, Lafuente A, Lafuente MJ, Grudzen C, Wrensch MR, Miike R, Ballesta A, Trias M. Aberrant methylation of p16INK4a in anatomic and gender-specific subtypes of sporadic colorectal cancer. *Cancer Epidemiol Biomarkers Prev* 1999; **8**: 501-506

12 **Esteller M**. Epigenetic lesions causing genetic lesions in human cancer: promoter hypermethylation of DNA repair genes. *Eur J Cancer* 2000; **36**: 2294-2300

13 **Verma M**, Srivastava S. Epigenetics in cancer: implications for early detection and prevention. *Lancet Oncol* 2002; **3**: 755-763

14 **Urosević N**, Krtolica K, Skaro-Milić A, Knezević-Usaj S, Dujić A. Prevalence of G-to-T transversions among K-ras oncogene mutations in human colorectal tumors in Yugoslavia. *Int J Cancer* 1993; **54**: 249-254

15 **Almoguera C**, Shibata D, Forrester K, Martin J, Arnheim N, Perucho M. Most human carcinomas of the exocrine pancreas contain mutant c-K-ras genes. *Cell* 1988; **53**: 549-554

16 **Herman JG**, Graff JR, Myöhänen S, Nelkin BD, Baylin SB. Methylation-specific PCR: a novel PCR assay for methylation status of CpG islands. *Proc Natl Acad Sci USA* 1996; **93**: 9821-9826

17 **Grunau C**, Clark SJ, Rosenthal A. Bisulfite genomic sequencing: systematic investigation of critical experimental parameters. *Nucleic Acids Res* 2001; **29**: E65-E65

18 **Bos JL**, Fearon ER, Hamilton SR, Verlaan-de Vries M, van Boom JH, van der Eb AJ, Vogelstein B. Prevalence of ras gene mutations in human colorectal cancers. *Nature* 1987; **327**: 293-297

19 **Burmer GC**, Loeb LA. Mutations in the KRAS2 oncogene during progressive stages of human colon carcinoma. *Proc Natl Acad Sci USA* 1989; **86**: 2403-2407

20 **Andreyev HJ**, Norman AR, Cunningham D, Oates JR, Clarke PA. Kirsten ras mutations in patients with colorectal cancer: the multicenter "RASCAL" study. *J Natl Cancer Inst* 1998; **90**: 675-684

21 **Maruyama K**, Ochiai A, Nakamura S, Baba S, Hirohashi S. Dysfunction of E-cadherin-catenin system in invasion and metastasis of colorectal cancer. *Nihon Geka Gakkai Zasshi* 1998; **99**: 402-408

22 **Bhatavdekar JM**, Patel DD, Chikhlikar PR, Trivedi TI, Gosalia NM, Ghosh N, Shah NG, Vora HH, Suthar TP. Overexpression of CD44: a useful independent predictor of prognosis in patients with colorectal carcinomas. *Ann Surg Oncol* 1998; **5**: 495-501

23 **Offerhaus GJ**, Giardiello FM, Bruijn JA, Stijnen T, Molyvas EN, Fleuren GJ. The value of immunohistochemistry for collagen IV expression in colorectal carcinomas. *Cancer* 1991; **67**: 99-105

24 **Choi HJ**, Jung IK, Kim SS, Hong SH. Proliferating cell nuclear antigen expression and its relationship to malignancy potential in invasive colorectal carcinomas. *Dis Colon Rectum* 1997; **40**: 51-59

25 **Olschwang S**, Hamelin R, Laurent-Puig P, Thuille B, De Rycke Y, Li YJ, Muzeau F, Girodet J, Salmon RJ, Thomas G. Alternative genetic pathways in colorectal carcinogenesis. *Proc Natl Acad Sci USA* 1997; **94**: 12122-12127

26 **Lengauer C**, Kinzler KW, Vogelstein B. Genetic instabilities in human cancers. *Nature* 1998; **396**: 643-649

27 **Toyota M**, Ohe-Toyota M, Ahuja N, Issa JP. Distinct genetic profiles in colorectal tumors with or without the CpG island methylator phenotype. *Proc Natl Acad Sci USA* 2000; **97**: 710-715
28 **Ionov Y**, Peinado MA, Malkhosyan S, Shibata D, Perucho M. Ubiquitous somatic mutations in simple repeated sequences reveal a new mechanism for colonic carcinogenesis. *Nature* 1993; **363**: 558-561
29 **Toyota M**, Ahuja N, Ohe-Toyota M, Herman JG, Baylin SB, Issa JP. CpG island methylator phenotype in colorectal cancer. *Proc Natl Acad Sci USA* 1999; **96**: 8681-8686
30 **van Rijnsoever M**, Grieu F, Elsaleh H, Joseph D, Iacopetta B. Characterisation of colorectal cancers showing hypermethylation at multiple CpG islands. *Gut* 2002; **51**: 797-802
31 **Wynter CV**, Walsh MD, Higuchi T, Leggett BA, Young J, Jass JR. Methylation patterns define two types of hyperplastic polyp associated with colorectal cancer. *Gut* 2004; **53**: 573-580
32 **Whitehall VL**, Walsh MD, Young J, Leggett BA, Jass JR. Methylation of O-6-methylguanine DNA methyltransferase characterizes a subset of colorectal cancer with low-level DNA microsatellite instability. *Cancer Res* 2001; **61**: 827-830
33 **Samowitz WS**, Holden JA, Curtin K, Edwards SL, Walker AR, Lin HA, Robertson MA, Nichols MF, Gruenthal KM, Lynch BJ, Leppert MF, Slattery ML. Inverse relationship between microsatellite instability and K-ras and p53 gene alterations in colon cancer. *Am J Pathol* 2001; **158**: 1517-1524
34 **Liang JT**, Chang KJ, Chen JC, Lee CC, Cheng YM, Hsu HC, Wu MS, Wang SM, Lin JT, Cheng AL. Hypermethylation of the p16 gene in sporadic T3N0M0 stage colorectal cancers: association with DNA replication error and shorter survival. *Oncology* 1999; **57**: 149-156
35 **Esteller M**, González S, Risques RA, Marcuello E, Mangues R, Germà JR, Herman JG, Capellà G, Peinado MA. K-ras and p16 aberrations confer poor prognosis in human colorectal cancer. *J Clin Oncol* 2001; **19**: 299-304
36 **Yi J**, Wang ZW, Cang H, Chen YY, Zhao R, Yu BM, Tang XM. p16 gene methylation in colorectal cancers associated with Duke's staging. *World J Gastroenterol* 2001; **7**: 722-725
37 **Maeda K**, Kawakami K, Ishida Y, Ishiguro K, Omura K, Watanabe G. Hypermethylation of the CDKN2A gene in colorectal cancer is associated with shorter survival. *Oncol Rep* 2003; **10**: 935-938
38 **Sanz-Casla MT**, Maestro ML, Vidaurreta M, Maestro C, Arroyo M, Cerdán J. p16 Gene methylation in colorectal tumors: correlation with clinicopathological features and prognostic value. *Dig Dis* 2005; **23**: 151-155
39 **Nagasaka T**, Sharp GB, Notohara K, Kambara T, Sasamoto H, Isozaki H, MacPhee DG, Jass JR, Tanaka N, Matsubara N. Hypermethylation of O6-methylguanine-DNA methyltransferase promoter may predict nonrecurrence after chemotherapy in colorectal cancer cases. *Clin Cancer Res* 2003; **9**: 5306-5312

S- Editor Liu Y **L- Editor** Lutze M **E- Editor** Zhou T

PO Box 2345, Beijing 100023, China
www.wjgnet.com
wjg@wjgnet.com

World J Gastroenterol 2007 February 28; 13(8): 1195-1203
World Journal of Gastroenterology ISSN 1007-9327

Quasispecies evolution in NS5A region of hepatitis C virus genotype 1b during interferon or combined interferon-ribavirin therapy

Pascal Veillon, Christopher Payan, Hélène Le Guillou-Guillemette, Catherine Gaudy, Françoise Lunel

Pascal Veillon, Hélène Le Guillou-Guillemette, Françoise Lunel, Laboratory of Virology, Angers University Hospital, 4 rue Larrey, 49933 Angers cedex 9, France
Christopher Payan, Departement of Microbiology, EA 3882, Brest University Hospital, 2 avenue Foch, 29609 Brest cedex, France
Catherine Gaudy, University Francois Rabelais, INSERM ERI 19, Faculty of Medecine, 10 Boulevard Tonnellé, BP 3223, 37032 Tours Cedex, France
Pascal Veillon, Hélène Le Guillou-Guillemette, Françoise Lunel, HIFIH Laboratory, UPRES EA 3859, IFR 132, University of Angers, rue de Haute Reculée, 49045 Angers, France
Supported by a grant from l'Agence National de la Recherche sur le Sida (ANRS grant 2001/011)
Correspondence to: Professor Françoise Lunel, Service de Bactériologie-Virologie et Hygiène Hospitalière, CHU ANGERS, 4 rue Larrey; 49933 ANGERS cedex 9,
France. frlunel-fabiani@chu-angers.fr
Telephone: +33-2-41355493 Fax: +33-2-41354164
Received: 2006-09-26 Accepted: 2006-12-09

Abstract

AIM: To evaluate the implication of substitutions in the hepatitis C virus (HCV) non-structural 5A (NS5A) protein in the resistance of HCV during mono-interferon (IFN) or combined IFN-ribavirin (IFN-R) therapy. Although NS5A has been reported to interact with the HCV RNA-dependent RNA polymerase, NS5B, as well as with many cellular proteins, the function of NS5A in the life cycle of HCV remains unclear.

METHODS: HCV quasispecies were studied by cloning and sequencing of sequential isolates from patients infected by HCV genotype 1b. Patients were treated by IFN-α2b for 3 mo followed by IFN-α2b alone or combined IFN-R therapy for 9 additional months. Patients were categorized intro two groups based on their response to the treatments: 7 with sustained virological response (SVR) (quasispecies = 150) and 3 non-responders (NR) to IFN-R (quasispecies = 106).

RESULTS: Prior to treatment, SVR patients displayed a lower complexity of quasispecies than NR patients. Most patients had a decrease in the complexity of quasispecies during therapy. Analysis of amino acids substitutions showed that the degree of the complexity of the interferon sensitivity-determining region (ISDR) and the V3 domain of NS5A protein was able to discriminate the two groups of patients. Moreover, SVR patients displayed more variability in the NS5A region than NR patients.

CONCLUSION: These results suggest that detailed molecular analysis of the NS5A region may be important for understanding its function in IFN response during HCV 1b infection.

Key words: Hepatitis C virus; Quasispecies; NS5A region; Interferon sensitivity-determining region; V3 domain

Veillon P, Payan C, Le Guillou-Guillemette H, Gaudy C, Lunel F. Quasispecies evolution in NS5A region of hepatitis C virus genotype 1b during interferon or combined interferon-ribavirin therapy. *World J Gastroenterol* 2007; 13(8): 1195-1203

http://www.wjgnet.com/1007-9327/13/1195.asp

INTRODUCTION

In Western countries, the hepatitis C virus (HCV) is the major cause of chronic hepatitis, cirrhosis and hepatocellular carcinoma[1]. HCV is a RNA virus belonging to the *Flaviviridae*. It has a single-stranded plus-sense genome of approximately 9.6 kb with a single open reading frame (ORF) encoding four structural (C, E1, E2 and p7) and six non-structural proteins (NS2, NS3, NS4A, NS4B, NS5A and NS5B). Current combination therapy of pegylated interferon (IFN) alpha and ribavirin (IFN-R) is not universally effective in patients with chronic hepatitis C; patients infected with genotypes 2 or 3 show a high rate of sustained virological response (SVR) (90%) whereas the HCV genotype 1 infected patients have the lowest level of SVR (40% to 50%)[2-4]. Factors that can predict the response to antiviral therapy are not well established; the accepted predictive parameters are: age, sex, pre-treatment viral load, fibrosis stage and HCV genotype[5]. Numerous studies have been undertaken to explain the resistance of genotype 1-infected patients to IFN therapy. Causes and mechanisms are not well understood, but several viral genomic regions have been suggested to antagonize the antiviral effect of IFN alpha, such as the E2, NS3/4A and NS5A regions[6].

The non-structural 5A (NS5A) protein is the ninth

protein coded by the ORF of HCV. It has a length of 447 amino acids (aa) for genotype 1b. An interaction with the double-stranded RNA protein kinase (PKR) has been described for NS5A within the codons 2209 and 2274 ($NS5A_{2209-2274}$)[7-9]. This interaction can block the IFN signalling pathway in cultured cells, and certain authors have suggested that this mechanism may be implicated in HCV resistance to IFN therapy. In 1995, Enomoto *et al*[10] described a correlation between the number of mutations within a 40 aa sequence of the NS5A region and the response to IFN therapy in genotype 1b-infected patients. This sequence has been termed the interferon sensitivity-determining region (ISDR). These results were then confirmed by other Japanese studies[11-15], but were never in accordance with most Western European[16-20] and American studies[21-23], in which most of the ISDR sequences harbored an intermediate profile. A recent meta-analysis focusing on the number of mutations within NS5A ISDR confirmed the predictive usefulness of ISDR, but a real geographical difference between Caucasian and Asiatic patients was underlined[24].

Recently, it was suggested that NS5A protein may also inhibit the antiviral effect of IFN in a PKR-independent manner in a human hepatocytic cell line[25]. Furthermore, another domain in the NS5A region, named V3 ($NS5A_{2356-2379}$)[26], could also be linked to IFN resistance. It has been suggested that mutations in the V3 domain may correlate with IFN response[17]. However, two reports have shown that insertion and deletion around the ISDR and the V3 domain had no impact on HCV RNA replication in cell culture[27,28].

In the present study, we examined mutations in the complete NS5A region, including its ISDR, PKR binding domain (PKRbd) and V3 domain, of HCV genotype 1b from patients treated with IFN or combined IFN-R therapy. HCV quasispecies of ten patients were selected for the analysis based on their response to the treatments combined IFN-R therapy.

MATERIALS AND METHODS

Study population

We analyzed PCR products from ten HCV genotype 1b infected patients included in a therapeutic trial[29]. Seven of them had SVR - three early and four slow responders according to HCV RNA clearance during therapy at mo 3 (M3) - and three were non-responders to IFN-R (NR). Patients were all studied at baseline (D0), M3 and M6, when gene amplification was possible (positive PCR). Patients received 6 million units of IFN-α2b three times weekly. If HCV RNA was still detectable at M2, ribavirin was combined with IFN at M3 and continued up to M12. SVR was defined as undetectable HCV RNA during treatment and six months after the end of therapy (EOT). Non-SVR was defined as detectable HCV RNA during treatment and six months after the EOT.

HCV RNA quantification

Quantification of serum HCV RNA was performed using VERSANT HCV RNA 3.0 assay (Bayer Diagnostics, Emeryville, CA, USA) with a detection threshold at 615 IU/mL (2.79 log IU/mL).

Table 1 Sequences of amplification and sequencing primers

Forward primers		Positions nt
E1	5' GAGGGGGCTGTGCAGTGGATG 3'	6057-6077
I3	5' TCCGGCTCGTGGCTAAGGGA 3'	6246-6265
S2	5' GGATTTCCACTACGTGACGGG 3'	6620-6640
S4	5' GGGTCTCCCCCCTCCTTGGCC 3'	6906-6926
S31	5' GGACTACGTCCCTCCGGTGG 3'	7241-7260
Reverse primers		
AS2	5' CGTCACGTAGTGGAAATCCCC 3'	6618-6638
AS32	5' GGGACGTAGTCCGGGTCCTTC 3'	7232-7252
I4	5' GCAGCAGACGAGATCCTCAC 3'	7567-7586
E2	5' GCTGCGAGATGTTGTGGCGTA 3'	7698-7718
Cloning primers	(pMOS vector)	
SeqS1	5' GGGAAAGCTTGCATGCCTGC 3'	
SeqAS2	5' GACGTTGTAAAACGACGGCC 3'	

Nucleotide positions are numbered according to the HCV-J sequence and the NS5A region is within positions 6246-7586.

RNA extraction and amplification by RT-PCR

HCV RNA was extracted from 200 μL of serum by guanidinium thiocyanate and silica method[30]. The full-length NS5A gene was amplified by nested RT-PCR. RT was combined with the first round of PCR with outer primers E1 and E2 while second amplification was performed with inner primers I3 and I4 as previously described (Table 1)[17,31]. PCR products were then subjected to electrophoresis in a 1% agarose gel (NuSieve GTG, FMC) and visualized by ethidium bromide staining before purification. In this study, we sequenced 343 296 nts from 256 clones of the complete NS5A region. According to *Taq* error rate (0.182×10^{-4})[32], 6.247 RT-PCR-introduced errors could have been analyzed as substitutions for all clones, i.e. 0.024 RT-PCR-introduced errors per clone.

PCR products cloning

PCR fragments cut out from the agarose gel were purified using a mini-column system (Wizard PCR Preps DNA purification system, Promega) and then were ligated into 50 ng of pMOS vector (pMOS*Blue* blunt-ended cloning kit, Amersham Bioscience). Transformants were grown on LB-agar plates containing 100 μg/mL ampicillin and 15 μg/mL tetracycline. The presence of HCV insert was confirmed by plasmid amplification using SeqS1 and SeqAS2 primers (Table 1). We produced between 4 and 17 clones per patient.

DNA sequencing

Cycle sequencing was performed using the CEQ 8000 Dye Terminator Cycle Sequencing kit following the manufacturer's instructions (Beckman Coulter) before automatic electrophoresis of the sequencing products using a CEQ 8000 (Beckman Coulter). Inner PCR primers S2, S4, S31, AS2 and AS32 were used as sequencing primers (Table 1). Sequences were analyzed using the CEQ 8000 software.

Sequence analysis

Multiple nucleotide (nt) sequence alignment and ambiguity were carried out with CLUSTAL X interface[33]. The nucleotide substitution rate over sites within each set of variants was estimated by using DAMBE software. The

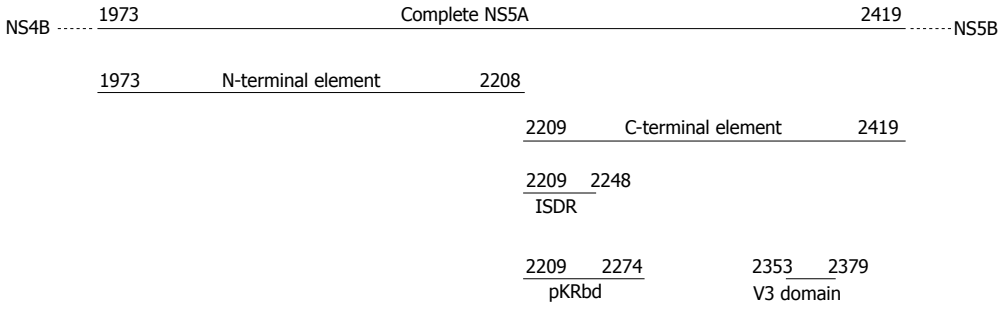

Figure 1 Schematic localisation of the six studied regions in NS5A protein. Amino acids positions are numbered according to the HCV-J polyprotein and the NS5A region is within positions 1973-2419.

Table 2 Clinical and virological characteristics of the 10 patients studied before and during treatment mean ± SD

Patient and time of treatment	Sex	Age	Viral load log IU/mL	*n*	NT substitutions/master sequence	AA substitutions/master sequence	Genetic distance
SVR1-D0	F	48	2.00	15	4.5 ± 2.3	2.5 ± 1.4	0.0065 ± 0.0008
SVR2-D0	F	53	4.55	13	5.1 ± 3.6	3.3 ± 2.1	0.0070 ± 0.0011
SVR3-D0	M	43	4.71	8	10.3 ± 3.6	4.7 ± 1.9	0.0105 ± 0.0018
SVR4-D0	M	59	6.24	16	15.4 ± 8.0	7.5 ± 4.9	0.0172 ± 0.0022
SVR4-M3	-	-	1.61	13	3.6 ± 2.1	1.8 ± 1.0	0.0051 ± 0.0008
SVR5-D0	F	65	5.44	15	10.1 ± 6.6	4.9 ± 2.0	0.0171 ± 0.0016
SVR5-M3	-	-	2.77	17	6.4 ± 2.4	3.3 ± 1.6	0.0070 ± 0.0010
SVR6-D0	M	47	7.26	17	15.9 ± 10.5	8.5 ± 5.1	0.0192 ± 0.0022
SVR6-M3	-	-	2.18	6	4.0 ± 1.7	2.4 ± 1.3	0.0062 ± 0.0012
SVR7-D0	F	51	6.61	15	29.3 ± 8.5	7.3 ± 2.7	0.0294 ± 0.0029
SVR7-M3	-	-	5.42	15	12.6 ± 4.2	4.6 ± 2.2	0.0156 ± 0.0016
NR1-D0	M	35	5.13	17	15.2 ± 4.3	3.5 ± 1.9	0.0181 ± 0.0020
NR1-M3	-	-	5.24	9	15.3 ± 4.4	4.8 ± 1.7	0.0143 ± 0.0020
NR1-M6	-	-	2.83	4	4.5 ± 3.1	2.0 ± 3.4	0.0041 ± 0.0013
NR2-D0	F	50	5.90	17	15.6 ± 6.4	5.2 ± 2.9	0.0181 ± 0.0020
NR2-M3	-	-	5.87	12	9.5 ± 3.6	3.9 ± 1.8	0.0125 ± 0.0013
NR2-M6	-	-	5.77	10	10.3 ± 3.3	4.0 ± 2.2	0.0274 ± 0.0020
NR3-D0	F	44	5.63	14	10.9 ± 3.7	4.4 ± 2.2	0.0279 ± 0.0021
NR3-M3	-	-	5.79	11	11.1 ± 2.7	4.0 ± 2.8	0.0157 ± 0.0017
NR3-M6	-	-	5.00	12	10.8 ± 3.3	4.4 ± 2.0	0.0154 ± 0.0015

F: Female; M: Male; *n*: number of PCR products analyzed; D0: beginning of the treatment; M3: 3 mo of treatment; SVR: Sustained Virological Responders; NR: Non-Responders to IFN-ribavirin therapy.

variability at each site i was measured by calculating the Shannon entropy at the site i (*Hi*) with the following formula: $Hi = -(\sum^{4}_{j=1} p_j \log_2 p_j)$, where j = 1, 2, 3, 4 corresponding to nucleotide A, C, G and T, and p_j is the proportion of nucleotide j at site i. The normalized entropy Sn was calculated as Sn = H/log N, where N is the total number of analysed sequences[34]. Types of mutational changes were also determined by means of MEGA 2.3 software. Genetic distances between pairs of sequences were performed using Kimura 2-parameters method[35]. The frequency of synonymous (dS) and non-synonymous (dN) substitutions per site were calculated with Nei-Gojobori method using the Jukes-Cantor correction to account for multiple substitution at the same site[36]. The dN/dS ratio is a measure of immunity pressure on a region. Construction of the phylogenetic tree of NS5A variants obtained from ten patients was performed using MEGA 2.3 software. The phylogenetic tree was constructed with the neighbour-joining method and bootstrap resampling (1000 replicates were used to test reliability of the tree topology)[37]. Master sequence was defined as the sequence obtained from direct sequencing of PCR products obtained before cloning.

A multiple alignment of the translated aa sequences was generated. Alignment analysis of nucleotides and proteins was performed using HCV-J (genotype 1b, D90208) as reference and HCV-H (genotype 1a, M67463) as out-group for the construction of the phylogenetic tree.

Six regions were studied: the ISDR ($NS5A_{2209-2248}$), PKR binding domain (PKRbd) ($NS5A_{2209-2274}$), V3 ($NS5A_{2353-2379}$), the N-terminal element of NS5A protein until ISDR ($NS5A_{1973-2208}$), the C-terminal element of NS5A protein from ISDR to the end ($NS5A_{2209-2419}$), and the complete sequence of NS5A ($NS5A_{1973-2419}$) (Figure 1).

Statistical analysis

Values for quantitative variables were expressed as means ± SD. Comparisons between groups were performed using the Student *T*-test or the non-parametric Mann-Whitney *U*-test or Kruskal-Wallis *K*-test for quantitative variables. The Pearson's correlation coefficient was used. A *P*-value of less than 0.05 was considered to be statistically significant.

RESULTS

Phylogenetic and heterogeneity analysis of HCV quasispecies

Characteristics of each patient are summarized in Table 2. We studied ten patients (four males and six females). Average

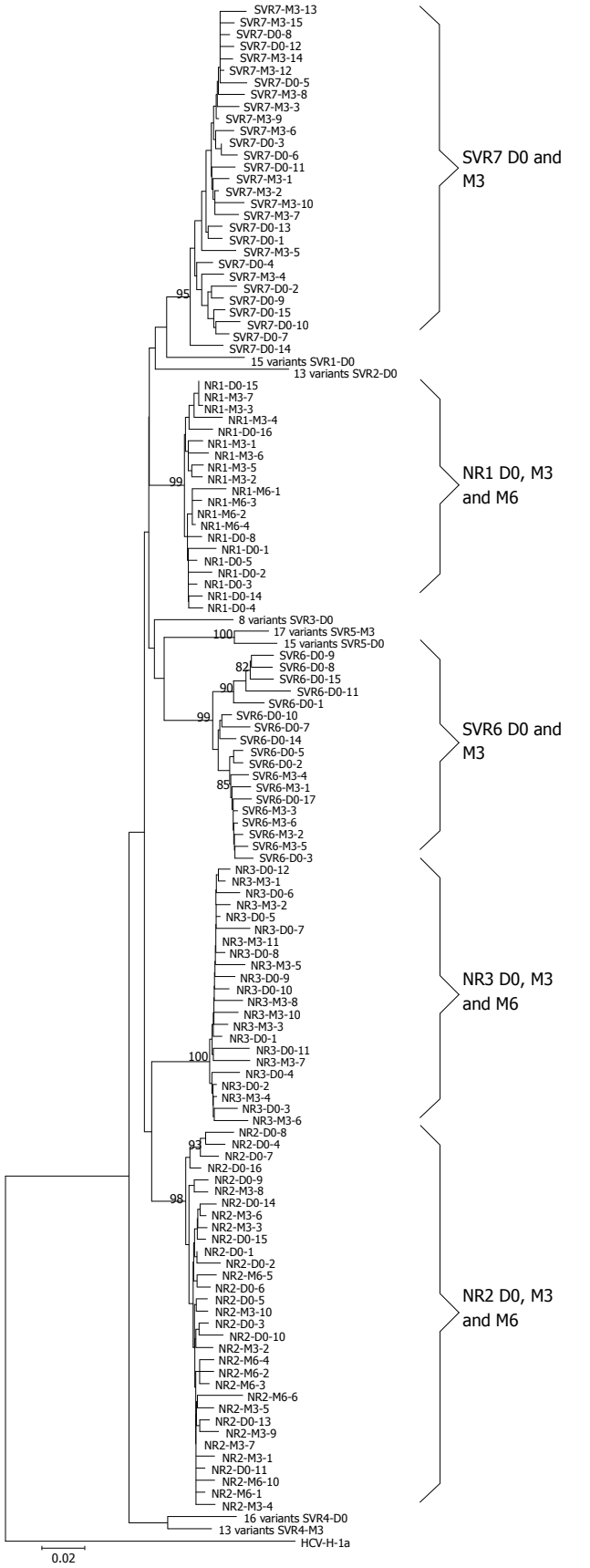

Figure 2 Phylogenetic tree of NS5A region (codon 1973-2419) of amino acids HCV variants obtained from ten patients at different time of treatment. D0: beginning of the treatment; M3: 3 mo of treatment; SVR: Sustained Virological Responders to IFN-ribavirin therapy; NR: Non-Responders to IFN-ribavirin therapy. HCV-H strain was used as outgroup. The internal node numbers represent the bootstrap values. Distance scale represents 2% of difference between sequences. When all NS5A sequences within a patient at one time point of treatment are grouped in a cluster, this cluster is presented by only one node.

Table 3 Characteristics of HCV quasispecies in pre-treatment isolates from SVR and NR patients

Region and patient type	Genetic distance	dS	dN	dN/dS	Num. amino acid mutations
NS5A					
SVR (n = 99)	0.1027	0.3239	0.039	0.120	33.9
NR (n = 48)	0.0698	0.1216	0.025	0.206	29.8
ISDR					
SVR (n = 99)	0.0834	0.3084	0.0295	0.096	1.3
NR (n = 48)	0.0765	0.2645	0.0271	0.102	1.9
PKRbd					
SVR (n = 99)	0.0934	0.2934	0.0424	0.145	5.3
NR (n = 48)	0.0815	0.2694	0.0332	0.123	5.7
V3					
SVR (n = 99)	0.1836	0.3264	0.1282	0.393	6.0
NR (n = 48)	0.1372	0.4482	0.0556	0.124	4.7

Values were calculated as described in methods; amino acids sequences were compared to HCV-J; n: number of PCR products analyzed; dS: frequency of synonymous substitutions per site; dN: frequency of non-synonymous substitutions per site; SV: Sustained Virological Responders; NR: Non-Responders to IFN-ribavirin therapy.

patient age was 49.5 years and HCV viral load was 5.35 log IU/mL (mean at baseline). We found a significant difference in viral load between the three groups of early, slow SVR and NR (P = 0.034), whereas no significant difference was found between the SVR and NR groups at baseline. The genetic variability of the NS5A region was confirmed by cloning NS5A PCR products obtained from the ten patients (7 SVR and 3 NR) into the pMOS vector. In total, PCR products from 256 clones of the NS5A region were analyzed (Table 2). No cluster in correlation with treatment response was observed in the phylogenetic tree (Figure 2). However, in two slow SVR patients (SVR4 and SVR5) two different clusters were individualized with two populations of variants (D0 and M3, respectively). In the two other slow SVR patients (SVR6 and SVR7) and in NR patients, we found mixed populations of variants at the beginning of treatment (D0) and during treatment (M3 or M6). Genetic complexity of nt and aa sequences calculated by Shannon entropy showed no significant difference between the two groups studied (Figure 3, A and B). Interestingly, when we looked at early SVR in comparison with slow SVR, we observed a significant difference between these three groups of patients, P = 0.026 and P = 0.024, respectively, for nt and aa complexity calculated by Shannon entropy. At baseline, we observed that PCR products from the SVR group displayed more frequently synonymous substitutions (dS) and non-synonymous substitutions (dN) than PCR products from the NR group along the NS5A region, ISDR and PKRbd domains, but not in the V3 domain for dS (Table 3, columns 3 and 4). dN/dS ratios were similar in the two groups in ISDR and PKRbd domains. This ratio was two times higher in SVR patients than in NR patients along the NS5A region and three times higher in the V3 domain (Table 3, column 5).

Among the aa sequences of the PKRbd and V3 domains, we observed that NR patients exhibited a higher variant complexity than SVR patients before initiation of IFN therapy in the three domains ISDR, PKRbd and V3 (Table 4). In ISDR, after three months of IFN therapy,

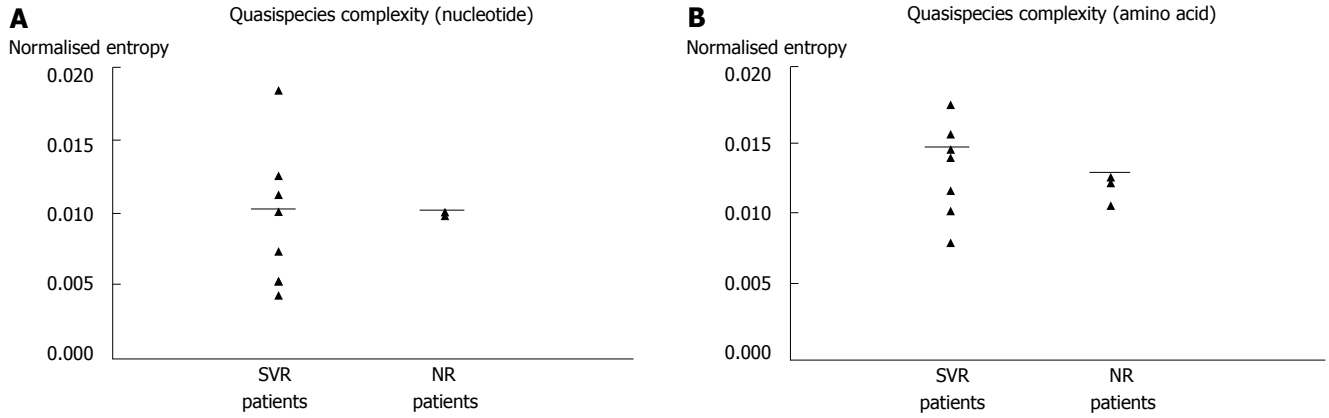

Figure 3 Genetic complexity of HCV quasispecies (**A**: nucleotide; **B**: amino acid) calculated by normalized entropy in seven sustained virological responders and three non-responders with median indicated by horizontal bar for each group. *P*-value calculated by Mann-Whitney *U*-test.

Table 4 Complexity evolution in HCV quasispecies from SVR and NR patients in ISDR, PKRbd and V3 domains

Patient	Time of treatment domains	D0 ISDR-PKRbd-V3	M3 ISDR-PKRbd-V3	M6 ISDR-PKRbd-V3
SVR1	*n* = 15	3–4–3	-	-
SVR2	*n* = 13	3–4–2	-	-
SVR3	*n* = 8	3–5–3	-	-
SVR4	*n* = 16–13	3–7–3	3–4–3	-
SVR5	*n* = 15–17	8–8–1	4–7–1	-
SVR6	*n* = 17–6	8–9–3	1–2–3	-
SVR7	*n* = 15–17	6–6–7	6–7–7	-
NR1	*n* = 17–9–4	6–8–7	3–4–4	1–3–2
NR2	*n* = 17–12–10	7–8–2	5–8–3	3–4–6
NR3	*n* = 14–11–12	6–7–4	5–7–3	4–5–2

Amino acids sequences were compared to HCV-J; *n*: number of PCR products analyzed.

two out of four slow SVR patients and the three NR patients showed a decrease in variant complexity (SVR5; SVR6; NR1; NR2 and NR10). The two other slow SVR patients displayed stability in variant complexity (SVR4 and SVR7). The three NR patients had a continuous decrease in the complexity under combined IFN-R regimen at M6 (NR1; NR2 and NR3).

Within PKRbd, after three months of IFN therapy, three out of four slow SVR patients and one out of three NR patients displayed a decrease in variant complexity (SVR4; SVR5; SVR6 and NR2) (Table 4). The two other NR patients exhibited stability in variant complexity (NR2 and NR3) and the fourth slow SVR patient showed an increase in variant complexity (SVR7). The three NR patients had a decrease in complexity under combined IFN-R therapy at M6.

After three months of IFN therapy, three out of four slow SVR patients (SVR4; SVR6 and SVR7) displayed a decrease in variant complexity in the V3 domain, as did two out of three NR patients (NR1 and NR3) (Table 4). The two other patients were found to contain an increase in variant complexity (SVR5 and NR2). Under combined IFN-R therapy, two NR patients had a low decrease in variant complexity (NR1 and NR3), whilst the third NR patient showed an increase (NR2) in variant complexity.

Variability in six different regions along the NS5A gene

Comparison to master sequence: Among the 256 PCR products studied, before and during treatment, we observed a mean of 11.7 ± 7.9 nt substitutions with a median of 10 nt substitutions.

At baseline, we observed 13.6 ± 9.1 nt substitutions (median of 12 nt substitutions) among the 147 clones analyzed, in comparison to the master sequence (Table 2, column 6). The aa variations were 4.8 ± 3.1 substitutions (with a median at 4) among all 256 clones and 5.4 ± 3.5 aa substitutions in clones analyzed before treatment, with a median of 5 aa substitutions. We also observed that all variants from SVR patients had a higher genetic diversity than all variants from NR patients in the four regions studied, including ISDR, PKRbd, V3 domain and complete NS5A (Table 3, column 2). Within patients, we observed that the 3 early SVR had a lower genetic diversity than the four slow SVR and the three NR.

We observed significantly more aa substitutions in SVR clones than in NR clones in two out of six regions (complete NS5A, $P = 0.013$; the first half of NS5A, $P = 0.032$). Interestingly, NR clones presented more aa substitutions in the V3 domain than SVR clones, but this was not statistically significant (Table 3).

During treatment, the genetic distance and numbers of substitutions (nt and aa) in SVR PCR products decreased between the baseline and M3 (Table 2, columns 6, 7 and 8). PCR products from NR patients also showed a decrease of the genetic distance, but this was lower than those from SVR patients. However, clones from NR patients had either stability or an increase in the number of aa substitutions observed under treatment. NS5A variants had a high heterogeneity without clonal selection of quasispecies and a low variation in ISDR and V3 domains during therapy.

Comparison to HCV-J sequence: Among the 256 clones analyzed, we observed a mean of 32.1 ± 5.2 aa substitutions. At baseline, a mean of 36.6 ± 5.6 aa substitutions (median at 32 aa substitutions) was observed among the 147 clones analyzed, in comparison to the

Table 5 Number of amino acids mutations observed in six different regions from NS5A protein, at baseline mean ± SD

NS5A region (aa range)	2 groups (D0) (*n* = 147)	SVR (D0) (*n* = 99)	NR (D0) (*n* = 48)	SVR (M3) (*n* = 51)	NR (M3) (*n* = 32)	NR (M6) (*n* = 26)
ISDR (2209-2248)	1.5 ± 1.6	1.3 ± 1.7	1.9 ± 1.1	0.8 ± 0.8	2.1 ± 1.0	1.8 ± 1.2
PKRbd (2209-2274)	5.4 ± 2.1	5.3 ± 2.4	5.7 ± 1.2	4.7 ± 1.6	6.1 ± 1.0	5.7 ± 1.3
V3 (2353-2379)	5.5 ± 1.4	6.0 ± 1.5	4.7 ± 0.6	6.1 ± 1.3	4.8 ± 0.7	5.1 ± 0.6
Complete NS5A (1973-2208)	32.6 ± 5.6	33.9 ± 6.0	29.8 ± 3.7	31.7 ± 5.3	30.8 ± 3.9	31.9 ± 2.9
N-terminal part of NS5A (1973-2208)	12.4 ± 3.1	12.9 ± 3.3	11.6 ± 2.4	11.7 ± 2.0	11.2 ± 2.1	12.8 ± 2.1
C-terminal part of NS5A (2209-2419)	20.1 ± 3.9	21.1 ± 4.1	18.2 ± 2.4	20.1 ± 4.2	19.6 ± 2.9	19.4 ± 3.4

n: number of PCR products analyzed; SVR: Sustained Responders; NR: Non-Responders to IFN-ribavirin therapy; D0: beginning of the treatment; M3: 3 mo of treatment; M6: 6 mo of treatment.

HCV-J sequence (Tables 2 and 5). Next, we determined for each group the level of aa substitutions in each site, with a threshold at 15 aa substitutions (this threshold was defined as half of the maximum (n = 31) of aa substitutions observed for the 256 clones; in position 2218). In ISDR, aa variations were found at positions 2218, 2224, 2232, 2234 and 2237, in the V3 domain at position 2377 and along NS5A protein at positions 2251 (PKRbd), 2280 and 2408.

At baseline, among the two group of patients (SVR and NR), the comparison of the different clone populations showed that all except one (PKRbd) of the six regions studied were able to differentiate the two groups (Table 5).

We observed more aa substitutions in SVR clones than in NR clones in four out of six regions (complete NS5A, $P < 0.001$; the first half of NS5A, $P = 0.010$; the second half of NS5A, $P < 0.001$ and V3, $P < 0.001$). Interestingly, NR clones presented more aa substitutions in ISDR than SVR clones, $P = 0.011$, and the PKRbd domain was not able to discriminate the two groups of patients. In contrast to previous findings, NR clones had more aa substitutions than SVR clones in ISDR and PKRbd regions. We did not find any correlation between HCV viral load and the number of mutations observed in ISDR and the V3 domains. A fair correlation was observed between HCV viral load and PKRbd ($r = 0.724$; $P = 0.018$). A good correlation was observed between HCV viral load and complete NS5A ($r = 0.855$; $P = 0.002$) and with the second half of NS5A ($r = 0.782$; $P = 0.008$).

During treatment, a decrease of aa substitutions occurred in the six studied regions for the two groups of patients. Only ISDR and the complete NS5A sequence showed a significant decrease in aa substitutions under treatment in comparison with populations studied at baseline ($P = 0.019$ and $P = 0.005$, respectively). In the NR clones, stability or a low decrease in aa substitutions was observed in the six regions, at baseline, M3 and M6.

Possible mutagenic effect of ribavirin during combination therapy

Among the three populations of clones from NR patients, we did not find any aa substitutions between M3 and M6 treatment points, as recently described in NS5A during ribavirin monotherapy[38]. No other specific aa substitutions were found in the NS5A protein.

DISCUSSION

Numerous viral and host factors have been described as predictors of response to therapy. HCV genotype 1, particularly genotype 1b, are most resistant to combined IFN-R therapy[5]. Among viral factors, genetic variability has been studied in many regions of the HCV genome, mainly in hypervariable region 1 (HVR1) and PKR-eIF2α phosphorylation homology domain (PePHD) of E2 region and in PKRbd (including ISDR) of NS5A[17,22,39-43]. However, few reports have studied the complete NS5A region[17,22]. Most of these studies examined patients treated by IFN monotherapy, with few studies of patients treated by combined IFN-R therapy.

A recent study examining viral sequence differences between African American and Caucasian patients treated by IFN with or without ribavirin found that the NS5A region did not cluster by race, but treatment response and IFN effectiveness did[44]. In this study, our analysis of the number of substitutions in the V3 domain showed a significant difference between the two groups of patients and a significant correlation between IFN effectiveness and a high number of mutations in the V3 domain[45].

In another study examining the second half of the NS5A region, especially ISDR, PKRbd and V3 domains, in patients treated by combined IFN-R therapy, the authors also found that the V3 domain showed more accumulation of substitutions than other domains in NS5A[45]. SVR patients had lower complexity and diversity than NR patients before treatment. During therapy, the investigators observed a decrease in complexity and diversity in SVR patients, and an increase in complexity with accumulation of non-synonymous mutations in NR patients.

In our study, we analyzed sequence variations of NS5A quasispecies in patients who received adapted therapy according to virological response during treatment. Among SVR patients, we analyzed three early SVR and four slow SVR patients compared to three NR patients. The construction of a phylogenetic tree did not allow us to distinguish the two groups of patients (SVR and NR). Before treatment, the analysis of genetic complexity and diversity did not show a significant difference between the seven SVR and the three NR patients. However, the genetic complexity and diversity were lower in early SVR than in the seven other SVR patients. The analysis of the immunity pressure in different domains of the NS5A gene did not show differences between the SVR and NR groups except for the V3 domain and the complete NS5A region where the SVR group presented a higher immunity pressure than NR patients. Generally, the analysis of mutations compared to the master sequence or HCV-J

sequences requires long fragments (a half or a complete NS5A protein) to distinguish SVR and NR. We did not observe any difference in specific aa substitutions between the two groups of patients.

During treatment, we observed a decrease of genetic complexity and diversity in slow SVR and NR patients. A very low complexity was found in the V3 domain in eight out of ten patients (6/7 of SVR and 2/3 of NR patients). In the PKRbd and V3 domains, we often observed complexity decrease or stability. Only one out of seven SVR and one out of three NR patients displayed complexity increase either under IFN therapy or under combined IFN-R therapy. Thus, we observed a different evolution of quasispecies under IFN alone or under combined therapy. This is in contrast to a recent study by Puig-Basagoti *et al*[45] where they observed a decrease in quasispecies complexity in SVR patients and a stability or increase in quasispecies complexity in NR patients. In this study, the analysis of the quasispecies was done at wk 1, 2 and 4, whereas in our study we analyzed quasispecies after a first three-month period of treatment under IFN alone and after a second three-month period under combined IFN-R therapy. We observed the same rate of appearance of aa substitutions in the ISDR domains for the two categories of patients. However, the instauration of a real modification of aa in a quasispecies was more often observed in SVR patients than in NR patients in the complete NS5A protein and in the PKRbd and V3 domains. Interestingly, in three slow SVR (SVR4-SVR5-SVR6) patients the main variant from the ISDR domain remained unchanged after three months of treatment. The same observation was made in two out of three NR patients who also exhibited complexity stability in the different NS5A regions.

Asahina *et al*[38] studied the possible mutagenic effect of ribavirin during a period of 28 days of ribavirin monotherapy before combined IFN-R therapy. During the first phase of ribavirin monotherapy, they observed an accumulation of non-synonymous substitutions located in NS5A. These substitutions were observed in ten patients and eight of them had SVR after treatment. In our study, we did not observe these substitutions in PKRbd nor in any part of NS5A. However, our treatment regimen was different and we only studied the effect of ribavirin during three months of combined therapy in NR patients. It is also possible that substitutions did arise during combined therapy, but were subsequently eliminated by the treatment.

In conclusion, our study reinforces the potential role of NS5A polymorphism, particularly in the V3 domain, in regulating HCV resistance to IFN treatment. Nevertheless, the underlying molecular mechanisms remain unclear. Mutations in the V3 domain may affect the interaction between NS5A and one or several IFN-induced antiviral effectors. Some studies found high mutation frequency in ISDR being associated with low HCV RNA titer, suggesting that NS5A may play a role in HCV replication. In our study, at baseline, we did not find any relationship between HCV viral load and the number of mutations observed in the ISDR and V3 domains. The number of mutations observed in PKRbd has shown a fair correlation with HCV viral load, but we found a better correlation when we analyzed the second half or the complete NS5A region. These results support the notion that mutations in the NS5A region may influence on HCV replication, and suggest that the entire NS5A region should be analyzed for mutations that may correlate with IFN response. Further clinical studies with new therapeutic approaches such as pegylated IFN, as well as the use of the recently developed HCV infection cell culture systems should further improve our understanding of the role of NS5A in regulation of the IFN response.

ACKNOWLEDGMENTS

The authors thank Schering-Plough for supporting the therapeutic protocol and all hepatologists and virologists of the Group of Fontevraud who participated to this therapeutic protocol. The authors thank Kevin L Erwin for his careful proofreading of the manuscript.

COMMENTS

Background

In this article, we analyzed NS5A HCV quasispecies evolution during antiviral treatment. Since the NS5A protein is implicated in HCV resistance, this study should enhance the knowledge of evolution of the resistance during treatment.

Research frontiers

Many previous articles focused on a small region(s) of NS5A without studying the complete gene. We believe that an analysis of the entire NS5A region is necessary because some sections of NS5A may be important for homologous and/or heterologous RNA-protein or protein-protein interactions and thus may play a role in conferring HCV resistance to IFN therapy.

Innovations and breakthroughs

To the best of our knowledge, only two reports studied quasisipecies along the complete NS5A region and did not observe quasispecies evolution during therapy. In contrast, our results suggest that V3 domain plays a role in HCV resistance to IFN therapy.

Applications

Our study may help identify mutations within the HCV genome that can be used to predict patients' response to IFN treatment or future new antiviral modalities, as well as provide molecular hints for the mechanisms underlying HCV resistance to the therapy.

Peer review

Study is important with findings suppporting previous results as well as novel findings. The biggest problem is the very small size of the patients analyzed. The paper is well written and consise.

REFERENCES

1 **Alberti A**, Chemello L, Benvegnù L. Natural history of hepatitis C. *J Hepatol* 1999; **31** Suppl 1: 17-24

2 **Zeuzem S**, Hultcrantz R, Bourliere M, Goeser T, Marcellin P, Sanchez-Tapias J, Sarrazin C, Harvey J, Brass C, Albrecht J. Peginterferon alfa-2b plus ribavirin for treatment of chronic hepatitis C in previously untreated patients infected with HCV genotypes 2 or 3. *J Hepatol* 2004; **40**: 993-999

3 **Manns MP**, McHutchison JG, Gordon SC, Rustgi VK, Shiffman M, Reindollar R, Goodman ZD, Koury K, Ling M, Albrecht JK. Peginterferon alfa-2b plus ribavirin compared with interferon alfa-2b plus ribavirin for initial treatment of chronic hepatitis C: a randomised trial. *Lancet* 2001; **358**: 958-965

4 **Fried MW**, Shiffman ML, Reddy KR, Smith C, Marinos G, Gonçales FL Jr, Häussinger D, Diago M, Carosi G, Dhumeaux

D, Craxi A, Lin A, Hoffman J, Yu J. Peginterferon alfa-2a plus ribavirin for chronic hepatitis C virus infection. *N Engl J Med* 2002; **347**: 975-982

5 **Poynard T**, McHutchison J, Goodman Z, Ling MH, Albrecht J. Is an "a la carte" combination interferon alfa-2b plus ribavirin regimen possible for the first line treatment in patients with chronic hepatitis C? The ALGOVIRC Project Group. *Hepatology* 2000; **31**: 211-218

6 **Hofmann WP**, Zeuzem S, Sarrazin C. Hepatitis C virus-related resistance mechanisms to interferon alpha-based antiviral therapy. *J Clin Virol* 2005; **32**: 86-91

7 **Gale M**, Katze MG. Molecular mechanisms of interferon resistance mediated by viral-directed inhibition of PKR, the interferon-induced protein kinase. *Pharmacol Ther* 1998; **78**: 29-46

8 **Tan SL**, Gale MJ, Katze MG. Double-stranded RNA-independent dimerization of interferon-induced protein kinase PKR and inhibition of dimerization by the cellular P58IPK inhibitor. *Mol Cell Biol* 1998; **18**: 2431-2443

9 **Gale MJ**, Korth MJ, Katze MG. Repression of the PKR protein kinase by the hepatitis C virus NS5A protein: a potential mechanism of interferon resistance. *Clin Diagn Virol* 1998; **10**: 157-162

10 **Enomoto N**, Sakuma I, Asahina Y, Kurosaki M, Murakami T, Yamamoto C, Izumi N, Marumo F, Sato C. Comparison of full-length sequences of interferon-sensitive and resistant hepatitis C virus 1b. Sensitivity to interferon is conferred by amino acid substitutions in the NS5A region. *J Clin Invest* 1995; **96**: 224-230

11 **Arase Y**, Ikeda K, Chayama K, Murashima N, Tsubota A, Suzuki Y, Saitoh S, Kobayashi M, Kobayashi M, Kobayashi M, Kumada H. Efficacy and changes of the nonstructural 5A GENE by prolonged interferon therapy for patients with hepatitis C virus genotype 1b and a high level of serum HCV-RNA. *Intern Med* 1999; **38**: 461-466

12 **Chayama K**, Tsubota A, Kobayashi M, Okamoto K, Hashimoto M, Miyano Y, Koike H, Kobayashi M, Koida I, Arase Y, Saitoh S, Suzuki Y, Murashima N, Ikeda K, Kumada H. Pretreatment virus load and multiple amino acid substitutions in the interferon sensitivity-determining region predict the outcome of interferon treatment in patients with chronic genotype 1b hepatitis C virus infection. *Hepatology* 1997; **25**: 745-749

13 **Enomoto N**, Sakuma I, Asahina Y, Kurosaki M, Murakami T, Yamamoto C, Ogura Y, Izumi N, Marumo F, Sato C. Mutations in the nonstructural protein 5A gene and response to interferon in patients with chronic hepatitis C virus 1b infection. *N Engl J Med* 1996; **334**: 77-81

14 **Kurosaki M**, Enomoto N, Murakami T, Sakuma I, Asahina Y, Yamamoto C, Ikeda T, Tozuka S, Izumi N, Marumo F, Sato C. Analysis of genotypes and amino acid residues 2209 to 2248 of the NS5A region of hepatitis C virus in relation to the response to interferon-beta therapy. *Hepatology* 1997; **25**: 750-753

15 **Nakano I**, Fukuda Y, Katano Y, Nakano S, Kumada T, Hayakawa T. Why is the interferon sensitivity-determining region (ISDR) system useful in Japan? *J Hepatol* 1999; **30**: 1014-1022

16 **Berg T**, Mas Marques A, Höhne M, Wiedenmann B, Hopf U, Schreier E. Mutations in the E2-PePHD and NS5A region of hepatitis C virus type 1 and the dynamics of hepatitis C viremia decline during interferon alfa treatment. *Hepatology* 2000; **32**: 1386-1395

17 **Duverlie G**, Khorsi H, Castelain S, Jaillon O, Izopet J, Lunel F, Eb F, Penin F, Wychowski C. Sequence analysis of the NS5A protein of European hepatitis C virus 1b isolates and relation to interferon sensitivity. *J Gen Virol* 1998; **79** (Pt 6): 1373-1381

18 **Sarrazin C**, Berg T, Lee JH, Rüster B, Kronenberger B, Roth WK, Zeuzem S. Mutations in the protein kinase-binding domain of the NS5A protein in patients infected with hepatitis C virus type 1a are associated with treatment response. *J Infect Dis* 2000; **181**: 432-441

19 **Squadrito G**, Orlando ME, Cacciola I, Rumi MG, Artini M, Picciotto A, Loiacono O, Siciliano R, Levrero M, Raimondo G. Long-term response to interferon alpha is unrelated to "interferon sensitivity determining region" variability in patients with chronic hepatitis C virus-1b infection. *J Hepatol* 1999; **30**: 1023-1027

20 **Zeuzem S**, Lee JH, Roth WK. Mutations in the nonstructural 5A gene of European hepatitis C virus isolates and response to interferon alfa. *Hepatology* 1997; **25**: 740-744

21 **Chung RT**, Monto A, Dienstag JL, Kaplan LM. Mutations in the NS5A region do not predict interferon-responsiveness in american patients infected with genotype 1b hepatitis C virus. *J Med Virol* 1999; **58**: 353-358

22 **Nousbaum J**, Polyak SJ, Ray SC, Sullivan DG, Larson AM, Carithers RL, Gretch DR. Prospective characterization of full-length hepatitis C virus NS5A quasispecies during induction and combination antiviral therapy. *J Virol* 2000; **74**: 9028-9038

23 **Murphy MD**, Rosen HR, Marousek GI, Chou S. Analysis of sequence configurations of the ISDR, PKR-binding domain, and V3 region as predictors of response to induction interferon-alpha and ribavirin therapy in chronic hepatitis C infection. *Dig Dis Sci* 2002; **47**: 1195-1205

24 **Pascu M**, Martus P, Höhne M, Wiedenmann B, Hopf U, Schreier E, Berg T. Sustained virological response in hepatitis C virus type 1b infected patients is predicted by the number of mutations within the NS5A-ISDR: a meta-analysis focused on geographical differences. *Gut* 2004; **53**: 1345-1351

25 **Podevin P**, Sabile A, Gajardo R, Delhem N, Abadie A, Lozach PY, Beretta L, Bréchot C. Expression of hepatitis C virus NS5A natural mutants in a hepatocytic cell line inhibits the antiviral effect of interferon in a PKR-independent manner. *Hepatology* 2001; **33**: 1503-1511

26 **Inchauspe G**, Zebedee S, Lee DH, Sugitani M, Nasoff M, Prince AM. Genomic structure of the human prototype strain H of hepatitis C virus: comparison with American and Japanese isolates. *Proc Natl Acad Sci USA* 1991; **88**: 10292-10296

27 **Liu S**, Ansari IH, Das SC, Pattnaik AK. Insertion and deletion analyses identify regions of non-structural protein 5A of Hepatitis C virus that are dispensable for viral genome replication. *J Gen Virol* 2006; **87**: 323-327

28 **Appel N**, Pietschmann T, Bartenschlager R. Mutational analysis of hepatitis C virus nonstructural protein 5A: potential role of differential phosphorylation in RNA replication and identification of a genetically flexible domain. *J Virol* 2005; **79**: 3187-3194

29 **Lunel F**, Veillon P, Fouchard-Hubert I, Loustaud-Ratti V, Abergel A, Silvain C, Rifflet H, Blanchi A, Causse X, Bacq Y, Payan C. Antiviral effect of ribavirin in early non-responders to interferon monotherapy assessed by kinetics of hepatitis C virus RNA and hepatitis C virus core antigen. *J Hepatol* 2003; 39: 826-833

30 **Boom R**, Sol CJ, Salimans MM, Jansen CL, Wertheim-van Dillen PM, van der Noordaa J. Rapid and simple method for purification of nucleic acids. *J Clin Microbiol* 1990; **28**: 495-503

31 **Payan C**, Véal N, Crescenzo-Chaigne B, Bélec L, Pillot J. New quantitative assay of hepatitis B and C viruses by competitive PCR using alternative internal sequences. *J Virol Methods* 1997; **65**: 299-305

32 **Malet I**, Belnard M, Agut H, Cahour A. From RNA to quasispecies: a DNA polymerase with proofreading activity is highly recommended for accurate assessment of viral diversity. *J Virol Methods* 2003; **109**: 161-170

33 **Thompson JD**, Gibson TJ, Plewniak F, Jeanmougin F, Higgins DG. The CLUSTAL_X windows interface: flexible strategies for multiple sequence alignment aided by quality analysis tools. *Nucleic Acids Res* 1997; **25**: 4876-4882

34 **Wolinsky SM**, Korber BT, Neumann AU, Daniels M, Kunstman KJ, Whetsell AJ, Furtado MR, Cao Y, Ho DD, Safrit JT. Adaptive evolution of human immunodeficiency virus-type 1 during the natural course of infection. *Science* 1996; **272**: 537-542

35 **Kimura M**. A simple method for estimating evolutionary rates of base substitutions through comparative studies of nucleotide sequences. *J Mol Evol* 1980; **16**: 111-120

36 **Nei M**, Gojobori T. Simple methods for estimating the numbers of synonymous and nonsynonymous nucleotide substitutions. *Mol Biol Evol* 1986; **3**: 418-426

37 **Gaudy C**, Moreau A, Veillon P, Temoin S, Lunel F, Goudeau

A. Significance of pretreatment analysis of hepatitis C virus genotype 1b hypervariable region 1 sequences to predict antiviral outcome. *J Clin Microbiol* 2003; **41**: 3615-3622

38 **Asahina Y**, Izumi N, Enomoto N, Uchihara M, Kurosaki M, Onuki Y, Nishimura Y, Ueda K, Tsuchiya K, Nakanishi H, Kitamura T, Miyake S. Mutagenic effects of ribavirin and response to interferon/ribavirin combination therapy in chronic hepatitis C. *J Hepatol* 2005; **43**: 623-629

39 **Gaudy C**, Lambelé M, Moreau A, Veillon P, Lunel F, Goudeau A. Mutations within the hepatitis C virus genotype 1b E2-PePHD domain do not correlate with treatment outcome. *J Clin Microbiol* 2005; **43**: 750-754

40 **Pawlotsky JM**, Pellerin M, Bouvier M, Roudot-Thoraval F, Germanidis G, Bastie A, Darthuy F, Rémiré J, Soussy CJ, Dhumeaux D. Genetic complexity of the hypervariable region 1 (HVR1) of hepatitis C virus (HCV): influence on the characteristics of the infection and responses to interferon alfa therapy in patients with chronic hepatitis C. *J Med Virol* 1998; **54**: 256-264

41 **Polyak SJ**, Nousbaum JB, Larson AM, Cotler S, Carithers RL, Gretch DR. The protein kinase-interacting domain in the hepatitis C virus envelope glycoprotein-2 gene is highly conserved in genotype 1-infected patients treated with interferon. *J Infect Dis* 2000; **182**: 397-404

42 **Ueda E**, Enomoto N, Sakamoto N, Hamano K, Sato C, Izumi N, Watanabe M. Changes of HCV quasispecies during combination therapy with interferon and ribavirin. *Hepatol Res* 2004; **29**: 89-96

43 **Gerotto M**, Dal Pero F, Pontisso P, Noventa F, Gatta A, Alberti A. Two PKR inhibitor HCV proteins correlate with early but not sustained response to interferon. *Gastroenterology* 2000; **119**: 1649-1655

44 **Layden-Almer JE**, Kuiken C, Ribeiro RM, Kunstman KJ, Perelson AS, Layden TJ, Wolinsky SM. Hepatitis C virus genotype 1a NS5A pretreatment sequence variation and viral kinetics in African American and white patients. *J Infect Dis* 2005; **192**: 1078-1087

45 **Puig-Basagoiti F**, Forns X, Furcić I, Ampurdanés S, Giménez-Barcons M, Franco S, Sánchez-Tapias JM, Saiz JC. Dynamics of hepatitis C virus NS5A quasispecies during interferon and ribavirin therapy in responder and non-responder patients with genotype 1b chronic hepatitis C. *J Gen Virol* 2005; **86**: 1067-1075

S- Editor Liu Y **L- Editor** Zhu LH **E- Editor** Lu W

PO Box 2345, Beijing 100023, China
www.wjgnet.com
wjg@wjgnet.com

World J Gastroenterol 2007 February 28; 13(8): 1204-1207
World Journal of Gastroenterology ISSN 1007-9327

VIRAL HEPATITIS

Epidemiology and transmission of hepatitis B and C viruses in Kazakhstan

Zhannat Z Nurgalieva, F Blaine Hollinger, David Y Graham, S Zhangabylova, Abai Zhangabylov

Zhannat Z Nurgalieva, S Zhangabylova, Abai Zhangabylov, Department of Faculty Therapy, Kazakh National Medical University named after SD Asfendiarov, Almaty, Kazakhstan
Zhannat Z Nurgalieva, F Blaine Hollinger, David Y Graham, Department of Medicine, VA Medical Center and Baylor College of Medicine, Baylor College of Medicine, Houston, TX, United States
F Blaine Hollinger, David Y Graham, Department of Molecular Virology and Microbiology Baylor College of Medicine, Houston, TX, United States
Supported by the Office of Research and Development Medical Research Service Department of Veterans Affairs; Public Health Service grant DK56338 which funds the Texas Gulf Coast Digestive Diseases Center; the Eugene B. Casey Foundation and the William and Sonya Carpenter Fund, Baylor College of Medicine
Correspondence to: David Y Graham, MD, Veterans Affairs Medical Center (111D), 2002 Holcombe Blvd. Houston, Texas 77030, United States. dgraham@bcm.tmc.edu
Telephone: +1-713-7950232 Fax: +1-713-7901040
Received: 2006-10-22 Accepted: 2007-01-26

Abstract

AIM: To investigate the epidemiology of hepatitis B virus (HBV) and hepatitis C virus (HCV) infection in the two major ethnic groups in Kazakhstan.

METHODS: A cross-sectional prospective study of HBV and HCV seroprevalence was performed among individuals born in Kazakhstan with no history of chronic hepatitis or liver disease.

RESULTS: There were 290 volunteers (140 Russians and 150 Kazakhs) aged 10 to 64 years, males accounted for 46%. Active HBV infection (HBsAg positive) was present in 3.8%, anti-HBc in 30%. The prevalence was similar in females and males (33% *vs* 25%) (P = 0.18). The prevalence of anti-HBc increased from 19% in 10-29 years old volunteers to 53% in 50-years and older volunteers. The prevalence of HBV infection was higher in married than in single adults (38% *vs* 26%, respectively) (P = 0.2) and more common in Kazakhs (35%) than in Russians (24%) (P = 0.07). HCV infection was present in 9 subjects (3.2%), 5 of them also were positive for anti-HBc in the absence of HBsAg.

CONCLUSION: The frequency of active HBV infection (3.8%) coupled with a high prevalence of HBV exposure in those > 50 years of age increases with age, which suggests that horizontal transmission likely relates to the use of contaminated needles. The low prevalence of HCV infection suggests that HBV and HCV are acquired differently in this group of subjects.

Key words: Viral hepatitis B; Viral hepatitis C; Hepatitis B virus; Transmission; Epidemiology; Sero-epidemiology; Kazakhstan

Nurgalieva ZZ, Hollinger FB, Graham DY, Zhangabylova S, Zhangabylov A. Epidemiology and transmission of hepatitis B and C viruses in Kazakhstan. *World J Gastroenterol* 2007; 13(8): 1204-1207

http://www.wjgnet.com/1007-9327/13/1204.asp

INTRODUCTION

Kazakhstan has two major ethnic groups: Kazakhs who trace their origins back to Genghis Khan, and ethnic Russians. Each constitutes approximately 40% of the population. The different ethnic groups share similar living and socioeconomic conditions.

Kazakhstan is part of a nine-country subregion in which the mortality due to chronic liver disease and cirrhosis has been estimated to be 21.8 per 100 000 population[1]. The mortality rate of hepatocellular carcinoma is also high, with liver cancer representing approximately 4% of all malignant neoplasms[2]. Hepatitis B virus (HBV) and hepatitis C virus (HCV) infections are both common causes of hepatocellular carcinoma. We conducted a cross-sectional study in Kazakhstan to examine the epidemiology and risk factors associated with HBV and HCV infections. We gave particular emphasis on possible relationships between chronic hepatitis B or C virus infections and a history of intravenous injections, blood transfusions, vaccinations, needle sticks, surgeries, having tattoos, and shared use of tooth brushes, body brushes and towels.

MATERIALS AND METHODS

We performed a cross-sectional seroepidemiologic study in Almaty, Kazakhstan. Both Russians and Kazakhs were entered if they were unrelated and born in Kazakhstan with no prior history of clinical hepatitis or chronic liver disease. An attempt was made to obtain an equal number

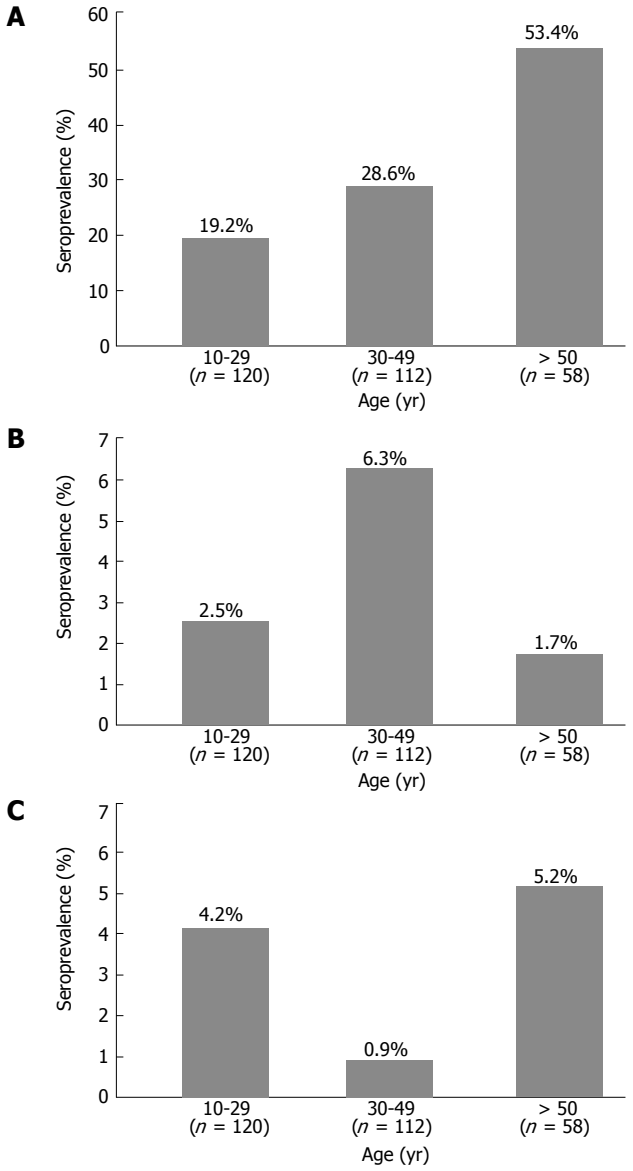

Figure 1 Prevalence of anti-HBc antibodies (**A**), HBsAg (**B**), and anti-HCV antibodies (**C**) in relation to age in Kazakhstan.

of volunteers per decade from each of these two major ethnic groups.

A trained physician interviewed each volunteer and completed a detailed questionnaire. Demographic data focusing on the environment during the subject's childhood included social and economic data (parent's education, occupation and family income) as well as histories of blood transfusions, intravenous injections, vaccinations, needle sticks, surgeries, having tattoos, and the shared use of tooth brushes, body brushes or towels. In women, we obtained data about miscarriages and abortions.

Serologic methods

Each volunteer provided a blood sample. Sera were stored at -20℃ until analyzed. Serum samples were tested for hepatitis A and B serology using kits (Abbott Diagnostic Laboratories, Abbott Park, IL), including enzyme immunoassays (EIA) for the qualitative detection of total antibody to hepatitis A virus (anti-HAV; HAVAB EIA), hepatitis B surface antigen (HBsAg; AUSZYME Monoclonal), and total antibody to hepatitis B core antigen (anti-HBc; Corzyme). Antibody to hepatitis B surface antigen (anti-HBs; AUSAB, human subtypes ad and ay) was evaluated by solid phase radioimmunoassay. Antibody to hepatitis C (anti-HCV; HCV Version 3.0, Ortho-Clinical Diagnostics, Inc, Raritan, NJ) was detected by EIA. The interpretation of the results was done according to the manufacturer's instructions.

Table 1 Concentration of anti-HBs in four HBsAg and anti-HBc positive subjects

I.D.	mIU/mL
11	16.1
180	3.4
249	4.0
143	5.7

RESULTS

Two hundred and ninety volunteers were enrolled in the study including 150 Kazakhs and 140 ethnic Russians ranging in age from 10 to 64 years. One hundred and thirty-four (46%) of the subjects were men.

Risk factors and prevalence of HBV

Total anti-HBc was found in 30% of the population, being similar in women (33.3%) and men (25.4%) ($P = 0.18$). There was an age-specific significant increase in the prevalence of anti-HBc antibody: from 19.2% in 10-29 years old individuals to 53.4% in those who were 50- years old and older (Figure 1A) ($P < 0.01$). The prevalence of anti-HBc was more common in Kazakhs (34.7%) than in Russians (24.3%) ($P = 0.07$). Among those who were 21-years old and older, the prevalence of hepatitis B infection was similar in married and single adults (38% *vs* 26%, $P = 0.2$) (data not shown).

The overall seroprevalence rate of active HBV infection (HBsAg positive) was 3.8% (11 of 290 subjects), none of these individuals tested was positive for anti-HCV. There was no significant difference in the prevalence of detectable HBsAg in men and women (3.7% of men *vs* 3.8% of women) ($P = 0.7$) nor between ethnic groups (4.3% of Russians *vs* 3.3% of Kazakhs) ($P = 0.9$). The prevalence of HBsAg peaked in those whose age was 30-49 years (6.3%) and was lower in those whose age was 10-29 years (2.5%) ($P = 0.3$) and lowest in those whose age was 50 years and more (1.7%) ($P = 0.4$, Figure 1B). Four of the 11 HBsAg positive individuals (36%) were anti-HBs positive. However, the concentrations of antibodies were low in this group of individuals (Table 1). Three of four individuals with concurrent HBsAg and anti-HBs positivity were Kazakhs, but gender distribution was equal.

Table 2 shows unadjusted and adjusted (for socio-economic status, gender, and ethnicity) incidence rates and risk factors possibly associated with acquisition of hepatitis B. The highest risks associated with hepatitis B infection were having been a blood donor or having a history of dental surgery. The risk factors for positive anti-HBc and

Table 2 Effect of selected risk factors on the incidence rate of anti-HBc in a study population from Kazakhstan (n = 86)

Risk factor	Unadjusted OR	P	95% CI	Adjusted[1] OR	P	95% CI
Blood transfusion	2.11	0.19	0.67-6.48	1.26	0.72	0.36-4.40
Blood donor	1.77	0.03	1.05-2.98	1.38	0.48	0.56-3.42
Tattoo	1.67	0.19	0.77-3.65	1.26	0.62	0.51-3.12
Ear piercing	1.43	0.16	0.87-2.39	1.20	0.57	0.64-2.24
Dental surgery	1.93	0.02	1.10-3.31	1.29	0.29	0.80-2.08

[1]Adjusted OR for socioeconomic status, ethnicity and gender.

Table 3 Effect of selected risk factors on the incidence rate of anti-HCV in a study population from Kazakhstan (n = 9)

Risk factor	Unadjusted OR	P	95% CI	Adjusted[1] OR	P	95% CI
Blood transfusion	2.48	0.41	0.29-21.20	1.42	0.76	0.15-13.38
Tattoo	4.02	0.05	0.90-16.44	14.40	0.01	1.76-118.32
Ear piercing	2.58	0.18	0.65-10.18	3.05	0.29	0.38-24.4
Dental surgery	1.65	0.48	0.42-6.52	1.46	0.64	0.29-7.26
Towel sharing	3.25	0.09	0.82-12.83	3.87	0.07	0.91-16.4

[1]Adjusted OR for socioeconomic status, ethnicity and gender.

HBsAg included dental surgery (73%), frequent injections (64%), and ear piercing (54%).

Risk factors and prevalence of viral hepatitis C

Anti-HCV was detected in only 9 subjects (3.2%) including 3 Kazakh women and 6 Russians (three women and three men). Five of the 9 subjects also had detectable levels of anti-HBc, but were negative for anti-HBs. Figure 1C and Table 3 display age-specific prevalence rates of anti-HCV in this study population and selected risk factors associated with anti-HCV seropositivity. A history of tattoos was a common risk factor for hepatitis C with a trend in risk toward towel sharing.

DISCUSSION

Almost 30% of the study population examined had evidence of current or past HBV infection which is similar to the results of a prior study in northwestern Kazakhstan, showing that 22% (n = 579) of the healthy population had detectable anti-HBc antibodies[3]. The prevalence of anti-HBc seropositivity in Kazakhstan is substantially lower than that reported in 110 Bukharian Jews who immigrated from Uzbekistan and Tajikistan (former Soviet Union) to Israel, 66% of them had evidence of exposure to HBV[4]. However, the prevalence of past or current hepatitis B infection is much higher in Central Asia than in Pakistan, Ethiopia, Sweden, England and Wales[5-8].

The primary mode of transmission of HBV in Kazakhstan is unsettled. The prevalence of infection increasing with age could result from either birth cohort effects and continuing gradual horizontal acquisition, or both. Demographic factors associated with risk of acquisition (i.e. history of blood donation and dental surgery) found in a recent study in Pakistan are blood transfusions and use of contaminated syringes, and contaminated dental and surgery equipment are the main risk factors for acquiring HBV infections[9]. However, in our study, adjustments for socioeconomic status, ethnicity and gender eliminated these significantly associated risk factors (Table 2).

In countries of European Region C, including Kazakhstan, the annual number of injections was reported to be 11.3 per person in 2000 and this estimate is the highest among countries recognized as having a global burden of disease. The same is true for the Russian Federation where the annual number of injections per person is also 11.3 and different from neighboring countries such as Kyrgyzstan and Uzbekistan where this estimate is 5.2 or China where the annual number of injections per person is only 2.4[10]. Several studies conducted in Russia showed that 85%-99% of injections are unnecessary with a ratio of 20:1 for injections being given with therapeutic intent compared to those for disease prevention[11,12]. In addition, the proportion of equipments being reused was reported to be 11%. Of interest in this study, the common factor for having both anti-HBc and HBsAg was a history of frequent injections.

In the current study, 4 of the 11 HBsAg positive subjects also had anti-HBs antibodies (36%). It was reported that the rate of concurrent HBsAg and anti-HBs positivity is between 21% and 32%[13-16] and is associated with evidence of viral replication and features of active inflammation[13] or with progressive liver disease[14]. Most probably, these discordant serologic results reflect a low concentration of non-complexed anti-HBs that fails to recognize insertions or deletions that occur in the pre-S/S region of the HBV genome[16,17]. Heterotypic antibody is often observed in these situations[13,15].

The prevalence of anti-HCV in this study population was 3.2% which is somewhat higher than the prevalence of anti-HCV antibodies observed in northwestern Kazakhstan (1.7%; P = 0.3)[3], or in Siberian natives from the Kamchatka Peninsula of Russia (1.4%, n = 348)[18]. In contrast, in the Republic of Azerbaijan[19], 8.7% of screened serum samples are anti-HCV reactive[20]. We feel certain that virtually all of our reactive samples represented a past or present infection with HCV based on strong EIA ratios of 3.0 or greater. However, we did not do HCV RNA testing to confirm its active infection. It also is possible that we underestimated the prevalence of hepatitis C in that a proportion of the population may have resolved their infection and subsequently lost their anti-HCV[21].

The risk factors related to HCV infection (Table 3) have very wide confidence intervals indicative of the small sample size which precludes making firm conclusions regarding transmission. However, the low prevalence of hepatitis C infection compared with the relatively high prevalence of HBV infection suggests that different modes of transmission are active in this population due to the sexual or vertical transmission of HBV and the

parenteral transmission of HCV. Overall, the use of unsafe (contaminated) needles remains of great concern in this population as a vehicle for transmission of these viruses.

REFERENCES

1 **The European health report**. World Health Organization 2005: Public health action for healthier children and populations. http://www.euro.who.int/ehr2005/20050809_1

2 **WHO Global Infobase Online: National/Subnational country profiles**. Kazakhstan: WHO Estimates of country level mortality. http://www.who.int/ncd_surveillance/infobase/web

3 **Kruglov IV**, Iashina TL, Tsvetova GV, Seliutina IA, Klimkin AIu, Aksenova NF, Sobina GV, Gerasimenko NA, Bakulin VS, Ivanov SV. The spread of hepatitis B and C markers and the etiological structure of the morbidity with acute viral hepatitis of the population in the Kuznetsk Basin and northwestern Kazakhstan. *Zh Mikrobiol Epidemiol Immunobiol* 1995; **6**: 36-37

4 **Glikberg F**, Brawer-Ostrovsky J, Ackerman Z. Very high prevalence of hepatitis B and C in Bukharian Jewish immigrants to Israel. *J Clin Gastroenterol* 1997; **24**: 30-33

5 **Hoffmann G**, Berglund G, Elmståhl S, Eriksson S, Verbaan H, Widell A, Lindgren S. Prevalence and clinical spectrum of chronic viral hepatitis in a middle-aged Swedish general urban population. *Scand J Gastroenterol* 2000; **35**: 861-865

6 **Gay NJ**, Hesketh LM, Osborne KP, Farrington CP, Morgan-Capner P, Miller E. The prevalence of hepatitis B infection in adults in England and Wales. *Epidemiol Infect* 1999; **122**: 133-138

7 **Tsega E**, Mengesha B, Hansson BG, Lindberg J, Nordenfelt E. Hepatitis A, B, and delta infection in Ethiopia: a serologic survey with demographic data. *Am J Epidemiol* 1986; **123**: 344-351

8 **Khan AJ**, Luby SP, Fikree F, Karim A, Obaid S, Dellawala S, Mirza S, Malik T, Fisher-Hoch S, McCormick JB. Unsafe injections and the transmission of hepatitis B and C in a periurban community in Pakistan. *Bull World Health Organ* 2000; **78**: 956-963

9 **Tassaduqe K**, Muhammad, Abdus S, Humera K, Asma S, Soban U. Studies on the prevalence of hepatitis B virus in relation to sex, age, promotive factors, associated symptoms and season among human urban population of Multan, Pakistan. *J Biol Sci* 2004; **4** :183-187

10 **Hutin YJ**, Hauri AM, Armstrong GL. Use of injections in healthcare settings worldwide, 2000: literature review and regional estimates. *BMJ* 2003; **327**: 1075

11 **Loukina TN**. Current treatment methods for the respiratory infections in children. Thesis for the degree of candidate of medical sciences. Moscow: Institute of Pediatrics, 1993

12 **Stekolschikova IA**. Diagnostic and treatment tactics in the management of ARI in children. Thesis for the degree of candidate of medical sciences. Moscow: Institute of Pediatrics, RAMS, 1993

13 **Shiels MT**, Taswell HF, Czaja AJ, Nelson C, Swenke P. Frequency and significance of concurrent hepatitis B surface antigen and antibody in acute and chronic hepatitis B. *Gastroenterology* 1987; **93**: 675-680

14 **Heijtink RA**, van Hattum J, Schalm SW, Masurel N. Co-occurrence of HBsAg and anti-HBs: two consecutive infections or a sign of advanced chronic liver disease? *J Med Virol* 1982; **10**: 83-90

15 **Tsang TK**, Blei AT, O'Reilly DJ, Decker R. Clinical significance of concurrent hepatitis B surface antigen and antibody positivity. *Dig Dis Sci* 1986; **31**: 620-624

16 **Wang YM**, Ng WC, Kang JY, Yap I, Seet BL, Teo J, Smith R, Guan R. Serological profiles of hepatitis B carrier patients in Singapore with special reference to the frequency and significance of concurrent presence of HBsAg and anti-HBs. *Singapore Med J* 1996; **37**: 150-152

17 **Ohba K**, Mizokami M, Kato T, Ueda R, Gurtsenvitch V, Senyuta N, Syrtsev A, Zoya K, Yamashita M, Hayami M. Seroprevalence of hepatitis B virus, hepatitis C virus and GB virus-C infections in Siberia. *Epidemiol Infect* 1999; **122**: 139-143

18 **Coleman PF**. Surveillance for hepatitis B surface antigen mutants. *J Med Virol* 2006; **78** Suppl 1: S56-S58

19 **Galetskiĭ SA**, Seniuta NB, Syrtsev AV, Abdullaev OM, Aliev DA, Kerimov AA, Yamashita M, Hayami M, Kato T, Mizokami M. Analysis of some viral infections, transmitted by parenteral and sexual routes, in the Republic of Azerbaijan. *Vopr Virusol* 1999; **44**: 232-236

20 **Pasha O**, Luby SP, Khan AJ, Shah SA, McCormick JB, Fisher-Hoch SP. Household members of hepatitis C virus-infected people in Hafizabad, Pakistan: infection by injections from health care providers. *Epidemiol Infect* 1999; **123**: 515-518

21 **Seeff LB**, Hollinger FB, Alter HJ, Wright EC, Cain CM, Buskell ZJ, Ishak KG, Iber FL, Toro D, Samanta A, Koretz RL, Perrillo RP, Goodman ZD, Knodell RG, Gitnick G, Morgan TR, Schiff ER, Lasky S, Stevens C, Vlahcevic RZ, Weinshel E, Tanwandee T, Lin HJ, Barbosa L. Long-term mortality and morbidity of transfusion-associated non-A, non-B, and type C hepatitis: A National Heart, Lung, and Blood Institute collaborative study. *Hepatology* 2001; **33**: 455-463

S- Editor Liu Y **L- Editor** Wang XL **E- Editor** Lu W

PO Box 2345, Beijing 100023, China
www.wjgnet.com
wjg@wjgnet.com

World J Gastroenterol 2007 February 28; 13(8): 1208-1213
World Journal of Gastroenterology ISSN 1007-9327

BASIC RESEARCH

Antisense oligonucleotide targeting midkine suppresses *in vivo* angiogenesis

Li-Cheng Dai, Xiang Wang, Xing Yao, Yong-Liang Lu, Jin-Liang Ping, Jian-Fang He

Li-Cheng Dai, Xiang Wang, Jian-Fang He, Huzhou Key Laboratory of Molecular Medicine, Huzhou Central Hospital, Huzhou 313000, Zhejiang Province, China
Xing Yao, Yong-Liang Lu, Department of General Surgery, Huzhou Central Hospital, Huzhou 313000, Zhejiang Province, China
Jin-Liang Ping, Department of Pathology, Huzhou Central Hospital, Huzhou 313000, Zhejiang Province, China
Supported by grants from Medical and Sanitary Research Foundation of Zhejiang Province, (No. 2003A077), Huzhou Natural Science Foundation, (No. 2004SZX07-11)
Correspondence to: Professor Li-Cheng Dai, Huzhou Key Laboratory of Molecular Medicine, Huzhou Central Hospital, Huzhou 313000, Zhejiang Province, China. dlc@hzhospital.com
Telephone: +86-572-2033020 Fax: +86-572-2033020
Received: 2006-12-25 Accepted: 2007-02-26

Abstract

AIM: To evaluate the effect of antisense oligonucleotide targeting midkine (MK-AS) on angiogenesis in chick chorioallantoic membrane (CAM) and *in situ* human hepatocellular carcinoma (HCC).

METHODS: An *in situ* human hepatocellular carcinoma (HCC) model and CAM assay were used in this experiment. The effect of MK-AS on angiogenesis was evaluated by cell proliferation assay and hematoxylin-eosin (HE) staining.

RESULTS: MK-AS significantly inhibited human umbilical vein endothelial cells (HUVEC) and *in situ* human HCC growth. At the same time, MK-AS suppressed the angiogenesis both in human hepatocellular carcinoma cell line (HEPG2)-induced CAM and *in situ* human HCC tissues.

CONCLUSION: MK-AS is an effective antiangiogenesis agent *in vivo*.

Key words: Midkine; Angiogenesis; Antisense oligonucleotide; Tumor; Chick chorioallantoic membrane assay; Hepatocellular carcinoma

Dai LC, Wang X, Yao X, Lu YL, Ping JL, He JF. Antisense oligonucleotide targeting midkine suppresses *in vivo* angiogenesis. *World J Gastroenterol* 2007; 13(8): 1208-1213

http://www.wjgnet.com/1007-9327/13/1208.asp

INTRODUCTION

Angiogenesis is a process leading to formation of new blood vessels, which plays a central role in survival of cancer cells, growth of local tumors, and development of distant metastasis[1]. It is believed that tumor cells require the ability to stimulate angiogenesis, and angiogenesis induced by tumor cells, leads to hypervascularization of tumor tissue[2]. More recently, it has been found that tumor cells also produce angiogenesis inhibitors[3]. The angiogenic phenotype of a solid tumor is accepted as a result of the net balance between the activities of angiogenesis promoters and inhibitors[4]. Preclinical testing of these antiangiogenic factors in animal models suggested that they can effectively suppress the growth and/or metastasis of experimental tumors[5-7]. Inevitably, identification of angiogenic inhibitors and demonstration of their angiostatic functions would provide rational foundations for the development of tumor-specific antiangiogenic therapy.

Up to now, different growth factors, such as basic fibroblast growth factor (bFGF), vascular endothelial growth factor (VEGF), transforming growth factor-alpha (TGF-α) and midkine (MK) have been identified as positive regulators of angiogenesis and are secreted by cancer cells to stimulate normal endothelial cell growth through paracrine mechanisms[8-11]. MK was first identified in early stage embryonal carcinoma cells during retinoic acid-induced differentiation[12]. MK and pleiotrophin comprise a family of heparin-binding growth/differentiation factors, which are different from other heparin-binding growth factors such as fibroblast growth factor and hepatocyte growth factor[13-15]. MK is over-expressed in various malignant tumors[16-24], and low or undetectable in normal adult tissues[13,24]. It is accepted that MK promotes the survival[25,26], growth[27,28] and migration[29-31] of many cells, involved in activating mitogen-activated protein kinase (MAPK), extracellular signal-regulated kinases 1 and 2 or protein kinase B (PKB/AKT) pathways[25,32]. Recently, it was reported that midkine binds to anaplastic lymphoma kinase (ALK) and acts as a growth factor for different cell types[33].

There is evidence that MK plays an important role in angiogenesis, which is an important event in tumor development and progression. It was reported that enhanced tumor growth in MCF-7 breast carcinoma cells due to high MK expression is correlated with increased vascular density and endothelial proliferation, implicating an angiogenic role of MK in tumor growth[11]. Additionally, MK, an angiogenic factor, is expressed in bladder cancer,

and its over-expression correlates with a poor outcome in patients with invasive cancers[20]. In fact, we have confirmed that MK-AS transfer can significantly inhibit the growth of hepatocellular carcinoma cells, which is associated with increased Caspase-3 activity[34]. The present study was to determine whether MK-AS can suppress angiogenesis, which is an important mechanism underlying inhibition of tumor cell proliferation.

MATERIALS AND METHODS

Antisense oligodeoxynucleotides

MK-AS (5'-CCCCGGGCCGCCCTTCTTCA-3') and MK-SEN phosphorothioate oligonucleotide (5'-TGAAGAAG GGCGGCCCGGGG-3') were synthesized with an applied biosystem model 391 DNA synthesizer using Oligo Pilot Ⅱ DNA (Amersham-Pharmacia, Piscataway, NJ, USA) and purified by high-performance liquid chromatography (HPLC) (Waters Delta Prep 4000, Milfordd, MA, USA) with SOURCE 15Q (Amersham Pharmacia, Piscataway, NJ, USA) as previously described[34].

Cultured cell lines

Human umbilical vein endothelial cells (HUVECs), a gift of the Chinese Academy of Medical Sciences, Beijing, China, were pooled after collagenase type Ⅰ treatment and seeded on cell culture plates. The cells were grown in RPMI 1640 medium (Invitrogen Corporation, CA, USA) supplemented with 20% fetal calf serum (FBS; GIBCO BRL, Grand Island, NY, USA), 100 U/mL penicillin and 100 μg/mL streptomycin at 37℃ in an atmosphere containing 5% CO_2.

Cell proliferation assay

A total of 3×10^3 cells were seeded in each well of a 96-well microtiter plate and allowed them to attach overnight. Oligonucleotides at the concentrations of 0.2, 0.4, 0.8 μmol/L were transfected into the cells with Lipofectin (Invitrogen, Carlsbad, CA, USA) following the manufacturer's instructions. Transfection medium was replaced by normal culture medium after 6 h. The effects of antisense oligodeoxynucleotide (ASODN) on cellular viability were measured by 3-[4, 5-dimethythiazol-2-yl]-5-[3-carboxymethoxyphenyl]-2-[4-sulfophenyl]-2H-tetrazolium, inner salt (MTS) assay. After 48 h of incubation following transfection, 20 μL MTS (Sigma, St Louis, MO, USA) was added to each well and incubated at 37℃ for 2 h. The absorbance value was determined at 490 nm by a MR600 microplate reader (Wallac 1420 Multilable counter, Wallac, Turku, Finland).

In vivo tumor studies

In situ HCC models were established as previously described[35]. Two days after *in situ* HCC models were established, mice were injected intravenously with saline (vehicle control) and MK-AS (25, 50 and 100 mg/kg per day) for 20 d. Body weight and general physical status of the animals were recorded daily. At the endpoint of the study, mice were killed by cervical dislocation and tumors were removed and weighed. Tumor sizes were monitored with calipers, the tumor volume (V, mm^3) was calculated as $(L \times W^2)/2$, where L = length (mm) and W = width (mm). The percentage of tumor growth inhibition was calculated as: inhibitory rate (%) = $(W_{control}-W_{treat})/W_{control} \times 100$.

Immunohistochemistry analysis for microvessel formation

Tumor specimens were fixed and frozen in tissue freezing medium (Triangle Biomedical Sciences, Durham, NC). Five-μm thick cryosections were cut and stained with HE for histopathological analysis. To analyze the microvessel formation in tumors, sections were stained with anti-CD34 monoclonal antibody (DAKO Corp., Carpinteria, CA) and subsequently with the avidin-biotin-peroxidase (ABC) method. Positively stained vascular endothelial cells (brown) were visualized and imaged using a digital camera attached to an Olympus microscope. Microvessel density was determined as previously described[36]. Briefly, regions of the highest vessel density ("hot spot" regions) were scanned at low magnification (× 40-100) and counted at higher magnification (× 200). Three such "hotspot" fields were counted in each tumor section, and the mean microvessel density value was recorded. Any endothelial cell or endothelial cell cluster that was clearly separated from adjacent microvessels was considered a single, countable microvessel. Positively stained vascular endothelial cells were visualized and imaged using a Magnifire camera (Olympus, Melville, NY) attached to an Olympus Provis microscope.

Western blot analysis

After transfection with MK-AS for 24 h, cells in the microplates were collected into 1.5 mL Eppendorf tubes on ice and centrifuged at 2000 r/min for 5 min at 4℃. Pellets were then lysed with lysis buffer [50 mmol/L Tris-HCl (pH 7.4), 0.5 mmol/L EDTA, 0.5% NP40, and 150 mmol/L NaCl] in the presence of protease inhibitors. Lysates were centrifuged at 12000 × *g* for 15 min to remove debris. Proteins (30 μg) were separated from samples by 12% sodium dodecyl sulfate-polyacrylamide gel electrophoresis (SDS-PAGE) and transferred onto hybond-polyvinylidene difluoride (PVDF) membranes (Amersham Biosciences). Midkine protein was identified using the primary antibody (Santa Cruz Biotechnology, Santa Cruz, CA, USA). The reactive band was visualized with an ECL-plus detection kit (Amersham Biosciences, Piscataway, NJ) and scanned by Gel Doc 1000 (Bio-Rad CA, USA). β-actin was used as a control.

Chick chorioallantoic membrane assay

Angiogenesis assay in chick chorioallantoic membranes (CAM) was performed as previously described[37]. Fertilized eggs were incubated at 38℃. On d 7, a window was opened on the eggshell to expose the CAM, and the window was covered with a tape for further incubation. Filter paper discs (0.5 cm in diameter) containing HepG2 cells (18000/disc) or PBS was placed on the surface of each CAM on d 8. After 24 h, 100 μL of 0.4 μmol/L MK-AS was given using a 30-gauge needle. Two days later, the CAM were fixed in 3.7% formaldehyde. Pictures were taken with a stereoscope, and the number of vessel

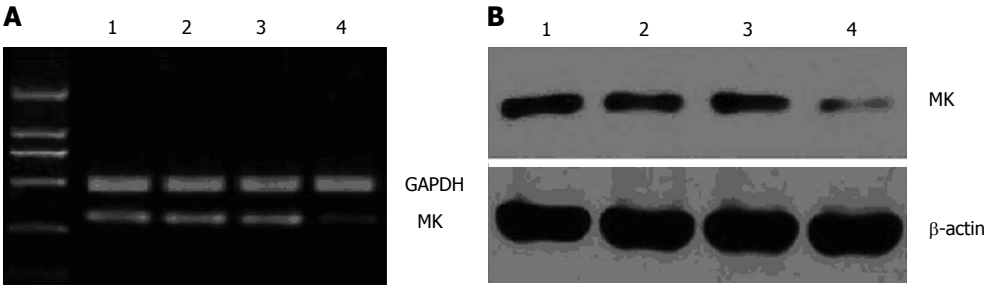

Figure 1 RT-PCR (**A**) and Western-blotting analysis (**B**) of MK expression in human umbilical vein endothelial cells (HUVEC) after transfection with 0.4 μmol/L MK-AS (lane 4), MK-SEN (lane 3), Lipofectin alone (lane 2) for 24 h. Lane 1 represents cells without transfection. GAPDH and β-actin were used as control respectively.

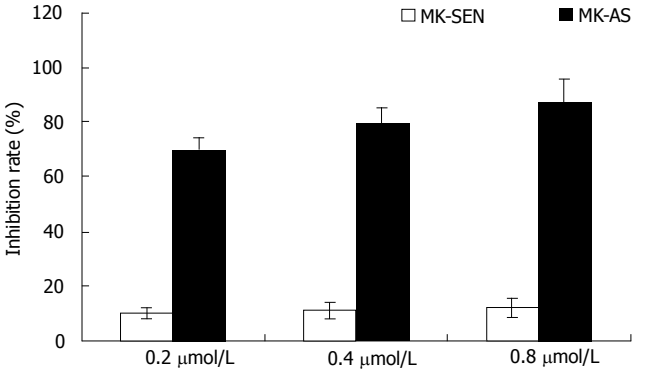

Figure 2 Effect of MK on growth of HUVEC. Cells after transfection with 0.4 μmol/L MK-AS or MK-SEN for 24 h were analyzed by MTS assay. Data were expressed as mean ± SD from four independent experiments.

branches was counted. Ten eggs were used for each experimental condition.

Statistical analysis

Data were expressed as mean ± SD, statistical analysis was carried out using Student's *t*-test (two tailed), $P < 0.05$ was considered statistically significant.

RESULTS

Effect of MK-AS on MK expression in HUVEC

Our previous studies showed that antisense oligonucleotide targeting MK down regulates MK expression in hepatocellular carcinoma cells[34]. In this study, we measured the effect of MK-AS on MK expression in HUVEC. After MK compounds were transfected for 24 h, total RNA and protein of HUVEC were extracted for analysis of the effect of MK-AS transfer on MK expression. Our results indicated that MK-AS could efficiently decrease the mRNA and protein content of MK in HUVEC (Figure 1A and B).

Effects of MK-AS treatment on HUVEC growth

To investigate the effect of MK-AS on endothelial cell proliferation, we analyzed the growth of HUVEC transfected with MK-SEN or MK-AS. MK-AS transfer significantly inhibited HUVEC proliferation (Figure 2), suggesting that MK signaling might directly contribute to endothelial cell growth. In contrast, no significant inhibition of HUVEC transfected with MK-SEN was observed.

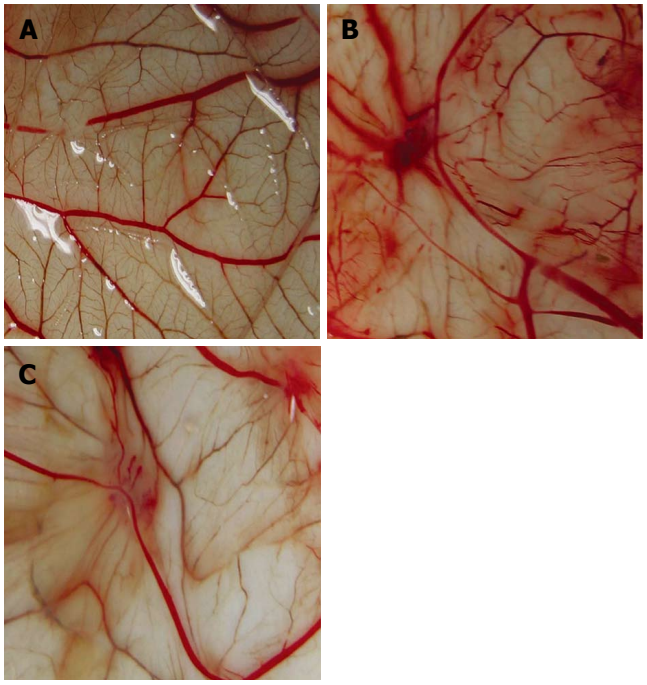

Figure 3 Angiogenesis in normal chick CAM (**A**), HepG2-induced CAM (**B**), and HepG2-induced CAM treated with 0.4 μmol/L MK-AS (**C**). Chick CAM assays were used to assess the impact of MK-AS on angiogenesis *in vivo*.

MK-AS inhibited angiogenesis in chick CAM

It is widely accepted that tumors can stimulate angiogenesis by releasing angiogenesis stimulators such as bFGF and VEGF[8,9]. HepG2 induced noticeable angiogenesis (Figure 3B). When paper discs absorbing PBS alone were placed onto the CAM, a few vessels occupied the CAM area covered by the paper discs (Figure 3A). Interestingly, when CAM implanted with HepG2 were treated with MK-AS (0.4 μmol/L), the number of vessels under the paper discs was significantly reduced (Figure 3C). Similar results were obtained when the mean vessel length was measured (data not shown). Chick embryos treated with MK-AS were alive and showed the same extent of motility as embryos from PBS-treated eggs at the end of the experiment.

Effects of MK-AS treatment on in situ HCC xenograft growth

We have reported that MK-AS inhibits tumor proliferation[38]. In the present study, an *in situ* HCC model of mice was used to evaluate the effect of MK-AS on *in vivo* tumor proliferation. MK-AS at 25 mg/kg, 50 mg/kg, 100

Table 1 Effect of MK-AS on weight and inhibition of *in situ* HCC

Treatment group	Tumor weight (g)	Inhibition rate (%)
Saline	1.29 ± 0.13	-
MK-AS 100 mg/kg per day	0.44 ± 0.18[b]	65.89
MK-AS 50 mg/kg per day	0.64 ± 0.18[b]	50.39
MK-AS 25 mg/kg per day	0.70 ± 0.14[b]	45.74
MK-Sen 50 mg/kg per day	1.04 ± 0.14[a]	19.38

[a]$P < 0.05$, [b]$P < 0.01$ *vs* control group.

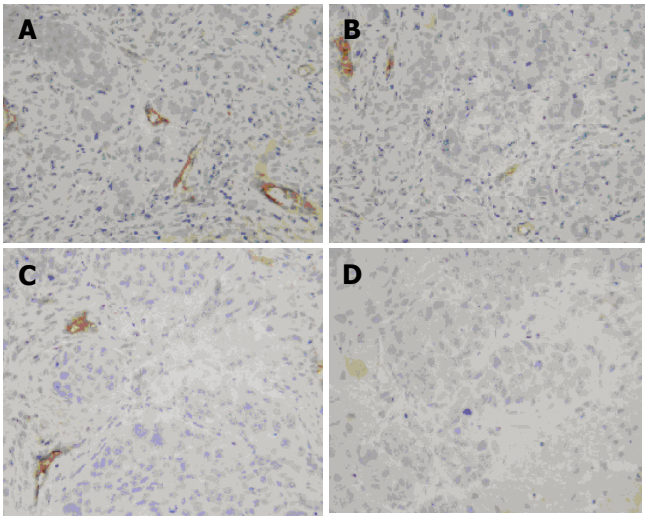

Figure 4 Immunohistochemical analysis of HCC xenograft angiogenesis after treatment with MK-SEN (**A**), 25 mg/kg of MK-AS per day (**B**), 50 mg/kg of MK-AS per day (**C**), and 100 mg/kg of MK-AS per day (**D**). Representative views of anti-CD34 antibody-stained vascular endothelium (brown) (x 200).

mg/kg per day and saline were intravenously administered for 20 d. Tumors were removed, measured and weighed. MK-AS treatment significantly inhibited tumor growth compared to saline treatment (Table 1). The highest inhibitory efficacy was 65.89% in MK-AS treatment group compared to saline treatment group. The effects of MK-AS on tumor growth are shown in Table 1. The final tumor volumes after 20-d treatment are shown in Table 2 ($P < 0.01$). No difference was found in the mean body weight of mice between the groups during the study (data not shown).

Effects of MK-AS treatment on in situ HCC xenograft angiogenesis

To determine whether the antitumor effect of MK-AS therapy is associated with angiogenesis suppression, the status of vessel formation in *in situ* HCC xenograft was assessed by immunohistochemistry with endothelial cell-specific CD34 staining. A representative result of immunostaining is shown in Figure 4. High density of microvessels was present in untreated tumor samples, whereas MK-AS treatment significantly reduced vascularization (Figures 4 and 5).

Table 2 Effect of MK-AS on growth of *in situ* human HCC

Treatment group	Tumor volume (mm^3)
Saline	807.75 ± 195.19
MK-AS 100 mg/kg per day	294.50 ± 70.66[b]
MK-AS 50 mg/kg per day	532.00 ± 121.57[b]
MK-AS 25 mg/kg per day	552.75 ± 84.38[b]
MK-Sen 50 mg/kg per day	630.88 ± 188.76[a]

[a]$P < 0.05$, [b]$P < 0.01$ *vs* control group.

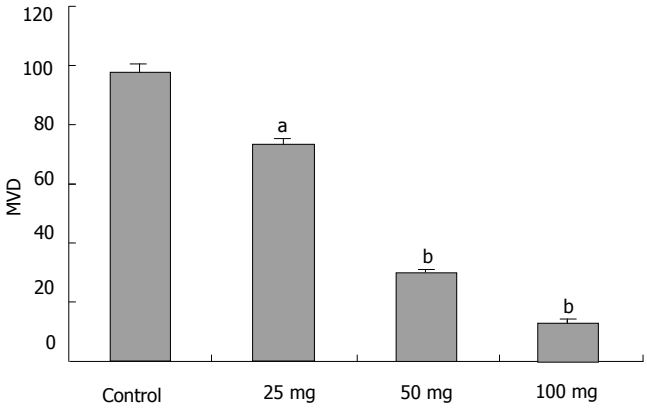

Figure 5 Tumors resected from mice at the experimental end point. Resected tumors were sectioned and stained as described in the text. Microvessel densities (MVD) were determined by counting CD34-positive endothelial cells in the sections and presented as mean ± SE positive cells/field from the three "hot-spot" fields. [a]$P < 0.05$, [b]$P < 0.01$ *vs* control group.

DISCUSSION

Tumor-induced neovascularization plays a key role in the development, progression and metastasis of neoplasm[39]. Angiogenesis is regulated by several endogenous stimulators and inhibitors of endothelial cell migration, proliferation and tube formation[4]. Tumor growth progression is correlated to the serum concentration of angiogenic mediators[40]. Furthermore, vascular density of tumor tissues is correlated to the clinical course of tumors[2]. MK is heparin binding to cytokines involved in neurogenesis, cell migration and mesoderm-epithelial interactions[41]. Choudhuri *et al*[11] reported that in vitro tumor cell growth is not affected by these growth factors, while *in vivo* tumor cell growth is correlated to increased vascular density of tumors. Since MK plays an important role in angiogenesis, it may be a possible therapy target to suppress angiogenesis of tumor proliferation.

Under physiological conditions the vasculature is quiescent in normal adults. Only 0.01% of endothelial cells in normal adult vessels are in the cell division cycle at any given time[42]. However, in response to an appropriate angiogenic stimulus, endothelial cells can be activated to grow new vessels. In the present study, down regulation of MK expression could restrain HUVEC proliferation, suggesting that endothelial cells can also inhibit angiogenesis *in vivo*. Chick CAM assay showed that MK-AS could inhibit local CAM vasculogenesis.

Furthermore, we developed an *in situ* HCC model of mice to determine the effect of MK-AS on tumor proliferation and angiogenesis *in vivo*. Our results indicate that MK-AS administration significantly inhibited tumor growth in the *in situ* HCC model of mice (Tables 1 and 2). Furthermore, Mk-AS administration also suppressed tumor angiogenesis *in vivo* (Figures 4 and 5). It should be noted that the tumor cell line originated from human HCC maintained the complete characteristics of human HCC tissue, such as AFP secretion, drug sensitivity. In addition, the pathological evidence also suggests that this model exhibits various features seen in clinical HCC patients, indicating that the information provided by this model can reflect the true clinic results of patients. In fact, angiogenesis suppressed by transfection with SiRNA targeting MK in human prostate cancer cell line (PC-3) has also been reported[43].

It has been well established that tumor growth and metastasis depend on the induction of new blood supply[44,45]. Angiogenic activity as determined by MVD, has been shown to correlate with worse prognosis in a number of solid tumors[46-48]. Therefore, antiangiogenic agents targeting either these factors or vascular endothelial cells can be used as promising therapeutic modalities in treatment of tumors[49]. In the present study, significant inhibition of angiogenesis was achieved using MK-AS, indicating that MK-AS is an effective antiangiogenesis agent.

COMMENTS

Background

Midkine (MK) is a 13kDa protein, a heparin-binding growth factor. Subsequent studies suggest that MK plays an important role in carcinogenesis.

Research frontiers

MK plays an important role in angiogenesis, which is an important event in tumor development and progression. Antisense oligonucleotide targeting MK is employed in cancer therapy as it can inhibit hypervascularization of tumors and is of great clinical interest.

Innovations and breakthroughs

In this study, MK inhibited angiogenesis in chicken chorioallantoic membrane and human hepatocellular carcinoma (HCC) xenograft. Meanwhile MK inhibited proliferation of human umbilical vein endothelial cells (HUVEC) and growth of HCC xenograft.

Applications

In this study, we addressed the potential therapeutic effect of MK on angiogenesis. Significant inhibition of angiogenesis was achieved using MK, indicating that MK is an effective anti-angiogenesis agent.

Peer review

The manuscript by Li-Cheng Dai *et al* describes the successful use of midkine to inhibit angiogenesis in chicken chorioallantoic membrane and human HCC xenograft. The results were found to be important for HCC therapy. The findings are of clinical interest.

REFERENCES

1 **Folkman J,** Tumor angiogenesis. In: Mendelsohn J, Howley P, Liotta LA, and Israel M, editors. The Molecular Basis of Cancer. Philadelphia: Saunders WB, 1995: 206–232
2 **Hanahan D**, Weinberg RA. The hallmarks of cancer. *Cell* 2000; **100**: 57-70
3 **Campbell SC**, Volpert OV, Ivanovich M, Bouck NP. Molecular mediators of angiogenesis in bladder cancer. *Cancer Res* 1998; **58**: 1298-1304
4 **Distler JH**, Hirth A, Kurowska-Stolarska M, Gay RE, Gay S, Distler O. Angiogenic and angiostatic factors in the molecular control of angiogenesis. *Q J Nucl Med* 2003; **47**: 149-161
5 **O'Reilly MS**, Boehm T, Shing Y, Fukai N, Vasios G, Lane WS, Flynn E, Birkhead JR, Olsen BR, Folkman J. Endostatin: an endogenous inhibitor of angiogenesis and tumor growth. *Cell* 1997; **88**: 277-285
6 **O'Reilly MS**, Holmgren L, Shing Y, Chen C, Rosenthal RA, Moses M, Lane WS, Cao Y, Sage EH, Folkman J. Angiostatin: a novel angiogenesis inhibitor that mediates the suppression of metastases by a Lewis lung carcinoma. *Cell* 1994; **79**: 315-328
7 **O'Reilly MS**, Pirie-Shepherd S, Lane WS, Folkman J. Antiangiogenic activity of the cleaved conformation of the serpin antithrombin. *Science* 1999; **285**: 1926-1928
8 **Goldfarb M**. The fibroblast growth factor family. *Cell Growth Differ* 1990; **1**: 439-445
9 **Ferrara N**, Houck K, Jakeman L, Leung DW. Molecular and biological properties of the vascular endothelial growth factor family of proteins. *Endocr Rev* 1992; **13**: 18-32
10 **Ferrara N**. The role of vascular endothelial growth factor in pathological angiogenesis. *Breast Cancer Res Treat* 1995; **36**: 127-137
11 **Choudhuri R**, Zhang HT, Donnini S, Ziche M, Bicknell R. An angiogenic role for the neurokines midkine and pleiotrophin in tumorigenesis. *Cancer Res* 1997; **57**: 1814-1819
12 **Kadomatsu K**, Tomomura M, Muramatsu T. cDNA cloning and sequencing of a new gene intensely expressed in early differentiation stages of embryonal carcinoma cells and in mid-gestation period of mouse embryogenesis. *Biochem Biophys Res Commun* 1988; **151**: 1312-1318
13 **Li YS**, Milner PG, Chauhan AK, Watson MA, Hoffman RM, Kodner CM, Milbrandt J, Deuel TF. Cloning and expression of a developmentally regulated protein that induces mitogenic and neurite outgrowth activity. *Science* 1990; **250**: 1690-1694
14 **Merenmies J**, Rauvala H. Molecular cloning of the 18-kDa growth-associated protein of developing brain. *J Biol Chem* 1990; **265**: 16721-16724
15 **Muramatsu T**. Midkine (MK), the product of a retinoic acid responsive gene, and pleiotrophin constitute a new protein family regulating growth and differentiation. *Int J Dev Biol* 1993; **37**: 183-188
16 **Garver RI**, Chan CS, Milner PG. Reciprocal expression of pleiotrophin and midkine in normal versus malignant lung tissues. *Am J Respir Cell Mol Biol* 1993; **9**: 463-466
17 **Garver RI**, Radford DM, Donis-Keller H, Wick MR, Milner PG. Midkine and pleiotrophin expression in normal and malignant breast tissue. *Cancer* 1994; **74**: 1584-1590
18 **Aridome K**, Tsutsui J, Takao S, Kadomatsu K, Ozawa M, Aikou T, Muramatsu T. Increased midkine gene expression in human gastrointestinal cancers. *Jpn J Cancer Res* 1995; **86**: 655-661
19 **Nakanishi T**, Kadomatsu K, Okamoto T, Tomoda Y, Muramatsu T. Expression of midkine and pleiotropin in ovarian tumors. *Obstet Gynecol* 1997; **90**: 285-290
20 **O'Brien T**, Cranston D, Fuggle S, Bicknell R, Harris AL. The angiogenic factor midkine is expressed in bladder cancer, and overexpression correlates with a poor outcome in patients with invasive cancers. *Cancer Res* 1996; **56**: 2515-2518
21 **Konishi N**, Nakamura M, Nakaoka S, Hiasa Y, Cho M, Uemura H, Hirao Y, Muramatsu T, Kadomatsu K. Immunohistochemical analysis of midkine expression in human prostate carcinoma. *Oncology* 1999; **57**: 253-257
22 **Mishima K**, Asai A, Kadomatsu K, Ino Y, Nomura K, Narita Y, Muramatsu T, Kirino T. Increased expression of midkine during the progression of human astrocytomas. *Neurosci Lett* 1997; **233**: 29-32
23 **Nakagawara A**, Milbrandt J, Muramatsu T, Deuel TF, Zhao H, Cnaan A, Brodeur GM. Differential expression of pleiotrophin and midkine in advanced neuroblastomas. *Cancer Res* 1995; **55**:

1792-1797
24 **Hidaka H**, Yagasaki H, Takahashi Y, Hama A, Nishio N, Tanaka M, Yoshida N, Villalobos IB, Wang Y, Xu Y, Horibe K, Chen S, Kadomatsu K, Kojima S. Increased midkine gene expression in childhood B-precursor acute lymphoblastic leukemia. *Leuk Res* 2007; 31: 1045-1051
25 **Owada K**, Sanjo N, Kobayashi T, Mizusawa H, Muramatsu H, Muramatsu T, Michikawa M. Midkine inhibits caspase-dependent apoptosis via the activation of mitogen-activated protein kinase and phosphatidylinositol 3-kinase in cultured neurons. *J Neurochem* 1999; **73**: 2084-2092
26 **Qi M**, Ikematsu S, Ichihara-Tanaka K, Sakuma S, Muramatsu T, Kadomatsu K. Midkine rescues Wilms' tumor cells from cisplatin-induced apoptosis: regulation of Bcl-2 expression by Midkine. *J Biochem* 2000; **127**: 269-277
27 **Muramatsu H**, Muramatsu T. Purification of recombinant midkine and examination of its biological activities: functional comparison of new heparin binding factors. *Biochem Biophys Res Commun* 1991; **177**: 652-658
28 **Muramatsu H**, Shirahama H, Yonezawa S, Maruta H, Muramatsu T. Midkine, a retinoic acid-inducible growth/differentiation factor: immunochemical evidence for the function and distribution. *Dev Biol* 1993; **159**: 392-402
29 **Takada T**, Toriyama K, Muramatsu H, Song XJ, Torii S, Muramatsu T. Midkine, a retinoic acid-inducible heparin-binding cytokine in inflammatory responses: chemotactic activity to neutrophils and association with inflammatory synovitis. *J Biochem* 1997; **122**: 453-458
30 **Maeda N**, Ichihara-Tanaka K, Kimura T, Kadomatsu K, Muramatsu T, Noda M. A receptor-like protein-tyrosine phosphatase PTPzeta/RPTPbeta binds a heparin-binding growth factor midkine. Involvement of arginine 78 of midkine in the high affinity binding to PTPzeta. *J Biol Chem* 1999; **274**: 12474-12479
31 **Horiba M**, Kadomatsu K, Nakamura E, Muramatsu H, Ikematsu S, Sakuma S, Hayashi K, Yuzawa Y, Matsuo S, Kuzuya M, Kaname T, Hirai M, Saito H, Muramatsu T. Neointima formation in a restenosis model is suppressed in midkine-deficient mice. *J Clin Invest* 2000; **105**: 489-495
32 **Sandra F**, Harada H, Nakamura N, Ohishi M. Midkine induced growth of ameloblastoma through MAPK and Akt pathways. *Oral Oncol* 2004; **40**: 274-280
33 **Stoica GE**, Kuo A, Powers C, Bowden ET, Sale EB, Riegel AT, Wellstein A. Midkine binds to anaplastic lymphoma kinase (ALK) and acts as a growth factor for different cell types. *J Biol Chem* 2002; **277**: 35990-35998
34 **Dai LC**, Wang X, Yao X, Lu YL, Ping JL, He JF. Antisense oligonucleotides targeting midkine induced apoptosis and increased chemosensitivity in hepatocellular carcinoma cells. *Acta Pharmacol Sin* 2006; **27**: 1630-1636
35 **Lin RX**, Tuo CW, Lü QJ, Zhang W, Wang SQ. Inhibition of tumor growth and metastasis with antisense oligonucleotides (Cantide) targeting hTERT in an *in situ* human hepatocellular carcinoma model. *Acta Pharmacol Sin* 2005; **26**: 762-768
36 **Weidner N**, Semple JP, Welch WR, Folkman J. Tumor angiogenesis and metastasis--correlation in invasive breast carcinoma. *N Engl J Med* 1991; **324**: 1-8
37 **Martins-Green M**, Feugate JE. The 9E3/CEF4 gene product is a chemotactic and angiogenic factor that can initiate the wound-healing cascade *in vivo*. *Cytokine* 1998; **10**: 522-535
38 **Dai LC**, Wang X, Yao X, Min LS, Ping JL, He JF. Antisense oligonucleotides targeting midkine inhibit tumor growth in an *in situ* human hepatocellular carcinoma model. *Acta Pharmacol Sin* 2007; **28**: 453-458
39 **Hahnfeldt P**, Panigrahy D, Folkman J, Hlatky L. Tumor development under angiogenic signaling: a dynamical theory of tumor growth, treatment response, and postvascular dormancy. *Cancer Res* 1999; **59**: 4770-4775
40 **Beecken WD**, Engl T, Hofmann J, Jonas D, Blaheta R. Clinical relevance of serum angiogenic activity in patients with transitional cell carcinoma of the bladder. *J Cell Mol Med* 2005; **9**: 655-661
41 **Zhang N**, Deuel TF. Pleiotrophin and midkine, a family of mitogenic and angiogenic heparin-binding growth and differentiation factors. *Curr Opin Hematol* 1999; **6**: 44-50
42 **Hobson B**, Denekamp J. Endothelial proliferation in tumours and normal tissues: continuous labelling studies. *Br J Cancer* 1984; **49**: 405-413
43 **Takei Y**, Kadomatsu K, Goto T, Muramatsu T. Combinational antitumor effect of siRNA against midkine and paclitaxel on growth of human prostate cancer xenografts. *Cancer* 2006; **107**: 864-873
44 **Plate KH**, Breier G, Risau W. Molecular mechanisms of developmental and tumor angiogenesis. *Brain Pathol* 1994; **4**: 207-218
45 **Hanahan D,** Folkman J. Patterns and emerging mechanisms of the angiogenic switch during tumorigenesis. *Cell* 1996; **86**: 353-364
46 **Brawer MK**, Deering RE, Brown M, Preston SD, Bigler SA. Predictors of pathologic stage in prostatic carcinoma. The role of neovascularity. *Cancer* 1994; **73**: 678-687
47 **Delahunt B**, Bethwaite PB, Thornton A. Prognostic significance of microscopic vascularity for clear cell renal cell carcinoma. *Br J Urol* 1997; **80**: 401-404
48 **Bochner BH**, Cote RJ, Weidner N, Groshen S, Chen SC, Skinner DG, Nichols PW. Angiogenesis in bladder cancer: relationship between microvessel density and tumor prognosis. *J Natl Cancer Inst* 1995; **87**: 1603-1612
49 **Streeter EH**, Harris AL. Angiogenesis in bladder cancer--prognostic marker and target for future therapy. *Surg Oncol* 2002; **11**: 85-100

S-Editor Liu Y **L-Editor** Wang XL **E-Editor** Zhou T

PO Box 2345, Beijing 100023, China
www.wjgnet.com
wjg@wjgnet.com

World J Gastroenterol 2007 February 28; 13(8): 1214-1220
World Journal of Gastroenterology ISSN 1007-9327

BASIC RESEARCH

Tetrandrine stimulates the apoptosis of hepatic stellate cells and ameliorates development of fibrosis in a thioacetamide rat model

Ming-Fu Yin, Li-Hua Lian, Dong-Ming Piao, Ji-Xing Nan

Ji-Xing Nan, Key Laboratory of Organism Functional Factors of the Changbai Mountain (Yanbian University), Ministry of Education and College of Pharmacy, Yanbian University, Yanji 133002 Jilin Province, China
Ming-Fu Yin, Li-Hua Lian, College of Pharmacy, Yanbian University, Yanji 133002 Jilin Province, China
Dong-Ming Piao, Department of Pathology, the Affiliated Hospital, Medical College, Yanbian University, Yanji 133002 Jilin Province, China
Supported by the National Natural Science Foundation of China, No. 32060127 and No. 30660225
Correspondence to: Dr. Ji-Xing Nan, Key Laboratory of Organism Functional Factors of the Changbai Mountain (Yanbian University), Ministry of Education, Yanji 133002, Jilin Province, China. jxnanybu@gmail.com
Telephone: +86-433-2732456 Fax: +86-433-2659795
Received: 2006-11-27 Accepted: 2007-01-05

Abstract

AIM: To investigate the therapeutic effect of tetrandrine on liver fibrosis induced by thioacetamide in rats *in vivo* and *in vitro*.

METHODS: *In vitro* study: we investigated the effect of tetrandrine on the apoptosis of rat hepatic stellate cells transformed by simian virus 40 (T-HSC/Cl-6), which retains the features of activated cells. *In vivo* study: hepatic fibrosis was induced in rats by thioacetamide. Tetrandrine was given orally to rats at doses of 5, 10 or 20 mg/kg for 4 wk compared with intraperitoneal injection of interferon-r.

RESULTS: *In vitro* study: 5, 10 or 25 μg/mL of tetrandrine-induced activation of caspase-3 in t-HSC/Cl-6 cells occurred dose-dependently. *In vivo* study: tetrandrine treatment as well as interferon-r significantly ameliorated the development of fibrosis as determined by lowered serum levels of aspartate aminotransferase (AST), alanine aminotransferase (ALT), total bilirubin (T-Bil) and the levels of liver hydroxyproline (Hyp), hyaluronic acid (HA), laminin (LN) and also improved histological findings. The effects of tetrandrine at the concentration of 20 mg/kg were better than the other concentration groups.

CONCLUSION: Tetrandrine promotes the apoptosis of activated HSCs *in vitro*. Tetrandrine administration can prevent liver fibrosis and liver damage induced by thioacetamide in rats *in vivo*, indicating that it might exert a direct effect on rat HSCs.

Key words: Tetrandrine; Apoptosis; Caspase-3; Liver fibrosis; Thioacetamide

Yin MF, Lian LH, Piao DM, Nan JX. Tetrandrine stimulates the apoptosis of hepatic stellate cells and ameliorates development of fibrosis in a thioacetamide rat model. *World J Gastroenterol* 2007; 13(8): 1214-1220

http://www.wjgnet.com/1007-9327/13/1214.asp

INTRODUCTION

Fibrosis represents the response of the liver to diverse chronic insults such as chronic viral infection, alcohol, immunological attack, hereditary metal overload, parasitic diseases and toxic damage. Because of the worldwide prevalence of these insults, liver fibrosis is common and ultimately results in cirrhosis that is associated with significant morbidity and mortality. Hepatic fibrosis, regardless of the causes, is characterized by an increase in extracellular matrix constituents, leading to complications of portal hypertension, esophageal varices and hepatic failure. The excessive accumulation of extracellular matrix is characteristic of hepatic fibrosis[1-3]. It is accepted that hepatic stellate cells (HSCs) play a central role in the development and resolution of liver fibrosis. HSCs are localized within the space of Disse and function to store retinoids in normal liver. In response to liver damage, HSCs are "activated" to a myofibroblast-like phenotype. It has recently been shown that recovery from established experimental fibrosis can occur through apoptosis of HSCs and is associated with reductions in liver collagen and expression of the tissue inhibitor of metalloproteinases. During chronic liver diseases, HSCs are activated into proliferative, fibrogenic, and smooth muscle α-actin (α-SMA) positive myofibroblasts, resulting in liver fibrosis[4,5]. Recently it was reported that during recovery from acute human and experimental liver injury, a number of activated HSCs undergo apoptosis, and there is a significant decrease in the extent of fibrosis within the same livers in association with this HSC apoptosis[6].

Therefore, induction of HSC apoptosis might be an important therapeutic strategy for hepatic fibrosis, while inhibition of HSC activation might have a role in the prevention of hepatic fibrosis. The development of approaches to prevent fibrotic changes in the liver or reverse the fibrosis is important[7]. However, therapeutic antifibrotic drugs are still at an experimental stage[8,9]. The major problems of antifibrotics are toxicity owing to the chronic administration and the lowered therapeutic effects of the agents used clinically as compared with *in vitro* studies. Therefore, developing antifibrotics from the natural products used in traditional medicine with little acute toxicity, may improve therapies[10].

Tetrandrine is a bis-benzyl isoquiniline alkaloid from the Chinese herb radix *Stephania tetrandra* S Moore. This compound has been characterized pharmacologically to exhibit hypotensive, anti-inflammatory, and immunosuppressive properties, to inhibit lipid peroxidation, and to have an antifibrogenic activity against pulmonary fibroblasts and an inhibitory effect on type I and Ⅲ collagen gene mRNA levels in the lung tissue of rats[11-13]. The dried root of *S. tetrandra* is one of the traditional Chinese medicines that have long been used to treat human liver fibrosis and cirrhosis[14]. Tetrandrine also shows a blocking action of calcium channels, which are known to play an important role in the regulation of hepatic stellate cell contractility, a marked phenotype of activated HSCs[15,16]. For many years, our laboratory has been screening candidate antifibrotic agents from natural products that have been used in traditional medicine to treat liver disease[10,17]. It was previously reported that tetrandrine has an antifibrotic function on liver fibrosis in rats induced by bile duct ligation and scission and tetrandrine exerts a direct inhibitory effect on rat HSCs[18]. We were intrigued to know if tetrandrine could improve the liver injury induced by thioacetamide (TAA). In a preliminary assay, we found that tetrandrine did induce apoptosis in HSCs. The aim of the present study was to explore the sequential pattern of apoptosis and the antifibrotic effect of tetrandrine on hepatic fibrosis induced by TAA in rats. Our results suggest that tetrandrine ameliorates development of fibrosis in a TAA rat model, accompanied by activation of caspase-3 and reduced number of activated HSCs.

MATERIALS AND METHODS

Reagents

Tetrandrine was purchased from Sigma-Aldrich (St Louis, MO, USA) and was dissolved in dimethyl sulphoxide (DMSO). The concentration of tetrandrine used for *in vitro* experiment was prepared by dilution with Williams' medium E (WME; Sigma-Aldrich). DMSO in cells was maintained at 0.5%. Thioacetamide (TAA) was also from Sigma-Aldrich. Hyaluronic acid RIA (HA) kit and laminin RIA (LN) kit were purchased from Shanghai HaiYan Medical Biotechnology Center. Interferon-r was from Livzon Biotechnology Co., Zhuhai, China.

Isolation of hepatic stellate cells and establishment of t-HSC/Cl-6 cell line

The transformed rat hepatic stellate cell line was generated as described by Kim *et al*[19] with some modifications. t-HSC/Cl-6 cells were cultured in WME medium supplemented with 10% fetal bovine serum (FBS; US Biotechnologies Inc., Parkerford, PA, USA) and 100 units/mL penicillin G and 100 μg/mL streptomycin (Gibco-Invitrogen Corp., Grand Island, NY, USA) and maintained at 37℃ with 5% CO_2/95% O_2. Cells were routinely passaged before reaching confluence.

Assay of caspase activity

After different treatments, cells were collected and washed with ice-cold phosphate-buffered saline (PBS). Cell lysates were prepared with caspase colorimetric assay kits (R&D Systems Inc.), according to the manufacturer's instructions. Protein concentrations in t-HSC/Cl-6 cell lysates were determined with a Bio-Rad DC Protein Assay kit (Bio-Rad Laboratories, Hercules, CA, USA). All of the samples were assayed in three independent experiments.

Tetrandrine treatment for TAA induced liver injury

Male Wistar rats (initial body weight 200-220 g) were purchased from the Animal Center of Changchun Agriculture University. All rats were housed and treated in accordance with the recommendations of the American Physiological Society (Council of Europe, 1982). On receipt, they received normal chow and water ad libitum and were maintained at 20℃-25℃, relative humidity of 50%-60% with a 12 h light/dark cycle throughout the experimentation. The rats were divided into six groups of 10 rats each. The hepatic fibrosis was established with TAA, which was diluted and administered to the rats by intraperitoneal injection (200 mg/kg mixed with water) twice weekly. Rats were given orally by gavage at a daily dose of 5, 10 or 20 mg/kg of tetrandrine group. Interferon-r group was given intraperitoneal injection of 5×10^4 U per rat every day. The normal and control groups received equal amounts of saline for 28 d. Three days after the last dose of TAA, the rats were anesthetized and sacrificed. Then blood was obtained by cardiac puncture for serum biochemical testing. Blood samples were kept at room temperature for 1 h and centrifuged at 3000 r/min for 30 min to obtain sera. The livers were immediately removed and a slice of the right lobe was fixed in formaldehyde solution. The rest were divided into equal parts, frozen in liquid nitrogen and stored at -70℃.

Determination of serum and liver biochemical indices

The level of serum aspartate aminotransferase (AST), alanine aminotransferase (ALT), and total bilirubin (T-bil) were measured on an Autodry chemistry analyzer (Spotchem SP4430, Arkray, Kyoto, Japan). While serum hyaluronic acid (HA) and laminin (LN) content in the liver were determined by radioimmunoassay. All procedures were in accordance to the instructions of the manual.

Determination of hydroxyproline contents in liver

The hydroxyproline content in the liver was determined by the method described by Jamall *et al*[20]. Briefly, specimens of the liver were weighed and completely hydrolyzed in 6 mol/L HCl. A fraction of the sample was derivatized using chloramine T solution and Erhlich's reagent, and optical

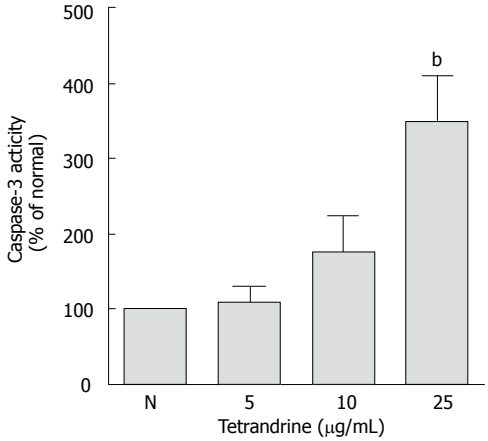

Figure 1 Caspase activity analysis. The caspase activity of normal cells was set at 100% and relative changes in activity are shown in association with drug doses. Values represent the results of three separate experiments. $^{b}P < 0.001$, *vs* normal control values.

density was measured at 558 nm. A standard calibration curve was prepared using trans-4-hydroxy-L-proline. The level of hydroxyproline reflects collagen in the liver.

Histological and immunohistochemical examinations

Liver specimens were preserved in 4% buffered paraformaldehyde and dehydrated in a graded alcohol series. Following xyline treatment, the specimens were embedded in paraffin blocks and cut into 5-μm thick sections, which were placed on plain glass microscopic slides. The sections were then stained with haematoxylin and eosin (HE) or Sirius-red staining, and observed under a light microscope.

Alpha-smooth muscle actin (α-SMA) for detection of activated HSCs was assessed immunohistochemically by the Polymer Detection System using an immunohistological staining kit and anti-α-SMA monoclonal antibodies.

Statistical analysis

All values are expressed as means ± SD. The results were evaluated by one-way ANOVA and Tukey's multiple comparison tests. Statistically significant differences between groups were defined as *P* values less than 0.05. Calculations were performed with the GraphPad Prism program (Graphpad Software, Inc, San Diego, USA).

RESULTS

Caspase-3 activation in tetrandrine -induced apoptosis

To assess the involvement of caspases in t-HSC/Cl-6 cell apoptosis, we detected the enzymatic activity of caspases-3, a downstream caspase. Activation of caspase-3 occurred dose dependently induced by the 5, 10 or 25 μg/mL of tetrandrine (Figure 1).

Liver/weight index

The conditions of rats did not change in control group, but the activity level of the rats was reduced. The general states of rats in other groups were much better than those in control group. Liver/weight index in model group was slightly higher than that in other groups, with no statistical significant difference (data not shown).

Table 1 Serum biochemical values in fibrotic rats induced by TAA treated with tetrandrine for 4 wk

Group	AST (IU/L)	ALT (IU/L)	T-Bil (μmol/L)
Normal	102 ± 24	34 ± 11	11.10 ± 1.29
TAA (200 mg/kg)	356 ± 70	198 ± 32	18.63 ± 2.50
TAA + tetrandrine (5 mg/kg)	266 ± 38[a]	142 ± 29[b]	15.70 ± 1.42[a]
TAA + tetrandrine (10 mg/kg)	259 ± 45[a]	139 ± 29[b]	15.11 ± 2.26[b]
TAA + tetrandrine (20 mg/kg)	227 ± 49[d]	115 ± 30[d]	14.89 ± 0.89[b]
TAA + interferon-r (5×10^4 U)	265 ± 38[a]	137 ± 25[b]	15.43 ± 1.36[a]

$^{a}P < 0.05$; $^{b}P < 0.01$; $^{d}P < 0.001$, *vs* control group.

Serum biochemical parameters

In rats treated with thioacetamide (TAA; 200 mg/kg, ip), serum levels of AST, ALT and T-Bil were increased to 349%, 618% and 168%, respectively, compared with that of normal rats (Table 1). Tetrandrine (5, 10 or 20 mg/kg per day, po, for 4 wk) significantly lowered serum AST, ALT and T-Bil levels in rats intoxicated by TAA. In 5 mg/kg tetrandrine-treated rats, serum AST, ALT and T-Bil levels were lowered to 74.7% ($P < 0.05$), 71.7% ($P < 0.01$) and 84.0% ($P < 0.05$) compared with that of control fibrotic rats, respectively. In 10 mg/kg tetrandrine treated rats, AST, ALT and T-Bil levels were lowered to 72.7% ($P < 0.05$), 70.2% ($P < 0.01$) and 81.1% ($P < 0.01$) compared with that of control fibrotic rats, respectively. In 20 mg/kg tetrandrine treated rats, AST, ALT and T-Bil levels were lowered to 63.7% ($P < 0.001$), 58.1% ($P < 0.001$) and 79.9% ($P < 0.01$) compared with that of control fibrotic rats, respectively. In interferon-r treated fibrotic rats, AST, ALT and T-Bil levels were lowered to 74.4% ($P < 0.05$), 69.1% ($P < 0.01$) and 82.8% ($P < 0.05$) compared with that of control fibrotic rats, respectively.

Hydroxyproline matrix contents in the liver

As shown in Figure 2A, liver contents of hydroxyproline increased to 229%, 4 wk after TAA-treatment ($P < 0.001$). Compared with the control fibrotic rats, in fibrotic rats treated with 5, 10 or 20 mg/kg tetrandrine, the hydroxyproline contents in the liver reduced to 73.3% ($P < 0.05$), 67.8% ($P < 0.01$) or 61.5% ($P < 0.001$), respectively. In interferon-r treated fibrotic rats, the hydroxyproline contents in the liver reduced to 64.6% ($P < 0.001$).

Extracellular matrix content in serum

As shown in Figures 2B and 2C, serum contents of HA and LN increased to 251% and 233%, 4 wk after TAA treatment ($P < 0.001$). In the fibrotic rats treated with 5, 10, 20 mg/kg tetrandrine or interferon-r, HA content in the serum reduced to 68.2% ($P < 0.05$), 62.32% ($P < 0.01$), 50.73% or 47.09% ($P < 0.001$), respectively, compared with the control fibrotic rats. Compared with the control fibrotic rats, in fibrotic rats treated with 5, 10, 20 mg/kg tetrandrine or interferon-r, LN content in the serum reduced to 53.59% ($P < 0.05$), 55.09% ($P < 0.01$), 65.09% ($P < 0.01$) or 68.30% ($P < 0.05$), respectively.

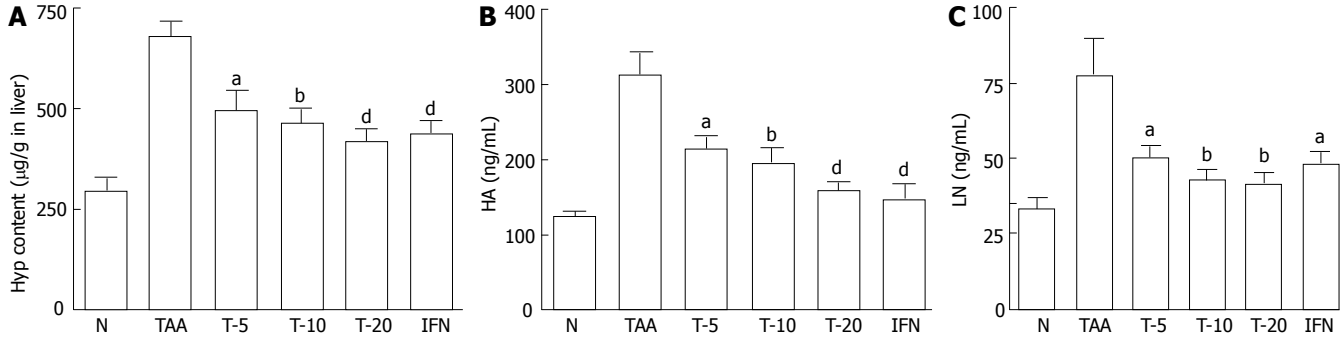

Figure 2 Liver hydroxyproline (**A**); HA (**B**) and LN (**C**) content of the TAA rats treated with tetrandrine. T-5: treated with 5 mg/kg tetrandrine; T-10: treated with 10 mg/kg tetrandrine; T-20: treated with 20 mg/kg tetrandrin; IFN: treated with interferon-r 5 × 10^4 U. Results represent the mean ± SD. $^aP < 0.05$; $^bP < 0.01$; $^dP < 0.001$, *vs* control group.

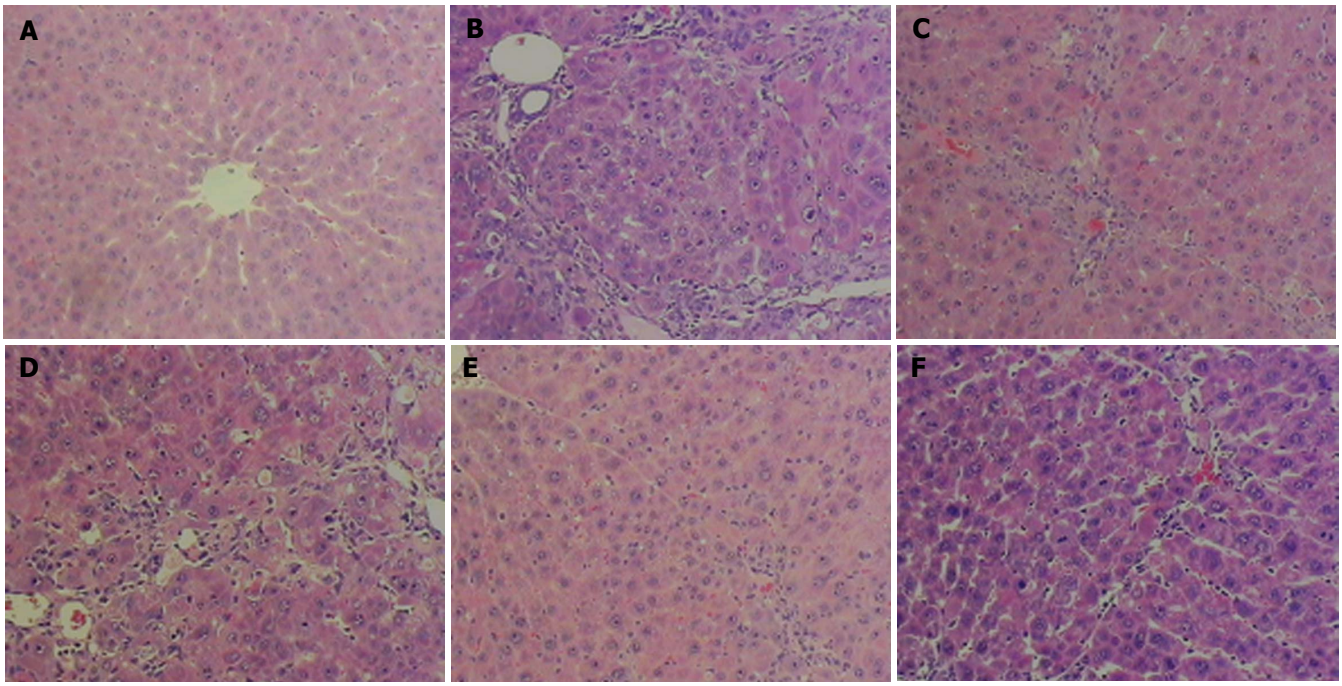

Figure 3 Light microscopic appearance (HE × 100) of fibrotic rat liver induced by TAA treated with tetrandrine for 4 wk. **A**: normal group; **B**: control group; **C**: TAA group with tetrandrine (5 mg/kg); **D**: TAA group with tetrandrine (10 mg/kg); **E**: TAA group with tetrandrine (20 mg/kg); **F**: TAA group with interferon-r (5 × 10^4 U).

Morphological changes in the liver

In control fibrotic group, the liver stained with HE and Sirius-red showed inflammation and an extensive accumulation of collagens (Figures 3B and 4B), fibrotic septa were increased and seen between areas of portal to portal and portal to central vein in some parts of liver lobules, and in some serious units pseudolobules presented. In tetrandrine and interferon-r treated fibrotic rats, there was a tendency towards less pronounced destruction of the liver architecture, compared with control fibrotic rat liver (Figure 3C-F, and Figure 4C-F).

As shown in Figures 3 and 4, TAA treatment for 4 wk resulted in liver injury, with loss of normal lobular architecture and a marked increase of collagen deposition throughout the liver. However, tetrandrine treatment resulted in reduced collagen deposition in the liver of TAA-treated rats.

HSC activation was examined immunohistochemically by determining α-SMA-positive areas in injured rat livers treated with TAA. Considerable expression was detected in areas of centrilobular and periportal fibrotic bands in TAA treated rats (Figure 5B). In normal livers, collagen was observed only around the central and portal veins (Figure 5A). Activated HSCs were characterized by expression of α-SMA. In tetrandrine-treated or interferon-r groups, the expression of α-SMA was much lower than that in control fibrotic group and the distribution of α-SMA positive cells was similar to that of collagen in the liver (Figure 5C-F). In contrast, 20 mg/kg tetrandrine-treated rats notably reduced the positive areas of α-SMA in the livers of rats treated with TAA.

DISCUSSION

Thioacetamide (TAA) is a thiono-sulfur containing compound, undergoing an extensive metabolism to acetamide and TAA-S-oxide. Whereas acetamide is devoid of liver-necrotizing properties, TAA-S-oxide

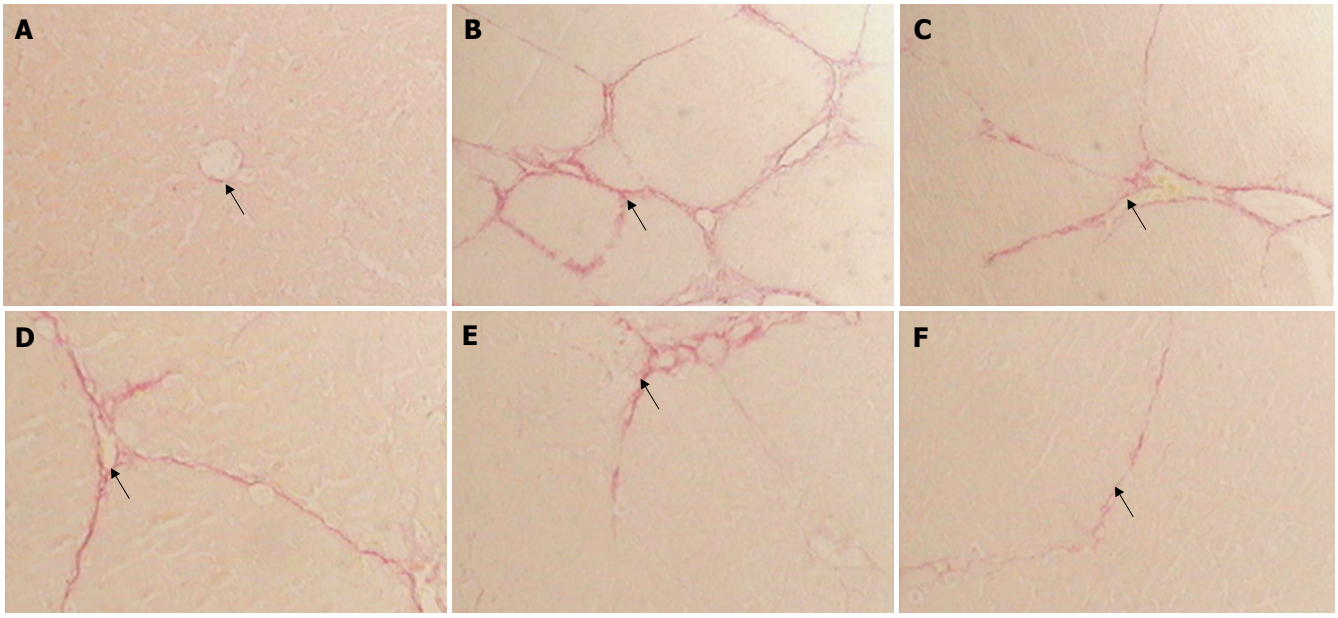

Figure 4 Light microscopical appearance (sirius red staining) of fibrotic rat liver induced by TAA treated with tetrandrine for 4 wk. Sirius red stains most hepatic collagens. **A**: normal group; **B**: control group; **C**: TAA group with tetrandrine (5 mg/kg); **D**: TAA group with tetrandrine (10 mg/kg); **E**: TAA group with tetrandrine (20 mg/kg); **F**: TAA group with interferon-r (5×10^4 U).

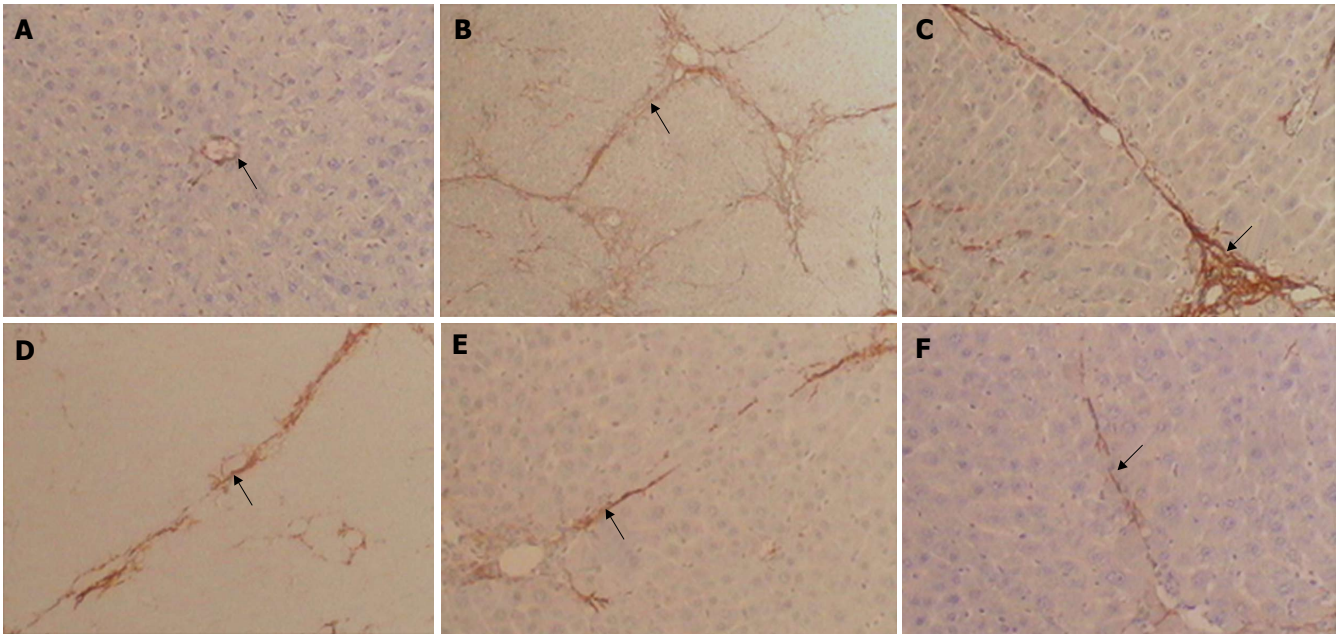

Figure 5 Representative liver section showing reaction of alpha-smooth muscle cell like actin (α-SMA) with mouse anti-α-SMA monoclonal antibody. α-SMA immunoreactivity (arrows) was seen in stellate cells in the fibrotic area. **A**: normal group; **B**: control group; **C**: TAA group with tetrandrine (5 mg/kg); **D**: TAA group with tetrandrine (10 mg/kg); **E**: TAA group with tetrandrine (20 mg/kg); **F**: TAA group with interferon-r (5×10^4 U).

is further metabolized, at least in part, by cytochrome P-450 monooxygenases to other products, including a polar product that is thought to be the sulfene, TAA-S-dioxide, a highly reactive compound[21]. Therefore, TAA is a typical hepatotoxin and causes centrilobular necrosis by generation of ROS. Although TAA is known mainly to cause necrosis in the liver, it has been reported recently that TAA induced apoptosis in rat liver within a few hours after its administration[22]. The present study showed that a low dose of TAA induced apoptosis in the pericentral areas, whereas a high dose of TAA induced necrosis. Excessive ROS causes necrosis.

The mechanism by which tetrandrine inhibits rat hepatic stellate cell activation is not clear. Tetrandrine administration has been shown to block the calcium channels in various cell types[23]. Moreover, activated hepatic stellate cells have receptors for a number of vasoconstrictor substances such as endotheline, angiotensin Ⅱ, vasopressin, thrombin and thromboxan A2[24-26]. Therefore, it is likely that the inhibitory effect of tetrandrine on hepatic stellate

cell activation is, at least in part, through the blocking of calcium channels. However, further study is needed to understand the precise mechanism of tetrandrine on activated hepatic stellate cells.

Here we showed that tetrandrine is toxic against t-HSC/Cl-6 cells and antifibrotic. Previous studies demonstrated that tetrandrine induced apoptosis in t-HSC/Cl-6 cells, and activated rat hepatic stellate cells transformed by SV40. The morphologies of tetrandrine-treated cells revealed the typical features of apoptosis and these apoptotic phenomena were further confirmed by DNA laddering and annexin v-propidium iodide double staining[27]. Previous reports have demonstrated that the caspase family proteases play essential roles in the process of apoptosis[28]. Caspase-3, which has a short prodomain and is localized near nuclei, cleaves substrates at the downstream end of the cascade[29]. This study demonstrated that the activation of caspase-3 is involved in tetrandrine-induced cell death including apoptosis. Moreover, we have shown that tetrandrine is also effective in mediating HSC apoptosis *in vivo* after the development of fibrosis. It suggests that apoptosis of activated HSCs plays a key role in resolution of hepatic fibrosis.

Our data provide evidence that tetrandrine will effectively induce HSC apoptosis. In addition, we have demonstrated evidence that induction of apoptosis in HSCs enhances the resolution of experimental fibrosis. Taken together, these observations suggest that a strategy based on inducing HSC apoptosis may be an effective antifibrotic approach. The effects of tetrandrine at 20 mg/kg dose are better than the other groups. In conclusion, our results demonstrate that tetrandrine administration could prevent liver fibrosis and liver damage induced by TAA in rats. In this study, tetrandrine reduced the degree of hepatocellular injury as determined by lower serum levels of AST, ALT, T-bil and liver hydroxyproline, serum HA and LN, and also improved morphological structure of the fibrotic liver. Our study shows a direct inhibitory effect on rat HSC activation and an antifibrogenic potential of tetrandrine in fibrotic rats induced by TAA. Tetrandrine may have therapeutic effects in human liver fibrosis.

COMMENTS

Background

Fibrosis represents the response of the liver to diverse chronic insults such as chronic viral infection, alcohol, immunological attack, hereditary metal overload, parasitic diseases and toxic damage. It is accepted that HSCs play a central role in the development and resolution of liver fibrosis. Recently it was reported that during recovery from acute human and experimental liver injury, a number of activated HSCs undergo apoptosis, and there is a significant decrease in the extent of fibrosis within the same livers in association with this HSCs apoptosis.

Research frontiers

Tetrandrine promotes HSC apoptosis in hepatic fibrosis. The study of its mechanism might lead to a new approach for fibrosis therapy. Further studies of the roles and regulation of HSC apoptosis and its possible mechanism are important for understanding the mechanism of resolution of liver fibrosis.

Innovations and breakthroughs

In this research, we investigated the effect of tetrandrine on the apoptotic death of rat HSCs *in vitro* and whether tetrandrine can prevent thioacetamide-induced fibrosis *in vivo*. The results showed that tetrandrine promotes the apoptosis of activated HSCs *in vitro* and prevent liver fibrosis and liver damage induced by thioacetamide in rats *in vivo*.

Applications

The results provide significant evidence illustrating the key feature of recovery from liver fibrosis is HSC apoptosis.

Terminology

HSCs: hepatic stellate cells; Caspase: Caspases, closely associated with apoptosis, are aspartate-specific cysteine proteases and members of the interleukin-1b-converting enzyme family. The activation and function of caspases, involved in the delicate caspase-cascade system, are regulated by various kinds of molecules, such as the inhibitor of apoptosis protein, Bcl-2 family proteins, calpain, and Ca^{2+}.

Peer review

In this manuscript by Yin *et al*, the authors report effect of tetrandrine on the treatment of liver fibrosis-induced by thioacetamide in rats *in vivo* and *in vitro*. They employed assay of caspase activity to observe the enzymatic activity of caspases-3, a downstream caspase, occurred dose-dependently and investigated tetrandrine treatment as well as interferon-r significantly ameliorates the development of fibrosis as determined by lowered serum levels of AST, ALT, T-Bil and the levels of liver hydroxyproline, HA, LN and also improved histological findings. Their data may be critical for the study of the mechanism of resolution of rat liver fibrosis and shed new light on the liver fibrosis therapy.

REFERENCES

1 **Gressner AM**, Bachem MG. Cellular sources of noncollagenous matrix proteins: role of fat-storing cells in fibrogenesis. *Semin Liver Dis* 1990; **10**: 30-46

2 **Kayano K**, Sakaida I, Uchida K, Okita K. Inhibitory effects of the herbal medicine Sho-saiko-to (TJ-9) on cell proliferation and procollagen gene expressions in cultured rat hepatic stellate cells. *J Hepatol* 1998; **29**: 642-649

3 **Friedman SL**. Seminars in medicine of the Beth Israel Hospital, Boston. The cellular basis of hepatic fibrosis. Mechanisms and treatment strategies. *N Engl J Med* 1993; **328**: 1828-1835

4 **Carloni V**, Pinzani M, Giusti S, Romanelli RG, Parola M, Bellomo G, Failli P, Hamilton AD, Sebti SM, Laffi G, Gentilini P. Tyrosine phosphorylation of focal adhesion kinase by PDGF is dependent on ras in human hepatic stellate cells. *Hepatology* 2000; **31**: 131-140

5 **Friedman SL**. Molecular regulation of hepatic fibrosis, an integrated cellular response to tissue injury. *J Biol Chem* 2000; **275**: 2247-2250

6 **Iredale JP**. Hepatic stellate cell behavior during resolution of liver injury. *Semin Liver Dis* 2001; **21**: 427-436

7 **Chojkier M**, Brenner DA. Therapeutic strategies for hepatic fibrosis. *Hepatology* 1988; **8**: 176-182

8 **Park EJ**, Ko G, Kim J, Sohn DH. Antifibrotic effects of a polysaccharide extracted from Ganoderma lucidum, glycyrrhizin, and pentoxifylline in rats with cirrhosis induced by biliary obstruction. *Biol Pharm Bull* 1997; **20**: 417-420

9 **Nan JX**, Park EJ, Kim HJ, Ko G, Sohn DH. Antifibrotic effects of the methanol extract of Polygonum aviculare in fibrotic rats induced by bile duct ligation and scission. *Biol Pharm Bull* 2000; **23**: 240-243

10 **Nan JX**, Park EJ, Kim YC, Ko G, Sohn DH. Scutellaria baicalensis inhibits liver fibrosis induced by bile duct ligation or carbon tetrachloride in rats. *J Pharm Pharmacol* 2002; **54**: 555-563

11 **Hui SC**, Chan TY, Chen YY. Tetrandrine inhibits lipid peroxidation but lacks reactivity towards superoxide anion and hydrogen peroxide. *Pharmacol Toxicol* 1996; **78**: 200-201

12 **Reist RH**, Dey RD, Durham JP, Rojanasakul Y, Castranova V. Inhibition of proliferative activity of pulmonary fibroblasts by tetrandrine. *Toxicol Appl Pharmacol* 1993; **122**: 70-76

13 **Liu BC**, He YX, Miao Q, Wang HH, You BR. The effects of tetrandrine (TT) and polyvinylpyridine-N-oxide (PVNO) on gene expression of type I and type III collagens during

experimental silicosis. *Biomed Environ Sci* 1994; **7**: 199-204
14 **Chen YJ**, Tu ML, Kuo HC, Chang KH, Lai YL, Chung CH, Chen ML. Protective effect of tetrandrine on normal human mononuclear cells against ionizing irradiation. *Biol Pharm Bull* 1997; **20**: 1160-1164
15 **Weinsberg F**, Bickmeyer U, Wiegand H. Effects of tetrandrine on calcium channel currents of bovine chromaffin cells. *Neuropharmacology* 1994; **33**: 885-890
16 **Berlin JR**. Spatiotemporal changes of Ca2+ during electrically evoked contractions in atrial and ventricular cells. *Am J Physiol* 1995; **269**: H1165-H1170
17 **Nan JX**, Park EJ, Kang HC, Park PH, Kim JY, Sohn DH. Anti-fibrotic effects of a hot-water extract from Salvia miltiorrhiza roots on liver fibrosis induced by biliary obstruction in rats. *J Pharm Pharmacol* 2001; **53**: 197-204
18 **Park PH**, Nan JX, Park EJ, Kang HC, Kim JY, Ko G, Sohn DH. Effect of tetrandrine on experimental hepatic fibrosis induced by bile duct ligation and scission in rats. *Pharmacol Toxicol* 2000; **87**: 261-268
19 **Kim JY**, Kim KM, Nan JX, Zhao YZ, Park PH, Lee SJ, Sohn DH. Induction of apoptosis by tanshinone I via cytochrome c release in activated hepatic stellate cells. *Pharmacol Toxicol* 2003; **92**: 195-200
20 **Jimenez W**, Parés A, Caballería J, Heredia D, Bruguera M, Torres M, Rojkind M, Rodés J. Measurement of fibrosis in needle liver biopsies: evaluation of a colorimetric method. *Hepatology* 1985; **5**: 815-818
21 **Hunter AL**, Holscher MA, Neal RA. Thioacetamide-induced hepatic necrosis. I. Involvement of the mixed-function oxidase enzyme system. *J Pharmacol Exp Ther* 1977; **200**: 439-448
22 **Ledda-Columbano GM**, Coni P, Curto M, Giacomini L, Faa G, Oliverio S, Piacentini M, Columbano A. Induction of two different modes of cell death, apoptosis and necrosis, in rat liver after a single dose of thioacetamide. *Am J Pathol* 1991; **139**: 1099-1109
23 **Chen J**, Wu Z, Chen S, Gong X, Zhong J, Zhang G. The effects of tetrandrine on the contractile function and microvascular permeability in the stunned myocardium of rats. *Jpn J Physiol* 1999; **49**: 499-506
24 **Kawada N**, Tran-Thi TA, Klein H, Decker K. The contraction of hepatic stellate (Ito) cells stimulated with vasoactive substances. Possible involvement of endothelin 1 and nitric oxide in the regulation of the sinusoidal tonus. *Eur J Biochem* 1993; **213**: 815-823
25 **Bataller R**, Nicolás JM, Ginès P, Esteve A, Nieves Görbig M, Garcia-Ramallo E, Pinzani M, Ros J, Jiménez W, Thomas AP, Arroyo V, Rodés J. Arginine vasopressin induces contraction and stimulates growth of cultured human hepatic stellate cells. *Gastroenterology* 1997; **113**: 615-624
26 **Rockey D**. The cellular pathogenesis of portal hypertension: stellate cell contractility, endothelin, and nitric oxide. *Hepatology* 1997; **25**: 2-5
27 **Zhao YZ**, Kim JY, Park EJ, Lee SH, Woo SW, Ko G, Sohn DH. Tetrandrine induces apoptosis in hepatic stellate cells. *Phytother Res* 2004; **18**: 306-309
28 **Roy MK**, Thalang VN, Trakoontivakorn G, Nakahara K. Mechanism of mahanine-induced apoptosis in human leukemia cells (HL-60). *Biochem Pharmacol* 2004; **67**: 41-51
29 **Shi Y**. Mechanisms of caspase activation and inhibition during apoptosis. *Mol Cell* 2002; **9**: 459-470

S- Editor Wang J **L- Editor** Zhu LH **E- Editor** Lu W

PO Box 2345, Beijing 100023, China
www.wjgnet.com
wjg@wjgnet.com

World J Gastroenterol 2007 February 28; 13(8): 1221-1229
World Journal of Gastroenterology ISSN 1007-9327

CLINICAL RESEARCH

Role of CARD15, DLG5 and OCTN genes polymorphisms in children with inflammatory bowel diseases

S Cucchiara, A Latiano, O Palmieri, AM Staiano, R D'Incà, G Guariso, G Vieni, V Rutigliano, O Borrelli, MR Valvano, V Annese

S Cucchiara, O Borrelli, Clinica Pediatrica, Università "La Sapienza", Roma, Italy
A Latiano, MR Valvano, V Annese, O Palmieri, U.O. Gastroenterologia, IRCCS "Casa Sollievo della Sofferenza", San Giovanni Rotondo, Italy
AM Staiano, Clinica Pediatrica Università di Napoli, Università di Padova, Italy
R D'Incà, Cattedra di Gastroenterologia, Università di Padova, Italy
G Guariso, Clinica Pediatrica Università di Padova, Italy
G Vieni, Clinica Pediatrica Università di Messina, Italy
V Rutigliano, Clinica Pediatrica Università di Bari, Italy
Supported by the Minister of Health, No. RC0503GA20
Correspondence to: Annese Vito, MD, U.O. Gastroenterologia, Ospedale IRCCS "Casa Sollievo della Sofferenza", Viale Cappuccini, 1-71013 S. Giovanni Rotondo, Italy. v.annese@operapadrepio.it
Telephone: +39-882-410335 Fax: +39-882-411879
Received: 2006-10-29 Accepted: 2007-01-12

Abstract

AIM: To investigate the contribution of variants of CARD15, OCTN1/2 and DLG5 genes in disease predisposition and phenotypes in a large Italian cohort of pediatric patients with inflammatory bowel diseases (IBD).

METHODS: Two hundred patients with Crohn's disease (CD), 186 ulcerative colitis (UC) patients, 434 parents (217 trios), and 347 healthy controls (HC) were studied. Polymorphisms of the three major variants of CARD15, 1672C/T and -207G/C SNPs for OCTN genes, IGR2096a_1 and IGR2198a_1 SNPs for the IBD5 locus, and 113G/A variant of the DLG5 gene were evaluated. Potential correlations with clinical sub-phenotypes were investigated.

RESULTS: Polymorphisms of CARD15 were significantly associated with CD, and at least one variant was found in 38% of patients (15% in HC, OR = 2.7, $P < 0.001$). Homozygosis for both OCTN1/2 variants was more common in CD patients (1672TT 24%, -207CC 29%) than in HC (16% and 21%, respectively; $P = 0.03$), with an increased frequency of the TC haplotype (44.8% *vs* 38.3% in HC, $P = 0.04$). No association with the DLG5 variant was found. CD carriers of OCTN1/2 and DLG5 variants more frequently had penetrating disease ($P = 0.04$ and $P = 0.01$), while carriers of CARD15 more frequently had ileal localization ($P = 0.03$). No gene-gene interaction was found. In UC patients, the TC haplotype was more frequent (45.4%, $P = 0.03$), but no genotype/phenotype correlation was observed.

CONCLUSION: Polymorphisms of CARD15 and OCTN genes, but not DLG5 are associated with pediatric onset of CD. Polymorphisms of CARD15, OCTN, and DLG5 genes exert a weak influence on CD phenotype.

Key words: Inflammatory bowel disease; Ulcerative colitis; Crohn's disease; CARD15; DLG5; Carnitine/organic cation transporter gene

Cucchiara S, Latiano A, Palmieri O, Staiano AM, D'Incà R, Guariso G, Vieni G, Rutigliano V, Borrelli O, Valvano MR, Annese V. Role of CARD15, DLG5 and OCTN genes polymorphisms in children with inflammatory bowel diseases. *World J Gastroenterol* 2007; 13(8): 1221-1229

http://www.wjgnet.com/1007-9327/13/1221.asp

INTRODUCTION

The inflammatory bowel diseases (IBD), Crohn's disease (CD) and ulcerative colitis (UC) have become increasingly common causes of morbidity in children[1,2]. Their prevalence has been on rise with children and adolescent currently accounting for approximately 30% of IBD patients[3,4]. Although the precise etiology of IBD remains elusive, both animal models and human studies point towards a strong genetic susceptibility.

The characterization of the NOD2/CARD15 gene at the IBD1 locus (16q12) in 2001 as the first gene conferring susceptibility to CD represented a milestone observation[5-7]. Although the role of NOD2 protein in CD remains under evaluation[8], it is surely involved in the innate immune response to bacterial pathogens[9,10]. CARD15 major variants are mostly associated with ileal disease and stricturing behaviour[7]. In pediatric series, a correlation with ileal localization[11-14], stricturing behaviour[12,13,15] early surgery[12,13] growth delay[13,14], and higher disease activity[13,16] has been reported, although with conflicting findings[17-19].

Functional polymorphisms in the carnitine organic cation transporter cluster (OCTN1/2)[20] on chromosome 5q31 and mutations in disc large gene 5 (DLG5)[21] on

the long arm of chromosome 10 (10q23) have also been reported to be associated with CD. Linkage on the 5q31 genomic area, the so-called IBD5 risk haplotype, was first reported by Rioux *et al*[22]. This 250-kilobase region contains 5 genes and multiple genetic variants with strong linkage disequilibrium[22]. A number of studies have confirmed the association of the IBD5 risk haplotype with CD[23-28] and UC[28,29]. Peltekova *et al*[20] found two novel single nucleotide polymorphisms (SNPs) with functional mutations, generating a 2-alleles risk haplotype (TC) predisposing to CD. Replication studies have found inconsistent genotype/phenotype correlation[30-34] with some concordance for presence of perianal fistulae[31,33], which is similar to that observed for the IBD5 risk haplotype[25,28]. More importantly, although Peltekova *et al*[20] in preliminary functional studies demonstrated that the OCTN1/2 variants resulted in impaired transport function of various organic cations and carnitine, but the precise link with IBD pathogenesis remains unexplained. All subsequent replication studies were unable to confirm the association of TC haplotype in the absence of the IBD5 risk haplotype[30-33], making the assumption of OCTN variants as causal genes still disputable[35].

Concerning the DLG5 gene, Hampe *et al*[36] initially described a susceptibility locus on chromosome 10 in a genome linkage study. Stoll *et al*[21] further narrowed down this risk region and identified two distinct haplotypes associated with IBD and CD. More specifically, the "risk haplotype D" was defined by a single non-synonymous SNP 113G→A; this nucleotide change resulting in the amino acid substitution R30Q, probably impedes scaffolding of the protein evaluated in silico analysis. A collaborative study[37], investigating two independent case-control cohorts and one family-based collection confirmed the association in 2 of the 3 cohorts, although with a modest effect on the relative risk to IBD (OR = 1.25). Other groups, however, reported negative findings[30,31,38]. More recently, a more thorough evaluation of the previously reported cohorts with other large control populations, has demonstrated that the DLG5 gene is a risk factor for CD only for men (OR = 2.49, CI 1.5-4), but not for women (OR = 1.01)[39]. Intriguingly, this difference is driven by a gender-dependent transmission ratio distortion among healthy controls (frequency of A allele: men 5.2%, women 11.3%).

In young patients, IBD might offer the opportunity to understand the pathopysiology of the diseases in a form that is closer to their underlying cause and mechanisms than in adult, because of a lower influence of environmental risk factor (i.e. smoking). Paradoxically, in contrast to the data in adults, there are studies mainly looking at CARD15 polymorphisms[11-19,40], while being scarce and conflicting on OCTN1/2 and DLG5 genes[41-44]. Moreover, many pediatric series are flawed by a small sample size[11,12,15,16,18,19,43,44], little information on UC patients[13,15,41], and lack of control populations[11,12,16,17,19].

In this study we have investigated the contribution of variants of CARD15, OCTN1/2 and DLG5 genes in IBD predisposition in a large Italian pediatric cohort. We also examined the genotype/phenotype relationships and gene-gene interactions.

MATERIALS AND METHODS

Study population

Patients under age of 18 at diagnosis were recruited into this study from 16 tertiary pediatric and gastroenterologic centres in Italy, in cooperation with a multicenter study endorsed by the SIGENP (Italian Society for Pediatric Gastroenterology, Hepatology and Nutrition). Ethical approval was obtained at all participating centres. All study participants were Caucasian and their parents gave a written informed consent.

The diagnosis of CD or UC was established by conventional clinical, radiological, endoscopic and histological criteria[45]. Indeterminate colitis was excluded from the study.

The recruited population was comprised of 200 patients with CD and 186 patients with UC. Blood samples were also taken from 434 parents, making 217 complete family trios (108 CD and 109 UC, respectively) available for analysis.

A total of 347 adult healthy unrelated blood donors (184 male, mean age 32 years, range 20-45) who served as controls were randomly recruited from their sites to minimize the potential geographic differences among San Giovanni Rotondo (Southern Italy, $n = 147$), Rome (Centre, $n = 100$) and Padova (Northern Italy, $n = 100$).

Data collection

Retrospective data were collected on patients using a standardized questionnaire obtaining information on patient and parental smoking details (at least one cigarette/d), ethnicity, and IBD family history. Additional clinical data were collected on patient demographics, age at IBD diagnosis, medications, extra-intestinal manifestations and need for resective surgery. Standard investigations employed in these patients were upper GI endoscopy, ileo-colonoscopy, and barium examination. CD disease location and behavior were categorized according to the Vienna classification[46]. Presence of perianal fistulae was analysed separately according to the Montreal's proposal[47].

In all patients, weight and height percentiles were calculated at diagnosis. Presence of growth retardation was defined as a reduction below the 5th percentile for weight, height or both.

Genotyping

Genomic DNA was extracted from peripheral blood leukocytes according to standard protocols[48], and genotyped in the laboratory of San Giovanni Rotondo Hospital.

Genotyping for Arg702Trp and Leu1007fsinsC common CARD15 variants was performed by DHPLC (denaturing high performance liquid chromatography, Wave System, Transgenomic Ltd, UK) and restriction fragment length polymorphisms (RFLP) assay was used for Gly908Arg (G/C). The 380 base pairs PCR product was digested with Hha I (New England Biolabs, Ipswich, MA), yielding 2 fragments of 138 and 242 base pairs in the presence of C allele and visualized on 2% (w/v) agarose gel. One hundred random samples were also confirmed by sequencing on ABI 310 DNA sequencer (Applied

Table 1 Primers sequences, methodology, and restriction enzymes used for genotyping

Gene locus	SNPs		Sequence	Methods/enzyme
CARD15	R702W	For	5′ACCTTCAGATCACAGCAGCC3′	DHPLC
		Rev	5′GCTCCCCCATACCTGAAC3′	
	G908R	For	5′AAGTCTGTAATGTAAAGCCAC3′	RFLP/Hha Ⅰ
		Rev	5′CCCAGCTCCTCCCTCTTC3′	
	L1007fsinsC	For	5′CTCACCATTGTATCTTCTTTTC3′	DHPLC
		Rev	5′GAATGTCAGAATCAGAAGGG3′	
IBD5	IGR2198a_1	For	5′GGGGCAATTCTATGAGGACA3′	RFLP/Nla Ⅲ
		Rev	5′CCAGAGACACTGGGACATCA3′	
	IGR2096a_1	For	5′GTAGCGAGAGGCTCCACAGT3′	RFLP/Dra Ⅰ
		Rev	5′TCCTCCATGCTACTGCTCTG3′	
OCTN1	C1672T	For	5′GGGTAGTCTGACTGTCCTGATTG3′	TaqMan
SLC22A4		Rev	5′TCTGGAAGAGTCATTCCCAAACTTTC3′	
		VIC	5′AAGGGTGAGGATTC3′	
		FAM	5′AAGGGTGAAGATTC3′	
OCTN2	G207C	For	5′CCGCTCTGCCTGCCA3′	TaqMan
SLC22A5		Rev	5′GCGGCTGGCCTTACATAGG3′	
		VIC	5′CAGGCCCGGAACC3′	
		FAM	5′CAGGCCCGCAACC3′	
DLG5	R30Q		C_7432738_10	TaqMan

DHPLC: Denaturing high performance liquid chromatography; RFLP: Restriction fragment length polymorphisms; TaqMan: ABI Prism 7700 sequencer detector.

Biosystems, Foster City, CA, USA) according to the manufacturer's recommendations.

For OCTN1/2 genotyping, the SLC22A4 1672C/T and SLC22A 5-207G/C primers were designed using Primer Express V 1.5 (Applied Biosystems). SNPs were genotyped using the Taqman system ABI PRISM 7700 (Applied Biosystems, Foster City, CA, USA) as previously described[33].

For the IBD5 locus, the IGR2096a_1 and IGR2198a_1 SPNs were selected from the haplotype originally described by J. Rioux[22] (http://www.genome.wi.mit.edu/IBD5). Genotyping was performed by restriction fragment analysis as previously described[28]. Results were confirmed by direct sequencing of representative samples for each genotype, using ABI cycle sequencing kit V 1.1 and the ABI 310 genetic analyzer.

For the DLG5 gene, we genotyped the 113 G→A variant (rs1248696) tagging the haplotype D, the over-transmitted haplotype in the study by Stoll *et al*[21], with 7700 TaqMan bi-allelic discrimination system. PCR reactions (15 mL) were performed in 1 × TaqMan Universal PCR Master Mix, 1 × Genotyping Assay Mix, and 50 ng of genomic DNA. After 2 min at 50℃, and 10 min at 94℃ initial denaturation, reaction was amplified for 40 cycles: 15 s at 94℃, and 60 s at 60℃.

A summary of primer sequences and methods is depicted in Table 1.

Detection of antibodies

Whenever serum samples were available, anti-nuclear cytoplasmatic antibodies (ANCA) were tested by a standard immuno-fluorescence technique[49]. In addition, presence of anti-saccharomyces cerevisiae antibodies (ASCA) was investigated by means of a commercial ELISA assay (Quanta Lite™ ASCA, Inova Diagnostics Inc, San Diego, USA)[50].

Data analysis

Comparison of allele and genotype frequencies was performed by Chi-square and Fisher exact tests when appropriate. Student's *t* test was used to compare means of continuous variables with the SPSS software ver. 11.5. Tests for Hardy-Weinberg equilibrium, linkage disequilibrium, haplotype frequency analysis and transmission disequilibrium were performed by the Haploview Software ver. 3.2 (http://www.broad.mit.edu/personal/jvbarret/haploview).

Power calculation was performed using the PS software (http://biostat.mc. vanderbilt. edu/twiki/bin/view/Main/PowerSampleSize).

Genotype-phenotype associations were analysed by means of univariate and multivariate stepwise logistic regression with the SPSS software. This approach allowed to take into account a dose-response effect (heterozygote or homozygote), the possible interactions between genes, and the effect of potential confounding variables (duration of follow-up, disease localization, etc.). The obtained *P* values were corrected (exact *P* value) for multiple comparisons. A possible interaction between CARD15, OCTN1/2, and DLG5 genes was also investigated.

RESULTS

Clinical findings

Main clinical characteristics of patients included in the study are depicted in Table 2.

The 200 CD patients had a mean age of 21 ± 8 years (range 1-18) with a slight male predominance (male/female = 115/85). The 186 UC patients had a mean age of 19 ± 9 years (range 1-18) with a female predominance (73/113). The mean age at diagnosis and the mean duration of follow-up (8-9 years) were similar between the two groups of patients. Eighteen percent

Table 2 Clinical and demographic characteristics of patients with CD and UC as evaluated in last follow-up (mean ± SD)

	Crohn's disease (n = 200)		Ulcerative colitis (n = 186)
Age (yr)	21 ± 8		19 ± 9
Age at diagnosis (yr)	12 ± 4		11 ± 5
Duration of follow-up (yr)	9 ± 7		8 ± 8
Sex (male/female)	115/85		73/113
Localization CD: n (%)			
- Ileum	38 (19)		
- Ileo-colon	116 (58)		
- Colon	45 (23)		
- Upper G-I tract	35 (18)[1]		
Localization UC: n (%)			
- Rectum-sigmoid			44 (24)
- Left colon			54 (29)
- Pancolitis			88 (47)
Disease type CD: n (%)	(Vienna)	(Montreal)	
- Inflammatory	104 (52)	135 (67)	
- Stricturing	40 (20)	45 (23)	
- Penetrating	56 (28)	20 (10)	
Growth delay: y/n (%)	60/84 (42)		21/126 (14)
Surgery: y/n (%)	51/149 (26)		13/137 (7)
EIM: y/n (%)	79/121 (40)		46/140 (25)
Perianal fistulae: y/n (%)	36/164 (18)		1/185 (0.5)
Family history: y/n (%)	18/182 (9)		22/164 (12)
ASCA: y/n (%)	77/32 (71)		18/57 (24)
ANCA: y/n (%)	18/86 (17)		65/50 (57)
Smoking y/n (%)	44/156 (22)		40/146 (21)

EIM: Extra-intestinal manifestations. [1]One patient had upper G-I involvement only.

of CD had an upper G-I involvement. The incidence of resective surgery (26% *vs* 7%, $P < 0.01$), extra-intestinal manifestations (40% *vs* 25%, $P = 0.002$), growth delay (42% *vs* 14%, $P < 0.001$) and perianal fistulae (18% *vs* 0.5%, $P < 0.001$) was significantly higher in CD than in UC patients. In the latter group, almost half of the patients had a pancolitis (47%). The incidence of ASCA and ANCA was 71% and 17% in CD patients, and 24% and 57% in UC patients, respectively, with a significant difference ($P < 0.0001$ and $P < 0.0001$, respectively).

Genotyping findings

The error rate of genotyping (defined as the percentages of disagreement in genotypes among 200 random samples tested in duplicate) was < 1% for all SNPs.

All genotypes in patients and healthy controls were in Hardy-Weinberg equilibrium. A strong linkage disequilibrium (D' > 91) was identified between the two OCTN1/2 variants, and between each OCTN1/2 variant and the IBD5 risk haplotype markers as well ($r^2 > 0.62$, $P < 0.001$) (Figure 1).

Table 3 summarizes the distribution of genotypes for the CARD15 variants (Arg702Trp, Gly908Arg and Leu1007fsinsC), OCTN1/2 variants (SLC22A4 and SLC22A5), the IBD5 risk haplotype SNPs (IGR2096a_1 and IGR2198a_1), and DLG5 gene polymorphism (113G→A).

Regarding the CARD15 gene, all three variants were frequently seen in CD patients as compared to controls ($P < 0.001$). By combining the three variants,

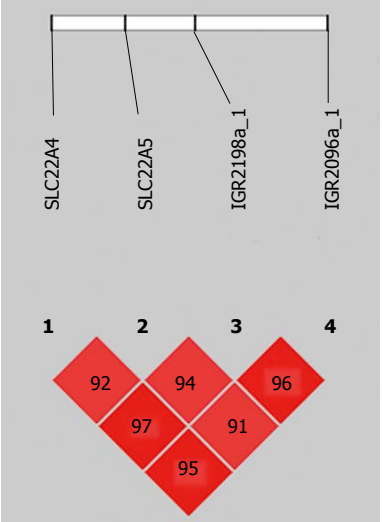

Figure 1 Evaluation of linkage disequilibrium in control subjects between IBD5 risk haplotype SNPs and OCTN1/2 variants ($r^2 > 0.62$; $P < 0.001$).

38% of CD patients had at least one mutation, and 15% had two mutations (homozygosis or compound heterozygosis). Respective figures in healthy controls were 15% and 1%. In carriers of one mutation, the odd risk was 2.7 (CI = 1.7-4.2; $P < 0.001$) while that for two mutations was 17 (CI = 5-58; $P < 0.001$).

As for the OCTN1 and OCTN2 variants, they were both significantly increased in CD patients for the homozygous genotype (1672TT: 24% *vs* 16% in controls, $P = 0.03$) (-207CC: 29% *vs* 21% in controls, $P = 0.03$). Moreover, the two-point haplotype, consisting of the 1672T and -207C alleles (OCTN-TC), was associated with CD (44.8% *vs* 38.3% in controls, $P = 0.043$). The 1672TT (22% *vs* 16% in controls) and -207CC (29% *vs* 21% in controls) genotypes were also increased in UC patients, the difference being statistically significant ($P = 0.10$ and $P = 0.05$, respectively). Accordingly, the frequency of TC haplotype was significantly increased also in UC patients (45.4% *vs* 38.3 in controls, $P = 0.03$).

The markers of IBD5 (IGR2096a_1 and IGR2198a_1) risk haplotype were both increased for the homozygous genotype in CD patients compared to controls, although with this sample size, only the AA genotype of the SNP IGR2096a_1 was significantly increased (23% *vs* 14% of controls, $P = 0.01$). Among individuals lacking the IBD5 risk haplotype (homozygous with respect to the non-risk associated allele of IGR2096a_1), only 7% of patients with CD and 5% of controls carried the TC haplotype, while in presence of the IBD5 risk haplotype, the TC haplotype was found in 61.9% of CD patients and 58.7% of controls. Similar data were obtained in UC patients (data not shown, available on request).

The distribution of 113G→A polymorphism of DLG5 was similar in patients and controls. No significant differences in allele or genotypes frequencies were noted. We also attempted to analyse the data based on gender of cases and controls based on the recent findings of male predominance[39], but results did not differ.

TDT analysis

TDT analysis of UC trios did not show significant transmission distortion of any genetic markers. As expected, a significant over-transmission towards affected

Table 3 Genotype distributions of CARD15, OCTN1-2, DLG5 genes, and IBD5 locus polymorphisms

SNPs	Genotype	Crohn's disease	*P* value OR 95% IC	Controls	*P* value OR 95% IC	Ulcerative colitis
CARD15			TT and CT *vs* CC			
R702W	TT	5 (3)	$P < 0.001$	1 (0)	NS	0 (0)
	CT	38 (19)	3.47 (2.06-5.86)	25 (7)		17 (9)
	CC	153 (78)		321 (93)		167 (91)
G908R	CC	2 (1)	CC and CG *vs* GG	0 (0)	NS	1 (1)
	CG	25 (13)	$P < 0.001$	18 (5)		12 (7)
	GG	170 (86)	2.90 (1.55-5.42)	329 (95)		171 (93)
1007fsInsC	CC	1 (1)	CC and CG *vs* GG	0 (0)	NS	0 (0)
	CG	25 (13)	$P = 0.0005$	11 (3)		10 (5)
	GG	172 (87)	4.62 (2.23-9.57)	336 (97)		176 (95)
OCTN1/2						
C1672T	TT	42 (24)	TT *vs* CT and CC	57 (16)	$P = 0.10$	36 (22)
	CT	79 (46)	$P = 0.03$	178 (51)		76 (47)
	CC	52 (30)	1.63 (1.04-2.56)	112 (32)		49 (30)
-G207C	CC	50 (29)	CC *vs* CG and GG	72 (21)	$P = 0.05$	46 (29)
	CG	84 (49)	$P = 0.035$	183 (53)		77 (48)
	GG	38 (22)	1.57 (1.03-2.38)	92 (27)		38 (24)
IBD5						
IGR2198a_1	GG	40 (21)	GG *vs* CG and CC	55 (16)	$P = 0.09$	39 (22)
	CG	93 (49)	$P = 0.13$	175 (50)		86 (48)
	CC	58 (30)		117 (34)		54 (30)
IGR2096a_1	AA	44 (23)	AA *vs* AC and CC	50 (14)	NS	32 (18)
	AC	89 (47)	$P = 0.01$	176 (51)		91 (51)
	CC	58 (30)	1.78 (1.13-2.79)	121 (35)		56 (31)
DLG5						
113G/A	AA	1 (1)	NS	2 (1)	NS	1 (1)
	AG	16 (10)		57 (16)		26 (15)
	GG	148 (90)		288 (83)		144 (84)

Table 4 Analysis of possible interaction between OCTN TC-haplotype and DLG5 variant with presence (or absence) of at least one CARD15 variant

		CD		UC		Controls	
CARD15		DLG5	OCTN TC haplotype (%)	DLG5	OCTN TC haplotype (%)	DLG5	OCTN TC haplotype (%)
CARD15+	DLG5+	5 (3)	42.6	7 (4)	35.2	11 (3)	44.8
	DLG5-	56 (34)		27 (16)		38 (12)	
CARD15-	DLG5+	12 (7)	46.2	20 (12)	48.7	44 (13)	39.1
	DLG5-	92 (56)		116 (68)		241 (72)	

DLG5-positive was defined as the AA or AG genotypes. Data expressed as absolute values or percentages (between brackets). All comparison had a *P* value > 0.05.

offspring was observed for CARD15 variants in CD trios: the Arg702Trp (transmitted/untrasmitted [T/U], 24/8, $P = 0.004$) and Leu1007fsinsC variants (T/U, 14/2, $P = 0.027$) were significantly over-transmitted. We did not observe distortion of transmission towards affected offspring for the Gly908Arg CARD15 variant, OCTN1/2 variants, and for the two IBD5 risk-haplotype-tagging SNPs IGR2198a_1 and IRG2096a_1. Regarding the DLG5 variant, an over-transmission of the wild-type allele of the 113G→A SNP towards affected offspring was found (T/U, 21/9, $P = 0.02$).

Gene-gene interaction

For the evaluation of gene-gene interactions, all subjects were stratified according to their CARD15 genotype. Genotypes and allele frequencies for the investigated variants of OCTN1/2 and TC haplotype, and for G113A variant of DLG5 were not different between CARD15-positive (carrying at least 1 CARD15 variant) and CARD15-negative subjects (Table 4). Similarly, no interactions between OCTN1/2 and DLG5 variants were found (data not shown, available on request).

Genotye-phenotype analysis

For the analysis of possible correlation between genotype and phenotype, patients were classified on the basis of presence or absence of at least one CARD15 variant, TC haplotype, and DLG5 risk genotype (carriers of the A allele). Data are shown in Table 5 and Table 6. CD patients carrying the CARD15 variants had more frequently ileal localization and less frequently a colonic localization (OR = 2.8, $P = 0.029$). Carriers of TC haplotype of OCTN1/2 variants had more occurrence of a penetrating disease (48.7% *vs* 43.5%) as compared with inflammatory/stricturing behaviour; this difference was statistically significant when perianal fistulae were not taken into account (62% *vs* 43%; $P = 0.038$) according to Montreal's classification. Similarly, a more frequent penetrating disease

Table 5 Genotype-phenotype correlation in CD patients evaluated by comparisons of carriers and non-carriers of at least one CARD15 variant (CARD15+), AA/AG genotypes of DLG5 variant (DLG5+) and presence of TC haplotype of OCTN1/2 variants (TC+)

CD *n* = 200	CARD15+ (*n* = 75)	CARD15- (*n* = 121)	DLG5+ (*n* = 17)	DLG5- (*n* = 148)	OCTN TC haplotype (%) +	-
Localization CD, *n* (%)						
Ileum	17 (23)	21 (17)	1 (6)	33 (22)	46	54
Ileo-colon	48 (64)	64 (53)	13 (76)	80 (54)	47	53
Colon	10 (13)	35 (29)	3 (18)	34 (23)	39	61
Upper G-I tract	16 (21)	18 (15)	3 (18)	29 (20)	53	47
Ileo *vs* colon	*P* = 0.029 OR 2.83 (1.10-7.33)					
Disease type CD, *n* (%)	Vienna-Montreal	Vienna-Montreal	Vienna-Montreal	Vienna-Montreal	V-M	V-M
- Inflammatory	37 (50) 48 (64)	66 (54) 86 (71)	7 41) 9 (52)	87 (59) 109 (74)	45/44	55/56
- Stenosing	19 (25) 21 (28)	19 (16) 22 (18)	4 (24) 4 (24)	26 (17) 30 (20)	40/41	60/59
- Penetrating	19 (25) 6 (8)	36 (30) 13 (11)	6 (35) 4 (24)	35 (24) 9 (6)	49/62	51/38
F *vs* S+ I (according to Montreal)			*P* = 0.011 OR 4.75 (1.29-17.57)		*P* = 0.038 OR 2.13 (1.03-4.4)	
Growth delay y/n, (%)	24/35 (41)	36/47 (43)	4/5 (44)	54/62 (47)	49/44	51/56
Resective surgery y/n, (%)	23/52 (31)	27/94 (22)	5/12 (29)	26/122 (18)	42/46	58/54
EIM y/n, (%)	27/48 (36)	49/72 (41)	9/8 (53)	58/90 (39)	40/48	60/52
Perianal fistulae y/n, (%)	13/62 (17)	23/98 (19)	2/15 (12)	26/122 (18)	45/45	55/55
ASCA (pos/neg), (%)	31/8 (79)	46/24 (66)	8/3 (73)	63/29 (68)	46/58	54/42
ANCA (pos/neg), (%)	5/26 (16)	13/59 (18)	1/11 (8)	15/66 (19)	44/49	56/51
Steroids need, y/n (%)	48/27 (64)	86/35 (71)	12/5(71)	96/52 (65)	43/48	57/52

P values are corrected for multiple comparisons.

Table 6 Genotype-phenotype correlation in UC patients evaluated by comparison of carriers vs non-carriers of at least one CARD15 variant (CARD15+), the AA/AG genotypes of DLG5 variant (DLG5+), and presence of TC haplotype of OCTN1/2 variants (TC+)

UC *n* = 186	CARD15+ (*n* = 36)	CARD15- (*n* = 148)	DLG5+ (*n* = 27)	DLG5- (*n* = 144)	OCTN TC haplotype (%) +	-
Localization UC, *n* (%)						
Rectum-sigmoid	7 (19)	36 (24)	9 (33)	28 (19)	45	55
Left colon	11 (31)	43 (29)	6 (22)	44 (31)	44	56
Pancolitis	18 (50)	69 (47)	12 (45)	72 (50)	47	53
Growth delay y/n, (%)	3/26 (10)	18/98 (16)	5/14 (26)	16/101 (14)	43/46	57/54
Resective surgery y/n, (%)	4/32 (11)	9/139 (6)	1/26 (4)	9/135 (6)	31/46	69/54
EIM y/n, (%)	9/27 (25)	37/111 (25)	4/23 (15)	40/104 (28)	51/44	49/56
ASCA (pos/neg), (%)	4/10 (29)	14/46 (23)	5/10 (33)	13/46 (22)	42/46	58/54
ANCA (pos/neg), (%)	13/6 (68)	52/43 (55)	11/8 (58)	52/40 (57)	43/40	57/60
Steroids need, y/n, (%)	26/10 (72)	109/39 (74)	21/6 (78)	105/39 (73)	46/46	54/54

(not including perianal fistulae) was found in CD patients with DLG5 risk variant (24% *vs* 6%; $P = 0.011$). No other significant differences were found between CD and UC patients (Table 6). No further correlation at this sample size could be observed when considering patients with two CARD15 variants, homozygous for TC haplotype or DLG5 variant. Similarly, no correlation could be found when evaluating subjects with all three concomitant gene variants (at least one CARD15 variant, OCTN TC-haplotype and DLG5 113G/A).

The correlations between at least one CARD15 variant with ileal localization (OR = 2.8, CI = 1.1-7.5; $P = 0.031$), OCTN TC-haplotype and DLG5 113G/A variant (OR = 4.05, CI = 1.05-15.5; $P = 0.041$) with penetrating disease were also confirmed at the stepwise logistic regression, after correction for potential confounders (duration of follow-up).

DISCUSSION

This study reports in the largest available cohort of pediatric IBD patients the contribution of variants of CARD15, OCTN1/2 and DLG5 genes on disease predisposition and correlation with phenotype. Reports of pediatric series to date available have been limited to mainly CARD15 variants[11-19], small number of subjects[11,12,15,16,18,19], and scarce information on UC patients[13,15,41].

The carriage rate of CARD15 variants in our pediatric population was 38% for CD patients and 20% for UC patients, not significantly different from figures in adult Italian population (36% for CD and 15% for UC, respectively)[51]. This finding is in agreement with previously reported frequencies in CD pediatric series ranging form 8.6% up to 60%, with lowest incidence in Swedish and Scottish population, similarly to the rates reported in corresponding adult population. Accordingly, this figure does not support the hypothesis of a stronger effect of CARD15 variants in early onset of CD. The relative contribution of each of the three common variants in our data is consistent with data from adult populations of IBD patients: 1007finsC confers the greatest risk (OR = 4.6, CI = 2.2-9.5) and G908R the least

(OR = 2.9, CI = 1.5-5.4). More specifically, the 1007finsC and R702W variants were associated with susceptibility to CD both in case control and family-based analysis, while the G908R variant was associated only in case control studies.

Homozygous carriers of OCTN1/2 variants were significantly more frequent in CD patients as compared to controls (OR = 1.6, $P = 0.03$). The TC haplotype was found in 44.8% of CD patients and 38.3% of controls ($P = 0.04$). No evidence of interaction with CARD15 gene was found since the frequency of TC haplotype was similar in CARD15-positive and CARD15-negative patients. Furthermore, a trend towards an increase of the homozygous carriers of OCTN1/2 variants was noticed in UC patients ($P = 0.05$), with a significant increase of TC haplotype (45.4%; $P = 0.03$), with similar finding in Italian adult population[33] and two other pediatric cohorts[41,42]. In contrast, no correlation of OCTN1/2 variants has been found in other pediatric series[43,44], perhaps for the smaller sample size of patients and controls. Our study confirmed the strong linkage disequilibrium between OCTN1/2 variants and SNPs tagging the IBD5 risk haplotype. Contrary to the Peltekova's study[20], the large majority of homozygous carriers of OCTN1/2 variants and TC haplotype were found in the background of IBD5-positive risk allele[35]. Although the possible causal role of the OCTN1/2 variants could not be excluded, further functional studies are needed to confirm and explain the role of these genes in IBD.

The DLG5 variant (G113A) was not correlated with pediatric IBD, even after stratifying patients and controls for gender in both the association study and family-based analysis. In addition, the A (risk) allele was significantly under-transmitted ($P = 0.02$), similarly to another adult series[31]. This might reflect a reduced effect of this variant in pediatric onset of IBD (5% *vs* > 10% in corresponding adult population)[39] and/or an insufficient power of the study sample. Based on the observed frequency of this variant in the control population (9%), our study sample could detect a ± 4.5% difference with a power of 90% and significance of 0.01.

No interaction between DLG5 variant and CARD15 or OCTN1/2 variants was found.

When the genotype-phenotype correlation was explored, there was only a weak correlation with ileal disease for CARD15 variants ($P < 0.03$) and penetrating disease for OCTN1/2 and DLG5 ($P < 0.04$, and $P < 0.02$, respectively). All these correlations were confirmed in the stepwise logistic regression analysis.

The correlation of CARD15 variants with ileal disease has been widely reported in most studies of adult[7] and child[11-14,41,44] Caucasian populations. Although some explanations for this consistent association have been put forward (e.g. presence of NOD2 in Paneth cells in terminal ileum, impaired regulation of Paneth-cell mediated antimicrobial response, perhaps through impaired production of α-defensin)[52], the clinical implications are unclear yet. Less than 50% of CD patients with ileal localization in this and other studies carry one CARD15 variant; moreover, carriers of this variant do not have a disease course and response to therapy, being different from non-carriers[53].

The association of OCTN1/2 and DLG5 variants with penetrating disease is intriguing since both genes are involved in maintaining mucosal integrity and permeability. A correlation between OCTN1/2 variants and penetrating disease has been reported in adult population[31-33], but not in the only two available studies in children with CD, in which no correlation[44] or only a correlation with growth delay was found[41]. Obviously, difference in selection of patients and duration of follow-up may explain this discrepancy. In our series, patients with penetrating disease were more than double than in the above-mentioned studies[41,44]. Moreover, our definition of growth delay (below 5th percentile) was more stringent than that of the Scottish study[41] (below 9th percentile). Nevertheless, when considering patients with both height and weight delay below the 5th percentile, a trend towards a correlation with TC-haplotype was found in our study ($P = 0.07$).

Regarding the correlation of DLG5 variant with penetrating disease, no reports are available so far in children with IBD. Moreover, data in adult population are very conflicting with no clear genotype-phenotype correlation demonstrated.

Finally, no correlation with age at diagnosis, family history, active and passive smoking, previous appendectomy, presence of ANCA and ASCA, growth delay, use of steroids, or need for surgery could be demonstrated in our series. Moreover, despite a significant increase of TC-haplotype of OCTN1/2 variants in UC patients, no correlation with any clinical phenotype was found. A potential limitation of this study lies in the large number of centres involved and the possible lack of reproducibility of clinical classification (disease behaviour). This choice allowed, however, to accomplish the study in the largest population of pediatric IBD patients so far for genetic purpose. Moreover, all patients were enrolled at academic referral centres and sorting of clinical features was obtained through a previously validated standardized questionnaire.

In conclusion, this study has demonstrated that the three common CARD15 variants and the recently described OCTN1/2 variants, but not the 113G/A DLG5 variant, are associated with susceptibility to CD in children. Furthermore, all three investigated genes exert a weak influence on clinical expression of CD; CARD15 variants (Arg702Trp, Gly908Arg and Leu1007fsinsC) are slightly more frequent in subjects with ileal localization, while OCTN (1672C/T and -207G/C) and DLG5 (113G/A) polymorphisms correlate with presence of penetrating behaviour.

ACKNOWLEDGMENTS

We thank Ms Ermelinda De Santo, Ms Tiziana Latiano, Ms Carla Zagaria and Mr Giuseppe Corritore for their skillful technical support. The following physicians contributed to the study by providing DNA samples and clinical information of their patients (number of probands between brackets): Roma: Cucchiara S, Borrelli O, Bascietto C (69); S. Giovanni Rotondo: Andriulli A, Annese V, Bossa F, Pastore M, D'Altilia M (75); Napoli:

Berni Canani E, Staiano AM (42); Padova: D'incà R, Sturniolo GC (36); Padova: Guariso G, Lodde V (33); Messina: Vieni G, Sferlazzas C (31); Bari: Rutigliano V, De Venuto D (15); Milano: Vecchi M, Saibeni S (15); Napoli: Riegler G (14); Parma: De Angelis GL (13); Roma: Caprilli R, Guagnozzi D (10); Reggio Calabria: Romano C (9); Palermo: Accomando S (8); Foggia: Campanozzi A (6), Firenze: Tonelli F (6) and Napoli: Castiglione F (4).

REFERENCES

1 **Armitage EL**, Aldhous MC, Anderson N, Drummond HE, Riemersma RA, Ghosh S, Satsangi J. Incidence of juvenile-onset Crohn's disease in Scotland: association with northern latitude and affluence. *Gastroenterology* 2004; **127**: 1051-1057

2 **Kugathasan S**, Judd RH, Hoffmann RG, Heikenen J, Telega G, Khan F, Weisdorf-Schindele S, San Pablo W, Perrault J, Park R, Yaffe M, Brown C, Rivera-Bennett MT, Halabi I, Martinez A, Blank E, Werlin SL, Rudolph CD, Binion DG. Epidemiologic and clinical characteristics of children with newly diagnosed inflammatory bowel disease in Wisconsin: a statewide population-based study. *J Pediatr* 2003; **143**: 525-531

3 **Hait E**, Bousvaros A, Grand R. Pediatric inflammatory bowel disease: what children can teach adults. *Inflamm Bowel Dis* 2005; **11**: 519-527

4 **Murch SH**, Baldassano R, Buller H, Chin S, Griffiths AM, Hildebrand H, Jasinsky C, Kong T, Moore D, Orsi M. Inflammatory bowel disease: Working Group report of the second World Congress of Pediatric Gastroenterology, Hepatology, and Nutrition. *J Pediatr Gastroenterol Nutr* 2004; **39** Suppl 2: S647-S654

5 **Hugot JP**, Chamaillard M, Zouali H, Lesage S, Cézard JP, Belaiche J, Almer S, Tysk C, O'Morain CA, Gassull M, Binder V, Finkel Y, Cortot A, Modigliani R, Laurent-Puig P, Gower-Rousseau C, Macry J, Colombel JF, Sahbatou M, Thomas G. Association of NOD2 leucine-rich repeat variants with susceptibility to Crohn's disease. *Nature* 2001; **411**: 599-603

6 **Ogura Y**, Bonen DK, Inohara N, Nicolae DL, Chen FF, Ramos R, Britton H, Moran T, Karaliuskas R, Duerr RH, Achkar JP, Brant SR, Bayless TM, Kirschner BS, Hanauer SB, Nuñez G, Cho JH. A frameshift mutation in NOD2 associated with susceptibility to Crohn's disease. *Nature* 2001; **411**: 603-606

7 **Economou M**, Trikalinos TA, Loizou KT, Tsianos EV, Ioannidis JP. Differential effects of NOD2 variants on Crohn's disease risk and phenotype in diverse populations: a metaanalysis. *Am J Gastroenterol* 2004; **99**: 2393-2404

8 **Kelsall B**. Getting to the guts of NOD2. *Nat Med* 2005; **11**: 383-384

9 **Hisamatsu T**, Suzuki M, Reinecker HC, Nadeau WJ, McCormick BA, Podolsky DK. CARD15/NOD2 functions as an antibacterial factor in human intestinal epithelial cells. *Gastroenterology* 2003; **124**: 993-1000

10 **Kobayashi KS**, Chamaillard M, Ogura Y, Henegariu O, Inohara N, Nuñez G, Flavell RA. Nod2-dependent regulation of innate and adaptive immunity in the intestinal tract. *Science* 2005; **307**: 731-734

11 **Wine E**, Reif SS, Leshinsky-Silver E, Weiss B, Shaoul RR, Shamir R, Wasserman D, Lerner A, Boaz M, Levine A. Pediatric Crohn's disease and growth retardation: the role of genotype, phenotype, and disease severity. *Pediatrics* 2004; **114**: 1281-1286

12 **Kugathasan S**, Collins N, Maresso K, Hoffmann RG, Stephens M, Werlin SL, Rudolph C, Broeckel U. CARD15 gene mutations and risk for early surgery in pediatric-onset Crohn's disease. *Clin Gastroenterol Hepatol* 2004; **2**: 1003-1009

13 **Russell RK**, Drummond HE, Nimmo EE, Anderson N, Smith L, Wilson DC, Gillett PM, McGrogan P, Hassan K, Weaver LT, Bisset M, Mahdi G, Satsangi J. Genotype-phenotype analysis in childhood-onset Crohn's disease: NOD2/CARD15 variants consistently predict phenotypic characteristics of severe disease. *Inflamm Bowel Dis* 2005; **11**: 955-964

14 **Tomer G**, Ceballos C, Concepcion E, Benkov KJ. NOD2/CARD15 variants are associated with lower weight at diagnosis in children with Crohn's disease. *Am J Gastroenterol* 2003; **98**: 2479-2484

15 **Ferraris A**, Knafelz D, Torres B, Fortina P, Castro M, Dallapiccola B. Analysis of CARD15 gene variants in Italian pediatric patients with inflammatory bowel diseases. *J Pediatr* 2005; **147**: 272-273

16 **Roesler J**, Thürigen A, Sun L, Koch R, Winkler U, Laass MW, Gahr M, Rösen-Wolff A, Henker J. Influence of CARD15 mutations on disease activity and response to therapy in 65 pediatric Crohn patients from Saxony, Germany. *J Pediatr Gastroenterol Nutr* 2005; **41**: 27-32

17 **Shaoul R**, Karban A, Weiss B, Reif S, Wasserman D, Pacht A, Eliakim R, Wardi J, Shirin H, Wine E, Leshinsky-Silver E, Levine A. NOD2/CARD15 mutations and presence of granulomas in pediatric and adult Crohn's disease. *Inflamm Bowel Dis* 2004; **10**: 709-714

18 **Weiss B**, Shamir R, Bujanover Y, Waterman M, Hartman C, Fradkin A, Berkowitz D, Weintraub I, Eliakim R, Karban A. NOD2/CARD15 mutation analysis and genotype-phenotype correlation in Jewish pediatric patients compared with adults with Crohn's disease. *J Pediatr* 2004; **145**: 208-212

19 **Ideström M**, Rubio C, Granath F, Finkel Y, Hugot JP. CARD15 mutations are rare in Swedish pediatric Crohn disease. *J Pediatr Gastroenterol Nutr* 2005; **40**: 456-460

20 **Peltekova VD**, Wintle RF, Rubin LA, Amos CI, Huang Q, Gu X, Newman B, Van Oene M, Cescon D, Greenberg G, Griffiths AM, St George-Hyslop PH, Siminovitch KA. Functional variants of OCTN cation transporter genes are associated with Crohn disease. *Nat Genet* 2004; **36**: 471-475

21 **Stoll M**, Corneliussen B, Costello CM, Waetzig GH, Mellgard B, Koch WA, Rosenstiel P, Albrecht M, Croucher PJ, Seegert D, Nikolaus S, Hampe J, Lengauer T, Pierrou S, Foelsch UR, Mathew CG, Lagerstrom-Fermer M, Schreiber S. Genetic variation in DLG5 is associated with inflammatory bowel disease. *Nat Genet* 2004; **36**: 476-480

22 **Rioux JD**, Daly MJ, Silverberg MS, Lindblad K, Steinhart H, Cohen Z, Delmonte T, Kocher K, Miller K, Guschwan S, Kulbokas EJ, O'Leary S, Winchester E, Dewar K, Green T, Stone V, Chow C, Cohen A, Langelier D, Lapointe G, Gaudet D, Faith J, Branco N, Bull SB, McLeod RS, Griffiths AM, Bitton A, Greenberg GR, Lander ES, Siminovitch KA, Hudson TJ. Genetic variation in the 5q31 cytokine gene cluster confers susceptibility to Crohn disease. *Nat Genet* 2001; **29**: 223-228

23 **Negoro K**, McGovern DP, Kinouchi Y, Takahashi S, Lench NJ, Shimosegawa T, Carey A, Cardon LR, Jewell DP, van Heel DA. Analysis of the IBD5 locus and potential gene-gene interactions in Crohn's disease. *Gut* 2003; **52**: 541-546

24 **Giallourakis C**, Stoll M, Miller K, Hampe J, Lander ES, Daly MJ, Schreiber S, Rioux JD. IBD5 is a general risk factor for inflammatory bowel disease: replication of association with Crohn disease and identification of a novel association with ulcerative colitis. *Am J Hum Genet* 2003; **73**: 205-211

25 **Armuzzi A**, Ahmad T, Ling KL, de Silva A, Cullen S, van Heel D, Orchard TR, Welsh KI, Marshall SE, Jewell DP. Genotype-phenotype analysis of the Crohn's disease susceptibility haplotype on chromosome 5q31. *Gut* 2003; **52**: 1133-1139

26 **Mirza MM**, Fisher SA, King K, Cuthbert AP, Hampe J, Sanderson J, Mansfield J, Donaldson P, Macpherson AJ, Forbes A, Schreiber S, Lewis CM, Mathew CG. Genetic evidence for interaction of the 5q31 cytokine locus and the CARD15 gene in Crohn disease. *Am J Hum Genet* 2003; **72**: 1018-1022

27 **Urcelay E**, Mendoza JL, Martinez A, Fernandez L, Taxonera C, Diaz-Rubio M, de la Concha EG. IBD5 polymorphisms in inflammatory bowel disease: association with response to infliximab. *World J Gastroenterol* 2005; **11**: 1187-1192

28 **Latiano A**, Palmieri O, Valvano RM, D'Incà R, Vecchi M, Ferraris A, Sturniolo GC, Spina L, Lombardi G, Dallapiccola B, Andriulli A, Devoto M, Annese V. Contribution of IBD5 locus to clinical features of IBD patients. *Am J Gastroenterol* 2006; **101**: 318-325

29 **McGovern DP**, Van Heel DA, Negoro K, Ahmad T, Jewell DP.

Further evidence of IBD5/CARD15 (NOD2) epistasis in the susceptibility to ulcerative colitis. *Am J Hum Genet* 2003; **73**: 1465-1466

30 **Török HP**, Glas J, Tonenchi L, Lohse P, Müller-Myhsok B, Limbersky O, Neugebauer C, Schnitzler F, Seiderer J, Tillack C, Brand S, Brünnler G, Jagiello P, Epplen JT, Griga T, Klein W, Schiemann U, Folwaczny M, Ochsenkühn T, Folwaczny C. Polymorphisms in the DLG5 and OCTN cation transporter genes in Crohn's disease. *Gut* 2005; **54**: 1421-1427

31 **Vermeire S**, Pierik M, Hlavaty T, Claessens G, van Schuerbeeck N, Joossens S, Ferrante M, Henckaerts L, Bueno de Mesquita M, Vlietinck R, Rutgeerts P. Association of organic cation transporter risk haplotype with perianal penetrating Crohn's disease but not with susceptibility to IBD. *Gastroenterology* 2005; **129**: 1845-1853

32 **Noble CL**, Nimmo ER, Drummond H, Ho GT, Tenesa A, Smith L, Anderson N, Arnott ID, Satsangi J. The contribution of OCTN1/2 variants within the IBD5 locus to disease susceptibility and severity in Crohn's disease. *Gastroenterology* 2005; **129**: 1854-1864

33 **Palmieri O**, Latiano A, Valvano R, D'Incà R, Vecchi M, Sturniolo GC, Saibeni S, Peyvandi F, Bossa F, Zagaria C, Andriulli A, Devoto M, Annese V. Variants of OCTN1-2 cation transporter genes are associated with both Crohn's disease and ulcerative colitis. *Aliment Pharmacol Ther* 2006; **23**: 497-506

34 **Newman B**, Gu X, Wintle R, Cescon D, Yazdanpanah M, Liu X, Peltekova V, Van Oene M, Amos CI, Siminovitch KA. A risk haplotype in the Solute Carrier Family 22A4/22A5 gene cluster influences phenotypic expression of Crohn's disease. *Gastroenterology* 2005; **128**: 260-269

35 **Reinhard C**, Rioux JD. Role of the IBD5 susceptibility locus in the inflammatory bowel diseases. *Inflamm Bowel Dis* 2006; **12**: 227-238

36 **Hampe J**, Schreiber S, Shaw SH, Lau KF, Bridger S, Macpherson AJ, Cardon LR, Sakul H, Harris TJ, Buckler A, Hall J, Stokkers P, van Deventer SJ, Nürnberg P, Mirza MM, Lee JC, Lennard-Jones JE, Mathew CG, Curran ME. A genomewide analysis provides evidence for novel linkages in inflammatory bowel disease in a large European cohort. *Am J Hum Genet* 1999; **64**: 808-816

37 **Daly MJ**, Pearce AV, Farwell L, Fisher SA, Latiano A, Prescott NJ, Forbes A, Mansfield J, Sanderson J, Langelier D, Cohen A, Bitton A, Wild G, Lewis CM, Annese V, Mathew CG, Rioux JD. Association of DLG5 R30Q variant with inflammatory bowel disease. *Eur J Hum Genet* 2005; **13**: 835-839

38 **Noble CL**, Nimmo ER, Drummond H, Smith L, Arnott ID, Satsangi J. DLG5 variants do not influence susceptibility to inflammatory bowel disease in the Scottish population. *Gut* 2005; **54**: 1416-1420

39 **Friedrichs F**, Brescianini S, Annese V, Latiano A, Berger K, Kugathasan S, Broeckel U, Nikolaus S, Daly MJ, Schreiber S, Rioux JD, Stoll M. Evidence of transmission ratio distortion of DLG5 R30Q variant in general and implication of an association with Crohn disease in men. *Hum Genet* 2006; **119**: 305-311

40 **Sun L**, Roesler J, Rösen-Wolff A, Winkler U, Koch R, Thürigen A, Henker J. CARD15 genotype and phenotype analysis in 55 pediatric patients with Crohn disease from Saxony, Germany. *J Pediatr Gastroenterol Nutr* 2003; **37**: 492-497

41 **Russell RK**, Drummond HE, Nimmo ER, Anderson NH, Noble CL, Wilson DC, Gillett PM, McGrogan P, Hassan K, Weaver LT, Bisset WM, Mahdi G, Satsangi J. Analysis of the influence of OCTN1/2 variants within the IBD5 locus on disease susceptibility and growth indices in early onset inflammatory bowel disease. *Gut* 2006; **55**: 1114-1123

42 **Babusukumar U**, Wang T, McGuire E, Broeckel U, Kugathasan S. Contribution of OCTN variants within the IBD5 locus to pediatric onset Crohn's disease. *Am J Gastroenterol* 2006; **101**: 1354-1361

43 **Bene J**, Magyari L, Talián G, Komlósi K, Gasztonyi B, Tari B, Várkonyi A, Mózsik G, Melegh B. Prevalence of SLC22A4, SLC22A5 and CARD15 gene mutations in Hungarian pediatric patients with Crohn's disease. *World J Gastroenterol* 2006; **12**: 5550-5553

44 **Ferraris A**, Torres B, Knafelz D, Barabino A, Lionetti P, de Angelis GL, Iacono G, Papadatou B, D'Amato G, Di Ciommo V, Dallapiccola B, Castro M. Relationship between CARD15, SLC22A4/5, and DLG5 polymorphisms and early-onset inflammatory bowel diseases: an Italian multicentric study. *Inflamm Bowel Dis* 2006; **12**: 355-361

45 **Podolsky DK**. Inflammatory bowel disease. *N Engl J Med* 2002; **347**: 417-429

46 **Gasche C**, Scholmerich J, Brynskov J, D'Haens G, Hanauer SB, Irvine EJ, Jewell DP, Rachmilewitz D, Sachar DB, Sandborn WJ, Sutherland LR. A simple classification of Crohn's disease: report of the Working Party for the World Congresses of Gastroenterology, Vienna 1998. *Inflamm Bowel Dis* 2000; **6**: 8-15

47 **Silverberg MS**, Satsangi J, Ahmad T, Arnott ID, Bernstein CN, Brant SR, Caprilli R, Colombel JF, Gasche C, Geboes K, Jewell DP, Karban A, Loftus EV, Peña AS, Riddell RH, Sachar DB, Schreiber S, Steinhart AH, Targan SR, Vermeire S, Warren BF. Toward an integrated clinical, molecular and serological classification of inflammatory bowel disease: report of a Working Party of the 2005 Montreal World Congress of Gastroenterology. *Can J Gastroenterol* 2005; **19** Suppl A: 5A-36A

48 **Sambrook J**, Fritsch EF, Maniatis F. Molecular cloning: a laboratory manual. Cold Spring Harbor, New York: Cold Spring Harbor Laboratory Press, 1989

49 **Lombardi G**, Annese V, Piepoli A, Bovio P, Latiano A, Napolitano G, Perri F, Conoscitore P, Andriulli A. Antineutrophil cytoplasmic antibodies in inflammatory bowel disease: clinical role and review of the literature. *Dis Colon Rectum* 2000; **43**: 999-1007

50 **Annese V**, Piepoli A, Perri F, Lombardi G, Latiano A, Napolitano G, Corritore G, Vandewalle P, Poulain D, Colombel JF, Andriulli A. Anti-Saccharomyces cerevisiae mannan antibodies in inflammatory bowel disease: comparison of different assays and correlation with clinical features. *Aliment Pharmacol Ther* 2004; **20**: 1143-1152

51 **Annese V**, Lombardi G, Perri F, D'Incà R, Ardizzone S, Riegler G, Giaccari S, Vecchi M, Castiglione F, Gionchetti P, Cocchiara E, Vigneri S, Latiano A, Palmieri O, Andriulli A. Variants of CARD15 are associated with an aggressive clinical course of Crohn's disease--an IG-IBD study. *Am J Gastroenterol* 2005; **100**: 84-92

52 **Strober W**, Murray PJ, Kitani A, Watanabe T. Signalling pathways and molecular interactions of NOD1 and NOD2. *Nat Rev Immunol* 2006; **6**: 9-20

53 **Louis E**, Michel V, Hugot JP, Reenaers C, Fontaine F, Delforge M, El Yafi F, Colombel JF, Belaiche J. Early development of stricturing or penetrating pattern in Crohn's disease is influenced by disease location, number of flares, and smoking but not by NOD2/CARD15 genotype. *Gut* 2003; **52**: 552-557

S- Editor Liu Y **L- Editor** Ma JY **E- Editor** Lu W

PO Box 2345, Beijing 100023, China
www.wjgnet.com
wjg@wjgnet.com

World J Gastroenterol 2007 February 28; 13(8): 1230-1235
World Journal of Gastroenterology ISSN 1007-9327

CLINICAL RESEARCH

Molecularly defined adult-type hypolactasia among working age people with reference to milk consumption and gastrointestinal symptoms

Sari R Anthoni, Heli A Rasinperä, Antti J Kotamies, Hanna A Komu, Harri K Pihlajamäki, Kaija-Leena Kolho, Irma E Järvelä

Sari R Anthoni, Kaija-Leena Kolho, Hospital for Children and Adolescents, University of Helsinki, Finland
Heli A Rasinperä, Hanna A Komu, Department of Medical Genetics, University of Helsinki, Finland
Antti J Kotamies, Helsinki Centre of Economic Research, Helsinki, Finland
Irma E Järvelä, Helsinki University Central Hospital, Laboratory of Molecular Genetics, Helsinki, Finland
Harri K Pihlajamäki, Central Military Hospital, Helsinki, Finland
Supported by the Sigrid Jusélius Foundation, Helsinki, Finland; the Foundation for Nutrition Research, Helsinki, Finland; the Research Foundation of Alfred Kordelin, Helsinki, Finland; Helsinki University Hospital Research Funding, Helsinki, Finland; the Foundation for Promoting Occupational Medicine in Finland, Helsinki, Finland; the Academy of Finland
Correspondence to: Dr. Irma Järvelä, University of Helsinki, Department of Medical Genetics Haartmaninkatu 8, FIN-00290 Helsinki, Finland. irma.jarvela@kolumbus.fi
Telephone: +358-50-5447030
Received: 2006-11-18 Accepted: 2007-02-08

Abstract

AIM: To study milk consumption and subjective milk-related symptoms in adults genotyped for adult-type hypolactasia.

METHODS: A total of 1900 Finnish adults were genotyped for the C/T$_{-13910}$ variant of adult-type hypolactasia and filled in a structured questionnaire concerning milk consumption and gastrointestinal problems.

RESULTS: The C/C$_{-13910}$ genotype of adult-type hypolactasia was present in 18% of the study population. The prevalence of the C/C$_{-13910}$ genotype was higher among subjects who were undergoing investigations because of abdominal symptoms (24%, $P < 0.05$). Those with the C/C$_{-13910}$ genotype drank less milk than subjects with either the C/T$_{-13910}$ or the T/T$_{-13910}$ genotype of lactase persistence (18% *vs* 38%; 18% *vs* 36%, $P < 0.01$). Subjects with the C/C$_{-13910}$ genotype had experienced more gastrointestinal symptoms (84%) during the preceding three-month period than those with the C/T$_{-13910}$ (79%, $P < 0.05$) or the T/T$_{-13910}$ genotype (78 %, $P < 0.05$). Only 9% (29/338) of the subjects with the C/C$_{-13910}$ genotype consumed milk and reported no symptoms from it.

CONCLUSION: Gastrointestinal symptoms are more common among adults with the C/C$_{-13910}$ genotype of adult-type hypolactasia than in those with genotypes of lactase persistence.

Key words: Lactase persistence; Lactose malabsorption; C/T$_{-13910}$ genotype; Abdominal symptoms; Milk consumption

Anthoni SR, Rasinperä HA, Kotamies AJ, Komu HA, Pihlajamäki HK, Kolho KL, Järvelä IE. Molecularly defined adult-type hypolactasia among working age people with reference to milk consumption and gastrointestinal symptoms. *World J Gastroenterol* 2007; 13(8): 1230-1235

http://www.wjgnet.com/1007-9327/13/1230.asp

INTRODUCTION

Gastrointestinal symptoms are a frequent cause for seeking medical advice in adult working age population[1]. Adult-type hypolactasia, characterised by the down regulation of lactase enzyme activity in the intestine during development is the most common enzyme deficiency in humans[2]. The symptoms caused by undigested lactose, bloating, diarrhoea and bowel gas are unspecific making the assessment of the diagnosis of adult-type hypolactasia a challenge to clinical practice. Symptoms vary greatly in severity and depend on the amount of lactose ingested and on individual sensitivity and may overlap with those of other gastrointestinal diseases such as irritable bowel syndrome (IBS) or diseases presenting with secondary lactose malabsorption, i.e. celiac disease[3]. Cases of individuals suspecting they have lactose intolerance are more common than the true prevalence of adult-type hypolactasia[4-9]. It has been shown that lactose-restricted diets improve symptoms markedly for example in IBS patients with lactose malabsorption and reduce the number of visits to the outpatient clinics[10]. Accurate diagnosis of lactose malabsorption, which is easily treatable by diet modification, would therefore be cost effective and time saving.

Diagnosis of adult-type hypolactasia has been based

on indirect methods, the lactose tolerance test (LTT) or breath hydrogen test (BHT). Specificity of the LTT ranges from 77% to 96%, and that of BHT from 89% to 100%. Sensitivities vary from 76% to 94% for LTT and from 69% to 100% for BHT[11]. These methods are time consuming for the patient and need substantial assistance by medical personnel. The determination of disaccharidase activities and lactase/sucrase ratios from the intestinal biopsy specimen would be the most accurate diagnostic method[12] but this invasive method is not suitable for everyday clinical practice.

It has been demonstrated that lactase non-persistence is inherited as an autosomal recessive trait. A proportion of the human population can digest lactose (lactase persistence) due to a mutation retaining lactase activity[13]. A single nucleotide polymorphism C to T located 13910 base pairs upstream the lactase gene is associated with the persistence/non-persistence trait in the Finnish families[14]. Analyses of several hundreds of intestinal biopsies have demonstrated that the C/C-13910 genotype is associated with low lactase activity (< 10 U/g/protein) and the C/T-13910 and T/T-13910 genotypes with high activity[14-16]. The prevalence of the C/T-13910 variant is compatible with the previously published figures for adult-type hypolactasia in European, Asian, African-American and Northern African populations[14-19]. It has been suggested, however, that in some African tribes the frequency of T-13910 allele does not parallel with the prevalence of lactase persistence[18]. Lactase mRNA transcribed from the C-13910 allele declines in the intestinal mucosa of children around five years of age[20], paralleling with the age of developmental down regulation of lactase enzyme activity[16]. *In vitro* -studies of the C/T-13910 variant have demonstrated greater increase in lactase promoter activity by the T-13910 variant[21,22]. This could possibly be explained by the recent finding of the T-13910 allele binding more strongly the transcription factor Oct-1 compared to the C-13910 allele[23]. Thus, the obtained functional data has given evidence for the use of the C/T-13910 variant as a robust marker for adult-type hypolactasia.

Here we have genotyped 1900 working-age people attending primary health care for the C/T-13910 variant associating with adult-type hypolactasia, and addressed the question about the prevalence and frequency of gastrointestinal symptoms as well as consumption of milk products.

MATERIALS AND METHODS

Participants

1902 adults from the capital area of Finland attending laboratory investigations in primary health care were asked to give a blood sample for genotyping of the C/T-13910 variant of adult-type hypolactasia and to fill in a questionnaire concerning the daily consumption of dairy products (normal and delactated milk, sour milk, yoghurt or ice cream, cheese) and possible milk related symptoms. The questions asked concerned whether or not a specific dairy product is included in the diet. Each participant was asked whether he/she had experienced any gastrointestinal complaints during the preceding three-month period. Frequency of gastrointestinal symptoms was also evaluated on daily and weekly basis. The questions on gastrointestinal symptoms covered: (1) the frequency of gastrointestinal symptoms such as flatulence, bloating, diarrhoea, heartburn, and constipation (2) the relation of their symptoms to meals, (3) correlation of the symptoms to different types of milk products or other foods, (4) previous diagnosis of lactose intolerance or a GI-disease such as colon cancer, celiac disease, or Helicobacter pylori infection. The age of the participants was ticked in questionnaire in three age groups (18-35 years, 36-51 years, and 52-64 years) due to the extensive number of study population. The formulated questionnaire was pre-tested on a small group of healthy adults. The collection of the questionnaires and blood samples occurred during a three-month period from February to May 2004. The study was approved by the Ethical Committee of the Helsinki University Central Hospital. All the subjects signed their written informed consent.

Genotyping

DNA of the study subjects (n = 1900) was isolated from peripheral blood samples by submerging a blank strip (Merck, Darmstadt, Germany) into EDTA blood. Strips were dried and heated in 1 × PCR reaction buffer (Dynazyme; Finnzymes, Espoo, Finland) containing 10 mmol/L Tris HCl (pH 8.8 at 25℃), 50 mmol/L KCl, 1.5 mmol/L $MgCl_2$, and 0.1% Triton X-100 to degrade proteins. After centrifuging 10 μL of the supernatant containing the DNA, the sample was amplified in a total volume of 50 μL, containing primers (one biotin-labeled 5'-(Biotin) CCTCGTTAATACCCACTGACCTA-3') (5 μmol/L) and one unmodified 5'-GTCACTTTGATATG ATGAGAGCA-3' (50 μmol/L), dNTPs (1000 μmol/L), 0.5 U of Taq polymerase (Dynazyme, Finnzymes) in a standard buffer. The PCR cycle conditions used were as following: an initial round of denaturation at 94℃ for 4 min, then 35 cycles at 94℃ for 30 s, 53℃ for 30 s, 72℃ for 1.15 min, and a final extension of 72℃ for 10 min. The resulting PCR products were analyzed by 1.5% agarose gel electrophoresis to verify the amplification and the size of the PCR product.

The C/T-13910 single nucleotide polymorphism was analysed using the solid-phase mini-sequencing method[24] that is based on the detection of tritium-labeled T-13910 and C-13910 alleles in the PCR reaction and measurement of their ratio using scintillation counter that directly reflects the ratio between the two sequences in the original sample. Briefly, in the mini-sequencing of the C/T-13910 single nucleotide polymorphism, two 10-μL aliquots of the biotin-labeled PCR product were captured to streptavidin coated microtitre wells (Thermo Electron, Helsinki, Finland). The reaction mixture contained 10 pmol of the detection primer (5'-GGCAATACAGATAAGATAATGT AG-3'), 0.1 μL of either ^{3}H-dCTP or ^{3}H-dTTP (Amersham Biosciences, Little Chalfont, Buckinghamshire, UK) and 0.05 U of DNA polymerase (Dynazyme Ⅱ, Finnzymes, Espoo, Finland). The reactions were allowed to occur for 15 min at 56℃ before washing off the unattached

label. Finally, the attached detection primer was eluted by NaOH treatment and the radioactivity measured in a liquid scintillation counter (Rackbeta 1209; Wallac, Turku, Finland).

Two samples of the 1902 were disqualified after being found infected with hepatitis B.

Statistical analyses

Statistical analyses were conducted using Tixel (version 8.1), which is a VBA-program for Excel. Descriptive analyses were conducted with simple logistic regression. Proportions were compared by using Chi-squared tests with continuity correction or Fisher's exact test when appropriate. Two-sided significance tests were used throughout.

RESULTS

The frequency of the C/C-13910 genotype associated with lactase non-persistence among the participants was 18% (Table 1). This figure corresponds to the earlier published prevalence of adult-type hypolactasia in the Finnish population[14-16], implying that the study population is representative for the general population. There was no difference in genotype distribution among male and female subjects, and no difference in separate age groups (data not shown).

The response rate for the questionnaire was high; a total of 99% (n = 1885) of the participants returned the questionnaire. A total of 42% of the patients reported a new, not gastrointestinal related disease as the reason for their laboratory visit. Earlier diagnosed diseases (25%) were the second most common cause for the visit, followed by gastrointestinal symptoms that were reported by 19% (348/1787) of the participants. Of these 348 subjects, the adult-type hypolactasia genotype C/C-13910 was observed in 24% (84/348), which was significantly more than in the study population ($P < 0.05$, Table 1).

Subjects with the C/C-13910 genotype had experienced more gastrointestinal symptoms (84%; 280/330) during the preceding three-month period than those with the C/T-13910 (79%; 698/885; $P < 0.05$) or the T/T-13910 genotype (78%; 501/641; $P < 0.05$, Table 2). Those with the C/C-13910 genotype reported more frequently gastrointestinal symptoms compared to C/T-13910 or T/T-13910 genotypes, but the difference was not significant (Table 2).

Gastrointestinal symptoms associated with lactose intolerance, namely flatulence, bloating and diarrhoea, were frequent among all genotype groups (Table 3). Flatulence was the only symptom significantly more frequent among the subjects with lactase non-persistent genotype compared to those with genotypes of lactase persistent ($P < 0.05$). Those with the C/C-13910 genotype experienced more bloating (61%) than those with the T/T-13910 genotype (55%) and C/T-13910 genotype (58%) but the difference did not reach statistical significance (Table 3).

As many as 45% of the participants informed having experienced gastrointestinal symptoms after drinking milk (Figure 1) and 25% of the participants reported symptoms from food containing milk. It is notable, that only 18% (60/338; $P < 0.01$)) of the subjects with the C/C-13910 genotype of adult-type hypolactasia informed drinking milk with meals, which is significantly less ($P < 0.01$) than those with the lactase persistent genotypes C/T-13910 (38%; 333/894) and T/T-13910 (36%; 236/653; Figure 1). The fat content of the milk was not questioned, but in Finland the vast majority of people use low-fat or fat-free milk as a drink. The number of people using low lactose containing milk as a drink was marginal according the questionnaire.

Table 1 Frequency of the C/T-13910 genotypes

Genotype	% (n)	GI-complaints % (n)	P
C/C-13910	18 (341)	24 (84)	< 0.05
C/T-13910	47 (901)	43 (148)	NS
T/T-13910	35 (658)	33 (116)	NS
Total	100 (1900)	100 (348)	

Only 9% (29/338) with the C/C-13910 genotype of adult-type hypolactasia consumed milk daily and reported no symptoms from milk. However, one third (18/60) of the milk drinkers with the C/C-13910 genotype did not answer the question about milk related symptoms. Most people with C/C-13910 genotype reporting GI-problems from milk (69%; 190/274) did not drink milk. The respective number of people with lactase persistence genotypes who reported milk-related problems and did not drink milk was 54% (299/554) for the C/T-13910 genotype and 50% (207/411) for the T/T-13910 genotype.

Cheese caused gastrointestinal symptoms for 11% of the participants according to their own judgment: for 17% of those with the C/C-13910 genotype, 10% of those with the C/T-13910 genotype and 9% of the ones with the T/T-13910 genotype ($P < 0.05$, Figure 2). Among all participants 14% experienced symptoms from cereal or bread, and 37% from ingested fat (Figure 1) and these were not related to the genotype of adult-type hypolactasia.

Among the study population, 15% (245/1649) reported having had a pathological LTT earlier: 36% (109/299) of those with the C/C-13910 genotype, 11% (82/777) with the C/T-13910 and 9% (54/573) with the T/T-13910 genotype.

A previous, pathological LTT was reported by 19% (64/341) of participants with the C/C-13910 genotype, by 10% (89/901) with the C/T-13910, and by 14% (91/658) with the T/T-13910 genotype. Five out of these 180 subjects with the C/T-13910 or T/T-13910 genotype with a pathological LTT reported a previously diagnosed possible secondary cause for hypolactasia i.e. celiac disease. An undiagnosed celiac disease in two other participants of these 180 subjects was suggested due to elevated level of transglutaminase antibodies in their sera[25].

DISCUSSION

The inability to absorb lactose is frequently suspected to underlie gastrointestinal symptoms in populations with high prevalence of adult-type hypolactasia and frequent dairy consumption. In this study we show that subjects with the C/C-13910 genotype, having low lactase activity in the intestinal wall[14-17,20] indeed do seek medical advice for

Table 2 The frequency of gastrointestinal symptoms according to the three genotype groups of lactase persistence/nonpersistence during previous three months

Abdominal complaints	C/C % (*n*)	C/T % (*n*)	T/T % (*n*)	OR C/C *vs* C/T (95% CI)	*P*	OR C/C *vs* T/T (95% CI)	*P*
During previous three months	84 (280/332)	79 (698/885)	78 (501/641)	1.44 (1.03-2.02)	< 0.05	1.50 (1.06-2.14)	< 0.05
Daily	23 (78/338)	22 (199/891)	19 (127/652)	1.04 (0.77-1.41)	NS	1.24 (0.90-1.71)	NS
Every other day	21 (72/338)	16 (145/891)	20 (129/652)	1.39 (1.02-1.91)	< 0.05	1.10 (0.79-1.52)	NS
Once a week	22 (74/338)	20 (176/891)	18 (115/652)	1.14 (0.84-1.55)	NS	1.31 (0.94-1.82)	NS
More seldom than once a week	17 (58/338)	20 (177/891)	21 (138/652)	0.84 (0.60-1.16)	NS	0.77 (0.55-1.08)	NS
No complaints	16 (52/332)	21 (187/885)	22 (140/641)	1.44 (1.03-2.02)	< 0.05	1.50 (1.06-2.13)	< 0.05

Table 3 The type of gastrointestinal symptoms among three genotype groups of lactase persistence/nonpersistence

Gastrointestinal symptoms	C/C % (*n* = 294)	C/T % (*n* = 725)	T/T % (*n* = 524)	OR C/C *vs* C/T (95% CI)	*P*	OR C/C *vs* T/T (95% CI)	*P*
Flatulence	79 (232)	73 (531)	73 (380)	1.37 (0.99-1.89)	< 0.05	1.42 (1.01-1.99)	< 0.05
Diarrhoea	40 (119)	38 (275)	40 (207)	1.11 (0.84-1.47)	NS	1.04 (0.78-1.39)	NS
Constipation	24 (72)	21 (152)	20 (107)	1.22 (0.89-1.68)	NS	1.26 (0.90-1.78)	NS
Bloating	61 (178)	58 (423)	55 (287)	1.10 (0.83-1.44)	NS	1.27 (0.94-1.69)	NS
Heartburn	32 (94)	37 (265)	38 (198)	0.82 (0.61-1.09)	NS	0.77 (0.57-1.04)	NS

Figure 1 Frequency of gastrointestinal symptoms experienced by various foods in the study population.

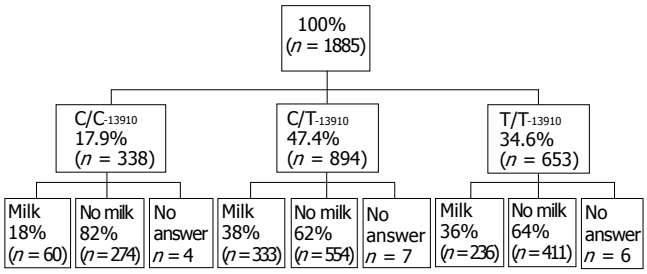

Figure 2 Flow-chart of the use of cow's milk as a drink in different genotype groups.

abdominal symptoms more often than subjects with high lactase activity. This occurred although they already had self restricted their milk consumption.

The response rate in this study was extremely high, 99%, thus the data about GI-symptoms was comprehensive. This exceptionally high response rate was achieved by the sound motivation of both the study subjects and the laboratory personnel. As expected, gastrointestinal symptoms were very common (80%) during the previous three months comparable to the earlier findings[1]. Flatulence was the only symptom that in this study was significantly more common among subjects with low lactase (C/C-13910 genotype). Diarrhoea and bloating, which according to earlier published studies are more common among lactose malabsorbers[4] were not more frequent among those with adult-type hypolactasia. These symptoms, however, were very common in the study population (40%-60%) pointing out the high prevalence of functional GI-symptoms[26].

The great majority of the study subjects did not drink milk at all. Milk consumption was rarest in the group of lactase non-persistent subjects: only 18% reported drinking milk daily, which might indicate that a natural aversion of milk has been developed by the subjects with low lactase activity. This is in agreement with our findings in a paediatric population in which children with the C/C-13910 genotype consumed less milk than children with a non-C/C-13910 genotype[16,27]. The majority of the children with the lactase non-persistent genotype C/C-13910 reported that they never drank milk[16]. At the age of 8-9 years, more than 40% of the subjects with the C/C-13910 genotype reported drinking less than one dl of milk daily, compared to 20% of the subjects with the C/T-13910 and T/T-13910 genotype, respectively[26].

Only 9% of those with the C/C-13910 genotype used daily milk and did not experience symptoms from ingested milk. This is in line with other studies[6,8,9] showing that not all individuals with lactose malabsorption report symptoms from food containing lactose. The colonic micro biota is variable[28] and the individual sensitivity to feel distension of the colon and to sense discomfort varies[29]. Accordingly, the recognition of the possible link between milk consumption and abdominal symptoms is not always easy[30]. The meal content has an effect on emptying of the stomach and thereby affects the lactose load in the

intestine[31,32]. Most lactose malabsorbers seem to tolerate small amounts of milk especially during meals[5,33]. Further studies are warranted to evaluate the amount of lactose tolerated by different genotype groups.

In this study population, 10% of those with the genotypes associated with lactase persistence (the C/T-13910 genotype or T/T-13910 genotype) reported that they had been earlier diagnosed lactose intolerant based on results of LTT. A possible cause for secondary hypolactasia, i.e. celiac disease, was found in 3% of these individuals. These findings imply that LTT, a commonly used method for diagnosis of lactose intolerance, produces high numbers of false positive test results as has been earlier observed[11]. One third of those with the C/C-13910 genotype associated with low lactase reported that they had previously had a positive LTT. Due to the way our question on earlier diagnosis of lactose intolerance was formulated, we do not know the extent of subjects with the C/C-13910 genotype who might have had a negative result for their LTT.

In conclusion, gastrointestinal symptoms are more common among adults with the C/C-13910 genotype of adult-type hypolactasia than in those with genotypes of lactase persistence. This was seen although individuals with the C/C-13910 genotype had restricted their milk consumption. Genotyping of the C/T-13910 polymorphism is a practical means for defining adult-type hypolactasia.

ACKNOWLEDGMENTS

We are grateful to the participants and the laboratory personnel of the outpatient clinics of the city of Espoo and the Central Military Hospital for their contribution.

REFERENCES

1 **Drossman DA**, Li Z, Andruzzi E, Temple RD, Talley NJ, Thompson WG, Whitehead WE, Janssens J, Funch-Jensen P, Corazziari E. U.S. householder survey of functional gastrointestinal disorders. Prevalence, sociodemography, and health impact. *Dig Dis Sci* 1993; **38**: 1569-1580
2 **Järvelä IE**. Molecular genetics of adult-type hypolactasia. *Ann Med* 2005; **37**: 179-185
3 **Tamm A**. Management of lactose intolerance. *Scand J Gastroenterol Suppl* 1994; **202**: 55-63
4 **Jussila J**, Launiala K, Gorbatow O. Lactase deficiency and a lactose-free diet in patients with "unspecific abdominal complaints". *Acta Med Scand* 1969; **186**: 217-222
5 **Vesa TH**, Korpela RA, Sahi T. Tolerance to small amounts of lactose in lactose maldigesters. *Am J Clin Nutr* 1996; **64**: 197-201
6 **Carroccio A**, Montalto G, Cavera G, Notarbatolo A. Lactose intolerance and self-reported milk intolerance: relationship with lactose maldigestion and nutrient intake. Lactase Deficiency Study Group. *J Am Coll Nutr* 1998; **17**: 631-636
7 **Saltzman JR**, Russell RM, Golner B, Barakat S, Dallal GE, Goldin BR. A randomized trial of Lactobacillus acidophilus BG2FO4 to treat lactose intolerance. *Am J Clin Nutr* 1999; **69**: 140-146
8 **de Vrese M**, Stegelmann A, Richter B, Fenselau S, Laue C, Schrezenmeir J. Probiotics--compensation for lactase insufficiency. *Am J Clin Nutr* 2001; **73**: 421S-429S
9 **Johnson AO**, Semenya JG, Buchowski MS, Enwonwu CO, Scrimshaw NS. Correlation of lactose maldigestion, lactose intolerance, and milk intolerance. *Am J Clin Nutr* 1993; **57**: 399-401
10 **Böhmer CJ**, Tuynman HA. The effect of a lactose-restricted diet in patients with a positive lactose tolerance test, earlier diagnosed as irritable bowel syndrome: a 5-year follow-up study. *Eur J Gastroenterol Hepatol* 2001; **13**: 941-944
11 **Arola H**. Diagnosis of hypolactasia and lactose malabsorption. *Scand J Gastroenterol Suppl* 1994; **202**: 26-35
12 **Dahlqvist A**. Assay of intestinal disaccharidases. *Scand J Clin Lab Invest* 1984; **44**: 169-172
13 **Sahi T**, Isokoski M, Jussila J, Launiala K, Pyörälä K. Recessive inheritance of adult-type lactose malabsorption. *Lancet* 1973; **2**: 823-826
14 **Enattah NS**, Sahi T, Savilahti E, Terwilliger JD, Peltonen L, Järvelä I. Identification of a variant associated with adult-type hypolactasia. *Nat Genet* 2002; **30**: 233-237
15 **Kuokkanen M**, Enattah NS, Oksanen A, Savilahti E, Orpana A, Järvelä I. Transcriptional regulation of the lactase-phlorizin hydrolase gene by polymorphisms associated with adult-type hypolactasia. *Gut* 2003; **52**: 647-652
16 **Rasinperä H**, Savilahti E, Enattah NS, Kuokkanen M, Tötterman N, Lindahl H, Järvelä I, Kolho KL. A genetic test which can be used to diagnose adult-type hypolactasia in children. *Gut* 2004; **53**: 1571-1576
17 **Swallow DM**. Genetics of lactase persistence and lactose intolerance. *Annu Rev Genet* 2003; **37**: 197-219
18 **Mulcare CA**, Weale ME, Jones AL, Connell B, Zeitlyn D, Tarekegn A, Swallow DM, Bradman N, Thomas MG. The T allele of a single-nucleotide polymorphism 13.9 kb upstream of the lactase gene (LCT) (C-13.9kbT) does not predict or cause the lactase-persistence phenotype in Africans. *Am J Hum Genet* 2004; **74**: 1102-1110
19 **Myles S**, Bouzekri N, Haverfield E, Cherkaoui M, Dugoujon JM, Ward R. Genetic evidence in support of a shared Eurasian-North African dairying origin. *Hum Genet* 2005; **117**: 34-42
20 **Rasinperä H**, Kuokkanen M, Kolho KL, Lindahl H, Enattah NS, Savilahti E, Orpana A, Järvelä I. Transcriptional downregulation of the lactase (LCT) gene during childhood. *Gut* 2005; **54**: 1660-1661
21 **Olds LC**, Sibley E. Lactase persistence DNA variant enhances lactase promoter activity in vitro: functional role as a cis regulatory element. *Hum Mol Genet* 2003; **12**: 2333-2340
22 **Troelsen JT**, Olsen J, Møller J, Sjöström H. An upstream polymorphism associated with lactase persistence has increased enhancer activity. *Gastroenterology* 2003; **125**: 1686-1694
23 **Lewinsky RH**, Jensen TG, Møller J, Stensballe A, Olsen J, Troelsen JT. T-13910 DNA variant associated with lactase persistence interacts with Oct-1 and stimulates lactase promoter activity in vitro. *Hum Mol Genet* 2005; **14**: 3945-3953
24 **Syvänen AC**, Aalto-Setälä K, Harju L, Kontula K, Söderlund H. A primer-guided nucleotide incorporation assay in the genotyping of apolipoprotein E. *Genomics* 1990; **8**: 684-692
25 **Tikkakoski S**, Savilahti E, Kolho KL. Undiagnosed coeliac disease and nutritional deficiencies in adults screened in primary health care. *Scand J Gastroenterol* 2007; **42**: 60-65
26 **Hillilä MT**, Färkkilä MA. Prevalence of irritable bowel syndrome according to different diagnostic criteria in a non-selected adult population. *Aliment Pharmacol Ther* 2004; **20**: 339-345
27 **Rasinpera H**, Saarinen K, Pelkonen A, Jarvela I, Savilahti E, Kolho KL. Molecularly defined adult-type hypolactasia in school-aged children with a previous history of cow's milk allergy. *World J Gastroenterol* 2006; **12**: 2264-2268
28 **Egert M**, de Graaf AA, Smidt H, de Vos WM, Venema K. Beyond diversity: functional microbiomics of the human colon. *Trends Microbiol* 2006; **14**: 86-91
29 **Vesa TH**, Seppo LM, Marteau PR, Sahi T, Korpela R. Role of irritable bowel syndrome in subjective lactose intolerance. *Am J Clin Nutr* 1998; **67**: 710-715
30 **Suarez FL**, Savaiano DA, Levitt MD. A comparison of symptoms after the consumption of milk or lactose-hydrolyzed milk by people with self-reported severe lactose

intolerance. *N Engl J Med* 1995; **333**: 1-4
31 **Martini MC**, Savaiano DA. Reduced intolerance symptoms from lactose consumed during a meal. *Am J Clin Nutr* 1988; **47**: 57-60
32 **Vesa TH**, Marteau PR, Briet FB, Boutron-Ruault MC, Rambaud JC. Raising milk energy content retards gastric emptying of lactose in lactose-intolerant humans with little effect on lactose digestion. *J Nutr* 1997; **127**: 2316-2320
33 **Vesa TH**, Marteau P, Korpela R. Lactose intolerance. *J Am Coll Nutr* 2000; **19**: 165S-175S

S- Editor Liu Y **L- Editor** Zhu LH **E- Editor** Lu W

PO Box 2345, Beijing 100023, China
www.wjgnet.com
wjg@wjgnet.com

World J Gastroenterol 2007 February 28; 13(8): 1236-1239
World Journal of Gastroenterology ISSN 1007-9327

RAPID COMMUNICATION

Clinical investigation of 41 patients with ischemic colitis accompanied by ulcer

Satohiro Matsumoto, Kenichiro Tsuji, Satoshi Shirahama

Satohiro Matsumoto, Kenichiro Tsuji, Satoshi Shirahama, Department of Internal Medicine, Kamigoto Hospital, Nagasaki, Japan
Correspondence to: Satohiro Matsumoto, MD, Department of Internal Medicine, Kamigoto Hospital, 1549-11 Aokata-gou, Shinkamigoto-cho, Minamimatsuura-gun, Nagasaki 8574404, Japan. hiyo-mana@gol.com
Telephone: +81-959-523000 Fax: +81-959-522981
Received: 2006-12-13 Accepted: 2007-01-29

Abstract

AIM: To investigate the relationship among the presence of ulcer lesions, underlying disease, and clinical course in patients with ischemic colitis.

METHODS: The subjects were 41 patients (10 male and 31 female; mean age 70 years) with ischemic colitis who were admitted to and received treatment in our hospital from 2000 to 2006. We compared their characteristics and analyzed the mean lengths of admission and fasting for 9 patients with ulcer lesions (ulcer group) and 32 without (non-ulcer group).

RESULTS: The groups with presence and absence of ulcer differed significantly only in white blood cell (WBC) count. Lengths of fasting and admission were 7.9 d and 17.9 d for the ulcer group and 4.4 d and 10.7 d for the non-ulcer group, respectively, and significantly longer in the ulcer group (P = 0.0057 and 0.0001). There was no correlation between presence of ulcer and presence of underlying diseases.

CONCLUSION: Lengths of fasting and admission were significantly longer in patients with ischemic colitis with ulcer than for those without ulcer.

Key words: Ischemic colitis; Ulcer; Fasting; Admission; White blood cell

Matsumoto S, Tsuji K, Shirahama S. Clinical investigation of 41 patients with ischemic colitis accompanied by ulcer. *World J Gastroenterol* 2007; 13(8): 1236-1239

http://www.wjgnet.com/1007-9327/13/1236.asp

INTRODUCTION

Ischemic colitis was first reported as a result of reversible vascular occlusion of the colon in 1963 by Boley *et al*[1], and in 1966 Marston *et al*[2] suggested the name "ischemic colitis" for it and clarified its clinical and histopathological features.

Marston *et al*[2] classified this disease into 3 forms, transient, strictures, and gangrene. It is defined as a "reversible condition caused by obstruction of blood flow in intestinal tract mucosa without apparent blockage of the main artery". In general, it is common in the elderly[3], and its prevalence increases with age, although it is seen in younger patients as well[4-6]. Its causes include vascular factors such as ischemia and embolus[7-9], intestinal factors such as constipation[5,10], irritable bowel syndrome[11,12] and history of intestinal surgery[13,14] as well as administration of drugs such as alosetron[11], cocaine[15], non-steroidal anti-inflammatory drugs[16], oral contraceptives[17] and oral laxatives[18].

While surgery is indicated for the gangrenous form of this disease, transient and stricturing forms are often ameliorated by bowel rest, fasting, and parenteral fluid administration alone. The lengths of fasting and admission vary among individuals. Significant prolongation of healing is sometimes observed, especially in patients with ulcer. We therefore examined the associations among etiology, clinical course, and presence of ulcer lesions in patients with transient and stricturing forms of ischemic colitis.

MATERIALS AND METHODS

The subjects were 41 patients (10 male and 31 female; mean age 70 years) with ischemic colitis who were admitted to and received treatment in our hospital from 2000 to 2006. Patients who developed ischemic colitis during admission for other diseases were excluded. Ischemic colitis was diagnosed comprehensively based on the essential criteria including lack of antibiotic administration, negative bacterial culture of feces or biopsy, lack of history of inflammatory bowel disease (IBD), as well as endoscopic and histopathological findings on biopsy. Age and mode of disease onset, symptoms and affected sites were included as complementary parameters.

Patients were divided into 2 groups by the presence of ulcer lesions and compared for age, gender, affected sites, hematological findings, performance status (0-4, 0: asymptomatic; 1: symptomatic but completely ambulant; 2: symptomatic, < 50% in bed during day time; 3:

Table 1 Clinical features of ischemic colitis patients: Comparison between ulcer and non-ulcer groups (mean ± SD)

Clinical features	Ulcer group (n = 9)	Non-ulcer group (n = 32)	Statistical significance
Age (mean, range, yr)	68 ± 19 (35-87)	71 ± 11 (42-92)	NS
Percentage of females (%)	77.8	75.0	NS
Lesion location: left colon (%)	88.9	100	NS
Performance status 0-1 (%)	77.8	87.5	NS
WBC ($\times 10^9$/L)	12.27 ± 4.67	8.44 ± 3.17	P = 0.0065
CRP (mg/dL)	2.6 ± 4.1	1.5 ± 2.3	NS
K (mEq/L)	3.8 ± 0.4	4.0 ± 0.5	NS
Total cholesterol (mg/dL)	179.3 ± 30.6	191.4 ± 35.6	NS
TG (mg/dL)	93.3 ± 41.0	73.2 ± 23.4	NS
LDH (IU/L)	190.0 ± 42.8	203.8 ± 37.8	NS
CPK (IU/L)	80.7 ± 38.9	82.7 ± 39.5	NS

Percentage of females and lesion location were evaluated with an χ-square test; Other data were evaluated with Student's t test after skewing with log transformation. CRP: C-reactive protein; K: potassium; TG: triglyceride; LDH: lactate dehydrogenase; CPK: creatinine phosphokinase.

Table 2 Underlying diseases: Comparison between ulcer and non-ulcer groups n (%)

	Ulcer group (n = 9)	Non-ulcer group (n = 32)	Statistical significance
Hypertension	6 (66.7)	19 (59.4)	NS
Hyperlipemia	0	6 (18.8)	NS
Diabetes mellitus	1 (11.1)	3 (9.4)	NS
Atrial fibrillation	1 (11.1)	1 (3.1)	NS
Cerebral infarction	1 (11.1)	2 (6.3)	NS
Chronic constipation	5 (55.6)	19 (59.4)	NS
Medications			
NSAIDS	0	1 (3.1)	NS
Antihypertensive agents	5 (55.6)	18 (56.3)	NS
Others	2 (22.2)	5 (15.6)	NS
History of abdominal surgery	4 (44.4)	14 (43.8)	NS

Percentages were evaluated with an χ-square test. NSAIDS: non-steroidal anti-inflammatory agents.

symptomatic, > 50% of time in bed, but not bed bound; 4: bed bound, using the WHO score criteria), underlying disease (hypertension, hyperlipemia, diabetes, chronic atrial fibrillation, cerebral infarction, constipation, and history of abdominal surgery), oral medications, and mean lengths of fasting and admission.

All patients underwent endoscopy of the lower gastrointestinal tract within 3 d after admission and 5 d after disease onset. As treatment, fasting and bowel rest with fluid replacement were used in all patients. Twenty-two (53.7%) patients received oral antiflatulents and 13 (31.7%) patients a combination with antibiotics. Total parenteral nutrition *via* a central venous line was performed in none of the patients. After disappearance of abdominal pain, patients were allowed to begin oral ingestion. Patients were discharged if they exhibited no relapse of symptoms after restarting oral ingestion.

Statistical analysis

Data are expressed as mean ± SD or percentage. Percentage of females, lesion location, performance status and underlying systemic diseases were evaluated with an X-square test. Other data were evaluated with Student's t test after skewing variable with log transformation. All data analysis was performed with the StatView 5.0. Statistical significance was set at $P < 0.05$.

RESULTS

Forty-one patients were analyzed (10 male and 31 female; mean age 70 years). Affected sites included the sigmoid colon (70.7%), descending colon (51.2%), transverse colon (12.2%), rectum (4.9%), and ascending colon (2.4%), with some overlap. The disease developed in 92.7% of the patients for the first time, and the remaining 7.3% for the second time. The disease was accompanied by ulcer in 9 (22.0%) patients.

Nine patients had ulcer (2 male and 7 female; mean age 66, range 35-87 years), the affected site was the left hemicolon in 8 patients. On the other hand, 32 patients had no ulcer (8 male and 24 female; mean age 71, range 42-92 years), the affected site was in the left hemicolon in all of them. In both groups, underlying diseases including hypertension, hyperlipemia, diabetes, atrial fibrillation, cerebral infarction, chronic constipation, and history of abdominal surgery, as well as oral medications, performance status, and hematological findings were examined as parameters. The significant difference was found between groups only in white blood cells (WBC), which was higher in the ulcer group (12.27×10^9/L) than in the non-ulcer group (8.44×10^9/L, P = 0.0065; Table 1). There were no statistically significant differences between groups in other parameters (Table 1 and Table 2).

Lengths of fasting and admission were 7.9 d and 17.9 d for the ulcer group and 4.4 and 10.7 d for the non-ulcer

Table 3 Durations of fasting and hospitalization: Comparison between ulcer and non-ulcer groups (mean ± SD)

	Ulcer group (n = 9)	Non-ulcer group (n = 32)	Statistical significance
Fasting (d)	7.9 ± 4.1	4.4 ± 2.9	P = 0.0057
Hospitalization (d)	17.9 ± 6.8	10.7 ± 3.6	P = 0.0001

group, respectively, being significantly longer in the ulcer group (P = 0.0057 and 0.0001; Table 3).

DISCUSSION

The etiology of ischemic colitis remains unclear. However, it may involve combination of vascular factors such as hypertension or hyperlipemia and intestinal factors such as chronic constipation and history of abdominal surgery. These may cause reduction of blood flow in the mucosa or wall of the intestinal tract, leading to ischemia. In the present study, patients with hypertension (61%), chronic constipation (58.5%), and history of abdominal surgery (43.9%) exhibited higher prevalence of ischemic colitis, which are consistent with previous reports[19,20].

Tohda *et al*[7] detected the correlation between arteriosclerosis and ischemic colitis using pulse wave velocity (PWV) as an indicator related to vascular factors, and reported higher PWV levels for the elderly. Similarly, we compared the contributions of vascular and intestinal factors to the occurrence of ischemic colitis in age, and observed that 2 (25%) patients developed the disease because of vascular factors and 7 (87.5%) patients because of intestinal factors among the eight younger patients aged less than 60 years. This indicates that vascular factors contribute predominantly to development of ischemic colitis.

In the present study, only WBC at admission was correlated with presence of ulcer. Notably, no difference in number of WBC between *H pylori*-infected patients with gastritis and those with ulcer has been noted[21]. Additionally, little difference has been reported in number of WBC between those with active disease and those with inactive disease in patients with inflammatory bowel disease[22]. Bjornestad *et al*[23] performed three routine laboratory tests (white blood cell count, hemoglobin concentration and erythrocyte volume fraction) in patients with four acute abdominal diseases (acute mesenteric ischemia: AMI, perforation of colon, perforation of peptic ulcer and intestinal obstruction). The WBC in patients with AMI was significantly higher than the normal range. The three variables were higher in AMI patients than in the other patients ($P < 0.001$). The discriminant analysis of the variables classified 80% of the patients correctly into AMI and non-AMI groups. This difference may reflect the inflammatory response in the acute stage and biological reactions associated with continued chronic inflammation.

This is the first report on lengths of fasting and admission in patients with ischemic colitis. In the present study, these lengths were 7.9 d and 17.9 d for the ulcer group and 4.4 d and 10.7 d for the non-ulcer group, respectively, being significantly longer in the ulcer group. Although we did not evaluate patient quality of life (QOL), stress on patients due to fasting and prolonged admission may cause a decrease in QOL. In addition, the costs associated with prolonged admission also causes a problem.

Strategies for the treatment of ischemic colitis are determined based on the severity of ischemia. Surgery is indicated for the gangrenous form of the disease. On the other hand, for transient and stricturing forms of the disease, younger patients may obtain prompt relief solely with follow-up, while older patients or those who have severe abdominal pain will require hospitalization, fasting, and management using parenteral fluid administration.

Lengths of fasting and admission were significantly longer in patients with ischemic colitis with ulcer than in those without ulcer. Ulcer associated with ischemic colitis is often localized in the left hemicolon. Noninvasive and local ulcer treatment such as use of enema preparations in addition to conventional treatment centering on bowel rest should be considered for ischemic enteritis accompanied by ulcer.

REFERENCES

1 **Boley SJ**, Schwartz S, Lash J, Sternhill V. Reversible vascular occlusion of the colon. *Surg Gynecol Obstet* 1963; **116**: 53-60
2 **Marston A**, Pheils MT, Thomas ML, Morson BC. Ischaemic colitis. *Gut* 1966; **7**: 1-15
3 **Higgins PD**, Davis KJ, Laine L. Systematic review: the epidemiology of ischaemic colitis. *Aliment Pharmacol Ther* 2004; **19**: 729-738
4 **Clark AW**, Lloyd-Mostyn RH, de Sadler MR. "Ischaemic" colitis in young adults. *Br Med J* 1972; **4**: 70-72
5 **Matsumoto T**, Iida M, Kimura Y, Nanbu T, Fujishima M. Clinical features in young adult patients with ischaemic colitis. *J Gastroenterol Hepatol* 1994; **9**: 572-575
6 **Shibata M**, Nakamuta H, Abe S, Kume K, Yoshikawa I, Murata I, Otsuki M. Ischemic colitis caused by strict dieting in an 18-year-old female: report of a case. *Dis Colon Rectum* 2002; **45**: 425-428
7 **Tohda G**, Higashi S, Sumiyoshi K, Sakumoto H, Kato C, Kane T. Evaluation of clinical features of ischemic colitis:comparison between young and elderly. *Dig Endoscopy* 2005; **17**: 123-130
8 **Collet T**, Even C, Bouin M, Lecluse E, Piquet MA, Crampon D, Grollier G, Dao T, Verwaerde JC. Prevalence of electrocardiographic and echocardiographic abnormalities in ambulatory ischemic colitis. *Dig Dis Sci* 2000; **45**: 23-25
9 **Hourmand-Ollivier I**, Bouin M, Saloux E, Morello R, Rousselot P, Piquet MA, Dao T, Verwaerde JC. Cardiac sources of embolism should be routinely screened in ischemic colitis. *Am J Gastroenterol* 2003; **98**: 1573-1577
10 **Habu Y**, Tahashi Y, Kiyota K, Matsumura K, Hirota M, Inokuchi H, Kawai K. Reevaluation of clinical features of ischemic colitis. Analysis of 68 consecutive cases diagnosed by early colonoscopy. *Scand J Gastroenterol* 1996; **31**: 881-886
11 **Friedel D**, Thomas R, Fisher RS. Ischemic colitis during treatment with alosetron. *Gastroenterology* 2001; **120**: 557-560
12 **Miller DP**, Alfredson T, Cook SF, Sands BE, Walker AM. Incidence of colonic ischemia, hospitalized complications of constipation, and bowel surgery in relation to use of alosetron

hydrochloride. *Am J Gastroenterol* 2003; **98**: 1117-1122
13 **Welch M**, Baguneid MS, McMahon RF, Dodd PD, Fulford PE, Griffiths GD, Walker MG. Histological study of colonic ischaemia after aortic surgery. *Br J Surg* 1998; **85**: 1095-1098
14 **Fanti L**, Masci E, Mariani A, Chiesa R, Jannello A, Melissano G, Castellano R, Guerini S, Tittobello A. Is endoscopy useful for early diagnosis of ischaemic colitis after aortic surgery? Results of a prospective trial. *Ital J Gastroenterol Hepatol* 1997; **29**: 357-360
15 **Linder JD**, Mönkemüller KE, Raijman I, Johnson L, Lazenby AJ, Wilcox CM. Cocaine-associated ischemic colitis. *South Med J* 2000; **93**: 909-913
16 **Appu S**, Thompson G. Gangrenous ischaemic colitis following non-steroidal anti-inflammatory drug overdose. *ANZ J Surg* 2001; **71**: 694-695
17 **Charles JA**, Pullicino PM, Stoopack PM, Shroff Y. Ischemic colitis associated with naratriptan and oral contraceptive use. *Headache* 2005; **45**: 386-389
18 **Lopez Morra HA**, Fine SN, Dickstein G. Colonic ischemia with laxative use in young adults. *Am J Gastroenterol* 2005; **100**: 2134-2136
19 **Medina C**, Vilaseca J, Videla S, Fabra R, Armengol-Miro JR, Malagelada JR. Outcome of patients with ischemic colitis: review of fifty-three cases. *Dis Colon Rectum* 2004; **47**: 180-184
20 **Green BT**, Tendler DA. Ischemic colitis: a clinical review. *South Med J* 2005; **98**: 217-222
21 **Schweeger I**, Fitscha P, Sinzinger H. Successful eradication of Helicobacter pylori as determined by ((13)) C-urea breath test does not alter fibrinogen and acute phase response markers. *Thromb Res* 2000; **97**: 411-420
22 **Kapsoritakis AN**, Potamianos SP, Sfiridaki AI, Koukourakis MI, Koutroubakis IE, Roussomoustakaki MI, Manousos ON, Kouroumalis EA. Elevated thrombopoietin serum levels in patients with inflammatory bowel disease. *Am J Gastroenterol* 2000; **95**: 3478-3481
23 **Bjørnestad E**, Lie RT, Janssen CW. The diagnostic potential of some routine laboratory tests. off. *Br J Clin Pract* 1993; **47**: 243-245

S- Editor Liu Y **L- Editor** Zhu LH **E- Editor** Che YB

PO Box 2345, Beijing 100023, China
www.wjgnet.com
wjg@wjgnet.com

World J Gastroenterol 2007 February 28; 13(8): 1240-1242
World Journal of Gastroenterology ISSN 1007-9327

RAPID COMMUNICATION

Effect of preoperative biliary drainage on outcome of classical pancreaticoduodenectomy

Chandra Shekhar Bhati, Chandrashekhar Kubal, Pankaj Kumar Sihag, Ankur Atal Gupta, Raj Kamal Jenav, Nicholas G Inston, Jagdish M Mehta

Chandra Shekhar Bhati, Pankaj Kumar Sihag, Ankur Atal Gupta, Raj Kamal Jenav, Jagdish M Mehta, Upgraded Department of Surgery, SMS Medical College, Jaipur, India
Chandra Shekhar Bhati, Chandrashekhar Kubal, Nicholas G Inston, Liver Unit, Queen Elizabeth Hospital, Birmingham, United Kingdom
Correspondence to: Chandra Shekhar Bhati, MS, MRCS, Research registrar, Department of HPB Surgery and Liver Transplantation, Queen Elizabeth Hospital, Birmingham, United Kingdom. c.s.bhati@bham.ac.uk
Telephone: +44-1216-271627
Received: 2006-11-28 Accepted: 2007-01-17

Abstract

AIM: To investigate the role of preoperative biliary drainage (PBD) in the outcome of classical pancreaticodu odenectomy.

METHODS: A 10-year retrospective data analysis was performed on patients (n = 48) undergoing pancreaticoduodenectomy from March 1994 to March 2004 in department of surgery at SMS medical college, Jaipur, India. Demographic variables, details of preoperative stenting, operative procedure and post operative complications were noted.

RESULTS: Preoperative biliary drainage was performed in 21 patients (43.5%). The incidence of septic complications was significantly higher in patients with biliary stent placement ($P < 0.05$, 0 *vs* 4). This group of patients also had a significantly higher minor biliary leak rate. Mortality and hospital stay in each group was comparable.

CONCLUSION: Within this study population the use of PBD by endoscopic stenting was associated with a high incidence of infective complications. These findings do not support the routine use of biliary stenting in patients prior to pancreatico-duodenectomy.

Key words: Whipple's operation; Preoperative stenting; Sepsis; Preoperative biliary drainage

Bhati CS, Kubal C, Sihag PK, Gupta AA, Jenav RK, Inston NG, Mehta JM. Effect of preoperative biliary drainage on outcome of classical pancreaticoduodenectomy. *World J Gastroenterol* 2007; 13(8): 1240-1242

http://www.wjgnet.com/1007-9327/13/1240.asp

INTRODUCTION

Pancreaticoduodenectomy is a challenging operation and is associated with high morbidity[1]. In the last two decades peri-operative mortality has decreased to less than 5% in published series from specialized centers[2,3]; although the morbidity remains high (25%-50%). The impact of jaundice on post-operative morbidity and mortality is well known. However the routine use of pre-operative biliary drainage (PBD) remains controversial[4]. The potential advantages of preoperative stenting include improved nutritional, metabolic and immune function, and the possibility of reduced postoperative morbidity and mortality rates[5-7]. Opponents of PBD argue that it increases infective complications and morbidity[8,9]. There are, however, certain clinical situations such as acute suppurative cholangitis and severe malnutrition where urgent biliary drainage is indicated and can be life-saving[10]. It is not clear whether the procedure itself or its complications influence the morbidity after pancreaticoduodenectomy. The optimal duration of preoperative drainage also remains unknown. Experimental studies have indicated that a period of 6 wk is necessary to obtain clinical benefit with PBD[11]. On the other hand, a clinical study has shown a higher incidence of morbidity and mortality when surgery was carried out within 6 wk of stent placement[12]. Although several reports have been published, still there are no clear guidelines regarding use of PBD in these patients. The aim of this study was to evaluate the effect of endoscopic PBD on morbidity and mortality after pancreatico-duodenectomy in a low volume center.

MATERIALS AND METHODS

Details of 48 patients who underwent Kosch-Whipple's pancreaticoduodenectomy for periampullary tumors (excluding tumor of the pancreatic head) from March 1994 to March 2004 were entered into a database that included patient characteristics, details of biliary stenting and stent-related infective complications, surgery, morbidity and mortality. Pancreaticoduodenectomy was performed in the Department of Surgery, S.M.S. Hospital, Jaipur by a single surgical team using a standard Kosch-Whipple's

Table 1 Patient variables in the stented and non stented groups

	PBD	No PBD	Significance
Patients (*n*)	21	27	0.453
Median age (yr)	50 (25-68)	48 (30-72)	0.446
Sex ratio (M:F)	10:11	15:12	0.588
Mean serum bilirubin (mg/dL)	7.85 (SD ± 5.59)	11.83 (SD ± 9.05)	0.561
Albumin (mg/dL)	3.34 (SD ± 0.7)	3.17 (SD ± 0.82)	0.872
Location of tumor			
Ampulla	18	25	0.439
Bile duct	0	1	0.373
Duodenum	3	1	0.188

Table 2 Morbidity and mortality in the two groups

	PBD	No PBD	Significance
Sepsis	4	0	0.018[a]
Wound infection	5	1	0.037[a]
Minor bile leak	3	0	0.043[a]
Pancreatic leak	6	2	0.106
Bleeding	1	0	0.252
Lymphorrhea	2	4	0.580
Median hospital stay (d)	13 (1-147)	12 (9-32)	0.943
Mortality	3	5	0.690

[a]$P < 0.05$, PBD *vs* No PBD.

technique. Before year 2000 most reconstructions involved a pancreatojejunostomy ($n = 17$), but after year 2000 pancreatogastrostomy ($n = 31$) was performed according to the surgeon's preference. Patients with chronic and benign diseases were excluded from this study. The data were collected retrospectively as well as prospectively and were reviewed.

Pancreatic leak was defined according to the criteria described by Yeo *et al*[9]: pancreatic fistula was diagnosed when more than 50 mL of drainage fluid with an amylase concentration of more than 3 fold the normal upper limit in serum was obtained on or after postoperative d 5, or when pancreatic anastomotic disruption was shown radiologically. Biliary leak was defined as more than 50 mL bile per day in the drain for at least three consecutive days after postoperative d 7. Biliary leak less than 50 mL per day in drain after postoperative d 3 was considered minor bile leak. Infectious morbidity was defined as any complication with evidence of associated localized or systemic infection indicated by fever, leucocytosis and positive culture.

Statistical analysis

Results are expressed as medians and ranges or as numbers and percentages of patients. Two tailed *t* test, chi-square test and binary logistic regression analysis were used for data analysis. SPSS statistical package was used (SPSS v13.0, Chicago, USA) for analysis. Differences were considered statistically significant at $P < 0.05$.

RESULTS

Forty eight patients had Whipple's operation for periampullary tumors. Twenty five patients (52.1%) were male and 23 (47.9%) were female. Median duration between onsets of symptoms to presentation was 3 mo (range 1 mo to 17 mo). The median age at presentation was 49 years (range 25 to 72). At admission 44 patients (91.7%) had jaundice [mean preoperative total bilirubin level was 10.09 mg/dL (SD ± 7.91)], 33 (68.8%) had abdominal pain, and 6 (12.5%) had a history of vomiting. Twenty-five (52.1%) patients noticed weight loss, and 27 (56.3%) had anemia. Preoperative liver function tests and other investigations are outlined in Table 1.

Forty three (89.6%) patients underwent side-viewing endoscopy for diagnosis. Preoperative histological diagnosis was obtained in 29 (60.4%) patients. Twenty one (43.8%) underwent preoperative biliary stenting at the time of preoperative instrumentation with drainage established successfully in all stented patients. All patients in stented group (21) underwent stenting by an endoscopical approach and plastic stents were used for drainage. There were no statistically significant differences in the demographics and pre-operative variables between patient groups with or without PBD (Table 2). Mean pre-operative serum bilirubin in the PBD group was 7.85 (SD ± 9.05) and 11.83 (SD ± 5.59) in non PBD group ($P \geqslant 0.05$).

Thirty one (64.6%) patients had pancreatico-gastrostomy and 17 (35.4%) patients had pancreatico-jejunostomy. The majority of the patients (43; 89.6%) had ampullary (ampula of Vater) carcinoma, whilst 4 (10.4%) patients had duodenal carcinoma and one patient had cholangiocarcinoma. Histopathological examinations of specimens revealed well differentiated tumors in 43 patients (89.6%); whilst other 5 were poorly differentiated. Only 8.3% of patients had lymph node involvement identified in surgical specimens and only 3% of the patients had positive resection margins.

All postoperative complications and subpopulation analyses between PBD and non-PBD groups are shown in Table 2. Postoperative sepsis occurred in 8.3% (4/48) of patients. Median hospital stay was 13 d (1-147 d) and overall mortality was 16.67%. One patient had postoperative bleeding that required re-exploration. There were 6 (12.5%) patients with wound infection and lymphorrhoea each and one patient developed delayed gastric emptying. Subpopulation analysis demonstrated a higher occurrence of infection and wound infection in PBD group ($P \geqslant 0.05$).

DISCUSSION

Pancreatico-duodenectomy is recognized as an acceptable surgical option in patients with pancreatic malignancies although the routine use of PBD remains controversial. In general, our unit's protocol is against PBD but within this series almost half of the patients (21/48) were already stented as they were referred from other centers. This may be reflected by the late presentation of patients in this series (the duration of symptoms varied from 1 mo to over one year).

There were some changes in the surgical technique in our study over the study period. During the initial years, classical pancreaticoduodenectomy was done with

pancreatico-jejunal (Dunking) anastomosis and 17 patients had pancreaticojejunal anastomosis (35.4%). Later on pancreatico-gastric direct duct to mucosa anastomosis was favoured in 31 patients. The morbidity and mortality rates were not significantly affected by the technique of pancreatic anastomosis to the gastrointestinal tract.

Half of the patients had bilirubin levels more than 10 mg% and only 4 cases (8%) presented without jaundice at the time of admission to our surgical unit. An average bilirubin level of 10 mg% at presentation has been reported in other studies. Earlier studies reported that there is an increased morbidity and mortality associated with severe jaundice (> 10 mg%)[13,14]. On the contrary, some recent studies have reported that the severity of jaundice has no influence on postoperative morbidity and mortality[15]. Povoski *et al*[8] concluded in their study that PBD, but not preoperative biliary instrumentation alone, was associated with increased morbidity and mortality rates in patients undergoing pancreatico-duodenectomy. In a prospective review, Sohn *et al*[9] reported the incidence of wound infection and pancreatic fistula to be significantly higher in stented patients.

The overall morbidity in our study of 48 cases was 35.41% (17 cases) and mortality was 16% (8 cases). In the first 5 years of our experience with pancreatico-duodenectomy, the operative mortality rate was 17.6%, which reduced to about 9% in last five years. Two patients died because of non surgical complications; one from dengue fever and one of myocardial infarction at the time of discharge. In our study, PBD was associated with increased morbidity following pancreatico-duodenectomy while mortality rates were unchanged. Although recent reports have shown that there is no change in infectious complication rates, notably wound infection, after PBD[16,17], our experience was different. The stented group had significantly higher morbidity (41%) in comparison to the non-stented group (30.7%). Wound infection, sepsis and minor bile leak were found to be main complications in the stented group. The wound infection rate was 27.2%, and fever 18.1%, both significantly higher in the stented group ($P \geqslant 0.05$). Minor biliary leak was significantly higher in the stented group ($n = 3$) ($P \geqslant 0.05$) (Table 2). Further regression analysis showed that PBD was associated with infective morbidity arising from stent placement. Larger prospective studies are needed to resolve the issue of duration of PBD. Other complications such as pancreatic leak, hemorrhage and lymphorrhoea were not influenced by stenting. The mean hospital stay in the two groups was comparable in spite of septic complications.

Some published studies suggest that stenting may have an effect on bile duct bacterial colonization and cause more infective complications[8,12]. Supporting the data above, our study confirms that PBD may have a negative impact on postoperative outcome after pancreatico-duodenectomy. However, judicious use may reduce the incidence of septic complications in selective patients. Randomized controlled trials in patient groups such as those with severe obstructive jaundice are required to address these controversies and improve outcomes and avoid unnecessary morbidity and mortality associated with PBD.

REFERENCES

1 **Sewnath ME**, Birjmohun RS, Rauws EA, Huibregtse K, Obertop H, Gouma DJ. The effect of preoperative biliary drainage on postoperative complications after pancreaticoduodenectomy. *J Am Coll Surg* 2001; **192**: 726-734

2 **Cameron JL**, Pitt HA, Yeo CJ, Lillemoe KD, Kaufman HS, Coleman J. One hundred and forty-five consecutive pancrea ticoduodenectomies without mortality. *Ann Surg* 1993; **217**: 430-435; discussion 435-438

3 **Trede M**, Schwall G, Saeger HD. Survival after pancreatoduodenectomy. 118 consecutive resections without an operative mortality. *Ann Surg* 1990; **211**: 447-458

4 **Isenberg G**, Gouma DJ, Pisters PW. The on-going debate about perioperative biliary drainage in jaundiced patients undergoing pancreaticoduodenectomy. *Gastrointest Endosc* 2002; **56**: 310-315

5 **Kimmings AN**, van Deventer SJ, Obertop H, Rauws EA, Huibregtse K, Gouma DJ. Endotoxin, cytokines, and endotoxin binding proteins in obstructive jaundice and after preoperative biliary drainage. *Gut* 2000; **46**: 725-731

6 **Gouma DJ**, Coelho JC, Schlegel JF, Li YF, Moody FG. The effect of preoperative internal and external biliary drainage on mortality of jaundiced rats. *Arch Surg* 1987; **122**: 731-734

7 **Gundry SR**, Strodel WE, Knol JA, Eckhauser FE, Thompson NW. Efficacy of preoperative biliary tract decompression in patients with obstructive jaundice. *Arch Surg* 1984; **119**: 703-708

8 **Povoski SP**, Karpeh MS, Conlon KC, Blumgart LH, Brennan MF. Preoperative biliary drainage: impact on intraoperative bile cultures and infectious morbidity and mortality after pancreaticoduodenectomy. *J Gastrointest Surg* 1999; **3**: 496-505

9 **Sohn TA**, Yeo CJ, Cameron JL, Pitt HA, Lillemoe KD. Do preoperative biliary stents increase postpancreaticoduode nectomy complications? *J Gastrointest Surg* 2000; **4**: 258-267; discussion 267-268

10 **Kumar R**, Sharma BC, Singh J, Sarin SK. Endoscopic biliary drainage for severe acute cholangitis in biliary obstruction as a result of malignant and benign diseases. *J Gastroenterol Hepatol* 2004; **19**: 994-997

11 **Krähenbühl L**, Schäfer M, Krähenbühl S. Reversibility of hepatic mitochondrial damage in rats with long-term cholestasis. *J Hepatol* 1998; **28**: 1000-1007

12 **Jagannath P**, Dhir V, Shrikhande S, Shah RC, Mullerpatan P, Mohandas KM. Effect of preoperative biliary stenting on immediate outcome after pancreaticoduodenectomy. *Br J Surg* 2005; **92**: 356-361

13 **Gilsdorf RB**, Spanos P. Factors influencing morbidity and mortality in pancreaticoduodenectomy. *Ann Surg* 1973; **177**: 332-337

14 **Dixon JM**, Armstrong CP, Duffy SW, Davies GC. Factors affecting morbidity and mortality after surgery for obstructive jaundice: a review of 373 patients. *Gut* 1983; **24**: 845-852

15 **Ceuterick M**, Gelin M, Rickaert F, Van de Stadt J, Devière J, Cremer M, Lambilliotte JP. Pancreaticoduodenal resection for pancreatic or periampullary tumors--a ten-year experience. *Hepatogastroenterology* 1989; **36**: 467-473

16 **Mullen JT**, Lee JH, Gomez HF, Ross WA, Fukami N, Wolff RA, Abdalla EK, Vauthey JN, Lee JE, Pisters PW, Evans DB. Pancreaticoduodenectomy after placement of endobiliary metal stents. *J Gastrointest Surg* 2005; **9**: 1094-1104; discussion 1104-1105

17 **Barnett SA**, Collier NA. Pancreaticoduodenectomy: does preoperative biliary drainage, method of pancreatic reconstruction or age influence perioperative outcome? A retrospective study of 104 consecutive cases. *ANZ J Surg* 2006; **76**: 563-568

S- Editor Liu Y **L- Editor** Zhu LH **E- Editor** Lu W

PO Box 2345, Beijing 100023, China
www.wjgnet.com
wjg@wjgnet.com

World J Gastroenterol 2007 February 28; 13(8): 1243-1246
World Journal of Gastroenterology ISSN 1007-9327

RAPID COMMUNICATION

Effects of the myeloperoxidase 463 gene polymorphisms on development of atrophy in *H pylori* infected or noninfected gastroduodenal disease

Ömer Yilmaz, Hakan Dursun, Nesrin Gürsan, İbrahim Pirim, Arif Yılmaz, Nihat Okcu

Ömer Yilmaz, Hakan Dursun, Arif Yılmaz, Nihat Okcu, Department of Gastroenterology, Faculty of Medicine, University of Atatürk, Erzurum 25070, Turkey
Nesrin Gürsan, Department of Pathology, Faculty of Medicine, University of Atatürk, Erzurum 25070, Turkey
İbrahim Pirim, Department of Medical Biology and Genetics, Faculty of Medicine, University of Atatürk, Erzurum 25070, Turkey
Correspondence to: Ömer Yilmaz, MD, Atatürk University, Medical Faculty, Department of Gastroenterology, Erzurum 25070, Turkey. yilmazo@atauni.edu.tr
Telephone: +90-442-2361212 Fax: +90-442-2361301
Received: 2006-11-03 Accepted: 2006-12-18

Abstract

AIM: To investigate the relationship between myeloperoxidase polymorphisms as a host-related factor and atrophy caused by *H pylori*.

METHODS: Our study enrolled 77 patients. Biopsy materials obtained during gastrointestinal endoscopies were evaluated for the presence of *H pylori*. Polymerase chain reaction-restriction fragment length polymorphism assay was used to characterize myeloperoxidase genotypes.

RESULTS: Forty four patients (57.1%) were *Hp* (+) and 33 (42.9%) were *Hp* (-). Sixty six (85.7%) had GG genotype, 10 (12.9%) had GA genotype and 1 (1.29%) had AA genotype. The change in atrophy in relation to neutrophil infiltration was significant in *Hp* (+) patients (P = 0.0001). The change in atrophy in relation to neutrophil infiltration in patients with GG genotype was significant (P = 0.002). However, the change in atrophy in relation to neutrophil infiltration was not significiant in patients with *Hp* (+) GG genotype (r = 0.066, P = 0.63).

CONCLUSION: Myeloperoxidase genotype is critical for development of atrophy in relation to the severity of inflammation. However, it is interesting to note that, *H pylori* does not show any additive effect on development of atrophy.

Key words: Gastritis; Gastroduodenal ulcer; Gastric cancer; Myeloperoxidase; *H pylori*

Yilmaz Ö, Dursun H, Gürsan N, Pirim İ, Yılmaz A, Okcu N. Effects of the myeloperoxidase 463 gene polymorphisms on development of atrophy in *H pylori* infected or noninfected gastroduodenal disease. *World J Gastroenterol* 2007; 13(8): 1243-1246

http://www.wjgnet.com/1007-9327/13/1243.asp

INTRODUCTION

H pylori is an agent that produces chronic infection in more than half of the world population[1]. The most important characteristic of *H pylori* infection is that it causes chronic active inflammation in the gastric mucosa, which involves neutrophils and monocytes[2]. While 100% of the persons carrying this microbe develops gastritis, the lifetime risk of peptic ulcer is 15%-20% and that of gastric cancer is 1%-3%[1].

The role of host-related factors in the pathogenesis of diseases caused by *H pylori* has been greatly ignored up to date[3,4]. It was demonstrated that the ability of the host to regulate the production of cytokines is influenced by the presence of polymorphisms in the promoter region of the relevant genes[5]. The polymorphisms in the genes affecting the production of cytokines might be one of the factors that lead to the interpersonal differences in the severity of gastric inflammation[3,5].

Myeloperoxidase (MPO) is a lysosomal enzyme found in the azurophilic granules of polymorphonuclear leukocytes (PNL)[6-9]. There are two promoter regions affecting MPO; -463G/A and -129G/A[10]. Allele A of this polymorphism reduces mRNA expression and thus, tissue damage in local inflammation is decreased[8,9,11]. Allele G has 25 times more transcriptional efficacies compared to allele A. The G/G genotype confers higher risk for persistent *H pylori* infection[12,13].

H pylori activates the oxidative metabolism in neutrophils[14]. Reactive oxygen products such as free oxygen radicals released from neutrophils, (O^{2-}), H_2O_2 and hydroxyl ion (OH) reacts with MPO and hypochloric acid (HOCI) is formed. Monochloroamines (NH_2CI) are formed when HOCI reacts with the ammonium produced by the urease enzyme of *H pylori*. Monochloroamines are oxidizing agents that are able to induce DNA fragmentation[4,8,14-16]. Thus, it has been advocated that

myeloperoxidase is involved in gastric damage induced by *H pylori*[4,11,17]. We assessed the association between neutrophil infiltration and atrophy caused by *H pylori* and MPO gene polymorphisms.

MATERIALS AND METHODS

We enrolled 77 patients (46 males, 31 females) who had undergone endoscopic examinations due to epigastric pain, dyspepsia, nausea and vomiting or weight loss. Patients who received antibiotic therapy, proton-pump inhibitors or non-steroid anti-inflammatory drugs within 3 mo prior to endoscopies were excluded.

Based on the endoscopic findings, 24 patients had gastritis, 26 had ulcers (duodenal or gastric ulcers) and 27 had gastric cancers. Diagnosis of patients who showed malignant findings in their endoscopies was confirmed by pathologic examination. In the light of endoscopic findings, two biopsies were obtained each from the antrum, angulus and corpus mucosa of the tissue adjacent to ulcer region and regions distant to malignant lesions. Biopsy materials were transferred into 3 separate small bottles containing formaldehyde and sent to the laboratory for evaluation of *H pylori* and pathologic examinations. Also, peripheral blood samples (3 mL) were collected from enrolled patients simultaneously and transferred into EDTA hemogram tubes. The tubes were transferred to the genetic laboratory under appropriate conditions avoiding coagulation.

Histopathologic examinations

The materials brought to the pathology laboratory were embedded in paraffin after follow-up procedures. Subsequently, cross-sections of 3-4 microns thick were obtained from the paraffin blocks. These cross-sections were stained by hematoxylin-eosin, Giemsa and Warthin-Starey stains, respectively. Preparations were divided into two groups as negative or positive based on the presence of *H Pylori* during direct visualization under a light microscope. Biopsy materials were staged according to neutrophilic activity, chronic inflammatory cell infiltration, glandular atrophy, intestinal metaplasia and *H pylori* density using criteria from the modified Sydney classification system. Each feature was evaluated as none (0), mild (1), moderate (2) or apparent (3)[18]. After all patients were scored according to 4 parameters of Sydney classification, sum of the parameters was calculated for three biopsy regions.

Myeloperoxidase genotyping

Patient blood samples transferred into EDTA tubes were used for DNA isolation. DNA isolation was performed using the column method (Gentra DNA isolation kit). Myeloperoxidase polymorphism analysis was performed by PCR and restriction fragment length polymorphism (RFLP) methods. Primers to be used were designed to detect Codone 463 of the myeloperoxidase gene.

Preparation of DNAs for PCR

Twenty microlitres DNA from each patient was transferred into 0.2 mL Eppendorf tubes. After addition of two different primers (forward pimer 5'-CCGTATAGGCAGA GAATGGTGAG-3' and reverse primer 5'-GCAATGGT TCAAGCGATTCTTC-3'), 1.5 μL; dNTP mix, 1 μL; Taq DNA polymerase, 1 μL; PCR buffer, 10 μL and distilled water, 15 μL, these tubes were placed into a PCR machine. PCR conditions were primer annealing at 56℃ for 1 min, polymerization at 72℃ for 1 min, and denaturation at 94℃ for 1 min. Thirty cycles were carried out[19]. The PCR product (amplicon) was incubated with *Acl*-I enzyme at 37℃ for 1.5 h and separated on a 2% agarose gel. DNA fragments on the gel were visualized after staining with 0.5 μg/mL ethidium bromide (EtBr).

Table 1 Distribution of myeloperoxidase genotypes in *Hp* (+) and *Hp* (-) patients according to endoscopic findings

	Hp (+)	*Hp* (-)	Total
n (%)	44 (57.1)	33 (42.9)	77 (100.0)
Gastritis	13	11	24
Ulcer (gastric or duodenum)	18	8	26
Gastric cancer	13	14	27
Myeloperoxidase GG	37	29	66
Myeloperoxidase GA	7	3	10
Myeloperoxidase AA	-	1	1
Neutrophil infiltration	2.80 ± 1.94[1]	0.88 ± 1.24	1.97 ± 1.91

Hp (+): *H pylori* positive group; *Hp* (-): *H pylori* negative group; $P < 0.0001$, *vs* the *Hp* (-) group. [1]Mean ± SD of a score of 0-3 according to the updated Sydney system.

Statistical analysis

Statistical analyses were performed using SPSS 11.0 for Windows statistical software, Kendall's Tau test and Linear regression analysis. P values < 0.05 were considered significant.

RESULTS

The mean age of the patients was 54.9 ± 14.1 years (19-82). Pathologic examination revealed that 44 of them were *Hp* (+) and 33 were *Hp* (-). Based on MPO gene polymorphism, 66 patients (85.7%) had GG genotype, 10 (12.9%) had GA and 1 (1.29%) had AA genotype. The patient with genotype A was an *Hp* (-) ulcer patient (Table 1).

There was a difference between *H pylori* (+) and *H pylori* (-) patients with respect to PNL infiltration (P = 0.0001). The change in atrophy in relation to neutrophil infiltration was significant in *Hp* (+) patients (y = 0.700x + 0.051) (P = 0.0001) (Figure 1). No such correlation was found for *Hp* (-) patients (y = 0.1214x + 0.50) (y: atrophy, x: neutrophil infiltration) (Figure 2) .

We found a significant correlation between atrophy and neutrophil infiltration in patients with GG genotype (n = 66) (y = 0.252x + 0.239) (P = 0.002). There was an insignificant correlation between atrophy and neutrophil infiltration in patients with GA genotype (n = 10) (y = 0.15x + 1.387) (P = 0.56).

Among the *Hp* (+) patients, the correlation between atrophy and neutrophil infiltration was insignificant for patients with both GG (n = 37) and GA genotypes (n = 7) (r = 0.066, P = 0.63; r = -0.474, P = 0.18, respectively).

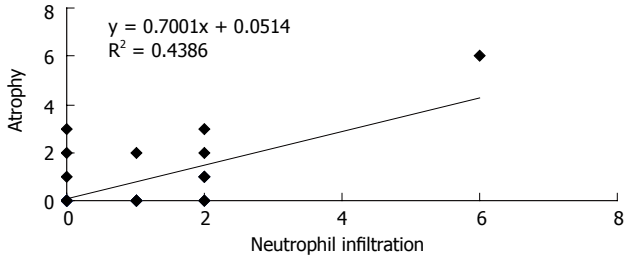

Figure 1 Changes in the atrophy in relation to neutrophil infiltration in *Hp* (+) patients.

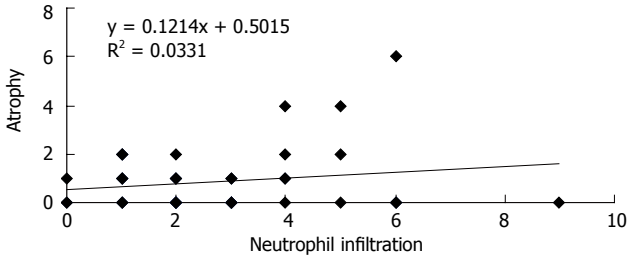

Figure 2 Changes in the atrophy in relation to neutrophil infiltration in *Hp* (-) patients.

Among the patients with *Hp* (-), we found an insignificant correlation between atrophy and neutrophil infiltration in patients with both GG (n = 29) and GA genotypes (n = 3) (r = 0.316, P = 0.06; r = 0.816, P = 0.22, respectively). Since our sample size was small, a statistical analysis for MPO AA (n = 1) genotype could not be performed.

DISCUSSION

About 60% of the world population is infected with *H pylori*[1]. Hyperproliferation induced by *H pylori* gastritis has been assumed as a starting point for events that trigger gastric cancer. Moreover, this hyperproliferation has been suggested to initiate changes in DNA[4,20,21]. The World Health Organization (WHO) has declared *H pylori* as the leading carcinogenic factor. In a cohort study conducted by WHO in 3 different regions, anti-*Hp* antibody levels were measured in blood samples obtained within the last 24 years from patients diagnosed with gastric cancer. It was stated that *H pylori* seropositivity increased the relative risk for developing gastric cancer[1]. Yamagato *et al*[22] reported that 3% of 1721 patients with *H pylori* developed gastric cancer during 9 years of follow up. Also, Uemura *et al*[23] reported that 2.9% of 1246 *Hp* (+) patients developed gastric cancer during 7.6 years of follow up. While there was a significant difference in *Hp* (+) patients with respect to atrophy and neutrophil infiltration, no such correlation was found for *Hp* (-) patients. Thus, inflammation induced by *H pylori* could be one of the predisposing factors in carcinogenesis.

Recently studies have been published on cytokine production in several conditions caused by *H pylori* infection as a host response and genetic polymorphisms[4]. Zambon *et al*[3] found that bacterial and virulence factors were associated with mucosal inflammation and severity of the illness. They found that *H pylori* virulence genes and a host genotype of IL-1 RN were directly correlated with peptic ulcer and intestinal metaplasia and they suggested that the interaction between cytokine genotypes and bacterial virulence factors are fundamental to development of *H pylori*-related lesions. Nardone *et al*[24] reported that, first atrophy localized in the antrum regresses or disappears subsequent to *H pylori* eradication. The changes seen in these lesions as a result of eradication show that, neutrophil infiltration plays a major role in these events above all.

Polymorphisms, defined as known changes in the genomic sequence, occur frequently throughout the human genome. It is known that in some cases, they modify the expression or function of gene products. Any polymorphism could affect susceptibilities to and outcome of an illness through the interaction of environment and genetics[25].

The question of how the variations in the genes associated with inflammation affect the inflammatory response induced by *H pylori* and accompanying gastric pathologies is an interesting one[26]. It has been stated that MPO itself might modulate susceptibilities to clinical outcomes of several illnesses where neutrophils are involved[10]. In a number of studies, the association between MPO polymorphisms and several conditions including chronic granulomatous illness, Alzheimer' s disease, malignancies such as the lung or pharyngeal cancer, some types of leukemia, atherosclerosis, periodontal diseases, multiple sclerosis and cystic fibrosis were reported[4,8,11-13]. Hamajima *et al*[12] investigated a myeloperoxidase genotype with low expression, which was negatively correlated with *H pylori* infection in 241 patients having complaints of dyspepsia, without a history of cancer. They found 79.7% of GG genotype, 19.5% of GA genotype and 0.8% of AA genotype. In another study assessing the association between MPO polymorphisms, atrophy and neutrophil infiltration, Roe *et al*[4] found 81.9% of GG genotype, 18.1% of GA genotype and 0.0% of AA genotype. It was indicated that while there was a positive correlation between the degree of atrophy and neutrophil infiltration in individuals with GG polymorphism, no such association was found in individuals with GA polymorphism. Also, in our study we found that while the correlation between atrophy and neutrophil infiltration was significant in patients with GG genotype, it was insignificant in patients with GA genotype.

Our results show that generally myeloperoxidase GG genotype is a critical host-related factor for development of atrophy that occurs in the setting of inflammation, and is considered as a cancer precursor. However, it is interesting to note that on the contrary to what is expected, GG genotype and *H pylori* positivity does not potentiate each other for development of atrophy. More studies are needed to elucidate this point in larger patient groups.

REFERENCES

1 **Sugiyama T**. Development of gastric cancer associated with Helicobacter pylori infection. *Cancer Chemother Pharmacol* 2004; **54** Suppl 1: S12-S20

2 **Kuwahara H**, Miyamoto Y, Akaike T, Kubota T, Sawa T,

Okamoto S, Maeda H. Helicobacter pylori urease suppresses bactericidal activity of peroxynitrite via carbon dioxide production. *Infect Immun* 2000; **68**: 4378-4383

3 **Zambon CF**, Basso D, Navaglia F, Germano G, Gallo N, Milazzo M, Greco E, Fogar P, Mazza S, Di Mario F, Basso G, Rugge M, Plebani M. Helicobacter pylori virulence genes and host IL-1RN and IL-1beta genes interplay in favouring the development of peptic ulcer and intestinal metaplasia. *Cytokine* 2002; **18**: 242-251

4 **Roe I**, Nam S, Kim J, Shin J, Bang W, Yang M. Association of the myeloperoxidase -463G-->A polymorphism with development of atrophy in Helicobacter pylori-infected gastritis. *Am J Gastroenterol* 2002; **97**: 1629-1634

5 **Hwang IR**, Hsu PI, Peterson LE, Gutierrez O, Kim JG, Graham DY, Yamaoka Y. Interleukin-6 genetic polymorphisms are not related to Helicobacter pylori-associated gastroduodenal diseases. *Helicobacter* 2003; **8**: 142-148

6 **Bombardier C**. An evidence-based evaluation of the gastrointestinal safety of coxibs. *Am J Cardiol* 2002; **89**: 3D-9D

7 **Smith WL**, Garavito RM, DeWitt DL. Prostaglandin endoperoxide H synthases (cyclooxygenases)-1 and -2. *J Biol Chem* 1996; **271**: 33157-33160

8 **Cascorbi I**, Henning S, Brockmöller J, Gephart J, Meisel C, Müller JM, Loddenkemper R, Roots I. Substantially reduced risk of cancer of the aerodigestive tract in subjects with variant--463A of the myeloperoxidase gene. *Cancer Res* 2000; **60**: 644-649

9 **Pakakasama S**, Chen TT, Frawley W, Muller CY, Douglass EC, Lee R, Pollock BH, Tomlinson GE. CCND1 polymorphism and age of onset of hepatoblastoma. *Oncogene* 2004; **23**: 4789-4792

10 **Rutgers A**, Heeringa P, Giesen JE, Theunissen RT, Jacobs H, Tervaert JW. Neutrophil myeloperoxidase activity and the influence of two single-nucleotide promoter polymorphisms. *Br J Haematol* 2003; **123**: 536-538

11 **Matsuo K,** Hamajima N, Suzuki R, Nakamura S, Seto M, Morishima Y, Tajima K. No substantial difference in genotype frequencies of interleukin and myeloperoxidase polymorphisms between malignant lymphoma patients and non-cancer controls. *Haematologica* 2001; **86**: 602-608

12 **Hamajima N**, Matsuo K, Suzuki T, Nakamura T, Matsuura A, Tajima K, Tominaga S. Low expression myeloperoxidase genotype negatively associated with Helicobacter pylori infection. *Jpn J Cancer Res* 2001; **92**: 488-493

13 **Katsuda N,** Hamajima N, Tamakoshi A, Wakai K, Matsuo K, Saito T, Tajima K, Tominaga S. Helicobacter pylori seropositivity and the myeloperoxidase G-463A polymorphism in combination with interleukin-1B C-31T in Japanese health checkup examinees. *Jpn J Clin Oncol* 2003; **33**: 192-197

14 **Mizuki I**, Shimoyama T, Fukuda S, Liu Q, Nakaji S, Munakata A. Association of gastric epithelial apoptosis with the ability of Helicobacter pylori to induce a neutrophil oxidative burst. *J Med Microbiol* 2000; **49**: 521-524

15 **Bhattacharjee M**, Bhattacharjee S, Gupta A, Banerjee RK. Critical role of an endogenous gastric peroxidase in controlling oxidative damage in H. pylori-mediated and nonmediated gastric ulcer. *Free Radic Biol Med* 2002; **32**: 731-743

16 **Karmeli F**, Okon E, Rachmilewitz D. Sulphydryl blocker induced gastric damage is ameliorated by scavenging of free radicals. *Gut* 1996; **38**: 826-831

17 **Tran CD**, Huynh H, van den Berg M, van der Pas M, Campbell MA, Philcox JC, Coyle P, Rofe AM, Butler RN. Helicobacter-induced gastritis in mice not expressing metallothionein-I and II. *Helicobacter* 2003; **8**: 533-541

18 **Dixon MF**, Genta RM, Yardley JH, Correa P. Classification and grading of gastritis. The updated Sydney System. International Workshop on the Histopathology of Gastritis, Houston 1994. *Am J Surg Pathol* 1996; **20**: 1161-1181

19 **Le Marchand L**, Seifried A, Lum A, Wilkens LR. Association of the myeloperoxidase -463G-->a polymorphism with lung cancer risk. *Cancer Epidemiol Biomarkers Prev* 2000; **9**: 181-184

20 **Meining A**, Riedl B, Stolte M. Features of gastritis predisposing to gastric adenoma and early gastric cancer. *J Clin Pathol* 2002; **55**: 770-773

21 **Cahill RJ**, Kilgallen C, Beattie S, Hamilton H, O'Morain C. Gastric epithelial cell kinetics in the progression from normal mucosa to gastric carcinoma. *Gut* 1996; **38**: 177-181

22 **Yamagata H**, Kiyohara Y, Aoyagi K, Kato I, Iwamoto H, Nakayama K, Shimizu H, Tanizaki Y, Arima H, Shinohara N, Kondo H, Matsumoto T, Fujishima M. Impact of Helicobacter pylori infection on gastric cancer incidence in a general Japanese population: the Hisayama study. *Arch Intern Med* 2000; **160**: 1962-1968

23 **Uemura N**, Okamoto S, Yamamoto S, Matsumura N, Yamaguchi S, Yamakido M, Taniyama K, Sasaki N, Schlemper RJ. Helicobacter pylori infection and the development of gastric cancer. *N Engl J Med* 2001; **345**: 784-789

24 **Nardone G**, Staibano S, Rocco A, Mezza E, D'armiento FP, Insabato L, Coppola A, Salvatore G, Lucariello A, Figura N, De Rosa G, Budillon G. Effect of Helicobacter pylori infection and its eradication on cell proliferation, DNA status, and oncogene expression in patients with chronic gastritis. *Gut* 1999; **44**: 789-799

25 **Foster CB**, Lehrnbecher T, Mol F, Steinberg SM, Venzon DJ, Walsh TJ, Noack D, Rae J, Winkelstein JA, Curnutte JT, Chanock SJ. Host defense molecule polymorphisms influence the risk for immune-mediated complications in chronic granulomatous disease. *J Clin Invest* 1998; **102**: 2146-2155

26 **Rad R**, Dossumbekova A, Neu B, Lang R, Bauer S, Saur D, Gerhard M, Prinz C. Cytokine gene polymorphisms influence mucosal cytokine expression, gastric inflammation, and host specific colonisation during Helicobacter pylori infection. *Gut* 2004; **53**: 1082-1089

S- Editor Liu Y **L- Editor** Zhu LH **E- Editor** Ma WH

PO Box 2345, Beijing 100023, China
www.wjgnet.com
wjg@wjgnet.com

World J Gastroenterol 2007 February 28; 13(8): 1247-1251
World Journal of Gastroenterology ISSN 1007-9327

RAPID COMMUNICATION

Prevalence of gastric varices and results of sclerotherapy with N-butyl 2 cyanoacrylate for controlling acute gastric variceal bleeding

Khalid Mumtaz, Shahid Majid, Hasnain A Shah, Kashif Hameed, Ashfaq Ahmed, Saeed Hamid, Wasim Jafri

Khalid Mumtaz, Shahid Majid, Hasnain A Shah, Kashif Hameed, Ashfaq Ahmed, Saeed Hamid, Wasim Jafri, Section of Gastroenterology, Aga Khan University Hospital, Karachi, Pakistan
Correspondence to: Dr. Hasnain A Shah, FRCP, Professor, Section of Gastroenterology, Department of Medicine, Aga Khan University Hospital, Stadium Road, Karachi, Pakistan. hasnain.alishah@aku.edu
Telephone: + 92-21-46864676
Received: 2006-11-06 Accepted: 2007-02-07

Abstract

AIM: To study the prevalence, predictors and control of bleeding following N-butyl 2 cyanoacrylate (NBC) sclerotherapy of gastric varix (GV).

METHODS: We analyzed case records of 1436 patients with portal hypertension, who underwent endoscopy during the past five years for variceal screening or upper gastrointestinal (GI) bleeding. Fifty patients with bleeding GV underwent sclerotherapy with a mean of 2 mL NBC for control of bleeding. Outcome parameters were primary hemostasis (bleeding control within the first 48 h), recurrent bleeding (after 48 h of esophago-gastro-duodenoscopy) and in-hospital mortality were analyzed.

RESULTS: The prevalence of GV in patients with portal hypertension was 15% (220/1436) and the incidence of bleeding was 22.7% (50/220). Out of the 50 bleeding GV patients, isolated gastric varices (IGV-I) were seen in 22 (44%), gastro-oesophageal varices (GOV) on lesser curvature (GOV-Ⅰ) in 16 (32%), and GOV on greater curvature (GOV-Ⅱ) in 15 (30%). IGV-Ⅰ was seen in 44% (22/50) patients who had bleeding as compared to 23% (39/170) who did not have bleeding (P < 0.003). Primary hemostasis was achieved with NBC in all patients. Re-bleeding occurred in 7 (14%) patients after 48 h of initial sclerotherapy. Secondary hemostasis was achieved with repeat NBC sclerotherapy in 4/7 (57%). Three patients died after repeat sclerotherapy, one during transjugular intrahepatic portosystemic stem shunt (TIPSS), one during surgery and one due to uncontrolled bleeding. Treatment failure-related mortality rate was 6% (3/50).

CONCLUSION: GV can be seen in 15% of patients with portal hypertension and the incidence of bleeding is 22.7%. NBC is highly effective in controlling GV bleeding. In hospital mortality of patients with bleeding GV is 6%.

Key words: Gastric varices; Portal hypertension; N-butyl cyanoacrylate; Bleeding; Sclerotherapy

Mumtaz K, Majid S, Shah HA, Hameed K, Ahmed A, Hamid S, Jafri W. Prevalence of gastric varices and results of sclerotherapy with N-butyl 2 cyanoacrylate for controlling acute gastric variceal bleeding. *World J Gastroenterol* 2007; 13(8): 1247-1251

http://www.wjgnet.com/1007-9327/13/1247.asp

INTRODUCTION

Gastric varix (GV) and its association with portal hypertension were first described in 1913[1]. Since then, there have been reports on different aspects of gastric varices including prevalence, bleed tendency and treatment options. The prevalence of GV in patients with portal hypertension varies from 18% to 70%[2,3], although the incidence of bleeding from gastric varices is relatively low ranging from 10% to 36%[3].

Management of GV presents is a challenging problem, because (1) since there is no consensus regarding the optimum treatment of GV, treatment tends to be empiric; (2) GV is not a homogeneous entity, and accurate classification defines its natural history and dictates its management; (3) although GV bleeding occurs less frequently than esophageal varix (EV) bleeding[4,5], whenever bleeding occurs it tends to be more severe and requires more red blood cell transfusions and has a higher mortality than EV bleeding[5]; (4) after control of acute bleeding, GV has a high rebleeding rate of 34% to 89%[6]; and (5) there is no consensus regarding subsequent sclerotherapy for prophylaxis against recurrent bleeding in GV patients. Optimal management of GV requires a multidisciplinary approach and close cooperation between gastroenterologists, interventional radiologists and the surgical team.

Sohendra *et al*[7] first reported in 1986 that bleeding from gastric varices could be controlled by sclerotherapy

using the tissue adhesive agent butyl cyanoacrylate. Since then several authors have used different sclerosing agents to achieve hemostasis in bleeding gastric varices, including N-butyl-2 cyanoacrylate (histoacryl)[4,8], 2-octyl cyanoacrylate[9], ethanolamine oleate injection[10], gastric variceal banding[11], thrombin[12], sodium tetradecyl sulfate[13]. However, N-butyl 2 cyanoacrylate (NBC) is the only promising agent.

Most reports on endoscopic treatment of bleeding gastric varices are small series, case reports, or retrospective reviews[14,15]. Not more than 1000 patients with bleeding GV have been treated with different sclerosing and coagulating agents. Cyanoacrylate injection can achieve primary hemostasis in 70% to 95% of patients with acute GV bleeding, with an early rebleeding rate ranging from 0% to 28% within 48 h[5,7,16]. Different doses of cyanoacrylate are used by different gastroenterologis ts[16,17]. Moreover, dilution ratio of NBC to lipoidal is different[18,19]. However, there is no consensus regarding effective dose and dilution of sclerosing agents.

This study was to analyze patients with GV in order to establish predictors of bleeding GV, and the efficacy and safety of NBC in treatment of bleeding GV.

Table 1 Clinical characteristics of patients with gastric varices

Characteristics	*n*	(%)
Number of patients	220	
Male:Female	141:79	(65:35)
Mean age (yr)	50 ± 11	
Etiology of GV		
HCV cirrhosis	155	(70)
HBV cirrhosis	38	(17.5)
NBNC	27	(12.5)
NCPHTN	9	
Alcoholism	5	
Budd-Chiari syndrome	1	
Wilson's disease	1	
Child-Pugh classification (A/B/C)	39/109/72	(18/49/33)
Types of gastric varices		
GOV-1	78	(35)
GOV-2	56	(25)
IGV-1	59	(27)
IGV-2	6	(03)
GOV-1 + GOV-2	14	(06)
GOV-2 + IGV-2	3	(1.5)
GOV 1+IGV 2	2	(01)
GOV 1 + IGV 1	2	(01)

MATERIALS AND METHODS

From March 2000 to March 2005, 1036 patients with portal hypertension underwent endoscopy in our hospital. Out of 220 GV patients with or without esophageal varices, 50 had active bleeding gastric varices which were treated with N-Butyl cyanoacrylate injection.

The cause of portal hypertension was defined on the basis of ultrasound and/or computed tomographic scan of abdomen along with Doppler ultrasound to study the patency and spleno-portal axis in all patients with bleeding GV.

The location of gastric varices was determined according to the classification described by Sarin and Kumar[3] and divided into gastroesophageal varices type 1 (GOV-1) GV continuing as an extension of esophageal varices on the lesser curve of the stomach), gastro-esophageal varices type 2 (GOV-2) on the greater curvature or fundal varices communicating with esophageal varices. Isolated gastric varices type 1 (IGV-1) and fundal varices within a few centimeters of the gastric cardia, or isolated gastric varices type 2 (IGV-2) and isolated ectopic gastric varices. Active bleeding was defined as bleeding or oozing of blood from a gastric varix, a clot or blackish ulcer or rent over a gastric varix, or the presence of distinct large gastric varices and absence of esophageal varices or other cause of gastrointestinal (GI) bleeding.

The clinical characteristics of patients including age, gender, Child-Pugh classification, type of varix, etiology and complications in patient with gastric varices were recorded and compared between groups with or without bleeding (Table 1).

Endoscopic sclerotherapy with n-butyl cyanoacrylate and lipoidal injection was performed by experienced endoscopists using a GIFQ160 gastroscope (Olympus, Tokyo, Japan). The sclerosant was injected into bleeding gastric varices using the 23 G disposable needle injector (Wilson Cook Medical Inc., Winston-Salem, NC).

The injection needle was primed with lipoidal (approximately 0.5 mL) to fill the dead space within the injection catheter. After the gastric varix lumen was punctured with the needle, 2 mL of NBC (histoacryl 100%) in aliquots of 1 mL, diluted in 0.5 mL lipoidal, was injected over 45-90 s, thus a dilution of 2:1 was achieved in all cases (Figure 1 and Figure 2). Distilled water was used to flush the injection needle before and after sclerotherapy. Additional NBC was not injected if bleeding was immediately controlled in patients. All patients received octreotide infusion (50 mg/per hour) at admission and continued for 3 d. All patients were given a proton pump inhibitor, initially intravenously for 48 h and then orally for 4-6 wk as per our endoscopy unit protocol.

Outcome measures

Primary hemostasis was defined as stability of vital clinical signs, no drop in hemoglobin concentration and no recurrent bleeding within the first 48 h after the initial sclerotherapy[16]. Re-bleeding was defined as hematemesis and/or melena, hypotension (a drop in systolic blood pressure of > 20 mmHg from baseline), fall in 2 gm/dL of hemoglobin and/or transfusion requirement of $\geqslant$ 2 units of packed red cells within that time.

Data analysis

Statistical interpretation of data was performed using Statistical Program for Social Sciences (SPSS) version 13. Results were expressed as mean ± SD for all continuous variables (e.g., age, gender, hospital stay, units of packed cells *etc.*) and numbers (percentage) for categorical data (e.g., gender, Child's class, *etc.*). Analysis was performed by using the independent *t*-test, chi-square test and Fisher's exact test wherever appropriate. $P < 0.05$ was considered statistically significant.

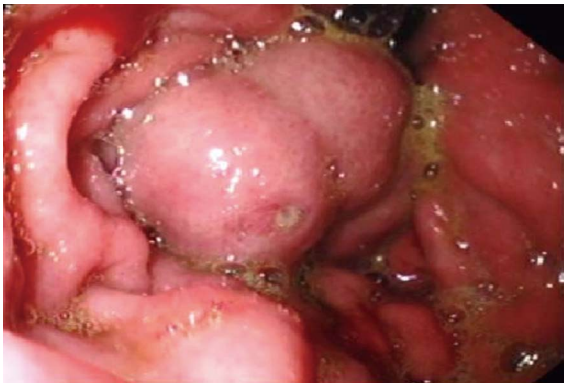

Figure 1 Isolated gastric varices with a nipple suggesting recent bleeding.

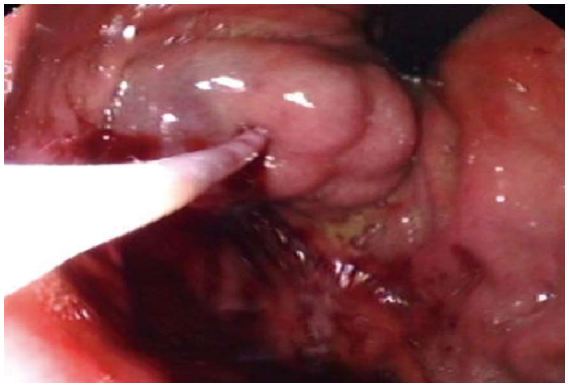

Figure 2 Injector needle with N- butyl cyanoacrylate in a large gastric fundal varix.

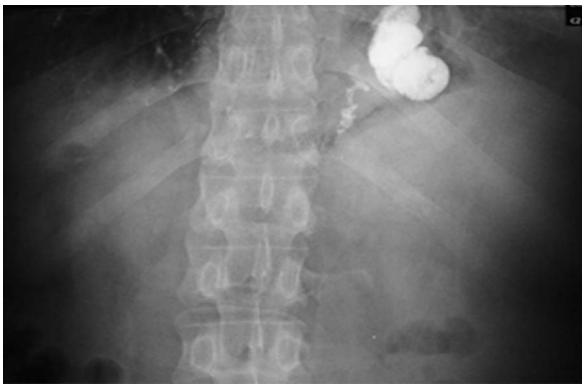

Figure 3 X-ray showing N-butylcyanoacrylate deposition in a gastric varix after sclerotherapy.

Table 2 Comparison between bleeding and non bleeding varices

Characteristics	Bleeding GV *n* (%)	Non bleeding GV *n* (%)	*P*
Age	50.48 ± 11.2	47.52 ± 12.7	0.14
Gender			
Male	30 (60)	111 (65.3)	
Female	20 (40)	59 (34.7)	0.49
Child Pugh class.			
A	12 (24)	27 (15.9)	
B	26 (52)	83 (48.8)	0.22
C	12 (24)	60 (35.3)	
Type of GV			
GOV- I	16 (32)	77 (45.3)	0.09
GOV-Ⅱ	15 (30)	58 (34.1)	0.58
IGV- I	22 (44)	39 (22.9)	< 0.01
IGV-II	0 (0)	11 (6.5)	0.06
Etiology of PHTN			
HBV	6 (12)	29 (17.1)	0.39
HCV	34 (68)	121 (71.2)	0.76
NBNC	6 (12)	21 (12.4)	0.94
Alcoholic	02 (2)	03 (1.8)	0.48
Non cirrhotic PHTN	01 (2)	08 (4.7)	0.59
Wilson's disease	01 (2)	00 (0)	0.06

RESULTS

The prevalence of bleeding gastric varices in patients with portal hypertension was 15% (220/1436) and the incidence of bleeding was 22.7% (50/220). The mean age of our patients with gastric varices was 50 ± 11 years, male patients accounting for 65% (141). The main etiology of bleeding gastric varices was hepatitis C-related cirrhosis in 34 (68%), followed by hepatitis B virus in 6 and non B non C cirrhosis in 6 (12%) patients, respectively. Alcoholic liver disease was found in 2 patients (4%), non cirrhotic portal hypertension in 1 patient and Wilson's disease in 1 patient, respectively. Twelve patients (24%) belonged to Child-Pugh A, 26 (52%) to Child-Pugh B, and 12 (24%) to Child-Pugh C.

Out of the 50 bleeding GV patients, IGV- I was seen in 22 patients (44%), GOV- I in 16 patients (32%), and GOV-Ⅱ in 15 patients (30%), concomitant GOV- I with GOV-Ⅱ in 3 patients. N-butyl cyanoacrylate (2 mL diluted in 1 cc lipoidal) was injected intravariceally in all patients with bleeding GV. The characteristics of bleeding and non bleeding gastric varices are shown in Table 2.

Among these 50 patients, 43 (86%) had active bleeding and 7 (14%) showed evidence of recent bleeding. Most varices (n = 48) were large (F3) according to Hashizume classification[20]. We compared bleeding and non bleeding GV and found that IGV- I was seen in 22/50 (44%) patients who had bleeding and in 39/170 patients (23%) patients who did not have bleeding (P < 0.003). Similarly, IGV-Ⅱ was observed in 0/50 (0%) and 11/170 (6.4%), GOV- I in 16/50 (32%) and 77/170 patients (45.2%) who did not have bleeding, GOV-Ⅱ in 15/50 (30%) and 50/170 patients (29.4%) who did not have bleeding from gastric varices, respectively.

The overall success rate for achieving primary hemostasis with NBC was 100% without recurrent bleeding within 48 h. A mean of 2.0 ± 0.5 cc NBC was injected in each patient.

Re-bleeding occurred in 7 (14%) patients after 48 h. Secondary hemostasis with repeat NBC sclerotherapy was achieved in 4 (57%) patients. Three patients died after repeat sclerotherapy: one during transjugular intrahepatic portosystemic stem shunt (TIPSS), one during surgery and one due to uncontrollable torrential bleeding. Treatment failure-related mortality rate was 6 % (3/50).

No major side effects occurred in most patients during and after NBC sclerotherapy. Three patients reported mild retrosternal chest pain which subsided within the next 24 h (Figure 3).

DISCUSSION

The overall incidence of gastric varices in patients with portal hypertension is 2%-70%[3]. Furthermore, we found that the incidence of bleeding from gastric varices in our patients is 22.7%, which is also similar to other reports[5].

In this study, the rate for primary hemostasis with NBC injection is consistent with the reported rate of 90% to 97% in other studies[8,14,16,21-23]. In our study, sclerotherapy with 2 mL NBC diluted in 1 mL lipoidal was effective in control of bleeding in all our patients during the first 48 h.

We used a higher dose of NBC with 2:1 dilution. Our technique avoids dilution of NBC, thus decreasing chances of migration and embolization as instantaneous polymerization is delayed.

It was reported that a hemostasis rate of 95% can be achieved without dilution of NBC, but serious side effects such as embolization may occur[24].

The risk of embolization increases with over dilution of cyanoacrylate which can slow down the process of polymerization. We avoided this problem by diluting 2 mL of NBC in 1 mL of lipoidal which was injected slowly over 45-90 s. Although the volume of injection was large, the side effects of a large volume were avoided and good hemostais was achieved by keeping a balanced dilution.

We also studied the predictors of the first gastric variceal bleeding, showing that the increased risk of bleeding is associated with larger varices including predominant IGV- I and GOV- I [5]. Kim *et al*[23] found that advanced Child-Pugh class and varix > 5 mm in size are associated with an increased risk of bleeding. Unlike esophageal varices, a high porto-systemic pressure > 12 mmHg does not cause GV bleeding, which is probably related to the high frequency of spontaneous gastro-renal shunts[17].

Cyanoacrylate therapy can improve and control re-bleeding. The high mortality rate is primarily a reflection of underlying advanced liver disease unaffected by the injection of cyanoacrylate[25,26]. This is further explained by a study of Kim *et al*[23] in which they prospectively followed a cohort of patients with gastric varices who did not undergo endoscopic therapy and found that the mortality rate is 35% over a median of 15 mo. Therefore, the role and efficacy of sclerotherapy for prophylaxis against recurrent bleeding are questionable.

In the present study, re-bleeding occurred after 48 h in 7 (14%) patients and was controllable in 4 (57%) with repeat injection of NBC. It was reported that the incidence of re-bleeding ranges from 23% to 35%[8,10,16]. However, Kind *et al*[14] reported that the incidence of re-bleeding is 15.5%.

Treatment failure-related mortality in our study was 6%, which is consistent with the reported mortality[16]. Another study showed that the mortality is 12.5% due to re-bleeding immediately after NBC sclerotherapy[8]. Kind *et al*[14] reported that the hospital mortality rate is 19.5% in patients with bleeding gastric varices.

In conclusion, endoscopic injection of NBC at a dilution of 2:1 appears to be effective and safe for the control of hemostasis in patients with bleeding gastric varices. If NBC is injected slowly, a large amount of NBC in proper dilution can be used without serious side effects.

REFERENCES

1 **Soehendra N**, Grimm H, Nam VC, Berger B. N-butyl-2-cyanoacrylate: a supplement to endoscopic sclerotherapy. *Endoscopy* 1987; **19**: 221-224

2 **Watanabe K**, Kimura K, Matsutani S, Ohto M, Okuda K. Portal hemodynamics in patients with gastric varices. A study in 230 patients with esophageal and/or gastric varices using portal vein catheterization. *Gastroenterology* 1988; **95**: 434-440

3 **Sarin SK**, Kumar A. Gastric varices: profile, classification, and management. *Am J Gastroenterol* 1989; **84**: 1244-1249

4 **Lo GH**, Lai KH, Cheng JS, Chen MH, Chiang HT. A prospective, randomized trial of butyl cyanoacrylate injection versus band ligation in the management of bleeding gastric varices. *Hepatology* 2001; **33**: 1060-1064

5 **Sarin SK**, Lahoti D, Saxena SP, Murthy NS, Makwana UK. Prevalence, classification and natural history of gastric varices: a long-term follow-up study in 568 portal hypertension patients. *Hepatology* 1992; **16**: 1343-1349

6 **Sarin SK**. Long-term follow-up of gastric variceal sclerotherapy: an eleven-year experience. *Gastrointest Endosc* 1997; **46**: 8-14

7 **Soehendra N**, Nam VC, Grimm H, Kempeneers I. Endoscopic obliteration of large esophagogastric varices with bucrylate. *Endoscopy* 1986; **18**: 25-26

8 **Huang YH**, Yeh HZ, Chen GH, Chang CS, Wu CY, Poon SK, Lien HC, Yang SS. Endoscopic treatment of bleeding gastric varices by N-butyl-2-cyanoacrylate (Histoacryl) injection: long-term efficacy and safety. *Gastrointest Endosc* 2000; **52**: 160-167

9 **Rengstorff DS**, Binmoeller KF. A pilot study of 2-octyl cyanoacrylate injection for treatment of gastric fundal varices in humans. *Gastrointest Endosc* 2004; **59**: 553-558

10 **Oho K**, Iwao T, Sumino M, Toyonaga A, Tanikawa K. Ethanolamine oleate versus butyl cyanoacrylate for bleeding gastric varices: a nonrandomized study. *Endoscopy* 1995; **27**: 349-354

11 **Shiha G**, El-Sayed SS. Gastric variceal ligation: a new technique. *Gastrointest Endosc* 1999; **49**: 437-441

12 **Yang WL**, Tripathi D, Therapondos G, Todd A, Hayes PC. Endoscopic use of human thrombin in bleeding gastric varices. *Am J Gastroenterol* 2002; **97**: 1381-1385

13 **Chiu KW**, Changchien CS, Chuah SK, Tai DI, Chiou SS, Lee CM, Chen JJ. Endoscopic injection sclerotherapy with 1.5% Sotradecol for bleeding cardiac varices. *J Clin Gastroenterol* 1997; **24**: 161-164

14 **Kind R**, Guglielmi A, Rodella L, Lombardo F, Catalano F, Ruzzenente A, Borzellino G, Girlanda R, Leopardi F, Pratticò F, Cordiano C. Bucrylate treatment of bleeding gastric varices: 12 years' experience. *Endoscopy* 2000; **32**: 512-519

15 **Dhiman RK**, Chawla Y, Taneja S, Biswas R, Sharma TR, Dilawari JB. Endoscopic sclerotherapy of gastric variceal bleeding with N-butyl-2-cyanoacrylate. *J Clin Gastroenterol* 2002; **35**: 222-227

16 **Akahoshi T**, Hashizume M, Shimabukuro R, Tanoue K, Tomikawa M, Okita K, Gotoh N, Konishi K, Tsutsumi N, Sugimachi K. Long-term results of endoscopic Histoacryl injection sclerotherapy for gastric variceal bleeding: a 10-year experience. *Surgery* 2002; **131**: S176-S181

17 **Stanley AJ**, Jalan R, Ireland HM, Redhead DN, Bouchier IA, Hayes PC. A comparison between gastric and oesophageal variceal haemorrhage treated with transjugular intrahepatic portosystemic stent shunt (TIPSS). *Aliment Pharmacol Ther* 1997; **11**: 171-176

18 **Miyazaki S**, Yoshida T, Harada T, Shigemitsu T, Takeo Y, Okita K. Injection sclerotherapy for gastric varices using N-butyl-2-cyanoacrylate and ethanolamine oleate. *Hepatogastroenterology* 1998; **45**: 1155-1158

19 **Lee YT**, Chan FK, Ng EK, Leung VK, Law KB, Yung MY,

Chung SC, Sung JJ. EUS-guided injection of cyanoacrylate for bleeding gastric varices. *Gastrointest Endosc* 2000; **52**: 168-174
20 **Hashizume M**, Kitano S, Yamaga H, Koyanagi N, Sugimachi K. Endoscopic classification of gastric varices. *Gastrointest Endosc* 1990; **36**: 276-280
21 **Quinn J**, Wells G, Sutcliffe T, Jarmuske M, Maw J, Stiell I, Johns P. A randomized trial comparing octylcyanoacrylate tissue adhesive and sutures in the management of lacerations. *JAMA* 1997; **277**: 1527-1530
22 **Nguyen AJ**, Baron TH, Burgart LJ, Leontovich O, Rajan E, Gostout CJ. 2-Octyl-cyanoacrylate (Dermabond), a new glue for variceal injection therapy: results of a preliminary animal study. *Gastrointest Endosc* 2002; **55**: 572-575
23 **Kim T**, Shijo H, Kokawa H, Tokumitsu H, Kubara K, Ota K, Akiyoshi N, Iida T, Yokoyama M, Okumura M. Risk factors for hemorrhage from gastric fundal varices. *Hepatology* 1997; **25**: 307-312
24 **D'Imperio N**, Piemontese A, Baroncini D, Billi P, Borioni D, Dal Monte PP, Borrello P. Evaluation of undiluted N-butyl-2-cyanoacrylate in the endoscopic treatment of upper gastrointestinal tract varices. *Endoscopy* 1996; **28**: 239-243
25 **Sarin SK**, Agarwal SR. Gastric varices and portal hypertensive gastropathy. *Clin Liver Dis* 2001; **5**: 727-767, x
26 **Pugh RN**, Murray-Lyon IM, Dawson JL, Pietroni MC, Williams R. Transection of the oesophagus for bleeding oesophageal varices. *Br J Surg* 1973; **60**: 646-649

S- Editor Liu Y **L- Editor** Wang XL **E- Editor** Lu W

PO Box 2345, Beijing 100023, China
www.wjgnet.com
wjg@wjgnet.com

World J Gastroenterol 2007 February 28; 13(8): 1252-1256
World Journal of Gastroenterology ISSN 1007-9327

RAPID COMMUNICATION

Detection of small hepatocellular carcinoma: Comparison of dynamic enhancement magnetic resonance imaging and multiphase multirow-detector helical CT scanning

Hong Zhao, Jin-Lin Yao, Ying Wang, Kang-Rong Zhou

Hong Zhao, Ying Wang, Department of Radiology, Affiliated Fifth Hospital, Zhongshan University, Zhuhai 519000, Guangdong Province, China
Jin-Lin Yao, Department of Surgery, Affiliated Fifth Hospital, Zhongshan University, Zhuhai 519000, Guangdong Province, China
Kang-Rong Zhou, Department of Radiology, Zhongshan Hospital, Fudan University, Shanghai 200032, Guangdong Province, China
Supported by a financial assistance from Zhuhai Technology Bureau, No. PC20052025
Correspondence to: Zhao Hong, Department of Radiology, Affiliated Fifth Hospital, Zhongshan University, Zhuhai 519000, Guangdong Province, China. zhaohongmd@sina.com
Telephone: +86-756-13924705561
Received: 2006-12-07 Accepted: 2007-01-23

Abstract

AIM: To compare the gadolinium-enhanced multiphase dynamic magnetic resonance imaging (MRI) and multiphase multirow-detector helical CT (MDCT) scanning for detection of small hepatocellular carcinoma (HCC).

METHODS: MDCT scanning and baseline MRI with SE T1-WI and T2-WI sequence combined with FMPSPGR sequence were performed in 37 patients with 43 small HCCs. Receiver operating characteristic (ROC) curves were plotted to analyze the results for modality.

RESULTS: The areas below ROC curve (Az) were calculated. There was no statistical difference in dynamic enhancement MDCT and MRI. The detection rate of small HCC was 97.5%-97.6% on multiphase MDCT scanning and 90.7%-94.7% on MRI, respectively. The sensitivity of detection for small HCC on MDCT scanning was higher than that on dynamic enhancement MRI. The sensitivity of detection for minute HCC (tumor diameter $\leqslant$ 1 cm) was 90.0%-95.0% on MDCT scanning and 70.0%-85.0% on MRI, respectively.

CONCLUSION: MDCT scanning should be performed for early detection and effective treatment of small HCC in patients with chronic hepatitis and cirrhosis during follow-up.

Key words: Hepatocellular carcinoma; X-ray computed tomography; Magnetic resonance imaging

Zhao H, Yao JL, Wang Y, Zhou KR. Detection of small hepatocellular carcinoma: Comparison of dynamic enhancement magnetic resonance imaging and multiphase multirow-detector helical CT scanning. *World J Gastroenterol* 2007; 13(8): 1252-1256

http://www.wjgnet.com/1007-9327/13/1252.asp

INTRODUCTION

Hepatocellular carcinoma (HCC) is the most common primary malignancy tumor of the liver. Dual-phase CT scanning is a sensitive method for the detection of HCC. The developments in rapid magnetic resonance imaging (MRI) in combination with gadolinium-enhanced multiphase multirow-detector helical CT (MDCT) scanning can obviously improve the detection of small HCC. However, MRI and MDCT have a lower sensitivity for detecting small HCC, especially minute HCC. MDCT scanning has a higher sensitivity for detection of small HCC[1-5]. The purpose of this study was to compare the dynamic enhancement MRI and MDCT for the detection of small HCC in patients with chronic liver disease and cirrhosis and to value the clinical role of new imaging technology in detection of small HCC.

MATERIALS AND METHODS

Patient Sample

Between October 2002 and December 2004, 37 patients (29 men, 8 women, mean age: 56 years, rang: 29-70 years) with chronic hepatic disease and cirrhosis who were suspected of having HCC during postoperative follow-up were included in this study. All the patients underwent multiphase contrast enhanced dynamic MDCT and gadolinium-enhanced dynamic MRI at 7 d intervals.

Lesion confirmation

Small HCC was confirmed in 24 of 37 patients. Fifteen of the 24 patients with 43 small HCCs underwent surgery and pathologic examination. Of the 15 patients undergoing surgery, small HCC was found in 2 by needle biopsy, in

Table 1 Area under the ROC curve and *P* value for MRI and MDCT in detecting HCC

	Observer 1		Observer 2	
Imaging techniques	A_z value	95% CI	A_z value	95% CI
MDCT	0.983	0.950-1.013	0.99	0.968-1.012
MRI	0.951	0.901-1.001	0.94	0.882-0.999
t value	-0.425		-0.956	
P value	0.672		0.348	

5 by digital subtraction angiography (DSA), and in 2 by iodized oil CT and elevated serum α-fetoprotein level (> 400 ng/mL) and ultrasound examination. Two out of 37 patients undergoing multiphase dynamic contrast enhanced MDCT and dynamic gadolinium enhancement MRI respectively, were suspected of having small HCC. Their serum α-fetoprotein level was decreased. Ultrasound examination one month after follow-up and multiphase dynamic contrast enhanced MDCT examination three months after follow-up showed that the lesions remained unchanged. Five out of 37 patients with liver cirrhosis undergoing gadolinium enhancement dynamic MRI scanning and multiphase dynamic contrast enhanced MDCT imaging were suspected of having small HCC. However, small HCC could not be found. Small HCC was not found in 3 of 5 patients who were followed up for 2-3 mo by contrast-enhanced MDCT, and in 2 of 5 patients who were followed up for 3 mouths by enhancement dynamic MRI. Multiphase dynamic contrast-enhanced MDCT and MRI examination displayed no new liver lesions in another 6 patients who were not diagnosed having small HCC during the tree-month follow-up period. The size of small HCC was ⩽ 1 cm in 20, and > 1 cm or ⩽ 3 cm in 23 of 43 small HCCs, respectively.

MDCT

All CT examinations were performed using a commercially available multidetector CT scanner (Marconi Mx 8000) with 0.5-0.75 s gantry rotation speed, 23.3 mm/s table speed, 5.0 mm-thick section, reconstruction interval 2.5 mm, 120 Kv and 200-250 mA.

Entire pre-contrast hepatic scanning was followed by a nonionic contrast enhancement (Omnipaque 300 mg I/mL) with 1.5 mL/kg and injection rate of 3 mL/s *via* an antecubital vein. Multiphase acquisitions were performed. The scanning delay set for early arterial phase (EAP), late arterial phase (LAP) and portal venous phase (PVP) was 21 s, 34 s and 85 s, respectively. Each of the entire liver scanning in cephalad-caudal orientation was completed in 4-8 s with patient's breath held.

MRI

MRI was performed with a GE Signa 1.5 T MR imaging system. A standard whole-body coil was used as the receiver coil for examinations. All the 37 patients underwent baseline MR imaging, including breath-hold spin-echo T1- weighted imaging(TR 500-700 ms, TE 14-20 ms), fat-suppressed fast spin-echo T2-weighted imaging (TR 2000-4000 ms, TE 80-120 ms) and gadolinium-enhanced triphasic dynamic gradient-recalled echo imaging with a fast multiplanar spoiled-gradient-recalled echo breath-hold imaging (FMPSPGR TR/TE/Flip Angle = 100-150 ms/4.6 ms/60-90°), matrix (256 × 128), 7 mm-thick section, and 1 acquisition. MR imaging was performed before and after gadolinium-enhanced dynamic gradient-recalled echo imaging (Gd-DTPA, Magnevist, Germany, NJ). Dynamic imaging was performed with a fast multiplanar spoiled-gradient-recalled echo breath-hold imaging. The contrast material was 0.2 mL/kg of body weight administered as a rapid IV bolus. After un-enhanced imaging, arterial phase image was obtained during 20-25 s. The second and third sets of images were obtained after approximately 60-90 s and 3 min, respectively.

Imaging analysis

All MRI and MDCT images were reviewed by two experienced radiologists, who knew that patients with liver cirrhosis were at risk of developing HCC, but were unaware of the presence and location of liver lesions and the result of other imaging examinations. The size and number of lesions were analyzed for the various multiphase dynamic contrast-enhanced MR sequences and MDCT imagines (early arterial, later arterial, portal phases) of the 37 patients.

The readers scored each imagine for the presence or absence of focal hepatic lesions, and assigned confidence levels to their observation: 1 = definite presence, 2 = probable presence, 3 = equivocal, 4 = probable absence, 5 = definite absence[6].

Statistical analysis

For each imaging method, a binomial receivor operationg characteristic (ROC) curve was fitted to each radiologist' s confidence rating using maximum likelihood estimation. The diagnostic accuracy of each imaging set for each observer and the composite data were calculated by measuring the area under the alternative free response ROC curve. The differences between imaging sets in terms of the mean Az value, were statistically analyzed using the two-tail Student's t test for paired data. The sensitivity and positive predictive values for each image set were then calculated. The sensitivity of each observer was determined by detecting the number of lesions assigned a confidence level of 1 or 2 from 42 HCCs. The degree of inter-observer agreement was calculated with chance-corrected kappa statistics. In general, a kappa statistic value greater than 0.75 is considered excellent agreement, 0.4-0.75 good agreement, and less than 0.4 poor agreement[6-8]. Statistical analyses were performed using the SPSS Statistical Programs, version 10.0. $P < 0.05$ was considered statistically different (Figure 1).

RESULTS

The kappa values were excellent between observers 1 and 2 for multiphase dynamic contrast-enhanced MDCT (κ value = 0.883) and MRI (κ value = 0.812). The A_z values calculated by each observer with multiphase dynamic contrast-enhanced MDCT and MRI for 42 lesions are shown in Table 1. For detection of lesions, two observers achieved a slightly higher diagnostic performance with

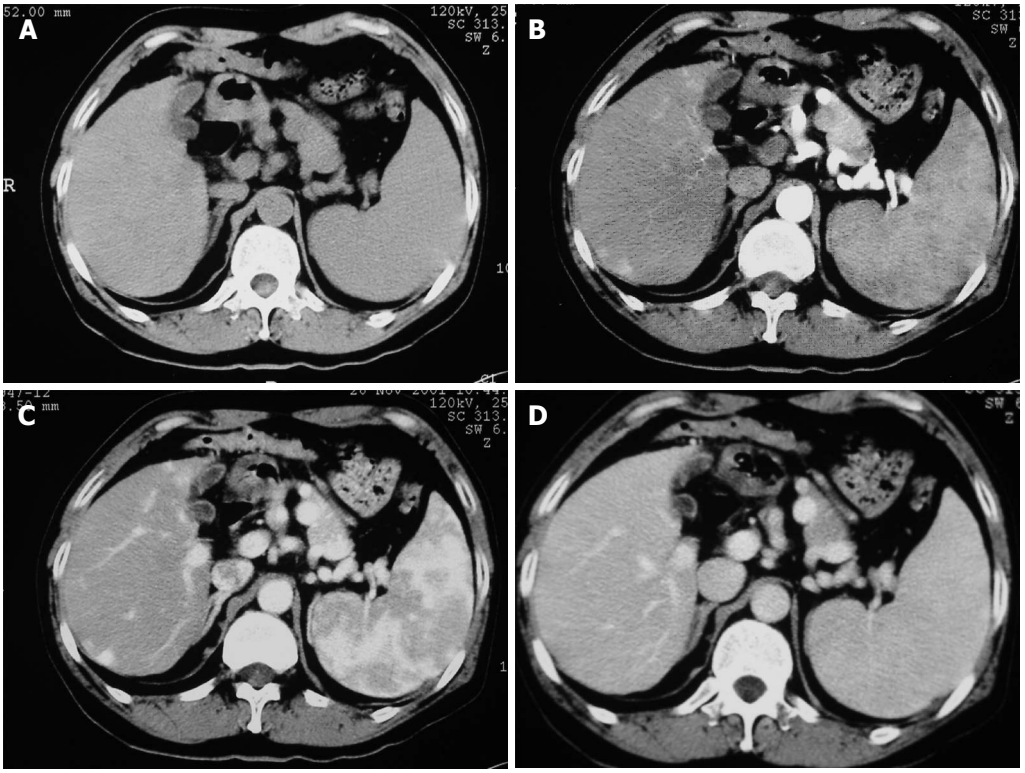

Figure 1 A 42-yr old man with pathologically proven hepatocellular carcinoma. **A**: Plan scanning; **B**: early arterial phase MDCT image showing slightly enhanced nodule in right lobe; **C**: later arterial phase MDCT image showing obvious enhanced lesion; **D**: on the portal venous phase MDCT image showing slight low attenuation.

Table 2 Sensitivity and positive predictive value for MRI and MDCT in detecting small HCC *n* (%)

Imaging Technique		Sensitivity (%)			Positive predictive value (%)
		≤ 1 cm SHCC *n* = 20	> 1 cm ≤ 3 cm SHCC *n* = 23	Total SHCC *n* = 43	*n* = 43
Observer 1	MDCT	19 (95.0)	22 (95.7)	41 (95.31)	97.6
	MRI	17 (85.0)	22 (95.72)	39 (90.7)	90.7
Observer 2	MDCT	18 (90.0)	21 (91.31)	39 (90.79)	97.5
	MRI	14 (70.0)	22 (95.7)	36 (83.7)	94.7

MDCT than with MRI, but the difference in the mean Az values of both imagine sets was not significant. The chance-corrected kappa values indicated the confidence levels for the imagine interpretation of the ROC analysis between the two observers.

The sensitivity and positive predictive values obtained with dynamic contrast-enhanced MDCT and MRI are shown in Table 2. For less than or equal to 1 cm minute HCC, the sensitivity of MRI was 85% and 70% , respectively for the two observers, but the sensitivity of MDCT for the two observers was higher than that of MRI (95% and 90%, respectively). The positive predictive value for MDCT was 97.5%-97.6% for MDCT and 90.7%-94.7% for MRI, respectively. There were less false-positive findings on MDCT.

DISCUSSION

Most HCCs occur in cirrhotic liver. Oka *et al*[9] in a 6-year follow-up study of 140 patients with cirrhosis, Oka *et al*[9] found that the cumulative incidence of HCC is 39% and its per year occurrence rate is 5.3%-8.8%. Small HCC results from cirrhosis. Early detection and diagnosis of small HCC are important in its effective treatment. Lim *et al*[10] have analyzed the sensitivity and specificity of double phase SCT in detecting small HCC. It was reported that imaging technology should be used in detecting small HCC[9,11].

Multiphase dynamic CT using a helical scanner has become the standard technology for detection and diagnosis of small HCC. The detection of hepatic nodular lesions by CT depends on the attenuation difference in the normal parenchyma and enhancement nodule lesions. Multiphase dynamic CT scanning can show the change between the tumor and its surrounding parenchyma. This may in part be a result of the difference in uptake and secretion of contrast material by hepatocytes of the normal liver parenchyma and HCC cells. Because the arterial phase is shorter than the portal venous phase, the scanning time of hepatic lesions is not the optimal time of tumors. Therefore, the dual-phase scanning is difficult to detect small HCC[7,9,11,12].

MRI is a less invasive and more feasible technique. The spin-echo sequence and gadolinium-enhanced triphasic dynamic breath-hold imaging are more effective. The advantage of contrast enhancement MRI is to deliver a small contrast material volume over a shorter period of time, which results in a tighter bolus. MRI has several advantages over dual-phase SCT in detection and characterization of small HCC, including greater soft-tissue contrast and sensitivity to intravascular contrast agent, and more types of sequences[6,14,16].

Tang *et al*[17] reported that 94% of small HCC can be found in cirrhotic liver by dynamic gadolinum-enhanced MRI. Yan *et al*[18] reported that 94.12% of small HCC (diameter < 1 cm) can be detected by MRI. Kim *et al*[19]

reported that 67% of small HCC (diameter < 1 cm) can be displayed by MRI.

The optimal imaging technology can detect most of small HCC. MDCT scanner recently has been introduced into clinical CT practice, and allows faster Z-axis coverage speed and hepatic imaging with thin image thickness in a very short time. MDCT can scan the entire liver during the double arterial phase. In addition, it improves the sensitivity of depicting small HCC and increases conspicuity for hypervascular lesions, and sensitivity of detecting small HCC[4,5,24].

The ROC curve analysis revealed that there was a higher validity for two imaging methods. Two observers achieved slightly higher diagnostic efficiency with multiphase contrast-enhanced MDCT than with dynamic enhanced MRI, but the difference in the areas below the ROC cure was not statistically significant (observer 1, $P = 0.672$; observer 2, $P = 0.348$). Multiphase contrast-enhanced MDCT had slightly higher predictive values than dynamic contrast enhanced MRI. The positive predictive value for MDCT and MRI by observer 1 was 97.6% and 90.7%, and 97.5% and 94.7% by observer 2, respectively. There were less false-positive findings on MDCT, but whether the diagnostic efficiency of multiphase contrast-enhanced MDCT is superior to dynamic contrast enhancement MRI needs further study with a large sample.

It was reported that the sensitivity of MRI in detection mall HCC is lower[20-22]. However, several factors can affect the visualization of primary focal hepatic lesions during contrast-enhanced or un-enhanced MRI, including the functionality of normal hepatic parenchyma, as well as the dimension, composition, and degree of visibility of the lesions, and the residual hepatic functionality of neoplastic cells themselves[23,24]. Since these factors tend to vary from patient to patient, it is often difficult to predict the behavior of a given lesion. There is a very good correlation between the blood supply and the degree of pathologic characteristics of hepatic lesions.

In our study, the sensitivity of MRI in detecting small HCC ($\leqslant$ 1 cm) was 70% and 85%, respectively. Seventy percent of 20 small HCCs showed isointensity, 4 demonstrated the signal change from isointensity to hyperintensity during arterial phase, portal venous phase, and delay phase. The other lesions displayed the signal change from hyperintensity to isointensity. These different findings may be due to the following reasons. First, cirrhotic liver has homogeneous or nonhomogeneous density, the signal intensity of cirrhotic liver parenchyma is higher than normal liver parenchyma, and the high patching signal intensity on T1-weigted imagines is due to fatty deposition or hepatitis. Second, since the degree of the liver parenchyma is lower because of hemosiderin deposition and large fibrous tissue in the liver parenchyma, the impaired hepatic cells could not absorb contrast material. Third, the portal hypertension splits liver blood flow into collateral vessels, thus reducing the contrast material in the liver parenchyma. Forth, since the time window of arterial phase is narrower and the imaging time of MRI is fixed at the arterial phase 20-25 s, portal venous phase 60-90 s, and delayed phase 120 s, it is difficult to show a real arterial phase[4].

In conclusion, small HCC often manifests as relatively small lesions in cirrhotic livers. There is an obviously enhanced small nodule in hepatic arterial phase whether it has homogeneous or nonhomogeneous density. The signal intensity and contrast enhancement patterns cannot be used in the final diagnosis of small HCC. It is important for patients with cirrhosis to undergo follow-up imaging more frequently. Nodule growth is highly predictive of small HCC[21,26]. Further study is needed since our study has some limitations.

REFERENCES

1 **Braga HJ**, Choti MA, Lee VS, Paulson EK, Siegelman ES, Bluemke DA. Liver lesions: manganese-enhanced MR and dual-phase helical CT for preoperative detection and characterization comparison with receiver operating characteristic analysis. *Radiology* 2002; **223**: 525-531

2 **Savci G**. The changing role of radiology in imaging liver tumors: an overview. *Eur J Radiol* 1999; **32**: 36-51

3 **Kawata S**, Murakami T, Kim T, Hori M, Federle MP, Kumano S, Sugihara E, Makino S, Nakamura H, Kudo M. Multidetector CT: diagnostic impact of slice thickness on detection of hypervascular hepatocellular carcinoma. *AJR Am J Roentgenol* 2002; **179**: 61-66

4 **Foley WD**, Mallisee TA, Hohenwalter MD, Wilson CR, Quiroz FA, Taylor AJ. Multiphase hepatic CT with a multirow-detector CT scanner. *AJR Am J Roentgenol* 2000; **175**: 679-685

5 **Murakami T**, Kim T, Takamura M, Hori M, Takahashi S, Federle MP, Tsuda K, Osuga K, Kawata S, Nakamura H, Kudo M. Hypervascular hepatocellular carcinoma: detection with double arterial phase multi-detector row helical CT. *Radiology* 2001; **218**: 763-767

6 **Kondo H**, Kanematsu M, Hoshi H, Murakami T, Kim T, Hori M, Matsuo M, Nakamura H. Preoperative detection of malignant hepatic tumors: comparison of combined methods of MR imaging with combined methods of CT. *AJR Am J Roentgenol* 2000; **174**: 947-954

7 **Yamashita Y**, Mitsuzaki K, Yi T, Ogata I, Nishiharu T, Urata J, Takahashi M. Small hepatocellular carcinoma in patients with chronic liver damage: prospective comparison of detection with dynamic MR imaging and helical CT of the whole liver. *Radiology* 1996; **200**: 79-84

8 **Ward J**, Guthrie JA, Scott DJ, Atchley J, Wilson D, Davies MH, Wyatt JI, Robinson PJ. Hepatocellular carcinoma in the cirrhotic liver: double-contrast MR imaging for diagnosis. *Radiology* 2000; **216**: 154-162

9 **Oka H**, Kurioka N, Kim K, Kanno T, Kuroki T, Mizoguchi Y, Kobayashi K. Prospective study of early detection of hepatocellular carcinoma in patients with cirrhosis. *Hepatology* 1990; **12**: 680-687.

10 **Lim JH**, Kim CK, Lee WJ, Park CK, Koh KC, Paik SW, Joh JW. Detection of hepatocellular carcinomas and dysplastic nodules in cirrhotic livers: accuracy of helical CT in transplant patients. *AJR Am J Roentgenol* 2000; **175**: 693-698

11 **Peterson MS**, Baron RL, Murakami T. Hepatic malignancies: usefulness of acquisition of multiple arterial and portal venous phase images at dynamic gadolinium-enhanced MR imaging. *Radiology* 1996; **201**: 337-345

12 **Furuta A**, Ito K, Fujita T, Koike S, Shimizu A, Matsunaga N. Hepatic enhancement in multiphasic contrast-enhanced MDCT: comparison of high- and low-iodine-concentration contrast medium in same patients with chronic liver disease. *AJR Am J Roentgenol* 2004; **183**: 157-162

13 **Francis IR**, Cohan RH, McNulty NJ, Platt JF, Korobkin M, Gebremariam A, Ragupathi KI. Multidetector CT of the liver and hepatic neoplasms: effect of multiphasic imaging on tumor conspicuity and vascular enhancement. *AJR Am J Roentgenol* 2003; **180**: 1217-1224

14 **Yu JS**, Kim KW, Kim EK, Lee JT, Yoo HS. Contrast

enhancement of small hepatocellular carcinoma: usefulness of three successive early image acquisitions during multiphase dynamic MR imaging. *AJR Am J Roentgenol* 1999; **173**: 597-604

15 **Semelka RC**, Martin DR, Balci C, Lance T. Focal liver lesions: comparison of dual-phase CT and multisequence multiplanar MR imaging including dynamic gadolinium enhancement. *J Magn Reson Imaging* 2001; **13**: 397-401

16 **Ito K**, Mitchell DG. Imaging diagnosis of cirrhosis and chronic hepatitis. *Intervirology* 2004; **47**: 134-143

17 **Tang Y**, Yamashita Y, Arakawa A, Namimoto T, Mitsuzaki K, Abe Y, Katahira K, Takahashi M. Detection of hepatocellular carcinoma arising in cirrhotic livers: comparison of gadolinium- and ferumoxides-enhanced MR imaging. *AJR Am J Roentgenol* 1999; **172**: 1547-1554

18 **Fu-Hua Y**, Jun Yang, Meng-Su Z. comparison of dynamic MRI ,and helical CT and ultrasonic imaging to diagnosis small hepatocellular carcinoma. *Zhongguo Yixue Jisuanji Chengxiang Zazi* 1997; **3**: 20-24

19 **Kim T**, Murakami T, Oi H, Matsushita M, Kishimoto H, Igarashi H, Nakamura H, Okamura J. Detection of hypervascular hepatocellular carcinoma by dynamic MRI and dynamic spiral CT. *J Comput Assist Tomogr* 1995; **19**: 948-954

20 **Krinsky GA**, Lee VS, Theise ND, Weinreb JC, Rofsky NM, Diflo T, Teperman LW. Hepatocellular carcinoma and dysplastic nodules in patients with cirrhosis: prospective diagnosis with MR imaging and explantation correlation. *Radiology* 2001; **219**: 445-454

21 **Jeong YY**, Mitchell DG, Kamishima T. Small (< 20 mm) enhancing hepatic nodules seen on arterial phase MR imaging of the cirrhotic liver: clinical implications. *AJR Am J Roentgenol* 2002; **178**: 1327-1334

22 **Kelekis NL**, Semelka RC, Worawattanakul S, de Lange EE, Ascher SM,Ahn IO, Reinhold C, Remer EM, Brown JJ, Bis KG, Woosley JT, Mitchell DG. Hepatocellular carcinoma in North America: a multiinstitutional study of appearance on T1-weighted, T2-weighted, and serial gadolinium-enhanced gradient-echo images. *AJR Am J Roentgenol* 1998; **170**: 1005-1013

23 **Grazioli L**, Morana G, Caudana R, Benetti A, Portolani N, Talamini G, Colombari R, Pirovano G, Kirchin MA, Spinazzi A. Hepatocellular carcinoma: correlation between gadobenate dimeglumine-enhanced MRI and pathologic findings. *Invest Radiol* 2000; **35**: 25-34

24 **Matsui O**, Kadoya M, Kameyama T, Yoshikawa J, Takashima T, Nakanuma Y, Unoura M, Kobayashi K, Izumi R, Ida M. Benign and malignant nodules in cirrhotic livers: distinction based on blood supply. *Radiology* 1991; **178**: 493-497

25 **Ichikawa T**, Kitamura T, Nakajima H, Sou H, Tsukamoto T, Ikenaga S, Araki T. Hypervascular hepatocellular carcinoma: can double arterial phase imaging with multidetector CT improve tumor depiction in the cirrhotic liver? *AJR Am J Roentgenol* 2002; **179**: 751-758

26 **Turnheim K**, Donath R, Weissel M, Kolassa N. Myocardial glucose uptake and breakdown during adenosine-induced vasodilation. *Pflugers Arch* 1976; **365**: 197-202

S- Editor Liu Y **L- Editor** Wang XL **E- Editor** Zhou T

PO Box 2345, Beijing 100023, China
www.wjgnet.com
wjg@wjgnet.com

World J Gastroenterol 2007 February 28; 13(8): 1257-1261
World Journal of Gastroenterology ISSN 1007-9327

RAPID COMMUNICATION

Aberrant expression of ether à go-go potassium channel in colorectal cancer patients and cell lines

Xiang-Wu Ding, Juan-Juan Yan, Ping An, Peng Lü, He-Sheng Luo

Xiang-Wu Ding, Juan-Juan Yan, Ping An, Peng Lü, He-Sheng Luo, Department of Gastroenterology, Renmin Hospital of Wuhan University, Wuhan 430060, Hubei Province, China
Xiang-Wu Ding, Department of Gastroenterology, Xiangfan Central Hospital, Xiangfan 441021, Hubei Province, China
Correspondence to: He-Sheng Luo, Department of Gastroenterology, Renmin Hospital of Wuhan University, Wuhan 430060, Hubei Province, China. xdong1971@163.com
Telephone: +86-27-88041911-2243 Fax: +86-27-88042292
Received: 2006-11-17 Accepted: 2006-12-06

Abstract

AIM: To study the expression of ether à go-go (Eag1) potassium channel in colorectal cancer and the relationship between their expression and clinico-pathological features.

METHODS: The expression levels of Eag1 protein were determined in 76 cancer tissues with paired non-cancerous matched tissues as well as 9 colorectal adenoma tissues by immunohistochemistry. Eag1 mRNA expression was detected in 13 colorectal cancer tissues with paired non-cancerous matched tissues and 4 colorectal adenoma tissues as well as two colorectal cancer cell lines (LoVo and HT-29) by reverse transcription PCR.

RESULTS: The frequency of positive expression of Eag1 protein was 76.3% (58/76) and Eag1 mRNA was 76.9% (10/13) in colorectal cancer tissue. Expression level of Eag1 protein was dependent on the tumor size, lymphatic node metastasis, other organ metastases and Dukes' stage ($P < 0.05$), while not dependent on age, sex, site and degree of differentiation. Eag1 protein and mRNA were negative in normal colorectal tissue, and absolutely negative in colorectal adenomas except that one case was positively stained for Eag1 protein.

CONCLUSION: Eag1 protein and mRNA are aberrantly expressed in colorectal cancer and occasionally expressed in colorectal adenoma. The high frequency of expression of Eag1 in tumors and the restriction of normal expression to the brain suggest the potential of this protein for diagnostic, prognostic and therapeutic purposes.

Key words: Colorectal cancer; Adenoma; Ether à go-go gene; Potassium channels

Ding XW, Yan JJ, An P, Lü P, Luo HS. Aberrant expression of ether à go-go potassium channel in colorectal cancer patients and cell lines. *World J Gastroenterol* 2007; 13(8): 1257-1261

http://www.wjgnet.com/1007-9327/13/1257.asp

INTRODUCTION

Ion channels play a vital role in the function of diverse cell types. In recent years, the concept of ion channels as therapeutic targets and diagnostic and prognostic biomarkers has attracted increasing interest, and trigged a wave of experimental results, identifying individual ion channels relevant with specific cancer types.

In 1969, several mutants from the fruit fly Drosophila melanogaster were produced following the treatment of adult males with ethyl methane sulfonate[1]. The mutants presented shaking of the legs under ether anesthesia and independent gene loci were found to be involved. One of these mutants exhibited a slow and rhythmic leg-shaking behavior; the locus involved was then named ether à go-go. Homology screening helped to identify other two sequences closely related to eag: the eag-related gene (erg) and the eag-like gene (elk); thus the EAG channels family comprises three subfamilies: EAG, ERG and ELK[2]. Two members for the eag subfamily, three for erg and two for elk are differentially expressed in different species including rat, bovine and humans. Two members of the eag subfamily are Eag1 (KCNH1, Kv10.1) and Eag2 (KCNH5, Kv10.2)[3].

Eag1 is detected only in the brain and placenta in the process of myoblast fusion, indicating that the channel is not expressed in differentiated peripheral tissues[4]. On the other hand, eag1 is expressed in several cell lines derived from human malignant tumors, such as neuroblastoma[5,6], melanoma[7], breast[5], and cervical carcinoma[5]. In these cell lines, Eag1 enhances the proliferation of the cells, and is required for the maintenance of growth. One of the most intriguing aspects of human eag1 channels is its relationship to cellular transformation. Cells transfected with Eag1 are able to grow in the absence of serum, lose contact inhibition, and induce aggressive tumors when implanted into immune-depressed mice[5]. Recently, functional expression of Eag1 has been described in clinical samples of cervical carcinoma[8]. Similarly, aberrant

expression of the channel has also been detected in sarcomas[9] and other tumors from diverse origins[12], while the surrounding tissues are devoid of Eag1 expression. Moreover, specific inhibition of Eag1 expression by antisense technique[5], siRNA[9,10] or by non-specific blockers[7,11] leads to a reduction in tumor cell proliferation *in vitro*.

The membrane protein Eag1 is accessible from the extracellular side and is predominantly present in tumor cells, represents a potential tumor marker and an interesting therapeutic target for cancer. For any potential clinical application it is an essential prerequisite that samples from human tumors overexpress the target Eag1. Colorectal cancer is a malignancy with a worldwide distribution, and the actual frequency of expression of Eag1 in colorectal tissue remained unknown. In this study, we explored the expression of Eag1 potassium channel in colorectal cancer and the relationship between their expression and clinicopathological features.

MATERIALS AND METHODS

Patients

Samples were obtained from Renmin Hospital of Wuhan University, according to a protocol approved by the Committee for the Conduct of Human Research. These patients had surgery between 2004 and 2005. Resected tissues were formalin-fixed and paraffin-embedded in the Department of Pathology. For immunohistochemical analysis, colorectal cancer tissue with paired non-cancerous matched tissue (NCMT) (n = 76) as well as colorectal adenoma tissue (from endoscopic biopsy) (n = 9) were obtained. For reverse transcription polymerase chain reaction, 13 colorectal cancer tissues with NCMT as well as 4 colorectal adenoma tissues (obtained from endoscopic biopsy) were examined during March to June 2006. These fresh specimens were kept in liquid nitrogen immediately after excision until use. Two pathologists screened histological sections and selected areas of the representative tumor cells. Tumor stage was classified according to Dukes' criteria.

Immunohistochemistry

For immunohistochemical analysis, 5 μm sections were sliced and mounted on poly-L-lysine-coated slides the day before use. Immunohistochemistry was conducted according to instructions of HistostainTM-Plus kits (Beijing Zhongshan Golden Bridge Biotechnology Co., LTD). The primary antibody Eag1 (Sigma-Aldrich, USA) was diluted 1:200 with 0.1% bovine serum albumin. As negative controls, the slides were treated by replacement of primary antibody with non-immune serum.

TTo achieve a semi-quantitative estimation of Eag1 expression levels, we used an immunohistochemical score method: Scores were 0, less than 10% of the tumor cells stained; 1+, faint staining in more than 10% of the cells; 2+, moderate staining in more than 10% of tumor cells; and 3+, strong staining in more than 10% of the cells. The immunohistochemical score was evaluated as negative (0), weakly positive (1+), and strongly positive (2+, 3+). Each stained slide was scored by two independent observers. There were no major disagreements regarding scoring and the average scoring was reported.

Cell culture

HT29 and LoVo cells (obtained from Cell Bank, Chinese Academy of Sciences) were maintained in T75 flasks in a humidified atmosphere at 37℃ with 50 ml/L carbon dioxide and passaged every 4-5 d. The HT-29 line was isolated from primary tumor, and LoVo line was isolated from metastatic tumor nodules in the left supraclavicular region. HT29 cells were cultured in McCoy's 5a medium (modified) with 1.5 mmol/L L-glutamine adjusted to contain 2.2 g/L 90% sodium bicarbonate, 10% fetal bovine serum. LoVo cells were grown in Ham's F12K medium with 2 mmol/L L-glutamine adjusted to contain 1.5 g/L 90% sodium bicarbonate, 10% fetal bovine serum. All media were also supplemented with 100 units/mL penicillin plus 100 μg/mL streptomycin.

RNA preparation and reverse transcription PCR

Total RNA was isolated from colorectal tissue and HT29 and LoVo cells using TRIZOL® reagent (Invitrogen Corporation, USA) following instructions of the TRIZOL kit.

We designed specific primers for Eag1 (Genbank accession: AF078741) and β-actin. The primers were as follows: For Eag1 (bp966-bp1441, 475 bp), sense primer 5' -GCTTTTGAGAACGTGGATGAG-3'; antisense primer 5'-CGAAGATGGTGGCATAGAGAA-3'. For β-actin (479 bp): sense primer 5'-TGACGGGGTCACCCACACT GTGCC-3'; antisense primer: 5'-CTGCAFCCTGTCGG CAATGCCAG-3' (479 bp). The primers were synthesized by Shanghai Sangon (China).

One step reverse transcription PCR (RT-PCR) was performed using One Step mRNA Selective PCR Kit 1.1 (TaKaRa Dalian, China) according to the manufacturer's specifications. The RT-PCR reaction mixture contained 25 μL of 2 × mRNA selective PCR buffer reaction buffer I, 10 μL of $MgCl_2$, 5 μL of dNTP/analog mixture, 1 μL of RNase Inhibitor, 1 μL of AMV Rtase XL, 1 μL of AMV-Optimized taq, 1 μL sense primer (20 μmol/L), 1 μL of antisense primer (20 μmol/L), 1 μL of total RNA, 4 μL of RNase free dH_2O to a final volume of 50 μL. Reactions without template RNA were used as a negative control. The RT-PCR for β-actin was used to check the quality of the RNA extraction and RT-PCR. The following RT-PCR conditions were used for Eag1: 1 cycle of 45℃ for 25 min; 30 cycles of 88℃ for 30 s, 50℃ for 45 s, and 72℃ for 1 min; and a final cycle of 72℃ for 7 min. The conditions for β-actin: 1 cycle of 50℃ for 15 min; 30 cycles of 85℃ for 30 s, 45℃ for 45 s, and 72℃ for 1 min; and a final cycle of 72℃ for 7 min.

Fifteen microliters of PCR products were analyzed by electrophoresis on a 1.5% agarose gel. DNA fragments were visualized and photographed under UV light after ethidium bromide staining. The expected band for each marker was identified by comigration of a DNA marker ladder electrophoresed in an adjacent lane.

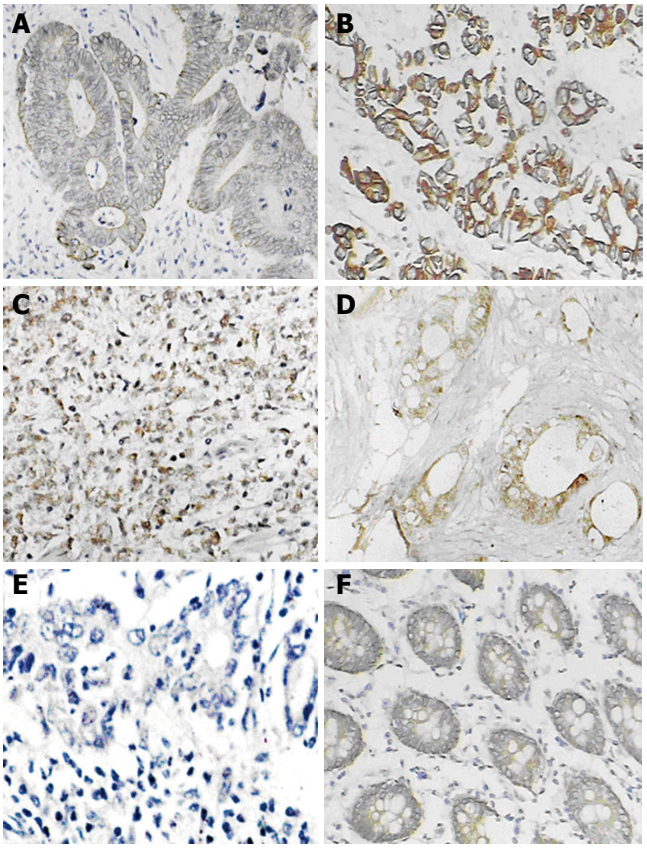

Figure 1 Typical immunohistochemical staining for Eag1 in colorectal cancer and adenoma. **A**, **B**, **C**: Positive staining of colorectal cancers; **D**: Positive staining of metastasis tissue from greater omentum; **E**: Negative control of colorectal cancer; **F**: Positive staining from one case of colonic adenoma.

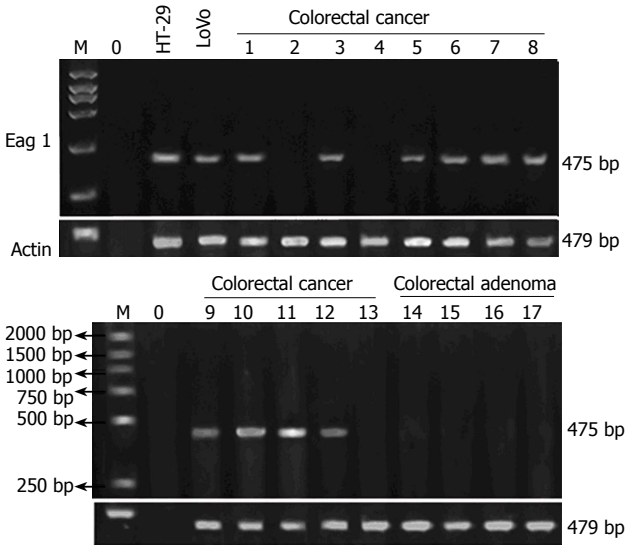

Figure 2 Eag1 mRNA expression in colorectal cancer and adenoma. Eag1 mRNA positively expressed in LoVo and HT29 cell lines and in 10/13 of colorectal cancer tissues, but negatively expressed in NCMT(not shown) and colorectal adenoma. M, molecular weight marker; 0, water.

Table 1 Eag1 immunoreactivity in the colorectal cancers

Stage	Eag1 expression[1]			Positive cases
	Negative	Weak	Strong	*n* (%)
A	3	2	2	4/7 (57.1)
B	13	14	12	26/39 (66.7)
C	2	5	9	14/16 (87.5)
D	0	5	9	14/14 (100)
Total	18	26	32	58/76 (76.3)

[1]Intensity of expression was interpreted as negative, weakly positive, and strongly positive, $P < 0.05$.

Statistical analysis

The χ^2-test was used for analysis. Differences between the values were considered significant when $P < 0.05$.

RESULTS

Eag1 channel is aberrantly expressed in colorectal cancer

Immunopositivity for Eag1 protein was clearly marked on the cytoplasm and/or membrane of cells. Using immunohistochemistry, aberrant expression of Eag1 was detected in tissue of colorectal cancer and negative expression was detected in NCMT. The frequency of expression of Eag1 in colorectal cancer averaged 76.3% (58/76) of the cases studied. Figure 1 shows representative positive expression of neoplastic tissue of colorectal cancer and metastatic cancer. Again, using reverse transcription PCR, positive expression of Eag1 was found in 10/13 (76.9%) of colorectal cancer samples and negative expression was found in 13 cases of NCMT (Figure 2, negative expression of NCMT was not shown here). Positive expression of Eag1 was also detected in HT29 and LoVo colorectal cancer cell lines (Figure 2).

Eag1 channel is occasionally expressed in colorectal adenoma

Nine cases of colorectal adenoma were also studied by immunohistochemistry, which were negative for Eag1 protein in most of the cases except that in 1 case weak positive expression was detected (Figure 1). In addition, Eag1 mRNA expression was not detected in 4 samples of colorectal adenomas by RT- PCR (Figure 2).

Relationship of Eag1 expression and clinic-pathological features

The immunohistochemistry results showed that no association was detected between Eag1 expression and sex, age, site, differentiation, while expression levels of Eag1 protein were found to be dependent on the tumor size, lymphatic node metastasis, other organ metastases and Dukes' stage ($P < 0.05$). Especially, all the tissues from metastatic cancer of other organ or Dukes' D stage cancer showed an intensively positive immunostaining (Figure 1 and Table 2). Table 1 summarizes the relationship of Eag1 protein expression with clinico-pathological features.

DISCUSSION

Because of its restricted distribution in normal tissue and its more ubiquitous distribution in cancer cells and its oncogenic properties, Eag1 channels have gained interest

Table 2 Clinico-pathological features and Eag1 protein expression

Clinico-pathological features	Number of tumor *n* (%)	Positive Eag1 expression *n* (%)	χ^2 value
Sex			0.70
Male	44 (57.9)	32(72.2)	
Female	32 (42.1)	26(81.3)	
Age (yr)			0.002
< 60	51 (67.1)	39 (76.5)	
⩾ 60	25 (32.9)	19 (76.0)	
Location			4.52
Recta	28 (36.8)	22 (78.6)	
Left colon	21 (27.6)	16 (76.2)	
Transverse colon	9 (11.8)	6 (66.7)	
Right colon	18 (23.7)	14 (77.8)	
Differentiation			2.09
High	18 (23.7)	12 (66.7)	
Moderate	22 (28.9)	16 (72.7)	
Low	29 (38.2)	24 (82.8)	
Undifferentiated	7 (9.2)	6 (85.7)	
Size			6.41[a]
< 5 cm	48 (63.2)	32 (66.7)	
⩾ 5 cm	28 (36.8)	26 (92.9)	
Lymphatic node metastasis			5.14[a]
N0	46 (60.5)	31 (67.4)	
N1	30 (39.5)	27 (90.0)	
Other organs metastasis			4.59[a]
M0	62 (81.6)	44 (71.0)	
M1	14 (18.4)	14 (100)	
Dukes' stage			8.89[a]
A	7 (9.2)	4 (57.1)	
B	39 (51.3)	26 (66.7)	
C	16 (21.1)	14 (87.5)	
D	14 (18.4)	14 (100)	

[a]$P < 0.05$.

as promising tools for the development of novel diagnostic and therapeutic methods of cancers.

Recently, a few published papers have documented the contribution of potassium channels in the pathological status of cells other than neural or lymphoid origin. A paper of Pardo's group represents a milestone in the link between Eag1 and cancer[5]. Furthermore, they found that Eag1 expression was limited outside the CNS, but was frequently expressed in clinic tumors from diverse origins, including colon carcinoma[12]. They reported that 6/8 of colon carcinomas were positively expressed. However, the actual frequency of expression of hEAG1 in colorectal cancer remained unknown. Here, we have provided that EAG1 protein and Eag1 mRNA were negatively expressed in normal colorectal tissue, but aberrantly expressed in a large fraction of colorectal cancer tissue and colorectal cell lines. These results strongly suggest the possibility of the use of Eag1 as a tool for the differential diagnosis of malignant transformation together with morphological criteria.

We also found that EAG1 protein was occasionally expressed in colorectal adenoma. Similar, Farias's group found one of negative pap smears of control cervical samples that presented human papilloma virus infection (the most important etiological factor for cervical cancer) was positive for Eag1 expression[8]. A plausible scenario is that the increase in Eag1 expression in precancer pathological changes could be an early sign of tumor development, namely, Eag1 may be involved in the early development of cancer.

We analyzed relationship of Eag1 expression detected by immunohistochemistry with clinico-pathological features, and found that there was no association between Eag1 expression and sex, age, site, differentiation, while expression of Eag1 was dependent on the tumor size, lymphatic node metastasis, metastases to other organs and Dukes' stage. Especially, all the tissues from metastatic cancers of other organ showed intensively positive immunostaining. Such a correlation would obviously be of great interest, since the channel could thus serve as a prognostic marker. These conclusions are somewhat different from opinions held by the Pardo's group. They found there were no correlations between Eag1 expression and demographic factors (sex, age, grade and site of tumor) of soft tissue sarcoma[9]. However, they also found that the tumors from patients who died over the two-year follow up period were much more likely to express significant levels of Eag1. To address this question precisely, quantitative studies of Eag1 expression and prospective studies with larger samples and longer time period will be needed.

Studies of Eag1 in cancer treatment have also provided some promising conclusions. Recently, the Pardo's group reported siRNA sequences acting specifically on Eag1, reproducibly induced a significant decrease in the proliferation of tumor cell lines while did not trigger any observable non-specific responses[10]. So, siRNA would serve as tools in the future to facilitate the elucidation of both the physiological and pathophysiological functions of this intriguing protein. We are also investigating the roles of Eag1-siRNAs served as tools in colorectal cancer therapy, and trying to clarify the effect of silencing the channel activity on tumor cells.

In conclusion, Eag1 potassium channels are aberrantly expressed in colorectal cancer patients and cell lines. These findings strongly suggest that Eag1 might be used as a potential diagnostic and prognostic marker as well as a potential membrane therapeutic target for colorectal cancer.

REFERENCES

1 **Kaplan WD**, Trout WE. The behavior of four neurological mutants of Drosophila. *Genetics* 1969; **61**: 399-409
2 **Warmke JW**, Ganetzky B. A family of potassium channel genes related to eag in Drosophila and mammals. *Proc Natl Acad Sci U S A* 1994; **91**: 3438-3442
3 **Bauer CK**, Schwarz JR. Physiology of EAG K+ channels. *J Membr Biol* 2001; **182**: 1-15
4 **Occhiodoro T**, Bernheim L, Liu JH, Bijlenga P, Sinnreich M, Bader CR, Fischer-Lougheed J. Cloning of a human ether-a-go-go potassium channel expressed in myoblasts at the onset of fusion. *FEBS Lett 1998*; **434**: 177-182
5 **Pardo LA**, del Camino D, Sánchez A, Alves F, Brüggemann A, Beckh S, Stühmer W. Oncogenic potential of EAG K(+) channels. *EMBO J* 1999; **18**: 5540-5547
6 **Meyer R**, Heinemann SH. Characterization of an eag-like potassium channel in human neuroblastoma cells. *J Physiol* 1998; **508** (Pt 1): 49-56
7 **Gavrilova-Ruch O**, Schönherr K, Gessner G, Schönherr

R, Klapperstück T, Wohlrab W, Heinemann SH. Effects of imipramine on ion channels and proliferation of IGR1 melanoma cells. *J Membr Biol* 2002; **188**: 137-149

8 **Farias LM**, Ocaña DB, Díaz L, Larrea F, Avila-Chávez E, Cadena A, Hinojosa LM, Lara G, Villanueva LA, Vargas C, Hernández-Gallegos E, Camacho-Arroyo I, Dueñas-González A, Pérez-Cárdenas E, Pardo LA, Morales A, Taja-Chayeb L, Escamilla J, Sánchez-Peña C, Camacho J. Ether a go-go potassium channels as human cervical cancer markers. *Cancer Res* 2004; **64**: 6996-7001

9 **Mello de Queiroz F**, Suarez-Kurtz G, Stühmer W, Pardo LA. Ether à go-go potassium channel expression in soft tissue sarcoma patients. *Mol Cancer* 2006; **5**: 42

10 **Weber C**, Mello de Queiroz F, Downie BR, Suckow A, Stühmer W, Pardo LA. Silencing the activity and proliferative properties of the human EagI Potassium Channel by RNA Interference. *J Biol Chem* 2006; **281**: 13030-13037

11 **Ouadid-Ahidouch H**, Le Bourhis X, Roudbaraki M, Toillon RA, Delcourt P, Prevarskaya N. Changes in the K+ current-density of MCF-7 cells during progression through the cell cycle: possible involvement of a h-ether.a-gogo K+ channel. *Receptors Channels* 2001; **7**: 345-356

12 **Hemmerlein B**, Weseloh RM, Mello de Queiroz F, Knötgen H, Sánchez A, Rubio ME, Martin S, Schliephacke T, Jenke M, Heinz-Joachim-Radzun, Stühmer W, Pardo LA. Overexpression of Eag1 potassium channels in clinical tumours. *Mol Cancer* 2006; **5**: 41

S- Editor Wang J **L- Editor** Zhu LH **E- Editor** Lu W

PO Box 2345, Beijing 100023, China
www.wjgnet.com
wjg@wjgnet.com

World J Gastroenterol 2007 February 28; 13(8): 1262-1267
World Journal of Gastroenterology ISSN 1007-9327

RAPID COMMUNICATION

Preventive effect of gelatinizedly-modified chitosan film on peritoneal adhesion of different types

Xie-Lai Zhou, Shan-Wen Chen, Guo-Dong Liao, Zhou-Jun Shen, Zhi-Liang Zhang, Li Sun, Yi-Jun Yu, Qiao-Ling Hu, Xiao-Dong Jin

Xie-Lai Zhou, Shan-Wen Chen, Guo-Dong Liao, Xiao-Dong Jin, Department of Urology, The First Affiliated Hospital, College of Medicine, Zhejiang University, Hangzhou 310003, Zhejiang Province, China
Zhou-Jun Shen, Department of Urology, Ruijin Hospital, School of Medicine, Shanghai Jiaotong University, Shanghai 200025, China
Xie-Lai Zhou, Zhi-Liang Zhang, Yi-Jun Yu, Surgical Department, Clinical Medical College of Hangzhou Teachers College, Hangzhou 310036, Zhejiang Province, China
Li Sun, Experimental Center of Medical Science, Hangzhou Teachers College, Hangzhou 310036, Zhejiang Province, China
Qiao-Ling Hu, Institute of Polymer Composites, Zhejiang University, Hangzhou 310027, Zhejiang Province, China
Supported by The National Natural Science Foundation of China, No. 50173023
Correspondence to: Xiao-Dong Jin, Department of Urology, The First Affiliated Hospital, College of Medicine, Zhejiang University, Hangzhou 310003, Zhejiang Province, China. addamm@mail.hz.zj.cn
Telephone: +86-571-87236833 Fax: +86-571-87236628
Received: 2006-12-21 Accepted: 2007-01-31

Abstract

AIM: To comparatively study the preventive effect of gelatinizedly-modified chitosan film on peritoneal adhesions induced by four different factors in rats.

METHODS: Chitosan was chemically modified by gelatinization, and made into films of 60 μm in thickness, and sterilized. Two hundred Sprague-Dawley rats were randomly divided into five groups, Sham-operation group (group A), wound-induced adhesion group (group B), purified talc-induced adhesion group (group C), vascular ligation-induced adhesion group (group D), and infection-induced adhesion group (group E), respectively. In each group, the rats were treated with different adhesion-inducing methods at the cecum of vermiform processes and then were divided into control and experimental subgroups. Serous membrane surface of vermiform processes were covered with the films in the experimental subgroups, and no films were used in the control subgroups. After 2 and 4 wk of treatments, the abdominal cavities were reopened and the adhesive severity was graded blindly according to Bhatia's method. The cecum of vermiform processes were resected for hydroxyproline (OHP) measurement and pathological examination.

RESULTS: Adhesion severity and OHP level: After 2 and 4 wk of the treatments, in the experimental subgroups, the adhesions were significantly lighter and the OHP levels were significantly lower than those of the control subgroups in group B (2 wk: 0.199 ± 0.026 *vs* 0.285 ± 0.041 μg/mg pr, $P < 0.001$; 4 wk: 0.183 ± 0.034 *vs* 0.276 ± 0.03 μg/mg pr, $P < 0.001$), D (2 wk: 0.216 ± 0.036 *vs* 0.274 ± 0.040 μg/mg pr, $P = 0.004$; 4 wk: 0.211 ± 0.044 *vs* 0.281 ± 0.047 μg/mg pr, $P = 0.003$) and E (2 wk: 0.259 ± 0.039 *vs* 0.371 ± 0.040 μg/mg pr, $P < 0.001$; 4 wk: 0.242 ± 0.045 *vs* 0.355 ± 0.029 μg/mg pr, $P < 0.001$), but there were no significant differences in groups A (2wk: 0.141 ± 0.028 *vs* 0.137 ± 0.026 μg/mg pr, $P = 0.737$; 4 wk: 0.132 ± 0.031 *vs* 0.150 ± 0.035 μg/mg pr, $P = 0.225$) and C (2 wk: 0.395 ± 0.044 *vs* 0.378 ± 0.043 μg/mg pr, $P = 0.387$; 4 wk: 0.370 ± 0.032 *vs* 0.367 ± 0.041 μg/mg pr, $P = 0.853$); Pathological changes: In group B, the main pathological changes were fibroplasias in the treated serous membrane surface and in group D, the fibroplasia was shown in the whole layer of the vermiform processes. In group E, the main pathological changes were acute and chronic suppurative inflammatory reactions. These changes were lighter in the experimental subgroups than those in the control subgroups in the three groups. In group C, the main changes were foreign body giant cell and granuloma reactions and fibroplasias in different degrees, with no apparent differences between the experimental and control subgroups.

CONCLUSION: The gelatinizedly-modified chitosan film is effective on preventing peritoneal adhesions induced by wound, ischemia and infection, but the effect is not apparent in foreign body-induced adhesion.

Key words: Chitosan; Gelatinization; Chemical modification; Peritoneum; Adhesion

Zhou XL, Chen SW, Liao GD, Shen ZJ, Zhang ZL, Sun L, Yu YJ, Hu QL, Jin XD. Preventive effect of gelatinizedly-modified chitosan film on peritoneal adhesion of different types. *World J Gastroenterol* 2007; 13(8): 1262-1267

http://www.wjgnet.com/1007-9327/13/1262.asp

INTRODUCTION

Peritoneal adhesion is a kind of defensive reaction to

peritoneal injury. However, it can also result in intestinal obstruction and cause severe clinical disorders. Therefore, it is important to prevent peritoneal adhesion in abdominal surgical operations. Unfortunately up to now, there have been no ideal methods to prevent peritoneal adhesion in clinical practice. Chitosan is a deacetylated derivate from chitin. Many previous studies showed that chitosan has effects of haemostasis, and sterilization, facilitates epithelial reparation and inhibits fibroblastic growth[1-3]. Chitosan has been used to prevent tissue adhesions, such as peritoneal adhesion, tendon adhesion and synarthrophysis[4-6]. In clinical application, it was found that the gel flows easily and is difficult to stay in the target regions for sufficient time, and the gel also degrades so fast that it could only maintain effectiveness for a short duration. In order to delay the degradation and decrease the fluidity of the gel, in our previous study, we processed the chitosan to films and transplanted it into the abdominal cavity of rats. But the film degraded too slowly and 8 wk after the transplantation, most of the films resided in the cavity. The residual film was encapsulated by the surrounding tissue and the peritoneal adhesion was worsened. In order to overcome these disadvantages, we mixed gelatin to chitosan and produced blending films. The blending film degraded much faster than the previous pure chitosan film, but it also produced foreign body reactions and formed severe foreign body granuloma around the blending film[7].

To solve the above problems and develop a useful chitosan film to prevent the peritoneal adhesion, in the present study we chemically modified the chitosan by gelatinization to develop a new sort of chitosan film, and comparatively studied the preventive effect of the film on peritoneal adhesions induced by wound, infection, ischemia and foreign body in rats.

MATERIALS AND METHODS

Animals and grouping

Two hundred Sprague-Dawley rats, one half for each gender, weighing 200-250 g, were provided by the Experimental Animal Center of Zhejiang Province. They were randomly divided into five groups: sham-operation group (group A), wound-induced adhesion group (group B), purified talc-induced adhesion group (group C), vascular ligation-induced adhesion group (group D), and infection-induced adhesion group (group E). Each of the above groups was subdivided into two subgroups, experimental and control subgroups (20 rats for each subgroup and one half for each gender). All the rats were fed under the same conditions: at 24-26℃ of environmental temperature, about 40% humidity, with an alternate 12 h light/dark cycle, and free access to food and water.

Preparation of chitosan film

The chitosan (from Yuhuan Aoxing Chitin Ltd., Zhejiang Province, China) was dissolved, purified, gelatinizedly modified, filtered and made into films. The films were dried and dissected to patches of 10 cm × 10 cm in size and 60 μm in thickness, and the film patches were sterilized by radiation of ^{60}Co for later use.

Surgical operation

Under general anaesthesia with intraperitoneal injection of 3% amobarbital (60-90 mg/kg), the rats were immobilized in dorsal position, routinely degermed, abdominally incised through a median incision of 2-3 cm long, and their vermiform processes were searched and pulled out of the incisions, then the terminal vermiform processes within a length of 3 cm were treated as follows: In group A, the vermiform processes were exposed to air for 5 min; in group B, the anterior surface of serous membrane was scraped slightly with surgical blade till obvious congestion and small bleeding drops appeared; in group C, 10 mg of talc powders were evenly smeared over the anterior surface of serous membrane; in group D, the vermiform artery stem was ligated with 0# surgical thread at a point of 3 cm from the dead end in the following way: loosely knotting the first loop, thrilling a thread with equivalent diameter to the vermiform artery stem through the first loop, tightening the first loop, pulling out the thrilled thread, and knotting and tightening the second loop of the ligation knot. The ligation resulted in a stricture of vermiform artery, which induced ischemia of the distal vermiform tissue from the ligation point. In group E, the dead end of the vermiform process was poked out with a hole using a 16# needle, a drop of intestinal content was extruded out and evenly smeared over the anterior surface of serous membrane, and then the remaining content in the vermiform process was pushed to the cecum. After the above treatments, for the experimental subgroups, the treated serous membranes were covered with the prepared chitosan films, and the vermiform processes were put back into the abdominal cavity, which were then closed. For the control subgroups, all the treatments were the same as those of the experimental subgroups except that the chitosan film was not placed. The duration from opening to closing the abdominal cavity was 5 min, so that the duration of exposure of intestines to air was the same for each rat.

At 2 and 4 wk after the surgery, 10 rats (5 female and 5 male) in each subgroup were randomly selected respectively and their abdominal cavities were reopened under anaesthesia, and the grades of peritoneal adhesion were evaluated, which existed between the treated vermiform processes and intestines, mesenteries and abdominal walls. After that, the vermiform processes with adhesions were resected and washed with normal saline, and then were divided into two segments for each resected process. The proximal segments were fixed with formalin and histopathologically examined, and the distal segments were stored at -80℃ for measurement of hydroxyproline (OHP).

Grading standard for peritoneal adhesion

According to Bhatia's[8] grading method of 5 levels and considering the characteristics of peritoneal adhesion in rats, we formulated the following grading standard:

Table 1 Comparison of peritoneal adhesive grades between experimental and control subgroups within each group

Group	Control group (n = 10)					Experimental group (n = 10)					U	P
	0	I	II	III	IV	0	I	II	III	IV		
Group A: sham-operation												
2 wk	9	1	0	0	0	10	0	0	0	0	45.000	0.317
4 wk	10	0	0	0	0	9	1	0	0	0	45.000	0.317
Group B: wound-induced adhesion												
2 wk	0	5	4	1	0	6	3	1	0	0	14.500	0.005
4 wk	0	5	5	0	0	7	3	0	0	0	7.500	0.001
Group C: purified talc-induced adhesion												
2 wk	0	0	1	3	6	0	0	1	2	7	45.500	0.687
4 wk	0	0	1	4	5	0	0	0	4	6	43.000	0.547
Group D: vascular ligation-induced adhesion												
2 wk	0	4	4	2	0	3	6	1	0	0	18.000	0.009
4 wk	1	4	4	1	0	5	4	1	0	0	21.500	0.023
Group E: infection-induced adhesion												
2 wk	0	0	1	4	5	0	4	5	1	0	5.500	0.001
4 wk	0	0	1	5	4	0	6	4	0	0	2.000	< 0.001

Grade 0: no adhesions; Grade I: the ratio of adhesive area/total treated area in the vermiform processes is < 50%, and the adhesion is easily to be dissected bluntly; Grade II: the ratio is ≥ 50%, and the adhesion is easily to be dissected bluntly; Grade III: area of the adhesion is out of consideration. Although blunt dissection for the adhesion can be carried out, it is difficult and the intestinal wall will be impaired after the blunt dissection; Grade IV: area of the adhesion is out of consideration. The adhesion is fast and cannot be bluntly dissected. Each rat was graded by three referees blindly and the average grade of the three was accepted as the adhesive grade of the rat.

Determination of total protein and OHP

The levels of total protein and OHP in the adhesive tissue were determined using the corresponding kits supplied by Nanjing Jiancheng Bioengineering Institute, China. The determining processes completely followed the instructions of the kits. Contents of OHP in the adhesive tissue were calculated as micrograms of OHP in each milligram of total protein (μg/mg pr).

Statistical analysis

All the data were processed with SPSS10.0. Mann-Whitney U test of non-parametric statistics for independent samples was used to analyze differences in the peritoneal adhesive grades and t-test was used to analyze differences in OHP levels between the experimental and control subgroups within each group.

RESULTS

Gross findings

Abdominal incisions healed in first grade in all rats of all groups. There was no obvious postoperative abdominal infection in groups A, B, C and D at 2 and 4 wk after the surgical operations. There was no residual chitosan film in the abdominal cavities of rats in all experimental subgroups.

Comparison of peritoneal adhesion grade

As it shows in Table 1, within group A (sham-operation group) and group C (talc-induced adhesion group), there was no significant difference in peritoneal adhesion between the experimental and control subgroups both at 2 and 4 wk ($P > 0.05$). Within group B (wound-induced adhesion group), group D (vascular ligation-induced adhesion group) and group E (infection-induced adhesion group), the peritoneal adhesion grades of experimental subgroups were significantly lower than those of corresponding control subgroups ($P < 0.05$) both at 2 and 4 wk after the surgical treatments. It indicates that the gelatinizedly modified chitosan film has remarkable effect on preventing peritoneal adhesions induced by wound, ischemia and infection, but no obvious effect on adhesion induced by talc powders. From the results in Table 1, we also concluded that in group E, the mean decreased adhesion grades were 1.7 and 1.4 from experimental to control group at 2 and 4 wk respectively. While in group B, the mean decreased grades were 1.1 and 1.2, and in group D, the mean decreased grades were 1.0 and 0.9. It suggests that the modified chitosan film is more effective on preventing infection-induced peritoneal adhesion than on wound and ischemia induced adhesion.

Comparison of OHP levels in adhesive tissue

As it shows in Table 2, in groups A and C, there were no significant differences in OHP levels between the experimental and control subgroups both at 2 and 4 wk ($P > 0.05$). In groups B, D and E, the OHP levels of experimental subgroups were significantly lower than those of corresponding control subgroups ($P < 0.05$) both at 2 and 4 wk after the surgical treatments. The changes in OHP levels were concordant with the changes in the adhesive grades, and it was confirmed to have a peritoneal adhesion-preventive effect when the gelatinizedly modified chitosan film was applied to regions with wound, ischemia and infection in abdominal surgical operations.

Comparison of pathological changes

In group A, there were no obvious pathological changes in vermiform processes of all rats. In groups B and D, there were obvious fibroplasias and sporadic infiltration of lymphocytes in serous membrane (group B) and the whole

Table 2 Comparison of OHP levels between experimental and control subgroups within each group (μg/mg pr)

Group	Control group (n = 10)	Experimental group (n = 10)	t	P
Group A: sham-operation				
2 wk	0.137 ± 0.026	0.141 ± 0.028	0.331	0.737
4 wk	0.150 ± 0.035	0.132 ± 0.031	1.217	0.225
Group B: wound-induced adhesion				
2 wk	0.285 ± 0.041	0.199 ± 0.026	5.602	< 0.001
4 wk	0.276 ± 0.038	0.183 ± 0.034	5.768	< 0.001
Group C: purified talc-induced adhesion				
2 wk	0.378 ± 0.043	0.395 ± 0.044	0.874	0.387
4 wk	0.367 ± 0.041	0.370 ± 0.032	0.182	0.853
Group D: vascular ligation-induced adhesion				
2 wk	0.274 ± 0.040	0.216 ± 0.036	3.408	0.004
4 wk	0.281 ± 0.047	0.211 ± 0.044	3.438	0.003
Group E: infection-induced adhesion				
2 wk	0.371 ± 0.040	0.259 ± 0.039	6.34	< 0.001
4 wk	0.355 ± 0.029	0.242 ± 0.045	6.675	< 0.001

layer (group D) of the adhesive vermiform processes at 2 wk, and the main pathological change was fibroplasia at 4 wk after the surgical treatments. The above pathological changes were milder in experimental subgroups than those in control subgroups except for changes in group D and at 4 wk. In group C at 2 wk, there occurred obvious foreign-body giant cell reactions, granuloma, fibroplasias and sporadic infiltration of lymphocytes at the treated serous membranes of adhesive vermiform processes, and the granuloma and fibroplasias became severer at 4 wk. There were no significant differences in the above pathological changes between the experimental and control subgroups. In group E, the main pathological change in the treated region was acute suppurative inflammation at 2 wk, and chronic inflammatory reaction characterized with granulation and fibroplasias at 4 wk after the surgical treatments. The above inflammatory reactions were milder in experimental subgroup than those in control subgroup both at 2 and 4 wk.

DISCUSSION

Chitosan is chemically termed β-(1, 4)-2-amino-2-deoxy-D-dextran, and its main component is glucosamine. Glucosamine is also a sort of internal substance in human bodies, therefore, chitosan is biocompatible. If the chitosan is introduced into animal or human bodies, it will be degraded into small molecules of oligosaccharides and absorbed by the bodies without causing any acute or chronic toxicity. Chitosan is a derivant of deacetylized chitin, and the chitin is the major component of outer shells of invertebrates. Because of these characteristics of chitosan, it is widely and deeply researched in areas of pharmaceutical preparations and medical polymer synthesis[9].

Peritoneal adhesion occurs in more than three fourths of patients following laparotomy. The outcomes of adhesion are unpredictable and diverse, causing a significant health care burden. Intestinal obstruction, infertility, problems at reoperative surgery and cumulative costs of care over many years are the key concerns[10]. The peritoneal adhesion develops only several hours after the abdominal surgical operations. At first, the serous fluid exudes from the injured sides of intestinal wall, and then fibrinogen in the serous fluid transforms to fibrin and coagulates, thereby membranous peritoneal adhesion in the injured intestinal wall is formed. After that, the fibrinolytic system is activated and the fibrin is lyzed, thereby the membranous peritoneal adhesion is gradually eliminated. If the fibrin cannot be totally lyzed, the left fibrin will be organized and develop fibrinous adhesion, which usually forms at 2 wk after the surgical operation[11]. Based on the mechanisms through which the chitosan prevents peritoneal adhesion: inhibiting growth of fibroblasts, facilitating reparation of the epithelium, and disinfection, it is concluded that the chitosan can only prevent against pre-fibrinous adhesion. Once the fibrinous adhesion is formed, chitosan is useless. Therefore, when we use chitosan film to prevent peritoneal adhesion, the optimal duration for the film to stay in the abdominal cavity is within 2 wk. Firstly, the film can exert an effect of mechanical isolation in a solid state before it is completely degraded; On the other hand, when the film is degraded, the released chitosan monomers can also take anti-adhesive effect. In the present study, we gelatinizedly modified the chitosan to develop a new sort of chitosan film, which can be slowly dissolved in water. The experiments demonstrated that, within 2 wk after the film was transplanted into the abdominal cavity of the rats, it was completely degraded and absorbed without any foreign-body granuloma reaction. This suggests that the gelatinizedly modified chitosan film has the potential to be biomaterial for adhesion-prevention.

There are many factors that can induce peritoneal adhesions, of which the main factors are wound, ischemia, infection and foreign bodies. In most cases of clinical peritoneal adhesion, the adhesions are caused by combined factors, among which one or several factors play major roles[11,12]. The present study utilized rat models to investigate effects of the gelatinizedly modified chitosan film on peritoneal adhesions induced by four different factors. The results demonstrated that, at 2 and 4 wk after the surgical operations, the chitosan films significantly reduced the adhesion grades in groups of wound, ischemia

and infection-induced adhesions. This suggests that the chitosan films have obvious preventing effects on wound, ischemia and infection-induced peritoneal adhesions. The results also demonstrated that the films are more effective on infection-induced peritoneal adhesion. The mechanism may be as follows: The chitosan film prevents infection-induced peritoneal adhesion not only through promoting the epithelium recovery and inhibiting the growth of fibrous tissue, but also through its anti-infection effect by inhibiting hyperplasia of granulation and fibrous tissue. Through the double pathways the chitosan may inhibit the adhesion more strongly. It also seemed that healing of the abdominal incisions is not obviously affected by the chitosan transplantation. With respect to effects of the chitosan film on intra-abdominal anastomotic stoma healing, it needs to be clarified further.

Within the talc powder-induced adhesion group, there were no significant differences in adhesive grades between the experimental and control subgroups both at 2 and 4 wk. This showed that the gelatinizedly modified chitosan film has no obvious preventive effect on foreign body-induced peritoneal adhesion. The reason is as follows: For the talc powder-induced adhesion, the main pathological changes are foreign-body granuloma complicated with a large quantity of fibroplasias, and these changes will maintain as long as the foreign bodies exist. However, the chitosan film degraded in a relative fast rate in the abdominal cavity and there was no obvious residual film at 2 wk after the transplantation. Therefore, the fast degraded film cannot exert a strong effect on a chronic and persistent foreign-body granuloma reaction.

There is a high content of OHP in collagen protein, a very low content in elastin protein, and none in other sorts of proteins. Ozogul *et al*[13] reported that there existed positive correlation between adhesive grades and OHP levels in the adhesive tissue, and concluded that OHP is a significant index to measure the adhesive degree of tissue, which is more sensitive and objective than the index of gross adhesive grade. In the present study, the OHP changing tendency within each group and differences in OHP levels between subgroups were concordant to those of adhesive grades. This further confirms the preventive effect of gelatinizedly modified chitosan film on wound, ischemia and infection-induced peritoneal adhesions.

COMMENTS

Background

Peritoneal adhesion can cause intestinal obstruction and other severe clinical disorders, so it is very important to prevent peritoneal adhesion in abdominal surgical operations. But up to now, there are still no ideal methods to prevent peritoneal adhesion in clinical practices. Chitosan is a deacetylated derivate from chitin. Many studies reported that chitosan was applied to prevent tissue adhesions, such as peritoneal adhesion, tendon adhesion and synarthrophysis, but the effect was not satisfactory.

Research frontiers

Chitosan is a sort of natural biological material and it has been processed into many forms for medical use. In the area of prevention of peritoneal adhesion with chitosan, the research hotspot is how to modify the chitosan by chemical and physical methods to improve its effectiveness on preventing the adhesion, and simultaneously reduce its adverse reactions.

Innovations and breakthroughs

In the previous application of chitosan gels to the prevention of peritoneal adhesion, it was found that the gel was much fluid and was difficult to stay in the target places for sufficient time, and moreover, the gel degraded so fast that it could only maintain the effectiveness for a short duration. In order to delay the degradation and decrease the fluidity of the gel, we processed pure chitosan into films, but the film degraded too slowly and the residual film was encapsulated by surrounding tissue and the peritoneal adhesion was worsened. In order to overcome these disadvantages, we mixed chitosan with gelatin and produced blending films. The blending film degraded much faster than the previous pure chitosan film, but it also created foreign body reaction and formed severe foreign body granuloma around the blending film. In the present study we chemically modified the chitosan in gelatinization to develop a new sort of chitosan film, and showed that the film is remarkably effective on preventing peritoneal adhesions induced by wound, ischemia and infection except the foreign body-induced adhesion.

Applications

The study results suggest that the gelatinizedly-chitosan film is a potential therapeutic material that could be used in preventing peritoneal adhesions induced by wound, ischemia and infection.

Terminology

Peritoneal adhesion: Peritoneal adhesion is a sort of defensive reaction to the peritoneal injury mainly including wound, infection, ischemia and foreign body, but it can also develop intestinal obstruction and cause severe clinical disorders; chitosan: Chitosan is a deacetylated derivate from chitin, and chitin is the second most abundant natural biopolymer derived from exoskeletons of crustaceans and also from cell walls of fungi and insects.

Peer review

This is a good descriptive study in which authors analyze the preventive effect of gelatinizedly-modified chitosan on peritoneal adhesions induced by different factors in rats. The results are interesting and suggest that gelatinizedly-chitosan is a potential therapeutic substance that could be used in preventing peritoneal adhesions induced by wound, ischemia and infection.

REFERENCES

1 **Rao SB**, Sharma CP. Use of chitosan as a biomaterial: studies on its safety and hemostatic potential. *J Biomed Mater Res* 1997; **34**: 21-28

2 Liu H, Du Y, Wang X, Sun L. Chitosan kills bacteria through cell membrane damage. *Int J Food Microbiol* 2004; **95**: 147-155

3 **Risbud M**, Hardikar A, Bhonde R. Growth modulation of fibroblasts by chitosan-polyvinyl pyrrolidone hydrogel: implications for wound management? *J Biosci* 2000; **25**: 25-31

4 **Xu RS**, Hou CL, Yin CH, Wang YS, Chen AM. Clinical study on chitosan in prevention of knee adhesion after patellar operation. *Zhongguo Xiufu Chongjian Waike Zazhi* 2002; **16**: 240-241

5 **Zhou J**, Elson C, Lee TD. Reduction in postoperative adhesion formation and re-formation after an abdominal operation with the use of N, O-carboxymethyl chitosan. *Surgery* 2004; **135**: 307-312

6 **Krause TJ**, Zazanis G, Malatesta P, Solina A. Prevention of pericardial adhesions with N-O carboxymethylchitosan in the rabbit model. *J Invest Surg* 2001; **14**: 93-97

7 **Zhang ZL**, Xu SW, Zhou XL. Preventive effects of chitosan on peritoneal adhesion in rats. *World J Gastroenterol* 2006; **12**: 4572-4577

8 **Bhatia DS**, Allen JE. The prevention of experimentally induced postoperative adhesions. *Am Surg* 1997; **63**: 775-777

9 **Kato Y**, Onishi H, Machida Y. Application of chitin and chitosan derivatives in the pharmaceutical field. *Curr Pharm Biotechnol* 2003; **4**: 303-309

10 **Senthilkumar MP**, Dreyer JS. Peritoneal adhesions: pathogenesis, assessment and effects. *Trop Gastroenterol* 2006;

27: 11-18
11 **Liakakos T**, Thomakos N, Fine PM, Dervenis C, Young RL. Peritoneal adhesions: etiology, pathophysiology, and clinical significance. Recent advances in prevention and management. *Dig Surg* 2001; **18**: 260-273
12 **Thompson J**. Pathogenesis and prevention of adhesion formation. *Dig Surg* 1998; **15**: 153-157
13 **Ozoğul Y**, Baykal A, Onat D, Renda N, Sayek I. An experimental study of the effect of aprotinin on intestinal adhesion formation. *Am J Surg* 1998; **175**: 137-141

S- Editor Liu Y **L- Editor** Zhu LH **E- Editor** Chin GJ

PO Box 2345, Beijing 100023, China
www.wjgnet.com
wjg@wjgnet.com

World J Gastroenterol 2007 February 28; 13(8): 1268-1270
World Journal of Gastroenterology ISSN 1007-9327

CASE REPORT

Endoscopic resection of an ampullary carcinoid presenting with upper gastrointestinal bleeding: A case report and review of the literature

Nooman Gilani, Francisco C Ramirez

Nooman Gilani, Francisco C Ramirez, Carl. T. Hayden Veterans Administration Medical Center, Phoenix, AZ, United States
Correspondence to: Nooman Gilani, MD, FACG, Department of Medicine and Research, Gastroenterology Section, Carl. T. Hayden VAMC, 650 E Indian School Rd, Phoenix, AZ 85012, United States. ngilani@pol.net
Telephone: +1-602-2775551-7618 Fax: +1-602-2226562
Received: 2006-10-12 Accepted: 2007-02-25

Abstract

Ampullary carcinoid is a rare tumor that can present with gastrointestinal bleeding, obstructive jaundice or pancreatitis. Some of these tumors are associated with Von Recklinghausen disease. The usual surgical options are a biliary-enteric anastomosis, Whipple procedure or rarely a local resection. The mean survival does not appear to be much different after a pancreaticoduodenectomy versus local surgical excision. We report a very rare case of a non-metastatic ampullary carcinoid causing upper gastrointestinal bleeding, which was managed by endoscopic ampullectomy.

Key words: Carcinoid; Ampulla of Vater; Ampullary tumor; Ampullectomy; Gastrointestinal bleeding

Gilani N, Ramirez FC. Endoscopic resection of an ampullary carcinoid presenting with upper gastrointestinal bleeding: A case report and review of the literature. *World J Gastroenterol* 2007; 13(8): 1268-1270

http://www.wjgnet.com/1007-9327/13/1268.asp

INTRODUCTION

Despite being rare, carcinoids are the most common neuroendocrine tumors of the gastrointestinal (GI) tract[1,2]. Carcinoid of the ampulla is an extremely rare tumor (0.05%) for which the correct pre-operative diagnosis is very low (14%) and very rarely they present with an ulceration of the overlying duodenal mucosa[2]. Less than 3% of ampullary carcinoids patients experience carcinoid syndrome[3]. These tumors generally have an indolent course, but more aggressive behavior in the form of distant metastases has been reported. We report a case of an ampullary carcinoid that manifested as an upper gastrointestinal bleeding and was managed with endoscopic snare resection of the ampulla of Vater.

CASE REPORT

A 71-year old man underwent upper endoscopy for the work up of a recent history of epigastric pain, melena and a 4 g decrease in hemoglobin. The esophagogastroduodenoscopy (EGD) was unremarkable except for a prominent ampullary area. A sideviewing scope showed an approximately 1.5 cm mass with an overlying superficial ulcer (Figure 1A). Biopsy specimen revealed a carcinoid tumor involving the muscularis propria (Figure 2A and B). The tumor lacked mitotic activity and psammoma bodies (sometimes associated with duodenal somatostatinomas). The tumor was positive for chromogranin, synaptophysin and somatostatin, and negative for gastrin, insulin, glucagon and human pancreatic polypeptide. The patient denied flushing, diarrhea, weight loss or wheezing. His liver enzymes were normal. A CT and an octreotide scan were unremarkable. EUS revealed no regional lymph nodes and tumor free pancreatic and common bile ducts. A serum serotonin level was normal at 80 ng/mL (22-180 ng/mL) and urinary 5-HIAA was 6.1 mg/24 h (normal up to 6 mg/24 h).

The patient declined aggressive surgical options but agreed to undergo an endoscopic ampullectomy with its modest risk of complications. After submucosal saline injection in the ampullary area, a snare assisted ampullectomy was performed with blended current (cut to coagulation ratio 5:1) at a setting of 150:30 watts using an electrosurgical unit (ERBE ICC-200, Tubingen, Germany). The tumor was removed piecemeal. A 5 Fr, 3 cm pancreatic stent was placed to prevent pancreatitis. The procedure was uneventful except for mild oozing which promptly stopped with local infiltration of 4 cc of 1/10000 epinephrine. The patient remained stable except for an asymptomatic transient elevation of transaminases and was discharged the next evening. The pancreatic stent was removed two weeks later and there was no residual tumor seen at this examination (Figure 1B). He did not have any further episodes of GI bleeding in the last three years. His hemoglobin and liver related tests were normal. Subsequent follow-up endoscopies using a side-viewing scope showed no residual tumor and biopsies (using jumbo

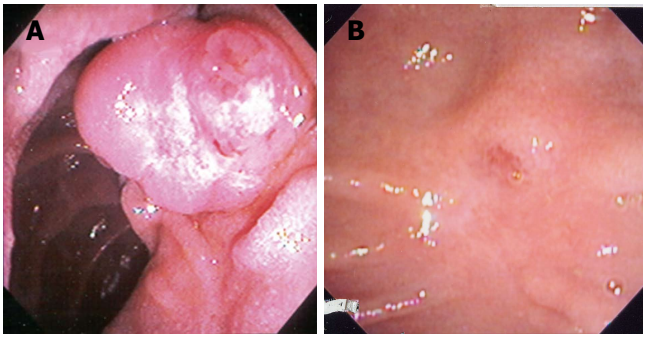

Figure 1 Endoscopic view showing an ampullary tumor (**A**) and the same area weeks after endoscopic resection of the tumor (**B**).

forceps) of the area remained negative for tumor cells. A follow-up EUS and two CT scans were also unremarkable.

DISCUSSION

Neuroendocrine neoplasms only rarely occur at the ampulla of Vater, and consist mostly of carcinoids and occasionally of poorly differentiated endocrine carcinomas (small cell carcinomas)[4]. Up to 26% of patients may have associated Von Recklinghausen disease[5]. There is a higher incidence (46%) of finding metastatic disease at diagnosis in carcinoids of the ampullary area. Jaundice (53%), pain (24%), pancreatitis (6%) and weight loss (3.6%) are common presenting symptoms[6] but upper GI bleeding from ulceration is rare[7]. Carcinoids have an intact overlying mucosa which may explain a high rate of false negative biopsies[2,6]. Examination using a side-viewing scope and obtaining deep excavating biopsies is essential towards establishing the diagnosis. The possibility of the bile duct involvement should be ascertained with ERCP and/or EUS. In detecting smaller tumors and for local angio-invasion, EUS could be extremely sensitive[8]. CT scan and MRI have a low sensitivity for the primary lesion[8]. Somatostatin receptor scan is 86% sensitive for duodenal carcinoids of $\geqslant$ 1 cm, in detecting both primary and metastatic disease[9]. A capsule endoscopy should be considered to rule out synchronous small bowel lesions.

Re-classified by WHO, carcinoids are now called neuroendocrine tumors. Ampullary carcinoids range from highly differentiated (probably benign) to well differentiated endocrine carcinomas and poorly differentiated carcinomas. The overall survival appears to be excellent at 90% for well differentiated tumors[2], but poor when these are not so well differentiated[10].

Choosing the best treatment option for ampullary carcinoids could be challenging. Although tumor size is not a good prognostic predictor[2,10], most experts still recommend either a Whipple or a pylorus preserving pancreatico-duodenectomy (PPPD) for tumors over 2 cm in size[11]. Metastatic disease has been found in 48% and 40% of the patients with tumor sizes of more than 2 cm and less than 2 cm, respectively[12]. Thus, some experts recommend a Whipple pancreatico-duodenectomy for all size tumors. On the other hand long-term survival has been achieved with local resection only[2,13]. In a study of

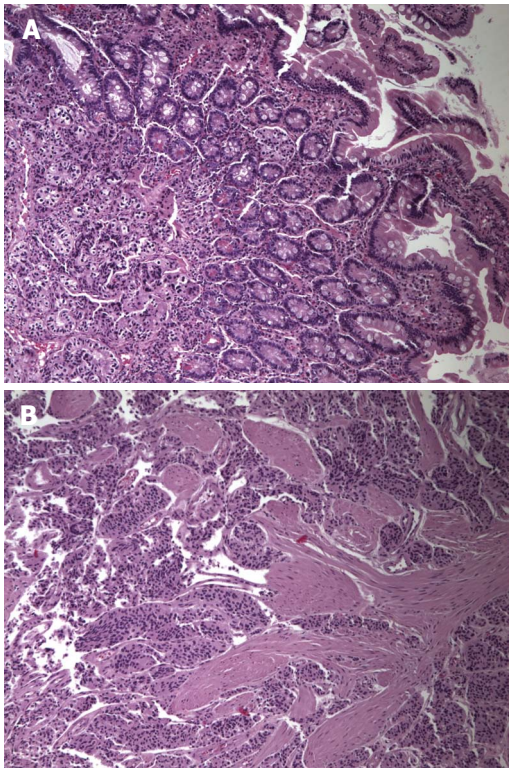

Figure 2 Histological examination of the resected specimen revealing carcinoid in the mucosa and submucosa, composed of discrete solid nests of round tumor cells with central nuclei and occasionally with gland-like lumina (**A**) and solid nests of tumor cells involving the musclaris propria (**B**) (HE, x 100).

90 patients with ampullary carcinoids, 52 had a PPPD (majority > 2 cm), while 22 underwent a local resection (majority < 2 cm). Post-operative mortality was 3/52 in the PPPD group compared to 0/22 in the group with local resection[14]. Therefore, less radical approaches should be considered in highly differentiated, slow growing tumors. In relatively high surgical risk patients with a small, non-metastatic tumor, local excision seems to be a reasonable operative choice, whereas the least invasive approach should be reserved for those who are not surgical candidates. An endoscopic ampullectomy which seems to be an effective treatment in the management of ampullary adenomas, could also be a viable option in selected patients with tumors *in situ* (Tis)[15] and carcinoids of the ampulla of Vater, without vascular invasion.

REFERENCES

1 **Godwin JD**. Carcinoid tumors. An analysis of 2,837 cases. *Cancer* 1975; **36**: 560-569
2 **Hatzitheoklitos E**, Büchler MW, Friess H, Poch B, Ebert M, Mohr W, Imaizumi T, Beger HG. Carcinoid of the ampulla of Vater. Clinical characteristics and morphologic features. *Cancer* 1994; **73**: 1580-1588
3 **Solcia E**, Fiocca R, Rindi G, Villani L, Luinetti O, Burrell M, Bosi F, Silini E. Endocrine tumors of the small and large intestine. *Pathol Res Pract* 1995; **191**: 366-372
4 **Van Eeden S**, Quaedvlieg PF, Taal BG, Offerhaus GJ, Lamers CB, Van Velthuysen ML. Classification of low-grade neuroendocrine tumors of midgut and unknown origin. *Hum Pathol* 2002; **33**: 1126-1132
5 **Hartel M**, Wente MN, Sido B, Friess H, Büchler MW. Carcinoid of the ampulla of Vater. *J Gastroenterol Hepatol* 2005;

20: 676-681
6 **Albizzatti V**, Casco C, Gastaminza M, Speroni A, Mauro G, Rubio HW. Endoscopic resection of two duodenal carcinoid tumors. *Endoscopy* 2000; **32**: S42
7 **Kim MH**, Lee SK, Seo DW, Won SY, Lee SS, Min YI. Tumors of the major duodenal papilla. *Gastrointest Endosc* 2001; **54**: 609-620
8 **Cannon ME**, Carpenter SL, Elta GH, Nostrant TT, Kochman ML, Ginsberg GG, Stotland B, Rosato EF, Morris JB, Eckhauser F, Scheiman JM. EUS compared with CT, magnetic resonance imaging, and angiography and the influence of biliary stenting on staging accuracy of ampullary neoplasms. *Gastrointest Endosc* 1999; **50**: 27-33
9 **Joseph K**, Stapp J, Reinecke J, Skamel HJ, Höffken H, Benning R, Neuhaus C, Lenze H, Trautmann ME, Arnold R. Receptor scintigraphy using 111In-pentetreotide in endocrine gastroenteropancreatic tumors. *Nuklearmedizin* 1993; **32**: 299-305
10 **Makhlouf HR**, Burke AP, Sobin LH. Carcinoid tumors of the ampulla of Vater: a comparison with duodenal carcinoid tumors. *Cancer* 1999; **85**: 1241-1249
11 **Roder JD**, Stein HJ, Hüttl W, Siewert JR. Pylorus-preserving versus standard pancreatico-duodenectomy: an analysis of 110 pancreatic and periampullary carcinomas. *Br J Surg* 1992; **79**: 152-155
12 **Anthony LB**, Martin W, Delbeke D, Sandler M. Somatostatin receptor imaging: predictive and prognostic considerations. *Digestion* 1996; **57** Suppl 1: 50-53
13 **Ricci JL**. Carcinoid of the ampulla of Vater. Local resection or pancreaticoduodenectomy. *Cancer* 1993; **71**: 686-690
14 **Clements WM**, Martin SP, Stemmerman G, Lowy AM. Ampullary carcinoid tumors: rationale for an aggressive surgical approach. *J Gastrointest Surg* 2003; **7**: 773-776
15 **Lee SY**, Jang KT, Lee KT, Lee JK, Choi SH, Heo JS, Paik SW, Rhee JC. Can endoscopic resection be applied for early stage ampulla of Vater cancer? *Gastrointest Endosc* 2006; **63**: 783-788

S- Editor Liu Y **L- Editor** Wang XL **E- Editor** Lu W

PO Box 2345, Beijing 100023, China
www.wjgnet.com
wjg@wjgnet.com

World J Gastroenterol 2007 February 28; 13(8): 1271-1274
World Journal of Gastroenterology ISSN 1007-9327

CASE REPORT

Multistep hepatocarcinogenesis from a dysplastic nodule to well-differentiated hepatocellular carcinoma in a patient with alcohol-related liver cirrhosis

Soo Ryang Kim, Hirotsugu Ikawa, Kenji Ando, Keiji Mita, Shuichi Fuki, Michiie Sakamoto, Yoshihiro Kanbara, Toshiyuki Matsuoka, Masatoshi Kudo, Yoshitake Hayashi

Soo Ryang Kim, Hirotsugu Ikawa, Kenji Ando, Keiji Mita, Shuichi Fuki, Department of Gastroenterology, Kobe Asahi Hospital, Japan
Michiie Sakamoto, Department of Pathology, Keio University School of Medicine, Japan
Yoshihiro Kanbara, Department of Surgery, Hyogo Medical Center for Adults, Japan
Toshiyuki Matsuoka, Department of Radiology, Osaka City University Medical School, Japan
Masatoshi Kudo, Department of Gastroenterology, Kinki University School of Medicine, Japan
Yoshitake Hayashi, Division of Molecular Medicine & Medical Genetics, International Center for Medical Research and Treatment, Kobe University Graduate School of Medicine, Japan
Correspondence to: Soo Ryang Kim, MD, Department of Gastroenterology, Kobe Asahi Hospital, 3-5-25 Bouoji-cho, Nagata-ku, Kobe 653-0801, Japan. info@kobe-asahi-hp.com
Telephone: +81-78-6125151 Fax: +81-78-6125152
Received: 2006-11-17 Accepted: 2007-01-29

Abstract

We describe a rare case of the transformation of a dysplastic nodule into well-differentiated hepatocellular carcinoma (HCC) in a 56-year-old man with alcoholrelated liver cirrhosis. Ultrasound (US) disclosed a 10 mm hypoechoic nodule and contrast enhanced US revealed a hypovascular nodule, both in segment seven. US-guided biopsy revealed a high-grade dysplastic nodule characterized by enhanced cellularity with a high N/C ratio, increased cytoplasmic eosinophilia, and slight cell atypia. One year later, the US pattern of the nodule changed from hypoechoic to hyperechoic without any change in size or hypovascularity. US-guided biopsy revealed well-differentiated HCC of the same features as shown in the first biopsy, but with additional pseudoglandular formation and moderate cell atypia. Moreover, immunohistochemical staining of cyclase-associated protein 2, a new molecular marker of well-differentiated HCC, turned positive. This is the first case of multistep hepatocarcinogenesis from a dysplastic nodule to well-differentiated HCC within one year in alcohol-related liver cirrhosis.

Key words: Multistep hepatocarcinogenesis; Dysplastic nodule; Well-differentiated hepatocellular carcinoma; Alcohol-related liver cirrhosis; Cyclase-associated protein 2

Kim SR, Ikawa H, Ando K, Mita K, Fuki S, Sakamoto M, Kanbara Y, Matsuoka T, Kudo M, Hayashi Y. Multistep hepatocarcinogenesis from dysplastic nodule to well-differentiated hepatocellular carcinoma in a patient with alcohol-related liver cirrhosis. *World J Gastroenterol* 2007; 13(8): 1271-1274

http://www.wjgnet.com/1007-9327/13/1271.asp

INTRODUCTION

In Western countries and in Japan, hepatocellular carcinoma (HCC) usually develops in close association with pre-existing liver cirrhosis (LC). The cirrhotic liver is therefore believed to have a precancerous lesion recognizable as a small nodule, referred to as the dysplastic nodule[1] or adenomatous hyperplasia[2]. The mean size of most dysplastic nodules is 7-8 mm, seldom larger than 20 mm in diameter. Among LC cases, the dysplastic nodule is usually hepatitis C virus (HCV)-related, rarely hepatitis B virus (HBV)-related, and has not been reported as alcohol-related. HCC usually develops in chronic liver diseases such as HCV and HBV. In Japan, HCC occurs in 81% of HCV and 14% of HBV carriers[3], but seldom in alcohol-related LC, whereas in the United States HCC occurs in 30% of alcohol-related LC[4]. Herein we describe a rare case of multistep hepatocarcinogenesis from a dysplastic nodule to well-differentiated HCC in a patient with alcohol-related LC.

CASE REPORT

A 56-year-old man was admitted to Kobe Asahi Hospital in April 2005 for further examination of a 10 mm hypoechoic nodule in the liver. In April 2001, histologic analysis of tissue obtained at biopsy because of his abnormal liver function had revealed alcohol-related LC (Figure 1); no nodule was detected. His alcohol consumption over 35 years was 120 mL/d. A physical examination on admission in April 2005 showed no remarkable abnormalities. There was no evidence of

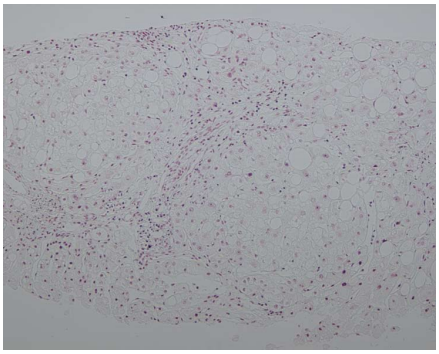

Figure 1 Histological features of liver biopsy (April 2001), alcohol-related liver cirrhosis, micronodular liver cirrhosis with fatty change (HE × 100).

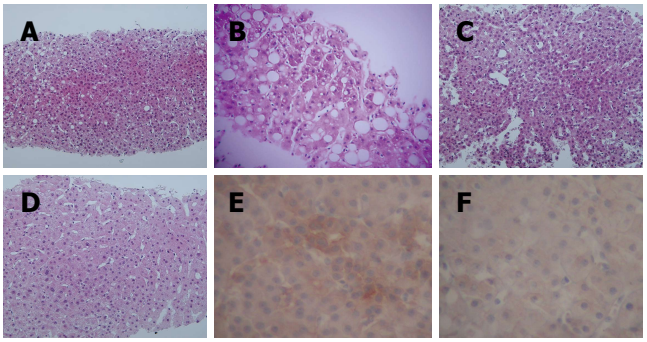

Figure 3 Histological features of US-guided liver biopsy of the liver. **A**: High grade dysplastic nodule (April 2005): increased cellularity with a high N/C ratio, increased cytoplasmic eosinophilia, and slight atypia (HE × 200); **B**: Non nodular lesion (HE × 200) (April 2005), well-differentiated HCC (May 2006): increased cellularity with a high N/C ratio, increased cytoplasmic eosinophilia, moderate atypia, and pseudoglandular formation (arrow) (HE × 200); **C**: Non-nodular lesion (May 2006); **D**: Immunohistochemical finding (May 2006) (HE × 200), CAP2 positive HCC cells are observed (more than 30%); **E**: Immunohistochemical finding (May 2006) (HE × 200): Liver cirrhosis is negative for CAP2; CAP2 positive HCC cells are observed (more than 30%); **F**: Immunohistochemical finding (May 2006) (HE × 200): Liver cirrhosis is negative for CAP2.

lymph adenopathy or splenomegaly. The serum was negative for HCV antibody (anti-HCV), hepatitis B surface antigen (HBsAg), and hepatitis B core antibody (anti-HBc). Laboratory data on admission in April 2005 disclosed the following abnormal values: platelets 7.1 × 10^4/μL (normal 13.1-36.2), aspartate aminotransferase 88 IU/L (8-38), γ-glutamyl transpeptidase (γ-GTP) 677 IU/L (16-84), total bilirubin 1.4 mg/dL (0.2-1.0), and indocyanine green (ICG) 15 min retention rate 35% (0%-10%). Alpha-fetoprotein (AFP), lens culinaris agglutinin A-reactive fraction of alpha fetoprotein (AFP L3) and protein-induced vitamin K absence (PIVKA Ⅱ) were within normal ranges. Immunological examinations revealed the following: IgG 1452 mg/dL (870-1700), IgM 235 mg/dL (33-190), IgA 207 mg/dL (110-410), B cell 8% (14%-13%), T cell 83% (66%-89%), CD4/CD8 ratio 2.08 (0.40-2.30), and NK cell activity 50% (18%-40%). Ultrasound (US) disclosed a 10 mm hypoechoic nodule in segment seven (S7) (Figure 2A). Plain computed tomography (CT) did not show any nodule, and contrast enhanced CT and magnetic resonance imaging (MRI) did not reveal any enhanced nodule. MRI revealed an isointensive nodule at both T1- and T2-weighted sequences. CT hepatic arteriography (CTA) did not show any enhanced nodule, and CT during arterial portography

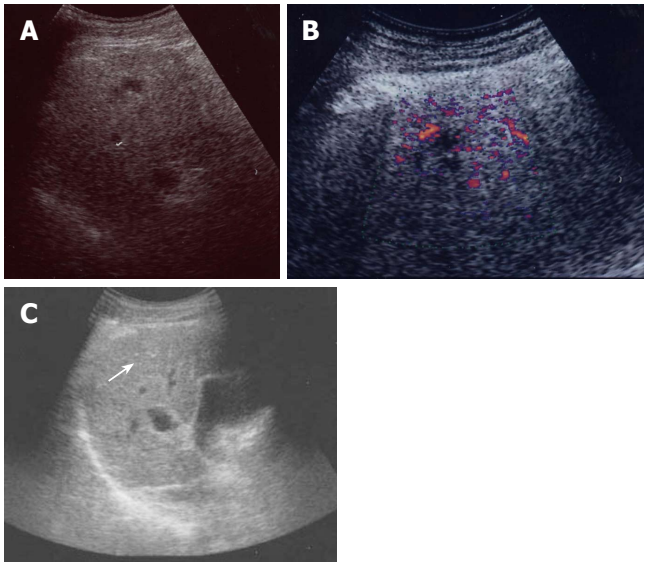

Figure 2 **A**: US imaging (April 2005). A 10 mm hypoechoic nodule in S7; **B**: contrast enhanced US (April 2005). Hypovascularity in the early phase; **C**: US imaging (May 2006). A 10 mm hyperechoic nodule in S7.

(CTAP) did not show any perfusion defect. Contrast enhanced US revealed a hypovascular nodule (Figure 2B). A US-guided biopsy revealed a high grade dysplastic nodule characterized by increased cellularity with a high N/C ratio, increased cytoplasmic eosinophilia, and slight cell atypia (Figure 3A and B). Immunohistochemical staining of both heat shock protein (HSP) 70 and cyclase-associated protein (CAP) 2 was negative.

In May 2006, the US pattern of the nodule changed from hypoechoic to hyperechoic (Figure 2C), although the size of the nodule did not change. Constant enhanced US revealed a hypovascular nodule, and AFP, AFP L3, and PIVKA Ⅱ were within normal ranges. The findings of imaging studies including contrast enhanced CT and MRI were all the same as in April 2005. A US-guided biopsy revealed well differentiated HCC of the same features as those in April 2005 with additional pseudoglandular formation and moderate cell atypia (Figure 3C and D). Immunohistochemical staining of CAP2 was over 30% positive (Figure 3E and F), although HSP70 staining was negative.

DISCUSSION

According to the classification by the International Working Party of the World Congress of Gastroenterology, hepatic nodules in patients with chronic liver diseases are subdivided into regenerative nodules (mono acinus and multi acinus), low-grade dysplastic nodules, high-grade dysplastic nodules, well-differentiated HCC, moderately-differentiated HCC, and poorly-differentiated HCC, in an ascending order of histologic grades, representing a sequence of multistep hepatocarcinogenesis[1].

It is often difficult-even for the hepatopathologist - to differentiate among regenerative nodules, precancerous lesions, and early HCC, especially from the examination of biopsy specimens. Therefore, the uncovering of an

objective molecular marker that would help to standardize histological diagnosis of early HCC and to lead to appropriate treatment is eagerly anticipated. Also, the molecular mechanisms of hepatocarcinogenesis are far from clear. A molecular understanding of multistep hepatocarcinogenesis is an important step toward the identification of additional biomarkers and new therapeutic targets of a greater specificity for HCC management. Diagnosis is based on histologic analysis of liver samples for identifying cytoarchitechtural features (cell atypia, increased cellularity, increased cytoplasmic eosinophilia, fatty change, pseudoglandular formation, trabecular thickness, etc) and on information from immunocytochemical staining, such as that with HSP70[5], and CAP2[6].

Chuma *et al*[5] have found several up-regulated genes involved in HCC progression by comparing expression profiles among early and progressed components of seven nodule-in-nodule-type HCCs (1 HBV-positive case, 5 HCV-positive cases and 1 negative for both B and C) and their corresponding non-cancerous liver tissues, with the use of an oligonucleotide array: HSP70 (a molecular marker of early HCC) and CAP2, with up-regulated expression in a stepwise manner in multistage hepatocarcinogenesis[6].

Immunohistochemically, HSP70 is significantly overexpressed in early HCC compared with its expression in dysplastic nodules, reaching 80% in most cases of well-differentiated HCC[5].

All cases of dysplastic nodules were negative or focally positive (about 5%-10% of the lesions) for CAP2; in contrast, most cases of HCC (27 of 29 cases) were positive for CAP2, to some extent. Of the lesions, 70%-100% were positive in the progressed components, and the positivity of well-differentiated HCC ranged from 10% to 100%[6].

In our case, although CAP2 staining of the first biopsy (April 2005) was negative, that of the second (May 2006) was positive over 30%. Histopathologically, the distinct difference between the two biopsies was the pseudoglandular formation and the moderate cell atypia of the second biopsy that are specific to well-differentiated HCC.

Consequently, we made the definite diagnosis of a high-grade dysplastic nodule after the first biopsy and a well-differentiated HCC after the second biopsy.

In our case, immunohistochemical staining of HSP70 was negative in the second biopsy, whereas that of CAP2 was positive. One explanation for this discrepancy is the difference in the positivity of immunohistochemical staining of well-differentiated HCC between HSP70 (72%)[5] and CAP2 (93%)[6].

It is well accepted that HCC can in a multistep manner develop from a dysplastic nodule[7,8] into HCC. Among LC cases, the dysplastic nodule is usually HCV-related, rarely HBV-related, and has not been reported as alcohol-related. Similarly, multistep hepatocarcinogenesis from a dysplastic nodule to well-differentiated HCC is usually HCV-related, rarely HBV-related, and has not been reported as alcohol-related[4].

In April 2001, no nodule was detected; in April 2005, a 10 mm hypoechoic nodule with the background of alcohol-related LC appeared in S7. Imaging studies by contrast enhanced US, CT, MRI, CTA, and CTAP revealed a hypovascular nodule compatible with a dysplastic nodule or well-differentiated HCC. The histopathological findings revealed a high-grade dysplastic nodule. In May 2006, the US pattern of the nodule changed from hypoechoic to hyperechoic without any change in size, and the imaging findings other than US were all the same as those in April 2005. Tumor markers such as AFP, AFP L3 and PIVKA Ⅱ were within normal ranges. The histopathological findings of the hyperechoic nodule revealed well-differentiated HCC. Alcohol abuse in some cases induces hyperplastic nodules that are usually associated with hypervascularity[9-11] and that are often misdiagnosed as HCC from imaging studies, as are dysplastic nodules from histopathological findings. Hyperplastic nodules do not, however, transform to HCC and often disappear subsequent to discontinued alcohol intake. The dysplastic nodule in our case is, in this respect, different from the hyperplastic nodule associated with hypervascularity. The clinical course of the patient showed multistep hepatocarcinogenesis from a dysplastic nodule to well-differentiated HCC within one year with the background of alcohol-related LC. The mechanism by which alcohol causes HCC is not known, but has been hypothesized to include oxidative stress, changes in retinoic acid metabolism and DNA methylation, decreased immune surveillance and genetic susceptibility[4]. The former three factors are common in patients with alcohol abuse. The latter two factors are specific to patients with individual differences of alcohol intake. In this case immunological examinations including immunoglobulin, the percentage of B cells and T cells, CD4/CD8 ratio, and NK cell activity were within almost normal limits. Therefore, one explanation for the transformation from a dysplastic nodule to an HCC may be genetic susceptibility that was not examined at the time.

To the best of our knowledge, this is the first case of multistep hepatocarcinogenesis from a dysplastic nodule to a well-differentiated HCC in alcohol-related LC.

Further study is needed to clarify the objective criteria for the definite diagnosis of dysplastic nodules and well-differentiated HCC, and the precise mechanism of hepatocarcinogenesis in alcohol-related LC.

REFERENCES

1 **Terminology of nodular hepatocellular lesions**. *Hepatology* 1995; **22**: 983-993

2 **Takayama T**, Makuuchi M, Hirohashi S, Sakamoto M, Okazaki N, Takayasu K, Kosuge T, Motoo Y, Yamazaki S, Hasegawa H. Malignant transformation of adenomatous hyperplasia to hepatocellular carcinoma. *Lancet* 1990; **336**: 1150-1153

3 **Ikai I**, Itai Y, Okita K, Omata M, Kojiro M, Kobayashi K, Nakanuma Y, Futagawa S, Makuuchi M, Yamaoka Y. Report of the 15th follow-up survey of primary liver cancer. *Hepatol Res* 2004; **28**: 21-29

4 **Morgan TR**, Mandayam S, Jamal MM. Alcohol and hepatocellular carcinoma. *Gastroenterology* 2004; **127**: S87-S96

5 **Chuma M**, Sakamoto M, Yamazaki K, Ohta T, Ohki M, Asaka M, Hirohashi S. Expression profiling in multistage hepatocarcinogenesis: identification of HSP70 as a molecular marker of early hepatocellular carcinoma. *Hepatology* 2003; **37**: 198-207

6 **Shibata R**, Mori T, Du W, Chuma M, Gotoh M, Shimazu M,

Ueda M, Hirohashi S, Sakamoto M. Overexpression of cyclase-associated protein 2 in multistage hepatocarcinogenesis. *Clin Cancer Res* 2006; **12**: 5363-5368

7 **Sakamoto M**, Hirohashi S, Shimosato Y. Early stages of multistep hepatocarcinogenesis: adenomatous hyperplasia and early hepatocellular carcinoma. *Hum Pathol* 1991; **22**: 172-178

8 **Kojiro M**, Shigetaka S, Nakashima O. Pathomorphologic characteristics of early hepatocellular carcinoma. In: Okuda K, Tobe T, Kitagawa T, editors. Early detection and treatment of liver cancer. *Gann Monogr Cancer Res* 1991; **38**: 29-37

9 **Nakashima O**, Watanabe J, Tanaka M, Fukukura Y, Kojiro M, Kurohiji T, Saitsu H, Adachi A, Nabeshima M, Miura K. Clinicopathologic study of hyperplastic nodules in patient with chronic alcoholic liver disease. *Kanzo* 1996; **37**: 704-713

10 **Kita R**, Osaki Y, Maruo T, Kimura T, Kokuryu H, Takamatsu S, Tomono N, Shimizu T. A case of severe alcoholic liver cirrhosis with multiple hyperplastic nodules. *Kanzo* 2001; **42**: 203-209

11 **Nagasue N**, Akamizu H, Yukaya H, Yuuki I. Hepatocellular pseudotumor in the cirrhotic liver. Report of three cases. *Cancer* 1984; **54**: 2487-2494

S- Editor Liu Y **L- Editor** Zhu LH **E- Editor** Chin GJ

PO Box 2345, Beijing 100023, China
www.wjgnet.com
wjg@wjgnet.com

World J Gastroenterol 2007 February 28; 13(8): 1275-1278
World Journal of Gastroenterology ISSN 1007-9327

CASE REPORT

Common bile duct schwannoma: A case report and review of literature

Luigi Fenoglio, Sara Severini, Paola Cena, Elena Migliore, Christian Bracco, Fulvio Pomero, Sergio Panzone, Giovan Battista Cavallero, Alberto Silvestri, Rodolfo Brizio, Felice Borghi

Luigi Fenoglio, Sara Severini, Paola Cena, Elena Migliore, Christian Bracco, Fulvio Pomero, Sergio Panzone ,Giovan Battista Cavallero, Alberto Silvestri, Department of Internal Medicine, Santa Croce and Carle Hospital, Cuneo, Italy
Rodolfo Brizio, Department of Pathology, Santa Croce and Carle Hospital, Cuneo, Italy
Felice Borghi, Department of General Surgery, Santa Croce and Carle Hospital, Cuneo, Italy
Correspondence to: Dr. Luigi Fenoglio, Santa Croce Hospital, Via Michele Coppino 26, Cuneo12100, Italy. fenoglio.l@ospedale.cuneo.it
Telephone: +39-338-5064398 Fax: +39-171-641615
Received: 2006-11-14 Accepted: 2007-02-12

Abstract

Schwannoma is a myelin sheath tumor complicated with neurofibroma, neurofibromatosis and neurogenic sarcoma. Peripheral nerve sheath tumors represent 2%-6% of gastrointestinal tract stromal tumors (GIST), but there are deficient data about location of neurogenic tumors in the biliary system and only nine cases of schwannoma of the extrahepatic biliary tract have been reported. These tumors are clinically non-specific. They are usually symptomatic by compressing the close or adjacent structures when being retroperitoneal, and their preoperative diagnosis is extremely difficult. This paper reviews the literature data and describes a case of schwannoma of the common bile duct associated with cholestasis in a healthy young woman, diagnosed and treated in our department. This case is of interest on account of the complexity of its diagnosis and the atypical macroscopic growth pattern of the tumor.

Key words: Schwannoma; Neurinoma; Common bile duct; Biliary tract

Fenoglio L, Severini S, Cena P, Migliore E, Bracco C, Pomero F, Panzone S, Cavallero GB, Silvestri A, Brizio R, Borghi F. Common bile duct schwannoma: A case report and review of literature. *World J Gastroenterol* 2007; 13(8): 1275-1278

http://www.wjgnet.com/1007-9327/13/1275.asp

INTRODUCTION

Myelin sheath tumors comprise schwannoma, neurofibroma, neurofibromatosis and neurogenic sarcoma. More than 90% are benign[1] and present in young to middle-aged subjects (twice in women than in men). They are usually asymptomatic and hence discovered incidentally[2]. Schwannoma is more common than neurofibroma. Its origin is often single. The 10% with a multiple origin[3] are classified as neurofibromatosis II, a disorder of autosomal dominant inheritance[4]. When located in gastrointestinal tract, schwannoma, leiomyoma, leiomyosarcoma and leiomyoblastoma constitute the gastrointestinal stromal tumors (GIST)[5]. Peripheral nerve sheath tumors account for 2%-6% of the GIST, but there are few reports of neurogenic tumors in the biliary system. The retroperitoneum is rarely involved[6]. Schwannomas arise only occasionally in the extrahepatic ducts and provoke symptoms by compressing adjacent structures[7]. Their symptoms were so varied to make their preoperative diagnosis very difficult. A cholestatic syndrome in a healthy woman is described in this report.

CASE REPORT

The patient was a 41-year-old woman who presented with ingravescent pruritus lasting one month, a 4 kg weight loss and scleral subicterus. Her clinical and family history were devoid of significance. There was no history of drug intake. The physical examination evidenced a normal spleen and the absence of lymphadenopathies in the explorable sites. There was evidence of diffuse scratching lesions on the lower limbs and subicteric sclerae.

Laboratory results: RBC 4.49 × 10^6/L (4.2-5.4), WBC 4.76 × 10^3/L (4-10), hemoglobin 14.4 g/dL (12-16), ESR 21 mm/s, PCR 0.76 mg/L (< 3), LDH 412 U/L (313-618), total proteins 8.7 g/dL (6.3-8.2), total bilirubin 2.1 mg/dL (0.2-1.3), conjugated bilirubin 1.4 mg/dL (0-0.4), bile acids 6.8 μmol/L (0-6), AST 90 U/L (< 40), ALT 161 U/L (9-56), GGT 290 U/L (12-58), ALPh 192 U/L (38-126), amylase 60 U/L (30-110), antimitocondrial antibody negative, CEA 1.3 ng/mL (< 5), CA 19-9 48.5 U/mL (< 37), CA-125 39.6 U/mL (< 35).

A CT scan (Figure 1A) revealed a lesion between the head of the pancreas and the gall bladder infundibulum near to the middle segment of the common bile duct. The mass was heterogeneous with a diameter of 3 cm. The upstream bile ducts were slightly dilated. The gall bladder was overdistended and contained a 2 cm stone in the fundus. Cholangio-MRI with the secretin test (Figure 1B-D) dislcosed a hypointensive signal in the weighted

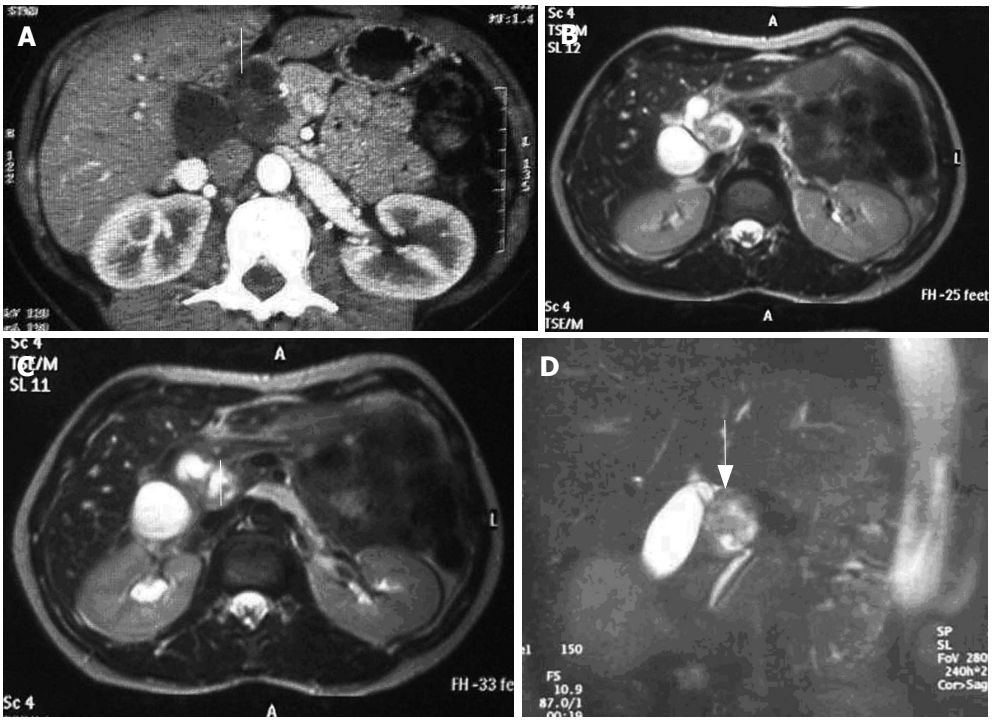

Figure 1 **A**: CT scan showing a very heterogeneous formation with a liquid content in close contiguity to the CBD (white arrow); **B**, **C**, **D**: Cholangio-MRI reveals a solid formation with a hypointensive signal in the weighted T1 sequences at the pancreatic isthmus (white arrows) with dilation of the upstream bile ducts.

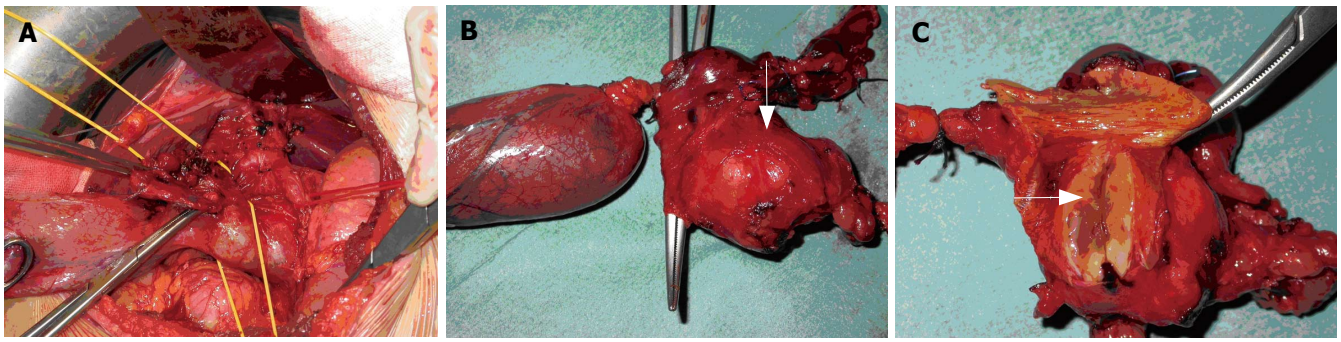

Figure 2 Intraoperative view of involvement of the intermediate tract of the common bile duct between its confluence with the cystic duct (**A**) and the prepancreatic tract (**B**) and (**C**) Gross inspection showing that the lesion (arrows) is solid and situated intramurally and below the mucosa in close contiguity with the CBD.

T1 sequences. The mass was assigned to the pancreatic isthmus. Its size and lack of uniformity were confirmed and a neoplastic origin was suspected. A good response to secretin showed that the function of the pancreas was unimpaired. Biliopancreatic echoendoscopy ruled out involvement of the pancreas, confirmed distention of the gall bladder and disclosed a solid, non-vascularised formation with many anaechogenic areas. Its contiguity with the portal axis rendered percutaneous biopsy inadvisable and exploratory laparotomy was performed. The formation involved the intermediate tract of the common bile duct between its confluence with the cystic duct and the prepancreatic tract (Figure 2A). The middle segment of the common bile duct was resected, together with the gall bladder (overdistended, but uninflamed) and the lymph nodes. A bilio-digestive Roux-en-Y anastomosis was performed on the loop. Gross inspection showed an intramural lesion under the mucosa with a diameter of 4 cm (Figure 2B and C). Histological examination revealed the proliferation of interwoven bundles of fused cells, occasionally separated by slacker, oedematous areas with a pseudocystic appearance (Figure 3A). There were also a few cells with an hyperchromic, atypical and bizarre nucleus (Figure 3B), ectatic, congested and partially thrombosed vessels (Figure 3C), and signs of perivascular hyalinisation (Figure 3D).

Immunohistochemical investigation showed that the tumor cells were vimentin and protein S-100 positive, and alpha-actin, desmin, CD34, cytokeratin pan (clone ARE1/E3) and CD117 negative. The postoperative course was uneventful. The cholestatic and hepatic cytolytic indices normalised after two months, with definite disappearance of pruritus, which continue to be normal after one year .

DISCUSSION

Schwannoma of the bile ducts is particularly rare, and it usually arises in the head, neck, spinal cord and the extremities[8], but rarely in retroperitoneum (6% of primary retroperitoneal tumors)[9]. It is usually located in the para-vertebral regions or in the pre-sacral pelvic zone[2,10]. The bladder and abdominal wall are occasionally involved.

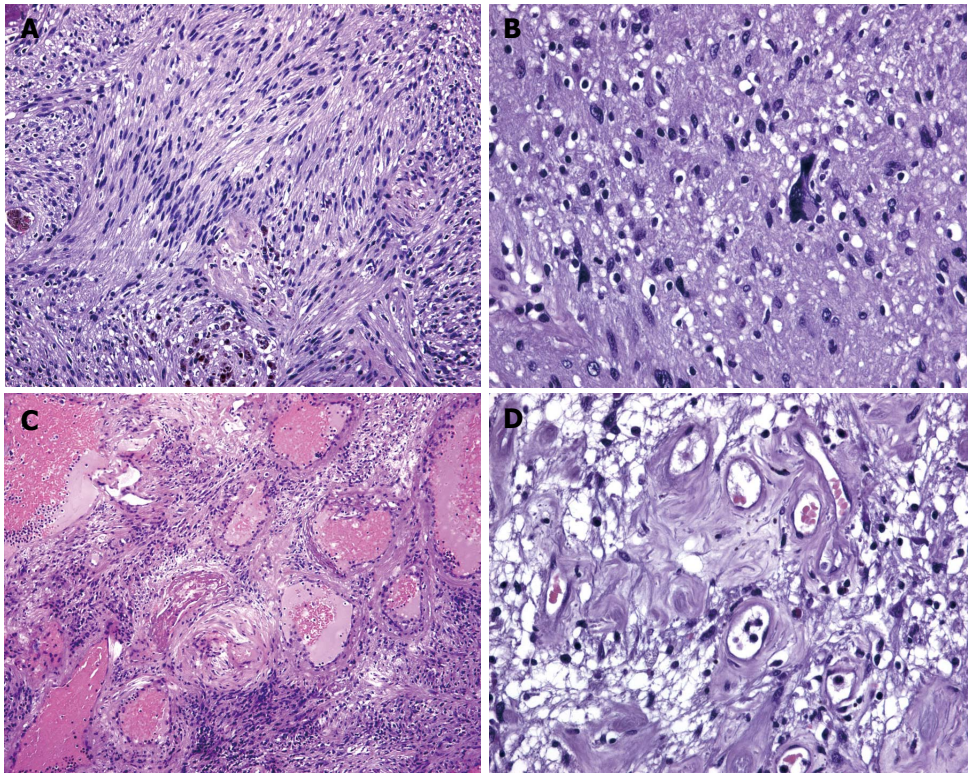

Figure 3 **A:** Histological examination showing that inter-woven bundles of fused cells separated by slacker, oedematous areas with a pseudocystic appearance (Antoni A schwannoma growth pattern); **B**: Histological examination showing a few cells with hyperchromic, atypical and bizarre nuclei.Histological examination showing a few cells with hyperchromic, atypical and bizarre nuclei; **C**: Histological examination showing hyalinisation and ectatic and partially thrombosed vessels; **D**: Histological examination showing perivascular hyalinisation.

Liver, rectal colon and esophageal involvement has been described[11-14], whereas only nine cases of schwannoma of the extrahepatic biliary tract and one case of benign schwannoma in the hepatoduodenal ligament have been reported since the 1970s[7,15-23]. Determination of tumor location must be done with great care when mass exists between the liver and the retroperitoneum, especially when the mass is hypovascular. Pre-surgical diagnosis of the tumor is very difficult because early clinical detection is limited until it gives a palpable mass or compresses the surrounding organs[6].

Diagnosis is usually entrusted to CT and MRI. The gastrointestinal schwannomas appeared as a round or oval homogeneously attenuating, well-defined mass with frequent signs of degeneration, such as cysts and calcifications on CT[24]. Recently it was reported that CTs do not reveal tumor capsule, cystic change, necrosis or calcification in any of the observed schwannomas[25]. Weighted T1 images disclose masses with low-medium signal intensity, whereas this is high in the weighted T2 images owing to alternation of the Antoni A and B areas and secondary degeneration[26].

In the present case, CT illustrated a hypodense and very heterogeneous formation initially referable to duodenal diverticulum. The MRI images were marked by slight weighted T2 hyperintensity due to the partially fluid content. A good response to secretin showed that the function of the pancreas was unimpaired.

We did not employ PET with fluorodeoxyglucose (FDG) uptake since it has been widely used to quantify the metabolism of malignant bone and soft-tissue malignant tumors, whereas little is known about FDG uptake in benign lesions. FDG PET is of limited value for the preoperative differentiation of schwannoma versus sarcoma[27]. Thus, a high FDG uptake is rather common in schwannoma[28].

The macroscopic growth pattern of the tumor mass was atypical. The two schwannoma growth patterns are called Antoni A and Antoni B. Elongated cells form an irregular, but compact palisade and the tissue arrangement is loose and there are cystic spaces between the cells[29]. In some cases, insufficient vascularisation of the mass may lead to degeneration in the form of cysts, calcifications, haemorrhages and hyalinisation[30]. These degenerative tumors are called "ancient schwannomas". Morphologic and immunophenotypic features of the lesion pointed to a so-called "ancient schwannoma", with reactive lymph nodes as described in the literature[31]. Digestive tract schwannomas are different from their soft tissue counterpart; they are not encapsulated and have an intramural growth pattern. Moreover, they are different both histologically and immunohistochimically from peripheral schwannomas. Gastrointestinal schwannomas, as in our case, are usually negative for CD34, CD117 and muscle cell markers, whereas they are strongly positive for vimentin and S100 protein. This typical combination differentiates schwannomas of the digestive tract from GIST. This differentiation is of practical importance. Gastrointestinal schwannomas are benign and associated with a good prognosis since post-surgical recurrences are unusual[32], even when treated only with enucleation. Gastrointestinal stromal tumors, on the other hand, present a negative course in more than 50% of the cases[33,34].

The distinctive feature of this case is the complexity of its diagnosis. Conventional radiography was unable to provide a precise picture of the nature and location of the mass. A diagnosis deduced from the instrumental finding often awaits intraoperative and definitive histological

confirmation[6]. Despite its complications, resection remains the treatment of choice. In the present case, only explorative laparotomy was able to demonstrate the seat and the nature of the lesion.

Lastly, in our case the postoperative course was uneventful and the cholestatic symptoms regressed two months after the operation.

REFERENCES

1 **Reed JC**, Hallet KK, Feigin DS. Neural tumors of the thorax: subject review from the AFIP. *Radiology* 1978; **126**: 9-17
2 **Kim SH**, Choi BI, Han MC, Kim YI. Retroperitoneal neurilemoma: CT and MR findings. *AJR Am J Roentgenol* 1992; **159**: 1023-1026
3 **Shields TW**, Reynolds M. Neurogenic tumors of the thorax. *Surg Clin North Am* 1988; **68**: 645-668
4 **MacCollin M**, Chiocca EA, Evans DG, Friedman JM, Horvitz R, Jaramillo D, Lev M, Mautner VF, Niimura M, Plotkin SR, Sang CN, Stemmer-Rachamimov A, Roach ES. Diagnostic criteria for schwannomatosis. *Neurology* 2005; **64**: 1838-1845
5 **Prévot S**, Bienvenu L, Vaillant JC, de Saint-Maur PP. Benign schwannoma of the digestive tract: a clinicopathologic and immunohistochemical study of five cases, including a case of esophageal tumor. *Am J Surg Pathol* 1999; **23**: 431-436
6 **de Diego Rodríguez E**, Roca Edreira A, Martín García B, Hernández Rodríguez R, Portillo Martín JA, Gutiérrez Baños JL, Correas Gómez MA, del Valle Schaan JI, Villanueva Peña A, Rado Velázquez MA, Torío Sánchez B. Retroperitoneal benign schwannoma. Report of a new case. *Actas Urol Esp* 2000; **24**: 685-688
7 **Honjo Y**, Kobayashi Y, Nakamura T, Takehira Y, Kitagawa M, Ikematsu Y, Ozawa T, Nakamura H. Extrahepatic biliary schwannoma. *Dig Dis Sci* 2003; **48**: 2221-2226
8 **Das Gupta TK**, Brasfield RD, Strong EW, Hajdu SI. Benign solitary Schwannomas (neurilemomas). *Cancer* 1969; **24**: 355-366
9 **Lane RH**, Stephens DH, Reiman HM. Primary retroperitoneal neoplasms: CT findings in 90 cases with clinical and pathologic correlation. *AJR Am J Roentgenol* 1989; **152**: 83-89
10 **Kinoshita T**, Naganuma H, Ishii K, Itoh H. CT features of retroperitoneal neurilemmoma. *Eur J Radiol* 1998; **27**: 67-71
11 **Daimaru Y**, Kido H, Hashimoto H, Enjoji M. Benign schwannoma of the gastrointestinal tract: a clinicopathologic and immunohistochemical study. *Hum Pathol* 1988; **19**: 257-264
12 **Wada Y**, Jimi A, Nakashima O, Kojiro M, Kurohiji T, Sai K. Schwannoma of the liver: report of two surgical cases. *Pathol Int* 1998; **48**: 611-617
13 **Fotiadis CI**, Kouerinis IA, Papandreou I, Zografos GC, Agapitos G. Sigmoid schwannoma: a rare case. *World J Gastroenterol* 2005; **11**: 5079-5081
14 **Nagai T**, Fujiyoshi K, Takahashi K, Torishima R, Nakashima H, Uchida A, Ookawara H, Fujitomi Y, Suzuki K, Yokoyama S, Sato R, Murakami K, Fujioka T. Ileal schwannoma in which blood loss scintigraphy was useful for diagnosis. *Intern Med* 2003; **42**: 1178-1182
15 **Wiermann H**, Wienbeck M. Benign tumors as the cause of extrahepatic occlusion syndrome. Report on a neuroma of the bile ducts. *Z Gastroenterol* 1975; **13**: 685-689
16 **Whisnant JD**, Bennett SE, Huffman SR, Weiss DL, Parker JC, Griffen WO. Common bile duct obstruction by granular cell tumor (schwannoma). *Am J Dig Dis* 1974; **19**: 471-476
17 **Silvestri F**. Neuroma of the common bile duct stump. *Chir Ital* 1965; **17**: 19-75
18 **ODEN B**. Neurinoma of the common bile duct; report of a case. *Acta Chir Scand* 1955; **108**: 393-397
19 **Ronchetti A**, Zanniello JM. Schwannoma of the common bile duct. Comments on a case. *Dia Med* 1962; **34**: 1365-1371
20 **Balart LA**, Hines C, Mitchell W. Granular cell schwannoma of the extrahepatic biliary system. *Am J Gastroenterol* 1983; **78**: 297-300
21 **Jakobs R**, Albert J, Schilling D, Nuesse T, Riemann JF. Schwannoma of the common bile duct: a rare cause of obstructive jaundice. *Endoscopy* 2003; **35**: 695-697
22 **Park MK**, Lee KT, Choi YS, Shin DH, Lee JY, Lee JK, Paik SW, Ko YH, Rhee JC. A case of benign schwannoma in the porta hepatis. *Korean J Gastroenterol* 2006; **47**: 164-167
23 **Häring RU**, Waninger J, Farthmann EH. Abdominal surgery in advanced age. Indications and prognosis exemplified by stomach, bile duct, colon and hernia surgery. *Fortschr Med* 1993; **111**: 98-101
24 **Rha SE**, Byun JY, Jung SE, Chun HJ, Lee HG, Lee JM. Neurogenic tumors in the abdomen: tumor types and imaging characteristics. *Radiographics* 2003; **23**: 29-43
25 **Levy AD**, Quiles AM, Miettinen M, Sobin LH. Gastrointestinal schwannomas: CT features with clinicopathologic correlation. *AJR Am J Roentgenol* 2005; **184**: 797-802
26 **Sakai F**, Sone S, Kiyono K, Maruyama A, Ueda H, Aoki J, Kawai T, Ishii K, Morimoto M, Haniuda M. Intrathoracic neurogenic tumors: MR-pathologic correlation. *AJR Am J Roentgenol* 1992; **159**: 279-283
27 **Ahmed AR**, Watanabe H, Aoki J, Shinozaki T, Takagishi K. Schwannoma of the extremities: the role of PET in preoperative planning. *Eur J Nucl Med* 2001; **28**: 1541-1551
28 **Beaulieu S**, Rubin B, Djang D, Conrad E, Turcotte E, Eary JF. Positron emission tomography of schwannomas: emphasizing its potential in preoperative planning. *AJR Am J Roentgenol* 2004; **182**: 971-974
29 **Rosai J**. Ackerman's surgical pathology. 6th ed. St. Louis, Mo: Mosby-Year Book, 1981: 1407-1479
30 **Enzinger FM**, Weiss SW. Soft tissue tumors. 2nd ed. St Louis, Mo: Mosby-Year Book, 1988: 719-860
31 **Hou YY**, Tan YS, Xu JF, Wang XN, Lu SH, Ji Y, Wang J, Zhu XZ. Schwannoma of the gastrointestinal tract: a clinicopathological, immunohistochemical and ultrastructural study of 33 cases. *Histopathology* 2006; **48**: 536-545
32 **Ben Moualli S**, Hajri M, Ben Amna M, Kolsi K, Chebil M, Ben Jilani S, Zaouech A, Ayed M. Retroperitoneal schwannoma. Case report. *Ann Urol* (Paris) 2001; **35**: 270-272
33 **Duffaud F**, Blay JY. Gastrointestinal stromal tumors: biology and treatment. *Oncology* 2003; **65**: 187-197
34 **Tran T**, Davila JA, El-Serag HB. The epidemiology of malignant gastrointestinal stromal tumors: an analysis of 1,458 cases from 1992 to 2000. *Am J Gastroenterol* 2005; **100**: 162-168

S- Editor Liu Y **L- Editor** Ma JY **E- Editor** Zhou T

PO Box 2345, Beijing 100023, China
www.wjgnet.com
wjg@wjgnet.com

World J Gastroenterol 2007 February 28; 13(8): 1279-1281
World Journal of Gastroenterology ISSN 1007-9327

CASE REPORT

Foregut duplication cysts of the stomach with respiratory epithelium

Theodosios Theodosopoulos, Athanasios Marinis, Konstantinos Karapanos, Georgios Vassilikostas, Nikolaos Dafnios, Lazaros Samanides, Eleni Carvounis

Theodosios Theodosopoulos, Athanasios Marinis, Konstantinos Karapanos, Georgios Vassilikostas, Nikolaos Dafnios, Lazaros Samanides, 2nd Department of Surgery, Areteion University Hospital, 76 Vasilisis Sofias av., Athens 11528, Greece
Eleni Carvounis, Department of Pathology, Areteion University Hospital, 76 Vasilisis Sofias av., Athens 11528, Greece
Correspondence to: Athanasios Marinis, MD, 2nd Department of Surgery, Areteion University Hospital, 40 Ptolemaidos str, 13674, Acharnes, Athens, Greece. sakisdoc@yahoo.com
Telephone: +30-210-7286128 Fax: +30-210-7286128
Received: 2006-12-01 Accepted: 2007-01-31

Abstract

Gastrointestinal duplication is a congenital rare disease entity. Gastric duplication cysts seem to appear even more rarely. Herein, two duplications cysts of the stomach in a 46 year-old female patient are presented. Abdominal computed tomography demonstrated a cystic lesion attached to the posterior aspect of the gastric fundus, while upper gastrointestinal endoscopy was negative. An exploratory laparotomy revealed a non-communicating cyst and a smaller similar cyst embedded in the gastrosplenic ligament. Excision of both cysts along with the spleen was performed and pathology reported two smooth muscle coated cysts with a pseudostratified ciliated epithelial lining (respiratory type).

Key words: Gastric; Cyst; Foregut; Duplication; Respiratory

Theodosopoulos T, Marinis A, Karapanos K, Vassilikostas G, Dafnios N, Samanides L, Carvounis E. Foregut duplication cysts of the stomach with respiratory epithelium. *World J Gastroenterol* 2007; 13(8): 1279-1281

http://www.wjgnet.com/1007-9327/13/1279.asp

INTRODUCTION

Gastrointestinal duplications are rare and even more exceptional are those occurring in the stomach. As a general definition, a gastrointestinal duplication is a spherical hollow structure with a smooth muscle coat, lined by a mucous membrane and attached to any part of the gastrointestinal (GI) tract from the base of the tongue to the anus[1]. These malformations are believed to be congenital and are formed before differentiation of the lining epithelium and, therefore, are named for the organs with which they are associated[2]. Foregut duplications may or may not communicate with the GI tract and usually are diagnosed in a younger age; in adults non-specific symptoms delay diagnosis, which is established during surgical exploration[3]. Herein, two gastric duplication cysts with respiratory epithelium are reported.

CASE REPORT

A 46-year-old female patient was admitted to our Surgical Department from another medical center, where the patient was evaluated for an episode of loss of consciousness. Past medical history, present status and physical examination were non disease-specific. Diagnostic workup included an abdominal computed tomography (CT) which demonstrated a cystic lesion measuring 6 cm × 6 cm × 7 cm attached to the posterior wall of the gastric fundus, was well circumscribed and had no contrast enhancement (Figure 1). Interestingly CT coronary sections revealed a pulmonary sequestration in the basal segment of the left lower lobe (Figure 2). Moreover, upper GI endoscopy showed a bulging deformation of the gastric fundus by an extrinsic mass, without any mucosal abnormalities. An exploratory laparotomy was performed and revealed two cystic lesions; the first was attached to the fundus of the stomach and the second was embedded within the gastrosplenic ligament, close to the spleen. Therefore, intact excision of both cysts and splenectomy were carried out. Postoperative course was uneventful and the patient has been asymptomatic since then.

Pathologic examination of the surgical specimens reported a large cyst, measuring 8 cm × 5.5 cm in diameter and 0.3 cm thick and a smaller cyst (removed from the gastrosplenic ligament), measuring 3 cm in diameter and 0.2 cm thick. Both consisted of a smooth muscular wall, were lined by a pseudostratified, ciliated and columnar (respiratory type) epithelium and contained a clear, gelatinous fluid. Sub-epithelium seromucous glands were microscopically identified (Figure 3), a histologic appearance reminiscent of bronchial wall; however no cartilage was present.

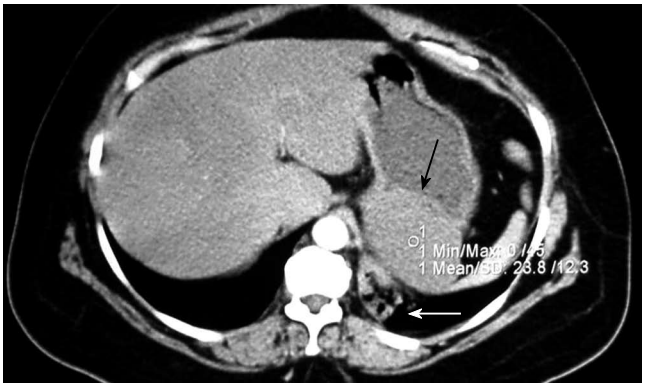

Figure 1 Abdominal CT scan demonstrating a cystic lesion attached to the posterior gastric wall (black arrow) and a pulmonary sequestration in the left pulmonary base (white arrow).

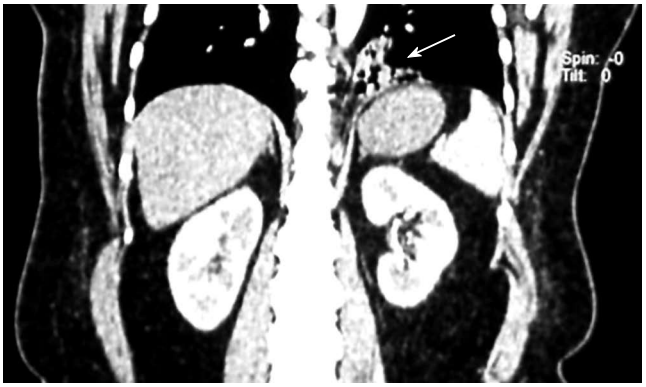

Figure 2 Coronary CT plate showing the pulmonary sequestration of the basal segment of the left lower lobe (arrow).

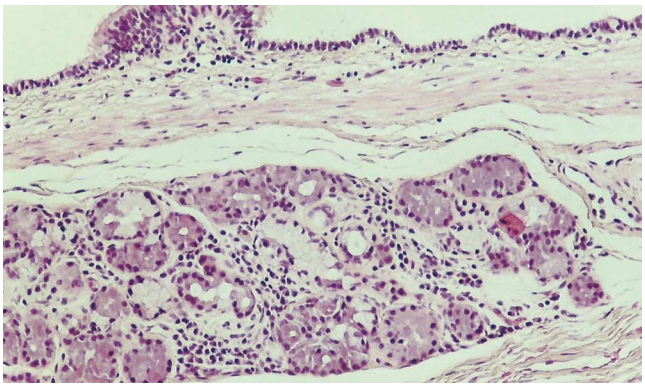

Figure 3 Histological section of the cyst wall lined by a respiratory-type epithelium and containing seromucinous glands (HE, x 100).

DISCUSSION

Gastric duplications account for between 3% and 20% of gastrointestinal duplications[2,4,5] and occur twice as frequent in females as in males. Controversy exists over the embryological origin of these anomalies. Duplications of the stomach are usually single, less than 12 cm in diameter and located on the greater curvature or on the posterior or anterior gastric wall[2]. Wieczorek *et al*[6] reported that gastric duplications can be tubular or cystic; the cystic type does not communicate with the gastric lumen (about 80% of gastric duplication cysts[7]). The first case report of a gastric duplication was published in 1911 by Wendel[8] and approximately 150 cases have been reported since then[2].

Due to their position and mass effect, gastric duplications cysts are usually diagnosed in a younger age. However, in adults diagnosis may be difficult. A wide range of symptoms and signs have been reported and vary from asymptomatic to non disease-specific presentations, e.g. vague abdominal complaints, nausea, vomiting, epigastric fullness, weight loss, anemia, dysphagia, dyspepsia, etc. Vomiting usually occurs due to partial or complete gastric outlet obstruction, while even more emergent cases have been reported such as pancreatitis[9], hemoptysis[10] and gastrointestinal hemorrhage[11]. In our case, the female patient presented with loss of consciousness due to dehydration occurring as a result of excessive vomiting and concomitant anemia. Associated pathologic conditions including pulmonary sequestration[12], multicystic kidney[13] and neoplasias[14] have been reported. The presence of respiratory type mucosa and seromucinous glands along with the presence of pulmonary sequestration in the lower lobe of the ipsilateral lung in our case supports the theory of embryologic origin from supernumerary foregut buds.

Foregut duplications cysts of the stomach are usually incidentally diagnosed. Although upper gastrointestinal series demonstrate external pressure on the stomach, preoperative workup mainly includes abdominal ultrasonography and computed tomography scans, as well as endoscopic ultrasonography and magnetic resonance imaging[15,16].

Due to malignant transformation and the report of gastric cancer arising in duplications of the stomach[17], surgical excision is considered to be the best treatment. Complete resection of the cyst is the ideal technique achieved with both open and laparoscopic[18] approaches. Unsuccessful approaches including percutaneous or endoscopic aspiration of cystic fluid have been reported[19], but are associated with complications, such as fistula formation and hemorrhage. When the recommended complete excision is not possible, converting both stomachs into one using a stapling device[20] or performing a segmental gastrectomy[21] are the possible alternatives.

In conclusion, foregut duplication cysts of the stomach are rare entities diagnosed incidentally and usually intraoperatively in adults and should be treated surgically by complete resection.

REFERENCES

1 **Glaser C**, Kuzinkovas V, Maurer C, Glättli A, Mouton WG, Baer HU. A large duplication cyst of the stomach in an adult presenting as pancreatic pseudocyst. *Dig Surg* 1998; **15**: 703-706
2 **Cunningham SC**, Hansel DE, Fishman EK, Cameron JL. Foregut duplication cyst of the stomach. *J Gastrointest Surg* 2006; **10**: 620-621
3 **Perek A**, Perek S, Kapan M, Göksoy E. Gastric duplication cyst. *Dig Surg* 2000; **17**: 634-636
4 **Pruksapong C**, Donovan RJ, Pinit A, Heldrich FJ. Gastric duplication. *J Pediatr Surg* 1979; **14**: 83-85
5 **Chawla A**, Gadaleta D, Kenigsberg K, Kahn E, Markowitz

J. Erosion through the posterior gastric wall by a pancreatic pseudocyst secondary to gastric duplication. *J Pediatr Gastroenterol Nutr* 1991; **13**: 115-118
6 **Wieczorek RL**, Seidman I, Ranson JH, Ruoff M. Congenital duplication of the stomach: case report and review of the English literature. *Am J Gastroenterol* 1984; **79**: 597-602
7 **Spivak H**, Pascal RR, Wood WC, Hunter JG. Enteric duplication presenting as cystic tumors of the pancreas. *Surgery* 1997; **121**: 597-600
8 **Wendel W**. Beschreibung eines operativ entfernten congenitalen Nebenmagens. *Arch Klin Chir* 1911; **96**: 895-898
9 **Katz W**, Annessa G, Read RC. Gastric duplication with pancreatic communication. Presenting as pancreatitis. *Minn Med* 1967; **50**: 1175-1179
10 **Menon P**, Rao KL, Saxena AK. Duplication cyst of the stomach presenting as hemoptysis. *Eur J Pediatr Surg* 2004; **14**: 429-431
11 **Stephen TC**, Bendon RW, Nagaraj HS, Sachdeva R. Antral duplication cyst: a cause of hypergastrinemia, recurrent peptic ulceration, and hemorrhage. *J Pediatr Gastroenterol Nutr* 1998; **26**: 216-218
12 **Mahour GH**, Woolley MM, Payne VC. Association of pulmonary sequestration and duplication of the stomach. *Int Surg* 1971; **56**: 224-227
13 **Liebert PS**. Gastric duplication and multicystic kidney associated with gonadal dysgenesis. *Clin Pediatr* (Phila) 1970; **9**: 60-62
14 **Mayo HW**, Mckee EE, Anderson RM. Carcinoma arising in reduplication of the stomach (gastrogenous cyst): a case report. *Ann Surg* 1955; **141**: 550-555
15 **Tanaka M**, Akahoshi K, Chijiiwa Y, Sasaki I, Nawata H. Diagnostic value of endoscopic ultrasonography in an unusual case of gastric cyst. *Am J Gastroenterol* 1995; **90**: 662-663
16 **Takahara T**, Torigoe T, Haga H, Yoshida H, Takeshima S, Sano S, Ishii Y, Furuya T, Nakamura E, Ishikawa M. Gastric duplication cyst: evaluation by endoscopic ultrasonography and magnetic resonance imaging. *J Gastroenterol* 1996; **31**: 420-424
17 **Kuraoka K**, Nakayama H, Kagawa T, Ichikawa T, Yasui W. Adenocarcinoma arising from a gastric duplication cyst with invasion to the stomach: a case report with literature review. *J Clin Pathol* 2004; **57**: 428-431
18 **Machado MA**, Santos VR, Martino RB, Makdissi F, Canedo L, Bacchella T, Machado MC. Laparoscopic resection of gastric duplication: successful treatment of a rare entity. *Surg Laparosc Endosc Percutan Tech* 2003; **13**: 268-270
19 **Ferrari AP**, Van Dam J, Carr-Locke DL. Endoscopic needle aspiration of a gastric duplication cyst. *Endoscopy* 1995; **27**: 270-272
20 **Izzidien al-Samarrai AY**, Crankson SJ, Sadiq S. The use of mechanical sutures in the treatment of gastric duplications. *Z Kinderchir* 1989; **44**: 186-187
21 **Holcomb GW**, Gheissari A, O'Neill JA, Shorter NA, Bishop HC. Surgical management of alimentary tract duplications. *Ann Surg* 1989; **209**: 167-174

S- Editor Liu Y **L- Editor** Zhu LH **E- Editor** Ma WH

PO Box 2345, Beijing 100023, China
www.wjgnet.com
wjg@wjgnet.com

World J Gastroenterol 2007 February 28; 13(8): 1282-1285
World Journal of Gastroenterology ISSN 1007-9327

CASE REPORT

Melena: A rare complication of duodenal metastases from primary carcinoma of the lung

Chrysoula Kostakou, Lubna Khaldi, Andrew Flossos, Andreas N Kapsoritakis, Spiros P Potamianos

Chrysoula Kostakou, Andrew Flossos, Andreas N Kapsoritakis, Spiros P Potamianos, Department of Gastroenterology, University Hospital of Larissa 41447, Greece
Lubna Khaldi, Department of Histopathology, University Hospital of Larissa 41447, Greece
Correspondence to: Dr. Spiros Potamianos, Department of Gastroenterology, 16 Sklirou St., Larissa 41447, Greece. spotam@med.uth.gr
Telephone: +30-2410-536823 Fax: +30-2410-670098
Received: 2006-12-12 Accepted: 2007-02-01

Abstract

Small bowel metastases from primary carcinoma of the lung are very uncommon and occur usually in patients with terminal stage disease. These metastases are usually asymptomatic, but may present as perforation, obstruction, malabsorption, or hemorrhage. Hemorrhage as a first presentation of small bowel metastases is extremely rare and is related to very poor patient survival. We describe a case of a 61- year old patient with primary adenocarcinoma of the lung, presenting with melena as the first manifestation of small bowel metastasis. Both primary tumor and metastatic lesions were diagnosed almost simultaneously. Upper gastrointestinal endoscopy performed with a colonoscope revealed active bleeding from a metastatic tumor involving the duodenum and the proximal jejunum. Histological examination and immunohistochemical staining of the biopsy specimen strongly supported the diagnosis of metastatic lung adenocarcinoma, suggesting that small bowel metastases from primary carcinoma of the lung occur usually in patients with terminal disease and rarely produce symptoms. Gastrointestinal bleeding from metastatic small intestinal lesions should be included in the differential diagnosis of gastrointestinal blood loss in a patient with a known bronchogenic tumor.

Key words: Melena; Duodenal metastases; Lung cancer

Kostakou C, Khaldi L, Flossos A, Kapsoritakis AN, Potamianos SP. Melena: A rare complication of duodenal metastases from primary carcinoma of the lung. *World J Gastroenterol* 2007; 13(8): 1282-1285

http://www.wjgnet.com/1007-9327/13/1282.asp

INTRODUCTION

Metastases affecting the small bowel and originating from carcinoma of the lung are rare, but recent reports suggest that they may be more frequent than previously thought as they rarely produce symptoms[1-3].

The majority of patients with metastases of the small bowel reported in the literature, present with bowel perforation[2-4]. Overt gastrointestinal hemorrhage has been described in a few cases as a prelude to bowel perforation, whilst it has been described only rarely as the main presentation[5-7].

We present a case of a 61-year old patient with upper gastrointestinal bleeding due to small bowel metastases from a primary adenocarcinoma of the lung with secondary deposits in the abdominal lymph nodes. Metastatic involvement of the duodenum presenting with melena has been described rarely in the literature.

CASE REPORT

A 61-year old man was admitted to our hospital with a two-day history of melena. He reported a four-month history of weakness, anorexia, 5 kg loss of weight, cough, dyspnea on exertion, and blood-stained sputum, and a two-month history of fatigue and altered bowel habits. He was a cigarette smoker with chronic obstructive airway disease and arterial hypertension.

On examination he was pale, with normal blood pressure and pulse rate. He had wheezy breathing and decreased breath sounds in the upper right lung region. Melena was proved by digital examination.

Hematocrit was 35% and hemoglobin 9.5 g/dL. Chest x-ray demonstrated a density in the upper region of the right lower lobe. Endoscopy of the upper gastrointestinal tract up to the second part of the duodenum revealed erosive antral gastritis, but no active bleeding site. CT scan of the thorax disclosed an irregularly-shaped nodular mass measuring 4 cm in diameter, in the upper region of the right lower lobe of the lung. Bronchial biopsy revealed the presence of blood clots and desquamated bronchial epithelial cells, without signs of malignancy. The results of cytological examination of bronchial excretions, however, proved positive for non-small cell carcinoma of the lung. Staging of the disease followed by CT scan of the upper and lower abdomen and the retroperitoneal space showed multiple, enlarged bilateral para-aortic, and mesenteric

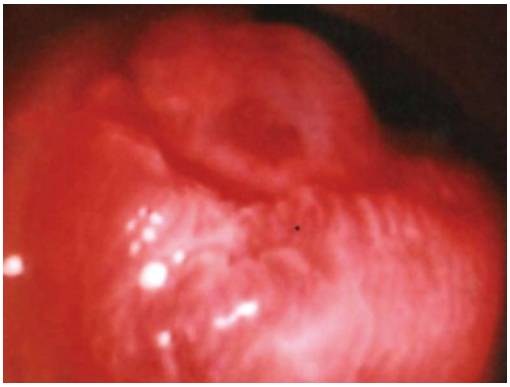

Figure 1 Endoscopic appearance of a large hemorrhagic polypoid mass at the proximal jejunum, representing metastatic lung carcinoma.

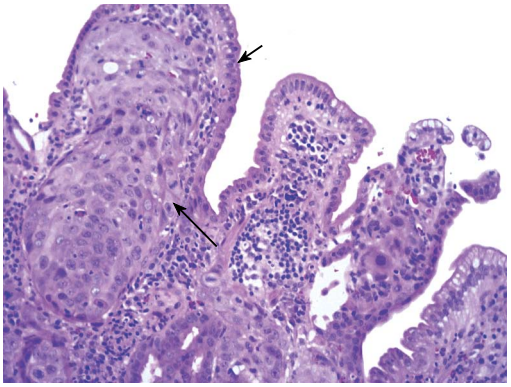

Figure 2 Gatherings of poorly-differentiated neoplastic cells invading the mucosal bed, and extending into the intestinal villi (long arrow), with sparing of the superficial epithelium (short arrow).

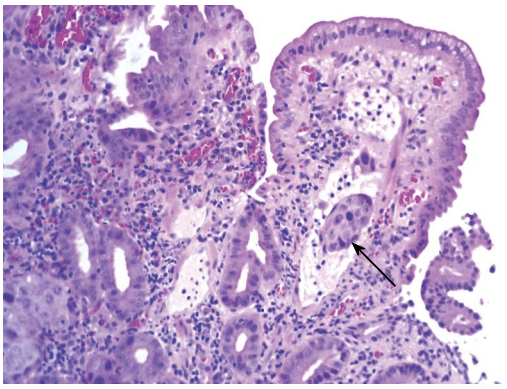

Figure 3 Embolus of neoplastic cells in lymph vessels of the intestinal villi.

lymph nodes.

The patient was started on combined chemotherapy with cisplatin and hydrochloric gemsitabine. His bowel motions became normal by the third day of hospitalization and he was subsequently discharged, denying further investigation.

During admission for the second round of chemotherapy and one month after diagnosis, the patient complained of diffuse abdominal pain and tenderness. Shortly afterwards this was accompanied with hemodynamic instability and tachypnea. Melena was proved by digital examination. Hematocrit fell from 34% to 26%, hemoglobin from 9 g/dL to 6 g/dL, and serum urea/creatinine ratio was greater than 40 (urea being 60mg/dL and creatinine 1.3 mg/dL). Plain abdominal X-ray showed no abnormalities and the patient underwent endoscopy of the upper and lower gastrointestinal tract using a Pentax© 160 cm colonoscope for both examinations. In the 4th part of the duodenum three irregular, nodular protrusions of the mucosa measuring 0.5-1.5 cm in diameter were observed. They were friable and slightly hemorrhagic. At the proximal jejunum there was a larger hemorrhagic polypoid mass about 2.5 cm in diameter (Figure 1). Biopsies of these lesions revealed gatherings of poorly-differentiated neoplastic cells invading the mucosal bed and extending into the intestinal villi with sparing of the superficial epithelium (Figure 2). Infiltration of the lymph vessels was also noted (Figure 3). These findings were consistent with metastatic disease. Immunohistochemical staining for keratins 8, 18, 19 and thyroid transcription factor 1 (TTF 1) as well as histochemical staining for periodic acid schiff (PAS) strongly supported the diagnosis of poorly-differentiated metastatic adenocarcinoma of the lung. Radiological examination of the small bowel was not completed due to patient discomfort. The patient was transfused with 3 units of packed erythrocytes and 3 units of fresh frozen plasma.

Only four cycles of chemotherapy were carried out due to deterioration of the patient. In addition, he received 4000 U of erythropoietin per week. Three months after his last episode of melena the patient continued to have occult upper gastrointestinal bleeding and was admitted on several occasions for blood transfusion. The patient died seven months after the diagnosis of end stage cancer of the lung.

DISCUSSION

Small bowel metastases usually originate from primary carcinomas of the gastrointestinal or genital organs, and more specifically from the large bowel, uterus, cervix, ovaries, and testes. Thoracic malignancies metastasize less frequently to the small bowel. Apart from carcinoma of the lung, these also include malignant melanoma, carcinoma of the breast, carcinoma of the salivary glands, carcinoma of the esophagus, and rhabdomyosarcoma of the lung[1,8,9].

Our patient had histologically-proven small intestinal lesions originating from primary lung adenocarcinoma. A review of the literature revealed few studies of patients with lung cancer and metastases to the small bowel. An extensive eleven-year study of patients with primary lung cancer revealed that at autopsy, 46 out of 431 patients (10.6%) had secondary deposits in the small bowel[1]. These patients had an average of 4.8 metastatic sites. A more recent study of patients with non-small cell carcinoma of the lung revealed small bowel metastases in 4.6% of cases[9]. It should be emphasized that all these cases had adenocarcinomas, with a disease stage greater than IIIA, as well as a minimum of two other metastatic sites before the development of bowel metastases. Another

large study involved 1399 patients with lung cancer who underwent surgical resection of the primary tumor[2]. This study revealed a much smaller percentage (0.5%) of symptomatic patients having small bowel metastases. In direct contrast to the previous study, which concludes that adenocarcinoma is the cell type resulting more frequently in small bowel metastasis, this study concludes that squamous cell carcinoma is the more frequent cause, accounting for 61% of cases.

Patients with primary lung cancer with metastases to the small bowel are usually asymptomatic[10,11]. Less frequently these metastases can cause symptoms which vary according to the way the metastatic tumor invades the bowel wall. Rapid tumor growth leads to symptoms of obstruction, although it seems that perforation occurs more commonly probably due to central tumor necrosis. Most cases of primary lung cancer and small bowel metastasis present with small bowel perforation[3,4,10]. According to a recent study, 98 cases of perforated lung cancer metastasis to the small intestine have been described in the literature since 1960[3]. When ulceration of the mucosa occurs the metastatic tumor may bleed, whilst large extension of tumor may lead to symptoms of malabsorption[1].

Hemorrhage from a metastatic tumor in the small bowel is uncommon, explaining the absence of large studies on this issue. A small number of isolated cases, however, have been described. They describe patients over the age of 55 years, with primary lung carcinoma of large or small cell types, who have already developed distant metastases, and these patients usually present with acute hemorrhage from ulceration of the metastatic tumor, and less frequently with iron deficiency anemia, or with non-specific abdominal symptoms before the onset of melena[12-15]. In one case report, the patient presented with iron-deficiency anemia and melena, and the diagnosis of primary lung cancer was made after surgical resection of the intestinal metastasis, as no tumor evidence was found on chest x-ray[2]. The presence of small bowel metastases in this patient was confirmed by CT scanning, as upper and lower gastrointestinal endoscopies were negative.

A very small number of cases of upper gastrointestinal bleeding due to duodenal metastases from lung cancer have been reported[5-7,12]. Small intestinal metastases have been reported to occur more frequently in the jejunum and terminal ileum than the duodenum[2,3,16]. As in our case, metastatic lesions of the small bowel from lung carcinoma are usually multiple[1,11].

Our patient is one of the very few cases described where melena as the first manifestation of small bowel metastasis, has arisen from the duodenum and jejunum[5-7,12,16]. Also it is interesting to note that the time interval was short between diagnosis of cancer and metastasis to the small bowel, as the patient presented with melena before the establishment of the diagnosis of lung carcinoma and was still in a good general state of health. The diagnosis of metastatic involvement of the small bowel was suspected, but not confirmed at the beginning. This emphasizes the importance of considering the presence of small bowel metastases in a patient with lung cancer displaying symptoms of hemodynamic instability, melena, or abdominal symptoms such as dyspepsia, distention and pain, even if the time elapsed from the time of diagnosis of cancer is short. It should be noted that occult gastrointestinal bleeding must be suspected if laboratory investigations reveal iron deficiency anemia, or a fall in hematocrit or hemoglobin, even in an asymptomatic patient.

Gastrointestinal hemorrhage can usually be managed conservatively with intravenous fluids and red blood cell transfusion until the patient is hemodynamically stable and hemorrhage ceases. However, cases requiring surgical resection of small bowel in order to control massive hemorrhage have also been reported[12,16]. Only a few patients have survived more than 9 mo after surgical resection of intestinal metastases, with the exception of one patient who survived 22 mo after peritonitis [2]. Perioperative mortality has decreased considerably, and the question of whether surgery should be considered as palliative therapy not only for symptomatic patients remains to be solved. After hemorrhage from small bowel metastases, patient survival varies between several weeks to several months[6,13]. It seems that hemorrhage originating from small bowel metastases, is related to a very poor patient survival. The patient we presented, survived for a considerably long time (7 mo after his first episode of bleeding). During this period of time he continued to have microscopic bleeding requiring occasional blood transfusion. Active gastrointestinal bleeding from small bowel metastases has never been described as the cause of death in patients suffering from carcinoma of the lung.

In conclusion, small bowel metastases from primary carcinoma of the lung occur usually in patients with terminal disease and rarely produce symptoms. Hemorrhage as a first presentation of small bowel metastases is extremely rare, especially when these are located in the duodenum, with a poor prognosis. Gastrointestinal bleeding from metastatic small intestinal lesions should be included in the differential diagnosis of gastrointestinal blood loss in a patient with a known bronchogenic tumor.

REFERENCES

1 **McNeill PM**, Wagman LD, Neifeld JP. Small bowel metastases from primary carcinoma of the lung. *Cancer* 1987; **59**: 1486-1489

2 **Berger A**, Cellier C, Daniel C, Kron C, Riquet M, Barbier JP, Cugnenc PH, Landi B. Small bowel metastases from primary carcinoma of the lung: clinical findings and outcome. *Am J Gastroenterol* 1999; **94**: 1884-1887

3 **Garwood RA**, Sawyer MD, Ledesma EJ, Foley E, Claridge JA. A case and review of bowel perforation secondary to metastatic lung cancer. *Am Surg* 2005; **71**: 110-116

4 **Savanis G**, Simatos G, Lekka I, Ammari S, Tsikkinis C, Mylonas A, Kafasis E, Nissiotis A. Abdominal metastases from lung cancer resulting in small bowel perforation: report of three cases. *Tumori* 2006; **92**: 185-187

5 **Steinhart AH**, Cohen LB, Hegele R, Saibil FG. Upper gastrointestinal bleeding due to superior mesenteric artery to duodenum fistula: rare complication of metastatic lung carcinoma. *Am J Gastroenterol* 1991; **86**: 771-774

6 **Hinoshita E**, Nakahashi H, Wakasugi K, Kaneko S, Hamatake M, Sugimachi K. Duodenal metastasis from large cell carcinoma of the lung: report of a case. *Surg Today* 1999; **29**:

799-802
7 **Kamiyoshihara M**, Otaki A, Nameki T, Kawashima O, Otani Y, Morishita Y. Duodenal metastasis from squamous cell carcinoma of the lung; report of a case. *Kyobu Geka* 2004; **57**: 151-153
8 **Stenbygaard LE**, Sørensen JB. Small bowel metastases in non-small cell lung cancer. *Lung Cancer* 1999; **26**: 95-101
9 **Ise N**, Kotanagi H, Morii M, Yasui O, Ito M, Koyama K, Sageshima M. Small bowel perforation caused by metastasis from an extra-abdominal malignancy: report of three cases. *Surg Today* 2001; **31**: 358-362
10 **Hillenbrand A**, Sträter J, Henne-Bruns D. Frequency, symptoms and outcome of intestinal metastases of bronchopulmonary cancer. Case report and review of the literature. *Int Semin Surg Oncol* 2005; **2**: 13
11 **Tomas D**, Ledinsky M, Belicza M, Kruslin B. Multiple metastases to the small bowel from large cell bronchial carcinomas. *World J Gastroenterol* 2005; **11**: 1399-1402
12 **Cremon C**, Barbara G, De Giorgio R, Salvioli B, Epifanio G, Gizzi G, Stanghellini V, Corinaldesi R. Upper gastrointestinal bleeding due to duodenal metastasis from primary lung carcinoma. *Dig Liver Dis* 2002; **34**: 141-143
13 **Kanemoto K**, Kurishima K, Ishikawa H, Shiotani S, Satoh H, Ohtsuka M. Small intestinal metastasis from small cell lung cancer. *Intern Med* 2006; **45**: 967-970
14 **Sanli Y**, Adalet I, Turkmen C, Kapran Y, Tamam M, Cantez S. Small bowel metastases from primary carcinoma of the lung: presenting with gastrointestinal hemorrhage. *Ann Nucl Med* 2005; **19**: 161-163
15 **Locher C**, Grivaux M, Locher C, Jeandel R, Blanchon F. Intestinal metastases from lung cancer. *Rev Mal Respir* 2006; **23**: 273-276
16 **Akahoshi K**, Chijiiwa Y, Hirota I, Ohogushi O, Motomatsu T, Nawata H, Sasaki I. Metastatic large-cell lung carcinoma presenting as gastrointestinal hemorrhage. *Acta Gastroenterol Belg* 1996; **59**: 217-219

S- Editor Liu Y **L- Editor** Wang XL **E- Editor** Ma WH

PO Box 2345, Beijing 100023, China
www.wjgnet.com
wjg@wjgnet.com

World J Gastroenterol 2007 February 28; 13(8): 1286-1288
World Journal of Gastroenterology ISSN 1007-9327

CASE REPORT

Liver toxicity of rosuvastatin therapy

Giuseppe Famularo, Luca Miele, Giovanni Minisola, Antonio Grieco

Giuseppe Famularo, Giovanni Minisola, Internal Medicine, San Camillo Hospital, Rome, Italy
Luca Miele, Antonio Grieco, Internal Medicine, Università Cattolica Sacro Cuore, Rome, Italy
Correspondence to: Dr. Giuseppe Famularo, Department of Internal Medicine, San Camillo Hospital, Circonvallazione Gianicolense, Rome 00152, Italy. gfamular@scamilloforlanini.rm.it
Telephone: +39-6-58704325 Fax: +39-6-58704325
Received: 2006-11-24 Accepted: 2007-01-29

Abstract

We report here a case of clinically significant liver toxicity after a brief course of rosuvastatin, which is the first statin approved by the regulatory authorities since the withdrawal of cerivastatin. Whether rosuvastatin has a greater potential compared with other statins to damage the liver is unclear and the involved mechanisms are also unknown. However, rosuvastatin is taken up by hepatocytes more selectively and more efficiently than other statins, and this may reasonably represent an important variable to explain the hepatotoxic potential of rosuvastatin. Our report supports the view that a clinically significant risk of liver toxicity should be considered even when rosuvastatin is given at the range of doses used in common clinical practice.

Key words: Rosuvastatin; Liver; Toxicity; Hepatitis; Statins

Famularo G, Miele L, Minisola G, Grieco A. Liver toxicity of rosuvastatin therapy. *World J Gastroenterol* 2007; 13(8): 1286-1288

http://www.wjgnet.com/1007-9327/13/1286.asp

INTRODUCTION

Liver toxicity is a well recognized adverse effect of treatment with statins[1]. However pre-marketing studies have suggested that rosuvastatin may have a lesser potential to cause liver toxicity as compared with other statins[2]. We report here a case of clinically significant liver toxicity after a brief course of rosuvastatin.

CASE REPORT

A 64-year-old man presented with a seven-days history of malaise, anorexia, upper abdominal discomfort, and jaundice. Four months earlier the patient had an acute myocardial infarction that was treated with angioplasty and stenting of a culprit lesion in the right coronary artery; liver function tests were normal and he was discharged on clopidogrel, aspirin, metoprolol, ramipril, and atorvastatin (40 mg daily). One week later, rosuvastatin (10 mg daily) was prescribed instead of atorvastatin as the patient reported an itching skin rash that developed soon after he took the second tablet of atorvastatin; at that time serum levels of aspartate aminotransferase (AST) and alanine aminotransferase (ALT) were 55 U/L and 45 U/L (normal range 10-36 U/L for both), respectively, with bilirubin, γ-glutamyltransferase (γ-GT), and alkaline phosphatase (AP) within the normal limits.

At the present admission, he was fully alert and oriented, apyrexial, with mild cutaneous and scleral jaundice, and no flapping tremor or stigmata of chronic liver disease; the remaining physical examination was normal. A laboratory work-up revealed AST 880 U/L, ALT 775 U/L, total bilirubin 2.6 mg/dL (normal range 0.2-1) with conjugated bilirubin 0.8 mg/dL; γ-GT, AP, ammonia, α-fetoprotein, electrolytes, hematologic and coagulation parameters, and renal function tests were normal. Serological screening for viral hepatitis (hepatitis A, B, C, E and G virus; cytomegalovirus; herpes simplex; and Epstein–Barr virus) was negative and HBV-DNA and HCV-RNA were not detected in the peripheral blood. Search for autoimmune liver disorders (antinuclear antibodies, anti-smooth-muscle antibodies, and antimitochondrial antibodies) was also negative as were results of iron, copper, ceruloplasmin metabolism and α1-antitrypsin concentrations.

Ultrasonography and contrast-enhanced computed tomography (CT) showed a normal liver and no expanded bile ducts or gallbladder abnormalities; there was no caval or portal thrombosis and no peri-hepatic or perisplenic intraperitoneal fluid. Echocardiography was also normal with no evidence of valvular disease, pericardial effusion, pulmonary hypertension, or left ventricular systolic or diastolic dysfunction.

The patient had an otherwise unremarkable medical record with no previous history of acute or chronic liver disease. He also denied toxic and alcoholic habits or using any other medications, including over-the-counter medications, or herbal remedies.

Rosuvastatin was withdrawn and AST and ALT levels fell to 216 U/L and 198 U/L, respectively, and bilirubin to 1.8 mg/dL on the 3rd day; ammonia and coagulation parameters remained within the normal range. Over the subsequent course symptoms gradually resolved, which

was paralleled by declining levels of liver enzymes and bilirubin; at no time were flapping tremor or other signs or symptoms of liver failure or encephalopathy observed and the patient was discharged on the 6th day with instructions for close follow-up as an outpatient. At that time, AST and ALT were 40 U/L and 32 U/L, respectively; bilirubin, ammonia, and coagulation parameters were normal. The patient refused a liver biopsy and a re-challenge test with rosuvastatin was not done for ethical reasons. At a follow-up visit two weeks later, he was doing well with normal liver function tests and a normal coagulation profile. The clinical and biochemical course of this patient is summarized in Figure 1.

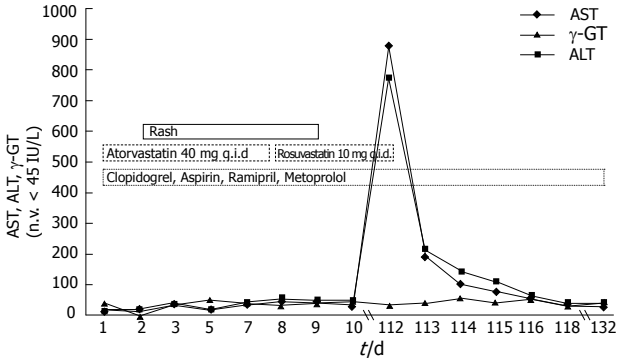

Figure 1 Course of liver enzymes and exposure to statins and other medications.

DISCUSSION

Until today the incidence of elevated serum liver enzymes among patients on treatment with statins generally ranges from 2% to 3%[1] while pre-marketing studies have shown a 20 to 30-fold lower incidence if rosuvastatin is used[2]. We report here a case of clinically significant liver toxicity after a brief course of rosuvastatin, which is the first statin approved by the regulatory authorities since the withdrawal of cerivastatin. According to the Naranjo probability scale our patient had a highly probable rosuvastatin-related adverse event[3]; furthermore, liver function tests were normal before statin treatment was started and we did not find any other plausible alternative cause to explain the onset of such a severe hepatitis in this case. As a matter of fact, we identified a clear temporal relationship between initiation of rosuvastatin therapy and the elevation of liver enzymes and the patient rapidly achieved a complete clinical and biochemical recovery after rosuvastatin was interrupted.

The episode of urticaria accompanied by a modest increase of liver enzymes after the patient was given atorvastatin, which was his first exposure to a statin, raises the view of an idiosyncratic or hypersensitivity cross-reaction between atorvastatin and rosuvastatin as an underlying mechanism of the liver injury that occurred during treatment with rosuvastatin. Even though the true correlation remains to be understood, we might reasonably conceive that allergic cross-reactions between the two statins might have contributed, at least to a certain extent, to the onset of severe liver damage in this case. Our patient had normal eosinophil count and remained apyrexial throughout the entire course. However all these features along with the absence of lymphadenopathy and the negative search for antinuclear and anti-smooth-muscle antibodies do not substantially argue against an allergic or immune-mediate mechanism of liver injury.

The patient was also receiving other medications in combination with rosuvastatin, but this is not a true confounding factor in our opinion. Our Medline search yielded only a few anecdotal reports of hepatitis associated with the use of clopidogrel or ramipril[4-7] and none of liver toxicity linked with metoprolol. In addition, aspirin-related hepatitis has been described, but this is a dose-related phenomenon caused by the intrinsic salicylate hepatotoxicity which generally does occur only when aspirin is given in full anti-inflammatory doses and not with the 75-300 mg used for anti-platelet indications[8]. One important point is that rosuvastatin is neither an inhibitor nor an inducer of cytochrome P450 isoenzymes and rosuvastatin itself is a poor substrate for these isoenzymes. It suggests that fewer drug interactions resulting from cytochrome P450-mediated metabolism should be expected with rosuvastatin compared with other statins[9,10]. There is no available evidence of any clinically significant pharmacokinetic interactions in subjects taking concomitant rosuvastatin and clopidogrel, ramipril, metoprolol, or aspirin.

Whether rosuvastatin has a greater potential compared with other statins to damage the liver is unclear and the involved mechanisms are also unknown. Results from a recent meta-analysis demonstrate that treatment with statins as a class is not associated with a significant risk of liver dysfunction and hepatitis, but studies with rosuvastatin were not included in this meta-analysis[1]. In contrast, a post-marketing analysis has shown that use of rosuvastatin, at least over its first year of marketing, was significantly more likely than atorvastatin, pravastatin, and simvastatin to be associated with a composite end point of adverse events including rhabdomyolysis, proteinuria, nephropathy, and renal failure, and there was also a significant trend in favor of an increased liver toxicity with rosuvastatin compared with the other statins even though this was not targeted as the primary end point of the study[11]. Furthermore, rosuvastatin is taken up by hepatocytes more selectively and more efficiently than other statins, and this may reasonably represent an important variable associated with the hepatotoxic potential of rosuvastatin[12].

Our report supports the view that a clinically significant risk of liver toxicity should be considered even when rosuvastatin is given at the range of doses used in common clinical practice.

REFERENCES

1 **de Denus S**, Spinler SA, Miller K, Peterson AM. Statins and liver toxicity: a meta-analysis. *Pharmacotherapy* 2004; **24**: 584-591

2 **Rosenson RS**. Rosuvastatin: a new inhibitor of HMG-coA reductase for the treatment of dyslipidemia. *Expert Rev Cardiovasc Ther* 2003; **1**: 495-505

3 **Naranjo CA**, Busto U, Sellers EM, Sandor P, Ruiz I, Roberts EA, Janecek E, Domecq C, Greenblatt DJ. A method for

estimating the probability of adverse drug reactions. *Clin Pharmacol Ther* 1981; **30**: 239-245
4 **Ramos Ramos JC**, Sanz Moreno J, Calvo Carrasco L, García Díaz Jde D. Clopidogrel-induced hepatotoxicity. *Med Clin* (Barc) 2003; **120**: 156-157
5 **Durán Quintana JA**, Jiménez Sáenz M, Montero AR, Gutiérrez MH. Clopidogrel probably induced hepatic toxicity. *Med Clin* (Barc) 2002; **119**: 37
6 **Willens HJ**. Clopidogrel-induced mixed hepatocellular and cholestatic liver injury. *Am J Ther* 2000; **7**: 317-318
7 **Yeung E**, Wong FS, Wanless IR, Shiota K, Guindi M, Joshi S, Gardiner G. Ramipril-associated hepatotoxicity. *Arch Pathol Lab Med* 2003; **127**: 1493-1497
8 **Fry SW**, Seeff LB. Hepatotoxicity of analgesics and anti-inflammatory agents. *Gastroenterol Clin North Am* 1995; **24**: 875-905
9 **White CM**. A review of the pharmacologic and pharmacokinetic aspects of rosuvastatin. *J Clin Pharmacol* 2002; **42**: 963-970
10 **Tornio A**, Pasanen MK, Laitila J, Neuvonen PJ, Backman JT. Comparison of 3-hydroxy-3-methylglutaryl coenzyme A (HMG-CoA) reductase inhibitors (statins) as inhibitors of cytochrome P450 2C8. *Basic Clin Pharmacol Toxicol* 2005; **97**: 104-108
11 **Alsheikh-Ali AA**, Ambrose MS, Kuvin JT, Karas RH. The safety of rosuvastatin as used in common clinical practice: a postmarketing analysis. *Circulation* 2005; **111**: 3051-3057
12 **Nezasa K**, Higaki K, Matsumura T, Inazawa K, Hasegawa H, Nakano M, Koike M. Liver-specific distribution of rosuvastatin in rats: comparison with pravastatin and simvastatin. *Drug Metab Dispos* 2002; **30**: 1158-1163

S- Editor Liu Y **L- Editor** Zhu LH **E- Editor** Lu W

PO Box 2345, Beijing 100023, China
www.wjgnet.com
wjg@wjgnet.com

World J Gastroenterol 2007 February 28; 13(8): 1289-1291
World Journal of Gastroenterology ISSN 1007-9327

CASE REPORT

Capsule endoscopy retention as a helpful tool in the management of a young patient with suspected small-bowel disease

Chryssostomos Kalantzis, Periklis Apostolopoulos, Panagiota Mavrogiannis, Dimitrios Theodorou, Xenofon Papacharalampous, Ioannis Bramis, Nikolaos Kalantzis

Chryssostomos Kalantzis, Periklis Apostolopoulos, Panagiota Mavrogiannis, Nikolaos Kalantzis, Gastroenterology Department, NIMTS Hospital, 10-12 Monis Petraki str. Athens, Greece
Dimitrios Theodorou, Ioannis Bramis, 1st Propedeutic Surgical Clinic, University of Athens Medical School, Hippocration Hospital, Athens, Greece
Xenophon Papaharalampous, Radiology Department, University of Athens Medical School, Areteion Hospital, Athens, Greece
Correspondence to: Dr. Periklis Apostolopoulos, NIMTS Hospital, Gastroenterology Department, 10-12 Monis Petraki str, Athens, Greece. periklisapo@yahoo.com
Telephone: +302-109613150
Received: 2006-12-10 Accepted: 2007-01-24

Abstract

Capsule endoscopy is an easy and painless procedure permitting visualization of the entire small-bowel during its normal peristalsis. However, important problems exist concerning capsule retention in patients at risk of small bowel obstruction. The present report describes a young patient who had recurrent episodes of overt gastrointestinal bleeding of obscure origin, 18 years after small bowel resection in infancy for ileal atresia. Capsule endoscopy was performed, resulting in capsule retention in the distal small bowel. However, this event contributed to patient management by clearly identifying the site of obstruction and can be used to guide surgical intervention, where an anastomotic ulcer is identified.

Key words: Capsule endoscopy; Retention; Small bowel obstruction; Obscure gastrointestinal bleeding; Surgery

Kalantzis C, Apostolopoulos P, Mavrogiannis P, Theodorou D, Papacharalampous X, Bramis I, Kalantzis N. Capsule endoscopy retention as a helpful tool in the management of a young patient with suspected small-bowel disease. *World J Gastroenterol* 2007; 13(8): 1289-1291

http://www.wjgnet.com/1007-9327/13/1289.asp

INTRODUCTION

Capsule endoscopy allows direct visualization of the entire small bowel in a noninvasive manner and has become the gold standard in evaluating suspected disease of the small bowel[1-4]. Capsule retention remains a major concern for physicians performing capsule endoscopy, since it can lead to a need for surgery to remove the capsule in a patient who otherwise might have been treated medically for the same illness. Nevertheless, it has been postulated that capsule endoscopy in certain patients with suspected small bowel obstruction, contributes to patient management by clearly identifying the site of obstruction and can be used to guide surgical intervention[5-7].

CASE REPORT

A 22-year old patient was admitted to our hospital for evaluation of recurrent episodes of overt gastrointestinal (GI) bleeding of obscure origin. The patient presented at birth with ileal atresia and underwent partial small bowel resection (excision of 30 cm of ileal loop sparing ileocaecal valve). He was reoperated three times during the first years of his life, initially due to anastomotic leak and subsequently twice for postoperative repair of fistulae. Since then, the patient had remained free of symptoms and developed normally. At the age of 18 years (in 2001), he had a severe episode of overt GI bleeding requiring blood transfusion, and two new bleeding episodes during the next two years. Upper and lower GI endoscopy, computed tomography of the abdomen, Meckel scintigraphy and enteroclysis, revealed no remarkable findings. In 2004 he had symptoms of incomplete intestinal obstruction, which resolved after conservative treatment. A new episode of GI bleeding with negative GI endoscopy requiring transfusion a few days before admission was the reason for referral to our unit, in order to carry out capsule endoscopy.

Because of his medical history, a patent capsule (Given Imaging Ltd., Yoqneam, Israel) was given prior to Pillcam SB, in order to avoid capsule retention. The patent capsule was impacted in the distal small bowel, causing temporary abdominal pain, which was confirmed by two abdominal X-rays on the second and forth day, as the patent capsule was detected at the lower abdomen to the middle line. On the sixth day, a new abdominal X-ray showed that the patent capsule was dissolved. Considering that the patent capsule stopped in a stenotic lesion, probably on the level of entero-enteric ileal anastomosis, surgical management

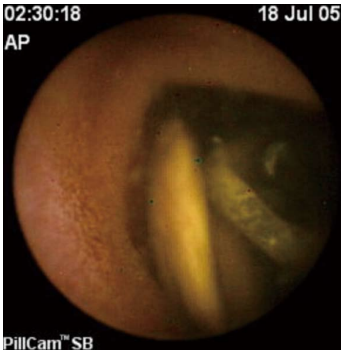

Figure 1 PillCam SB enteroscopy showing the point of capsule retention (Bezoar).

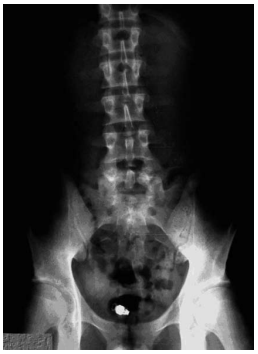

Figure 2 Plain abdominal film on the fifth day after capsule ingestion.

was decided. After discussion with the surgeons and based on data supporting that capsule endoscopy in patients with suspected small bowel obstruction can guide surgical intervention by identifying the site of obstruction[5], capsule endoscopy was carried out after a written consent was obtained from the patient. Four sachets of PEG preparation were given the day before capsule endoscopy procedure was performed.

The capsule passed through the stomach, duodenum and jejunum in 2 h and 30 min, with no evidence of disease and remained impacted in an ileal loop, where a food bezoar was observed (Figure 1). Abdominal X-rays after 24 h and on the fifth day confirmed capsule retention (Figure 2). The patient was operated on the sixth day. Loose adhesions were identified and resected. The capsule was palpated 50 cm proximal to the ileocaecal valve, on the level of the entero-enteric anastomosis and an anastomotic ulcer causing stenosis was found after incision. Intraoperative enteroscopy through the incision point was performed in order to examine the ileal segment from the stenosis to the ileocaecal valve that was found normal. The lesion was resected (Figure 3) and histology demonstrated focal ulceration with chronic inflammation, but no evidence of granulomata, crypt abscesses or malignancy. The patient was discharged on the fifth postoperative day and remained asymptomatic 12 mo post-surgery.

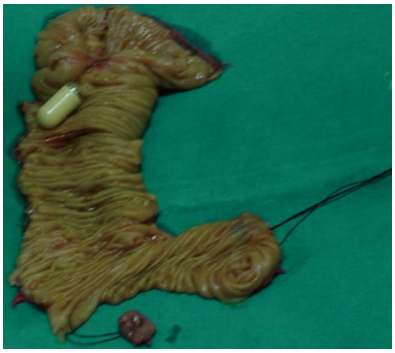

Figure 3 Surgical specimen with ulceration and retained PillCam SB capsule.

DISCUSSION

Atresia and stenosis are common birth defects affecting the small intestine, but few population-based studies have examined the epidemiology of small intestinal atresia and stenosis. It was reported that the rate of small intestinal atresia and stenosis is 2.9 per 10 000 live births (I 95% CI = 2.3-3.6)[8]. Current operative techniques and contemporary neonatal critical care result in a 5% morbidity and mortality rate, with late complications not uncommon[9]. Protein-losing enteropathy and gastrointestinal bleeding due to anastomotic ulcer after 4-12 years have been reported[10]. Actually, gastrointestinal bleeding occurred in our patient due to anastomotic ulcer 18 years after small bowel resection. For these reasons, follow-up of these patients in their adulthood is recommended and physicians must be aware to identify and address these late occurrences[9].

Capsule endoscopy is currently the preferred test for mucosal imaging of the entire small intestine[4]. When integrated into a global approach to the patient, capsule endoscopy can achieve effective decision-making, concerning subsequent investigations and treatments. Capsule retention remains the major concern for physicians performing capsule endoscopy, since retention could lead to a need for an otherwise unnecessary surgery to remove the capsule. As there is no accepted imaging method for completely avoiding capsule retention, it is clear that obtaining a good medical history is the best single method[11].

Our patient had two risk factors for capsule retention: a history of previous small-bowel resection and a distant history of partial small-bowel obstruction. For these reasons, a patent capsule was given initially to the patient. The retention of patent capsule in the small intestine, confirmed our suspicions. Nevertheless, Cheifetz *et al*[5] showed that capsule retention in the small intestine could help a pre-decided operation by guiding the surgeons to clearly indentify the site of obstruction in patients with suspected small-bowel obstruction. Even though capsule endoscopy did not help us to diagnose a definite lesion, as we did not take clear images of the site of capsule retention, palpation of the capsule by the surgeons during operation, could lead them directly to the site of stenosis.

In conclusion, capsule retention is not always an adverse event, as in certain patients with suspected small bowel obstruction, the retained capsule can be used as a "guiding point" for a pre-decided surgical intervention.

REFERENCES

1 **Iddan G**, Meron G, Glukhovsky A, Swain P. Wireless capsule endoscopy. *Nature* 2000; **405**: 417
2 **Appleyard M**, Glukhovsky A, Swain P. Wireless-capsule diagnostic endoscopy for recurrent small-bowel bleeding. *N Engl J Med* 2001; **344**: 232-233
3 **Mishkin DS**, Chuttani R, Croffie J, Disario J, Liu J, Shah

R, Somogyi L, Tierney W, Song LM, Petersen BT. ASGE Technology Status Evaluation Report: wireless capsule endoscopy. *Gastrointest Endosc* 2006; **63**: 539-545
4 **Leighton JA**, Goldstein J, Hirota W, Jacobson BC, Johanson JF, Mallery JS, Peterson K, Waring JP, Fanelli RD, Wheeler-Harbaugh J, Baron TH, Faigel DO. Obscure gastrointestinal bleeding. *Gastrointest Endosc* 2003; **58**: 650-655
5 **Cheifetz A**, Sachar D, Lewis B. Small bowel obstruction: indication or contraindication for capsule endoscopy. *Gastrointest Endosc* 2004; **59**: 461
6 **Cheifetz AS**, Lewis BS. Capsule endoscopy retention: is it a complication? *J Clin Gastroenterol* 2006; **40**: 688-691
7 **Baichi MM**, Arifuddin RM, Mantry PS. What we have learned from 5 cases of permanent capsule retention. *Gastrointest Endosc* 2006; **64**: 283-287
8 **Forrester MB**, Merz RD. Population-based study of small intestinal atresia and stenosis, Hawaii, 1986-2000. *Public Health* 2004; **118**: 434-438
9 **Escobar MA**, Ladd AP, Grosfeld JL, West KW, Rescorla FJ, Scherer LR, Engum SA, Rouse TM, Billmire DF. Duodenal atresia and stenosis: long-term follow-up over 30 years. *J Pediatr Surg* 2004; **39**: 867-871; discussion 867-871
10 **Couper RT**, Durie PR, Stafford SE, Filler RM, Marcon MA, Forstner GG. Late gastrointestinal bleeding and protein loss after distal small-bowel resection in infancy. *J Pediatr Gastroenterol Nutr* 1989; **9**: 454-460
11 **Cave D**, Legnani P, de Franchis R, Lewis BS. ICCE consensus for capsule retention. *Endoscopy* 2005; **37**: 1065-1067

S- Editor Liu Y **L- Editor** Zhu LH **E- Editor** Lu W

PO Box 2345, Beijing 100023, China
www.wjgnet.com
wjg@wjgnet.com

World J Gastroenterol 2007 February 28; 13(8): 1292-1294
World Journal of Gastroenterology ISSN 1007-9327

CASE REPORT

Simultaneous development of diabetic ketoacidosis and Hashitoxicosis in a patient treated with pegylated interferon-alpha for chronic hepatitis C

Aspasia S Soultati, Spyridon P Dourakis, Alexandra Alexopoulou, Melanie Deutsch, Athanasios J Archimandritis

Aspasia S Soultati, Spyridon P Dourakis, Alexandra Alexopoulou, Melanie Deutsch, Athanasios J Archimandritis, 2nd Department of Internal Medicine, University of Athens, Medical School, Hippokration General Hospital, 114 Vas Sofias Avenues, Athens 11527, Greece
Correspondence to: Spyridon P Dourakis, 28 Achaias st, Athens 11523, Greece. spdour@med.uoa.gr
Telephone: +30-210-6918464 Fax: +30-210-6993693
Received: 2006-07-24 Accepted: 2007-01-12

Abstract

Classical interferon-alpha has been shown to be correlated with the development of a variety of autoimmune disorders. A 38 year-old female patient developed simultaneously diabetic ketoacidosis and hyperthyroidism 5 mo following initiation of treatment with pegylated interferon-α and ribavirin for chronic hepatitis C. High titers of glutamic acid decarboxylase, antinuclear and thyroid (thyroid peroxidase and thyroglobulin) antibodies were detected. Antiviral treatment was withdrawn and the patient was treated with insulin for insulin-dependent diabetes mellitus and propranolol for hyperthyroidism. Twelve months after cessation of pegylated interferon-α therapy the patient was euthyroid without any medication but remained insulin-dependent.

Key words: Autoimmune thyroiditis; Insulin dependent diabetes mellitus; Pegylated interferon-alpha; Chronic hepatitis C

Soultati AS, Dourakis SP, Alexopoulou A, Deutsch M, Archimandritis AJ. Simultaneous development of diabetic ketoacidosis and Hashitoxicosis in a patient treated with pegylated interferon-alpha for chronic hepatitis C. *World J Gastroenterol* 2007; 13(8): 1292-1294

http://www.wjgnet.com/1007-9327/13/1292.asp

INTRODUCTION

Interferon-alpha (IFN-α), a natural protein with anti-viral, anti-proliferative and immunomodulatory effects is routinely administered in chronic hepatitis C (CHC). Classical IFN-α has been correlated with the development of a variety of autoimmune disorders including Hashimoto thyroiditis, immune-mediated thrombocytopenia, hemolytic anemia, psoriasis, rheumatoid arthritis, systemic lupus-like syndromes, primary biliary cirrhosis and sarcoidosis. The reported cumulative incidence of all autoimmune disorders ranged from 1% to 3%[1,2].

Clinical thyroid disease has been reported to develop in 10%-15% of patients treated with IFN-α for CHC[3,4]. However, it was not established whether IFN-α treatment is associated with the development of insulin dependent diabetes mellitus (IDDM). The prevalence of diabetes mellitus development in patients receiving classical IFN-α for CHC is very low ranging from 0.08% to 0.7%[1,2]. The prevalence of pancreatic auto-antibodies appeared to rise from 3% to 7% prior to and following initiation of IFN-α treatment, respectively, in a review of 9 relative studies by Fabris *et al*[5]. In those studies different types of IFN-α and variable schedules were used.

Pegylated IFN-α has been recently approved for the treatment of CHC and has been associated with only a few cases of autoimmune thyroiditis[6]. We herein describe the simultaneous development of diabetic ketoacidosis and Hashitoxicosis in a patient treated with pegylated IFN-α for CHC.

CASE REPORT

A 38-year-old female patient presented with a two fold increase of aminotransferases and positive hepatitis C virus (HCV) antibodies. HCV RNA was high (> 1 000 000 copies/mL, genotype 1b) and liver histology revealed an activity grade of 4/18 and a fibrosis score of 3/6 according to Ishak's modified HAI classification system[7]. Treatment with pegylated IFN-α-2α 180 μg/wk, in combination with oral ribavirin 1000 mg/d was initiated in February 2004. During treatment alanine aminotransferase (ALT) flares did not occur. Virological response (negative HCV RNA) was achieved at the fourth week of treatment.

In July 2004 the patient developed weakness and rapid weight loss up to 12 kg within 2 wk. Thyroid function tests revealed hyperthyroidism of autoimmune etiology, i.e. thyroid stimulating hormone (TSH): 0.008 μIU/mL (normal values: 0.15-6.1), free triiodothyronine (FT_3): 6.90 pg/mL (normal values: 2.03-4.6), free thyroxine (FT_4): 1.8 ng/dL (normal values: 0.9-1.7), positive thyroid peroxidase

(anti-TPO > 1300 IU/mL, normal values < 2 IU/mL), thyroglobulin (anti-Tg 18.6 IU/mL, normal values < 2 IU/mL) and thyroid stimulating immunoglobulin antibodies (TSI 96%, normal values: 0.02%-15%). Propranolol was administered. A few days later the patient was admitted with clinical and laboratory features indicating diabetic ketoacidosis (blood glucose: 470 mg/dl, pH: 7.08, HCO_3: 5 mmol/L). The antiviral treatment was withdrawn. Her clinical condition was improved with i.v. fluids and insulin therapy. Following normalization of the acute metabolic profile, intensive insulin therapy was recommended. The patient had no family history of diabetes mellitus. The HLA class Ⅱ typing revealed a genetic predisposition to IDDM as demonstrated by the presence of type 1 diabetes associated DRB1*03 (A*01, A*02/B*08, B*35/Cw*04, Cw*07, DRB1*03, DRB1*03/DQB1*02) haplotype (Diabetes, Pathogenesis of type 1A Diabetes In: http://www-endotext.com). Glutamic acid decarboxylase (GAD) antibodies were strongly elevated (725.52 RU/units) whereas insulin autoantibodies (IA-2) were undetectable at the onset of IDDM (< 5.3 RU/units). Additional immunological profile showed positive antinuclear antibodies (> 1:640). All the other auto-antibodies including anti-smooth muscle, anti-dsDNA, anti-ENA, anti-RNP, anti-SSA, anti-SSB, p-ANCA, c-ANCA, anti-MPO, anti-PR3, anti-LF, anti-mitochondrial were negative. The value of plasma C peptide with test glucagon was 0.61 ng/mL and 0.76 ng/mL at 0 and 6 min, respectively (normal values: 0.5-3.2 ng/mL), indicating an insulin secretion deficiency.

Twelve months after cessation of pegylated IFN-α and ribavirin therapy, the patient remained insulin dependent with a daily requirement of insulin 35 units (C-peptide levels remained low), but no medication was required for the thyroid. Last thyroid evaluation revealed a reversible condition with a decrease in the anti-TPO titers (109.5 IU/mL) and normal TSH. HCV RNA in serum was undetectable.

DISCUSSION

Classical IFN-α has been reported to induce insulin resistance[8-11] although there are also reports suggesting a beneficial effect on glucose metabolism[12-14]. However, the potential of classical IFN-α to induce IDDM has not been well established.

There have been a variety of mechanisms that may account for the effect of IFN-α on pancreatic beta cell dysfunction in patients with CHC. First, it has been reported that viral dsRNA activates the toll-like receptor-3 and the nuclear factor NFnB to induce pancreatic beta cell apoptosis and also the production of IFN-α, which is directly cytotoxic to beta cells of the pancreas. Second, IFN-α activates the oligoadenylate synthase-RnaseL pathway and the protein kinase R pathway thus inducing apoptosis of pancreatic beta cells[15]. Third, IFN-α may stimulate a counter regulatory hormone secretion (growth hormone, glucagon, etc.), thus resulting in impaired glucose tolerance[8]. Regarding IDDM, IFN-α may favour the development of Th1 immune reaction and thereby contribute to the development of autoimmune disease by the activation of CD4 lymphocytes secreting interleukin IL-2, IFN-gamma, and tumor necrosis factor[15]. IFN-α expression has also been associated with over-expression of MHC class Ⅰ antigens in human islets of pancreas[16].

Thirty five cases of IFN-α related IDDM had been reported[17-20] up to 2005. In 2003 Fabris *et al*[5] reviewed 31 cases of classical IFN-α related IDDM. A family history of IDDM was present in 3 cases and HLA haplotypes conferring susceptibility to IDDM were present in 89% of the reviewed cases. A time-period of 10 d to 4 years elapsed between the onset of treatment and the clinical development of IDDM. Fifty percent of the patients were positive for at least one pancreatic autoantibody before therapy. The rate increased to 77% during IFN-α treatment whereas 5 patients initially negative for pancreatic autoimmunity were seroconverted during therapy. Clinical manifestations included polyuria, polydipsia and weight loss in the vast majority of patients. Permanent insulin administration was required in 75% of the cases[5].

To date, the development of IDDM during pegylated IFN-α and ribavirin therapy for CHC was documented in only two cases in the English literature[21,22]. In the case reported by Jabr *et al*[21], pegylated IFN-α and ribavirin were administered in a patient with CHC and human immunodeficiency virus infection. Seven months following initiation of treatment, polyuria, generalized weakness, increased thirst and loss of appetite were manifested. Hyperosmolarity and ketoacidosis eventually developed. The patient required permanent insulin therapy thereafter. Pancreatic autoimmunity markers were not assessed. In the case presented by Cozzolongoa *et al*[22], IDDM developed following a 3-mo treatment with pegylated IFN-α-2b and ribavirin for CHC. An increase in the titers of islet-cell and glutamic acid decarboxylase antibodies before the start of therapy and 2 mo after the diagnosis of diabetes mellitus was documented. HLA class Ⅱ typing showed a predisposition to IDDM. The patient eventually required permanent insulin therapy.

Diabetic ketoacidosis was reported in a few classical IFN-α related cases[23-26], in one pegylated IFN-α related case[21] and the case herein described. The development of diabetic ketoacidosis and the permanent insulin dependency thereafter indicated a severe metabolic disturbance, which may be attributed to a rapidly developing Th1-mediated pathogenic reaction[23].

Co-existence of positive thyroid and pancreatic autoimmunity markers was documented in a few cases in the literature[23,27-29]. In the case presented by Bosi *et al*[23], clinical features of autoimmune hyperthyroidism and IDDM coexisted. In the current case the multiple autoimmune manifestations, ie. IDDM and Hashitoxicosis with highly elevated GAD and anti-TPO antibodies and additional autoimmunity markers, illustrated a vigorous triggering of the immune system by pegylated IFN-α in a genetically predisposed individual.

Gogas *et al*[30] have suggested a predictive model to identify patients with a predisposition to autoimmunity disease before the start of IFN-α therapy for melanoma. Prospective identification of the individual benefit/risk ratio would facilitate personalized treatment strategies

when IFN-α treatment is planned.

In conclusion, it seems that pegylated IFN-α shares common features with classical IFN-α as far as autoimmunity is concerned. A high clinical awareness is recommended in patients with known genetic susceptibility or positive autoimmunity markers prior to or during IFN-α therapy.

REFERENCES

1 **Okanoue T**, Sakamoto S, Itoh Y, Minami M, Yasui K, Sakamoto M, Nishioji K, Katagishi T, Nakagawa Y, Tada H, Sawa Y, Mizuno M, Kagawa K, Kashima K. Side effects of high-dose interferon therapy for chronic hepatitis C. *J Hepatol* 1996; **25**: 283-291

2 **Fattovich G**, Giustina G, Favarato S, Ruol A. A survey of adverse events in 11,241 patients with chronic viral hepatitis treated with alfa interferon. *J Hepatol* 1996; **24**: 38-47

3 **Deutsch M**, Dourakis S, Manesis EK, Gioustozi A, Hess G, Horsch A, Hadziyannis S. Thyroid abnormalities in chronic viral hepatitis and their relationship to interferon alfa therapy. *Hepatology* 1997; **26**: 206-210

4 **Mandac JC**, Chaudhry S, Sherman KE, Tomer Y. The clinical and physiological spectrum of interferon-alpha induced thyroiditis: toward a new classification. *Hepatology* 2006; **43**: 661-672

5 **Fabris P**, Floreani A, Tositti G, Vergani D, De Lalla F, Betterle C. Type 1 diabetes mellitus in patients with chronic hepatitis C before and after interferon therapy. *Aliment Pharmacol Ther* 2003; **18**: 549-558

6 **Maede Y**, Morishita K, Iwamura K, Takayama Y, Tsukada Y, Kishino M, Shimizu T, Matsushima S, Komatsu T, Kasagi Y. Chronic hepatitis C with early complication of Grave's disease during the treatment of pegylated interferon alpha-2a. *Nihon Naika Gakkai Zasshi* 2005; **94**: 2600-2602

7 **Ishak K**, Baptista A, Bianchi L, Callea F, De Groote J, Gudat F, Denk H, Desmet V, Korb G, MacSween RN. Histological grading and staging of chronic hepatitis. *J Hepatol* 1995; **22**: 696-699

8 **Koivisto VA**, Pelkonen R, Cantell K. Effect of interferon on glucose tolerance and insulin sensitivity. *Diabetes* 1989; **38**: 641-647

9 **Ishigami Y**, Kanda T, Wada M, Shimizu Y. Glucose intolerance during interferon therapy in patients with chronic hepatitis type C. *Nihon Rinsho* 1994; **52**: 1901-1904

10 **Imano E**, Kanda T, Ishigami Y, Kubota M, Ikeda M, Matsuhisa M, Kawamori R, Yamasaki Y. Interferon induces insulin resistance in patients with chronic active hepatitis C. *J Hepatol* 1998; **28**: 189-193

11 **Chatterjee S**. Massive increase of insulin resistance in a patient with chronic hepatitis C after treatment with interferon. *J Assoc Physicians India* 2004; **52**: 514

12 **Ito Y**, Takeda N, Ishimori M, Akai A, Miura K, Yasuda K. Effects of long-term interferon-alpha treatment on glucose tolerance in patients with chronic hepatitis C. *J Hepatol* 1999; **31**: 215-220

13 **Konrad T**, Zeuzem S, Vicini P, Toffolo G, Briem D, Lormann J, Herrmann G, Berger A, Kusterer K, Teuber G, Cobelli C, Usadel KH. Evaluation of factors controlling glucose tolerance in patients with HCV infection before and after 4 months therapy with interferon-alpha. *Eur J Clin Invest* 2000; **30**: 111-121

14 **Tai TY**, Lu JY, Chen CL, Lai MY, Chen PJ, Kao JH, Lee CZ, Lee HS, Chuang LM, Jeng YM. Interferon-alpha reduces insulin resistance and beta-cell secretion in responders among patients with chronic hepatitis B and C. *J Endocrinol* 2003; **178**: 457-465

15 **Devendra D**, Eisenbarth GS. Interferon alpha--a potential link in the pathogenesis of viral-induced type 1 diabetes and autoimmunity. *Clin Immunol* 2004; **111**: 225-233

16 **Foulis AK**. Interferon-alpha and IDDM: comment. *Diabetologia* 1996; **39**: 127

17 **Sasso FC**, Carbonara O, Di Micco P, Coppola L, Torella R, Niglio A. A case of autoimmune polyglandular syndrome developed after interferon-alpha therapy. *Br J Clin Pharmacol* 2003; **56**: 238-239

18 **Christensen UB**, Krogsgaard K. Onset of type 1 diabetes mellitus during combination therapy of chronic hepatitis C with interferon-alpha and ribavirin. *Ugeskr Laeger* 2004; **166**: 1024-1025

19 **Schories M**, Peters T, Rasenack J, Reincke M. Autoantibodies against islet cell antigens and type 1 diabetes after treatment with interferon-alpha. *Dtsch Med Wochenschr* 2004; **129**: 1120-1124

20 **Radhakrishnan S**, Upadhyay A, Mohan N, Dhar A, Walia HK, Zubaidi G. Late development of diabetes mellitus after interferon-alfa and ribavirin therapy for chronic hepatitis C: a case report. *Med Princ Pract* 2005; **14**: 281-283

21 **Jabr FI**, Ordinario MM. Sudden onset of diabetic ketoacidosis during pegylated interferon alfa therapy. *Am J Med* 2003; **115**: 158-159

22 **Cozzolongo R**, Betterle C, Fabris P, Paola Albergoni M, Lanzilotta E, Manghisi OG. Onset of type 1 diabetes mellitus during peginterferon alpha-2b plus ribavirin treatment for chronic hepatitis C. *Eur J Gastroenterol Hepatol* 2006; **18**: 689-692

23 **Bosi E**, Minelli R, Bazzigaluppi E, Salvi M. Fulminant autoimmune Type 1 diabetes during interferon-alpha therapy: a case of Th1-mediated disease? *Diabet Med* 2001; **18**: 329-332

24 **Bhatti A**, McGarrity TJ, Gabbay R. Diabetic ketoacidosis induced by alpha interferon and ribavirin treatment in a patient with hepatitis C. *Am J Gastroenterol* 2001; **96**: 604-605

25 **Recasens M**, Aguilera E, Ampurdanés S, Sánchez Tapias JM, Simó O, Casamitjana R, Conget I. Abrupt onset of diabetes during interferon-alpha therapy in patients with chronic hepatitis C. *Diabet Med* 2001; **18**: 764-767

26 **Mofredj A**, Howaizi M, Grasset D, Licht H, Loison S, Devergie B, Demontis R, Cadranel JF. Diabetes mellitus during interferon therapy for chronic viral hepatitis. *Dig Dis Sci* 2002; **47**: 1649-1654

27 **Fabris P**, Betterle C, Floreani A, Greggio NA, de Lazzari F, Naccarato R, Chiaramonte M. Development of type 1 diabetes mellitus during interferon alfa therapy for chronic HCV hepatitis. *Lancet* 1992; **340**: 548

28 **Fabris P**, Betterle C, Greggio NA, Zanchetta R, Bosi E, Biasin MR, de Lalla F. Insulin-dependent diabetes mellitus during alpha-interferon therapy for chronic viral hepatitis. *J Hepatol* 1998; **28**: 514-517

29 **Seifarth C**, Benninger J, Böhm BO, Wiest-Ladenburger U, Hahn EG, Hensen J. Augmentation of the immune response to islet cell antigens with development of diabetes mellitus caused by interferon-alpha therapy in chronic hepatitis C. *Z Gastroenterol* 1999; **37**: 235-239

30 **Gogas H**, Ioannovich J, Dafni U, Stavropoulou-Giokas C, Frangia K, Tsoutsos D, Panagiotou P, Polyzos A, Papadopoulos O, Stratigos A, Markopoulos C, Bafaloukos D, Pectasides D, Fountzilas G, Kirkwood JM. Prognostic significance of autoimmunity during treatment of melanoma with interferon. *N Engl J Med* 2006; **354**: 709-718

S- Editor Liu Y **L- Editor** Zhu LH **E- Editor** Lu W

PO Box 2345, Beijing 100023, China
www.wjgnet.com
wjg@wjgnet.com

World J Gastroenterol 2007 February 28; 13(8): 1295-1298
World Journal of Gastroenterology ISSN 1007-9327

CASE REPORT

Gallstone ileus: Report of two cases and review of the literature

Jen-Wei Chou, Chang-Hu Hsu, Kuan-Fu Liao, Hsueh-Chou Lai, Ken-Sheng Cheng, Cheng-Yuan Peng, Mei-Due Yang, Yung-Fang Chen

Jen-Wei Chou, Chang-Hu Hsu, Kuan-Fu Liao, Hsueh-Chou Lai, Ken-Sheng Cheng, Cheng-Yuan Peng, Division of Gastroenterology, Department of Internal Medicine, China Medical University Hospital, Taichung 40447, Taiwan, China
Mei-Due Yang, Department of Surgery, China Medical University Hospital, Taichung 40447, Taiwan, China
Yung-Fang Chen, Department of Radiology, China Medical University Hospital, Taichung 40447, Taiwan, China
Correspondence to: Dr. Hsueh-Chou Lai, MD, Division of Gastroenterology, Department of Internal Medicine, China Medical University Hospital, No.2, Yuh-Der Road, North District, Taichung 40447, Taiwan,
China. adenocarcinomalai@yahoo.com.tw
Telephone: +886-4-22052121-2220 Fax: +886-4-22023119
Received: 2006-11-08 Accepted: 2007-02-12

Abstract

Gallstone ileus is a rare disease and accounts for 1%-4% of all cases of mechanical intestinal obstruction. It usually occurs in the elderly with a female predominance and may result in a high mortality rate. Its diagnosis is difficult and early diagnosis could reduce the mortality. Surgery remains the mainstay of treatment. We report two cases of gallstone ileus. The first was a 78-year old woman who had a 2-d history of vomiting and epigastralgia. Plain abdominal film suggested small bowel obstruction clinically attributed to adhesions. Later on, gallstone ileus was diagnosed by abdominal computed tomography (CT) based on the presence of pneumobilia, bowel obstruction, and an ectopic stone within the jejunum. She underwent emergent laparotomy with a one-stage procedure of enterolithotomy, cholecystectomy and fistula repair. The second case was a 76-year old man with a 1-wk history of epigastralgia. Plain abdominal film showed two round calcified stones in the right upper quadrant. Fistulography confirmed the presence of a cholecystoduodenal fistula and gallstone ileus was also diagnosed by abdominal CT. We attempted to remove the stones endoscopically, but failed leading to an emergent laparotomy and the same one-stage procedure as for the first case. The postoperative courses of the two cases were uneventful. Inspired by these 2 cases we reviewed the literature on the cause, diagnosis and treatment of gallstone ileus.

Key words: Gallstone ileus; Intestinal obstruction; Pneumobilia; One-stage procedure; Enterolithotomy; Cholecystoduodenal fistula

Chou JW, Hsu CH, Liao KF, Lai HC, Cheng KS, Peng CY, Yang MD, Chen YF. Gallstone ileus: Report of two cases and review the literature. *World J Gastroenterol* 2007; 13(8): 1295-1298

http://www.wjgnet.com/1007-9327/13/1295.asp

INTRODUCTION

The cause of mechanical small bowel intestinal obstruction includes gallstones, foreign bodies, bezoars, tumors, adhesions, congenital abnormity, intussusceptions, and volvulus[1]. Among these causes, a gallstone-induced intestinal obstruction is also referred to as a "gallstone ileus". Gallstone ileus is a rare and potentially serious complication of cholelithiasis[2]. It accounts for 1%-4% of all cases of mechanical intestinal obstruction, but for up to 25% of those in patients over 65 years of age with a female to male ratio of 3.5-6.0:1[3-6]. The morbidity and mortality rate of gallstone ileus remain very high, partly because of misdiagnosis and delayed diagnosis[7]. Thus, early diagnosis and prompt treatment could reduce the mortality rate. Here, we report two cases of gallstone ileus and review the literature of this rare disease.

CASE REPORTS

Case 1

A 78-year old woman presented to our emergency department (ED) with a 2-d history of vomiting and epigastric pain. She had a past medical history of hypertension and underwent a hystectomy for a myoma at the age of 38. On physical examination, her abdomen was mildly distended without tenderness or rebound or Murphy's sign. The white blood count was 16 630/μL with 87.6% neutrophils, blood urea nitrogen 67 mg/dL, 2.3 mg/dL creatinine 2.3 mg/dL and k 2.7 mmol/L. The other tests were unremarkable. A plain abdominal film demonstrated mildly dilated bowel loops, but a vague stone was not identified in the left iliac fossa (Figure 1). The diagnostic impression was ileus due to adhesions. Abdominal ultrasound (US) disclosed a shrunken gallbladder with internal air, but without stones. An abdominal computed tomography was performed, demonstrating air in the biliary tree (Figure 2A). Moreover,

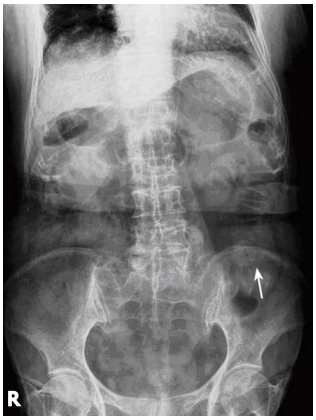

Figure 1 Plain abdominal film showing a vague stone not identified in the left iliac fossa (arrow).

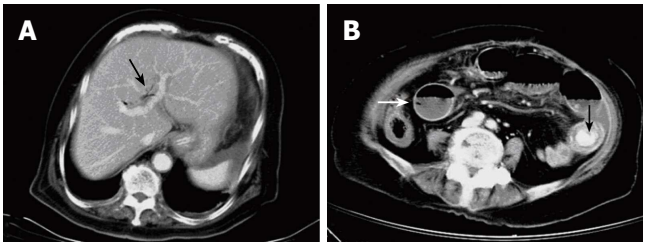

Figure 2 Abdominal computed tomography scan showing air in the biliary tree (arrow) (**A**) and an ectopic stone (arrow) impacting the jejunal lumen accompanying dilatation of proximal small bowel loops (white arrow) (**B**).

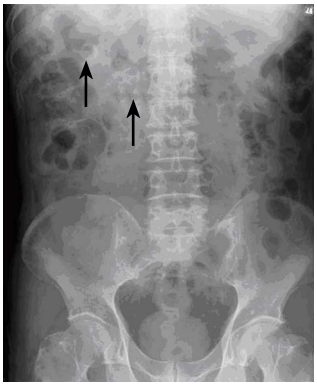

Figure 3 Plain abdominal film showing two round calcified stones in the right upper quadrant of abdomen (arrow).

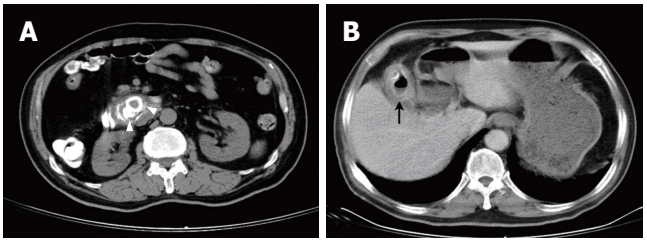

Figure 4 Abdominal computed tomography scan showing two round calcified stones impacting the proximal third portion of the duodenum (arrowhead) (**A**) and a thickened wall gallbladder with internal air and small calcified content (arrow) (**B**).

an ectopic stone impacted in the jejunal lumen was seen in the left lower quadrant along with dilatation of the proximal small bowel (Figure 2B). The diagnosis of gallstone ileus was made and she underwent an emergent laparotomy. At operation a small shrunken gallbladder with dense adhesion to the stomach was found. After lysis of adhesion, a fistula between the gallbladder dome and the lesser curvature of gastric antrum was confirmed. Moreover, a stone was palpated in the jejunum about 140 cm distal to the ligament of Treitz causing total obstruction of the lumen. When the jejunum was opened, the stone was laminated and cylinder shaped, measuring 3 cm × 3 cm × 2 cm in diameter. Enterolithotomy, cholecystectomy and repair of the cholecystogastric fistula were performed. The pathology showed chronic cholecystitis and a fistula walled by granulation tissue. The postoperative course was uneventful except for mild wound infection, and she remained in good health after one-year follow-up.

Case 2

A 76-year old man was brought to our ED because of epigastric pain for one week. He denied any history of abdominal surgery or biliary disease. On physical examination his abdomen was soft, but tender in the epigastric area. Laboratory tests were unremarkable. Abdominal X-ray showed two round calcified stones in the right upper quadrant of the abdomen (Figure 3). An EGD disclosed a deep hole in the posterior wall of the duodenal bulb, but no stone was identified. Fistulography confirmed the presence of a cholecystoduodenal fistula. An abdominal CT was performed, showing two round calcified stones located in the proximal third portion of the duodenum causing dilatation of proximal bowel lumen (Figure 4A). There was a thickened wall gallbladder with internal gas and small calcified content was also discovered (Figure 4B). Duodenoscopy was performed again, showing two stones impacted in the proximal third portion of the duodenum. We attempted to catch the stones with a Dormia basket, but failed because of their larger size. Therefore, he was referred to our department of surgery for emergent laparotomy. Laparotomy displayed that the gallbladder was adhered to the duodenum accompanying a cholecystoduodenal fistula. A large black stone, measuring 5 cm × 4 cm × 3 cm in diameter, impacted the proximal third portion of the duodenum. No other stones were found in the gastrointestinal (GI) tract. Enterolithotomy, cholecystectomy, duodenorrhaphy, feeding jejunostomy, and repair of the cholecystoduodenal fistula were performed. Microscopically, the gallbladder showed cholelithiasis with acute and chronic inflammation and a fistula walled by fibrous and granulation tissue. The postoperative course was complicated by a wound infection, and he was discharged 2 mo later.

DISCUSSION

Gallstone is a common disease with a prevalence in 10% of the adult population in the United States[8]. However, it is only symptomatic in 20%-30% of patients, with biliary colic being the most common symptom[9]. The most common complications of gallstone disease include acute cholecystitis, acute pancreatitis, choledocholithiasis with or without cholangitis, and a gangrenous gallbladder. Other uncommon complications include Mirizzi syndrome,

cholecystocholedochal fistula, and gallstone ileus[2,10].

The term "gallstone ileus" was first coined by Bartolin in 1654 and referred to the mechanical intestinal obstruction due to impaction of one or more large gallstones within the GI tract. Biliary-enteric fistula is the major pathologic mechanism of gallstone ileus[11]. The gallstone enters the GI tract through a fistula between a gangrenous gallbladder and the GI tract. Occasionally a stone may enter the intestine through a fistulous communication between the common bile duct and the GI tract. Although the gallstone can impact anywhere in the GI tract, its size should be at least 2 cm to 2.5 cm in diameter to cause obstruction[6]. Reisner and Cohen[5] reviewed 1001 cases of gallstone ileus and reported that the most common locations of impaction of gallstone are the terminal ileum and the ileocecal valve because of the anatomical small diameter and less active peristalsis. They also found that the less common locations for impaction are the jejunum, the ligament of Treitz, and the stomach, while the duodenum and colon are the rare locations for impaction[5].

The clinical manifestations of gallstone ileus are variable and usually depend on the site of obstruction. The onset may be manifested as acute, intermittent or chronic episodes[12]. The most common symptoms include nausea, vomiting and epigastric pain. Moreover, a small portion of patients may present with hematemesis secondary to duodenal erosions. Laboratory studies may show an obstructive pattern with elevated values of bilirubin and alkaline phosphophatase.

The diagnosis of gallstone ileus is difficult, usually depending on the radiographic findings. In 50% of cases the diagnosis is often only made at laparotomy[5]. The classic Rigler's triad of radiography includes mechanical bowel obstruction, pneumobilia, and an ectopic gallstone within bowel lumen. However, air in the gallbladder is also a frequent finding in gallstone ileus[13]. Plain abdominal films usually show non-specific findings because only 10% of gallstones are sufficiently calcified to be visualized radiographically. For example, in our first case, although the ectopic gallstone appeared on the initial plain abdominal film, it was misdiagnosed as fecal material due to insufficient calcification. But in our second case, two gallstones were definitely identified on a plain abdominal film. Upper or lower GI barium studies occasionally identify the site of obstruction or fistula. Abdominal US is useful to confirm the presence of cholelithiasis and may identify fistula, if present[14]. Abdominal CT becomes the more important modality in diagnosing gallstone ileus because of its better resolution. By comparing with plain abdominal film and abdominal US, it can provide a more rapid and specific diagnosis in emergency use. Lassandro *et al*[15] compared the clinical value of plain abdominal film, abdominal US and abdominal CT in diagnosing 27 cases of gallstone ileus, and found that the Rigler's triad presents 14.81% in plain abdominal film, 11.11% in abdominal US, and 77.78% in abdominal CT, respectively. Additionally, Yu *et al*[16] studied the value of abdominal CT in the diagnosis and management of gallstone ileus and concluded that the abdominal CT offers crucial evidence not only for the diagnosis of gallstone ileus but also for decision making in management strategy[16]. Rarely, laparoscopy is used to diagnose this disease[17].

Gallstone ileus usually requires emergent surgery to relieve intestinal obstruction. Bowel resection is only indicated when there is intestinal perforation or ischemia[18]. There is no uniform surgical procedure for this disease because of its low incidence. Although enterolithotomy alone remains the popular operative method in most reports, the one-stage procedure composed of enterolithotomy, cholecystectomy and repair of fistula is necessary, if indicated[19]. Tan *et al*[20] compared the two surgical strategies of enterolithotomy alone and enterolithotomy with cholecystectomy for the emergent treatment of gallstone ileus, and concluded that both procedures are safe with no mortality, but the better surgical option is enterolithotomy. Doko *et al*[21] agreed that the one-stage procedure should be reserved only for highly selected patients with absolute indications. Recently, laparoscopy-guided enterolithotomy has become the preferred surgical approach in treating gallstone ileus[22]. Additionally, the non-surgical treatment of gallstone ileus has been suggested, including endoscopic removal and shockwave lithotripsy, but this depends on the location of obstruction[23,24]. In our second case, the two stones were detected by radiography preoperatively, but they were not found on the first EGD. The second duodenoscopy revealed two stones impacting the third portion of the duodenum. We attempted to remove them endoscopically, but failed due to their larger size.

The prognosis of gallstone ileus is usually poor and worsens with age. Previous studies reported that the mortality rate is 7.5%-15%[5,6], largely due to delayed diagnosis and concomitant conditions such as cardiorespiratory disease, obesity and diabetes mellitus. The postoperative recurrence rate of gallstone ileus is 4.7% and only 10% of patients require secondary biliary surgery for recurrent biliary symptoms[5,25].

In conclusion, gallstone ileus is a rare cause of intestinal obstruction. It must be considered in intestinal obstruction patients with a past history of gallstone, especially in elderly females. Abdominal CT is the preferred modality because of its rapid diagnosis of gallstone ileus. Surgical treatment is emergent when the radiological finding is highly or even suspicious or confirmed.

REFERENCES

1 **Richards WO**, Williams LF. Obstruction of the large and small intestine. *Surg Clin North Am* 1988; **68**: 355-376
2 **Abou-Saif A**, Al-Kawas FH. Complications of gallstone disease: Mirizzi syndrome, cholecystocholedochal fistula, and gallstone ileus. *Am J Gastroenterol* 2002; **97**: 249-254
3 **Kurtz RJ**, Heimann TM, Kurtz AB. Gallstone ileus: a diagnostic problem. *Am J Surg* 1983; **146**: 314-317
4 **Clavien PA**, Richon J, Burgan S, Rohner A. Gallstone ileus. *Br J Surg* 1990; **77**: 737-742
5 **Reisner RM**, Cohen JR. Gallstone ileus: a review of 1001 reported cases. *Am Surg* 1994; **60**: 441-446
6 **Rodríguez Hermosa JI**, Codina Cazador A, Gironès Vilà J, Roig García J, Figa Francesch M, Acero Fernández D. Gallstone Ileus: results of analysis of a series of 40 patients. *Gastroenterol Hepatol* 2001; **24**: 489-494
7 **Lobo DN**, Jobling JC, Balfour TW. Gallstone ileus: diagnostic

pitfalls and therapeutic successes. *J Clin Gastroenterol* 2000; **30**: 72-76
8 **Everhart JE**, Khare M, Hill M, Maurer KR. Prevalence and ethnic differences in gallbladder disease in the United States. *Gastroenterology* 1999; **117**: 632-639
9 **Berger MY**, van der Velden JJ, Lijmer JG, de Kort H, Prins A, Bohnen AM. Abdominal symptoms: do they predict gallstones? A systematic review. *Scand J Gastroenterol* 2000; **35**: 70-76
10 **Newman HF**, Northup JD, Rosenblum M, Abrams H. Complications of cholelithiasis. *Am J Gastroenterol* 1968; **50**: 476-496
11 **Glenn F**, Reed C, Grafe WR. Biliary enteric fistula. *Surg Gynecol Obstet* 1981; **153**: 527-531
12 **Kasahara Y**, Umemura H, Shiraha S, Kuyama T, Sakata K, Kubota H. Gallstone ileus. Review of 112 patients in the Japanese literature. *Am J Surg* 1980; **140**: 437-440
13 **Balthazar EJ**, Schechter LS. Air in gallbladder: a frequent finding in gallstone ileus. *AJR Am J Roentgenol* 1978; **131**: 219-222
14 **Lasson A**, Lorén I, Nilsson A, Nirhov N, Nilsson P. Ultrasonography in gallstone ileus: a diagnostic challenge. *Eur J Surg* 1995; **161**: 259-263
15 **Lassandro F**, Gagliardi N, Scuderi M, Pinto A, Gatta G, Mazzeo R. Gallstone ileus analysis of radiological findings in 27 patients. *Eur J Radiol* 2004; **50**: 23-29
16 **Yu CY**, Lin CC, Shyu RY, Hsieh CB, Wu HS, Tyan YS, Hwang JI, Liou CH, Chang WC, Chen CY. Value of CT in the diagnosis and management of gallstone ileus. *World J Gastroenterol* 2005; **11**: 2142-2147
17 **Agresta F**, Bedin N. Gallstone ileus as a complication of acute cholecystitis. Laparoscopic diagnosis and treatment. *Surg Endosc* 2002; **16**: 1637
18 **Syme RG**. Management of gallstone ileus. *Can J Surg* 1989; **32**: 61-64
19 **Zuegel N**, Hehl A, Lindemann F, Witte J. Advantages of one-stage repair in case of gallstone ileus. *Hepatogastroenterology* 1997; **44**: 59-62
20 **Tan YM**, Wong WK, Ooi LL. A comparison of two surgical strategies for the emergency treatment of gallstone ileus. *Singapore Med J* 2004; **45**: 69-72
21 **Doko M**, Zovak M, Kopljar M, Glavan E, Ljubicic N, Hochstädter H. Comparison of surgical treatments of gallstone ileus: preliminary report. *World J Surg* 2003; **27**: 400-404
22 **Franklin ME**, Dorman JP, Schuessler WW. Laparoscopic treatment of gallstone ileus: a case report and review of the literature. *J Laparoendosc Surg* 1994; **4**: 265-272
23 **Dumonceau JM**, Delhaye M, Devière J, Baize M, Cremer M. Endoscopic treatment of gastric outlet obstruction caused by a gallstone (Bouveret's syndrome) after extracorporeal shock-wave lithotripsy. *Endoscopy* 1997; **29**: 319-321
24 **Meyenberger C**, Michel C, Metzger U, Koelz HR. Gallstone ileus treated by extracorporeal shockwave lithotripsy. *Gastrointest Endosc* 1996; **43**: 508-511
25 **van Hillo M**, van der Vliet JA, Wiggers T, Obertop H, Terpstra OT, Greep JM. Gallstone obstruction of the intestine: an analysis of ten patients and a review of the literature. *Surgery* 1987; **101**: 273-276

S- Editor Liu Y **L- Editor** Wang XL **E- Editor** Chin GJ

PO Box 2345, Beijing 100023, China
www.wjgnet.com
wjg@wjgnet.com

World J Gastroenterol 2007 February 28; 13(8): 1299-1302
World Journal of Gastroenterology ISSN 1007-9327

CASE REPORT

Primary intestinal malignant fibrous histiocytoma: Two case reports

De-Liang Fu, Feng Yang, Ashish Maskay, Jiang Long, Chen Jin, Xian-Jun Yu, Jin Xu, Zhong-Wen Zhou, Quan-Xing Ni

De-Liang Fu, Feng Yang, Ashish Maskay, Jiang Long, Chen Jin, Xian-Jun Yu, Jin Xu, Quan-Xing Ni, Department of General Surgery, Huashan Hospital, Shanghai Medical College, Fudan University, Shanghai 200040, China
Zhong-Wen Zhou, Department of Pathology, Huashan Hospital, Shanghai Medical College, Fudan University, Shanghai 200040, China
Correspondence to: De-Liang Fu, Department of General Surgery, Huashan Hospital, 12 Central Urumqi Road, Shanghai 200040, China. surgeonfu@yahoo.com.cn
Telephone: +86-21-62489999-6062 Fax: +86-21-62489743
Received: 2006-11-08 Accepted: 2007-01-04

Abstract

Malignant fibrous histiocytoma (MFH) occurs most commonly in the extremities and trunk, but rarely in the intestine. Here we report two cases of primary intestinal MFH. The first case was a 70-year old man admitted for recurrent right lower quadrant abdominal pain. At laparotomy, a tumor was found originating from the cecum, with a suspicious metastatic nodule on the surface of the right lobe of the liver. A right hemicolectomy was performed followed by an ileotransverse end-to-end anastomotic reconstruction. The second case was a 43-year old man with intussusceptions of the small intestine. An emergent laparotomy revealed 4 pedunculated masses in the small bowel and a partial resection of the small intestine was performed. Though the symptoms were not typical, based on histological and immunohistochemical studies, the patients were diagnosed as MFH of the intestine. They were not treated with chemotherapy or radiotherapy and both died within 3 mo. MFH of the intestine is an extremely rare neoplasm with an aggressive biological behavior. The pathogenesis of this disease has not been clarified to date. Complete surgical excision is preferred, adjuvant chemotherapy or radiotherapy may be advisable.

Key words: Malignant fibrous histiocytoma; Intestinal neoplasms; Abdominal pain

Fu DL, Yang F, Maskay A, Long J, Jin C, Yu XJ, Xu J, Zhou ZW, Ni QX. Primary intestinal malignant fibrous histiocytoma: Two case reports. *World J Gastroenterol* 2007; 13(8): 1299-1302

http://www.wjgnet.com/1007-9327/13/1299.asp

INTRODUCTION

Malignant fibrous histiocytoma (MFH) is a common soft tissue sarcoma, usually occurring in the extremities. Primary intestinal MFH is a very rare neoplasm, with not more than 40 cases reported in international literatures[1-5]. Here we report two cases of primary intestinal MFH and review other reported cases.

CASE REPORTS

Case 1

A 70-year old man was admitted for recurrent right lower quadrant abdominal pain for about 50 d. He had no recent history of fever, vomiting, diarrhea, or constipation. Physical examination revealed a slightly tender fist-size mass in the right lower quadrant of the abdomen. Laboratory examination showed a white blood cell count of 5.02×10^9/L, and a neutrophil count of 68.3%. Abdominal ultrasonography revealed a large hypoechoic mass in the right lower quadrant and an abdominal computed tomography demonstrated a large soft-tissue mass in the right lumbar region and iliac fossa (Figure 1A). Chest X-ray and computed tomography showed a mass on the hilum of the right lung (Figure 1B). Barium enema and colonofiberscopy were not performed owing to the patient's abdominal pain. At laparotomy, a tumor was found originating from the cecum and infiltrating into the right lateral peritoneum. There was a suspicious metastatic nodule located on the surface of the right lobe of the liver. A right hemicolectomy was carried out, and reconstruction was performed by an ileotransverse end-to-end anastomosis. Grossly, an ulcerative annular tumor undergone necrosis was seen in the cecum, measuring 12 cm × 10 cm. There was a tumor nodule on the mesentery, measuring 3 cm × 2 cm. On cut section, the tumor was soft in consistency, solid and grayish-white in color. Microscopic examination revealed that the tumor was pleomorphic and consisted of spindle-shaped cells, oval cells, pleomorphic giant cells, and inflammatory cells. There were involvements of two lymph nodes. Immunohistochemical stains were positive for vimentin (Figure 2), KP-1, α 1-antitrypsin, LYS, P53, Ki67, and

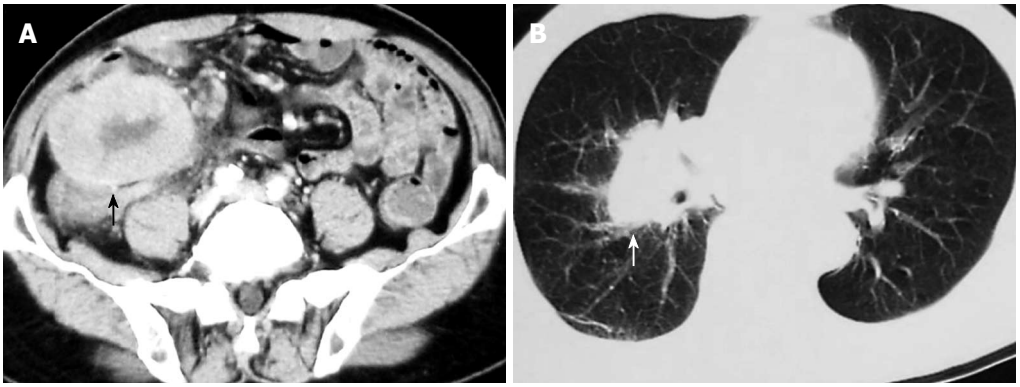

Figure 1 Computed tomography showing a large soft-tissue mass (black arrow) in the right lumbar region and iliac fossa (**A**) and a mass (white arrow) on the hilum of the right lung (**B**).

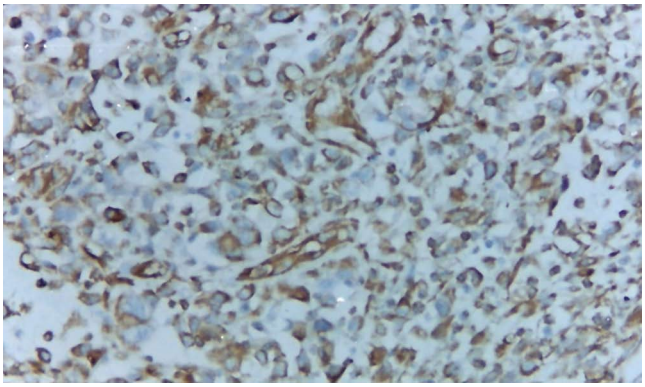

Figure 2 Tumor cells showing positive staining for vimentin (EnVision × 200).

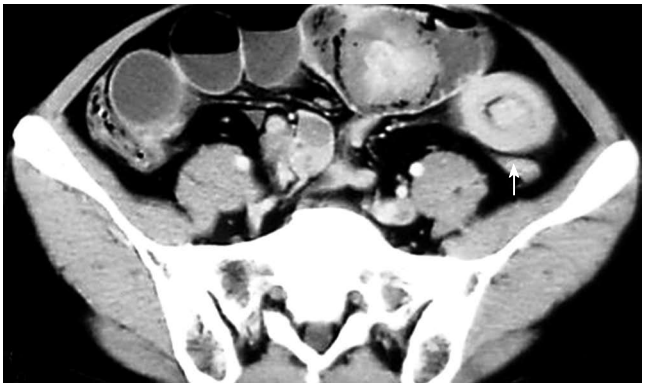

Figure 3 Computed tomography showing features of multiple intussusceptions in the small intestine (white arrow).

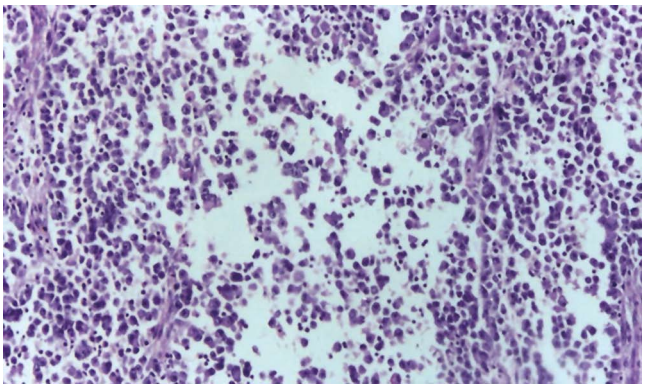

Figure 4 Histology revealing tumor cells consisting of fibroblast-like cells, histiocyte-like cells and pleomorphic giant cells (HE, × 40).

negative for S-100, CD1a, CD34, CD117, HMB45, CK, and SMA. The final histopathological diagnosis was MFH of the cecum. Postoperatively, the patient developed pyrexia for about one week which was subsequently followed by breathlessness as a result of lung metastasis. He was not treated with chemotherapy or radiotherapy, and died a month later.

Case 2

A 43-year old man with a history of melena for 10 d had intermittent abdominal pain, fever, vomiting and diarrhea. Physical examination revealed a slightly distended tender abdomen. Laboratory findings showed a white blood cell count of 23.39 × 10^9/L, and an elevated C-reactive protein level of 193.0 mg/L. Plain abdominal X-ray films showed small bowel obstruction. Computed tomography demonstrated features of multiple intussusceptions, i.e. some portions of the small intestine were seen invaginating into contiguous segments (Figure 3). Chest X-ray and computed tomography showed a mass on the apex of the right lung. The diagnosis of intussusceptions of the small intestine was made, and an emergency operation was performed. At laparotomy, 4 masses measuring 8, 5, 5, 3 cm in diameter were seen in the small bowel and local partial resections of the small intestine were performed. The resected specimens contained pedunculated tumors. Some metastatic nodules were also noted on the mesentery. Microscopic examination demonstrated fibroblast-like cells, histiocyte-like cells and pleomorphic giant cells within the tumor substance (Figure 4). Immunohistochemical stains were positive for vimentin, Ki67 (Figure 5A), P53 (Figure 5B), CK, KP-1 (Figure 5C), LYS, and negative for ER, PR, c-erbB2, MMP2, MMP9, S-100 and HMB45. The pathological findings were compatible with MFH of the small intestine. Postoperatively, the patient had high fever, vomiting and abdominal pain. White blood cell count varied from 26.64 × 10^9/L to 55.5 × 10^9/L, and plain abdominal X-ray films demonstrated partial bowel obstruction. The patient was not treated with chemotherapy or radiotherapy, and died 2 mo later.

DISCUSSION

Malignant fibrous histiocytoma (MFH) was first described

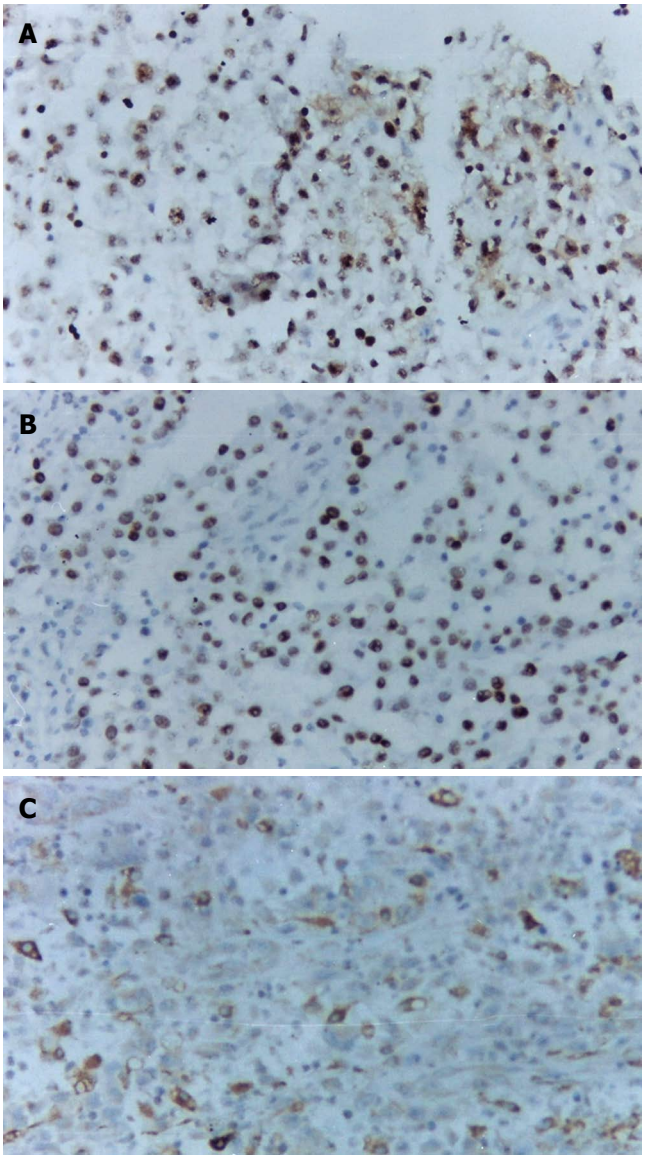

Figure 5 Tumor cells showing positive staining for Ki67 (**A**), P53 (**B**), and KP-1 (**C**) (EnVision × 200).

as malignant histiocytoma and fibrous xanthoma by Ozello *et al* in 1963, and was established by O'Brien and Stout in 1964 to describe soft tissue sarcomas arising from fibroblasts and histiocytes[3,5]. The peak incidence of extraintestinal MFH occurs in the sixth and seventh decades of life. It usually occurs in the extremities, presenting as a painless mass, and less commonly in the retroperitoneal space, associated with weight loss and increased intra-abdominal pressure[6]. Five histological subtypes of MFH have been described: pleomorphic storiform, myxoid, giant cell, inflammatory, and angiomatoid; the most common being pleomorphic storiform and myxoid types. The first two subtypes tend to be high-grade neoplasms, while the others are usually low-grade sarcomas[7]. The karyotypic abnormalities in MFH are usually complex, with multiple numerical and structural rearrangements[8]. Schmidt[9] reported that chromosomes 1, 3, 6, 9, 12, 16, 18, and 20 are involved in structural aberrations, and that the breakpoint regions are most frequently observed in 1p32, 3p25, and in the centromeric region of chromosomes 1 and 16. The pathogenesis of MFH has not been clarified to date. However, it has been recognized as a complication of radiation, resulting from chronic postoperative repair, trauma, surgical incisions or burn scars[10-13].

Primary MFH of the intestine is very rare. Not more than 40 cases have been reported in international literatures[1-4]. We reviewed the total 37 cases of intestinal MFH, including ours, and summarized the findings as follow. The ratio of men to women was 2.4:1, with an average age of 54.2 years and a range of 12-84 years. The tumor originated from the duodenum in 2 patients, the jejunum in 5, the ileum in 6, the jejunum and the ileum in 1, the cecum in 4, the ascending colon in 6, the transverse colon in 5, the descending colon in 2, the sigmoid colon in 2, the rectum in 3, and from the anal canal in 1. In most patients, the tumor was solitary, while in 4 cases multiple tumors were observed. The distribution of the colorectal MFH was different from that of carcinoma. Despite the fact that most of the tumors were large, ranging from 2 to 19 cm in diameter, their early detection was difficult. The symptoms were not typical: most patients complained of abdominal pain, fever, anorexia, bloody stools and diarrhea, but few had constipation. Thirty-five of the patients were treated surgically, 3 received adjuvant chemotherapy, one was given radiotherapy, and one underwent chemoradiation. In some patients, initial laparatomy revealed metastatic masses, especially in the regional lymph nodes, liver and lungs. Local recurrence was the most common pattern of recurrence in MFH of the intestine. Several patients died of local recurrence or metastasis including our reported two cases.

The diagnosis of MFH depends on an accurate differential diagnosis from other sarcomas, observation of karyomorphism and differential figures, and positive results on immunohistological staining. It was reported that MFH frequently expresses vimentin, actin, CD-68, and α 1-antitrypsin and α 1-antichymotrypsin[14]. Thus, the final diagnosis of our patients was MFH. The differential diagnosis of MFH should include pleomorphic liposarcoma and rhabdomyosarcoma. The former lacks the storiform pattern and shows evidence of cellular differentiation, while the latter shows cross striations on histological examination.

Murata[15] reported that colorectal MFH of the inflammatory type produces granulocyte colony-stimulating factor (G-CSF). Liesveld[16] reported that patients with MFH have leukocytosis, leukemoid reaction, and paraneoplastic syndrome because of various cytokines produced by tumor cells. Thus, postoperative recurrent leukocytosis and elevated CRP level might be predictors for recurrence of MFH. The second case presented to our center had leukocytosis and leukemoid reaction postoperatively.

The treatment for MFH is early and complete surgical excision with en-bloc regional lymph node dissection. Postoperatively, our patients were not given chemotherapy due to their poor general condition. Chemotherapy and radiotherapy were used, but without success. Zagars[17] reported that adjuvant chemotherapy cannot minimize the rate of metastasis. Patients with myxoid tumors do

not require systemic therapy. However, patients with nonmyxoid disease exceeding 5 cm are at a significant risk of developing metastases and the development of effective adjuvant treatment is an important research goal. Another report stated that inadequate peritumoral excision is a cause for recurrence[18].

Most of the reports suggest that the prognosis associated with colonic MFH is poor. Weiss and Einzinger's analysis of MFH[6] showed that the 2-year survival rate of patients with pleomorphic/storiform type of MFH is 60% and the rate of metastases is 42%. Tumor site (extremity *vs* nonextremity), location (proximal *vs* distal), size ($\leqslant$ 5 cm *vs* > 5 cm), and histology (myxoid *vs* nonmyxoid) are not significant determinants for final outcome [17]. For metastatic relapse, the major determinants were histology (myxoid *vs* nonmyxoid) and tumor size. Myxoid tumors have a low metastatic propensity (13% 10-year metastatic rate) compared to nonmyxoid tumors (40% 10-year metastatic rate).

In conclusion, primary intestinal MFH is an extremely rare neoplasm with an aggressive biological behavior. Clinicians and pathologists must consider the possibility of this tumor and include it in the differential diagnoses of intestinal lesions. Complete surgical excision is preferred and adjuvant chemotherapy or radiotherapy may be advisable. Due to the high recurrence, life-long surveillance should be carried out.

REFERENCES

1 **Udaka T**, Suzuki Y, Kimura H, Miyashita K, Suwaki T, Yoshino T. Primary malignant fibrous histiocytoma of the ascending colon: report of a case. *Surg Today* 1999; **29**: 160-164
2 **Singh DR**, Aryya NC, Sahi UP, Shukla VK. Malignant fibrous histiocytoma of the rectum. *Eur J Surg Oncol* 1999; **25**: 447-448
3 **Okubo H**, Ozeki K, Tanaka T, Matsuo T, Mochinaga N. Primary malignant fibrous histiocytoma of the ascending colon: report of a case. *Surg Today* 2005; **35**: 323-327
4 **Hiraoka N**, Mukai M, Suzuki M, Maeda K, Nakajima K, Hashimoto M, Hosoda Y, Hata J. Malignant fibrous histiocytoma of the cecum: report of a case and review of the literature. *Pathol Int* 1997; **47**: 718-724
5 **Hasegawa S**, Kawachi H, Kurosawa H, Obi Y, Yamanaka K, Nakamura K, Abe T. Malignant fibrous histiocytoma in the ileum associated with intussusception. *Dig Dis Sci* 2004; **49**: 1156-1160
6 **Weiss SW**, Enzinger FM. Malignant fibrous histiocytoma: an analysis of 200 cases. *Cancer* 1978; **41**: 2250-2266
7 **Anagnostopoulos G**, Sakorafas GH, Grigoriadis K, Kostopoulos P. Malignant fibrous histiocytoma of the liver: a case report and review of the literature. *Mt Sinai J Med* 2005; **72**: 50-52
8 **Szymanska J**, Tarkkanen M, Wiklund T, Virolainen M, Blomqvist C, Asko-Seljavaara S, Tukiainen E, Elomaa I, Knuutila S. A cytogenetic study of malignant fibrous histiocytoma. *Cancer Genet Cytogenet* 1995; **85**: 91-96
9 **Schmidt H**, Körber S, Hinze R, Taubert H, Meye A, Würl P, Holzhausen HJ, Dralle H, Rath FW. Cytogenetic characterization of ten malignant fibrous histiocytomas. *Cancer Genet Cytogenet* 1998; **100**: 134-142
10 **Fukunaga M**, Endo Y, Ushigome S. Radiation-induced inflammatory malignant fibrous histiocytoma of the ileum. *APMIS* 1999; **107**: 837-842
11 **Froehner M**, Gaertner HJ, Hakenberg OW, Wirth MP. Malignant fibrous histiocytoma of the ileum at a site of previous surgery: report of a case. *Surg Today* 2001; **31**: 242-245
12 **Kim GI**, Lee JH, Kim HK, Park SH, Kim CH. Malignant fibrous histiocytoma in a chronic burn scar: a rare case report and review of the literature. *Burns* 2004; **30**: 742-745
13 **Yücel A**, Yazar S, Demirkesen C, Durak H, Dervişoğlu S, Altintaş M. An unusual long-term complication of burn injury: malignant fibrous histiocytoma developed in chronic burn scar. *Burns* 2000; **26**: 305-310
14 **Rosenberg AE**. Malignant fibrous histiocytoma: past, present, and future. *Skeletal Radiol* 2003; **32**: 613-618
15 **Murata I**, Makiyama K, Miyazaki K, Kawamoto AS, Yoshida N, Muta K, Itsuno M, Hara K, Nakagoe T, Tomita M. A case of inflammatory malignant fibrous histiocytoma of the colon. *Gastroenterol Jpn* 1993; **28**: 554-563
16 **Liesveld JL**, Rush S, Kempski MC, Turner AR, Brennan JK, Gasson JC, Abboud CN. Phenotypic characterization of the human fibrous histiocytoma giant cell tumor (GCT) cell line and its cytokine repertoire. *Exp Hematol* 1993; **21**: 1342-1352
17 **Zagars GK**, Mullen JR, Pollack A. Malignant fibrous histiocytoma: outcome and prognostic factors following conservation surgery and radiotherapy. *Int J Radiat Oncol Biol Phys* 1996; **34**: 983-994
18 **Matsumoto S**, Ahmed AR, Kawaguchi N, Manabe J, Matsushita Y. Results of surgery for malignant fibrous histiocytomas of soft tissue. *Int J Clin Oncol* 2003; **8**: 104-109

S- Editor Wang J **L- Editor** Wang XL **E- Editor** Ma WH

PO Box 2345, Beijing 100023, China
www.wjgnet.com
wjg@wjgnet.com

World J Gastroenterol 2007 February 28; 13(8): 1303-1305
World Journal of Gastroenterology ISSN 1007-9327

CASE REPORT

Eosinophilic gastroenteritis with ascites and hepatic dysfunction

Hai-Bo Zhou, Jin-Ming Chen, Qin Du

Hai-Bo Zhou, Jin-Ming Chen, Qin Du, Department of Gastroenterology, Second Affiliated Hospital of Zhejiang University, Hangzhou 310009, Zhejiang Province, China
Correspondence to: Dr. Hai-Bo Zhou, Department of Gastroenterology, Second Affiliated Hospital of Zhejiang University, Hangzhou 310009, Zhejiang Province, China. zhouhaibohz@163.com
Telephone: +86-571-87783564
Received: 2006-12-06 Accepted: 2007-01-08

Abstract

Eosinophilic gastroenteritis is a rare gastrointestinal disorder with eosinophilic infiltration of the gastrointestinal wall and various gastrointestinal dysfunctions. Diagnosis requires a high index of suspicion and exclusion of various disorders that are associated with peripheral eosinophilia. We report a case of eosinophilic gastroenteritis, which had features of the predominant subserosal type presenting with ascites and hepatic dysfunction, and which responded to a course of low-dose steroid.

Key words: Ascites; Eosinophilia; Gastroenteritis

Zhou HB, Chen JM, Du Q. Eosinophilic gastroenteritis with ascites and hepatic dysfunction. *World J Gastroenterol* 2007; 13(8): 1303-1305

http://www.wjgnet.com/1007-9327/13/1303.asp

INTRODUCTION

Eosinophilic gastroenteritis, first reported by Kaijser in 1937, is a rare gastrointestinal disorder that can present with various gastrointestinal manifestations, depending on the specific site of the affected gastrointestinal wall. Klein *et al*[1] have demonstrated that this disorder could be pathologically classified into three major types: predominant mucosal layer, predominant muscle layer, and predominant subserosal layer. However, its clinical features, etiology, and treatment have not yet been definitely established. We report a case of eosinophilic gastroenteritis with features of the predominant subserosal type, including ascites and liver dysfunction.

CASE REPORT

In July 2006, a 33-year-old man presented with mild upper abdominal pain and, three days later, with abdominal distention, frequency of bowel motion and fever. His temperature was 38.5℃. He had no past history of ulcer pain and never had any abdominal operation. There had been no weight loss and neither blood nor mucus was present in the stool. The patient denied taking any drugs or herbal medicine. There was a history of allergy to levofloxacin. Chest examination showed no abnormality. Abdominal examination revealed a soft, mildly tender abdomen, and shifting abdominal dullness.

The patient was admitted to the Second Affiliated Hospital of Zhejiang University in July 2006. The hemoglobin level was 13.0 g/L(normal range, male, 11-16 g/L) and white cell count was 13.6 × 10^9/L, with 41.1% neutrophils, 27.9% lymphocytes, 8% monocytes and 22.5% eosinophils. The platelet count was 138 × 10^9/L, and the sedimentation rate was 8 mm/h. The tests for antinuclear factor, rheumatoid factor, serum hepatitis B surface antigen and serum hepatitis A, C, E antibodies gave negative results. The alanine aminotransferase level was 337 U/L (normal range, 0-50 U/L) and the aspartate aminotransferase was 223 U/L (normal range, 0-40 U/L). The anti-amoebic titer was negative and stool microscopy for ova and cysts was negative. Ultrasonography of the abdomen revealed a moderate amount of ascites (Figure 1). Gastroscopy showed mild antral gastritis. Biopsy of gastric antrum and proximal duodenum revealed inflammation with marked eosinophilic infiltration (Figure 2 and Figure 3). Colonoscopy showed mild proctitis and sigmoid colitis.

After excluding the possibilities of a malignancy, parasitic disease, and autoimmune disease, eosinophilic gastroenteritis was diagnosed. This diagnosis was supported by the presence of peripheral eosinophilia and eosinophilic infiltration of the serosa and subserosa of the gastric antrum and proximal duodenum. A small daily dose of steroid (prednisolone 20 mg) was given. Four days later, the patient recovered from his symptoms. The white cell count was 9.5 × 10^9/L, with 49.1% neutrophils, 27.2% lymphocytes, 7.7% monocytes and 15% eosinophils. Seven days later, the alanine aminotransferase level was 128 U/L and the aspartate aminotransferase was 38 U/L. Ultrasonography of the abdomen revealed no ascites. Steroid treatment was gradually tapered and eventually terminated after 4 wk.

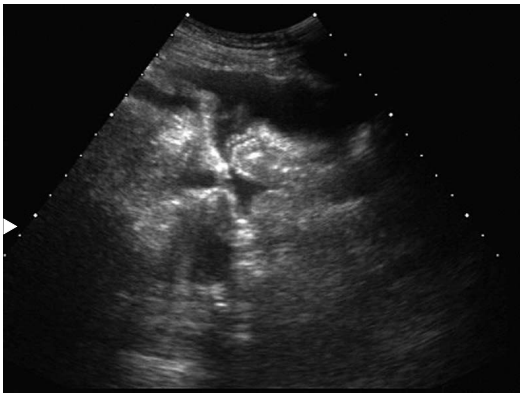

Figure 1 Ultrasonography of the abdomen revealed a moderate amount of ascites.

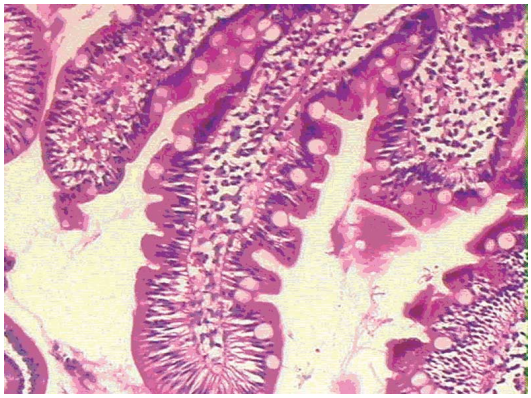

Figure 2 Histologic section of proximal duodenum showed inflammation with marked eosinophilic infiltration (HE, × 100).

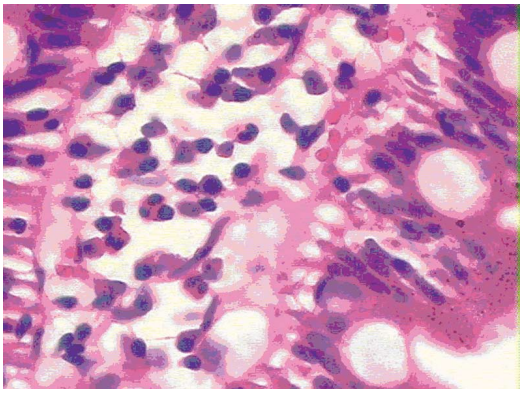

Figure 3 Histologic section of proximal duodenum showed inflammation with marked eosinophilic infiltration (HE, × 400).

DISCUSSION

The important feature in this case of eosinophilic gastroenteritis is the extremely high eosinophil count in the peripheral blood and the serosa and subserosa of the gastric antrum and proximal duodenum. The diagnosis of eosinophilic gastroenteritis was confirmed after the exclusion of other disorders that have similar features, such as gut lymphoma, parasitic infection, carcinoma, inflammatory bowel disease, and allergy.

Eosinophilic gastroenteritis is a rare disease, which was first reported by Kaijser in 1937. In 1970, Klein demonstrated that this disorder could be pathologically classified into three major types: predominant mucosal, predominant muscle layer, and predominant subserosal. The involvement of different layers usually gives rise to different clinical manifestations. Mucosal disease generally presents with bleeding, protein-losing enteropathy, or malabsorption. Involvement of the muscle layer may cause bowel wall thickening and subsequent intestinal obstruction. The subserosal form usually presents with peritonitis and eosinophilic ascites, which was the case in this patient.

Eosinophilic gastroenteritis can involve any part of the gastrointestinal tract from the esophagus down to the rectum. The stomach and duodenum, however, are the most common sites of involvement[2-5]. The etiology of eosinophilic gastroenteritis is currently unknown. Allergies to certain foods or immunological abnormalities have been speculated as its etiology[6-8]. On the other hand, some investigators[9,10]have demonstrated that the etiology of this disorder is not associated with allergic reactions. In our case, there was a past history of levofloxacin allergy. However, the patient denied taking any drugs or herbal medicine. The finding of high eosinophil count in the peripheral blood suggested allergic disorder or parasitic disorders, or abdominal lymphoma. The likelihood of parasitic disorders and abdominal lymphoma was remote because of the history of the patient's illness, the physical findings, and the findings on gastroscopy, colonoscopy and ultrasonography.

In the mucosal form of eosinophilic gastroenteritis, multiple biopsies must be taken during endoscopy, because mucosal involvement is often patchy in nature. When there is a submucosal disease, biopsy of the mucosal layer sometimes fails to expose eosinophilic gastroenteritis. Laparotomy or laparoscopy is often required to make a diagnosis in such cases.

Treatment with a steroid is the mainstay in the management of eosinophilic gastroenteritis. Clinical improvement usually is seen after treatment with a low dose of steroid. Surgical intervention may sometimes be required for patients with complicating obstruction or when performing a full thickness intestinal biopsy to establish the diagnosis.

REFERENCES

1 **Klein NC**, Hargrove RL, Sleisenger MH, Jeffries GH. Eosinophilic gastroenteritis. *Medicine* (Baltimore) 1970; **49**: 299-319
2 **Liacouras CA**. Eosinophilic esophagitis: treatment in 2005. *Curr Opin Gastroenterol* 2006; **22**: 147-152
3 **Straumann A**, Simon HU. Eosinophilic esophagitis: escalating epidemiology? *J Allergy Clin Immunol* 2005; **115**: 418-419
4 **Repiso Ortega A**, Alcántara Torres M, González de Frutos C, de Artaza Varasa T, Rodríguez Merlo R, Valle Muñoz J, Martínez Potenciano JL. Gastrointestinal anisakiasis. Study of a series of 25 patients. *Gastroenterol Hepatol* 2003; **26**: 341-346
5 **Caldwell JH**. Eosinophilic Gastroenteritis. *Curr Treat Options Gastroenterol* 2002; **5**: 9-16
6 **Liacouras CA**. Eosinophilic esophagitis in children and adults. *J Pediatr Gastroenterol Nutr* 2003; **37** Suppl 1: S23-S28
7 **Kweon MN**, Kiyono H. Eosinophilic gastroenteritis: a problem

of the mucosal immune system? *Curr Allergy Asthma Rep* 2003; **3**: 79-85

8 **Cordero Miranda MA**, Blandón Vijil V, Reyes Ruiz NI, Avila Castañón L, del Río Navarro BE, García Aranda JA, Blanco Rodríguez G, Sienra Monge JJ. Eosinophilic proctocolitis induced by foods. Report of a case. *Rev Alerg Mex* 2002; **49**: 196-199

9 **Seibold F**. Food-induced immune responses as origin of bowel disease? *Digestion* 2005; **71**: 251-260

10 **Barbie DA**, Mangi AA, Lauwers GY. Eosinophilic gastroenteritis associated with systemic lupus erythematosus. *J Clin Gastroenterol* 2004; **38**: 883-886

S- Editor Liu Y **L- Editor** Zhu LH **E- Editor** Zhou T

PO Box 2345, Beijing 100023, China
www.wjgnet.com
wjg@wjgnet.com

World J Gastroenterol 2007 February 28; 13(8): 1306-1307
World Journal of Gastroenterology ISSN 1007-9327

LETTERS TO THE EDITOR

What caused the increase of autoimmune and allergic diseases: A decreased or an increased exposure to luminal microbial components?

Xiaofa Qin

Xiaofa Qin, Department of Surgery, UMDNJ-New Jersey Medical School, Newark, New Jersey 07103, United States
Correspondence to: Xiaofa Qin, MD, PhD, Department of Surgery, UMDNJ-New Jersey Medical School, 185 South Orange Avenue, Newark, NJ 07103, United States. qinxi@umdnj.edu
Telephone: +1-973-9722896 Fax: +1-973-9726803
Received: 2006-12- 06 Accepted: 2007-01-16

Key words: Autoimmune disease; Allergic diseases; Hygiene hypothesis; Intestinal permeability; Luminal microbial components

Qin X. What caused the increase of autoimmune and allergic diseases: A decreased or an increased exposure to luminal microbial components? *World J Gastroenterol* 2007; 13(8): 1306-1307

http://www.wjgnet.com/1007-9327/13/1306.asp

TO THE EDITOR

The dramatic increase of allergic and autoimmune diseases such as asthma, atopic dermatitis (eczema), allergic rhinitis, inflammatory bowel disease (IBD, including both Crohn's disease and ulcerative colitis), multiple sclerosis, and insulin-dependent diabetes mellitus (type I diabetes) in the developed countries in the last century[1-3] is a big puzle. "Hygiene Hypothesis" was proposed more than two decades ago and it suggested that the increase in these allergic and autoimmune diseases is caused by the aberrant development and response of the immune system due to a reduced exposure to microorganisms along with the improved hygiene[2-4]. Interestingly, recent studies revealed that these allergic and autoimmune diseases are closely related to the microbes in the gut[5]. For instance, even asthma, an allergic reaction of the lung to inhaled antigens, is closely related to a reduced exposure to foodborne and orofaecal microbes, rather than the amount of allergens in the air or the exposure to airborne microbes[5-7]. It is known that bacteria in the gut could be 10 times in number of the eukaryotic cells of the body[8]. Therefore, it would be not too surprising that microbes in the gut may have a great impact on these autoimmune and allergic diseases.

On the other hand, many studies revealed that an increase in intestinal permeability was shown in patients with these autoimmune and allergic diseases, such as those with IBD[9,10], multiple sclerosis[11], type I [12,13] (but not type Ⅱ[14]) diabetes, asthma[15,16], and atopic eczema[17,18]. The increased intestinal permeability in these patients seems to be a prerequisite rather than a consequence of these diseases, as it could precede the clinical onset of these diseases[12,19,20]. In addition, increased intestinal permeability was also seen not only in healthy relatives[10,21], but also in spouses of these patients[10,22]. An increase in intestinal permeability would result in an increased infiltration of the luminal components. Therefore, it would be reasonable to ask what have caused the increase of these autoimmune and allergic diseases: is it a deceased exposure to luminal microbial components due to the improved hygiene, or an increased exposure to luminal microbial components due to the increased intestinal permeability?

There is a large amount of microbes in the gut. The endotoxin in gut bacteria could be enough to kill the host thousands of times over[23]. Therefore, it would be more likely that the tightness of the gut barrier would have played a more important role in determining the extent of exposure rather than the absolute number of microbes in the gut. Actually, there could be an intrinsic link between the increased intestinal permeability and improved hygiene. An effective inactivation of the digestive proteases depends on gut bacteria[24,25]. The increased intestinal permeability could be a result of the improved hygiene and a reduction in gut bacteria, by a mechanism such as the impaired inactivation of digestive proteases by gut bacteria, and thus an over-digestion of gut barrier. A reduction in gut bacteria not only can be the result of improved sanitary conditions, along with the more clean food and water, it also can be caused by an inhibition of gut bacteria by factors such as the widely used sweetener saccharin[26]. Interestingly, saccharin consumption correlated well with the ups and downs of the IBD, and probably had played a causative role in IBD[27,28]. This would lead us to raise a more general question: Will the improved hygiene and thus a reduction in gut bacteria necessarily result in a decreased exposure to luminal microbial components, the fundamental assumption of the "Hygiene Hypothesis"[29,30]. Further study in this area would be worthwhile. It would help better understand why both Th1 type diseases such as Crohn's diseases and type I diabetes, and Th2 type diseases such as ulcerative colitis and atopic diseases increase with the improved hygiene[29,30].

REFERENCES

1 **Hopkin JM**. Mechanisms of enhanced prevalence of asthma and atopy in developed countries. *Curr Opin Immunol* 1997; **9**: 788-792
2 **Von Hertzen LC**, Haahtela T. Asthma and atopy - the price of affluence? *Allergy* 2004; **59**: 124-137
3 **Bach JF**. The effect of infections on susceptibility to autoimmune and allergic diseases. *N Engl J Med* 2002; **347**: 911-920
4 **Strachan DP**. Hay fever, hygiene, and household size. *BMJ* 1989; **299**: 1259-1260
5 **Noverr MC**, Huffnagle GB. Does the microbiota regulate immune responses outside the gut? *Trends Microbiol* 2004; **12**: 562-568
6 **Matricardi PM**, Rosmini F, Riondino S, Fortini M, Ferrigno L, Rapicetta M, Bonini S. Exposure to foodborne and orofecal microbes versus airborne viruses in relation to atopy and allergic asthma: epidemiological study. *BMJ* 2000; **320**: 412-417
7 **Matricardi PM**, Rosmini F, Panetta V, Ferrigno L, Bonini S. Hay fever and asthma in relation to markers of infection in the United States. *J Allergy Clin Immunol* 2002; **110**: 381-387
8 **Guarner F**, Malagelada JR. Gut flora in health and disease. *Lancet* 2003; **361**: 512-519
9 **Hollander D**, Vadheim CM, Brettholz E, Petersen GM, Delahunty T, Rotter JI. Increased intestinal permeability in patients with Crohn's disease and their relatives. A possible etiologic factor. *Ann Intern Med* 1986; **105**: 883-885
10 **Söderholm JD**, Olaison G, Lindberg E, Hannestad U, Vindels A, Tysk C, Järnerot G, Sjödahl R. Different intestinal permeability patterns in relatives and spouses of patients with Crohn's disease: an inherited defect in mucosal defence? *Gut* 1999; **44**: 96-100
11 **Yacyshyn B**, Meddings J, Sadowski D, Bowen-Yacyshyn MB. Multiple sclerosis patients have peripheral blood CD45RO+ B cells and increased intestinal permeability. *Dig Dis Sci* 1996; **41**: 2493-2498
12 **Bosi E**, Molteni L, Radaelli MG, Folini L, Fermo I, Bazzigaluppi E, Piemonti L, Pastore MR, Paroni R. Increased intestinal permeability precedes clinical onset of type 1 diabetes. *Diabetologia* 2006; **49**: 2824-2827
13 **Carratù R**, Secondulfo M, de Magistris L, Iafusco D, Urio A, Carbone MG, Pontoni G, Cartenì M, Prisco F. Altered intestinal permeability to mannitol in diabetes mellitus type I. *J Pediatr Gastroenterol Nutr* 1999; **28**: 264-269
14 **Secondulfo M**, de Magistris L, Sapone A, Di Monda G, Esposito P, Carratù R. Intestinal permeability and diabetes mellitus type 2. *Minerva Gastroenterol Dietol* 1999; **45**: 187-192
15 **Hijazi Z**, Molla AM, Al-Habashi H, Muawad WM, Molla AM, Sharma PN. Intestinal permeability is increased in bronchial asthma. *Arch Dis Child* 2004; **89**: 227-229
16 **Benard A**, Desreumeaux P, Huglo D, Hoorelbeke A, Tonnel AB, Wallaert B. Increased intestinal permeability in bronchial asthma. *J Allergy Clin Immunol* 1996; **97**: 1173-1178
17 **Pike MG**, Heddle RJ, Boulton P, Turner MW, Atherton DJ. Increased intestinal permeability in atopic eczema. *J Invest Dermatol* 1986; **86**: 101-104
18 **Ukabam SO**, Mann RJ, Cooper BT. Small intestinal permeability to sugars in patients with atopic eczema. *Br J Dermatol* 1984; **110**: 649-652
19 **Irvine EJ**, Marshall JK. Increased intestinal permeability precedes the onset of Crohn's disease in a subject with familial risk. *Gastroenterology* 2000; **119**: 1740-1744
20 **Wyatt J**, Vogelsang H, Hübl W, Waldhöer T, Lochs H. Intestinal permeability and the prediction of relapse in Crohn's disease. *Lancet* 1993; **341**: 1437-1439
21 **Katz KD**, Hollander D, Vadheim CM, McElree C, Delahunty T, Dadufalza VD, Krugliak P, Rotter JI. Intestinal permeability in patients with Crohn's disease and their healthy relatives. *Gastroenterology* 1989; **97**: 927-931
22 **Breslin NP**, Nash C, Hilsden RJ, Hershfield NB, Price LM, Meddings JB, Sutherland LR. Intestinal permeability is increased in a proportion of spouses of patients with Crohn's disease. *Am J Gastroenterol* 2001; **96**: 2934-2938
23 **Magnotti LJ**, Deitch EA. Burns, bacterial translocation, gut barrier function, and failure. *J Burn Care Rehabil* 2005; **26**: 383-391
24 **Norin KE**, Gustafsson BE, Midtvedt T. Strain differences in faecal tryptic activity of germ-free and conventional rats. *Lab Anim* 1986; **20**: 67-69
25 **Norin KE**, Midtvedt T, Gustafsson BE. Influence of intestinal microflora on the tryptic activity during lactation in rats. *Lab Anim* 1986; **20**: 234-237
26 **Anderson RL**, Kirkland JJ. The effect of sodium saccharin in the diet on caecal microflora. *Food Cosmet Toxicol* 1980; **18**: 353-355
27 **Qin XF**. Impaired inactivation of digestive proteases by deconjugated bilirubin: the possible mechanism for inflammatory bowel disease. *Med Hypotheses* 2002; **59**: 159-163
28 **Qin X**. Is the incidence of inflammatory bowel disease in the developed countries increasing again? Is that surprising? *Inflamm Bowel Dis* 2007; 13: 804-805
29 **Guarner F**, Bourdet-Sicard R, Brandtzaeg P, Gill HS, McGuirk P, van Eden W, Versalovic J, Weinstock JV, Rook GA. Mechanisms of disease: the hygiene hypothesis revisited. *Nat Clin Pract Gastroenterol Hepatol* 2006; **3**: 275-284
30 **Schaub B**, Lauener R, von Mutius E. The many faces of the hygiene hypothesis. *J Allergy Clin Immunol* 2006; **117**: 969-977; quiz 978

S- Editor Liu Y **L- Editor** Ma JY **E- Editor** Lu W

PO Box 2345, Beijing 100023, China
www.wjgnet.com
wjg@wjgnet.com

World J Gastroenterol 2007 February 28; 13(8): 1308
World Journal of Gastroenterology ISSN 1007-9327

ACKNOWLEDGMENTS

Acknowledgments to Reviewers of *World Journal of Gastroenterology*

Many reviewers have contributed their expertise and time to the peer review, a critical process to ensure the quality of *World Journal of Gastroenterology*. The editors and authors of the articles submitted to the journal are grateful to the following reviewers for evaluating the articles (including those published in this issue and those rejected for this issue) during the last editing time period.

Daniel Lindsay Worthley, Dr
Department of Gastroenterology and Hepatology,Flinders Medical Centre, Room 3D230, Bedford Park, SA 5042, Australia

Abraham Rami Eliakim, Professor
Gastroenterology, Rambam Medical Center, Technion School of Medicine, PO Box 9602, Haifa 31096, Israel

Nikolaus Gassler, Professor
Institute of Pathology, University Hospital RWTH Aachen, Pauwelsstrasse 30, 52074 Aachen, Germany

Shinn-Jang Hwang, Professor
Department of Family Medicine, Taipei Veterans General Hospital, VGH, 201, Shih-Pai Road, Section 2, 11217, Taiwan, China

Limas Kupcinskas
Gastroenterology of Kaunas University of Medicine, Mickeviciaus 9, Kaunas LT 44307, Lithuania

Dieter Glebe, PhD
Institute for Medical Virology, Justus Liebig University Giessen, Frankfurter Str. 107, Giessen 35392, Germany

Serdar Karakose, Dr, Professor
Department of Radiology, Meram Medical Faculty, Selcuk University, Konya 42080, Turkey

John Frank Di Mari, Assistant Professor
Internal Medicine, Gastroenterology , 9.138 MRB 301 University Blvd. Galveston, Texas 77555-1064, United States

Richard A Rippe, Dr
Department of Medicine, The University of North Carolina at Chapel Hill, Chapel Hill, NC 27599-7038, United States

Seng-Lai Tan
Principal Scientist, Eli Lilly and Company, Indianapolis 46285, United States

Chris Jacob Johan Mulder, Professor
Department of Gastroenterology, VU University Medical Center, PO Box 7057, 1007 MB Amsterdam, The Netherlands

Hiroki Sasaki, PhD
Genetics Division, National Cancer Center Research Institute, 1-1, Tsukiji 5-chome, Chuo-ku, Tokyo 104-0045, Japan

John Frank Di Mari, Assistant Professor
Internal Medicine, Gastroenterology ,9.138 MRB 301 University Blvd. Galveston, Texas 77555-1064, United States

Jesus K Yamamoto-Furusho, Dr
Instituto Nacional de Ciencias Medicas y Nutricion, Vasco de Quiroga 15, Col. seccion XVI, Mexico 14000, Mexico

Florian Obermeier
Internal Medicine I, University of Regensburg, Franz-Josef-Strauss Allee11, Regensburg 93053, Germany

María Isabel Torres López, Professor
Experimental Biology, University of Jaen, araje de las Lagunillas s/n, Jaén 23071, Spain

Jay Pravda, MD
Inflammatory Disease Research Center, Gainesville, Florida, 32614-2181, United States

Marek Hartleb
Gastroenterology, CSK, ul. Medyków 14, 40-752 Katowice, Poland

Amedeo Columbano
Dipartimento di Tossicologia, Sezione di Oncologia e Patologia Molecolare, Via Porcell 4, 09124 Cagliari, Italy

John K Marshall, MD
Division of Gastroenterology (4W8), McMaster University Medical Centre, 1200 Main Street West, Hamilton, Ontario L8N 3Z5, Canada

Ton Lisman, PhD
Department of Haematology G.03.550, University Medical Centre, Heidelberglaan 100, 3584 CX Utrecht, The Netherlands

Takuji Torimura, MD
Second Department of Medicine, Kurume University School of Medicine, 67 Asahi-machi, Kurume City, Fukuoka 830-0011, Japan

Ramsey Chi-man Cheung, MD, Professor
ivision of GI & Hepatology, VAPAHCS(154C), 3801 Miranda Ave, Stanford University School of Medicine, Palo Alto, CA 94304, United States

Gisela Sparmann, MD
Division of Gastroenterology, Department of Internal Medicine, University of Rostock, Ernst-Heydemann-Str. 6, Rostock D-18057, Germany

Silvana Zanlungo, Professor
Departamento de Gastroenterología, Pontificia Universidad Católica de Chile, Marcoleta 367, Casilla 114-D, Santiago, Chile

Jean Louis Frossard, Dr
Division of gastroenterology, Geneva University Hospital, Rue Micheli du Crest, 1211 Geneva 14, Switzerland

Yukihiro Shimizu, Dr
Kyoto Katsura Hospital, 17 Yamada-Hirao, Nishikyo, Kyoto 615-8256, Japan

Nikolaus Gassler, Professor
Institute of Pathology, University Hospital RWTH Aachen, Pauwelsstrasse 30, 52074 Aachen, Germany

Khek-Yu Ho, Professor
Department of Medicine, National University Hospital, 119074, Singapore

Wendy Michelle Mars, PhD
Department of Pathology , University of Pittsburgh , S-411B South Biomedical Science Tower Pittsburgh , PA 15261, United States

James Neuberger, Professor
Liver Unit, Queen Elizabeth Hospital, Birmingham B15 2TH, United Kingdom

Zahariy Krastev, Professor
Department of Gastroneterology, Universiti Hospital "St. Ivan Rilski",#15, blvd "Acad. Ivan Geshov", Sofia 1431, Bulgaria

Paolo Del Poggio, Dr
Hepatology Unit, Department of Internal Medicine, Treviglio Hospital, Piazza Ospedale 1, Treviglio Bg 24047, Italy

Valerio Nobili, Dr
Liver Unit, Research Institute, Bambino Gesù Children's Hospital, S. Onofrio 4 Square, 00165 Rome

Martin Hennenberg
Dipl-Biol, Medizinische Klinik & Poliklinik I, Uni-Klinik Bonn, Sigmund-Freud Str. 25, 53105 Bonn, Martin

Claudia Veltkamp, MD
2Department of Gastroenterology, University of Heidelberg, INF 410, 69120 Heidelberg, Germany

PO Box 2345, Beijing 100023, China
www.wjgnet.com
wjg@wjgnet.com

World J Gastroenterol 2007 February 28; 13(8): 1309
World Journal of Gastroenterology ISSN 1007-9327

Meetings

MAJOR MEETINGS COMING UP

Meeting Falk Research Workshop: Morphogenesis and Cancerogenesis of the Liver
25-26 January 2007
Goettingen
symposia@falkfoundation.de

Meeting Canadian Digestive Diseases Week (CDDW)
16-20 February 2007
Banff-AB
cagoffice@cag-acg.org
www.cag-acg.org/cddw/cddw2007.htm

Meeting Falk Symposium 158: Intestinal Inflammation and Colorectal Cancer
23-24 March 2007
Sevilla
symposia@falkfoundation.de

Meeting BSG Annual Meeting
26-29 March 2007
Glasgow
www.bsg.org.uk/

NEXT 6 MONTHS

Meeting 42nd Annual Meeting of the European Association for the Study of the Liver
11-15 April 2007
Barcelona
easl2007@easl.ch
www.easl.ch/liver-meeting/

Meeting Falk Symposium 159: IBD 2007 - Achievements in Research and Clinical Practice
4-5 May 2007
Istanbul
symposia@falkfoundation.de

Meeting European Society for Paediatric Gastroenterology, Hepatology and Nutrition Congress 2007
9-12 May 2007
Barcelona
espghan2007@colloquium.fr

Digestive Disease Week
19-24 May 2007
Washington Convention Center, Washington DC

Meeting Gastrointestinal Endoscopy Best Practices: Today and Tomorrow, ASGE Annual Postgraduate Course at DDW
23-24 May 2007
Washington-DC
tkoral@asge.org

Meeting ESGAR 2007 18th Annual Meeting and Postgraduate Course
12-15 June 2007
Lisbon
fca@netvisao.pt

Meeting Falk Symposium 160: Pathogenesis and Clinical Practice in Gastroenterology
15-16 June 2007
Portoroz
symposia@falkfoundation.de

Meeting ILTS 13th Annual International Congress
20-23 June 2007
Rio De Janeiro
www.ilts.org

Meeting 9th World Congress on Gastrointestinal Cancer
27-30 June 2007
Barcelona
meetings@imedex.com

EVENTS AND MEETINGS IN 2007

Meeting Falk Research Workshop: Morphogenesis and Cancerogenesis of the Liver
25-26 January 2007
Goettingen
symposia@falkfoundation.de

Meeting Canadian Digestive Diseases Week (CDDW)
16-20 February 2007
Banff-AB
cagoffice@cag-acg.org
www.cag-acg.org/cddw/cddw2007.htm

Meeting Falk Symposium 158: Intestinal Inflammation and Colorectal Cancer
23-24 March 2007
Sevilla
symposia@falkfoundation.de

Meeting BSG Annual Meeting
26-29 March 2007
Glasgow
www.bsg.org.uk/

Meeting 42nd Annual Meeting of the European Association for the Study of the Liver
11-15 April 2007
Barcelona
easl2007@easl.ch
www.easl.ch/liver-meeting/

Meeting Falk Symposium 159: IBD 2007 - Achievements in Research and Clinical Practice
4-5 May 2007
Istanbul
symposia@falkfoundation.de

Meeting European Society for Paediatric Gastroenterology, Hepatology and Nutrition Congress 2007
9-12 May 2007
Barcelona
espghan2007@colloquium.fr

Meeting Gastrointestinal Endoscopy Best Practices: Today and Tomorrow, ASGE Annual Postgraduate Course at DDW
23-24 May 2007
Washington-DC
tkoral@asge.org

Meeting ESGAR 2007 18th Annual Meeting and Postgraduate Course
12-15 June 2007
Lisbon
fca@netvisao.pt

Meeting Falk Symposium 160: Pathogenesis and Clinical Practice in Gastroenterology
15-16 June 2007
Portoroz
symposia@falkfoundation.de

Meeting ILTS 13th Annual International Congress
20-23 June 2007
Rio De Janeiro
www.ilts.org

Meeting 9th World Congress on Gastrointestinal Cancer
27-30 June 2007
Barcelona
meetings@imedex.com

Meeting 15th International Congress of the European Association for Endoscopic Surgery
4-7 July 2007
Athens
info@eaes-eur.org
congresses.eaes-eur.org/

Meeting 39th Meeting of the European Pancreatic Club
4-7 July 2007
Newcastle
www.e-p-c2007.com

Meeting XXth International Workshop on Heliobacter and related bacteria in cronic degistive inflammation
20-22 September 2007
Istanbul
www.heliobacter.org

Meeting Falk Workshop: Mechanisms of Intestinal Inflammation
10 October 2007
Dresden
symposia@falkfoundation.de

Meeting Falk Symposium 161: Future Perspectives in Gastroenterology
11-12 October 2007
Dresden
symposia@falkfoundation.de

Meeting Falk Symposium 162: Liver Cirrhosis - From Pathophysiology to Disease Management
13-14 October 2007
Dresden
symposia@falkfoundation.de

American College of Gastroenterology Annual Scientific Meeting
12-17 October 2007
Pennsylvania Convention Center
Philadelphia, PA

Meeting APDW 2007 - Asian Pacific Digestive Disease Week 2007
15-18 October 2007
Kobe
apdw@convention.co.jp
www.apdw2007.org

15th United European Gastroenterology Week, UEGW
27-31 October 2007
Le Palais des Congrès de Paris, Paris, France

Meeting The Liver Meeting® 2007 - 57th Annual Meeting of the American Association for the Study of Liver Diseases
2-6 November 2007
Boston-MA
www.aasld.org

Gastro 2009, World Congress of Gastroenterology and Endoscopy London, United Kingdom 2009

PO Box 2345, Beijing 100023, China
www.wjgnet.com
wjg@wjgnet.com

World J Gastroenterol 2007 February 28; 13(8): 1310-1312
World Journal of Gastroenterology ISSN 1007-9327

Instructions to authors

GENERAL INFORMATION

World Journal of Gastroenterology (*WJG, World J Gastroenterol* ISSN 1007-9327 CN 14-1219/R) is a weekly journal of more than 48 000 circulation, published on the 7th, 14th, 21st and 28th of every month.

Original Research, Clinical Trials, Reviews, Comments, and Case Reports in esophageal cancer, gastric cancer, colon cancer, liver cancer, viral liver diseases, *etc*., from all over the world are welcome on the condition that they have not been published previously and have not been submitted simultaneously elsewhere.

Indexed and abstracted in

Current Contents®/Clinical Medicine, Science Citation Index Expanded (also known as SciSearch®) and Journal Citation Reports/Science Edition, *Index Medicus*, MEDLINE and PubMed, Chemical Abstracts, EMBASE/Excerpta Medica, Abstracts Journals, *Nature Clinical Practice Gastroenterology and Hepatology*, CAB Abstracts and Global Health. ISI JCR 2003-2000 IF: 3.318, 2.532, 1.445 and 0.993.

Published by

The WJG Press

SUBMISSION OF MANUSCRIPTS

Manuscripts should be typed double-spaced on A4 (297 mm × 210 mm) white paper with outer margins of 2.5 cm. Number all pages consecutively, and start each of the following sections on a new page: Title Page , Abstract, Introduction, Materials and Methods, Results, Discussion, acknowledgements, References, Tables, Figures and Figure Legends. Neither the editors nor the Publisher is responsible for the opinions expressed by contributors. Manuscripts formally accepted for publication become the permanent property of The WJG Press, and may not be reproduced by any means, in whole or in part without the written permission of both the authors and the Publisher. We reserve the right to put onto our website and copy-edit accepted manuscripts. Authors should also follow the guidelines for the care and use of laboratory animals of their institution or national animal welfare committee.

Authors should retain one copy of the text, tables, photographs and illustrations, as rejected manuscripts will not be returned to the author(s) and the editors will not be responsible for the loss or damage to photographs and illustrations in mailing process.

Online submission

Online submission is strongly advised. Manuscripts should be submitted through the Online Submission System at: http://www.wjgnet.com/index.jsp. Authors are highly recommended to consult the ONLINE INSTRUCTIONS TO AUTHORS (http://www.wjgnet.com/wjg/help/instructions.jsp) before attempting to submit online. Authors encountering problems with the Online Submission System may send an email you describing the problem to wjg@wjgnet.com for assistance. If you submit your manuscript online, do not make a postal contribution. A repeated online submission for the same manuscript is strictly prohibited.

Postal submission

Send 3 duplicate hard copies of the full-text manuscript typed double-spaced on A4 (297 mm × 210 mm) white paper together with any original photographs or illustrations and a 3.5 inch computer diskette or CD-ROM containing an electronic copy of the manuscript including all the figures, graphs and tables in native Microsoft Word format or *.rtf format to:

Editorial Office

World Journal of Gastroenterology
Editorial Department: Apartment 1066, Yishou Garden,
58 North Langxinzhuang Road,
PO Box 2345, Beijing 100023, China
E-mail: wjg@wjgnet.com
http: //www.wjgnet.com
Telephone: +86-10-85381892
Fax: +86-10-85381893

MANUSCRIPT PREPARATION

All contributions should be written in English. All articles must be submitted using a word-processing software. All submissions must be typed in 1.5 line spacing and in word size 12 with ample margins. The letter font is Tahoma. For authors from China, one copy of the Chinese translation of the manuscript is also required (excluding references). Style should conform to our house format. Required information for each of the manuscript sections is as follows:

Title page

Full manuscript title, running title, all author(s) name(s), affiliations, institution(s) and/or department(s) where the work was accomplished, disclosure of any financial support for the research, and the name, full address, telephone and fax numbers and email address of the corresponding author should be included. Titles should be concise and informative (removing all unnecessary words), emphasize what is new, and avoid abbreviations. A short running title of less than 40 letters should be provided. List the author(s)' name(s) as follows: initial and/or first name, middle name or initial(s) and full family name.

Abstract

An informative, structured abstract of no more than 250 words should accompany each manuscript. Abstracts for original contributions should be structured into the following sections: AIM: Only the purpose should be included. METHODS: The materials, techniques, instruments and equipments, and the experimental procedures should be included. RESULTS: The observatory and experimental results, including data, effects, outcome, *etc*. should be included. Authors should present *P* value where necessary, and the significant data should accompany. CONCLUSION: Accurate view and the value of the results should be included.

The format of structured abstracts is at: http://www.wjgnet.com/wjg/help/11.doc

Key words

Please list 5-10 key words that could reflect content of the study mainly from *Index Medicus*.

Text

For most article types, the main text should be structured into the following sections: INTRODUCTION, MATERIALS AND METHODS, RESULTS and DISCUSSION, and should include in appropriate Figures and Tables. Data should be presented in the body text or in Figures and Tables, but not in both.

Illustrations

Figures should be numbered as 1, 2, 3 and so on, and mentioned clearly in the main text. Provide a brief title for each figure on a separate page. No detailed legend should be involved under the figures. This part should be added into the text where the figures are applicable. Digital images: black and white photographs should be scanned and saved in TIFF format at a resolution of 300 dpi; color images should be saved as CMYK (print files) but not as RGB (screen-viewing files). Place each photograph in a separate file. Print images: supply images of size no smaller than 126 mm × 85 mm printed on smooth surface paper; label the image by writing the Figure number and orientation using an arrow. Photomicrographs: indicate the original magnification and stain in the legend. Digital Drawings: supply files in EPS if created by freehand and illustrator, or TIFF from photoshops. EPS files must be accompanied by a version in native file format for editing purposes. Existing line drawings should be scanned at a resolution of 1200 dpi and as close as possible to the size where they will appear when printed. Please use uniform legends for the same subjects. For example: Figure 1 Pathological changes of atrophic gastritis after treatment. A: ...; B: ...; C: ...; D: ...; E: ...; F: ...; G: ...

Tables

Three-line tables should be numbered as 1, 2, 3 and so on, and mentioned clearly in the main text. Provide a brief title for each table. No detailed legend should be included under the tables. This part should be added into the text where the tables are applicable. The information should complement but not duplicate that contained in the text. Use one horizontal line under the title, a second under the column heads, and a third below the Table, above any footnotes. Vertical and italic lines should be omitted.

Notes in tables and illustrations

Data that are not statistically significant should not be noted. $^{a}P<0.05$, $^{b}P<0.01$ should be noted ($P>0.05$ should not be noted). If there are other series of *P* values, $^{c}P<0.05$ and $^{d}P<0.01$ are used. Third series of *P* values can be expressed as $^{e}P<0.05$ and $^{f}P<0.01$. Other notes in tables or under

illustrations should be expressed as ^1F, ^2F, ^3F; or some other symbols with a superscript (Arabic numerals) in the upper left corner. In a multi-curve illustration, each curve should be labeled with ●, ○, ■, □, ▲, △, *etc.* in a certain sequence.

Acknowledgments

Brief acknowledgments of persons who have made genuine contributions to the manuscripts and who endorse the data and conclusions are included. Authors are responsible for obtaining written permission to use any copyrighted text and/or illustrations.

REFERENCES

Coding system

The author should code the references according the citation order in text in Arabic numerals, put references codes in square brackets, superscript it at the end of citation content or the author name of the citation. For those citation content as the narrate part, the coding number and square brackets should be typeset normally. For example, Crohn's disease (CD) is associated with increased intestinal permeability[1,2]. If references are directly cited in the text, they would be put together with the text, for example, from references [19,22-24], we know that...

When the authors code the references, please ensure that the order in text is the same as in reference part and also insure the spelling accuracy of the first author's name. Do not code the same citation twice.

PMID requirement

PMID roots in the abstract serial number indexed by PubMed (http://www.ncbi.nlm.nih.gov/entrez/query.fcgi?db=PubMed). The author should supply the PMID for journal citation. For those references that have not been indexed by PubMed, a printed copy of the first page of the full reference should be submitted.

The accuracy of the information of the journal citations is very important. Through reference testing system, the authors and editor could check the authors name, title, journal title, publication date, volume number, start page, and end page. We will interlink all references with PubMed in ASP file so that the readers can read the abstract of the citations online immediately.

Style for journal references

Authors: the first author should be typed in bold-faced letter. The surname of all authors should be typed with the initial letter capitalized and followed by their name in abbreviation (For example, Lian-Sheng Ma is abbreviated as Ma LS, Bo-Rong Pan as Pan BR). Title of the cited article and italicized journal title (Journal title should be in its abbreviation form as shown in PubMed), publication date, volume number (in black), start page, and end page [PMID: 11819634]

Note: The author should test the references through reference testing system (http://www.wjgnet.com/cgi-bin/index.pl)

Style for book references

Authors: the first author should be typed in bold-faced letter. The surname of all authors should be typed with the initial letter capitalized and followed by their name in abbreviation (For example, Lian-Sheng Ma is abbreviated as Ma LS, Bo-Rong Pan as Pan BR) Book title. Publication number. Publication place: Publication press, Year: start page and end page.

Format

Journals

English journal article (list all authors and include the PMID where applicable)

1 **Grover VP**, Dresner MA, Forton DM, Counsell S, Larkman DJ, Patel N, Thomas HC, Taylor-Robinson SD. Current and future applications of magnetic resonance imaging and spectroscopy of the brain in hepatic encephalopathy. *World J Gastroenterol* 2006; **12**: 2969-2978 [PMID: 16718775]

Chinese journal article (list all authors and include the PMID where applicable)

2 **Lin GZ**, Wang XZ, Wang P, Lin J, Yang FD. Immunologic effect of Jianpi Yishen decoction in treatment of Pixu-diarrhoea. *Shijie Huaren Xiaohua Zazhi* 1999; **7**: 285-287

In press

3 **Tian D**, Araki H, Stahl E, Bergelson J, Kreitman M. Signature of balancing selection in Arabidopsis. *Proc Natl Acad Sci U S A* 2006; In press

Organization as author

4 **Diabetes Prevention Program Research Group**. Hypertension, insulin, and proinsulin in participants with impaired glucose tolerance. *Hypertension* 2002; **40**: 679-686 [PMID: 12411462]

Both personal authors and an organization as author

5 **Vallancien G**, Emberton M, Harving N, van Moorselaar RJ; Alf-One Study Group. Sexual dysfunction in 1, 274 European men suffering from lower urinary tract symptoms. *J Urol* 2003; **169**: 2257-2261 [PMID: 12771764]

No author given

6 21st century heart solution may have a sting in the tail. *BMJ* 2002; **325**: 184 [PMID: 12142303]

Volume with supplement

7 **Geraud G**, Spierings EL, Keywood C. Tolerability and safety of frovatriptan with short- and long-term use for treatment of migraine and in comparison with sumatriptan. *Headache* 2002; **42** Suppl 2: S93-99 [PMID: 12028325]

Issue with no volume

8 **Banit DM**, Kaufer H, Hartford JM. Intraoperative frozen section analysis in revision total joint arthroplasty. *Clin Orthop Relat Res* 2002; (**401**): 230-238 [PMID: 12151900]

No volume or issue

9 Outreach: bringing HIV-positive individuals into care. *HRSA Careaction* 2002; 1-6 [PMID: 12154804]

Books

Personal author(s)

10 **Sherlock S**, Dooley J. Diseases of the liver and billiary system. 9th ed. Oxford: Blackwell Sci Pub, 1993: 258-296

Chapter in a book (list all authors)

11 **Lam SK**. Academic investigator's perspectives of medical treatment for peptic ulcer. In: Swabb EA, Azabo S. Ulcer disease: investigation and basis for therapy. New York: Marcel Dekker, 1991: 431-450

Author(s) and editor(s)

12 **Breedlove GK**, Schorfheide AM. Adolescent pregnancy. 2nd ed. Wieczorek RR, editor. White Plains (NY): March of Dimes Education Services, 2001: 20-34

Conference proceedings

13 **Harnden P**, Joffe JK, Jones WG, editors. Germ cell tumours V. Proceedings of the 5th Germ Cell Tumour Conference; 2001 Sep 13-15; Leeds, UK. New York: Springer, 2002: 30-56

Conference paper

14 **Christensen S**, Oppacher F. An analysis of Koza's computational effort statistic for genetic programming. In: Foster JA, Lutton E, Miller J, Ryan C, Tettamanzi AG, editors. Genetic programming. EuroGP 2002: Proceedings of the 5th European Conference on Genetic Programming; 2002 Apr 3-5; Kinsdale, Ireland. Berlin: Springer, 2002: 182-191

Electronic journal (list all authors)

Morse SS. Factors in the emergence of infectious diseases. Emerg Infect Dis serial online, 1995-01-03, cited 1996-06-05; 1(1): 24 screens. Available from: URL: http//www.cdc.gov/ncidod/EID/eid.htm

Patent (list all authors)

16 **Pagedas AC**, inventor; Ancel Surgical R&D Inc., assignee. Flexible endoscopic grasping and cutting device and positioning tool assembly. United States patent US 20020103498. 2002 Aug 1

Inappropriate references

Authors should always cite references that are relevant to their article, and avoid any inappropriate references. Inappropriate references include those that are linked with a hyphen and the difference between the two numbers at two sides of the hyphen is more than 5. For example, [1-6], [2-14] and [1, 3, 4-10, 22] are all considered as inappropriate references. Authors should not cite their own unrelated published articles.

Statistical data

Present as mean ± SD or mean ± SE.

Statistical expression

Express t test as t (in italics), F test as F (in italics), chi square test as χ^2 (in Greek), related coefficient as r (in italics), degree of freedom as γ (in Greek), sample number as n (in italics), and probability as P (in italics).

Units

Use SI units. For example: body mass, m (B) = 78 kg; blood pressure, p(B) = 16.2/12.3 kPa; incubation time, t (incubation) = 96 h, blood glucose concentration, c (glucose) 6.4 ± 2.1 mmol/L; blood CEA mass concentration, p (CEA) = 8.6 24.5 μg/L; CO_2 volume fraction, 50 mL/L CO_2 not 5% CO_2; likewise for 40 g/L formaldehyde, not 10% formalin; and mass fraction, 8 ng/g, *etc.* Arabic numerals such as 23, 243, 641 should be read 23 243 641.

The format about how to accurately write common units and quantum is at: http://www.wjgnet.com/wjg/help/15.doc

Abbreviations

Standard abbreviations should be defined in the abstract and on first mention in the text. In general, terms should not be abbreviated unless they are used repeatedly and the abbreviation is helpful to the reader. Permissible abbreviations are listed in Units, Symbols and Abbreviations: A Guide for Biological and Medical Editors and Authors (Ed. Baron DN, 1988) published by The Royal Society of Medicine, London. Certain commonly used abbreviations, such as DNA, RNA, HIV, LD50, PCR, HBV, ECG, WBC, RBC, CT, ESR, CSF, IgG, ELISA, PBS, ATP, EDTA, mAb, can be used directly without further mention.

Italics

Quantities: *t* time or temperature, *c* concentration, *A* area, *l* length, *m* mass, *V* volume.
Genotypes: *gyr*A, *arg* 1, *c myc*, *c fos*, *etc.*
Restriction enzymes: *Eco*RI, *Hin*dI, *Bam*HI, *Kbo* I, *Kpn* I, *etc.*
Biology: *H pylori, E coli, etc.*

SUBMISSION OF THE REVISED MANUSCRIPTS AFTER ACCEPTED

Please revise your article according to the revision policies of *WJG*. The revised version including manuscript and high-resolution image figures (if any) should be copied on a floppy or compact disk. Author should send the revised manuscript, along with printed high-resolution color or black and white photos, copyright transfer letter, the final check list for authors, and responses to reviewers by a courier (such as EMS) (submission of revised manuscript by e-mail or on the *WJG* Editorial Office Online System is NOT available at present).

Language evaluation

The language of a manuscript will be graded before sending for revision. (1) Grade A: priority publishing; (2) Grade B: minor language polishing; (3) Grade C: a great deal of language polishing; (4) Grade D: rejected. The revised articles should be in grade B or grade A.

Copyright assignment form

Please downloaded CAF from http://www.wjgnet.com/wjg/help/9.doc.

We certify that the material contained in this manuscript:

Ms:

Title:

is original, except when appropriately referenced to other sources, and that written permission has been granted by any existing copyright holders. We agree to transfer to WJG all rights of our manuscript, including: (1) all copyright ownership in all print and electronic formats; (2) the right to grant permission to republish or reprint the stated material in whole or in part, with or without a fee; (3) the right to print copies for free distribution or sale; (4) the right to republish the stated material in a collection of articles or in any other format. We also agree that our article be put on the Internet.

Criteria for authorship: The WJG requests and publishes information about contributions of each author named to the submitted study. Authorship credit should be based on (1)direct participation in the study, including substantial contributions to conception and design of study, or acquisition of data, or analysis and interpretation of data; (2) manuscript writing, including drafting the article, or revising it critically for important intellectual content; (3)supportive work, including statistical analysis of data, or acquisition of funding, or administration, technology and materials support, or supervision, or supportive contributions. Authors should meet at least one of the three conditions. The WJG does not publish co-first authors and co-corresponding authors.

We hereby assign copyright transfer to WJG if this paper is accepted.

Author Name in full (Full names should be provided, with first name first, followed by middle names and family name at the last, eg, Eamonn MM Quigley). Handwritten names are not accepted.

Author Name in abbreviation (Family name is put first in full, followed by middle names and first name in abbreviation with first letter in capital, eg, Quigley EMM). Handwritten names are not accepted.

1 Full Name: _____

Abbreviation Name: _____

Signed: _____

Date: _____

2 Full Name: _____

Abbreviation Name: _____

Signed: _____

Date: _____

3 Full Name: _____

Abbreviation Name: _____

Signed: _____

Date: _____

4 Full Name: _____

Abbreviation Name: _____

Signed: _____

Date: _____

5 Full Name: _____

Abbreviation Name: _____

Signed: _____

Date: _____

6 Full Name: _____

Abbreviation Name: _____

Signed: _____

Date: _____

7 Full Name: _____

Abbreviation Name: _____

Signed: _____

Date: _____

8 Full Name: _____

Abbreviation Name: _____

Signed: _____

Date: _____

9 Full Name: _____

Abbreviation Name: _____

Signed: _____

Date: _____

10 Full Name: _____

Abbreviation Name: _____

Signed: _____

Date: _____

Final check list for authors

The format is at: http://www.wjgnet.com/wjg/help/13.doc

Responses to reviewers

Please revise your article according to the comments/suggestions of reviewers. The format for responses to the reviewers' comments is at: http://www.wjgnet.com/wjg/help/10.doc

Proof of financial support

For paper supported by a foundation, authors should provide a copy of the document and serial number of the foundation.

Publication fee

Authors of accepted articles must pay publication fee.
EDITORIAL and LETTERS TO THE EDITOR are free of change.